

Handbook of Extractive Metallurgy

Edited by Fathi Habashi

Volume I: The Metal Industry
Ferrous Metals

 **WILEY-VCH**

Weinheim • Chichester • New York • Toronto • Brisbane • Singapore

Professor Fathi Habashi
Université Laval
Département de Mines et de Métallurgie
Québec G1K 7P4
Canada

This book was carefully produced. Nevertheless, the editor, the authors and publisher do not warrant the information contained therein to be free of errors. Readers are advised to keep in mind that statements, data, illustrations, procedural details or other items may inadvertently be inaccurate.

Editorial Directors: Karin Sora, Ilse Bedrich
Production Manager: Peter J. Biel
Cover Illustration: Michel Meyer/mmad

Library of Congress Card No. applied for
A CIP catalogue record for this book is available from the British Library

Die Deutsche Bibliothek – CIP-Einheitsaufnahme
Handbook of extractive metallurgy / ed. by Fathi Habashi. –
Weinheim ; New York ; Chichester ; Brisbane ; Singapore ; Toronto :
WILEY-VCH ISBN 3-527-28792-2

Vol. 1. The metal industry, ferrous metals. – 1997

Vol. 2. Primary metals, secondary metals, light metals. – 1997

Vol. 3. Precious metals, refractory metals, scattered metals, radioactive metals, rare earth metals. – 1997

Vol. 4. Ferroalloy metals, alkali metals, alkaline earth metals; Name index; Subject index. – 1997

© VCH Verlagsgesellschaft mbH – A Wiley company,
D-69451 Weinheim, Federal Republic of Germany, 1997

Printed on acid-free and low-chlorine paper

All rights reserved (including those of translation into other languages). No part of this book may be reproduced in any form – by photoprinting, microfilm, or any other means – nor transmitted or translated into a machine language without written permission from the publishers. Registered names, trademarks, etc. used in this book, even when not specifically marked as such, are not to be considered unprotected by law.

Composition: Jean François Morin, Québec, Canada
Printing: Strauss Offsetdruck GmbH, D-69509 Mörlenbach
Bookbinding: Wilhelm Oswald & Co., D-67433 Neustadt/Weinstraße

Printed in the Federal Republic of Germany

Preface

Extractive metallurgy is that branch of metallurgy that deals with ores as raw material and metals as finished products. It is an ancient art that has been transformed into a modern science as a result of developments in chemistry and chemical engineering. The present volume is a collective work of a number of authors in which metals, their history, properties, extraction technology, and most important inorganic compounds and toxicology are systematically described.

Metals are neither arranged by alphabetical order as in an encyclopedia, nor according to the Periodic Table as in chemistry textbooks. The system used here is according to an economic classification which reflects mainly the uses, the occurrence, and the economic value of metals. First, the ferrous metals, i.e., the production of iron, steel, and ferroalloys are outlined. Then, nonferrous metals are subdivided into primary, secondary, light, precious, refractory, scattered, radioactive, rare earths, ferroalloy metals, the alkali, and the alkaline earth metals.

Although the general tendency today in teaching extractive metallurgy is based on the fundamental aspects rather than on a systematic description of metal extraction processes, it has been found by experience that the two approaches are complementary. The student must have a basic knowledge of metal extraction processes: hydro-, pyro-, and electrometallurgy, and at the same time he must have at his disposal a description of how a particular metal is extracted industrially from different raw materials and know what are its important compounds. It is for this reason, that this *Handbook* has been conceived.

The *Handbook* is the first of its type for extractive metallurgy. Chemical engineers have already had their Perry's *Chemical Engineers' Handbook* for over fifty years, and physical metallurgists have an impressive 18-volume *ASM Metals Handbook*. It is hoped that the

present four volumes will fill the gap for modern extractive metallurgy.

The *Handbook* is an updated collection of more than a hundred entries in *Ullmann's Encyclopedia of Industrial Chemistry* written by over 200 specialists. Some articles were written specifically for the *Handbook*. Some problems are certainly faced when preparing such a vast amount of material. The following may be mentioned:

- Although arsenic, antimony, bismuth, boron, germanium, silicon, selenium, and tellurium are metalloids because they have covalent and not metallic bonds, they are included here because most of them are produced in metallurgical plants, either in the elemental form or as ferroalloys.
- Each chapter contains the articles on the metal in question and its most important inorganic compounds. However, there are certain compounds that are conveniently described together and not under the metals in question for a variety of reasons. These are: the hydrides, carbides, nitrides, cyano compounds, peroxo compounds, nitrates, nitrites, silicates, fluorine compounds, bromides, iodides, sulfites, thiosulfates, dithionites, and phosphates. These are collected together in a special supplement entitled *Special Topics*, under preparation.
- Because of limitation of space, it was not possible to include the alloys of metals in the present work. Another supplement entitled *Alloys* is under preparation.
- Since the largest amount of coke is consumed in iron production as compared to other metals, the articles "Coal" and "Coal Pyrolysis" are included in the chapter dealing with iron.

I am grateful to the editors at VCH Verlagsgesellschaft for their excellent cooperation, in particular Mrs. Karin Sora who followed the project since its conception in 1994, and to

Jean-François Morin at Laval University for his expertise in word processing.

The present work should be useful as a reference work for the practising engineers and the students of metallurgy, chemistry, chemical engineering, geology, mining, and mineral beneficiation. Extractive metallurgy and the chemical industry are closely related; this *Handbook* will

therefore be useful to industrial chemists as well. It can also be useful to engineers and scientists from other disciplines, but it is an essential aid for the extractive metallurgist.

Fathi Habashi

Table of Contents

<i>Volume I</i>		<i>Part Seven</i>	Refractory Metals
<i>Part One</i>	The Metal Industry		26 Tungsten.....1329
	1 The Economic Classification of Metals.....1		27 Molybdenum.....1361
	2 Metal Production.....15		28 Niobium.....1403
	3 Recycling of Metals.....21		29 Tantalum.....1417
	4 By-Product Metals.....23		30 Zirconium.....1431
<i>Part Two</i>	Ferrous Metals		31 Hafnium.....1459
	5 Iron.....29		32 Vanadium.....1471
	6 Steel.....269	<i>Part Eight</i>	Scattered Metals
	7 Ferroalloys.....403		34 Germanium.....1505
<i>Volume II</i>			35 Gallium.....1523
<i>Part Three</i>	Primary Metals		36 Indium.....1531
	8 Copper.....491		37 Thallium.....1543
	9 Lead.....581		38 Selenium.....1557
	10 Zinc.....641	<i>Part Nine</i>	Radioactive Metals
	11 Tin.....683		40 General.....1585
	12 Nickel.....715		41 Uranium.....1599
<i>Part Four</i>	Secondary Metals		42 Thorium.....1649
	13 Arsenic.....795		43 Plutonium.....1685
	14 Antimony.....823	<i>Part Ten</i>	Rare Earth Metals
	15 Bismuth.....845		44 General.....1695
	16 Cadmium.....869		45 Cerium.....1743
	17 Mercury.....891	<i>Volume IV</i>	
	18 Cobalt.....923	<i>Part Eleven</i>	Ferroalloy Metals
<i>Part Five</i>	Light Metals		46 Chromium.....1761
	19 Beryllium.....955		47 Manganese.....1813
	20 Magnesium.....981		48 Silicon.....1861
	21 Aluminum.....1039		49 Boron.....1985
	22 Titanium.....1129	<i>Part Twelve</i>	Alkali Metals
<i>Volume III</i>			50 Lithium.....2029
<i>Part Six</i>	Precious Metals		51 Sodium.....2053
	23 Gold.....1183		52 Potassium.....2141
	24 Silver.....1215		53 Rubidium.....2211
	25 Platinum Group Metals.....1269		54 Cesium.....2215

	55 Alkali Sulfur Compounds.....	2221
<i>Part</i>	Alkaline Earth Metals	
<i>Thirteen</i>	56 Calcium.....	2249
	57 Strontium.....	2329
	58 Barium.....	2337
	Authors.....	2355
	Name Index.....	2375
	Subject Index.....	2379

Part One

The Metal Industry

																Nonmetals				H	He
Li	Be											Metalloids		B	C	N	O	F	Ne		
Na	Mg	Al	Metals										Si	P	S	Cl	Ar				
K	Ca	Sc	Ti	V	Cr	Mn	Fe	Co	Ni	Cu	Zn	Ga	Ge	As	Se	Br	Kr				
Rb	Sr	Y	Zr	Nb	Mo	Tc	Ru	Rh	Pd	Ag	Cd	In	Sn	Sb	Te	I	Xe				
Cs	Ba	La [†]	Hf	Ta	W	Re	Os	Ir	Pt	Au	Hg	Tl	Pb	Bi	Po	At	Rn				
Fr	Ra	Ac [†]																			
†	Ce	Pr	Nd	Pm	Sm	Eu	Gd	Tb	Dy	Ho	Er	Tm	Yb	Lu							
‡	Th	Pa	U	Np	Pu	Am	Cm	Bk	Cf	Es	Fm	Md	No	Lr							

1 The Economic Classification of Metals

FATHI HABASHI

1.1	Introduction.....	1	1.3.4	Precious Metals	8
1.2	Ferrous Metals	1	1.3.5	Refractory Metals.....	8
1.2.1	Steel.....	1	1.3.6	Scattered Metals.....	10
1.2.2	Wrought Iron	2	1.3.7	Radioactive Metals.....	10
1.2.3	Cast Irons.....	2	1.3.8	Rare Earths.....	12
1.2.4	Pure Iron	3	1.3.9	Ferroalloy Metals.....	12
1.3	Nonferrous Metals.....	3	1.3.10	Alkali Metals	12
1.3.1	Primary Metals	3	1.3.11	Alkaline Earth Metals.....	13
1.3.2	Secondary Metals	5	1.4	References	13
1.3.3	Light Metals.....	6			

1.1 Introduction

While the Periodic Table classifies metals, metalloids, and nonmetals according to their chemical properties, it does not indicate their relative economic value. The fact that iron and its alloys, e.g., steel, are by far the most important metals from the point of view of production and use, has resulted in the classification of metals as ferrous (iron and its alloys) and nonferrous (all other metals and metalloids). This classification is well justified: the annual production of iron in one year exceeds the production of all other metals combined in ten years.

1.2 Ferrous Metals

Iron produced in the blast furnace (pig iron) is converted into the following commercial products: Steel, wrought iron, cast irons, and pure iron. Table 1.1 shows typical analysis of these products; steel is the most important product. Chemically pure iron is prepared on a small scale because of its limited use.

Table 1.1: Typical analysis of ferrous materials.

	Pig iron	Cast iron	White cast iron	Steel	Wrought iron
C	3.5-4.25	2.50-3.75	1.75-2.70	0.10	0.02
Si	1.25	0.50-3.00	0.8-1.20	0.02	0.15
Mn	0.90-2.50	0.40-1.00	< 0.4	0.40	0.03
S	0.04	0.01-0.18	0.07-0.15	0.03	0.02
P	0.06-3.00	0.12-1.10	< 0.02	0.03	0.12
Slag	0	0	0	0	3.00

1.2.1 Steel

Steel is made on a large scale by blowing oxygen and powdered lime through molten iron to oxidize the impurities. According to their use, steels are divided into three main groups:

Constructional Steel. This is used for the manufacture of machine parts, motor cars, building elements, sky scrapers, ships, bridges, war instruments (cannons, tanks, etc.), and containers. It can be carbon or alloy steel. The mechanical properties of alloy steel are considerably higher than those of carbon steel. Chromium and nickel are the main alloying elements used in this category.

Tool Steel. This is used for the manufacture of tools (lathe knives, chisels, cutters, etc.). It is either carbon (0.7-1.2% C), or chromium, manganese, silicon, or tungsten alloy steel. Manganese alloy steels are used to make machines such as rock crushers and power shovels, which must withstand extremely hard use.

Special-Quality Steel. These include corrosion-resisting, stainless, acid-resisting, and heat-resisting steels. Stainless steel, which contains chromium and sometimes nickel and manganese, is a hard, strong alloy that resists heat and corrosion. Stainless steels are used for such things as jet engines, automobile parts, knives, forks, spoons, and kitchen equipment.

1.2.2 Wrought Iron

Wrought iron was known since antiquity and was the major ferrous material produced until the nineteenth Century; it is produced now in limited amounts. Wrought iron is practically pure iron, low in carbon, manganese, sulfur, and phosphorus, but contains an appreciable amount of slag in mechanical admixture. Its desirable properties are due to the fibrous structure of this slag which gives it excellent resistance to shock and vibration, making it particularly suitable for the manufacture of such products as engine bolts, crane hooks, lifting chains and couplings. Wrought iron is readily welded, and the presence of slag makes it self-fluxing. It is readily machinable and cuttings are sharp and clean because the chips crumble and clear the dies instead of forming long spirals. Wrought iron is made from pig iron by melting in a furnace lined with ferrous oxide. Under these conditions, the entire carbon content of the pig iron is oxidized and removed, as well as most of the other impurities while silicon forms slag. As a result, the melting point of the mass increases and a sticky lump is obtained saturated with slag. The lump, which weighs about 200 kg is removed from the furnace then put through a squeezer to remove as much slag as possible.

1.2.3 Cast Irons

Cast iron is a series of iron-carbon alloys containing more than 1.5% C, together with silicon, manganese, phosphorus, and sulfur which are impurities from the raw material and are not alloying elements. The form in

which carbon is present in the cast iron determines its properties.

Grey Cast Iron. Produced by melting pig iron, scrap iron, and steel mixture to give the cast iron composition. The slow cooling and the high silicon content favors the decomposition of cementite into iron and free carbon in the form of flakes. Gray cast iron is characterized by its power to damp vibrations and by the wear resistance imparted by the lubricating effect of graphite. Both properties make it a useful material for the construction of machinery by casting. It is readily machinable (due to graphite flakes) and is an economic material since it has a low melting point of about 1200 °C. It has, however, poor toughness and limited tensile strength.

White Cast Iron. Produced by melting pig iron and steel scrap. After solidification no carbon is precipitated but remains in combination as iron carbide. It is hard, brittle, and unmachinable. It is used for making grinding balls, dies, car wheels, but mostly used for making malleable cast iron.

Malleable Cast Iron. Prepared from white cast iron by annealing for several days, whereby iron carbide is decomposed into iron and graphite in form of nodules. It is more ductile and more resistant to shock than grey cast iron. It is used in large quantities for such materials as pipes and pipe fittings and the automotive industry requiring higher mechanical properties.

Ductile Cast Iron. It is a high-carbon ferrous product containing graphite in the form of spheroids. The spheroid is a single polycrystalline particle, whereas the nodule is composed of an aggregate of fine flakes. Ductile cast iron has all the advantages of cast iron, e.g., low melting point, good fluidity and castability, ready machinability, and low cost, plus the additional advantages of high yield strength, high elasticity, and a substantial amount of ductility. It is used by the automotive, agricultural instruments and railroad industries, pumps, compressors, valves, and textile machinery. Ductile cast iron is pro-

duced from any cast iron by introducing a small amount of magnesium (in form of a magnesium-nickel alloy containing 50–80% Ni), or cerium into the molten iron while in the ladle, shortly before casting. This addition catalyzes the decomposition of carbon into spheroids and not flakes.

1.2.4 Pure Iron

High-purity iron possesses temporary magnetism, i.e., when the magnetic field is removed, the magnetism disappears. Carbon-iron alloys on the other hand, show permanent magnetism. For this as well as for other reasons, e.g., studying the physical properties of the metal, the preparation of high-purity iron is of scientific interest. Preparation of pure iron is a tedious process that requires special techniques and numerous operations.

1.3 Nonferrous Metals

The nonferrous metals are divided into numerous groups according to their production,

properties, use, and occurrence (Table 1.2). This classification is arbitrary since one metal may be placed in two groups, e.g., titanium is both a light and a refractory metal, rhenium is both scattered and refractory; similarly hafnium. The term "rare metals" is sometimes applied to the refractory, scattered, radioactive, and the lanthanides collectively. This terminology is misleading because such metals are not rare; it may be the difficulty in their extraction and uncommon utilization that give the impression that they are rare.

1.3.1 Primary Metals

While iron is the most widely used metal, it lacks important properties such as corrosion resistance. From the beginning of the Nineteenth Century, copper, nickel, lead, zinc, and tin and their alloys found use as substitutes for iron in industrial applications that required particular properties in which cast irons and steels were lacking. That is one reason why these metals are known as primary metals. (Table 1.3).

Table 1.2: Commercial classification of nonferrous metals and metalloids.

Group	Metals	Remarks
Primary	Cu, Pb, Zn, Sn, Ni	Extensively used; second in importance to iron.
Secondary	As, Sb, Bi, Cd, Hg, Co	Mainly by-products of primary metals but also form their own deposits. Used in almost equal amounts (10–20 thousand tons annually).
Light	Be, Mg, Al, Ti	Low specific gravity (below 4.5), used mainly as material of construction.
Precious	Au, Ag, Pt, Os, Ir, Ru, Rh, Pd	Do not rust; highly priced.
Refractory	W, Mo, Nb, Ta, Ti, Zr, Hf, V, Re, Cr	Melting points above 1650 °C. Mainly used as alloying elements in steel but also used in the elemental form. Some resist high temperature without oxidation.
Scattered	Sc, Ge, Ga, In, Tl, Hf, Re, Se, Te	Do not form minerals of their own. Distributed in extremely minute amounts in the earth's crust.
Radioactive	Po, Ra, Ac, Th, Pa, U, Pu	Undergo radioactive decay. Some of them (U, Pu, and Th) undergo fission. Plutonium prepared artificially in nuclear reactors.
Rare earths	Y, La, Ce, Pr, Nd, Sm, Eu, Gd, Tb, Dy, Ho, Er, Tm, Yb, Lu	Always occur together, similar chemical properties. Not rare as the name implies.
Ferroalloy metals	Cr, Mn, Si, B	Were once mainly used as alloying elements to steel, but now also used in elemental form.
Alkali	Li, Na, K, Rb, Cs	Soft and highly reactive.
Alkaline earths	Be, Mg, Ca, Sr, Ba	Higher melting point and less reactive than the alkali metals

Table 1.3: Typical uses of primary metals.

Metal	Use	%
Copper	Electrical	50
	Buildings	20
	Engineering and transport	25
	Other	5
		100
Lead	Batteries	35
	Pipes, sheets	15
	Gasoline additive	12
	Cable sheathing	10
	Pigments, chemicals	10
	Alloys, solder	10
	Other	7
		100
Zinc	Galvanizing	40
	Die casting	27
	Alloys	18
	Sheet, wire, etc.	8
	Zinc compounds	5
	Other	2
		100
Tin	Tinplate	50
	Solder	20
	Alloys	15
	Chemicals	3
	Other	12
		100
Nickel	Stainless steel	28
	Cast irons and alloy steels	20
	Nonferrous alloys	20
	High-temperature alloys	12
	Electroplating	16
	Catalysts	1
	Other	3
		100

Copper. The high heat conductivity of copper makes it a suitable material of construction for heat conducting devices such as heating or cooling coils, boiling kettles, and other parts of chemical engineering apparatus. Because of its high electrical conductivity it became the chief material for conductors, contacts, and other electroconductive parts. It is used only as a pure metal since traces of impurities greatly reduce this property. However, pure copper is too soft for structural components of machines and apparatus. Its alloys with other metals are much stronger and many of them surpass copper in other properties, e.g., in corrosion resistance.

Alloys of copper with 10 to 40% Zn are called brass. They are cheaper than pure cop-

per, can readily be shaped and machined, and are strong, hard and resistant to corrosion. They find extensive application in chemical and general machine-building, ship-building and military engineering. Bronze is an alloy of copper with 6 to 20% tin that found extensive use because of its excellent mechanical, anti-friction, and anticorrosion properties. Alloys similar to bronze are prepared by admixing metals other than tin to copper, e.g., aluminum (5–11%), lead (25–33%), silicon (4–5%), and beryllium (1.8–2.3%). Aluminum bronzes with additions of lead are suitable for bearings while beryllium bronzes are used in the manufacture of springs. Copper-nickel alloys (5–35% Ni) and German silver (5–30% Ni and 13–45% Zn) are particularly resistant to attack by aggressive media. They are used to make medical instruments, home appliances, and works of art. Copper was the first among non-ferrous metals in world output until 1958 when it was moved to second place by aluminum. In electrical engineering, copper is more and more being replaced by aluminum, which is less electroconductive, but lighter.

Nickel. As compared to other heavy nonferrous metals, nickel is stronger, harder, more refractory and more corrosion resistant. Similar to iron and cobalt, it is ferromagnetic. It is relatively expensive and its consumption as a pure metal is low. Nickel is used for plating metals with a view to protect them against corrosion and for ornamental purposes. Nickel sheets, pipes, and wire are used for special components of apparatus and instruments in the chemical industry. Nickel is also required for the manufacture of certain types of batteries which are lighter, more compact and dependable in operation than lead batteries. Nickel catalysts find their application in many chemical processes.

More than half of nickel is consumed in the manufacture of nickel-iron alloys. Chromium-nickel, stainless, and acid-resistant steels, commonly containing up to 8% Ni and with admixtures of chromium and other metals, are widely used in the chemical industry, machine tool manufacture, building of durable

structures, general machine building, and military engineering. Strong and wear-resistant nickel cast irons, alloyed with chromium, molybdenum, and copper, are necessary for the manufacture of heavy internal combustion engines for locomotives and of special machine tools and dies.

Many nickel alloys are chemically resistant and can withstand temperatures up to 600 °C. They are used for turbines of jet aircraft, gas turbine power plants, and in nuclear reactors. Nichrome (75–85% Ni, 10–20% Cr, the balance iron) and other similar thermoelectric nickel alloys are not only refractory, but possess high electrical resistance and are suitable for wire or strip resistor heaters. Strongly, magnetic alloys of nickel with iron (permalloys) and other similar alloys find extensive application in electrical and radio engineering. Alloys of nickel with copper have been mentioned earlier.

Lead. Lead was used to make coins, ornaments, miscellaneous vessels, and water pipes. With the invention of gun powder, it found use for the manufacture of case-shot, bullets, and shot. Abilities of lead to resist attack by dilute sulfuric and hydrochloric acids and many other chemicals have made the metal the chief material for the chemical industry in the 19th century. Lead is amenable to rolling: sheets 2 to 10 mm thick are suitable for anti-corrosion coating of various apparatus. Sheaths of electric cables intended for prolonged underground service, in water or moist surroundings are made from lead blended with small amounts of other metals to enhance its plasticity. Lead storage batteries are necessary to start internal combustion engines. About half of the lead produced is used in the manufacture of electric cables and storage batteries. In nuclear engineering, lead serves as a shield against γ -rays.

Lead alloys differ from the pure metal either by greater strength and hardness or by anti-friction properties, and most of the alloys are resistant to corrosion. Printing alloys for casting type contain antimony, tin, and copper in addition to lead. Antimony makes the alloys

hard, while tin greatly improves their castability. Alloys of lead and antimony, hard and corrosion-resistant, find extensive use in chemical engineering. In soldering alloys, or solders, lead may partly replace tin.

Zinc. Zinc protects iron against corrosion in the air and in cold water. More than half of zinc output is consumed for this purpose. Zinc-plating (galvanizing) is considerably cheaper than tin-plating or nickel-plating. Another important field of application is the manufacture of alloys, inclusive of the already mentioned brases and German silver. Zinc-based alloys, partly employed instead of bronzes and low-friction alloys in bearings, contain aluminium (8–11%), copper (1–2% and magnesium (0.03–0.06%). Identical components, but in a different ratio to zinc, are contained in printing alloys, similar in properties to lead-antimony alloys.

Tin. Used in tin-plating, solders, bronze and other alloys. At one time was used for wrapping purposed in form of tinfoil.

1.3.2 Secondary Metals

This group includes the metals cadmium, cobalt, and mercury and the metalloids arsenic, antimony, and bismuth. They are mainly by-products of the primary metals but also form their own deposits. They are used worldwide in almost equal amounts of about 20 000 tons annually (Table 1.4).

Cadmium. Cadmium is used in the metallic form in electroplating and alloying. Cadmium compounds are used in paints and pigments; cadmium sulfide is yellow, and cadmium selenide is red. Cadmium compounds are toxic and therefore care must be taken during processing cadmium and its compounds to avoid inhalation or dispersal of cadmium fumes and dust or the release of cadmium-bearing effluents into the environment.

Cobalt. This metal is used principally in heat and corrosion-resistant alloys, in jet engine parts, and in magnets. It also serves as a binder material in tungsten and other carbide cutting

tools, and in hardfacing alloys. Nonmetallic applications (paint drier, ceramics, and catalysts) account for about 20% of its consumption.

Table 1.4: Typical uses of secondary metals.

Metal	Use	%
Antimony	Batteries	47
	Pigments, chemicals	18
	Fire retardants	11
	Rubber, plastics	8
	Glass, ceramics	6
	Bearing alloys	4
	Other	6
		100
Cadmium	Cadmium plating	50
	Plastics stabilizer	20
	Pigments	15
	Ni-Cd batteries	7
	Other	8
		100
Cobalt	Alloys	45
	Magnets	30
	Paint driers	10
	Ceramics	5
	Catalysts	5
	Other	5
		100
Mercury	Caustic-chlorine cells	35
	Batteries, electrical	28
	Biocidal paints	14
	Instruments	10
	Dental	5
	Agriculture	3
	Other	6
		100

Mercury. In older times mercury was principally used for the recovery of gold and silver from their ores by amalgamation, a process that is now obsolete because of the poisonous nature of the metal vapor. It is now used as a liquid cathode in chlorine and sodium hydroxide manufacture. The mercury lamps use and electric discharge tube that contains mercury vapor; they are more efficient as a light source. Mercury is also used in electrical switching devices, in thermometers and barometers, as an alloy with silver and tin for dental applications. Nonmetallic applications include mercuric oxide in batteries, in certain organic preparations as fungicide, bactericide, or preservative.

Arsenic. Arsenic is regarded as a troublesome impurity in smelting and refining and must be removed during the recovery of the primary metals. Its compounds are toxic and therefore their handling in a plant is costly because of the strict anti-contamination measures. Its consumption in the metallic form is only 3% of the total; it is mostly used as compounds. As metal, it is used as a minor additive in non-ferrous alloys (copper and lead based) to improve their strength, and sometimes to improve corrosion resistance. In the electronic industry, high-purity arsenic is combined with gallium and/or indium for making semiconductors, solar cells, infrared detectors, light-emitting diodes, and lasers. Arsenic compounds are mainly used as herbicides and insecticides.

Antimony. Antimony is mainly used as an alloying constituent of lead, e.g., to harden lead for storage batteries, and as alloying element in bearings, type metal, and solder. In compound form antimony trioxide is used in ceramic enamels in plastics, as a white pigment, and as flame retardant.

Bismuth. Bismuth is mainly used for the manufacture of low-melting alloys (m.p. as low as 60 °C) which are used for making safety plugs.

1.3.3 Light Metals

These are beryllium, aluminum, magnesium, and titanium. They are used in pure state and in alloys, characterized by light weight and high strength hence they are valuable materials of construction (Table 1.5). They are reactive metals and difficult to prepare and became known in the metallic state relatively recent.

Beryllium. Beryllium is an expensive metal used in small and specialized industries. Its dust and fumes as well as vapors of its compounds are poisonous to inhale. It is fabricated by powder metallurgy techniques because coarse grains tend to develop in the castings causing brittleness and low tensile strength. About 10% of the metal is used in the metallic

form, 80% in form of beryllium-copper alloys (containing about 2% Be), or other master alloys, and the remaining 10% is used as a refractory oxide. In the metallic form it is used as a moderator to slow down fast neutrons in nuclear reactors because of its low atomic weight and low neutron cross section. As an alloy with copper, it is particularly important in springs because such alloys possess high elasticity and great endurance.

Table 1.5: Typical uses of light metals.

Metal	Use	%
Beryllium	Electric industry	37
	Electronic industry	16
	Nuclear reactors	20
	Aerospace	18
	Others	9
		100
Aluminum	Buildings	30
	Transportation (automotive, aircrafts)	20
	Electrical	15
	Packaging	15
	Others (reducing agent, paint)	20
		100
Titanium	Jet engine	84
	Chemical industry	16
		100
Magnesium	As metal and alloy (reducing agent)	65
	As oxide for refractories	7
	Fertilizer, paper, etc.	28
		100

Aluminum. Pure aluminum often replaces copper in electrical engineering. Although its electrical conductivity is only 65% that of copper, the density of aluminum is almost three times as less (Cu 8.95, Al 2.7). This means a lesser consumption of the metal. Also suspension of aluminum conductors requires fewer poles than that for copper. Pure aluminum is soft, but, if alloyed with small additions of other elements its mechanical strength increases. Aluminum alloys combine strength, lightness, and corrosion resistance. Its large scale production started in the first quarter of this century when aeronautics was then making its first steps. Today it finds wide application in building construction. Aluminum alloys containing silicon are used in casting, cylinders, pistons, and other parts of

aircraft and automotive engines as they readily reproduce mould configuration; they are also light and strong.

The surface of aluminum and of its alloys is always coated by a thin but strong layer of Al_2O_3 which protects it against further oxidation. The film is extra strong if it is obtained by anodic oxidation. The film can readily be dyed in many colors and this is widely used. The strength of the surface films and its harmlessness to users make aluminum suitable for the manufacture of various equipment in the food industry. In the form of foil it is used for packing foodstuffs. Aluminum powder is also used in the manufacture of paint. The strong affinity of aluminum makes it suitable for preparing metals from their oxides. Because of its abundance in the Earth's crust, the metal is more likely to be used as a substitute to wood, plastics, and other construction materials. Nonmetallic applications of aluminum account for about 10% of the element. Bauxite and alumina are used as refractories, fused alumina is used in abrasives, aluminum sulfate is used in water treatment.

Magnesium. Magnesium is lighter than aluminum resists poorly the action of atmospheric air, particularly when moist but its alloys with aluminum, zinc, and manganese are adequately corrosion resistant. These alloys, readily castable and machinable, have a wide application in the manufacture of aircraft, automotive industry, and in rockets. The high affinity of magnesium for oxygen allows its use as a reducing agent for metallothermic reactions, e.g., production of titanium and uranium. The high affinity of magnesium for oxygen and its ability to burn in the air with evolution of large quantities of heat and light makes it suitable in the manufacture of incendiary shells and flares. The main application of magnesium at present is an oxide used as a refractory brick for furnace lining. A large amount of this material is prepared from sea water.

Titanium. Titanium is somewhat heavier than magnesium and aluminum, but it is stronger and very resistant to corrosion. Titanium and

its alloys resist heat up to 450 °C, whereas aluminum and magnesium alloys tend to fail at about 300 °C. That is why titanium alloys became the basic materials for jet aircraft. Titanium alloys are used for the manufacture of jet engines, rockets, and shells of satellites. The largest application of titanium is an oxide used as a white pigment.

1.3.4 Precious Metals

This group of metals is composed of gold, silver, and the six platinum group metals: platinum, osmium, iridium, ruthenium, rhodium, and palladium. They are all common in that they do not rust, and are highly priced (Table 1.6).

Table 1.6: Typical uses of precious metals.

Metal	Use	%
Gold	Jewelry and arts	70
	Dental	9
	Space and defence	8
	Other	13
		100
Silver	Silverware	29
	Photography	28
	Electrical	22
	Brazes, solder	10
	Silver batteries	3
	Other	8
		100
Platinum	Catalysts	60
	Electrical	17
	Glass forming	9
	Dental, medical	5
	Jewelry, etc.	4
	Other	5
		100

Gold. A large part of the world's gold supply is held by governments and central banks, to provide stability for paper currency, and as a medium for settling international trade balances. The unit of gold purity is called karat, it is 1/24¹. A 22-karat gold, for example, is an alloy containing 22 parts gold and 2 parts other ingredients, usually silver; hence it contains 91.67% gold and 8.33% silver. A large part is also used in jewellery, arts, in dentistry, and in coins.

¹ A carat is also the unit of trade (200 mg) of diamonds.

- All the gold ever mined in the world would fit into a store room measuring 17 metres long, 17 metres high, and 17 metres wide.
- The American Federal Reserve Bank on Wall Street is the biggest repository of gold in the world: some 13 000 tons of gold are kept behind 90 ton steel doors in vaults blasted out of solid granite.
- Gold is used in the electronics industry to make more than 10 billion tiny electrical contacts every year.
- Of the estimated 100 000 tons of refined gold in the world – bullion, jewellery, coin – no less than 40 000 tons, or 40% was mined in South Africa since 1886.
- Over 50 tons of gold are used every year by the world's dentists.
- Italy is by far the biggest user of gold for the manufacture of jewellery: about 250 tons annually, enough to make 100 million wedding rings.

Silver. Pure silver is too soft for many applications and an alloy of silver and copper is commonly used. Silver is used as an ornamental metal for tableware and in coins. It is also commonly used in plating articles made of cheaper metals, in fabricating mirrors, and in preparation of silver salts used in photography.

Platinum. Platinum is an important contact catalyst in the chemical industry e.g., oxidation of ammonia. It has also important uses in the electrical industry, in dentistry, in jewellery, and in laboratory ware.

1.3.5 Refractory Metals

This group of metals is composed of the transition metals tungsten, molybdenum, niobium, tantalum, titanium, zirconium, hafnium, vanadium, rhenium, and chromium. All these metals have high melting points. For example, tungsten melts at 3380 °C, rhenium at 3180 °C, molybdenum at 2610 °C. They are mainly used as alloying elements in steel but also are used in the elemental form. Some resist high temperature without oxidation, and

some are very hard, having excellent wear and abrasion resistance (Table 1.7).

Table 1.7: Typical uses of refractory metals.

Metal	Use	%
Vanadium	Ferrous alloys	80
	Nonferrous alloys	10
	Catalyst (V ₂ O ₅)	10
		100
Chromium	Metallurgical (stainless steel)	58
	Refractories (oxide)	30
	Chemical industry (tanning of leather, electroplating)	12
		100
Molybdenum	Steel industry	80
	Chemicals	20
		100
Tungsten	Tungsten carbides	53
	Alloy steels	23
	Electrical lamps	13
	Chemicals	4
	Other	7
		100

Tungsten. Tungsten has the highest melting point of all metals; it also has one of the highest densities. When combined with carbon, it becomes one of the hardest man-made materials. While the tungsten filaments for light bulbs are widely used, its most common and most valuable use is in metal cutting, mining, and oil drilling tools. Although tungsten can be used at high temperatures, an oxide film forms which is volatile above temperature of approximately 540 °C. So, for use at extremely high temperatures, tungsten parts must be coated, used in a vacuum, or be surrounded by a protective atmosphere. Typical uses involving protective atmospheres – or vacuum – include incandescent lamp filaments, electron tube electrodes, and various types of heating elements. Silicide coating and noble metal cladding are effective oxidation-resisting coatings, for example, cladding the tungsten with a platinum gold alloys.

Tungsten is resistant to many severe environments which readily attack other metals. It resists nitric, sulfuric, and hydrofluoric acids at room temperatures. It is only subject to slight attack by hot alkaline solutions such as potassium, sodium, and ammonium hydroxides. Tungsten also has good resistance to sev-

eral liquid metals including sodium, mercury, gallium, and magnesium; to oxide ceramics such as alumina, magnesia, zirconia and thorium. It is often used for crucibles to melt these materials in an inert atmosphere.

Molybdenum. Molybdenum is hard with respect to tensile stresses. Its electric and heat conductivities are somewhat lower than those of tungsten. When heated without access of air, it is readily amenable to mechanical working and can be drawn into a thin wire. It retains strength up to temperatures of about 1000 °C. It is used in parts of vacuum apparatus, e.g., hooks for filaments in electric bulbs, targets of X-ray tubes, heaters of high-temperature furnaces, plates of generator and rectifier tubes. Molybdenum steels possess a high mechanical strength, wearability and impact strength. Because molybdenum oxidizes rapidly at about 600 °C in air, a protective coating is needed in hot air applications. Many coatings involve formation of a thin layer of MoSi₂ on the surface of the molybdenum part. The compound has outstanding oxidation resistance up to about 1650 °C. In vacuum, uncoated molybdenum has a virtually unlimited life at high temperature.

Vanadium is mainly used as an alloying element in steel, in titanium alloys, and in some high-temperature alloys. In form of V₂O₅ it is used as a catalyst for oxidation reactions (SO₂ to SO₃).

Niobium. The major use of niobium is as an alloying element for steel. It also offers lower density and low thermal neutron cross section compared to other refractory metals, which makes niobium useful in atomic reactors. At ordinary temperatures niobium will resist attack by all mineral acids, with the exception of hydrofluoric acid, and it is not affected by mixed acids such as aqua regia.

Tantalum. Tantalum is one of the most corrosion resistant materials available. It forms stable anodic oxide films which make excellent electronic capacitors.

Rhenium. Rhenium has a melting point exceeded only by tungsten, density exceeded

approximately 10% the industrial demand. At the beginning of this century, shortly after the discovery of radioactivity, uranium ores were exclusively treated for their radium content to be used for medical purposes while uranium was rejected. It was only after the discovery of fission that this tendency was reversed. Highly enriched uranium, used for weapons needs, has more than 90% ^{235}U .

1.3.8 Rare Earths

This group of 13 metals always occur together and have similar chemical properties. These are cerium, praseodymium, neodymium, samarium, europium, gadolinium, terbium, dysprosium, holmium, erbium, thulium, ytterbium, and lutetium. Another member of this group is promethium, whose position in the Periodic Table is between neodymium and samarium does not occur in nature but is found in the fission products of uranium. To this group is always added lanthanum and yttrium because they also have similar properties and are associated with these metals in nature. These metals are not rare – they are widely distributed in nature and it is preferable to call them the lanthanides in reference to the first member of the group. They form their own ore deposits and also occur in phosphate rock, in iron ores, and others.

The annual consumption of lanthanides is about 30 000 tons. They are finding use as deoxidizers, in alloys, in the production of cast iron and steel, as catalysts, in lighter flints and flares, in the glass and ceramic industry, in optical glass as well as glass polishers, in the manufacture of ferrites for use as magnetic materials for electric motors, electronic circuits, and computers. Europium and yttrium are used in the manufacture of phosphors, producing the bright reds and greens of color television. Because of neutron-absorption properties they are used in the manufacture of control rods in nuclear reactors. They have many other applications, e.g., in the production of more efficient fluorescent lighting, portable X-ray sources, better X-ray screens, fiber

optics, quick-drying paints, synthetic gems, and others.

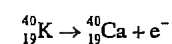
1.3.9 Ferroalloy Metals

This group of metals is composed of chromium, manganese, silicon, and boron. They were once mainly used as alloying elements to steel in form of ferroalloys but now are also used in the elemental form. Thus chromium is used as a protective coating by electroplating on iron, silicon is used in the preparation of semiconductors and to convert energy from the sun directly into electricity. Manganese is used as an alloying element with aluminum and copper. Manganese dioxide is a powerful oxidizing agent. Boron carbide and boron nitride are hard materials second only to diamond.

1.3.10 Alkali Metals

This is the first group in the Periodic Table. Their name is derived from fact that when reacted with water they form alkalies. Soft and highly reactive, usually not used as metals except lithium as an alloying element for aluminum, sodium as a reducing agent either alone or as an amalgam, and an alloy of 50% Na and 50% K known as NaK is used as a coolant in nuclear reactors. Sodium salts have a variety of applications, e.g., NaCl is a source of chlorine, potassium salts are used as fertilizers.

The economic deposits of the alkali metals are mainly found in nature as salt deposits or in surface and subsurface waters except lithium which may also be found as a silicate; the last member of the group, francium, does not occur in nature. At one time sodium carbonate was recovered from the ashes left after burning wood by leaching with water, while potassium carbonate was recovered similarly but from ashes left after burning seaweeds. One of potassium isotopes that is naturally occurring is radioactive.



1.3.11 Alkaline Earth Metals

This is the second group of the Periodic Table whose name originates from the fact that these metals form stable oxides (earths) that have alkaline reaction. For example, calcium forms the oxide CaO which dissolves in water to form calcium hydroxide. The first two members beryllium and magnesium are of useful mechanical properties and being light, are used as light metals. The last member, radium is radioactive and of no importance as a metal. At the beginning of this century, radium salts were used for treating cancer and for painting phosphorescent watch dials. Of the remaining three, calcium is the most important being used sometimes as a reducing agent. Calcium compounds CaCO_3 (limestone), $\text{CaSO}_4 \cdot 2\text{H}_2\text{O}$ gypsum, and $\text{Ca}_{10}(\text{PO}_4)_6\text{F}_2$ (fluorapatite, the main component of phosphate rock) occur in nature in great amounts and the first two are widely used as material of construction while the third is a source of fertilizers. The pyramids of Egypt were constructed of limestone.

Magnesium is like calcium in forming large deposits, for example, dolomite and magnesite. It is also found in relatively large amounts in sea water. Besides being a light metal it is also used as a reducing agent. Strontium and barium on the other hand, are of limited use.

1.4 References

1. F. Habashi, *Metallurgical Chemistry*, American Chemical Society, Washington, DC, 1987. Audio course (5 cassettes, 5 hours playing time) and manual.
2. F. Habashi, *Principles of Extractive Metallurgy*, volume 1: "General Principles" (1969, reprinted 1980); vol. 2: "Hydrometallurgy" (1970, reprinted 1980); vol. 3: "Pyrometallurgy" (1986, reprinted 1992). Gordon & Breach, Langhorne, PA.
3. N. Sevryukov, B. Kuzmin, Y. Chelishchev, *General Metallurgy*, translated from Russian, Mir Publishers, Moscow 1969.
4. A. Zelikman, O. E. Krein, G. V. Samsonov, *Metallurgy of Rare Metals*, translated from Russian, Israel Program for Scientific Translations, Jerusalem 1966.
5. N. L. Weiss (ed.): *SME Mineral Processing Handbook*, Society of Mining Engineers, AIME, New York 1985.

2 Metal Production

FATHI HABASHI

2.1 The Logarithmic Law	15	2.3 Prices	18
2.1.1 Growth Rate	16	2.4 Metal-Producing Associations and cartels	19
2.1.2 Doubling Period	17	2.5 References	19
2.2 Production Patterns	17		

2.1 The Logarithmic Law

There is usually a gradual increase in the production of most metals. This is due to new ore discoveries, increased population, and the natural development in society.

For most metals, the rate of increase of production follows a logarithmic law (Figures 2.1 and 2.2) and is constant within a certain period of time:

$$\log W_2 - \log W_1 = k(t_2 - t_1)$$

where W_2 and W_1 are the weights of metal produced in time t_2 and t_1 respectively, and k is a constant. This logarithmic law is the same as population growth (Figure 2.3) which is de-

rived from the relation: rate of increase of population at a certain moment is proportional to the number of people at that moment:

$$\frac{dN}{dt} = kN$$

$$\int_{N_1}^{N_2} \frac{dN}{N} = k \int_{t_1}^{t_2} dt$$

$$2.303 \log \frac{N_2}{N_1} = k(t_2 - t_1)$$

Statistical information on metal production are useful in projection of future needs. Some facts can also be deduced from these curves:

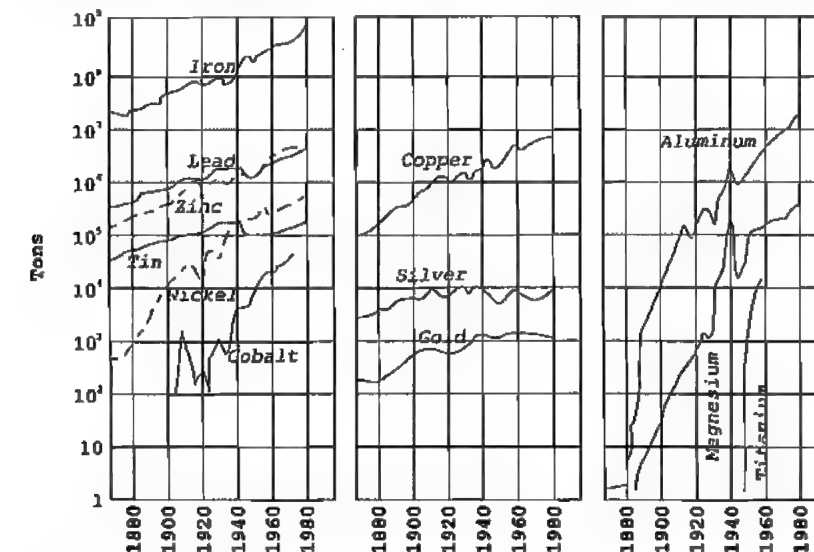


Figure 2.1: Production of metals.

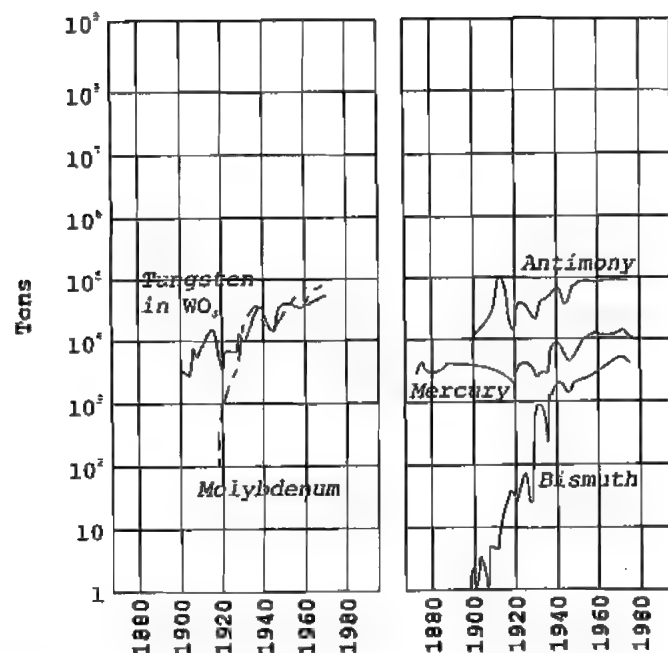


Figure 2.2: Production of metals (continued).

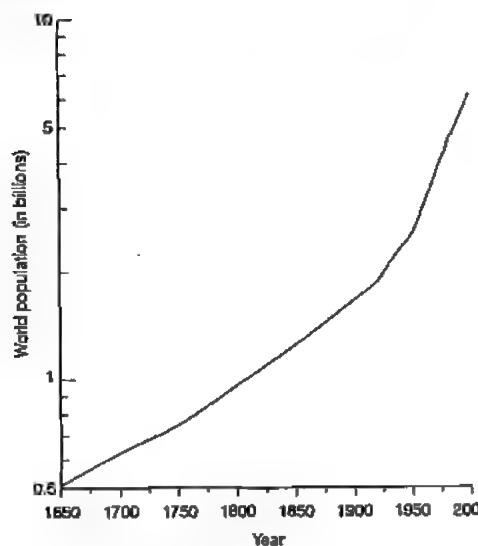


Figure 2.3: World population.

2.1.1 Growth Rate

The constant $k \times 100$, which is the slope of the curves shown in Figures and during a certain period, is called the *growth rate* and is ex-

pressed in percent. For example, the growth rate of copper during the period 1870 to 1910 was 5%, i.e., copper production increased by 5% every year during the period mentioned. The growth rate for metals are not the same; some metals, especially the new ones grow at a faster rate than the old metals. For example:

- The growth rate of nickel is higher than that for lead. The reason for this is that an old metal like lead, once used extensively for constructing equipment for chemical plants, e.g., lead chambers in sulfuric acid plants, is now giving way to the new metal, nickel, which is finding increasing use in the form of stainless steels and for constructing corrosion resistant equipment.
- The growth rate of aluminum is higher than that for copper. The two metals are good electrical and heat conductors, easily worked or machined, and resistant to atmospheric corrosion. Aluminum became cheaper than copper after World War II and is now replacing it in power cables.

2.1.2 Doubling Period

Another way of expressing the rate of growth is the *doubling period*, Δt , i.e., the time required for a certain metal to double its production. This is related to the growth rate by the relation:

$$\Delta t = \frac{2.303 \log 2}{k} = \frac{0.69}{k}$$

Thus, in the case of copper mentioned above, a growth rate of 5%, i.e. $k = 0.05$ means that copper production doubles every 14 years ($\Delta t = 0.69/0.05 \approx 14$) during that period.

2.2 Production Patterns

The maxima in the curves in Figures 2.1 and 2.2 are due to the exceptionally high production rates in time of wars to meet military needs and for stockpiling. On the other hand in time of crises, the curves show exceptionally low production rates, e.g., 1921 and the early 1930s.

With the exception of iron ores and aluminum ores, most ores are complex, i.e., they may yield more than one metal. As a result, the production pattern of a certain metal may also be complex. Table 2.1 shows the production pattern for silver. It can be seen that only 20% of the world's silver comes from silver ores and the rest is by-product of lead, copper, copper-nickel, gold, and tin ores.

Table 2.1: Sources of silver produced worldwide.

Origin	%
Silver ores	20
Lead ores	45
Cu, Cu-Ni ores	18
Gold ores	15
Tin ores	2
	100

A metal may follow the production pattern of another if both occur together in ores. For example:

- Gold and silver usually follow each other because a large part of silver is a by-product of gold production.

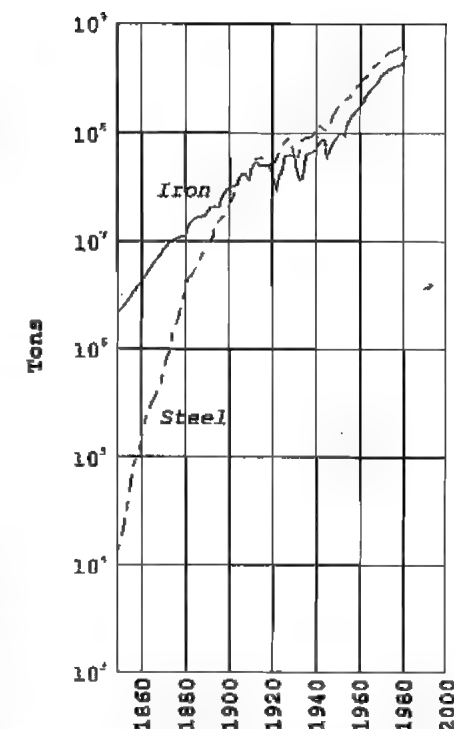


Figure 2.4: World production of iron and steel.

- Lead and zinc have nearly the same production level (as well as the same price). The two metals are closely related in the sense that they always occur together in ores; thus a zinc plant usually produces lead as by-product and vice versa.

Production patterns of metals change as a result of the following factors:

- *Changing technology.* Steel was produced in small amounts until the discovery of the Bessemer Process in 1850s (Figure 2.4). Similarly, the production of aluminum increased rapidly after the discovery of the electrolytic process in 1886, and that of gold after the discovery of the cyanidation process in 1887.
- *Changing application.* The curve for silver shows a slight decrease in production during the past 40 years. It is not so much used as a coinage metal since the introduction of nickel. Otherwise it has the same growth rate as gold.

2.3 Prices

Prices of metals vary from few cents/kg, e.g., iron, aluminum, and lead, to tens of thousands of dollars/kg, e.g., gold and platinum. The price of a metal varies also with the purity, the form whether in powder, ingot, pellets, etc., and the amount sold. There are many factors that control the price of a metal. For example:

Availability of rich deposits. Large iron deposits containing 60% iron are common, while a gold deposit is usually 0.001%. It would, therefore, be expected that iron is cheaper than gold.

Easiness in extraction. A metal that can be extracted by reduction with carbon is usually cheaper than metal that must be extracted by reduction with metallic magnesium (or other metal). For example, lead oxide is reduced by coke while beryllium fluoride is reduced by magnesium. Evidently, lead will be cheaper than beryllium.

Easiness in refining. A metal that can be refined from aqueous solution or can be handled in air when molten will be usually cheaper than a metal that must be refined from fused salts or must be handled in inert atmosphere because of its reactivity. Thus nickel, for example, is cheaper than titanium.

However, there are many exceptions to the above. For example:

- Copper is actually easier to produce than aluminum, yet it is more expensive.
- Tellurium occurs in ores in nearly the same concentration as gold, yet, it is much cheaper.
- Lead is more difficult to refine than nickel, yet, it is cheaper.
- Sodium is more difficult to handle than zinc, yet, it is cheaper.

All these factors combine to give a simple relation: The price of a metal varies inversely with its production. Metals produced in large tonnage are less expensive than those produced in small tonnage. Iron is the cheapest metal while the platinum metals are the most

expensive. Expressed in a different way, cheaper metals are consumed in greater quantities than more expensive ones. Many other commodities fall on the same straight line.

This straight line cannot be explained by the law of supply and demand because if a metal is in great demand its price should rise. This is not the case: iron is in great demand yet its price is the lowest of all metals. The law of supply and demand, however, applies temporarily within certain periods when the production level of a metal is changed. For example, a shut down in the steel industry may lead to an increased price of the metal because of the temporary shortage in supply. When the price reaches a certain high level, production is resumed. This is usually the case when there is a labor conflict. The price of the metal, however, usually does not come back to its original level before the conflict because of the increased cost of its production. Soon after, other industries follow suite, and the prices adjust themselves.

A natural phenomenon in pricing metals is that new metals start with high price, and their price gradually decreases as time goes on due to development in the extractive processes, and also to increase in its production due to increased demand. For example, aluminum started as a very expensive metal, now it is a cheap metal.

The price of the lanthanides (rare earths) requires some clarification. There metals always occur together. To separate a member of the group it is necessary to separate all the others and stock pile them. The cost of producing a desired member is therefore very high. If for instance a use is found for the stock piled material, then price would decrease.

Once the price of an expensive metal is reduced and approaches another metal, substitution for a particular use becomes possible without sacrificing a loss in the end use. For example, aluminum foil replaced tin foil in wrapping, aluminum busbars replaced copper in electrical industry, and aluminum beverage cans replaced tinned steel.

The price of copper was once about three times that of either lead or zinc. In the last 30

years it has only been double their price. This can be explained when comparing the production patterns; it was only 30 years ago that copper production approached that of lead or zinc and started to surpass them.

2.4 Metal-Producing Associations and cartels

A great demand for a metal causes a shortage in the market, and as a result, the price tends to rise. To meet the shortage and hold the price constant, cartels are formed. These can be either private or government sponsored. For example, the tin cartel which was composed of seven producing countries as members and controlled 94% of the production in the Western World fixed the price of the metal by creating a stock of the metal furnished by the members. Should the price of the metal increase, the cartel offers its stock for sale thus lowering the price and vice versa: should the price decrease the cartel buys metal from the market until the price is stabilized at the desired value. The tin cartel, however, broke down few years ago because a non-member producing country increased its production of the metal and the cartel was unable to buy a

large stock of the metal available on the market.

Associations are usually formed between producers of a certain metal world-wide. For example:

- Aluminum Association
- Cobalt Development Institute
- International Copper Association
- International Lead-Zinc Research Organization
- Nickel Development Institute
- Tantalum-Niobium International Study Center

The purpose of these associations is to promote the use of the metal in question through diffusing information, subsidizing research in potential applications, etc. Metal producing companies participate by paying the cost of operations. They also sponsor holding conferences and publish bulletins about their activities.

2.5 References

1. *Canadian Minerals Yearbook*, Communications Canada, Ottawa 1996.
2. *Minerals Yearbook*, volume 1: "Metals and Minerals"; volume 2: "Area Reports"; volume 3: "International Review". US Bureau of Mines, Washington, DC, 1992.

3 Recycling of Metals

FATHI HABASHI

3.1 Introduction	21	3.3 Nonferrous Metals	21
3.2 Ferrous Metals	21	3.4 References	22

3.1 Introduction

Recovery of a metal from scrap requires much less energy than starting from ore. For example, the remelting of steel scrap to produce reusable steel saves about 74% of the energy that would be required to produce the same quantity of steel from iron ores. In the case of aluminum, it is even higher – it reaches 96% (Table 3.1). Recycling of metals has two important effects on society.

- Conservation of natural resources
- Decreasing pollution of the environment.

As a result, there is a great effort nowadays to collect and recycle old metals.

Table 3.1: Energy savings through recycling of metals.

Metal	Energy saving, %
Aluminum	96
Copper	87
Iron and steel	74
Zinc	63
Lead	60

3.2 Ferrous Metals

There are small-scale steel plants that operate solely on scrap; these usually use electric furnaces for melting. Other steelmaking processes based on raw iron as a starting material also use scrap to a variable degree (Figure 3.1). The use of scrap in certain steelmaking processes is necessary because it is used to control the temperature in the converter during steelmaking. As a result of oxidizing the impurities in the pig iron, the temperature rises because of the exothermic nature of the reaction. To prevent the rapid deterioration of refractories, scrap is added to cool down the charge. On the average, the steel industry consumes 50% raw iron and 50% scrap. Steel

scrap for steelmaking comes from two main sources:

- **Local.** This is scrap produced locally in a steelmaking plant during shaping. In a steel plant, about one third of the steel produced is returned as scrap.
- **External.** This is old automobiles, farm equipment, railroad rails, ships, etc., that is purchased from outside sources.

Steel scrap in form of tin cans is usually sold to the copper industry to be used for precipitating copper from leach solutions by the reaction:



It is first heated to remove tin by volatilization before use (detinning).

A shortage of scrap is expected in the future as a result of introducing continuous casting method which produces less local scrap. This shortage, however, can be overcome by producing a certain quantity of iron by "direct reduction" methods. This iron is not produced in the blast furnace but in less expensive equipment such as a rotary kiln, a static bed, or a fluidized bed. It differs from blast furnace iron in being not subjected to melting, and is suitable as a substitute for scrap. Usually steel produced from such iron is made in electric furnaces (Figure 3.1).

3.3 Nonferrous Metals

Great efforts are now being made to collect and recycle scrap of aluminum (e.g., beverage cans), copper (e.g., electric wires), lead (e.g., old automobile batteries), silver (e.g., used photographic films, table ware), nickel from hydrogenation catalysts, platinum from auto-

mobile exhaust gas catalyst and ammonia oxidation catalyst, etc. As a result, new technologies are constantly emerging for treating and purifying such scrap.

3.4 References

1. S. A. Bortz, R. S. De Cesare, *Accomplishments in Waste Utilization*, Information Circular 8884, U.S. Bureau of Mines, Washington, DC, 1982.
2. S. A. Bortz, K. B. Higbie (eds.): *Materials Recycling*, Information Circular 8826, U.S. Bureau of Mines, Washington DC, 1980.
3. R. K. Collings, *Mineral Waste Resources of Canada*, a series of reports issued by CANMET, Ottawa 1977-1980.
4. P. Mehant et al. (eds.): *Resource Conservation and Environmental Technologies in Metallurgical Industry*, Canadian Institute of Mining, Metallurgy, and Petroleum, Montréal 1994.
5. S. R. Rao et al., *Waste Processing and Recycling in Mining and Metallurgical Industries*, Canadian In-

stitute of Mining, Metallurgy, and Petroleum, Montréal 1992.

6. S. R. Rao, T. J. Veasey, *Second International Symposium on Waste Processing and Recycling in the Mining and Metallurgical Industries*, Canadian Institute of Mining, Metallurgy, and Petroleum, Montréal 1995.
7. R. F. Rolsten (ed.), *Materials: Dispose or Recycle?*, Wright Company, Dayton, OH, 1977.
8. M. Sittig, *Metal and Inorganic Waste Reclaiming Encyclopedia*, Noyes Data Corporation, Park Ridge, NJ.
9. M. J. Spendlove, *Recycling Trends in the United States*, Information Circular 8771, U.S. Bureau of Mines, Washington, DC, 1976.
10. M. J. Spendlove, *Bureau of Mines Research on Resource Recovery*, Information Circular 8750, U.S. Bureau of Mines, Washington, DC, 1977.
11. P. R. Taylor, H. Y. Sohn, N. Jarret (eds.), *Recycle and Secondary Recovery of Metals*, The Minerals, Metals and Materials Society, Warrendale, PA, 1985.
12. K. J. Thome-Kozmiensky (ed.), *Recycling International: Recovery of Energy and Material from Residues and Waste*, Freitag-Verlag, Berlin 1982.

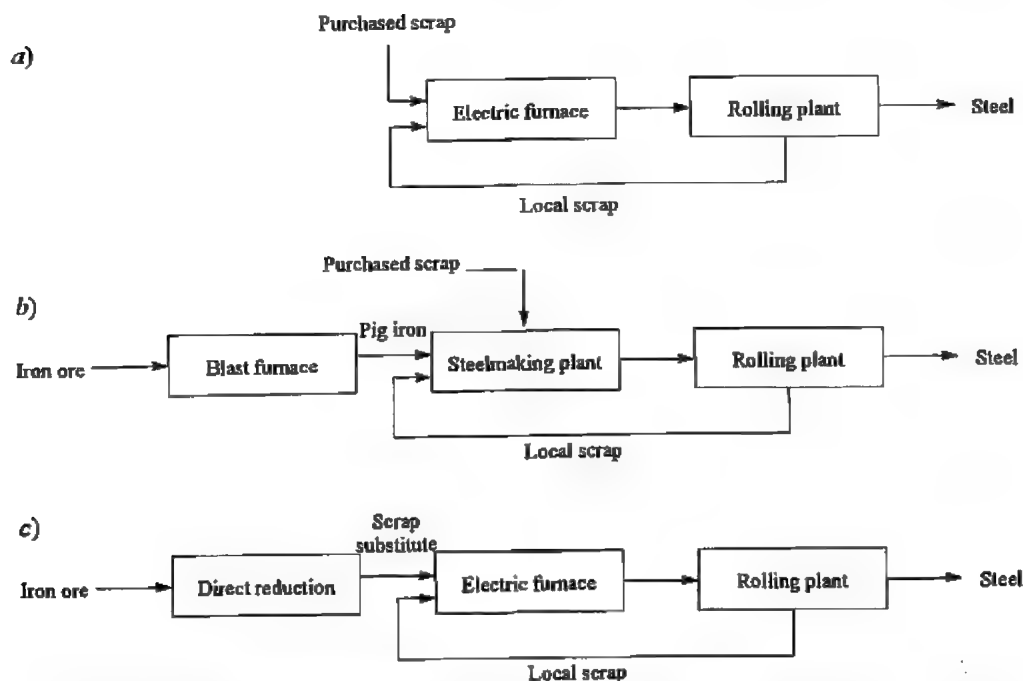


Figure 3.1: The role of scrap and scrap substitutes in the steel industry: (a) Steel industry based solely on scrap; (b) Steel industry based on $\approx 50\%$ raw iron and $\approx 50\%$ scrap; (c) Steel industry based on scrap substitutes.

4 By-Product Metals

FATHI HABASHI

4.1 Introduction.....	23	4.5 Rhenium from Porphyry Copper Ores	24
4.2 Uranium from Phosphate Rock	23	4.6 Cadmium from Zinc Concentrates..	24
4.3 Vanadium from Fuel Oil.....	23	4.7 Gallium from Aluminum Ores	25
4.4 Precious Metals from Copper Ores .	23	4.8 References	25

4.1 Introduction

It is often possible to recover certain metals as by-products during the processing of ores. This is often aided by the fact that metals found in exceedingly small amount in a feed material to a chemical or a metallurgical process are enriched in certain fractions during processing i.e.g. dust, slimes and residues and therefore can be economically recovered as by-products. In some cases this may be a means to conserve the natural resources, in others it may be an essential purification step.

4.2 Uranium from Phosphate Rock

Phosphate rock contains on the average 150 ppm uranium. During the processing of the rock for fertilizer manufacture, uranium is enriched in the phosphoric acid produced as an intermediate product and is usually recovered as a by-product without interfering with the manufacturing process (Figure 4.1).

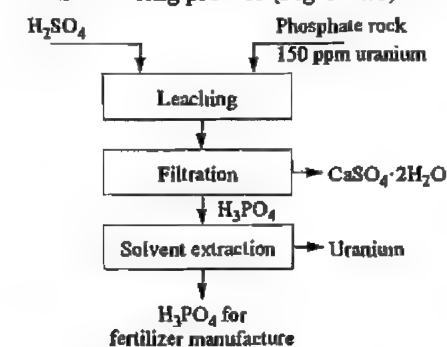


Figure 4.1: Recovery of uranium from phosphate rock.

4.3 Vanadium from Fuel Oil

Fuel oil contains on the average 100 ppm vanadium. During burning in boilers to generate steam, the dust collected in the gas treatment section is rich in vanadium (Figure 4.2).

4.4 Precious Metals from Copper Ores

A copper ore containing 1 to 2% Cu that may be beneficiated to a concentrate containing 20 to 40% Cu, when smelted yields raw metal containing about 97% Cu. During the electrolytic refining step to get 99.9% Cu, the impurities behave differently: some remain in solution and can be crystallized, for example nickel sulfate, while the others remain at the bottom of the tank as insoluble residue called slimes (Figure 4.3). These are an important source of the precious metals as well as selenium and tellurium originally present in the ore.

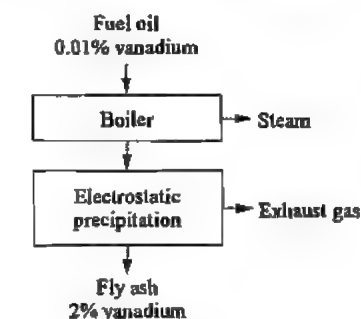


Figure 4.2: Recovery of vanadium from fuel oil.

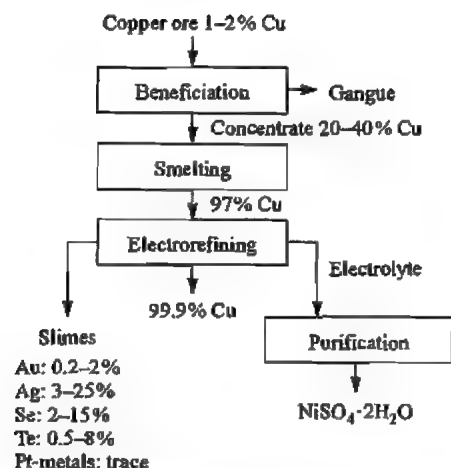


Figure 4.3: Enrichment of traces of metals present in copper ore during the production of the metal.

4.5 Rhenium from Porphyry Copper Ores

Chalcopyrite concentrate from porphyry copper ores contains on the average 0.05% molybdenite. This is usually separated by selective flotation. The molybdenite concentrate obtained contains about 700 ppm rhenium which is enriched in the dust fraction during oxidation (Figure 4.4). This is the principal source of rhenium.

4.6 Cadmium from Zinc Concentrates

During the production of zinc by the hydrometallurgical route small amounts of cadmium are present in the leach solution and these must be removed before the electrowinning step (Figure 4.5). This is an important source of cadmium. At the same time germanium, indium, and thallium are retained in the leach residue and are recovered.

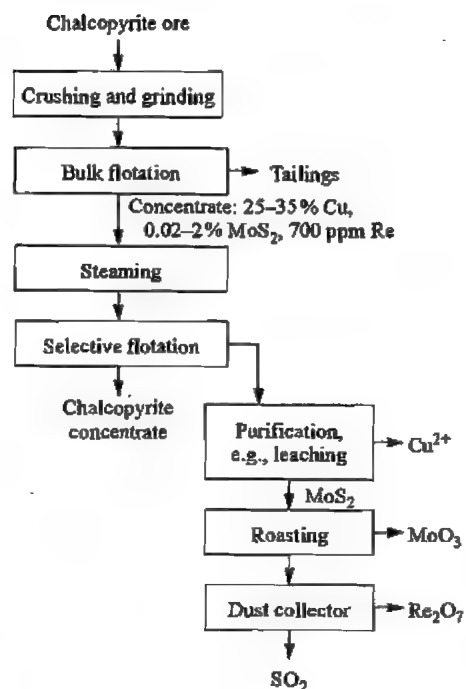


Figure 4.4: Chalcopyrite – a major source of rhenium.

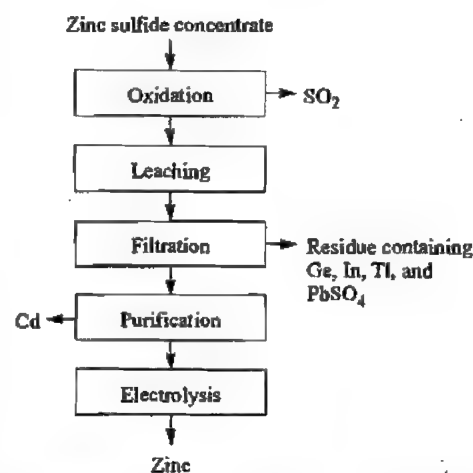


Figure 4.5: Recovery of cadmium as a by-product of the zinc industry.

4.7 Gallium from Aluminum Ores

Traces of gallium found in bauxite, the principal source of aluminum, are usually recovered from a bleed of the aluminate leach solution (Figure 4.6).

4.8 References

1. W. Schreiter, *Seltene Metalle*, 3 volumes, VEB Deutscher Verlag für Grundstoffindustrie, Leipzig 1961-1963.
2. R. Kieffe, G. Jangg, P. Ertmayer, *Sondermetalle*, Springer-Verlag, Vienna 1971.
3. A. Patrick et al., *The Economics of By-Product Metals*, 2 parts, US Bureau of Mines Information Circulars 8569, 8570 (1973).
4. J. G. Parker, *Occurrence and Recovery of Certain Minor Metals in the Smelting-Refining of Copper*, US Bureau of Mines Information Circular 8778 (1978).
5. L. A. Haas, D. R. Weir (eds.): *Hydrometallurgy of Copper, its By-Products, and Rarer Metals*, Society of Mining Engineers AIME, New York 1983.

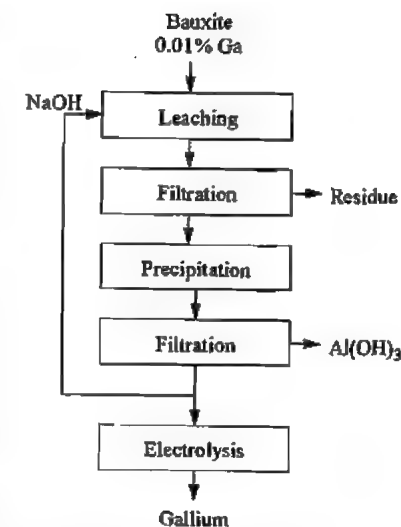


Figure 4.6: Recovery of gallium from bauxite as a by-product of the aluminum industry.

Part Two

Ferrous Metals

																H	He			
Li	Be													B	C	N	O	F	Ne	
Na	Mg	Al														Si	P	S	Cl	Ar
K	Ca	Sc	Ti	V	Cr	Mn	Fe	Co	Ni	Cu	Zn	Ga	Ge	As	Se	Br	Kr			
Rb	Sr	Y	Zr	Nb	Mo	Tc	Ru	Rh	Pd	Ag	Cd	In	Sn	Sb	Te	I	Xe			
Cs	Ba	La [†]	Hf	Ta	W	Re	Os	Ir	Pt	Au	Hg	Tl	Pb	Bi	Po	At	Rn			
Fr	Ra	Ac [‡]																		

†	Ce	Pr	Nd	Pm	Sm	Eu	Gd	Tb	Dy	Ho	Er	Tm	Yb	Lu
---	----	----	----	----	----	----	----	----	----	----	----	----	----	----

†	Th	Pa	U	Np	Pu	Am	Cm	Bk	Cf	Es	Fm	Md	No	Lr
---	----	----	---	----	----	----	----	----	----	----	----	----	----	----

5 Iron

FATMI HABASHI (§§ 5.1, 5.2, 5.4–5.6 EXCEPT 5.5.6–5.5.11, 5.8–5.9 EXCEPT 5.9.1, 5.14–5.16, 5.17.1, 5.18–5.19); HEINRICH MEIER (§ 5.3); JUN-ICHIRO YAGI (§§ 5.5.6–5.5.11); ANDREAS BUHR, MANFRED KOLTERMANN (§ 5.7); LOTHAR FORMANEK, FRITZ ROSE (§ 5.10 EXCEPT 5.10.1); KLAUS WESSEPE (§ 5.10.1); JORGEN FLICKENSCHILD, ROLF HAUKE (§ 5.11); GERNOT MAYER-SCHWINNING, REINER SKROCH (§ 5.12); HEINZ-LOTHAR BÖNNAGEL, HANS-GEORG HOFF (§ 5.13); EGON WILDERMUTH (§§ 5.17.2–5.17.3); HANS STARK (§§ 5.17.4–5.17.5); FRANZ LUDWIG EBENHÖCH (RETIRED), GABRIELE FRIEDRICH (§ 5.17.6); BRIGITTE KOHBORTH (§ 5.17.6, TOXICOLOGY AND OCCUPATIONAL HEALTH); JACK SILVER (§ 5.17.7); RAFAEL RITUPER (§ 5.20); GÜNTER BUXBAUM, HELMUT PRINTZEN (§ 5.21.1); HORST FERCH, WILFRIED MAYER, KLAUS SCHNEIDER, HEINRICH WINKLER (§ 5.21.2); HENDRIK KATHREIN, LUTZ LEITNER (§§ 5.21.3.1–5.21.3.3); HELMUT JAKUSCH, MANFRED ÖHLINGER, ECKEHARD SCHWAB, RONALD J. VEITCH (§ 5.21.3.4); GÜNTER ETZRODT (§ 5.21.4); RALF EMMERT, KLAUS-DIETER FRANZ, HARTMUT HÄRTNER, KATSUHISA NITTA, GERHARD PFAFF (§ 5.21.5); HARALD GAEDCKE (§§ 5.21.6–5.21.7); JOHN C. CRELLING (§§ 5.22.1–5.22.4, 5.22.9–5.22.11); DIETER SAUTER (§§ 5.22.5, 5.22.8); DIETER LEININGER † (§ 5.22.6); UDO BERTMANN, BERNHARD BONN (§ 5.22.7); RAINER REDMERT (§ 5.22.8); WOLFGANG GATZKA (§ 5.22.12); SEMIH ESER, RASHID KHAN, LJUBISA R. RADOVIC, ALAN SCARONI (§ 5.22.13)

5.1	Introduction	31	5.5.7	Effective Utilization of Energy ...	67
5.2	Occurrence	31	5.5.8	Blast Furnace Productivity Criteria	77
5.2.1	Native Metal	31	5.5.9	Use of Blast Furnace Products ...	80
5.2.2	Oxide Minerals	32	5.5.10	Process Control	81
5.2.3	Complex Oxides	33	5.5.11	Hot-Metal Desulfurization	90
5.2.4	Carbonates	33	5.6	Plant Layout	96
5.2.5	Sulfides, Disulfides, and Complex Sulfides	33	5.6.1	Dust-Recovery System	96
5.2.6	Phosphates	34	5.6.1.1	Dust Catchers	96
5.3	Ores	35	5.6.1.2	Cyclones	97
5.3.1	Ore Deposits	35	5.6.1.3	Spray Towers	97
5.3.2	Supply of Iron Ore	36	5.6.1.4	Venturi Scrubbers	98
5.3.3	Most Important Iron-Producing Countries	37	5.6.1.5	Electrostatic Precipitators	98
5.3.4	Beneficiation of Iron Ore	39	5.6.2	Heat Economy System	100
5.3.5	Agglomeration	43	5.7	Refractory Materials	101
5.4	Reduction of Iron Oxides	49	5.8	Iron from Pyrite Cinder	102
5.4.1	Chemical Aspects	49	5.8.1	The Chloride Route	102
5.4.2	Technical Aspects	50	5.8.2	The Sulfate Route	103
5.4.3	Raw Materials	52	5.9	Iron from Ilmenite	103
5.4.3.1	Iron Ores	53	5.10	Direct Reduction Processes	104
5.4.3.2	Coke	53	5.10.1	Fuels and Reducing Agents	106
5.4.3.3	Limestone	54	5.10.2	Shaft Furnace Processes for Direct Reduction	110
5.4.3.4	Air	54	5.10.3	Retort Processes	114
5.4.4	Products	54	5.10.4	Fluidized-Bed Processes	115
5.4.4.1	Pig Iron	54	5.10.5	Rotary Kiln Processes	118
5.4.4.2	Slag	54	5.11	Smelting-Reduction Processes	123
5.4.4.3	Gas	55	5.11.1	Processes Using Electrical Energy	124
5.4.4.4	Flue Dust	55	5.11.2	Char-Coke-Bed Melter-Gasifiers	127
5.4.5	Behavior of Impurities	55	5.11.3	Converter-Type Melters	130
5.5	The Blast Furnace	56	5.12	Aspects of Environmental Protection	132
5.5.1	General Description	56	5.12.1	Air Pollution Control	133
5.5.2	Operation	59	5.12.2	Prevention of Water Pollution	136
5.5.3	Operating Difficulties	60	5.12.3	Noise Reduction	136
5.5.4	Shutdown	61	5.12.4	Waste Management	137
5.5.5	Efficient Operation and Improvements	61	5.13	Economic Aspects	137
5.5.6	Engineering Aspects	63	5.14	Pure Iron	143

5.15 Iron-Carbon System	144	5.21.4 Iron Phosphide	189
5.16 Technical Varieties of Iron	146	5.21.5 Iron Oxide-Mica Pigment	189
5.17 Compounds	147	5.21.6 Transparent Iron Oxides	190
5.17.1 General	147	5.21.7 Transparent Iron Blue	191
5.17.1.1 Ferrous Compounds	147	5.22 Coal and Coal Pyrolysis	191
5.17.1.2 Ferric Compounds	147	5.22.1 Coal Petrology	191
5.17.1.3 Complex Compounds	148	5.22.2 Coalification	195
5.17.2 Iron(II) Sulfate	149	5.22.3 Occurrence	196
5.17.3 Iron(III) Sulfate	150	5.22.4 Classification	198
5.17.4 Iron(III) Chloride	150	5.22.5 Chemical Structure of Coal	200
5.17.5 Iron(II) Chloride	153	5.22.5.1 Characterization of Coals	202
5.17.6 Iron Pentacarbonyl	153	5.22.5.2 Structural Deductions from	
5.17.7 Iron Compounds, Miscellaneous ..	160	Analytical and Bench-Scale Data ..	204
5.18 Relationships Between the		5.22.5.3 Bonding of Elements in Coal	204
Different Forms of Iron Oxides	162	5.22.5.4 Structural Evidence of Coals	205
5.19 The Aqueous Oxidation of Iron		5.22.6 Hard Coal Preparation	205
Sulfides	164	5.22.6.1 Preliminary Treatment and	
5.19.1 Pyrite	164	Classification of Raw Coal	205
5.19.2 Arsenopyrite	165	5.22.6.2 Wet Treatment	206
5.19.3 Pyrrhotite	165	5.22.6.3 Dewatering	207
5.20 Regeneration of Iron-Containing		5.22.6.4 Decantation and Thickening of the	
Pickling Baths	166	Process Water	208
5.20.1 Sulfuric Acid Pickling Solutions ..	166	5.22.6.5 Dosing and Blending	208
5.20.1.1 Crystallization	166	5.22.6.6 Removal of Pyritic Sulfur	209
5.20.1.2 Electrolysis	168	5.22.6.7 Thermal Drying	209
5.20.2 Hydrochloric Acid Pickling		5.22.7 Coal Conversion (Uses)	210
Solutions	168	5.22.7.1 Preparation	210
5.20.3 Nitric and Hydrofluoric Acid		5.22.7.2 Briquetting	210
Pickling Solutions	169	5.22.7.3 Carbonization and Coking	211
5.21 Pigments	171	5.22.7.4 Pyrolysis	211
5.21.1 Iron Oxide Pigments	171	5.22.7.5 Coal Liquefaction	212
5.21.1.1 Natural Iron Oxide Pigments	172	5.22.7.6 Coal Gasification	213
5.21.1.2 Synthetic Iron Oxide Pigments	172	5.22.7.7 Coal Combustion	215
5.21.1.3 Toxicology and Environmental		5.22.7.8 Conversion of Coal for Purposes	
Aspects	177	Other Than the Generation of	
5.21.1.4 Quality	177	Energy	215
5.21.1.5 Uses	178	5.22.8 Agglomeration	215
5.21.1.6 Economic Aspects	178	5.22.9 Transportation	216
5.21.2 Iron Blue Pigments	179	5.22.10 Coal Storage	217
5.21.2.1 Structure	179	5.22.11 Quality and Quality Testing	218
5.21.2.2 Production	179	5.22.12 Economic Aspects	220
5.21.2.3 Properties	180	5.22.12.1 World Outlook	220
5.21.2.4 Uses	182	5.22.12.2 Some Major Coal-Producing	
5.21.2.5 Toxicology and Environmental		Countries	221
Aspects	184	5.22.13 Coal Pyrolysis	224
5.21.3 Iron Magnetic Pigments	185	5.22.13.1 Thermoplastic Properties of Coal ..	224
5.21.3.1 Iron Oxide Magnetic Pigments	185	5.22.13.2 Yield and Distribution of Pyrolysis	
5.21.3.2 Cobalt-Containing Iron Oxide		Products	238
Pigments	187	5.22.13.3 Kinetics	245
5.21.3.3 Metallic Iron Pigments	187	5.22.13.4 Hydrometallurgy	247
5.21.3.4 Barium Ferrite Pigments	188	5.22.13.5 Pyrolysis Processes	248
		5.23 References	257

5.1 Introduction¹

Iron is an Anglo-Saxon word; the symbol, Fe, comes from Latin *ferrum*. The French term *siderurgie*, i.e., iron technology, comes from *σιδηρος* the Greek word for iron. Also *sideritis* is the Latin word for lodestone.

The use of iron has been known since the earliest times; it was prepared by the so-called bloomery hearth, or Catalan forge. Iron ores were heated in a shallow trench with a large excess of wood charcoal, fanned by bellows. Lumps (blooms) of wrought iron were obtained, and were welded together by hammering. As technology advanced during the Middle Ages, the trench was replaced by a small shaft furnace, and from this the present day blast furnace has developed. The use of water power to operate the blast was introduced during the 14th century. The consequent considerable increase in furnace temperature resulted in the production of iron with a much higher carbon content than formerly, namely cast iron. This was not malleable but it was soon discovered how this might be converted into malleable iron by a second heating in an ample supply of air (refining). The iron industry received a great impetus at the end of the 18th century, when the demand for iron began to increase as a result of the invention of the steam engine and the railway. The shortage of wood charcoal led to the introduction of coke, as fuel and as reducing agent. Coke was first used in the blast furnace by Abraham Darby, in 1732. The refining process underwent fundamental improvements during the 19th century, through the introduction of the blast refining method (Bessemer process, 1855; Thomas-Gilchrist process, 1878) and of regenerative heating (Siemens-Martin process 1865). Later, smelting in the electric furnace has been introduced for the production of certain high-grade steels.

Iron is the cheapest and most widely used metal. Its annual production exceeds by far that of all other metals combined. It comprises

approximately 93% of the tonnage of all the metals used.

5.2 Occurrence

Iron is a relatively abundant element in the universe. It is found in the sun and many stars in considerable quantity. Iron is found native as a principal component of a class of meteorites known as siderites. The core of the earth is thought to be largely composed of iron. The metal is the fourth most abundant element in the earth's crust: about 5% is iron. Iron is a vital constituent of plant and animal life, and appears in hemoglobin.

5.2.1 Native Metal

Iron occurs in the native state in two forms [1]:

Telluric Iron. This form of iron is known as telluric iron, i.e., terrestrial, to distinguish it from meteoric, i.e., coming from outer space. The difference in nickel, cobalt, carbon, and basalt content clearly distinguishes one from the other (Table 5.1). Although both types may look alike and may occur as large boulders 20 to 80 tons, there is another way to distinguish between the two, besides chemical analysis, is the Widmanstätten structure that appears in meteoric iron when a piece is polished, etched and examined by the optical microscope. The large crystals indicating slow cooling is characteristic of meteoric iron. The major occurrence of telluric iron is in association with the basalts² of Western Greenland. Large boulders are on exhibit at the Natural History Museums in Stockholm, Copenhagen, and Helsinki. Telluric iron is found also as small millimeter-sized pea-shaped grains disseminated in the basalt, characterized of their low carbon content, usually less than 0.7%. These were extracted from the basalt by the natives by crushing and then cold-hammering the collected metallic particles into coin-sized

¹ For History of Iron, see Section 6.2.

² Basalt is a heavy dark grey or black basic igneous rock composed mainly of finely divided pyroxene, feldspar, and sometimes olivine.

flakes to insert them into groves in bone and use them as knives.

Table 5.1: Typical analysis of telluric and meteoritic iron.

	Telluric, %	Meteoritic, %
Nickel	0.5–4	5–20
Cobalt	0.1–0.4	0.5–0.7
Carbon	0.2–4.5	0.03–0.10
Basalt	5–10	nil

Ferronickel. Ferronickel is an iron–nickel alloy that occurs in nature as the mineral awaruaite, FeNi_3 (named after Awarua Bay in New Zealand, where it was first discovered), and josephinite, FeNi_2 (named after Josephine County, Oregon where it was first discovered). Both minerals contain cobalt, usually in the ratio $\text{Ni}:\text{Co} = 10:1$. Ferronickel also occurs as

microscopic lamellae in association with asbestos, as microscopic crystals in association with serpentine, or as microscopic particles associated with the minerals pentlandite, $(\text{Fe}, \text{Ni})\text{S}$, and hazelwoodite, NiS , in serpentine rocks (Figure 5.1). Thus it occurs in most asbestos formations and can be recovered from the asbestos tailings by magnetic methods.

5.2.2 Oxide Minerals

Iron ores of sedimentary origin account for nearly 80% of the world's reserves; the remaining 20% is of magmatic origin such as magnetite. The most important oxide minerals are the following:

- **Hematite, Fe_2O_3 .** Occurs in nature in the following forms:
 - Specular hematite: black to steel grey crystals with metallic luster
 - Micaceous hematite: occurs in thin flakes resembling mica; they may be so thin as to be translucent and they are then deep red
 - Common red hematite is dark red in massive, granular or earthy (red ocher) form
 - Magnetic. This is the $\gamma\text{-Fe}_2\text{O}_3$ which occurs in the Ural as the mineral maghemite. It is like Fe_3O_4 , a cubic spinel type.
- **Magnetite, Fe_3O_4 .** It is brittle with a dark grey to black opaque color, with metallic luster, strongly magnetic.

Geological Terms

- **Limonite** is a geologic term signifying certain deposits of hydrated iron oxides which vary in color from brown to yellow. It is formed by the weathering and alteration of other iron-bearing compounds. When present in a loose, porous and earthy deposits in swamps, it is known as bog iron ore. When mixed with clay it forms what is known as yellow ocher. Most limonite ores require washing to remove clay, and drying to remove moisture, before shipping or reduction.
- **Taconite** is another geological term signifying an iron ore deposit consisting of fine grains of hematite and magnetite embedded in a matrix of silica. It is difficult to drill and blast but easy to grind. Large deposits of this type occur in the Lake Superior region containing 25–35% Fe. Enrichment can be effected by magnetic methods to separate magnetite, and flotation to separate hematite to achieve a concentrate containing 63% Fe.
- **Laterite** is a limonite containing 1–2% Ni and about 0.1% Co. At present these are used as nickel and not as iron ore, e.g., in Cuba.
- **Oolitic ironstone** is iron carbonate which has replaced the CaCO_3 of an oolitic limestone retaining the texture of the original rock. The rock consists of small round grains resembling the roe of fish.

Table 5.2: Complex oxides of iron.

Chromite	$\text{Cr}_2\text{O}_3 \cdot \text{FeO}$
Columbite	$\text{Nb}_2\text{O}_5 \cdot (\text{Fe}, \text{Mn})\text{O}$
Tantalite	$\text{Ta}_2\text{O}_5 \cdot (\text{Fe}, \text{Mn})\text{O}$
Ilmenite	$\text{TiO}_2 \cdot \text{FeO}$
Wolframite	$\text{WO}_3 \cdot \text{FeO}$

5.2.3 Complex Oxides

Iron occurs in combination with other metals in form of complex oxides (Table 5.2). It is only recovered from ilmenite concentrates as a by-product of the manufacture of titanium slag, e.g., Sorelslag used for making TiO_2 pigment.

5.2.4 Carbonates

Siderite, FeCO_3 . When occurring in economic deposits it represents a low-grade iron ore since the pure mineral contains only 48.3% Fe. It crystallizes in rhombohedra like calcite, which dissolves in water containing carbonic acid, with the formation of iron(II) hydrogen carbonate, $\text{Fe}(\text{HCO}_3)_2$. Such waters rapidly deposit iron(III) oxide hydrate when exposed to air, since the excess carbon dioxide escapes, the carbonate deposited is hydrolyzed, and is oxidized by atmospheric oxygen.

5.2.5 Sulfides, Disulfides, and Complex Sulfides

Iron(II) sulfide occurs in nature as pyrrhotite, FeS , iron(II) disulfide as pyrite and marcasite, FeS_2 . It also occurs in combination with arsenic as the mineral arsenopyrite, FeAsS . Iron(III) sulfide occurs in the form of double sulfides, especially with copper(I) sulfide — e.g., chalcopyrite, CuFeS_2 or $\text{Cu}_2\text{S} \cdot \text{Fe}_2\text{S}_3$, and bornite, Cu_3FeS_3 or $3\text{Cu}_2\text{S} \cdot \text{Fe}_2\text{S}_3$. These are the major copper minerals.

Iron monosulfide (ferrous sulfide), FeS . Iron sulfide, crystallized in the hexagonal system, is magnetic. The iron sulfide occurring in meteorites, with the same crystal structure, is called troilite. Pyrrhotite almost always contains nickel, and is therefore of importance as a nickel ore. The sulfur content of pyrrhotite is usually 1 to 2% higher than corresponds with

Figure 5.1: Photomicrograph of polished sections. A) Lamella of ferronickel in asbestos deposit 0.05–0.5 mm in size (70 ×); B) Microscopic crystals of ferronickel (560 ×); C) Microscopic particles of ferronickel (F) cemented with pentlandite (P) from serpentine rock (210 ×).

the formula FeS, the excess sulfur being built into the crystal lattice. Its ability to take up a certain excess of sulfur arises from the fact that a proportion of the positions which should be occupied by Fe atoms may remain vacant. The density of FeS varies between 4.5 and 5.

Pyrite (iron disulfide), FeS₂. Pyrite is widely distributed in nature. The ore is not a source of iron but a source of sulfur. However, the residue of roasting from the manufacture of sulfuric acid is smelted for iron, after the impurities which are undesirable for this purpose, although often valuable in themselves, have been removed in special refineries: silver and gold are present as well as copper and zinc. The disulfide also occurs as marcasite.

Pyrite and marcasite have a brassy yellow color and metallic luster. They differ in their crystal structures. Pyrite, which is commonly found in well formed large crystals (usually cubes or pentagonal dodecahedra, or combinations of these forms), belongs to the pentagonal hemihedral class of the cubic system. Marcasite is orthorhombic.

Pyrite and arsenopyrite are different from other sulfide minerals since they contain the

disulfide ion, S₂²⁻; arsenopyrite contains in addition the diarsenide ion, As₂²⁻. In pyrite, FeS₂, the iron atoms are in a face-centered cubic arrangement with pairs of the sulfur atoms located on the cube diagonals. In arsenopyrite, FeAsS, the iron atoms are also in a face-centered cubic arrangement like in pyrite but half of the diagonal positions are occupied by pairs of the sulfur atoms and the other half by pairs of arsenic atoms.

Pyrite and arsenopyrite have received great attention recently because in some gold ores called "refractory", they entrap gold in their crystal structure and render the metal unextractable by cyanide solution unless the mineral structure is destroyed by thermal or aqueous oxidation prior to cyanidation. Pyrite is also the major sulfur-bearing impurity mineral in coal. Attempts to upgrade the coal include the aqueous oxidation of the pyrite.

5.2.6 Phosphates

Vivianite. Hydrated iron(II) orthophosphate, Fe₃(PO₄)₂·8H₂O, is the main source of phosphorus impurity in iron ores.

Table 5.3: Important minerals in iron ores.

Mineral	Chemical formula	Density, g/cm ³	Hardness (I)	Specific susceptibility (order of magnitude)
Iron (for comparison)	Fe	7.88	4-5	
Magnetite	Fe ₃ O ₄	5.2	5.5	10 ⁻¹ -1
Specularite ("hematite")	Fe ₂ O ₃	5.2-5.3	6.5	10 ⁻⁴
Limonite				
Needle ore	α-FeOOH	4.3	5-5.5	10 ⁻⁶ -10 ⁻⁵
Ruby mica	β-FeOOH	4.0	5	10 ⁻⁶ -10 ⁻⁵
Siderite	FeCO ₃	3.7-3.9	4-4.5	10 ⁻⁶
Pyrite	FeS ₂	5.0-5.2	6-6.5	10 ⁻⁶
Pyrrhotite	FeS	4.6	4	10 ⁻³ -10 ⁻⁴
Chalcocopyrite	CuFeS ₂	4.1-4.3	3.5-4	10 ⁻⁵ -10 ⁻⁶
Apatite	Ca ₃ F(PO ₄) ₃	3.2	5	-10 ⁻⁶
Vivianite	Fe ₃ (PO ₄) ₂ ·8H ₂ O	2.6-2.77	3	
Quartz	SiO ₂	2.65	7	-10 ⁻⁶
Orthoclase	KAlSi ₃ O ₈	2.55	6	10 ⁻⁶
Plagioclase	NaAlSi ₃ O ₈ /CaAl ₂ Si ₂ O ₈	2.6-2.8	2-2.5	10 ⁻² -10 ⁻⁵
Kaolinite, dickite	Al ₂ (OH) ₄ Si ₂ O ₁₀	2.6	1	
Muskovite	KAl ₂ (OH) ₂ F ₂ [AlSi ₃ O ₁₀]	2.6-2.8	2-2.5	10 ⁻² -10 ⁻⁵
Pyrolusite	MnO ₂	5	1-6	10 ⁻⁶
Calcite	CaCO ₃	2.6-2.8	3	-10 ⁻⁶
Ilmenite	FeTiO ₃	4.5-5	5-6	10 ⁻⁴

5.3 Ores [2, 3]

Iron is found in high concentration in ore deposits, where it occurs mainly as oxide. Table 5.3 lists the iron minerals of greatest industrial importance (along with some accompanying gangue minerals) and their relevant properties.

The only minerals of worldwide importance are hematite (specularite, Fe₂O₃), magnetite (Fe₃O₄) and limonite (FeOOH). Siderite (FeCO₃) finds limited use on a local basis. Other ores such as chamosite (an iron magnesium aluminosilicate) or pyrite are virtually not important for iron production anymore.

5.3.1 Ore Deposits

Of the variety of classification systems that have been proposed for iron-ore deposits, the one from the United Nations Survey is used here [4]. The criterion is the physical appearance of the deposit; the main types are bedded (A), massive (B), residual (C), by-product (D) and other (E)

A Bedded Deposits

A-1 Iron formation

Lake Superior Type

Chiefly Precambrian; primarily as sedimentary deposits, heavily metamorphosed (itabirite, taconite, jaspilite or quartz-banded ore); enriched by weathering processes (Mesabi, Minas Gerais, Carajas, Venezuela, Labrador and Quebec, Krivoi Rog)

Algoma Type

Primarily as thinly-banded quartzite with interlayers of iron ore; enriched as limonite hematite weathering ore

A-2 Ironstone formation

Mainly marine sedimentary deposits of minette type; Clinton, Wabana; chiefly mesozoic, with limonite as the most important mineral

A-3 Other Iron-Ore Sediments

Examples: clastic deposits, ferruginous sandstone, and iron shale; also alluvial deposits and unconsolidated clastic sediments

B Massive Deposits

B-1 Bilbao Type

Deposits from weathering of siderite rock, with limonite and hematite in the weathering zone

B-2 Magnitnaya Type

Contact-metasomatic replacement deposits

B-3 Kiruna Type

Magnetite intrusion, usually with apatite

B-4 Taberg Type

Syngenetic titanomagnetite bodies and deposits of finely intergrown ilmenite ores

C Residual Deposits

C-1 Laterite and iron-ore caps as a result of weathering of underlying iron-bearing rocks

C-2 Fluvial deposits and bog ore

C-3 Other residual ores, e.g., caps of sulfide ore deposits (gossan, "iron hat"), unconsolidated clastic deposits

D By-products

Recoverable values in by-product iron oxide

E Other Types of Deposits

e.g. Iode-type deposits (Siegerland)

Bedded deposits are stratigraphic members enriched in iron by a factor of ca. 4-12 above average. They occur in all geologic ages; including ores which originate from them, they account for ca. nine-tenths of potential iron reserves. Names applied to Precambrian metamorphic ore beds are itabirite, taconite, Lake Superior type, quartz-banded ore, jaspilite, magnetite quartzite, hematite quartzite, etc. More recent formations are known as minette (Jurassic), Salzgitter type, and other local names. In general, the term bedded deposits is used for iron-mineral enrichments in which ore minerals are more or less closely laminated with quartz, jasper or carbonate rock and the iron-bearing sediments lie conformably to the under- and overlying beds of igneous or metasedimentary rock. Thus, iron formations can be chemical rocks, clastic sediments, or rock beds that have been replaced by iron mineral during diagenesis or in their subsequent history.

Massive iron-ore deposits are ore bodies of irregular shape, discordantly embedded in the enclosing rock. They include:

- Replacement deposits in carbonate rocks (Bilbao type) with siderite, hematite or limonite (the last two in the weathering zone above the water table)
- Contact-metasomatic deposits in the contact region of acidic intrusive rocks with magnetite and, to a lesser extent, hematite, siderite, pyrite, pyrrhotite and copper sulfide (Magnitnaya type)
- Magnetite intrusions in acidic magmatic rock (Kiruna type)
- Massive or intergrown titanomagnetite or ilmenite concentrations in basic rock (Taberg type).

The most important type of *residual deposit* is laterite, which occurs as a cap overlying a

wide variety of rocks. It is the product of weathering in tropical and subtropical climatic regions. The iron content of these ores is usually low (limonite, hematite), the alumina content high, and undesirable accessory constituents such as chromium, phosphorus, and nickel are frequently present (e.g., at Vogelsberg, Germany). Thus, laterite has largely ceased to be an important iron ore except where the lateritic caps of other iron ore deposits have secondary enrichments of up to 69% iron. On the other hand, nickel-bearing laterites are the most important nickel ores of the future (Cuba, New Caledonia, the Philippines). Extended fluvial deposits, such as the Robe River deposit in Western Australia, should also be mentioned. Bog ores, in contrast, form deposits of small extent that were formerly locally important. They are precipitation products from iron-containing solutions. The weathering cap of sulfide deposits (gossan or "iron hat"), which are usually separated from the primary sulfides by an indistinct boundary, are of some importance.

5.3.2 Supply of Iron Ore

Until about the 1950s, ironworks were mainly supplied from their own deposits; ore and concentrate were transported over short distances. Since that time a fundamental change has occurred as a result of (1) the greater demand because of increased production, (2) the drop in the cost of overseas transport because of larger ship capacities, and (3) the need for higher productivity because of continually rising labor and energy costs. The iron ore demand of the most important steel-producing regions is essentially met by a few large ore-producing regions.

Medium-sized and small ironworks located at deposit are now found only in case of large deposits (northeast India, the Ukraine and other areas of the former Soviet Union, northeast China). Table 5.4, listing world iron-ore reserves, also shows, from the tonnage standpoint, that only a few countries play important roles in ore supply. The short descrip-

tions below are limited to the most important deposit areas and supplier countries.

Production figures for iron ore, ore concentrate, and ore agglomerate appear in Table 5.5.

Table 5.4: World iron ore reserves [5].

	Reserves, $t \times 10^6$	Iron content, %
Former Soviet Union	110 750	25.4
China	42 000	30.0
Brazil	34 540	56.9
Canada	26 417	31.6
United States	25 400	20.7
Australia	17 781	60.0
India	13 500	61.5
South Africa	6 300	59.1
France	4 064	40.2
Sweden	3 353	59.1
Venezuela	2 337	54.4
Liberia	1 668	39.5
Other	2 235	28.4
World total	290 235	35.4

Table 5.5: World iron ore production, ore, concentrate and agglomerate (1975–1986) ($t \times 10^6$) [6].

	1975	1980	1986	1993
North America	132.0	127.1	82.8	96.0
Canada	46.9	48.8	36.1	32.3
Mexico	5.1	7.6	7.3	8.0
United States	80.1	70.7	39.4	55.7
South America	134.3	146.1	164.7	189.8
Brazil	89.9	114.7	132.0	159.4
Chile	11.0	8.6	7.0	7.0
Peru	7.8	5.7	5.0	5.2
Venezuela	24.8	16.1	19.1	15.5
Europe	355.5	335.3	313.6	184.2
Austria	3.8	3.2	3.1	1.4
France	49.6	29.0	12.4	3.5
Germany	3.3	1.9	0.7	0.1
Norway	4.1	3.9	3.7	2.2
Spain	7.6	9.2	6.1	2.5
Sweden	30.9	27.2	20.5	18.7
Soviet Union/CIS	232.8	244.7	249.9	154.0
United Kingdom	4.5	0.9	0.3	—
Former Yugoslavia	5.2	4.5	6.7	0.3
Asia	122.7	122.8	151.9	303.8
China	65.0	68.1	90.0	224.7
India	41.4	41.9	47.8	56.0
North Korea	9.4	8.0	8.0	10.0
Turkey	2.4	2.6	4.0	5.1
Africa	57.7	60.8	55.8	44.2
Algeria	3.2	3.5	3.4	2.6
Liberia	24.0	18.2	15.3	—
Mauretania	8.7	8.9	8.9	9.2
South Africa	12.3	26.3	24.5	29.4
Oceania	99.9	99.2	92.5	123.7
Australia	97.6	95.5	90.0	121.4
New Zealand	2.3	3.6	2.4	2.3
World total	902.0	891.3	861.3	941.7

It is striking that the most important supply sources are type A deposits (bedded), and among these the metamorphic deposits of Itabira type (under that or some other local name), chiefly of Precambrian age.

Especially important are the enrichment or weathering zones of these deposits, where the mobilization of silica and alumina has produced rich ores that can be forwarded to ironworks without preliminary beneficiation. Table 5.5 also shows that ores expensive to produce and those whose beneficiation does not yield concentrates with at least ca. 60% iron have lost much of their importance. In fact, most of them will no longer be in production after a few years. Examples are the Mesozoic deposits in France, Belgium and Luxembourg (minettes), in the United Kingdom (home ore), and in Germany (Salzgitter, Siegerland, Lahn-Dill, Oberpfalz).

The important producer countries rank as follows by tonnage output (1993 production, tonnes $\times 10^6$):

China	224.7
Brazil	159.4
Former Soviet Union	154.0
Australia	121.4
India	55.0
United States	55.7
Canada	32.3
Sweden	18.7
Venezuela	17.5

5.3.3 Most Important Iron-Producing Countries [4–8]

Brazil. Brazil is currently the biggest producer of ore for *overseas shipment*. Two ore districts are now in production. The "iron quadrangle" ("Quadrilatero ferrifero") in Minas Gerais state is the more important. It supplies several local ironworks, but most of the product is exported.

The ores occur in three successive beds, Precambrian in age and strongly metamorphosed, called (from shallowest to deepest) Rio das Velhas, Minas Gerais, and Itacolomi [4]. The ore is thought to consist of marine sedimentary deposits. The ore beds contain 35%–60% iron.

Various ore types are distinguished:

- Hematite enrichments (lump to powder ore), > 64% iron
- Silica-rich hematite ore, 60–64% iron
- Itabirite, 35–60% iron, occurring in compact, soft and powder forms and typical of the Minas Gerais series
- Canga, (60–68% iron), a conglomerate-like ore that often consists of rounded fragments in a limonite matrix

Capacity is ca. 130×10^6 t/a of ore shipped; about a tenth is shipped as lump ore, 24×10^6 t/a as pellets, and the remainder as sinter fine ore ("sinter feed").

The second large ore district is Carajas, with a production target of 35×10^6 t/a, 10–20% of this being lump ore. The Carajas ore also lies within Precambrian beds and has been enriched by secondary processes to 60–67% iron.

Venezuela [4, 8]. The most important iron-ore district is the Imataca belt, including the well-known Cerro Bolivar, El Pao, and San Isidro deposits. The belt is part of the Precambrian Guyana Shield. The ores occur in a sequence of metamorphic rocks with gneiss, shales, and taconite-like iron-banded quartzite. Secondary processes have created rich ore deposits, partly through the precipitation of iron hydroxide in cavities. At the surface, a hematite-rich laterite cap, 1–50 m thick has formed; this is still the main source of ore. In 1987, ore output was 17.2×10^6 t, of which 5.5×10^6 t was consumed domestically.

Lump ore, sintered fine ore and pellet feed containing 62–67% iron, 0.6–6% silica, 2% alumina and 2–5% loss on ignition are produced. To meet the needs of direct reduction units (Midrex, HyL) at the Matanza ironworks, a 6 600 000 t/a pellet plant has been erected.

Canada. The Labrador geosyncline is the most important ore district. Precambrian deposits of the Lake Superior type are regarded genetically as continental shelf deposits that have undergone various degrees of metamorphism. There are weathered rich ores containing over 60% Fe and having high limonite

contents; weathered, relatively coarse-grained magnetite hematite ores containing 20–50% quartz; and unweathered banded ore.

United States—Lake Superior. Most of the known iron-ore reserves in the United States are found in the Lake Superior area, in Minnesota, Wisconsin, and Michigan. About three-quarters of U.S. ore production comes from this region; the output goes to ironworks south of the Great Lakes (Ohio, Pennsylvania). The deposits occur in Lower and Middle Precambrian strata. Iron oxide, carbonate, silicate and sulfides are thinly banded with gel quartz and other gangue minerals. The thickness is between 15 and 300 m. Fine-grained magnetite and hematite are the principal ore minerals.

In weathering zones locally enriched lump ores exist containing ca. 60% Fe; these consist of hematite and limonite. Mining is limited to these rich ores and magnetite-bearing beds, which are relatively easy to beneficiate by magnetic separation.

Australia. The large iron-ore reserves of this continent are concentrated in the north of Western Australia, in the Pilbara district. The Precambrian banded itabirite ores contain magnetite, quartz, carbonate, and stilpnomelane. The near-surface region includes hematite and limonite weathering ores. Besides these in situ enrichments, conglomerate and residual ores are also found; the latter have a high limonite content and occur chiefly in old Tertiary riverbeds.

India. In India the most important ore deposits are enclosed in the strata of a Precambrian geosyncline, which runs parallel to the east coast over a significant part of the subcontinent. The ore is mainly of itabirite type; lateritic weathering has produced rich ore with a high alumina content in the gangue, which extends to a considerable depth. Locally, quartz-banded lean ore and similar primary ores have also been exploited. Hematite ore containing > 60% iron is worked; it is partly lump ore and partly sinter fine ore. Hematite-limonite ore also occurs. The lateritic hard-ore cap is often underlain by blue dust. This ore consists of

medium- to fine-grained primary specularite, martite and, locally, primary magnetite as weathering residue, and contains only small amounts of quartz, kaolin minerals, and gibbsite as gangue.

China. China has many isolated ore deposits, most of which form the basis for local iron and steel industries. The largest concentration of reserves, however, is in the provinces of Liaoning (northeast China) and Hebei (eastern central China). The ores are of itabirite type, mainly with hematite-quartzite ores containing 50% iron. Large rich ore reserves are obviously nonexistent in China. Of the ores now being mined, it is known that beneficiation is often difficult and costly. Exceptions are the various magnetite deposits of Magnitnaya type. Some ores contain undesirable secondary constituents such as tin, fluor spar and finely intergrown apatite. Despite the potential reserves, cost considerations may cause China to import iron-rich ore; the recently observed construction of steelworks at coastal sites is an indication of this policy.

Former Soviet Union. The former Soviet Union has more than 20 iron-ore regions. The most important reserves are in the regions of Kursk, western Siberia, and the Ukrainian crystalline shield. The first two areas account for ca. 30% each, the last for some 10% of the Soviet Union's total reserves [4]. The most important production region is the Ukrainian Shield, with the Krivoi Rog syncline as its center ("Krivbas"). The Precambrian strata here contain both magnetite-quartzite and hematite-martite quartzite ores.

In the area of the *Kursk Magnetic Anomaly*, three basins are distinguished: Belgorod in the west, Kursk-Orel in the center, and Staryi Oskol in the east. Near-surface rich ore with hematite and martite has been exploited for some time. The horizontal quartzite magnetite beds are of increasing economic importance. From the geological standpoint, the iron-bearing beds form part of the Precambrian basement of the Central Russian shield.

In the *western Siberian* ore province, three districts exist. However, only the *Kuznetsk-*

Sayan area has acquired economic importance. It consists of a large number of contact-metasomatic magnetite ore bodies of slight and moderate thickness, which also contain iron sulfide and zinc sulfide. The deposits are thought to have originated in the time of the Caledonian orogenesis.

The *Gornyi Altai* district has limited reserves in Clinton-type deposits (sedimentary deposits with partial secondary enrichment), which date from the Variscan orogenesis.

The western Siberian district, in a narrower sense, has considerable reserves of minette-type sedimentary ore deposits that have not been much explored; these had their genesis as marine coastal deposits in the Upper Cretaceous and the Eocene.

Sweden. For a long time, Sweden was the most important ore supplier for the Central European and, in part, the Western European iron industry. Quartz-banded magnetite-hematite ores of the Lake Superior type were mined in central Sweden. However, the chief source of ore for export is northern Lapland, in a district centered around Kiruna and Malmberget, where Kiruna-type magnetite deposits (massive intrusions in granite-like enclosing rock, with a relatively high apatite content) occur. Reserves are more than 2×10^9 t, with ca. 60% iron and 0.04–5% phosphorus. The phosphorus content is reduced to 0.04% by beneficiation, because hardly any Bessemer pig iron is produced in western Europe anymore.

5.3.4 Beneficiation of Iron Ore

The purpose of beneficiation is to render the ore more suitable for transport and for various reduction and smelting processes in the production of pig iron or steel.

The only processing steps used for ores mined from rich deposits (rich ores) are crushing and screening. Such ores come mainly from the weathering zones of itabirite deposits. At some mines, washing is combined with the screening of fines (< 6–8 mm) for sintering; very fine material containing kaolin is thus separated, and the alumina content is reduced. Low-grade ore is concentrated to lower

transport costs and bring about a chemical composition suitable for the subsequent reduction step. In this enrichment process, the gangue is reduced and, in many cases, its composition improved. Current reduction and smelting processes require a basic slag ($\text{CaO}:\text{SiO}_2 > 1$), but the gangue, of nearly every type of iron ore, is "acidic", that is, it contains an excess of silica. Beneficiation lowers the silica level to 5–8% in the concentrate.

Harmful components present in the ore must be removed. Such components include phosphorus, arsenic, chromium, copper, vanadium, alkali, sulfur and titanium; these either make metallurgical processing more difficult or degrade the iron and steel quality. A small quantity of titanium (< 0.5%) is, however, added to the burden at some ironworks, because it has been found to increase the life of the blast-furnace brickwork.

The basic methods of beneficiation for iron ores are usually the same as for nonferrous ores and industrial minerals. Naturally some peculiarities exist because of the mineralogy and the type of intergrowth.

Crushing. Conventional equipment is employed for crushing. Primary crushing takes place in gyratory crushers (up to 3500 t/h) or jaw crushers. Mobile versions of the latter are now employed directly at the mines. Cone crushers are common for the second and third stages of crushing. They are however, increasingly replaced by semiautogenous grinding (SAG). Here steel balls, 100 mm or greater in diameter are added in a quantity of up to 6 vol% to aid the comminuting action. Autogenous mills are tumbling mills of large diameter and relatively short length, roughly 0.4–1.2 times the diameter. Fine grinding takes place in rod and ball mills, usually in a closed circuit with classification by hydrocyclones. Both dry and wet comminution are practiced; the wet process is more common when this step is followed by concentration.

Another option is autogenous or semi-autogenous primary crushing followed by fine grinding in a pebble mill; a tumbling mill which does not contain steel balls but lumps of ore of ca. 75–30 mm in diameter. This is possi-

ble only with hard ore that yields enough "pebbles" in the first crushing stage. This process has the advantage that no grinding balls are needed, but the energy requirement for grinding often increases if the conditions in the mill are not optimal.

Screening. Vibration screens with elliptical or linear oscillations have been widely adopted for screening. Multilevel screens of the Mogensen design are increasingly used.

Concentration. The concentration of iron ore is generally based on physical differences between the iron-bearing and gangue minerals (Table 5.3). *Flotation* and *electrostatic concentration* utilize physicochemical differences. The iron minerals have a higher specific gravity than the gangue minerals, so in many cases *gravity* or *centrifugal concentration* is possible. The *dense-media separation* process for coarse particles (≥ 3 mm) in drum or tank separators is also used. For medium-sized material, ca. 15–0.5 mm, cyclone separators or the cylindrical "Dyna Whirlpool" can be employed. Both use a centrifugal force field for separation. Gravity separators for fines (roughly 2–0.075 mm) include the Humphreys' spiral concentrator and the Reichert cone separator.

The Reichert cone separator has been adopted in the past two decades mainly for the beneficiation of placer ore, but it is used more and more for fine-grained weathering iron ores.

The *magnetic concentration* of magnetite ore takes place in drum-type separators with a low-intensity magnetic field. Dry separators are fed from the top and discharge the non-magnetics, in wet separation the ferromagnetics are picked up from the feed pulp (underfeed). Ferrite-based permanent magnets have almost completely replaced ALNICO and electromagnets. The magnetic flux density is up to 0.15 T. Wet separators include drums up to 1500 mm in diameter and 3600 mm wide, with throughput capacities of 50–200 t/h. The drums, with up to five poles, are arranged in appropriately designed tanks for cocurrent or countercurrent operation. In addition, high-intensity wet magnetic separators

have been employed since ca. 1970 in the concentration of weakly magnetic ore. The Jones design is most common. Here the separating elements are arranged in a ring which rotates carousel-fashion through a strong field generated by electromagnets. The magnetic flux density in the separation zone is 0.1–0.5 T; because of the tip configuration of the separating elements, it is concentrated at the tips to much higher values with a strong convergence of the field lines. The carousel design permits semi-continuous operation.

High-intensity dry magnetic separators are generally not used in beneficiation any longer. Electrostatic drum type separators are employed only for the recleaning of the concentrate, where they remove mainly quartz-bearing gangue. The process is restricted to grain sizes in the range of 1–0.05 mm.

Flotation has been used for iron-ore beneficiation since ca. 1950. The first two systems in Michigan were built for "direct" flotation (values in froth) of fine-grained specularite ore. Tall oil and diesel oil were added as collectors. "Hot flotation" enabled concentrates to float with only a few percent of silica. The rougher concentrate in pulp form was heated to $> 90^\circ\text{C}$, then recleaned in several stages after cooling. "Indirect" or "reverse" flotation is most commonly used today; the gangue goes into the froth and the iron ore into the underflow. Conditions are controlled so as to prevent the ore from flotation. As depressants for iron ore, starches or dextrin are used in conjunction with a basic pH. The collectors employed for gangue depend on the gangue minerals: oleic acid or oleates (e.g., for apatite) or amine salts (for quartz and feldspar). In general, the goal is first to enrich the ore as much as possible by less expensive means (gravity, magnetic separation), using relatively expensive flotation only for the final beneficiation stage. In the case of rich ores, however, flotation can also be employed as the sole concentration process when only a little gangue is to be removed.

A process of limited importance is *magnetizing roasting* followed by low-intensity magnetic separation. The iron minerals are

thermally converted to magnetite with solid, liquid or gaseous reducing agents. The process is used in shaft furnaces in China and rotary kilns in the former Soviet Union.

A *thermal beneficiation* process is the roasting of siderite ore. The purpose of this process is to save weight for transport and to relieve the blast furnace of the carbon dioxide load. Shaft furnaces or sintering machines are employed. In the latter case, agglomeration is combined with calcination.

Figure 5.2 presents a general flowsheet for the beneficiation of iron ore. Currently almost all the crude ore comes from large-scale open pit mines with capacities between 10 000 and 100 000 t/d. Only in Swedish Lapland, the former Soviet Union and China are high-capacity underground mines operated. Depending on the iron content and other requirements, the ore is processed into lumps, sinter or pellets; Table 5.6 lists the fractions of these products in blast furnace burdens in several areas. Table 5.7 gives some analyses of ores that are of commercial importance.

The beneficiation of an Indian laterite ore is shown schematically in Figure 5.3. The ore is a decomposition product containing limonite and hematite values along with kaolin, quartz and alumina minerals as gangue. By washing in a drum and then removing the finest fraction, the iron content is elevated by ca. 3% units and the Al_2O_3 content is lowered from 3–4% to $< 1.7\%$.

Table 5.6: Lump ore and agglomerate in blast-furnace charge, 1986, % [8].

	Germany	Western Europe	Japan	United States	Total
Lump ore	9.8	12.1	16.8	5.3	12.5
Sinter	64.4	70.5	73.6	22.5	62.4
Pellets	25.8	17.4	9.6	72.2	25.1
Total	100.0	100.0	100.0	100.0	100.0

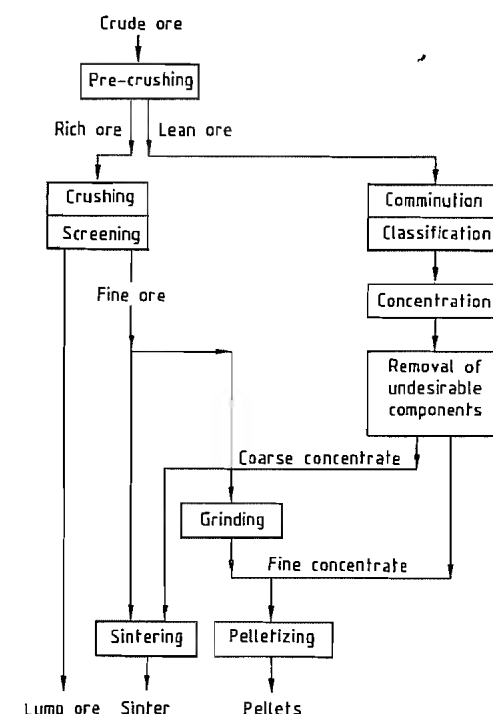


Figure 5.2: Schematic diagram of iron-ore processing.

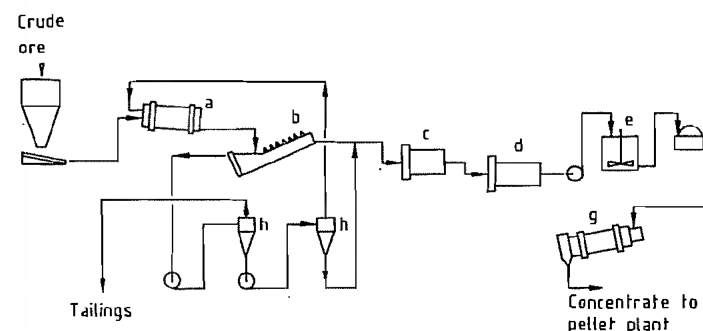


Figure 5.3: Flowsheet of Pale beneficiation plant, India: a) Washing drum; b) Spiral classifier; c) Rod mill; d) Ball mills; e) Slurry tank; f) Disk filter; g) Rotary dryer; h) Hydrocyclones.

Table 5.7: Analyses of iron ores [9, 10].

	Fe _{tot}	SiO ₂	Al ₂ O ₃	CaO	MgO	Ignition loss
Lump ores						
Hamersley Iron	65.0	2.9	1.6	0.1	0.1	2.7
Mt. Newman Mining	65.7	3.4	1.2	0.1	0.1	1.5
CVRD-Itabira	67.7	1.1	1.0	0.0	0.0	0.4
CVRD-Carajas	67.6	0.7	1.1	0.1	0.0	1.3
Ferteco Feijao	67.3	1.8	1.0	0.1	0.0	0.9
MBR-Aguas Claras	68.4	0.6	0.7	0.1	0.1	0.8
Chowgule	60.1	3.5	2.8	0.0	0.0	not known
Bellary-Hospet	66.9	2.1	1.9	0.1	0.1	0.8
SNIM-Mauretania	63.1	6.8	1.3	0.0	0.0	not known
ISCOR-Sishen	66.5	3.1	1.1	0.1	0.1	0.6
ISCOR-Thabazimbi	64.0	6.0	1.0	0.2	0.4	1.2
Cerro Bolivar	64.2	1.3	1.0	0.1	0.1	5.5
Fine ores						
Hamersley Iron	62.5	4.4	2.6	0.1	0.1	3.2
Mt. Newman	62.6	5.5	2.4	0.0	0.0	4.7
Robe River	57.2	5.6	2.7	0.1	0.1	9.2
CVRD-Sinter Fines	64.4	5.0	1.2	0.1	0.1	1.5
CVRD-Carajas	67.9	0.6	0.7	0.1	0.1	1.4
Ferteco-Fabrica	64.3	3.1	1.9	0.1	0.1	2.7
Romeral	65.4	4.4	0.9	0.9	1.0	0.8
Mifergui-Nimba	67.5	2.3	1.0	0.1	0.0	1.0
Sesa Goa	60.6	3.5	4.2	0.1	0.1	3.8
NMDC-Bailadila	65.4	2.1	1.9	0.0	0.0	not known
Carol Lake	65.8	4.5	0.1	0.5	0.4	0.3
Bong Mining Co.	64.7	7.5	0.3	0.2	0.3	0.3
LAMCO	64.7	4.7	1.0	0.0	0.0	1.7
LKAB-Kiruna KBF	69.7	1.2	0.2	0.6	0.5	0.2
LKAB-Kiruna KDF	62.0	4.6	0.8	3.6	1.2	0.6
Co. Andaluza de Minas	55.0	4.4	1.1	4.3	0.4	not known
ISCOR-SISHEN	65.5	3.7	1.6	0.1	0.1	0.7
C.V.G.-El Pao	64.5	3.7	1.4	0.1	0.1	1.9
Pellets						
Evelth Mines	65.6	4.9	0.1	0.8	0.4	
Kiruna	66.1	2.5	0.3	0.3	2.0	
Malmberget	66.7	2.2	0.8	0.2	1.6	
CVRD	65.3	2.8	0.5	3.0	0.1	
Ferteco	65.0	3.3	0.9	2.5	0.0	
Samarco	65.1	2.6	1.2	2.2	0.2	
Kudremukh	66.1	2.8	0.3	2.3	0.1	
Carol Lake	65.6	4.9	0.3	0.5	0.3	
Cartier Mining Co.	65.2	5.2	0.5	0.4	0.3	
Wabush Lake	65.8	3.0	0.4	0.1	0.0	
Bong Mining Co.	64.1	7.0	0.3	0.3	0.3	
Las Encinas	66.8	1.5	0.7	1.6	0.8	
Empire CCL	65.3	5.6	0.4	0.2	0.3	
Empire CCL	59.5	5.3	0.4	7.0	1.9	
Minntac	65.6	5.4	0.2	0.2	0.3	

This simple way of improving the composition of iron-rich fine ore is often used in India and Brazil. A basically similar process with washing troughs or log washers was formerly used for high-alumina ores in many other regions (Salzgitter, Ilsede, Mesabi Range). If much of the alumina present is associated with limonite, a rod mill is employed instead of a

washing drum. Applying 3–4 kWh/t on comminution frequently results in satisfactory removal of alumina. Figure 5.4 illustrates the beneficiation of a magnetite ore from a Magnitnaya-type deposit. Secondary and tertiary crushing and primary grinding are replaced by an autogenous mill.

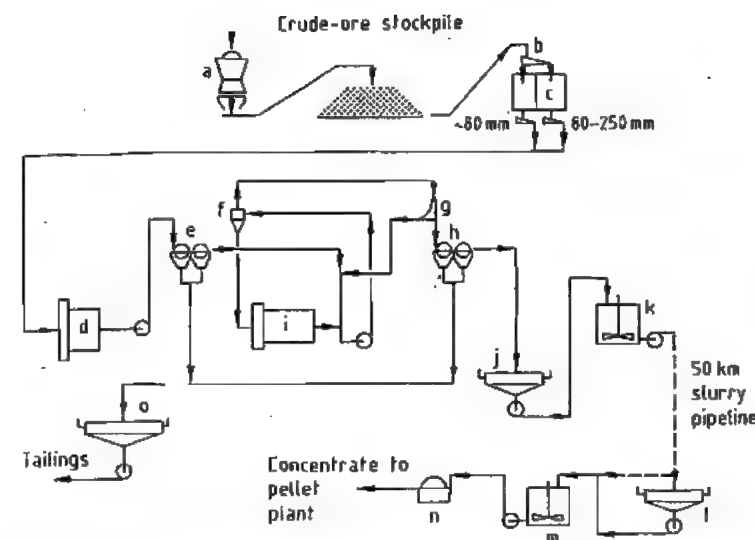


Figure 5.4: Flowsheet of Pena Colorado beneficiation plant, Mexico: a) Primary crusher; b) Crude-ore screen; c) Crude-ore bins; d) Autogenous mill; e) Primary magnetic separation; f) Hydrocyclones; g) Sieve bend; h) Secondary magnetic separation; i) Ball mill; j) Concentrate thickener; k) Slurry tank; l) Concentrate thickener; m) Slurry tanks; n) Disk filter; o) Tailings thickener.

The concentrate has ca. 69% iron; with a particle-size distribution of ca. 80% <0.045 mm, which is fine enough for pipeline transportation and pelletizing. Numerous beneficiation plants for magnetite ore from other deposit types have been designed in a similar way, for example in the former Soviet Union (Krivoi Rog, Kursk, Olenogorsk), in the Lake Superior area, and in northern Sweden. Older installations still employ conventional comminution (three stages of crushing and two to three stages of grinding).

For hematite ore, the first grinding stage is followed by gravity separation or, in the case of fine grained ore, further grinding is followed by high-intensity wet magnetic separation or flotation. In many cases, however, the principal iron minerals in such ores from weathering zones include not only hematite but martite (which is only a little less magnetizable than magnetite) with residual magnetite. In this case, complex flowsheets must be adopted, including low- and high-intensity magnetic separation, flotation, classification and slurry treatment for dewatering of the concentrate. This is also the case if undesirable constituents are present (e.g., apatite).

Finally, the *selective dispersion* process should be mentioned. In one Michigan plant, this operation is a preliminary to flotation. After grinding to the liberation size, sodium hydroxide and starch are added to the ore pulp (sodium hydroxide to disperse aluminous and limonitic constituents, starch to flocculate the specularite) and the flocculated agglomerates are separated from the dispersed minerals in a hydroseparator. The downstream flotation removes coarse quartz which is discharged in a conventional manner, with amine salts as collectors.

5.3.5 Agglomeration

In present-day smelting technology, very fine material is undesirable in the reduction equipment. The blast furnace is the dominant type of equipment for the production of iron metal. Only in exceptional cases (small furnaces with capacities up to ca. 100–150 t/d of pig iron) is unscreened crude ore used (after primary crushing if necessary). Modern high-performance blast furnaces require physical and metallurgical preparation of the burden. Formerly agglomeration was used in a purely

physical way, as a process of size enlargement aimed at improving the permeability of the blast-furnace burden; however, developments in recent years have shifted part of the slagging into the fine-ore or concentrate sintering step. On the other hand, the requirements for physical and chemical quality of the blast furnace burden have become more stringent, and mining companies that supply ore to several ironworks (as the large ones generally do) now prepare a variety of concentrate or fine ore qualities from the same or similar crude ores.

As a rule, blast-furnace burden contains lump ore, sinter, and pellets. Pellets are made from both concentrate and iron-rich fine ore. If the beneficiation process yields very fine-grained concentrates (e.g., <0.1 mm), these are usually converted to pellets at the mine and transported in this form. Sinter is generally produced at the ironworks. The varying loads imposed on material during transport to the blast furnace mean that pellets must satisfy stringent mechanical strength requirements. Pellets are also nearly always made from one well-defined ore or concentrate, whereas sinter is produced from predesigned mixtures of ores and additives. There are exceptions, such as pellets made at ironworks from mixed ore, or sinter made from a single ore or concentrate quality where an ironworks uses ore from a single deposit. Blast furnaces are also sometimes operated with lump ore alone, sinter alone, or pellets alone. Sponge iron plants are generally fed with a single iron source.

Sinter and pellets differ in the way the particles are bound into the agglomerate. In pellets, the ore particles are connected chiefly by bridges of ore. When magnetite is oxidized at temperatures >900 °C during hardening of pellets, these bridges arise through mobilization of lattice constituents during recrystallization into the hematite lattice. In the case of hematite ores, mobilization is less pronounced, because the crystal lattice structure does not change. The formation of iron oxide bridges is supported by additional slag bridges; it must be remembered that the quantity of slag in many pellet qualities is only 3–4% (corresponding to 6–7 vol %).

Sinter consists of a calcium ferrite matrix, with siliceous and aluminous constituents dissolved and primary hematite embedded in it. Whereas pellets are thoroughly oxidized (a maximum of 0.5% FeO), sinter contains 4–6% FeO, which is linked to silica and alumina in the matrix.

Pellets are burned at a temperature below the melting points of the constituents. Their strength gain is adequate only when the reaction temperature is controlled to ± 10 °C over long time periods. For this reason, hot gas is used to supply heat; it can be generated by the combustion of fuel gas, oil, or even coal. In sintering, on the other hand, the constituents of the mixture are melted. This happens at temperatures so high that the reaction itself goes to completion within minutes, but in a thin layer that continuously advances through the material bed concurrently to the gas. The fuel is coke breeze, or occasionally non-gassing coal fines, evenly distributed in the sinter mixture.

Pelletizing. Iron-ore pellets are made in two steps. The concentrate to be pelleted must have a sufficiently fine particle-size distribution (65–85% <0.045 mm) and a specific surface area of at least $1600 \text{ cm}^2/\text{g}$ as measured by a permeability method (Blaine, Fisher Sub-sieve Sizer).

Spherical *green pellets* (green balls) of appropriate size (ca. 9–16 mm in diameter) are formed by a pelletizing disk or drum. The particles are bound together by capillary forces acting through water bridges between them. This means that green pellets can be obtained only at a narrow range of moisture content. If the water content in the fine ore (which is usually recovered as a filter cake) is too high, water-absorbent materials such as bentonite can be used to correct it within narrow limits. If the water content is low (ideal case) it is useful to hold it in the filter cake ca. 0.5–1% lower than the green pellet moisture content to suppress the premature formation of undersize pellets ("micropellets") in the granulator.

Prior to (or during) the formation of green pellets, substances are added to the fines to render them stable against the stresses that oc-

cur in the hardening process. In addition to bentonite, whose active constituent is strongly water-absorbent montmorillonite, organic binders such as Peridur have come into use recently. The latter are advantageous in that they can be burned off during hardening, whereas bentonite elevates the silica and alumina content of the pellets.

Purchasers usually prescribe the gangue composition of pellets to fit the operating requirements of the particular blast furnace and the chemical composition of the other iron sources to be used. This composition, which also governs the chemical and metallurgical properties of the pellets, is controlled with additives, the most important being slaked lime, limestone, dolomite and olivine. These are

added in a grain size corresponding to that of the fines.

The second operation is the thermal *hardening* of the pellets at 1200–1320 °C. Non-thermal hardening is employed only in a few unimportant cases. Three distinct heat hardening systems exist: the traveling grate (Figure 5.5), the combination of preheating traveling grate and rotary kiln (grate-kiln) (Figure 5.6), and the shaft furnace. The shaft furnace is mainly suitable for magnetite concentrates and low capacities (up to ca. 500 000 t/a) and has lost much of its market share in the past 15 years. The traveling grate and the grate-kiln combination each share ca. 50% of the market.

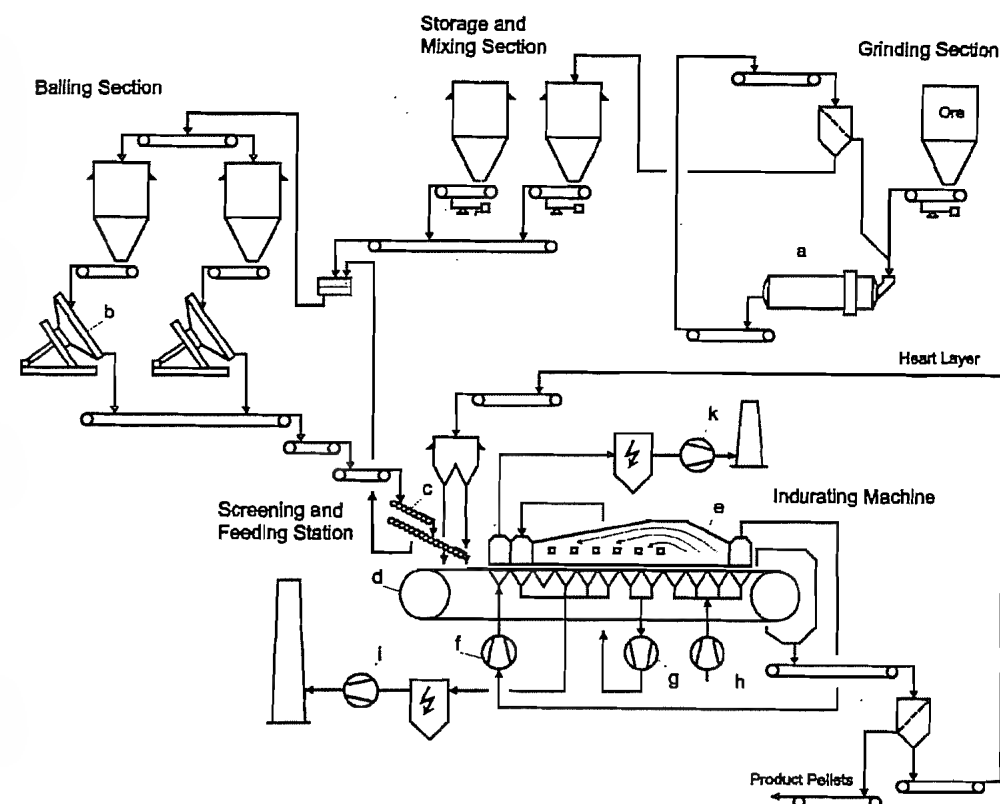


Figure 5.5: Flowsheet of Lurgi-Darvo travelling grate pelletizing process: a) Grinding mill; b) Pelletizing discs; c) Roller feeders; d) Travelling grate; e) Firing hood; f) Updraft Drying fan; g) Recuperation fan; h) Cooling air fan; i) Waste gas fan; k) Hood exhaust fan.

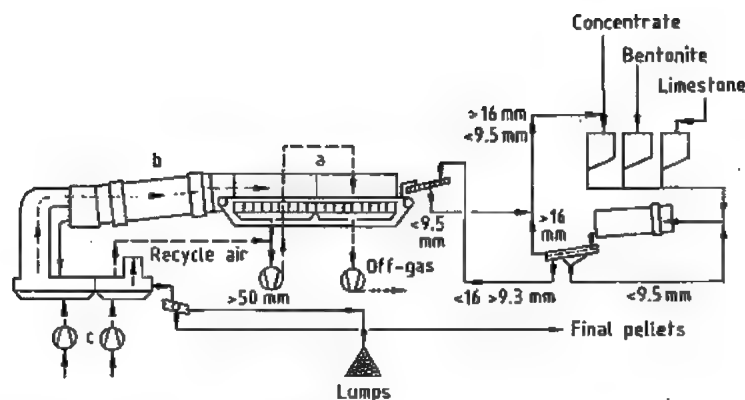


Figure 5.6: Flowsheet of combined traveling grate/rotary kiln ("grate kiln") process: a) Traveling grate; b) Rotary kiln; c) Annular coolers.

The "basicity" of the final pellets, expressed as the ratio $(\text{CaO} + \text{MgO}) : (\text{SiO}_2 + \text{Al}_2\text{O}_3)$, is < 0.1 for "acid pellets" or up to 1.3 for "basic pellets". Each range of values offers certain advantages and disadvantages with respect to mechanical strength and metallurgical qualities.

After a number of years of declining pellet production and the shutdown of several plants, the western world had, at the end of 1987, a pellet capacity of roughly 163×10^6 t/a (100 units using the three hardening processes).

According to present information, the former Soviet Union has 20 traveling-grate plants and 5 grate-kiln plants. The first group has a total reaction area of ca. 6500 m^2 , which might correspond to a pellet capacity of ca. 50×10^6 t/a. Grate-kiln plants add an estimated capacity of ca. 107 t/a .

While the former Soviet Union has a large number of pellet plants, up to now this has not been the case for China.

For the assessment of the mechanical and metallurgical properties of burned pellets, a number of parameters are determined in more-or-less standardized tests. The most important are:

● Cold Compression Strength

Individual pellets 10–12 mm in diameter are compressed to failure between two plane or slightly concave faces of a hydraulic press, and the crushing force is measured (values

found in practice are usually $> 3000 \text{ N}$ per pellet).

● Abrasion Resistance

The abrasion resistance is determined in the ISO tumble test. Under standardized conditions, pellets are tumbled in a drum and the $> 6.3 \text{ mm}$ and $< 0.6 \text{ mm}$ fractions are determined. The values should be at least 95% and at most 4%, respectively.

● Low-Temperature Disintegration test

This test indicates how the pellets will behave, for example, in the blast furnace in the critical range of temperatures around 500°C . In an electrically heated rotary kiln, pellets are heated to $500 \pm 10^\circ\text{C}$ and held at this temperature for 60 min under reducing conditions. After cooling, the pellets are screened to determine the $> 6.3 \text{ mm}$ and $< 0.5 \text{ mm}$ fractions. The degree of reduction is determined. The values for the $> 6.3 \text{ mm}$ fraction are usually between 60 and 80%; those for $< 0.5 \text{ mm}$ usually 10–20%.

● Free Swelling

In a vertical tubular furnace, 18 pellets are reduced with a carbon monoxide hydrogen mixture at 1000°C . The weight loss during reduction yields the degree of reduction. The volume change in the pellets indicates the swelling, which should be 20% at maximum. The compression strength measured in a hydraulic press should be $> 500 \text{ N}$ per pellet.

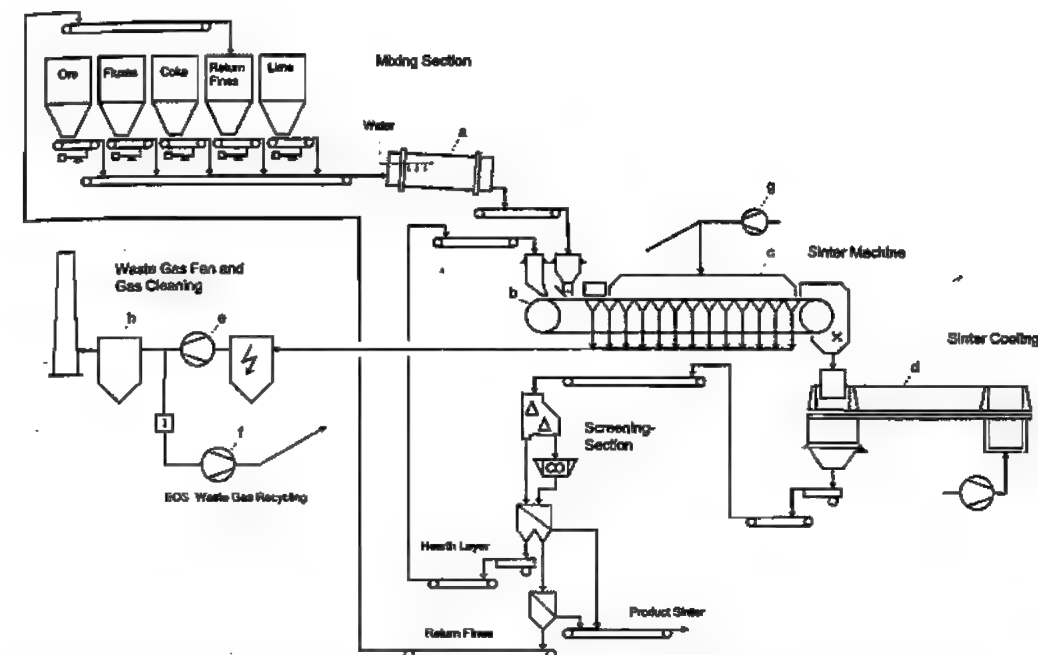


Figure 5.7: Flowsheet of sintering: a) Mixing drum; b) Travelling grate; c) Gas distribution hood (EOS only); d) Annular cooler; e) Waste gas fan; f) EOS recycling gas fan; g) Fresh air blower (EOS only); h) Waste gas final cleaning.

● Reduction under Load (RUL)

In an upright retort, pellets are heated to 1050°C , placed under a mechanical load of 5 N/cm^2 , and exposed to a reducing atmosphere. The pressure drop of the reducing gas across the bed and the reduction rate are determined. A low pressure drop indicates pellets stable in reduction. The pressure drop should not exceed 100 Pa.

The reduction rate at 40% reduction is an important parameter of reducibility; dR/dt_{40} should be at least 1% per minute.

Special test methods have been devised for pellets used in various direct-reduction processes (HyL reduction test in an upright retort, Midrex test, and testing for the SL/RN process in an electrically heated laboratory rotary kiln). In the test for the SL/RN process, pellets and reducing agent (usually coal) are investigated at the same time. A number of different or modified test procedures are employed in individual countries or at individual iron works.

Sintering. Iron ore sinters are virtually all produced in travelling-grate installations (Figure 5.7). The rotary kiln and pan-sintering processes formerly in use are no longer important. Likewise, cooling of the hot sinter at the last section of the grate has become obsolete. Standard is now the straight-grate "Dwight-Lloyd-Process". Straight-grate as well as annular coolers are in use. Quite some efforts are being made to reduce solid and gaseous contaminants contained in the sintering off-gas (dust, SO_2 , NO_x). A new development recently introduced by Lurgi in industrial plants is "EOS" (Emission Optimised Sintering) process. It is characterized by recirculating approximately half of the off-gas of the sintering grate back to the gas distribution hood, where it is mixed with fresh air and used as oxygen carrier and for heat transportation through the sinter bed. The advantages are reduction of the final waste gas volume (allows for smaller gas cleaning facilities), and substantial reduction of waste gas pollutants (dust, SO_2 , NO_x , dioxines, furanes). Fuel consumption is reduced by

about 5 kg/t of sinter, whereas the electric energy consumption is increased by about 1.5 kWh/t.

As a rule, several ores are processed in one unit; a "monosinter" from just one ore is the exception. Along with ore and concentrate, the mixture for sintering also contains recycle material from the ironworks, provided no buildup of undesirable or detrimental substances results. Undersize sinter from the screening step is also recycled. The basicity of the sinter has been substantially increased in recent years. Originally sintering was considered only as a means to deal with fine ore with respect to improved handling and permeability of the blast furnace burden ("physical burden processing"). The overall chemical composition of the blast furnace feed (including coke ash) was adjusted by addition of suitable materials in the form of lumps (limestone, dolomite, manganese ore if necessary). Thus, the basicity of sinter and lump ore generally was < 1 (exception minette ore with high calcite content of the gangue).

Today these additives are generally added to the sinter mix as fines (< 5 mm) and sometimes precalcined (burnt lime instead of limestone). The basicity of the sinter is generally higher than that of the blast furnace slag to compensate (1) for the "acid" coke ash, (2) the gangue of the lump ore, and (3) slag components of the iron-ore pellets.

Increasing the basicity also improves the quality of the basic sinter as well as the heat economy. Many plants today produce sinter with a basicity of > 1.5. The slag analysis is controlled by addition of limestone or burnt lime, dolomite (to control CaO and MgO), olivine (to control MgO and SiO₂), and quartz sand. The most common fuel is coke breeze. To ignite the mixture gas or oil heating is applied. The total heat consumption for an iron-rich basic sinter is between 1.3 and 1.7 MJ per tonne of final sinter. When low-iron ore mixtures (e.g., those containing minettes) or ores containing high levels of alumina (2–4% Al₂O₃) are sintered, the heat consumption is higher (up to 2.5 MJ/t). Analyses of sinter

from German ironworks fall in the following approximate ranges (in %):

Fe _{tot}	55.5–55.8
Fe(II)	4.5–6
SiO ₂	5–6
CaO	9–11
MgO	1.2–3.2
Al ₂ O ₃	1.2–2
CaO:SiO ₂	1.4–1.9

Ironworks in Germany use imported ores almost exclusively; some heat-consumption and analysis figures for other European ironworks differ from the ones cited, because low-iron domestic ores still are processed there. In contrast, sintering plants in Japan operate under conditions similar to those in Germany. The basicity of the sinter in Japan, however, is nearly always > 1.8.

In the United States, the fraction of sinter in the burden is only 22.5% (1986; Table 5.6), much lower than in Europe and Japan. The fraction of pellets, on the other hand, is very high (72.2%). Thus, in the United States improvement in pellet quality, above all in metallurgical properties, have been the focus of attention, with the result that basic pellets with CaO:SiO₂ ratios of ca. 1.5 have been sought.

Few details are known about current sintering technology in the former Soviet Union and China. Rich fine ores are rare in both countries, and agglomerates are made chiefly from concentrates. In some works, blast furnaces are operated on 100% sinter. Since the basicity of the sinter in these cases must be adapted to the requirements for blast-furnace operation, the basicity values are often too low for a sinter of truly good quality. One remedy might be to pellet part of the concentrate at a low basicity and raise the basicity of the sinter to 1.6–1.8.

A variety of test methods are used for sinter quality control; some of the techniques are similar to the ones for pellets. The methods include:

● Shatter Test

The shatter test has been standardized only in Japan. At Lurgi, 150 kg of sinter (grain size > 8 mm) is dropped three times from a height of 2 m onto a steel plate; then the

> 20 mm, 20–8 mm, 8–2 mm, and < 2 mm fractions are determined.

● Tumble Test

The shatter test is often replaced by the tumble test, which follows the same guidelines as described above for pellets. The fraction < 6.3 mm should be at least 70%; at German ironworks it is between 70 and 85%.

● Low-Temperature Disintegration

This test is not one of the standard ones; it is performed in a similar way to the test on pellets.

● Reduction Degradation Index (RDI)

The reduction degradation index is now regarded as the most important quality criterion for sinter. In the test, 500 g of sinter (grain size 20–16 mm) in a stationary bed is reduced for 30 min at 550 °C by a gas mixture comprising 30 vol%, carbon monoxide and 70 vol% nitrogen.

After cooling, the sample is placed in a drum (130 mm in diameter and 200 mm long and provided with two lifters) and subjected to 900 revolutions at 30 rpm. The material is then screened at 6.3 mm, 3.15 mm and 0.5 mm. The RDI is the fraction < 3.15 mm. This should be 35% if possible; at ironworks, in Germany it is between 30 and 40%.

● Relative Reducibility

Ironworks use very different methods for the relative reducibility test. A sample is reduced at 900 °C using a carbon monoxide nitrogen mixture similar to RDI. The index reported is the degree of reduction at the end of the test. In addition, a test as set forth in ISO 4695 is carried out to determine the reduction rate at 40%, reduction, which is usually ca. 1.5% per minute.

5.4 Reduction of Iron Oxides [11]

5.4.1 Chemical Aspects

The reduction of iron oxide ores takes place at an appreciable rate only at temperatures

above 900 °C. Below this temperature, a dark porous mass is obtained having the same shape as the original lumps or particles, and reduction is usually incomplete. Figure 5.8 shows a particle of Fe₂O₃ before and after reduction by hydrogen at 700 °C showing the porous nature of the product. In general, reduction follows the scheme



If reduction is conducted below 570 °C, the reaction follows the scheme



Figure 5.8: A 20-μm Fe₂O₃ sphere before and after reduction by hydrogen at 700 °C (2500 x).

since FeO is unstable below 570 °C. When a hard dense oxide is reduced, metallographic examination usually shows a layered structure: Fe₂O₃ in the core, surrounded by Fe₃O₄, FeO, and finally Fe as can be seen in Figure

5.9. For porous oxides, however, no distinct interfaces are observed, except a gradual transformation from Fe on the outside to Fe_2O_3 in the center. This is because the reducing gas can penetrate faster than it can react at any oxide interface.

Between 950 and 1000 °C complete reduction in a reasonable length of time usually takes place. At 1000 °C, sintering of the particles starts and a product having the form of a sponge is obtained. At about 1200 °C a pasty porous mass is formed due to the presence of impurities. If reduction is carried out in the presence of carbon, the iron absorbs it rapidly and the product begins to melt at 1300 °C. Iron containing 4.5% carbon melts at 1125 °C which is far below the melting point of pure iron (1530 °C). Table 5.8 summarizes these points.

Figure 5.9: Cross section of a partially reduced dense iron ore in hydrogen at 850 °C for 35 minutes. Sample etched to show the multilayer structure of products.

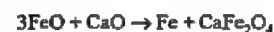
Table 5.8: Effect of temperature on the reduction of iron oxide ores.

Temperature, °C	Product
900	Dark grey porous mass has the same shape as the original particles; reduction usually incomplete.
950–1000	Complete reduction in a reasonable length of time.
1000	Sintering of product starts; the product has the shape of a sponge.
1200	A pasty porous mass is formed.
1300	If reduction is carried out in presence of carbon, the iron absorbs it rapidly and the product begins to melt.

Ferric oxide, Fe_2O_3 , is generally reduced with a higher velocity than Fe_3O_4 . Also, hy-

drogen is more effective than CO as a reducing agent. Like any other heterogeneous reaction, the rate of reduction is influenced by the stagnant boundary layer of gas which surrounds each oxide particle (the Nernst boundary layer). This factor depends on the rate of flow of the reducing gas past the oxide particle, i.e., it is a function of the design and operation of the apparatus used for reduction. The resistance of the boundary layer may be eliminated by increasing the rate of flow of gas, but this way may not be economically feasible because unreacted gas will escape in the stack, or the carry over of dust particles will be excessive.

Swelling or shrinkage may accompany the reduction. Swelling is due to the formation of whiskers which in turn is related to the phenomena of nucleation and crystal growth. Shrinkage is due to volume change when the oxide is reduced to metal as well as due to sintering. Both are influenced by impurities. Calcium oxide, for example, was found to prevent swelling and to increase the rate especially when conducted at or below 700 °C. The width of the FeO layer formed when Fe_2O_3 -CaO mixture is reduced is much less than when pure Fe_2O_3 is reduced, all other conditions being equal. It seems that FeO reacts with CaO forming Fe and a ferrite according to



Calcium ferrite formed is then reduced directly to Fe and CaO without producing FeO. Calcium carbonate increases the rate of reduction in the same way as CaO with the added advantage that during sintering prior to reduction, CO_2 is given off thus creating a porous product which enhances reduction. Small amounts (0.1–1%) of Na_2CO_3 or K_2CO_3 cause extensive swelling.

5.4.2 Technical Aspects

It was not until the 14th century that furnaces were developed that could not only produce iron but at the same time melt it so that the product called pig iron could be tapped

from the furnace in a molten form, thus allowing large scale production and continuous operation. Such a furnace is called a blast furnace because of the blast of air introduced. Figure 5.10 shows a typical view of a blast furnace plant. At present, most pig iron is transferred in molten state to steelmaking plants and in this form it is referred to as hot metal. Sometimes, it is required in solid form

for convenient handling and therefore is cast into molds where it solidifies to form what is referred to as pigs. Processes taking place in the furnace are:

- Reduction of the iron compounds present in the ore
- Separation of the resulting iron from the slag.

Figure 5.10: Typical view of a blast furnace plant. The blast furnace at the center, the three towers on the left are the stoves.

Figure 5.11: Hot metal mixer.

Steel is the most important commercial form of iron because of its high tensile strength. Molten pig iron from the blast furnace is usually stored in a hot-metal mixer before transferring it to the steelmaking plant (Figure 5.12). A hot-metal mixer is a cylindrical vessel up to 1500 tons capacity, lined with fire bricks (about 0.6 m thickness) and mounted horizontally such that it can be tilted to pour the desired amount of metal into a transfer ladle for transport to the steelmaking plant (Figure 5.11). The functions of the hot-metal mixer are therefore the following:

- To conserve the heat in pig iron, keeping it molten for long periods.
- To promote uniformity of iron by mixing the products of several blast furnaces. This permits delivery of iron of more uniform compositions and temperatures.
- To permit independent operations between the blast furnaces and the steelmaking plant because of its large capacity.

Table 5.9 shows the raw materials and the products of a modern blast furnace.

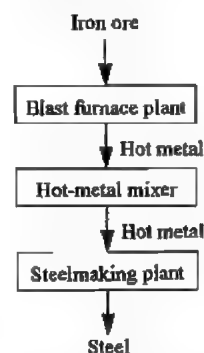


Figure 5.12: Schematic representation for the flow of raw material for steelmaking.

5.4.3 Raw Materials

Iron ores are the most important raw material charged to blast furnace. Other minor material are the following:

- Mill scale (Fe_3O_4 by-product of hot-rolling)

Table 5.9: Raw materials and products of a blast furnace per ton of pig iron (in tons).

Raw materials	
Ore	1.7
Coke	0.5–0.65
Flux (limestone)	0.25
Air	1.8–2.0
Products	
Pig iron	1.0
Slag	0.2–0.4
Flue dust	0.05
Blast furnace gas	2.5–3.5

Table 5.10: Typical analysis of Lake Superior ore.

	%
Fe	55.6
SiO_2	5.9
Mn	0.2
P	0.6
Al_2O_3	3.6
CaO	1.2
MgO	0.9
SO_3	0.06
$\text{Na}_2\text{O} + \text{K}_2\text{O}$	trace
TiO	0.02
H_2O	12.1

- Blast furnace flue dust after sintering
- Pyrite cinder after leaching away of the non-ferrous metals it contained

5.4.3.1 Iron Ores

High-grade ores contain 60–70% Fe, medium-grade 40–60% Fe, and low-grade < 40% Fe. The world's main supply of iron is obtained from ores containing hematite; those containing magnetite supply only about 5% of the world's iron and the most important source of such ores is Sweden and the Urals. The most important ore containing siderite is in Erzberg, Austria. A typical analysis of an iron ore is shown in Table 5.10.

5.4.3.2 Coke¹

Coke in the blast furnace has two functions:

- As a fuel producing the heat required for reduction and melting the iron.
- To supply the reducing agent (mainly CO).

¹ For the manufacture of coke, see Section 5.22.

Table 5.11: Typical analysis of coke.

	%
C	90.0
SiO_2	4.4
Fe	1.3
Mn	0.07
P	0.03
Al_2O_3	2.8
CaO	0.3
MgO	0.2
S	0.9
H_2O	1.5

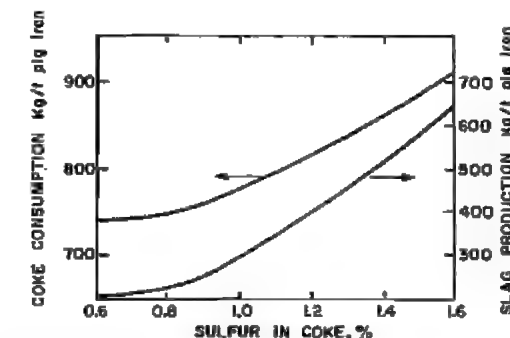


Figure 5.13: Effect of sulfur in coke on coke consumption and slag volume.

Besides, a small amount of carbon dissolves in the hot metal, thus lowering its melting point. Main requirement for coke are: high calorific value, high mechanical strength, and low impurities. A typical analysis of coke is given in Table 5.11. Coke burns intensively near the tuyères; temperatures in this region reach 1700 °C. At this temperature, CO_2 reacts immediately with carbon to form CO:

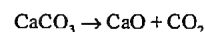


Sulfur in the coke accounts for about 90% of the total sulfur entering the blast furnace. About half of this sulfur is volatilized as H_2S or COS when the coke is burned and leaves with the blast furnace gas. The remaining sulfur is partially eliminated in the slag, and a small amount enters the metal. When coke contains excess sulfur, large amounts of limestone must be added to insure that the sulfur content of the pig iron is maintained at a low level. This will result in a large volume of slag, and a correspondingly large consumption

of coke because the decomposition of limestone is an endothermic reaction, as shown in Figure 5.13. Furthermore, the productivity of the furnace decreases.

5.4.3.3 Limestone

The function of limestone is to render the gangue in the ore and the ash of the coke, mainly SiO_2 and Al_2O_3 which have high melting points, easily fusible. In the blast furnace, limestone is decomposed starting at 800 °C as follows:



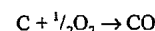
It is used in pieces 5–10 cm in size; a typical analysis is shown in Table 5.12.

Table 5.12: Typical analysis of limestone.

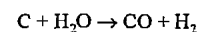
	%
CaO	51.5
MgO	1.7
CO ₂	41.4
SiO ₂	3.4
Fe	0.3
Mn	0.1
P	0.006
Al ₂ O ₃	0.9
SO ₃	0.06
Na ₂ O + K ₂ O	trace
H ₂ O	0.5

5.4.3.4 Air

Air for the blast furnace has to be preheated to 500–1000 °C and compressed to 200–300 kPa to burn the necessary amount of coke to furnish the required temperature for the reaction:



Air always contains a certain amount of moisture depending on the atmospheric humidity. Near the tuyères zone, any moisture in the air will react with coke as follows:



Since this reaction is endothermic, variation in atmospheric humidity greatly affects the thermal balance of the furnace to such an extent that it would cause wide variation in the chemical composition of the iron produced. Some plants installed units to separate the moisture

from the air by refrigeration before entering the furnace.

Table 5.13: Typical analysis of pig iron.

	%
C	3.5–4.25
Si	≈ 1.25
Mn	0.9–2.5
S	≈ 0.04
P	0.06–3.00
Fe	≈ 94

5.4.4 Products

5.4.4.1 Pig Iron

Pig iron is transferred molten as hot metal or molded in pig-machine. A typical analysis of pig iron is given in Table 5.13. The hearth temperature influences the carbon content in pig iron.

5.4.4.2 Slag

Slag formed in the blast furnace serves two purposes:

- To collect the impurities in the molten metal
- To protect the metal from oxidation by the furnace atmosphere

Analysis of a typical blast furnace slag is given in Table 5.14. About 1% of the slag containing about 60% Fe is recovered by magnetic separation and is returned to the blast furnace. Molten slag from a blast furnace is usually treated in one of the following ways:

- It is poured into a pit and after solidifying and cooling it is excavated, crushed, and screened. The product is called air-cooled slag and is used in concrete and railroads.
- It is either allowed to run directly into a pit of water producing a coarse, friable product, or a stream of molten slag is broken up by a high-pressure water jet as it falls into the pit. The product in both cases is called granulated slag and is used in making building blocks.
- If limited amounts of water are applied to the molten slag, a dry cellular lump of product called lightweight expanded slag is formed. In this case the amount of water

should be less than that required for granulation. This slag has a relatively high structural strength with good insulating and acoustical properties and is therefore used in making acoustical tile and for other structural purposes.

- Slag fines are used as filling material in road construction since they have excellent binding properties with bitumen.

Table 5.14: Analysis of a typical blast furnace slag.

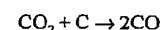
	%
SiO ₂	35
CaO	44
Al ₂ O ₃	15
MgO	3
FeO	1
MnO	1
S	1
Total	100

Table 5.15: Typical analysis of blast furnace gas.

	vol%
CO	27
CO ₂	12
N ₂	60
H ₂	1
(CN) ₂	trace
Total	100

5.4.4.3 Gas

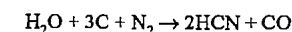
Gas coming out of furnace top is more than that introduced at the bottom due to the gasification of carbon. A typical analysis of the gas is given in Table 5.15. The CO content in the gas is due to the reaction:



About 20% of the total fuel requirement is consumed in this manner. This reaction not only consumes coke but also consumes heat since it is endothermic. Carbon dioxide is a product of ore reduction and CaCO_3 decomposition. Because of its CO content, the blast furnace gas is used as a fuel to preheat the air blast and to generate power (boilers, etc.). The gas leaves the furnace at 120–370 °C.

During the manufacture of iron in the blast furnace, some hydrogen cyanide, HCN, and cyanogen gas, (CN)₂, are formed as a result of the reaction of nitrogen in the blast with coke.

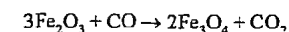
These gases are extremely poisonous. Their formation is thought to be catalyzed by alkali oxides:



Blast furnace gas contains 200–2000 mg/m³ of these cyano compounds. In the dust collecting system, the gases are scrubbed with water and some of this water finds its way in waste disposal. Before discharging this water, cyanide compounds dissolved in it must be destroyed.

5.4.4.4 Flue Dust

This material is composed of about 15% carbonaceous material, 15% gangue, and 70% Fe_3O_4 though only Fe_2O_3 may have been charged; the reason is that the reaction at the top of furnace is



Flue dust is collected as a mud in the venturi scrubbers and Cottrell precipitators; it contains about 40% solids. It is transferred to thickeners where it is thickened to 60% solids, then filtered. The filtrate returns to the thickeners and the filter cake containing about 25% moisture is transferred to the sintering plant where it is agglomerated into a product suitable for charging to the furnace.

5.4.5 Behavior of Impurities

Impurities in the raw materials play an important role in the blast furnace because they influence the quality of the product and the life of the refractory lining. Although some of these impurities may be in trace amounts, yet they will represent hundreds of thousands of tons when considering the continuous operation of the furnace for 5 to 7 years through which millions of tons of ore have been reduced. The behavior of impurities varies considerably and can be divided as follows:

- Unobjectionable impurities are those which are not reduced, e.g., Al_2O_3 and MgO. They are also valuable fluxes.
- Impurities that completely enter the pig iron; these are phosphorus, copper, tin, nickel, and vanadium. The reduction of the

compounds of these elements takes place readily. Of these the most serious is phosphorus since it has to be completely removed to make an acceptable steel.

- Impurities that partially enter the pig iron: these are manganese, silicon, titanium, and sulfur. The reduction of MnO_2 , SiO_2 , and TiO_2 takes place only at high temperatures. Therefore, the presence of the respective metals in pig iron will be a function of the temperature in the hearth; usually about 70% of these metals enter the pig iron. Titanium is especially undesirable because its presence in the slag, even in small amounts, increases its viscosity. Manganese, silicon, and sulfur have to be removed later in the steelmaking process.

- Impurities that accumulate in the furnace: these are the alkali metals and zinc. Compounds of these metals are readily reduced. As the charge descends into the hotter region of the furnace they are reduced to metals; these metals are volatile under the conditions of operations in the furnace. As vapors, they travel upward, where they react with CO_2 and deposit as oxides on the surfaces of the cooler particles of the charge and are again returned to the hotter region of the furnace as the charge descends. The process is repeated and thus these metals will never leave the furnace. They accumulate in large amounts and the vapors penetrate the refractories and partially condense in the pores and cracks thus causing their disintegration. To minimize difficulties in furnace operation such as fluctuating hot metal temperature or sulfur content and to avoid the build-up of alkali in the furnace, the amount of alkali entering the furnace is carefully monitored and maintained at a fixed low level. Slag basicity and hot metal temperature are also adjusted to ensure maximum removal of alkali in the slag. The tendency is approximately as follows:

- As the alkali content increases, slag basicity should be decreased for any given temperature of iron.

- As the temperature of molten iron increases, slag basicity should be decreased for any given alkali loading.

These conditions are opposite to those needed for hot metal sulfur content, and therefore a compromise has to be made.

5.5 The Blast Furnace

5.5.1 General Description [11–14]

The blast furnace is composed of a hearth and a stack on the top. Such furnace is also known as a shaft or a vertical furnace (Figure 5.14). The name is due to the fact that air is blown or “blasted” through the charge. The furnace has the following characteristics:

- The charge enters at the top of the stack and the products get out at the bottom. Any gases formed are discharged from the top.
- Heating is conducted by burning coke which is incorporated in the charge. It is ignited by air blown in near the bottom of the furnace. The hot gases pass upward through the descending cold charge.
- The charge must consist of coarse material that is strong enough to withstand the static pressure in the shaft without crumbling into powder. Powders are objectionable because they will be easily blown outside the furnace by the gases. Also, they cause channelling to take place in the furnace, i.e., the reacting gases will go only through certain channels in the bed thus decreasing greatly the furnace efficiency. The charge must be permeable so that the rising gases can pass freely through all of its parts.
- At one time, the top of the furnace was left open causing great heat loss. Later, it was closed and opened only during charging. Today furnaces have at the top the double bell system which keeps the furnace closed at all times thus preventing the escape of gases even during charging. This system (Figure 5.15) is composed of two bells: one small and one large. When both are in the closed position, the charge is dumped in the hopper above the small bell. The large bell remains

closed while the small bell is opened to admit the charge to the large bell hopper. The small bell is then closed to prevent the escape of gas into the atmosphere, and the large bell is opened to admit the charge to the furnace. The large bell is again closed and the process repeated. It should be noted that the rod supporting the large bell passes through a hollow rod supporting the small

bell, thus permitting the independent operation of bells. The opening and closing of the bells is fully automated.

- High temperature can be attained in a furnace without damaging the refractory lining by inserting hollow wedge-shaped plates in the outer side of the refractory lining which are water-cooled.

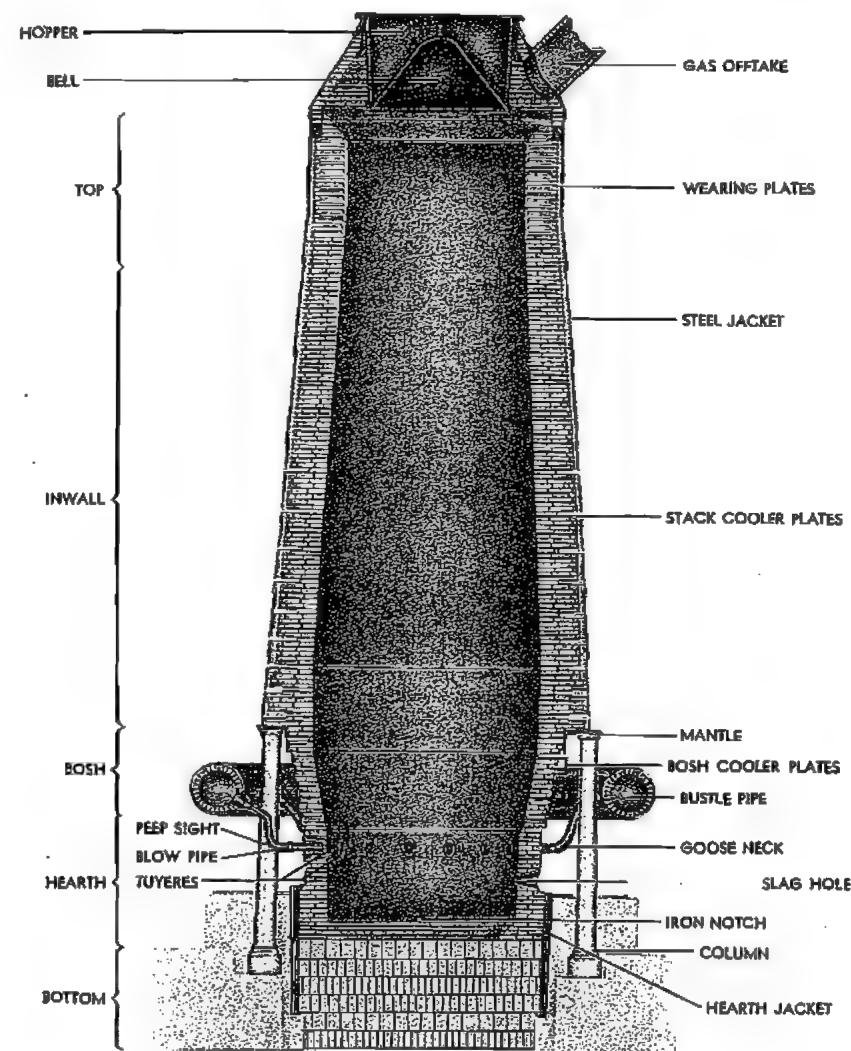


Figure 5.14: A vertical furnace — the iron blast furnace.

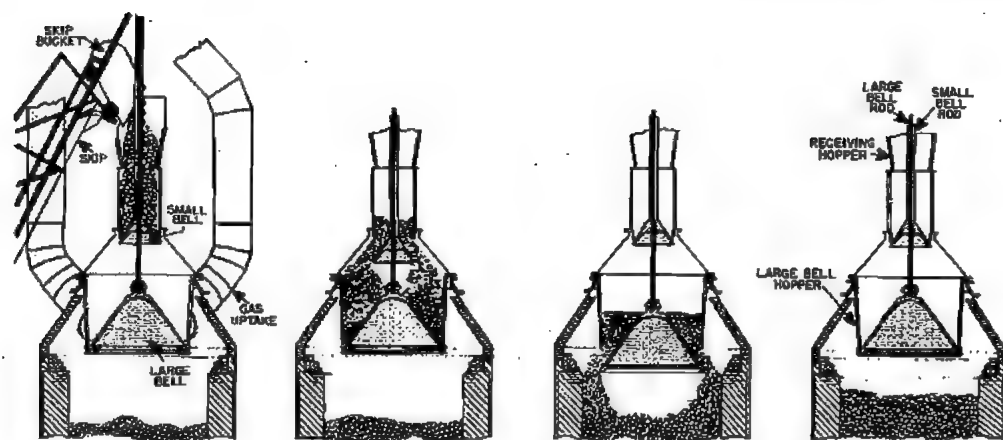


Figure 5.15: Double bell system for charging a blast furnace without permitting an escape of gases.

- Air for the furnace is introduced at the lower part. Figure 5.16 shows a section through the bosh and upper part of the hearth wall showing details of connections between the tuyère and the bustle pipe in a large blast furnace. The bustle pipe is a large circular, refractory-lined pipe that encircles the furnace at about the mantle level and distributes the air blast from the hot-blast main to the furnace. The blowpipe, a horizontal, ceramic-lined steel pipe about 1.5 m long, carries the hot blast from the bustle pipe through the tuyère stock and gooseneck to the tuyères. The tuyères are nozzle-like copper castings about 20 in number, spaced equally around the hearth about 30 cm below the top of the hearth. Each tuyère fits into a tuyère cooler casting through which cold water circulates. The gooseneck is lined with fire brick, and has a small opening closed by the tuyère cap through which a small rod may be inserted to clean out the tuyères without removing the blow pipe. A small glass-covered opening called the peep sight is placed in front of the tuyères to allow the inspection of the interior of the furnace directly.
- The furnace acts as a countercurrent heat exchanger: the cold charge is descending while the hot gases are ascending in the furnace. Thus, coke will be preheated in the upper part of the furnace so that when it

reaches the lower portion and comes in contact with the hot air blast at the tuyères, it will burn with great intensity. In the upper part of the furnace, the ore also loses its water content and is preheated.

- The liquid products formed settle to the bottom from where they can be removed. New material is charged at the top in quantities sufficient to keep the charge level relatively constant.
- Tapping a molten material from the furnace, e.g., a molten metal is usually conducted in the following way. The notch which is closed with clay is opened by drilling into the clay with a pneumatic drill until the skull of metal is met, then an oxygen lance is used to form a hole through it. The metal flows into the main trough which has a skimmer located near its end. The skimmer separates any slag flowing with the metal and drives it into the slag ladles. The metal continues to flow down the main runner from which it is diverted at intervals into the metal ladles by means of gates. At the end of tapping, the hole is closed by means of the clay gun. The nose of the gun enters the metal notch and clay is forced from the gun by a plunger or a screw operated electrically or by steam. The slag notch can be opened or closed by means of a steel cone-shaped knob on the end of a long steel bar. Figure 5.17 shows a section through the slag notch.

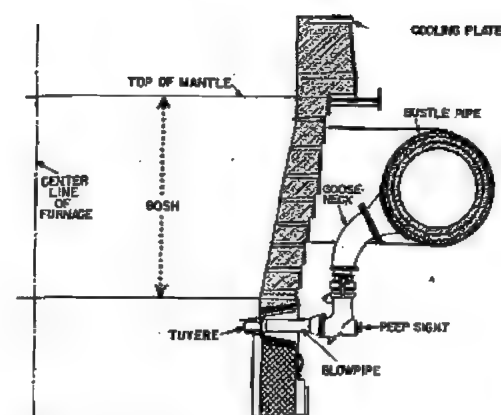


Figure 5.16: Section through the bosh and upper part of the hearth wall of a blast furnace.

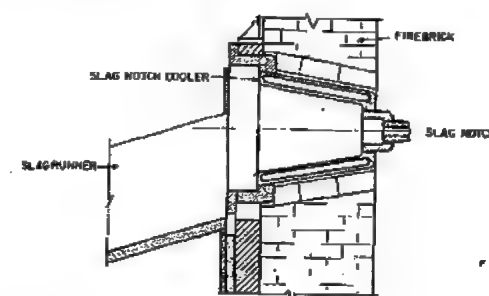


Figure 5.17: Section through slag notch of a blast furnace.

- The furnace is lined with refractory materials which must have a high melting point to withstand high temperatures. Alumina-silica refractories are usually used for lining the stacks. The percentage of Al_2O_3 in the bricks increases in the lower part of the stack. Graphite is one of the most refractory substances known but oxidizes slowly at high temperatures; it is usually used for lining the hearth.
- The furnaces are fully automated and may produce 10 000 tons of iron per day. They are huge structures over 60 m high. The column of material inside the furnace is about 25 m high that varies in temperature between 190 and 1760 °C. A furnace is designed to operate continuously for 5–7 years with a total production of about 14 million tons.

- To support a large furnace, a reinforced concrete pad about 3 m thick and 18 m diameter is built. A circular heat-resistant concrete pad about 6 cm thick is laid over the foundation (Figure 5.18). A large furnace requires 8–10 supporting columns which are anchored to the concrete foundation. A heavy, horizontal steel ring 5–10 cm thick called mantle rests on the top of the supporting columns. It supports the furnace shell and brickwork so that, when necessary, the hearth and bosh brickwork may be removed without much trouble.

5.5.2 Operation

Starting a New Furnace. Bringing a newly built furnace into routine operation is called "blowing-in". This process requires the skill and cooperation of a large number of people, and it takes probably more than a month to achieve this goal. Once a furnace goes into operation it is expected to continue for 5 to 7 years during which about 8 million tons of iron are produced before a major shutdown. The steps involved are:

- Drying the lining of furnace and stoves. This operation is carried out for the following reasons:
 - To drive off the vast amount of water absorbed by the brick during construction, and contained in the slurry used in brick-laying.
 - To avoid as much as possible thermal shock to the structure. Drying is carried out by burning natural gas or wood in the stoves and circulating the hot gases to the furnace. Heating should be increased gradually and it usually takes 10 to 14 days. During this stage intensive checking of pipes, connections, etc., takes place.
- Filling the furnace. Usually the hearth and bosh are filled with coke, then about an equal charge of coke, limestone, and siliceous material are mixed together and added on top. Then comes a charge composed of a small amount of ore and coke.

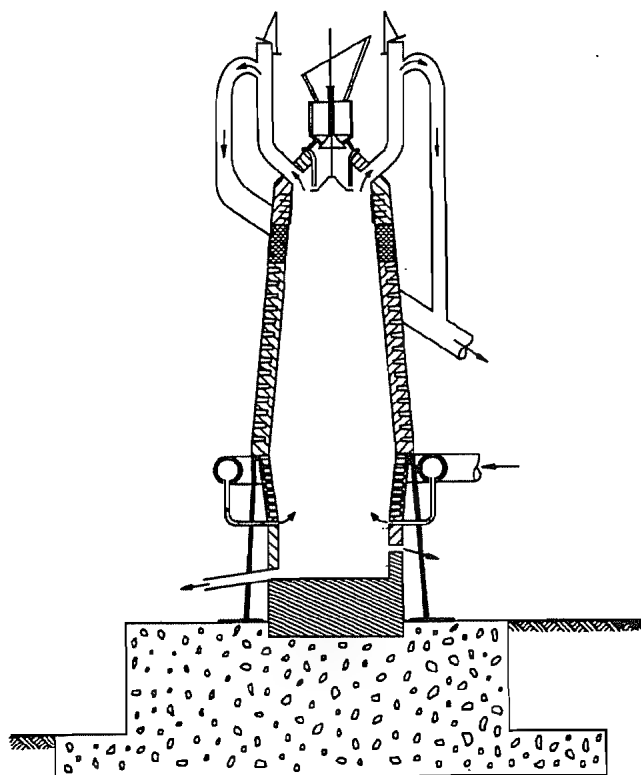
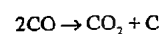


Figure 5.18: General view of the iron blast furnace showing top details and concrete foundation.

- **Lighting the charge.** This is done by blowing small volumes of hot blast at 1000 °C.
- **First stages of operation.** Once the coke in the furnace is ignited, it is important to ignite the gas leaving the furnace otherwise it will cause a health hazard to the environment due to the CO content. Gradually the hot blast volume entering the furnace is increased. After the initial coke charge is consumed, slag will begin to accumulate in the hot hearth. Charging at the top continues and at the same time the percentage of the ore is gradually increased. Once there is indication that enough slag accumulated, the slag notch is closed. Tapping of slag takes place 6 to 8 hours after the air was blown in, while iron tapping takes place after 24 to 28 hours. It takes 5 to 6 days until the iron produced is according to the specifications.

5.5.3 Operating Difficulties

An important difficulty in operation is when the charge in the upper part of the stack is cemented together into a large impervious mass (bridge) while the material underneath continues to move downward thus creating a void. The void tends to increase until the bridge collapses, causing a sudden downward movement of the charge which is known as "slip". In severe cases, this causes a sudden increase in gas pressure and an effect like an explosion. Reasons for this slip may be due to alkali vapors that condense at the top of the furnace and cement the solid material together, or it may be due to fine carbon depositions which results from the reaction



5.5.4 Shutdown

Temporary shutdown for an emergency or otherwise is called "banking", and it involves reducing the combustion rate, thus preserving the charge for future use. The air blast is stopped, the blowpipes are dropped, and the tuyères openings are plugged with clay. If the shutdown is planned for a few days, coke may be charged without flux, and charging continues, until the coke descends to the bosh. The final tapping is made and then air is cut off. A heavy blanket of ore is dumped in the furnace to cover the upper burden surface and reduce the natural draft. At the conclusion of the tapping, the tapping holes are plugged and the furnace isolated. In this way the charge in the furnace can be kept for an indefinite time until blowing-in is required.

Extended shutdown is called "blowing out" and usually takes place when the lining is worn. Sometimes, however, business conditions may necessitate that production is no more required and an extended shutdown is necessary. Subsequent to blowing out and when the furnace is to be completely relined, the hot metal must be completely drained. A hole is drilled into the furnace bottom below the hearth staves, and a runner for iron is installed. A long oxygen lance is inserted in the hole to open the remaining brick and allow the iron to flow. This residual iron is called "salamander", and may be 400 to 600 tons.

Starting an empty furnace from cold is generally faster and requires less effort than starting it from a shutdown. However, the cost of blowing out, raking out, and cleaning prior to starting is more expensive than a temporary shutdown.

5.5.5 Efficient Operation and Improvements

In the past 50 years blast furnace production increased from an average of 800 t/day to 8000 t/day with some furnaces operating at 10 000 t/day. It seems, however, that the size of a blast furnace is limited by two factors:

- The large capital cost which will be difficult to raise
- The limited mechanical strength of coke to withstand the static pressure of a tall furnace.

The great increase in the blast furnace output is due to the following:

Beneficiated Feed. A feed to a blast furnace should fulfill the following conditions:

- Uniform size to allow gases to flow through without channelling.
- Mechanically strong to withstand handling, the high temperature, and the high static pressure in the furnace without crushing or disintegration.
- Free from fines to minimize the dust blown out of the furnace.
- Fairly permeable to enhance the reduction process.

For these reasons high quality coke sized to about 50 mm is usually used. Ore is also prepared and sized between 10 and 25 mm. Powdered feed material is compacted and sized before charging. Since high temperatures are usually applied in the compaction process, a part of the limestone required for the charge to the furnace is incorporated into the compacted material. In this way, the calcination CaCO_3 takes place outside the furnace, thus increasing its capacity and at the same time decreasing the volume of the exit gases. This process is known as "self fluxing sinter".

Increased Blast Temperature. When the air blast temperature is increased by preheating, the coke consumption will decrease and as a result the furnace capacity will increase. Since a certain amount of heat enters the furnace with the preheated air, the furnace efficiency increases. The higher the air temperature the higher the economy will be for the following reasons:

- The amount of coke required per unit metal produced is reduced.
- As a result of decreased fuel consumption, the air volume per unit metal produced will also decrease.

- As a result of the previous two points, the volume of gas leaving the furnace per unit metal produced will also decrease. This results in the decreased size of gas ducts and dust collecting system, etc.
- The reaction rate is increased as a result of increased air temperature, thereby lowering the reaction time of the process, i.e., increased productivity.

Oxygen Enrichment. Air is composed of 21% oxygen and 79% nitrogen. The advantages gained by using pure oxygen or oxygen-enriched air in oxidation processes offsets the cost of liquefaction of air and separating the nitrogen. The reasons for that are the following:

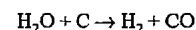
- Nitrogen acts as a diluent and absorbs large amounts of the combustion heat. When oxygen or oxygen-enriched air is used, the amount of heat lost by nitrogen is therefore decreased. As a result, the temperature of the furnace rises, and consequently production is increased. Or, coke consumption/ton of material processed is reduced.
- The total volume of gases passing through the furnace would be considerably less than in normal practice. Therefore, the erosion of the refractories should be reduced and the size of furnace and dust-collecting units reduced.
- High-melting-point slags can be used, i.e., slags containing lime. In this case sulfur can be eliminated.

Nitrogen-Free Operation. Instead of using a high temperature air blast it has been suggested to use cold oxygen. In this way the temperature in the furnace could be kept high and the inconveniences due to nitrogen could be eliminated. The cold tuyères facilitate the injection of coal in the furnace and in this way coke will be used only as a reducing agent and not as a fuel, which represents a great saving. Further, the top gas could be cleaned, treated to remove CO_2 , and the remaining CO recycled for use as a fuel.

Fuel Injection. When a sufficiently hot blast is available, a portion of a cheap fuel (pulver-

ized coal, fuel oil, natural gas) can be injected to replace some of the expensive coke. This results in increased production because it permits the removal of some coke from the charge. It is also a means for controlling the flame temperature since the fuel is injected cold. Generally, when tuyère-injected fuels are used, the moisture content of the blast must be decreased. The choice of the fuel depends on its cost and also on the cost of equipment for its injection. The equipment for gas injection is the least expensive and that for pulverized coal is the most.

Blast Humidity Control. By adding moisture to the blast in the form of steam, it is possible to control the flame temperature and to achieve a smooth furnace operation because the reaction of steam with coke is endothermic:

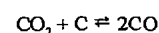


The products of this reaction are themselves reducing agents.

Pressure Operation. There is a recent tendency to operate the blast furnace under a slight pressure. This results in increased furnace capacity and decreased coke consumption. Operating under pressure, however, results in several difficulties. The furnace must be air tight at the top. Also charging equipment must have a special mechanism to allow the bell to be lowered. On the other hand, flue gases, being at high pressure, may be recovered in a turbine to be used, for example, in blast blowing.

Operating the blast furnace under pressure can be achieved by introducing a throttling valve in the gas system. This results in the following advantages:

- Larger amounts of air can be blown and consequently increased production rate.
- Increased pressure shifts the equilibrium of the following reaction to the left:



This reaction is responsible for the consumption of unnecessary amounts of coke. As a result, operating a furnace at 200 kPa

results in a decreased coke consumption of about 10%.

- As a result of decreased coke consumption, the available volume in the furnace will increase and more ore can be reduced.

5.5.6 Engineering Aspects

The iron produced in the blast furnace is saturated with carbon and is in the molten state. Depending on burden composition and operation technique of the blast furnace, the molten iron produced contains varying amounts of other elements such as silicon, manganese, phosphorus and sulfur. The blast furnace can produce pig iron but not steel.

The blast furnace is operated to achieve the following three major objectives:

- *Lowest energy consumption*, particularly the lowest coke rate;
- *Highest productivity*, i.e., highest production rate per unit volume of the furnace;
- *Composition and temperature* of the molten pig iron produced must meet the requirements of the steel shop and must be constant.

Table 5.16 shows the simplified mass and heat balances of the reactions that proceed sequentially during the descent of the burden in the blast furnace. All figures in the table are based on 1 mol Fe_2O_3 , 1/4 mol CaCO_3 as a flux, and k mol of coke as fuel and reductant.

Hematite is first reduced via magnetite to wustite by the gas. Because the heat requirement of the reactions are small, the heat content of the gas is sufficient for heating the burden (see Figure 5.20). The gas composition prevailing in the upper part of the furnace (below 1000 °C) has the reducing potential for hematite and magnetite as depicted in Figure 5.21. Only a portion x of the wustite is reduced to iron because of kinetic limitation. The deviation of the gas composition from the Boudouard equilibrium above 650 °C is due to the low reactivity of coke. Thus, carbon dioxide is not adequately converted to carbon monoxide. Deviation below 650 °C is caused by suppression of the carbon deposition reaction, $2\text{CO} \rightleftharpoons \text{CO}_2 + \text{C}$. For coke saving, the former deviation from equilibrium is desirable, however, the latter undesirable.

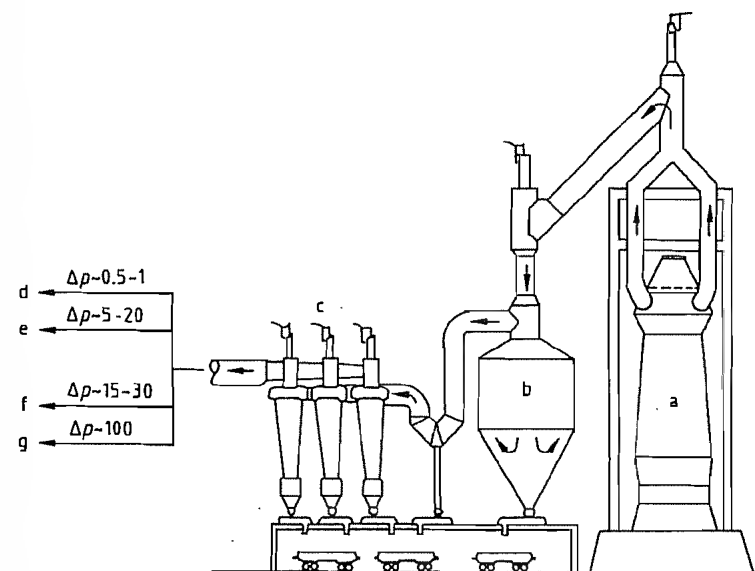


Figure 5.19: Top gas cleaning system [15]: a) Blast furnace; b) Dust catcher; c) Cyclone; d) To electric precipitator; e) To hurdle scrubber; f) To bag filter; g) To venturi scrubber.

Table 5.16: Simplified mass and heat balances in the blast furnace as a countercurrent reactor [21]: increase (+), decrease (-).

	C	Fe ₂ O ₃	FeO	Fe	CaCO ₃	CaO	CO	CO ₂	O ₂	N ₂	Heat*
1 Charge consisting of 1 mol Fe ₂ O ₃ , 1/4 mol CaCO ₃ , & mol carbon	+k	+1			+1/4						
2 Indirect reduction hematite → wustite Fe ₂ O ₃ + CO → 2FeO + CO ₂		-1	+2				-1	+1			negligible
3 Indirect reduction wustite → iron x(2FeO + CO → 2Fe + 2CO ₂)			-2x	+2x			-2x	+2x			negligible
4 Decomposition of limestones					-1/4	+1/4		+1/4			ΔH _d for 1 CaCO ₃ = 67.2 kJ at > 700 °C
5 Direct reduction of remaining wustite (1-x)(2FeO + 2C → 2Fe + 2CO)	-2(1-x)		-2(1-x)	+2(1-x)			+2(1-x)				ΔH _{cp} for 2 FeO = 315(1-x) kJ at 1100 °C (heat of reaction)
6 Melting of iron and slag											ΔH _m for 2 Fe = 42 kJ at 1300 °C
7 Combustion of carbon y(C + 1/2 O ₂ + 2N ₂ → CO + 2N ₂)	-y						y		-1/2		ΔH _c for 1 C = -111 kJ
8 Hot blast 1/2 y mol									+1/2	+2y	ΔH _f for 5/2 mol air = -0.884(t ₃ - t ₄) kJ
Input at top	+k	+1			+1/4					+2y	
Input at bottom			0				y + 1 - 4x	1.25 + 2x			
Output at top	k - 2(1-x) - y = 0	0	0	+2	0	+1/4					
Output at bottom											

*Heat of reaction not based on reaction temperature.

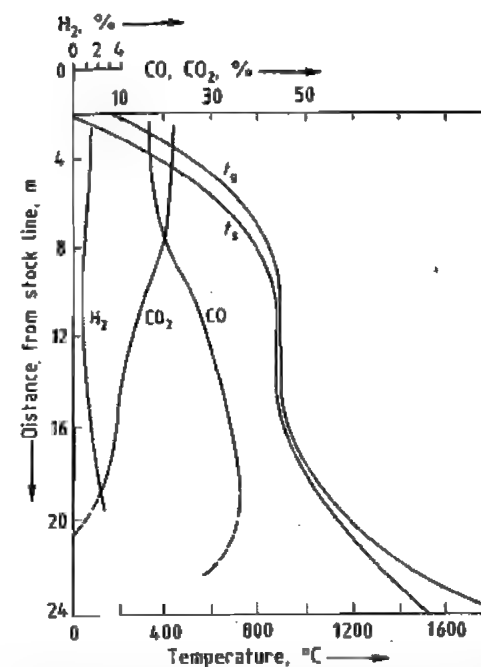
t₃ = Hot blast temperature; t₄ = Temperature at which the direct reduction is assumed to proceed.

Figure 5.20: Schematic profile of temperature and gas composition in the longitudinal direction of the blast furnace.

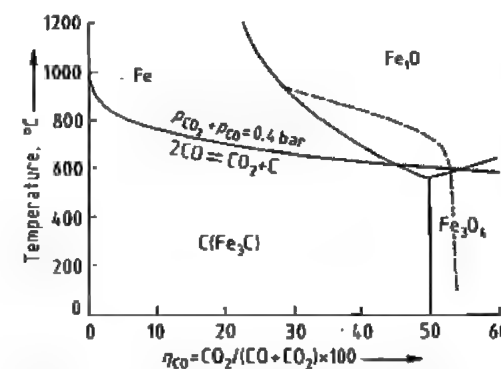


Figure 5.21: Variation of temperature and gas composition in a typical operation of the blast furnace superimposed on the reduction equilibrium diagram of iron oxide.

During descent of the burden, limestone starts to decompose at ca. 700 °C. This reaction requires heat and releases carbon dioxide, therefore the gas is cooled and its carbon dioxide content increases. Consequently, the reduction rate of iron oxide decreases and the value of x in Table 5.16 decreases. A lower

value of x corresponds to a higher coke rate according to the balance shown in Table 5.16. The wustite that has not yet been indirectly reduced by the gas to iron must be reduced directly with carbon. This reaction requires a great amount of heat. For simplicity it has been assumed in Table 5.16 that direct reduction of wustite proceeds at 1100 °C. This zone of the furnace is critical for the completion of the entire process. The amount of oxygen which must still be removed from the ore in this part of the furnace depends on the degree of reduction achieved in its upper part. Therefore the residual amount of oxygen depends on the reducibility of the ore. On the other hand, the amount of oxygen which can be removed from the ore in this zone depends on the enthalpy that is delivered by the gas at 1100 °C. This enthalpy, in turn, depends on the amount of coke that is available for combustion in front of the tuyères.

If excess heat is available, a higher top-gas temperature is found. However, the utilization degree of the gas η_{CO} decreases because the excess heat is supplied by combustion of coke to carbon monoxide. This phenomenon can be controlled by decreasing the coke rate of the burden materials fed at the top of the bed. However, the action will only be effective after 4–6 h when the burden charged at new rates comes to the tuyère zone. An immediate effect is obtained if the heat input to the lower part of the furnace is decreased by increasing the moisture content or decreasing the temperature of the blast.

It is more difficult to compensate an enthalpy shortage in the lower part of the furnace. An increase in the coke rate is effective only after several hours. It is often not possible to increase the temperature of the blast because the blast temperature is usually at its maximum for economic reasons. The maximum blast temperature is limited by the capacity of the stoves and also by the maximum allowable temperature of the blast furnace. A short-term solution to compensate an enthalpy shortage is to inject fuels such as hydrocarbons, natural gas, oil, or pulverized coal together with an oxygen enrichment of the blast.

Upon further descent of the burden, the enthalpy $\Delta H_{E.S}$ needed to melt iron and slag must be supplied. For simplicity, they are assumed to melt down at 1300 °C (see column 6 in Table 5.16).

The various heat sinks are compensated by the equal amount of heat supplied from the combustion of the coke and from the hot blast as described in columns 7 and 8 in Table 5.16. This requirement almost determines the coke rate for various conditions. This is an approximate calculation because the coke requirement for the reduction of molten wustite, silica, and manganese oxide as well as that for the carbon dissolved in the metal has not been taken into account. To consider the heat and mass balances, the furnace is divided into two parts by a boundary line which is drawn in the thermal and chemical reserve zone. In this zone, the temperature is almost constant (ca. 900 °C) and no reduction of iron ores occurs.

The coke rate is determined by the enthalpy requirement of the lower furnace. The quantity of carbon y (mol of carbon per moles of hematite to be reduced) needed to supply the heat is given by Equation (1) (for symbols see Table 5.16):

$$y = -\Delta H_{E.S} + \frac{(1-x)\Delta H_{CO}}{\Delta H_C + \Delta H_L} \quad (1)$$

The total amount of carbon required k is given by (see Table 5.16):

$$k = y - 2x + 2 \quad (2)$$

The amount of carbon required for direct reduction is:

$$k - y = -2x + 2$$

Substitution of the figures listed in Table 5.16 gives the carbon rate as a function of the hot blast temperature t_B and the amount of wustite reduced indirectly x , assuming that the direct reduction proceeds primarily at $t_R = 1100$ °C

$$k = \frac{357}{111 + 0.084(t_B - 1100)} - \frac{2 + 315}{111 + 0.084(t_B - 1100)} x + 2$$

The coke rate Q is then given by:

$$Q = 118k$$

on the basis of a carbon content of the coke of 85% and on iron content of the hot metal of 93.5%.

The *fraction of indirect reduction* r_{CO} indicates how much oxygen has been removed from the ore by indirect reduction. Taken together with the fraction of direct reduction r_C , the sum should be equal to unity:

$$r_{CO} + r_C = 1 \quad (3)$$

For reduction of hematite, the following relation is valid (Table 5.16, columns 2 and 3):

$$r_{CO} = \frac{O_{removed}}{O_{total}} = 1 + \frac{2x}{3} \quad (4)$$

On the basis of the *balance* shown in Table 5.16, it is not possible to assign a value to x (amount of wustite indirectly reduced). The maximum value of x can be determined thermodynamically. If the value of x is given, then r_{CO} is obtained from Equation (4). In fact, the value of x is determined by the rate of the indirect reduction of iron ore and by the reactivity of the coke which, in turn, determines the degree to which the Boudouard reaction proceeds. The value of x can be evaluated from the composition of the top gas if the operational data are available. The gas utilization factor is defined by Equation (5):

$$\eta_{CO} = \frac{\% CO_2}{\% CO_2 + \% CO} \quad (5)$$

Substitution of the values in Table 5.16 provides the following Equation:

$$\eta_{CO} = \frac{1 + 2x}{2(1 - x) + y} \quad (6)$$

Since y depends only on the enthalpies and x for a given blast temperature (see Equation 1), the value of x can be determined if the decomposition of limestone is neglected. In practice, r_{CO} is between 0.45 and 0.65 and the corresponding values of x are between 0.175 and 0.475.

The *amount of air* l required per mole of hematite and the *amount of off-gas* generated g_G , are obtained from Table 5.16:

$$l = \frac{5y}{2} \quad (\text{amount of air}) \quad (7)$$

$$g_G = 3y - 2x + 2 \quad (\text{amount of off-gas}) \quad (8)$$

These equations are approximate expressions and should be improved for more accurate calculations—particularly when the calculated results are to be used for furnace control to keep the composition and temperature of the hot metal constant. For this purpose it is necessary to formulate the heat and mass balances on hydrogen from water vapor and hydrocarbons and on the solutes in the iron (e.g., carbon, silicon, manganese, and phosphorus).

5.5.7 Effective Utilization of Energy

The high thermal efficiency of the blast furnace (Table 5.17) directly leads to a low coke rate. Heat losses through the wall amount to ca. 5%. Additionally 2–5% of thermal energy is lost in the form of off-gas enthalpy. These values decrease with increasing furnace size so that the total loss of thermal energy is < 6%. Compared to the low *thermal energy loss* of the blast furnace, the *chemical energy* of the off-gas is rather large and amounts to ca. half of the thermal energy used effectively in the furnace.

Table 5.17: An example of enthalpy balance for the modern blast furnace (no. 6BF at Chiba works of Kawasaki Steel Corp.).

Enthalpy	¥ 103 kJ per ton of pig iron	%
Input		
Raw materials	519	3
Coke	14 412	83
Blast	1 411	8
Electricity	1 093	6
Total	17 439	100
Output		
Top gas	5 389	31
	(chemical: 4966; thermal: 423)	
Pig iron	9 697	56
Slag	908	5
Dust	255	1
TRT's recovery ^a	536	3
Wall, heat loss	653	4
Total	17 439	100

^a TRT: Top-gas pressure recovery turbine.

The thermal energy supplied by the hot blast (Table 5.17) should be partly subtracted from the total energy required for the blast furnace operation because the blast is primarily heated by the off-gas. Even in modern blast furnaces ca. 30% of the primary energy supplied by coke leaves the process in the form of carbon monoxide and hydrogen in the off-gas. A heat loss of 3–7% is caused by *slag enthalpy*. With these considerations in mind, lowering of the energy requirement can be accomplished as follows:

- use the chemical energy of the off-gas as efficiently as possible in the process system,
- decrease the specific slag volume,
- prepare the burden (operation of the stack), i.e., carry out dehydration and decarbonization outside the blast furnace by utilizing inexpensive energy sources.

Additionally, efforts exist to replace metallurgical coke by other inexpensive energy sources because of high cost and shortage of coking coal.

Blast Furnace Operation and Physical Properties of Burden Materials. The heat required to produce 1 t of hot metal substantially depends on the physical properties of the iron ores. In modern blast furnace operation, processed ores like sinter and pellets are usually fed to the furnace to conduct stable operation for pursuing higher productivity and lower coke rate. Physical properties which significantly affect the blast furnace operation are reducibility and reduction disintegration. *Higher reducibility* contributes to the increase in indirect reduction in the stack region thereby increasing the utilization factor η_{CO} and decreasing the coke rate because of a decrease in direct reduction. *Reduction disintegration* directly affects the gas permeability of the burden beds and may cause flow maldistribution which negatively affects the reduction of iron ore and gas utilization. Therefore, the physical properties of the sinter should be controlled appropriately. A lower FeO content in the sinter enhances the reducibility, however, a higher content improves the reduction disintegration as shown in Figures 5.22 and 5.23.

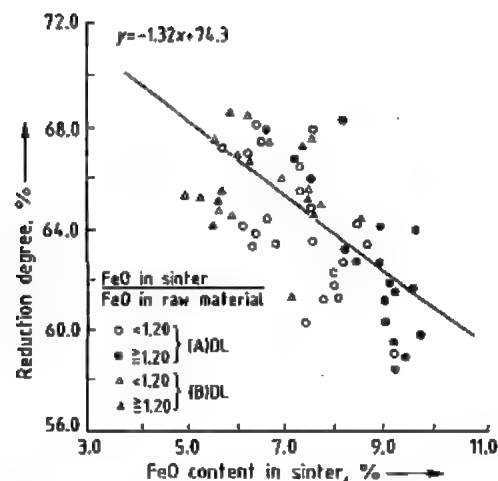


Figure 5.22: Influence of FeO content in sinter on the reducibility [22] (Courtesy of The Iron and Steel Institute of Japan).

A low gangue content of the burden materials also contributes significantly to the coke savings by decreasing the slag volume.

Chemical Energy of the Off-Gas. Burden materials with a high reducibility and a low reduction disintegration provide a low coke rate, but a high gas utilization factor η_{CO} . A better burden preparation allows the use of a larger portion of the off-gas for heating the blast. These circumstances significantly decrease the waste energy that leaves the blast furnace process in the form of off-gas. Figure 5.24 illustrates the decrease in the coke rate in Germany and in Japan by improving the physical properties of the burden materials and utilization of the off-gas. Figure 5.24 also shows the effect of replacing coke by oil and pulverized coal on the coke rate. The theoretical limits of the coke rate for a fully oxidized burden and a burden that has been 60% and 100% prereduced are also indicated in this diagram. When 100% prereduced burden is used, the blast furnace is operated as a melting furnace like a cupola that produces cast iron. In this case, a gas with a very high calorific value is produced because the blast furnace works as an iron and gas producer.

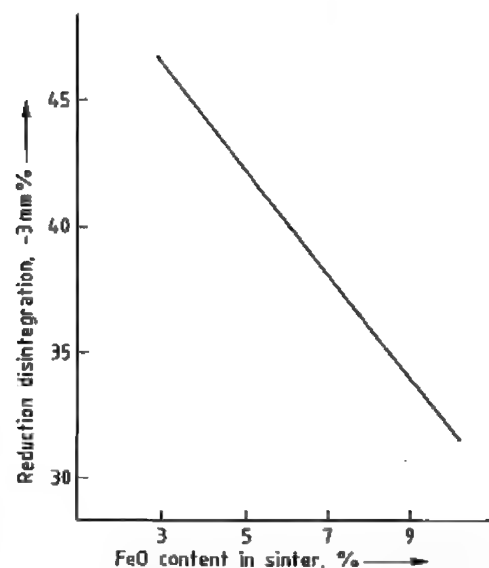


Figure 5.23: Relation between FeO content in sinter and reduction disintegration degree [23] (Courtesy of The Iron and Steel Institute of Japan).

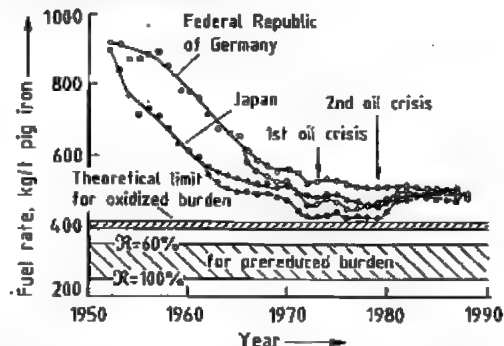


Figure 5.24: Specific fuel rate for the production of 1 t hot metal in Japan and Germany: — Fuel rate; -- Coal rate.

Figure 5.25 shows that the calorific value of the off-gas decreases with decreasing coke rate, which favors the cost effective operation of the blast furnace. On the other hand, it may be necessary to increase the calorific value of the off-gas by increasing the coke rate when the calorific value of the off-gas is not sufficient to heat other furnaces in the steep plant or the hot blast stoves and when a cheaper energy source is not available. In the case, the blast furnace also has a function as a gas producer.

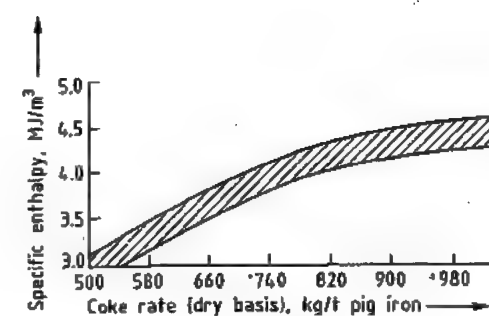


Figure 5.25: Relationship between specific enthalpy of top gas and coke rate [24] (Courtesy of Verlag Stahleisen mbH).

In spite of the successful efforts to decrease the coke rate and to use substitutive fuels since the 1950s, the problem to what limit the coke rate can be lowered is still not solved. Sufficient coke must be present in front of the tuyères to form a dead man through which the gaseous products can ascend. In addition, the coke consumed in the dead man must be replaced. If the quantity of coke required for these portions of the process is not available, then the characteristics of the process change and it can no longer be called a blast furnace process.

Figure 5.26 gives a schematic illustration of the processes occurring in the combustion zone in front of the tuyères [24]. According to direct observations, coke particles are entrained in the turbulent air flow immediately in front of the tuyère opening and fly on circular trajectories within the raceway.

The coke particles are primarily gasified in the raceway. According to the gaseous composition distribution in the raceway shown in Figure 5.27, coke burns with the gas at first forming carbon dioxide, and then carbon dioxide is reduced to carbon monoxide in an area near the coke-filled bed. A typical gas composition change from the tuyère via the raceway to the packed bed calculated by a two-dimensional model [27] is shown in Figure 5.28. From this figure the gasification reaction has almost gone to completion in the raceway region, therefore a very small quantity of CO_2 is

left for the coke packed bed around the raceway.

Moreover, the direct observations indicate that a shower of iron and slag droplets descends in front of the tuyères, together with coke particles falling through the air flow. In addition, in no other part of the raceway roof was the burden observed to descend. On the basis of these observations it is assumed that the molten iron and slag trickles down in the space between the individual tuyères and within the dead man. This phenomenon has been proven by dissection of blast furnaces [28, 29].

Fluid flow studies have shown that the adequate quantity of gas cannot flow through the cohesive layers or through the layers which hold up the molten materials unless a sufficient volume of coke bed (which has a high permeability) is present inside the furnace.

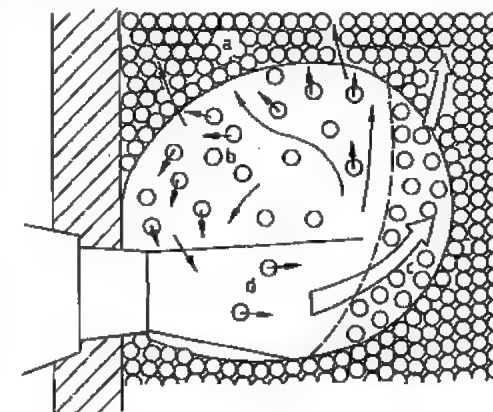


Figure 5.26: Movement of coke particles in front of the tuyère and location of combustion zone: a) Packed zone; b) Coke fluidizing zone; c) Coke slow moving zone; d) Blast jet.

Basic Concept to Improve Blast Furnace Performance. The following technologies or their combinations have been principally approved to decrease the coke rate and to increase the productivity of the blast furnace:

- Pretreatment of iron ores improves the reducibility and permeability and hence, increases the gas utilization η_{CO} . Examples are *sintering* or *pelletizing* of the ore and screening to separate the fines.

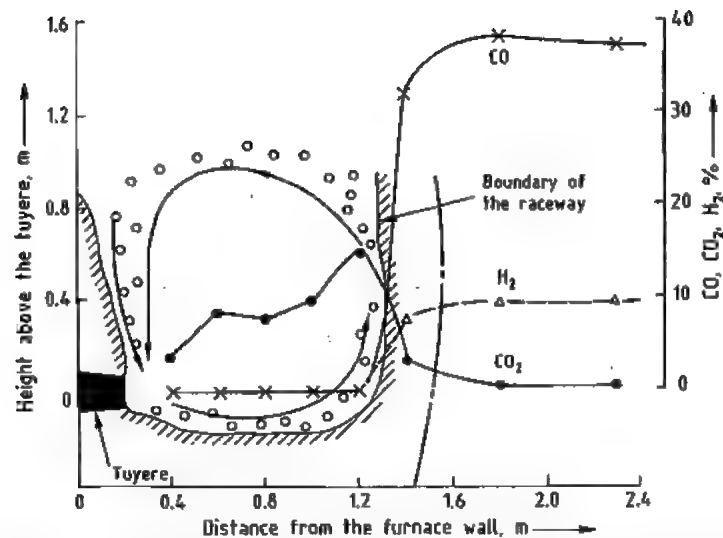


Figure 5.27: Combustion of coke in the raceway [25] (Courtesy of The Iron and Steel Institute of Japan).

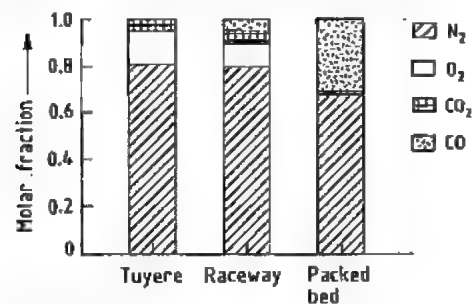


Figure 5.28: Change of gas composition from the tuyere to the packed bed.

- Injection of *auxiliary fuels* such as hydrocarbons, oil, and pulverized coal replaces coke for heating and reduction purposes.
- Oxygen enrichment of the blast together with fuel injection decreases the amount of blast; this decreases the amount of off-gas per tonne of coke and increases the furnace efficiency.
- Increase in the blast temperature reduces the amount of coke required for heating.
- High pressure operation allows the introduction of a larger amount of blast per unit time.
- Reducing gas injection in the lower part of the stack lowers the amount of coke required for reduction.

- The use of *partially reduced ore* results in a decrease in the coke rate and an increase in the productivity of the furnace.

The effect of these various technologies on the coke rate and their limits of applicability can be summarized with the aid of the extended Rist diagrams shown in Figures 5.29, 5.30 and 5.32.

Table 5.18 lists quantitative results obtained from operational data concerning the technologies applied to decrease the coke rate on the basis of the Rist diagram and to increase the productivity.

Curve 1 in Figure 5.29 represents the conditions in a blast furnace without additional technologies. Heat is liberated during the oxidation of carbon (coke for heating) by the hot blast (E to F). The segment FG represents the reduction of elements dissolved in iron and segment GK corresponds to direct reduction. The indirect reduction is represented by the segment AK. The diagram allows the determination of the amount of carbon required per mole of iron (C/Fe) and the amount of coke (85% C) required per tonne of hot metal (93.4% Fe). For this purpose, the operating line 1 is shifted to the line 1a which goes through the origin. The intersection of 1a with the abscissa in the upper part of the diagram

together with curves I or II gives the carbon consumption (C/Fe) on the ordinates I or II on the left side, while the coke consumption can be read from the ordinate on the right. The lower abscissa (0–100%) is valid for the segment between E and K. It shows the coke consumption for heating (EF), for reduction (GK), and for the reduction of minor constituents in the burden (FG). For the blast furnace operation in accordance with line 1 the coke rate is 550 kg per tonne of hot metal which is equivalent to a C:Fe ratio of 2.3. The consumption ratio is 60% for heating, 25% for direct reduction, and 15% for the reduction of the minor constituents in the burden.

Lines 2 and 3 are theoretical operating lines for obtaining the limits of the coke rate. Line 2

(no coke used for reduction) is based on the assumption that the reactivity of the coke is so poor that the Boudouard reaction and the direct reduction are suppressed completely. However, it is also assumed that a gaseous composition is reached which corresponds to the reduction equilibrium from wustite to iron (point W). In this case the entire quantity of carbon monoxide required for the reduction must be generated by the combustion of coke. This condition causes the extremely high coke rate (line 2a) of ca. 1000 kg per tonne of hot metal, a lower gas utilization η_{CO} as well as higher temperatures of off-gas and molten iron.

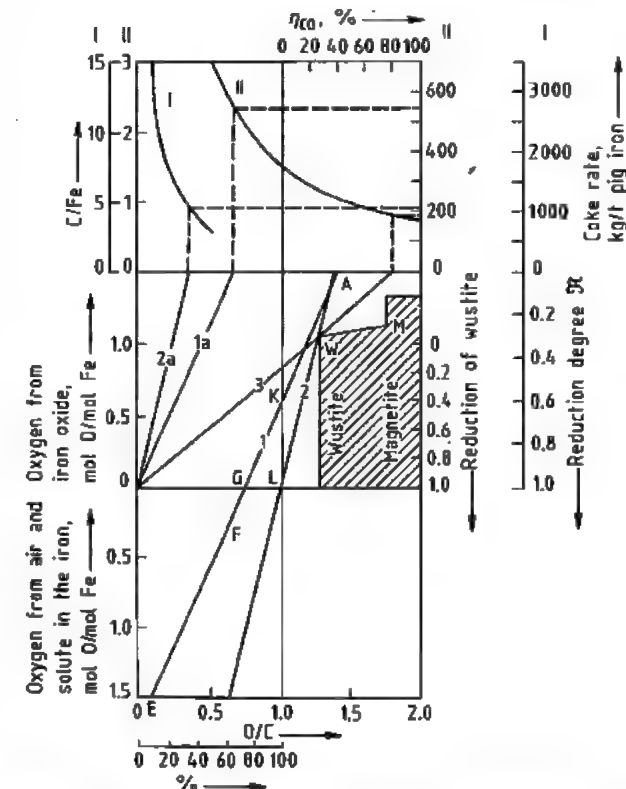


Figure 5.29: Extended Rist diagram [20]. Line 1: normal blast furnace operation (standard); Lines 2 and 3: hypothetical operation (Line 2: coke for reduction = 0, line 3: coke for heating = 0).

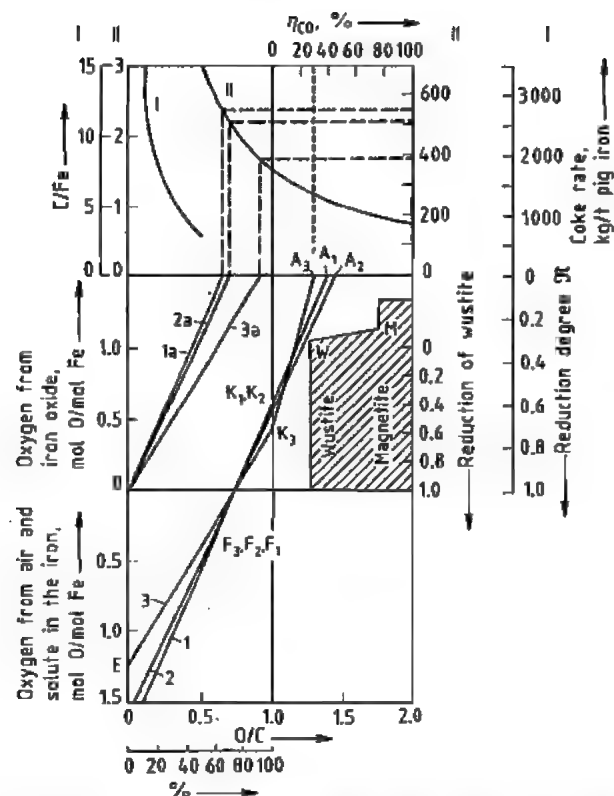


Figure 5.30: Effect of measures to decrease the coke rate and to increase the productivity of the blast furnace estimated by the Rist diagram [20]. Line 1: normal blast furnace operation (standard); Line 2: improvement in gas permeability and reducibility; Line 3: improvement in indirect reduction (K_3) by injecting reducing gas into the stack.

Line 3 is based on the assumption that no coke is required for heating and that the total heat required is supplied by a hot inert gas. In that case the coke rate would be ca. 200 kg per tonne of hot metal while the gas utilization would be 80%.

Line 2 in Figure 5.30 shows the decrease of the coke rate caused by the improvement of gas permeability and reducibility compared with the standard case (line 1). Line 2 gives an improvement of 5% in gas utilization thereby close approaching the equilibrium point W in the wustite field. In addition, the degree of direct reduction (K_2) decreases which leads to a coke saving of 30 kg per tonne of hot metal (thm). The reducibility of various burdens are

shown in Figure 5.31, which were measured according to Japanese industrial standard.

It is evident from Figure 5.30 that improvement in the physical properties of burdens does not result in a large decrease in the coke rate but can probably contribute much to the stable operation of the blast furnace. A lower coke rate (i.e., a lower slope of the operating line in Figure 5.30) could only be achieved if it were possible to increase the degree of direct reduction together with the gas utilization. This method would lead to an increase in the heat requirement that must be supplied by a hotter blast if coke is to be saved. However, the hot blast temperatures have already reached their technological limit.

Table 5.18: Effect of various parameters on the coke rate and the productivity of the blast furnace, based on 1 t of hot metal [21].

Parameter	Range	Change	Effect on coke rate kg per tonne of hot metal
Slag volume, kg/t	250–350	–100	–15 to 25
Partially reduced pellets ^a , % of burden	0–30	+10	–1.5 to 2.0
Fully reduced pellets ^b , kg/t	0–20	+10	–2 to 3
Scrap, kg/t		+10	–4
Gas velocity in stack ^c , m/s	2.5–5.0	–0.1	–2.5 to 3.0
Hot metal silicon, %	0.5–1.5	–0.1	–4 to 7
Fines in burden, % < 5 mm	0–7	–1	–4 to 7
Crushed ore, % of burden			
8–40 to 8–30 mm	0–40	40	–10 to 13
8–30 to 10–25 mm	0–40	40	–5 to 7
Coke ash content, %	6–12	–1	–5 to 10
Pellet content of burden, %	0–100	+10	–5 to 10
Sinter content of burden, %	0–100	+10	–5 to 10
Blast moisture content ^d , g/m ³		–10	–6 to 10
Blast temperature, °C	900–1350	+100	–8 to 20
Oil injection, kg/t	50–100	+1	–0.9 to 1.4
Blast oxygen enrichment, %		+1	+2 to 3% ^e
Top gas pressure, kPa	10–250	+10	+1 to 2% ^e

^a With 68% Fe, 40% metallic iron.

^b Fully metallized.

^c With respect to empty stack (superficial velocity).

^d Air at standard conditions.

^e Increase in melting rate.

Fuel injection through the tuyères (e.g., pulverized coal or hydrocarbons) can supply a part of the heat requirement. In some cases, the blast is also enriched with oxygen to increase the combustion efficiency. The best record achieved up to now with the blast furnace in the Kimitsu Works of Nippon Steel are shown by line 2 in Figure 5.32. The coke rate is 390 kg/t for a heavy oil addition of 60 kg/t (gas utilization of ca. 45%, indirect reduction of ca. 75%). There is a slight break in the line at K_2 which indicates that the quantity of reducing gas is larger as a result of the oil addition than in the case of carbon gasification alone.

Auxiliary fuels injected into the blast furnace can replace coke only up to a certain limit. In the raceway the hydrocarbons are only combusted to carbon monoxide and hydrogen, liberating less heat than coke per equal quantity of oxygen.

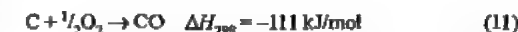
Natural gas



Oil



Coke



Thus a given quantity of heating coke can only be replaced by a larger quantity of hydrocarbons if the same amount of heat has to be generated. In other words, the replacement ratio, defined by hydrocarbons:coke is > 1 . However, twice to three times the amount of reducing gas including hydrogen is produced per mole of combustion air (Equations 9 and 10) compared to the combustion of coke (Equation 11).

The addition of hydrocarbons increases the degree of indirect reduction because the reduction rate of hydrogen is higher than that of carbon monoxide. Thus, the degree of direct reduction and its enthalpy requirement decrease. Consequently, the overall effect of hydrocarbon injection on the replacement ratio increases, thereby giving an overall hydrocarbon coke replacement ratio < 1 . The enthalpy deficiency which suppresses further increase of indirect reduction becomes increasingly noticeable whenever more coke is replaced by increasingly larger amounts of hydrocarbons.

The advantage of the lower fuel cost, therefore, becomes gradually less. However, a more serious problem is the decrease in the furnace productivity. Fuel injection can be made more cost-effective by increasing the oxygen enrichment of the blast or the hot blast temperature. Modern practice makes use of the theoretical and actual flame temperatures to control the replacement ratio. Japanese furnaces are operated on the basis of a theoretical flame temperature of ca. 2200 °C.

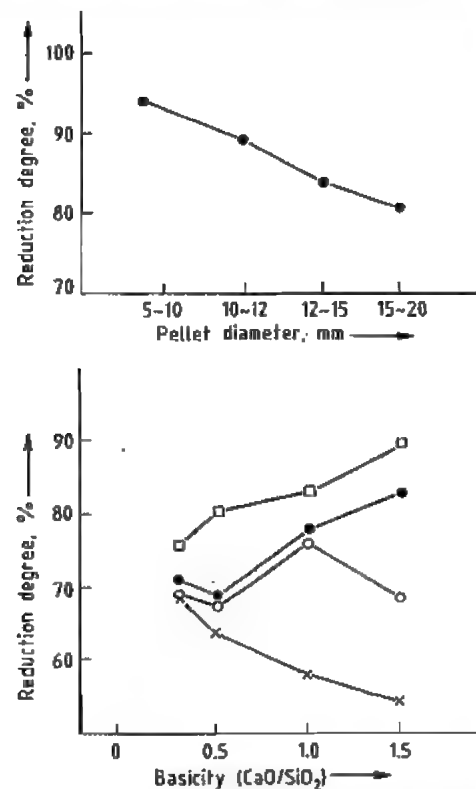


Figure 5.31: Influence of basicity and pellet diameter on reduction degree [31] (Courtesy of The Iron and Steel Institute of Japan): —□— 1200 °C; —●— 1250 °C; —○— 1300 °C; —×— 1350 °C.

Cost effectiveness considerations should take into account the fact that the sulfur content of the hot metal increases as a result of oil injections. This leads to a cost increase associated with the desulfurization of hot metal. Ad-

ditions of up to 70 kg/t have been tried and were technically feasible. However, the oil crises of 1973 and 79 made oil very expensive. Therefore almost all blast furnaces operated in Japan changed the injection fuel from oil to pulverized coal. Figure 5.33 illustrates the replacement ratio of coke by pulverized coal. Pulverized coal is more difficult to inject into the blast furnace than oil because it is in the solid not in the fluid state and it contains ash. A successful technology for pulverized coal injection has been developed to inject up to 150 kg/t by using low ash coal crushed to < 200 mesh (74 μm) [33]. However oil or natural gas injection is also conducted depending on local energy conditions all over the world.

Line 3 in Figure 5.30 shows a break which represents the operation of *injecting a reducing gas* into the stack to promote indirect reduction. This leads to the heating and reducing coke requirement of 390 kg/t (line 3a). However, inherent to the low coke rate is a low gas utilization η_{CO} of only 30%. The break in line 3 at K_3 is the result of an increase in the quantity of the gas at the point of injection. This technology has not been accepted for widespread application because of the poor gas utilization and the large amount of top gas. However, the reducing gas injection in the stack region is an important technology for the operation of the blast furnace with pure oxygen [34], which is currently being developed for the super high productivity of the blast furnace process.

Line 3 in Figure 5.32 represents a blast furnace operation using *prereduced ore* with a metallization degree of 50%. This procedure leads to a decrease in the coke rate to 310 kg/t. In this case, gas utilization is only ca. 30%. Therefore, such an operation is only recommended when the blast furnace capacity is insufficient to satisfy a sudden increase in hot metal demand. The productivity of the blast furnace increases significantly by using prereduced material although it is more expensive.

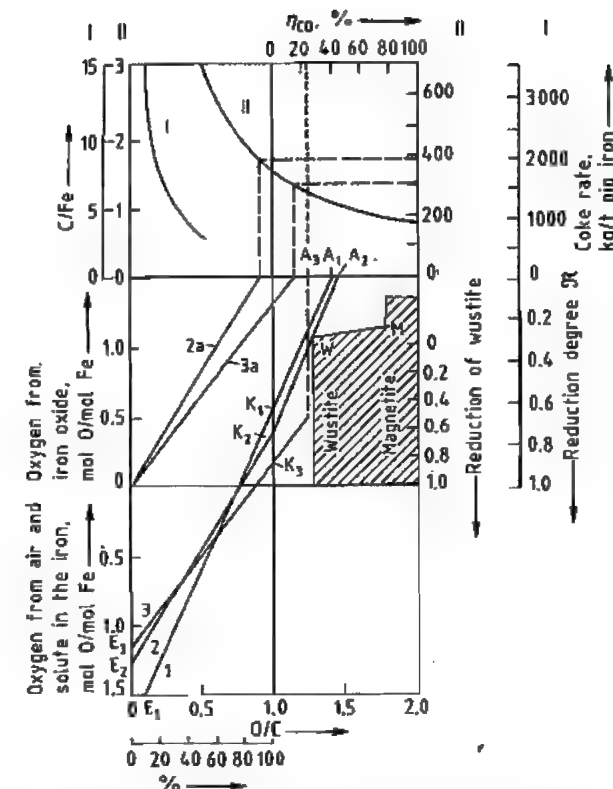


Figure 5.32: Effect of measures to decrease the coke ratio and to increase the productivity of the blast furnace estimated by the Rist diagram [20]. Line 1: blast furnace operation (standard); Line 2: decrease in the coke ratio through injection of inexpensive energy (best values achieved with Japanese furnaces); Line 3: operation with prereduced ore.

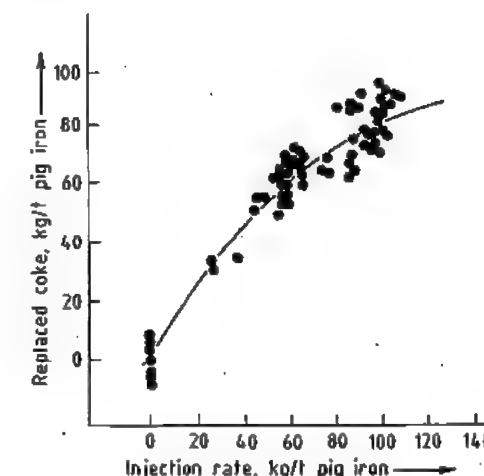


Figure 5.33: Coke replacement with pulverized coal injection [32] (Courtesy of The Iron and Steel Institute of Japan).

Slag Practices. The slag must meet the following requirements:

- It should absorb all unreduced non-volatile components of the burden and remove them from the blast furnace.
- It should be a liquid of low viscosity.
- It should be able to absorb the sulfur primarily contained in the fuels and it should contain as little iron oxide as possible to increase the yield of hot metal.
- The slag volume should be as low as possible without impairing the desulfurization.
- The temperature range where the burden components become cohesive should be narrow to ensure better permeability of the burden column.
- Finally, the slag should be converted to saleable material.

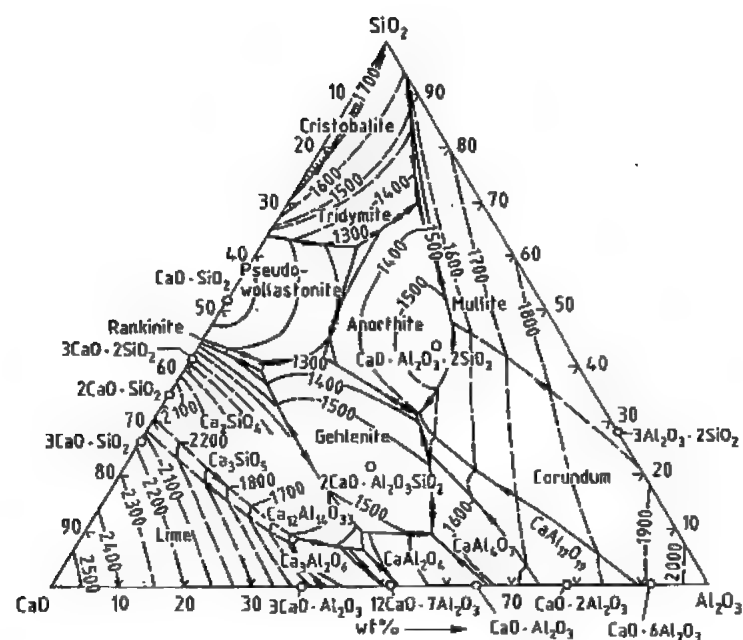


Figure 5.34: Phase diagrams of the system $\text{CaO}-\text{Al}_2\text{O}_3-\text{SiO}_2$ [35].

These requirements are in part complementary and in part mutually exclusive. It is therefore necessary to state priorities.

About 95% of the slag consists of SiO_2 , CaO , MgO , and Al_2O_3 . The requirement of low viscosity can be met by a variety of components in this quaternary system. Ignoring the presence of MgO , the phase diagram of the ternary system $\text{CaO}-\text{Al}_2\text{O}_3-\text{SiO}_2$ illustrated in Figure 5.34 shows a low melting temperature region which is parallel to the $\text{CaO}-\text{SiO}_2$ binary for low Al_2O_3 content. This region extends from high SiO_2 content to the saturation isotherm for $2\text{CaO} \cdot \text{SiO}_2$ and then for essentially constant CaO content toward high Al_2O_3 content. The MgO content of the slag does not substantially affect the relative position of the low melting temperature region and only affects the absolute values of the melting temperatures. The compositions of blast furnace slags as encountered under various operating conditions are shown in Figure 5.35.

The desulfurization of the hot metal increases with slag basicity, i.e., with increasing CaO and/or MgO content. Region 1 in Figure

5.35 can, therefore, be used only for processing low sulfur burden (e.g., in Brazil where very low sulfur content charcoal is often used as reductant). Because the gangue constituents usually form a low basicity slag, region 1 largely represents the slag composition without addition of fluxes. The furnace can be operated at a relatively low temperature because of the low melting points. Region 2 is reached for low iron content burden with acid gangue constituents. This mode of operation prevails, for example, in Salzgitter and requires extensive desulfurization of the hot metal outside of the blast furnace. The attainment of a basicity that would result in adequate desulfurization within the furnace would require a large lime addition which leads to a high slag volume and consequently to higher coke rate. Region 3 represents the worldwide preferred slag compositions for large blast furnaces. In this case, depending on the alumina content, dolomite must be added to satisfy the required MgO contents (see Table 5.19).

Slags with higher basicities B as shown in Table 5.19 would favor optimum softening

conditions. The softening and melting range of the gangue constituents is ca. 80–130 °C for $B = 0.5$ and ca. 20–50 °C for $B = 2.0$. Because of the higher melting temperature of the highly basic slag and of extra energy required due to the larger quantity of flux addition, hence, the slag basicity is maintained at ca. 1.2.

Table 5.19: Optimum composition of blast furnace slag in % [35].

Al_2O_3	CaO	MgO	SiO_2
5	43	16	36
10	44	14	32
15	44	12.5	28.5
20	45	11	24
25	48	8	19
30	56	5	9
35	54	4	7

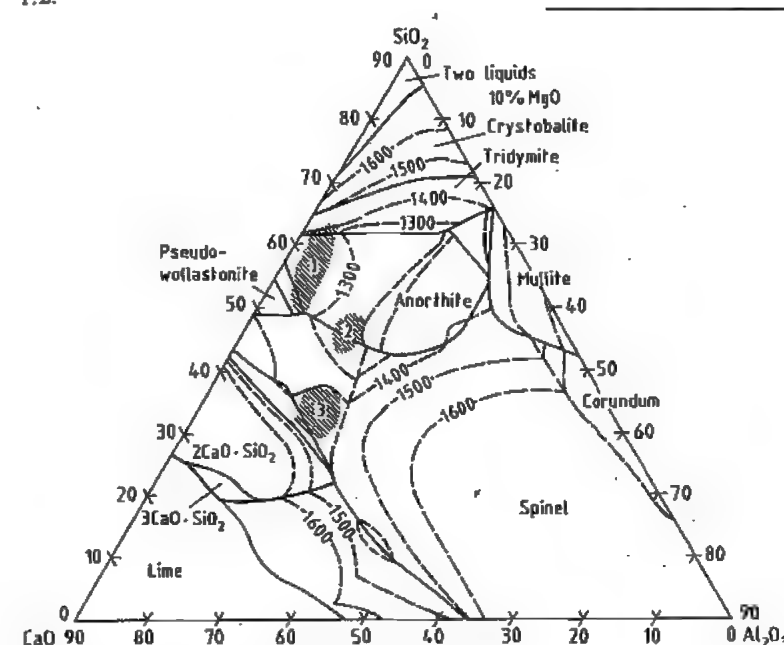


Figure 5.35: Composition of typical blast furnace slags on the $\text{CaO}-\text{Al}_2\text{O}_3-\text{SiO}_2$ phase diagram (see Figure 5.34) [20] (for explanation of regions 1, 2, and 3 see text).

5.5.8 Blast Furnace Productivity Criteria

The production rate P (t/d) of a blast furnace has been linked in various ways with the constructive data of the blast furnace and with metallurgical properties of the burden to give the specific furnace productivity. To date, no consensus has been reached to define a parameter which characterizes the furnace size and can be used in the calculation of the productivity. The characteristic parameters proposed up to now are (1) the hearth diameter, (2) the hearth bustle area that determines the depth of penetration of the blast in front of the tuyères,

(3) the square of the hearth diameter, (4) the hearth area, and (5) the working volume of the furnace. In Germany the hearth area is mostly used as a characteristic parameter for the furnace size, whereas in Japan the inner volume of the furnace is often used.

To compare various furnaces, the coke consumption with respect to the hearth diameter is often used. The coke consumption is a criterion (typical parameter) to express the productivity in the furnace which is operated in a given mode. The amount of coke consumed in the furnace is determined stoichiometrically by the constant blast volume blown. If the quantity of blast exceeds the limit, unfavor-

able phenomena such as hanging of the burden or variations in hot metal composition occur. The following relations have been proposed between hearth diameter and coke consumption:

$$D = \sqrt{4Q/\pi R}$$

$$Q = 30.673 \times 1.829(D - 1.829 - 2L_p)$$

$$Q = \gamma D^2 \quad (12)$$

$$\log Q = 2.59 \times \log d + 0.73$$

$$Q = 9.06D^{2.22}$$

where γ is the productivity factor, D is the hearth diameter and R a constant. The production of hot metal P is related to coke consumption per day Q (t coke per day) by the coke rate K (t of coke consumed for producing 1 t of hot metal) and is indirectly evaluated from the quantity of blast blown or the coke consumed:

$$P = Q/K \quad (13)$$

Blast furnaces which are well operated have a specific hot metal production rate $p = P/A$ of $65 \text{ t m}^{-2} \text{ d}^{-1}$ at a coke rate of 470 kg/t m , a slag volume of 300 kg/t m , a superficial gas velocity at the top of 3 m/s and a blast temperature of 1100°C . In Japan specific production rates of $80 \text{ t m}^{-2} \text{ d}^{-1}$ together with slag volume of 180 kg/t m have been achieved. Productivities based on the hearth area should be interpreted carefully, because the hearth diameter increases during the course of a furnace campaign by the wear of the lining. Therefore, the productivity should be evaluated by using the actual hearth area.

The coke consumption Q is shown as a function of the hearth diameter in Figure 5.36 for a productivity factor γ between 10 and 25. The daily production rate of some blast furnaces, as a function of the hearth diameter is shown in Figure 5.37. Curves for the specific hot metal productivity p are also shown for comparison. In practice it has been observed that the specific iron productivity does not increase proportionally for extremely high coke rates because for hard driven furnaces the coke rate K in Equation (13) increases with decreasing gas utilization.

Table 5.20: Values of constants in Equation (14) [39] (Courtesy of The Iron and Steel Institute of Japan).

	l	m	n
$P_1 \leq 1000$	0	2.0	500
$1000 < P_1 \leq 1500$	0.10	1.5	1000
$1500 < P_1 \leq 2000$	0.175	1.2	1500
$2000 < P_1$	0.235	1.0	2000

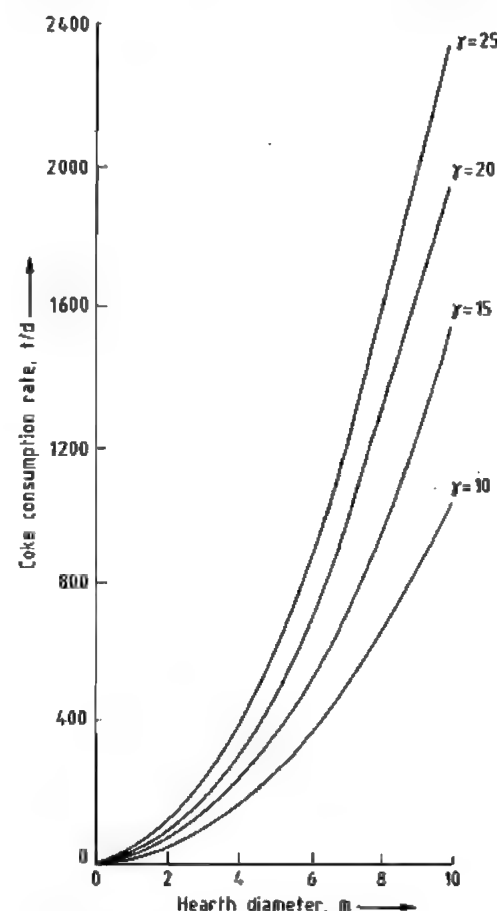


Figure 5.36: Change of coke consumption with the hearth diameter D and productivity factor γ [37].

Formulae for the calculation of the productivity based on empirical observation of operating furnaces have been derived with the aid of regression analysis [38]. These formulae are used to compare various furnaces or for the design of new furnaces. A regression formula on productivity is given for the blast furnace which produce pig iron for steelmaking.

Table 5.21: Characteristic data for modern large blast furnaces.

	Japan		Germany	France
	No. 2 Oita NSC	No. 5 Fukuyama NKK	No. 1 Schweilger Thyssen Stahl AG	No. 4 Dunkerque SOLLAC
Blown in date, month-year	10-1976	02-1986	02-1973	11-1987
Hearth diameter, m	14.8	14.4	13.6	14.0
Working volume, m ³	5070	4664	3596	3648
Number of tuyères	40	42	40	40
Number of tap holes	5	3	4	4
Number of cinder notch	0	0	0	0
Bell and hopper arrangement ^a	2B + V	4B	PW	PW
Top gas pressure, kPa	max. 300	230	330	max. 250
Hot blast stoves (number-type) ^b	4/ECS	4/ECS	3/ECS	4/ECS
Blast blower	electr.	electr.	electr.	electr.
Gas cleaning ^c	DC/2VS	DC VS EP	DC C VS	DC VS C
Production, t/d	10 150	9295	8700	8250
Load on hearth area, t m ⁻² d ⁻¹	59.0	57.1	60.7	54
Net burden weight, kg/t m	—	1640	1600	1631
Slag weight, kg/t m	321	309	255	314
Coke rate (dry), kg/t m	493	512	337	345
Pulverized coal injection (dry), kg/t m	0	0	145	127
Blast temperature, °C	1097	995	1150	1185
Blast volume (standard conditions), m ³	1110	1151	1100	1062
Oxygen enrichment, %	0	1.05	0	0

^aB = bell; V = valves; PW = Paul Worth top without a bell.

^bECS = external combustion stack.

^cDC = dust catcher; VS = venturi scrubber; EP = electric precipitator; C = cyclone.

^dt m = tonne of hot metal.

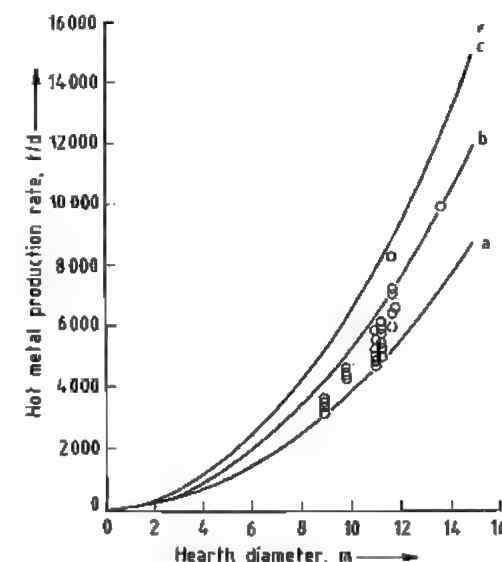


Figure 5.37: Relationship between hot metal production rate and the hearth diameter. The curves are for different specific hot metal production rates [38]. a) $50 \text{ t m}^{-2} \text{ d}^{-1}$; b) $68 \text{ t m}^{-2} \text{ d}^{-1}$; c) $85 \text{ t m}^{-2} \text{ d}^{-1}$.

$$P = A \frac{\left[9241 + \frac{(4.5(O_2 - 2.20))/100}{1 + \frac{(m/100)(P_1 - n)}{100}} \right]}{\left[489 - 0.10(t_b - 1132) + 10(\text{Ash} - 10.8) \right.} \\ \left. 0.2(\text{SV} - 304) - 0.9[(\text{SR} - \text{SFPe}) - 71.7] - 0.5(\text{OPe} - 91) \right]} \quad (14)$$

where P is the productivity ($\text{t d}^{-1} \text{ m}^{-2}$); A a constant ($0.85-1.15$); O_2 the oxygen enrichment of the blast (%); P_1 the top-gas pressure ($\text{gf/cm}^2 = \text{gram force per square centimeter} = 98.0665 \text{ Pa}$); l, m, n are constants given in Table 5.20, t the blast temperature ($^\circ \text{C}$); Ash the ash content in coke (%); SV the slag volume, (kg per tonne of pig iron); SR the sinter ratio (%); SFPe the self fluxing pellet ratio (%), OPe the acid pellet ratio (%).

The disadvantage of this formula is that it is entirely empirical. It does not predict productivity increases with technological improve-

ments. Important operational data for some large blast furnaces are summarized in Table 5.21.

5.5.9 Use of Blast Furnace Products

Hot metal, slag and top gas are the products of the blast furnace.

Hot Metal. Most of the hot metal is processed to steel by means of the LD (Linz Donawitz) oxygen top-blowing processes. The hot metal used for the LD or open hearth (Siemens-Martin) steelmaking process is known as *low-phosphorus* hot metal. It is characterized by low phosphorus and low sulfur contents. *High phosphorus* hot metal (Thomas iron) can also be refined to steel by means of the oxygen steelmaking (LD/AC) process. Other types of hot metal are further processed in foundries to *cast iron* or are used as alloys in the steel shop or in the foundry because of their high alloy content (e.g., manganese, silicon). The composition of the common types of hot metal are listed in Table 5.22. The Bessemer (Thomas) and open hearth processes have been replaced by the oxygen top-blowing processes.

Slags. Depending on the conditions during solidification, the slags produced by the blast furnace are further processed to:

- Air-cooled slag (solidification in slag pots or pouring pads),
- Granulated slag (spraying of the liquid slag with water),
- Pumice slag (foaming with water), or
- Slag wool (blowing of the liquid slag with air or steam)

Granulated slag can be in the form of pebbles or can have a porous structure depending on the granulation process. The different structure affects the hydraulic-bonding properties, the grindability, and the strength. Granulated slag is used as a material for making blast furnace cement by mixing it with Portland cement after pulverization. It is also used as a fertilizer.

Pumice slag is used in porous form as an insulation and filler material in heavy concrete and as a replacement for other bulk additions.

Air-cooled slag is either ground, such as granulated slag, or crushed and screened to be used as ballast or aggregate.

Slag wool is used in the form of pads for thermal insulation.

The relative quantities of the various products made from blast furnace slag for the various application are listed in Table 5.23 [40].

Table 5.22: Average composition of various kinds of hot metal (%) [36].

	C	Si	Mn	P	S
Low phosphorus iron	3.8-4.5	0.5-1.0	1.5-5.0	0.05-0.12	<0.05
LD hot metal	3.8-4.4	1.0	0.8-1.2	0.01	<0.04
Thomas (Bessemer) iron	3.5-3.9	ca. 0.3	ca. 0.8	ca. 1.8	<0.055
Hematite hot metal	3.5-4.2	1.5-3.5	0.7-1.0	<0.12	<0.04
Foundry iron I	3.5-4.5	1.5-3.5	1.0	0.5-0.7	<0.04
Foundry iron III	3.5-4.5	1.5-3.5	1.0	0.7-1.0	<0.06
Foundry iron IV A	3.5-4.5	1.5-3.5	0.7	1.0-1.4	<0.06
Foundry iron IV B	3.5-4.5	1.5-3.5	0.7	1.4-2.0	<0.06
Specialty and malleable cast iron	3.4-4.3	0.3-4.0	0.2-1.0	0.05-0.10	<0.05
Specialty metal (high carbon)	4.0-4.8	<2.5	0.3-0.6	0.08-0.15	<0.05
Specialty metal for the production of nodular cast iron	2.8-4.3	<2.0	<0.2	<0.06	<0.02
Sievertland specialty metal	2.8-3.4	2-3.5	2-4	<0.1	<0.05
Spiegel iron	4.0-5.0	<1.0	6-30	0.1-0.15	<0.04
Ferro manganese (75%)	6.0-7.0	<1.0	70-80	<0.25	<0.03
Ferro silicon	1.4-2.2	8-13	0.5-0.7	<0.15	<0.04
Charcoal hot metal	3.6-4.2	0.25-2.75	<1.0	ca. 0.03	ca. 0.015

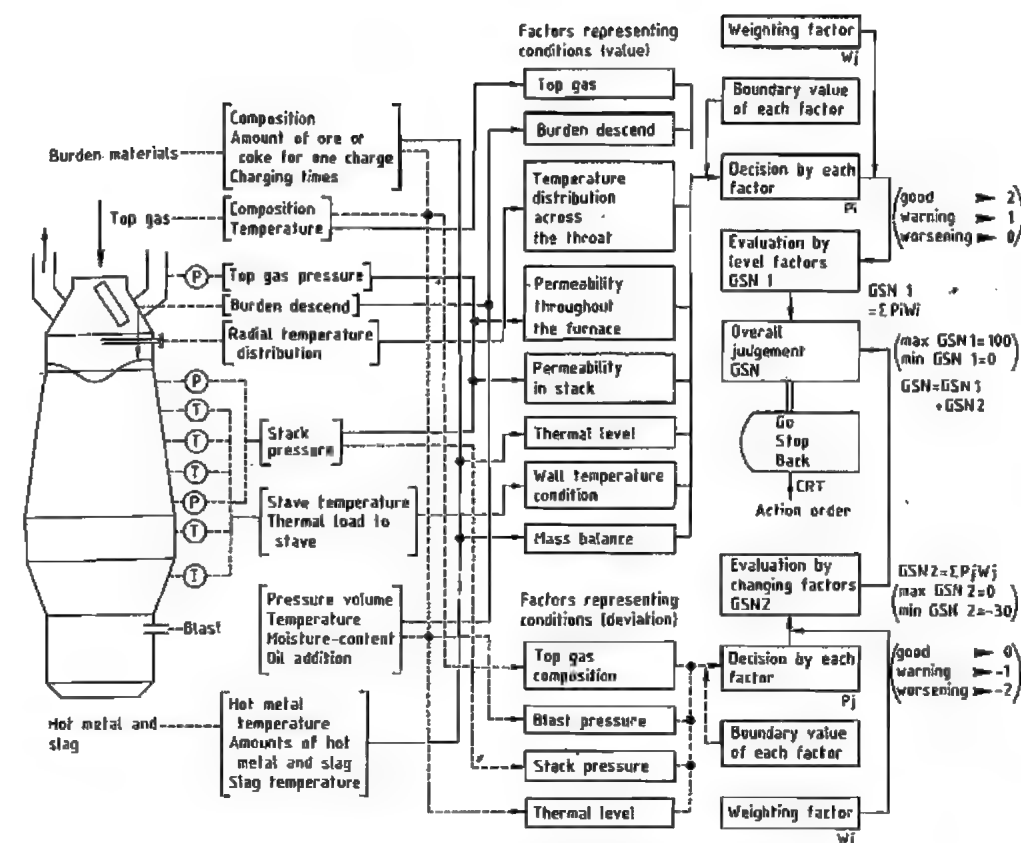


Figure 5.38: A control system of blast furnace developed by Kawasaki Steel Corp. [41] (Courtesy of The Iron and Steel Institute of Japan).

Table 5.23: Slag production and use in Japan in 1987 [40].

	10 ³ t	%
Slag production from blast furnace	23 842	
Slag use		
Road-bed construction	6 328	26.54
Improvement of ground	174	0.73
Engineering works	1 666	6.99
Cement	12 064	50.60
Concrete	1 496	6.27
Manure and improvement of soil	423	1.77
Building	603	2.53
Others	1 088	4.56

Top-Gas. The top-gas consists mainly of N₂, CO₂, CO and H₂. The utilization degree of the top gas is usually ca. 50% therefore it is a lean gas whose calorific value is between 2850 and 3560 kJ/m³ (STP). This value is very low compared to those of coke oven gas and LD

gas. Almost all the top gas is used in the iron and steel plant itself which has been extensively discussed (see Figures 5.7, 5.20, and 5.25).

5.5.10 Process Control

Thirty years ago, the blast furnace process was operated completely by manual control. Relatively few measuring devices were available for process monitoring purposes. Since the 1950s the productivity of a typical furnace has increased by ca. 20 times. This improvement in operation increased the importance of the process control. Modern blast furnaces are, therefore, equipped with a sophisticated system of measuring and controlling devices, and are directly linked to the process computer

(Figure 5.38). The latter is often incorporated into the total control system of the whole plant via a larger business computer.

The computer control of the blast furnace process for the optimization of the quality and costs started ca. twenty years ago. Research in this area is still being carried out. Much information can be obtained about the process by measuring the in- and outflows of mass and energy and also about many phenomena taking place inside the furnace. However, the basic problem is to convert these informations into control variables to serve the control circuit. The algorithm to evaluate the control variables from the measured values are based on various mathematical models.

Static and Dynamic Models Based on Statistics. In these models the blast furnace is considered to be a black box. The effect of certain deliberate changes in the input variables (e.g., coke addition, pulverized coal injection, moisture content of the blast, back pressure at the top) on productivity, hot metal composition, top gas utilization, etc. is evaluated. With the aid of statistical models, this leads to regression expressions containing the desired algorithms for the determination of the control variables. These statistical blast furnace models that have already been applied successfully do not, in principle, require any knowledge concerning the phenomena occurring inside the blast furnace. An example of such a regression expression is the productivity formula (see Equation 14) which should only be used for control purposes based on the values of a particular furnace and not based on values collected from various furnace operations. Although it is relatively simple to derive such an expression representing a blast furnace model from operational data, its application is limited. If such a model is applied to new operating conditions, then its predictions deviate from reality, the more the new operating conditions deviate from those which are described by the statistical data. Optimization of the operating conditions becomes stringently conservative when applying statistical models.

Static models based on statistics allow predictions concerning the steady state of the furnace only. **Dynamic models** based on statistics allow predictions concerning the behavior during a transient when passing from one steady state condition to another.

Models Based on Overall Balances. Models derived by taking overall balances represent the internal phenomena of the blast furnace on the basis of two-stage heat and mass balances. The procedure is principally similar to that described in section 5.5.6 in which the application of the Rist diagram and the heat and mass transfer phenomena (Table 5.16) were discussed. However, the models are more exact and detailed. A disadvantage of these blast furnace models is that they are unable to predict time-dependent phenomena in the furnace, although data concerning phenomena occurring in the blast furnace are evaluated. For the evaluation of the control variables it is, therefore, necessary to make assumptions concerning the *thermal equilibrium* between gas and solids in the thermal reserve zone and the *chemical equilibrium* between gaseous components (CO and CO₂) and solid component (iron and wustite), in the chemical reserve zone. The assumption corresponds to point W in the Rist diagram.

In the overall balance model, a *direct* relationship exists between input and output variables. This is a definite difference to the statistical model. The overall balance model has only one apparent degree of freedom which is the *degree of indirect reduction*. The existence of this apparent degree of freedom is caused by a lack of knowledge and will disappear when the internal phenomena of the blast furnace can be measured exactly and incorporated in the model. Under the fixed technological boundary condition the function of the blast furnace is *determined* by these phenomena in combination with certain pretreatment of ore and coke as well as a given hot metal composition.

Kinetic-Dynamic Model. The kinetic-dynamic model in its most extensive form is based on a knowledge of all phenomena that

constitute the entire blast furnace process. The phenomena include thermodynamic equilibrium and the kinetic relationships that govern the momentum, heat and mass transfer. The model is also based on the knowledge of the behavior of burden materials (e.g., size distribution at the top of the furnace, descending movement, softening and melting), coke gasification, and gas permeability. The model can simulate the behavior of a blast furnace for any given situation with a large computer. All the data required for the model can be determined in the laboratory and essentially need not be corrected with data based on actual operating conditions. The model thus constructed has proved to be advantageous for the study of new processing conditions and the predictions of the operating results without performing costly experiments with the blast furnace. Its disadvantage is the requirement of great amount of expenditure to complete information on all the important phenomena occurring in the furnace. For routine blast furnace control, the model must be simplified to reduce computer loads.

The most important kinetic phenomena for constructing the mathematical model by taking differential balances around a control volume are the chemical reactions (e.g., reduction of iron oxide, coke gasification, water gas shift reaction, and reduction of silica). The reduction rate of iron oxide by carbon monoxide or hydrogen can be expressed in terms of the three-interface unreacted-core shrinking model which is represented in Figure 83. Rate and equilibrium constants needed for the rate equation are given in reference [42]. For *silica reduction*, a mechanism via the intermediate formation of SiO gas has recently been proposed [43]. A rate equation has been derived for the transfer of silicon from the SiO gas to the hot metal in accordance with the mechanism as described by Equation (15).

$$\frac{d[\%Si]}{dt} = k_s(A/M)P_{SiO} \quad (15)$$

where k_s designates the reaction rate constant, A/M the specific area, and P_{SiO} the partial pressure of SiO.

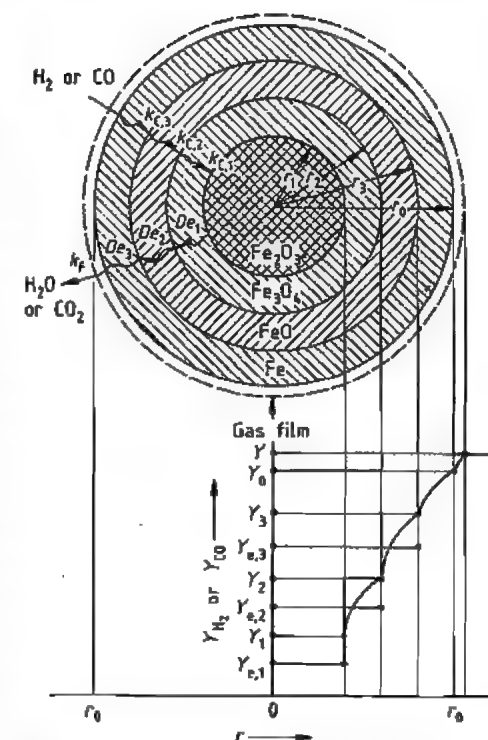


Figure 5.39: Three-interface unreacted core model [41] (Courtesy of The Iron and Steel Institute of Japan): De_i = intraparticle diffusivity in i -th phase; k_{ci} = rate constant of i -th chemical reaction; k_f = mass transfer coefficient through gas film; r = radial coordinate; Y = molar fraction of gas.

This mechanism has been found to give excellent simulation results when it is incorporated into the mathematical model.

The *heat transfer* between the different phases in a packed bed is usually expressed in the form of convection heat transfer. The estimation of the heat transfer coefficient is mainly based on the Ranz Equation [45]:

$$Nu = 2.0 + 0.6(9Re_p)^{1/2}Pr^{1/3} \quad (16)$$

where Nu , Re_p , and Pr designate Nusselt, particle Reynolds, and Prandtl numbers.

However, this equation sometimes gives an inappropriate value. The rate of heat exchange in a packed bed is currently being studied. *Flow maldistribution* of gas in a packed bed can be estimated by using the Ergun equation,

a potential flow mechanism is often applied to the solid flow [46].

On the basis of the principal concepts mentioned above, one-dimensional [47], or two-dimensional [46, 48, 49] mathematical models were derived. On the other hand, dynamic changes in the internal situation of a blast furnace were also simulated by an unsteady-state mathematical model [50, 51].

Even if a supercomputer is available for the simulation computation of a whole blast furnace, it is still quite difficult to obtain detailed results which include all the phenomena occurring in a blast furnace. Mathematical models presenting some specified phenomena in a blast furnace are effective when detailed information is requested. Such models are developed for analyzing burden distribution at the top of a blast furnace [52], gas flow and heat

transfer in the cohesive zone [53], raceway phenomena [27], fluid flow in the hearth [54] and so on.

Some examples of the simulation results are shown in Figures 5.40, 5.41, and 5.42. Figure 5.40 depicts a one-dimensional distribution of process variables such as temperature, pressure, concentration, and fractional reduction for two different top-gas pressure.

Temperature and gas-concentration distributions reveal the existence of thermal and chemical inactive zones and characteristic distribution of CO concentration which shows maximum value at the position where the CO₂ concentration is zero. The simulation results agree well with the principal behaviors of the process variables previously shown in Figure 5.20.

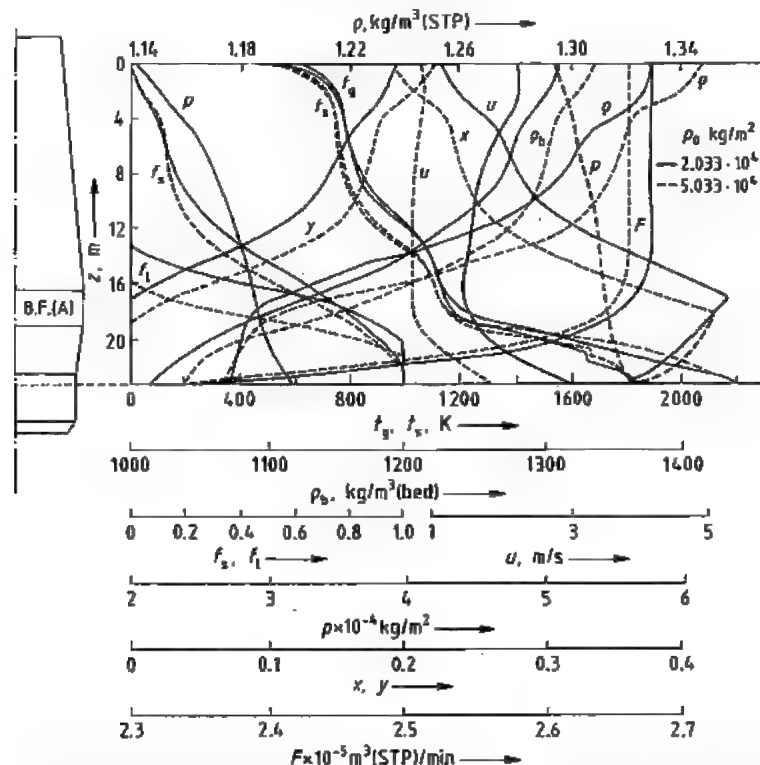


Figure 5.40: Longitudinal distribution of process variables in blast furnace (A) for the case of high-pressure operations [46] (Courtesy of The Iron and Steel Institute of Japan); t_g , t_s = temperatures of gas and solid; f_i = fractional reduction of iron oxide; f_s = fractional decomposition of limestone; u = superficial gas velocity; p = gas pressure; p_0 = top gas pressure; x , y = molar fraction of CO and CO₂; F = volume flow rate of gas; ρ = gas density; ρ_b = bulk density of burden bed.

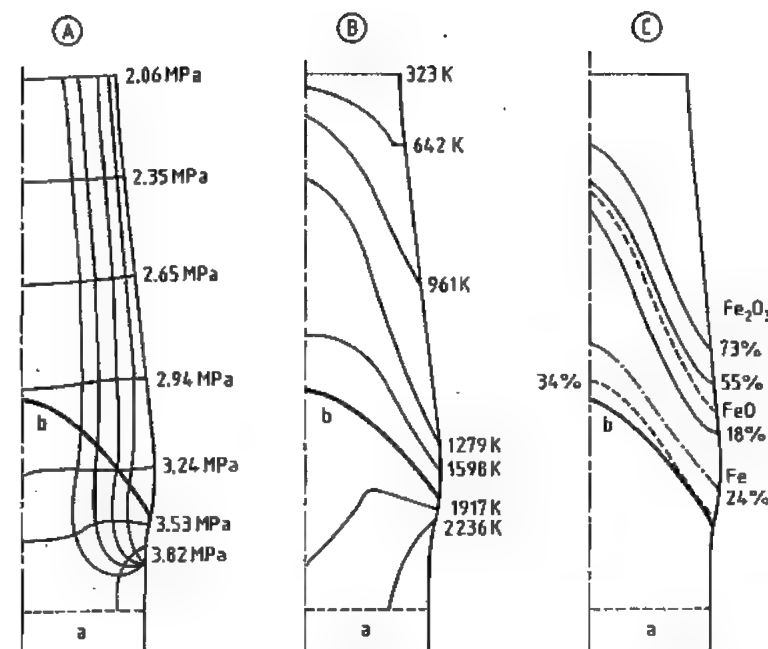


Figure 5.41: Two dimensional simulation results by finite difference method [48] (Courtesy of The Iron and Steel Institute of Japan): A) Streamlines and isobars; B) Isotherms of solid; C) Reduction of ore; a) Liquid; b) Fusion zone.

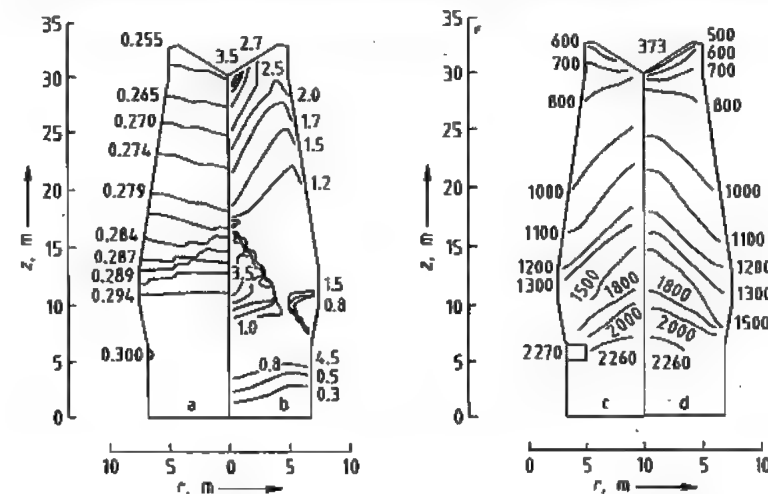


Figure 5.42: Two dimensional simulation result by finite element method [46] (Courtesy of The Iron and Steel Institute of Japan): a) Isobars (P in MPa); b) Contour lines of average mass velocity of gas ($\text{kgm}^{-2}\text{s}^{-1}$); c) Isotherms of gas (t_g in K); d) Isotherms of solid (t_s in K).

Figure 5.41 shows the streamline of gas, as well as the radial distribution of pressure, temperature and reduction degree, which show a considerable nonuniformity. One of the impor-

tant problems is how to control or utilize the nonuniformity to improve productivity.

Figure 5.42 shows computed radial profiles of pressure, gas velocity, and temperatures of

gas and solids. In this computation, the layer-by-layer structure of the packed beds and the radial particle size distribution were considered, which markedly affect the gas permeability and then gas flow and temperature distributions.

Complete measurement of the internal state of a blast furnace is very difficult because of its huge size. Simulation technology in combination with operating and some measured data is very important to understand the behavior of the blast furnace.

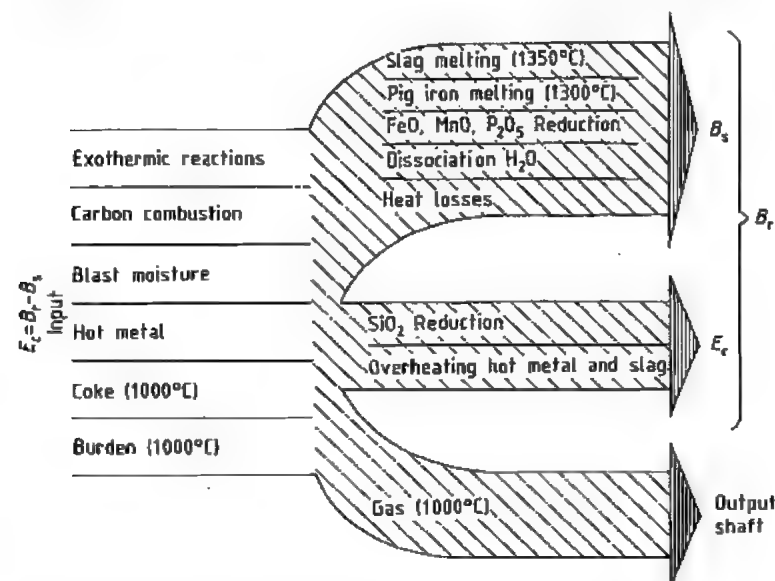


Figure 5.43: Heat balance for calculating value of E_c —heat required for the reduction of silicon and for the overheating of iron and slag [55] (Courtesy of The Institution of Mining and Metallurgy).

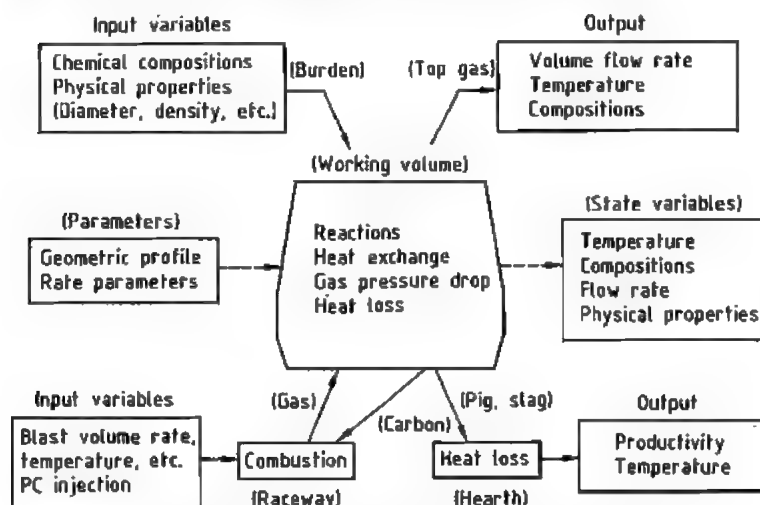


Figure 5.44: Schematic diagram of a dynamic simulation model of blast furnace [51] (Courtesy of The Iron and Steel Institute of Japan).

Application of the Models. The purpose of the blast furnace control during continuous operation is the increase in productivity by stabilizing the furnace operation and the production of high quality pig iron of appropriate temperature and composition. The control variables are (1) ore: coke ratio and burden distribution at the top of the furnace, (2) flow rate and temperature of blast, water vapor addition, and oxygen injection, pulverized coal, oil and fine ore injection.

Originally, attention was paid to the *thermal condition* in the lower part of the blast furnace for the stable operation. The so-called *Wu model* was proposed by the Institut de recherches sidérurgiques (IRSID) in France. In the model, the heat input into the lower part of the furnace is calculated from blast volume and composition, tuyère injection, and the off-gas analysis. The amount of heat W_u is that required for the melting of iron and slag, the reduction of the alloying elements, and compensation for heat loss. The value of W_u can be calculated by subtracting the heat consumed by direct reduction of the iron oxides from the total heat supplied to the lower part of the furnace. By maintaining W_u at a constant set value pig iron of a constant composition can be produced.

At the Centre de recherches métallurgiques (CNRM) in Belgium, a somewhat different model of the same basic type was developed for automatic regulation of the thermal condition of the furnace. In this model, the heat input per ton of pig iron into the high-temperature zone of the furnace was calculated from the temperature and composition of the top gas, the blast volume, blast temperature, and blast composition. The value obtained is called the heat requirement. The term E_c was defined as the difference between the actual (B_r) and the standard heat requirements (B_s). The latter quantity represents the amount of heat needed to produce a pig iron at 1300 °C containing 0% Si.

The value of E_c corresponds to the heat required for silica reduction and for overheating slag and metal. The heat balance to calculate E_c is shown in Figure 5.43.

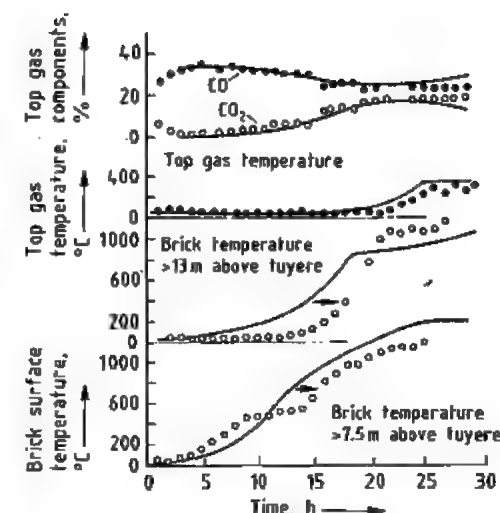


Figure 5.45: Comparison between measured and simulated changes of process variables in blow-in operation of Kokura no. 2 blast furnace, Sumitomo Metal Industries, Ltd. [51] (Courtesy of The Iron and Steel Institute of Japan): — Predicted; ● Measured.

A *one-dimensional dynamic model* was applied to the *unsteady-state* blast furnace operation such as the shut down, the blow-in, and the blow-out together with a *two-dimensional gas flow* model. A schematic diagram is shown in Figure 5.44. Figure 5.45 shows the simulation results for the blow-in operation of the blast furnace according to the scheduled increase in blast volume and temperature as shown in Figure 5.46. The initial condition given to the mathematical model was obtained from the actual filling condition of coke and burden before the start of the blow-in. The results confirm the effectiveness of the model application to the planning of the blow-in operation of the blast furnace. Another successful example for the application of a dynamic model to the actual operation has been reported for the blow-out of the blast furnace. The content of the blast furnace was blown out with the decrease of stock level from the top to the upper bosh under the schedule predicted by the mathematical model. Actual changes of the operation conditions are shown in Figure 5.47 in comparison with the scheduled ones. The actual results are in reasonable agreement with the schedule (see Table 5.24). Some im-

provements to the mathematical model are necessary for obtaining a satisfactory agreement. However, principally such a kinetic-dynamic model is found to be effective not only for steady-state but also for unsteady-state operations.

The most precise mathematical model of a blast furnace to date is the two-dimensional steady-state kinetic model developed by Sugiyama et al. [57] (Nippon Steel Corp.). It includes models for operational design, burden distribution, gas, solid and liquid flow, for the reaction rate of seven chemical reactions, for heat transfer and a total combination model. When operational conditions and a blast furnace profile are given, this model provides (1) streamlines of gas, liquid and solids, (2) pressure distribution, (3) reduction degree of iron oxides, (4) gas, solid and liquid temperature, and (5) location of the cohesive zone.

An integrated process computer system in the entire ironmaking department is being developed for increasing flexibility and productivity in the ironmaking systems which consist essentially of coke ovens, sintering machines, hot stoves, and blast furnaces.

The three-layer hierarchical system shown in Figure 5.48 is used for integrated control. In the system, *microcomputers* can accept the operating data directly from the plant and can control it. A *process computer* which eventually controls the overall ironmaking system is installed to provide sufficient information to the operator for realizing effective operation. Finally, a central *business computer* is connected to the process computers for optimal control of the overall iron and steel production

system. Chiba works of Kawasaki Steel Corp. constructed this three layers system for two sintering plants and achieved effective operational control.

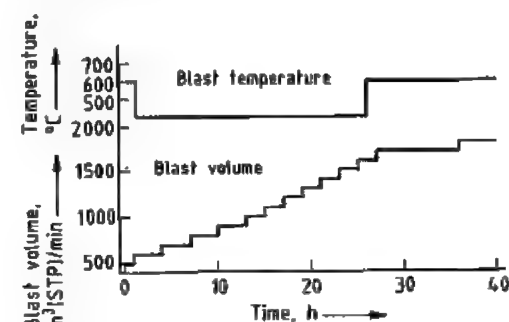


Figure 5.46: Schedule of the blow-in operation for the Kokura no. 2 blast furnace based on a dynamic model [51] (Courtesy of The Iron and Steel Institute of Japan).

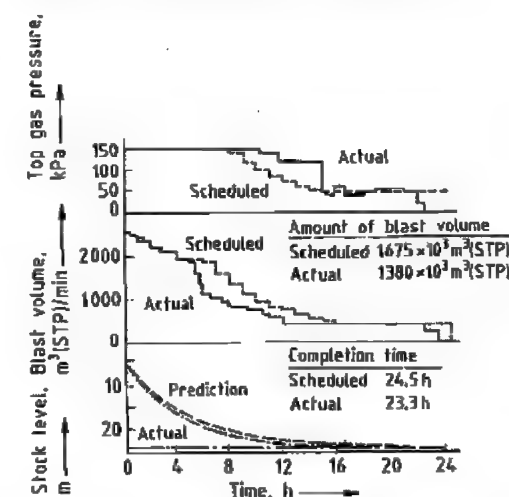


Figure 5.47: Results of the empty blow-out operation of the Kokura no. 2 blast furnace [56] (Courtesy of The Iron and Steel Institute of Japan).

Table 5.24: Results of the empty blow-out operation of the Kokura no. 2 blast furnace in Sumitomo Metal Industries [56] (Courtesy of The Iron and Steel Institute of Japan).

	Actual results	Schedule	Difference, %
Blow-out operation time, h	23.3	24.5	-5
Accumulated amount of blast volume, $m^3 \times 10^3$ (STP)	1380	1675	-18
Accumulated amount of water-spray, t	694	716	-3
Pig iron produced during blow-out, t	880	998	-12
Amount of total coke consumption, t	550	690	-20
Coke consumption per blast volume, $t/m^3 \times 10^3$ (STP)	0.40	0.41	-2

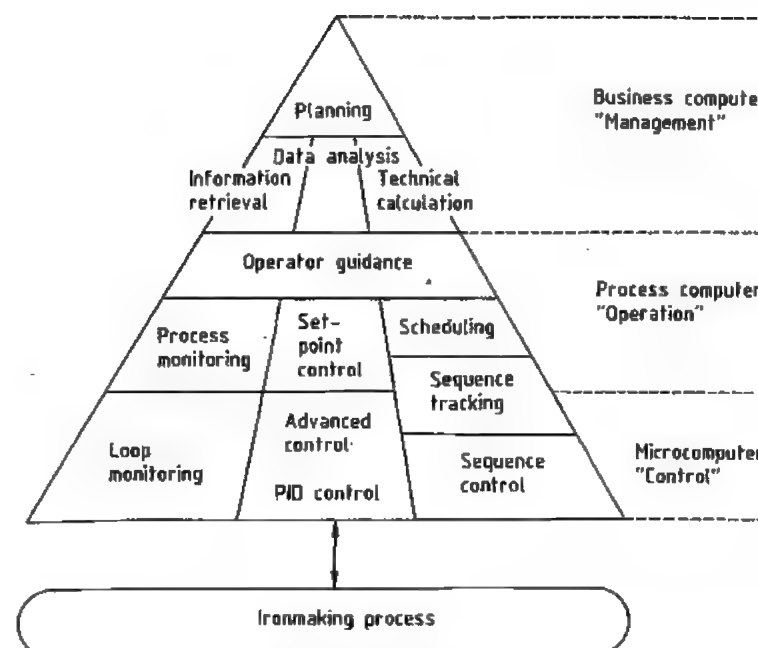


Figure 5.48: Functional hierarchy of the ironmaking information system [37] (Courtesy of The Iron and Steel Institute of Japan).

Table 5.25: Summation of net exergy losses in the blast furnace ironmaking system [60] (Courtesy of The Iron and Steel Institute of Japan).

Process	Case A-1			Case A-2, MJ/thm		
	Inflow	Outflow	Net loss	Inflow	Outflow	Net loss
Blast furnace	17 054	15 175	1 879 (20.8%)	16 920	14 736	2184 (24.1%)
Coke oven	22 657	18 580	4 077 (45.1%)	20 110	16 491	3619 (39.9%)
Hot stove	1 983	1 276	707 (7.8%)	2 100	1 423	677 (7.5%)
Sintering machine	3 014	764	2250 (24.9%)	3 074	733	2341 (25.8%)
Rotary kiln	138	33	105 (1.2%)	339	79	260 (2.9%)
Curing of nonfired pellets	190	170	20 (0.2%)			
Total	45 036	35 998	9038 (100%)	42 543	33 462	9081 (100%)

Although great progress has been made in the computer control of blast furnaces by introducing mathematical models, control is still incomplete. Recently, artificial intelligence has been introduced into blast-furnace control. The principal strategy of this technology is based on operational data [59]. Therefore, the question how to accumulate the operating data is most important. Some trials have been made to couple the artificial intelligence (Expert system) with a mathematical model.

Energy Recovery. After the oil crisis, energy cost increased drastically. Therefore in high-

energy consuming industries, energy saving has been examined from various points of view. In Japan 1.9×10^7 kJ energy is currently consumed to produce 1 t crude steel in the blast furnace ironmaking process. This value is 20% lower than 10 years ago. The energy savings are still conducted in each ironmaking process. In the blast furnace, a lot of energy is saved by using top-pressure recovery turbines. Figure 5.49 illustrates the development of energy savings in the ironmaking department of NSC during the last 15 years.

To pursue further energy savings, an exergy analysis was conducted on the basis of actual

operation data of a blast furnace ironmaking system which produced ca. 7000 t pig iron per day. Very high net exergy losses occur in the coke oven and the sintering machine (see Table 5.25). Compared to these processes the blast furnace destructs less exergy. Net exergy losses in the conventional blast furnace, the direct reduction electric furnace, and the smelting reduction systems are compared in Figure 5.50. The exergy analysis for the conventional and the direct reduction iron-electric furnace systems was performed on the basis of operation data but in case of the smelting reduction system, the data were obtained by taking heat and material balances. However, no definite difference among the net exergy losses were found. Further energy savings will probably lower exergy losses even further.

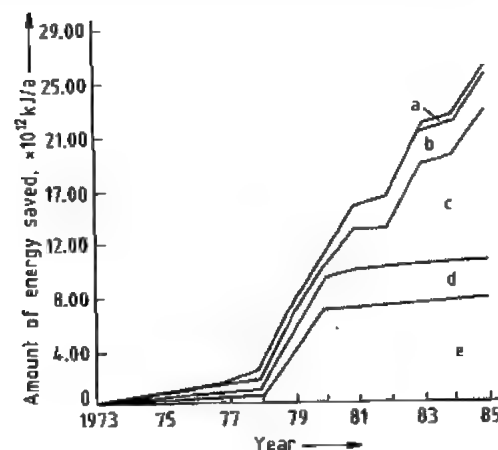


Figure 5.49: Chronological change in the amount of energy saved by main waste heat recovery process in Nippon Steel Corp. (60) (Courtesy of The Japan Iron and Steel Institute): a) Recovery of sensible heat from coke oven gas; b) Recovery of waste heat from sinter cooler; c) Coke dry quenching; d) Recovery of sensible heat from hot stove; e) Top gas pressure recovery turbine.

5.5.11 Hot-Metal Desulfurization

The sulfur content of the hot metal produced depends on the sulfur content of the fuels, the slag basicity, the slag volume, and the silicon content of the hot metal. The sulfur transfer mechanism in the blast furnace is

shown schematically in Figure 5.51. After the hot metal is separated from slag, the former is desulfurized by gas metal and slag-metal reactions. However, in the upper part of the cohesive zone, the sulfur compounds present in the gas phase are absorbed partly by solid iron ores.

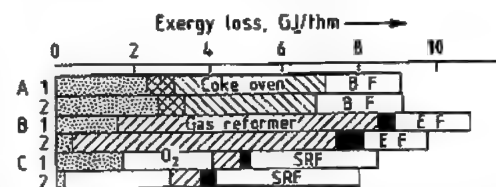


Figure 5.50: Summation of net exergy losses in different ironmaking systems [61] (Courtesy of The Iron and Steel Institute of Japan): A) Blast furnace ironmaking (1 = standard, 2 = pulverized coal injection); B) Direct reduction-electric furnace ironmaking (1 = fired pellet, 2 = nonfired pellet); C) Smelting reduction ironmaking (1 = shaft furnace, 2 = fluidized bed). O₂ = oxygen production; BF = blast furnace; EF = Electric furnace; SRF = Smelting reduction furnace. □ Pretreatment, agglomeration of raw materials; ■ Shaft furnace, fluidized beds; ▨ Hot stove.

The steelmaking process requires a sulfur content of the hot metal of $< 0.025\text{--}0.035\%$, because desulfurization is difficult in the steelmaking process. Except for the desulfurization of the coke, sulfur can be removed in the blast furnace, between the blast furnace and the steel shop, and in the steel shop. The cost is reported to be the lowest for desulfurization between the blast furnace and the steel shop [62].

Desulfurization in the *blast furnace* requires an increase in the limestone additions. This leads to the additional costs associated with the limestone itself and the increased coke rate because more heat is needed for melting the slag and for decomposing the limestone. In addition to this, the carbon dioxide generated from limestone must be compensated.

Desulfurization in the *steel-producing vessel* requires a large slag volume even for highly basic slags because of the unfavorable sulfur distribution ratio under oxidizing conditions. Iron losses to the slag increase because of the large slag volume.

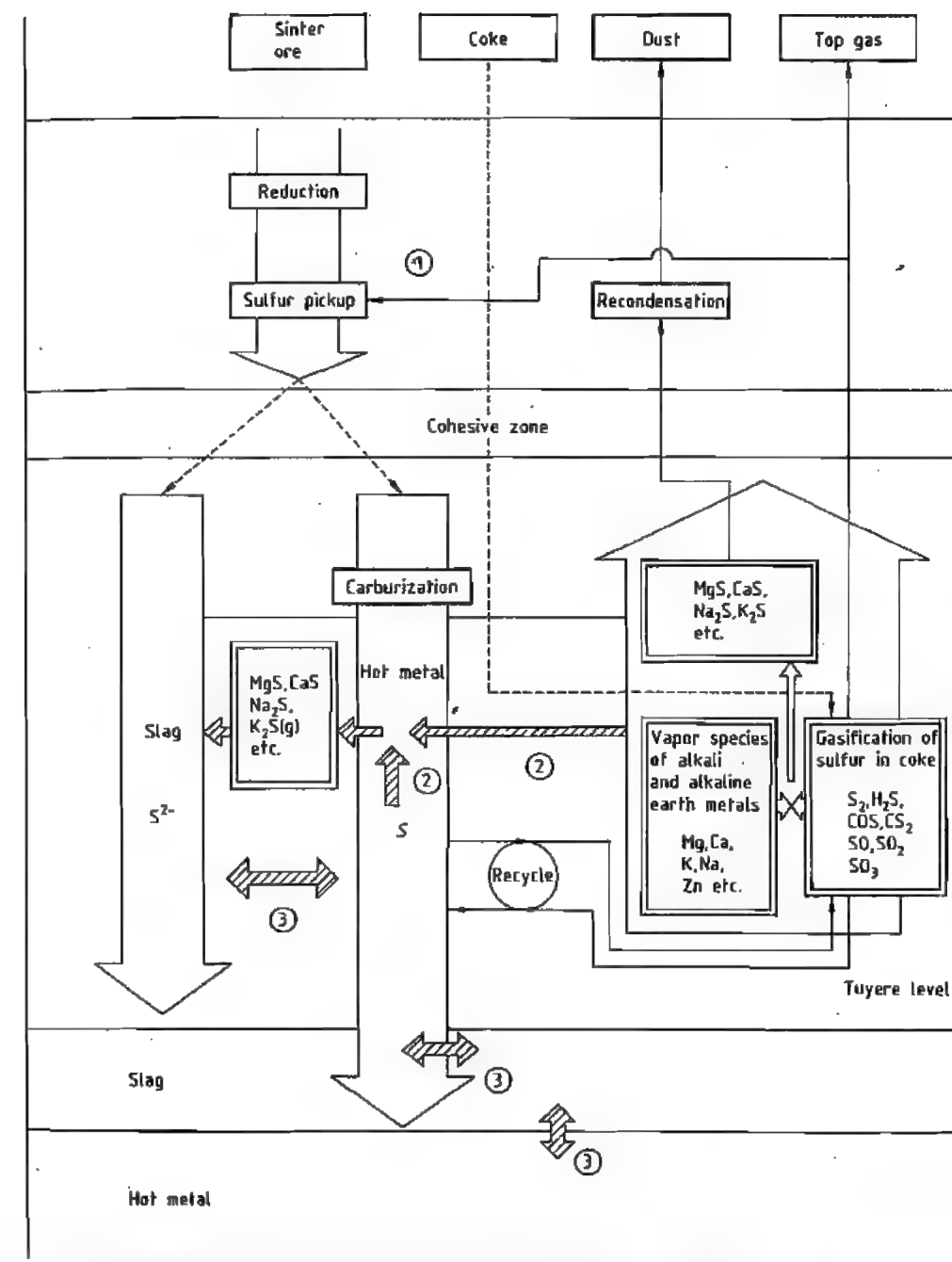


Figure 5.51: Schematic representation of sulfur transfer routes in the blast furnace [65] (Courtesy of The Iron and Steel Institute of Japan).

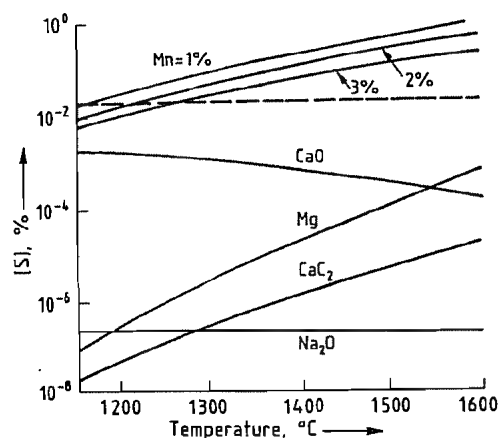


Figure 5.52: Temperature dependence of equilibrium sulfur content of carbon-saturated hot metal [63] (Courtesy of The Iron and Steel Institute of Japan).

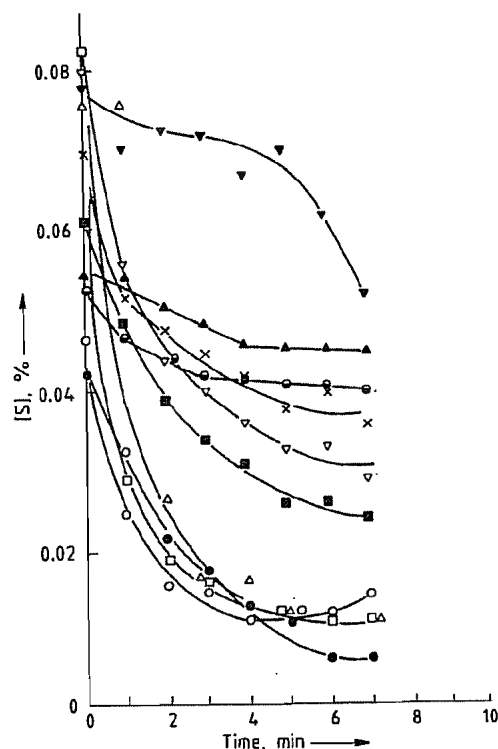


Figure 5.53: Changes of sulfur content with time in bottom-blowing ladle desulfurization process for variable fluxes (amount of flux addition 10 kg/thm) [63] (Courtesy of The Iron and Steel Institute of Japan): ● CaC_2 ; ▲ CaO ; ■ Ca(CN)_2 ; □ Na_2CO_3 ; △ NaOH ; ○ KOH ; × NaCl ; ▽ NaF ; ● Na_3AlF_6 .

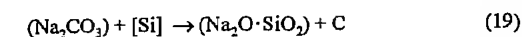
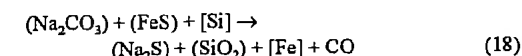
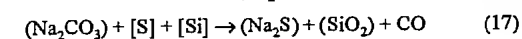
At present, it is advantageous to desulfurize at least a portion of the hot metal during *transportation to the steel shop*. After mixing with hot metal which is not desulfurized outside the blast furnace, an input sulfur content of ≤ 0.02% can be delivered to the steel shop.

Desulfurizing Fluxes include calcium compounds which are in the solid state or half melting conditions at the hot metal temperature (e.g., CaO , CaC_2 , Ca(CN)_2 , and CaF_2), alkaline compounds in the liquid state (e.g., KOH , NaCl , and NaF), and magnesium and its alloys in the gaseous state.

Their desulfurization ability is remarkably affected by treatment conditions such as (1) mixing, (2) atmosphere (oxidizing or reducing), (3) composition of hot metal, and (4) property and amount of blast furnace slag. Figure 5.52 shows the equilibrium sulfur content obtained by each desulfurizing flux. Actual desulfurization curves for the *bottom blowing* method with nitrogen are shown in Figure 5.53.

According to these figures, desulfurization degree, method, cost, and workability should be considered when selecting of a desulfurizing flux in addition to its desulfurizing ability.

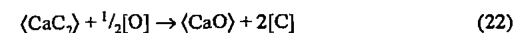
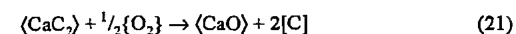
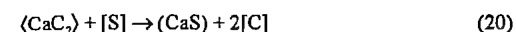
The equation for the desulfurization reaction with *soda ash* [64] and of concurrent reactions are as follows (Equations 17–19):



Furthermore, Na_2CO_3 reacts easily with SiO_2 from the refractories forming $2\text{Na}_2\text{O} \cdot \text{SiO}_2$, $\text{Na}_2\text{O} \cdot \text{SiO}_2$, and $\text{Na}_2\text{O} \cdot 2\text{SiO}_2$. The vaporization loss of Na_2CO_3 is ca. 6% at 1250 °C. This value increases to 35% at 1350 °C, therefore the effect of desulfurization decreases sharply at temperatures > 1300 °C. The disadvantages of desulfurization with soda ash are its corrosive action to the vessel lining and the environmental problems related to discarding slags which contain high alkaline contents. Environmental problems arise from sodium oxide-containing fumes and from the reaction

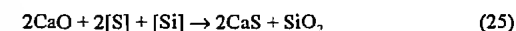
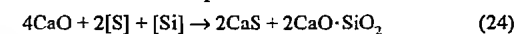
of the sodium sulfide contained in the slag with water to produce hydrogen sulfide and sodium hydroxide.

The desulfurization reactions of hot metal with *calcium carbide* are as follows:



As calcium carbide is easily oxidized (see Equations 21 and 22) the desulfurization should take place under controlled atmosphere. The reaction product CaS which has a high melting temperature of 2450 °C forms the solid slag. The diffusion of sulfur in the hot metal to the boundary between hot metal and calcium carbide is the rate-determining step of the desulfurization reaction. In the sulfur-transfer mechanism, mixing strongly affects the degree of desulfurization. When calcium carbide particles are injected with an inert carrier gas, a calcium sulfide layer grows at the outer surface of the particle as the reaction proceeds. The reactivity of each particle decreases with increasing thickness of this layer. Thus, the efficiency of this flux is relatively low. Its advantage is that a very low residual sulfur content of the hot metal can be achieved irrespective of its initial sulfur content.

When *lime* is used, the following desulfurization reactions proceed:



The reaction given by Equation (25) occurs at 1300 °C even if the silicon content of the hot metal is only 0.05%. If the silicon in the hot metal is oxidized to silicon dioxide in this process, it reacts with lime to form $2\text{CaO} \cdot \text{SiO}_2$. This reaction decreases the amount of lime available for desulfurization. Therefore oxidation of silica should be prevented by using the inert or reducing atmospheres or airtight vessels.

Magnesium is sometimes used as a desulfurizing flux because it has a very strong affinity for sulfur. Equations (26), (27), and (28) represent the desulfurization by magnesium and the

oxidation of magnesium which occurs in the desulfurization process.



The vaporization temperature of magnesium is relatively low (1107 °C). Therefore, magnesium evaporates upon contact with the hot metal and the desulfurization efficiency decreases. It is therefore necessary to control the vaporization (see below).

Table 5.26: Typical desulfurization processes outside the blast furnace [18] (Courtesy of The Iron and Steel Institute of Japan).

Method	Process
Soda-ash paving	soda-ash paving process reladling process ladle with siphon process
Shaking ladle	shaking ladle process DM converter process rotating drum process
Stirrer	Demag-Östberg process Rheinstahl process KR process
Injection	(ladle process) (torpedo-car process)
Gas bubbling	bottom blowing process top blowing process
Gas-lift mixing reactor	GMR process
Desulfurization with magnesium	injection process plunging bell process
Continuous desulfurization in the blast-furnace runner	turbulator process powder injection process paddle-type stirrer process electromagnetic stirrer process

Desulfurization Processes. To produce low-sulfur or ultra-low sulfur steel, a number of desulfurization processes have been developed. Typical processes for desulfurization *outside* the blast furnace are listed in Table 5.26. In each process, acceleration of the desulfurization reaction is achieved by increasing the contact area between the desulfurizing fluxes and the hot metal. This is carried out by employing improved stirring techniques. The other requirements for the processes are as follows: (1) inexpensive desulfurizing fluxes, (2) high reproducibility with regard to the de-

gree of desulfurization, (3) small decrease of the hot metal temperature, (4) low iron loss to the slag, and (5) an easy and inexpensive disposal of the slag.

Desulfurization in the *blast-furnace runner* is not widely accepted at present despite the favorable surface:volume ratio and the low degree of technical expenditure required. The reasons are the corrosive attack of the slag on the runner material, the hazardous exposure of the workers to alkaline fume, and the poor reproducibility with respect to the degree of desulfurization.

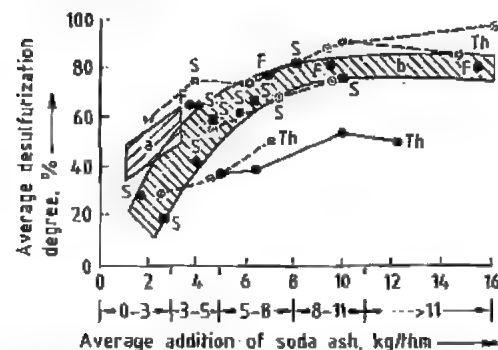


Figure 5.54: Effect of the amount of soda ash addition on the desulfurization of hot metal in various desulfurization processes [66] (Courtesy of Verlag Stahleisen mbH): ○ Blast-furnace runner; ■ Transportation ladle; ⊙ Mixer-ladle; ⊕ Mixer-ladle-ladle; ⊗ Torpedo car ladle, ladle with siphon; S = pig iron for steelmaking; Th = Thomas pig iron; F = pig iron for foundry. a) Ladle with siphon; b) furnace-runner and transportation ladle.

The soda-ash paving method is frequently used for desulfurization in the *transport ladle* because of its simplicity. The transport ladle is used to transport the hot metal from the blast furnace to the hot-metal mixer located in the steel shop. In this method, the desulfurizing flux is placed in the ladle prior to filling it with hot metal. Good mixing is achieved by formation of carbon dioxide and by the falling hot-metal stream. The slag is removed from the filled ladle. Figure 5.54 illustrates the relationship between the final degree of desulfurization and the amount of soda ash added. The final desulfurization degree increases with increasing soda-ash addition up to a value of 80%, which is obtained at 8 kg "soda-ash addition" per ton of hot metal. After that the des-

ulfurization degree in most cases reaches a plateau level.

Efforts to improve the mass transfer of the sulfur by moving the vessel containing the hot metal involved trials with rotating drums (Kalling-Dommarvet process [67]) and *shaking* or *rotating ladles*. In the shaking ladle, the ladle axis rotates around a circular path at ca. 70 rpm. By reversing the direction of the movement, the mixing effect can be enhanced (Kobe Steel process [65]).

Figure 5.55 shows desulfurization processes with mechanical stirrers. The stirrer proposed by ÖSTBERG (see Figure 5.55A) has a *hollow stirrer* which discharges the *hot metal* through horizontal tubes by centrifugal forces and absorbs hot metal from the bottom of the vertical tube. The simple stirrer proposed by KRAEMER in Rheinstahl Hüttenwerk (Figure 5.55B) is made of refractory. This stirrer mixes in *desulfurizing fluxes* into the hot metal. The stirrer developed by Nippon Steel (Figure 5.55C) is an impeller which produces eddy flow of the *hot metal*. Results of plant experiments for this stirrer are shown in Figure 5.56. According to this figure the process is highly effective for desulfurization. The stirrer method is widely used in North America, Europe, and Japan for the production of low-sulfur steel or ultra-low sulfur steel.

The *injection method* of hot metal desulfurization is widely accepted for the desulfurization in a ladle or a torpedo-car. In this method the flux powder of desulfurization is injected with a gas stream. As flux powder CaC_2 , $\text{Ca}(\text{CN})_2$, CaO and soda ash are widely used. Currently magnesium is also used. The injection lance is better for dipping into the hot metal bath. The dipping depth should be 1/2 to 3/4 of the bath depth. NSC [76] and TSAG [77] developed the respective process for desulfurization by using the injection method.

In the *gas-bubbling* method, the desulfurizing flux is at first added to the surface of the hot metal and then mixing is started by the injection of gas into the hot metal. The injection is made through the lance dipped into the hot metal (top-blowing method) or through the porous plug at the bottom (bottom-blowing

method). Figure 5.57 represents schematically the bottom-blowing desulfurization ladle. Ultra-low sulfur steel containing 0.001–0.002% S can only be produced by this method if the second addition of calcium carbide is made after the slag of the first treatment is removed.

The *gas-lift mixing reactor* method (GMR method) was proposed by Kobe Steel. The ba-

sic principle of this method is to use the buoyancy force of the gas injected at the bottom of the riser as driving force for a circulatory motion of the hot metal as illustrated in Figure 5.58. This method removes sulfur in hot metal to <0.002% by adding 5 kg of CaC_2 per tonne of hot metal.

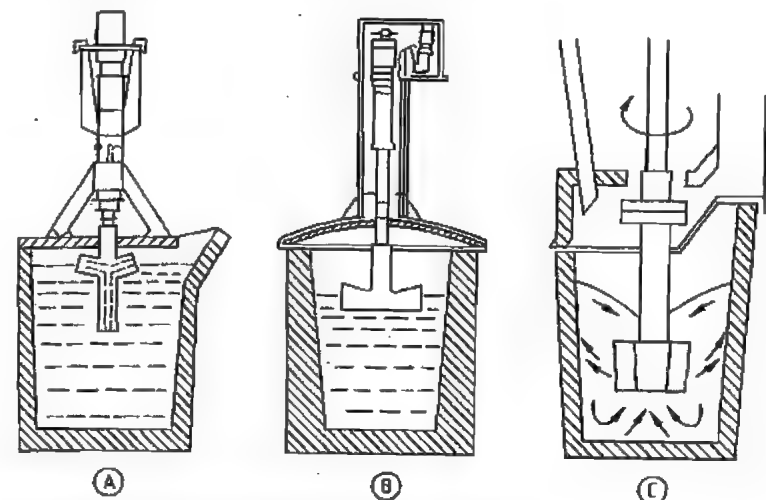


Figure 5.55: Stirrers for desulfurization of hot metal [75] (Courtesy of The Iron and Steel Institute of Japan): A) Demag-Östberg process; B) Rheinstahl process; C) KR process.

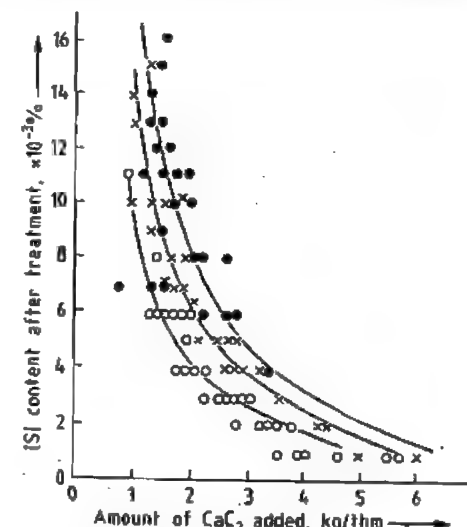


Figure 5.56: Relation between amount of CaC_2 added and [S] content after treatment [75] (Courtesy of The Iron and Steel Institute of Japan). [S] content before treatment (1350 °C): ○ 0.02%; × 0.03%; ● 0.04%.

If magnesium is used as a desulfurizing flux, magnesium-coke [80], a plunging bell [80–82] injection of a magnesium-aluminum alloy, surface-coated magnesium, or a mixture of CaO and Mg with gas [83–85] are used to suppress the vaporization loss of magnesium.

Since some problems remain unsolved in magnesium desulfurization (such as violent scattering of hot metal and resulfurization which requires a too long treatment time) the operation techniques must be improved. The advantages of this method in comparison to other methods are the very small amounts of flux required, ca. 1 kg/t, and the easy disposal of the slag.

It is very difficult to compare the various desulfurization processes for the pretreatment of hot metal, because many factors such as facility cost, operation cost, amount and cost of desulfurizing flux, degree of desulfurization, workability, and iron loss must be considered.

Figure 5.59 shows the relationship between degree of desulfurization and operation cost. To reduce the cost of desulfurization, effective and inexpensive desulfurization fluxes and desulfurization processes requiring less flux must be developed.

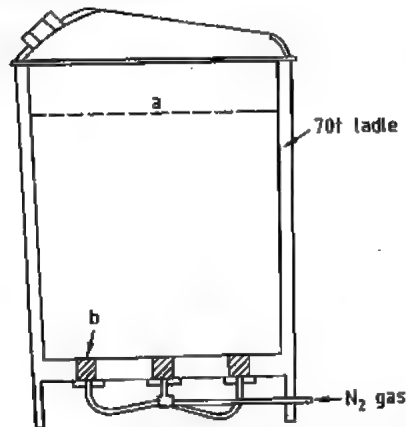


Figure 5.57: Desulfurization ladle with porous plugs [78] (Courtesy of The Iron and Steel Institute of Japan): a) Surface of hot metal; b) Porous plugs.

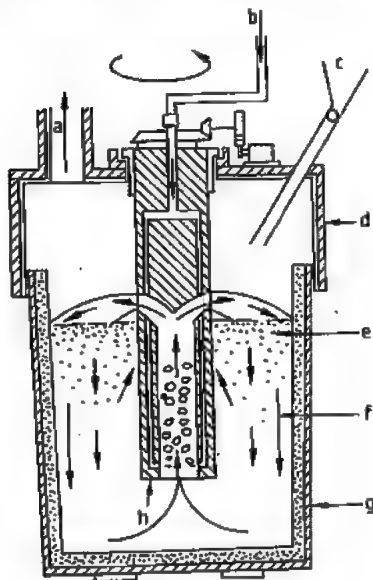


Figure 5.58: Schematic diagram of the gas lift mixing reactor for desulfurization [79] (Courtesy of The Iron and Steel Institute of Japan): a) Dust collecting duct; b) Compressed nitrogen; c) Inlet of flux; d) Cover for dust catch; e) Desulfurizing flux; f) Hot metal; g) Ladle; h) Main part of gas-lift mixing reactor.

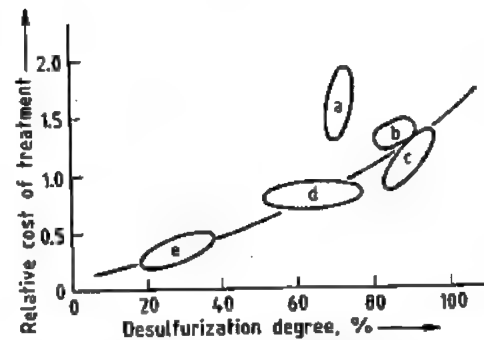


Figure 5.59: Relation between desulfurization degree and relative cost of treatment [76] (Courtesy of Dept. of Materials Science and Engineering, McMaster University, Hamilton, Canada). Sulfur content before treatment: 0.030%. a) Mag-coke process; b) Porous plug process; c) KR process; d) Top blowing process; e) Soda-ash pouring process.

5.6 Plant Layout

A blast furnace plant consists of numerous units beside the furnace itself (Figure 5.60). The most important units are the following:

5.6.1 Dust-Recovery System

The blast furnace gas may contain up to 170 kg of dust per-ton of pig iron produced. This dust must be captured for two reasons:

- To recover its valuable metal content
- To prevent pollution of the environment.

Gas cleaning is conducted in two steps:

- Removal of large particles in dust catchers followed by cyclones.
- Removal of fine particles in spray towers, venturi scrubbers, or electrostatic precipitators.

5.6.1.1 Dust Catchers

The gas is allowed to pass through a large chamber to reduce its velocity and cause the dust to drop out by gravity. To enhance the separation, the direction of gas flow is reverse. A typical gravity chamber is shown in Figure 5.61. It is a 10–12-m diameter, brick-lined vessel.

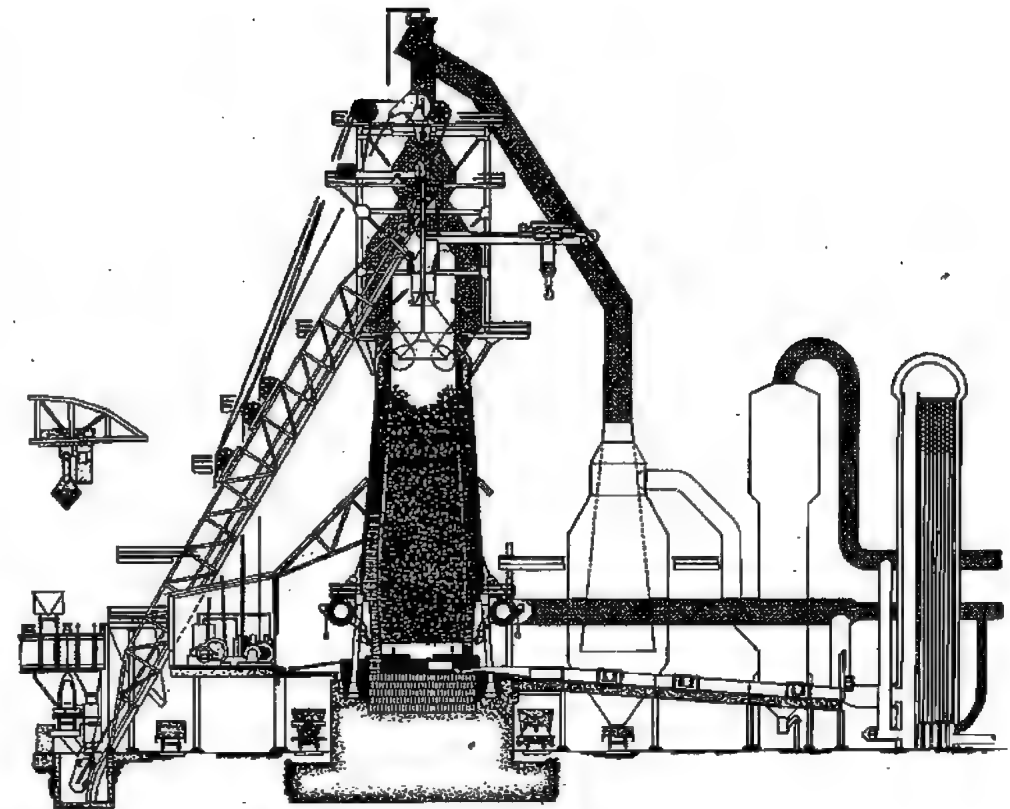


Figure 5.60: Blast furnace plant.

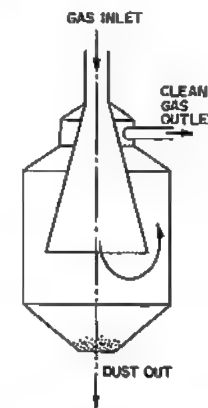


Figure 5.61: Dust catcher.

5.6.1.2 Cyclones

This equipment is more efficient than the previous type and occupies less space. The

dust-laden gas enters a cylindrical or conical chamber tangentially. The centrifugal force causes the dust particles to travel outward to the wall of the chamber, where they collide and fall downward to a receiver at the bottom, while the gas escapes from an opening at the top (Figure 5.62).

5.6.1.3 Spray Towers

In these towers (Figure 5.63) the gas passes upwards countercurrent to a descending spray of water. To increase the contact between the two phases, the tower is packed with wooden grates, ceramic tiles, or metal spirals. The part of the tower above the water spray is for separating the water droplets from the exit gases. A typical unit consists of a contact zone where the dust laden gas and the water are brought together, followed by a separation zone where

the gas is separated from the wetted slurry. In the contact zone, the particles increase their weight and size and adhere together when they are moistened thus making their separation easy.

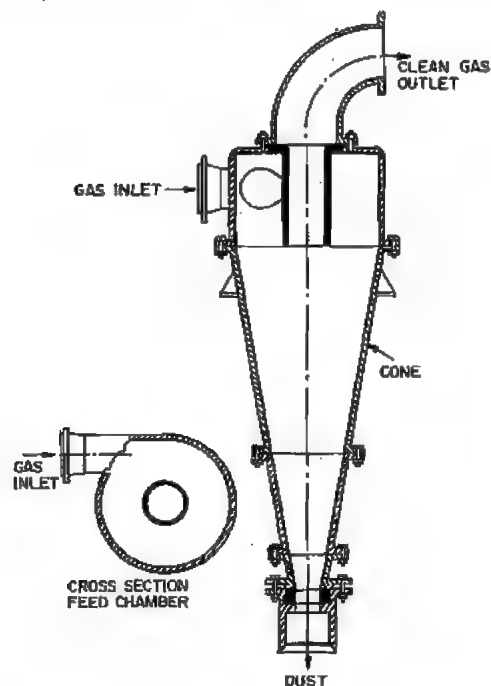


Figure 5.62: Dust-collecting cyclone.

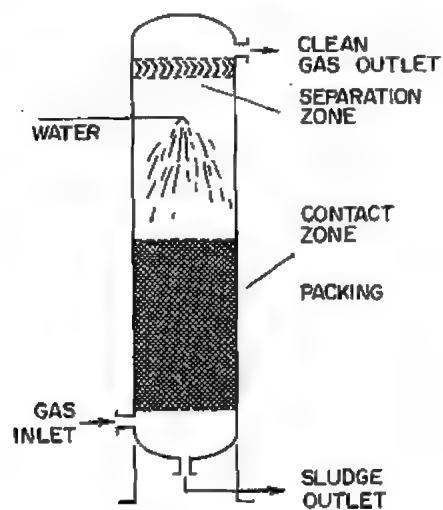


Figure 5.63: Spray towers for dust removal.

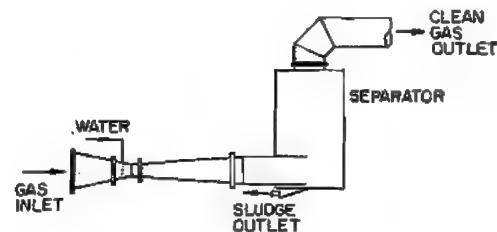


Figure 5.64: Venturi scrubber.

5.6.1.4 Venturi Scrubbers

In this system, water is introduced at the throat of a venturi perpendicular to gas flow and is atomized into tiny droplets; thus a large surface area is created. The venturi is followed by a separating section usually in the form of a centrifugal eliminator for the removal of the entrained droplets and collected dust particles (Figure 5.64).

5.6.1.5 Electrostatic Precipitators

Dust separation in this equipment is based on the fact that if the solid particles carried in a gas are given an electrical charge, they will be attracted to a collection device carrying the opposite charge. The type most commonly employed consists of a series of ionizing electrodes and an oppositely charged series of collecting electrodes housed in a chamber through which the exhaust gas is routed (Figure 5.65). The ionizing electrodes are rods while the collecting electrodes are grounded plates or shells that have a large surface area compared to the ionizing electrodes. A high voltage of 50 000 to 80 000 volts is applied across the two sets of electrodes to maintain the highest electrostatic field without sparking.

Under the influence of the electrostatic field, the gas molecules get electrically charged and move away from these electrodes toward the collecting electrodes. As the suspended dust particles collide with these molecules, the electric charge is transferred to the dust.

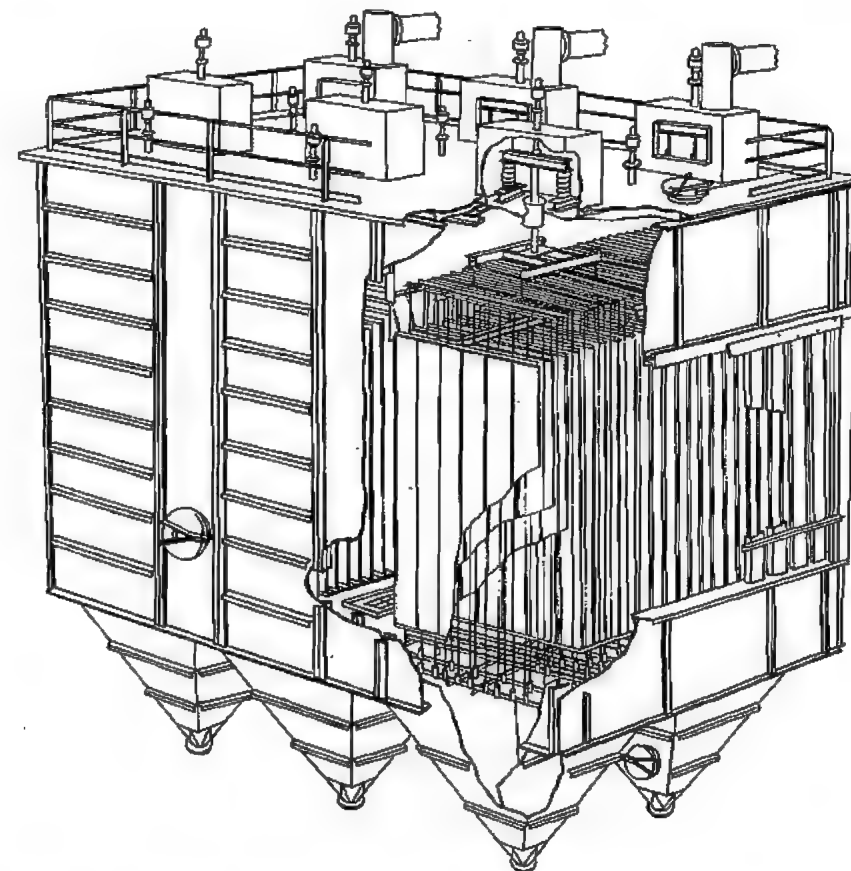
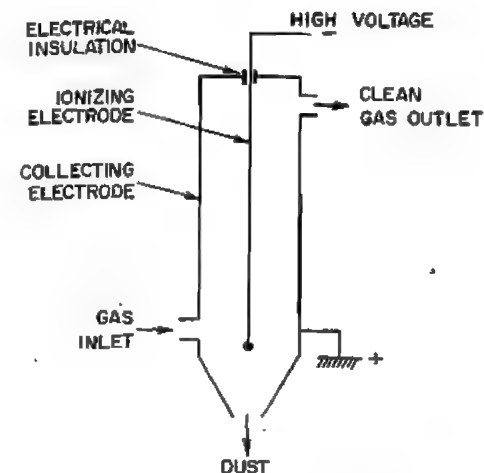


Figure 5.65: Electrostatic precipitator. A) Principle; B) Industrial installation.

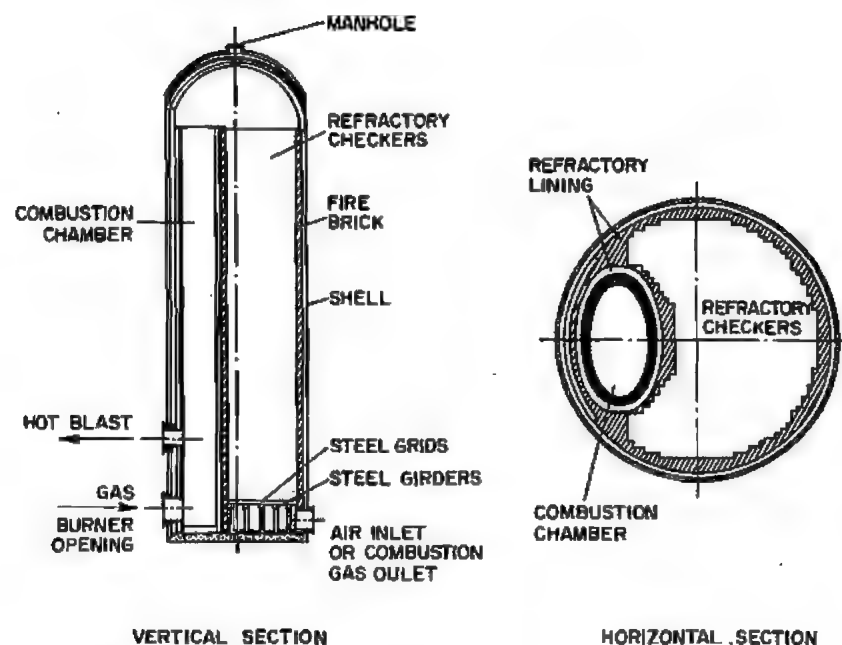


Figure 5.66: Stoves for heat recovery from blast furnace gas.

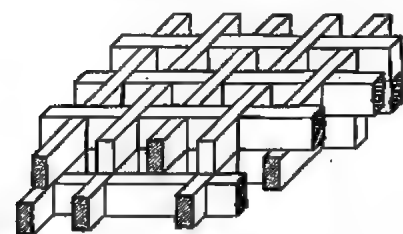


Figure 5.67: Arrangement of refractory brick in a regenerator.

The particles are then attracted to the collecting electrodes, where they lose their charge and fall into hoppers below, or become dislodged by automatic intermittent tapping. Electrostatic precipitations are expensive but efficient equipment.

5.6.2 Heat Economy System

Gases leaving a blast furnace are not at high temperature but have a high calorific value due to their CO content. The gases after being purified of their dust content are then burned in stoves and the heat of combustion is used to heat fire brick chambers. Once the chambers

are hot, the blast furnace gas is switched over to another stove and air is introduced in the hot chamber to take away the heat before entering the furnace. The cycle is then repeated. A typical unit is 7–9 m diameter and about 36 m high with a dome-shaped top and consists of two parts (Figure 5.66):

- The combustion chamber where the blast furnace gas is burned.
- The refractory chamber where the hot combustion gases pass before their exit (Figure 5.67).

The heating surface in the chambers is usually 22 000–25 000 m². There are usually 3 units per furnace, and they are provided with a common stack. The air blast for the furnace passes through the heated stove countercurrent to the gas. One stove is “on blast” for 1 to 2 hours at a time while the other two stoves are “on gas” for 2 to 4 hours. This is achieved by means of automatic valves. With the advancement of gas cleaning, the use of refractory bricks with small openings became feasible, thus resulting in a high efficiency.

5.7 Refractory Materials

Refractory materials must meet the following requirements:

- Mechanical stability under load at high temperatures (up to and beyond 1800 °C, depending on quality),
- Resistance to slags and dusts at high temperature, and
- Specific thermal properties, such as thermal conductivity, specific heat, and resistance to sudden temperature changes, depending on application.

These properties can be tested in the laboratory under conditions similar to the service conditions. Some methods are internationally standardized (PRE, i.e., Fédération européenne de produits réfractaires and ISO recommended test methods) [86]. Refractories are classified by chemical-mineralogical criteria and by process requirements. The basic distinction is between shaped products (bricks) and unshaped ones (mixtures, mortars, castables). Another basis for classification is the type of binding. Here a distinction must be made between fired products (firing temperatures 800–1800 °C) and unfired, chemically bonded refractories (phosphate binders, resin binders, refractory cements, water glass, magnesium sulfate).

In the iron and steel industry in Germany, the classification of the “Steel and Iron Material Data Sheets” (Stahl-Eisen-Werkstoffblätter) is used.

Table 5.27 shows the consumption of refractory materials (kg per tonne of crude steel) for Germany and Japan in 1970, 1980, 1990, and 1993. The steep decline is mainly accounted for by new steelmaking technologies (oxygen-injection process replacing the Siemens-Martin furnace, introduction of continuous casting) and by improvements in refractory qualities.

This progression is also clear from Table 5.28, which lists the outputs of the main qualities of refractory bricks in Japan. The 1970 and 1993 figures show the decrease in fireclay brick and silicate brick production and the in-

crease in high-grade refractories (magnesia-carbon, high-alumina castable).

The world steel industry is the principal consumer of refractories (ca. 60%).

Pig-iron production includes (1) blast furnaces with hot blast stoves, and (2) torpedo ladles, with a molding capacity of 150 600 t of molten pig iron, as transport containers from the blast furnace to the steelworks. This sector employs mainly the following refractory qualities: carbon and graphite bricks, silicon carbide bricks, materials containing more than 50% alumina, fireclay, and silica.

In *steelworks* the most important qualities are magnesia-carbon bricks, bricks and mixtures based on magnesia and dolomite, zircon material, and high-alumina castables.

Table 5.27: Consumption of refractories in Germany and Japan (kg per tonne of crude steel).

	Germany				Japan			
	1970	1980	1990	1993	1970	1980	1990	1993
Bricks	19	12.9	8.8	7.1	24	9.5	5.5	4.9
Mixtures	16	10.5	5.9	6.3	5	5.8	6.0	6.4
Total	35	23.4	14.7	13.4	29	15.3	11.5	11.3

Table 5.28: Production of refractories in Japan in 1000 t.

	Bricks	1970	1980	1990	1993
Fireclay		1800	829	325	280
50% Al ₂ O ₃		191	173	155	125
Silica		260	66	7	5
Chrome-magnesia		284	278	126	99
Magnesia-carbon			52	123	107
Dolomite-magnesia		251	104	13	8
Zircon		61	91	52	31
Silicon carbide			53	27	18
Insulants		88	55	27	15
Others		75	44	35	37
Unshaped Products (Mixtures)		570	907	836	845

Blast Furnaces. Molten pig iron and slag are present in the lower part of the blast furnace (bottom and hearth). Repairs cannot be made to this part of the furnace during operation. Chemical and mechanical attacks on the refractory material occur here. Graphite and carbon bricks are the most important structural refractories for this portion of the blast furnace. Carbon bricks have a higher cold-crushing strength than graphite bricks and those containing some graphite (part-graphite and semi-graphite bricks). Carbon bricks have a

lower porosity than graphite bricks. Microporous carbon and part-graphite bricks with additions of alumina and silicon have higher alkali and pig-iron resistance [91, 98].

The current state of the art is the "ceramic cup", which comprises sintered mullite bricks placed in front of the carbon on the bottom, and large-size prefabricated panels of corundum concrete in front of the carbon on the wall. This type of lining protects the carbon bricks and prolongs their service life greatly. In the other zones of the blast furnace (bosh, belly, stack), a variety of brick qualities are used. These include bricks containing over 50% alumina, corundum bricks, and silicon carbide bricks with various binders. Hard fire-clay bricks are usually employed in the stack. Furnaces often differ greatly in their refractory linings. The properties of some refractory structural materials are given in Table 5.29.

Runner and Taphole Mixtures. Tar-free unshaped products containing > 50% alumina, silicon carbide, and carbon are used in cast, vibrated or rammed form. Numerous and very different mixtures are in use, including spinel ($MgAl_2O_4$)-containing material in the metal level and mixtures up to 80% SiC in the slag level.

Hot Blast Stoves. The standard lining consists of silica bricks in the dome (temperatures up to 1500 °C), bricks with > 50% alumina in the combustion chamber, and silica and fireclay bricks (depending on thermal stress) in the checkerwork shaft.

Torpedo Ladles [90, 99]. In the lining design, the following factors relating to stresses on the refractory must be considered: temperature of pig iron (1450–1520 °C), distance transported, slag composition, and metallurgical reactions such as desiliconization, dephosphorization and desulfurization in the ladle.

Lining bricks mostly contain > 50% Al_2O_3 (andalusite and bauxite bricks). If the slag has a CaO:SiO₂ ratio > 1, unfired pitch-bonded dolomite bricks can also be used with success. The increase in metallurgical reactions in torpedo ladles has led to new types of lining, which have been adopted in an attempt to extend the service life (100 000–400 000 t pig iron transported). In zone lining, resin-bonded corundum-carbon-silicon carbide bricks are used in the slag zone (especially in Japan), with resin-bonded andalusite carbon bricks in the bottom. Linings differ from plant to plant, depending on service conditions.

5.8 Iron from Pyrite Cinder [74]

Pyrite is mainly used for the manufacture of sulfuric acid. It is oxidized in fluidized bed reactors whereby the following reaction takes place:



While SO_2 can be readily converted to SO_3 and then to H_2SO_4 , iron oxide (called cinder) cannot be used directly for manufacturing iron because of the presence of impurity metals. Table 5.30 shows analysis of cinder. As a result, methods have been developed to purify the cinder and at the same time to recover the nonferrous metals present. The recovery of nonferrous metals from the cinder is achieved by two routes: the chloride and the sulfate processes.

5.8.1 The Chloride Route

In this route, the nonferrous metals are transformed into water-soluble chlorides by heating with a solid chloride. At low temperature the chlorides remain in the residue while at high temperature they are volatilized.

Table 5.29: Properties of blast-furnace lining bricks.

	Carbon	Microporous carbon (10% Al_2O_3 , 15% Si)	Graphite	Mullite (70% Al_2O_3)	Corundum concrete (90% Al_2O_3)
Bulk density, g/cm ³	1.53–1.57	1.63–1.73	1.55–1.60	2.45	3.30
Open porosity, %	14–18	14–18	25–28	15–18	9–12
Micro porosity > 1 μm, %	8–11	≤ 2			
Ash, %	< 7	35–40	< 1		
Cold compression strength, N/mm ²	30–40	60–90	15–25	70	60
Thermal conductivity, Wm ⁻¹ K ⁻¹ ,					
at 20 °C	3–8	5–7	130	2	5
at 500 °C	5–12	8–10	95	1.8	4
at 1000 °C	8–14	11–13	65	1.7	3

Table 5.30: Typical analysis of pyrite cinder.

Main components, %		Trace metals, ppm	
Fe	54–58	Co	300–1500
Gangue	6–10	Ag	25–50
Cu	0.8–1.5	Au	0.5–1.5
Zn	2.0–3.5	Cd	40–100
S	2.5–4.0	Ni	15–1500
Pb	0.3–0.7	Mn	300–3000

Table 5.31: Data on the treatment of pyrite cinder by Kowa-Seiko process.

	Dry pellets, %	Heated pellets, %	Volatilization, %
Cu	0.47	0.04	91
Pb	0.18	0.01	92
Zn	0.59	0.01	97
As	0.05	0.05	—
S	0.61	0.03	96.5
Fe	59.2	61.5	—
Au (g/t)	0.94	0.05	95
Ag (g/t)	33.6	7.00	80

DK Process. This process has been used in Germany for nearly a century at the Duisburger Kupferhütte in Duisburg (operations ceased in 1980s). The pyrite cinder is mixed with NaCl and heated continuously in a multiple hearth furnace at 800 °C to transform nonferrous metals into water-soluble chlorides. Each batch requires about 2 days for leaching in vats. The concentrated leach solution obtained in the first 15 to 20 hours is sent for copper and other metals recovery, while that subsequently obtained, being poor in metal content, is recycled. The residue, called purple ore, now a high-grade iron ore (61–63% Fe), is sintered and delivered to the blast furnace.

Kowa-Seiko Process. This is a Japanese process in which the cinder is mixed with calcium chloride, pelletized, then heated in a rotary kiln at 1100 °C to volatilize nonferrous metal

chlorides (Table 5.31). These are scrubbed in water from the exit gases and the solution treated for metal recovery.

5.8.2 The Sulfate Route

This route is mainly used for the recovery of cobalt from the cinder. It is based on a careful temperature control during the oxidation of pyrite. If the temperature is kept at 550 °C, cobalt in the pyrite will be converted to sulfate and therefore can be leached directly from the cinder with water. At least two plants are using this process:

- At the Bethlehem Steel plant, Sparrows Point, Maryland, the hot pyrite cinder is quenched with water to give a slurry containing 6–8% solids. When the solids are filtered off, the solution contains 20–25 g/L Co; it is processed further for metal recovery. In the cinder the Fe:Co ratio is 50:1; in solution it is 1:1. This plant supplies the only domestic source of cobalt in USA.
- In Finland at the Outokumpu Company plant, the sulfated pyrite cinder contains 0.8–0.9% Co and other nonferrous metals. It is leached with water to get a solution at pH 1.5 analyzing 20 g/L Co, 6–8 Ni, 7–8 Cu, 10–12 Zn, and trace amounts of iron, which is treated for metal recovery.

5.9 Iron from Ilmenite [11]

Ilmenite, $FeTiO_3$, is the major titanium mineral. It represents 90% of the world titanium ore reserves while rutile, TiO_2 , accounts for the remaining 10%. Ilmenite occurs either

as massive deposits, e.g., in the Province of Quebec, or as sand at the mouth of rivers, e.g., in India. The Quebec deposits are one of the largest in the world. However, when compared with other ilmenite ores, the Quebec ore is a low-grade ore (Table 5.32). It is beneficiated by physical methods to a concentrate containing 36.8% TiO_2 , 41.8% Fe (total), and a small amount of sulfur.

Table 5.32: Analysis of ilmenite ores.

	%
TiO_2	43–59
FeO	9–38
Fe_2O_3	5–25
SiO_2	0.4–4
Al_2O_3	1.3–3.3
MgO + CaO	0.1–1.4
V	0.4–2

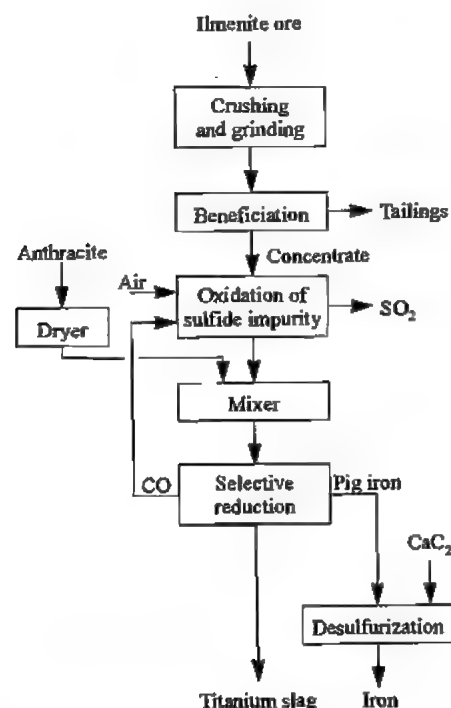


Figure 5.68: Selective reduction of ilmenite.

The concentrate is mixed with a certain amount of carbon which is just enough to reduce the iron oxide component of the ore, then charged in an electric furnace at 1650 °C where iron oxide is reduced to metal while titanium is separated as a slag (Figure 5.68). This method is used by the QIT Fer et Titane incorporation at its plant in Sorel near Montréal and at Richards Bay in South Africa. It is also used in Ukraine at Zaporozhye and in Japan.

A small amount of TiO_2 is reduced to Ti_2O_3 and will be found in the slag. The slag is mainly titanates of iron, magnesium, and calcium together with some calcium and aluminum silicates; its titanium dioxide content varies between 72 and 98%. The analysis of iron produced at Sorel is given in Table 5.33. The slag is high in titanium and low in iron and is therefore preferable to ilmenite in manufacturing TiO_2 pigment or titanium metal.

5.10 Direct Reduction Processes

The name "direct reduction" is misleading, because these reduction processes do not constitute a "more direct" route to steel than does the blast furnace. Nor does the term have anything to do with direct reduction in the blast furnace. Despite all these objections, however, the term has become accepted in international usage.

Table 5.34 lists the plants for direct reduction of iron ore that were in operation or under construction in 1995, together with their locations and the processes employed.

Table 5.33: Analysis of iron produced from Quebec ilmenite at Sorel (also known as Sorelmetal).

	%
C	1.8–2.5
S	0.11
P_2O_5	0.025
MnO	trace
V_2O_5	0.4
Cr	0.05
Si	0.08
TiO_2	trace

Table 5.34: World direct reduction plants (plant list is correct as of December 31, 1995) [102] This list does not include plants that are inoperable or have been dismantled.

Process	Plant	Location	Capacity, Mt/year	Modules	Start-up	Status*
Midrex	Georgetown Steel	Georgetown, SC, USA	0.40	1	1971	O
	Hamburger Stahlwerke	Hamburg, Germany	0.40	1		O
	Sidbec Dosco 1	Contrecoeur, QC, Canada	0.40	1	1973	O
	SIDERCA	Campana, Argentina	0.40	1	1976	O
	Sidbec Dosco 2	Contrecoeur, QC, Canada	0.60	1	1977	O
	SIDOR I	Matanzas, Venezuela	0.35	1		O
	ACINDAR	Villa Constitución, Argentina	0.60	1	1978	O
	Qatar Steel Co.	Umm Said, Qatar	0.40	1		O
	British Steel	Hunterston, Scotland	0.80	2	1979	I
	SIDOR II	Matanzas, Venezuela	1.27	3		O
	CIL	Point Lisas, Trinidad & Tobago	0.84	2	1980–1982	O
	Delta Steel	Warri, Nigeria	1.02	2	1982	O/I
	Hadeed I	Al-Jubail, Saudi Arabia	0.80	2	1982–1983	O
	OEMK	Stary Oksol, Russia	1.67	4	1983–1988	O
	Amsteel Mills	Labuan Island, Malaysia	0.65	1	1984	O
	ASCO	Ahwaz, Iran	1.20	3	1985–1992	O
	ANSDK I	El Dikheila, Egypt	0.72	1	1986	O
	LISCO	Misurata, Libya	1.10	2	1989–1990	O
	Essar Steel I & II	Hazira (India)	0.88	2	1990	O
	MINORCA (OPCO)	Puerto Ordaz, Venezuela	0.83	1		O
	VENPRECAR	Matanzas, Venezuela	0.66	1		O
	Essar Steel III	Hazira, India	0.44	1	1992	O
	NISCO	Mobarakeh, Iran	3.20	5	1992–1994	O
	Hadeed II	Al-Jubail, Saudi Arabia	0.65	1	1992	O
	HDIL	Raigad, India	1.00	1	1994	O
	ANSDK II	El Dikheila, Egypt	0.80	1	1997	C
	Hanbo Steel	Asan Bay, South Korea	0.80	1		C
	IMEXSA	Lázaro Cárdenas, Mexico	1.20	1		C
	Total		24.08	45		
HyL-III	Hylsa 2M5	Monterrey, Mexico	0.25	1	1979	O
	Hylsa 3M5	Monterrey, Mexico	0.50	1	1983	O
	IMEXSA	Lázaro Cárdenas, Mexico	2.00	4	1988–1990	O
	Grasim	Raigad, India	0.75	1	1993	O
	PT Krakatau Steel	Kota Baja, Indonesia	1.35	2	1993–1994	O
	PSSB	Kemaman, Malaysia	1.20	2	1993	O
	Usiba	Salvador, Bahia, Brazil	0.31	1	1994	O
	Hylsa 2P5	Puebla, Mexico	0.61	1	1995	O
	Total		6.97	13		
HyL-I	Tamsa	Veracruz, Mexico	0.28	1	1967	I
	SIDOR I	Matanzas, Venezuela	0.36	1	1976	O
	Hylsa 2P	Puebla, Mexico	0.63	1	1977	O
	PT Krakatau Steel	Kota Baja, Indonesia	1.68	3	1978–1982	O/I
	SIDOR II	Matanzas, Venezuela	1.70	3	1980–1981	O
	ASCO	Ahwaz, Iran	1.03	3	1993–1995	O
	Total		5.68	12		
SL/RN	Piratini	Charquedas, Brazil	0.06	1	1973	I
	SIL	Paloncha, India	0.03	1	1980	O
	Siderperu	Chimbote, Peru	0.09	3		O
	ISCOR	Vanderbijlpark, South Africa	0.72	4	1984	O
	BSIL I	Chandil, India	0.15	1	1989	O
	Prakash Industries I	Champa, India	0.15	1	1993	O
	Nova Iron & Steel	Bilaspur, India	0.15	1	1994	O
	Prakash Industries II	Champa, India	0.15	1	1996	C
	BSIL II	Chandil, India	0.15	1	1998	C
	Total		1.65	14		

Process	Plant	Location	Capacity, Mt/year	Modules	Start-up	Status*
Jindal	Jindal Strips	Raigarh, India	0.40	4	1993-1995	O
	Monnet Ispat I	Raipur, India	0.10	1	1993	O
	Jindal Strips	Raigarh, India	0.20	2	1996-1997	C
	Monnet Ispat II	Raipur, India	0.10	1	1997	C
	Total		0.80	8		
DRC	Scaw Metals I	Germiston, South Africa	0.18	2	1983-1989	O
	Tianjin Iron & Steel	Tianjin, China	0.30	2	1996	C
	Scaw Metals II	Germiston, South Africa	0.15	1		C
	Total		0.63	5		
Codir	Dunswart	Benoni, South Africa	0.15	1	1973	O
	Sunflag	Bhandara, India	0.15	1	1989	O
	Goldstar	Mallividu, India	0.22	2	1992	O
	Total		0.52	4		
Fior	Fior de Venezuela	Matanzas, Venezuela	0.40	1	1976	O
OSIL	OSIL	Keonjhar, India	0.10	1	1983	O
	Lloyd's Steel	Ghugus, India	0.30	2	1996-1997	C
	Total		0.40	3		
Purofer	ASCO	Ahwaz, Iran	0.33	1	1977	O
SIL	SIL	Paloncha, India	0.06	2	1980-1985	O
	Bellary Steels	Bellary, India	0.06	2	1992-1993	O
	HEG	Borai, India	0.06	2	1992	O
	Kumar Met.	Naigonda, India	0.03	1	1993	O
	Raipur Alloys	Raipur, India	0.03	1		O
	Tamilnadu Sponge	Salem, India	0.03	1		O
	Aceros Arequipa	Pisco, Peru	0.06	2	1996	C
	Total		0.33	11		
Iron Carbide Nucor Steel		Point Lisas, Trinidad & Tobago	0.30	1	1994	O
Tisco	Ipatata I	Joda, India	0.12	1	1986	O
	Ipatata II	Joda, India	0.12	1	1998	C
	Total		0.24	2		
Dav	Davsteel	Cullinan, South Africa	0.04	1	1985	O
Kinglor-Metor	No. 3 Mining Enterprise	Maymo, Burma	0.04	2	1981-1984	O

* Status codes: O = operating; I = idle; C = under construction.

Table 5.36 contains technical data for the direct reduction processes described in this chapter and certain other processes. The stated capacities should be regarded as approximate, as some of the processes have been further developed. The annual plant outputs often vary from the original design capacity. In particular, the demand of the client (i.e., of the electric steel mill), a low scrap price, or a shortage of spare parts may lower the annual output.

In most direct reduction processes, up to 92-95% of the iron oxide is reduced to metallic iron. The degree of metallization $Fe_{\text{metallic}}/Fe_{\text{total}}$ in % is an important variable for characterizing the direct-reduced iron (DRI) produced by the process in question.

5.10.1 Fuels and Reducing Agents [103, 104]

A considerable amount of heat input is required in the production of iron, because essentially all the processes involved are pyrometallurgical. Part of the heat is used to heat up the raw materials to be processed and part of it is required for endothermic chemical reactions. The majority of this energy is obtained by combustion of fossil fuels. Approximately one-quarter of the annual output of steel is derived from scrap in electric arc furnaces which pose a correspondingly high demand for thermoelectric energy.

Fuels. Fossil fuel, especially in the form of coke constitutes the primary reducing agent in blast furnaces; this coke cannot be replaced arbitrarily by substitutes such as coal. Coke functions both as a support material and as a matrix through which gas circulates in the stock column. A portion of the fuel can be introduced into the tuyere along with the air supply. Figure 5.69 provides detailed insight into the demand for the fossil fuels in iron manufacture, indicating its percentage distribution by various fuel types and consumers.

The illustration is based on an integrated production facility in which all the coke and a portion of the required electrical energy is produced on site, the extent of the latter being a function of the availability of excess off-gas [105].

All energy data in Figure 5.69 relate to total energy input, including that from external sources of electricity. Approximately 88% of the imported energy is derived ultimately from

coal, 83% of which is converted into coke. Gas is derived as a by-product: 15% from the coke ovens, 20% from the blast furnace, and 4% from the steel mill. This gas is in turn processed in the coke oven plant and distributed to power plants and other appropriate units within the facility for subsequent processing.

A number of requirements must be met by coke that is intended for use in iron manufacture:

- The ash, moisture, and sulfur content should be as low as possible, and should show little variation.
- Coke strength should be consistently high with the lowest possible variation.
- The coke should be as unreactive as possible, in particular toward carbon dioxide and steam.
- Particle size should be kept in the range of 40-80 mm, but at least in the range of 20-80 mm.

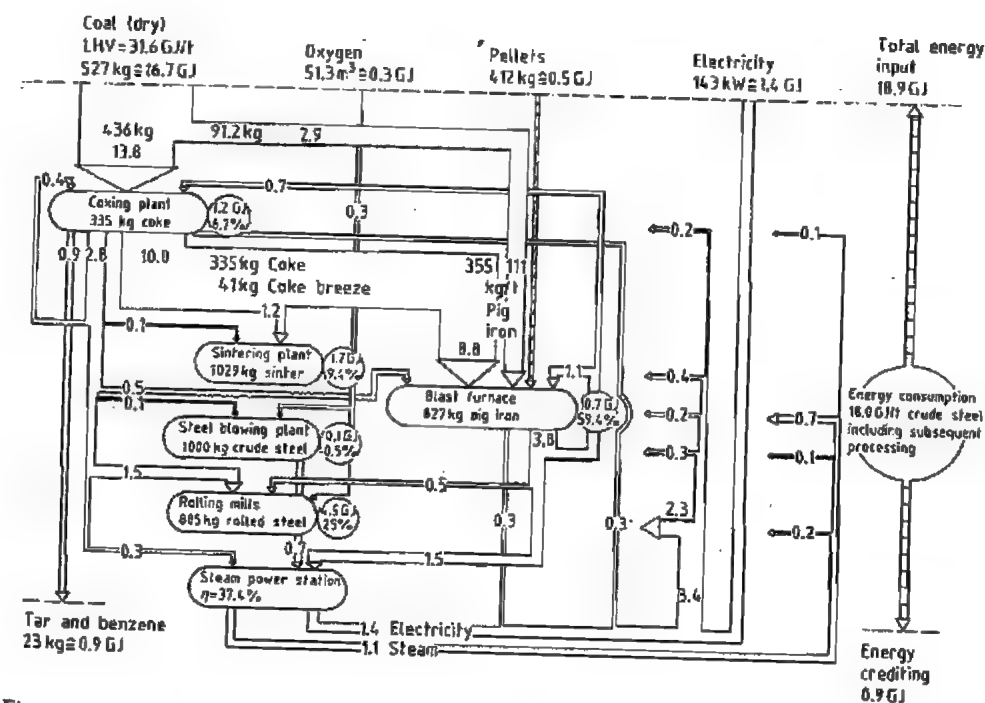


Figure 5.69: Energy demand distribution in an integrated steel mill based on 1 t of crude steel.

Table 5.35: Important characteristics of coke.

Blast furnace coke	
Drum index ^a (%)	> 90
Dust M 10 ^a (%)	< 6
Moisture (%) ^b	< 5
Ash (%) ^b	< 10
Sulfur (%) ^c	< 1
Volatiles (%) ^c	

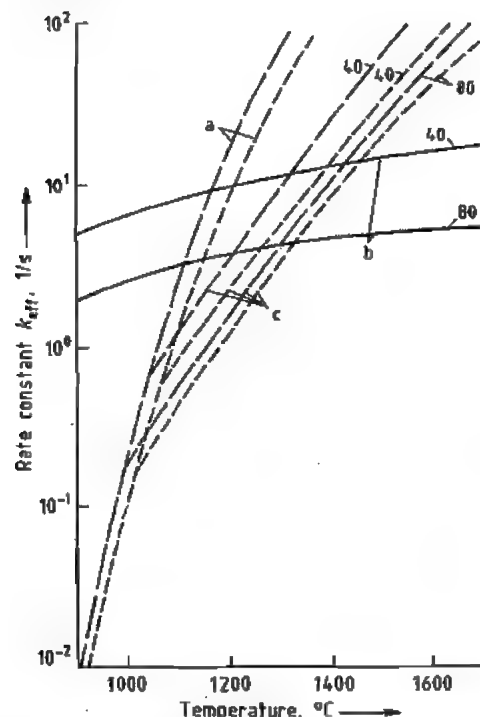
^aBased on DIN 51 717, equivalent to ISOIR 556.^b% of crude weight.^cOf dry weight.

Figure 5.70: Limiting curves for the effective rate constant in the Boudouard reaction shown for two types of coke; — coke type a; --- coke type b (the curve parameter is the grain diameter in mm): a) Chemical surface reaction; b) Boundary layer diffusion; c) Pore diffusion.

Coke characteristics are the subject of numerous norms, including ISOIR 556, DIN 51 717–51 719, DIN 51729, and DIN 51730. Typical values for coke intended for iron manufacture (reflecting these norms) are presented in Table 5.35.

Coke reactivity is determined on the basis of the norm ST/ECE/Cool/12. Specifications supplied with respect to ash and sulfur content

are applicable not only to coke but also to injection coal.

Depending on coke temperature and particle size, the principal determinant in the rate of the Boudouard reaction



is the varying resistance to reactivity. In the case of blast-furnace coke with a particle size between 40 and 80 mm, and at low temperature (< 1050 °C), the limiting factor is the resistance of the interfacial reaction. For particles < 8 mm in diameter the resistance of the interfacial reaction is rate-limiting up to ca 1200 °C. Between 1050 and ca. 1350 °C the resistance of pore diffusion becomes the rate-determining factor in the Boudouard reaction. Above 1350 °C the rate of reaction is governed by the diffusion of carbon dioxide through the gaseous layers adhering to the coke particles. The corresponding relationships are illustrated in detail in Figure 5.70.

Carbon conversion r_c in $\text{mol m}^{-3} \text{s}^{-1}$ may be computed on the basis of the rate constant k_{eff} derived from Figure 5.70 [103]

$$r_c = \frac{dn_c}{dt} = k_{\text{eff}}(n_{\text{CO}_2}^0 - n_{\text{CO}_2}^{\text{eq}}) \quad (30)$$

where $n_{\text{CO}_2}^0$ is the CO_2 concentration in the gas phase (mol/cm^3) and $n_{\text{CO}_2}^{\text{eq}}$ the CO_2 concentration in equilibrium with C and CO (Boudouard reaction).

Furthermore

$$k_{\text{eff}} = k_m \cdot m_c \cdot \eta \quad (31)$$

where m_c is the mass of carbon (g) per cubic meter of charge and η the pore utilization factor according to Thiele. Within the temperature range in which the interfacial reaction is rate determining

$$k_m = H_C \cdot e^{-360/RT} \text{ g}^{-1} \text{ s}^{-1} \quad (32)$$

where H_C is the reactivity factor. Moreover, because $n = 1$

$$k_{\text{eff}} = m_c \cdot H_C \cdot e^{-360/RT} \text{ s}^{-1} \quad (33)$$

The activation energy of 360 kJ/mol is uniformly applicable with respect to any fuel [86]. Depending on reactivity and charge size,

the product $m_c \times H_C$ may range from $0.4 \times 10^{13} \text{ s}^{-1}$ to $0.4 \times 10^{15} \text{ s}^{-1}$.

Gaseous and liquid fuels used in iron manufacture are described elsewhere.

Reducing Agents. Assuming that iron oxide is present in the solid state, industrial-scale reduction of iron ore with carbon monoxide or hydrogen takes place according to



If iron oxide is present as a liquid, a second reaction is also possible:



Carbon monoxide is produced in the blast furnace from the reaction of oxygen in the blast air with hot coke and other reducing agents such as injected coal or oil



Carbon monoxide is also the product of the Boudouard reaction

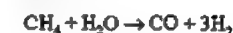


Carbon dioxide required by Equation (29) is formed during the reduction of iron oxide according to Equation (34). In some cases, coal is utilized as the reducing agent, which means that the gases actually responsible for reduction arise both from coal pyrolysis and from coal gasification inside the reduction reactor.

Coal pyrolysis may lead to varying quantities of hydrogen and hydrocarbons, which in turn serve partly as reducing agent and partly as fuel. The majority of the reducing gas in such a case originates from the solid carbon contained in the coal, where ore reduction and the Boudouard reaction are linked through Equations (29) and (34).

Gaseous reducing agents other than those formed in the reduction reactor itself are derived from natural gas, oil, or coal. Stoichiometrically, the large number of processes that are actually suitable for gas production, is limited significantly because a low content of steam and carbon dioxide as well as a specific hydrogen:carbon monoxide ratio is required in the reducing gas.

An appropriate gas for reduction above the decomposition temperature of carbon monoxide is that produced by steam reforming, with a composition of 73% hydrogen, 13% carbon monoxide, 1% water, 8% carbon dioxide, and 5% methane:



In the *Midrex process* a 1.5:1 ratio of hydrogen and carbon monoxide is required. This ratio is achieved by reaction of natural with blast furnace top gas which results in a better utilization of input energy (composition after condensation of steam: 20% CO_2 with the balance being CO and H_2O at equal ratios):



Reduction gas should contain as little steam and carbon dioxide as possible. Even relatively small amounts of these substances drastically limit the utility of the gas, because according to Equation (34) the reduction of iron oxide itself produces carbon dioxide and water. Their presence in the reduction gas would therefore shift the equilibrium to the side of iron oxide. At the temperatures normally employed for converting iron oxide to iron, the ratio $\text{CO}:\text{CO}_2$ or $\text{H}_2:\text{H}_2\text{O}$ must not fall significantly below 2.3. In addition, reduction gas should contain as little undecomposed hydrocarbons as possible.

The use of fossil fuels in iron manufacture is currently the subject of careful reevaluation, and new reduction techniques are in the development stage. It is quite likely that coal will come to play an increasingly important role as a source of reduction gas. This can be accomplished by partially combusting coal with oxygen in an iron bath. The resulting hot gas is then used to reduce iron oxide in a separate vessel (see the equations above). Then the reduced iron is itself transferred to the iron bath where it is melted. Gas generation on the basis of nuclear energy is expected to remain economic for many years, although some effort is currently being directed toward the use of a plasma arc for converting carbon sources into reduction gas.

5.10.2 Shaft Furnace Processes for Direct Reduction

Wiberg-Söderfors Process. The oldest shaft furnace process for direct reduction of iron ore, the Swedish Wiberg process, is based on a patent issued in 1918. Up to the end of the 1950s, it was technologically improved and adapted to changed conditions on the ore and fuel markets. Nowadays, the Wiberg process is only of historical significance.

The development of the process was promoted above all by the growing shortage of very low-sulfur charcoal pig iron, the raw material for Swedish high-quality steel. In addition,

it was intended that coke would only be used for the reduction process, the process heat being supplied by cheap electricity available because of the geographical location.

In the Wiberg process (Figure 5.71) the iron ore is preheated in the top section of the furnace (a) to the reduction temperature of ca. 950 °C by hot gases generated by combustion of part of the so-called excess gas. In the zone immediately below, the ore is reduced to wustite with ca. one third of the reducing gas volume. The reduction to metallic iron takes place in the bottom section of the furnace at ca. 950 °C with ca. 1300 m³ (STP) gas/t DRI.

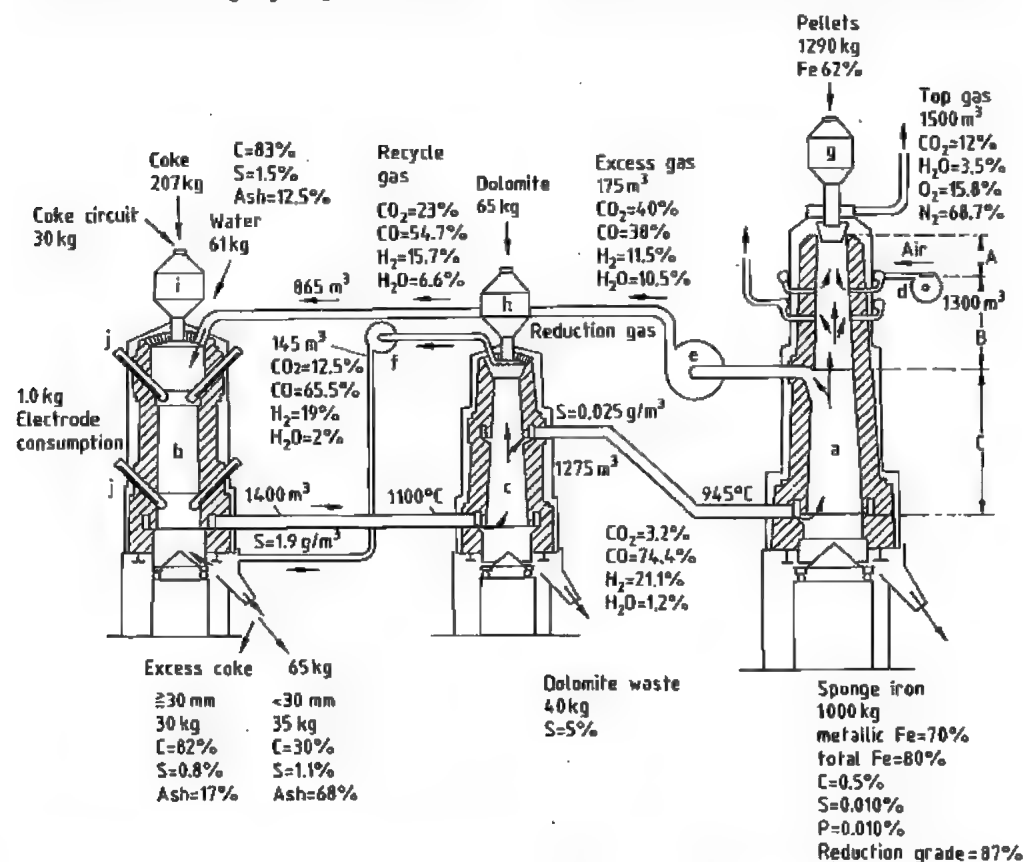


Figure 5.71: Flow Sheet and material balance (based on 1 t sponge iron) of the Wiberg process. All volumetric values of the gases refer to standard conditions [101]. a) Reduction shaft; b) Carburetor; c) Desulfurization shaft; d, e, f) Fans; g, h, i) Charging bins for pellets, dolomite, and coke; j) Electrodes; A) Preheating zone; B) Pre-reduction zone; C) Main reduction zone.

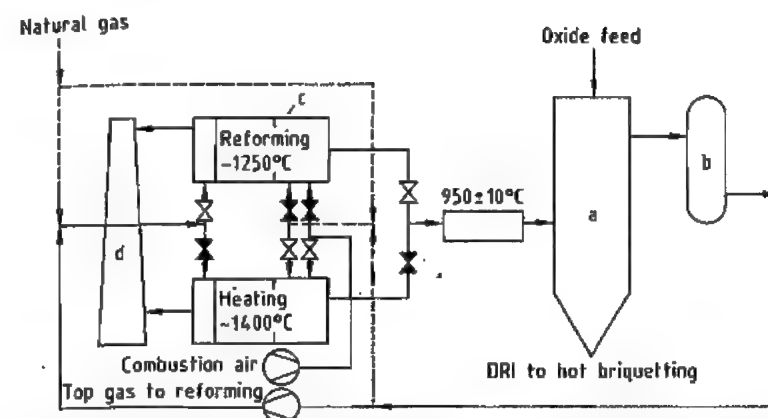


Figure 5.72: Schematic of the Purofer process: a) Shaft furnace; b) Top-gas scrubber; c) Gas reformer; d) Stack.

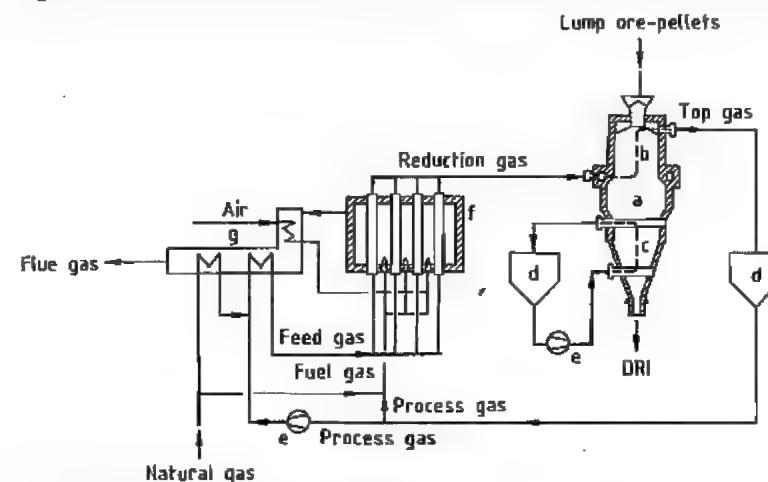
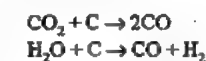


Figure 5.73: Schematic of the Midrex process: a) Shaft furnace; b) Reduction zone; c) Cooling zone; d) Scrubber; e) Gas compressor; f) Gas reformer; g) Recuperator.

Table 5.36: Typical consumption figures for direct reduction processes.

Process	Reductant	Consumption, GJ/t DRI	Electrical energy, kWh/t DRI	Metallization, %
Midrex	natural gas	10.0	100	92-94
HyL I	natural gas	18.9		85
HyL III	natural gas	10.5		90-93
Purofer	natural gas, oil	14.3	93	95
Nippon steel	natural gas	10.5		90-92
Fior	natural gas	16.0		90
SL/RN	coal	14.8	80	93

in the carburetor (b) over a hot column of coke. The energy required for the endothermic reactions



is supplied by resistance-heating electrodes.

The gas, which is contaminated with sulfur from coke, is passed through dolomite in a shaft furnace for desulfurization (c). The reducing gas contains 95% carbon monoxide and hydrogen in a ratio of ca. 3:1.

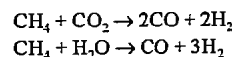
The Wiberg process, which was developed for the special conditions of the Swedish iron industry, was a pioneering technology. The

Two thirds of the reducing gas is withdrawn by means of a hot gas fan (e) and regenerated

high cost of coke and electrical energy to generate the reducing gas is the reason why this process is no longer in use.

The principle of generating the reducing gas by a chemical reaction between the off-gas of the reduction shaft (the top gas) and natural gas has been applied in two processes: the Purofer and the Midrex process.

Purofer Process. This process (Figure 5.72) was developed at Hüttenwerke Oberhausen (later Thyssen Niederrhein); the ICEM process developed by the Romanian Research Institute for Metallurgy is similar to it. The ore (preferably pelletized) passes vertically downward through the shaft furnace in countercurrent to the hot reducing gas. The gas is used for heating the charge and for reduction. The reducing gas is generated catalytically in regenerative-type gas generators. After cooling and purification, the top gas is used partly for heating up the gas generators and partly for chemical conversion of the natural gas at 900–1000 °C to reducing gas according to the equations



The carbon from methane reforming that is deposited on the catalyst of the regenerator during reducing-gas production is burned off during heating-up. This regenerative phase causes slight variations in reducing gas temperature and composition. In the Purofer process, the DRI is discharged hot and can be transported in containers either directly to an electric steel mill or to a hot briquetting plant.

In addition to the pilot plant in Oberhausen (capacity 500 t/d), one plant was built in Brazil (but with a Texaco heavy-oil gasifier as gas generator) which is now dismantled. The only plant in operation in Iran is designed for operation with natural gas.

Midrex Process. The most successful gas-based direct reduction process is the Midrex process developed by Midland-Ross Corp. of Toledo, Ohio (Figure 5.73) [107].

In this process, natural gas continually undergoes catalytic conversion to hydrogen and

carbon monoxide (ratio ca. 1.5:1) at ca. 900 °C using a partial stream (ca. 2/3) of the top gas, which is cleaned and cooled to lower its water-vapor content. Reduction is accomplished in the cylindrical part of the shaft furnace at 780–900 °C, depending on the temperature at which sintering ("sticking") of the reduced ore or the pellets occurs. In the conical discharge section of the shaft furnace, the DRI is cooled to ca. 45 °C by recirculated cooling gas. Here, the carbon content of the product can also be adjusted to between 1.2 and 2.5%. There are also Midrex plants featuring hot discharge followed by hot briquetting.

One third of the top gas is used to heat the gas reformer, whereas the hot flue gases serve to preheat the combustion air and the feed gas mixture prior to reforming.

With increasing heat recovery in the recuperator and reduction temperatures of ca. 900 °C, energy consumption per tonne of DRI may fall to 9.6 GJ in the Midrex process.

The reducing gas can also be generated by *steam reforming* of natural gas. The first shaft furnace direct-reduction process to employ steam reforming was the *Armco process*. Here natural gas undergoes continuous catalytic conversion with excess steam according to the reaction:



After removal of the water vapor, the top gas is used as cooling gas.

Only one commercial plant was ever built because of the difficulty of achieving complete mixing of the cooling gases entering the lower part of the shaft with the hot top gases from the reduction zone, the low reducing potential of the gases, and a range of technical problems.

Nippon Steel (NSC) Process. The reducing gas containing over 95% carbon monoxide and hydrogen is generated by steam reforming with only a slight excess of water vapor and addition of top gas freed from water and carbon dioxide (see Figure 5.74). Like the Purofer process, the NSC process has a hot discharge facility, from which DRI can be filled into containers and taken either directly

to a steel mill or to a hot briquetting plant. Only one plant in Malaysia with a design capacity of 1000 t/d has been built which was later modified into an HyL-III plant.

HyL-III Process. Hojalata y Lamina S.A. (HyL) of Mexico has also developed a shaft-furnace process based on steam reforming of natural gas (HyL-III process, Figure 5.75). This process represents a further development of HyL's retort process (see Section 5.10.3). Because of the large quantity of excess steam

produced in continuous catalytic conversion of the natural gas, the generated gas must first be cooled to remove the excess water vapor. After addition of water- and carbon dioxide-free top gas and indirect heating to ca. 850 °C, the reducing gas is fed into the reduction shaft. In the bottom section of the shaft furnace, the DRI is cooled down to < 50 °C as in the Midrex process. HyL-III plants can also be operated with hot discharge and hot briquetting.

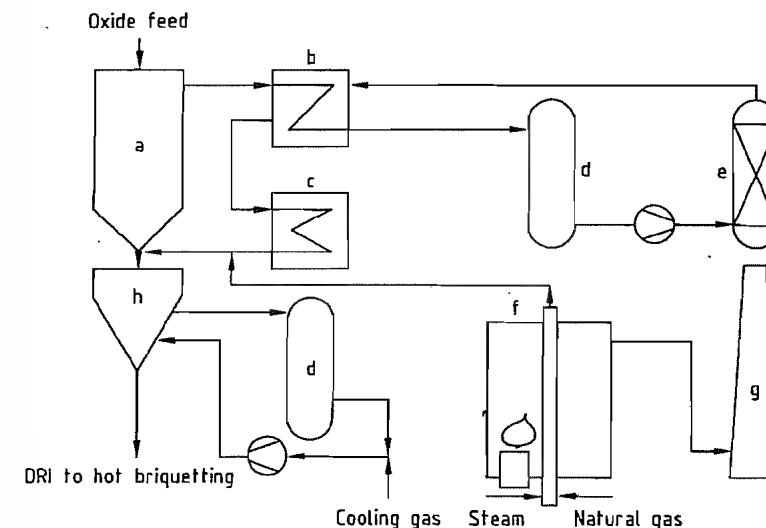


Figure 5.74: Schematic of the Nippon Steel process: a) Shaft furnace; b) Heat exchanger; c) Gas heater; d) Dust remover; e) CO₂ scrubber; f) Reformer; g) Stack; h) Cooling zone.

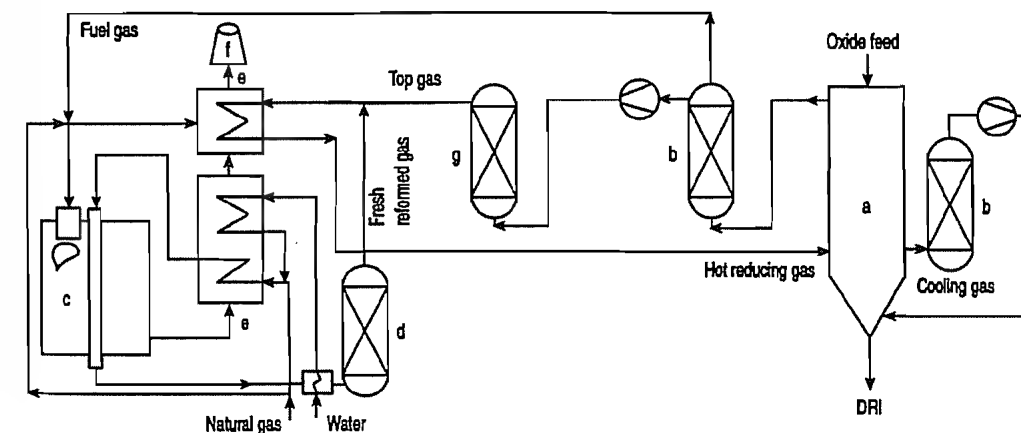


Figure 5.75: Schematic of the HyL-III process: a) Shaft furnace; b) Gas scrubber; c) Reformer; d) Cooler; e) Recuperator; f) Stack; g) CO₂ scrubber.

The degree of metallization of the DRI produced by the various shaft furnace processes ranges from 92–95%. The carbon content is usually 1.5–2%.

5.10.3 Retort Processes

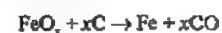
HyL Process (HyL-I Process). A number of plants employing this process were built up to 1975 before the shaft-furnace processes became established. The development of this process began in 1951 at Hojalata y Lamina S.A., Monterrey (Mexico). It operates with four reactors simultaneously, each one being at a different point in the reduction cycle at a particular time. Figure 5.76 shows the stage at which product DRI is cooled with cold reducing gas in retort 1. At this point, the carbon content of the DRI is adjusted to ca. 2%. After cooling and water-vapor condensation, the off-gas from this retort is reheated to reduction temperature and passed through retort II, where pre-reduced material is fully reduced. The gas is then recooled to remove any newly formed water vapor, reheated and fed to retort III containing freshly charged ore, which is then pre-reduced. The off-gas from this stage is cooled and freed from water vapor; it is then available for use as fuel gas for steam raising. Retort IV is simultaneously emptied from DRI and charged with ore.

As lump ore or pellets are stationary in the retorts during reduction, the risk of sticking is high. Sophisticated removal devices are required for emptying the retorts.

The degree of metallization of the DRI is often lower at the bottom of the retorts than in the upper layers. Thus the target average degree of metallization is often only ca. 86%. As gas generation is carried out with a large excess of steam and cooling and reheating of each retort is very costly, an energy consumption of ca. 21 GJ per tonne DRI must be taken into account.

Höganäs Process. This process has been in operation since 1911 and has undergone no significant technical modifications since the 1950s, nor has its use become any more widespread. In this process, iron ore is reduced with coal in hermetically sealed crucibles with indirect heating (by combustion of the carbon monoxide escaping from the crucibles). The sulfur content of the DRI is minimized by adding limestone or dolomite to the charge mix and rapidly cooling the product. It is thus suitable for use in powder metallurgy or stainless-steel production. The capacity of plants operating on the Höganäs process is relatively low, ca. 35 000 t/a.

Kinglor-Metor Process. This process occupies a category between the shaft furnace and the retort processes. The development of this process (Figure 5.77) by Co. Kinglor-Metor S.p.a., Mineraria & Metallurgica, Italy, began in 1971 but was based on the Echeverria process which had been in operation in Spain since 1957 [108]. Like the rotary kiln processes (see Section 5.10.5) and in contrast to the gas-based direct reduction processes described so far, it uses a solid carbon-containing reductant, which is charged together with the ore (6–25 mm size) and, where applicable, limestone or dolomite is used for desulfurization. The heat for the strongly endothermic reaction



which in this case takes place at ca. 1050 °C, is supplied through the wall of the shaft furnace, which must therefore have a high thermal conductivity. Silicon carbide satisfies the requirements as to thermal conductivity, heat resistance, and abrasion resistance. The shaft heating burners are designed for gaseous and liquid fuels. The reduced material is indirectly cooled with gas in the bottom zone of the shaft. Commercial plants consist of a group of six reduction chambers, each with a capacity of ca. 20 t/d DRI.

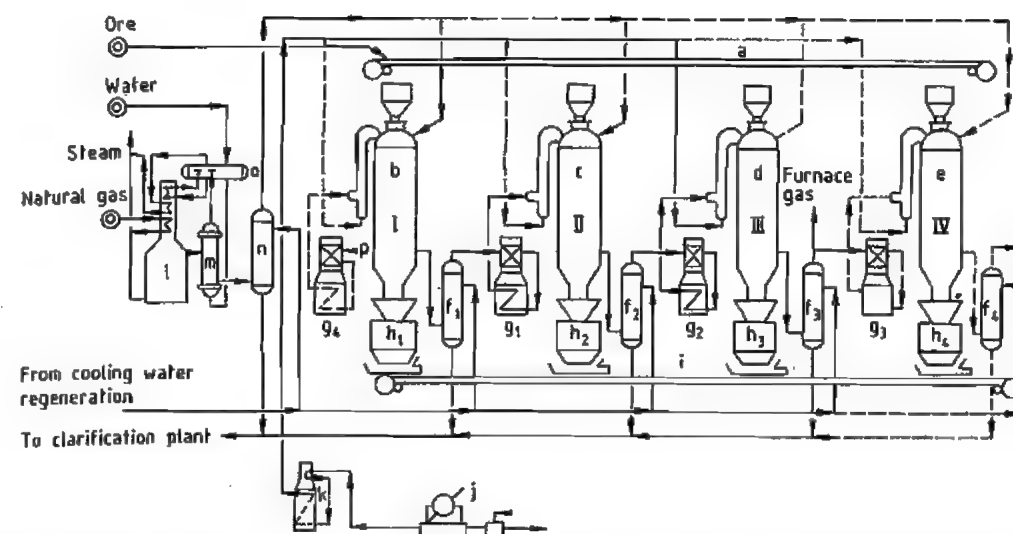


Figure 5.76: Flow sheet of the HyL-I process: a) Ore conveyor belt; b) Retort I at cooling stage; c) Retort II at final reduction stage; d) Retort III at pre-reduction stage; e) Retort IV at discharging and charging stage; f₁–f₄) Cooler; g₁–g₄) Gas preheating; h₁–h₄) Intermediate container for sponge iron; i) Conveyor belt for sponge iron; j) Air compressor; k) Air preheating; l) Reduction gas generator; m) Superheated steam generator; n) Cooler; o) Saturated steam generator; p) Connection between cooler l₄ and preheater g₄.

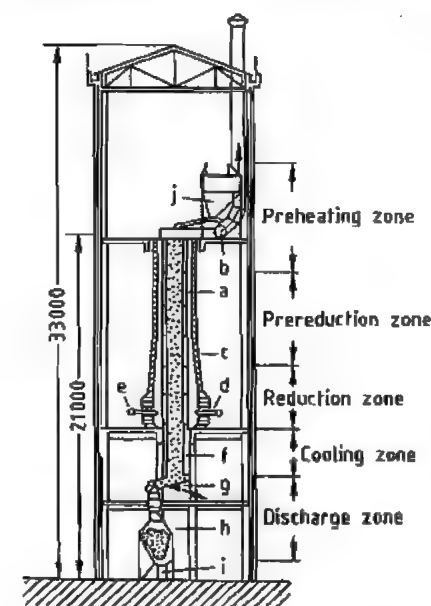


Figure 5.77: Shaft furnace of the Kinglor-Metor process (dimensions in mm): a) Silicon carbide shaft; b) Gas discharge pipe; c) Fireclay outer wall; d) Burner; e) Gas or oil pipe; f) Air cooling; g) Extruding screw discharge; h) Hopper; i) Sponge iron discharge; j) Charging hopper.

5.10.4 Fluidized-Bed Processes

Fluidized-bed processes for direct reduction exploit the lower cost of fine ores compared with lump ores and pellets. However, the disadvantages of these processes are that (1) the fine ores have a tendency towards sticking above ca. 700 °C and that (2) below 600 °C the susceptibility to reoxidation of the DRI is so high that it must be stored under inert gas or hot-briquetted.

Fluidized-bed processes that operated with pure hydrogen were the *Novalfer process* and the *H-Iron process*; however, they did not attain any major technological significance. In the *HIB-process*, reduction was carried out in several stages with a gas containing ca. 85% hydrogen. The ore of 0.2 mm size underwent only ca. 65% metallization and was then hot-briquetted. The sole commercial plant has been converted by Midrex Corp. into a shaft furnace plant with hot discharge/hot briquetting.

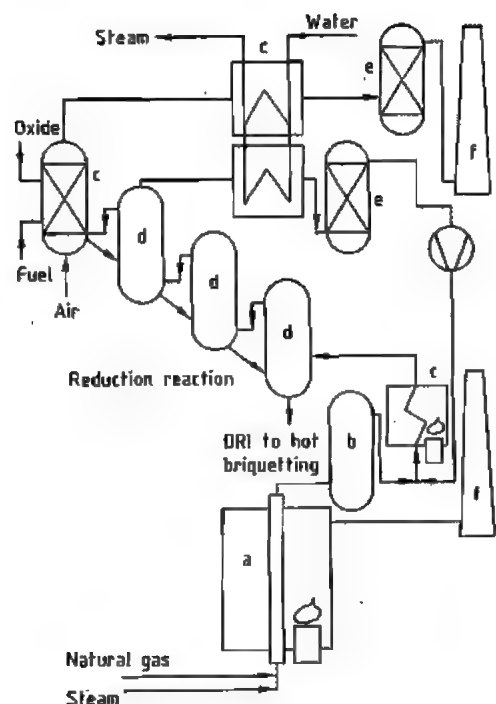


Figure 5.78: Schematic of the Fior process: a) Reformer; b) Gas cooler; c) Heater; d) Fluidized-bed reactor; e) Scrubber; f) Stack.

Fior (Fluidized Iron Ore Reduction) Process. Development of the Fior process (Figure 5.78) started in the 1950s at Esso Research and Engineering in collaboration with Arthur D. Little. Following the building and operation of a 300 t/d pilot plant in Dartmouth, Nova Scotia, from 1965 to 1969, a 400 000 t/a commercial plant operating on this process was built in Puerto Ordaz, Venezuela.

After drying and preheating to ca. 880 °C, the fine ore (mostly < 5 mm) is metallized to a degree of ca. 92% in a three-stage fluidized bed. The reducing gas is generated by steam reforming of natural gas in continuously operating catalytic reformers. The reduced fine ore is hot-briquetted, the briquettes being cooled and shipped to the end-users without further passivation.

The Finmet process is a further development of the Fior process, taking advantage of the experience gained in more than 10 years of Fior plant operation.

Iron Carbide Process (Figure 5.79) [109]. In NUCOR's Iron Carbide process, fine iron oxide (0.1–1 mm) is reduced by a hydrogen- and methane-containing gas to iron carbide according to:



The iron oxide is heated to 700 °C prior to feeding into the fluidized bed reactor in which the reduction of the iron oxide and the formation of iron carbide occurs at a temperature of approx. 570 °C and at a pressure of approx. 3 bar(g).

In the fluidized bed reactor baffles are arranged, which cause the solids to move from the inlet to the outlet. The relatively low reduction temperature required to form iron carbide results in a retention time of about 16 hours in the first 900-t/day plant built in Trinidad. At a gas-to-solids ratio of about 10 000 Nm³/t oxide, the gas volumes to be handled are very high compared to shaft-furnace processes.

The fines carried over with the reduction gases are partially recovered in a cyclone and recycled into the reactor. After heat exchange with the cold reduction gas, the off-gases are scrubbed, cooled for water condensation, compressed, and recycled via heat exchanger and a gas heater. Make-up gas is hydrogen. The reduction gas consists of 60% CH₄, 34% H₂, 2% CO, 1% H₂O, and minor amounts of CO₂ and N₂. The iron carbide formed in NUCOR's plant contains 90% Fe total (90% as Fe₃C, 8% as FeO, 2% as Fe metal), 6.2% C, 2% gangue.

Iron carbide is listed as a nonpyrophoric material, therefore handling and shipping do not require briquetting or other treatment to avoid reoxidation.

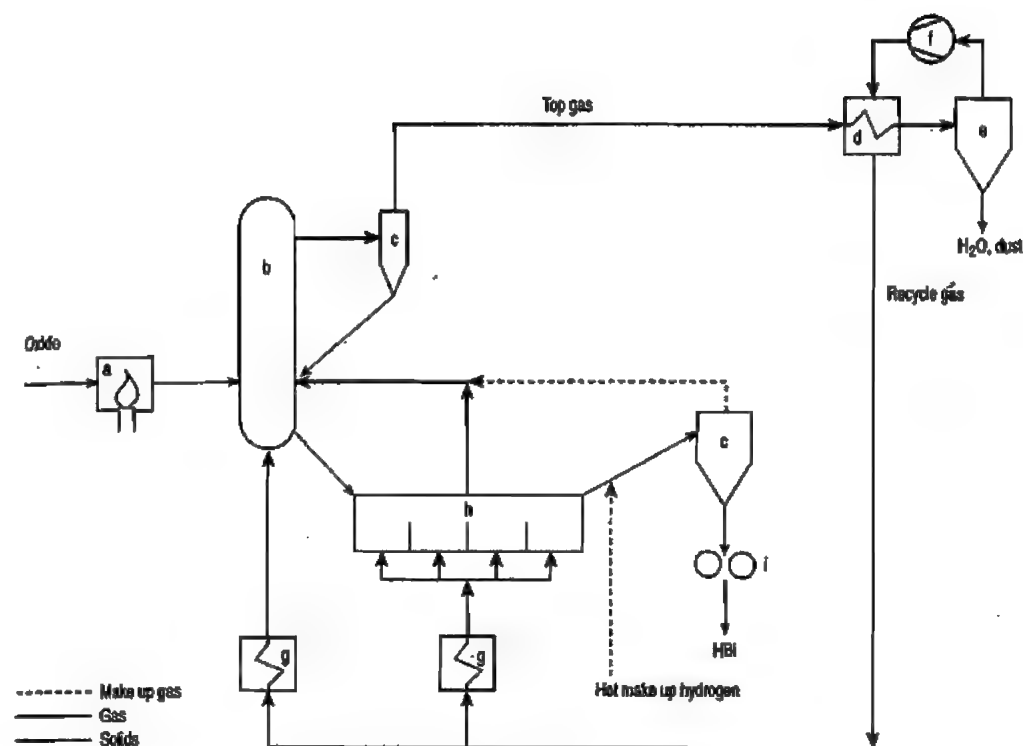
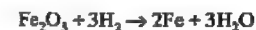


Figure 5.79: Flowsheet of the Iron Carbide process: a) Oxide heater; b) Reduction reactor; c) Cyclone; d) Heat exchanger; e) Scrubber/cooler; f) After-cooler; g) Compressor; h) Gas heater; i) Product cooling.

Circored® Process (Figure 5.80) [110]. In Lurgi's Circored® process fine iron oxide ores (0.1–1 mm) are reduced by hydrogen according to:



The ore, preheated to approx. 800 °C, is first prereduced to about 65% metallization in a circulating fluidized-bed reactor (CFB) within 20 minutes.

The final reduction to 90–93% metallization is achieved in a following fluidized-bed reactor (FB) with several compartments at lower gas velocities over a period of up to 4 hours — depending on the desired metallization and the reducibility of the oxides.

The reactors are operated at temperatures generally below 650 °C to avoid sticking. The off-gases from the final reduction step in the FB as well as make-up hydrogen are passed

into the CFB reactor. Most of the solids in the off-gases from the CFB are recovered in the recycle cyclone.

The gases are then passed through a heat exchanger, dedusted, cooled for water vapor condensation, and compressed to the plant pressure of approx. 4 bar(g). After heat exchange with the hot off-gases from the CFB the reduction gas is heated to 750 °C before being reintroduced into the two reduction reactors.

Hot make-up hydrogen is first used to transport and further heat up the reduced fines from the FB into a briquetting plant before being passed into the CFB. The reduced DRI fines are hot briquetted if the product is intended for export. It is also possible to directly charge it into smelting furnaces.

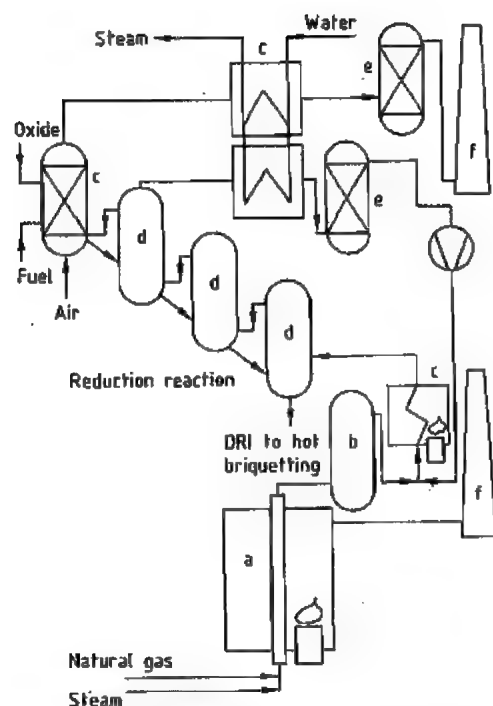


Figure 5.78: Schematic of the FIOR process: a) Reformer; b) Gas cooler; c) Heater; d) Fluidized-bed reactor; e) Scrubber; f) Stack.

FIOR (Fluidized Iron Ore Reduction) Process. Development of the FIOR process (Figure 5.78) started in the 1950s at Esso Research and Engineering in collaboration with Arthur D. Little. Following the building and operation of a 300 t/d pilot plant in Dartmouth, Nova Scotia, from 1965 to 1969, a 400 000 t/a commercial plant operating on this process was built in Puerto Ordaz, Venezuela.

After drying and preheating to ca. 880 °C, the fine ore (mostly < 5 mm) is metallized to a degree of ca. 92% in a three-stage fluidized bed. The reducing gas is generated by steam reforming of natural gas in continuously operating catalytic reformers. The reduced fine ore is hot-briquetted, the briquettes being cooled and shipped to the end-users without further passivation.

The Finmet process is a further development of the FIOR process, taking advantage of the experience gained in more than 10 years of FIOR plant operation.

Iron Carbide Process (Figure 5.79) [109]. In NUCOR's Iron Carbide process, fine iron oxide (0.1–1 mm) is reduced by a hydrogen- and methane-containing gas to iron carbide according to:



The iron oxide is heated to 700 °C prior to feeding into the fluidized bed reactor in which the reduction of the iron oxide and the formation of iron carbide occurs at a temperature of approx. 570 °C and at a pressure of approx. 3 bar(g).

In the fluidized bed reactor baffles are arranged, which cause the solids to move from the inlet to the outlet. The relatively low reduction temperature required to form iron carbide results in a retention time of about 16 hours in the first 900-t/day plant built in Trinidad. At a gas-to-solids ratio of about 10 000 Nm³/t oxide, the gas volumes to be handled are very high compared to shaft-furnace processes.

The fines carried over with the reduction gases are partially recovered in a cyclone and recycled into the reactor. After heat exchange with the cold reduction gas, the off-gases are scrubbed, cooled for water condensation, compressed, and recycled via heat exchanger and a gas heater. Make-up gas is hydrogen. The reduction gas consists of 60% CH₄, 34% H₂, 2% CO, 1% H₂O, and minor amounts of CO₂ and N₂. The iron carbide formed in NUCOR's plant contains 90% Fe total (90% as Fe₃C, 8% as FeO, 2% as Fe metal), 6.2% C, 2% gangue.

Iron carbide is listed as a nonpyrophoric material, therefore handling and shipping do not require briquetting or other treatment to avoid reoxidation.

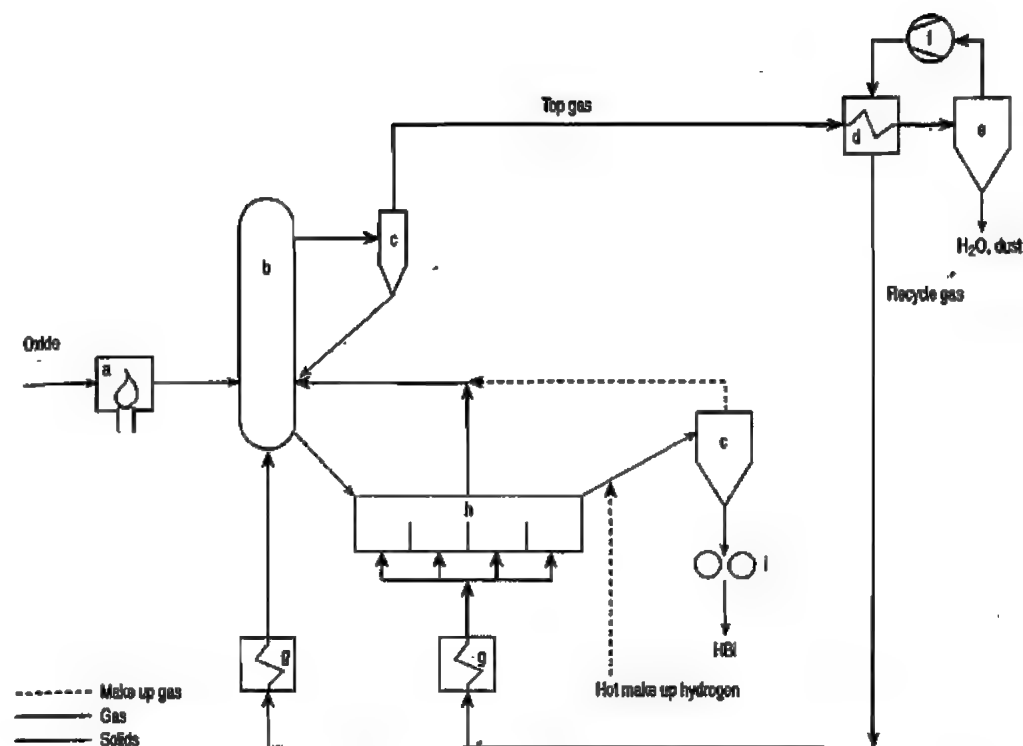


Figure 5.79: Flowsheet of the Iron Carbide process: a) Oxide heater; b) Reduction reactor; c) Cyclone; d) Heat exchanger; e) Scrubber/cooler; f) After-cooler; g) Compressor; h) Gas heater; i) Product cooling.

Circored® Process (Figure 5.80) [110]. In Lurgi's Circored® process fine iron oxide ores (0.1–1 mm) are reduced by hydrogen according to:



The ore, preheated to approx. 800 °C, is first prereduced to about 65% metallization in a circulating fluidized-bed reactor (CFB) within 20 minutes.

The final reduction to 90–93% metallization is achieved in a following fluidized-bed reactor (FB) with several compartments at lower gas velocities over a period of up to 4 hours — depending on the desired metallization and the reducibility of the oxides.

The reactors are operated at temperatures generally below 650 °C to avoid sticking. The off-gases from the final reduction step in the FB as well as make-up hydrogen are passed

into the CFB reactor. Most of the solids in the off-gases from the CFB are recovered in the recycle cyclone.

The gases are then passed through a heat exchanger, dedusted, cooled for water vapor condensation, and compressed to the plant pressure of approx. 4 bar(g). After heat exchange with the hot off-gases from the CFB the reduction gas is heated to 750 °C before being reintroduced into the two reduction reactors.

Hot make-up hydrogen is first used to transport and further heat up the reduced fines from the FB into a briquetting plant before being passed into the CFB. The reduced DRI fines are hot briquetted if the product is intended for export. It is also possible to directly charge it into smelting furnaces.

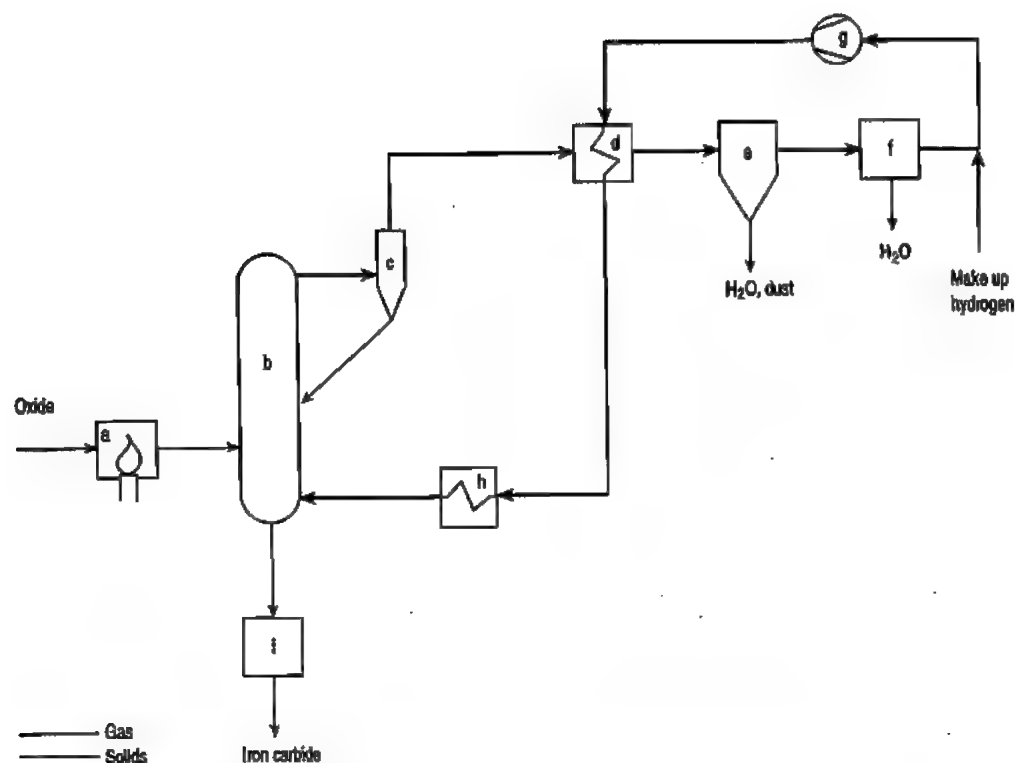


Figure 5.80: Flowsheet of the Circored® process: a) Oxide heater; b) Circulation in fluidized bed; c) Cyclone; d) Heat exchanger; e) Scrubber/cooler; f) Compressor; g) Gas heaters; h) Fluidized bed; i) Briquetting machine.

A 500 000-tpy Circored® plant is under construction in Trinidad. By using a CO/CH₄-containing reduction gas, the Circored® process can also be applied for production of a carbon containing HBI with approx. 1–3% C or iron carbide with approx. 6.5% C.

Circofer® Process (Figure 5.81). Another fluidized bed process developed by Lurgi Metallurgie operating with a CFB prereduction and a final FB reduction step is based on coal as the basic energy source. Fine coal is partially burned in a "gasifier/heater" and the semicoke produced is used as a heat carrier into the CFB as well as to prevent sticking of the iron particles at the reduction temperature of > 900 °C. The final reduction is achieved at lower temperatures in the FB with recycled off-gases from the CFB. The gas treatment is rather sim-

ilar to the Circored® process, however, a CO₂-absorber step had to be included as the reduction is achieved mainly with CO-containing gases. No commercial plant has been built so far.

5.10.5 Rotary Kiln Processes

The internal kiln temperature is continuously recorded by thermocouples installed along the entire length of the kiln and projecting into the kiln freeboard. The power supply to the shell fans and the transmission of the data recorded by the individual thermocouples is accomplished by means of slip rings mounted on the kiln shell. Devices for taking samples of material during operation are also mounted on the kiln shell.

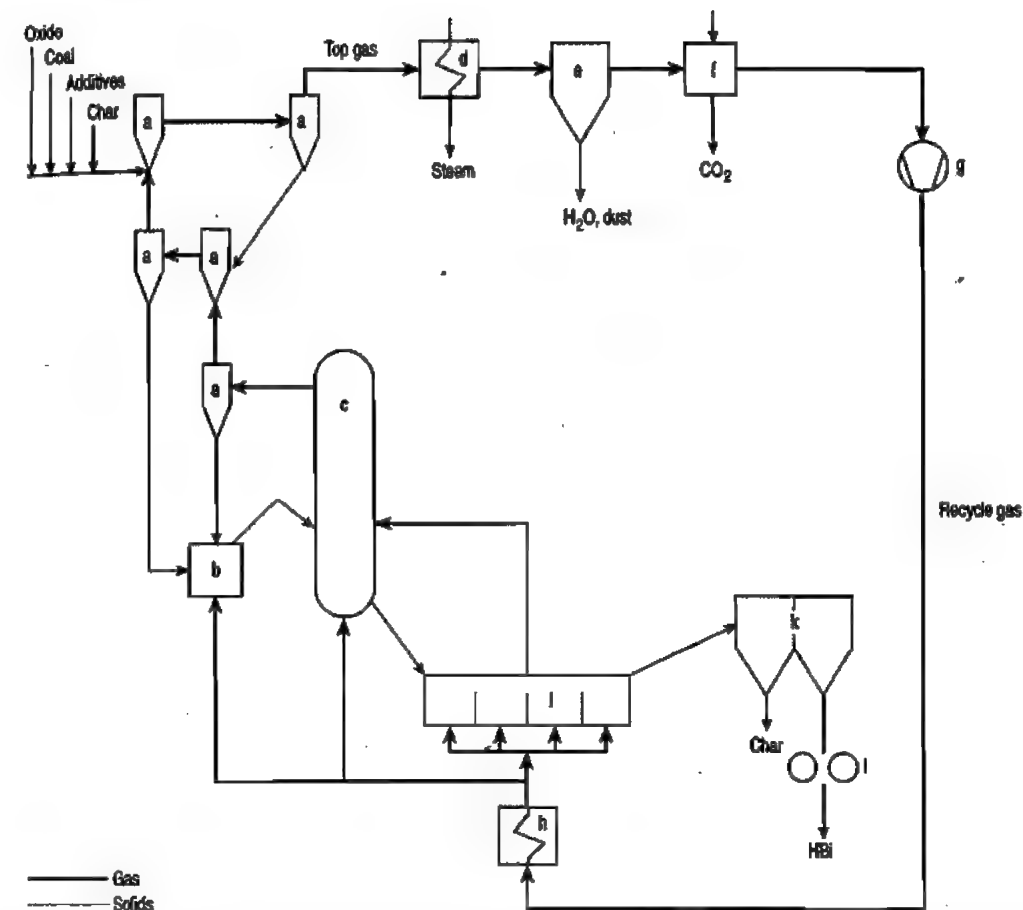


Figure 5.81: Flowsheet of the Circofer® process: a) Preheating cyclone system; b) ---; c) Circulating fluidized bed; d) Heat exchanger; e) Scrubber/cooler; f) CO₂ removal; g) Compressor; h) Gas heater; i) Fluidized bed; k) Magnetic separation; l) Briquetting machine.

Rotary kiln processes for direct reduction of iron oxides are based on coal as reductant. Typical features of rotary kiln processes are their high flexibility with regard to feedstocks and their capability for economic production of even small quantities of DRI. All non-caking coals ranging from lignite through bituminous coals up to anthracite or coke breeze are suitable as reductants. In addition to the pellets and lump ores that are the main iron-bearing materials, iron sands, and ilmenite concentrates are also industrially used.

Of the various rotary kiln processes [111], the *Krupp Codir process* and the *Lurgi SL/RN*

process have attained the greatest technological significance. The two processes operate according to similar principles. As most of the DRI currently produced in rotary kilns worldwide is manufactured by the SL/RN process (see Table 5.36), the principle of the rotary kiln processes will be explained with reference to this process.

The SL/RN process was developed in 1964 out of the combination of two separate processes: the Stelco-Lurgi (SL) process for producing DRI from *high-grade ores* and the Republic Steel National Lead (RN) process for beneficiation of *low-grade ores*.

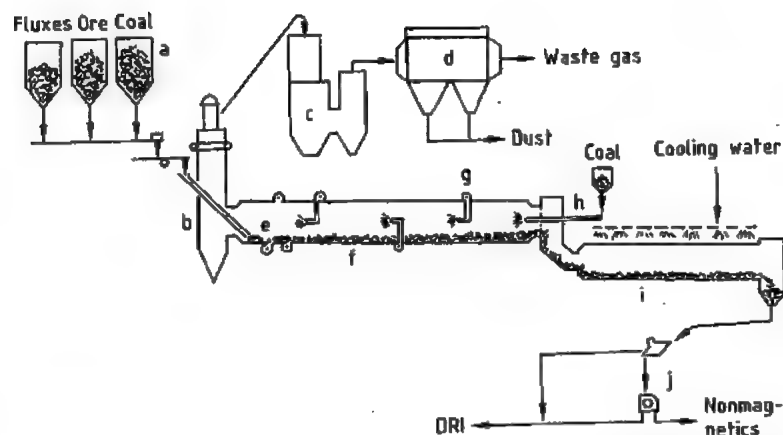


Figure 5.82: Lurgi SL/RN process: a) Bins for raw materials; b) Afterburning chamber; c) Waste-heat boiler; d) Gas cleaning; e) Underbed air injection; f) Rotary kiln; g) Air tubes; h) Injection coal; i) Rotary cooler; j) Product separation.

In the SL/RN process (Figure 5.82), reduction of iron oxide is carried out in a refractory-lined rotary kiln (f) inclined from the feed to the discharge end. The slope of the kiln is ca. 1.5–2.5% depending on the feed materials.

The kiln is equipped at both ends with special seals between the rotating kiln and the fixed feed and discharge heads. These seals essentially prevent inleakage of air and thus reoxidation. A number of fans are installed on the shell of the kiln; these supply the necessary process air via so-called air tubes or via air injection nozzles in the feed zone of the rotary kiln.

The *central burner* installed at the kiln discharge end is used to dry out the refractory kiln lining during the initial start-up and to heat up the system after a shutdown. Under normal operating conditions, only air without fuel is fed through the central burner. However, if low-reactivity coals (anthracite) are used, it may be necessary to continuously fire a small amount of supplementary fuel via the central burner to satisfy the overall heat requirement.

Fresh coal, recycle carbon, ore or pellets, and dolomite or limestone as desulfurizing agent are charged in a predetermined ratio at the kiln feed end by a gastight charging system.

Up to ca. 35% of the total fresh coal required is fed into the kiln from the discharge end with a special pneumatic injection system (h). This improves the utilization of the energy contained in the coal volatiles and prevents depletion of carbon in the material bed, especially in the case of very long kilns.

The charge passes through the kiln in ca. 8–12 h. The retention time mainly depends on the slope, degree of filling, and the rotational speed of the kiln. For each combination of iron-bearing material and reductant, a minimum retention time is necessary to achieve the desired degree of metallization; this is determined with laboratory tests.

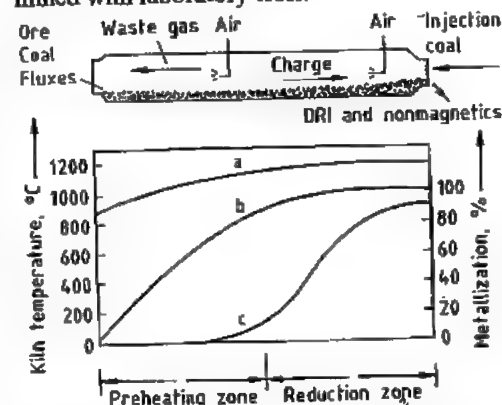


Figure 5.83: Temperature and degree of metallization as a function of the location in the kiln: a) Gas temperature; b) Charge temperature; c) Metallization.

Table 5.37: Iron ores and coals processed in SL/RN plants.

Plant	City	Country	Type	Iron ore				Coal			
				Fe	SiO ₂	CaO	Others	Fixed carbon	Volatiles matter	Ash	Sulfur
Highveld ^a	Witbank	South Africa	Mapochs lump ore	54	2.1		13.2 TiO ₂ 1.7 V ₂ O ₅ 8 TiO ₂	54	31	15	0.6
NZS	Glenbrook	New Zealand	Iron sand	58	1.1	0.2		51	43	35	0.3
Piratiní	Charqueadas	Brazil	Itabira pellets	67	2.4	1.6		40	25	18	0.4
Siderperu	Chimbote	Peru	Marcona pellets	66	2.2	1.0		81	3	25	0.7
SIL	Paloncha	India	Bayaram lump ore	63	4.5	0.1		44	31	14	0.3
Iscor	Vanderbijipark	South Africa	Sishen lump ore	66	2.5	0.2		59	26	25	0.6
BSIL	Chandil	India	Bihar lump ore	67.4	1.5	0.1		51	24	25	0.7

^a Prereduction only.

For example, the necessary retention time for a combination of "porous" pellets and highly reactive lignite is low, whereas that for "compact" lump ores and low-reactive anthracite is high.

In simplified terms, the rotary kiln can be divided into a preheating and a reduction zone (Figure 5.83).

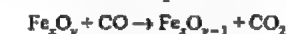
In the preheating zone, the feed materials are dried, and coal volatiles escape, and the charge is heated to reducing temperature (ca. 950–1100 °C).

An overview of the coals and ores used in SL/RN plants is given in Table 5.37. The usual grain sizes of the feed materials are < 15 mm for the reductant, < 25 mm for the iron-bearing materials and < 3 mm for the desulfurizing agent.

The charge is heated through exchange of heat with the kiln waste gases flowing counter-currently to the charge. The energy is supplied by the sensible heat of the waste gases from the reduction zone, by the partial combustion of the coal volatiles, and by direct burning of carbon in the preheating zone.

If high-volatile coals are used, injection of air into the charge can bring about partial combustion of the volatiles within the charge, which accelerates preheating.

In the preheating zone, a certain degree of prereduction is accomplished through the coal volatiles. However, the greater part of the reduction occurs in the *reduction zone* at near-constant temperature according to



The carbon dioxide formed during reduction reacts within the charge with fixed carbon according to the Boudouard reaction



and forms the carbon monoxide required for the reduction process.

The necessary heat in the reduction zone is supplied through combustion of the surplus carbon monoxide from reduction, of the volatiles in the injected coal, and of fixed carbon.

The desired temperature profile is established by controlled addition of combustion air along the length of the kiln.

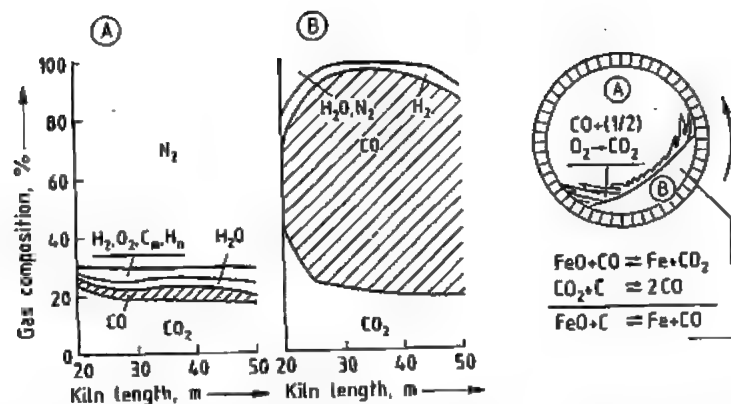


Figure 5.84: Gas composition in the kiln freeboard (A) and kiln charge (B) measured in an industrial kiln of 50 m length.

Inside the kiln, an *oxidizing atmosphere* above the charge and a *reducing atmosphere* within the charge prevail in close proximity (Figure 5.84). Accordingly, the reactions occurring above the charge in the kiln freeboard are exothermic and those taking place in the material bed are endothermic. Separation of the two atmospheres is ensured by the gas generated in the material bed, which also prevents reoxidation of particles of DRI at the charge surface.

After leaving the rotary kiln, the DRI is cooled to ca. 100 °C together with the excess coal in an indirectly cooled rotary cooler. The DRI is separated from the nonmagnetic kiln discharge material by *screening* and *magnetic separation*.

The > 3 mm fraction of the *magnetic portion* can be directly used for steel production, the < 3 mm fraction is normally briquetted before further use.

The > 3 mm fraction of the *nonmagnetic portion* is mostly char and can be recycled to the process. The < 3 mm fraction, containing ash, calcined desulfurizing agent, and char, is disposed of.

In particular cases, e.g., if the ash content of the coal is very low, it is advantageous to charge the entire kiln discharge material directly into a downstream electric furnace without cooling and separation. This brings considerable savings in electric energy for the melting down process.

The waste gases leave the kiln at the feed end at ca. 850–1000 °C. They pass through a dust-settling chamber to remove coarse dust and enter an afterburning chamber, where combustible gases and carbon particles are burnt off. The waste gases are then cooled, cleaned and discharged to the atmosphere. Alternatively, the sensible heat of the gases leaving the afterburning chamber may be recovered in a downstream steam boiler for generation of process steam or combined for production of steam and electric power.

Since 1984, a four-strand SL/RN plant with a capacity of 600 000 t/a DRI and waste-heat recovery has been in operation at the Vanderbijlpark Works of ISCOR in South Africa. Approximately 1.9 t of process steam (1.6 MPa, 260 °C) per tonne of DRI are generated for the steel mill.

Taking into account a variety of reducing agents, the energy requirement (without char recycling) referred to as the lower heating value of the coals, is ca. 19.3 GJ/t DRI for lignite briquettes (A), ca. 18.4 GJ for bituminous coal (B), and ca. 17.8 GJ for a mixture consisting of 70% anthracite (C) and 30% bituminous coal (B) [112]. The analyses of these coals are shown in Table 5.38.

If a combination C:B = 50:50 with recycled char is used, the energy requirement is only 14.8 GJ/t DRI [112].

Further typical consumption figures are given below:

Ore or pellets (Fe_{tot} 67%) 1.42–1.44 t

Fixed carbon	380–475 kg
Electric power	70–90 kWh
Water	1.5–2.5 m ³
Manpower	0.4–0.6 man hours
Repair and maintenance	\$8–10

In addition to DRI production, SL/RN rotary kilns are commercially used for prereduction of iron ore at Highveld Steel in Witbank, South Africa (13 units with an ore capacity of 200 000 t/a each, 30–35% metallization) and for reduction of ilmenite concentrates at Westralian Sands Ltd. in Capel, Western Australia (one unit, ilmenite throughput 180 000 t/a, 95–97% metallization).

Table 5.38: Coal analyses.

Coal	A	B	C
Fixed carbon, %	44	59	88
Volatile matter, %	51	27	8
Ash, %	5	14	4
Lower heating value (dry), GJ/kg	23.3	27.0	32.7

5.11 Smelting-Reduction Processes

Smelting-reduction processes are multi-stage processes where hot metal is produced directly with coal, particularly noncoking coal.

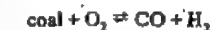
The main reasons for developing smelt-reduction processes (since 1970) was to find processes which produce *liquid iron* economically at low capacity and use *coal directly*. The processes should be more flexible regarding raw material and operation and should cause less pollution than a blast furnace.

The ore, fine ore, or lump ore is prereduced with the gas produced in the melting vessel. The prereduced ore (sponge iron) is melted down in a melting vessel where melting energy is generated by oxidation of coal. Some processes use also electrical energy in the melting stage.

Simulations with computer models were performed for different smelt reduction process configurations [113–115] to find an optimum process and to estimate the influence of postcombustion and prereduction on coal consumption. (Postcombustion is defined as the partial oxidation of a gas previously generated in the melting vessel, whereby the energy pro-

duced by this combustion is transferred to the bath with high efficiency.) Economical and technical comparison can be found in the literature [116–118].

Characteristics of Coals for the Smelting-Reduction Processes. The most important property of the coal for the smelting reduction processes is its volatile content, because this determines the gasification temperature of the reaction



Coals with *low volatile* content generate a high temperature when gasified with oxygen, the released energy being used for sponge iron melting. Gasification of coals with a high volatile content such as lignite results in a low temperature because the volatile hydrocarbons must be cracked before gasification can occur.

Figure 5.85 shows the calculated adiabatic gasification temperature (gasification to CO + H₂) as a function of the H:C and O:C molar ratio of the coal. The higher the gasification temperature the better the coal is suited for smelt reduction process, i.e., the lower is the coal consumption. The classification of coals by the aforementioned molar ratio is more accurate than by volatile content because coals with the same volatile content can show remarkable differences in their gasification temperature. The coal rank classification shown in Figure 5.85 gives only a rough estimation.

For *converter-type* melters the degree of postcombustion must be increased when using highvolatile coal, but there are some limitations with respect to the movement of the bath. For processes with countercurrent flow of coal and gas, besides energetic limitation, problems with tar formation can also occur.

The *ash content* of the coal is less critical than its volatile content. The mainly acidic ashes of the coal must be compensated for by additives so that basic slags can be formed. Thus, processes which require a high slag basicity are more sensitive to the ash content. The additives (limestone, dolomite) enter the melter stage in most cases in the calcined form. Otherwise the influence of the ash con-

tent on the coal consumption is too high and extra energy for calcining the additives and for the endothermic Boudouard reaction is needed.

The moisture content of the coal (ca. 10%) decreases the gasification temperature drastically because of the endothermic water-gas reaction. Hence, most of the processes use dried coal.

Other properties of the coal such as the melting behavior of the ash, the swelling index, or the reactivity are of little or no concern. The Hardgrove index influences the grinding cost when grinding is necessary (converter processes).

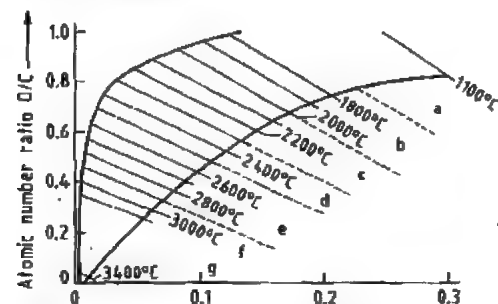


Figure 5.85: Adiabatic gasification temperatures ($H_2 + CO$) for coals in dependence on the atomic number ratio: a) Lignite; b) Subbituminous coal; c) High volatile bituminous coal; d) Medium volatile bituminous coal; e) Low volatile bituminous coal; f) Anthracite; g) Coke.

The sulfur content of the coal should be of course as low as possible ($\leq 1\%$). However, the tolerable range must be evaluated for each smelt reduction process separately.

Classification of Smelting-Reduction Processes. The first developments in smelting reduction on a laboratory scale failed in the 1960s because the conversion of coal and fine ore in a melting vessel was tried without prereduction [119]. The next development was in Sweden in the 1970s, where the energy was introduced into the melting vessel in the form of electrical energy. Further developments were the converter processes with and without postcombustion. Processes which are closest to the blast furnace are those with a char-or coke-bed melter-gasifier (Table 5.39).

Processes which only modify the blast furnace technique such as the oxygen-coal blast furnace of BSC and NKK or the plasmaheated blast furnace Pirogas [117] are not discussed here.

In the case of processes using fine ore generally only the smelting reactor is developed. The integration of the fine-ore reduction into the process and therefore directly into the smelting reactor has not yet been realized in any of the existing pilot plants.

5.11.1 Processes Using Electrical Energy

These processes were developed in Sweden and consist of a prerelution stage of the fine ore and a final reduction which use electrical energy. The electrical energy is introduced via plasma burners (Plasmamelt), electric arc (El-red), or electric resistance heating (Inred). The only process which has a technical application is the Plasmamelt process in a modified form (Plasmadust and Plasmachrome). Because of the high electricity consumption these processes can only be considered for iron production in countries with cheap electricity.

Plasmamelt. The Plasmamelt process [142, 137] was developed by SKF Steel Engineering AB. The flow sheet is shown in Figure 5.86. Fine ore is prereluted with a reduction gas generated in the smelting reduction stage. The prereluted material (reduction degree 50–60%) is injected together with powdered coal into a coke-filled shaft furnace (melter) provided with plasma generators. Recycled process gas is used as injection gas. The final reduction and melting occur inside the coke column which also protects the refractory. A proportion of the spent reduction off-gases is combusted to dry and preheat the ore fines.

The Plasmamelt process requires a low coke intake (consumption 50–100 kg per tonne of hot metal), 1100 kWh of electricity and 200 kg coal per tonne of hot metal. The prerelution stage was developed separately in a 1 t/h pilot plant. Integrated operation of melting and reduction has not yet been tested.

Table 5.39: Smelting-reduction processes [118].

Process	Ore type	Fuel	Prerelution (reduction degree)	Final reduction	Development stage	References
Char or coke bed melter-gasifier						
Corex	lump	lump coal	shaft furnace (90%)	fluidized bed	1000 t/d	[120–123]
Sumitomo SC	lump	coke (30%) fine coal	shaft furnace (60%)	cupola	8 t/d	[124, 125]
Kawasaki XR	fine	lump coal	circulating fluidized bed (40–80%)	fluidized bed	10 t/d	[126, 127]
Converter with postcombustion						
Hismelt (CRA)	fine	fine coal	fluidized bed	horizontal cylindrical converter (C-injection)	10 t	[128–130]
MIP and melting cyclone	fine	fine coal	hot and melting cyclone (30%)	horizontal cylindrical converter (C-injection)	20 t	[131]
NKK	fine	fine coal	fluidized bed (15%)	converter (C-top blowing)	5 t	[132, 133]
NSC	fine	fine coal	circulating fluidized bed (30%)	converter (C-top blowing)	5 t	[134]
Kobe Steel	lump	fine coal, CH_4	shaft furnace	converter (C-injection)	0.5 t	[117]
Without postcombustion						
Coin (Krupp)	fine	fine coal	circulating fluidized bed (> 90%)	converter (C-injection)	3 t	[135–137]
CBF (British Steel/Hoogovens)	lump	fine coal	shaft furnace (> 90%)	two-stage converter (C-top blowing)		[117]
Process with electrical energy						
ELRED (ASEA)	fine	fine coal	circulating fluidized bed	d.c. arc furnace	8 t/h melting, 0.5 t/h red.	[138, 139]
Inred (Boliden)	fine	fine coal	melting chamber	arc furnace	8 t/h	[140, 141]
Combimelt (Lurgi)	lump	lump coal	rotary kiln	submerged electric furnace		
Plasmamelt (SKF)	fine	fine coal coke fine coal	fluidized bed	shaft furnace	8 t/h melting	[142, 143]

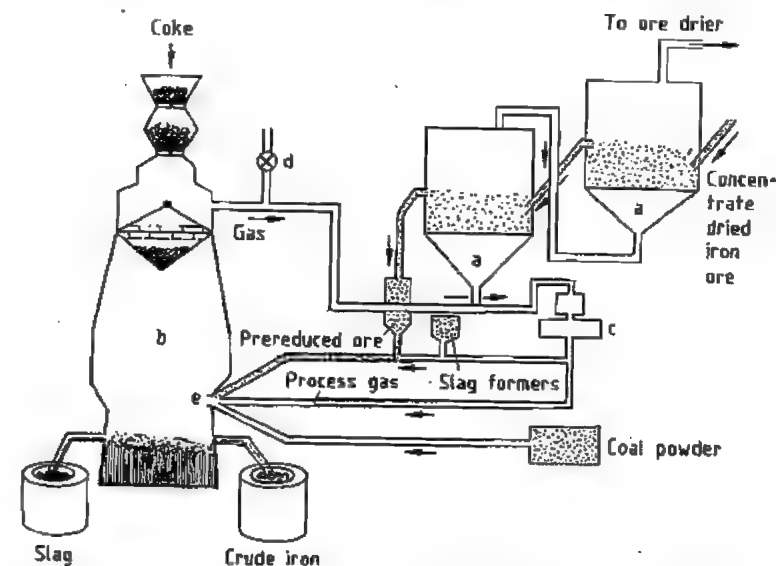


Figure 5.86: The Plasmamelt process: a) Prerelution; b) Shaft furnace; c) Compressor; d) Pressure control; e) Plasma generator.

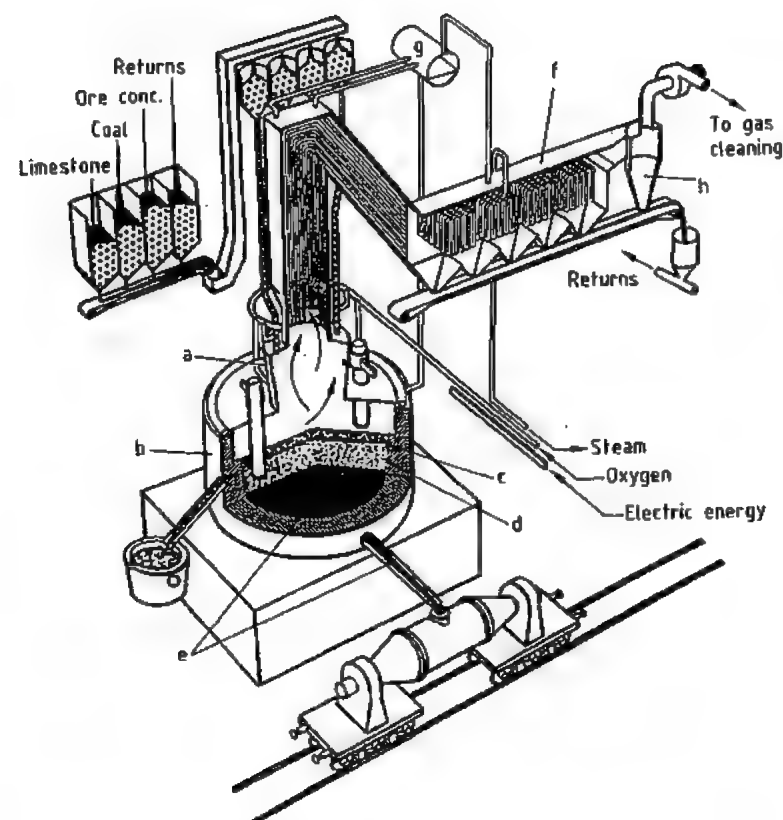


Figure 5.87: The Inred process: a) Flash-smelting chamber; b) Submerged-arc furnace; c) Coke bed with sponge iron and slag; d) Slag; e) Iron; f) Waste-heat boiler; g) Boiler drum; h) Cyclone.

A melter with a capacity of 8 t/h is integrated in a modified process (Plasma dust) where waste oxides from steelworks are processed in Southern Sweden.

The *Inred* process [140, 141] was developed by Boliden and tested from 1982–1984 in a pilot plant with a capacity of 8 t/h. Fine ore, coal, and fluxes are fed together with oxygen in a flash-melting chamber giving temperatures of 1900 °C. Superheated liquid FeO together with some coal char fall into the electric furnace with submerged arc, where final reduction takes place (Figure 5.87). Because of the high FeO content in the slag (7–8%) a sulfur content of 0.15–0.2% must be expected for a commercial plant.

In the *Elred* process [138, 139] fine ore is prereduced to 60–70% in a single-stage fast-

fluidized bed at 950–1000 °C before being melted down in an electric arc furnace (hollow Söderberg electrode). The reducing gas is produced by partial combustion of coal with air within the fluidized bed. The prereduction pilot plant was built by Lurgi with a capacity of 500 kg/h and the electric arc furnace by ASEA (capacity 8 t/h) (Figure 5.88). Up to now this process has found no technical application for iron production.

The *Combismelt* process combines the Lurgi prereduction rotary kiln and a submerged electric arc furnace (DEMAG). The electric energy is generated by waste heat and off-gas.

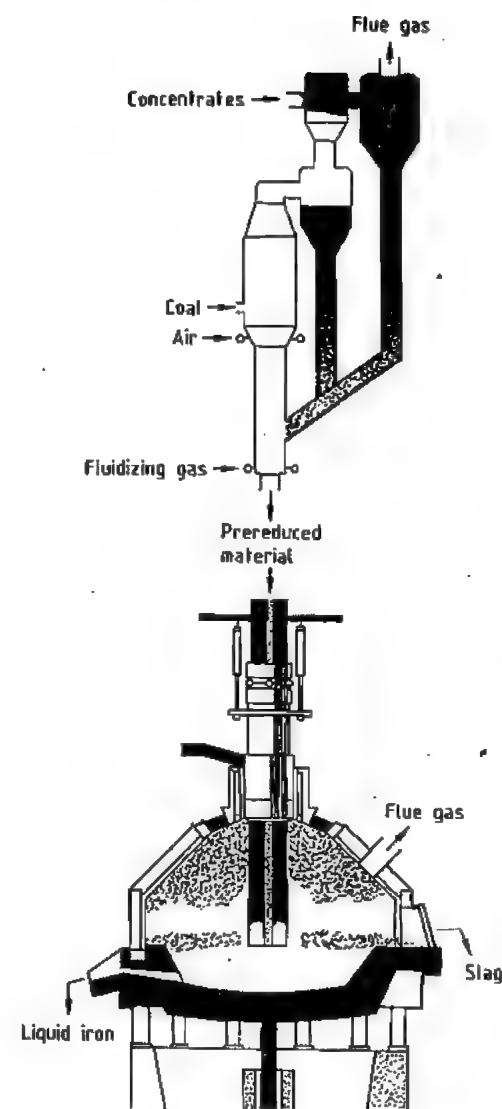


Figure 5.88: The Elred process.

5.11.2 Char-Coke-Bed Melter-Gasifiers

In these processes the melting stage is a fixed bed or fluidized bed of char or coke. Prereduction is performed in a shaft furnace (Corex, Sumitomo) or fluidized bed (Kawasaki).

The Corex process (formerly called KR process) is the most advanced smelting reduction process with a 1000 t/d plant in operation in South Africa since 1988 [120–123]. This process was developed by Deutsche Voest-Alpine Industrieanlagenbau (formerly Korf Engineering) and its parent company Voest-Alpine in Austria to a 60 000 t/a pilot plant from 1981 to 1987.

The Corex process (Figure 5.89) separates the iron-ore reduction and melting steps into two reactors:

- Generation of reducing gas and liberation of energy from coal for melting occur in the melter-gasifier.
- Reduction of iron ore occurs in a shaft furnace.

The Corex process is designed to operate under elevated pressure, up to 0.5 MPa.

Coal is fed into the gasifier (a) where it comes into contact with a reducing gas atmosphere at a temperature of ca. 1000–1100 °C. Instantaneous drying and degasification of the coal particles occur in this upper portion of the melter-gasifier. Reducing gas is generated in a fluidized bed, by the partial oxidation of coal.

At first carbon is oxidized to carbon dioxide. Then, carbon dioxide reacts with free carbon to form carbon monoxide. The gas temperature in the fluidized bed is in the range of 1600–1700 °C. The temperature conditions in the freeboard zone above the fluidized bed guarantee production of a high-quality reducing gas which contains ca. 65–70% carbon monoxide, 20–25% hydrogen, and 2–4% carbon dioxide. The remaining constituents are methane, nitrogen and steam.

After leaving the melter-gasifier, the hot gas is mixed with cooling gas to obtain a temperature suitable for direct reduction, ca. 850–900 °C. The gas is then cleaned in hot cyclones (d) and fed to the shaft furnace as reducing gas. A small amount of the cleaned gas is converted to cooling gas in a gas cooler. The fines captured in the hot cyclone are reinjected into the melter-gasifier.

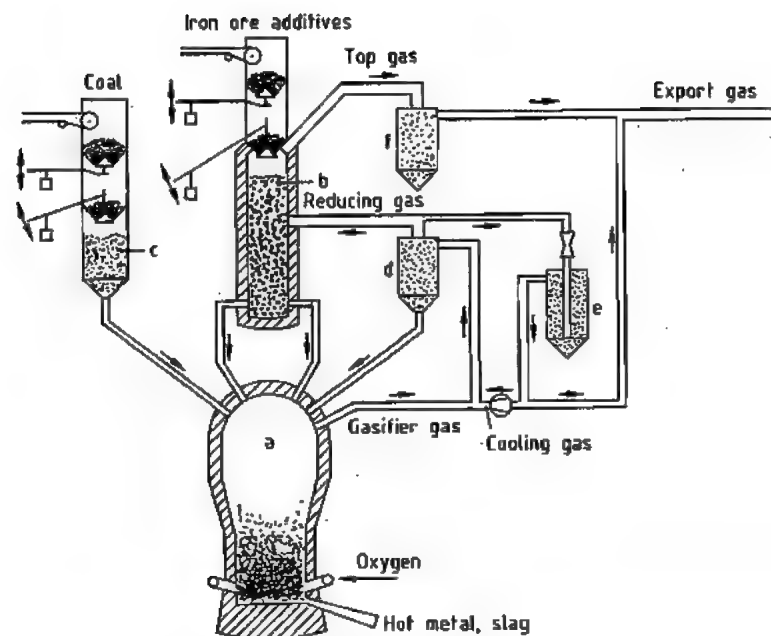


Figure 5.89: The Corex process, basic flow sheet with export gas: a) Melter-gasifier; b) Reduction shaft furnace; c) Coal feed system; d) Hot dust cyclone; e) Cooling-gas scrubber; f) Top-gas scrubber.

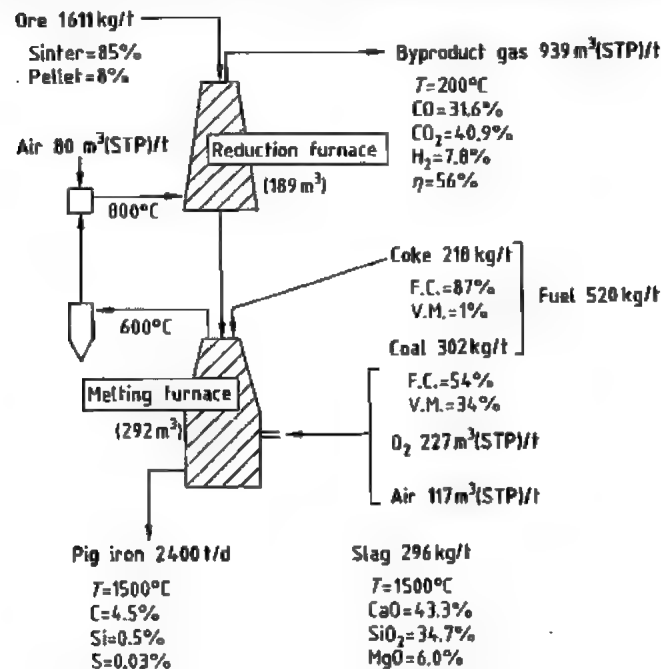


Figure 5.90: Expected material flow sheet for a Sumitomo SC commercial plant (F.C. = fixed carbon; V.M. = volatile matter).

The reducing gas is fed into the reduction furnace and countercurrently ascends through the iron burden.

The iron ore, charged into the shaft furnace through a lock hopper system, descends by gravity. The reduction reaction in the shaft furnace, using gas with ca. 70% carbon monoxide and 25% hydrogen is exothermic, leading to temperatures in the burden which are above the reducing gas temperature. Because of carbon monoxide decomposition, carbon deposits will form on the iron and act as a lubricant. Formation of Fe_3C occurs as well and cluster formation is avoided. The top gas is cleaned and cooled in a scrubber, and is then available for various purposes. Metallization of the DRI averages 90–95%, and its carbon content is in the range of 3–5%, depending on the raw material used and operating conditions.

The continuous transfer of the hot DRI (temperature 800–900 °C) from the reduction furnace to the melter gasifier is carried out by a special controllable transport system which discharges into connected downcomers. The velocity of the descending sponge iron particles is lowered in the fluidized bed, further reduction is completed, heating and melting occurs. Hot metal and slag drop to the bottom of the melter-gasifier. Analogous to the practice in the blast furnace hot metal and slag are discharged by conventional tapping procedures. Tapping is carried out every 2.5–3 h on an average. For a good desulfurization a slag basicity > 1 is required.

Temperature and silica content of the hot metal can be adjusted by various process parameters, i.e., coal particle size, height of the fluidized bed, system pressure, and rate of hot metal production.

The melter-gasifier may generate a certain amount of surplus gas depending on the coal selected. This surplus gas becomes part of the cooling gas stream, and can be either used separately or mixed with the top gas from the shaft furnace. When using a high volatile bituminous coal, the resulting gas mixture (export gas) approximates 1800 m³ (STP) per tonne of hot metal with a lower heating value of ca. 8000 kJ/m³ (STP).

According to the composition and quality of the coal, the specific oxygen consumption is ca. 450–550 m³ (STP) per tonne of hot metal. The energy for the oxygen production can be supplied from about one third of the export gas of the Corex plant. The coal consumption depends on the coal quality and is ca. 0.5–0.7 t fixed carbon per tonne of hot metal.

If the export gas cannot be used economically, it is converted to reducing gas by removal of carbon dioxide and recycled. This process route offers the advantage of a lower coal and oxygen consumption.

The Sumitomo SC process [124–125] uses a combination of two shaft furnaces (Figure 5.90), the reduction furnace which produces DRI from lump ore and a coke-bed melting furnace which generates the reducing gas. Oxygen, air, and pulverized coal are blown into the coke bed. Low-grade coke is charged at the top of the melting furnace which corresponds to the lower part of a blast furnace or a cupola.

The gas coming out of the melting furnace with a temperature of 600 °C is cleaned in a cyclone, then it must be heated up by partial combustion with air to the reducing temperature of 800 °C.

The melting furnace was developed in a pilot plant with a capacity of 8 t/d in 1982. In 1984 the reduction furnace was integrated. Expected consumption figures (Figure 5.90) for a commercial plant are given on the basis of the result obtained by the pilot plant. The expected coke consumption of 218 kg per tonne of hot metal (in the pilot plant much higher) is nearly as high as that of a modern blast furnace with a high coal-injection rate. So the goal of a cokeless process is not achieved.

Kawasaki developed a smelting reduction process for ferrochrome production on the basis of a coke-bed melter with two-stage tuyères, the XR process [126, 127]. Powdered ore was prereduced in a fluidized-bed reactor and injected into the furnace through the upper tuyère. For iron production, this process was

modified to feed coal from the top as schematically shown in Figure 5.91.

Small-size degassed coal forms a fluidized bed in the upper part of the furnace and the lumpy char forms a packed bed in the lower part. The pilot plant for the XR process with a capacity of 10 t/d was started 1987. It is planned to reduce the fines in a circulating fluidized bed to a reduction degree of 80%.

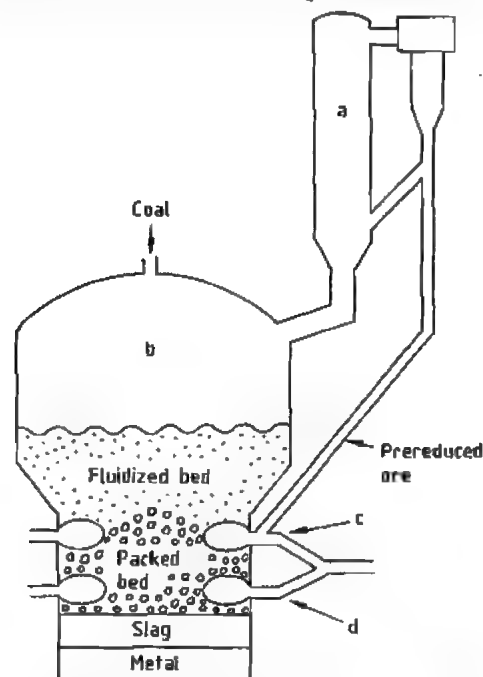


Figure 5.91: The Kawasaki XR process: a) Fluidized bed prereduction furnace; b) Coke-bed melter; c) Upper tuyère; d) Lower tuyère.

5.11.3 Converter-Type Melters

The converter-type melters are under development from the experience of the oxygen LD-BOF converter for steelmaking. Coal is injected with or without oxygen in a liquid iron bath.

In most of the processes the carbon monoxide hydrogen gas mixture coming out of the melt is partially combusted (postcombusted) to generate heat (up to 1900 °C) which is transferred to the bath. Processes using fine ore prereduce the ore in fluidized beds to a re-

duction degree of 15–90%. In most cases the process pressure is low (ca. 50 kPa). At present only the melting stage is developed for most of the processes. *Integrated operation* of melting and reduction has not been tested. Apart from the latter the most critical areas of these processes are refractory lifetime, gas-handling system (accretions), and foaming and splashing of the melt. Because of the high FeO-content in the slag the sulfur content of the hot metal is higher and the silicon content lower than in the blast furnace process.

Processes with Postcombustion. The most advanced converter process has been developed by Klöckner, Germany, and CRA, Australia, since 1981 [128–130]. After pretests a pilot 10 t-converter started operation in 1984 with a capacity of 4 t/h where especially postcombustion was investigated. The prereduction stage was not tested in this plant. In 1987 Klockner was bought out and CRA formed a joint venture with Midrex to further develop the process under the name *Hismelt*. The flowsheet of the Hismelt process is shown in Figure 5.92. Coal is injected from the bottom into the melt. The energy for melting and final reduction is generated by partial combustion of the converter gas with preheated air. The converter off-gas is used for prereduction of the fine ore. Because of the high oxidation degree of the gas it is only possible to reduce the ore to iron(II) oxide which is separated in a cyclone and fed to the converter. The main problem of this process is whether the high postcombustion degrees, up to 65% depending on coal quality, and reduction degree can be maintained for continuous operation and whether the huge amount of hot gas can be handled.

The *NKK process* [132, 133] is another converter type process which also operates with a high postcombustion degree (see Figure 5.93). Coal and oxygen are blown in from the top to the bath. The fine ore is prereduced only to a low degree.

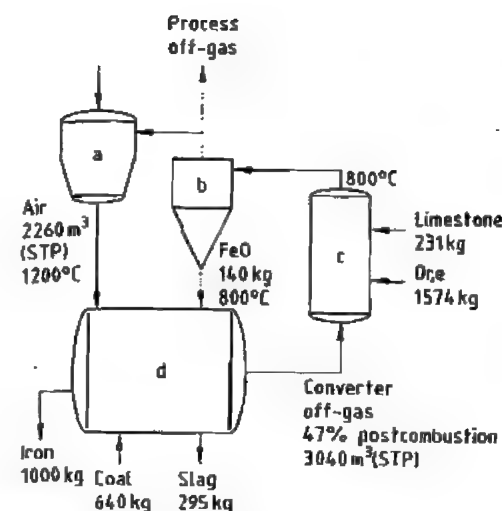


Figure 5.92: Flowsheet of Hismelt process for the case 47% postcombustion and reduction to FeO: a) Air pre-heaters; b) Cyclone; c) Prereducer; d) Hismelt converter.

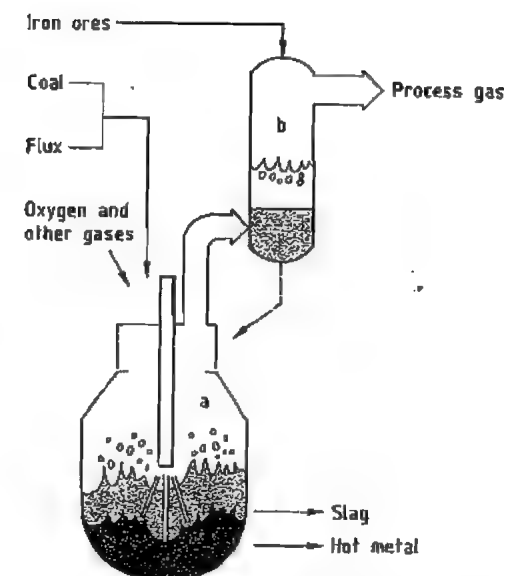


Figure 5.93: The NKK's smelting reduction process for ironmaking: a) Smelting reduction furnace; b) Preheating and prereduction furnace.

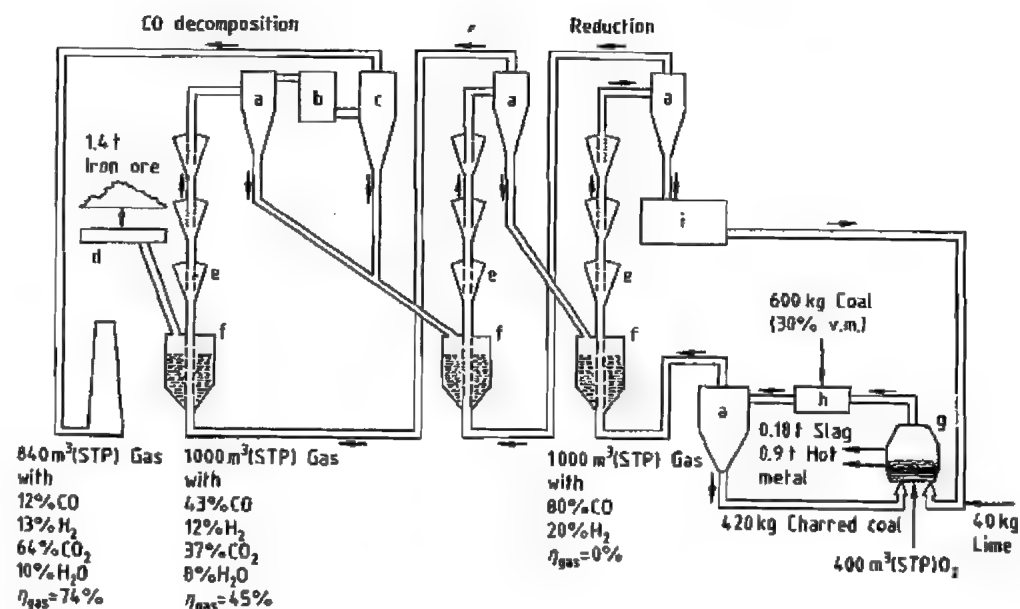


Figure 5.94: COIN concept of a coal-based smelting reduction process for iron ore fines: a) Hot cyclone; b) Gas cooler; c) Bag filter; d) Screw conveyor; e) Whirl box; f) Pneumatic conveyor; g) Melter-gasifier; h) Charring; i) 1 t directly reduced iron and 85 kg carbon.

Since 1986 tests have been performed in a 5 t-converter. In 1988 a prereduction stage was integrated in the pilot plant with a capacity of 100 t/d.

Processes Without Postcombustion. The Coin process [135–136] developed by Krupp operates without post combustion and with a high reduction degree. In the first published flow sheets the prereduction stage was a shaft furnace. The latest one (see Figure 5.94) shows a multistage prereduction of fine ore which was tested separately in a pilot plant. The prereduction stage is a combination of entrained-bed and fluidized-bed reactors.

The converter pilot plant is a 3 t-converter. To achieve a high degree of metallization a high reduction temperature is needed. Sticking of the ore is prevented by carbon monoxide decomposition in a prereduction stage at 500–600 °C. Oxygen and degassed coal is blown into the bath from the bottom. As no postcombustion delivers energy, the coal (especially high volatile coal) must be preheated and charred by injecting in the converter off-gas and recycling via a cyclone. The process is very complex and integration of the multistage prereduction, the coal devolatilizer, and the converter is not easy.

5.12 Aspects of Environmental Protection

In the recent past, the rapidly increasing environmental consciousness has led to considerably tightened environmental standards in many countries. In Germany, for instance, a limiting value for dust emissions of 150 mg/m³ (STP) was stipulated as early as 1974 in the TA Luft for the prevention of air pollution. The amendment to the TA Luft in 1986 further reduced dust emissions in waste gases to 50 mg/m³ (STP) [144]. This limit applies to total dust emissions. Lower limits have been set for individual components, such as heavy metals, e.g., 0.2 mg/m³ (STP) for cadmium, mercury, and thallium; 1 mg/m³ (STP) for arsenic, cobalt, nickel, selenium, and tellurium; and 5 mg/m³ (STP) for antimony, lead, chro-

mium, manganese, vanadium, and copper as well as cyanide and fluoride. Urged by stringent requirements, the steel industry has made substantial investments in environmental technology in recent years [145]. In Germany, for instance, from 1975 to 1984 ca. 2.4×10^9 DM (10% of the steel industry's resources for new investments) were spent on environmental protection. The lowering of dust emissions from 10 kg per tonne of raw steel in 1960 to the present value of 1.4 kg per tonne of crude steel serves as an example for the success of new techniques in controlling air pollution [146].

The endeavors towards pollution control are not limited to the *air pollution control*, but also include *water pollution control*, *reduction of noise*, and *waste management*. The division of capital expenditure between the individual areas in Germany (1975–1984) is as follows:

Air pollution control	67.7%
Water pollution control	21.4%
Noise reduction	9.5%
Waste management	1.4%
Total	2354×10^6 DM

It can be seen that the investment in air-pollution control represents two thirds of the total capital expenditure.

Apart from the *direct measures* taken to control pollution, the *saving or recovery of energy* also has a favorable effect on the environment because the corresponding amounts of energy can only be produced at the expense of the environment. The most important examples of these measures are (1) the reduction of the specific fuel consumption during sintering by half since the 1950s, (2) the expansion of blast-furnace top gas in turbines and its utilization for heating, (3) dry coke quenching, and (4) CO gas recovery.

Pollution-control techniques being currently employed in pig-iron production and in related auxiliary plants will be described with a series of examples. However, in view of the diversity of processes available, a complete survey cannot be presented here.

5.12.1 Air Pollution Control

Virtually all areas of ironworks make use of gas dedusting techniques. Apart from mechanical and filtering dust separators and scrubbers, electrostatic precipitators are frequently used today [147–149].

Sintering Plants. In the past, dust separation from off-gases in iron-ore sintering plants was carried out with cyclones. Today's demands are essentially fulfilled by three-field horizontal dry electrostatic precipitators, which are operated on the suction side of the sinter waste-gas fan. The waste-gas flow rate of a sinter belt with a reaction area of e.g., 400 m² is in the range of 1.8×10^6 m³/h. As shown in Figure 5.95, the waste-gas dedusting in that case is achieved in two parallel electrostatic precipitators.

The electrical resistance of sinter dust, which in most cases is very high, frequently impedes electrostatic dust precipitation [150]. Increasing the humidity of the gas, by adding water either to the off-gas or to the sinter belt, can improve dust separation by reducing the *electrical resistance* of the dust. Dust emission can be reduced by 20–50% of the starting values by conditioning the waste gas with sulfur trioxide [149]. In this process sulfur dioxide, obtained, e.g., by combustion of sulfur, is oxidized to sulfur trioxide and added to the waste gas in front of the electrostatic filter. A level of 10–30 ppm of sulfur trioxide in the waste gas is sufficient to reduce the electrical resistance of dust and thus cause the improvement in dedusting efficiency mentioned above. The required amount of sulfur trioxide is so low that

only ca. 33 kg/h of sulfur are needed to produce e.g., 20 ppm of sulfur trioxide for the conditioning of the waste gas of a 400 m² sinter belt. Extra sulfur trioxide emission does not occur because it is bound to the dust by chemisorption (sulfate formation). The effect of this process depends on the basicity of the sinter feed and on the composition of the raw material.

Simple housings at feeding points, at the sinter discharge end, at screening machines and at numerous transport devices cannot effectively prevent the escape of dust into the surroundings. For this reason, *suction hoods* are installed that are connected by means of branched ducts to a central dedusting system, which is often an electrostatic precipitator. The schematic of a so-called room dedusting system of this type is presented in Figure 5.96. In many cases, the dust-laden off-gas from the sinter cooler is passed through the room dedusting plant, however, it may sometimes be led to a separate electrostatic precipitator.

Blast Furnace. A blast furnace with an open top is not used any longer. Dedusting systems have allowed the cleaning of top-gas to dust loading values of < 10 mg/m³ (STP), and thus have permitted the utilization of the energy contained in this gas in turbines and for the heating of hot blast stoves. Apart from the direct protection of the environment brought about by top-gas purification compared to an open top, an indirect effect is achieved by saving energy which would have to be produced at the expense of the environment.

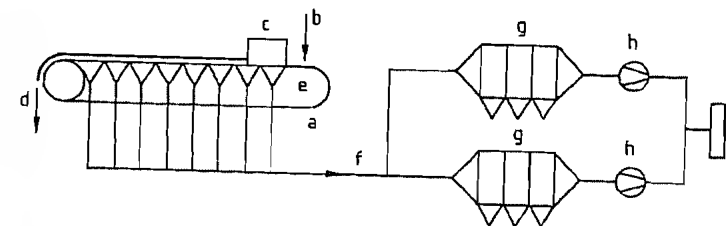


Figure 5.95: Sinter plant waste-gas dedusting: a) Sintering machine; b) Feed point; c) Igniter; d) Sinter; e) Wind boxes; f) Manifold; g) Electrostatic precipitator; h) Fan; i) Stack.

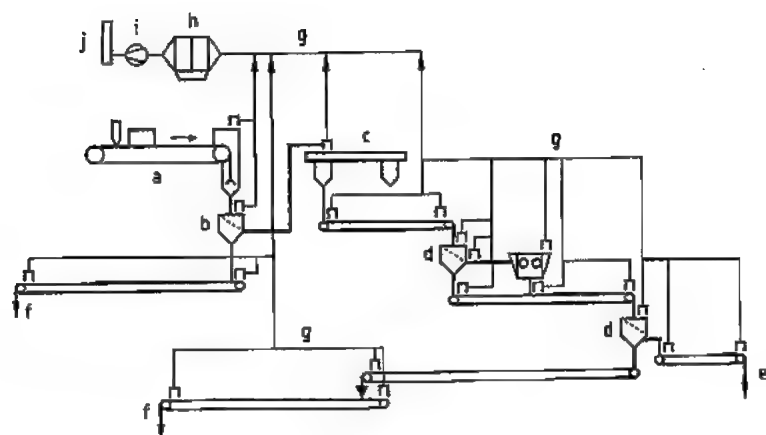


Figure 5.96: Sinter plant room dedusting: a) Sintering machine; b) Hot screening; c) Cooler; d) Cold screening and crushing; e) Sinter product; f) Return fines; g) Suction system; h) Electrostatic precipitator; i) Fan; j) Stack.

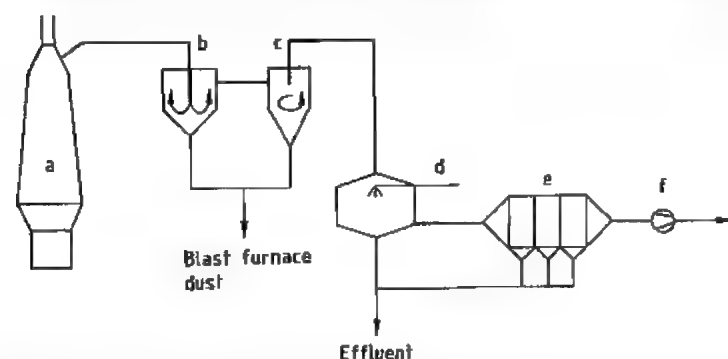


Figure 5.97: Top-gas cleaning: a) Blast furnace; b) Gravity dust catcher; c) Cyclone; d) Scrubber; e) Wet electrostatic precipitator; f) Fan.

The top-gas leaving the blast furnace (a) is loaded with 10–40 g/m³ (STP) of dust. The volumetric flow rate of a blast furnace that has, e.g., an output of 5000 t of hot metal per day is ca. 420 000 m³/h (STP). Figure 5.97 shows the components of the top-gas purification plant of a blast furnace that is operated at a slight overpressure. The larger particles of dust are first separated in a gravity dust catcher (b), i.e., a settling chamber with flow deflection, and subsequently in a cyclone (c). Further cleaning of the blast-furnace gas occurs in a single- or multiple-stage scrubber (d) and in a wet electrostatic precipitator (e), which carries out both fine purification as well as removal of droplets. If the top-gas volumet-

ric flow rates are very high, several purification plants are installed in parallel.

The top-gases from blast furnaces that are operated at higher pressures can be freed from dust to the desired degree of purity by using a pressure difference of ca. 20 kPa in high performance scrubbers without an electrostatic precipitator. Another method of top-gas dust separation, which has been repeatedly and successfully used recently, is dry dust removal in electrostatic precipitators. This method has the advantage of involving low pressure losses and consequently has a lower energy requirement for gas transport and, in addition, water and sludge treatments are no longer necessary. Dry top-gas purification represents the latest technological development.

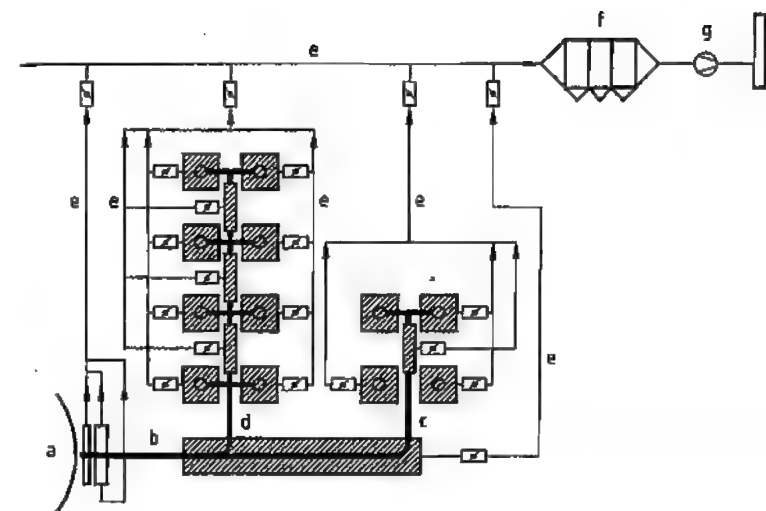


Figure 5.98: Cast house dedusting: a) Blast furnace, area of tapping hole; b) Main runner with skimmer; c) Hot metal runner with transfer points; d) Slag runner with transfer points; e) Suction lines; f) Electrostatic precipitator; g) Fan; h) Stack.

In the area of raw material handling a room dedusting plant prevents dust emissions. The burden bunkers and conveyors are connected by a suction system to a bag filter or an electrostatic precipitator.

The smoke that arises during the tapping of the blast furnace represents a minor environmental problem as far as emission protection is concerned. However, it is a nuisance for the operating personnel and makes working conditions on the casting platforms very difficult. *Cast house dedusting* is being carried out for some years now to improve working conditions. In fact, even older blast furnaces are being equipped with dedusting systems [151, 152]. The enclosing of the skimmer, iron, and slag runners and their points of transfer with easily removable hoods having fire-proof linings is characteristic for a casting house dedusting plant. The enclosed areas are connected to suction lines, which are preferably installed below the casting platform. The region of the tapping hole cannot be enclosed because it has to remain accessible to the drilling and plugging machines. In this case, smoke is usually caught with a suction hood placed near the tapping hole and then led to the precipitator. The flow diagram of the main,

hot metal, and slag runners on a casting platform as well as the suction system is shown in Figure 5.98. The hatched parts of the diagram represent the enclosed areas. It can be seen that each suction point has a damper. When the plant is in operation, only the suction points at which smoke is to be trapped are opened. For instance, if no slag is discharged in the first phase of tapping, all the dampers on the slag runner remain closed.

In blast furnace tapping, the flow volume that has to be trapped, dedusted, and transported is 500 000–800 000 m³/h. The power consumption of a casting house dedusting system can reach 0.8 MW, hence, modern plants are automatically controlled. Control dampers in the suction lines and variable-speed blowers draw off as little air as necessary. For example, a minimum amount of air is withdrawn during tapping pauses and maximum amounts at the start and termination of tapping. Bag filters or electrostatic precipitators are employed as dust collectors. The advantages of electrostatic precipitators are the substantially lower pressure loss and the fact that they can be operated during tapping pauses with minimal power input.

Dry Coke Quenching. As mentioned above, dry quenching of coke also has a positive effect on the environment, because of the fact that, in contrast to wet quenching, the waste heat of the coke is utilized and no cooling clouds are produced. The heat is removed from the coke with the help of recirculating gas and used for steam generation in a waste-heat boiler. In an ironworks in Germany, two 70 t/h dry coke quenching plants produce 36 t/h of steam each, which is then used as a fuel substitute in a neighbouring power plant [153]. The fuel saved in this way contributes to environmental protection. An equivalent of > 20 MW of electrical power is produced.

Direct Reduction Plants. In direct reduction plants the waste gases leaving the furnace are freed from dust in an electrostatic precipitator, bag filter or scrubber, depending on the requirements in the operational areas. Electrostatic precipitators or bag filters are used for room dedusting plants.

Regarding the emissions of the dust components mentioned above, cadmium, lead, and possibly manganese can be of relevance in the making of pig iron, however, the limiting values for these metals are generally adhered to.

5.12.2 Prevention of Water Pollution

In the course of pig iron production, modern ironworks cause practically neither water pollution, nor warming up of waters. Only small amounts of water are required in *sintering plants* for rolling the burden and, if necessary, for sinter cooling or gas conditioning. The water used is released into the atmosphere in the gaseous state through the waste gas stack. Generally, direct *reduction plants* do not produce wastewater.

Blast furnaces, on the other hand, have a considerable water requirement for cooling. In the past, up to 60 m³ of water were consumed per tonne of pig iron [154]. Another water-consuming process pertaining to the blast furnace is wet top-gas purification. It is becoming

increasingly rare today that the wastewater of this process is released into the atmosphere. In fact, the introduction of a closed water circulation with the appropriate water conditioning plant [155, 156] for top-gas purification and blast furnace cooling contributes to the marked decrease in the water requirement for steelmaking, which is today ca. 30 m³ per tonne of raw steel [146].

Blast-furnace cooling with a closed circulation requires water-cooling plants. Usually the circulation water is evaporated in the blast furnace coolers and condensed and cooled in cooling towers.

The essential components of a scrubber/precipitator effluent for top-gas purification are shown in Figure 5.99. The clarification of the effluent can be carried out in a thickener and the dewatering of the sludge in a filter press. However, other dewatering machines, such as drum or rotary disk filters may be applied.

5.12.3 Noise Reduction

As in other industrial plants, numerous sources of noise exist in ironworks, which contribute to the total noise emission. Many of these noise sources are not specific to the production of pig iron. These include fans, compressors, pumps and ore-dressing plants. The noise abatement measures consist of, e.g., the use of low-vibration motors, the enclosing of machines or other apparatus, or even entire parts of the plant, such as the sinter waste-gas fans [157].

Special measures are required to dampen the feeding and expansion noises at hot blast stoves. Considerable noise reduction can be achieved here by covering the valves and the expansion line with a sound-absorbing material and by using sound absorbers or perforated disks in the blowoff line [158]. Emission values of ca. 40 dB(A) can be achieved at a distance of 1000 m from a blast furnace or sintering plant if noise damping measures are used consistently [159].

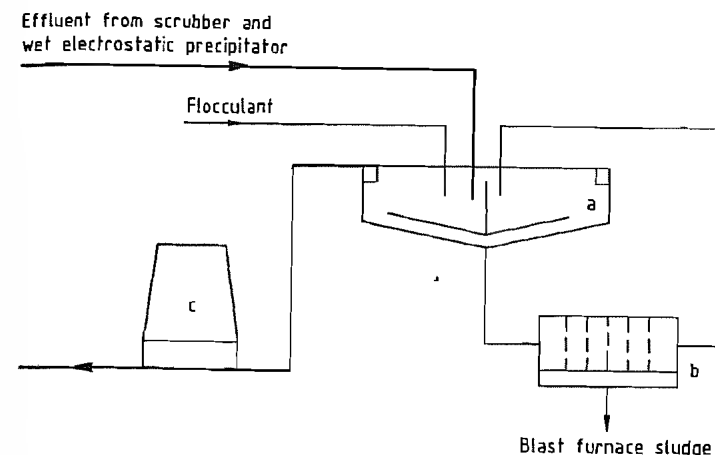


Figure 5.99: Effluent treatment for top-gas cleaning: a) Thickener, b) Filter press; c) Cooling tower.

5.12.4 Waste Management

Blast furnace slag is quantitatively the most important waste material created in the production of pig iron. This material is completely utilized. About two thirds of the total amount is employed in road construction. The remainder is used by the cement industry for the production of blast furnace cement [160].

The recycling of the *dry dust* obtained in top gas purification also causes no problems because it can be recycled to the sintering plant. However, *blast furnace sludge* is for the most part still being dumped, in amounts of 130 000 t/a in Germany [161]. The reason for this is the high content of lead, zinc, and alkali found in the sludge. If the sludge were recirculated, these substances would accumulate in the blast furnace. Today, various processes are available which reduce the environmental impact caused by these dumps by allowing the recycling of blast furnace sludge and other waste containing lead and zinc.

One way of expelling the unwanted accompanying substances is the reprocessing of dusts and sludge in rotary kilns [162–165]. The product thus obtained consists essentially of metallic iron, which can, e.g., be briquetted and returned to the pig iron production [166].

Most of the dust separated in the waste-gas precipitators of sintering plants can usually be led back into the process. Only the dust arising

in the last field of the electrostatic precipitator must be removed from the circulation because of alkali enrichment.

The prime goal is always the avoidance or minimizing of residual substances. For example the specific amount of slag has decreased from 800 kg/t at the beginning of the 1950s to 300–350 kg/t of pig iron today. In a modern steel plant, ca. 90% of the total amount of waste products is recycled.

5.13 Economic Aspects

Pig Iron. The conventional and by far the most common approach to iron manufacture involves reducing and smelting the iron ore in a blast furnace together with coke, the immediate product being pig iron. Pig iron, in turn, is the principal raw material for the manufacture of commercial iron and steel. Production of a tonne of steel requires ca. 700 kg of pig iron in addition to scrap and flux.

World production of pig iron in 1988 reached a level of 532×10^6 t, derived from ca. 960×10^6 t of iron ore (Tables 5.40 and 5.41) [167]. The European Community alone produced 93.7×10^6 t of pig iron in 1988, using 142×10^6 t of ore and sinter together with 44×10^6 t of coke [168]. The major cost factors in pig iron manufacture are related to raw materials (41%), fuel (34%), and processing (25%).

Table 5.40: Iron ore production and fraction of world output, reported by country.

Country	Fe content, %	Production, 10 ⁶ t			% of World Output		
		1986	1987	1988 ^a	1986	1987	1988 ^a
France	30	12.6	11.3	10.0	1.3	1.2	1.0
United Kingdom	28	0.3	0.3	0.2	0	0	0
Germany	30	0.7	0.2	0.1	0.1	0	0
Spain	46	6.1	3.3	3.9	0.6	0.4	0.4
Sweden	64	20.5	19.6	20.4	2.1	2.1	2.1
Turkey	57	4.0	4.5	4.8	0.4	0.4	0.5
Norway	64	3.5	3.1	2.6	0.4	0.4	0.3
Austria	30	3.1	3.1	2.3	0.3	0.3	0.2
Finland	39	0.7	0.7	0.6	0.1	0.1	0.1
United States	62	39.6	47.0	57.4	4.1	5.1	6.0
Canada	64	37.3	37.8	40.2	3.9	4.1	4.2
Brazil	65	129.5	134.0	145.0	13.6	14.5	15.1
Venezuela	64	16.7	17.2	18.2	1.7	1.9	1.9
Mexico	62	8.0	7.0	8.5	0.8	0.8	0.9
Peru	67	5.3	5.4	4.3	0.6	0.6	0.4
Chile	60	6.3	6.2	7.3	0.7	0.7	0.8
Argentina	39	0.6	0.7	0.7	0.1	0.1	0.1
Other Latin America		0.4	0.6	0.6	0	0.1	0.1
South Africa	64	24.5	22.0	22.7	2.6	2.4	2.4
Liberia	60	15.6	13.8	12.8	1.6	1.5	1.3
Mauretania	61	9.2	9.0	9.7	1.0	1.0	1.0
Algeria	50	3.4	3.4	3.5	0.4	0.4	0.4
Egypt	44	2.0	2.0	2.0	0.2	0.2	0.2
Tunisia	50	0.3	0.3	0.3	0	0	0
Morocco	63	0.2	0.2	0.1	0	0	0
Zimbabwe	64	0.8	0.9	1.0	0.1	0.1	0.1
India	63	48.8	48.4	52.5	5.1	5.3	5.5
Iran	46	0.3	0.3	0.5	0	0	0.1
South Korea	48	0.5	0.5	0.8	0.1	0.1	0.1
Japan	50	0.3	0.3	0.2	0	0	0
Other Asia		0.3	0.3	0.3	0	0	0
Australia	62	97.3	104.6	95.4	10.2	11.3	9.9
New Zealand	57	2.6	2.3	3.0	0.3	0.3	0.3
Former Soviet Union	60	250.0	251.0	250.4	26.2	27.2	26.1
China	60	142.5	157.0	153.8	14.9	17.0	16.0
North Korea	48	8.0	8.0	8.0	0.8	0.9	0.8
Yugoslavia	35	6.8	4.2	5.6	0.7	0.5	0.6
Romania	26	2.0	2.0	2.0	0.2	0.2	0.2
Bulgaria	33	2.1	1.9	2.1	0.2	0.2	0.2
Former Czechoslovakia	26	1.8	1.8	1.8	0.2	0.2	0.2
Hungary	24						
Albania	50	0.8	0.8	0.8	0.1	0.1	0.1
EEC		19.7	16.5	14.2	2.1	1.8	1.5
Western nations		501.1	495.2	535.5	52.5	53.7	55.8
Socialist nations		433.7	426.7	424.5	45.4	46.3	44.2
World total		934.5	921.9	960.0	100	100	100

^aPreliminary figures, in some cases estimates.

Table 5.41: Pig iron production and fraction of world output, by country.

Country	Production, 10 ⁶ t			% of World Output		
	1986	1987	1988 ^a	1986	1987	1988 ^a
EEC	85 324	85 603	93 681	17.45	16.94	17.62
Germany	29 018	28 517	32 453	5.94	5.64	6.11
Belgium/Luxembourg	10 724	10 559	9 182	2.19	2.09	1.73
France	13 982	13 449	14 786	2.86	2.66	2.78
United Kingdom	9 812	11 914	13 235	2.01	2.36	2.49
Italy	11 886	11 355	11 376	2.43	2.25	2.14
The Netherlands	4 628	4 575	4 994	0.95	0.91	0.94
Portugal	463	431	445	0.09	0.08	0.08
Spain	4 811	4 804	4 691	0.98	0.95	0.88
Finland	1 978	2 063	2 173	0.41	0.41	0.41
Norway	570	370	367	0.12	0.07	0.07
Austria	3 349	3 451	3 664	0.69	0.68	0.69
Sweden	2 435	2 314	2 494	0.50	0.46	0.47
Switzerland	65	70	70	0.01	0.01	0.01
Turkey	3 666	4 068	4 437	0.75	0.81	0.83
United States	39 772	43 917	50 457	8.14	8.68	9.49
Canada	9 249	9 719	9 486	1.89	1.92	1.78
Japan	74 651	73 418	79 295	15.27	14.53	14.92
Australia	5 853	5 579	5 723	1.20	1.10	1.08
OECD Nations	232 181	230 497	251 837	47.50	45.61	47.38
Former Soviet Union	113 600	113 900	114 000	23.24	22.53	21.45
German Democratic Republic	2 625	2 743	2 750	0.54	0.54	0.52
Bulgaria	1 600	1 656	1 650	0.33	0.33	0.31
Poland	10 200	10 023	10 000	2.09	1.98	1.88
Romania	9 500	9 500	9 500	1.94	1.88	1.79
Former Czechoslovakia	9 600	9 788	9 800	1.96	1.94	1.84
Hungary	2 075	2 109	2 050	0.42	0.42	0.39
Comecon Nations	149 200	149 770	149 750	30.52	29.64	28.17
Former Yugoslavia	3 067	2 868	2 912	0.64	0.57	0.55
South Africa	5 774	6 317	6 112	1.18	1.25	1.15
Zimbabwe	644	560	545	0.13	0.11	0.10
Argentina	1 639	1 752	1 610	0.34	0.35	0.30
Brazil	15 838	21 335	23 627	3.24	4.22	4.44
Chile	591	617	778	0.12	0.12	0.15
Colombia	319	326	310	0.07	0.06	0.06
Mexico	3 728	3 698	3 642	0.76	0.73	0.69
Peru	216	179	202	0.05	0.04	0.04
Venezuela	491	471	506	0.10	0.09	0.10
China	47 000	50 200	51 000	9.62	9.93	9.59
India	10 509	10 920	11 709	2.15	2.16	2.20
North Korea	5 750	5 900	5 900	1.18	1.17	1.11
South Korea	9 003	11 057	12 585	1.84	2.19	2.36
World	488 836	505 514	531 575	100	100	100

^aPreliminary figures, in some cases estimates. Source for EEC data: SAEG; for all other nations: ISI.

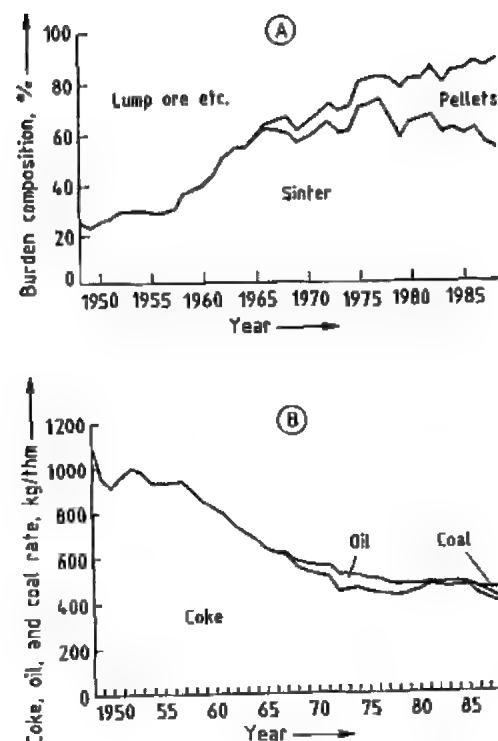


Figure 5.100: Development of blast furnace burden composition (A) and fuel rate (B) in Germany since 1950 for basic pig iron.

In view of the massive requirements for raw material and energy, and investment costs, the potential for savings through optimization of scale and exploitation of more economical sources of raw material is extremely attractive. Environmental protection measures have also come to play an increasingly important economic role in iron manufacture in recent years.

Careful organization and quality control on the input side of pig iron production is also important with respect to the properties of the principal end product—steel—and consequently on the market picture as it relates to steel vs. alternative materials. Economic factors and quality are therefore closely linked.

Several recent developments deserve special mention as determinants of the competitiveness of steel, especially from the standpoint of cost reduction:

- Increased emphasis on major sources of ore displaying a high iron content, a consideration which helps to minimize fluctuations in ore quality.
- Significant improvement in the facilities for handling and transporting ore in increasingly large unit amounts. Intercontinental marine ore transport today involves units as large as 350 000 dwt (i.e., dead weight), representing a three-fold increase in maximum load in the course of 20 years.
- Steady improvement in the preparation of the furnace charge in terms of ore classification, sintering, and pelleting. For example, the use of lump ore has decreased in Germany from 35% in 1970 to < 10% currently. Sinter input, on the other hand, has increased to 60%, and pelletized ore—virtually unknown before 1965—now represents 30% of the charge (Figure 5.100).
- Significant reduction in fuel consumption and more variety in the nature of the fuel employed for reduction.

Fuel consumption has dropped by a total of ca. 20% over the last 20 years, now amounting to only 480 kg per tonne of pig iron. Coke continues to constitute the major source of fuel (415 kg/t), although since about 1986 inexpensive coal has increasingly been used as a coke substitute (40 kg/t). Petroleum fuel currently accounts for ca. 25 kg/t.

By far the largest part of the pig iron output goes into steel production: ca. 91×10^6 t (97%) in the case of the EEC with an additional 2×10^6 t consumed by foundries. About 0.7×10^6 t in the form of spiegel eisen and high-carbon ferromanganese are being used for the production of alloyed steel.

In Europe essentially no open market exists for basic pig iron, because the steel industry is effectively self-supporting. Iron of this type is purchased only rarely and in times of shortage, as when demand is particularly strong or some industrial mishap causes supply problems. By contrast, there is a lively trade in such products as foundry iron, hematite iron, and spherical pig iron. The list price of foundry iron, for example, remained steady in the range of

55–75\$/t for nearly 20 years. It finally began to climb at the time of the 1974 oil crisis as a result of increasing energy prices, subsequently reaching a level of 190–260\$/t.

The largest exporter of pig iron, and by a wide margin, is Brazil at 2×10^6 t/a, followed by Canada and Germany with ca. 0.5×10^6 t/a each (Table 5.42) [169].

Sponge Iron. The direct reduction process (see Section 5.10) has recently provided the market with a new form of pig iron: sponge iron, available in significant quantity since the 1970s and produced from lump ore or pellets. Current world output of sponge iron is estimated at 14×10^6 t/a.

Table 5.42: Development of import and export of pig iron (worldwide).

Country	1981	1982	1983	1984	1985	1986	1987	1988
Import^a								
EEC ^b	1550	1672	1430	1541	1698	1885	1906	2363
Germany	285	303	279	295	348	379	364	324
Belgium/Luxembourg	172	132	89	135	160	159	182	309
Denmark	52	66	31	38	61	77	79	113
France	435	399	385	447	505	413	424	325
United Kingdom	148	165	168	102	124	148	119	233
Ireland	1	2	1	1	1	1	1	3
Italy	348	437	319	400	335	475	530	745
Netherlands	51	50	39	64	62	61	60	72
Greece	17	14	17	7	14	25	21	
Spain	41	104	102	52	88	147	126	8
Austria	95	89	51	66	67	52	42	62
Sweden	64	83	61	64	69	77	62	25
Switzerland	65	74	72	71	78	42	34	46
Former Czechoslovakia	843	901	780	745	869	809	717	685
Japan	1068	1337	952	777	604	921	1443	2917
United States	857	633	456	925	307	603	378	811
Poland	1449	1273	1135	1188	1354	1323 ^c	1338	
Hungary	291	235	295	281	321	255	263	
Former Yugoslavia	71	99	65	75	57	57 ^c	27	
Export^a								
EEC ^b	1420	1013	996	1145	1281	690	697	713
Germany	821	622	497	590	705	542	540	464
Belgium/Luxembourg	19	17	16	27	26	23	30	38
Denmark		1						
France	538	332	389	475	451	12 ^d	54	55
United Kingdom	35	31	60	34	59	33	43	31
Ireland			2			1		
Italy	1	3	22	10	22	61	20	37
Netherlands	6	5	12	9	18	18	10	4
Norway	280	213	183	160	212	185	191	134
Austria					1	1	7	
Sweden	45	30	27	3	7	10	3	12
Australia	158	300	350	150				
Japan	12	61	341	285	1083	1058	51	30
Canada	523	526	389	449	654	602	523	388
United States	33	59	14	61	40	50	53	70
Hungary			5	21				
Brazil	714	693	1801	2473	2476	2369	2445	2532

^aPig iron including spiegel iron and blast furnace ferromanganese.

^bIncluding internal exchange, 1988 without Greece.

^cPreliminary.

^dExport not totally broken down because of security reasons.

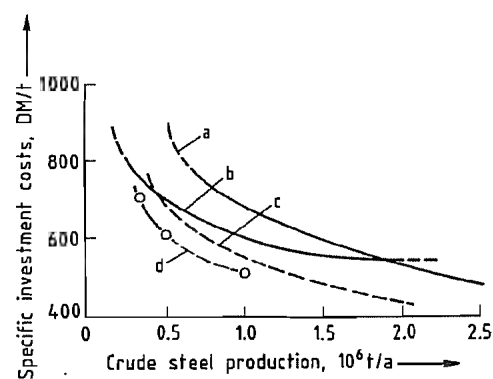


Figure 5.101: Specific investment costs for steel mills based on coal.

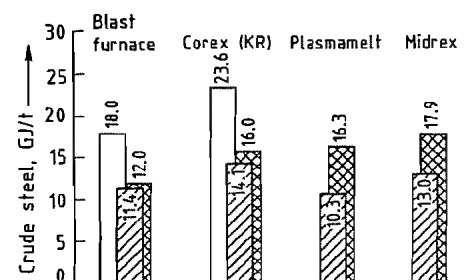


Figure 5.102: Comparison of specific gross energy consumption (□), net energy consumption (▨), and consumption of primary energy referred to net energy (▤) for different production processes (for the production of 1 t of crude steel based on ore).

This newer production method represents a significantly more economical route to pig iron than that involving coke when alternative forms of energy are available in abundance (e.g., natural gas, as in the case of Indonesia, Malaysia, the Middle East, Mexico, and Venezuela). Indeed, sponge iron can often be produced for 120\$/t under appropriate conditions, and most of the direct reduction facilities currently in operation are located in the regions cited [170].

Sponge iron is devoid of elemental silicon and phosphorus, and it contains only little carbon i.e., it lacks any source of energy for the subsequent conversion to steel. In this sense it is comparable to steel scrap, and it is highly priced as a charge for electric furnaces where these can be operated economically.

Alternative Production Methods. So far, no other alternative routes to iron manufacture have achieved any significance. The current trend in technical innovation is suggested by the Corex method utilizing a melter-gasifier which was developed in Germany and first introduced in South Africa in 1988. One important advantage of the process is a significant reduction in environmental pollution, and it also avoids the expensive construction of coking pelletizing, and sintering facilities. The potential cost saving has been estimated at as much as 30%.

Size of the Production Facility. One way of classifying the various manufacturing methods is in terms of dimension (scale, capacity). For example, *blast furnaces* today may be as large as 15 m in diameter, with a working volume of 5580 m³ (Cherepovets, Novolipetsk). Nevertheless, massive facilities such as these are not always optimal from an economic standpoint, nor do they necessarily match the needs in a given situation. Local factors and a desire for flexibility may well dictate smaller units. Thus, the average blast furnace in Japan has a diameter of 12 m, while in Germany 9 m is more typical.

For technical reasons, *direct reduction* facilities are much smaller, with a typical maximum annual output of 600 000 t. The first *smelting reduction* Corex units are currently producing only ca. 300 000 t/a.

Lower investment costs are responsible for the fact that smaller steel mills in particular (i.e., those with an annual output < 1 × 10⁶ t) tend to utilize a direct-reduction or smelting-reduction iron process (Figure 5.101) in contrast to the blast furnaces at larger integrated steel mills, where the *lower fuel consumption* associated with a conventional blast furnace is the decisive factor [171] (Figure 5.102).

The principal economic factors addressed here with respect to iron intended as a precursor to steel—performance of the production unit, investment costs, energy consumption, advantages of scale—all suggest that the blast furnace will continue to retain its primacy over the long term. Only where unusual local

conditions favor other sources (through cheap sources of energy or limited demand) is the otherwise efficient and economical blast furnace likely to be displaced.

5.14 Pure Iron [172, 173]

The pure metal is not often encountered in commerce, but is usually alloyed with carbon or other metals. Chemically pure iron can be prepared either by the reduction of pure iron oxide (best obtained for this purpose by heating the oxalate in air) with hydrogen, or by the electrolysis of aqueous solutions of iron(II) salts, e.g., of iron(II) ammonium oxalate. On the technical scale, pure iron is prepared chiefly by the thermal decomposition of iron pentacarbonyl. The so-called "carbonyl iron" prepared in this way initially contains some carbon and oxygen in solid solution. These impurities can be removed by suitable after treatment.

Table 5.43: Some physical properties of iron.

Density at 20 °C, g/cm ³	7.874
Thermal expansion coefficient at 20 °C	11.7 × 10 ⁻⁶
Lattice constant, cm	2.861 × 10 ⁻⁸
Melting point, °C	1539
Boiling point, °C	≈ 3200
Temp. of α, γ transformation (A ₃) on heating, °C	910
Temp. of γ, δ transformation (A ₄) on cooling, °C	1400
Resistivity at 20 °C, Ωcm	9.7 × 10 ⁻⁶
for commercial iron	11 × 10 ⁻⁶
Temperature coefficient of resistance	0.0065
Compressibility, cm ² /kg	0.60 × 10 ⁻⁶
Specific heat, cal g ⁻¹ K ⁻¹	0.105
Heat of fusion, cal/g	64.9
Heat of α, γ transformation, cal/g	3.86
Heat of γ, δ transformation, cal/g	1.7
Linear correction at α, γ on heating	0.0026
Linear correction at γ, δ on heating	0.001–0.003
Modulus of elasticity, lb/in ²	30 × 10 ⁶
dynes/cm ²	21 × 10 ¹¹
Modulus of rigidity, lb/in ²	12 × 10 ⁶
Proportional limit for annealed iron, lb/in ²	19 × 10 ³
Tensile strength, lb/in ²	25–100 × 10 ³
Brinell hardness number (annealed)	50–90

Pure iron is a lustrous, rather soft metal (hardness 4.5). Some of its physical properties are given in Table 5.43. Iron is ferromagnetic, i.e., it is strongly magnetized when placed in a

magnetic field. Unlike iron which contains carbon, pure iron has a very low remanence, i.e., it instantly loses its magnetization when the applied electric field is removed. For this reason it finds certain applications in electro-technology, e.g., for electric motors and transformers, in which rapid fluctuations must occur in the magnetism of an iron core. In the solid state, iron can have several allotropic forms depending primarily on its temperature. These are:

- **α-Iron:** magnetic and stable to 768 °C, crystallizes in a body centered cubic lattice, i.e., iron atoms are arranged at the centre and the apexes of unit cubes. It dissolves very little carbon (0.025% at 721 °C). Alpha iron with the carbon traces dissolved in it is called *ferrite*.
- **β-Iron:** it is a form stable between 768 and 910 °C. It is alpha iron that has lost its magnetism. It does not dissolve carbon.
- **γ-Iron:** this form is stable between 910 and 1390 °C. The crystallographic appearance is a face centered cubic lattice, i.e., iron atoms are arranged at the apexes and centers of the sides of unit cubes. It is nonmagnetic and dissolves 2% carbon at 1102 °C. Gamma iron with carbon in solution is called *austenite*.
- **δ-Iron:** the last of the allotropic forms, it is nonmagnetic and stable between 1391 and 1537 °C, melting point. The crystallographic arrangement is in the form of a body-centered cubic lattice.

The physical properties of iron are changed by the presence of foreign elements (metalloids or metals) in very small amounts.

Iron has a great affinity for oxygen. It rusts in moist air, i.e., the surface gradually becomes converted into iron oxide hydrate. Compact iron reacts with dry air only above 150 °C. When heated in air it forms the intermediate oxide, Fe₃O₄, which is also formed during the forging of red hot wrought iron. In a very finely divided state — such as is obtained, for example, when iron oxalate is heated in hydrogen — iron is pyrophoric.

Iron objects are protected from rusting by covering them with coatings of other metals (e.g., zinc, tin, chromium, nickel) or with paint (red lead). A particularly effective protection from rust can be achieved by converting the iron superficially to iron(II) phosphate ("phosphatizing"). This is done by treatment with a solution of acid manganese or zinc phosphate, $Mn(H_2PO_4)_2$ or $Zn(H_2PO_4)_2$. Iron dissolves in dilute acids with the evolution of hydrogen and the formation of iron(II) salts. The normal potential of iron in contact with iron(II) salt solutions is +0.440 V at 25 °C, relative to the normal hydrogen electrode. If iron is dipped into a copper sulfate solution, it becomes covered with metallic copper:



At ordinary temperature, iron is hardly attacked by air-free water. If air has access, however, the porous iron(III) oxide hydrate is formed, and corrosion goes on continuously as a result. Concentrated sodium hydroxide attacks iron, fairly strongly, even in the absence of air, especially at high temperatures, since the $Fe(OH)_2$ goes into solution through the formation of hydroxo salts.

Iron combines energetically with chlorine when heated, and also with sulfur and phosphorus, but not directly with nitrogen. It has a strong tendency, however, to unite or alloy with carbon and silicon. These alloys are most important for the properties of technical iron. Oxygen is dissolved by molten iron, as FeO ; some of this is retained in solid solution on cooling (δ -iron can dissolve up to 0.12%, α -iron only up to 0.04% of O in solid solution). The oxygen content of iron reduces its workability when hot. Nitrogen is absorbed from the air by molten iron only in minimal amounts. However, if iron is heated in ammonia gas, an iron-nitrogen compound, Fe_3N , is formed, which displays a considerable solubility in solid iron, and confers great hardness. This property is utilized in the surface-hardening of iron articles, by heating them in ammonia (nitriding process). In addition to the foregoing, there is a second compound, Fe_4N , with a rather narrow range of homogeneity.

Above 660 °C, this is transformed without change of composition into crystals of Fe_3N , in which only one half of the available lattice positions are occupied by nitrogen atoms.

Hydrogen is also absorbed by iron at a red heat. The amount absorbed is small, and is proportional to the square root of the pressure. Electrolytic iron, however, may contain larger amounts of hydrogen, which make it hard and brittle. The hydrogen is driven off on heating, and the iron then becomes ductile.

5.15 Iron-Carbon System

A variety of textural constituents can be distinguished in solidified iron containing carbon. The most important are the following:

Austenite, a solid solution of carbon in iron (more precisely, in γ -iron). The formation of austenite depends on the fact that carbon atoms can take up positions at the center and in the middle of the cell edges of the unit cube of γ -iron (Figure 5.103). If these sites were occupied in every unit cell, a compound FeC , with 50 atom% C, would be produced. However, the crystal lattice of austenite is stable only below 8 atom% C. The C atoms thus built into the crystal lattice distribute themselves statistically between the cell centers and cell edges, and austenite has the characteristics of a "solid solution". The crystal lattice of γ -iron is expanded uniformly in all directions by the incorporation of the C atoms, but the expansion is small.

Martensite, a metastable conversion product of austenite, formed by rapid cooling, can be regarded as a (supersaturated) solid solution of carbon in α -iron. Like all supersaturated solutions, it is unstable (or metastable). As shown in Figure 5.103, only a fraction of the sites available for C atoms is occupied in the martensite structure also. If all lattice positions were occupied, a compound FeC would result in this case also. As compared with the α -iron structure, the crystal lattice of martensite has undergone tetragonal distortion; it is stretched in one direction, and contracted a little in the two others.

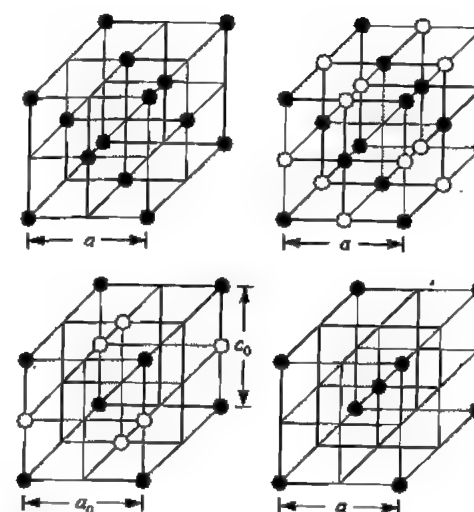


Figure 5.103: Detailed structure of the textural constituents in iron-carbon system. γ -iron: $a = 3.59$ Å (extrapolated to room temperature); austenite: $a = 3.63$ Å (for 8 atom% C); martensite: $a_0 = 2.84$, $c_0 = 3.00$ Å (for 6 atom% C); $\alpha(\delta)$ -iron: $a = 2.86$ Å.

Cementite, a compound of iron and carbon, Fe_3C (contains 6.68% C), has a considerably more complex structure; the Fe atoms form prisms, with the C atoms located at their midpoints.

Ledeburite, an eutectic mixture of cementite with austenite (saturated with carbon). An eutectic is formed by the cooling of a melt.

Pearlite, an eutectoid mixture of ferrite and cementite. An eutectoid is applied to a mixture which is formed in the solid state.

Figure 5.104 represents the phase diagram of the iron-carbon system up to a content of 5% by weight of C. The melting point of iron is first lowered by the addition of carbon, from A to E, and is then raised again with further increase of carbon content. The eutectic point E corresponds to 4.2% C, and a temperature of 1140 °C. A melt of iron containing 4.2% of carbon solidifies in the form of ledeburite. From melts with a lower carbon content, mixed crystals of γ -iron with carbon (austenite) first separate. The mixed crystals have a lower carbon content than the melt, so that a melt having the composition corresponding to the point b on the liquidus curve AE is in equi-

librium with mixed crystals having the composition given by the point a on the solidus curve AC. The melt is thus enriched in carbon through the deposition of austenite. At the same time, the concentration of carbon in the austenite deposited rises continuously until, at the point C, with a carbon content of 1.7% C, this phase is saturated with carbon. The melt has then reached the point E, and the remaining melt solidifies as ledeburite.

Melts containing up to 1.7% of carbon therefore yield only austenite, and those with a higher content (up to 4.2%) give ledeburite as well. Austenite, however, is only stable at high temperatures. When the alloy is slowly cooled, it undergoes transformation into a mixture of ferrite and pearlite, at temperatures between F (the transformation temperature of γ -iron into δ -iron) and H (or D), depending on its carbon content (G is the transformation temperature of δ -iron into α -iron). Martensite, which is characterized by its extreme hardness, is formed as an intermediate product in this transformation, and persists at ordinary temperature if cooling is effected rapidly ("quenching"). Under microscopic examination on a polished section, martensite stands out clearly in the form of dark needles from the light, not yet transformed austenite.

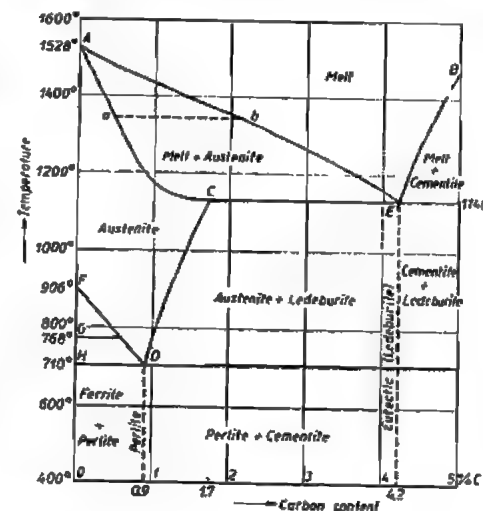


Figure 5.104: Phase diagram of iron-carbon alloys (simplified).

On passing to a melt with more than 4.2% of carbon, cementite, Fe_3C , first separates on rapid cooling. When the carbon content of the residual melt has thereby been reduced to 4.2%, the rest solidifies as ledeburite. If cooling is allowed to take place slowly, however, graphite crystallizes out, for the most part, in place of cementite. This is because, at temperatures below the melting point, a mixture of iron and graphite is more stable than a mixture of iron and cementite. Hence the latter is slowly converted into the former at about 1000 °C. As a result of this transformation within the solid alloy, the graphite is deposited in an extremely finely divided state ("temper carbon"). This fact, as already mentioned, is taken advantage of in malleabilizing.

5.16 Technical Varieties of Iron

Ordinary technical iron contains silicon, manganese, and other impurities, as well as carbon, and the properties of the iron-carbon alloys may be modified to a considerable extent by these other constituents. Thus silicon represses the formation of cementite and favors the deposition of graphite, whereas manganese acts in the opposite manner. The influence of silicon, manganese, etc. on the range of existence of the various modifications of iron, becomes practically important only when these elements are present in considerable concentration, as in the special steels.

Pig Iron or Cast Iron. This is iron which contains more than 2.3%, and usually 5–10% of foreign constituents, with a carbon content of 2–5%. It melts without previous softening, and therefore cannot be forged, but it casts well, since it fills the molds sharply. The melting point of pig iron lies between 1100 and 1200 °C. Pig iron is brittle at ordinary temperature. Ordinary grey cast iron contains the carbon chiefly in the form of graphite (typically 0.9% "combined carbon", 2.8% graphite). White cast iron, contains its carbon essentially as cementite (e.g., 3% "combined carbon",

0.1% graphite). Since it is harder and more brittle than grey cast iron, it is less suitable for castings (except for malleable cast iron), and is used almost exclusively as raw material for the production of malleable iron.

Malleable iron has a lower carbon content than pig iron, and contains fewer impurities. The carbon content is usually between 0.04 and 1.5%. Malleable iron melts at a higher temperature than pig iron. It softens gradually at high temperatures, and can therefore be forged and welded, as well as rolled or stretched into wires.

Soft Iron. This iron contains 0.5% of carbon at the most. It is tough and relatively soft, and can therefore be worked particularly well. It approaches pure iron in its properties, but differs from the latter in that, when magnetized, it loses its magnetism with a greater or less delay (hysteresis).

Steel. Steel has a higher carbon content than soft iron — usually between 0.5 and 1%. It can be forged and welded less readily than soft iron. It is also harder than the latter, and not tough but elastic at ordinary temperature. The most important characteristic of steel is that it may be hardened. If it is heated to bright redness, and suddenly cooled (by plunging it into water or oil), it becomes extraordinarily hard and brittle. The brittleness can be removed without any reduction in hardness, by "tempering" the steel — that is, by heating it carefully for a short time to a moderately high temperature (250–300 °C).

The possibility of hardening steel is based on the fact that iron-carbon alloys with a carbon content below 1.7% can be converted into austenite by heating them. When this is suddenly cooled ("quenched") it passes over, partially or completely, into the very hard martensite. As follows from the phase diagram (Figure 5.104), the temperature necessary for hardening varies, according to the carbon content of the steel. It is usually about 900 °C. The effect of tempering is to release or diminish the internal strains that result from quenching.

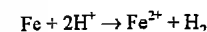
If, in course of tempering, the temperature is raised higher, so that pearlite begins to separate out in a state of very fine subdivision, the hardness decreases to some extent but the tensile strength is increased. It is essential, however, that the heat treatment should not be continued so long that the martensite decomposes completely into pearlite, as the hardness and strength would then be lost once more.

5.17 Compounds

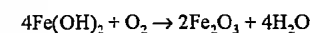
5.17.1 General

5.17.1.1 Ferrous Compounds

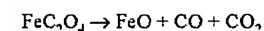
When iron is dissolved in nonoxidizing acids such as hydrochloric or dilute sulfuric, solutions containing ferrous ion are obtained.



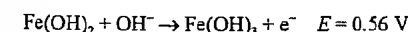
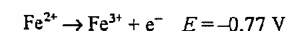
When a solution of a pure ferrous salt is treated with an alkali hydroxide, a white, gelatinous precipitate of ferrous hydroxide, $\text{Fe}(\text{OH})_2$, is formed. In the presence of air, ferrous hydroxide quickly turns green, and then slowly becomes reddish-brown as it is oxidized to hydrous ferric oxide.



Because of this fact it is difficult to obtain pure white ferrous hydroxide, and ferrous oxide, FeO , is prepared by the thermal decomposition of ferrous oxalate:



rather than by the dehydration of ferrous hydroxide. Solutions containing ferrous ion have a pale green color. In the presence of air, ferrous ion is slowly oxidized to ferric. This oxidation takes place much more readily in alkaline than in acidic solution, as is indicated by the standard potentials for the following half-reactions:



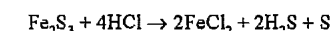
The most important ferrous compound is the sulfate, which crystallizes from aqueous solution as the heptahydrate, $\text{FeSO}_4 \cdot 7\text{H}_2\text{O}$.

Because of the ease with which ferrous compounds are oxidized, particularly in alkaline solution, ferrous sulfate is widely used in chemical industry and in the laboratory as a reducing agent.

When equimolar proportions of ferrous sulfate and ammonium sulfate are brought together in aqueous solution, and the solution is evaporated until crystallization takes place, a double salt of the formula $(\text{NH}_4)_2\text{SO}_4 \cdot \text{FeSO}_4 \cdot 6\text{H}_2\text{O}$, known as Mohr's salt, is obtained. In the solid state, Mohr's salt is not oxidized by the air, and it is useful, therefore, as a dependable source of ferrous ion free from ferric.

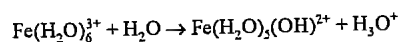
The ferrous halides are most readily prepared by the action of solutions of the corresponding hydrogen halides upon metallic iron. The chloride crystallizes as the green hydrate $\text{FeCl}_2 \cdot 4\text{H}_2\text{O}$ when its solution is evaporated out of contact with the air.

Ferrous sulfide, FeS , is obtained either by direct union of iron and sulfur or by the action of hydrogen sulfide on neutral or basic solutions of ferrous ion. The black precipitate of FeS obtained in this reaction is readily soluble in even weakly acidic solutions. A black precipitate is obtained by the action of S^{2-} ions on iron(III) salt solutions. This is practically insoluble in water, but is soluble in dilute acids, and has a composition corresponding to the formula Fe_2S_3 . It decomposes readily in air when it is moist, with the formation of iron oxide hydrate and the deposition of sulfur. Sulfur is also deposited when the precipitate is treated with hydrochloric acid:



5.17.1.2 Ferric Compounds

The iron atom has only two electrons in its outer (4s) shell. It may, however, lose or share in addition an electron from the incomplete 3d subshell, thereby attaining an oxidation state of 3+. Solutions of many ferric salts contain the hydrated ferric ion, $\text{Fe}(\text{H}_2\text{O})_6^{3+}$. Because of the small size and high charge on the ferric ion, the hydrated ion reacts with water to give acid solutions.



When solutions of ferric salts are boiled, basic ferric salts or hydrous ferric oxide may be precipitated. The yellow color of solutions of ferric salts is due to complex hydrated ions or to colloidal hydrous ferric oxide. When a solution of a ferric salt is treated with ammonia, or with a soluble hydroxide, a red-brown gelatinous precipitate of hydrous ferric oxide is obtained which readily goes into the colloidal condition. Since its composition varies with the method of preparation. It is best represented as $\text{Fe}_2\text{O}_3 \cdot x\text{H}_2\text{O}$. Hydrous ferric oxide does not dissolve in basic solutions.

When hydrous ferric oxide is strongly heated, it loses all its water and yields the anhydrous oxide, Fe_2O_3 . This oxide exists in a number of crystalline modifications, the particular form depending upon the method by which it is obtained. As the mineral hematite, ferric oxide occurs in large quantities in the earth's crust. Finely divided ferric oxide obtained by the burning of pyrite is used as a red pigment or as a mild abrasive under the names of Venetian red. When ferric oxide is heated to a very high temperature, or when iron burns in oxygen or is heated in steam, ferroxoferric oxide, Fe_3O_4 , is obtained. This compound occurs naturally as the ore called magnetite, some samples of which are highly paramagnetic and are known as lodestones. This oxide may also be regarded as ferrous ferrite, and its formula accordingly may be written $\text{Fe}(\text{FeO})_2$.

The most important salt of ferric ion is ferric chloride. It is a true salt only when hydrated; the physical properties of the anhydrous form indicate that it is covalent. Anhydrous ferric halides are obtained by the passage of a current of the corresponding halogen gas over heated iron. Under these conditions, ferric chloride, for example, crystallizes in black crystals in the cold parts of the tube. The density of the vapor formed when these crystals are volatilized (280 °C) indicates that the compound is Fe_2Cl_6 . Anhydrous ferric chloride dissolves readily in water to yield a yellow solution of the hydrated com-

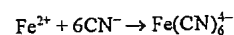
pound. Several solid hydrates are obtainable, the most familiar being $\text{FeCl}_3 \cdot 6\text{H}_2\text{O}$.

On evaporation of solutions containing equimolar proportions of ferric sulfate and the sulfate of an alkali metal or ammonium, violet-colored ferric alums are obtained, e.g., $(\text{NH}_4)_2\text{SO}_4 \cdot \text{Fe}_2(\text{SO}_4)_3 \cdot 24\text{H}_2\text{O}$. Ferric nitrate, also, may be obtained in violet-colored crystals, having the formula $\text{Fe}(\text{NO}_3)_3 \cdot 9\text{H}_2\text{O}$.

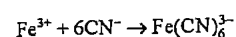
5.17.1.3 Complex Compounds

Iron in both the 2+ and 3+ oxidation states forms many complex compounds. Of these, the complex cyanides, because of their high stability, are particularly important.

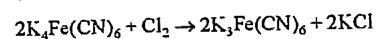
When solutions containing ferrous ion are treated with an excess of cyanide ion, the pale yellow complex ferrocyanide ion is obtained. This ion is so stable that solutions of ferrocyanides have none of the properties either of ferrous or of cyanide ion:



The most familiar ferrocyanides are the readily soluble sodium and potassium salts, $\text{Na}_4\text{Fe}(\text{CN})_6 \cdot 10\text{H}_2\text{O}$ and $\text{K}_4\text{Fe}(\text{CN})_6 \cdot 3\text{H}_2\text{O}$. Likewise, when solutions containing ferric ion are treated with an excess of cyanide ion, the very stable red ferricyanide complex is obtained:



The most important ferricyanide is the potassium salt $\text{K}_3\text{Fe}(\text{CN})_6$, which is obtained industrially by the oxidation of the ferrocyanide with chlorine:



These complex cyanide ions form precipitates with a number of metal ions and are therefore useful in analytical chemistry. When a solution of a ferrocyanide reacts with a soluble ferric salt, a dark blue precipitate of complex structure, called Prussian blue, is obtained. Likewise, when a solution of a ferricyanide is treated with a soluble ferrous salt, a complex dark blue precipitate known as Turnbull's blue is obtained. The compositions of these precipitates vary considerably with the

conditions under which the reaction is carried out. The important fact, however, is that ferrous ion reacts with ferricyanide ion to give a dark blue precipitate, whereas ferric ion reacts with ferrocyanide ion to give a precipitate of practically identical color. On the other hand, pure ferrous ion forms a white precipitate with ferrocyanide ion, and ferric ion reacts with ferricyanide ion to yield a brown solution containing a complex of unknown composition. These reactions provide a convenient method for testing for ferrous and ferric ions and for distinguishing between them.

The addition of a solution containing thiocyanate ion, SCN^- , to a solution containing ferric ion produces a deep red color. More than one colored complex ion is formed but in each of these complexes, thiocyanate ions are coordinated to the ferric ion. This reaction constitutes a very sensitive test for ferric.

5.17.2 Iron(II) Sulfate

Properties. Iron(II) sulfate heptahydrate, ferrous sulfate, copperas, green vitriol, $\text{FeSO}_4 \cdot 7\text{H}_2\text{O}$, *mp* 64 °C, *p* 1.898 g/cm³, crystallizes from aqueous solution as green, monoclinic crystals, which are readily soluble in water and glycol but insoluble in alcohol, acetone, and methyl acetate. On being heated to 60–70 °C, 3 mol of water is driven off to form the tetrahydrate, $\text{FeSO}_4 \cdot 4\text{H}_2\text{O}$. In the absence of air, at ca. 300 °C, iron(II) sulfate monohydrate, a white powder, is formed. When heated to ca. 260 °C in the presence of air, the monohydrate is oxidized to iron(III) sulfate. Decomposition of iron(II) sulfate begins at about 480 °C. Iron(II) sulfate is efflorescent in dry air. In moist air, the surface of the crystals becomes covered with brownish basic iron(III) sulfate. Aqueous solutions of iron(II) sulfate are slightly acidic due to hydrolysis. The rate of oxidation by air increases in alkaline solution and on raising the temperature. Iron(II) sulfate reduces copper(II) ions to copper(I) ions and gold or silver ions to the corresponding metal. With univalent cations (e.g., K, Rb, Cs, NH_4 , and Tl) and divalent cations (e.g., Cd, Zn, Mn, and Mg), double salts (alums) are

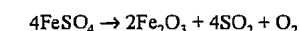
readily formed; an example is Mohr's salt, iron(II) ammonium sulfate, $\text{FeSO}_4(\text{NH}_4)_2\text{SO}_4 \cdot 6\text{H}_2\text{O}$. This green salt is soluble in water, easily purified, and more stable to oxidation than iron(II) sulfate heptahydrate.

Production. Iron(II) sulfate is produced by dissolving scrap iron in dilute sulfuric acid or by oxidizing moist pyrites in air.

Iron(II) sulfate is also obtained as a byproduct from steel pickling and from the production of titanium dioxide (sulfate process, with ilmenite as raw material). It is recovered from pickling liquors in a relatively pure form. The purity of iron(II) sulfate from the production of titanium dioxide depends on the source of the ilmenite. A typical composition is 87–90% $\text{FeSO}_4 \cdot 7\text{H}_2\text{O}$, 6–7% $\text{MgSO}_4 \cdot 7\text{H}_2\text{O}$, 0.6–0.7% TiOSO_4 , 0.2% $\text{MnSO}_4 \cdot 7\text{H}_2\text{O}$, 3–6% water, and depending upon the type of ilmenite used, traces of nickel, chromium(III), vanadium, copper, zirconium, and others.

Uses. Iron(II) sulfate is used for the preparation of other iron compounds. It is employed to a lesser extent in writing inks, wood preservatives, desulfurizing coal gas, and the production of Turnbull's blue, Prussian blue, and other iron pigments; as an etchant for aluminum; for process engraving and lithography; and as an additive to fodder.

As sensitivity to environmental protection increased, other uses had to be found for iron(II) sulfate, because the above mentioned applications did not consume the amounts available as a byproduct from industrial processes. Large amounts of iron(II) sulfate are used for the clarification of community effluents. With an additional clarification step, up to 90% of the phosphate in the effluent can be eliminated. Sludge formed in clarification tanks may be used as fertilizer [174–175]. Iron(II) sulfate can also be recycled. After drying to the monohydrate, it is decomposed in a calciner:



Sulfur dioxide is converted by the contact process to sulfuric acid [176]. The conversion of iron(II) sulfate to gypsum and iron(II) chloride

by treatment with calcium chloride has also been proposed. The iron(II) chloride is then decomposed to iron(III) oxide and hydrochloric acid [177]. To convert surplus iron(II) sulfate to a product that can be disposed on a dump site, it can be neutralized with one equivalent of calcium hydroxide. The conversion is reportedly 97% [178]. To regulate the setting characteristics of cement, gypsum can be replaced by iron(II) sulfate [179]. As an additive to cement, iron(II) sulfate can reduce the content of water-soluble chromates substantially [180]. Iron(II) sulfate solutions can be used to eliminate chlorine in waste gases [181]. Effluents containing cyanides and chromates may be decontaminated with iron(II) sulfate [182]. Iron(II) sulfate can be used to combat chlorosis, a disease of vines [179]. It is also used to treat alkaline soil and to destroy moss [179].

Toxicology. If swallowed, iron(II) sulfate can cause disturbances of the gastrointestinal tract. Ingestion of large quantities by children may cause vomiting, hematemesis, hepatic damage, and peripheral vascular collapse [183].

The acute oral toxicity (LD50) of iron(II) sulfate in the rat is 1389–2778 mg/kg, and the in rabbit, 2778 mg/kg [184].

5.17.3 Iron(III) Sulfate

Properties. Anhydrous iron(III) sulfate, ferric sulfate, $\text{Fe}_2(\text{SO}_4)_3$, is a yellowish-white solid. It dissolves in water, hydrolyzing at the same time, to yield a brownish solution. Basic iron(III) sulfate precipitates when the solution is boiled. With alkali metal (M) sulfates, iron(III) sulfate forms alums, $\text{M}^+\text{Fe}(\text{SO}_4)_2 \cdot 12\text{H}_2\text{O}$. Alums are almost colorless but normally have a violet tinge.

Production. Iron(III) sulfate is prepared by treating iron(II) sulfate with boiling concentrated sulfuric acid, or by evaporating a mixture of iron(III) oxide and sulfuric acid. Iron(III) sulfate solutions are produced industrially by injecting chlorine gas into an iron(II) sulfate solution [185]. The solution thus ob-

tained contains a mixture of iron(III) sulfate and iron(III) chloride.

Uses. Ferric sulfate is used to prepare alums and iron oxide pigments, and as a coagulant for the treatment of liquid effluents. Ammonium ferric sulfate is used for tanning. Solutions of iron(III) compounds are used to reduce the volume of sludge from effluent treatment plants. By using a mixture of iron(III) sulfate, iron(III) chloride, and calcium hydroxide it is possible to achieve a dry-matter content of the sludge, after filtration, of at least 35% [186].

5.17.4 Iron(III) Chloride

Iron(III) chloride, ferric chloride, is a by-product of some metallurgical and chemical processes, such as the chlorinating decomposition of iron-bearing oxide ores. Its ready availability and the cheap feeds used to produce it (iron and chlorine) have made iron(III) chloride, especially its aqueous solution, a significant feed stock for many industries, in particular, water treatment and the production of iron oxides or other iron compounds.

Properties. Iron(III) chloride, FeCl_3 , sublimation temperature ca. 305 °C, *bp* 332 °C [2.1]; ΔH_f° (25 °C) –399.67 kJ/mol [187], ρ (25 °C) 2.89 g/cm³ [188], is an almost black crystalline solid.

It is dimeric (Fe_2Cl_6) in the gas phase up to about 400 °C, dissociates at higher temperature, and is monomeric at 750 °C in the presence of excess chlorine. If chlorine is not present in excess, the compound decomposes to iron(II) chloride and chlorine above 200 °C [189].

Anhydrous iron(III) chloride has a hexagonal layer structure and forms dark, almost black, microcrystalline platelets with a metallic luster. The strongly hygroscopic crystals form a series of hydrates in humid air ($\text{FeCl}_3 \cdot x\text{H}_2\text{O}$, $x = 6, 3.5, 2.5, 2$) [190] and deliquesce on absorbing more moisture. The crystalline commercial product is iron(III) chloride hexahydrate, $\text{FeCl}_3 \cdot 6\text{H}_2\text{O}$, *mp* ca.

37 °C. It forms yellow crystals and occurs as $[\text{FeCl}_2(\text{H}_2\text{O})_4]^+\text{Cl}^- \cdot 2\text{H}_2\text{O}$.

Iron(III) chloride is very soluble in water: 430 g of FeCl_3 per kilogram of solution at 0 °C, 480 g/kg at 20 °C, and 743 g/kg at 40 °C [191]. The enthalpy of solution of anhydrous iron(III) chloride is 95 kJ/mol for the formation of a 40% solution at 20 °C. The aqueous solution is strongly acidic. If a solution of iron(III) chloride is diluted and neutralized slowly with alkali, $[\text{Fe}(\text{H}_2\text{O})_6]^{3+}$ is deprotonated to give yellow $[\text{Fe}(\text{OH})(\text{H}_2\text{O})_5]^{2+}$ and dimeric $[\text{Fe}_2(\text{OH})_2(\text{H}_2\text{O})_8]^{4+}$. Brown, colloidal $\beta\text{-FeOOH}$ is formed upon further neutralization; at higher temperature, iron hydroxide precipitates [192].

Iron(III) chloride is readily soluble in liquids having donor properties, such as alcohols, ketones, ethers, nitriles, amines, and liquid sulfur dioxide, but only sparingly soluble in nonpolar solvents such as benzene and hexane. The reaction of iron(III) chloride with hydrochloric acid or chlorides yields the tetrachloroferrates $[\text{FeCl}_4]^-$ and $[\text{FeCl}_4(\text{H}_2\text{O})_2]^-$. Because complexes are also formed with donor solvents, iron(III) chloride can be extracted from aqueous solutions in the presence of hydrochloric acid by using ether [193].

Iron(III) chloride is a strong oxidizing agent. Thus, many metals (for example, Fe, Cu, Ni, Pd, Pt, Mn, Pb, and Sn) are dissolved by aqueous iron(III) chloride, with the formation of iron(II) chloride; magnesium dissolves with evolution of hydrogen. Iron(III) chloride solution liberates carbon dioxide from alkali-metal carbonates. When iron(III) chloride is heated in air, iron(III) oxide and chlorine are produced. Above 200 °C, iron(III) chloride is rapidly reduced by hydrogen to iron. It is also reduced by coal.

Production. Anhydrous iron(III) chloride is produced industrially by reaction of dry chlorine with scrap iron at 500–700 °C [194]. The process is known as direct chlorination. Preheated scrap is charged into the top of a water-cooled iron shaft furnace, while chlorine (or a mixture of chlorine and nitrogen) is admitted at the bottom. To prevent formation of iron(II)

chloride, a 10–30% excess of chlorine is used. Iron scrap is added continuously at a rate depending on the reaction temperature and the amount of chlorine remaining in the exit gas. The iron(III) chloride vapor produced passes through water- or air-cooled condensation chambers. The crystals obtained are removed continuously from the walls by vibration or knocking. They are then ground, screened, and packaged with exclusion of moisture. Chlorine in the waste gas is removed either by scrubbing with iron(II) chloride solution, to give iron(III) chloride, or by reacting with sodium hydroxide solution, to yield sodium hypochlorite and sodium chloride.

In another process, carried out in a reactor with an acid-resistant liner, iron scrap and dry chlorine gas react in a eutectic melt of iron(III) chloride and potassium or sodium chloride (e.g., 70% FeCl_3 and 30% KCl) [195]. First, iron scrap is dissolved in the melt at 600 °C and oxidized to iron(II) chloride by iron(III) chloride. Iron(II) chloride then reacts with chlorine to yield iron(III) chloride, which sublimes and is collected in cooled condensation chambers.

The advantages of direct chlorination include higher space time yields, lower capital cost, and less waste. The melt process gives a purer product because impurities remain largely in the melt; however, for this reason the melt must be changed and disposed of frequently.

Iron(III) chloride solutions are prepared by dissolving iron in hydrochloric acid and oxidizing the resulting iron(II) chloride with chlorine. In a continuous, closed-cycle process, iron(III) chloride solution is reduced with iron and the resulting iron(II) chloride solution is reoxidized with chlorine. Iron(III) chloride solution is also produced by solving iron(III) oxide in hydrochloric acid. Solid iron(III) chloride hexahydrate is crystallized by cooling a hot concentrated solution.

Quality Specifications and Analysis. Commercial forms of iron(III) chloride include sublimed anhydrous iron(III) chloride ($\geq 99\%$ FeCl_3), iron(III) chloride hexahydrate (ca.

60% FeCl_3), and iron(III) chloride solution (ca. 40% FeCl_3). Iron(III) chloride for potable water treatment must comply with DIN 19602 (February 1987).

Trivalent iron is determined by iodometric titration with sodium thiosulfate; chloride ion is determined by argentometry.

Occupational Health. Iron(III) chloride irritates the skin and, especially, eyes. Therefore, workers handling it must wear protective glasses, facial protection, and rubber gloves. The TLV for iron(III) chloride is that for soluble iron salts: 1 mg of iron per cubic meter.

Storage and Transportation. Anhydrous iron(III) chloride can be stored in standard steel containers. It is shipped airtight in sheet-iron drums or plastic barrels, and loose in tank trucks. Moist iron(III) chloride and iron(III) chloride solutions attack ordinary metals. The following materials are suitable for containers to hold iron chloride solutions: rubberized steel; plastics such as polyethylene, poly(vinyl chloride), and polytetrafluoroethylene; fiber-reinforced plastics; glass; stoneware; porcelain; and enamel. The only suitable metallic materials are titanium, tantalum, and Hastelloy C.

The transport classification for anhydrous iron(III) chloride is UN No. 1773, RID-ADR Class 8.11c and for iron(III) chloride solution, UN No. 2582, RID-ADR Class 8.5c.

Iron(III) chloride spilled by accident must be collected and forwarded to a sewage plant for disposal. Contaminated soil must be cleaned with a large amount of water and neutralized with lime. Iron(III) chloride is a Class 1 hazard to water quality.

Uses. Anhydrous iron(III) chloride is used in organic chemistry as a chlorinating agent for aliphatic hydrocarbons and for aromatic compounds. It also acts as a catalyst in Friedel-Crafts syntheses and condensation reactions. Iron(III) chloride is also used occasionally as an oxidizing agent [196, 197].

Because solutions of iron(III) chloride dissolve metals such as copper and zinc without troublesome evolution of hydrogen, they are

used for the etching or surface treatment of metals (e.g., in the manufacture of electronic printed circuits, copperplate rotogravure printing, textile printing rolls), and for making signs. Iron(III) chloride solutions are also used in leaching the copper ore chalcopryrite.

Iron(III) chloride is used as a starting material in the preparation of other iron compounds, particularly oxides and hydroxides. However, most iron(III) oxide pigments obtained by hydrolysis of iron(III) chloride at high temperature have weak colors and a bluish cast, so these processes have not achieved commercial importance.

The largest use of iron chloride is in the form of dilute solutions that are employed as flocculating and precipitating agents in water treatment [198]. In processing surface waters into potable and process water, 5–40 g of iron(III) chloride is added to 1 m³ of crude water at pH 6–7. The precipitated iron(III) hydroxide adsorbs finely divided solids and colloids (e.g., clays and humic acids). If decarbonization or the precipitation of heavy metals is to be carried out at the same time, slaked lime is added to adjust the pH to 9–11.

In municipal and industrial wastewater treatment, iron(III) chloride is particularly effective because it precipitates heavy metals and sulfides, whereas contaminants such as oils and polymers, which are difficult to degrade, are adsorbed on the iron hydroxide flocs. Phosphates are also lowered to a level of ca. 1 mg of phosphorus per liter of water in the clarifier discharge. Preliminary treatment with iron(III) chloride can increase the capacity of overloaded clarifier plants.

Sludge conditioning with iron(III) chloride and lime improves the dewatering of filter sludge, so that drier sludges, better suited to disposal or incineration, are obtained.

Consumption of iron(III) chloride in the United States in 1994 was as follows [199]:

Sewage and wastewater treatment: 65%

Water treatment: 25%

Catalyst, etchant, and other: 10%

Solutions of iron chlorosulfate, FeClSO_4 , obtained by chlorinating iron(II) sulfate, are

also used extensively as flocculents in water treatment [201].

Economic Aspects. Of the few anhydrous iron(III) chloride producers worldwide, the most important in Europe is BASF. Most of the iron(III) chloride is obtained as a by-product when iron-bearing raw materials are chlorinated or when steels are pickled with hydrochloric acid; the major commercial form is the 40% solution.

Outputs (by year, as 100% FeCl_3) and major producers are

Europe (1994)	estimated 150 000 t (Solvay, Atochem, BASF, SIDRA)
USA (1994) [199]	200 000 t (Du Pont, PVS, Imperial West Chem.)
Japan (1987) [200]	322 000 t

The most important European producers of iron chlorosulfate are Kronos Titan and Thann et Mulhouse SA.

5.17.5 Iron(II) Chloride

Iron(II) chloride, ferrous chloride, is much less important industrially than iron(III) chloride. The etching of steel with hydrochloric acid yields large amounts of iron(II) chloride, which is chlorinated in solution or thermally decomposed to iron oxide and hydrochloric acid. A solution of iron(II) chloride is also obtained as a by-product from the chloride process for the production of titanium dioxide.

Properties. Iron(II) chloride, FeCl_2 , mp 677 °C, bp 1074 °C, ΔH_f° (25 °C) –342.1 kJ/mol, ρ (25 °C) 3.16 g/cm³, forms pale green, rhombohedral crystals which are readily soluble in water, alcohol, and acetone, but only sparingly soluble in ether and benzene. The compound occurs naturally as the mineral lawrencite. It forms several hydrates, $\text{FeCl}_2 \cdot x\text{H}_2\text{O}$ ($x = 1, 2, 4, 6$).

When heated in air, iron(II) chloride forms iron(III) chloride and iron oxides. Iron(II) chloride solution undergoes virtually no hydrolysis; it is oxidized readily by air.

Production. Anhydrous iron(II) chloride is produced from iron filings heated to red heat in a stream of hydrogen chloride or from iron and chlorine at 700 °C. The product is ob-

tained as a sublimable white mass. Iron(II) chloride can also be prepared by passing hydrogen over heated iron(II) chloride.

Solutions of iron(II) chloride are prepared by dissolving iron in hydrochloric acid or by reducing iron(III) chloride solutions with iron. When a hot saturated solution is cooled to 0 °C, pale green, monoclinic crystals of the hexahydrate are obtained; cooling to room temperature yields the blue-green tetrahydrate. If the solution is concentrated at 90 °C, the green dihydrate is obtained; above 120 °C or on vacuum evaporation, the dihydrate is converted to the monohydrate, $\text{FeCl}_2 \cdot \text{H}_2\text{O}$. In the absence of air, the monohydrate is converted to anhydrous iron(II) chloride at 230 °C [202].

Quality Specifications. Iron(II) chloride is sold as an anhydrous powder ($\geq 96\%$ FeCl_2), as the dihydrate ($> 75\%$ FeCl_2), as the tetrahydrate ($> 60\%$ FeCl_2), and as an aqueous solution (ca. 30% FeCl_2).

Transportation. Solid iron(II) chloride is shipped in sheet-iron drums, plastic bags, or glass containers, and its solution is transported in rubberized containers or plastic barrels.

Uses. Iron(II) chloride is used as a reducing agent and for the production of other iron compounds. Increasingly, iron(II) chloride solution serves as a precipitating and flocculating agent with reducing properties for use in water treatment; it is especially effective with wastewater containing chromate, for example.

Pure iron(II) chloride solution is an important starting material for the preparation of acicular goethite, $\alpha\text{-FeOOH}$, and lepidocrocite, $\gamma\text{-FeOOH}$, which are further processed to $\gamma\text{-Fe}_2\text{O}_3$ magnetic pigments. Pure iron(II) chloride is also employed in the preparation of pure iron.

5.17.6 Iron Pentacarbonyl

Metal carbonyls are complexes in which carbon monoxide is coordinated to the central metal atom. Of the iron carbonyls, only iron pentacarbonyl, $\text{Fe}(\text{CO})_5$, is economically significant.

M. BERTHELOT [203] and, independently, L. MOND and L. QUINCKE [204] discovered iron pentacarbonyl in 1891 [205]. Only after BASF had developed high-pressure technology for ammonia synthesis was its industrial production feasible. In 1925, a large plant was built in Germany by BASF to make iron pentacarbonyl which had proved to be a very effective antiknock agent for gasoline engines. When the compound was replaced shortly afterwards by lead alkyls, which were beneficial to motors, the production of iron powder from iron pentacarbonyl came to the fore.

In 1940, GAF began producing the pentacarbonyl in the United States under license from BASF. A BASF plant was moved to the Soviet Union in 1945. Plants built in England (1944) and France (1952) have ceased production. In addition to iron powder, BASF has been producing pure iron oxide from the carbonyl since about 1930.

Physical Properties. Iron pentacarbonyl is a clear, yellow, mobile liquid with an indistinctive odor. The molecule has a trigonal-bipyramidal structure [206].

Endothermic decomposition to iron and carbon monoxide begins at ca. 60 °C. Although decomposition becomes marked at the boiling point, iron pentacarbonyl can be distilled at atmospheric pressure with slight losses.

Some physical properties of iron pentacarbonyl are as follows:

<i>mp</i>	-20 °C
<i>bp</i>	103 °C
Critical temperature	285–288 °C
Critical pressure	2.90 MPa
Heat of fusion	69.4 kJ/kg
Heat of vaporization	190 kJ/kg
Specific heat (20 °C)	1.2 kJkg ⁻¹ K ⁻¹
Viscosity (20 °C)	76 mPa·s
Surface tension (20 °C)	0.022 N/m
Coefficient of linear expansion (20 °C)	0.00125
Refractive index (<i>n</i> _D ²⁵)	1.518
Thermal conductivity	0.139 Wm ⁻¹ K ⁻¹
Enthalpy of dissociation (vapor)	994 kJ/kg
Heat of combustion (to CO ₂ and Fe ₂ O ₃)	-8200 kJ/kg
Density, g/cm ³	
at 0 °C	1.495
at 20 °C	1.457
at 40 °C	1.419
at 60 °C	1.380

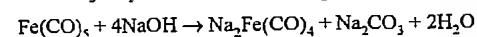
Vapor pressure, kPa	
at 20 °C	3.49
at 60 °C	21.33
at 100 °C	87.58

Iron pentacarbonyl is completely miscible with petroleum ether, hexane, benzene, pentanol and higher alcohols, ethyl ether, acetone, acetic acid, and ethyl acetate. It is partially miscible with paraffin oil and lower alcohols up to butanol [207].

Water solubility data for iron pentacarbonyl are contradictory; a value of 50–100 mg/L can be assumed [208]. The solubility of water in iron pentacarbonyl is 200–400 mg/kg.

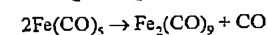
The most complete documentation on iron pentacarbonyl is given in [209]; for earlier literature, see [210].

Chemical Properties. Iron pentacarbonyl is an easily combustible substance. It does not react with water or with weak or dilute acids. With concentrated acids, the corresponding iron salts are formed with the evolution of carbon monoxide and hydrogen. Reactions with halogens yield iron halides. Iron pentacarbonyl also reduces organic compounds; for example, nitrobenzene is reduced to aniline; a ketone, to an alcohol; and indigo, to indigo white. The Hieber base reaction yields iron carbonyl hydride or its salts [212–216]:



The salt Na₂Fe(CO)₄ is a strong reducing agent.

Visible-light photolysis of pure iron pentacarbonyl or its solutions yields diiron nonacarbonyl, which precipitates as golden hexagonal platelets [217, 218]:



The trinuclear iron carbonyl Fe₃(CO)₁₂ is also known [219–224].

As a highly reactive and readily available compound, iron pentacarbonyl is used for the preparation of many complexes, but these are not very significant industrially [211].

The most important industrial reactions of iron pentacarbonyl are thermal decomposition in the absence of air, yielding iron powder and carbon monoxide, and combustion to iron(III) oxide, Fe₂O₃.

Table 5.44: Equilibrium data for the formation of iron pentacarbonyl.

<i>T</i> , °C	<i>P</i> _{CO} , bar	Fe(CO) ₅ , vol% (at equilibrium)	$K = \frac{P_{\text{Fe}}^5}{P_{\text{Fe}(\text{CO})_5}}$	
			Observed	Calculated
60	0.69	22.4	0.86	0.363
80	1.47	21.8	20.1	3.39
160	38.83	9.0	2.4×10^7	1.0×10^5
200	132.68	5.7	5.5×10^9	1.26×10^5

Production. Although nickel carbonyl can be obtained from nickel and carbon monoxide at atmospheric pressure and moderate temperature, the production of iron pentacarbonyl requires a pressure of 5–30 MPa, a temperature of 150–200 °C, and the presence of reactive iron.

Values reported for the reaction equilibrium are not in good agreement with those calculated [225–228]. Table 5.44 lists experimental data for the equilibrium constant along with values calculated from the Nernst approximation [228].

Even at high temperature and pressure, massive iron reacts sluggishly with carbon monoxide, so iron sponge, with its greater surface area, is used as starting material [229]. Better yields are said to be obtained with iron quenched and granulated from the melt and containing 2–4% sulfur [230], which has a catalytic action [231]. For the reaction kinetics, see [232].

The exothermic reaction



is carried out in high-pressure batch equipment with a vertical reactor charged with iron. The gas, circulated by a pump, is preheated and admitted to the reactor. It leaves the reactor hot and loaded with iron pentacarbonyl which is condensed in a heat exchanger and allowed to expand into the unpressurized purification system under low pressure. To maintain the pressure in the system, the carbon monoxide used is replaced with fresh gas. Most of this is obtained when the carbonyl is decomposed to iron powder. This closed operating cycle removes carbonyl from the reaction equilibrium [233].

Carbon monoxide pressure, temperature, and flow rate are controlled carefully throughout the batch to avoid spontaneous decomposition of carbon monoxide, which would result in a sharp temperature increase and the deposition of carbon black [234].

The liquid carbonyl contains some lubricating oil (from the pump), water, and iron dust. Depending on the starting material, volatile carbonyls of nickel, chromium, molybdenum, and tungsten may also be present. These are removed by distillation.

The batch process is rather expensive and requires inert gas purging at the beginning and end of each batch. Nonetheless, other approaches have not been implemented. In a wet process, carbon monoxide was reacted with solutions of iron(II) salts in aqueous ammonia at 11.5 MPa and 80 °C, giving iron pentacarbonyl in yields of 40–50% [235, 236]. A solution of iron(II) chloride in methanol containing a sulfur compound and Mn powder is said to form iron pentacarbonyl on reaction with carbon monoxide [237]. Another process uses three fluidized beds in series, for iron ore (e.g., hematite) reduction, high-pressure carbonylation, and carbonyl decomposition; however, the process has not been adopted commercially [238, 239].

Quality Specifications and Analysis. Commercial pure iron pentacarbonyl is brought to high purity by double distillation. The levels of contaminants, metals that form volatile carbonyls, and sulfur are at or below the threshold of detectability [208].

To test for trace contaminants, a sample is solidified by cooling, treated with excess bromine, and brought slowly to room temperature. After the reaction stops, the residue is dissolved in dilute nitric acid. Techniques suitable for analyzing the solution (e.g., for Cr, Ni, Mo, or Pb) are atomic absorption spectroscopy and emission spectroscopy with inductively coupled plasma. Iron pentacarbonyl can be analyzed in a similar fashion after being dissolved in concentrated nitric acid.

Iron pentacarbonyl in gases, including air, can be oxidized with a hydrogen peroxide

methanol mixture and analyzed as iron hydroxide [208]. Bromine water and concentrated nitric acid are also suitable as oxidizing agents. The exposure of individual workers to iron pentacarbonyl is measured using a personal air sampler, consisting of a charcoal-filled tube and a small battery operated gas pump. The iron pentacarbonyl is catalytically oxidized on the activated charcoal to give iron oxide, which can be determined as iron after combustion of the charcoal. The average content of iron pentacarbonyl in the air is then calculated.

Indoor air can be continuously monitored by radiometry with ionization detectors. Iron pentacarbonyl is atomized to an aerosol in a measuring chamber at 150 °C; the aerosol diminishes the ionization current generated by a radioactive source. The change in current is a measure of the carbonyl concentration. The detection threshold is ca. 0.1 ppm [240].

Gas chromatography with an electron-capture detector has been used to determine iron pentacarbonyl and nickel tetracarbonyl in synthesis gas. The limit of detection for nickel tetracarbonyl has been found to be 0.001 ppm and that for iron pentacarbonyl somewhat less [241].

Safety. Two potential hazards must be considered in relation to iron pentacarbonyl: toxicity and combustion. These can be controlled only if the product is handled in sealed equipment [208]. The fire hazard can be summarized as follows:

Flash point	< -15 °C
Ignition point	< 65 °C
Lower explosion limit	2.6–4.5 vol%

On substances with a high surface area, such as activated charcoal, ignition is possible even at room temperature.

Because the heat of combustion of iron pentacarbonyl is only one-fifth that of fuel oil, iron pentacarbonyl fires are easy to extinguish. The best extinguishing agent is water, which removes heat and forms an airtight cover. Water that has been used to extinguish fires must not be discharged into natural waters.

Iron pentacarbonyl burns completely to iron(III) oxide and carbon dioxide only when it is atomized with air. Open combustion (e.g., in a dish) does not go to completion, and carbon monoxide is formed.

The best protection against the occurrence of iron pentacarbonyl concentrations that might present a danger of poisoning or explosion is continuous air monitoring. Carbon monoxide alarms respond only at much higher, toxic concentrations.

Storage. At industrial plants, iron pentacarbonyl is stored and processed in the absence of air in metallic (usually steel) equipment. Suitable seals and fittings are recommended by the carbonyl producer [208].

In unpressurized tanks, the carbonyl is covered with a protective gas (CO, N₂, Ar, CO₂). Tanks are connected to a gas reservoir so that the pressure does not drop below atmospheric even when the tank is cooled.

When the product is stored in pressurized vessels, the liquid is withdrawn through a submerged tube, not through valves in the tank bottom.

Tanks and pumps are installed in liquid-tight collecting basins.

Cleaning of Equipment and Disposal. Process equipment can be cleaned before opening by flushing with steam and then condensing the iron pentacarbonyl and water.

Carbonyl residues are collected and reused whenever possible. Because of the density difference, the product can easily be separated from water.

Laboratory carbonyl residues can be collected in a bottle partly filled with water. Glassware is washed several times with a small amount of acetone, which is poured into water for phase separation.

Small amounts of iron pentacarbonyl can be disposed of by burning in a sheet-metal tub. The presence of carbon monoxide in the off-gas must be taken into account.

Transportation. Because of fire and toxicity hazards, stringent regulations apply to the

transportation of iron pentacarbonyl. Containers must be airtight and stable.

In Germany, the same regulations apply as in the case of nickel carbonyl. Both substances are assigned to Class 6.1, No. 3 under RID and GGVE for rail shipment, and under ADR and GGVS for road shipment. These regulations allow pressurized containers up to 250 L rated at 1 MPa. They are subject to inspection as pressure vessels (e.g., by TÜV) before being placed in service and at five-year intervals thereafter. The contents are limited to 1 kg of iron pentacarbonyl per liter of capacity. Every pressurized container must bear a nameplate with the following information: name of substance, owner, empty weight, year of first inspection and year of most recent inspection, inspector's stamp, maximum filling weight, and rated pressure.

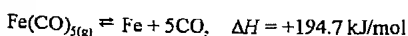
The largest producer of iron pentacarbonyl, BASF, sells it in 20- and 250-kg pressurized containers. Each container has two valves or a double valve, so that liquid can be withdrawn through a submerged tube.

Also used as nonreturnable packaging in Europe are 1-L pressurized aluminum bottles, with a rated pressure of 1 MPa and a filling weight of 1 kg.

For international shipment by sea, iron pentacarbonyl is classified as follows: UN No. 1994, Class 6.1, IMDG Code. Air shipment and mailing are forbidden.

Similar regulations now apply in the United States. Although iron pentacarbonyl is a Poison B, because of the risk of inhalation it must be packaged in gas containers under pressure as prescribed for a Poison A under DOT Hazardous Materials Regulations. The containers hold 300 pounds of carbonyl.

Carbonyl Iron Powder. By far the largest use of iron pentacarbonyl is for the production of carbonyl iron powder. The equilibrium reaction



goes from left to right at standard pressure above 200 °C. The iron deposited on hot surfaces is brittle hard, and not commercially us-

able. In hot liquids such as paraffin oil, finely dispersed iron is obtained [242]. The only process that has become industrially important is decomposition in cavity decomposers, which yields spherical iron particles of 1–10 µm diameter [243].

The decomposer is a pipe, externally heated by electricity or gas, into which iron pentacarbonyl vapor is admitted from the top. The carbonyl decomposes not on the wall, which is heated to > 300 °C, but on iron particles circulating in the gas stream. These particles grow to 3–8 µm and are then discharged along with the carbon monoxide generated. Carbon and oxygen produced by the decomposition of carbon monoxide are incorporated in the iron. Addition of ammonia reduces the carbon and oxygen content but leads to incorporation of nitrogen in the iron particles.

The cavity decomposer, invented by BASF in 1924, has not changed fundamentally. A variety of practices have been adopted to control the product, above all its particle size. Zinc particles are obtained by admitting oil vapor into the decomposer [244], by diluting the carbonyl vapor with recycled carbon monoxide gas [245], or by applying a temperature gradient from the top to the bottom of the decomposer [246]. Fine particles result if the rate of flow of iron pentacarbonyl is high; larger ones, if the rate is low [247]. Inlet velocity is also a factor [248].

Carbon, nitrogen, and oxygen can be largely eliminated from the iron powder by treatment with hydrogen at ca. 450 °C [249]. The spheres, which were previously very hard (Vickers Lardness 800–900), become soft (100–150 Vickers) and can be deformed by pressure. Hard and soft types are marketed for diverse applications [250].

Carbonyl iron powder is made into magnetic cores for electronic components [251, 252]. In powder metallurgy, pure iron and iron alloys are made into parts by pressing [253, 254] and by metal injection molding [255, 256], carbonyl iron powder being an important component of powders and feedstocks [257, 258]. Carbonyl iron powder is also employed for the fortification of foods such as

white bread and in the production of iron-containing pharmaceuticals. It is used as a reducing agent in organic chemistry, and is incorporated in rubber or plastic sheets that are used for microwave attenuation [259–261]. For preparation, use, particle-size distribution, and behavior on heat treatment, see [262–266].

Carbonyl Iron Oxide. Only BASF converts iron pentacarbonyl to iron oxides. The processes are harmless to the environment, because the only by-product is carbon dioxide, and no pollution of the wastewater with salts occurs, unlike when iron oxides are precipitated from solutions of iron salts.

Red iron oxide, in a finely divided form similar to carbon black, is obtained by atomizing iron pentacarbonyl and burning it in an excess of air [267]. By varying temperature and residence time in the reactor, transparent or highly transparent red pigments can be produced [268–270]. The highly transparent pigments are nearly X-ray amorphous and have BET surface areas of 80–160 m²/g. The less transparent grades have surface areas of 10–35 m²/g and clearly show a hematite structure. The iron oxide is used to make high-quality ferrites and similar ceramic materials. Because the content of other metals and electrolytes is extremely low and little energy is needed for dispersion, the oxide is particularly suitable for use as a lightfast, UV-blocking red pigment for paints, wood varnishes, fiber dyeing, and color printing.

Water injection [271] and passage through an intense centrifugal force field [272] during production improve both separation and compactibility.

Air oxidation of iron pentacarbonyl to magnetite is possible at higher temperature [273]. At 100–400 °C, magnetic black Fe₃O₄ or brown γ-Fe₂O₃ can be obtained, as desired. The carbon monoxide formed undergoes virtually no oxidation if the reaction takes place in a mechanically agitated fluidized bed of product oxide [274]. Finely dispersed γ-Fe₂O₃ pigments and Fe₃O₄ pigments (particle size 2 to 200 nm) are produced by BASF to be used

in aqueous suspension as contrasting agents in nuclear magnetic resonance tomography [275].

To obtain mixed oxides with iron as primary component, iron pentacarbonyl is atomized together with a compound of the other metal (in liquid or dissolved form) that is converted to the oxide at high temperature. For example, by atomizing the carbonyl with an aqueous solution of chromic acid, iron chromium oxide can be obtained for use as a catalyst or as a brown pigment [276, 277].

Other Uses. Polycrystalline iron whiskers can be made by decomposing iron pentacarbonyl in a magnetic field [278–288]. The whiskers are remarkably strong and said to be suitable for making composites or for catalysts. Another process for producing iron whiskers employs an empty space decomposer at temperatures higher than 360 °C for thermal decomposition of iron pentacarbonyl [289].

Novel effect pigments ranging from bright yellow to brilliant red are prepared in a fluidized bed of aluminum powder, which is coated with iron oxide when iron pentacarbonyl vapor and air are admitted [290, 291]. Novel brilliant pigments are produced by coating aluminum flakes with nanometer films of hematite deposited from iron pentacarbonyl and optionally a second layer of colorless metal oxide [292]. Other pigments are made on a mica base [293]. These pigments are lightfast and corrosion resistant and are therefore suitable for use in automobile paints.

Carriers for the toner in photocopiers are obtained by coating fine spherical particles of iron or glass [294], respirable plastics [295], or porous silico-containing material [296]. Colored single component toner powders are made of dispersions of carbonyl iron powder, reflecting pigments or dyes and other substances in a binder [297, 298].

Suspensions of finely divided iron [299] or its alloys [300] are prepared by decomposing iron pentacarbonyl in solution. This process can be used to produce magnetic liquids [301].

If iron pentacarbonyl is decomposed on, for example, gold ore, the iron deposits preferen-

tially on the metal, which could then be recovered by magnetic separation [302].

Iron pentacarbonyl is not an important industrial catalyst [303]; for its use as a catalyst in organic chemistry, see [304]. Iron pentacarbonyl has been described as a catalyst for the hydrogenation of coal [305, 306]. The catalysis of partial subsurface combustion of heavy crude oil by iron pentacarbonyl, with the aim of lowering the viscosity, has been reported [307, 308].

The complex Na₂Fe(CO)₄ formed in solution by the Hieber base reaction [309], recommended long ago for reducing vat dyes [310], has met with renewed interest. For example, chlorate can be removed from diaphragm-cell caustic soda with this product [311]. The use of Na₂Fe(CO)₄ to reduce organic compounds has been described [312]. Operation of a fuel cell using iron pentacarbonyl and an aqueous alkali hydroxide of pH < 9 has been proposed [313].

If iron carbonyl is added during thermal degradation of hydrocarbons to carbon fibers, subsequent high-temperature treatment gives a higher yield of better graphitized, more conductive fibers [314].

Pyrite films are obtained from iron pentacarbonyl and sulfur or hydrogen sulfide by chemical vapor deposition. The films are photoactive and can be used to make solar cells [315].

Economic Aspects. Three companies produce iron pentacarbonyl: BASF (Germany) with a capacity of over 9000 t/a, GAF (Huntsville, Alabama) with an estimated 1500–2000 t/a, and a plant in the former Soviet Union.

These plants also produce carbonyl iron powder, with capacities of ca. 1500 t/a (BASF) and 500 t/a (GAF). The BASF plant has an iron oxide capacity of ca. 1000 t/a.

Consumption of the carbonyl for other purposes is insignificant compared to inplant consumption.

Toxicology and Occupational Health. Based upon the limited data that is available from laboratory animal studies, iron pentacarbonyl must be classified as highly toxic.

The first laboratory study demonstrated that a 45.5 min inhalative exposure to 0.025 vol% (250 ppm) of iron pentacarbonyl is fatal to rabbits [316]. Studies by BASF showed that 30-min exposure to 40 ppm of iron pentacarbonyl is already lethal to rabbits [317]. Cats reacted with considerably less sensitivity and survived exposure to 300 ppm. In guinea pigs, rats, and mice, fatalities began after exposure to 140 ppm. After 30-min exposure, LC₅₀ values of 2.190 mg/m³ (275 ppm) for mice and 910 mg/m³ (115 ppm) for rats were found in later acute toxicity studies [318]. The four-hour median lethal concentration was determined to be 10 ppm in rats [319].

The oral LD₅₀ of iron pentacarbonyl is 0.012 mL/kg (0.018 mg/kg) in rabbits and 0.22 mL/kg (0.033 mg/kg) in guinea pigs [320]. After percutaneous application, the LD₅₀ in rabbits is 0.24 mL/kg [320]. In BASF experiments, the following LD₅₀ values were determined for acute oral toxicity: rabbit, 20 mg/kg; rat, 25 mg/kg; mouse, 100 mg/kg; cat, 100 mg/kg. Iron pentacarbonyl was found to be not mutagen in an Ames test. No skin and eye irritation was observed in OECD 404, OECD 405 tests [317].

Depending on carbonyl concentration, lethargy, respiratory symptoms, and lung edema were found in rats in further inhalation experiments [321]. No data are available on the chronic toxicity of iron pentacarbonyl. Only one six-month feeding study with rats, in which 13 mg/d did not lead to any toxic effects, has been reported [322]. The clinical symptomatology of iron pentacarbonyl intoxication is similar to that of nickel carbonyl poisoning. It is marked by immediate onset of disorientation and vomiting. Fever, coughing, and difficulty in breathing occur after 12–36 h. Fatalities usually occur 4–11 d after exposure to a lethal dose. Pathological lesions are found in the lungs and in the vascular and nervous systems [323]. Although iron pentacarbonyl and nickel carbonyl intoxications have similar symptoms, iron pentacarbonyl is probably less toxic (see Table 5.45) [324]. Furthermore, the use of iron pentacarbonyl should result in less

exposure than nickel carbonyl because of its lower vapor pressure.

Safety precautions are, however, required when working with iron pentacarbonyl to prevent oral, inhalatory, and dermal exposure, because of the relatively high acute toxicity. The MAK value for iron pentacarbonyl is 0.1 ppm. The TLV-TWA is 0.1 ppm (0.8 mg/m³), as Fe.

Table 5.45: Acute rat inhalation toxicity.

Substance	LC ₅₀ , mg/m ³	Exposure time, min
Ni(CO) ₄	240	30
Fe(CO) ₅	910	30

5.17.7 Iron Compounds, Miscellaneous

Iron Acetates. When scrap iron reacts with acetic acid, it dissolves to form acetate salts [325]. If the initial black solution is concentrated to 12%, solid iron acetate can be obtained. This salt is a mixture of iron(II) and iron(III) oxidation states of indefinite proportions best formulated as Fe_x(CH₃COO)_y. It is used as a catalyst for acetylation and carbonylation reactions.

Iron(II) acetate, Fe(C₂H₃O₂)₂, is colorless. It is used in textile dyeing as an iron base for dark brown, dark blue, and black colors.

Iron(III) acetate, Fe(C₂H₃O₂)₃, is prepared industrially by reacting scrap iron with acetic acid, followed by oxidation of the solution with air; it is very sensitive to light. Iron(III) acetate is used for dyeing and printing textiles, as a mordant in dyeing, as a catalyst in organic oxidation reactions, and in dyeing chamois leather.

Basic iron(III) acetate, Fe(OH)(C₂H₃O₂)₂, is obtained by boiling a solution of iron(III) acetate and allowing the hydroxy salt to precipitate. This brownish-red compound is used as a mordant in dyeing, for weighting silk and felt, as a conservation additive for timber, and as a colorant for leather.

Iron(II) carbonate, FeCO₃, forms as a white precipitate when solutions of alkali-metal carbonate salts are added to solutions of iron(II) salts. It is used as a supplement in animal diets and as a flame retardant [325].

Iron Citrates. Iron citrate is a complex of indefinite formula, containing both iron(II) and iron(III). *Iron(II) citrate* and *iron(III) citrate* are also of indefinite stoichiometry. *Iron(III) citrate* (1:1 Fe-citric acid) is also known. Iron citrates are readily soluble in hot water and exhibit complex solution chemistry. These compounds have been used as supplements to animal diets and to soil.

Iron(III) ammonium citrate also has an indefinite formula. The brown hydrated form contains 16.5–18.5% iron, ca. 9% ammonia, and 65% citric acid, whereas the green hydrated form contains 14.5–16% iron, ca. 7.5% ammonia, and 75% citric acid [325]. Iron ammonium citrates are very soluble in water but insoluble in ethanol. They are used as iron additives in food for human consumption (e.g., bread and milk) and for the treatment of iron deficiency in small animals and cattle. They are sensitive to light and are used in light-sensitive paper [325].

Iron Halides. The iron(II) halides (fluoride, bromide, and iodide) are used as catalysts for fluorination, bromination, and iodination in organic reactions. Iron(II) iodide is used as a source of iron and iodine in veterinary medicine.

Iron(III) fluoride is used as a catalyst in organic reactions. Iron(III) bromide is used in the catalytic bromination of aromatic compounds.

Iron Nitrates. *Iron(II) nitrate hexahydrate*, Fe(NO₃)₂·6H₂O, mp 60.5 °C, forms green, rhombohedral crystals. It is prepared by dissolving iron in cold nitric acid (*d* < 1.034 g/cm³). With increasing density, a greater proportion of iron is oxidized to iron(III). Iron(II) nitrate is used as a catalyst for reductions.

Iron(III) nitrate nonahydrate, Fe(NO₃)₃·9H₂O, forms colorless or pale violet monoclinic crystals. It is made by dissolving iron in nitric acid (*d* > 1.115 g/cm³).

Iron(III) nitrate hexahydrate, Fe(NO₃)₃·6H₂O, forms colorless, cubic crystals (mp 35 °C). Iron(III) nitrate is used as a mordant, in tanning, and as a catalyst for oxidation reactions.

Iron(II) phthalocyanine is synthesized from 1,2-dicyanobenzene and an iron(II) complex in refluxing 1-chloronaphthalene and is purified by sublimation at 450 °C. This green compound is insoluble in most solvents. Because it can exist in many oxidation states, iron(II) phthalocyanine is used as a catalyst for a variety of chemical and electrochemical redox reactions. It is also an important pigment [326].

Iron Compounds for the Treatment of Anemia [327, 328]. Sufficient iron in the diet of humans and animals is essential for tissue growth. Iron is found at the active site of many important proteins in the human body. These include hemoglobin (oxygen transport), myoglobin (storage of oxygen), cytochrome c oxidase (converts oxygen to water), cytochrome P450 (hydroxylation of poisonous or unwanted chemicals), and other cytochromes such as cytochrome c (part of the electron-transport system). In addition, iron is necessary for the biosynthesis of iron-sulfur proteins such as rubredoxin.

Although a sufficient amount of iron can usually be found in the diet, the level of absorption of this element from food is generally low. Therefore, the supply of iron can become critical in a variety of conditions. Iron-deficiency anemia is commonly encountered in pregnant women and may also be a problem in the newborn, especially in animal species such as the pig. Some diseases (e.g., rheumatoid arthritis, hemolytic diseases, and cancer) result in poor distribution of iron in the body and thus lead to chronic anemia.

More than 34 iron-containing preparations are used as hematinics for the treatment of iron-deficiency anemia [328]. Oral iron therapy is usually the preferred method of treatment unless good reasons exist for using another route. The daily oral dosage of elemental iron should be 100–200 mg. Iron(II) salts are more commonly used than iron(III) salts because they are assumed to be more soluble in the pH range 3–7. Solubility is essential if the compound is to permeate cell membranes. The rate of regeneration of hemo-

globin appears to be independent of the salt used, provided sufficient iron is given. Factors affecting the choice of preparation are the incidence of side effects and the cost. If side effects occur, an alternative iron preparation or a reduced dosage can be tried. The main iron compounds used in iron supplements are iron(II) fumarate, iron(II) gluconate, iron(II) sulfate, iron(II) succinate, iron(III) chloride solution, and iron(III) ammonium citrate. In addition, iron dextran and iron sorbital are used in injectable hematinics. Iron(II) sulfate is often preferred because it is the cheapest form and is at least as effective as any other. A number of oral preparations contain ascorbic acid (vitamin C) to stabilize the iron(II) state. However, the therapeutic advantage is minimal and the cost may be increased. Folic acid is used in conjunction with an iron salt for the prevention of anemia in pregnant women.

Iron(II) complexes have a major disadvantage, however, in that they are sensitive to oxidation, especially in aqueous environments. This can be hindered initially by protectively coating iron(II) compounds in tablet form. However, when they dissolve in the gut, oxidation still occurs to give insoluble iron(III) salts (containing hydroxide). These frequently cause irritation and gastrointestinal distress. Such side effects are often severe, because large doses are necessary to ensure that enough iron is absorbed. Nausea and epigastric pain may occur and are said to be dose-related, although the relationship between altered bowel behavior (constipation) and dosage is unclear [328].

Soluble iron(III) complexes are thus preferred (because oxidation is not a problem). Unfortunately, such complexes are likely to be charged (which is unsatisfactory for passive membrane diffusion). Even if these complexes were neutral, they may still be toxic.

The ideal properties of an iron(III) chelation complex for treating iron-deficiency anemia are: (1) solubility in the pH range 6–9, (2) a ligand with a high affinity for iron(III), (3) a neutral iron(III) complex, and (4) nontoxicity. Furthermore, after absorption into the body the complex must enter into an equilibrium

with transferring (the iron-transport protein) so that iron is available for utilization in metabolic pathways. This means that the chelator must be metabolized rapidly to ensure that iron is freshly available.

One such complex currently under trial is iron(III) maltol, $[\text{FeL}_3]$ (maltol(HL) = 3-hydroxy-2-methyl-4H-pyran-4-one). Recently, iron(III) maltol and similar complexes [328–332] have been shown to possess the desirable properties outlined above for the treatment of iron-deficiency-related diseases.

Another iron-related disease in humans is severe tissue iron overload. This may occur during the treatment of anemia, mainly as a result of a large number of blood transfusions. This condition is treated by injections of desferrioxamine mesylate, which is a good chelating agent for iron(III), and is also used to treat cases of accidental iron poisoning.

5.18 Relationships Between the Different Forms of Iron Oxides

Fe_2O_3 loses oxygen on heating at about 1390 °C to give Fe_3O_4 :



Fe_3O_4 can be considered as a compound of ferrous oxide, FeO , and ferric oxide, Fe_2O_3 . It crystallizes in the cubic system and can be obtained by heating iron fillings in air. It is also formed during the forging of red hot wrought iron. In pure water in the absence of oxygen, steel forms a film of Fe_3O_4 at about 50 °C:



It is a black powder, insoluble in dilute acids, strongly ferromagnetic, and has a high electrical conductivity. That is why it is sometimes used as electrodes.

It was once thought that synthetic Fe_3O_4 behaves differently from natural magnetite on oxidation in that an intermediate phase $\gamma\text{-Fe}_2\text{O}_3$ is observed in the synthetic sample but not in the natural mineral:



This was later resolved when it was found that the oxidation is dependent on the particle size of Fe_3O_4 ; only extremely fine particles 3000 Å yield $\gamma\text{-Fe}_2\text{O}_3$.

Ferrous oxide, FeO , is known as the wüstite phase, Fe_{1-x}O , after its discover Fritz Wüst. It has a cubic lattice of NaCl type, and unstable below 570 °C when it decomposes as follows:



However, it can be cooled rapidly to prevent the decomposition. It can be obtained as a black pyrophoric powder in the following ways:

- Heating ferrous oxalate in the absence of air:



- Heating stoichiometric amounts of Fe and Fe_3O_4 in an inert atmosphere at 1100 °C, then cooling rapidly:



Iron(II) hydroxide, $\text{Fe}(\text{OH})_2$ or $\text{FeO} \cdot \text{H}_2\text{O}$, is formed by treating iron(II) salts with alkali hydroxide in absolutely air-free solution. It precipitates as a white flocculent material which has a great affinity for oxygen. It thereby turn green, which progressively darkens and eventually passes into the red brown color of iron(III) oxide hydrate. The green color may be an intermediate product such as $\text{Fe}(\text{OH})_2 \cdot \text{FeOOH}$. Pure $\text{Fe}(\text{OH})_2$ when washed and dried in the absence of air decomposes at 200 °C to give FeO with some Fe_3O_4 . It is slightly soluble in concentrated NaOH forming sodium hydroxoferrate, $\text{Na}_2[\text{Fe}(\text{OH})_4]$. If oxygen is passed through a strongly alkaline suspension of $\text{Fe}(\text{OH})_2$, $\alpha\text{-FeOOH}$ is produced.

Iron(III) hydroxide, $\text{Fe}(\text{OH})_3$, is formed by adding ammonia to iron(III) salt solutions, as a red-brown slimy precipitate which yields a gel of variable water content when it is dried. When freshly precipitated, it is amorphous to x-rays. It dissolves readily in dilute acids, and also dissolves to some extent in hot concentrated NaOH forming sodium ferrite, NaFeO_2 .

As aging takes place, the diffraction pattern characteristic to FeOOH develops but is never complete:



Two types of iron oxide hydroxide can be obtained in this way: $\alpha\text{-FeOOH}$ from sulfate, nitrate (Figure 5.105), and $\beta\text{-FeOOH}$ from chloride and fluoride solutions (Figure 5.105).

Freshly precipitated ferric hydroxide when filtered and washed, then examined by differential thermal analysis shows endothermic peak at low temperatures (100–250 °C) due to the loss of water, followed by exothermic peak at about 300 °C. X-ray diffraction before 300 °C shows no pattern, but after 300 °C shows that of $\alpha\text{-Fe}_2\text{O}_3$, thus indicating that the exothermic peak is due to the crystallization of $\alpha\text{-Fe}_2\text{O}_3$:



A sample aged for 28 months showed similar behavior, but the transition amorphous to crystalline took place at about 400 °C and is less defined, demonstrating that during aging only partial crystallization took place.

If the oxide hydrate is prepared at room temperature by precipitation, the transition temperature of crystallization is about 300 °C as indicated previously; but, if prepared at 90 °C by hydrolysis, the transition temperature is about 450 °C. Electron micrographic

studies showed that the transition process amorphous–crystalline is accompanied by an increase in the particle size from below 50 Å to about 300 Å. This phenomena is not restricted to iron oxides but to other oxides as well.

$\beta\text{-FeOOH}$ is obtained as a light brown deposit when a ferric solution containing Cl^- ion is hydrolyzed by boiling. It entraps variable amounts of Cl^- ions within its crystal structure which can be partly washed with water. The amount of Cl^- has an important influence on the thermal behavior of the material and its infrared spectrum but not on the x-ray diffraction pattern.

$\gamma\text{-FeOOH}$ occurs in nature to a minor extent as the mineral lepidocrocite. When heated below 500 °C it loses water giving $\gamma\text{-Fe}_2\text{O}_3$:



It is artificially prepared by adding NaOH to dilute FeSO_4 solutions until pH 6 followed by blowing air through the solution for 2 hours and is then allowed to age for 2 days. The differential thermal analysis pattern of $\gamma\text{-FeOOH}$ shows an endothermic dehydration peak at 330 °C followed by the exothermic transformation of $\gamma\text{-Fe}_2\text{O}_3$ to $\alpha\text{-Fe}_2\text{O}_3$ at 535 °C. At room temperature and in weak acid or neutral medium, FeS is oxidized slowly to $\gamma\text{-FeOOH}$ as follows:

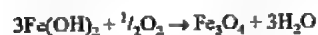
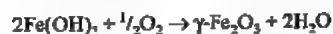
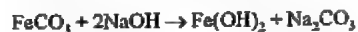


Figure 5.105: Left: $\alpha\text{-FeOOH}$ obtained by aging iron hydroxide gel for 155 days (precipitation took place at pH 10); Right: $\beta\text{-FeOOH}$.

Oxidation of Fe_3O_4 below 400 °C also yields $\gamma\text{-Fe}_2\text{O}_3$.

$\delta\text{-FeOOH}$ is obtained from $\text{Fe}(\text{OH})_2$ by rapid oxidation with an excess of H_2O_2 or ammonium persulfate. It is a brown strongly magnetic material that loses about 10% of its water at 100 °C and is partially transformed to hematite; complete transformation takes place at 200 °C.

FeCO_3 can be formed artificially when $(\text{NH}_4)_2\text{CO}_3$ is added to a ferrous solution. Freshly precipitated ferrous carbonate when oxidized by excess H_2O_2 is transformed to $\text{Fe}(\text{OH})_3$; however, this hydroxide is dark yellow instead of red brown. It also undergoes crystallization during aging to $\alpha\text{-FeOOH}$. Ferrous carbonate reacts with NaOH to form a surface layer of $\text{Fe}(\text{OH})_2$ which on oxidation results in the formation of magnetic iron oxides:



This is the basis of a beneficiation method for low-grade siderite ore, whereby the magnetic iron oxides formed are separated from the gangue minerals by magnetic methods.

5.19 The Aqueous Oxidation of Iron Sulfides [333]

The behavior of pyrite and arsenopyrite during leaching is different from other sulfides due to the presence of the disulfide ion, S_2^{2-} . Arsenopyrite contains in addition, the diarsenide ion, As_2^{2-} . The presence of the disulfide ions is manifested on heating the minerals in absence of air: pyrite loses an atom of sulfur, while arsenopyrite loses an atom of arsenic:



5.19.1 Pyrite

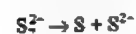
Pyrite dissociates in water as follows:



When the disulfide ion reacts further, the equilibrium is shifted to the right, and more pyrite goes into solution. Disulfide ion is similar to peroxide ion, O_2^{2-} , which may undergo autooxidation¹ to elemental sulfur and sulfide ion:



Overall reaction:



Hence, three paths may arise depending on the conditions:

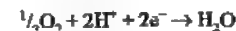
- High acidity and the absence of oxygen. In this case H_2S is formed:



or



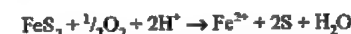
- High acidity and low oxygen concentration. In this case, elemental sulfur is formed:



Overall reaction:



or

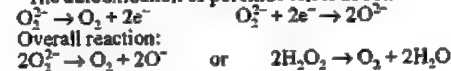


In this case, the aqueous oxidation of pyrite may be considered to take place by an electrochemical mechanism like other sulfides in acid medium and can be represented by:

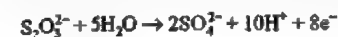


- In neutral medium and high oxygen concentration: In this case, it seems that the autooxidation of the disulfide ion does not take place because in neutral medium, thiosulfates and other lower oxidation products were identified. Thiosulfates may, therefore, form directly from the disulfide ion by the following reaction:

¹ The autooxidation of peroxide ion is as follows:



which oxidizes further to sulfate:



The overall reaction in this case is:



which leads to the global oxidation reaction of pyrite in neutral medium



or



Two points should be noted from the above scheme:

- Pyrite takes up one eighth of its oxygen required for oxidation to sulfate from the water and the remaining from molecular oxygen. This was confirmed experimentally by using radioactive oxygen in following up the reaction.
- Under certain conditions hydroxyl ions are formed during the oxidation. This was confirmed when pyrite was in contact with water containing agar-agar thus minimizing the diffusion of OH^- ions. Cathodic regions form on pyrite whereby oxygen is reduced according to:



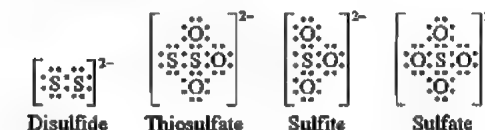
while at the anodic zone the following reactions would take place:



The presence of thiosulfates in waste solutions raises an environmental problem because these are usually not precipitated by standard methods like sulfates, e.g., when adding $\text{Ca}(\text{OH})_2$. Hence they escape the mine site and may contaminate surface waters. This topic was the subject of an extensive research project in Canada.

Sulfites were also identified in deaerated solutions. The relation between disulfide,

thiosulfate, sulfites, and sulfate ions is shown schematically below:

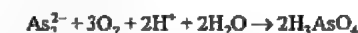


5.19.2 Arsenopyrite

Arsenopyrite may dissociate in water as follows:



The behavior of disulfide ion is probably the same as in the case of pyrite in acid and in neutral medium, while the diarsenide ion forms arsenic acid:



The overall reactions are:

- In acid medium:



- In neutral medium:



Ferrous ion formed in the above reactions oxidizes further to form ferric arsenate precipitates:



5.19.3 Pyrrhotite

Pyrrhotite is slowly solubilized in water at 110 °C and 200 kPa oxygen pressure as ferrous sulfate:



If, however, the reaction is conducted in presence of dilute acid (0.1 M), the formation of elemental sulfur and ferric oxide takes place:



It will be also observed that the acid initially added will be present unchanged at the end of reaction. In fact the acid is consumed at the initial stage of the reaction and then regenerated later. The reason is that the oxidation of

ferrous ion to ferric is possible only in presence of acid:



Hydrolysis of ferric ion then follows with generation of acid:



That is why FeS suspended in water will yield only a solution of FeSO_4 when oxidized but in presence of acid the formation of Fe^{3+} becomes possible. Because of hydrolysis, Fe_2O_3 is formed and the acid is regenerated. It should be observed that the oxygen utilization in the presence of acid is less than in the first case.

5.20 Regeneration of Iron-Containing Pickling Baths

In Germany in 1987, the output of rolled steel products from base, high-grade, and stainless steels averaged 2.0×10^6 t per month. Approximately 60% of this is pickled at least once.

Pickling removes the oxide layer that adheres to the steel surface. The oxide layer arises as scale in heat-treatment processes or as rust through the corrosive action of water, with its load of dissolved substances, or through humid atmospheric corrosion.

Whereas rust consists largely of Fe_2O_3 , scale is made up of the three iron oxides (wustite FeO , magnetite Fe_3O_4 , and hematite Fe_2O_3) in a ratio that depends on steel composition, annealing conditions (temperature, heating time, furnace atmosphere), final temperature of rolling, and rate of cooling after rolling.

The "picklability" of a steel and the acid consumption for pickling also depend on many factors: adherence of scale, composition of the steel, mode and magnitude of mechanical working, type and composition of pickling solution, and pickling conditions. The selection of pickling acid is dictated by the required surface quality and by economic factors. The most important pickling acids for iron and steel are sulfuric and hydrochloric. Phospho-

ric, nitric, and hydrofluoric acids are used for special purposes and stainless steels.

Iron(III) ions that dissolve during pickling are reduced by metallic iron, so that the pickling acid contains primarily iron (II) salts. The quantity of iron dissolved during pickling is called chemical pickling loss; it accounts for 0.2–1.2% of the iron or steel being pickled and accounts for approximately three-quarters of the weight loss during pickling.

If iron salts are removed from the pickling liquor, the unconsumed pickling solution can be returned to the pickling unit after the addition of an amount of acid equivalent to the quantity of salts precipitated.

The acid consumed in pickling can also be completely regenerated from the iron salts. The pickling liquor recycled between the pickling tanks and the regeneration unit is thus not consumed, apart from evaporation losses.

5.20.1 Sulfuric Acid Pickling Solutions

When steel is pickled with sulfuric acid, the scale oxides dissolve to give iron sulfates. The rate of dissolution of the three oxides in sulfuric acid increases in the order Fe_2O_3 , Fe_3O_4 , FeO . The reaction of sulfuric acid with metallic iron to give iron(II) sulfate and hydrogen is inhibited by pickling additives (inhibitors).

Two processes are employed to regenerate sulfuric acid pickling liquor, whose description follows.

5.20.1.1 Crystallization

In industrial plants, spent pickling solution is usually cooled by using brine. The cooling effect depends strongly on the cleanliness of the cooling surface, on which salt crust can easily form. These systems, therefore, require very careful upkeep. Frequent shutdowns must be expected.

Vacuum Crystallization (Figure 5.106). A vacuum equal to the vapor pressure of water at the desired final temperature is maintained in the crystallization vessel.

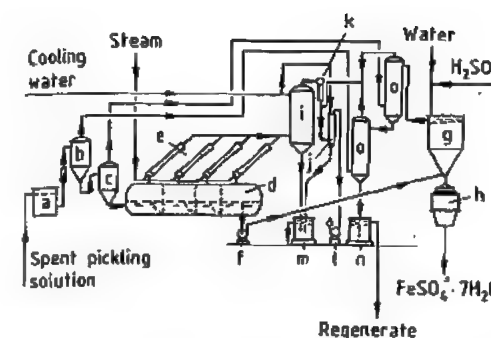


Figure 5.106: Vacuum crystallization (Keramchemie/Lurgi): a) Suction tank; b, c) Precoolers; d) Crystallizer; e) Steam-jet compressor; f) Salt-slurry pump; g) Thickener; h) Centrifuge; i) Direct-contact condenser; j) Auxiliary condenser; k) Steam-jet venting device; l) Vacuum pump; m) Water receiver; n) Pickling solution receiver; o) Acid direct-contact condensers.

Part of the pickling solution is pumped continuously from the pickling tank to the vacuum crystallizer, where it is cooled evaporatively to 5 °C and then to 0 °C to crystallize iron(II) sulfate. Water vapor flows directly, or after compression in a high-performance steam-jet apparatus, to a direct-contact condenser. The salt-liquid mixture is removed continuously by a salt-slurry pump and separated in a centrifuge. After the mother liquor has been freshened with concentrated sulfuric acid and water, it is returned to the pickling tank. The vacuum in the evaporator is maintained by a vacuum pump connected to the direct-contact condenser.

A modified design omits the steamjet apparatus; therefore, only electrical energy is needed for its operation, which may be an economic advantage because in this case no fuel is required for steam generation.

Cyclone Crystallization (Figure 5.107). In the cyclone crystallizer (b), fine droplets of spent pickling solution are sprayed counter-current to a stream of air. In this way, rapid evaporation and cooling are accomplished. If the iron content of the pickling solution is to be kept low, a second cooling stage is added. Indirect cooling with water or brine takes place in the cooling vessel (c). A blower injects air to prevent the crystals from settling and forming a crust on the vessel wall. Iron(II)

sulfate crystals are separated in the centrifuge (d); the filtrate (regenerate) is returned to the pickling plant.

The iron(II) heptahydrate can be used in the production of cyanoferrates, as a flocculent in wastewater treatment, in the production of gas adsorbents, as a pesticide, as a chemical fertilizer, and in the production of iron-oxide pigments.

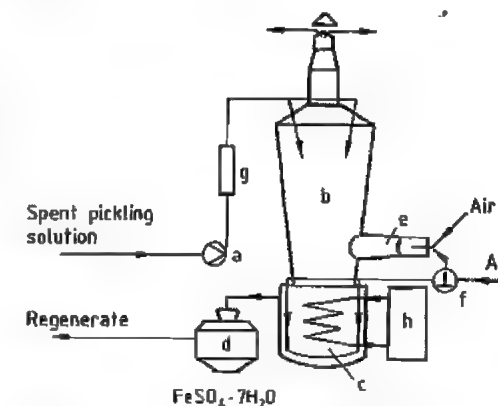


Figure 5.107: Cyclone crystallizer (Andritz-Ruthner): a) Acid pump; b) Cyclone crystallizer; c) Cooling vessel; d) Centrifuge; e) Vent; f) Blower; g) Pickling liquor tank; h) Cooling system.

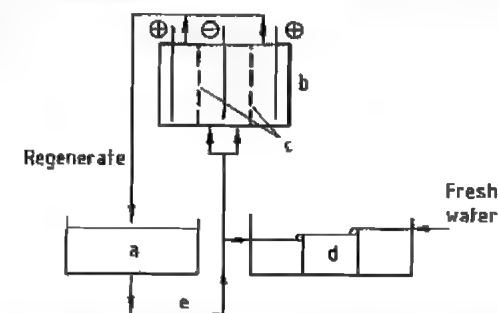


Figure 5.108: Regeneration by electrolysis: a) Pickling tank; b) Electrolysis cell; c) Diaphragm; d) Cascade rinsing; e) Spent pickling solution.

The heptahydrate can also be converted to the monohydrate. A continuous apparatus for the preparation of very pure monohydrate is built by Mannesmann Anlagenbau/Messo-Chemietechnik.

The heptahydrate is dehydrated to the monohydrate at a well-defined acid concentration at ca. 90 °C. After separation of the crys-

talline monohydrate in a centrifuge, iron sulfate-poor mother liquor is returned to the reactor. The water vapor resulting from the dehydration is removed from the cycle.

5.20.1.2 Electrolysis

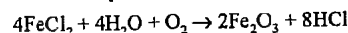
An electrolytic process has recently been developed [334]. Cathode and anode compartments are separated by a diaphragm (Figure 5.108). Metallic iron is deposited at the cathode; sulfuric acid and oxygen are produced at the anode. Electrolysis is facilitated by addition of an electrolyte, which is not consumed and does not affect the pickling process, but allows iron to be recovered most effectively from the acidic solution. Sulfuric acid either flows directly from the anode compartment back to the pickling tank or is detained temporarily in a holding tank.

Evaporation and electrochemical decomposition result in a continual loss of water. Using multiple countercurrent cascade rinsing after pickling allows the quantity of water to be adjusted so that no wastewater is produced. The unit is marketed by Keramchemie.

5.20.2 Hydrochloric Acid Pickling Solutions

Because of its technical advantages, hydrochloric acid has largely replaced sulfuric acid in pickling baths, especially in large plants.

Hydrogen is produced when iron is dissolved. Iron(III) chloride, formed by dissolution of Fe_3O_4 and Fe_2O_3 , is reduced by the hydrogen to yield FeCl_2 , so that virtually the only chloride present in the pickling liquor is iron(II) chloride. Spent pickling solution can be regenerated completely by thermal decomposition. Iron chloride is converted to iron oxide and hydrochloric acid:



Gas or oil is used as fuel. The heat consumption is ca. 3 MJ for the simultaneous regeneration of 1 L of pickling solution and 1 L of rinse liquor.

In large-scale operations, the two processes that have found widespread application are (1)

the fluidized-bed process and (2) the spray-roasting process.

Each is employed in more than 100 industrial plants. The efficiency of the acid recovery is ca. 99%.

Fluidized-Bed Process. In the Lurgi-Keramchemie fluidized-bed regeneration process [335] (Figure 5.109), spent pickling solution is led via the settling tank and the venturi loop into the fluidized bed in the reactor. The bed consists of granulated iron oxide. Residual acid and water are evaporated at 850 °C, and iron chloride is converted to iron oxide and hydrogen chloride. Growth and new formation of iron oxide grains in the fluidized bed are controlled so that a dust-free granulated product is obtained, with a particle diameter of 1–2 mm and a bulk density of ca. 3.5 g/cm³. The granular product is discharged continuously at the bottom of the reactor and transported by a vibrating cooling chute and a vibrating spiral conveyor to the storage bin. In smaller units, the granular product can also be discharged directly into shipping containers.

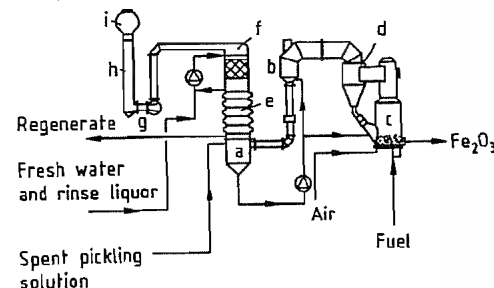


Figure 5.109: Fluidized-bed process for regeneration of hydrochloric acid pickling solutions: a) Separating tank; b) Venturi scrubber; c) Cyclone; d) Absorber; e) Scrubbing stage; g) Off-gas blower; h) Stack; i) Mist collector.

The hot gases from the reactor contain hydrogen chloride and a small amount of iron oxide dust, which is collected in the cyclone and returned to the fluidized bed. In the venturi scrubber, the off-gas is then cooled to ca. 100 °C. The thermal energy of the off-gases is used to concentrate the pickling solution by evaporation before it is fed to the reactor. Fine dust particles in the gas stream are removed by scrubbing.

From the venturi scrubber, the cooled gas stream goes to the absorber, where hydrogen chloride is absorbed adiabatically with rinse liquor and fresh water. The hydrochloric acid thus produced has a concentration of ca. 18%. It is recycled to the pickling unit or held in a storage tank. After passing through a scrubbing stage and a mist collector, the off-gas is virtually free of hydrochloric acid and is released to the atmosphere.

Spray-Roast Process. The spray-roast process is often employed for the recovery of metal oxides from metal chloride solutions. It can also be used for the regeneration of iron chloride-laden hydrochloric acid solution [336]. The pure spray-roast oxide obtained in this way is used in the ferrite industry (150 000 t in 1987).

As shown in Figure 5.110, spent pickling solution goes to the venturi scrubber where hot gases concentrate it by evaporation of water. In the next step, the highly concentrated pickling liquor is injected into the spray-roast reactor at a pressure of 0.3–0.5 MPa as a fine spray either cocurrent or countercurrent to hot combustion gases. The cocurrent arrangement is common for pickling acids that contain zinc and lead, because their chlorides have high vapor pressures and are separated after a shorter retention time.

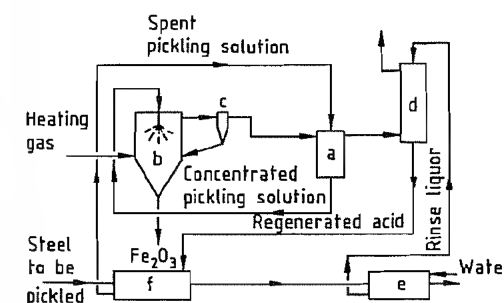


Figure 5.110: Spray-roast process for regeneration of hydrochloric acid pickling solutions: a) Venturi scrubber; b) Spray-roast reactor; c) Cyclone; d) Absorber; e) Rinse tanks; f) Pickling tanks.

The temperature of the roasting gas outlet from the spray tower is about 400 °C. The gases proceed to the cyclone. Fine iron oxide powder, together with the oxide collected in

the cyclone, is discharged continuously (bulk density 0.3–0.4 g/cm³).

When some silicon-rich steels are pickled, the silicon dioxide content of the pickling solution does not permit the iron(III) oxide product to be used in the ferrite industry. The quantity of silica can be reduced in an additional precleaning step [337], in which silica is selectively removed from the pickling solution.

After passing through the cyclone, the roasting gases are cooled and scrubbed in the venturi scrubber before going to the absorber, where hydrogen chloride is absorbed to produce 18–20% hydrochloric acid. The acidic iron chloride solution, which is generated when the pickled steel is rinsed, is used as the absorption liquor. Hydrochloric acid is recycled to the pickling tank. Residual gases, with a low hydrochloric acid content, are discharged to the atmosphere.

Spray-roast plants have unit capacities of 0.3–25 m³/h of pickling acid and a similar amount of rinse liquor.

The Fe_2O_3 generated in the thermal decomposition process can be used as raw material in various industries. The most important options are the production of magnetic materials (e.g., soft and hard ferrites), the production of iron powder for the fabrication of sintered parts and welding electrodes, and use as an additive in the manufacture of magnetic tapes, abrasives, tiles, glass, cosmetics, and pigments.

5.20.3 Nitric and Hydrofluoric Acid Pickling Solutions

Stainless and acid-resistant steels are usually pickled with a mixture of nitric and hydrofluoric acids. Nitric acid serves as an oxidizing agent, whereas hydrofluoric acid forms complexes with metal ions. In contrast to the pickling of carbon steel, the permissible iron concentration in a pickling solution for special steels is limited by the tendency of iron and the alloy components to form fluoride complexes and thus reduce the concentration of fluoride ions in solution. Severe inhibition of the pickling process occurs at a total metal

concentration of 50 g/L, so that pickling solutions must be topped up with fresh hydrofluoric acid, and eventually neutralized and discarded, even though only about half the acid content has been consumed.

When the pickling bath is neutralized with calcium hydroxide, the resulting metal hydroxides and calcium fluoride form a sludge that can be disposed of without treatment, but nitrates remain in solution and contribute to eutrophication in receiving waters.

The following regeneration processes have been devised in recent years.

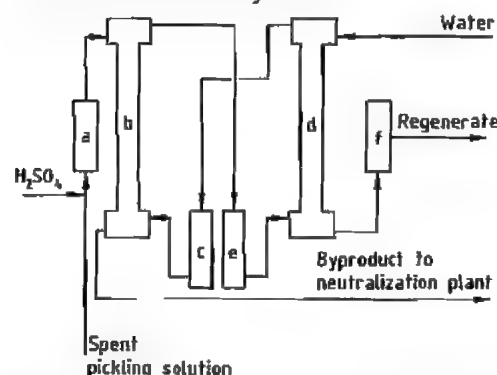


Figure 5.111: Regeneration of HF-HNO₃ pickling liquors by liquid-liquid extraction: a) Heat exchanger; b) Extraction column; c) Storage tank; d) Reextraction column; e) Storage tank; f) Adsorber.

Liquid-Liquid Extraction. Liquid-liquid extraction [338] makes use of the fact that nitric and hydrofluoric acids form adducts with tributyl phosphate that are soluble in hydrocarbon solvents. Addition of sulfuric acid also renders extractable acid anions bound in the form of metal salts. Around 93% of the nitric acid and 60% of the hydrofluoric acid can be recovered. The flow sheet for the process is shown in Figure 5.111.

After sulfuric acid has been added to the spent pickling solution and the mixture has been cooled, it is directed to the top of an extraction tower; the organic phase enters at the bottom. The aqueous raffinate, containing sulfuric acid, is discharged at the bottom. From the top of the tower, the organic phase, laden with extracted acid, goes to the foot of a re-extraction tower. The water inlet at the top

washes out the acids. The organic phase discharged at the top goes back to the extraction tower. In an adsorber, traces of tributyl phosphate are removed from the aqueous regenerate before it is returned to the pickling tank. The tributyl phosphate is returned to the tank (c).

Fluoride-Crystallization. In this process, the recovery of nitric acid is ca. 90% (Figure 5.112) and that of hydrofluoric acid, 55%, despite the fact that metals precipitate as fluorides, so that corresponding amounts of hydrofluoric acid are consumed. The filter residue can be employed as a feedstock for the production of hydrofluoric acid or for the recovery of nickel.

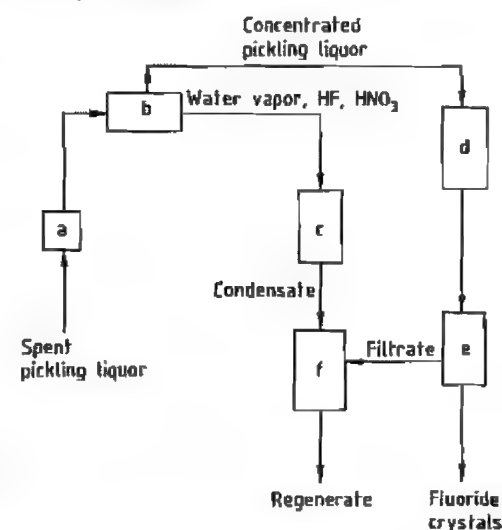


Figure 5.112: Regeneration of HNO₃-HF pickling solutions by fluoride crystallization: a) Particle collector; b) Flow-through evaporator; c) Condenser; d) Crystallization tanks; e) Filter; f) Storage tank.

Spent pickling solution is led through a particulate collector and a flow-through evaporator, where it is evaporated within minutes to about half its volume by electrical heating. The water vapor, which contains part of the nitric and hydrofluoric acids, is condensed by indirect cooling. The sparingly soluble fluorides of iron and of the alloy constituents precipitate from the concentrated, supersaturated solution in crystallization tanks and are re-

moved periodically by filtration. The filtrate is led to a storage vessel where it is combined with condensate from the condenser. After addition of fresh nitric and hydrofluoric acid, the liquor is returned to the pickling tank.

Bipolar Membrane Process. In the bipolar membrane process [339] (Figure 5.113), the free acids are first recovered in an electrodialysis cell and then returned to the pickling tank. Metal ions are then precipitated as metal hydroxides by neutralization with potassium hydroxide. Metal hydroxide sludge is collected in the downstream filter press. The filtered salt solution (potassium fluoride and potassium nitrate) goes to a bipolar membrane module where HF, HNO₃, and KOH are separated from the potassium salts. The acid mixture is returned to the pickling tank, whereas potassium hydroxide is reused for neutralization. The dilute salt solution (KF, KNO₃) is desalted by reverse osmosis. Part of it is used as wash liquor for the filter press, and the rest is recycled to the membrane unit to obtain the highest possible yield of acids and potassium hydroxide. The residue from the filter can be reused as raw material in iron and steel works, depending on its content of metal hydroxides.

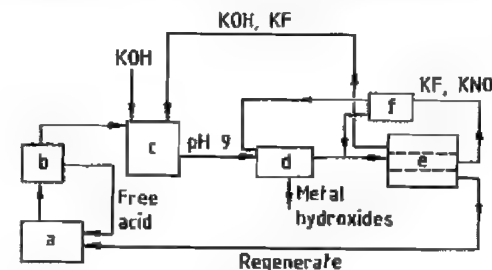


Figure 5.113: Regeneration of HNO₃-HF pickling solutions in a bipolar membrane cell: a) Pickling tank; b) Electrodialysis cell; c) Neutralization; d) Filter press; e) Bipolar membrane module (Aquatech cell); f) Reverse osmosis.

Retardation Process. The retardation process can generally be employed for separating strong inorganic acids from their salts. By loading a strongly basic ion-exchange resin with spent pickling solution and then eluting with water, separation into a high-salt fraction and a subsequent high-acid fraction is

achieved. The flow sheet for the process is shown in Figure 5.114.

Acid retardation can probably be accounted for by diffusion of undissociated acid into the ion-exchange resin grains so that upon elution with water, it must diffuse back out; the result is that elution of acid is retarded [340].

For nitric and hydrofluoric acid pickling solutions, most of the free acids can be recovered in this way. Partial regeneration of pickling solutions reduces disposal costs.

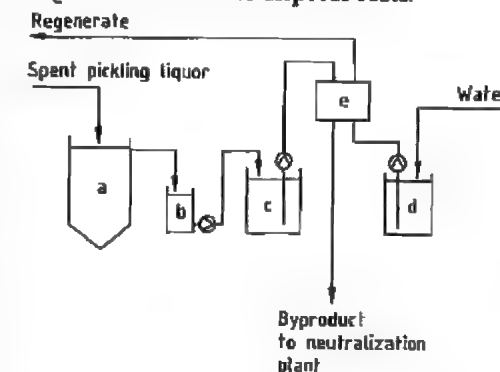


Figure 5.114: Regeneration of HNO₃-HF pickling solutions by acid retardation: a) Sedimentation tank; b) Buffer tank; c) Pickling-liquor metering tank; d) Water metering tank; e) Resin bed.

5.21 Pigments

5.21.1 Iron Oxide Pigments

The continually increasing importance of iron oxide pigments is based on their nontoxicity; chemical stability; wide variety of colors ranging from yellow, orange, red, brown, to black; and low price. Natural and synthetic iron oxide pigments consist of well-defined compounds with known crystal structures:

- α -FeOOH, goethite, diasporite structure, color changes with increasing particle size from green-yellow to brown-yellow
- γ -FeOOH, lepidocrocite, boehmite structure, color changes with increasing particle size from yellow to orange
- α -Fe₂O₃, hematite, corundum structure, color changes with increasing particle size from light red to dark violet

• $\gamma\text{-Fe}_2\text{O}_3$, maghemite, spinel super structure, ferrimagnetic, color: brown

• Fe_3O_4 , magnetite, spinel structure, ferrimagnetic, color: black

Mixed metal oxide pigments containing iron oxide are also used. Magnetic iron oxide pigments and transparent iron oxide pigments are described later.

5.21.1.1 Natural Iron Oxide Pigments

Naturally occurring iron oxides and iron oxide hydroxides were used as pigments in prehistoric times (Altamira cave paintings) [341]. They were also used as coloring materials by the Egyptians, Greeks, and ancient Romans.

Hematite ($\alpha\text{-Fe}_2\text{O}_3$) has attained economic importance as a red pigment, goethite ($\alpha\text{-FeOOH}$) as yellow, and the umbers and siennas as brown pigments. Deposits with high iron oxide contents are exploited preferentially. Naturally occurring magnetite (Fe_3O_4) has poor tinting strength as a black pigment, and has found little application in the pigment industry.

Hematite is found in large quantities in the vicinity of Málaga in Spain (Spanish red) and near the Persian Gulf (Persian red). The Spanish reds have a brown undertone. Their water-soluble salt content is very low and their Fe_2O_3 content often exceeds 90%. The Persian reds have a pure hue, but their water-soluble salt content is disadvantageous for some applications. Other natural hematite deposits are of only local importance. A special variety occurs in the form of platelets and is extracted in large quantities in Kärnten (Austria). This micaceous iron oxide, is mainly used in corrosion protection coatings.

Goethite is the colored component of yellow ocher, a weathering product mainly of siderite, sulfidic ores, and feldspar. It occurs in workable amounts mainly in South Africa and France. The Fe_2O_3 content gives an indication of the iron oxide hydroxide content of the

ocher, and is ca. 20% in the French deposits and ca. 55% in the South African.

Umbers are mainly found in Cyprus. In addition to Fe_2O_3 (45–70%), they contain considerable amounts of manganese dioxide (5–20%). In the raw state, they are deep brown to greenish brown and when calcined are dark brown with a red undertone (burnt umbers).

Siennas, mainly found in Tuscany, have an average Fe_2O_3 content of ca. 50%, and contain < 1% manganese dioxide. They are yellow-brown in the natural state and red-brown when calcined [342].

The processing of natural iron oxide pigments depends on their composition. They are either washed, slurried, dried, ground, or dried immediately and then ground in ball mills, or more often in disintegrators or impact mills [343].

Siennas and umbers are calcined in a directly fired furnace, and water is driven off. The hue of the products is determined by the calcination period, temperature, and raw material composition [344].

Natural iron oxide pigments are mostly used as inexpensive marine coatings or in coatings with a glue, oil, or lime base. They are also employed to color cement, artificial stone, and wallpaper. Ocher and sienna pigments are used in the production of crayons, drawing pastels, and chalks [345].

The economic importance of the natural iron oxide pigments has decreased in recent years in comparison with the synthetic materials.

5.21.1.2 Synthetic Iron Oxide Pigments

Synthetic iron oxide pigments have become increasingly important due to their pure hue, consistent properties, and tinting strength. Single-component forms are mainly produced with red, yellow, orange, and black colors. Their composition corresponds to that of the minerals hematite, goethite, lepidocrocite, and magnetite. Brown pigments usually consist of mixtures of red and/or yellow and/or black; homogeneous brown phases are also pro-

duced, e.g., $(\text{Fe}, \text{Mn})_2\text{O}_3$ and $\gamma\text{-Fe}_2\text{O}_3$, but quantities are small in comparison to the mixed materials. Ferrimagnetic $\gamma\text{-Fe}_2\text{O}_3$ is of great importance for magnetic recording materials.

Several processes are available for producing high-quality iron oxide pigments with controlled mean particle size, particle size distribution, particle shape, etc. (Table 5.46):

- Solid-state reactions (red, black, brown)
- Precipitation and hydrolysis of solutions of iron salts (yellow, red, orange, black)
- Laux process involving reduction of nitrobenzene (black, yellow, red)

The raw materials are mainly by-products from other industries: steel scrap obtained from deep drawing, grindings from cast iron, $\text{FeSO}_4 \cdot 7\text{H}_2\text{O}$ from TiO_2 production or from steel pickling, and FeCl_2 also from steel pickling.

Iron oxides obtained after flame spraying of spent hydrochloric acid pickle liquor, red mud from bauxite processing, and the product of pyrites combustion are no longer of importance. They yield pigments with inferior color properties that contain considerable amounts

of water-soluble salts. They can therefore only be used in low-grade applications.

Solid-State Reactions of Iron Compounds. Black iron oxides obtained from the Laux process (see below) or other processes may be calcined in rotary kilns with an oxidizing atmosphere under countercurrent flow to produce a wide range of different red colors, depending on the starting material. The pigments are ground to the desired particle size in pendular mills, pin mills, or jet mills, depending on their hardness and intended use.

The calcination of yellow iron oxide produces pure red iron oxide pigments with a high tinting strength. Further processing is similar to that of calcined black pigments.

High-quality pigments called copperas reds are obtained by the thermal decomposition of $\text{FeSO}_4 \cdot 7\text{H}_2\text{O}$ in a multistage process (Figure 5.115). If an alkaline-earth oxide or carbonate is included during calcination, the sulfate can be reduced with coal or carbon-containing compounds to produce sulfur dioxide, which is oxidized with air to give sulfuric acid [346–349]. The waste gases and the dissolved impurities that are leached out in the final stage present ecological problems, however.

Table 5.46: Reaction equations for the production of iron oxide pigments.

Color	Reaction	Process
Red	$6\text{FeSO}_4 \cdot x\text{H}_2\text{O} + \frac{3}{2}\text{O}_2 \rightarrow \text{Fe}_2\text{O}_3 + 2\text{Fe}_2(\text{SO}_4)_3 + 6\text{H}_2\text{O}$	copperas process
	$2\text{Fe}_2(\text{SO}_4)_3 \rightarrow 2\text{Fe}_2\text{O}_3 + 6\text{SO}_3$	
	$2\text{Fe}_3\text{O}_4 + \frac{1}{2}\text{O}_2 \rightarrow 3\text{Fe}_2\text{O}_3$	calcination
	$2\text{FeOOH} \rightarrow \text{Fe}_2\text{O}_3 + \text{H}_2\text{O}$	calcination
	$2\text{FeCl}_2 + 2\text{H}_2\text{O} + \frac{1}{2}\text{O}_2 \rightarrow \text{Fe}_2\text{O}_3 + 4\text{HCl}$	Ruthner process
Yellow	$2\text{FeSO}_4 + \frac{1}{2}\text{O}_2 + 4\text{NaOH} \rightarrow \text{Fe}_2\text{O}_3 + 2\text{Na}_2\text{SO}_4 + 2\text{H}_2\text{O}$	precipitation
	$2\text{FeSO}_4 + 4\text{NaOH} + \frac{1}{2}\text{O}_2 \rightarrow 2\alpha\text{-FeOOH} + 2\text{Na}_2\text{SO}_4 + \text{H}_2\text{O}$	precipitation
	$2\text{Fe} + 2\text{H}_2\text{SO}_4 \rightarrow 2\text{FeSO}_4 + 2\text{H}_2$	
	$2\text{FeSO}_4 + \frac{1}{2}\text{O}_2 + 3\text{H}_2\text{O} \rightarrow 2\alpha\text{-FeOOH} + 2\text{H}_2\text{SO}_4$	Penniman process
	$2\text{Fe} + \frac{1}{2}\text{O}_2 + 3\text{H}_2\text{O} \rightarrow 2\alpha\text{-FeOOH} + 2\text{H}_2$	
Orange	$2\text{Fe} + \text{C}_6\text{H}_5\text{NO}_2 + 2\text{H}_2\text{O} \rightarrow 2\alpha\text{-FeOOH} + \text{C}_6\text{H}_5\text{NH}_2$	Laux process
	$2\text{FeSO}_4 + 4\text{NaOH} + \frac{1}{2}\text{O}_2 \rightarrow 2\gamma\text{-FeOOH} + 2\text{Na}_2\text{SO}_4 + \text{H}_2\text{O}$	precipitation
Black	$3\text{FeSO}_4 + 6\text{NaOH} + \frac{1}{4}\text{O}_2 \rightarrow \text{Fe}_3\text{O}_4 + 3\text{Na}_2\text{SO}_4 + 3\text{H}_2\text{O}$	1-step precipitation
	$2\text{FeOOH} + \text{FeSO}_4 + 2\text{NaOH} \rightarrow \text{Fe}_3\text{O}_4 + \text{Na}_2\text{SO}_4 + 2\text{H}_2\text{O}$	2-step precipitation
	$9\text{Fe} + 4\text{C}_6\text{H}_5\text{NO}_2 + 4\text{H}_2\text{O} \rightarrow 3\text{Fe}_3\text{O}_4 + 4\text{C}_6\text{H}_5\text{NH}_2$	Laux process
	$3\text{Fe}_2\text{O}_3 + \text{H}_2 \rightarrow 2\text{Fe}_3\text{O}_4 + \text{H}_2\text{O}$	reduction
Brown	$2\text{Fe}_2\text{O}_3 + \frac{1}{2}\text{O}_2 \rightarrow 3\gamma\text{-Fe}_2\text{O}_3$	calcination
	$3\text{Fe}_3\text{O}_4 + \text{Fe}_2\text{O}_3 + \text{MnO}_2 + \frac{1}{2}\text{O}_2 \rightarrow (\text{Fe}_{11}\text{Mn})\text{O}_{18}$	calcination

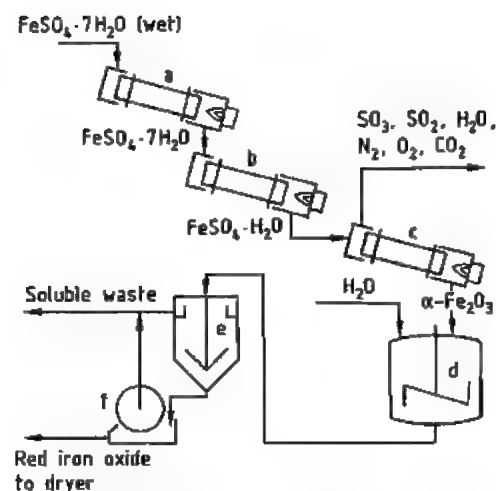


Figure 5.115: Production of copperas red: a) Dryer; b) Rotary kiln (dewatering); c) Rotary kiln; d) Tank; e) Thickener; f) Filter.

Lower quality products can be obtained by single-stage calcination of iron(II) sulfate heptahydrate in an oxidizing atmosphere. The pigments have a relatively poor tinting strength and a blue tinge. Decomposition of iron(II) chloride monohydrate in air at high temperatures also yields a low-quality red iron oxide pigment [350].

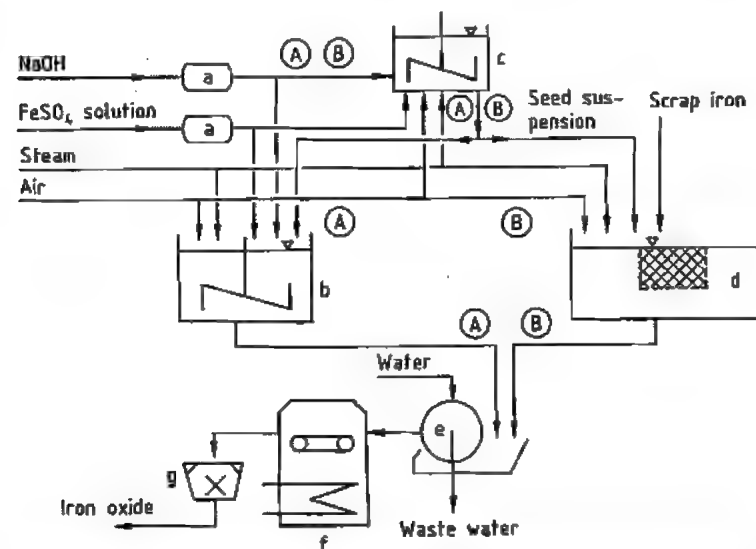


Figure 5.116: Production of yellow iron oxide by the precipitation (A) and Penniman (B) processes: a) Tank; b) Pigment reactor; c) Seed reactor; d) Pigment reactor with scrap basket; e) Filter; f) Dryer; g) Mill.

In a new process, micaceous iron oxide is obtained in high yield by reacting iron(III) chloride and iron at 500–1000 °C in an oxidizing atmosphere in a tubular reactor [351].

Black Fe_3O_4 pigments with a high tinting strength can be prepared by calcining iron salts under reducing conditions [352]. This process is not used industrially because of the furnace gases produced.

Controlled oxidation of Fe_3O_4 at ca. 500 °C produces a single-phase brown $\gamma\text{-Fe}_2\text{O}_3$ with a neutral hue [353].

Calcination of $\alpha\text{-FeOOH}$ with small quantities of manganese compounds gives homogeneous brown pigments with the composition $(\text{Fe}, \text{Mn})_2\text{O}_3$ [354]. Calcination of iron and chromium compounds that decompose at elevated temperatures yields corresponding pigments with the composition $(\text{Fe}, \text{Cr})_2\text{O}_3$ [355].

Precipitation Processes. In principle, all iron oxide hydroxide phases can be prepared from aqueous solutions of iron salts (Table 5.46). However, precipitation with alkali produces neutral salts (e.g., Na_2SO_4 , NaCl) as by-products which enter the wastewater.

Precipitation is especially suitable for producing soft pigments with a pure, bright hue. The manufacture of $\alpha\text{-FeOOH}$ yellow is described as an example. The raw materials are iron(II) sulfate ($\text{FeSO}_4 \cdot 7\text{H}_2\text{O}$) or liquors from the pickling of iron and steel, and alkali [NaOH , $\text{Ca}(\text{OH})_2$, ammonia, or magnesite]. The pickle liquors usually contain appreciable quantities of free acid, and are therefore first optionally neutralized by reaction with scrap iron. Other metallic ions should not be present in large amounts, because they have an adverse effect on the hue of the iron oxide pigments.

The solutions of the iron salts are first mixed with alkali in open reaction vessels (Figure 5.116 Route A) and oxidized, usually with air. The quantity of alkali used is such that the pH remains acidic. The reaction time (ca. 10–100 h) depends on the temperature (10–90 °C) and on the desired particle size of the pigment. This method yields yellow pigments ($\alpha\text{-FeOOH}$) [356, 357]. If yellow nuclei are produced in a separate reaction (Route A in Figure 5.116, tank c), highly consistent yellow iron oxide pigments with a pure color can be obtained [358].

If precipitation is carried out at ca. 90 °C while air is passed into the mixture at ca. pH ≥ 7 , black iron oxide pigments with a magnetite structure and a good tinting strength are obtained when the reaction is stopped at a $\text{FeO}:\text{Fe}_2\text{O}_3$ ratio of ca. 1:1. The process can be accelerated by operating at 150 °C under pressure; this technique also improves pigment quality [359]. Rapid heating of a suspension of iron oxide hydroxide with the necessary quantity of $\text{Fe}(\text{OH})_2$ to ca. 90 °C also produces black iron oxide of pigment quality [360, 361].

Orange iron oxide with the lepidocrocite structure ($\gamma\text{-FeOOH}$) is obtained if dilute solutions of the iron(II) salt are precipitated with sodium hydroxide solution or other alkalis until almost neutral. The suspension is then heated for a short period, rapidly cooled, and oxidized [362, 363].

Very soft iron oxide pigments with a pure red color may be obtained by first preparing

$\alpha\text{-Fe}_2\text{O}_3$ nuclei, and then continuously adding solutions of iron(II) salt with atmospheric oxidation at 80 °C. The hydrogen ions liberated by oxidation and hydrolysis are neutralized by adding alkali and keeping the pH constant [364]. Pigment-quality $\alpha\text{-Fe}_2\text{O}_3$ is also obtained when solutions of an iron(II) salt, preferably in the presence of small amounts of other cations, are reacted at 60–95 °C with excess sodium hydroxide and oxidized with air [365].

The Penniman process is probably the most widely used production method for yellow iron oxide pigments [366, 367]. This method considerably reduces the quantity of neutral salts formed as by-products. The raw materials are iron(II) sulfate, sodium hydroxide solution, and scrap iron. If the sulfate contains appreciable quantities of salt impurities, these must be removed by partial precipitation. The iron must be free of alloying components. The process usually consists of two stages (Route B in Figure 5.116).

In the first stage, nuclei are prepared by precipitating iron(II) sulfate with alkali (e.g., sodium hydroxide solution) at 20–50 °C with aeration (c). Depending on the conditions, yellow, orange, or red nuclei may be obtained. The suspension of nuclei is pumped into vessels charged with scrap iron (d) and diluted with water. Here, the process is completed by growing the iron oxide hydroxide or oxide onto the nuclei. The residual iron(II) sulfate in the nuclei suspension is oxidized to iron(III) sulfate by blasting with air at 75–90 °C. The iron(III) sulfate is then hydrolyzed to form FeOOH or $\alpha\text{-Fe}_2\text{O}_3$. The liberated sulfuric acid reacts with the scrap iron to form iron(II) sulfate, which is also oxidized with air. The reaction time can vary from ca. two days to several weeks, depending on the conditions chosen and the desired pigment. At the end of the reaction, metallic impurities and coarse particles are removed from the solid with sieves or hydrocyclones; water-soluble salts are removed by washing. Drying is carried out with band or spray dryers (f) and disintegrators or jet mills are used for grinding (g). The

main advantage of this process over the precipitation process lies in the small quantity of alkali and iron(II) sulfate required. The bases are only used to form the nuclei and the relatively small amount of iron(II) sulfate required initially is continually renewed by dissolving the iron by reaction with the sulfuric acid liberated by hydrolysis. The process is thus considered environmentally friendly. The iron oxide pigments produced by the Penniman process are soft, have good wetting properties, and a very low flocculation tendency [366–374].

Under suitable conditions the Penniman process can also be used to produce reds directly. The residual scrap iron and coarse particles are removed from the pigment, which is then dried [375] and ground using disintegrators or jet mills. These pigments have unsurpassed softness. They usually have purer color than the harder red pigments produced by calcination.

The Laux Process. The Béchamp reaction (i.e., the reduction of aromatic nitro compounds with antimony or iron) which has been known since 1854, normally yields a black-gray iron oxide that is unsuitable as an inorganic pigment. By adding iron(II) chloride or aluminum chloride solutions, sulfuric acid, and phosphoric acid, LAUX modified the process to yield high-quality iron oxide pigments [376]. Many types of pigments can be obtained by varying the reaction conditions. The range extends from yellow to brown (mixtures of α -FeOOH and/or α -Fe₂O₃ and/or Fe₃O₄) and from red to black. If, for example, iron(II) chloride is added, a black pigment with very high tinting strength is produced [376]. However, if the nitro compounds are reduced in the presence of aluminum chloride, high-quality yellow pigments are obtained [377]. Addition of phosphoric acid leads to the formation of light to dark brown pigments with good tinting strength [378]. Calcination of these products (e.g., in rotary kilns) gives light red to dark violet pigments. The processes are illustrated in Figure 5.117.

The type and quality of the pigment are determined not only by the nature and concentration of the additives, but also by the reaction rate. The rate depends on the grades of iron used, their particle size, the rates of addition of the iron and nitrobenzene (or another nitro compound), and the pH value. No bases are required to precipitate the iron compounds. Only ca. 3% of the theoretical amount of acid is required to dissolve all of the iron. The aromatic nitro compound oxidizes the Fe²⁺ to Fe³⁺ ions, acid is liberated during hydrolysis and pigment formation, and more metallic iron is dissolved by the liberated acid to form iron(II) salts; consequently, no additional acid is necessary.

The iron raw materials used are grindings from iron casting or forging that must be virtually free of oil and grease. The required fineness is obtained by size reduction in edge runner mills and classification with vibratory sieves. The iron and the nitro compound are added gradually via a metering device to a stirred tank (a) containing the other reactants (e.g., iron(II) chloride, aluminum chloride, sulfuric acid, and phosphoric acid). The system rapidly heats up to ca. 100 °C and remains at this temperature for the reaction period. The nitro compound is reduced to form an amine (e.g., aniline from nitrobenzene) which is removed by steam distillation. Unreacted iron is also removed (e.g., in shaking tables, c). The pigment slurry is diluted with water in settling tanks (d) and the pigment is washed to remove salts, and filtered on rotary filters (e). It may then be dried on band, pneumatic conveyor, or spray dryers to form yellow or black pigments, or calcined in rotary kilns (h) in an oxidizing atmosphere to give red or brown pigments. Calcination in a nonoxidizing atmosphere at 500–700 °C improves the tinting strength [379]. The pigments are then ground to the desired fineness in pendular mills, pin mills, or jet mills, depending on their hardness and application.

The Laux process is a very important method for producing iron oxide because of the coproduction of aniline; it does not generate by-products that harm the environment.

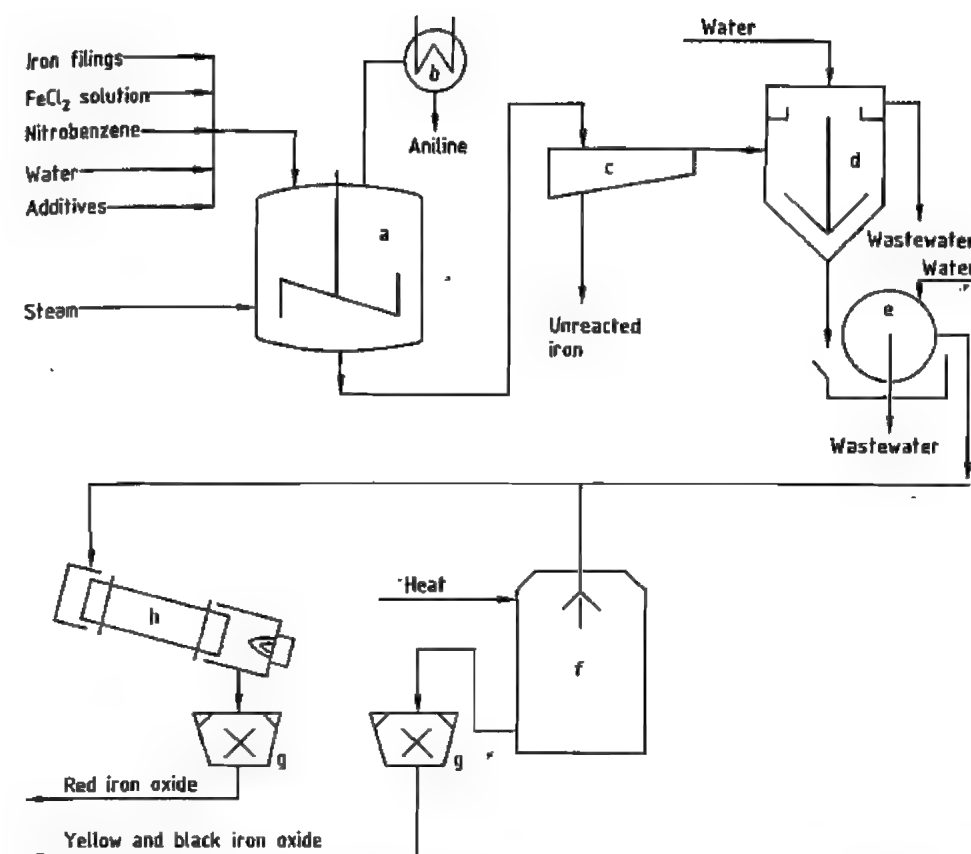


Figure 5.117: Production of iron oxide pigment by the Laux process: a) Reactor; b) Condenser; c) Classifier; d) Thickener; e) Filter; f) Dryer; g) Mill; h) Rotary kiln.

Other Production Processes. The three processes already described are the only ones that are used on a large scale. The following processes are used on a small scale for special applications:

- Thermal decomposition of Fe(CO)₅ to form transparent iron oxides [380]
- Hydrothermal crystallization for the production of α -Fe₂O₃ in platelet form [381]

5.21.1.3 Toxicology and Environmental Aspects

The Berufsgenossenschaft der Chemischen Industrie (Germany) has recommended that all iron oxide pigments should be classified as inert fine dusts with an MAK value of 6

mg/m³. This is the highest value proposed for fine dusts.

Iron oxide pigments produced from pure starting materials may be used as colorants for food and pharmaceutical products [382]. Synthetic iron oxides do not contain crystalline silica and therefore are not considered to be toxic, even under strict Californian regulations.

5.21.1.4 Quality

The red and black iron oxide pigments produced by the methods described have an Fe₂O₃ content of 92–96%. For special applications (e.g., ferrites) analytically pure pigments with Fe₂O₃ contents of 99.5–99.8% are produced.

The Fe_2O_3 content of yellow and orange pigments lies between 85 and 87% corresponding to FeOOH contents of 96–97%. Variations of 1–2% are of no importance with respect to the quality of the pigments. Pigment quality is mainly determined by the quantity and nature of the water-soluble salts, the particle size distribution (hue and tinting strength are effected) and the average particle size of the ground product. The hue of red iron oxide is determined by the particle diameter, which is ca. 0.1 μm for red oxides with a yellow tinge and ca. 1.0 μm for violet hues.

The optical properties of the yellow, usually needle-shaped, iron oxide pigments depend not only on the particle size, but also on the length to width ratio (e.g., length = 0.3–0.8 μm , diameter = 0.05–0.2 μm , length: diameter ratio = ca. 1.5–8). In applications for which needle-shaped particles are unsuitable, spheroidal pigments are available [383]. Black iron oxide pigments (Fe_3O_4) have a particle diameter of ca. 0.1–0.6 μm .

Some iron oxide pigments have a limited stability on heating. Red iron oxide is stable up to 1200 °C in air. In the presence of oxygen, black iron oxide changes into brown $\gamma\text{-Fe}_2\text{O}_3$ at ca. 180 °C and then into red $\alpha\text{-Fe}_2\text{O}_3$ above 350 °C. Yellow iron oxide decomposes above ca. 180 °C to form red $\alpha\text{-Fe}_2\text{O}_3$ with liberation of water. This temperature limit can be increased to ca. 260 °C by stabilization with basic aluminum compounds. The thermal behavior of brown iron oxides produced by mixing depends on their composition.

5.21.1.5 Uses

All synthetic iron oxides possess good tinting strength and excellent hiding power. They are also lightfast and resistant to alkalis. These properties are responsible for their versatility. The principle areas of use are shown in Table 5.47.

Iron oxide pigments have long been used for coloring construction materials. Concrete roof tiles, paving bricks, fibrous cement, bitumen, mortar, rendering, etc. can be colored with small amounts of pigment that do not af-

fect the setting time, compression strength, or tensile strength of the construction materials. Synthetic pigments are superior to the natural pigments due to their better tinting power and purer hue.

Natural rubber can only be colored with iron oxides that contain very low levels of copper and manganese ($\text{Cu} < 0.005\%$, $\text{Mn} < 0.02\%$). Synthetic rubber is less sensitive.

In the paint and coating industries, iron oxide pigments can be incorporated in many types of binders. Some reasons for their wide applicability in this sector are pure hue, good hiding power, good abrasion resistance, and low settling tendency. Their high temperature resistance allows them to be used in enamels.

The use of iron oxide as a polishing medium for plate glass manufacture has decreased now that other methods of glass production are available.

Table 5.47: Main areas of use for natural and synthetic iron oxide pigments.

Use	Amount, %		
	Europe	United States	World
Coloring construction materials	64	37	60
Paints and coatings	30	48	29
Plastics and rubber	4	14	6
Miscellaneous	2	1	5

5.21.1.6 Economic Aspects

Accurate production figures for natural and synthetic iron oxide pigments are difficult to obtain, because statistics also include non-pigmentary oxides (e.g., red mud from bauxite treatment, intermediate products used in ferrite production). World production of synthetic iron oxides in 1985 was estimated to be between 500 000 and 600 000 t; production of natural oxides was ca. 100 000 t. The most important producing countries for synthetic pigments are Germany, the United States, the United Kingdom, Italy, Brazil, and Japan. The natural oxides are mainly produced in France, Spain, Cyprus, Iran, Italy, and Austria.

The most important manufacturers are Bayer, Deanshanger, SILO (Europe); Colum-

bian Chemicals, Harcross, Miles (USA); Globo (Brazil); and Toda (Japan).

5.21.2 Iron Blue Pigments

The term iron blue pigments as defined in ISO 2495 has largely replaced a variety of older names which were either related to the place where the compound was produced or represented particular optical properties, e.g., Berlin blue, Bronze blue, Chinese blue, Milori blue, Non-bronze blue, Paris blue, Prussian blue, Toning blue, and Turnbull's blue. These names usually stood for insoluble pigments based on microcrystalline Fe(II)Fe(III) cyano complexes which do not differ significantly in their composition; many were associated with specific hues. A standardized naming system has been demanded by users and welcomed by manufacturers, and has led to a reduction in the number of names [384].

Iron blue, C.I. Pigment Blue 27:77510 (soluble blue is C.I. Pigment Blue 27:77520), was discovered in 1704 by DIESBACH in Berlin by a precipitation reaction, and can be regarded as the oldest synthetic coordination compound.

MILORI was the first to produce it as a pigment on an industrial scale in the early nineteenth century [385].

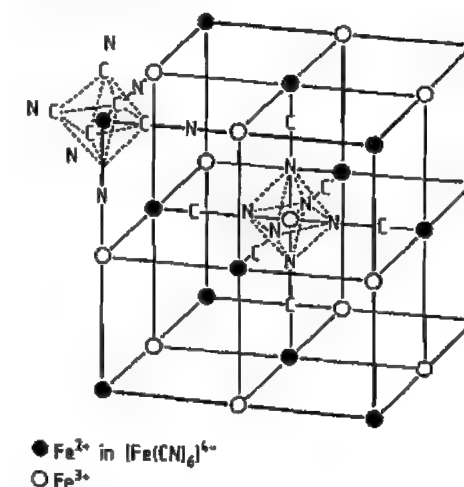


Figure 5.118: Crystal structure of iron blue [388].

5.21.2.1 Structure

X-Ray and infrared spectroscopy show that iron blue pigments have the formula $\text{M}^{\text{I}}\text{Fe}^{\text{II}}\text{Fe}^{\text{III}}(\text{CN})_6 \cdot \text{H}_2\text{O}$ [386]. M^{I} represents potassium, ammonium, or sodium, of which the potassium and ammonium ions are preferred because they produce excellent hues in industrial manufacture.

The crystal structure of the $\text{Fe}^{\text{II}}\text{Fe}^{\text{III}}(\text{CN})_6$ grouping is shown in Figure 5.118. A face-centered cubic lattice of Fe^{2+} is interlocked with another face-centered cubic lattice of Fe^{3+} to give a cubic lattice with the corners occupied by iron ions. The CN^- ions are located at the edges of the cubes between each Fe^{2+} ion and the neighboring Fe^{3+} ; the carbon atom of the cyanide is bonded to the Fe^{2+} ion and the nitrogen atom is coordinatively bonded to the Fe^{3+} ion. According to [387] the deep blue colour is the result of electron transfer from iron(II) and iron(III) with the absorption of light energy ("Charge Transfer Complex").

The wide-mesh lattice of the crystal contains relatively large spaces which can be occupied alternately by alkali ions and water molecules. In order to retain the crystal structure — and also the optical properties — water molecules must be present. Loss of water beyond a certain limit brings about fundamental changes in the pigment properties. A bonding mechanism for the coordinating water molecules assumes that both zeolitic and adsorptive states are possible.

Many investigations helped to elucidate the structure of iron blue [390–393].

5.21.2.2 Production

Iron blue pigments are produced by the precipitation of complex iron(II) cyanides by iron(II) salts in aqueous solution. The product is a whitish precipitate of iron(II) hexacyanoferrate(II) $\text{M}_2^{\text{I}}\text{Fe}^{\text{II}}[\text{Fe}^{\text{II}}(\text{CN})_6]$ or $\text{M}^{\text{I}}\text{Fe}^{\text{II}}[\text{Fe}^{\text{II}}(\text{CN})_6]$ (Berlin white), as an intermediate stage, which is aged and then oxidized to the blue pigment [388].

Potassium hexacyanoferrate(II) or sodium hexacyanoferrate(II) or mixtures of these salts

are usually used. When the pure sodium salt or a calcium hexacyanoferrate(II) solution is used, the pigment properties are obtained by adding a potassium or ammonium salt during the precipitation of the white paste product or prior to the oxidation stage.

The iron(II) salt used is crystalline iron(II) sulfate or iron(II) chloride solution. The oxidizing agent can be hydrogen peroxide, alkali chlorates, or alkali dichromates. Industrial precipitation is carried out batchwise in large stirred tanks by simultaneous or sequential addition of aqueous solutions of potassium hexacyanoferrate(II) and iron(II) sulfate to a dilute acid. The filtrate from the white paste product must contain a slight excess of iron. Temperature, pH, and concentration of the starting solutions have a decisive influence on the size and shape of the precipitated particles. The suspension of white paste is aged by heating. The ageing period varies in length and temperature depending on the required properties of the finished pigment. This is followed by the oxidation to form the blue pigment by adding hydrochloric acid and sodium or potassium chlorate [394]. Finally, the suspension of the blue pigments is pumped into filter presses either immediately or after having been washed with cold water and decanted. After filtering, it is washed until free of acid and salt.

Depending on the pigment type, the filter press-cakes (35–60% solids) are either moulded into cylindrical pellets and dried to a finished dust-free product, or liquefied and spray dried, or dried and then ground to form a powder pigment.

Dispersibility can be improved by adding organic compounds to the pigment suspension before filtering to prevent the particles from agglomerating too strongly on drying [395, 396]. In another method (the Flushing process), the water in the wet pigment paste is replaced by a hydrophobic binder [397]. Although these and other methods of pigment preparation produce fully dispersible products consisting mainly of iron blue and a binder [398–400], they have not become established on the market.

A "water-soluble" blue can be manufactured by adding peptizing agents (the latter improve the water solubility via an emulsifying action). This forms a transparent colloidal solution in water without the use of high shear forces [388].

5.21.2.3 Properties

Hue, relative tinting strength, dispersibility, and rheological behavior are the properties of iron blue pigments with the most practical significance. Other important properties are the volatiles content at 60 °C, the water-soluble fraction, and acidity (ISO 2495). Pure blue pigments are usually used singly (e.g., in printing inks) and do not need any additives to improve them. Finely divided iron blue pigments impart a pure black tone to printing ink.

Owing to their small particle size (see Table 5.48 and Figures 5.119 and 5.120), iron blue pigments are very difficult to disperse. A graph of particle size distribution is given in Figure 5.121 for a commercial quality iron blue and for a micronized grade with similar primary particle size. The micronized grade gives greater tinting strength in dry mixtures than the blues obtained from standard grinding. The average size of the aggregates in the micronized material is ca. 10 µm compared with ca. 35 µm for the normal quality product.

Iron blue pigments are thermally stable for short periods at temperatures up to 180 °C, and therefore can be used in stoving finishes. The powdered material presents an explosion hazard, the ignition point is 600–625 °C (ASTM D 93-52). The pigments are combustible in powder form, ignition in air being possible above 140 °C [388].

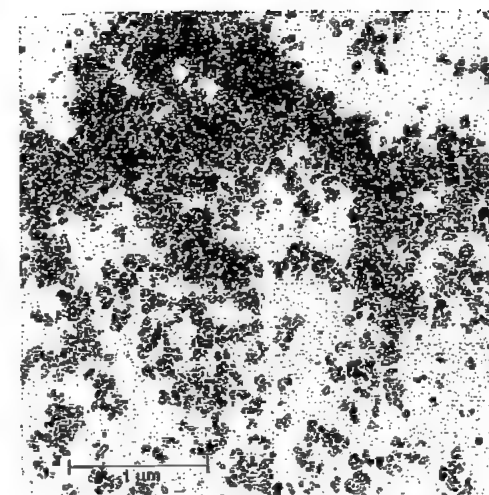


Figure 5.119: Electron micrograph of an iron blue pigment of small particle size (Manox Blue® 460 D).

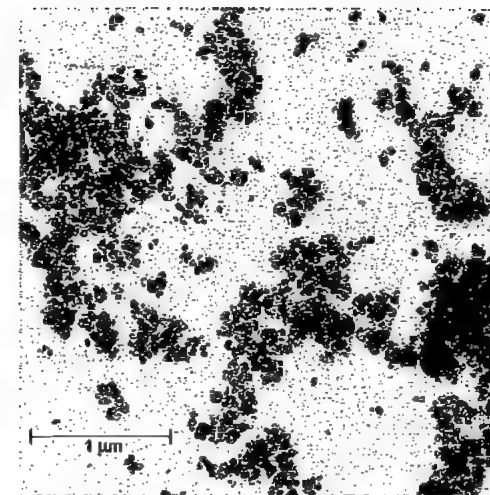


Figure 5.120: Electron micrograph of an iron-blue pigment of normal particle size (Vossen-Blau® 705).

Table 5.48: Physical and chemical properties of iron blue pigments (Vossen-Blau® and Manox® grades).

Type	Vossen-Blau® 705	Vossen-Blau® 705 LS*	Vossen-Blau® 724	Manox® Blue 480 D	Manox Easisperse® HSB 2
Colour Index Number	77510	77510	77510	77510	77510
Colour Index Pigment	27	27	27	27	27
Tinting strength ^b	100	100	100	115	95 ^c
Hue	pure blue	pure blue	pure blue	pure blue	pure blue
Oil absorption ^d , g/100 g	36–42	40–50	36–42	53–63	22–28
Weight loss on drying ^e , %	2–6	2–6	2–6	2–6	2–6
Tamped density ^f , g/L	500	200	500	500	550
Density ^g , g/cm ³	1.9	1.9	1.9	1.8	1.8
Mean diameter of primary particles, nm	70	70	70	40	80
Specific surface area ^h , m ² /g	35	35	35	80	30
Thermal stability, °C	150	150	150	150	150
Resistance to acids	very good	very good	very good	very good	very good
Resistance to alkalis	poor	poor	poor	poor	poor
Resistance to solvents	very good	very good	very good	very good	very good
Resistance to bleeding	very good	very good	very good	very good	very good

*LS = Luftstrahlmühle (air jet mill).

^bDIN ISO 787/CVI and DIN ISO 787/XCIV.

^cSurface-treated easily dispersible type.

^dDIN ISO 787/V, ASTM D 281, or JIS K 5101/19 (JIS: Japanese Industrial Standard).

^eDIN ISO 787/II, ASTM D 280, or JIS K 5101/21.

^fDIN ISO 787/XI or JIS K 5101/18.

^gDIN ISO 787/X or JIS K 5101/17.

^hDIN 66131.

Iron blue pigments have excellent light- and weatherfastness. When mixed with white pigments, these properties can disappear [401]. Recent investigations have shown that a topcoat (as commonly applied in automobile manufacture) overcomes this problem [402]. Figure 5.122 shows changes in residual gloss

and color after a short weathering period. The pigments are resistant to dilute acid and oxidizing agents, and do not bleed. They are decomposed by hot, concentrated acid and alkali. Other properties are listed in Table 5.48.

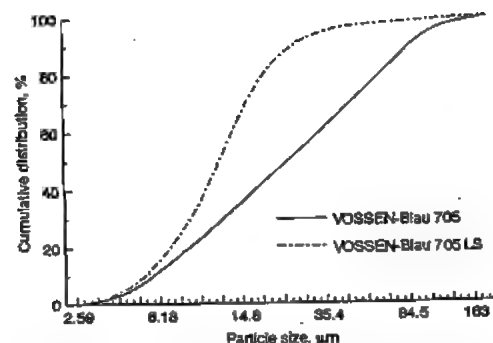


Figure 5.121: Cumulative particle size distribution curve of a normal (705) and a micronized (705 LS) iron blue pigment of equal primary particle size. LS = Luftstrahlmühle (air jet mill).

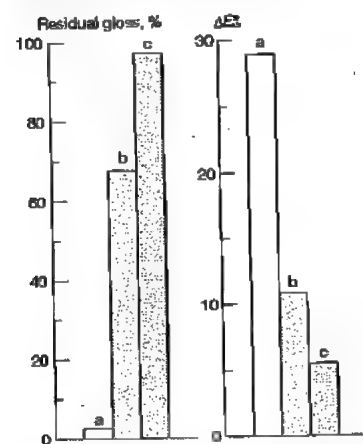


Figure 5.122: Residual gloss and ΔE^*_{ab} values for isocyanate-cross-linked polyacrylate resins that contain 15% Vossen-Blau® 2000 (older pigment type which has been replaced by Manox® Blue 460 D) relative to the binder and 15% TiO_2 (rutile) relative to the iron blue pigment after 1000 h fast exposure to UV [402]: a) Without clearcoat; b) With clearcoat but without UV protection; c) With clearcoat and UV protection.

5.21.2.4 Uses

Total production of iron blue in 1975 was ca. 25 000 t/a, but in 1991 it was only ca. 15 000 t/a. The main consumer in Europe and the United States is the printing industry. The second largest use in Europe, especially of micronized iron blue pigments, is for coloring fungicides, but use in the paint industry is decreasing.

Printing Ink Industry. Iron blue pigments are very important in printing, especially roto-gravure, because of their deep hue, good hiding power, and economic cost/performance basis. Iron blue is often mixed with phthalocyanine pigments for multicolor printing. Another important use is in controlling the shade of black printing inks. Typical amounts used are 5–8% for full-shade retogravure inks and 2–8% for toning black gravure and offset inks.

Iron blue pigments are used in the manufacture of single- and multiple-use carbon papers and blue copying papers, both for toning the carbon black and as blue pigments in their own right [388].

Toning of Black Gravure Inks. For the toning of black gravure inks, for example, 2 to 6% of Vossen-Blau 705 are used together with 6 to 12% of carbon black. Combinations with red pigments with a blue undertone are also common. When using organic pigments, resistance to solvents must be taken in account. Because of the poor dispersibility of iron blue compared with carbon black it is both economical and practical to disperse the blue pigment in a separate step.

While the visual judgement of black is influenced by the individual ability of the observer to distinguish small colour differences in deep black, it is possible, with the help of photometric measurements, to graphically interpret objective evaluations by means of physical data [389].

Figure 5.123 illustrates the colour changes of a low structure LCF-type carbon black by addition of Pigment Blue 27 (Vossen-Blau 705) and Pigment Violet 27 or by toning with a 4:1 combination of Pigment Blue 27 and Pigment Red 57:1. A mixture of asphalt resin, calcium/zinc resinate and phenol resin was used as a binder. The pigment concentration for all was 13.2%. The toner was added in 2.2% steps up to 6.6% with a simultaneous reduction from 13.2 to 6.6%.

Toning of Black Offset Printing Inks. The basic requirements for the successful use of iron blue as a toning agent in offset printing inks are resistance to damping or "fountain"

solutions and good dispersibility. "Resistance" is understood here as the hydrophobic characteristics of the pigment.

This property prevents wetting of the pigment by water and therefore its peptization. Non-resistant iron blue can render the ink useless by adsorbing water to above the normal content. A negative side-effect of peptization is the "dissolution" of the blue pigment from the printing ink and the resulting blue colouration of the fountain solution with the familiar problems of printing-plate contamination, also known as scumming or toning.

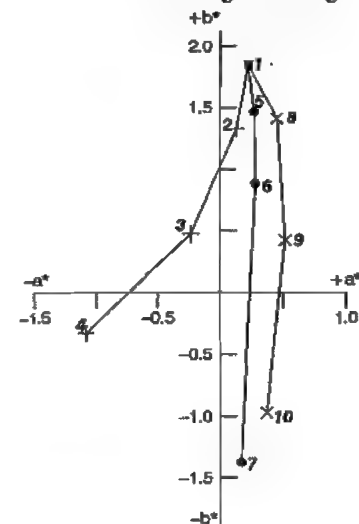


Figure 5.123: Colour coordinates of black gravure inks with different toning. + 2–4: Pigment Black LCF/Vossen-Blau 705; ● 5–7: Pigment Black LCF/[VB 705–Pigment Red 57:1(4:1)]; × 8–10: Pigment Black LCF/[VB 705 Pigment Violet 27 (2:1)]; ■ 1: Pigment Black LCF = Printex 35.

The combined dispersion of pigments is only practical with colourants of similar dispersibility. Toning agents with a considerable higher resistance to dispersion than carbon black are therefore delivered by the manufacturer in the form of a predispersed paste or must be ground separately by the user.

Developments in the fields of iron blue technology have overcome these problems. A new generation of pigments has been generated which covers both the demand for a sufficient resistance against damping solutions and the request for a good dispersibility. Easily

dispersible iron blue is preferred to be used for combined dispersion with carbon black in the so-called "Co-Grinding" process.

In the following section, the coloristic effects of those iron blue pigments are described, as obtained in toning experiments involving a LCF-type carbon black, in comparison with Pigment Blue 15:3 and Pigment Blue 61.

The pigment concentration of the inks is 24%, i.e. the amount of carbon black was reduced correspondingly with the addition of 3, 6, or 9% of blue pigment. Black inks containing 15 to 24% of carbon black are excluded from this experiment, and are presented to give an additional coloristic description of "pigment" black as regards the development of the hue when used as a self-colour pigment in increasing concentrations.

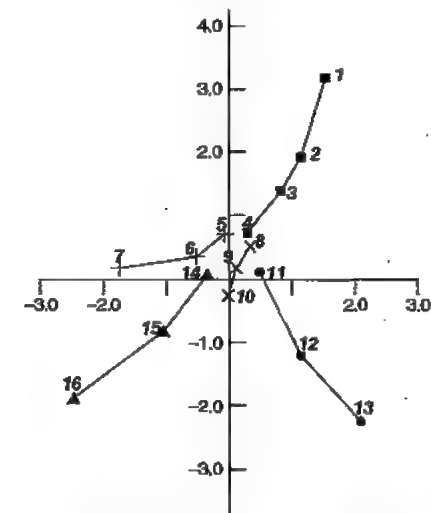


Figure 5.124: Colour locations of black offset printing inks with different toning. ■ 1–4: Pigment Black LCF (= Printex 35); + 5–7: Pigment Black LCF/Manox Easiperse; × 8–10: Pigment Black LCF/[Manox Easiperse/Pigment Red 57:1(4:1)]; ● 11–13: Pigment Black LCF/Pigment Blue 61; ▲ 14–16: Pigment Black LCF/Pigment Blue 15:3.

In the visual and the colorimetric evaluation the colour location change of the carbon black when used as a self-colour pigment is noticeable since there is a tendency to a black with a blue undertone at higher pigment concentration, even without the addition of toning

agent. In Figure 5.124 these are the colour locations 1–4, starting with 15% carbon black and in increasing additions in steps of 3% to a maximum concentration of 24%.

However, it is also clear that without the addition of a blue pigment the achromatic point cannot be achieved.

By adding various toning agents the desired colour hue is achieved - although with varying red/green spread. Iron blue (Manox Easisperse 154) brings about a clear shift towards green with a relatively small shift in the blue direction (see colour locations 5–7). The required target is more successfully achieved by the use of a mixture of iron blue and Pigment Red 57:1 in the ratio 4:1. The colour locations 8–10 illustrate useful ways of approaching the achromatic point with the addition of 3%, 6%, and 9% of the mixture.

The addition of 3% of Pigment Blue 61 already results in a significant step towards blue/red and shows almost identical incremental changes with further additions (see colour locations 11–13). In addition, the bronze effect occurs which intensifies with increasing distance from the achromatic point. With Pigment Blue 15:3 in numerically equivalent increments, the hue of the black ink moves towards blue/green in the opposite direction from the achromatic point and with a negative shift (colour locations 14–16).

Agriculture. Since ca. 1935 and especially in Mediterranean countries, blue inorganic fungicides based on copper and used for treating vines have largely been replaced by colorless organic compounds. Micronized iron blue pigments are used to color these fungicides (normally at a concentration of 3–8%), so that even small amounts become visible due to the high color intensity, and precise control is possible. The fungicide is usually milled or mixed with a micronized iron blue pigment [403].

A welcome side effect of treating fungi (e.g., *peronospora plasmopara viticola*) with iron blue is the fertilizing of vines in soils that give rise to chlorosis. Leaf color is intensified, aging of the leaves is retarded, and wood quality ("ripeness") is also improved [404–

406]. Iron is necessary for chlorophyll synthesis, which improves grape quality and yield. Other iron salts do not have this effect [405].

Paints and Coatings. Iron blue pigments are used in the paint industry, especially for full, dark blue colors for automotive finishes. A full shade with good hiding power is produced by 4–8% iron blue pigments.

Paper. Blue paper can be produced by adding "water-soluble" iron blue pigment directly to the aqueous phase. Alternatively, a suitable iron blue pigment can be ground together with a water-soluble binder, applied to the paper, dried, and glazed (quantity applied: ca. 8% in the finished product).

Pigment Industry. The importance of iron blue in the production of chrome green and zinc green pigments has greatly increased worldwide (see Section 46.10.2.3).

Medical Applications. Iron blue has become important as an agent for decontaminating persons who have ingested radioactive material. The isotope ^{137}Cs which would otherwise be freely absorbed via the human or animal digestive tract exchanges with the iron(II) of the iron blue [407, 408] and is then excreted in the feces [409]. Gelatin capsules containing 500 mg iron blue are marketed as Radiogardase-Cs (Heyl). Thallium ions have been found to behave similarly [410–412]. The gelatin capsules for this purpose are sold as "Antidotum Thalii" (Heyl) [413].

5.21.2.5 Toxicology and Environmental Aspects

Blue pigment compounds show no toxicity in animal studies therefore it is not expected to cause any adverse effects on human health. No toxic effects were reported in humans when blue pigment compounds were used experimentally or therapeutically.

Toxicokinetic studies showed, that the adsorption of iron blue pigments is very low. Following intravenous injection of a ^{59}Fe -radio labelled iron blue pigment, the $[\text{Fe}(\text{CN})_6]^{4-}$ ion was rapidly and virtually

completely excreted with the urine. After oral administration of ferric cyanoferrate (^{59}Fe) approx. 2% of the labelled hexacyanoferrate ion was absorbed by the gastro-intestinal tract [414]. Most of the substance is excreted with the feces [415] and there was no evidence of its decomposition.

The decomposition of blue pigment salts to toxic cyanide in aqueous systems is very low. The CN-release of $\text{KFe}[\text{Fe}(\text{CN})_6]$ in artificial gastric or intestinal juice was 141 or 26 $\mu\text{g}/(\text{g} \cdot 5 \text{ hours})$ respectively and in water 37 $\mu\text{g}/(\text{g} \cdot 5 \text{ hours})$. The corresponding figure of $\text{Fe}_4[\text{Fe}(\text{CN})_6]_3$ were 64, 15 and 22 $\mu\text{g}/(\text{g} \cdot 5 \text{ hours})$ [416].

In the breath of rats after i.p. injection of ^{14}C -labelled $\text{KFe}[\text{Fe}(\text{CN})_6]$ less than 0.01% (detection limit) was found, whereas in another study 0.04–0.08% of the orally administered dose was found in the exhaled air [417]. It can be concluded, that the hexacyanoferrate(II) complex disintegrates only to a small extent in the intestinal tract after oral administration. This is confirmed by the results of acute oral toxicity studies which show in high doses no clinical symptoms or lethality. The LD_{50} values are above 5000–15 000 mg/kg (limit tests) [418–420].

In primary irritation tests no or only slight effects were seen at the skin or in the eyes of the treated rabbits respectively [420, 421]. No skin sensitisation occurred in a Guinea pig maximisation test [418].

The subchronic (90–120 days) consumption of iron blue pigments at concentrations of 1–2% in the food or drinking water influenced slightly the body weight gain, but no other clinical signs or histopathological changes were observed [422–425]. After the administration of daily doses of 200 or 400 mg/kg for ten days to dogs the body weight gained and the general condition remained unaffected [426].

In a bacterial test system (ames test) no increase of mutagenicity was detected without or in presence of a metabolic system [420].

In human volunteers who received 1.5 or 3.0 g ferric cyanoferrate for up to 22 days ap-

part from a slight obstipation no effects were reported [426, 427].

$\text{Fe}_4[\text{Fe}(\text{CN})_6]_3$ can bind cesium therefore iron blue pigments are used in clinical practice as an antidote for the treatment of humans contaminated with radioactive cesium (see also section 5.21.2.4). Clinical use of iron(III) ferrocyanide in doses up to 20 g/d for decontaminations of persons exposed to radio cesium has not been associated with any reported toxicity [428].

Blue pigment salts are also used as an effective antidote for thallium intoxications. Ferric cyanoferrate interferes with the enterosystemic circulation of thallium ions and enhances their faecal excretion [429].

In a semistatic acute fish toxicity test (*Leuciscus idus*, melanotus, fresh water fish) a saturated solution with different blue pigment compounds (with unsolved material on the bottom or filtrated solution) no death occurred within 96 hours. Based on the quantity weighed the *No Observed Effect Level* (NOEL) is greater than 1000 mg/L (nominal concentrations) [430].

The bacterial toxicity was measured according DEV, DIN 38 412, L3 (TTC [2,3,5-triphenyl-2H-tetrazolium chlorid] test). The result gives an EC_{50} (effective concentration) varying between 2290 and 14 700 mg/L, and estimated NOEC values in the range of < 10 to 100 mg/L [431].

There are no harmful effects on fish, but the toxic effects on bacteria constitute a slight hazard when iron blue pigments are present in water.

5.21.3 Iron Magnetic Pigments

5.21.3.1 Iron Oxide Magnetic Pigments

Ferrimagnetic iron oxide pigments are used in magnetic information storage systems such as audio and videocassettes, floppy disks, hard disks, and computer tapes. Cobalt-free iron(III) oxide and nonstoichiometric mixed-phase pigments have been used since the early

days of magnetic tape technology. Currently, $\gamma\text{-Fe}_2\text{O}_3$ and Fe_3O_4 (the latter in small amounts) are mainly used in the production of low-bias audio cassettes [iron oxide operating point IEC I standard (International Electrotechnical Commission)], and studio, broadcasting, and computer tapes.

Production. The shape of the pigment particle is extremely important for ensuring good magnetic properties. Isometric iron oxide pigments produced by direct precipitation are seldom used. Since 1947, needle-shaped $\gamma\text{-Fe}_2\text{O}_3$ pigments have been prepared with a length to width ratio of ca. 5:1 to 20:1 and a crystal length of 0.1–1 μm [432].

Anisometric forms of Fe_3O_4 with the spinel structure or $\gamma\text{-Fe}_2\text{O}_3$ with a tetragonal superlattice structure do not crystallize directly. They are obtained from iron compounds that form needle-shaped crystals (usually α - and $\gamma\text{-FeOOH}$) [433–435]. The oxyhydroxides are converted to Fe_3O_4 by dehydration and reduction. Reducing agents may be gases (hydrogen, carbon monoxide) or organic compounds (e.g., fatty acids). The particle geometry is retained during this process.

Since the pigments are subjected to considerable thermal stress during this conversion, the FeOOH particles are stabilized with a protective

coating of sintered material (usually silicates [436], phosphates [437], chromates [438], or organic compounds such as fatty acids [439]).

Finely divided stoichiometric Fe_3O_4 pigments are not stable to atmospheric oxidation. They are therefore stabilized by partial oxidation or by complete oxidation to $\gamma\text{-Fe}_2\text{O}_3$ below 500 °C.

In an alternative process, the starting material consists of needle-shaped particles of $\alpha\text{-Fe}_2\text{O}_3$ instead of FeOOH pigments [440, 441]. The synthesis is carried out in a hydrothermal reactor, starting from a suspension of $\text{Fe}(\text{OH})_3$, and crystal growth is controlled by means of organic modifiers.

Properties. Magnetic pigments with very different morphological and magnetic properties that depend on the field of application and quality of the recording medium, are used. The largest particles (length ca. 0.6 μm) are used in computer tapes. The noise level of the magnetic tape decreases with decreasing particle size. Fine pigments are therefore being used increasingly for better quality compact cassettes.

The magnetic properties may be determined by measurement of hysteresis curves on the powder or magnetic tape.

Table 5.49: Some quality requirements for iron oxide and metallic iron magnetic pigments.

Field of application	Pigment type	Approximate particle length, mm	Specific surface area, m^2/g	Coercive field strength H_c , kA/m	Saturation magnetization M_s , $\text{mT} \cdot \text{m}^3/\text{kg}$	M_r/M_s
Computer tapes	$\gamma\text{-Fe}_2\text{O}_3$	0.60	13–17	23–25	y	0.80–0.85
Studio radio tapes	$\gamma\text{-Fe}_2\text{O}_3$	0.40	17–20	23–27	85–92	0.80–0.85
IEC I compact cassettes standard (iron oxide operating point)	$\gamma\text{-Fe}_2\text{O}_3$	0.35	20–25	27–30	87–92	0.80–0.90
high grade	$\text{Co-}\gamma\text{-Fe}_2\text{O}_3$	0.30	25–37	29–32	92–98	0.80–0.90
IEC II compact cassettes (CrO_2 operating point)	$\text{Co-}\gamma\text{-Fe}_2\text{O}_3$, $\text{Co-Fe}_3\text{O}_4$	0.30	30–40	52–57	94–98	0.85–0.92
IEC IV compact cassettes (metal operating point)	metallic iron	0.35	35–40	88–95	130–160	0.85–0.90
Digital audio (R-DAT)*	metallic iron	0.25	50–60	115–127	130–160	0.85–0.90
1/2" Video	$\text{Co-}\gamma\text{-Fe}_2\text{O}_3$, $\text{Co-Fe}_3\text{O}_4$	0.30	25–40	52–57	94–98	0.80–0.90
Super-VHS video	$\text{Co-}\gamma\text{-Fe}_2\text{O}_3$	0.20	45–50	64–72	94–96	0.80–0.85
8-mm video	metallic iron	0.25	50–60	115–127	130–160	0.85–0.90

*R-DAT: rotary digital audio tape.

Table 5.49 shows some quality requirements for the most important applications of magnetic pigments. Column 4 gives the coercive field strength (H_c) required for information storage materials. The coercive field is the magnetic field required to demagnetize the sample.

The saturation magnetization M_s is a specific constant for the material and for magnetic iron oxides is principally determined by the Fe^{2+} ion content. The ratio of remanent magnetization to saturation magnetization (M_r/M_s) for the tape depends mainly on the orientation of the pigment needles with respect to the longitudinal direction of the tape, and should approach the theoretical maximum value of unity as closely as possible.

Apart from the morphological and magnetic properties, usual pigment properties such as pH value, tap density, soluble salt content, oil absorption, dispersibility, and chemical stability are of great importance for the manufacture of magnetic recording materials.

Producers of magnetic iron oxides include BASF and Bayer (Germany); Ishihara, Sakai, Showa Denko, Titan K., and Toda K (Japan); 3M, Magnox (USA); and Saehan Media (Korea).

World production of cobalt-free magnetic iron oxides in 1990 was ca. 24 000 t, of which ca. 74% was used in compact cassettes and audio tapes, and ca. 25% in computer tapes.

5.21.3.2 Cobalt-Containing Iron Oxide Pigments

Cobalt-containing iron oxides form the largest proportion (ca. 60%) of magnetic pigments produced today. Due to their high coercivity they can be used as an alternative to chromium dioxide for the production of video tapes, high-bias audio tapes (CrO_2 operating point), and high-density floppy disks.

Production. The iron oxide pigments described above are either doped or coated with cobalt:

- Body-doped pigments contain 2–5% cobalt that is uniformly distributed throughout the

hulk of the pigment particles. It is either incorporated during production of the FeOOH precursor or precipitated as the hydroxide onto one of the intermediate products [442] using cobalt(II) salts as the cobalt source.

- Cobalt-coated pigment particles (2–4% Co) consist of a core of $\gamma\text{-Fe}_2\text{O}_3$ or nonstoichiometric iron oxide phase, and a 1–2 nm coating of cobalt ferrite with a high coercivity [443]. The coating can be produced by adsorption of cobalt hydroxide, or epitaxial precipitation of cobalt ferrite in a strongly alkaline medium [444, 445]. Surface-coated pigments show better magnetic stability than doped pigments.

Properties. Pigments with a coercive field strength of 50–56 kA/m are used in video cassettes, high-bias audio cassettes (chromium dioxide operating point IEC II), and high-density floppy disks. Depending on the quality of the tape, the particle size varies between 0.2 and 0.4 μm (Table 5.49).

Pigments with a higher coercive field strength (ca. 70 kA/m) and smaller particle size (particle length ca. 0.15–0.2 μm) are used for super VHS cassettes.

Pigments treated with only small amounts of cobalt (0.5% Co, coercive field strength ca. 31 kA/m) are used as an alternative to cobalt-free $\gamma\text{-Fe}_2\text{O}_3$ pigments for high-quality low-bias audio cassettes.

Cobalt-containing pigments are mainly produced by the magnetic iron oxide producers. World production for 1990 was 45 000 t, of which the highest proportion (ca. 85%) was used for video tapes.

5.21.3.3 Metallic Iron Pigments

The magnetization of iron is more than three times higher than that of iron oxides. Metallic iron pigments can have a coercive field strength as high as 150 kA/m, depending on particle size. These properties are highly suitable for high-density recording media. Oxidation-resistant products based on metallic pigments first became available in the late 1970s.

Production. Metallic iron pigments are commercially produced by the reduction of acicular (needle-shaped) iron compounds [446]. As in the production of magnetic iron oxide pigments, the starting materials are iron oxide hydroxides or iron oxalates, which are reduced to iron in a stream of hydrogen either directly or via oxidic intermediates.

Due to their high specific surface area, metallic pigments are pyrophoric, so that passivation is necessary. This can be achieved by slow, controlled oxidation of the particle surface [447].

Properties. The coercive field strength of metallic iron pigments is primarily determined by their particle shape and size, and can be varied between 30 and 150 kA/m. Pigments for analog music cassettes ($H_c \approx 90$ kA/m) usually have a particle length of 0.35 μm (Table 5.49). The length to width ratio of the pigment needles is ca. 10:1. Finely divided pigments (particle length ca. 0.25 μm) with a coercive field strength of 120 kA/m are used for 8-mm video and digital audio cassettes (R-DAT), tapes used by television organizations (ED Beta, Betacam SP MP, M II, Digital Video D2), and for master video cassettes (mirror master tapes). In the field of data storage, a small quantity is used in micro floppy disks.

Metallic pigments have a higher specific surface area (up to 60 m^2/g) and a higher saturation magnetization than oxidic magnetic pigments. Their capacity for particle alignment corresponds to that of the oxides (Table 5.49).

Economic Aspects. The largest producers of metallic iron pigments are Chisso, Dowa Mining, Kanto Denka K., Mitsui Toatsu, and Nisan Chemicals (Japan).

World consumption in 1990 was ca. 1000 t, of which ca. 75% was used in the manufacture of video tapes and ca. 25% for audio tapes. Consumption is expected to increase.

5.21.3.4 Barium Ferrite Pigments

Barium ferrite pigments have been considered for several years for high-density digital

storage media [448, 449]. They are very suitable for preparing unoriented (e.g., floppy disks), longitudinally oriented (conventional tapes), and perpendicularly oriented media. In the latter the magnetization is oriented perpendicular to the coating surface. They are required for perpendicular recording systems which promise extremely high data densities, especially on floppy disks. Barium and strontium ferrites are also used to prevent forgery of magnetic stripes, e.g., in cheque and identity cards.

Properties. Hexagonal ferrites have a wide range of structures distinguished by different stacking arrangements of three basic elements known as M, S, and Y blocks [450]. For magnetic pigments, the M-type structure (barium hexaferrite $\text{BaFe}_{12}\text{O}_{19}$) is the most important. The magnetic properties of M-ferrite can be controlled over a fairly wide range by partial substitution of the Fe^{3+} ions, usually with combinations of di- and tetravalent ions such as Co and Ti. Barium ferrite crystallizes in the form of small hexagonal platelets. The preferred direction of magnetization is parallel to the c-axis and is therefore perpendicular to the surface of the platelet. The specific saturation magnetization of the undoped material is ca. 72 Am^2/kg and is therefore somewhat lower than that of other magnetic oxide pigments. In barium ferrite the coercive field strength is primarily determined by the magnetocrystalline anisotropy and only to a limited extent by particle morphology. This is the reason why barium ferrite can be obtained with extremely uniform magnetic properties. Barium ferrite pigments have a brown color and chemical properties similar to those of the iron oxides.

Production. There are three important methods for manufacturing barium ferrite on an industrial scale: the ceramic, hydrothermal, and glass crystallization methods. The main producers are Toshiba and Toda.

Ceramic Method. Mixtures of barium carbonate and iron oxide are reacted at 1200–1350 $^\circ\text{C}$ to produce crystalline agglomerates which are ground to a particle size of ca. 1 μm .

This method is only suitable for the high-coercivity pigments required for magnetic strips [451].

Hydrothermal Method. Iron $[\text{Fe}(\text{III})]$, barium, and the dopants are precipitated as their hydroxides and reacted with an excess of sodium hydroxide solution (up to 6 mol/L) at 250–350 $^\circ\text{C}$ in an autoclave. This is generally followed by an annealing treatment at 750–800 $^\circ\text{C}$ to obtain products with the desired magnetic properties. Many variations of the process have been described [452–456], the earliest report being from 1969 [457]. In later processes, hydrothermal synthesis is followed by coating with cubic ferrites, a process resembling the cobalt modification of iron oxides. The object is to increase the saturation magnetization of the material [458–460].

Glass Crystallization Method. This process was developed by Toshiba [461]. The starting materials for barium ferrite production are dissolved in a borate glass melt. The molten material at ca. 1200 $^\circ\text{C}$ is quenched by pouring it onto rotating cold copper wheels to produce glass flakes. The flakes are then annealed to crystallize the ferrite in the glass matrix. In the final stage the glass matrix is dissolved in acid. In a variation of this process, the glass matrix is produced by spray drying [462].

Magnetic Recording Properties. Typical values of physical properties of barium ferrite pigments used in magnetic recording are given in Table 5.50.

Barium ferrite is highly suitable for high-density digital recording mainly because of its very small particle size and its very narrow switching field distribution. It also has a high anhysteretic susceptibility and is difficult to overwrite [463]. This is partly explained by positive interaction fields between particles in the coating layer [464]. The high anhysteretic

susceptibility makes barium ferrite media particularly suitable for the anhysteretic (bias field) duplicating process [465]. Unlike many other magnetic materials used in high-density recording, barium ferrite, being an oxide, is not affected by corrosion [466]. Processing of the pigment can be problematic, e.g., applying orienting fields can easily lead to unwanted stacking of the particles which has adverse effects on the noise level and the coercive field strength of the magnetic tape. A marked temperature dependence of the magnetic properties was a problem in the early days, but this can be overcome by appropriate doping [467].

5.21.4 Iron Phosphide

Commercial iron phosphide anticorrosive pigments usually consist of Fe_2P with traces of FeP and SiO_2 . The pigment is a powder with a metallic gray color and contains 70% Fe, 24% P, 2.5% Si, and 3.0% Mn. The density is 6.53 g/cm^3 and the mean particle size is ca. 3–5 μm .

Iron phosphide anticorrosive pigments are recommended by manufacturers as replacement materials for zinc dust to reduce the price of zinc-rich paints [468].

A trade name for iron phosphide is Ferrophos (Hooker Chemicals & Plastics Corp., USA).

5.21.5 Iron Oxide–Mica Pigment [469–474]

Mica can be coated not only with TiO_2 but also with other metal oxides that are deposited from hydrolyzable metal salts [469–474]. Iron(III) oxide is highly suitable because it combines a high refractive index (metallic luster) with good hiding power and excellent weather resistance [475].

Table 5.50: Typical properties of barium ferrite pigments.

Application	Specific surface area, m^2/g	Platelet diameter, nm	Platelet thickness, nm	H_c , kA/m	M_s/p , Am^2/kg
Unoriented (floppy disk)	25–40	40–70	15–30	50–65	50–65
Oriented	25–60	40–120	10–30	55–100	50–65
Magnetic strips	12–15	100–300	50–100	220–440	60–70

Aqueous precipitation reactions are used for production of commercial Fe_2O_3 -mica pigments, starting from Fe^{2+} or Fe^{3+} with subsequent calcination at 700–900 °C.

Pigments can also be produced by a direct CVD fluidized-bed process based on oxidation of iron pentacarbonyl and deposition of Fe_2O_3 on mica and other platelet substrates [476, 477].

Brilliant, intense colors are obtained with 50–150 nm layers of Fe_2O_3 (hematite) on muscovite. Absorption and interference colors are produced simultaneously and vary with layer thickness. Especially the red shades are more intense than those of TiO_2 -mica pigments because interference and absorption enhance each other. An intense green-red flop with different viewing angles is possible at a Fe_2O_3 layer thickness producing green interference [478]. A theoretical investigation is given in [479, 480].

On account of their good hiding power, high chemical inertness, lack of toxicity, and brilliant intense color in the bronze, copper, and red ranges, these pigments are becoming increasingly important in sophisticated end uses such as automotive coatings and cosmetics.

5.21.6 Transparent Iron Oxides

Transparent yellow iron oxide has the α - $\text{FeO}(\text{OH})$ (goethite) structure; on heating it is converted into transparent red iron oxide with the α - Fe_2O_3 (hematite) structure. Differential thermogravimetric analysis shows a weight loss at 275 °C. Orange hues develop after brief thermal treatment of yellow iron oxide and can also be obtained by blending directly the yellow and red iron oxide powders.

Production. *Transparent yellow iron oxide*, C.I. Pigment Yellow 42:77492, is obtained by the precipitation of iron(II) hydroxide or carbonate with alkali from iron(II) salt solutions and subsequent oxidation to $\text{FeO}(\text{OH})$. On an industrial scale, oxidation is usually carried out by introducing atmospheric oxygen into the reaction vessel. Important factors for good transparency are high dilution during precipi-

tation, a temperature of < 25 °C during oxidation, and short oxidation times (< 5 h). Oxidation can be carried out under acidic or basic conditions [481, 482]. The best results are obtained by using 6% iron(II) sulfate solutions and precipitation with ca. 85% sodium carbonate as a 10% solution. The starting material is usually crystalline $\text{FeSO}_4 \cdot 7\text{H}_2\text{O}$, obtained as a by-product from ilmenite in the pickling of iron or in the production of titanium dioxide according to the sulfate procedure. In order to improve pigment properties, the suspension is matured for about a day before filtration. It is then filtered, dried, and carefully ground to a powder. The primary particles are needle-shaped and have an average length of 50–100 nm, a width of 10–20 nm, and a thickness of 2–5 nm.

Transparent red iron oxide, C.I. Pigment Red 101:77491, is obtained by heating the yellow pigment (e.g., in a cylindrical rotary kiln) at 400–500 °C (Figure 5.125).

Figure 5.125: Electron micrograph of a transparent red iron oxide pigment (Sicotrans Red 2815).

Transparent red iron oxides containing iron oxide hydrate can also be produced directly by precipitation. A hematite content of > 85% can be obtained when iron(II) hydroxide or iron(II) carbonate is precipitated from iron(II) salt solutions at ca. 30 °C and when oxidation is carried out to completion with aeration and seeding additives (e.g., chlorides of magnesium, calcium, or aluminum) [483]. Transparent iron oxides can also be synthesized by

heating finely atomized liquid pentacarbonyl iron in the presence of excess air at 580–800 °C [484, 485]. The products have a primary particle size of ca. 10 nm, are X-ray amorphous, and have an isometric particle form. Hues ranging from red to orange can be obtained with this procedure, however, it is not suitable for yellow hues.

Transparent brown iron oxides are produced by precipitating iron(II) salt solutions with dilute alkali (sodium hydroxide or sodium carbonate) and oxidizing with air. Only two-thirds of the precipitated iron hydroxide, oxide hydrate, or carbonate is oxidized. Alternatively, the iron oxides can be produced by complete oxidation of the precipitate iron compounds and subsequent addition of half the amount of the initial iron salt solution and precipitation as hydroxide [486, 487]. However, these products have the composition $\text{FeO} \cdot \text{Fe}_2\text{O}_3$ and are ferromagnetic; they are not of practical importance.

Properties and Uses. As far as resistance to light, weather, and chemicals is concerned, transparent iron oxides behave in a similar manner to the opaque iron oxides. In addition, they show a high UV absorption, which is exploited in applications such as the coloring of plastic bottles and films used in the packaging of UV-sensitive foods [488, 489].

Worldwide consumption of transparent iron oxides is 2000 t/a. They are mainly used in the production of metallic paint in combination with flaky aluminum pigments and in the coloring of plastics for bottles and fibers.

Toxicology. Special toxicological studies on transparent iron oxides have not yet been carried out. The results of opaque iron oxides are applicable.

Trade names and producers include Capelle (Gebroeders Cappelle N.V., Belgium), Fastona Transparent Iron Oxide (Blythe Colours Ltd., UK), Sicotrans (BASF and BASF Lacke + Farben, Germany), and Trans Oxide (Hilton Davis, USA).

5.21.7 Transparent Iron Blue

Iron blue, C.I. Pigment Blue 27:77520 (Milor blue), also occurs in finely dispersed forms (primary particle size < 20 nm, specific surface area 100 m²/g) that are more transparent than the conventional iron blue pigments. They are generally produced by the same procedure as the less transparent iron blue pigments but a higher dilution factor is used. The transparency of these pigments is exploited solely in the production of printing inks (illustration gravure).

Trade names include Manox Iron Blue (Manox, UK), and Vossen-Blue 2000 (Degussa, Germany). Transparent iron blue pigments are also produced by Dainichiseika (Japan).

5.22 Coal and Coal Pyrolysis

5.22.1 Coal Petrology

Coal Characterization. Coal is an extremely heterogeneous, complex material that is difficult to characterize. Coal is a rock formed by geological processes and is composed of a number of distinct organic entities (macerals) and lesser amounts of inorganic substances (minerals). Each of the coal macerals and minerals has a unique set of physical and chemical properties; these in turn control the overall behavior of coal. Although much is known about the properties of minerals in coal, for example, the crystal chemistry, crystallography, and magnetic and electrical properties, surprisingly little is known about the properties of individual coal macerals. Even though coal is composed of macerals and minerals, it is not a uniform mixture of these substances. The macerals and minerals occur in distinct associations called lithotypes, and each lithotype has a set of physical and chemical properties that also affect coal behavior.

Coal seams, the basic units in which coal occurs, are in turn composed of layers of coal lithotypes, and individual coal seams may also have their own sets of physical and chemical properties. For example, even if two coal

seams have the same maceral and mineral composition, the seams may have significantly different properties if the maceral associations in lithotypes in the two seams are different. The enclosing rocks immediately adjacent to a coal seam can also affect the properties of the coal. This aspect is particularly important in mine design, production, and strata control. The compositional characterization of a coal seam must cover the nature of the macerals, the lithotypes, the entire seam, and the association of the seam with the neighboring strata.

In addition to compositional factors, coal properties also change with the rank or the degree of coalification of a given sample of coal. Coal is part of a metamorphic series ranging from peat, through lignite and subbituminous and bituminous coal, to anthracite. Temperature, pressure, and time alter the original precursors of coal through this metamorphic series. As the rank of the coal changes, the properties of the coal macerals change progressively and, therefore, so also do the properties of lithotypes and the entire seam.

Because of these factors, coal characterization requires a detailed knowledge of both the maceral composition and the rank of the coal. All coal properties are ultimately a function of these two factors.

The Maceral Concept. The term maceral was introduced by STOPES to distinguish the organic components of coal (macerals) from the inorganic components (minerals) [490]. The term is now interpreted in two conflicting ways. The interpretation of the International Committee for Coal Petrology (ICCP) is that a maceral is the smallest microscopically recognizable component of coal [491]. This conception, generally held by most European coal petrographers, is based on morphology and other criteria such as size, shape, botanical affinity, and occurrence. The ICCP concept implies that the properties of the macerals change with rank. Thus, the same maceral, vit-

rinite, can exist in a bituminous coal as well as in an anthracite.

In contrast, the maceral concept of SPACKMAN (commonly held in North America) is based on the idea that macerals are substances with distinctive sets of properties [492]. Thus, vitrinite in a bituminous coal is viewed as a different maceral than vitrinite in an anthracite because the two materials have different properties.

The basis of the petrographic study of coal composition is the idea that coal is composed of a number of distinct macerals. The entire body of coal petrographic literature supports this idea and is in direct contrast to the earlier chemical concept of coal being composed of a single unique molecular substance. Although the concept and the term "coal molecule" may once have been useful, modern chemical studies of coal recognize coal's heterogeneous maceral composition.

Maceral Types and Properties. A large number of different macerals have been named and classified in various systems. The ICCP system is given in part in Table 5.51. Although this system is useful for some purposes, it is impractical for routine maceral analysis because of the large number of terms. For such routine analysis, classification systems with a limited number of terms are needed. In the standard method for maceral analysis D 2799 of the American Society for Testing and Materials (ASTM), only six terms are required, although some additional terms are defined in ASTM Standard D 2796 (see Table 5.52).

Although there is no standard method for the analysis of fluorescent macerals, some additional terms, listed in Table 5.52, are used for this type of analysis.

As shown in Table 5.52, coal macerals fall into three distinct groups: vitrinite, liptinite, and inertinite. Vitrinite macerals are generally the most abundant, commonly making up 50–90% of North American coals. This group is not as abundant in coals that originate in the southern hemisphere.

Table 5.51: Survey of the macerals of hard coal, according to the ICCP system.

Maceral group	Maceral	Maceral type ^a	Maceral variety ^a	Kryptomaceral ^a
Vitrinite	telinite		cordaitelinite fungotelinite xylotelinite	
	collinite	telocollinite gelocollinite desmocollinite corpocollinite		kryptotelinite kryptocorpocollinite
	vitrodetrinite			
Exinite	sporinite		tenuisporinite crassisporinite microsporinite macrosporinite	
	cutinite resinite alginite liptodetrinite			
Inertinite	micrinite macrinite semifusinite fusinite			
	sclerotinite	pyrofusinite degradofusinite		
			plectenchyminite corposclerotinite pseudocorposclerotinite	
	inertodetrinite			

^a Incomplete, can be arbitrarily extended.

Table 5.52: Classification of macerals, according to the ASTM system, for routine analysis.

Maceral group	Maceral ASTM D 2799	Additional ASTM D 2796	Terms used in fluorescence analyses
Vitrinite	vitrite	pseudo-vitrite	fluorescing vitrite
Liptinite	exinite resinite	sporinite cutinite alginite	fluorinite bituminite exudatinitite
Inertinite	micrinite semifusinite fusinite	macrinite sclerotinitite	

Most vitrinite macerals are derived from the cell wall material (woody tissue) of plants. Although the details of the vitrification process are not well understood, it is generally believed that during the coalification process the plant cell wall material is chemically altered and broken down into colloidal particles that are later deposited and desiccated. This process commonly homogenizes the components so that the resulting macerals are structureless. The variation in vitrinite macerals is usually thought to be due to differences in the original plant material or to different conditions of al-

teration at the peat stage or during later coalification.

Under the microscope, vitrinite macerals have a reflectance (brightness) between that of the liptinite and inertinite macerals. Because the reflectance of the vitrinite macerals shows a more or less uniform increase with coal rank, reflectance measurements for the determination of rank are always taken exclusively on vitrinite macerals. The reflectance of vitrinite macerals is also anisotropic, so that in most orientations a particle of vitrinite will display two maxima and two minima with complete rotation. Two types of vitrinite are usually distinguished in North American coals. Normal vitrinite is almost always the most abundant maceral present and makes up the groundmass in which the various liptinite and inertinite macerals are dispersed. It has a uniform gray color and is always anisotropic. With UV excitation, some normal vitrinites will fluoresce. Pseudovitrinite always has a slightly higher reflectance than normal vitrinite in the same coal. It also tends to occur in large particles that are usually free of other macerals and py-

rite. Pseudovitrinite particles commonly show brecciated corners, serrated edges, wedge-shaped fractures, and slitted structures. Pseudovitrinite does not fluoresce under UV light.

In international practice, the terms desmocollinite, heterocollinite, and vitrinite B are used to describe normal vitrinite, and telocollinite, homocollinite, and vitrinite A are used for pseudovitrinite.

Liptinite macerals are derived from the waxy and resinous parts of plants, i.e., the spores, cuticles, and resins. This group generally makes up 5–15% of most North American coals, although it dominates some unusual types of coal such as cannel and boghead. In any given coal, liptinite macerals have the lowest reflectance. Liptinite macerals are the most resistant to alteration or metamorphism in the early stages of coalification; thus, the reflectance changes are slight up to the rank of medium-volatile coal. In this range the reflectance of liptinite macerals increases rapidly until it matches or exceeds the reflectance of vitrinite macerals in the same coal and, thus, essentially disappears. Sporinite is the most common of the liptinite macerals and is derived from the waxy coating of fossil spores and pollen. It generally has the form of a flattened spheroid with upper and lower hemispheres compressed until they fuse. The outer surfaces of the sporinite macerals often show various kinds of ornamentation. In Paleozoic coals, two sizes of spores are common. The smaller ones, usually < 100 μm in diameter, are called microspores, and the larger ones, ranging up to several millimeters in diameter, are called megaspores. Cutinite, found as a minor component in most coals, is derived from the waxy outer coating of leaves, roots, and stems. It occurs as long stringers, which often have one fairly flat surface and another that is crenulated. Cutinite usually has a reflectance equal to that of sporinite. Occasionally the stringers of cutinite are distorted. Resinite is also common in most coals and usually occurs as ovoid bodies with a reflectance slightly greater than that of sporinite and cutinite but still less than that of vitrinite.

Some of the larger pieces of resinite may appear to be translucent with an orange color. In some coals, particularly in those from the western United States, a number of different forms of resinite may be distinguished by using fluorescent microscopy. Alginite is derived from fossil algæ colonies. It is rare in most coals and is often difficult to distinguish from mineral matter. However, in UV light it fluoresces with a brilliant yellow color and can display a distinctive flower-like appearance.

Newly Defined Fluorescent Macerals. With the use of fluorescence microscopy, TEICHMÜLLER defined three new macerals: fluorinite, bituminite, and exudatinite [493]. Although these macerals have some characteristic features in normal white-light microscopy, they can be properly identified only by their fluorescence properties.

Fluorinite usually occurs as very dark lenses that may show internal reflections. Fluorinite is also commonly associated with cutinite. Fluorinite fluoresces with a very intense yellow color.

Bituminite is difficult to detect in white light and is often mistaken for mineral matter. It is common in vitrinite-poor detrital coals. It occurs as stringers and shreads and fluoresces weakly with an orange to brown color. This material is similar to what organic petrologists call amorphous organic matter (AOM).

Exudatinite is a secondary maceral which appears as an oil-like void filling. It has no shape of its own, and can usually only be detected by its weak orange to brown fluorescence in UV light.

The *inertinite* maceral groups are derived from plant material, usually woody tissue, that has been strongly altered by charring in a forest fire or by biochemical processes such as composting either before or shortly after deposition. These macerals can make up 5–40% of most North American coals, with the higher amounts occurring in Appalachian coals. In southern hemisphere coals, this group commonly is more abundant than vitrinite. The inertinite macerals have the highest magnitude

and greatest range of reflectance of all the macerals. They are distinguished by their relative reflectances and by the presence of cell texture.

Fusinite is seen in most coals and has a charcoal-like structure. It is always the highest reflecting maceral present and is distinguished by a cell texture that is commonly broken into small shards and fragments.

Semifusinite has the cell texture and general features of fusinite except that it is of lower reflectance. In fact, semifusinite has the largest range of reflectance of any of the various coal macerals. Semifusinite is also the most abundant of the inertinite macerals in most coals.

Macrinite is a very minor component of most coals and usually occurs as structureless ovoid bodies with the same reflectance as fusinite.

Micrinite occurs as very fine granular particles of high reflectance. [It is commonly associated with the liptinite macerals and sometimes gives the appearance of actually replacing the liptinite.]

5.22.2 Coalification

A unique and often troublesome feature of coal that distinguishes it from other fuels and bulk commodities is its property of rank. All coal starts out as peat, which is then changed into progressively higher ranks of coal. This transformation is generally divided into two phases. The first, which occurs in the peat stage, is called diagenesis or biochemical coalification. In this phase most of the plant material making up the peat is biochemically broken down. Specifically, most of the cellulose in the plant material is digested away by bacteria, and the lignin in the plant material is transformed into humic acids and humic compounds, humins. Some plant material is also thermally altered by partial combustion or biochemical charring. Still other plant material, such as spores and pollen, survive the diagenesis stage without much change. After diagenesis is complete and the altered peat is buried,

geological forces begin to act in the geological or metamorphic phase of coalification.

Because of the common occurrence of high-rank coals in geologically deformed areas, for example, anthracite in the eastern Appalachian Mountains and low-volatile bituminous coal in the folded and faulted Canadian Rocky Mountains, it was assumed that tectonic pressure was responsible for the high rank of most coals. However, this position has now lost most of its support because recent studies in the folded coal seams of the Ruhr Basin show that isorank lines (isovols) follow the folds in the seams [495]. This shows that the coal achieved its rank before the structural deformation and was not altered during or after such deformation. Similar studies of stratigraphic relationships in the Canadian Rocky Mountains showed that the higher rank coals correlated with increasing depth of burial and not tectonism [496]. Laboratory experiments using increased confining pressure have not led to increased coalification [497].

The majority of the geological evidence suggests that temperature is the major factor in coalification and that the temperature range in which most coalification takes place is 50–150 °C. The depth at which these temperatures occur is a function of the natural geothermal gradient (dT/dZ), which ranges from 0.8 °C/100 m to 4 °C/100 m. Therefore, at these two geothermal gradient extremes, the depth at which 150 °C would be reached, if a surface temperature of 20 °C is assumed, is 16.25 km (53 300 feet, 10.1 miles) for the lowest gradient and 3.25 km (10 700 feet, 2.02 miles) for the highest. The major lines of evidence for the importance of temperature in coalification are as follows:

- An increase in coal rank and temperature with depth is confirmed by thousands of bore holes.
- Lines of equal rank contour igneous intrusions and show an increase in rank in the direction of the intrusion. In some cases, natural coke is found at the contact of a coal seam with an intrusion.

- Laboratory experiments show that wood can be coalified by heating in an inert atmosphere. Increasing the pressure alone has no effect on the coalification of wood.
- When thermodynamic factors are considered, it is clear that temperature should have more of an effect than pressure. While an increase in temperature will encourage most coalification reactions by increasing the available energy, an increase in pressure may often inhibit such reactions by raising the energy requirements for such reactions to take place.

It was long thought that time was not a factor in coalification, and the example of the Russian paper coals of lignite rank and Carboniferous age was often cited as evidence. However, it is now believed that if the peat has been buried deeply enough to effect coalification, then time does have a "soaking effect". For example, in Venezuela there is a subbituminous coal of Eocene age that has been buried at a depth of 1120–1220 m at 125 °C for $(10-20) \times 10^6$ years. In Germany there is a coal that has been at the same depth and temperature for 300×10^6 years and is of anthracite rank [495]. Numerous other examples have been found and a number of correlation charts relating depths of burial, temperature, rank, and time are based on this type of data.

Changes in the coal rank correspond to changes in most of the properties of the coal. For example, as rank increases, moisture, volatile matter, and ultimate oxygen and hydrogen decrease, whereas fixed and ultimate carbon, calorific value, and reflectance increase. All of these measurements and even some combinations of these have been used as measures of coal rank. However, with the exception of reflectance, they all suffer from two major drawbacks. First, none actually change uniformly across the rank range of coal. Second, they are all bulk properties of coal and, thus, can be significantly affected by changes in maceral composition having nothing to do with rank. For example, a coal with a higher-than-normal content of liptinite macerals can have a higher-than-normal hydrogen content

and, therefore, appear to have a lower rank than it actually does on the basis of a rank parameter independent of composition such as reflectance. The reflectance parameter of coal is based on the amount of light reflected from the vitrinite macerals in a coal compared to a glass standard of known refractive index and reflectance. The vitrinite reflectance of coal changes uniformly across most of the coal rank range. However, it is not very sensitive in the lowest rank range (lignite to lower subbituminous).

5.22.3 Occurrence

Coal Seam Occurrence. Although coal particles are scattered throughout many rock units, most coal occurs in seams, which can range in thickness from a few millimeters to over 30 m. In North America and, indeed, most of the world, anthracite and bituminous coals occur in thinner seams of 1–2 m while the lower rank coals, lignite and subbituminous, commonly occur in thicker seams of up to 20–30 m. While many seams, even minable seams, are of a limited size area, some seams continuously underlie large areas. The Pittsburgh coal seam extends over 77 700 km² in Pennsylvania, Ohio, West Virginia, and Maryland, and it is of minable thickness for over 15 540 km².

Although there are hundreds of named coal seams in the United States, relatively few are of the quality, thickness, and size of area to be extensively exploited commercially. In the Appalachian anthracite region, the Mammoth seam is the major source of production. In the northern Appalachian field, the major minable seams are the Pittsburgh, Lower Kittanning (No. 5 Block), Upper Freeport, Campbell Creek (No. 2 Gas), Upper Elkhorn (No. 3), Fireclay, Pocahontas, and Sewell seams. All of these seams are suitable for use in making coke. In the southern Appalachians, the Sewanee, Mary Lee, and Pratt seams are the most important, and the latter two are used extensively as coking coals. In the Illinois Basin, the Harrisburg Springfield No. 5 and the Herrin No. 6 are of a minable thickness of over 38 800–51 800 km². In the Oklahoma, Kan-

sas, Missouri, and Arkansas region, the Weir-Pittsburg and Lower Hartshorne seams are the most important. In the Powder River Basin, the Anderson-D-Wyodak seam is continuously exposed for 193 km and is estimated to contain at least 91 Gt of coal. In Utah the Lower Sunnyside and Hiawatha seams have produced the most coal. The former is of coking quality, and the latter is characterized by a high resin content, which itself has been exploited. In Colorado the Wadge, Raton-Walsen, and Wheeler A, B, C, and D are the most important coal seams and some production from the Raton-Walsen and Wheeler seams has been used for coking. Finally, in Washington state the Roslyn (No. 5) is the most mined coal seam. Production from these seams accounts for ca. 75–80% of the cumulative past United States coal production [499].

Coal Seam Structures. All coal seams have a number of structural features, including partings, splits, rolls, cutouts, cleats, faults, folds, and alterations caused by igneous intrusions. These features strongly affect the mining and economical recovery of the coal. *Partings* are layers of rock, usually shale or sandstone, that occur within a coal seam and were caused by an influx of sediment into the original coal swamp. In commercial seams, the partings must, of necessity, be few and thin (a few centimeters). However, even in such seams the partings can be very extensive. For example, near the base of the Herrin No. 6 seam, there is a parting known as the blue band that is found throughout the entire Illinois Basin. When the thickness of a layer of rock within a seam increases to the point where it is no longer practical to mine the parting with the coal, the seam can be considered to have *split*. Although some seams like the Hiawatha in Utah split into three or more minable seams, the splitting of one seam into multiple seams can present serious problems in mining, including correlation (i.e., tracing a given seam across a zone, e.g., a valley, where it is missing) and loss of minable thickness.

In addition to partings and splits within the coal seam, the upper and lower surfaces of a

seam often pinch and swell to change the coal seam thickness. Such features have been called *pinches*, *rolls*, *horsebacks*, and *swells*, and their occurrence at the base of a seam is usually attributed to differential compaction. Roof rolls are common and the protrusion of rock into the coal causes some serious problems with mine roof stability. *Cutouts* or stream washouts are the extreme cases where the protrusion actually eliminates the coal seam. These features are clearly the result of nondeposition or erosion by ancient streams associated with the coal swamps.

Another important feature of coal seams, especially in bituminous coals, is the presence of closely spaced fractures within the coal. These fractures, called *cleats*, are usually perpendicular to the bedding plane of the coal and commonly occur in two sets perpendicular to each other. This gives the coal a tendency to break into blocks. The cleat controls the ease with which the coal breaks up, and it has long been used in coal mining. The most prominent cleat is called the face cleat because the working face of a mine is often parallel to it. The other cleat is called the butt cleat. Cleats give coal high permeability to gas and groundwater and also act as sites of mineral deposition. Calcite and pyrite are the most common cleat-filling minerals, although other minerals including gypsum can occur.

Faulting and *folding* of coal seams by geological forces can also be important features. Seams that are faulted or folded usually cannot be mined by surface methods and are more expensive to mine than flat seams. When faulting is extensive, even thick seams of high quality may be too discontinuous to mine. On the other hand, folding can double the minable thickness of some seams, thereby increasing their value, as with the anthracite seams in eastern Pennsylvania.

The *alteration* of coal seams by igneous intrusions is widespread and is a serious problem in some coal fields, such as those in the Rocky Mountains of the United States. The alteration is thermal and causes an increase in carbon content and a decrease in hydrogen, moisture, and volatile matter. In the contact

zone, the coal may be transformed into natural coke. Although such contact zones are usually small, extensive amounts of natural coke are known and have been commercially exploited in some areas such as the Raton Mesa of Colorado.

Coal Seam Distribution. Although coal seams are found in rocks of all geologic ages since the Devonian, the age distribution is not even. Major coal deposits of Carboniferous age occur in eastern and central North America, in the British Isles, and on the European continent. Major deposits of Permian age occur in South Africa, India, South America, and Antarctica. In Jurassic times the major coal accumulation was in Australia, New Zealand, and parts of Russia and China. The last great period of coal deposition was at the end of the Cretaceous period and the beginning of the Tertiary period. Coals originating at this time are found in the Rocky Mountains of North America, in Japan, Australia, New Zealand, and in parts of Europe and Africa. Because they are younger, these coals tend to be of lower rank, usually subbituminous, than the Carboniferous coals. Since the Cretaceous some coal has been deposited in scattered locations more or less continuously and tends to be lignite or brown coal.

The distribution of coal seams throughout the world is also not uniform. As shown in Figure 5.126, most of the world's coal is located in only three countries, the United States, the former Soviet Union, and China. Although the figures vary from source to source, each of these countries has about 25% of the total coal resources, while the rest of the world shares the remaining 25%. In the United States, bituminous coal seams are concentrated in the Appalachian and Illinois Basins. Most of the subbituminous coal occurs in the various smaller basins in the Rocky Mountain region, and the lignite seams are concentrated in the northern Great Plains and the Gulf Coast area.



Figure 5.126: Geographic location of the world's coal.

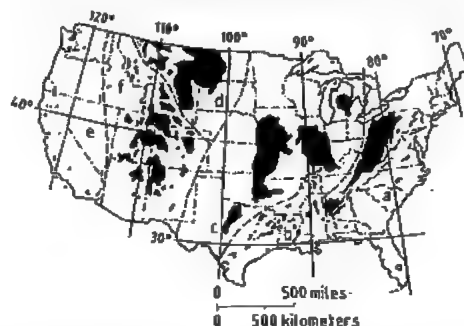


Figure 5.127: Coal provinces of the conterminous United States: a) Eastern; b) Gulf; c) Interior; d) Northern Great Plains; e) Pacific Coast; f) Rocky Mountains.

5.22.4 Classification

Coal is combustible and should be composed of more than 50% carbonaceous material [500]. Commercially, coal is classified in a number of ways on the basis of:

- The original plant or maceral composition, sometimes called coal type
- The degree of maturity or metamorphism, called coal rank
- The amount of impurities such as ash or sulfur, called coal grade
- The industrial properties such as coking or agglomeration.

One of the main classifications by composition used by the United States Bureau of Mines is based on the relative amounts of petrographic entities detected in thin-section analysis, including anthraxylon (translucent material roughly equivalent to vitrinite), translucent attritus (roughly equivalent to liptinite), and opaque attritus and fusain (roughly equivalent to inertinite) [501, 502]. Under this system, coals are divided into two groups: **banded coals**, with > 5% anthraxylon, and **nonbanded coals**, with < 5% anthraxylon. The banded coals are subdivided into three types: *bright coal*, consisting mainly of anthraxylon and translucent attritus with < 20% opaque matter, *semisplint coal*, consisting mainly of translucent and opaque attritus with 20–30% opaque matter, and *splint coal*, consisting mainly of opaque attritus with > 30% opaque matter. The nonbanded coals are divided into *cannel coal*, consisting of attritus with spores, and *boghead coal*, consisting of attritus with algae.

The various bands or layers in coal evident to the unaided eye have also been classified into four types [503]. *Vitrinite* layers appear bright and vitreous; *clarain* appears as relatively less bright, striated layers; *durain* is dull and featureless; *fusain* layers are dull gray and like charcoal. Although these terms (all ending in *ain*) are megascopic terms meant to be applied to hand-specimen samples, they do

have some compositional implications at the microscopic level. For example, vitrinite layers contain mainly vitrinite macerals, fusain layers contain mainly inertinite macerals, and clarain and durain are mixtures of all three maceral types.

The most important classification for commercial purposes in the United States is the ASTM classification by rank. It is the basis on which most of the coal in the United States is bought and sold. This classification, ASTM Standard D 388 shown in Table 5.53, divides coals into 4 classes, anthracite, bituminous, subbituminous, and lignitic, which are further subdivided into 13 groups on the basis of fixed carbon and volatile matter content, calorific value, and agglomerating character. The fixed carbon and volatile matter values are on a dry, mineral-matter-free basis and the calorific values are on a moist, mineral-matter-free basis. In this system, coals with ≥ 69% fixed carbon are classified by fixed carbon content and those with < 69% fixed carbon content are classified by calorific value.

Table 5.53: Classification of coal by rank. This classification does not include a few coals, principally nonbanded varieties, which have unusual physical and chemical properties and which come within the limits of fixed carbon or calorific value of the high-volatile bituminous and subbituminous ranks. All of these coals either contain < 48% dry, mineral-matter-free fixed carbon or have > 15 500 Btu/lb moist, mineral-matter-free.

Class	Group	Fixed carbon limits, % (dry, mineral-matter-free basis)	Volatile matter limits, % (dry, mineral-matter-free basis)	Calorific value limits, Btu/lb (moist, mineral-matter-free basis) ^a	Agglomerating character
Anthracite	metaanthracite	≥ 98	≤ 2	—	non-agglomerating
	anthracite	≥ 92 < 98	> 2 ≤ 8	—	
	semianthracite ^b	≥ 86 < 92	> 8 ≤ 14	—	
Bituminous	low-volatile bituminous coal	≥ 78 < 86	> 14 ≤ 22	—	commonly agglomerating ^c
	medium-volatile bituminous coal	≥ 69 < 78	> 22 ≤ 31	—	
	high-volatile A bituminous coal	— < 69	> 31	—	
	high-volatile B bituminous coal	—	—	≥ 14 000 ^c < 14 000 ^c	
	high-volatile C bituminous coal	—	0	≥ 11 500 < 13 000 ^c	
Subbituminous	subbituminous A coal	—	—	≥ 10 500 < 11 500	non-agglomerating
	subbituminous B coal	—	—	≥ 9 500 < 10 500	
	subbituminous C coal	—	—	≥ 8 300 < 9 500	
Lignitic	lignite A	—	—	≥ 6 300 < 8 300	
	lignite B	—	—	< 6 300	

^a Moist refers to coal containing its natural inherent moisture but not including visible water on the surface of the coal.

^b If agglomerating, classify in low-volatile group of the bituminous class.

^c Coals having 69% or more fixed carbon on the dry, mineral-matter-free basis shall be classified according to fixed carbon, regardless of calorific value.

^d It is recognized that there may be nonagglomerating varieties in these groups of the bituminous class, and there are notable exceptions in high-volatile C bituminous group.

Thus, all lignitic and subbituminous coals and the lower rank bituminous coals are classified by their calorific value. It is also important to note that not all coals can be fitted into this system. This is especially true of coals with a high liptinitic maceral content, such as cannel and boghead types.

The other important classification system is the international system of the ISO. In this system, coals are divided into two types: hard coals with greater than 23.86 MJ/kg (10260 Btu/lb) and brown coals and lignites with calorific values less than that amount. In the hard coal classification shown in Table 5.54, the coals are divided into classes, groups, and subgroups. The classes are similar to ASTM groups and based on dry, ash-free volatile matter and moist, ash-free calorific value. The classes are numbered as 0 to 9. The classes are divided into four groups, numbered 0 to 3 on the basis of the swelling properties (free-swelling index, also called crucible swelling number, and Roga index). These groups are further broken down into six subgroups numbered 0–5 on the basis of their Audibert–Arnu dilatation number and Gray–King coke type. The system is set up in such a way that all coals are classified with a three-digit number, in which the first digit is the class, the second digit is the group, and the third digit is the subgroup.

The lignites and brown coals are only divided into classes and groups. The classes, numbered from 1 to 6, are based on ash-free moisture; the groups, based on dry, ash-free tar yield, are numbered from 0 to 4. This classification is shown in Table 5.55.

Although the ASTM and International Systems are different, there is a reasonable correspondence between the ASTM group names and the International System class numbers. This is shown in Table 5.56.

5.22.5 Chemical Structure of Coal

The organic components of coal consist of a complex mixture of macromolecular carbon compounds of varied chemical constitution. The heterogeneity of coal is well-known from optical studies of thin coal sections. The microscopically distinct and distinguishable maceral groups of vitrinite, liptinite, and inertinite, their proportions, and the association of macerals of several groups with each other are essentially responsible for the physical, chemical, and technological properties of a particular coal. Preformed macerals derived from transformation of the original lipidic, woody, and waxy plant matter under varying oxidizing and reducing conditions and processes are present in peat and soft lignites. Temperature-induced chemical changes of these macerals and increased pressures influencing the physical structure of the material undergoing coalification have led to the formation of lignitic, subbituminous, bituminous, and anthracitic coals, forming the basis of coal classification by rank [504, 505].

The minerals of coal play a considerable part in the industrial use of coals of all ranks. The mineral content, its distribution within the coal and its composition may affect carbonization, gasification, combustion, and liquefaction processes by modifying the process of coal depolymerization and influencing hydrogenation and the thermal behavior of the resulting ash under both oxidizing and reducing conditions.

Besides microscopically unidentifiable plant ash, coals contain varying amounts of *syngenetic* and *epigenetic* minerals, which entered the organic coal substance during the first or second phase of coalification, respectively. They have either grown together with the organic substance or are physically separable. Generally, medium to high ash coals contain epigenetic minerals. Structure and hardness bear considerable influence on the distribution in the various fractions of the crushed coal from coal preparation plants.

Table 5.54: International classification of hard coal by type. Where the ash content of coal is too high to allow classification according to the present system, it must be reduced by laboratory float-and-sink method (or any other appropriate means). The specific gravity selected for flotation should allow a maximum yield of coal with 5–10% of ash.

Group (caking properties)	Group number	Free-swelling index	Roga index	Code numbers ^a										Subgroups (caking properties)	
				Code numbers ^a										Subgroup number	Gray–King
3	> 4	> 45		435	535	635								5	> G ₄
				334	434	534	634							4	G ₃ –G ₆
				333	433	533	633	733						3	G ₂ –G ₄
				332 ^b	432	532	632	732	832					2	E–G
2	2.5–4	20–45		323	423	523	623	723	823					3	G ₁ –G ₄
				322	422	522	622	722	822					2	E–G
				321	421	521	621	721	821					1	contraction B–D
1	1–2	5–20		212	312	412	512	612	712	812				2	E–G
				211	311	411	511	611	711	811				1	contraction B–D
0	0–0.5	0–5		100	100	200	300	400	500	600	700	800	900	.0	nonsoftening A
Class number ^c				0	1A	1B	2	3	4	5	6	7	8	9	
Volatile matter, % (dry, ash-free)	0–3	3–6.5	6.5–10	10–14	14–20	20–28	28–33	> 33	> 33	> 33	> 33	> 33	> 33	> 33	
Calorific parameter ^d															

^a First digit class, second digit group, third digit subgroup.

^b 332a: volatile matter 14–16% and 332b: volatile matter 16–20%.

^c Approximate volatile matter content 33–41% (class 6), 33–44% (class 7), 35–40% (class 8), and 42–50% (class 9).

^d Gross calorific value on moist ash-free basis (30 °C, 96% relative humidity) in Btu/lb.

Table 5.55: Classification of brown coal according to ISO 2950-1974-(E).

Group parameter: yield of tar on a dry, ash-free basis, %		Group number		Code number	
> 25	4	14	24	34	44
20–25	3	13	23	33	43
15–20	2	12	22	32	42
10–15	1	11	21	31	41
≤ 10	0	10	20	30	40
Class number		1	2	3	4
Class parameter: total moisture content of mined coal on an ash-free basis, %		≤ 20	20–30	30–40	40–50
					50–60
					60–70

Therefore, it is often necessary to evaluate coal properties further by subjecting samples to thermal, extractive, and mechanical tests, assessing on a small scale the expected behavior and at the same time providing for study of the types and compositions of specific reaction products.

Such experiments that yield fragmental decomposition compounds can also be employed for the structural identification of coals.

The determinations include, e.g., pyrolytic or progressive devolatilization tests, extraction or solubility studies, performance of selected coking tests, reactivity measurements on specially prepared cokes, grain stability evaluation, and ash slagging behavior.

Petrographic Studies

The determination of the petrographic composition of coals by maceral group analysis is a valuable tool for assessing structural aspects and predicting coal behavior. Usually it also incorporates the determination of the degree of coalification by measuring the reflectance of the vitrinite as the most important and abundant group of macerals. This method allows a ranking or classification of coals by their degree of coalification and, hence, identifies the type of coal. It also reveals specific phenomena that may have induced structural coal changes within the geochemical stage of coal formation, such as aging or contact coalification due to inflowing magma.

5.22.5.2 Structural Deductions from Analytical and Bench-Scale Data

The results of coal analyses predict thermal decomposition products (proximate analysis, carbonization assay, caking and coking tests) and the element composition (ultimate analysis). Furthermore, the moisture level of run-of-mine coals is indicative of the capillary structure, allowing a first tentative classification of a particular coal. The lack of moisture holding capacity of highly coalified coals is proof of

an increasingly densified structure. The element ratio, particularly that of H/C and its change to lower values as coalification progresses, points toward the aromatization of structural groups. Likewise, the dramatic decrease in oxygen within the series peat to anthracite strongly suggests the loss of functional end groups.

The softening properties of bituminous coals (caking and coking tests) reveal the mobility of fragmented decomposition products, observed particularly in coals with high hydrogen and, hence, high vitrinite and liptinite contents. On the other hand, oxygen-rich coals, i.e., low-rank coals with an associated appreciable inertinite content or highly aromatic coals with a high degree of cross-linkage, yield recondensed solid depolymerization products. The tar and gas composition (carbonization assay, devolatilization, caking, and coking tests) shows that hydrogen preferentially enters liquid and gaseous components due to rearrangement [506].

Stable fragments, obtained from specific pyrolysis or hydropyrolysis studies, indicate the major types and the volatility of aromatic molecules present in a particular coal. Liquid-phase treatment produces larger unit fragments, which can be determined analytically. A petrographic survey permits selective composition analyses and structural identification of individual major maceral groups such as vitrinite.

5.22.5.3 Bonding of Elements in Coal

Thermal depolymerization by controlled slow or flash pyrolysis of coals, oxidation, hydrogenation, liquefaction of coals, supercritical and selective solvent extraction, as well as the application of modern physical techniques such as X-ray diffraction, IR spectroscopy, nuclear magnetic resonance, or pyrolysis mass spectrometry have furnished extensive data on the bonding of elements in coals. Major findings from these investigations are [507]:

Carbon: The aromaticity increases from 40–50% C in subbituminous coals to 70–80%

C in bituminous coals and is over 90% C in anthracites.

Hydrogen: Aromatic bonding to carbon and as aliphatic hydrogen in, e.g., methylene ($-\text{CH}_2-$) and methyl ($-\text{CH}_3$) groups occurs.

Oxygen: Major functional groups are hydroxyl ($-\text{OH}$), carboxyl ($-\text{COOH}$), carbonyl ($>\text{C}=\text{O}$), etheric ($-\text{O}-$) and heterocyclic oxygen.

Sulfur: Bonding is predominantly as thiophenes, also in the thiolic form ($\text{R}-\text{SH}$), decreasing with higher rank coals; up to ca. 25% S is present as aliphatic sulfides ($\text{R}-\text{S}-\text{R}$). Heterocyclic sulfur compounds are also known to exist.

Nitrogen: Very little information on organic nitrogen bonding is available. It appears to occur in heterocycles.

5.22.5.4 Structural Evidence of Coals

Much data on the structural aspects of coal has been accumulated and published by numerous authors, with the aid of the chemical and physical techniques available to modern science [508, 509].

The overall picture, however, is still very incomplete. The difficulty is that coal is a highly heterogeneous mixture and, as such, is not a clearly defined macromolecular aromatic compound of uniform molecular mass and structure. Thus, evaluated structural parameters refer to isolated fragments, components (vitrinite), or constituents. According to the current level of understanding, however, coal may be described structurally as a three-dimensional skeleton of generally four to five highly stable condensed aromatic and hydroaromatic units with cross-linkage by weaker short-chain aliphatic groups. Reactive functional end groups and aliphatic structures are attached to the aromatic skeleton. The average molecular mass distribution is ca. 500–800 for low-rank coals, increasing to ca. 3000–6000 for bituminous coals, and possibly values in excess of 100 000 for anthracites.

Various overall models for the complex organic structure of coals, combining available

experimental data on structural fragment analysis, have been tentatively proposed. However, none as yet fully accounts for all the phenomenological characteristics [507].

5.22.6 Hard Coal Preparation

The ROM (run of mine) coal brought to the surface contains various types of accompanying minerals and interstratifications, which must be removed to obtain a coal that complies with market demands for the different types and grades. Grain size, ash content, and moisture content can be controlled within a narrow range by applying mechanical and physical cleaning methods. The ROM coal is subjected almost exclusively to mechanical wet treatments that are more difficult and expensive if the feed is intimately intergrown.

5.22.6.1 Preliminary Treatment and Classification of Raw Coal

The upper grain size of raw coal is defined by the dimensions of the coal cleaning equipment. Before being fed to that equipment, the coal is subjected to preliminary screening and crushing to a diameter of 120–150 mm; foreign matter is simultaneously removed. Coarse dirt is normally reduced in particle size along with the coal, and only in exceptional cases is it removed by preliminary treatment. Such preliminary removal of coarse dirt is done exclusively in drum or inclined separators. Dual eccentric and resonance screens are used for lump coal; each of these machines has a throughput of up to 2 kt/h.

After preliminary screening and removal of foreign matter, the coal in the 0–150 (or 0–120) mm diameter range is defined as raw feed coal. To an increasing extent, this coal is fed to a storage and homogenization plant without further treatment. Homogenization then produces a consistent grain size and uniform contents of moisture, dirt, and volatile materials. The uniform quality of the coal feed makes possible a uniform product and optimal utilization of the washery capacity [510].

Homogenization of the raw feed coal can be carried out in blending silos or on blending yards. Figure 5.132 shows the homogenization results of a silo. A critical factor in homogenization is the size of the storage location for containing one day's output.

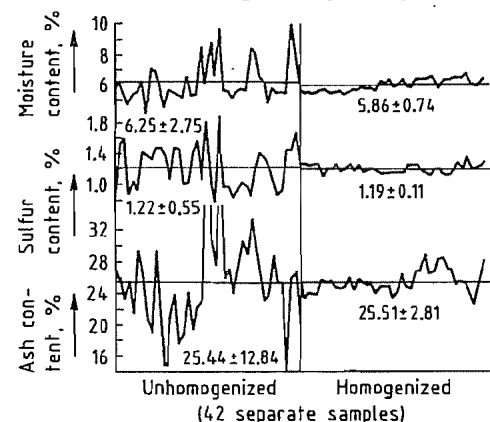


Figure 5.132: Homogenization of raw coal in a blending silo.

In the washery the coal is first classified to ensure optimal utilization of the subsequent cleaning equipment for coarse coal and smalls. Normally the raw feed coal is screened off between 10 and 12 mm and subdivided into coarse raw coal and raw smalls. Such classification is carried out either on vibrating screens or on tensioned screens equipped with varying types of bottoms of perforated plate or tissue. The throughput for a unit may be as high as 1 kt/h [511]. The raw coarse fraction is then subjected to wet mechanical cleaning, which completely removes adhering smalls and ultrafines by spraying.

Prior to cleaning of the raw smalls 0–12 (or 0–10) mm, the ultrafines are removed by a complex method. Normally an air separation method, e.g., dry classifying, or wet desliming on screens is used. Among the air separators, cyclone separators with mechanical dust discharge have proven to be most successful. These are designed for throughputs of up to 700 t/h. Vibrating separators are used in some exceptional cases where dust must be removed from all of the raw feed 0–150 (or 0–120) mm [512]. With some rare exceptions, the separa-

tor dust is added unscreened to the saleable products; in the future, however, an increasing proportion of the dust will need to be cleaned.

5.22.6.2 Wet Treatment

Cleaning of the raw feed is done by wet treatment in jigs and dense-medium separators, which separate according to differences in density or flotation (surface) properties.

Cleaning in Jigs

Almost all of the jigs used in Germany are of the air-pulse type or, in exceptional cases, of the wash-box type [513, 514]. They usually yield three products. Separation is accomplished by density, under the action of a pulsating flow of water. Pulsation may be applied either by a simple stroke or a superimposed double stroke.

During recent years, the Batac jig with compressed air chamber underneath the bed proved to be the most successful machine. With such a system, all of the machine width, including the chamber width, is available for jigging. An electronic valve control or a mechanical rotational valve is used to adjust the compressed-air load. Air pulsation coupled to the hydraulic inductive discharge controls enables the operator to modify the cut point by simply actuating a selector. This allows the cleaning of two different coal types successively in the same jig. The jigs usually accept coarse coal 10–150 (or 10–120) mm in diameter and smalls < 10 mm.

Cleaning in Dense-Media Separators

The coarse fraction is also cleaned by dense media, particularly in star-wheel extractors or inclined separators [515].

Whereas previously baryte, clay, ultrafine dirt, loess, and pyrite were used as dense media, the more recent equipment runs almost exclusively on magnetite and ilmenite. Selection of the dense medium depends on the method of regeneration (magnetic separation or gravity). The regeneration method also depends on the grain size of the dense medium.

A jig can be controlled by using either floaters or a layer of a given weight. It can also be fully automatic, controlled by gamma-ray counters. Dense-media equipment is controlled by maintaining the densities constant via automatic addition of the dense liquid. This adjustment can be set so precisely that it approximates separation by a true solution. While the cut point with dense-media cleaning is, in general, more precise than that with jigs, the latest achievements in jig cleaning have resulted in the widely expanded use of jigs within Germany because the coal normally is highly amenable to jig cleaning and because machine expenditure and costs are lower.

Cleaning by Flotation

Currently, some 14% of the raw coal feed in Germany is subjected to flotation. The diverging degrees of wettability of different mineral components allow cleaning of very fine particles by means of air bubbles. The bubbles are created by dispersion of the air feed in the dense medium; they remove the coal particles that have been rendered hydrophobic by flotation agents [516]. Flotation is applied to slurries if they contain an excessive percentage of mineral components so that their inclusion in the high-grade product is economically impossible.

Flotation plants consist of five to seven separate cells or flotation troughs with the corresponding number of stirrers. Each cell is between 5 and 14 m³ and has a throughput up to 100 t/h particulate matter corresponding to 1000 m³/h of pulp. Flotation is done either in one or two steps. The current flotation agent is of the collecting and foaming type. A ton of particulate matter requires 0.3–0.8 kg of flotation agent for the process.

Other Cleaning Methods

Cleaning on tables and in dense-media cyclones has been used in certain cases to reduce the sulfur content of the product and to obtain a coal extremely low in ash.

5.22.6.3 Dewatering

Moisture must be removed after wet cleaning [516–519]. There are static and dynamic methods. Among the dynamic methods are screen dewatering of nut-size coal and preliminary dewatering of small products on stationary screening tables or in refuse elevators. The static methods are being replaced by dynamic ones (centrifuge, vacuum, and pressurized dewatering) because of the demand for low final moisture content. The concurrent higher ultrafine and moisture contents in the raw coal have necessitated additional process steps.

Smalls are normally dewatered on vibrating screen centrifuges. Several improvements in their design particularly the conversion from vertical to horizontal arrangements have allowed high throughputs and easy repair and maintenance. Centrifuges with drum diameters of 1.3 m and rated capacities of 250 t/h (water-free) are the best. The smalls are dewatered down to 5 or 7% at centrifugal forces of 80–100 g, depending on grain size distribution.

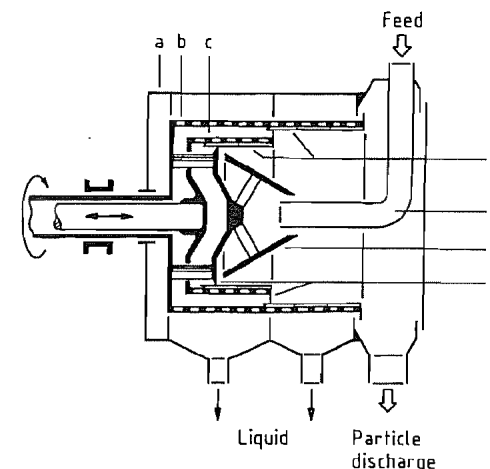


Figure 5.133: Two-step pusher screen: a) Enclosure; b) External screen drum; c) Internal screen drum; d) Slot screens; e) Feed pipe; f) Vortex; g) Pusher rings.

Coarse slurries are dewatered in pusher screens where the centrifuge forces (400–500 g) are higher than in vibrating screen centrifuges and where residences are considerably longer. Figure 5.133 shows a pusher screen. A

first (comparatively short) step provides preliminary dewatering and an even distribution of particles on the drum periphery. This is followed by the secondary dewatering step. Recent pusher screen designs have drum diameters up to 1.2 m with a rated throughput of coarse slurring of more than 40 t/h. The coarse slurry is dewatered to 9–15%, depending on grain size distribution.

Drum filters with surface areas up to 120 m² and disk filters of up to 500 m² are available for ultrafine dewatering. With this equipment, specific feed rates of 100–800 kgm⁻²h⁻¹ (wf) and moisture contents of 18–28% are attainable.

The flotation concentrate is also dewatered by means of a solid-bowl screen centrifuge where a solid-bowl section is followed by a cylindrical screen section, which dewateres the pre-thickened feed under favorable conditions independent of the particle concentration in the feed medium. Such a solid-bowl centrifuge is depicted in Figure 5.134. Flotation tailings are dewatered either by chamber filter presses or by solid-bowl centrifuges. More recently, screen belt presses have also been used. The selection of these alternatives depends on the desired moisture content of the waste.

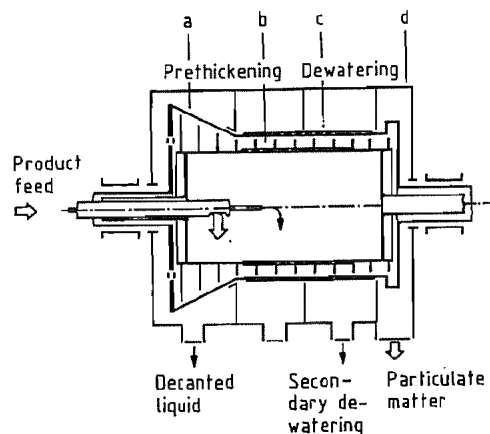


Figure 5.134: Solid-bowl centrifuge: a) Solid bowl; b) Conveyor screw; c) Screen bowl; d) Enclosure.

5.22.6.4 Decantation and Thickening of the Process Water

Wet-type coal preparation plants involve a number of particle-water circuits where up to 6000 m³/h medium are circulated. If the water is to be reused for further cleaning steps, the particulate matter must be removed from it as far as possible. Decantation units, which usually consist of circular thickeners with diameters up to 40 m, are used. Rectangular thickeners are used less often. Water circulation varies, depending on the mechanical equipment, and can be as high as 6 m³ per ton of raw feed coal. Water consumption oscillates near 0.2 m³/t feed for a closed circuit. It can rise to as high as 1 m³/t feed if, e.g., salt content is excessive or if the flotation waste must be discharged to an external disposal site.

The decantation units are meant to bring about simultaneously a desirable degree of thickening for subsequent dewatering or cleaning procedures. Thickener outputs fluctuate between final concentrations of 120 g/L for flotation feed and 650 g/L for pusher screen dewatering. About 0.5 g of organic sedimentation accelerators are added per cubic meter to promote sedimentation for wash-water decantation.

5.22.6.5 Dosing and Blending

The products from coal preparation (nuts, dewatered smalls, air separation dust, flotation concentrate, and middlings, i.e., product that has a high content of intergrown material) are stored separately in bunkers. The demand for nut-size particles has been declining, and they are reduced to < 10 mm diameter by impact or hammer mills. They then serve as a constituent of high-grade coals. The cleaned products are withdrawn from the bunkers and blended according to a set program. During this operation, the ash contents can be monitored or adjusted by automatic rapid-measuring instruments. The addition of those components that are highest in ash (air separation dust) is adjusted, depending on the measurements, so that the final product is brought to

the desired ash content. Instruments for rapid and continuous measurement of moisture content will soon be introduced. Other mechanical equipment used for dose-feeding and blending includes filling-level indicators, dose-feeding devices, and belt weighers.

5.22.6.6 Removal of Pyritic Sulfur

Sulfur may be present in hard coal as elementary sulfur, sulfate, organic sulfur, or sulfide (pyrite).

Pyritic sulfur is removed by modern cleaning procedures [520, 521]. The raw coal is screened off at ca. 40 mm. The dirt of the > 40 mm product is removed in a jig. The jig floatings are reduced to < 40 mm, fed along with the < 40 mm product from sizing to a blending yard, and homogenized. The product is then cleaned in another jig; the coal and intergrowth of this step are reduced to a diameter of < 10 mm and fed to dense-media cyclones to yield, at low separation density, a raw coal

low in sulfur. The intergrowth from the cyclone is reduced to a diameter < 3 mm and then classified in cyclones at 0.063 mm and subjected to secondary cleaning on tables. The < 0.063 mm product is then subjected to flotation. Dewatering of the intermediate products is done in vibrating screen centrifuges, pusher screens, and solid-bowl screen centrifuges.

5.22.6.7 Thermal Drying

Thermal drying is restricted to a few special cases in the treatment of coking and power station coals because the procedure involves high costs. The continuing increase of the ultrafine proportion, which is difficult to dewater, and the increasingly stringent quality demands necessitate more advanced dissociation and cleaning of ultrafines, as well as novel techniques of coal extraction, haulage, and treatment. These factors have led to increasing reliance on thermal drying in the aforementioned sectors [521].

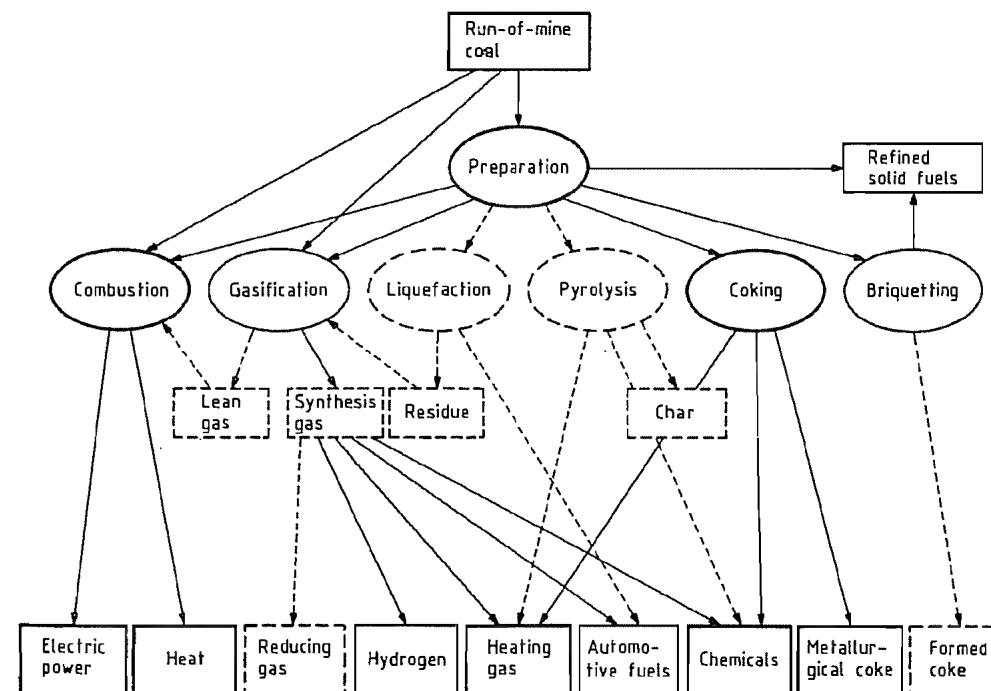


Figure 5.135: Coal conversion processes and end uses.

Drum-type dryers are usually superior to the gas suspension dryers in terms of energy balance. The current quality requirements for coals for coking and power stations require that only part of the coal volumes be dried to stay within the moisture tolerances required for the final smalls product. Less drying also reduces problems of dust.

5.22.7 Coal Conversion (Uses)

Coal conversion processes may be divided into three groups. *Mechanical conversion processes* include coal preparation and briquetting. *Processes for transforming coal into secondary fuels* include coking, gasification, liquefaction, and combustion. *Processes for the conversion of coal for purposes other than the generation of energy* include the recovery of by-products during coking, the production of active carbon, and the preparation of coal-based materials.

In Figure 5.135 the individual conversion processes are shown by ellipses, and the intermediates and end products are depicted by rectangles. Because there are so many variations of the processes, only the most important routes are depicted. The dark lines show processes and common applications. The thinner lines represent less common routes, and the broken lines show those that are still under development or have not yet found commercial application.

5.22.7.1 Preparation

Coal preparation is part of the colliery operation and is intended to turn the raw coal into more saleable products with defined characteristics. The choice of preparation process depends on the *raw material* and its technological properties, the *market requirements* for quantity, type, and quality, and *economic and environmental considerations*.

Coal preparation is used to differing extents in different countries. In Germany, all of the coal obtained by underground mining is subjected to preparation, whereas ca. 85–90% of the lignite, which is obtained exclusively by

open-cast mining, is used for power generation without preparation. The lignites and sub-bituminous coals in the United States and Australia are also used without preparation. These two countries only submit coal to full preparation if it is to be used for coking. Probably about half of the coal used throughout the world undergoes preparation.

The water, ash, and sulfur contents, the size, and the volatile constituents are all important properties of coal that can be affected by preparation. Reduction of the sulfur content is especially significant because there is a worldwide concern about pollution.

Comminution, screening, grading (the true focal point of the preparation process), dewatering, settling, thickening, storage, proportioning, and mixing to blend the finished products are all important preparation processes.

The production and stabilization of suspensions of coal in water and coal in oil, which can be used to replace fuel oil in power stations and industrial boilers, are not considered to lie within the normal scope of preparation. The application of suspensions of coal in water to the transport of coal in pipelines is being examined as an alternative to other types of transport [523–525].

5.22.7.2 Briquetting

Lignites or low-volatile coals of a particle diameter < 6 mm that are not suitable for coking and are not used in power stations can be burned in grate stokers only if they are converted to lump form. This can be carried out commercially by briquetting. Binding agents are used for low-volatile coals, but these are not required for lignites. Less common methods of compacting include hot briquetting, in which a coking coal is used as the binding agent, and pelletizing. With some exceptions, such as in the former German Democratic Republic, briquetting is of only minor significance in the sales of coal to private and industrial users. Since the mid-1950s, oil and natural gas have effectively replaced coal as a

means of heating in other countries because of their cost and convenience.

5.22.7.3 Carbonization and Coking

Low-temperature carbonization and coking involve heating of coal with the exclusion of air. This process removes the condensable hydrocarbons (pitch, tar, and oil), gas, and gas liquor, leaving a solid residue of coke. Low-temperature carbonization (up to 800 °C) and coking (> 900 °C) are differentiated by the final temperature. The two processes also differ sharply in the rate of heating of the coal and in the residence time in the reactor. These parameters have a direct effect on the product yields. Low-temperature carbonization produces fine coke and fairly large quantities of liquid and gaseous products, whereas high-temperature coking is used primarily for the production of a high-temperature lump coke. After the oil crisis of 1973, attempts were made to submit the coal used in power stations to preliminary low-temperature carbonization. The coal by-products were then to be refined while the coke was used for firing. However, the process could not be made profitable.

Currently, high-temperature coking of coal is carried out entirely in batch-operated coke ovens, of which the majority are of the horizontal chamber type. The feedstock is a coking coal of given size composition. The coking properties depend chiefly on softening and resolidification temperatures and on swelling behavior. Coking takes place at a temperature of 1000–1400 °C. The coking time of 15–30 h depends on the operating conditions and type of oven. The main product is metallurgical coke required for the production of pig iron. It is characterized by its suitable size and high resistance to abrasion even under blast furnace conditions. Coke oven gas and liquid by-products are also produced. In Western Europe, these have considerable influence on the economy of coking and, therefore, are reprocessed. However, in many coke oven plants in the United States, the by-products are burned.

Considerable technical improvements in coke production have occurred in recent years. These have led to greater cost effectiveness. They include mechanization and automation of oven operation, reduction of coking time and increase of specific throughput by the use of thinner bricks of higher thermal conductivity, and increased oven sizes.

Coking in horizontal chamber ovens is becoming increasingly difficult for the long term due to the deteriorating quality of coal feedstocks. Therefore, coking technology must be assisted with additives and auxiliary technology. Potential additives include petroleum coke, bitumen, and oil. Among the auxiliary technologies to be considered are the ramming operation, such as is used in Germany and some East European countries, and the various modifications of coal preheating, which are used in Western Europe, the United States, and Japan.

Dry cooling of coke has recently found increased use in Western Europe to recover stored heat. For climatic reasons this technique has been used for a considerable time in the former Soviet Union. Dry cooling of coke leads to considerable savings in energy and pollution, especially when used in combination with preheating.

At the start of the 1960s, many countries considered developing a continuous production process for formed coke in expectation of a further worldwide increase in demand for coke for steel production. Numerous process developments, such as briquette coking or hot briquetting of a mixture of char and caking coal, have been demonstrated on an industrial scale. Even so, these processes have not been able to gain acceptance. This is partly because unexpected improvements in chamber coking have been realized and partly because the steel industry has been having difficulty for more than a decade, and thus, the anticipated shortage of coking coal has not yet occurred.

5.22.7.4 Pyrolysis

Pyrolysis includes carbonization and coking. It is also the starting reaction in gasifica-

tion, combustion, and direct liquefaction processes. As the modern coal conversion processes have come to involve higher pressures, e.g., to increase the reaction rates and reduce the vessel dimensions, pyrolysis under pressure and in different gas atmospheres has been systematically studied.

Laboratory-scale trials show that under high hydrogen pressure, coal can be converted to gaseous and liquid products, especially BTX aromatics (benzene, toluene, and xylene), with good yield. In addition, the process results in a residue char that must be either burned or gasified. The technology is called *hydropyrolysis*. It is classified as gasification or liquefaction, according to temperature and pressure (800 °C, 100 MPa). An extended research and development program on hydropyrolysis is funded by the International Energy Agency. After successful laboratory trials, a process development unit has begun operation.

5.22.7.5 Coal Liquefaction

Coal liquefaction can be accomplished in two ways. Treating coal suspended in suitable oils with hydrogen in the presence of a catalyst or with hydrogenating solvents yields oil products and some unreactive residue. This technology is called *direct liquefaction* or *coal hydrogenation*. In addition, coal can be gasified with steam and oxygen to yield a mixture of hydrogen and carbon monoxide (synthesis gas) from which liquid products can be synthesized. This technology is usually called *indirect liquefaction*. Both routes were developed into industrial-scale processes during the 1930s. However, (indirect) coal liquefaction is currently employed on an industrial scale only in South Africa (Sasol plants I, II, and III). Further developments took place in 1975–1985 mainly in Germany, the United States, and Japan.

Direct Liquefaction

Coal hydrogenation is a hydrogenating digestion of the coal molecule. Hydrogenation

using a solvent brings about depolymerization at ca. 15 MPa and 430–460 °C to yield an asphalt-like product. This product can have the ash removed, e.g., by hot filtration, and it can serve as a boiler fuel or as a feedstock, e.g., for the production of high-quality carbon products. However, many development schemes went on to further hydrogenate the extract in a separate stage and thereby produce a synthetic oil that can be distilled and refined into marketable products [527, 528]. New examples of this technology are the American EDS (Exxon donor solvent) [529] and SRC (solvent refined coal) [530] processes and several Japanese developments on a pilot-plant scale [531]. In the new American development of ITSL (integrated two stage liquefaction), extraction and further hydrogenation are combined in one process [532].

Catalytic hydrogenation of coal usually requires a pressure of tens of megapascals and a temperature of 450–480 °C. These strong reaction conditions yield a light oil fraction that can be further refined. This technology is used, e.g., in the Kohleöl process (Germany), in the H-Coal process (United States), and in Japanese developments. For the Kohleöl process a demonstration plant of 200 t/d coal throughput has been in operation since 1981. The Japanese are just completing a demonstration plant in Australia. These new processes surpass the prewar Bergius–Pier process by increased selectivity and yield of useful liquid products, by a considerable reduction in operating pressure to 20–30 MPa from ca. 70 MPa, by increased volumetric reactor throughput, by improved availability of the plant, and last but not least, by having the unreacted residue conditioned in such a way as to make it accessible to steam gasification for hydrogen production. The very recent German development of integrated raffination in which part of the downstream processing of the Kohleöl has been incorporated into the hydrogenation process has led to further substantial improvements and may even constitute an entirely new liquefaction process.

Direct liquefaction also reduces the sulfur and nitrogen contents of the liquid products

compared to those of the reactant feed coal. Thus, extractive hydrogenation is also considered as a means of obtaining a clean boiler fuel from coal. However, the economic prospects that complete hydrogenation will produce a synthetic crude oil are more promising. Further refinement into light fuel oil, automotive fuels, and chemical feedstocks essentially follows petrochemical technology although coal oils require an adaptation of the refining catalysts.

Indirect Liquefaction

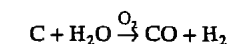
The synthesis of hydrocarbons from synthesis gas is called indirect liquefaction. This technology is also named the Fischer Tropsch synthesis after its discoverers. The process was developed in prewar Germany and was used extensively during World War II. After the war, the process could not compete with cheap oil from the Middle East. New capacity was erected only in South Africa, where it was set up downstream of Lurgi fixed-bed coal gasifiers. In the Sasol I plant, two different Fischer Tropsch process technologies are employed, the fixed-bed Arge process (Lurgi Ruhrchemie) and the entrained-flow Synthol process (Kellogg–Sasol). The Arge process produces mainly gasoline, fuel oil, and waxes, whereas the Synthol process yields a larger fraction of gasoline and low molecular mass products (methane and propylene). The Sasol II and III plants, built in the late 1970s, use only the Synthol process. On an energy basis the total liquid product yield obtained by indirect liquefaction of coal in the Sasol II plant is ca. 32%.

5.22.7.6 Coal Gasification

Systematic development of coal gasification began in the first half of the 19th century. A mixture of carbon monoxide and hydrogen was produced. This was generally used for chemical purposes, which remained the main application of coal gasification for nearly 100 years. Many communities relied on coke oven gas to supply town gas for illumination, cook-

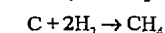
ing, and heating into the second half of this century. However, coal or coke gasification was also employed mainly for peak shaving in large gas schemes and also for the supply of gas to industrial furnaces. These applications provided strong development incentives. Natural gas and mineral oil in large amounts and at low cost replaced gas manufactured from coal not only in the heating market, but also in the chemical industry in most countries. The oil crisis of 1973–1974, with its sudden steep increase in prices of mineral oil and natural gas and the subsequent supply shortages, triggered new interest in coal gasification.

Gasification can be accomplished by reacting coal with oxidizing or reducing agents. Using oxygen (or air) and steam as gasifying agents yields water gas.



The composition chosen for the blast depends on individual process conditions and governs the carbon monoxide:hydrogen ratio of the product. Varying the steam:oxygen ratio in the blast is a very sensitive and convenient means of controlling the reaction temperature.

Gasification with hydrogen (hydrogasification) leads primarily to methane.



However, hydrogasification is usually incomplete and produces a char residue, which cannot economically be converted with hydrogen. Thus, reductive gasification is considered as only a preliminary step in the complete gasification of coal. However, it is a very favorable step if a gas with a high heating value, e.g., substitute natural gas (SNG), is to be produced. Hydrogasification is also involved in most fixed-bed countercurrent-flow gasification processes, contributing to the methane content of the product. Several other reactions take place simultaneously, including the Boudouard reaction, complete combustion of carbon, and methane formation from carbon monoxide and hydrogen.

In coal gasification processes, it is necessary to optimize heat transfer, mass transfer,

and chemical reaction conditions between huge flows of solid and gaseous agents and to achieve a high throughput and optimal energy economy at the same time. Many varieties of coal gasification processes have been developed, reflecting compromises of the many constraints and conditions.

First consideration must be given to the intended use of the product gas. Current interest focuses on the preparation of the following:

- A gas with a high heating value, e.g., SNG
- A fuel gas, e.g., a clean boiler or turbine fuel
- Synthesis gas, for the production of commodity chemicals
- Hydrogen, for ammonia production or for energy purposes
- Reducing gas, for direct reduction of iron ore

A second, equally important, consideration applies to the available coal. Of particular importance are coal rank, grain size, caking properties, ash content, and ash melting behavior. Third, environmental regulations, site specific infrastructure, etc. have to be taken into account. Considering all these factors, a decision in favor of fixed-bed, fluidized-bed, or entrained-flow gasification can be made.

In a *fixed-bed* gasifier, coal and blast are usually contacted in countercurrent flow. This leads to the splitting of the overall gasification reaction into several zones with favorable conditions for the various reaction steps involved. Fixed-bed gasification usually results in excellent carbon utilization and high efficiency. It is applicable to coals of all ranks. However, it requires lump, noncaking or weakly caking coal with a high ash softening temperature. The product contains tars and other liquid by-products that complicate the gas treatment. Atmospheric fixed-bed gasifiers of various design are still occasionally found in small-scale industrial use. On a large scale, some Lurgi fixed-bed pressurized gasification plants are operating commercially, e.g., in South Africa (Sasol I, II, and III).

Fluidized-bed gasification, invented in 1922 by WINKLER at BASF, has the advantage of fairly simple reactor design and very high

reactor throughputs even at atmospheric pressure. However, reaction temperature is limited by the need to avoid ash agglomeration so that fluidized gasification is restricted to very reactive fuels such as subbituminous coals or lignite. Winkler gasifiers operating at atmospheric pressure produce synthesis gas in the former German Democratic Republic and in India. In Germany, further development to Winkler gasification at high pressure has taken place, and a first demonstration unit has been completed [533, 534].

Entrained-flow gasification takes place in a flamelike reaction zone, usually at a very high temperature to produce a liquid slag. For economical operation, a high-standard heat recovery system is mandatory, but the product gas is free of methane, tars, etc., thereby considerably simplifying gas and water treatment.

Entrained-flow gasifiers of the Koppers-Totzek design operated at atmospheric pressure are used industrially in many countries to produce hydrogen or synthesis gas. The Texaco partial-oxidation process recently has been adapted to coal gasification in a pressurized entrained-flow reactor. Industrial-scale plants operate or are under construction in the United States, Germany, and Japan.

Apart from these well-established or highly developed processes, further intense development is under way on existing processes, as well as on new concepts. During the last decade most of the existing processes have been modernized or modified by incorporating new process engineering, materials, and control technology. Such new concepts as pressurized gasification in various modes, hydrogasification, multistage processes, slag bath and molten iron processes, and allothermal processes, e.g., using process heat from gas-cooled nuclear reactors, have been proposed and tested [535-540].

Some of the new development projects have subsequently been terminated or shelved because of the present availability of mineral oil and natural gas. However, the long-term incentive of securing and diversifying the world energy supply is still valid. Environmental considerations may favor converting coal into

a clean fuel gas that can be used either conventionally or in highly efficient technologies like fuel cells or combined cycle power plants. Furthermore, low-quality coals, which are located in remote places and are therefore not marketable as such, can be gasified and converted on site into transportable products such as commodity chemicals or hydrocarbons and thereby contribute to worldwide supplies.

5.22.7.7 Coal Combustion

In combustion the energy content of the fuel is completely released and can be recovered as sensible heat. The combustion products are usually considered to be useless waste products. Therefore, coal combustion is not classically considered to be a coal conversion or refining process, but rather an energy conversion process. However, modern combustion systems, e.g., two-stage combustion or low-nitrogen oxide burners, involve clearly distinguishable reaction steps such as pyrolysis and partial oxidation (gasification), which are classical conversion reactions. In the fluidized-bed combustion of coal, sulfur dioxide is removed from the flue gas during the combustion process by adding limestone sorbent to the feed coal. This enables low-grade coal to be burned cleanly, eliminating the need for preliminary upgrading steps.

5.22.7.8 Conversion of Coal for Purposes Other Than the Generation of Energy

Coal Tar Chemical Industry

Considerable quantities of aromatic chemical feedstocks are still prepared by reprocessing the coal tar that is produced during coking at a worldwide rate of ca. 16 Mt/a (tar and pitch). The tar components are reprocessed into dyes, pesticides, varnishes, vitamins, and textile auxiliaries. Tar oils are used for the production of carbon black, e.g., for tire manufacture, and for the production of impregnating oils. Special pitches recovered from coal tar

are used for the production of special coke, e.g., that used for electrodes.

Until the early 1950s, industrial production of aliphatic hydrocarbons was based on acetylene produced from calcium carbide. This coal-based chemical feedstock was subsequently replaced by the more economical ethylene produced from crude oil. Research into the production of acetylene is again being carried out worldwide, and new methods using carbide and plasma arcs are being investigated. Special attention is given to reducing the high energy requirement.

Production and Use of Activated Carbon

Precise thermal and chemical treatment of lignite or coal can produce activated carbon with a specific pore system. Activated carbons made from coal are particularly noted for their high ignition temperatures and good resistance to abrasion. Therefore, they are suitable for use in industrial processes for removing sulfur and nitrogen compounds from the flue gases emitted by coal-fired power stations, for wastewater purification, for separation of various mixtures of gases, and for solvent recovery, etc.

5.22.8 Agglomeration

Numerous industrial processes require coal in its coarse state for handling and transportation and as a feed for such thermal applications as combustion, gasification, iron ore reduction, and carbonization. However, highly mechanized mining operations, coal preparation, and beneficiation yield a high proportion of fines. Upgrading of such coal fines by agglomeration is frequently applied and considered [541-546].

The choice of agglomeration process and of a possible binder depends very much on the degree of coalification of the coal and the intended application.

The agglomeration ability of a coal is mainly influenced by its moisture-holding capacity, ash content and composition, hydro-

phobicity, size distribution, and plastic or elastic behavior.

Fundamental coal agglomeration methods are grouped into

- Briquetting and extrusion [542, 546–550];
- Balling and tumbling [542, 544, 545, 551–554].

In the processes of the first group, a compressive force is applied to a prepared coal or a coal and binder mixture.

The double-roll hydraulic press and extrusion presses of various designs are the most common mechanical devices used. Binderless briquetting or extrusion requires that a high pressure be exerted on the coal. Therefore, its applicability is generally limited to predried peat or soft lignites sized to particle diameters < 1 or 0.5 mm that exhibit defined plastic properties. Ash contents should be low to prevent excessive erosion [550].

Binder briquetting or extrusion exercised at low to medium pressures is applied to coal with insufficient plastic properties, but essentially elastic properties, i.e., subbituminous, bituminous, and anthracitic coals usually of particle sizes < 3 mm. Organic binders such as pitch, bitumen, starch, molasses, lignosulfonates, or inorganic additives, e.g., clay minerals, are used in quantities of 2–8%. Briquettes produced with water-soluble binders require a subsequent drying step to attain final strength [546, 555, 556].

Hot briquetting techniques utilizing the softening of bituminous coals at a temperature of 350–450 °C are employed for the production of hot briquettes from mixtures of coal and coke.

Balling of finely ground prepared coal generally smaller than 0.315 mm in particle diameter with 2–6% of organic or inorganic binders has only recently evolved as a commercially viable coal agglomeration technique by using pelletizing disks designed for light bulk materials [544, 554, 557]. Both moist and dry pellets may be used industrially. Although the disk produces pellets of almost uniform size, tumbling in, e.g., rotary drums or mixers yields pellets of a wide size distribution. This

mode of agglomeration is preferentially applied to subbituminous, bituminous, and anthracitic coals of both low and high ash contents, but predried lignites can also be pelletized [542, 551, 552]. Drying and thermal treatment of these pellets, however, cause severe cracking and significant losses in strength and stability.

Coal agglomerates must withstand mechanical and thermal treatment when used in industry. The type and severity of stress depend on the particular use and mode of treatment which mainly include transportation, drying, thermal shock, pyrolysis, gasification, and combustion [546, 549, 551]. Suitable procedures for the agglomeration step may be developed and selected from bench-scale simulation studies. Subsequent handling and thermal experiments with these agglomerates lead to a final, optimized product, which may be tested on a larger scale in pilot or commercial plants.

5.22.9 Transportation

The large amount of coal that is mined every year is a major commodity for the transportation industry and one that requires a significant capital investment. In the United States, ca. 50% of the 700–800 Mt of coal produced per year is shipped by rail; 18% is shipped by river barges; and the rest is handled by trucks, conveyor belts, and pipelines. The actual cost of long-distance shipping is usually quite modest, but the loading and unloading of the coal adds greatly to the total cost of shipping. In a typical surface mining operation, for example, coal is moved from the mine by truck or conveyor belt to a nearby preparation plant, where it is loaded onto a unit train for rail shipment to a utility or port facility. At the port it may then be loaded onto river barges or ocean-going bulk carriers.

Although some of the coal transported by rail is shipped at single car or bulk rates, most is carried at lower rates in unit trains of up to 100 cars that travel continuously to a single destination and return. The unit train carries only coal and each car can carry up to 100 t.

The cars are of either the bottom-dumping or roll-over type, and each car can be unloaded in 1.5–5 min in modern processing facilities, which have a capacity of 2000–6000 t/h.

The least expensive means of transporting coal is by *river barges*, whereby the cost is as low as \$0.005 per mile (\$0.003 per km). The barges have open tops and commonly hold up to 1000–1500 t each. They are moved in groups or tows of 20–30 barges powered by a single towboat. Although there can be some problems with delivery schedules due to congestion, the ease and economy of river transport are major factors in the location of many coal-burning utilities along inland waterways in the United States and in Europe.

In the United States, ca. 12% of coal production is carried by *trucks*. Much of this is done at surface mines, where the coal is hauled from the working face to preparation plants. This is usually done with dedicated high-capacity vehicles; however, significant amounts of coal are hauled by trucks on public highways. *Conveyor belts* are also used for transporting coal from mines to preparation plants, as well as for short cross-country hauls of over 10 miles (16 km) to loading points. Because they are dependable and economical, conveyor belts are also widely used for in-mine coal transport.

Although > 80% of the coal mined in the United States is used domestically as steam coal, some of the metallurgical coal production is shipped overseas. This coal is shipped in dry bulk carriers that can be loaded and unloaded in modern port facilities at rates of up to 100 000 t/h. These ocean-going ships are usually in the 60 000 t range, although some are larger. In addition, some smaller vessels in the 30 000 t range that are self-unloading are also in service. These ships have the advantage of being able to use a much greater number of ports.

The transportation of coal by *slurry pipeline* has been demonstrated to be dependable and economical, even though there are only a few such pipelines in use around the world. In this technique the coal is reduced to a diameter of < 1 mm, treated with chemicals to prevent

corrosion and improve flow characteristics, and mixed with water. It is then pumped as a slurry at a velocity of 1.5–2 m/s. The fact that pipelines can be built above ground or buried eliminates some environmental problems, but their high water requirements can be a serious drawback. Sustained delivery rates of > 600 t/h have been demonstrated.

5.22.10 Coal Storage

The use of any bulk commodity requires the storage of sufficient material to ensure efficient operations. In the case of coal, this requirement varies from a few days supply at the mine to a few months supply at a power plant. Although some covered storage in bins or silos is practical at mines and small operations, most of the larger volumes of coal are stored in open piles, where it is exposed to the air and precipitation. When coal is exposed to air, it loses moisture and begins to oxidize. This oxidation can degrade coal quality, and more important, it can cause spontaneous combustion that destroys the coal. The main coal properties that influence oxidation are the particle size, pyrite content, and rank. Coal oxidation leading to spontaneous combustion is enhanced as the particle size decreases and as the pyrite content increases. Low-rank coals such as lignite and subbituminous coal are very difficult to store because of their strong tendency toward spontaneous combustion, and care must be taken even with the lower rank bituminous coals. Repeated wetting and drying also exacerbate oxidation. The continued oxidation generates more heat than can be dissipated, and this leads to hot spots, which eventually ignite.

In a stockpile even mild oxidation can lead to a degradation of coal quality. For steam coals there can be some loss in calorific value, but in coking coals there can be a total loss of quality. The fluid properties can be destroyed, and the heat transfer properties and coke production yields can also be reduced. The quality of coke made from oxidized coal is also seriously altered. The prime coke property, coke strength or stability, is reduced, and this

can result in the loss of iron production in the blast furnace. Oxidized coal also increases the reactivity of coke and leads to higher coke consumption in the blast furnace. Because all of the effects of oxidation are undesirable, every effort should be made to prevent it.

The main steps to prevent oxidation involve limiting the access of air and protection from wind and precipitation. Stacking the coal to eliminate size segregation and compaction of the pile with earth-moving equipment to reduce pore space have proven helpful. Coating the pile with a sealant also helps protect it from air and moisture, although this may be expensive. Another costly but useful step is to provide the storage piles with some kind of wind protection. The wind not only enhances oxidation, but it also removes the fine particles from the coal pile and can thereby create environmental problems.

Another aspect of coal storage is the need to mix and blend the stockpile coal to homogenize the product coal reclaimed from it, so that a consistent, uniform product can be delivered to the plant. This can be a serious concern in cases where coal is coming into an operation from a number of sources. The usual way to solve this problem is to develop a bedding and blending system. A typical system consists of a plan to build a stockpile with long, thin layers of the various incoming coals and to reclaim the coal from the pile with vertical cuts across these layers. The key design factors are the variability of a target blending parameter such as ash or sulfur content and the desired degree of homogeneity. These are evaluated to determine the necessary pile parameters such as individual layer thickness.

5.22.11 Quality and Quality Testing

Because coal is so variable in its maceral and mineral composition, its suitability for a given use must be determined by a variety of tests. Although some tests such as chemical analysis are quite general in nature, others such as ash fusion are specific for particular uses.

Chemical Analyses. Although coal is composed of a large number of organic chemical components, no true standard organic chemical test exists for coal. The two major kinds of chemical analyses used are the proximate analysis and ultimate analysis, which are standard tests defined by the American Society for Testing and Materials.

The *proximate analysis* (ASTM D 3172) consists of a determination of the moisture, ash, and volatile matter, and a calculation of the fixed carbon value. The *moisture* is determined by heating the sample at 104–110 °C to a constant weight. The percent weight loss is reported as the moisture value. The *ash* in this analysis is the incombustible residue after the coal is burned to a constant weight. It should be noted that the ash value is not a measure of the kinds or relative amounts of the minerals in the coal. The *volatile matter* is a measure of the amount of gas and tar in a coal sample. It is reported as the weight loss minus the moisture after the coal is heated in the absence of air at 950 °C for 7 min. The *fixed carbon* is not a distinct chemical entity. It is reported as the difference between 100% and the sum of the moisture, ash, and volatile matter values. While the proximate analysis as described above is a rather simple assay of the chemical nature of coal, its value as a quality parameter is well established and is widely used in commerce.

The *ultimate analysis* (ASTM D 3176) consists of direct determinations of ash, carbon, hydrogen, nitrogen, sulfur, and an indirect determination of the oxygen. The ash is determined as in the proximate analysis, and because all of the values are reported on a moisture-free basis, moisture must also be determined.

Both proximate and ultimate analyses are reported in a number of different ways, and care must be taken to be certain of the method of reporting. On the "as-received" basis, the results are based on the moisture state of the coal sample as it was received for testing. With the "dry" basis, the results are calculated back to a condition of no moisture, and with the "dry, ash-free" basis, the results are calcu-

lated to a condition of no moisture and no ash. These calculations are done so that different coals can be compared on their inherent organic nature. The reporting basis can cause significant changes in the values reported, and it is essential that a target value and the value of a sample in question be on the same basis. For example, for a given coal with a moisture of 10%, an ash value of 15%, a volatile matter of 30%, and a fixed carbon content of 45%, the volatile matter content would be 33.3% on a dry basis and 40% on a dry, ash-free basis. The corresponding fixed carbon values are 50% and 60%, respectively.

Because some components of the minerals such as water from the clays and carbon dioxide from calcite are lost in the high-temperature ashing process, the ash value determined is less than the actual mineral matter in the raw coal. A number of corrections for this loss are in use, but the one most used in the United States is the Parr formula, where the corrected mineral matter is equal to 1.08 times the ash percentage plus 0.55 times the sulfur percentage. Results reported with this correction are considered to be on a dry, mineral-matter-free basis.

Mineral Matter. The mineral matter content of a coal is the actual weight percent of the minerals present. It is the best measure of the inorganic content of a coal, but it is difficult to determine. Although there is no standard test for mineral matter, low-temperature ashing (< 150 °C) with an oxygen plasma device is widely used for this purpose. The X-ray diffraction analysis of the low-temperature ash is used to identify the actual minerals in the ash. However, with present techniques it is impossible to accurately determine the amounts of the various minerals present in a given coal.

Although a large number of different minerals have been identified in coal, the four most common are clays, pyrite, calcite, and quartz. The minerals get into the coal in a variety of ways. Some can be part of the original plant material itself. Silica (quartz) is present in some of the saw grasses of modern swamps, and similar types of plants are known from an-

cient swamps. Certainly much of the mineral matter is transported into the coal-forming swamp from the environment. Much of the clays and quartz minerals were brought into the coal swamp as clastic material in streams or in airborne dust. Most of the common minerals could be chemically precipitated from solution under conditions that can exist in swamps. Some minerals such as calcite and pyrite can also be precipitated into cleats and fractures in coal after it has formed and coalified beyond the peat stage.

The presence of sulfur in coal is of great interest because of the problems it causes in utilization, especially air pollution. There are three commonly recognized forms of sulfur in coal. Pyrite sulfur is the sulfur tied up in the mineral pyrite, FeS_2 ; it is determined by leaching with nitric acid. Sulfate sulfur is of minor importance and thought to be formed by the weathering of pyrite; it is determined by leaching with hydrochloric acid. Organic sulfur is that portion of the total sulfur that is organically bound with the various coal macerals; it is determined indirectly by difference. There also may be some minor elemental sulfur present in coal. The forms of sulfur are determined in accordance with the ASTM standard D 2492.

The occurrence of pyrite in coal is of special interest because it is the only form of sulfur that can usually be removed by mechanical cleaning methods and because it is a major source of air and water pollution. Although some pyrite is formed by the chemical combination of the sulfur and iron that occur naturally in peat, most of the pyrite found in coal is thought to form from Fe(III) ions absorbed on clay minerals that are transported into coal swamps, and from sulfate ions that are introduced into the swamp in seawater. Marine water usually has about two orders of magnitude more sulfate ions than fresh water. In the swamp the ferric Fe(III) is reduced to Fe(II) , which combines with the sulfur in the sulfate ions to form pyrite. While this process is clearly not the only way that pyrite can form in coal seams, it is a good model for many United States coal seams, especially those in

the Illinois Basin. In these seams it is reported [558–560] that both the total sulfur and pyritic sulfur contents are controlled by the nature of overlying rocks; they are both high under marine rocks and low under nonmarine rocks.

Pyrite can occur in coal in a number of forms such as single crystals, void fillings, irregular and dendritic masses, and framboids (raspberry-like clusters). The most significant forms are the more massive ones, which are easier to remove from the coal by washing, and the framboidal forms, which are more chemically active because of their high surface area. When pyrite is exposed to air and water, it oxidizes in a series of chemical reactions that generate sulfuric acid and cause acid mine drainage. In fact, the reaction of 1 mol of pyrite with air and water results in the generation of 2 mol of sulfuric acid.

Thermal Properties. The most widely used thermal property is the calorific value, which is a measure of the heat produced by combustion of a unit quantity of coal under given conditions (ASTM D 3286). It is usually reported on a moist, mineral-matter-free basis and is used this way in the ASTM classification of coals by rank. The major use of the calorific value is in the evaluation of coals for use in steam generation. In many utility company contracts, coal is bought on the basis of total calorific value per unit mass.

5.22.12 Economic Aspects

5.22.12.1 World Outlook

Reserves. The world's proven recoverable reserves of coal are an estimated 520×10^9 t of hard coal (anthracite and bituminous) and 512×10^9 t of brown coal (subbituminous and lignite). Proven reserves are those which geological and engineering information indicate with reasonable certainty can be recovered in the future from known deposits under existing economic conditions.

Production. Total production of hard coal (anthracite and bituminous) worldwide has remained on the same level since 1988. How-

ever, the individual regions of production have developed to different extents. For instance, production in Europe has been reduced, while the coal output of countries such as Australia, China, India, Indonesia, and South Africa has increased, in some areas considerably. In 1994, production of hard coal reached 3.2×10^9 t (Table 5.58). World production of brown coal (subbituminous and lignite) has been increasing continuously, and in 1994 output amounted to ca. 1.3×10^9 t (Table 5.59). This amount yields approximately the same heat as 0.9×10^9 t of hard coal.

Consumption. Approximately 20% of the 3.2×10^9 t of hard coal used in the world is allocated to coking coal and 80% to steam coal. Virtually all brown coal is used in power stations. The largest growth in both production and consumption in the period 1984 to 1994 has been in Australia and Asia.

Trade. Most coal is consumed in the regions of production. World trade in hard coal amounts to only 12% of world production. Nevertheless, since some important consumer countries are without adequate resources of their own, trade in hard coal has assumed worldwide proportions (Table 5.61). Australia, North America, and South Africa are the main net exporting regions, Japan, Western Europe, and Korea are the main importing regions. Brown coal is not traded over long distances.

Table 5.58: Proven recoverable world coal reserves as of end 1994 [561].

Region	Quantity, Mt	
	Anthracite and bituminous	Subbituminous and lignite
Africa	60 405	1 267
Canada & United States	111 004	138 177
Latin America	6 509	4 899
Asia	133 173	94 599
Eastern Europe ^a	135 422	180 091
Western Europe	27 476	47 529
Australia & New Zealand	45 369	45 690
Total	519 358	512 252

^aIncluding the former Soviet Union.

5.22.12.2 Some Major Coal-Producing Countries

United States of America

Reserves. The United States possess economically recoverable hard coal reserves of ca. 107×10^9 t — one fifth of the total world reserves. For brown coal the respective figures are 134×10^9 t and 25%.

Table 5.59: World hard coal production in 1994 [562].

Region or country	Quantity, $\times 10^6$ t	Proportion, %
Africa		
South Africa	195.3	6.1
Others	7.9	0.3
Africa total	203.2	6.4
Americas		
United States	605.0	19.0
Canada	36.6	1.2
Brazil	4.4	0.1
Colombia	23.5	0.7
Mexico	6.7	0.2
Others	6.3	0.2
America total	682.5	21.4
Asia		
China	1110.0	34.9
India	248.0	7.8
Indonesia	30.5	1.0
Japan	6.9	0.2
South Korea	7.4	0.2
Pakistan	3.1	0.1
Turkey ^a	5.0	0.2
Others	51.5	1.6
Asia total	1462.4	46.0
Europe		
Bulgaria	0.2	0.0
Czech Rep. & Slovakia	17.4	0.5
Hungary	1.0	0.0
Poland	133.6	4.2
Romania	4.3	0.1
Former Soviet Union ^b	369.2	11.7
Other Eastern Europe	0.2	0.0
Eastern Europe total	525.9	16.5
France	7.5	0.2
Germany	52.0	1.7
Spain	14.4	0.5
United Kingdom	48.0	1.5
Other Western Europe	0.6	0.0
Western Europe total	122.5	3.9
Europe total	648.4	20.4
Australia & New Zealand	184.7	5.8
World	3181.2	100.0

^aIncludes the part in Europe.

^bIncludes the part in Asia.

Production. The United States have maintained a high level of production for decades, producing one fourth of the world's coal. Long-wall mining accounts for an increasing proportion of underground coal production.

Consumption. Domestic coal consumption, which absorbs nearly 90% of the production, has varied little in the past few years, with power stations being the main consumers. Exports have fallen due to heavy competition from newcomers.

Australia

Reserves. Australia possesses economically recoverable reserves of 45×10^9 t of hard coal and 45×10^9 t of brown coal, each representing 9% of world reserves.

Table 5.60: World brown coal production in 1994 [562].

Region or country	Quantity, $\times 10^6$ t	Proportion, %
America		
United States	330.0	26.0
Canada	36.2	2.8
America total	366.2	28.8
Asia		
China	100.0	7.8
India	19.0	1.5
Turkey ^a	45.0	3.5
Others	38.4	3.0
Asia total	202.4	15.9
Europe		
Bulgaria	28.6	2.2
Czech Rep. & Slovakia	65.8	5.2
Hungary	12.4	1.0
Poland	66.8	5.3
Romania	36.3	2.9
Former Soviet Union ^b	105.8	8.3
Other Eastern Europe	53.6	4.2
Eastern Europe total	369.3	29.1
Austria	1.4	0.1
France	1.5	0.1
Germany	207.1	16.4
Greece	57.3	4.5
Italy	0.5	0.0
Spain	15.7	1.2
Western Europe total	283.5	22.3
Europe total	652.8	51.4
Australia & New Zealand	48.8	3.9
World	1270.2	100.0

^aIncludes the part in Europe.

^bIncludes the part in Asia.

Table 5.61: World trade in hard coal in 1983. [563].

Country	Quantity, $\times 10^3$ t	
	Exports	Imports
United States	67 603	6 631
Canada	28 225	8 402
Colombia	18 400	
Venezuela	3 600	
China	18 000	1 350
India	99	6 278
Indonesia	18 833	251
Israel		5 381
Japan		111 404
Korea		35 977
Turkey		5 640
Belgium	645	11 894
Czech Republic	5 301	1 939
Denmark	24	10 467
Finland		5 933
France	622	14 231
Germany	970	13 090
Italy		14 299
Netherlands	2 242	15 121
Poland	22 968	129
Russia	27 400	28 300
Spain		12 726
Ukraine	4 126	8 930
United Kingdom	1 095	18 400
South Africa	42 650	
Australia	128 405	
Others	37 692	101 933
Total	428 900	438 706

Production. Coal production has risen steadily during the last few decades and is expected to do so in future.

Consumption. The high-quality coals found in Queensland and New South Wales are of value as steam and metallurgical coals, and most of production is for export. In 1984 Australia became the world's foremost hard-coal exporter with 61×10^6 t. In 1993 exports even doubled these figures. Production from Western Australia, Victoria, and South Australia (bituminous and subbituminous coal, lignite) is geared to local thermal electricity generation.

Germany

Reserves. Due to its very large deposits of brown coal, unified Germany possesses nearly

8% of the world's economically recoverable coal reserves.

Production. Output of hard coal has fallen from a peak of 150×10^6 t in 1957 to 52×10^6 t in 1994, and further reductions are planned. Brown-coal production dropped continuously with the closure of mines in the eastern Länder. Nevertheless, with $> 200 \times 10^6$ t, Germany is still the second largest producer of brown coal in the world.

Consumption. The majority of the hard coal (65%) and nearly all of the brown coal is channeled into the generation of electricity. The second largest consumer is the steel industry. Hard-coal imports have not varied much in recent years.

Poland

Reserves. Polish recoverable coal reserves amount to 29×10^9 t of hard coal and 13×10^9 t of brown coal.

Production. Poland boosted its production for export reasons for a long period. In mid-1980s government officials expected to increase hard-coal output to 205×10^6 t and its brown coal output to 100×10^6 t by the year 2000. Instead, production in 1994 fell to 133×10^6 t of hard coal and 67×10^6 t of brown coal.

Consumption. Inland consumption decreased every year from 1984 to 1994 and may decrease even further. In the meantime, Poland tried to maintain its exports. In 1984, when it was able to export 45×10^6 t, thereby attaining a 14% share of world trade, Poland set its intermediate export goal at 42×10^6 t/a of hard coal. During the last years, exports reached only 20×10^6 t.

South Africa

Reserves. South Africa has recoverable reserves of ca. 55×10^9 t of hard coal, which at current production levels would last 300 years.

Production. Production has remained fairly constant at ca. 190×10^6 t/a.

Consumption. The slight increase in production in the last years was initiated by higher internal demand. Coal is the main primary energy for the generation of electricity (95%). In addition, South Africa still uses coal as a raw material for the production of liquid and gaseous fuels. Exports are estimated at a rather constant 43×10^6 t/a.

China

Reserves. China accounts for ca. 11% of world recoverable coal reserves. Hard-coal reserves are concentrated in the north and northwest of the country. Substantial lignite deposits are distributed throughout the country.

Production. Production has been increased steadily, so that China is now the world's largest producer (1994: 1110×10^6 t hard coal; 100×10^6 t lignite and brown coal).

Consumption. China is very dependent on its vast coal reserves. In the period 1984 to 1994 China's coal demand has increased by 50% and now accounts for ca. 75% of primary energy requirements. Transportation of coal is a major problem, with a significant proportion of production being in the north, but with the most rapidly growing demand in the southern and eastern regions. Therefore, China is investigating the transport of coal by pipeline. High-capacity electricity transmission to the south is another option under consideration. Only minor quantities (20×10^6 t/a) of coal are exported, the bulk being used internally for electricity and heat generation.

India

Reserves. India possesses ca. 7% of world reserves, mostly bituminous coal.

Production. Coal is the main source of energy and vital for India's economic development. Efforts to develop the industry have resulted in a steady increase of production to ca. 250×10^6 t of hard coal.

Consumption almost doubled in the period 1984 to 1994. Despite increased production,

some coal is imported, mainly for quality reasons.

Indonesia

Reserves. Indonesia has vast resources of high-quality accessible coal. In terms of tonnage, southern Sumatra contains the highest proportion although much of it is lignite. The coal from Kalimantan includes some deposits of very high quality (low ash and sulfur, high volatile matter).

Production. In the period 1984 to 1994, production has risen dramatically.

Consumption. A major export market has developed and exports are expected to grow and to gain a substantial market share for high-quality coals in Europe, the Far East, and possibly the United States. However, Indonesia is expected to become a net importer of oil early in the 21st century. The national policy is therefore to expand internal use. The target is for 80% of electricity to be generated from coal-fired plants.

United Kingdom

Reserves. In its 1992–1993 annual accounts, British Coal estimated that 190×10^9 t of coal resources lie under the United Kingdom in seams over 0.6 m thick and less than 1200 m deep, of which 2×10^9 t were regarded as economically recoverable. A reasonable estimate for lignite resources in Northern Ireland is ca. 10^9 t.

Production. Due to the high cost of extracting the coal, production had to be steadily reduced and will be cut even further.

Consumption. The United Kingdom is still among the major consumers of coal in the world, but with competition from other energy resources, especially oil and gas from the North Sea, a further decline is expected.

Former Soviet Union

Reserves. With 241×10^9 t of recoverable coal reserves, 104×10^9 t of which hard coal, the

former Soviet Union accounts for 25% of the total world reserves.

Production. Due to its vast resources the Soviet Union ranked third among world producers. The political changes were followed by major economic disruptions which affected coal production in particular. In 1994 coal production in Russia reached only 65% of the 1984 level. The Ukrainian production dropped by 40%.

Consumption. Coal consumption has mirrored reduced production. Major changes will depend on future political developments.

5.22.13 Coal Pyrolysis

Coal pyrolysis is the heating of coal to produce gases, liquids, and a solid residue (char or coke). Pyrolysis occurs in all coal utilization processes, i.e., combustion, gasification, liquefaction, and carbonization. The nature of pyrolysis and of the products is intimately related to the operating conditions and to the composition and properties of the coal. Consequently, control of pyrolysis is important in coal utilization processes.

The thermal decomposition (or devolatilization) of coal is illustrated using Wiser's model of coal structure (Figure 5.136) [564]. This model, one of many in the literature, represents the types of structures found in coals. Although it does not necessarily depict the structure of a particular coal, it is consistent with current knowledge of coal physics and chemistry.

Pyrolytic rupture of functional groups attached to aromatic and hydroaromatic units of the coal structure leads to the formation of gases (CO , CO_2 , H_2O , CH_4 , C_2H_4 , etc.). In addition the cross-links (indicated by arrows in Figure 5.136) break and release reactive free radicals (fragments). The fate of these radicals controls the overall yield and distribution of products. Stabilization of the fragments with hydrogen gives primary volatile products and favors a high yield of gases and liquids (Figure 5.137). Some primary products are also obtained by release of low molecular mass spe-

cies (the so-called mobile phase), which are believed to be trapped within the coal network [565]. However, if the fragments undergo secondary cracking, polymerization, or condensation reactions, part of the primary product is converted to char.

The four fundamental aspects of this complex process are the following:

- The thermoplastic behavior of some coals;
- The yield and distribution of pyrolysis products;
- The temperature and time dependency (kinetics) of the pyrolysis process;
- The source of hydrogen for the stabilization of reactive fragments.

5.22.13.1 Thermoplastic Properties of Coal

When bituminous coal is heated, it undergoes marked chemical and physical changes, which are influenced by rank, petrographic composition, particle size, heating rate, temperature, and the atmosphere in which pyrolysis occurs. Bituminous coal softens and melts at 350–400 °C. In contrast, lignite, subbituminous coal, and anthracite do not soften when heated. Fusion and agglomeration may produce a fluid mass. Concurrently, thermal decomposition may liberate gases and vapors, producing a foamlike material with significant volume change. At some point, the foam solidifies.

These macroscopic changes are accompanied by microstructural rearrangements within the fluid phase, which govern the properties of the resulting coke. Development of the coke microstructure often involves formation of an intermediate phase called carbonaceous mesophase.

Volume changes (expansion and contraction) occur in some bituminous coals on heating. Initial softening at temperature T_s produces a fluid. As softening increases, pores and voids are eliminated and the material undergoes volume contraction, reaching a minimum V_c at temperature T_c . At this point, rapid gas evolution leads to expansion, producing a

maximum V_s at temperature T_s . With a further increase in temperature, the fluid coal resolidifies at temperature T_r ; the corresponding volume is V_r . These phenomena, i.e., softening, swelling, and resolidification are collectively referred to as the *thermoplastic properties* of a coal, otherwise called the softening, plastic, fluid, agglomerating, caking, and coking properties of coal.

The terms "caking" and "coking" are sometimes used incorrectly as synonyms. In a strict sense, caking describes softening and agglomeration of coal on heating, without any implications about the nature of the resulting solid. Caking coals, on the other hand, are those that form strong, coherent solids (metallurgical cokes) on softening and resolidifying in conventional coke ovens. In other words, all caking coals exhibit caking behavior, but not all caking coals can be coked. Coal that does not become fluid when heated is generally termed nonswelling or noncaking.

Continued heating of a semicoke, i.e., a solid residue still containing appreciable volatile matter, to ca. 1000 °C leads to further decomposition with formation of a solid residue termed coke. Coke contains little or no volatile matter and undergoes little further volume change when heated. The volume changes occurring during the transformation of a coal

into a semicoke depend on the fluidity of the plastic mass and its resistance to the escape of gases and vapors.

An understanding of the thermoplastic behavior of coal is important for nearly all coal conversion and coke-making processes. For example, plasticity development and agglomeration may create severe operating difficulties in gasifiers.

In a *moving-bed gasifier*, as the coal proceeds down the (sometimes pressurized) reactor, it devolatilizes at relatively low heating rates (25–65 °C/min) in the presence of a reducing atmosphere. Under these conditions, bituminous coal undergoes, in varying degrees, thermoplastic transformations that can lead to the formation of coke masses. These are detrimental to the flow of gases and solids, resulting in poor operation of the gasifier. In the extreme, coke agglomerates can completely plug the reactor.

In a *fluidized-bed gasifier*, an agglomerated mass may disrupt the fluidization. As a complicating factor, highly swollen coke may greatly reduce the bed density and lower the throughput. As a further complication, a highly swollen coke mass tends to disintegrate when it is fluidized, producing excessive fines that are carried from the bed and must be separated from the exhaust gas.

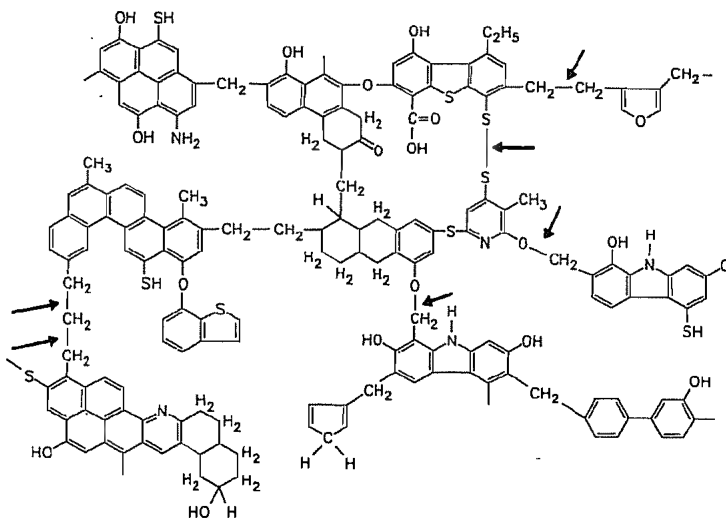


Figure 5.136: Wiser's model of coal structure [564].

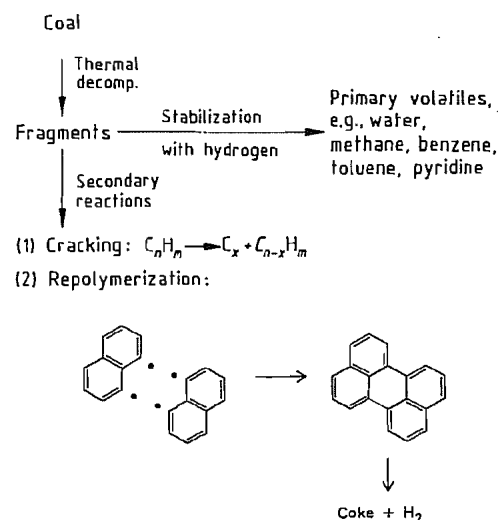


Figure 5.137: Primary and secondary reactions in coal pyrolysis.

In contrast to the general objectives in gasification and combustion, extensive plasticity development is essential during carbonization to produce metallurgical coke. The main objective of the coking industry is to produce coke for blast furnace operation. In this context, recent research has focused on the identification of coke microconstituents and the mechanism of their formation. The improvement of coke microstructure depends largely on the ability to modify the thermoplastic properties of the coal feedstocks and the associated mesophase. This is of particular significance because of the interest in the plastic behavior of weakly caking coal as a supplement to the reserves of prime coking coal.

Experimental Techniques

The industrial importance of the thermoplastic properties of coal is reflected in the many methods available for its characterization [566]. A common objective of these techniques is to predict the behavior of coal in various processes.

The *free-swelling index* (Gray-King) provides a visual comparison of cokes carbonized under well-defined conditions. The method is inexpensive, rapid, and reproducible, but lacks

flexibility. *Hot-stage optical microscopy* permits the visual observation of morphological changes caused by heat. The *Foxwell gas flow method* measures the resistance to the flow of a highly purified gas through a bed of coal during continuous heating; the pressure drop indirectly measures the fluidity of the plastic mass. The *constant torque plastometer* records the velocity, as a function of temperature, of a rotating shaft passing through a bed of coal. In the variable torque plastometer, the velocity is kept constant and the required torque measured as a function of temperature. The resulting measurements of fluidity provide a sensitive index of oxidation or weathering, but not of swelling. The heating rate is limited to ca. 3 °C/min. In the *dilatometer*, the volume change on solidification is measured as a function of temperature. This is applicable over a wide range of heating rates and provides data on dilation parameters and transition temperatures, but not on fluidity changes.

These empirical tests require that experimental conditions be specified when results are reported. Furthermore, these tests measure different aspects of thermoplastic behavior; therefore, there is no single best method or technique that can predict the changes which occur in all industrial processes. Selection of a test method depends on the utilization process.

Experimental Variables

The thermoplasticity of a coal is a complicated phenomenon. It is affected by softening and rheological properties and by formation of gas bubbles [570], which are strongly influenced by pyrolysis conditions and feedstocks.

Coal Rank and Petrographic Composition

The thermoplastic properties of coal vary widely as a function of rank. Moreover, the plastic properties of some bituminous coals serve to differentiate them from others of similar rank. A number of attempts have been made to *correlate plastic properties with rank*. Swelling, measured by dilatometry, exhibits a maximum for a volatile-matter content of ca. 25–28%; the Gieseler fluidity reaches a maxi-

mum at ca. 28–32% of volatile matter [568]. Correlation of the free-swelling index (FSI) with the maximum Gieseler fluidity is poor, which is not surprising; rather, it illustrates the heterogeneity of coal [567]. Some variations can be expected because of the obvious differences in test conditions. In the FSI test, a 1-g sample of coal (250 µm particle size or 60 mesh) is heated in a silica crucible at 820 ± 2 °C for 2.5 min; the swelling is compared to that of a standard. The Gieseler fluidity test measures the rotary speed (in dial division per minute, ddpm) of a stirrer under a constant torque in a compacted 5-g charge, heated at 3 ± 0.1 °C/min from 300 °C until it resolidifies. However, the FSI does not increase monotonically with increasing Gieseler fluidity. In any case, the data support the concept of an optimum fluidity that is essential for maximum swelling.

The principal maceral responsible for coal plasticity is *vitritine*, the predominant petrographic constituent of most United States coals. Exinite differs from vitritine of the same rank by containing more hydrogen and volatile matter. Exinite exhibits a lower softening temperature, wider plastic range, greater Gieseler fluidity, and higher dilatometric swelling than vitritines (Figure 5.138) [566].

Inertinite is infusible and inert, regardless of coal rank. It is distinguished from vitritine of the same rank by its higher density and lower hydrogen and volatile matter contents [568].

Plasticity usually reflects the properties of the constituent macerals, but it also depends on the dispersion of exinite and inertinite within the vitritine. This dispersion determines the degree of interaction between the different macerals. Consequently, predicting the thermoplastic behavior of a coal from its petrographic (maceral) analysis alone is impossible.

Heating Rate

The thermoplasticity of coals increases as the heating rate is increased [569]. Shock heating rates (above 100 °C/min) significantly in-

crease the maximum swelling [569]. However, beyond a limiting heating rate (100–300 °C/min) a further increase does not increase swelling. On the other hand, at a low heating rate (below 3 °C/min), even a highly plastic coal may not soften or swell.

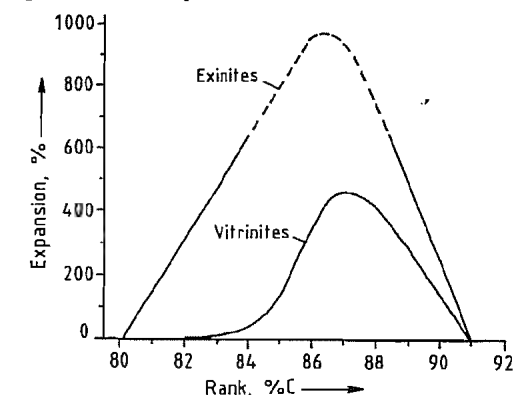


Figure 5.138: Expansion of vitritines and exinites [566].

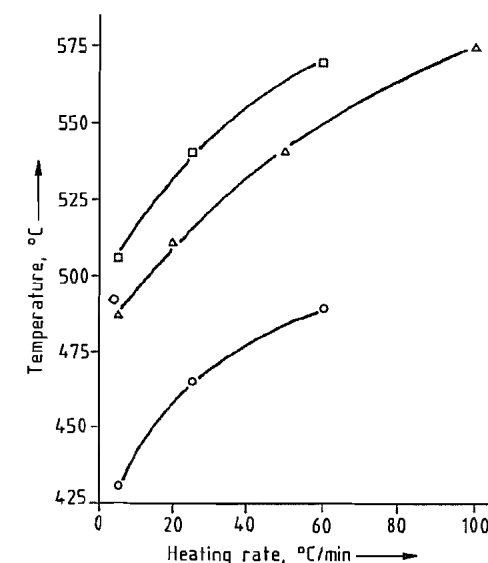


Figure 5.139: Effect of heating rate on the characteristic temperatures of a low-volatile bituminous coal (particle size: 74 µm; pressure: 101.3 kPa of He) [567]. ○ Softening temperature; △ Temperature of maximum devolatilization; ◇ Temperature of maximum fluidity [570]; □ Temperature of maximum swelling (dilatometry).

The effect of heating rate can be explained in terms of a competition between evolution of volatile matter and thermal decomposition. At

a higher heating rate, reactive components of the volatile matter, which would otherwise be lost before plasticity develops, can participate in secondary reactions that promote fluidity.

With an increase in heating rate, the characteristic temperatures (for softening, maximum swelling, and maximum fluidity) increase, as measured by plastometry or dilatometry (see Figure 5.139). Because these temperatures do not shift to the same extent, the temperature range over which the coal is plastic is generally widened.

An important effect of heating rate on the thermoplastic properties of coals is related to the maximum rate of devolatilization [566]. As the heating rate increases from ca. 1 to ca. 7 °C/min, the maximum swelling, maximum Gieseler fluidity, and maximum devolatilization rate all increase [567]. An increase in the heating rate produces a linear increase in the maximum rate of devolatilization. In addition, the maximum swelling increases with increasing heating rate, although this parameter is dependent on particle size. The maximum rate of devolatilization is slightly lower for the larger fraction.

The sequence of events occurring during coal pyrolysis is a function of heating rate. Softening is preceded by a rapid increase in evolution of volatile matter. Within the same temperature range, the viscosity of the sample reaches a minimum [570]. In response to this rapid rise in formation of volatile substances the coal particles and coal bed expand, producing the maximum swelling, determined by dilatometry, and the maximum rate of devolatilization, determined by thermogravimetric analysis [567].

Particle Size

The effect of particle-size variations on the thermoplastic properties of coal has not been widely reported. The data published before 1980 conflict. A few investigations have suggested that extremely fine grinding of the coal particles reduces thermoplastic properties. However, these results are possibly due to increased ease of weathering and oxidation of

the more finely ground coal, or to maceral and mineral segregation that occurs during grinding.

Experimental data on particle size must be interpreted with caution. Studies conducted in a Hoffmann dilatometer, which accommodates coarse samples, have shown that the effect of particle size varies according to coal type and petrographic constituents [568].

The effect of particle size is dependent on heating rate [567]. At a high rate (60 °C/min), a considerable decrease in the particle size resulted in a significant increase in swelling. This confirmed earlier findings that, at a higher heating rate, the maximum swelling was greatest for the smallest size fraction [571, 572]. The behavior at 60 °C/min has been explained as follows: the smaller coal particles, with their greater surface: volume ratio, fuse more easily with the neighboring particles and produce a homogeneous mixed phase [567]. In contrast, the larger coal particles tend to maintain their individuality [567, 569].

With slower heating (5 °C/min), the swelling parameter for the smaller fraction (~74 µm) was less than that at 60 °C/min. This was attributed to slower devolatilization at 5 °C/min, resulting in a lower swelling pressure, i.e., the pressure generated inside the particles. In addition, the diffusion distance (the distance traveled by the volatile substances before escaping) is shorter for smaller particles. Therefore, an increase in particle size with slower heating results in greater swelling.

A particle-size effect is also noted in the contraction parameter. In general, the initial contraction of the coal particles is significantly greater for the smallest fraction [567, 571, 572]. This is explained by the suggestion that larger coal particles fuse less than smaller ones because of their lower surface: volume ratios.

Pressure

Until recently, little work had been published on the effects of inert gas pressure on

the thermoplastic properties of coal. In the absence of data at elevated pressure, the behavior of coal under typical gasification conditions (elevated pressure and reducing atmosphere) has generally been extrapolated from data obtained at atmospheric pressure. However, this treatment has serious deficiencies.

Several investigations have shown that pressure increases the coke and gas yields at the expense of tar production. This has been attributed to an increased residence time of volatile and plasticizing substances in the coal melt and to a corresponding effect on rheological behavior. Pyrolysis of bituminous coal at elevated pressure has also been shown to increase the Gieseler fluidity (Figure 5.140) [573].

Swelling of coal in dilatometers results from a balance between opposing forces and occurs when the internal (intraparticle or intrabed) gas pressure (swelling pressure) generated in the plastic state is higher than the applied forces that tend to contain it. This internal pressure depends on the coal type, particle size, heating rate, and temperature. Consequently, at elevated pressure, coal swelling depends largely on experimental conditions. For a range of bituminous coals, the rank dependency of the effect of pressure on the maximum swelling parameters was highly variable [567]. In addition, the extent of maximum swelling varied markedly.

Other observed effects of pressure, irrespective of coal rank, were an increased contraction parameter and an expanded plastic range. In contrast, with vacuum pyrolysis, maximum swelling, contraction, and plastic range were significantly reduced [567]. The effects of pressure can be explained qualitatively by invoking the concept of optimum fluidity, which is essential for high expansion. If the melted coal is very fluid, swelling is not extensive because the volatile substances escape easily. At the other extreme, minimum fluidity is essential for the material to fuse and entrap volatile material. This implies that an optimum fluidity exists, which is necessary to permit a high degree of swelling. Under vac-

uum, for example, volatile and plasticizing components are readily removed before sufficient fluidity or swelling pressure can develop. Hence, thermoplastic behavior is inhibited [567].

Production of volatile matter during pyrolysis is a necessary but insufficient condition for a coal to become plastic and swell. The combined effects of the generated volatile matter and the rheological properties of coal determine thermoplastic behavior [567, 572, 574].

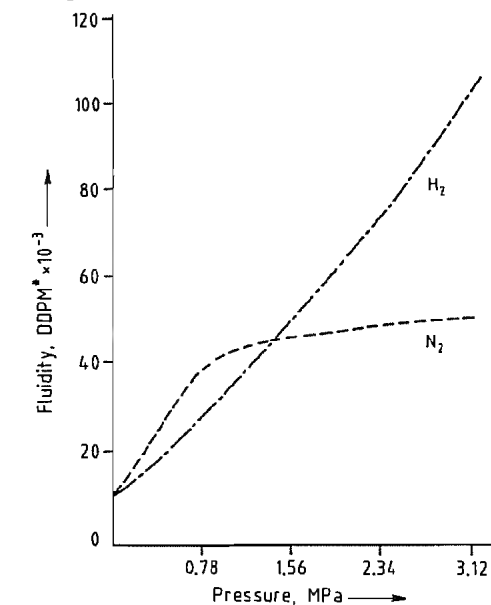


Figure 5.140: Effect of pressure on the Gieseler fluidity of a bituminous coal [573]. *DDPM = dial divisions per minute.

Gaseous Atmosphere

The effects of a gaseous atmosphere on the thermoplastic properties of coal are of interest because in many processes devolatilization occurs in the presence of reactive gases, e.g., H₂, CO/H₂, or CO₂.

The effects of H₂ and He depend on the conditions. However, an increase in the maximum swelling parameter can be correlated with the degree of hydrogenation. At heating rates above 60 °C/min in a high-pressure microdilometer, the thermoplastic properties of

a low-volatile bituminous coal were not significantly different in atmospheres of H₂ or He [567]. The total loss of mass during pyrolysis at ca. 630 °C in these two gases was similar, indicating little hydrogenation at high heating rates.

In contrast, at a low heating rate of 5 °C/min, the maximum swelling is significantly greater at elevated H₂ pressure compared to He. The loss of mass during pyrolysis is also significantly greater in H₂ than in He, indicating some hydrogenation at this heating rate [567].

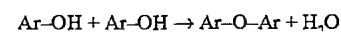
The maximum Gieseler fluidity (heating rate, 5 °C/min) of a weakly swelling coal (FSI = 0.5) at atmospheric pressure was markedly greater in H₂ than in He or N₂ [573, 575].

Preoxidation

In many processes, thermoplastic behavior of bituminous coals can have undesirable consequences. Caking can be reduced or eliminated by low-temperature (below the softening point) preoxidation, which can destroy thermoplastic properties [568, 569, 576, 577]. In addition, carbonization of preoxidized bituminous coal produces a char with a higher gasification reactivity and surface area than coke produced from untreated coal [578].

Although many studies have been conducted on oxidized or weathered coals, oxidation mechanisms are still poorly understood. Small amounts of oxygen (0.01–0.02%) can produce substantial changes in coal plasticity [579]. The first stage of oxidation was postulated as peroxide formation; however, this has not been confirmed experimentally. It was further suggested that the peroxide is unstable above 70 °C and decomposes to yield more stable coal oxygen complexes with evolution of CO₂, CO, and H₂O.

Another proposed mechanism was that oxidation increases hydroxyl, carboxyl, and carbonyl content [566]. As the temperature rises the hydroxyl groups can condense with the liberation of water:



where Ar is an aromatic radical.

Fourier transform infrared (FTIR) studies suggest that in the early stages of oxidation, the main functional groups formed are carbonyl and carboxyl [580]. At higher degrees of oxidation, evidence indicates a significant increase in ether, ester, and phenolic groups. Loss of plastic properties on oxidation is attributed to the formation of ether and ester cross-links. The decline in fluid behavior on oxidation can be correlated to a reduction in the aliphatic hydrogen content [581].

The swelling of a highly fluid coal increased on mild oxidation [568, 569, 571]. More severe oxidation sharply reduced swelling.

Little work has been done on carbonization of preoxidized coal under the pressure of a reducing gas. Successful operation of fixed- and fluidized-bed processes depends on the behavior of preoxidized coal when it is devolatilized under these conditions.

A preoxidized coal shows a higher loss of mass during pyrolysis in H₂ than in N₂ [567]. The thermoplastic properties of preoxidized coal are highly dependent on pressure, and maximum swelling increases significantly at an elevated pressure of H₂ or He [567, 582, 583]. This suggests that if preoxidized coal is used as a feed material for a pressurized process, where devolatilization occurs in a reducing atmosphere, the effects of preoxidation are reduced.

Although oxidation is an inexpensive technique for reducing the plastic behavior of coal, deleterious consequences have been reported [567]. Preoxidation results in an overall loss of carbon (as CO₂) and hydrogen (as H₂O); hence, the heating value is significantly reduced. Consequently, other means of reducing thermoplastic properties are being investigated.

Additives

Inorganic additives are an alternative to preoxidation. They reduce the caking of coal carbonized at atmospheric pressure (Table 5.62); however, they have economic and operational drawbacks.

Table 5.62: Effects of additives on thermoplastic behavior of coal [584].

Additive	Concentration	Pretreatment	Caking index ^a	Changes in caking index	
				Before	After
Dry sand	20%	dry mixed	FSI	4.5	4.1
NaOH	20%	dry mixed	FSI	4.5	1.0
Na ₂ CO ₃	20%	dry mixed	FSI	4.5	1.8
Na ₂ CO ₃	10%	dry mixed	FSI	4.5	3.0
Na ₂ CO ₃	5%	dry mixed	dpm	275	15
K ₂ CO ₃	20%	dry mixed	FSI	7.0	1.5
Boric acid	2%	dry mixed	BS swelling no.	8.0	0.5
NaCl	1 N solution	20 g of coal in 200 mL of solution dried at 105 °C for 40 min	FSI	4.5	2.0
Na ₂ CO ₃	1 N solution		FSI	4.5	1.3
NaHCO ₃	1 N solution		FSI	4.5	1.5
NaOH	1 N solution		FSI	4.5	1.0
BF ₃	0.25 mmol	gravimetric gas sorption at saturated pressure	FSI	8.0	2.0
BF ₃	BF ₃ /100 g		FSI	8.0	2.0
BF ₃	0.27		FSI	9.0	2.0
BF ₃	0.21		FSI	7.0	2.5
AlCl ₃ , (CH ₃) ₂ CHCl ^b	—	—	coke inspection	agglomerated	powder
HCl	not stated	1 h at 150 °C	coke inspection	agglomerated	powder
Excess tri- <i>n</i> -butyl borate	—	—	BS swelling no.	8.0	0
Phosphorylation ^c	—	—	BS swelling no.	8.0	0.5
Acetylation ^c	—	—	BS swelling no.	8.0	2.5
NH ₃ solution with Ni catalyst 3–3.5% Ni	—	autoclaved with liquid NH ₃ at 120 °C for 4 h	swelling no.	2.2	1.1

^aFSI = Free Swelling Index; dpm = Divisions per minute as determined by a Gieseler plastomer; BS = British Standard.

^bFriedel-Crafts alkylation.

^cEsterification of phenolic hydroxyl groups.

The mechanism of decaking is not known. In general, an additive may function as an inert diluent or in a more active role by chemically interacting with the softened coal. Some inert additives may provide sites for complex reactions of the coal. Some inert additives reduce fluidity by adsorbing primary decomposition products. Removal of 2–3% of the extractable bitumen prevents caking completely [568].

Additives may also increase the permeability to gas flow and, therefore, reduce swelling in the coal melt. Compounds like SiO₂, however, serve simply as diluents.

Additives may also react chemically with the pyrolysis products. Substances, such as K₂CO₃, KOH, CaO, Fe₂O₃, Fe₃O₄, HCl, and BF₃, reduce the swelling of coal at atmospheric pressure.

The effectiveness of additives in decaking under gasification conditions has been examined [567, 585, 586]. Compounds of K, Ca, or

Fe significantly reduced thermoplasticity under most conditions. Although K₂CO₃ and KOH are effective decaking agents, KCl is not. Similarly, CaO and Ca(OCOCH₃)₂ were more effective than CaCO₃. Both Fe₂O₃ and Fe₃O₄ destroyed thermoplasticity at 0.1 MPa (H₂ or He), even at ca. 5%.

Effective additives may promote char formation during pyrolysis. Pyrolysis at elevated hydrogen pressure usually increases *V_s*. This was attributed to a reduction of char-forming reactions, thereby increasing fluidity of the system [567].

Development of Thermoplasticity

Softening

Although thermoplastic properties of coal have been studied for many years, softening still lacks a satisfactory explanation. However, a general pattern has been established.

Direct microscopic observations are revealing. Between 325 and 450 °C, depending on coal rank and experimental conditions, visible softening is manifested as follows [569]:

- Coal particles become mobile and fill the bed space. Larger particles, which soften less than smaller ones, fuse with the smaller particles.
- So-called fusion pores begin to form as softening continues, depending on particle size and nature of the coal. However, with further softening, the material becomes more homogeneous, making distinction between pores formed by fusion and those formed by devolatilization difficult. As softening continues, viscosity decreases, particle boundaries disappear, and gas evolution increases.
- With a further increase in temperature, viscosity increases until resolidification occurs, pore volume and vitrinite reflectance increase, and in some cases, anisotropy increases.

Softening can be measured in a dilatometric test by the onset of contraction when a bed of coal is heated under a weighted plunger. A more precise measurement is given by the attainment of a specific degree of fluidity within the plastometer. In all theories of plasticity, it is acknowledged that a fusible material is formed during softening, but differences of opinion exist as to the origin, nature, and function of this material [572].

The homogeneous-melt theory, for example, proposes that coal undergoes pastelike melting throughout the entire mass, but decomposes at the same time, giving rise to gas and an infusible solid [587, 588]; the composition of this mixture depends on time and temperature. Resolidification is observed when the transformation to infusible material is complete. If decomposition proceeds too rapidly before the inception of softening, fusion does not occur and char is formed. On the other hand, if softening occurs before the evolution of volatiles, a coal fuses and swells to form a coke.

According to the *partial-melt theory*, only a fraction of the coal melts and the remainder is

plasticized. The fusible fraction, the coking principle or bitumen, has been identified in benzene and chloroform extracts.

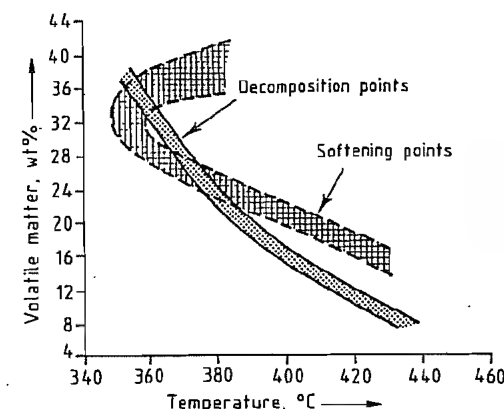


Figure 5.141: Relationship of volatile matter content to softening points and decomposition points of coal [589].

In the *thermobitumen theory*, softening is defined as a consequence of pyrolysis that transforms coal into fluid products. The appearance of these fluid products causes softening and plasticity. Their disappearance by evaporation or thermal decomposition results in resolidification. The fluid products are termed metaplast or thermobitumen, implying that they are the products of pyrolysis.

The *physical and physicochemical theory* proposes that thermal softening is initially a physical process of partial melting of the coal substance to a fluid mass. However, the rheological properties of this mass are subsequently modified by chemical reactions during decomposition. Therefore, development of fluidity is believed to be the result of both physical and physicochemical processes.

In noncaking coal, the decomposition point is lower than the softening point. The rank dependency of these temperatures is illustrated in Figure 5.141, which shows that plastic coals occupy only a narrow range of rank. Other theories suggest that the fraction of a coal that fuses plasticizes the remainder [589–598].

Thermal softening of coal is apparently not related to physical melting but instead to kinetic phenomena [566, 599]. The development of fluidity may be the result of physical

and physicochemical processes without appreciable rupture of covalent bonds during pyrolysis. After melting of the mass, the properties are modified by pyrolytic reactions [594]. This mechanism is consistent with three conditions that have been proposed as being necessary and sufficient for plasticity development [600]:

- Lamellar bridging structures that can be thermally broken
- A supply of hydroaromatic hydrogen
- Intrinsic ability of micelles and lamellae to become mobile, i.e., ability of the coal to melt independent of thermal bond rupture.

Swelling

Investigators agree that the softening of coal particles is caused by the melting or solvation of low molecular mass substances or by primary pyrolytic decomposition [568]. Softening causes swelling and the formation and liberation of gas. The gas cannot escape rapidly because of the low permeability of the plastic mass. Hence, gas bubbles are formed with high internal pressures. In response to this internal pressure, the viscous plastic mass swells like baker's dough. The formation of an impermeable plastic mass is a precondition for swelling.

Swelling can be observed in coal particles individually or collectively. *Intraparticle* (single-particle) swelling results from the formation of a plastic mass that eliminates the fissures and macropores through which gas could escape. The resulting internal pressure swells the plastic mass. Swelling of particle beds, i.e., *interparticle swelling*, is caused similarly when the plastic mass fills the interparticle spaces, preventing gas from escaping.

The importance of each type of swelling depends on the particle size and the nature of the coal. Intraparticle swelling is only important for weakly coking coal. For coal to form a coherent and strong coke, interparticle swelling is necessary. In highly plastic coal distinction between the two types of swelling is often impossible [585].

The extent of swelling depends on the rate of devolatilization [566, 567]. A minimum fluidity is essential to reduce the permeability of the plastic mass to gas flow and generate swelling pressure. However, if the plastic mass is too fluid, gas bubbles escape at low pressure.

Swelling has been viewed as a process independent of softening [596, 597, 601]. In this light, swelling is a consequence of the pore structure of the starting coal. It is caused by the pressure of the evolved gas trapped within the micropores.

Porosity exhibits a minimum for the higher rank bituminous coals, for which swelling is at a maximum. This mechanism explains intraparticle swelling, but not interparticle swelling. Because microporosity is a prominent feature of agglomerating coal, an empirical relationship between swelling and porosity may exist without necessarily implying that swelling is a consequence of porosity. In fact, swelling and porosity may be consequences of a third factor, such as cross-linking density.

Resolidification

Resolidification is usually attributed to a series of cracking reactions followed by condensation and polymerization. A large number of free radicals and small molecules are generated by cracking. This is consistent with the observation that the original solvating agent, the bitumen, decomposes at ca. 480 °C, before resolidification of the coal to form a semicoke [594]. Because of the loss of hydrogen-donating and solvating agents, which would otherwise stabilize the free radicals, the solid material polymerizes forming semi-coke. This viewpoint is supported by the fact that the semicoke is deficient in hydrogen compared to the precursor.

Coke Microstructure and Mesophase Formation

The properties of cokes are determined by their microstructural characteristics. The structure property relationship is, however,

difficult to establish for coke because of its extreme heterogeneity in chemical constitution and physical structure. Nevertheless, considerable progress has been made since the 1920s, primarily with the aid of optical microscopy.

The most significant industrial use of coke is in the production of iron and steel. Only prime coking coal produces coke appropriate for blast furnaces, where reactivity and stability under thermal stress are required [602, 603]. These requirements are met by metallurgical coke.

In general, the principal feature of the coke microstructure is the anisotropy of the organic coke substance as observed by optical microscopy [604–608]. The critical role of an intermediate plastic phase (carbonaceous mesophase) in the development of the characteristic anisotropic structures was first recognized in 1965 [609, 610]. Subsequent research has been devoted to the significance of mesophase formation during the carbonization of coking coal [611], the effect of coal rank and chemical constitution on mesophase formation [612–616], the use of optical and scanning electron microscopy [617], and the chemistry of mesophase formation [618–622]. These investigations may help to improve coke manufacture by modifying the microstructure through the development of a carbonaceous mesophase.

Microscopic Characterization

Optical microscopy is the principal means of analyzing coke morphology and anisotropic structures [617, 620]. The resolution limit of the optical microscope is ca. 0.2 μm . Optical anisotropy is an expression of structural anisotropy on the same scale [623].

For microscopic examinations, polished coke sections are viewed in plane-polarized light [624]. The appearance of the polished surface is termed the optical texture. Isotropic and anisotropic structures can be distinguished on the basis of different behavior [625, 626]. A common technique employs *reflection interference colors* [626]. These are

yellow, blue, and dark purple for anisotropic materials and light purple for isotropic materials. Thus, cokes can be characterized by color and the shape and size of the isochromatic areas [617].

Differences in optical activity between isotropic and anisotropic cokes are due to differences in the range of crystallographic order [618]. The crystallographic order of isotropic coke is considered to be only small in scale; i.e., the parallelism of associated constituent lamellar molecules extends over short distances (ca. 1–5 nm). Although the structure can be claimed to be anisotropic for 1–5 nm, it is essentially isotropic to the light beam because this range is far below the resolution of the optical microscope (ca. 200 nm). However, for anisotropic coke, the range of crystallographic order extends from 0.3 to ca. 200 μm ; in the light beam, the material has bulk anisotropy [618].

An optical microscopic classification of the organic solid residues derived from the hydrogenation of bituminous coal can be applied to coke obtained by carbonization. Table 5.63 includes the type of macerals and the transient phases responsible for coke microstructures. The formation of the transient, fluid phases (vitroplast and mesophase) is indicative of fusion (or plasticity) during carbonization and is limited to certain bituminous coals.

The term *vitroplast* designates a plastic or formerly plastic carbonization product of vitrinite that, unlike the starting material, is optically isotropic. In coke it is characterized by flow structures and spherical morphologies.

The semifusinite maceral can also make a small contribution to the formation of spherical vitroplast. Further alteration of vitrinite and the spherical vitroplast derived from it is seen in the development of cenospheres. This term was first used to designate structures formed by rapid heating of pulverized coal [628, 629]. A cenosphere is defined as a reticulated hollow sphere composed of ribs or frames and windows. Cenospheres are formed by the gas liberated within vitroplast spheres during the plastic stage [627].

Table 5.63: Optical microscopic classification of solid carbonization products [627].

Classification	Optical nature	Intermediate fluid phase	Maceral precursor
Vitroplast (VP ^a)	isotropic	vitroplast	vitrinite, semifusinite
Cenosphere (CS ^a)	isotropic and anisotropic	vitroplast	vitrinite
Semicoke (SC ^a)	anisotropic	mesophase	vitrinite, semifusinite
Unreacted or slightly altered vitrinite (UV ^a)	anisotropic	—	vitrinite
fusinite (FS ^a)	isotropic	—	fusinite

^a Abbreviation.

In contrast to vitroplasts, the mesophase is optically anisotropic and represents the main route for the formation of anisotropic structures in coke. It is considered to be a unique, ordered, fluid system consisting of high molecular mass, planar molecules.

The solid product formed via a mesophase is called a semicoke, a term used in a more general sense for the solid products of low-temperature (500–600 °C) carbonization of coking coals or heavy hydrocarbon feedstocks, such as coal-tar and petroleum pitches.

Both vitroplasts and cenospheres may develop intrinsic anisotropic structures (depending on the conditions of carbonization) while retaining their characteristic morphology. Another type of anisotropy in coke is associated with the unreacted vitrinite fragments. The distinction among these anisotropic microconstituents has a significant bearing on coke properties [627].

Scanning electron microscopy (SEM) is also useful for examining the microstructural characteristics of solids [630]. Its high resolution (ca. 3 nm) and depth of focus permit characterization of surface topography at very low and high magnifications (up to $\times 200\,000$). Specimens are examined by sweeping a finely focused electron beam across the surface. The resulting signals include secondary electrons, backscattered electrons, and characteristic X-rays.

In the examination of coke, the most useful signal is the variation in secondary electron emission with changing surface topography. Optical microscopy and SEM are complementary techniques for coke characterization, providing structural and topographical information, respectively [618].

Carbonaceous Mesophase

The important properties of cokes, including mechanical strength and reactivity, are governed by the arrangement of the constituent carbon atoms. The principal features of the atomic arrangement are the alignment and size of *carbon crystallites*. The highest degree of alignment is seen in natural graphite crystals, which consist of extended layers of fused hexagonal rings of carbon atoms. This structure, with an interlayer spacing of 0.3354 nm, is approached by certain carbons manufactured from coal tar and petroleum pitches and by polynuclear aromatic hydrocarbons on heating at 2500–3000 °C. Depending on their behavior when heat-treated, carbonaceous solids can be classified as graphitizing or nongraphitizing, e.g., coke and char, respectively, in the case of coal-derived solids.

Although the crystallite alignment in carbonaceous solids is only observable after heating at 1000 °C, crystallite alignment starts during carbonization over a narrow temperature range near 450 °C [620]. This stage, coincident with plasticity development, is characterized by the formation of carbonaceous mesophase, which leads to the anisotropic structures found in cokes. The shape and size of these anisotropic structures usually determine the behavior of the coke [631]. Substances that form graphitizing coke via a mesophase include the vitrinites of medium-volatile coking coal, coal-tar and petroleum pitches, polymers such as poly(vinyl chloride), and polynuclear aromatic compounds such as anthracene.

Lignites, thermosetting resins, polymers such as poly(vinylidene chloride), and hydrocarbons such as biphenyl do not form me-

sophase; instead, they produce isotropic nongraphitizing coke commonly referred to as *char* [620].

An outstanding characteristic of carbonaceous mesophase is the prevailing *molecular order*, which represents an intermediate state between totally isotropic liquids and anisotropic solid crystals. A crystal is characterized by long-range order. Isotropic liquids, on the other hand, possess no long-range order [632]. In liquid crystals, some but not all of the long-range order is maintained. The state is neither crystalline nor strictly liquid, and in 1922 the term mesophase was proposed [633–635]. The plastic, anisotropic phase formed during carbonization is designated interchangeably as liquid crystal or (carbonaceous) mesophase.

Of the several types of *liquid crystals*, the nematic (threadlike) type is the most relevant to carbonaceous mesophase [636]. Nematic liquid crystals separate from the isotropic liquid as anisotropic spherical droplets that eventually coalesce to give nematic domains. The molecular arrangement is envisaged as rod-shaped, similarly sized molecules lying parallel to each other but with no stacking order.

The parallel alignment of the molecules in carbonaceous mesophase and the separation from the isotropic liquid in the form of spheres suggest the behavior of nematic liquid crystals. The molecular units of carbonaceous mesophase are, however, disk-shaped and widely varied in size [637]. Furthermore, the formation of carbonaceous mesophase usually involves irreversible chemical processes, in contrast to the physical and reversible formation of nematic liquid crystals. Carbonaceous mesophase consists essentially of large polynuclear aromatic hydrocarbons [638]. Mesophase spheres formed during the carbonization of pitch may contain smaller molecules incorporated in the matrix of planar condensed-ring compounds (Figure 5.142) [637]. This gives a molecular mass distribution in the range of 400–3000 or even more.

The most commonly observed arrangement of molecules in mesophase spheres is the *Brooks–Taylor configuration*, in which layers of planar molecules lie parallel to the equato-

rial plane around the polar axis, but curve to reach the surface at an angle [620, 640]. Other configurations have been observed, especially in the presence of induced magnetic fields and solid particles, e.g., carbon black [641, 642]. These configurations apparently show no different properties.

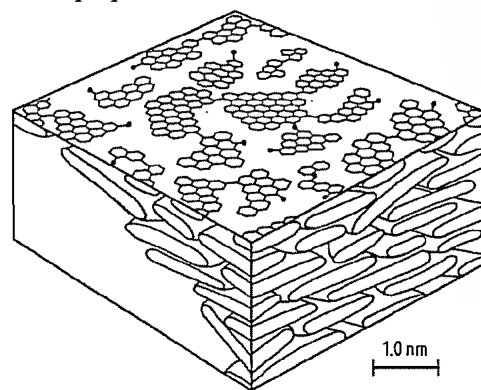


Figure 5.142: Nematic molecular order of carbonaceous mesophase comprised of methyl-substituted polynuclear aromatic compounds connected by methylene bridges and biaryl linkages [637, 639].

The uninhibited *formation and development of mesophase* occurs in three sequential stages: nucleation, growth, and coalescence. This progression, although clearly seen with the optical microscope in pitch and aromatic hydrocarbons, is not always observed during coal carbonization because of the inhibition of growth and coalescence or the very rapid formation of the final texture of the semicoke.

Nucleation is observed as the separation of anisotropic spheres from the isotropic melt, when they become sufficiently large (ca. 0.3 μm in diameter) to be visible. This is a homogeneous process that does not require a specific site. Under favorable conditions, the spheres can grow at the expense of the isotropic melt and coalesce to form large domains of ordered regions, which eventually solidify to semicoke. This type of extensive mesophase development (flow domains) leads to highly graphitizable coke.

If growth and coalescence are inhibited, irregularly shaped anisotropic spheres of small-scale order (0.3–10 μm grain size) are formed. These structures, frequently encountered in

coal carbonization, are termed *mosaics*. A widely used classification, based on the shape and size of the anisotropic structures found in coke, is as follows [614]:

<i>Isotropic</i>	no optical activity, uniform, light purple color on the surface
<i>Anisotropic</i>	
Via mesophase	dark purple, yellow and blue areas of varying shape and size
Fine-grained mosaics	irregularly shaped, isochromatic areas (ISIA), 0.5–1.5 μm long
Medium-grained mosaics	ISIA, 1.5–5.0 μm long
Coarse-grained mosaics	ISIA, 5.0–10 μm long
Coarse flow	rectangular, flow-type structures 30–60 μm long; > 10 μm wide
Flow domains	flow-type structures > 60 μm long; > 10 μm wide
Domains	isometric structures > 60 μm in diameter
<i>Basic anisotropy</i>	flat, featureless anisotropy associated with the parent unreacted (or slightly altered) vitrains from high-rank coals

The sequential formation of mesophase is apparently not the sole mechanism leading to anisotropic structures in coal-derived coke. *Vitrains* from high-rank coals behave somewhat differently from coking and caking coals [612]. The inherent (basic) anisotropy of vitrain, which is rather featureless, is unchanged or converted directly to flow-type anisotropy. In this respect, it does not follow the progressive development of flow-type anisotropy.

Mesophase formation results from extremely complex and interdependent *physical and chemical processes* occurring during carbonization. The first chemical process is the rupture of weak bonds, breaking down the molecular network and forming free radicals, followed by such reactions as cyclization, aromatization, and polymerization.

The *fluid carbonization medium* at this stage can be envisaged as a dynamic chemical system, with increasing molecular mass and size [618]. When the planar molecules reach a critical concentration and size, van der Waals forces become sufficiently strong to establish parallel orientation. The resultant anisotropic miscellae separate from the isotropic fluid phase in the form of spheres. If the molecules are not sufficiently planar, parallel stacking is

sterically hindered. The spherical shape of the separated anisotropic miscella results from the usual requirement of minimum surface area and surface energy at the interface of a two-phase system [618].

The principles governing mesophase formation can be summarized as follows:

- Heteroatoms and alkyl groups inhibit mesophase formation by cross-linking reactions, which impair planarity.
- Naphthenic hydrogen promotes mesophase formation via hydrogen-transfer reactions, which retard cross-linking and increase fluidity.
- Aromatic systems promote mesophase formation by virtue of their planarity and low reactivity.

These findings are based on studies of model compounds thought to resemble the building blocks of bituminous coal and petroleum feedstocks [619, 622, 643, 644]. In addition, mesophase formation depends on carbonization conditions.

The carbonization of coal of different rank produces coke with corresponding optical properties [616]. Low-rank coals (lignite and subbituminous) do not soften during carbonization, thus producing isotropic chars [617].

The size of the anisotropic structures in coke generally increases with increasing coal rank (Figure 5.143) [51]. Whole coal behaves like vitrain. Caking coal with high volatile content forms isotropic coke containing small amounts of fine-grained mosaics. With increasing rank up to the prime coking coals, these anisotropic structures become larger (5–10 μm) and more numerous.

In coke from prime coking coal, the optical texture (apart from inorganic and infusible organic petrographic components) is essentially and continuously anisotropic, with structures varying in size from fine-grained mosaics to coarse particles up to 20 μm . The anisotropic structures in coke from fusing coal (high-to-low-volatile-content bituminous) develop mostly via mesophase formation.

Semianthracites, anthracites, and some noncaking low-volatile bituminous coals

have no fluid stage during carbonization. The large anisotropic structures found in these cokes originate from the inherent anisotropy of the parent coal [612].

The variations in the optical texture of coke from coals of different rank reflect the differences in mesophase formation. These differences can be explained in terms of the variations in chemical constitution.

Coals become more aromatic with increasing rank, which is also associated with decreasing oxygen content and increasing incorporation of oxygen into cyclic structures [645–647].

In low-rank coal, most oxygen is in the form of carboxyl ($-\text{COOH}$) and hydroxyl ($-\text{OH}$) groups; both are reactive cross-linking agents. Oxygen in cyclic structures does not participate in cross-linking. In light of the principles discussed in this section, increasing aromaticity and decreasing oxygen content can explain the improvement in mesophase formation with increasing coal rank.

Carbonization conditions also affect mesophase formation. These effects are due to changes in the rate of chemical and physical processes [648, 649].

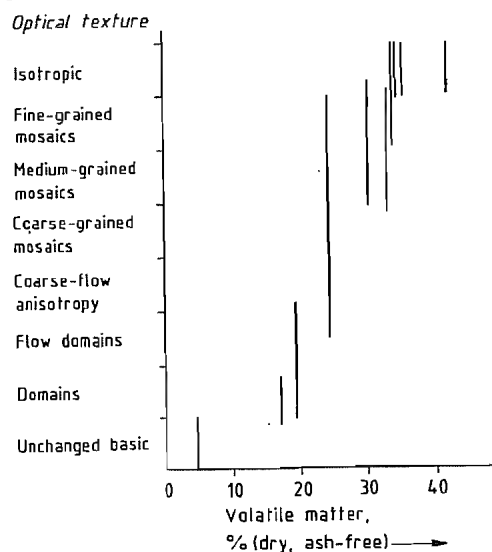


Figure 5.143: Variation of coke optical texture with volatile matter content of the parent vitrains [614].

Modification of Optical Texture and Properties

The most significant feature of the microstructure of metallurgical coke is the unique anisotropy that is associated with low porosity and takes the form of mosaics bridged by small flowtype structures in the pore wall [616]. Most macropores are hundreds of micrometers in size; the pore wall is of significant thickness [616]. The limited porosity provides a coke density suitable for blast furnace operations, whereas the bonding of the small growth units of the anisotropic structures strengthens the coke. In addition, the anisotropic and nonporous nature of the coke reduces reactivity toward carbon dioxide, as is desired in blast furnace operations.

Consequently, coke properties can be modified by altering the optical texture and morphology. This makes possible manufacture of metallurgical coke from the large reserves of noncoking coal of low rank.

Modification of mesophase formation has therefore, great value in improving coke. The coking of noncoking coal with coking coal or pitch is also useful [650, 651].

5.22.13.2 Yield and Distribution of Pyrolysis Products

Experimental Methods

The yield of pyrolysis products (gases, liquids, and solids) is determined by monitoring the loss of coal mass or the quantity of gas evolved. In the traditional determination of proximate volatile matter (e.g., ASTM or DIN), the yield is measured as the mass lost from a fixed bed at standard conditions. Deviations from these conditions can change mass losses significantly (Figure 5.144). Smaller samples in a standard crucible (shorter bed depths) and higher heating rates and temperatures increase volatile yield.

Yields are also increased by reducing gas pressure and particle size. Thus, the volatile-matter content is highly dependent on pyrolysis conditions and can exceed 150% of the

ASTM value (e.g., last line, Table 5.64). When volatile products are desired, increased yield is of great interest. Furthermore, factors that influence the product distribution are important because in many processes the liquids (not the gases) are of primary interest.

In contrast to coal gasification, for example, with its few and easily identified products, the prediction of yield and product distribution in coal pyrolysis is difficult. The extreme complexity of coal pyrolysis precludes accurate thermodynamic analysis. Moreover, the temperature and pressure are often ill-defined. In rapid pyrolysis, internal pressures as high as 100 MPa have been estimated [652]. The design of reactors and processes is usually based on experimental determination of the yield and product distribution as functions of temperature, heating rate, pressure, particle size, and coal rank [653].

Experimental Variables

Time and Temperature

The determination of temperature and residence time in entrained-flow reactors presents special problems. Particle temperature is usually estimated from measurements of gas temperature (by suction pyrometry) with the aid of a heat-transfer model. Particle residence time (≤ 1 s) is calculated from known or assumed trajectories by using an appropriate model for the fluid and solid dynamics. The

total yield of volatile substances, when not obtained from material balances, is frequently determined from the mineral matter or ash in the coal or char. The distribution of volatile products is usually determined by gas chromatography or mass spectrometry.

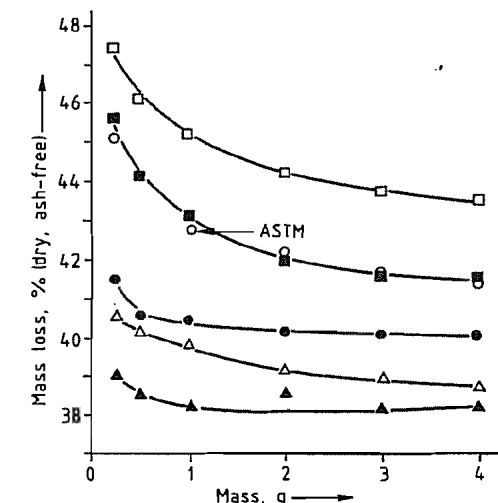


Figure 5.144: Effect of sample mass (bed depth), heating rate, and pyrolysis temperature on mass loss [652].

Symbol	Heating rate, °C/s	Temperature, °C
Δ	6	750
\circ^a	14	950
\square	22	1150
\blacktriangle	0.5	750
\bullet	0.5	950
\blacksquare	0.5	1150

^a Standard ASTM volatile matter test.

Table 5.64: Comparison of experimental pyrolysis yields with proximate volatile matter [653].

Conditions	Coal rank	Proximate analysis ^a , VM, %	Experimental yield, V ^a , %	V ^a /VM ^b
Dry basis, heated to 950 °C at 600 °C/s	medium-volatile bituminous (mvb)	25.3	19	0.75
	high-volatile A bituminous (hvAb)	31.6	36	1.14
	high-volatile A bituminous (hvAb)	37.7	49	1.30
	subbituminous	40.7	48	1.17
	high-volatile bituminous (hvb)	44.0	41	0.93
Dry, ash-free basis, heated to 1000 °C at 10 ³ °C/s	bituminous	46.2	53.7	1.16
	lignite	44.3	44.7	1.01
	bituminous	44.6	52.2	1.17
	bituminous	42.5	65	1.53

^a ASTM method.

^b V^a = total volatile matter; VM = proximate volatile matter.

Table 5.65: Distribution of volatile products in coal pyrolysis [653].

Method	Coal type	Volatile products, % (dry)			
		Tar ^a	Gas	Water	T ^b
Fischer assay, 600 °C	Furst Leopold	11.2	10.0	8.1	29.3
Stirred bed, 600 °C		18.7	7.0	7.5	33.2
Slow heating, 0.08 °C/s	Moscow brown coal	4.6	11.9	6.0	22.5
Rapid heating to 500 °C		4.0	8.1	9.6	21.7
Thin layer of particles heated to 1050–1100 °C at 1500 °C/s	Maigre Oignies no. 2	1.8	5.1	1.5	8.4
	Bergmannsgluck	41.7	5.9	3.0	23.6
	Emma fines	15.9	6.2	2.4	24.5
	Lens-Lievin no. 10	17.1	7.0	2.6	26.7
	Flenus de Bruay	25.2	9.6	4.4	39.2
	Wendell III	22.5	7.9	4.1	34.5
	Faulquemont	18.9	12.6	5.2	36.7
Entrained flow, 600 °C	West Virginia, mvb ^c	18.7	1.8	6.5 ^e	27.0
	Illinois, mvb ^c	19.6	19.7	4.6 ^c	43.9
	Pittsburgh, hvAb ^d	31.5	22.0	8.0 ^e	61.5
	Wyoming, subbituminous B	11.0	26.4	5.6 ^e	43.0
Fischer assay, 500 °C	Western Kentucky	16.3	5.0	9.4	30.7
Flow tube, 530–650 °C	hvBb ^c	33.0	6.6	1.7	41.3
Thin layer of particles heated to 1000 °C at 1000 °C/s	Pittsburgh, hvAb ^d	25.8	11.3	6.5	43.6
	Montana lignite	6.8	22.7	10.4	39.9

^a Volatiles condensable at 20 °C.^b Combined volatiles from tar, gas, and water.^c See Table 5.64 for abbreviation.^d High-volatile A bituminous.^e Estimated as mass difference between original dry coal and combined tar, gas, and char yields.

Table 5.66: Composition of gaseous products in coal pyrolysis [653].

Conditions	Temperature, °C	Volatiles, %	Gas composition, vol % (dry)			
			CO ₂	CO	H ₂	CH ₄
Thin layer of particles	105–1100 (at 1500 °C/s)	8.4	2.2	10.1	66.2	8.6
		18.1	1.6	5.0	67.2	21.4
		20.4	2.0	6.0	62.9	20.3
		24.4	3.8	9.6	64.2	21.0
		31.0	4.1	15.8	54.3	16.9
		33.9	2.4	10.0	52.8	21.8
		36.4	6.1	20.6	60.3	13.1
Fluidized bed	600	31	12.0	12.3	14.7	50.5
Fischer assay	600	31	10.3	8.7	22.4	54.2
Entrained flow	600	31.6	9.2	3.6	19.4	24.7
		34.6	11.7	0.0	23.0	40.7
		37.7	9.5	9.5	17.1	42.9
		40.7	16.0	10.5	25.6	33.9
Flow tube	530–650	41	10.6	4.9	25	42.3
Thin layer of particles	1000 (at 1000 °C/s)	39.5	3.2	9.9	57.8	17.8
		39.6	24.0	37.2	27.8	8.8

The yield of volatile products in the pyrolysis of coals of different rank under different heating rates increases continuously with increasing temperature. This results from the existence of a hierarchy of bond energies in the structure of coals (Figure 5.136). In most cases, even at heating rates as high as 10 000 °C/s in

entrained-flow reactors, pyrolysis is complete at ca. 1000 °C. For a longer residence time, a lower temperature is needed to achieve a particular yield, in accordance with Arrhenius-type behavior. In particular, the yield is a sensitive function of temperature for short residence times in entrained-flow reactors.

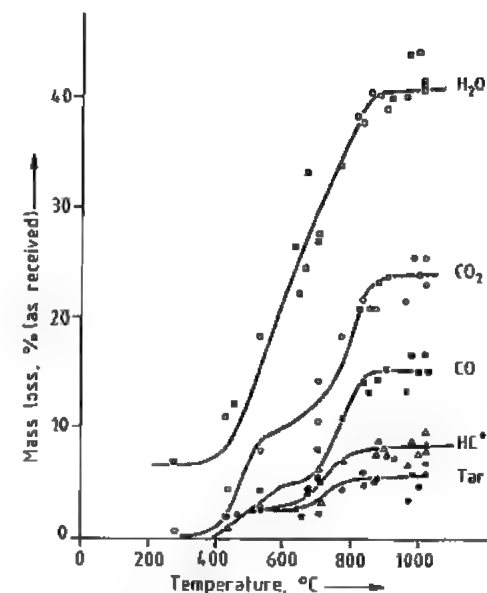


Figure 5.145: Effect of temperature on the distribution of volatile products from a lignite (pressure: 101.3 kPa of He; mean particle diameter: 74 µm; heating rate: 270–10 000 °C/s). □ Total; ○ Tar + HC gases and H₂ + CO + CO₂; ■ Tar + HC gases and H₂ + CO; △ Tar + HC gases and H₂; ● Tar [653]. * HC = Hydrocarbon.

The effect of temperature, the most important influence on product distribution, is illustrated in Tables 5.65 and 5.66, and Figures 5.145 and 5.146. The influence of temperature on the distribution of volatiles obtained from rapid pyrolysis of a lignite (270–10 000 °C/s) is clearly seen in Figure 5.145. The yield of tars reaches a low maximum at relatively low temperature. The hydrocarbon gases consist mainly of methane, ethylene, and hydrogen. The oxygen-containing products, water, carbon dioxide, and carbon monoxide, dominate the gas composition. A result of this temperature dependence is that the pyrolysis products have a range of heating values. This is illustrated in Figure 5.147 for lignite and is typical of the problems associated with obtaining clean-burning fuel from low-rank coals.

In contrast, a high yield of tar and other combustible matter is obtained by the rapid pyrolysis of bituminous coal (Figure 5.146). In both cases, as in all pyrolysis processes, the

yield of char or coke is substantial, even at 1000 °C.

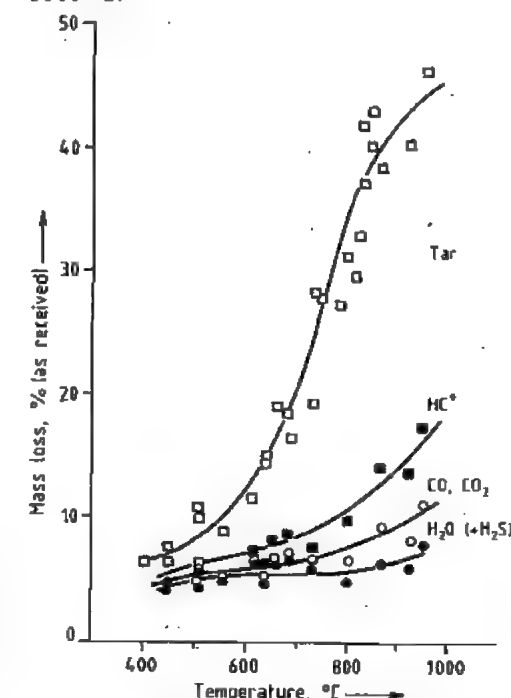


Figure 5.146: Effect of temperature on the distribution of volatile products from a bituminous coal (pressure: 101.3 kPa of He; mean particle diameter: 74 µm; heating rate: 1000 °C/s). □ Total; ■ HC gases and H₂ + CO and CO₂ + H₂O and H₂S; ○ CO and CO₂ + H₂O and H₂S; ● H₂O and H₂S [653]. * HC = Hydrocarbon.

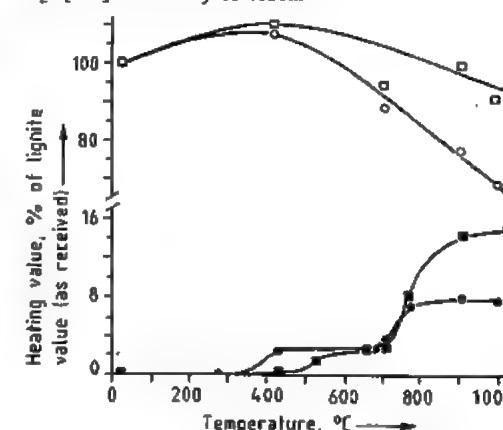
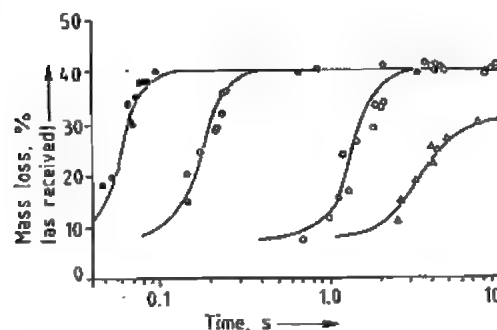


Figure 5.147: Effect of temperature on the distribution of heating value among the products of pyrolysis of a lignite (pressure: 101.3 kPa of He; heating rate: 1000 °C/s). □ Total; ○ Char; ■ Gas; ● Tar [653].

Table 5.67: Effect of heating rate on product distribution from bituminous coals [653].

Product	Yield, % (as received)		
	350–450 °C/s	1000 °C/s	13 000–15 000 °C/s
CO	2.4	2.4	2.3
CO ₂	1.6	1.2	1.7
H ₂ O	7.6	7.8	7.7
CH ₄	2.2	2.5	2.4
C ₂ H ₄	0.40	0.83	0.66
C ₂ H ₆	0.59	0.51	0.59
C ₃ S	1.1	1.3	1.2
Other HC gas	1.1	1.3	1.4
Light HC liquid	2.3	2.4	2.7
Tar	22.4	23.0	23.0
H ₂	—	1.0	—
Char	54.0	53.0	53.0
Total	95.69	97.24	96.65
Error (loss)	4.3	2.8	3.3
Number of runs	3	20	2

**Figure 5.148:** Effect of time on pyrolysis mass loss from a lignite (pressure: 101.3 kPa of He; final temperature (if attained): 1000 °C; mean particle diameter: 70 μm). ● 10⁴ °C/s; ○ 3000 °C/s; □ 650 °C/s; △ 180 °C/s [653].

Heating Rate

The effect of heating rate on coal pyrolysis has often been misunderstood. If slow heating (e.g., 10 °C/min in fixed-bed reactors) is compared with rapid heating (e.g., 10 000 °C/s in entrained-flow reactors), the latter usually gives a better yield. In most such comparisons, however, the heating rate is not the only variable. A change from a fixed-bed reactor to an entrained-flow reactor involves a sharp decrease in the density of the pyrolyzing medium, with important implications for secondary char-forming reactions. However, when the only change is an increased heating rate (Table 5.67 and Figure 5.148), yield and

product distribution are unaffected [653], but the time required to reach a given yield is reduced.

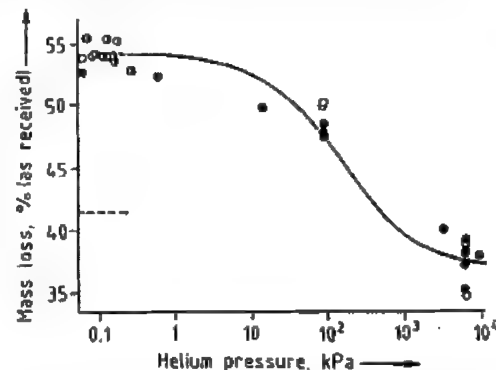
Pressure

In the rapid pyrolysis of bituminous coal yield usually decreases with increasing pressure (Figure 5.149). A drop in the yield of tar is not compensated by an increase in the yield of hydrocarbon gases, such as methane (Figure 5.150 and Table 5.68). Increased pressure evidently favors char-forming reactions, particularly cracking and polymerization.

Particle Size

As with heating rate, the effect of coal particle size has been difficult to determine. Changes in particle size are usually accompanied by changes in temperature and residence time. In entrained-flow systems, the calculated residence time is dependent on particle size. Obtaining identical temperature time histories for a range of sizes is difficult; therefore, reports in the literature are conflicting.

As might be intuitively expected (see Section 5.22.13.2), larger particles give a lower yield of volatiles. Increase in char formation (due to tar cracking or polymerization) is not compensated by increased yield of hydrocarbon gas (Figure 5.151 and Table 5.69).

**Figure 5.149:** Effect of pressure on pyrolysis mass loss from a bituminous coal (final temperature: 1000 °C; mean particle diameter: 70 μm; residence time: 5–20 s). Nominal heating rate, °C/s: ● 650–750; □ 3000; ○ 10 000. ----- Proximate volatile matter (ASTM).**Table 5.68:** Effect of pressure on product distribution from lignite and bituminous coal [653].

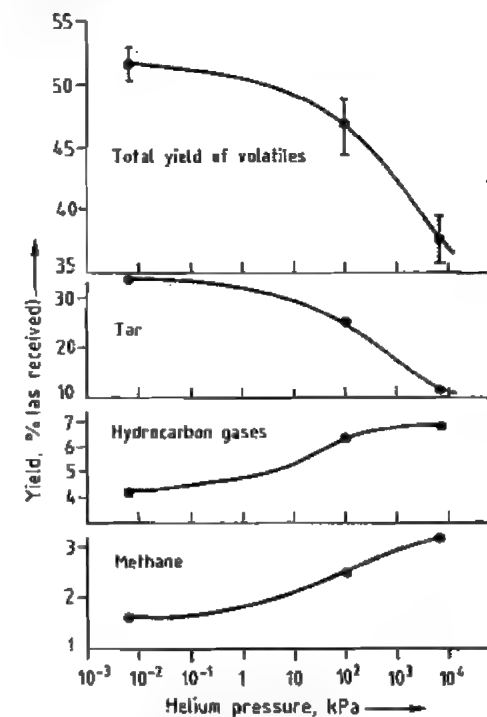
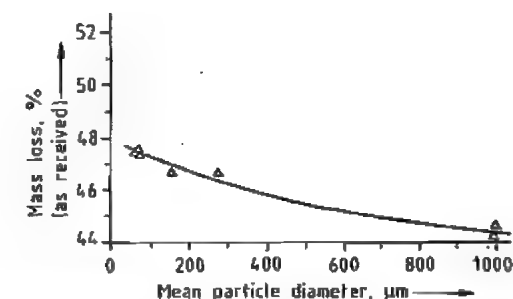
Product	Yield, % (as received)					
	Lignite			Bituminous ^a		
	6.6 Pa of He ^b	0.1 MPa of He ^b	6.9 MPa of He ^a	6.6 Pa of He	0.1 MPa of He	6.9 MPa of He
CO	6.1	7.1	9.0	2.0	2.4	2.5
CO ₂	7.6	8.4	10.6	1.4	1.2	1.7
H ₂ O ^c	17.7	16.5	13.4	6.8	7.8	9.5
H ₂	—	0.50	—	0.75	1.0	—
CH ₄	0.94	1.3	2.5	1.6	2.5	3.2
C ₂ H ₄	0.43	0.56	0.55	0.45	0.83	0.46
C ₂ H ₆	0.21	0.18	0.17	0.44	0.51	0.89
C ₃ H ₈ + C ₃ H ₁₀	0.46	0.37	0.38	0.71	1.3	0.71
Other HC ^d gases	0.60	0.47	0.21	0.98	1.3	1.6
Light HC ^d liquids	0.81	—	1.1	1.6	2.4	2.0
Tar	6.9	5.4	2.8	31.9	23.0	12.0
Char	55.2	58.7	59.0	48.5	53.0	62.4
Total	97.0	99.5	99.7	97.1	97.2	97.0
Error (loss)	3.0	0.5	0.3	2.9	2.8	3.0

^aFinal temperature: 850–1070 °C; mean particle diameter: 74 μm; heating rate: 1000 °C/s; residence time: 2–10 s.

^bFinal temperature: 900–1035 °C; no residence time.

^cIncludes coal moisture (lignite: 6.8%; bituminous: 1.4%); may include H₂S.

^dHC = Hydrocarbon.

**Figure 5.150:** Effect of pressure on the yield and distribution of volatile products from a bituminous coal (final temperature: 1000 °C; mean particle diameter: 74 μm; heating rate: 1000 °C/s; residence time: 2–10 s) [653].**Figure 5.151:** Effect of particle size on pyrolysis mass loss from a bituminous coal (pressure: 101.3 kPa of He; final temperature: 1000 °C; heating rate: 650–750 °C/s; residence time: 5–20 s) [653].

Coal Rank

Coals over a wide range of rank can give yields of pyrolysis products that are higher than their standard content of volatile matter (as determined by ASTM proximate analysis) (see Figures 5.145 and 5.146, Tables 5.65 and 5.70). The most important result is the high tar yield given by entrained-flow pyrolysis of bituminous coal.

Table 5.69: Effect of particle size on product distribution from a bituminous coal (pressure: 101.3 kPa of He; final temperature: 850–1070 °C; heating rate: 1000 °C/s; residence time: 3–10 s) [653].

Product	Yield, % (as received)			
	53–88 µm (average, 74 µm)	< 300 µm ^a	300–830 µm	830–900 µm
CO	2.4	2.7	3.2	3.0
CO ₂	1.2	1.1	1.2	1.3
H ₂ O ^b	78	5.4	5.3	7.2
H ₂	1.0	—	—	0.99
CH ₄	2.5	2.9	3.0	3.2
C ₂ H ₄	0.83	1.0	1.1	1.3
C ₂ H ₆	0.51	0.50	0.55	0.63
C ₃ S	1.3	0.92	0.84	1.1
Other HC ^c gases	1.3	1.4	1.1	1.2
Light HC ^c liquids	2.4	2.5	2.6	2.7
Tar	23.00	24.2	21.3	18.4
Char	53.0	57.1	56.5	55.8
Total	97.2	99.7	96.7	96.8
Error (loss)	2.8	0.3	3.3	3.2
Number of runs	20	1	2	3

^a 830–990-µm sample ground to pass 297-µm sieve (50 mesh).^b Includes coal moisture (1.4%); may include some H₂S.^c HC = Hydrocarbon.**Table 5.70:** Effect of coal type on yields of gaseous pyrolysis products [653].

Element/compound	Composition, %		
	Lignite	Subbituminous	Bituminous
<i>Coal analysis (as received)</i>			
C ^a	71.2	73.5	77.7
H ^a	4.6	5.8	5.5
N ^a	1.1	1.2	1.5
S ^a	1.3	0.81	6.1
O ^a , by difference	21.8	18.7	9.2
H ₂ O	6.8	34.7	1.4
Ash, dry	10.6	9.1	11.5
VM ^a	44.3	—	11.5
<i>Product analysis^a</i>			
CO	8.5	5.8	2.8
CO ₂	10.10	11.3	1.4
H ₂ O	11.6	—	7.4
H ₂	0.60	1.1	1.2
N ₂	—	—	—
CH ₄	1.6	4.8	2.9
C ₂ H ₄	0.67	0.24	0.95
C ₂ H ₆	0.24	0.89	0.58
C ₃ H ₈	0.17	0.47	1.5 ^b
Total	33.5	24.6	18.7

^a Dry, ash-free.^b Includes C₃H₆.

Mechanism

The objective of most coal pyrolysis processes, whether fuels or chemicals are being produced, is to maximize the yield of gaseous

and liquid products (coke production is a notable exception). This is achieved by reducing secondary char-forming reactions (cracking and polymerization) of high molecular mass products.

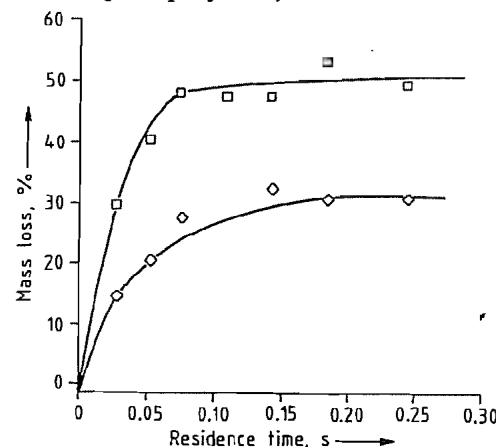
Cracking and polymerization can occur within and between the coal particles. These reactions are usually subject to surface catalytic effects and to the nature of the medium to which the primary products are exposed [654].

Volatile material can be driven from the interior of a coal particle by increasing the internal pressure or by reducing the external (ambient) pressure. High pressure gradients accelerate volatilization, thus reducing residence time within the particle, which decreases the probability of secondary reactions and char formation. This explains the effect of external pressure (shown in Figure 5.149) and of high heating rates, which result in rapid heat transfer and a high rate of thermal decomposition. This higher rate of formation of volatiles increases the internal pressure and reduces char formation.

Minimizing interparticle secondary reactions also is important for a maximum yield of volatiles. This is achieved by minimizing particle loading. In entrained-flow reactors, particle loading is far lower than in fixed-bed

reactors and the heating rate is far higher. Fluidized-bed reactors are intermediate between these two types.

When pyrolyzed, low-rank coal yields much less tar than bituminous coal. In part this is due to the presence of high molecular mass aromatic units in high-rank coal, which form liquid rather than gaseous products. Another factor is the presence of cations in low-rank coal. Acid washing removes these cations and substantially increases the yield of volatiles (Figure 5.152). This is attributed to a higher tar yield and the elimination of char-forming reactions catalyzed by the highly dispersed cations (principally Ca²⁺).

**Figure 5.152:** Effect of cations on pyrolysis mass loss from a lignite (pressure: 101.3 kPa of N₂; final temperature: 900 °C; mean particle diameter: 70 µm; heating rate: 104 °C/s). □ Acid-washed; ◇ As received [655].

Various options are available when selecting the operating conditions of a pyrolysis reactor [656]. Residence times of 0.1 s or less are attainable only in entrained-flow reactors; at the other extreme, residence times of 100 000 s or more are practical only in fixed-bed reactors. At low temperature (ca. 525 °C), the total yield of volatiles is low because thermal decomposition is incomplete. Entrained-flow conditions minimize secondary reactions and give the highest overall yield. Furthermore, high molecular mass products are stable at low temperature, and the product distribution favors liquids. At ca. 1000 °C, volatilization is complete, with a correspondingly

high yield. Again, entrained-flow conditions reduce secondary reactions and increase overall yield. However, even under dilute conditions in entrained-flow reactors, high temperature causes substantial cracking and gives gas as the principal volatile product.

5.22.13.3 Kinetics

The practical importance of the kinetics of the processes described in section 5.22.13.2 depends on the reactor type [653, 657, 658]. In *fixed-bed reactors*, such as coke ovens where the heating rate is ca. 100 °C/min or less, kinetics are not important. The time required for complete pyrolysis is much less than the time required for heating to the final temperature, which determines yield and product distribution.

On the other hand, residence time at pyrolysis temperatures is important in *entrained-flow reactors*, such as pulverized-coal combustors and some modern pyrolysis reactors, which are increasingly important.

A simple kinetic treatment for determining the rate constants that define the size of a reactor or reaction zone is to assume first-order decomposition of the volatile matter in the coal:

$$\frac{dV}{dt} = k(V' - V) \quad (37)$$

where k = rate constant (s⁻¹), V = fraction of volatiles evolved at time t , and V' = total amount of volatiles in the coal.

The magnitude of the effect of coal rank is debatable. In one report the kinetics of pyrolysis were found to be insensitive to changes in rank from lignite to bituminous coal [657]. A possible explanation for this observation is that rapid pyrolysis rates are not determined by the chemical process of bond rupture, but by the physical processes of heat or mass transfer.

The modeling of the complex pyrolysis process by a single first-order reaction is an oversimplification. Many alternative kinetic schemes, proposed to represent more closely the actual mechanism of coal pyrolysis, range from 2 independent parallel reactions corre-

sponding to the postulated 2 components in coals [659], to 42 reactions of the postulated 14 different functional groups in coal [660].

A reasonable compromise, which incorporates process complexity and is a mathematically adequate yet physically reasonable kinetic model [661], is based on a hierarchy of bond energies in the coal structure (Figure 5.136). The pyrolysis is assumed to consist of a large number, i , of independent chemical reactions representing the rupture of various bonds within the coal structure:

$$\frac{dV_i}{dt} = k_i(V_i' - V_i) \quad (38)$$

where the symbols are analogous to those of Equation (37), with the subscript i denoting a particular reaction. The rate constants k_i are assumed to be of Arrhenius form and to differ only in the values of their activation energies. The number of reactions is assumed to be large enough to permit the activation energies E_i to be expressed as a continuous Gaussian distribution function

$$f(E) = \frac{1}{\sigma(2\pi)^{1/2}} \exp\left[-\frac{(E-E_0)^2}{2\sigma^2}\right]$$

with

$$\int_0^\infty f(E)dE = 1$$

where E_0 = mean activation energy and σ = standard deviation.

The term $f(E)dE$ represents the fraction of potential volatiles that have an activation energy between E and $E + dE$,

$$\frac{dV'}{V'} = f(E)dE \quad (39)$$

The total amount of volatiles remaining in the coal is obtained by combining the contribution from each reaction, i.e., by integrating Equation (38) over all values of E by using Equation (39):

$$\frac{V' - V}{V'} = \int_0^\infty \exp\left[-A \int_0^t \left(-\frac{E}{RT}\right) dt - \frac{(E-E_0)^2}{2\sigma^2}\right] dE \quad (40)$$

or

$$\frac{V' - V}{V'} \quad (41)$$

$$= \frac{1}{\sigma\sqrt{2\pi}} \int_0^\infty \exp\left[-A \int_0^t e^{-\frac{E}{RT}} dt - \frac{(E-E_0)^2}{2\sigma^2}\right] dE$$

Equations (40) and (41) show that in addition to the temperature time history, four parameters are needed to correlate coal pyrolysis data. The total yield of volatiles, V' , should be determined experimentally and is not necessarily equal to the ASTM volatile matter content.

This model represents a significant improvement over the single first-order reaction scheme. Curves drawn through the experimental points in Figures 5.145 and 5.146 were obtained by using this model.

If, for simplicity and convenience, the single first-order reaction model of coal pyrolysis is assumed, the treatment that in the past has been applied to complex continuous reaction mixtures [662] and more recently to model coal liquefaction [663] should be used. It results in a temporal distribution of activation energies rather than the spatial distribution just described. It considers coal to be composed of constituents C_i ; pyrolysis results in products P_i

$$\sum C_i \rightarrow \sum P_i$$

where the pyrolysis of each constituent is a first-order reaction:

$$-\frac{dC_i}{dt} = k_i(T)f(C_i)$$

Because C_i and P_i are not identifiable chemical species, a grouping procedure is used:

$$\sum C_i = V$$

The first-order rate expression, analogous to Equation (37), becomes [664]

$$-\frac{dV}{dt} = k(T, V)f(V)$$

Thus, the first-order rate constant k is not only a function of temperature, but also of the concentration of the volatiles, i.e., of conver-

sion or time of pyrolysis. Limited experimental evidence [665] suggests that k decreases with conversion because of an increase in the observed activation energy. This can be interpreted as the intuitively reasonable initial predominance of the rupture of relatively weak bonds in the coal structure.

The main conclusion from this brief analysis is that some of the variation in rate constants can be attributed to the fact that the constants may not have been compared at the same level of conversion.

For optimization of product distribution, having rate parameters for the total yield of volatiles and for individual compounds is desirable. The principal issue is the number of reactions necessary to describe the pyrolysis. In particular, determination of tar evolution rates is difficult because the rates are dependent on the transport properties of the experimental system. In one report these rate constants seem to correlate equally well the pyrolysis of lignite, subbituminous coal, and bituminous coal [657]. This means that pyrolysis rates may be dependent only on the quantity of the various functional groups in the coal and not on its origin or type. This conclusion, if established as generally valid for chemically rather than physically controlled pyrolysis processes, would simplify the design of pyrolysis reactors.

5.22.13.4 Hydropyrolysis

Most coal conversion processes involve hydrogen transfer reactions; pyrolysis involves *hydrogen redistribution*. Free radicals formed by bond rupture usually capture hydrogen atoms (Figure 5.137). Under entrained-flow pyrolysis conditions, the total yield of volatiles is typically 20–40% higher than the ASTM volatile content of the coal, i.e., at least 30–40% of the product is a solid. The available hydrogen is used primarily to stabilize gaseous radicals, such as methyl or ethyl, leaving the higher molecular mass radicals to polymerize and form char.

To reduce char formation and increase volatile yield, the coal is pyrolyzed in the presence of hydrogen [666]. The effect is more pronounced at higher hydrogen pressure, but is not observed if pyrolysis in an inert atmosphere is followed by exposure to hydrogen. Coal can be converted completely to methane in a few seconds at 950 °C and 50 MPa of hydrogen [667]. These effects are not fully understood, but seem to resemble the effect of hydrogen in coal liquefaction, where external hydrogen stabilizes the free radicals formed by bond scission and inhibits char formation. Another possible role of hydrogen in hydropyrolysis is to attack the highly reactive, but transient nascent carbon sites. Aromatic carbon radicals are formed by cleavage of functional groups. Hydrogen reacts with these active sites eventually forming methane, and, thus, the overall yield of volatiles is increased.

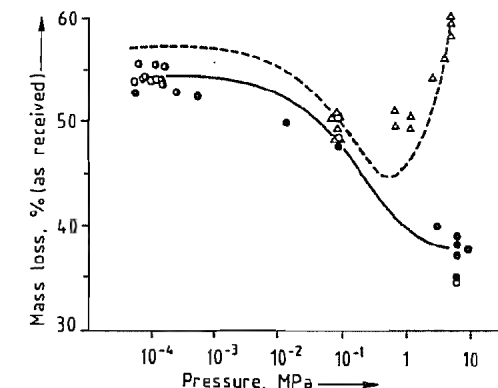


Figure 5.153: Effect of helium and hydrogen pressure on pyrolysis mass loss from a bituminous coal (final temperature: 1000 °C; mean particle diameter: 70 μm; residence time: 5–20 s). ○ He (104 °C/s); ● He (3000 °C/s); ● He (650–750 °C/s); △ H₂ (750 °C/s) [653].

The effects of hydrogen pressure on the yield and distribution of pyrolysis products is illustrated in Figures 5.153 and 5.154 (see also Table 5.71). As discussed previously, an increase in the pressure of an inert gas reduces the yield of volatiles. With hydrogen, however, the yield first drops (Figure 5.153), and then increases with an increase in pressure.

Table 5.71: Yields from pyrolysis and hydrolypyrolysis of bituminous coal (final temperature: 850–1070 °C; mean particle diameter: 74 µm; heating rate: 1000 °C/s) [653].

Product	Yield, % (as received)					
	0.1 MPa of He ^a		6.9 MPa of He ^a		6.9 MPa of H ₂ ^b	
	Bituminous ^c	Lignite ^d	Bituminous ^c	Lignite ^d	Bituminous ^c	Lignite ^d
CO	2.4	9.4	2.5	9.0	—	7.1
CO ₂	1.2	9.5	1.7	10.6	1.3	8.5
H ₂ O	6.8	16.5	9.5	12.9	—	16.0
CH ₄	2.85	1.3	3.2	2.5	23.2	9.5
C ₂ H ₄	0.8	0.6	0.5	0.6	0.4	0.2
C ₂ H ₆	0.5	0.2	0.9	0.2	2.3	1.4
C ₃ H ₆ + C ₃ H ₈	1.3	—	0.7	—	0.7	—
Other HC ^e gases	1.3	—	1.6	—	2.0	—
Light HC ^e liquids	2.4	—	2.0	—	5.3	—
Tar	23	5.4	12	3	12	8
Char	53.0	56.0	62.4	59.8	40.2	48.5

^aPyrolysis.

^bHydrolypyrolysis.

^cResidence time: 2–20 s.

^dResidence time: 3–10 s.

^eHC = Hydrocarbon.

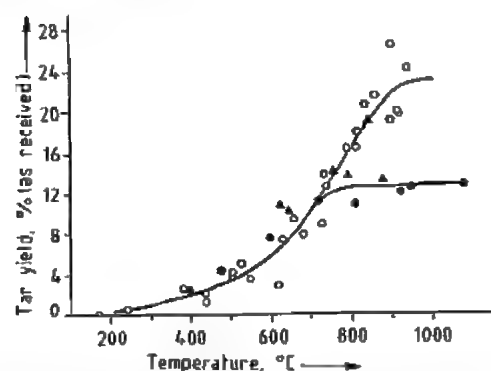


Figure 5.154: Comparison of tar yields from pyrolysis and hydrolypyrolysis of a bituminous coal (mean particle diameter: 74 µm; heating rate: 1000 °C/s). ○ 0.1 MPa of He; ● 6.9 MPa of He; ▲ 6.9 MPa of H₂ [653].

Experimental evidence suggests that the principal effect of H₂ is not in preventing secondary char-forming reactions (Figure 5.154). The yield of tar under the experimental conditions employed decreased under high hydrogen pressure. In this instance, the detrimental effect of a high external pressure overcame the beneficial stabilizing effect of hydrogen. In the case of a bituminous coal and a lignite, the overall yield enhancement was due to an increase in methane production (see Table 5.71).

On thermal decomposition, the pores of coal particles are filled with reactive (e.g., rad-

icals) and less reactive volatiles. The latter escape unchanged, whereas the former are either quenched and escape, are cracked, or polymerize. Active char (or coke) contains active sites that react with H₂ to give methane. The deactivated sites contribute little or nothing to the overall volatile yield. The corresponding kinetic expressions are given below [653]:

Pyrolysis:

$$V' = V_{\text{ar}}'' + V_{\text{r}}'' \frac{K_c}{K_c + k_1} = V_{\text{ar}}'' + V_{\text{r}}'' \frac{1}{1 + k_1 P / k_c}$$

Hydrolypyrolysis:

$$V' = V_{\text{ar}}'' + V_{\text{r}}'' \frac{K_c + k_2 P_{\text{H}_2}}{K_c + k_2 P_{\text{H}_2} + k_1} + k_3 P_{\text{H}_2}$$

The curves in Figure 5.153 were obtained by using these expressions.

5.22.13.5 Pyrolysis Processes

Pyrolysis and hydrolypyrolysis give gaseous, liquid, and solid products; a further hydrogenation step may be required. Fixed-bed processes (low heating rate) give the highest quality coke. They predominate commercially and are often referred to as carbonization processes. Dilute-phase fluidized-bed and entrained-flow processes (high heating rate), suitable for high yield of gaseous and liquid

products, are at various stages of precommercial development.

Pyrolysis processes can be classified as early (Table 5.72) [668] or contemporary (ad-

vanced). The *early processes* generally involved low-cost systems and were intended to produce solids (coke or char) rather than liquids.

Table 5.72: Early pyrolysis processes [668].

Pyrolysis process	Final temp., °C	Products	Processes
Low temperature	500–700	more coke, high tar yield	Rexco (700 °C), cylindrical vertical retorts; coalite (650 °C), vertical tubes
Medium temperature	700–900	more coke, high gas yield, domestic briquettes	Town gas (obsolete) and coke, phumacite, using low-volatile steaming coal, pitch-bound briquettes carbonized at 800 °C
High temperature	900–1050	hard, unreactive coke for metallurgical use	foundry coke (900 °C); blast furnace coke (950–1050 °C)

Table 5.73: Low-temperature batch processes [670].

	Process						
	Krupp-Lurgi	Brennstoff-Technik	Otto	Weber	Phumacite	Parker retort	Rexco
Country (year)	Germany (1930s)	Germany (1940s)	Germany (1940s)	Germany (1940s)	United Kingdom (1940s)	United Kingdom (1920s)	United Kingdom (1920s)
Objective	char production	lumpy char from weakly coking coals	char and gas production	char production	smokeless domestic fuel	smokeless domestic fuel	smokeless domestic fuel
Plants (year)	Wanne-Eickel (1943)	Berlin-Neukölln (1944)	—	—	South Wales (1942)	Barnsley (1927), Bolsover (1936)	Nottingham, England (1936)
Yields							
Char	2.04 × 10 ⁸ kg/a	0.75 kg/kg dry coal	—	—	0.7 kg/kg coal	—	—
Tar	1.2 × 10 ⁶ kg fuel oil/a 1.9 × 10 ⁶ kg motor fuel/a	0.1 L/kg dry coal	—	—	0.06 kg/kg coal	0.08 L/kg coal	0.08 L/kg coal
Gas	105 L/kg coal	142 L/kg dry coal	—	—	—	125 L/kg coal	unknown
Gas HV ^a	—	(2.5–3) × 10 ⁴ kJ/m ³	—	—	—	26 000 kJ/m ³	5200 kJ/m ³
Reactor	vertical fixed-bed retort	vertical fixed-bed retort	vertical fixed-bed retort	vertical fixed-bed retort	vertical fixed-bed retort	vertical fixed-bed retort	vertical fixed-bed retort
Capacity	270 kg/d	10 ⁵ kg briquettes/d	3600 kg/d	unknown	11 340 kg/d	0.3 kg/kg charge	50 000 kg/d
Heating	indirect hot gas recycling	indirect hot gas recycling	indirect heating by gas burned in flues	unknown	indirect heating by recycling hot combustion gas	indirect radiant heat by combustion gas	direct heat by combustion gas
Temperature range	560–620 °C	650 °C	—	—	—	650 °C	650 °C
Residence time	2–3 h	2–4 h	—	—	4 h	4.5 h	13.5 h
Current status	—	semicommercial closed plant still may be operating in the former GDR ^b	—	—	—	—	—

^aHV = heating value.

^bGDR = German Democratic Republic.

Table 5.74: Low-temperature continuous processes [670].

	Process			
	Coalite & Chemical Products	Lurgi-Spallgas	Disco	Koppers continuous vertical ovens
Country (year)	United Kingdom (1950s)	Germany (1930s)	United States (1930s)	Germany (1940s)
Objective	char, liquid fuels	char, automotive fuels	lump char	char
Plants (year)	Bolsover, England (1952)	Offleben, Germany, Japan (1941), New Zealand (1931), Lehigh, North Dakota (1940)	Pittsburgh, PA	Kattowitz (1945)
Yields				
Char	0.74 kg/kg coal	0.45 kg/kg briquette	6.8×10^3 kg/d	1.5×10^4 kg/d-retort
Tar	0.06 L/kg coal	0.125 kg/kg briquette	—	2.1×10^3 kg/d retort
Gas	111 L/kg coal	144 L/kg briquette	—	0.32 L/kg coal
Gas HV ^a	26 000 kJ/m ³	8380 kJ/m ³	—	1.8×10^4 kJ/m ³
Reactor	Parker vertical retort	continuous vertical retort	continuous rotating horizontal retort	continuous vertical retort
Capacity	0.3 kg coal charge	2.7×10^3 kg briquettes/d	1.4×10^3 kg/d	25 000 kg/d
Heating	radiant heat supplied by combustion gas	direct contact with combustion gas	indirect heating by circulating hot combustion gas through flues built in hearths	indirect and direct heating by passing hot gases alternately upward and downward through flues and regenerators
Temperature range	combustion chamber held between 600 and 700 °C	600–700 °C	550 °C	700 °C
Residence time	coal carbonized for 4 h	20 h	1.5 h	21 h/retort
Current status	in operation	—	closed	—

^a HV = heating value.

Contemporary processes, on the other hand, have been designed to maximize production of liquid by using conditions (e.g., dilute phase, pressurized H₂, and rapid heating and quenching) that minimize secondary pyrolysis reactions. This requires more expensive equipment and severer operating conditions [656, 669].

Low-Temperature Pyrolysis Processes

Early Processes

Low-temperature pyrolysis (below 700 °C) was developed mainly to supply gas for public lighting and smokeless (devolatilized) solid fuel for home use. By-product tars were valuable as chemical feedstocks and could be converted to gasolines, heating oils, and lubricants. Commercial low-temperature coal pyrolysis was utilized extensively in Europe, but was almost abandoned after 1945 as oil and natural gas became widely available.

Rising oil prices have reactivated interest in this process.

The many low-temperature processes developed in Europe can be classified as batch or continuous, vertical or horizontal, and directly or indirectly heated (Tables 5.73 [670] and 5.74).

Retorts or by-product coke ovens were employed. Horizontal retorts (D retorts), 2.5–6 m long, were usually grouped together to form a bank heated by flue gas, with manual loading and unloading. Vertical retorts, both batch and continuous, were preferred in the United States and Europe because they permit gravity loading and unloading [671].

Rates of heat-transfer and carbonization were increased by using steel refractories as materials of construction. Internal heating was sometimes necessary to accelerate heat transfer by circulating hot gas. Only noncaking or weakly caking coals were used in continuous vertical retorts because caking coal softens

and flows, forming large masses of coke that stick to the retort walls.

Two noteworthy low-temperature pyrolysis processes are the Disco and Coalite processes. These were successful when most low-temperature processes failed [671, 672].

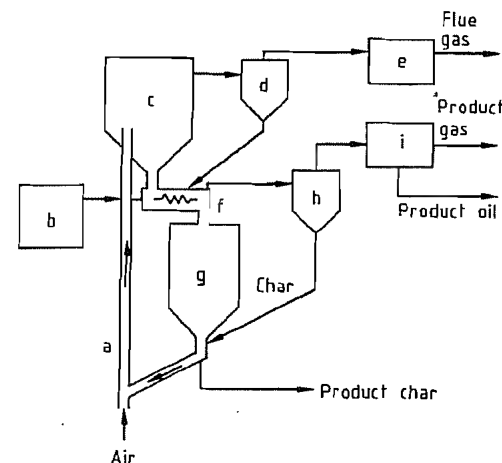


Figure 5.155: Lurgi-Ruhrgas process: a) Transport reactor and lift line; b) Coal preparation; c) Collecting bin; d) Cyclone; e) Heat recovery; f) Mixer-carbonizer; g) Surge hopper; h) Cyclone; i) Condenser.

Contemporary Processes

Lurgi-Ruhrgas Process. The Lurgi-Ruhr-gas process (Figure 5.155) for the low-temperature production of liquids from low-rank coals is currently in commercial use in Europe.

Crushed coal is rapidly heated in a mixer (f) to 450–600 °C by contact with recirculating char particles that have been heated by partial oxidation in an entrained-flow reactor. The gas from the mixer is freed of particulate matter in a cyclone (h) and is passed through a series of condensers (i) to collect the liquid products, the latter are hydrogenated to yield stable products.

The char constitutes ca. 50% of the products, whereas liquid yield is ca. 18%; the remaining 32% is gas with a heating value of $(26\text{--}31) \times 10^6$ J/m³.

Toscoal Process. The Toscoal process, an adaptation of the Toscoal II oil-shale retorting

process, was developed at a pilot plant near Golden, Colorado, with a capacity of 22.5×10^3 kg/d.

Crushed dry coal is preheated in lift pipes with flue gas from a ball heater and is fed to a rotating pyrolysis drum containing hot ceramic balls. Pyrolysis at ca. 500 °C produces char and hydrocarbon vapors. The char is separated by a trommel screen and withdrawn. The balls are reheated and returned to the drum. Pyrolysis products are cooled and condensed to recover light gases and coal liquids.

High-Temperature Processes (Coke-Making)

Coke Ovens

High-temperature carbonization is employed primarily to produce blast-furnace and foundry cokes for use in iron and steel manufacture. The process is carried out in coke ovens at ca. 900 °C.

In the 16th century, coke was found to burn hotter and cleaner than coal [673]. The earliest type of coke oven, the so-called *beehive oven*, was developed in the 1850s; its main characteristic is that the heat necessary for coking is produced by burning the volatile coal constituents within the oven [674, 675]. All the gaseous and liquid by-products are lost, together with large amounts of heat.

Beehive ovens have persisted well into the 20th century with progressive improvements in design and operation, such as heat recovery systems and vertical flues to supply process heat to the coking chamber.

A parallel development during the 19th century led to *slot ovens*. At first, these were simple rectangular firebrick structures holding a layer of coal ca. 1 m deep; later they were equipped with external heating flues [650]. In a further development, volatile by-products were collected and used as fuel.

By the 1940s, the basic design of *modern coke ovens* had been developed. The ovens were ca. 12 m long, 4 m high, and 0.5 m wide, equipped with doors on both sides. The air supply was preheated by the hot exit gas. The

recovery of the waste heat created higher temperatures and increased coking rates [676]. Since the 1940s, the process has been mechanized and the construction materials have been improved without significant design modifications. Current assemblies may contain up to 60 ovens as large as 14 m long and 6 m high. Because of heat transfer considerations, widths have remained 0.3–0.6 m. Each oven in the battery holds up to 30 t of coal and operates on a 15-h cycle [677].

The coking process illustrated in Figure 5.156. The coal is conveyed from storage bunkers (a) to blending (b) and crushing (c) units, and then to the coke oven bunker (d). The ovens are loaded from a mobile larry car (e) located on top of the battery. Coking takes place in completely sealed ovens (f). The by-product vapors and gases are collected and sent to recovery and processing units.

After carbonization, the oven doors are opened and the ram (g) pushes the red-hot coke into a quenching car. The coke is transported to the quenching unit (h) and then dumped on a sloping wharf (i) for cooling and drying. The dry coke is transferred to the screening and loading unit (j).

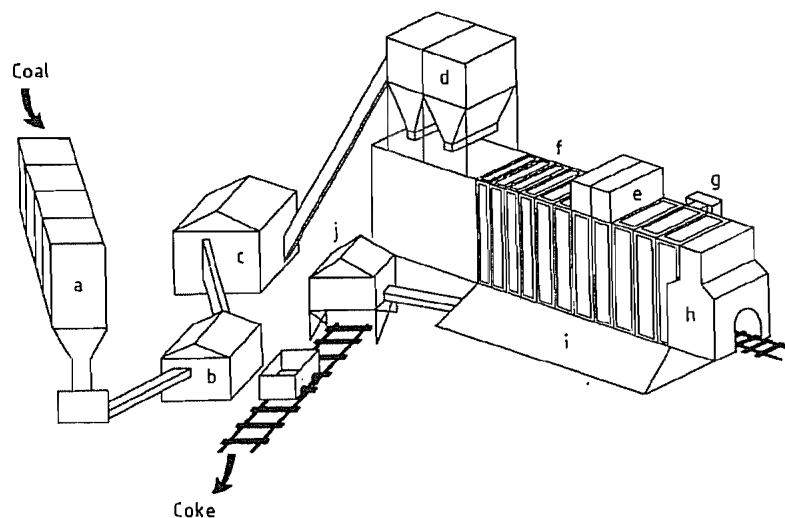


Figure 5.156: Coke-making process [650]: a) Storage bunkers; b) Blending plant; c) Crusher; d) Service bunker; e) Charging car; f) Coke oven; g) Ram machine; h) Cooling tower; i) Cooling wharf; j) Coke screen.

Coke Properties

The properties of coke depend on the coal and the processing conditions employed. The particle size, mineral matter, and moisture content, which can be controlled, affect the bulk density of the coal. Rank and maceral composition determine the fluidity of the plastic phase formed at intermediate temperatures. Significant process conditions include the wall temperature, coking time, and oven width; the heating rate and final temperature also affect coke structure.

The coal is prepared for coking by washing, drying, sizing, preheating, briquetting, and blending, with or without addition of pitch or breeze (fine coke particles) [674]. Foreign matter is removed mechanically and particle size is adjusted. Preheating (up to ca. 600 °C) increases production by ca. 50% and reduces coking time without loss of quality [674].

Briquetting, with or without binder, increases the strength of the coke produced and permits noncoking or poorly coking coals to be used to make metallurgical coke. Cold briquetting is performed below the softening point of the coal (ca. 400 °C) and hot briquetting above the softening point (450–520 °C) [676].

Coal blending improves coke properties and yield and permits the use of noncoking or weakly coking coals [678]. Blending may also prevent damage to ovens when high coking pressure develops.

By-Products

Carbonization by-products were important in the development of the organic chemicals industry, but their use has greatly diminished because of competition from petroleum-based products. The principal by-products are tar and coke-oven gas. Gas produced in the early slot ovens was used for domestic heating. Coal tar can be processed by petroleum-refining techniques. High-temperature tar can be fractionally distilled; three oil cuts are taken and a solid residue remains [596, 679]:

- *Light oil* ($bp < 200$ °C), composed primarily of benzene, toluene, xylenes, and styrene.
- *Middle oil* ($bp < 370$ °C), containing tar acids (phenols), tar bases (e.g., pyridine, anilines, and quinolines), and neutral oils (naphthalene).
- *Heavy oil* ($bp < 550$ °C), containing aromatic compounds, such as anthracene, phenanthrene, carbazole, and chrysene.

- *Coal tar pitch* (solid residue), consisting of a wide range of polycondensed aromatic compounds; it can be used as a binder for coal briquetting.

By-products that are obtained more cheaply from petroleum are no longer recovered exhaustively from coal tar.

Formed-Coke Processes

The preparation techniques and reactor configurations employed by some of the coking processes developed since the 1960s are different. Among these processes, the formed-coke ones have been the most successful (see Table 5.75). The term “formed coke” is used to describe cokes obtained by the carbonization of briquettes of weakly coking or noncoking coals. These processes provide the possibility of using weakly coking or noncoking coals, of controlling coke size to improve blast furnace operation, and of continuous operation in a contained system.

Blast furnace tests of these cokes have been successful. They are usually higher in moisture, volatile matter, sulfur, and reactivity to carbon dioxide, and lower in abrasion resistance than conventional metallurgical cokes [650].

Table 5.75: Formed-coke processes [650, 676, 680].

Process (country)	Raw materials	Process steps
FMC (USA)	noncoking or coking coals and tar	1) Oxidation and carbonization of coal in fluidized beds 2) cold briquetting of char with tar 3) preheating and carbonization of briquettes
DKS (Japan)	noncoking, coking coals and pitch	1) cold briquetting of coal with pitch 2) carbonization of briquettes
HPNC (France)	weakly coking, coking coals and pitch	1) cold briquetting of coal with pitch 2) carbonization of briquettes
BFL (Germany)	high-volatile noncoking coals and coking coals or pitch	1) carbonization of noncoking coal 2) hot briquetting of char with coking coal or pitch 3) carbonization of briquettes
ANCIT (Germany)	low-volatile noncoking coals and coking coals	1) flash heating of low-volatile noncoking coal 2) hot briquetting of char with coking coal 3) reheating of briquettes
Sapozhnikov (Russia)	high-volatile weakly coking coals and low-volatile weakly coking coals	1) flash heating of coal 2) hot briquetting 3) carbonization of briquettes
CCC-BNR (USA)	high-volatile noncoking coals and coking coals on pitch as binder	1) preheating of high-volatile coal 2) hot briquetting of char with binder 3) carbonization of briquettes

Environmental Aspects

Coking plants create environmental problems like other large installations producing dusty materials and gaseous and liquid effluents [649]. Gas and volatile emissions may arise from leaks. Coal and coke particulates may be discharged during loading and unloading, and water used for quenching may be contaminated.

Particulate, volatile, and gas emissions can be reduced by using sheds or traveling hoods with dust and fume collectors [650]. Polluted water must be treated in wastewater plants. In some plants, dry quenching is used instead of water quenching, and the coke is cooled by gas or steam in a closed system. A further advantage of this process is that energy can be recovered via sensible heat and combustible gases.

In addition to air pollution, machinery and working conditions are hazardous. Plant location and accident prevention require serious consideration.

Contemporary Hydropyrolysis and Pyrolysis Processes

The three processes shown in Table 5.76 illustrate the principles described in section 5.22.13.2. Their main objective is production of liquid hydrocarbons, for which entrained-flow conditions are the most favorable. However, char or coke is still the principal product in all three processes; its efficient use is one of the main issues in their economic analysis. The use of hydrogen in the Rockwell process reduces char production to some extent but as discussed in Chapter 5.22.13.4, this is achieved primarily by increasing the yield of gas, not liquids.

Table 5.76: Characteristics of selected pyrolysis processes [656].

Process	Reactors	Temperature, °C	Pressure, MPa	Yield, % (dry)			
				Coke	Tar and oil	Gas	H ₂ O
COED	fluidized-bed	290–565	0.12–0.19	62	21	14	3
Occidental	entrained-flow	610	0.3	56	35	7	2
Rockwell	entrained-flow	845	3.5	46	38	16	—

The *Coal Oil Energy Development (COED) process* (Figure 5.157), is a part of the CO-GAS process for complete conversion of coal to gases and liquids. The residual char from pyrolysis reacts with H₂O and O₂ in a fluidized-bed gasifier (g) to produce the hot synthesis gas, a mixture of CO and H₂. The synthesis gas serves as fluidizing and heat-transfer medium in the pyrolysis reactors (p₁–p₄).

The conditions in the gasifier do not permit complete conversion to gases. Part of the char that leaves is recycled to the pyrolysis section, where it provides additional heat for the endothermic devolatilization. The entrained fine particles and the remaining char are burned in a combustor (c). The hot flue gas is also recycled to the pyrolysis section to provide more heat.

This brief description illustrates the principal technical issues involved in the evaluation of pyrolysis processes: the type of contact between solids and fluids; the method of supplying heat; and the amount and fate of the residual char. In this context, several features of the COED process increase the production of liquids. The countercurrent flow of solids and gases (or vapors) and the increasing operating temperatures in the various pyrolysis stages help to reduce cracking by avoiding subsequent exposure to higher temperatures. The relatively dilute medium in the fluidized beds also helps to reduce the probability of secondary interparticle reactions.

The low final temperature favors production of liquids. However, the heating rates are relatively low and intraparticle secondary reactions may still occur. The use of internally generated and recirculated hot gas and char to provide energy for devolatilization has the advantage of efficiency but it introduces a degree of complexity.

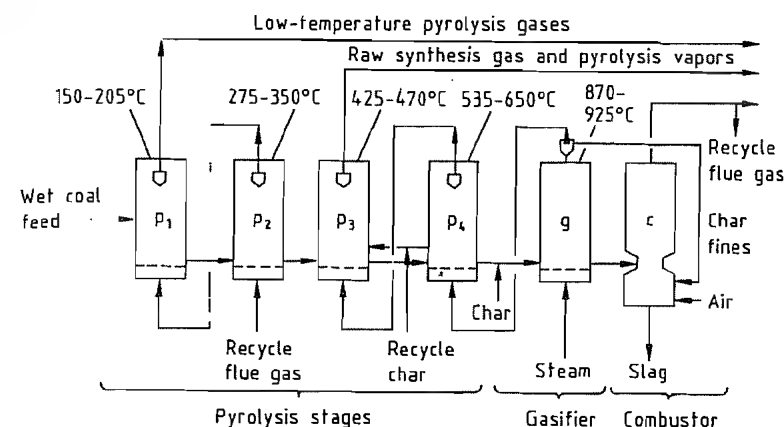


Figure 5.157: COED pyrolysis process [656]. p₁–p₄ = Pyrolysis reactors; g = Fluidized-bed gasifier; c = Combustor.

The complete internal utilization of the coal is a virtue of the COED/COGAS process. The relatively low final pyrolysis temperature forms a char that is highly reactive and, thus, suitable for gasification with steam. The resulting synthesis gas is a highly valuable and versatile product that can be converted, for example, to a natural gas substitute by methanation.

Entrained-flow reactors are favored by a new generation of coal-conversion processes for several reasons. Both fixed-bed and fluidized-bed reactors need auxiliary equipment to avoid difficulties in processing of agglomerating bituminous coal. The fusion of coal particles during pyrolysis can block these reactors. In the COED process (Figure 5.157), for example, where bituminous coal is the preferred feedstock because of its potentially high liquid yield, one of the stages (p₂) introduces oxygen cross-links into the coal structure and subsequently reduces or eliminates thermoplasticity, thus preventing agglomeration.

High throughputs are possible in entrained-flow reactors. The very dilute medium reduces the probability of particle agglomeration. Furthermore, rapid heating and a short residence time sharply reduce the importance of the plastic phase of pyrolysis of bituminous coals.

Finally, these conditions maximize the yield of volatiles and favor production of chars that may be sufficiently reactive to give

valuable products, as in the COGAS process. Less reactive chars serve as fuel.

In the *Occidental process* (Figure 5.158) [681], the reactor operates at ca. 625 °C, thus maximizing production of liquids. Heat is supplied by mixing the coal with recirculated char that is made incandescent by partial combustion. The conditions for entrained flow require particles smaller than 200 μm (typically 80% passing through a 60 mesh screen) and, thus, pulverization is necessary in contrast to fixed-bed and fluidized-bed processes. The residual char is usually desulfurized for sale as "smokeless" fuel.

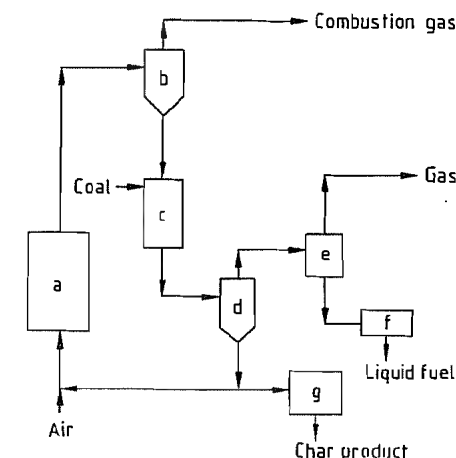


Figure 5.158: Occidental pyrolysis process [681]: a) Char burner; b) Cyclone; c) Reactor; d) Cyclone; e) Oil collection system; f) Liquid upgrading; g) Char desulfurization plant.

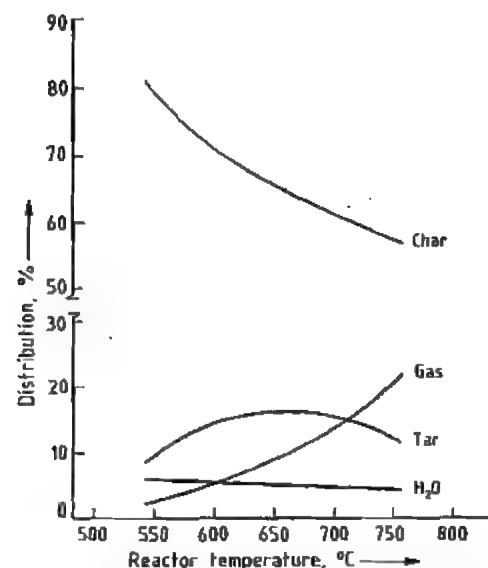


Figure 5.159: Effect of temperature on the distribution of products from a subbituminous coal in the Occidental process (pressure: 21 kPa of N_2 ; particle size: 80% passing a 250 μm screen, 60 mesh; residence time: 1.5 s) [681].

The effect of temperature and residence time on product distribution is shown in Figures 5.159 and 5.160.

The Rockwell hydropyrolysis process (Figure 5.161) incorporates the entrained-flow re-

actor as a minor component; other operations are similar to those encountered in petroleum refining. The hydrogen feed is preheated by partial combustion. After hydropyrolysis lasting 0.02–0.2 s, the products are rapidly quenched to prevent secondary char formation. A maximum liquid yield is obtained at an intermediate reactor temperature [682].

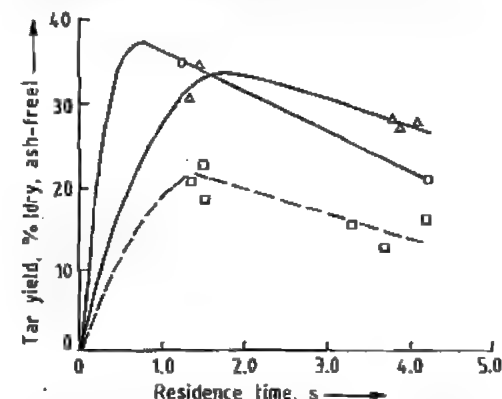


Figure 5.160: Effect of residence time on tar yield in the Occidental process (pressure: 21 kPa of N_2 ; particle size: 80% passing a 250 μm screen, 60 mesh). \square Subbituminous coal (649 °C); Δ Bituminous coal (607 °C); \circ Bituminous coal (660 °C) [681].

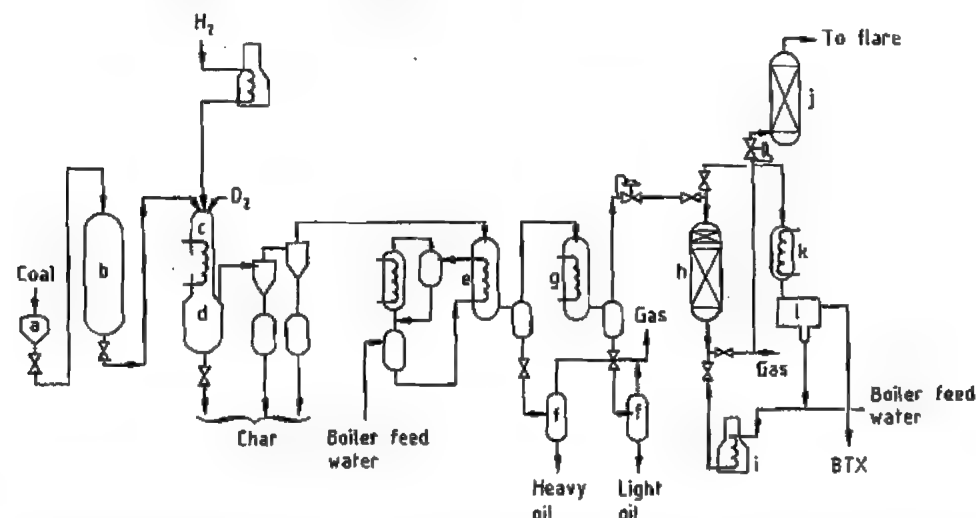


Figure 5.161: Rockwell hydropyrolysis process [682]: a) Loading feeder; b) Coal feeder; c) Reactor; d) Char-vapor separator; e) Heavy oil condenser; f) Flash drum; g) Light oil condenser; h) BTX adsorber; i) Boiler; j) Scrubber; k) BTX-steam condenser; l) Decanter.

Changing hydrogen pressure affects product distribution, but not the yield of liquids; very high pressure is apparently needed to stabilize the reactive fragments in the absence of a solvent [682].

5.23 References

1. F. Habashi, "Native Metals" in R. G. Reddy, R. N. Weizenbach (eds.), *International Symposium Extractive Metallurgy of Copper, Nickel, and Cobalt*, volume 1, The Minerals, Metals & Materials Society, Warrendale, PA, 1993, pp. 1147–1153.
2. United Nations Conference on Trade and Development Review of Iron Ore Statistics, GF.94-53266, 1994.
3. H. J. Werz et al.: *Environmental Protection in Iron Ore Sintering by Waste Gas Recirculation*, Stahleisen 1995, pp. 120–126.
4. United Nations, Survey of World Iron Ore Resources, New York 1970.
5. *Skilling's Mining Review* 75 (1986) no. 39, 4.
6. *Iron Ore 1986*, American Iron Ore Association, Cleveland, OH 1987.
7. *Skilling's Mining Review* 77 (1988) no. 17, pp. 4–5, 17.
8. K. J. Pieper, *Handel und Verbrauchsentwicklung von Eisenerzpellets in der westlichen Welt*, lecture at VDEh Düsseldorf, 10.6.1987.
9. R. C. Anderson et al. *Skilling's Mining Review* 76 (1987) no. 33, pp. 6–9.
10. Exploration and Berghau GmbH, personal communication 1988.
11. F. Habashi, *Principles of Extractive Metallurgy*, volume 3 — Pyrometallurgy, Gordon & Breach, New York 1986.
12. H. E. McCannan (ed.), *The Making, Shaping, and Treating of Steel*, United Steel, Pittsburgh, PA, 1964.
13. J. H. Strassburger et al. (editors), *Blast Furnace. Theory and Practice*, 2 volumes, Gordon & Breach, New York 1969.
14. Gmelin-Durrer, *Metallurgy of Iron/Metallurgie des Eisens*, volumes 1–4, Springer Verlag, Berlin 1964–1972.
15. Gmelin-Durrer: *Metallurgie des Eisens*, 4th ed. vols. 2a, b, Verlag Chemie, Weinheim 1964.
16. M. Higuchi, M. Izuka, T. Shibuya: *Developments in Ironmaking Practice*, The Iron and Steel Institute, London 1973 p. 98.
17. G. Heynert, E. Legille, in [16] p. 109.
18. Iron and Steel Inst. Japan: *Handbook of Iron and Steel*, vol. 2, Maruzen Publishing Co., Tokyo 1979, p. 295.
19. in Ref. [18] p. 306.
20. *Ullmann*, 4th ed., 10, 370.
21. M. Manes, J. S. Maikay, *J. Metal.* 14 (1962) 308–314.
22. in Ref. [18] p. 110.
23. in Ref. [18] p. 120.
24. G. Heynert, P. Ischebeck, W. V. Spee, *Eisen* 81 (1961) 1–12.
25. M. Nakamura, T. Sugiyama, T. Uno, Y. Hara, S. Kondo, *Tetsu to Hagane* 63 (1977) 28–36.
26. M. Hatano, B. Hiraoka, M. Fukuda, T. Masuike, *Trans. Iron Steel Inst. Jpn.* 17 (1977) 102–109.
27. M. Hatano, K. Kurita, T. Yanaka: *Int'l Blast Furnace Hearth and Raceway Symposium*, Newcastle AIMM 1981, p. 4.1–4.10.
28. K. Kanbara et al., *Trans. Iron Steel Inst. Jpn.* 17 (1977) 371–380.
29. K. Takeda et al., *Proc. Ironmaking Conf.* 46 (1987) 191–198.
30. H. Lackmann: *4. Dozentenseminar des Vereins Deutscher Eisenhüttenleute, Gelsenkirchen* 1973.
31. in Ref. [18] pp. 159, 160.
32. M. Izuka: *116th and 117th Nishiyama Memorial Seminar organized by Iron Steel Institute Japan*, 1987, pp. 1–38.
33. J. Cappel, M. Geerdes, K. Hangner, H. B. Lungen, *Stahl Eisen* 108 (1988) 459–468.
34. Y. Ohno et al., *7th Process tech. Conf. Proceedings*, Toronto 1988, pp. 195–201.
35. in [15] 1972, vols. 4a, b.
36. in [15] vols. 4a, b.
37. H. Schenk, *Stahl Eisen* 83 (1963) 1683–1690.
38. H. Wysocki, *Vorlesung Entwerfen von Hüttenwerksanlagen*, Techn. Univ. Berlin 1975.
39. in Ref. [18] pp. 278–300.
40. Japan Institute of Iron and Steel Slags: *Annual Report of Iron and Steel Slags Statistics* 1988.
41. M. Saino: *116th and 117th Nishiyama Memorial Seminar organized by Iron Steel Institute, Japan* 1987, pp. 237–278.
42. Y. Hara, M. Sakawa, S. Kondo, *Tetsu to Hagane* 62 (1976) 315–323.
43. Iron and Steel Inst. Japan: *Blast Furnace Phenomena and Modeling*, Elsevier, London 1987, pp. 121–127, pp. 132–133.
44. N. Tsuchiya, M. Tokuda, M. Ohtani, *Tetsu to Hagane* 58 (1972) 1927–1939.
45. W. E. Ranz, *Chem. Eng. Prog.* 48 (1952) 247–253.
46. J. Kudoh, J. Yagi, *Tetsu to Hagane* 73 (1987) 2020–2027.
47. J. Yagi, I. Muchi, *Trans. Iron Steel Inst. Jpn.* 10 (1970) 392–405.
48. M. Hatano, K. Kurita, *Tetsu to Hagane* 66 (1980) 1898–1907.
49. M. Kuwabara et al., *Proc. Joint Symp. of Iron Steel Inst. Jpn. and Australasian Institute Mining and Metallurgy*, Tokyo 1983, pp. 193–204.
50. S. Taguchi et al., *Tetsu to Hagane* 68 (1982) 2302–2310.
51. M. Hatano, K. Kurita, H. Yamaoka, T. Yokoi, *Trans. Iron Steel Inst. Jpn.* 25 (1985) 911–940.
52. Y. Okuno et al., *Tetsu to Hagane* 73 (1987) 91–98.
53. T. Sugiyama, J. Yagi, Y. Omori: *Proc. 3rd Int'l Iron Steel Congr.*, 1978 Chicago, pp. 479–488.
54. J. Ohno et al., *International Blast Furnace Hearth & Raceway Symposium*, Newcastle, Australia 1981, pp. 10–12.
55. A. Poos: *Heat and Mass Transfer in Process Metallurgy*, A. W. D. Hills, 1967, pp. 1–38.
56. M. Hatano, K. Kurita, H. Yamaoka, T. Yokoi, in [50] pp. 941–948.
57. T. Sugiyama et al., *Curr. Adv. Mater. Proc.* (in Japanese), 1 (1988) 22–25.

58. A. Kato, *Tetsu to Hagane* 73 (1987) 461–468.
59. J. Yagi, T. Akiyama, *Curr. Adv. Mater. Proc.* (in Japanese) 2 (1989) 2.
60. A. Nakagawa, *Tekkoku* (1986) no. 6, 5–9, issued by The Japan Iron and Steel Federation.
61. T. Akiyama, J. Yagi, *Process Tech.* 74 (1988) *Conf. Proc.* ISS-AIME, vol. 7, Toronto, 1988, pp. 179–193.
62. M. Wahlster, H. P. Schulz, J. Thein, *Stahl Eisen* 89 (1969) 478–486.
63. in Ref. [18] p. 450.
64. W. Domalski, K. Fabian, D. Nolle, *Stahl Eisen* 88 (1968) 906–919.
65. in Ref. [18] p. 443.
66. H. P. Schulz, *Stahl Eisen* 89 (1969) 249–262.
67. S. Eketorp, B. Kalling, *Gießerei* 46 (1959) 905–912.
68. T. Okuro, *Tetsu to Hagane* 52 (1966) no. 2, 120–139.
69. in Ref. [18] p. 446.
70. H. Kajioaka in W. K. Lu (ed.): *Symposium on External Desulphurizations of Hot Metal*, p. 15-1–15-35 McMaster Univ., Hamilton, Canada, 1975.
71. W. Meichsner, K. H. Peters, W. Ullrich, H. Knahl, *J. Met.* 26 (1974) no. 4, 55–58.
72. in Ref. [18] p. 441.
73. in Ref. [18] p. 448.
74. F. Habashi, *A Textbook of Hydrometallurgy*, Métallurgie extractive Québec, Sainte-Foy 1993.
75. Iron and Steel Inst. Japan: *Handbook of Iron and Steel*, vol. 2, Maruzen Publishing Co., Tokyo 1979, p. 446.
76. H. Kajioaka in W. K. Lu (ed.): *Symposium on External Desulphurizations of Hot Metal*, p. 15-1–15-35 McMaster Univ., Hamilton, Canada, 1975.
77. W. Meichsner, K. H. Peters, W. Ullrich, H. Knahl, *J. Met.* 26 (1974) no. 4, 55–58.
78. in [75] p. 441.
79. in [75] p. 448.
80. H. Nashiwa, S. Yamaguchi, M. Takano, M. Iwami, *Sumitomo Kinkoku* 27 (1975) 207–211.
81. W. H. Duquette: *Open Hearth Conf. Proc.*, TMS-AIME, 56 (1973) 79.
82. P. F. Potocic, K. G. Leewis, *Gießerei* 46 (1959), pp. 3-1–3-19.
83. W. A. Voronova, *Steel USSR* 4 (1974) 261.
84. L. G. Nelson, *Proc. Ironmaking Conf.* 34 (1975) 451–459.
85. P. Koros, R. G. Petrushka, in [80], pp. 7-1–7-25.
86. Fédération européenne de produits réfractaires PRE *Refractory Materials*, PRE Administrative Secretariat, Rue de Colonies 18–24, Boîte 17, B 1000, Brussels.
87. *Stahleisen-Werkstoffblätter* 912 bis 917, Verlag Stahleisen, Düsseldorf 1984.
88. *Refractory Engineering — Materials, design, construction*, Vulkan-Verlag, Essen 1996.
89. M. Koltermann, "Refractories from the European View Point. Development and Trend of Refractories in the Steel Industry", *Taikabutsu Overseas* 4 (1984) no. 3, pp. 3–13.
90. Y. Naruse: *Future Trend and Development of Refractories Industry in Japan*, Proceedings of 2nd International Conference on Refractories, The Technical Association of Refractories Japan, Tokyo 1987, pp. 3–60.
91. Institut für Gesteinshüttenkunde der RWTH Aachen, *Feuerfeste Werkstoffe für die Herstellung und den Transport von Roh Eisen*, 31. Internationales Feuerfestkolloquium, Aachen, 10.–11. Oktober 1988.
92. M. Koltermann, "Feuerfeste Stoffe für Hochtemperaturwinderhitzer", *Stahl Eisen* 95 (1975) 847–850.
93. M. Koltermann, "Torpedo ladle Refractories in West Germany", *Taikabutsu Overseas* 5 (1985) no. 2, 35–40.
94. M. Koltermann, "Feuerfeste Baustoffe 1980 bis 1990 — Rückblick und Prognosen", *Stahl und Eisen* 111 (1991) no. 8, 41–48.
95. M. Koltermann, "Steelplant Refractories — Tendency in Production, Consumption, Ladle Lining", *Proceedings of the 2nd International Symposium on Refractories*, Beijing, China, November 1992, 135–148.
96. N. Nameishi, B. Nagai, T. Matsumoto, "Overview of refractory technology in the nineties in Japan", *Proceedings of the 2nd International Symposium on Refractories*, Beijing, China, November 1992, 79–105.
97. S. Kataoka, "Refractories for steelmaking in Japan", *UNITECR Proceedings*, vol. 1, Kyoto 1995, 1–27.
98. H. Nakamura, "Carbon-containing bricks for blast furnaces", *Taikabutsu Overseas* 15 (1995) 13–18.
99. H. Nishio, A. Matsuo, "Al₂O₃-SiC-C bricks for torpedo car", *Taikabutsu Overseas* 15 (1995) 39–46.
100. "Statistics", *Taikabutsu Overseas* 16 (1996) no. 3, 58.
101. Ullmann 4th ed., 10, 395.
102. Midrex Corporation, *Direct from Midrex*, vol. 21, no. 3, 2nd quarter, 1996, Charlotte, NC.
103. L. v. Bogdandy, H. J. Engell: *Die Reduktion der Eisenerze*, Springer Verlag, Berlin/Verlag Stahleisen mbH, Düsseldorf 1967.
104. Energie- und Betriebswirtschaftsstelle des Vereins Deutscher Eisenhüttenleute (eds.): *Inhaltszahlen für die Wärmewirtschaft in Eisenhüttenwerken*, 6th ed., Verlag Stahleisen mbH, Düsseldorf 1968.
105. *Energy and the Steel Industry*, International Iron and Steel Institute, Committee on Technology, Brussels 1982.
106. Fédération européenne de produits réfractaires PRE *Refractory Materials*; Recommendations 1985, PRE-Sekretariat, CH-8023 Zürich, Löwenstr. 31.
107. Midrex Corporation, *Direct from Midrex*, vol. 13, no. 4, 3rd quarter 1988, Charlotte, NC.
108. R. Ferrari, F. Colanti, *Iron Steel Eng.* 53 (1975) 57–60.
109. R. Garraway, *Iron & Steelmaker*, June 1996, pp. 27–30.
110. M. Hirsch, R. Husain, P. Weber, H. Eichberger, paper presented at the International Conference "Pre-reduced Products in Europe", Milan, Italy, Sept. 23–24, 1996.
111. R. L. Stephenson, R. M. Smailer: "Direct Reduced Iron, Iron and Steel" *AIME Annu. Meet. Proc. Sess.* (Warrendale, PA) 1980.
112. L. Formanek, H. Eichberger: *Direktreduktion im Drehrohrofen*, European economic community research project for coal and steel; Document no. 7210-BA/101, 1985.
113. F. Oeters, A. Saatci, *Proc. Tech. Proc. ISS* 6 (1986) 1021.
114. F. Oeters, A. Saatci: *Stahl Eisen Report*, "Mass and Heat Balances", Verlag Stahleisen GmbH, Düsseldorf 1987.
115. R. J. Fruehan, K. Ito, B. Ozturk: "Analysis of bath smelting processes for producing iron", *Steel Res.* 60 (1989) no. 3/4, 129–137.
116. J. O. Edström: "Alternative Ironmaking Processes", *European Ironmaking Congress*, Aachen 1986.
117. R. B. Smith, M. J. Corbett: "Coal based iron making process", *7th Process Techn. Conf. Proc.*, AIME, Toronto 1988, 147–178.
118. F. Oeters, R. Steffen: "Entwicklungslinien der Schmelzreduktion und des Einschmelzens", *4. Kohle-Stahl-Kolloquium*, TU Berlin 1989.
119. S. Eketorp: "Smelting reduction", *Process Ironmaking Conference, Metallurg. Soc. AIME* 27 (1968) 36–39.
120. G. Papst, R. Hauk, W. Kepplinger, F. Ottenschläger: "The Corex process", *Metal. Plant. Technol.* 9 (1986) no. 6, 24, 26, 28, 29.
121. R. Hauk, J. Flickenschild, F. Ottenschläger: "KR-Process hot metal production on the basis of coals", *6th Process Techn. Conf. Proc.*, AIME, Washington 1986, pp. 1031–1039.
122. H. Feichtner, W. Maschlanka, F. Helten: "The COREX-process", *Skilling's Min. Rev.* 78 (1989) no. 2, 20–27.
123. H. van der Merwe, W. Kepplinger, R. Hauk, B. Vuletic: "Operation results in the first commercial COREX-plant at ISCOR Pretoria Works", *International Congr. New developments in metallurgical processing Proc.*, vol. 1, VDEh, Düsseldorf 1989.
124. M. Hatano, T. Miyazaki, H. Yamaoka, Y. Kamei: "New Ironmaking process by use of pulverized coal and oxygen", *6th Process Techn. Conf. Proc.*, AIME, Washington 1986 pp. 1049–1055.
125. T. Miyazaki, H. Yamaoka, Y. Kamei, F. Nakamura: "A new ironmaking process consisted of shaft type reduction, furnace and cupola type melting furnace", *Trans. Iron Steel Inst. Jpn.* 27 (1987) 618–625.
126. T. Hamada et al.: "Development of Kawasaki smelting reduction process for the reduction of iron and ferroalloys", *Proceedings of the pyrometallurgy 1987 London* 1987, pp. 435–459.
127. H. Itaya et al.: "Development of the XR-process", *7th Process Techn. Conf. Proc.*, AIME, Toronto 1988, pp. 209–216.
128. L. von Bogdandy, K. Brotzmann, K. Schäfer, H.-G. Geck: *Stahl Eisen* 104 (1984) no. 22, 1143–1148.
129. K. Brotzmann: "New concept and methods for iron and steel production", *70th Steelmaking Conference Proceedings, ISS-AIME*; Pittsburgh 1987, pp. 3–12.
130. J. A. Innes, J. P. Moodie, I. D. Webb, K. Brotzmann: "Direct smelting of iron ore in a liquid iron bath — the HI-smell process", *Process Techn. Conf. Proc.*, AIME, Toronto 1988, pp. 225–231.
131. J. Barin, M. Lemperle, M. Modigell: "Smelting reduction of iron ore", *Steel Res.* 60 (1989) no. 3/4, 120–121.
132. K. Iwasa et al.: *Curr. Adv. Mat. Proc.* 1 (1988) no. 4, 1085.
133. K. Iwasaki, H. Kawata, K. Yamada, T. Kitagawa: "Integrated test plant work on smelting reduction iron-making process", *International Congr. New Developments in Metallurgical Processing Proc.*, vol. 1, VDEh, Düsseldorf 1989.
134. N. Tokumitsu et al.: "Development of smelting reduction process using an iron bath", *7th Process Techn. Conf. Proc.*, AIME, Toronto 1988, pp. 99–107.
135. J. Harwig, D. Neuschütz, D. Radke, F. Seelig: "Entwicklung eines Einschmelzverfahrens mit kombinierter Direktreduktion unter Einsatz beliebiger Feinkohlen", *Stahl Eisen* 100 (1980), 535–543.
136. J. Harwig, D. Neuschütz, D. Radke, W. D. Röpke: "The Krupp COIN Process Combined with Direct Reduction", *UNECE Seminar*, Noordwijkerhout, Netherlands, May 1983.
137. D. Neuschütz, T. Hoster: "Concept and present state of a coal-based smelting reduction process for iron ore fines", *Steel Res.* 60 (1989) no. 3/4, 113–119.
138. P. Collin, H. Stickler: "Ironmaking alternative paves the way to cheaper steel", *Iron Steel Int.* 53 (1980) 81–86.
139. H. Stickler: "Varianten des Elred-Verfahrens", *Stahl Eisen* 104 (1984) 539–541.
140. H. I. Elvander, R. A. Westman: *Iron Steel Eng.* 59 (1982) no. 4, 57–60.
141. H. Elvander, G. Omberg: "Das Inred-Iron-Verfahren für die Roheisenerzeugung", *Stahl Eisen* 104 (1984) 864–866.
142. H. G. Herlitz, B. Johansson, S. O. Santen: "A new family of reduction processes based on plasma technology", *Iron Steel Eng.* 61 (1984) 39–44.
143. J. Feinmann (ed.): *Plasma Technology in metallurgical processing*, Iron and Steel Society, Warrendale 1987, p. 111.
144. *Erste Allgemeine Verwaltungsvorschrift zum Bundes-Immissionsschutzgesetz* (Technische Anleitung zur Reinhaltung der Luft) 27. Febr. 1985.
145. D. Eickelpasch et al., *Stahl Eisen* 100 (1980) no. 6, 260–270.
146. J. A. Philipp et al., *Stahl Eisen* 107 (1987) no. 11, 507–514.
147. H. J. White: *Industrial Electrostatic Precipitation*, Addison-Wesley Publishing Company, Inc., Reading, MA 1963.
148. G. Mayer-Schwinnig, R. Rennhack, *Chem.-Ing.-Techn.* 52 (1980) no. 5, 375–383.
149. S. Oglesby, Jr., G. B. Nichols: *Electrostatic Precipitation* (Pollution engineering and technology; 8), Marcel Dekker, New York 1978.
150. R. Bothe, *Stahl Eisen* 88 (1968) no. 25, 1414–1422.
151. H. Kahnwald, *Stahl Eisen* 104 (1984) no. 7, 351–356.
152. P. O. Spawn, T. J. Maslany, *JAPC* 31 (1981) 1060.
153. B. Bussmann et al., *Stahl Eisen* 105 (1985) no. 3, 121–130.
154. R. Görgen, W. Theobald, *Stahl Eisen* 97 (1977) no. 14, 657–664.
155. W. Theobald, G. Schnegelsberg, *Berghüttenmann Monatsh.* 116 (1971) no. 9, 328–340.
156. G. Metcalf, G. Eddy: *Wastewater Engineering*, McGraw-Hill Book Company, Boston 1979.
157. L. L. Beranek: *Noise Reduction*, McGraw-Hill Book Company, London 1960.

158. K. Althoff, *Stahl Eisen* 107 (1987) no. 22, 1071–1075.
159. H. U. Haering et al., *Stahl Eisen* 102 (1982) no. 15/16, 749–754.
160. J. A. Philipp, H. Maas, *Stahl Eisen* 104 (1984) no. 8, 403–407.
161. E. Mertins, *Erzmetall* 39 (1986) no. 7/8, 399–404.
162. H. Serbent, *Techn. Mitt.* 71 (1978) no. 11/12, 569–575.
163. G. Meyer et al., *Stahl Eisen* 96 (1976) no. 24, 1228–1233.
164. H. Maczek, R. Kola, *J. Met.* 32 (1980) no. 1, 53–58.
165. G. Kossek et al., *Erzmetall* 32 (1979) no. 3, 135–139.
166. W. Kaas et al., *Stahl Eisen* 98 (1978) no. 24, 1277–1281.
167. *Statistisches Jahrbuch Stahl*, WV 1988, p. 292, 297.
168. K.-H. Peters, H.-B. Lungen, *Stahl Eisen* 110 (1989) to be published.
169. Ref. [167] p. 318.
170. R. Steffen, H.-B. Lungen, *Stahl Eisen* 108 (1988) no. 7, p. 67–71.
171. E. Steinmetz, R. Steffen, R. Thielmann, *Stahl Eisen* 106 (1986) no. 9, 37–45.
172. H. E. Cleaves and J. G. Thompson, *The Metal Iron*, McGraw-Hill, New York 1935.
173. H. Remy, *Lehrbuch der anorganischen Chemie*, volume 2, Akademische Verlagsgesellschaft, Leipzig 1961, pp. 299–344.
174. K. Mudrak, G. Stobbe, "Anwendung der Simultanfällung zur Phosphatelimination", *Wasser Luft Betr.* 18 (1974) no. 5, 289–293.
175. K. I. Dahlquist, L. Hall, L. Bergmann: "Eliminierung von Phosphaten mit zweiwertigem Eisensulfat in der Kläranlage Käppala (S)", *Wasser Luft Betr.* 20 (1976) no. 5, 107–112.
176. A. Heitmann, P. Reher, *Chem. Ing. Tech.* 46 (1974) 592–593.
177. Standard Messo, DE-OS 30 30 964 A1, 1980 (H. D. Kutta).
178. Enteco Impianti SpA, DE-OS 29 37 131, 1979 (L. Piccolo, A. Paolinelli, A. Rovele).
179. K. H. Linder et al.: *Materialien*, "Rückstände aus der Titan Dioxid Produktion", vol. 2/76, Umweltbundesamt, Berlin 1982, pp. 96 ff.
180. Aktieselskabet Aalborg Portland Cement Fabrik, EP 01 60 747, 1981 (P. L. Rasmussen).
181. J. Latorezai, I. Nagy, I. Kalo, J. Mihaleczku, HU 24 384, 1979.
182. M. Munemori, T. Aoki, Y. Inove, in K. B. Pojasek (ed.): *Toxic and Hazardous Waste Disposal*, "Simultaneous removal of hazardous metals from waste water and disposal of the resultant sludge", Ann Arbor Science Publishers, Ann Arbor 1980, pp. 97–105.
183. *Dangerous Prop. Ind. Mater. Rep.* 7 (1987) no. 1, 55–60.
184. W. S. Spector: *Handbook of Toxicology*, vol. 1, W. B. Saunders Co., Philadelphia–London 1956.
185. Kronos Titan GmbH, DE 27 10 969, 1977 (A. Hartmann, A. Kulling, D. Schinkitz, E. Klein).
186. Kronos Titan GmbH, DE 30 30 558, 1980 (A. Hartmann, D. Schinkitz).
187. JANAF, *Thermochemical Tables*, NSRDS-NBS 37, 2nd ed., National Bureau of Standards, Washington, DC, 1971.
188. R. C. Weast et al.: *Handbook of Chemistry and Physics*, 68th ed., CRC Press, Boca Raton, FL, 1987–1988.
189. H. Schäfer, *Z. Anorg. Allg. Chem.* 266 (1951) 269–274.
190. Gmelin, System no. 59 "Eisen", part B, pp. 239–241.
191. R. K. Freier: *Daten für Anorg. und Org. Verb.*, vols. 1 + 2, "Wässrige Lösungen", Walter de Gruyter, Berlin–New York 1978.
192. W. Feitknecht, R. Giovanoli, W. Michaelis, M. Müller, *Helv. Chim. Acta* 56 Fasc. 8 (1973) no. 293, 2847–2856.
193. D. E. Chalkey, R. J. P. Williams, *J. Chem. Soc.* 1955, 1920–1926.
194. BASF, DE 1 592 222, 1967 (K. Opp et al.).
195. BASF, DE 830 787, 1948 (H. Schlecht).
196. Houben-Weyl, "Halogenverbindungen", V/3.
197. *Synthetica Merck*, vol. I, Merck AG, Darmstadt 1969, pp. 182–189.
198. R. Klute, *Entsorgungspraxis* 11 (1987) 536–548.
199. *Chemical Economics Handbook*, SRI International, Nov. 1995.
200. *Jpn Chem. Week*, Sept. 9, 1987, p. 2.
201. G. von Hagel, *Korresp. Abwasser* 33 (1969) no. 10, 908–915.
202. DOW, US 1 938 461, 1932 (C. F. Prutton).
203. M. Berthelot, *C. R. Hebd. Seances Acad. Sci.* 112 (1891) 1343.
204. L. Mond, L. Quincke, *J. Chem. Soc.* 1891, 604.
205. W. A. Herrmann, *Chem. Unserer Zeit* 22 (1988) no. 4, 113–122.
206. R. Boese, D. Blaeser, *Z. Kristallogr.* 193 (1990) nos. 3–4, 289–290.
207. D. Braga, F. Grepioni, A. G. Orpen, *Organometallics* 12 (1993) no. 4, 1481–1483.
208. Produkt-Merkblatt GAF 1977.
209. F. L. Ebenhöch: *Pentacarbonyl Iron Brochure*, BASF Aktiengesellschaft, Ludwigshafen 1988.
210. Gmelin, Eisenorganische Verbindungen, B3, pp. 1–247.
211. Gmelin, no. 59, Eisen, Teil B, pp. 486–498.
212. Ullmann, 4th ed., 10, 417–418.
213. Greenwood–Earnshaw: *Chemie der Elemente*, VCH Verlagsgesellschaft, Weinheim 1988.
214. W. Hieber, F. Leutert, *Ber. Dtsch. Chem. Ges.* 64 (1931) 2831.
215. W. Hieber, F. Leutert, *Naturwissenschaften* 19 (1931) 360.
216. W. Hieber, F. Leutert, *Z. Anorg. Allg. Chem.* 204 (1932) 145.
217. W. Hieber, *Z. Anorg. Allg. Chem.* 204 (1932) 165.
218. Ch. Eischenbroich, A. Salzer: *Organometallicchemie*, Teubner, Stuttgart 1986, pp. 243–245.
219. J. Dewar, H. O. Jones, *Proc. R. Soc. (London) Ser. A* 76 (1905) 558–577.
220. E. Speyer, H. Wolf, *Chem. Ber.* 60 (1927) 1424.
221. J. Dewar, H. O. Jones, *Proc. R. Soc. (London) Ser. A* 79 (1907) 66.
222. H. Freundlich, E. J. Cuy, *Chem. Ber.* 56 (1923) 2264.
223. P. Chini, *Inorg. Chim. Acta Rev.* 2 (1968) 31–51.

224. W. Hieber, G. Brendel, *Z. Anorg. Allg. Chem.* 289 (1957) 324.
225. BASF, DE 928 044, 1953.
226. BASF, DE 948 058, 1952.
227. A. Mittasch, *Angew. Chem.* 41 (1928) 827.
228. H. Pichler, H. Walenda, *Brennst. Chem.* 21 (1940) 134.
229. L. W. Ross, F. H. Haynie, R. F. Hochmann, *J. Chem. Eng. Data* 9 (1964) 339–340.
230. H. E. Charlton, J. H. Oxley, *AIChEJ* 11 (1965) no. 1, 79–84.
231. BASF, DE 499 296, 1924 (A. Mittasch, M. Müller-Cunradi, A. Pross).
232. BASF, DE 634 283, 1934 (L. Schlecht, H. Naumann).
233. W. Hieber, O. Geisenberger, *Z. Anorg. Allg. Chem.* 262 (1950) 15.
234. E. M. Vigdorchik, R. A. Shvartsman, P. P. Shukvostov: *Issled. V. Obl. Metall. Nikelya i Kobalta*, Leningrad 1983, pp. 125–132.
235. BASF, DE 485 886, 1925 (A. Mittasch, C. Müller, L. Schlecht).
236. BASF, DE 442 718, 1925 (M. Müller-Cunradi).
237. W. Reppe, *Justus Liebigs Ann. Chem.* 582 (1953) 116.
238. BASF, DE 753 618, 1940.
239. Montecatini, IT 728074, 1966.
240. C. Dufour-Berte, E. Pasero, IT 887 928, 1971.
241. C. Dufour-Berte, E. Pasero, *Chim. Ind. (Milan)* 49 (1967) no. 4, 347–354.
242. Mine Safety Appliances Comp., DE 1 086 460, 1957 (R. A. Morris, R. Heine-Geldern).
243. W. Schäfer, *Fresenius Z. Anal. Chem.* 335 (1989) no. 7, 785–790.
244. BASF, DE 493 874, 1926 (A. Mittasch, C. Müller, E. Linckh).
245. BASF, DE 500 692, 1924 (A. Mittasch, W. Schubardt, C. Müller).
246. GAF, US 2 612 440, 1950 (G. O. Altmann).
247. GAF, US 2 914 537, 1957 (D. J. Randall).
248. V. G. Syrkina, I. S. Tolmashy, SU, 1 186 398, 1964.
249. BASF, US 2 851 347, 1956 (L. Schlecht, E. Österreicher, F. Bergmann).
250. BASF, DE 3 428 121, 1984; US 4 652 305, 1985 (F. L. Ebenhöch, R. Schlegel).
251. BASF, DE 528 463, 1927 (W. Meiser, W. Schubardt, O. Kramer).
252. BASF Broschüre, "Carbonyleisenpulver", Ludwigshafen 1994.
253. BASF, US 1 840 286, 1926 (E. Hochheim).
254. C. Heck: *Magnetische Werkstoffe und ihre technische Verwendung*, Heidelberg 1975, pp. 79–81, 397–415.
255. F. Durtschmid, L. Schlecht, W. Schubardt, *Stahl Eisen* 52 (1932) 845–849.
256. F. V. Lenel: *Powder Metallurgy*, MPIF Princeton, NJ 1980.
257. L. F. Pease, *Metal Powder Report* 43 (1988) no. 4, 242–254.
258. M. Blömacher, D. Weinand, *Metal Powder Report* 43 (1988) no. 5, 328–330.
259. M. Blömacher, D. Weinand, M. Schwarz, E. Langer, *Powder Injection Molding, Advances in Powder Metallurgy & Particulate Materials — 1993*, Vol. 5, Metal Powder Industries Federation, Princeton, NJ.
260. E.-M. Langer, M. Schwarz, H. Wohlfrom, M. Blömacher, D. Weinand, *Prakt. Metallogr.* 33 (1996) 5.
261. Whittaker Corp., US 4 173 018, 1979 (M. Dawson, L. Saffredial).
262. The Dow Corp., US 4 414 339, 1982 (J. Sole, R. R. Harris).
263. H. Dominik, E. Eckert, *Nachricht. Z.* 41 (1988) 280–283.
264. A. Mittasch, *Angew. Chem.* 41 (1928) 827–833.
265. G. Böhm, (BASF) *World Steel & Metalworking* (1982/83).
266. F. L. Ebenhöch, *Prog. Powder Metall.* 42 (1986) 133–140.
267. F. L. Ebenhöch, *Metal Powder Report* 42 (1987) no. 1, 12–14.
268. GAF, *Metal Powder Report* 43 (1988) no. 5, 338–340.
269. BASF, DE 422269, 1924 (A. Mittasch).
270. BASF, DE 2210279, 1972 (F. L. Ebenhöch, K. P. Hansen, H. Stark).
271. BASF, DE 2344196, 1973 (W. Ostertag et al.).
272. W. Ostertag, F. L. Ebenhöch, K. Bittler, G. Wunsch, *Defazet Aktuell* (1979) no. 12, 434–435.
273. BASF, DE 1116643, 1959 (H. Klippel).
274. BASF, DE 2619084, 1976 (W. Ostertag et al.).
275. BASF, DE 830946, 1949 (L. Schlecht, G. Trageser).
276. BASF, DE 3208325, 1982 (M. Appl, F. L. Ebenhöch, R. Schlegel, E. Völkl).
277. BASF, WO-A-96/06891, 1994.
278. BASF, DE 1953518, 1969 (F. L. Ebenhöch et al.).
279. BASF, DP 2517713, 1974 (W. Ostertag, G. Wunsch, F. Ebenhöch, E. Völkl, G. Bock).
280. US 3 441 408, 1964 (H. J. Schladitz).
281. US 3 570 829, 1971 (H. J. Schladitz).
282. H. J. Schladitz, *Z. Metall.* 59 (1968) 18.
283. H. J. Schladitz, W. A. Jessor, D. S. Lashmore, *Z. Appl. Phys.* 48 (1977) 478.
284. Klöckner-Werke AG, US 3955962, 1975 (W. Dawihl, W. Eicke).
285. Klöckner-Werke AG, US 4002464, 1975 (W. Dawihl, W. Eicke).
286. Klöckner-Werke AG, DE-OS 2603951, 1976 (H. Schön, R. Gustke).
287. Fa. W. M. Müller, DE 3206838, 1982 (F. Unterreithmeier).
288. W. Dawihl, W. Eicke, *Powder Metall. Int.* 3 (1971) 75.
289. L. E. Mürr, O. T. Inal, *J. Appl. Phys.* 42 (1971) 3887.
290. H. G. F. Wilsdorf, O. T. Inal, L. E. Mürr, *Z. Metall.* 69 (1978) no. 11, 701–705.
291. BASF, US 5085690, 1992.
292. BASF, FR 3003352, 1981 (W. Ostertag, K. Bittler, G. Bock).
293. W. Ostertag, N. Mronga, P. Hauser, *Farbe Lack* 93 (1987) no. 12, 973.
294. BASF, EP 05580022, 1992.
295. BASF, US 4344987, 1981 (W. Ostertag, K. Bittler, G. Bock).
296. Xerox Corp., US 4 238 558, 1980 (R. F. Ziolo).
297. Xerox Corp., US 4 245 026, 1981 (R. F. Ziolo).
298. Xerox Corp., GB 1 577 257, 1980 (R. F. Ziolo).
299. BASF, US 4803143, 1989.
300. Océ, US 4443527, 1984.
301. Xerox Corp., US 4 252 671, 1981 (T. W. Smith).

300. Hitachi Maxell Ltd., JP-Kokai 58/137202, 1983.
301. J. M. Ginder, *Encyclopedia of Applied Physics*, Vol. 16, VCH Publishers Inc., 1996.
302. Hazen Research Inc., US 4 229 209, 1980 (J. K. Kindig, R. L. Turner).
303. Ullmann, 4th ed., 10, 417-418.
304. H. Alper in T. Wender, P. Pino (eds.): *Organic Syntheses via Metal Carbonyls*, vol. 2, Wiley Interscience, New York 1977, pp. 545-593.
305. T. Suzuki, O. Yamada, Y. Takahashi, Y. Watanabe, *Fuel Process Technol.* **10** (1985) no. 1, 33-43.
306. Pentanyl Corp., US 4451351, 1984 (C. R. Porter, H. D. Kaesz).
307. D. Racz, I. Lorincz, B. Toth, A. Kassay, HU 15890, 1975.
308. P. Kolocsa, D. Danoczy, K. Heberger, D. Racz, HU 35768, 1983.
309. BASF, DE 441179, 1925 (M. Müller-Cunradi).
310. BASF, DE 486596, 1927 (A. Schneevoigt).
311. BASF, DE 3707713, 1988 (W. Kochanek, B. Leutner, D. Schläfer).
312. J. P. Collmann, *Acc. Chem. Res.* **8** (1975) 342-347.
313. BASF, DE 3837309, 1988.
314. Asahi Chem. Ind., JP 86/225320-225328, 1985 (K. Nahamura, Y. Komatsu).
315. H. Tributsch et al., *Mater. Res. Bull.* **21** (1986) 1481-1487.
316. H. W. Armit, *J. Hyg.* **8** (1908) 565.
317. Letter from BASF Corporation to USEPA submitting enclosed follow-up information concerning enclosed reports and studies on iron pentacarbonyl with attachments (1991) NTIS order No.: NTIS/OTS0529732.
318. F. W. Sundermann et al., *Arch. Ind. Health* **19** (1959) 11.
319. Initial submission: an acute inhalation toxicity study of iron pentacarbonyl in the rat (final report) with attachments and cover letter dated 022792 (1992) NTIS order No.: NTIS/OTS0535889.
320. W. B. Deichmann, H. W. Gerarde: *Toxicology of Drugs and Chemicals*, Academic Press, New York-London 1969, p. 335.
321. J. C. Gage, *Br. J. Ind. Med.* **27** (1970) 1-18.
322. P. V. Sacks, D. N. Houchin, *Am. J. Clin. Nutr.* **31** (1978) 566-573.
323. R. S. Brief et al., *Am. Ind. Hyg. Assoc. J.* **28** (1967) 21.
324. H. E. Stokinger in: *Patty*, vol. IIA, pp. 1797-1799.
325. *Kirk-Othmer*, **13**, 764-788.
326. Ullmann, 4th ed., **10**, 426-428.
327. A. B. Prasad (ed.): *British National Formulary*, British Medical Association and The Pharmaceutical Society of Great Britain, Norwich 1986, pp. 282-288.
328. M. T. Ahmet, C. S. Frampton, J. Silver, *J. Chem. Soc. Dalton Trans.* **1988**, 1159.
329. R. C. Hider, G. Kontoghiorghes, J. Silver, M. A. Stockham, GB-A 2117766, 1983.
330. R. C. Hider, G. Kontoghiorghes, M. A. Stockham, FP-A 107458, 1984.
331. R. C. Hider, H. Kontoghiorghes, J. Silver, M. A. Stockham, EP-A 138421, 1985.
332. R. C. Hider, G. Kontoghiorghes, J. Silver, M. A. Stockham, FP-A 138420, 1985.
333. F. Habashi, "The Aqueous Oxidation of Pyrite, Covellite, and Arsenopyrite" in *Process Mineralogy XII*, edited by R.D. Hagni, The Minerals, Metals & Materials Society, Warrendale, PA, 1995, pp. 343-350.
334. Keramchemie GmbH, DE 3206538, 1986 (H. J. Heimhard, H. J. Simon).
335. H. J. Heimhard, G. Hitzemann, *Stahl Eisen* **105** (1985) 1222-1228.
336. G. Diez, P. Nieder, *Ind. Anz.* **87** (1965) no. 56, 1303-1311.
337. Andritz-Ruthner Division, AT 380675, 1984 (H. Krivanec, B. Wasserbauer, D. Gausriegler).
338. H. Mühlberg, J. Mensler, P. Björklund, *Stahl Eisen* **95** (1975) 639-642.
339. Company brochure, Allied Signal Inc. USA, 1987.
340. R. Rituper, *Metall* **43** (1989) no. 9, 854-858.
341. J. L. W. Jolly, C. T. Collins: "Natural Iron Oxide Pigments", *Iron Oxide Pigments*, part 2, Information Circular-Bureau of Mines 8813, Washington 1980.
342. H. Kittel: *Lehrbuch der Lacke und Beschichtungen*, vol. II, Verlag, W. A. Colomb Berlin 1974, p. 109.
343. E. Ack, *Farben Ztg.* **28** (1922/23) 493.
344. M. A. Bouchonnet, *Bull. Soc. Chim. Fr.* (1912) 9 345.
345. H. Wagner, R. Haug: "Gelbe Eisenoxydfarben", **8d**, Veröffentlichung des Fachausschusses für Anstrich-technik bei VDI und VDCh, VDI-Verlag, Düsseldorf 1934.
346. I. G. Farbenind., US 1813649, 1929 (P. Weise).
347. Minnesota Mining & Manuf. Co., US 2634193, 1947 (G. E. Noponen).
348. Minnesota Mining & Manuf. Co., US 2452608, 1941 (G. B. Smith).
349. Verein Österr. Eisen- und Stahlwerke, OE 176206, 1952 (E. Petzel).
350. The Nitralloy Corp., US 2592580, 1945 (H. Loevenstein).
351. E. V. Carter, R. D. Laundon, *J. Oil Colour Chem. Ass.*, 1990 (1) 7-15.
352. Bayer, DE 2653765, 1976 (B. Stephan, G. Winter).
353. Bayer, DE 3820499, 1988 (B. Kröckert, G. Buxbaum, A. Westerhaus, H. Brunn).
354. Bayer, DE-AS 1191063, 1963 (F. Hund, H. Köller, D. Rade, H. Quast).
355. BASF, DE-OS 2517713, 1975 (W. Ostertag et al.).
356. Magnetic Pigment Co., US 1424635, 1919 (P. Fireman).
357. Ault & Wiberg Co., US 1726851, 1922 (E. H. McLeod).
358. Interchem. Corp., US 2388659, 1943 (L. W. Ryan, H. L. Sanders).
359. C. K. Williams & Co., US 3133267, 1934.
360. Reconstruction Finance Corp., US 2631085, 1947 (L. M. Bennetch).
361. Reymers Holms Gamla Ind., GB 668929, 1950 (T. G. H. Holst, K. A. H. Björmed).
362. Glemser, DE 704295, 1937 (O. Glemser).
363. Pfizer, DE-OS 2212435, 1972 (L. M. Bennetch, H. S. Greiner, K. R. Hancock, M. Hoffman).
364. Hollnagel, Kühn, DL 26901, 1960 (M. Hollnagel, E. Kühn).
365. C. K. Williams & Co., US 2620261, 1947 (T. Toxby).

366. West Coast Kalsomine Co., US 1327061, 1917 (R. S. Penniman, N. M. Zoph).
367. National Ferrite Co., US 1368748, 1920 (R. S. Penniman, N. M. Zoph).
368. Frazee, US 1923362, 1927 (V. Frazee).
369. Magnetic Pigment Co., US 2090476, 1936 (P. Fireman).
370. C. K. Williams & Co., US 2111726, 1932 (G. Plews); US 2111727, 1937 (G. Plews).
371. Magnetic Pigment Co., US 2127907, 1937 (P. Fireman).
372. Bayer, DE 902163, 1951 (B. H. Marsh).
373. C. K. Williams & Co., US 2785991, 1952 (L. M. Bennetch).
374. Bayer, FR 1085635, 1953 (F. Hund); DE 1040155 1954 (F. Hund).
375. Mineral Pigments, US 2633407, 1947 (D. W. Marsh).
376. I. G. Farbenind., DE 463773, 1925 (J. Laux).
377. I. G. Farbenind., DE 515758 1925 (J. Laux).
378. I. G. Farbenind., DE 551255, 1930 (U. Haberland).
379. Bayer, EP 0249843, 1987 (A. Westerhaus, K. W. Ganter, G. Buxbaum).
380. I. G. Farbenind., DE 466463, 1926 (W. Schubardt, M. Grote).
381. Bayer, EP0014382, 1980 (G. Franz, F. Hund).
382. R. C. Rowe, *Pharm. Int.* **9** (1984) 221-224.
383. Bayer, DE 3326632, 1983 (W. Burrow, H. Printzen, H. Brunn, K. Nollen).
384. Ullmann, 4th ed. **18**, 623.
385. C. Clauss, E. Gratzfeld in H. Kittel (ed.): *Pigmente*, 3rd ed. Wissenschaftl. Verlags GmbH, Stuttgart 1960.
386. M. F. Dix, A.D. Rae, *J. Oil Colour Chem. Assoc.* **61** (1978) 69.
387. A. Ludi, "Berliner Blau", *Chemie in unserer Zeit* **4** (1988) 22.
388. Degussa *Vossen-Blau-Pigmente*, Frankfurt/M. 1973.
389. "Fotometrische Messung tiefschwarzer Systeme", *Schriftenreihe Pigmente* Nr. 24, Degussa AG, 60287 Frankfurt/M. 1989.
390. G. K. Wertheim et al., *J. Chem. Phys.* **54** (1971) 3235.
391. H. Buser et al., *J. Chem. Soc. Chem. Commun.* **23** (1972) 1299.
392. M. L. Napijalo, V. Stefancic, *Fizika (Zagreb)* **8** Suppl. (1976) 16.
393. R. J. Emrich et al., *J. Vac. Sci. Techn. A* **5** (1987) 1307.
394. F. Herren et al., *Inorg. Chem.* **19** (1980) 956.
395. A. Ludi, *Chem. Unserer Zeit* **22** (1988) 123.
396. Degussa AG, DE 1188232, 1964 (E. Gratzfeld).
397. Degussa AG, DE 976599, 1952 (H. Verbeek, E. Gratzfeld).
398. Chem. Fabrik Wesseling AG, DE 1061935, 1955 (H. Verbeek, E. Gratzfeld).
399. Degussa AG, DE 233669, 1962 (E. Gratzfeld).
400. Degussa AG, DE-OS 1792418, 1968 (E. Gratzfeld, E. Clausen, E. Ott).
401. Degussa AG, DE 1937832, 1969 (E. Gratzfeld).
402. Degussa AG, DE 1949720, 1969 (E. Gratzfeld, E. Kühn).
403. L. Müller-Fokken, *Farbe + Lack* **84** (1978) 489.
404. H. Ferch, H. Schäfer: *18th AFTPV-Kongressbuch*, Nice 1989, p. 315.

403. "Vossen-Blau zur Färbung von Fungiziden", *Schriftenreihe Pigmente* Nr. 50, Degussa AG, Frankfurt/M. 1985.
404. W. Koblet, *Schweiz. Z. Obst Weinbau* **1** (1965) 8.
405. H. Wiedmer et al.: *Agro-Dok* no. D4341; Sandoz AG, Basel 1977.
406. R. Ciferri: "Le 4 Stagioni" (Montecatini) **4** (1963) no. 2, 2.
407. V. Nigrovic, *Int. J. Rad. Biol.* **7** (1963) 307.
408. V. Nigrovic, *Phys. Med. Biol.* **10** (1965) 81.
409. I. V. Tananayev, *Zh. Neorg. Khim.* **1** (1956) 66.
410. P. Dvorak, *Z. Gesamte Exp. Med.* **89** (1969) 151.
411. P. Dvorak, *Arzneim. Forsch.* **20** (1970) 1886.
412. P. Dvorak, *Z. Naturforsch. B* **26** (1971) 277.
413. V. Nigrovic, F. Böhne, K. Madshus, *Strahlentherapie* **130** (1966) 413.
414. P. Dvorak, *Z. ges. exp. Med.* **151** (1969) 89-92.
415. T. A. Shashina et al., *Gig. Tr. Prof. Zabol.* **1** (1991) 35-36.
416. J. M. Verzijl et al., *Clinical Toxicol.* **31** (1993) 553-562.
417. B. D. Nielsen et al., *Z. Naturforsch.* **45** (1990) 681-690.
418. Degussa AG, unpublished report: Degussa AG US-IT-Nr. 84-0074-DKT (1984) and 88-0083-DKT, 88-0084-DKT (1988a).
419. *NPIRI (National Printing Ink Research Institute Raw Materials Data Handbook)* **4** (1983) 21, Napim, New York.
420. Degussa AG, unpublished report: Degussa AG US-IT-Nr. 77-0069-FKT (1977).
421. Degussa AG, unpublished report: Degussa AG US-IT-Nr. 85-0081-DKT, 85-0080-DKT (1985a), 87-0038-DKT, 87-0039-DKT, 87-0040-DKT (1987) and 88-0085-DKT (1988b).
422. F. Leuschner, H. Otto, unpublished (1967); in: *Kosmetische Färbemittel*, Harald Boldt Verlag KG, Boppard 1977.
423. V. Nigrovic et al., *Strahlentherapie* **130** (1966) 413-419.
424. M. Günther, Kernforschungszentrum Karlsruhe, KFK 1326, Gesellschaft für Kernforschung m.b.H., Karlsruhe, unpublished report US-IT-Nr. 70-0001-FKT (1970).
425. P. Dvorak et al., *Naunyn-Schmiedeberg's Arch. Pharmacol.* **269** (1971) 48-56.
426. K. Madshus et al., *Int. J. Radiation Biol.* **10** (1966) 519-520.
427. A. K. Madshus, A. Strömme, *Z. Naturforsch.* **A23** (1968) 391-392.
428. J. P. Mulkey et al., *Vet. Human Toxicol.* **35** (1993) 445-453.
429. V. Pai, *West Indian Med. J.* **36** (1987) 256-258.
430. Degussa AG, unpublished report: Degussa AG US-IT-Nr. 85-0082-DGO, 85-0085-DGO, 85-0088-DGO, 85-0078-DGO (1985b).
431. Degussa AG, unpublished report: Degussa AG US-IT-Nr. 79-0046-DKO, 79-0047-DKO, 79-0088-DKO (1979), 85-0079-DKO, 85-0083-DGO (1985c).
432. Armour Research Foundation, US 2694656, 1947 (M. Camras).
433. Bayer, DE 1061760, 1957 (F. Hund).
434. EMI, GB 765464, 1953 (W. Soby).
435. BASF, DE 1204644, 1962 (W. Balz, K. C. Malle).

436. VEB Elektrochemisches Kombinat, Bitterfeld, DD 48590, 1965 (W. Baronius, F. Henneberger, W. Geidel).
437. Agfa-Gevaert, DE 1592214, 1967 (W. Abeck, H. Kober, B. Seidel).
438. Bayer, DE 1803783, 1968 (F. Rodi, H. Zimigbl).
439. Pfizer, US 3498748, 1967 (H. S. Greiner).
440. Sakai Chemical Industries, US 4202871, 1980 (S. Matsumoto, T. Koga, K. Fukai, S. Nakatani).
441. A. R. Corradi et al., *IEEE Trans. Magn.* **MAG-20** (1984) 33–38.
442. Bayer, DE 1266997, 1959 (W. Abeck, F. Hund).
443. Y. Imaoka, S. Umeki, Y. Kubota, Y. Tokunaka, *IEEE Trans. Magn.* **MAG-14** (1978) 649.
444. 3M, US 3573980, 1968 (W. D. Haller, R. M. Col-line).
445. Hitachi Maxell, DE 2235383, 1972 (Okazoe, Akira).
446. G. Bate, *J. Appl. Phys.* **52** (1981) 2447.
447. M. Kishimoto, S. Kitahata, M. Amwmiya, *IEEE Trans. Magn.* **MAG-22** (1986) 732–734.
448. T. Fujiwara, *IEEE Trans. Magn.* **MAG-23** (1987) 3125.
449. D. E. Spiliotis, *IEEE Trans. Magn.* **MAG-25** (1988) 4048.
450. H. Hibst, *Angew. Chem.* **94** (1982) 263.
451. H. Stäblein in F. E. Wohlfarth (ed.): *Ferromagnetic Materials*, vol. 3, North Holland Publ., Amsterdam, Oxford, New York, Tokyo 1982.
452. Toshiba, EP-A 39773, 1980 (H. Endo et al.).
453. Toda, EP-A 150580, 1983 (N. Nagai et al.).
454. Dow Mining, DE-OS 3527478, 1984 (K. Aoki).
455. Sakai Chemical, DE-OS 3529756, 1984 (S. Jwasaki et al.).
456. Ishihara, EP-A 299332, 1987 (K. Nakata et al.).
457. Uguine Kuhlmann, DE-OS 2003438, 1969 (M. G. de Bellay).
458. Toda, EP-A 164251, 1984 (N. Nagai et al.).
459. Toda, EP-A 232131, 1986 (N. Nagai et al.).
460. Matsushita, EP-A 290263, 1987 (H. Torii et al.).
461. Toshiba, DE 3041960, 1979 (O. Kubo et al.).
462. BASF, DE-OS 3702036, 1987 (G. Mair).
463. R. E. Fayling, *IEEE Trans. Magn.* **MAG-15** (1979) 1567.
464. R. J. Veitch, *IEEE Trans. Magn.* **MAG-26** (1990) 1876.
465. Y. Okazaki et al., *IEEE Trans. Magn.* **MAG-24** (1989) 4057.
466. D. E. Spiliotis, *IEEE Trans. Magn.* **MAG-26** (1990).
467. O. Kubo et al., *IEEE Trans. Magn.* **MAG-24** (1988) 2859.
468. Hooker Chemicals & Plastics Corp.: *Ferrophos*, company information, Niagara Falls, NY, and D. E. de Jong bv. Apeldoorn, Holland, 1976.
469. W. Bäumer, *Farbe + Lack* **79** (1973) p. 747.
470. L. M. Greenstein in *Pigment Handbook*, 2nd ed., Vol. 1, J. P. Wiley & Sons, New York 1988, p. 846.
471. K. D. Franz, H. Härtner, R. Emmert, K. Nitta in *Ullmann's Encyclopedia of Industrial Chemistry*, Vol. A20, VCH Verlagsgesellschaft mbH, Weinheim 1992, p. 353.
472. K. D. Franz, R. Emmert, K. Nitta, *Kontakte (Darmstadt)* **2** (1992) p. 3.
473. G. Pfaff, R. Maisch, *Farbe + Lack* **101** (1995) p. 89.
474. R. Glausch, M. Kieser, R. Maisch, G. Pfaff, J. Weitzel in *Periglanzpigmente*, Curt R. Vincentz Verlag, Hannover 1996, pp. 42–46.
475. Merck KGaA, US 3926659, 1975 (R. Esselborn, H. Bernhard).
476. BASF, US 4344987, 1982 (W. Ostertag, K. Bittler, G. Bock).
477. W. Ostertag, *Nachr. Chem. Techn. Lab.* **42** (1994) p. 849.
478. G. Gehrenkemper, F. Hofmeister, R. Maisch, *Eur. Coat. J.* **3** (1990) p. 80.
479. P. Hauser, N. Mronga, W. Ostertag, *Adv. Org. Coat. Sci. Technol. Ser.* **13** (1991) p. 414.
480. C. Schmidt, M. Friz, *Kontakte (Darmstadt)* **2** (1992) p. 15.
481. US 2558302, 1951 (G. C. Marcot et al.).
482. US 2558304, 1951 (G. C. Marcot et al.).
483. Bayer, DE-OS 2508932, 1975 (F. Hund, G. Linde).
484. Bayer, DE 2210279, 1973 (F. L. Ebenhöch, K.-P. Hansen, H. Stark).
485. BASF, DE 2344196, 1973 (F. L. Ebenhöch, D. Werner, G. Bock).
486. BASF F + F AG, DE-OS 2228555, 1972 (H. Gae-decke, R. Bauer).
487. Magnetic Pigment Comp., US 1424635, 1922 (P. Fireman).
488. Reichard-Coulston Inc., US 2574459, 1947 (L. H. Bennetch).
489. F. Finus, *Farbe + Lack* **7** (1975) 604–607.
490. G. Narvuglio, R. F. Sharrock, R. J. Kennedy, *Oil J., Col. Chem. Assoc.* **61** (1978) 79–85.
491. M. C. Stopes: "On the petrology of banded bitumi-nous coals", *Fuel* **14** (1935) 4–13.
492. International Committee for Coal Petrology: *Hand-book of coal petrography*, 2nd ed., Centre national de la recherche scientifique, Paris 1963.
493. W. Spackman: "The maceral concept and the study of modern environments as a means of understand-ing the Nature of Coal", *Trans. N. Y. Acad. Sci.* **20** (1958) no. 5, 411–423.
494. M. Teichmüller: "Über neue Macerale der Liptinit-Gruppe und die Entstehung von Micrinit", *Fortschr. Geol. Rheinl. Westfalen* **24** (1974) 37–64.
495. W. H. Ode, W. H. Frederic: "The International Sys-tem of Hard-Coal Classification and Its Application to American Coals", *U.S. Bur. Mines Rep. Invest.* **5435** (1958).
496. M. Teichmüller, R. Teichmüller: "Geological cause of coalification", in R. F. Gould (ed.): "Coal Sci-ence", *Adv. Chem. Ser.* **55** (1966) 133–163.
497. P. A. Hacquebard, J. D. Donaldson: "Rank studies of coal in the Rocky Mountains and Inner Foothills Belt Canada", in R. R. Dutcher, P. A. Hacquebard, J. M. Schopf, J. A. Simon (eds.): "Carbonaceous ma-terials as indicators of metamorphism", *Spec. Pap. Geol. Soc. Am.* **153** (1974) 75–93.
498. E. Hryckowian, R. R. Dutcher, F. Dacheille: "Experi-mental studies of anthracite coals at high pressures and temperatures", *Econ. Geol.* **62** (1967) no. 4, 517–539.
499. G. H. Wood, T. M. Kehn, M. D. Carter, W. C. Cul-bertson: "Coal resource classification system of the U.S. Geological Survey", *Geol. Surv. Circ.* **891** (1983) 65 p.
500. P. Averitt: "Coal resources of the United States", *U.S. Geol. Surv. Bull.* **1412** (1975).
501. J. M. Schopf: "A definition of coal", *Econ. Geol.* **51** (1956) 521–527.
502. R. Thiessen: "What is coal?", *Int. Circ. U.S. Bur. Mines* **7397** (1947) 48 p.
503. B. C. Parks, H. J. O'Donnell: "Petrography of American coals", *Bull. U.S. Bur. Mines* **550** (1956) 193 p.
504. M. C. Stopes: "On the four visible ingredients in banded bituminous coals", *Proc. R. Soc. London Ser. B* **90** (1919) 470.
505. M. L. Gorbaty, K. Ouchi (eds.): "Coal Structure", *Adv. Chem. Ser.* **192**, American Chemical Society, Washington, DC, 1981.
506. R. C. Neavel: "Origin, Petrography and Classifica-tion of Coal", in M. A. Elliot (ed.): *Chemistry of Coal Utilization*, 2nd suppl. vol., Chap. 3, J. Wiley & Sons, New York, Chichester, Brisbane, Toronto 1981, pp. 91–158.
507. D. W. van Krevelen: *Coal and Its Properties Re-lated to Conversion*, Int. Conference on Coal Con-VERSION, Pretoria, RSA, 16–20 August 1982.
508. R. M. Davidson: *Molecular Structure of Coal*, Rep. No. ICTIS/TR 08, Jan. 1980, IEA Coal Research, London.
509. G. R. Gavalas, P. H.-K. Cheong, R. Jain, *Ind. Eng. Chem. Fundam.* **20** (1981) 113–122.
510. G. J. Pitt, G. R. Millward: *Coal and Modern Coal Processing*, An Introduction, Academic Press, Lon-don, New York, San Francisco 1979.
511. R. von der Gathen, K.-H. Kubitz, B. Bogen-schneider: "Die Auswirkungen der Vergleichmäßi-gung von Rohförderkohle auf Kosten und Produkte der Aufbereitung", *Glückauf* **119** (1983) 22–27.
512. M. Hampel: "Großsiebmaschinen für die Vorklas-sierung in Steinkohlensortierungsanlagen", *Glückauf* **113** (1977) 80–85.
513. K.-H. Kubitz, P. Wilczynski: "Trockene Feinst-kornabscheidung in Siebtern: neuere Entwick-lungen bei der Ruhrkohle AG", *Glückauf* **110** (1974) 480–484.
514. E. Fellensiek: "Das Setzverhalten unterbettgepulster Feinkorn-Großsetzmaschinen", *Glückauf-For-schungsh.* **39** (1978) 207–212.
515. E. Fellensiek: "Feinkornsortierung auf einer neuar-tigen, in Doppelfrequenz gepulsten Durchsetz-maschine", *Glückauf-Forschungsh.* **42** (1981) 130–136.
516. S. Heintges: "Die Entwicklung der Schwertrübesor-tierung von Steinkohlen in der Bundesrepublik Deutschland", *Glückauf* **109** (1973) 955–960.
517. M. Becker: "Der Weg zu den Großraumflotations-anlagen bei der Ruhrkohle AG", *Glückauf* **113** (1977) 952–955.
518. W. Blankmeister, B. Bogenschneider, K.-H. Ku-bitza, D. Leininger, L. Angerstein, R. Köhling: "Op-timierung der Fein- und Feinstkohlenentwässerung im Bereich unter 10 mm", *Glückauf* **112** (1976) 758–762.
519. W. Erdmann: "Neuere Entwicklungen bei der Ent-wässerung von fein- und feinstkörnigen Stein-kohlenerzeugnissen", *Aufbereit. Tech.* **26** (1985) 249–258.
520. D. Leininger, P. Wilczynski, R. Köhling, W. Erd-mann, T. Schieder: "Behandlung und Verwertung von Flotationsbergen in der Bundesrepublik Deutschland", *Glückauf* **115** (1979) 467–472.
521. R. von der Gathen: "Möglichkeiten und Grenzen der Entschwefelung von Steinkohle", *Glückauf* **115** (1979) 112–118.
522. W. P. Bethe, G. Koch: "Neue Bauformen für Auf-bereitungsanlagen", *Glückauf* **119** (1983) 368–373.
523. W. Erdmann: "Die thermische Trocknung in der Steinkohlensortierung der Bundesrepublik Deutschland", *Aufbereit. Tech.* **19** (1978) 581–586.
524. D. Rebb: "Latest Design in Coal Pipelining", *Can. Min. J.* **104** (1983) no. 3, 20–22.
525. T. Wheeler: "Hydraulic Transport of Coal: Slurry Pipelines", *Mine Quarry* **14** (1985) 35–38.
526. J. R. Siemon: "Economic Potential of Coal-Water Mixtures", *IEA Coal Res.*, London, Sept. 1985.
527. S. Furfari: "Hydrolysis of Coal", *IEA Coal Res.*, London, Oct. 1982.
528. E. Ahland, F. Friedrich, I. Romey, B. Strobel, H. Weber, *Erdöl Erdgas* **102** (1986) no. 3, 148–154.
529. A. G. Comalli, J. B. MacArthur, H. H. Stotler: "H-Coal Process Demonstrations, Development and Research Activities", *Prepr. Pap. Am. Chem. Soc. Div. Fuel Chem.* **27** (1982) no. 3/4, 104–113.
530. D. T. Wade, L. L. Ansell, W. R. Epperly: "Coal liq-uefaction", *CHEMTECH* **1982**, no. 4, 242–249.
531. W. G. Schützendübel: "SRC II", *Energie* **32** (1980) no. 6/7, 254–259.
532. K. Uesugi: "The Status of Coal Liquefaction Tech-nology Development in Japan", *Int. Working Forum of Coal Liquefaction*, Atlanta, GA, Apr. 4–9, 1986.
533. J. M. Lee, R. V. Nalitham, C. W. Lamb: "Recent de-velopments in Two-Stage Coal Liquefaction at Wil-sonville", *Prepr. Pap. Am. Chem. Soc. Div. Fuel Chem.* **31** (1986) no. 2, 316–324.
534. G. Franken, W. Adlhoeh, W. Koch, *Chern. Ing. Tech.* **52** (1980) 324–327.
535. K. A. Theis, E. Nilschke: "Make Syngas from Lign-ite", *Hydrocarbon Process.* **66** (1982) no. 9, 233–237.
536. H.-D. Schilling, B. Bonn, U. Krauß: *Kohlenver-gasung*, 3rd ed., vol. 22: "Bergbau, Rohstoffe, Ener-gie", Verlag Glückauf, Essen 1982.
537. H.-D. Schilling, B. Bonn, U. Krauß: "Coal Gasifica-tion", Graham & Trotmann, London 1981.
538. R. Specks, *Glückauf* **119** (1983) no. 23, 1147–1159.
539. P. Nowacki (ed.): "Coal Gasification Processes", *Energy Technology Review No. 70*, Noyes Data Corp., Park Ridge, NJ, 1981.
540. H. Teggers, H. Jüntgen, *Erdöl Kohle Erdgas Petro-chem. J.* **37** (1984) no. 4, 163–173.
541. J. M. Caffin: "Industrial Coal Gasification; Technol-ogy, Applications and Economics", *Energy Prog.* **4** (1984) no. 3, 131–137.
542. M. Teper, D. F. Hemming, W. C. Ulrich, EAS-Re-port E2/80, London, January 1983.
543. S. A. Elmquist et al., DOE/FE/05147-1488, May 1983.
544. M. K. Schad, C. F. Hafke, CEP May 1983, 45–51.
545. K. V. S. Sastry, D. W. Fuerstenau, EPRI CS-2198, Project 1030-1, January 1982.
546. F. P. Calhoun, *Min. Congr. J.* **49** (1962) 38–39.
547. N. Galbenis, O. Abel, J. Lehmann, W. Peters, *Erdöl Kohle Erdgas Petrochem.* **34** (1981) 59–65.
548. F. H. Beckmann, *Stahl Eisen* **100** (1980) 803–813.

548. E. Dunger, P. Dittmann, H. Reißmann, *Neue Bergbautech.* **10** (1980) 427-430.
549. H. Krug, W. Naundorf, *Energietechnik* **31** (1981) 62-68, 228-232.
550. R. Kurtz, *Braunkohle (Düsseldorf)* **32** (1980) 368-372, 443-448.
551. A. F. Baker, R. E. McKeever, A. W. Deurbrouck, DOE, RI-PMTC-12 (82), March 1982.
552. M. A. Colaluca, TENRAC/EDF-043, July 1981.
553. H. P. Hudson, J. E. Landon, J. H. Walsh: *The Canadian Mining and Metallurgical Bull. for January 1964*, Montréal, pp. 52-58.
554. K. V. S. Sastry, V. P. Mehrotra, 3rd Int. Symp. Agglomeration, Nürnberg, May 1981, H 36-38.
555. E. Ahland, J. Lehmann, *Erdöl Kohle Erdgas Petrochem.* **34** (1981) 402-407.
556. H.-G. Schäfer, 3rd Int. Symp. Agglomeration, Nürnberg, May 1981, S 53-55.
557. M. Schad, D. Sauter et al., BMFT-FB-T-85, Oct. 1985, pp. 108-109.
558. G. H. Cady, *Illinois Geological Survey Report of Investigations*, no. 35, 1935, pp. 25-39.
559. H. J. Gluskoter, J. A. Simon, *Illinois Geological Survey Circular*, no. 432, 1968, p. 28.
560. C. N. Kravits, J. C. Crelling, *Int. J. Coal Geol.* **1** (1981) 195-212.
561. *Survey of Energy Resources*, World Energy Council.
562. *BP Statistical Review of World Energy*, June 1995.
563. *1993 Energy Statistics Yearbook*, United Nations, 1995.
564. D. D. Whitehurst, T. O. Mitchell, M. Farcasiu: *Coal Liquefaction*, Academic Press, New York 1980.
565. T. Green, J. Kovac, D. Brenner, J. Larsen in R. A. Meyers (ed.): *Coal Structure*, Academic Press, New York 1982, pp. 199-282.
566. D. W. Van Krevelen: *Coal: Typology-Chemistry-Physics-Constitution*, Elsevier, Amsterdam 1961.
567. M. R. Khan, Ph. D. Thesis, The Pennsylvania State Univ., 1985.
568. R. Loison, A. Peytavy, A. Boyer, R. Grillot in H. H. Lowry (ed.): *Chemistry of Coal Utilization*, Suppl. vol., J. Wiley & Sons, New York 1963, pp. 150-201.
569. D. Hebermehl, F. Orywal, H. Beyer in M. A. Elliott (ed.): *Chemistry of Coal Utilization*, 2nd Suppl. vol., J. Wiley & Sons, New York 1981, pp. 317-351.
570. J. T. Senftle, Ph. D. Thesis, The Pennsylvania State Univ., 1982.
571. D. J. Maloney, M. S. Thesis, The Pennsylvania State Univ., 1980.
572. M. R. Khan, M. S. Thesis, The Pennsylvania State Univ., 1985.
573. M. S. Lancet, F. A. Sim, *Am. Chem. Soc., Div. Fuel Chem., Prepr.* **26** (1981) no. 3, 167.
574. M. R. Khan, R. G. Jenkins, *Fuel* **63** (1984) 109-115.
575. M. Kaiho, Y. Toda, *Fuel* **58** (1979) 397.
576. D. J. Maloney, Ph. D. Thesis, The Pennsylvania State Univ., 1983.
577. A. F. Boyer: *Proc. International Conference on Chemical Engineering in Coal Industry*, Pergamon Press, Paris 1957, p. 141.
578. O. P. Mahajan, M. Komatsu, P. L. Walker, Jr., *Fuel* **59** (1980) 3.
579. B. S. Ignasiak, A. J. Szladow, D. S. Montgomery, *Fuel* **53** (1974) 12.
580. P. C. Painter, M. M. Coleman, R. W. Snyder, O. P. Mahajan et al., *Appl. Spectrosc.* **35** (1981) 106.
581. C. Rhoads, J. T. Senftle, M. M. Coleman, A. Davis et al., *Fuel* **63** (1984) 245-250.
582. M. R. Khan, R. G. Jenkins, *Fuel* **65** (1986) 1291.
583. M. R. Khan, R. C. Jenkins, *Fuel* **65** (1986) 1203.
584. S. K. Chakrabartty, S. Parkash, N. Berkowitz, *Fuel* **55** (1976) 270.
- G. F. Crewe, U. Gat, V. Dhir, *Fuel* **54** (1975) 20.
- A. C. Cunningham, W. F. Wyss, *Fuel* **46** (1967) 137.
- W. R. Epperly, H. M. Siegel: *Proc. of 11th Symposium Intersociety Energy Conversion Engineering Conference*, State Line, Nevada, Sept. 12-17, 1976, pp. 249-267.
- Y. Nishiyama, Y. Tamai, *Fuel* **57** (1978) 559.
- J. W. Patrick, F. H. Shaw, *Fuel* **51** (1972) 69.
- R. H. Schlosberg, M. L. Gorbaty, R. L. Lang, *Fuel* **57** (1978) 424.
585. M. R. Khan, R. G. Jenkins: *Proc. International Conference on Coal Science*, Int. Energy Agency (IEA), Pittsburgh, PA, 1983, pp. 495-498.
586. M. R. Khan, R. G. Jenkins, *Fuel Process. Technol.* **8** (1984) 307-311.
587. E. Audibert, *Fuel* **5** (1926) 229.
588. E. Audibert, L. Delmas, *Fuel* **6** (1927) 131-140, 182-189.
589. J. G. Bennett, *J. Inst. Fuel* **14** (1941) 175.
590. S. R. Illingworth, *Fuel* **1** (1922) 3-6, 17-19, 33-35, 65-67.
591. R. Thiessen, *Ind. Eng. Chem.* **24** (1932) 1032.
592. R. G. Atkinson, R. E. Brewer, J. D. Davis, *Ind. Eng. Chem.* **29** (1937) 840-844.
593. H. L. Riley, H. E. Blayden, J. Gibson: *Proc. Conference Ultrafine Structure of Coals and Cokes*, British Coal Utilization Research Assn. (BCURA), London 1943, pp. 176-231.
594. H. R. Brown, P. L. Waters, *Fuel* **45** (1966) 17-41.
595. W. Hirst in [593], pp. 80-94.
596. N. Berkowitz: *An Introduction to Coal Technology*, Academic Press, New York 1979.
597. D. H. Bangham, F. A. P. Maggs: *Proc. Conference Ultrafine Structure of Coals and Cokes*, BCURA, 1944, p. 118.
598. I. G. C. Dryden, M. Griffith, *BCURA Rev.* **134** (1954) 62.
599. D. Fitzgerald, *Trans. Faraday Soc.* **52** (1956) 362-369.
600. R. C. Neavel in M. L. Gorbaty, J. W. Larsen, I. Wender (eds.): *Coal Science*, vol. 1, Academic Press, New York 1982, pp. 1-19.
601. P. H. Given: *Coal Agglomeration and Conversion Symposium*, Morgantown, WV, 1975.
602. L. Grainger: *Coke Oven Managers Association Yearbook*, Mexborough U.K., 1975, p. 282.
603. J. Dartnell, *Ironmaking Steelmaking* **1** (1978) 18-24.
604. P. Ramdohr, *Eisenhüttenwesen* **1** (1928) 669.
605. C. E. Marshall, *Fuel* **24** (1945) 120.
606. E. Stach in H. Freund (ed.): *Handbuch der Mikroskopie in der Technik*, vol. 2, Verlag Umschau, Frankfurt 1952, Part 1, p. 411.
607. C. Abramski, M. T. Mackowsky in [606], p. 311.
608. B. Alper, *Brennst. Chem.* **37** (1956) 194.
609. G. H. Taylor, *Fuel* **40** (1961) 465.
610. J. D. Brooks, G. H. Taylor, *Carbon* **3** (1965) 185.
611. H. Marsh, *Fuel* **52** (1973) 205.
612. J. W. Patrick, M. J. Reynolds, F. H. Shaw, *Fuel* **52** (1973) 198.
613. H. Marsh, F. Dacheille, M. Iley, P. L. Walker, Jr. et al., *Fuel* **52** (1973) 253.
614. A. Grint, U. Sweitlik, H. Marsh, *Fuel* **58** (1979) 642.
615. A. Grint, H. Marsh, *Fuel* **60** (1981) 1115.
616. H. Marsh, P. L. Walker, Jr., *Fuel Process. Technol.* **2** (1979) 61-75.
617. H. Marsh, J. Smith in C. Karr (ed.): *Analytical Methods for Coal and Coal Products*, vol. 2, Academic Press, New York 1978, pp. 371-414.
618. H. Marsh, P. L. Walker, Jr. in P. L. Walker, Jr., P. A. Thrower (eds.): *Chemistry and Physics of Carbon*, vol. 15, Marcel Dekker, New York 1979, pp. 229-286.
619. E. Fitzer, K. Müller, W. Schäfer, in P. L. Walker, Jr. (ed.): *Chemistry and Physics of Carbon*, vol. 7, Marcel Dekker, New York 1971, pp. 237-383.
620. J. D. Brooks, G. H. Taylor, *Chemistry and Physics of Carbon*, vol. 4, Marcel Dekker, New York 1968, pp. 243-286.
621. H. Marsh, R. C. Neavel, *Fuel* **59** (1980) 511.
622. I. C. Lewis, *Carbon* **20** (1982) 519.
623. W. J. Schmidt in H. Freund (ed.): *Handbuch der Mikroskopie in der Technik*, vol. 1, Verlag Umschau, Frankfurt 1957, Part 1, p. 147.
624. E. A. Rosauer: *Instruments for Materials Analysis*, Iowa State Univ. Press, Ames 1981.
625. J. L. White in J. O. McCaldin, G. Somorjai (eds.): *Progress in Solid-State Chemistry*, vol. 9, Pergamon Press, Oxford 1974, pp. 59-104.
626. R. A. Forrest, H. Marsh, *Carbon* **15** (1977) 348.
627. G. D. Mitchell, A. Davis, W. Spackman in R. T. Ellington (ed.): *Liquid Fuels from Coal*, Academic Press, New York 1977, pp. 255-270.
628. H. E. Newall, F. S. Sinnatt, *Fuel* **3** (1924) 424.
629. P. J. Street, R. P. Weight, P. Lightman, *Fuel* **48** (1969) 342.
630. M. Von Heimendahl: *Electron Microscopy of Materials - An Introduction*, Academic Press, New York 1980.
631. H. Marsh, C. Cornford in M. L. Deviney, T. M. O'Grady (eds.): *Petroleum Derived Carbons*, *Amer. Chem. Soc. Symposium Series* **21**, Amer. Chem. Soc., Washington, DC, 1976, pp. 266-281.
632. J. N. Murrell, E. A. Boucher: *Properties of Liquids and Solutions*, J. Wiley & Sons, New York 1982, pp. 92-95.
633. F. Reinitzer, *Monatsh. Chem.* **9** (1888) 421.
634. O. Lehmann, *Z. Phys. Chem. (Frankfurt am Main)* **4** (1889) 462.
635. G. Friedel, *Ann. Phys. (Paris)* **18** (1922) 273.
636. F. D. Saeva (ed.): *Liquid Crystals*, Marcel Dekker, New York 1979.
637. I. Mochida, K. Maeda, K. Takeshita, *Carbon* **16** (1978) 459.
638. I. C. Lewis, *Carbon* **16** (1978) 503.
639. J. L. White in M. L. Deviney, T. M. O'Grady (eds.): *Petroleum Derived Carbons*, *Amer. Chem. Soc. Symposium Series* **21**, Amer. Chem. Soc., Washington, DC, 1976, pp. 282-314.
640. J. Dubois, C. Agache, J. L. White, *Metallography* **3** (1970) 337-369.
641. T. Imamura, Y. Yamada, S. Oi, H. Honda, *Carbon* **16** (1978) 481.
642. K. J. Hüttinger, *Carbon* **10** (1972) 5.
643. I. C. Lewis, L. S. Singer in P. L. Walker, Jr. (ed.): *Chemistry and Physics of Carbon*, vol. 17, Marcel Dekker, New York 1981, pp. 1-88.
644. T. Yokono, H. Marsh in H. D. Shultz (ed.): *Coal Liquefaction Products*, vol. 1, J. Wiley & Sons, New York 1983, pp. 125-138.
645. Ref. [566], pp. 445-452.
646. I. G. C. Dryden in [568], pp. 262-268.
647. P. H. Given, *Fuel* **39** (1960) 147.
648. J. W. Patrick, M. J. Reynolds, F. H. Shaw, *Carbon* **13** (1975) 509.
649. F. Goodarzi, D. G. Murchison, *Fuel* **57** (1978) 273.
650. L. Grainger, J. Gibson: *Coal Utilization Technology, Economy and Policy*, Holsted Press, London 1981, pp. 137-150.
651. M. Forrest, H. Marsh in E. L. Fuller, Jr. (ed.): *Coal and Coal Products: Analytical Characterization Techniques*, *Amer. Chem. Soc. Symposium Series* **205**, Amer. Chem. Soc., Washington, DC, 1982, pp. 1-25.
652. R. H. Essenhigh in C. Y. Wen, E. S. Lee (eds.): *Coal Conversion Technology*, Addison-Wesley, Reading, MA, 1979, Chapter 3.
653. J. B. Howard in [569], Chapter 12.
654. A. W. Scaroni, P. L. Walker, Jr., R. G. Jenkins, *Fuel* **60** (1981) 558.
655. M. E. Morgan, R. G. Jenkins in H. H. Shoberg (ed.): *The Chemistry of Low-Rank Coals*, *Amer. Chem. Soc. Symposium Series* **264**, Amer. Chem. Soc., Washington, DC, 1984, p. 213.
656. R. F. Probst, R. E. Hicks: *Synthetic Fuels*, McGraw-Hill, New York 1982.
657. P. R. Solomon, D. G. Hamblen, *Prog. Energy Combust. Sci.* **9** (1983) 323.
658. H. Jüntgen, K. H. van Heek, *Fuel Process. Technol.* **2** (1979) 261.
659. N. Y. Nsakala, R. H. Essenhigh, P. L. Walker, Jr., *Combust. Sci. Technol.* **16** (1977) 153.
660. G. R. Gavalas, P. H. K. Cheong, R. Jain, *Ind. Eng. Chem., Fundam.* **20** (1981) 113.
661. D. B. Anthony, J. B. Howard, *AIChE J.* **22** (1976) 625.
662. R. Aris, G. R. Gavalas, *Philos. Trans. R. Soc. London. Ser. A* **260** (1966) 43.
663. A. Szladow, P. Given, *Ind. Eng. Chem. Process Des. Dev.* **20** (1981) 27.
664. S. V. Golikeri, D. Luss, *AIChE J.* **18** (1972) 277.
665. P. L. Walker, Jr., R. G. Jenkins, L. R. Radovic: "Importance of Active Sites for Char Gasification in Oxygen (Air) and CO₂", Final Report, Gas Research Institute, Chicago, Oct., 1982.
666. J. L. Johnson in [569], Chapter 23.
667. F. Moseley, D. Paterson, *J. Inst. Fuel* **40** (1967) 523.
668. G. J. Pitt, G. R. Millward (eds.): *Coal and Modern Coal Processing. An Introduction*, Academic Press, New York 1979, p. 152.
669. L. Seglin, S. A. Bresler in [569], pp. 785-846.
670. M. R. Khan, T. Kurata: "The Feasibility of Mild Gasification of Coal: Research Needs", U.S. Dept. of Energy, Morgantown Energy Technology Center, Technical Note TM-85/4019, 1985, NTIS DE 85013625.

671. P. J. Wilson, Jr., D. D. Clendenin in [568], Chapter 10.
 672. G. S. Pound, *J. Inst. Fuel* 25 (1952) 355.
 673. M. O. Holwatey in R. A. Meyers (ed.): *Coal Handbook*, Marcel Dekker, New York 1981, Chapter 9.
 674. F. Denig in H. H. Lowry (ed.): *Chemistry of Coal Utilization*, vol. 1, J. Wiley & Sons, New York 1945, Chapter 24.
 675. J. Speight in J. Falbe (ed.): *The Chemistry and Technology of Coal*, Marcel Dekker, New York 1983, Chapter 12.
 676. E. Ahland, G. Nashan, W. Peters, W. Weskamp in J. Falbe (ed.): *Chemical Feedstocks from Coal*, J. Wiley & Sons, New York 1982, pp. 12-77.
 677. A. E. Williams, L. O. Smith, K. A. König, K. A. Basciani, *Iron Steel Eng.* 60 (1983, May) 45.
 678. N. Nakamura, Y. Togino, T. Adachi, *Ironmaking Steelmaking* 5 (1978) no. 2, 49-60.
 679. T. F. Edgar: *Coal Processing and Pollution Control*, Gulf Publ. Co., Houston 1983, Chapter 6.
 680. W. Eisenhut in [569], Chapter 14.
 681. P. W. Chang, K. Durai-Swamy, F. W. Knell, *Coal Process. Technol.* 6 (1980) 20.
 682. C. L. Oberg, A. Y. Falk, *Coal Process. Technol.* 6 (1980) 159.

6 Steel

DIETER SCHAUWINHOLD (§§ 6.1, 6.7.1); MANFRED TONCOURT (§ 6.2); ROLF STEFFEN (§ 6.3.1); DIETER JANKE (§ 6.3.2); KLAUS SCHÄFER (§§ 6.3.3-6.3.4); RUDOLF HAMMER †, HATTO JACOB† (§§ 6.3.5.1-6.3.5.3); ROBERT HENTRICH (§ 6.3.5.4); LOTHAR KUCHARCIK (§ 6.3.5.5); ROGER PANKERT (§§ 6.4-6.5); HANS HOUARDY (§ 6.6.1); HANS-JÖRGEN GRABKE (§ 6.6.2); WINFRIED DAHL (§ 6.6.3); REINHARD WINKELGRUND (§ 6.7.2); VOLKER BROCKMANN, HEINZ-LOTHAR BONNAGEL (§ 6.8)

6.1 Introduction	270	6.5 Surface Coating	351
6.2 History	274	6.5.1 Introduction	351
6.2.1 From Prehistoric Times to the Middle Ages	274	6.5.2 Hot-Dip Coating	351
6.2.1.1 Native Iron	274	6.5.2.1 Plant and Processes	351
6.2.1.2 Iron from Ores	274	6.5.2.2 Other Coating Processes	353
6.2.1.3 Technology of Iron Production	274	6.5.3 Electrolytic Coating (Electroplating)	356
6.2.2 From the Middle Ages to the 1800s	275	6.5.3.1 Plant and Processes	356
6.2.2.1 Bloomery Furnaces	275	6.5.3.2 Electroplating Cells	357
6.2.2.2 Blast Furnaces	276	6.5.3.3 Coating Types	359
6.2.2.3 Metal Shaping	277	6.5.4 Vacuum Vapor Deposition	359
6.2.3 The Industrial Age	277	6.5.4.1 Plant and Processes	359
6.2.3.1 Pig Iron Production	278	6.5.4.2 Further Developments	360
6.2.3.2 Steel Production	278	6.5.5 Coil Coating	360
6.2.3.3 Rolled Steel Production	281	6.5.5.1 Plant and Processes	360
6.3 Crude Steel Production	282	6.5.5.2 Coating Systems	361
6.3.1 Raw Materials	282	6.5.6 Roll-Bonded Cladding	362
6.3.1.1 Hot Metal	284	6.5.6.1 Principles	362
6.3.1.2 Scrap	285	6.5.6.2 The Process	362
6.3.1.3 Sponge Iron	286	6.5.6.3 Variations	362
6.3.1.4 Lime	288	6.5.7 Summary	362
6.3.2 Physical and Chemical Fundamentals	290	6.6 Uses	363
6.3.2.1 Thermodynamics	290	6.6.1 Introduction	363
6.3.2.2 Kinetics and Mass Transfer	299	6.6.2 Chemical Properties	363
6.3.3 Production Processes	301	6.6.2.1 Introduction	363
6.3.3.1 Oxygen-Blowing Processes	302	6.6.2.2 Uniform Corrosion	364
6.3.3.2 Electric Steel Process	306	6.6.2.3 Atmospheric Corrosion	365
6.3.3.3 Production of Stainless Steels	310	6.6.2.4 Passivation	365
6.3.4 Secondary Metallurgy	312	6.6.2.5 Pitting Corrosion	366
6.3.4.1 Steel Treatment at Atmospheric Pressure	313	6.6.2.6 Crevice Corrosion	366
6.3.4.2 Vacuum Treatment	316	6.6.2.7 Intergranular Corrosion of Stainless Steels	366
6.3.5 Casting and Solidification	318	6.6.2.8 Stress Corrosion Cracking	367
6.3.5.1 Fundamentals	317	6.6.2.9 Hydrogen Absorption and Hydrogen Embrittlement	367
6.3.5.1 Ingot Casting	323	6.6.2.10 Oxidation of Iron	368
6.3.5.2 Continuous Casting	327	6.6.2.11 Oxidation of Carbon Steels and Low-Alloy Steels	368
6.3.5.3 Consumable Electrode Remelting Processes	336	6.6.2.12 High-Temperature Steels	369
6.3.5.4 Cast Steel and Cast Iron	338	6.6.2.13 Effects of Chlorine in Oxidation	370
6.4 Forming	344	6.6.2.14 Sulfidation of Iron and Steel	370
6.4.1 Pickling	344	6.6.2.15 Carburtization	370
6.4.2 Rolling	345	6.6.2.16 Nitriding	371
6.4.3 Annealing	347	6.6.2.17 Decarburization, Denitriding, and Hydrogen Attack	372
6.4.4 Skin-Pass Rolling	348	6.6.3 Physical Properties	372
6.4.5 Stainless Steels	349	6.6.3.1 Pure Iron	372
6.4.6 Future Developments	349	6.6.3.2 α -Iron Solid Solutions	375

6.6.3.3 γ -Iron Solid Solutions	376	6.7.2.4 Factors Influencing Recycling	385
6.6.3.4 Other Effects of Structure	376	6.7.2.5 Economic and Logistic Aspects	387
6.7 Environmental Protection	377	6.8 Economic Aspects	388
6.7.1 Environmental Aspects of Steel Production and Processing	377	6.8.1 World Steel Production, Consumption, and Trade	388
6.7.1.1 Production of Steel and Steel Products	377	6.8.2 Steel Intensity and Weight Saving in Steel	391
6.7.1.2 Steel Processing and Steel in Use ..	380	6.8.3 Capital Investment and Subsidies ..	393
6.7.2 Steel Recycling	381	6.8.4 Future Prospects	395
6.7.2.1 The Tradition of Steel Recycling ...	381	6.9 References	395
6.7.2.2 Types of Scrap	381		
6.7.2.3 Scrap Processing	384		

6.1 Introduction

Nowadays the term steel is understood to include not only all forgeable iron-based materials, but also all highly alloyed metallic materials in which the element iron is an important component, but which are not necessarily forgeable. With few exceptions, the carbon content is $< 2\%$.

For over 3000 years, steel has made a major contribution to human development, e.g., in tools for cultivating the soil and processing stone and almost all other materials, as a construction material for steel and reinforced concrete structures, in transport technology, for the generation and distribution of energy, for the fabrication of machinery and equipment (including equipment for the manufacture of plastics), in the household, and in medicine. It remains, for the foreseeable future, by far the most important material for the maintenance and improvement of our quality of life.

The outstanding importance of steel is the result of its ready availability and its versatility. The earth's crust contains ca. 5% iron, making it the fourth most abundant element after oxygen (46%), silicon (28%), and aluminum (8%). Rich deposits of iron ores are available in many parts of the world. Moreover, the free energy required to isolate iron from its oxidic ores is less than half of that required for aluminum [1]. The versatility of steel is due to the polymorphism of the iron crystal and its ability to alloy with other elements, forming solid solutions or compounds. The microstructure of steel in a finished com-

ponent can be adjusted by means of the chemical composition, the forming conditions and a wide variety of possible heat treatments. The attainable tensile strength ranges from ca. 300 N/mm² for deep-drawing sheet steel (e.g., for automotive body parts that are difficult to draw) to > 2000 N/mm² for critical components in aircraft. Tensile strengths as high as 2600 N/mm² are achieved in 0.15 mm diameter drawn wire for steel cord used in radial tires.

Cryogenic steels with high strength and good toughness at very low temperatures are used for the transport and storage of liquefied gases at temperatures of < -200 °C. Other steels with good properties at temperatures of 650–700 °C and above are used in power station equipment and gas turbines.

Highly developed soft magnetic steels are essential in the construction of transformers. Steel is also used to make permanent magnets. Nonmagnetizable steels have also been developed for use in electrical technology, shipbuilding, and physics research. Wear-resistant steels are used in rock-crushing machines and in industrial stirring equipment. Machine tools, used for metal cutting, require steels of the highest possible hardness to endow stability to the cutting edge. Other steels with very good machinability have been developed and are used for the economic manufacture of complex turned parts, or for mass production on high-speed automated equipment. Chemically resistant steels are essential in the chemical and foods industries, as well as in household equipment. For the majority of

steel grades—more than 2500 are available today—very good welding properties are important, and here steel has an advantage over competing materials.

Modern knowledge of controlling the microstructure of steel, and hence its properties, offer opportunities to match steel products to new sets of requirements [2].

Unlike brick or concrete buildings, steel structures can be dismantled relatively easily. Furthermore, almost 100% of the steel can be recovered from steel-containing products and can be remelted to yield steels of similar or higher quality. In this respect, iron and steel are superior to all competitive materials.

The great importance of steel in the world's economy is also exemplified by production figures. In the early 1900s, total world production of steel was less than 35×10^6 t/a. In 1940 it was 140×10^6 t/a. The figures for the period after 1950 (Figure 6.1) indicate a surprisingly large growth in world crude steel production after World War II. Up to the mid-1970s, this was mostly due to those developed countries with the greatest rate of economic growth, such as Japan, the six founding countries of the European Community, and also the Soviet Union. In the United States, growth had already ceased by the mid-1960s due to market saturation.

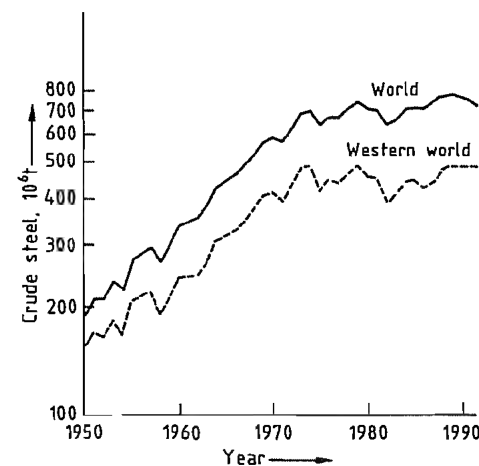


Figure 6.1: World crude steel production 1950–1991.

A rapid increase in steel production also took place in some Latin American countries, continuing until the mid-1980s. In many countries in Asia, Africa, and the Middle East, new steel industries were built up, or existing capacity was increased. The developments in some Asian countries during the last 16 years are remarkable (Table 6.1).

The relationship between total economic development and steel production can be seen clearly from these figures. Figure 6.1 also shows that world production of crude steel has stagnated since the mid-1970s, apart from the usual market fluctuations. A sharp rise in crude steel production in countries with rapidly increasing industrialization contrasts with zero or even negative growth in steel production in countries that are already highly industrialized (e.g., the United States). Several reasons can be suggested:

Table 6.1: Development of crude steel production in Asian countries (Source: International Iron and Steel Institute).

Country	Production, 10 ³ t/a		
	1975	1985	1991
China	23 903	46 700	70 400
South Korea	1 994	13 539	26 000
Taiwan	680	5 088	11 000
India	7 991	11 140	17 100

The steel consumption of a country is determined by the "specific market demand", i.e., production plus imports minus exports of steel product s expressed in kilograms crude steel per capita. In industrialized countries, this reaches saturation at ca. 600 ± 100 kg, which can only be exceeded in special circumstances. If there are sections of industry with extremely high steel consumption (shipbuilding or automotive industries), and if these are strongly export oriented, a value of > 700 kg per capita can be reached because the exported finished products do not remain in that country. Figure 6.2 shows that the saturation value of 600 kg was reached as early as 1950 in the United States. Other industrialized countries reached this figure in the 1970s, and this reduced the growth of steel production. Also, the expansion of the steel industry in countries

which had been importing rolled steel made it impossible for steel exports from the industrialized countries to grow. Extrapolation of the Figure 6.2 into the 1980s is problematical because the figure "kilogram crude steel per capita" is now no longer comparable with figures up to ca. 1975 due to technical developments (described below) in rolled steel products.

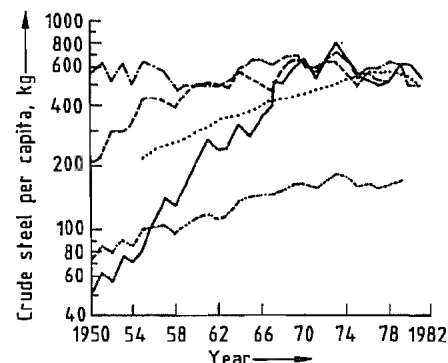


Figure 6.2: Specific market demand for crude steel (production + imports - exports) [1]: — = United States; — = Germany; = Former Soviet Union; — = Japan; - - - = World.

Table 6.2: Countries with a crude steel output $> 10 \times 10^6$ t/a (1991 and 1992) with portion of continuously cast steel shown (Source: International Iron and Steel Institute, 1992).

Country	Production, 10^6 t/a		Portion of continuously cast steel, %	
	1991	1992	1991	1992
Soviet Union	132.8	116.8	17.7	17.1
Japan	109.6	98.1	94.4	95.4
United States	79.7	84.3	75.7	78.9
China	70.4	80.0	26.5	30.0
Germany	42.2	39.7	89.5	92.0
South Korea	26.0	28.0	96.4	96.8
Italy	25.1	24.9	95.1	96.1
Brazil	22.6	23.9	56.0	58.6
France	18.4	18.0	95.0	95.2
India	17.1	18.1	14.3	
United Kingdom	16.5	16.1	85.5	87.0
Canada	13.0	13.9	83.6	86.5
Spain	12.9	12.3	91.8	93.2
Czechoslovakia	12.1	11.1	17.0	21.9
Belgium	11.3	10.3	92.2	93.9
Taiwan	11.0	10.7	94.6	94.9
Poland	10.4	9.8	8.6	9.1

From the second half of the 1960s, use of the continuous casting process in steelworks increased, approaching 20% by 1975 world-

wide. By 1991, the proportion of continuously cast steel reached 67% worldwide. This process gives an increase in yield of ca. 12–15% of crude steel for rolled steel products, compared with ingot casting. Hence, up to 15% less crude steel is required to produce the same amount of rolled steel product for the steel processing industry. Other improvements in yield productivity in steel plants and in steel-consuming industries also reduced the consumption of crude steel without jeopardizing the use of steel for a particular end product.

Table 6.2 lists all countries with a crude steel output of more than 10^6 t/a during 1991 and 1992 and gives the percentage of continuously cast steel.

In 1978, however, for the countries represented in Figure 6.2, the percentages of continuously cast steel were:

Former Soviet Union	9.5%
Japan	46.2%
United States	15.2%
Germany	38.0%

The large differences between the 1978 and 1991 figures, means that comparison of the number of kilograms crude steel per capita is of questionable value.

Below a continuously cast steel portion of ca. 85–90% "kilograms crude steel per capita" is an indication of the state of modernization of the steel industry of a country. Above this range, the production program and the proportion of steel products not produced by continuous casting (e.g., steel castings, heavy forgings) play an important part in crude steel production. Only countries with a crude steel output in 1991 of max. 10^6 t/a (e.g., Switzerland and New Zealand) produce 100% of their steel by continuous casting.

A further reason for the absence of the usual growth in crude steel production in the 1960s in the industrialized countries, must be attributed to the development of higher strength steel grades. In the last 15–20 years, these grades of steel have been increasingly used by steel processors. Especially in the motor vehicle industry, high-strength steels have been used to improve constructional design

through weight reduction. Consequently, there is a decrease in the amount of steel used, in addition to that achieved with the replacement of steel by competing materials such as aluminum or plastics.

When assessing the technological and economic significance of steel, it is interesting to examine the different finished steel products and how their share of the total production of rolled steel has changed over the years. There are two groups: "long products" (i.e., beams, steel shapes, steel bars, railway-track material, piling sections, and wire rod) and "flat products" (i.e., plates, sheets, strip-steel and universal-plate).

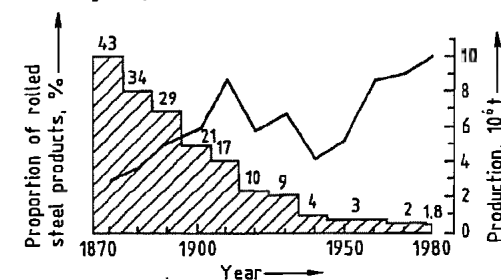


Figure 6.3: World production of steel for railway-track material lines. Solid line: total production of railway-track material; Hatched area: railway-track material as percentage of the total world production of rolled steel.

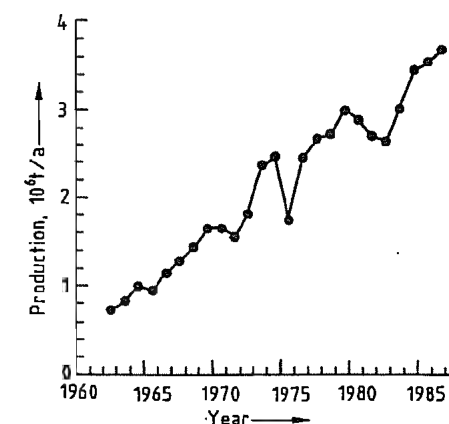


Figure 6.4: Production of cold-rolled stainless steel strip by western countries.

In 1870 3×10^6 t of railway-track material accounted for 43% of total world production of rolled steel products (Figure 6.3), while in 1991 the output of railway-track material,

which underwent a threefold increase to 9×10^6 t, accounted for barely 1.2% of total production. In modern industrialized countries, 60–70% of rolled steel production consists of flat products, mainly hot- and cold-rolled strip and sheet, coated sheet, tinplate and electric sheet, all with thicknesses in the range of 0.15–3 mm. The production of cold-rolled stainless steel strip has increased sharply during the last 25 years, as shown in Figure 6.4.

There is intensive world trade in products of the steel industry, especially among major steel producing countries. Only in a few cases does this involve special products or special steel grades, for which some producers have a leading position. International competition is severe, and producers must offer consistently high-quality products. The large producers have therefore built up comprehensive quality assurance systems over many years, conforming to ISO Standard 9002 and local regulations such as ASME in the United States, Lloyds Register in the United Kingdom, and TUV in Germany. The aim is to control all steps of the manufacturing process, and to use statistical methods to ensure that the finished product has the desired properties, dimensional tolerances, and a defect-free surface finish. The intensive testing of finished products that was formerly carried out can then be largely dispensed with, and replaced by the testing of random samples, the results of which form part of the control loop.

Such quality-assured production is a prerequisite for the direct processing of sheet coils on automatic press lines without any inspection (even for exposed autobody parts).

A further important aid to international trade in steel is the existence of common standard specifications and terms of delivery. Specifications for steel products have been formulated by ISO over many years. However, these are often only the first steps toward harmonization of the various interpretations and technical possibilities. In Europe, since 1986, EN Standards for all steel products and testing methods have been compiled by the ECIS (European Committee for Iron and Steel Standardization). These standards must be adopted

via CEN (Comité européen de normalisation) into the national standards of all European nations. They will certainly achieve importance outside Europe, too.

6.2 History

6.2.1 From Prehistoric Times to the Middle Ages

6.2.1.1 Native Iron

Since the earliest times, humans have used iron, the second most abundant metal in the earth after aluminum. It was first discovered in the form of the native element, which occurs only rarely as tellurian iron of volcanic origin, and mainly as meteoric iron. The Egyptians, Sumerians, Khatti, and Hittites must have had knowledge of its origin, as they called it ore, or metal, from heaven. Meteoric iron can be identified from its high nickel content (ca. 5–25%), and the typical Widmanstätten structure, formed on solidification. The oldest known examples of worked meteoric iron are beads from Gerzeh (3500 B.C.) and a dagger from Ur (3000 B.C.).

6.2.1.2 Iron from Ores

It is not known when, where, or how iron was first deliberately produced from its ores. It is often said that the technique of extracting iron was developed from observations made during copper extraction, and that the idea suggested itself simultaneously in many places with a long tradition of copper smelting. A geographical analysis can be carried out from linguistic similarities, archeological finds, and documents. According to present knowledge, iron was first smelted in eastern Asia Minor and northern Mesopotamia around 2000–1500 B.C., and possibly also in the plains north of the Caucasus. As the Chinese were the first to produce a high-carbon, high-phosphorus (up to 7%) liquid castable iron, it is conceivable that they also succeeded in winning iron from its ores at a very early date.

Around 500 B.C., knowledge of iron winning spread through Asia Minor to North Africa, parts of Asia, and all of Europe.

6.2.1.3 Technology of Iron Production

At first, the iron was smelted in a bloomery fire, later in a bloomery hearth furnace, and crucibles. The iron ore was charged with charcoal, and later, according to the type of gangue material, with other fluxes, into a hearth or the shaft of a furnace. The charcoal was burned by a blast caused either by a natural draught (convection) or by hand- or foot-operated bellows. The rising combustion gases dry the materials (Figure 6.5), and reduce the ore at ca. 900–1100 °C, forming a primary slag of wustite (FeO). From the gangue, a molten liquid slag forms, from which, in a further reduction stage, pure solid iron separates out, with formation of secondary slag. Since no appreciable carbonization of the iron takes place, it does not liquefy, even in the lower part of the furnace (temperature ca. 1200–1300 °C). The product, the so-called bloom, consists of iron with slag inclusions and residual charcoal. These were separated, and the blooms were reheated and forged into bars. Up to the late Middle Ages iron, or rather steel, was obtained exclusively by this process directly from the ore, except in China. As a result of improved bellow technology, the furnace volume grew. About 900 years ago, this development culminated in bloomery furnaces with reached heights of 4 m, thanks to the wind pressure from waterwheel-powered bellows.

In addition to the technique of iron winning, knowledge of the properties of iron and how to modify them also developed empirically and involved little understanding of cause and effect, even up to the 1700s. It was recognized at an early stage that iron could be hardened by heating (with carburization) followed by rapid cooling. As early as the 900s B.C. crucible furnaces were used for carburizing iron in Gerar, Palestine. Moreover, the technique of combining high- and low-carbon steels was used to achieve a desired combina-

tion of properties, such as toughness and hardness, e.g., in the production of Damascus steels.

6.2.2 From the Middle Ages to the 1800s

In the 900s, technology was revolutionized by the waterwheel, with far-reaching effects on iron production. Water power became more important than the availability of ore when choosing the location for iron smelters. Thus, the preferred smelter location changed from the mountains, with proximity to ore and wood, to the river valleys, with their availability of flowing water.

The blast produced by water-driven bellows enabled larger furnaces to be operated. These were originally bloomery furnaces, but became flowing furnaces in the 1100s and 1200s. Water power was also used to operate tail hammers, lift hammers, etc. This development took place almost simultaneously in the alpine regions, and in western and northern Europe, which is not surprising in view of the

extensive trade in medieval Europe. The historical development of iron and steel production equipment, and the growth of total world steel production, is summarized in Figure 6.6.

6.2.2.1 Bloomery Furnaces

In principle, bloomery furnaces were simply an increase in furnace size. They were up to 6 m high, operated batchwise, and produced a bloom up to 100 kg after ca. 15 h operation. The earlier furnaces produced a bloom of only 20 kg. Refining the blooms is a two-stage operation: a metallurgical treatment in the refining furnace (slag removal, homogenization, and, if necessary, decarburization); followed by hammering into bars, and a mechanical mixing operation in which bars of steel of various qualities are hammered together, forming a fairly uniform product. Bloomery furnaces, like the small Corsican and Catalan forges that used the same principle, were still producing a small fraction of the total production up to the 1800s. The production of steel by the direct method is currently undergoing a renaissance.

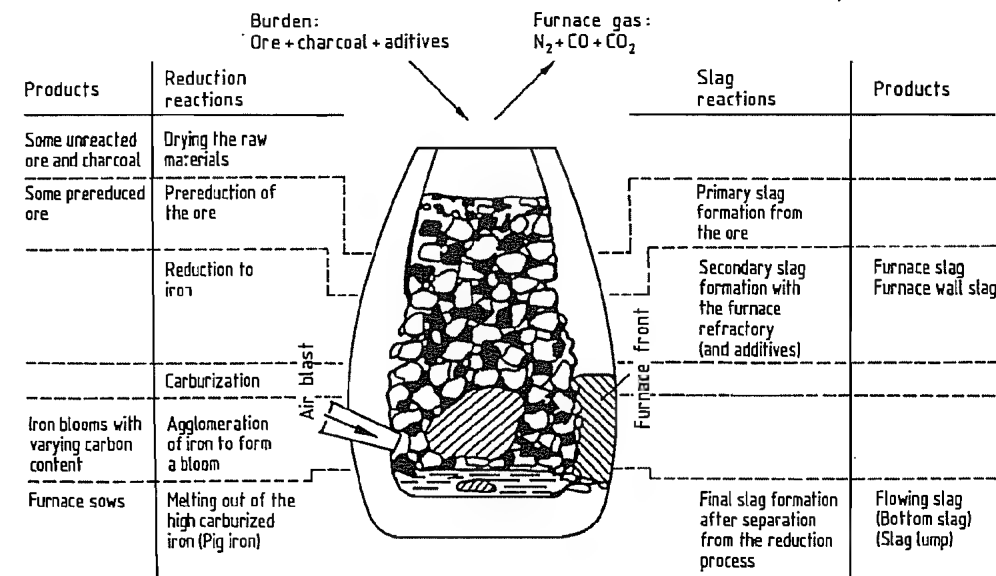


Figure 6.5: Furnace reactions for the production of iron by the direct method in a bloomery furnace (after D. HORSTMANN).

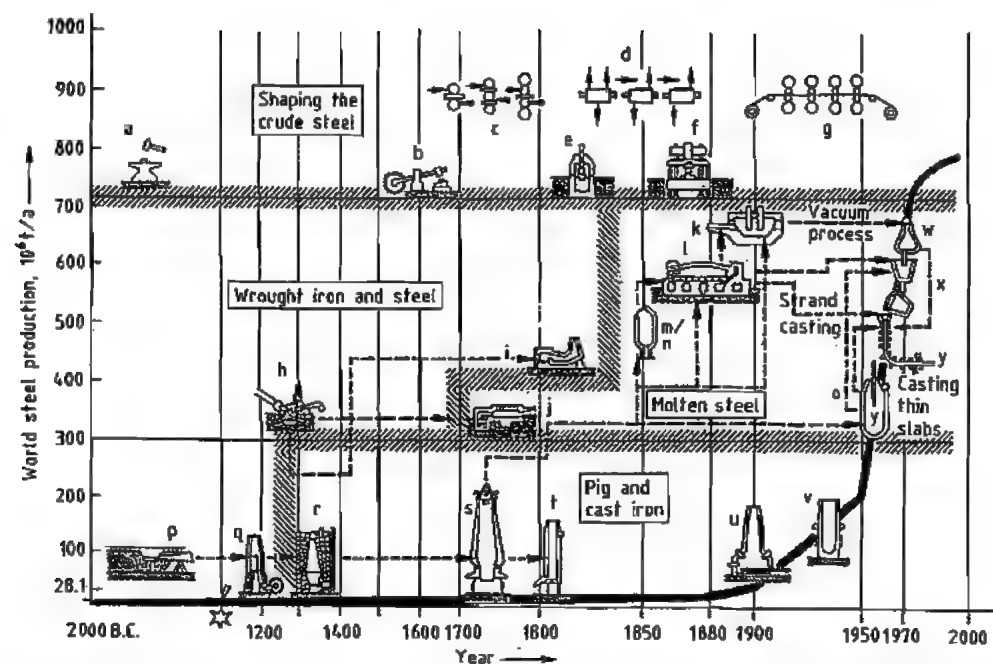


Figure 6.6: Development of steel production processes and forming, with a graph of annual steel production [13]: a) Hammer and anvil; b) Tail hammer; c) Two-, three-, and four-high rolling stands; d) Open rolling mill; e) Steam hammer; f) Forging press; g) Continuous rolling mill; h) Finery fire; i) Puddling furnace; j) Crucible furnace; k) Electric furnace; l) Open hearth furnace; m) Bessemer converter (acid lining); n) Thomas converter (basic lining); o) Oxygen steelmaking converter; p) Finery fire; q) Bloom furnace; r) Charcoal blast furnace; s) Coke blast furnace; t) Cupola furnace; u) Electric shaft furnace; v) Low shaft furnace; w) Vacuum degassing; x) Continuous casting; y) Thin slab casting.

6.2.2.2 Blast Furnaces

Together with the use of water power, the main revolution in iron smelting in Europe was the discovery of the two-stage indirect production of steel – the method still used today. In the first stage, liquid pig iron with a high carbon content is produced in the blast furnace. In the second stage, this pig iron is decarburized and refined to steel in a finery fire. The improved air pressure and flow rate enabled furnace temperatures $> 1200^\circ\text{C}$ to be achieved. The furnace volume could be increased, leading to a longer dwell time for the burden as it passed down the furnace shaft. This led to improved reduction of the iron ore (the yield increasing from 50 to $> 85\%$), and carburization of ca. 2.5–5.0%. The lowering of the melting point led to the production of liquid pig iron for the first time, and consider-

ably improved output. The furnaces could be charged without interrupting the process, and the liquid iron was directly cast into finished products (furnace plates and cannon balls) or bars for sale or captive processing in the finery shown. Here, the crushed pig iron was smelted in the finery hearth and decarburized under an oxidizing slag. Steel blooms were formed from the molten metal as it thickened, and these were then hammer forged into semifinished products. The furnace workers were able in some degree to control the properties of the product, but their empirical knowledge was mainly limited to processing certain types of ore or pig iron. An example is Osemund iron, which was ductile and, therefore, used for wire production. Steel production and processing centers were established in Austria, France, Belgium, United Kingdom, Germany, Sweden, and Russia. Iron production in Eu-

rope increased from 20 000–30 000 t/a (when small blast furnaces were introduced in ca. 1200 A.D.) to ca. 150 000 t/a at the inception of coke-based metallurgy in the mid-1700s.

6.2.2.3 Metal Shaping

Up to the 1500s, iron was processed only by forging and drawing, but, as the indirect method of iron production became widespread, water-powered rolling mills came into use. However, production rates of the blast furnace, the finery fire, and the hammer forge were roughly comparable, and hot rolling was unable to produce a product comparable to forged steel. Therefore, hot rolling was only occasionally used for the treatment of forged material. Its most important application emerged later in the so-called iron-splitting works, in which strips were produced from steel sheet (e.g., for nail production). These operations were common in almost all iron-producing countries until the mid-1600s.

The range of rolled products increased during the early 1700s. In Sweden, CHRISTOPH POLHEMUS was able to produce rolled steel with various profiles for knife blades and files. In England, JOHN HANBURY produced thin steel sheet on a pillar rolling mill for tinplate manufacture. This type of equipment was being used for the manufacture of steel sheet for steam boilers by 1764 at the latest. In the same year, JOHN PAYNET obtained a patent for the preforming of flat bar by grooved rolls, and JOHN WESTWOOD was awarded a patent for cold rolling in 1783. In 1778, the Frenchman FLEUR described a four-stand rolling mill with closed passes which he used for wire production. Proposals for continuous rolling were also published.

Apart from the iron bearings, rollers, cutting rings, and spacers, the rolling mills were constructed of wood. In the mid-1700s, gear wheels and pillars were all of cast iron. Energy was supplied by one or two waterwheels, depending on the size of the rolling mill. The upper and lower rolls were generally driven separately, but pinion stands were also used. The mechanical and thermal stresses on the

rolls were large. At first the rolls were made by welding a hardenable steel sheet around the forged roll body. Later, cast iron rolls were used. A further development was the casting of steel around a bar which was used as roll neck.

Rolling mills did not yet replace hammer forges, as their use was limited by the quality of the engineering and the availability of power.

6.2.3 The Industrial Age

The 1700s saw the development of mechanical power (steam engines), transport (railways, bridges), and the increasing use of machinery, all of which was made possible only by the almost complete replacement of wood by steel as a construction material. The resulting enormous increase in demand provided the impetus for the development of new methods for bulk steel production.

Iron and steel were produced exclusively from charcoal up to the 1700s, but by the end of the century, processes had been developed that enabled charcoal to be replaced by coal. These were coke-based metallurgy and the crucible steel and puddling process, supplemented by the development of the hot rolling process. They formed the basis for the economic mass production of this universal construction material, which satisfied the broad requirements of the approaching industrial era.

During the preindustrial epoch, most of the improvements in steel production methods took place on the European mainland, but the inventions that led to the industrial revolution were made in Britain. These are linked with the following names:

- ABRAHAM DARBY II (1711–1763) who introduced the first true coke-based blast furnace (1735) and the first use of steam engines (1742) to steel production
- BENJAMIN HUNTSMAN (1704–1776) – crucible steel casting (1742)
- HENRY CORT (1740–1800) – development of the puddling process (1783–1784)

- JEAN BEAUMONT NEILSON (1792–1865) – hot air blast (1829)
 - JAMES NASMYTH (1808–1890) – steam hammers (1839), first installed at Creusot (1841)
 - HENRY BESSEMER (1813–1898) – acid air refining process (1856–1860)
 - SIDNEY G. THOMAS (1850–1885) and PERCY C. GILCHRIST (1851–1935) – basic refining process (1878)
 - WILHELM SIEMENS (1823–1892) and FRIEDRICH SIEMENS (1826–1904) – regenerative heating (1861)
- Important innovators in other countries include:
- FABER DU FAUR (1786–1855) – blast heating (1832)
 - PIERRE-ÉMILE MARTIN (1824–1915) – open hearth process (1864)
 - RAINER DAELEN (1813–1887) – universal mill stand (1848)
 - CHARLES MORGAN (1831–1911) – rolling mill technology (from 1865)
 - GEORGE BEDSON – continuous rolling mills (1860)
 - REINHARD MANNESMANN (1856–1922) and MAX MANNESMANN (1857–1915) – rolling seamless tubes (1890)
 - PAUL HÉROULT (1863–1914) electric arc furnace (1900)

These innovations were gradually introduced into the most important iron-producing countries, including the United Kingdom, Belgium, France, Germany, Austria, and the United States, all of which made their own contributions to the further development of iron and steel technology. Historically, the last pioneering inventions are the basic oxygen steelmaking process, secondary metallurgy, and continuous casting, which were developed in the 1940s and 1950s.

6.2.3.1 Pig Iron Production

The cradle of coke-based metallurgy was Coalbrookdale, where ABRAHAM DARBY I (1678–1717), who had invented the process of casting iron in sand molds in 1707, probably began the production of pig iron using coke in 1709. His son, ABRAHAM DARBY II, was the

first to operate a blast furnace fueled entirely with coke in 1735. Coke-based metallurgy spread to the rest of the United Kingdom only slowly at first (in 1750, 3 of 74 blast furnaces were coke based; in 1760, 14 of 78; in 1791, 85 of 107). The real breakthrough came with the development of the puddling process for converting pig iron into steel, the production rate matching that of the iron-making process. In mainland Europe, these new technologies were adopted in a dilatory fashion. The first coke-based blast furnaces were operated in France by CREUSOT in 1785, and in Germany in Gleiwitz (1796). Whereas pig iron production in the U.K. was almost exclusively based on coke in the early 1800s, Germany reached this stage only at the end of the century.

From the early 1800s, coke-based metallurgy was accompanied by research and development, with increases in productivity and profitability. Developments were mainly concerned with the design and size of blast furnaces, including blast and power supplies, increasing the efficiency of energy utilization, and improving yield and quality through better understanding of the metallurgical processes, enabling the control of the blast furnace process to be improved, culminating in computer control. This development can be demonstrated by data for selected blast furnaces (Table 6.3).

6.2.3.2 Steel Production

After the invention of the pig iron furnace, forgeable and hardenable iron (steel) was produced both from almost carbon-free wrought iron and from highly carburized pig iron.

Wrought iron, in the form of soft iron bar, was carburized to steels with a higher carbon content from the early 1600s (originally in 1601 in Nuremberg by PAULUS HANNIBAL) by heating in carbon-containing powders with exclusion of air. This so-called cemented steel had a wide range of uses, e.g., for springs, knives, and files. In the 1700s, the steel industry in Sheffield was founded on the use of this process for the treatment of imported Swedish iron bars. Here, 205 cementation furnaces pro-

duced almost 80 000 t steel in 1862. The last of these went out of production in 1951. This cemented steel (blister steel), which was inhomogeneously surface-carburized and blistered, was homogenized by hammering out (sometimes repeatedly) bundles of cemented steel rods to form “shear steel”. Although this led to some equalization in material properties, this steel met the increasing quality requirements only to a limited extent.

Crucible Steel

The first decisive step toward production of nearly homogeneous and slag-free steel was taken by BENJAMIN HUNTSMAN in 1740, with the production of liquid steel by melting together cement steel with added bar iron and glass in refractory crucibles. The productivity of this process was later increased by improvements to the crucible material (graphite). Crucible steel opened up completely new perspectives. The steel was both castable and forgeable. By pouring the contents of several crucibles into one mold, ingots and castings of large mass were produced for the first time. As alloying was possible, steel developed into a universal construction material. As this process was more economical than the production of shear steel, it spreads relatively rapidly.

Puddled Steel

Pig iron from the small furnaces that later developed into blast furnaces was cast, either directly or after remelting, in a cupola furnace

to give finished products (e.g., machine parts, construction elements, household articles) or was decarburized to forgeable steel. The steel produced by decarburizing coke pig iron tended to be brittle (owing to sulfur and phosphorus) compared with that produced from charcoal pig iron. The low productivity of decarburization in open charcoal-fired finery fire became a problem, owing to the increasing rate of production of pig iron; steel producers sought a more effective fining process that would operate with coal or coke. The breakthrough was achieved by HENRY CORT with his patented method (1783–1784) for producing wrought steel – the puddling process. This consisted of remelting the pig iron and fining with the combustion gases from the coal- or coke-fired reverberatory furnace (Figure 6.7), followed by mechanical slag removal and welding together of the lumps of steel by means of a steam hammer or squeezer to form blooms of very variable chemical analysis. These were rolled in a rolling mill to form “crude” flat iron. To produce a homogeneous rolled steel, fagots of flats were placed together, heated in a welding furnace, and rolled. This step could be carried out several times. The process met all requirements of the time, i.e., increase in productivity (tenfold), replacement of charcoal by coal, and reduction of production costs. It spread relatively rapidly into all iron-producing countries. In Germany, the first puddling plant was started in the Rasselstein iron works in 1824. The last puddling operation ceased in the 1940s.

Table 6.3: Development of blast furnaces.

Year and location	Hearth area, m ²	Coke consumption per tonne iron, kg	Iron output, t/d
1796 (Gleiwitz)	0.3	3500	1–2 (later 4)
1801–1815 (U.K.)		2500	5–7
1856 (Hasslinghausen)	3.6	1600	20–23
1880 (United States)	8.8	1510	120
1901 (United States)	15.3	1000	464
1929 (Bruckhausen)	33.2	740	1100
1993 (Schwelgern 2)	174.9	480*	10 600

* Fuel consumption.

Ingot Steel

With time the puddling process also became unable to meet the increasing demand for steel. In 1856, HENRY BESSEMER invented his autothermic air refining process, which made it possible for the first time in the history of iron production to convert pig iron directly into liquid steel, increasing productivity by a factor of 70 (Figure 6.8). In the Bessemer process, molten pig iron is blown with air from below in a tiltable converter. The molten metal is decarburized by oxidation, which also removes silicon and manganese. The heat liberated causes the temperature to rise well above the melting point. As the original lining of the converter was acidic, only low-phosphorus pig iron could be treated, and the use of the process was therefore limited. This problem was solved in 1878 by SIDNEY G. THOMAS and PERCY C. GILCHRIST by the use of basic dolomite as converter lining. Thus, phosphorus could be removed by means of a basic slag, which later became an important fertilizer (Thomas slag). The Thomas process was widely used, especially on the European mainland, where the ores, e.g., minette (oolitic iron ore), often have a high phosphorus content. In

Germany, the first Thomas steelwork was operated in 1879. The last one was shut down only very recently.

Ingot steel production by air refining became the most important steel production process worldwide with the introduction of the basic oxygen (LD, Linz-Donawitz) process in 1952.

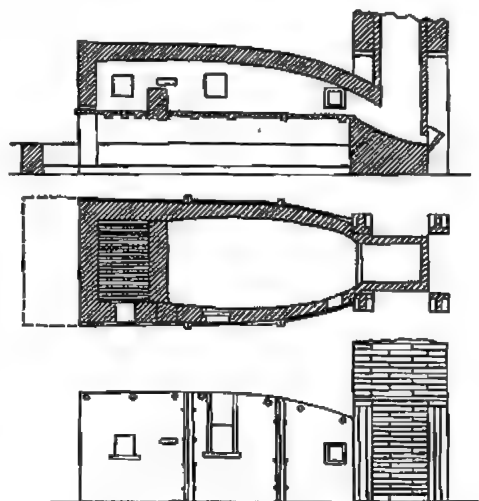


Figure 6.7: Puddling furnace with iron hearth and cast iron shell (1830) [14].

Figure 6.8: Bessemer steel works with circular casting pit (Friedrich Krupp, Historical Archive, 1970).

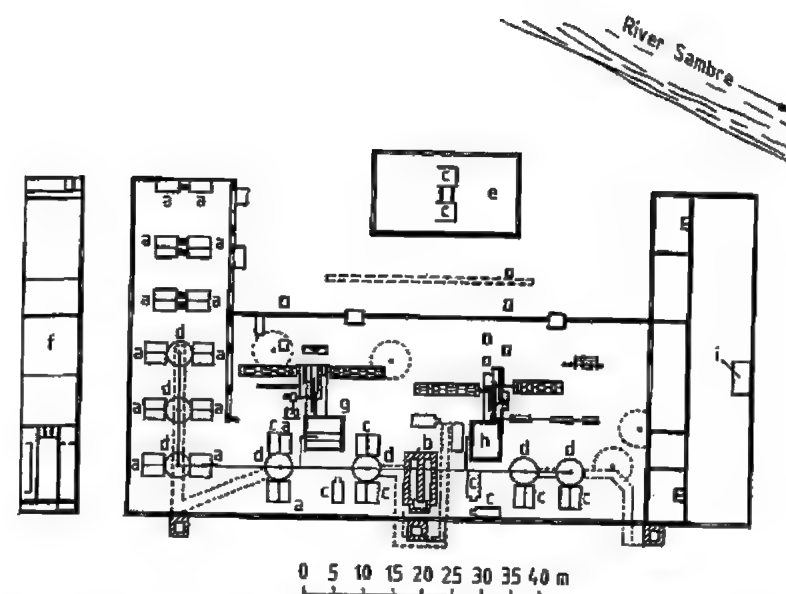


Figure 6.9: Ground plan of rolling mill at Couillet (1835) [15]: a) Puddling furnace; b) Coal-fired boiler; c) Welding furnaces; d) Waste heat boilers; e) Finishing drop; f) Workshops; g) Machine 1; h) Machine 2; i) Stores.

In parallel with the air-refining processes, the aliothermic hearth process was also developed. In 1864, F. and W. SIEMENS together with E. and P. MARTIN succeeded in melting pig iron and steel scrap, using regenerative heating in a reverberatory furnace. The Siemens-Martin process at first achieved great importance for the recovery of scrap. Later, pig iron was melted with iron ore, with or without the addition of steel scrap. Until the breakthrough achieved by the oxygen refining process, this was the most important steel production process, accounting for up to 60% of all steel production.

After the 1850s, electrical energy became available, and attempts were made to build electric hearth melting furnaces. The electric arc furnace developed by HÉROULT was especially successful, and was first operated full-scale in Germany in 1906. Although it was initially used for the production of special steels, it is now increasingly used only for steel melting, owing to the availability of cheap electricity, and the introduction of secondary metallurgy.

6.2.3.3 Rolled Steel Production

Puddled Steel and Steam Power

Following the discovery of (1) the puddling process, which enabled iron to be converted to the finished product by a rolling operation; and (2) the introduction of the steam engine, the technology of the rolling mill became an integral part of steel production.

Although this new technology was quickly adopted and further developed in England, this only happened in a few places, owing to the high cost of steam engines. As early as 1784, J. WILKINSON started the first steam-driven rolling mill in his iron works in Bradbury, and replaced the hammer forge by a blooming mill with self-adjusting rolls. This was patented in 1792. There followed improvements in rolling equipment, by making it more powerful (the production of cast machine components of ever-increasing size, and the development of techniques for gearing and driving). This can be seen from the dimensions of the rolls, which reached diameters of 300 mm and body widths of 1200 mm.

On the basis of these new methods, England's iron and steel industry occupied a leading position throughout the 1800s. Continental iron producers were able to adopt the new technology only later, sometimes only by industrial espionage or by the enticement of specialist personnel. The major economic incentive was the immense demand for railway track.

The plan view (Figure 6.9) of the rolling mills at Couillet (1835) shows the layout of a typical works of that time. The puddling and rolling plants formed a single unit. The steam engines were at the heart of the ironworks. They drove the puddling plant and rail mill, the three-stand sheet mill, the six-stand bar mill, a two-stand mill for rolling-cutting, and an auxiliary plants. This works produced ca. 10 000 t rolled steel in 1840.

Ingot Steel and Mass Production

The further development of rolling mills took place against the background of the developing mass production of ingot steel. The first product became the cast steel ingot. Developments took place particularly in drive technology and the construction of specialized rolling stands and mills (and also auxiliary machinery and reheating furnaces which are not considered in this article). The realization of reversible operation of rolling stands driven by steam engines was the trigger for the further improvement of the driving machinery. In the 1870s, hydraulic friction coupling for reversible operation was successfully designed and constructed. However, almost 30 years of development were required before the problem of reversing the steam-driven rolling mill engine was solved by CLEMENS KISSELBACH in 1891. The use of electrical driving machinery, which began in 1900, increased, especially after the invention of the reversible electrically driven rolling mill engine by ILGNER in 1902.

The design and construction of rolling mills and plant was driven by the demand for mass production, with increasing throughput, size, and range of products. The American, JOHN

FRITZ, in 1857, eliminated the need for reversible rolls by designing and successfully operating a three-high rolling stand for rail production. In 1848, RAINER DAELLEN built the first universal rolling stand, which found wide application, especially in the United States. Using this equipment, finishing of I-beams was first achieved in 1866. In 1883, I. J. SEAMAN and H. SACK separately applied for patents for universal rolling mills for rolling beams. Wire and rod steel products were rolled in open rolling trains. The introduction of mechanical loopers in 1877 led to a considerable increase in performance. At the end of the 1860s, G. BEDSON constructed the first continuous finishing train for wire, with 16 alternately horizontal and vertical rolling stands. This type of train was further developed, mainly by C. MORGAN in the United States. In 1905, in Gary, Indiana, the first train operating completely continuously from ingot to finished product was commissioned. From the early 1800s, a large number of proposals for the production of seamless tubes by rolling were made. However, the breakthrough was an invention by M. and R. MANNESMANN, in which a hollow body was produced by skew rolling (1886), with subsequent expansion to form a seamless thin-walled tube in the Pilger step-by-step-type seamless tube rolling mill (1890). The development of flat rolling aimed to increase the dimensions of strip and sheet, the weight of charge, and productivity. The United States led the way, and the first continuous hot strip mill went into operation during the 1920s. These mills constitute as important a development for modern steel production as the oxygen steelmaking process, secondary metallurgy, and continuous casting.

6.3 Crude Steel Production

6.3.1 Raw Materials

The following iron-bearing materials are used for crude steel production (Table 6.4) [16]:

- Molten iron from blast furnaces (hot metal), mainly used for steel production by the basic oxygen furnace (BOF) process
- Scrap, sponge iron, and solidified blast-furnace iron (pig iron), mainly used for melting steel in electric furnaces

Another important raw material is lime for slag formation. Alloying elements, such as chromium, nickel, molybdenum, titanium, vanadium, and niobium, and elements used as deoxidizing agents (e.g., manganese, silicon, and aluminum) are not discussed in detail here.

The most important iron-bearing material is hot metal. Of the total world crude steel production of 770–720 t/a in the early 1990s, ca. 60% was produced from hot metal obtained by reducing iron ore, and ca. 40% from steel scrap. Steel scrap is of increasing importance as a raw material because of the lower primary energy consumption and lower CO₂ emissions, compared with the blast furnace–converter production route. Figure 6.10 compares the total specific primary energy consumption per tonne of steel produced from ore with that for steel produced from scrap [17].

Table 6.4: Properties of hot metal, sponge iron, and scrap [16].

	Hot metal	Sponge iron	Scrap
Raw materials	poor to rich ores, low or high in phosphorus	ores with low gangue content	internal scrap production scrap collected scrap
Availability	almost unlimited	limited to low gangue ores or pellets	depends on steel consumption and crude steel production
Production and processing	classification, sintering, pelletizing blast furnace	classification or pelletizing shaft furnace rotary furnace retort fluidized bed	shears (cutting–burning)
Primary energy consumption (GJ/t)	14	12 (shaft furnace)	0.6 (shredder)
State of aggregation	liquid	solid	solid
Storage and transport	severely limited	special techniques may be necessary (e.g., briquetting)	good
Type of furnace using this material	oxygen-blowing furnace (BOF) (electric furnace)	electric furnace (as cooling agent in oxygen furnace)	electric furnace Siemens–Martin furnace (as cooling agent in oxygen furnace)
Price	depends on production costs	depends on production costs, market price, or agreed price	market price
Chemical properties			
Composition	constant	constant	variable
Unwanted elements	sulfur phosphorus (depends on application)	none phosphorus (depends on application)	depends on process
Type of gangue		depends on ore	
Physical properties	liquid	bulk material	variable shredded scrap (in bulk)
Bulk density		> 12 t/m ³	fluctuates around 1.2 t/m ³ depending on type of scrap
Thermal conductivity		low	high

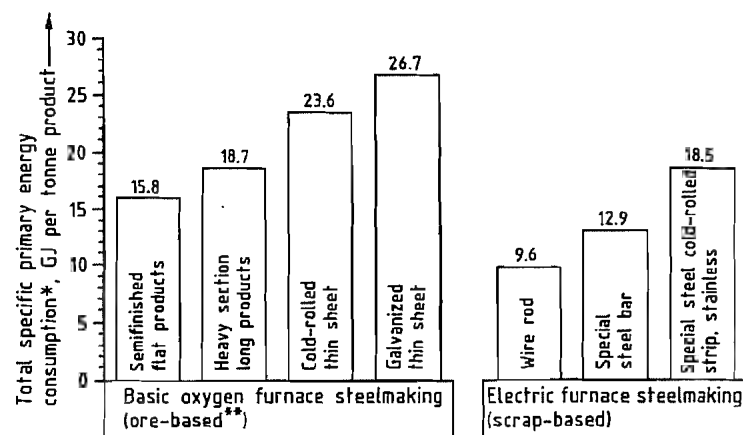


Figure 6.10: Comparison of total specific primary energy consumption for steel products made from ore and scrap [17].
* Including primary energy consumption for generating electricity in thermal power stations, and energy-intensive materials (oxygen, steam, compressed air, cooling water, etc.); ** Including added scrap for cooling.

Table 6.5: Characteristic compositions of grades.

Type of pig iron	C, %	Si, %	Mn, %	P, %	S, %
Low-phosphorus	4.0–4.5	0.30–0.70	0.20–0.70	0.05–0.12	0.03–0.06
High-phosphorus	3.2–4.0	0.30–0.70	0.25–1.20	1.50–2.20	0.03–0.06
Foundry	3.5–4.2	1.80–2.50	0.70–1.00	0.50–0.70	0.03–0.06

6.3.1.1 Hot Metal

Hot metal is produced by reduction of iron ore in a blast furnace. Modern furnaces produce 5000–12 000 t/d. Immediate transfer of the hot metal to the converter for refining to crude steel requires the blast furnace and the steelworks to be in close proximity.

Iron ore is charged to the blast furnace in lump form or as agglomerated fine ore (sintered or pelletized), and reduced. Coke and injected coal are used as reducing agents, and these react with the hot air blast, liberating energy. The molten product, known as hot metal, separates from the liquid slag. It can be pre-treated before transfer to the steelworks, to reduce the content of undesired accompanying elements such as sulfur, silicon, and phosphorus.

Various types of hot metal are produced, depending on the composition of the ore fed to the blast furnace (burden) and the method of furnace operation. They include low-phosphorus hot metal, (Thomas) hot metal (high in phosphorus), and foundry hot metal (high in

silicon). The chemical compositions of several grades of hot metal are listed in Table 6.5.

Low-phosphorus hot metal is important for steelmaking. Typical temperatures for tapping the blast furnace are 1350–1450 °C. Carbon content is typically high (4–4.5%), as is sulfur content, these elements being picked up from the coke and the injected coal. A pretreatment of the hot metal, e.g., with lime-magnesium mixtures, reduces the sulfur content from ca. 0.040% to <0.010%.

Pig iron is also used to a limited extent as an iron-bearing material for steel production involving melting; the hot metal, after tapping from the blast furnace, is cooled in sand molds to form pigs which can be used like scrap in steel production.

Hot metal is produced not only by the blast furnace method, but also in coke-free processes in smaller units by smelting reduction, e.g., the Correx process, which produces 1000–2000 t/d [18].

6.3.1.2 Scrap

Steel scrap is traded worldwide [19]. It is mainly melted in electric furnaces, but to a limited extent is also added as a cooling agent to converters used in steel production by blowing processes. In 1992, ca. 350×10^6 t steel scrap was used worldwide for steel production, the specific scrap consumption being ca. 445 kg per tonne of crude steel. Specific scrap consumption differs widely between countries, depending on the structure of the steel industry [20, 21]. In Italy, where the proportion of electric steel production is 50%, the proportion of scrap used, ca. 650 kg per tonne of crude steel, is naturally larger than in Germany (ca. 380 kg/t), which has 21% electric steel production (Figure 6.11).

The total quantity of scrap handled on world markets is ca. 50×10^6 t/a. A survey of the most important exporting and importing countries is given in Table 6.6. The price of scrap fluctuates widely, depending on supply and demand. Figure 6.12 gives an example of the fluctuations in the price of a particular grade of scrap in the Ruhr region.

Scrap is classified according to its origin: internally recycled scrap; production scrap from the steel processing industry, also known as new scrap; and collected scrap, also known as old scrap.

Internally Recycled Scrap. Improvements in the utilization of materials and technological changes, e.g., the introduction of the strand casting process, have steadily reduced the availability of internally recycled scrap in recent years (Figure 6.13) [22].

New and Old Scrap. To meet the requirements of steelworks, internally recycled scrap is supplemented by the purchase of new and old scrap. To maintain steel production quality, the quality of these purchased materials is controlled by lists of scrap grades. Criteria include the metallic iron content (e.g., > 92%), the lump size, the bulk density (e.g., > 0.9 t/m³), and the density of bundles (e.g., > 1.3 t/m³).

Current proportions are ca. 50% from old scrap, 15–20% from new scrap, and 30–35% from internally recycled scrap.

The quantity of scrap available worldwide depends on the quantity of crude steel produced, although there is a time delay. Whereas internally recycled and new scrap are immediately returned to the system, an average of ca. 70% of used steel products are returned as old scrap after ca. 20 years [19, 20]. On the basis of this assumption, H. W. KREUTZER has shown how the total world supply of old scrap has changed with time (Figure 6.14). In line with steel production figures which increased steadily in former years, the availability of old scrap at first continues to increase, but then levels out after ca. 20 years.

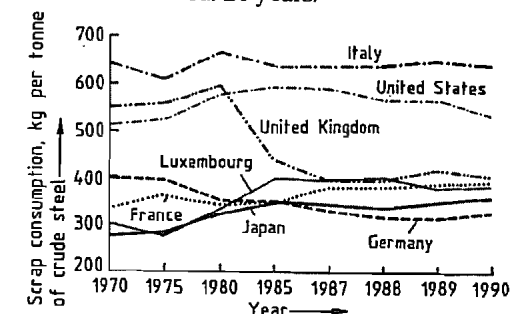


Figure 6.11: Average specific scrap consumption for crude steel production in various countries [21].

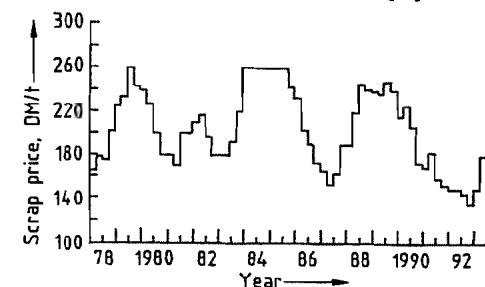


Figure 6.12: Variations in scrap prices since 1978 [20].

Table 6.6: Balance of exports and imports for several countries in 1991 [21].

	Export balance, 10^6 t	Import balance, 10^6 t
United States	8.28	
Germany	7.63 ^a	
United Kingdom	3.12	
France	2.31	
Japan	1.48 ^a	
European Community	1.96	
Taiwan		2.19
South Korea		3.49
Spain		4.27
Turkey		4.44
Italy		6.03
Developing countries		10.30

^aData for 1992.

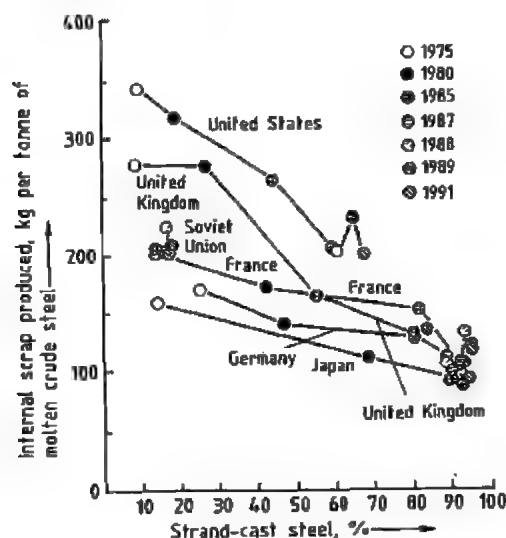


Figure 6.13: Variations in the specific amount of internal scrap produced in various industrialized countries as a function of the percentage of strand casting [22].

It is important that scrap should not introduce unwanted elements into the steel, thereby impairing its quality. Pretreatment of the scrap by size reduction and sorting, e.g., with the aid of a shredder, is therefore very important. It is essential not to introduce elements that cannot be removed from the crude steel, or whose removal is costly, e.g., copper, nickel, molybdenum, or tin. In some steel products, a copper content of 0.40% is tolerable, but in high-

quality products, e.g., thin steel strip, the copper content is normally $< 0.01\%$. Therefore, when recycling scrap automobiles, copper-containing components such as electric motors and cables must be stripped out before scrapping. On the other hand, when zinc-coated car bodies are recycled, the zinc becomes concentrated in the steelworks dust, and can be easily recycled, if the levels of zinc in the dust are high enough (ca. $> 20\%$). So far, this has been achieved in electric steelworks owing to the high input of scrap [23]. The zinc is recovered from the dust in nonferrous metal smelting works.

Table 6.7 shows the maximum tolerable total content of Cu, Sn, Ni, Cr, and Mo for a number of steel products, and some typical concentrations of these elements in the raw materials pig iron, sponge iron, and five different types of scrap.

6.3.1.3 Sponge Iron

Another solid raw material for the steel industry is sponge iron, also known as DRI (direct reduced iron). Because of its purity and suitability for controlled feeding, it is becoming of increasing importance.

Table 6.7: Residuals in steel and its raw materials [24].

	Cu + Sn + Ni + Cr + Mo, %
<i>Typical maximum residual limits of carbon steels</i>	
Thinplate for draw and iron cans	0.12
Extra deep drawing quality sheet	0.14
Drawing quality and enameling steels	0.16
Commercial quality sheet	0.22
Fine wire grades	0.25
Special bar quality	0.35
Merchant bar quality	0.50
<i>Typical residual content of charge materials</i>	
Direct reduced iron	0.02
Pig iron	0.06
No. 1 factory bundles	0.13
Bushelling	0.13
No. 1 heavy melting	0.20
Shredded auto	0.51
No. 2 heavy melting	0.73

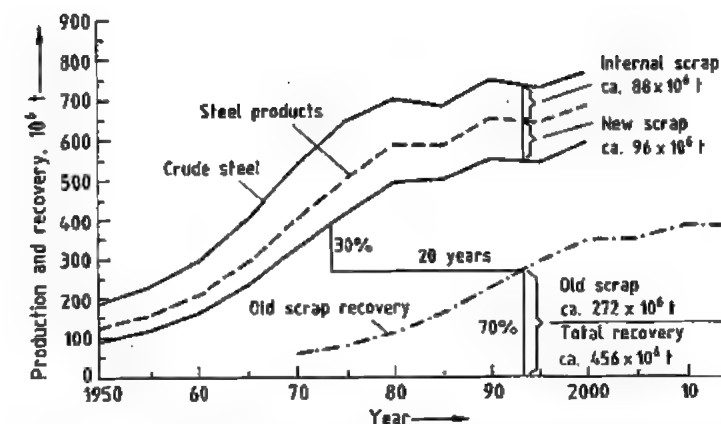


Figure 6.14: World crude steel production, with a forecast of old scrap availability up to 2015 [20].

Table 6.8: Processes for the direct reduction of iron ores.

Reduction by gases	Reduction by solids
Shaft furnace: Midrex Hyl III	Rotary kiln: SL/RN Krupp-Codir
Fluidized bed: FIOR Iron carbide	Rotary hearth furnace: Inmetco Fastmet

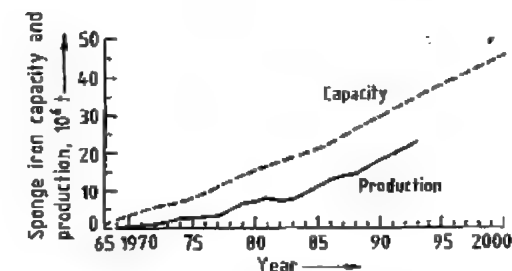


Figure 6.15: Growth of production capacity and production of sponge iron [25].

Sponge iron is produced by reduction of iron ore in the solid phase, by means of (1) reduction gas (obtained from natural gas with varying hydrogen and carbon monoxide content); or (2) coal. Of the direct reduction processes listed in Table 6.8, the Midrex and Hyl processes are the most important. Gas reduction processes account for 92% of world sponge iron production. Direct reduction processes are operated where cheap energy is available (natural gas, coal), e.g., Mexico, Venezuela, Saudi Arabia, Iran, Malaysia, Indonesia, India, and South Africa.

Figure 6.15 shows the growth of the capacity and production rate of sponge iron [25]. In 1993, total production was 23.9×10^6 t while capacity was ca. 35×10^6 t, i.e., production plants were only 68% utilized. A further increase in world sponge iron capacity of at least 12×10^6 t/a is forecast for the year 2000.

The sponge iron produced is mainly melted in adjoining steelworks, so that amounts available on the world market are limited. Approximately 3.4×10^6 t sponge iron was exported in 1992 [26]. However, there is an increasing trend toward the construction of "merchant plants", e.g., in Malaysia and Venezuela.

These types of sponge iron could be of great interest for reducing levels of unwanted elements by replacing some of the scrap used in the production of scrap-based, high-grade steel products, especially flat products produced in minimills.

Because trade in these materials has so far been small, no lists of grades or general regulations exist for sponge iron supplies, such as apply to scrap. Important characteristics include the total iron content, the ratio of metallic iron to total iron, the gangue content, and the carbon content. As all the gangue constituents report to the sponge iron, ores low in gangue, or specially produced pellets, are used. Otherwise, additional energy must be used to melt the gangue when melting sponge iron. The metallic iron/total iron ratio should, therefore, preferably be $> 92\%$. The carbon

content of sponge iron from the gas reduction process is 1–2.5%, which is higher than the typical value for sponge iron produced by the coal reduction process (0.1–0.2%). A high carbon content can help to reduce the consumption of electrical energy for melting if the carbon is burned with air or oxygen to form carbon monoxide, which is post-combusted in the melting plant. New developments in direct reduction involve the production of iron carbide, which should give a carbon content of > 5% of the DRI [27].

Table 6.9 gives typical figures for the composition of a Midrex sponge iron (gas reduction in a shaft furnace) and an SL/RN sponge iron (solid state reduction with coal in a rotary kiln). Table 6.10 gives typical figures for bulk density, lump density, and porosity of sponge iron produced from lump or pelletized ore, and for briquetted sponge iron [16].

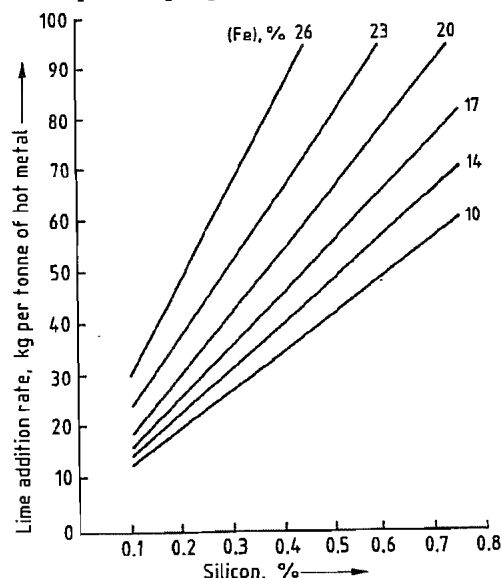


Figure 6.16: Required rate of addition of lime as a function of the silicon content of pig iron and iron content of slag [29].

When transporting and storing porous sponge iron, attention must be paid to its tendency to reoxidize exothermically, owing to the large surface: volume ratio. The heat given off can lead to ignition of the sponge iron and to a fire, e.g., during transport. This reoxida-

tion behavior, typical of many types of sponge iron, can be characterized by determining the ignition temperature, the rusting behavior, and the evolution of hydrogen in a moist atmosphere. Safety precautions must always be taken for the transport, loading, unloading, and storage of sponge iron. Regulations and other information relevant to transport by sea have been published by insurance companies. The tendency to reoxidation can be reduced by passivation of the sponge iron. The best method of limiting transport hazards is briquetting.

Table 6.9: Chemical composition of sponge iron [25].

	Midrex	SL/RN
Fe, %	91–93	90.4–93.7
Metallic Fe/total Fe, %	92–95	92–93
SiO ₂ , %	2.0–3.5	2.4–5.8
Al ₂ O ₃ , %	0.5–1.5	1.8
CaO, %	0.2–1.6	0.05–0.3
MgO, %	0.3–1.1	≤ 0.05
C, %	1.0–2.5	0.1–0.2

Table 6.10: Properties of sponge iron [16].

Form	Bulk density, t/m ³	Lump density, g/cm ³	Porosity, %
Lumps	1.9	2–3.5	70–50
Pellets	1.7		
Briquettes	2.5	4.5–6	35–15

6.3.1.4 Lime

Lime is used as a reagent and slag former in steel production. It is the main constituent of the most metallurgically effective slags that combine with the unwanted elements in the steel.

Lime (CaO) is formed on calcination of limestone (CaCO₃) at ca. 1000 °C. Depending on the calcination temperature, calcination time, dwell time in the furnace, and type of gas flow through the furnace, various qualities of CaO can be produced, e.g., soft- or hard-burned lime [28]. The quality requirements of the steel industry include high purity (94–97% CaO), well-defined chemical composition, optimum grain size, and rapid dissolution in the

slag. Calcined (soft-burned) dolomitic limestone is also used in steel production.

In steel production by top blowing with oxygen, the hot metal composition is of the greatest significance when determining the quantity of lime to be added for refining in the converter. The amount required to produce a slag that is slightly supersaturated with respect to lime is illustrated in Figure 6.16, which also shows the iron content of the slag [29]. As well as decreasing the silicon and sulfur content of hot metal, the changes brought about by the introduction of the combined blowing process in the mid-1980s had a further effect in reducing lime content [30, 31]. By bottom blowing with an inert gas to give agitation during oxygen blowing, the reactions approach equilibrium much more closely, and hence a better utilization of the slag is achieved. Figure 6.17 illustrates this trend toward a reduction in specific lime consumption, using German BOF steelmaking as an example. Between 1970 and 1990, specific lime addition was reduced from ca. 70 to ca. 45 kg per tonne of crude steel.

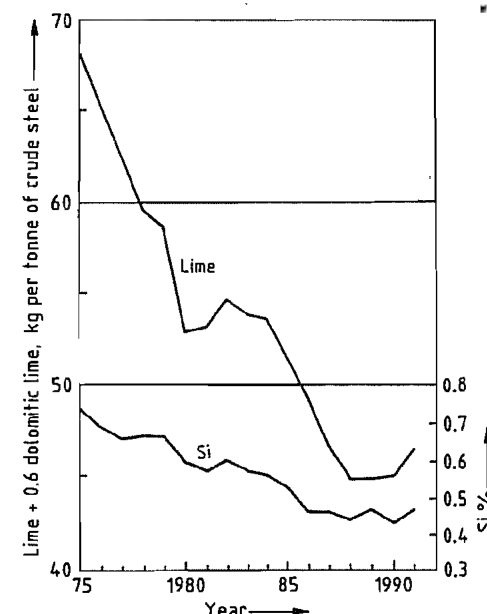


Figure 6.17: Variation in the specific consumption of lime and the silicon content of low-phosphorus pig iron in an oxygen steelmaking plant in Germany (1975–1990).

In electric steel production with scrap addition, the process in the 1970s was mainly to add an oxidizing slag, and then to change to a refining slag. Today, both low- and medium-alloyed steels are produced under one slag. The oxidizing treatment is followed by a reduction phase by the slag. All the other metallurgical operations have been moved to the later processing stages of the secondary metallurgy. Specific lime consumption in steel production in the electric arc furnace is currently 35–40 kg/t. Soft-burned lime usually has lump size 10–30 mm, and should have a sulfur content < 0.02%. With sponge iron instead of scrap, the amount of slag increases, because of the silica introduced with the gangue materials in the sponge iron. The amount of lime added depends on the amount of SiO₂ that is to be re-acted. The slag basicity (CaO/SiO₂) should be 1.5–2.

Modern developments in secondary metallurgy have led to new process steps in the operations that take place between the steelworks and the strand casting plant. Slags, which have become reactive contact phases, are now at the heart of metallurgical research and development. As there are many aims of secondary metallurgy, the slags used can differ widely. Lime-containing slags mostly consist of reactive CaO–CaF₂–Al₂O₃ mixtures for steel treatment in the ladle furnace, for intensive blowing in the ladle, or as a basic covering slag. The compositions of desulfurizing slags are ca. 55–60% CaO, 5–10% CaF₂ and Al₂O₃. Typical lime addition rates are therefore, 10–15 kg/t. As well as the intensive stirring process with synthetic slag, the injection of CaO–CaF₂ mixtures at the rate of 3–5 kg/t is common.

Metallurgical lime must fulfill special requirements for utilization of waste slag from the steelworks [32]. Steelworks slags, when used as hydratable components of building materials, should contain only such levels of lime and free magnesium oxide that volume stability can be absolutely guaranteed. For this reason the relevant specifications limit the free lime content to < 7% or < 4%, according to

the intended use (volume of intergranular free space).

The interests of the steelworks and the slag users coincide with respect to lime [32]. The steelworks require a readily soluble lime for metallurgical reasons. The slag user has problems with volume stability if the solid slag contains lime that failed to dissolve when it was liquid. Therefore, reactive, soft-burned lime should be used for slag utilization reasons.

6.3.2 Physical and Chemical Fundamentals

6.3.2.1 Thermodynamics

Metallic Systems Based on Iron

In steelmaking, the most common accompanying elements in molten iron are C, Si, Mn, P, S, and the gaseous elements H and N. In the reactions that take place when oxygen is brought into contact with the molten materials, the concentrations of the unwanted elements in the iron are reduced to the levels required in the steel produced. The thermodynamic data for metallic systems based on iron, such as solubility and activity, are of fundamental importance for the control of these reactions.

The state of carbon in Fe-C alloys can be seen from the phase diagram (Figure 6.18) [33]. Carbon dissolves in both molten and solid iron. Its solubility in the latter varies according to the crystal structure of the iron. Although carbon dissolves to only a very small extent in α -Fe and δ -Fe, its solubility in γ -Fe at 1153 °C is 2.1%. The solid solution of γ -Fe-C is known as austenite. The solubility of carbon in molten iron is given by the equation [34, 35]:

$$[\%C]_{\max} = 1.30 \times 2.57 \times 10^{-3} t \quad (1)$$

$$t = 1152 - 2000 \text{ } ^\circ\text{C}$$

The solubility of carbon in molten iron is also influenced by other elements present (Figure 6.19) [34].

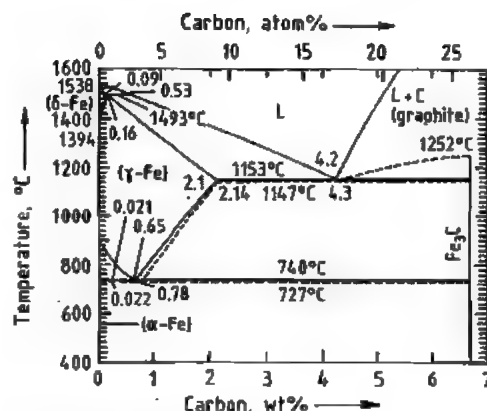


Figure 6.18: Phase diagram for Fe-C alloys.

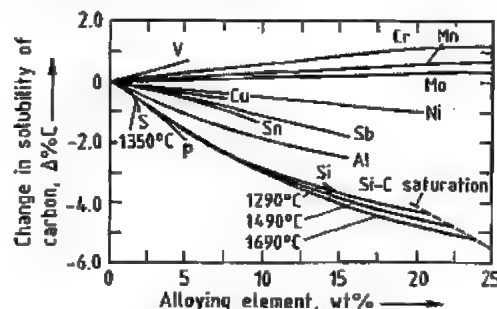


Figure 6.19: Effect of alloying elements on the solubility of carbon in molten iron alloys [34].

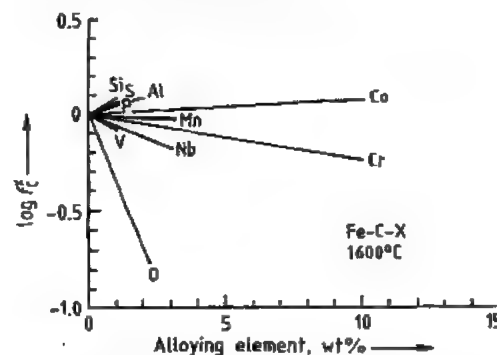
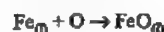


Figure 6.20: Effect of alloying elements on the activity coefficient of carbon in molten iron alloys [36].

The effect of other elements on the activity of the carbon in molten iron can be represented by the interaction parameters e_C^C and e_C^X . The value of e_C^C at 1600 °C is 0.14 [36]. The activity of the carbon is only slightly dependent on temperature. The effect of other el-

ements on the activity coefficient of carbon is shown in Figure 6.20 [36].

The Fe-O phase diagram is shown in Figure 6.21 [37]. The liquid region, in which molten iron is in equilibrium with molten iron(II) oxide, is relevant to the steelmaking process. The solubility of oxygen in molten iron is limited by the precipitation of molten FeO in the reaction:



The solubility of oxygen varies with temperature according to the equation [38]:

$$\log [\%O]_{\max} = -\frac{6320}{T} + 2.734 \quad (2)$$

in the range 1530–1700 °C. Equation (2) corresponds to the line BB' in Figure 6.21.

There have been many experimental determinations of oxygen activities in the system Fe-O and of the effect of other elements X in the system Fe-O-X. The temperature dependence of e_O^O is [36]:

$$e_O^O = -\frac{1750}{T} + 0.794 \quad (3)$$

The effect of various alloying elements and other additives on the activity coefficient f_O^X at 1600 °C is shown in Figure 6.22 [39].

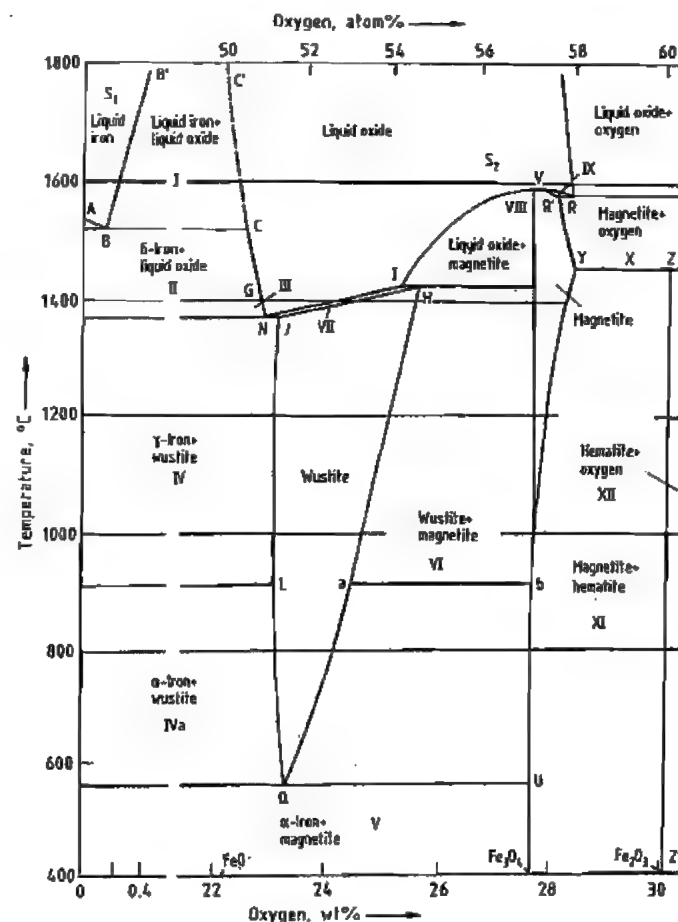


Figure 6.21: Phase diagram for Fe-O [37].

	T, °C	O ₂ , %	P _{CO₂} /P _{CO}
A	1536		
B	1528	0.16	0.209
C	1528	22.60	0.209
G	1400 ^a	22.84	0.263
H	1424	25.60	16.2
I	1424	25.31	16.2
J	1371	23.16	0.281
L	911 ^a	23.10	0.447
N	1371	22.91	0.282
Q	560	23.26	1.05
R	1583	28.30 ^b	
R'	1583	28.07 ^b	
S	1424	27.64	16.2
V	1597	27.64 ^c	
Y	1457	28.36 ^c	
Z	1457	30.04 ^b	
Z'		30.06	

^a Value for pure iron.

^b P_{O₂} = 0.1 MPa.

^c 5.75 kPa.

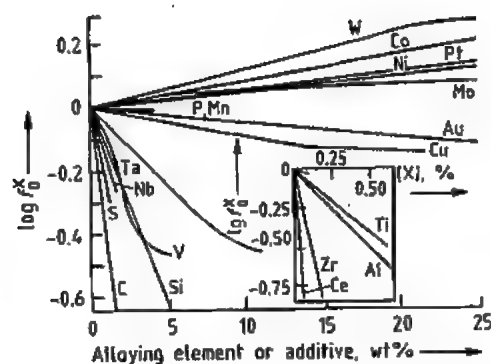


Figure 6.22: Effects of alloying elements and other additives on the activity coefficient of oxygen in molten iron alloys at 1600 °C [39].

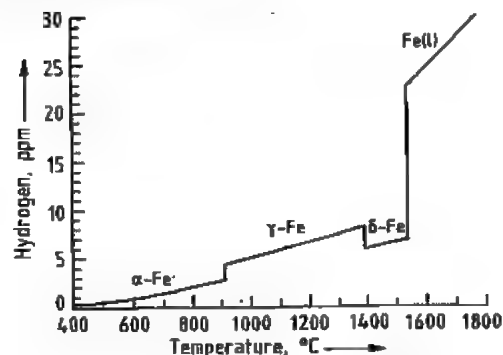


Figure 6.23: Effect of temperature on the solubility of hydrogen in pure iron at 0.1 MPa [40].

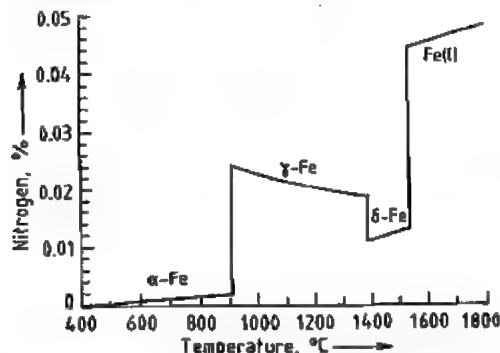


Figure 6.24: Effect of temperature on the solubility of nitrogen in pure iron at 0.1 MPa [40].

Hydrogen and nitrogen can have adverse effects on the properties of solid and liquid metals. During the process of steelmaking, hydrogen from atmospheric moisture usually enters the steel. The most important source of

nitrogen during steelmaking is atmospheric air. Nitrogen is also absorbed during oxygen blowing, the N_2 content of the O_2 used being ca. 3%.

The solubility of H and N in iron obeys the Sievert square root law:

$$[\% \text{H}] = K_{\text{H}} \sqrt{p(\text{H}_2)} \quad (4)$$

$$[\% \text{N}] = K_{\text{N}} \sqrt{p(\text{N}_2)} \quad (5)$$

where p represents partial pressure.

The effect of temperature on solubility is reflected in variations of the equilibrium constants K_{H} and K_{N} . The solubility of hydrogen and nitrogen in pure iron at partial pressure 0.1 MPa (1 bar) is shown as a function of temperature in Figures 6.23 and 6.24 [40]. For hydrogen, the solution process is endothermic over the whole temperature range 400–1800 °C. Nitrogen dissolves exothermically in the γ -phase.

The solubility of hydrogen and nitrogen is changed by the presence of a third element, mainly by affecting the activity coefficient of the dissolved gas (Figures 6.25–6.28) [41–43].

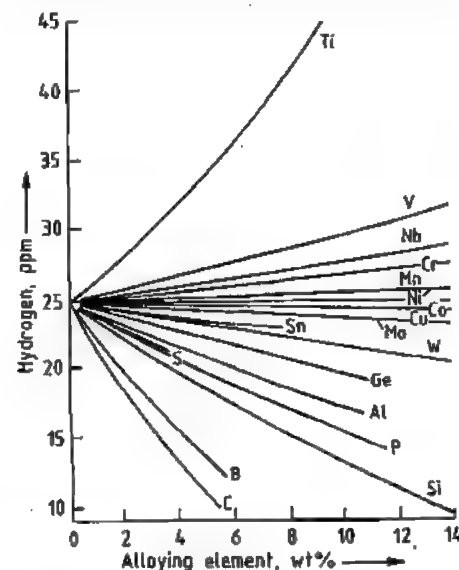


Figure 6.25: Effect of alloying elements on the solubility of hydrogen in iron alloys at ca. 1600 °C and $p(\text{H}_2) = 0.1$ MPa [41].

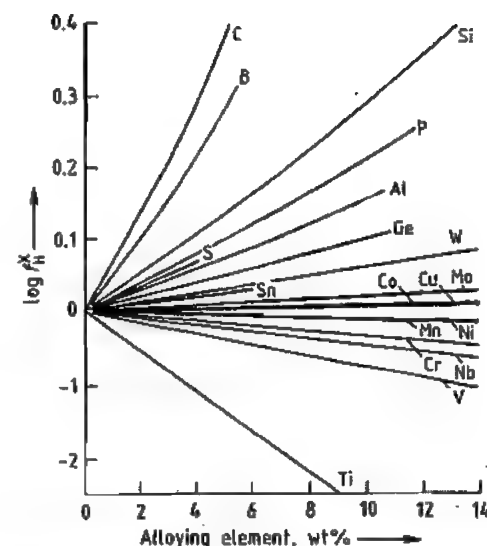


Figure 6.26: Effect of alloying elements on the activity coefficient of hydrogen in molten iron alloys at ca. 1600 °C and $p(\text{H}_2) = 0.1$ MPa [41].

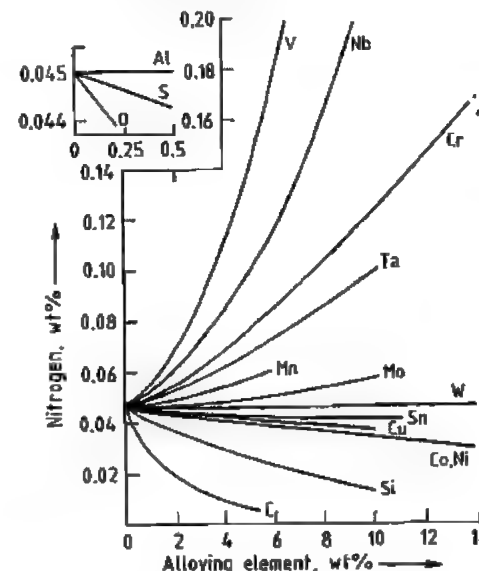


Figure 6.27: Effect of alloying elements on the solubility of nitrogen in molten iron alloys at ca. 1600 °C and $p(\text{N}_2) = 0.1$ MPa [42].

Slag Systems

In the steelmaking process, slags are formed as products of the refining reaction

and by the addition of materials such as lime. It is extremely important that the slag forms quickly, enabling the important reactions between metal and slag, e.g., desulfurization and dephosphorization, to proceed until the required low levels of sulfur and phosphorus are obtained in the finished steel.

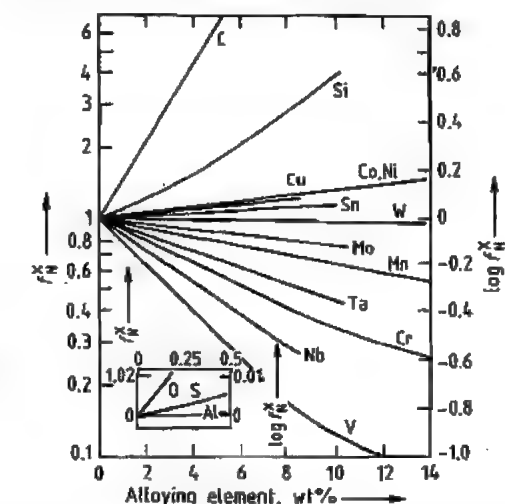


Figure 6.28: Effect of alloying elements on the activity coefficient of nitrogen in molten iron alloys at ca. 1600 °C and $p(\text{N}_2) = 0.1$ MPa [43].

Calcium silicate slags are important in the metallurgy of steelmaking when the raw materials have a low phosphorus content. The essential system is $\text{FeO}-\text{CaO}-\text{SiO}_2$ (Figure 6.29) [44]. In general, the total of these three components is $> 80\%$, the remainder consisting mainly of MnO , with smaller amounts of P_2O_5 , MgO , Al_2O_3 , and Cr_2O_3 . Figure 6.29 shows the solid phases in equilibrium with the melt at various surfaces of the precipitate. Continuous lines separate the saturation surfaces of individual solid phases from each other, at which more than one phase is precipitated on cooling. The isotherms are shown as broken lines. For steelworks slags, the most important region includes the stability zones of the liquid slags, dicalcium silicate, tricalcium silicate, and lime. An important isothermal diagram for steel manufacture is that at 1600 °C (Figure 6.30) [45], which shows lines of equal FeO activity for the equilibrium with

metallic iron. In the area a-b-c-d-e-f, the slags are liquid at 1600 °C. All other areas consist of more than two phases. The activity of FeO gives a measure of the tendency of the slag to oxidize, and from it the corresponding oxygen content of the melt can be deduced. The FeO activity is also important in desulfurization and dephosphorization.

Metal-Slag Reactions

Refining Reactions

In the refining treatment of molten pig iron to make steel, carbon is removed along with other elements, e.g., Si and Mn, by blowing the molten metal with oxygen. The thermodynamics of the reactions are independent of the process used; differences between the various processes affect only the kinetics of the individual reactions. Typical concentration changes in the steel melt during oxygen blowing in a basic oxygen converter are shown in Figure 6.31 [46]. The main aim is to reduce the carbon content to the desired value in the

shortest possible time. However, the time must be long enough to enable the slag to form, the desired tapping temperature to be achieved, and phosphorus and sulfur to be removed from the system until the desired levels are reached.

Decarburization is achieved by the reaction:



The CO bubbles promote homogenization of the melt, and the elements H and N dissolved in the melt are picked up in the bubbles as they ascend. The equilibrium constant of the decarburization reaction [47] is given by:

$$\log K = \frac{1160}{T} + 2.003 \quad (7)$$

In practical decarburization processes, a simplified expression for the equilibrium between C and O is used

$$[\%C][\%O] = 0.0025 P(\text{CO}) \quad (8)$$

at 1600 °C.

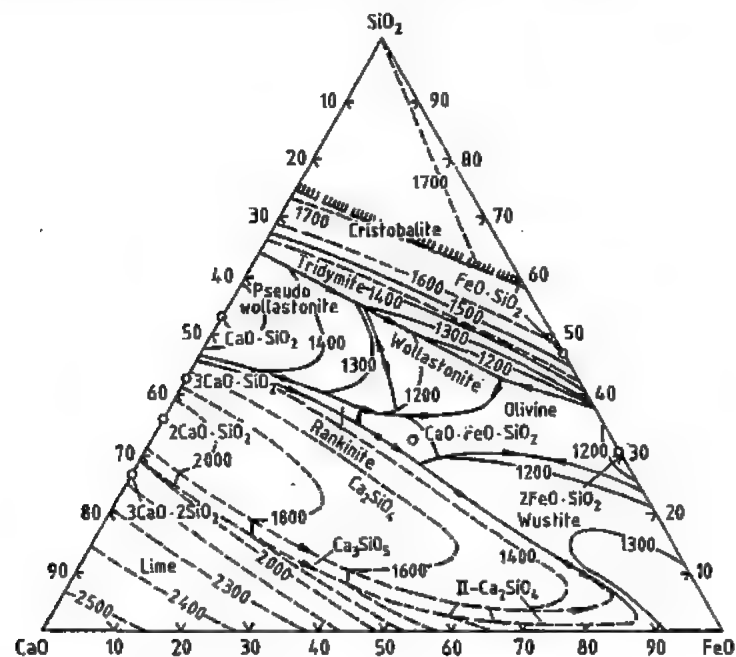


Figure 6.29: Phase diagram for CaO-FeO-SiO₂ [44].

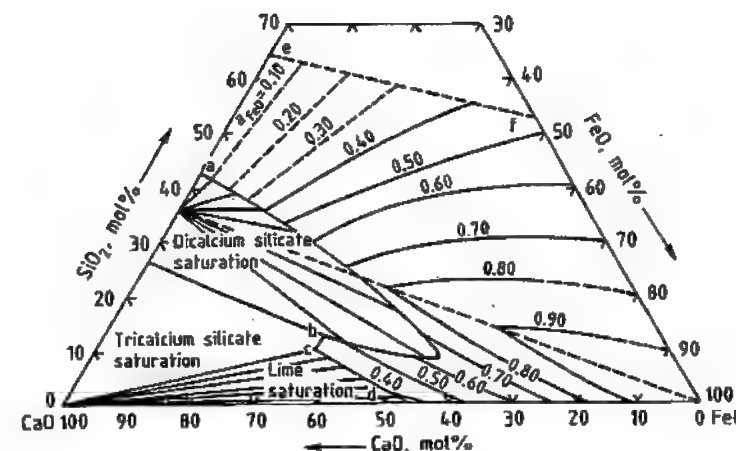


Figure 6.30: Phase diagram for CaO-FeO-SiO₂ with lines of equal activity for FeO at 1600 °C [45].

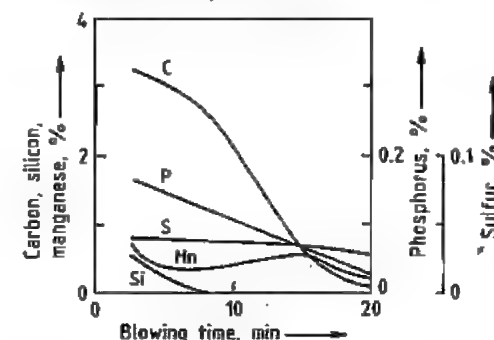


Figure 6.31: Changes in melt composition during the blow in a basic oxygen steelmaking converter (idealized) [46].

Silicon is rapidly removed during the oxidation process, owing to its high affinity for oxygen, and combines with the lime in the slag; oxidation takes place by the reaction:



The equilibrium constant for this reaction is:

$$\log K = \log \frac{a_{\text{SiO}_2}}{a_{\text{Si}} a_{\text{O}}^2} = \frac{30110}{T} - 11.4 \quad (10)$$

The exothermic oxidation of silicon provides a large proportion of the process heat. The oxidation product SiO₂, together with FeO, forms the first slag. This reduces the melting point of the added lime to such an extent that a reactive liquid slag can be formed. Therefore, the amount of CaO added and the

amount of slag formed are mainly determined by the Si content.

Manganese is removed at the beginning of the oxidation process, mostly in parallel with silicon. Oxidation of manganese can be represented by the equation:



The equilibrium constant is given by

$$\log K = \log \frac{a_{\text{MnO}}}{a_{\text{Mn}} a_{\text{O}}} = \frac{12590}{T} - 5.53 \quad (12)$$

Toward the end of the silicon oxidation, the increased melt temperature leads to the reduction by carbon of the manganese oxide in the slag, according to the equation:



However, at the end of the blow, the manganese content decreases continuously, owing to oxidation of the manganese, mainly by FeO in the slag:



Dephosphorization

The conditions in steelmaking processes favor dephosphorization of iron, which takes place by oxidation of phosphorus and combination with a basic slag. The reaction proceeds as follows:



Slag composition:
MnO=6%; MgO=2%
CaO + SiO₂ + P₂O₅ + FeO_n + MnO=100%

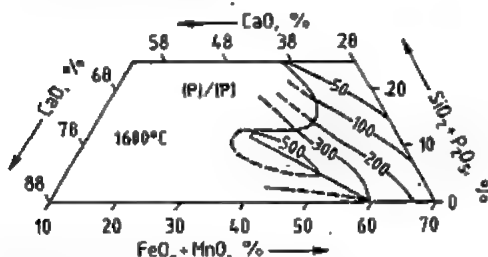


Figure 6.32: Lines of equal phosphorus distribution in the system CaO-(SiO₂ + P₂O₅)-(FeO_n + MnO) [48].

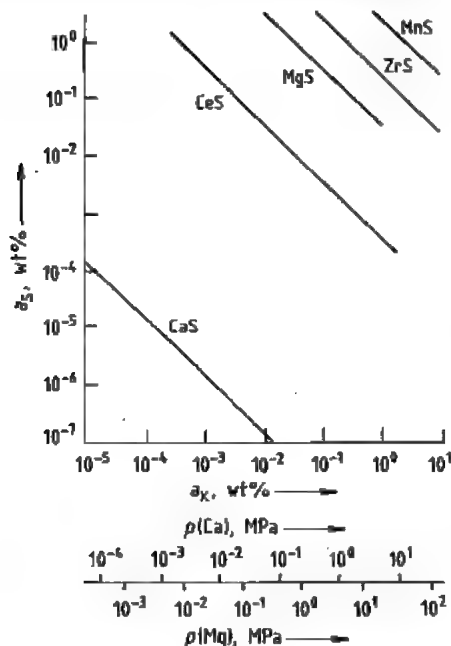


Figure 6.33: Equilibria between sulfur and various metallic elements in molten iron. [49].

The equilibrium constant is given by:

$$\log K = \log \frac{a_{\text{CaO}} \cdot p_{\text{O}_2}}{a_{\text{CaO}}^2 a_{\text{Fe}}^2 a_{\text{O}}^2} = \frac{61\,100}{T} - 23.3 \quad (16)$$

This expression shows that the conditions for oxidative dephosphorization are: (1) oxidizing slag (high FeO activity); (2) high activity of lime in the slag; and (3) low temperature, as reaction (15) is exothermic. These conditions

are particularly well satisfied at the start of the process.

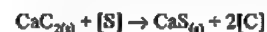
In low-phosphorus pig iron, the type most commonly produced today, the slag formed during steelmaking consists mainly of CaO, SiO₂, and FeO_n, with P₂O₅ content ca. 1–2%. The phosphorus equilibrium in this type of slag has been thoroughly investigated. In Figure 6.32, lines of equal phosphorus distribution at 1600 °C are shown for the system CaO-(SiO₂ + P₂O₅)-(FeO_n + MnO), with 6% MnO and 2% MgO. As expected, the lines are approximately parallel to the lime saturation line.

Desulfurization

Unlike dephosphorization, desulfurization is a reduction reaction. Since the oxidizing conditions in the converter do not favor the removal of sulfur from the melt, desulfurization is mainly carried out by treatment of the pig iron or of the metal in the ladle.

Desulfurization can be carried out by means of the precipitation reaction that occurs when elements with a high affinity for sulfur are added, either by taking up the sulfur into the slag phase, or by transferring it into the gas phase.

The affinity for sulfur of a desulfurizing agent is indicated by the solubility product of its sulfide in molten iron (Figure 6.33) [49], the most stable of these being calcium sulfide. Although the alkaline earths and rare earths form relatively stable sulfides, their oxides are much more stable; the sulfides are formed only if the dissolved oxygen has been removed. The most commonly used desulfurizing agents are added to the steel in the form of alloys (CaSi, CaC₂, CaAl, etc.), by special techniques. The desulfurization reaction can be represented by the typical equation:



for which

$$\Delta G^\circ = -359\,000 + 109.47 T/\text{mol} \quad (17)$$

Desulfurization by slag treatment is represented by the following equation, according to the ionic theory for slags:



$$\Delta G^\circ = 71\,965 - 387 T/\text{mol} \quad (18)$$

The most favorable thermodynamic conditions for slag desulfurization are: (1) high basicity of the slag; (2) low oxygen content in the slag or melt; and (3) high temperature.

Figure 6.34 shows the partition of sulfur between aluminum-containing steel and CaO-Al₂O₃-SiO₂-MnO slag containing 5% MgO at 1625 °C [50]. Slags of this type are used for the desulfurization of steel in ladle metallurgy. The sulfur in pig iron can also be removed by Na₂CO₃. The desulfurization reaction is:



or



The Na₂S formed can be oxidized by air:

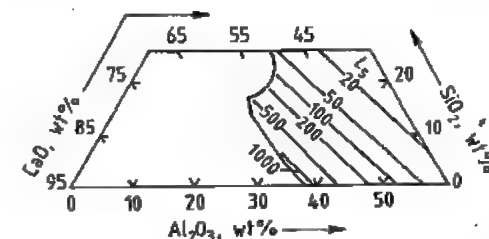
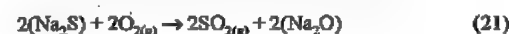


Figure 6.34: Sulfur partition coefficient L_S between aluminum-containing steel ($a_{\text{Al}} = 0.07\%$) and CaO-Al₂O₃-SiO₂-MgO slags containing 5% MgO at 1625 °C [50].

Deoxidation

At the end of the refining process, there is a considerable amount of oxygen dissolved in the molten steel; this can be removed by adding elements with a sufficient affinity for oxygen (precipitation deoxidation), or by slags which take up an amount of oxygen from the melt corresponding approximately to the equilibrium distribution (diffusion deoxidation).

The reaction between oxygen and a metal M in precipitation deoxidation can be represented by the equation:



The equilibrium constant is:

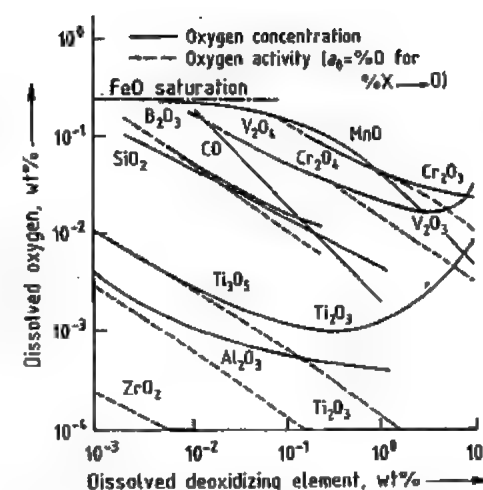


Figure 6.35: Deoxidation equilibria in molten iron at 1600 °C [51].

$$K = \frac{a_{\text{M}_x\text{O}_y}}{a_{\text{M}}^x a_{\text{O}}^y} \quad (23)$$

In practice, either the deoxidation constant $K' = a_{\text{M}_x\text{O}_y} / a_{\text{M}}^x$ or the solubility product $K'' = [\%M]^x [\%O]^y$ is usually used. Small values of K' or K'' correspond to high deoxidizing power. The relative deoxidizing powers of various elements are shown in Figure 6.35 [51]. The activities, or concentrations, of oxygen are plotted against those of the deoxidation elements on a logarithmic scale. The three deoxidation elements most commonly used, in increasing order of effectiveness, are Mn < Si < Al. Aluminum is one of the most powerful deoxidation elements.

Deoxidation elements are often used in combination; the advantage of this lies partly in lowering the thermodynamic activity of the oxides formed, owing to compound formation, or dilution in the slag, and partly in the formation of oxidic slags with lower melting points, which separate more readily from the steel melt, or can be shaped at the rolling temperature. Figure 6.36 is a graphical representation of deoxidation with Al-Si. Various deoxidation products (alumina, mullite, and silicate) are formed, depending on the $[a_{\text{Al}}]/[a_{\text{Si}}]$ ratio.

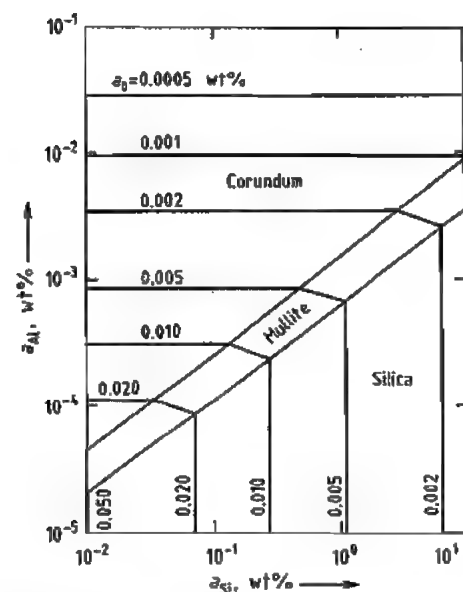


Figure 6.36: Deoxidation diagram for Al-Si-O at 1600 °C [49].

In diffusion deoxidation, no inclusions are formed in the melt, but long reaction times are necessary to remove the oxygen. The reaction can be represented by:



Decreasing the FeO content of the slag leads to removal of oxygen from the melt. Diffusion deoxidation is being replaced by precipitation deoxidation.

Metal-Gas Reactions

If there is no slag on the surface of the molten metal, or if gas bubbles are formed within the melt, metallurgical reactions between the metal and gas phases take place. These include decarburization and degassing, either under reduced pressure, or by bubbling an inert gas such as argon through the melt.

As mentioned earlier, the concentrations of the gases dissolved in the iron depend on their partial pressures (Figure 6.37). Pressure reduction can cause hydrogen and nitrogen to be removed from the melt, but this is not the case with oxygen. Although the solubility of oxy-

gen varies with pressure according to the equation:

$$[\%O] = K_O \sqrt{p(O_2)}$$

it is not feasible to remove oxygen simply by pressure reduction, as the required oxygen partial pressure is less than that attainable in vacuum vessels (10 Pa). However, it is possible to use vacuum in conjunction with reaction (6) in the melt between carbon and oxygen to form the gaseous deoxidation product CO. The equilibrium constant:

$$K = \frac{p(CO)}{a_C a_O}$$

explains the strong pressure dependence. Figure 6.38 shows the equilibrium between oxygen and carbon as a function of $p(CO)$ [3.37]. A decrease in $p(CO)$ leads to simultaneous decarburization and deoxidation.

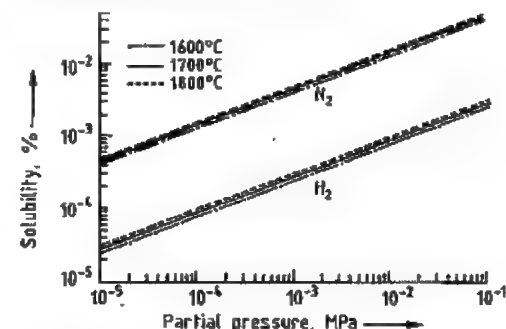


Figure 6.37: Solubility of nitrogen and hydrogen in molten iron [40].

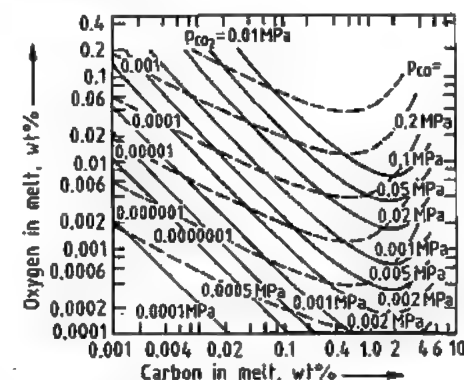


Figure 6.38: Equilibria between carbon and oxygen dissolved in molten iron with CO and CO₂ at various pressures and 1600 °C [52].

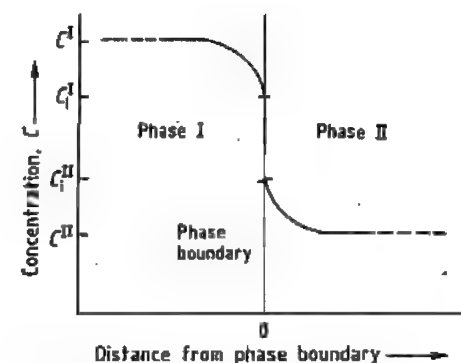


Figure 6.39: Schematic concentration profiles across a phase boundary.

Dissolved hydrogen and nitrogen can also be removed without vacuum degassing by bubbling an inert gas through the melt. As the partial pressures of the hydrogen and nitrogen in the bubbles of inert gas are almost zero, hydrogen and nitrogen diffuse from the melt into the bubbles, owing to the concentration difference, and ascend with them.

6.3.2.2 Kinetics and Mass Transfer

Kinetics of Heterogeneous Reactions

In the metallurgy of steel production, the kinetics of the heterogeneous reactions are of interest because the individual homogeneous phases are usually in local thermodynamic equilibrium, so that macroscopic reactions do not occur. Heterogeneous reactions occur between the various phases that are not in thermodynamic equilibrium with each other. Figure 6.39 shows the concentration profile of a substance in two phases in contact with each other. The total reaction is made up of several steps:

- Transport of the reactants to the phase boundary
- Chemical reaction at the phase boundary
- Transport of the reaction products from the phase boundary

The overall rate depends on the rate of the slowest step, known as the rate-determining

step. If the overall process is considered, the mass flux density j is:

$$j = \frac{C^I - \frac{C^{II}}{K}}{\frac{1}{\beta_I} + \frac{1}{k} + \frac{1}{K\beta_{II}}} \quad (25)$$

where C^I , C^{II} are concentrations in phases I and II, K is the equilibrium constant of the heterogeneous reaction, β_I , β_{II} are mass transfer coefficients, and k is the reaction rate constant. The equation:

$$\frac{1}{\beta_{tot}} = \frac{1}{\beta_I} + \frac{1}{k} + \frac{1}{K\beta_{II}} \quad (26)$$

defines the overall mass transfer coefficient β_{tot} . Therefore, from Equation (25):

$$j = \beta_{tot} \left(C^I - \frac{C^{II}}{K} \right) \quad (27)$$

The mass transfer coefficients β_I and β_{II} are obtained from theory of mass transfer by using experimental data. The rate constant k is obtained from the chemical kinetics of phase boundary reactions for metallurgical systems. These rate constants are usually greater than the mass transfer coefficients of the transport processes that take place before and after the chemical reactions. The overall rate is therefore determined by mass transfer. Equation (27) gives the rate of mass transfer to a phase boundary when the mass transfer coefficient is known. To obtain an expression for the variation with time of the concentration of a dissolved substance in the mother phase, a mass balance must be carried out which takes account of the nature of the phase contact and the characteristic parameters for emulsified systems [53].

Flow and Mass Transfer Coefficients

Mass transfer into a phase is made up of diffusion and convection. In the interior of the phase, sufficient flow takes place to give a uniform concentration. Concentration gradients exist only near the phase boundary. As there is no flow at this boundary layer, mass

transport takes place by diffusion, and Fick's first law applies:

$$j = D \frac{C^I - C^*}{\delta_N} \quad (28)$$

where the asterisk indicates the phase boundary.

If this is combined with the flow equation $j = \beta(C^I - C^*)$, the equation $\beta = D/\delta_N$ is obtained. Here, δ_N denotes the thickness of the boundary layer, and D the diffusion coefficient of the overlying material. To determine β , it is necessary to determine the boundary layer thickness, whose value depends on flow conditions. Theoretical analysis and experimental investigation of the various flow fields that occur in metallurgical processes yield a formula for calculating the mass transfer coefficient in dimensionless form.

Metal-Gas Phase Boundaries with Nonturbulent Flow

The flow field is represented in Figure 6.40. The flow from the interior of the melt is first deflected at a stagnation point, e.g., the top of a column of bubbles or the middle of an inductively agitated melt, flows parallel to the upper surface, and is again deflected at a later stagnation point, e.g., the wall, and flows back into the interior. In this way, the surface is continuously renewed. The diffusion process takes place between the gas phase and the metal flowing to the surface. A mean mass transfer coefficient for this condition can be calculated in the form of a Sherwood number Sh , as a function of the Reynolds number Re and the Schmidt number Sc :

$$Sh = \frac{2}{\sqrt{\pi}} Re^{1/2} Sc^{1/2} \quad (29)$$

where $Sh = \beta l/D$, $Re = ul/\nu$, $Sc = \nu/D$; β is the mean mass transfer coefficient (cm/s), l the flow length (cm), u the flow rate (cm/s), ν the kinematic viscosity of the melt (cm²/s), and D the diffusion coefficient of the overlying material (cm²/s).

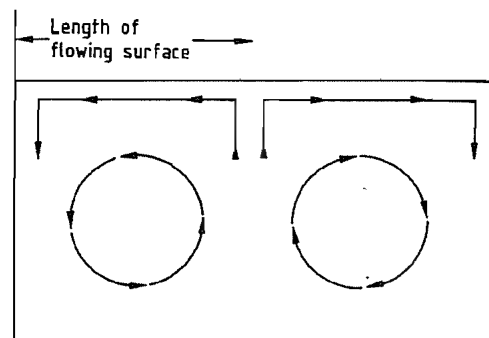


Figure 6.40: Mass transfer with continuous renewal of the free surface (schematic).

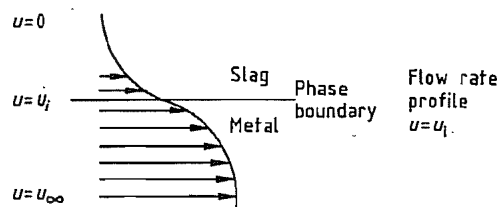


Figure 6.41: Flow field at a liquid-liquid phase boundary.

Metal-Slag Phase Boundaries with Nonturbulent Flow

This flow field is represented in Figure 6.41. Friction takes place between the slag and the metal. The phase boundary moves at a velocity u_i during mass transfer. In the determination of the mass transfer, momentum transfer due to friction must be taken into account. Equations for the flow film thicknesses on the metal and slag sides are first obtained. By including the condition that the shearing forces on each side of the phase boundary must be equal, the velocity of the phase boundary obtained and the mass transfer calculated.

Solid (Metal or Slag)-Liquid Phase Boundaries with Nonturbulent Flow

This condition represents, e.g., the processes of dissolution of alloys, or the solution abrasion of refractory materials. Mass transfer takes place on the liquid side. As shown in Figure 6.42, the flow rate, which is u_∞ within the melt, falls to zero at the boundary layer, and both the flow boundary layer and the dif-

fusion boundary layer must be considered on the side of the melt. The mass transfer coefficient can be obtained by theoretical calculations from the equation:

$$Sh = 0.664 Re^{1/2} Sc^{1/3} \quad (30)$$

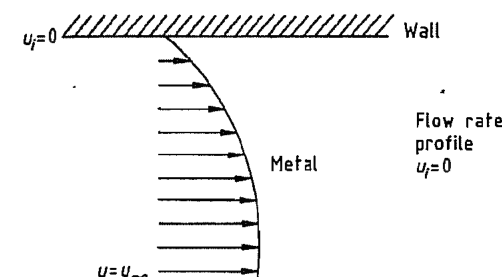


Figure 6.42: Mass transfer at a wall.

Mass Transfer with Turbulent Flow

In metallurgical vessels, turbulent flow is usually present, caused by ascending CO bubbles and/or blowing with oxygen. In turbulent flow, turbulence spheres at the phase boundary contribute additional mass transfer by their flow components perpendicular to the phase boundary. This mass transfer can be regarded as turbulent diffusion, leading to an increased value of the diffusion coefficient. To calculate the mass transfer at a solid wall with turbulent flow, the following equation can be used [54]:

$$Sh = 0.037 Re^{0.8} Sc^{0.2} \quad (31)$$

At free surfaces [53, 54]:

$$Sh = 0.32 \left(\frac{D \rho u_\infty^2}{\sigma_{equiv}} \right)^{1/2} \quad (32)$$

where D is the diffusion coefficient, ρ the density of the melt, σ_{equiv} the equivalent interfacial tension of the melt, and u_∞ the shearing force rate for turbulent flow.

The equivalent interfacial tension differs from the normal interfacial tension in that the back pressure, caused by the irregularity of the boundary surface, is expressed as the sum of the effects of interfacial and gravitational forces [54]. For steel melts, which have high

interfacial tensions, σ_{equiv} can be assumed equal to the interfacial tension of the melt. The shearing force rate u_∞ is a measure of the degree of turbulence. The value must be determined by turbulence measurements. For steel melts, this can at present only be investigated with the aid of mathematical models.

Equation (32) is also valid for metal-slag phase boundaries with turbulent flow, if there is no turbulence in the slags, and if the full weight of the stationary slag layer on the melt is considered when calculating the equivalent interfacial tension. If there is any turbulence in the slag, this should be included. However, it is often negligible.

6.3.3 Production Processes

Steel production depends on the availability of raw materials such as pig iron, scrap, and sponge iron. There are two fundamentally different methods (Figure 6.43) [55]: blowing oxygen into liquid iron (mainly pig iron), and smelting iron-containing materials, such as scrap and sponge iron.

A typical example of the first method is the oxygen converter. In the electric furnace, and (now of less importance) the open hearth furnace, large amounts of scrap and sponge iron can be melted together. Depending on local conditions, mixed methods can also be used, in which various proportions of scrap and pig iron are processed, e.g., the KMS (Klöckner-Maxhütte-Stahlerzeugungsverfahren, and EOF (energy-optimized furnace) processes.

The object of all steel production processes is the removal of unwanted metallic, nonmetallic, and gas-forming elements from the raw materials, and the controlled addition of alloying elements to obtain the required characteristics of the various grades of steel.

The growth of world crude steel production, and the proportional contributions of the various processes are shown in Figures 6.44 and 6.45 [56, 57].

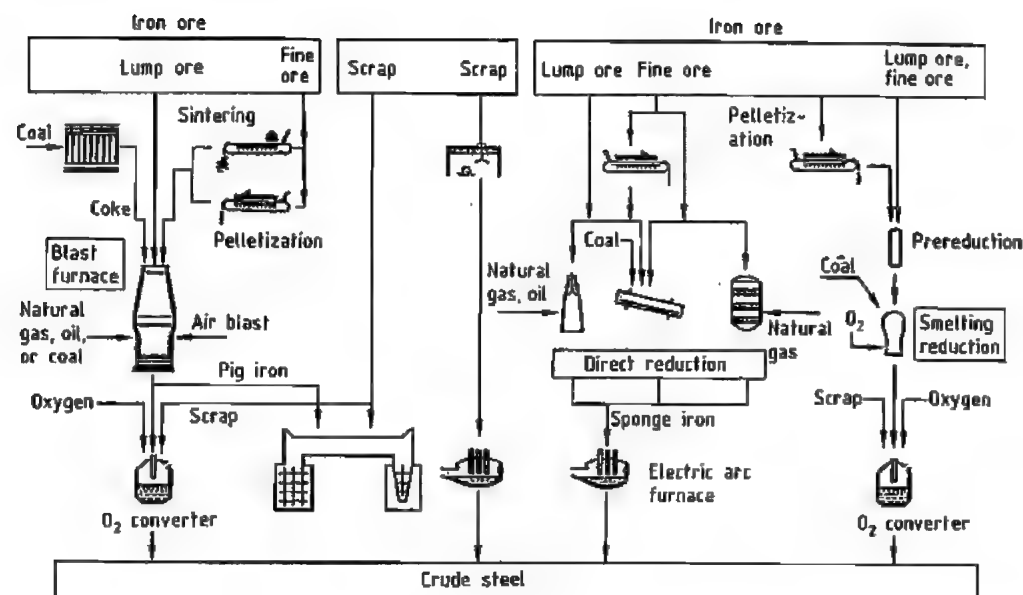


Figure 6.43: Crude steel production methods.

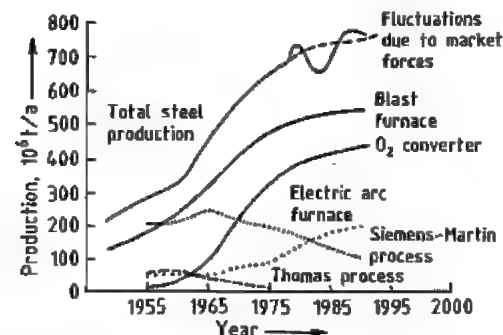


Figure 6.44: Growth of world pig iron and crude steel production by various processes.

6.3.3.1 Oxygen-Blowing Processes

Unwanted elements in pig iron (and sometimes in scrap), principally carbon, silicon, and phosphorus, are removed by the oxidation reactions and transferred into the gas or slag phases (decarburization).

The carbon monoxide produced is a source of thermal energy. After thorough purification, it is collected in gasholders and burned to provide heat for associated production plant. The oxides SiO_2 and P_2O_5 dissolve in the liquid slags formed from the added lime and the iron

oxide produced during the oxidative decarburization processes.

The energy required to raise the temperature and melt the raw materials during the blowing process comes from the enthalpies of the oxidation reactions:

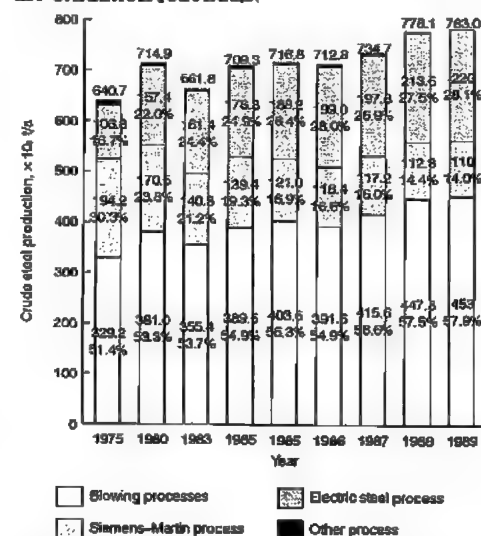


Figure 6.45: Growth of crude steel production, with contributions of the various production processes. * Estimated.

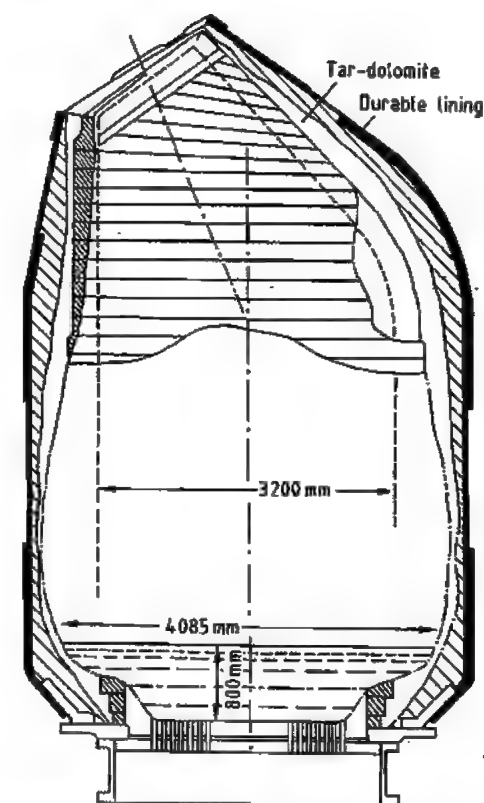


Figure 6.46: Section through a Thomas converter after 400 melts.



From ca. 1870, conversion of pig iron to liquid crude steel was carried out by blowing air, the oxidizing agent, through tuyères in the base of a bottom-blown converter (tiltable steel vessel with refractory lining) containing a 20–80 t charge. Steel production processes using air blowing can be subdivided into the Bessemer process (only for low-phosphorus pig iron) and the Thomas process (capable of removing phosphorus). In the Bessemer process, the converter was lined with silica bricks. It was not possible to use a lime-containing slag to combine with the P_2O_5 owing to the acidic lining. In the Thomas process (Figure 6.46),

dolomite was used to line the converter, and a lime-based slag could then be used to treat phosphorus-containing pig iron [58].

The nitrogen in air dissolved to some extent in the liquid steel, and has a detrimental effect on its properties. Increasing quality requirements (aging stability, etc.) and the unfavorable economics of this process led to its discontinuation.

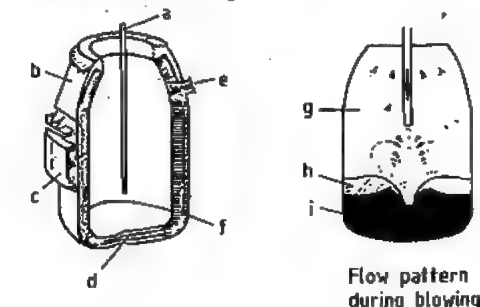


Figure 6.47: Top-blown oxygen converter: a) Oxygen lance; b) Converter top; c) Supporting ring; d) Converter bottom; e) Taping hole; f) Refractory lining; g) Gas space; h) Slag layer; i) Molten metal.

LD and OBM Processes

The first LD (Linz–Donawitz) converter, with a capacity of 30 t, was operated in Linz in 1952. The decarburization reaction is greatly speeded up by the use of pure oxygen, giving blowing times of 10–20 min. The oxidation enthalpies result in lower heat losses and enable more scrap or ore to be added. The converters have total charge 50–400 t, and are lined with dolomite or magnesite bricks [55].

Oxygen is injected from above through a water-cooled lance with several nozzles, onto the surface of the melt (Figure 6.47). The high-pressure jets of oxygen (up to 1.2 MPa) oxidize the iron, carbon, and other elements at rates depending on their affinity for oxygen. The gas reactions cause thorough mixing of the molten materials, and this is maintained after completion of the blowing process by purging bricks built into the base of the vessel. Temperatures of 2500–3000 °C are produced in the central reaction zone, and a reactive slag is rapidly formed from the added lime and the oxidized iron. The thermodynamic and kinetic

processes are described in Sections 6.3.2.1 and 6.3.2.2. The heat and mass transfer processes take place according to the rules given earlier.

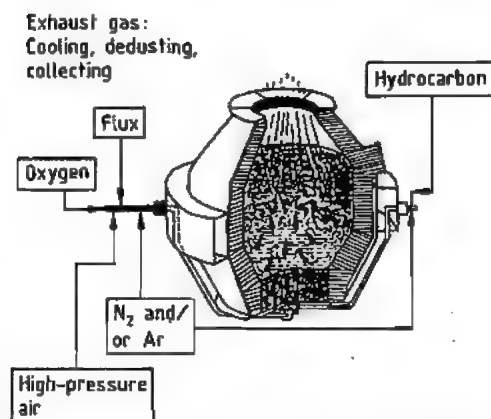


Figure 6.48: Section through an OBM converter. Oxygen is injected from below, through tuyères cooled by hydrocarbons blown into the melt.

The OBM (oxygen-blowing technique) (Figure 6.48), a modification of the air blast processes, was developed in 1968–1969 in Sulzbach-Rosenberg [55]. Pure oxygen is passed through bottom tuyères into the melt. These tuyères are highly stressed, and are stabilized by cooling them with hydrocarbons. The cooling effect is a result of the endothermic decomposition of the hydrocarbons by the hot melt. The OBM process causes more intensive mixing of the steel and the slag compared with the method of blowing in the oxygen from above. This gives improved reaction kinetics and yield, owing to the lower iron content of the slag. The advantages of the more rapid slag formation and the less violent blow can be enhanced by adding powdered lime through the bottom of the converter, along with the oxygen. However, the capacity of the OBM process for melting scrap is limited in comparison with the LD process, owing to the lesser extent of afterburning of the waste gases, and the smaller amount of iron oxidation.

The combined blowing technique in general use today (Figure 6.49) has been devel-

oped from the top-blowing process and past experience of the bottom-blowing process [55]. The combined process provides:

- Homogeneous melts due to rapid breakdown of the scrap
- Reduction of the blowing cycle time by 25%
- Higher yield of iron and alloying elements
- Better control of the chemical composition
- Improved purity
- Lower quantity of slag and reduced tendency for it to be ejected
- Increased lifetime of the converter lining
- More favorable conditions for the measuring systems for process control

Plant layouts do not differ greatly from one another. Figure 6.50 shows a side view of the converters and continuous casting plant of a steelworks [55].

Depending on the products required, the pig iron in the torpedo ladle car or filling pit is desulfurized by blowing with slag formers containing lime and/or magnesium. In Japan, for steel products with a very low phosphorus content, it is also usual to remove the silicon and phosphorus [59]. In this case, the converter simply removes carbon from the melt (Figure 6.51).

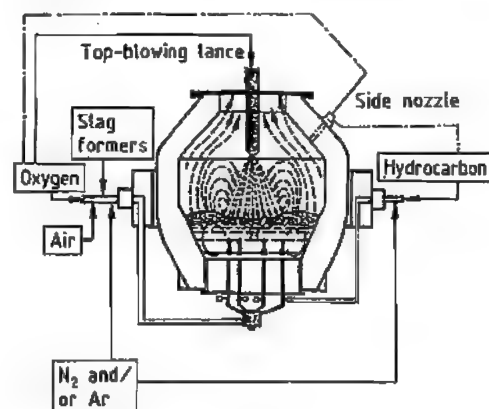


Figure 6.49: Combined blowing technique with top-blowing lance or side tuyère.

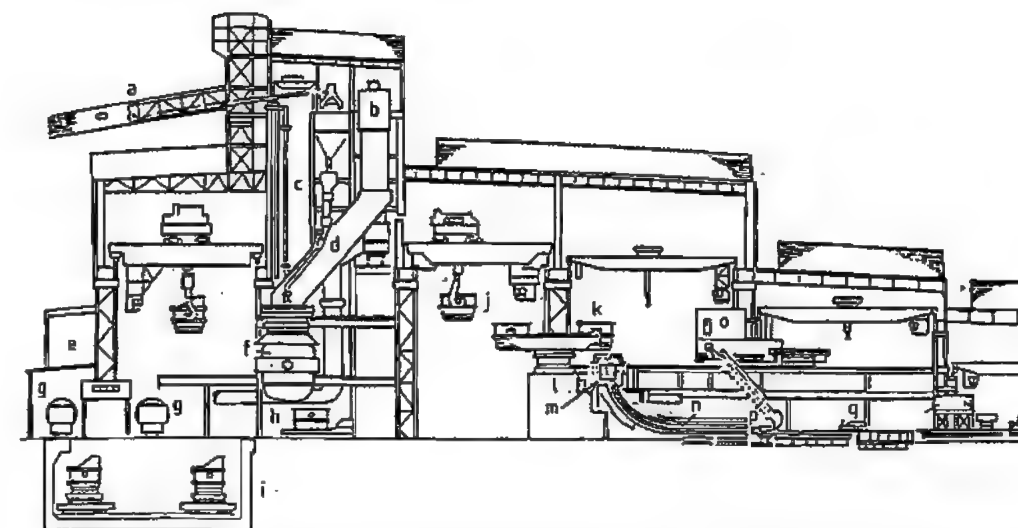


Figure 6.50: Converter and continuous casting plant: a) Feeder conveyor belt; b) High bunker; c) Blowing lance; d) Chute; e) Control room; f) 310 t converter; g) 600 t torpedo ladle car; h) Ladle transporter; i) Pig iron filling pit; j) Filled ladle; k) Pouring ladle; l) Ladle turret; m, n) Continuous casting machine; o) Continuous casting control room; p) Dummy bar; q) Cutting.

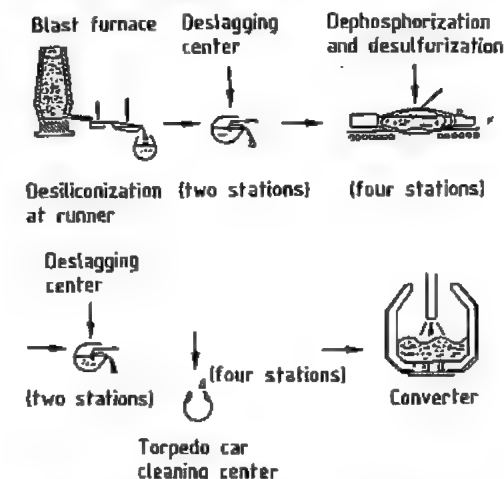


Figure 6.51: Hot metal pretreatment process at Mizushima works.

The mathematical model of the process calculates the quantities of pig iron, scrap, and lime for the melt (based on the composition and temperature of the raw materials); the nominal tapping temperature; and the analysis of the crude steel, and starts the oxygen addition after the scrap and pig iron have been charged. Distribution of the oxygen and con-

trol of the height of the lance are computer controlled. The course of the blowing operation is set by the dynamic process control, which requires occasional fine adjustments based on "sub-lance measurements", that give the temperature and the carbon and oxygen content of the melt. Other elements may also be determined if required. Figure 6.52 shows how the melt temperature and composition change during the blowing operation. Here, the final composition is 0.059% C, 0.031% Mn, 0.018% P, 0.019% S, 0.003% N, and 0.083% O. Figure 6.53 shows the corresponding changes in the composition of the slag [60].

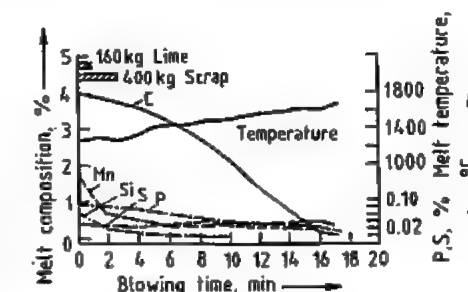


Figure 6.52: Changes in melt temperature and composition during blowing.

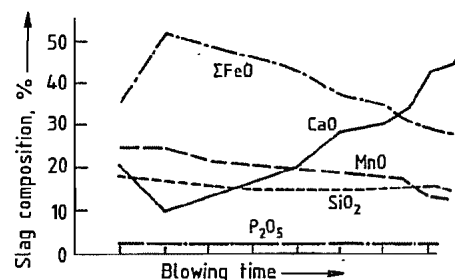


Figure 6.53: Changes in slag composition during blowing.

At the end of the oxygen treatment, the converter is tilted and the steel is tapped into a ladle (a steel container with bottom-pouring facility and refractory lining). The steel is separated from the slag during emptying of the converter by means of a floating stopper introduced into the tapping spout. This prevents the slag, which is of lower density, from running out. Alternatively, an electromagnetic measurement in the tapping system can give a signal for the emptying process to be stopped.

To prevent emission of dust in the waste gases, all sources of dust, such as the pig iron handling and charging operations, lime feeding equipment, etc., are linked to a filtering system, usually cloth filters. The physical and chemical heat of the converter waste gases are utilized by installing a waste heat steam boiler with associated electrostatic filter or scrubber. The waste gases, at 1400–1600 °C, supply heat to the steam generation system, and the cooled gases, calorific value ca. 7000 kJ/m³, are collected in a gasholder after purification. The dust collected in the filters or scrubbers can be recycled to the process, after suitable treatment.

Other Developments

Steel production processes based on an air or oxygen blast are autothermic, i.e., the energy requirement is provided by the physical and chemical heat from the pig iron. The use of scrap is limited by the composition and temperature of the pig iron, and varies between 0 and 20%, depending on process variations and quality requirements.

Higher additions of scrap require the use of an allothermic process, with added fuel. In the KMS (Klöckner–Maxhütte–Steelmaking Process) process, additional energy is provided by adding hydrocarbons during scrap preheating, or powdered coal or coke during the blowing operation. This process is extremely flexible with regard to the metallic materials used, i.e., scrap, pig iron, and sponge iron.

In the KS process, the use of pig iron is completely eliminated. In the first phase, a carbon-rich melt is produced by melting scrap and adding carbon by a blowing process, together with an equivalent amount of oxygen. Heat transfer is optimized by afterburning the reaction gases. In the second phase, conversion of the carbon-rich melt to steel is completed by the further addition of scrap.

In the Tula process (developed in the former Soviet Union), a carbon-containing material in lump form is added from above to a combined blowing converter. This provides the energy required for melting the scrap.

The EOF furnace (energy-optimized furnace) uses combustion of the waste gas and continuous preheating of the scrap in the hot waste gas stream to minimize the additional fuel requirements for an increased proportion of scrap in the melt. This has enabled up to 60% steel scrap to be used.

6.3.3.2 Electric Steel Process

In the electric steel process, the heat required is obtained not by oxygen combustion of the accompanying elements in the pig iron, but from electrical energy. The conversion of electrical energy into heat can be achieved by an electric arc, induction, or plasma furnace. Electric steel processes are based on the use of scrap, with small amounts of solid pig iron. For a long time, the use of these processes was limited to the production of special steels, as energy consumption was high and the economics were unfavorable. Increases in the size of power stations and the capacity of electrical distribution systems have enabled batch weights to be increased, and the costs of energy, electrodes, refractory material, and capi-

tal investment to be reduced. Today, this process is second in importance only to the oxygen-blowing process in world crude steel production (Figure 6.47).

Over 90% of all electric steel produced is by the use of the a.c. electric arc furnace [61]. Three graphite electrodes carry the current through the furnace roof into the charge of metal. The electric arc formed melts the charge at temperatures up to 3500 °C. The furnace has the following essential components: the vessel or shell with a furnace door and a tapping hole; the roof which can be removed for charging; electrode arms which support the electrodes; tilting equipment for emptying the furnace; the furnace transformer, and the measuring and control equipment.

The melting procedure for the electric arc furnace comprises the following stages:

- Charging
- Melting
- Oxidization (decarburization), with an increase in temperature
- Tapping

The raw materials (scrap, sponge iron, pig iron, alloying elements, etc.) together with the required additives (lime, coal, ore, etc.) are loaded into special charging buckets which are then emptied into the furnace through a bottom opening. To fill the furnace, two or three charging operations are required, between which the scrap is partially melted.

The melting process begins with switching on the current and striking the arc. A supplementary blow with oxygen and fuel oxygen mixtures accelerates melting and reduces current consumption. The duration of the melting period is determined by the electric power limit and the maximum heat load of the furnace shell.

Oxidation of elements, such as silicon, manganese, carbon, phosphorus, and sulfur begins during the melting phase as the liquid reactants, steel and slag, react with the added

oxygen. The gaseous carbon monoxide formed from the reaction between the iron oxide and the carbon causes bubbling in the melt and purges the hydrogen and nitrogen. Removal of the phosphorus as calcium phosphate in the slag during the oxidation phase is important, and all the other metallurgical processes take place during the reductive secondary metallurgical treatment in the ladle or ladle furnace.

After the steel has reached the required temperature, the tap hole is opened and the furnace is tilted to empty it into the ladle below.

The development of the modern electric steel process began early in 1960, using powerful transformers and blowing with oxygen (Figure 6.54) [62]. Modern furnace design and process control techniques have made it possible to increase the specific transformer power from 300–400 kVA/t to 800–1000 kVA/t. The electric furnaces of this new generation are operated at a power factor of 0.8–0.86, and enable tap-to-tap times of 50–80 min, and throughputs of > 100 t/h to be achieved (Figure 6.55).

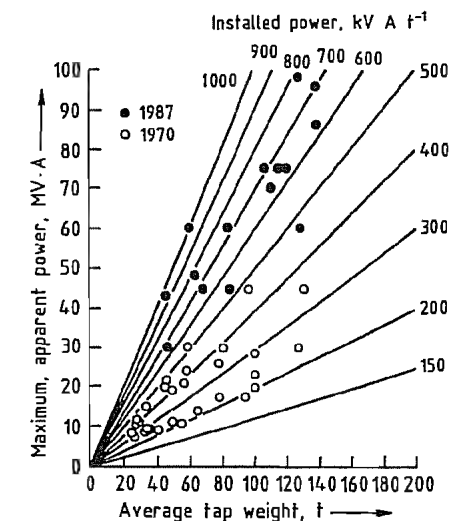


Figure 6.54: Development of specific installed power.

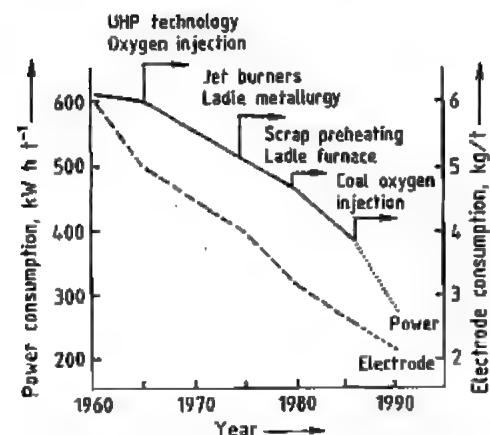


Figure 6.55: Effects of developments in electric arc furnace technology since 1965 on specific power and electrode consumption.

The essential characteristics of modern electric steel production are:

- Process automation
- Enclosure of the furnace
- Preheating of the scrap
- Water-cooled wall and roof elements
- Gas/oil-oxygen jet burners
- Foam slugging
- Current-carrying supporting arms for the electrodes
- Electrode cooling
- Facilities for charging through the furnace roof
- Bottom stirring devices
- Slag-free tapping (eccentric bottom tap hole)

Owing to their high energy input, modern electric furnaces produce considerable quantities of smoke and waste gas. To minimize environmental pollution, the furnaces are enclosed. Conditions in the workplace and surroundings can thus be maintained to a standard that meets legal requirements.

The waste gases produced in the furnace are extracted through an aperture in the furnace roof, and the dust from various sources in the furnace area is collected in the upper part

of the housing. This is constructed from sound-insulating elements, and reduces the noise level from the furnace to 20–25 dB. The waste gas is passed through a cooler which can also serve to recover the heat, and is then dedusted by cloth filters. In some operating conditions, the dust from the electric furnace can contain considerable quantities of heavy metals, such as zinc and lead, and so it is worth recovering them.

The slags produced consist of calcium silicate with 10–15% iron oxide. These are quite stable, and can be used as fill for road and dam construction.

The very rapid development of the d.c. electric arc furnace began in the middle of 1985 (Figure 6.56) [63]. Important advantages are:

- Lower electrode consumption
- Savings in electrical energy
- Smaller effect on the electricity supply system
- Symmetrical distribution of heating in the melt
- Stirring effect on the melt

The central electrode becomes the cathode, and the melt the anode, the bottom of the furnace vessel being insulated from the wall. Current-carrying elements are built into the hearth, and provide an electrical connection to the melt.

The d.c. arc acts as a jet pump, directing the gases in and around the electric arc plasma toward the melt, causing efficient heat transfer from the electrode to the melt. The largest d.c. furnace operating has a capacity of 130 t, with a transformer power of 100 MV·A, and a steel output of 10^6 t/a.

An important feature of modern electric steel production is computer control. The supervision and control of the production units, combined with precise data collection, leads to improved material flow and more efficient utilization of energy and alloying metals, and ensures high and reproducible quality.

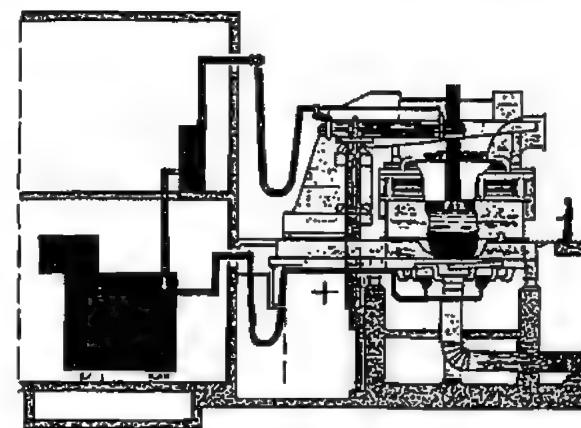


Figure 6.56: The bottom is made of electrically conducting refractory material to ensure reliable and durable continuity.

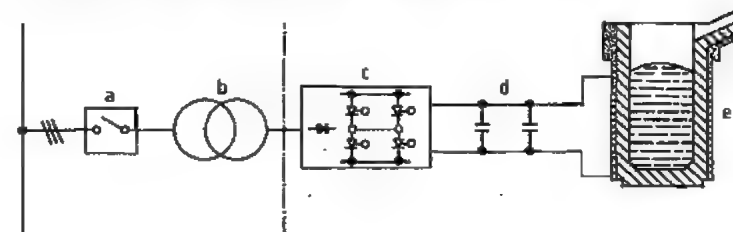


Figure 6.57: Electric induction furnace: a) Circuit breaker; b) Transformer; c) Frequency converter; d) Capacitor bank; e) Induction furnace. Melting capacities of 15 t/h can be achieved at current densities of 1 MW/t in an 8 t medium-frequency furnace.

Special Processes

In foundries, induction furnaces are widely used for melting and holding steel and nonferrous alloys [63]. The water-cooled, current-carrying coil surrounds a refractory-lined crucible (Figure 6.57) that holds the material to be melted. Electricity is supplied by a medium-frequency (MF) frequency converter, fed from a high- or low-voltage transformer. The current density can be 1 MW/t, and an output of 15 t/h can be obtained from an MF furnace with a capacity of 8 t.

Since the development of high-power plasma burners, it has become possible to use plasma melting furnaces for the production of special steels in 40 t batches. The energy is supplied by adjustable d.c. argon plasma burners, built into the furnace shell. The burner produces a plasma (ionized gas) in the electric arc, at temperatures 3000–5000 °C, and this

melts the furnace contents. The use of inert gases for the plasma protects the melt against reactions with oxygen, nitrogen, hydrogen, etc., thereby ensuring a high yield of alloy. Carburization of the melt does not occur, as there are no graphite electrodes. Vacuum treatment of the steel is not necessary.

For the production of special alloys containing high proportions of alloying elements with a high affinity for oxygen (Al, Ti, etc.), it is common to use inductively heated or electron beam vacuum furnaces.

The Siemens–Martin Open Hearth Process

In 1960, the Siemens–Martin open hearth process (Figure 6.58) produced ca. 70% of the world's crude steel, but this rapidly declined following the growth of the oxygen-blowing

and electric steel processes, and ceased operation after a few years.

It was developed for melting scrap, and was characterized by its great flexibility with respect to the proportions of pig iron and scrap used. The tank-shaped furnaces are heated by fossil fuels such as gas or oil, burned in hot air. The regenerative air preheating invented by Siemens takes place in "checker chambers" that contain refractory bricks heated by the waste gas, and are situated under the furnace. The combustion temperatures achieved enable steel scrap to be melted.

The capacity of these furnaces is 50–1000 t. The use of air for the combustion leads to the production of large quantities of waste gas, whose purification, sometimes including desulfurization, is difficult and expensive. Additional oxygen, introduced through lances or burners (tandem furnaces), has been used to improve operation, but this leads to severe erosion of the refractory furnace lining. The open hearth process has in general lost its importance, as it cannot achieve either the output or flexibility of blowing processes.

6.3.3.3 Production of Stainless Steels

Although world steel production is subject to very severe fluctuations dictated by market conditions, the average growth rate of stainless steels (i.e., resistant to rust, acid, and heat) between 1950 and 1985 was 6%. In 1990, total output reached 10^7 t. Special metallurgical processes have been developed for steels with a chromium content 12–28% and low carbon content [65].

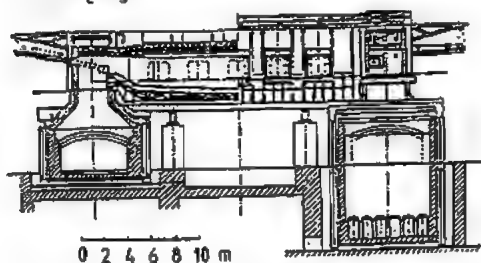


Figure 6.58: German-American design for a 250 t furnace for gas and oil firing [64].

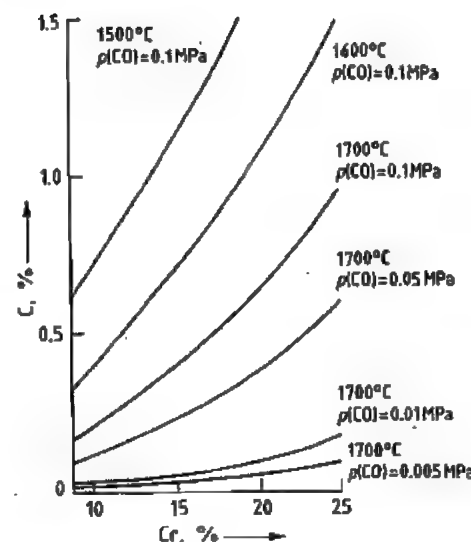


Figure 6.59: The Fe-C-Cr-O system.

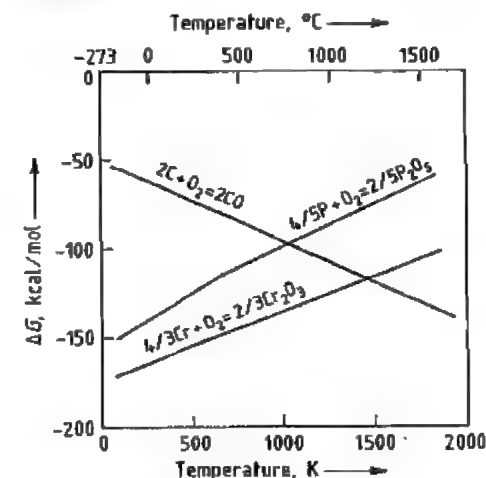


Figure 6.60: Free energy of oxidation of Cr, P, and C as a function of temperature.

Production conditions are determined by the thermodynamic equilibria of the reactions of oxygen with carbon and chromium (Figures 6.59, 6.60).

In the first process variation, which is mainly used in western countries, an electric furnace is used to melt scrap and alloying elements. The composition of the molten metal used corresponds approximately to that of the desired steel product, apart from the carbon

content. Decarburization and desulfurization are carried out, either in a converter or a ladle in vacuum, or in a combination of the two (Figure 6.61).

The converters are operated by the combined blowing technique (i.e., via top lance and bottom tuyères) to increase the rate of decarburization. Nitrogen is used as the protective gas for the bottom tuyères and to reduce the oxygen partial pressure. Argon is used to give low carbon contents and to avoid nitro-

gen pick up of the steel. After decarburization, the Cr_2O_3 -containing slag is reduced with silicon, and the sulfur combines with the lime-based slag. In an alternative process, the pre-melt is poured from the electric furnace into a ladle placed in a vacuum chamber. Decarburization is then achieved by a stream of oxygen which enters via the lid of the vacuum chamber as the pressure is reduced, and is then blown through a lance into or over the melt.

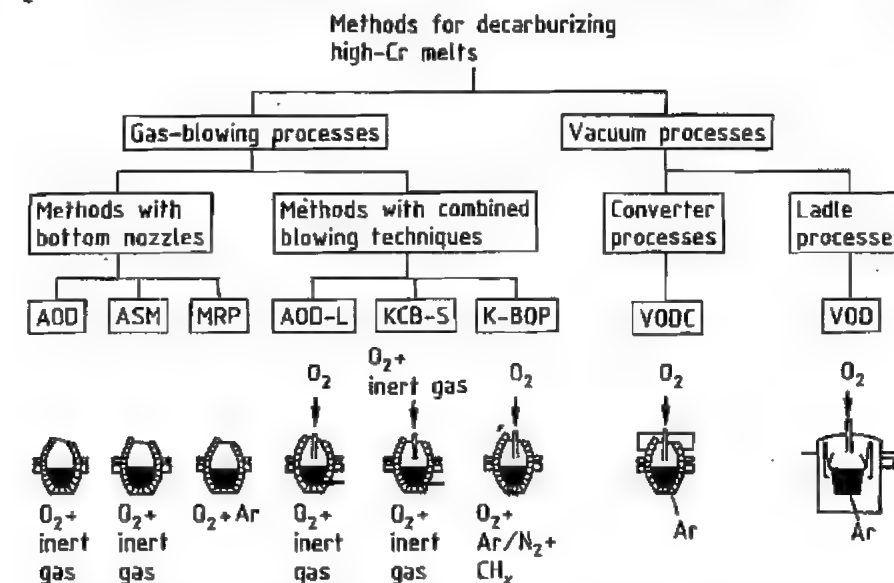


Figure 6.61: Methods for decarburizing high-chromium melts: AOD = argon-oxygen decarburization; ASM = argon secondary metallurgy; MRP = metal refining process; AOD-L = argon-oxygen decarburization lance; KCB-S = Krupp combined blowing stainless; K-BOP = Kawasaki basic oxygen process; VODC = vacuum-oxygen decarburization converter; VOD = vacuum-oxygen decarburization.

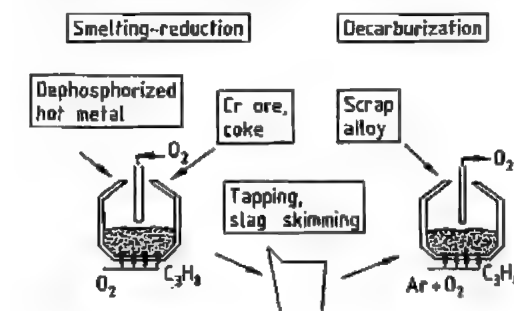


Figure 6.62: Two-stage stainless steel production (smelting-reduction) process.

In the vacuum process, the rate of decarburization reaches 0.03%/min, a considerably lower figure than that achieved by the converter processes. The latter give high productivity and favorable economics and are therefore, used for high-volume production of crude stainless steels. Vacuum processes are especially suitable for the production of special steels with very low carbon content (30 ppm), and low levels of nitrogen and hydrogen.

A combination of both processes utilizes the high decarburization rate of the converter in the high-carbon content region, and the low

carbon levels achievable by the vacuum process.

In Japan, a two-stage process is used for the melt reduction of chromium ores to produce stainless steels (Figure 6.62) [66]. Two 85 t combined blowing converters are used. In the first of these, chromium ore is added to a dephosphorized pig iron bath where it is reduced to chromium with coal and oxygen. The carbon-containing chromium melt is tapped and, after slag removal, charged to the second converter, where it is decarburized. The heat of reaction enables added scrap and alloying metals to be melted. The advantage of the combined blowing converter is that, as well as passing oxygen and argon through the bottom tuyères, it is also possible to decarburize with pure oxygen, as the tuyères are cooled with hydrocarbons.

6.3.4 Secondary Metallurgy

The steelmaking processes described earlier with the exception of plasma furnaces, take place in oxidizing atmospheres, and are designed to maximize the output and cost-effectiveness of crude steel production.

The secondary metallurgical treatment processes produce the specific properties required for the various applications of the steels concerned. They include:

- Adjustment of alloy composition
- Deoxidation
- Homogenization of temperature and composition
- Temperature adjustment
- Decarburization
- Desulfurization
- Degassing
- Control of inclusion shape
- Adjustment of purity

The processes take place in the steel ladle, so that the steel production equipment is not involved, and correspond to the quality program and the production plan (Figure 6.63) [55].

It is essential that the slag produced during the oxidation processes should be separated cleanly, and that the refractory lining of the ladle should not act as a source of oxygen during the reduction phase, or have a detrimental effect on the composition of the reaction slag.

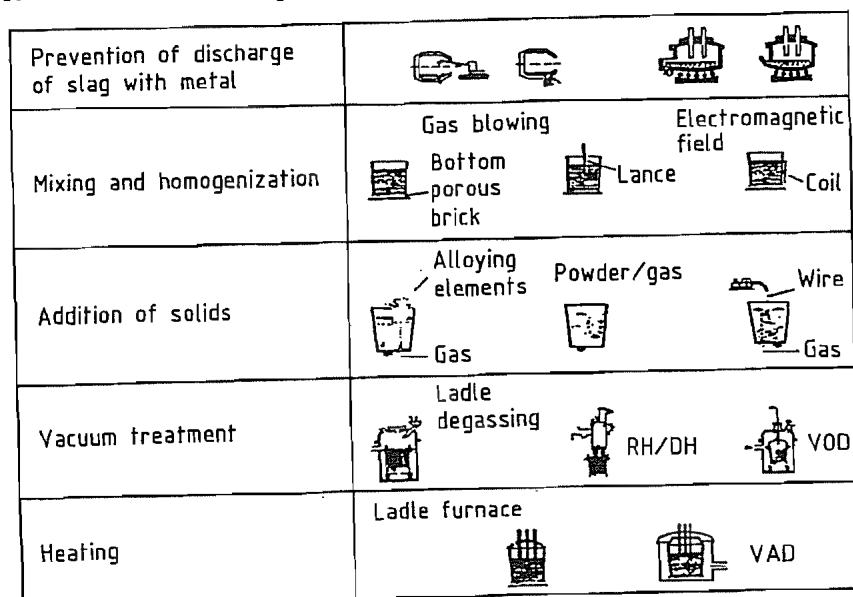


Figure 6.63: Secondary metallurgy processes in steel production. VAD = vacuum arc decarburization.

To hold back the slag formed during the oxygen-blowing process, floating stoppers are used to close off the tap hole. Their function depends on the different densities of the steel and slag; alternatively, mechanical or pneumatic devices can be used. In electric furnaces, there is a curved region or syphon near the tapping hole, or an oval hearth is provided so that no slag is discharged, provided that a residue of 15–20% steel is retained in the furnace.

6.3.4.1 Steel Treatment at Atmospheric Pressure

Secondary metallurgy requires mixing in the ladle. This is achieved by passing gases through porous bricks in the bottom of the ladle, or by injecting them through refractory-covered lances dipping into the melt, thus producing a rising stream of bubbles. A possible alternative is to use the stirring effect of electromagnetic fields acting through the nonmagnetic walls of the ladle. Depending on the amount of mixing energy generated, this can cause circulation and homogenization of the steel under the slag layer, or mixing of the steel with the slag with chemical reaction, e.g., desulfurization. If ladle covers are used, the steel can be protected from reoxidation and falling temperature.

The solid materials can be added in lump form through openings in the ladle lid, or injected in powder form through lances, using a gas as transport medium. For exactly measured additions, solid wire can be added (e.g., aluminum), or wire filled with other substances (e.g., CaSi), which can be added almost without loss of material.

Deoxidation

As well as alloy addition, deoxidation (removal of residual oxygen) is necessary in the production of quality steels. Depending on the carbon content of the steel, it can contain 100–300 ppm dissolved oxygen, and this is removed by adding elements with an affinity for oxygen (e.g., silicon or aluminum, to form sil-

ica or alumina). These oxides are of lower density than steel, but their particle size also greatly affects their upward movement. The deoxidation products are encouraged to coagulate by agitating the steel in the ladle with argon or nitrogen. The ascending reaction products take up the liquid reactive ladle slag. The amount of these materials remaining in the steel determines its oxide content, and affects its mechanical properties. By using a combination of deoxidizing metals, a very low level of oxygen in the steel can be achieved (Figure 6.64) [68].

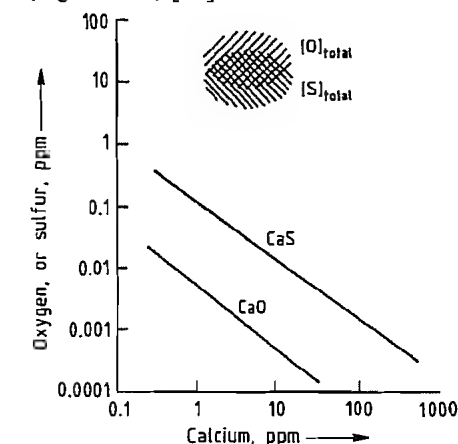


Figure 6.64: Equilibrium of calcium and sulfur or oxygen in liquid iron at unit activity of CaS and CaO [66, 67].

Desulfurization

For high rates of steel production, only a limited amount of desulfurization can be carried out in the blast furnace. When a blast furnace process is optimized for low fuel consumption, the sulfur distribution coefficient between the slag and the pig iron is 20, which, for current mass ratios, leads to a sulfur content of 500 ppm in the pig iron (Figure 6.65). Depending on quality requirements, the first step is the injection of lime and other calcium-magnesium compounds into the pig iron ladle. The relatively poor sulfur partition coefficient (ca. 5) in the oxygen injection steel-making process is due to the oxidizing reactions. However, if the steel has a high enough aluminum content after deoxidation,

this gives good reducing conditions. If the correct desulfurizing agents are chosen (CaO , Mg , CaC_2 , CaSi), or lime-saturated desulfurizing slags are used, sulfur distribution coefficients of 1000 can be achieved [69]. The desulfurization of the pig iron and steel, especially if both these processes are used, enables the required quality to be achieved flexibly and economically. The use of desulfurizing slags requires intensive mixing of the steel and the slag under reducing conditions.

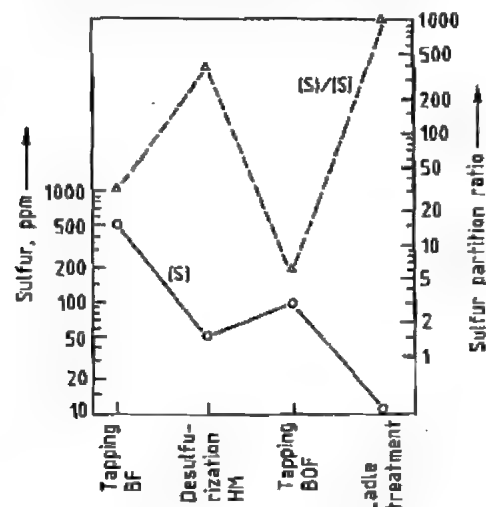


Figure 6.65: Process stages for adjustment of low sulfur content in liquid steel.

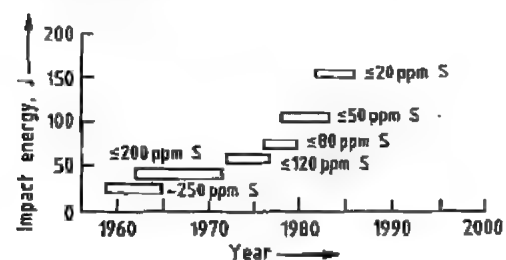


Figure 6.66: Development of toughness and sulfur content.

Figure 6.66 shows the changes in sulfur content in steel produced on a large scale over a number of years [68]. In this example, which refers to steel used for pipes, the development of toughness and sulfur content is shown. The use of calcium compounds under certain conditions leads to the formation of spheroidal in-

clusions that are not deformed during the rolling process. This has enabled high-strength steels with good toughness properties to be developed.

Dephosphorization

Phosphorus removal is carried out under oxidizing conditions during production of the crude steel, and is influenced by the lime saturation, the P_2O_5 content, and the temperature of the slag produced during decarburization (Section 6.3.3). The production of low-phosphorus steel requires low-P, low-Mn pig iron, and effective removal of the P_2O_5 -containing slag produced during decarburization and before deoxidation.

Temperature Control

The temperature changes during steel production affect the course of the reaction (as shown by the example of dephosphorization), and also affect the economics (wear of the refractory linings of furnaces and ladles). The secondary metallurgical operations: alloying, desulfurization, degassing, etc., require time, and therefore involve heat losses. Without ladle heating, this would necessitate the use of unfeasibly high tapping temperatures. Electrically heated ladle furnaces are increasingly used in steelworks—initially in EF steel plants and then in BOF plants—to ensure an optimum temperature regime during the process.

Figure 6.67 illustrates the increasing use of ladle furnaces [67]. The furnaces consist of an assembly of two or three a.c. or d.c. electrodes, and a water-cooled roof, with fume extraction equipment, and a working door for adding materials and for the control equipment (Figure 6.68) [69].

The transformer capacity is ca. 150 kV·A per tonne ladle contents, and gives a heating rate of 5 °C/min. The diameter of the pitch circle has been reduced to 600–700 mm in new designs to protect the refractory ladle lining. Agitation of the steel and slag to homogenize the steel, and to promote the steel-slag reactions, is very important in the operation of the

ladle furnace. The electricity consumption for treatment time ca. 40 min is 30–40 KWh/t, and the amount of electrode material consumed is 0.3 kg per tonne of steel. With a ladle furnace, the temperature at which the steel is tapped can be reduced by 100 °C without affecting the secondary metallurgical reactions.

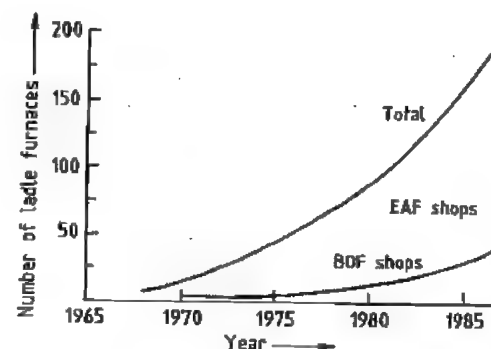


Figure 6.67: Ladle furnace development.

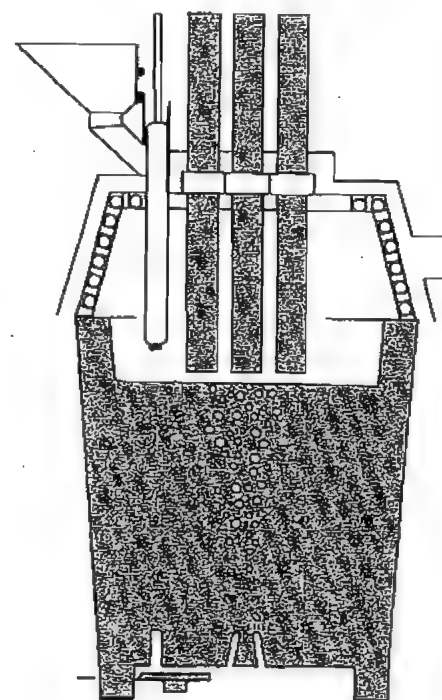


Figure 6.68: Typical layout for a ladle furnace.

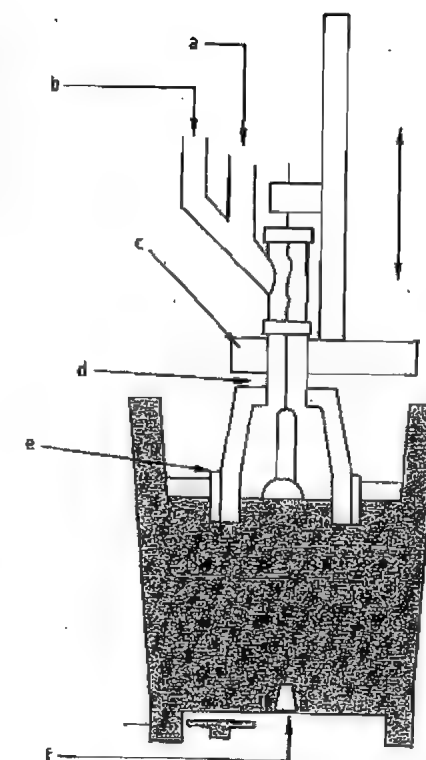


Figure 6.69: Equipment for the CAS process: a) Dust-collecting hood; b) Alloy chute; c) Snorkel raising and lowering unit; d) Oxygen lance; e) Bell; f) Porous plug.

An alternative to the ladle furnace is the CAS/CAS-OB (Composition Adjustment by Sealed Argon Bubbling) developed by Nippon Steel [69], the IR-UT (Injection Refining-Up Temperature) process proposed by Sumitomo. The heat evolved by the oxidation of aluminum or silicon is used to heat the steel, instead of electrical energy. The process is suitable for producing flat products that are insensitive to hydrogen. After the slag-free steel has been tapped, it is agitated by inert gas, and alloyed in a bell (Figure 6.69). If the temperature has decreased too much, the melt can be heated to the required pouring temperature by adding aluminum and oxidizing it with oxygen. The addition of O_2 at a rate of $11 \text{ m}^3 \text{h}^{-1} \text{t}^{-1}$ gives a heating rate of 7 °C/min.

6.3.4.2 Vacuum Treatment

The vacuum treatment of steel is used increasingly owing to its versatility and special advantages, and is indispensable for removal of gases dissolved in the steel, such as hydrogen and nitrogen. The reactions proceed at very low pressure (0.5 hPa). The various processes are shown in Figure 6.70 [55]. They can be divided into three groups: recirculating treatment of small quantities of metal; ladle treatment; and treatment of a stream of molten metal.

The recirculating processes are characterized by high throughputs. In the RH plant, two refractory-clad snorkels dip into the steel being treated; in the DH plant only one snorkel is used. Whereas in the RH process, the steel is transferred into the vacuum vessel by blowing inert gas via a nozzle (gas lift), in the DH plant the movement of the steel in the vessel is achieved by the up-and-down motion of the vessel. In both processes, oxygen lances can be provided.

Decarburization

The decarburization reaction is strongly pressure dependent, so that when it is carried out under vacuum, fine decarburization is the result. As shown in Figure 6.71, carbon content < 50 ppm can be achieved reproducibly under optimal process conditions [68].

The required treatment time is strongly pressure dependent. A rapid decrease in pressure is only feasible if the vacuum vessel is fairly large, as the melt splashes severely. If the amount of oxygen dissolved in the steel is insufficient for the decarburization reaction, oxygen is blown in with a lance, liberating heat.

Nitrogen Removal

High nitrogen content has a detrimental effect on the deep-drawing properties of continuously annealed mild steel, and also reduces the resistance of tube steels to hydrogen-induced cracking (HIC). The change in nitrogen

content during oxygen blowing is shown in Figure 6.72 [68].

If the nitrogen content in the pig iron is low, nitrogen levels of 30 ppm in plain carbon steels can be achieved. However, steel can pick up nitrogen if nitrogen-containing alloying elements are used, and nitrogen removal may then be necessary. This can be carried out by vacuum treatment under controlled conditions [68]. Nitrogen removal by ladle degassing (after desulfurization) can give a nitrogen content ca. 50 ppm (Figure 6.73). Sulfur interferes with nitrogen removal.

The ladle degassing operation gives intensive phase contact between the steel and the slag, which has a beneficial effect on desulfurization. With 10 ppm sulfur and low oxygen content, a nitrogen level of 30 ppm in the steel can be achieved, whether the starting level is 50 or 110 ppm.

Dehydrogenation

To avoid flaking (material separation) in the steel, the hydrogen content must be lower than its maximum solubility. For large cross sections, i.e., conditions favoring segregation, it is necessary to reduce the hydrogen content of the liquid steel to < 0.8 ppm. The diffusion reaction is controlled by the difference between the hydrogen partial pressure in the steel and that in the gas at the phase boundary, and therefore proceeds more rapidly as the pressure in the vessel decreases. The formation of new surfaces by intensive purging with inert gas, or otherwise agitating the steel in RH and DH equipment promotes hydrogen removal, as shown in Figure 6.74 [70].

The choice of steel production and secondary metallurgical processes depends on the product, the production rate, the raw material, and the energy situation. In Europe, high-quality flat products are produced by the route: blast furnace – oxygen blowing – RH or DH vacuum treatment – continuous casting. Long products are mainly produced by the route: electric furnace – ladle furnace – continuous casting. New developments such as COREX–EOF–KES and continuous casting to give

cast-to-shape products, promise technological and economic stimuli, especially with respect to the environment.

6.3.4.3 Fundamentals

All processes of casting and solidification depend on the basic processes of heat transfer, mass transfer, and interface kinetics. This applies not only to ingot casting, continuous casting, and foundry work, but also to remelting and spraying processes, crystal growth, the production of composite materials from a melt, and rapid solidification to give a crystalline or amorphous structure. These basic prin-

ciples are valid for all metals and alloys, and the theory is very advanced [71–76].

Nevertheless, steel is special material, having its own characteristic casting and solidification properties that differ from those of both light and heavy nonferrous metals. The peculiarities of steel include: high melting point, low thermal conductivity, phase transformations of the iron, high density, and strong affinity for oxygen. The wide variety of alloy compositions of steel is also reflected in its solidification properties, i.e., the way in which the thermal processes and structure formation take place [77].

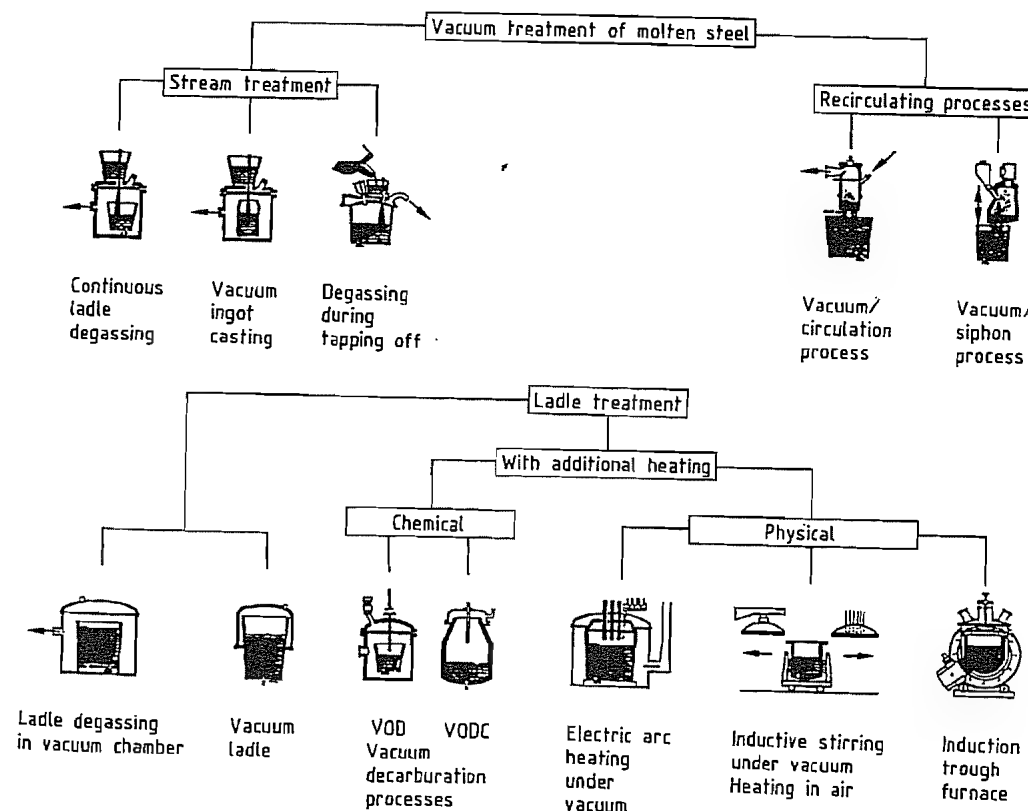


Figure 6.70: Vacuum treatment of steel.

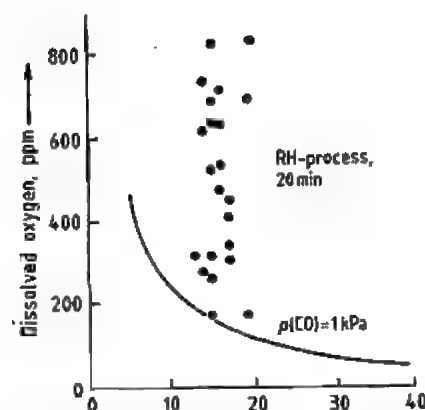


Figure 6.71: Final carbon content as a function of dissolved oxygen.

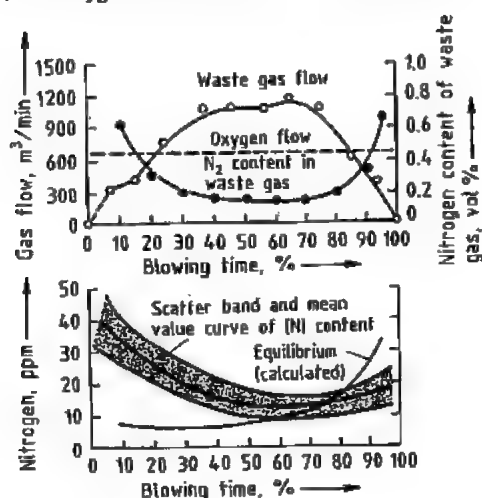


Figure 6.72: Nitrogen removal.

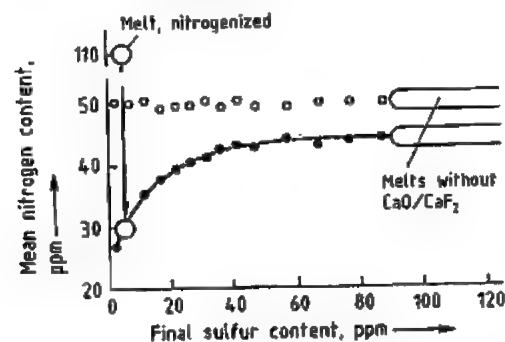


Figure 6.73: Mean nitrogen content before and after vacuum treatment. \circ = [N] before ladle degassing; \bullet = [N] after ladle degassing.

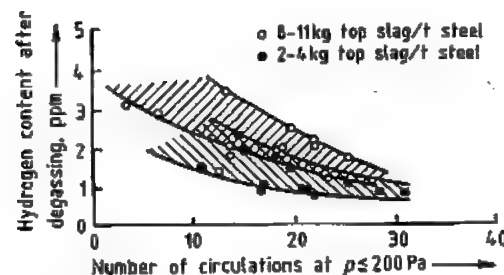


Figure 6.74: Hydrogen removal.

A rigorous scientific treatment of heat and mass transfer and interface kinetics cannot be given here, but their most important consequences are indicated, including solidification morphology, micro- and macrosegregation phenomena, sulfide precipitation, and the formation of inclusions by deoxidation. Thermal stress and mechanical deformation also merit consideration, as they particularly affect the quality of the product; processing techniques and mechanical engineering are tailored to suit them.

6.3.5 Casting and Solidification

Solidification Morphology of Steel. The general criteria for the stability of a nominally planar solidification front are: high superheat, convection, low rate of solidification, low content of alloying elements, and a high partition ratio. These conditions are seldom met in casting operations in the steel industry. Much more frequently, there is "constitutional undercooling" at the solidification front, so that steel almost always solidifies dendritically.

Figure 6.75 shows a scanning electron micrograph of a "quasi-decanted" dendritic solidification front from the central shrinkage cavity of a continuously cast billet of high-temperature steel.

The dendritic crystals consist of primary, secondary, and tertiary arms, all with crystallographic growth direction [100]. The dendritic growth mainly determines the spatial pattern of segregation.

Primary and secondary dendrite arm spacings in a typical continuously cast steel slab are shown in Figure 6.76. Plots of these spac-

ings against distance from a surface of the slab are parabolic, with the widest spacings in the center of the slab.

By the method of steady-state unidirectional solidification, typical values for the growth variables affecting the dendrite arm spacings can be determined [78, 79]. In the equations:

$$\lambda = cR^mG^n$$

and

$$\lambda = c\theta_f$$

R represents the solidification rate, G the temperature gradient, and θ_f the local solidification time.

Figure 6.77 shows such a correlation for the primary arm spacings in a steel with 0.15% C and 1.44% Mn. Further values of these parameters for selected steels are given in Table 6.11. These show that high-alloy steels have a finer dendritic structure than low-alloy steels. Figure 6.78 shows that, for four low-alloy steels (I-IV), the data are in good agreement with equations of the form:

$$\lambda_2 = c\theta_f$$

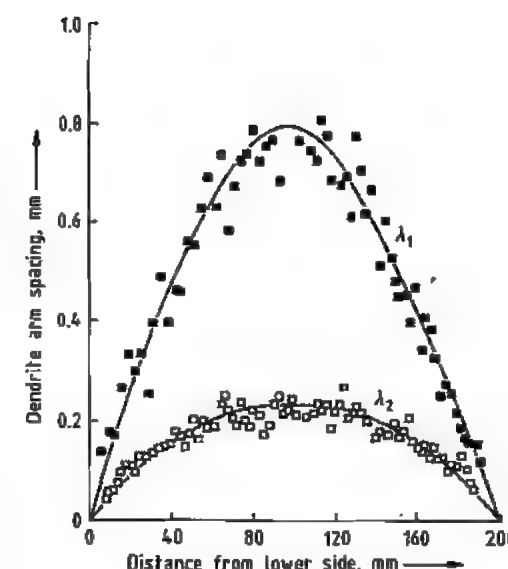


Figure 6.76: Variation of dendrite arm spacing in a continuously cast slab of steel, grade API X60, 0.14% C, 1.50% Mn.

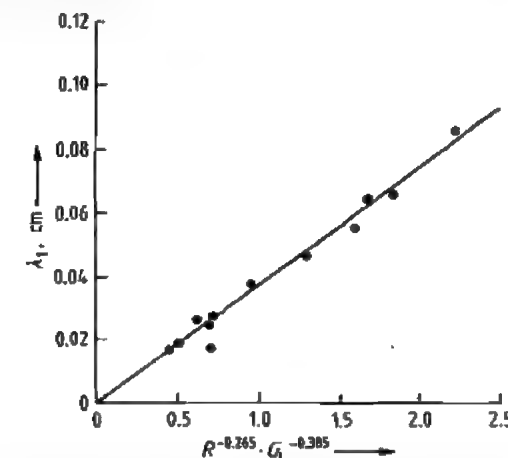


Figure 6.77: Correlation of primary arm spacing λ_1 with R and G_L for steel II with 0.15% C, 1.44% Mn. $\lambda_1 = 0.0368R^{0.263}G_L^{-0.385}$, λ_1 in cm; R in cm/s; G_L (K/cm) is the temperature gradient at the liquidus temperature.

Figure 6.75: Dendrite morphology in center of a continuously cast billet of steel, grade 10 CrMo 910.

Table 6.11: Equations for dendrite arm spacings λ (cm) as a function of growth variables R (cm/s), G ($^{\circ}\text{C}/\text{cm}$), and θ_f (s).

Type	Steel composition	Primary arms	Secondary arms	
I	0.09% C, 1.36% Mn	$\lambda_1 = 0.0367R^{0.29}G^{-0.43}$	$\lambda_2 = 0.01487R^{0.41}G^{-0.51}$	$\lambda_3 = 0.00280\theta_f^{0.507}$
II	0.15% C, 1.44% Mn	$\lambda_1 = 0.0368R^{0.27}G^{-0.39}$	$\lambda_2 = 0.00645R^{0.43}G^{-0.40}$	$\lambda_3 = 0.00168\theta_f^{0.43}$
III	0.59% C, 1.10% Mn	$\lambda_1 = 0.1900R^{0.26}G^{-0.72}$	$\lambda_2 = 0.01500R^{0.41}G^{-0.51}$	$\lambda_3 = 0.00158\theta_f^{0.447}$
IV	1.48% C, 1.14% Mn	$\lambda_1 = 0.2700R^{0.24}G^{-0.72}$	$\lambda_2 = 0.01000R^{0.49}G^{-0.51}$	$\lambda_3 = 0.00072\theta_f^{0.50}$
V	0.63% C, 24.9% Mn	$\lambda_1 = 0.0610R^{0.17}G^{-0.36}$	$\lambda_2 = 0.00360R^{0.41}G^{-0.37}$	$\lambda_3 = 0.00058\theta_f^{0.44}$
VI	0.68% C, 28.3% Cr	$\lambda_1 = 0.0280R^{0.25}G^{-0.51}$	$\lambda_2 = 0.00320R^{0.41}G^{-0.37}$	$\lambda_3 = 0.00052\theta_f^{0.39}$

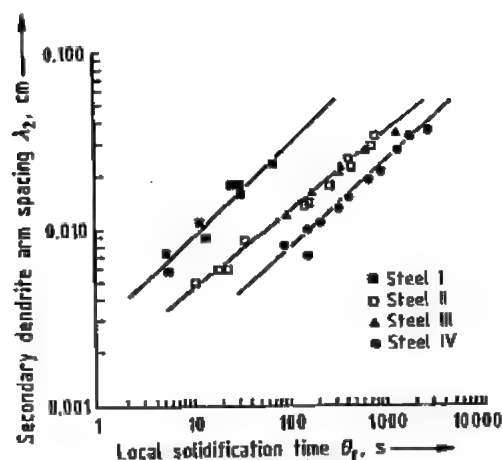


Figure 6.78: Correlation of secondary arm spacing λ_2 with local solidification time θ_x .

Figure 6.79: Formation of free crystals in a steel melt continuously cast with undercooling.

If R , G , and θ_f are known, the segregation spacings can be predicted. Conversely, local cooling rates can be found by measuring the segregation spacings.

If molten metal is undercooled during casting, free crystallites can be generated. This can take place by heterogeneous nucleation, or by the detachment of dendrite arms, which can be caused by a small degree of superheat, or by inoculation, stirring, jolting, or vibration.

A suspension of crystals in molten steel is shown in Figure 6.79. The crystallites can redissolve and become globular in form. The globulites settle out during casting and appear, e.g., at the bottom of an ingot or the lower side or central zone of a continuously cast strand.

An advantage of this equiaxed structure is that its properties are isotropic.

Interdendritic Microsegregation. The thermodynamic basis for microsegregation is the change in concentration that accompanies a phase change from liquid to solid, and is expressed by the partition ratios k of the solute elements present in the iron. Kinetic factors include enrichment of the dissolved elements in front of the phase boundary, which depends on mass transfer in the liquid, and the extent of diffusional equilibration in the solid. The degree of concentration enrichment at the phase boundary C_s^* , in the case of layer crystal formation without diffusion in the solid, is given by:

$$C_s^* = kC_0(1-f_s)^{1/k-1}$$

where C_0 is the starting concentration, and f_s the extent of solidification in the dendritic volume element. The degree of solute rejection is, therefore, determined by k . Typical values of k for the more important elements found in steel are given in Table 6.12. The elements S, P, and C segregate strongly. With carbon, some concentration equilibration takes place by diffusion.

Table 6.12: Equilibrium partition ratio k of solute element at solid-liquid interface for δ - or γ -iron.

	k^{δ}	k^{γ}
C	0.20	0.35
Si	0.77	0.52
Mn	0.75	0.75
P	0.13	0.06
S	0.06	0.025

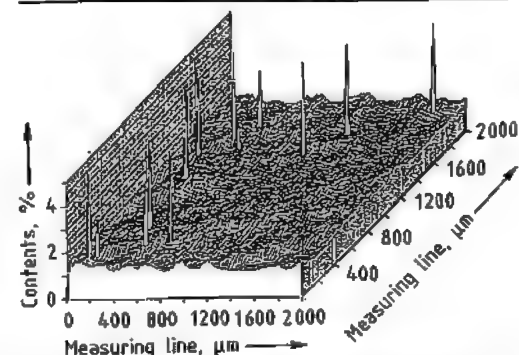


Figure 6.80: Concentration profile of the microsegregation of Mn in a 2.8 t ingot of steel, grade 25 CrMo 4.

Segregation can be measured over a large area by computer-controlled automatic electron beam microanalysis. For example, Figure 6.80 shows a three-dimensional relief map of the manganese concentration in a 25 CrMo 4 steel [80]. The scattered high peaks are caused by MnS inclusions.

Modern microanalytical techniques can produce up to 10^6 point measurements within 24 h. In a typical manganese determination, the area investigated can be 80×80 mm, the number of points measured 600 000, the time required 13 h, and the beam diameter $100 \mu\text{m}$ [81].

Formation of Macrosegregations. Macrosegregations extend over considerably greater distances than dendrite branches. Typical ranges are between the edge and the center or between the top and the bottom of an ingot. The distinction must be made between enrichment and depletion. A systematic discussion of segregation phenomena, including a theoretical treatment, is given in [82].

Positive A- and V-type segregations in cast ingots result from natural convection due to density differences in the enriched liquid over the cross section of the cast material. Stable flow channels can be formed. Sometimes, V-type segregation can also occur in the center of continuously cast strands with equiaxed solidification structure.

In the two-dimensional solidification of continuously cast billets, segregation can take place along the axis of the core. This is associated with shrinkage, and is caused by the growth of dendrites that periodically form bridges that partially seal off the lower part of the liquid metal. Owing to the volume deficit, a powerful suction force is produced toward the crater end. This type of flow restriction does not occur during the one-dimensional solidification of slabs.

Segregation can also be caused by deformation of the outer shell of a strand, e.g., by nonsteady-state bulging outward and rolling back again [83]. This causes a pumping effect in the remaining liquid metal, and leads to so-called central segregation in the slab. Tensile

strains at the heterogeneous solidification front cause segregated internal cracking if critical stresses are exceeded. "Soft" or "hard" reduction, to densify the central zone must, therefore, not lead to overstressing of the material below the solidus.

If there is forced convection at the solidification front, e.g., caused by rimming action during ingot casting of unkill steel or by electromagnetic agitation, a washing effect occurs. A depleted streaky layer is produced. With continuous casting, "white bands" are formed.

Depletion is also caused by sedimentation of suspended crystallites, as these are purer than the melt. The accumulation of a conical heap of crystals at the bottom of the ingot therefore leads to "negative" segregation, whereby the axial concentration of alloying elements increases toward the top of the ingot. This happens, e.g., with heavy forging grade ingots.

Sulfide Precipitation. With modern ladle metallurgical treatment, the sulfur content can be brought below 10 ppm, albeit at some cost, by transferring the sulfur into the slag. Any dissolved residual sulfur can be combined with calcium to form stable calcium sulfide, which has no harmful effects on the properties of the product.

However, it is not always necessary to have the lowest possible sulfur content, so desulfurization and calcium treatment of the steel can often be omitted. The sulfur then becomes concentrated in the interdendritic spaces, owing to its low k value, and eventually precipitates as MnS. The course of the reaction, and hence the form of the sulfide, are determined by the degree of deoxidation and alloy content of the melt, and the local processes of solute redistribution and mass transfer. The various sulfide types in the cast product are [84, 85]:

Type I. Globular oxysulfides that were originally liquid. Formation mechanism: monotectic degeneration. Steel grades: unkill, semikilled.

tic. Steel grades: fully killed, high-alloy, containing C, Si, P, Cr, Zr.

The scanning electron micrographs in Figure 6.81 show typical examples of these morphologies. Types intermediate between II and III can have faceted shapes with branched dendrites.

The size of the sulfide inclusions depends on the local precipitation rate and hence indirectly on the rate of cooling at the solidus temperature. This correlation is illustrated by the log-log plot in Figure 6.82 [86].

Figure 6.81: Variation of sulfide morphologies in as-cast steel: A) Type I; B, C) Type II; D, E) Transitional types; F) Type III.

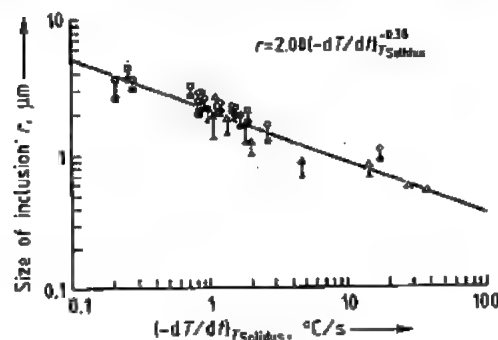


Figure 6.82: Mean size of sulfide inclusions in steel ingots with 0.55% C, 2.00% Mn, 0.009–0.039% S.

Type II. Coral-shaped chain-like sulfide colonies. Formation mechanism: eutectic. Steel grades: killed, low alloy.

Type III. Angular, crystalline sulfide particles. Formation mechanism: "divorced" eutec-

Figure 6.83: Growth morphologies of alumina inclusions in Al-killed steel.

Formation of Inclusions by Deoxidation. In contrast to sulfide formation during solidification, oxide inclusions are precipitated in the liquid steel at an earlier stage by deoxidation. The amount of dissolved oxygen is reduced to the equilibrium value in a few seconds after the addition of aluminum [87]. As deoxidation proceeds, the inclusions agglomerate or coagulate, and mostly go into the slag. This flotation leads to a reduction in so-called total oxygen.

When aluminum is used for deoxidation, alumina inclusions are formed with a spheroidal or dendritic morphology (Figure 6.83) [88]. The coral-like shapes are formed by agglomeration of particles, 2–5 μm in size. In steelworks these clusters are referred to as "nests" or "clouds".

The various growth shapes that can be formed under different supersaturation condi-

tions and activities of the oxygen and aluminum are shown in Figure 6.84 [89]. From left to right, the oxygen level decreases and the aluminum activity increases. At low oxygen levels, the spheroidal oxides initially formed become covered with radiating, stalky, or compact nitrides.

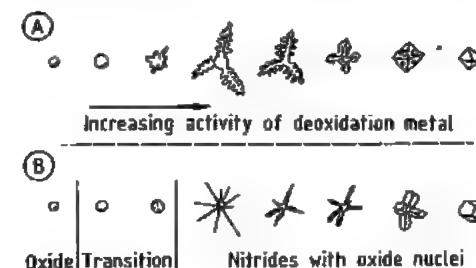


Figure 6.84: Schematic representation of oxide and nitride morphologies as a function of oxygen level.

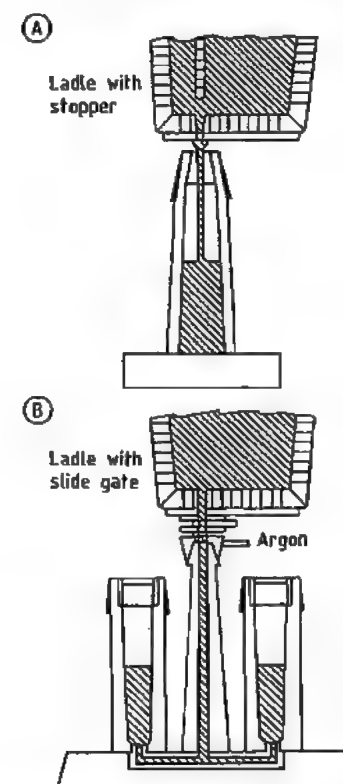


Figure 6.85: Top pouring (A) and bottom (B) pouring during ingot casting [90].

6.3.5.1 Ingot Casting

The transition of steel from liquid to solid is mainly achieved by continuous casting. Nevertheless, the older ingot casting process is still used in steelworks all over the world. The molten steel is poured into ingot molds, where it solidifies.

The steel is poured (teemed) from the refractory-lined ladle via a ceramic, closable outlet nozzle. There are two methods of filling the ingot mold. In the top-pouring method, the steel is poured from above directly into the mold, and in the bottom-pouring method, it passes down a central funnel, then through a system of refractory passageways built into a thick steel plate, and passes from below into the ingot molds standing on the plate (Figure 6.85) [90].

The molds can have a rectangular, square, circular, or polygonal interior cross section, depending on the cross section of the profile to be produced by rolling. To facilitate removal of the solid ingot, the mold tapers slightly outward, with the wider end either at the bottom (big-end-down molds) or top (big-end-up molds) (Figure 6.86) [91]. Ingots can be 0.1–40 t for rolled steel, and up to 500 t for forged steel.

Apart from the cross-sectional shape, the type of ingot mold, and the pouring method, ingots are also characterized according to the physical, thermodynamic, and chemical processes that take place during solidification. Several gases are present in solution in liquid steel. The solvent power of the steel decreases as the temperature decreases, and as the steel solidifies. In ingot casting, oxygen is of particular significance for the solidification process. If oxygen is liberated during solidification, it reacts with the carbon in the steel to form carbon monoxide. This can be partially or completely prevented by combining the oxygen with deoxidants such as aluminum, silicon, or titanium.

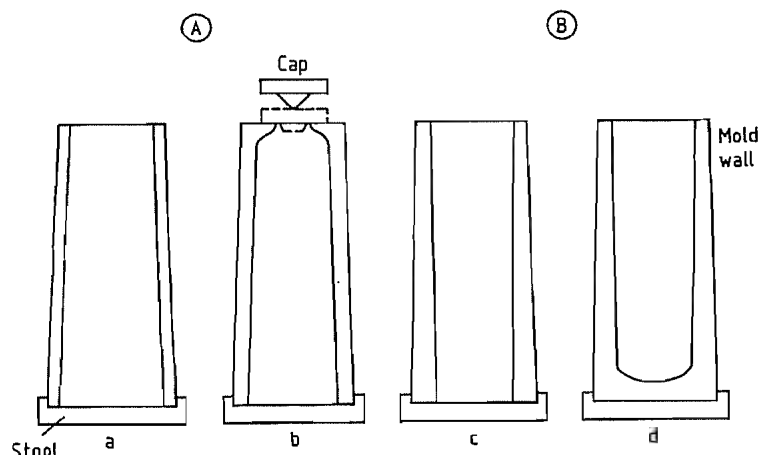


Figure 6.86: Cross sections (not to scale) of the principal types of ingot mold [91]. A) Big-end-down-molds: open top (a) and bottle top (b); B) Big-end-up-molds: open top (c) and closed top (d).

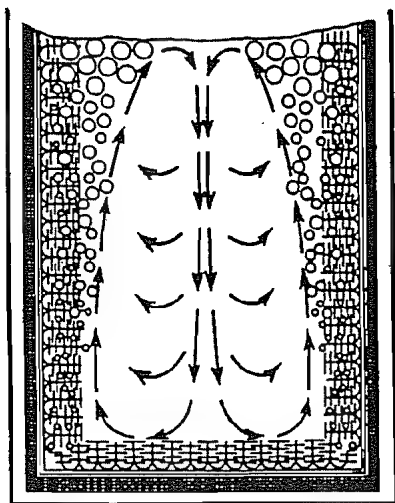


Figure 6.87: Flow pattern in a rimming steel ingot during solidification [97].

If the oxygen is allowed to react with the carbon, the steel product is known as rimming steel. Partial deoxidation leads to "semikilled" steel, and complete deoxidation to "killed steel". Deoxidation to semikilled or killed steel is carried out in the ladle. There is also a combined rimming and killed steel, obtained by first allowing the melt to solidify for some time, and then deoxidizing it in the mold, after which it solidifies completely like a killed steel. This produces "ingot-killed steel".

Rimming Steel. As soon as the liquid steel comes into contact with the walls of the mold and the bottom plate, a thin skin of solid steel is formed. This grows rapidly at first, as the cold mold and bottom plate rapidly absorb heat, and, much later, release it to the atmosphere. After a short time, this compact layer of steel becomes detached from the ingot wall as the solid steel contracts. The gap formed reduces the heat transfer rate from the steel to the mold, and hence the rate of loss of heat to the surroundings. Consequently, the steel solidifies more slowly [92–96].

As the steel changes from liquid to solid, the solubility of oxygen decreases, so that it is liberated and reacts with the carbon present to form carbon monoxide. In addition to the dissolved oxygen present at the start of the pouring process, atmospheric oxygen is picked up by the liquid steel during pouring, and during its subsequent solidification; this also reacts with the carbon in the steel. The CO gas bubbles are partly entrapped between the growing steel dendrites, forming so-called edge blow holes, but most of them ascend in the region of the solidification front, combining with other bubbles on their way up. This leads to the formation of a rim of bubbles at the edge of the steel, and an upward gas flow which causes an upward flow of the liquid steel. Thus, the steel in the ingot flows strongly upward at the solid-

ification front and downward in the center (Figure 6.87) [97]. This rimming action has led to the name "rimming steel".

In the production of rimming steel, CO should be produced rapidly from the start of solidification, giving a strong flow. If the flow is weak, CO bubbles remain entrapped by the growing dendrites. This causes excessive formation of a ring of bubbles not far below the outer surface of the ingot, which results in the appearance of surface defects resembling cracks when the ingot is processed in the rolling mill.

Apart from oxygen, other elements that are less soluble in the solid state are released at the solidification front. This solute rejection is known as segregation (see Section 6.3.4.3). The elements that separate out are carried away by the flow of steel, and are concentrated in the remaining melt. This leads to a rim layer of greater chemical purity and enrichment of the segregated elements in the interior.

After a time, the process of gas release (rimming action) is deliberately stopped by placing a heavy steel cover on top of the ingot, or a steel plate, over which water is sprayed. The steel solidifies on the underside of the cover, and forms a dense cap. In the interior of the ingot, gas formation ceases, owing to the increase in gas pressure, and the flow of steel gradually subsides. In the part that still remains liquid, there are detached crystals of very pure iron, formed by redistribution of solute elements. These suspended solid particles sink to the lower part of the ingot, as their density is higher than that of the remaining liquid metal. This sedimentation results in an equiaxed zone, with a reduced level of impurity elements in the lower part of the ingot. At the top of the ingot, enrichment of elements occurs, e.g., phosphorus and sulfur, which can have a harmful effect on the properties of the rolled product. This marked concentration of elements at the top of the ingot is called macrosegregation.

The ring of gas bubbles formed during the rimming action, and those formed even after the ingot has been closed off, tend to compen-

sate for the difference between the specific volume of the liquid and that of the solid steel. The walls of these cavities have a clean and bright metallic surface, and weld together during subsequent rolling.

These processes during solidification cause the ingot of rimming steel to have a clean edge zone, a rim of bubbles in the lower region, a chemically pure equiaxed region at the bottom end of the interior, and a strongly segregated upper region (Figure 6.88) [98].

Thus, the ingot of rimming steel has a very inhomogeneous structure. Owing to its clean edge region, it can be used in applications that require a good surface. However, it cannot be used for manufacturing components where a large amount of deformation is involved. This is due to its great inhomogeneity and its aging properties, owing to the residual nitrogen. It is also unsuitable if great importance is attached to welding properties [97–110].

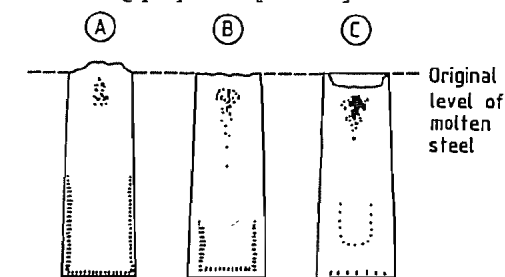


Figure 6.88: Distribution of blow holes in rimming steel ingots [98]. A) After slight rimming action: low oxygen content; B) After moderate rimming action: medium oxygen content; C) After vigorous rimming action: high oxygen content.

Killed Steel. If the dissolved oxygen content in the steel is reduced by deoxidation until it is significantly less than the carbon present, no carbon monoxide gas can form during solidification, and the steel is said to be killed. In killed steel, there is redistribution of those elements whose solubility in solid steel is lower than that in liquid steel. Some of these segregated elements are enclosed between the growing crystals (dendrites). This is termed microsegregation (see Section 6.3.4.3).

Convection of the molten metal also takes place during solidification of killed steel. However, this is considerably less intense than

in rimming steel, and takes place in the opposite flow direction. In front of the solidification interface, free crystallites move downward along with the liquid steel. The solid particles of steel settle at the bottom end of the ingot, while liquid steel flows upward in the center. As the descending crystals are chemically purer than the remaining liquid steel, a depleted conical heap forms at the bottom of the ingot. Here, the concentration of solute elements is lower than it was in the steel before pouring, whereas the concentration of the solute elements in the upper part of the ingot is correspondingly higher. Thus, there is so-called negative segregation in the lower part, and positive segregation in the upper part of the ingot. This is generally referred to as ingot segregation, and becomes more marked as the ingot cross section increases.

As well as ingot segregation, so-called A- or V-type segregation can take place when killed steel ingots solidify (see Section 6.3.4.3). Unsteady flow through the network of dendrites sometimes leads to the formation of channels, in which enriched liquid metal solidifies. On longitudinal cross sections of the ingot, these channels appear as A- or V-shaped segregation. The intensity of this type of segregation is dependent on the morphology of the solidified ingot. The finer the dendritic structure, the less marked is A- and V-type segregation.

To prevent the uncontrolled formation of shrinkage cavities in the interior of ingots of killed steel, the steel at the upper part of the ingot (the ingot head) is kept in the liquid state as long as possible. The liquid steel can then flow downward to compensate for the shrinkage of the solidifying region, and cavity formation is prevented.

The reservoir of liquid steel is maintained by reducing the heat transfer from the top part of the ingot to the mold by lining the latter with refractory, thermally insulating, and often slightly exothermic plates. The loss of heat in an upward direction to the atmosphere is reduced by applying an insulating and/or exothermic powder. Figure 6.89 shows typical longitudinal sections of steel ingots poured

into normal big-end-up and big-end-down ingot molds, with and without a feeder head, or "hot top", of this type [91]. In big-end-down ingots, through-solidification occurs earlier in the upper part than in the lower part of the ingot. This produces axial porosity, which under no circumstance should connect with the outside atmosphere, as this leads to oxide formation in the interior, preventing welding during subsequent rolling operations. Unless the top of the ingot is thermally insulated (hot topping), ingots produced in big-end-up molds form shrinkage cavities which extend deep into the ingot, so that the yield of good material is poor. An ingot from a big-end-down mold without a hot top will have axial porosity.

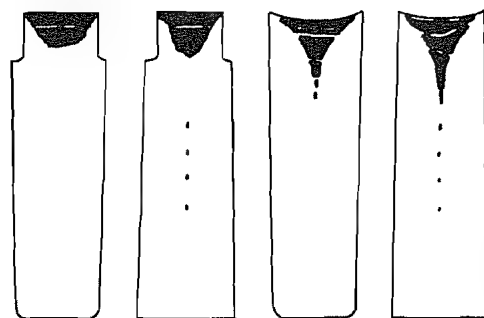


Figure 6.89: Types of killed ingot [91]. A) Big-end-up, hot-topped; B) Big-end-down, hot-topped; C) Big-end-up, not hot-topped; D) Big-end-down, not hot-topped.

When steels are to be used in applications that require an absolute minimum of interior defects, a hot top of adequate size is essential. For example, when heavy ingots are produced for forging, and are cast big-end-up, a feeder head of thermally insulating material is placed on top, with a volume large enough to prevent formation of a shrinkage cavity in the ingot. Segregation of the remaining molten material then takes place in the feeder head inside the hot top. This part is later separated from the good part of the ingot.

As killed steel is mostly used for demanding applications, there must be as few nonmetallic inclusions as possible. Modern ladle metallurgy, combined with a very high standard of pouring practice, have brought great improvements. If any nonmetallic inclusions

remain entrapped, however, these consist mainly of oxidic and sulfidic materials. These can originate from the products of deoxidation, from insulating materials, or are formed during solidification by reactions of the segregation elements. Inclusions in killed steel are mainly found entrapped in the region of the cone of sedimented equiaxed material, at the bottom of the ingot [91, 111–119].

Semikilled Steel. In this type of steel, the ratio of oxygen to carbon content is set by controlled deoxidation, so that the ingot at first solidifies, like killed steel. After a time, the carbon and oxygen become enriched in the remaining liquid, so that the solubility product is exceeded and carbon monoxide is formed. Meanwhile, the ingot head has solidified and is therefore dense, so that blow holes are formed in the interior of the ingot, owing to shrinkage (Figure 6.90) [91].

Semikilled steels are not used for applications with high demands on internal purity and defect-free surface properties [91, 120–122].

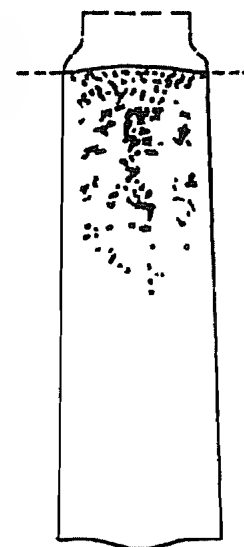


Figure 6.90: Longitudinal section through a semikilled steel ingot [91].

Ingot killed steel was developed to combine the clean surface of rimming steel with the low degree of macrosegregation and good aging stability of killed steel. The tops of the ingot

molds are provided with insulating tiles, as with killed steel. The steel is poured undeoxidized into the mold until the insulated region contains a few centimeters of steel. A second and possibly a third mold is then filled in the same way. During this time, rimming takes place in the first mold, as well as solidification of an outer shell of steel, several centimeters thick, which consists of very clean unkill steel, free of inclusions and segregation. The first ingot mold is then completely filled, while simultaneously adding aluminum in granular form to the stream of metal, thereby mixing it into the liquid part of the ingot. Carried by the central downward flow of rimming steel, the aluminum is transported to the lower part of the ingot. The dissolved aluminum reacts with the oxygen to form coarse Al_2O_3 particles, which rapidly ascend into the highest part of the ingot, owing to their low density. The ingot then solidifies like a killed steel. All the ingots from a heat are poured in this piece-meal fashion. This process produces an ingot with an outer layer of clean rimming steel, ca. 30 mm thick, and a larger inner region of nonaging killed steel with little macrosegregation (Figure 6.91) [123]. This steel can be used when a defect-free surface is required on a nonaging material [123].

6.3.5.2 Continuous Casting

In the historical development of continuous casting (strand casting), a breakthrough was achieved in large-scale production by S. JUNGHANS with the invention of the oscillating mold in 1949. This became widely used during the 1970s [124, 125]. By definition, strand casting is a steady-state process in which a strand is continuously drawn out of a mold [126–130]. After the 1980s, development of the conventional continuous casting process virtually came to an end [131–143]. The rolled products produced from continuously cast strand sections are characterized by their extremely good finish and functional properties, are not subject to any particular limitations, and are suitable for a wide range of applications [144].

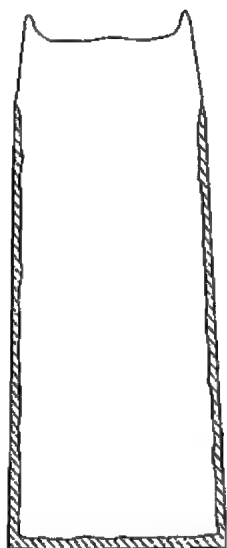


Figure 6.91: Longitudinal section through an ingot of steel killed in the mold [123].

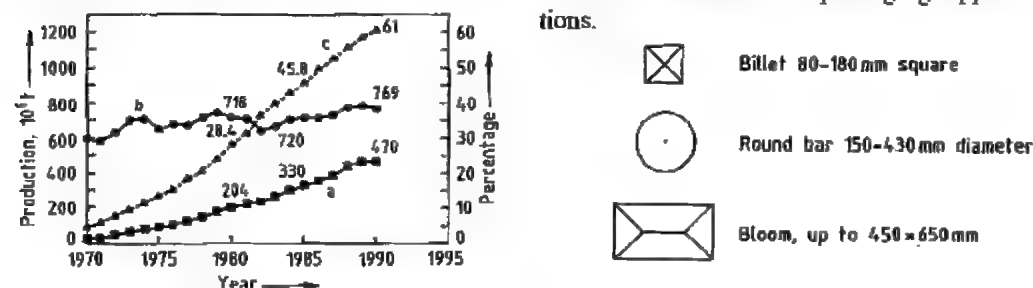


Figure 6.92: Development of world steel production, CC output and CC ratio 1970-1980: a) World CC-production; b) World crude steel production; c) Share of CC-production, %.

The Growth of Strand Casting

The growth of strand casting worldwide is illustrated in Figure 6.92. It has already reached > 60% of the total. Up to the 1980s, the competitiveness of steel producers was measured by the proportion of strand casting used. Today, many steelworks use the process exclusively. In many industrialized countries, the proportion is > 90%, but in some regions, it is only 20% [144].

The strand casting technique replaces individually cast ingots, blooming and slabbing mills, and semifinished mills. The yield of

rolled products per tonne molten steel is increased by 10-18% (see section 6.1). This technological change has resulted in an excess of crude steel capacity, but has greatly contributed to energy savings.

Figure 6.93 shows the shapes and dimensions of some typical strands, with size ranges. Billets are used to manufacture wire or rod. Round bar products are used as the starting material for seamless tubes. Continuously cast blooms are used in the production of profile steel and rails. Case hardening and heat-treatable steels, cold-heading and cold-extruding steels, spring steels, chain steels, rolling bearing steels, and free cutting steels are routinely produced [145]. Slabs are converted into thick plate for pipeline or vessel construction, or processed into hot-rolled wide strip and products made from this, such as cold-rolled thin sheet, which may be surface treated for automobile construction or packaging applications.

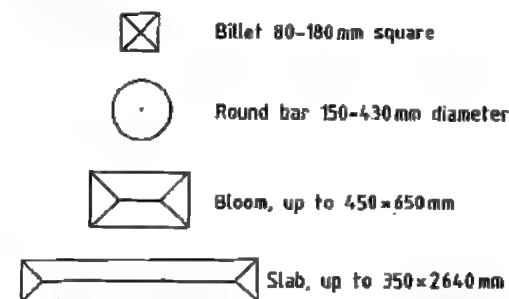


Figure 6.93: Typical cross sections and dimensions of continuously cast strands.

Productivity

If strand casting accounts for 100% of the total output of a steelworks, productivity rates become very important. The capacities of the melting, ladle treatment, and casting process must be matched as precisely as possible. If the mix of steel types produced is variable, it must be possible to react to changes with great flexibility.

Modern strand casting plants are characterized by high availability. The utilization ratio, i.e., the ratio of casting time to time available, is 40-90%. In sequential casting, one melt is

cast immediately after another without interruption. The ladles are mounted on a turret which swivels, raises, and lowers the ladle (Figure 6.94). The molten steel passes through the following items of plant or process steps: ladle-tundish-mold-secondary cooling zone-straightening and withdrawal machine-runout rollers.

For high productivity, it is also necessary to have a high rate of withdrawal and a long length of the liquid pool. High outputs can only be achieved when bow type casters are used, where the strand, which still has a molten interior, is cast on a circular arc and then straightened to the horizontal position. Figure 6.95 shows the various types of plant used during the development of the process. Vertical plants (V) have a limited output, owing to the height required. The most usual system is the circular arc plant with a curved mold (CAC), with several straightening points. In a circular arc machine with straight mold (CAS), the strand, with its molten center, is first bent into an arc, and then straightened. The bending and straightening take place pro-

gressively. Extremely precise mechanical technology is used to minimize stressing of the cast material.

The production rate for a single strand depends on the format, dimensions, and casting speed (Figure 6.96) [144]. For slabs, a rate of 5.5 t/min is possible. This must be matched to the batch time of the basic oxygen furnace. For blooms and billets, the number of strands must be increased to four or six to match this batch time.

Plant availability can be improved by: insertion of the dummy bar from above; design of mold and runout rollers as a quick change unit; flying tundish changeover by means of a swivel device; uninterrupted casting of different steels one after the other without forming a mixed zone the old strand being joined to the new by a cage-and-anchor joint; and computer-controlled automatic width adjustment of the strand. A high standard of control technology and automations necessary in the casting plant. Regular inspection and preventive maintenance ensure problem-free casting.

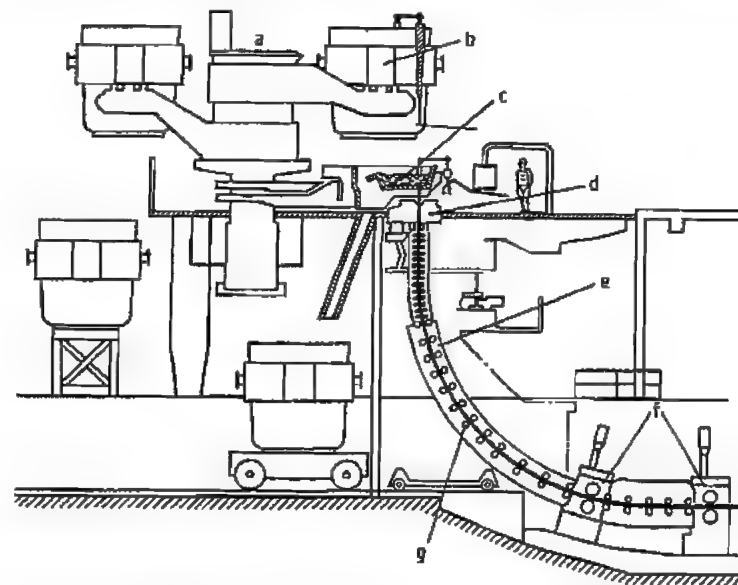


Figure 6.94: Blown caster with ladle turret: a) Ladle turret; b) Ladle; c) Tundish; d) Mold; e) Secondary cooling zone; f) Straightening and withdrawal; g) Guide rollers.

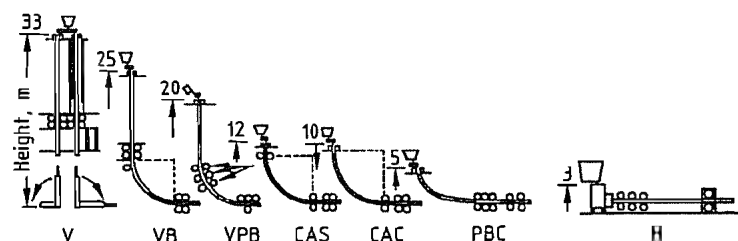


Figure 6.95: Principal types of continuous casting machines for steel: V = vertical; VB = vertical with bending; VPB = vertical with progressive bending; CAS = circular arc with straight mold; CAC = circular arc with curved mold; PBC = progressive bending with curved mold; H = horizontal.

With slabs and blooms, an average run of nine heats is usual, and with billets, five heats [44]. More flexibility in the production program is provided by a device for longitudinal cutting of slabs, especially for "jumbo" slabs, up to 2640 mm in width. Double and triple casting can also be provided for.

Mold Oscillation and Shell Formation

The most important invention in the technical development of strand casting was mold oscillation, which gives the product a good surface finish. Figure 6.97 shows how the molten steel from the tundish passes through a submerged entry nozzle into a slab mold. The steel flows sideways during slab casting, but vertically downward with square or round mold shapes. The pouring temperature is controlled within a very narrow range.

The oscillation of the mold is illustrated in Figure 6.98. The movement is usually sinusoidal. Stroke and frequency are so adjusted that the mold briefly overtakes the strand during the downward movement. During this so-called negative strip time, the skin of the casting is briefly upset. Any surface damage is completely healed. The negative strip time t_N (an important control parameter) is given by the following formula:

$$t_N = \frac{1}{\pi f} \arccos \frac{v_g}{\pi f h}$$

where t_N is in s, the frequency f is in s^{-1} , the casting speed v_g in mm/s, and the stroke h in mm. If $t_N \rightarrow 0$, tearing of the shell occurs, and if it is too large (> 0.2 s) deep oscillation marks are produced, and lubrication in the gap

between the mold and the strand is impaired. When changes to the casting rate occur during unsteady phases, such as the start of casting or ladle changes, the frequency is adjusted. Amplitudes are kept constant at 2–6 mm, but frequencies vary around $6 s^{-1}$. A curved mold oscillates precisely along the arc.

Molds are usually 700–900 mm long, and are made of high-strength, copper-based materials. To maximize operating life, the surface is coated with chrome (60–80 μm) or nickel (0.5–4.0 mm). For small cross sections, tube molds are usual, and for large cross sections, plates are mounted on stable steel frames. To accommodate the contraction of the steel, the molds taper inward. For plants with high casting rates for billets and blooms, very close geometrical tolerances must be adhered to. For sensitive steels with high sulfur content or wide solidification range, the casting speed is reduced.

Control of Molten Steel Level and Gap Lubrication

For problem-free strand withdrawal from the mold, the cycle must be optimized, the meniscus level of molten steel kept constant, and an appropriate casting powder must be used to lubricate the gap.

The flow of steel is controlled by sliding gates (Figure 6.97) or stoppers. The steel level is detected with the aid of radioactive sources, ^{60}Co or ^{137}Cs , or eddy current detectors, and is controlled within ± 5 mm, or even ± 2 mm, depending on the sophistication of the control equipment, the format of the strands, and the casting rate.

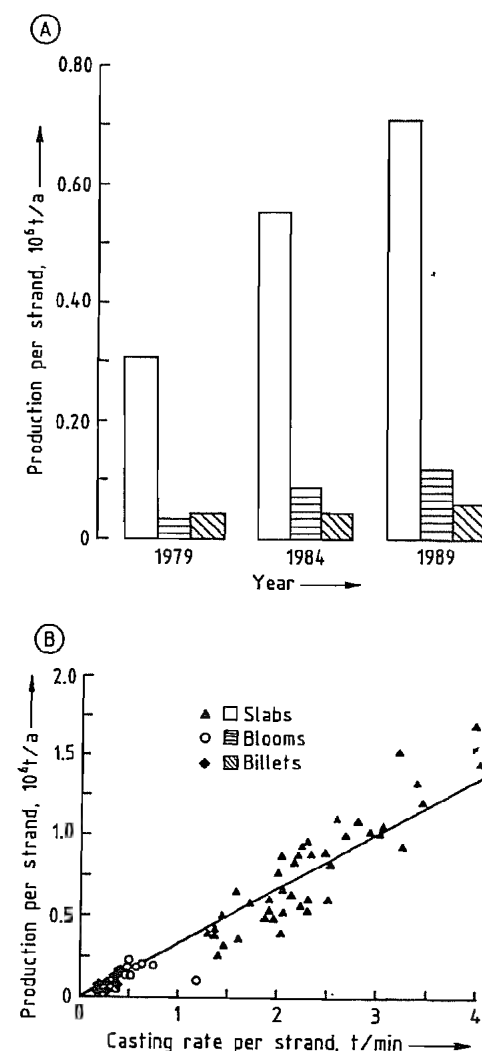


Figure 6.96: Annual production per strand of European casters (A) as a function of the casting rate per strand for different strand sections (B).

The casting powders used must be appropriate for the types of steel and the casting conditions. On contact with the surface of the steel, they should melt promptly at 1100–1200 $^{\circ}C$, and form a lubricating film between the strand and the mold. Penetration into the gap plays a key role in the formation of the steel surface for high withdrawal speeds [145].

Casting powders consist of CaO , SiO_2 , and Al_2O_3 . CaF_2 , Na_2O , or Li_2O are added to lower the viscosity. Carbon particles in the form of powdered coke or soot retard the melting. The basicity of the slags is given by:

$$CaO/SiO_2 = 0.8 \text{ to } 1.2$$

The amount of casting powder required depends on the oscillation cycle, the casting speed, the geometry of the gap, and the viscosity. Slabs are cast by means of low-viscosity slags: 0.1–0.3 $Pa \cdot s$ (1300 $^{\circ}C$). For blooms, viscosities must be somewhat higher: 0.4–1.5 $Pa \cdot s$ (1300 $^{\circ}C$).

Casting powders protect the molten steel from radiation heat loss, prevent contact with atmospheric oxygen, and absorb oxide inclusions that rise to the surface, especially Al_2O_3 . Powders and granules (nowadays preferred) can be added automatically in the fluidized state.

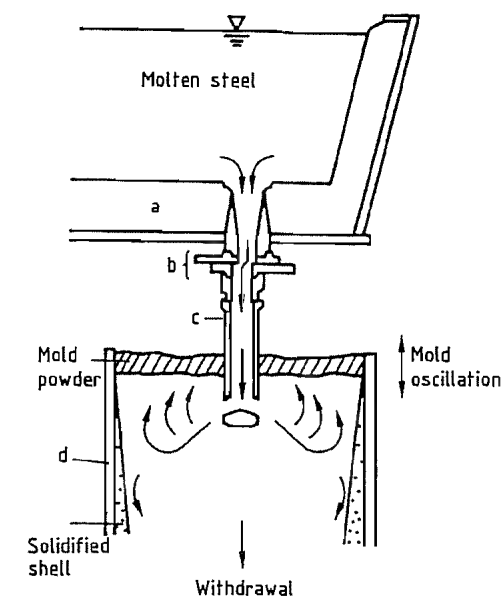


Figure 6.97: Steel flow from tundish into an oscillating slab mold: a) Tundish; b) Sliding gate; c) Submerged entry nozzle; d) Copper mold plate.

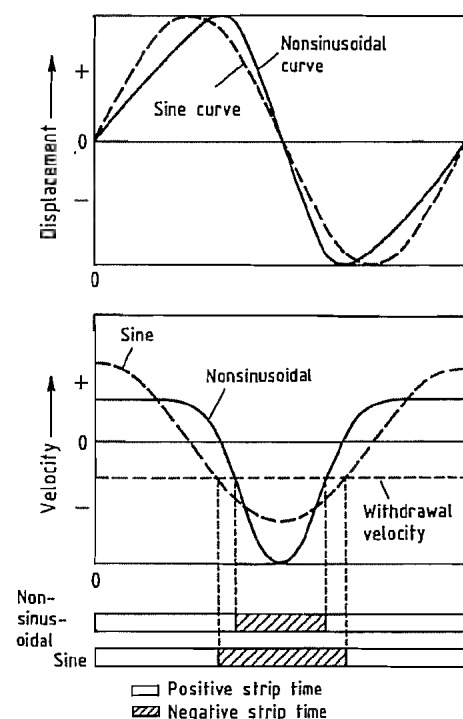


Figure 6.98: Mold oscillation with definition of positive and negative strip times.

Support Roller Apron and Secondary Cooling Zone

At the mold exit, the skin of the strand is sometimes quite thin, e.g., 10–12 mm, depending on the withdrawal velocity, and is ductile and deformable under the conditions of high temperature and ferrostatic pressure. Whereas billets and round bars are dimensionally stable, the wide faces of slabs and blooms tend to bulge, and must be supported by rollers [146].

To prevent excessive thermal stress on the rollers, they are cooled internally. The helirollers contain a spiral channel for circulating the water, and are stable and long-lasting [138]. Divided rollers with intermediate bearings are of smaller diameter and can accommodate narrower gaps between them. Where bending and straightening of the strand is carried out, deviation of the rollers from the ideal line

must not exceed 1 mm. Loose-fitting and worn rollers must not cause this limit to be exceeded.

In the secondary cooling zone, the strand is cooled with water sprays. There are various jet systems to provide different flow rates of water impingement. In the extreme, the surface can be sprayed “black”. In the early days, large quantities of water were used for fear of break-outs of molten steel. Since then, the water rate has been limited to the minimum required for the necessary cooling intensity. Air/water mixtures are used to achieve gentle and uniform cooling. Specific consumptions of spray water are 0.7 L per kilogram of steel for spray cooling, and 0.1–0.2 L/kg for air-mist cooling.

Automation

Today, almost all the functions of a casting machine are automatically controlled. Figure 6.99 gives an overview of the individual processes [132]. Secondary cooling is dynamically controlled. The spray water is adjusted according to the casting speed to prevent undercooling. Cooling water circulation, hydraulic, and lubrication systems are computer controlled. The rate of steel casting is measured by weighing, and cutting of the strand into lengths is optimized with respect to the heads and tail pieces.

Quality

The quality of continuously cast steel as a semifinished material for rolled steel production can be assessed by four criteria:

- Homogeneity of chemical composition
- Uniformity of steel structure
- Extremely high purity
- Defect-free surface

The above requirements are met if the process is trouble free. Solidification can be controlled to be columnar or equiaxed by means of temperature control and the stirring effect of electromagnetic fields, enabling the blooms and billets to have isotropic properties

throughout. With slabs, soft reduction is carried out by conical compression of the center.

Contact of air with the steel is prevented by shrouding systems and by covering the molten metal in tundish and mold with powder. Carry-over of slag along with the steel from the casting ladle is detected and prevented. The flow of steel in the tundish is controlled such that oxide inclusions separate out. It is also necessary to use stable refractory materials and refined pouring techniques to ensure a high-purity product. For high-output plants, a vertical part of 2–3 m in height enhances the flotation of inclusions and gas bubbles.

Materials technology has elucidated the high-temperature ductility of steel from its molten state to the γ - α transformation, and mechanical engineering has provided the necessary data on permissible material stresses during casting. By progressive bending and straightening, and suitable roller distances, tensile strain at the solidification front can be kept $< 0.3\%$. Critical temperature zones susceptible to surface cracking are avoided by appropriate cooling. Harmful elements, e.g., N and S, are removed from the steel, or chemically combined to form stable compounds.

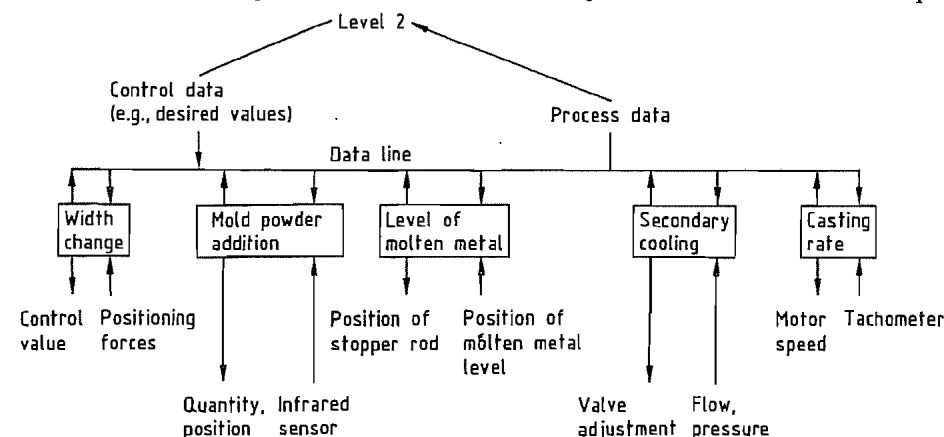


Figure 6.99: Instrumentation and automatic process control of a continuous casting machine.

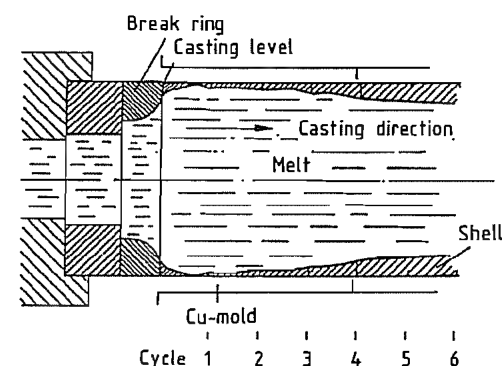


Figure 6.100: Creating an artificial meniscus during solidification in a horizontal casting mold.

Horizontal Strand Casting

Horizontal strand casting has replaced ingot mold casting for several types of steel which have hitherto been regarded as unsuitable for strand casting [137, 147]. The capital cost of a horizontal strand casting plant is small. The tundish and mold form a single unit, giving complete exclusion of air. The horizontal strand requires neither bending nor straightening.

The special feature of the process is the creation of an “artificial meniscus” at the break ring, where the skin of the casting first forms (Figure 6.100) [148]. The strand is withdrawn stepwise, and the short frozen sections are welded together. The cycle comprises three phases: pulling out, pushing back, and pause. The pushing-back stage allows healing to oc-

cur. The design of the machinery must enable the large mass of the strand to be moved with very high precision with respect to both distance and time [149, 150]. Typical round bar dimensions are 150–350 mm in diameter.

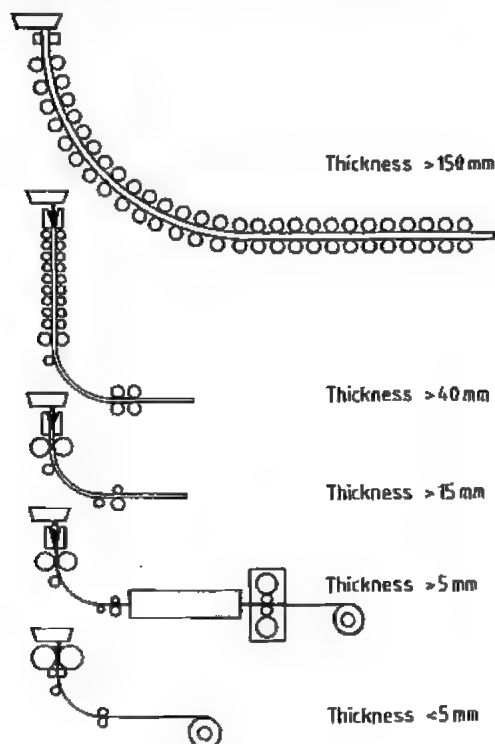


Figure 6.101: New processes for the production of thin slabs and hot strip.

The breaking ring is made of BN, and is not wettable. Useful lives for this item of 4–7 h have been reported. The formation of the solidified skin is precisely controlled with the aid of thermocouples. The casting parameters and mold taper must be precisely matched. Nevertheless, the process is flexible with regard to the formats and steel types. It is of interest for small-scale operations, e.g., 3000 t/month in 100 different grades of mild, stainless, or high-temperature steel [132, 149].

Hot Charging or Direct Rolling

Not only is conventional strand casting a fully developed process, guaranteeing a high

productive capacity, but it offers the opportunity for energy savings by integration with the rolling mill, i.e., utilizing the heat of the strand by hot charging or direct rolling [139]. For this, the operation of the rolling mill must synchronize with the flow of material from the melting shop, the secondary metallurgical processes, and the strand casting plant. The temperature of the cast product is not allowed to fall below 1200 °C. The surface and the interior must be of high quality.

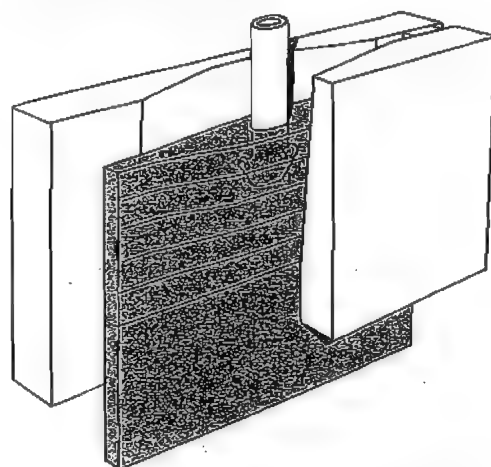


Figure 6.102: Schematic representation of casting mold for thin slabs.

Casting Thin Slabs

Under the heading “near net shape casting”, the development of casting technology since 1983 has aimed to match the thickness of continuously cast slabs more closely to that of the end product [151, 152], i.e., to reduce the amount of metal forming required, and hence to economize on plant equipment [153–155]. Processes for the production of thin slabs or strip are illustrated schematically in Figure 6.101.

At the heart of thin slab technology is the funnel-shaped mold into which a narrow submerged entry nozzle with side exit openings is inserted (Figure 6.102) [153]. The shell of the strand is smoothly deformed in a controlled manner until it leaves the mold, and the gentle contours keep the bending stress small. The

strand leaves the mold with plane parallel surfaces in its wide dimension. Thin slab technology is otherwise similar to conventional strand casting, e.g., control of the level of molten steel, supporting rollers, secondary cooling, etc.

New Processes for Hot Steel Strip Production

For integrated “mini-steelworks”, various processes have been devised for the production of hot steel strip, based on thin slab casting technology. It is generally agreed that a direct link between casting and rolling to produce a finished product in an in-line, multi-stand rolling mill is impossible, because the casting and rolling speeds cannot be matched. A buffer can be provided between these processes by operating them in two stages.

A compact strip production (CSP) plant consists of a casting machine, a conveying and linking system designed as a roller hearth furnace, and a hot finish rolling mill [154, 155]. The casting machine is vertical, with bending facility. The casting format is 50 × 1600 mm; the casting speed is 5 m/min. The strand is cut

into 45 m lengths, which are loaded at nearly 1100 °C into an annealing furnace, 162 m long. The final rolling temperature is 880 °C.

In-line strip production (ISP) is shown in Figure 6.103. The thin slab, with a liquid core, is softly reduced in thickness from 60 to 43 mm immediately after the mold [142, 156, 157]. After through-solidification, the strand passes through three graded stands of high-reduction rolling units. Its thickness is reduced to 15–25 mm, and it is made into 28 t coils. Before coiling, it can be reheated by inductive heating to a temperature of 1150 °C. The coils are kept hot in furnaces, ready for the finish rolling mills. The hot steel strip has a final thickness of 1.8–12.5 mm and can be intensively cooled.

The casting pressing-rolling (CPR) process (Figure 6.104), combines a conventional oscillating thin slab mold of the type described above, with a powerful pair of compression rollers to reduce the thickness of the strand, which has a liquid interior, to 15–25 mm in a single step [158]. The hot strand is then rolled to its final dimensions at 1300 °C in a four-high stand.

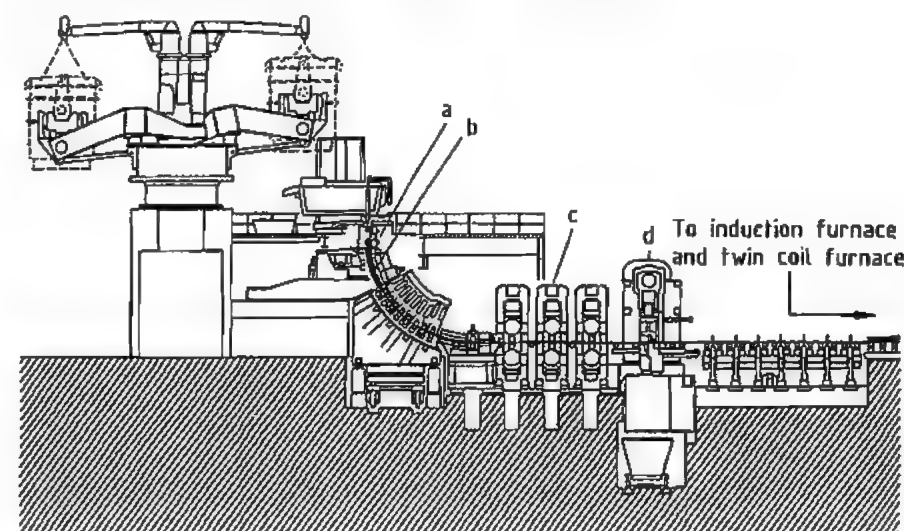


Figure 6.103: Caster for in-line strip production (ISP): a) Vertical bow-type mold; b) Soft reduction; c) High reduction (three stands); d) Pendulum shear.

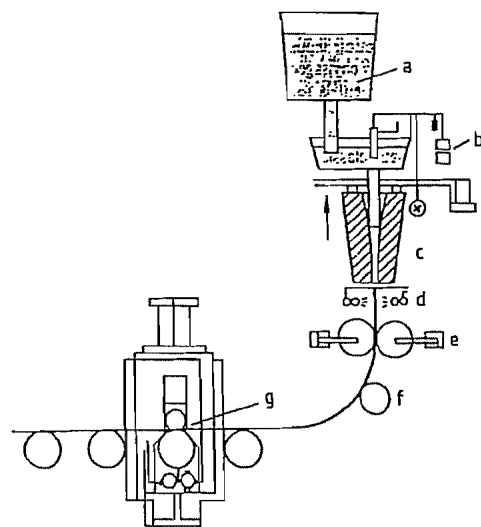


Figure 6.104: Casting-press-rolling process: a) Ladle; b) Tundish; c) Mold; d) Descaling; e) Press rollers; f) Bending roller; g) Straightening unit.

Rationalization

The new processes of hot steel strip production may replace some of the classical "thick slab hot strip steel mills", but not completely [155]. Hot strip steel produced by the standard method can be divided into: mild steel for cold forming and cold rolling (76.2%); weldable construction steels (10.5%); high-strength carbon steels (1.7%); microalloyed weldable fine grain and tube steels (6.4%); stainless steels (3.3%); and silicon steels for electric sheet (1.9%).

Assuming sufficiently good surface properties of the mild steels produced by the new casting-rolling processes, their suitability for cold forming and cold rolling is beyond question [155]. Of the total amount of hot steel strip listed above, 75% could be produced more economically. A considerable fraction of the total production could be transferred from large integrated steelworks to mini-steelworks. The forming properties of 21% of this total are difficult or critical. Further development work is needed; in particular, the alloy compositions of these materials must be matched to the new casting-rolling processes.

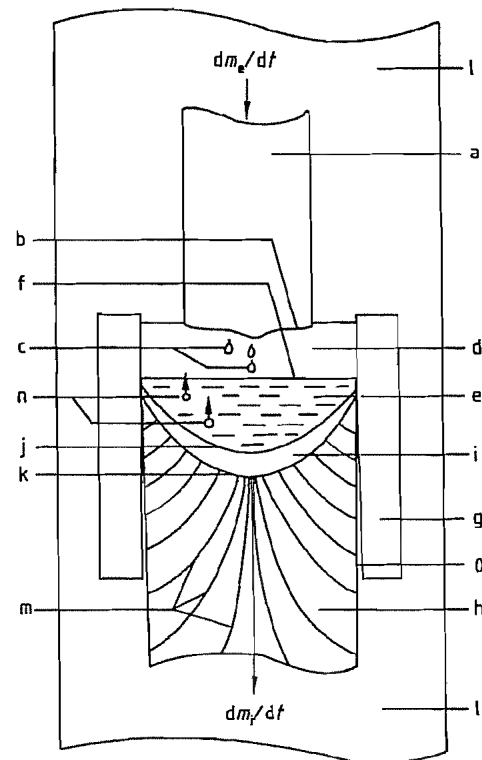


Figure 6.105: Consumable electrode remelting: a) Electrode = metal to be remelted; b) Electrode surface heated above m_p ; c) Metal droplets; d) Remelting environment (vacuum, liquid slag, plasma); e) Liquid metal pool; f) Surface of liquid metal pool; g) Crystallizer (water-cooled mold); h) Remelted ingot; i) Mushy zone; j) Liquidus isotherm; k) Solidus isotherm; l) External environment (vacuum, air, inert gas); m) Solidification direction; n) Inclusion in liquid pool.

6.3.5.3 Consumable Electrode Remelting Processes

Remelting processes are used for upgrading the quality of steels and Fe-, Co-, and Ni-based superalloys; conventionally made metal bars are transformed, by simultaneous remelting and resolidification, into new materials with superior properties.

Remelting Processes

Figure 6.105 outlines the remelting process for steel and superalloys. The metal to be re-

melted is first produced by primary melting, secondary refining, and casting processes, including vacuum induction (VIM) and plasma melting and casting. It is introduced into the remelting process as a so-called "electrode", which is normally shaped by direct ingot casting, with or without subsequent rolling or forging, or by continuous casting. Compound electrodes, such as bundles of bars or continuously cast billets may be used, as well as several individual electrodes to be remelted simultaneously. Addition of deoxidizers or alloying elements (e.g., Al wire, Ti strip, high-nitrogen alloy compacts) to an electrode, to form a compound electrode, is common.

The electrode is heated at one end above the liquidus temperature so that liquid metal droplets are formed. These fall through the reactive environment of the remelting zone to the liquid metal pool, the surface of which is also heated above the liquidus temperature. The liquid metal pool is confined by a heat-extracting crystallizer, usually a water-cooled copper (or steel) mold. Heat extraction causes the liquid pool to solidify slowly into a new ingot, the "remelted ingot". A "mushy zone" is maintained between the pool and the fully solidified ingot.

The remelting rate dm_e/dt of the electrode(s) practically equals the mold-filling rate dm_f/dt of the remelted ingot. This rate is one or two orders of magnitude smaller than in conventional ingot or continuous casting. A typical value for round remelted ingots of diameter D_i is:

$$dm_f/dt = (1000 \text{ kg h}^{-1} \text{ m}^{-1}) D_i$$

A typical ingot for the rolling mill of mass 3000 kg and diameter 0.5 m thus needs a remelting time of 6 h, a big forging ingot (180 000 kg, 2.4 m) needs 75 h; the time is further increased by the necessary "hot topping" at the end of remelting.

General Aims of Remelting

Ingot Structure. One aim of remelting is improvement of ingot structure and homogeniza-

tion of longitudinal and transverse mechanical properties.

Conventionally cast ingots and strands have a predominant direction of solidification, from the surface to the center, with consequent voids and center segregations. To achieve homogeneous and acceptable mechanical properties, high reduction during hot forming is necessary, which limits the final dimensions of the finished products. Because of their low solidification rate, remelted ingots solidify mainly from the bottom to the top (Figure 6.105), which presents center voids and segregations and leads to an extremely sound and homogeneous ingot structure. Less reduction is necessary to achieve a sound product, which increases the final dimensions attainable with a given hot forming device (rolling mill, forge).

Cleanliness. The second aim of remelting is the improvement of metal cleanliness, two mechanisms being effective:

- The heated metal surfaces and the droplets react with the reactive environment. If the reactive environment is high vacuum, degassing and vacuum deoxidation reactions take place, lowering the content of hydrogen, oxides, nitrides, and volatile metallic residual elements (Cu, Pb, Zn, etc.); if it is reactive slag, complex deoxidation, denitrogenation, and desulfurization take place, together with retention of inclusions from the electrode in the slag.
- Large inclusions, finding their way into the liquid pool, have time to rise slowly to the top, where they are eliminated by various mechanisms. By reaction with the liquid metal, many of the rising inclusions are reduced in size; below a certain particle diameter rising stops, and these inclusions are retained in the solidifying matrix. The remelted ingot has not only a lower total inclusion content, but the maximum inclusion size of the remaining inclusions is much lower than in the electrode material.

Other Aims. Through the introduction of remelting, these processes have often had the

special aim of making products previously not possible by conventional means. An important application is the production of high-nitrogen steels, with high-pressure nitrogen (e.g., 5 MPa) as the remelting environment. Another application is production of sound hollow ingots of steels which are difficult to hot-work, by remelting multiple electrodes into a common annular mold.

Remelting Apparatus

Table 6.13 lists the main processes. Most units for general applications are ESR units, followed by VAR units, EBR, PESR, VADER, and PAR are used for special applications. Details of remelting apparatus construction (electrode feeding; round, square, rectangular, and hollow molds; ingot withdrawal; slags; alloy addition devices; automation, etc.) and other processes are given in the references [159–166].

Results and Applications

The high cleanliness of remelted steels makes them useful for surgical implants, highly polishable pressing sheets for laminate production, etc. The homogeneity of mechanical properties is good for thick products of ultra-strength structural steels, tool steels, etc.

The soundness of the ingot allows large forgings, up to 100 t or more, to be made from a much smaller ingot, compared with the conventional route. Some high-temperature alloys exhibit improved forgeability. High-nitrogen, fully austenitic PESR steels are used for production of large, nonmagnetic retaining rings for electrical power generators. Further applications are listed in [159–166].

During the last decade, steady improvements in conventional melting and casting technologies regarding cleanliness and soundness have taken over many applications; the more economic route of melting, secondary refining, and continuous casting is favored over remelting processes. For sound ingots of up to a few tonnes, the powder metallurgy route has become a competing, albeit more expensive process.

6.3.5.4 Cast Steel and Cast Iron

Cast Steel

Many grades of steel, of various composition, are suitable for casting. The carbon content can be as high as 2%, but is usually 0.02–0.4%. Casting consists of pouring into refractory molds, and allowing to solidify.

In the production of steel castings, all types of molds and casting processes are used, including hand- and machine-made molds, shell molds, and ceramic molds. Other processes include precision casting by the lost wax process, the full mold process, and centrifugal casting. Castable steel is melted by methods similar to those for rolling and forging steel, mostly in electric arc furnaces lined with a basic refractory, and, less commonly, in induction-heated, crucible furnaces. The processes of secondary metallurgy in oxygen/argon converters or specially designed gas-purged ladles are increasingly important.

In Germany, of all the crude steel produced, 0.6% is cast. The proportion is similar in other industrialized countries.

Cast Steel for General Applications. These materials are used for components intended for use between -10 and 300°C , which are subject to moderate dynamic and impact stresses, e.g., parts for general machinery, wheels and wheel bearings, rolling equipment, and ships' anchors. The most common material in this group is mild steel, though some low-alloy steels are also used. Steels with a low carbon content have good welding properties, which has ensured a wide range of applications for steel castings. It is common to improve the welding properties by reducing the carbon content, and to compensate for this by increasing the manganese content.

Figure 6.106 shows the temperature dependence of the mechanical properties of unalloyed cast steel.

Cast Steel for Special Applications. Cast steel was formerly at a disadvantage compared with forged and rolled steel for welded construction, in that high-strength grades with adequate welding properties were unavailable. Metallurgical advances in steel production, especially secondary metallurgy, have enabled the production of steels which, after casting and heat treatment have tensile strengths of ca. 800 N/mm^2 . They are thus equivalent to rolled and forged steels, and can be welded to them (Figure 6.107).

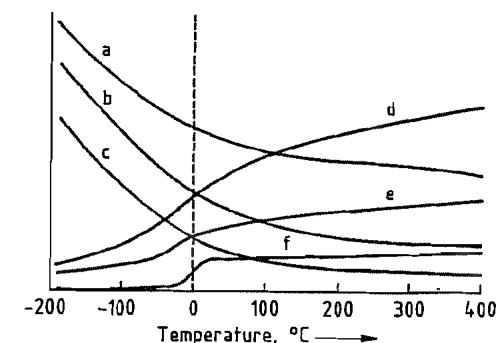


Figure 6.106: Mechanical properties of unalloyed cast steel as a function of temperature: a) Tensile strength; b) 0.2% yield strength; c) Flexural fatigue strength; d) Constriction; e) Elongation; f) Notched impact strength.

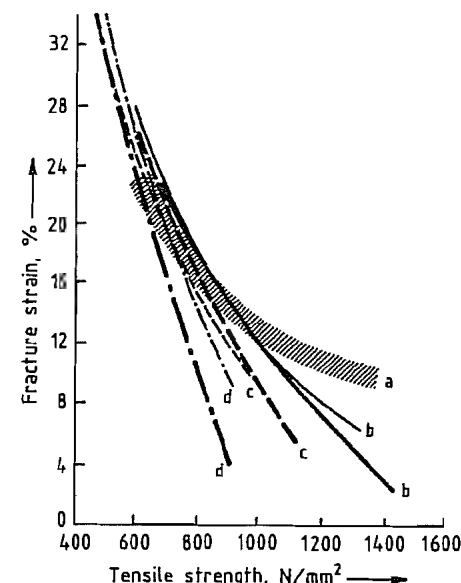


Figure 6.107: Correlation between fracture strain and tensile strength of tempered cast steel compared with rolled and forged steels: a) Steel values from DIN 17200; b) Tempered structure; c) Mixed structure; d) Ferritic-pearlitic structure. — = Cast steel valves from Steel Castings Handbook; --- = Experimental cast steel valves.

With these properties, the high-strength weldable and castable grades of steel now available are suitable for welded designs in many areas of engineering. Grades suitable for turbines and steam power stations can be used to make castings up to 100 t.

Alloying costs are not high, but they need to have a carbon content of ca. 0.2% for good

Table 6.13: Consumable electrode remelting processes.

Process	Name	Energy input	Remelting environment	External environment	References
ESR	electro-slag remelting	high-current a.c. (or d.c.) resistance heating of liquid slag	liquid slag of CaF_2 - CaO - Al_2O_3 or similar type, heated above metal m_p	air or inert gas	[159, 162, 163]
VAR	vacuum arc remelting	high-current d.c. arc between electrode and pool surface	low-vacuum plasma	high vacuum	[160–163]
EBR	electron-beam remelting	high-voltage electron beams hitting electrode tip and pool surface	high-vacuum plasma	high vacuum	[160, 162, 164]
PESR	pressure electro-slag remelting	see ESR	see ESR	high-pressure inert gas, mostly N_2 plus additions	[165]
VADER	vacuum arc double-electrode remelting	high-current d.c. arc between two electrodes	vacuum plasma	vacuum	[161–163]
PAR	plasma arc remelting	plasma beams from d.c. or a.c. plasma burner(s)	plasma gas	vacuum, normal or high-pressure inert or reactive gas	[162, 166]

welding properties. To ensure that components of all types will have the properties desired, including welding properties, martensitic and lower bainitic structures must be produced, for uniform strength and toughness.

For plain carbon steel castings, the limit of the wall thickness for through-tempering is ca. 20 mm. By the use of suitable alloying elements, this can be extended to ca. 500 mm, although the welding properties are somewhat affected.

Hot-strength, low-temperature, and stainless grades of cast steel, including austenitic and duplex steels, are produced in a similar way to the rolling and forging steels.

The tendency of low-temperature nickel steels to give a coarse-grained structure on solidification makes them less suitable for casting. It is, therefore, recommended that Cr-Mo or Ni-Cr-Mo alloy steels should be used, if possible.

Typical grades of steel for casting have heat and abrasion-resistance properties which cannot be matched by rolling and forging steels.

Cast steel is regarded as a high-temperature steel if it effectively resists the scaling effect of gases at $> 600^\circ\text{C}$. Heat-resistant steels can be divided into ferritic and austenitic grades, and alloys based on nickel and cobalt. Ferritic steels are alloys containing 7–28% Cr and 1.7% Si, and austenitic steels contain 18–30% Cr and 10–37% Ni. High-temperature steels (Figure 6.108) are used for components that are highly stressed, both thermally and mechanically, and are subjected, either continuously or intermittently, to corrosive gases at ca. 600 – 1150°C . These materials have made the continuous operation of industrial furnaces an economic possibility. Other areas of use include ore treatment (roasting furnaces), and the cement, petroleum, and petrochemical industries. Heat-resistant cast steel is used for valve cages, and combustion chambers in diesel engines.

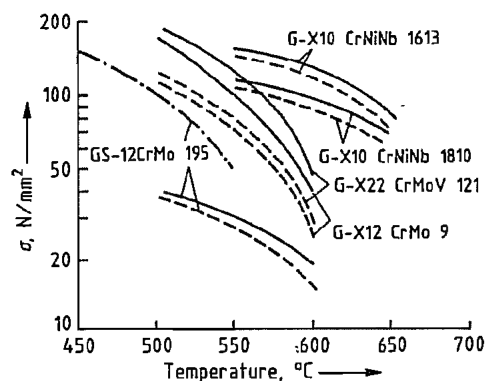


Figure 6.108: High-temperature cast steel for working temperatures above 540°C . — = $\sigma_{B/100\,000}$; — — = $\sigma_{1/100\,000}$; — — — = DVM (Deutscher Verband für Materialprüfung der Technik) creep limit.

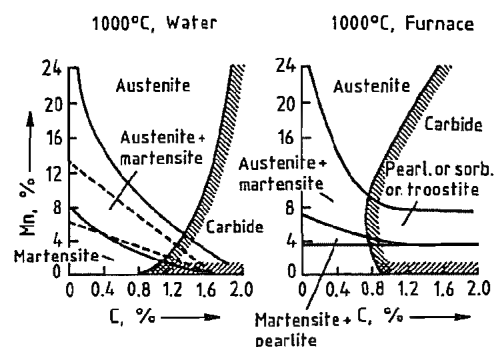


Figure 6.109: Structure of cast hard manganese steel as a function of cooling rate.

Cast hard manganese steel (Figure 6.109), which contains 1.0–1.4% C and 12% Mn, was first described in 1888, and has retained its importance up to the present day. In order to develop its maximum abrasion-resistance properties, a cold-hardening process is required, e.g., by impact or pressure working, which can increase the hardness of the abrasion-resistant surfaces from 250–300 to 500 HB (Brinell hardness scale). Good toughness properties can be produced by a solution annealing process at 1050°C , with water quenching.

Hard manganese steel is unsatisfactory under conditions of abrasive wear without impact and pressure work hardening, as under these conditions no cold hardening occurs.

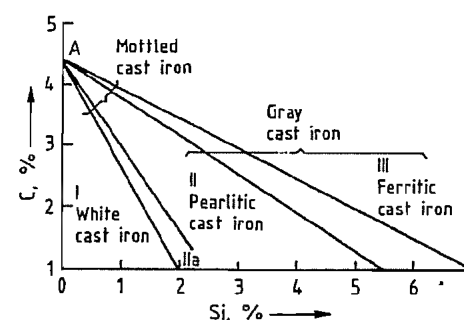


Figure 6.110: Structure zones of cast iron.

Tempering steels are used where components and workpieces undergo mainly abrasion, but are also subjected to impact stress.

Abrasion-resistant cast hard chrome steels have the highest abrasion resistance of all cast steels. They contain 2.5–3.5% C and 15–27% Cr, and attain their highest abrasion resistance after hardening at 900 – 1050°C , with either accelerated or static air quenching. This group has the lowest toughness of all the abrasion-resistant materials. Components made of this material must not be subjected to transverse stress. Hard chromium steel is used under conditions of predominantly frictional abrasion, and where impact and pressure stresses are small.

Cast Iron

Cast iron includes iron carbon alloys with carbon content ca. 2.8–4%. The carbon is for the most part not chemically bonded to the iron, but is present in elemental form.

Gray Iron. Cast iron with flake graphite, also known as gray iron, is an iron-based material in which the carbon is nearly all in the form of microscopic graphite flakes with a ferritic-pearlitic structure (Figure 6.110). In Germany, this material falls under the DIN 1691 standard, which specifies tensile strengths of 150–350 N/mm². In the United Kingdom, BS 1452 applies, and in the United States, ASTM A48.

Formation of the graphite and its primary structure, and hence the strength and hardness of the product, depend very much on the cooling and solidification rate, and hence on the

wall thickness. However, heat treatment of gray iron is not normally practicable, so this relationship is less important than the correct choice of chemical composition. For gray iron components, the design can only specify the wall thicknesses and the required strength the choice of chemical composition must be left to the foundry.

Cast iron is poured at ca. 1300 – 1450°C . When molten, it can completely fill complicated thin-walled molds, reproducing pattern details exactly. Other important characteristics include its property of damping vibration, its good resistance to corrosion by weathering, and its good machining properties.

The amount of cast iron exceeds that of all other cast materials; ca. 40% is used in the automobile industry. Other applications include mechanical engineering, the building industry (radiators, boilers, sanitary ware, pipes), chemical plant, shipbuilding, and mining. The former demand by steelworks for cast iron ingot molds has been greatly diminished by the introduction of the continuous casting process.

Spheroidal Graphite (SG) Cast Iron. In spheroidal graphite, also known as ductile iron or nodular iron, the free graphite in the ferritic-pearlitic matrix is almost completely in spheroidal form. This is achieved by treating the melt with magnesium. The formation of spheroidal graphite gives very good ductility, unlike the brittle properties of gray iron.

This material, first produced in 1948, is now the subject of the German DIN 1693, BS 2789 in the United Kingdom, and ASTM A 536 in the United States. Its hardness can be increased by heat treatment and tempering. Its mechanical and physical properties place it between lamellar cast iron and cast steel, though it more closely resembles cast steel.

A large consumer of SG iron is the gas and water pipe industry, which produces centrifugally cast pressure pipes and special pieces (elbows, Y-pieces, T-pieces, etc.). The automobile and general engineering industries have an even greater and increasing demand. Rollers, ingot molds, and heavy, thick-walled

storage containers for the disposal of radioactive waste are manufactured from SG iron.

A special development, austempered ductile iron (ADI), also known (somewhat inappropriately) as "bainitic" cast iron, has interesting mechanical properties. When its tensile strength is 900 N/mm², its breaking elongation is 5–12%; when its tensile strength is 1400 N/mm², its breaking elongation is 1–2%. These materials also have very good abrasion properties. The bainitic hardening is carried out in a salt bath at ca. 300–500 °C for 20 min to ca. 2 h. As yet there is no standard specification in Germany, the United States, Japan, or Sweden. A European standard is in course of preparation.

Cast Iron with Vermicular Graphite. In this type of cast iron, the graphite that separates out is mainly in vermicular form. The connection between this type of cast iron and the mineral vermiculite, a magnesium aluminum silicate, is only conceptual. On heating and expanding, vermiculite swells up to worm-like shapes (Latin: *vermis*, worm). Expanded vermiculite is used in the building industry as a sound, and thermal insulator, and has no connection with cast iron.

The basic structure of cast iron with vermicular graphite can be ferritic, pearlitic, or a mixed structure. The mechanical properties of the material lie somewhere between those of gray iron and SG iron. Vermicular graphite has been known since the discovery of spheroidal graphite in 1948. Any vermicular graphite in the SG iron structure was regarded as having a harmful effect on properties. Its occurrence indicated the presence of troublesome elements (principally titanium), which limited the formation of spheroidal graphite if the standing time of the melt was inadequate or excessive. This led to fading of the effects of the magnesium treatment, and imperfect formation of the graphite in the interior of thick-walled SG iron castings.

There is no German standard for this material, but local standards exist.

Alloyed Cast Iron. The properties of cast iron can be modified within wide limits by adding

elements such as nickel, chromium, manganese, copper, and silicon, which change the metallic structure. Corrosion-resistant and high-temperature grades are used, e.g., in the chemical industry, in furnaces, and in the automobile industry. The cryogenics industry uses low-temperature grades that do not become brittle at temperatures far below 0 °C. The electrical industry has wide-ranging requirements for nonmagnetic materials, and materials with high electrical resistivity.

In Germany, these materials are covered by DIN 1694 (austenitic cast iron) and DIN 1695 (abrasion-resistant alloyed cast iron), in the United Kingdom by BS 3468, and in the United States by ASTM A439.

White Cast Iron and Roll Casting. In these special grades of cast iron, the carbon in the structure is not graphite, but iron carbide. White cast iron is extremely resistant to abrasion by frictional and grinding effects. These grades are used in a wide range of rolling operations, and in grinding and mixing processes. As these materials are normally not heat treated, the mechanical properties depend only on the chemical composition, even for very heavy and thick-walled components (rolls).

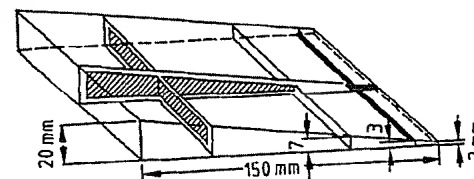
Malleable Iron. Malleable iron castings acquire their special properties by a tempering heat treatment. Malleable iron is formed from an iron-carbon alloy (DIN 1692) whose chemical composition is such that, after solidification, the carbon in the metallic structure of the casting is not free graphite, but chemically combined as iron carbide, Fe₃C. In this condition, the material is hard and brittle, and almost useless. The tempering process causes a transformation of the white iron by decomposition of the iron carbide at the high temperature used. Elemental carbon is precipitated, and is then present in the structure as compact nodules or flakes.

Depending on the heat treatment, two types of malleable iron can be produced: "white heart" malleable iron in which the heat treatment removes the carbon (Figure 6.111), and

"black heart" malleable iron in which it does not.

Malleable iron can be produced only in castings of limited mass and wall thickness. Mass varies between a few grams and ca. 100 kg. The good machining properties and especially the uniformity and consistency of the useful properties of malleable iron make it highly suitable for production foundries.

Most of the malleable iron castings produced (65%) go to the automobile industry. In second place comes the building industry (fittings and pipe connectors). Other consumers include the general engineering and electrical industries, and manufacturers of locks.



Carbon, %		
Bound: Total:		
≤0.1	≤0.1	Ferrite
0.1–0.7	0.1–2	Ferrite + pearlite + temper carbon
0.7	2–3	Pearlite + temper carbon

Figure 6.111: Distribution of carbon and development of the structure in white heart malleable iron of various wall thicknesses.

Melting of Cast Iron. The oldest and most widely used melting furnace in iron foundries is the cupola furnace. It was developed from the early charcoal furnaces, which were sometimes provided with a cover to keep off snow and rain.

The modern cupola furnace is a shaft furnace with height approximately six times its diameter. The inside diameter is ca. 800–3000 cm. Most cupola furnaces have melting capacities of 6–12 t (Figure 6.112), but the largest cupola furnaces produce 80 t/h. Pig iron, alloying elements, scrap castings, and steel scrap, together with coke (the fuel) and limestone to liquefy the slag and combine with the sulfur in the coke, are all charged in weighed batches into the cupola furnace.

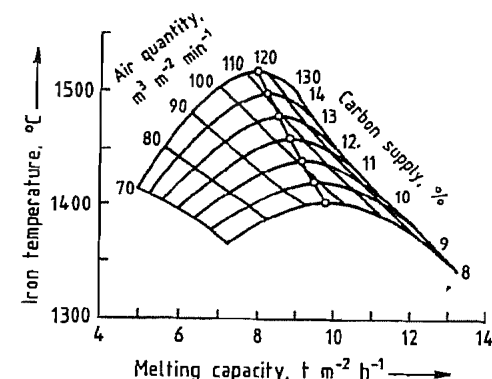


Figure 6.112: Iron temperature and melting rate as a function of air blast and available carbon for a cupola furnace with specific cross-sectional area 1 m².

The cupola furnace consists of a strong cylindrical steel sheet outer cover, lined with a thick layer of refractory bricks and rammed refractory material. In the bottom part of the furnace shaft, ring-shaped nozzles (tuyères) blow air into the incandescent layers of coke, iron, and other materials.

In the melting zone, the metallic raw materials, selected so that the molten cast iron has the desired composition when it flows from the furnace, are mixed. Molten cast iron at ca. 1500 °C and molten slag are then tapped from separate openings into separate containers. The cast iron is usually collected in a large, refractory-lined holding vessel in front of the cupola furnace. The casting ladles can then be filled from this as required. The slag flows into a cast iron skip, and, after solidification, is disposed of on a waste tip. It is sometimes granulated by adding water, or is used to produce slag wool, used as an insulating material.

Modern cupola furnaces use the hot blast system, in which the combustion air is preheated and sometimes enriched with oxygen. This increases the temperature and melting capacity.

In another type of cupola furnace, firing is by gas or oil. The furnace is provided with burners instead of tuyères. The column of metal is supported in the shaft by a water-cooled grate, located above the burner zone. Ceramic spheres on the grate increase heat transfer by convection, and the molten iron

passes over these and drips into the hearth. The cupola furnace is an economic method of melting large amounts of iron of constant or slightly varying composition. The molten iron can be continuously removed from the furnace. To an increasing extent, induction crucible furnaces are used in iron foundries, usually operating at mains frequency (50 Hz) with iron capacities up to 80 t, although most are in the range 3–25 t. Furnaces of this type do not absorb electrical energy when empty, and absorb very little when charged with material in small pieces, because no appreciable induced current is produced under these circumstances. Hence, low-frequency crucible furnaces must always have a quantity of molten metal in the furnace (25% of the total crucible capacity). To start up the furnace, a precast starting block that matches the shape of the crucible is placed in the crucible by means of a crane.

Medium-frequency induction crucible furnaces, operated at 500–1000 Hz, are similar to the mains frequency furnaces, except that their capacities are considerably less for electrical reasons. Medium-frequency furnaces are used if rapid melting and heating, melting without starting blocks, or frequent changes of metal grade are required.

6.4 Forming

Metals, including steel, can be subjected to plastic deformation in the solid state by the application of external forces, i.e., they can be formed into new permanent shapes. Here, the term “forming” or “metal forming” means the intentional and controlled change of the geometry of a workpiece, usually from a simple geometry to a complex one with regard to the shape, size, accuracy and tolerances, appearance and properties. The mass, composition, and state of the material remain unchanged. If, however, the plastic limit is exceeded so that the change in geometry is not controlled, forming with defects occurs, and the desired product is not obtained.

For many applications, the products of hot rolling are unsatisfactory, e.g., with respect to cross section, surface quality, dimensional accuracy, and general finish, so that cold rolling is necessary, i.e., reduction of the thickness of the hot-rolled strip between two working rolls without additional heating. Cold rolling of steel is mainly used in the production of light-section, thin sheet, and stainless steel sheet of thickness 0.1–3.0 mm.

The production cycles in a cold rolling mill differ considerably from those in a hot rolling mill. The raw material is first descaled, rolled, and then heated. Further steps are slitting, coiling, inspection, skin-pass rolling and packing.

6.4.1 Pickling

Hot-rolled steel sheet always has a layer of scale of variable structure on its surface, depending on the hot rolling conditions (Figure 6.113). The method of descaling depends on the composition of the scale. For high-grade steels, chemical descaling is carried out in hydrochloric or sulfuric acid, while stainless steels are normally pickled in a nitric acid mixture. Purely chemical descaling is often a long process, but it can be accelerated by preliminary mechanical descaling, e.g., stretching, leveling abrasive blasting, or rolling. Effective descaling requires the scale to be broken down.

Pickling is carried out in continuously operating plants (Figure 6.114). There are usually two pay-off reels from which the strip is run. It is first cut by cropping shears to form the beginnings and ends of the strips, and the start of the band is machine welded to the end of the previous band. Great care must be taken in the production of the weld bead, as this is rolled in the cold rolling mill, and must not be torn off. So that the actual pickling process can take place continuously during this interruption to the flow, there is a storage looper between the welding machine and the pickling plant. After welding, the storage looper is refilled at ca. 2.5 times the pickling speed.

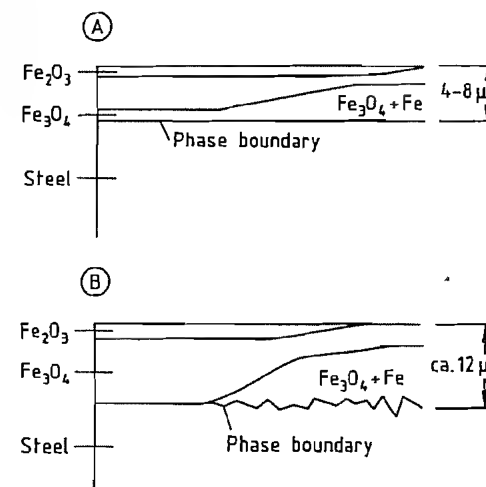
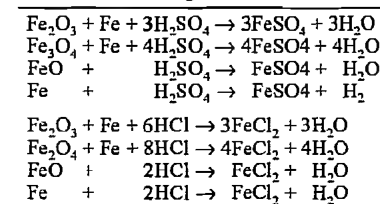


Figure 6.113: Structure of the scale layer on hot-rolled unalloyed or low-alloyed steel: A) Coil temperature ca. 570 °C; B) Coil temperature ca. 750 °C.

Before the actual pickling process, there is usually a stretcher bend-leveling device which also causes mechanical descaling. This preliminary descaling is very important, as there must be a certain percentage of free iron surface in the pickling bath, so that pickling can start. Normal steels are usually pickled in 20–25% sulfuric acid at 95–100 °C, or 15–20% hydrochloric acid at 60–70 °C in three or four fully enclosed pickling baths. For strip speed 240 m/min, the dwell time in the bath is ca. 20–30 s. The pickling time depends not only on the steel composition and hot rolling conditions, but is also a function of acid concentration, temperature, and concentration of iron(II) salt, which increases as the dissolution of scale proceeds.

The chemical reactions during pickling are described in the literature [175–179]. Individual pickling reactions are given in Table 6.14.

Table 6.14: Pickling reactions.



As the area of the clean steel surface increases, the pickling time decreases until a point known as the critical free surface is reached. For hydrochloric acid, this is ca. 15%, and for sulfuric acid, ca. 2%.

After leaving the acid baths, the strip is washed, dried, oiled, and coiled to form rolls of the required mass. The storage looper compensates for interruptions to the process. All pickling plants are provided with trimming shears, normally located at the exit, though in some plants at the inlet.

The used acid can be regenerated, in the case of sulfuric acid by precipitating iron sulfate as its heptahydrate in a crystallizer (see Section 5.20).

Hydrochloric acid can be regenerated by decomposing the iron chloride to hydrochloric acid and iron oxide, by a spray process at 450 °C, or in a fluidized bed at 850 °C [180].

6.4.2 Rolling

After pickling, the descaled hot-rolled strip is cold rolled, reducing its thickness (1.5–5 mm) by up to 90%. Many types of stands are used in the production of cold-rolled strip, e.g., two-high, four-high, or larger. In reversing stands, one roll pass can be immediately followed by another by reversing the direction of the rollers. Reversing stands with many rolls exert a high pressure on the strip because the diameters of the working rolls are small. These stands are therefore mainly used for steels with work-hardening properties, e.g., stainless steels and electric sheet steels.

Some 4–6 four-high stands can be installed one after the other to form a so-called tandem cold rolling mill (Figure 6.115). These mills have the advantage that the strip reaches its final thickness by going in one pass from the pay-off reel through all the stands. Strip speeds at the exit can reach 2400 m/min.

The gap is lubricated with an oil-water emulsion to enable a high degree of deformation (thickness reduction) to be achieved at high rolling speeds. The oil provides lubrication, and the water absorbs the heat produced in the rolling process.

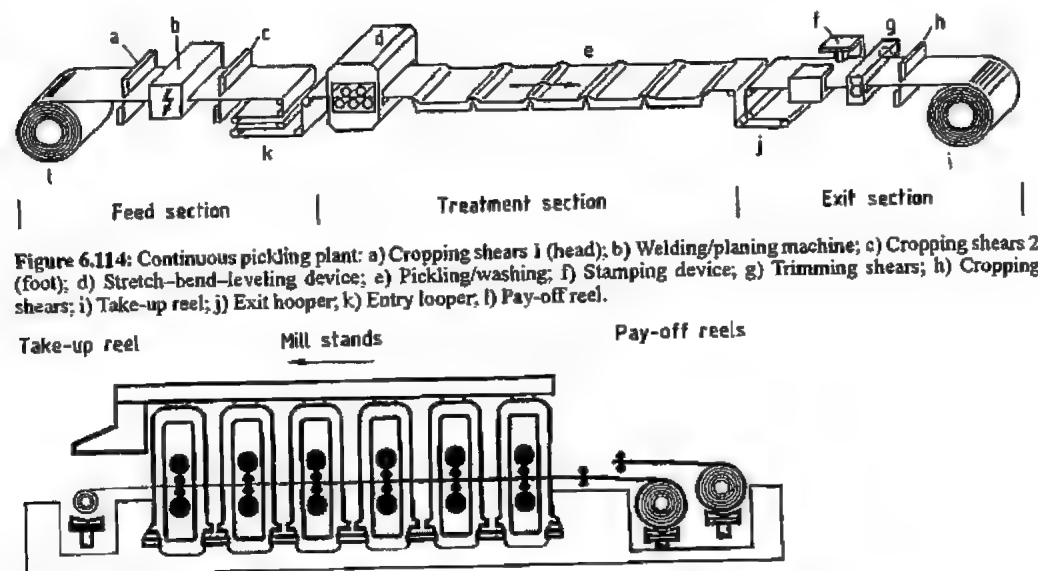


Figure 6.114: Continuous pickling plant: a) Cropping shears 1 (head); b) Welding/planning machine; c) Cropping shears 2 (foot); d) Stretch-bend-leveling device; e) Pickling/washing; f) Stamping device; g) Trimming shears; h) Cropping shears; i) Take-up reel; j) Exit looper; k) Entry looper; l) Pay-off reel.

Figure 6.115: Six-stand tandem cold rolling mill.

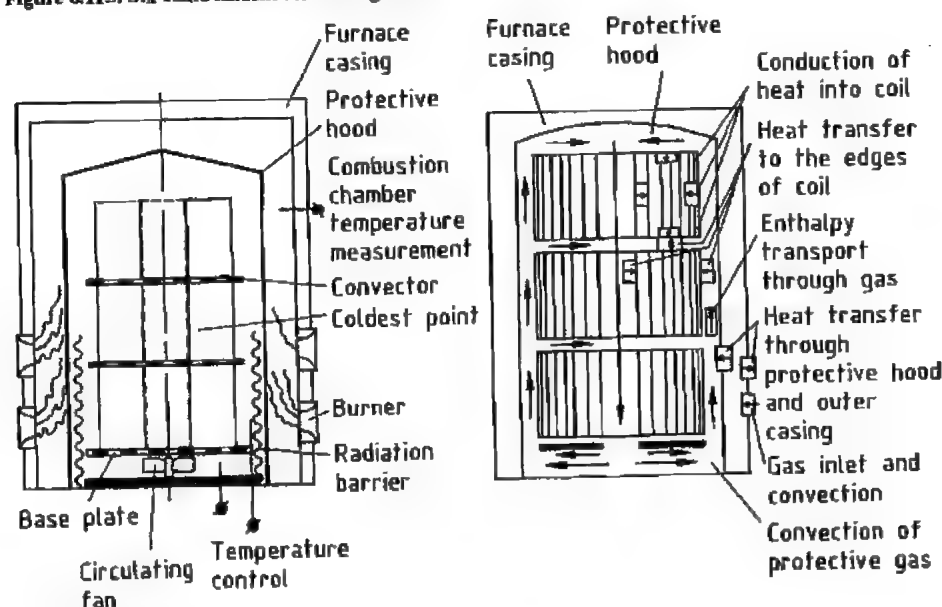


Figure 6.116: Hood furnace with heat transfer and gas flow indicated.

Experiments have shown that it is not possible to change the profile in a cold rolling mill, so the hot-rolled strip profile must be produced to close tolerances. If the shape of the gap between the rolls does not correspond to the profile of the strip being rolled, flatness

defects can occur (differences in the length of individual fibers) [181].

The control elements usually used to adjust the flatness are:

- Curved working rolls, both positively and negatively. Gap correction up to 180 μm can be achieved.
- Adjustable intermediate rolls. This system requires six stands.
- Thermal changes to the crowning of the roll. The degree of thermal expansion of the roll body can be changed locally by adjusting the cooling, but this can only produce extremely small changes.
- Continuously variable crown systems (universal profile control). The rolls can be adjusted to produce a convex or concave gap; the range of control here is ca. 400 μm .

With the aid of precisely controlled strip tensions between the stands and highly developed measuring and automation technology, it is possible to provide a gap shape appropriate for the shape of the strip. With this system, flat cold-rolled strip with thickness variations of only a few thousandths of a millimeter and high-quality surface finish can be produced.

Cold rolling causes work-hardening of the steel. This is reduced by an annealing stage.

6.4.3 Annealing

The cold-rolled coiled strip is stacked in a hood furnace for annealing (Figure 6.116). The combustion chamber is heated by oil or gas burners. The heat passes through the protective hood into the space where the steel coils are stacked. A circulating fan provides as uniform a temperature distribution as possible. The atmosphere in conventional plants is usually HNX gas (a nitrogen-hydrogen mixture in which the hydrogen content is close to the flammability limit).

The heat passes into the coils through their outer edges, so that these areas are always hotter than the inner windings, especially during heating up.

This heat treatment causes the organic residues of the emulsion to burn off without leaving a residue, in accordance with the reactions given in Table 6.15 [182–184]. The strip is then heated to the recrystallization temperature, and annealed under the protective gas at

ca. 700 °C. This treatment produces a complete recrystallization of the cold-rolled steel. The coils are cooled by removing the outer casing. As the annealing space is then hotter than its surroundings, heat passes out of the protective hood in the reverse direction. The outer windings of the coil cool more quickly than the inner windings. If the cooling is too rapid, tensions due to shrinking occur, and these can cause diffusion welding of the windings (stickers).

Table 6.15: Annealing reactions.

$\text{CO}_2 + \text{C} \rightleftharpoons 2\text{CO}$	Boudouard reaction
$\text{CO} + \text{H}_2\text{O} \rightleftharpoons \text{CO}_2 + \text{H}_2$	Water gas reaction
$\text{Fe} + x\text{CO}_2 \rightleftharpoons \text{FeO}_x + x\text{CO}$	Oxidation of iron due to CO_2/CO ratio
$\text{Fe} + x\text{H}_2\text{O} \rightleftharpoons \text{FeO}_x + x\text{H}_2$	Oxidation of iron due to $\text{H}_2\text{O}/\text{H}_2$ ratio
$\text{C} + 2\text{H}_2 \rightleftharpoons \text{CH}_4$	Methane reaction

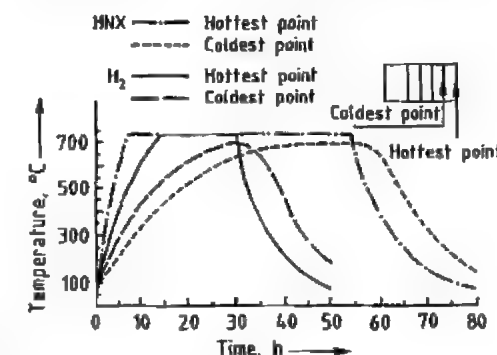


Figure 6.117: Comparison of annealing times in a hood furnace under HNX and H_2 atmospheres.

Annealing in this type of furnace was formerly very slow. Another serious limitation was the limited rate of cooling attainable, so that certain grades of steel were very difficult to produce in this furnace. An annealing process in a 100% hydrogen atmosphere with improved convection has been developed in recent years. This gives shorter annealing times (mainly owing to the rapid cooling), and more uniform mechanical properties. The hydrogen easily diffuses into the coil windings, and its conductivity is a factor of seven greater. Moreover, the smaller H_2 molecules

enable more rapid circulation of the atmosphere (high convection, Figure 6.117).

The continuous strip annealing process was developed in Japan in the 1970s (Figure 6.118). At the feed end there are: a double-feeder pay-off reel, a welding machine, a cleaning zone, and a storage looper (required if coils need to be welded together to give continuous operation). The strip then passes through the heat treatment zone: heating chamber, annealing chamber, cooling unit, tempering zone, and second cooling chamber. These are followed by the exit looper, the skin pass mill, the side-cutting shears, the inspection area, the cut-to-length line, and the double-coiling reel. As the treatment time for the material is short (ca. 10 min), the annealing temperature is higher than in the batch annealing process.

There are four continuous annealing processes which compete worldwide, differing mainly in the cooling equipment used, and the cooling rates achieved [185].

The recrystallizing annealing process eliminates the hardening produced by cold working, but the mechanical properties of the annealed strip are poor: low tensile strength, low yield point, high fracture strain, etc. Annealed thin strip has a marked upper yield point and a large extension at the lower yield point.

There are two basically different annealing cycles for continuous annealing furnaces (Fig-

ure 6.119). In the first, the strip is heated to the annealing temperature, held at this temperature, cooled to the dwell temperature, held again, and then cooled to room temperature. The other alternative consists of heating to the annealing temperature, cooling with gas jets to an intermediate temperature, and quenching in water to room temperature. The strip is then brought up to the aging temperature, and finally cooled again to room temperature. Treatment at the aging temperature is not necessary for dual-phase steels.

Quenching is produced by the rapid cooling of the strip in the continuous annealing process, so that the carbon remains in solution. For this reason, continuous annealing is very suitable for producing high-strength, dual-phase, and IF (interstitial-free) steels.

6.4.4 Skin-Pass Rolling

As stated above, the annealed material must be rolled (skin-pass rolling) to prevent flow lines owing to the distinct upper and lower yield points. This also produces the roughness which customers require. This is of great importance for deep drawing or coating the steel. For example, if complex deep-drawn parts are required, e.g., for automobile construction, the surface of the steel should be rough in order to retain the lubricant. Good coating properties require a surface with a large number of peaks, which should be randomly distributed.

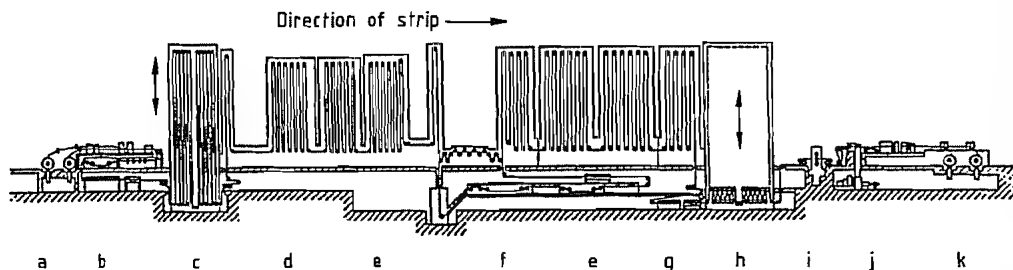


Figure 6.118: Continuous annealing plant: a) Pay-off reel; b) Strip cleaning; c) Entry looper; d) Heating zone; e) Tempering zone; f) Reheating zone; g) Cooling; h) Exit looper; i) Skin-pass rolling; j) Inspection/oil treatment; k) Take-up reel.

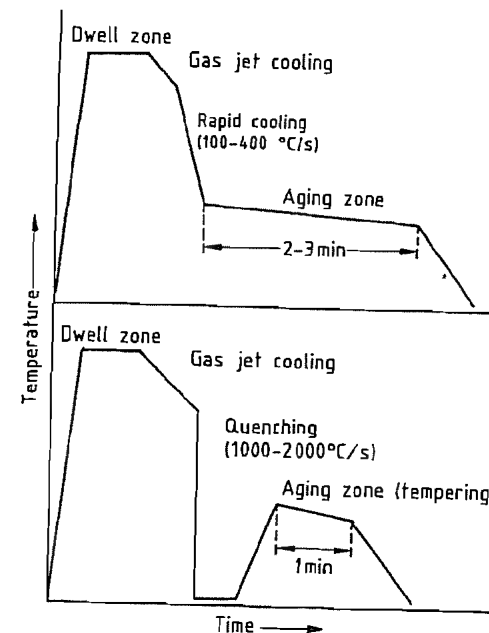


Figure 6.119: Heating cycles of continuous annealing.

Various steel grades can be produced in these two annealing cycles.

6.4.5 Stainless Steels

The processing of stainless steel in a cold rolling mill is quite different (Figure 6.120). Austenitic stainless steel behaves differently from ferritic stainless steel. The hot-rolled strip is first annealed. This is necessary because, after the hot rolling process, the strip cools slowly, and carbon tends to precipitate at the grain boundaries, owing to its reduced solubility at lower temperature. Annealing causes the carbon to go back into solution. Rapid cooling of the strip then prevents the carbon from precipitation by diffusion. Although the annealing time required to bring the carbon into solution is short for austenite, a long time is necessary for ferritic steels, so that batch annealing is necessary. In the continuous furnace, annealing is carried out in an oxidizing atmosphere to produce a scale with a high oxygen content, thereby assisting the pickling process. This does not apply to high-grade

steels. The strip is then quenched, by air-water cooling.

Annealing in the hood furnace is successful because of the increase in throughput obtainable under the reducing atmosphere. Considerable increases in throughput have been achieved by the use of hydrogen, even though its concentration is only 25%.

A high proportion of the scale is removed by abrasive blasting. Although the abrasive particles are mainly spheroidal, a high degree of roughness is produced. This must be removed by rolling, another cause of the high deformation strain in high-grade steel mills.

Sodium sulfate is used in electrolytic pickling. The electrolytic pickle liquor is in effect self-regenerating.

Conventional pickling is carried out with a mixture of nitric (12–14%) and hydrofluoric acid (2–4%). Pickling temperatures are usually 40–60 °C. Unlike sulfuric acid or hydrochloric acid pickling solutions, regeneration is not possible, so that the spent acids must be rendered harmless and disposed off.

After pickling, the strip is usually rolled on "Sendzimir" rolling mills (more rarely on four- and six-high stands).

The strip is then annealed to convert the steel from the work-hardened state produced by cold rolling into a recrystallized and stress-relieved state, to enable further treatment of the strip to be carried out.

Stainless steels are to an increasing extent being annealed in bright annealing plants [186], as this process enables the bright surface produced by cold rolling, and typical of special steels, to be retained (Figure 6.121).

The strip is finally rolled again (skin-pass rolling).

6.4.6 Future Developments

The extent of automation in cold rolling mills has raised the possibility of linking the individual process steps. For instance, attempts are being made to link the pickling stage with the tandem rolling operation. This requires the outputs of the two operations to match. In Japan, a cold rolling mill is being

operated in which pickling, rolling, and continuous annealing have been combined, despite the fact that the outputs of the continuous annealing process and the rolling mill do not

correspond. The maximum economic output of a continuous annealing plant is 800 000 t/a, while tandem rolling mills can easily achieve twice this production rate.

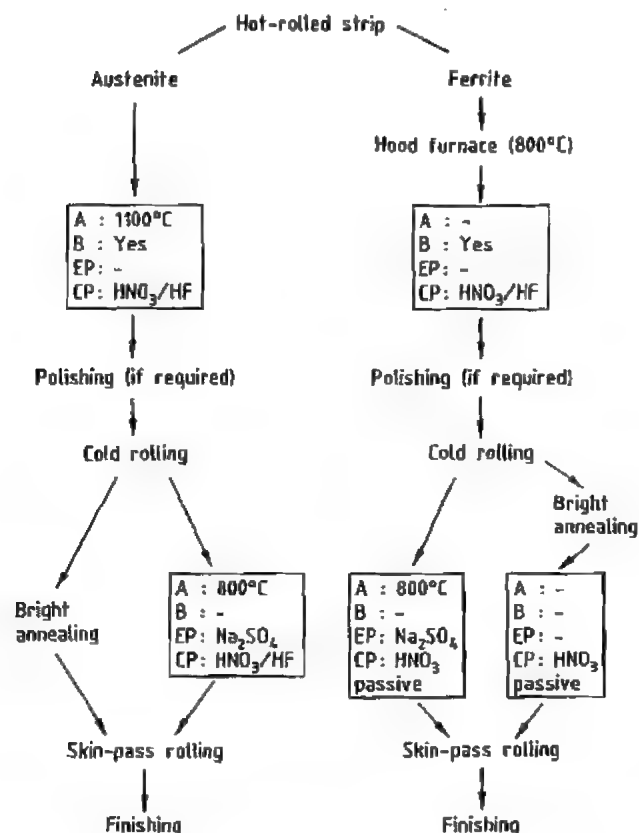


Figure 6.120: Flow diagram of a combined annealing/pickling line. A = annealing; B = abrasive blasting; EP = electrolytic pickling; CP = chemical pickling.

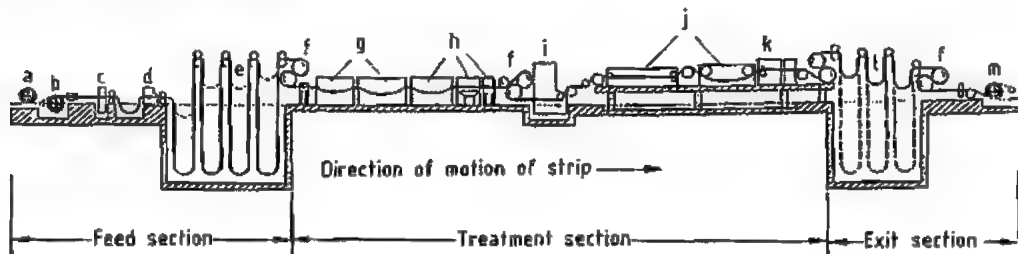


Figure 6.121: Annealing/pickling line for stainless steel: a) Pay-off reel 1; b) Pay-off reel 2; c) Welding machine; d) Trimming shears; e) Looper 1; f) Roll stand; g) Furnaces; h) Cooling zone; i) Abrasive blasting; j) Pickling; k) Spray washing; l) Looper; m) Take-up reel.

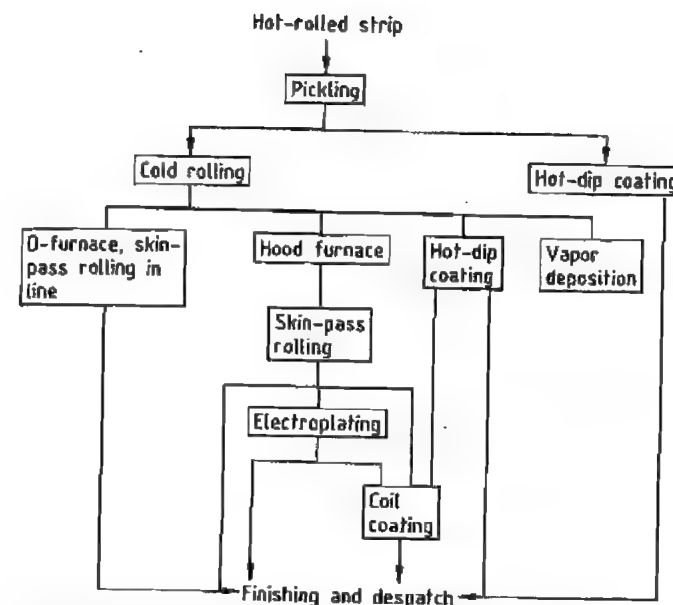


Figure 6.122: Surface coating in relation to other production processes.

6.5 Surface Coating

6.5.1 Introduction

Technical developments in recent years have greatly increased the output of surface-coated steel strip. The demand for improved corrosion protection is not the only driving force. The properties of coated strip, such as the yield point, expansion properties, and cold workability needed to be improved before these products could be used, e.g., in the automotive industry. New processes had to be developed to improve welding and paint application properties for large-scale industrial manufacture. These involved close cooperation between the producers and consumers of coated steel sheet. Within the steel industry the continuous surface coating processes used include hot dipping, electrolytic techniques, vapor treatment, and coil coating.

The status of surface coating in relation to other production processes within the steel industry is shown in Figure 6.122.

The design of surface coating plants for wide steel strip essentially consists of the me-

chanical entry section, the process itself, and the exit section. The input and output sections are provided with pay-off reels, coiling reels, leveling machines, shears, welding machines, loopers, regulating and pulling rolls, etc.

This equipment produces a continuous strip, and enables treatment to be carried out at constant strip speed, under stable process conditions. Inspection areas for quality assurance are usually situated at the exit end.

As well as coated strip, the steel industry also produces clad steel sheet. This is a composite material that combines the properties of a carrier material which is usually cheap (e.g., carbon steel) with those of a metal more suitable for the conditions of use (e.g., corrosion-resistant steel).

6.5.2 Hot-Dip Coating

6.5.2.1 Plant and Processes

In the hot-dip coating process, the steel strip is continuously passed through molten metal. An alloying reaction between the two

metals takes place, leading to a good bond between coating and substrate.

Cold-rolled wide strip is usually used for hot-dip coating, but this is contaminated with rolling lubricant emulsion and of abraded iron fines. To ensure a good bond between the metal coating and the substrate, the surface of the strip must be thoroughly cleaned before dipping in the molten metal.

The important parts of the hot-dip coating process (Figure 6.123) are [187]: the continuous furnace; the treatment zone where the metal coating is applied; cooling and final treatment.

Older plants usually have a horizontal continuous furnace which comprises a directly heated preheating furnace and indirectly heated reduction and holding zones with reducing H_2/N_2 atmospheres, followed by cooling zones. In the preheating furnace, the strip is rapidly heated to $> 550^\circ\text{C}$, and is cleaned by burning off the oil emulsion residues. In the reduction and holding zones, the strip is heated to cause recrystallization or normalization, according to the grade of steel, to give the cold-rolled, work-hardened substrate material the desired mechanical properties.

For normal grades of thin steel strip, temperatures are $700\text{--}750^\circ\text{C}$, and for IF (interstitial free) steels $> 800^\circ\text{C}$.

The strip is cooled in the cooling zones to a temperature slightly above that of the molten

metal, with static cooling elements and rapid coolers.

After leaving the continuous furnace, the cleaned and heated strip, under a protective gas, is fed by means of a so-called snout into the molten metal (Figure 6.124), which is contained in a heated metal or ceramic vessel. Immediately after this, jet processing is carried out by blowing a gaseous medium through a slit, of the same length as the width of the strip, onto the upper and lower sides of the strip. This enables different coatings to be produced on the two sides. The coating thickness ($7\text{--}45\text{ }\mu\text{m}$, or $50\text{--}300\text{ g/m}^2$) is a function of gas pressure, strip speed, nozzle-strip distance, nozzle aperture, jet angle, and the viscosity and density of the metal being removed.

The thickness of the metal coating is continuously monitored, and controlled by adjustments to the jet processing equipment.

After jet processing, the liquid metal coating passes through air cooling equipment, so that it solidifies before it comes into contact with the first roller that deflects it from the vertical.

The strip then passes through more processing equipment. It is rolled in the finishing stand to improve its technical properties or to give a uniform surface appearance. The flatness of the strip is then improved by stretch-leveling equipment.

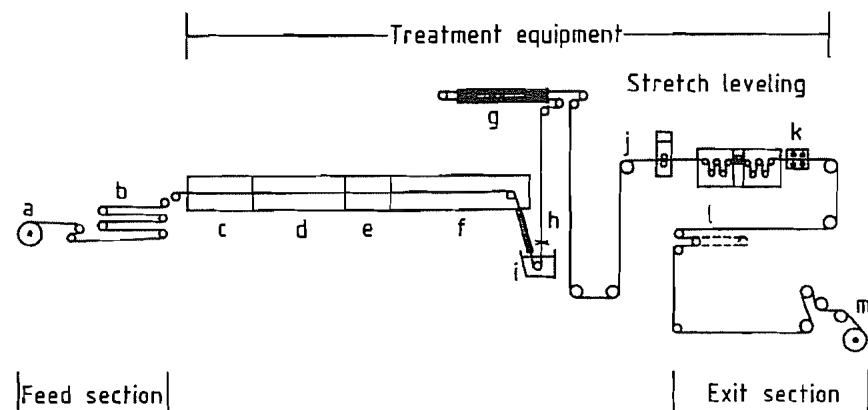


Figure 6.123: Hot-dip coating plant: a) Pay-off reel; b) Entry looper; c) Preheater; d) Reduction zones; e) Holding zone; f) Cooling zones; g) Strip cooling; h) Nozzle; i) Molten metal bath; j) Skin-pass rolling; k) Final chemical treatment; l) Exit looper; m) Take-up reel.

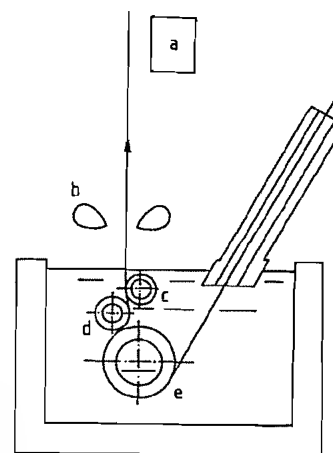


Figure 6.124: Control of coating thickness: a) Coating thickness measurement; b) Jet processing nozzle (slit); c) Pass line roll; d) Stabilizing roll; e) Bottom roll.

Further chemical treatment—chromate passivation and/or oil treatment, for temporary protection of the surface against “white rust” is sometimes carried out.

In new plants (Figure 6.125), the continuous furnace is usually vertical, which reduces the number of contacts between the easily damaged strip and the carrier rollers. These plants also have alkaline cleaning equipment, with brushing and rinsing zones to remove both the emulsion residues and most of the particles of abraded iron. The preheater in these plants is usually indirectly heated, as the emulsion residues are removed in the alkaline cleaning.

6.5.2.2 Other Coating Processes

Up to the late 1960s, only zinc and aluminum were used to coat steel. Corrosion resistance and working properties were later improved by using coatings based on a composite zinc-aluminum system. Table 6.16 lists the most important coatings, with compositions, coating thicknesses, and bath temperatures.

Zinc in the presence of moisture provides cathodic protection of the steel substrate. This is effective, even in the region of the uncoated edges, up to a steel thickness ca. 1 mm.

Aluminum has a dense outer oxide layer which reduces loss rates in various atmospheres, and gives better corrosion protection, especially at higher temperatures. The zinc-aluminum combination is selected to give the best coating properties for each application.

In the hot-dip zinc coating process, when the oxide-free steel surface is dipped, a multi-layer Fe-Zn diffusion zone is formed which is then covered with a layer of zinc on removing the sheet from the bath. In batch galvanizing, uncontrolled growth of the Fe-Zn layer leads to a thick and very brittle coating with several component layers (Figure 6.126) that does not readily undergo forming processes. On the other hand, a continuous zinc coating process involves short contact times between the strip and the molten zinc. Aluminum is added to reduce the speed of the Fe-Zn reaction, leading to a relatively thin alloy layer. Compared with batch processes, this composite system permits an extreme degree of deformation without detachment of the coating.

When the zinc coating solidifies, the well-known zinc spangle appears, caused by lead in the zinc bath (usually 0.10–0.15%). Hot zinc-coated thin strip with good forming and paint application properties must have zinc crystals that are as small and uniform as possible over the length and width of the strip. Crystal size can be controlled by nucleation or by the composition of the bath.

Control of the number of nuclei by the introduction of foreign nuclei has been used for some years (Figure 6.127). Nuclei in the form of water, water vapor, water-soluble salts, or zinc dust are blown onto the liquid coating surface. The success of the operation depends on uniformity over the whole width of the strip.

The third method of reducing zinc spangle is to reduce the lead content (Figure 6.128). As the solubility of lead in the zinc crystals is low, separate crystals tend to appear. If the lead content is $< 0.05\%$, the crystals are hardly visible macroscopically.

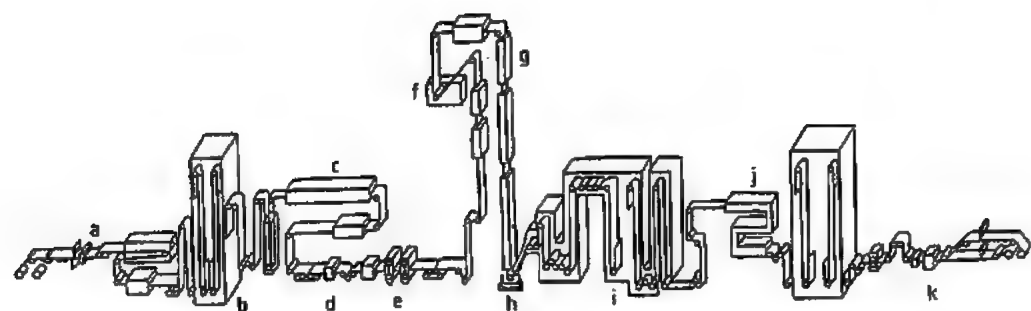


Figure 6.125: Hot-dip zinc coating plant at the Kawasaki Mizushima works: a) Exit section; b) Chromate passivation; c) Iron flash (electrolytic); d) Stretcher-roller leveling equipment; e) Measurement and control equipment; f) Skin-pass rolling; g) Zinc bath; h) Galvannealing furnace; i) Furnace; j) Pretreatment; k) Entry section.

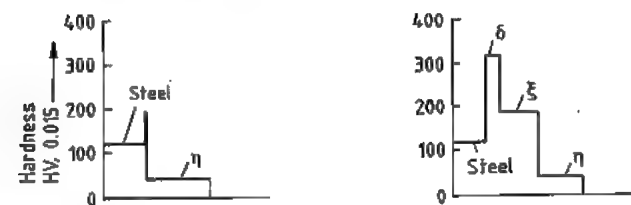
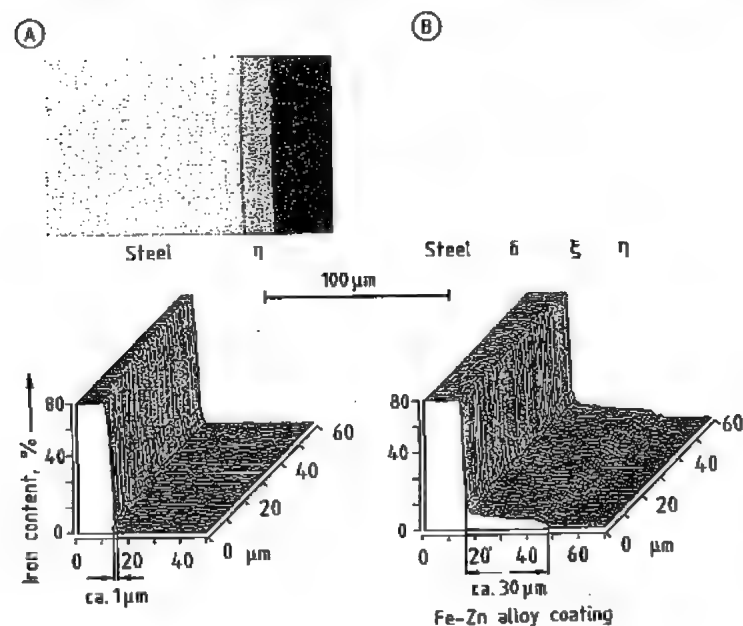


Figure 6.126: Coating structure, Fe content, and hardness of hot-dipped steel: A) Continuous galvanization; B) Batch galvanization.

Table 6.16: Composition and temperature of hot-dip coating baths and coating thicknesses produced.

Coating	Zn, %	Al, %	Si, %	Bath temperature, °C	Coating thickness, μm
Zinc coating					
Monogal	99.5	0.12-0.30		450-480	7-45
Galvannealed					7-15
Galfan	95	5		420-450	7-25
Galvalume	43.4	55	1.6	600-620	13-28
Aluminum coating (type 1)		90	10	660-680	17-45

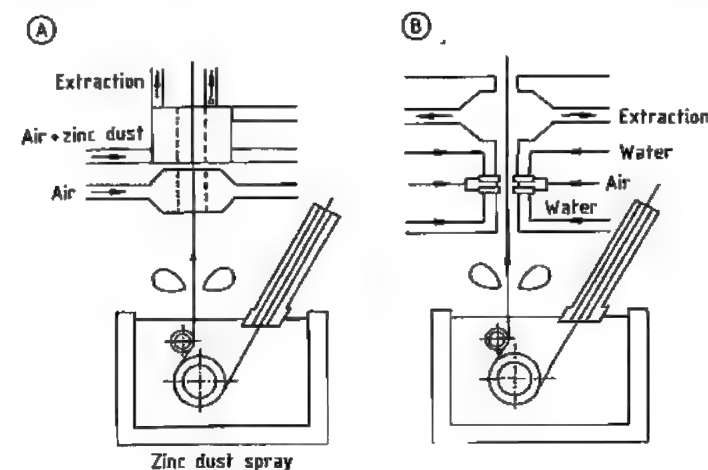


Figure 6.127: Control of crystal size in hot-dip zinc coatings by adding foreign nuclei: A) Zinc dust spray; B) Water-air spray.

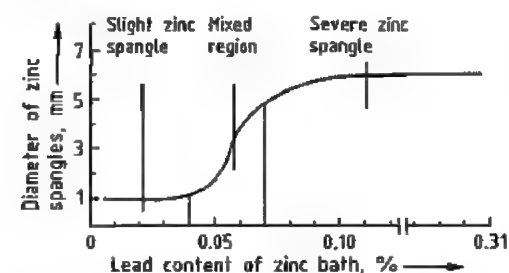


Figure 6.128: Zinc spangle diameter as a function of lead content of the coating bath.

Steel strip coated with zinc on one side only, the other side having similar properties to those of cold-rolled strip, is required in small amounts by the automotive industry.

In the process shown in Figure 6.129, liquid zinc is transferred to the strip under a nitrogen atmosphere by means of a carrier roll. In the Monogal process, the zinc coating is removed from one side of the strip by brushing in the opposite direction with a metal brush (Figure 6.130), and is removed by a fume extraction

system. A residual layer remains on the brushed side, consisting of ca. 10 g/m² material in the form of an Fe-Zn layer. The result resembles material that has been coated by applying a hot melt to one side only.

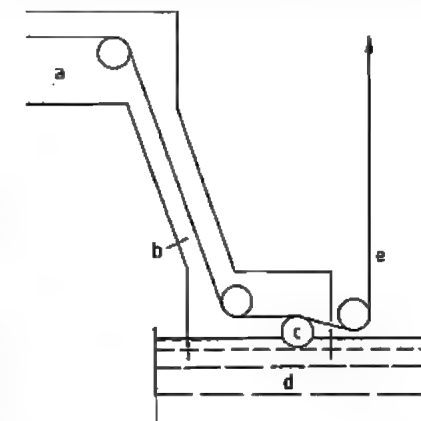


Figure 6.129: Coating steel strip on one side only (Nippon Steel): a) Furnace; b) N₂ atmosphere; c) Coating roller; d) Zinc bath; e) Stripping nozzle.

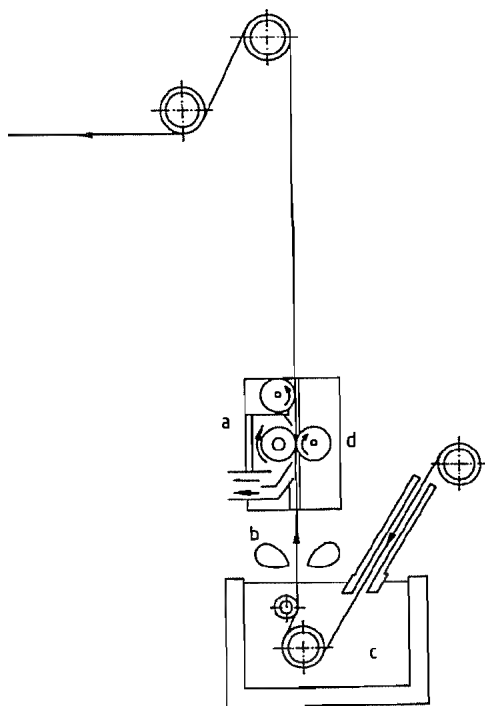


Figure 6.130: Hot-dip zinc coating by the Monogal process: a) Reverse-direction metal brush with zinc dust extraction; b) Nozzles; c) Zinc bath; d) Pass line roller.

In the Galvannealed process (Figure 6.131), on-line treatment of the strip is carried out immediately after zinc coating. After solidification, the coating (30–90 g/m², 5–12 μm) is heated briefly at 460–600 °C, inductively or with gas. This converts the zinc coating to a penetrating Fe–Zn alloy layer, which should have Fe content 9–11% for maximum forming properties. Compared with a pure zinc coating, Fe–Zn alloy coating gives improved welding and paint adhesion properties. If the Galvannealed strip is not painted, its corrosion resistance is less good.

A coating with the trade name Galfan was developed by the Centre de recherches métallurgiques in 1980. The zinc is alloyed with ca. 5% aluminum to give a eutectic composition with melting point ca. 380 °C. Wettability of the steel strip is improved by including small amounts of cerium and lanthanum in the melt bath. The Galfan coating has a lower loss rate

and improved forming properties (for comparable coating thicknesses) when used without a paint coating in an industrial atmosphere.

An Al–Zn alloy (ca. 55% Al, ca. 43% Zn, and 1.6% Si) was introduced by Bethlehem Steel in 1963 under the trade name Galvalume. It has a low loss rate, especially in maritime climates.

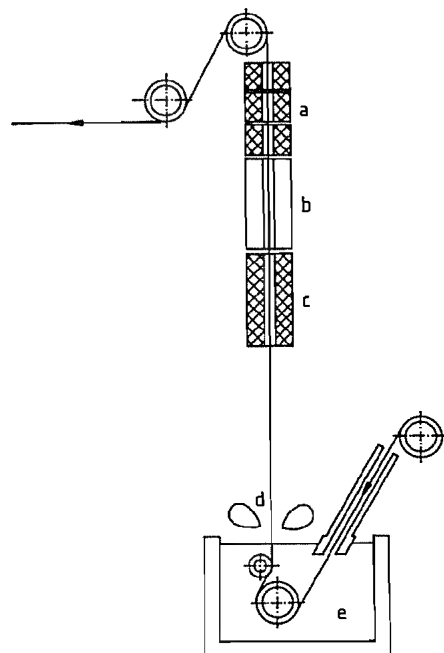


Figure 6.131: Hot-dip zinc coating by the Galvannealed process: a) Cooling zone; b) Holding zone; c) Heating zone; d) Nozzles; e) Zinc bath.

6.5.3 Electrolytic Coating (Electroplating)

6.5.3.1 Plant and Processes

In electrolytic coating (electroplating), the steel strip, which has been annealed and rolled (skin-pass rolling), is continuously passed through an aqueous electrolyte containing zinc ions (Figure 6.132) [188]. An electric current causes the zinc ions to be deposited on the steel strip, which forms the cathode. The process takes place at 55–75 °C, so that there is no alloying with the steel strip, and the me-

chanical properties of the substrate are not affected. The desired coating thickness is achieved by controlling current and strip speed.

In an electroplating plant (Figure 6.133), the equipment at the feed end is similar to that used for hot-dip coating, and only those features that differ from hot dipping are described here.

The surface of the cold-rolled strip must be clean so that an adherent, optically defect-free metallic coating is produced. Electrolytic coating plants have facilities for cleaning the strip, normally a combination of spray, brush, and electrolytic cleaning with alkaline cleaning solutions at 80 °C.

In cleaning facilities that use chemical solutions, multistage rinsing with brushing equipment is always provided, so that residues from the treatment solutions are removed as completely as possible.

After cleaning, many plants include stretch-leveling equipment to ensure that the strip is flat. This is necessary so that the distance between the anode and the strip can be kept small, while avoiding contact between the two (short circuits), thus minimizing electricity costs.

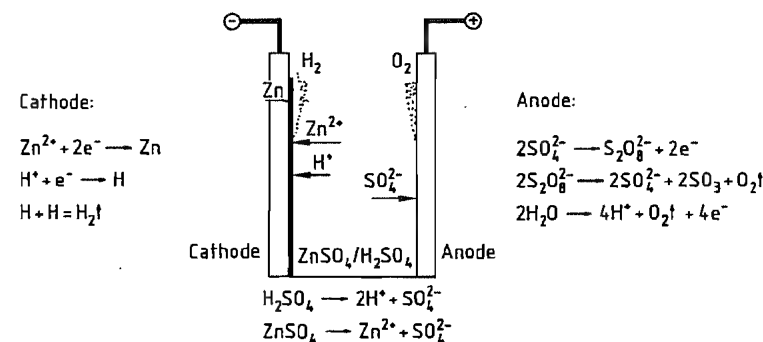


Figure 6.132: Electrolytic coating with zinc.

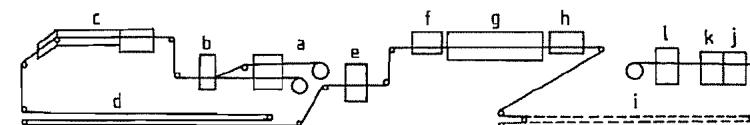


Figure 6.133: Electrolytic coating plant: a) Pay-off reels; b) Welding machine; c) Alkaline cleaning; d) Entry loop; e) Stretch-leveler; f) Pickling; g) Electroplating; h) Aftertreatment; i) Exit loop; j) Trimming shears; k) Oil treatment; l) Take-up reel.

In the electrolytic pickling process, the strip is activated before the zinc coating stage. After cleaning and pickling, the strip enters the coating facility, in which the number of electrolytic cells is sufficient to enable the production rate to match that of the rest of the plant.

The strip can be treated to give additional temporary corrosion protection, most commonly by phosphating and/or chromate passivation.

A strip drier is always provided at the exit end of the treatment zones of an electrolytic coating plant. In the discontinuous part of the exit area, there are usually trimming shears to ensure the correct strip width.

6.5.3.2 Electroplating Cells

In steel strip electroplating plants, coating takes place in the electroplating cells. The strip is connected to the negative pole of a rectifier, and forms the cathode. The conduction rollers have a highly wear-resistant cladding of special steel, and have to be cooled, owing to the high current which they carry. Compression rollers ensure good electrical contact. The anodes are situated on both sides of the strip, as near the strip as possible.

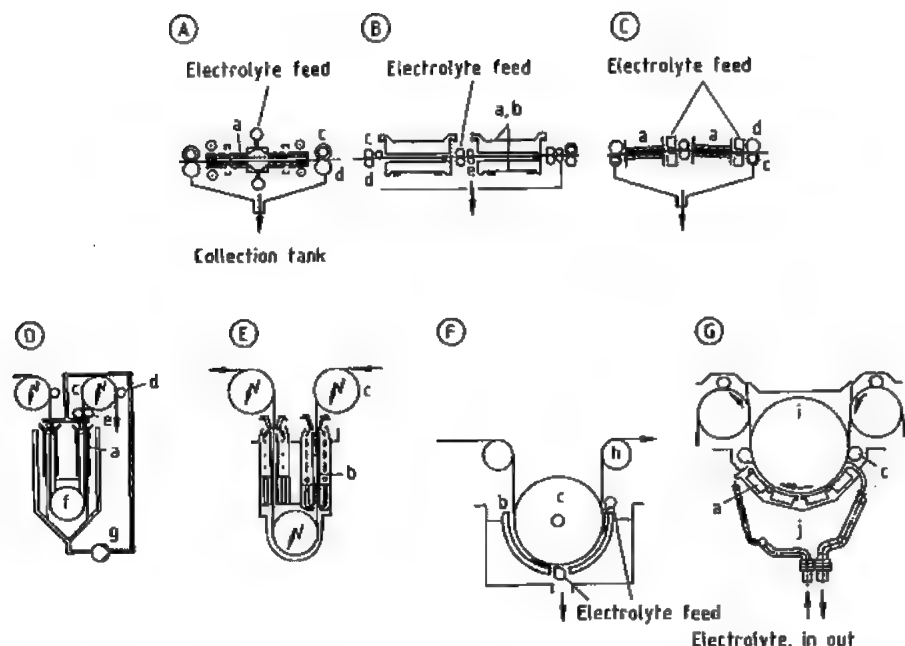


Figure 6.134: Electroplating cells: A) LCC-H (insoluble electrode, sulfate electrolyte; horizontal cell); B) NKK (soluble/insoluble anode; chloride/sulfate electrolyte; horizontal cell); C) Krupp/SEH (insoluble anode, sulfate electrolyte, horizontal cell); D) Gravitel (insoluble Ti anode, sulfate electrolyte, vertical cell); E) HS (soluble anode, sulfate electrolyte, vertical cell); F) Carosel (soluble anode, chloride electrolyte, radial cell); G) KC (insoluble anode, sulfate electrolyte, radial cell). a) Insoluble anode; b) Soluble anode; c) Current-carrying roller; d) Pressure roller; e) Squeeze rollers; f) Dipping rollers; g) Pump; h) Deflecting roller; i) Top roller; j) Edge mask.

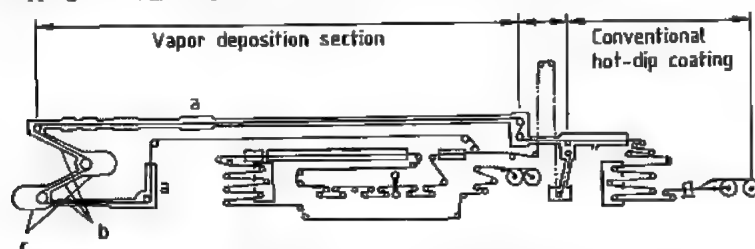


Figure 6.135: Zinc vapor deposition plant at the Nisshin Sakai works: a) Gas jet cooler; b) Vacuum system; c) Vaporization chambers.

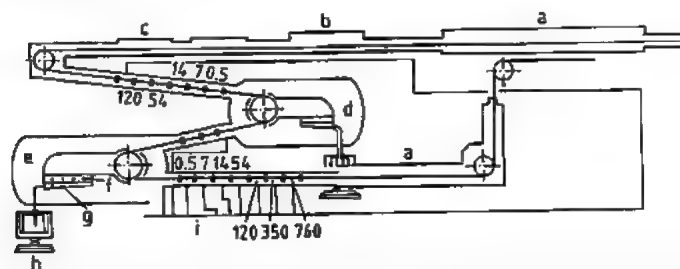


Figure 6.136: Vacuum system for the zinc vapor deposition plant: a) Gas jet cooler; b) N_2 gas; c) Edge heater; d, e) Vaporization chambers (2.66 Pa); f) Heating coils; g) Vaporizer; h) Zn melt; i) Vacuum pumps.

There are two types of anode:

- Solid anodes of the metal being coated dissolve at a rate proportional to the current and must be replaced at regular intervals.
- With insoluble anodes made of lead alloys, or titanium plates coated with noble metals. Zinc solutions must be added to the electrolyte.

To produce zinc or alloy coatings, sulfuric or hydrochloric acid electrolytes and soluble anodes are most often used. Addition of conducting salts, e.g., Na_2SO_4 or $(NH_4)_2SO_4$, ensures high conductivity, with current densities $> 100 A/dm^2$.

Three types of cell can be used for electroplating (Figure 6.134); horizontal and vertical cells are used for coating one or both sides, while radial cells coat one side only.

6.5.3.3 Coating Types

Zinc Electroplated Thin Steel Strip. Corrosion protection increases with increasing coating thickness, but workability and weldability deteriorate. A coating thickness of ca. $7.5 \mu m$ represents a good compromise.

Zinc-Nickel Coatings with $11 \pm 1\%$ Nickel.

This material has good corrosion properties, but mechanical properties are sometimes inferior to those of pure zinc coatings. Sealed Zn-Ni coatings (Durasteel) give improved workability.

Zinc-Iron Coatings. These give cathodic protection up to an iron content of 85% in the coating. Anticorrosion and workability properties are good with iron content 15–25%, while good paint application properties are obtained with iron content $> 50\%$. This has led to the development of a two-layer coating, the first with 10–25% Fe, (the rest being Zn), the outer coating containing $> 60\%$ Fe.

As well as these established types of coating, Zn-Co and Zn-Mn alloys are being investigated. Cobalt also shows interesting properties, even at low concentration, and can be plated at high current densities. Manganese is of great interest owing to the formation of a protective surface layer of Mn_2O_3 .

Tin and Lead-Tin Coatings. Lead-tin coatings containing 10% Sn (Terne) are mainly used to plate steel sheet for gasoline tanks. It has indifferent electrochemical behavior towards chemicals, but displays good corrosion behavior as well as good paint application properties for selected paint systems.

Tinplate is steel strip, 0.1–0.5 mm thick, with a tin coating of ca. $2.4 g/m^2$. A solution of tin fluoroborate can be used as electrolyte. The thin strip, which forms the cathode, is passed between two rows of thin anodes. After coating, the strip is heated above $232^\circ C$ (mp tin), and quenched in water to give the brilliant luster of electrolytically produced tinplate. Strip speeds $> 650 m/min$ can be reached. Tinplate is used in packaging (painted, foil-covered, or printed).

Electrolytic chromium-coated steel (ECCS) is a special type of chromium-plated thin steel strip, and is produced in a similar process. In many applications, ECCS has replaced tinplate.

6.5.4 Vacuum Vapor Deposition

6.5.4.1 Plant and Processes

In the vacuum vapor deposition process, the coating metal is deposited onto the "cold" steel strip from the vapor phase [189]. Vacuum vapor deposition is not yet established on a large scale in the steel industry, and is operated at only one location so far, where a hot-dip plant has been converted to a vapor deposition plant (Figures 6.135, 6.136).

Vaporization is simply carried out in the zinc melting vessel. The plant has only a directly heated preheater, without alkaline cleaning. This degree of cleanliness of the strip is often adequate for the vapor process. Coating takes place in two chambers, both operating at 2.66 Pa; the vaporization capacity of the first is 350 kg/h, and that of the second chamber is 500 kg/h. Molten zinc at $460^\circ C$ is pumped into the vaporization chamber where it immediately vaporizes at the low pressure. The strip must be cooled to ca. $250^\circ C$ in the

vacuum chamber so that the zinc precipitates onto the cold strip. The operating pressure is reached by successive reduction of the atmospheric pressure by squeeze rollers.

While the hot-dip process is mainly suitable for producing zinc coatings with thickness $> 60 \text{ g/m}^2$, zinc vaporization produces coatings with thickness ca. 30 g/m^2 , often more cheaply than the electrolytic process.

6.5.4.2 Further Developments

[190, 191]

Vacuum vapor technology is mainly suitable for coating with pure metals, alloys, chemical compounds, and composite layers that cannot be produced by hot-dip or electrolytic coating. Potential coating materials under investigation are listed below:

Metals

Zinc
Aluminum
Chromium
Titanium
Nickel
Copper
Silicon

Alloys

Nickel chromium
Zinc alloys, e.g., Zn-Mg, Zn-Cr, Zn-Al, Zn-Ni, Zn-Ti

Chemical compounds

TiN, TiC
 Al_2O_3
 SiO_2

Composites

Al-Ti, Al-Cr
TiN-Cr
Zn-Al
Zn-Zn alloys

With a sufficient number of vaporizing chambers vapor coating could be carried out at rates of 350–400 m/min. A vaporizing plant could be incorporated into an existing continuous annealing furnace, adding to the production capacity for coated steel strip. As only one side is coated in each chamber, it would be possible to coat either one side or both.

6.5.5 Coil Coating

6.5.5.1 Plant and Processes

In the production of coil-coated thin sheet [192], the substrate material can be cold-rolled strip, zinc-coated thin sheet (hot-dip or electroplated), aluminum strip, or special steel strip. Liquid paint or foil is applied to these carrier materials by rolling.

A coil coating plant (Figure 6.137) consists of the feeding equipment, strip cleaning, chemical pretreatment, coating areas for primer and topcoat with the associated drying ovens, and the exit equipment. The strip is cleaned by methods similar to those used in zinc electroplating, but in this case the surface is then phosphated or chromated. For this, the solutions are sprayed at ca. 40°C , under pressure. The strip is then cooled with deionized water and passivated. The chromate or phosphate coating provides corrosion protection for the whole system, and improves adhesion of the polymer coating. Before the strip is introduced into the coating station, this precoat is dried with hot air.

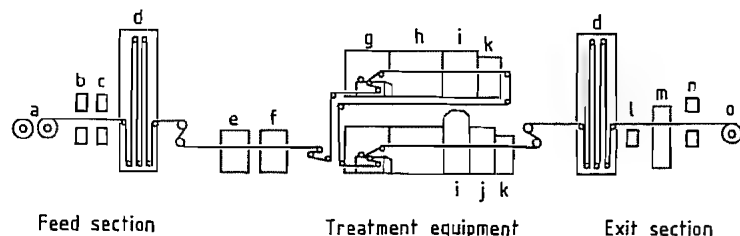


Figure 6.137: Coil coating plant: a) Pay-off reel; b) Cropping shears; c) Tack welding machine; d) Storage looper; e) Strip cleaning; f) Chemical pretreatment; g) Coating equipment; h) Furnace; i) Lamination equipment; j) Air cooler; k) Water quenching; l) Inspection table; m) Protective foil application; n) Edging shears; o) Coiling reel.

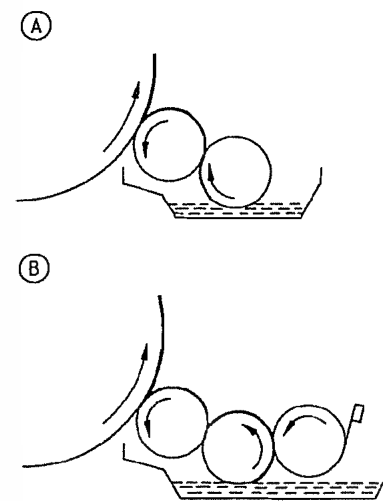


Figure 6.138: Typical coil coating systems: A) Two rollers, reverse rotation; B) Three rollers, complete reverse rotation.

Primer or undercoat is applied at the first coating station (Figure 6.138). The paint is usually applied by typical rolling machines, running in the opposite direction to the strip, one on each side of the strip, each paint roller having two or three feed rollers, depending on the coating material. As a rule, a chromium-plated dipping roller supplies the paint from a tank to a rubber-coated roller running in the opposite direction to the strip, and applies a paint film at a rate controlled by a special roller. The primer can be applied to the upper and lower side of the strip. The strip then usually passes into the first drying oven in which it hangs freely, and is heated to ca. $200\text{--}240^\circ\text{C}$, depending on the coating system. The strip with its coat of primer is then cooled by air and water, and passes to the second coating station. The topcoat is applied on one or both sides, usually only the upper side. The coating is then backed in the second drying oven at ca. $240\text{--}260^\circ\text{C}$. Before the strip passes to the air or water cooling area, it can be provided with a decorative and/or protective film. These laminates are applied under very precise conditions of temperature and pressure. If a decorative foil is used, an adhesive is applied instead of the top coat in the second coating station.

Table 6.17: Coating materials and thickness ranges of coating films.

Coating materials	Abbreviation	Usual range of film thickness, μm
<i>Liquid coating materials</i>		
<i>Standard systems</i>		
Polyesters	SP	5–25
Acrylics (resin)	AY	5–25
Silicone-modified polyesters	SP-SI	15–25
Epoxy resins	EP	3–15
Polyurethanes	PUR	10–25
Poly(vinylidene fluoride)	PVDF	20–25
Poly(vinyl chloride) organosol	PVC(O)	30–60
Poly(vinyl chloride) plastisol	PVC(P)	80–400
<i>Special systems</i>		
Weldable zinc dust primer	ZP	10–20
Heat-resistant nonstick system	HRNS	5–15
<i>Film coatings</i>		
Polyacrylate	PMMA(F)	50–75
Poly(vinyl chloride)	PVC(F)	100–300
Poly(vinyl fluoride)	PVF(F)	38
Polyethylene	PE(F)	100–300

Coating thicknesses, which depend on the coating system, are continuously monitored over short distances by integrating thickness measuring equipment, and are maintained within very close tolerances by varying the rotation speed or the application pressure of the coating rollers.

6.5.5.2 Coating Systems (Figure 6.139, Table 6.17)

The liquid coatings used are paints, based on polyester and acrylic resins, poly(vinyl chloride) plastisols, and poly(vinylidene fluoride). More recently, polyurethane paint systems have been used in special applications. Zincrometal and Inmozinc consist of thin steel sheet coated with zinc dust colors. Printed or single color poly(vinyl chloride) films are applied by rolling with an adhesive activated by hot air, and the same process is used for poly(vinyl fluoride) films. The coated or laminated material can be provided with additional protection against handling and assembly operations by means of adhesive polyethylene

protective films, applied hot or cold. Coating thicknesses are usually 15–300 μm .

6.5.6 Roll-Bonded Cladding

[193, 194]

6.5.6.1 Principles

In roll-bonding (cladding), two or more materials, which are usually flat, are pressure welded together. The process can be carried out with cold or preheated materials (cold roll-bonding or hot roll-bonding).

In continuous cold pressure welding of strip material, two metallic solids are bonded strongly together by high pressure, which causes plastic deformation. The adhesive bond can only be assured if the surfaces are clean and have a well defined surface structure (roughness).

The surfaces must be brought together under pressure until their distance apart is of the order of interatomic distances. As surfaces of technical quality are always covered with a very thin oxide layer, these layers must be broken by deformation. In roll-bonding, it is therefore necessary to stretch the surface, with exclusion of gas, so that new reactive surfaces are exposed by plastic flow. These are then brought into contact at interatomic distances, so that a strong bond can be formed by adhesion. The bond strength is increased by subsequent annealing homogenization.

6.5.6.2 The Process (Figure 6.140)

In the production of roll-bonded steels, surface pretreatment is very important. The necessary conditions are:

- Complete absence of grease
- A clean, freshly activated metal surface
- A roughened surface, produced by stretching

After pretreatment, the freshly brushed steel is fed, with the cladding material, into the roll nip, and deformed in one roll pass, the extent of deformation being 50–70%.

6.5.6.3 Variations

In roll-bonding, a composite material is produced which often combines the special properties of the individual components in an ideal manner. For cost effectiveness, a cheap substrate material is often plated with an expensive, corrosion-resistant, acid-resistant, or heat-resistant material (Table 6.18).

Table 6.18: Substrate cladding materials for cold roll-bonding.

Substrate materials	Cladding materials
Iron	Corrosion-resistant steels
Steel	High-temperature steels Ni and Ni alloys Cu and Cu alloys Aluminum Noble metals Special metals (Ti, Ta, Mo)

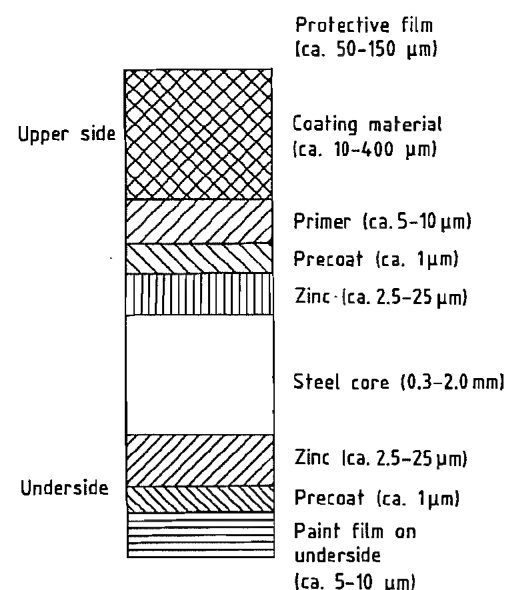


Figure 6.139: Cross section of coated steel strip.

6.5.7 Summary

Surface-coated thin steel strip was developed to improve, e.g., the corrosion properties of the steel, or to provide a decorative appearance. The user must consider a range of properties, such as workability, welding properties, adhesive properties, and paint application

properties. Each type of surface treatment has strengths and weaknesses compared with competitive processes.

Other surface treatment methods are likely to become available, including electro- and plasma polymerization, electrolytic deposition of Al and Ti from organic solutions, plasma spraying, ion implantation, and cathodic sputtering.

6.6 Uses

6.6.1 Introduction

(Section 6.6.1 is reprinted from Ullmann's Encyclopedia of Industrial Chemistry, 5th Edition)

"At room temperature, pure iron has a body-centered cubic structure. The solubility of carbon is <0.001% in this phase, which is known as α -iron. On heating, α -iron is transformed at 911 °C into the face-centered cubic γ -phase. This γ -iron can dissolve ca. 2% carbon as a solid solution. On cooling this, transformation of γ -iron to α -iron occurs and carbon is precipitated as carbide Fe_3C . In the heat treatment of transformable steels, they are heated until the γ -phase is formed, so when this is cooled more or less quickly, metastable states may be produced, and the precipitation of Fe_3C , which in equilibrium is associated with the formation of α -phase, is more or less suppressed. The range of applications of steel depends on the fact that

heat treatment can induce all the transitions between the metastable states, and those states effectively correspond to equilibrium conditions, so that a large number of microstructures and combinations of properties can be produced [195, 196]. Another method of modifying steel consists of adding alloying elements to stabilize the α -phase up to the melting point, or conversely to cause the γ -phase to be stable down to room temperature. These possibilities are mainly used to improve corrosion resistance or to achieve particular physical properties."

6.6.2 Chemical Properties

6.6.2.1 Introduction

Iron is the most widely used metallic material and, alloyed with different elements, it is the basis of a wide variety of steels, with a range of mechanical properties and chemical stability. Iron itself is rather reactive, readily forming oxides, hydroxides, sulfides, etc. It undergoes an electrochemical reaction with humid air (rusting) which can rapidly consume unprotected unalloyed steel. The rust layer is not protective, unlike the thin, dense oxide layer on aluminum or zinc, but similar behavior can be attained by alloying Fe with Cr (> 12% Cr gives stainless steels).

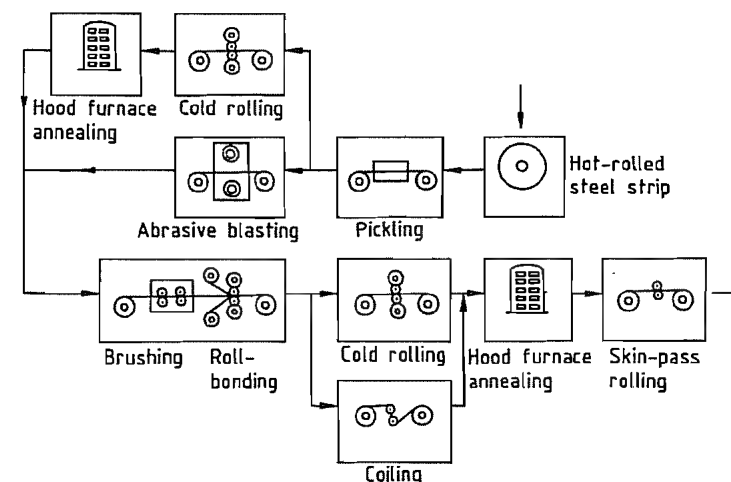


Figure 6.140: Production of roll-bonded steel strip.

Iron is also very susceptible to oxidation or sulfidation at high temperature; FeO and FeS show a wide homogeneity range, correlated to high concentrations of lattice defects (cation vacancies), high diffusivities in the lattice, and high growth rates. Alloying can lead to high oxidation resistance; Cr steels or Ni–Cr steels with ca. 20% Cr can be used up to 1000 °C, and Fe–Cr–Al alloys at even higher temperatures, since they form slow-growing oxide layers, which also give limited protection in environments which are sulfidizing, carburizing, or chloriding (heat exchangers in combustion or gasification atmospheres).

The chemical behavior of iron and steels is of greatest interest in connection with corrosion problems; in the following, reactions and corrosion processes are described only briefly, emphasizing the special points of chemical behavior of iron and steels.

6.6.2.2 Uniform Corrosion

Corrosion of iron in aqueous electrolytes results from the anodic dissolution process:



and the simultaneous, independent cathodic reduction of an oxidizing agent, in most cases either hydrogen ions:



or oxygen molecules dissolved in the electrolyte:



The potential dependence of reactions (33) and (34) is described by the Volmer–Butler equation, an exponential relation; oxygen reduction is mostly controlled by diffusion of molecular oxygen to the metal surface, independent of potential. The overlap of anodic and cathodic reactions is shown in Figure 6.141. The corrosion potential U_k is established at a negative value, where the current density of anodic dissolution i_a and oxygen reduction i_k are equal. The anodic dissolution is further dependent on the concentration of defects in the metal surface, and especially for

iron, is enhanced with increasing concentration of OH^- [198], and also SH^- or NH_4^+ [199].

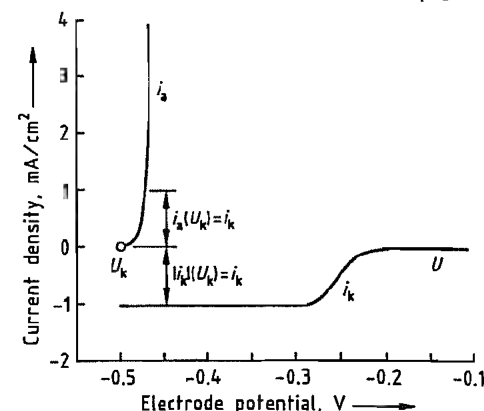
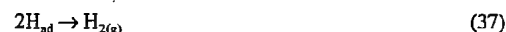


Figure 6.141: Electrochemistry of iron corrosion.

The reduction of H^+ occurs in several steps; electron transfer occurs by the Volmer reaction:



The adsorbed H_{ad} atoms can react to H_2 , according to the Tafel reaction:



or the Heyrowski reaction:



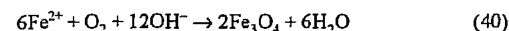
Adsorbed H atoms also can enter the metal, which leads to hydrogen-induced cracking (HIC) or hydrogen-induced stress corrosion cracking (HISCC).

In neutral water, the corrosion rate is determined by H^+ diffusion to the metal surface, and the anodic dissolution rate is restricted to $0.2 \mu\text{A}/\text{cm}^2$, corresponding to $2 \times 10^{-4} \text{ cm/a}$. Since the exchange current densities i_0 of the Volmer and Tafel reactions are very low, and since that of the Heyrowski reaction is negligibly small [200], iron does not corrode in neutral water free of oxygen. In contrast, the corrosion of iron in neutral water saturated with oxygen (in equilibrium with air) is rapid—the calculation assuming rate-controlling O_2 diffusion in a slowly flowing electrolyte yields $0.15 \text{ mA}/\text{cm}^2$, corresponding to a corrosion loss of 0.15 cm/a . This high value is not reached under natural conditions, since

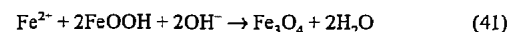
rust is formed, and the oxygen must diffuse through the pores of this corrosion product.

6.6.2.3 Atmospheric Corrosion

In corrosion by oxygen-containing electrolytes, Fe^{2+} is oxidized to Fe^{3+} , and oxides and oxyhydrates are precipitated on the metal surface:



These reactions occur on the surface of the solid corrosion products and not in the electrolyte. Atmospheric corrosion (rusting) in the presence of a liquid electrolyte film [201] on the metal leads to Fe_3O_4 at the iron surface, and FeOOH and Fe_2O_3 at the phase boundary with the atmosphere. With restricted oxygen access, when all pores of the rust are filled with water, Fe^{2+} formed at the inner phase boundary [202] can react with FeOOH :



On drying the rust layer, allowing better access of oxygen, Fe_3O_4 is oxidized again, to FeOOH . Atmospheric corrosion can be retarded by certain alloying elements: Cu, P, Cr, and Ni, which are added to rust-resistant steels, e.g., Corten. Sulfur dioxide strongly accelerates rusting of steels by initiating the reaction sequence [203]:

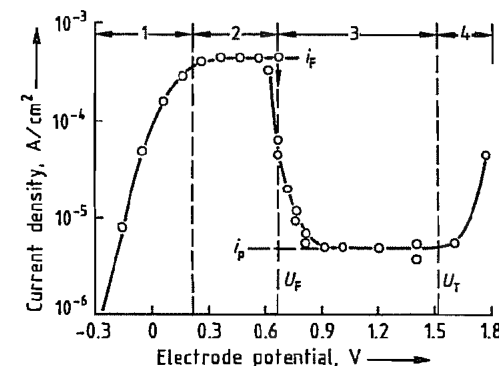
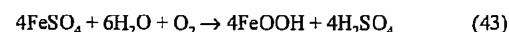
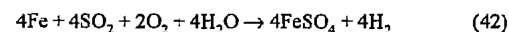


Figure 6.142: Electrochemistry of passivation of iron in HCl 1 mol/L at 25 °C. U_T = transpassivation potential.

In this reaction sequence, one SO_2 molecule can transfer 15–150 Fe atoms into the rust [204] by its catalytic action, until the reaction is stopped by formation of insoluble basic iron sulfates.

6.6.2.4 Passivation

The passivation behavior of iron is shown in Figure 6.142 [205]. In region 1, the current–potential curve describes active anodic dissolution; according to the Butler–Volmer equation, the increase in current is exponential. In region 2, the increase is limited since the solubility limit of FeSO_4 is approached at the metal surface—corrosion is controlled by outward diffusion of the Fe^{2+} through the diffusion boundary layer, independent of potential. At the passivation (Flade) potential U_F the current density abruptly decreases, owing to formation of a passive layer, i.e., a very thin oxide layer, most probably $\gamma\text{-Fe}_2\text{O}_3$ [206], a few nanometers thick, depending on potential and temperature. In the passive region 3, a steady state of continuous film growth and dissolution is established, at current density i_p , ca. $10^{-5} \text{ A}/\text{cm}^2$, corresponding to a corrosion rate 0.1 mm/a . In the transpassive region 4, enhanced iron dissolution and oxygen formation occur simultaneously. For the passivation potential of iron in the acidic region (in V):

$$U_F = 0.5 - 0.005\text{pH} \quad (44)$$

Iron is passivated at $\text{pH} > 10$ by oxygen in the electrolyte, this is important for the use of reinforcing steel in concrete, because the electrolyte in the pores of the concrete is saturated with $\text{Ca}(\text{OH})_2$ at $\text{pH} 12.5$. Iron can also be passivated in strong oxidizing acids such as HNO_3 .

The current–voltage curve for nickel [207] is similar to that for iron; for chromium [208] the passivation potential is shifted to more negative potentials, and current density in the passive state is $< 10^{-7} \text{ A}/\text{cm}^2$ (Figure 6.143). In the passive region, Cr^{3+} is formed and very slowly dissolved, in the transpassive region, formation of chromate and dichromate with hexavalent Cr begins. This behavior is re-

flected in the passivation of Fe–Cr and Fe–Ni–Cr steels [209]; with increasing Cr content the passivation potential is shifted to lower values and the current density in the passive region is decreased, so stainless steels are passive over a wide range of conditions. The breakthrough potential at which Cr^{6+} formation starts, is virtually independent of Cr content.

6.6.2.5 Pitting Corrosion

If a passive layer is destroyed locally, the layer may heal under passivating conditions or, in the presence of halide ions, pitting may occur, i.e., local attack with formation of hemispherical pits. During pitting, active and passive regions are stable in the immediate neighborhood. The active areas are stabilized by the potential drop, caused by a high dissolution current through the electrolyte in the pit (the bottom of the pit is at potentials below passivation potential and the surrounding passive film is at a higher potential) [210]. Pitting occurs if the value of the pitting potential U_p is exceeded, and if the corrosive ions have a critical concentration c_L . For Fe–Cr and Fe–Ni–Cr steels, the pitting potential increases with Cr and Mo content (Mo is more effective than Cr). Since then, N has been found to be even more effective [211]. Pitting can start in Cr-depleted zones, e.g., after carbide precipitation at grain boundaries [212].

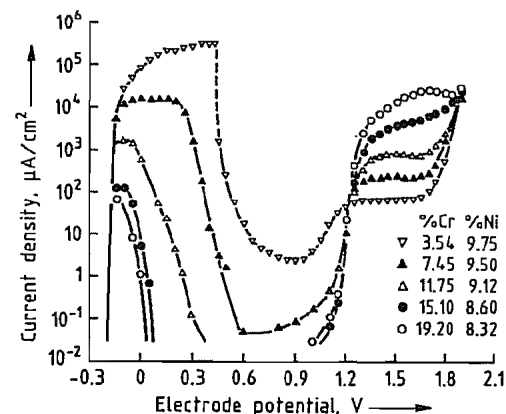
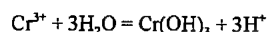


Figure 6.143: Electrochemistry of iron passivation at various concentrations of Cr and Ni.

6.6.2.6 Crevice Corrosion

If there are crevices between a metal and a second phase, or in the metal itself, the onset of corrosion is often observed in the crevice, owing to retardation of the electrolyte exchange into and out of the crevice. When the transport of oxidizing agent into the crevice is retarded, leading to depletion of, e.g., dissolved oxygen, the potential may fall below the passivation potential and iron and low-alloy steels may start to corrode. Also, the transport of corrosion products out of the crevice is inhibited, and their hydrolysis may lower the pH, e.g., by the reaction:



The increasing acidity reduces the activation and pitting potentials, so active corrosion or pitting may start [213, 214].

6.6.2.7 Intergranular Corrosion of Stainless Steels

Ferritic chromium steels and austenitic Cr–Ni steels are susceptible to intergranular corrosion after sensitization, i.e., after precipitation of carbides at 450–750 °C. Precipitation at grain boundaries [215, 216] leads to chromium depletion nearby. If the potential is in the range between the passivation potentials of the steel and iron, rapid dissolution of the metal phase occurs along the grain boundaries. Potentials in this range are established in the Strauss test [217], where the sample is in contact with Cu and immersed in CuSO_4 – H_2SO_4 solution, so that sensitized materials undergo intergranular disintegration. In the temperature–time diagram, the conditions for sensitization are limited by curves for the onset of carbide precipitation, which tends to shorter times at higher C concentration and longer times at lower temperature, and by curves for the end of carbide precipitation, which also needs shorter times at higher temperature. After the end of precipitation, the chromium concentration equalizes and the material becomes corrosion resistant again.

This intergranular corrosion of stainless steels can be suppressed by very low carbon

concentrations < 0.01% (Figure 6.144), or by addition of stabilizing elements, such as Ti and Nb, which tie up carbon in very stable carbides [218, 219]. Precipitation of TiC and NbC can be induced by heat treatment at 900–950 °C (stabilization), where the chromium carbides dissolve and the solubility of TiC and NbC is still very low; such treatment is important after welding of steels.

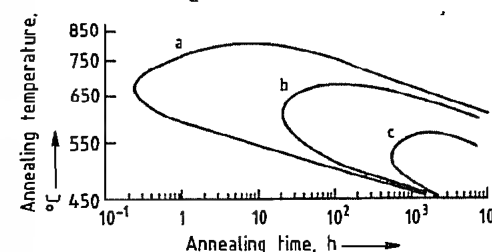


Figure 6.144: Annealing behavior of steel at various carbon concentrations: a) 0.04% C; b) 0.02% C; c) 0.01% C.

6.6.2.8 Stress Corrosion Cracking

The preconditions for stress corrosion cracking (SCC) are: (1) the stress causes a shear or strain of the material; and (2) the electrolyte induces formation of a passive or protective layer [220, 221]. The strain leads to failure of the passive layer at a slip step; there the free material is rapidly attacked under anodic dissolution. Repeated failure at this spot initiates crack growth. The electrolyte forms a new protective film at the walls of the crack and only the crack tip stays active, leading to deep cracks. Strain rate and passivation rate must obey certain relations to obtain SCC; if, for example, the passivation rate is too high, this leads to immediate passivation of the whole crack and termination of crack growth, whereas too slow passivation leads to strong truncation of the crack, or widening to a deep groove. SCC is observed in the following cases:

- Austenitic steels in chloride solutions—transgranular crack growth [222–226]
- Ferritic and ferritic-pearlitic structural steels in hot concentrated alkali carbonate and nitrate solutions—intergranular crack growth [227–231]

The latter type of SCC is enhanced by the presence of impurity elements, such as P, at grain boundaries, similar to the intergranular corrosion of iron and ferritic steels in nitrates at elevated potentials [231]. Under stress conditions, the selective corrosion of the crack tip causes SCC at low P concentrations and without anodic polarization.

6.6.2.9 Hydrogen Absorption and Hydrogen Embrittlement

On the surface of iron or steel, immersed in aqueous solution, the interplay of reactions (33)–(38) establishes coverage with adsorbed hydrogen H_{ad} , which may correspond to a high hydrogen activity ($a_{\text{H}} = 1$ at $p(\text{H}_2) = 100$ kPa), depending on electrochemical potential E and pH:

$$\log a_{\text{H}} = \frac{E - F}{2.3RT} + \text{pH} = \frac{E}{0.059} + \text{pH} \quad (45)$$

especially if the Tafel reaction (37) is poisoned by inhibitors, such as arsenic acid in the electrolyte. In a neutral NaCl solution free of oxygen, the corrosion potential E of iron is -0.6 V, and hydrogen activity can reach 10^3 . Correspondingly, hydrogen is absorbed into the iron matrix in much higher concentration than its solubility at $p(\text{H}_2) = 100$ kPa, which at 25 °C is ca. 3 atoms per 10^8 iron atoms [232, 233]. Not all hydrogen in steels is dissolved, i.e., distributed on interstitial sites; most is in special sites (traps) where its energy is decreased, owing to stress fields in the lattice around dislocations, inclusions, etc. [234]. High hydrogen concentration in steels causes hydrogen embrittlement, i.e., decrease of toughness and brittle fracture. This effect of hydrogen is explained by H enrichment at the crack tip, where it weakens the Fe–Fe bonds in the already strained regions at the tip, and decreases the surface energy of the newly formed surface in the crack [235]. By this mechanism the presence of hydrogen can cause hydrogen-induced cracking (HIC), and aggravate stress corrosion cracking (HISCC). High-strength steels are especially susceptible.

6.6.2.10 Oxidation of Iron

Iron forms three oxides, hematite Fe_2O_3 , magnetite Fe_3O_4 , and wustite FeO which is stable only above 570°C [236–238]. FeO has a wide range of homogeneity, due to cation vacancies V_{Fe}^{\times} , for which the concentration is dependent on oxygen pressure. Oxidation of iron at temperatures $> 570^\circ\text{C}$ yields fast-growing oxide layers composed of an outer layer of Fe_2O_3 , then Fe_3O_4 , and a thick inner layer of FeO [239, 240]. The oxides grow mainly by outward diffusion of iron via cation vacancies, which move inward. Since the cation vacancy concentration is highest in FeO , the diffusivity of Fe^{2+} is high, and the growth rate is most rapid.

Owing to the high oxide growth rate, unalloyed steels cannot be applied at temperatures $> 570^\circ\text{C}$, but perform reasonably well at lower temperatures, since the scale of hematite and magnetite grows slowly enough. In CO_2 – CO and H_2O – H_2 mixtures at high temperatures, oxygen partial pressures are effective at which only FeO or a $\text{Fe}_3\text{O}_4/\text{FeO}$ layer is formed. Under such conditions, the growth rate of FeO up to a thickness of about $100\ \mu\text{m}$ is controlled by the phase boundary reaction on the outer surface [241–243], where the oxygen is transferred from the gases:



In this stage of oxidation, a linear rate law applies for the increase of scale thickness:

$$\frac{dx}{dt} = k_l \quad (48)$$

where the linear rate constant k_l is a function of the partial pressures, the oxygen activity at the surface, and the distance from equilibrium [243–245]. There is a gradual transition from phase boundary reaction control to diffusion-controlled growth, where the rate is inversely proportional to the thickness x :

$$\frac{dx}{dt} = \frac{k_p}{x} \quad (49)$$

This results in the parabolic law:

$$x^2 = 2k_p t \quad (50)$$

which leads to growth rate decreasing with time. Such parabolic behavior is characteristic of most metals and alloys used at high temperatures, the lower the value of k_p , the slower the growth of the scale. Values of k_p can be deduced according to the theory of C. WAGNER [246] from data on the diffusivities of cations and anions or electric conductivity and transference numbers of the ions.

6.6.2.11 Oxidation of Carbon Steels and Low-Alloy Steels

On heat treatment and hot rolling, steels are oxidized and decarburized [247–249]. Oxidation is described by a linear law in CO_2 and a parabolic law in O_2 ; both reactions behave additively. At first only iron is oxidized and carbon is enriched in the metal below the scale. With continued scale growth, vacancies condense at the interface to form voids in which CO_2 and CO are formed in equilibrium with FeO . This gas diffuses outward through cracks and pores of the scale, which leads to carbon loss. Carbon diffusion through the solid oxide is impossible. After some time, a steady state is established in which the carbon supply to the interface is controlled by diffusion in the metal. Thus, after a brief oxidation, carbon enrichment is observed, but after long-term oxidation, the steel is always decarburized.

Some other more noble alloying (or impurity) elements in steels, e.g., Ni, Co, Cu, Sn, Pb, As, and Sb also enrich beneath the scale during oxidation. Enrichment of Cu, Sn, As, or Sb decreases the melting point, which can lead to difficulties in hot rolling. Specifically Cu, sometimes in combination with Sn, causes “hot shortness” by formation of a melt which penetrates into grain boundaries. If other elements are enriched beneath the scale, the iron must diffuse through this zone to the oxide-metal interface before it is oxidized. Especially for Fe–Ni and high-Ni steels [250–252], this causes inward growth of protrusions from the oxide into the metal which leads to a rugged, strongly interlocked interface; the oxide

scale is strongly adherent to the metal and difficult to remove, e.g., after hot rolling. With increasing Ni content, enhanced temperature and oxygen partial pressure, the formation of FeO on Fe–Ni alloys is suppressed in favor of the more slowly growing spinel $(\text{Fe,Ni})_3\text{O}_4$.

6.6.2.12 High-Temperature Steels

Steels to resist heat and oxidation must be alloyed with sufficient concentrations of Cr and/or Al. The slowly growing oxides Cr_2O_3 or Al_2O_3 , which have a small degree of disorder, can form a protective scale. Iron–chromium alloys are the base materials for many ferritic steels. The oxidation behavior as a function of Cr content is shown in Figure 6.145 [253]. At Cr concentrations $< 2\%$, the oxidation rate is increased since dissolution of Cr_2O_3 in FeO may even increase the amount of cation vacancies (Wagner–Hauffe doping effect); trivalent Cr replaces divalent Fe, this is equalized by negatively charged vacancies. With increasing Cr content wustite formation is suppressed, the spinel $(\text{Fe,Cr})_3\text{O}_4$ is formed, for which the growth rate decreases with Cr content. At Cr content 15–30%, the mixed oxide $(\text{Fe,Cr})_2\text{O}_3$ is formed on the metal surface, its growth rate shows a minimum at 20–25% Cr in the alloy [254]. Many ferritic steels have Cr content 17–25%; they are oxidation resistant, but there may be chromium depletion beneath the scale, and if the scale is damaged outgrowth of wustite may occur with formation of “rosettes”.

This effect is suppressed in the Cr–Ni steels where, instead of wustite, a Fe,Ni spinel is formed. Such austenitic steels, with 20–27% Cr and 12–32% Ni, are widely used for high-temperature processes, since, in contrast to ferritic Fe–Cr steels, they have higher mechanical strength and do not show embrittlement by σ -phase formation. Additional alloying with 12% Si improves resistance to oxidation and especially carburization, since an inner film of SiO_2 below the Cr_2O_3 retards oxidation and carburization.

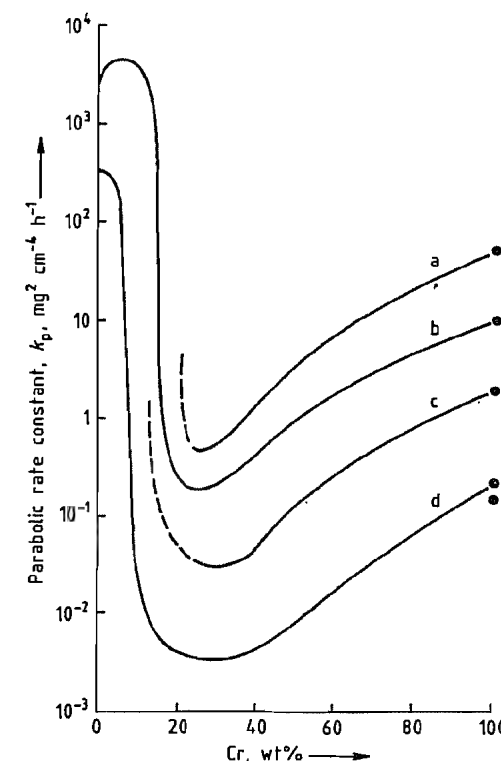


Figure 6.145: Oxidation kinetics as a function of Cr content: a) 1200°C ; b) 1100°C ; c) 1000°C ; d) 900°C .

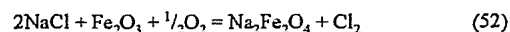
Iron–aluminum alloys need 6–8% Al to form a protective Al_2O_3 layer [255, 256], but only at temperatures $> 900^\circ\text{C}$ is the most protective $\alpha\text{-Al}_2\text{O}_3$ generated. Formation of Al_2O_3 and suppression of internal oxidation is favored by chromium; Fe–Cr–Al alloys with ca. 20% Cr and 4–5% Al are used for heating elements and other highly oxidation-resistant components. The lifetime of the heating elements is greatly increased by small additions of rare earths, e.g., Ce, Y, La, which strongly improve the adherence of the Al_2O_3 scale. The use of such additives also helps to improve other high-temperature alloys, in terms of nucleation, stability, and adherence of protective scales.

Silica layers may also serve as protective scales, but Fe–Si alloys are not used as high-temperature materials. Formation of Fe_2SiO_4 and an inner layer of SiO_2 plays a role in the

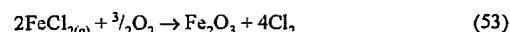
annealing of silicon sheet for electrical applications.

6.6.2.13 Effects of Chlorine in Oxidation

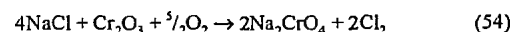
The presence of chlorine may cause acceleration of oxidation, so-called "active oxidation" [257–260]. Especially in waste PVC and NaCl-containing coal incineration, HCl and chlorides from combustion react with the oxide scale on steels to form chlorine



The chlorine penetrates the scale and reacts at the oxide-metal interface to form FeCl_2 which evaporates and oxidizes according to



The chlorine partially diffuses inward and reacts again, thus establishing a circuit, in which Cl_2 catalyzes the "active corrosion" (active, since no dense oxide layer passivates the steel). This process causes problems in waste incineration and other processes in oxidizing, chloridizing atmospheres. Not only are low-alloy steels strongly attacked, but also chromia-forming high-alloy steels, due to the reaction



The chlorine produced penetrates the scale and causes formation of volatile chlorides of the alloy components.

6.6.2.14 Sulfidation of Iron and Steel

The main sulfidation products of iron in sulfidizing environments are pyrrhotite FeS and pyrite FeS_2 . Pyrrhotite, like FeO , is highly nonstoichiometric, owing to cation vacancies, their concentration being dependent on sulfur partial pressure and temperature [261, 262]. Accordingly, the diffusivity of Fe in FeS is high and the FeS growth rate is very rapid, even at relatively low temperature. As in the case of FeO , the linear rate law (Equation 47) applies for growth in H_2S – H_2 atmospheres

[263, 264]; k_1 depends on $p(\text{H}_2\text{S})$ and is inversely proportional to the sulfur activity on the sulfide surface. The rate-controlling step is transfer of S_{ad} from H_2S to the surface, which is retarded with increasing sulfur activity. Upon sulfidation, rate control gradually changes to solid-state diffusion and to the parabolic rate law [265]. Corrosion by H_2S is a problem in the petrochemical and chemical industries, and is not easily suppressed. Even steels with Cr content up to 17% do not behave much better than low-alloy steels [266].

During corrosion of iron in SO_2 or Ar-SO_2 mixtures at 600–1000 °C, the phases FeO and FeS grow simultaneously on the metal surface [267–269], if the transport in the gas phase or the phase boundary reaction is rate determining. Owing to the high diffusivities of cations in FeS , lamellae of FeO and FeS grow side by side up to a layer thickness of ca. 150 μm , following a linear law. In the application of steels in flue gases, a scale of $\text{Fe}_2\text{O}_3/\text{Fe}_3\text{O}_4$ is stable on the steel surfaces and SO_2 should have no effect on oxidation. However, if SO_2 penetrates the scale, at the interface sulfides can be formed. The mass action law for the reaction $\text{SO}_2 = \frac{1}{2}\text{S}_2 + \text{O}_2$ predicts that very high sulfur pressures are possible at the oxide-metal interface, since $p(\text{O}_2)$ is very low there. This is especially dangerous in high-Ni alloys, since $\text{Ni-Ni}_3\text{S}_2$ forms a liquid eutectic at 645 °C, and the presence of such melts strongly aggravates corrosion.

Sulfidation of heat exchangers is a problem in coal gasifiers; chromia-forming steels have been tested at 700–800 °C [270–274] but fail after lifetimes of some hundreds or thousands of hours. Preoxidation has been used to improve protection, but the chromia layers generated can also fail after similar lifetimes, either by external sulfidation, i.e., growth of sulfides of Fe, Ni, and Mn on the chromia scale, or by internal sulfidation, formation of sulfides of Cr and Mn beneath the scale.

6.6.2.15 Carburization

Carburization in gas atmospheres is a technical process for case hardening of steels, a

specified carbon content is established in the surface and the carburized components are quenched in oil for hardening [275, 276]. Carburization can also be an unwanted process in the high-temperature corrosion of materials, e.g., cracking tubes in petrochemistry, and heating tubes or grates in industrial furnaces. In this process, carbon diffuses into the alloy and carbides are precipitated, mainly chromium carbides M_7C_3 and M_{23}C_6 , with loss of both ductility and oxidation resistance [277, 278].

In both cases, the carbon transfer is by reactions in which CO , CH_4 or hydrocarbons decompose on the metal surface [279, 280], the transfer is very fast by the reaction:



less fast by:



and very slow by:



Rate equations and rate constants for these reactions have been determined for iron and binary iron alloys. The reactions are strongly retarded by sulfur [281].

In gas carburization for case hardening, the process is jointly controlled by the phase boundary reaction and inward diffusion of carbon; this has been studied in detail, and can be controlled well, to obtain certain penetration profiles of carbon in different steels and corresponding hardness profiles [282].

The unwanted carburization of cracking tubes [277, 278, 283] is generally suppressed, or at least retarded, by the oxide layer on the high-Cr–Ni steels used, only small amounts of carbon are transferred through pores or cracks formed on creep of the tubes. However, failure occurs if the tubes are heated above 1050 °C; the coke in the tubes reacts with Cr_2O_3 to chromium carbides which are no longer protective, and relatively fast carburization takes place [278]. This may happen during decoking of the tubes in H_2O – H_2 mixtures, when the temperature is not sufficiently controlled. Under these conditions, materials with 1–2% Si are resistant because of the protective effect of an

inner SiO_2 layer beneath the chromia layer. Small amounts of sulfur in the atmosphere can also retard carburization.

Metal dusting [284–288] is the disintegration of steels into a dust of metal particles and carbon, occurring in atmospheres of $a_C > 1$ (carbon activity $a_C = 1$ means equilibrium with graphite) and in recent years has become problematic. The reaction sequence: (1) supersaturation of the metal with dissolved C; (2) formation of metastable carbide at $a_C > 1$; (3) deposition of graphite on this carbide ($a_C \rightarrow 1$); (4) decomposition of the carbide to carbon and metal particles; and (5) deposition of further graphite from the atmosphere on the metal particles. This leads to metal wastage and the formation of the loose corrosion product "coke", which is easily removed by fast gas flow in the plants, leaving pits and holes. Protection is possible by the chromia layer on high-alloy steels—their resistance depends on their ability to form oxide layers and healing. Furthermore, sulfur can protect since adsorbed sulfur effectively poisons steps (1), (3), and (5) of the reaction sequence, however, addition of sulfur is not possible with synthesis gas ($\text{CO} + \text{H}_2$) for the production of methanol, hydrocarbons, etc.

6.6.2.16 Nitriding

Similar to carburization, there is a technical process of nitriding for surface hardening, and an unwanted corrosion process at high temperatures which leads to nitride formation in steels and losses in ductility and oxidation resistance.

The nitrogen transfer can be from N_2 , NH_3 – H_2 mixtures, or by plasma nitriding in a glow discharge. The latter process is performed since N_2 is rather inert; nitrogen transfer:



is slow, with high activation energy [289]. Much faster is:



So NH_3 – H_2 mixtures can be used for nitriding and nitrocarburizing (with CO) at relatively low temperature. Their nitrogen partial pres-

tures are [289] very high as calculated from the mass action law; the equilibrium values are of the order of 10^5 kPa N_2 . This may lead to deterioration of the nitrated case, by void formation with condensation of dissolved N at lattice defects to molecular N_2 , which can develop high pressure, corresponding to the N_2 partial pressure of the NH_3 - H_2 mixture, and form small bubbles in the material.

Nitriding for surface hardening leads to a layer of ϵ -nitride on the steels.

Nitriding of high-alloy steels happens only at high temperature $> 1000^\circ\text{C}$, e.g., on burner tubes [290, 291] and after failure of the oxide scale by cracking or spalling; mainly chromium nitrides Cr_2N are formed in the metal matrix.

6.6.2.17 Decarburization, Denitriding, and Hydrogen Attack

Thorough decarburization of steel is necessary for several applications, e.g., sheet for single-layer enameling, deep drawing steels, and silicon steels for use in generators and transformers. Decarburization is performed at 700 – 900°C in wet hydrogen, and is controlled by carbon diffusion to the surface. The product c_D (solubility \times diffusivity) is critical, and has a maximum at ca. 800°C [292, 293]. The surface reactions are the formation of CO and CH_4 , i.e., the back reactions of Equations (55) and (57), CH_4 formation being negligible.

Denitrogenation [294, 295] is also important for deep drawing and electric sheet, this is also conducted in wet H_2 at ca. 750°C , and occurs by NH_3 formation and N_2 desorption, the back reactions of Equations (54) and (55). The presence of some H_2O accelerates the rate of NH_3 formation [296, 297], but electric sheet with Si cannot be denitrogenated in wet hydrogen since SiO_2 formation retards the process.

In processes which involve high hydrogen partial pressures at elevated temperatures (hydrogenation reactions, ammonia synthesis), considerable amounts of atomic hydrogen enter the walls of steel vessels, and the cementite in unalloyed steels is attacked and methane is

formed. Dissolution of the Fe_3C and precipitation of CH_4 and H_2 at interfaces and defects in the steel cause weakening and embrittlement of carbon steels. The more stable carbides in low-alloy Cr and Cr-Mo steels are resistant to hydrogen attack in the usual temperature range for the processes in question; the stability ranges of different steels as functions of temperature and hydrogen partial pressure are compiled in Nelson diagrams [298].

6.6.3 Physical Properties

Knowledge of the physical properties of steel is important for controlling its structure, and hence its properties. In this Section, the physical properties of pure iron are described first, followed by those of the solid solutions of the various iron modifications, and finally some other factors that influence structure [299].

6.6.3.1 Pure Iron

Crystal Structure. Iron occurs both in body-centered cubic (bcc) and face-centered cubic (fcc) structures. The bcc α -phase, which is stable at lower temperatures, is ferromagnetic up to the Curie temperature $T_c = 1041$ K, and is transformed into the paramagnetic state at higher temperatures (above the A_2 point). At 1184 K, the A_3 point, α -iron is transformed into the fcc form, γ -iron. The stability range extends up to 1665 K (A_4 point). Between 1665 and 1807 K, iron has a bcc structure, again δ -iron. Pure iron melts at 1807 K.

The crystal structures of α - and γ -iron are shown in Figure 6.146. The number of atoms in the unit cell is 2 in the bcc structure and 4 in the fcc structure. The number of nearest neighbors is 8 and 12 respectively, and of next nearest neighbors 6. The lattice constant of α -iron at room temperature $a_{RT} = 0.28662$ nm. Thermal expansion data are shown in Figures 6.147 and 6.148. In Figure 6.147, the difference in the y -axis scales for the bcc and fcc structures is due to the difference in the number of atoms per unit cell. The calculated density is $\rho = 7.876$ g/cm³.

The coefficient of linear thermal expansion α (Figure 6.149) increases with increasing temperature, and is higher for the fcc than for the bcc phase. The hatched area between the measured and calculated curves is due to a magnetostrictive effect in the region of the Curie temperature.

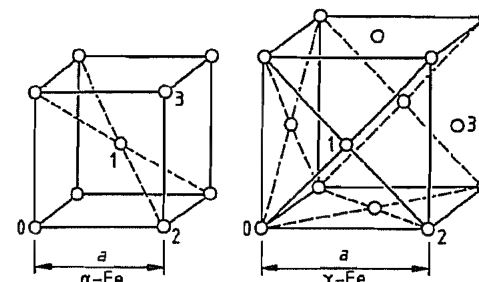


Figure 6.146: Crystal structure of α - and γ -iron.

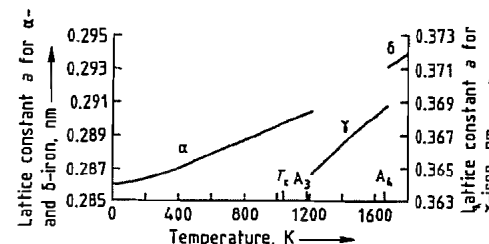


Figure 6.147: Effect of temperature on the lattice constant of iron.

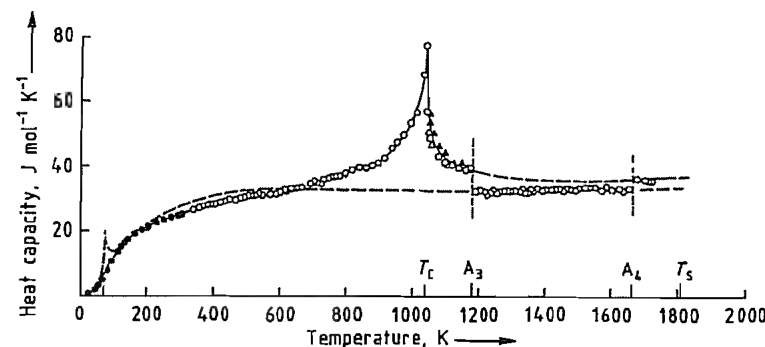


Figure 6.150: Effect of temperature on the molar heat capacity of iron. Solid line, most probable values; dashed line, values calculated for the instability ranges of α - and γ -iron. \bullet According to [301]; \triangle According to [302]; \blacktriangle According to [303]; \circ According to [304].

Specific Heat Capacity. The specific heat capacity of a substance is the heat required to increase the temperature of unit mass by 1 K. The effect of temperature on its value is of

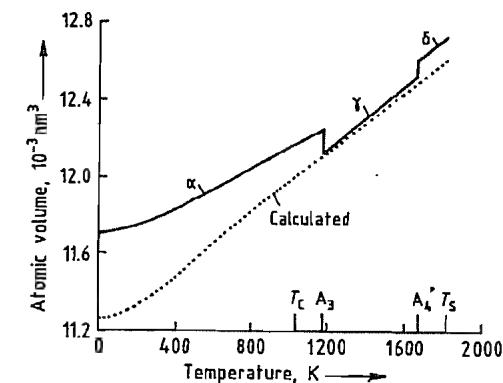


Figure 6.148: Effect of temperature on the atomic volume of iron.

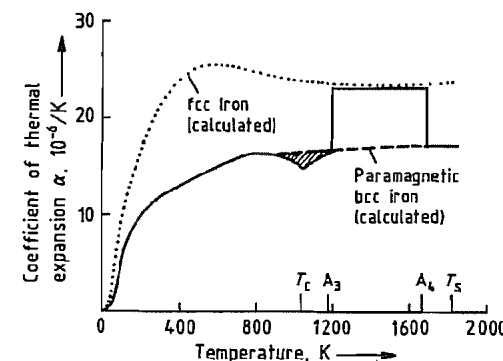


Figure 6.149: Effect of temperature on the thermal expansion coefficient of iron.

fundamental importance, as the specific heat capacity is used in the calculation of enthalpy and entropy. The results of recent determinations are plotted in Figure 6.150, with the most

probable values indicated by a continuous curve [300]. The broken curves refer to the region of instability of the bcc and fcc phases.

The heat capacity is the sum of various components. There is a sharply defined maximum in bcc iron in the region of the Curie temperature. This represents the magnetic component, due to the energy required to destroy the magnetic ordering that occurs during the ferromagnetic-paramagnetic transition.

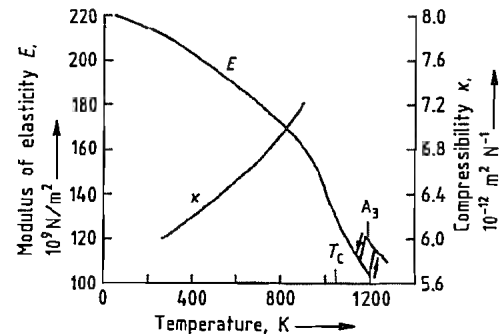


Figure 6.151: Moduli of elasticity and compressibility of iron [305].

Elastic Properties. The modulus of elasticity (Young's modulus E) represents the relationship between the elastic extension or strain and an applied tension or stress σ . This obeys Hooke's law $\sigma = E\epsilon$. The effect of temperature on E is illustrated in Figure 6.151 (the values were determined for polycrystalline iron). In single crystals, the modulus of elasticity is strongly dependent on the crystallographic orientation of the sample (anisotropy). This anisotropy is also apparent in materials with a well-defined texture.

Volume changes under hydrostatic pressure are described by the compressibility κ , shown as a function of temperature in Figure 6.151.

Magnetic Properties. Individual iron atoms have a permanent magnetic moment. At temperatures above the Curie temperature, the directions of the magnetic moments are randomly distributed, and the material is paramagnetic. There is a linear relationship between field strength and polarization, represented by the volume susceptibility.

Below the Curie temperature, the magnetic moments of neighboring atoms in the bcc lat-

tice are arranged parallel to each other, and the iron is ferromagnetic. Within the Weiss zones (magnetic domains) the moments are all in the same direction. This direction may differ from the direction within neighboring domains, so that they cancel each other.

The properties of a ferromagnetic material can be represented by the magnetization curve (Figure 6.152). With increasing field strength H , the polarization increases as the number of favorably oriented magnetic domains increases, and the magnetic moments align in the direction of the applied field. The maximum value is the saturation polarization. If the applied field is removed, the residual polarization at $H = 0$ is the remanence. The coercive field strength is the applied field which reduces the polarization to zero.

The saturation polarization varies with temperature, and disappears at the Curie temperature [306, 307]. The magnetization curve for single crystals varies with crystal orientation, being steepest in the [100] direction, and considerably less steep in the [111] direction. This effect is utilized in the manufacture of textured electroplated steel.

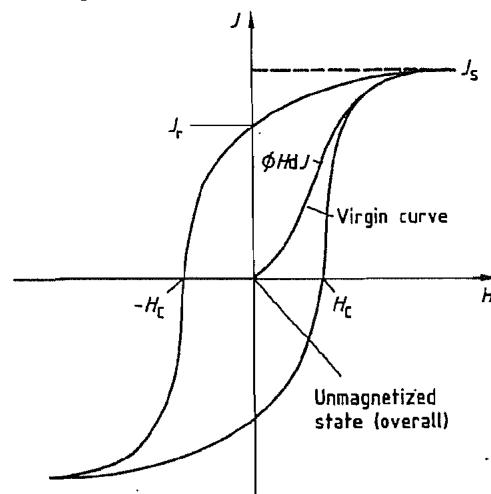


Figure 6.152: Magnetization curve of a ferromagnetic material. H = field strength; J = polarization ($B = J + \mu_0 H$ = induction); J_s = saturation polarization; J_r = remanence; H_c = coercive field strength; $\phi H dJ$, the area of the hysteresis loop, gives the amount of energy liberated as heat on reversal of the direction of magnetization. This is the hysteresis loss, quoted per unit mass.

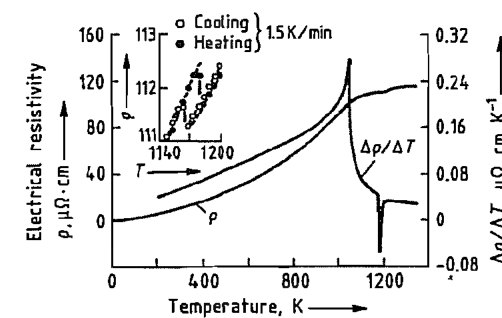


Figure 6.153: Effect of temperature on the electrical resistivity of pure iron.

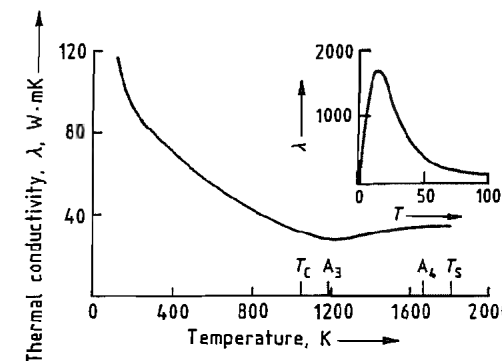


Figure 6.154: Effect of temperature on the thermal conductivity of pure iron.

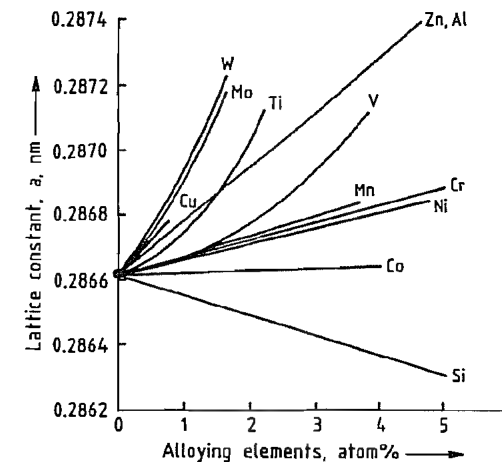


Figure 6.155: Effect of alloying elements on the lattice constant of α -iron.

Electrical Properties. The high electrical conductivity of iron is due to the great mobility of the free electrons, but their movement is

scattered by deviations from the periodic lattice potential or by the electrons of unfilled shells. All crystal defects, e.g., holes, dislocations, stacking faults, impurity atoms, and precipitates, lead to energy losses by the motion of free electrons, and hence to an electrical resistance that falls to the so-called residual resistance at absolute zero. According to the Matthiessen rule, resistance is made up of a temperature-dependent part, due to lattice vibrations, and a residual resistance which is independent of temperature. The effects of the magnetic and the α - γ transitions can also be seen in Figure 6.153.

At high temperatures, thermal conductivity is a result of the same processes that lead to electrical conductivity. The thermal conductivity-temperature curve is similarly affected by the magnetic transformation as shown in Figure 6.154 [300, 308]. According to the Wiedemann-Franz-Lorenz law, the ratio of thermal conductivity to electrical conductivity is directly proportional to temperature. From this relationship, thermal conductivity can be calculated from electrical conductivity even at high temperatures when direct determination is difficult.

6.6.3.2 α -Iron Solid Solutions

Alloying elements can be divided into those that restrict the γ -region, and those that stabilize the γ -phase and extend its limits [309]. The effect of alloying additives on the transformation behavior of steel can be understood only from knowledge of the effect on various properties. Almost all alloying elements cause a volume increase. Figure 6.155 shows their effect on the lattice constant of α -iron. Only silicon leads to a contraction. Electrical resistance increases in proportion to the concentration of the alloying element (Figure 6.156). The most significant effect of alloying elements on magnetic properties is on the Curie temperature, as this affects the temperature of the transformation from γ - to α -iron. Figure 6.157 shows the effects of various elements. The large increase caused by cobalt is of special interest.

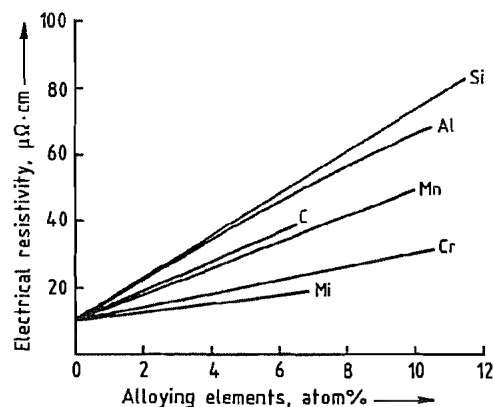


Figure 6.156: Increase in the decimal resistivity of α -iron by alloying elements.

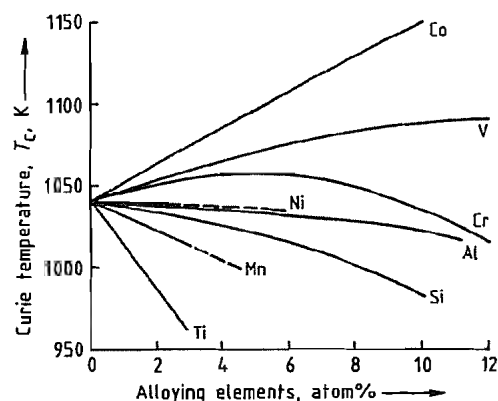


Figure 6.157: Effect of alloying elements on the Curie temperature of α -iron.

The temperature dependence of the physical properties of α -iron mixed crystals is closely linked to their magnetic behavior, and is not significantly different from that of pure iron. For example, the heat capacity of iron-chromium alloys is essentially constant if the temperature scale is based on the Curie temperature.

Ferritic iron-silicon alloys are of special importance, as these have low magnetization losses [306, 310]. Silicon addition increases electrical resistance, and hence reduces eddy current losses. The crystal anisotropy energies and the consequent hysteresis losses are reduced. Addition of $> 4.5\%$ Si prevents the α - γ transformation, and enables a coarse grain

structure to be produced. Texturing allows the magnetic anisotropy to be exploited.

6.6.3.3 γ -Iron Solid Solutions

The magnetic properties of austenitic iron alloys are complex—as ferromagnetism, anti-ferromagnetism, and paramagnetism can occur. Iron-manganese [311], iron-nickel [312], and iron-nickel-manganese alloys [313] are of industrial importance.

The thermal expansion coefficients of paramagnetic γ -alloys (e.g., iron-manganese-nickel and iron-nickel-chromium alloys) are relatively high at room temperature. This is utilized in bimetallic systems [314]. Conversely, a large volume magnetostriction in magnetically ordered alloys compensates for thermally induced changes to the lattice dimensions; only a small amount of thermal expansion takes place over a certain temperature range [315]. Iron alloys containing 35% nickel are examples of Invar alloys of this type.

6.6.3.4 Other Effects of Structure

In general, physical properties are influenced by lattice defects. Density is somewhat decreased by lattice defects. All lattice defects increase the residual electrical resistance, whereas lattice vibrations are the main cause of resistance at high temperatures. Spontaneous magnetization and the Curie temperature depend mainly on lattice structure and composition. However, the magnetization curve is strongly influenced by the structure; lattice defects tend to prevent movement of the domain walls, and hence increase the remanence and coercive field strength.

In multiphase structures, the different properties of the phases must also be considered. These properties combine in proportion to the volume ratios in only the simplest cases, e.g., density, heat capacity, heat of transformation, and heat of formation, provided that the phases are in a coarse state of subdivision. A systematic treatment is not yet possible. Probably the most important industrial application

is represented by the “hard” or permanent magnetic materials, with high coercive field strengths and a high BH value.

6.7 Environmental Protection

6.7.1 Environmental Aspects of Steel Production and Processing

6.7.1.1 Production of Steel and Steel Products

Large quantities of raw additive and auxiliary materials are used in the production of crude steel and rolled steel products, and large amounts of energy are used in these processes. Substances in the solid, liquid, and gaseous states are potential sources of environmental pollution.

For reasons of economy, the steel industry, especially in Europe, has always attempted to use as little primary energy as possible, to limit the consumption of auxiliary materials, e.g., water, by means of complex recycling systems, and to utilize or recycle by-products or residues, e.g., slags and mill scale. From the early 1900s, integrated steel plants, in close association with coking plants and rolling mills, have optimized the use of CO-containing blast furnace top gas according to the current state of technology. The use of blast furnace slag for cement and for road construction is very much older than the general interest in environmental pollution. In the last 20–30 years, the ever-increasing severity of environmental controls have led to technological developments within the steel industry which have been very successful [318]. However, some of the regulations imposed demand additional capital investment and operating costs whose justification may be dubious, especially when in some countries the regulations imposed are different and, thereby, distort competition. The following discussion is based mainly on available data for the steel industry,

and particularly, individual steel plants in the western part of Germany.

Environmental aspects of the production of pig iron in a blast furnace have already been described. Further numerical data on developments during the last 30 years are given here. Figure 6.158 shows the considerable decrease in the consumption of carbon for reduction purposes in pig iron production [318]; Figure 6.159 shows the continuous decrease in the specific amount of blast furnace slag, and its 100% use in various applications [319]. The generation of electrical energy from expansion turbines running on blast furnace top gas (Figure 6.160) is a further contribution to environmental protection [320].

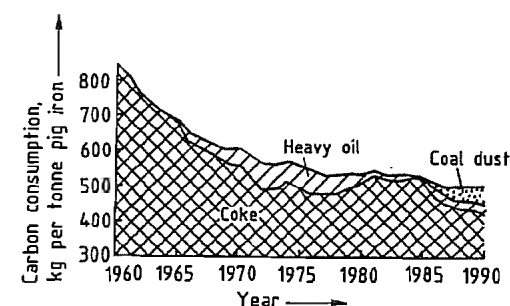


Figure 6.158: Carbon consumption in pig iron production.

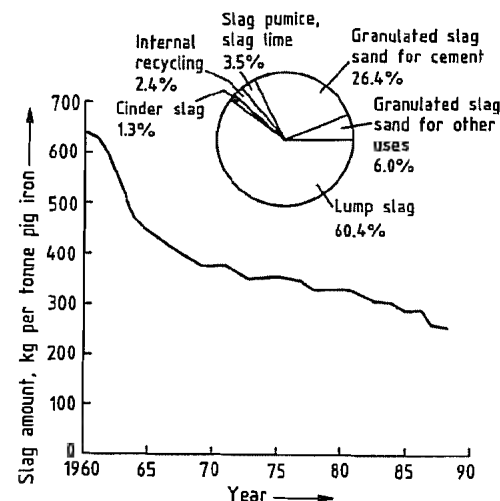


Figure 6.159: Development of the specific amount of blast furnace slag and its utilization.

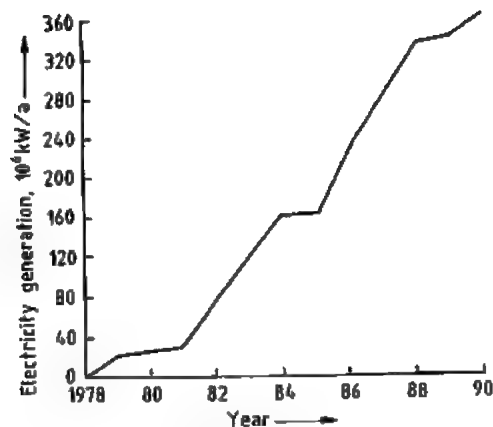


Figure 6.160: Electricity generation by expansion turbines from blast furnace top gas.

In a steel melting shop, the amount of dust formed and the possibility of its recovery depend very much on the different steel melting processes, which have undergone many changes (Section 6.3.3). The changeover to the oxygen blast process and improvements in dedusting equipment, including secondary dedusting, have led to an emission rate of only 0.7 kg per tonne crude steel in the melting shops of the German steel industry (Figure 6.161) [321]. Secondary dedusting, comparable to the "cast house dedusting" at the blast furnace, involves the additional dedusting equipment at different operation points located before and after the converters, e.g., pig

iron transfer pit, mixers, deslagging stands; the dedusting equipment consists of stationary or movable hoods and skirts. Figure 6.162 illustrates the complexity of this additional dust collection in a steel melting shop with three converters [322].

A comprehensive study has shown that the total quantity of dust and sludge collected in the steel plants in North Rhine/Westphalia is 41 kg per tonne crude steel (Figure 6.163), of which more than 80% is reused [320].

The hot waste gas formed in an oxygen converter is used to produce steam in a waste heat boiler in the primary dedusting installation [321, 322]. After further purification and cooling (Figure 6.164), it is collected so that its high CO content (68–70%) can be used sometimes after mixing with other gases. Figure 6.165 shows the significant energy generation which has been achieved in Germany [319].

Slag, an inevitable by-product in steelworks has been further reduced in recent years, reaching 121 kg per tonne crude steel in 1991, of which 87.5% was utilized [320].

The mill scale occurring in hot rolling mills is a pure iron oxide, and can be reused in sintering plants. However, oil-containing mill scale sludge must be pretreated. Rotary kiln installations to be used for this purpose are in the experimental stage [322].

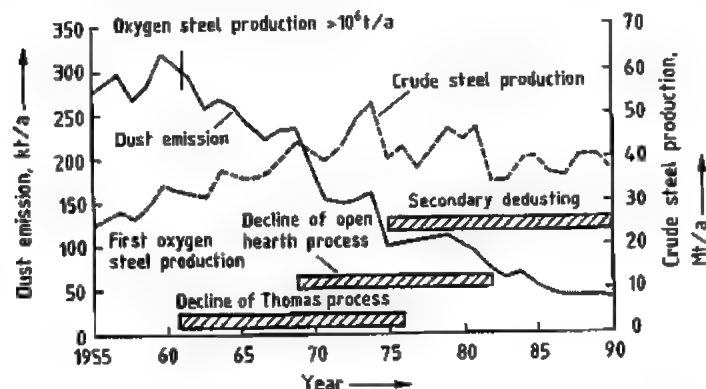


Figure 6.161: Development of crude steel production and dust emission by the German steel industry.

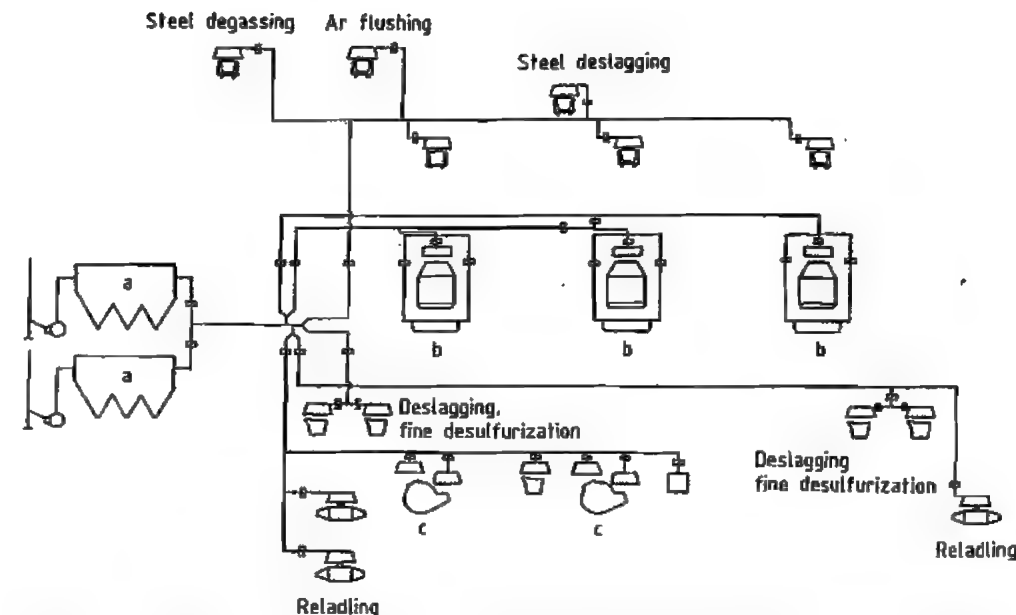


Figure 6.162: Dust collection in a three-converter steelshop: a) Electrostatic precipitator; b) Converters; c) Mixers.

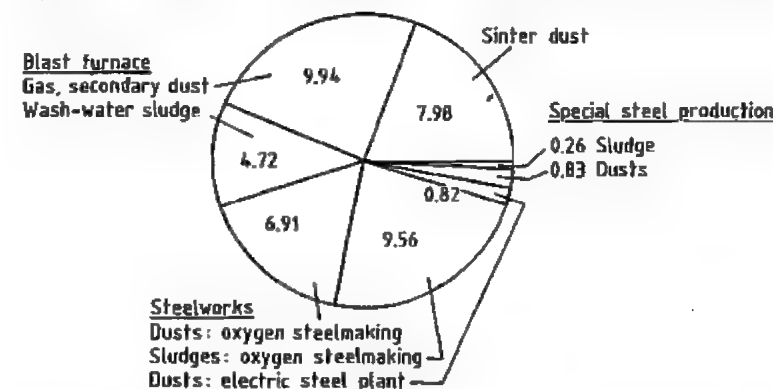


Figure 6.163: Origins of dusts and sludges in pig iron and steel production in North Rhine/Westphalia. Amounts in kg per tonne crude steel.

Control of water consumption in a steel plant is also very important from the environmental point of view. All parts of the production operation involve the consumption of water, sometimes in very large quantities, e.g., for cooling the installations and the products. Attention has always been paid to the development and use of methods for saving water, e.g., the treatment and reuse of water in com-

plex recirculating systems. In 1989, in a steel-plant situated near the Rhine, only 3% of the process water used was fresh water, i.e., 2.5 m³ fresh water per tonne crude steel (Figure 6.166) [318]; the remaining 97% came from the recirculation system. Some 83% of the water used in the steel industry is surface water.

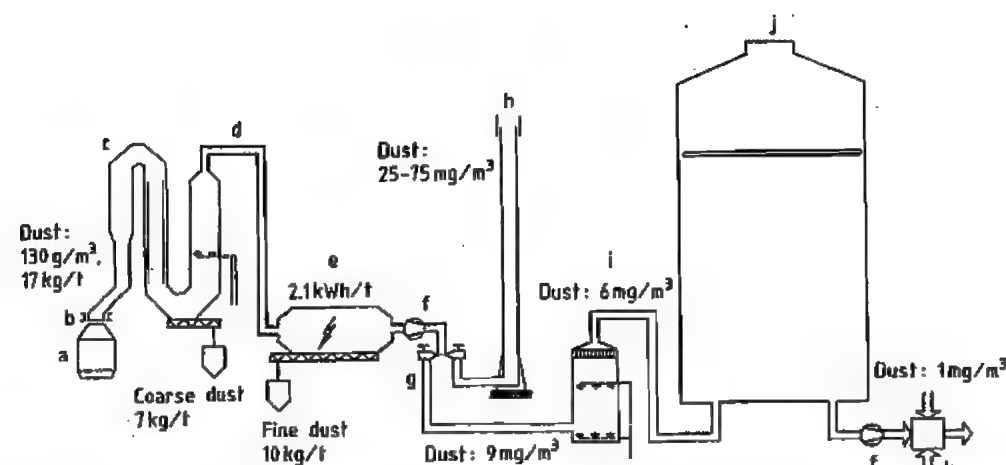


Figure 6.164: Converter gas cleaning and recovery system: a) Converter; b) Skirt; c) Steam boiler; d) Evaporation cooler; e) Dry electrostatic precipitator; f) Fan; g) Reversing valve; h) Flare stack; i) Gas cooler; j) Gas holder; k) Gas mixing station.

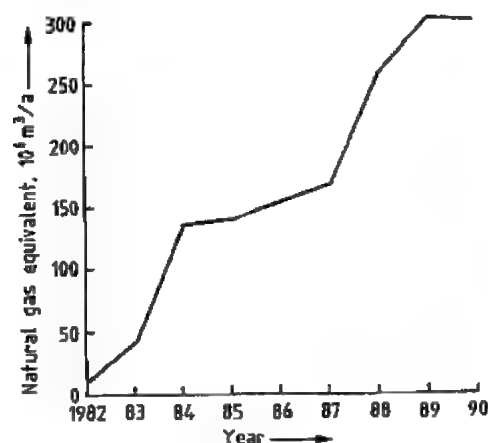


Figure 6.165: Energy production by the use of converter gas.

A high proportion of rolled steel production is cold-rolled or coated steel sheet, tinplate, black plate, and cold-rolled electric sheet. The hot-rolled strip for these finished products must be treated in continuous pickling lines to remove the adhering mill scale before the cold-rolling process. The used pickling solution is also treated in a recirculating system in which an iron salt, e.g., sulfate, crystallizes, and fresh acid is added, so that only a small fraction of the solution leaves the plant after neutralization. The iron hydroxide sludge,

which contains gypsum, cannot be used any further. This also applies to the wash-water in the pickling line, but the amount of wash-water used can be much reduced by appropriate techniques.

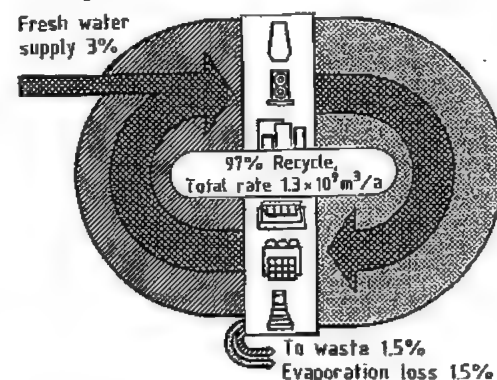


Figure 6.166: Internal water circulation.

6.7.1.2 Steel Processing and Steel in Use

Steel used in manufacturing as described in earlier sections, is environmentally a very friendly material.

The processing of steel can certainly involve sound emissions, e.g., during hammering, sheet metal working, and forging. Gases

can result when flame cutting and welding steel. However, in both these cases, it is possible to protect personnel at the workplace without great cost and without causing too much inconvenience to the individual. In certain heat treatment processes, e.g., those using molten salt baths, the advice of the manufacturers of the salts or other substances used should be followed, and relevant legal requirements must be observed relating to their handling and disposal.

Environmental problems associated with the use of steel products are practically nonexistent, since steel is a highly recyclable material. Even tinplate is environmentally a friendly packaging material, as it can be separated from waste materials or residues, e.g., from garbage incineration plants, by virtue of the ferromagnetic properties of the steel, and can then be reused.

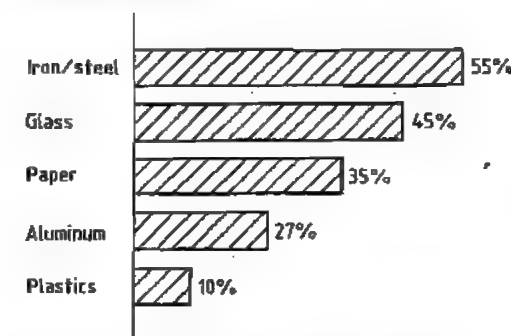


Figure 6.167: Extent of recycling of various materials.

Figure 6.167 illustrates the extent to which construction materials are recycled, and in the case of steel this can easily be increased further [323]. The reuse of steel scrap is of great importance for the overall economy. Approximately 60% less primary energy is required for melting scrap for steel production, than for the smelting of ores [323].

In the last 15 years, the use of sheet with a surface coating, mostly zinc, has increased considerably, both in automotive body manufacture and in other applications. Doubts about the use of zinc-coated steel scrap from these sources are unjustified. Most of the zinc vaporizes during crude steel production, and is recovered in the dust from the filters in the de-

dusting equipment. If manufacturers dispose of moderately zinc-rich scrap separately, this can be processed and used in suitable electric steel plants, and the zinc can be economically recycled. For this there must be at least 16% Zn in the filter dust [324].

6.7.2 Steel Recycling

6.7.2.1 The Tradition of Steel Recycling

More than 3000 years ago, iron had already been the material foundation for cultural development. It has given its name to an entire epoch. The industrialization is closely linked with the development of the iron and steel industry. Almost all other industries have been directly or indirectly dependent on advances in steel production.

On 28 October 1865, the first iron was smelted by the Siemens-Martin open hearth process using 70% scrap, so beginning the industrial utilization of scrap [325].

For over a hundred years, a technically and economically viable high-tonnage recycling system has existed for handling production waste and worn-out capital equipment and consumables made of steel and cast iron. For steel scrap, there is a completely closed system for recycling worn-out steel products, any number of times. The recycling process continually yields high quality steel grades without downgrading.

As industrialization progressed and steel production increased toward the 1890s, the demand for raw materials rose. By then, scrap was already an important substitute for the usual raw material in the iron- and steel-producing industry.

6.7.2.2 Types of Scrap

Listings. In order to provide precise descriptions of the physical and chemical properties required in reusable scrap, an agreed list of scrap grades has been prepared by the steel and steel recycling industry in Germany (Table 6.19).

Table 6.19: Extract from the German list of scrap grades (1 September 1993) (Source: Bundesverband der Deutschen Schrott-Recycling-Wirtschaft e.V., Düsseldorf).

Category	Specifi- cation	Description	Dimensions	Density	Steriles ^a
Old scrap	E3	Old thick steel scrap, predominantly more than 6 mm thick in sizes not exceeding 1.5 × 0.5 × 0.5 m, prepared in a manner to ensure direct charging. May include tubes and hollow sections. Excludes vehicle body scrap and wheels from light vehicles. Must be free of rebars and merchant bars, free of metallic copper, tin, lead (and alloys), mechanical pieces and steriles to meet the aimed analytical contents. Refer to points (B) and (C) of the general conditions.	Thickness ≥ 6 mm < 1.5 × 0.5 × 0.5 m	≥ 0.6	≤ 1 %
	E1	Old thin steel scrap predominantly less than 6 mm thick in sizes not exceeding 1.5 × 0.5 × 0.5 m prepared in a manner to ensure direct charging. If greater density is required it is recommended that maximum 1 metre is specified. May include light vehicle wheels, but must exclude vehicle body scrap and domestic appliances. Must be free of rebars and merchant bars, free of metallic copper, tin, lead (and alloys), mechanical pieces and steriles to meet the aimed analytical contents. Refer to points (B) and (C) of the general conditions.	Thickness < 6 mm < 1.5 × 0.5 × 0.5 m	≥ 0.5	< 1.5 %
New scrap (low residuals, uncoated) ^b	E2	Thick new production steel scrap predominantly more than 3 mm thick prepared in a manner to ensure direct charging. The steel scrap must be uncoated unless permitted by joint agreement and be free of rebars and merchant bars even from new production. Must be free of metallic copper, tin, lead (and alloys), mechanical pieces and steriles to meet the aimed analytical contents. Refer to points (B) and (C) of the general conditions.	Thickness ≥ 3 mm < 1.5 × 0.5 × 0.5 m	≥ 0.6	< 0.3 %
	E8	Thin new production steel scrap predominantly less than 3 mm thick prepared in a manner to ensure direct charging. The steel scrap must be uncoated unless permitted by joint agreement and be free of unbound ribbons to avoid trouble when charging. Must be free of metallic copper, tin, lead (and alloys), mechanical pieces and steriles to meet the aimed analytical contents. Refer to points (B) and (C) of the general conditions.	Thickness ≥ 3 mm 1.5 × 0.5 × 0.5 m (except bound ribbons)	≥ 0.4	< 0.3 %
	E6	New production thin steel scrap (less than 3 mm thick) compressed or firmly baled in a manner to ensure direct charging. The steel scrap must be uncoated unless permitted by joint agreement. Must be free of metallic copper, tin, lead (and alloys), mechanical pieces and steriles to meet the aimed analytical contents. Refer to points (B) and (C) of the general conditions.		≥ 1	< 0.3 %
Shredded	E40	Shredded steel scrap. Old steel scrap fragmentized into pieces not exceeding 200 mm in any direction for 95 % of the load. No piece, in the remaining 5 %, shall exceed 1000 mm. Should be prepared in a manner to ensure direct charging. The scrap shall be free of excessive moisture, loose cast iron and incinerator material (especially tin cans). Must be free of metallic copper, tin, lead (and alloys), and steriles to meet the aimed analytical contents. Refer to points (B) and (C) of the general conditions.		> 0.9	< 0.4 %

Category	Specifi- cation	Description	Dimensions	Density	Steriles ^a
Steel turn- ings ^c	ESH	Homogeneous lots of carbon steel turnings of known origin, free from excessive bushy. Should be prepared in a manner to ensure direct charging. Turnings from Free Turning Steel must be clearly identified. The turnings must be free from all contaminants such as nonferrous metals, scale, grinding dust, and heavily oxidized turnings or other materials from chemical industries. Prior chemical analysis could be required.			^d
	ESM	Mixed lots of carbon steel turnings, free from excessive bushy and free from turnings from Free Cutting Steel. Should be prepared in a manner to ensure direct charging. The turnings must be free from all contaminants such as nonferrous metals, scale, grinding dust, and heavily oxidized turnings or others materials from chemical industries.			^d
High resid- ual scrap	EHRB ^e	Old and new steel scrap consisting mainly of rebars and merchant bars prepared in a manner to ensure direct charging. May be cut, sheared, or baled and must be free of excessive concrete or other construction material. Must be free of metallic copper, tin, lead (and alloys), mechanical pieces and steriles to meet the aimed analytical contents. Refer to points (B) and (C) of the general conditions.	Max. 1.5 × 0.5 × 0.5 m	≥ 0.5	< 1.5 %
	ENRM ^f	Old and new mechanical pieces and components not accepted in the other grades prepared in a manner to ensure direct charging. May include cast iron pieces (mainly the housings of the mechanical components). Must be free of metallic copper, tin, lead (and alloys), and pieces such as bearing shells, bronze rings, and others as well as steriles, to meet the aimed analytical contents. Refer to points (B) and (C) of the general conditions.	Max. 1.5 × 0.5 × 0.5 m	≥ 0.6	< 0.7 %
Fragment- ized scrap from incin- eration	E46	Fragmentized incinerator scrap. Loose steel scrap processed through an incinerating plant for household waste followed by magnetic separation, fragmentized into pieces not exceeding 200 mm in any direction and consisting partly of tin-coated steel cans. Should be prepared in a manner to ensure direct charging. The scrap shall be free of excessive moisture and rust. Must be free of excessive metallic copper, tin, lead (and alloys), and steriles to meet the aimed analytical contents. Refer to points (B) and (C) of the general conditions.		≥ 0.8	Fe content ≥ 92 %

^a Corresponds to the weight of steriles, not adhering to the scrap, remaining at the bottom of the vehicle after unloading by magnet.

^b Coated Material must be notified.

^c Free from all contaminants (nonferrous metals, scale, grinding dust, chemical materials, excess oil).

^d To date, no clear method to determine these values.

^e Rebar and Merchant Bar must be classified apart due essentially to the copper content which could place them out with old scrap and new scrap low residual grades.

^f Mechanical and engine components must be classified apart principally due to their Ni, Cr, and Mo content which could place them out with the thick old scrap and heavy new scrap low residual grades.

These defined grades apply only to carbon steel scrap. The following general requirements are included in the European list of scrap grades of 1 July 1995. The scrap must be:

- Prepared in a manner to ensure direct charging

- Handleable magnetically
- Free from elements harmful to the smelting process

Plant Scrap. Plant scrap is produced in the manufacture of steel and of rolled finished products. It is directly reused in the steel-works.

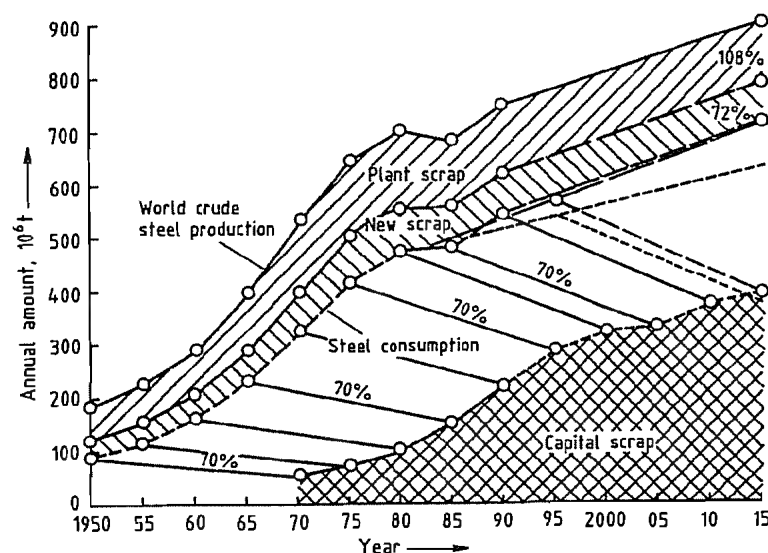


Figure 6.168: Development of arisings of plant scrap, new, and capital scrap, with estimated future figures.

New Scrap. New scrap arises in steel processing industries as production waste. It is usually returned to steelworks and foundries by the recycling industry.

Capital Scrap. Capital scrap is composed of steel, cast steel, and cast iron originating from used commodity and industrial goods. There are three types, classified according to origin:

- Demolition scrap
- Automobile scrap
- Collected scrap

The development of the amounts of plant scrap, new scrap, and capital scrap is illustrated in Figure 6.168, with estimated future figures, assuming that 70% of steel consumption is returned to the material cycle after a period of 20 years.

6.7.2.3 Scrap Processing

Separation

Steel is used in engineering, plant construction, vehicles, building industry, shipbuilding, household appliances, packaging, etc. When products that consist mainly of steel are no longer usable, they are usually processed by the steel recycling industry. The composition

and dimensions of scrap are usually such that it cannot be used in steelworks and foundries in its original state. Appropriate processes must therefore be used for:

- Size reduction
- Separation from other materials
- Classification into grades

A unique characteristic of steel and iron scrap is that it can easily be recovered from accompanying materials by its magnetic properties, enabling the iron-containing constituents to be returned to steelworks and foundries in a high state of purity.

Shearing Machines

Large pieces of scrap can be size-reduced by shearing machines. Even before the World War I guillotine shears were used for this purpose.

Further developments led to the larger and faster alligator shears, and then to the hydraulic machines used today, where the scrap is charged by a crane into a feeding bed. The feeding bed is usually provided with a prepress which compresses the scrap so that even bulky material can be pushed under the blades of the shears. Size reduction of, e.g., freight

cars industrial equipment, and large components, including material from shipbreaking and other heavy demolition work, is carried out with shears with a compression force of up to 2000 t and blades up to 2.50 m wide [326].

Presses

Scrap presses are used to densify clean steel scrap, e.g., production waste from rolling mills and steel processing industries, to facilitate transportation and charging, and to reduce it to the specified dimensions.

In the early 1920s, slow mechanical screw presses with large vertical boxes and small charging holes were developed. These were able to bale light collected scrap and new sheet scrap.

Mechanical baling presses were followed by high-pressure hydraulic presses with large charging boxes. This hydraulic equipment produces high-density bales of the size needed for steel production plants, e.g., converters and electric furnaces, and for the melting facilities of the foundry industry. The usual bale sizes are: 30 × 30 × 30 cm and 40 × 40 × 60 cm for the foundry industry, and 60 × 60 × 150 cm for the steel industry [327].

Shredders

Increasingly, scrap is no longer in pure form, but combined with other materials. Examples include old vehicles and household appliances, which contain considerable amounts of plastics, glass, rubber, nonferrous metals, and other materials. Shredders (Figure 6.169) have been used by the steel recycling industry since the mid 1960s to produce automobile and collected scrap that meets the requirements of the steelworks.

A shredder functions on the principle of the swing-hammer mill. The products fed to the shredder are broken down to pieces not larger than fist-sized, and are then fed to an air separator to remove the light waste fraction, which includes plastics, textiles, and cardboard. An electromagnetic drum or band separator separates the steel scrap from the nonferrous met-

als and coarse impurities (heavy waste fraction). The materials removed by the air separator, which cannot, at present, be recycled (shredder residues) must be disposed of. This is expensive, and is likely to become more so. Shredding provides a means of recovering the iron and steel from used products with purity ca. 98%, so that they can be returned to the raw material cycle.

6.7.2.4 Factors Influencing Recycling

Alloy Steels

In steel production, the properties of various grades of steel are achieved by adding alloying elements. Alloy steel can also be returned to the material cycle, if it is sorted according to chemical composition. The alloying elements are retained when the scrap is melted, and new alloy steels can be produced from this metal.

Surface Coatings

Steel is surface coated to give the properties required, i.e., surface quality, stress condition, and corrosion protection. Surface coatings can be either metallic (e.g., zinc) or nonmetallic. The latter include organic coatings (plastic or paints) and inorganic coatings (cement mortar or enamel) [328].

Smelting of zinc-coated steel scrap during steel production is the present state of the art. As zinc boils at 907 °C and steel melts at 1400–1500 °C, the zinc vaporizes from the melt and is collected as zinc oxide in dedusting plants. If the zinc content of the steelworks dust is ca. 16%, it is profitable to recover the zinc [329, 330].

Before scrap recovered from steel with a nonmetallic coating can be returned to steel production, it is usually processed by shredding, or cold shock treatment to remove adhering materials from the scrap, as these are harmful to the smelting process, or can lead to inadmissible emissions.

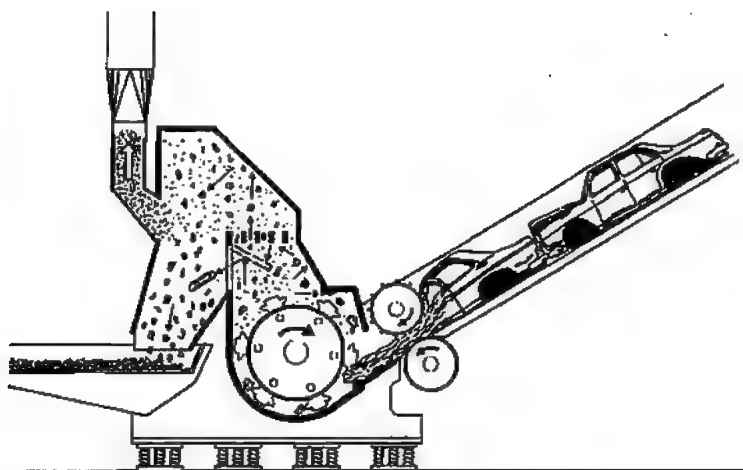


Figure 6.169: Operating principle of a shredder.

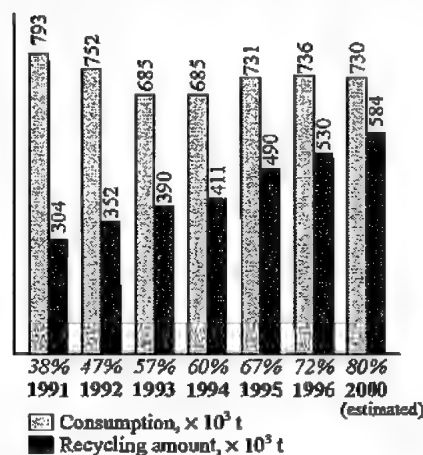


Figure 6.170: Consumption and partial recycling of tinplate packaging in Germany.

Pretreatment of Used Steel Products

Steel products and components at the end of their lives are often associated with impurities, or are attached to other materials. To prevent the unwanted materials from being returned to steel production along with the scrap, pretreatment and purification are necessary, e.g., removal of oil from chips arising from the processing of steel, which are classified as new scrap.

Pretreatment of used products that consist mainly of steel is often also necessary for dis-

posing of or recycling the other materials in the products, e.g., the disposal of old cars. In the initial dismantling, the batteries of the old vehicles are removed to return the lead to a separate material cycle. This also prevents the lead from contaminating waste tips when the shredder residues are dumped. For the same reason, fuel, oil, gear, differential, and shock absorbers, and brake fluid and coolant are recovered before the old cars are shredded. In refrigerators, freezers, and air conditioning equipment, the cooling liquids are recovered to prevent their escape into the atmosphere.

Tinplate packaging, e.g., for foodstuffs, consists of very thin tinned steel sheet. The scrap from tinplate cans is processed by the steel recycling industry, and returned to steel production where it is used without problems. The consumption of tinplate packaging and the extent of its recovery for recycling in Germany is shown in Figure 6.170.

Steel sheet packaging for commercial use, e.g., barrels or canisters, can be contaminated with organic or inorganic residues from the filling (paints, varnishes, oils, or adhesives). They must be emptied as far as possible and then processed by, e.g., shredding, cold shock treatment, or centrifuging, enabling the scrap to remain in the material cycle, provided that the chemical and physical quality requirements of the steel industry are met.

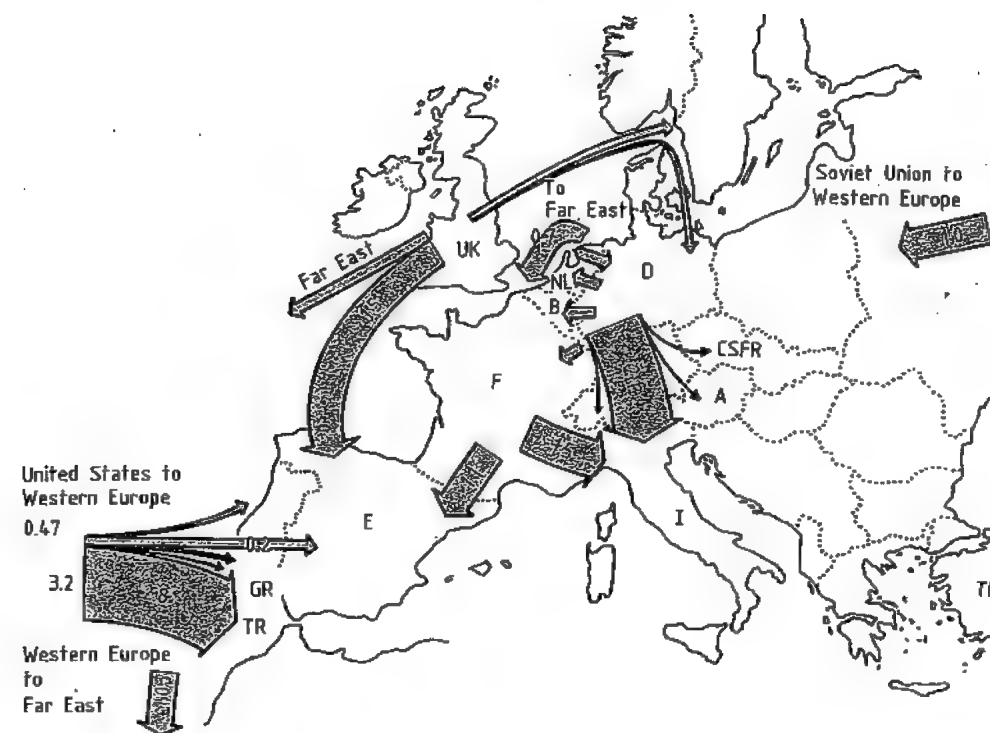


Figure 6.171: World trade in scrap 1990.

6.7.2.5 Economic and Logistic Aspects

Scrap Consumption

According to the International Iron and Steel Institute (IISI), total world consumption of scrap, including scrap used in foundries, was 360×10^6 t in 1994. Most of this (330×10^6 t) was used in steel production. In 1994, total world crude steel production was 728×10^6 t [331]. Hence, the average consumption of scrap per tonne crude steel produced was ca. 450 kg. Electric steel plants accounted for 223×10^6 t scrap. Thus, ca. 60% of scrap was consumed by electric steel plants.

World Market for Scrap

Scrap is an international commodity with a free price structure. Scrap arisings and consumption vary greatly from one country to an-

other. The proportions of the various steel production processes in different countries have a considerable influence on scrap consumption, and hence on the flow of imports and exports. In electric steelworks, 100% scrap can be used for steel production. In 1995, the average usage of scrap in German electric steelworks was 1004 kg per tonne crude steel.

In oxygen steel production, pig iron produced in the blast furnace is oxidized together with scrap in a converter. The average usage of scrap in 1995 in Germany was 181 kg per tonne crude steel for this process [332]. In the production of high quality steel grades shredded scrap for cooling is preferred because of its high purity and the small lump size.

The most important flows of scrap in world trade in 1990 are illustrated in Figure 6.171.

Infrastructure and Logistics

The task of the steel recycling industry is to take responsibility for iron and steel scrap, i.e., to transport, store, process, and deliver to steelworks and foundries a high-quality raw material.

The recycling system offers one particular advantage: The collecting points are installed in all countries. They collect scrap according to its origin, lump size, and impurity levels. The structure of these organizations varies:

- Small-scale and collection service
- Medium-sized scrap wholesale traders
- Organizations supplying scrap to steelworks

Scrap is transported by rail, water, and road. To enable prompt delivery, the steel recycling industry has made considerable investments in handling and transportation facilities.

The demand for scrap is not constant, so the scrap recycling industry maintains stocks containing the equivalent of the purchasing requirements of steelworks for ca. 2 months. Thus, the industry has taken over an important function in balancing scrap arisings with consumption [333].

6.8 Economic Aspects

6.8.1 World Steel Production, Consumption, and Trade

From the World War II to the early 1970s, world crude steel production grew at an average annual rate of ca. 5.5%. Since then, the rate has been only 1% (Figure 6.172). The number of steel-producing countries increased from ca. 30 to ca. 90.

The largest steel-producing companies, with their 1992 production, are shown in Table 6.20.

Of the total world crude steel production, 721×10^6 t in 1992, 345×10^6 t (48%) was produced by 50 companies in the western world. There are also large steelworks in the countries of the former Soviet Union. Some of these are listed in Table 6.21.

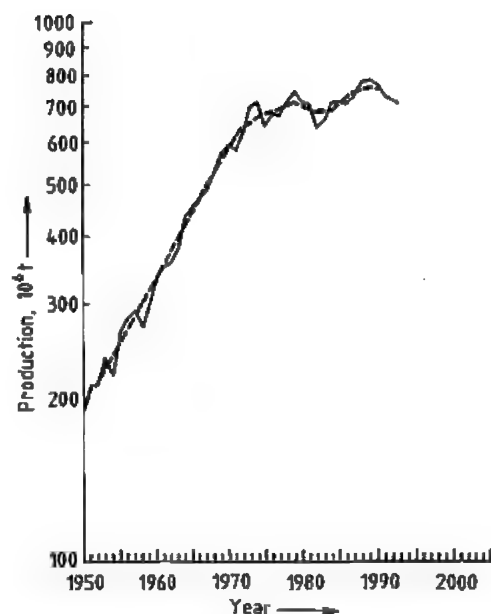


Figure 6.172: World steel production from 1950 (selected regions). Smooth curve is 5-year average. Data Supplied by the Statistisches Bundesamt (German Federal Bureau of Statistics) and the International Iron and Steel Institute (IISI).

Table 6.20: Leading steel producers 1992.

Company	Country	Production, 10^6 t
Nippon Steel	Japan	25.10
Usinor Sacilor	France	21.10
PoSCO	Korea	20.01
British Steel	United Kingdom	12.39
NKK	Japan	10.89
Ilva	Italy	10.60
Thyssen	Germany	10.13
Kawasaki	Japan	10.00
Sumitomo Metals	Japan	9.97
Sail	India	9.70
Bethlehem	United States	9.60
US Steel	United States	9.50

Table 6.21: Steel production in the former Soviet Union.

Steelworks	Country	Capacity, 10^6 t/a
Magnitogorsk	Russia	16.2
Cherepovets	Russia	14.0
Krivoy Rog	Ukraine	13.9
Lipetsk	Russia	9.9
Nizhny Tagil	Russia	8.3

After the political changes of the early 1990s, steel production in these countries decreased considerably, i.e., from 216×10^6 t in 1987 to 124×10^6 t in 1993.

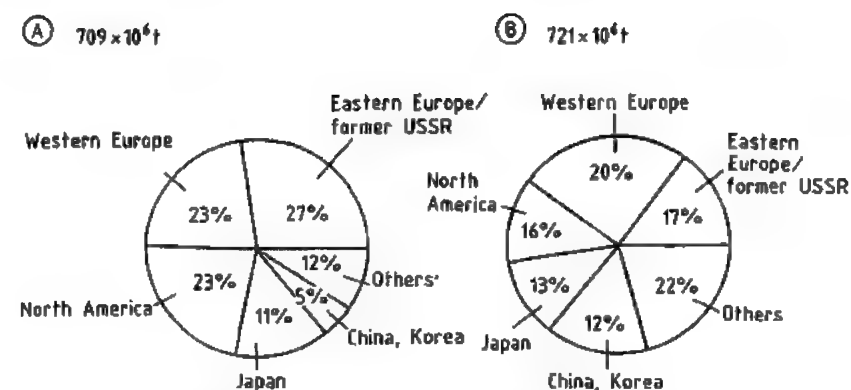


Figure 6.173: Steel consumption: A) 1974; B) 1992. Source: IISI, Brussels.

Table 6.22: Steel production and consumption 1970–1992.

Region	Production Consumption Balance, 10^6 t			Production Consumption Balance, 10^6 t			Production Consumption Balance, 10^6 t		
	1970			1980			1992		
European Community	146.2	132.9	13.3	141.9	119.9	22.0	129.1	115.2	13.9
Western Europe	161.9	153.9	8.0	161.2	142.1	19.1	153.8	135.3	18.5
United States	119.3	127.3	-8.0	101.5	118.6	-17.1	84.3	100.3	-16.0
Japan	93.3	69.9	23.4	111.4	79.0	32.4	98.1	84.0	14.1
Industrialized countries	397.4	374.0	23.4	406.9	366.2	40.7	366.9	340.4	26.5
Developing countries	22.1	42.2	-20.1	56.7	94.4	-37.7	117.2	147.7	-30.5
Brazil	5.4	6.0	-0.6	15.3	14.3	1.0	23.9	9.1	14.8
Eastern Europe	40.1	41.5	-1.4	61.2	59.6	1.6	32.4	21.1	11.3
Former Soviet Union	115.9	110.2	5.7	147.9	150.4	-2.5	117.0	115.0	2.0
China	18.0	22.5	-4.5	37.1	43.2	-6.1	80.0	83.1	-3.1
World	595.7	592.8	2.9	715.9	718.8	-2.9	720.5	714.8	5.7

Table 6.23: World trade in steel 1991.

Country	Exports, 10^6 t	Country	Imports, 10^6 t
Germany	19.6	Germany	16.8
Japan	17.9	United States	14.3
Belgium/Luxembourg	14.3	France	10.3
France	12.0	Italy	10.3
Brazil	10.9	Japan	9.0
Italy	9.0	Taiwan	8.7
United Kingdom	8.0	South Korea	8.5
Korea	7.7	United Kingdom	5.6
United States	5.8	Iran	5.5
Netherlands	5.7	Netherlands	5.2
Soviet Union	5.4	Belgium/Luxembourg	4.7
Spain	4.8	Soviet Union	4.6

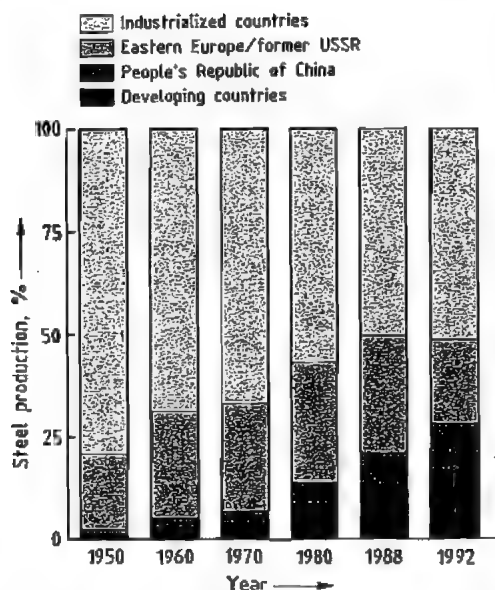


Figure 6.174: Crude steel production by region 1950–1992.

The strong growth of the world steel industry starting in the 1970s was due to the high demand for steel in western Europe, Japan, and eastern Europe. In these regions, steel consumption expanded by almost 7% per annum. In the United States, the rate was only 2%. Consumption by the developing countries grew rapidly from small beginnings, at > 8.5% per annum.

In the last 30 years, considerable regional changes in steel consumption and production have occurred. Approximately one-fifth of steel consumption and 15% of steel production is associated with the developing regions (Figure 6.173). China has also moved ahead. Japan improved its position until the early 1970s, but its share of the world volume has stagnated since then. Europe and the United States are producing a considerably lower proportion than 20 years ago.

Regional shifts have increased the extent to which the developing countries have become self-sufficient, but in recent years, demand has grown more rapidly than supply. The traditional exporters, e.g., Japan and the European Community, have relied more strongly on

their domestic markets. The United States has been a net importer since 1959. The relationship between production and market supply has developed as shown in Table 6.22.

Brazil has become one of the largest net exporters. Meanwhile, the contribution by eastern Europe and the former Soviet Union to the world total has decreased since the end of the communist planned economy (Figure 6.174).

World steel exports have grown more rapidly than world production (Figure 6.175) because of variations in the regional distribution of demand and production. In the 1970s and early 1980s, the volume of international trade in steel tended to grow at the same rate as general world trade, but in recent years, the volume of steel trade has not increased. The increasing self-sufficiency of new producing countries tends to have a braking effect, but in the area of products and grades, and as a result of competition for customers by the manufacturing companies, active interchange across national boundaries is likely in future.

Steel exports from Japan have decreased from > 30×10^6 t in the mid-1980s to 18×10^6 t in 1991. Most significant is the collapse of trade among the former COMECON countries—ca. 15×10^6 t reduction in the exchange volume. As shown by the high uptake by China from the international market in late 1992/early 1993, relatively large fluctuations in world steel exports are likely.

A summary of the largest exporting and importing countries in 1991 is given in Table 6.23.

An important feature of the steel industry that affects investment decisions is the extent of export orientation of steel manufacturers. In the industrialized countries, the important steel consumers, e.g., engineering and motor vehicle manufacturers, export a high proportion of their steel-containing products (Table 6.24).

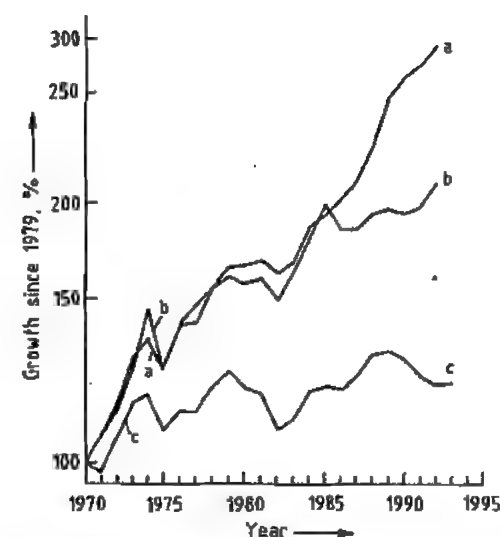


Figure 6.175: World steel exports, production, and trade from 1970. 1970 figures = 100%. a) World trade (all products); b) Steel exports; c) Crude steel production. Source: IISI; Dresdner Bank.

Table 6.24: Direct and indirect steel exports of selected regions.

	Direct export	Indirect export	Direct production, %	Indirect production, %
10^6 t rolled steel				
<i>European Community</i>				
1979	65.7	32.0	53.4	32.4
1990	70.2	37.7	5839	35.8
<i>Japan</i>				
1979	30.7	12.0	30.8	17.1
1990	16.6	20.4	16.9	23.0

Table 6.25: Steel consumption in selected countries 1990.

Country	Consumption, kg rolled steel per capita
West Germany	482
France	285
United Kingdom	244
Sweden	336
Japan	751
Brazil	60

In countries with very high steel exports, e.g., Germany and Japan, the so-called indirect foreign steel trade affects the trend of development of steel consumption and per capita steel consumption considerably (Table 6.25). For these two countries in 1990, indirect ex-

ports and imports of rolled steel resulted in a net balance, estimated at 9.3 and 19.4×10^6 t. These examples show the importance of the basic conditions for fair international trade.

The demand for steel, the most important construction material for industry (including the construction industry) and handicrafts, is mainly determined by overall economic development, and hence by capital investment and external trade in steel-containing goods. The optimism which, in the early 1970s, led to investment in steel capacity was considerably dampened after the first oil crisis of 1974–75. The second large increase in the price of oil in 1979, and the increased attention to environmental problems slowed down the economic growth of the western industrialized countries, where the standard of living had reached a remarkably high level. Future growth is likely to be essentially calmer.

6.8.2 Steel Intensity and Weight Saving in Steel

Steel consumption depends on the state of the overall national economy, especially on investments and foreign trade. In the early stages of industrialization, steel consumption grows at a rate out of proportion to that of the national product. Later, the so-called steel intensity decreases, and steel consumption grows more slowly than the national product (Figure 6.176). The most important reasons include:

- Weight savings in steel manufacture by design optimization, making use of lighter and qualitatively superior steels. The 320 m Eiffel Tower was built of 7000 t steel in 1889, but today would require only 2000 t. A 165 m mast for a radio link station can be built today with only 210 t steel.
- The use of different materials within the broad area of rolled steel products, e.g., greater use of flat products in place of long products, and the use of increasingly thin sheet for flat products (Figure 6.177).

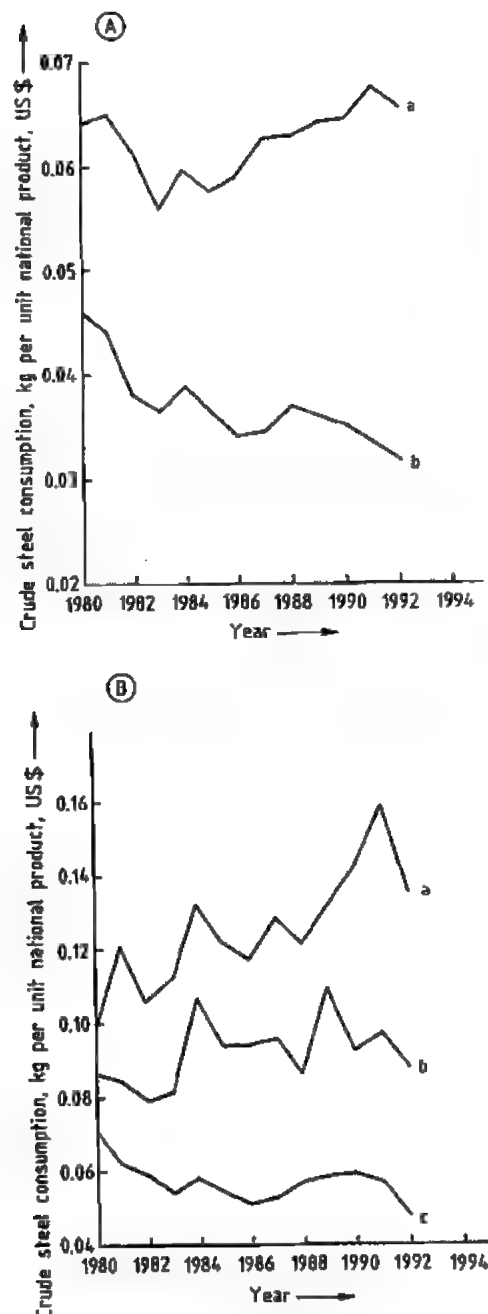


Figure 6.176: Steel consumption from 1980: A) Developing countries (a); Industrialized countries (b); B) Korea (a); Turkey (b); Japan (c). From calculations supplied by IISI.

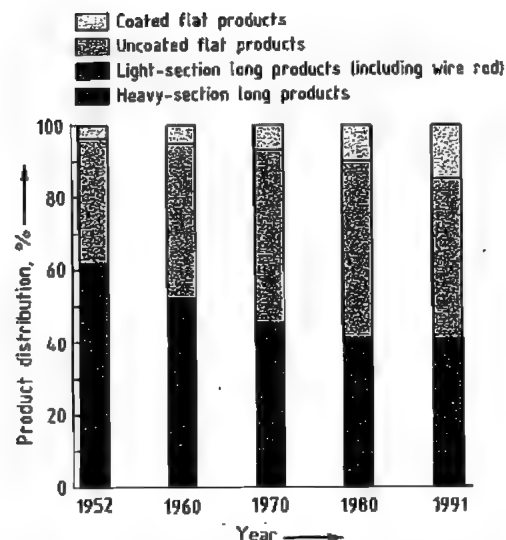


Figure 6.177: Distribution of rolled steel finished products in the European Community. Source: Eurostat.

- Replacement of steel by other materials, e.g., light metals or plastics, e.g., in automobiles. The proportion of steel and iron has decreased from 75% in the 1970s to 65% in the early 1990s. The aluminum content has grown from 3% to 5%, and plastics from 6% to 10%. It is likely that steel will continue to be the most important constituent of automobiles, remaining at ca. 60%.
- A combination of steel with other materials is often the best solution (e.g., sandwich construction).
- The reason for most of the reduction in specific steel consumption is the improved productivity of the steel industry itself, and not the replacement of materials.
- With increasing maturity of a national economy, the fraction of the total national product accounted for by commercial services increases, and the fraction accounted for by manufacturing and heavy basic materials decreases. In 1960, the proportion of the West German national product accounted for by manufacturing was 53%, in 1980 it was 43%, and in 1992, 37%. Mining, basic materials, and manufactured goods contributed 32%, 30%, and 23% to the turnover of manufacturing business in these years.

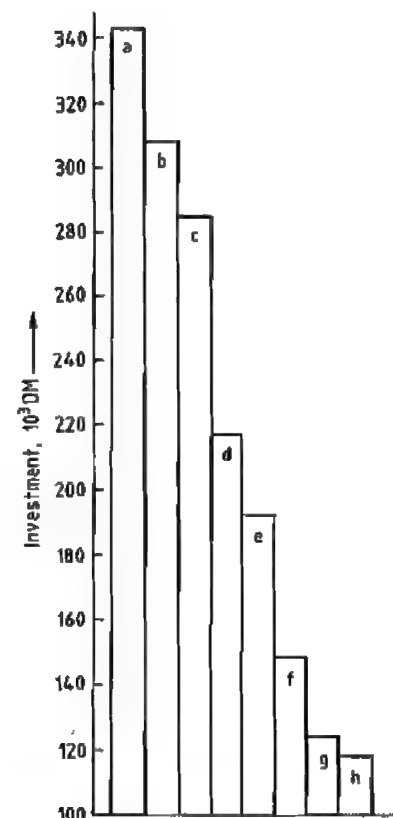


Figure 6.178: Capital investment per installation, West Germany 1990: a) Steel; b) Chemicals; c) Quarrying, extraction, and working up of stone and earths; d) Industry (total); e) Road vehicles; f) Food industry; g) Electrical industry; h) Mechanical engineering. Source: IW, Cologne.

6.8.3 Capital Investment and Subsidies

The steel industry, a capital-, energy-, and raw-material-intensive industry, has always striven to improve productivity and cost effectiveness. Improvements in industrial plant design production methods, and installations for recovering or recycling waste heat, waste gases, electricity, and water have been of central importance. The high intensity of capital investment brought steep cost reductions whenever it was possible to fully utilize the capacities of very large installations. Consequently, from the 1950s to the 1970s, large in-

tegrated steelworks were central to strategic planning. Optimization of locations with respect to raw material supplies (coastal steelworks) or large marketing regions (Rhine, Ruhr) was emphasized. Technical development at that time mainly provided the measurement and control techniques essential for large blast furnaces, large converters, strand casting plants, and large rolling mills, and the electronic support for the organization of production. Innovations and improvements have contributed to reductions in the capital cost per tonne steel produced, in specific energy consumption, in raw and auxiliary materials costs, and in general running costs.

In modern steelworks, the production of 1 tonne rolled steel requires 1.1 t crude steel, whereas 20 years ago it required 1.3 t. Consequent savings of raw steel are ca. 80×10^6 t/a worldwide. There is a further possible saving of 40×10^6 t by further modernization, assuming the same volume of rolled steel.

However, intensity of capital investment compared with other branches of industry is still relatively high. In 1990, it was 340 000 DM per installation, which compares with only 118 000 DM in engineering (Figure 6.178). Capital investment constitutes just 20% of the cost of steel produced in West Germany. Personnel costs account for ca. 25%. The sum of these costs is only slightly influenced by short-term market fluctuations. Large production units cannot be throttled back at will. However, as the steel market reacts extremely strongly to economic change (rising demand in boom periods, falling demand during recessions), suppliers have problems in matching supply to demand, especially in times of weak markets. The result is intense competition between suppliers for small market volumes at falling prices. As long as businesses can build up a financial reserve in good economic times, short-term falls in demand can be coped with. However, this becomes much more difficult if medium-term demand forecasts are over-optimistic.

For a long time, so-called mini-steelworks have become the cost and price leaders among producers of light-section steel products (e.g.,

rod and wire rod). For this product area, the favored production scheme is electrosteel processing of scrap and small rolling mills. This reduces capital costs, and gives flexibility in matching market fluctuations.

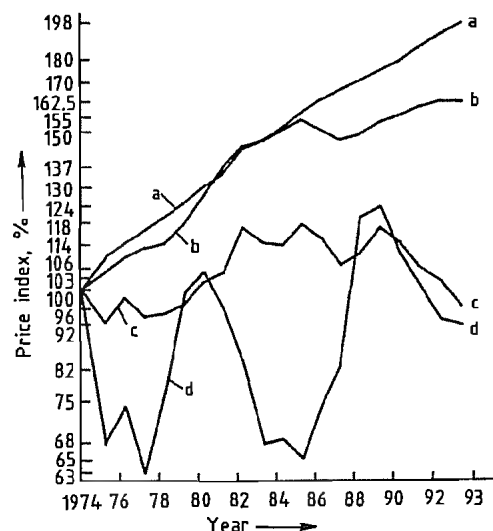


Figure 6.179: Price fluctuation in selected branches of the West German business economy 1974–1993. 1985 index recalculated to set 1974 figures = 100%. a) Producers' prices, motor vehicle construction; b) Commercial products (total); c) Rolled steel; d) Export prices, Western Europe (steel bars). Data supplied by the Statistisches Bundesamt (German Federal Bureau of Statistics).

New technology, organization systems, and the resulting increase in productivity and economic efficiency have also influenced price. Steel prices have risen considerably more slowly than those of the average industrial product. In recent years they have even fallen, and the severe fluctuations in international quotations during economic cycles have at least been no worse than those of 20 years ago (Figure 6.179).

There are very high barriers preventing steel making installations with overcapacity from getting out of the market. In western Europe since the mid 1970s these have become even higher, as state intervention distorts competition, making reduction in capacity very difficult. Large subsidies have ensured survival, especially of nationalized undertakings (Figure 6.180). Reduction in capacity is lag-

ging behind the true need, and finance for capital investment in modernization has continued to be available (Table 6.26).

Private undertakings can only combat such subsidized competition for a limited period, if there is no countervailing policy to avoid subsidized companies increasing their market share.

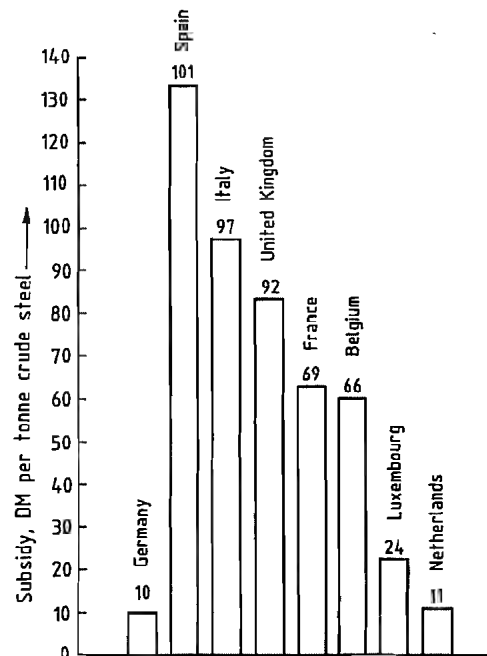


Figure 6.180: Distortion of competition by subsidies 1975–1993. Figures for Spain from 1984. Source: Wirtschaftsvereinigung Stahl (Industrial Association for Steel).

Table 6.26: Capital investment and subsidies in selected countries 1975–1991. Average figures, DM per tonne crude steel produced.

	West Germany	France	United Kingdom	Italy
Subsidies	10	69	92	97
Capital investment	47	63	70	67

The steel politics of the European Community since the middle 1970s exemplify the disastrous effects of state intervention in a market economy. The decisions of the European Commission and the Council of Ministers during the steel crisis of 1991–1993 show that there is a gulf between the broad political

aims of a European Union and the real economic, financial, and structural politics of the member countries.

In some steel-producing countries (e.g., the United Kingdom and Brazil) governments have become unwilling to pay high subsidies, on the grounds that they block the possibilities for investment in alternative projects. Privatization of nationalized steel undertakings has gone ahead.

6.8.4 Future Prospects

New perspectives are opening up in the steel industry through further technical developments in casting and rolling technology. A new generation of continuous production lines, from crude steel to products close to final dimensions, may considerably reduce the specific capital costs both of flat steel products and of heavy profiles, increasing the flexibility of undertakings to match economic fluctuations. At the same time, productivity can be significantly improved. Different configurations of the supply structure are likely to become available to the large suppliers of flat steel products, who are themselves advancing these technical developments, i.e., independent small and medium manufacturing units, or a combination of several plants with an efficient source of crude iron and steel from large units.

In recent years, small and medium-sized steelworks, mainly based on scrap, have been in favor, but there are limits to this development. Increasing amounts of scrap are available for steel production, but growing world steel demand is likely to require the smelting of iron ore.

Thus, from the economic point of view, many opportunities present themselves for steel as a competitive material for the future.

6.9 References

1. H.-J. Engell: *Stahl – Prinzipien seines Aufbaus und Aufgaben künftiger Entwicklungen*, Jahrbuch der Akademie der Wissenschaften in Göttingen, 1982.
2. Verein Deutscher Eisenhüttenleute (ed.): "Fundamentals", *Steel—A Handbook for Materials Re-*

- search and Engineering, vol. 1, Springer Verlag, Berlin 1992.
3. International Iron and Steel Institute (IISI): *World steel in Figures*, Brussels 1992.
4. K. A. Zimmermann: "Renaissance der Eisenbahn – eine Realität?" *IISI – Jahrestagung*, Colorado Springs 1978.
5. R. Grundmann, H. M. Mozek, K. H. Michel, H. Mülders: "Warmband und Kaltband aus nichtrostenden Stählen", *Stahl u. Eisen* 107 (1987) 1221–1227.
6. J. G. L. Blumhof: *Versuch einer Enzyklopädie der Eisenhüttenkunde*, vol. 1–4, G. F. Heyer, Gießen 1816–1821.
7. L. Beck: *Geschichte des Eisens*, vol. 1–5, Vieweg & Sohn, Braunschweig 1891–1903.
8. O. Johannsen: *Geschichte des Eisens*, 3rd ed., Verl. Stahlisen, Düsseldorf 1953.
9. R. F. Tylecote: *A History of Metallurgy*, 2nd ed., Inst. of Materials, London 1992.
10. A. Paulinyi: *Das Puddeln*, Oldenbourg, München 1987.
11. K. C. Barraclough: "Blister Steel", vol. 1; "Crucible Steel", vol. 2; *Steelmaking Before Bessemer*, Metals Society, London 1984.
12. K. C. Barraclough: *Steelmaking 1850–1900*, Inst. of Metals, London 1990.
13. O. Johannsen: "Die geschichtliche Entwicklung der Walzwerkstechnik", in J. Puppe, G. Stauder (eds.): *Walzwerkswesen*, vol. 1, Verl. Stahlisen, Düsseldorf, Springer Verlag, Berlin 1929, pp. 252–337.
14. *Stahlfibel*, Verlag Stahlisen, Düsseldorf 1989, p. 135.
15. O. Johannsen: *Geschichte des Eisens*, 3rd ed., Verlag Stahlisen, Düsseldorf 1953, p. 331.
16. Valerius-Hartmann: *Handbuch der Stahlisen Fabrikation*, J. G. Engelhardt, Freiberg 1985, Figure 1.
17. W. Rosenbleck, H. W. Kreutzer, R. Steffen, W. Schäfer, R. Willeke, *Stahl u. Eisen* 101 (1981) no. 7, 463–471.
18. D. Springorum, *Stahl u. Eisen* 112 (1992) no. 12, 45.
19. H. M. W. Delport, *Ironmaking Steelmaking* 19 (1992) no. 3, 183–189.
20. H. W. Kreutzer: "Schrotteinsatz in der Eisen- und Stahlindustrie", paper presented at "Rückstandsoptimierte Werkstoff- und Produktionstechnik am Beispiel des Automobils". RWTH, Aachen, Germany, Nov. 25, 1993.
21. R. Willeke, R. Ewers, H. W. Kreutzer, *Stahl u. Eisen* 114 (1994) no. 5, 83–88.
22. Verein Deutscher Eisenhüttenleute (VDEh) (eds.): *Jahrbuch Stahl* 1994, vol. 1, p. 216.
23. H. W. Kreutzer, *Stahl u. Eisen* 112 (1992) no. 5, 65–69.
24. W. Ullrich, H. Schicks, *Stahl u. Eisen* 111 (1991) no. 11, 85–92.
25. J. W. Brown, R. L. Reddy, P. J. Salomon: "Economic Problems Related to Creation of Steelplants Using Direct Reduction", Economic Commission for Europe (ECE), Seminar given at the Steel Committee, May 16–20, 1983, Noordwijkerhout, Report R30.
26. R. Steffen, H.-B. Lungen, *Stahl u. Eisen* 114 (1994) no. 6, 85–92.

26. Midrex Corp.: Midrex News Release, Charlotte, N.C. 1993.
27. F. A. Stephens, *Steel Times Int.*, March 1993, 11–12.
28. K. H. Zepfer, F. Daube, *Stahl u. Eisen* 103 (1983) no. 7, 319–324.
29. N. Bannenber, *Stahl u. Eisen* 111 (1991) no. 7, 71–76.
30. E. Höffken: "Entwicklungstrend des Oxygenstahlverfahrens", *Freiberg. Forschungsh. B* 229 (1982) 57–66.
31. W. Florin, R. Hammer, E. Höffken, W. Ullrich, H. Schicks, *Stahl u. Eisen* 105 (1985) no. 9, 531–536.
32. J. Geiseler, *Stahl u. Eisen* 111 (1991) no. 1, 531–536.
33. T. B. Massalski (ed.): *Binary Alloy Phase Diagrams*, 2nd ed., vol. 1, ASM Int., Materials Information Society, Ohio 1990.
34. F. Neumann, H. Schenck, *Arch. Eisenhüttenwes.* 30 (1959) 477–483.
35. M. G. Benz, J. F. Elliott, *Trans. Am. Inst. Min. Metall. Pet. Eng.* 221 (1961) 303–332.
36. G. K. Sigworth, J. F. Elliott, *Met. Sci.* 8 (1974) 298–310.
37. L. S. Darken, R. W. Gurry, *J. Chem. Soc. A* 68 (1946) 798–816.
38. C. R. Taylor, J. Chipman, *Trans. Am. Inst. Min. Metall. Pet. Eng.* 154 (1943) 228–247.
39. Z. Buzek, A. Hulta, *Freiberg. Forschungsh. B* 117 (1969) 59–73.
40. The Japan Society for the Promotion of Science, The 19th Committee on Steelmaking. *Steelmaking Data Sourcebook*, Gordon and Breach, New York 1988.
41. H. D. Kunze, E. Schürmann, *Gießereiforschung* 20 (1968) 35–48.
42. R. D. Pehlke, J. F. Elliott, *Trans. Am. Inst. Min. Metall. Pet. Eng.* 218 (1960) 1088–1101.
43. M. Ohtani, *Tetsu to Hagane* 54 (1968) 1381–1407.
44. E. Schürmann, F. Winterfeld, *Thyssenforschung* 4 (1972) 118–132.
45. F. Oeters: *Die physikalische Chemie der Eisen- und Stahlerzeugung*, Verlag Stahleisen, Düsseldorf 1964, 156–211.
46. R. D. Walker, D. Anderson, *Iron Steel* 45 (1972) 271–276.
47. S. Banya, S. Matoba in G. R. St. Pierre (ed.): *Physical Chemistry of Process Metallurgy*, part 1, Interscience Publisher, New York 1959, pp. 373–401.
48. P. Hammerschmid, D. Janke, H. W. Kreutzer, E. Reichenstein, R. Steffen, *Stahl u. Eisen* 105 (1985) 433–442.
49. M. Olette, C. Gatellier, R. Vasse: "Progress in Ladle Steel Refining", *Proc. Int. symp. Phys. Chem. Iron Steelmaking* 1982, art. VII-1.
50. P. V. Riboud, C. Gatellier, *Ironmaking Steelmaking* 12 (1985) 79–86.
51. E. T. Turkdogan, *Arch. Eisenhüttenwes.* 54 (1983) 1–10.
52. E. Steinmetz, *Rödx Rundschau* 1969, 605–617.
53. F. Oeters: *Metallurgie der Stahlerzeugung*, Springer Verlag, Berlin, Verlag Stahleisen, Düsseldorf 1989.
54. V. G. Levitch: *Physicochemical Hydrodynamics*, Prentice Hall, Englewood Cliffs 1962.
55. A.-K. Bolbrinker in Verein Deutscher Eisenhüttenleute (ed.): *Stahlfibel*, Verlag Stahleisen, Düsseldorf 1989.
56. R. Weber, L.-A. Mersolotto, H.-W. Gudenau, F.-H. Gradien, *Stahl u. Eisen* 110 (1990) no. 12, 98.
57. Verein Deutscher Eisenhüttenleute (ed.): *Jahrbuch Stahl*, Verlag Stahleisen, Düsseldorf 1990.
58. H. Voge, E. Eickworth, *Stahl u. Eisen* 79 (1959) no. 23, 1716.
59. T. Shima in: *Proc. Sixth IJSC*, Nagoya 1990.
60. E. Plöckinger, W. Wahlster, *Stahl u. Eisen* 80 (1960) 407–416.
61. L.-P. Pesce, H. Todzy, H. Schnitzer, *Int. Steel Mat. Mag.* (1989) 591.
62. R. Heinke et al., *Steel Techn. Int.* 1988.
63. ABB Publikation: "Direct Current Arc Furnace".
64. Verein Deutscher Eisenhüttenleute (ed.): *Eisenhütte*, 5th ed., Verlag Stahleisen, Düsseldorf 1961.
65. H.-U. Lindenberg, K.-H. Schubert, H. Zorcher, *Stahl u. Eisen* 107 (1987) 1192.
66. G. K. Sigworth, J. F. Elliott, *Metal Science* (1971), p. 298, 310.
67. I. Barin, O. Knacke: *Thermodynamical Properties of Inorganic Substances*, Springer-Verlag, Heidelberg 1973.
68. H. Legrand, M. Amblard in: *Int. Conf. Sec. Met.* 1987, p. 452.
69. F. Oeters, E. Görl, *Steel research* 61 (1990) no. 9.
70. G. Stolte, R. Teworte, *33 Met. Prod.* 11 (1991) 18/19.
71. D. Nolle, U. Eulenburg, A. Jahns, H. Miska in: *Int. Conf. Sec. Met.* 1987, p. 275.
72. B. Chalmers: *Principles of Solidification*, J. Wiley & Sons, New York 1964.
73. M. C. Flemings: *Solidification Processing*, McGraw-Hill, New York 1974.
74. W. Kurz, D. J. Fisher: *Fundamentals of Solidification*, Trans Tech SA, Aedermannsdorf, Switzerland 1984.
75. B. W. Berry (ed.), "Solidification of Metals", *Proc. Int. Conf.*, Brighton, 4–7 December 1967, The Iron and Steel Institute, London 1968.
76. "Solidification and Casting of Metals", *Proc. Int. Conf. Solidification*, Sheffield, 18–21 July 1977, The Metal Society, London 1979.
77. The University of Sheffield and The Institute of Metals (eds.): "Solidification Processing 1987, Preprints", *Int. Conf.*, Sheffield, United Kingdom, Sept. 21–24, 1987.
78. G. Grünbaum et al.: *A Guide to the Solidification of Steels*, Jernkontoret, Stockholm 1977.
79. H. Jacobi, K. Schwerdtfeger, *Metall. Trans.* 7A (1976) 811–820.
80. M. A. Taha, H. Jacobi, M. Imagumbai, K. Schwerdtfeger, *Metall. Trans.* 13A (1982) 2131–2141.
81. E. Schürmann, S. Baumgartl, L. Nedeljkovic, M. Tripkovic, *Steel Research* 58 (1987) no. 11, 498–502.
82. K. Miyamura, I. Taguchi, H. Soga, *Trans. Iron Steel Inst. Jpn.* 24 (1984) 883–890.
83. K. Schwerdtfeger: *Metallurgie des Stranggießens, Gießen und Erstarren von Stahl*, Verlag Stahleisen, Düsseldorf 1992, pp. 171–202.
84. K. Wünnenberg, *Stahl u. Eisen* 98 (1978) no. 6, 254–259.

85. W. Dahi, H. Hengstenberg, C. Düren, *Stahl u. Eisen* 86 (1966) no. 13, 782–795.
86. E. Steinmetz, H.-U. Lindenberg, *Arch. Eisenhüttenwes.* 47 (1976) no. 9, 521–524; no. 12, 713–718.
87. K. Schwerdtfeger, *Arch. Eisenhüttenwes.* 41 (1970) no. 9, 923–937; 43 (1972) no. 3, 201–205.
88. F. Oeters, H.-J. Selenz, E. Förster, *Stahl u. Eisen* 99 (1979) no. 8, 389–397.
89. E. Steinmetz, H.-U. Lindenberg, W. Mörsdorf, P. Hammerschmid, *Stahl u. Eisen* 97 (1977) no. 23, 1154–1159.
90. E. Steinmetz, H.-U. Lindenberg, *Arch. Eisenhüttenwes.* 47 (1976) no. 4, 199–204.
91. Ullmann, 4th Ed., 22, 14–16.
92. *The Making, Shaping and Treating of Steel*, 10th ed., United States Steel Corp., Pittsburgh, Ass. Iron Steel Eng. (1985) 691–740.
93. G. Lepie, H. Rellermeyer: "Untersuchungen über den Erstarrungsverlauf in Gußblöcken", *Arch. Eisenhüttenwes.* 37 (1966) no. 12, 925–934.
94. K.-K. Aschendorff, E. Köhler, H. Schroer, B. Abel: "Seigerungen in unberuhigten Stahlblöcken", *Stahl u. Eisen* 82 (1962) no. 20, 1356–1366.
95. H. F. Bishop, F. A. Brandt, W. S. Pellini: "Solidification Mechanism of Steel Ingots", *J. Met.* 4 (1952) 44–54.
96. A. Diener, A. Drastik, W. Haumann: "Untersuchung über den Wärmeübergang zwischen Block und Kokille beim Erstarren von Stahl", *Arch. Eisenhüttenwes.* 43 (1972) 525–533.
97. F. Oeters, K. Sardemann: "Untersuchung zum zeitlichen Verlauf der Erstarrung in der Randzone und zur Spaltbildung zwischen Block und Kokille", *Int. Iron Steel Congr.*, Düsseldorf 1974, vol. 3 VDEh, Düsseldorf 1974.
98. H.-J. Langhammer, H. G. Geck: "Vorgänge beim Gießen und Erstarren von unberuhigtem Stahl", in: *Gießen und Erstarren von Stahl*, Verlag Stahleisen, Düsseldorf 1967, pp. 33–75.
99. W. Recknagel, H. Oppenhoff: "Was der Blasstahlerwerker von seiner Arbeit wissen muß", *Stahleisen-Schriften*, 2nd ed., vol. 6, Verlag Stahleisen, Düsseldorf 1977, p. 120.
100. H. C. Vacher, E. H. Hamilton, *Trans. Am. Inst. Min. Metall. Eng. Iron Steel Div.* 95 (1931) 124–140.
101. A. Hultgren, G. Phragmén, *Trans. Am. Inst. Min. Metall. Eng. Iron Steel Div.* 135 (1939) 133–244.
102. H. Rellermeyer: "Vorgänge bei der Blockerstarung", in: *Die physikalische Chemie der Eisen- und Stahlerzeugung*, Verlag Stahleisen, Düsseldorf 1964, pp. 350–376.
103. H. Rellermeyer, R. Hammer: "Metallurgische Fragen beim Vergießen und Erstarren von unberuhigtem Stahl", *Stahl u. Eisen* 78 (1958) no. 22, 1505–1513.
104. K. Asano, T. Otiashi, *Tetsu to Hagane* 54 (1968) 74–75, 643–673.
105. P. Nilles: "Theoretical Study of the Solidification of Rimming Steel", *J. Iron Steel Inst. London* 202 (1964) 601–609.
106. P. Nilles, F. Becker, A. Thill: "Untersuchung über die Erstarrung von unberuhigt vergossenem Stahl", *Stahl u. Eisen* 85 (1965) 1025–1032.
107. H.-J. Langhammer, H. G. Geck: "Vorgänge beim Gießen und Erstarren von unberuhigtem Stahl", in: *Gießen und Erstarren von Stahl*, Verlag Stahleisen, Düsseldorf 1967, pp. 33–75.
108. E. Steinmetz, H.-U. Lindenberg, *Arch. Eisenhüttenwes.* 47 (1976) no. 9, 521–524; no. 12, 713–718.
109. K. Schwerdtfeger, *Arch. Eisenhüttenwes.* 41 (1970) no. 9, 923–937; 43 (1972) no. 3, 201–205.
110. F. Oeters, H.-J. Selenz, E. Förster, *Stahl u. Eisen* 99 (1979) no. 8, 389–397.
111. E. Steinmetz, H.-U. Lindenberg, W. Mörsdorf, P. Hammerschmid, *Stahl u. Eisen* 97 (1977) no. 23, 1154–1159.
112. E. Steinmetz, H.-U. Lindenberg, *Arch. Eisenhüttenwes.* 47 (1976) no. 4, 199–204.
113. Ullmann, 4th Ed., 22, 14–16.
114. *The Making, Shaping and Treating of Steel*, 10th ed., United States Steel Corp., Pittsburgh, Ass. Iron Steel Eng. (1985) 691–740.
115. G. Lepie, H. Rellermeyer: "Untersuchungen über den Erstarrungsverlauf in Gußblöcken", *Arch. Eisenhüttenwes.* 37 (1966) no. 12, 925–934.
116. K.-K. Aschendorff, E. Köhler, H. Schroer, B. Abel: "Seigerungen in unberuhigten Stahlblöcken", *Stahl u. Eisen* 82 (1962) no. 20, 1356–1366.
117. H. F. Bishop, F. A. Brandt, W. S. Pellini: "Solidification Mechanism of Steel Ingots", *J. Met.* 4 (1952) 44–54.
118. A. Diener, A. Drastik, W. Haumann: "Untersuchung über den Wärmeübergang zwischen Block und Kokille beim Erstarren von Stahl", *Arch. Eisenhüttenwes.* 43 (1972) 525–533.
119. F. Oeters, K. Sardemann: "Untersuchung zum zeitlichen Verlauf der Erstarrung in der Randzone und zur Spaltbildung zwischen Block und Kokille", *Int. Iron Steel Congr.*, Düsseldorf 1974, vol. 3 VDEh, Düsseldorf 1974.
120. H.-J. Langhammer, H. G. Geck: "Vorgänge beim Gießen und Erstarren von unberuhigtem Stahl", in: *Gießen und Erstarren von Stahl*, Verlag Stahleisen, Düsseldorf 1967, pp. 33–75.
121. W. Recknagel, H. Oppenhoff: "Was der Blasstahlerwerker von seiner Arbeit wissen muß", *Stahleisen-Schriften*, 2nd ed., vol. 6, Verlag Stahleisen, Düsseldorf 1977, p. 120.
122. H. C. Vacher, E. H. Hamilton, *Trans. Am. Inst. Min. Metall. Eng. Iron Steel Div.* 95 (1931) 124–140.
123. A. Hultgren, G. Phragmén, *Trans. Am. Inst. Min. Metall. Eng. Iron Steel Div.* 135 (1939) 133–244.
124. H. Rellermeyer: "Vorgänge bei der Blockerstarung", in: *Die physikalische Chemie der Eisen- und Stahlerzeugung*, Verlag Stahleisen, Düsseldorf 1964, pp. 350–376.
125. H. Rellermeyer, R. Hammer: "Metallurgische Fragen beim Vergießen und Erstarren von unberuhigtem Stahl", *Stahl u. Eisen* 78 (1958) no. 22, 1505–1513.
126. K. Asano, T. Otiashi, *Tetsu to Hagane* 54 (1968) 74–75, 643–673.
127. P. Nilles: "Theoretical Study of the Solidification of Rimming Steel", *J. Iron Steel Inst. London* 202 (1964) 601–609.
128. P. Nilles, F. Becker, A. Thill: "Untersuchung über die Erstarrung von unberuhigt vergossenem Stahl", *Stahl u. Eisen* 85 (1965) 1025–1032.
129. H.-J. Langhammer, H. G. Geck: "Vorgänge beim Gießen und Erstarren von unberuhigtem Stahl", in: *Gießen und Erstarren von Stahl*, Verlag Stahleisen, Düsseldorf 1967, pp. 33–75.
130. E. Steinmetz, H.-U. Lindenberg, *Arch. Eisenhüttenwes.* 47 (1976) no. 9, 521–524; no. 12, 713–718.
131. K. Schwerdtfeger, *Arch. Eisenhüttenwes.* 41 (1970) no. 9, 923–937; 43 (1972) no. 3, 201–205.
132. F. Oeters, H.-J. Selenz, E. Förster, *Stahl u. Eisen* 99 (1979) no. 8, 389–397.
133. E. Steinmetz, H.-U. Lindenberg, W. Mörsdorf, P. Hammerschmid, *Stahl u. Eisen* 97 (1977) no. 23, 1154–1159.
134. E. Steinmetz, H.-U. Lindenberg, *Arch. Eisenhüttenwes.* 47 (1976) no. 4, 199–204.
135. Ullmann, 4th Ed., 22, 14–16.
136. *The Making, Shaping and Treating of Steel*, 10th ed., United States Steel Corp., Pittsburgh, Ass. Iron Steel Eng. (1985) 691–740.
137. G. Lepie, H. Rellermeyer: "Untersuchungen über den Erstarrungsverlauf in Gußblöcken", *Arch. Eisenhüttenwes.* 37 (1966) no. 12, 925–934.
138. K.-K. Aschendorff, E. Köhler, H. Schroer, B. Abel: "Seigerungen in unberuhigten Stahlblöcken", *Stahl u. Eisen* 82 (1962) no. 20, 1356–1366.
139. H. F. Bishop, F. A. Brandt, W. S. Pellini: "Solidification Mechanism of Steel Ingots", *J. Met.* 4 (1952) 44–54.
140. A. Diener, A. Drastik, W. Haumann: "Untersuchung über den Wärmeübergang zwischen Block und Kokille beim Erstarren von Stahl", *Arch. Eisenhüttenwes.* 43 (1972) 525–533.
141. F. Oeters, K. Sardemann: "Untersuchung zum zeitlichen Verlauf der Erstarrung in der Randzone und zur Spaltbildung zwischen Block und Kokille", *Int. Iron Steel Congr.*, Düsseldorf 1974, vol. 3 VDEh, Düsseldorf 1974.
142. H.-J. Langhammer, H. G. Geck: "Vorgänge beim Gießen und Erstarren von unberuhigtem Stahl", in: *Gießen und Erstarren von Stahl*, Verlag Stahleisen, Düsseldorf 1967, pp. 33–75.
143. W. Recknagel, H. Oppenhoff: "Was der Blasstahlerwerker von seiner Arbeit wissen muß", *Stahleisen-Schriften*, 2nd ed., vol. 6, Verlag Stahleisen, Düsseldorf 1977, p. 120.
144. H. C. Vacher, E. H. Hamilton, *Trans. Am. Inst. Min. Metall. Eng. Iron Steel Div.* 95 (1931) 124–140.
145. A. Hultgren, G. Phragmén, *Trans. Am. Inst. Min. Metall. Eng. Iron Steel Div.* 135 (1939) 133–244.
146. H. Rellermeyer: "Vorgänge bei der Blockerstarung", in: *Die physikalische Chemie der Eisen- und Stahlerzeugung*, Verlag Stahleisen, Düsseldorf 1964, pp. 350–376.
147. H. Rellermeyer, R. Hammer: "Metallurgische Fragen beim Vergießen und Erstarren von unberuhigtem Stahl", *Stahl u. Eisen* 78 (1958) no. 22, 1505–1513.
148. K. Asano, T. Otiashi, *Tetsu to Hagane* 54 (1968) 74–75, 643–673.
149. P. Nilles: "Theoretical Study of the Solidification of Rimming Steel", *J. Iron Steel Inst. London* 202 (1964) 601–609.
150. P. Nilles, F. Becker, A. Thill: "Untersuchung über die Erstarrung von unberuhigt vergossenem Stahl", *Stahl u. Eisen* 85 (1965) 1025–1032.
151. H.-J. Langhammer, H. G. Geck: "Vorgänge beim Gießen und Erstarren von unberuhigtem Stahl", in: *Gießen und Erstarren von Stahl*, Verlag Stahleisen, Düsseldorf 1967, pp. 33–75.
152. E. Steinmetz, H.-U. Lindenberg, *Arch. Eisenhüttenwes.* 47 (1976) no. 9, 521–524; no. 12, 713–718.
153. K. Schwerdtfeger, *Arch. Eisenhüttenwes.* 41 (1970) no. 9, 923–937; 43 (1972) no. 3, 201–205.
154. F. Oeters, H.-J. Selenz, E. Förster, *Stahl u. Eisen* 99 (1979) no. 8, 389–397.
155. E. Steinmetz, H.-U. Lindenberg, W. Mörsdorf, P. Hammerschmid, *Stahl u. Eisen* 97 (1977) no. 23, 1154–1159.
156. E. Steinmetz, H.-U. Lindenberg, *Arch. Eisenhüttenwes.* 47 (1976) no. 4, 199–204.
157. Ullmann, 4th Ed., 22, 14–16.
158. *The Making, Shaping and Treating of Steel*, 10th ed., United States Steel Corp., Pittsburgh, Ass. Iron Steel Eng. (1985) 691–740.
159. G. Lepie, H. Rellermeyer: "Untersuchungen über den Erstarrungsverlauf in Gußblöcken", *Arch. Eisenhüttenwes.* 37 (1966) no. 12, 925–934.
160. K.-K. Aschendorff, E. Köhler, H. Schroer, B. Abel: "Seigerungen in unberuhigten Stahlblöcken", *Stahl u. Eisen* 82 (1962) no. 20, 1356–1366.
161. H. F. Bishop, F. A. Brandt, W. S. Pellini: "Solidification Mechanism of Steel Ingots", *J. Met.* 4 (1952) 44–54.
162. A. Diener, A. Drastik, W. Haumann: "Untersuchung über den Wärmeübergang zwischen Block und Kokille beim Erstarren von Stahl", *Arch. Eisenhüttenwes.* 43 (1972) 525–533.
163. F. Oeters, K. Sardemann: "Untersuchung zum zeitlichen Verlauf der Erstarrung in der Randzone und zur Spaltbildung zwischen Block und Kokille", *Int. Iron Steel Congr.*, Düsseldorf 1974, vol. 3 VDEh, Düsseldorf 1974.
164. H.-J. Langhammer, H. G. Geck: "Vorgänge beim Gießen und Erstarren von unberuhigtem Stahl", in: *Gießen und Erstarren von Stahl*, Verlag Stahleisen, Düsseldorf 1967, pp. 33–75.
165. W. Recknagel, H. Oppenhoff: "Was der Blasstahlerwerker von seiner Arbeit wissen muß", *Stahleisen-Schriften*, 2nd ed., vol. 6, Verlag Stahleisen, Düsseldorf 1977, p. 120.
166. H. C. Vacher, E. H. Hamilton, *Trans. Am. Inst. Min. Metall. Eng. Iron Steel Div.* 95 (1931) 124–140.
167. A. Hultgren, G. Phragmén, *Trans. Am. Inst. Min. Metall. Eng. Iron Steel Div.* 135 (1939) 133–244.
168. H. Rellermeyer: "Vorgänge bei der Blockerstarung", in: *Die physikalische Chemie der Eisen- und Stahlerzeugung*, Verlag Stahleisen, Düsseldorf 1964, pp. 350–376.
169. H. Rellermeyer, R. Hammer: "Metallurgische Fragen beim Vergießen und Erstarren von unberuhigtem Stahl", *Stahl u. Eisen* 78 (1958) no. 22, 1505–1513.
170. K. Asano, T. Otiashi, *Tetsu to Hagane* 54 (1968) 74–75, 643–673.
171. P. Nilles: "Theoretical Study of the Solidification of Rimming Steel", *J. Iron Steel Inst. London* 202 (1964) 601–609.
172. P. Nilles, F. Becker, A. Thill: "Untersuchung über die Erstarrung von unberuhigt vergossenem Stahl", *Stahl u. Eisen* 85 (1965) 1025–1032.
173. H.-J. Langhammer, H. G. Geck: "Vorgänge beim Gießen und Erstarren von unberuhigtem Stahl", in: *Gießen und Erstarren von Stahl*, Verlag Stahleisen, Düsseldorf 1967, pp. 33–75.
174. E. Steinmetz, H.-U. Lindenberg, *Arch. Eisenhüttenwes.* 47 (1976) no. 9, 521–524; no. 12, 713–718.
175. K. Schwerdtfeger, *Arch. Eisenhüttenwes.* 41 (1970) no. 9, 923–937; 43 (1972) no. 3, 201–205.
176. F. Oeters, H.-J. Selenz, E. Förster, *Stahl u. Eisen* 99 (1979) no. 8, 389–397.
177. E. Steinmetz, H.-U. Lindenberg, W. Mörsdorf, P. Hammerschmid, *Stahl u. Eisen* 97 (1977) no. 23, 1154–1159.
178. E. Steinmetz, H.-U. Lindenberg, *Arch. Eisenhüttenwes.* 47 (1976) no. 4, 199–204.
179. Ullmann, 4th Ed., 22, 14–16.
180. *The Making, Shaping and Treating of Steel*, 10th ed., United States Steel Corp., Pittsburgh, Ass. Iron Steel Eng. (1985) 691–740.
181. G. Lepie, H. Rellermeyer: "Untersuchungen über den Erstarrungsverlauf in Gußblöcken", *Arch. Eisenhüttenwes.* 37 (1966) no. 12, 925–934.
182. K.-K. Aschendorff, E. Köhler, H. Schroer, B. Abel: "Seigerungen in unberuhigten Stahlblöcken", *Stahl u. Eisen* 82 (1962) no. 20, 1356–1366.
183. H. F. Bishop, F. A. Brandt, W. S. Pellini: "Solidification Mechanism of Steel Ingots", *J. Met.* 4 (1952) 44–54.
184. A. Diener, A. Drastik, W. Haumann: "Untersuchung über den Wärmeübergang zwischen Block und Kokille beim Erstarren von Stahl", *Arch. Eisenhüttenwes.* 43 (1972) 525–533.
185. F. Oeters, K. Sardemann: "Untersuchung zum zeitlichen Verlauf der Erstarrung in der Randzone und zur Spaltbildung zwischen Block und Kokille", *Int. Iron Steel Congr.*, Düsseldorf 1974, vol. 3 VDEh, Düsseldorf 1974.
186. H.-J. Langhammer, H. G. Geck: "Vorgänge beim Gießen und Erstarren von unberuhigtem Stahl", in: *Gießen und Erstarren von Stahl*, Verlag Stahleisen, Düsseldorf 1967, pp. 33–75.
187. W. Recknagel, H. Oppenhoff: "Was der Blasstahlerwerker von seiner Arbeit wissen muß", *Stahleisen-Schriften*, 2nd ed., vol. 6, Verlag Stahleisen, Düsseldorf 1977, p. 120.
188. H. C. Vacher, E. H. Hamilton, *Trans. Am. Inst. Min. Metall. Eng. Iron Steel Div.* 95 (1931) 124–140.
189. A. Hultgren, G. Phragmén, *Trans. Am. Inst. Min. Metall. Eng. Iron Steel Div.* 135 (1939) 133–244.
190. H. Rellermeyer: "Vorgänge bei der Blockerstarung", in: *Die physikalische Chemie der Eisen- und Stahlerzeugung*, Verlag Stahleisen, Düsseldorf 1964, pp. 350–376.
191. H. Rellermeyer, R. Hammer: "Metallurgische Fragen beim Vergießen und Erstarren von unberuhigtem Stahl", *Stahl u. Eisen* 78 (1958) no. 22, 1505–1513.
192. K. Asano, T. Otiashi, *Tetsu to Hagane* 54 (1968) 74–75, 643–673.
193. P. Nilles: "Theoretical Study of the Solidification of Rimming Steel", *J. Iron Steel Inst. London* 202 (1964) 601–609.
194. P. Nilles, F. Becker, A. Thill: "Untersuchung über die Erstarrung von unberuhigt vergossenem Stahl", *Stahl u. Eisen* 85 (1965) 1025–1032.
195. H.-J. Langhammer, H. G. Geck: "Vorgänge beim Gießen und Erstarren von unberuhigtem Stahl", in: *Gießen und Erstarren von Stahl*, Verlag Stahleisen, Düsseldorf 1967, pp. 33–75.
196. E. Steinmetz, H.-U. Lindenberg, *Arch. Eisenhüttenwes.* 47 (1976) no. 9, 521–524; no. 12, 713–718.
197. K. Schwerdtfeger, *Arch. Eisenhüttenwes.* 41 (1970) no. 9, 923–937; 43 (1972) no. 3, 201–205.
198. F. Oeters, H.-J. Selenz, E. Förster, *Stahl u. Eisen* 99 (1979) no. 8, 389–397.
199. E. Steinmetz, H.-U. Lindenberg, W. Mörsdorf, P. Hammerschmid, *Stahl u. Eisen* 97 (1977) no. 23, 1154–1159.
200. E. Steinmetz, H.-U. Lindenberg, *Arch. Eisenhüttenwes.* 47 (1976) no. 4, 199–204.
201. Ullmann, 4th Ed., 22, 14–16.
202. *The Making, Shaping and Treating of Steel*, 10th ed., United States Steel Corp., Pittsburgh, Ass. Iron Steel Eng. (1985) 691–740.
203. G. Lepie, H. Rellermeyer: "Untersuchungen über den Erstarrungsverlauf in Gußblöcken", *Arch. Eisenhüttenwes.* 37 (1966) no. 12, 925–934.
204. K.-K. Aschendorff, E. Köhler, H. Schroer, B. Abel: "Seigerungen in unberuhigten Stahlblöcken", *Stahl u. Eisen* 82 (1962) no. 20, 1356–1366.
205. H. F. Bishop, F. A. Brandt, W. S. Pellini: "Solidification Mechanism of Steel Ingots", *J. Met.* 4 (1952) 44–54.
206. A. Diener, A. Drastik, W. Haumann: "Untersuchung über den Wärmeübergang zwischen Block und Kokille beim Erstarren von Stahl", *Arch. Eisenhüttenwes.* 43 (1972) 525–533.
207. F. Oeters, K. Sardemann: "Untersuchung zum zeitlichen Verlauf der Erstarrung in der Randzone und zur Spaltbildung zwischen Block und Kokille", *Int. Iron Steel Congr.*, Düsseldorf 1974, vol. 3 VDEh, Düsseldorf 1974.
208. H.-J. Langhammer, H. G. Geck: "Vorgänge beim Gießen und Erstarren von unberuhigtem Stahl", in: *Gießen und Erstarren von Stahl*, Verlag Stahleisen, Düsseldorf 1967, pp. 33–75.
209. W. Recknagel, H. Oppenhoff: "Was der Blasstahlerwerker von seiner Arbeit wissen muß", *Stahleisen-Schriften*, 2nd ed., vol. 6, Verlag Stahleisen, Düsseldorf 1977, p. 120.
210. H. C. Vacher, E. H. Hamilton, *Trans. Am. Inst. Min. Metall. Eng. Iron Steel Div.* 95 (1931) 124–140.
211. A. Hultgren, G. Phragmén, *Trans. Am. Inst. Min. Metall. Eng. Iron Steel Div.* 135 (1939) 133–244.
212. H. Rellermeyer: "Vorgänge bei der Blockerstarung", in: *Die physikalische Chemie der Eisen- und Stahlerzeugung*, Verlag Stahleisen, Düsseldorf 1964, pp. 350–376.
213. H. Rellermeyer, R. Hammer: "Metallurgische Fragen beim Vergießen und Erstarren von unberuhigtem Stahl", *Stahl u. Eisen* 78 (1958) no. 22, 1505–1513.
214. K. Asano, T. Otiashi, *Tetsu to Hagane* 54 (1968) 74–75, 643–673.
215. P. Nilles: "Theoretical Study of the Solidification of Rimming Steel", *J. Iron Steel Inst. London* 202 (1964) 601–609.
216. P. Nilles, F. Becker, A. Thill: "Untersuchung über die Erstarrung von unberuhigt vergossenem Stahl", *Stahl u. Eisen* 85 (1965) 1025–1032.
217. H.-J. Langhammer, H. G. Geck: "Vorgänge beim Gießen und Erstarren von unberuhigtem Stahl", in: *Gießen und Erstarren von Stahl*, Verlag Stahleisen, Düsseldorf 1967, pp. 33–75.
218. E. Steinmetz, H.-U. Lindenberg, *Arch. Eisenhüttenwes.* 47 (1976) no. 9, 521–524; no. 12, 713–718.
219. K. Schwerdtfeger, *Arch. Eisenhüttenwes.* 41 (1970) no. 9, 923–937; 43 (1972) no. 3, 201–205.
220. F. Oeters, H.-J. Selenz, E. Förster, *Stahl u. Eisen* 99 (1979) no. 8, 389–397

126. Contin. Cast. Steel, Proc. Int. Conf., Biarritz, 31 May–2 June 1976, The Metals Society, London 1977.
127. "Continuous Casting", Proc. Int. Iron Steel Congr. 4th, London, May 12–14, 1982.
128. Continuous Casting '85, London, 22–24 May 1985, The Institute of Metals London 1985.
129. CRM and VDEh (eds.): 4th international Conference Continuous Casting, ICC '88, Brussels, 17–19 May 1988, Stahleisen, Düsseldorf 1988.
130. AIM (ed.): 1st European Conference on Continuous Casting, Florence, 23–25 Sept. 1991, Milano 1991.
131. H. Schrewe: Stranggießen von Stahl, Einführung und Grundlagen, Verlag Stahleisen, Düsseldorf 1987.
132. K. Schwerdtfeger: Metallurgie des Stranggießens, Gießen und Erstarren von Stahl, Verlag Stahleisen, Düsseldorf 1992.
133. L. J. Heaslip, A. McLean, I. D. Sommerville: "Chemical and Physical Interactions During Transfer Operations", Continuous Casting, vol. 1, ISS-AIME, Warrendale 1983.
134. J. K. Brimacombe, I. V. Samarasekera, J. E. Lait: "Heat Flow, Solidification and Crack Formation", Continuous Casting, vol. 2, ISS-AIME, Warrendale 1984.
135. J. J. Moore: "The Application of Electromagnetic Stirring (EMS) in the Continuous Casting of Steel", Continuous Casting, vol. 3, ISS-AIME Warrendale 1984.
136. T. B. Harabuchi, R. D. Pehlke: "Design and Operations", Continuous Casting, vol. 4, ISS-TMS, Warrendale 1988.
137. R. A. Heard, A. McLean: "Horizontal Continuous Casting", Continuous Casting, vol. 5, ISS-TMS, Warrendale 1988.
138. H. Schrewe et al., Stahl u. Eisen 108 (1988) no. 9, 427–436.
139. "Progress of the Iron and Steel Technologies in Japan in the Past Decade, III: Steelmaking", Transactions ISIJ 25 (1985) 627–710.
140. E. Höffken et al., Stahl u. Eisen 105 (1985) no. 22, 1167–1175.
141. G. Holleis, R. Scheidl, W. Dutzler, Fachber. Hüttenprax. Metallverarbeit. 25 (1987) no. 10, 959–967.
142. D. Kothe, F.-P. Pleschitschnigg, F. Boshl, MPT Metallurg. Plant and Technol. 13 (1990) no. 1, 1226.
143. P. Nilles, A. Étienne, 1st European Conf. on Continuous Casting, vol. 1, Florence 1991, pp. 1.1–1.16.
144. D. Schauwinhold, Stahl u. Eisen 102 (1982) no. 21, 1077–1082.
145. P. Riboud in K. Schwerdtfeger (ed.): Metallurgie des Stranggießens, Gießen und Erstarren von Stahl, Verlag Stahleisen, Düsseldorf 1992, pp. 233–255.
146. K. Wünnenberg, Stahl u. Eisen 98 (1978) no. 6, 254–259.
147. R. Thielmann, R. Steffen, Stahl u. Eisen 100 (1980) no. 7, 401–407.
148. P. Voss-Spilker, W. Reichelt, Iron Steel Eng. 1983 June, 32–38.
149. P. Stadler, J. von Schnakenburg, Stahl u. Eisen 109 (1989) no. 9, 463–469.
150. T. Nozaki, S. Itoyama, Trans. Iron Steel Inst. Jpn. 27 (1987) 321–331.
151. The Korean Institute of Metals, The Institute of Metals, UK, Preprints 2 (eds.): "SRNC-90 Near Net Shape Casting", Internat. Conf., RIST, Pohang, Korea, Oct. 14–19, 1990.
152. J.-P. Birat, R. Steffen, MPT Metallurg. Plant Technol. 14 (1991) no. 3, 44–57.
153. E. Höffken, P. Kappes, H. Lax, Stahl u. Eisen 106 (1986) no. 23, 1253–1259.
154. F. K. Iverson, K. Busse, Stahl u. Eisen 111 (1991) no. 1, 37–45.
155. W. Rohde, H. Wladika, Stahl u. Eisen 111 (1991) no. 1, 47–61.
156. H.-J. Ehrenberg, L. Parschat, F.-P. Pleschitschnigg, C. Praßer, W. Rahmfeld, Stahl u. Eisen 109 (1989) no. 9/10, 453–462.
157. F.-P. Pleschitschnigg et al., MPT Metallurg. Plant Technol. 15 (1992) no. 2, 66–82.
158. E. Höffken, Stahl u. Eisen 113 (1993) no. 2, 49–54.
159. W. E. Duckworth, G. Hoyle: Electro-Slag Refining, Chapman and Hall, London 1969.
160. H. C. Child, G. E. Oldfield, R. Bakish, A. Lawley: "Vacuum Melting" in O. Winkler, R. Bakish (eds.): Vacuum Metallurgy, Chap. V, Elsevier, Amsterdam 1971, pp. 517–642.
161. W. H. Sutton: "Progress in the Vacuum (VIM, VAR) Melting of High Performance Alloys", Proc. Int. Conf. Vac. Metall. 7th, Nov. 26–30, 1982, Tokyo, The Iron and Steel Institute of Japan, Tokyo 1982, pp. 904–915.
162. L. W. Lherbier: "Melting and Refining", in C. T. Sims, N. S. Stoloff, W. C. Hagel (eds.): Superalloys II, Chap. 14, J. Wiley & Sons, New York 1987, pp. 387–410.
163. A. Choudhury: "State of the Art of Superalloy Production for Aerospace and Other Applications Using VIM/VAR or VIM/ESR", ISIJ Int. 32 (1992) no. 5, 563–574.
164. A. Choudhury, E. Hengsberger: "Electron Beam Melting and Refining of Metals and Alloys", ISIJ Int. 32 (1992) no. 5, 673–681.
165. J. Menzel, G. Stein, R. Dahlmann: "Manufacture of N-Alloyed Steels in a 20 t PESR-Furnace", in High Nitrogen Steels HNS90, Aachen, Oct. 10–12, 1990, Verlag Stahleisen, Düsseldorf 1990, pp. 365–375.
166. G. K. Bhat: "Plasma Arc Remelting" in J. Feinman (ed.): Plasma Technology in Metallurgical Processing, Chap. 13, Iron and Steel Society, Warrendale 1987, pp. 163–174.
167. K. Roesch, H. Zeuner, K. Zimmermann: Stahlguß, 2nd ed., Verlag Stahleisen, Düsseldorf 1982.
168. H. Wübbenhorst, G. Engels: 5000 Jahre Gießen von Metallen, Gießerei-Verlag, Düsseldorf 1989.
169. F. Roll: Handbuch der Gießerei-Technik, Springer Verlag Berlin 1959.
170. H. G. Gerhard, O. Nickel, K. Röhrig, D. Wolters: Legiertes Gußeisen, vol. 1, 1970, vol. 2, 1974, Gießerei-Verlag, Düsseldorf.
171. G. Oehlstör, J. Jäckel, Stahl u. Eisen 112 (1992) 53–60.
172. W. Krämer, J. Schnyder, H. Feldmann, G. Kirchmann, Stahl u. Eisen 110 (1990) no. 6, 59–64.

173. A. Hensel, P. Poluchin (eds.): Technologie der Metallformung, Deutscher Verlag für Grundstoffindustrie, Leipzig 1991, p. 476.
174. W. Schupe, G. Thaler: "Überblick über den Entwicklungsstand der Ofenführung durch Rechnerunterstützung", Stahl u. Eisen 107 (1987) no. 20, 37–42.
175. L. Prümmer in VDEh (ed.): Grundlagen des Beizens in Herstellung von kaltgewalztem Band, Verlag Stahleisen, Düsseldorf 1970.
176. W. Bumbullis, G. Köhler, B. Schweinsberg: "Kaltwalzen auf flacher Bahn", Beizeinrichtungen in Kontaktstudium Umformtechnik, part II, seminar preprint, Verlag Stahleisen, Düsseldorf 1981.
177. B. Frisch, W. R. Thiele, Stahl u. Eisen 101 (1981) no. 9, 577–585.
178. B. Frisch, W. R. Thiele, D. Prediger, Arch. Eisenhüttenwes. 54 (1983) no. 8, 311–380.
179. B. Frisch, W. R. Thiele, C. Messerschmidt, Arch. Eisenhüttenwes. 54 (1983) no. 9, 375–380.
180. H. J. Heimhard, G. Hitzemann, Stahl u. Eisen 105 (1985) 1222–1228.
181. E. Neuschütz: "Planheitsmessung und -regelung beim Warm- und Kaltwalzen von Bändern", Symposium DGM "Walzen von Flachprodukten", DGM-Informationsgesellschaft, Oberursel 1987.
182. B. Chatelain: "Einfluß der Glühparameter auf die Gas-Metall-Reaktion bei fest gewickelten Ringen", EGKS-Bericht EUR 12 115 FR.
183. B. Chatelain, V. Leroy: "Gas-Metall-Reaktionen beim Haubenglühen, Einfluß die Oberflächeneigenschaften des Blechs", EGKS-Abschlußbericht Nr. 7210/KB/204.
184. B. Chatelain et al.: "Beurteilung des Glühens von kohlenstoffarmen Stählen mit Wasserstoff-Gas-Metall-Reaktionen", Rev. Metall. CII, Feb. (1988) 173–180.
185. R. Pankert: "Durchlaufglühverfahren für Feibleche im Vergleich", Stahl u. Eisen 105 (1985) 889 ff.
186. H. W. Honervogt et al.: "Blankglühanlage für nichtrostende und säurebeständige Kaltbänder", Stahl u. Eisen 107 (1987) no. 9, 267.
187. J. Albrecht et al.: "Stand der Technik bei der Herstellung von Schmelztauchüberzügen", Stahl u. Eisen 107 (1987) no. 21, 973 ff.
188. J. H. Meyer zu Bexten, G. Gessner, K. F. Hüttebräucker, K. P. Mohr: "Elektrolytisch verzinktes Feiblech – Die Situation in Deutschland", Stahl u. Eisen 108 (1988) no. 21, 975 ff.
189. B. Meuthen, R. Pankert: "Stand der Breitbandverzinkung in Japan", Stahl u. Eisen 110 (1990) no. 6, 75 ff.
190. H. Lämmermann, K. Frommann: "Oberflächenveredelung von Band", Vakuumbeschichtung von Stahlband, Berichtsband, Verlag Stahleisen, Düsseldorf 1990.
191. W. Dürr, G. Höltsch, J. Kuhn, W. Schlump: "Aus der Dampfphase beschichtetes Blech und Band", Stahl u. Eisen 113 (1993) no. 5, 79–87.
192. P. von Laer, H. Hülsmann: Herstellung von bandbeschichtetem Feiblech – Eigenschaften, Verarbeitung, Anwendung, VDEh, DVV, Düsseldorf 1987.
193. P. Funke, H. R. Priebe, H. Buddenberg: "Die Untersuchung von Verfahrensparametern beim Walzplattieren", Stahl u. Eisen 110 (1990) no. 6, 67 ff.
194. H. Buddenberg, P. Funke, W. Gebel, R. Theile: "Herstellung und Eigenschaften NE-metallplattierter Stahlbänder für die Automobilindustrie", Stahl u. Eisen 111 (1991) no. 7, 93 ff.
195. Verein Deutscher Eisenhüttenleute (ed.): "Fundamentals", Steel – A Handbook for Materials Research and Engineering, vol. 1, Springer Verlag, Verlag Stahleisen, Düsseldorf 1992, p. 17.
196. G. Krauss in F. B. Pickering (ed.): Microstructure and Transformations in Steel, vol. 7, VCH Verlagsgesellschaft, Weinheim 1992, p. 1.
197. A. von den Steinen: Gasturbinen, Probleme und Anwendungen, Verlag Stahleisen, Düsseldorf, 1967, pp. 131–146.
198. K. E. Heusler, Z. Electrochem. 62 (1958) 582.
199. T. Ramachandran, K. Bohnenkamp, Werkst. Korros. 30 (1979) 43.
200. E. G. Daff, K. Bohnenkamp, H.-J. Engell, Corros. Sci. 19 (1979) 591.
201. M. Stratmann, Ber. Bundesges. Phys. Chem. 94 (1990) 626.
202. U. R. Evans, C. A. J. Taylor, Corros. Sci. 12 (1972) 227.
203. K. Bohnenkamp, Arch. Eisenhüttenwes. 47 (1976) 751.
204. G. Schikorr, Werkst. Korros. 14 (1963) 69.
205. G. Herbsleb, H.-J. Engell, Z. Elektrochem. 65 (1961) 881.
206. C. Wagner, Ber. Bunsenges. Phys. Chem. 77 (1973) 1090.
207. N. Sato, G. Okamoto, J. Electrochem. Soc. 110 (1963) 605.
208. Y. M. Kolotykin, Z. Elektrochem. 62 (1958) 664.
209. K. Osazawa, H.-J. Engell, Corros. Sci. 6 (1966) 389.
210. K. J. Vetter, H.-H. Strehlow, Ber. Bunsenges. Phys. Chem. 74 (1970) 1024.
211. J. E. Truman in J. Foct, A. Hendry (eds.): Proc. I. Int. Conf. High Nitrogen Steels, Institute of Metals, London 1989, p. 225.
212. R. Stefek, F. Franz, A. Holecek, Werkst. Korros. 30 (1979) 189.
213. N. Lukomski, K. Bohnenkamp, Werkst. Korros. 30 (1979) 482.
214. J. W. Oldfield, W. H. Sutton, Br. Corros. J. 13 (1978) 13.
215. K. Bungardt, E. Kunze, E. Horn, Arch. Eisenhüttenwes. 29 (1958) 193.
216. J. J. Demo, A. P. Bond, Corrosion (Houston) 31 (1975) 21.
217. B. Strauß, H. Schottky, J. Hinnüber, Z. Anorg. Chem. 188 (1930) 309.
218. I. Class, H. Gräfe, Werkst. Korros. 11 (1960) 5–29.
219. G. Herbsleb, Werkst. Korros. 19 (1968) 406.
220. D. L. Davidson, F. F. Lyle, Corrosion (Houston) 31 (1975) 135.
221. H.-J. Engell in J. C. Scully (ed.): The Theory of Stress Corrosion Cracking in Alloys, published by NATO Scientific Affairs Division, Brussels 1971, p. 86.
222. E. Brauns, H. Ternes, Werkst. Korros. 19 (1968) 1.
223. M. Ahlers, E. Riecke, Corros. sci. 18 (1978) 21.
224. M. Marek, R. F. Hochmann, Corrosion (Houston) 27 (1971) 361.
225. H. E. Hänninen, Int. Met. Rev. 24 (1979) 85.
226. M. O. Speidel, Corrosion (Houston) 33 (1977) 199.

227. A. Bäuml, H.-J. Engell, *Arch. Eisenhüttenwes.* **32** (1961) 379.
228. K. Bohnenkamp, *Arch. Eisenhüttenwes.* **39** (1968) 361.
229. E. Wendler-Kalsch, *Werkst. Korros.* **31** (1980) 534.
230. W. Radecker, B. N. Mishra, *Werkst. Korros.* **17** (1966) 193.
231. J. Küpper, H. Erhart, H. J. Grabke, *Corros. Sci.* **21** (1981) 227.
232. E. Riecke, *Werkst. Korros.* **29** (1978) 106.
233. E. Riecke, *Met. Corros. Proc. Int. Congr. Met. Corros. 8th 1981*, no. 1, 605.
234. J. P. Hirth, *Metall. Trans.* **11A** (1980) 861.
235. R. A. Oriani, *Ber. Bunsenges. Phys. Chem.* **76** (1972) 848.
236. L. S. Darken, R. W. Gurry, *J. Am. Chem. Soc.* **67** (1945) 1398.
237. J. Spencer, O. Kubaschewski, *CALPHAD Comput. Coupling Phase Diagrams Thermochem.* **2** (1978) 147.
238. B. E. F. Fender, F. D. Riley, *J. Phys. Chem. Solids* **30** (1969) 793.
239. A. Rahmel: in *Chemical Metallurgy of Iron and Steel*. ISI Publ., no. 146, London 1973, p. 395.
240. H.-J. Engell, *Acta Metall.* **6** (1958) 439.
241. K. Hauffe, H. Pfeiffer, *Z. Metallkd.* **44** (1953) 27.
242. E. T. Turkdogan, W. M. McKewan, L. Zwell, *J. Phys. Chem.* **69** (1965) 327.
243. F. S. Pettit, R. Yinger, J. B. Wagner, Jr., *Acta Metall.* **8** (1960) 617.
244. H. J. Grabke, *Ber. Bunsenges. Phys. Chem.* **69** (1965) 48.
245. H. J. Grabke, K. J. Best, A. Gala, *Werkst. Korros.* **21** (1970) 911.
246. C. Wagner, *Z. Phys. Chem. Abt. B* **21** (1933) 25; **32** (1936) 447.
247. K. Bohnenkamp, H.-J. Engell, *Arch. Eisenhüttenwes.* **33** (1962) 359.
248. H. Meurer, H. Schmalzried, *Arch. Eisenhüttenwes.* **42** (1971) 87.
249. W. Koenigsmann, F. Oeters, *Werkst. Korros.* **29** (1978) 10.
250. L. A. Morris, W. W. Smeltzer, *Acta Metall.* **15** (1967) 1591.
251. A. D. Dalvi, W. W. Smeltzer, *J. Electrochem. Soc.* **121** (1974) 386.
252. C. Wagner, *Corros. Sci.* **9** (1969) 91.
253. G. C. Wood, I. G. Wright, T. Hodgkiess, D. P. Whittle, *Werkst. Korros.* **21** (1970) 900.
254. K. A. Hay, F. G. Hicks, D. R. Holmes, *Werkst. Korros.* **21** (1970) 917.
255. W. C. Hagel, *Corrosion (Houston)* **21** (1965) 316.
256. P. Tomaszewicz, G. R. Wallwork, *Corrosion (Houston)* **40** (1984) 152.
257. M. J. McNallan, W. W. Liang, S. H. Kim, C. T. King in R. A. Rapp (ed.): "High Temperature Corrosion", NACE 1983, 316.
258. H. J. Grabke, E. M. Müller, *Werkst. Korros.* **41** (1990) 227.
259. D. Bramhoff, H. J. Grabke, E. Reese, H. P. Schmidt, *Werkst. Korros.* **41** (1990) 303.
260. E. Reese, H. J. Grabke, *Werkst. Korros.* **43** (1992) 547.
261. G. H. Geiger, R. L. Levin, J. B. Wagner, Jr., *J. Phys. Chem. Solids* **27** (1966) 947.
262. B. Swaroop, J. B. Wagner, Jr., *Trans. Metall. Soc. AIME* **239** (1967) 1215.
263. K. Hauffe, A. Rahmel, *Z. Phys. Chem. (Leipzig)* **199** (1951) 152.
264. R. A. Meussner, C. E. Birchenall, *Corrosion (Houston)* **13** (1957) 677.
265. E. T. Turkdogan, *Trans. Metall. Soc. AIME* **242** (1968) 1665.
266. W. L. Worrell, E. T. Turkdogan, *Trans. Metall. Soc. AIME* **242** (1968) 1673.
267. W. Auer, *Met. Corros. Proc. Int. Congr. Met. Corros. 8th 1981*, no. 2, 649.
268. A. Rahmel, *Oxid. Met.* **9** (1975) 401.
269. T. Flatley, N. Birks, *J. Iron Steel Inst.* **209** (1971) 523.
270. R. P. Salisburg, N. Birks, *J. Iron Steel Inst.* **209** (1971) 534.
271. B. A. Gordon, V. Nagarajan, *Oxid. Met.* **13** (1979) 197.
272. R. A. Perkins in R. A. Rapp (ed.): *High temperature corrosion*, NACE, Houston, Texas 1981.
273. F. H. Stott, F. M. F. Chong in D. B. Meadowcroft, M. J. Manning (eds.): *Proc. Conf. Corrosion Resistant Materials for Coal Conversion Systems*, Applied Science, London 1983, p. 491.
274. J. Stringer, "Sulfidation as Industrial Problem and Limiting Factor", Workshop on The High Temperature Corrosion of Alloys in Sulfur Containing Environments, Petten, Dec. 1985.
275. R. E. Lobnig, H. J. Grabke, *Corros. Sci.* **30** (1990) 1045.
276. F. Neumann, U. Wyss, *HTM Härterei Tech. Mitt.* **25** (1970) 253.
277. C. A. Stickels, C. M. Mack, M. Brachaczek, *Metall. Trans.* **11B** (1980) 471.
278. H. J. Grabke, U. Gravenhorst, W. Steinkusch, *Werkst. Korros.* **27** (1976) 291.
279. A. Schnaas, H. J. Grabke, *Oxid. Met.* **12** (1978) 387.
280. H. J. Grabke, *Arch. Eisenhüttenwes.* **46** (1973) 603.
281. H. J. Grabke, *HTM Härterei Tech. Mitt.* **45** (1990) 110.
282. H. J. Grabke, *Mater. Sci. Eng.* **42** (1980) 91.
283. J. Wünnig, *Härterei Tech. Mitt.* **23** (1968) 101; *HTM Härterei Tech. Mitt.* **39** (1984) 50.
284. K. Ledjeff, A. Rahmel, M. Schorr, *Werkst. Korros.* **30** (1979) 767, **31** (1980) 83.
285. G. M. Lai in: *High Temperature Corrosion of Engineering Alloys*, American Society for Metals, Materials Park, Ohio 1990, pp. 68–71.
286. J. C. Nava Paz, H. J. Grabke, *Oxid. Met.* **39** (1993) 437.
287. H. J. Grabke, R. Krajak, J. C. Nava Paz, *Corros. Sci.* **35** (1993) 1141.
288. H. J. Grabke, R. Krajak, E. M. Müller-Lorenz, *Werkst. Korros.* **44** (1993) 89.
289. H. J. Grabke, C. B. Bracho-Troconis, E. M. Müller-Lorenz, *Werkst. Korros.* **45** (1994) 215.
290. H. J. Grabke, *Ber. Bunsenges. Phys. Chem.* **72** (1968) 533, 541.
291. I. Aydin, H.-E. Bühler, A. Rahmel, *Werkst. Korros.* **31** (1980) 675.
292. W. Steinkusch, *Werkst. Korros.* **27** (1976) 91.
293. K. Lücke, *Arch. Eisenhüttenwes.* **25** (1954) 181.
294. A. Mayer, *Stahl u. Eisen* **83** (1963) 1169.

294. W. Oelsen, K.-H. Sauer, *Arch. Eisenhüttenwes.* **38** (1967) 141.
295. W.-D. Jentzsch, S. Böhmer, *Neue Hütte* **11** (1974) 647.
296. R. M. Hudson, *Trans. Metall. Soc. AIME* **230** (1964) 1138.
297. G. J. Kor, J. F. van Rump, *J. Iron Steel Inst.* **207** (1969) 1377.
298. G. A. Nelson: *Steels for Hydrogen Service at Elevated Temperatures and Pressures in Petroleum Refineries and Petrochemical Plants*, API Publication 941, Washington, May 1983.
299. W. Pepperhoff: "Physikalische Eigenschaften", in Verein Deutscher Eisenhüttenleute (ed.): *Werkstoffkunde Stahl*, vol. 1. "Grundlagen", Düsseldorf 1984, pp. 401–433.
300. W. Pepperhoff: "Physical Properties", in Verein Deutscher Eisenhüttenleute (ed.): *Steel*, vol. 1, "Fundamentals", Düsseldorf 1992, pp. 379–411.
301. Landolt-Börnstein, 6th ed., 4, 2a, 131–300.
302. K. K. Kelley, *J. Chem. Phys.* **11** (1943) 16–18.
303. D. C. Wallace, P. N. Siddles, G. C. Danielson, *J. Appl. Phys.* **31** (1960) 168–176.
304. M. Braun: "Über die spezifische Wärme von Eisen, Kobalt und Nickel im Bereich hoher Temperaturen", Dissertation, Universität Köln 1964.
305. W. Bendick, W. Pepperhoff, *Acta Metall.* **30** (1982) 679–684.
306. H. M. Ledbetter, R. P. Reed, *J. Phys. Chem. Ref. Data* **2** (1974) 531–618.
307. K. M. Koch, W. Jellinghaus: *Einführung in die Physik magnetischer Werkstoffe*, Deuticke, Wien 1957.
308. E. Kneller: *Ferromagnetismus*, Springer Verlag, Berlin 1962.
309. R. Kohlhaus, F. Richter, *Arch. Eisenhüttenwes.* **33** (1962) 291–299.
310. W. Oelsen, *Stahl u. Eisen* **69** (1949) 468–475.
311. R. M. Bozorth: *Ferromagnetism*, Van Nostrand, New York 1955.
312. Y. Endoh, Y. Ishikawa, *J. Phys. Soc. Jpn.* **30** (1971) 1614–1627.
313. L. Kaulman, M. Cohen, *J. Met.* **8** (1956) 1393–1400.

313. H.-H. Ettwig, W. Pepperhoff, *Phys. Status Solidi A* **23** (1974) 105–111.
314. W. Bendick, H.-H. Ettwig, F. Richter, W. Pepperhoff, *Z. Metallkd.* **68** (1977) 103–107.
315. F. Richter, W. Pepperhoff, *Arch. Eisenhüttenwes.* **47** (1976) 45–50.
316. H. P. Hougardy: *Umwandlung und Gefüge unlegierter Stähle. Eine Einführung*, Ind ed., Verlag Stahlisen, Düsseldorf 1990.
317. *Atlas zur Wärmebehandlung der Stähle*, vol. 1, Verlag Stahlisen, Düsseldorf 1961.
318. E. Schulz, *Jahrestagung IISI*, Montreal, Canada, 7 Oct. 1991, *Stahl u. Eisen* **112** (1992) no. 5, 43–51.
319. K. A. Zimmermann, *Stahl u. Eisen* **111** (1991) no. 12, 36–40.
320. J. A. Philipp et al., *Stahl u. Eisen* **112** (1992) no. 12, 75–86.
321. J. A. Philipp, *World Steel & Metalworking Annu.* **1988**, 101–104 (SPG-Coburg).
322. J. A. Philipp, *World Steel Rev.* **1** (1991) 62–73.
323. E. Schulz, *Stahl u. Eisen* **113** (1993) no. 2, 25–33.
324. E. Höfken, J. Wolf, P. Kühn, *Thyssen Tech. ber.* **24** (1992) 119–127.
325. Verein Deutscher Eisenhüttenleute (eds.): *Stahlfibel*, Verlag Stahlisen, Düsseldorf 1989, p. 134.
326. Bundesverband der Deutschen Schrott-Recycling-Wirtschaft e.V. (ed.): *Vom Schrott zum Stahl*, Düsseldorf 1984, pp. 37, 38, 39.
327. Bundesverband der Deutschen Schrott-Recycling-Wirtschaft e.V. (ed.): *Vom Schrott zum Stahl*, Düsseldorf 1984, pp. 36, 37.
328. W. Ullrich, H. Schicks: "Aspekte zum Recycling von metallisch beschichtetem Stahl", *Stahl u. Eisen* **111** (1991) no. 11, 85, 86.
329. J.-P. Kleingarn: "Rückgewinnung von Zink aus verzinktem Stahlschrott", *Feuerverzinken* **15** (1986) no. 3, Beratung Feuerverzinken, Düsseldorf.
330. In [324] pp. 121, 124.
331. International Iron and Steel Institute, Brussels.
332. Bundesverband der deutschen Stahl-Recycling-Wirtschaft e.V., Düsseldorf.
333. Bundesverband der Deutschen Schrott-Recycling-Wirtschaft e.V. (ed.): *Vom Schrott zum Stahl*, Düsseldorf 1984, pp. 11, 12.

7 Ferroalloys

RUDOLF FICHTE (§§ 7.1, 7.5, 7.9); FATHI HABASHI (§ 7.2, INTRODUCTORY PARAGRAPH); FRED W. HALL (§ 7.2, EXCEPT INTRODUCTORY PARAGRAPH); BERND NEUER, GERHARD RAU (§ 7.3); PETER M. CRAVEN, JOHN W. WAUDBY, DAVID BRUCE WELLBELOVED (§ 7.4); DEREK G. E. KERFOOT (§ 7.6); HERBERT DISKOWSKI (§ 7.7); EBERHARD LÜDERITZ (§ 7.8); JOACHIM ECKERT (§ 7.10); VOLKER GÜTHER, OSKAR RÖDL (§§ 7.11–7.12); GÜNTER BAUER (RETIRED), HANS HESS, ANDREAS OTTO, HEINZ ROLLER, SIEGFRIED SATTELBERGER (§ 7.12); HARTMUT MEYER-GRÜNOW (§ 7.13)

7.1	Introduction	404	7.6	Ferronickel	454
7.2	Carbothermic and Metallothermic Processes	405	7.6.1	Rotary Kiln–Electric Furnace Process	454
7.2.1	General Considerations	405	7.6.2	Ugine Ferronickel Process	457
7.2.1.1	Introduction	405	7.6.3	Falcondo Ferronickel Process	458
7.2.1.2	Basic Metallurgy	407	7.6.4	Refining of Ferronickel	459
7.2.1.3	Commercial Production	411	7.7	Ferrophosphorus	460
7.2.1.4	Other Uses of Aluminothermic Processes	415	7.8	Ferrotungsten	460
7.2.1.5	Possible Further Developments	415	7.8.1	Composition	460
7.3	Ferrosilicon	415	7.8.2	Uses	461
7.4	Ferromanganese	420	7.8.3	Production	462
7.4.1	High-Carbon Ferromanganese	423	7.8.3.1	Carbothermic Production	463
7.4.1.1	Production of Ferromanganese in Blast Furnaces	423	7.8.3.2	Carbothermic and Silicothermic Production	463
7.4.1.2	Production of Ferromanganese in Electric Arc Furnaces	425	7.8.3.3	Metallothermic Production	464
7.4.2	Production of Silicomanganese	432	7.9	Ferroboron	465
7.4.3	Production of Medium-Carbon Ferromanganese	434	7.9.1	Physical Properties	465
7.4.3.1	Production of Medium-Carbon Ferromanganese by Oxygen Refining of High-Carbon Ferromanganese	435	7.9.2	Chemical Properties	466
7.4.3.2	Silicothermic Production of Medium-Carbon Ferromanganese	436	7.9.3	Raw Materials	466
7.4.4	Production of Low-Carbon Ferromanganese	436	7.9.4	Production	466
7.4.5	Gas Cleaning	437	7.9.4.1	Carbothermic Production	467
7.4.6	Recent Developments and Future Trends	437	7.9.4.2	Aluminothermic Production	467
7.5	Ferrochromium	438	7.9.5	Quality Specifications for Commercial Grades	469
7.5.1	Physical and Chemical Properties	439	7.9.6	Storage and Shipment	470
7.5.2	Raw Materials	439	7.9.7	Chemical Analysis	470
7.5.3	Production	440	7.9.8	Pollution Control	471
7.5.3.1	High-Carbon Ferrochromium	442	7.9.9	Uses	471
7.5.3.2	Medium-Carbon Ferrochromium	444	7.9.10	Economic Aspects	471
7.5.3.3	Low-Carbon Ferrochromium	445	7.9.11	Toxicology and Industrial Hygiene	472
7.5.3.4	Nitrogen-Containing Low-Carbon Ferrochromium	448	7.10	Ferroniobium	472
7.5.3.5	Other Chromium Master Alloys	448	7.10.1	Production	472
7.5.4	Quality Specifications, Storage and Transportation, and Trade Names	449	7.10.2	Uses of Ferroniobium	472
7.5.5	Uses	451	7.11	Ferrotitanium	473
7.5.6	Economic Aspects	452	7.11.1	Composition and Uses	473
7.5.7	Environmental Protection; Toxicology and Occupational Health	453	7.11.2	Production	474
			7.11.3	Economic Aspects	476
			7.12	Ferrovandium	476
			7.12.1	Production from Vanadium Oxides	476
			7.12.2	Direct Production from Slags and Residues	477
			7.13	Ferromolybdenum	477
			7.13.1	Submerged Arc Furnace Carbothermic Reduction	478
			7.13.2	Metallothermic Reduction	480
			7.14	References	483

7.1 Introduction

Ferroalloys are master alloys containing elements that are more or less soluble in molten iron and that improve the properties of iron and steel. These alloys usually contain a significant amount of iron. Ferroalloys have been used for the last 100 years, principally in the production of cast iron and steel [1]. As additives, they give iron and steel improved properties, especially increased tensile strength, wear resistance, and corrosion resistance. These effects come about through one or more of the following:

- A change in the chemical composition of the steel
- The removal or the tying up of harmful impurities such as oxygen, nitrogen, sulfur, or hydrogen
- A change in the nature of the solidification, for example, upon inoculation [2]

Ferroalloys are also used as starting materials in the preparation of chemicals and pure metal; as reducing agents (e.g., the use of ferrosilicon to reduce rich slags); as alloying elements in nonferrous alloys; as starting materials for special products such as amorphous metals. Table 7.1 lists some commercial ferroalloys.

Over the years, the binary ferroalloys have been modified by the addition of further components. For example, magnesium is regularly added to ferrosilicon, which, when used in cast iron, produces a spheroidal graphite; and manganese or zirconium can be added to calcium-silicon.

Production. Generally, ferroalloys are prepared by direct reduction of oxidic ores or concentrates with carbon (carbothermic), silicon (silicothermic), or aluminum (aluminothermic, closely related to the Goldschmidt reaction; see section 7.2). However, roasted ores (e.g., for ferromolybdenum) and pure technical-grade oxides (for ferromolybdenum, and ferroboration) are also used as starting materials.

The large-volume ferroalloys — *ferrosilicon*, *ferromanganese*, *ferrochromium* — are

prepared continuously by carbothermic reduction in large, submerged-arc furnaces. The carbon is provided by coke, and the power supply ranges from 15 to 100 MVA. Ferromanganese is also produced in blast furnaces. Both ferromanganese and ferrochromium, because of their affinity for carbon, contain high concentrations of carbon (7–8%). In contrast, ferrosilicon contains little carbon; in fact, the carbon concentration decreases as the silicon concentration is increased, e.g., ferrosilicon containing 25% Si contains 1% C, while that containing 75% Si contains only 0.1% C.

Table 7.1: Ferroalloys.

Alloy	Composition, %
Calcium-silicon	28–35 Ca 60–65 Si 6 Fe
Calcium-silicon-aluminum	15–25 Ca 10–40 Al 35–50 Si
Calcium-silicon-barium	15–20 Ca 14–18 Ba 55–60 Si
Calcium-silicon-magnesium	25–30 Ca 10–15 Mg 50–55 Si
Calcium-manganese-silicon	16–20 Ca 14–18 Mn 58–59 Si
Calcium-silicon-zirconium	15–20 Ca 15–20 Zr 50–55 Si
Ferroboration	12–14 B
Ferrochromium	45–95 Cr 0.01–10 C
Ferrosilicochromium	40–65 Cr 45–20 Si
Ferromanganese	75–92 Mn 0.05–8.0 C
Ferrosilicomanganese	58–75 Mn 35–15 Si
Ferromolybdenum	62–70 Mo
Ferronickel	20–60 Ni
Ferroniobium	55–70 Nb
Ferroniobiumtantalum	55–70 Nb 2–8 Ta
Ferrophosphorus	ca. 25 P
Ferroselenium	ca. 50 Se
Ferrosilicon	8–95 Si
Ferrotitanium	20–75 Ti
Ferrotungsten	70–85 W
Ferrovandium	35–80 V
Ferrozirconium	ca. 85 Zr
Ferrosilicozirconium	35–42 Zr ca. 50 Si

Low-carbon ferromanganese (0.1–2% C) or ferrochromium (0.02–2% C) is produced in the following way: a silicon-containing alloy, ferrosilicomanganese or ferrosilicochromium, is made by carbothermic reduction of an appropriate ore and quartzite in a submerged-arc furnace. Then this silicon alloy is used for the silicothermic reduction of an appropriate ore in an electric-arc refining furnace. Oxygen is seldom used to reduce the carbon content.

Ferrophosphorus is a by-product of the carbothermic production of phosphorus. *Ferrotungsten* is produced carbothermically in small, high-power electric furnaces. *Ferroboration* is produced from carbon, iron, and boron oxide or boric acid in one- and three-phase electric furnaces. *Zirconium-containing ferrosilicon* is made carbothermically in electric furnaces from zircon (ZrSiO_4) or baddeleyite (ZrO_2); ferrosilicon, with either 75 or 90% Si, is added.

Silicothermic reduction, with the addition of some aluminum, is used to prepare *ferromolybdenum* in refractory-lined reaction vessels. The energy released in the reaction is adequate to melt both metal and slag, and the solidified block of ferromolybdenum can be recovered easily. *Ferronickel* is also mainly produced by silicothermic reduction. Aluminothermic reduction is the method of choice for the production of *ferrovanadium*. The starting materials are vanadium(V) oxide, aluminum, and iron turnings, chips, stampings, or nail bits. The reaction is carried out in refractory-lined reaction vessels. The reaction produces enough heat to melt both metal and slag. In fact, inert materials must be added to keep the peak temperature lower. Ferrotitanium and ferroboration are also produced aluminothermically.

The production and use of titanium as a large-volume construction material yields enough scrap for *ferrotitanium* containing ca. 70% Ti to be made by melting iron and titanium scrap together. *Ferrozirconium* containing 80–85% Zr is also made by melting metal scrap and iron together. *Ferroselenium* is pro-

duced by the exothermic reaction of iron and selenium powders.

The production of ferroalloys is of great economic importance, especially in countries that have the raw materials and the energy supply. Alloy steels constitute an ever growing fraction of total steel production because of their superior properties. As an example of the importance of ferroalloys, an estimated 1.8×10^9 DM (ca. $\$0.8 \times 10^9$) of ferroalloys were consumed in 1986 by the steel industry in Germany.

Environmental Aspects. During the production of ferroalloys, the emission of undesirable substances into the environment must be kept under control. There are guidelines for this, e.g., see [3].

7.2 Carbothermic and Metallothermic Processes

Carbothermic processes are mainly used for the large-scale production of ferrosilicon, ferromanganese, ferrochromium, ferronickel, and ferrotungsten. Ferrophosphorus is a by-product of elemental phosphorus production by the carbothermic reduction of phosphate rock. Carbothermic processes for the production of ferroboration, ferrotitanium, ferrovanadium, and ferromolybdenum have been largely replaced by metallothermic processes, mainly aluminothermic and silicothermic.

7.2.1 General Considerations

7.2.1.1 Introduction¹

The usual method of reduction by carbon is inapplicable to the reduction of refractory oxides and ores. The products commonly covered under this title are usually required to be low in carbon and they are avid carbide formers. Also, no conventional refractories would stand up to the long reduction times at the high temperatures required. For such products, ad-

¹ For the production of chromium by the aluminothermic process, see Chapter 46.

vantage is taken of the high temperatures achieved and the rapidity of metallothermic reactions using reactive metals, notably Al.

Early examples of such reactions are BERZELIUS' reduction of K_2TaF_7 by Na and WÖHLER's reduction of $AlCl_3$ by Na, in 1825 and 1828, respectively. However, the father of aluminothermic processes was undoubtedly GOLDSCHMIDT who, in 1898, described the production of low-carbon, high melting-point metals, without extraneous heat, by feeding an exothermic mix into an already ignited first portion [4].

The term "aluminothermic processes" can cover a wide field. For the present purposes it is taken, as is generally understood, to be the manufacture, by Al reduction of refractory oxides or ores, of metals and alloys mainly used in the steel and superalloy industries. Because some important alloys are produced aluminosilicothermally, they are included in the survey.

The main alloys under discussion are FeB, FeMo, FeNb, FeTi, FeV, and FeW. There are many minor variations, such as CrC, where superior purity or the absence of Fe is required for alloys used in superalloy production, and FeNb from Nb_2O_5 instead of ore, where extra purity is required, again for superalloys.

Aluminothermic Mn, formerly of importance, has been superseded by electrolytic Mn, and aluminothermic production of FeTi has largely given way to induction furnace melting of Fe and Ti scraps. The latter method also now substitutes for the former, dangerous, highly exothermic production of 55–60% TiAl and 55–60% ZrAl. When possible, combined electroaluminothermic methods can be used.

Because most basic reactions require extra heat this is provided by Al and a vigorous oxidant. Aluminum is an expensive fuel. At an Al powder price of \$1400/t and a small-scale electricity cost of 4.9 C/kWh the heating effect of Al combustion costs about three times that of electricity.

Although a minor proportion of production, some FeB, FeNb, FeTi, and FeV is produced in the arc furnace. In view of the small ton-

nages involved, such productions usually occur only where an arc furnace exists for other purposes.

Apart from the necessity of metallothermic reduction advantages of the process as compared to conventional reduction processes are:

- Very rapid reaction with less heat loss by radiation and convection
- Much less gas volume
- Easy accommodation of diverse productions
- Small plant investment (important, considering the small production).

A disadvantage of metallothermic production is that no refining of the metal is possible. It is important to leave the slag in situ to allow metal drops to settle into the regulus, so that one is faced with a large depth of slag quickly crusting over. Alternatively, if the slag is tapped, requiring subsequent ore dressing processes to recover included metal, the metal regulus quickly becomes sluggish. Therefore, the composition of the mix must be regulated very carefully to produce the optimum combination of oxygen and reactant metal levels in the product, and all ingredients must be low in harmful impurities. Obvious ones are C, S, and P. Other impurities in the various ores used for different products are As, Sn, Pb, Sb, and Cu. Nitrogen is not usually a problem because the metal regulus formed is protected by the slag layer. Chromium metal, used in superalloys and electric heating elements, is an extreme case, where, apart from low impurities generally, certain impurities, such as Ga, Pb, and B, must be kept down to a few parts per million.

Table 7.2: Production of metal and alloys by aluminothermic processes.

	t/a	Expressed as
FeB	1 350	18% B
FeMo ^a	40 500	65% Mo
FeNb	16 300	65% Nb
FeV	25 000	80% V
FeW	4 000	80% W

^a The FeMo represents about one third of the total Mo used in the steel industry; the remaining two thirds are used as MoO_3 .

The worldwide – excluding the former USSR and China – production of ferroalloys

by aluminothermic processes is shown in Table 7.2.

7.2.1.2 Basic Metallurgy

A metallothermic reduction of a metal compound is possible when the reductant metal has a greater affinity for the nonmetal element of the compound than the desired metal. In various branches of metallurgy the nonmetal may be a halogen, sulfur, or oxygen. Aluminothermic processes, as previously defined, depend upon the high affinity of Al for oxygen as compared to that of many other metals.

Thermochemistry

Aluminum has a high affinity for oxygen, and the ease of reduction of a metal oxide depends on the difference in oxygen affinity of Al and the metal. The affinity for oxygen is indicated by its heat of formation, ΔH , expressed for comparison purposes as ΔH per mol/oxygen (kJ/mol O). Table 7.3 gives a selection of ΔH values at the standard temperature of 298 K.

A quantitative measure for the stability of an oxide is the Gibbs free energy of formation, ΔG , which is related to the heat of formation by the formula:

$$\Delta G_T^0 = \Delta H - T\Delta S$$

Table 7.3: Heats of formation of oxides [5].

Oxide	$-\Delta H_{298}$, kJ/mol oxide	$-\Delta H_{298}$, kJ/mol O
CaO	634.7	634.7
MgO	601.7	601.7
Al_2O_3	1678.5	559.4
ZrO ₂	1101.5	550.6
TiO ₂	945.4	472.7
SiO ₂	911.0	455.5
B ₂ O ₃	1272.8	424.1
Na ₂ O	415.3	415.3
Ta ₂ O ₅	2047.3	409.5
Nb ₂ O ₅	1900.8	380.2
Cr ₂ O ₃	1130.4	376.8
V ₂ O ₅	1551.6	310.2
WO ₃	843.2	280.9
Fe ₃ O ₄	1117.5	279.3
Fe ₂ O ₃	821.9	273.8
FeO	264.6	264.6
MoO ₃	745.7	248.7

where S is the entropy and is always zero or positive because it corresponds with the increasing atomic disorder of the system with temperature. Figure 7.1 shows the free energy of formation of the oxides of interest at high temperatures. All oxides become less stable as temperature increases. The more negative the free energy of formation at a given temperature the greater the tendency for that metal to reduce an oxide of less negative free energy.

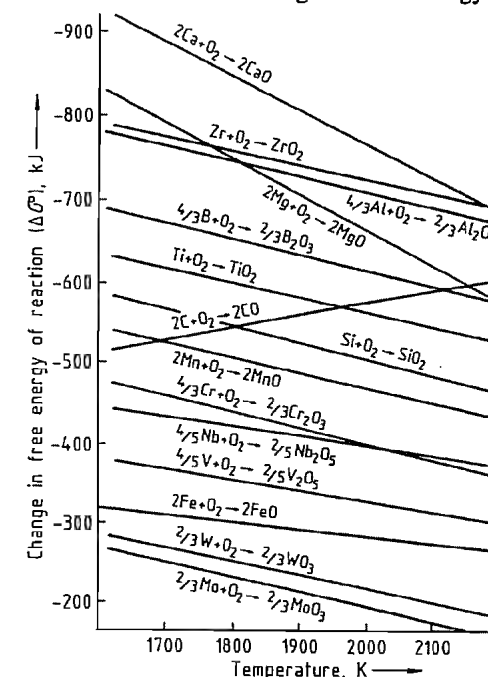


Figure 7.1: Change in free energy of oxide formation reactions [6].

The free energies of reaction of oxides with Al and Si are given in Figures 7.2 and 7.3.

Although the free energy of reaction is a quantitative measure, not all data necessary for such complex reactions as commercial metallothermic reactions are readily available and it is usual for the practicing metallurgist to rely on heats of formation for calculation of heats of reaction.

Fundamental Reactions

Although Ca and Mg may be the most suitable reactants, they are not used in the reduc-

tions under review. Their basic costs are high compared to Al and Si and 16 parts by weight O require 40 parts Ca, 24 parts Mg, 18 parts Al, or 14 parts Si. Furthermore, the boiling points of Ca and Mg are 1484 °C and 1090 °C, respectively. The heats of reaction of the oxides of interest with Al and Si are given in Table 7.4.

A guide for a successful aluminothermic reaction, permitting adequate separation of metal and slag, is a $-\Delta H_{298}$ higher than 300 kJ/mol [7]. This is confirmed in practice: additional heat is required for Cr production, whereas the reaction producing 80% FeV is so vigorous that it requires cooling. This guide does not apply to silicothermic reactions.

Auxiliary Reactions

Many reactions require additional heat to produce fully liquid metal and slag. Except for producing pure Cr, the first step is to make an addition of iron oxide plus reactant, giving a higher average heat of reaction. This also has the advantage of producing significantly lower melting points (Table 7.5).

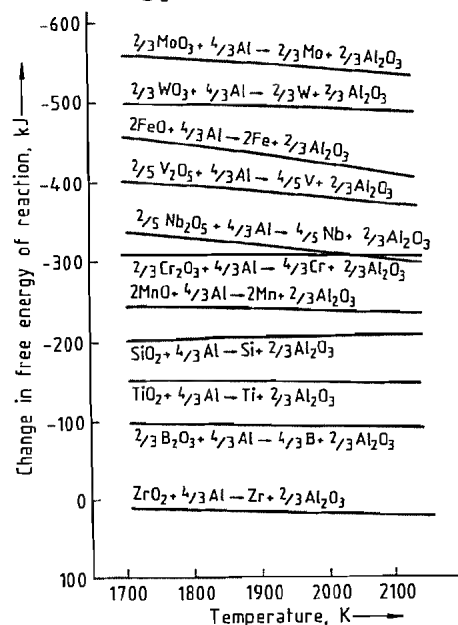


Figure 7.2: Change in free energy of reaction in the reduction of oxides by aluminum.

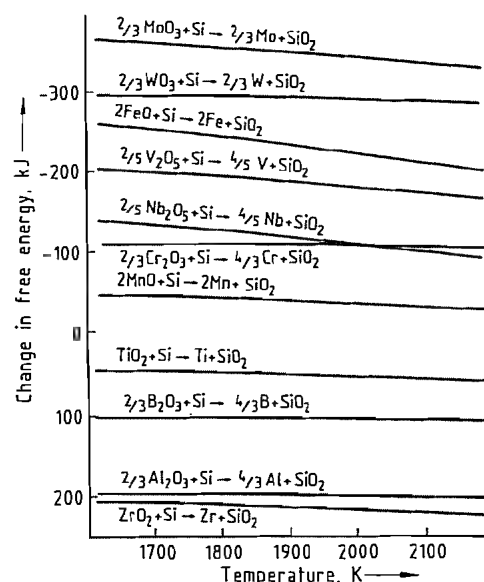


Figure 7.3: Change in free energy of reaction in the reduction of oxides by silicon.

Table 7.4: Heats of reaction per mole reductant.

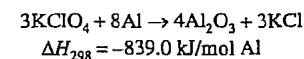
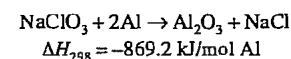
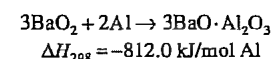
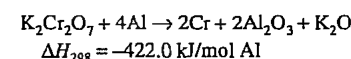
	$-\Delta H_{298}$, kJ
$\frac{1}{2}\text{TiO}_2 + \text{Al} \rightarrow \frac{3}{4}\text{Ti} + \frac{1}{2}\text{Al}_2\text{O}_3$	130.2
$\frac{1}{2}\text{SiO}_2 + \text{Al} \rightarrow \frac{3}{4}\text{Si} + \frac{1}{2}\text{Al}_2\text{O}_3$	156.0
$\frac{1}{2}\text{B}_2\text{O}_3 + \text{Al} \rightarrow \text{B} + \frac{1}{2}\text{Al}_2\text{O}_3$	202.6
$\frac{3}{10}\text{Nb}_2\text{O}_5 + \text{Al} \rightarrow \text{B} + \frac{1}{2}\text{Al}_2\text{O}_3$	268.8
$\frac{1}{2}\text{Cr}_2\text{O}_3 + \text{Al} \rightarrow \text{Cr} + \frac{1}{2}\text{Al}_2\text{O}_3$	273.8
$\frac{3}{10}\text{V}_2\text{O}_5 + \text{Al} \rightarrow \frac{3}{5}\text{V} + \frac{1}{2}\text{Al}_2\text{O}_3$	373.9
$\frac{1}{2}\text{WO}_3 + \text{Al} \rightarrow \frac{1}{2}\text{W} + \frac{1}{2}\text{Al}_2\text{O}_3$	417.4
$\frac{3}{8}\text{Fe}_3\text{O}_4 + \text{Al} \rightarrow \frac{9}{8}\text{Fe} + \frac{1}{2}\text{Al}_2\text{O}_3$	420.2
$\frac{1}{2}\text{Fe}_2\text{O}_3 + \text{Al} \rightarrow \text{Fe} + \frac{1}{2}\text{Al}_2\text{O}_3$	428.3
$\frac{3}{2}\text{FeO} + \text{Al} \rightarrow \frac{3}{2}\text{Fe} + \frac{1}{2}\text{Al}_2\text{O}_3$	442.1
$\frac{1}{2}\text{MoO}_3 + \text{Al} \rightarrow \frac{1}{2}\text{Mo} + \frac{1}{2}\text{Al}_2\text{O}_3$	466.4
$\frac{2}{3}\text{WO}_3 + \text{Si} \rightarrow \frac{2}{3}\text{W} + \text{SiO}_2$	348.8
$\frac{1}{2}\text{Fe}_3\text{O}_4 + \text{Si} \rightarrow \frac{3}{2}\text{Fe} + \text{SiO}_2$	352.1
$\frac{2}{3}\text{Fe}_2\text{O}_3 + \text{Si} \rightarrow \frac{4}{3}\text{Fe} + \text{SiO}_2$	363.0
$2\text{FeO} + \text{Si} \rightarrow 2\text{Fe} + \text{SiO}_2$	381.8
$\frac{2}{3}\text{MoO}_3 + \text{Si} \rightarrow \frac{2}{3}\text{Mo} + \text{SiO}_2$	414.1

Table 7.5: Melting points of some metals (in °C) and of alloys of these metals with iron.

V	1902	80% FeV	1770
B	2180	16% FeB	1550
Nb	2468	65% FeNb	1560
Mo	2620	65% FeMo	1900
W	3410	80% FeW	2500

In silicothermic reactions, a proportion of Al is usually used to increase the exothermicity particularly, because the products, e.g., FeW and FeMo, have such high melting points.

Because the alloy specifications have become traditional, although not necessarily ideal, there is a limit to the amount of iron oxide and Al to be added, and, indeed, it may be more economical to increase the heat content of the mixture further, by using highly oxidic compounds plus Al. The reactions and the heats of reaction (in kJ/mol Al) for the additives most commonly used are:



In some cases additional heat was applied formerly extraneously by preheating the charge. This has been given up because of practical difficulties of heating a mixture of low heat conductivity and the danger of premature ignition, with loss of the charge and damage to the preheating equipment.

The cheap nitrates are not used now because products low in nitrogen are required and the metals in question are avid nitride formers. BaO_2 is useful because it not only acts as an oxidant, but is a strong base and assists the progress of the reaction by combining with the Al_2O_3 produced. However, its high molecular mass and its one available oxygen atom make it a very expensive oxidant, and its use is confined to highly exothermic mixes, e.g., for TiAl and ZrAl, where it helps to smooth the reaction. The common oxidant is NaClO_3 , but KClO_4 is to be preferred because it is more stable and NaClO_3 is hygroscopic. In Cr mixes, $\text{K}_2\text{Cr}_2\text{O}_7$ is used and is preferred to CrO_3 on health grounds as well as expense.

Fluxes

Both Al_2O_3 and SiO_2 have high melting points, 2050 °C and 1722 °C, respectively. The aim in metallothermic reactions is to produce a fluid slag, so as to permit good separation of slag and metal. In the case of aluminosilico reactions, residual iron oxide and Al_2O_3 are already good fluxes, and lime also is used because the strongly basic CaO , apart from fluxing, lowers the activity of Al_2O_3 and SiO_2 .

In aluminothermic reactions residual oxides may play a part, the compound $\text{Al}_2\text{O}_3 \cdot \text{TiO}_2$ having a melting point of 1590 °C; Na_2O and K_2O , not completely vaporized, also assist. The usual flux is CaO which has a pronounced effect on the melting point of Al_2O_3 . It is not used in Cr manufacture as it spoils the slag for use in refractories and calcium chromite is a stable compound.

Figure 7.4 shows the effect on melting point of additions of several oxides to Al_2O_3 .

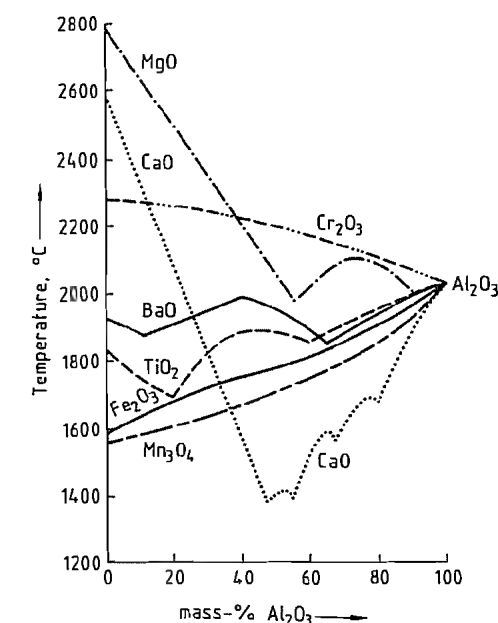


Figure 7.4: Melting point curves of binary alumina slags.

Table 7.6: Heats of formation of compound oxides.

Compound	$-\Delta H_{298}$, kJ/mol
$\text{Al}_2\text{O}_3 \cdot \text{SiO}_2$	192.6
$2\text{Al}_2\text{O}_3 \cdot \text{B}_2\text{O}_3$	69.5
$\text{BaO} \cdot \text{Al}_2\text{O}_3$	100.5
$\text{CaO} \cdot \text{Al}_2\text{O}_3$	15.1
$\text{CaO} \cdot \text{SiO}_2$	89.2

Table 7.7: Heats of formation of intermetallic compounds.

Compound	ΔH_{298} , kJ/mol
FeTi	40.6
FeB	29.3
FeAl ₃	112.2
FeSi	77.0
TiAl	80.8
CaSi	150.7
AlB	67.0

The energy required to fuse the flux is partially compensated by the heats of formation of the compound oxide (Table 7.6).

Formation of Intermetallic Compounds

The heat of reaction of the mixture can be increased by the formation of intermetallic compounds. Table 7.7 gives some examples. However, this is restricted in that most of the higher heats of formation belong to unwanted compounds because the usual aim is to keep residual elements, such as Al and Si, to a minimum. Of the alloys considered it is only in the case of FeTi and to a lesser extent in that of FeB that aluminides have some significance.

All reactions are equilibria. Commercial alloys must be low in oxygen and most alloys can be produced at 1% Al or Si without appreciable oxygen content. This is not the case with FeTi, where the equilibrium cannot be driven further than Al levels of 4–6%.

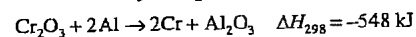
Thermochemistry in Practice

A commercial metallothermic reaction must provide sufficient heat to drive the reaction as far to the right side of the equation as possible, plus that heat required to bring the products to a temperature sufficiently high to permit separation of metal and slag and to provide for heat losses. The amount of total heat

must be the minimum required, because heat is expensive and because excess heat supplied to an exothermic reaction moves the equilibrium in the undesired direction.

Heats of formation have not always been determined at the high operating temperatures. Working on heats of formation at 298 K requires knowing the specific heats, latent heats, and, in charges employing sodium salts and chlorates, the heats of vaporization. Slags can be complex so that little idea can be had of their heats of formation. The amount of heat losses cannot be forecast and varies with the size of charge. Losses can be established and compensated for only by trial and error.

Therefore, available information is used as much as possible, accompanied by intelligent extrapolations of such information. Final adjustments to the charge are a matter of trial and error. A very simple example is:



Heat required for products at 2000 °C:

Al_2O_3	$H_{2273} - H_{298}$	356 kJ
2Cr	$H_{2273} - H_{298}$	184 kJ
amounts to:		540 kJ

According to this, there is a heat balance, so there should be a satisfactory result. However, it is found in practice that 125 kJ extra heat are required, provided by Al plus $\text{K}_2\text{Cr}_2\text{O}_7$ and/or KClO_4 . This 125 kJ (for a certain size of charge) is a measure of the heat losses. More would be required for small charges and less for bigger charges. It is interesting that this conforms with the guide.

Chemical composition of ores is some guide to improving the heat balance. Generally the higher the state of the oxide in the ore, the higher the heat of reaction with Al or Si. A classical example was that of Mn ore where the reaction $3\text{MnO} + 2\text{Al} \rightarrow 3\text{Mn} + \text{Al}_2\text{O}_3$ did not supply sufficient heat. A preoxidation to Mn_3O_4 produced a satisfactory result. Preoxidation also is found beneficial to some ilmenites.

There are many other factors affecting the fine control of an exothermic reaction, and it is not always economic to indulge in laboratory control of all of them. They mainly affect the

speed of the reaction, which should be an optimum to minimize heat losses but not to create excess heat with its adverse effect on the equilibrium.

Granulometry. If the charge is to be reacted in bulk then the ideal would be a charge of concrete-type granulometry, giving maximum contact and minimum air inclusion. However, to provide effective heat control, charges usually are fed. There should be an optimum particle size of the ingredients, therefore, coarse enough to minimize dust losses but fine enough to give an adequate speed of reaction. Aluminum powder can be controlled, because suppliers will supply within reasonable size ranges. In some cases, such as the highly exothermic FeV reaction, Al pellets and turnings can be used and they are used also to some extent in the very competitive production of the cheap alloy FeTi. These are crude raw materials and different parcels require slight adjustments to the mix. Ores are a different matter. These must usually be used as they arise; the coarser they are in any one production, the more the amount of heat required. Where ores are extremely fine, leading to high dust losses, it may be economical to pelletize.

Mineralogic Structure of Ores. Complex ores, such as pyrochlore, can vary widely in structure, and different parcels require adjustments to the mix.

Bulk Density. This is related to granulometry, but even in Cr_2O_3 , which would be expected to be uniform from parcel to parcel and where grain sizes are of a few microns, variations in the supplier's final calcination temperature can affect the bulk density greatly and hence the recovery.

Mass of Charge. The percentage of heat losses varies inversely with the size of charge. These losses cannot be measured, but when the mass of a charge is increased, less heat per unit charge is required; this decrease can be obtained by an intelligent estimate finalized by trial and error.

Rate of Feeding. This is very much an art and efficient feeding can minimize some of the

above mentioned difficulties. The general aim is to maintain a cover of unreacted mix on the surface of the liquid slag, so as to minimize radiation losses but not to feed too fast and produce too hot a reaction.

It can be seen from the above that whereas thermochemistry plays a vital role in providing the basic knowledge for any metallothermic production, there are other "fine tuning" adjustments that are a matter of experience.

7.2.1.3 Commercial Production

There are two methods of promoting the reaction. One is to fill the reaction vessel with the charge and ignite it via an easily ignitable mixture, such as BaO_2 or Na_2O_2 plus aluminum; the reaction then proceeds from top to bottom of the charge. This is a wasteful method because only approximately one third of the capacity of the reaction vessel is used. The mix calculation must be very accurate because no control of the speed of reaction can be exercised. Because the charge is always covered by liquid slag, dust losses should be low, but there can be considerable loss by splashing owing to the violence of the reaction. The short reaction time should mean low heat losses, but this advantage is counteracted by the intense radiation from an always liquid surface. This method is seldom used, but there are some reactions that are so exothermic that they are dangerous and practically impossible to feed, such as those for the minor products 55–60% TiAl and ZrAl. This "firing down" method is used sometimes also for FeW production, where the extra heat supplied to achieve the high melting point requires a highly exothermic reaction near the limit of feedability.

The second method, almost universal, is to use a charge slightly more exothermic than that for "firing down", to ignite a small portion in the reaction vessel, and to feed the remaining charge. By doing so, the full capacity of the vessel is used so that vessel preparation costs per unit production are approx. one third those of the "firing-down" method. Another great advantage is that the speed of the reac-

tion can be controlled by varying the feeding rate so that it gets neither too hot nor too cold. As mentioned previously, this is quite an art, but it is surprising how soon a skilled worker becomes used to visual control of the temperature of the reaction.

There are also two types of reaction vessel. One is a mobile steel pot, lined with refractory. The other is a sand bed into which cylindrical holes are dug and lined with firebrick. This latter method usually is confined to aluminosilico reactions, such as those for FeW and FeMo.

Pot reactions are carried out in firing chambers, where the under pressure, as compared to that outside, is kept to the minimum required for complete exhaust of fume consistent with the charge feeder's need to observe the reaction but to keep dust losses to a minimum. *Sand bed reactions* are usually under a movable hood connected to the main flue. Whereas tall chimneys were once the solution to disposal of fume, modern conceptions of pollution control demand efficient dust collection. Owing to the volatility of MoO_3 , this production demands its separate dust collector, the recovery from which makes the difference between profit and loss on the operation. For other productions, because of the small tonnage of individual products and because the fume is largely Al_2O_3 , CaO , NaOH , etc., with low contents of valuable oxide, a communal collector is used. Collectors are of many types, but the most efficient is the reverse-jet filter. Because of the presence of CaO , NaOH , etc., the filter, when not in use, must always be kept above 100°C to prevent caking of the fume on the bags.

Figure 7.5 shows the arrangement, in principle, for feeding, reaction in a chamber, and fume extraction. After firing, the reaction pots must be left to cool to allow final settling out of metal droplets and eventual solidification. Depending on the size of the reaction, solidification can take a long time, but 24 h, which often fits in with the overall routine of the production, is usually sufficient. The pot is then stripped, leaving a block of metal with

adherent block of slag. The whole is then carefully quenched in a water tank, which causes the slag block to separate and embrittles the metal to some extent, facilitating subsequent crushing.

The sides of the metal block are surrounded by an adherent mixture of metal and slag created by penetration into the refractory lining. This easily breaks away and is consumed in the next reaction. The top surface, containing pockets of very adherent slag, requires removal by automatic hammers and, in the last resort, by hand chipping hammers. The bottom of the block usually requires less attention. Final cleaning of the whole block is by shot blasting.

The block is coarsely broken up by a mobile hammer of the pile driver type and crushed to desired size in jaw crushers and/or rotary crushers with intermediate screenings. There is immense variety in customer's size requirements, ranging from, say, 15-cm lumps for bulk users down to graded powders for welding rod manufacturers. An increasing demand is for bags of 6 mm and down alloy, each containing a fixed weight of the desired alloying element.

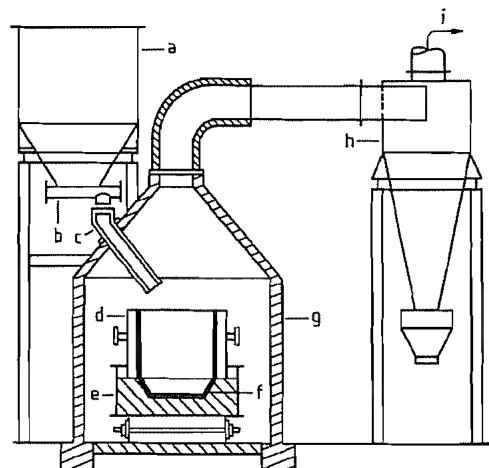


Figure 7.5: Reaction chamber with feeding hopper, reaction vessel, and dust collector: a) Feeding hopper; b) Feed-regulating valve; c) Feeding chute; d) Separable refractory-lined steel plate cylinder; e) Refractory-lined base; f) Optional magnesite inner lining; g) Firebrick-lined chamber; h) Filter; i) Offtake to chimney.

Pot Design and Construction

Although there is theoretically no limit to the size of the charge, as compared to steel production, the weights are small for the following reasons:

- **Costs.** Overall, raw materials are expensive. It is the aim of a producer to try to keep pace evenly with sales, holding modest stocks of raw materials and finished product. The total annual production of any one producer is small and diverse, with, in some cases, several specifications for one product.
- **Handling Facilities.** The total weight of a refractory-lined pot full of metal and slag is about three times that of the metal produced. Crane size is limited by cost and the small building required for carrying out the reactions, and for total operation lift trucks are convenient.
- **Preliminary Metal Breaking.** The small tonnages involved preclude a very expensive, large, preliminary breaking plant. Some alloys, particularly FeMo, are very tough and metal block thickness is usually limited to 30–35 cm.
- **Metal Specification.** Some residual specifications are very tight, notably that for Al in Cr metal. A mishap in the weighing of the charge can produce an off-grade block that may be in stock for a long time.
- **Refractory Failure.** Although rare, there can be an occasional failure of the refractory, producing breakout of metal and slag at high economic loss.

Therefore, metal block weights usually vary between 1000 and 2500 kg and, depending on the density of metal and slag, two pot sizes suffice. A small pot of ca. 200 kg metal capacity is useful for intermediate size investigations on new raw materials. A typical pot covering 1000–1750 kg metal would have internal dimensions of ca. 100 cm diameter and 125 cm height and one for 2500 kg would have the same height but be of 120 cm diameter in order to avoid too thick a metal block.

The outer construction consists of a plate steel cylinder attached to a heavy steel base by

quick-acting lugs. The base may be on wheels or adapted for lift truck operation. The lining is of moistened, crushed slag from chromium or ferrovanadium production, because this is a reasonably pure corundum. To ease cleaning of the metal block, magnesite tiles may be used in the metal zone, particularly for the hotter reactions. After preparation of the refractory base, either from bricks or ramming of crushed slag, the sides are rammed around a tapered, withdrawable template. Ramming is by hand, by pneumatic or electric hammer, or by jolting on a foundry jolt molding machine. The lining must then be dried for several hours to remove moisture. It is taken up to a dull red heat.

Basic sand bed operation is to construct a well in the sand bed from unmortared firebricks which takes the whole molten charge. After sufficient time is allowed for metal to settle out, a channel is made through the sand at the slag–metal interface level and the slag tapped off. A variation is to use a similar well in the sand bed sufficient to accommodate only the metal, topped by a firebrick-lined steel shell to accommodate the slag, with ample sand seal at the junction. After the reaction, the slag is tapped at the junction and the shell used several times.

Charge and Charge Preparation

Ideally, there would be an optimum size for raw materials, fine enough for a successful reaction but as coarse as possible to minimize dust losses. Fortunately, most oxides and ores are of reasonable size in these respects. Wolfram ores may have to be ground sometimes and it is known that very fine ores, such as pyrochlore, have been pelletized. Chromium oxide, at a grain size of a few μm , can be expected to give high dust losses but the grains have a strong tendency to self-adherence so that the particles are much larger. Even so, there is a slightly noticeable difference in recovery when different oxides are used, this varying directly with the final calcining of the oxide during its manufacture. The calcination increases grain size and density.

Auxiliary oxidants are of satisfactory grain size with the proviso that NaClO_3 tends to agglomerate on storage and must be sieved down to max. 1 mm before use. The minimum size of Al is limited by dust losses and the risk of dust explosions. It should not be below ca. $\text{BSS } 240 = 64 \mu\text{m}$. The size used in exothermic reactions then depends on the reaction. For chromium it is on the order of average 0.25 mm, for FeB and FeNb, 0.45 mm, and the Al powder can be partially substituted by cheaper foil powder. In the highly exothermic FeV reaction, where the V_2O_5 is in the form of flakes or lumps, only a little coarse powder is used to assist the start of the reaction, the bulk being pellets, chopped wire, and/or pure turnings. Despite the fine size of ilmenite and rutile, the same applies to FeTi production. Owing to the relative cheapness of the ores, Al is the most expensive ingredient, and cheap aluminum is used at the expense of Ti recovery.

In aluminosilico reductions only powders are used, in the case of FeMo because the ore is fine, in the case of FeW to obtain maximum speed of reaction so as to achieve the high temperature required. The reductants are Al powder and 75% FeSi, on the order of 0.25 mm average.

The amount of flux used is kept to a minimum in aluminothermic charges. Where sodium salts are used as auxiliary oxidants, residual Na_2O already lowers the melting point of the slag. A calcium salt is the usual flux because it has such a significant effect on the melting point of Al_2O_3 (Figure 7.4). Instead of CaO, CaF_2 often is used as its low melting point of 1418°C assists in promoting a smooth reaction. The amount used is often 1–2% of the total charge, never more than 5%.

Significant quantities of CaO– CaF_2 are used in aluminosilico thermic reactions because it is important for their success to tie the SiO_2 produced. As can be seen from Table 7.5, CaO has a strong affinity for SiO_2 .

After the components have been weighed out accurately, they are mixed completely in a gently acting mixer, such as a drum with lifters, V blender, or rotating cube. Duration of

mixing can be determined only by practice and can be determined initially by analyzing samples taken at intervals.

The charge is then dropped into a feeding hopper.

Feeding

When a charge has been prepared accurately to produce the desired result, success depends on the efficiency of feeding. The usual method is to control the exit valve of the feeding hopper according to the visual observation of the speed of the reaction, making slight adjustments to compensate for momentary coldness or hotness. Additional finer control is often applied by means of a handrake in the feeding chute. A fast reaction, such as that for FeV, often requires cooling, and a second small hopper may be used to feed a portion of crushed FeV slag. A FeW reaction is fed as fast as possible.

Further Processing

Pot stripping, block cleaning, and crushing require no further description than given earlier, except to emphasize the importance of avoiding cross contamination. This is particularly the case with FeB. A small amount of B is very beneficial to a steel designed for it but an unknown amount can be disastrous.

Safety Precautions

It must be realized that exothermic production, inadequately supervised, can be a very dangerous operation. Aluminum powder and oxidants are themselves fire hazards, and risk is magnified, when they are in contact, maybe to explosive proportions.

Aluminum powder and oxidants must be stored separately and the latter kept clear of carbonaceous material. Only sufficient for a single charge should be brought to the mixing department, and, during weighing, the oxide or ore should be sandwiched between the Al powder and the auxiliary oxidant to avoid direct, concentrated contact.

Mixing plants should be grounded to avoid buildup of static electricity. During firing, overfeeding can cause violent eruptions. Lumpy NaClO_3 can cause explosions. In case of an inadvertent lining failure, a large enough well should be provided to accept all the charge.

The main causes of disastrous explosions are Al dust explosions, either primary, because of careless handling, or secondary, over an overfed reaction. It also has been known for the metal and slag, apparently solid, to be quenched while still liquid internally, creating a disastrous explosion.

Employees must be protected from inhalation of dust and physical contact with charge components. This is particularly the case with hexavalent compounds of Cr, which can cause the well-known chrome ulcers.

Housekeeping must be exceptional. Fine dust accumulated on roof beams has been known to combust spontaneously.

7.2.1.4 Other Uses of Aluminothermic Processes

A significant use of an aluminothermic process is the welding of railway and tramway line joints, where the reaction takes place in a small crucible, and the steel produced is tapped onto the joint. In a similar manner, heavy cracked steel components, such as rolls, are welded and worn parts are built up and remachined. Developments over the last few years are the repair of ingot mold stools, where the steel stream has worn a cavity, and of cracked ingot mold lugs.

The use of exothermic reactions in incendiary bombs, where the intense Fe_2O_3 –Al reaction ignites the magnesium casing, is well known. Other military uses are for flares, which in the case of sea rescue give off colored smokes.

Milder reactions, damped down by insulating materials, are used in feeder head compounds, which are spread over the surface of liquid steel ingots in order to conserve the heat and minimize piping. For steel castings, similar compositions are formed into sleeves in-

serted in the sand mold to insure liquidity over the whole of the pouring time. Where large amounts of alloying addition are made to steel in the ladle, the cooling effect of the addition may be counteracted by the use of exothermic briquettes composed of alloy, Al, and oxidant. Minor uses are for jointing of Al and Cu cables by a CuO–Al reaction, and as slow reactions for hand warmers and food cans for explorers.

7.2.1.5 Possible Further Developments

Wherever alloys with low content are required, aluminothermic processes are necessary, and they have been brought to such an efficiency that little further improvement can be foreseen. Improved refractories may permit further transfer of some reactions to the arc furnace, saving Al plus auxiliary oxidant, but at present, those which can be envisaged possibly to stand up to the longer exposure are very expensive and have to compete with the self-produced refractory from an exothermic reaction.

Plasma processes are a possibility, the very high temperatures encouraging the oxide carbon reaction, but up to now there has been no success in driving the reaction to low C levels. Here again, refractories are a problem.

A relaxation of maximum impurity levels would be of mutual economic benefit to alloy maker and steel maker. Stringent specifications for superalloys are obvious, but when the small proportion of alloy used in many steels and the wealth of purification methods used in bulk steel production are considered, then some relaxation in impurity levels should be possible, enabling use of cheaper, more impure ores. Higher Al and/or Si levels would give better recovery and, where present specifications are very low, lower oxygen levels.

7.3 Ferrosilicon [10, 11]

The term ferrosilicon refers to iron–silicon alloys with Si contents of 8–95%.

Table 7.8: Composition of ferrosilicons (ISO 5445).

Designation	Chemical composition									
	Si		Al		P (max.)	S (max.)	C (max.)	Mn (max.)	Cr (max.)	Ti (max.)
	Over	Up to and including	Over	Up to and including						
FeSi 10	8.0	13.0		0.2	0.15	0.06	2.0	3.0	0.8	0.30
FeSi 15	14.0	20.0		1.0	0.15	0.06	1.5	1.5	0.8	0.30
FeSi 25	20.0	30.0		1.5	0.15	0.06	1.0	1.0	0.8	0.30
FeSi 45	41.0	47.0		2.0	0.05	0.05	0.20	1.0	0.5	0.30
FeSi 50	47.0	51.0		1.5	0.05	0.05	0.20	0.8	0.5	0.30
FeSi 65	63.0	68.0		2.0	0.05	0.04	0.20	0.4	0.4	0.30
FeSi 75 Al 1	72.0	80.0		1.0	0.05	0.04	0.15	0.5	0.3	0.20
FeSi 75 Al 1.5	72.0	80.0	1.0	1.5	0.05	0.04	0.15	0.5	0.3	0.20
FeSi 75 Al 2	72.0	80.0	1.5	2.0	0.05	0.04	0.20	0.5	0.3	0.30
FeSi 75 Al 3	72.0	80.0	2.0	3.0	0.05	0.04	0.20	0.5	0.5	0.30
FeSi 90 Al 1	87.0	95.0		1.5	0.04	0.04	0.15	0.5	0.2	0.30
FeSi 90 Al 2	87.0	95.0	1.5	3.0	0.04	0.04	0.15	0.5	0.2	0.30

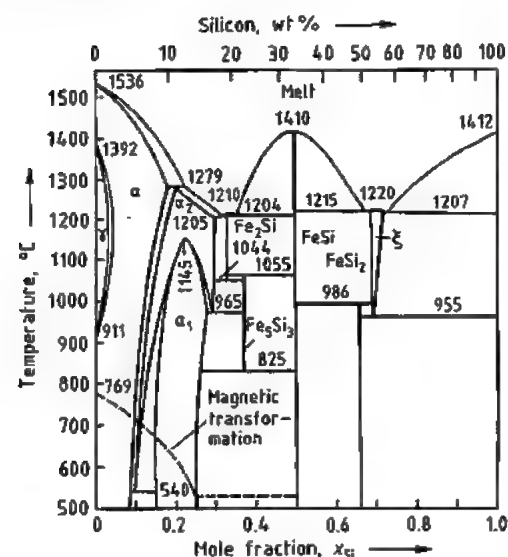


Figure 7.6: Iron-silicon phase diagram [12].

Table 7.8 lists the composition of commercial ferrosilicons.

FeSi75 is commercially the most important, although FeSi45 is still produced in large quantities for the North American market. Alloys containing > 95 % silicon are classified as silicon metal.

Physical Properties. The Fe-Si phase diagram (Figure 7.6) shows the existence of four compounds: Fe₂Si, Fe₃Si₂, FeSi, and FeSi₂ [12]. Commercial alloys differ from the com-

pounds shown in the phase diagram with regard to their stoichiometry.

During solidification of the standard grade, FeSi75, silicon crystallizes initially, followed by solidification of the ζ-phase—the high-temperature phase of FeSi₂—at 1207 °C. FeSi45 is composed of initially separated FeSi and FeSi₂, which is stable below 955 °C [13].

Transformation of the ζ-phase to stable FeSi₂ is accompanied by an increase in volume, which can lead to disintegration of the alloy in the range of 45–65 % silicon. The transformation and thus the disintegration can be suppressed by supercooling (i.e., rapid solidification in shallow molds).

Structural data for the iron silicides are summarized in Table 7.9. Table 7.10 lists the densities and melting ranges of commercial alloys.

Table 7.9: Crystal structure of iron silicides.

Compound	Crystal structure	Lattice constants, pm
Fe ₂ Si ₃	hexagonal	$a = 675.5, c = 471.7$
FeSi	cubic	$a = 448.9$
FeSi ₂	tetragonal	$a = 269.2, c = 513.7$

Table 7.10: Density and melting range of commercial FeSi alloys.

Alloy	$\rho, \text{g/cm}^3$	Melting range, °C
FeSi 10	7.3	1280–1350
FeSi 25	6.5	1270–1350
FeSi 45	5.1	1250–1350
FeSi 75	3.2	1250–1350
FeSi 90	2.5	1300–1400

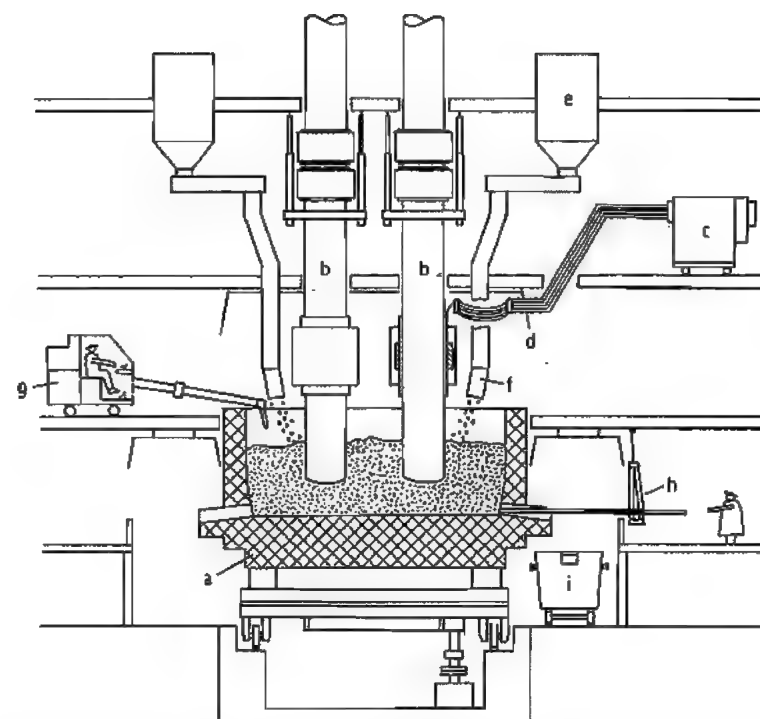


Figure 7.7: Submerged arc furnace: a) Furnace casing with lining (rotatable); b) Electrodes; c) Transformers; d) Secondary power supply; e) Raw material bunker; f) Charging pipes; g) Stoker machine; h) Burning-out unit; i) Tapping-off ladle.

Raw Materials. Pure quartzes with SiO₂ content > 98 % are used for the production of FeSi45 to FeSi90. Such quartzes occur naturally as pebbles or rock (vein quartz, quartzite). Quartz sands are processed into briquettes, in which the reducing coal required for a quasi-self-fluxing burden can be incorporated. For good gas flow through the furnace, the starting materials should be free of fine particles, which also requires that they remain dimensionally stable on heating and do not deprecipitate too early.

Depending on the location, high-quality iron ore or scrap iron is used as the iron source. In industrialized countries, washed and dried unalloyed steel turnings are generally used.

Flaming coals with low ash content, metallurgical coke, high-temperature brown coal coke, petroleum coke, brown coal briquettes, or wood chips are employed as reducing

agent, depending on availability. In calculating the amount of reducing agent required, the carbon resulting from consumption of the Söderberg electrodes must be taken into account; the electrodes supply 5–10 % of the total requirement.

The trend is toward the use of finer-grained quartz and coal. For quartz (previously 15–100 mm) the particle size now used is 8–40 mm; for coal, 2–20 mm.

Production. Ferrosilicon is produced in three-phase, submerged arc furnaces with power consumptions of 10–70 MW, corresponding to an annual capacity between 9×10^3 and 60×10^3 t per furnace.

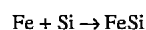
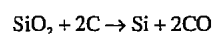
Figure 7.7 shows a schematic of such a furnace. With few exceptions, production is carried out in open furnaces, which allow the burden surface to be poked with stoker machines to prevent crust formation and thus maintain uniform gas flow through the fur-

nace. In modern furnaces the furnace casing can be rotated to reduce encrustation in the lower areas.

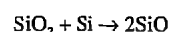
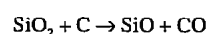
Closed furnaces must be built with a rotating furnace vessel to avoid sintering of the burden, since stoker machines can no longer be used. Closed furnaces operate more efficiently (cheaper) because the carbon monoxide gas formed can be used. However, this requires a more elaborate construction of the furnace: with a rotatable hearth and extensive dedusting of the hot off-gases [14].

Generally, large furnaces with capacities of > 40 MW present additional construction and operational problems. The thermal stress of the refractory materials and the off-gas losses also increase because these furnaces have higher operating temperatures [15, 16].

Reactions in the furnace occur according to the simplified scheme:



Side reactions also occur that result in a lower yield of the desired product, especially when insufficient carbon is used:



Gaseous SiO is oxidized by atmospheric oxygen at the burden surface to give SiO₂ dust, which is carried out of the furnace with the off-gas.

An excess of carbon leads to the formation of SiC, which also lowers the yield.

Specific material and energy requirements for the production of FeSi45 and FeSi75 are summarized in Table 7.11.

Table 7.11: Specific material and energy consumption for FeSi production.

	FeSi 45	FeSi 75
Quartz, kg/t	1200–1300	1800–2000
Iron turnings, kg/t	550–650	230–260
Carbon, kg/t	450–520	700–900
Söderberg paste, kg/t	40–50	55–70
Energy consumption, kWh/t	5800–6500	8500–10 000

Heating the batch to the reaction temperature of up to 1800 °C is achieved mainly by electrical energy (ca. 80 %). The energy up-

take of the batch depends on the so-called hearth resistance, whereby the conductivity of the FeSi burden is provided mainly by the coal. Thus, changing the type of coal influences the resistance. The grain size also plays a role: the smaller the grain, the higher is the resistance. The hearth resistance automatically regulates the depth of insertion of the Söderberg electrodes and thus the power consumption of the furnace. A uniformly high hearth resistance and low electrodes are desirable.

The liquid alloy, that accumulates in the hearth is tapped off to pouring ladles at regular intervals (about once an hour) and poured into shallow molds.

Ferrosilicon production is a slag-free process, which means that all the impurities present in the raw materials are transferred to the product. To obtain high purities the alloy must be purified by further treatment outside the furnace.

Aluminum and calcium impurities are removed by oxidation:

- By injection of gaseous oxygen through immersed lances or through nozzles or sparging blocks in the base of the pouring ladle
- By treatment with oxidizing siliceous slag, which can be stirred or blown in

Treatments used to obtain the lowest aluminum and calcium concentrations (in the extreme case, 0.02 % max.) also result in silicon losses. The silicon content for these grades drops from 75 to ca. 65 %.

Due to the low affinity of titanium for oxygen, the content of titanium impurities cannot be lowered metallurgically. Low Ti contents must be obtained by using raw materials that contain as little titanium as possible.

Environmental Protection. Silicon monoxide vapor is formed in the reduction process. The SiO is oxidized in air to produce extremely fine SiO₂ dust (particle size 0.1–1 µm), which is carried out of the furnace with the off-gas. Furthermore, small amounts of fine particles from the burden are also entrained. A total of 250–350 kg of dust is produced per tonne of FeSi75 [17].

The off-gas from the furnace can be cleaned in filter chambers (bag filters) to the maximum values allowed by TA Luft (20 mg/m³). The collected dust is sometimes dumped but is now mainly sold as a raw material. Pure SiO₂ dusts are used as cement additives, for example [18, 19].

Since the FeSi process is slag free, it has the advantage of having no slag that must be disposed of.

Quality Specifications. Quality requirements and terms of delivery are summarized in ISO 5445 (see Table 7.8) and DIN 17560. In addition, numerous customer specifications exist, some of which require drastically reduced impurity contents. The sieve analysis of ferroalloys is set out in ISO 4551; sampling is described in ISO 4552; and chemical analysis, in ISO 4139 and ISO 4158. Recognized analysis methods are also described in [20–22].

Storage, Transport, and Toxicology. Ferrosilicons produce hydrogen on contact with water. Alloys containing 30–70 % Si are classified as dangerous substances, Class 4.3, for transport by road and rail according to GGVS/GGVE and RID/ADR. Alloys with < 30 % and > 70 % Si are excluded from this regulation for land transportation. All commercial FeSi alloys are classified as dangerous goods, Class 4.3, for transportation by ship (IMDG Code) and by air (UN no. t408, IATA-DGR: Class 4.3).

Ferrosilicon itself is nontoxic. For handling the dust the general MAK values for fine dust (6 mg/m³) are applicable [23], as well as the usual safety measures such as goggles and face masks.

On contact with water, traces of toxic gases such as phosphine can be formed by reaction with slag adhering to the ferrosilicon. However, if stored in ventilated rooms in accordance with regulations, the critical MAK concentrations are rarely attained (PH₃: MAK 0.1 ppm) [23].

Uses. Approximately 75 % of the FeSi produced is used in the steel industry, where a requirement of 3–3.5 kg of FeSi75 per tonne of

steel can be considered normal. For melting almost all grades of steel, silicon is added as a deoxidizer and alloying agent. Silicon binds oxygen dissolved in steel melts, leading to noncritical concentrations. To increase this effect, FeSi is generally added together with other deoxidizers such as aluminum, calcium, and manganese.

Silicon that is not consumed in deoxidation dissolves as an alloying element in the steel and increases its strength and yield point [24]. Conventional construction steels contain 0.2–0.4 % silicon. More highly alloyed grades include tool steels, in which silicon improves the hardenability and wear resistance; hot-work steels that contain silicon for better tempering properties; spring steels (up to 2 % Si); and transformer and electro steels (up to 4.5 % Si). Low hysteresis losses are characteristic of the latter materials. Since the magnetic losses depend on the purity of the steel, high-purity FeSi, with drastically reduced content of aluminum, carbon, and titanium, is used.

Foundries consume almost 25 % of the ferrosilicon produced worldwide. Normal cast iron contains 2–3 % silicon for improved precipitation of graphite and increased strength.

Ferrosilicon alloys are also used as carrier alloys for metals such as barium, strontium, calcium, and titanium, usually in amounts of 2–4 %. These treatment alloys for gray cast iron are added to the ladle or mold to improve the precipitation of graphite. Ferrosilicon is also the prealloy for FeSiMg alloys; magnesium causes the formation of spherical graphite in spherulitic graphite iron.

Economic Aspects. In 1990, world consumption of ferrosilicon, calculated as FeSi75, was 3.4 × 10⁶ t, which compared to a capacity of 5.5 × 10⁶ t. Thus capacities were utilized only to ca. 62 %. Usually, the rate of utilization varies between 65 and 75 %. Thus, the economic situation at the beginning of the 1990s was characterized by marked pressure on prices and by the closure of unprofitable operations. However new capacities of ca. 250 × 10³ t/a are now planned, with almost 200 × 10³ t/a in Venezuela alone.

The choice of plant location depends less on the raw materials (quartz, coal) than on the availability of cheap electricity. Production is spread worldwide; the CIS and China are important producers (each with a capacity of ca. 10^6 t/a), followed by Norway, the United States and Brazil (each ca. 0.5×10^6 t/a).

7.4 Ferromanganese

A number of manganese-containing ferroalloys are manufactured which are used

Table 7.12: Types of ferromanganese and their general compositions [27].

Alloy	Composition, %		
	Manganese	Carbon	Silicon
High-carbon ferromanganese (carbure)	72–80	7.5	<1.25
Medium-carbon ferromanganese (affiné)	75–85	<2.0	
Low-carbon ferromanganese (suraffiné)	76–92	0.5–0.75	
Silicomanganese	65–75	<2.5	15–25
Ferromanganese silicon	58–72	0.08	23–35
Spiegeleisen	16–28	<6.5	11–45

largely in the mild steel, foundry, and stainless steel industries [25–27]. The names and typical compositions of these alloys are given in Table 7.12, and the international standards for the most commonly used alloys, namely high-carbon ferromanganese HC FeMn and silicomanganese FeSiMn, are given in Table 7.13 [25]. These are generally classified as intermediate products and the range of their end uses is shown in Figure 7.8.

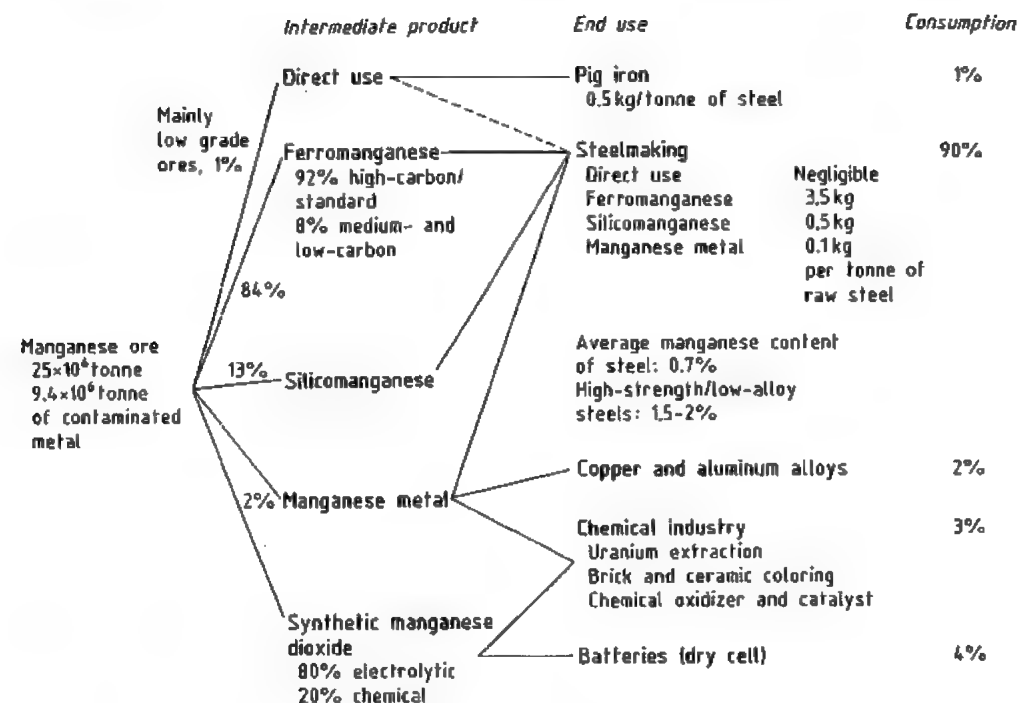


Figure 7.8: Manganese intermediate products and end uses.

Generally, high-carbon ferromanganese and silicomanganese are produced from a blend of manganese-containing ores, and in the case of silicomanganese, slags and silica are added. Ferromanganese can be produced in either electric submerged furnaces or blast furnaces, although only four blast furnace producers exist in the Western world [26], whereas silicomanganese is largely produced

in submerged arc furnaces. Producers of high-carbon ferromanganese and silicomanganese are listed in Table 7.14. High-carbon ferromanganese can be converted to medium-carbon manganese by an oxygen blowing process, and silicomanganese can be further refined into medium- or low-carbon ferromanganese as well as manganese metal (Figure 7.9).

Table 7.13: Ferromanganese standards [25].

Alloy	Country or organization	Standard	Reference
FeMn	International Standards Organization	DIS	5446
	France	AFNOR NF	A-15-020
	Japan	JIS	G 2301
	United States	ASTM	A 99-66
	Former Soviet Union	GOST	4755-70
	Germany	DIN	17564
FeSiMn	International Standards Organization	DIS	5447
	France	AFNOR NF	A-13-030
	Japan	JIS	G 2304
	United States	ASTM	A 701
	Former Soviet Union	GOST	4756-70
	Germany	DIN	17564

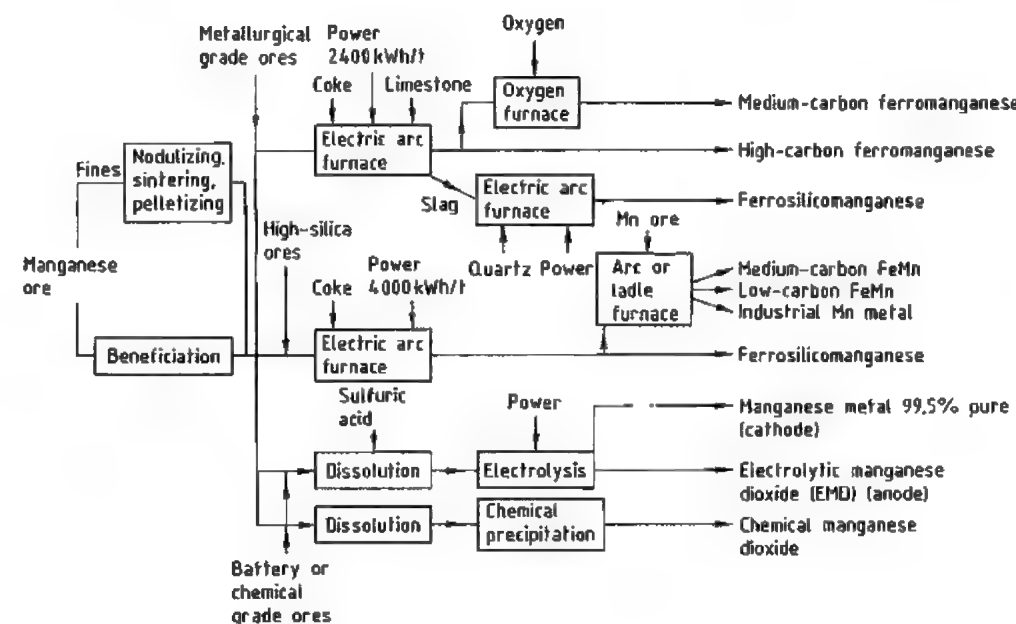


Figure 7.9: Summary of process routes.

Table 7.14: Producers of high-carbon ferromanganese and silicomanganese (producers of 10 000 t/a of either ferroalloy in 1988) [26].

Country	Company	Site	Capacity, $\times 10^3$ t (1995)		Production, $\times 10^3$ t (1995)	
			FeMn	SiMn	FeMn	SiMn
South Africa	Samancor	Meyerton	365	180	304	125
	Transalloys	Witbank	0	140	0	141
India	Ferroalloys	Cato Ridge	170	0	129	0
	Tisco	Keonjhar	18	12	13	9
	Facor	Shreeramnagar	21	0	12	0
	Khandelwal	Khandelwal Nagar	30	10	11	6
	Sandur Manganese	Hospet	40	5	36	3
	UF & A	Maneck Nagar	18	50	15	35
Japan	Maharashtra Electrosmit	Chandrapur	72	18	40	18
	Nippon Denko	Hidaka	0	19	0	6
	Kobe Steel	Kakogawa	61	31	41	29
	Mizushima	Hurashiki	156	0	155	0
	Chuo Denki Kogyo	Kashima	85	57	71	33
	Nippon Denko KK	Tokushima	95	53	73	8
Korea	JMC	Takaoka	85	7	55	3
	Korea Ferroalloy	Pohang	37	48	37	27
	Dongil Chungong	Pohang	30	35	28	25
Taiwan	Dongbu Industry	Tonghae	55	42	51	37
	Chen Hsing Industrial	Taipei	30	20	15	0
Belgium	Sadaci	Gent	19	10	15	10
France	SFPO	Boulogne	390	0	337	0
Italy	Pechiney	Dunkerque	0	60	0	55
	Carlo Tassara	Breno	10	45	8	39
Norway	Italghisa	Bagnolo Meila	15	33	11	32
	Elkem	Porsgrunn	150	50	104	24
	Tinfos Jernverk	Kvinesdal	0	135	0	120
Spain	Elkem	Sauda	150	60	127	65
	Hidro Nitro	Monzón	0	40	0	10
	Fyesa	Boo de Guarnizo	35	46	30	30
Argentina	Carburos Metálicos	Cee	50	46	18	28
	Grassi	Malargue	27	24	10	20
Brazil	Paulista/Sibra	Various	163	255	122	230
	Maringa	Itapeva	20	30	10	24
Mexico	Minera Autlan	Teziutlan	0	28	0	19
	Minera Autlan	Tamos	86	65	78	65
Venezuela	Hevensa	Puerto Ordaz	0	70	0	52
USA	Elkem Metals	Marietta	120	80	112	56
Australia	Temco	Bell Bay	105	95	93	94
Total, Africa			535	320	433	266
Total, Asia			833	407	653	239
Total, Europe			819	525	650	413
Total, Latin America			296	472	220	410
Total, North America			120	80	112	56
Total, Australia			105	95	93	94
World Total			2708	1899	2161	1478

Table 7.15: Composition of the former Soviet blast-furnace high-carbon ferromanganese [27].

Grade and official grade coke	Mn content, %	Si, %	Deleterious elements, not to exceed		
			P, % (group A ^a)	P, % (group B ^a)	S, %
Mn-5	75.0	2.0	0.35	0.45	0.03
Mn-6	70.0–75.0	2.0	0.35	0.45	0.03
Mn-7	70.0–75.0	1.0	0.35	0.45	0.03

^aFurnace.

7.4.1 High-Carbon Ferromanganese

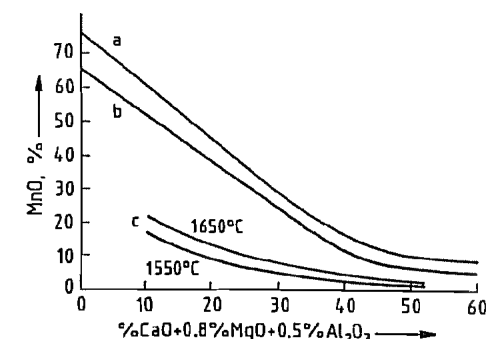
7.4.1.1 Production of Ferromanganese in Blast Furnaces [26–30]

Ferromanganese can be produced in blast furnaces in a manner similar to pig iron and spiegeleisen; however, in the Western world only four producers employ this method. These are Thyssen Stahl (Germany), BSC Cleveland (United Kingdom), SFPO (France), and Mizushima (Japan) (see Table 7.16, page 426), [26]. In the former Soviet Union, the majority of the high-carbon ferromanganese is produced in blast furnaces [27]. The choice of the use of blast furnaces over electric furnaces is based on the relative price of coke and electricity. Blast furnaces are usually used where the cost of power is high in relation to coke. In blast furnaces, coke is used both as a reductant and as the energy source. The coke rate in blast furnaces is higher than in submerged arc furnaces, which use electricity as the power source [28]. An exception to this is SFPO, where off-gases from the furnace are used to produce electricity, which is sold back to the local power supplier.

The product produced from blast furnaces generally contains 76% Mn and 16% Fe; the ferromanganese produced in the former Soviet Union is generally of a lower grade (Table 7.15) [27].

Raw Material Selection and Pretreatment. The raw materials required for the production of high-carbon ferromanganese are manganese ores, fluxes such as limestone, dolomite, or silica, and solid fuels and reductants such as coke.

In order to produce ferromanganese of the required grade a single ore is seldom suitable because the desired Mn/Fe ratio of the charge determines the Mn content of the final product [28]. Ores from various sources are therefore blended to achieve the ideal ratio and to limit the contents of the deleterious components silica, alumina, and phosphorus in the raw material mix.

**Figure 7.10:** Variation of equilibrium MnO content of slag for high-carbon ferromanganese and silicomanganese production [31].

The raw material is crushed and screened to ca. 5–30 mm. Alternatively, sintered or pelletized fine ore can be used (see Section 47.4). Some deleterious components can be partially removed from the ore prior to melting by dense-medium separation or flotation. Slagging components (dolomite or limestone) can be added to the sintered or pelletized ore, which results in cost savings in the blast furnace. Partial reduction of the higher manganese oxides may also occur during sintering.

Blast Furnace Operation. In comparison to iron making, high gas temperatures are required in ferromanganese production because the reduction of manganese(II) oxide takes place at a higher temperature than is required for the reduction of wustite [29]. This is achieved by oxygen enrichment of the hot blast or, in the case of SFPO, by heating the blast with nontransferred arc plasma torches [30]. The plasma arc increases the flame temperature from 2200 to 2800 °C and considerably reduces the coke consumption, which usually ranges from 1270 to 2000 kg/t.

The recovery of manganese in the alloy is usually 75–85%. This is influenced by the MnO content of the slag, the slag-to-metal ratio, and losses in the flue gases. The MnO content of the slag is highly dependent on the basicity ratio (CaO + MgO)/SiO₂ (Figure 7.10) [31], which can be controlled by the choice of ore and addition of flux. Losses to the flue gas can generally be recovered in the gas cleaning section (see Section 7.4.5). These

materials can then be agglomerated and returned to the furnace.

At the Mizushima works, the double bell valve of the conventional blast furnace has been replaced with an arrangement incorporating a distribution chute (Figure 7.11) [32]. This results in a better distribution of the burden in the shaft and therefore a more even flow of gas through the burden (Figure 7.12). The incorporation of a distribution chute lowers the coke consumption of the furnace.

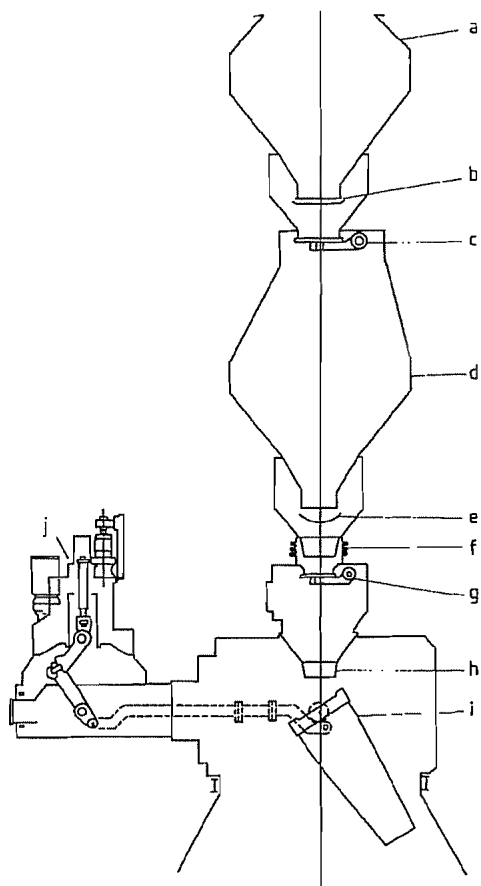


Figure 7.11: The cardan distributor on the blast furnace [32]: a) Upper bunker; b) Gate valve; c) Upper seal valve; d) Lower bunker; e) Material flow control gate; f) Expansion joint; g) Lower seal valve; h) Vertical chute; i) Distribution chute; j) Driving apparatus.

In spite of the innovations mentioned above the raw material costs of blast furnaces remain higher than those of submerged arc furnaces

[26] due to the high cost of coke. With the exception of SFPO, blast furnace production costs are higher than the average production cost of ferromanganese in electric furnaces.

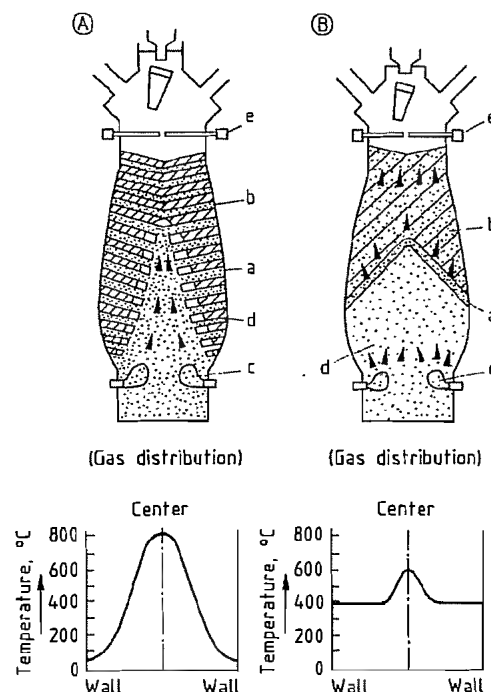
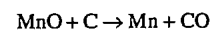


Figure 7.12: Effect of mixing on the distribution of gas in a blast furnace [32]. A) For layer by layer charging; B) For perfect-mixed charging. a) Cohesive zone; b) Lumpy zone; c) Raceway; d) Dead man; e) Throat sonde.

The Reduction Process in the Blast Furnace. The reduction of the higher manganese oxides to manganese(II) oxide takes place in the upper zone of the shaft according to the reactions given earlier. These generally occur below 900 °C and are indirect. The reactions are exothermic, and the heat generated causes high top temperatures and necessitates water cooling of the furnace top.

The reduction of manganese(II) oxide



is highly endothermic, in contrast to the weakly endothermic reduction of wustite. This requires higher temperatures and, consequently, higher coke rates are required for the smelting of ferromanganese in blast furnaces.

7.4.1.2 Production of Ferromanganese in Electric Arc Furnaces

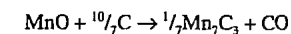
The majority of producers of ferromanganese in the Western world use submerged arc electric furnaces (Table 7.16). Although electric furnaces have lower capacities than blast furnaces they have the advantage that the heat requirement is provided by electricity, and coke and coal are added to the feed only as reductants. Consequently the coke consumption is lower in electric furnaces than in blast furnaces, which is a considerable advantage in the light of dramatically increasing coke prices. An additional advantage is that the process is not entirely dependent on high-strength coke, unlike blast furnaces, and a portion of the carbon requirement can be supplied in the form of coal. In South Africa, where coking coal is in short supply, up to 70% of the carbon for the production of ferro- and silicomanganese is supplied in the form of bituminous coal.

Originally electric furnaces were small (3–8 MVA); however, furnaces have grown progressively larger with time [33]. Recently built electric furnaces have capacities of 75–90 MVA. Smaller furnaces are still popular with producers because they offer flexibility in that they can be switched more easily between different products than their larger counterparts [34]. The larger size and more stable operation of modern electric furnaces, due largely to computer control, have resulted in lower electricity consumption. Electric furnaces used in the production of manganese alloys are generally circular and have three electrodes, each coupled to a separate electrical phase (Figure 7.13) [35]. The diameters of these furnaces range from 2 to 20 m.

In modern electric arc furnaces the raw material is usually fed by gravity from bunkers above the furnace. Fresh burden therefore automatically enters the furnace as the raw materials are melted and slag and metal are removed from the system. In older furnaces

use is still made of charging cars to introduce raw materials to the top of the units.

As the raw materials move down the furnace, the higher oxides of manganese are reduced to MnO by the gas leaving the furnace. The reduction of manganese(II) oxide occurs by the contact of carbon with the molten oxide in the slag phase. The overall reaction is:



for which

$$G^\theta = 265.7 - 0.18T \text{ kJ [36]}$$

The heat required for this endothermic reaction, for heating the burden, and to compensate for heat losses is supplied by the electrical input to the furnace. Heating takes place by the flow of electricity from the tips of the electrodes, which are submerged in the burden, through the burden and slag to the metal, as well as through the flow of electricity between the electrodes [36].

Design and Operation of Electric Furnaces

The degree of heating depends on the electrical current flow as well as the resistance provided by the burden and the slag to the flow of electricity. In the production of ferromanganese the resistivity of the burden is low, hence low voltages between the electrodes are necessary to maintain satisfactory penetration of the electrodes in the charge. The vapor pressure of manganese is high; therefore overheating of the charge must be avoided. The current densities on the electrodes should accordingly be lower for ferromanganese production than for other ferroalloys [37]. The diameters of the electrodes are therefore larger in ferromanganese furnaces than in other ferroalloy furnaces to facilitate the high currents required for low voltage operation. The distance between electrode centers is usually larger than in other furnaces, hence the furnace diameters tend to be greater. The values of these design parameters for a number of operating furnaces are given in Table 7.17.

Table 7.16: Profiles of manganese alloy producers [26].

Country	Company (location)	Furnaces utilized on ferromanganese	Furnaces utilized on silicomanganese
Argentina	Industrias Siderúrgicas Grassi (El Nihuil)	1 × 5 MVA	1 × 5 MVA
	(Blanco Encalada)	1 × 3 MVA	1 × 3 MVA
Australia	Temco (Bell Bay)	1 × 27 MVA	1 × 29 MVA
			1 × 35 MVA
			1 × 45 MVA
Belgium	Sadaci (Gent)	1 × 25 MVA	
Brazil	Companhia Ferroligas do Amapá (Santana)	1 × 13 MVA	
	Cia de Cimento Portland Maringa (Itapeva)	1 × 7 MVA	1 × 7 MVA, 1 × 3 MVA.
			1 × 15 MVA
France	Usinor Sacilor (Dunkirk)	102 × MVA	
	SFPO (Boulogne)	blast furnaces	
	Pechiney Électrometallurgie (Dunkirk)		1 × 45 MVA
Georgia	Zestafoni Ferroalloys (Zestafoni)	22 furnaces	1 × 600 MVA
India	Andhra Ferro Alloys (Kottavalasa)	1 × 4 MVA	
	Facor (Shree Ramnagar)	1 × 17 MVA	
	GMR Vasavi Industries (Tekkali)		2 × 19 MVA
	Nava Bharat Ferroalloys (Paloncha)		1 × 17 MVA
	Ispat Alloys (Balasore)	1 × 15 MVA	2 × 15 MVA
	Tata Iron & Steel Co. (Joda)	1 × 17 MVA	1 × 9 MVA
	Crescent Ferroalloys (Seoni)		1 × 3 MVA
	Hira Ferroalloys (Raipur)	1 × 7 MVA	
	Jain Carbide & Chemicals (Raipur)		2 × 3 MVA
	Jalan Ispat Castings (Meghnagar)		1 × 9 MVA
	Nav Chrome (Raipur)	1 × 4 MVA	
	Quality Steel & Forging (Meghnagar)		1 × 4 MVA
	Shree Ganesh Ferroalloys (Raigarh)	1 × 4 MVA	interchangeable to SiMn
	Sri Girija Smelters (Raipur) ^a	1 × 4 MVA	
	Srinivasa Ferroalloys (Raipur) ^a	1 × 4 MVA	
	Standard Ferroalloys (Raipur)		1 × 8 MVA
	Vika Ferroalloys (Raipur)	1 × 3 MVA	interchangeable to SiMn
	Dandeli Steel & Ferroalloys (Dandeli)	1 × 4 MVA	interchangeable to SiMn
	Sandur Manganese (Vyasankere)	1 × 18 MVA	interchangeable to SiMn
	Visvesvaraya Iron & Steel (Bhadravati)	2 × 22 MVA	
	Balaji Electro Smelters (Yotmal)	1 × 4 MVA	interchangeable to SiMn
	Kandelwal Ferroalloys (Kanhari)	1 × 9 MVA	1 × 9 MVA
	Maharashtra Elektrosmit (Chandrapur)	1 × 33 MVA	1 × 33 MVA
	Universal Ferro & Allied Chemicals (Tumsar)	1 × 17 MVA	1 × 17 MVA, 2 × 9 MVA
Italy	Italgisa (Bagnolo Mella)		1 × 15 MVA
	Fornileghe (Breno)	2 × 10 MVA	1 × 10 MVA
Japan	Chuo Denki Kogyo (Kashima)	1 × 40 MVA	1 × 50 MVA
	Kobe Steel (Kakogawa)	1 × 20 MVA	1 × 20 MVA
	Mizushima (Mizushima)	1 blast furnace	
	Nippon Denko (Samani)		1 × 8 MVA
	(Miyako)		1 × 5 MVA
	(Tokushima)	1 × 40 MVA	
	Yahagi Iron (Nagoya)	1 blast furnace	
Kazakhstan	Yermak (Yermak) ^a		27 furnaces
Korea	Dongbu Corporation (Donghae City)	1 × 8 MVA	1 × 8 MVA
	Dongil Industries (Pohang)	1 × 8 MVA	1 × 12 MVA, 1 × 8 MVA
	Hanhap Corporation (Pohang)	1 × 13 MVA	1 × 16 MVA
Mexico	Minera Autlan (Tamos)	1 × 33 MVA	
	(Teziutlan)	1 × 33 MVA, 2 × 15 MVA	1 × 12 MVA, 2 × 6 MVA
			1 × 5 MVA
	Ferroalmex (Gómez Palacio)		2 × 15 MVA

Country	Company (location)	Furnaces utilized on ferromanganese	Furnaces utilized on silicomanganese
Norway	Elkem (Porsgrunn)	1 × 45 MVA, 1 × 39 MVA, 1 × 18 MVA	interchangeable to SiMn
	Elkem (Saude)	1 × 5 MVA, 1 × 36 MVA, 1 × 30 MVA, 1 × 24 MVA, 1 × 10 MVA, 2 × 6 MVA	interchangeable to SiMn
South Africa	Tinfos Jernverk (Kvinesdal)		2 × 45 MVA
	Ferro Alloys (Cato Ridge)	2 × 24 MVA, 2 × 12 MVA	
	Samancor (Meyerton)	2 × 75 MVA, 1 × 81 MVA	2 × 18 MVA, 2 × 21 MVA, 3 × 10 MVA
	Transalloys (Witbank)		1 × 21 MVA, 1 × 23 MVA, 2 × 49 MVA
Spain	Ferroatlántica (Boo)	1 × 20 MVA	1 × 30 MVA, 2 × 13 MVA
	(Cee)	1 × 17 MVA	3 × 24 MVA
	(Monzón)		1 × 45 MVA
Taiwan	Chen Hsing Industrial (Hsi-Chih)	1 × 10 MVA	interchangeable to SiMn
Ukraine	Nikopol Ferroalloys (Nikopol)	16 furnaces	29 furnaces
	Zaporozhye Ferroalloys (Zaporozhye)	1 × 1050 MVA	
USA	Elkem Metals (Marietta)	2 × 40 MVA	1 × 50 MVA
Venezuela	Havensa (Matanzas)		1 × 11 MVA, 2 × 9 MVA, 2 × 3 MVA, 1 × 15 MVA

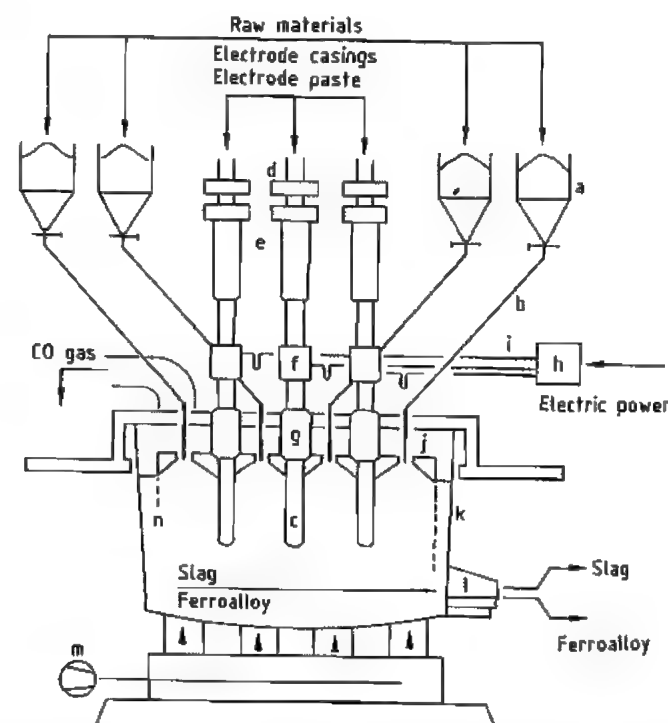
^a Interchangeable to FeCr.

Figure 7.13: Layout of an electric arc furnace [35]: a) Charging bins; b) Charging tubes; c) Electrodes; d) Electrode slipping device; e) Electrode positioning devices; f) Current transmission to electrodes; g) Electrodes sealing; h) Furnace transformer; i) Current bus bar system; j) Furnace cover; k) Furnace shell; l) Tap hole; m) Furnace bottom cooling; n) Re-fractory material.

Table 7.17: Furnace design parameters.

	Elkem Beauharnois	Elkem Sauda	Temco Bellbay	Samancor Meyerton M 10	Samancor Meyerton M 4	Former So- viet Union PRO 2.5	Former So- viet Union PKZ 33
Inside shell diameter, m	15.1	12.5	10.0	16.0	9.8	2.7	6.7
Shell height, m	8.8	6.0	5.2	8.0	5.7	1.2	3.0
Electrode diameter, m	1.90	1.90	1.4	1.90	1.20	0.30	1.5
Tapholes	2 Metal, 2 Slag		2 Metal, 1 Slag	2 Metal, 1 Slag	2 Metal, 1 Slag		
Megawatt rating	4.5	30	13	46	20	2.5	33

Most electric furnaces have two tapholes offset by 60 °C which are used alternately to tap both slag and metal. The slag and metal are then separated either in the ladle or by means of a skimmer plate in the runner between the furnace and the ladle [38]. In larger furnaces, separate tapholes are included for metal and slag [34]. Tapholes are usually opened by taphole drills and closed with automatic mud guns.

An important feature in the design of submerged arc furnaces is the Söderberg electrodes. These are used because the large electrode diameters required for the production of manganese alloys make the use of pre-baked electrodes uneconomic. The Söderberg electrode consists of a mild steel or stainless steel casing which is stiffened with internal fins and is filled with a carbonaceous paste, consisting of a solid aggregate, usually calcined anthracite, and a binder of coal-tar pitch [34]. The paste becomes plastic when hot and fills the entire volume of the casing. On further heating of the electrode by the electric current and furnace heat, the paste is baked and becomes solid. As the electrode is consumed, additional casings are welded onto the top. The current carrying capacity and strength of an electrode is a function of the quality of the paste, the electrode baking rate, and the cross-sectional area. Breakages of Söderberg electrodes are a major cause of downtime in electric furnaces, and proper management of the electrodes is therefore essential for efficient production [34].

A number of devices are commercially available to control the electrodes' movement and slipping rate (rate at which the electrode is allowed to move through the rings to compen-

sate for its consumption in the furnace). One of these is designed and manufactured by Elkem [38]. The electrode is clamped by hydraulically operated rings and is moved up and down on hydraulic cylinders. Current is fed to the electrode through brass contact shoes clamped around its diameter.

Large electric furnaces are usually completely closed at the top, and the CO-rich gas leaves the furnace at approximately 290 °C and is cleaned in cyclones and venturi scrubbers. The gas is then either flamed off to the atmosphere or, more recently, is used to generate electricity. This is the case of SFPO [26] and at Tinfos in Norway [39]. At Elkem's plant in Canada the off-gases are used to fuel auxiliary equipment in the plant [40]. Smaller furnaces are either open or closed. In the case of open furnaces the gas is usually withdrawn by fans and cleaned in a bag-filter plant. In this case the gases are completely burnt in the furnace and have no commercial value.

Raw materials are usually batch weighed and blended according to a predetermined recipe and are then fed to bunkers above the furnace. The mix then gravitates into the furnace through feed chutes. To ensure an even distribution of material over the furnace, up to ten feed chutes are radially distributed around each electrode and one is positioned in the center of the furnace.

After the metal is tapped from the furnace it is cast into molds formed from ferromanganese fines or cast iron and allowed to solidify. The alloy is then removed, crushed, and screened into various size fractions, depending on the requirements of the user. An alternative to this practice is the use of a casting machine. In this case the metal is tapped di-

rectly onto a moving train consisting of small molds. The metal then solidifies and is ejected from the mold at the end of the strand. The advantage of this process is that the product is more even in size and cubical in shape. The generation of fines (<6 mm), which are generally unsalable, is also minimized. To date Elkem, Samancor, Transalloys, Chuo Denki, and Mizushima use casting machines for a portion of their products.

Raw Materials Required for the Manufacture of High-Carbon Ferromanganese

Manganese ores from different sources vary widely in their contents of manganese, iron, silica, alumina, lime, magnesia, and phosphorus. To produce standard ferromanganese (78% Mn) and a slag containing 30% MnO, the manganese to iron ratio in the charge must be 6:5. Since a single manganese ore of this ratio is seldom available, blending of ores from different sources is common practice to reach the desired manganese to iron ratio and to control the level of deleterious elements, particularly phosphorus. The ore mixes used in some operations are shown in Table 7.18 [37]. The use of sinter as a source of manganese is becoming increasingly popular. In the sintering process a degree of prereduction is achieved, reducing the energy requirement in the furnace. The additional advantage of sinter is that fine ores, which are otherwise unusable, are agglomerated in the sintering process. Bag-house dust and sludge from gas cleaning plants can also be recycled to the furnace in the form of sinter. The maximum amount of sinter that can be fed to the furnace is a moot point and depends on its mineralogy and state of prereduction. When sinter replaces ore of high MnO₂ content, the energy required in the furnace increases because the highly exothermic reduction of MnO₂, Mn₂O₃, and Mn₃O₄, (see Section 47.5.2) no longer takes place in the furnace [37]. The use of Mamatwan sinter, in place of Mamatwan ore, results in power savings be-

cause the calcination of the carbonates in Mamatwan ore is energy consuming [41]. At the Zestafori ferralloy works in the former Soviet Union, up to 100% sinter is used in the furnaces [42]. The bottom size of ore is also important because close packing of the ore in the furnace must be avoided [37]. This can result in the formation of calcined bridges in the furnace, which disrupt the distribution of gas and can cause eruptions when the gas entrained under a bridge is suddenly released on its collapse [34]. Generally ores larger than 6 mm are used in large furnaces. The addition of small amounts of <6 mm material to small furnaces is possible. Generally, ore is screened prior to batch weighing of the furnace mix.

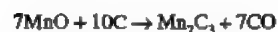
The carbon required in the furnace is generally added in the form of coke. The size of the reductant is important. Coke and coal of too small a size can also cause close packing as well as affecting the resistivity of the burden. To maintain electrode penetration at Elkem Sauda [43] coke nuts (10–20 mm) are used. This is a compromise between the resistivity and the necessity of maintaining a coke bed at the bottom of the furnace.

Limestone, dolomite, or silica are added to the process as fluxes to adjust the basicity of the slag. The amount and type of flux added depends on the blend of ores and whether a discard- or high-slag practice is used. At Elkem's operation in Beauharnois the use of alumina as a flux makes the operation of the furnace possible with 100% Moanda ore from Comilog [44].

Chemistry of the Process

A dig out of a 75 MVA ferromanganese furnace at the Metalloys operation in South Africa showed that nine distinct zones exist around each electrode (Figure 7.14) [45]. This study showed that material descends rapidly down the side of the electrode (a) into the semi-active zone (b), where prereduction of higher manganese oxides to MnO takes place. Thereafter, the material moves into the active zones of the furnace (c, f), where reactions

take place between the manganese(II) oxide in the melt and the coke particles in the coke bed:



Equilibrium between the slag and metal was thought to exist under each electrode, and further from the electrode, layers of unreacted ore and coke were found to be present (h). This suggests that heat is concentrated under each electrode. The path of electrical transfer was deduced to be from the electrode tip through the coke bed and into the alloy layer (g).

The efficient production of high-carbon ferromanganese therefore depends on the degree of reduction of MnO by carbon as well as the prereduction that occurs in the upper re-

gion of the furnace. The ratio of CO and CO₂ in the off-gas is important and can be used to monitor the condition of the furnace. The higher the CO₂ content of the off-gas, the higher is the energy efficiency of the process, because the reducing potential of the gas is being more fully utilized (Figure 7.15) [43, 45]. Good operation of the furnace is indicated by a CO₂/(CO₂ + CO) ratio of 0.55. This ratio, as well as the MnO content of the slag, can be used to control the coke rate of the furnace. Undercoking of the furnace is indicated by high MnO content of the slag and a low CO₂ content in the off-gas [43].

Table 7.18: Operating parameters of some ferromanganese electric arc furnaces.

		Temco Bellbay	Elkem Porsgrunn	Elkem Beauharnois	Facor Sheermnagar	Soman- cor M 10	Soman- cor M 2
Raw material additions, tonnes/tonne alloy							
Manganese ore:	Groote Eylandt	1.171	(18%)				
	South Africa: high grade	0.780	(31%)			0.927	0.926
	medium						
	Mamatwan ore		(51%)			0.345	
	Mamatwan sinter					0.884	0.176
	Gabon: Moanda ore			(78%)			
	Moanda sinter			(22%)			
	India: average 44% Mn				2.18–2.23		
Operating results							
Average operating load, MW		13	25	34.4	5	45	16
Operating time, %			98	99		99	98
Specific energy consumption, kWh/t		2430	2399	2050	3100	2560	2710
Manganese recovery, %			77.3	75	79	77	74
Slag practice		high slag	high slag	high slag	discard slag	discard slag	discard slag
Slag composition, %							
MnO		40.4	43.1	44.7	20.0	20.0	20.0
MgO		1.8	4.4		2.5	7.3	7.4
Al ₂ O ₃		13.8	11.1	28.8	9.00	4.3	3.8
CaO		15.2	11.9	1.0	32.5	35.6	34.8
SiO ₂		28.2	24.2		30.5	32.4	31.5
Metal analysis, %							
Mn		78	78	78	74.5	76.5	76.5
Fe			14.6		17.6	15.4	15.4
Si		0.25	0.08		0.50	0.20	0.20
P		0.14	0.16		0.35	0.09	0.09
C		6.7	6.89		6.7	6.9	6.9
Ratios							
Slag/metal ratio		0.514				0.68	0.80
Basicity ratio (mass)		0.68			1.35	1.35	
Basicity ratio (molar)		1.9					

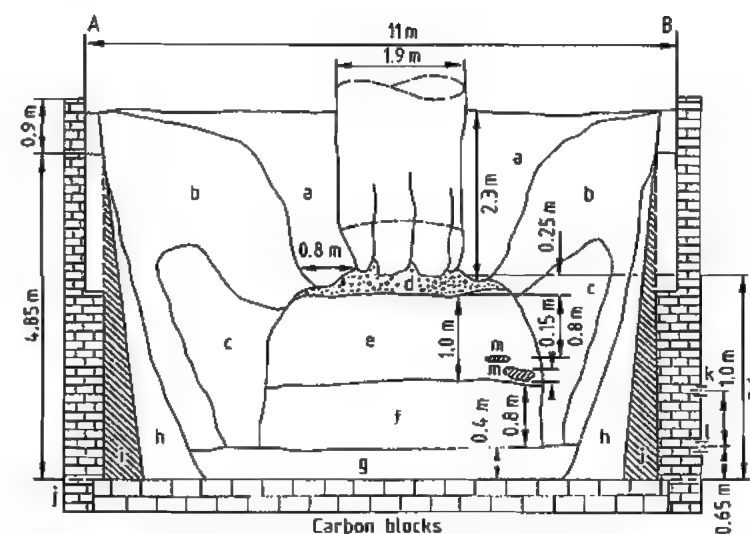


Figure 7.14: Zones in a ferromanganese furnace [36]: a) Loosely sintered burden; b) Loosely sintered material enriched in carbonaceous reducing agents; c) Coke and slag region, showing the active zone away from the electrode; d) Coke bed; e) Coke-enriched layer, with CaO–MnO–SiO₂ slag; f) MnO melt layer with some slag, coke, and additional carbonaceous reducing agent; g) Ferromanganese alloy layer intermixed with MnO melt; h) Graphitized and carbon-rich material; i) Carbon lining; j) Brick lining; k) Slag taphole level; l) Metal taphole level; m) Pieces of electrode.

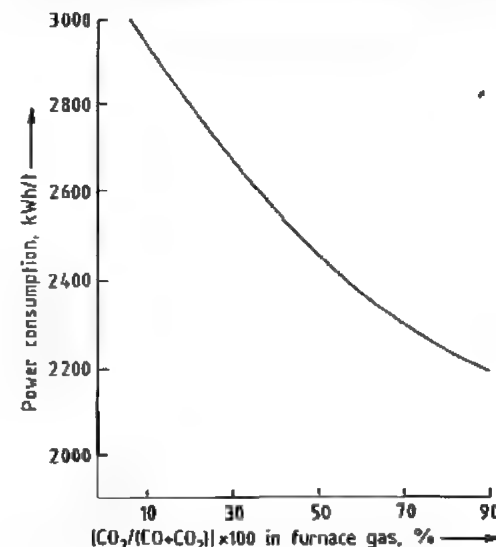


Figure 7.15: Relationship between off-gas composition and power consumption for ferromanganese production [43].

A further influence on the MnO content of the slag is the basicity ratio (CaO + MgO):SiO₂. Generally the addition of basic oxides increases the melting point of the slag. The hotter slag improves the reaction between

the slag and the coke and, consequently, more MnO is reduced. Increasing the basicity of the slag thus decreases the residual MnO content (Figure 7.10). The MnO content of the slag is also reduced by increasing the penetration of the electrodes, which also increases the slag temperature. The target MnO content of the slag depends on whether a discard- or high-slag process is used.

Discard-Slag Practice

Discard slags generally have MnO contents of 8–12%. Slag is produced by the silica and other basic oxides entrained in the ore. Manganese(II) oxide is entrained in the silicate network and is released by addition of CaO or MgO. By increasing the basicity of the slag the recovery of manganese as metal is increased; however, consumption of carbon and electricity also increases. The discard-slag process is therefore only used where power is relatively cheap and the delivered cost of manganese ore is high [37]. The recovery of manganese to the metal is between 70 and 75% when this practice is used. The practice usu-

ally involves the addition of limestone or dolomite to the furnace. However, in South Africa where high proportions of Mamatwan ore are used, a basic slag is produced without the addition of limestone, due to the high CaO content of the ore. In India the discard-slag practice is used because high recoveries of manganese are necessary to produce 74 % Mn from lower grade ores.

High-Slag Practice

In the high-slag practice less coke is required for reduction and little or no basic fluxes are used because the MnO content of the slag satisfies the requirement for basic oxides. Slags of this nature tend to contain more than 25 % MnO. In the high MnO practice the power consumption is reduced because a higher proportion of the reduction occurs by the gases and less MnO is reduced by solid carbon. Maximum use is therefore made of the exothermic nature of the prereduction reactions. The recovery of manganese is low in the ferromanganese furnace, but the overall recovery of manganese is high because the slag is usually used for the production of silicomanganese [37].

An additional attraction of the high-slag process is that an artificial ore, with a manganese to iron ratio of up to 100:1, can be made from relatively low-grade ores. This artificial ore can then be used to produce the highest grade of ferromanganese without the need to purchase costly high-grade ores. An additional benefit is the extremely low phosphorus content of the slag, which hence lowers the phosphorus content of any mix in which it is used. In countries having only ores with high phosphorus contents, the first stage of the process is the production of a slag high in MnO and a low-manganese alloy [46].

Since the energy input in the production of ferromanganese by the high-slag process is lower than that of the discard-slag process, it

is used by most producers. Slag compositions for various producers are shown in Table 7.18.

7.4.2 Production of Silicomanganese

Unlike ferromanganese, silicomanganese is only produced in electric arc furnaces, most of which can be used interchangeably to produce either of the manganese-containing alloys. Silicomanganese is used either as a substitute for ferromanganese and ferrosilicon in steelmaking or as a raw material for the production of medium- and low-carbon ferromanganese and industrial manganese metal. The composition of silicomanganese produced in the Western world is given in Table 7.12 and of that produced in the former Soviet Union in Table 7.19. Although silicomanganese generally contains 14–19 % Si, grades containing up to 35 % are produced for the production of extremely low-carbon alloys.

The solubility of carbon in the alloy decreases with increasing silicon content (Figure 7.16) [47]. On cooling, sparingly soluble SiC comes out of solution.

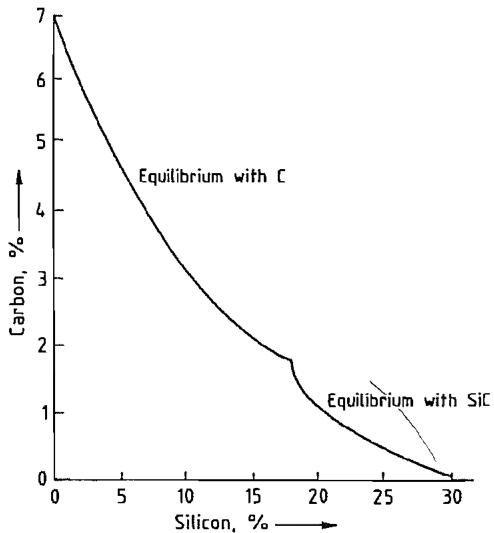


Figure 7.16: Carbon solubility in the Fe–Mn–Si–C system (50–80 % Mn) at 1420 °C [47].

Table 7.19: Composition of Soviet silicomanganese [27].

Grade and official grade code	Si ^a , %	Mn minimum, %	C, %	Deleterious elements, not to exceed		
				P, % (group A ^b)	P, % (group B ^b)	S, %
CMn26	26.0	60.0	0.2	0.1	0.05	0.03
CMn20	20.0–25.9	65.0	1.0	0.3	0.25	0.03
CMn17	17.0–19.9	65.0	1.7	0.3	0.35	0.03
CMn14	14.0–16.9	65.0	2.5	0.3	0.35	0.03
CMn10	10.0–13.9	65.0	3.5	0.3	0.35	0.03

^a As reported.
^b Furnaces.

Table 7.20: Operating parameters for silicomanganese production.

		Temco Bellbay	Elkem Porsgrunn	Elkem Beauharnois
Raw material additions, tonnes/tonne alloy				
Manganese ore:	Groote Eylandt	0.227		
	South Africa: medium grade		0.536	0.942
	Mamatwan ore		0.647	
	Mamatwan sinter			0.754
Ferromanganese slag		0.227		
Remelt metal		0.091		
Reductants:	coke	0.141	0.198	
	coal		0.566	0.836
Fluxes:	limestone			
	magnesite			
	quartz	0.127	0.610	0.814
Operating results				
Average operating load, MW		28	46	11
Operating time, %		94	97	98
Specific energy consumption, kWh/t		4400	3870	3900
Manganese recovery, %		85	74	67
Slag composition, %				
MnO			78.0	15.0
MgO			3.9	4.5
Al ₂ O ₃		29.7	7.7	6.1
CaO			20.9	21.1
SiO ₂		33.8	48.5	47.0
Metal analysis, %				
Mn		65.9	67.7	65.5
Fe			16.0	15.5
Si		19.1	17.5	17.8
P			0.09	0.09
C		1.38	1.18	1.15
Ratios				
Slag/metal ratio			0.72	1.17
Basicity ratio		1.0	0.54	0.55

There are three general routes for the production of silicomanganese:

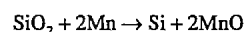
- Reduction of manganese ores and silica with coke and coal
- Reduction of MnO-rich slags from ferromanganese production and quartzite with coke and coal
- Reaction of standard ferromanganese and quartzite with coke

The first two processes are used for the production of alloys containing 15–25 % Si and can be carried out in the same furnaces used for ferromanganese production. The third method is used to produce alloys containing 30–35 % Si and is generally performed in smaller furnaces.

Raw Materials. The raw materials used in silicomanganese production are similar to those

used in making ferromanganese. Silica is added to the furnace as quartz or quartzite, and ferromanganese slag can be used as an alternative additional source of manganese instead of manganese ore or sinter. As in the case of ferromanganese, production advantages can be gained by using sintered ore (particularly from Matatwan). At the Kashima works of Chuo Denki, 40 % of the ore feed is in the form of sinter. The raw materials used to produce silicomanganese are given in Table 7.20.

Chemistry of the Process. In a dig out of a small electric arc furnace [48], four zones were distinguished: the burden zone, the zone of the coke bed, the melting zone, and the metal layer. In the burden zone, the higher oxides of manganese are reduced to MnO , while the higher oxides of iron are reduced to FeO and partially to metallic iron. Manganese(II) oxide is converted to complex silicates, which begin to melt at the bottom of the burden zone. Fine metallic particles exist in the coke bed zone, which are possibly caused by condensation of silicon and manganese in the hot areas under the electrodes. In the upper and lower parts of the melt zone, the reduction of manganese and silicon oxides occurs. The equilibrium is determined by the following reaction [31]:



This equation is important in determining the silicon and manganese contents of the metal that collects in the lowest part of the furnace and is influenced by the slag chemistry and the temperature of the process. Increasing the CaO content of the slag reduces the silicon content of the metal. The basicity requirement of the slag is therefore better supplied in the form of MgO . Higher temperatures tend to drive Si into the metal at the expense of Mn. Higher temperatures are therefore required in the production of silicomanganese than in the production of ferromanganese.

Silicomanganese is produced by most manufacturers of manganese alloys, and the slag and metal compositions and operating parameters of some producers are given in Table 7.20. To produce manganese metal of 97 %

Mn by the silicothermic method, a silicomanganese containing 28 % Si is required that is particularly low in phosphorus and iron. This is made from a manganese slag produced from the partial reduction of manganese ore.

Operation of the Furnace. The operation of the furnace for silicomanganese production is similar to that of ferromanganese production. However, deeper penetration of the electrodes is necessary to provide the higher temperature required to drive the reduction of silicon [31]. The resistivity of the burden is therefore important, and the size and the activity of the reductant is critical for stable operation of the furnace.

7.4.3 Production of Medium-Carbon Ferromanganese

Medium-carbon ferromanganese contains 1–1.5 % carbon and has a manganese content of 75–85 % (Table 7.12). Medium-carbon ferromanganese can be produced either by refining high-carbon ferromanganese with oxygen or by the silicothermic route, whereby the silicon in silicomanganese is used to reduce additional MnO added as ore or slag. The former process has considerable advantages [47] and is used by most producers. Elkem Metals in Norway and the United States use their patented manganese oxygen refining (MOR) process to refine high-carbon ferromanganese in plants having capacities of 5000 t/month and have closed their silicothermic plant in the United States. A similar facility was sold under license to the Torros plant of Minera Autlan in Mexico. Thyssen Stahl (Germany) uses a similar process to produce medium-carbon ferromanganese from the high-carbon ferromanganese produced in their blast furnaces. Samancor (South Africa) and Usinor Sacilor (France) have patented a similar process, but have not yet built a plant [49].

Transalloys (South Africa) produces 20 000 t/a of medium-carbon ferromanganese by the silicothermic route and appears to be the only producer in the Western world to do so. In the former Soviet Union, medium- and

low-carbon ferromanganese are produced silicothermically with manganese recoveries of 59–63 % [27]. The silicothermic and MOR processes are shown schematically in Figure 7.17.

7.4.3.1 Production of Medium-Carbon Ferromanganese by Oxygen Refining of High-Carbon Ferromanganese

In the MOR process patented by Union Carbide, high-carbon ferromanganese is decarburized in a similar manner to the steel-making process in the basic oxygen furnace [47]. However, several distinctive differences are encountered in the case of ferromanganese:

- A final temperature of 1750 °C compared to 1550 °C
- Refractory attack is more severe
- Difficult casting of the final alloy
- The higher vapor pressure of manganese,
- The higher volume and temperature of the off-gas

In the MOR process, oxygen is blown into the molten high-carbon ferromanganese and the temperature is increased from its tapping value of 1300 to 1750 °C. The heat required is supplied by the oxidation of manganese to manganese(II) oxide and carbon to carbon monoxide. The need to increase the temperature is shown by the carbon temperature relationship in Figure 7.18. In the early part of the blowing process, most of the oxygen is consumed by oxidation of manganese, and the temperature of the melt increases from 1300 to 1550 °C. Hereafter, carbon is rapidly oxidized and the temperature rises to 1650 °C. Above this temperature, the rate of carbon removal decreases and manganese is once again oxidized. The process is stopped at 1750 °C, which corresponds to a carbon content of 1.3 %. Further reductions in carbon content result in unacceptably high losses of manganese. In the MOR process, the recovery of manganese is ca. 80 % and the distribution of manganese can be broken down as follows [47]:

Alloy MC FeMn	80 %
Fume formed by vaporization	13 %
Slag formed by oxidation of Mn	5 %
Other losses, splashing	2 %

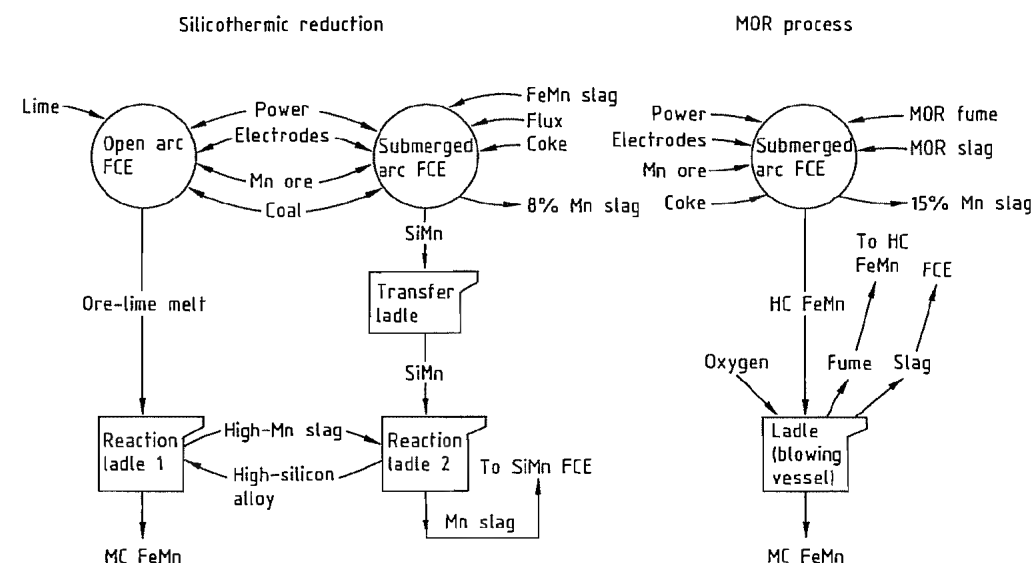


Figure 7.17: Process flow sheet comparison for silicothermic reduction and the MOR process [47].

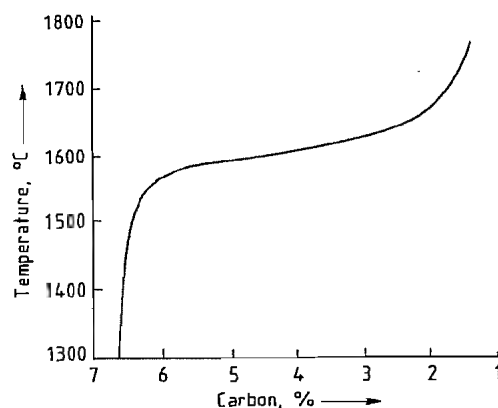


Figure 7.18: Dependence of carbon content on temperature for a ferromanganese alloy (Mn:Fe, 6:1) at 101.3 kPa [47].

The manganese lost in the fume is recovered in the gas cleaning plant and is then pelletized and returned to the high-carbon ferromanganese furnace. The slag, which contains about 65% MnO, is also returned to the high-carbon ferromanganese furnace. The successful operation of this process depends on the design of the blowing vessel and oxygen lance as well as giving careful attention to operational procedures. In the joint patent of Samancor and Usinor Sacilor, a bottom blown converter is used and steam is injected at the end of the blow as a coolant [49].

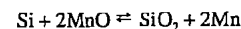
The MOR process has many advantages over the silicothermic process: lower energy consumption, lower capital investment, lower production cost, and greater flexibility.

The main disadvantage of the process is that its use is limited to production of medium-carbon ferromanganese because the carbon content cannot be reduced to below 1.3%.

7.4.3.2 Silicothermic Production of Medium-Carbon Ferromanganese

In the silicothermic production of medium-carbon ferromanganese, a high-grade slag or a melt containing manganese ore and lime is contacted with silicomanganese containing 16–30.1% silicon [50]. The silicon in the alloy acts as the reducing agent in the process,

which reduces the manganese(II) oxide in the melt. Similarly to silicomanganese production, the equilibrium is determined by the reaction:



The purpose of the lime is to reduce the activity of the SiO_2 in the melt, thus forcing the above reaction as far to the right as possible. The ratio of CaO to SiO_2 in the slag should be greater than 1.4 to ensure a sufficient reduction in the activity of SiO_2 . The carbon entering the process in the silicomanganese remains entirely in the metal phase and is therefore found in the product. Thus, to produce a medium-carbon ferromanganese containing 1% C, a silicomanganese containing 20% Si is necessary (Figure 7.16).

The heat produced by the silicothermic reduction is not sufficient to sustain the process; hence it is usually carried out in an electric arc furnace. These furnaces are usually small and, unlike ferromanganese furnaces, are lined with magnesite bricks, which are fairly resistant to the highly basic slag. The power consumption is between 1000 and 3000 kW. These furnaces can be tilted so that the slag can be separated from the metal. At Transalloys (South Africa) the process is carried out in a mixing ladle.

Although the silicothermic reduction process is more energy intensive than the decarburization of high-carbon ferromanganese, it has the advantage that the final carbon content is limited only by the carbon content of the initial silicomanganese. The silicothermic process can therefore be used to produce low-carbon ferromanganese and industrial manganese metal.

7.4.4 Production of Low-Carbon Ferromanganese

Low-carbon ferromanganese contains 76–92% Mn and 0.5–0.75% C (see Table 7.12). The production of low-carbon silicomanganese is not possible by the decarburization of high-carbon ferromanganese without incurring extremely high losses of manganese [50].

Use must accordingly be made of a silicothermic reduction process.

The process is similar to that used in the silicothermic production of medium-carbon ferromanganese. High-purity ores are used and in particular ores containing iron and phosphorus should be avoided. An artificial manganese ore, produced as a high-grade slag, is particularly suitable because of its low impurity level and because all the manganese is present as MnO. The reduction of the higher oxides of manganese is therefore unnecessary.

The operating figures for 1 t of ferromanganese containing 85–92% Mn, 0.1% C, and 1% Si with a manganese recovery of 75% are:

Calcined manganese ore	1250–1350 kg
Silicomanganese (32–33% Si)	800–850 kg
Quicklime	1000–1100 kg
Electrodes	10–12 kg
Electricity	1800–2500 kWh

Since the required silicon content of the metal is low, a slag high in MnO is necessary. The MnO content of the slag can, however, be reduced by the use of a two-stage refining operation. In the first stage, an excess of silicomanganese is maintained and a slag containing 6–8% Mn is teemed and discarded. The second refining stage with manganese ore and lime results in a slag containing 10–14% Mn, which is returned to the silicomanganese furnace.

7.4.5 Gas Cleaning

In all the processes described in this chapter, large volumes of gas are generated. These gases consist generally of CO, CO_2 , and N_2 , and contain large quantities of dust from the raw materials and condensed manganese droplets. These gases require cleaning prior to their venting to the atmosphere. In open furnaces, in which the gas is totally combusted, hoods are incorporated in the design through which the gas is removed. This gas is cooled in trombone coolers to ca. 200 °C and the dust is removed in bag filters. Ideally, after recovery the dust should be agglomerated and returned to the furnace. In closed furnaces, the gas is usually cleaned in cyclones and venturi

scrubbers prior to combustion to the atmosphere or used in downstream processes. At Elkem Sauda in Norway, gas from the 36 MVA furnace is cleaned by two wet venturi scrubbers. The gas has an initial dust loading of 150 g/m³ which is reduced to a maximum of 50 mg/m³ [38]. The dust recovered from the cleaning plant is filtered, sintered and returned to the process. At Samancor's Meyerton works in South Africa the gas from the 81 MVA and two 75 MVA closed furnaces is cleaned by a cyclone followed by two venturi scrubbers. A mist eliminator is included in the gas plant of the 81 MVA furnace to reduce the moisture content because the gas is used for heating in other areas of the plant. The emissions from the gas plants are less than 50 mg/m³, which is the statutory maximum. The gas from the remaining open furnaces is cleaned in a bag filter plant. Investigations are under way to briquette the dust from this plant due to its high manganese content and high manganese to iron ratio.

It is expected that dust limits will be reduced to 25 mg/m³. In addition to this the exposure limits allowed in the working environment in manganese producing facilities have been reduced due to the toxicity of manganese dust; the following limits apply:

United States, United Kingdom, Australia,	
Belgium, Brazil, Germany	5 mg/m ³
Yugoslavia	2 mg/m ³
Former Soviet Union, Poland	0.3 mg/m ³
Bulgaria	0.02 mg/m ³

7.4.6 Recent Developments and Future Trends

Energy-Saving Measures. In regions with high electricity prices recent developments have concentrated on the saving of energy. This is of particular importance to Japanese producers of manganese alloys that use electric furnaces. Developments include the use of the off-gas from the furnace to preheat and mildly prerreduce the ore, either in a rotary kiln or in a shaft kiln above the furnace.

The former process is used at the Kashima Works of Chuo Denki, where the feed to the

40 MVA ferromanganese furnace is heated to 950 °C in a rotary kiln and the higher oxides of the manganese ore are partially reduced. The ore loses 23 % of its mass during this process [51]. The use of this system has resulted in savings in power, and an additional advantage is that coal can be used instead of coke to satisfy the carbon requirement of the furnace. Care must be taken to avoid rapid heating and consequent decrepitation of the ore in the kiln.

The process in which a shaft kiln is positioned above the furnace was invented by NASU [52]. In this process the gas from the furnace is burnt under the furnace roof and the hot burnt gas leaves the furnace through a vertical shaft. The raw ore mix is introduced to the top of the shaft and is heated in a counter-current fashion by the exhaust gas. The ore is then fed to the furnace, where further heating takes place as the ore is exposed to the radiant heat produced by the burning gas in the roof. Two furnaces of this type are in operation at the Mizushima plant and their operation has resulted in power savings.

Computer Control of Electric Furnaces. Computer control of electric furnaces is practiced by Elkem at Suada in Norway, at Marietta in Ohio, and at Beauharnois in Canada. Temco in Tasmania and Samancor in South Africa also use computer control [53]. The following improvements in operating parameters have been realized by computer control at Elkem's plant at Beauharnois:

Operating power level (MV)	5% improvement
Power cost reduction from increased load	3% improvement
Manpower cost reduction	9% improvement
Statistical process control	lower variation in product

Elkem is investigating the potential of enhancing their process control system by the incorporation of an expert system. This system, based on artificial intelligence, will incorporate the experience of the operator in the process control system and will be used to diagnose reasons for poor furnace performance. Possible changes to improve the operation will be suggested by the expert system [54].

Use of Plasma Furnaces. Non-transferred arc plasma furnaces have been used successfully in the production of charge chrome. Attempts to produce ferromanganese in plasma furnaces have not been economically successful due to the high losses of manganese caused by volatilization in the arc attachment zone. In addition, no preheating of the ore takes place in a plasma furnace, unlike in the burden zone of the submerged arc furnace. In an effort to solve these problems and to utilize the higher specific throughputs that are obtainable in a plasma unit, a combined plasma/shaft furnace is being jointly developed by Voest Alpina and Samancor [55].

7.5 Ferrochromium

Ferrochromium is a master alloy of iron and chromium, containing 45–95% Cr and various amounts of iron, carbon, and other elements. The ferrochromium alloys are classified by their carbon content and are known by their French names because basic work in this field was carried out mainly in France:

- *High-carbon ferrochromium* (HC ferrochromium) with 4–10% C, “ferrochrome carbure”
- *Medium-carbon ferrochromium* (MC ferrochromium) with 0.5–4% C, “ferrochrome affiné”
- *Low-carbon ferrochromium* (LC ferrochromium) with 0.01–0.5% C, “ferrochrome suraffiné”

The mechanical and chemical properties of steel can be improved by alloying it with ferrochromium. Chromium combined with nickel gives stainless steel excellent chemical resistance.

The first industrial use of ferrochromium in producing low-chromium alloy steels was in 1860–1870 in France. Previously P. BERTHIER (1821) and E. FREMY (1857) produced small quantities of high-carbon ferrochromium in crucibles by reducing chromite or combinations of chromium and iron oxides with charcoal. This direct reduction process was transferred to the blast furnace or cupola to

produce low-chromium alloys with 7–8% Cr, and later on alloys with 30–40% Cr. In the United States (1869), Sweden (1886), and Russia (1875), similar processes were developed for producing high-carbon ferrochromium [56, pp. 1–3; 57].

The fundamental work by MOISSAN (1893) on using the electric arc furnace and its industrial application for the direct carbothermic production of high-carbon ferrochromium by HÉROULT (1899) were major improvements over the blast furnace that led to the modern large-scale production.

The reduction of chromite by silicon for the production of low-carbon ferrochromium was developed by F. M. BECKETT (1907) and improved by G. JEAN (1909).

The aluminothermic production of low-carbon ferrochromium has proved to be too expensive and the method is seldom used now.

7.5.1 Physical and Chemical Properties

Low-carbon ferrochromium has a bright silvery appearance; as carbon content increases, the metal turns from gray to dark gray. The density and melting range for different grades of ferrochromium are summarized in Table 7.21 [58].

The Fe–Cr phase diagram (Figure 7.19, [59]) exhibits a continuous series of solid solutions at higher temperature and a σ -phase at lower temperature. This brittle σ -phase has a

tetragonal structure ($a = 8.7995 \times 10^{-10}$ m, $c = 4.5442 \times 10^{-10}$ m).

Commercial ferrochromium contains mainly carbon as a constituent element because of the high affinity of chromium for the carbon used in the reduction process. The constitution and structure of the C–Cr–Fe system has been reviewed [60]. A projection of the liquidus temperatures and solid-phase equilibrium by isothermal sections from 1150 to 600 °C have been published [60].

7.5.2 Raw Materials

The only raw materials for the production of ferrochromium are chromite ores. The mineral chromite has a spinel structure and its formula may be written as $(\text{Fe}^{2+}, \text{Mg})\text{O} \cdot (\text{Cr}, \text{Al}, \text{Fe}^{3+})_2\text{O}_3$. A high Cr:Fe ratio is advantageous to produce an alloy with high chromium content. Chromite ores are classified as follows [61]:

- Ores rich in chromium: > 46% Cr_2O_3 , Cr:Fe > 2:1; for the production of ferrochromium
- Ores rich in iron: 40–46% Cr_2O_3 , Cr:Fe < 2:1; for the production of charge chrome and for the chemical industry
- Ores rich in aluminum: > 60% $(\text{Cr}_2\text{O}_3 + \text{Al}_2\text{O}_3)$, > 20% Al_2O_3 ; for refractories

Metallurgical-grade chromite ores are classified as hard lumpy or friable lump types, fines, and concentrates. Concentrates are produced by mechanical upgrading of lean ores or fines [62].

Table 7.21: Some physical properties of ferrochromium and ferrosilicochromium [58].

Alloy	Density ρ , g/cm ³	Melting range, °C	
		Liquidus	Solidus
Chromium metal (electrolytic)	7.2		1900
Chromium metal (aluminothermic)	7.2		1850
Low-carbon ferrochromium (72% Cr, 0.01% C)	7.35	1690	1660
Low-carbon ferrochromium (72% Cr, 0.05% C)	7.35	1670	1639
Low-carbon ferrochromium (69% Cr, 0.1% C)	7.35	1604	1343
High-carbon ferrochromium (69% Cr, 4–6% C, 1% Si)	7.2	1500	1350
High-carbon ferrochromium (64% Cr, 5% C, 1% Si)	7.1	1450	1340
Ferrochromium, charge grade (63% Cr, 5.5% C, 7% Si) ^a	6.7	1500	1400
Ferrochromium, charge grade (56% Cr, 6% C, 5% Si) ^a	6.8	1493	1660
Ferrochromium silicon (36%, 40% Si)	5.3	1388	1360

^a Charge chrome (see Table 7.27).

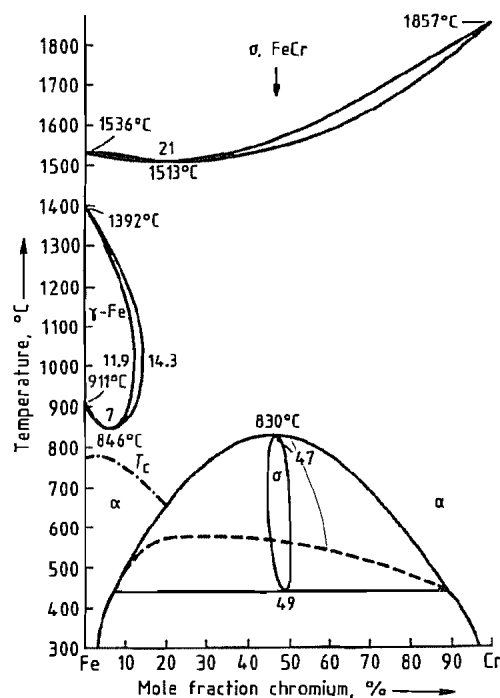


Figure 7.19: Fe-Cr phase diagram [59].

In the production of high-carbon ferrochromium, which is by far the alloy in greatest demand, generally a lumpy type of chromite ore is necessary. The submerged arc smelting of high-carbon ferrochromium by direct reduction of carbon in large low-shaft electric furnaces generally requires lumpy chromite ores to allow the reaction gases to pass from the lower reaction zone to the top of the furnace, where the burden (i.e., charge) is continuously charged.

About 80% of chromite ores in the western world are fines (< 10 mm). Therefore, efforts have been made to agglomerate these fines, by either sintering, briquetting, or pelletizing [63]. Fines of chromite ores can be used to produce low-carbon ferrochromium.

Typical analyses of some important metallurgical chromite ores are summarized in Table 7.22 [64].

The reducing agent for chromite is usually carbon in the form of coke (gas coke, coal, or charcoal); its contents of S and P should be

low. Silicon as a reducing agent is used in the form of ferrosilicochromium or ferrosilicon to produce low-carbon ferrochromium. Fluxing agents, e.g., quartzite or alumina (corundum or bauxite) and lime, are charged with the burden for slag formation. In the carbothermic production of ferrosilicochromium, chromite and quartzite are used as the raw materials.

7.5.3 Production

The oxides of iron and chromium present in the chromite can be readily reduced at high temperature with carbon. Because of the tendency of chromium to form carbides, a carbon-containing alloy is always obtained. The oxides can also be reduced with silicon, aluminum, or magnesium. However, only carbothermic and silicothermic reductions are used commercially. The reducibility of chromite depends on its composition. A chromite rich in iron ($\text{FeO} \cdot \text{Cr}_2\text{O}_3$) can be reduced by carbon at lower temperature than one rich in magnesium ($\text{MgO} \cdot \text{Cr}_2\text{O}_3$) [65, 66]. Iron oxide is reduced by carbon at a lower temperature than chromium oxide.

A thermodynamic analysis of carbothermic reactions in the field of ferroalloys has been performed [67]. For the carbothermic reduction of FeO , Cr_2O_3 , and SiO_2 , equilibrium temperatures at different CO pressures were calculated. The values in Table 7.23 were found at 101.3 kPa. Carbides with higher carbon content formed initially at lower temperature react at higher temperature with Cr_2O_3 and form carbides with lower carbon content; finally, reduction of SiO_2 starts at higher temperature. Therefore, production of ferrosilicochromium alloys requires high temperature.

In practice the reactions are somewhat more complicated because iron-containing chromium carbides are formed. In high-carbon ferrochromium, the double carbide $(\text{Cr}, \text{Fe})_7\text{C}_3$ is present. In this compound, two to four Cr atoms can be substituted by iron atoms. Equilibrium temperatures have been calculated for the FeO reduction in chromite [66]:

Table 7.22: Analyses of some chromite ores, metallurgical grade.

Compound	Chromite ore, %				
	Tranvaal lump ^a	Zimbabwe friable ^b	USSR lump ^c	Turkey lump ^d	Albania lump
Cr_2O_3	42.55	49.53	53.73	47.58	40.5
FeO	21.85	11.6	8.5	9.45	11.4
Fe_2O_3	4.85	2.2	4.3	3.1	—
MgO	9.26	17.52	17.3	18.7	23.3
Al_2O_3	15.5	7.3	9.4	8.8	7.3
SiO_2	5.54	5.14	4.3	8.33	12.6
L.O.I. ^e	0.2	2.3	2.1	2.25	3.4
Cr:Fe	1.43	3.20	3.81	3.42	3.13

^a Bushveldmassiv [64].

^b Great Dyke (friable lump) [64].

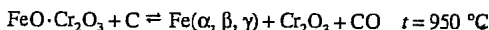
^c Kempirsajski [64].

^d Anatolia (Fethiye) [64].

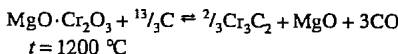
^e Loss on ignition.

Table 7.23: Equilibrium temperatures for various carbothermic reduction reactions [67].

Condensed reactants	Condensed products	Gases	Equilibrium temperature, °C
FeO, C	Fe	CO_2, CO	670
$\text{Cr}_2\text{O}_3, \text{C}$	Cr_3C_2	CO	1150
$\text{Cr}_2\text{O}_3, \text{Cr}_3\text{C}_2$	Cr_7C_3	CO	1190
$\text{Cr}_2\text{O}_3, \text{Cr}_7\text{C}_3$	Cr_{23}C_6	CO	1530
$\text{Cr}_2\text{O}_3, \text{Cr}_{23}\text{C}_6$	Cr	CO	1810
SiO_2, C	SiC	CO	1480
SiO_2	Si	CO, Si	1710



For the Cr_2O_3 reduction:

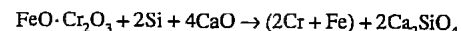


Because the difference in temperature between these two reactions is slight and because iron also facilitates reduction of chromium oxide, selective reduction of iron is difficult. In solid-state reduction studies on Transvaal chromite, the amount of iron and chromium found in the metallic state at 1000 °C was 11.0% of the iron and 1.3% of the chromium, and at 1200 °C was 98.3% of the iron and 38.5% of the chromium [64].

In the carbothermic reduction process, unreduced oxides from the chromite (MgO , Al_2O_3) and from the gangue (SiO_2 in serpentine and olivine) are collected in a slag, which generally contains 30% SiO_2 , 30% MgO , and 30% Al_2O_3 . The remaining 10% is composed of Cr_2O_3 , CaO , MnO , and FeO [65]. Control of slag composition is important with respect to melting temperature and fluidity. The ap-

proximate melting temperature may be derived from the ternary diagram for $\text{MgO}-\text{Al}_2\text{O}_3-\text{SiO}_2$ [68].

Low-carbon ferrochromium is produced by the silicothermic reduction of chromite ore. Silicon is used in the form of ferrosilicochromium, which is produced in submerged arc furnaces (as is high-carbon ferrochromium) by carbon reduction of chromite ore and quartzite. The solubility of carbon in the FeSiCr alloy depends on the silicon content; if the silicon content is higher, the carbon content is lower. The carbon solubility at different silicon contents and temperatures is shown in Table 7.24 [69]. The reduction of Cr_2O_3 by Si is enhanced by addition of lime (CaO), which reduces the activity of SiO_2 in the slag. The reduction may be written as follows:



Special chromium master alloys like CrMo , CrW , and CrNb are produced aluminothermically by coreduction of the relevant oxides together with chromium oxide.

Table 7.24: Solubility of carbon in ferrosilicochromium as a function of temperature, calculated from equations given in [69].

Silicon content ^a , %	Carbon content, %			
	1550 °C	1450 °C	1350 °C	1300 °C
20	2.34	2.21	2.08	2.02
30	0.66	0.60	0.54	(solid)
40	0.07	0.05	0.03	0.02
50	0.03	0.02	(solid)	(solid)

^a Cr:Fe = 2.67.

7.5.3.1 High-Carbon Ferrochromium

High-carbon ferrochromium is produced by direct reduction of chromite ores with carbon (coke, coal, or charcoal) in large, three-phase submerged arc furnaces with 10–50 MV A capacity (corresponding to 15 000–60 000 t/a of ferrochromium production). Elkem in Sweden operates the largest known electric arc furnace with 105 MV A capacity. This furnace is used to produce high-carbon ferrochromium and ferrosilicochromium.

Submerged arc furnaces work continuously as a low-shaft electric furnace, where the burden is charged around the self-burning Söderberg electrodes. These electrodes are deeply immersed in the burden column and discharge to the reduced liquid products, i.e., the metal and slag, on the bottom of the furnace. Metal and slag are tapped at regular intervals through tapholes near the furnace bottom; they flow into a ladle with a slag overflow leading to another ladle or to a slag pan. After the slag has been skimmed, the metal is poured into heavy, flat cast-iron molds lined with sand or into sand molds. The furnace hearth and the walls in the reaction zone are normally lined with carbon blocks or a ramming mix; in special cases, magnesite is used. The walls of the shaft are lined with fireclay or magnesite.

In older plants with relatively small submerged arc furnaces, the CO reaction gas is burned at the top of the furnace and then scrubbed. Modern submerged arc furnaces with high capacities are totally closed, and the unburned reaction gas (ca. 90% CO) is scrubbed. Thus, the volume of the off-gas can be minimized (by a factor of 10–20 compared to that of the open top furnace), and the investment costs for the gas-cleaning plant are correspondingly lower. Furthermore, the combustible gas can be used as a fuel for processes, such as calcining the limestone and drying and preheating the ore or the whole burden, or for producing energy.

The coke rate is calculated on the basis of the stoichiometric requirement of the oxides and on the amount of dissolved carbon in the

alloy; allowance is made for some combustion at the top of the furnace and for reaction with moisture. The slag composition is important to produce metal of desired quality and to maintain smooth furnace operation. Therefore, the slag is analyzed from tap to tap or once per shift, and the additives are altered accordingly. In modern plants, calculation of the burden and collection of data from the furnace are computerized [70].

The silicon content in high-carbon ferrochromium is dependent on the reduction temperature. High-melting slags lead to higher silicon content in the alloy (ferrochromium with 4–6% C). A typical slag composition is 30–33% SiO₂, 26–28% Al₂O₃, 20–25% MgO, 3–7% CaO, and 8–13% Cr₂O₃ for charge chrome containing 52–54% Cr, 6–7% C, and 2–4% Si produced from Transvaal ore or charge chrome containing 63–67% Cr, 5–7% C, and 3–6% Si produced from Zimbabwe ore.

The lumpiness of the ore and the coke quality are important to maintain a proper submerged arc process. Because of the high coke rate (ca. 25%), the coke properties (size, bulk density, volatile matter, and fixed carbon) are mainly responsible for the electrical resistance of the burden.

The current/potential ratio (*I/U*) is particularly important for large furnaces to maintain a reasonable power factor [71]; as a rule, *I/U* is approximately 200. Therefore, the electric power must be supplied at high current and low potential (e.g., 50 kA at 250 V). Specially constructed leads to the electrodes are necessary to carry the secondary current in order to avoid self-induction and energy losses [72].

Because more than 80% of chromite ores mined in the western world are finer than 10 mm, agglomeration processes have been adopted to provide a good burden porosity in the electric arc furnaces, especially in the larger ones [63]. In some ferrochromium plants, fines and lumpy ores are blended in ratios between 1:1 and 4:1. Thus, Union Carbide in Tubatse, South Africa, produces 120 000 t/a of charge chrome in three open submerged arc furnaces, each with a capacity

of 30 MV A. A blend of 80% fines and 20% lumpy ore is used. A submerged arc process can be maintained by using raking machines to break the crusts that are formed [73]. A Cr recovery of 75% was achieved for the production of a charge chrome containing 52.5% Cr, 6.4% C, 3.5% Si, 0.04% S, and 0.02% P, and a slag containing 38% SiO₂, 25.5% MgO, 4.5% CaO, 32% Al₂O₃, and 13% Cr₂O₃. The power consumption was 4000 kWh/t of alloy.

Middelburg Steel & Alloys in South Africa installed a briquetting plant with a capacity of 250 000 t/a. The use of briquettes improved the furnace performance and resulted in higher productivity and lower specific energy consumption. In two semiclosed submerged arc furnaces, each with a capacity of 30 MV A, 100 000 t/a of charge chrome (53.5% Cr, 7.4% C, 2–3% Si, 0.015% S, and 0.015% P) was produced with a power consumption of 3800 kW h/t of alloy [74].

Pelletizing of chromite fines and concentrates as an agglomeration process has been adopted by Gesellschaft für Elektrometallurgie (GfE) in Germany using the Lepol (grate kiln) process [75], and by Ferrolegeringar in Trollhättan, Sweden, using the Cobo (cold bond) process [76]. These pellets can be used for the production of ferrochromium and silicochromium.

Sintered chrome ore fines were used successfully in Japan. However, briquetting is the main agglomeration method used [63].

Figure 7.20 shows the new process developed by Outokumpu Oy in Finland for the production of ferrochromium from their own chromite-containing deposit near the town of Kemi [77, 78].

The chromite concentrate is pelletized, using bentonite as a binder. After sintering in a shaft furnace, the pellets are blended with fluxes and coke. This burden is then preheated in a rotary kiln at 1000–1100 °C and charged to a fully closed 24 MV A submerged arc furnace producing 60 000 t/a of charge chrome (53.5% Cr, 7% C, and 2.5% Si) and slag (30.2% SiO₂, 24.9% MgO, 6.8% CaO, 25.9% Al₂O₃, 6.8% Cr, and 1.8% Fe); Cr recovery is 84%. The off-gas from the furnace (ca. 90%

CO) has a heat value of 3.07 kWh/m³ (STP) and is used as a fuel for the shaft furnace and for heating the kiln.

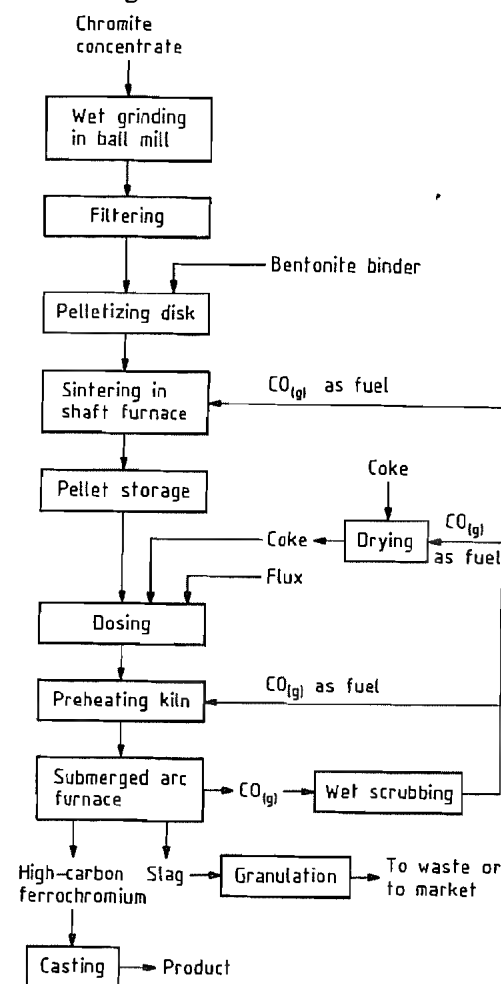


Figure 7.20: Outokumpu Oy high-carbon ferrochromium process [77, 78].

This technology results in a low specific energy consumption of 2600–2800 kWh/t of charge chrome. The process has been adopted in other countries (Orissa Mining in India, Elazig in Turkey, Hellenic Ferroalloys in Greece, and Ferrochrome Philippines in the Philippines). Ferrochrome Philippines successfully began production in 1984 in a 20 MV A furnace rated for 50 000 t/a of high-carbon ferrochromium [79].

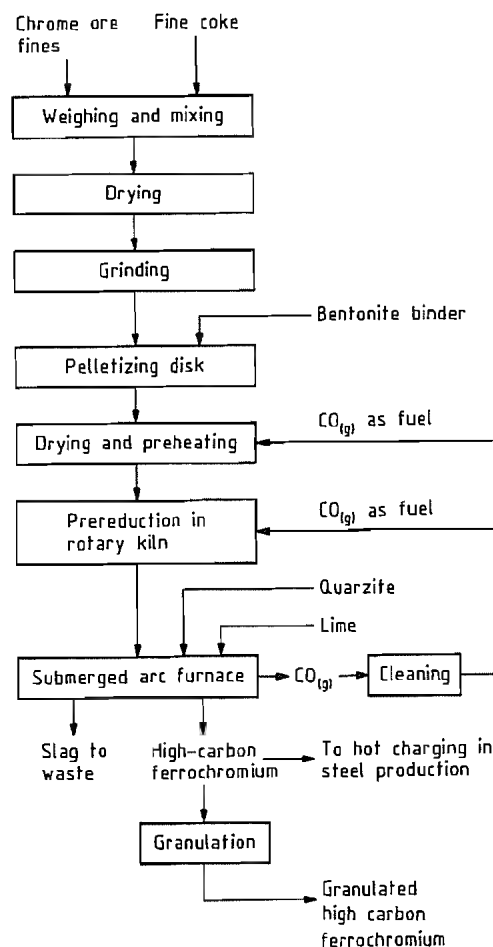
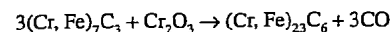


Figure 7.21: Showa Denko high-carbon ferrochromium process [80, 81].

A further improvement in specific energy consumption was achieved by the SRC process (solid-state reduction of chrome ores), developed by Showa Denko K. K. in Japan [80, 81]. This process is shown in Figure 7.21. The addition of carbon and flux during pelletizing resulted in a reduction of iron oxide and a partial reduction of chromium oxide during sintering in a rotary kiln at 1350–1450 °C. Hot charging a burden containing 60% prereduced pellets in a closed 18 MV·A submerged arc furnace required an energy consumption of 2000–2100 kWh/t of alloy for an annual production of 50 000 t high-carbon ferrochromium.

mium (57–60% Cr, ca. 8% C, and ca. 3% Si). This process was also adopted by Johannesburg Consolidated Investment (South Africa) in a 180 000 t/a ferrochromium plant.

A special ferrochromium 4–6% C grade with 60–72% Cr and max. 1.5% Si was used for many years in the steel industry before inexpensive charge chrome from South Africa became more attractive. This ferrochromium is not saturated with carbon. It is produced the same way as charge chrome in large submerged arc furnaces, but with a magnesite lining instead of a carbon lining. This process has been improved by using chromite ore mixes containing a definite fraction of hard and lumpy refractory ores with a high MgO content to produce a high-melting slag (e.g., 29–32% SiO₂, 32–35% MgO, 29–32% Al₂O₃, and 3.5–6.0% Cr₂O₃) [82, 83]. At a higher reduction temperature of 1500–1700 °C, the following refining reaction of the refractory ore takes place [66]:



Because of the low sulfur specification (< 0.05%) in this grade, coke with low sulfur content is used as the reductant; 30–35% of the sulfur in the coke is transferred to the metal. Alternatively, desulfurizing slags may be used. The ferrochromium can be poured into a highly basic fluid slag, e.g., slag from the LC-ferrochromium process. The sulfur forms CaS, which is removed in the slag.

A new process for producing ferrochromium with 5% C and < 1% Si from unagglomerated chromite fines in a transferred arc plasma furnace has been developed by Tetronics Research & Development [84]. Commercialization of this process has been accomplished in South Africa, where a 10.8 MV·A plasma furnace has been built [85].

7.5.3.2 Medium-Carbon Ferrochromium

Medium-carbon ferrochromium with 0.5–4% C can be produced by refining high-carbon ferrochromium or by silicothermic reduction of chromite ores. Batch refining of high-

carbon ferrochromium with refractory chromite ores in an electric arc furnace is no longer used because of the high power consumption of 8000–9000 kWh/t of ferrochromium [72].

Decarburization of high-carbon ferrochromium in an oxygen-blown converter is more economical, especially on a large scale. In the United States and Japan, a top-blowing process with oxygen using water-cooled lances to the metal surface was used. In Germany, a bottom-blowing process (OBM = oxygen bottom Maxhütte or Q-BOP) was introduced in the 1970s [86]. This process is characterized by oxygen injection from the bottom into the metal bath with the oxygen jet, resulting in a high decarburization rate of ca 0.3% C/min. Because of the high bath temperature (1800–1850 °C), mainly the carbon is oxidized. Chromium recovery is high; for example, recovery of product with 0.8–1% C is 85%, and it is improved to 90–93% by adding silicochromium and lime. A typical sequence for a blow is shown in Figure 7.22 [87].

Because demand for medium-carbon ferrochromium is small compared to demand for the high-carbon material, the decarburization processes are rarely used. However, reduction of chromite ores with silicon in the form of silicochromium is used and is an economical production method for medium-carbon ferrochromium because the low-carbon grade can be produced as well. To make ferrochromium with 1–2% C, a silicochromium alloy with a Si content of 25–30% can be used (see Table 7.24). The power consumption, including the energy for silicochromium, amounts to 5000–6000 kWh/t of ferrochromium.

7.5.3.3 Low-Carbon Ferrochromium

Low-carbon ferrochromium is produced mainly by silicothermic reduction of chromite ores. This process dates back to the Swedish three-step process introduced in 1920 by A. B. Ferrolegeringar in Trollhättan [72].

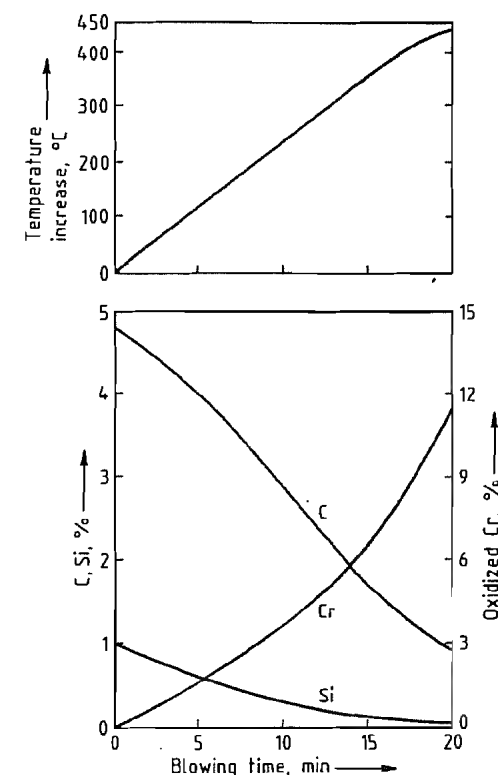


Figure 7.22: Sequence of an OBM-oxygen blow of carbon ferrochromium [87].

In step one, chromite ore was totally reduced with carbon in an electric arc furnace to an intermediate ferrochromium (Halbprodukt) with 60–65% Cr, 5–6% C, and 5–7% Si, and a discard slag. In step two, this intermediate ferrochromium was smelted with quartzite and coke in a slagless process to produce silicochromium (40–45% Si, ca. 40% Cr, and < 0.5% C). Finally, this silicochromium was used as a reductant in the third step; the crushed alloy was thrown onto the surface of a chrome ore-lime melt in an arc furnace. The tapped ferrochromium contained ca. 70% Cr, ca. 1% Si, and 0.03–0.05% C. The slag, which contained 20–25% Cr₂O₃, was returned to the first step to improve Cr recovery.

This Swedish process was modified, especially when the direct silicochromium production by carbothermic coreduction of chromite ore and quartzite in large submerged arc fur-

naces in one step proved more economical than the slagless process. Furthermore, the silicothermic conversion was improved by adding more lime to form a highly basic slag (CaO/SiO_2 ratio of ca. 2). Thus, ferrochromium with < 1.5% Si was produced with a lean slag (ca. 5% Cr_2O_3) in one step. Residual elements, i.e., S and N, were low (< 0.01% and < 0.02%, respectively). The power consumption was 3000–3500 kWh/t of ferrochromium for the silicothermic process (arc furnaces with 2–10 MV·A capacity) and, including the power consumption for the silicochromium production, was 8000–9000 kWh/t ferrochromium.

Currently, the most important process for the production of LC ferrochromium is the Perrin process, developed in 1937 by the Société Ugine in France [88]. This process combines the direct reduction of silicochromium in a submerged arc furnace with a countercurrent silicothermic reduction of a chrome ore-lime melt (produced in an arc furnace) in a reaction ladle.

Production of Silicochromium. Silicochromium is not only used as a reductant in the production of LC ferrochromium, but also as an alloying and deoxidizing agent in the steel industry.

Silicochromium is made in large three-phase submerged arc furnaces of 10–36 MV·A capacity. These furnaces are of the same type as those used to produce HC ferrochromium. The lower reaction zone is lined with carbon and the upper side walls of the furnace shaft are lined with fireclay bricks. Maintaining the Söderberg electrodes deep in the burden column (30–50 cm above the hearth) is important to reduce the SiO_2 to Si. Therefore, coke with low electric conductivity and low bulk density (< 400 kg/m³) is used (e.g., gas coke).

The electrical conditions in silicochromium furnaces are somewhat different from those in furnaces used to produce HC ferrochromium; e.g., the current/potential ratio is higher (I/U = ca. 500) [72]. The volume of $\text{CO}_{(g)}$ from silicochromium production is much higher than

from HC ferrochromium production. Therefore, a porous burden is essential. To scrub the huge volumes of $\text{CO}_{(g)}$ produced, modern silicochromium furnaces are closed systems, and the unburned gas is used as a fuel.

To produce an alloy composed of 45% Si, 40% Cr, and 0.02% C, a burden containing 100 parts of a refractory chromite (high Cr/Fe ratio of ca. 3 and a $\text{MgO/Al}_2\text{O}_3$ ratio of 1.2–1.4), 110 parts of quartzite, and 65 parts of coke (85% fixed C) is continuously charged to the submerged arc furnace. Metal and slag are tapped every few hours. The slag contains 48–50% SiO_2 , 25–27% MgO , 19–21% Al_2O_3 , and 1–3% Cr_2O_3 . The Cr recovery is 93–95%, and the power consumption is 7500–8500 kWh/t of alloy (45% Si). The power consumption is primarily dependent on the Si content of the alloy. For a silicochromium with 40% Si and 45% Cr, the power consumption is 6500–7500 kWh/t.

Production of LC Ferrochromium by the Perrin Process. Single-stage silicochromium production is one portion of the Perrin process. This process requires two furnaces: a submerged arc furnace to produce silicochromium and an open-top electric arc furnace to melt a chromite ore-lime slag. A flow sheet of the entire process is shown in Figure 7.23.

The silicochromium and slag from the submerged arc furnace are tapped to a lined segregating ladle and are allowed to settle for 1–2 h. Dissolved SiC floats to the top. The separated alloy (40–45% Si, 45–40% Cr, and 0.05–0.02% C) is removed through a taphole at the bottom of the ladle. The alloy is reacted with an intermediate liquid slag (8–10% Cr_2O_3) in a second basic-lined reaction ladle to produce an intermediate alloy and a discard slag. The intermediate alloy (20–25% Si, 60–55% Cr, and 0.05–0.03% C) is allowed to solidify and is separated from the slag (< 1% Cr_2O_3). Because of its high basicity, the slag disintegrates to powder (falling slag).

The rich slag (chrome ore lime melt with 25–27% Cr_2O_3 , 7–8% FeO , 2–3% SiO_2 , and 45–48% CaO) is tapped from the open-top electric arc furnace in weighed amounts to an-

other basic-lined reaction ladle. Crushed intermediate alloy from the first reaction ladle is added to form the desired LC ferrochromium (ca. 70% Cr, < 1.5% Si, and 0.02–0.05% C) and an intermediate slag (8–10% Cr_2O_3). This slag is reacted with silicochromium to lower the Cr_2O_3 content to < 1%.

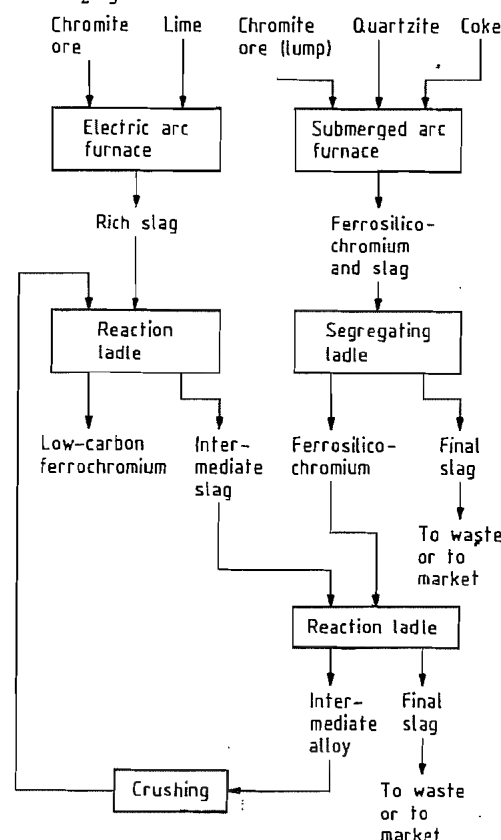


Figure 7.23: Low-carbon ferrochromium production by the Perrin process [88] (according to [65]).

Production of 1 t of silicochromium by this process typically requires 1450 kg of chrome ore, 1500 kg of quartzite, 870 kg of coke, 32–35 kg of electrodes, and 7700 kWh power [65]. Production of 1 t of ferrochromium requires 1440 kg of chrome ore, 1250 kg of lime, 660 kg of silicochromium (45% Si and 40% Cr), 22 kg of electrodes, and 3200 kWh power.

Therefore, the total energy consumed to produce 1 t of LC ferrochromium, including

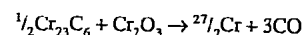
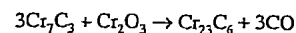
silicochromium production, is 8200 kW·h. The overall recovery of Cr by the Perrin process is 90–92%.

Low-carbon ferrochromium is tough and difficult to break. Therefore, it is poured into flat molds, sometimes filled with liquid slag to protect the mold. Quenching the hot alloy in water facilitates breaking it into small lumps, which is performed with heavy pneumatic hammers.

Many variations of the Perrin process have been developed. For example, chrome ore or lime have been added to the exothermic reactions, which occur in the two reaction ladles (Figure 7.23), to “dampen” the reaction and to save energy. Another variation is the selective reduction of FeO , producing an iron-rich alloy; the remaining slag, high in Cr_2O_3 , is reacted with silicochromium high in Si, to give LC ferrochromium (80–90% Cr). By selectively reducing FeO , CoO is also reduced in the iron-rich alloy and a Co-free ferrochromium can be produced. This is used to produce alloyed steels for atomic energy plants.

Production of LC Ferrochromium by the Simplex Process. From 1943 to 1953 Union Carbide developed a new production process for LC ferrochromium, the so-called Simplex process, in which finely ground HC ferrochromium was decarburized in the solid state with oxidized ferrochromium by vacuum annealing [89–91]. The plant in Marietta, Ohio, went into production in 1953 and is now managed by Elkem Metals Co., Pittsburgh, Pennsylvania. The flow sheet of the process is shown in Figure 7.24.

High-carbon ferrochromium is crushed, pulverized in ball mills, and then oxidized in suspension in a vertical gas- or oil-fired shaft furnace [92]. The proper stoichiometric C/O ratio for decarburizing is attained by mixing the oxidized material with HC ferrochromium powder according to the following reactions:



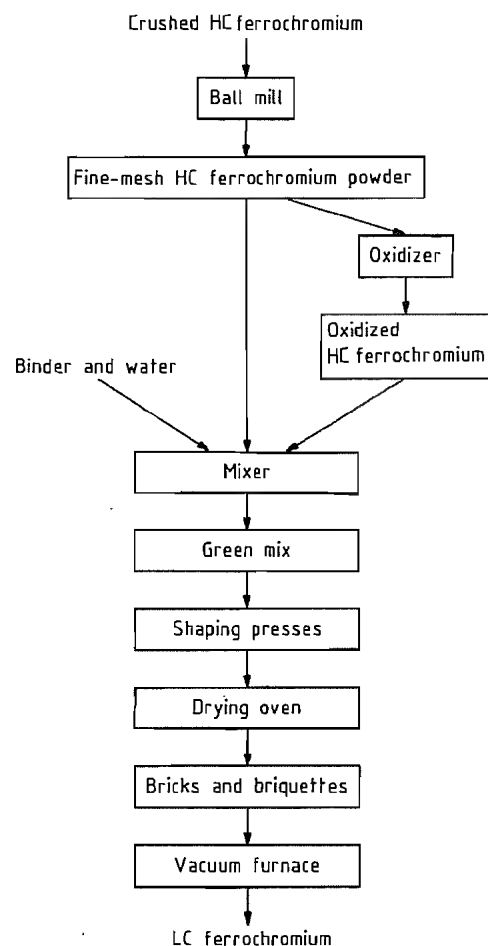


Figure 7.24: Production of low-carbon ferrochromium by the Simplex process [90].

The mixture is either formed into briquettes or loosely packed in corrugated pasteboard boxes, placed on a refractory topped bogie hearth (33.5 m × 3.35 m), and rolled into the vacuum chamber, which is a horizontal steel cylinder (43 m in length × 4.6 m in diameter). The graphite resistance heating elements are suspended above the charge from the refractory-lined roof. The vacuum (0.01–0.4 kPa) is generated by multistage steam ejectors. The process requires a special heating program up to 1370 °C, which follows the progress of decarburization. When the decarburization of the

charge is complete, the power is shut off and the furnace is cooled by flooding with argon.

A complete reaction cycle requires 4–5 d; ca. 100 t of material is produced. A typical analysis of LC ferrochromium from the Simplex process is ca. 70% Cr, ca. 1% Si, and 0.008–0.010% C. Oxygen is higher (ca. 1%) than in LC ferrochromium from the Perrin process (ca. 0.2%).

7.5.3.4 Nitrogen-Containing Low-Carbon Ferrochromium

Chromium has a high affinity for nitrogen and forms the nitrides Cr_2N and CrN . Low-carbon ferrochromium can form nitrides either in the solid or in the liquid state. These alloys with up to 10% N are used in steel containing nitrogen as well as chromium [58]. The Simplex process is convenient for forming nitrides in LC ferrochromium in the solid state. During the cooling cycle, nitrogen is added to the vacuum vessel and the optimum temperature range of 1200–800 °C is held over a longer period to produce an alloy with 7–10% N.

Silicothermically produced LC ferrochromium can form nitrides when pulverized and heated in boxes in a continuous annealing furnace at 1000 °C under nitrogen [93]. The sintered product (ρ 5–6 g/cm³) contains 5–10% N as Cr_2N .

On the other hand, LC ferrochromium can form nitrides in the liquid state with nitrogen gas in a melting furnace, e.g., an induction furnace [94]. The tapped alloy contains 2–4% N and is very homogeneous (ρ 7.0 g/cm³) [95].

7.5.3.5 Other Chromium Master Alloys

Chromium master alloys other than ferrochromium are produced in much smaller amounts. They are used mainly to produce heat-resistant alloys, based on nickel or cobalt (superalloys), and abrasion-resistant materials, and are used to alloy small amounts of chromium to copper or aluminum.

Nickel–chromium master alloys containing 50–80% chromium may be made by alumin-

thermic processes or by melting chromium metal and nickel in induction-heated furnaces. The aluminothermic process must be performed in water-cooled molds in an inert atmosphere because of the high quality required of these master alloys [96]. For direct melting of chromium metal and nickel, a vacuum induction furnace or an inert gas atmosphere is also preferred; refining occurs simultaneously during melting [97].

Binary chromium master alloys, such as *chromium–molybdenum* (with 30% Mo) or *chromium–niobium* (with 30–80% Nb) [98, 99], are made by aluminothermic reduction of the corresponding oxides. Master alloys containing more than two metals, e.g., *cobalt–chromium–tungsten* (ca. 43% Co, ca. 37% Cr, ca. 16% W, ca. 3% C), or *cobalt–chromium–molybdenum* (26–30% Cr, 4–5% Mo, rest Co) [99], are made by direct melting of the metals in an inert atmosphere or in vacuum induction furnaces. *Copper–chromium* master alloys containing up to 10% Cr, e.g., V–CuCr 10 [100], are made by directly alloying chromium with an oxygen-free copper melt; the resulting alloy is quickly cast into flat pigs. The same method is used for the production of *aluminum–chromium* master alloys with 5, 10, or 20% Cr by alloying comminuted chromium metal with a superheated aluminum melt. The master alloy containing 5–6% Al is standard in Germany, i.e., V–AlCr 5 [101]. Another aluminum chromium master alloy containing ca. 50% Cr and 50% Al is made for special purposes [99].

7.5.4 Quality Specifications, Storage and Transportation, and Trade Names

International standards of specifications and conditions of delivery for ferrochromium and ferrosilicochromium are given in ISO 5448 [102] and ISO 5449 [103], respectively. The following specifications are contained in tables in reference [102]:

- Chromium content of ferrochromium alloys ranges from 45 to 95% [102, Table 1]; e.g.,

the designation is FeCr 50 for 45–55% Cr content.

- Composition of HC ferrochromiums with normal phosphorus [102, Table 2] and with low phosphorus content [102, Table 3]; e.g., FeCr 50 C 50 (45–55% Cr, 4–6% C, max. 1.5% Si, max. 0.050% P, and max. 0.10% S), or FeCr 60 C 50 Si 2 LP (55–65% Cr, 4–6% C, 1.5–3% Si, and max. 0.03–% P). HC ferrochromium is standardized to 10% C. Ferrochromium with low sulfur content is designated LS (low sulfur, i.e., max. 0.05%).
- Analysis of MC ferrochromiums with normal phosphorus [102, Table 4] and with low phosphorus [102, Table 5]; carbon content ranges from 0.5–1.0%, 1.0–2.0%, up to 2.0–4.0%, e.g., FeCr 70 C 20 (65–75% Cr, 1.0–2.0% C, max. 1.5% Si, max. 0.050% P, and max. 0.050% S); or FeCr 60 C 10 LP (55–65% Cr, 0.5–1.0% C, max. 1.5% Si, max. 0.03% P, and max. 0.050% S).
- Standard chemical composition of LC ferrochromium for normal [102, Table 6] and for low [102, Table 7] phosphorus alloys; carbon content ranges from less than 0.015%, 0.015–0.030%, up to 0.25–0.50%; e.g., FeCr 60 C 05 (55–65% Cr, 0.03–0.05% C, max. 1.5% Si, max. 0.050% P, max. 0.030% S, and max. 0.15% N) or FeCr 70 C 03 LP (65–75% Cr, 0.015–0.03% C, max. 1.5% Si, max. 0.03% P, max. 0.03% S, and max. 0.15% N).
- LC ferrochromium with high chromium content (75–95%) [102, Table 8]; e.g., FeCr 90 C 03 (85–95% Cr, 0.015–0.03% C, max. 1.5% Si, max. 0.020% P, max. 0.03% S, max. 0.02% Co, and max. 0.20% N).
- Nitrogenated LC ferrochromiums [102, Table 9]; the three given are smelted FeCr...C1 N3, sintered FeCr–C1 N7, and sintered FeCr...C1 N7 Si. The Cr contents given in [102, Table 1] are valid for these alloys. The nitrogen contents are 2–4% in the smelted qualities and 4–10% in the sintered qualities.

- Particle size ranges for ferrochromium deliveries [102, Table 9]; there are seven classes from 100–315 mm (Class 1) to ≤ 3.15 mm (Class 7).

ISO Standard 5448 [102] also covers testing (sampling and chemical analysis) as well as storage and transportation according to international regulations. ISO Standard 5449 [103] for ferrosilicochromium specifications and conditions of delivery recognizes 12 different compositions with increasing Si content, ranging from FeCrSi 15 (min. 55% Cr, 10%–18% Si, max. 6% C, max. 0.05% P, and max. 0.03% S) up to FeCrSi 50 (min. 20% Cr, 45–60% Si, max. 0.1% C, max. 0.03% P, and max. 0.03% S). Low-carbon and low-phosphorus grades are FeCrSi 50 LC (max. 0.05% C) and FeCrSi 48 LP (min. 35% Cr, 42–55% Si, max. 0.05% C, max. 0.02% P, and max. 0.01% S). The particle size of ferrosilicochromium deliveries is specified in seven classes as for ferrochromium. Ferrochromium and ferrosilicochromium are shipped in bulk or packaged in containers or steel drums.

In the United States, standards for ferrochromium and ferrosilicochromium are specified in ASTM A 101–73 [104] and ASTM A 482–76 [105]. Also recommended are methods for sampling (ASTM–E32) and chemical analyses (ASTM–E31). Comparisons between the standards in Germany for ferrochromium and ferrosilicochromium in DIN17565 [106]

and the ISO standards are given in Tables 7.25 and 7.26 [107].

Internationally approved methods for sampling [108] and analytical determination of chromium in ferrochromium and ferrosilicochromium [109] and of silicon in ferrosilicochromium [110] are available as a draft.

Table 7.27 contains trade names and the relevant analyses of special and nonstandardized ferrochromium and ferrosilicochromium alloys. Charge chrome is a relatively cheap high-carbon ferrochromium with no definite specification. It can be added to a basic oxygen-blown stainless steel charge [65]. Extra-high-carbon (EHC) ferrochromium is supplied as a powder for abrasive surface-welding purposes. Simplex ferrochromium is a low-carbon ferrochromium produced by the Simplex process. Low-carbon and -nitrogen (LCN) and low-carbon, -nitrogen, and -silicon (LCNSi) ferrochromium are trade names for special grades used to manufacture corrosion- and heat-resistant steel. A low-carbon ferrochromium reactor grade is used to make corrosion- and heat-resistant steel for nuclear equipment. Cromax is a low-carbon, high-chromium ferrochromium used to produce heat-, corrosion-, and wear-resistant special steel. The high-chromium alloys can partly replace chromium metal in superalloys. Silicochrom 40 is mainly used for deoxidizing steel and for Cr₂O₃ reduction in slags; silicochrom 60 for alloying corrosion- and heat-resistant steel.

Table 7.25: Comparison of the chemical composition of ferrochromium ISO 5448 and DIN 17565 [107].

Designation	% Cr		% C		% Si		% P max.		% S max.	
	SIN	ISO	DIN	ISO	DIN	ISO	DIN	ISO	DIN	ISO
FeCr 70 C 5	60–72	—	4.0–6.0	—	< 1.5	—	0.030	—	0.50	—
FeCr 50/60/70 C 50	—	45–75 ^a	—	4.0–6.0	—	< 1.5	—	0.050	—	0.10
FeCr 50/60/70 LSLP	—	45–75 ^a	—	4.0–6.0	—	< 1.5	—	0.030	—	0.05
FeCr 70 C	65–75	—	0.5–4.0 ^b	—	< 1.5	—	0.030	—	0.050	—
Fe 50/60/70 C	—	45–75 ^a	—	0.5–4.0 ^b	—	< 1.5	—	0.050	—	0.050
FeCr 70 C ^c	65–75	—	0.01–0.50 ^d	—	< 1.5	—	0.030	—	0.010	—
FeCr 50/60/70 C	—	45–75 ^a	—	0.015–0.50 ^e	—	< 1.5	—	0.050	—	0.030

^a FeCr 50 means 45–55% Cr, FeCr 60 means 55–65% Cr, FeCr 70 means 65–75% Cr.

^b In four grades.

^c 0.15% N.

^d In seven grades.

^e In six grades.

Table 7.26: Comparison of the chemical composition of ferrosilicochromium ISO 5449 and DIN 17565 [107].

Designation	% Cr		% C		% Si		% P max.		% S max.	
	SIN	ISO	DIN	ISO	DIN	ISO	DIN	ISO	DIN	ISO
FeCrSi 15	—	> 55.0	—	10.0–18.0	—	6.0	—	0.050	—	0.030
FeCrSi 20/22	55–65	> 55.0	25–20	20.0–25.0	0.50	0.05	0.020	0.030	0.010	0.030
FeCrSi 23	—	> 45.0	—	18.0–28.0	—	3.5	—	0.050	—	0.030
FeCrSi 26	—	> 45.0	—	24.0–28.0	—	1.5	—	0.030	—	0.030
FeCrSi 33	—	> 43.0	—	28.0–38.0	—	1.0	—	0.050	—	0.030
FeCrSi 40	40–45	> 35.0	45–35	35.0–40.0	0.050	0.2	0.020	0.030	0.010	0.030
FeCrSi 45	—	> 28.0	—	40.0–45.0	—	0.1	—	0.030	—	0.030
FeCrSi 50 LC	—	> 20.0	—	45.0–60.0	—	0.05	—	0.030	—	0.030
FeCrSi 55	—	> 28.0	—	50.0–55.0	—	0.03	—	0.030	—	0.030
FeCrSi 48 LP	—	> 35.0	—	42.0–55.0	—	0.05	—	0.020	—	0.010

Table 7.27: Special and nonstandardized ferrochromium and ferrosilicochromium alloys.

Trade name	Analysis, %							Producer
	Cr	C	Si	P	S	N	Co	
Charge chrome ^a	53–58	5–8	6–3	—	—	—	—	—
EHC ferrochromium	min. 66	min. 9.0	0.5–1.0	max. 0.03	max. 0.05	—	—	GfE/EWW ^b
Simplex ferrochromium	ca. 70	max. 0.01	ca. 1.0	—	—	—	—	Union Carbide/Elkem
LCN ferrochromium	ca. 70	max. 0.05	max. 1.5	—	—	max. 0.020	—	GfE/EWW ^b
LCNSi ferrochromium	ca. 70	max. 0.05 max. 0.03	max. 0.30 max. 0.20	—	—	max. 0.020	—	GfE/EWW ^b
Ferrochromium reactor grade	80–85	max. 0.06 max. 0.05	max. 2.5 max. 1.50	—	—	max. 0.20	max. 0.02	ABF/FTA ^c
Cromax-90 chrome	85–90	max. 0.06 max. 0.03	max. 1.0 max. 0.5	max. 0.015 min. 0.007	max. 0.015 min. 0.007	—	—	Showa Denko
Silicochrom 40	35–40	max. 0.05	35–40	max. 0.03	—	—	—	GfE/EWW ^b
Silicochrom 60	55–65	max. 0.05	20–25	max. 0.03	—	—	—	GfE/EWW ^b

^a Alloy has no definite specification.

^b Gesellschaft für Elektrometallurgie/Elektrowerk Weisweiler.

^c Aktiebolaget Ferrolegeringar/Trollhätteverken.

7.5.5 Uses

Ferrochromium is used principally as a master alloy to produce Cr-containing steel and cast iron [58]. Chromium alloyed in steel imparts oxidation and corrosion resistance because of the formation of a thin, continuous, impervious chromium oxide film on the steel surface.

Most ferrochromium is used to manufacture stainless steel. Martensitic grades with ca. 13% Cr are used for applications such as knives, whereas ferritic grades with 18–22% Cr are used as deep-drawing sheets. Austenitic CrNi steels exhibit especially good corrosion (acid) resistance and are used for equipment in

the chemical industry as well as for food-processing machinery. The most widely known type is AISI 302, which contains 18% Cr and 8% Ni. A small amount of molybdenum further improves the acid resistance. Heat-resistant steel (24–26% Cr and 19–21% Ni) is used in power stations for steam boilers and heat exchangers; superalloys based on nickel or cobalt (ca. 30% Cr) are used for gas turbine parts.

Chromium addition to steel also improves its mechanical properties (ability to harden, wear resistance, and retention of strength at elevated temperature). Steel with 0.5–2.0% Cr is widely used in the automotive industry as

case-hardening steel ($\leq 0.2\%$ C and 1.4–2.1% Ni) and heat-treatable steel (0.2–0.5% C, 0.9–2.1% Ni, and 0.15–0.35% Mo). Abrasion-resistant steel for ball bearings is alloyed with 0.5–1.6% Cr (ca. 1% C and 0.2% Mo). Permanent magnetic steel contains 1–3% Cr (1.0–1.3% C). In tool steel for cold and hot working and high-speed steel, up to 14% Cr is alloyed as carbide (in addition to carbides of W, Mo, and V). Stellites (35–70% Co, 25–33% Cr, 10–25% W, and 2–4% C) are highly resistant to abrasion and are used for cutting tools.

Addition of up to 30% chromium to cast iron improves hardness and heat resistance. Powdered ferrochromium (mainly the high-carbon grade) is used for chromizing the surface of steel or cast iron parts (pack-chromizing or case-chromizing. A high-carbon ferrochromium with extra-high-carbon content is used in powdered form for abrasive surface welding (Table 7.27, EHC Ferrochromium).

7.5.6 Economic Aspects

Ferrochromium is mainly consumed in highly industrialized countries producing a major amount of high-grade (stainless) steel, e.g., the United States, Europe, and Japan. However, production is shifting from these consuming countries to those with large ore resources; 93% of the known potential chromite reserves of the world are in Africa, mainly in South Africa, and ca. 3% in the former USSR and Albania [111] (see Table 46.1). This shift is a consequence of modern oxygen-blowing processes in combination with argon and vacuum treatment, i.e., argon-oxygen decarburization and vacuum-oxygen decarburization, for the production of stainless steel. These processes allow the use of cheap HC ferrochromium (charge chrome) instead of LC grades. Formerly only LC ferrochromium could be used. Because power consumption for production of HC ferrochromium is only about half that of the LC grade, the availability of cheap hydroelectric power in Scandinavia is no longer as advantageous. The change in

ferrochromium consumption from LC to HC grades first took place in the United States and later, in the 1970s, in Europe [112].

In 1984, world production of marketable, i.e., lumpy, ore and concentrates was 9.2×10^6 t, 11% of which was produced in Western Europe, Finland, Turkey, Greece, and Cyprus, 37% in Eastern Europe (former USSR and Albania), 4% in Latin America (Brazil and Cuba), 9% in Asia (Philippines, India, Iran, Vietnam, Japan, and Pakistan), and 38% in Africa (South Africa, Zimbabwe, Madagascar and Sudan) [113]. In 1984, the world production of chromite ore and concentrates was 9.9×10^6 t, 72% of which was consumed for metallurgical, 12% for refractory, and 17% for chemical purposes.

The metallurgical industry was the main user of chromium and consumed the following amounts in 1980 (based on United States statistics) [114]: 72% for wrought stainless and heat-resistant steels, 13% for wrought alloy steel, 3% for tool steel, 7% for cast iron and cast steel, and 5% for other uses. In 1984, the total consumption of primary chromium units (from ferrochromium) in the United States was 195 380 t of which 79% was for the production of stainless and heat-resisting steels, i.e., 96 kg of chromium units per ton of stainless and heat-resisting steels produced [115]. The ferrochromium consumption in Germany was 263 300 t in 1985. The change in consumption of LC to HC ferrochromium over the last 25 years is evident from Table 7.28.

In 1981, consumption of ferrochromium in the western world was estimated to be $(1.32\text{--}1.36) \times 10^6$ t; ca. 0.5×10^6 t of this was consumed in the European Economic Community (EEC). In 1982, consumption fell drastically because of the recession in the steel industry. Consumption in the western world has since increased to ca. 2×10^6 t [116]. In 1981, the production capacity for ferrochromium plants in the western world was 3.1×10^6 t [86].

Prices of ferrochromium and ferrosilicochromium are reported weekly in *Metal Bulletin* (London). *Erzmetall* (published monthly) reports prices twice a year for raw materials and for ferrochromium. *American Metal Mar-*

ket is a daily publication that also gives chromium ore and alloy prices.

Because the United States does not possess chromite deposits, most of the ferrochromium consumed is imported, mainly from Africa [117].

7.5.7 Environmental Protection; Toxicology and Occupational Health

Considerable attention must be paid to environmental protection during ferrochromium production. Dust evolution from ores and raw materials must be controlled during transportation and storage, and also during preparatory processes.

The off-gas from the electric arc furnaces is cleaned by using devices, such as bag filters, scrubbers, and electrostatic precipitators [72]. Bag filters are mainly used in preparatory processes, e.g., grinding, drying, briquetting [74], and pelletizing [75], and in open or semiclosed submerged arc furnaces [73, 74]. Scrubbers (Venturi and disintegrators) are preferred for cleaning unburned CO gas from closed submerged arc furnaces [77]. Effluent water from the scrubber is treated to meet wastewater regulations. Electrostatic precipitators (Cottrell filters) are also used for cleaning the off-gas from submerged arc furnaces for HC ferrochromium [118] and ferrosilicochromium [119] production. Gas from the chrome ore-lime melting furnace and from the ladle reactions during the Perrin process are cleaned with bag filters [120]. The dust content can be lowered from 150 to 20 mg/m³ and the emis-

sion of Cr(VI) to < 1 mg/m³ by optimizing the working conditions.

Chromium(VI) is mainly responsible for the toxicity of chromium and its compounds. Chromic acid, CrO₃, is carcinogenic. Germany has enacted an emission protection law and a technical guidance for clean air (TA-Luft) [121]. The TA-Luft restricts the mass of carcinogenic substances, i.e., Cr(VI) compounds (specified as Cr), in respirative form to 1 mg/m³ (Class II). The total dust concentration in emissions is limited to 20 mg/m³, and other inorganic materials in dust form, i.e., chromium and its compounds (Class III), to 5 mg/m³. The maximum allowable concentration (MAK) of CrO₃ (measured as CrO₃) in the air at the workplace is 0.1 mg/m³ [122].

In the United States the Clean Air Act Amendments, enacted in 1970, mandated the states set standards to limit air pollution. In pursuing this amendment, the U.S. Environmental Protection Agency (EPA) in a joint effort with the Ferroalloys Association studied dust emissions from alloy plants to establish ambient air quality standards [123, 124]. The states enacted process weight regulations and applied them to ferroalloy furnaces. The EPA published their studies "Engineering and Cost Study of the Ferroalloy Industry" and proposed New Source Performance Standards (NSPS) for new furnaces. A comparison of the state regulations and the NSPS (promulgated October, 1974) limitations for HC ferrochromium, charge chrome, and ferrosilicochromium for a 30-MW furnace are shown in Table 7.29 [124].

Table 7.28: Ferrochromium consumption in Germany.

	Consumption, t/a					
	1960	1965	1970	1973	1983	1985
LC ferrochromium	43 450	34 650	44 500	33 550	13 000	14 350
MC ferrochromium	20 300	24 400	16 700	18 400	7 500	11 600
HC ferrochromium	7 500	17 550	70 600	113 150	210 000	237 350
Total	71 250	76 600	131 800	165 100	220 500	263 300

Table 7.29: Comparison of NSPS limitations and state regulations for ferrochromium dust emissions [124].

Material	NSPS limitation		State regulation	
	kg/(mw·h)	kg/h	Most stringent	Least stringent
HC ferrochromium	0.23	6.94	13.00	17.55
Charge chrome	0.23	6.94	13.00	17.55
Ferrosilicochromium	0.23	6.94	8.29	10.80

Regulations on water pollution control (the federal act was passed in 1972) were also proposed by the Ferroalloys Association Environmental Committee and EPA [124]. Finally, the disposal of solid waste (slags, dusts, etc.) is also subject to regulations.

The TLV-TWA (1985–1986), which have been adopted, are as follows [125]: 0.5 mg/m³ for chromium metal and chromium(II) and chromium(III) compounds, and 0.05 mg/m³ for chromite ore processing (chromate) as Cr and chromium(VI) compounds as Cr. Chromite ore processing and certain water-insoluble Cr(VI) compounds are listed in Appendix A1a as human carcinogens.

7.6 Ferronickel

The rotary kiln electric furnace smelting process is now used almost universally for the production of ferronickel from oxide ores. Nippon Mining shut down the last blast furnace producing ferronickel, at Saganoseki in Japan, in 1985 [131]. Variations on the electric furnace ferronickel process, which were developed in the 1950s by Ugine (France) and by Falconbridge in the 1960s, made it possible to achieve a more selective reduction of nickel, and thereby produce higher nickel grade products from lower grade ores.

The first commercial scale electric furnaces to produce ferronickel were the 10.5 MVA units installed by SLN at its Doniambo smelter in New Caledonia in 1958. The largest units currently (1989) in operation are a 51 MVA unit at Cerro Matoso in Colombia and a 60 MVA furnace at Pacific Metals at Hachinohe in Japan.

7.6.1 Rotary Kiln–Electric Furnace Process [130]

In the earliest plants, the function of the rotary kiln was limited to drying and dehydrating the ore, and furnace operating temperatures did not exceed 700 °C. The hot calcine was then blended with reductant, usually coal, and transferred to the electric furnace where reduction of the metals occurred.

In the electric furnace the calcined ore was smelted with the reductant to form immiscible layers of slag and ferronickel. The New Caledonian ores, with their high magnesia and silica contents (2.5% Ni, 10–15% Fe), require no additional flux for slag formation. Virtually all the nickel and 60–70% of the iron in the ore are reduced to metal to yield a ferronickel grading about 20% Ni; the slag contains only 0.1% Ni. The energy consumption in the electric furnace for this mode of operation is 2.0–2.2 GJ per tonne of dry ore (550–600 kWh/t).

As the process was developed and applied to a wider range of nickel laterite ores, several improvements in design and operating technique were made. The operating temperature of the rotary kiln was increased to 900–1000 °C, and reductant was added to the kiln feed to ensure a more complete dehydration of the ore and to allow a partial reduction of the metals to occur in the kiln. As a result energy consumption in the electric furnace was reduced to 1.8–2.0 GJ/t (500–550 kWh/t).

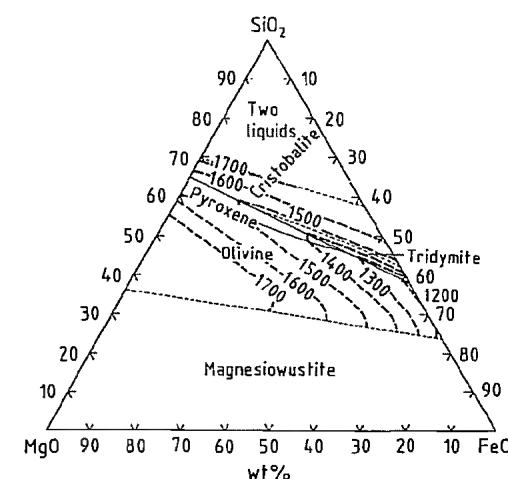
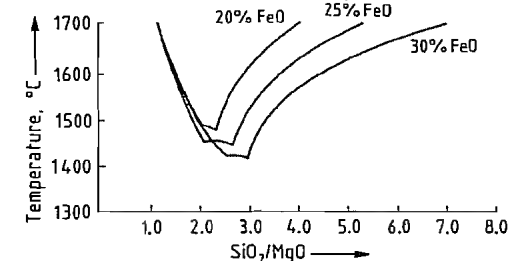
The degree of reduction achieved in the kiln depends on the composition of the ore and on the reactivity of the reductant. Iron and nickel silicate minerals are generally less reactive than nickel oxide minerals. Usually lignites and charcoal are the most reactive reductants, and high-volatile coals are more reactive than low-volatile coals, anthracite, or coke. Typically, under optimum conditions, up to 40% of the nickel is reduced to metal in the kiln, while the iron oxides are reduced to iron(II) oxide (FeO).

In the electric furnace the charge must be heated to 1400–1650 °C to permit the separation of distinct slag and metal phases. The energy input to the charge is provided by

radiation from the electric arcs around the tips of the electrodes and by the heat generated in the slag by resistance heating due to the flow of current through the slag layer between the electrodes. Since the electrical resistivity of the metal layer is much lower than that of the slag, very little heat is generated in the metal layer, which must therefore receive heat by conduction and convection transfer from the overlying slag layer. For satisfactory heat transfer, the temperature differential between slag and metal layers should be at least 100 °C.

The mode of operation of the electric furnace is largely determined by the melting temperature of the slag. Except for the limonitic ores, where the alumina and lime contents have a significant effect, the slag melting temperatures for a particular ore can be estimated from the FeO–MgO–SiO₂ equilibrium phase diagram (Figure 7.25) [132]. For SiO₂/MgO weight ratios of less than 2:1, the slag melting temperatures are essentially independent of the FeO content. At high SiO₂/MgO weight ratios the slags are close to saturation with SiO₂, and the slag melting temperatures are then a function of the FeO content (Figure 7.26) [129]. High iron contents, which normally occur with low-magnesia ores, result in the formation of highly corrosive low-melting (1350–1450 °C) slags. Since the use of magnesia or silica fluxes is usually uneconomic, the problem of low-melting slags must be overcome in the design and operating mode of the furnace [133].

Operation of the electric furnace is simplest when the slag melting temperature is higher than the metal melting temperature (1300–1400 °C). For such a system the furnace is operated with a covered bath (Figure 7.27A). The hot ore charge is allowed to build up on top of the molten slag, and the electrodes are not immersed in the slag layer. Under these conditions much of the reduction reaction occurs in the hot charge layer before it melts.

**Figure 7.25:** The FeO–MgO–SiO₂ phase diagram.**Figure 7.26:** Slag melting point as a function of FeO content.

The high-iron limonite ores, which produce slags with melting points well below the melting point of the metal phase, can be smelted if the distance between the electrode tips and the slag–metal interface is reduced significantly. The electrodes must therefore penetrate deeply into the molten slag layer (Figure 7.27B). A vertical temperature gradient is then set up in the slag layer, with the highest temperature around the electrode tips. Under these conditions it is possible to operate the furnace with a metal tapping temperature higher than the slag tapping temperature. However the deep immersion of the electrodes in the slag results in a significant reaction between the carbon of the electrodes and metal oxides in the slag, with the evolution of carbon monoxide around the electrodes. The evolution of gases makes covered bath operation of the furnace impractical, and necessitates open bath

operation (Figure 7.27B) with the slag surface exposed around the electrodes [130].

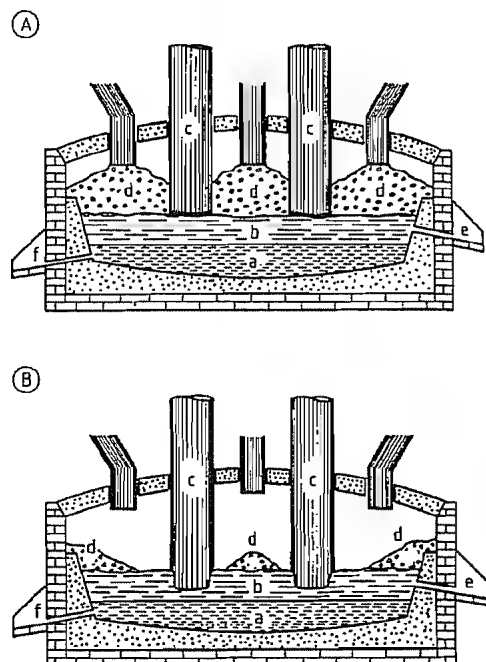


Figure 7.27: Electric furnace operation. A) Covered bath; B) Open bath. a) Metal pool; b) Slag bath; c) Electrodes; d) Solid charge; e) Slag tap hole; f) Metal tap hole.

The ferronickel grade produced in the electric furnace smelting operation can be closely controlled by the amount of solid reductant added to the process. For a given addition of reductant, nickel recovery is highest, followed by cobalt, and iron recovery to the metal phase is lowest. Generally as much as 60–70% of the iron is reduced from silicate ores, while only 10–15% of the iron is reduced from high iron limonitic ores.

Normal operating practice is to produce up to 25% Ni ferronickel from silicate ores and 15–20% Ni ferronickel from limonitic ores. Nickel losses to the electric furnace slag under these conditions are quite low (0.1% Ni in the slag). Nickel losses to slag increase with nickel grade, although grades with 35–45% Ni can normally be produced from most ores without excessive losses (0.15–0.20% Ni in the slag). Above 45% Ni in ferronickel, slag losses increase rapidly. Where higher grades

are required, the ferronickel electric furnace product can be upgraded by removing iron by oxidation and slagging in an oxygen-blown converter, and the high Ni content slag is recycled to the electric furnace. Ferronickel grades as high as 90% nickel can be achieved with two stages of converter upgrading.

Current industrial practice is illustrated by the following descriptions of specific operations. In the Doniambo smelter of SLN in New Caledonia, which was built in 1958, the wet ores are carefully blended and screened to produce a smelter feed with an average composition of 2.5–3.0% Ni and Co, 20–28% MgO, 15–20% Fe₂O₃, and 30–40% SiO₂. The ore is blended with anthracite as a reductant and heated in a rotary kiln to 950 °C. Only a minor degree of reduction occurs in the kiln. The hot calcine is transferred to an electric furnace (one of eight 10.5 MVA or three 33 MVA units). Smelting is carried out with a charge covered bath, although the electrodes dip about 30 mm into the slag layer. Energy consumption is 90 MJ/kg Ni (2.35 GJ/t ore or 650 kWh/t ore) and electrode consumption is 1.5 kg/kg Ni (39 kg/t ore). Nickel and iron recoveries from ore to ferronickel product are 95 and 50%, respectively. The slag tapping temperature is 1550–1600 °C, while the metal is tapped at 1450 °C. The slag, which typically contains 0.1–0.2% Ni, is granulated and discarded [134, 135].

The crude ferronickel contains 24% Ni, 69% Fe, 2% C, 3% Si, 1.5% Cu, and 0.25% S. It is either cast into ingots for market, converted to nickel matte, or desulfurized and refined to higher quality ferronickel. Ferronickel is marketed by SLN as 25 kg ingots and as granules.

Much the same process is used by the three Japanese ferronickel smelters, Pacific Metals at Hachinohe [136], Sumitomo at Hyuga [137], and Nippon Mining at Saganoseki, by Morro do Niquel in Brazil [138], by PT Aneka Tambang in Indonesia, and by Cerro Matoso in Colombia [139, 140]. All these operations process ores with relatively low Fe/Ni ratios of 6:1 or less. Representative ore and slag compositions are given in Table 7.30.

Table 7.30: Silicate ore and slag compositions [129].

Smelter	Ore composition, %				Slag composition, %		
	Ni	Fe	MgO	SiO ₂	FeO	SiO ₂	MgO
SLN	2.7	14–15	20–28	35–40	12	45	30
Hyuga	2.4	9–14	22–29	35–43	8	52	36
Morro de Niquel	1.25	6.5	30	43	7	50	30
Aneka Tambang	2.25	13	24	45	5	56	29
Cerro Matoso	2.9	14	15	46	22	59	20

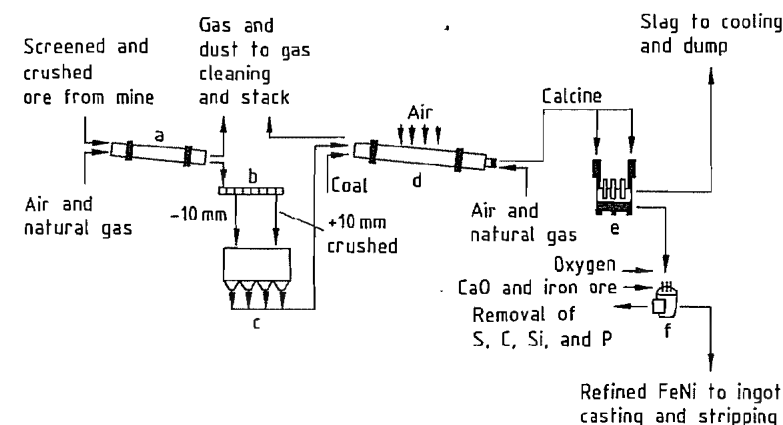


Figure 7.28: Flow sheet of the Cerro Matoso ferronickel smelter: a) Drying kiln; b) Screen; c) Batch bins; d) Reduction kiln; e) Electric furnace; f) ASEA/SKF Fe-Ni refining.

The most recently built plant is that of Cerro Matoso (1982) which treats an ore with the exceptionally high SiO₂/MgO ratio of 3:1. The resulting acid slags have proved to be highly corrosive to furnace refractories. The dried ore (12% moisture) is ground, blended with coal, and pelletized prior to entering the rotary kiln (Figure 7.28). The kiln is operated at 900–950 °C with an oxidizing atmosphere and a reducing bed to achieve prereduction of 20% of the nickel to metal, and up to 95% of the iron oxide to the divalent state (FeO). Smelting is carried out in a single 51 MVA electric furnace. The ferronickel, grading over 40% Ni, is tapped at 1420–1440 °C, while the slag, containing 0.2% Ni, is tapped at 1600–1630 °C. The ferronickel is refined and upgraded to 43% Ni prior to being cast into 22 kg ingots, or granulated [139].

The operation of LARCO at Larymna in Greece is an example of ferronickel production from a very low grade limonitic ore (1.2–1.3% Ni, 31–35% Fe). In this case a high degree of prereduction in the rotary kiln is essen-

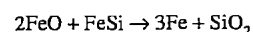
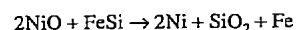
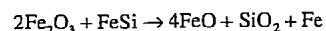
tial. The ground ore is blended with lignite, coal, and heavy fuel oil, and heated to 920 °C in one of two countercurrently fired rotary kilns. The kiln discharge still contains about 3% carbon, but is reported to contain no metallic nickel, while most of the iron oxides are reduced to FeO. The calcine is smelted in one of four electric furnaces (13–16 MVA) to produce a metal phase containing 15% Ni, 0.02% C, and 0.25% S. The metal is tapped at 1520 °C and upgraded to 28% Ni in an oxygen-blown converter. This treatment also reduces the sulfur content to 0.06%. Energy consumption for the electric furnace is 125 MJ/kg Ni (1.6 MJ/t ore or 440 kWh/t ore) and electrode consumption is 0.4 kg/kg Ni (5 kg/t ore) [141].

7.6.2 Uginé Ferronickel Process

In the rotary kiln–electric furnace process excess carbon is normally added to the furnace charge to ensure quantitative reduction of nickel oxide. As a result more iron oxide is re-

duced to metal than is desirable, decreasing the ferronickel grade and leaving a high residual carbon level, typically 1–3% in the product. The excess iron and carbon are subsequently removed by oxidation with air or oxygen. Consequently the process is not particularly economical in terms of energy consumption.

A more selective method of nickel oxide reduction was developed by the French company Ugine in the early 1950s and applied commercially by Hanna Mining in their plant in Riddle, Oregon, in 1954. In this process the ore is dried and calcined in a rotary kiln and melted in an electric furnace without addition of reductant to produce a melt of iron and nickel oxides. No slag metal separation occurs in the electric furnace. The molten ore is transferred to a ladle furnace where it is reduced by reaction with ferrosilicon at 1650 °C. The two phases are mixed by repeated pouring of the mixture from one ladle furnace to another. The nickel oxide and some of the iron oxide are reduced to metal. The balance of the iron is removed as slag.



The reduced ferronickel contains 30–50% Ni and very low levels of carbon and sulfur. The major impurity is phosphorus, which is removed by oxidation with iron ore and slagging with lime.

7.6.3 Falcondo Ferronickel Process [142]

The Falconbridge ferronickel operation in the Dominican Republic treats a low-grade ore (1.5% Ni, 17% Fe, 24% MgO, and 35% SiO₂) by means of a specially developed process designed to provide a more selective reduction of nickel relative to iron than is possible in the rotary kiln–electric furnace process. Reduction of briquetted ore is carried out in shaft furnaces fired with a reducing gas, generated by cracking low-sulfur naphtha. No solid or

liquid reductants are added to the furnace feed. A high degree of reduction of the ore is achieved in the shaft furnace, and the subsequent electric furnace step is required to do little more than melt the reduced calcine to allow separation of the metal and slag phases. The ferronickel produced is high grade (38% Ni) and contains low impurity levels (< 0.04% C and Si).

The Falcondo plant, which has a capacity of 35 000 t/a Ni, was commissioned in 1971. The ore is carefully blended to maintain a constant chemical composition, particle size, and moisture content, so that it can be briquetted without a binder. The briquettes are calcined and reduced in twelve open-top shaft furnaces. Each furnace is equipped with its own gasification reactor in which low-sulfur naphtha is cracked by combustion with a deficiency of air to produce reducing gas (CO + H₂). The hot reducing gas at 1250 °C is first cooled to 1150 °C before being supplied to the shaft furnace through the primary tuyères. The gas flows upwards, countercurrent to the ore briquettes which are fed to the open top of the furnace. The gas reduces the nickel oxides to metal and the iron oxides to FeO. A portion of the partly reacted reducing gas is taken off from the top of the furnace, where it is mixed with a controlled amount of air and fed back into the furnace through secondary tuyères located 1.8 m above the primary tuyères. This stream provides the combustion fuel to dry and calcine the ore feed in the upper section of the shaft.

The hot reduced briquettes are discharged from the bottom of the shaft furnace at 800 °C and are transferred to one of three 55 MVA electric furnaces. The furnace operation consumes only 1.6 GJ/t (440 kWh/t) of charge. The crude ferronickel, which is tapped at 1475–1500 °C, contains 32–40% Ni. The slag, containing about 0.15% Ni, is tapped at 1500–1600 °C. The crude ferronickel, which typically contains only 0.15% S, 0.03% P, 0.04% Si, and 0.02% C, is refined to remove sulfur and phosphorus.

Table 7.31: Impurities in ferronickel [129].

Smelter	Crude Fe–Ni, %				Refined Fe–Ni, %			
	C	S	Si	P	C	S	Si	P
SLN	2.5	0.40	1.50	0.150	0.03	0.02	0.02	0.02
Cerro Matoso	0.17	0.45	1.45	0.024	0.03	0.03	0.70	0.03
Falcondo	0.02	0.15	0.04	0.030	0.06	0.08	0.30	0.01

7.6.4 Refining of Ferronickel

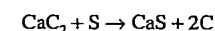
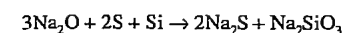
The refining of ferronickel resembles that of steel in that the principal impurities are sulfur carbon, silicon, phosphorus, and oxygen. Typical impurity levels in crude and refined ferronickel are shown in Table 7.31.

Crude ferronickel produced by the conventional rotary kiln–electric furnace process usually contains high levels of carbon and sulfur. These ferronickels are first treated under reducing conditions to remove sulfur and are then refined sequentially under oxidizing conditions with suitable fluxes to remove carbon, silicon, and phosphorus. Ferronickel produced by the selective reduction processes, such as the Ugine or Falcondo processes, which typically contain very low levels (< 0.04%) of carbon and silicon, are normally treated first for phosphorus and then for sulfur removal. The Falcondo ferronickel is not refined to remove carbon or silicon, and in fact the levels of these impurities increase during refining.

A variety of equipment is used for the refining of ferronickel, including electric arc furnaces, shaking ladles, and low-frequency induction furnaces for desulfurization, and oxygen-blown converters (both L-D and side-blown) for silicon, carbon, and phosphorus removal. The ASEA–SKF ladle furnace, which incorporates an electric arc furnace roof carrying three carbon electrodes and induction stirring of the melt, is used in a number of plants including Cerro Matoso and Falcondo.

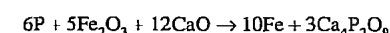
Sulfur is generally removed under reducing conditions by adding soda ash, lime, or calcium carbide to the molten ferronickel. Good agitation of the melt is essential to ensure effective mixing of the reagent with the metal phase, and this can be achieved by adding the reagent to the ladle during furnace tapping, by using a shaking ladle, or by providing electri-

cal induction stirring. In some plants poling with greenwood poles is used to provide additional agitation and reductant. Sulfur reacts with the fluxes to form sodium or calcium sulfides, which are slagged off with the silicates formed by reaction of flux with silicon:



The melt cools during this treatment and oxygen is blown into the melt to reheat it to tapping temperature. Two stages of fluxing are often necessary to desulfurize the ferronickel to the required level (0.02%). The Falcondo smelter uses a complex combination of ferrosilicon, aluminum, silicocalcium, lime, and fluorspar to desulfurize its low-carbon ferronickel.

Removal of silicon, carbon, and phosphorus is normally conducted in an oxygen-blown converter or an oxygen lanced ladle. Carbon is removed simply by oxidation with oxygen to carbon monoxide. Silicon is removed by oxidation with oxygen and fluxing with lime and fluorspar. Phosphorus is oxidized either by blowing the melt with oxygen or by adding iron ore and fluxing the phosphorus(V) oxide with lime:



The slags are removed by skimming after each refining step. If necessary the ferronickel can be deoxidized by addition of ferrosilicon, although this practice increases the silicon content.

Ferronickel is not usually treated to remove cobalt, copper, or arsenic, which may be present in significant amounts. Refined nickel can be produced by the electrolysis of 90% ferronickel in a chloride sulfate electrolyte, but this process has not found wide application [141].

7.7 Ferrophosphorus

During the production of elemental phosphorus by reduction of phosphate rock in an electric furnace, ferrophosphorus collects under the slag. The ferrophosphorus is tapped off, usually once per day, through a hole in one of the carbon blocks, which is opened with an oxygen lance and closed again with a clay plug. The ferrophosphorus, together with some slag, flows into a crucible, from which the lighter slag overflows into a bed of sand. When the tapping off is completed the ferrophosphorus is poured from the crucible into a bed of sand, and, after cooling, is broken into pieces [143].

Every time the ferrophosphorus is tapped off, its radioactivity is measured. If a ^{60}Co source becomes dislodged as the furnace lining wears away, the ^{60}Co is transferred quantitatively into the ferrophosphorus. The radiation supervisor decides in each case whether the ferrophosphorus should be sold, placed in short term storage, or stored indefinitely.

Fume extraction operates in the areas surrounding the furnace tapping and sand beds. The waste gases are purified by wet methods. For new installations, the following emission levels are not exceeded [144]:

Dust	50 mg/m ³
Phosphoric acid (as P_2O_5)	20 mg/m ³

Depending on the method of furnace operation, the ferrophosphorus contains between 15 and 28% P, corresponding approximately to the formula Fe_2P . The more extensively the phosphate rock is reduced, the more silica is converted into silicon, which reduces the phosphorus content of the ferrophosphorus. The combined content of P and Si is 25–30%. Ferrophosphorus with a low silicon content (< 3%) has a fairly good market potential, and is used in the manufacture of phosphorus-containing alloys. The grades with a low phosphorus content are not in great demand, but can be used in smelting low-phosphorus iron ores or to increase the P_2O_5 content of basic Thomas slag.

Ferrophosphorus is stored in the open, and supplied either loose or in drums. The other metals present in the ferrophosphorus in addition to the Fe, P, and Si depend on the composition of the phosphate rock. Examples of compositions of ferrophosphorus are given in Table 7.32.

Valuable metals such as vanadium, can be recovered economically from the ferrophosphorus if they are present in unusually high concentrations. Vanadium is recovered together with chromium by blowing with oxygen. Both metals accumulate in the slag.

Older processes for treating ferrophosphorus, which are however no longer of importance, are described in [145].

Table 7.32: Composition of ferrophosphorus (%).

Process	P	Si	Ti	Cr	V	Mn
Höchst high percentage	26.6	0.3	4.5	0.2	0.6	0.5
Höchst low percentage	20.0	9.5	5.8	0.2	0.5	0.7
TVA	24.0	1.7	1.7	0.2	0.3	1.1
FMC	27.1	0.2	0.3	4.5	5.4	0.5

7.8 Ferrotungsten

7.8.1 Composition

Commercial ferrotungsten is a tungsten-iron alloy containing at least 75% W, and having a very fine-grained structure and a steel-gray appearance. It is supplied in 80–100 mm lumps in accordance with DIN/ISO standard specifications. Special sizes can be produced by further size reduction to suit customers' requirements. The standardized compositions are listed in Table 7.33 [146].

The binary phase diagram for Fe–W is shown in Figure 7.29. The phases Fe_7W_6 (μ) and FeW (δ) exist close to the edge phases. However, ferrotungsten occurs in the equilibrium state only after prolonged high-temperature treatment. Therefore, in commercial ferrotungsten, the phase Fe_2W (λ) should still be present alongside the δ -phase. The melting temperature of ferrotungsten containing ca. 80% W is very high, the liquidus temperature

being > 2500 °C and the solidus temperature ca. 1640 °C. The density of ferrotungsten is 15.4 g/cm³.

7.8.2 Uses

Ferrotungsten and tungsten melting base are mainly used as alloying materials in the steel industry as they dissolve more readily than pure tungsten in molten steel, owing to their lower melting points, and are also cheaper.

Tungsten additions increase the hardness yield strength, and ultimate tensile strength of the steel without reducing the elongation, area reduction on breaking, and notched bar fracture toughness [148].

In steel, tungsten forms stable carbides that increase hot strength and wear resistance. Tungsten-containing alloys are therefore mainly used in the production of tool steels, especially high-speed steels [149].

High-speed steels represent the main application area for ferrotungsten. These steels are highly alloyed with tungsten, molybdenum, vanadium, and chromium. After the correct heat treatment, they have high hardness and wear resistance, and are mainly used for machining at high cutting rates and temperatures up to 600 °C. The alloying elements and the carbon form hard, wear-resistant carbides in a matrix with good hardness retention properties. The standard high-speed steels specified in DIN 17350 contain 6–18.5% tungsten [150].

Table 7.33: Specifications of the composition of ferrotungsten, DIN 17562 and ISO 5450 [146] (impurities: 0.6–1.0% Si; 0.6–1.0% Mn; 0.20–0.25% Cu; 0.05–0.06% S; 0.05–0.06% P).

	% W		% C max.		% Al max.		% Sn max.		% As max.		% Sb max.		% Mo max.	
	DIN	ISO	DIN/ISO	DIN/ISO	DIN/ISO	DIN/ISO	DIN/ISO	DIN/ISO	DIN	ISO	DIN	ISO	DIN	ISO
FeW 80	75–80		1.0				0.10		0.10		0.08			
FeW 80		70–85	1.0	0.10			0.10		0.10		0.05		1.0	
FeW 80 LC		70–85	0.1	0.10			0.10		0.10		0.05		0.5	

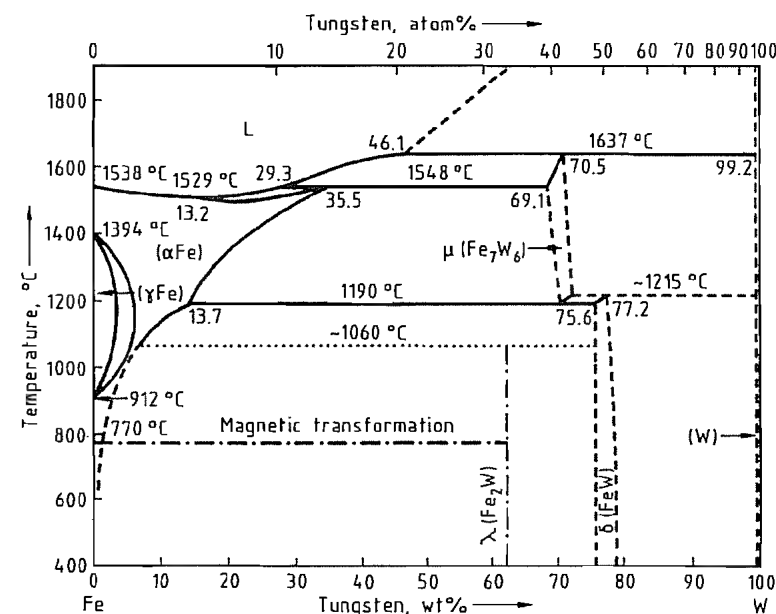


Figure 7.29: Binary phase diagram of the Fe–W system [147].

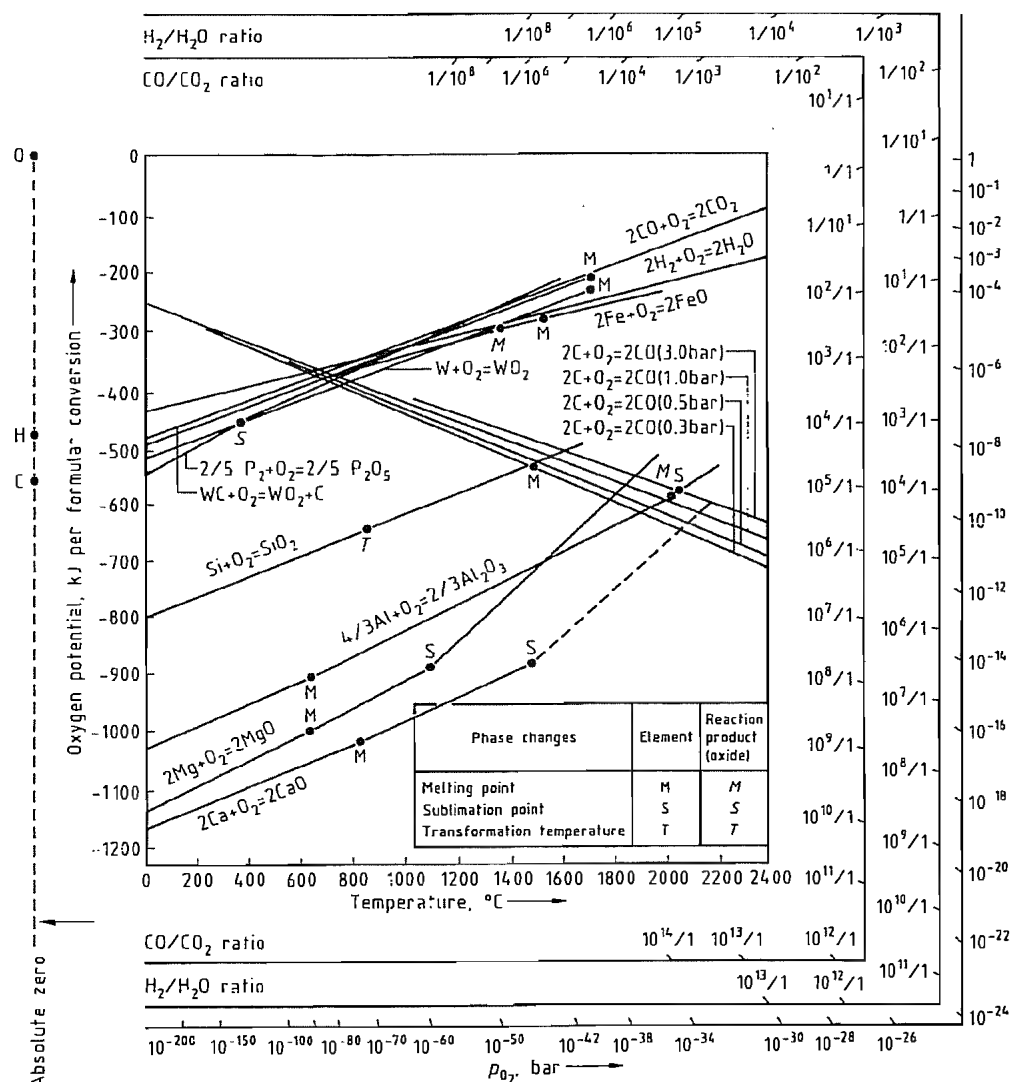


Figure 7.30: Effect of temperature on the oxygen potentials of oxides [151].

7.8.3 Production

The raw materials used for ferrotungsten production are rich ores or concentrates containing the minerals wolframite, hübnerite, ferberite, and scheelite. "Synthetic scheelite", a precipitated calcium tungstate, is also used.

These raw materials contain tungsten in the form of WO_3 , which can be relatively easily reduced either with carbon or silicon and/or

aluminum. Reduction with magnesium and calcium is also possible, but is of no industrial importance for cost reasons. Figure 7.30 shows the effect of temperature on the oxygen potentials of metal oxides. Although tungsten forms carbides with carbon, the formation of tungsten carbide in the finished product can be virtually prevented by suitably controlling the $CO:CO_2$ ratio, so that a low-carbon ferrotung-

sten with a maximum carbon content of 1% is produced. Tungsten oxides are reduced in preference to iron oxides, so that ferrotungsten with a high tungsten content can be produced, even if the ore has a high FeO content.

Thus, ferrotungsten can be produced by carbothermic reduction in an electric arc furnace or by metallothermic reduction aluminum.

The carbothermic or silicocarbothermic method is preferred for cost reasons. Moreover, higher impurity contents (tin and arsenic) can be tolerated in the raw materials.

When high levels of arsenic and tin are present in the concentrates, these can be vaporized by roasting in rotary tube furnaces.

7.8.3.1 Carbothermic Production

Because of the high melting point of ferrotungsten, the so-called solid block melting process is normally used, as tapping off is not possible at the furnace temperatures that are required.

In this process, the ferrotungsten accumulates in the hearth of the furnace vessel, which is constructed in sections. After the desired weight has been produced, the furnace lining is removed and the metal ingot can be removed after cooling. The solid block is cleaned, crushed, and sorted. The cleaned-off material and skin of the ingot are returned to the furnace for remelting.

The use of several melting vessels enables the process to be semicontinuous.

The process is usually operated in two stages, as an excess of tungsten ore is used in the ingot melting process (refining stage), producing a WO_3 -rich slag that must be processed in a second (reduction) stage to give ferrotungsten with a low W content and a low- WO_3 slag.

The low-W ferrotungsten is reused in the refining stage. The slag, which contains < 1% WO_3 , can be dumped. The flow diagram of this two-stage process is shown in Figure 7.31 [152].

In the three-phase electric arc furnaces usually used today, the pitch circle diameter of the electrodes is small to ensure adequate energy concentration. Typical furnace data for a three-phase electric arc furnace for the production of FeW 80 are [153]:

Power	2000–3000 kVA
Refractory lining	monolithic rammed carbon
Electrode material	
refining stage	graphite
reduction stage	Söderberg
Energy consumption per tonne FeW	7500–8500 kWh
FeW ingot weight	11–12 t

The electric arc furnaces are provided with waste-gas purification plants both for environmental reasons and to realize the value of the WO_3 in the flue dust. This dust, enriched in arsenic and tin vaporized from the concentrates is usually added to the reduction stage or processed in special batches. The resulting secondary dust must either be chemically processed to obtain tungsten compounds or disposed of as a special waste if it cannot be sold.

7.8.3.2 Carbothermic and Silicothermic Production

In 1937, V. N. GUSAROV developed a continuous process for the production of ferrotungsten containing ca. 75% W. This was used in the former Soviet Union and former Czechoslovakia [154, 155]. It is presumably now used in the Czech Republic.

This metallurgically interesting process is carried out in three successive stages in a three-phase electric arc furnace lined with magnesite. Of the oxygen in the WO_3 , 60% reacts with carbon and 40% with silicon (as ferrosilicon containing 75% Si). In the first stage, ferrotungsten (75% W) is produced by substoichiometric carbon reduction. This ferrotungsten is formed in a pasty consistency under a WO_3 -rich slag, and can be scooped out with ladles. Details of the individual processes are as follows:

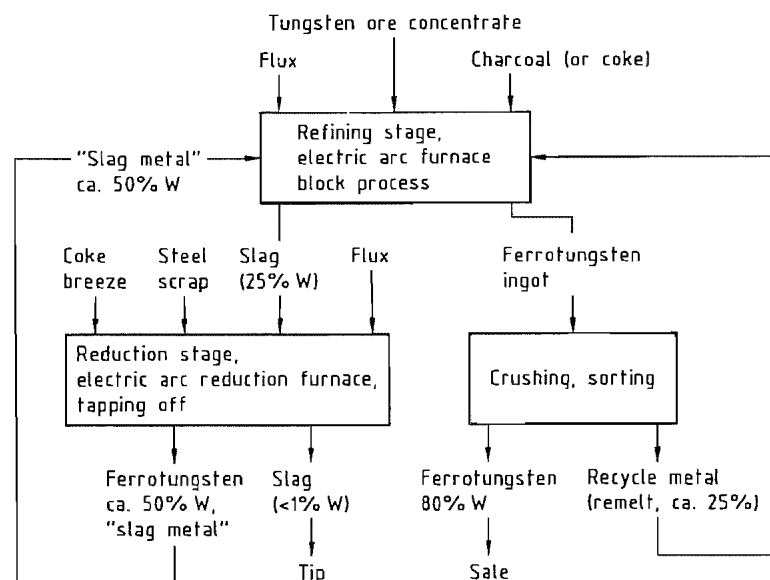


Figure 7.31: Carbothermic production of ferrotungsten.

Tungsten yields of 97–98% can be obtained in the solid block process.

Stage 1. Reduction of tungsten ore concentrates by carbon under a WO_3 -rich slag (10–16% WO_3 , 26–28% FeO , 15–17% MnO), and scooping out the ferrotungsten (e.g., 73.3% W, 0.4% Mn, 0.43% Si, 0.05% P, 0.06% S, 25.2% Fe).

Stage 2. Reduction of the WO_3 -rich slag with $FeSi$ 75 and addition of scrap iron (to reduce the tungsten content of the ferrotungsten produced). Tapping off the low- WO_3 slag (e.g., 0.3% WO_3 , 20.8% MnO , 51% SiO_2 , 2.7% FeO , 3.6% Al_2O_3 , 21.1% CaO). The metal, with a reduced tungsten content (54–70% W, 3–8% Si, 1–2% Mn) remains in the furnace.

Stage 3. Refining of the low-tungsten metal by adding tungsten concentrates. A WO_3 -rich refining slag (18–25% WO_3) is formed, and the tungsten content of the metal increases.

The advantage of the process is the continuous method of operation; thus the furnace can be operated for considerably longer periods without interruption for relining than in the solid block process. A further advantage is the lower energy consumption, i.e., ca. 4000 kWh

per tonne of ferrotungsten. The tungsten yield is 98%, approximately the same as for the solid block process.

Disadvantages include the heavy labor of the scooping operation and the accumulation of some of the ferrotungsten in a “furnace sow” or “salamander”. This ferrotungsten can be retrieved only after furnace relining, and is recovered as product after remelting.

7.8.3.3 Metallurgical Production

Tungsten oxide can be reduced by silicon and/or aluminum (Figure 7.30). Compared with carbothermic reduction, metallurgical production of ferrotungsten requires purer raw materials, as the reactions proceed very rapidly, and the impurities are chemically reduced as well as the raw materials. In this process, about 50% of the tin and arsenic present, most of which would be vaporized during the longer carbothermic process, end up in the ferrotungsten.

The tungsten concentrates in finely divided form are mixed with coarsely powdered aluminum and silicon. Pure silicon or ferrosilicon cannot be used, as these would not give a self-sustaining reaction, the heat evolved being in-

sufficient to melt the ferrotungsten and slag formed. Aluminum and silicon in the ratio 70:30 are therefore used.

The reaction mixture is charged into a refractory-lined furnace vessel and preheated to 400–500 °C. The preheating can be omitted if Fe_2O_3 and Al are mixed into the reaction mixture as a booster.

The reaction is started at the top by igniting initiators, which are mixtures of, e.g., BaO_2 and aluminum powder. A purely aluminothermic mixture burns completely in a few minutes, but silicothermic–aluminothermic mixtures react more slowly. After cooling, the furnace vessel is removed, and the blocks of metal and slag are separated. This method produces ferrotungsten ingots of 700–2000 kg. The metal ingot is cleaned, crushed, and sorted. Pieces with adhering slag are sent back for remelting.

The metallurgical production process has lost much of its importance in recent years, owing to the high costs of the aluminum and silicon reducing agents, and the necessity for using pure and therefore expensive raw materials.

The process is suitable only for special customer requirements, and for operations which also produce other alloys by the aluminothermic principle.

Advantages of the process include the simple, low-cost plant, and the minimal tying-up of materials resulting from the short processing time. The tungsten yield is ca. 96%.

M. Riss and Y. KHODOROVSKY have described the electroaluminothermic production of ferrotungsten from scheelite [155]. The reaction time is extended by melting in an electric arc furnace, and separation of the metal from the slag is improved.

7.9 Ferroboration

Ferroboration is basically an iron–boron alloy containing 10–20% B. It is used mainly in the steel industry. Ferroboration was first produced in 1893, by HENRI MOISSAN [156], from boric acid, iron, and carbon in a single-phase

electric-arc furnace lined with carbon. Ferroboration produced in this way contains carbon. The introduction of the thermite reaction by GOLDSCHMIDT in 1898 led to the aluminothermic reduction of boric oxide to ferroboration, for years the main commercial method for producing ferroboration. Recently though the carbothermic process has again found use for the production of ferroboration, now as a raw material for the manufacture of amorphous metals. Aluminothermic ferroboration contains residual aluminum, which causes severe casting problems.

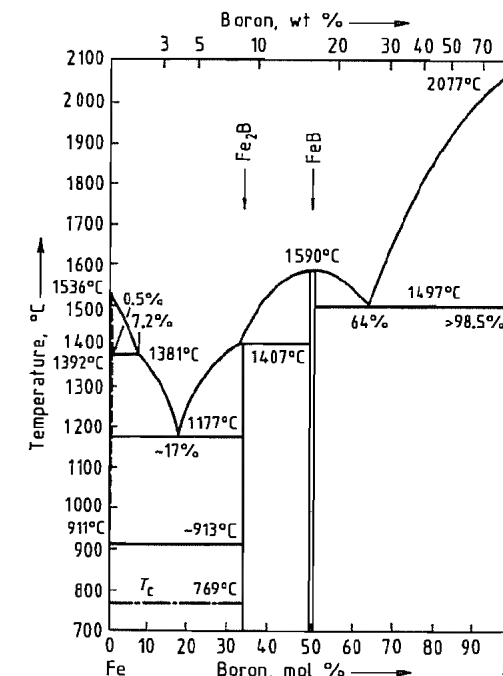


Figure 7.32: Phase diagram of iron–boron [157].

7.9.1 Physical Properties

In the system iron–boron, shown in Figure 7.32 [157], there are two intermetallic compounds, FeB and Fe_2B (ρ 6.3 and 7.3 g/cm³, respectively). The crystal structure of FeB is orthorhombic ($a = 0.5502$, $b = 0.2948$, $c = 0.4057$ nm), whereas that of Fe_2B is tetragonal ($a = 0.5109$, $c = 0.4249$ nm). Additional physical properties of the two iron borides are summarized in Table 7.34. Also see [161].

The enthalpies of formation at 1385 K have been determined by high-temperature solution calorimetry [162]: -67.87 ± 8.05 kJ/mol for Fe_2B , and -64.63 ± 4.34 kJ/mol for FeB .

Commercial ferrobaboron alloys, either aluminothermic or carbothermic, are bright silver and brittle with a fine or coarse crystalline fracture. The density depends mainly on the boron content:

boron, %	20.2	17.9
aluminum, %	2.7	0.8
density, g/cm ³	6.02	6.41

Table 7.34: Properties of Fe_2B and FeB [158–160].

Property	Fe_2B	FeB
Microhardness, Vickers, 100 g, kN/mm ²	13.24	16.19
Thermal conductivity, $\text{W cm}^{-1} \text{K}^{-1}$	0.2–0.3	0.1–0.2
Electrical resistivity, at room temperature, $\mu\Omega \text{cm}$	≈ 10	≈ 20
Temperature coefficient of resistance, $\mu\Omega/\text{K}$	0.18	0.4
Curie temperature, K	1015	598
Coefficient of linear expansion (300–1000 K), K^{-1}	8×10^{-6}	$10\text{--}16 \times 10^{-6}$

7.9.2 Chemical Properties

Commercial ferrobaboron changes in appearance over prolonged exposure to humid air; its bright silver disappears, the surface turning dull gray, with almost red “rusty” stains. Ferrobaboron dissolves in mineral acids (Section 7.9.7). Distilled hot water may react slightly with ferrobaboron [163]. Some contradictory statements about the chemical behavior of ferrobaboron in the literature are probably due to other elements in the alloy. Fe_2B dissolves in HCl (1:2), hydrogen and boranes evolving, the latter hydrolyzing into suboxides [164, 165]. FeB is resistant to HCl ($\rho = 1.19$ g/cm³) and H_2SO_4 ($\rho = 1.84$ g/cm³), both at room temperature and at their boiling point. FeB dissolves completely in HNO_3 . Both FeB and Fe_2B react with nitrogen at temperatures above 350 °C to give boron nitride [158].

The behavior of boronized steels, i.e., steel with thin layers of FeB on the surfaces, was discussed by A. MATUSCHKA [159]. Such steels are oxidation resistant up to 700–900 °C. The boronized steel CK45 (AISI 1042) is resistant to 20% HCl , 10% H_3PO_4 , and 10% H_2SO_4 at

56 °C. Stainless steels, such as X10CrNiTi 18 9 (Werkstoff Nr. 1.4541, AISI 321, SAE 30321) can be made more resistant to attack by 20% HCl or 10% H_2SO_4 at 56 °C by boronizing the surface.

7.9.3 Raw Materials

The following boron minerals can be used for the manufacture of ferrobaboron: colemanite (51% B_2O_3), pandermite (48% B_2O_3), pricite (51% B_2O_3), and boracite (62% B_2O_3). However, the raw materials most commonly used are boric oxide ($\approx 99\%$ B_2O_3) and boric acid ($\approx 57\%$ B_2O_3).

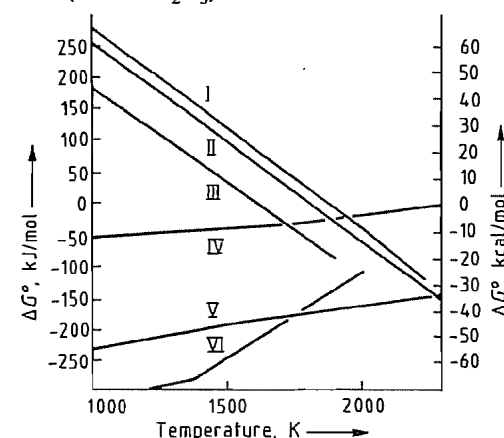


Figure 7.33: Free energies ΔG° of reactions reducing boric oxide as a function of temperature.
 I — $\frac{2}{3}\text{B}_2\text{O}_3 + 2\text{C} \rightarrow \frac{4}{3}\text{B} + 2\text{CO}$
 II — $\frac{2}{3}\text{B}_2\text{O}_3 + \frac{1}{3}\text{C} \rightarrow \frac{1}{3}\text{B}_4\text{C} + 2\text{CO}$
 III — $\frac{2}{3}\text{B}_2\text{O}_3 + \frac{4}{3}\text{Fe} + 2\text{C} \rightarrow \frac{4}{3}\text{FeB} + 2\text{CO}$
 IV — $\frac{2}{3}\text{B}_2\text{O}_3 + \text{Si} \rightarrow \frac{4}{3}\text{B} + \text{SiO}_2$
 V — $\frac{2}{3}\text{B}_2\text{O}_3 + \frac{4}{3}\text{Al} \rightarrow \frac{4}{3}\text{B} + \frac{2}{3}\text{Al}_2\text{O}_3$
 VI — $\frac{2}{3}\text{B}_2\text{O}_3 + 2\text{Mg} \rightarrow \frac{4}{3}\text{B} + 2\text{MgO}$

7.9.4 Production

Boric oxide can be reduced by carbon, aluminum, or magnesium. Reduction by silicon is incomplete. Figure 7.33 shows the calculated free energies of the corresponding reactions as a function of temperature [160]. For commercial production, either reduction by carbon (carbothermic or endothermic) or reduction by aluminum, sometimes with some magnesium (aluminothermic or exothermic) is usual. The coreduction of iron and boric oxide proceeds

more readily than the reduction of either alone because of the formation of the borides Fe_2B and FeB . Iron can be replaced by other boride-forming metals, manganese, nickel, or cobalt. In carbothermic reduction there is a tendency to form boron carbide, thus leading to a carbon-containing ferrobaboron.

Aluminum and boron also form borides, and this results in residual aluminum in aluminothermic ferrobaboron.

7.9.4.1 Carbothermic Production

In order to produce a carbothermic ferrobaboron with a low carbon content the boron content must be high, i.e., the higher the boron content the lower the carbon solubility and thus carbon pick-up.

The reduction of boric oxide by carbon requires high temperature; therefore, the process is carried out in an electric-arc furnace (single- or three-phase type) of capacities up to 1500 kVA. These are relatively small production units, for the worldwide demand for ferrobaboron is low compared with that for other electrothermic ferroalloys.

The London & Scandinavian Metallurgical Co., United Kingdom, produces a ferrobaboron with 16–18% B, 0.5% C, and < 0.15% Al by carbothermic reduction of boric oxide.

In a Japanese patent [166] the carbothermic production of ferrobaboron from boric acid, iron powder, and charcoal in a Héroult-type electric-arc furnace with carbon lining is claimed. One example describes the production of an alloy with 10.3% B, 2% Si, and 0.98% C in a 350-kW three-phase electric-arc furnace. The mix is 100 parts boric acid, 135.8 parts iron powder (92.9% Fe), and 57 parts charcoal powder. The boron recovery is 81.7%, and the power consumption 4550 kWh per tonne of alloy. Another example describes the small-scale production of an alloy containing 15.3% B. Another Japanese patent [167] claims the carbothermic production of a B- and Si-containing alloy, e.g. 3.3% B, 2.9% Si, and 3.0% C, in a special vertical blast furnace. The ferrobaboron is intended for use in the manufacture of amorphous alloys.

The production of ferrobaboron from pig iron and boric acid in an electric-arc furnace with a final oxygen blow leads to an alloy with 16.3% B, 0.03–0.06% Al, and 0.03–0.06% C. The boron recovery in small-scale runs is said to be 60–65%; the power consumption, 16 500 kWh per tonne of alloy [168]. Silicon-containing boron alloy can be produced by carbothermic reduction. The process is described by K. D. FRANK in [169]. A mixture of 100 parts colemanite, 100 parts quartzite, 40 parts iron turnings, and 60 parts low-temperature coke is charged to a 1000-kW electric-arc furnace. A metal containing 5.35% B, 37.2% Si, and 0.21% C is tapped. Boron recovery is 70%, and the power consumption is 6000 kWh per tonne of alloy.

Gesellschaft für Elektrometallurgie mbH, Düsseldorf, Germany, has developed a process for the carbothermic production of ferrobaboron containing 15–20% B and < 0.1% Al in a three-phase submerged arc furnace, whereby boric oxide and iron oxide are simultaneously reduced by charcoal and other low-density carbonaceous materials, e.g., wood chips [170].

Nickel boron can also be produced carbothermically. Boric oxide and/or boric acid and nickel are the raw materials. London and Scandinavian Metallurgical Co., London, United Kingdom, produces a nickel boron containing 15–18% B; 0.5 and 0.15% C (max.); and 0.20% Al (max.) in the electric-arc furnace by carbon reduction.

7.9.4.2 Aluminothermic Production

Ferrobaboron can be made batchwise in a convenient way by the reduction of boric oxide and iron oxide with aluminum powder. Some magnesium in the aluminothermic mix is beneficial: Magnesium is the stronger reducing agent at temperatures below its boiling point, whereas aluminum is more effective above the boiling point of magnesium, where such metallothermic reactions generally take place. The aluminothermic coreduction of boric oxide and iron oxide (Fe_2O_3) is highly exo-

thermic, and only a little additional energy is necessary for a self-propagating reaction. The thoroughly mixed compounds are charged into a refractory-lined pot and ignited, either the whole mix (top firing) or by igniting a starting mix, the rest then charged as the reaction proceeds over a few minutes. The liquid metal and slag separate on account of differing densities, and after cooling the metal button, up to 1500 kg, is removed. After mechanical cleaning, the metal button is broken and crushed to the desired size. The companies of the Metallurg Group [171], who produce ferrobaboron from boric oxide, iron oxide, and aluminum powder, obtain boron recoveries of 70–75% for the 18–20% B grade and 80–85% for the 15–18% B grade by optimizing process parameters. The aluminum consumption can be as low as 4.8–5 kg Al per kg of B.

N. A. CHIRKOV et al. [172] investigated heat balances for an electro-aluminothermic ferrobaboron process using either 1) boric oxide or

2) boric acid as the raw material. Three different mixes — igniting, main, and precipitation — are charged consecutively into a three-phase electric-arc furnace and reacted to produce a ferrobaboron melt with $\approx 20\%$ B. The composition of the charges and the results are summarized in Table 7.35. The heat balances for these two cases are shown in Table 7.36. The investigators are convinced that the process can be optimized to improve the boron recovery and the consumption figures.

When borate ores such as boracite or colemanite are used as raw materials, instead of boric oxide, the aluminothermic process gives boron recoveries as low as 40–50% [173–175]. The specific aluminum consumption is normally higher because the process needs additional energy, in form of either a booster (peroxides or chlorates plus aluminum powder) or in the form of electricity by smelting the mix in the electric-arc furnace (electro-aluminothermic process).

Table 7.35: Charge composition during electro-aluminothermic production of ferrobaboron using boric oxide and boric acid raw materials [172].

	Mix 1			Mix 2		
	Igniting	Main	Precipitation	Igniting	Main	Precipitation
Raw materials						
Boric oxide, kg	—	1200	—	—	—	—
Boric acid, kg	—	—	—	—	1800	—
Iron ore, kg	200	200	1000	200	180	950
Al powder, kg	65	820	282	65	820	262
Lime, kg	70	100	170	70	450	170
Total, kg	335	2320	1452	335	3250	1382
Time, min	30	98	32	3	114	23
Power consumption, kWh		1130			1980	
Products						
Ferrobaboron, kg		1200 ^a			1100 ^a	
% B		20			18	
% Al		3			3.9	
% Si		1.13			1.7	
Slag, kg		2900 ^a			2080 ^a	
% B ₂ O ₃		14–15 ^a			10–12 ^a	
Boron recovery, %		64			63	
Aluminum consumption, kg per tonne of ferrobaboron		973			1043	
Energy consumption, kWh per tonne of ferrobaboron		940			1800	

^aEstimated.

Table 7.36: Heat balances for the electro-aluminothermic production of ferrobaboron using boric oxide and boric acid as raw materials [172].

Input and consumption	From B ₂ O ₃		From H ₃ BO ₃	
	ΔH , 10 ⁶ J	%	ΔH , 10 ⁶ J	%
1. Chemical reactions	13 182	69.0	12 345	58.3
2. Electric power	4 072	21.3	7 143	33.7
3. Side reactions	1 833	9.7	1 699	8.0
Total input	19 087		21 186	
1. Heat content of slag	9 515	49.3	9 237	42.9
2. Heat content of metal	3 235	16.7	2 907	13.5
3. Heat content of dust	63	0.3	125	0.6
4. Dehydration of acid	48	0.2	1 084	5.0
5. Decomposition of carbonates	60	0.3	98	0.5
6. Heat content of gases	141	0.7	2 805	13.1
7. Accumulation of heat by furnace brickwork	4 678	24.2	4 212	19.6
8. Radiation	1 581	8.3	1 045	4.8
Total consumption ^a	19 319		21 514	

^aThe discrepancies between input and consumption are 232×10^6 J (1.2%) and 328×10^6 J (1.5%).

Table 7.37: German Standards 17567 [180].

Designation	Composition							
	B, %	Al, max. %	Si	C	Mn	P	S	Co
FeB16	15–18	4.0	1.0	0.10	0.50	0.005	0.001	0.005
FeB18	18–20	2.0	2.0					
FeB12C	10–14	0.50	4.0	2.0	0.50	0.005	0.1	0.005
FeB17C	14–19							

Table 7.38: United States standards [181].

Grade	Composition, %				
	Boron min.	Boron max.	Carbon max.	Silicon max.	Aluminum max.
A1	12.0	14.0	1.5	4.0	0.5
A2	12.0	14.0	1.5	4.0	8.0
B1	17.5	19.0	1.5	4.0	0.5
B2	17.5	19.0	1.5	4.0	8.0
C1	19.0	24.0	1.5	4.0	0.5
C2	19.0	24.0	1.5	4.0	8.0

Complex boron additives for steel, which contain boron in a dilute alloy together with protective elements, are produced from ferrobaboron and other alloying elements by a melting process (see Table 7.39, and [176]). Other boron master alloys such as nickel boron and cobalt boron with $\approx 15\%$ B and 0.1% or 1.0% Al (max.) can be produced aluminothermically using boric oxide and nickel or cobalt (as metal and/or oxide) [177]. Copper boron with ca. 2% B is commercially produced by Gesellschaft für Elektrometallurgie [178], using an electromagnesianthermic process with copper and boric oxide as raw mate-

rials. Aluminum master alloys with 2.5–4.5% B and 5% Ti + 1% B are produced in an induction furnace by adding potassium boron fluoride and potassium titanium fluoride to an aluminum bath [179].

7.9.5 Quality Specifications for Commercial Grades

Quality standards are specified in Germany by DIN 17567 [180], which also describes sizing, sampling, analytical methods, shipment, and storage. Analyses of the standard grades are summarized in Table 7.37. The American ASTM recognizes six grades of ferrobaboron; analyses are given in Table 7.38. Ferrobaboron is shipped in various sizes. In Europe pieces of fist size and in the United States sizes such as 2 in or 1 in x Down are commercial. Ferrobaboron can also be ground to powder of desired size (e.g., 20 mesh x D, i.e., less than 0.84 mm). In the United States, where the use of boron in steel is fast growing, and also in the United Kingdom, special boron alloys

have been developed as hardenability intensifiers (Table 7.39). These complex alloys contain elements to protect boron against oxidation (Al, Si) and boron nitride formation (Ti, Zr) [182]. Boron-containing aluminum master alloys (Table 7.40) are standardized in Germany [183]. Nickel boron, cobalt boron, and copper boron are not standardized. Typical analyses for commercial alloys are given in Table 7.40.

In the United States and the United Kingdom special boron additives for the steel industry have been developed. The *trade names*, e.g., BATS (abbreviation for boron-aluminum-titanium-silicon), are shown in Table 7.39.

7.9.6 Storage and Shipment

Ferroboration and other boron master alloys are generally not toxic, and there is no special legislation on use and handling. Ferroboration is generally packed in steel drums marked with material grade, size, lot number, and producer. The shipment is accompanied by a data sheet on safe handling including physical and chem-

ical properties, sale storage, and handling directions, e.g., use of protective gloves or dust respirators. Ferroboration and other boron master alloys and additives should be stored in a dry area in their original containers.

7.9.7 Chemical Analysis

For the determination of boron in ferroboration the sample is dissolved in HCl (1:1) or H₂SO₄ (1:1) containing a few drops of HNO₃ and refluxed. Residues rich in boron are fused with sodium peroxide. The solution is passed through an ion-exchange column, neutralized, diluted with polyalcohol, and titrated with sodium hydroxide [184–186]. Small amounts of boron in steel are determined by special methods [182]. One photometric determination of boron in steel is the curcumin method. A fully automated determination of boron in ferroboration, aluminum, and complex ferroalloys by neutron transmission is a convenient method for routine analyses [187]. Standard analytical methods in the United States and the United Kingdom [188, 189] have been described.

Table 7.39: Complex boron alloy "hardenability intensifiers" [176, 182].

Designation	Composition ^a , %						
	B	Al	Ti	Si	Zr	Mn	C
BATS 50 ^b	0.50	13	20	7	5	8	—
BATS TT ^b	1.60	11	58	—	3.5	5	—
BATS 2Z ^b	2.50	11	36	8	6	—	—
BATS Wire	2.3	89.7	8	—	—	—	—
CARBOTAM ^b	2.0	3.0	15–20	4	—	—	0.50
BALCORE 101 ^c	2.5	25	—	—	—	—	—
BALCORE 102 ^c	3.4	34	—	—	—	—	—

^a The remainder is iron.

^b BATS 50, BATS TT, BATS 2Z, and CARBOTAM are registered trademarks of the Shieldalloy Corp., Newfield, NJ.

^c BALCORE is a registered trademark of the LSM Co., London. The size of BALCORE 101 wire is 3.2 mm (34 g/m). The size of BALCORE 12 wire is 5 mm (75 g/m).

Table 7.40: Composition of boron master alloys [176–178].

Alloy	Analysis, %					
	B	Ti	Al	Si	C	Others
Aluminum boron V-Al B 3	2.5–3.4	—	rest	max. 0.2	—	^a
V-Al B 4	3.5–4.5	—	rest	max. 0.2	—	^a
Aluminum-titanium-boron V-Al Ti 5 B 1	0.9–1.4	5.0–6.2	rest	max. 0.2	—	^a
Nickel boron	15–18	—	0.1–1.0	max. 0.8	0.1–0.5	rest Ni
Cobalt boron	15–18	—	max. 1.0	—	—	rest Co
Copper boron	≈ 2	—	—	—	—	rest Cu

^a See DIN 1725 [183].

7.9.8 Pollution Control

During production the usual proscriptions on pollution have to be obeyed.

In both the carbothermic and the exothermic reduction processes the dust off-gases have to be cleaned, either dry in bag filters or electrostatic dust precipitators or wet in disintegrators or Venturi scrubbers (O. RENZ in [169]). A special combined dry-wet cleaning plant for the off-gases of an aluminothermic plant is described by SEYBOLD [190].

7.9.9 Uses

The main use of ferroboration is in steel [182, 191]. Very small amounts of boron improve the hardenability of both plain carbon and alloyed steels. Boron acts as a hardenability intensifier of other hardening elements, such as carbon, manganese, chromium, molybdenum, etc. The boron should be present in the concentration range of 5–15 ppm (max. 30 ppm). Thus the use of boron saves the expense of more costly alloying elements. Because of the high affinity of boron for oxygen and nitrogen, also that dissolved in steel, boron has to be protected from these two elements. Therefore, good predeoxidation by calcium, aluminum, or silicon and denitrification by titanium or zirconium are necessary. In the United States and the United Kingdom complex boron master alloys that contain these protective elements have been developed and have proved very effective for controlled boron addition to steels. In case-hardened steels, boron exhibits better hardenability and strength; in nonaging steels, especially for the automotive industry, the sheet-forming properties are improved. Boron also offers benefits in high-strength low-alloy (HSLA) steels, and it improves the cutting properties in high-speed steels.

In stainless steels of the chrome-nickel type (ASTM 316), 0.004–0.009% B significantly improves the ductility in the hot forming range (950–1250 °C). In very low concentration (0.002–0.005%) boron is beneficial to creep properties in austenitic heat-resistant stainless steels, as well as in ferritic

steels, then in combination with titanium, molybdenum, or niobium. Steels with boron contents up to 2.5% are used for control rods in nuclear reactors because the thermal neutron cross section of boron is so high. Boron is also used in hardfacing and abrasion-resistant alloys; e.g., Colmonoy, a Ni–Cr–Si–B alloy containing up to 3% B, and Stellite, an abrasion-resistant Co–Cr–W alloy containing up to 2.5% B.

The copper-boron master alloy is the best agent for deoxidizing copper for the production of a highly conducting metal. Aluminum is treated with aluminum boron master alloy to increase the electrical conductivity and with aluminum-titanium-boron master alloy to refine the grain [179].

A new field of boron usage is the production of amorphous alloys or metallic glasses. Intensive development has been carried out by Allied Chemical Corp. [192]. These alloys consist of a transition metal (Fe, Ni, or Co) and about 20 mol % of a metalloid (B, C, Si, or P). They exhibit extraordinary physical properties, especially the magnetic properties, and may be used for low-hysteresis-loss transformer cores [193].

7.9.10 Economic Aspects

The consumption of ferroboration is relatively low due to the small concentrations necessary in steel. In the Western World and Japan, ferroboration production was ≈ 1400 t/a in 1982 and ≈ 2000 t/a in 1983, showing an increasing tendency. In 1981 only 2% of the total boron consumption in the United States was for the metallurgy and nuclear fields [194]. According to American Metal Market (28 Dec. 1983), ferroboration costs \$3.89 per pound (one pound = 454 g); nickel boron, \$5.57 per pound of the regular grade, \$5.67 per pound for the low-aluminum grade, and \$6.30 per pound for the low-carbon grade.

7.9.11 Toxicology and Industrial Hygiene

Ferroboron and boron master alloys are generally not toxic, but in the handling of raw materials for their production protective measures must be taken, e.g., the use of protective gloves and glasses as well as dust respirators when handling boric acid. In the production facilities the usual protective measures (clothing, glasses, dust respirators) must also be taken.

7.10 Ferroniobium

Approximately 85–90% of the total niobium production is used in the steel industry in the form of iron niobium alloy (ferroniobium) containing 40–70% niobium. Depending on the application, the alloy can also contain small amounts of Ta (ferroniobium tantalum), e.g., FeNb65Ta2, which contains 65% Nb and 2% Ta. Other alloy specifications are given in [195].

7.10.1 Production

Ferroniobium is usually produced by aluminothermic reduction of niobium oxide ores, with the addition of iron oxides if the niobium ore used contains insufficient iron. The starting materials are mainly columbites and pyrochlore concentrates.

The enthalpy of the reaction between Nb_2O_5 and Al is -276.1 kJ/mol Al , which is lower than the threshold value for self-sustaining aluminothermic reactions. The mixture must therefore either be preheated or mixed with oxygen-releasing compounds such as BaO_2 , CaO_2 , KClO_4 , KClO_3 or NaNO_3 .

Concentrates with lower percentages of niobium (ca. 40%) can also be treated by the aluminothermic process in an electric arc furnace. Also, a two-stage electroaluminothermic process for the production of ferroniobium from columbite has been developed [196].

The method of operation is to charge the mixture of niobium concentrate with the additives to refractory lined reaction vessels. Ei-

ther the whole mixture is reacted, or a small amount is set aside, ignited with a special exothermic mixture, and added to the bulk mixture. The molten reaction product is allowed to solidify in the furnace, and the block of metal separates from the slag. After cooling, it is broken into pieces of the required size.

In the aluminothermic process operated at Araxa, Fe–Nb blocks of metal up to 11 t in weight are produced. The yield of niobium metal is 96–97%. The typical composition of a reaction charge is as follows:

Pyrochlore concentrate	18 000 kg (60% Nb_2O_5)
Iron oxide	4000 kg (68% Fe)
Aluminum powder	6000 kg
Fluorspar	750 kg
Lime	500 kg

The reaction gives ca. 11 000 kg of ferroniobium of composition:

Nb	66.0%
Fe	30.5%
Si	1.5%
Al	0.5%
Ti	0.1%
P	0.1%
S	0.04%
C	0.08%
Pb	0.02%

and ca. 20 000 kg of slag containing:

Al_2O_3	48%
CaO	25.0%
TiO_2	4.0%
BaO	2.0%
Re_2O_3	4.0%
Nb_2O_5	trace
ThO_2	2.0%
U_3O_8	0.05%

Special niobium alloys, e.g., nickel–niobium, cobalt–niobium, aluminum–niobium, and chromium–niobium, are also manufactured by the aluminothermic process. For these alloys, which have various niobium contents [197], niobium oxide is the only raw material used.

7.10.2 Uses of Ferroniobium

Niobium has very marked carbide and nitride forming properties and is therefore mainly used in the production of steels and gray iron [198]. The addition of niobium prevents intercrystalline corrosion in stainless austenitic chromium nickel steels and improves corrosion resistance, weldability, ductility, and toughness in ferritic chromium

steels [199]. Ferroniobium is also used as a trace additive in large quantities for the production of high-strength low-alloy (HSLA) steels used in automobile body manufacture, structural steels, concrete reinforcing steel, and pipelines. Superalloys containing up to 5% niobium are used for gas turbine components. These materials have high hot strength [200, 201], and mostly have a nickel or copper base. The niobium is added in the form of nickel niobium or cobalt niobium.

7.11 Ferrotitanium

7.11.1 Composition and Uses

Ferrotitanium is described in DIN 17566 as a master alloy containing at least 28% Ti, obtained by reduction of the corresponding raw

materials or their concentrates. The International Standard for ferrotitanium is ISO 5454-1980 (E), which specifies a Ti content of at least 20% and allows greater variation in the Al content (up to 10% Al) than DIN 17566. The Standards specify not only the chemical composition (Table 7.41) but the condition, testing methods (sampling and analysis), shipping, and storage. Ferrotitanium in "normal lump form" usually means lumps up to 25 kg in weight. Ferrotitanium can also be supplied on demand as crushed material and/or sieved as agreed. It is supplied in sealed steel drums.

Melting points and densities of some commercial ferrotitanium alloys are listed in Table 7.42.

The binary titanium–iron phase diagram is shown in Figure 7.34 [202].

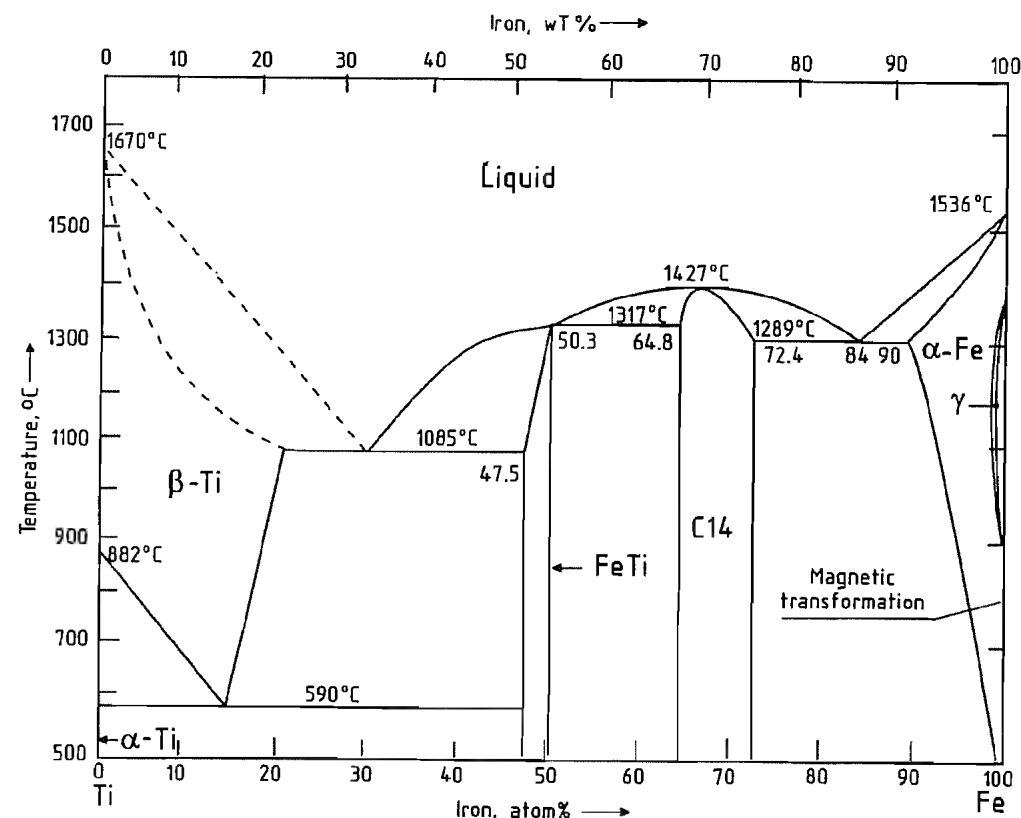


Figure 7.34: Ti–Fe phase diagram [202].

7.9.11 Toxicology and Industrial Hygiene

Ferroboreon and boron master alloys are generally not toxic, but in the handling of raw materials for their production protective measures must be taken, e.g., the use of protective gloves and glasses as well as dust respirators when handling boric acid. In the production facilities the usual protective measures (clothing, glasses, dust respirators) must also be taken.

7.10 Ferroniobium

Approximately 85–90% of the total niobium production is used in the steel industry in the form of iron niobium alloy (ferroniobium) containing 40–70% niobium. Depending on the application, the alloy can also contain small amounts of Ta (ferroniobium tantalum), e.g., FeNb65Ta2, which contains 65% Nb and 2% Ta. Other alloy specifications are given in [195].

7.10.1 Production

Ferroniobium is usually produced by aluminothermic reduction of niobium oxide ores, with the addition of iron oxides if the niobium ore used contains insufficient iron. The starting materials are mainly columbites and pyrochlore concentrates.

The enthalpy of the reaction between Nb_2O_5 and Al is -276.1 kJ/mol Al , which is lower than the threshold value for self-sustaining aluminothermic reactions. The mixture must therefore either be preheated or mixed with oxygen-releasing compounds such as BaO_2 , CaO_2 , KClO_4 , KClO_3 or NaNO_3 .

Concentrates with lower percentages of niobium (ca. 40%) can also be treated by the aluminothermic process in an electric arc furnace. Also, a two-stage electroaluminothermic process for the production of ferroniobium from columbite has been developed [196].

The method of operation is to charge the mixture of niobium concentrate with the additives to refractory lined reaction vessels. Ei-

ther the whole mixture is reacted, or a small amount is set aside, ignited with a special exothermic mixture, and added to the bulk mixture. The molten reaction product is allowed to solidify in the furnace, and the block of metal separates from the slag. After cooling, it is broken into pieces of the required size.

In the aluminothermic process operated at Araxa, Fe–Nb blocks of metal up to 11 t in weight are produced. The yield of niobium metal is 96–97%. The typical composition of a reaction charge is as follows:

Pyrochlore concentrate	18 000 kg (60% Nb_2O_5)
Iron oxide	4000 kg (68% Fe)
Aluminum powder	6000 kg
Fluorspar	750 kg
Lime	500 kg

The reaction gives ca. 11 000 kg of ferroniobium of composition:

Nb	66.0%
Fe	30.5%
Si	1.5%
Al	0.5%
Ti	0.1%
P	0.1%
S	0.04%
C	0.08%
Pb	0.02%

and ca. 20 000 kg of slag containing:

Al_2O_3	48%
CaO	25.0%
TiO_2	4.0%
BaO	2.0%
Fe_2O_3	4.0%
Nb_2O_5	trace
ThO_2	2.0%
U_3O_8	0.05%

Special niobium alloys, e.g., nickel–niobium, cobalt–niobium, aluminum–niobium, and chromium–niobium, are also manufactured by the aluminothermic process. For these alloys, which have various niobium contents [197], niobium oxide is the only raw material used.

7.10.2 Uses of Ferroniobium

Niobium has very marked carbide and nitride forming properties and is therefore mainly used in the production of steels and gray iron [198]. The addition of niobium prevents intercrystalline corrosion in stainless austenitic chromium nickel steels and improves corrosion resistance, weldability, ductility, and toughness in ferritic chromium

steels [199]. Ferroniobium is also used as a trace additive in large quantities for the production of high-strength low-alloy (HSLA) steels used in automobile body manufacture, structural steels, concrete reinforcing steel, and pipelines. Superalloys containing up to 5% niobium are used for gas turbine components. These materials have high hot strength [200, 201], and mostly have a nickel or copper base. The niobium is added in the form of nickel niobium or cobalt niobium.

7.11 Ferrotitanium

7.11.1 Composition and Uses

Ferrotitanium is described in DIN 17566 as a master alloy containing at least 28% Ti, obtained by reduction of the corresponding raw

materials or their concentrates. The International Standard for ferrotitanium is ISO 5454-1980 (E), which specifies a Ti content of at least 20% and allows greater variation in the Al content (up to 10% Al) than DIN 17566. The Standards specify not only the chemical composition (Table 7.41) but the condition, testing methods (sampling and analysis), shipping, and storage. Ferrotitanium in "normal lump form" usually means lumps up to 25 kg in weight. Ferrotitanium can also be supplied on demand as crushed material and/or sieved as agreed. It is supplied in sealed steel drums.

Melting points and densities of some commercial ferrotitanium alloys are listed in Table 7.42.

The binary titanium–iron phase diagram is shown in Figure 7.34 [202].

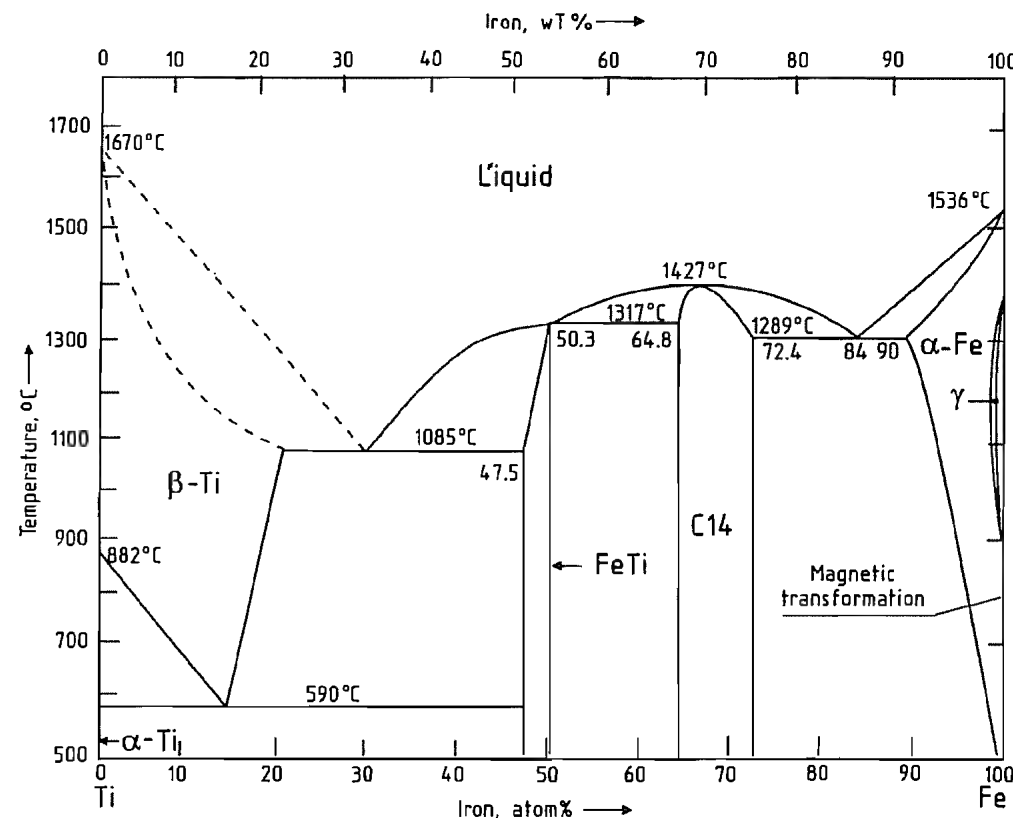


Figure 7.34: Ti–Fe phase diagram [202].

Table 7.41: Composition of commercial ferrotitanium alloys DIN 17566.

Alloy grade	Alloy number ^a	Chemical composition, %						
		Ti ^b	Total Al max.	Si max.	Mn Max.	C max.	P max.	S max.
FeTi 30	0.4530	28–32	4.5	4.0	1.5	0.10	0.050	0.060
FeTi 40	0.4540	36–40	6.0	4.5	1.5	0.10	0.10	0.060
FeTi 50	0.4550	46–50	75	4.0	1.0	0.10	0.10	0.060
FeTi 70	0.4570	65–75	2.0	0.20	1.0	0.20	0.040	0.030
FeTi 70 VB (vacuum treated)	0.4571	65–75	0.50	0.10	0.20	0.20	0.030	0.030

^a In accordance with DIN 17007, Sheet 3 (draft).^b Variation within a batch must not exceed ±2%.**Applications in the Iron and Steel Industry.**

Compared with pure titanium, ferrotitanium has the advantages of better solubility (lower melting point and higher density) and lower price. Titanium is useful mainly because of its ability to form a carbide. However, as the affinity of titanium for oxygen is considerably higher than for carbon, the steel must be effectively deoxidized before titanium is added. Titanium is only used for this deoxidation in special cases. Titanium is also used for nitrogen removal and for bonding with sulfur [203].

Table 7.42: Melting points and densities of some commercial ferrotitanium alloys.

Composition, %			mp, °C	ρ, g/cm ³
Ti	Al	Si		
30.6	4.0	3.7	1325–1500	6.2
39.1	5.8	4.0	1325–1480	5.9
46.6	7.6	3.2	1305–1480	5.5
70.0	0.1–0.5		1070–1135	5.4

In the production of stainless austenitic chromium–nickel steels, titanium is added to combine with the small amount of carbon present to form TiC (“stabilization”), thereby preventing intergranular corrosion (e.g., adjacent to welds).

Deoxidation of killed steel with titanium improves its quality by minimizing oxidic inclusions. Depending on the carbon content, it also reduces cracking tendency (grain refinement of austenite) and increases yield strength (titanium-containing ferrite). Titanium addition also minimizes segregation in the upper part of the ingot on casting, thus improving the yield.

Addition of titanium to tool steels gives a finer grain and reduces the depth of hardening

and hence the cracking tendency. In sulfur-containing free-cutting steels, especially highly alloyed stainless chrome and chromium–nickel steels, the sulfur is bonded to the titanium. This prevents red shortness and improves ductility.

Some complex master alloys with boron contain titanium and other elements (BATS = boron–aluminum–titanium–silicon). The boron is added in small amounts to the steel to improve the hardening properties and grain refinement, and the titanium is added to protect the boron from nitrogen (by forming TiN).

High-temperature hardenable alloys based on iron and especially nickel (e.g., nimonic alloys) contain up to 4.5% Ti [204]. Here, the titanium reacts with the aluminum and nickel to form coherent particles with the composition Ni₃(Ti, Al), which cause precipitation hardening. Titanium is also used as a microalloying element in high-strength, low-alloy (HSLA) steels [205].

The addition of titanium to cast iron causes the formation of finer graphite on supercooling, thereby improving the mechanical properties.

Powdered ferrotitanium and ferrosilicon–titanium alloys, sometimes with higher aluminum contents, are used as coatings on welding electrodes. Also, welding wires for HSLA steels are alloyed with ca. 0.5% Ti to give a fine-grained weld bead.

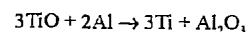
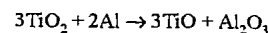
7.11.2 Production

The starting materials for the production of ferrotitanium are ilmenite, leucoxene, perovskite, and slag concentrates produced from il-

menite. Because of the increasing availability of titanium scrap, this also is used to an increasing extent for the production of ferrotitanium (mostly > 70% Ti) and other titanium master alloys.

Reduction with Carbon. Carbothermic production in electric arc furnaces leads to high carbon contents in the ferrotitanium. However, as the main use of ferrotitanium is to combine with the carbon in steel, the presence of carbon in the ferrotitanium is undesirable, and this production method is therefore now hardly used. The carbothermic production of ferrotitanium containing 15–18% Ti, 5–8% C, 1–3% Si, and 1–2% Al, and of ferrosilicon titanium containing ca. 30% Ti, ca. 30% Si, up to 0.3% C, and 1–3% Al is described in [206].

Metallothermic Production. DIN 17566 specifies grades of ferrotitanium containing 28–50% Ti and 4.5–7% Al. These are mainly produced by the aluminothermic process. The reduction of TiO₂ by Al proceeds via TiO.



If there is too much TiO₂ in the reaction mixture, TiO can be formed as a third phase besides the metal and slag [207]. In the aluminothermic production of ferrotitanium there is a high consumption of aluminum, as it reacts both with the iron oxide in the ilmenite and with the oxygen-producing substances added to increase the exothermicity.

An aluminothermic mixture, consisting, for example, of 4320 kg Australian ilmenite (58.55% TiO₂), 480 kg rutile (96.7% TiO₂), 190 kg calcined limestone, 107 kg potassium perchlorate, and 1693 kg Al powder, is placed in a refractory-lined combustion vessel and ignited to start the reaction. After cooling, a 2250 kg block of ferrotitanium is obtained containing 39.8% Ti, 6.7% Al, 3.4% Si, and 0.02% C, which separates well from the slag. The titanium yield is 50%, and the specific consumption of aluminum (based on the Ti in the ferrotitanium) is 1.89 kg Al/kg Ti.

In the electro-aluminothermic process, which is carried out in an arc furnace, the raw

materials contain as little iron oxide as possible, so that most of the aluminum is used to reduce titanium oxide. The consequent lack of exothermicity is compensated by electrical energy. A process developed in France is now widely used [208]. Here, an ilmenite concentrate, after addition of lime, is partially reduced with carbon in an electric-arc furnace to give a slag concentrate with a high concentration of titanium oxide, and the reduced iron is tapped off. The molten slag is then reduced in several stages by blowing in aluminum and iron, producing ferrotitanium of the desired composition.

In a process developed by the Gesellschaft für Elektrometallurgie [209], a calcium oxide/titanium oxide melt containing ca. 75% TiO₂ is first produced from prerduced ilmenite, from rutile and lime, or from perovskite with addition of iron scrap, and is reacted with a molten aluminum iron alloy containing 60–70% Al in a reaction ladle to give ferrotitanium and slag. Yields of titanium of 60–67% are obtained, and the specific aluminum consumption is 1.0–1.1 kg Al/kg Ti.

Production from Titanium Scrap and Sponge. As the availability of titanium scrap is increasing with the growth in the consumption of titanium, it is being increasingly used for the production of ferrotitanium (mainly high-grade material containing 65–75% Ti) and ferrotitanium–silicon. Because of its low melting point (ca. 1100 °C) the alloy containing 70% titanium melts comparatively readily when alloyed with iron in an induction furnace, in an arc furnace with consumable electrodes under vacuum or argon, or in an electroslag melting furnace. Contact of the melt with air must be prevented because of the strong affinity of titanium for oxygen and nitrogen. Ferrotitanium can also react with refractory crucibles [210]. The high-grade ferrotitanium alloys produced by melting under vacuum are designated FeTi 70 VB in DIN 17566.

Calcium–silicon–titanium alloys are produced by melting together commercial cal-

cium silicon and titanium sponge or scrap in an induction furnace [206, p. 579].

7.11.3 Economic Aspects

The prices of ferrotitanium are published in the London "Metal Bulletin", and the monthly average prices (from the Metal Bulletin), with the corresponding exchange rates, have been published since 1979 in the journal *Erzmetall* [211].

7.12 Ferrovandium

According to DIN 17563 [212], ferrovandium is "a master alloy with a vanadium content of at least 50% produced by reduction of the corresponding raw materials or their concentrates". In the United States alloys with lower vanadium contents are also commercially available. The iron vanadium and vanadium aluminum master alloys and the commercial grades of vanadium alloys are listed in Table 7.43.

Table 7.43: Commercial grades of vanadium master alloys [213, 214].

Ferrovandium	% V	% C	% Si	% Al
Fe V 40	35–48	0.5	2.0	0.5
Fe V 50	48–60	0.5	2.0	0.3
Fe V 60	50–65	<0.15	<1.5	<2.0
Fe V 80	78–82	0.15	1.5	<1.5

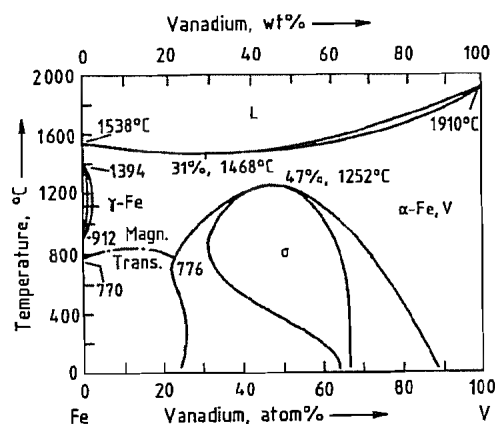


Figure 7.35: Phase diagram Fe-V [215].

The Fe-V phase diagram (Figure 7.35) shows almost complete mutual solubility of

the elements. At compositions approximating to FeV below 1200 °C, a σ -phase exists which forms tetragonal crystals.

7.12.1 Production from Vanadium Oxides

The reduction of vanadium oxides is assisted by the presence of iron, as the activity of the vanadium is reduced, and the solubility of oxygen in vanadium-iron is much lower than in pure vanadium, because of the lower melting point [216]. The vanadium oxides can therefore be reduced with carbon, silicon, and aluminum in the presence of iron, the product being ferrovandium.

Reduction with Carbon. The high affinity of vanadium for carbon leads to carbide formation, so that carbothermic reduction can only be used when there is no requirement for vanadium with low carbon content. The Union Carbide Corporation has developed a process that gives a V_2C -containing alloy known as Carvan [217], with a C content in the range 10–13% [213].

Reduction with Silicon. Under today's conditions for the processing of V_2O_5 , silicothermic reduction is no longer generally profitable, as the process has multiple stages and gives a poor vanadium yield in the form of a low-vanadium ferrovandium. The vanadium losses in this process are 10–25% [218].

Reduction with Aluminum. The high-vanadium grades of ferrovandium, FeV 60, FeV 80, and FeV 90, are now usually produced by aluminothermic treatment of V_2O_5 . The aluminothermic process can readily be controlled on a large scale. It is especially suitable for the treatment of vanadium pentoxide because it gives a high yield of high-grade ferrovandium in a single process step.

After ignition, the reaction of V_2O_5 with aluminum is self-sustaining. Some of the mixture of V_2O_5 flakes, aluminum powder or granules, fine steel shot, and an initiating mixture (e.g., $BaO_2 + Al$ powder) is ignited, and further quantities of the mixture are then added. The combustion time for the usual

batch size (to produce 0.5–1 t metal) is only a few minutes. After cooling for 2–3 d, the furnace is dismantled, and the block of metal at the bottom is cleaned and crushed or ground to the commercially desired particle size.

As the reaction proceeds very rapidly, the aluminum in the metal and the vanadium oxide in the slag may not attain equilibrium, so that the vanadium content of the slag may be too high. To prevent this, an electric arc is ignited after completion of the aluminothermic reaction to maintain the molten state of the melt and the slag until reaction is complete [219].

7.12.2 Direct Production from Slags and Residues

Enriched vanadium-containing oxidation slags can also be processed directly to a technical-grade ferrovandium. In the method of Christiania Spigerverk [220], a 50% ferrovandium is obtained in an electric arc furnace by a two-stage reduction process. In the first stage, the FeO fraction of the slag is reduced with ferrosilicon (FeSi 75) with addition of lime, and in the second stage the slag obtained in the first stage is reduced with 90% silicon to give a ferrovandium alloy. The vanadium yield is 80%, and the FeV still contains traces of Si, Cr, Mn and Ti.

Ferrovandium can be obtained by the electrosilicothermic treatment of high-vanadium boiler ashes and enriched fly ash, either alone or in combination with vanadium-containing oxidation slags, depending on their composition. As oil residues and fly ash contain only small amounts of iron, the iron removal stage normally necessary with oxidation slags can be omitted.

7.13 Ferromolybdenum

In the steel and foundry industry molybdenum is added to melts, either as technical ox-

ide or in the form of ferromolybdenum. Table 7.44 summarizes the internationally standardized ferromolybdenum alloys; the typical molybdenum content ranges from 55 to 75%. Compared to pure molybdenum, ferromolybdenum dissolves much more easily in the steel melt and is cheaper to produce. Practical experience has shown that alloys with up to 75% molybdenum do not cause any dissolution problems. Nevertheless there is still a demand for 65% molybdenum alloys which are even less critical as regards dissolution characteristics. The Fe-Mo phase diagram is shown in Figure 7.36. Due to the limited information available, the melting temperatures of the alloy at high molybdenum concentrations can only be estimated. In practice they are likely to be considerably lower than indicated by the phase diagram because of significant concentrations of silicon and other impurities.

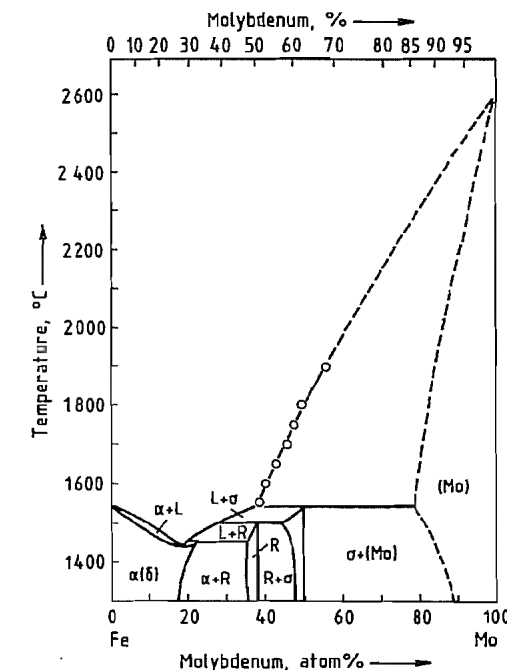


Figure 7.36: Fe-Mo phase diagram showing estimated liquidus (L) compositions at higher molybdenum concentrations [221]. α , δ , and R are intermetallic phases.

Table 7.44: International specifications for ferromolybdenum.

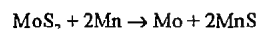
Specification	Symbol/designation	Composition, %							
		Mo	Si (max.)	C (max.)	S (max.)	P (max.)	Cu (max.)	Pb (max.)	Sn (max.)
ASTM A 132-74 (reapproved 1979)	Ferromolybdenum (formerly grade B)	60.0 min.	1.0	0.10	0.15	0.05	1.0	0.01	0.01
DIN 17561	FeMo 70 (0.4270 ^a)	60–75 ^b	1.0	0.10	0.10	0.10	0.5		
	FeMo 62 (0.4262 ^a)	58–65 ^b	2.0	0.50	0.10	0.10	1.0		
ISO 5452	FeMo 60	55.0–65.0 ^c	1.0	0.10	0.10	0.05	0.5		
	FeMo 60 Cu 1	55.0–65.0	1.5	0.10	0.10	0.05	1.0		
	FeMo 60 Cu 1.5	55.0–65.0	2.0	0.50	0.15	0.05	1.5		
	FeMo 70	65.0–75.0 ^c	1.5	0.10	0.10	0.05	0.5		
	FeMo 70 Cu 1	65.0–75.0	2.0	0.10	0.10	0.05	1.0		
	FeMo 70 Cu 1.5	65.0–75.0	2.5	0.10	0.20	0.10	1.5		
Japanese Industrial Standard, JIS G 2307 1978									
Class:									
High-carbon ferro- molybdenum	FMoH	55.0–65.0 ^c	3.0	6.0	0.20	0.10	0.5		
Low-carbon ferro- molybdenum	FMoL	60.0–70.0 ^c	2.0	0.10	0.10	0.06	0.5		

^aMaterial numbers in preparation, proposed numbers.

^bThe range of variation within a lot may not exceed $\pm 2\%$.

^cThe range of variation within a graded lot should not exceed 3% absolute.

The principal raw materials used for ferromolybdenum production are molybdenum concentrates and technical-grade molybdenum trioxide. One method proposed for the production of ferromolybdenum used molybdenum concentrates which were reacted with ferromanganese to form ferromolybdenum and manganese sulfide [222]:



Due to the high Gibbs free energy of manganese(II) sulfide formation, this reaction is claimed to yield ferromolybdenum with a relatively low sulfur concentration, but a further sulfur removal step appears to be necessary. This process is not, however, used on a commercial basis.

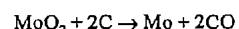
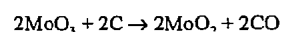
Technical-grade molybdenum trioxide is commonly used as the molybdenum raw material. Because of its high value and the fact that MoO_3 starts to sublime at 700 °C, electrostatic precipitators or bag houses must be used to collect the molybdenum dust and sublimates for recirculation. Good housekeeping is also essential to minimize molybdenum handling losses.

Two principal processes are used for molybdenum oxide reduction: carbothermic re-

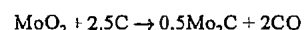
duction in a submerged arc furnace and metallothermic reduction. The most commonly applied method is the silicothermic reduction, a type of metallothermic reduction.

7.13.1 Submerged Arc Furnace Carbothermic Reduction

The carbothermic reduction of MoO_3 can proceed as follows:



or with formation of molybdenum carbide:



The Gibbs free energies of oxide and carbide formation are shown in Figure 7.37 as a function of temperature. The reduction of MoO_3 starts at fairly low temperatures. If the process were run at these temperatures (i.e., < 600 °C) then Mo_2C would be formed because it is more stable than molybdenum. However, since the process is run at 1700–2000 °C, any intermediately formed molybdenum carbide reacts to form molybdenum metal:

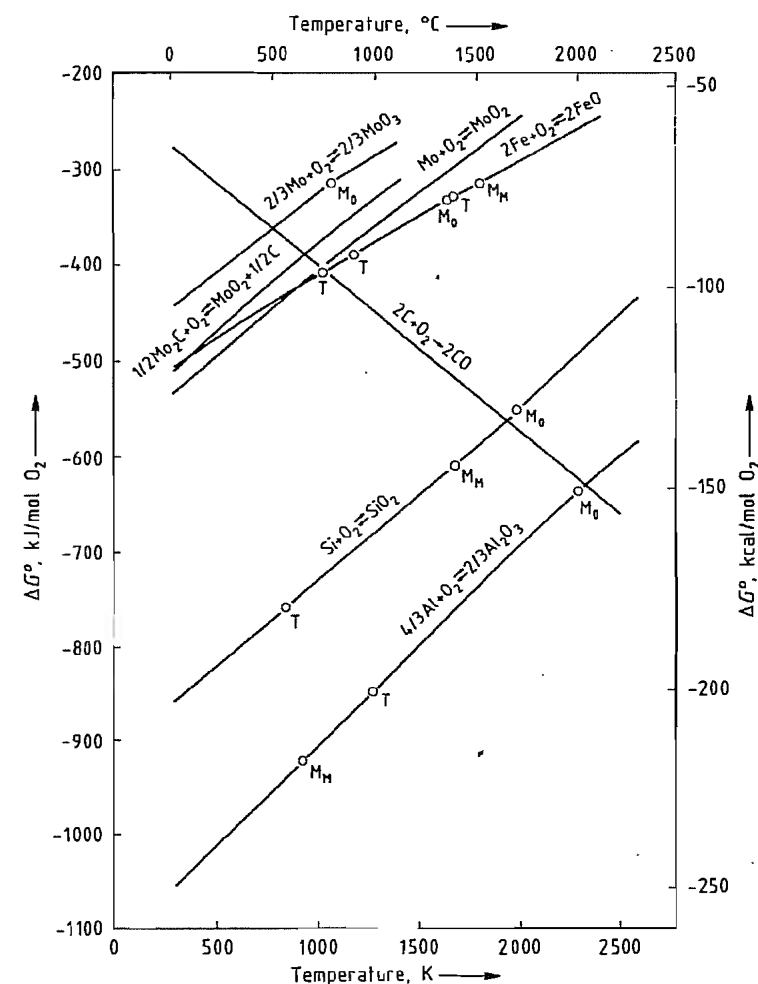
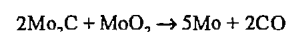


Figure 7.37: Gibbs free energy of oxide and carbide formation [223]. T = transformation point; M_M = melting point of metal; M_O = melting point of oxide.

Under practical conditions the resulting metal alloy is low in carbon.

Because of the commercial disadvantages of the process, detailed literature describing the process is limited [224–227]. The process was previously run in single-phase 300–500 kW and three-phase 1500–2000 kW electric arc furnaces. The use of the single-phase arc furnace seems to have been more successful because of its higher energy density within the furnace. A single-phase system with a cylindrical magnesite or carbon-based rammed furnace body and equipped with a bottom carbon

electrode is shown in Figure 7.38. The top electrode is adjustable and the whole furnace arrangement runs on tracks so that it can easily be replaced with a new unit. The process is run batchwise, producing a semimolten metal block and a slag. The slag contains up to 10% molybdenum oxide and must be retreated by remelting. Melting of a 1.5–2 t metal block takes about 20–28 h. To separate metal and slag, the furnace assembly must be stripped and later rebuilt for reuse.

Raw materials are technical-grade molybdenum oxide; iron ore or millscale, steel

punchings, nail nips or turnings; lime and fluorspar as fluxing agents; and charcoal as reducing agent. To minimize MoO_3 sublimation, the concentrate and carbon material are briquetted. The reaction is started by melting slag from a previous reaction and adding the briquetted mixture to the slag to avoid molybdenum sublimation. Once the initial reduction to MoO_2 has taken place, sublimation is avoided. The resulting slag consists of some unreduced MoO_2 and FeO which has a higher Gibbs free energy than MoO_2 (Figure 7.37). To improve metal-slag separation, lime and fluorspar are added. The slag should be fluid and is tapped toward the end of the reduction cycle. The metal block is stripped while it is still red hot and quenched in water to aid subsequent crushing. The metal must be hand-sorted to recycle any parts of the block contaminated with slag. The resulting molybdenum-rich slag has to be remelted in a separate process into a low-molybdenum, high-carbon intermediate alloy which is recycled.

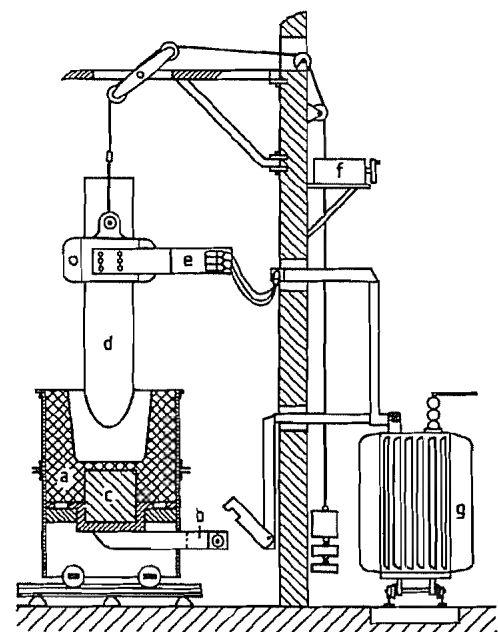


Figure 7.38: Single-phase submerged arc furnace [227]: a) Furnace with rammed lining; b) Bottom electrode power supply bar; c) Bottom electrode (carbon); d) Top electrode; e) Electrode clamp with power supply cables; f) Electrode control; g) Transformer.

Table 7.45: Consumables required to produce 1 t of ferromolybdenum in the carbothermic process [227].

Consumable	Single-phase furnace 300 kW	Three-phase furnace, 1500 kW
Roasted Mo concentrate, kg	1160	1420
Remelt material, kg	280	330
Slag treatment metal, kg	165	168
Nail nips, kg	172	230
Platescale, kg	290	102
Lime, kg	150	178
Fluorspar, kg	150	178
Charcoal, kg	255	310
Electrodes, kg	95	135
Power, kWh	4300	4450
Products		
Ferromolybdenum, kg	1000	1000
Remelt, kg	270	250
Dust, kg	66	

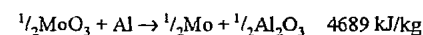
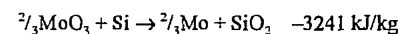
Table 7.45 shows the consumption of electric energy and ingredients required to produce ferromolybdenum using the carbothermic process.

7.13.2 Metallothermic Reduction

Metallothermic reduction in which silicon (or aluminum) is used to reduce the MoO_3 is the commonly used production process for ferromolybdenum today. Its advantages are that it is a single-step process which results in a saleable metal and a low-molybdenum slag and that it requires only basic process equipment. Due to the large difference in the Gibbs free energy for aluminum oxide and silicon dioxide formation compared to molybdenum oxide formation (Figure 7.37), the reduction process approaches 100% molybdenum reduction.

An aluminothermic or silicothermic reaction must be sufficiently exothermic to melt all the reaction constituents resulting in satisfactory separation of the liquid metal and liquid slag phases before cooling. According to SHEMTCHUSHNY, a minimum specific heat of reaction of -2700 kJ/kg is required for a reaction to be self-sustained [228]. This assumes that no additional heat is added to the reaction (e.g., by preheating the charge or by adding booster oxides and further reducing metal). Consideration of the specific heats of reaction shows that both aluminum and silicon can be

used to reduce MoO_3 in self-sustained reactions:



If aluminum is reacted with MoO_3 , the resulting heat of reaction is very high, leading to excessive evaporation of MoO_3 and the danger of an explosion of the reaction mixture.

Consequently, silicon is the preferred reducing element. Furthermore, less silicon is necessary compared to aluminum (stoichiometric consumption is 0.439 kg silicon per kilogram of molybdenum, compared to 0.562 kg aluminum per kilogram of molybdenum) and silicon in the form of ferrosilicon is considerably cheaper than aluminum.

Practical experience, even when using charges much larger than a 200 kg, shows that silicon alone does not result in a self-sustained reaction. Some of the silicon must therefore be replaced with aluminum or other elements with a similar oxygen affinity. Some of the required iron is often added in the form of millscale or iron ore concentrates which react with silicon or aluminum to generate additional heat. Part of the iron remains as FeO in the slag and acts as a fluxing agent. Further fluxing agents are lime and fluorspar, which are necessary to ensure good separation of metal and slag and low molybdenum concentrations (typically $< 1\%$) in the slag. The dust generated in the process can contain up to 5% of the molybdenum in the charge. Any dust and sublimed MoO_3 must be extracted, recovered, and recycled to achieve an overall molybdenum yield of 97–99%.

To achieve reproducible reactions, a homogeneous mixture of the precisely weighed reaction ingredients is required. All ingredients must be dry, well-calcined, and ideally their particle size should be $< 1 \text{ mm}$. A typical firing arrangement is shown in Figure 7.39. The crucible unit consists of a circular or square, sand- or brick-lined base section and a cylindrical refractory-lined, steel section that contains the reaction slag. The mix feeding arrangement allows part of the reaction mixture to be placed into the well-dried crucible

unit. The reaction is started by adding a small amount of a mixture of barium peroxide and aluminum to a special starter mix which tends to be more exothermic than the main mix. Once the main mix has started to react, the bulk of the reaction mix is continuously fed into the crucible arrangement. Total reaction times of 30–60 min for metal block weights of 1–4 t can be expected. After completion of the reaction, metal and slag are allowed to segregate for another 30–60 min before the bulk of the slag is tapped off. The red-hot metal block is then stripped off the furnace base and quenched in water to aid crushing. Jaw crushers are commonly used for crushing the metal. Considerable care has to be taken when sampling the metal for molybdenum content because the molybdenum tends to segregate within the block. Any highly segregated metal and metal contaminated with slag inclusions is recycled for remelting. Good housekeeping is necessary to recycle all splashings, floor sweepings, etc. and achieve a good total molybdenum yield.

In a process modification used by Duval Corporation, Duval Sierrita [230], the entire reaction mix is charged into the reaction crucible before ignition. The advantage is that controlled addition of the reaction mix is not required. The disadvantages are that the reaction speed cannot be controlled by varying the feed rate and that a larger crucible unit is required to contain the initial mixture.

Recent developments have centered on improving process economics. Automatic handling and weighing of the raw materials as well as finished metal and ferromolybdenum slag is one area of activity. Other activities center around the optimization of ingredient and consumable costs.

Metallothermic mixtures used to produce ferromolybdenum are summarized in Table 7.46. Mixtures A–D represent different possibilities of increasing the reaction heat by using aluminum or calcium in the form of a calcium-silicon or a ferrosilicon-aluminum alloy [227]. Reaction D can be regarded as a fairly typical ferromolybdenum reaction mix; it

gives 87 kg ferromolybdenum with 67–73% molybdenum, 0.05–0.08% carbon, 0.03–0.05% sulfur, 0.25–0.6% silicon and 5 kg remelt metal as well as a slag containing 0.34% MoO₃, 13.85% Fe₂O₃, 7.4% CaO, 9.9%

Al₂O₃, and 64.5% SiO₂. The reaction mix also contains recycled dust and metal remelt which is normal practice when continuously producing ferromolybdenum.

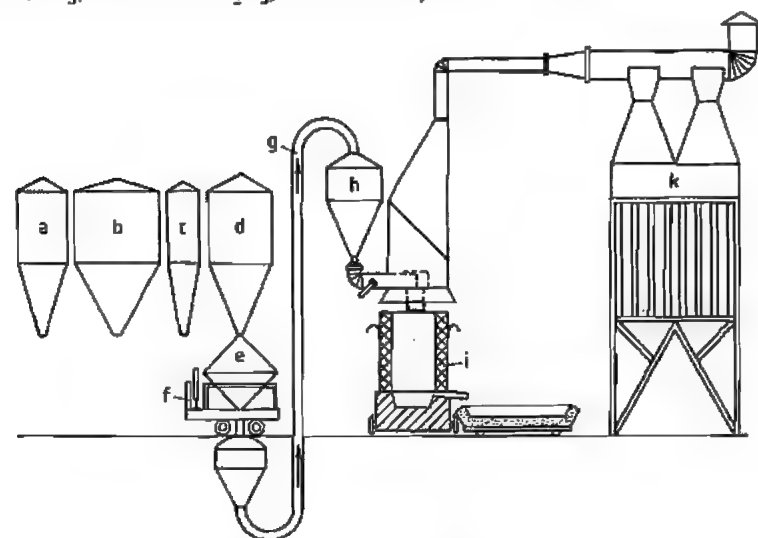


Figure 7.39: Metallothermic firing arrangement [229]: a) Storage hopper for iron ore or millscale; b) Storage hopper for roasted Mo concentrate; c) Storage hopper for fluorspar; d) Storage hopper for aluminum and ferrosilicon (75% Si) powder; e) Mixing hopper; f) Balance; g) Air lift system; h) Firing hopper; i) Reaction vessel; k) Electrostatic precipitator.

Table 7.46: Reaction mixtures used for ferromolybdenum production.

Component	DURRER, VOLKERT [227]				Climax Molybdenum			Literature from the former Soviet Union		
	A	B	C	D	[231]	[232]	[232]	[233]	[234]	[235]
Roasted Mo concentrate, kg	100	100	100	100	100	100	100	100	100	100
MoO ₃ concentration, %	ca. 90	ca. 90	ca. 90	ca. 90	85	85	85	81.7–84	80.3	85
Platescale, kg	29	16–18	35	51		24.2	22.5			
Fe ore, kg					26.9			26	22	29.6
Fe concentration, %					69				65.7	67.1
Fe turnings, kg	5–6	18						19.5		
Fe scrap, kg						17.3 ^d	5.2 ^d		19	19.2
Ferrosilicon, kg	31.5	21–23	65 ^c	38	48.9	20.8	31.2	35.1	31.6	36.8
Si concentration, %	75	75	45	75	50	75	75	75	77	73.6
Ca–Si alloy, kg		17–18								
Al powder, kg	9.0			5	5.1	12.1	6.9	3.7	4.3	3.8
Al concentration, %	99.5			99.5	93				93	99
Lime, kg				2.5	7	8.7		3.0		3
Fluorspar, kg			7	7.5	2.2		5.2	2.0	3	2
CaF ₂ concentration, %					95					
Dust, kg				9.5			5.2			
Remelt, kg				5.5			6.9			

^aUp to 36 mixes used in one reaction.

^bMix preheated to 150 °C.

^cCalculated mix.

^dFe shot.

^eFeSi 45 Al 10 alloy.

Mixtures E–G have been reported to have been used by Climax Molybdenum in their Langeloth (USA) plant [231]. The mixtures are based on 100 kg technical molybdenum oxide input with 85% MoO₃ in the technical oxide. Reaction E can be regarded as a typical reaction mix for a ferromolybdenum with 58–64% molybdenum. The maximum impurity levels quoted were 0.1% carbon, 0.25% sulfur, 0.5% copper, and 1% silicon. Reaction G can be regarded as a typical reaction mix yielding an approximately 70% molybdenum alloy.

Mixtures H–J have been taken from literature from the former Soviet Union [233–235]. Mixture H gives ferromolybdenum containing 60–65% molybdenum, 0.15–0.9% silicon, 0.04% phosphorus, 0.08% sulfur, 0.05% carbon, and ca. 0.5% copper and slag containing 0.06–0.17% molybdenum, 67–70% SiO₂, 7–11% FeO, 10–13% Al₂O₃, 6–8% CaO, and 1–3% MgO. Mixture I uses a mix preheating to 150 °C, and should have resulted in a ferromolybdenum with ca. 56% molybdenum (calculated). Mixture J is part of a calculated formulation according to Elyutin [235]. The calculation is based on 96.8 kg ferromolybdenum containing 58.14% molybdenum, 0.53% silicon, and 0.07% carbon and 87 kg slag containing 65.65% silicon oxide, 10.06% aluminum oxide, and 24.28% iron(II) oxide. A heat balance has been calculated for this formulation. The total heat generated is 422.45 MJ. This heat is assumed to be consumed to provide the latent and melting heat for the metal (25%), the slag (50%), and to cover the heat losses of 25%.

7.14 References

1. R. Fichte, H.-J. Retelsdorf: "Stahlveredler" in *Winnacker-Küchler*, vol. 4, pp. 198–234. Durrer-Volkert: *Metallurgie der Ferrolegierungen*, 2nd ed., Springer Verlag, Berlin-Heidelberg-New York 1972.
2. P. D. Deeley, K.-J. A. Kundig, H. R. Spendlow, Jr.: *Ferroalloys and Alloying Additives Handbook*, Shieldalloy Corp., Newfield, N. J., Metallurg Alloy Corp., New York 1981.
3. VDI-Richtlinien VDI 2576 (May 1983): *Emissionsminderung – Elektrothermische und metallothermische Erzeugung von Ferrolegierungen* (Emission Control – Electrothermic and Metallothermic Ferroalloy Production), vol. 2 of *VDI-Handbuch Reinhaltung der Luft*, Beuth Verlag, Berlin-Köln 1983.
4. H. Goldschmidt, *Justus Liebigs Ann. Chem.* 301(1898) 19–28.
5. O. Kubaschewski, C. B. Alcock: *Metallurgical Thermochemistry*, 5th ed., Pergamon Press, London-New York 1979.
6. N. P. Elyutin et al.: *Production of Ferroalloys*, 2nd ed., Israel Programme for Scientific Translations, S. Monon, Jerusalem 1961.
7. W. Dautzenberg, in: Durrer & Frank, (G. Volkert, K.-D. Frank, eds.): *Metallurgie der Ferrolegierungen*, 2nd ed., Springer Verlag, Berlin-Göttingen-Heidelberg-New York 1972.
8. E. M. Levin et al.: *Phase Diagrams for Ceramists*, American Ceramic Society Inc., Columbus, 1964, Supplement 1969.
9. W. G. Moffatt: *Handbook of Binary Phase Diagrams*, General Electric Corp, Schenectady 1973 (plus updates).
10. K. A. Feldmann, K. D. Frank in R. Durrer, G. Volkert (eds.): *Metallurgie der Ferrolegierungen*, Springer Verlag, Berlin 1972.
11. W. P. Eljutin, I. A. Palow, B. E. Levin: *Ferrolegierungen*, VEB Verlag Technik, Berlin 1953.
12. E. Schürmann, N. Hensgen, *Arch. Eisenhüttenwes.* 51 (1980) no. 1, 1–4.
13. J. A. De Huff, V. D. Coppolecchia, A. Lesnewich, *Electr. Furn. Proc.* 27 (1969) 167–174.
14. H. Krogrund, *ISLAF Conference*, Acapulco 1978.
15. DEMAG company brochure, Submerged Arc Furnaces, Duisburg 1979.
16. T. W. Lopuszynski, J. P. Trunco, W. L. Wilbern, *Electr. Furn. Proc.* 30 (1972) 89–93.
17. U.S. Environmental Protection Agency Office of Air and Waste Management Research Triangle Park, N. C., 27711 EPA 450/2-74-008, 1974.
18. G. Rau, *Erzmetall* 44 (1991) no. 11, 557–559.
19. P. C. Aitcin, *Electr. Furn. Proc.* 42 (1984) 301–310.
20. ASTM Designation: *Annual Book of ASTM Standards*, E 360 – 70 T, ASTM, Philadelphia, 1970.
21. *Handbuch für Eisenhüttenlaboratorium*, vol. 2, Verlag Stahl Eisen mbH, Düsseldorf.
22. *Analyse der Metalle*, vol. 1, Springer Verlag, Berlin 1980.
23. DFG: *Maximale Arbeitsplatzkonzentration und Biologische Arbeitsstofftoleranzwerte*, VCH Verlagsgesellschaft, Weinheim 1991.
24. E. Houdremont: *Handbuch der Sonderstahlkunde*, Springer Verlag, Berlin 1956.
25. J. S. Stanko: *Steel Makers Guide to Manganese*, Mintek, Randburg 1989.
26. Commodities Research Unit: *The Costs of Producing Ferroalloys*, vol. 2, London 1989.
27. V. V. Strishkov, R. M. Levine: *The Manganese Industry in the U.S.S.R.*, U.S. Bureau of Mines, Washington 1986.
28. H. Bromet: "Technical and Economic Comparison of the Various Furnaces used for Ferro and Silico

- Manganese", *INFACON 80, Proc. Int. Ferro-Alloys Congr.* 2nd, 1980.
29. O. Kubaschewski, C. D. Alcock: *Metallurgical Thermochemistry*, 5th ed., Pergamon Press, Oxford 1979.
 30. *Plasma Torches in Blast Furnaces*, Société du ferromanganèse de Paris, Outreau 1986.
 31. W. J. Rankin: "Si-Mn Equilibrium in Ferromanganese Production", *J. S. Afr. Inst. Min. Metall.* 79 (1979) Sept., c167-c174.
 32. S. Sakurai: *Recent Operational Results of the Shaft Type Ferro-Manganese Smelting Furnace*, Mizushima Ferro-Alloy Company Japan, Mizushima 1986.
 33. A. G. Amesén, B. Asphaug: "Computer Control of Electric Smelting Furnaces", *Proc. Int. Ferro Alloy Conf.*, Johannesburg 1974.
 34. Z. Van der Walt, W. A. Gericke: "The Effect of the Magnitude of Scale on Various Operating Characteristics in the Production of High-Carbon Ferromanganese", *Proc. Lat. Am. Inst. Iron and Steel*, Seminar Ferroalloys, 1975.
 35. G. Glöckler, H. G. Müller: "A Comparison of the Electric Submerged Arc Furnace and the Plasma Smelting Furnace", *BHM Berg-Hüttenmänn. Monatsh.* 134 (1989) no. 5.
 36. A. Kousaris, J. B. See: "Reactions in the Production of High Carbon Ferromanganese from Mamatwan Ore", *J. S. Afr. Inst. Min. Metall.* 19 (1979) 149-158.
 37. R. T. Hooper: "The Production of Ferromanganese", *Electr. Furn. Conf. Proc.* 24 (1967) 141-145.
 38. L. Rossenmyr: "Manganese Alloy Production in Large Submerged Arc Furnaces", *Electr. Furn. Conf. Proc.* 27 (1970) 121-124.
 39. Tinfos Company Brochure, Tinfos Jernverk AS, Oyestronda, Norway 1989.
 40. "Electric Furnaces Beats Pollution", *Mod. Power Eng.*, May 1974.
 41. W. Gericke: "The Establishment of a 500 000 t/a Sinter Plant at Samancor's Mamatwan Manganese Ore Mine", *Proc. Int. Ferroalloys Congr. 5th* (1987) April.
 42. A. A. Tskilishvili: "Production of High-Carbon Ferromanganese from Manganese Iron Sinter", *Stal'* (1975) no. 9, 816-817.
 43. E. Svana: "Ferro Manganese Smelting", *Elkem Seminar on Smelting*, New Delhi 1974.
 44. R. G. Rotzloff: "High Carbon Ferromanganese Production on the High Alumina Practice", *Electr. Furn. Conf. Proc.* 44 (1987) 169-173.
 45. H. W. Wise: "High Carbon Ferromanganese Metallurgical Variables", *Electr. Furn. Conf. Proc.* 24 (1968) 88-92.
 46. J. F. Dery: "Metallurgical Calculations for Ore Evaluation and Operational Planning in the Electric Furnace Smelting of High Carbon Ferromanganese", unpublished paper (1964).
 47. D. S. Kozak, L. R. Matricardi: "Production of Refined Ferromanganese Alloy by Oxygen Refining of High Carbon Ferromanganese", *Electr. Furn. Conf. Proc.* 38 (1980) 123-127.
 48. R. Ando, T. Yamagishi, T. F. Fukusima, K. Kawasaki: "A Study on the Silicomanganese Process", *Electr. Furn. Conf. Proc.* 34 (1974) 107-115.
 49. Creusot-Loire and S. A. Manganese Amcor Ltd., FR 79 0169, 1979.
 50. N. A. Barcza, D. P. O'Shaughnessy: "Optimum Slag - Alloy Relationships for the Production of Medium to Low Carbon Ferromanganese", *Can. Metall. Q.* 20 (1981) no. 3, 285-294.
 51. T. Chisaki, K. Takervchi: "Electric Smelting of High Carbon Ferromanganese with Preheated Pre-reduced Materials at Kashima Works", Kashima 1971.
 52. I. Tanabe: "Preheating of Ore for a Ferromanganese Furnace. A Recent Trend in Japan", *Electr. Furn. Conf. Proc.* 23 (1967) 131-138.
 53. C. T. Ray, A. H. Olsen: "Computer Control of Four Furnaces in Tasmania", *Electr. Furn. Conf. Proc.* 44 (1987) 217-223.
 54. T. K. Leonard: "Expert Systems Can Control Ferroalloy Processes", *Proc. Int. Ferroalloy Congr. 5th* (1989) 267-279.
 55. H. Muller, D. B. Wellbeloved: "Examples of Plasma Potential for Industrial Applications", *Symp. Proc. Int. Symp. Plasma Chem.* 1989.
 56. A. H. Sully, E. A. Brandes: *Metallurgy of the Rare-Earth Metals - Chromium*, 2nd ed., Butterworth, London 1967.
 57. A. Coutagne: *La fabrication des ferro-alliages*, Baillière Fils, Paris 1924.
 58. P. D. Deeley, K. J. A. Kundig, H. R. Spendelow, Jr.: *Ferroalloys and Alloying Additives Handbook*, 1st ed., Shieldalloy Corp., Newfield, N.J., 1982 Metallurgy Alloy Corp., New York, NY, 1981.
 59. O. Kubaschewski: *Iron-Binary Phase Diagrams*, Springer-Verlag, Berlin-Heidelberg-New York and Verlag Stahleisen mbH, Düsseldorf 1982, pp. 31-34.
 60. V. G. Rivlin, *Int. Metal. Rev.* 29 (1984) no. 4, 299-327.
 61. P. Wille, *Stahl Eisen* 103 (1983) no. 3, 127-132.
 62. F. Ergunalp, *Trans. Inst. Min. Metall.* 89 (1980, Oct.) A179-A184.
 63. D. P. O'Shaughnessy, *Mining Mag.* 147 (1982, Oct.) 291-299.
 64. H. Fuchs: "Untersuchung des Petrographischen und Mineralogischen Aufbaus von Chromerzen für die Metallurgische Verwertung und ihrer Reduzierbarkeit mit dem Ziel der Aufstellung von Bewertungsrichtlinien", Dissertation Rheinisch-Westfälische-Technische-Hochschule (RWTH), Aachen 1962.
 65. A. G. E. Robiette: *Electric Smelting Processes*, C. Griffin Co., London 1973, pp. 150-178.
 66. K. Willand: "Untersuchungen zur Herstellung von Ferrochrom mit 4-6% Kohlenstoff", Dissertation RWTH, Aachen 1971.
 67. J. H. Downing: "Theoretical Basis for Smelting Ferroalloys", *34th Electric Furnace Conference*, St. Louis, Miss., Dec., 1976.
 68. E. M. Levin, C. R. Robbins, H. F. McMurdie in M. K. Reser (ed.): *Phase Diagrams for Ceramists*, 2nd ed., compiled at National Bureau of Standards, American Ceramic Society, Columbus, OH, 1969, p. 246 (Fig. 712).
 69. F. Breuer: "Untersuchungen über das System Chrom-Eisen-Silizium-Kohlenstoff und ihre Nutzanwendung im Bereich der Technischen Siliko-

- chrom-Legierungen", Dissertation RWTH, Aachen 1961.
70. M. S. Rennie, *Electr. Furn. Conf. Proc.* 37 (1979), 202-209.
 71. J. H. Downing, L. Urban, *J. Met.* 18 (1966) 337-344.
 72. G. Volkert, W. Dautzenberg, J. Willems, G. Zieger et al.: "Ferrochrom und Chrommetall", in Durrer, G. Volkert, K.-D. Frank: *Metallurgie der Ferrolegierungen*, 2nd ed., Springer, Berlin-Heidelberg-New York 1972, pp. 292-365.
 73. H. D. Rowley, D. M. Legg: "Construction and Operation of Charge Chrome Facilities at Tubatsé Ferrochrome (Pty.), Steelport, Transvaal, South Africa", *35th Electric Furnace Conference*, Chicago, Dec. 1977, Special Arc Prepr.
 74. W. D. Winship: "Briquetting - An Economic Solution for the Production of Ferro-Chrome in South Africa", *Proc. of the 15th Biennial Conf.*, Inst. for Briquetting and Agglomeration, Montréal, Québec, 1977, pp. 139-152.
 75. E. Lankes, W. Böhm: "Experience Made and Operational Results Obtained with a Chrome Ore Pelletizing Plant Working on the LEPOL Process", *Int. Ferroalloy Conf. (INFACON)*, Johannesburg, South Africa, Apr., 1974.
 76. N. G. Lindberg, T. S. Falk, *CIM Bull.* 69 (1976, Sept.) 117-126.
 77. J. Relander, M. Honkaniemi: "Production of Ferrochrome from Low-Grade Ores", *Symposium on Extraction of Steel Alloying Metals*, Technical Univ. of Lulea, Sweden, Mar. 15-18, 1983, Prepr. pp. 295-301.
 78. H. Tuovinen, J. Relander, M. Honkaniemi, *Electr. Furn. Conf. Proc.* 36 (1978) 127-133.
 79. W. Schiffler, *Stahl Eisen* 104 (1984) no. 21, 1099-1101.
 80. Y. Kanoh, *Met. Bull. (London)*, Ferro Alloys Special Issue, 1971, 83-85.
 81. K. Ichikawa, *Chem. Eng.* 81 (1974, Apr.) 36-37.
 82. R. A. Leeper, T. J. Dyrdek, *Electr. Furn. Conf. Proc.* 23 (1965) 110-114.
 83. H.-J. Retelsdorf, R. M. Fichte, F. Breuer, H. Zimmermann, *Metall (Berlin)* 36 (1982) 140-143.
 84. N. A. Barcza, T. R. Curr, W. D. Winship, C. P. Heanley, *Electr. Furn. Conf. Proc.* 39 (1981) 243-260.
 85. *Met. Bull. Mon.* 151 (1983, Jul.) 91-93.
 86. Ges. f. Elektrometallurgie mbH, DE 2201388, 1972 (F. Breuer, K. Brotzmann, G. Duderstadt, R. Fichte et al.); DE 2 531034, 1975 (F. Breuer, G. Duderstadt, G. Nassauer, W. M. Dresler et al.); DE 2540290, 1975 (F. Breuer, G. Duderstadt, W. Dresler, R. Fichte et al.).
 87. H. Franke, G. Duderstadt: "Production of Medium Carbon Ferrochromium in a Bottom Blowing Converter and its Application in Stainless Steel Production", *Int. Ferroalloy Conf. (INFACON)*, Johannesburg, South Africa, Apr. 1974.
 88. Soc. d'électrochimie, d'électrometallurgie et aciéries électriques d'Ugine, US 2100265, 1932 (P. Perrin).
 89. Electric Furnace Products Co., DE 860073, 1950 (H. de Wet Erasmus, H. R. Spendelow, Jr.).
 90. C. G. Chadwick, *J. Met.* 13 (1961) 806-808.
 91. J. Krüger in O. Winkler, R. Bakish (eds.): *Vacuum Metallurgy*, Elsevier, Amsterdam-London-New York 1971, pp. 265-268.
 92. Union Carbide Corp., DE 1302764, 1961 (F. D. Hamilton, Jr., O. B. Chamberlain, Jr.).
 93. Gesellschaft für Elektrometallurgie mbH, DE 1558500, 1967 (R. Fichte, H. Franke, H.-J. Retelsdorf).
 94. V. P. Nemchenko et al., *Stal'* 1982, no. 7, 37-39 (Engl. Transl. from Russ. BISI 21593).
 95. GfE-Lieferprogramm, 1974.
 96. Reading Alloys, US 4 331475, 1982 (F. H. Perfect).
 97. R. Hahn, H. Andörfer, H.-J. Retelsdorf, *Erzmetall* 36 (1983) 459-465.
 98. Shieldalloy Corp., Product Specifications MA-104, MA-106, Newfield, NJ, 1979.
 99. GfE, Legierungen - Legierungsmetalle, Gesellschaft für Elektrometallurgie mbH, Düsseldorf, Mar., 1980.
 100. DIN 17657, Kupfer-Vorlegierungen, 1973.
 101. DIN 1725 Blatt 3, Aluminiumlegierungen - Vorlegierungen, 1973.
 102. International Standard ISO 5448, Ferrochromium-Specification and Conditions of Delivery, International Organization for Standardization, 1981.
 103. International Standard ISO 5449, Ferrosilicochromium-Specification and Conditions of Delivery, International Organization for Standardization, 1980.
 104. ASTM Designation, A101-73, Standard Specification for Ferrochromium, American National Standard G68.1, American National Standards Institute, 1973.
 105. ASTM Designation, A482.76, Standard Specification for Ferrochrome-Silicon, American National Standard G76.1, American National Standards Institute, 1976.
 106. DIN 17565, Ferrochrom, Ferrochrom-Silizium und Chrom. Technische Lieferbedingungen, Arbeitsausschuß Ferrolegerungen im Deutschen Normenausschuß (DNA), 1968.
 107. H.-J. Fischer, K.-D. Frank: *Erzmetall* 35 (1982) 403-409.
 108. International Standard ISO 3713, Draft Proposal, Ferroalloys Sampling and Preparation of Samples, General Rules, ed. Dec., 1985.
 109. Draft International Standard ISO/DIS 4140, Ferrochromium and Ferrosilicochromium Determination of Chromium Content Potentiometric Method, International Organization for Standardization, 1978.
 110. Draft International Standard ISO/DIS 4158, Ferrosilicon, Ferrosilicomanganese and Ferrosilicochromium Determination of Silicon Content Gravimetric, International Organization for Standardization, 1977.
 111. W.-H. Grebe, H. Kästner, C. Kippenberger, U. Krauß et al.: *Untersuchungen über Angebot und Nachfrage Mineralischer Rohstoffe, VII Chrom*. Bundesanstalt für Geowissenschaften & Rohstoffe, Hannover; Deutsches Institut für Wirtschaftsforschung, Berlin 1975, 147 pp.
 112. P. Wille, *Stahl Eisen* 103 (1983) 127-132.
 113. B. M. Coope, "Chromite", *Mining Annual Review* 1984, 65-68, published by *Min. J. (London)* 1984 (June).
 114. *Chromium Review* (1983, Apr.) no. 1, 13.

115. D. P. O'Shaughnessy, *J. Met.* 37 (1985, July) 57–58.
116. *Erzmetall* 37 (1984) 478–479.
117. *Met. Bull. Mon.* 131 (1981, Nov.) 59–63.
118. J. W. Scott, *Electr. Furn. Conf. Proc.* 29 (1971) 80–82.
119. H.-J. Retelsdorf, E. Hodapp, N. Endell, *Electr. Furn. Conf. Proc.* 27 (1969) 109–114.
120. D. Liesegang, *Erzmetall* 37 (1984) 18–21.
121. Erste Allgemeine Verwaltungsvorschrift zum Bundes-Immissionsschutzgesetz, TA-Luft (Technische Anleitung zur Reinhaltung der Luft) Feb. 27, 1986.
122. D. Henschler (ed.): *Gesundheitsschädliche Arbeitsstoffe. Chrom und seine Verbindungen*, Verlag Chemie, Weinheim 1983, Part 9.
123. R. A. Person, *Electr. Furn. Conf. Proc.* 33 (1975) 39–46.
124. R. Wintersteen, *Electr. Furn. Conf. Proc.* 39 (1981) 221–225.
125. ACGIH (ed.): *Threshold Limit Values (TLV) for Chemical Substances in the Work Environment*, ACGIH, Cincinnati, OH, 1985–1986.
126. G. P. Tyroler, C. A. Landolt (eds.): *Extractive Metallurgy of Nickel and Cobalt*, The Metallurgical Society of AIME, Warrendale, PA, 1988.
127. D. J. I. Evans, R. S. Shoemaker, H. Veltman (eds.): *International Laterite Symposium*, SME-AIME, New York 1979.
128. Y. Ogura, I. Doi (eds.): "Proceedings of International Symposium on Laterite", *Int. J. Miner. Process.* 19 (1987) 1–4.
129. C. M. Diaz et al. in [126, pp. 211–239].
C. M. Diaz et al., *J. Met.* 40 (1988) no. 9, 28–33.
130. A. A. Dor, H. Skretting in [127, pp. 459–490].
131. K. Ishii in [128, pp. 15–24].
132. E. F. Osborn, A. Muan in M. K. Reser (ed.): *Phase Diagrams for Ceramists*, American Ceramic Society, Columbus, OH, 1964, p. 236.
133. B. Wasmund, G. G. Hatch, "Systematic Approach to the Design of a High Power Electric Matte Furnace", *World Electrotechnical Congress*, Moscow 1977.
134. M. de Vernon in J. N. Anderson, P. E. Queneau (eds.): *Pyrometallurgical Processes in Non-Ferrous Metallurgy*, TMS, vol. 39, Gordon and Breach, New York 1967.
135. *Min. Mag.* 130 (1974) May, 336–349.
136. K. Yamada, T. Hiyama in [128, pp. 215–221].
137. T. Ogura, K. Kuwayama, A. Ono, Y. Yamada in [128, pp. 189–198].
138. E. Langer in [127, pp. 397–411].
139. S. C. C. Barnett, I. Patino, F. A. Perez, J. G. Schofield in *Extraction Metallurgy '85*, Inst. Min. Metall., London 1985.
140. R. R. Roberlson, I. P. Vargas, *Eng. Min. J.* 186 (1985) no. 5, 18–22.
141. *Min. Mag.* 129 (1973) July, 12–19.
142. I. H. Keith et al. in [127, pp. 123–242].
143. Knapsack, DE 2127251, 1971 (U. Thümmel, J. Rothkamp).
144. VDI-Richtlinie: *Phosphor und anorganische Phosphorverbindungen, ausgenommen Düngemittel*, VDI 3450, May 1989.
145. *Ullmann*, 3rd ed., 13, 515.
146. H. J. Fischer, K.-D. Frank, *Erzmetall* 35 (1982) 403–409.
147. T. Massalski: *ASM Binary Alloy Phase Diagrams*, 2nd ed., American Society for Metals, Materials Park, OH, 1992.
148. *Ullmann*, 4th ed., A22, 54.
149. *Winnacker-Küchler*, 4th ed., 4, 180–182.
150. J. Eube in: *Stahl, Tabellenbuch für Auswahl und Anwendung*, DIN, 1st ed., Verlag Stahlisen, Düsseldorf 1992.
151. VDEH (eds.): *Grundlagen des Hochofenverfahrens*, Verlag Stahlisen, Düsseldorf 1973.
152. A. G. E. Robiette: *Electric Smelting Processes*, Charles Griffin, London 1973.
153. R. Durrer, G. Volkert: *Metallurgie der Ferrolegierungen*, 2nd ed., Springer Verlag, Berlin-Heidelberg-New York 1972.
154. V. P. Elyutin, Y. A. Pavlov, B. E. Levin, E. M. Alekseev: *Production of Ferroalloys-Electrometallurgy*, 2nd ed., MIR Publ., Moscow 1957.
155. M. Riss, Y. Khodorovsky: *Production of Ferroalloys*, MIR Publ., Moscow 1967.
156. J. Escard: *Les fours électriques industriels et les fabrications électrothermiques*, 2nd ed., Dunod, Paris 1924, p. 458.
157. O. Kubaschewski: *Iron-Binary Phase Diagrams*, Springer Verlag, Berlin-Heidelberg-New York, Verlag Stahlisen, Düsseldorf 1982.
158. G. V. Samsonov: *Handbook of High Temperature Materials*, no. 2: *Properties Index*, Plenum Press, New York 1964.
159. A. Graf v. Matschka: *Borieren*, Hanser Verlag, München-Wien 1977.
160. I. Barin, O. Knacke: *Thermochemical Properties of Inorganic Substances*, Springer Verlag, Berlin, Verlag Stahlisen, Düsseldorf 1973, supplement (authors: I. Barin, O. Knacke, O. Kubaschewski) 1977.
161. H. Pastor, F. Thevenot, *Inf. Chim.* 1978, no. 178, 151–170.
162. S. Sato, O. J. Kleppa, *Metall. Trans. B* 13B (1982) 251–257.
163. *Gmelin*, Iron (system no. 59), main A2 (1929) 1177–1178.
164. L. Y. Markovskii, G. V. Kaputovskaja, *Zh. Prikl. Khim. (Leningrad)* 33 (1960) 569–577.
165. L. Y. Markovskii, E. T. Bezruk, *Zh. Prikl. Khim. (Leningrad)* 35 (1962) 491–498.
166. Mitsui Mining & Smelting Co., JP 60016/73, 1971 (T. Masuyama et al.).
167. Kawasaki Steel Corp., DE-OS 3228593, 1982, Prior. JP 174960-81 (T. Hamada et al.).
168. Mitsui Mining & Smelting Co., JP 5826025, 1981.
169. G. Volkert, K. D. Frank (ed.): *Metallurgie der Ferrolegierungen*, 2nd ed., Springer Verlag, Berlin 1972.
170. Gesellschaft für Elektrometallurgie, DE 3409311-7, 1984.
171. Metallurg Alloy Corp., New York, NY, USA; Shieldalloy Corp., Newfield, NJ; London & Scandinavian Metallurgical Co., Ltd., London, England; Gesellschaft für Elektrometallurgie mbH, Düsseldorf, Germany (private communication).
172. N. A. Chirkov et al., *Stal'* 1967, 325–327, Transl. BISI 14535 (August 1976).

173. V. P. Elyutin, Y. A. Pavlov, B. E. Levin, E. M. Alekseev: *Production of Ferroalloys - Electrometallurgy*, 2nd ed., National Science Foundation, Washington, D.C., and the Department of the Interior, translated from Russian by the Israel Program for Scientific Translations (1961).
174. M. Riss, Y. Khodorovsky: *Production of Ferroalloys*, MIR Publishers, Moscow 1967 (transl. from the Russian by I. V. Savin).
175. G. V. Samsonov, *Vopr. Poroshk. Metall. Prochn. Mater.* 1960, no. 8, 8–23; *Chem. Abstr.* 57 (1962) 8274c.
176. Shieldalloy Corp., Newfield, NJ: *Product Specification Data Sheet* (1979).
177. London & Scandinavian Metallurgical Co., London: *The Metallurg Companies, Products etc.* (July 1975).
178. Gesellschaft für Elektrometallurgie, Düsseldorf: *Legierungen und Legierungsmetalle*, Prospectus 1980.
179. G. P. Jones, J. Pearson, *Metall. Trans. B* 7B (1976) 223–234.
180. DIN 17567: *Ferrobor - Technische Lieferbedingungen* (Jan. 1970).
181. ANSI/ASTM A 323-76: *Standard Specification for Ferroboron*.
182. P. D. Deeley, K. J. A. Kundig: *Review of Metallurgical Applications of Boron in Steel*, Shieldalloy Corp., Newfield, NJ, Metallurg Alloy Corp., New York 1982.
183. DIN 1725 Blatt 3: *Aluminiumlegierungen - Vorlegierungen* (June 1973).
184. Chemikerausschuß der GDMB: *Analyse der Metalle. I. Schiedsanalysen*, 3rd ed. (1966); *II. Betriebsanalysen*, 2nd ed. (1961), Springer Verlag, Berlin.
185. *Handbuch für das Eisenhütten-Laboratorium*, vol. 2a, Verlag Stahlisen, Düsseldorf 1982.
186. G. Wünsch, F. Umland in W. Fresenius, G. Jander (ed.): *Handbuch der analytischen Chemie*, 3rd part: *Quantitative Analyse*, vol. III: "Elemente der dritten Hauptgruppe. Bor", 2nd ed., Springer Verlag, Berlin-Heidelberg-New York 1971.
187. H. L. Giles, G. M. Holmes, *J. Radioanal. Chem.* 48 (1979) 65–72.
188. British Standard 1121: *Methods for the Analysis of Iron and Steel*, part 49: *Boron in Ferro-Boron*, Volumetric, 1966.
189. ASTM (E 31): *Chemical Analysis of Ferro-Alloys, Ferroboron*.
190. C. F. Seybold, *Electr. Furn. Proc.* 27 (1969) 99–108.
191. P. D. Deeley, K. J. A. Kundig, H. R. Spendlow Jr.: *Ferroalloys & Alloying Additives Handbook*, Shieldalloy Corp., Newfield, NJ, Metallurg Alloy Corp., New York, NY, 1981.
192. Allied, DE-OS 3011152, 1980.
193. W. Jaschinski, W. Wolf, *Metall (Berlin)* 36 (1982) 782–783.
194. E. W. Fajans: *Mining Annual Review - 1982*, Min. J., London, June, 1982, pp. 112–113.
195. R. Durrer, G. Volkert in G. Volkert, K.-D. Frank (eds.): *Metallurgie der Ferrolegierungen*, Springer Verlag, Berlin-Göttingen-Heidelberg 1972.
196. Vanadium Corp., US 2909427, 1958 (H. W. Rathman, J. O. Staggers, H. K. Bruner).
197. Gesellschaft für Elektrometallurgie mbH, Düsseldorf, Lieferprogramm 1989.
198. A. J. DeArdo, J. M. Gray, L. Meyer: "Fundamental Metallurgy of Niobium in Steel" in H. Stuart (ed.): *Niobium-Proceedings of the International Symposium*, New York 1984, pp. 685–759.
199. S. R. Keown, F. B. Pickering: "Niobium in Stainless Steels" in H. Stuart (ed.): *Niobium-Proceedings of the International Symposium*, New York 1984, pp. 1113–1141.
200. C. T. Sims: "A Perspective of Niobium in Superalloys" in H. Stuart (ed.): *Niobium-Proceedings of the International Symposium*, New York 1984, pp. 1169–1220.
201. J. K. Tien, J. P. Collier: "Current Status and Future Developments of the Niobium and Tantalum Containing Superalloys", *Proceedings of International Symposium on Tantalum and Niobium* 1988, Tantalum-Niobium International Study Center, Brussels, Belgium, pp. 657–679.
202. J. L. Murray, *Bull. Alloy Phase Diagrams* 2 (1981) no. 3, 393.
203. London & Scandinavian Metallurgical Co.: *Legierungselemente*, Ges. f. Elektrometallurgie, Düsseldorf 1962.
Leitner-Plöckinger in E. Plöckinger, H. Straube (eds.): *Die Edeltahlerzeugung*, 2nd Ed., Springer-Verlag, Berlin 1965.
204. T. Sims, W. C. Hagel: *The Superalloys*, Wiley, New York 1972.
205. "Micro Alloying" *75th Proceedings of an International Symposium on HSLA-Steels* 1975, Union Carbide Corp., New York 1977.
206. W. Dautzenberg, G. Volkert: "Ferrotitan", in G. Volkert, K. D. Frank (eds.): *Metallurgie der Ferrolegierungen*, 2nd ed., Springer-Verlag, Berlin 1972.
207. H.-G. Brandsteller, Ph.D. Thesis RWTH Aachen 1956.
208. Pêchiney Compagnie de produits chimiques et électrometallurgiques, FR 1321503, 1962; DE-AS 1245134, 1972.
209. Gesellschaft für Elektrometallurgie, DE 2242352, 1972.
210. G. Duderstadt, Ph.D. Thesis RWTH Aachen 1960.
211. *Erzmetall* 32 (1979) 107, 251, 354, 461; 33 (1980) 63, 241, 421, 521; 34 (1981) 50, 224, 439, 566; 35 (1982) 59, 212, 412, 549.
212. DIN 17563: *Ferrovandium*, Technische Lieferbedingungen, Dec. 1965.
213. G. Roethe, W. Gocht: *Handbuch der Metallmärkte*, Springer Verlag, Berlin 1974.
214. GfE Gesellschaft für Elektrometallurgie mbH, company brochure, Nürnberg, Aug., 94.
215. J. F. Smith: *Phase Diagrams of Binary Vanadium Alloys*, American Society for Metals Int., Met. Park, OH, 1989.
216. W. Schmidt: "Untersuchungen an Vanadiummetall und seinen aluminothermisch hergestellten Legierungen mit Aluminium und Eisen", Ph. D. Thesis, RWTH Aachen 1969.
217. UCC, US 3334992, 1962.
218. O. Smetana: "Ferrovandium und Vanadinmetall", in *Durrer-Volkert: Metallurgie der Ferrolegierungen*, 2nd ed., Springer Verlag, Berlin 1972.
219. F. Goebel, OE 169315, 1951.

220. Christiania Spigerverk, NO 115556, 1967.
221. J. K. Thorne, J. M. Dahle, L. H. Van Vlack, *Met. Trans.* 1 (1970) 2125-2132.
222. Ferrolegeringar Trollhättäverken AB, DE-OS 2716591, 1977 (J. Wallen).
223. I. Barin, O. Knacke: *Thermochemical Properties of Inorganic Substances*, Springer Verlag, Berlin and Verlag Stahleisen mbH, Düsseldorf 1973.
224. L. Northcott: *Molybdenum*, Butterworth, London 1956.
225. A. G. E. Robiette: *Electric Smelting Processes*, Charles Griffin & Co. Ltd., London 1973.
226. British Intelligence Objectives Sub-Committee: *The German Ferro-Alloy Industry*, B.I.O.S. Final Report No. 798, Trip No. RAT 71/72 Dec., 1945.
227. R. Durrer, G. Volkert in G. Volkert, K. D. Frank (eds.): *Metallurgie der Ferrolegerungen*, 2nd ed., Springer Verlag, Berlin 1972.
228. *Ullmann*, 4th ed. 7, 355.
229. H. Haag, *Erzmetall* 15 (1962) 229-234.
230. *Eng. Min. J.* 176 (1975) no. 6, 98-99.
231. M. W. Murphy, E. S. Wheeler, A. Linz, *Min. Metall* 27 (1946) 350-352.
232. J. H. Young Jr.: *Comparison of Electric Smelting Processes with Thermite Process*, Preprint von ILAFA-Latin American Seminar on Ferroalloys, Salvador de Bahia, June 22-27, 1975.
233. M. Riss, Y. Khodorovsky: *Production of Ferroalloys*, MIR Publishers, Moscow 1967.
234. V. I. Vasil'ev et al, *Sb. Tr. Chelyab. Elektrometall. Komb.* 4 (1975) 55-59; *Chem. Abstr.* 84 (1976) 138 836t.
235. V. P. Elyutin, Y. A. Pavlov, B. E. Levin, E. M. Alekseev: *Production of Ferroalloys Electrometallurgy*, 2nd ed, Israel Program for Scientific Translations, Jerusalem 1957.

Handbook of Extractive Metallurgy

Edited by Fathi Habashi

**Volume II: Primary Metals
Secondary Metals
Light Metals**

 **WILEY-VCH**

Weinheim • Chichester • New York • Toronto • Brisbane • Singapore

Professor Fathi Habashi
Université Laval
Département de Mines et de Métallurgie
Québec G1K 7P4
Canada

This book was carefully produced. Nevertheless, the editor, the authors and publisher do not warrant the information contained therein to be free of errors. Readers are advised to keep in mind that statements, data, illustrations, procedural details or other items may inadvertently be inaccurate.

Editorial Directors: Karin Sora, Ilse Bedrich
Production Manager: Peter J. Biel
Cover Illustration: Michel Meyer/mmad

Library of Congress Card No. applied for
A CIP catalogue record for this book is available from the British Library

Die Deutsche Bibliothek – CIP-Einheitsaufnahme
Handbook of extractive metallurgy / ed. by Fathi Habashi. –
Weinheim ; New York ; Chichester ; Brisbane ; Singapore ; Toronto :
WILEY-VCH ISBN 3-527-28792-2

Vol. 1. The metal industry, ferrous metals. – 1997

Vol. 2. Primary metals, secondary metals, light metals. – 1997

Vol. 3. Precious metals, refractory metals, scattered metals, radioactive metals, rare earth metals. – 1997

Vol. 4. Ferroalloy metals, alkali metals, alkaline earth metals; Name index; Subject index. – 1997

© VCH Verlagsgesellschaft mbH – A Wiley company,
D-69451 Weinheim, Federal Republic of Germany, 1997

Printed on acid-free and low-chlorine paper

All rights reserved (including those of translation into other languages). No part of this book may be reproduced in any form – by photoprinting, microfilm, or any other means – nor transmitted or translated into a machine language without written permission from the publishers. Registered names, trademarks, etc. used in this book, even when not specifically marked as such, are not to be considered unprotected by law.

Composition: Jean François Morin, Québec, Canada
Printing : Strauss Offsetdruck GmbH, D-69509 Mörlenbach
Bookbinding: Wilhelm Oswald & Co., D-67433 Neustadt/WeinstraÙe

Printed in the Federal Republic of Germany

Preface

Extractive metallurgy is that branch of metallurgy that deals with ores as raw material and metals as finished products. It is an ancient art that has been transformed into a modern science as a result of developments in chemistry and chemical engineering. The present volume is a collective work of a number of authors in which metals, their history, properties, extraction technology, and most important inorganic compounds and toxicology are systematically described.

Metals are neither arranged by alphabetical order as in an encyclopedia, nor according to the Periodic Table as in chemistry textbooks. The system used here is according to an economic classification which reflects mainly the uses, the occurrence, and the economic value of metals. First, the ferrous metals, i.e., the production of iron, steel, and ferroalloys are outlined. Then, nonferrous metals are subdivided into primary, secondary, light, precious, refractory, scattered, radioactive, rare earths, ferroalloy metals, the alkali, and the alkaline earth metals.

Although the general tendency today in teaching extractive metallurgy is based on the fundamental aspects rather than on a systematic description of metal extraction processes, it has been found by experience that the two approaches are complementary. The student must have a basic knowledge of metal extraction processes: hydro-, pyro-, and electrometallurgy, and at the same time he must have at his disposal a description of how a particular metal is extracted industrially from different raw materials and know what are its important compounds. It is for this reason, that this *Handbook* has been conceived.

The *Handbook* is the first of its type for extractive metallurgy. Chemical engineers have already had their Perry's *Chemical Engineers' Handbook* for over fifty years, and physical metallurgists have an impressive 18-volume *ASM Metals Handbook*. It is hoped that the

present four volumes will fill the gap for modern extractive metallurgy.

The *Handbook* is an updated collection of more than a hundred entries in *Ullmann's Encyclopedia of Industrial Chemistry* written by over 200 specialists. Some articles were written specifically for the *Handbook*. Some problems are certainly faced when preparing such a vast amount of material. The following may be mentioned:

- Although arsenic, antimony, bismuth, boron, germanium, silicon, selenium, and tellurium are metalloids because they have covalent and not metallic bonds, they are included here because most of them are produced in metallurgical plants, either in the elemental form or as ferroalloys.
- Each chapter contains the articles on the metal in question and its most important inorganic compounds. However, there are certain compounds that are conveniently described together and not under the metals in question for a variety of reasons. These are: the hydrides, carbides, nitrides, cyano compounds, peroxo compounds, nitrates, nitrites, silicates, fluorine compounds, bromides, iodides, sulfites, thiosulfates, dithionites, and phosphates. These are collected together in a special supplement entitled *Special Topics*, under preparation.
- Because of limitation of space, it was not possible to include the alloys of metals in the present work. Another supplement entitled *Alloys* is under preparation.
- Since the largest amount of coke is consumed in iron production as compared to other metals, the articles "Coal" and "Coal Pyrolysis" are included in the chapter dealing with iron.

I am grateful to the editors at VCH Verlagsgesellschaft for their excellent cooperation, in particular Mrs. Karin Sora who followed the project since its conception in 1994, and to

Jean-François Morin at Laval University for his expertise in word processing.

The present work should be useful as a reference work for the practising engineers and the students of metallurgy, chemistry, chemical engineering, geology, mining, and mineral beneficiation. Extractive metallurgy and the chemical industry are closely related; this *Handbook* will

therefore be useful to industrial chemists as well. It can also be useful to engineers and scientists from other disciplines, but it is an essential aid for the extractive metallurgist.

Fathi Habashi

Table of Contents

Volume I		Part Seven	Refractory Metals
Part One	The Metal Industry		26 Tungsten.....1329
	1 The Economic Classification of Metals.....1		27 Molybdenum.....1361
	2 Metal Production.....15		28 Niobium.....1403
	3 Recycling of Metals....21		29 Tantalum.....1417
	4 By-Product Metals.....23		30 Zirconium.....1431
Part Two	Ferrous Metals		31 Hafnium.....1459
	5 Iron.....29		32 Vanadium.....1471
	6 Steel.....269	Part Eight	Scattered Metals
	7 Ferroalloys.....403		33 Rhenium.....1491
Volume II			34 Germanium.....1505
Part Three	Primary Metals		35 Gallium.....1523
	8 Copper.....491		36 Indium.....1531
	9 Lead.....581		37 Thallium.....1543
	10 Zinc.....641		38 Selenium.....1557
	11 Tin.....683		39 Tellurium.....1571
	12 Nickel.....715	Part Nine	Radioactive Metals
Part Four	Secondary Metals		40 General.....1585
	13 Arsenic.....795		41 Uranium.....1599
	14 Antimony.....823		42 Thorium.....1649
	15 Bismuth.....845		43 Plutonium.....1685
	16 Cadmium.....869	Part Ten	Rare Earth Metals
	17 Mercury.....891		44 General.....1695
	18 Cobalt.....923		45 Cerium.....1743
Part Five	Light Metals	Volume IV	
	19 Beryllium.....955	Part Eleven	Ferroalloy Metals
	20 Magnesium.....981		46 Chromium.....1761
	21 Aluminum.....1039		47 Manganese.....1813
	22 Titanium.....1129		48 Silicon.....1861
			49 Boron.....1985
Volume III		Part Twelve	Alkali Metals
Part Six	Precious Metals		50 Lithium.....2029
	23 Gold.....1183		51 Sodium.....2053
	24 Silver.....1215		52 Potassium.....2141
	25 Platinum Group Metals.....1269		53 Rubidium.....2211
			54 Cesium.....2215

	55 Alkali Sulfur Compounds.....	2221
<i>Part</i>	Alkaline Earth Metals	
<i>Thirteen</i>	56 Calcium.....	2249
	57 Strontium.....	2329
	58 Barium.....	2337
	Authors.....	2355
	Name Index.....	2375
	Subject Index.....	2379

Part Three

Primary Metals

																H	⁺ He
Li	Be											B	C	N	O	F	Ne
Na	Mg	Al											Si	P	S	Cl	Ar
K	Ca	Sc	Ti	V	Cr	Mn	Fe	Co	Ni	Cu	Zn	Ga	Ge	As	Se	Br	Kr
Rb	Sr	Y	Zr	Nb	Mo	Tc	Ru	Rh	Pd	Ag	Cd	In	Sn	Sb	Te	I	Xe
Cs	Ba	La [†]	Hf	Ta	W	Re	Os	Ir	Pt	Au	Hg	Tl	Pb	Bi	Po	At	Rn
Fr	Ra	Ac [‡]															
			†	Ce	Pr	Nd	Pm	Sm	Eu	Gd	Tb	Dy	Ho	Er	Tm	Yb	Lu
			‡	Th	Pa	U	Np	Pu	Am	Cm	Bk	Cf	Es	Fm	Md	No	Lr

8 Copper

HARALD FABIAN † (§§ 8.1–8.10); HUGH WAYNE RICHARDSON (§ 8.11 EXCEPT 8.11.3.4); FATHI HABASHI (§ 8.11.3.4); ROBERT BESOLD (§ 8.12)

8.1	Introduction	492	8.6.1.2	Continuous Fire Refining	531
8.2	Physical Properties	493	8.6.1.3	Casting of Anodes	531
8.3	Chemical Properties	495	8.6.2	Electrolytic	531
8.4	Occurrence	497	8.6.2.1	Principles	532
8.4.1	Copper Minerals	497	8.6.2.2	Practice	534
8.4.2	Origin of Copper Ores	498	8.6.3	Melting and Casting	536
8.4.3	Copper Ore Deposits	499	8.6.3.1	Remelting of Cathodes	536
8.4.4	Copper Resources	500	8.6.3.2	Discontinuous Casting	536
8.4.5	Mining	500	8.6.3.3	Continuous Casting	536
8.5	Production	501	8.6.3.4	Continuous Rod Casting and Rolling	537
8.5.1	Beneficiation	501	8.6.4	Copper Powder	538
8.5.2	Segregation	503	8.6.5	Copper Grades and Standardization	539
8.5.3	Roasting	503	8.6.6	Quality Control and Analysis	540
8.5.4	Pyrometallurgical Principles	505	8.7	Processing	541
8.5.4.1	Behavior of the Components	505	8.7.1	Working Processes	541
8.5.4.2	Matte	505	8.7.2	Other Fabricating Methods	541
8.5.4.3	Slags	506	8.7.3	Uses	542
8.5.4.4	Oxidizing Smelting Processes	507	8.8	Economic Aspects	543
8.5.4.5	Proposals	509	8.9	Environmental Protection	545
8.5.5	Traditional Bath Smelting	510	8.10	Toxicology	546
8.5.5.1	Blast Furnace Smelting	510	8.11	Compounds	546
8.5.5.2	Reverberatory Furnace Smelting	510	8.11.1	The Copper Ions	547
8.5.5.3	Modern Reverberatory Smelting	512	8.11.2	Basic Copper Compounds	548
8.5.5.4	Electric Furnace Smelting	512	8.11.2.1	Copper(I) Oxide	548
8.5.6	Autogenous Smelting	513	8.11.2.2	Copper(II) Oxide	549
8.5.6.1	Outokumpu Flash Smelting	514	8.11.2.3	Copper(II) Hydroxide	550
8.5.6.2	INCO Flash Smelting	515	8.11.2.4	Copper(II) Carbonate Hydroxide	552
8.5.6.3	KIVCET Cyclone Smelting	516	8.11.3	Salts and Basic Salts	553
8.5.6.4	Flame Cyclone Smelting	517	8.11.3.1	Copper(I) Chloride	553
8.5.7	Converting	518	8.11.3.2	Copper(II) Chloride	555
8.5.7.1	Discontinuous Converting	518	8.11.3.3	Copper(II) Oxychloride	556
8.5.7.2	Continuous Converting	521	8.11.3.4	Copper(I) Sulfate	557
8.5.8	Continuous Smelting and Converting	521	8.11.3.5	Copper(II) Sulfates	557
8.5.8.1	Mitsubishi Process	521	8.11.4	Compounds and Complexes of Minor Importance	563
8.5.8.2	Noranda Process	522	8.11.4.1	Compounds	563
8.5.8.3	Other Processes	523	8.11.4.2	Complexes	567
8.5.9	Recovery of Copper from Secondary Materials	524	8.11.5	Reclamation	568
8.5.10	Hydrometallurgical Extraction	525	8.11.6	Copper and the Environment	569
8.5.10.1	Principles	526	8.11.7	Economic Aspects	570
8.5.10.2	Processes	528	8.11.8	Toxicology and Occupational Health	571
8.6	Refining	529	8.12	Copper Pigments	571
8.6.1	Pyrometallurgical	529	8.13	References	572
8.6.1.1	Discontinuous Fire Refining	529			

8.1 Introduction

Copper, the red metal, apart from gold the only metallic element with a color different from a gray tone, has been known since the early days of the human race. It has always been one of the significant materials, and today it is the most frequently used heavy non-ferrous metal. The utility of pure copper is based on its physical and chemical properties, above all, its electrical and thermal conductivity (exceeded only by silver), its outstanding ductility and thus excellent workability, and its corrosion resistance (a chemical behavior making it a half-noble metal).

Its common alloys, particularly brass and bronze, are of great practical importance. Copper compounds ores are distinguished by bright coloration, especially reds, greens, and blues. Copper in soil is an essential trace element for most creatures, including humans.

Etymology. According to mythology, the goddess Venus (or Aphrodite) was born on the Mediterranean island of Cyprus, formerly Κύπρος (Greek), where copper was exploited millennia before Christ. Therefore, in early times the Romans named it *cuprium*, later called *cuprum*. This name is the origin of *copper* and of the corresponding words in most Romance and Germanic languages, e.g., *cobre* (Spanish and Portuguese), *cuiivre* (French), *Kupfer* (German), *koper* (Dutch), and *koppar* (Swedish).

A "cross with handle", from the Egyptian epoch, was called the mirror of Venus. In the alchemistic period, this sign meant the metal copper. Even now in astronomy it designates the planet Venus and in biology stands for "female".

History [21–24]. The first metals found by Neolithic man were gold and copper, later silver and meteoric iron. The earliest findings of copper are presumed to be nearly nine millennia old and came from the region near Konya in southern Anatolia (Turkey). Until recently the six-millennia-old copper implements from Iran (Tele Sialk) were presumed to be the

oldest. In the Old World, copper has been worked and used since approximately:

7000 B.C.	Anatolia
4000 B.C.	Egypt, Mesopotamia, Palestine, Iran, and Turkestan
3000 B.C.	Aegean, India
2600 B.C.	Cyprus
2500 B.C.	Iberia, Transcaucasia, and China
2200 B.C.	Central Europe
2000 B.C.	British Isles
1500 B.C.	Scandinavia

Empirical experience over millennia has led to an astonishing knowledge of copper metallurgical operations:

- Native copper was hardened by hammering (cold working) and softened by moderate heating (annealing).
- Heating to higher temperatures (charcoal and bellows) produced molten copper and made possible the founding into forms of stone, clay, and later metal.
- Similar treatment of the conspicuously colored oxidized copper ores formed copper metal.
- The treatment of sulfide copper ores (chalcocopyrite), however, did not result in copper metal, but in copper matte (a sulfidic intermediate). Not before 2000 B.C. did people succeed in converting the matte into copper by repeated roasting and smelting.
- In early times, bronze (copper–tin alloy) was won from complex ores, the Bronze Age beginning ca. 2800 B.C. At first, copper ores were smelted with tin ores; later, bronze was produced from metallic copper and tin. Brass (copper–zinc alloy) was known ca. 1000 B.C. and became widely used in the era of the Roman Empire.

In Roman times, most copper ore was mined in Spain (Rio Tinto) and Cyprus. With the fall of the Roman Empire, mining in Europe came to a virtual halt. In Germany (Saxony), mining activities were not resumed until 920 A.D. During the Middle Ages, mining and winning of metals expanded from Germany over the rest of Europe. In the middle of the 16th century, the current knowledge of metals was compiled in a detailed publication [23] by Georgius Agricola, *De Re Metallica* (1556).

Independent of the Old World, the Indians of North America had formed utensils by working native copper long before the time of Christ, although the skills of smelting and casting were unknown to them. On the other hand, the skill of copper casting was known in Peru ca. 500 A.D., and in the 15th century the Incas knew how to win the metal from sulfide ores.

Around 1500, Germany was the world leader in copper production, and the Fugger family dominated world copper trade. By 1800, England had gained first place, processing ores from her own sources and foreign pits into metal. Near 1850, Chile became the most important producer of copper ores, and toward the end of the last century, the United States had taken the world lead in mining copper ores and in production of refined copper.

Technical development in the copper industry has made enormous progress in the last 120 years. The blast furnace, based on the oldest principle of copper production, was continually developed into more efficient units. Nevertheless, after World War I, it was increasingly replaced by the reverberatory furnace, first constructed in the United States. Since the end of World War II, this furnace has been superseded slowly by the flash smelting furnace invented in Finland. Recently, several even more modern methods, especially from Canada and Japan, have begun to compete with the older processes.

An important development in producing crude metal was the application of the Bessemer converter concept to copper metallurgy by Manhès and David (France, 1880): this principle is still the most widely used method for copper converting in the world.

Over time the requirements for copper purity have become increasingly stringent. The invention and development of electrolysis by J. B. Elkington (England, 1865) and E. Wohlwill (Germany, 1876) made refining of high-purity copper possible.

In addition, the quantity of copper produced has increased immensely (Table 8.1). Since 1880, ca. 275×10^6 t was mined between 1800 and 1900.

Table 8.1: World mine production of copper (approximate, from several sources).

Year	Production, 10^3 t	Year	Production, 10^3 t
1700	9	1960	4200
1800	17	1965	5000
1850	57	1970	6400
1900	450	1975	7300
1950	2500	1980	7900
1955	3100	1984	8100

8.2 Physical Properties

Most properties of metallic copper depend on the degree of purity and on the source of the metal. Variations in properties are caused by:

- Grade of copper, i.e., the oxygen content: tough-pitch, deoxidized copper, oxygen-free copper
- Content of native impurities (e.g., arsenic) or remnants of additives (e.g., phosphorus), which form solid solutions or separate phases at the grain boundaries
- Thermal and mechanical pretreatment of the metal, which lead to states such as cast copper, hot-rolled copper, cold-worked (hard) copper, annealed (soft) copper, and sintered copper

These property differences are caused by the defects in the crystal lattice. Two groups of properties are to be distinguished:

- Low dependence on crystal lattice defects, e.g., caloric and thermodynamic properties, magnetic behavior, and nuclear characteristics
- High dependence on defects, e.g., electrical and thermal conductivity, plastic behavior, kinetic phenomena, and resistance to corrosion

The variations in properties are caused either by physical lattice imperfections (dislocations, lattice voids, and interstitial atoms) or by chemical imperfections (substitutional solid solutions).

Atomic and Nuclear Properties. The atomic number of copper is 29, and the atomic mass A , is 63.546 ± 0.003 (IUPAC, 1983). Copper consists of two natural isotopes, ^{63}Cu (68.94%) and ^{65}Cu (31.06%). There are also

nine synthetic radioactive isotopes with atomic masses between 59 and 68, of which ^{67}Cu has the longest half-life, ca. 58.5 h.

Crystal Structure. At moderate pressures, copper crystallizes from low temperatures up to its melting point in a cubic-closest-packed (ccp) lattice, type A1 (also F^1 or Cu) with the coordination number 12. X-ray structure analysis yields the following dimensions (at 20 °C):

Lattice constant	0.36152 nm
Minimum interatomic distance	0.2551 nm
Atomic radius	0.1276 nm
Atomic volume	7.114 cm ³ /mol

Density. The theoretical density at 20 °C, computed from lattice constant and atomic mass is 8.93 g/cm³. The international standard was fixed at 8.89 g/cm³ in 1913 by the IEC (International Electrotechnical Commission). The maximum value for 99.999% copper reaches nearly 8.96 g/cm³.

The density of commercial copper depends on its composition, especially the oxygen content, its mechanical and thermal pretreatment, and the temperature. At 20 °C, a wide range of values are found:

Cold-worked and annealed copper	8.89–8.93 g/cm ³
Cast tough-pitch electrolytic copper	8.30–8.70 g/cm ³
Cast oxygen-free electrolytic copper	8.85–8.93 g/cm ³

The values for cold-worked copper are higher than those of castings because the castings have pores and gas cavities.

The density of copper is nearly a linear function of temperature, with a discontinuity at the melting point:

t , °C	ρ , g/cm ³
solid copper: 20	8.93
600	8.68
900	8.47
1083	8.32
liquid copper: 1083	7.99
1200	7.81

The solidification shrinkage is 4%; the specific volume at 20 °C is 0.112 cm³/g.

Mechanical Properties. Important mechanical values are given in Table 8.2. High-purity copper is an extremely ductile metal. Cold working increases the hardness and tensile strength (hard or hard-worked copper); subse-

quent annealing eliminates the hardening and strengthening so that the original soft state can be reproduced (soft copper). The working processes are based on this behavior. Impurities that form solid solutions of the substitutional type likewise increase hardness and tensile strength.

Table 8.2: Mechanical properties of copper at room temperature.

Property	Unit	Annealed (soft) copper	Cold-worked (hard) copper
Elastic modulus	GPa	100–120	120–130
Shearing modulus	GPa	40–45	45–50
Poisson's ratio		0.35	
Tensile strength	MPa	200–250	300–360
Yield strength	MPa	40–120	250–320
Elongation	%	30–40	3–5
Brinell hardness (HB)		40–50	80–110
Vickers hardness (HV)		45–55	90–120
Scratch hardness		≈ 3	

Pure copper has outstanding hot workability without hot brittleness, but the high-temperature strength is low. Detrimental impurities, those that decrease the strength at high temperatures, are principally lead, bismuth, antimony, selenium, tellurium, and sulfur. The concentration of oxides of such elements at the grain boundaries during heating causes the embrittlement. However, such an effect can be desirable when free cutting is required. At subzero temperatures, copper is a high-strength material without cold brittleness.

The changes in typical mechanical properties such as tensile strength, elongation, and hardness by heat treatment result from recrystallization [25]. The dependence of recrystallization temperature and grain size on the duration of heating the amount of previous cold deformation and the degree of purity of copper can be determined from diagrams. The recrystallization temperature is ca. 140 °C for high-purity copper and is 200–300 °C for common types of copper. A low recrystallization temperature is usually advantageous, but higher values are required to maintain strength and hardness if the metal is heated during use.

Thermal Properties. Important thermal values are compiled in Table 8.3. The thermal

conductivity of copper is the highest of all metals except silver.

Table 8.3: Thermal properties of copper.

Property	Unit	Value
Melting point	K	1356 (1083 °C)
Boiling point	K	2868 (2595 °C)
Heat of fusion	J/g	210
Heat of vaporization	J/g	4810
Vapor pressure (at mp)	Pa	0.073
Specific heat capacity at 293 K (20 °C) and 100 kPa (1 bar)	J g ⁻¹ K ⁻¹	0.385
at 1230 K (957 °C) and 100 kPa		0.494
Average specific heat 273–573 K (0–300 °C) at 100 kPa (1 bar)	J g ⁻¹ K ⁻¹	0.411
273–1273 K (0–1000 °C) at 100 kPa		0.437
Coefficient of linear thermal expansion 273–373 K (0–100 °C)	K ⁻¹	16.9 × 10 ⁻⁶
273–673 K (0–400 °C)		17.9 × 10 ⁻⁶
between 273 and 1173 K (0–900 °C)		19.8 × 10 ⁻⁶
Thermal conductivity at 293 K (20 °C)	W m ⁻¹ K ⁻¹	394

Electrical properties. In practice, the most important property of copper is its high electrical conductivity; among all metals only silver is a better conductor. Both electrical conductivity and thermal conductivity are connected with the Wiedemann–Franz relation and show strong dependence on temperature (Table 8.4). The old American standard, 100% IACS (International Annealed Copper Standard), corresponds to 58.0 MS/m at 20 °C, and it is still widely used in the United States. The corresponding electrical resistivity (ρ) is $1.7241 \times 10^{-8} \Omega \cdot \text{cm}$, and the less usual resistivity based on weight (density of 8.89 g/cm³, IEC) is $0.1533 \text{ W} \cdot \text{g} \cdot \text{m}^{-1}$. The corresponding temperature coefficients are $0.0068 \times 10^{-8} \Omega \text{m K}^{-1} (\text{dp/dT})$ and $0.00393 \text{ K}^{-1} (\rho^{-1} \text{dp/dT})$. The theoretical conductivity at 20 °C is nearly 60.0 MS/m or 103.4% IACS, and today commercial oxygen-free copper (e.g. C10200 or Cu–OF) has a conductivity of 101% IACS.

The factors that increase the strength decrease electrical conductivity: cold working and elements that form solid solutions. Ele-

ments that form oxidic compounds that separate at grain boundaries affect electrical properties only slightly. Copper may lose up to ca. 3% of its conductivity by cold working; however, subsequent annealing restores the original value. There is a simple rule: the harder the copper, the lower is its conductivity.

Other Properties. High-purity copper is diamagnetic with a mass susceptibility of $-0.085 \times 10^{-6} \text{ cm}^3/\text{g}$ at room temperature. The dependence on temperature is small. However, a very low content of iron can strongly affect the magnetic properties of copper.

The lower the frequency of light, the higher the reflectivity of copper. The color of a clean, solid surface of high-purity copper is typically salmon red.

The surface tension of molten copper is $11.25 \times 10^{-3} \text{ N/cm}$ at 1150 °C, and the dynamic viscosity is $3.5 \times 10^{-3} \text{ Pa} \cdot \text{s}$ at 1100 °C. Detailed physical-property information and data are to be found in the literature, particularly as tabular compilations [25–30].

Table 8.4: Temperature dependence of thermal and electrical conductivity of copper.

Temperature		Thermal conductivity, W m ⁻¹ K ⁻¹	Electrical conductivity, MS/m
K	°C		
17	-256	5000	
73	-200	574	460
113	-160	450	
173	-100	435	110
273	0	398	60
293	20	394	58
373	100	385	44
473	200	381	34
573	300	377	27
973	700	338	15

8.3 Chemical Properties

In the periodic table, copper is placed in period 4 and subgroup IB (together with silver and gold); therefore, it behaves as a typical transition metal. It appears in oxidation states +1 to +4, its compounds are colored, and it tends to form complex ions.

At relatively low temperature, copper(II) is the most stable state, but above 800 °C, copper(I) predominates, which is significant for pyrometallurgical processes; oxidation states

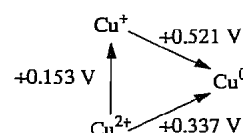
+3 and +4 were discovered in recent years in some coordination compounds.

The distribution of the 29 electrons is $1s^2 2s^2 2p^6 3s^2 3p^6 3d^{10} 4s^1$. From this electron configuration, $[\text{Ar}]3d^{10}4s^1$, is derived the copper(I) ion (Cu^+) with a complete M shell (18 electrons). The copper(II) ion (Cu^{2+}) originates from the configuration $[\text{Ar}]3d^9 4s^2$, which has a slightly higher energy level.

The valence states and their radii determine the space lattice of alloys and compounds:

Species	Coordination number	Radius, nm
Cu^0	12	0.128
Cu^+	6	0.096
Cu^{2+}	6	0.072

The standard electrode potentials (at 25 °C) of copper correspond to the relative stabilities of the three species:



These values [31], or thermochemical data [32], in comparison with those of other elements, establish copper as a relatively noble metal.

Behavior in Air. Copper in dry air at room temperature slowly develops a thin protective film of copper(I) oxide. On heating to a high temperature in the presence of oxygen, copper forms first copper(I) oxide, then copper(II) oxide, both of which cover the metal as a loose scale.

In the atmosphere, the surface of copper oxidizes in the course of years to a mixture of green basic salts, the patina, which consists chiefly of the basic sulfate, with some basic carbonate. (In a marine atmosphere, there is also some basic chloride.) Such covering layers protect the metal.

Behavior versus Diverse Substances. While many substances scarcely react with copper under dry conditions, the rate of attack increases considerably in the presence of moisture. Copper has a high affinity for free halogens, molten sulfur, or hydrogen sulfide.

Therefore, copper is essentially not attacked by nonoxidizing acids, such as dilute sulfuric, hydrochloric, phosphoric, or acetic and other organic acids.

Dissolution of copper is possible either by oxidation or by formation of complexed copper ions. Thus, copper is soluble in oxidizing acids, such as nitric acid, hot concentrated sulfuric acid, and chromic acid, or in nonoxidizing acids containing an oxidizing agent such as oxygen or hydrogen peroxide. For example, acetic acid attacks copper in the presence of atmospheric oxygen to form verdigris, a green or greenish-blue pigment. In hydrometallurgical practice, metal compounds such as iron(III) sulfate, iron(III) chloride, and copper(II) chloride are suitable oxidizing agents.

The other method of dissolving copper is through formation of complex ions. The best reagents for this purpose are aqueous solutions of ammonia and ammonium salts or alkali-metal cyanides. However copper is essentially not attacked by alkali-metal hydroxide solutions.

Fresh water has practically no corrosive effect on copper, and seawater has only a small effect but wastewater containing organic sulfur-bearing compounds can be corrosive.

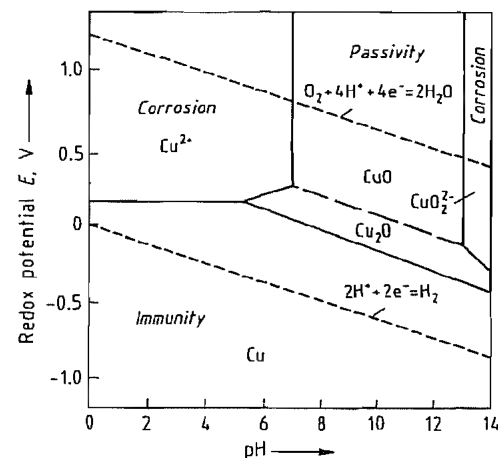


Figure 8.1: Pourbaix diagram for copper in highly dilute aqueous solution at normal temperature [35].

Corrosion [33–34]. M. J. N. Pourbaix has developed potential pH equilibrium diagrams for metals in dilute aqueous solutions [35]. Such

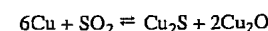
graphs give a rough indication of the feasibility of electrochemical reactions. Figure 8.1 shows the behavior of copper at room temperature and atmospheric pressure. The $\text{Cu-H}_2\text{O}$ system contains three fields of different character:

- Corrosion, in which the metal is attacked
- Immunity, in which reaction is thermodynamically impossible
- Passivity, in which there is no cause of kinetic phenomena

Gases and Copper [36–37]. An exact knowledge of the behavior of solid and liquid copper toward gases is important for production and use of the metal. With the exception of hydrogen, the solubility of gases in molten copper follows Henry's law: the solubility is proportional to the partial pressure.

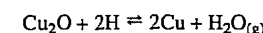
Oxygen dissolves in molten copper as copper(I) oxide up to a concentration of 12.65% Cu_2O (corresponding to 1.4% O) (also see Figure 8.22). Copper(I) oxide in solid copper forms a separate solid phase.

Sulfur dioxide dissolves in molten copper and reacts:



Hydrogen is considerably soluble in liquid copper, and after solidification some remains dissolved in the solid metal, although copper does not form a hydride. The solubility follows Sievert's law, being proportional to the square root of the partial pressure because the H_2 molecules dissociate into H atoms on dissolution. Hydrogen has high diffusibility because of its extremely small atomic volume.

Hydrogen dissolved in oxygen-bearing copper reacts with copper(I) oxide at high temperatures to form steam:



Steam is not soluble in copper; therefore, it either escapes or forms micropores.

Nitrogen, carbon monoxide, and carbon dioxide are practically insoluble in liquid or solid copper. Hydrocarbons generally do not react with copper. An exception, acetylene (ethyne), reacts at room temperature to form the highly explosive copper acetylides Cu_2C_2 and CuC_2 ; therefore, acetylene gas cylinders must not be equipped with copper fittings.

Table 8.5: Typical copper contents of natural materials.

Mineral	Content, ppm
Basalt	85
Diorite	30
Granite	10
Sandstone	1
Copper ores (poor)	5 000
Copper ores (rich)	50 000
Native copper	950 000
Seawater	0.003
Deep-sea clays	200
Manganese nodules	10 000
Marine ore sludges	10 000
Earth's crust (average)	50
Meteorites (average)	180

8.4 Occurrence

In the upper part of the earth's crust (16 km deep), the average copper content is ca. 50 ppm. Older estimates were nearly 100 ppm, while recent spectral analysis values are 30–40 ppm. Copper is 26th in order of abundance of the elements in the accessible sphere of the earth. Table 8.5 shows average copper contents in natural materials.

8.4.1 Copper Minerals

More than 200 minerals contain copper in definable amounts, but only ca. 20 are of importance as copper ores (Table 8.6) or as semiprecious stones (turquoise and malachite). Copper is a typical chalcophilic element; therefore, its principal minerals are sulfides, mostly chalcopyrite, bornite, and chalcocite, often accompanied by pyrite, galena, or sphalerite.

Table 8.6: The most important copper minerals.

Mineral	Formula	Copper	Crystal system	Density, g/cm ³
Native copper	Cu	≤ 99.92	cubic	8.9
Chalcocite	Cu ₂ S	79.9	orthorhombic	5.5–5.8
Digenite	Cu ₉ S ₅	78.0	cubic	5.6
Covellite	CuS	66.5	hexagonal	4.7
Chalcopyrite	CuFeS ₂	34.6	tetragonal	4.1–4.3
Bornite	Cu ₅ FeS ₄ /Cu ₃ FeS ₃	55.5–69.7	tetragonal	4.9–5.3
Tennantite	Cu ₁₂ As ₄ S ₁₃	42–52	cubic	4.4–4.8
Tetraedrite	Cu ₁₂ Sb ₄ S ₁₃	30–45	cubic	4.6–5.1
Enargite	Cu ₃ As ₄	48.4	orthorhombic	4.4–4.5
Bourmonite	CuPbSbS ₃	13.0	orthorhombic	5.7–5.9
Cuprite	Cu ₂ O	88.8	cubic	6.15
Tenonite	CuO	79.9	monoclinic	6.4
Malachite	CuCO ₃ ·Cu(OH) ₂	57.5	monoclinic	4.0
Azurite	2CuCO ₃ ·Cu(OH) ₂	55.3	monoclinic	3.8
Chrysocolla	CuSiO ₃ ·nH ₂ O	30–36	(amorphous)	1.9–2.3
Diopside	Cu ₆ [Si ₆ O ₁₈]·6H ₂ O	40.3	rhombohedral	3.3
Brochantite	CuSO ₄ ·3Cu(OH) ₂	56.2	monoclinic	4.0
Antlerite	CuSO ₄ ·2Cu(OH) ₂	53.8	orthorhombic	3.9
Chalcanthite	CuSO ₄ ·5H ₂ O	25.5	triclinic	2.2–2.3
Atacamite	CuCl ₂ ·3Cu(OH) ₂	59.5	orthorhombic	3.75

Secondary minerals are formed in sulfide ore bodies near the earth's surface in two stages. In the oxidation zone, oxygen-containing water forms copper oxides, subsalts (subcarbonates and subsulfates), and silicates. In the deeper cementation zone, copper-bearing solutions from these salts are transformed into secondary copper sulfides (chalcocite and covellite) and even native copper of often high purity, e.g., in the Michigan copper district (Keweenaw Peninsula).

Other metallic elements frequently found in copper ores are iron, lead, zinc, antimony, and arsenic; less common are selenium, tellurium, bismuth, silver, and gold. Substantial enrichments sometimes occur in complex ores. For example, ores from Sudbury, Ontario, in Canada contain nickel and copper in nearly the same concentrations, as well as considerable amounts of platinum metals. The copper ores from Zaire and Zambia are useful sources of cobalt. Many porphyry copper ores in America contain significant amounts of molybdenum and are the most important single source of rhenium. The extraction of precious metals and other rare elements can be decisive for the profitability of copper mines, smelters, and refineries.

8.4.2 Origin of Copper Ores

Ore deposits are classified according to their mode of formation, but the origin of copper ores is geologically difficult to unravel, and some of the proposed origins are controversial. The classification distinguishes two main groups, the magmatic series and the sedimentary series.

Magmatic Ore Formation. This involves magma crystallization and comprises the following groups:

- Liquid magmatic ore deposits originate by segregation of the molten mass so that the heavier sulfides (corresponding to matte) separate from the silicates (corresponding to slag) and form intrusive ore bodies. Examples: Sudbury, Ontario; Norilsk, western Siberia.
- Pegmatitic-pneumatolytic ore deposits develop during the cooling of magma to ca. 374 °C, the critical temperature of water. Examples: Bisbee, Arizona; Cananea, Mexico.
- Hydrothermal ore deposits result by further cooling of the hot, dilute metal-bearing solutions from ca. 350 °C downward, i.e., below the critical temperature of water. Such deposits contain copper primarily as chalcocopyrite and satisfy ca. 50% of the demand

in the Western world. There are many examples of different types of hydrothermal deposits. Examples: Butte, Montana (gangue deposit); Tsumeb, Namibia (metasomatic deposit); Bingham Canyon, Utah; Chuquibambilla, Chile; Toquepala, Peru; Bougainville, Solomon Islands (impregnation deposits). Impregnation deposits are also called disseminated copper ores or porphyry copper ores (or simply porphyries) because of their fine particle size.

- Exhalative sedimentary ore deposits originate from submarine volcanic exhalations and thermal springs that enter into seawater, and constitute a transitional type to sedimentary deposits. These ores are third in economic importance in the Western world. The actual formation of such sulfidic precipitations can be observed, for example, the marine ore slimes in the Red Sea. Examples: Mount Isa, Queensland; Rio Tinto, Spain; Kammelsberg (Harz), Germany.

Sedimentary Ore Formation. The origin of sedimentary ore occurs in the exogenous cycle of rocks and may be subdivided into the following groups:

- Arid sediment in sandstones and conglomerates occur widely in Russia as widespread continental zones of weathering with uneven mineralization. Examples: Dsheskasgan, Kazakhstan; Exótica, Chile.
- Partly metamorphized sedimentary ores in shales, marls, and dolomites form large strata-bound ore deposits, especially in the African copper belt, and represent the second most important source of copper to the Western world, as well as supplying nearly 75% of its cobalt. Examples: Zaire (oxidation zone, oxidized ores ≤ 6% Cu); Zambia (cementation zone, secondary sulfide ores, ≤ 4% Cu).
- Marine precipitates have formed sedimentary ore deposits similar to the present phenomenon of sulfide precipitation by sulfur bacteria in the depths of the Black Sea. Examples: Mansfeld (copper schist), Germany; Silesia (copper marl), Poland.

- Deep-sea concretions lie in abundance on the bottom of the oceans, especially the Pacific Ocean. These so-called manganese nodules could also be a source of copper in the future.

8.4.3 Copper Ore Deposits

Geologically, the main regions of copper ore deposits are found in two formations: the Precambrian shields and the Tertiary fold mountains and archipelagos. There are major producing countries on every continent [38].

- North America: United States (Arizona, Utah, New Mexico, Montana, Nevada, and Michigan), Canada (Ontario, Quebec, British Columbia, and Manitoba), and Mexico (Sonora)
- South America: Chile, Peru, and Brazil
- Africa: Zaire, Zambia, Zimbabwe, South Africa, and Namibia
- Australia and Oceania: Queensland, Papua New Guinea
- Asia: Russia (Siberia, Kazakhstan, and Uzbekistan), Japan, Philippines, Indonesia, India, Iran, and Turkey
- Europe: Poland (Silesia), Yugoslavia, Spain (Huelva), Norway, Sweden, and Finland

Antarctica may be an important copper ores in the foreseeable future.

Table 8.7: Copper ore reserves in 1983 of the most important producing countries of the Western world [41–42].

Country	Ore reserves, × 10 ⁶ t	Percentage of world reserves
United States	99.6	21.1
Chile	96.5	20.5
Peru	30.6	6.5
Zambia	30.3	6.4
Zaire	29.6	6.3
Canada	27.4	5.8
Mexico	23.1	4.9
Australia	16.1	3.4
Panama	12.7	2.7
Philippines	11.9	2.5
Papua New Guinea	10.8	2.3
Brazil	10.0	2.1
Total	398.6	84.5

8.4.4 Copper Resources

The copper contents of the worldwide primary copper reserves are listed in Table 8.7. Reserves are the identified (measured, indicated, and inferred) resources and do not include undiscovered (hypothetical and speculative) resources. In the course of time, the available reserves increase in consequence of both technological progress in the processing of ores with low copper content or undesirable impurities and the discovery of new ore deposits [39–40]. In 1982 the world reserves were estimated at 505×10^6 t of copper. The total land-based resources were estimated at 1.6×10^9 t of copper. In addition there is an estimated 700×10^6 t of copper in deep-sea nodules.

If one assumes that total production will remain stable, the identified resources would last until ca. 2050, which is the static outlook. In contrast, the dynamic approach which assumes that production will increase at the rate it has in recent years, would reduce the duration of known reserves by nearly half. If one considers all copper resources, these times would be at least doubled. However, all of these forecasts are quite unreliable. In addition, the forecasts do not take into consideration secondary copper (recycling scrap).

8.4.5 Mining

Exploration, which is the search for ore deposits and their subsequent detailed investigation, is required to ascertain the commercial feasibility of a potential mine. Many geological, geochemical, and geobotanical methods are available, but all are complicated and expensive. Often legal and political factors are more decisive than technological aspects. The average copper content of ores is an essential factor. In 1900, this content worldwide was ca. 5% Cu. Today it is ca. 1%; nevertheless, this represents a ca. 200-fold enrichment of the average in the earth's crust. High-grade deposits (> 6% Cu) are largely exhausted.

For economic reasons, modern copper mining must have high capacity, which means ex-

tensive mechanization. The high cost of mining and of ore beneficiation contributes up to two-thirds of the final price of copper.

There are several methods of mining copper ores:

- Open-pit (surface) mining
- Underground (deep) mining
- In situ leaching (solution mining)
- Ocean mining

At present, the greatest part of primary copper comes from open-pit mines, mostly from porphyry ores. The first open-pit mine was started at Bingham Canyon, Utah, early in this century; other big mines are found in Chuquibambilla, Chile and Toquepala, Peru. Profitable open-pit production requires large ore bodies near the surface with a minimum copper content of 0.5% (in some cases, as low as 0.3%) in sulfidic form for subsequent beneficiating by froth flotation.

Underground mining has been practiced for millennia. However, in the last few decades the competition of open-pit mining has made such older underground methods as overhand and underhand stoping uneconomical. Newer procedures such as open stoping or block caving can be used if good ores occur in deep deposits. The copper concentration should exceed 1%, and some content of other profitable metals is desirable.

In situ leaching is a hydrometallurgical process in which copper is extracted by chemical dissolution in sulfuric acid. This method is suitable for low-grade copper ore bodies for which customary mining operations would be uneconomical as well as for the leaching of remnant ores from abandoned mines. In some cases, the ore body must be broken before leaching by blasting with explosives to increase the surface area for chemical reaction.

A recent development is ocean mining, which involves obtaining metalliferous raw materials from the deep oceanic zones. Two groups of substances are of interest: deep-sea nodules [43] and marine ore slimes [44]. The nodules (manganese nodules) contain, in addition to iron oxides, ca. 25% Mn, 1% Ni, 0.35% Co, and 0.5% (max. 1.4%) Cu. Spe-

cially equipped ships have collected and lifted these nodules from depths of 3000–5000 m; specific metallurgical and chemical methods for processing the nodules have been developed in pilot plants. Because of the extremely high expenses, large-scale operations of this type have not yet been undertaken. Marine ore slimes from the Red Sea (2200-m depth) average ca. 4% Zn, 1% Cu, and a little silver. Although methods for processing these slimes have been investigated, this resource is not now economically important.

8.5 Production

Over the years copper production methods have been subjected to a continual selection process because of the need [45] for (1) increased productivity through rationalization, (2) lower energy consumption, (3) increased environmental protection, (4) increased reliability of operation, and (5) improved safety in operation. During this development a number of tendencies have become apparent:

- Decrease in the number of process steps
- Preference for continuous processes over batch processes
- Autogenous operation
- Use of oxygen or oxygen-enriched air
- Tendency toward electrometallurgical methods
- Increased energy concentration per unit of volume and time
- Electronic automation, measurement, and control
- Recovery of sulfur for sale or disposal
- Recovery of valuable byproducts

The selection of a particular production method depends essentially on the type of available raw materials, which is usually ore or concentrate and on the conditions at the plant location.

About 80% of the primary copper in the world comes from low-grade or poor sulfide ores, which are usually treated by pyrometallurgical methods, generally in the following sequence:

- Beneficiation by froth flotation to get a concentrate
- Optional partial roasting to obtain oxidized material or calcines
- Two-stage pyrometallurgical treatment
 - a) smelting concentrates to matte
 - b) converting matte by oxidation to crude (converter or blister) copper
- Refining the crude copper, usually in two steps
 - a) pyrometallurgically to fire-refined copper
 - b) electrolytically to high-purity electrolytic copper

About 15% of the primary copper originates from low-grade oxidized (oxide) or mixed (oxidized and sulfidic) ores. Such materials are generally treated by hydrometallurgical methods.

The very few high-grade or rich copper ores still available can be processed by traditional smelting in a shaft furnace. This process is also used for recovering copper from secondary materials such as intermediate products scrap and wastes.

Figure 8.2 illustrates the most important operations in copper extraction from various copper ores.

8.5.1 Beneficiation

Most sulfide copper ores must be beneficiated to increase the metal content. The essential operation is froth flotation, which is usually carried out in two successive steps: the first is collective or bulk flotation for concentrating all the metal-containing minerals, and the second, if necessary, is selective flotation to separate the various minerals [47].

Figure 8.3 shows the reduction in total mass with simultaneous enrichment of copper content in the steps from ore to metal. Modern dressing plants are always built near the mines to reduce the transportation costs and are constructed in a relatively uniform manner. The first operation is the comminution of lumpy ores to a pulp in the following stages:

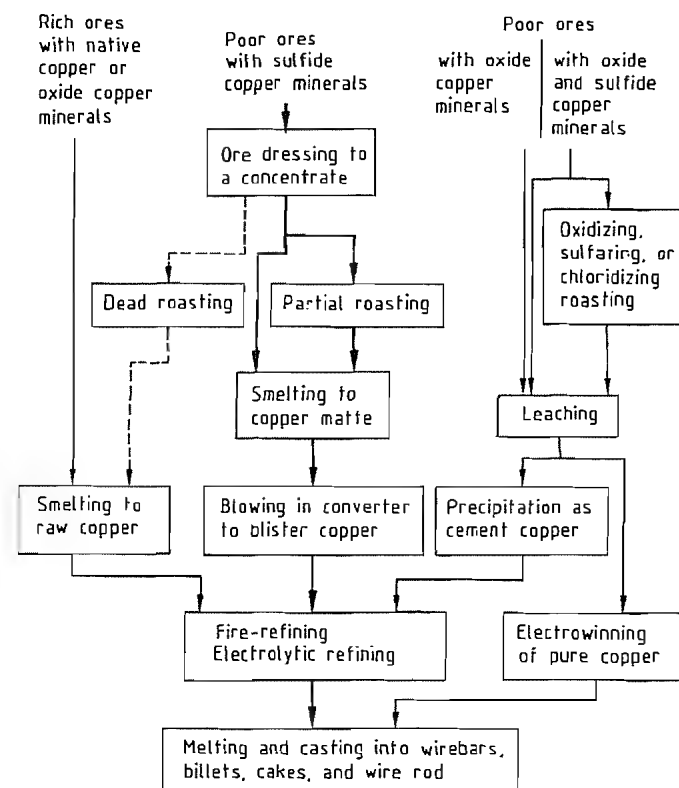


Figure 8.2: The most important stages in copper production [46].

- Crushing in jaw, gyratory, and cone crushers
- Sizing on vibrating screens
- Wet grinding in rod and ball mills or, more recently, by autogenous milling

- Classifying in classifiers and hydrocyclones

The separation of the feed pulp into metal sulfides and gangue or into different sulfide groups is done by froth flotation using frothers, collectors, activators, depressers, and reagents to control the pH (e.g., lime). In simple cases, the flotation cells are combined into three groups with three distinct functions:

- Rougher flotation for sorting into preconcentrate and tailings
- Cleaner flotation for posttreatment of preconcentrate
- Scavenger flotation for posttreatment of the tailings from the first step

Figure 8.4 illustrates the relationship among these three operations, omitting the intermediate grinding steps.

The next step is solid-fluid separation by sedimentation in settlers and thickeners with subsequent vacuum filtering by drum and disk filters. The residual moisture is 8–12% and the concentrates are usually shipped in this condition. In a few cases, the pulp is conveyed in pipelines. Dewatered concentrates may heat spontaneously or even catch fire; therefore, appropriate precautions must be taken [48].

The copper content of dried chalcopyrite concentrates (CuFeS_2) averages 20–30%, rarely less, but considerably more if chalcocite (Cu_2S) is present. The average particle size is determined by the flotation conditions and is generally between 0.25 and 0.01 mm.

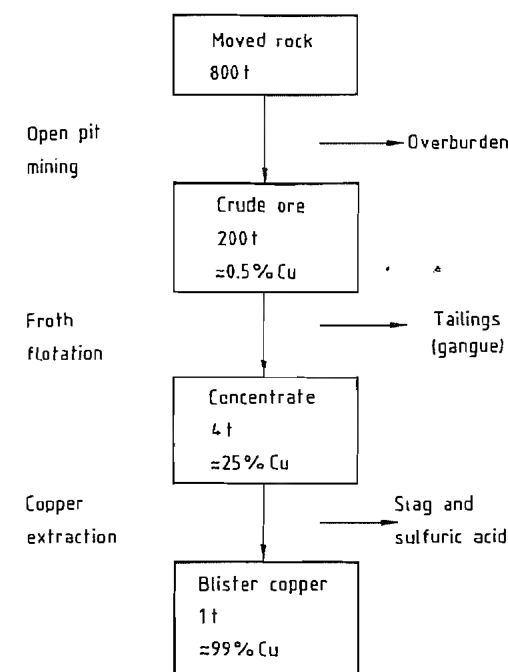


Figure 8.3: Enrichment of copper from ore to metal.

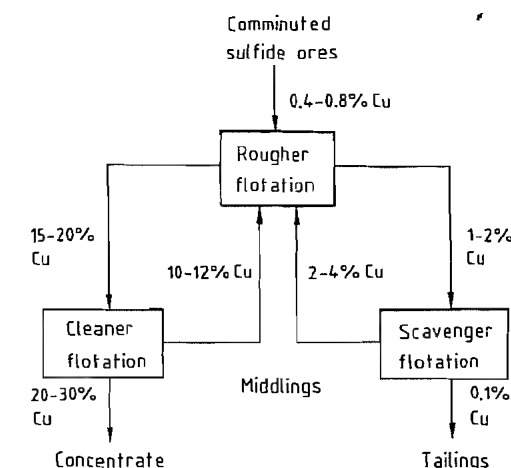


Figure 8.4: Froth flotation of sulfide copper ores.

8.5.2 Segregation

Special low-grade oxidized copper ores that are not economically usable by current methods, especially hydrometallurgical processes, occur in large ore bodies in Africa and

America. These contain copper mostly as silicates (chrysocolla and diopside), and because of their high content of silica and often limestone, they are treated by segregation, a process known for more than 60 years and recently used sporadically in the so-called TORCO (treatment of refractory copper ores) process. The chemical reactions are complicated: ore, gangue, and furnace gases react with added sodium chloride and pulverized coal or coke to form copper(I) chloride and then metallic copper, which is sulfidized and collected by flotation. TORCO [50] plants were built in Zambia and Mauretania, and a variant, the Mitsui segregation process, has been installed in Peru [51].

8.5.3 Roasting

Roasting may be used to prepare sulfide concentrates for subsequent pyrometallurgical or hydrometallurgical operation. For pyrometallurgical processing, the purpose of roasting is to decrease the sulfur content to an optimum level for smelting to copper matte. In many modern processes, however, roasting is not a separate step, but is combined with matte smelting. For hydrometallurgical extraction, roasting forms compounds that can be leached out.

The roasting process, which produces the so-called calcines, has several effects:

- Drying the concentrates
- Oxidizing a part of the iron present
- Controlling the sulfur content
- Partially removing volatile impurities, especially arsenic
- Preheating the calcined feed with added fluxes, chiefly silica and limestone

Chemical Reactions. When the moist concentrates, which contain many impurity elements are heated, a multitude of chemical reactions occur. Because analysis of the many thermodynamic equilibria is not practical, a few fundamental systems are usually chosen. The most important is the ternary copper–oxygen–sulfur system (Figure 8.5). The next most important system is the ternary iron–oxygen–

sulfur system because most sulfidic copper ores contain significant amounts of iron.

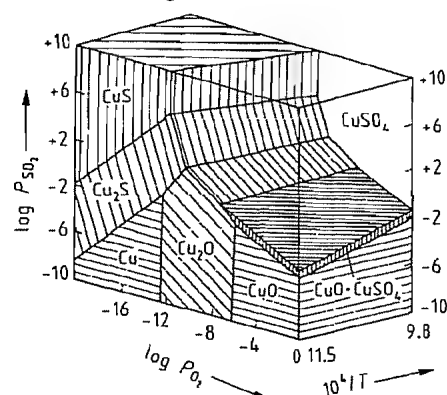
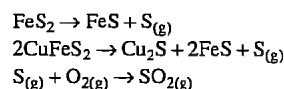
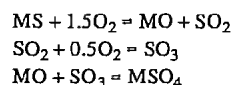


Figure 8.5: Partial phase diagram of the ternary Cu-O-S system [52].

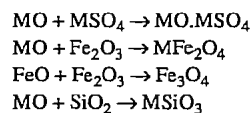
Initially, sulfides such as pyrite and chalcopyrite decompose and generate sulfur vapor, which reacts with oxygen to form sulfur dioxide:



The principal reactions, i.e., the formation of metal (= M) oxides, sulfur trioxide, and metal sulfates, are exothermic.



In addition, there are secondary reactions such as the formation of basic sulfates, ferrites (especially magnetite), and silicates, the last providing most of the slag in the subsequent smelting:



Methods. There are several important roasting methods; all involve oxidation at an elevated temperature, generally between 500 and 850 °C:

- **Partial (oxidizing) roasting** is the conventional way of extracting copper from sulfide concentrates. At 800–850 °C, the degree of roasting is determined by controlling the ac-

cess of air. A predetermined amount of sulfur is removed and only part of the iron sulfide is oxidized. The copper sulfide is relatively unchanged. These conditions are important for the formation of a suitable matte.

- **Total, or dead, roasting** is occasionally used for complete oxidation of all sulfides for a subsequent reduction process or for special hydrometallurgical operations.
- **Sulfatizing roasting** is carried out at 550–565 °C to form sulfates. This method yields calcines well-suited for hydrometallurgical treatment.
- **Chloridizing roasting** involves sulfatizing roasting with addition of sodium chloride. The temperature should not exceed 600 °C to avoid loss of copper(I) chloride. This treatment, which was developed by the Duisburger Kupferhütte, Germany, is limited to pyrite cinders for subsequent leaching and precipitating [53]; however, the process was discontinued several years ago.
- **Chloridizing volatilization** involves heating to ca. 1200 °C in the presence of calcium chloride so that various metal chlorides and other volatile compounds can be separated. The Finnish Vuoksenniska process, which used this procedure, was discontinued years ago. Recently a Japanese company started up a similar procedure.

The roasted product is obtained in one of three states, depending on the maximum roasting temperature:

- **Low temperature.** The roasted concentrates remain in the same state as before (solidus range).
- **Intermediate temperature.** A sinter forms if some liquid phase appears (range of softening).
- **High temperature.** The whole feed melts during roasting (liquidus range).

Roasters. Only a few roaster designs are now used.

- **Multiple-hearth furnaces**, which produce pulverous calcines, were the most widely used type (in various models, e.g., the well-known Herreshoff furnace) until the middle

of the 20th century. Since then, they have been increasingly displaced by the fluidized-bed roaster.

- **Fluidized-bed reactors**, the most modern type, also yield pulverous calcines. Their two key advantages are exploitation of waste heat and high productivity in consequence of favorable kinetic reaction conditions. The reactors are 5–12 m high and have a diameter of 4–8 m. Examples: Anaconda Co., Butte, Montana; RTB Bor, Bor, Yugoslavia.
- **Sintering (blast) roasters** are used only if concentrates are to be processed in blast furnaces (see the *Blast Furnace Smelting* section). The most important type is the Dwight-Lloyd sinterer. Example: Lubumbashi smelter Zambia.
- **Flash smelting furnaces** combine roasting and smelting in the same unit (see the *Autogenous Smelting* section).

The average residence time of concentrate in the various roasters is very different:

multiple-hearth furnace	a few hours
sintering apparatus	a few minutes
fluidized-bed reactor	a few seconds

The roaster gases that are generated contain sulfur dioxide, which is generally converted to sulfuric acid in contact acid plants. The SO₂ content in the roast gas is ca.

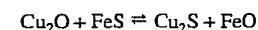
5–8 vol % for multiple-hearth furnaces
8–15 vol % for fluidized-bed reactors

8.5.4 Pyrometallurgical Principles

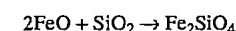
Smelting of unroasted or partially roasted sulfide ore concentrates produces two immiscible molten phases: a heavier sulfide phase containing most of the copper, the *matte*, and an oxide phase, the *slag*. In most copper extraction processes matte is an intermediate.

8.5.4.1 Behavior of the Components

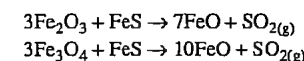
The most important equilibrium matte smelting is that between the oxides and sulfides of copper and iron:



Iron(II) oxide reacts with added silica flux to form fayalite, a ferrous silicate that is the main component of slag:



Liquid iron sulfide reduces higher iron oxides to iron(II) oxide:



The second reaction serves to remove magnetite, which complicates furnace operations because of its high melting point (1590 °C) [55].

The pyrometallurgical production of copper from sulfide ore concentrates may be considered as a rough separation of the three main elements as crude copper, iron(II) silicate slag, and sulfur dioxide. About 20 accompanying elements must be removed from the copper by subsequent refining. Table 8.8 shows the distribution of important impurities among matte slag and flue dust. Precious metals, such as silver gold, platinum, and palladium, collect almost entirely in the matte, whereas calcium, magnesium, and aluminum go into the slag.

Table 8.8: Average percentage distribution of the accompanying elements in copper smelting [20].

Element	Matte	Slag	Flue dust
Arsenic	35	55	10
Antimony	30	55	15
Bismuth	10	10	80
Selenium	40	—	60
Tellurium	40	—	60
Nickel	98	2	—
Cobalt	95	5	—
Lead	30	10	60
Zinc	40	50	10
Tin	10	50	40
Silver and gold	99	1	—

8.5.4.2 Matte

The ternary Cu-Fe-S system is discussed in detail in the literature [56–58]. Figure 8.6 shows the composition of the pyrometallurgically important copper mattes and the liquid-phase immiscibility gap between matte and the metallic phase. In the liquid state, copper matte is essentially a homogeneous mixture of copper(I) and iron(II) sulfides: the pseudobinary Cu₂S–FeS system.

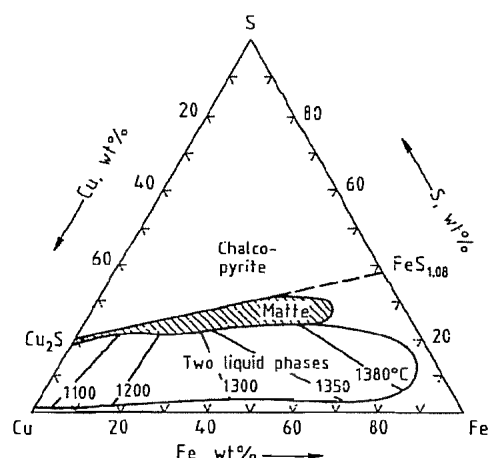


Figure 8.6: Ternary Cu-Fe-S diagram showing copper mattes and the miscibility gap [56].

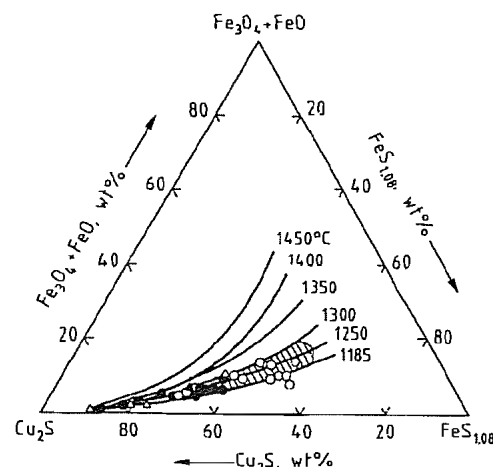


Figure 8.7: Partial ternary $\text{Cu}_2\text{S}-\text{FeS}_{1.08}-(\text{Fe}_3\text{O}_4 + \text{FeO})$ diagram [59] showing mattes from various processes. ○ Reverberatory furnace; △ Flash smelting furnace; ▲ Electric furnace; ● Blast furnace; ■ Converter.

Arsenides and antimonides are soluble in molten matte, but their solubility decreases with an increasing percentage of copper in the matte. Accordingly, when the arsenic concentration is high, a special phase, the so-called *speiss*, can separate. It is produced under reducing conditions in the blast furnace, and its decomposition is complicated.

Compositions of several copper mattes are shown in the partial diagram $\text{Cu}_2\text{S}-\text{FeS}-(\text{Fe}_3\text{O}_4 + \text{FeO})$ (Figure 8.7), which is a section

of the quaternary Cu-Fe-O-S system. The density of solid copper mattes ranges between 4.8 g/cm^3 (FeS) and 5.8 g/cm^3 (Cu_2S); liquid mattes have the following densities: 4.1 g/cm^3 (30% Cu, 40% Fe, 30% S), 4.6 g/cm^3 (50% Cu, 24% Fe, 26% S), and 5.2 g/cm^3 (80% Cu, 20% S).

8.5.4.3 Slags

Slags from copper matte smelting contain 30–40% iron in the form of oxides and about the same percentage of silica (SiO_2), mostly as iron(II) silicate. Such slags can be considered as complex oxides in the $\text{CaO}-\text{FeO}-\text{SiO}_2$ system [60] or, because of the relatively low CaO content of most slags, in the partial diagram $\text{FeO}-\text{Fe}_2\text{O}_3-\text{SiO}_2$ [61] (Figure 8.8). Ternary systems of these and other pertinent oxide systems are found in the literature [62–63]. Table 8.9 shows the general composition of some slag types. Important properties of copper slag systems are compiled in [64].

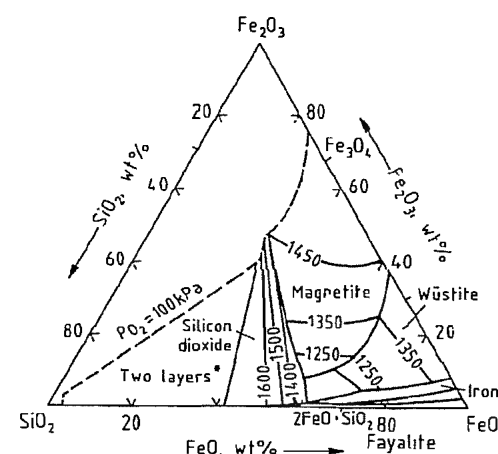


Figure 8.8: Ternary $\text{FeO}-\text{Fe}_2\text{O}_3-\text{SiO}_2$ diagram [61].

The objectives of matte smelting are to achieve a rapid complete separation of matte and slag, the two immiscible phases, and a minimal copper content in the slag. The differing properties of slag and matte affect this separation:

- the low, narrow melting interval of slag

- the low density of liquid slag (ca. $3.1\text{--}3.6 \text{ g/cm}^3$) and the difference in density between molten matte and slag of ca. 1 g/cm^3

- the low viscosity and high surface tension of the slag

The ratio of the weight percent of copper in matte to that of copper in slag should be between 50 and 100. High matte grades generally cause high copper losses in 'slag'. Such losses depend on the mass ratio of slag to copper produced, which is usually between 2 and 3. Copper in slags occurs in various forms, including suspended matte, dissolved copper(I) sulfide, and slagged copper(I) oxide, partially as a silicate, which is typical of nonequilibrium processing.

Slags containing < 0.8% copper are either discarded as waste or sold as products with properties similar to those of natural basalt (crystalline) or obsidian (amorphous). When liquid slag is cooled slowly, it forms a dense, hard crystalline product that can be used as a large-size fill for riverbank protection or dike construction and as a medium-size crushed fill for roadbeds or railway ballast. Quick solidification, by pouring molten slag into water, gives amorphous granulated slag, an excellent abrasive that has partially supplanted quartz sand. Ground granulated slag is used as a trace element fertilizer because of its copper and other nonferrous metals.

Most of the newer copper smelting processes produce high-grade mattes, and the short residence time of the materials in the reaction chamber results in an incomplete approach to chemical equilibrium. Both factors lead to high amounts of copper in the slag, generally > 1%. Such slags must be treated by special methods for copper recovery.

Table 8.9: Composition (%) of typical copper smelter slags [65].

Component	Reverberatory furnace	Flash furnace	Noranda reactor	Peirce-Smith converter
Copper	0.4–0.6	1–1.5	8–10	3–5
Iron (total)	35	40	35	50
Silica	38	30	21	25
Magnetite	7–12	13	25–29	25
Ratio of Fe to SiO_2	0.92	1.33	1.67	2.0

8.5.4.4 Oxidizing Smelting Processes

Nearly all pyrometallurgical copper processes are based on the principle of partial oxidation of the sulfide ore concentrates. Methods based on the total oxidation of sulfide ores with subsequent reduction to metal, avoiding the formation of copper matte, are used only rarely because of high fuel consumption, formation of copper-rich slags, and production of crude copper with a high level of impurities.

Prior to the 1960s, the most important way of producing copper was roasting sulfide concentrates smelting the calcines in reverberatory furnaces and converting the matte in Peirce-Smith converters. Since that time, the modern flash smelting process with subsequent converting has become predominant. Figure 8.9 shows the flow sheet of a modern copper smelter from concentrate to pure cathode copper, including the use of oxygen, recovery of waste heat, and environmental protection. Table 8.10 compares the important stages and processes of copper production, showing the range of the matte composition for each process.

Cost. Both capital and operating costs for copper smelters must be estimated with care because the published data vary considerably [68–69]. The costs depend on the plant location, generally increasing with

- the leanness of the raw material—the lower the copper content the higher the costs
- the price and demand for energy
- rigorous environmental protection
- inflation
- low foreign exchange rates

Table 8.10: Survey of pyrometallurgical processes for copper production [67].

Process	Matte composition										Description, final product
	% S % Fe % Cu	10	20	32	48	30	28	26	24	22	% S % Fe % Cu
Roasting											solid-state desulfurization
Smelting											melting, natural-grade matte
Reverb smelting (Green feed) (calcine feed)											oxygen flash smelting, medium-grade matte
Electric smelting											flash smelting, high-grade matte
INCO oxygen flash smelting											
KIVCET process											
Reverb (oxygen sprinkle smelting)											
Outokumpu flash smelting											
Noranda process (matte mode)											
El Teniente reactor											
Converting											converting
Peirce-Smith											
Hoboken											
TBRC											
Continuous smelting and converting											
KHD Contop process											
Mitsubishi process											
Q-S process											
Noranda process (copper mode)											
TBRC											
Refining											
Fire refining											

The amount of energy required to produce copper pyrometallurgically depends on the process (Table 8.11).

Table 8.11: Energy required for pyrometallurgical production of copper [13].

Process	Energy required per 1 t Cu, GJ
INCO Flash smelting (95% O ₂)	1.7
Electric furnace	6.7
Noranda process (30% O ₂)	6.7
Outokumpu flash smelting	8.4
Mitsubishi process	10.1
Reverberatory furnace with roasted concentrate (calcine feed)	13.4
Brixlegg process	19.3
Reverberatory furnace with raw concentrate (green feed)	21.8

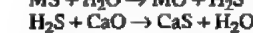
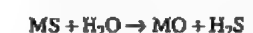
8.5.4.5 Proposals

Numerous laboratory experiments and pilot-plant runs have been carried out to develop smelting methods based on elements other than oxygen. Two lines of development have dominated reduction with hydrogen and chlorination, however, without leading to commercialization.

Reduction. A potential process involves the reduction of chalcopryrite [73, 74]:



The reduction by hydrogen is endothermic, but the overall reaction with calcium oxide is exothermic. A similar proposal is based on the reaction of a metal sulfide with steam in the presence of calcium oxide:



Chlorination. The reactions of chalcopryrite with chlorine are also of interest [75]:



followed by electrolysis of the molten copper(I) chloride.

The recently proposed thermoelectron chlorination process is another variation [76]:

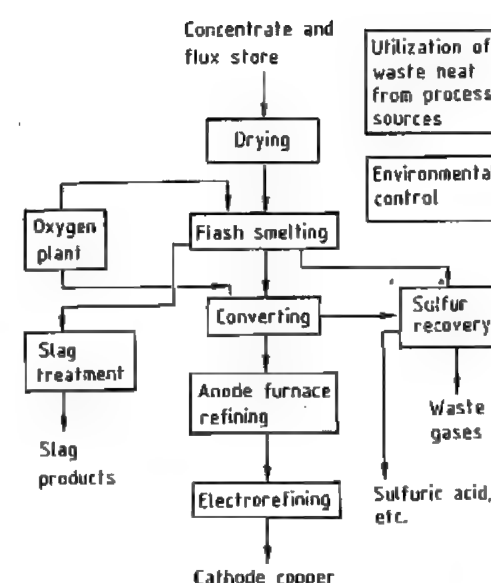
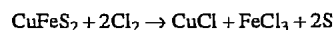


Figure 8.9: Typical flow sheet for pyrometallurgical copper production from ore concentrates [66].

The flash smelting process is the most efficient pyrometallurgical method, costing as little as one-third the conventional processes. The costs of hydrometallurgical processing also depend on the copper content, but generally the capital costs are up to 50% lower than conventional processing.

Energy requirements have a large effect on operating costs. There are publications on comparative power demands [70–72]; however, the data vary widely and must be used with care. The step that uses the largest fraction of the energy needed to produce copper pyrometallurgically is the smelting itself [13]:

Step	Energy required per 1 t Cu, GJ	Deviation, %
Mining	5.5	35
Beneficiation	3.8	35
Smelting (Outokumpu flash)	8.4	20
Converting	0.0	
Anode casting	0.2	10
Electrolysis	1.3	10
Cathode casting	1.7	10
Total	ca. 21.0	



Electrolysis. Another approach, to avoid converting, proposed the electrolysis copper matte [77].

8.5.5 Traditional Bath Smelting

At the end of the Middle Ages, copper was produced by the German or Swedish smelting process that involved roasting reduction with up to seven process steps in small shaft furnaces. Around 1700, reverberatory furnaces were constructed in which the ore was processed by roasting reaction, the so-called English or Welsh copper smelting process, originally with ten process steps.

The large blast and reverberatory furnaces of the 20th century were derived from these principles. Later, the electric furnace for matte smelting was developed.

8.5.5.1 Blast Furnace Smelting

The blast or shaft furnace is well-suited for smelting high-grade, lumpy copper ore. If only fine concentrates are available, they must first be agglomerated by briquetting, pelletizing, or sintering. Because of this additional step and its overall low efficiency, in the last decades, the blast furnace lost its importance for primary copper production and currently is obsolete and, thus, used in only a few places.

Smaller types of blast furnace, however, are used to process such copper-containing materials as intermediate products (e.g., cement copper or copper(I) oxide precipitates), reverts (e.g., converter slag, refining slag, or flue dusts), and copper-alloy scrap.

The construction of the furnace is basically related to that of the iron blast furnace, but there are considerable differences in design, especially in size and shape: the copper blast furnace is lower and smaller, and its cross section is rectangular. Recent developments in the steel industry have been adopted, including use of preheated air (hot blast), oxygen-enriched air, and injection of liquid fuels.

The furnace is charged with alternate additions of mixture (copper-containing materials

and accessory fluxes such as silica, limestone, and dolomite) and coke (which serves as both fuel and reducing agent). There are three zones in the furnace:

- In the heating zone (the uppermost), water evaporates and less stable substances dissociate.
- In the reduction zone, heterogeneous reactions between gases and the solid charge take place.
- In the smelting zone, liquid phases react.

The usual mode of operation is *reducing smelting*, which yields two main products. Sulfide ores are used to produce a matte (40–50% Cu) and a disposal slag (ca. 0.5% Cu). In contrast, oxide ores are processed directly to impure black copper ($\leq 95\%$ Cu) and to a copper-rich slag. The two ore types can be smelted together to produce matte and a slag with low copper content. Another product is top gas, which contains flue dust. Ores that contain high concentrations of arsenic and antimony also form speiss, which is difficult to decompose.

Oxidizing smelting in blast furnaces has been discontinued—not only the older processes such as pyrite and semipryrite smelting, but also the comparatively new Momoda process developed in Japan (1955) and operated in Spain (Rio Tinto) as well.

Examples of operating matte blast furnaces include Lubumbashi, Zaire; VEB Mansfeld Kombinat, Germany; Glogow, Silesia, Poland.

8.5.5.2 Reverberatory Furnace Smelting

Parallel to the increasing production of fine concentrates in the first half of the 20th century, the reverberatory furnace (reverb) became the main producer of copper matte. About 1960, there were nearly 100 large units in operation, mainly in the United States, Canada, Chile, Zaire, Zambia, Australia, Japan, and Russia. Since that time, the number has declined as a result of severe competition from modern autogenous smelting processes. The reverberatory furnace erected in Sar Chesh-

meh, Iran, a few years ago was probably the last of its type.

The largest units, with hearth areas up to 380 m², are up to 38 m long, 11 m wide, and ca. 4 m high. The construction scheme is shown in Figure 8.10. The internal furnace walls have a refractory lining of basic brick, preferably magnesite brick, for prolonged operating life; in addition, water jackets are provided for protection of sidewalls, and the suspended arch is made with exchangeable bricks. Throughput can attain 1000 t/d and consists of concentrates with fluxes (silica and limestone) and copper-rich converter slag.

The treatment of sulfide concentrates depends on the sulfur:copper ratio. If the sulfur content is too high, the material must be partially roasted to remove excess sulfur and to obtain an optimum composition for the formation of matte. This process is called a hot-calcine-charged operation. On the other hand, if the S:Cu ratio is in the proper range, no special pretreatment of the concentrate is required and the cold-wet-charged (or green-charged) operation can be used. A combined action of the two methods has been demonstrated [78].

The charge is passed into the part of the furnace near the burners, either through central or lateral openings in the roof or through the sidewalls, as shown in Figure 8.10. Fuel (pulverized coal heavy fuel oil or natural gas) and combustion air are injected at the front; the maximum flame temperature exceeds

1500 °C, and heat is transferred by radiation. In contrast to the reducing operation in a blast furnace, the reverberatory furnace atmosphere is slightly oxidizing or neutral. The off-gas (1200–1300 °C) flows through a waste-heat boiler for steam generation and then a gas purification plant.

The front part of the furnace functions as a melting zone, and the back half as a settler where matte and slag separate. The copper content of such mattes is generally controlled to 35–50%. The depth of the molten bath is generally 40–50 cm for slag and 60–80 cm for matte.

A special problem with reverberatory furnaces is the formation of high-melting magnetite, which can lead to operational problems and even furnace shutdown. Because of roasting, calcine charging produces more magnetite than does green charging.

The concentration of sulfur dioxide in the waste gases, < 1 vol% in calcine-charged smelting and ca. 2 vol% in green-charged smelting, is too low for the production of sulfuric acid.

The reverberatory process has the highest energy consumption of all proven pyrometallurgical copper matte smelting methods. A green-charged furnace consumes ca. 60% more fuel than a calcine-charged unit for the same smelting capacity, and nearly thrice the energy input of the Outokumpu flash smelting furnace.

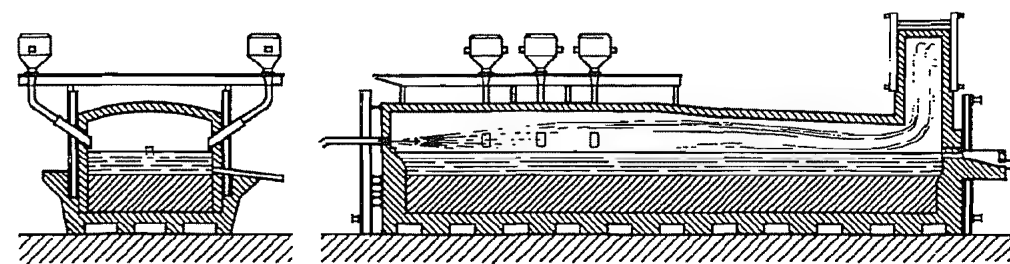


Figure 8.10: Schematic longitudinal and cross-section views through a reverberatory furnace [46].

8.5.5.3 Modern Reverberatory Smelting

Conventional reverberatory smelting is thermally inefficient and produces a large volume of low-SO₂ waste gas that is unsuitable for producing sulfuric acid. New developments derived from the principle of reverberatory smelting eliminate these disadvantages, chiefly by using oxygen and rebuilding extant furnaces. Some of these developments are the following:

- **Conventional-burner oxygen enrichment.** The improvement in efficiency is achieved by increasing the oxygen concentration in the combustion air of conventional front burners to 30–40 vol% O₂, saving energy and increasing the concentration of sulfur dioxide in the off-gas to the point that the off-gas is suitable for sulfuric acid production.
- **Oxy-fuel reverberatory smelting** [79]. Special oxy-fuel burners mounted in the furnace roof fire vertically downward onto the charge with up to 60% oxygen-enriched combustion air. The smelting rate may increase to 50%, and the concentration of sulfur dioxide in the off-gas may increase to 7 vol%, adequate for producing sulfuric acid. Several plants have been built on this principle: Onahama smelter, Japan; Caletones smelter, El Teniente, Chile; and smelters in Canada and Russia.
- **Oxygen sprinkle smelting.** A recent invention [80] that involves installation of three or four sprinkler burners in the furnace roof for feeding concentrates fluxes fuel (pulverized coal) and oxygen (98%) produces a high-grade matte containing ca. 75% Cu.

While the conventional reverberatory furnace is primarily a physical melting apparatus, the new variant is an efficient chemical reactor. This operation was a transition stage to the autogenous flash smelting processes and was first employed at the Morenci smelter. Phelps Dodge Corp., New Mexico, United States.

- **Bai-Yin copper smelting process (BYCSP).** A new concept originating from the Bai-Yin Non-Ferrous Metals Co. [81], China, uses a furnace divided by a partition wall into a roasting/smelting zone and a settling zone. The molten bath is intensively agitated by air, which is blown through tuyères arranged in series. This method is said to have twice the smelting capacity of conventional operations.

8.5.5.4 Electric Furnace Smelting

In regions where relatively cheap electrical power was available, electric furnaces were built. The Scandinavian countries were the first to do electric matte smelting: 1929 at Sullitjelma, Norway; 1938 at Imatra, Finland, and 1949 at Rönnskär, Sweden. Approximately 30 electric matte smelting furnaces are now in operation in Scandinavia, the United States, Canada, Zambia, South Africa, and Russia.

Electric furnaces have the rectangular ground plan and the dimensions of larger reverberatory furnaces. Along the centerline, up to six Soderberg continuous self-baking electrodes are used with alternating current (Table 8.12). The largest furnace of this type in the world, at the Inspiration smelter in Arizona, has an electrical power input of 51 000 kVA [82–83].

Table 8.12: Two examples of electric matte smelting furnaces.

Company and plant location	Electrical load, kVA	Inside dimensions, m			Hearth area, m ²	Electrodes		Furnace input, t/d
		Length	Width	Height		Number	Diameter, m	
Boliden, Rönnskär, Sweden	12 000	24	6	3	144	3	1.2	500
Inspiration, Inspiration, Arizona, United States	51 000	36	10	5	360	6	1.8	1650

The smelting process in such units is similar to the operation in reverbs, but the concentrate is usually dried–rarely roasted–before charging. The converter slag is returned to the furnace. The composition of matte and slag resembles that of the reverb products, but the content of magnetite is lower because the roasting process is omitted. No fuel is burned and the volume of waste gases and the quantity of flue dust are small. The SO₂ content of the waste gas can be 10%. The off-gas also contains carbon oxides from the consumption of the graphite electrodes.

A significant difference between the electric furnace and the reverb is the inversion of the temperature gradient in the furnace cavity. In the reverb, the combustion gases have the highest temperature, whereas in electric matte smelting, the waste gases are ca. 500 °C cooler than the slag phase, which is heated by the electric energy. Accordingly, in the electric furnace, cheap refractories are sufficient for lining the walls above the slag zone and the roof; only a common arch is required.

The temperatures of both molten phases depend on the submergence of the electrodes, and the required heat is controlled by the electrical power supplied. Heat transfer takes place chiefly by convection, which causes intense circulation in the molten bath.

The current is divided into two partial circuits, through slag and through matte. The difference in conductivity is great, slag:matte ratio of 1:102 to 1:103; therefore, the depth of immersion of the electrodes into the liquid slag must be precisely controlled. As the electrodes immerse deeper into the slag, more current flows through the matte. If they touch the matte layer, a short circuit occurs. These considerations lead to an approximate relation between the electrical power input and the depth of the slag layer: 6000 kVA and 0.5 m, 30 000 kW and 1.0 m, and 50 000 kW and 1.5 m.

The matte layer reaches a maximum height of ca. 0.8 m. The smelting capacity of electrical furnaces is higher than that of reverbs, averaging 3–4 t m⁻² d⁻¹.

Brixlegg Process. Lurgi developed [84] and practiced at Brixlegg, Tirol, Austria, a modification of the old roasting reaction process. Nearly dead-roasted concentrates are reduced in batches by coal in a small special circular electric furnace (2500 kVA, 5-m diameter). The crude copper averaged only 95% Cu, and the operation has been discontinued.

8.5.6 Autogenous Smelting

Autogenous smelting involves the use of combustion heat generated by reactions of the feed in an oxidizing atmosphere in which the sulfide concentrate acts partly as a fuel. The formerly separate steps of roasting and smelting are combined into a roast-smelting process. The spatial and temporal coupling of exothermic and endothermic reactions leads to an economical process, but the sensible heat of nitrogen in the air causes a deficit in the heat balance. In practice, various measures must be taken:

- Preheating combustion air with waste heat or in a preheater
- Increasing the oxygen content of the combustion air and even using pure oxygen
- Combustion of natural gas, fuel oil, or pulverized coal in supplementary burners

To achieve autogenous operation and prevent agglomeration of the feed, the moisture in the concentrate must be removed by drying before charging. The quantity of added fluxes is minimized as far as practical to save energy.

Because the residence time of the sulfide particles in the reaction chamber is only a few seconds, kinetic conditions predominate over the thermodynamic equilibrium. The reactants form a heterogeneous system, with the feed suspended in the gas flow, thus the term smelting in suspension. These processes have several advantages:

- High rate of reaction, increasing the production rate
- Energy savings
- Low volume of off-gas and correspondingly high concentration of SO₂ and low quantity of flue dust if oxygen is used

However, a typical disadvantage is the high copper content of the slags.

8.5.6.1 Outokumpu Flash Smelting

After a preliminary test in 1946, the first full-scale flash smelting furnace was started in 1949 by Outokumpu Oy in Harjavalta, Finland. In recent years this process has partially replaced reverberatory smelting, and it will probably become the most important method in the future. At present, more than 30 Outokumpu furnaces are in operation, with a total capacity of nearly one-third of the world primary copper production. In Japan alone there are seven Outokumpu units. The Outokumpu process is easily converted to computer control [85].

Furnace Design (Figure 8.11). A flash furnace has been developed from a reverb with a mounted roaster in which smelting takes place simultaneously. Large units comprise three sections with approximate dimensions as follows:

- Circular reaction shaft for roasting and smelting dried concentrates in suspension; 6–7 m in diameter and 7–9 m high
- Settling hearth for collecting the molten droplets and separating matte from slag; 120–160 m² hearth area and up to 24 m long, 6–7 m wide, and 3 m high

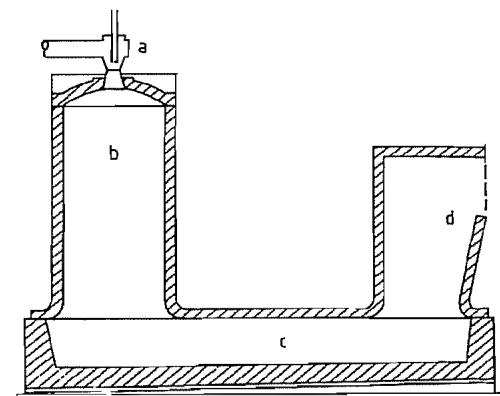


Figure 8.11: Outokumpu flash smelting furnace, longitudinal section [86]: a) Concentrate burners; b) Reaction shaft; c) Settler; d) Offtake shaft.

- Rectangular uptake shaft for waste gas and flue dust; 6–7 m long, 3 m wide, and 6–7 m high

Operation [87]. Various sorts of concentrates ($\leq 10\%$ H₂O) and a few fluxes (mainly silica) are mixed and dried in rotary dryers or in flash dryers. The dried feed is conveyed to the top of the reaction shaft, where three or four special concentrate burners are mounted. Measures required to maintain autogenous conditions include preheating of combustion air in special air preheaters up to ca. 500 °C, oxygen enrichment, and conventional burners for additional firing. The oxygen:concentrates ratio determines the final copper content in the matte. The heterogeneous mixture of gas and particles or gas and droplets remains in the reaction shaft only a few seconds before reaching the settler; the liquid matte and slag separate at ca. 1200 °C, and the matte is tapped for converting. Outokumpu mattes, which contain 50–70% Cu, result in slags that contain up to 2% Cu. Typical operating data are shown in Table 8.13.

Table 8.13: Outokumpu process, Ashio plant (Furukawa Co.), Japan [88].

	Air (21 vol% O ₂)	Oxygen-enriched air (41.5 vol% O ₂)
Concentrate throughput, t/d	440	550
Process air, m ³ /h	22 000	9600
Copper matte grade, % Cu	48	60
Heavy oil consumption, L/t	65	10
Off-gas		
SO ₂ content, %	11.5	33
O ₂ content, %	1.0	1.5
Flue dust, %	8.8	5.2
Production		
Blister copper, t/d	95	120
Sulfuric acid, t/d	250	330
Relative electric power consumption, %	100	128
Total consumption of heavy oil, %	100	35

Slag Cleaning. In practice two methods are used: froth flotation and treatment in small circular electric slag furnaces. The decision for one or the other is determined by economics. In froth flotation the slag concentrate is returned to the feed, and the tailings are dis-

carded. The second method involves the reduction of flash furnace slags in an electric furnace, which yields a matte and slag that is suitable for sale.

Off-gas and Flue Dust. The waste gases are separated from part of the flue dust at ca. 1250 °C in the offtake shaft and pass through a waste heat boiler for generating steam, and subsequently to an electrostatic (Cottrell) precipitator for separating the mass of flue dust, which is recycled to the feed. The precleaned off-gas with SO₂ content of > 8% is usually processed to sulfuric acid.

The flue dust consists chiefly of sulfates and basic sulfates of copper lead and zinc as well as some volatile compounds of arsenic, antimony, bismuth, and selenium. Repeated recycling makes it possible to enrich selected elements for later extraction. The quantity of flue dust can reach ca. 10% of the input.

In large furnaces the throughput is ca. 60 t of concentrate per hour, corresponding to a copper production of nearly 150 000 t/a.

Special Operations. There are several recent variations of Outokumpu flash smelting, especially in Japanese smelters:

- Ashio smelter (Furukawa Co.), Japan. The flash furnace has been rebuilt with the shortest reaction shaft of all Outokumpu units, only 4.7 m high, to minimize heat loss. A special burner and use of high oxygen content in the blast air compensate for this short reaction zone [88].
- Saganoseki smelter (Nippon Mining Co.), Japan. The smelter operates two Outokumpu units in which hot oxygen-enriched blast air is used. Heating of the input air to 1000–1200 °C takes place in special hot-blast stoves. The overall energy efficiency is reported to exceed that of the conventional Outokumpu process [89].
- Tamano smelter (Hibi Kyodo Smelting Co.), Japan. To eliminate the slag cleaning furnace, electrodes are inserted into the settler of the flash furnace. This mode is termed the FSFE (flash smelting furnace with electrodes) process [90]. A second

plant, the PASAR smelter, has been erected recently in the Philippines.

- Glogow smelter, Silesia, Poland. The concentrates used here have an unusual composition: 17–32% Cu, 1–3% Pb, only 2–5% Fe, 7–10% S, and even 5–8% organic carbon. Air that is highly enriched with oxygen (up to 80 vol% O₂) is used, which permits the direct production of blister copper. The two disadvantages are the high content of impurities (lead, arsenic, and bismuth) in the copper and the extremely high percentage of copper (7–16%) in the slag, both depending on the level of oxygen enrichment [91].
- Hidalgo smelter (Phelps Dodge Corp.), New Mexico, United States. This new plant is intended to produce elemental sulfur instead of sulfuric acid by reducing the SO₂ in the offtake shaft with pulverized coal and hydrocarbons [92].

Trends. The diversity of modified furnace constructions and operating methods shows the adaptability of the Outokumpu process to different raw materials and smelter locations. As increasing oxygen content has been used in the blast air, the process has approached the principle of INCO flash smelting. On the other hand, newer developments aim at the production of blister copper or white metal (75–80% Cu) from concentrates in only one vessel, thereby approaching continuous smelting and converting as in the Noranda process.

8.5.6.2 INCO Flash Smelting

INCO Metals Co., Canada, was the first company in the nonferrous metal industry to use commercially pure oxygen, which it did in autogenous flash smelting. After tests in the late 1940s, two smaller furnaces were put into operation in 1952–1953, and a rebuilt unit with a capacity of ca. 1400 t/d has been operating since 1968 [93].

The construction is similar to that of a medium-sized reverb (about 23 m × 6 m with a maximum height of 5 m), but feed and oxygen (95–98 vol%) are blown horizontally through

burners at both ends of the furnace. The offtake is arranged at the center of the roof. A sheet steel encasing keeps the furnace nearly gastight. The matte contains ca. 50% Cu and the slag 0.7% Cu.

The advantages of the process rest on the use of pure oxygen and relate particularly to handling off-gas. Because of the relatively small gas volume, the dust formation is negligible, and the cooling and dust-collecting system can be small. On the other hand, the SO_2 content of the off-gas is ca. 80%, so that liquid sulfur dioxide can be produced. Other advantages are the relatively low energy requirement and the simple design. Figures 8.12 and 8.13 give the heat balance for INCO flash smelting and a sketch of the furnace.

However, the INCO process is employed only to a small extent. Apart from an older plant in Almalyk, Uzbekistan [94], only two companies in the United States have chosen this process in recent years for modernizing their facilities: Hayden smelter (ASARCO), Arizona and Hurley smelter (Kennecott Copper Corp.), New Mexico.

8.5.6.3 KIVCET Cyclone Smelting

Developments in power-plant technology have led to adoption of the cyclone principle

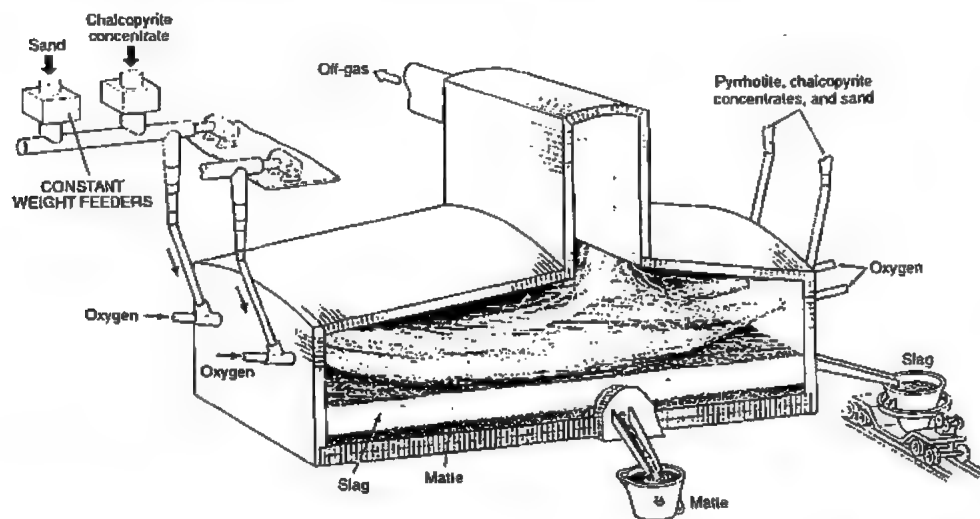


Figure 8.13: Principle of INCO flash smelting furnace.

by the metallurgical industry. The acronym KIVCET uses the initial letters of the following Russian terms: oxygen, vortex, cyclone, electrothermic. The development began in 1963, and the first plant was operated by Irtysh Polymetal Combine in Glubokoe, Kazakhstan; other ex-USSR plants are under construction [95].

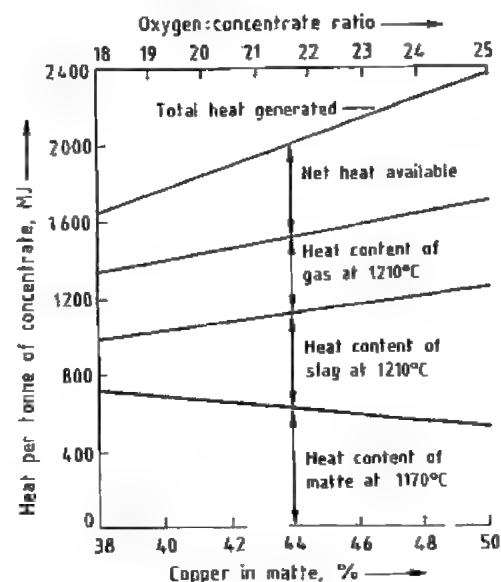


Figure 8.12: Heat balance of INCO flash smelting [93].

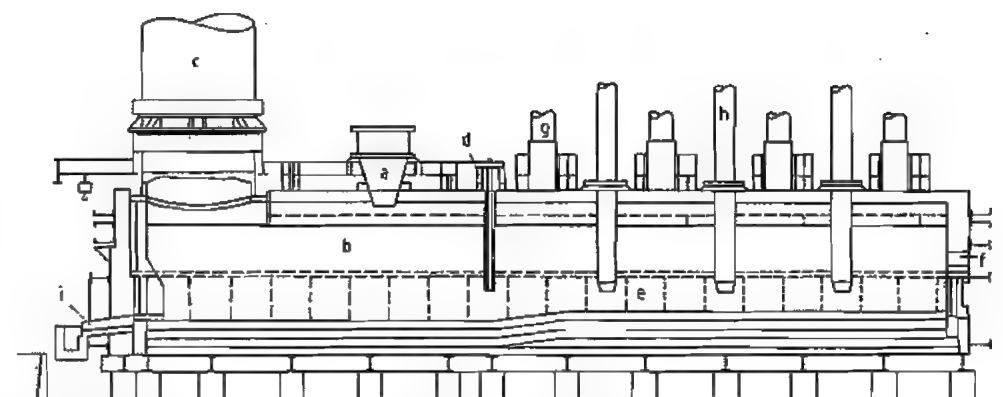


Figure 8.14: KIVCET furnace [95]: a) Smelting cyclone; b) Separating chamber; c) Cyclone waste-gas offtake; d) Partition wall; e) Settling reduction hearth; f) Slag tap hole; g) Feed of reductant and offtake for waste gas from the hearth; h) Electrical resistance heating; i) Matte taphole.

Table 8.14: KIVCET process: analysis and yield [95].

Analysis and yield	Metal		
	Cu, %	Zn, %	Pb, %
Analysis			
Concentrate ^a	25.60	10.0	1.7
Copper matte	50.00	2.5	2.0
Slag	0.35	3.5	0.2
Yield			
In matte	99.1	12.7	60.0
In oxidic condensate	—	71.0	34.1

^a Also 24.0% Fe and 33.0% S.

The method is aimed at processing copper sulfide concentrates that contain considerable amounts of other metals. The essential part of the continuously operated plant is the smelting cyclone, in which the concentrates are fed vertically, and technical-grade oxygen ($\leq 95\%$) is blown in horizontally, so that reaction takes place rapidly above 1500°C .

The furnace is divided to allow separating and settling of the reaction products, in this respect similar to a reverb. In contrast to the separation chamber, the atmosphere in the electrically heated settler is maintained in a reducing state so that the slag does not need special posttreatment.

The off-gas volume is small, and the percentage of SO_2 can be up to ca. 80%. Metals are recovered from the flue dust of both the separating chamber and the settler. Table 8.14 and Figure 8.14 explain the process.

Using a KIVCET license, KHD Humboldt Wedag AG, Köln (Cologne), is developing the combined Contop process [96] (Section on Other Processes).

8.5.6.4 Flame Cyclone Smelting

The flame cyclone reactor (FCR) process was suggested by LURGI and Deutsche Babcock AG ca. 1975 and has been demonstrated at a pilot plant of Norddeutsche Affinerie in Hamburg with a capacity of ca. 10 t/h. It is a high-temperature ($> 1500^\circ\text{C}$) reaction for autogenous smelting of copper sulfide concentrates in a high-oxygen atmosphere (up to ca. 75%). A second characteristic is the simultaneous removal of volatile compounds of other elements, such as zinc, cadmium, tin, lead, arsenic, antimony, and bismuth, as oxides and basic salts, in the flue dust. The SO_2 content of the off-gas is greater than 50%. The products are a high-grade matte containing up to 80% Cu and slag, which separates in a settler [97].

The principle of this method differs from that of the KIVCET process in that the reaction in the FCR process takes place in a special chamber situated before the cyclone, where the molten droplets are separated by centrifugal force. The process is well-suited for processing complex or dirty concentrates, the raw material of the future.

8.5.7 Converting

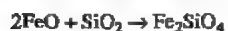
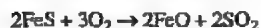
Matte produced by smelting processes is treated in the molten state by blowing with air; this stage of concentration is known as converting. Copper and iron sulfides, the main constituents of matte, are oxidized to a crude copper, ferrous silicate slag, and sulfur dioxide.

The batch converting process has been employed for many decades in two operating steps at ca. 1200 °C in the same vessel. Investigations and development of continuous methods are being made [98–99].

8.5.7.1 Discontinuous Converting

The conventional converting of matte is a batch process that yields in the first step an impure copper(I) sulfide containing ca. 75–80% Cu, the so-called white metal, and in the second step the converter, or blister, copper averaging 98–99% Cu. The name blister copper derives from the SO₂-containing blisters that are enclosed in the solidified metal.

First Step. The main reactions are oxidation of iron(II) sulfide and slagging of iron(II) oxide by added silica flux:

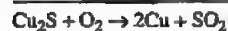
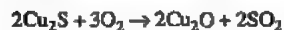


Formation of magnetite occurs near the tuyères:



In Figure 8.6, the first step corresponds to moving along the pseudobinary Cu₂S–FeS line to form an impure copper(I) sulfide.

Second Step. Continuing oxidation occurs as in a typical roasting reaction process:



In Figure 8.6 and Figure 8.15, the composition moves along the Cu₂S–Cu line from the copper(I) sulfide to crude metallic copper, the two phases being immiscible.

The blister copper contains < 0.1% S, ca. 0.5% O, and traces of other impurities.

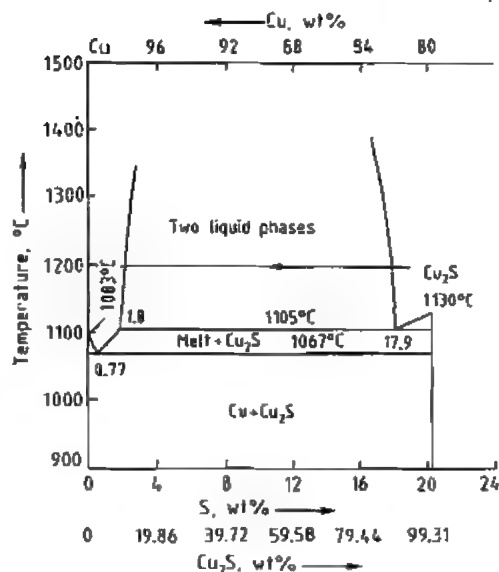


Figure 8.15: The Cu–Cu₂S system [100].

Converter Slags. The slags from the first step are iron(II) silicates (40–50% Fe) with high magnetite content (15–30% Fe₃O₄). The initial copper content of 3–8% can increase up to 15% at the end of the reaction by formation of copper(I) oxide. This slag can be decopperized by returning it to the smelting unit or by froth flotation.

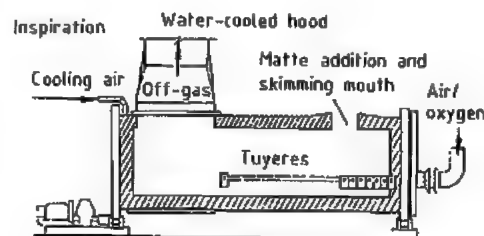
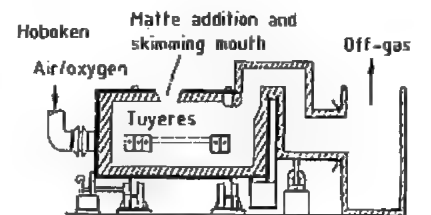
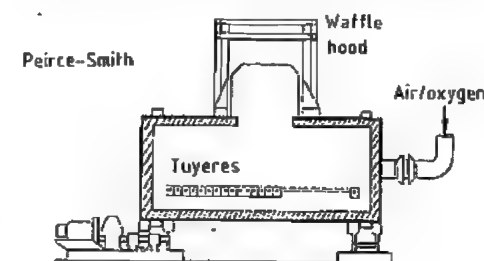
The high-viscosity small-volume converter slags from the second step have a high copper content (20–40%) in the form of copper(I) oxide or silicate. When enough slag has accumulated, it is returned to the first converting stage.

Temperature. Converting is a strongly exothermic process that can overheat during oxidation of iron-rich mattes. The temperature must be held ca. 1200 °C by adding fluxes, copper scrap, precipitates from hydrometallurgical treatment (e.g., cement copper), or concentrates. The off-gas (5–8 vol% SO₂) is transferred to a sulfuric acid plant.

The blowing time per batch is a few hours; however, as the copper content of the matte increases, the converting time decreases. Occasionally, oxygen-enriched air is used to increase the throughput.

Impurities. The distribution of other elements among the phases during converting is as follows:

- Noble metals and most of the nickel, cobalt, selenium, and tellurium collect in white metal and then in blister copper.
- The bulk of zinc and some nickel and cobalt collect in converter slag.
- The oxides and sulfates of arsenic, antimony, bismuth, tin, and the basic sulfates of lead are found in flue dust.



Converter Types. The copper converter was invented in 1880 by Manhès and David, based on the Bessemer converter, which had been used in the steel industry since 1855. This development led to the incorrect name “copper bessemerizing”, although the true Bessemer process is a refining step. Originally, the copper converter was upright, and such obsolete units were in operation until the early 1980s, e.g., the Great Falls converter developed by Anaconda Mining Co., United States.

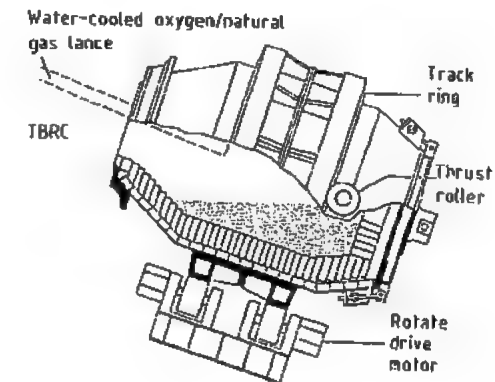
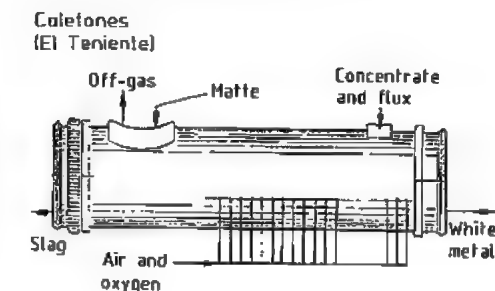
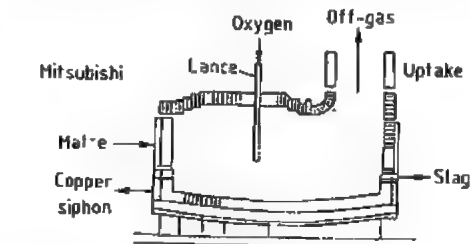


Figure 8.16: The evolution of the copper converter [101].

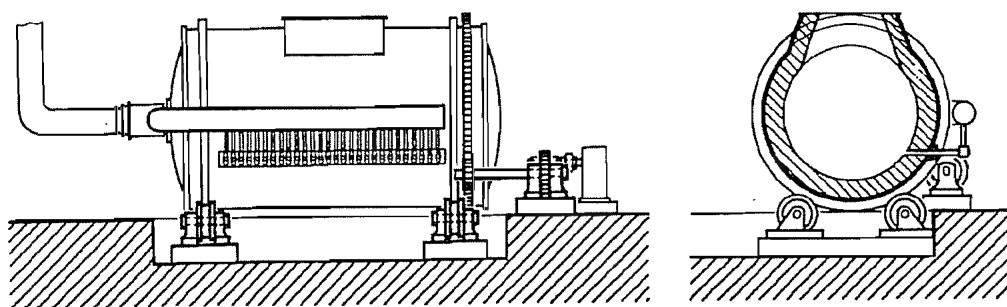


Figure 8.17: Schematic cross section and back view of a Peirce-Smith converter [45].

The following types are in use currently (Figure 8.16):

- Peirce-Smith converter. The P-S type has been the most important apparatus for converting for many decades, and the number in operation may be in the range of a thousand. It is a horizontal cylinder lined with basic bricks (magnesite, chrome magnesite) that can be rotated about its long axis (Figure 8.17); blast air is blown through a horizontal row of tuyères. In practice, the punching of tuyères with special devices is necessary to maintain the flow of air. The largest vessels are 9–11 m long with a diameter of 4–4.5 m.
- Hoboken or syphon converter [102]. This variation of the P-S type was developed years ago by Metallurgie Hoboken N.V., Belgium, but is now used by only a few smelters in Europe and in North and South America; larger units are operated at Gliogow smelter in Silesia, Poland; Inspiration smelter in Arizona; and Paipote smelter (ENAMI), Chile [103]. Its advantage is its freedom from sucking in air, so the off-gas can attain SO_2 levels up to 12%. Special features of the design are the small converter mouth and the syphon or goose neck that guides the off-gas and flue dust flow.
- Inspiration converter [104]. The construction of the Inspiration Consolidated Mines, Arizona, United States, is the most recent development in converter technology. Its design is similar to the Caletones type as it also has two mouths, the smaller for charging, the larger for the off-gas. The latter is well hooded in all operating positions.
- Caletones or El Teniente modified converter. Another modification longer than the P-S converter is the TMC [105]. The main design differences are two separated mouths for charging and off-gas flow, and the lateral tapholes for liquid slag and white metal. The latter is converted to blister copper in a conventional P-S converter. Further characteristics are testing for the direct smelting of concentrates in the converter with oxygen and the tendency to continuous operation. There are two units at Caletones smelter (ENAMI), El Teniente, Chile.
- Top-blown rotary converter [106]. The TBRC, which is known in the steel industry as the Kaldo converter, was adopted by the nonferrous industry (first by INCO, Canada) because of its great flexibility. Air, oxygen-enriched air, or on occasion, commercial oxygen is blown through a suspended water-cooled lance onto the surface of a charge of copper-containing materials. In practice, the TBRC is used batchwise for special operations on a small scale:
 - Converting copper matte with high levels of such impurities as bismuth and arsenic took place at the Tennant Creek smelter (Peko-Wallsend Ltd.), Australia, but it has been discontinued.
 - Direct smelting of concentrates (clean, complex, or dirty) to white metal or blister copper is performed at Rönnskär smelter (Boliden Metall AB), Sweden.
 - Slags from sulfide concentrate smelting and native copper are treated at Kamloops

smelter (Afton Mines Ltd.), British Columbia, Canada.

– Copper extraction from copper scrap and other secondary materials is also carried out.

- Siros melt process [107]. A new development, the Siros melt process (not shown in Figure 8.16) operates batchwise, similar to the TBRC process when used for direct smelting and subsequent converting (cf. *b*) above). Pelletized concentrates, air, and fuel are fed through a submerged lance into a special stationary furnace of circular design. After withdrawal of the primary slag, the matte is converted to white metal and then to blister copper in the same reactor. This concept of CSIRO, Australia, needs more testing before commercialization.

8.5.7.2 Continuous Converting

While continuous copper smelting processes have been in operation for many years, continuous converting of matte has come into use only slowly. In the Western world, however, these trends have recently led to a novel combination of continuous smelting and converting methods (Section on Continuous Smelting and Converting). The Eastern bloc has also been investigating continuous converting [108–109].

Among the newer concepts originating from companies in Canada and the United States is the flash converting method developed by Kennecott Copper Corp., United States [110], termed the SMOC (solid matte oxygen converting) process. Solidified matte from a smelting furnace is comminuted; the finely powdered matte is oxidized in a flash furnace with commercial oxygen to give blister copper slag, and an off-gas containing ca. 75 vol % SO_2 .

8.5.8 Continuous Smelting and Converting

Recently, copper metallurgists have tried to combine operation steps into simplified en-

ergy-saving processes. There are now two modern methods in use: the multistep Mitsubishi process and the single-step Noranda process. The Outokumpu process has recently been modified to produce blister copper [91]. Attempts have been made to employ continuous production, autogenous operation, and the use of oxygen. Apart from furnace design, the various processes differ in the following important details:

- Blowing the combustion air through tuyères into the molten bath or through lances onto the charge
- Mode of streaming of the two liquid phases (matte and slag) in uniflow or countercurrent
- Method of slag decopperizing

8.5.8.1 Mitsubishi Process

Mitsubishi Metals Corp., Japan, tested the new concept in 1961 and started a commercial plant in Naoshima in 1974 with an annual capacity of 70 000 t of copper [111]. The principle of the process is the interconnecting of three furnaces, as shown in Figure 8.18:

- Smelting or S-furnace. Dried concentrates, fluxes (silica and limestone), pulverized coal, basic return converter slag, and flue dust are smelted with fuel oil and unpreheated oxygen-enriched air to produce matte.
- Slag cleaning or CL-furnace. Separation of matte from slag is effected in this electric furnace by addition of coke and some pyrite for decopperizing the slag, which is then discarded.
- Converting or C-furnace. Blister copper is produced by continuously oxidizing the high-grade matte. A special basic slag ($\text{Fe}_3\text{O}_4\text{--CaO--Cu}_2\text{O}$) is formed by addition of small amounts of limestone. This slag is returned to the S furnace after granulation.

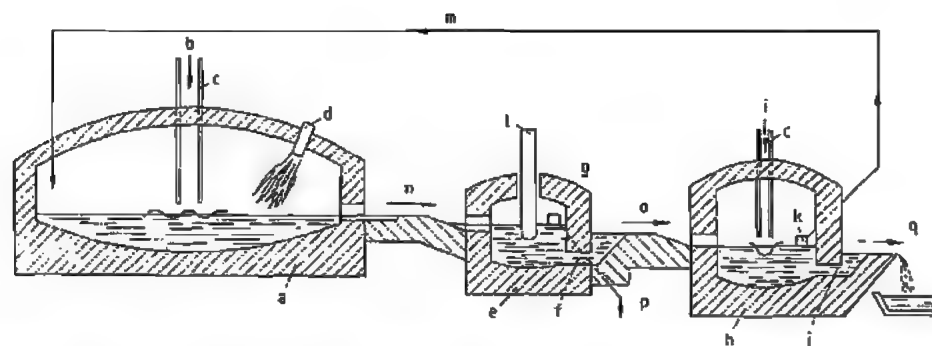


Figure 8.18: Mitsubishi process [112]. Furnaces and furnace parts: a) Smelting furnace; b) Charging part for dried concentrates and fluxes; c) Lances for blowing air and oxygen; d) Burners; e) Slag cleaning furnace; f) Matte syphon; g) Slag overflow; h) Converting furnace; i) Charging part for limestone; j) Blister copper syphon; k) Revert slag overflow; l) Anodes; m) Slag return system. Material flow: n) Matte and slag; o) Matte; p) Slag to granulator; q) Blister copper.

Table 8.15: Mitsubishi process: composition of smelting products at the Naoshima, Japan, plant [113].

Material	Composition, %					
	Cu	Fe	S	SiO ₂	CaO	Al ₂ O ₃
Concentrates	27.5	27.5	31.0	5.5	0.5	1.5
Matte	65.0	11.0	22.0			
Discarded slag	0.5	42.0	0.7	30.2	4.2	3.3
Converter slag	15.0	44.0	0.1	0.2	15.0	0.2
Blister copper	98.5		0.1			
Copper anodes	99.4					

Table 8.15 contains typical analytical data on the intermediate products. The off-gas contains ca. 15 vol% SO₂ and is used to produce sulfuric acid; the flue dust comprises 2–3% of the charged concentrates. The energy consumption is about the same as that of the Outokumpu process, but the investment and personnel costs are lower.

A new plant of this design was put into use in 1981 by Kidd Creek Mines Ltd. at Timmins smelter, Northern Ontario, Canada [114], which is to increase in capacity from 60 000 to 90 000 t/a.

8.5.8.2 Noranda Process

The tests of this first single-step continuous copper smelting process began in 1964, and a large-scale plant was put into use in 1973 at Horne smelter (Noranda Mines Ltd.) in Noranda, Quebec, Canada. The original annual capacity of 70 000 t/a has since been increased to ca. 100 000 t/a [115].

The Noranda reactor is a rotatable horizontal cylinder up to 21 m long with a diameter of ca. 5 m and lined with chrome–magnesite bricks. Its longitudinal section is shown in Figure 8.19. In normal operation the vessel remains stationary with 50–60 tuyères on a level with the molten matte. If the process is interrupted, the reactor must be revolved to raise the tuyères.

The furnace is continuously charged at one end with pellets consisting of wet sulfide concentrates ($\leq 10\%$ H₂O), silica flux, and pulverized coal. The slag is very viscous as a result of the high percentage of magnetite (20–30%) and contains 10–15% copper because liquid matte and slag move in unflow, the copper content in both phases increasing during the reaction. The slag is decopperized by flotation. The slag concentrates containing 50–55% Cu are returned to the reactor as additional feed with all flue dusts. The tailings (ca. 0.5% Cu) are discarded. Blister copper collects as a third liquid layer in the lowest part of the reactor.

The burners at both ends of the reactor are fed by gas or oil and oxygen-enriched air. The SO₂ content of flue gas is between 8 and 15 vol%, depending on the oxygen content of the combustion air and the fuel quantity.

Apart from the advantages of continuous and partially autogenous operation, the Noranda process suffers several disadvantages in its original mode:

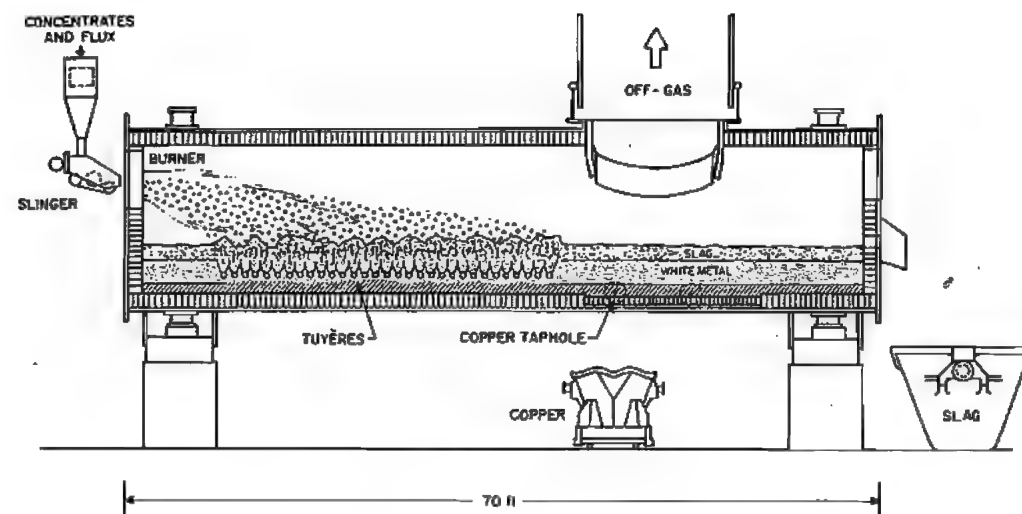


Figure 8.19: Noranda Process prototype reactor [116].

- High copper content in the slag
- High sulfur content in the blister copper (1–2%, only ca. 0.1% in batch converting)
- Large amounts of such impurities as arsenic, antimony, and bismuth in blister copper if dirty concentrates are charged

The isolated steps of conventional methods are better suited for treating ores with high levels of impurities. Therefore, the blister mode of the Noranda process was replaced by the matte mode to produce white metal, which is converted to blister copper in P–S converters. The copper content of the Noranda slag is cut in half. Table 8.16 shows the distribution of impurities in the intermediate products starting with a concentrate containing 25% Cu, 29% Fe, and 32% S.

In 1978, the Utah Copper Division of Kennecott Copper Corp. started three Noranda reactors in its Garfield smelter in Utah, United States.

8.5.8.3 Other Processes

WORCRA Process. The acronym comes from the inventor (H. K. Worner) and the company (Conzinc Rio-Tinto of Australia). In a pilot plant at Port Kembla, New South Wales, the process was demonstrated in 1968 and at-

tained a capacity of ca. 8000 t of blister copper per year. In spite of initial progress, the method was not technically successful, and the tests were dropped. However, reports in the literature [118] imply that the principle may be revived.

The process differs from the Noranda process in that the stationary furnace is U-shaped, dried concentrates are charged, and the liquid matte and slag flow in a countercurrent. The slag contains only ca. 0.5% Cu and needs no subsequent treatment. The energy consumption and the required space are greater. The principal problem was the rapid deterioration of the injection lances, which are immersed in the molten slag.

Q–S Process. A method invented by P. E. Queneau and R. Schuhmann, Jr. [119] and under development since 1981 for the extraction of lead from sulfide concentrates in a pilot plant at Berzelius Metallhütten GmbH, Duisburg, Germany, is to be tested for the production of blister copper or white metal. The Q–S reactor is similar to the Noranda design with a rotating nearly cylindrical vessel. The flow of molten matte and slag is countercurrent; thus, it produces a low-grade slag. The copper content of this slag is lowered to 0.2% Cu by a re-

ducing treatment with carbon monoxide in the same reactor, called deconverting.

KHD-Contop Process. Another recent project for the direct production of copper or lead from sulfide concentrates has been developed by KHD Humboldt Wedag AG, Köln (Cologne). The acronym Contop stands for continuous top-blowing process [120]. The process involves a series of steps in a stationary double-furnace system, each divided into several sections for different tasks. The concentrates and fluxes are continuously charged into a cyclone flash smelter resembling the KIVCET reactor, where the raw material reacts with pure oxygen at 1500–1700 °C. This heating, and slag fuming by top-blowing a mixture of pure oxygen and gaseous fuel through lances into the adjoining settling and slag cleaning reactor, remove most of the impurities by volatilization.

Thus the process provides relatively pure metal from dirty concentrates in one continuous operation. High-grade matte (75–80% Cu) flows into the second part of the reactor, which uses the HCCR process. The final product is fire-refined copper suitable for anode casting. The slag does not need posttreatment, and the off-gas can contain up to 20 vol% SO₂.

Two other proposals, the Britcosmaco process [121] of G. J. Brittingham, Australia, and the BM Autogenous process [122] of the U.S. Bureau of Mines, require special stationary furnaces in which molten matte and slag flow in a countercurrent. Tests of these processes have been discontinued.

8.5.9 Recovery of Copper from Secondary Materials

Copper is recovered from materials, including copper and copper-alloy scrap, as well as substances that contain oxidized copper, such as slag, flue dust, dross, ash, residue, and sludge.

New scrap (fabricating waste) can be recycled to the appropriate melting and casting plant. Old scrap (used copper), however, must be sorted and sampled to select the most suitable sequence of recovery operations in a smelter or refinery. The recovery of metals from copper alloys is complicated because of separation problems. In practice, pyrometallurgical treatments employing a blast furnace and converter are preferred.

Converter-Blast Furnace Method. The original so-called Knudsen process was patented in 1915 and its variants became the conventional method. Copper-alloy scrap, such as brass, bronze, gunmetal, and nickel alloys, is melted in small converters with coke and iron scrap (but no silica) during air blowing. The iron performs the three functions of reducing agent, fuel, and component for slag formation. Iron also minimizes the oxidation of copper and, thus, lowers the copper content of the nevertheless copper-rich slag. Unlike the large matte converter, the scrap converter operates under reducing conditions above the molten bath [123].

Table 8.16: Noranda process: distribution of accompanying elements in the material flow [117].

Element	Mode of operation								
	Converting to matte with atmospheric air			Converting to blister copper with atmospheric air			Converting to blister copper with O ₂ -enriched air (30 vol% O ₂)		
	Off-gas (flue dust)	Reactor slag	Matte (70% Cu)	Off-gas (flue dust)	Reactor slag	Blister copper	Off-gas (flue dust)	Reactor slag	Blister copper
Lead	74	13	13	24	74	2	21	77	2
Zinc	27	67	6	21	78.9	0.1	14	85.8	0.2
Cadmium	—	—	—	95.5	4	0.5	95	4.5	0.5
Arsenic	85	7	8	19	27	54	39	14	47
Antimony	57	28	15	29	36	35	18	52	30
Bismuth	70	21	9	52	30	18	43	42	15
Selenium	—	—	—	78	7	15	60	21	19

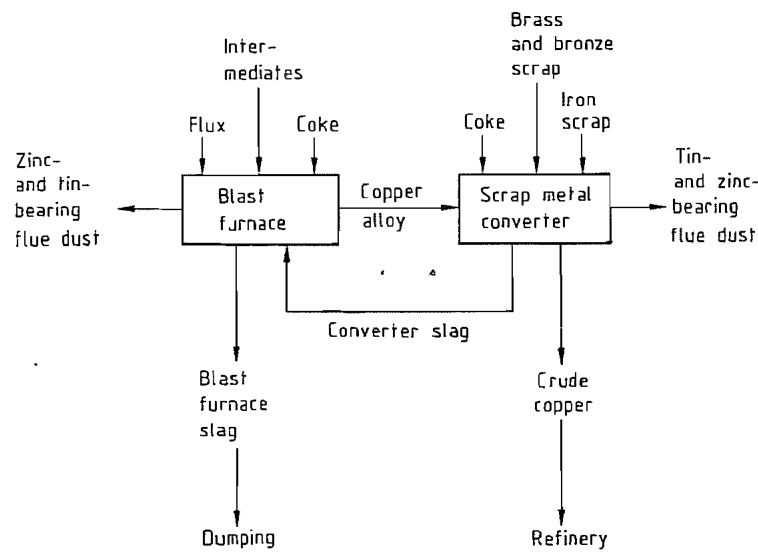


Figure 8.20: Converter-blast furnace method: scheme for the recovery of copper from scrap [123].

Zinc and tin are volatilized as zinc vapor and SnO and burn in the converter hood to ZnO and SnO₂. Lead is also oxidized, and the PbO is partly volatilized and partly collected in the slag. The volatile compounds collect in flue dust, from which they are recovered.

Crude copper in the converter contains some impurities and must be retained. The copper-rich slag must be processed by reducing blast furnace smelting to yield black copper (Figure 8.20).

Blast Furnace-Converter Method. The reversed process is well-suited for smelting oxidized secondary materials [124]. This method of processing brass scrap produces zinc oxide, which is utilized as a raw material for zinc white or zinc metal. Bronze and gunmetal scrap yield mixtures of oxides from which tin lead solder is made.

The treatment of nickel alloys (e.g., German silver, a Cu–Ni–Zn alloy) is difficult because of the tendency of nickel to form slag. Methods have been developed that let the nickel pass into the electrolyte during copper electrolysis (see Chapter 12).

Summary. There is no satisfactory general method for the processing of alloy scrap despite many proposals [125–129]. Secondary

metal reserves are becoming increasingly important, as are processes for the recovery of metals from them [130–131].

8.5.10 Hydrometallurgical Extraction

Most “new” hydrometallurgical methods are derived from well-known reactions of analytical chemistry. While pyrometallurgical processes readily handle raw materials of variable composition, hydrometallurgical methods have advantages of specific adaptability and high selectivity. They are particularly suitable for processing low-copper-content oxidized or combined oxide-sulfide copper ores, dump stocks, residues, or intermediate products.

Disadvantages are the relative slowness of leaching, the large volume of solution per unit mass of copper, and the complicated extraction of precious metals that remain in the leaching residues. Another problem is the removal of sulfur from sulfide ores. Although sulfur dioxide is not generated, dilute solutions containing sulfate ion, which must be precipitated as gypsum to avoid water pollution, are formed. Newer developments are aimed at direct separation as elemental sulfur.

Currently, ca. 15% of the primary world copper is produced by hydrometallurgical extraction. The main products are electrowon pure copper and crude cement copper.

8.5.10.1 Principles

The following is only a brief survey of hydrometallurgical processes; details are to be found in the literature, e.g., [132–133].

Basic Process Steps. Hydrometallurgical processes can generally be subdivided into the following steps:

- Pretreatment, physical (e.g., comminution) or chemical (e.g., roasting)
- Leaching, chiefly with sulfuric acid or ammoniacal solutions, sometimes under oxidizing conditions
- Solution purification, e.g., by precipitation of impurities and filtration or selective enrichment of copper by solvent extraction or ion exchange
- Separation, precipitation of copper metal or copper compounds such as Cu_2O , CuS , CuCl , CuI , CuCN , or $\text{CuSO}_4 \cdot 5\text{H}_2\text{O}$ (crystallization)
- Posttreatment, e.g., fire-refining of crude cement copper or thermal reduction of copper compounds

Leaching. In copper production, leaching is used in a number of ways:

- In situ leaching, applied in loose ore bodies
- Dump or heap leaching of lumpy material
- Vat or percolation leaching of small-sized material
- Agitation or slime leaching of fine-grade material without pressure
- Pressure leaching of fine-grade material or without oxygen

In practice, only a few proven chemicals, *lixiviants*, are used:

- Dilute sulfuric acid, suitable for leaching oxidized copper ore such as oxides, basic carbonates and sulfates, and silicates
- Solutions of iron (III) salts, especially iron(III) sulfate, as oxidizing agents in sul-

furic acid if sulfide copper minerals are also present

- Ammoniacal solutions of ammonium salts, especially ammonium carbonate for oxidized ores, as well as for native copper if the accompanying gangue is soluble in acids

Other lixiviants have been proposed and occasionally used, e.g., hydrochloric acid, nitric acid, concentrated sulfuric acid, and solutions of iron(III) chloride, copper(II) chloride, or dichromates. In pressure leaching of sulfide ores, oxygen is advantageously applied to oxidize the sulfide to sulfate or elemental sulfur. Economic aspects are decisive for the choice of a lixiviant.

A recent development is the *bacteria-assisted leaching* of low-grade copper ores and industrial wastes. Certain autotrophic bacteria accelerate the oxidation of copper and iron sulfides. Typical species are *Thiobacillus thiooxidans*, which oxidizes sulfide to sulfate, and *Thiobacillus ferrooxidans*, which oxidizes iron(II) to iron(III). The $\text{Fe(II)} \rightarrow \text{Fe(III)}$ reaction takes place slowly in atmospheric oxygen, but the bacteria catalyze it.

The reaction rate depends on the living conditions of the bacteria. Bacterial leaching of sulfide copper ores is carried out at temperatures between 25 and 40 °C, pH (sulfuric acid) of 1.5–3.5, a definite concentration of metal ions, access to oxygen, and no direct exposure to sunlight.

Currently, species of bacteria can be developed and cultured for the performance of specific tasks. It seems likely that such biotechnological methods may assume increased importance because of their lack of environmental problems and their low energy consumption [134–135].

Solvent or Liquid-Liquid Extraction [136–137]. The solvent extraction of dilute copper solutions from leaching processes concentrates copper and eliminates impurities. This operation is based on the immiscibility of liquid aqueous and organic phases, with a high solubility of copper, but not of impurities, in the organic phase.

The solvent extraction process comprises two steps: selective extraction of copper from an aqueous leach solution into an organic phase (extraction circuit) and the reextraction or stripping of the copper into dilute sulfuric acid to give a solution suitable for electrowinning (stripping circuit).

There are two important groups of proven organic chemicals for solvent extraction: LIX types (Henkel Corporation, formerly General Mills Chemicals, United States) and KELEX types (Ashland Chemical, United States). The improved selectivity of newly developed reagents has increased the importance of solvent extraction.

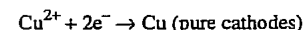
Ion Exchange [138]. Resins for selective absorption of copper have been used only in special cases, e.g., for recovery of dissolved metals from electroplating wastewater [139].

Cementation. The reduction and precipitation of copper from dilute sulfuric acid leach solutions by iron is the oldest hydrometallurgical method. In practice, iron scrap, if possible sheet iron, or sponge iron produced by reduction of iron oxides so that a large surface area is available, is used. The precipitation is carried out in vessels such as launders, cells, tanks, and special cone precipitators [140].

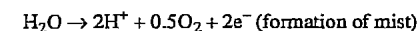
The precipitate, cement copper, is an impure copper, from ca. 60% to >90% Cu. Further treatment is usually by a pyrometallurgical process. Relatively pure cement copper can be used as a raw material for the production of copper sulfate.

Electrowinning [141]. The electrolytic deposition of copper from its solutions differs from the electrolytic refining process in two important ways: the use of insoluble anodes instead of soluble ones and, consequently, much higher voltage (ca. 2–2.4 V), with a resultant power consumption of 2000–2600 kWh t^{-1} .

The cathodic half-reaction is the same as in electrolytic refining:



The anodic half-reaction results in the generation of oxygen and hydrogen ions:



The reformed acid is returned to the leaching or the extraction circuit. Because of the insolubility of anodes, anode slime does not form.

Various types of anodes have been developed [142], e.g.:

- Lead-antimony (hard lead) anodes, the conventional type
- Chiles ex anodes (copper-silicon alloy), an older development from Chuquicamata, Chile
- Titanium anodes—a new type—coated with a layer containing platinum metals to decrease the high overpotential of oxygen

The use of titanium avoids the disadvantages of lead anodes. Titanium anodes have high corrosion resistance, do not contaminate copper cathodes with lead, and save energy because of the lower oxygen overpotential.

In this way, the current efficiency (usually 80–90%) can be improved. Impurities from anodes and from the electrolyte lead to higher energy consumption, secondary redox reactions, and the necessity for keeping the current density below 200 A/m^2 . Newer developments allow the use of high current densities [143].

The electrolyte can be obtained in two ways. High-value pregnant copper solutions (containing 30–40 g/L) from agitation and pressure leaching are suitable for direct electrowinning after solution cleaning. Low-value pregnant copper solutions (containing < 10 g/L) from in situ, dump, heap, and vat leaching must be enriched and cleaned by solvent extraction.

Electrowinning plants are constructed, equipped, and operated like electrolytic refineries. Their production capacity, however, is relatively small, apart from one exception in Zambia. Several plants exist in the United States, Chile, Peru, Zambia, and Zaire.

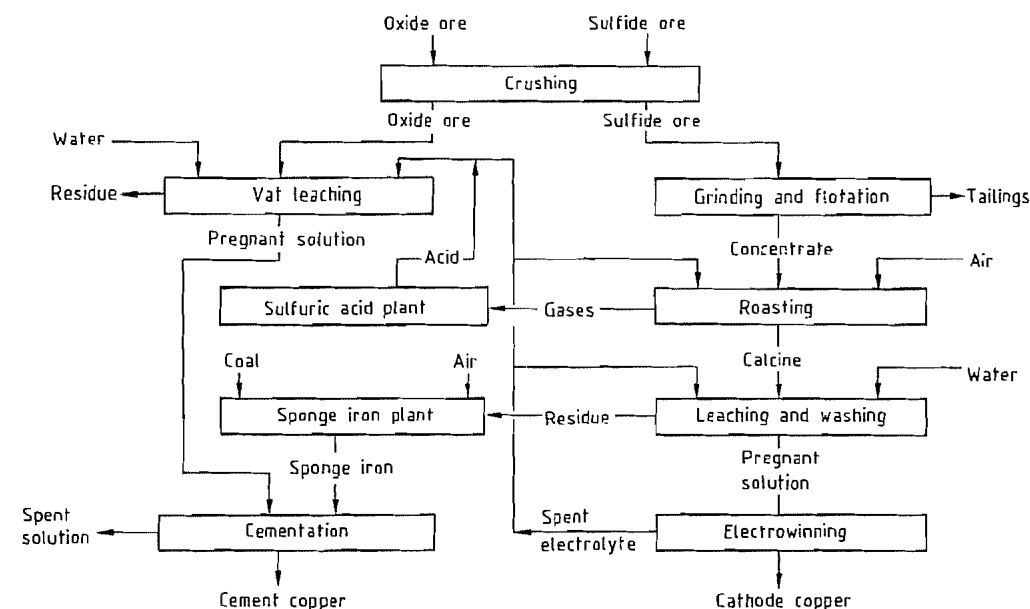


Figure 8.21: Typical flow sheet for hydrometallurgical copper production from ores [145].

Precipitation by Reducing Gases. A third way to precipitate copper from dilute solutions is reduction with gases under pressure at high temperature, usually with hydrogen, to produce metal powder. However, there is no commercial production of copper powder by this technique [144].

8.5.10.2 Processes

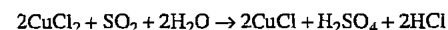
Of the great number of proposed hydrometallurgical methods, only a few have found their way into industrial practice (Figure 8.21). Numerous examples of proven and unproven processes can be found in the literature [145–147].

Processing of Oxidic Copper Ores. The most widespread method, used for many decades at Chuquibambilla, Chile, involves leaching of oxidized ores, such as copper subcarbonates, subsulfates, and silicates, in dilute sulfuric acid and the separation of metallic copper by cementation with scrap iron or by electrowinning.

A new example is the technique of the large copper oxide processing plant of the Anamax

Mining Co. at Twin Buttes, Arizona, which was started up 1975 [148]. This operation comprises ore leaching in dilute sulfuric acid, solvent extraction, and electrowinning. This succession of process steps has proven to be an advantageous combination.

Chlorine-containing oxidic ores, such as atacamite, are treated at Mantos Blancos, Chile [149], by leaching with a mixture of sulfuric and hydrochloric acids to produce a solution of copper(II) chloride, from which copper(I) chloride is precipitated by reduction with sulfur dioxide. The acid mixture is regenerated:



Refined copper is obtained from the precipitate pyrometallurgically.

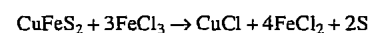
Processing of Sulfide Copper Ores. There are numerous possibilities for treating sulfide ore concentrates by hydrometallurgical methods, with or without pretreatment by roasting. The following examples of commercial processes are arranged according to the final state of sulfur (sulfur dioxide; sulfates, including

thiosulfates and dithionates, or elemental sulfur).

One of the oldest methods is the *RLE process* [145], which involves roasting, leaching, and electrowinning. After roasting concentrates in fluidized-bed reactors and generating sulfur dioxide, the calcines are leached with sulfuric acid spent electrolyte, and pure copper is separated by electrowinning. This process, developed by Hecla Mining Co., was applied at Lakeshore Mine, Arizona, and later at Chambishi, Zambia and Shituru, Zaire.

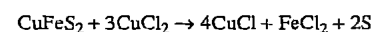
The *Arbiter process* [150] of the Anaconda Copper Co. uses countercurrent leaching of concentrates with ammonia solution under an oxygen atmosphere at low pressure and low temperature. Copper is produced by solvent extraction and electrowinning. The sulfur is recovered as ammonium sulfate, or the ammonia can be regenerated.

The *Cymet process* [151], based on recovering elemental sulfur, has been developed by the Cyprus Mines Corp. and has undergone some variations, such as combination with anodic dissolution of chalcopryrite. A preferred technique consists of leaching concentrates with an iron(III) and copper(II) chloride solution and separating solid copper(I) chloride:



The intermediate copper(I) chloride is reduced to metallic copper with hydrogen in a fluidized-bed reactor.

Another chloride leaching operation is the *CLEAR* (copper leaching, extraction, and refining) process [152], developed by the Duval Corp. at their plant in Sieritta, Arizona. The concentrate is treated with boiling copper(II) chloride solution:



A high concentration of sodium chloride is maintained to keep copper(I) in solution as a complex. Coarse copper powder is produced by electrolyzing the purified solution.

8.6 Refining

Conventional refining comprises three stages: (1) pyrometallurgical or fire refining, (2) electrolytic refining, and (3) remelting of cathodes and casting of shapes. Refining without electrolysis is adequate if the fire-refined copper has the necessary purity and if the content of precious metals can be neglected. Extremely high-purity copper is occasionally needed for research purposes; in such cases, zone melting or repeated electrolysis of cathodes is used.

8.6.1 Pyrometallurgical

Fire refining is applied to crude copper such as blister copper from converters (97–99% Cu), black copper from blast furnaces (ca. 90–95% Cu), cement copper from hydrometallurgical operations (85–90% Cu), anode scrap from electrolytic refining, and high-grade copper scrap, chiefly unalloyed wire scrap.

The refining of molten copper to anode copper for electrolysis or commercial fire-refined copper has the following functions:

- Removing impurities by slagging and volatilization with the precious metals remaining entirely in the metallic copper
- Reducing the sulfur content to ca. 0.003% by oxidation
- Decreasing the oxygen content to < 0.1% by reduction (poling) to get a flat surface as a result of the water–gas equilibrium in molten copper

8.6.1.1 Discontinuous Fire Refining

Two different furnace types are available for batch copper refining, the older reverberatory furnace and the more modern rotary furnace. The former, which resembles smaller reverbs for matte smelting from concentrates, has a capacity of 200–400 t of copper per charge and can be fed with molten or solid copper. Rotary furnaces hold up to 350 t of

molten metal per charge and are generally fed only with liquid copper. An extra melting furnace, e.g., anode shaft type, can be required for remelting of solid materials (scrap and anode rests).

Low-sulfur pulverized coal, fuel oil, natural gas, or reformed natural gas serve as fuel. The refractory lining consists of basic bricks, such as magnesite or the more spall-resistant chrome magnesite bricks.

After charging and possibly melting, oxidation and reduction stages are carried out in sequence. At the beginning of the oxidation period, air is blown into the melt, partly slagging and partly volatilizing the impurities. During this blowing step, a part of the copper is oxidized to copper(I) oxide, which dissolves in the liquid metal (Figure 8.22). If the content of Cu_2O in copper ca. 10% (corresponding to $\geq 1\%$ O), it acts as a selective oxidizing agent:

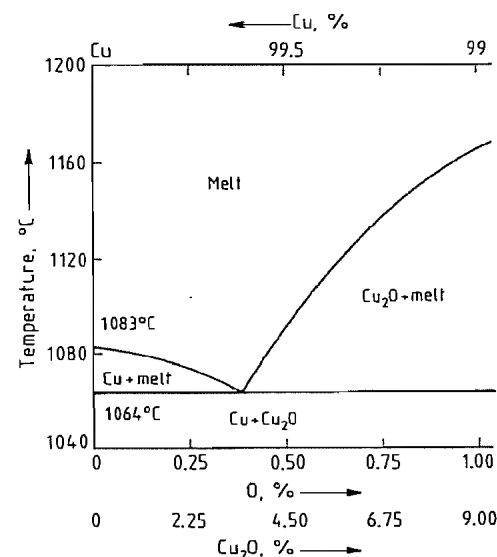
$$\text{Cu}_2\text{S} + 2\text{Cu}_2\text{O} \rightarrow 6\text{Cu} + \text{SO}_2$$


Figure 8.22: Partial phase diagram of the Cu- Cu_2O system.

In practice, large amounts of SO_2 are generated so that this final stage of the oxidation period is termed boiling. Reduction of the sulfur content limits SO_2 blisters in the solid copper.

The subsequent poling with wood is a centuries-old method that is still employed in

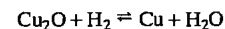
older reverb plants. Large tree trunks (poles) of beech, birch, eucalyptus, etc. are plunged under the surface of the melt to generate reducing gases and steam by dry distillation of the wood. The escaping gas mixture reacts with copper(I) oxide and mixes the molten bath [1, p. 441; 2, p. 392].

This awkward operation has been largely displaced by gas poling [153] in rotary furnaces: natural gas (CH_4), reformed gas (CO , H_2 , and N_2), propane, or ammonia [154] is blown into the copper melt through tuyères. This new process has been introduced at several large smelters in North America, Europe and Japan.

The poling operation proceeds in two steps. During tight poling, the remaining sulfur dioxide from copper(I) sulfide is almost entirely flushed out by the escaping gas a sample of liquid copper at the end of this stage solidifying without blisters or cavities. Next comes the poling tough pitch, which is necessary to reduce the copper(I) oxide and achieve the required low oxygen content. High Cu_2O content in the solidified metal causes brittleness and decreased strength; moreover Cu_2O disproportionates to copper metal and cupric ions in sulfuric acid electrolytes which disturbs the electrolytic refining operation.

The final oxygen content in fire-refined tough-pitch copper must be 0.02–0.05%; for anodes it can be 0.05–0.3%. The fire-refining process can be understood from the Cu-O system [155] (see Figure 8.22); the system Cu-O-S is important in the oxidation period (see Figure 8.5) and the Cu-H-O system for the reduction or poling period.

When a copper melt solidifies, a shrinkage of ca. 5 vol% occurs, but a flat surface can be achieved by careful control of the equilibrium



The steam of micropores can compensate the volume difference and a flat set cast is obtained.

Surface and fracture of small samples of solidified copper from the molten bath are observed during the refining process to ascertain the current state. Recently it has become pos-

sible to measure the oxygen content of the copper melt potentiometrically.

A special problem is the extremely high copper content (up to ca. 40% Cu, chiefly as Cu_2O) in refining slags. Such products are treated as high-grade oxidized copper ores.

8.6.1.2 Continuous Fire Refining

As in converting processes, the development of continuous pyrometallurgical refining has begun.

HCCR Process [156]. In the HCCR (Humboldt continuous copper refining) process, a special stationary top-blown furnace accomplishes the following functions in three sections:

- Charging or melting of solid or liquid crude copper in the first chamber
- Oxidizing the flowing copper melt by oxygen in the second chamber
- Deoxidizing the metal by reducing gases such as methane or propane in the third chamber.

All gases are blown through lances as supersonic jets onto the surface of the melt.

Contimelt Process [157]. A two-stage process for copper melting and refining was developed in 1968 by Norddeutsche Affinerie at Hamburg, in cooperation with Metallurgie Hoboken-Overpelt in Olen, Belgium. The first stage began operation in 1979, and the complete process has been operated since 1982 on a commercial scale. The continuous operations are performed successively in two units connected by launders. First is the anode shaft furnace, where charging, melting, and oxidation of crude copper take place. Second is the small drum-type furnace, where poling and casting of anodes are carried out. The oxygen content of copper from the anode shaft furnace averages 0.6%, with 0.15% after poling. A feature of the shaft furnace is the additional equipment with oxygen burners for regulating the composition of the furnace atmosphere and the overheating of copper. In comparison with conventional fire refining, the Contimelt

process provides savings in energy and labor. Increased throughput to 100 t/h is planned.

8.6.1.3 Casting of Anodes

The conventional method of producing anodes is the discontinuous casting on casting wheel machines. The pure copper molds must be sprayed with a slurry that prevents the sticking of solidified anodes; baryte, alumina, or silica flour are suitable. (Calcium-containing material is not suitable because it forms gypsum, which is partially soluble in the electrolyte.) The casting rate can reach 80 t/h. The anode weights vary between 160 and 400 kg, depending on the refinery. Anodes from modern plants usually have the following dimensions: 0.9–1.1 m long; 0.9–1.0 m wide; and 3.5–5.0 cm thick. They weigh 300–400 kg. Economic considerations call for anodes of nearly the same weight within a plant; therefore, discontinuous casting is best controlled by electronic systems.

Contilanol Process. A recent development produces uniform anodes by using the continuous Hazelett twin-belt casting system. A special method developed by Metallurgie Hoboken-Overpelt in Olen, Belgium, in cooperation with Norddeutsche Affinerie in Hamburg, is called the Contilanol process [158]. The continuous cast strip of anode copper formed between two belts and damblock chains is 1 m wide and 1.5–6 cm thick; special cutting equipment separates the strip into individual anodes 1 m long. Some refining plants use the new method, e.g., White Pine, Michigan, United States; Onahama, Japan.

8.6.2 Electrolytic

About 80% of the world copper production is refined by electrolysis. This treatment yields copper with high electrical conductivity and provides for separation of valuable impurities, especially the precious metals.

The basic patent for galvanic deposition of metals was awarded to J. B. Elkington in 1865. The most important technical problems were solved by E. Wohlwill at the Norddeut-

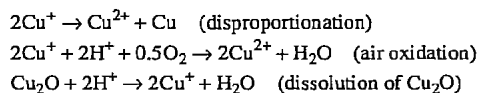
sche Affinerie in Hamburg, Germany, in 1876, and this method has been used ever since. The first electrolytic copper refinery in the United States was operated from 1883 to 1918 by the Balbach Smelting and Refining Co., Newark, New Jersey.

8.6.2.1 Principles [159–160]

Several possible half-reactions can occur at the electrodes.

Anode reactions	Cathode reactions	Standard electrode potential E^0 (25 °C), V
$\text{Cu} \rightarrow \text{Cu}^{2+} + 2e^-$	$\text{Cu}^{2+} + 2e^- \rightarrow \text{Cu}$	0.337
$\text{Cu} \rightarrow \text{Cu}^+ + e^-$	$\text{Cu}^+ + e^- \rightarrow \text{Cu}$	0.521
$\text{Cu}^+ \rightarrow \text{Cu}^{2+} + e^-$	$\text{Cu}^{2+} + e^- \rightarrow \text{Cu}^+$	0.153

Secondary reactions occur in the electrolyte:



Oxidation by air and disproportionation of copper(I) ions yield a surplus of copper(II) ions in the electrolyte. The copper metal powder formed by the disproportionation of Cu^+ contributes to the accumulation of the anode slime.

The electrochemical equivalent of copper depends on the oxidation state of the copper:

Species	$\text{g A}^{-1} \text{h}^{-1}$	mg/L
Cu^{2+}	1.185	0.3294
Cu^+	2.371	0.6588

The greater electrochemical equivalent of copper(I) suggests the use of solutions of copper(I) ions instead of copper(II) ions. However, this concept has not been put into practice because of enormous industrial difficulties [161].

The two most important electrical parameters in electrolytic copper refining operations are the cell voltage and the current density. The cell voltage, which usually ranges between 0.25 and 0.3 V, is determined by several factors:

- Ohmic resistance of the electrolyte, depending on composition, temperature, electrode distance, and cell construction
- Polarization, especially concentration polarization of electrodes, which depends on the rate of electrolyte circulation
- Overpotential because of organic additives (e.g., an inhibitor for achieving uniform electrocrystallization of copper)
- Voltage loss in the circuit
- Anode passivity, which may occur at high current densities

The interaction of these effects is difficult to predict. At any particular electrolytic facility, a continuing effort is made to optimize parameters the cell voltage. The voltage loss in the conductors and contacts is minimized by good plant design and use of special contacts (Baltimore grooves, Whitehead contacts, wet contacts, etc.).

The second important parameter is the cathodic current density, which is 180–280 A/m^2 in conventional electrolytic copper refining. With increasing current density the production of copper increases and the current efficiency decreases because the cathode potential depends on the current density.

Impurities. The behavior of impurities depends on their position in the electrochemical series: elements more electropositive than copper are insoluble, while less electropositive ones dissolve in or react with the electrolyte. For that reason, the anode material is distributed by electrolysis among three phases: cathode copper, electrolyte, and anode slime (Table 8.17) [162].

Copper Cathodes. Cathode copper is produced currently in a purity between 99.97 and 99.99%. Silver can be deposited in traces; however, this can be avoided by precipitating the silver from the electrolyte with chloride ion. Other impurities, such as suspended slime or droplets of the electrolyte, may be mechanically occluded. The following measures are taken to produce copper of high purity:

- Maintenance of the optimum current density, to prevent cathodic deposition of other elements (e.g., arsenic)
- Addition of organic inhibitors to avoid the formation of nodules on the cathode surface
- Removal of impurities such as arsenic, antimony, and bismuth from the electrolyte by adsorption or chemisorption
- Prevention or elimination of suspended slimes by regulating the electrolyte flow and occasionally filtering it.

Table 8.17: Electrolytic copper refining: distribution of elements in cathodes and electrolyte [162].

	Anode, % ^a	Cathode, ppm [*]	Electrolyte, g/L
Cu	99.5	99.99%	45
Au	25.5 ppm	0.1	
Ag	399 ppm	5.0	
Pb	0.076	1.3	
Zn	0.001	0.3	0.43
Fe	0.025	2.4	0.92
Ni	0.070	0.7	16
Se	0.030	0.4	
Te	0.006	0.3	
As	0.044	0.4	3.58
Sb	0.011	0.8	0.34
Bi	0.006	0.3	0.1
Sn	0.002	0.4	0.001
S	0.007	4	
Insolubles	0.020	—	
H_2SO_4	—	—	200

^a Unless otherwise stated.

Electrolyte. The composition of copper electrolytes from various plants is generally similar: ca. 35–45 g of copper and 150–220 g of sulfuric acid per liter at an operating temperature of 55–65 °C (see Table 8.17). As a result of secondary reactions during electrolysis, the concentration of copper(II) ions increases slowly; therefore, this copper surplus must be recovered by cathodic deposition in a few (ca. 2%) liberator cells equipped with insoluble anodes, usually of antimonial lead. Soluble impurities, such as iron, cobalt, zinc, manganese, most of the nickel, and some arsenic and antimony, are also enriched in the electrolyte.

The upper limits of impurity content are ca 10 g/L for arsenic and 20–25 g/L for nickel. Part of the electrolyte is withdrawn continuously from the circuit for purification, and the volume is compensated by adding sulfuric

acid and cathode wash water. There are two methods of purification. In the first, the solution can be completely decopperized in a system of special liberator cells with insoluble anodes; arsenic and antimony are almost completely deposited and returned to pyrometallurgical operations. The electrolyte is then concentrated by vacuum evaporation to yield concentrated sulfuric acid and crude nickel sulfate, from which pure nickel sulfate or nickel metal can be produced.

The second method of purification is by producing copper sulfate. For this purpose, the sulfuric acid is usually neutralized by addition of copper shot in the presence of air. The copper sulfate is obtained by crystallization, and the mother liquor is cemented with iron scrap.

Anode Slimes [163–164]. The content of insoluble substances is < 1% of the anode weight, and they collect on the bottom of cells as anode slime. They contain precious metals (silver, gold, and platinum); selenides and tellurides of copper and silver; lead sulfate; stannic [tin(IV)] oxide hydrate; and complex compounds of arsenic, antimony, and bismuth (the undesired floating slimes). The main component is copper. In addition, gypsum and silica, alumina, or baryte from anode casting are present.

The distribution of the elements (in %) varies over wide ranges:

copper	20–50
nickel	0.5–2
lead	5–10
arsenic	0.5–5
antimony	0.5–5
bismuth	0.5–2
selenium	5–20
tellurium	1–4
silver	≤ 25
gold	≤ 4

Although the separation techniques differ greatly from plant to plant, anode slimes are generally treated as follows:

- Oxidizing leaching of copper with dilute sulfuric acid
- Recovery of selenium and tellurium by pyrometallurgical or hydrometallurgical methods

- Removal of detrimental elements and production of silver alloy (Doré bullion)
- Separation of precious metals by electrolysis (silver and gold) and fractional precipitation (platinum metals)

The greatest part of the world selenium production comes from processing copper anode slimes.

8.6.2.2 Practice [165–167]

Figure 8.23 gives a schematic flowsheet of a conventional plant. A modern example is the Amarillo, Texas, plant of ASARCO [169] with a capacity of 420 000 t/a, the second largest plant in the world, constructed in 1973–1975.

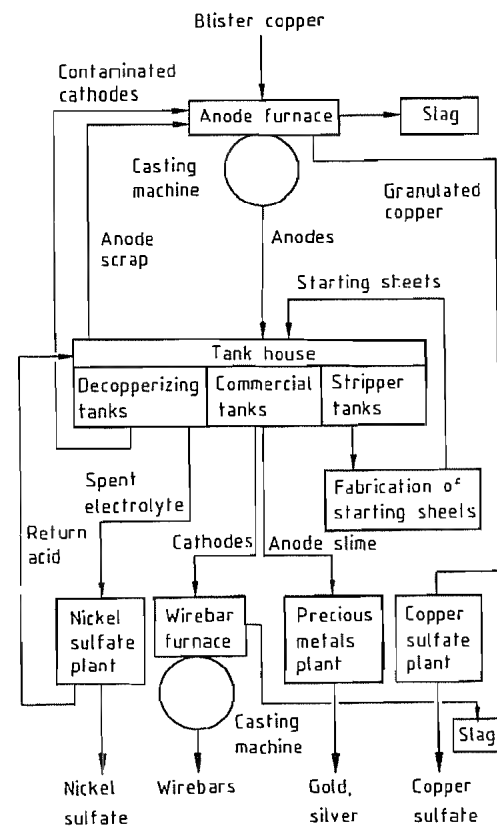


Figure 8.23: Flow sheet for electrolytic refining of copper [168].

Cells and Cell operation. The cells or electrolytic tanks are generally constructed of reinforced concrete lined with antimonial lead sheet or a plastic such as hard poly(vinyl chloride). The cells are rectangular, ca. 3.5–5 m long, 0.8–1.2 m wide, and 1.2–1.5 m deep.

Copper anodes and starting sheet cathodes are suspended alternately in the cells with precise spacing. Commercial cells contain between 30 and 50 electrodes of each type. The distance between the surfaces of two adjacent electrodes should be small (ca. 2 cm) to avoid voltage loss, but not so small that the deposited copper is contaminated with anode slime.

The anodes remain in the cell for 20–28 d, the anode life. During this time the cathodes are usually changed twice so that their weight is only 60–160 kg. The anode scrap, ca. 15 % of the total anode mass, is returned to fire refining.

Stripper tank groups for producing starting sheets are in a special section of the tank house. A stripper tank contains copper anodes and stripper blanks (cold-rolled copper plates) as cathodes. Copper is electrodeposited on the surface of these blanks and forms a metallic layer < 1 mm thick in 1 d. The stripper blanks must be swabbed with a film of mineral oil to make it possible to strip off the thin copper sheets from which the final starting sheets are fabricated. Techniques have been developed for separating copper sheets from copper blanks and also for fabricating the final starting sheets. The starting sheet preparation machine constructed by the Swedish company Wennberg [170] is one example.

In recent years, the copper stripper have been slowly replaced by titanium blanks [171], which offer the advantages of not requiring lubrication with oil, easy separation of the metals, providing a smoother surface of the deposited copper sheet, and excellent corrosion resistance. The higher price of titanium is a disadvantage.

Electrical System. The energy consumption per tonne of copper ranges from 220 to 280 kWh in conventional plants; the current efficiency is between 92 and 98 %. Short circuits,

caused primarily by faulty suspension of starting sheets, decrease the output of cathodes. Short circuits are frequently or continuously monitored by checking for a temperature increase with infrared scanning or older electrical and magnetic methods.

Two electrical connection systems have been developed, the multiple system and the series system. In the series system the electrodes are connected in series, each acting as an anode on one side and a cathode on the other. This system is no longer used commercially, but the combination of this connection with high current density shows promise [172].

The multiple system is employed exclusively in 70 large refineries. The anodes and the cathodes within one cell are connected in parallel, and a group of such cells are connected in series. Each cell usually has 30–50 anodes and the same number of cathodes.

The direct current is converted from alternating current by rectifiers; the older types have been largely replaced by silicon rectifiers.

Electrocrystallization [173]. The structure of an electrodeposited cathode surface can be influenced by adsorption of molecules on the crystallites. The addition of colloids or special organic compounds improves cathode quality by yielding an evenly grained copper deposition. Important surface-active additives, or inhibitors, are bone glue, gelatine, avitane A (sulfonated aliphatic hydrocarbons), goulac, or bindarene (sulfonated wood fibers). Effective substances with definite composition are thiourea and its derivatives and other sulfur-nitrogen compounds. These inhibitors, mostly in combination, are added to the electrolyte in extremely small amounts, although more is added at higher current density. Inhibitors increase the voltage and, therefore, the energy consumption.

New Developments. In addition to continuous casting of anodes by the Contilnod system and remelting of cathodes in the ASARCO shaft furnace, the following are innovations in operating techniques:

- Extensive mechanization of the handling and preparation of electrodes. Examples: Outokumpu Oy, Finland; Metallurgie Hoboken-Overpelt, Belgium; Onahama Smelting and Refining, Japan; and Phelps Dodge, United States [174].
- Jumbo tanks instead of conventional cells, first installed in 1972 at the Onahama plant in Japan [175]. The capacity of the new plant is nearly 100 000 t/a. Jumbo tanks with ca. 20 times the effective volume of usual cells, contain relatively light anodes (130 kg). Anode and cathode lives are the same, only 10 d; accordingly, the amount of anode scrap that must be returned to the anode furnace is increased 30 %. In contrast to the conventional process, the electrolyte flows parallel to the electrode surfaces, which are separated by only 10 mm. A newer jumbo tank installation is at the Timmins plant (Kidd Creek Mines), Northern Ontario, Canada.
- Higher current density (300–400 A/m²) for increased production capacity. A consequence is higher anodic and cathodic overpotentials because of anodic passivation and concentration polarization, with the resultant risk of cathodic impurities. These disadvantages can be overcome by use of periodic current reversal (PCR or PRC process) [176], developed by Kombinat G. Damjanow at Pirdov, Bulgaria. This innovation involves reversal of current flow for a few seconds every few minutes (e.g., 100 s forward and 5 s reverse). The procedure reduces overpotentials without deterioration in cathode quality. The switching is precisely controlled by equipment with thyristoformers. At present only a few refineries, e.g., in Japan and Austria (Brixlegg), employ the PCR process.
- The ISA system [177] introduced at the Townsville plant (Copper Refineries Pty.), Australia. The use of copper starting sheets has been eliminated by the use of permanent stainless steel starting sheets as cathodes. This decreases production time and cuts material costs. After 8–10 d, the copper deposit

is easily removed from the steel sheets, which are equipped with special plastic edge strips. The flat and stable sheets allow close spacing between the electrodes, thereby decreasing the electrical resistance in the cell and lowering the energy consumption. The ISA system is also used at the White Pine refinery, Michigan, United States.

8.6.3 Melting and Casting

Copper cathodes must be remelted and cast to shapes because the structure of copper formed by electrocrystallization is not suitable for working to semifinished products. Cathodes are remelted in several types of special furnaces that perform the tasks of melting, postrefining (if necessary), holding, and casting. Casting can be carried out by the older discontinuous methods or by modern continuous casting.

8.6.3.1 Remelting of Cathodes

There are various kinds of furnaces that use either fossil fuels (coal, coke, fuel oil, natural gas, or reformed natural gas) or electric energy:

- Small coke-fired crucible furnaces
- Gas- or oil-fired rotary furnaces
- Large hearth furnaces (reverbs)
- Electric-arc furnaces
- Low-frequency induction furnaces
- Cathode shaft furnaces (e.g., ASARCO type)

Copper ready for pouring must be nearly free of sulfur, at most 10–3% (10 ppm) S, because a higher content affects detrimentally the mechanical properties of the metal.

In practice, copper is treated in two ways:

- After melting cathodes with sulfur-containing fuels, the copper melt must be fire-refined like blister copper, by oxidation and poling. This is the case when hearth furnaces are employed for casting wire bars.

- Use of electric power or sulfur-free fuels allows the use of continuous units, such as induction or ASARCO furnaces.

The ASARCO shaft furnace, constructed by American Smelting and Refining Co. [178–179], has a cylindrical shaft consisting of a steel jacket with a brick lining. Cathodes are charged near the top, and the combustion gases ascend in countercurrent now from groups of burners; the liquid metal is collected in a holding furnace. Apart from its effectiveness and high productivity, a distinct advantage is the maintenance of a constant, slightly reducing atmosphere by automatic control. The largest types (1.8 m diameter and 8 m high) can have a throughput up to 80 t/h. Worldwide ca. 200 units are in operation.

8.6.3.2 Discontinuous Casting

The discontinuous casting of various shapes on horizontal casting wheels with open ingot molds, analogous to the casting of anodes, was formerly the most important casting method. It is being replaced by continuous casting processes.

The capacity of the largest casting wheels is nearly 100 t/h. They are usually operated in combination with large hearth furnaces holding up to 650 t of liquid copper. The molds consist of pure copper, usually sprayed with a bone ash slurry to avoid sticking. The major product is still the 90–136 kg horizontally cast wire bar [180], or occasionally ingots and ingot bars.

8.6.3.3 Continuous Casting

Since the end of World War II, several continuous casting methods have been developed. A comprehensive synopsis, including patents, has been published [181].

Continuous casting has several technological and economic advantages over the older casting processes, such as excellent surface quality, uniform grain structure without blisters and shrinkage cavities, and energy savings.

The principle is simple, but actual practice proved difficult. Molten copper flows continuously into a relatively short water-cooled chill, usually lined with graphite and open at both top and bottom. The solidifying metal itself forms the lower closure. The shape is steadily withdrawn by clamping rolls and cooled by spraying with water.

There are three main continuously cast shapes: circular billets with a diameter up to 500 mm (for extrusion presses or tube rolling mills), square bars, and rectangular cakes with cross sections up to 1200 × 200 mm (for rolling to sheets and strips). Seamless tubes and other hollow shapes are occasionally produced. Continuous casting shapes are automatically sawn off by flying saws when they reach the required lengths (up to 6 m). In semi-continuous casting, the process must be interrupted, but the shapes can be up to ca. 12 m long.

The kind of chill is generally independent of the furnace: the liquid metal stream free-

falls into the chill (e.g., Junghans system), or the less frequent fixed connection of chill with the furnace (e.g., ASARCO casting system).

Recent methods employ a joint moving in unison with the solidifying metal and a mold with traveling parts forming a gap of the required cross section. (An example is the Hazlett process employed for continuous casting of anodes. Such casting methods are particularly suitable for continuous production of shapes with a small cross section.

8.6.3.4 Continuous Rod Casting and Rolling

The continuous production of cast and rolled wire rod [182–183] involves considerable energy savings because the solidified hot metal can be rolled immediately. Several plants use such a direct process starting from molten electrolytic tough-pitch copper. Worldwide > 100 plants are in operation, using the following systems:

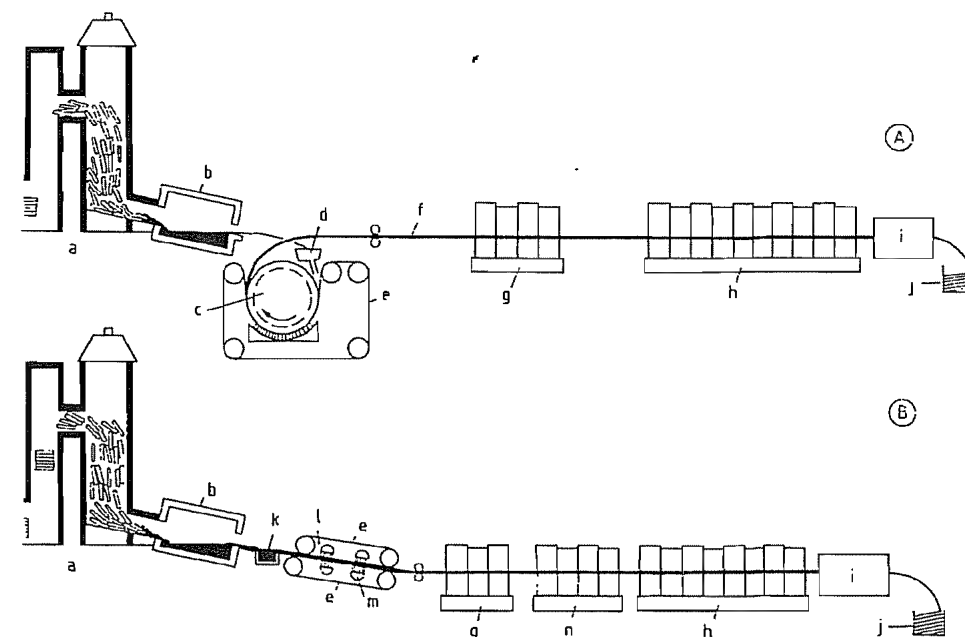


Figure 8.24: Scheme of continuous rod casting and rolling [186]. A) Southwire process; B) Contirod process. a) Melting furnace (ASARCO); b) Holding furnace; c) Wheel; d) Tundish; e) Steel band; f) Continuously cast copper bar; g) Preliminary rolling mill train; h) Finishing rolling mill train; i) Pickler; j) Coiler; k) Casting receptacle; l) Casting canal; m) Stationary edge dams; n) Middle rolling mill train.

- Properzi process [184]. The first continuous copper rod caster was constructed in 1960 following developments for other nonferrous metals. It operates on the wheel-belt casting principle, i.e., casting into the gap between the periphery of the casting wheel and the closing steel belt. About ten plants are in operation with a capacity up to 30 t/h.

- Southwire process [185]. Started in 1963 as a further development of the wheel-belt casting principle with capacity up to ca. 50 t/h. the Southwire process directly introduces the continuous cast bar into the rolling mill (Figure 8.24). After rolling, the rod, which is oxidized on the surface, is continuously treated by pickling with dilute sulfuric acid, water or steam rinsing, and wax coating. The saleable product (8–16 mm diameter) is formed into “coils” of up to 5 t, which are packaged. About 30 plants exist at present.

- Secor process [187]. Only two factories (Australia and Spain) use this modified wheel-belt casting concept, dating from 1975, with a capacity up to ca. 10 t/h.

- Contirod or Krupp-Hazelett process [188]. As a variant of the Hazelett twin-belt process similar to the Contilnod process (Section on Casting of Anodes), the continuous cast bar solidifies between two belts and damblock chains and is directly moved to the rolling mill (Figure 8.24). Metallurgie Hoboken-Overpelt, Belgium, developed this system in the 1960s; the capacity of the largest units is ca. 50 t/h. At present ca. 16 plants are operated.

- General Electric dip forming process [189]. A process based on the “candlestick” principle has been operated since about 1970. A copper core rod is pulled upward through liquid copper so that its diameter increases, the thickened rod moves immediately to rolling. Oxygen-free copper can be produced by using a reducing atmosphere. The capacity is ca 10 t/h. Nearly 20 plants exist at present.

- Outokumpu up-cast process [190]. A new upward casting system developed in 1969 draws copper upward through a vertical die cooler with a cooled graphite mouthpiece dipping into the melt. The caster, comprising 8 or 12 strands, yields oxygen-free copper at the rate of ca. 2 t/h per line. Because of the small cross section (8–25 mm diameter), hot rolling is not required. Approximately 20 plants are in operation.

8.6.4 Copper Powder

Copper and copper-alloy powders are required for products prepared by powder metallurgical techniques, including friction materials, carbon brushes, self-lubricating bronze bearings, special filters, and other sintered components.

The principal methods for producing copper powders are electrolytic deposition at high current densities and the atomization of molten metal, the latter more for copper-alloy powders. Copper powders are also formed by cementation or by pressured precipitation from aqueous solutions, but such precipitates are of little commercial interest.

Atomizing is done by spraying a melt into a pressured air or water flow. Various grain shapes are formed, depending on the cooling rate and on additives that change the surface tension. Additives that decrease surface tension, e.g., magnesium, form irregular powders; those that increase it, e.g., lead or phosphorus, yield globular particles. Spongy powders can be obtained by reduction of oxidized copper powders with hydrogen.

Electrolytically deposited powder particles have dendritic shape; a typical flow sheet is shown in Figure 8.25. For this purpose electrolysis is used as a shaping process rather than for refining because high-purity copper cathodes are the anodes. The main parameters of powder electrolysis are, as Figure 8.26 shows, the following [191]:

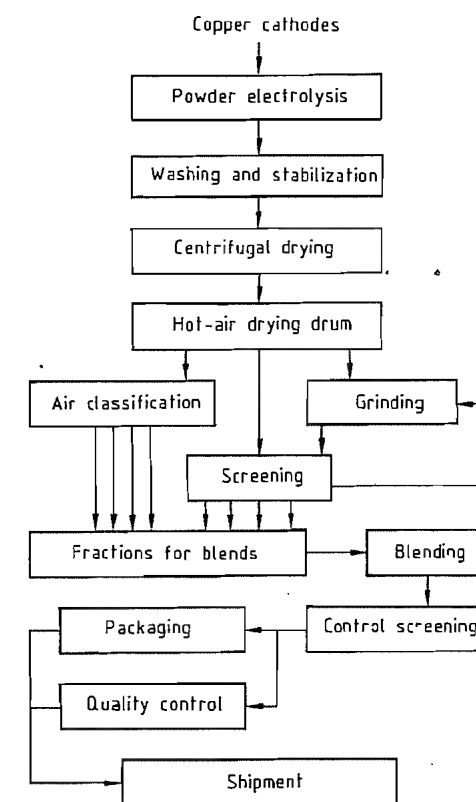


Figure 8.25: Flow sheet for electrolytic copper powder production [191].

- Cathodic current density
- Electrolyte temperature
- Concentration of copper(II) ions
- Concentration of chloride ions

Varying these reactors markedly change particle shapes and apparent densities.

Anodic and cathodic current densities differ. The former is normally 300–600 A/m², and the latter is 2000–4000 A/m², which is 10–20 times higher than the cathodic values in conventional electrolytic copper refining. This effect is obtained by using copper rod cathodes and platelike anodes. The energy consumption in powder electrolysis averages nearly 2 kWh/kg⁻¹. The powders are generally posttreated for various purposes. Electrolytic copper powders are characterized by dendritic particle shape, high purity, low oxygen con-

tent, favorable resistance to oxidation, and good green strength.

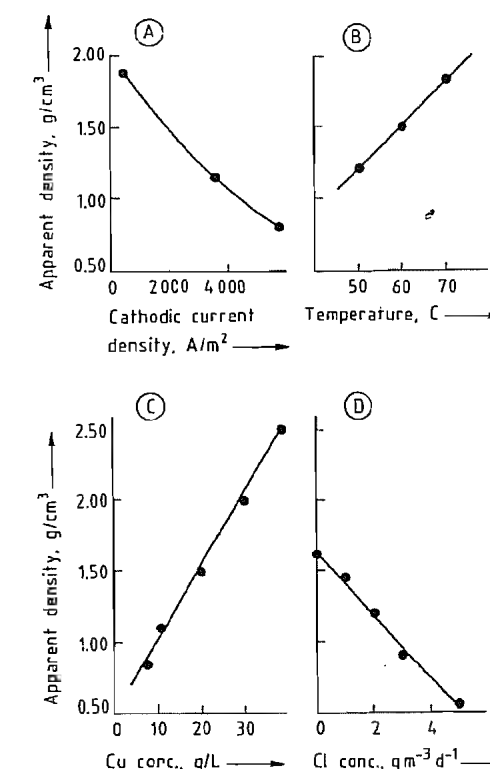


Figure 8.26: Apparent density of electrolytic copper powder as a function of four electrolysis parameters [191]. Other conditions: A) Cu 6 g/L, no Cl, 60 °C; B) Cu 17 g/L, no Cl, 3600 A/m²; C) no Cl, 50 °C, 3600 A/m²; D) Cu 13 g/L, 50 °C, 3600 A/m².

8.6.5 Copper Grades and Standardization

The three main grades of refined copper are (1) tough-pitch copper, (2) de-oxidized copper, and (3) oxygen-free copper.

- **Tough-pitch copper** normally contains 0.02–0.04% (as Cu₂O) and ca. 0.01% total of other impurities. This grade is easily worked and has an electrical conductivity of ≥ 100% IACS, but it is unsuitable for welding and brazing because of the danger of hydrogen embrittlement. About 80% of the world production of refined copper is tough pitch,

mostly electrolytic tough-pitch copper (ETP).

- **Deoxidized copper**, with no oxygen content is produced by addition of nonmetallic or metallic reducing agents, usually copper phosphide. As a result of the absence of oxygen, hydrogen embrittlement cannot occur, and such copper is well suited for welding and brazing. The content of residual phosphorus, however, increases the electrical resistivity. Deoxidized copper with low residual phosphorus (DLP, ca. 0.005 % P) is required if the metal is to be used as a conductor. Copper with high residual phosphorus (DHP, ca. 0.04 % P) can be employed for nonelectrical purposes.
- **Oxygen-free (OF) copper** is a special quality produced by keeping oxygen away from the copper melt in a controlled atmosphere. Copper of this type with an oxygen content less than 0.001 %, is suited for purposes requiring weldability and high electrical conductivity, especially electronics. OFHC, oxygen-free high-conductivity copper, is internationally known.

Standardization [14, 192–193]. Most industrial countries have established standards for copper; these national specifications include detailed specifications for chemical composition, physical properties, and geometrical dimensions, but differences exist. Table 8.18 indicates the rough equivalent between international and some national specifications for the most important copper properties.

Table 8.18: Comparison of international and selected national standards [14].

Germany DIN 1708 DIN 1787	International ISO R 1337	United States ASTM B 224	Great Britain BS 2872, etc. ^a
KE-Cu	Cu-CATH	CATH	
E1-Cu 58	Cu-ETP	ETP	C 101
E2-Cu 58	Cu-FRHC	FRHC	C 102
E-Cu 57	Cu-FRHC	FRHC	
F-Cu	Cu-FRTP	FRTP	104
OF-Cu	Cu-OF	OF	C 103
SW-Cu	Cu-DLP	DLP	
SF-Cu	Cu-DHP	DHP	C 106

^a Also BS 1036, BS 1037, BS 1038, BS 1172, and BS 1861.

8.6.6 Quality Control and Analysis

Tests for quality control of copper are carried out on samples of both refinery shapes and semifinished products. There is need to standardize the testing methods, but currently only some of them are fixed in national specifications. The most important tests are the measurement of electrical conductivity, mechanical properties, and quality of the metal surface.

The electrical conductivity is very sensitive to impurities and crystal lattice imperfections. Mechanical tests measure hardness, tensile strength, elongation at failure, and torsional fatigue strength. The spiral elongation test [194] is a complicated test method that assesses the purity and the mechanical behavior of the sample. Defects on the surface and subsurface can occur in various forms, e.g., folds, splashes, cracks, inclusions, and voids. The voids are caused by gas porosity, shrinkage porosity, and shrinkage cavities.

Nondestructive testing procedures, such as radiography, ultrasonic examination, or eddy-current technique can be used. Metallographic methods (polishing and etching) give information by microscopic examination.

Analytical methods are of interest for determining the impurity level of copper products. Both wet chemical procedures and physicochemical procedures, such as atomic absorption spectrometry, optical emission spectroscopy, and X-ray fluorescence spectroscopy, are employed, the latter essentially for quick analysis of solid and liquid co- and byproducts [195–196]. The classical analytical methods are gradually being superseded by the modern automatic instrumental techniques. It is especially important to analyze the oxygen content, and one effective modernized method is available, hot extraction, i.e., melting a copper sample in a small graphite crucible and determining the CO formed by IR absorption spectroscopy.

8.7 Processing

The pure metal produced in refineries or melting plants is manufactured into semifabricated products.

8.7.1 Working Processes

Usually copper is treated initially by non-cutting, shaping processes to obtain semifinished products or “semis”. These processes are subdivided into hot working, cold working and, if necessary, process annealing.

Hot working means plastic forming above the recrystallization temperature. Generally copper is preheated to 800–900 °C, and the subsequent hot forming is finished at ca. 400 °C. Cast bars from modern combined continuous casting/rod-rolling systems already have sufficient temperature, thus saving thermal energy. After cooling, the hot-worked copper is soft copper. Its mechanical and electrical properties are scarcely changed, but its density has increased to nearly 8.9.

The next step is cold working, which involves plastic forming below the recrystallization temperature. In practice, the operation is done at room temperature. Unlike hot working, this procedure entails an essential strain hardening of the metal by increasing the number of lattice defects; however, simultaneously formed lattice voids cause a considerable decrease of electrical and thermal conductivity. After cold working, the metal is hard copper.

Process annealing is a heat treatment that is necessary if the hardened copper must be softened again, either for continued working or for producing (soft) copper with high electrical conductivity. Special furnaces are used for the purpose of steady heating and cooling of the metal—often in a nonoxidizing atmosphere. To achieve the intended microstructural change, the recrystallization temperature of 200–300 °C must be exceeded: in practice, the metal is heated to 400–500 °C for accelerated recrystallization. Copper products with exactly defined properties can be obtained if all annealing conditions are carefully controlled.

The engineering techniques are versatile. The following working methods are of special importance:

Hot working hot rolling extrusion drop forging	Cold working cold rolling cold drawing cupping
---	---

Foils only ca. 0.002 mm thick are manufactured by rolling, and wires to 0.004 mm diameter by drawing. Many products of varying size are fabricated by modern variants of the extrusion process [197]. The fabrication of tubes is also quite diverse [198]. The most widely used working processes are compiled in Table 8.19.

Table 8.19: Important fabricating processes for copper products.

Refinery shapes	Hot-working process	Cold-working process	Semi-finished products
Cakes	hot rolling	→ cold rolling	sheets/strip
Wirebars or square bars	hot rolling	→ wire drawing	wires
Billets	extruding	→ cold drawing	tubes/pipes
Billets	extruding or hot rotary piercing	→ cold drawing or cold pilger rolling	tubes/pipes

8.7.2 Other Fabricating Methods

In many cases, machining operations are required, e.g., cutting, turning, planing, drilling, and sawing. However, these are more important for copper alloys than for pure copper because of copper's tendency to gum. Non-continuous casting processes are likewise more suitable for copper alloys because copper has a disadvantageous coulability. These include sand mold casting, permanent mold casting, gravity die casting, pressure die casting, and centrifugal casting. Continuous or semicontinuous casting processes, however, are well-suited for pure copper.

Galvanoplasty is an electrolytic operation for manufacturing complicated objects that require high precision and flawless surfaces such as hollow bodies, disk matrices, and elec-

prototypes. A special galvanic method is copper plating, which involves electrolytic deposition of a thin layer of copper on another metal either for surface protection or as a base layer for electroplating with another metal.

Powder-metallurgical techniques are used primarily for the mass production of small pieces, especially intricate forms such as electrotechnical and mechanical structural parts. The metal powders are first compacted by pressure and then sintered in a controlled atmosphere. The copper powder is often mixed with other powdered metals, including those that do not form common copper alloys.

There are other important fabricating methods [199]. Joining is usually carried out above room temperature by soldering, brazing, or welding. Soldering may be used for all sorts of copper, owing to the low temperature. However, welding and brazing are feasible only with deoxidized or oxygen-free copper.

When tough-pitch copper is heated in an atmosphere containing hydrogen, the steam generated collects within the grain boundaries at high pressure and can destroy the grain structure by forming cracks. This phenomenon is known as "hydrogen embrittlement".

Mechanical joining and metal bonding are also possible ways of joining copper with other materials.

Surface treatment of copper is a group of operations for surface protection or surface refinement. These include mechanical, electrical, or electrochemical handling, e.g., polishing, matte finishing, pickling by dilute sulfuric or nitric acid, metal coating or electroplating (with nickel, nickel and chromium, tin, silver, gold, or platinum metals), lacquering or coating with synthetic plastics (mainly for electrical insulation), enameling of objects (applied art), and chemical or electrochemical coloring (decoration). Coloration is effected by chemicals, mostly specially formulated metal salt solutions which form thin layers of insoluble green, red, brown, or black compounds.

8.7.3 Uses

Copper is a useful material with a wide range of applications because of its combination of properties. Because of its excellent electrical conductivity, it is the dominant conductor material. Copper is used primarily as round wire or rods, bare or insulated, for current generation, transmission, and conduction; various sorts of cables are produced for special applications. Substantial quantities of copper are made into generators, motors, transformers, and other electrical appliances. About 50 % of the world consumption of copper is for electrical purposes. As a result of its high thermal conductivity, copper is well-suited for vessels and pipes, especially for heating, cooling, and heat exchange.

While high-conductivity copper is required for electrotechnical and electronic uses, special copper qualities are chosen for other uses. About 30% of world copper production is used for alloying. Copper alloys are usually cold-worked; only ca. 10% of them are cast.

Copper is frequently used in the chemical and food industries because of its high resistance to corrosion. There is substantial use of copper in mechanical engineering, by fabricators of precision implements, in vehicle construction, and in ship building. There is increasing interest in copper building construction as a material for installation, wall lining, and roofing. Hydraulic engineers use copper sheets for tightening on dams, sluices (floodgates), and bridges.

Other areas of application are in the fabrication of household articles, art objects, coins and medals, and in military hardware as ammunition. There is a smaller demand for other purposes, such as electrodeposition; powder-metallurgical copper, special materials for brakes and self-lubricating bearings, small precision parts, filters, graphite brushes; and alloying additives for aluminum, iron, and steel. Use in copper compounds, chiefly copper sulfate and copper oxides, consumes only 1–2 % of the primary world production.

Table 8.20 lists the distribution of copper consumption among various industries. This

distribution is effectively determined by the specific useful properties of copper. The use of copper (including alloys) in the United States in 1982, based on essential properties, can be broken down as follows [201]:

Electrical conductivity	57.0%
Corrosion resistance	21.9%
Thermal conductivity	12.1%
Constructional behavior	7.4%
Aesthetic effects	1.6%

Table 8.20: Industrial use of copper (including alloys) in the Western world in 1981, percentage by country [200].

Branch	United States	United Kingdom	Germany	Japan
Electrical and electronic industry	46	55	52	52
Industrial machinery and equipment	19	12	14	15
Building construction	16	11	15	9
Transportation	10	13	11	17
Other	9	9	8	7

Substitution and Miniaturization. Several materials compete with copper and may substitute for it, depending on the relative costs. Copper is partly replaced by aluminum in automotive radiators and in transmission cables, high-voltage long-distance lines, and household wiring. Copper wires and cables for telecommunications are being displaced by microwave technology and fiber optics. Copper is being replaced by plastics for water pipes in both residential and commercial construction. In the area of corrosion-resistant materials, in addition to plastics there are also stainless steel and titanium.

The movement toward making smaller and smaller parts has been one of the most pervasive and continuing pressures on the copper market. A dramatic drop in the use of copper has occurred in the widespread acceptance of printed circuits. The use of wire has plummeted. The number and size of the connectors have dropped. On the other hand, miniaturization has steadily decreased the cost of the final products, thus increasing the number of units sold.

The average cross section of parts has steadily decreased. At one time, 0.813 mm was a base point for metal thickness, but this has decreased generally to 0.250 mm and in

electronics even to 0.250 mm. In electronics, formerly 4500 kg of metal was necessary to furnish products to a consumer market that currently requires less than 900 kg.

Table 8.21: Mine production of copper [202].

Country or region	Copper content ($\times 10^3$ t)			Percentage (1983)
	1973	1978	1983 ^a	
Chile	735	1034	1257	15.3
United States	1559	1358	1038	12.6
Canada	824	659	625	7.6
Zambia	707	643	543	6.6
Zaire	489	424	502	6.1
Peru	208	376	322	3.9
Others	1516	1605	1924	23.4
Western world	6038	6099	6211	75.5
Eastern countries	1473	1754	2009	24.5
World total	7511	7853	8220	100

^a The 1983 mine production is given for more countries and regions in Table 8.22.

At the same time, however, this drive towards miniaturization, whether in the thickness of an automotive radiator or in the size of an electronic component, is a challenge to the copper industry to produce purer copper and more useful alloys and to the copper fabricating industry to produce the new miniaturized products.

8.8 Economic Aspects

There are numerous tabular compilations of statistics on copper resources, production, and consumption [202–206]. Many books deal with economic relations and commercial problems, e.g., [207–210]. Compilations of companies in the nonferrous metal industry [211] and the mining industry [212] are published at irregular intervals.

Production and Consumption. The copper production of mines, smelters, and refineries and the consumption by country and region are given in Tables 8.21 and 8.22. Production and consumption per capita are listed in Table 8.23. Over the decades, the annual per capita consumption of primary copper in the United States has grown [205]:

Late twenties	7.5 kg
Early thirties	2.5 kg
World War II	9.5 kg
Postwar period	7.5 kg
1970	13.3 kg
1979	14.6 kg

During the 1980s, there has been no increase in consumption in America and Europe and only a small increase worldwide.

Prices. The development of copper prices since 1850 is shown in Figure 8.27. The fluctuation caused by political and economic events after World War II are conspicuous.

Table 8.22: Production and consumption of copper in 1983 ($\times 10^3$ t) [202].

Country or region	Production			Consumption of refined copper
	Mine	Smelter	Refinery	
Austria			41.9	21.9
Belgium-Luxembourg		2.8	404.6	258.2
Finland	37.8	70.1	55.4	65.8
France	0.1		43.9	390.0
Germany	1.2	159.1	420.3	737.0
Italy	1.6		31.2	325.0
Norway	26.2	26.5	22.7	9.0
Portugal	2.4	2.8	4.6	12.3
Sweden	64.0	78.8	63.4	113.0
Spain	63.9	89.0	158.6	122.5
United Kingdom				
Yugoslavia	0.7		144.4	358.0
Other ^a	129.5	86.8	123.7	133.5
	2.6	2.8		53.4
Europe*	327.5	515.9	1514.7	2599.6
India	43.8	35.4	28.1	96.0
Indonesia	78.6			16.7
Iran	65.0	47.0	10.0	
Japan	46.0	944.6	1091.9	1216.3
Korea (South)	2.6	113.0	134.8	152.3
Malaysia	29.1			17.9
Oman	11.0	7.6	3.8	
Philippines	271.4	38.8	38.8	5.0
Taiwan		37.9	38.0	104.8
Turkey	24.9	18.3	31.8	57.9
Other	1.5			20.8
Asia*	573.9	1242.6	1377.2	1687.7
South Africa	211.8	192.3	157.7	73.6
Botswana	20.3			
Morocco	24.2			
Namibia	52.1	54.2		
Zaire	502.2	465.8	226.9	23.5
Zambia	542.8	562.7	575.4	
Zimbabwe	23.7	31.2	25.4	
Other	0.3		2.4	
Africa	1377.4	1306.2	987.8	97.1

Country or region	Production			Consumption of refined copper
	Mine	Smelter	Refinery	
United States	1038.1	927.7	1583.7	1775.4
Argentina				37.0
Brazil	33.0	63.1	88.5	148.4
Canada	625.0	336.9	464.3	195.0
Chile	1257.1	1058.1	833.4	23.8
Mexico	206.1	66.9	80.2	79.2
Peru	322.2	295.9	190.6	18.3
Other ^b	2.8			6.0
America[†]	3484.3	2748.6	3240.7	2283.0
Australia	264.2	173.6	201.9	114.8
New Zealand				0.4
Papua New Guinea	183.2			
Australia and Oceania	447.4	173.6	201.9	115.2
Western world	6210.5	5986.9	7322.3	6782.6
USSR	1180.0	1280.0	1500.0	1360.0
Bulgaria	80.0	60.0	62.0	62.0
Germany (DDR)	12.0	17.0	50.0	115.0
Poland	402.3	320.0	360.1	176.6
Romania	28.0	40.2	47.0	68.0
China	175.0	195.0	310.0	410.0
Korea (North)	10.0	35.0	35.0	17.0
Mongolia	95.0			
Other	27.0	22.5	47.9	124.4
Eastern countries and Cuba	2009.3	1969.7	2412.0	2333.0
Total	8219.8	7956.6	9734.3	9115.6

^a Excluding Eastern countries.

^b Excluding Cuba.

Table 8.23: Per capita production and consumption of copper, kilograms per person, in 1979 [205].

Country or region	Production	Consumption
United States	9.0	14.6
Japan	8.5	15.1
Germany	6.2	16.5
Economic Community (EEC)	3.6	11.6
Western world	2.4	3.4
USSR	5.6	—
World	2.2	—

Prices are set primarily at two metal exchanges: the London Metal Exchange (LME) and the New York Commodity Exchange (Comex).

Product Promotion. Two international organizations deal with copper promotion, re-

search, and development: the Conseil international pour le développement du cuivre (CIDEC) and the International Copper Research Association (INCRA).

Three European Institutions are the Deutsches Kupfer-Institut e.V. (DKI), Berlin; the Copper Development Association (CDA), London; and the Centre d'information cuivre, laitons et alliages, Paris.

In 1968, four developing countries that are among the main copper ore exporters in the world—Chile, Peru, Zambia, and Zaire—formed an association, CIPEC (Conseil intergouvernemental des pays exportateurs de cuivre). Some other countries have since joined.

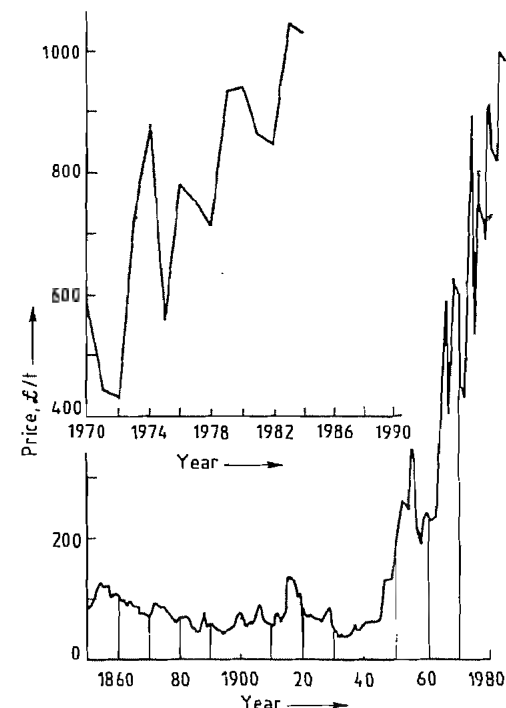


Figure 8.27: Annual average copper prices in London between 1850 and 1984 [202].

8.9 Environmental Protection

The worldwide growth of industry and population has caused a series of environmental problems, particularly the following: (1) emis-

sion control; (2) water protection; (3) solid-waste disposal.

Emission Control. There are two important tasks in the treatment of off-gas from pyrometallurgical processes in copper metallurgy: the removal of sulfur dioxide and the containment of flue dust.

Because most copper comes from sulfide ores, sulfur is the main problem in copper extraction. In pyrometallurgical operations, it appears as sulfur dioxide (Table 8.24) [214–215]. The mass ratio of sulfur to copper in sulfidic concentrates is usually between 0.8 and 1.6. Consequently, a large quantity of sulfur dioxide must be captured because of its harmful effects on health, vegetation, and property. In most cases, sulfuric acid is produced from the SO_2 -containing off-gas [216].

Flue dust can be separated from off-gas to a high degree in modern gas-cleaning systems such as electrostatic precipitators, baghouses, cyclones, and wet scrubbers. This metal-containing dust is recycled.

A growing problem is caused by the increasing arsenic content of available copper ores—the so-called dirty copper ores. Much of the arsenic is removed as arsenic trioxide during pyrometallurgical operations by volatilization and can be captured with flue dust [217].

Table 8.24: Comparison of SO_2 concentrations in copper smelting off-gas [213].

Process	SO_2 , vol %
Multiple-hearth roasting	5–8
Fluidized-bed roasting	8–15
Sinter roasting	1–2
Blast furnace smelting	2–5
Reverberatory furnace smelting	0.5–2.5
Electric furnace smelting	0.5–5
Outokumpu flash smelting	10–30
INCO flash smelting	75–80
KIVCET process	80–85
Peirce-Smith converter	5–12
Hoboken converter	7–17
TBRC process	1–15
Mitsubishi process	15–20
Noranda process	10–20

Water Protection. Harmful wastewater does not usually result from pyrometallurgical copper production but water for direct or indirect cooling of furnaces, casting machines, and

cast copper products is required on a large scale. This cooling water is moderately warmed, but does not acquire chemical impurities. Closed circulation is used as much as possible in modern plants.

Hydrometallurgical operations for the extraction of copper from ores or concentrates present the risk of water pollution. These solutions, of various compositions, must be post-treated if they cannot be recycled. Such post-treatment consists of neutralization or precipitation of specific ions, chiefly anions bearing sulfur and the cations of heavy metals. Lime is an excellent precipitant. Thus, the sulfate ion in sulfuric acid solutions formed during hydrometallurgical extraction is precipitated as gypsum [218].

Solid-Waste Disposal. The following means are used for handling solid residues:

- Recycling
 - Exploitation as raw material for the preparation of useful products
 - Dumping in deposits
- One example of each method follows:
- Flue dust from pyrometallurgical operations, e.g., from the Outokumpu flash smelting process, are added to the feed and recycled into suitable furnaces and occasionally into blast furnaces after agglomeration. Zinc-containing flue dusts can be processed into zinc and zinc compounds.
 - Discarded slags with low copper content from some copper smelting processes can be sold after suitable treatment.
 - Hydrometallurgical techniques yield various precipitates such as elemental sulfur or impure gypsum, which can easily be deposited.

8.10 Toxicology

Copper is a vital trace element for humans, most animals, and plants. For higher organisms, the compact metal is completely harmless. However protista, especially bacteria, die in contact with metallic surfaces of copper and

many of its alloys (oligodynamic effect) [219–220].

Continued exposure to the metal dust or fumes can irritate mucuous membranes. The following exposure limits have been established:

Form	Germany	United States
Metal dust	MAK 1 mg/m ³	TLV/STEL 2 mg/m ³
Metal fumes	MAK 0.1 mg/m ³	TLV/TWA 0.2 mg/m ³

8.11 Compounds

Copper compounds, although they represent a small fraction of total copper production, play an important and varied role in industry and agriculture. One of the oldest known fungicides was copper-based and was used extensively in the early part of the century. The last 20 years have brought about a resurgence in the use of copper-based fungicides partly because of a lack of tolerance by fungi to copper and also because of its relatively low toxicity to higher plants and animals. Although copper is an essential trace element for higher plants and animals, it is acutely toxic in higher doses. Copper compounds are used as nutritional additives in animal feeds and fertilizers, and are found in a variety of dietary supplements. Copper salts are used in the control of algae in lakes and ponds, and the oxides are used in antifouling paints and coatings. Copper acetoarsenite, Paris green, is used as an insecticide, and copper chromium arsenate is an effective alternative to creosote for the preservation of wood.

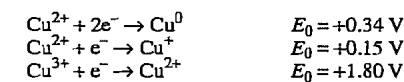
Copper and its compounds are used catalytically in numerous organic reactions, e.g., polymerization, isomerization, and cracking reactions. They are used in the textile and dye industries in the preparation of rayon and acrylonitrile, as mordants and oxidants in textile dyeing and printing, and in the preparation of azo dyes. Copper compounds are used as pigments in glass, ceramics, porcelains, varnishes, and artificial gems, and in the manufacture of the copper phthalocyanine pigments. Copper salt solutions are used for

electroplating, in brazing and burnishing preparations, and as brighteners for aluminum. Solutions of copper(I) complexes are used to selectively absorb carbon monoxide, butadiene, and alkenes from gas streams. In the petroleum industry, copper compounds are used as deodorizing (desulfurization) and purifying agents. Copper(II) carbonate is used in drilling muds to protect against release of poisonous hydrogen sulfide gas, and copper(I) iodide is used in acid muds to bind corrosion inhibitors to the iron drills. More recent applications of copper compounds are in pollution control and solar technology.

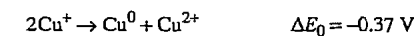
The multitude of applications of copper compounds in the biosphere is largely responsible for the extent of academic interest in them. Also, the facile reduction–oxidation of the copper(I)–copper(II) couple, the ease of theoretical treatment of the d^9 copper(II) system, and the varied stereochemistries and magnetic behaviors associated with copper ions enhance their theoretical appeal. Since this treatment of copper compounds is primarily from an industrial perspective, the reader whose interest is academic is referred to the classic references [221–224] as well as to more recent materials [225–231] that are attune to the subtle chemistries of copper and its compounds. Compounds of primary industrial importance are distinguished from compounds of minor importance in this section.

8.11.1 The Copper Ions

Copper, $[\text{Ar}] 3d^{10} 4s^1$, is a member of the first transition series. It is classified as a transition element in the broader definition because the copper(II) valence state, $[\text{Ar}] 3d^9$, comprises such a large proportion of the defined chemistry of copper. Copper in its compounds exists primarily in two oxidation states, 1+ and 2+. Although copper(0) and copper(III) compounds have been identified, they are not presently of commercial importance. The stabilities of the various valence states of copper are illustrated by the following standard reduction potentials:



From the above, it is seen that



with $pK = -5.95$

In other words, the free copper(I) ion does not exist to any appreciable extent in aqueous solution. In the presence of ligands such as ammonia, chloride, or cyanide, solutions of copper(I) can be prepared that are stable with respect to disproportionation. For example, the colorless solution of tetraamminecopper(I) sulfate is prepared readily by contact of blue tetraamminecopper(II) sulfate with metallic copper in the absence of air. Upon acidification with sulfuric acid, copper powder and a copper(II) ammonium sulfate solution are produced. The insoluble copper(I) chloride can be produced by sulfuric acid acidification of a copper(I) ammine chloride solution. If the solution is acidified with hydrochloric acid, a solution of $[\text{CuCl}_2]^-$, $[\text{CuCl}_3]^{2-}$, or $[\text{CuCl}_4]^{3-}$ species is produced, depending on chloride concentration. Copper(I) chloride is stable to water because of its insolubility, which is a result of the polymeric structure that arises from the chloride's ability to bridge copper. This contrasts with the sulfate's inability to coordinate or bridge strongly. Consequently, copper(I) sulfate can be produced only in nonaqueous media.

The electronic structure of the copper(I) ion is $[\text{Ar}] 3d^{10}$. The compounds are diamagnetic and colorless except where charge-transfer bands arise. Copper(I) is isoelectronic with zinc(II) and the preferred stereochemistries are similar. As a result of the filled 3d level, no ligand field stabilization occurs and electronic distortions are minimized. The stereochemistry around the copper(I) ion is determined mainly by the size of the anions, as well as by the electrostatic and covalent bonding forces. The preferred stereochemistry is tetrahedral, with linear and trigonal planar compounds also being common.

The majority of copper(II) compounds exhibit square planar or distorted octahedral configurations about the copper ion. The $3d^9$

electronic structure gives rise to the classic example of Jahn–Teller distortion in which the four planar metal–ligand distances are smaller than the two axial distances. Copper(II) ions are also found in distorted tetrahedral and various five-coordinate environments.

The copper(II) ion, $[\text{Ar}] 3d^9$, is predominantly blue or green, and the unpaired $3d$ electron results in magnetic phenomena. In most copper compounds, the unpaired electrons of the copper ions are sufficiently isolated from each other so that the compounds exhibit paramagnetic behavior. However, there are many polynuclear copper compounds in which the spins are coupled, which lowers the magnetic moment. The coupling may be so weak that it must be observed near the absolute zero of temperature, or it may be strong enough to render the compound diamagnetic at room temperature or above.

8.11.2 Basic Copper Compounds

8.11.2.1 Copper(I) Oxide

Cu_2O , m_p 1235 °C, d_4^{25} 5.8–6.2, decomposes above 1800 °C. It occurs in nature as the red or reddish brown mineral cuprite with a cubic or octahedral crystal morphology. Depending on the method of preparation and particle size, the synthetic material is yellow, orange, red, or purple. The yellow material has erroneously been referred to as copper(I) hydroxide, but X-ray diffraction patterns indicate that there are no differences in the crystal structures of the colored forms. Their thermodynamic data are as follows: c_p (298 K) 429.8 $\text{J kg}^{-1}\text{K}^{-1}$, c_p (290–814 K) 519.2 $\text{J kg}^{-1}\text{K}^{-1}$, c_p (290–1223 K) 565.2 $\text{J kg}^{-1}\text{K}^{-1}$, ΔH^0 (25 °C) –166.6 kJ/mol. Copper(I) oxide is stable in dry air but slowly oxidizes to copper(II) oxide in moist air. It is practically insoluble in water but dissolves in aqueous ammonia. In excess hydrochloric acid, soluble copper(I) chloride complexes are formed; however, in dilute sulfuric or nitric acids, disproportionation to the soluble copper(II) salts and copper powder results.

Production. Copper(I) oxide is produced easily by a variety of methods; its instability with respect to oxidation requires careful consideration. Copper(I) oxide produced pyrometallurgically is usually coated with isophthalic acid or pine oil to preserve its integrity [232]. Hydrometallurgically produced material can be stabilized by mixing the particle slurry with glue, gelatin, casein, or dextrin before drying [233–236].

Pyrometallurgical Processes. Copper(I) oxide is formed when copper powder is heated above 1030 °C in air; to prevent further oxidation, it must be cooled quickly in an inert atmosphere. To allow for lower temperature production of copper(I) oxide, carbon can be blended with copper(II) oxide and heated to 750 °C in an inert atmosphere. The material must be stabilized by coating the formed particles with isophthalic acid or pine oil [232]. A more stable copper(I) oxide results when stoichiometric amounts of copper powder and copper(II) oxide are blended, heated to 800–900 °C in an inert atmosphere, and allowed to cool. The production can be effected at lower temperature if ammonia or certain ammonium salts are added to the blend [237–239]. The autoclave oxidation of copper metal at 120 °C and about 0.6 MPa gauge pressure with air in the presence of water and small amounts of sulfuric and hydrochloric acids produces a red, pigment-grade product [240]. By varying the pressure and temperature, considerable differences in particle size, coloring, apparent bulk density, and buoyancy have been found.

Hydrometallurgical Processes. Tetraamminedicopper(I) sulfate, $\text{Cu}_2(\text{NH}_3)_4\text{SO}_4$, prepared by leaching an excess of copper with a solution of ammonia and ammonium sulfate, with air as the oxidant, yields a red copper(I) oxide upon acidification to pH 3–5 [241]. The less corrosive ammonium carbonate leach system in which $\text{Cu}_2(\text{NH}_3)_4\text{CO}_3$ is produced is more common. Upon vacuum distillation, a very stable red Cu_2O product remains [241]. If sodium hydroxide is added to the leach liquor, a yellow microcrystalline powder is precipitated [242]. When the yellow Cu_2O is heated in an excess of sodium hydroxide, it is con-

verted to an orange material of somewhat larger particle size.

Steam stripping of the copper(I) ammine carbonate solution yields a brown, impure product [243] which can be converted to a red material by washing it in an organic acid, e.g., formic or acetic acid [244]. An impure, brown product can also be converted to a red material by boiling it in 20% sodium hydroxide solution [245].

If a saturated solution of copper(I) ammine carbonate is agitated over copper metal, a layer of red copper(I) oxide is continuously produced which can be broken loose and recovered [246]. When copper salts are leached with chelating agents such as ethylenediaminetetraacetic acid [247] or ammonia [248] under pressure of carbon monoxide or hydrogen, and sodium hydroxide is subsequently added, a relatively stable, yellow copper(I) oxide is obtained; the reaction is catalyzed by an alkali metal iodide [249].

The reduction of a boiling slurry of basic copper(II) sulfate with sulfur dioxide at a pH of about 3 produces a reddish product [250]. Red copper(I) oxide has also been prepared by mixing a slurry of basic copper(II) sulfate with neutral copper(II) sulfate and adding sodium sulfite to a pH of 5.2. The mixture is then acidified to pH 3.5–5 and heated to boiling. The intermediate copper(I) sulfite slurry is decomposed to copper(I) oxide and sulfurous acid. Alkali is subsequently added to maintain a pH of 2.6–2.8 [251].

When a solution of copper(I) chloride and sodium chloride is neutralized with sodium hydroxide and then heated to 138 °C under pressure, a red copper(I) oxide is obtained which has an average particle diameter of about 2.5 μm [252]; an orange product (about 1- μm particles) is prepared by neutralizing the solution to pH 8.5 at 60 °C [253]. Simultaneous mixing of copper(I) chloride solutions with sodium chloride and sodium hydroxide solution in the presence of copper(I) oxide seed crystals at a controlled pH of 10.0, 55 °C, and under nitrogen, gives a reddish purple material (average diameter 48 μm). At pH 7.0, a

yellow material is obtained with an average particle size of 0.4 μm [254].

The electrolytic production of copper(I) oxide between copper electrodes in brine yields a yellow product at room temperature. At higher temperature, an orange or red material is produced.

Uses. The largest commercial use of copper(I) oxide is in antifouling paints for boat and ship bottoms; it is an effective control for barnacles and algae. The yellow or orange copper(I) oxide is used as a seed and crop fungicide, and the red material is used as a pigment in ceramic glazes and glass. Copper(I) oxide is also used in rectifiers and in brazing. Numerous organic reactions are catalyzed by copper(I) oxide, and it is an effective absorbent for carbon monoxide.

Analysis and Specifications. The ASTM approved analysis and specification for pigment-grade copper(I) oxide [255] and the military specification for the pigment grade [256] are listed in Table 8.25.

Table 8.25: Specifications for pigment-grade copper(I) oxide (%).

Assay	Navy I [256, 257]	Navy II [256]
Copper(I) oxide	97.0	90.0
Total copper (min.)	86.0	80.0
Reducing power (min.)	97.0	90.0
Nitric acid-insolubles (max.)	0.3	0.3
Chloride (max.)	0.4	0.4
Sulfate (max.)	0.1	0.1
Zinc oxide (max.)	—	10.0
Other metals (max.)	0.5	0.5
Acetone-soluble material (max.)	0.5	0.5

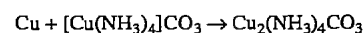
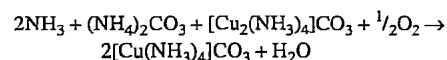
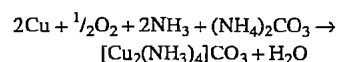
8.11.2.2 Copper(II) Oxide

CuO , m_p 1330 °C, d_4^{25} 6.48, occurs in nature as the black minerals tenorite (triclinic crystals) and paramelaconite (tetrahedral, cubic crystals). Commercially produced copper(II) oxide is usually black, although a brown product (particle size < 10^{–6} m) can also be produced. Thermodynamic data: c_p (298 K) 531.1 $\text{J kg}^{-1}\text{K}^{-1}$, c_p (290–1253 K) 682.4 $\text{J kg}^{-1}\text{K}^{-1}$, ΔH^0 (25 °C) –155.3 kJ/mol. Copper(II) oxide is stable to air and moisture at room temperature. It is virtually insoluble in

water or alcohols. Copper(II) oxide dissolves slowly in ammonia solution but quickly in ammonium carbonate solution; it is dissolved by alkali metal cyanides and by strong acid solutions. Hot formic acid and boiling acetic acid solutions readily dissolve the oxide. Copper(II) oxide is decomposed to copper(I) oxide and oxygen at 1030 °C and atmospheric pressure; the reduction can proceed at lower temperature in a vacuum. Hydrogen and carbon monoxide reduce copper(II) oxide to the metal at 250 °C and to copper(I) oxide at about 150 °C. Ammonia gas reduces copper(II) oxide to copper metal and copper(I) oxide at 425–700 °C [237].

Production. Copper(II) oxide can be prepared pyrometallurgically by heating copper metal above 300 °C in air; preferably, 800 °C is employed. Molten copper is oxidized to copper(II) oxide when sprayed into an oxygen-containing gas [257]. Ignition of copper(II) nitrate trihydrate at about 100–200 °C produces a black oxide. Basic copper(II) carbonate, when heated above 250 °C, produces a black oxide if a dense carbonate is employed; a brown material is produced when the light and fluffy carbonate is used. An alkali-free oxide can be prepared by ignition of copper(II) carbonate produced from ammonium carbonate and a copper(II) salt solution. Copper(II) hydroxide, when heated above 100 °C, is converted to the oxide.

Hydrometallurgy is the most common method for the production of copper(II) oxide. A solution of ammonia and ammonium carbonate in the presence of air effectively leaches metallic copper; the process is represented by the following reactions:



The second and third reactions proceed readily; the first is slow. Consequently, in batch operations the leach is usually begun with a small charge of the copper solution, but

continuous operations offer significantly improved rates. The leach liquor is then filtered to remove iron impurities and metallic copper, and is subsequently oxidized by air sparging. If necessary, lead and tin are removed by treatment with strontium, barium, or calcium salts [258–261]. The solution is filtered again and stripped of ammonia and carbon dioxide by steam injection or pressurized boiling to produce a black copper(II) oxide [258]. The ammonia and carbon dioxide are recycled for further use. The process is illustrated in Figure 8.28. Alternatively, the leach liquor can be treated with strong alkali to precipitate the intermediate copper(II) hydroxide, and then boiled to remove ammonia, with subsequent decomposition of the hydroxide to the black oxide.

Flue dust can be separated from off-gas to a high degree in modern gas-cleaning systems such as electrostatic precipitators, baghouses, cyclones, and wet scrubbers. This metal-containing dust is recycled.

A growing problem is caused by the increasing arsenic content of available copper ores—the so-called dirty copper ores. Much of the arsenic is removed as arsenic trioxide during pyrometallurgical operations by volatilization and can be captured with flue dust [217].

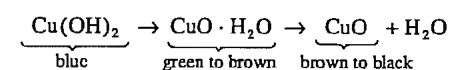
Flue dust can be separated from off-gas to a high degree in modern gas-cleaning systems such as electrostatic precipitators, baghouses, cyclones, and wet scrubbers. This metal-containing dust is recycled.

A growing problem is caused by the increasing arsenic content of available copper ores—the so-called dirty copper ores. Much of the arsenic is removed as arsenic trioxide during pyrometallurgical operations by volatilization and can be captured with flue dust [217].

8.11.2.3 Copper(II) Hydroxide

$\text{Cu}(\text{OH})_2$, d_4^{25} 3.37, ΔH^0 (25 °C) 446.7 kJ/mol, decomposes over 100 °C or over 50 °C in the presence of an excess of alkali. Copper(II) hydroxide is virtually insoluble in water (0.003 mg/L), and decomposes in hot

water to the more stable copper(II) oxide and water:



Copper(II) hydroxide is readily soluble in mineral acids and ammonia solution. When freshly precipitated, it is soluble in concentrated alkali, with the formation of $[\text{Cu}(\text{OH})_3]^-$ or $[\text{Cu}(\text{OH})_4]^{2-}$. Copper(II) hydroxide is inherently unstable but can be kinetically stabilized by a suitable production method.

Production. There are two classes of copper(II) hydroxide. The first is stoichiometrically rather precise, with a copper content as high as 64%; the theoretical copper content of $\text{Cu}(\text{OH})_2$ is 65.14%. This class is produced by the ammonia process [272–275], which yields a pure product of relatively good stability and large particle size. The best product results from the addition of strong alkali to the soluble copper(II) ammine complex [272, 275]. A relatively large particle-size product, deep blue in color and high in copper content, is precipitated below 35 °C. The resulting material is fairly stable or can be coated with gelatin to enhance its stability [276].

In the copper(II) hydroxide made by the ammonia process, the solubility of the copper(II) ammine complexes provides for crys-

tallite growth. This affords a large particle size, a limited surface area (point of dehydration), and hence a relatively stable product, in contrast with the unstable product (valuable assay) that results from the addition of hydroxide solutions to copper(II) salt solutions at 20 °C or above. The reaction with hydroxide is diffusion-controlled, allowing essentially no time for crystallite growth. The product is obtained as a gelatinous, voluminous precipitate with a large surface area, which is quite unstable and difficult to wash free of impurities. If the same reaction, with the same order of addition, is allowed to occur at 0–10 °C, a product of defined particle size and measurable surface area results, with greater stability but low assay.

The second class of copper(II) hydroxide, which represents a “stable” product but has lower assay and greater impurity, is produced from an insoluble precursor such as basic copper(II) carbonate or copper(II) phosphate. The first stable copper(II) hydroxide of this kind was made from copper(II) phosphate with alternate additions of copper(II) sulfate and sodium hydroxide solutions [277]. The process is illustrated by the following series of reactions:

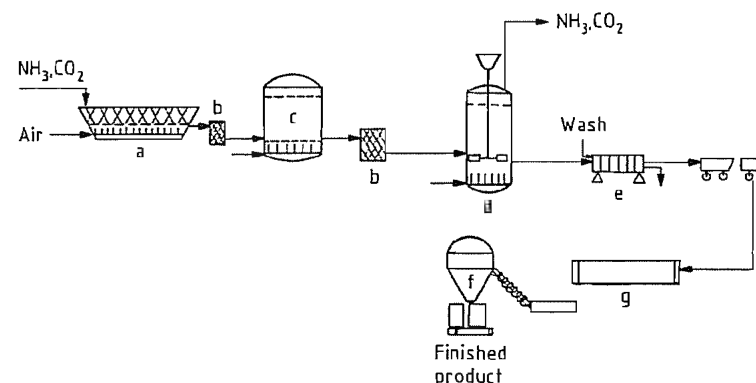
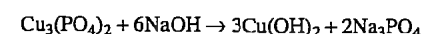
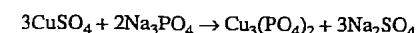


Figure 8.28: Process flow diagram for production of copper(II) oxide from ammonia–ammonium carbonate leach: a) Leach vat; b) Filter; c) Treatment tank; d) Strip tank; e) Press; f) Bag house; g) Drying kiln.

The alternate copper(II) sulfate sodium hydroxide addition is continued through 15 or 20 cycles and yields a stable product with 58–59% copper and 3–5% phosphate. The product has a small particle size and a high surface area, and is used as an agricultural fungicide.

Other stable copper(II) hydroxides of high surface area and fine particle size have been produced more recently [278–280]; the processes include the use of a copper(II) oxychloride precursor in the presence of an anionic surfactant [279] or a magnesium sulfate-precipitated precursor [278]. An electrolytically produced material has also been made by using trisodium phosphate as the electrolyte [281].

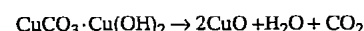
The classic Bordeaux slurry of copper(II) sulfate and lime in water has been replaced by a powdered stabilized product. This is obtained by mixing copper(II) nitrate solution and lime, adding cellulose pitch liquor (a waste product of the paper industry), and drying to yield a powder which is effective as a fungicide [282]. Sodium carbonate can be used as the precipitating agent instead of lime [283].

Uses. Copper(II) hydroxide is used as an active precursor in the production of copper(II) compounds. Ammonia-processed copper(II) hydroxide is used in the production of copper(II) naphthenate, copper(II) 2-ethylhexanoate, and copper soaps. Ammonia-processed copper(II) hydroxide is also used in the production of rayon (Schweitzer's reagent) and in the stabilization of nylon. Copper(II) hydroxides of the second class are often used as fungicides because of their small particle size. Copper(II) hydroxide is also used as a feed additive, a catalyst in the vulcanization of polysulfide rubber, and an antifouling pigment.

Analysis and Specifications. Copper is determined iodometrically with sodium thiosulfate [271]. The analysis of typical ammonia-processed copper(II) hydroxide (mass fractions in %) is copper 63.0, iron 0.05, zinc 0.05, lead 0.05, naphthenic acid-insoluble material 2.0, sulfate 0.3.

8.11.2.4 Copper(II) Carbonate Hydroxide

Copper(II) carbonate hydroxide, also called basic copper(II) carbonate, occurs in nature as the metastable mineral *azurite*, also called *chessylite*, a blue, monoclinic crystalline or amorphous powder with a formula approximating $2\text{CuCO}_3 \cdot \text{Cu}(\text{OH})_2$, d_4^{24} 3.8, ΔH^0 (20 °C) -87.4 kJ/mol, and *malachite*, green, monoclinic crystals with a formula approximating $\text{CuCO}_3 \cdot \text{Cu}(\text{OH})_2$, d_4^{25} 3.9–4.0, ΔH^0 (20 °C) -57.7 kJ/mol. The copper(II) carbonate of commerce, malachite, is also known as Bremen green. Pure copper(II) carbonate, CuCO_3 , has not been isolated. Copper(II) carbonate is virtually insoluble in water but dissolves readily in aqueous ammonia and alkali metal cyanide solutions. Copper(II) carbonate dissolves quickly in mineral acid solutions and warm acetic acid solution, with the formation of the corresponding copper(II) salt. Malachite is much more stable than copper(II) hydroxide but slowly decomposes to the oxide according to the following reaction:



Malachite is rapidly decomposed to the oxide above 200 °C.

Production. Two grades of copper(II) carbonate are available commercially, the light and the dense. The light grade is a fluffy product of high surface area. It is precipitated by adding a copper(II) salt solution, usually copper(II) sulfate solution, to a concentrated solution of sodium carbonate at 45–65 °C. Azurite is formed initially, and complete conversion to malachite usually occurs within two hours. The conversion is accelerated by the addition of malachite nuclei to the reactor.

A dark green, dense product results when a copper(II) salt solution is added to a solution of sodium hydrogen carbonate at 45–65 °C; conversion to malachite requires about one hour in this case. The density is maximized if the reactor is washed with acid prior to the precipitation to prevent premature nucleation on malachite nuclei. (A less dense product would be produced if malachite nuclei are

added to the slurry of azurite.) Solutions of copper(II) salt and sodium carbonate can also be added simultaneously at a pH of 6.5–7.0 and a temperature between 45 and 65 °C; conversion to malachite is usually complete within one hour. When a solution of copper(II) ammonium carbonate is boiled, ammonia and carbon dioxide are expelled from the solution, and a deep green, dense copper(II) carbonate precipitates [258].

Uses. Copper(II) carbonate is used as a precursor in the production of copper salts and soaps. It is used in animal feeds as a source of copper, in the sweetening of petroleum, and in electroplating for the control of pH. Copper(II) carbonate is used as a hydrogenation catalyst and as an accelerator in polymerization reactions. The light grade is somewhat effective as a fungicide and is used as a seed protectant.

Analysis and Specifications. Copper is analyzed by iodometric titration with sodium thiosulfate solution [271]. Table 8.26 gives typical analyses of light and dense technical-grade copper(II) carbonates.

Table 8.26: Typical analysis of commercially available copper(II) carbonate hydroxides.

Assay	Light, %	Dense, %
Copper	55.5	55.0
Sulfate	0.6	0.6
Iron	0.1	0.1
Zinc	0.01	0.02
Lead	0.003	0.005
Hydrochloric acid-insoluble material	0.05	0.05
Water	1.0	2.0

8.11.3 Salts and Basic Salts

8.11.3.1 Copper(I) Chloride

Copper(I) chloride, CuCl , *mp* 422 °C, *bp* 1367 °C, d_4^{25} 4.14, ΔH^0 (25 °C) -134.6 kJ/mol, occurs in nature as the colorless or gray cubic-crystal *nantokite*. The commercially available product is white to gray to green and of variable purity. Copper(I) chloride is fairly stable in air or light if the relative humidity is less than about 50%. In the presence of moisture and air, the product is oxi-

dized and hydrolyzed to a green product that approaches copper(II) oxychloride, $\text{CuCl}_2 \cdot 3\text{Cu}(\text{OH})_2$. In the presence of light and moisture, a brown or blue product is obtained. Copper(I) chloride is slightly soluble to insoluble in water, with values from 0.001 to 0.1 g/L being reported. It is readily hydrolyzed to copper(I) oxide by hot water. Copper(I) chloride is insoluble in dilute sulfuric and nitric acids, ketones, alcohols, and ethers, but it quickly dissolves in hydrochloric acid, alkali halide, or ammonia solutions with the formation of complex compounds that are readily oxidized by air. Copper(I) chloride is soluble in solutions of alkali metal cyanides or thiosulfates and of coordinating amines, pyridines, and nitriles, notably, acetonitrile [284]. The increase in solubility of copper(I) chloride with chloride ion concentration illustrated in Figure 8.29 [285]. When the chloride concentration is decreased by dilution with water, the pure white copper(I) chloride precipitates.

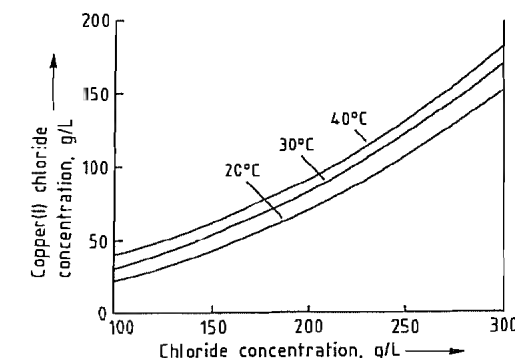
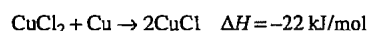
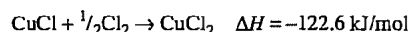
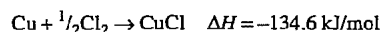


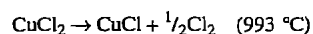
Figure 8.29: Solubility of copper(I) chloride in excess chloride ion solution at different temperatures.

Production. The direct combination of the elements is the most common method of production. The reaction of copper metal and chlorine is not spontaneous at ambient temperature. Once the metal is heated to red heat in the presence of chlorine, the reaction is self-sustaining and requires external cooling to prevent the metal from melting. A number of similar patents exist [286–289] in which copper metal is reacted with chlorine gas to produce a molten copper(I) chloride that is cast and pulverized. The primary difference in con-

ditions is the use of a shaft furnace [286] as opposed to the use of crucibles. The recommended process temperature varies from 450 to 800 °C [286, 287] or 500 to 700 °C [288, 289]. The conditions required for the high-temperature production of a pure copper(I) chloride can be illustrated by the following:



Higher temperature and excessive contact with copper metal favor the production of a very pure copper(I) chloride. The lowest possible temperature is obviously 422 °C, the melting point of copper(I) chloride. As the temperature approaches the decomposition temperature for the reaction



a product of higher purity is obtained. Operationally, a temperature between 750 and 900 °C is ideal, and results in a product of > 98% purity. The process of Degussa [287] illustrates a commonly used commercial process for the high-temperature production of copper(I) chloride; Figure 8.30 shows a suitable crucible for the production of technical-grade copper(I) chloride. Once the reaction is initiated, chlorine and copper metal (shot, chopped wire, or briquettes) are added continuously. As the molten product is formed on the surface of the upper metal layer, it flows by gravity down through the porous copper bed to effect further reduction of any copper(II) chloride, and out the exit port onto a rotating table where the product is allowed to cool and solidify. The flakes that form are packaged as is or ground to a powder and packaged. Because of the high temperature during the reaction and the volatility of copper(I) chloride, the exit port must be vented to a caustic scrubber. When the molten product is allowed to fall onto a high-speed, horizontally rotating disk constructed of quartz, graphite, or porcelain, small prills of uniform size are produced [290]. The product is spun out onto a water

cooled diaphragm and collected. If the copper is contaminated with oxides, hydrogen chloride gas should be added to the chlorine gas stream to prevent the production of basic copper(II) chlorides that would contaminate the product [286].

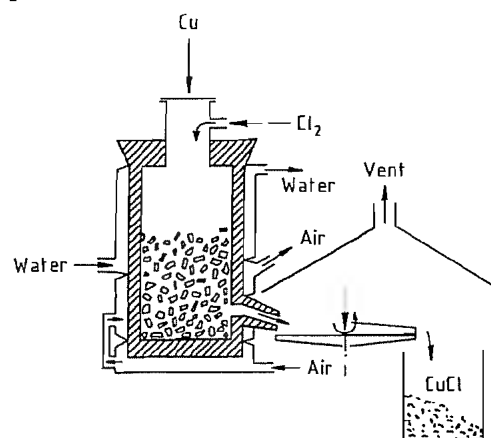
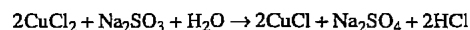


Figure 8.30: Crucible used in the production of copper(I) chloride.

If the product is packaged quickly and sealed properly, no extreme precautions are required. Otherwise, the product must be stored under nitrogen to preserve its integrity or coated with mineral oil as a barrier to moisture. Copper(I) chloride is also produced hydrometallurgically by the reduction of copper(II) in the presence of chloride ions [291]:



Other reducing agents can be used, such as metallic copper, sulfurous acid, hydroxylamine, hydrazine, or phosphorous acid. The copper(I) chloride solution is produced, for example, by mixing a copper(II) chloride solution with metallic copper in the presence of hydrochloric acid or sodium chloride. The colorless to brown solution is stable only in the absence of air. Continuous preparations of copper(I) chloride solutions have been developed [292, 293]. When they are diluted with water, a white crystalline material precipitates which can be vacuum dried or washed with sulfurous acid, then with alcohol and ether, and carefully dried. Zinc has also been used as

a reducing agent in a more recent process [294].

Production of copper(I) chloride by treatment of ores with iron(III) chloride solutions [295, 296] and recovery of the product through chlorination in pit furnaces above 800 °C [297] have also been attempted.

Uses. Copper(I) chloride is used as a precursor in the production of copper(II) oxychloride and copper(I) oxide, as well as fine copper powder [298]. The production of silicone polymers, the vulcanization of ethylene-propene rubbers (EPDM) [299], and acrylonitrile production are other applications. Copper(I) chloride is also used in the purification of carbon monoxide gas [300–303] and the production of phthalocyanine pigments [304, 305]. More recently, copper(I) chloride has been found to be an effective catalyst in the production of dialkyl carbonates [306–308].

Analysis and Specifications. Copper(I) chloride is analyzed according to [271]. Table 8.27 lists specifications for technical- and reagent-grade material.

Table 8.27: Specifications for copper(I) chloride.

Assay	Technical-grade, %	Reagent-grade, %
Copper (min.)	97.0	90.0
Acid-insolubles (max.)	0.1	0.02
Iron (max.)	0.01	0.005
Sulfate (max.)	0.3	0.10
Arsenic (max.)	—	0.001
Not precipitated by H ₂ S as sulfate (max.)	—	0.2

8.11.3.2 Copper(II) Chloride

Copper(II) chloride, CuCl_2 , *mp* (extrapolated) 630 °C, d_4^{25} 3.39, begins to decompose to copper(I) chloride and chlorine at about 300 °C. The often reported melting point of 498 °C is actually a melt of a mixture of copper(I) chloride and copper(II) chloride. Decomposition to copper(I) chloride and chlorine is complete at 993 °C. The deliquescent monoclinic crystals are yellow to brown when pure; their thermodynamic data are as follows: c_p (298 K) $-579.2 \text{ J kg}^{-1} \text{ K}^{-1}$, c_p (288–473 K) $-621.7 \text{ J kg}^{-1} \text{ K}^{-1}$, c_p (288–773 K)

$-661.9 \text{ J kg}^{-1} \text{ K}^{-1}$, ΔH^0 (25 °C) -247.2 kJ/mol . In moist air, the dihydrate is formed. Figure 8.31 shows the solubility of copper(II) chloride in water and hydrochloric acid at two temperatures [309]. At higher concentrations of hydrogen chloride, $[\text{CuCl}_3]^-$ and $[\text{CuCl}_4]^{2-}$ complexes are formed. Copper(II) chloride is easily soluble in methanol and ethanol and moderately soluble in acetone.

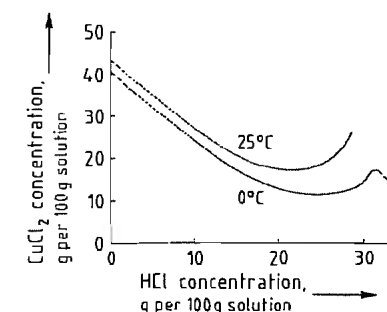


Figure 8.31: Solubility of copper(II) chloride in hydrochloric acid solutions at different temperatures.

The more common commercial form of copper(II) chloride is the dihydrate, $\text{CuCl}_2 \cdot 2\text{H}_2\text{O}$, *mp* around 100 °C (with decomposition to the anhydrous form). This occurs in nature as blue-green orthorhombic, bipyramidal crystals of eriochalcite, d_4^{25} 2.51. Its solubility characteristics are proportionally similar to those of the anhydrous form. In moist air the dihydrate deliquesces, and in dry air it effloresces.

Production. Because of the relative stabilities of copper(I) chloride and copper(II) chloride at high temperature, it is improbable that a pure anhydrous copper(II) chloride can be prepared by excessive chlorination of copper in a melt, even though such methods have been reported. The most common method for the production of anhydrous copper(II) chloride is by dehydration of the dihydrate at 120 °C. The product must be packaged in air-tight or desiccated containers.

The dihydrate can be prepared by the reaction of copper(II) oxide, copper(II) carbonate, or copper(II) hydroxide with hydrochloric acid and subsequent crystallization. Commercial production of copper(II) chloride dihy-

drate uses a tower packed with copper. An aqueous solution is circulated through the tower. Sufficient chlorine is passed into the bottom of the tower to oxidize the copper completely [292, 293]; to prevent hydrolysis [precipitation of copper(II) oxychloride] of concentrated copper(II) chloride solutions, they are kept acidic with hydrochloric acid. The tower can be operated batchwise or continuously; Figure 8.32 shows the continuous operation. A hot, concentrated liquor is circulated continuously through the tower, and the overflow from the tower is passed through a crystallizer where the liquor is cooled; the product is then centrifuged, dried, and packaged. The addition of hydrogen chloride is pH controlled; the addition of water is controlled by specific gravity. Copper is added daily or twice daily, as needed.

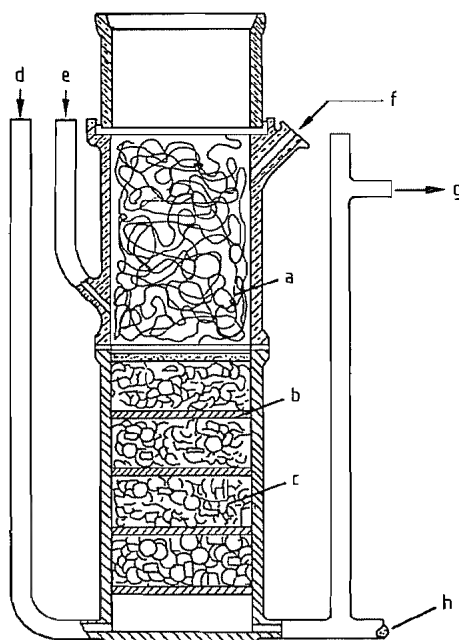


Figure 8.32: Reactor for the production of copper(II) chloride solutions: a) Copper metal; b) Porous plates; c) Raschig rings; d) Chlorine inlet; e) Steam inlet; f) Solution recycle; g) Solution to crystallizer; h) Drain.

Uses. Copper(II) chloride dihydrate is used in the preparation of copper(II) oxychloride [310, 311]. It serves as a catalyst in numerous organic chlorination reactions such as the pro-

duction of vinyl chloride [312] or 1,2-dichloroethane [313]. Copper(II) chloride dihydrate is used in the textile industry as a mordant and in the petroleum industry to sweeten sulfidic crude oil. Copper(II) chloride solutions are used for plating copper on aluminum, and in tinting baths for tin and germanium. Copper(II) chloride dihydrate is used as a pigment in glass and ceramics, as a wood preservative, and in water treatment.

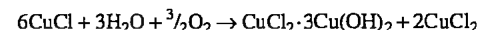
Analysis and Specifications. Copper is analyzed iodometrically with sodium thiosulfate [271]. A typical analysis of technical-grade copper(II) chloride dihydrate (in %) is as follows: copper(II) chloride dihydrate 99.0 (min.), iron 0.02, zinc 0.05, sulfate 0.05, water-insoluble material 0.01, material not precipitated by hydrogen sulfide as sulfate 0.15.

8.11.3.3 Copper(II) Oxychloride

Copper(II) oxychloride, $\text{Cu}_2\text{Cl}(\text{OH})_3$, is usually written as $\text{CuCl}_2 \cdot 3\text{Cu}(\text{OH})_2$. The trade name is copper oxychloride or basic copper chloride; the internationally accepted name (IUPAC) is dicopper chloride trihydroxide. Copper oxychloride is found in nature as the minerals paratacamite, green hexagonal crystals, and atacamite, green rhombic crystals, d_4^{25} 3.72–3.76 [314]. It is virtually insoluble in water, dissolves readily in mineral acids or warm acetic acid, and is soluble in ammonia and alkali-metal cyanide solutions. The green oxychloride is converted into blue copper(II) hydroxide in cold sodium hydroxide solution [279] and into the oxide in hot sodium hydroxide solution. With a lime suspension, copper oxychloride is converted into the blue calcium tetracuproxochloride, calcium tetracopper(II) chloride tetrahydroxide, $\text{CaCl}_2 \cdot 4\text{Cu}(\text{OH})_2$ [315]. It is decomposed to the oxide at 200 °C.

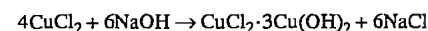
Production. Copper(II) oxychloride is most often prepared commercially by air oxidation of copper(I) chloride solutions [310, 311, 316, 317]. For this purpose, a concentrated sodium chloride solution containing about 50 g/L copper(II) is contacted with copper metal to produce a solution containing about 100 g/L

copper(I). The copper(I) chloride sodium chloride solution with or without the copper metal, is then heated to 60–90 °C and aerated to effect oxidation:

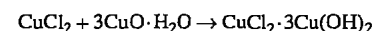
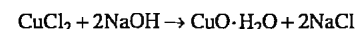


The mother liquor is separated from the precipitate and recycled into the process. The particles that are obtained by the above process are generally less than 4 µm in diameter and are suitable as crop fungicides. The particle size can be reduced further by increasing the agitation during oxidation and by utilizing a lower temperature [316]. Also, spray-drying of the product slurry gives a micronized product [318] as a result of deagglomeration of the material.

Copper(II) oxychloride can also be prepared by reaction of a copper(II) chloride solution with sodium hydroxide [314]:



or by reaction of a copper(II) chloride solution with freshly precipitated, hydrated copper(II) oxide [319]:



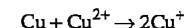
Copper oxychloride has also been produced as a by-product in the electrolytic production of copper(I) chloride [320].

Uses. Copper oxychloride is used primarily as a foliar fungicide [310, [321–325]; it is also used as a pigment.

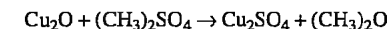
Analysis and Specifications. A typical analysis of technical-grade copper(II) oxychloride (in %) is as follows: copper 56.0, chloride 14.0 15.0, sulfate 2.0 2.5, hydroxide 22.5–23.5, water 3.0–6.0. Copper is analyzed by iodometric titration with sodium thiosulfate [271].

8.11.3.4 Copper(I) Sulfate

Cu_2SO_4 can be prepared in solution by dissolving metallic copper in a solution of CuSO_4 in absence of air:



Solid Cu_2SO_4 , however, cannot be crystallized from such solution because decomposition takes place during this operation. Solid Cu_2SO_4 can be prepared according to Recoura's method [326] by the reaction of Cu_2O with dimethyl sulfate:

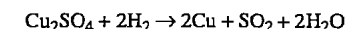


Cu_2SO_4 so prepared must be washed with ether and dried at 60 °C in a stream of argon for 24 h; it is pale beige in color. Reagent grade Cu_2O is not suitable for this purpose because it contains CuO. Freshly prepared Cu_2O from Fehling's solution is suitable. The product is about 75% pure; the remaining 25% is CuSO_4 .

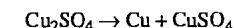
Cu_2SO_4 is also formed during the hydrogen-reduction of CuSO_4 at about 220 °C [327–332]:



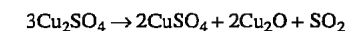
However, the product will always be contaminated with unreacted CuSO_4 . If the reaction time is longer or at a higher temperature (250–300 °C), the product will be contaminated with metallic copper due to the reaction:



Cu_2SO_4 is fairly stable in dry air at room temperature but decomposes rapidly in presence of moisture:



On heating in argon, Cu_2SO_4 decomposes at about 400 °C according to:

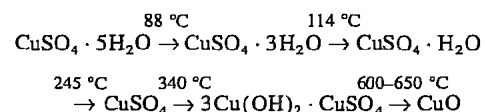


8.11.3.5 Copper(II) Sulfates

Copper(II) Sulfate Pentahydrate

$\text{CuSO}_4 \cdot 5\text{H}_2\text{O}$, d_4^{25} 2.285, c_p (273–291 K) 1126 J/kg⁻¹K⁻¹, ΔH_f^0 (25 °C) –850.8 kJ/mol, bluestone, blue vitriol, is found in nature as the mineral chalcantite, blue triclinic crystals that can be ground to a light blue powder. Copper(II) sulfate pentahydrate slowly effloresces in dry air or above 30.6 °C with the formation of the trihydrate, $\text{CuSO}_4 \cdot 3\text{H}_2\text{O}$. At 88–100 °C the trihydrate is produced more

quickly. Thermal analysis of the pentahydrate gives the following:

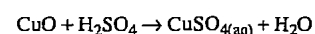


Above about 114 °C, the monohydrate is formed, and between about 245 and 340 °C, the anhydrous product CuSO_4 results. Figures 8.33A and 8.33B show solubility of CuSO_4 in water and density of the solution as a function of temperature and sulfuric acid concentration [333, 334]. The pentahydrate can be crystallized from the solution either by addition of sulfuric acid or by evaporation. Although the addition of sulfuric acid appears to be more economical, the concentration of the solution by evaporation is preferred because the crystals obtained from a "neutral" (pH 3.5–4.0) medium are less prone to hard cake formation than the acid crystals. As the particle size of the pentahydrate decreases, the tendency toward hard cake formation increases, and the necessity to increase the pH during crystallization is enforced. When a free-flowing, commercial product of fine particle size is required, such alkaline additives as calcium oxide or calcium stearate must be incorporated

into the final product to assure flowability. The incorporation of excess acid into the product accelerates the in situ dehydration of the pentahydrate and promotes hard cake formation. Lower temperature and lower humidity slow the caking process.

Copper(II) sulfate pentahydrate is soluble in methanol (15.6 g/100 mL solution) but insoluble in ethanol. It readily forms soluble alkaline complexes at sufficiently high concentrations of amines or alkali cyanides, but basic sulfates are precipitated from solution by ammonia at an intermediate pH (about 4.2–6.8). Copper(II) sulfate pentahydrate is the most commonly used copper compound because of the economics and the availability of starting materials, the ease of production, and the extent of by-product utilization (primarily copper electrowinning liquors).

Production. Copper(II) sulfate pentahydrate is prepared most easily by the reaction of a basic copper(II) compound with a sulfuric acid solution (100–200 g/L H_2SO_4), e.g.:



Copper metal, sulfuric acid, and air are the most common starting materials for the production of copper sulfate pentahydrate:

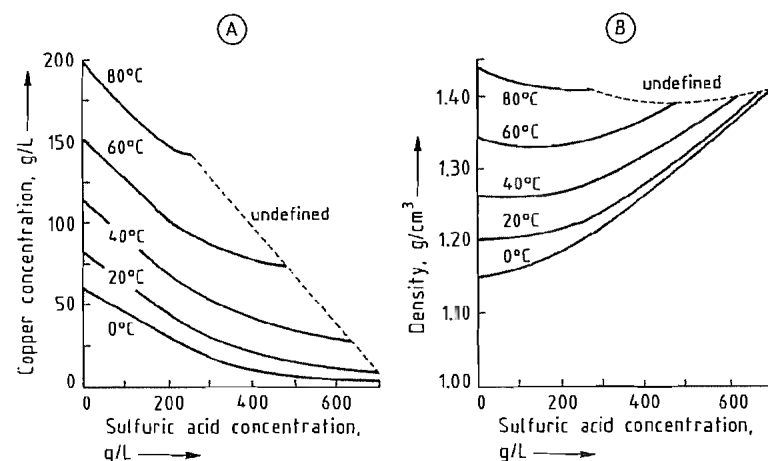
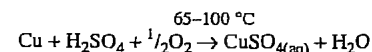


Figure 8.33: Saturated solutions of copper(II) sulfate. A) Solubility of copper(II) sulfate (as copper) as a function of sulfuric acid concentration and temperature; B) Density of copper(II) sulfate solutions as a function of sulfuric acid concentration and temperature. Reprinted with permission [334].



Harike Process. The Harike process [335] is the best commercial example of the preceding reaction (Figure 8.34). Blister shot copper up to 25 mm in diameter is added to the reaction tower (2.9 m² cross sectional area) to give a bed of copper metal 2.74-m high. Two different reaction conditions are given in Table 8.28. Condition A allows for the production of concentrated copper(II) sulfate solutions and subsequent crystallization from acid media. Condition B gives a concentrated neutral solution of copper(II) sulfate that can be crystallized or diluted with water and used for direct production of other copper products. The rate of oxygen consumption by the system is directly proportional to the mass of copper metal dissolved. Air flows of 46 m³h⁻¹m⁻² are used in order to fill with air the voids that are created by the packing of the copper shot. The solution is circulated cocurrently with the air flow to wet the particles continuously and en-

hance mixing of the solution with the copper metal. If the air flow is decreased and the voids in the copper metal bed are not filled sufficiently, the hot acid solution oxidizes the copper metal in the absence of air with the formation of a copper sulfide film. This film renders the copper metal inert to further oxidation and would lower the efficiency of the tower. On the other hand, an increase in air flow above 46 m³h⁻¹m⁻² decreases the fraction of oxygen consumed and would also result in a lowered efficiency of the tower. If an increased production (greater oxygen consumption) with good tower efficiencies is required, the height of the tower must be increased. This would also be necessary if a copper metal of lower surface area was used such as scrap copper instead of the blister shot copper. The use of cement copper and fine chopped wire creates insufficient voids for adequate air passage; such fine copper must be leached in agitated vessels.

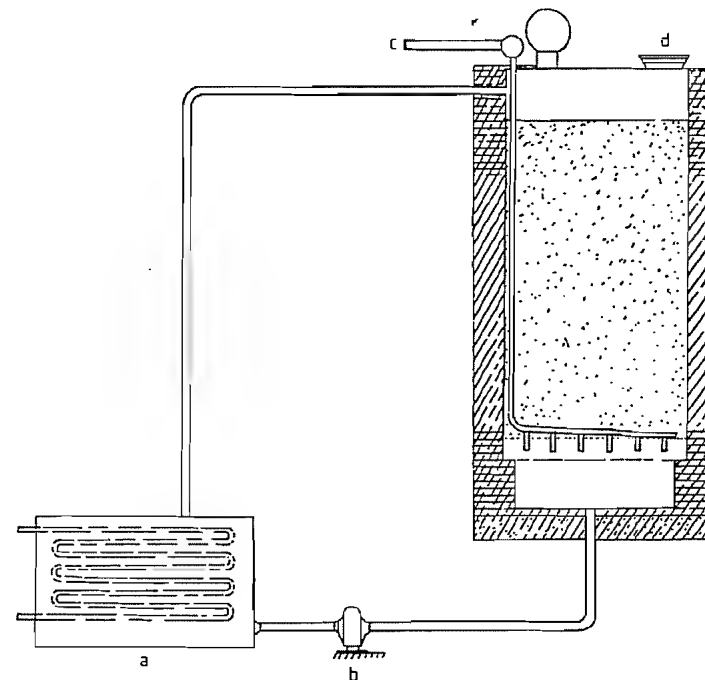


Figure 8.34: Harike tower process for production of copper(II) sulfate solutions: a) Heat exchanger; b) Circulation pump; c) Air inlet; d) Copper input.

Table 8.30: Specifications of electroless-grade copper(II) sulfate pentahydrate.

Assay	%
Copper	25.1
Iron	<0.0015
Lead	<0.003
Nickel	<0.001
Manganese	<0.0005
Chromium	<0.0005
Chlorine	nil
Water-insolubles	0.01

Anhydrous Copper Sulfate

CuSO_4 occurs in nature as the mineral hydrocyanite. It is gray to white and has a rhombic crystal morphology. It decomposes to the green basic copper(II) sulfate at 340 °C, and at 600–650 °C it decomposes to copper(II) oxide. Some of the properties of the anhydrous salt are as follows: d_4^{25} 3.6, c_p (273–291 K) 631.8 J kg⁻¹ K⁻¹, c_p (273–373 K) 657.3 J kg⁻¹ K⁻¹, ΔH^0 (25 °C) -771.6 kJ/mol. The compound is soluble in water, somewhat soluble in methanol (1.1 g/100 mL), but insoluble in ethanol. It readily dissolves in aqueous ammonia and excess alkali metal cyanides, with the formation of complexes. The material is hygroscopic, with conversion to the pentahydrate in moist air below 30 °C.

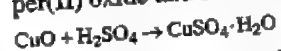
The anhydrous salt is prepared by careful heating of the pentahydrate salt to 250 °C. It can also be prepared by the reaction of hot concentrated sulfuric acid with copper metal, but purification is rather difficult.

The compound has limited commercial use but it can be used as a desiccant for removing water from organic solvents and is a sensitive indicator of the presence of moisture in such solvents.

Copper(II) Sulfate Monohydrate

$\text{CuSO}_4 \cdot \text{H}_2\text{O}$, d_4^{20} 3.25, is a whitish powder. The solubility of the monohydrate in water is identical to the pentahydrate on a copper basis. The product is hygroscopic and must be packaged in containers with moisture barriers. It is commercially produced by dehydration of the pentahydrate at 120–150 °C. A novel prepara-

tion is to triturate stoichiometric ratios of copper(II) oxide and sulfuric acid:



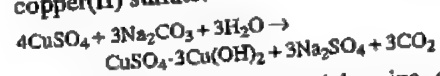
The uses of the monohydrate are analogous to those of the pentahydrate. Although there can be slight economic advantages (primarily freight costs) in using the monohydrate, market acceptance has not been great. Presently, less than 5% (copper basis) of copper(II) sulfate is marketed in the monohydrate form.

Basic Copper(II) Sulfates

Four distinct basic copper(II) sulfates can be identified by potentiometric titration of a copper(II) sulfate solution with sodium carbonate or sodium hydroxide solution [342, 343]: $\text{CuSO}_4 \cdot 3\text{Cu}(\text{OH})_2 \cdot \text{H}_2\text{O}$ (langite), $\text{CuSO}_4 \cdot 2\text{Cu}(\text{OH})_2$ (antlerite), $\text{CuSO}_4 \cdot 3\text{Cu}(\text{OH})_2$ (brochantite), and $\text{CuSO}_4 \cdot \text{Cu} \cdot 2\text{Cu}(\text{OH})_2 \cdot x\text{H}_2\text{O}$. Their unique crystal morphologies are confirmed by X-ray diffraction.

The most important commercial basic copper(II) sulfate, commonly referred to as *tribasic copper sulfate*, is $\text{CuSO}_4 \cdot 3\text{Cu}(\text{OH})_2$, mp ca. 380 °C (decomp.), d_4^{25} 3.78, occurs in nature as the green monoclinic mineral brochantite. It is readily soluble in mineral acids, acetic acid solution, and ammonia solution; it is insoluble in water. Above 650 °C it decomposes to copper(II) oxide. If anhydrous copper(II) sulfate is heated cautiously to 650 °C, another naturally occurring mineral is obtained, dolerophane, $\text{CuSO}_4 \cdot \text{CuO}$, which reacts readily with water at 20 °C to form $\text{CuSO}_4 \cdot 3\text{Cu}(\text{OH})_2 \cdot \text{H}_2\text{O}$ or at 100 °C to form $\text{CuSO}_4 \cdot 2\text{Cu}(\text{OH})_2$ [344].

Production. Tribasic copper(II) sulfate, the commercially available basic copper(II) sulfate, is most often prepared by the addition of sodium carbonate solution to hot solutions of copper(II) sulfate:

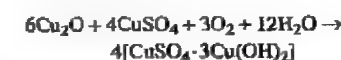
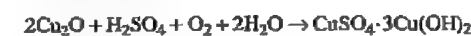


Great variation of particle size can be achieved by control of the precipitation temperature. As the temperature is increased, larger particles with greater bulk density are

formed. If a small particle size is desired, lower precipitation temperature should be used. However, as the precipitation temperature is lowered, multiple hydrates and larger amounts of sulfate are incorporated into the product; e.g., around 50 °C, the dried product contains only about 50% copper. A precipitation temperature around 90 °C is required to make a pure tribasic copper(II) sulfate.

The single largest use of the compound is as a crop fungicide, and small particles are preferred because they give a greater degree of coverage. These small particles can be obtained by high-energy attrition of the product or by carefully controlled precipitation conditions.

Another method of making tribasic copper(II) sulfate is the aeration of a suspension of copper(I) oxide in the presence of stoichiometric quantities of sulfuric acid or copper(II) sulfate [345]:



A purified, concentrated solution of copper(II) sulfate containing ammonium sulfate can be neutralized to pH 6.0–6.5 with ammonia to give a blue precipitate of approximate stoichiometry $4\text{CuSO}_4 \cdot 12\text{Cu}(\text{OH})_2 \cdot 5\text{H}_2\text{O}$. When this is dried, a green tribasic copper(II) sulfate is formed with up to 1 mol of hydration water per mole of tribasic salt [346]; the water content depends on the drying temperature.

A continuous process has been developed in which copper(II) sulfate solutions are neutralized to pH 5.9 at 30 °C by addition of gaseous ammonia to an agitated vessel [347]. A unique, germicidally active, basic copper(II) sulfate whose X-ray diffraction pattern differs from langite and brochantite has been prepared in this way [348].

Reaction of copper(II) sulfate with $\text{Na}_3\text{PO}_4 \cdot 12\text{H}_2\text{O}$ and sodium hydroxide in aqueous solution gives a fine, blue, basic copper(II) sulfate powder (16% SO_4 , 2.6% PO_4 , and 54.9% Cu) that is formulated into a germicidal powder.

Tribasic copper(II) sulfate can also be prepared by cautiously heating copper(II) sulfate to 340 °C or by the aeration of a hot copper(II) sulfate solution in contact with copper metal.

Other basic copper(II) sulfates of commercial interest are the classic fungicidal mixtures, Bordeaux and Burgundy slurries, in which copper(II) sulfate solution is mixed with lime and soda ash, respectively. They are of variable stoichiometry. More recently, the aqueous Bordeaux suspension has been dried to yield a stable basic copper(II) sulfate powder of variable composition [349].

Uses. As stated earlier, basic copper(II) sulfate is primarily used as a crop fungicide [350, 351]. It has also been utilized as a precursor in the separation of copper from metallic impurities [352].

Analysis and Specifications. The analysis of a typical technical-grade tribasic copper(II) sulfate is (mass fractions in %) as follows: copper 53.5, iron 0.08, sulfate 19.0, carbonate 2.0, water 2.0–5.0. This is analyzed according to [271].

8.11.4 Compounds and Complexes of Minor Importance

8.11.4.1 Compounds

Copper(I) acetate, CuCH_3COO , is obtained as white crystals which are stable when dry but decompose on exposure to water. The product is obtained by reducing an ammoniacal solution of copper(II) acetate; on acidification with acetic acid, the crystals precipitate. Ammoniacal solutions of copper(I) acetate are used commercially to absorb olefins.

Copper(II) acetate monohydrate, neutral verdigris, $\text{Cu}(\text{CH}_3\text{COO})_2 \cdot \text{H}_2\text{O}$, mp 115 °C, d_4^{25} 1.88, decomposes at 240 °C; it forms dark green, monoclinic crystals; its solubility in water at 25 °C is 6.8 g/100 g solution; the compound is slightly soluble in methanol, diethyl ether, and acetone.

Copper(II) acetate monohydrate is produced by the reaction of copper(II) carbonate

or copper(II) hydroxide with a solution of acetic acid or by the reaction of copper(II) oxide with hot dilute acetic acid. Alternatively, the material can be made by refluxing aqueous acetic acid in the presence of copper metal and air. The technical product is generally 99% pure.

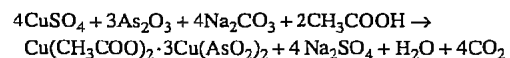
Copper(II) acetate monohydrate is used in textile dyeing and as a ceramic pigment. It is used as a fungicide, as a precursor in the production of Paris green [copper(II) acetoarsenite], and as a polymerization catalyst in organic reactions.

Basic copper(II) acetate, $\text{Cu}(\text{CH}_3\text{COO})_2 \cdot \text{CuO} \cdot 6\text{H}_2\text{O}$ (variable), exists as blue to green salts, depending on the amount of water of hydration. Blue verdigris has the above formula, while green verdigris has fewer molecules of water of hydration. The salts are slightly soluble in water or ethanol, and soluble in dilute mineral acid or aqueous ammonia.

The basic salts are produced by neutralizing copper(II) acetate solutions. They can also be prepared by refluxing acetic acid over copper in the presence of air until the basic salt precipitates.

The basic copper(II) acetates are used as precursors in the manufacture of Paris green [copper(II) acetoarsenite] and as fungicides. They are used as pigments in oil- and water-based paints and in textile dyeing.

Copper(II) acetoarsenite, (acetato)tri-metaarsenitodicopper(II), $\text{Cu}(\text{CH}_3\text{COO})_2 \cdot 3\text{Cu}(\text{AsO}_2)_2$ (variable), also known as Paris green, is an emerald green, poisonous powder. It is virtually insoluble in water and ethanol but dissolves in dilute mineral acids and aqueous ammonia. Copper(II) acetoarsenite is primarily made by the reaction of a solution of copper(II) sulfate with arsenic(III) oxide, sodium carbonate, and acetic acid



or by the reaction of copper(II) oxide with a hot solution of acetic acid and arsenic(III) oxide. A solution of copper(II) acetate or a suspension of basic copper(II) acetate can also

react with arsenic(III) oxide. The product is used as an insecticide, in the preservation of wood, and as an antifouling pigment.

Copper(II) arsenate, $\text{Cu}_3(\text{AsO}_4)_2 \cdot 4\text{H}_2\text{O}$ (variable), is a blue-green to blue insoluble powder. It is most often prepared by reaction of copper(II) sulfate solutions with arsenic(V) oxide and sodium hydroxide. Copper(II) arsenate is used as an insecticide, fungicide, rodenticide, wood preservative, and antifouling pigment.

Copper(II) arsenite, CuHAsO_3 (variable), Scheele's green, an insoluble green powder, is prepared by the reaction of a copper(II) sulfate solution with arsenic(III) oxide and sodium hydroxide and is used as pigment and insecticide.

Copper(I) bromide, CuBr , *mp* 504 °C, *bp* 1345 °C, d_4^{25} 4.72, forms white cubic crystals that slowly decompose on exposure to light or to moist air; it is soluble in hydrochloric and hydrobromic acids and in aqueous ammonia, but very slightly soluble in water. This compound is prepared pyrometallurgically [see copper(I) chloride, or by reducing a copper(II) sulfate solution in the presence of sodium bromide, usually with sulfur dioxide or metallic copper. Copper(I) bromide is used as a polymerization catalyst for organic reactions.

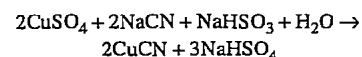
Copper(II) bromide, CuBr_2 , *mp* 498 °C, d_4^{25} 4.77, crystallizes from warm solution as black, deliquescent, monoclinic crystals. Below 29 °C, the green tetrahydrate, $\text{CuBr}_2 \cdot 4\text{H}_2\text{O}$, results. The anhydrous product is very soluble in water (55.7 g/100 g solution) and soluble in ethanol and acetone. It is insoluble in diethyl ether, benzene, or concentrated sulfuric acid. Copper(II) bromide is most conveniently prepared by dissolving copper(II) oxide in hydrobromic acid; it can also be prepared by the direct action of bromine water on metallic copper. Copper(II) bromide is used as a brominating reagent and catalyst in organic synthesis and as an intensifier in photography.

Copper(II) chromate(VI), CuCrO_4 , is obtained as reddish brown crystals. Numerous insoluble basic salts can be formed from solu-

tions. Neutral copper(II) chromate is prepared by direct heating of a mixture of copper(II) oxide and chromium(VI) oxide. It decomposes around 400 °C, with the formation of copper(II) chromate(III). Copper(II) chromate(VI) is used in wood preservation and in the weatherproofing of textiles.

Copper(II) chromate(III), CuCr_2O_4 , forms black, tetragonal crystals which are insoluble in water. It is prepared by heating neutral copper(II) chromate(VI) to 400 °C. Copper(II) chromate(III) is used as a hydrogenation catalyst.

Copper(I) cyanide, CuCN , *mp* 474 °C (in nitrogen), d_4^{25} 2.92, is usually a white to cream-colored powder, which is practically insoluble in water, cold dilute acids, and ethanol, but dissolves in ammonia and alkali cyanide solutions with the formation of complexes. Copper(I) cyanide is produced by the addition of an alkali cyanide and sodium hydrogensulfite to a solution of copper(II) sulfate:



Copper(I) cyanide is very poisonous and must be handled cautiously. It is used in electroplating and in organic reactions as a polymerization catalyst or as a means of introducing the cyanide moiety. Copper(I) cyanide has also been used as an antifouling pigment for marine paints and is an active fungicide and insecticide.

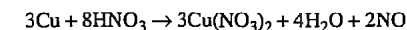
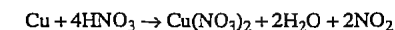
Copper(II) formate, $\text{Cu}(\text{HCOO})_2$, *mp* ca. 200 °C (decomp.), d_4^{25} 1.831, is soluble in water and slightly soluble in ethanol. The reaction of copper(II) oxide, carbonate, or hydroxide with formic acid is used to prepare the product. The most common commercial form, a royal blue material, is prepared by crystallization from water at 75–85 °C. A metastable dihydrate is produced by crystallization at 50–60 °C. Copper(II) formate tetrahydrate is prepared by crystallization from cool solutions. Copper(II) formate is used to prevent bacterial and mildew growth in cellulosic materials.

Copper(I) iodide, CuI , *mp* 605 °C, *bp* 1290 °C, d_4^{25} 5.62, occurs in nature as the mineral marshite, white to reddish brown cubic crystals. It is virtually insoluble in water but dissolves in ammonia solution, alkali iodide and cyanide solutions, and dilute hydrochloric acid. Copper(I) iodide is manufactured pyrometallurgically by the reaction of hot copper with iodine vapor. Alternatively, copper(II) salt solutions are reacted with alkali iodides to precipitate copper(I) iodide.

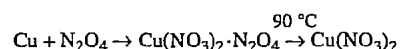
Copper(I) iodide is used as a heat and light stabilizer in polymers, photographic emulsions, and light-sensitive papers, and in oil drilling to aid in corrosion inhibition in highly acid environments. It is also used as a feed additive, in cloud seeding, and as a double salt with mercury(II) iodide as a temperature indicator.

Copper(II) nitrate trihydrate, $\text{Cu}(\text{NO}_3)_2 \cdot 3\text{H}_2\text{O}$, *mp* 114.5 °C, d_4^{25} 2.32, is a blue, deliquescent salt that crystallizes as rhombic plates. It is very soluble in water (77.4 g/100 g solution) and ethanol. When crystallized from solution below the transition point (26.4 °C), the hexahydrate is produced, $\text{Cu}(\text{NO}_3)_2 \cdot 6\text{H}_2\text{O}$, *mp* 26.4 °C (with loss of 3 mol of water of hydration), d_4^{24} 2.07, blue, deliquescent, prismatic crystals. The anhydrous nitrate is not produced by heating the hydrates; instead, decomposition to the basic copper(II) nitrate, $\text{Cu}_2(\text{NO}_3)(\text{OH})_3$, begins around 80 °C. Conversion to copper(II) oxide is complete at 180 °C.

Copper(II) nitrates are obtained by dissolving copper(II) oxide, basic copper(II) carbonate, or copper(II) hydroxide in nitric acid solution. The various hydrate crystals obtained depend on the conditions of crystallization. Basic copper(II) nitrate can be precipitated directly from solution by neutralization. Copper(II) nitrate salts are often produced by dissolving copper metal in nitric acid solution. The reaction is vigorous, and oxides of nitrogen are evolved:



The second reaction is favored by a lower temperature and dilute acid. Anhydrous copper(II) nitrate can be produced in ethyl acetate:



It is not available commercially.

The hydrates of copper(II) nitrate are used in the textile industry as oxidants and mordants in dyeing. They are used to prepare a copper(II) oxide of high surface area, which is useful as a catalyst in numerous organic reactions. The nitrate salts are used as colorants in ceramics, in the preparation of light-sensitive papers, and in the burnishing of iron, as well as the browning of zinc and brightening of aluminum. They are also used in pyrotechnics and as an oxidative component in solid rocket fuels.

Copper(II) oxalate, CuC_2O_4 , is a blue-white powder, which is very slightly soluble in water. Copper(II) oxalate is prepared by precipitation from a mixture of a copper(II) salt and sodium oxalate solution. The product is used as a stabilizer for acetylated polyformaldehyde and as a catalyst in organic reactions.

Copper(II) phosphate trihydrate, $\text{Cu}_3(\text{PO}_4)_2 \cdot 3\text{H}_2\text{O}$, is a light blue powder which is insoluble in cold water, slightly soluble in hot water, and soluble in ammonia solution and mineral acids. This compound is prepared by reaction of copper(II) sulfate solution with soluble alkali phosphates; it precipitates as a voluminous, almost gelatinous, product. Copper(II) phosphate trihydrate is used as a fungicide and corrosion inhibitor.

Copper(II) diphosphate hydrate, $\text{Cu}_2\text{P}_2\text{O}_7 \cdot x\text{H}_2\text{O}$ (variable), has the following typical analysis: Cu 33–36%, P_2O_7 45–49%. Copper(II) pyrophosphate is a light blue powder which is insoluble in water, but soluble in solutions containing an excess of diphosphate. It is prepared by the precipitation reaction of solutions of copper(II) sulfate and alkali diphosphate. Solutions are used for plating copper on plastics, aluminum, and zinc.

Copper(II) selenide, CuSe , *mp* not defined, d_4^{25} 6.0, decomposes at dull red heat; it is in-

soluble in water but dissolves in hydrochloric acid with evolution of H_2Se . Copper(II) selenide is prepared by reducing copper(II) selenite with hydrazine. It is used as a catalyst in the digestion of organic chemicals by the Kjeldahl method.

Copper(II) soaps are water-insoluble copper salts of long-chain fatty acids. They are usually sold as 6–10% copper solutions in a kerosene diluent. The copper(II) soaps are commonly prepared by direct reaction of the fatty acid with copper(II) hydroxide or basic copper(II) carbonate in an organic diluent, or by precipitation from aqueous media when copper(II) sulfate solution is mixed with the sodium salt of the respective fatty acid. The common commercially available soaps, concentrations, and uses follow.

Copper(II) naphthenate contains 8% copper and is used as a mildewcide in textiles, woods, and paints, and to prevent barnacle growth on ship bottoms.

Copper(II) oleate (9-octadecenoate) contains between 6 and 9% copper, and is used as a combustion improver in fuel oils, as an emulsifier and dispersant, and as an antifouling coating for fish nets and lines.

Copper(II) stearate (octadecanoate) contains 10% copper, and is used in antifouling paints and in the preservation of wood and textiles.

Copper(I) sulfide, Cu_2S , *mp* 1100 °C, d_4^{25} 5.6, occurs in nature as the mineral chalcocite, blue to gray rhombic crystals, also known as copper glance. It has a lustrous metallic look. Copper(I) sulfide is virtually insoluble in water, but is soluble with decomposition in nitric acid and concentrated sulfuric acid, and soluble in alkali cyanide solution through complex formation. It is decomposed to copper(II) oxide, copper(II) sulfate, and sulfur dioxide by heating in air, and to copper(II) sulfide and copper by heating in the absence of air. Copper(I) sulfide is prepared by heating copper and sulfur in a hydrogen atmosphere or by precipitation with hydrogen sulfide from an ammoniacal copper(II) salt solution. It is used in

luminous paints, lubricants, solar cells, thermoelements, and semiconductors.

Copper(II) sulfide, CuS , d_4^{25} 4.6, decomposes at 220 °C and occurs in nature as the mineral covellite, as blue-black hexagonal or monoclinic crystals. It is virtually insoluble in water, but soluble in alkali cyanides and in ammonia solution with complex ion formation. This compound is decomposed by hot nitric acid. It is stable in dry air, but is slowly oxidized to copper(II) sulfate in moist air. Copper(II) sulfide can be prepared by melting an excess of sulfur with copper(I) sulfide or by precipitation with hydrogen sulfide from a solution of anhydrous copper(II) chloride in anhydrous ethanol. It is used in the dye industry for the preparation of aniline black dyes and as an antifouling pigment.

Copper(II) tetrafluoroborate, $\text{Cu}(\text{BF}_4)_2$, is prepared commercially by the neutralization of tetrafluoroboric acid with copper(II) hydroxide or basic copper(II) carbonate. It is generally produced as a concentrated solution and is used in the production of printed circuits and in copper plating.

Copper(I) thiocyanate, CuSCN , *mp* 1084 °C (under nitrogen), d_4^{25} 2.84, is a white to yellow amorphous powder, which is very slightly soluble in water and dilute mineral acids, and soluble in ammonia solution, alkali thiocyanate solutions, and diethyl ether. It is stable to dry air but slowly decomposes in moist air. The material is prepared by reacting a copper(I) chloride solution with an alkali metal thiocyanate at 80–90 °C. The recovered product is dried under nitrogen. Copper(I) thiocyanate is used as an antifouling pigment.

8.11.4.2 Complexes

Copper(I) and copper(II) ions form many stable complexes with halides, amines, azo compounds, cyanides, and other complexing media. This, in part, accounts for the fact that more X-ray crystal structures have been determined for copper complexes than for any other first-row transition metal ion. Many of these complexes are of great commercial sig-

nificance. The dissociation constants for a number of copper complexes are given in Table 8.31.

Table 8.31: Dissociation constants of copper(I) and copper(II) complexes ($\text{p}K = -\log K$).

Complex ion	Dissociation products	$\text{p}K$
$[\text{CuCl}_3]^-$	$\text{CuCl} + 2\text{Cl}^-$	–2.0
$[\text{CuCl}_2]^-$	$\text{Cu}^+ + 2\text{Cl}^-$	4.7
$[\text{CuBr}_2]^-$	$\text{CuBr} + \text{Br}^-$	–3.3 to –2.3
$[\text{CuBr}_2]^-$	$\text{Cu}^+ + 2\text{Br}^-$	5 to 6
$[\text{Cu}(\text{CN})_3]^{2-}$	$[\text{Cu}(\text{CN})_2]^- + \text{CN}^-$	11.3
$[\text{Cu}(\text{CN})_2]^-$	$\text{Cu}^+ + 2\text{CN}^-$	16
$[\text{Cu}(\text{NH}_3)_2]^+$	$\text{Cu}^+ + 2\text{NH}_3$	10.8
$[\text{Cu}(\text{NH}_3)_2]^{2+}$	$\text{Cu}^{2+} + \text{NH}_3$	4.1
$[\text{Cu}(\text{NH}_3)_2]^{2+}$	$\text{Cu}^{2+} + 2\text{NH}_3$	3.5
$[\text{Cu}(\text{NH}_3)_3]^{2+}$	$\text{Cu}^{2+} + 3\text{NH}_3$	2.9
$[\text{Cu}(\text{NH}_3)_4]^{2+}$	$\text{Cu}^{2+} + 4\text{NH}_3$	2.1
$[\text{Cu}(\text{NH}_3)_5]^{2+}$	$\text{Cu}^{2+} + 5\text{NH}_3$	–0.5
$[\text{CuCl}_4]^{2-}$	$[\text{CuCl}_3]^- + \text{Cl}^-$	0.01
$[\text{CuCl}_3]^-$	$\text{CuCl}_2 + \text{Cl}^-$	0.06
CuCl_2	$\text{CuCl}^+ + \text{Cl}^-$	0.4
CuCl^+	$\text{Cu}^{2+} + \text{Cl}^-$	1
$[\text{Cu}(\text{OH})_4]^{2-}$	$[\text{Cu}(\text{OH})_3]^- + \text{OH}^-$	0.9
$[\text{Cu}(\text{OH})_3]^-$	$\text{Cu}(\text{OH})_2 + \text{OH}^-$	–5

Copper Ammine Complexes. Copper(II) salts form complexes of the type $[\text{Cu}(\text{NH}_3)_n]^{2+}$ where $n = 1$ –5. The pentaammine complex is favored only in concentrated ammonia solution (Table 8.31). The hexaammine complex is formed only in anhydrous ammonia. The tetraammine complex of copper(II) is favored at low ammonia concentrations. For the copper(I) complexes of ammonia, the diammine complex is favored. Tetraammine copper(II) hydroxide, $[\text{Cu}(\text{NH}_3)_4](\text{OH})_2$, Schweitzer's reagent, is used in the dissolution of cellulose and in the production of rayon. Copper(I) diammine salt solutions are used in the absorption of olefins and carbon monoxide. Many copper circuit boards are etched with ammoniacal ammonium salt solutions; copper ammine solutions, which can be used in the production of copper compounds, are by-products of this process.

Copper Chloride Complexes. Copper(I) and copper(II) ions form complexes with hydrochloric acid or soluble metal chlorides. Dilute solutions of copper(II) chloride are blue. As

the chloride concentration increases, the color of the solution shifts toward green, intensifying as the concentration of the distorted tetrahedral $[\text{CuCl}_4]^{2-}$ ion increases. Copper(II) compounds have been isolated that contain either the $[\text{CuCl}_4]^{2-}$ anion or the $[\text{CuCl}_3]^-$ anion, e.g., CsCuCl_4 and KCuCl_3 , respectively.

The insoluble copper(I) chloride can be solubilized by chloride-containing solutions, with the formation of the $[\text{CuCl}_2]^-$ ion. The benzene-insoluble copper(I) chloride dissolves readily in the presence of anhydrous aluminum chloride with formation of the $\text{Al}[\text{CuCl}_4]$ complex. In acetonitrile, copper(I) chloride is solubilized with the formation of the isolable $[\text{Cu}(\text{CH}_3\text{CN})_4]\text{Cl}$ complex.

Copper(I) Cyanide Complexes. Alkali cyanides readily dissolve copper(I) cyanide, with the formation of $[\text{Cu}(\text{CN})_2]^-$ and $[\text{Cu}(\text{CN})_3]^{2-}$ complexes. Solutions or the complexes are of great importance in the electroplating industry because of their versatility. From saturated copper and sodium cyanide baths, crystals of the double salt $\text{Na}_2\text{Cu}(\text{CN})_3 \cdot 2\text{H}_2\text{O}$ can be obtained readily.

Other Copper Complexes of Industrial Significance. Solvent extraction of copper(II) ions relies on the ability of copper to form complexes and to break those complexes as a function of pH [337, 353, 354]. The most common reagents used commercially are substituted salicylaldoximes, 1,8-hydroxyquinolines, and α -hydroxyoximes.

Copper(II) is solubilized in alkaline media by complex formation with tartrates for use as Fehling's solution, which is utilized in the analysis of reducing sugars. Copper(II) *bis*-(1,8-dihydroxyquinoline) is used as a textile fungicide and as a pigment. Copper phthalocyanines [355, 356] are exceptionally stable blue and green pigments, as are the azo dye complexes of copper.

8.11.5 Reclamation

The reclamation or recycling of copper wastes and by-products is environmentally imperative and, in many cases, economically

sound. Better technologies have been developed to produce useful materials from wastes and by-products, many of which are now considered hazardous wastes. The establishment of the Resource Conservation and Recovery Act by the EPA defined procedures to assure proper disposal or reclamation of hazardous wastes [357]. However, no distinction is made between waste buried in an approved landfill and waste recovered as useful products. Unfortunately, in many cases this encourages the burial of recyclable waste materials.

The largest sources of reclaimable by-product copper are the electronics and plating industries, as well as spent electrowinning baths [340]. Electrowinning baths are most often crystallized or precipitated as tribasic copper(II) sulfate for use in agriculture.

In the manufacture of circuit boards, a copper laminate is selectively dissolved (etched). This dissolution process yields the desired circuit board and a by-product copper solution, the spent etchant. The earliest etching solutions used iron(III) chloride-hydrogen chloride or chromium trioxide sulfuric acid solutions which were difficult to recycle. Later, the sulfuric acid etchants that used hydrogen peroxide [358, 359] or persulfate [360–362] as oxidants were developed. Recycling of the copper is achieved through crystallization, precipitation [362], ion exchange [363], or cementation [364, 365]. Alkaline etchants utilized a mixture of ammonia and ammonium sulfate with persulfate as the oxidant [366] or a mixture of ammonia and ammonium chloride with chlorite as the oxidant [367]. The primary etchants used today are the ammonia ammonium chloride system with air as the oxidant and the hydrochloric acid system with stabilized hydrogen peroxide as the oxidant [368].

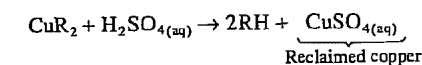
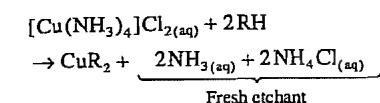
Copper is recovered from the acid chloride etchants:

- By neutralization and precipitation of copper(II) oxychloride or copper(II) oxide [262]
- By reduction with sodium hydrogensulfite, for example, to precipitate copper(I) chlo-

ride which can then be converted to copper(I) oxide by sodium hydroxide treatment [369]

- By cementation with scrap iron [370]. From the alkaline etchants, copper is recovered:
- By distillation to strip ammonia and precipitate copper(II) oxide [371]
- By addition of base to precipitate copper(II) hydroxide, followed by steam stripping of the ammonia [372]
- By reduction to copper with formaldehyde [373] or $\text{Na}_2\text{S}_2\text{O}_4$ [374]
- By electrolysis [375].

One of the more elegant methods for the recovery of copper from ammonia ammonium chloride etchants utilizes solvent extraction [376] (Figure 8.35). Not only is the copper recovered, but the etchant is simultaneously regenerated:



where R is an α -hydroxyoxime as shown by equation (1).

The copper can be further reclaimed by crystallization or electrowinning.

8.11.6 Copper and the Environment

The reclamation of copper by-products and wastes and the regulation of plant effluents and sanitary waters have resulted in lower indiscriminate release of copper into natural waters [377]. Where large quantities of copper in high concentration exist, recovery of the copper can, in many cases, be economical. Regulations have been established to control or limit altogether the introduction of copper into waters [378–382]. The Federal Water Pollution Control Act Amendments of 1972 set up a comprehensive program to "restore and main-

tain the chemical, physical, and biological integrity of the nation's waters" [378].

Limitations of copper in drinking water have also been established: the World Health Organization recommends 0.05–1.5 mg/L [383]. No specific drinking water standards for copper have been established by the Environmental Protection Agency [384].

A variety of technologies presently exist for the removal of copper from wastewaters and drinking water [385, 386]. The most common treatment methods include direct precipitation [378–380, 387–390] or electrolysis [391, 392].

Although copper is toxic in exceedingly low concentrations to certain lower life forms, notably fungi and algæ, it is a necessary constituent of higher plants and animals. Copper plays a necessary role as an oxidation catalyst and oxygen carrier, probably second only to iron in importance [393]. Copper aids plants in photosynthesis and other oxidative processes. In higher animals, it is responsible for oxidative processes and is present in many proteins such as phenolase, hemocyanin, galactose oxidase, superoxide dismutase, ceruloplasmin, tyrosinase, monoamine oxidase, and dopamine β -hydroxylase [394, 395].

Copper compounds are regularly applied for their nutrient value to agricultural crops in European countries [396–398]. In the United States, more emphasis is now being placed on the value of copper as a nutritional feed additive [396, 399, 400]: it increases the rate of gain and feed efficiencies of the animals. The increased use of copper as a feed additive has caused concern about the environmental impact of high levels of copper in manure [401, 402]. The recently approved maximum total copper content in animal feeds for Western European countries is shown in Table 8.32 [396].

Table 8.32: Maximum copper levels in Western European animal feeds.

Use	Total copper, mg/kg
Fattening pigs, up to 16 weeks	175
Fattening pigs, 17th week to 6th months	100
Fattening pigs, over 6 months	50
Breeding pigs	50
Calves, fed milk-based products	30
Calves, other feeds	50
Sheep	20
Other animals	50

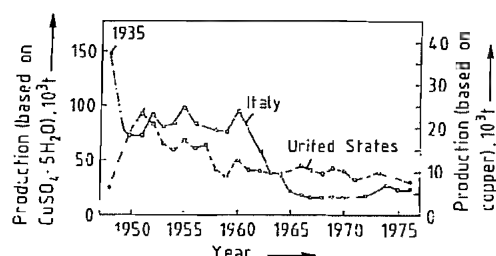
The largest single application of copper compounds is as an agricultural fungicide. Although copper is a necessary constituent of higher plants and animals, it is highly toxic to certain fungi. In human medicine, the importance of copper as a nutrient in proper development and growth is receiving increased study [394, 403]. Also, copper is being used in the production of new copper antibiotics and copper anti-inflammatory drugs [403]. The recommended daily requirement of copper is as follows [403]:

Humans	2.5–5.0 mg
Cattle	50–70 mg
Horses	50–60 mg
Sheep	10–15 mg
Swine	10–20 mg

8.11.7 Economic Aspects

The world's production of copper compounds represents less than 2% of the total production of primary metal [285]. In 1974, 7.65×10^6 t of primary copper was produced, with 1.3% (100 000 t) used in the production of copper compounds. Of these 100 000 t, 80% is used to prepare copper(II) sulfate pentahydrate.

Historically, the United States and Italy have led the world in producing copper sulfate pentahydrate (Figure 8.36) [285]. The U.S. production and valuation of copper sulfate pentahydrate are given in Table 8.33 [404].

**Figure 8.36:** Production of copper(II) sulfate pentahydrate in Italy and the United States (1950–1976).**Table 8.33:** Production and valuation of copper(II) sulfate pentahydrate in the United States.

Year	Production		Price of copper(II) sulfate pentahydrate, US\$/kg
	Quantity, t	Copper content, t	
1978	31 800	8551	1.04
1979	35 005	9286	1.18
1980	31 010	8445	1.23
1981	35 640	9413	1.14
1982	32 230	8385	1.08

Table 8.34: Estimate of current annual use of copper in agriculture [396].

Country	Total, t	Fungicide, %	Animal feed, %	Crop nutrient, %
<i>Europe</i>				
France	5 380	83.6	14.9	0.9
Germany	2 800	35.7	28.6	35.7
Greece	1 410	97.9	1.4	0.7
Italy	6 220	96.5	3.2	0.3
Portugal	1 120	89.3	8.9	1.8
Spain	2 800	89.3	10.7	0.0
Others	15 563	49.8	34.5	15.8
<i>Asia and Australia</i>				
Australia	1 556	19.3	6.4	74.3
India	3 500	0.0	0.0	100.0
Japan	2 040	98.0	1.2	0.7
Others	1 811	78.7	0.6	20.3
<i>Africa</i>				
Algeria	1 750	100.0	0.0	0.0
Kenya	1 000	100.0	0.0	0.0
Tanzania	2 000	100.0	0.0	0.0
Others	2 635	96.4	0.6	3.0
<i>America</i>				
Brazil	7 160	97.8	1.4	0.8
Mexico	1 650	100.0	0.0	0.0
United States	6 400	46.9	9.4	43.8
Others	3 540	40.7	2.8	56.6
Total	70 305	76.4	12.1	11.4

According to estimates about 70% (70 000 t) of the total world's production of copper compounds is used in agriculture [396]. Table 8.34 gives a breakdown by region, country,

and use. Copper sulfate pentahydrate can be blended directly with feed or fertilizers for animal feeds or crop nutrients, respectively. For application as a foliar fungicide, it must be rendered insoluble to prevent it from being easily washed off the leaf. The first copper fungicide on the market was Bordeaux mixture (1882), a combination of lime and copper sulfate [405]. The inherent phytotoxicity of Bordeaux mixture led to the development of the "fixed coppers" in the 1920s and 1930s. The fixed coppers are grouped into four categories: (1) basic sulfates, (2) basic chlorides, (3) oxides, and (4) miscellaneous — silicates, phosphates, etc. [406, 407]. To enhance their performance, the fixed coppers are usually blended with wetting agents, dispersants, sticking agents, and diluents. Since better coverage and enhanced efficacy are obtained with smaller particles, the basic coppers are usually ground before packaging [408]. Table 8.35 gives a partial list of available fixed copper fungicides.

8.11.8 Toxicology and Occupational Health

Copper is an essential trace element in humans. In larger quantities it can be lethal. The salts are usually considered to be more toxic than the metal. The acute oral toxicity in humans, LD_{50} , is about 100 mg/kg; however, recovery has occurred after ingestion of up to 600 mg/kg. The symptoms of copper poisoning include nausea, vomiting, gastric disturbances, apathy, anemia, cramps, convulsions, coma, and death.

Many reported cases of illness were once attributed to chronic copper poisoning, but they are now thought to be caused by impurities in the refining of copper, e.g., lead, arsenic, and selenium [409, 410]. The question of chronic poisoning is still open to debate. Prolonged exposure to copper dust can cause

skin irritation and discoloration of skin and hair. Whether pathological changes occur is uncertain, although there is evidence of accumulation of copper in the liver. Attempts to induce chronic copper poisoning in animals have been unsuccessful.

The inhalation of dusts of copper compounds irritates the upper respiratory tract [411, 412]. Ulceration and perforation of the nasal septum have occurred. Workers exposed to dusts of copper salts complained of metallic tastes and irritation of the oral and nasal mucosa. Smokers complained of an intense sweet taste during inhalation of the smoke. Long-term exposure to copper-containing dust has resulted in atrophic changes in the mucous membranes. Mild nasal discomfort was noted in workplace concentrations as low as 0.08 mg/m³. A very small fraction of the workers exhibited allergic skin reactions from exposure to copper-containing dust [413, 414].

Copper compounds embedded in the eye produce a pronounced foreign body reaction with discoloration of the ocular tissue. Conjunctivitis, ulceration, and turbidity have been reported [415, 416].

The current workplace standard for copper dust concentration in air, MAK and TLV, is 1 mg/m³ [417–419]. Copper fume standards are 0.2 mg/m³ [417] and 0.1 mg/m³ [418, 419]. A number of reviews and books of a more specific nature report detailed animal and workplace studies [420–424].

8.12 Copper Pigments

Copper and gold bronze pigments (powdered copper–zinc alloys) are usually produced by dry milling. Depending on the alloy composition, the following "natural shades" are produced:

Copper	100% copper
Pale gold	ca. 90% copper and 10% zinc
Rich pale gold	ca. 85% copper and 15% zinc
Rich gold	ca. 75% copper and 25% zinc

Table 8.35: Commercially available fixed coppers.

Manufacturer/representative	Trade name	Active ingredient	Cu, %
BASF	BASF-Grünkupfer	copper oxychloride	45
	Kauritil	copper oxychloride	47
Bayer	Cupravit-Spezial	copper oxychloride	45
	Cupravit-Forte	copper oxychloride	50
CP Chemicals	Basic Copper Sulfate	tribasic copper sulfate	53
	Champion WP	copper hydroxide	50
Cuproquim	Hydrox	copper hydroxide	50
Hoechst	Vitigran, Conc.	copper oxychloride	45
Kocide/Griffin	Kocide 101	copper hydroxide	50
Merck	Perenox	copper(I) oxide	50
Norddeutsche-Affinerie	Cobre Nordox	copper(I) oxide	50
Phelps-Dodge	Tribasic Copper Sulfate	tribasic copper sulfate	53
Sandoz	Cobre Sandoz	copper(I) oxide	50
Simplot	Blue Shield	copper hydroxide	50
Spieß Urania	Funguran	copper oxychloride	45
	Cuprasol	copper oxychloride	50
Tennessee Copper	Tribasic Copper Sulfate	tribasic copper sulfate	53
Wacker	Wacker-Kupferkalk	copper oxychloride	15–18

Copper–zinc alloys with a higher zinc content (brass) cannot be ground or formed into flake pigments on account of their brittleness. Controlled oxidation of “natural” bronze powders converts them into “fired” bronze powders. These shades (e.g., English green, lemon, ducat gold, fire red) are produced as a result of interference effects that depend on the thickness of the oxide coating.

Copper and gold bronze pigments are not as colorfast as aluminum pigments because they decompose to produce colored oxides and corrosion products. However, stabilized pigments (e.g., with a silica coating) are also available for critical applications in binders with high acid values or that react with copper or zinc.

The classical fields of application for the gold bronze pigments are the graphics industry (bronzing); printing (offset, gravure, flexographic, and screen printing); and coloring plastics. They are also used in the paint industry for decorative finishes (e.g., dip coatings for candles).

Gold bronze pigments are nontoxic. In Germany they are permitted in food packaging materials provided that they do not lead to contamination of the food. They are also allowed for printing on cigarette paper and filter tips according to the tobacco regulations if the zinc content does not exceed 15%. Similar

regulations apply in the United States and other countries.

8.13 References

- V. Tafel: *Lehrbuch der Metallhüttenkunde*, 2nd edition, vol. 1, Hirzel, Leipzig 1951.
- A. Butts: *Copper – The Science and Technology of the Metal, Its Alloys and Compounds*, Reinhold Publ. Co., New York 1954.
- N. N. Muratsch: *Handbuch des Metallhüttenmannes*, vol. 1, VEB-Verlag Technik, Berlin, 1954.
- Gmelin, system no. 60, “Kupfer”, Part A (1955).
- H. Grothe (ed.): *Lueger-Lexikon der Technik*, 4th edition (*Lexikon der Hüttenkunde*), Deutsche Verlagsanstalt, Stuttgart 1963.
- A. Sutulov: *Copper Production in Russia*, University of Concepción, Chile, 1967.
- R. P. Ehrlich: “Copper in Metallurgy”, *Symposium of the Metallurgical Society*, Denver, CO, Feb. 15–19, 1970.
- M. J. Jones (ed.): “Advances in Extractive Metallurgy and Refining”, *Symposium of the Institution of Mining and Metallurgy*, London, Oct. 4–6, 1971.
- Winnacker-Küchler, 4th edition, vol. 4, p. 350.
- A. Sutulov: *Copper Porphyries*, University of Utah, Salt Lake City 1974.
- M. J. Jones (ed.): “Copper Metallurgy – Practice and Theory”, *Symposium of the Institution of Mining and Metallurgy*, Brussels, Feb. 11, 1975.
- J. C. Yannopoulos, J. C. Agarwal (eds.): *Extractive Metallurgy of Copper*, vol. 1: “Pyrometallurgy and Electrolytic Refining”, The Metallurgical Society of AIME, New York, NY, 1976; (AIME Annual Meeting, Las Vegas 1976).
- A. K. Biswas, W. G. Davenport: *Extractive Metallurgy of Copper*, 3rd edition, Pergamon Press, Oxford–New York 1995.
- Deutsches Kupfer-Institut: *Kupfer*, 2nd edition, Berlin 1980.
- C. B. Gill: *Nonferrous Extractive Metallurgy*, J. Wiley & Sons, New York 1980.
- D. B. George, J. C. Taylor (eds.): *Copper Smelting – An Update*, The Metallurgical Society of AIME, Warrendale, PA, 1981.
- E. G. West: *Copper and Its Alloys*, Ellis Horwood Ltd., Chichester, England, 1982.
- T. K. Corwin, T. W. Devitt, M. A. Taft, A. C. Worrell: *International Technology for the Nonferrous Smelting Industry*, Noyes Data Corp., Park Ridge, NJ, 1982.
- H. Y. Sohn, D. E. George, A. D. Zunkel (eds.): *Advances in Sulfide Smelting*, vol. 1 (*Basic Principles*), vol. 2 (*Technology and Practice*), The Metallurgical Society of AIME, Warrendale, PA, 1983.
- F. Pawlek: *Metallhüttenkunde*, De Gruyter, Berlin–New York 1983.
- L. Aitchison: *A History of Metals*, vols. 1 and 2, MacDonald & Evans Ltd., London 1960.
- R. F. Tylecote: *History of Metallurgy*, The Institute of Metals, London 1976.
- Georgius Agricola: *Zwölf Bücher vom Berg- und Hüttenwesen* (1556), 5th edition, VDI-Verlag, Düsseldorf 1978.
- L. Suhling: *Der Seigerhüttenprozeß*, Riederer-Verlag, Stuttgart 1976.
- Landolt-Börnstein, IV 2b, 639–648, 668–719.
- Deutsche Ges. f. Metallkunde u. Verein Deutscher Ingenieure (eds.): *Werkstoff-Handbuch Nichteisenmetalle*, 2nd edition, part 3, VDI-Verlag, Düsseldorf 1960.
- American Society of Metals (eds.): *Metals Handbook*, 8th edition, vol. 1, Metals Park, Ohio, 1961.
- K. Dies: *Kupfer und Kupferlegierungen in der Technik*, Springer Verlag, Berlin 1961.
- D’Ans-Lax: *Taschenbuch für Chemiker und Physiker*, 3rd edition, vol. 1, Springer Verlag, Berlin 1967.
- Copper Development Assoc.: *CDA Technical Note TN 20: Copper Data*, London 1975.
- J. O’M. Bockris, A. K. N. Reddy: *Modern Electrochemistry*, 6th edition, vols. 1 and 2, Plenum Press, New York 1977.
- E. G. King, A. D. Mah, L. B. Pankratz: *Thermodynamic Data of Copper and Its Inorganic Compounds*, Int. Copper Res. Assoc., New York 1973.
- H. Käsche: *Die Korrosion der Metalle*, 2nd edition, Springer Verlag, Berlin 1979.
- S. K. Coburn (ed.): *Corrosion Source Book*, American Society for Metals, Metals Park, Ohio, 1984.
- M. Pourbaix: *Atlas of Electrochemical Equilibria in Aqueous Solutions*, Pergamon Press, Oxford 1966.
- P. Klare: *Kupfer-Sauerstoff-Wasserstoff, Auszüge aus dem Schrifttum der letzten hundert Jahre*, Ges. Deutscher Metallhütten- und Bergleute, Clausthal-Zellerfeld 1962.
- E. Fromm, E. Gebhardt (eds.): *Gase und Kohlenstoff in Metallen*, Springer Verlag, Berlin 1976.
- E. Kraume: *Die metallischen Rohstoffe*, 2nd edition, vol. 4: Kupfer, Enke Verlag, Stuttgart 1964.
- Bundesanstalt für Bodenforschung, Hannover, Deutsches Institut für Wirtschaftsforschung, Berlin: *Untersuchungen über Angebot und Nachfrage mineralischer Rohstoffe*, vol. 2: Kupfer (1972).
- W. Gocht: *Handbuch für Metallmärkte*, 2nd edition, Springer Verlag, Berlin 1985.
- Source: *Economic Studies Division*, CIPEC, Neuilly-sur-Seine, French, 1984.
- Z. S. Vukmanovic, *Metall (Berlin)* 38 (1984) 238.
- Metallgesellschaft: *Mitteilungen aus dem Arbeitsbereich Nr. 18: Manganknollen – Metalle aus dem Meer*, Frankfurt/Main 1975.
- D. Neuschütz, U. Scheffler, *Erzmetall* 30 (1977) 152–157.
- U. Kuxmann, *Erzmetall* 27 (1974) 55–64.
- Norddeutsche Affinerie: *Kupfer in Natur, Technik, Kunst und Wissenschaft*, Hamburg 1966.
- K. S. E. Forssberg (ed.): *Flotation of Sulfide Minerals*, Elsevier Sci. Publ., New York 1985.
- N. W. Kirshenbaum: *Transport and Handling of Sulfide Concentrates*, Stanford, CA, 1967.
- J. De Cuyper, *Erzmetall* 30 (1977) 88–94.
- F. Pawlek, *Erzmetall* 22 (1969) 413–414.
- M. Kaneko, *Eng. Min. J.* 175 (1974) no. 12, 61–64.
- R. O. Thomas, D. W. Hopkins in [11, p. 1–5].
- H. Schackmann, *Erzmetall* 20 (1967) 499–511.
- D. MacAskill, *Eng. Min. J.* 174 (1973) no. 7, 82–86.
- S. D. Michaelson et al., *J. Met.* 18 (1966) 172–180.
- H. Schlegel, A. Schüller, *Freiberg. Forschungsh. B* 1952, no. 2, 2–31.
- W. A. Krivsky, R. Schuhmann, *Trans. Am. Inst. Min. Metall. Pet. Eng.* 209 (1957) 981–988.
- Y. A. Chang, Y. E. Lee, J. P. Neumann in [12, vol. 1, p. 21–48].
- F. Johannsen, H. Knahl, *Erzmetall* 16 (1963) 611–621.
- E. M. Levin et al.: *Phase Diagrams for Ceramists*, vols. 1 and 2, The American Ceramic Soc., Columbus, OH, 1964; Suppl. 1969.
- P. Röntgen, R. Winterhager, R. Kammel, *Erzmetall* 9 (1956) 207–214.
- W. Wiese, *Erzmetall* 17 (1964) 298–305.
- J. M. Floyd, P. J. Mackey: *Extraction Metallurgy '81* (Symposium), The Institution of Mining and Metallurgy, London 1981.
- C. Diaz: “The Thermodynamic Properties of Copper–Slag Systems”, *INCRA Monogr. III*, USA, 1974.
- K. N. Subramanian, J. J. Themelis, *J. Met.* 24 (1972) no. 4, 33–38.
- B. T. Andersson, P. Paarni in [19, p. 1005].
- J. G. Eacott in [19, p. 583].
- W. Schwartz, *Erzmetall* 26 (1973) 113–120.
- M. Leiponen in [16, p. 323–339].
- H. H. Kellogg, *Eng. Min. J.* 178 (1977) no. 4, 61–64.
- H. Hilbrans, P. Paschen, *Erzmetall* 34 (1981) 639–644.
- Ch. H. Pitt, M. E. Wadsworth, *J. Met.* 33 (1981) 25–34.
- F. Habashi, R. Dugdale, *Met. Trans.* 4B (1973) no. 8, 1865–1871.
- F. Habashi, B. I. Yostos, *J. Met.* 29 (1977) no. 7, 11–16.
- R. S. Olsen et al., *Trans. Soc. Min. Eng. AIME* 254 (1973) no. 4, 301–305.
- K. Parameswaran et al. in [16, p. 294–295].
- G. Dobbert, W. Wiese: *Periodische Wechsel-Reduktionselektrolyse von Spurstein unter Gewinnung von*

- umformfähigem Elektrolytkupfer und Elementarschwefel, Forschungsberichte Nordrhein-Westfalen, Westdeutscher Verlag, Opladen 1977.
78. A. H. Kinneberg in [7, p. 173-176].
 79. Onahama Smelting & Refining Co., US4001013, 1977 (M. Goto et al.).
 80. K. Cormack, *Eng. Min. J.* **185** (1985) no. 6, 44-48.
 81. Ch. Baiqi, T. Xiangtin, J. Xigen, M. Yuebo: *Bai-Yin Copper Smelting Process*, Paper of the Bai-Yin Non-Ferrous Metals Co., China (1984).
 82. B. Ydstie: "The Electric Copper Matte Furnace", *104th AIME Annual Meeting*, New York, February 1975.
 83. I. S. Blair, K. G. Jones, I. Slaughter in [19, vol. 2, p. 817-838].
 84. Metallgesellschaft, DE855770, 1950 (C. A. Mæzler).
 85. P. Bryk, *Radex Rundsch.* **1952**, no. 1, 7-19.
 86. A. Lange, *Erzmetall* **13** (1960) 151.
 87. S. V. Härkki, J. T. Juusela: *New Developments in Outokumpu Flash Smelting Method*, Metallurgical Soc. of AIME, New York 1974, paper no. A 74-16.
 88. O. Fujii, M. Shima in [16, p. 165-171].
 89. M. Yasuda, T. Yuki, M. Kato, Y. Kawasaki in [16, p. 251-263].
 90. S. Okada, M. Miyake, A. Hara, M. Uekawa in [19, vol. 2, p. 855-874].
 91. Outokumpu Oy, DE 2 536 392, 1975 (O. A. Aaltonen, B. T. Andersson et al.).
 92. Outokumpu Oy, US 3 948 639, 1973 (E. O. Nermes, T. T. Talonen).
 93. T. N. Antonioni, C. M. Díaz, H. C. Garven, C. A. Landolt in [16, p. 17-31].
 94. K. I. Ushakov et al., *Tsvetn. Met. (N.Y.)* **16** (1975) no. 2, 5-9.
 95. G. Melcher, E. Müller, H. Weigel, *J. Met.* **28** (1976) 4-8.
 96. Humboldt Wedag's Cyclone, *Eng. Min. J.* **178** (1977) no. 10, 45, 49.
 97. G. Berndt, K. Emicke: *Extraction Metallurgy '85*, The Institution of Mining and Metallurgy, London 1985.
 98. F. E. Lathe, L. Hodnett: "Data on Copper Converter Practice in Various Countries", *Trans. TMS-AIME* **212** (1958) 603-617.
 99. R. E. Johnson (ed.): *Copper and Nickel Converters*, The Metallurgical Soc. of AIME, Warrendale, PA, 1979.
 100. F. Johannsen, H. Vollmer, *Erzmetall* **13** (1960) 313.
 101. P. J. Mackey, P. Tarasoff in [19, vol. 2, p. 408].
 102. J. Leroy, P. J. Lenoir: "Hoboken Type of Copper Converter and Its Operation", *Institution of Mining and Metallurgy, Symposium*, London, April 1967 (Paper 15).
 103. J. D. Gomez in [98, p. 291-311].
 104. Inspiration Consolidated Copper Co., GB 2 089 011 A, 1981 (A. F. Tittes et al.).
 105. R. Campos, C. Queirolo in [98, p. 257-273].
 106. G. Lindquist, P.-L. Nystedt, S. Petersson in [16, p. 41-49].
 107. J. M. Floyd, N. C. Grave, B. W. Lightfoot: *Extractive Metallurgy Symposium 1980*, The Australian Institute of Mining and Metallurgy, Melbourne, Australia, 1980, p. 63-74.
 108. D. A. Diomidovskii et al., *Tsvetn. Met. (Moscow)* **32** (1959) no. 2, 27-34.
 109. F. Sehnalek, J. Holeczy, J. Schmiedl, *J. Met.* **16** (1964) 416-420.
 110. K. J. Richards, D. G. George, L. K. Bailey in [19, p. 489-498].
 111. M. Goto, N. Kikumoto: "Process Analysis of Mitsubishi Continuous Smelting and Converting Process", *110th AIME Annual Meeting*, Chicago, February 1981.
 112. T. Suzuki, T. Nanago: "Development of New Continuous Copper Smelting Process", *Jt. MMIJ-AIME Meet.* Tokyo, May 1972.
 113. T. Suzuki et al. in [16, p. 60].
 114. M. P. Amsden, R. M. Sweetin, D. G. Treilhard, *J. Met.* **30** (1974) no. 7, 16-26.
 115. J. B. W. Bailey, A. G. Storey: "The Noranda Process after Six Years' Operation", *18th Annual CIM Conference of Metallurgists*, Sudbury, Ontario, August 1979.
 116. P. Tarasoff, "Process R & D — The Noranda Process", *Met. Trans. B* **15B** (1984) September, 417.
 117. P. J. Mackey, G. C. McKerrow, P. Tarasoff: "Minor Elements in the Noranda Process", *104th AIME Annual Meeting*, New York, February 1975.
 118. H. K. Worner, *Eng. Min. J.* **172** (1971) no. 8, 64-68.
 119. R. Schuhmann, P. E. Queneau: "Thermodynamics of the Q-S Oxygen Process for Coppermaking", *AIME Annual Meeting*, Las Vegas 1976.
 120. N. Torres, G. Melcher, *CIM Bull.* **77** (1984) no. 871, 86-91.
 121. G. J. Brittingham, DE 1 280 479, 1964.
 122. R. B. Worthington, *Rep. Invest. U.S. Bur. Mines* **1973**, 7705.
 123. G. Fleischer, R. Kammel, U. Lembke, *Metall (Berlin)* **32** (1978) 29-34.
 124. W. S. Nemes, *Trans. Inst. Min. Metall. Sect. C* **93** (1984) 180-192.
 125. W. S. Nemes, J. A. Charles, A. G. Cowen, *J. Met.* **13** (1961) 216-220.
 126. J. S. Jacobi, *J. Met.* **32** (1980) no. 2, 10-14.
 127. W. Schwartz, *Metall (Berlin)* **34** (1980) 121-124.
 128. H. P. Rajevic, W. R. Opie, *J. Met.* **34** (1982) no. 3, 54-56.
 129. R. Hubrich, K. Hein, *Neue Hütte* **28** (1983) 452-456.
 130. A. Bahr, *Erzmetall* **33** (1980) 324-330.
 131. J. Julius, *Metall (Berlin)* **38** (1984) 758-762.
 132. J. C. Yannopoulos, J. C. Agarwal (eds.): *Extractive Metallurgy of Copper*, vol. 2: "Hydrometallurgy and Electrowinning", The Metallurgical Society of AIME, New York, NY, 1976 (AIME Annual Meeting, Las Vegas 1976).
 133. L. A. Haas, R. Weir (eds.): "Hydrometallurgy of Copper, its Byproducts and Rarer Metals", The Metallurgical Society of AIME, New York 1983.
 134. A. Pinches et al., *Hydrometallurgy* **2** (1976) 87-103.
 135. W. Grote et al., *Proc. Australas. Inst. Min. Metall.* **278** (1981) 37-40.
 136. D. S. Flett, *Trans. Inst. Min. Metall. Sect. C* **83** (1974) 30-38.
 137. M. G. Atmore, K. J. Severs, R. B. G. Voyzey: "Past, Present and Future of Solvent Extraction of Copper", *Inst. Min. Metall. and Chinese Soc. of Metals, Internat. Conference*, Kunming, Yunnan, China, October 1984.
 138. R. R. Greenstead, *J. Met.* **31** (1979) no. 3, 13-16.
 139. R. Kammel, H.-W. Lieber, *Galvanotechnik* **68** (1977) 413-418.
 140. A. E. Back, *J. Met.* **31** (1979) no. 3, 13-16.
 141. W. R. Hopkins, G. Eggett, J. B. Scuffham: "Electrowinning of Copper from Solvent Extraction Electrolytes — Problems and Possibilities", in: *International Symposium on Hydrometallurgy* AIME, New York 1973, p. 127-144.
 142. D. J. Robinson, St. E. James (eds.): *Anodes for Electrowinning*, TMS-AIME, Warrendale, PA, 1984.
 143. W. C. Cooper: "Recent Advances and Future Prospects in Copper Electrowinning", *22nd Annual CIM Conference of Metallurgists*, Edmonton, Alberta, August 1983.
 144. *Eng. Min. J.* **168** (1967) no. 1, 97-100.
 145. W. A. Griffith, H. E. Day, T. S. Jordan, V. C. Nyman, *J. Met.* **27** (1975) no. 2, 17-25.
 146. R. G. Bautista (ed.): *Hydrometallurgical Process Fundamentals*, Plenum Press, New York 1984.
 147. K. Osseo-Asare, J. D. Miller (eds.): "Hydrometallurgy — Research, Development and Plant Practice", *12th AIME Annual Meeting*, Atlanta, GA, March 1983.
 148. W. R. Hopkins, A. J. Lynch, *Eng. Min. J.* **178** (1977) no. 2, 56-64.
 149. W. Schwartz, R. Michels, *Erzmetall* **17** (1964) 117-124.
 150. M. C. Kuhn, N. Arbiter, H. Kling, *CIM Bull.* **67** (1974) no. 742, 62-73.
 151. P. R. Kruesi, E. S. Allen, J. L. Lake, *CIM Bull.* **66** (1973) no. 734, 81-87.
 152. G. E. Atwood, R. W. Livingston, *Erzmetall* **33** (1980) 251-255.
 153. J. J. Oudiz, *J. Met.* **25** (1973) no. 12, 35-38.
 154. R. Henych, F. Kadlec, V. Sedlacek, *J. Met.* **17** (1965) 386-388.
 155. J. Osterwald, H. Sadat-Darbandi, *Metall (Berlin)* **30** (1976) 1057-1058.
 156. G. Melcher, F. Sauert, *Erzmetall* **33** (1980) 451-455.
 157. G. Kapell, W. Leutloff, *J. Met.* **32** (1980) no. 9, 36-40.
 158. J. M. Dompas, *Min. Mag. (London)* (1983) no. 9, 169-175.
 159. V. T. Isakov: *The Electrolytic Refining of Copper*, Technocopy, Stonehouse, Glos., England 1973.
 160. GDMB Gesellschaft Deutscher Metallhütten- und Bergleute (ed.): *Elektrolyse der Nichteisenmetalle*, Verlag Chemie, Weinheim-Deerfeld Beach-Basel 1982.
 161. A. P. Brown et al., *J. Met.* **33** (1981) no. 7, 49-57.
 162. H. Ykeda, Y. Matsubara, in [12, vol. 1, p. 601 (1970)].
 163. I. Fujimura, A. Katan, The Met. Soc. AIME, TMS Paper Selection A 82-12, 1982.
 164. J. Sato, T. Imamura, M. Hojo, T. Suzuki, *Nippon Kogyo Kaishi* 1046 (1975) no. 97, 258.
 165. J. C. Jenkins: "Copper Tank House Technology Reviewed and Assessed", *Symposium May 1985, Australas. Inst. Min. Metall.*, Victoria, Australia.
 166. M. J. Jaskula, *Electrochim. Acta* **28** (1983) 1395-1406.
 167. T. B. Braun, *J. Met.* **33** (1981) no. 2, 59-67.
 168. B. Rühl in: *Metallgesellschaft AG, Frankfurt a. M., Review of the Activities* no. 11 (1968) p. 48.
 169. Amarillo Copper Refining, *Eng. Min. J.* **182** (1981) no. 9, 67-78.
 170. Wennberg, DE 2 618 679, 1976 (R. Bengtsson).
 171. *Eng. Min. J.* **176** (1975) no. 4, 101.
 172. W. W. Harvey, M. R. Randlett, K. I. Bangerskis, *J. Met.* **27** (1975) no. 7, 19-25.
 173. R. Winand, *Trans. Inst. Min. Metall. Sect. C* **84** (1975) 67-75.
 174. K. Rinne, in [160, p. 72-76 (1982)].
 175. M. P. Amsten et al., *J. Met.* **30** (1978) no. 7, 16-26.
 176. J. Bertha, J. Schwimann, H. Wöbking, H. Wörz, *Erzmetall* **32** (1979) 335-337.
 177. I. J. Perry, J. O'Kane: "A Review of Five Years of Commercial Operations of the ISA Electrorefining Process at Townsville, Australia", *Jt. GDMB-IMM Symposium*, Hamburg, October 1983.
 178. Asarco Inc., US 3 199 977, 1965 (A. J. Philipps, R. Baier).
 179. C. L. Thomas, *Metal Bull. Monthly* (August 1983), 17-22.
 180. K. Sczimarowsky, *Draht-Welt* **46** (1960) 329-335.
 181. E. Herrmann: *Handbook on Continuous Casting*, Aluminium-Verlag, Düsseldorf 1980.
 182. L. W. Collins, Jr. (ed.): *Nonferrous Wire Handbook*, vol. 1: "Nonferrous Wire Rod", The Wire Assoc. Int. Inc., Guilford, CT, 1977.
 183. H.-D. Hirschfelder, *Draht* **29** (1978) 164-170.
 184. L. Properzi, A. Ossani, *Draht-Welt* **66** (1980) 456-458.
 185. E. H. Chia, R. D. Adams, *J. Met.* **33** (1981) no. 2, 68-74.
 186. P. Wincierz, *Z. Metallkd.* **66** (1975) 235-248.
 187. I. A. Dundurs, D. W. Hoey, C. W. Walter, *Wire J.* **13** (1980) no. 9, 120-125.
 188. J.-P. Dosdat, J. M. Dompas, *Wire J.* **13** (1980) no. 8, 90-95.
 189. B. Hansson, K.-G. Soderlund, E. Martinsson, *J. Inst. Met.* **98** (1970) 234-237.
 190. M. Rantanen, *Wire J.* **13** (1980) no. 3, 102-104.
 191. E. Peissker, Int. J. *Powder Metall. Powder Technol.* **20** (1984) no. 2, 87-101.
 192. *1984 Annual Book of ASTM Standards*, vol. 02.01: "Copper and Copper Alloys", ASTM, Philadelphia (published annually).
 193. DIN Taschenbuch 26: *Nichteisenmetalle, Normen über Kupfer und Kupfermetalllegierungen*, 3rd edition, Beuth-Verlag, Berlin 1984.
 194. ISO Technical Report 4745 (E), High Conductivity, Copper — Spiral Elongation Test (1978).
 195. GDMB and VDEh (eds.): *Analyse der Metalle*, vol. 1: "Scheidsanalysen", Springer Verlag, Berlin 1966; Supplement volume (Erg.-Bd.) 1980.
 196. C. Engelmann, G. Kraft, J. Pauwels, C. Vandecasteele: *Modern Methods for the Determination of Non-Metals in Non-Ferrous Metals*, De Gruyter, Berlin-New York 1985.
 197. M. Bauser, *Metall (Berlin)* **38** (1984) 513-516.
 198. E. Tuschy, *Z. Metallkd.* **61** (1970) 488-492.
 199. *Source Book on Copper and Copper Alloys*, American Soc. of Metals, Metals Park, Ohio, 1979.
 200. Source: Commodities Research Unit, London.

201. Source: Copper Development Assoc. Inc., New York.
202. Metallgesellschaft AG (ed.): *Metallstatistik 1974-1984*, vol. 72, Frankfurt/M. 1985.
203. World Bureau of Metal Statistics (ed.): *World Metal Statistics 1984*, London.
204. Service Études et Statistiques (ed.): *Annuaire Minemet 1984, Statistiques Annual*, Groupe Métal, Paris.
205. American Metal Market (ed.): *Metal Statistics 1984, The Purchasing Guide of the Metal Industries*, New York.
206. C. J. Schmitz: *World Nonferrous Metal Production and Prices 1700-1976*, Frank Cass & Co., London 1979.
207. H. P. Münster, G. Kirchner: *Taschenbuch des Metallhandels*, 7th edition, Metall Verlag, Berlin-Heldelberg 1982.
208. R. F. Mikesell: *The World Copper Industry - Structure and Economic Analysis*, J. Hopkins University Press, Baltimore-London 1979.
209. Metal Bulletin Conferences Ltd.: *Metal Bulletin's 2nd International Copper Conference*, London, April 1984, Surrey, England.
210. *Metall Bulletin Handbook '85*, Metal Bulletin Books Ltd., Surrey, England.
211. R. M. Serjeantson (ed.): *Non-Ferrous Metal Works of the World*, Met. Bull. Books Ltd., London 1985.
212. *Mining Companies of the World*, Mining Journal Books Ltd., London 1975.
213. J. G. Eacott in [16, p. 101].
214. T. D. Chatwin, N. Kikumoto (eds.): *Sulfur Dioxide Control in Pyrometallurgy*, Metallurg. Soc. AIME, Warrendale, PA, 1982.
215. CS Survey: Sulfur Dioxide Emission Control in the Copper Industry, *Copper Studies* 12 (1985) no. 12 (June), 1-3, Commodities Research Unit Ltd., London.
216. L. J. Friedman in [19, p. 1023-1040].
217. I. J. Weisenberg, P. S. Bakshi, A. E. Vervært, *J. Met.* 31 (1979) no. 10, 38-44.
218. J. G. Eacott in [16, p. 127-128].
219. *Committee on Medical and Biological Effects of Environmental Pollutants: Copper*, Nat. Academy of Sci., Washington 1977.
220. G. D. Clayton, F. E. Clayton (eds.): *Patty's Industrial Hygiene and Toxicology*, 3rd edition, vol. 2A, Wiley-Interscience, New York 1981, p. 1620.
221. *Gmelin*, System No. 60 "Kupfer", Teil A (1955), Teil B (1958-66), Teil C (1978), Teil D (1963).
222. P. Pascal in *Nouveau Traité de chimie minérale*, vol. 3, Masson et Cie, Paris 1957, pp. 155-421.
223. J. Mellor: *A Comprehensive Treatise on Inorg. and Theoretical Chemistry*, vol. 3, Longman's and Green Co., New York 1923, pp. 49-294.
224. A. Butts (ed.): *Copper - The Science and Technology of the Metal, its Alloys and Compounds*, ACS Monograph 122, Reinhold Publ. Co., New York 1954.
225. W. Hatfield, R. Whyman in R. Carlin (ed.): *Transition Metal Chemistry*, vol. 5, Marcel Dekker, New York 1969, pp. 47-179.
226. M. Kalo, H. Jonassen, J. Fanning, *Chem. Rev.* 64 (1964) 99.
227. B. Hathaway, D. Billig, *Coord. Chem. Rev.* 5 (1970) 1-43.
228. H. Sigel, *Angew. Chem. Int. Ed. Engl.* 13 (1974) 394.
229. R. Doedens, *Prog. Inorg. Chem.* 21 (1976) 209.
230. M. Bruce, *J. Organomet. Chem.* 44 (1972) 209.
231. F. Jardine, *Adv. Inorg. Chem. Radiochem.* 17 (1975) 116.
232. C. K. Williams Co., US 2554319, 1953 (J. Ayers).
233. Rohm and Haas, US 2184617, 1939 (L. Hurd).
234. Rohm and Haas, US 2273708, 1942 (L. Hurd).
235. K. Hauffe, P. Kofstad, *Z. Elektrochem.* 59 (1955) 399.
236. Merck, US 2409413, 1951 (H. Becker).
237. Calumet and Hecla, US 3466143, 1969 (H. Day).
238. Glidden, US 2758014, 1956 (J. Drapeau, P. Johnson).
239. Glidden, US 2891842, 1959 (J. Drapeau, P. Johnson).
240. Norddeutsche Aff., GB 772846, 1957; DE 1020010, 1957 (E. Klumpp).
241. S. Mahalla, US 3492115, 1970.
242. Lake Chem. Co., US 2474497, 1949 (P. Rowe).
243. G. E. Co., US 3186833, 1965 (R. Cech).
244. Lake Chem Co., US 2474533, 1949 (L. Klein).
245. Glidden, US 2817579, 1957 (J. Drapeau, P. Johnson).
246. Tennessee Corp., US 3457035, 1969 (J. Barker).
247. USA, Secretary of the Interior, US 3716615, 1973 (D. Bauer, P. Haskett, R. Lindstrom).
248. USA, Secretary of the Interior, US 3833717, 1974 (P. Haskett, D. Bauer, R. Lindstrom, C. Elges).
249. S. Titova, V. Golodov, D. Sokol'skii, SU 488788, 1975; *Chem. Abstr.* 84 (1976) 124057c.
250. Mountain Copper, US 2665192, 1954 (P. Rowe).
251. Mountain Copper, US 2977195, 1961 (C. Matzinger).
252. Nippon Chem., JP-Kokai 80/71629, 1980.
253. ICI, GB 936922, 1963 (A. Campbell, A. Taylor).
254. Nippon Chem., JP-Kokai 78/133775, 1978; *Chem. Abstr.* 93 (1981) 116652 p.
255. ASTM: *Standard Methods of Chemical Analysis of Dry Cuprous Oxide and Copper Pigments*, D283-52 (reapproved 1978) Philadelphia, pp. 89-94.
256. Military Specification: *Pigment, Cuprous Oxide* MIL-P-15169B (Ships), 1963; Amendment - 1 MIL-P-15169B (Ships), 1969.
257. Metallgesellschaft, DE 1007307, 1957 (J. Dornauf).
258. W. Kunda, H. Veltman, D. Evans, *Copper Met. Proc. Extr. Met. Div. Symp.* 1970, 27-69.
259. Fluor Corp., US 2927018, 1960 (C. Redemann).
260. Fluor Corp., US 2923618, 1960 (C. Redemann, H. Tschimer).
261. Sherritt Gordon Mines, US 3127264, 1964 (H. Tschimer, L. Williams).
262. Ruehl, Erich, Chem. Fabrik, DE 3115436, 1982 (W. Jagusch, H. Reichelt).
263. Jap. Bur. Ind. Tech., DE 2047372, 1971 (Y. Moriya).
264. Kachita Co., DE 2028791, 1970 (T. Tamura, A. Sakamoto, T. Kato).
265. TDK Electronics, JP-Kokai 75/131668, 1975 (S. Adachi, T. Miyakoshi, M. Hattori).
266. Fordwerke, DE 2046180, 1971 (J. Jones, E. Weaver).

267. Mitsui Toatsu Chem., JP-Kokai 74/72179, 1974 (T. Kobayagawa, Y. Nakajima).
268. Oxy. Catalyst, FR 1402087, 1965.
269. Lonza, DE 2012250, 1970 (T. Voelker, K. Hering).
270. Philips Gloelampen Fabrik., DE 2103538, 1971 (C. Esveltdt, N. Slijkerman).
271. C. Freedenthal: *Copper Compounds, Encyclopedia of Industrial Chemical Analysis*, J. Wiley & Sons, New York 1970, pp. 651-680.
272. Cellocilk Co., US 1800828, 1931 (W. Furness).
273. D. Marsh, B. Marsh, US 2104754, 1938.
274. Mountain Copper, US 2536096, 1951 (P. Rowe).
275. Lake Chem. Co., US 2525242, 1950 (P. Rowe).
276. H. Neville, C. Oswald, *J. Phys. Chem.* 35 (1931) 60-72.
277. Copper Research, US 24324, 1957 (W. Furness).
278. Rohm and Haas, US 3231464, 1966 (E. Dettwiler, J. Fillietaz).
279. Cuproquim S.A., US 4418056, 1983 (M. Gonzalez).
280. Giuliani Aldolfomer Ind., BR 83/01912, 1983 (J. Giuliani, A. Meyer).
281. Kennecott Copper, DE 1592441, 1965 (W. Furness); US 3194749, 1965.
282. Hoechst, DE 824199, 1951 (K. Pfaff, A. Voigt).
283. Hoechst, DE 824200, 1951 (K. Pfaff, A. Voigt).
284. E. Gimsey, D. Muir, A. Parker, *Proc. Australas. Inst. Min. Metall.* 273 (1980) 21-25.
285. *Ullmann*, 4th ed. 15, 564.
286. Degussa, DE 1000361, 1955 (F. Bittner).
287. Degussa, FR 2009852, 1969.
288. Norddeutsche Affinerie, DE 1813891, 1958.
289. Norddeutsche Affinerie, US 3679359, 1972 (E. Haberland, W. Perkow).
290. Mitsubishi Metal Corp., JP-Kokai 80/60003, 1980.
291. R. Keller, H. Wycoff, *Inorg. Synth.* 2 (1946) 1-4.
292. Schering, DE 1080088, 1958 (H. Niemann, K. Herrmann).
293. Harshaw, US 2367153, 1945 (C. Swinehart).
294. Goldschmidt, DE 3305545, 1983 (E. Mack, L. Witzke).
295. Cyprus Metallurg., DE 2607299, 1976 (D. Goens, P. Kruesi).
296. Cyprus Metallurg., US 3972711, 1976 (D. Goens, P. Kruesi).
297. Metallgesellschaft, DE 1174996, 1963 (K. Meyer, H. Ransch, H. Pietsch); DE 1180946, 1963; DE 1160622, 1963.
298. Duisburger Kupferhütte, US 3353950, 1967 (H. Junghaus); DE 1200545, 1965.
299. Nitto Elec. Ind., JP-Kokai 78/65348, 1978.
300. Jap. Pure Hydrogen Co., JP-Kokai 70/48693, 1970 (T. Yamamoto).
301. Phillips Petro. Co., US 3658463, 1972 (W. Billigs).
302. Tenneco Chem. DE 2414800, 1974 (R. Turnbo, D. Keyworth).
303. H. Allgood, *Fert. Sci. Technol. Ser.* 2 (1974) 289-309.
304. DuPont, US 3230231, 1966 (H. Burtolo, J. Braun, C. Winter).
305. DuPont, US 4035383, 1977 (R. Sweet).
306. Anic S.p.A., DE 2743690, 1978 (U. Romano, R. Tessi, G. Cipriani, L. Micucci); US 4218391, 1980.
307. Ube Industries, JP-Kokai 79/106429, 1979 (H. Itatani, S. Dano).
308. Anic S.p.A., DE 3045767, 1981 (U. Romano, F. Rivetti, N. Muzio); US 4318862, 1983.
309. As reported in A. Siedell (ed.): *Solubilities of Inorganic and Metal Organic Compounds*, vol. 1, D. Van Nostrand, New York 1940, p. 478.
310. Sudhir Chem. Co., US 3202478, 1965 (A. Hindle, S. Raval, S. Damani, H. Damani, K. Damani); GB 912125, 1962.
311. N. V. Koninklijke Ned. Zoutindustrie, FR 957457, 1947.
312. Hoechst, DE 1931393, 1969 (H. Kreckler, H. Kukertz).
313. Distillers Co., BE 616762, 1962; GB 932180, 1962.
314. W. Feitknecht, K. Maget, *Helv. Chim. Acta* 32 (1949) 1639-1653.
315. Wacker, DE 1083794, 1960 (H. Baumgartner).
316. Bayer, DE 1159914, 1963 (E. Podschus).
317. Instytut Przemysłu Org., PL 55953, 1968.
318. Bayer, DE 1161871, 1963 (E. Podschus, W. Joseph); US 3230035, 1965.
319. Ciba, Ltd., CH 243271, 1946.
320. Sirco, A.G., CH 256414, 1947.
321. Fisons Pest Control, US 2907691, 1959 (G. Hartley, P. Park).
322. Fahlberg-List GmbH, WE 1920963, 1970 (G. Günter, F. Schülde, K. Schoeyen).
323. Riedel-de-Haen, DE 1142724, 1963.
324. P. Ramos, E. Esteban, V. Callao, *Arts. Pharm.* 12 (1971) 471-477.
325. W. Feitknecht, K. Maget, *Helv. Chim. Acta* 32 (1949) 1639-1653.
326. A. Recoura, *C.R.* 148 (1909) 1105.
327. F. Habashi, R. Dugdale, *Met. Trans.* 4 (1973) 1429-1430.
328. K. Vo Van, F. Habashi, *Can. J. Chem.* 23 (1972) 3872-3875.
329. M. Nagamori, F. Habashi, *Met. Trans.* 5 (1974) 523-524.
330. K. Vo Van, F. Habashi, *Can. J. Chem. Eng.* 52 (1974) 369-373.
331. F. Habashi, S. A. Mikhail, K. Vo Van, *Can. J. Chem.* 23 (1976) 3646-3650.
332. F. Habashi, S. A. Mikhail, *Can. J. Chem.* 23 (1976) 3651-3657.
333. As reported in W. Linke (ed.): *Solubilities of Inorganic and Metal Org. Compounds*, 4th ed., vol. 1, Amer. Chem. Soc., Washington, D.C. 1958, pp. 965-968.
334. H. Moyer, *AIME Annual Meeting*, New Orleans, Feb. 18-22, 1979.
335. Tennessee Copper, US 2533245, 1950 (G. Harike).
336. C. Merigold, D. Agers, J. House, *Int. Solvent Extr. Conf.* 1971.
337. General Mills, US 3224873 (Swanson).
338. Dow, US 4031038, 1977 (R. Grinstead); US 4098867, 1978.
339. S. Tataru, RO 67946, 1979.
340. F. Lowenstein, M. Moran in *Faith, Keyes and Clark's Industrial Chemicals*, 4th ed., John Wiley and Sons, New York 1975, pp. 280-283.
341. Hitachi Chem., JP-Kokai 76/03396, 1976 (T. Senda, T. Umehara); JP-Kokai 76/03395, 1976.
342. L. Markov, K. Balarev, *Izv. Khim.* 15 (1982) 472-481.

343. H. Weiser, W. Milligan, E. Cook, *J. Am. Chem. Soc.* **64** (1942) 503-508.
344. A. Binder, *Compt. Rend.* **198** (1934) 653, 2167.
345. Cities Service, US 3725535, 1973 (J. Barker).
346. Vereinigte Metallwerke, DE 2701253, 1977 (J. Bertha).
347. Compagnie de Saint-Gobain, FR 1302445, 1962 (M. Provost).
348. Takeda Chem. Ind., FR 1452608, 1966.
349. INCRA, US 3846545, 1970 (S. Foschi); FR 2001428, 1969 (E. Hess, D. Kennedy, C. Whitham).
350. J. Horsfall, J. Heuberger, *Phytopathology* **32** (1942) 226-232.
351. J. Horsfall: *Fungicides and their Action*, Chronica Botanica Co., Waltham, MA 1945.
352. Duisburger Kupferhütte, DE 2602448, 1977 (W. Roever, K. Lippert).
353. A. Biswas, W. Davenport: *Extractive Metallurgy of Copper*, Pergamon Press, Oxford-New York 1976.
354. G. Ritcey, A. Ashbrook: *Solvent Extraction*, Part II, Elsevier, Amsterdam 1979, pp. 197-248.
355. DuPont, US 3230231, 1966 (H. Bartolo, J. Braun, C. Winter).
356. DuPont, US 4035383, 1977 (R. Sweet).
357. USEPA, *Environmental Protection Agency*, Code of Federal Regulation 40CFR, parts 240-299, 1983.
358. Mitsubishi, US 3597290, 1971 (A. Naito, Y. Masuda, S. Osawa).
359. Dart Ind., US 4158593, 1979 (J. Allan, P. Readio).
360. Denka, US 3770530, 1973 (O. Fujimoto).
361. Denka, US 3936332, 1976 (A. Matsumoto, K. Itani); US 3939089, 1976; Tokai Electro-Chem., US 3839534, 1974 (A. Matsumoto, O. Fujimoto).
362. FMC, GB 873583, 1959 (P. Margulies, J. Kressbach, H. Wehrfritz); DE 1160270, 1959.
363. K. Jones, R. Pyper, *J. Met.* **31** (1979) no. 4, 19-25.
364. Micro Copper Corp., US 3679399, 1972 (D. Linton, A. Zinkl, J. Ballam).
365. Showa Electric Wire and Cable, JP-Kokai 75/84415, 1975 (Y. Kogane).
366. FMC, US 3837945, 1974 (J. Chiang).
367. FMC, US 3844857, 1974 (J. Chiang).
368. P. Fintschenko, *Met. Finish. J.* **20** (1974) 138-139.
369. Nippon Chem. Ind., JP-Kokai 83/140321, 1983.
370. A. Celi, DE 3208609, 1983.
371. D. Klein, DE 3204815, 1983.
372. J. Leroy, Contribution to International Recycling Congress (IRC), Berlin 1982, 592-595.
373. Western Electric, US 4428773, 1984 (K. Krotz).
374. Hitachi Cable, JP-Kokai 80/159895, 1980.
375. Western Electric, US 3843504, 1974 (B. Nayder).
376. Criterion, US 4083758, 1978 (W. Hamby, M. Slade).
377. F. Harrison, *Gov. Rep. Announce. Index (U.S.)* **84** (1984) 42-139.
378. USEPA: *Development Document for Effluent Limitations Guidelines and Standards for the Inorganic Chemicals Point Source Category*, Phase II, 440/1-83/007-6 (1983).
379. USEPA: *Nonferrous metals manufacturing point source category; effluent limitations guidelines, pretreatment standards, and new source performance standards*, *Fed. Regist.* **49** (1984) 8742-8831.
380. USEPA: *Clean water; Inorganic chemicals manufacturing point source category, effluent limitations, guidelines, pretreatment standards and new source performance standards*, *Fed. Regist.* **49** (1984) 33402-33429.
381. *Wasserhaushaltsgesetz - WHG - vom 27.7.1957 in der Fassung vom 26.4.1976*, BGBl. I (1976).
382. EG - *Gewässerschutzrichtlinie vom 4.5.1976* - Amtsblatt der EB Nr. L 129/23 vom 18.5.1976, hier Anhang Stoffliste II u. a. mit Kupfer.
383. WHO: *International Standards for Drinking Water*, Monograph Series No. 3 (1971) 40.
384. USEPA: "Interim Primary Drinking Water Standards", *Fed. Regist.* **40** (1975) 11994.
385. J. Hallowell, J. Shea, G. Smithson, A. Tripler, B. Gonser, *Gov. Rep. Announce (U.S.)* **74** (1974) 89-161.
386. F. Pierrot, D. Vanel, *Galvano-Organo Trait. Surf.* **52** (1983) 726-728.
387. C. Roy, US 3816306, 1974.
388. Höllmüller Maschinenbau, DE 2257364, 1974 (E. Lendle, G. Wartenberg).
389. BASF, DE 2255402, 1974 (H. Hiller, A. Schuhmacher, H. Schmidt).
390. M. Manafont, ES 397046, 1974.
391. Nippon Electric, JP-Kokai 84/22694, 1984.
392. R. Spearot, J. Peck, *Environ. Prog.* **3** (1984) 124-128.
393. D. Kertesz, R. Zito, F. Ghirelli in O. Hayaishi (ed.): *Oxygenases*, Academic Press, London 1962.
394. Ciba Foundation Symposium: *Biological Roles of Copper*, no. 79, Excerpta Medica and Elsevier-North Holland, Amsterdam 1980, p. 343.
395. H. Sigel (ed.): *Metal Ions in Biological Systems*, vol. 12, Properties of Copper, Marcel Dekker 1981, p. 384.
396. INCRA: V. Shorrocks, Planning Study, *Use of Copper as a Micronutrient for Crops*, Part 1, New York, July 1984.
397. W. Ernst, *Schwermetallvegetation der Erde*, G. Fischer Verlag, Stuttgart 1974.
398. *Micronutrients in Agriculture*, Soil Sci. Soc. of Amer., Inc., Madison, WI 1972.
399. G. Cromwell, T. Stahly, W. Williams, *Feedstuffs* **53** (1982) 30, 32, 35-36.
400. L. DeGoey, R. Wahlstrom, R. Emerick, *J. Anim. Sci.* **33** (1971) 52-57.
401. INCRA: *Environmental Impact Analysis Report*, Copper Salts in Animal Feed, Int. Copper Res. Assoc., Inc., New York-London 1974.
402. USEPA: "Registration on the Level of Copper in Animal feed", *Fed. Regist.* **38** (1973) 178.
403. INCRA: *A Critical Review of Copper in Medicine*, Report No. 234, Int. Copper Res. Assoc., Inc., Göteborg-New York 1975.
404. U.S. Dept. of Interior: *Minerals Yearbook 1982*, vol. 1, U.S. Govt. Printing Office, Washington, D.C., 1983, p. 209.
405. G. Johnson, *Agricult. History* **9** (1935) 67-79.
406. D. Frear in *Chemistry of Insecticides, Fungicides, and Herbicides*, 2nd ed., D. Van Nostrand, New York 1948, pp. 211-228.
407. E. R. de Ong in *Chemistry and Uses of Pesticides*, 2nd ed., Reinhold Publ. Co., New York 1956, pp. 31-47.
408. S. Gunther, *Chem Ing. Tech.* **31** (1959) 731-734.
409. E. Browning: *Toxicity of Industrial Metals*, 2nd ed., Butterworths, London 1969.
410. R. Fabre, R. Truhaut: *Précis de toxicologie*, Centre doc. univ., Paris 1960.
411. A. Askergren, M. Mellgren, *Scand. J. Work, Environ. Health* **1** (1975) 45-49.
412. R. Gleason, *Am. Ind. Hyg. Assoc. J.* **29** (1968) 461-462.
413. Y. Kambe, Matsushima, T. Kuroume, S. Suzuki, *Proc. Fourth Int. Congr. Rural Med.*, Zürich 1970, 55-57.
414. E. Saltzer, J. Wilson, *Arch. Dermatol.* **98** (1968) 375-376.
415. *Documentation of Threshold Limit Values for Substances in Workroom Air*, 3rd ed., Cincinnati 1974.
416. W. Grant: *Toxicology of the Eye*, 2nd ed., C. C. Thomas, Springfield, IL 1974.
417. NIOSH: *Manual of Industrial Chemicals*, U.S. Dept. of Labor, September 1978.
418. D. Henschler: *Gesundheitsschädliche Arbeitsstoffe, Toxikologisch-arbeitsmedizinische Begründung von MAK-Werten*, Verlag Chemie, Weinheim 1972/77.
419. DFG: *Maximale Arbeitsplatzkonzentration*, Verlag H. Boldt, Boppard 1976.
420. H. E. Stokinger in *Patty*, vol. 2A, pp. 1620-1630 (1981).
421. S. Cohen, *JOM, J. Occup. Med.* **16** (1974) 621-624.
422. Int. Labor Office: *Encyclopedia of Occupational Health and Safety*, McGraw-Hill, New York 1971.
423. N. Sax: *Dangerous Properties of Ind. Materials*, 4th ed., Van Nostrand, New York 1982.
424. W. Dreichmann, H. Gerarde: *Toxicology of Drugs and Chemicals*, Academic Press, New York 1969.

9 Lead

ALBERT MELIN (§§ 9.1–9.6); EDWARD F. MILNER, CHARLES A. SUTHERLAND (§§ 9.1–9.9); ROBERT C. KERBY (§§ 9.6.2, 9.11); HERBERT TEINDL (§ 9.10); DAVID PRENGAMAN (§ 9.12); DODD S. CARR (§ 9.13); GÜNTER ETZRODT (§§ 9.14.1–9.14.4); RALF EMMERT, KLAUS-DIETER FRANZ, HARTMUT HÄRTNER, KATSUHISA NITTA, GERHARD PFAFF (§ 9.14.5)

9.1 Introduction	581	9.7.4 Future Trends	618
9.2 History	582	9.8 Uses	618
9.3 Properties	582	9.9 Economic Aspects	620
9.4 Occurrence	584	9.9.1 Lead Concentrate Schedules	620
9.5 Production	585	9.9.2 Lead Statistics	621
9.5.1 Ore Concentration	585	9.10 Toxicology and Occupational Health	623
9.5.2 Smelting	585	9.10.1 Sources of Lead Exposure	623
9.5.2.1 Sintering Reduction Process	585	9.10.2 Absorption and Excretion	625
9.5.2.2 Reduction in the Blast Furnace	591	9.10.3 Effects	625
9.5.3 Roast Reaction Processes	596	9.10.4 Indices for Monitoring Lead Exposure	625
9.5.4 Direct Smelting Reduction Processes	596	9.11 Control of Lead Emissions	626
9.5.4.1 Air Flash Smelting	597	9.11.1 In-Plant Lead Emissions	626
9.5.4.2 Oxygen Flash Smelting	597	9.11.2 Ambient Lead Emissions	627
9.5.4.3 Air-Slag Bath Smelting, the Isasmelt Process	600	9.12 Alloys	627
9.5.4.4 Oxygen-Slag Bath Smelting, QSL Process	601	9.13 Compounds	628
9.5.5 Other Lead Processes	603	9.13.1 Salts and Oxides	628
9.6 Refining of Lead Bullion	603	9.13.1.1 Acetates	628
9.6.1 Pyrometallurgical Refining	604	9.13.1.2 Carbonates	629
9.6.1.1 Decoppering	604	9.13.1.3 Halides	630
9.6.1.2 Removal of Arsenic, Tin, and Antimony	607	9.13.1.4 Oxides	630
9.6.1.3 Removal of Noble Metals	608	9.13.1.5 Silicates	632
9.6.1.4 Dezincing	609	9.13.1.6 Sulfates	632
9.6.1.5 Debismuthizing	610	9.13.1.7 Other Salts	632
9.6.1.6 Final Refining and Casting of Lead	610	9.13.2 Organolead Compounds	633
9.6.1.7 Processing of Intermediate Products of Pyrometallurgical Refining	611	9.13.3 Occupational Health	634
9.6.2 Electrolytic Refining of Lead Bullion	613	9.14 Pigments	635
9.7 Recovery of Secondary Lead from Scrap Materials	615	9.14.1 Lead Cyanamide	635
9.7.1 Battery Types and Composition	616	9.14.2 Red Lead	635
9.7.2 Battery Breaking and Processing Feed Preparation	616	9.14.3 Calcium Plumbate	635
9.7.3 Smelting of Battery Scrap Materials	616	9.14.4 Lead Powder	635
		9.14.5 Basic Lead Carbonate	636
		9.15 References	636

9.1 Introduction

The metal lead remains a major nonferrous commodity in modern industry as it has been from antiquity. In 1988 lead consumption in the nonsocialist world was estimated to be 4.2×10^6 t, which is well below the capacity of the primary producing and recycling plants. Con-

cern about the toxicity of lead has brought about substitutions in some uses and proscriptions in others; consequently, the lead market is now dependent on the lead storage battery. Growth in the transportation field, principally in conventional internal combustion engine automobiles, has been the main factor in sustaining a modest growth in lead consumption

of around 2.4% in 1988. The consumption of lead in other use areas (including the drastically reduced gasoline additive market, pigments, ammunition, solders, plumbing, and shielding) amounts to less than that in the battery market. Recent discoveries in North America, Australia, South Africa, and China have brought economic lead ore reserves to a level comfortably above expected consumption.

9.2 History

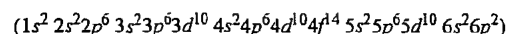
The knowledge and use of lead goes back as far as 5000 B.C. to the ancient Egyptians. The metal was used extensively by the Phoenicians, Romans, Indians, and Chinese. The first lead mines in Spain were operated around 2000 B.C. The uses of the metal included weight standards, coinage (ultimately replaced by silver), statuary, sheathing and lining, trinkets, anchoring of iron rods, and making of seals. The Greeks operated lead mines at Laurium in the fifth century B.C. and the Romans mined in the Rio Tinto region of Spain in 300 B.C. The Romans used lead extensively for water piping; indeed latin "plumbum" for lead came from the word for a water spout, and from it has come the name plumber. They also used lead for soldering, in sheets for inscribed lettering, and for preparation of lead oxides. Lead uses increased in the Middle Ages with supporting mines appearing in England, Germany, Bohemia, and other parts of Europe. Lead roofing, lead "comes" in stained glass windows, guttering, drain pipes, and later type founding were additional uses that continue today. Lead received considerable attention from the alchemists. Older uses of lead as material for projectiles expanded considerably with the invention of firearms.

In the nineteenth century, the United States entered the lead production industry because of its major natural resources, and was followed by Australia and Canada. In the twentieth century the appearance of the automobile, chemical, and machine industries created large new uses for lead in gasoline antiknock

additives, bearing and plumbing alloys, accumulator batteries, and chemical equipment. Modern uses include glass making, sound attenuation, and radiation shielding.

9.3 Properties

The element lead is a lustrous metal. When freshly cut, surfaces are bluish white but oxidize readily to the familiar dull grey color. Lead is located in group 14 of the periodic table. The element displays valences of 2+ and 4+ as indicated by its electronic configuration:



This permits attainment of stability by donation of two or four electrons.

Lead Isotopes. Lead (atomic number 82) has four naturally occurring isotopes; mass numbers listed in order of abundance are 208 (51–53%), 206 (23.5–27%), 207 (20.5–23%), and 204 (1.35–1.5%). Variations in isotopic concentration can cause a difference of 0.15 in the normal atomic mass A_r of 207.21. Three of the natural isotopes are radioactive: ^{208}Pb is the end product of thorium decay, while ^{206}Pb and ^{207}Pb are formed from the uranium series via actinium and radium, respectively. A number of unstable radioactive isotopes exist with mass numbers of 200–203, 205, 209–214. Lead is a preferred shielding material against gamma rays and X-rays because of its high density and atomic number; if sufficiently pure, it does not become radioactive when used for shielding against neutron sources.

Physical and Mechanical Properties. The outstanding physical properties of lead are its low melting point, high density, softness, and malleability. The metal can readily be worked by rolling and extruding, and is slightly ductile. The physical and mechanical properties of lead follow:

<i>Physical Properties:</i>	
<i>mp</i> , °C	327.4
Latent heat of fusion, J/g	23.4
<i>bp</i> , °C	1741
Latent heat of vaporization, J/g	862
Vapor pressure, kPa	
980 °C	0.133
1160 °C	1.33

Lead

1420 °C	13.33
1500 °C	26.7
1600 °C	53.3
<i>Density, g/cm³</i>	
20 °C	11.336
327.4 °C (solid)	11.005
327.4 °C (liquid)	10.686
400 °C	10.597
500 °C	10.447
<i>Mean specific heat, J g⁻¹ K⁻¹</i>	
–200–0 °C	0.1202
0–100 °C	0.131
0–200 °C	0.134
0–300 °C	0.136
<i>Specific electrical resistance, Ω/cm</i>	
20 °C	20.65
100 °C	27.02
200 °C	36.48
300 °C	47.94
<i>Thermal conductivity, W m⁻¹ K⁻¹</i>	
–100 °C	0.371
0 °C	0.355
100 °C	0.342
200 °C	0.329
300 °C	0.316
327.4 °C (solid)	0.313
327.4 °C (liquid)	0.155
<i>Surface tension of liquid lead, mN/m</i>	
327.4 °C	444
350 °C	442
400 °C	438
500 °C	431
600 °C	424
800 °C	410
<i>Dynamic viscosity of liquid lead, mPa·s</i>	
327.4 °C	2.75
350 °C	2.60
400 °C	2.34
450 °C	2.12
500 °C	1.96
550 °C	1.70
<i>Magnetic susceptibility (20 °C), H m⁻¹ kg⁻¹</i>	
–1.5 × 10 ⁻⁹	
<i>Coefficient of linear expansion, K⁻¹</i>	
at 20 °C	29.1 × 10 ⁻⁶
mean 20–300 °C	31.3 × 10 ⁻⁶
<i>Mechanical Properties:</i>	
Brinell hardness (20 °C)	2.5–3.0
Transverse contraction coefficient (20 °C)	0.45
Young's modulus, GPa	16.5
Elongation (in 5-cm gauge length), %	50–60
Velocity of sound in lead, m/s	1227
<i>Tensile strength, kPa</i>	
–100 °C	42 000
20 °C	14 000
150 °C	5 000

Chemical Properties. Fresh cut or cast lead surfaces undergo oxidation and tarnish rapidly to form an insoluble protective layer of basic lead carbonate. Lead is attacked by water in the presence of oxygen, but again an insoluble carbonate or silicate protective layer is formed if dissolved carbonates or silicates are present in the water. This resistance of the metal to

corrosion by air, water, and soil has been exploited in the historical uses of lead in plumbing and piping. Lead might be expected to dissolve in acids with liberation of hydrogen, but this is prevented by the high hydrogen overvoltage, and attack occurs only when the combination of oxidizing conditions and soluble salt species exists. Thus the metal resists hydrochloric acid corrosion to quite high concentrations, sulfuric acid to 60 °Bé (ca. 13.3 mol/L), and hydrofluoric acid totally; however, it dissolves readily in warm, dilute nitric acid to form soluble lead nitrate. Lead is also corroded by weak organic acids, such as acetic or tartaric acid, in the presence of oxygen. The protective coating formed by oxidation is removed by alkali with formation of soluble plumbites and plumbates.

Crystal Structure. Lead crystals are face-centered and cubic with the following dimensions:

Atomic radius, nm	0.175
Atoms per unit cell	4
Lattice constant (edge of unit cell), nm	0.49389

Electrochemical Properties.

Electrochemical equivalent, g A ⁻¹ h ⁻¹	3.865
Ionic radius, Pb ²⁺ , nm	0.118
Pb ⁴⁺ , nm	0.070
Metallic radius, nm	0.17502
Covalent radius (sp ³), nm	0.144
<i>Ionization potentials, eV</i>	
1st	7.415
2nd	14.97
<i>Standard oxidation potentials (25 °C), V</i>	
Pb → Pb ²⁺ + 2e ⁻	0.126
Pb ²⁺ + 2H ₂ O → PbO ₂ + 4H ⁺ + 2e ⁻	–1.456
Pb + 2OH ⁻ → PbO + H ₂ O + 2e ⁻	0.576
Pb + 3OH ⁻ → HPbO ₂ ⁻ + H ₂ O + 2e ⁻	0.54

Lead forms two series of compounds corresponding to valence states of 2+ and 4+, lead(II) compounds are electrovalent (ionic), while those of lead(IV) are essentially covalent. The metal is amphoteric and forms lead salts, plumbites, and plumbates. When melted in air, lead oxidizes readily to its monoxide PbO (also called litharge or simply lead oxide); oxidation (drossing) can be promoted or inhibited by dissolved metallic impurities. Other lead oxides are the dioxide PbO₂ (actually sesquioxide Pb₂O₄) and red lead Pb₃O₄ (the orthoplumbate Pb·Pb₂O₄). All the lead(III) halides are known, and are consider-

ably more soluble in hot water than in cold they also form double chlorides with alkali metals and a series of oxyhalides, the oxychlorides being the most familiar. Other common compounds of lead are the soluble nitrate and acetate; lead chromate (chrome yellow) used as a pigment along with red lead; lead borate used along with oxides in glass making; lead sulfide (galena), which is the principal naturally occurring form of the metal; and lead sulfate that is readily formed by sulfating a soluble lead salt and by natural oxidation of galena.

9.4 Occurrence

Lead, like copper and zinc, is a markedly chalcophilic element. Its mean abundance in the Earth's crust is 16 g/t (0.0016%). Enrichments occur only in the pneumatolytic and especially the hydrothermal sulfide phase in the form of vein (lode), impregnated, and particularly metasomatic deposits. Sedimentary enrichments are of little importance.

Lead Minerals. Galena or lead sulfide, PbS, theoretically 86.6% Pb, is by far the most important lead mineral and the sole primary one. Other common forms of naturally occurring lead are usually associated with or derived from galena deposits. They include mixed sulfides such as jamesonite, $\text{Pb}_4(\text{Sb,Fe})_7\text{S}_{14}$ (ca. 40% Pb) and boulangerite, $\text{Pb}_5\text{Sb}_4\text{S}_{11}$ (ca. 58% Pb); anglesite, PbSO_4 (68.3% Pb), a product of galena oxidation; cerussite or white lead ore, PbCO_3 (77.5% Pb), a decomposition product of galena; pyromorphite, also qualified as green, brown or variegated lead ore, $\text{Pb}_5(\text{PO}_4)_3\text{Cl}$ (76% Pb); vanadinite, $\text{Pb}_5(\text{VO}_4)_3\text{Cl}$; wullenite or yellow lead ore, PbMoO_4 (56% Pb); crocoite, PbCrO_4 ; and phosgenite or horn lead, $\text{Pb}_2\text{Cl}_2\text{CO}_3$. Frequent impurities in lead minerals are zinc, copper, arsenic, tin, antimony, silver, gold, and bismuth.

Deposits. The most important mineable lead ore is galena, which occurs chiefly in association with other minerals, mainly zinc ores. Lead deposits can be classified as follows:

- Hydrothermal vein, impregnation, and replacement deposits (e.g., Broken Hill, Australia; Anvil Mine, Canada; and numerous deposits of the Cordilleran-Andean Orogeny);
- Volcanogenic sedimentary deposits, some occurring as massive bodies of rich ore, others as impregnations (e.g., Sullivan Mine, Canada; Rammelsberg, Germany; Mount Isa and Hellyer, Australia);
- Hydrothermal or marine sedimentary deposits, typically in calcareous or dolomitic formations of the North American and European platforms (e.g., Pine Point, Canada; the New Lead Belt in the Missouri district, United States; Red Dog, Alaska).

In world mining output, mixed lead-zinc ore deposits are most important and account for ca. 70% of total production of both metals. In second place are deposits that contain predominantly lead ores (ca. 20% of total production), and the remainder (ca. 10%) is obtained as a by-product from zinc, copper-zinc, and other deposits.

Table 9.1: World lead ore reserves (millions of tonnes contained lead) (U.S. Bureau of Mines, Division of Mineral Commodities, January 1989).

Country	Reserves ^a	Reserve base ^b
Australia	16	28
United States	11	22
Canada	8	15
South Africa	4	6
Mexico	3	4
Peru	2	3
Former Yugoslavia	2	3
Other market economy countries	9	14
Centrally planned economies	20	30
Total	75	125

^a Estimated currently economically recoverable lead.

^b Reserves augmented by marginally economic ores, some currently uneconomic but with potential, and also some provision made for determination of additional reserves in known ore bodies.

An important by-product of lead ore production is silver, which is incorporated into the lattice of galena, and is recovered with the lead when concentrates are smelted. Some 70% of world silver production comes from lead concentrates. Valuable amounts of gold

are also contained in some lead deposits. Another by-product from lead ore is copper, but the amount is a very small part of the total world copper output.

Reserves. Total world lead reserves were reported in 1987 as 75×10^6 t lead content (Table 9.1). Western countries owned about 73% of the total.

The United States has extensive lead deposits in the southeast of Missouri (New Lead Belt). These deposits and the new Red Dog lead-zinc orebody in Alaska are located in bedded marine-sedimentary or hydrothermal deposits. Further reserves are found in the Rocky Mountains (Idaho, Utah, Colorado) in the form of hydrothermal vein and replacement deposits. Canadian reserves are also substantial but of generally lower grade, and are located in the Appalachian region of New Brunswick, the Rocky Mountain trench, and the Yukon. North and South America, including the Latin American countries, hold about 35% of known reserves.

Australia has the most substantial lead resources amounting to about 21% of the world total; they are concentrated in Mount Isa (Queensland), Broken Hill (New South Wales), and Tasmania.

The remaining western reserves are found in many places in Europe, Africa, and Southern and Eastern Asia. The largest known European reserves are in Yugoslavia.

Most Eastern Bloc reserves (ca. 27% of world reserves) lie in the former Soviet Union (Kazakhstan and the Altai and Karatau regions). Only little information is available on these reserves and recent discoveries in China.

Data on exploitable reserves are only valid in the short-term, because they are subject to long-term economic fluctuations. The growth of world reserves of lead ore through new discoveries can be expected to outstrip the increase in primary metal production. Recycling of lead, already a major source of the metal, particularly for battery making, can be expected to suppress production from primary sources.

9.5 Production

9.5.1 Ore Concentration

The most common feed for lead production is sulfidic lead concentrate, which contains an average of 50–60% lead (occasionally as high as 70–80% or as low as 30%). Oxide lead concentrates are of secondary importance.

Lead ores in deposits are usually intergrown with other minerals and with host rock. These crude ores are not smeltable and must first be beneficiated into concentrates of much higher lead content but with minimum loss of lead.

Ore beneficiation normally includes crushing, dense-medium separation, grinding, froth flotation, and drying of concentrate. Lead flotation is usually the first step in the separation of lead-zinc and lead-zinc-copper ores.

9.5.2 Smelting

The major process for the production of primary lead from a sulfide concentrate is the sinter oxidation-blast furnace reduction route. Older processes involving direct oxidation of lead sulfide to lead or the roast reaction between lead sulfide and the oxidation products lead oxide and lead sulfate are now of little importance. In the last two decades new oxygen metallurgy processes featuring sulfide oxidation in a flash flame or by oxygen injection into a slag bath, followed by reduction of the lead oxide slag, have advanced to industrial application.

In the Imperial Smelting Furnace process, lead is produced simultaneously with zinc. This process will not be considered here, for details see Chapter 10.

9.5.2.1 Sintering Reduction Process

The sintering reduction process involves two steps:

- A sintering oxidative roast to remove sulfur with production of PbO

● Blast furnace reduction of the sinter product.

The objective of sintering lead concentrates is to remove as much sulfur as possible from the galena and the accompanying iron, zinc, and copper sulfides, while producing lump agglomerate of adequate strength combined with porosity for subsequent reduction in the blast furnace. The sulfur dioxide content of the sintering gases is often recovered and used in sulfuric acid production. The chemistry of the roast sintering process is complex because it involves many oxygen- and sulfur-containing lead compounds.

The Pb-S-O System. The Pb-S-O system was investigated comprehensively by KELLOGG and BASU [7] whose results were later confirmed by many investigators. WILLIS provides an excellent summary of the physical chemistry of the oxidation of lead sulfide [8]. Lead in sinter occurs mainly as lead monoxide or lead silicate. The temperature of the sinter charge must be high enough to attain the area of PbO predominance (i.e., > 950 °C, see Figure 9.1).

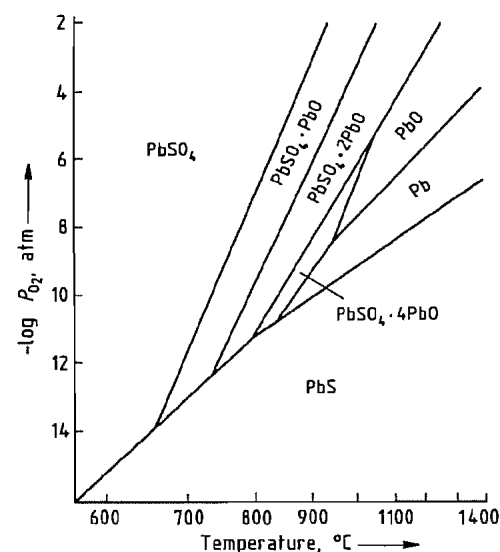


Figure 9.1: Phase relations in the Pb-S-O ternary system with air as the oxidizer and a partial sulfur dioxide pressure of 0.2 atm [9]. * 1 atm = 0.1013 MPa.

Oxidation starts with the formation of lead sulfate, which is the stable reaction product at the oxygen and sulfur dioxide partial pressures and temperatures commonly used in sintering. Lead sulfate then reacts further with lead sulfide, decomposing to increasingly basic sulfates and ultimately to lead monoxide. Lead in dust carried out by the sintering gas is totally sulfated.

The composition of the sinter is important as regards its behavior in the blast furnace. The lead monoxide and lead silicate which account for most of the lead content are readily fusible and reducible. The integrity of the sinter thus depends on the presence and quantity of other constituents, typically silicates of zinc, iron, and calcium, and ferrites. These substances are much more refractory than the lead compounds and provide a framework that keeps the sinter lump from disintegrating after the lead compounds have been removed.

Sinter Roasting Techniques. The development of sinter roasting goes back to work by HUNTINGTON and HEBERLEIN (1896), who proposed that lead ores mixed with limestone chips be roasted in a converter with an air blast (blast roasting). Implementation of this idea became the basis of the modern sintering technique, which combines roasting with agglomeration of the charge in the sintering step.

A continuous sintering machine with a sintering bell was devised in 1905–1908 by DWIGHT and LLOYD. At about the same time, von SCHLIPPENBACH introduced the circular sintering machine.

A distinction is made between *downdraft sinter roasting*, where the air required for roasting is drawn downwards through the sinter mixture, and *updraft sintering*, in which the air is blown upwards through the bed. Updraft sintering is preferred because it produces lower gas volumes of higher sulfur dioxide content that are suitable for sulfuric acid production.

Downdraft Sintering

The original downdraft process proposed by DWIGHT and LLOYD was the conventional

technique for the sinter roasting of lead ores until about 1955. It has now been superseded by updraft sintering. In downdraft sintering the nodulized charge blend is fed continuously onto a traveling grate, and sulfides are ignited on the surface of the charge bed by burners. As the ignited charge moves away from the ignition zone, air is drawn downward through the charge. The sulfur is burned on a downward advancing front, and incipient fusion of solids agglomerates the nodules of desulfurized charge into a porous sinter product.

A characteristic of downdraft sintering of lead ores is the low sulfur dioxide concentration of the roasting gases (Figure 9.2). Since off-gases containing 1–2 vol% sulfur dioxide occur at the end of the sintering machine and cannot generally be discharged into the atmosphere, recirculation of the gas or chemical scrubbing is necessary. Even with gas recirculation, the production of acid-strength gas causes problems due to the formation of liquid phases during sintering that reduce the gas permeability of the bed, and in particular to the metallic lead formed by the reaction of lead sulfide with lead sulfate. The molten lead flows downward through the sinter bed along with the gas stream and forms a very tight layer immediately above the grate. Part of the lead also drops through the grate into the wind boxes. Removal of the lead from the wind boxes is expensive and causes long downtimes. Water-bath quenching of wind-box lead and conveyor belt cleaning have been practised to overcome this problem. With downdraft sintering the maximum lead content of the sinter mix is limited to about 40% to avoid excessive production of wind-box lead.

Updraft Sintering

Principles. The difficulties encountered in downdraft sintering are avoided in updraft sintering in which sintering takes place in an ascending gas stream (Figure 9.3). Roasting air is supplied to the machine from below through

the wind boxes, and the gas flows upward through the sinter bed. To initiate roasting, a 2–3 cm layer of feed is placed on the grate and ignited in a downdraft ignition box (Figure 9.3A). The main sinter bed (d) is then distributed onto the burning ignition layer (b), the direction of gas flow is reversed (Figure 9.3B), and air is forced upward through the sinter bed. The main layer is ignited from the first layer, and sinter roasting advances upward. To prevent caking of the ignition layer on the grate bars during downdraft ignition, the grate is usually covered with a hearth layer of return sinter (c) before the ignition layer is placed.

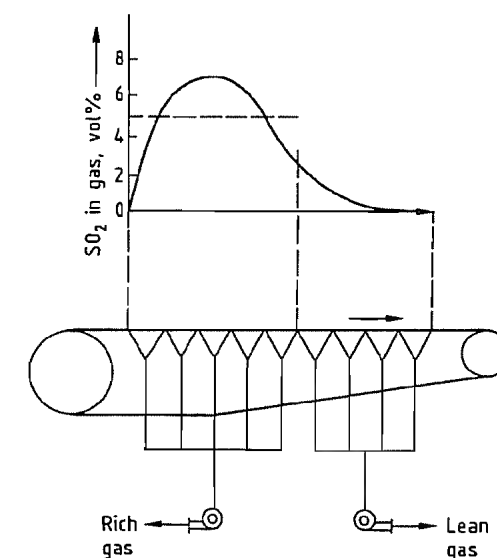


Figure 9.2: Variation in sulfur dioxide content of sintering gases along a downdraft sintering machine.

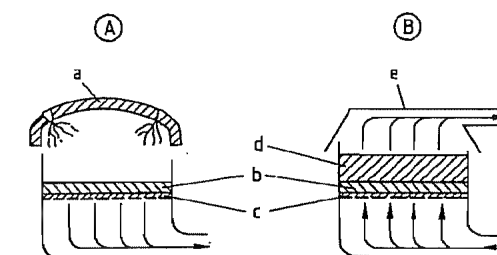


Figure 9.3: Updraft sintering. A) Downdraft ignition; B) Sintering. a) Ignition hood; b) Ignition layer; c) Hearth layer; d) Sinter bed; e) Exhaust hood.

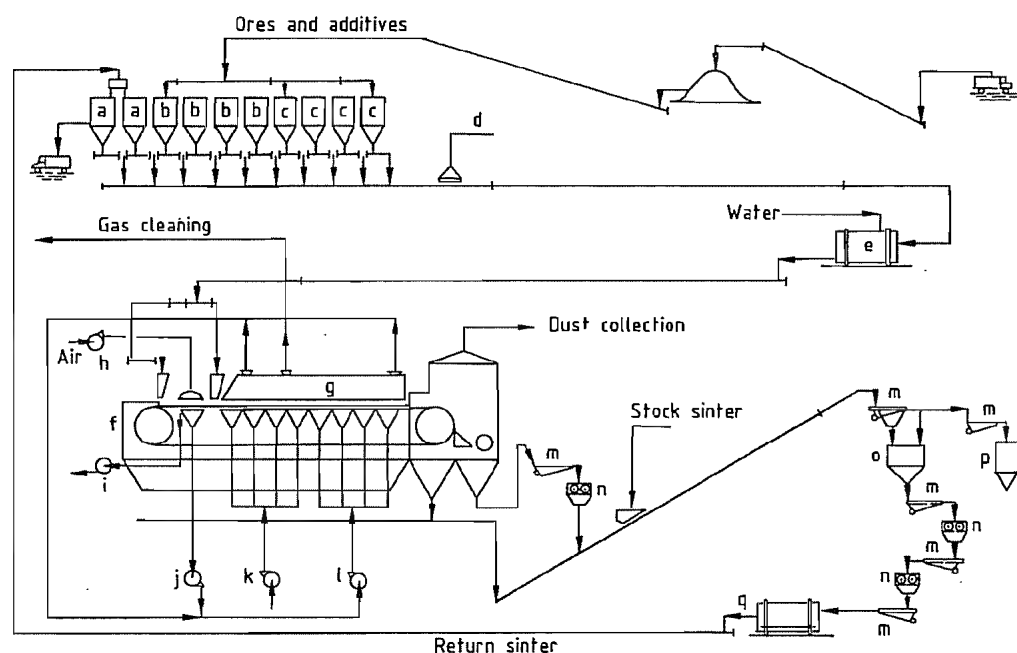


Figure 9.4: Flowsheet of an updraft sinter plant for lead ores: a) Return sinter bins; b) Lead concentrate bins; c) Flux and other charge material bins (silica, limestone, leach residues, etc.); d) Magnet; e) Mixing-nodulizing drum; f) Sinter machine; g) Sinter grate; h) Ignition air blower; i) Ventilation air blower; j) Ignition exhaust fan; k) Sintering air blower; l) Sinter gas recycle blower; m) Sinter screens; n) Roll crushers; o) Undersize sinter bin; p) Product sinter bin; q) Return fines cooling drum.

Since cold air flows into the sinter bed from below, any metallic lead that forms is immediately cooled and solidifies while still in the bed. This makes for good permeability of the bed, lower gas flow, and uniform sintering. Higher sulfur dioxide levels in the roast gases can thus be achieved, and sinter charges containing up to 50% lead can be managed.

Plant Design. The development of updraft sintering began in 1950–1955 at the Port Pirie lead smelter in Australia and at Lurgi Gesellschaft für Chemie und Hüttenwesen, Germany. The process has since been adopted worldwide. All recently constructed sintering plants have been designed for updraft sintering and a large number of downdraft plants have been reconstructed. Updraft sintering became an essential component of the Imperial Smelting zinc process because of the exacting requirements for satisfactory operation (i.e., low sulfur and high sinter hardness).

The flowsheet of a plant of modern design is shown in Figure 9.4. Recent developments have concerned not only increases in the size of updraft sintering machines, but also improvements in capacity, automation, and of working conditions. Dust-collection systems and gas-cleaning systems must comply with increasingly strict regulations on air and water pollution control.

An updraft sintering plant comprises many devices and machines, which employ a logical system of electrical interfaces. Precise control of process performance is difficult, primarily because lag times from entry of the feed to appearance of the product from the sinter strand are long and sampling of the feed and product sinter are difficult. Consistent feed preparation, either by means of large-scale bedding operations or very accurate weigh feeders for the concentrates and fluxes, can provide a high precision of feed-forward control.

Feed Mixture. A charge moisture content of 4.5–5.5% is of utmost importance for achieving good bed permeability during combustion. The desired moisture content of the feed mixture is attained by adding water to the tumbling and mixing drum. Two drums usually operate continuously to achieve good control. If feed material moisture is too high, charge drying is required.

Crushed recycle sinter is required to control the fuel content of the charge and to enhance bed permeability. Cooling of recycle sinter is necessary for mechanical reasons and to minimize dust production. The main difficulties encountered in return sinter cooling are caused by irregular discharge of the sinter strand combined with the handling of moist ventilation gases produced in water quench cooling drums.

Because sinter quality and plant capacity are strongly affected by the physical quality of the recycled sinter, comminution of the returns is very important. The desired size distribution of the lump sinter that is to be reduced in the blast furnace is obtained by two-stage crushing and screening. The returns needed for the sinter charge are also broken down to the requisite particle size (normally 6 mm) by using roll crushers in a two-stage process.

Dust Collection. Dust collection is a major problem in updraft sintering plants. The plant comprises many machines and devices, some of which must transport, screen, and crush hot material; lead-containing dust is produced at all transfer points. Proper ventilation is essential to provide satisfactory in-plant hygiene, and efficient cleaning of exhaust gas is required to control lead emissions. High volumes of ventilation air have to be handled at considerable extra cost. Dust recovered from baghouses and wet scrubbers must be recycled to the process.

Because sintering plants emit both dry and wet dust-laden gases, gas cleaning design has been constantly improved. The most recent plants employ a combination of wet scrubbing and dry baghouse gas cleaning. The cooling drum ventilation and the hot gases from the

sintering machine are cleaned in water scrubbers. Discharge gas temperatures are too high for bag filters. The other dust-collection points (crushing and screening) are combined in a common baghouse. Dust recovered from baghouses is added to the thickener slime that is supplied as coolant to the cooling drum. The dust load in the process sulfur dioxide from the sintering machine is usually collected in high-temperature electrostatic precipitators, moistened, and added directly to the sinter mixture.

Recovery of Sulfur. For optimal operation of the sintering machine, some 15–20 m³m⁻² min⁻¹ of air (at STP) must be delivered along its whole length. The combined exhaust gases have an average sulfur dioxide content of 4–5 vol%. However, since peak sulfur dioxide levels of over 10% occur at the front end of the sintering machine, a rich gas stream with a relatively high sulfur dioxide content can be separated and the balance tail gas is recycled to the front-end wind boxes. In this way, a rich gas containing 6–6.5 vol% sulfur dioxide can be delivered to a sulfuric acid plant. The technique involves a certain deliberate loss of capacity resulting from the injection of hot recycled lean gas at 300–350 °C.

Size and Capacity of Sintering Plant. Standard sizes have been adopted for updraft sintering machines. Size is defined chiefly by smelting capacity and by the quantity of sulfur to be combusted.

Roasting capacities of 1.3–1.5 td⁻¹m⁻² are achieved with modern updraft sintering and are over 50% higher than those of older downdraft systems. For normal lead sintering an annual lead production capacity of 70 000–100 000 t requires a sinter machine of 50–70 m² updraft area. Machines up to 90 m² are employed in Imperial Smelting process plants. These rates and sizes are material-dependent and must be confirmed by tests for each proposed charge. Data for the updraft sinter plant at Port Pirie, Australia are listed below:

Number of sinter machines	1
Roasting surface	
total, m ²	70.5
effective, m ²	62.3

Sinter production, tm^2d^{-1}	20.1
Throughput, t/d	4500
Feed blend, %	
new materials	36
return sinter	64
Sulfur content, %	
concentrates	16–27
new materials	11
return sinter	2.5
total feed blend	5.5
product sinter	1.8
Lead in sinter, %	45
Thickness of ignition layer, mm	35
Total bed thickness, mm	300
Strand speed, m/min	1.42
Ignition method	downdraft
Ignition burners	
number	2
fuel	natural gas
usage, m^3/h	30
Wind boxes	
number	9
bed area, m^2	4.9 (no. 1)
	8.2 (nos. 2–9)
pressure, kPa	5.0 (no. 1)
	4.5 (no. 2)
	3.5 (no. 3)
	2.0 (nos. 4–9)
maximum air flow, $\text{m}^3\text{min}^{-1}\text{m}^{-2}$	38.8
SO_2 concentration, vol%	4–6
Sulfuric acid production	yes

Sintering for the Imperial Smelting Process. Lead–zinc concentrates or mixtures of lead and zinc concentrates for the Imperial Smelting Furnace process must be desulfurized and sintered before reduction in the zinc vaporizing blast furnace. The sinter must incorporate recycled intermediate products from the sinter plant and blast furnace and also the fluxes needed to obtain the desired slag balance. The sinter must be chemically uniform, well desulfurized, as well as hard and abrasion-resistant to avoid formation of lines in the furnace. It must also have a high porosity and a narrow particle-size range.

These requirements can be satisfied only by carefully controlled updraft sintering with feed sulfur held between 5 and 6.5%, moisture at 4–7% and return sinter sizing between 1 and 5 mm. For further details, see Chapter 10.

Products of Sinter Roasting

Sinter. Product sinter should be agglomerated in large lumps that are strong enough to prevent decrepitation during handling. The sinter

should have a cellular, porous structure without pockets of unroasted ore or very dense regions.

Sintering Gases. The sulfur dioxide concentration in the sintering gases is lower than that found in the roasting of zinc or copper ores, especially when high-lead concentrates containing as little as 14–16% sulfur are processed. In the sintering of lead concentrates, the sulfur dioxide level fluctuates between 4 and 6 vol% under favorable conditions and with gas recycling. Release of the lean gases into the atmosphere is unacceptable, although this is still done in a few instances. The roasting gases contain a small amount of sulfur trioxide; their dust content is usually 2–5 g/m^3 , but may reach 20 g/m^3 in exceptional cases. Extensive cleaning is always necessary if the gas is to be processed into sulfuric acid. Pollution control laws require that metal losses be kept to a minimum. The typical gas cleaning train consists of dry electrostatic precipitators, a wet scrubber, followed by wet electrostatic cleaning.

The cleaned sintering gases are generally forwarded to sulfuric acid production. They are sometimes processed into liquid sulfur dioxide after absorption in an organic solvent. In rare cases they are scrubbed with ammonia to produce ammonium sulfate and high-strength sulfur dioxide for recycle or liquid sulfur dioxide production.

Sulfuric acid derived from lead-sintering plants is produced as “black acid”. Its black color is due to carbon particles from the volatile organic constituents of flotation reagents. The color can be removed with hydrogen peroxide at additional expense.

Flue Dusts. Flue dusts from lead sintering plants contain 60–70% lead, about 10% sulfur, and varying amounts of zinc, cadmium, arsenic, antimony, and mercury. The lead is predominantly in the form of lead sulfate or basic lead sulfate, with a minor quantity of lead sulfide. Flue dusts are recycled to the sinter blend.

9.5.2.2 Reduction in the Blast Furnace

The second part of the roast reduction process is carried out in a blast furnace. Where the lead content of the sinter (mainly lead oxide) is reduced to metallic lead, other metals such as copper, antimony, arsenic, and noble metals are also produced. Other constituents (gangues) contained in the sinter and the flux are carried off as silicate slag. In lead blast-furnace smelting, zinc remains in the slag, but in the Imperial Smelting process the furnace top is hot and gaseous zinc leaves the furnace along with the off-gases and is then condensed to liquid zinc metal.

The charge to the blast furnace comprises

- Sinter, which incorporates the roasted concentrate and fluxes
- Other oxygen-containing lead materials such as oxides and silicates
- Metallurgical lump coke as the reducing and heating fuel

Process Description

The lead blast furnace is a countercurrent reactor in which a charge (sinter and coke) moves through a vertical shaft in countercurrent to the ascending gas flow. The descending charge successively passes through the preheating zone (to ca. 200 °C), the reaction or reduction zone (to ca. 900 °C), the melting zone (to ca. 1150 °C), and finally the combustion zone (tuyère zone). The liquid reaction products collect in the furnace crucible, which is located below the tuyère zone.

Principles. In the combustion zone, atmospheric oxygen blown in through the tuyères reacts with the coke to form carbon dioxide with extensive release of heat. This hot gas ascends through a coke-rich layer (arch) and is reduced to carbon monoxide, the main reductant. In the melting zone and in the overlying reduction zone, heat is transferred from the gas and liquid slag is formed from the fluxes and sinter gangue. Most of the metal-forming reactions take place in the softening-melting

zone, even though the residence time in this zone is relatively short. Before fusion, heterogeneous gas–solid reactions and heat transfer processes take place. Free moisture and water of crystallization are driven off in the preheating zone.

The rates of coke combustion and conversion of carbon dioxide to carbon monoxide (Boudouard reaction equilibrium) must be in accordance with the rate of reduction in the reaction zone and with the rate of heat transfer. If the combustion rate exceeds the rate of heat transfer to the charge, the coke burns more rapidly than the charge melts causing the melting zone to rise in the furnace. If the combustion rate is lower than the rate of heat transfer, the coke burns so slowly that it prevents the charge from descending and slows down the performance of the furnace. If the rates of combustion and heat transport are in good agreement, the melting zone and thus the plastic region are narrow. The charge material then flows through at a uniform speed and gas channeling and blow holes are minimized.

For optimal heat and mass transport in the reaction zone, gas velocity should be high and the resistance to gas flow low. The physical and chemical characteristics of the sinter should ensure adequate solids integrity in the reaction zone. Finally, the blast furnace charge should be as physically homogeneous as possible.

Behavior of Sinter Components. The exothermic reduction of lead oxide by carbon, carbon monoxide, and hydrogen begins at relatively low temperature. Other oxygen-containing lead species (e.g., aluminates, silicates, and ferrites) require more intense reducing conditions. Lead sulfate and the basic lead sulfates are converted chiefly by reaction with silicates, but they can also react with sulfides to yield metallic lead. Lead sulfide partly reacts with sulfates to form metallic lead.

The noble metals are largely dissolved in the lead product (*bullion*), with small amounts distributed to sulfide matte and slag.

The copper content of the sinter is captured in the matte in sulfide form, provided suffi-

cient sulfur is present. If, however, the sulfur level is insufficient, the copper is reduced and goes into solution in the lead bullion. A small portion of the copper is always incorporated into the slag in either oxide or sulfide form.

Zinc oxide is located in the slag, and to keep it in solution the slag must be rich in iron(II) oxide. Zinc levels in slag exceeding 18–20% cause slag viscosity problems and some hearth accretions. Part of the zinc oxide is reduced to zinc vapor above the tuyère zone, but the vapor is immediately reoxidized to zinc oxide in the colder zone (zinc circulation in the blast furnace). Zinc sulfide, charged in the sinter or formed from metallic zinc, is notorious because it promotes the formation of accretions on the walls of the smelting shaft. If a matte is formed, it can dissolve a certain amount of the zinc sulfide, but then its melting point rises and the physical separation of the slag becomes more difficult.

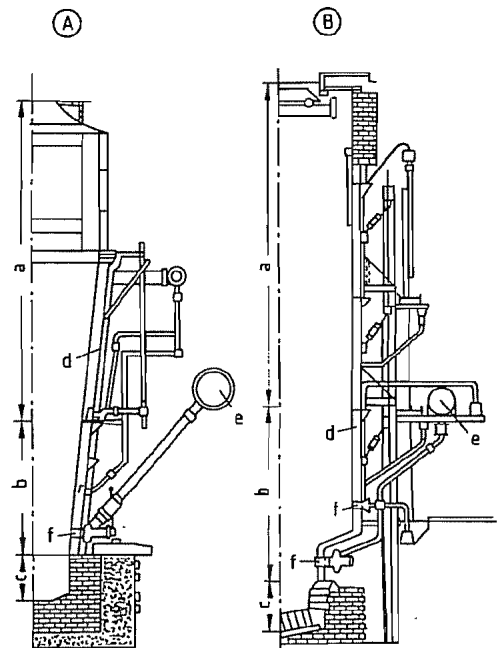


Figure 9.5: Blast furnace profiles. A) Single-level tuyère furnace; B) Double-level tuyère furnace. a) Upper shaft (preheating); b) Lower shaft (melting, reduction, tuyère zone); c) Crucible (slag, lead); d) Shaft and tuyère water jackets; e) Blast air bustle pipe; f) Blast tuyères.

Antimony and arsenic compounds are reduced to the respective metals which dissolve in the lead bullion. If the amount of arsenic is too large to be absorbed by the matte, and if copper, iron, and nickel are also present, metal arsenides (*speisses*) may be formed. Some arsenic is also volatilized and some is slagged. Tin is partly reduced into the lead bullion.

Separation of the fused products leaving the furnace hearth is based on their low mutual solubility and their differing densities (lead bullion about 10.5, matte 4.5–5.0, slag 3.5–3.8 g/cm³).

Lead Blast Furnaces

Lead blast furnaces are classed in two groups: round (*mushroom furnaces*) and rectangular (*Rachette furnaces*). The round design is only used in special low-capacity operations. The Rachette furnace is the standard type of lead blast furnace, and often has rounded corners. The *chair-jacket furnace* is a modification of the Rachette design and has two rows of tuyères, one above the other. Figure 9.5 shows two conventional blast-furnace profiles.

A typical lead blast furnace has a rectangular cross section 5–8.5 m above the tuyères, a water-cooled melting zone, and a syphon tapper for continuous lead discharge. For a given charge, furnace capacity can be increased only by enlarging the cross section. The area of the tuyère zone is the controlling factor. The world's largest furnace, employed by the Broken Hill Associated Smelters, Port Pirie, Australia, has a tuyère zone length of 10 m. Structural and operating data for this furnace are listed below:

Number of furnaces	1
Type	Rachette type with chair jackets
Furnace feed	
sinter, t/d	1250
total, t/d	1415
coke as % of sinter	9.5
Bullion production, t/d	550
Blast air	
rate, m ³ /min	510
pressure, kPa	120
Hearth area	
lower, m ²	17.13

upper, m ²	30.34
Number of tuyères	
sides	81
ends	10
Tuyère diameter, mm	122
Nozzle diameter, mm	65
Elevation of bottom tuyères above hearth, mm	742
Furnace coke	
fixed carbon, %	82
carbon combustion rate, t m ⁻² d ⁻¹	3.3
Top gases, m ³ m ⁻² min ⁻¹ (STP)	16.2
Type of lead tapper	Asarco-Roy

The tuyère zone width can be increased only as long as the blast can penetrate from both sides, generally to around 1.5 m. The furnace can be widened if two offset rows of tuyères are placed one above the other such that the center ("dead zone") of the charge is brought to the melting point in the narrower bottom tuyère zone. Since the penetration depth of the blast in the furnace permits a maximum width of 1.8 m in the bottom tuyère zone, the top tuyère zone has a maximum width of 3.6 m. Widths of 1.5 and 3 m have been achieved in practice. The cooling jackets have the shape of a chair, which gives this configuration its name (Figure 9.5B).

The furnace shaft was formerly constructed of refractory bricks, but in modern furnaces a series of supported water jackets form the shaft, which may be either vertical (Figure 9.5B) or taper toward the bottom (Figure 9.5A). The hearth is subjected to the highest temperature and is cooled by one or more rows of replaceable cooling jackets set one on top of another.

The jackets are cooled with water that is either pumped in a closed cycle or circulated by the thermosiphon principle (i.e., natural convection). Jacket cooling by evaporative cooling (steam generation) is practised in the former Soviet Union. The water jackets have openings for the tuyères through which the blast enters. Combustion air must be at a pressure between 5 and 20 kPa. The resistance of the furnace depends not only on the quantity of blast injected but also on the permeability of the charge. Blowers whose delivery is valuable but independent of the furnace back-pressure are most suitable. These requirements are best met by positive blowers with a variable

speed, but equipment wear often dictates their replacement by centrifugal blowers.

Tests at several lead smelters have demonstrated that enrichment of the blast with oxygen increases throughput (ca. 5% increase for each additional 1% oxygen in the blast). When oxygen replaces part of the blast air, a higher combustion zone temperature is achieved, gas flow per unit of lead is reduced, and the furnace operates more smoothly. Benefits include increased production, a reduction in coke consumption, lower off-gas temperatures, and lower dust generation. Similar results have been achieved with preheated blast air. Whether oxygen enrichment or blast preheating is preferable depends only on economics. Oxygen enrichment has become more popular, especially since low-cost oxygen production has become increasingly common. However, as yet the degree of enrichment of the lead furnace blast is very modest: only 2–3%.

A crucible located below the tuyères serves to separate the liquid products and collect the lead. In large production units, lead is withdrawn continuously, and in smaller ones tapped at intervals. If the lead bullion has a high copper content, the continuous syphon tapper runs into accretion problems. It should be replaced by a discontinuous tapper placed just above the bottom of the crucible, so that it is always covered with molten lead to protect it against deposits. With the Asarco (Roy) continuous tapper the liquid phases are separated outside the furnace [10]. Lead and slag are discharged together into an external settler attached to the furnace, in which the liquid phases are separated. The Asarco tapper gives higher capacities with lower investment and maintenance costs, along with more hygienic workplace conditions. It has the drawback of a higher lead level in the slag. North American smelters employ the Asarco tapper; some European smelters use the Arents syphon tapper.

If a separate matte phase is formed, slag and matte can be separated in a heated launder, where the matte with its higher relative density settles and the slag floats. If the slag is to be discarded or kilned for zinc recovery, it is

usually granulated. It may, however, also be transported in the molten state to a zinc fuming furnace.

The charging of blast furnaces is largely automated. Charging devices for open-top furnaces may be bucket elevators and skips or a variable discharge conveyor belt. Tipping or bottom dump charge buckets are used for the more common closed-top furnaces. Various alternating charging techniques are employed to achieve layers or blends of coke and sinter in the shaft. Blast-furnace top gases are drawn off the furnace top by an exhaust fan and passed through a baghouse for dust removal.

Products of the Lead Blast Furnace

The lead blast furnace yields the following products:

- **Lead bullion**, which must be further refined.
- **Slag**, which may contain large amounts of zinc and must then be further processed.
- **Flue dusts and baghouse dusts**, which consist of fumes and dust particles carried over by the furnace top gases. Cadmium tends to accumulate in this dust, and sometimes a special cadmium separation leach is carried out before the dust is recycled to sintering.
- **Top gas**. Blast furnace top gas usually contains 3–4% carbon monoxide, which represents an unavoidable energy loss. With normal heat exchange between gas and solids in the shaft the top gas is too cold for practical heat recovery, so after dust removal it is released to atmosphere.
- **Matte**, a sulfidic product of blast-furnace smelting, forms only if the burden contains enough sulfur. In general, provided the charge does not contain too much copper or sulfur, matte phase formation is avoided with the copper remaining in solution in the lead bullion and slag. Subsequent reverberatory melting of lead bullion drosses yields copper matte, lead metal, and slag. The copper matte can contain varying amounts of lead, iron, zinc, and noble metals. Copper matte is usually sold to special copper smelters, but processing of matte to copper

sulfate or copper metal is becoming more common.

- **Speiss** is only formed when the burden contains amounts of arsenic, nickel, cobalt, and antimony that are so large that they can no longer be taken up by the matte. Speiss is undesirable, because it dissolves large quantities of noble metals and also requires expensive refining.

Composition and Processing of Slag. The slag consists of gangue, fluxes, and the zinc contained in the charge. It also contains dissolved and suspended metals (lead, copper, silver), which are a potential economic loss. The chemical and physical properties of the slag have a considerable effect on furnace throughput, product separation, metal recovery, and coke consumption in the furnace. Lead blast furnace slag should have a low melting point, be adequately fluid (low viscosity) at the furnace bottom temperature [11], and have minimal density. Slags are compounded to attain these properties by fluxing to selected component ratios. Thus, in the ternary system CaO-FeO-SiO_2 almost all lead blast furnace slag compositions lie in an area that is bounded by weight ratios of 1:1 to 4:1 for $\text{SiO}_2:\text{CaO}$ and 1:2 to 3:2 for $\text{SiO}_2:\text{FeO}$ (Figure 9.6). This is further illustrated in Figure 9.7 for a number of North American and Australian lead blast furnaces.

Lead blast-furnace slag often contains sufficient zinc to make recovery profitable by rotary kiln or submerged combustion slag fuming. In both cases zinc oxide in the slag is reduced to metallic zinc (vapor) by carbon, oxidized by secondary air, and carried out in the furnace gases for recovery of zinc oxide dust.

Zinc recovery rotary kilns (Waelz kilns) are up to 95 m long with an internal diameter of up to 4.5 m and they are lined with refractory material. The granulated blast-furnace slag is mixed with other zinc intermediates (steel dusts, etc.) and solid fuel reductant; it travels down the kiln and is heated to reaction temperature by combustion gases from a burner at the discharge end. The stripped slag is usually

close to its melting point at discharge, and normally contains 2–3% zinc and < 0.25% lead. Production from a Waelz kiln is about 120–155 kg of zinc per day per cubic meter of furnace volume, declining with increasing furnace size. The captured dust contains roughly 75% zinc and lead. Zinc recovery is 88–95% and lead recovery is about 90–98%.

In the *slag-fuming process* a mixture of coal dust and air is injected through tuyères into a liquid blast-furnace slag at 1150–1250 °C in a water-jacketed furnace. The slag is delivered in liquid form directly from the lead blast furnace and may have up to 30% of solid granulated slag or slag skulls added to it. The process is typically operated in batch mode in furnaces of 50–100 t capacity.

At the Plovdiv lead smelter in Bulgaria, slag is tapped continuously from the lead blast furnace through a slag syphon. It then flows through a preheating electric furnace (+ 100 °C) and enters the continuous slag fuming furnace. Heavy fuel oil is used as reductant

rather than the more conventional pulverized coal.

Metal recoveries in slag fuming plants are about the same as in Waelz kilns. Slag fuming furnaces normally recover heat from the hot gases in waste heat boilers or air heat exchangers.

Imperial Smelting Process

In the Imperial Smelting process, lead and zinc are produced together in a single blast furnace operation. This is basically a zinc production process in which lead is also obtained. It is especially well-suited to processing lead-zinc mixed concentrates. The zinc to lead ratio in the sinter mixture is usually 2:1. The furnace design is similar to that of conventional lead blast furnaces of the chair-jacket type, but there is only one row of tuyères. The top is closed by a double-bell system. For process principles and description, see Chapter 10.

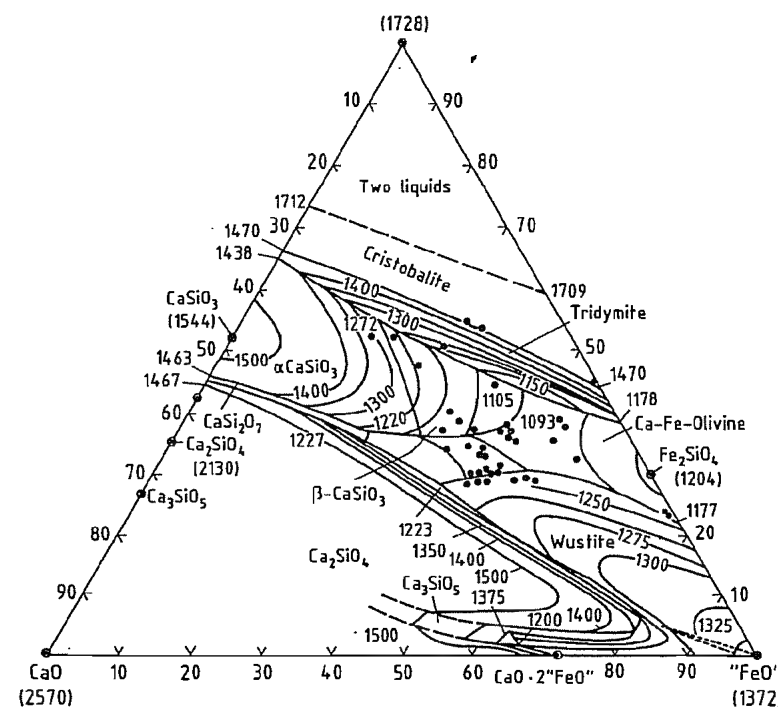


Figure 9.6: The $\text{FeO-SiO}_2\text{-CaO}$ ternary system, showing compositions of several lead blast furnace slags (•) [12].

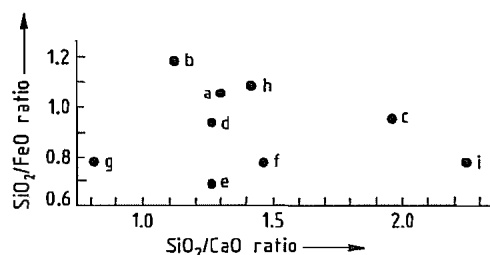
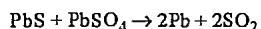
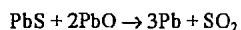


Figure 9.7: SiO₂:FeO and SiO₂:CaO weight percentage ratios in blast furnace slags [13]: a) Asarco, East Helena; b) Asarco, El Paso; c) Asarco Glover; d) Amax; e) Brunswick M&S; f) Cominco; g) Mount Isa; h) BHAS, Port Pine; i) St. Joe Lead.

9.5.3 Roast Reaction Processes

Lead sulfide reacts with lead oxide or lead sulfate to form metallic lead and sulfur dioxide in the roast reaction:



A number of processes dating from the earliest times have been used to recover lead by partial air oxidation of lead sulfide. These processes are categorized as excess sulfur or excess oxygen, depending on whether the reaction series exhausts the oxide and sulfate or the sulfide species, respectively. High-grade lead concentrates are required in order to maximize the activities of the lead species and, therefore, lead recovery.

The principal commercial example of the excess sulfur type is the *Boliden electric furnace process*. Since this process contains elements of flash smelting, it is described in Section 9.5.4.

An example of the excess oxygen roast reaction chemistry is the *Scotch (Newnham) hearth process*, one of the earliest lead-making techniques. The old furnace design was improved and automated in the Bleiberg Bergwerks Union (Schlippenbach) rotary hearth [14]. This process produces a small quantity of high-lead (grey) slag which requires separate recovery treatment, and low-strength sulfur dioxide gas, unsuitable for production of sulfuric acid. The hearth processes

are now antiquated and are responsible for a very small amount of lead production.

9.5.4 Direct Smelting Reduction Processes

The fundamental problems encountered in the sinter, oxidation-blast furnace method of lead production (e.g., high process and hygiene ventilation gas volumes, high maintenance costs for sintering machinery, and expensive coke fuel for reduction) have long been recognized. The quest for a simpler, more direct smelting system has been pursued for many years, and several new processes have now achieved industrial application.

Table 9.2 summarizes the key features of the most prominent new lead smelting processes. They can be classified into two principal categories: *flash smelting* of dried feed mixtures using air or oxygen, and *bath smelting* of undried feed mixtures also with air or oxygen. Oxidation of the feed produces a medium-strength sulfur dioxide gas, a variable amount of lead bullion, a slag rich in lead monoxide, and a lead sulfate flue dust which must be recirculated.

The strength of the sulfur dioxide gas produced depends on the degree of oxygen enrichment and the amount of auxiliary fuel required for autogenous operation of the oxidation step. With the use of oxygen, sulfur dioxide gas contents of 20–30% are typical.

The amount of direct-smelt lead bullion produced during the oxidation step depends on the thermal balance. In the case of direct smelting of a very high-grade lead concentrate, up to 80% of the lead in the charge can be obtained as direct bullion with the remaining 20% as a slag rich in lead monoxide. With low-grade feed charges requiring auxiliary fuel, all lead can be oxidized to a high-lead slag, with no direct bullion production.

The second step in direct smelting processes is reduction of lead from the high-lead slag (25–40% Pb). Slag has been successfully reduced by submerged fuel combustion or injection, reduction assisted by an electric furnace, and a combination of these techniques.

Table 9.2: Summary of direct smelting lead processes.

Process	Smelting type	Source of oxygen	Special features
Boliden Electric furnace	dry charge flash smelting continuous	enriched air	flash oxidation in freeboard of electric furnace; slag reduction by coke breeze in electric furnace; lead bullion is high in sulfur requiring special treatment
Kivcet	dry charge flash smelting continuous	technical oxygen	an electric furnace freeboard is separated into an oxidation flash smelting shaft and a slag reduction section by a partition wall extending into the slag bath; majority of slag reduction is done by coke checker at bottom of smelting shaft
Boliden Kaldo	batch dry charge flash smelting into TBRC vessel	technical oxygen	batch oxidation is followed by slag reduction in same vessel using PbS followed by coke reductant
Outokumpu	dry charge flash smelting continuous	technical oxygen	slag reduction done in separate electric furnace employing powdered coal injection with nitrogen through lance
Isasmelt	moist charge slag bath smelting continuous	air or enriched air	air is injected into slag batch by Siros melt lance; feed dropped into slag bath; slag reduction by coal in a similar lance-vessel unit
QSL	moist charge slag bath smelting continuous	technical oxygen	horizontal cylindrical reactor divided into oxidation and reduction sections by refractory wall; oxygen injected into lead-slag bath through nitrogen shrouded tuyères; moist feed dropped into slag bath; slag reduction by submerged combustion of oxygen fuel in gas shrouded tuyères

9.5.4.1 Air Flash Smelting

Boliden Process [15]. Dry, high-grade galena concentrate (65–75% Pb) is blown into an electric furnace with oxygen-enriched air. Limestone flux and coke breeze are also included in the feed charge. Suspended lead sulfide particles react to produce lead monoxide and lead metal, which collect in the furnace hearth along with the fused slag constituents. Desulfurization is not complete. The furnace products are lead bullion containing 2–3% sulfur, slag containing 4–5% lead, and flue dust. Desulfurization of bullion is completed by air blowing in a downstream converter.

The Boliden electric furnace process has operated successfully since 1963 at the Rönnskär Smelter in Skelleftehamn, Sweden. The 8000-kVA smelting furnace employs four Söderberg electrodes. Product slag is treated in a slag fuming furnace along with copper slag for zinc and lead recovery. A section of the electric furnace is shown in Figure 9.8 and typical daily furnace charge and production figures are listed below:

Charge	
concentrate	280 t
limestone	40 t
iron oxide	7 t
coke breeze	7 t
recycle flue dust	140 t

drosses	15 t
oxygen enrichment	25% O ₂
Products	
slag	70 t (34% CaO, 17% Zn)
bullion	280 t

Several drawbacks have prevented wider industrial application — high-grade lead concentrate is required, flue dust production is high, and bullion treatment is required to remove residual sulfur.

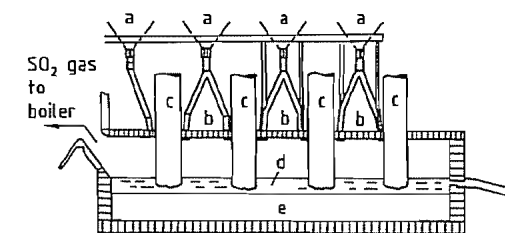


Figure 9.8: Boliden lead smelting electric furnace: a) Dry feed hoppers; b) Dry feed-air injection ports; c) Söderberg electrodes; d) Slag bath; e) Lead bullion.

9.5.4.2 Oxygen Flash Smelting

The most prominent oxygen flash smelting processes for lead production are the Kivcet CS process developed in the former Soviet Union [16], the Kaldo process developed by Boliden in Sweden [17], and the Outokumpu process developed in Finland [18]. In all these processes, very complete desulfurization of

the charge is effected through the production of a strongly oxidizing slag. The required oxygen potential can only be achieved with lead monoxide when its weight fraction is high (> 35% lead in the initial slag) [19]. The other major slag components are in ratios very similar to those found in blast-furnace slag.

Kivcet Process

The Kivcet process was developed at the Vniitvetmet Institute, Ust Kamenogorsk, former Soviet Union. Of the recently developed smelting processes, the Kivcet process is the most advanced, with industrial plants operating at the Ust Kamenogorsk Lead-Zinc Combine and at the Samim lead-zinc metallurgical complex in Portovesme, Sardinia. The Kivcet furnace at the Samim plant is a sophisticated structure, employing extensive water-cooling on the furnace side walls and in the smelting shaft. The general process flows are shown in Figure 9.9. Figure 9.10 shows a section of the smelting furnace at Portovesme.

As shown in Figure 9.10, the oxidation section of the electric furnace freeboard is separated from the reduction section by a water-cooled, gastight wall (d) which dips into the furnace slag bath. Dried and blended charge components consisting of lead concentrate and other lead-bearing materials, required fluxes, recycle flue dust, and oxygen are fed through burners (a) at the top of the oxidation shaft (b). Combustion of charge constituents at a temperature up to 1400 °C and a shaft height of 3–5 m permits almost complete desulfurization before collection of the reaction products in the slag bath (f).

Reduction of the lead monoxide from charge combustion is accomplished mainly by using a layer of coke particles floating on the slag bath under the submerged partition wall (d) into the reduction section of the electric furnace where reduction of lead monoxide is

completed to produce a slag containing 2–3% lead. If desired, additional coke breeze reductant and electrical energy can be used to fume zinc. In this mode of operation, product slag containing 3–4% zinc and 1–2% lead can be obtained. Zinc fumed in the electric furnace can theoretically be recovered as metal using a lead splash condenser, but a simpler approach is to burn the zinc vapor to zinc oxide in a combustion flue (h) and recover an oxidized flue dust for further zinc recovery processing.

Lead bullion is removed from the furnace by a syphon and slag is withdrawn continuously from a weir overflow.

Sulfur dioxide gas from the combustion shaft passes under a water-cooled partition wall before rising in an extended vertical wall boiler duct. Cooling of the sulfur dioxide gas flue dust mixture to 450 °C is accomplished in the vertical boiler stack (e) before the gases enter an electrostatic precipitator for separation of the lead sulfate fumes. Flue dust production is moderate, about 10–20% of the feed charge weight.

The Kivcet process can smelt oxidic charge materials such as zinc leach residues. Extra auxiliary fuel for adequate flame temperature and sufficient shaft height for adequate retention time must be provided to achieve the required degree of desulfurization.

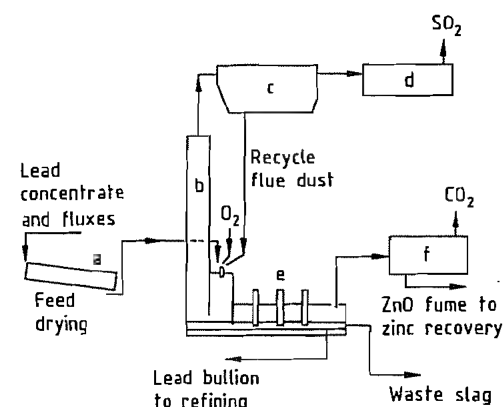


Figure 9.9: Kivcet lead smelting process: a) Feed drying; b) SO₂ gas cooler; c) SO₂ gas cleaning electrostatic precipitator; d) SO₂ gas scrubber; e) Flash smelting furnace; f) Electric furnace gas cleaning.

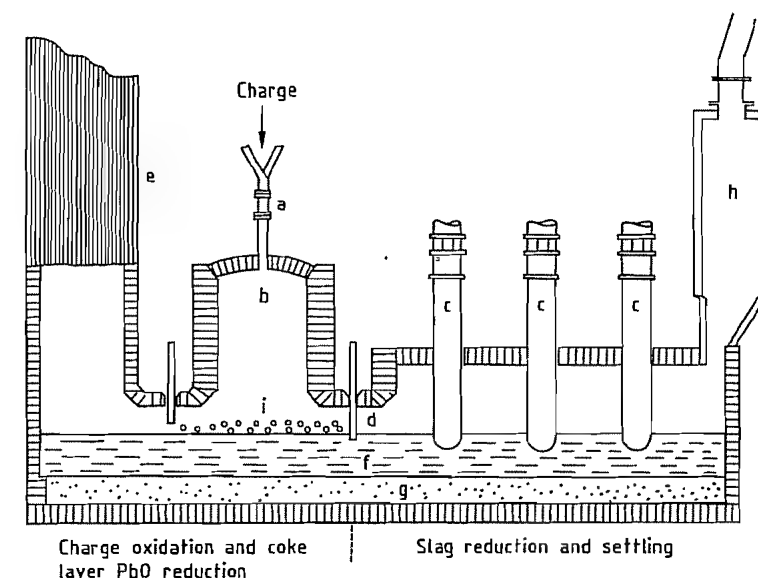


Figure 9.10: Kivcet lead smelting furnace (Portovesme, Italy): a) Oxygen burner for dry feed; b) Flash smelting shaft; c) Furnace electrodes; d) Partition wall; e) Membrane wall SO₂ gas cooler; f) Slag bath; g) Lead bullion; h) Zinc fume combustor-cooler; i) PbO reduction coke layer.

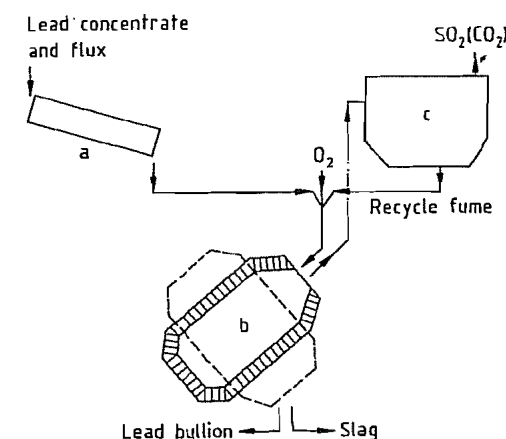


Figure 9.11: Boliden Kaldor process: a) Feed drying; b) Kaldor vessel; c) Gas cooling and cleaning.

Boliden Kaldor Process

The Boliden Kaldor process employs a top-blown rotary converter in a batch manner. A cycle starts with oxygen combustion of dry charge constituents into a preheated empty vessel. Figure 9.11 shows the process flows. Charge combustion is continued until lead

bullion and high-lead slag have accumulated to the limit of vessel weight or volume capacity. Charge combustion is then stopped and slag reduction commences. Lead sulfide concentrate is used to reduce a major portion of the lead monoxide in the slag, followed by coke breeze reduction to discharge slag composition. The vessel's slag and bullion contents are then poured into ladles, and the smelting cycle repeated.

The Boliden Kaldor process can handle a variety of lead-containing charge materials such as secondary scrap and flue dusts. The cyclic production of sulfur dioxide bearing gas and barren reduction gas introduces some complications to the gas handling and sulfur dioxide recovery system.

Outokumpu Process

Outokumpu Oy of Finland pioneered the air flash smelting of copper concentrates in the late 1940s, and this process has become standard worldwide. Experimental work on air flash smelting of lead concentrate in pilot plants was carried out in the 1960s. Little

commercial interest was shown at that time, and pilot-plant testing on several types of lead concentrates was not resumed until the late 1970s, when oxygen rather than air was used for the flash smelt. Full-scale lead smelter engineering studies have been carried out, but to date no production plants have been constructed.

The process scheme of the Outokumpu lead flash smelting process is shown in Figure 9.12. Lead concentrate and flux are dried in a rotary dryer (a), mixed with recycle flue dust, and then flash smelted with oxygen in the oxidation furnace smelting shaft (b). High-lead slag and lead bullion collected in the furnace hearth may be tapped separately to provide a direct lead bullion product. Alternatively, if direct lead bullion production is small, slag and bullion are tapped together into a separate electric slag reduction furnace (d). In the electric furnace, pulverized coal is injected with nitrogen into the slag bath to reduce lead monoxide.

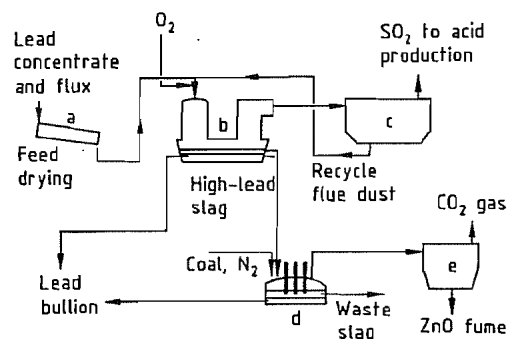


Figure 9.12: Outokumpu lead smelting process: a) Feed drying; b) Flash smelting furnace; c) SO_2 gas cooling and cleaning; d) Electric slag reduction furnace; e) Electric furnace gas cleaning.

The pilot-plant equipment consisted of a rotary dryer, dry concentrate bins, pneumatic conveyors for concentrate and recycle flue dust, a flash furnace (15 m^3), a waste heat boiler (3 t/h steam), an electrostatic precipitator, and a 2 MVA electric furnace.

The pilot plant processed 3–5 t/h of concentrate ranging from 47% to 75% lead content. Bullion and slag were continuously tapped to

the electric furnace for slag reduction. About 10 000 t of lead concentrate were processed.

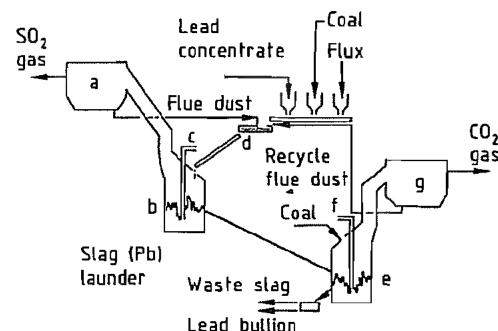


Figure 9.13: Isasmelt lead process: a) SO_2 cooling and cleaning; b) Oxidation; c) Lance for oil and air; d) Feed mixing; e) Reduction furnace; f) Lance for oil and air; g) Reduction gas cooling and cleaning.

9.5.4.3 Air-Slag Bath Smelting, the Isasmelt Process

The Isasmelt process (Figure 9.13) consists of two stages and was developed by Mount Isa Mines and Csiro in Australia [20]. Both stages, the charge oxidation stage and the slag reduction stage, employ a stationary, cylindrical, refractory-lined reaction vessel. The process features the Sirosmelt lance, which is a steel pipe that is cooled by the high-velocity process air which it injects into the melt. In the oxidation vessel (b), air or oxygen-enriched air and supplementary oil fuel are injected through a Sirosmelt lance (c) into the center of the vessel. The blended feed materials (d), lead concentrate, fluxes, and moist recycle flue dust are dropped into the slag bath and agitated by the lance burner. Virtually all the charge lead content is oxidized to a high-lead monoxide slag. The slag is transferred to the reduction vessel (e), which employs a similar air fuel lance (f), with additional lump coal charged separately as reductant.

Starting in 1983, a 5 t/h concentrate feed demonstration plant was used to prove the smelting stage of the process. In the first year of operation, 21 000 t of lead concentrate were treated to produce high-lead monoxide slag, which was subsequently processed by sintering and blast furnace reduction. In 1985, con-

struction of the second-stage reduction vessel demonstration plant was started. At the present time the installation of a full-scale production plant at Mount Isa is being studied.

A cross-section of the oxidation furnace is shown in Figure 9.13 (b). The furnace consists of a cylindrical steel shell, 2.7 m in diameter and 4.5 m high, lined with chrome magnesite bricks backed with an insulation lining. Typical analyses are given in Table 9.3. Operating conditions for the demonstration plant are as follows:

Lead concentrate rate	4 t/h
Smelting temperature	1030 °C
Air:concentrate ratio	125% of theoretical
Fume rate	10% of lead in feed
Flux addition	12% of concentrate rate
Oil requirement	25 kg per tonne of concentrate

Table 9.3: Typical analyses from the Isasmelt demonstration plant oxidation vessel.

Component	Lead concentrate, %	Slag product, %
Pb	47.3	51.8
Zn	7.0	7.6
Fe	12.4	13.6
SiO_2	2.8	9.8
CaO	0.9	1.5
S	23.8	0.3

9.5.4.4 Oxygen-Slag Bath Smelting, QSL Process

The QSL Process is named after its inventors, P. E. QUENEAU and R. SCHUHMAN JR., as well as the process developers Lurgi Chemie [21]. Development of the process progressed through bench-scale tests in 1974–1975, pilot-plant operation in 1976–1979, and a demonstration plant operation at Metallhüttenwerke, Berzelius, Duisburg, Germany from 1981 to 1985. Three commercial plants were constructed: in Trail, Canada (Cominco Ltd.), in Germany (Berzelius Binsfeldhammer Smelter), and in China. The Canadian plant was shut down and dismantled after a brief operation.

Figure 9.14 shows the general scheme of a QSL process lead smelter. Lead concentrate, fluxes, auxiliary coal fuel, recycle flue dust, and other charge components are blended (b) in a moist condition to form a single feed

charge to the QSL reactor. The reaction vessel is a horizontal refractory-lined cylinder that is divided by a partition wall into an oxidation section (c) and a slag reduction section (d). The working dimensions of the demonstration plant reactor (10 t concentrate per hour, 30 000 t of lead per year) were 2.5 m (diameter) by 22 m (length, 7 m of which is occupied by the oxidation zone). Nitrogen-shrouded tuyères on the bottom of the reactor injected oxygen into the oxidation section. Similar shrouded tuyères were employed for submerged combustion of oxygen-coal or oxygen-natural gas reduction mixtures. Blended feed was charged through ports at the top of the oxidation reaction section into the injection-agitated lead and slag bath.

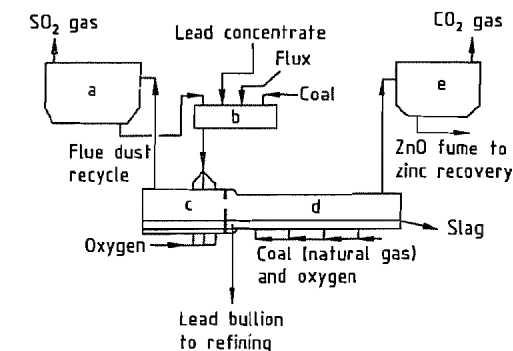


Figure 9.14: QSL lead smelting process: a) Oxidation gas cooling and cleaning; b) Feed mixing; c) Oxidation section; d) Slag reduction section; e) Reduction gas cooling and cleaning.

The oxidation products in the QSL process are high-lead slag, sulfur dioxide gas, flue dust, and lead bullion. The amount of lead produced in the oxidation zone depends on the charge makeup and lead concentrate grade. Slag from the oxidation zone flows through an underflow port in the vessel partition wall into the slag reduction zone (d). Lead bullion is removed by a lead syphon at the side of the vessel. The smelting vessel is rotated by 90° during stoppages to bring the injection tuyère systems above the vessel slag level. Inspection of the refractory and tuyère maintenance can be carried out with the vessel in this standby position.

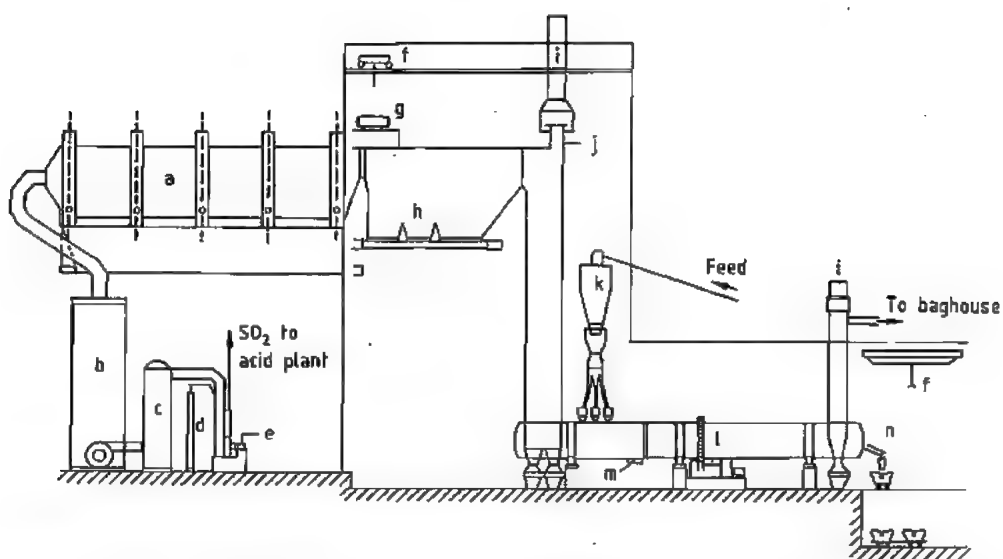


Figure 9.15: QSL lead smelting plant (Trail, Canada): a) Electrostatic precipitator; b) Spray tower; c) Cooling tower; d) Stripper; e) SO₂ fan; f) Crane; g) Steam drum; h) Waste heat boiler; i) Emergency stack; j) Cooling channel; k) Feed bin; l) Reactor; m) Lead syphon; n) Slag tap.

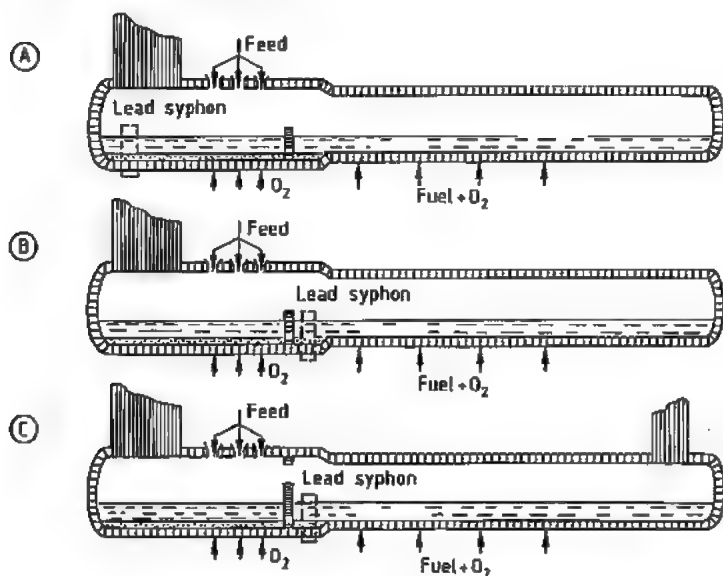


Figure 9.16: QSL smelting vessel configurations. A) Conventional, low arsenic-antimony bullion; B) Increased arsenic-antimony recovery in bullion; C) Recovery of zinc oxide fume.

Figure 9.15 shows the QSL smelting plant in Trail, Canada. The reaction vessel has dimensions of 4.5 m (diameter) by 12.5 m (length) in the oxidation section, and 4.0 m (diameter) by 28 m (length) in the reduction

section. Nominal plant capacity is 160 000 t/a of lead and 230 000 t/a of reduced slag. Reduction is performed with partially combusted natural gas. Three smelting vessel configuration options are shown in Figure 9.16.

Figure 9.16A. This is the simplest smelting configuration and is employed at the Duisburg demonstration plant. Reduction gas and oxidation gas flow into the same gas cooling system. Reduction and fuming of zinc in the reduction zone is controlled to limit zinc circulation in recycle flue dust. Lead bullion produced in the reduction zone flows countercurrent to oxidation slag through the partition wall underflow port. The product lead bullion is withdrawn from the oxidation end of the furnace. With this configuration the arsenic and antimony contents are minimized in the bullion and maximized in the reduced slag.

Figure 9.16B. This differs from the previous option in that the product bullion syphon is located on the reduction side of the slag partition wall. Arsenic and antimony in bullion are maximized with this option.

Figure 9.16C. This smelting vessel configuration has an auxiliary gas offtake at the reduction end of the vessel for withdrawing a zinc-bearing reduction fume. The lead syphon is located on the reduction side of the partition wall for maximum arsenic and antimony deportment to bullion. This design is employed in the Cominco Trail smelter.

9.5.5 Other Lead Processes

Several other lead processes have been tested on small and pilot scales but none has been commercialized. The *Halkyn process* involves the fused-salt electrolysis of lead sulfide dissolved in molten lead chloride; it has been modified and improved, most recently by the U.S. Bureau of Mines [22]. Trouble-free fused-salt electrolysis is feasible only with high-quality lead concentrates; high contents of impurities (e.g., copper) cause the formation of barrier layers and cell complications.

Wet processes have not succeeded although many have been investigated in the chloride, nitrate, sulfate systems, and with selective alkylamine leaching of lead sulfate followed by carbonation of lead. An alternate leaching system employs ammoniacal ammonium sul-

fate, which also dissolves lead sulfate well and is cheaper than the amine solutions.

9.6 Refining of Lead Bullion

Production lead, known as bullion, contains numerous dissolved impurities. Molten lead is an excellent solvent for a variety of metals and compounds, and raw bullion commonly contains copper, iron, zinc, sulfur, arsenic, tin, antimony, bismuth, noble metals (silver, gold, platinum group metals), oxygen, and occasionally nickel, cobalt, and tellurium. The lead content varies between about 90 and 99.9% depending on the process and feed quality. The percentages of impurity contents for blast-furnace lead bullion treated in refining plants are as follows:

Cu	0.2–4.0
Fe	0–0.5
Zn	0–0.5
Ni	0–0.1
Co	0–0.1
Co	0–0.1
As	0–2.0
Sb	0–6.0 (usually < 2.0)
Ag	0–2.0
Bi	0–6.0 (usually < 2.0)
Sn	0–4.0 (usually < 1.0)
S	typically 0.2–0.3
O	typically 0.1

The object of lead bullion refining is to produce pure commercial lead metal and to separate the valuable impurity metals into their most valuable marketable form. The two main refining routes used are pyrometallurgical and electrolytic. The latter is generally reserved for higher levels of impurities (especially bismuth).

Pyrometallurgical processes are generally operated in a batch manner; however, continuous operation is being applied to many of the process steps. The advantage of pyrometallurgical refining lies in the consecutive selective recovery of impurity metals.

In *electrolytic refining*, all the impurities are concentrated in the anode slime and must be separated by a relatively complicated process. On the other hand, electrolysis yields lead that is very low in bismuth (< 10 g of bismuth per tonne of lead), which cannot be eco-

nomically produced by the pyrometallurgical route. Over 90% of installed capacity for lead-bullion refining worldwide is based on pyrometallurgical methods.

9.6.1 Pyrometallurgical Refining

Principles. When metals are refined pyrometallurgically, impurities dissolved in the parent metal are enriched in a phase that is insoluble (or sparingly insoluble) in the parent metal. Enrichment can be achieved by adding reagents, by controlling the pressure and temperature, or by a combination of both techniques. Methods are classified as chemical, precipitation, and distillation processes.

Attention to the kinetics of the unit operations involved in lead refining is of the utmost importance. Kinetic reactors can govern the degree of refining that is attainable when the system is far removed from the theoretical chemical or physical equilibrium. In other systems the chemical equilibrium is approached closely. A good review of the physical chemistry is given in [23].

Chemical Processes. A reagent added to the parent metal reacts with one or more impurities to form a compound that is insoluble in the parent metal. Occasionally, fluxes are also used, for example to cause oxides formed in the solid phase to go into a liquid slag. Reagents include oxygen (atmospheric oxygen or oxygen-evolving salts), sulfur, and chlorine. The refining step is then referred to as selective oxidation, sulfurization, or chlorination. Reagent selection is based on a comparison of the free energy of formation of the oxides, sulfides, or chlorides of the parent metal and of the impurities in question.

Precipitation Processes. Generally, impurities become less soluble in the host metal as the temperature falls, and can be rejected either directly from the melt (e.g., copper from the binary system copper-lead), or as a compound with the parent metal (e.g., iron as FeZn_3 from iron-zinc solutions). Alternatively, suitable reagents can form insoluble compounds that can be skimmed off (e.g., bismuth from lead-bismuth solutions after addi-

tion of calcium and magnesium); this is really a chemical process that involves the formation of insoluble intermetallic compounds.

Distillation Processes. Distillation processes are employed when a large difference in vapor pressure exists between the parent metal and the impurity (e.g., in the separation of residual zinc from lead bullion after Parkes desilvering).

Process Steps. All of the above processes are used in the pyrometallurgical refining of lead bullion. A typical pyrorefining scheme is as follows:

- **Removal of copper** is a two-stage operation. The first stage is primary decoppering by *drossing* (precipitation). The second is *selective sulfidizing* of copper by the Colcord process, which involves the addition of sulfur (a chemical process).
- **Removal of arsenic, tin, and antimony** by selective oxidation with injected air or with oxidizing agents such as sodium nitrate in a caustic slag (Harris process).
- **Removal of noble metals** is usually called desilvering or desilvering and involves intermetallic precipitation with zinc by the Parkes process.
- **Removal of zinc** remaining after desilvering is achieved by vacuum distillation.
- **Debismuthizing.** If required to meet refined lead specifications, bismuth is removed by precipitation with alkali metals and/or alkaline earth metals, for example with calcium and magnesium in the Kroll-Betterton process.
- **Removal of alkali metals and alkaline earth metals** remaining after debismuthizing is called final refining and is performed by selective oxidation with air under a salt slag cover.

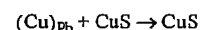
9.6.1.1 Decoppering

Drossing (Liquation). Copper is soluble to several percent in hot lead bullion but to only 0.06% at the freezing point. When the lead cools, copper and other impurities precipitate as a lead-rich *copper dross*. This process is al-

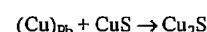
ways the first step in any lead refining operation. In the first phase of cooling to about 950 °C, nearly all dissolved iron and zinc are precipitated as oxides, magnetites, or spinels. The noble metals and other impurities with higher solubilities (e.g., copper, arsenic, antimony, tin, bismuth) remain dissolved in the lead.

In the next cooling stage, the copper compounds of sulfur, arsenic, antimony, and tin separate, along with considerable lead sulfide and entrained metallic lead. The large lead content must be separated by a dross retreatment process. Nickel and cobalt, if present, separate similarly to copper.

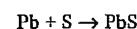
Fine decoppering may also be referred to as sulfur decoppering or sulfur drossing (Colcord process). After drossing, elemental sulfur is mixed into the molten lead bullion at the lowest possible temperature (320 °C) for selective sulfidization of copper. Lead(II) sulfide and copper(II) sulfide form stable phases in the ternary system Pb-Cu-S when liquid or gaseous sulfur is present. The copper sulfide can be produced by the reaction between copper-lead alloy and liquid or gaseous sulfur whenever there is a local excess of sulfur:



Copper(II) sulfide can decopper lead by the reaction



Sulfur simultaneously reacts with lead, but much more slowly than with copper:



The lead corner of the Pb-Cu-S system is shown in Figure 9.17 and suggests that the copper level can in theory only be decreased to about 0.05% by sulfur precipitation. With cooling, however, lead sulfide forms as well as copper(I) sulfide (Cu_2S). In fact copper levels of 0.001–0.002% can be achieved if minor amounts of silver or tin are also present and attention is paid to good shear stirring and gradual addition of sulfur [23]. This is because silver and tin slow down the reaction between lead and sulfur. Without silver or tin, 0.01% copper can be attained only by repeated sulfur

additions and with prohibitive sulfiding of lead.

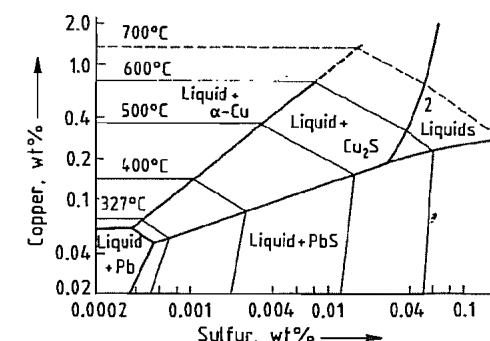


Figure 9.17: Lead corner of the Pb-Cu-S ternary system [23].

Process Engineering. Decoppering of lead bullion usually takes place immediately after the bullion is discharged from the blast furnace. In batch decoppering, drossing is carried out in kettles with capacities of up to 300 t. Powerful stirrers help separate the phases, allowing the formation of a "dry" dross containing little entrained lead metal. The dry dross is removed from the melt surface by skimming, usually with mechanically or pneumatically driven perforated scoops, or by suction. In industrial drossing, final copper contents of 0.06–0.12% are reached. This level of copper would greatly increase the zinc requirement for Parkes process desilvering, and therefore fine (sulfur) decoppering is always necessary.

An important advance is *continuous decoppering*, which combines decoppering and reprocessing of the copper dross in a single stage. Continuous drossing has several advantages over the batch process of dry stirring in kettles. Effective lead drossing by cooling is combined with the formation of matte and slag in a single process step. Handling of dusty copper dross is eliminated, which permits a major improvement in plant hygiene. Success in the development of a continuous drossing process has been achieved in Australia and the former Soviet Union by using a deep lead bath reverberatory furnace. The process is also employed at Cominco's lead smelter in Trail, Canada.

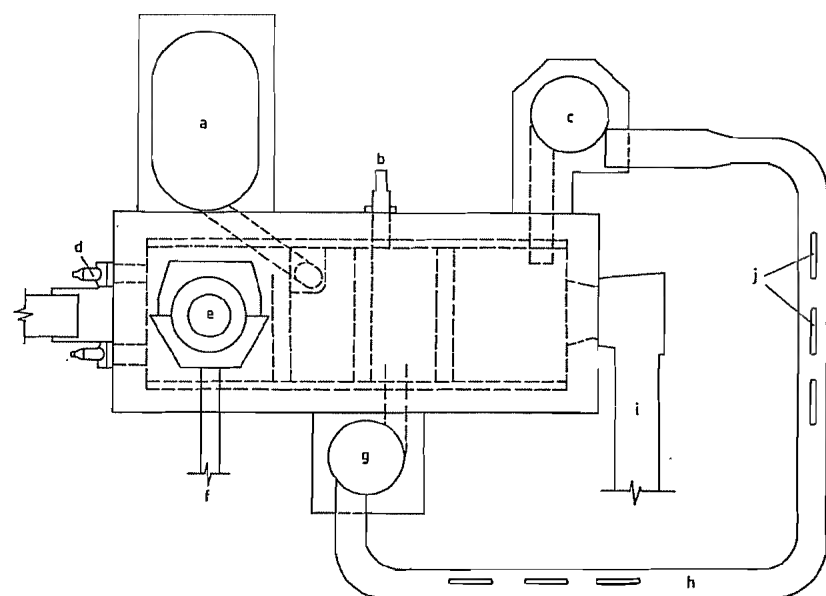


Figure 9.18: Plan view of the continuous dressing furnace of Broken Hill Associated Smelters (BHAS) at Port Pirie, Australia: a) Product dressed lead; b) Slag and matte tapping spout; c) Circulating pump pot; d) Gas burners; e) Charge port; f) Ventilation; g) Return launder pot; h) Cooling launder; i) Water-cooled flue; j) Water-cooled plates.

Figure 9.18 shows the furnace used by Broken Hill Associated Smelters (BHAS) in Port Pirie, Australia. The gas-fired furnace has an external bullion cooling launder (h) with immersible water-cooled plates (j). Hot bullion from the blast furnace is charged to the dressing furnace and is cooled by mixing with colder lead from the cooling launder. Dross formed rises to the heated surface and is melted to matte and slag. The third-generation furnace now used at Port Pirie has hearth dimensions of 6.15 m by 2.0 m and a depth of 1.7 m [24]. The process is best suited to refining lead with a fairly uniform impurity content. An important operating criterion is the ratio of copper to sulfur in the bullion. A high ratio causes the formation of high melting point speiss crusts in the furnace. Recent development has allowed addition of elemental sulfur to the furnace permitting satisfactory operation at bullion copper levels approaching three percent.

In the Russian continuous dressing process, bullion cooling is achieved by indirect water-cooling through the furnace bottom. Copper

drossing and cooling are finished in batch kettles, dross being recycled to the dressing furnace. Soda ash is added to the furnace to produce a low lead soda matte.

Sulfur Dressing. *Final decoppering* (sulfur dressing) is carried out *batchwise* in most plants in kettles fitted with a powerful stirrer. Fine sulfur is added in increments to the lead vortex at 330–340 °C, and the formed copper dross is skimmed, usually with the aid of sawdust. This dross is much lower in copper (and higher in sulfur) than primary decoppering dross and is returned to a convenient point in the smelting process. In industrial operation, about 1 kg of sulfur is added per kilogram of copper; the end copper content must be less than 50 g/t if possible. Several sulfur treatments are needed to achieve this.

A *continuous sulfur dressing system* has been developed by BHAS at Port Pirie [24] and has been operating since 1981. The process employs a series of small stirred kettles [23]. A continuous flow of bullion from the copper dressing furnace is cooled, treated with elemental sulfur, and mechanically drossed.

9.6.1.2 Removal of Arsenic, Tin, and Antimony

The removal of arsenic, tin, and antimony is called *softening*. Two processes are in use: selective oxidation with air in fired furnaces and the Harris process.

Oxidation in Air-Blown Furnaces. This method is based on the fact that tin, arsenic, and antimony react more readily with oxygen than lead, and are oxidized (in the order listed) before lead at 700–750 °C. Air is injected through vertical lances onto the surface of a lead bath in a rectangular oil- or gas-fired reverberatory furnace. The oxides of tin, arsenic, antimony, and lead form a fluid slag, which is periodically removed from the surface of the lead bath. A considerable amount of lead is oxidized and the slag generally contains 50–60% lead monoxide. In batch reverberatory softening, segregation of slag skimmings into high arsenic–tin and high antimony lots is possible, but not usually practised.

The oxides float on the molten lead and are withdrawn as softening slag. Refining time depends on the amount of impurities in the charged bullion and also on the air-lancing method. Impurity oxidation rates in the order of $4 \text{ kg m}^{-2} \text{ h}^{-1}$ are typical.

Continuous bullion softening is operated by BHAS, Port Pirie, Australia. Drossed lead is pumped continuously into a softening reverberatory furnace fitted with an air-lance system similar to a batch softening furnace. The rate of bullion feed and the rate of arsenic and antimony oxidation are such that the antimony content is maintained at 0.02–0.05%. Antimony oxidation rates of $40 \text{ kg m}^{-2} \text{ h}^{-1}$ are achieved, about an order of magnitude greater than in batch softening.

Harris Process. The Harris process employs molten sodium hydroxide as a medium for the oxidation of arsenic, tin, and antimony from lead bullion. Metallurgie Hoboken–Overpelt, Hoboken, Belgium [25] and the Norddeutsche Affinerie, Hamburg, Germany [26], use this process. Harris refining is performed

batchwise using a reaction cylinder holding molten sodium hydroxide installed in a lead kettle. Figure 9.19 shows one half of a dual kettle Harris reactor as employed at the Hoboken smelter. Bullion is pumped through the Harris reactor caustic charge until the required degree of impurity removal is achieved. A valve at the bottom of the caustic vessel is then closed allowing the loaded caustic to be discharged to a transport ladle for subsequent hydrometallurgical processing. Fresh molten caustic recovered from the salt processing plant is charged to the reactor by ladle for the next refining cycle.

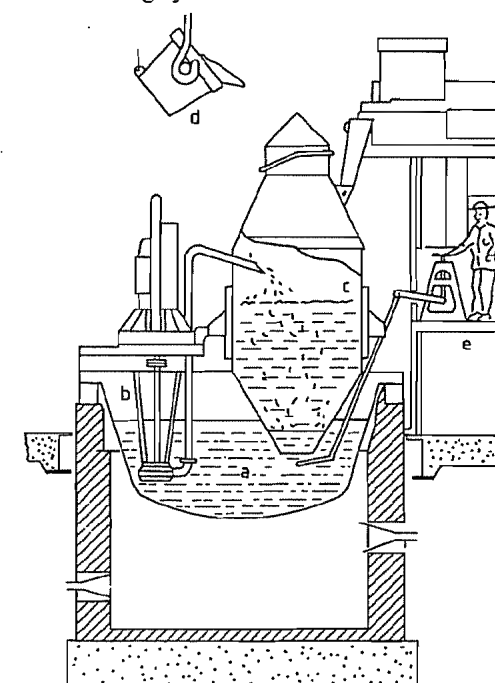
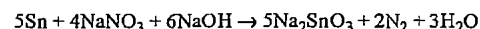
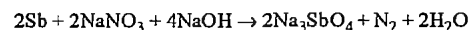
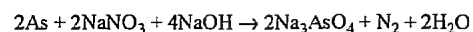


Figure 9.19: Harris reactor at Metallurgie Hoboken–Overpelt S.A. [25]. One half of the dual reactor is shown. a) Lead bullion; b) Lead bullion pump; c) Molten caustic holding vessel; d) Molten caustic supply ladle; e) Reactor control system.

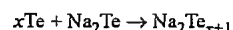
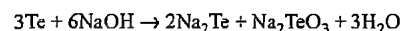
The Harris process is the preferred softening process for lead bullion containing high levels of impurities. The plant at Hoboken can remove up to 400 t of arsenic, tin, and antimony from lead bullion per month.

Harris softening involves the oxidation of arsenic, tin, and antimony by air or by sodium

nitrate added to the caustic bath. The oxidation products, in order of their formation, are sodium arsenate, sodium stannate, and sodium antimonate:



Tellurium is oxidized to sodium tellurate and telluride:



The arsenic salt is soluble in the molten caustic whereas the salts of tin and antimony form a solid suspension. Because of the reversibility of the oxidation chemistry (e.g., Na_3SbO_3 will oxidize arsenic and tin from bullion), a loaded caustic salt is produced that is high in arsenic and tin, followed by a salt containing primarily antimony. Table 9.4 gives the distribution of arsenic, tin, and antimony in the products of the Harris refining process at the Hoboken lead smelter. A flow sheet is given in Section 9.6.1.7 (Figure 9.24).

Table 9.4: Distribution of metals in products separated by the Harris process at Metallurgie Hoboken-Overpelt S.A. [23].

Product ^a	Metal, %		
	As	Sn	Sb
Lead particles As-Sn	5.5	5.0	2.1
Lead particles Sb	0.2	0.1	4.0
Black antimonate ^b	0.5	2.5	3.8
Calcium stannate	2.2	91.8	0.2
Calcium arsenate	91.6	0.5	0.3
White antimonate		0.1	89.6

^a For origin of products, see Figure 9.24.

^b Contains more than 80% of extracted Te, Se, and In.

9.6.1.3 Removal of Noble Metals

Noble metals and residual copper are removed from lead by the Parkes process in which zinc metal is added to the molten silver-bearing lead and the mixture is cooled (see also Chapter 24) Silver-zinc mixed crystals precipitate out and rise to the bath surface as a crust (Parkes process crust). The intermetallic compounds have a higher melting point than

lead and are virtually insoluble in zinc-saturated lead.

The metallurgical operations in the Parkes process are based on the lead corner of the ternary system Ag-Pb-Zn (Figure 9.20). Most of the silver removal takes place in the liquid + ϵ -phase Ag-Zn crystals region; the last crop of crystals in the latter part of the second stage comes from the liquid + η -phase region. Silver removal is very efficient and depends on the quantity of zinc and the number of stages used, but it is usually not economical to use more than two stages.

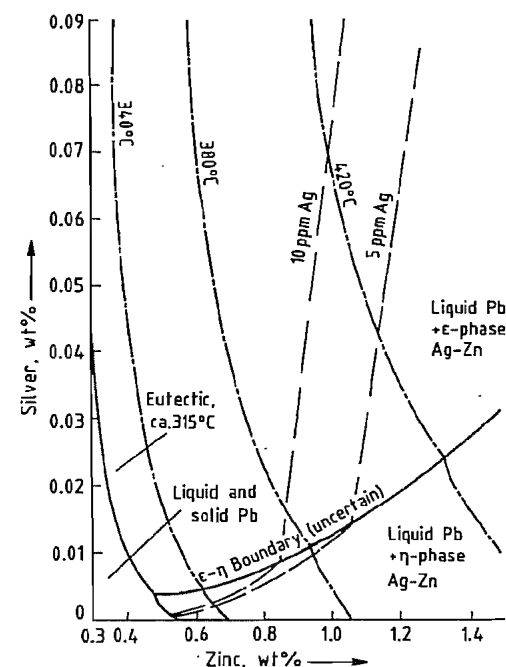


Figure 9.20: Lead corner of the Pb-Ag-Zn system in rectangular coordinates [23]. The isotherms (—) indicate how much zinc can be dissolved in the lead. The cooling curves (---) indicate the course of desilvering in the batchwise two-stage process for final silver concentrations of 5 and 10 ppm.

Process Engineering of Desilvering. In the *batch process*, desilvering is performed in two stages in kettles with capacities of up to 300 t. In the first stage “lean crust” from the preceding charge is added along with other recycle zinc and stirred into new softened lead at 460 °C. The “rich crust” is skimmed off for

silver recovery. In the second stage, zinc metal is added with stirring; more zinc silver crystals form, and the bath is then cooled to near freezing at about 370 °C so that the last crystals separate. At this point, the silver content of the near-freezing lead is 5–10 ppm.

The *Williams continuous desilvering process*, developed at Port Pirie, employs a deep kettle surrounded by heating jackets, which impose a vertical temperature gradient on the lead column from 600 °C at the top to the temperature of the ternary Ag-Pb-Zn eutectic at the bottom. The upper part of the column contains ports for the intake of lead, addition of zinc, and removal of the ternary alloy. A siphon for discharging the desilvered lead has its intake just above the bottom of the kettle.

The softened silver-bearing lead is brought to 650 °C in a conditioning furnace and then flows continuously into the desilvering kettle. The lead flows through the zinc layer in the upper part of the kettle, and becomes saturated with zinc. As it descends down the kettle, it is cooled along the imposed temperature gradient. When it approaches the freezing temperature, silver-zinc crystals precipitate and rise to the zinc layer at the lead surface. The desilvered lead contains about 3 ppm Ag and 0.6% Zn, and leaves the kettle through the siphon.

The composition of a fresh zinc layer changes, becoming enriched in silver (and lead). When it approaches about 15% silver, 20% lead, it begins to freeze. The mushy alloy is then ladled out and replaced with fresh zinc. Residual copper and any gold are removed very efficiently along with the silver. Continuous desilvering produces only a single silver-zinc crust which can be sent directly to distillation — an advantage over two-stage desilvering. The modern batch operation, however, uses less zinc and has lower operating costs.

9.6.1.4 Dezincing

The desilvered lead still contains about 0.55–0.6% zinc which must be removed. Older methods used air and steam, caustic soda, or chlorine, all of which oxidized the zinc metal. These have been replaced by vac-

uum distillation of zinc from the desilvered lead. The large difference in vapor pressure between the host lead and dissolved zinc permits the volatilization of about 95% of the zinc from the desilvered lead when a vacuum of about 0.133 Pa is applied at about 600 °C. A condensing surface placed close to the surface of the lead allows kinetic control of the distillation. The zinc content of the vapor exceeds the mole fraction in the melt by over 500% [23].

Process Engineering. Batch dezincing is performed in a kettle: a water-cooled bell is sealed vacuum-tight on the kettle and distillation is carried out at about 600 °C and a vacuum of about 0.133 Pa (measured at the pump). The lead is circulated by a stirring mechanism, also sealed vacuum-tight. Crystalline zinc precipitates on the bottom of the water-cooled vacuum bell and is struck off after the termination of the process. Adequate sealing was originally achieved by letting the bell dip into the lead bath (barometric seal); today, water-cooled gaskets are preferred.

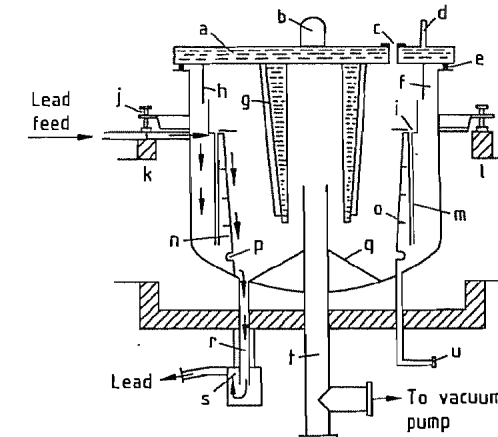


Figure 9.21: Continuous vacuum dezincing: a) Water-cooled cover; b) Hook; c) Window; d) Cooling water connections; e) Rubber gasket; f) Baffle; g) Cooling fins; h) Weir plate; i) Lead trough; j) Level control; k, l) Furnace setting gas entry and exit; m) Lead inlet to trough; n) Evaporation surface; o) Reinforcement; p) Flexible connection; q) False bottom; r) Lead siphon; s) Lead outlet; t) Vacuum connection; u) Drain.

At Port Pirie, continuous dezincing has also been developed. The dezincing apparatus

(Figure 9.21) consists of a thin-film evaporator with roughly 0.75 m^2 of evaporating surface. It can dezinc 16–37 t/h of Parkes lead, and 90–95% of the zinc content is recovered on a water-cooled fin condenser. When about 3 t of zinc has been collected, the condenser is replaced. The deposited zinc is melted and returned to the desilvering operation.

The lead is heated to 590–620 °C in a pre-heat furnace, before entering the vacuum kettle. After dezincing, it leaves the unit at 540–560 °C with a zinc content of about 0.03%. The pressure inside the kettle is 3–7 Pa. The residual zinc in the lead bullion is removed during final refining.

9.6.1.5 Debismuthizing

Debismuthizing is the last step of lead-bullion refining. It is applied when the bismuth content of the ore is so high that it restricts the use of the soft lead smelted from it. When possible, bismuth-rich and bismuth-poor ores are smelted separately in order to refine the minimum amount of lead bullion with the maximum bismuth content.

Bismuth is less reactive than lead, therefore it cannot be removed with oxygen, chlorine, or sulfur. It is customarily separated by addition of an alkali metal or alkaline earth metal forming a bismuthide M_xBi , but this only permits a minimum bismuth content of 0.03%, which is not adequate for many requirements. The removal of bismuth to < 0.01% can be achieved by the *Kroll-Betterton process*, which uses calcium and magnesium and also by the *Jollivet-Penarroya process*, which uses potassium and magnesium. Only the former remains in use; the metallurgical reactions take place in the lead corner of the corresponding quaternary system (Figure 9.22). Bismuth separates as a crust of the double bismuthide, CaMg_2Bi_2 .

The lowest attainable bismuth content is around 0.002% at the quaternary eutectic point. Further addition of calcium and magnesium does not improve bismuth removal. The reagent requirement is given by the total calcium and magnesium needed for precipitation

as the double bismuthide and for saturation of the lead.

Process Engineering. The Kroll-Betterton batch debismuthizing process is carried out in kettles. Magnesium and calcium (in lead) are stirred into the lead bath at a temperature of about 420 °C. The bath is then cooled to near the solidification point with slow stirring. The crust (enriched about 10:1 in bismuth) is removed in a similar manner to the Parkes process. The crust grade can be improved considerably by stirring into the next batch of lead. Both batch and continuous versions of the Kroll-Betterton refining are practiced. A procedure is also used for secondary, fine debismuthizing by antimony addition [27].

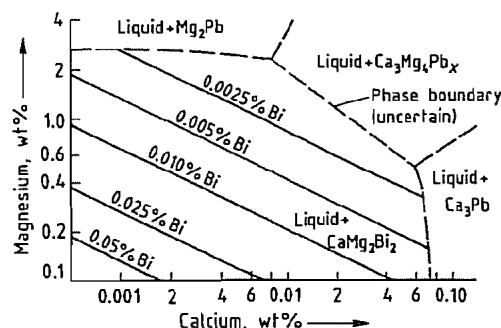


Figure 9.22: Lead corner liquidus of the quaternary Pb-Bi-Ca-Mg system [23].

9.6.1.6 Final Refining and Casting of Lead

Refined lead contains arsenic, antimony, and tin at a level of 10–20 g/t; zinc corresponding to the final content in vacuum dezincing (ca. 30 g/t); and (if debismuthizing has been performed) calcium and magnesium corresponding to the saturation limit. These impurities are removed down to below 1 g/t by treatment with caustic soda and, in some instances, with sodium nitrate.

Most casting today is done automatically in strip or (less often) bench form, in machines provided with automatic stacking devices. The casting temperature is around 400 °C. Immediately after admission to the chill mold, the thin oxide surface film is skimmed off. The

cast lead has a coarsely crystalline surface; if final refining and casting techniques are correct, there are no temper colors.

9.6.1.7 Processing of Intermediate Products of Pyrometallurgical Refining

Copper Dross. Copper dross is a complex mixture of compounds and contains a substantial amount of sulfidic and metallic lead. Melting the dross in a retreatment furnace frees the metallic lead and forms a matte phase, consisting mainly of lead and copper sulfides, and a slag which contains metal oxides and often requires silicate fluxing. If arsenic is available and sulfur is deficient, a copper arsenide speiss product is formed. The slag is returned to the smelter, but the matte is a product for sale or further processing.

All constituents of the dross deport to the four possible liquated phases lead, speiss, matte, and slag. If large amounts of arsenic are present, a speiss forms in which nickel, arsenic, and part of the copper are preferentially concentrated. If copper and arsenic levels in the dross are low, the matte and speiss must be enriched by a further treatment. In dross retreatment, it is desirable to minimize the lead content of the final matte. If the iron and sulfur contents are known, the final lead content can be approximately estimated from Figure 9.23: % Fe is equated to % (Fe + Zn) in the lead-free matte and % S can be determined from the lead-free sum, $\text{Fe} + \text{Zn} + \text{Cu} + \text{S} = 100\%$. For example, for a lead-free matte containing 7% Fe, 1% Zn, 24% S, and 68% Cu, the lead content predicted from Figure 23 is 20%. The final matte would then contain 20% Pb, 5.6% Fe, 0.8% Zn, 19.2% S, and 54.4% Cu. This is a fair estimate only for low alkali mattes. Sodium or calcium additions lower lead solubility in the matte substantially; at 5% sodium or calcium the solubility is reduced to less than 20% of that in the same matte without alkali. This is the basis of the soda matte process used by Asarco (El Paso) and St. Joe Lead at Hercules, in which about 5% soda ash is added

to the dross during melting and produces a copper enriched matte.

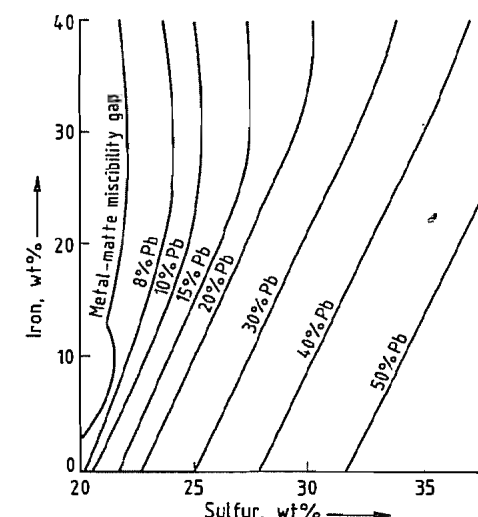


Figure 9.23: Solubility of lead in Cu-Fe-S mattes [23].

The recovered lead contains most of the noble metals. Matte, and particularly speiss if present, also hold significant amounts of precious metals. Fume from the furnace is enriched in indium, tin, arsenic, and zinc. Slag, matte and speiss are normally granulated.

Hydrometallurgical methods for treating copper dross involve solubilizing the copper for electrowinning either by pressure oxidation leaching in sulfuric acid or by ammoniacal leaching and solvent extraction.

Softening Slags and Drosses. Softening slag and skimmings with variable contents of tin, arsenic, and antimony are usually reduced to hard lead. An effort is made to slag off part of the arsenic during reduction. The process is normally carried out in a rotary furnace, but can also be done in a blast furnace.

In the short rotary furnace at Port Pirie, 7 t of softening slag are reduced batchwise with the addition of 5% soda, 7% charcoal, and 6% "caustic slag" from subsequent refining. The charcoal is added in two portions. After the first portion is reacted, a lead bullion containing 2–3% antimony is tapped off and recycled. After the second reduction, about 85% of the

feed antimony is tapped off as an alloy containing 25–30% antimony.

Harris Salt Slags. Harris slags are processed to recover a large portion of the valuable minor metals as black antimonate (Sn, Sb, Te, Se, In) and sodium antimonate (Sb); to precipitate the tin as calcium stannate and arsenic as calcium arsenate; and to recover caustic soda for reuse. The flowsheet of Metallurgie Hoboken–Overpelt is shown in Figure 9.24.

Silver–Zinc Rich Crusts for Desilvering. The purpose of processing the silver–zinc-rich crusts is to recover a malleable rich lead that contains all the noble metals. Some of the lead and as much as possible of the zinc must be removed; the latter is reused. Removal is achieved by expression and/or liquation with

production of a dry or liquated crust, followed by zinc distillation.

Expression is commonly carried out in an air-driven Howard press submerged in a liquid lead bath, and the lead content of the compressed crust is brought to 50–60%.

Liquation. Alternatively the crust may be melted at about 600 °C under a salt cover and separated into a lead-rich lower layer, which is returned to desilvering, and a zinc-rich upper layer which passes to zinc removal.

Distillation allows the zinc content of the liquated rich crusts to be recovered in metallic form so that it can be reused for desilvering lead bullion. Distillation can be performed either at STP in the Faber du Faur furnace or under vacuum in the Leferrer furnace.

In the older *Faber du Faur* furnace, liquated zinc-rich crust is placed in inclined bottle-shaped graphite retorts and heated to 1000–1500 °C. Zinc condenses in a separate receiver in liquid form and is tapped off periodically. A certain amount of dross (zinc dust) is also formed; since this contains noble metals, it is recycled to the process.

A more modern method is the *Penarroya–Leferrer vacuum distillation* with radiation heating. This runs at a temperature (600 °C) well below the melting point of silver and considerable lead must be added to the crust to hold the silver in solution when most of the zinc has gone. The zinc condenses as a liquid. Low frequency induction furnaces are also used.

The distillation residue consists of silver containing other precious metals, zinc, lead, and copper. Zinc, lead, and copper are removed by cupellation (air oxidation), and the silver bullion is separated from gold by electrolysis. The cathode silver can be further refined by chlorination.

Bismuth Drosses. Bismuth dross can be processed by either pyrometallurgical or electrolytic methods. In either case, the reagents calcium and magnesium are first removed, so that the subsequent operations are always performed on a pure lead–bismuth alloy.

Lead is removed by selective chlorination of the lead–bismuth alloy with chlorine gas, lead being converted to lead chloride with virtually no loss of bismuth. The rate of lead chlorination in lead bismuth alloys with > 85% bismuth is extremely high at 700–800 °C. In practice, chlorine is injected into an alloy already enriched to this level, and lean material is simultaneously added. Operation is thus continuous and material throughput is constant. The crude bismuth usually has a low foreign element content (copper, noble metals), which is removed by a process similar to that used for the refining of lead bullion.

In comparison with the pyrometallurgical technique, the electrolytic method has the advantage that the lead is deposited in pure form at the cathode (generally as fine lead). The an-

ode slime from electrolytic lead–bismuth separation is subjected to reduction melting; the product is an alloy containing > 90% bismuth along with lead, copper, and noble metals. This alloy can be processed pyrometallurgically (selective chlorination) or by bismuth electrolysis.

9.6.2 Electrolytic Refining of Lead Bullion

The electrolytic refining of lead bullion from soluble anodes has been practised for years in a number of large plants. Because the poor solubility of lead sulfate rules out sulfate electrolysis, the only candidate electrolytes are the few readily soluble lead salts. In practice, solutions used have been restricted to the lead salts of fluosilicic acid (H_2SiF_6), fluoboric acid (HBF_4), and amidosulfuric (sulfamic) acid ($\text{H}_2\text{NSO}_3\text{H}$). The most important of these is the fluosilicate electrolyte.

Metals with a higher electrochemical potential than lead (silver, gold, copper, bismuth, antimony, arsenic, and germanium) remain essentially undissolved and accumulate in the anode slime, which is processed to recover them. Metals with a lower potential, such as iron, nickel, and zinc do go into solution, but the feed lead bullion contains such low levels of them that enrichment in the electrolyte is insignificant. The deposition potential of tin, -0.140 V, is close to that of lead, -0.126 V. Tin is therefore deposited along with lead from both fluosilicate and fluoborate electrolytes. The amidosulfate electrolyte, on the other hand, allows separation of lead and tin because of the low solubility of tin sulfamate.

The undissolved impurities, if they are present in large enough quantities, form a porous skeletal coating (slime). The slime adheres to the anode and retains its initial form, so that cells need not be regularly cleaned and deslimed. The mechanical strength of the slime depends on the content of foreign metals in the anode. Higher contents of bismuth and antimony enhance strength; increasing copper leads to a dense slime, so that the feed must be decoppered to < 400 g/t copper. The produc-

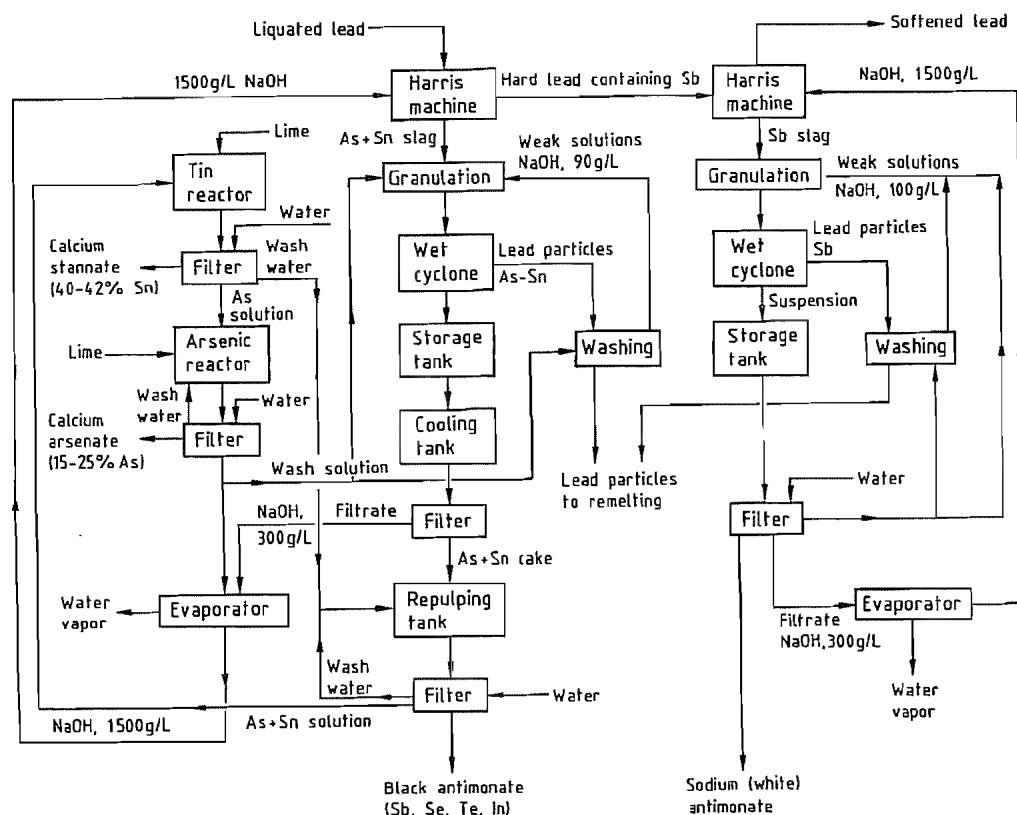
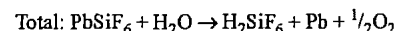
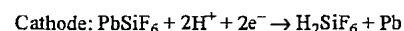
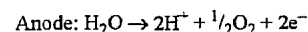


Figure 9.24: Treatment of Harris salt slags at Metallurgie Hoboken–Overpelt S.A. [25].

tion of adherent anode slimes requires a minimum antimony and bismuth content of 1–1.2%. The cell voltage rises with increasing thickness of the slime coating and may reach up to twice the initial voltage; thus, energy consumption imposes an economic limitation. In addition, the increasing voltage can lead to dissolution of antimony, arsenic, and bismuth from the slime. The residence time of the anodes in the cell, is governed by this rise in cell voltage and thus by the concentration of impurities in the anode lead.

In industrial electrolytic lead refining, the *Betts process*, an aqueous solution of fluosilicic acid and lead fluosilicate (PbSiF_6) is electrolyzed. One liter of electrolyte contains 60–100 g lead as fluosilicate and 70–120 g free H_2SiF_6 . Glue and/or other organic inhibitors (300–500 g per tonne of electrolytic lead) are added to obtain smooth deposits. Electrolyte losses result from the decomposition of H_2SiF_6 and entrainment in the anode slime.

The consumption of H_2SiF_6 is around 2 kg per tonne of electrolytic lead. The lead content of the electrolyte rises slowly because of the difference in current efficiency between anode and cathode. This increase is sometimes offset by precipitation of lead sulfate after addition of sulfuric acid. However, the lead content is usually held at the desired level by electrolysis in separate cells with insoluble graphite anodes. The following reactions take place:



Cathode blanks are made of electrolytic lead and are 0.8–1 mm thick. They are fabricated either by casting over an inclined plane (older procedure) or with a water-cooled drum that dips into the lead bath. One or two cath-

ode changes are generally required per anode. Current densities are 150–240 A/m^2 at the anode and 130–220 A/m^2 at the cathode. Current efficiency is 85–95% and energy consumption about 190 kWh per tonne of electrolyte lead. After electrolysis has been completed the anodes have about 30–40% of their starting weight and are melted down into new anodes. The cathodes are thoroughly cleaned, melted down, refined with soda in a kettle to eliminate residual antimony, arsenic, and tin, and cast into ingots.

The size and weight of the electrodes used for lead electrolysis at the Cominco lead refinery in Trail, Canada are given in Table 9.5. Other important data follow [28]:

Lead electrorefining data, Cominco Trail plant

Electrorefining cells	
Number	800
Dimensions (length × width × height), mm	2750 × 800 × 1250
Capacity, m^3	2.7
Material	polymer-containing concrete

Typical operating data

(based on lead production of t/a 120 000)

Anodes per cell	24
Cathodes per cell	25
Anode to anode spacing, mm	110
Current density, A/m^2	
Cathodes	130–220
Anodes	150–240
Current efficiency, %	80–90
Refining cycle, d	5
Cell voltage, V	0.3–0.5
Power consumption for electrolysis, kWh/t	168
Power consumption for other purposes, kWh/t	50
Hydrofluosilicic acid consumption, kg/t	2
Aloes extract consumption, kg/t	0.17
Lignin sulfonate consumption, kg/t	
Electrolyte temperature, °C	35–42
Electrolyte circulation to cell, L/min	20–25

Analyses

Anode, %	1.0–1.2 Sb, 0.3–0.6 As, 0.04–0.07 Cu, 0.1–0.2 Bi, 0.1–0.6 Ag
Cathode, g/t	3Cu, 8Bi
Anode slime, %	40–50 Sb, 20–30 As, 10–20 Pb, 5–15 Bi, 5–15 Ag
Electrolyte, g/L	60–70 Pb, 80–100 H_2SiF_6

Table 9.5: Size and weight of anodes and cathodes used at the Cominco lead refinery.

Immersion dimensions	Starter cathode	Plated cathode	Starter anode	Corroded anode
Length, mm	900	910	860	850
Width, mm	660	680	660	650
Thickness, mm	1	20	30	10
Area, m^2	1.2	1.25	1.2	1.15
Approximate weight, kg	6	140	200	60

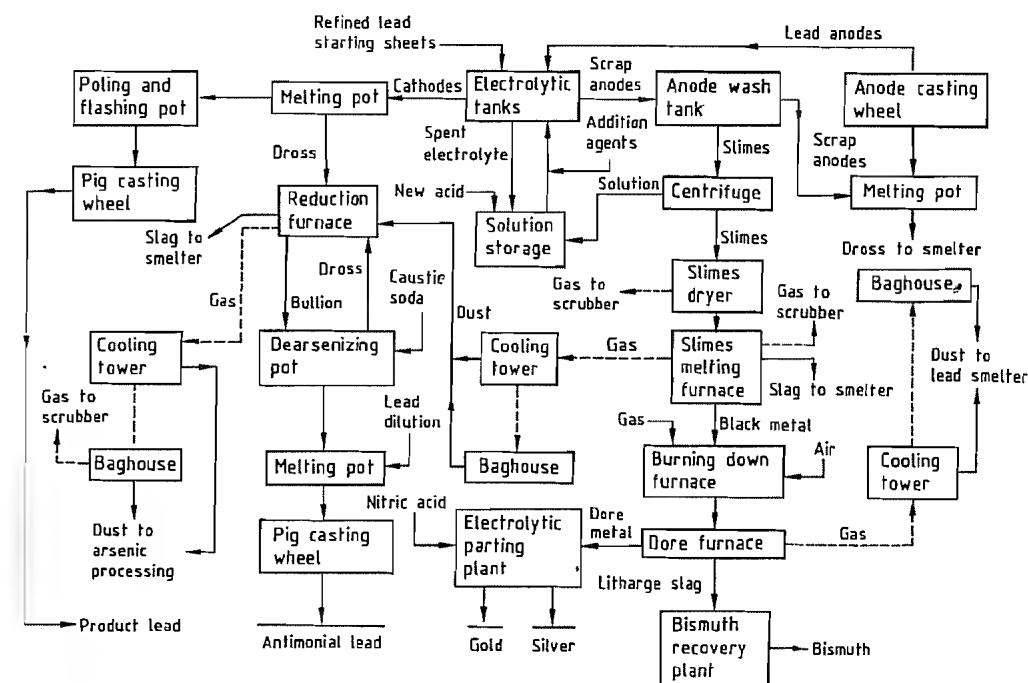


Figure 9.25: Flowsheet for electrolytic lead refining and slime treatment of Cominco Ltd. (Trail, Canada).

Processing of Anode Slime. The composition of the anode slime depends directly on the impurities in the anode lead. In general, anode slime contains not only noble metals but also high levels of bismuth and antimony. Different compositions are seen at plants that have modified their operation for bismuth recovery. For example, at the Norddeutsche Affinerie, the anode lead consists of bismuth drosses and high-bismuth lead that has gone through the entire thermal refining process except for Kroll–Betterton debismuthizing.

No single processing method has been devised for such diverse intermediate products. By way of example, Figure 9.25 presents the flowsheet of the Cominco refinery in Trail. The combination of proven pyrometallurgical processes yields product lead, doré (gold–silver), antimonial (hard) lead, and bismuth metal. The complexity of anode-slime processing places some restrictions on the inherently elegant electrolytic refining technique.

9.7 Recovery of Secondary Lead from Scrap Materials

The total world production of refined lead in 1987 was estimated to be 5.6×10^6 t. Of this approximately 60% was primary lead from lead ores and concentrates; the remainder (40%) was secondary lead produced from scrap materials. As the consumption of lead for sheet, pipe, and cable sheathing has declined and consumption for lead acid storage batteries has increased, the secondary lead industry is primarily concerned with the processing of scrap batteries. In recent years the industry in the United States, and to a lesser extent in Europe, has experienced new, more stringent environmental regulations, and very low lead prices in the mid-1980s. These factors have brought about the closure of a large number of small-scale secondary processing operations, and provided the impetus for the development of improved technology. Besides improving plant working conditions and re-

ducing ambient lead emissions, an important objective of new environmental regulations is to force the efficient recycling of lead-acid batteries and prevent disposal in municipal waste sites. The potential generation of acetic acid and contamination of ground water with soluble lead acetate is the basis for this regulatory pressure. In Germany the efficiency of spent battery recycling is claimed to be 90%.

9.7.1 Battery Types and Composition

Lead-acid storage batteries are of three general types:

- SLI (Starting, Lighting, Ignition) batteries, the bulk of which are automotive;
- Traction vehicle batteries; and
- Stationary batteries for supplying emergency power.

The key components in all these types are:

- a polypropylene containment box
- grids, connectors, and poles of lead alloy
- electrode paste: mixture of lead sulfate and lead oxides
- grid separators of poly(vinyl chloride) (PVC)
- sulfuric acid

The approximate composition of these materials on a weight percentage basis is:

Lead alloy components	21
Lead oxide	16
Lead sulfate	24.5
Water and sulfuric acid	24
Polypropylene	7.7
Poly(vinyl chloride)	3.8
Others	3.0

9.7.2 Battery Breaking and Processing Feed Preparation

Scrap battery preparation has progressed through four levels:

1. Acid drainage followed by pyrometallurgical processing of the entire battery and case. This blast furnace smelting approach became increasingly difficult with

the change from bakelite to easily-fused polypropylene battery cases [27].

2. Separation of acid and case, both of which went to waste as gypsum (after neutralization with lime) and plastic garbage, respectively. The remaining mixture of poles, grids, grid paste, and PVC separators became secondary smelter feed.
3. Mechanical shredding of batteries followed by heavy medium separation to produce
 - Drainage acid for sale or limerock neutralization to produce gypsum as waste
 - Clean polypropylene for sale and recycle
 - A clean metallic fraction which can be smelted at low temperature
 - Battery paste mixture of PbSO_4 and PbO_x
 - Clean PVC plastic to waste or recycle
4. The same as (3) except that battery paste and drainage acid are reacted with sodium carbonate to produce dry crystals of sodium sulfate, a saleable product [28]. This system has several advantages. The sulfur content of the lead-bearing feed materials is largely eliminated, thus simplifying the subsequent smelting processes and reducing the amount of waste sulfur and lead-bearing slag. Figure 9.26 shows the flow-sheet of the Tonolli CX process as an example.

9.7.3 Smelting of Battery Scrap Materials

The metallurgical equipment used for treating battery scrap consists of blast furnaces, reverberatory furnaces, rotary kilns, and short rotary furnaces.

Blast Furnace Treatment of Battery Scrap [29–32]. Typical blast furnace charge consists of cased batteries and battery plates with paste, limestone flux, scrap iron, metallurgical coke, and miscellaneous recycle drosses and slags.

Blast furnaces used for battery scrap smelting are smaller than primary lead industry blast furnaces. Typical hearth areas are in the range of 2–5 m². Smelting products are lead

bullion containing most of the antimony content of the charge, iron matte containing most of the sulfur in the charge, slag, and flue dust which must be melted or agglomerated for recycle.

Plastic materials in the charge can, through fusion, impede the flow of material in the furnace shaft. This adverse effect is controlled by recirculating crushed slag in the furnace charge. Volatile organics in the off-gas must be combusted in an afterburner to prevent bag-house operating problems.

With advanced battery feed preparation systems, the role of the blast furnace in the industry is expected to decline in favor of reverberatory or rotary furnace reduction of lead carbonate-oxide sludge and metallic grid products.

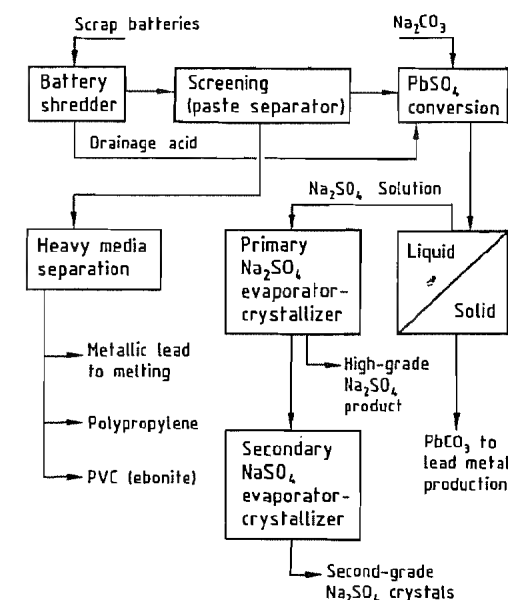


Figure 9.26: CX scrap battery components recovery plant.

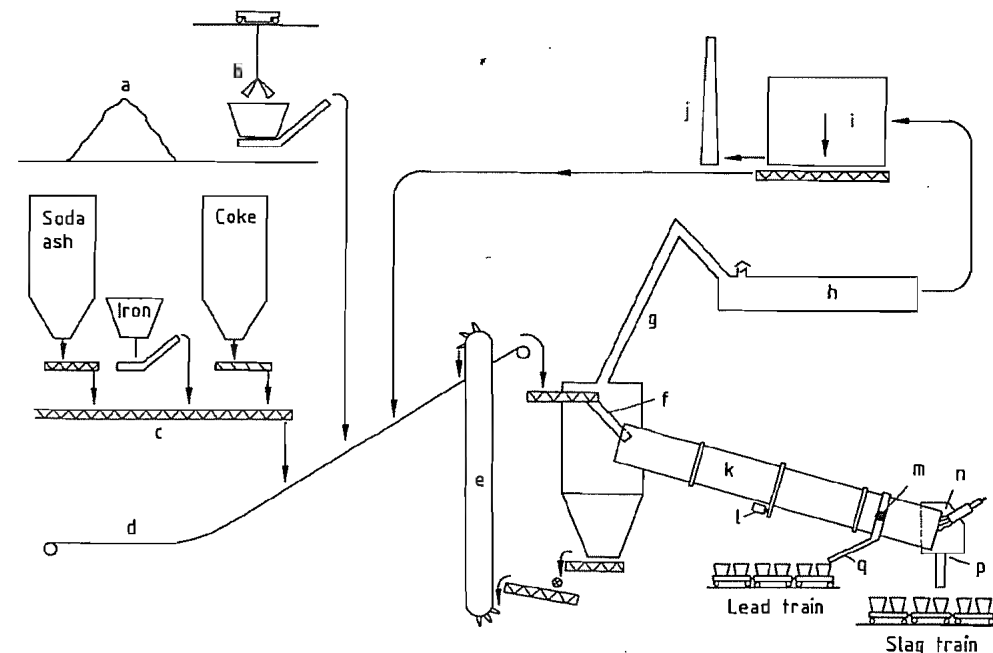


Figure 9.27: Rotary kiln scrap battery smelting plant: a) Buffer storage building; b) Bucket crane; c) Flux feed conveyor; d) Main feed conveyor; e) Bucket elevator; f) Feed chute; g) Vee duct; h) Balloon screw; i) Baghouse; j) Stack; k) Kiln; l) Kiln drive; m) Tap hole; n) Burner head; o) Burner; p) Slag chute; q) Lead launder.

Rotary Kiln Smelting of Secondary Lead.

Continuous processing with long rotary kilns was developed by Preussag AG, Goslar, Germany, and is practised in several other locations [33]. A typical equipment layout for this type of plant is shown in Figure 9.27. The kiln charge consists of a plastic-free mixture of sulfate, lead posts, grids, metallic iron, soda ash, coke breeze, and recycle flue dust. Products are lead bullion and a mixed matte slag material for discard.

Short Rotary Furnace Smelting. The short rotary furnace is extensively used for smelting battery scrap materials [34]. Typical furnace dimensions are a diameter of 3.5–4.0 m and a length of 4–5 m. Reverse-flow firing is usually employed with the combustion burner and gas offtake at one end of the furnace. The charge components and general metallurgy are very similar to the rotary kiln process. The main difference is batch rather than continuous operation, which allows the use of different charges for the production of high- or low-antimony bullion products.

Reverberatory Furnace Smelting. The reverberatory furnace, although generally less productive than rotary furnaces, provides good control of the reduction potential required to produce low-antimony bullion and retain antimony in slag for subsequent reduction to high-antimony bullion. Reduction of desulfurized battery paste is also readily achieved at low temperature in reverberatory furnaces.

9.7.4 Future Trends

Increased environmental pressure is expected to continue to force innovation in secondary lead recovery. Slags produced by thermal reduction processes are classified as hazardous waste in the United States. Further electric furnace reduction of slag is now being practiced by the RSR Corporation in the United States to make slags acceptable for non hazardous disposal.

The lead–acid (SLI) battery industry is changing to sealed low-maintenance designs which require high-purity lead for the calcium lead alloy grids. The secondary industry has been forced to produce an increasing percentage of high-purity lead compared to the grades of antimonial lead produced in the past. Removal of antimony by kettle caustic softening is costly. The incentive to separate battery scrap into low-antimony paste and high-antimony metallic components for separate processing is thus expected to increase.

The search for nonthermal processes for high-purity lead recovery, particularly from desulfurized battery paste, is expected to intensify. Research work by the U.S. Bureau of Mines [35], and the RSR Corporation in the United States and Technologic Tonolli (Italy) on a fluosilicic acid leach electrowin method of treating lead carbonate oxide paste is expected to be used commercially in the early 1990s.

9.8 Uses

The trend in end-use consumption of lead over the period 1977–1987 is illustrated in Table 9.6 for the United States, Japan, and Western Europe. A more thorough breakdown compiled by the Lead Development Association and the Lead Zinc Study Group for presentation to the “Metals 2000” Conference is drawn upon for the following analysis.

Lead batteries were responsible for 60% of refined lead consumption in the Western world in 1987 (ca. 2.5×10^6 t). The battery market is by far the largest end use of lead. It has shown a steady growth rate of 6% from 1984 to 1989, corresponding to the increase in the number of automobiles worldwide. Automotive batteries for starting, lighting and ignition (SLI), traction batteries, and stationary batteries account for 75, 10, and 15% of total battery lead consumption, respectively.

Table 9.6: Consumption of lead by end-use (%) (Source: Metallstatistik 1977–1987).

Use	United States		Japan		Europe ^a	
	1977	1987	1977	1987	1977	1987
Batteries	59.8	77.5	49.6	68.7	38.4	44.6
Cables	0.9	1.6	10.1	1.7	11.0	7.0
Semifinished	7.0	6.7	8.2	3.0	16.8	17.5
Pigments and chemicals ^b	21.0	7.6	15.0	16.2	25.4	22.3
Alloys	7.2	4.4	5.1	4.6	4.4	3.4
Other	4.1	2.2	12.0	5.8	4.0	5.2
Total	100.0	100.0	100.0	100.0	100.0	100.0
Total, 10^6 t	1.436	1.230	0.334	0.378	1.164	1.131

^a Germany, France, United Kingdom, Italy.

^b Includes antiknock compounds.

SLI batteries represent the predominant use of lead. In 1987 about 160×10^6 batteries were used in new cars and for replacements in a world car population of over 500×10^6 . The number of vehicles is expected to increase, and so should lead use in batteries. The content of lead and lead compounds in battery walls, grids, and coatings has been steadily reduced to improve performance, minimize weight, and extend lifetimes. This has contributed to much better operating economics. The vehicle battery market is obviously vulnerable to substitution by other elemental couples and chemistry, but so far no competition appears likely to have a serious impact. Other factors that could affect future SLI battery use are increasing power requirements of cars and haulage vehicles, which would demand more powerful batteries and the possible use of higher voltages.

Traction batteries are used to power electric vehicles which have low running costs and are quiet and pollution-free. The vehicles are commonly used in short-range commercial delivery applications, in airports, and as fork lifts. The heavy weight and limited capacity of the conventional lead acid battery seriously restrict vehicle speed and operating range between charges. It is unlikely that the lead battery will power a successful design of passenger vehicle.

Stationary batteries are used for standby and emergency power supply. Besides emergency lighting, special applications involve computer installations, process control sys-

tems, and emergency power in aircraft and trains. The market is growing. A new market is developing for small, sealed cells used in safety and security systems and personal computers.

Pigments and Lead Compounds. After batteries, the next largest use of about 14% of refined lead is in glass making, ceramic glazes, plastic stabilizers, and paints. Lead glass has desirable optical, electrical, and radiation shielding properties, and lead crystal glass in particular is in great demand. Although ceramic glazes for tiles, tableware, and fine china have declined in application because of concern about lead's toxicity, they remain a significant part of the compound market. Lead compounds used for stabilizing PVC against temperature and UV light are finding intensive competition from other, more environmentally acceptable stabilizers. The lead pigment market is now very small.

Semifinished Products. Rolled and extruded lead, mainly sheet and pipe, account for about 8% of total lead use. Piping was formerly the greater part of this sector, but toxicity concerns and substitution by plastics and copper have reduced the market considerably. The use of lead sheet for roofing, restoration of old buildings, sound insulation, radiation shielding, and chemically resistant linings is now greater than that for piping and is growing steadily.

Cable Sheathing. A major area of lead use was in the protection of electrical and tele-

communications cables, but this market has declined drastically since the early 1960s due to substitution by aluminum and plastics. Nevertheless, this application still accounts for about 5% of total lead use, and there now appears to be a return to thin lead sheathing as a total moisture barrier in association with plastic sheathing.

Lead Alloys. Solders, type metal, bearing alloys containing lead still account for about 4% of the lead consumption. Type metal usage has nearly disappeared, but the bearing metal market is still reasonable in spite of some substitution. Uses of lead-base solder are growing, as electronic products find increasing markets which outweigh the trend to miniaturization and inroads made by tin.

Gasoline Additives. In 1972 the use of tetraethyl lead for improving the octane rating of gasoline was nearly 400 000 t/a. Since then, this sector has declined dramatically by 70%, principally in the United States. The reason has been the proscription of lead antiknock compounds by environmental legislation. The tetraethyl lead market, now 3% of lead use, can be expected to disappear with the eventual departure of older vehicle engines that require leaded gasoline.

Shot and Ammunition. Shot and ammunition account for about 2% of lead consumption and represent a steady market. Lead shot is used in alloying steel and brass to free machining metals, and for shotgun cartridges.

Miscellaneous. Uses that do not fall into the above categories account for about 4% of lead use, and include products featuring the high density of lead such as wheel weights, yacht keels, ornamental items, stained glass, and massive radiation shielding.

Much work is being done by lead concerns to identify and develop new applications for the metal. Promising new uses include lead levelling battery banks used by utilities or by major power consumers to reduce high-cost peak power consumption; lead containers for disposal of radioactive waste; and asphalt sta-

bilizers for retarding road paving deterioration.

9.9 Economic Aspects

9.9.1 Lead Concentrate Schedules

Most lead smelters operate with a concentrate supply from associated mines. A few "custom" smelters (e.g., at Hoboken) purchase essentially all feed materials on the open market. In rare cases a smelter will agree to "toll" a concentrate, whereby the concentrate supplier pays for the processing of his material as part of the smelter's overall charge, and receives the recovered metal for his own use.

Lead concentrate from the beneficiation of lead-zinc or lead-zinc-copper ores is the primary feed for blast furnace and flash smelters. Smelters employing the Imperial Smelting process generally use mixed lead-zinc concentrates. Conventional lead concentrates consist of galena in a sulfide matrix; the lead content is usually well over 60%. The concentrate may also contain zinc and iron sulfides; gangues such as silicon dioxide, calcium oxide, magnesium oxide, and aluminum oxide; and a number of minor metal impurities that may be partially or totally recovered and which may also cause smelting or refining problems. The price assigned to a concentrate by a smelter reflects its own priorities and the suitability of the concentrate for the operation, as regards its valuable components and impurities. Smelters reject concentrates with elements that adversely affect metallurgy or refining practice. Examples are rejection of a high-sulfur (low-lead) concentrate by a down-draft sintering operation or of a bismuthic concentrate by a refinery without a capability for bismuth removal and recovery.

In compounding the aggregate feed and in selecting concentrates for purchase, lead smelter metallurgists and ore buyers balance the inputs of all valuable and harmful elements to create a charge that can be handled effectively and consistently within the limits of the operating processes, and with maximum

profit. The pattern is set by the major concentrate supplies, usually from in-company sources: other raw materials are obtained to fit objectives of output, quality, cost, and timing.

A lead smelter's purchase schedule for lead concentrates comprises identifications and rules that govern payments for certain components, penalties levied on the presence of others, occasional bonus payments or penalties for desirable or undesirable combinations, and a treatment charge designed to cover smelting and refining costs and allow for profit. Most smelters can make available a general or "open" schedule set out in sufficient detail to cover a wide range of raw materials, but this is applied only to small lots. Major long-term purchases are normally made on the basis of a negotiated schedule. The schedule of purchase terms also covers sampling, assay of constituents and moisture, settlement of disputes, reference metal prices for determination of paid values, currency exchange, escalation of costs and prices, and payment terms.

Through its applied schedules, a lead smelter always pays for lead, silver, and gold, often for copper and zinc, sometimes for bismuth, and very rarely for antimony, platinum, palladium, or indium. Lead payment is offered on about 95–97% of the contained lead at a defined lead price. A blast furnace or flash smelter prefers lead content > 60%, but an ISP smelter accepts lower lead content, particularly with associated substantial copper value. Silver and gold are routinely recovered at high efficiency by lead refineries, and are paid for at current prices subject to minimum deduction from the assayed content, reflecting the minor losses, and to a treatment charge.

A payment may be offered for contained zinc if the smelter processes high-zinc charges by slag forming but additional costs for fluxes and fuel are assessed against the payment. The ISP smelters routinely pay for zinc subject to minimum deduction and a treatment charge. Iron is a major component of lead smelting slag and is of particular value in fluxing zinc, but may be present in excess of requirement and would then incur a modest penalty.

Most blast furnace and ISP smelters pay for copper, which is usually recovered in drossing as matte, subject to minimum deduction and treatment charge. ISP smelters can handle higher copper inputs than other lead smelters.

Arsenic is always heavily penalized under lead smelter schedule terms from levels as low as 0.05%; this reflects the uncompensated problems arsenic creates in refining, hygiene, and environmentally acceptable disposal. Antimony is usually neither paid for nor penalized.

Bismuth's treatment in a lead smelter schedule depends on whether the refinery can separate and recover the metal comprehensively (as in electrolytic refining) or by pyrometallurgical debismuthizing at high unit cost. More often it would be a reason for rejection of the concentrate. Certain smelters can recover tin, indium, cadmium and thallium in the sintering, drossing, and refining circuits but these elements are never paid for. Thallium may be the cause of rejection by an electrolytic refinery and tin by an ISP zinc-lead smelter.

Lime and silica are desirable fluxes in lead smelting and are usually assigned minor credits in a lead schedule. Blast furnace smelters may penalize alumina for its deleterious effect on slag; ISP smelters can take higher aluminum oxide but are concerned with magnesium oxide content.

Other materials that are treated in lead smelters for lead and other values are scrap lead, scrap batteries, lead ashes and sludges, and zinc smelter leach residues. Metal and battery scrap are the normal feeds for secondary smelters under specific purchase terms. Zinc residues contain substantial lead and silver values in addition to substantial undissolved zinc, and are handled at high cost in additional fuel, fluxes, and slag fuming furnace operation in joint lead-zinc smelters such as the one at Trail.

9.9.2 Lead Statistics

World mine production of lead has been steady at $(3.4\text{--}3.5) \times 10^6$ t/a of contained lead

since the early 1970s. Production since 1925 in millions of tonnes is as follows:

1925	1501	1985	3581
1950	1686	1986	3378
1960	2376	1987	3389
1970	3433	1988	3400
1980	3470		

Table 9.7: World production (primary and secondary) and consumption of refined lead.

Year	Production, $\times 10^6$ t	Consumption, $\times 10^6$ t
1977	5.388	5.466
1985	5.634	5.460
1986	5.464	5.551
1987	5.631	5.623

The estimates of world lead resources shown in Table 9.1 represent a comfortable reserve against expected consumption requirements for the future, and there are excellent prospects for further economic discoveries.

Production (primary and secondary) and consumption of refined lead in the last ten years are shown in Table 9.7, and by area and

Table 9.8: Lead statistics for most important lead producing and consuming countries, 1987 (Source: Metallstatistik 1977–1987).

	Mine production (contained Pb), 10^3 t	Refined production (primary and secondary), 10^3 t	Refined consumption, 10^3 t
Germany	24.5	340.4	344.6
France	2.2	245.5	207.5
Italy	12.2	168.3	244.0
United Kingdom	0.7	347.0	287.5
Former Yugoslavia	82.0	124.6	129.4
Spain	83.2	122.7	105.8
Rest of Europe	156.1	265.4	311.8
<i>Total Europe</i>	<i>360.9</i>	<i>1613.9</i>	<i>1630.6</i>
Japan	27.9	338.5	377.9
Rest of Asia	111.8	244.2	407.3
<i>Total Asia</i>	<i>139.7</i>	<i>582.7</i>	<i>785.2</i>
Africa	214.6	159.9	111.4
United States	318.3	1027.9	1202.8
Canada	413.4	225.8	102.9
Mexico	177.1	185.1	99.6
Peru	192.0	70.8	21.9
Other South America	73.4	140.7	162.6
<i>Total America</i>	<i>1174.2</i>	<i>1650.3</i>	<i>1589.8</i>
Australia, Oceania	186.2	220.7	65.0
<i>Total Western World</i>	<i>2375.6</i>	<i>4227.5</i>	<i>4182.0</i>
Former Soviet Union	510.0	780.0	775.0
Other Eastern Bloc	503.7	623.9	665.5
<i>Total Eastern Bloc</i>	<i>1013.7</i>	<i>1403.9</i>	<i>1440.5</i>
<i>Total World</i>	<i>3389.3</i>	<i>5631.4</i>	<i>5622.5</i>

trading bloc for 1987 in Table 9.8. About one-third of current refined lead production is from recycled materials.

Lead ranked first in production among non-ferrous metals in the first quarter of the twentieth century, but now ranks fourth after aluminum, copper, and zinc. This is due more to consumption growth for the other metals than to decline in lead use. Lead has suffered the loss of some major markets in pigments, water piping, and lead alkyls caused by legislation reflecting concern for its toxicity and environmental impact, from substitutions by plastics and aluminum, and the decrease in requirement for type metal. These losses now appear to have stabilized. They have been more than offset by the growth in production of lead batteries for automobile and transport use. The lead battery represents the dominant use of production and recycled lead and is the mainstay of the lead industry.

Of very considerable concern to the industry has been the slump in lead price, which reflects but far transcends the worldwide industrial recession in the first half of the 1980s (Table 9.9). The price of lead reached its lowest point in recorded history in terms of the real value of money in 1985. The period from 1982 to 1986 saw dismally inadequate returns and outright losses, with the abandonment of many producing mines and severe retrenchment or closure of smelting plants. Since the mid 1980s the price of lead has recovered by over 50%. This has encouraged many lead producers to modernize or replace old smelting plants by the new flash-smelting technologies that are better able to meet the stringent hygiene and environmental regulations that govern plant operation.

Table 9.9: Annual average producer price of lead in the United States (Source: Metallstatistik 1977–1987).

Year	Price (U.S. cents/kg)
1978	74.28
1979	116.20
1980	93.73
1981	80.57
1982	56.38
1983	47.86
1984	56.40
1985	42.10
1986	48.74
1987	79.20
1988	81.08

9.10 Toxicology and Occupational Health

Lead is one of the seven metals used in antiquity by the Euroasian civilization. Its uses were varied. Physicians prescribed various forms of lead to heal ailments ranging from constipation to infectious diseases such as the plague. Lead was also used to preserve or sweeten wine, for water pipes, cosmetics, and ceramic glazes.

The symptoms of lead poisoning have been recognized for centuries. HIPPOCRATES described lead colic in 370 B.C. and PLINY reported poisoning among lead workers in about

50 A.D. In 1700 RAMAZZINI [36] noted the illness of potters who worked with lead. In 1933 KEHOE and his coworkers [37], brought to light the important consideration that lead is very widely found in the environment. Their studies showed that although lead is not an essential element for the body, a measurable amount exists in all adult body tissues and fluids.

Today, there is considerable literature on the effects of lead, ranging from overt signs and symptoms of lead poisoning to subtle effects such as reduced intelligence quotient scores, behavioral effects, and impaired hearing. The relevance of these effects and the definition of lead exposure levels are subjects of extensive debate.

9.10.1 Sources of Lead Exposure

Many sources of lead exposure affect the workplace and the general population.

Drinking Water. Drinking water can be a significant contribution to lead intake, especially for young children.

Lead can enter the aquatic system through fallout and surface runoff, from natural sources or from lead-lined tanks, lead pipes, and lead solder joints.

The lead content of drinking water is controlled in the European Economic Community (EEC) and North America by water quality standards, and is subject to revision. The EEC [38] specifies 50 $\mu\text{g/L}$ as a maximum allowable lead concentration in water for human consumption; the Environmental Protection Agency (EPA) of the United States is contemplating lowering its current lead-in-water standards from 50 to 5 $\mu\text{g/L}$ [39].

Lead concentrations in drinking water exceeding 300 $\mu\text{g/L}$ have been reported [40]. Such high contents can be attributed to very soft water, low pH, and high temperature; for example, samples of soft, hot or stagnant 'first draw' water exposed to lead or lead in pipes usually have a high lead content.

Atmosphere. Worldwide natural lead emissions to the atmosphere from natural sources

have been estimated to be 24×10^3 t/a, compared to $(350-450) \times 10^3$ t/a from anthropogenic sources. By far the greatest contribution comes from automotive lead emissions. A determined effort has been made in most countries to reduce the amount of allowable lead in gasoline. The EEC currently stipulates a limit of 0.15 g/L for added lead (the lead is added as tetraethyl lead). A more stringent position has been taken by the United States, where the EPA regulated lead content in gasoline at 0.29 g/L in 1982 and then to 0.026 g/L in 1986.

The lowering of lead in gasoline has been cited by the Center for Disease Control (CDC) in the United States as the major reason for the 37% decrease in children's blood lead levels, based on a nation-wide survey conducted between 1976 and 1980 [42]. Another view is that the effect is attributable mainly to socioeconomic improvements.

Lead emissions from industrial sites such as smelters and metal recovery operations also contribute to atmospheric lead. However, fallout from these sources is localized and is estimated to contribute only about 10% of the overall lead emission. Ambient lead levels in the proximity of primary and secondary smelters can be significant. At El Paso, Texas, mean lead levels in 1971 ranged from 0.46–2.72 $\mu\text{g}/\text{m}^3$ with peak values as high as 22 $\mu\text{g}/\text{m}^3$ [43]. Sampling data from Yugoslavia recorded peak levels in excess of 200 $\mu\text{g}/\text{m}^3$ [44]. Typical levels near point source areas are 0.1–1 $\mu\text{g}/\text{m}^3$ and for rural areas ≤ 0.1 $\mu\text{g}/\text{m}^3$. Community air quality criteria are set in the range of 1.5–2.0 $\mu\text{g}/\text{m}^3$ with a view to lowering these levels. For example, EPA is proposing tightening their current standard from 1.5 $\mu\text{g}/\text{m}^3$ standard to 0.5 $\mu\text{g}/\text{m}^3$.

Soil. Natural soil can contain from 2 to 200 ppm and can be greatly influenced by anthropogenic sources. There are few standards for lead in soil; however, many countries have guidelines with suggested maximum levels of ca. 500–1000 ppm.

Lead-bearing dust can be especially dangerous to very young children because of a high level of ingestion through their play and

eating habits. The concentration of lead in street dust and surface soil can be very high, especially if located near a major freeway. Soil samples from areas of Vancouver, Canada taken near heavy traffic areas were similar to samples taken 1.6 km from a large primary lead smelter complex (1545 and 1662 ppm, respectively) [45]. A survey of street dust in 77 midwestern U.S. cities showed a mean lead content of 1600 ppm in residential areas and 2400 ppm in industrial areas [46].

Diet. Lead (mainly organic compounds) can enter the human body through the skin, by inhalation, or by ingestion. Ingestion in food is generally the major source of lead intake. Lead in the diet can come from numerous sources such as uptake of lead into plants; deposition onto vegetables; from soil or water; and from lead solder in canned goods.

Absorption of lead from the gastrointestinal tract by adults is estimated to be about 5–10%, but 25–55% by young children [47]. Ingestion of lead-based paint by children is still considered the most frequent cause of lead intoxication in the United States [48]. The amount of lead absorbed through the digestive system is greatly influenced by stress, fasting, and the solubility of the lead compound; for example, lead acetate is 25 times more soluble in intestinal fluid than lead sulfide [49].

Occupational Exposure. Workers employed in primary and secondary lead smelters, as well as in the production of lead metal and lead compounds are exposed to lead absorption hazards. Because of the fine particle size of lead fume and its solubility, it can readily enter the respiratory system and be absorbed in the blood stream.

The workplace lead standard in the EEC and North America have been tightened to the current range of 0.05–0.15 mg/m^3 . The MAK value is 0.1 mg/m^3 and the TLV-TWA value is 0.15 mg/m^3 . This has been strong motivation for the development of new process technology, improvement of engineering controls, and stricter use of personal protective equipment by industry to reduce worker exposure.

9.10.2 Absorption and Excretion

Absorption of lead into the body is greatly affected by the size of the lead-containing particle and its solubility.

Retention through the respiratory system is 20–60% [50]. Particles of 0.1–1 μm are small enough to reach the alveoli where absorption into the blood stream can take place; particles larger than 1–2 μm may be deposited in the naso-pharyngeal area, trachea, or bronchi and leave by swallowing or expectoration. Thus, fine lead fume has a much greater influence on a worker's blood lead value than coarser dust.

Gastrointestinal absorption of lead has been discussed earlier. Absorption through the skin is not considered to be important for inorganic lead compounds, but organic lead compounds such as tetraethyl lead or lead naphthenate are readily absorbed across the skin barrier.

Approximately 90% of ingested lead is not absorbed and eliminated in the feces. Lead absorbed into the blood stream deposits to soft tissue and gradually accumulates in bone. Some is excreted in urine. With consistent intake of lead, a steady state between lead concentrations in blood, soft tissue and bone is established [51].

9.10.3 Effects

Acute Effects. The total average daily lead intake for adults is estimated to be 150–300 μg , which is reflected in a blood lead level of 10–25 $\mu\text{g}/\text{dL}$. Blood taken from 'normal' persons in 16 countries in the 1960s showed an average of 17 $\mu\text{g}/\text{dL}$.

Hematological Effects. One of the more deleterious effects of lead is on blood and blood-forming tissue. Lead can inhibit almost all steps in the biosynthesis of hemoglobin and globulin [52].

Neurological Effects. In the early part of this century, excessive prolonged exposure to lead was reflected in brain disease and muscle weakness in lead workers and children. These extreme exposures have long been eliminated.

Today the greatest concerns relate to neurological effects on young children. Neurobe-

havioral deficits have been correlated with lead content in teeth [53], and blood lead levels in children, which were formerly considered to be acceptable, are now being reviewed in many countries. In the United States the tolerable maximum blood lead in children was reduced from 40 to 25 $\mu\text{g}/\text{dL}$ in 1985.

Renal Effects. The kidney is the major route for the excretion of lead that has been absorbed into the body, and it is also one of the organs affected by lead toxicity [54]. In most situations renal dysfunction occurring as a result of chronic lead exposure is reversible provided serious tissue damage has not occurred. However, irreversible renal damage may result from a prolonged, very high lead body burden. Hypertension can also follow.

Reproduction Effects. Toxic levels of lead can cause sterility in men, and miscarriages and spontaneous abortions in women. The fetus is especially vulnerable because lead can cross the placental barrier. Men with blood lead levels $> 60-70$ $\mu\text{g}/\text{dL}$ may have reduced sperm count and mobility [55], but data are not conclusive.

Carcinogenicity. Lead and its compounds are currently under close scrutiny by the EPA with respect to its potential as a cancer-causing agent. The international Agency for Research on Cancer has listed inorganic lead compounds in Group 2B (agents that are possibly carcinogenic to humans), but this is a wide generalization from observations limited to lead acetate and phosphate [56].

9.10.4 Indices for Monitoring Lead Exposure

Biological monitoring of workers provides an assessment of overall exposure to a chemical or compound, and sets guidelines for the evaluation of potential health hazards. Several of the more common indices for evaluation of overall lead absorption are outlined below.

Lead in Blood. Lead in blood is generally considered the best indicator of the lead con-

centration in soft tissue and is an effective means of assessing exposure to lead. Some investigators have been able to predict increases in blood lead after low lead exposures with some accuracy [57]. Blood lead levels of 60–70 µg/dL in male workers have generally been considered acceptable [58], but some authorities such as OSHA have established a limit of 50 µg/dL, and the World Health Organization is proposing an upper limit of 40 µg/dL for males and 30 µg/dL for females.

Lead in Urine. Lead in urine best reflects a sudden, recent exposure and is a sharper index than the subsequent, more gradual change in blood lead concentration. Although correlation between blood and urinary lead levels is often poor, under stable conditions a urinary lead value of 150 µg per gram of creatinine corresponds to a blood lead of 60 µg/dL.

Urinary ALA. Urinary δ -aminolevulinic acid (ALA) found considerable success as a means of screening suspected lead intoxication or lead poisoning in the late 1960s and early 1970s. This nonspecific test measures the effect lead has on the hematopoietic system. The analysis is cumbersome and has been gradually replaced by other tests.

Zinc Protoporphyrin. Lead can block normal hematopoiesis by inhibiting the enzyme ferrochelatase and this causes elevation of zinc protoporphyrin (ZPP) in red cells [59]. Assessment of the ratio of ZPP to hemoglobin can be made by measuring ZPP fluorescence. This nonspecific screening test for lead toxicity has been available since the early 1970s.

Teeth and Hair. Lead content in teeth, particularly dentine, has been used to assess exposure and measure psychological deficits in children but is not practical for second-growth teeth. Hair has also been suggested as a method of evaluating lead absorption, but it is almost impossible to discern between intrinsic lead and that absorbed on the surface from external sources.

9.11 Control of Lead Emissions

The adverse effects of lead ingestion on the health of humans and animals make control of lead emissions a major operating challenge in all primary, secondary, and processing production industries. This overall problem has a dual focus:

- The effect of emissions on in-plant atmospheric contamination and lead absorption by production workers.
- The effect of plant emissions on ambient air lead levels and accumulative lead dust fallout on areas around the production site.

This challenge has long been part of the lead production industry, but since the 1970s improved diagnosis of biological problems related to lead and the resulting increased government regulatory pressure have greatly increased the demand for reduction of overall emission. Improved engineering controls and total process revisions are the broad approaches that have been taken to achieve compliance. Much progress has been made worldwide; however, the degree of success largely depends on the regulatory standards which have been set or proposed. In the United States, the proposed levels of 50 µg/m³ for in-plant air and an annual mean of 1.5 µg/m³ for lead in air outside the plant boundaries represent perhaps the most difficult industrial challenge.

9.11.1 In-Plant Lead Emissions

Engineering Controls. Assuming major process gas flows are handled by efficient dust removal equipment and discharged in high stacks, in-plant lead levels are mainly influenced by fugitive process emissions. Well-engineered ventilation systems are required to control dust and fume emissions from hot sinter or molten slags. The provision of effective ventilation is costly in terms of energy usage and capital cost.

Personal Respirators. The use of personal respirators by plant workers is almost univer-

sal practise to reduce respiratory lead intake from the plant atmosphere. The use of respirators is often construed as evidence of inadequate engineering control of fugitive emissions. Certainly the elimination of respirator use for most production jobs other than special maintenance work is a desirable objective, but, it is not being achieved in most plants at present. Personal hygiene habits are increasingly recognized as critical to controlling lead intake by workers. Measures such as provision of clean clothing, compulsory washing, no smoking or eating on the job, and clean eating facilities are common.

Process Revisions. The new oxygen smelting processes described in Section 9.5.4 are attractive because they have inherent advantages for lead emission control. The traditional sintering and blast furnace method of lead production is a most difficult engineering challenge for achieving good control of in-plant emissions. The sinter operation involves large recirculating flows of hot, dusty, abrasive sinter requiring large ventilation volumes. Blast furnace reduction can be an erratic operation often troubled by a hot top and blowing and accompanying fugitive emissions from the gas collection system.

The new oxygen smelting processes have the following favorable characteristics:

- Inherent lower process gas volume with oxygen usage giving less cleaning and reduced emissions
- Recirculating loads requiring separate ventilation are minimized
- Equipment is relatively compact and well sealed

The introduction of these new pyrometallurgical processes over the next one to two decades should have a major beneficial impact on the in-plant and ambient lead emission problems of today's primary lead smelters.

9.11.2 Ambient Lead Emissions

Ambient lead emissions originate from residual lead after cleaning of process and ventilation gas and general fugitive lead emissions.

The accumulation of ambient lead fallout on vegetation eaten by cattle or the buildup of an objectional concentration of lead in the top soil is the most serious aspect of ambient emissions. The current use of high-efficiency baghouses for cleaning process and ventilation gases, combined with curtailment of fugitive emissions of dust and fume from process equipment, roads, and stock yards, have made major reductions in ambient emissions at most primary and secondary lead smelters.

9.12 Alloys

Lead is one of the oldest known metals. Its use was known before 3000 B.C. All early civilizations used lead extensively for ornamental and structural uses. The use of lead pipes for the transportation of water by the Romans, one of the early uses of lead, endures to the present.

The primary and most important mineral for recovery of lead is galena, PbS. Lead ores are found on every continent, usually in combination with zinc, copper, and silver. The United States is the leading lead-producing country followed by Canada and Australia. Total annual production of lead and lead alloys in 1987 was about 4.3×10^6 t. Recycling of lead scrap, mainly from batteries, lead sheet, and cable sheathing, provided 2.1×10^6 t.

About 40% of lead is used as pure lead, lead oxides, or lead chemicals; the remainder is used in the form of lead alloys. The major uses of lead alloys are: lead acid batteries, ammunition, cable sheathing, building construction (sheets, pipes, and solders), bearings, gaskets, specialty castings, anodes, fusible alloys, shielding, and weights.

Lead is a heavy, soft, bluish gray metal which has a low melting point and a high boiling point. The density, malleability, lubricity, flexibility, and coefficient of thermal expansion are quite high. The elastic modulus, elastic limit, tensile and compression strength, hardness, and electrical conductivity are relatively low. Lead has excellent resistance to

corrosion in a wide variety of media. Lead is easily alloyed with many other metals. Because lead alloys have low melting points, they can be cast into many shapes by using a variety of molding materials and casting processes.

Lead is very ductile and malleable, and can be fabricated into various shapes by rolling, extruding, forging, spinning, and hammering. The low tensile strength and very low creep strength of lead make it unsuitable for use without the addition of alloying elements. The major alloying elements used to strengthen lead are antimony, calcium, tin, copper, tellurium, arsenic, and silver. Minor alloying elements are selenium, sulfur, bismuth, cadmium, indium, aluminum, and strontium.

9.13 Compounds

Lead is one of the oldest known metals, dating from about 3000 B.C. The Romans used lead extensively for water pipes, while in ancient Egypt, lead compounds were employed for glazing pottery and ornamental objects, a purpose for which they are still used today. Now, the largest single use of lead compounds, mainly lead oxide, is for the manufacture of lead acid storage batteries. Other industrially important uses of lead compounds range from antiknock additives in gasoline to lead crystal glasses and stabilizers for plastics during thermal processing.

9.13.1 Salts and Oxides

Lead is an amphoteric element, which forms lead salts with acids as well as metal salts of plumbic acid with alkalies. Lead forms many salts, oxides, and organometallic compounds. Although lead has four electrons in its outer (or valence) shell, the usual valence of lead is 2+, rather than 4+, because of the reluctance of its two 6s electrons to ionize. Also, the divalent plumbous ion differs from the other group 14 divalent ions, such as the stannous ion (Sn^{2+}), in that it does not have reducing properties.

Many inorganic lead compounds have two or more crystalline forms with different properties. As a result, the oxides and sulfide of divalent lead often appear colored because of their state of crystallization. Thus, pure, tetragonal α -PbO is red; orthorhombic β -PbO is yellow; and crystals of lead sulfide, PbS, have a black, metallic luster. On the other hand, the carbonates, sulfates, nitrates, and halides (except for the yellow iodide) are colorless.

Highly crystalline basic lead salts, both anhydrous and hydrated, are readily formed. For example, tetrabasic lead sulfate, $4\text{PbO} \cdot \text{PbSO}_4$, and the tribasic lead sulfate hydrate, $3\text{PbO} \cdot \text{PbSO}_4 \cdot \text{H}_2\text{O}$, are prepared by boiling suspensions of lead oxide and lead sulfate in water. Moreover, complex mixed salts, such as white lead, $2\text{PbCO}_3 \cdot \text{Pb}(\text{OH})_2$, are readily formed.

Most lead compounds are derived from pig lead (refined metal), usually via conversion to lead monoxide (PbO), commonly known as litharge. In general, lead compounds may be formed by the reaction of a slurry of litharge and the appropriate acid, by the reaction of a solution of a lead salt with an acid, or by fusion of litharge with the appropriate metal oxide. In the latter case, for example, the ease with which lead monoxide combines with silicon dioxide to form a low-melting silicate has been utilized in the ceramics industry for producing glasses and glazes.

9.13.1.1 Acetates

Lead reacts readily with acetic acid to form four different lead acetate compounds: anhydrous, basic, trihydrate, and tetraacetate. Some physical properties of the lead acetates are summarized in Table 9.10.

Anhydrous lead acetate, plumbous acetate, $\text{Pb}(\text{C}_2\text{H}_3\text{O}_2)_2$, is a white, crystalline solid that is very soluble in water. It is made by dissolving lead monoxide or lead carbonate in concentrated acetic acid. Solutions of lead acetate are often used to prepare other lead salts.

Table 9.10: Physical properties of lead acetates [67].

Compound	mp, °C	ρ , g/cm ³	Solubility, g/100 mL H ₂ O (t, °C)
$\text{Pb}(\text{C}_2\text{H}_3\text{O}_2)_2$	280	3.25	44.3 (20), 221 (50)
$2\text{Pb}(\text{OH})_2 \cdot \text{Pb}(\text{C}_2\text{H}_3\text{O}_2)_2$	75 (dec. 200)		6.25 (15), 25 (100)
$\text{Pb}(\text{C}_2\text{H}_3\text{O}_2)_2 \cdot 3\text{H}_2\text{O}$	75 (dec. 200)	2.55	45.6 (15), 200 (100)
$\text{Pb}(\text{C}_2\text{H}_3\text{O}_2)_2$	175	2.228	dec.

Basic lead acetate, lead subacetate, $2\text{Pb}(\text{OH})_2 \cdot \text{Pb}(\text{C}_2\text{H}_3\text{O}_2)_2$, is a heavy white powder that is very soluble in water and soluble in ethanol. It is prepared by dissolving lead monoxide in dilute acetic acid. Basic lead acetate is used for sugar analysis.

Lead acetate trihydrate, sugar of lead, $\text{Pb}(\text{C}_2\text{H}_3\text{O}_2)_2 \cdot 3\text{H}_2\text{O}$, is a white, monoclinic crystalline solid having a refractive index (along the β axis) of 1.567. It is very soluble in water, but insoluble in ethanol. Lead acetate trihydrate is prepared by dissolving lead monoxide in hot dilute acetic acid; large, long crystals separate upon cooling. Although the crystals are intensely sweet, they are poisonous. Lead acetate trihydrate is the usual commercial form of lead acetate and it is available in technical and reagent grades. It is used to make other lead compounds (for example, basic lead carbonate, lead chromate, and lead salts of higher fatty acids), as a mordant for cotton dyes, as a water repellent, and as a processing agent in the cosmetic, perfume, and toiletry industries.

Lead tetraacetate, plumbic acetate, $\text{Pb}(\text{C}_2\text{H}_3\text{O}_2)_4$, is a colorless, monoclinic crystalline solid that is soluble in chloroform and in hot acetic acid, but decomposes in cold water and in ethanol. Lead tetraacetate is prepared by adding warm, anhydrous, glacial acetic acid to red lead (Pb_3O_4) and subsequently cooling the solution. It is available in laboratory quantities as colorless to faintly pink crystals stored under glacial acetic acid. Lead tetraacetate is often used as an oxidizing agent in organic syntheses because it is highly selective in cleaving vicinal glycols. It also readily cleaves α -hydroxy acids, such as ox-

alic acid, at room temperature. Another use is for the introduction of acetoxy groups in organic molecules [68].

9.13.1.2 Carbonates

Lead carbonate, PbCO_3 , ρ 6.6 g/cm³, forms colorless orthorhombic crystals having refractive indices of 1.804, 2.076, and 2.078. It is slightly soluble in cold water (1.1 mg/L at 20 °C), is soluble in acids and alkalies, but is insoluble in aqueous ammonia and ethanol. Lead carbonate is produced by passing carbon dioxide into a cold dilute solution of lead acetate, or by shaking a suspension of a lead salt (less soluble than the carbonate) with ammonium carbonate at low temperature to avoid formation of basic lead carbonate. Lead carbonate is used in the catalytic polymerization of formaldehyde to give high molecular mass crystalline poly(oxyethylene) [69], to improve the bonding of polychloroprene to metals in wire-reinforced hoses [70], as a component of high-pressure lubricating greases [71], and as a lubricant and stabilizer for poly(vinyl chloride) [72].

Basic lead carbonate, white lead, $2\text{PbCO}_3 \cdot \text{Pb}(\text{OH})_2$, ρ 6.14 g/cm³, forms white hexagonal crystals that decompose at 400 °C. It is insoluble in water, slightly soluble in carbonated water, soluble in nitric acid, and insoluble in ethanol. Basic lead carbonate is made by reacting soluble lead acetate with carbon dioxide in the presence of air. It is no longer used as a white hiding pigment in paints because of its toxicity, but it has many other uses. For example, basic lead carbonate is used as a component of ceramic glazes, as a curing agent with peroxides to form improved polyethylene wire insulation [73], as a color-changing component of temperature-sensitive inks [74], as a component of lubricating grease [75], and as a component of weighted nylon-reinforced fish nets made of poly(vinyl chloride) fibers [76].

9.13.1.3 Halides

Lead combines with the halogens to form the corresponding fluoride, chloride, bromide, and iodide. Some physical properties of the lead halides are listed in Table 9.11.

Table 9.11: Physical properties of lead halides [67].

Compound	mp, °C	bp, °C	ρ , g/cm ³	Solubility at 20 °C, g/100 mL H ₂ O
PbF ₂	855	1290	8.24	0.064
PbCl ₂	501	950	5.85	0.99
PbBr ₂	373	916	6.66	0.844
PbI ₂	402	954	6.16	0.063

Lead fluoride, lead difluoride, PbF₂, is a colorless, orthorhombic crystalline compound up to ca. 220 °C, above which it transforms into the cubic form. Lead fluoride dissolves in nitric acid, but is insoluble in acetone and aqueous ammonia. It is prepared by reacting lead hydroxide or lead carbonate with hydrofluoric acid, or by the reaction of lead nitrate with potassium fluoride. Lead fluoride is used in glass sealing disks for IR sensors [77]; in wear resistant automotive shock absorbers [78]; for the electroless deposition of lead [79]; as a flux for brazing of aluminum and its alloys [80]; in optical glass fibers for IR transmission [81]; and in thin-film batteries [82].

Lead chloride, lead dichloride, PbCl₂, forms white orthorhombic needles having refractive indices of 2.199, 2.217, and 2.260. It is slightly soluble in dilute hydrochloric acid and in aqueous ammonia, but is insoluble in ethanol. It is made by reacting lead monoxide or basic lead carbonate with hydrochloric acid, or by treating a solution of lead acetate with hydrochloric acid and allowing the precipitate to settle. Upon heating in air, lead chloride readily forms basic chlorides, for example, PbCl₂·Pb(OH)₂, which is known as Pattinson's lead white, an artist's pigment. Other uses of lead chloride include: a precursor of organolead compounds [83]; seawater-activable batteries [84]; expanding polymer-based mortar [85]; flux for soldering cast iron and cast brass [86]; sound-insulating rubber sealants [87]; corrosion inhibitor for galvanized

steel [88]; and infrared-transmitting glasses for CO₂ lasers [89].

Lead bromide, lead dibromide, PbBr₂, forms white orthorhombic crystals that are slightly soluble in aqueous ammonia, soluble in acids and in aqueous potassium bromide (due to complex formation), but insoluble in ethanol. Lead bromide decomposes slowly when exposed to light and darkens due to the formation of lead. It is prepared by reaction of hydrobromic acid with lead monoxide or lead carbonate. Lead bromide is used industrially as a filler for name-resistant polypropylene [90], in glass optical waveguides for infrared thermometers [91], and for catalysts for producing polyesters [92].

Lead iodide, lead diiodide, PbI₂, forms a powder of yellow hexagonal crystals that dissolve in alkalis and in aqueous potassium iodide, but not in ethanol. Lead iodide is made by reacting a water-soluble lead compound with hydroiodic acid or with a soluble metal iodide. It is readily purified by recrystallization from water. Lead iodide is used in aerosols for cloud seeding to produce rain artificially [93]; for making high-contrast photographic images of laser radiation [94]; for high capacity cathodes in lithium batteries [95]; and in low-temperature thermographic copying materials [96].

9.13.1.4 Oxides

There are two main oxides of lead, lead monoxide (PbO) and lead dioxide (PbO₂), in which it is divalent and tetravalent, respectively. In addition, lead forms a mixed oxide, Pb₃O₄, and a black oxide which normally contains 60–80% lead monoxide, the remainder being finely divided metallic lead. The largest market for lead oxides is in the lead acid battery industry, where lead monoxide is used to prepare the active paste for the electrode grids. The next largest market for lead oxides is the ceramics industry, which employs these compounds for the production of glasses, glazes, and vitreous enamels. Other major markets for lead oxides are the paint and rubber industries.

Another important outlet for lead oxide is for the production of lead salts, particularly those used as heat stabilizers for poly(vinyl chloride) resins, especially basic lead salts. In 1979, the U.S. plastics market consumed ca. 9500 t of lead salts [97]. Because of its electrical and electronic properties, lead oxide is used in the production of capacitors, electrophotographic plates, transducers, and ferromagnetic and ferroelectric materials. Examples of the latter include mixed oxides, such as lead zirconate–lead titanate, and lead metaniobate.

Some physical properties of the lead oxides are given in Table 9.12.

Table 9.12: Physical properties of lead oxides [67].

Compound	Decomp., °C	ρ , g/cm ³
PbO	1472 (bp)	9.53
PbO ₂	290	9.375
Pb ₂ O ₃	370	
Pb ₃ O ₄	500	9.1

Lead monoxide, litharge, PbO, exists in a red-dish alpha form up to 489 °C; it then transforms to a yellow beta form (massicot), which is stable at high temperatures. It has a water solubility of 17 mg/L at 20 °C, and is soluble in nitric acid, alkalis, lead acetate, ammonium chloride, and chlorides of calcium and strontium. In alkalis, it forms the plumbite ion, PbO₂²⁻. Lead oxides are produced industrially by thermal processes in which lead is directly oxidized with air. In the ball-mill process, metallic lead balls are tumbled in air to produce a "leady" oxide, which typically contains 20–35% free lead. The Barton pot process oxidizes droplets of molten lead at ca. 430 °C to produce either litharge or leady litharge.

The principal use of lead monoxide is in the manufacture of pastes for the grids used in lead acid batteries. It is also widely used in optical, electrical, and electronic glasses, as well as in glazes for fine tableware. To render the lead compounds insoluble in foods, the glazes and vitreous enamels are prepared from frits, in which the lead monoxide is converted to lead bisilicate, for example. Litharge is also used in rubber as a vulcanizing agent, in lead

soaps employed as driers in varnishes, in high-temperature lubricants as a neutralizing agent in organic syntheses, as a heat stabilizer in plastics, and as a starting material in the production of pigments [99]. The preparation, properties, and other uses of lead oxide are described in [100]. The consumption of litharge in the United States is summarized in Table 9.13 according to end-use.

Table 9.13: Litharge consumption in the United States [98].

Industry	Litharge consumption, t			
	1982	1983	1984	1985
Ceramics	30 980	36 782	37 960	65 413
Chrome pigments	6 591	5 973	4 367	3 794
Paints	3 052	3 256	3 635	3 397
Rubber	787	933	1 016	739
Other	10 267	9 596	9 920	10 590
Total	51 677	56 540	56 898	83 933

Lead dioxide, lead peroxide, plattnerite, PbO₂, is a brownish-black crystalline powder consisting of fine flakes in either the orthorhombic alpha or the tetragonal beta form. Lead dioxide decomposes to lead monoxide when heated above 290 °C. Lead dioxide is practically insoluble in water or alkaline solutions. It dissolves slowly in acetic acid or aqueous ammonium acetate, but more rapidly in hydrochloric acid and in a mixture of nitric acid and hydrogen peroxide. It is produced industrially by the oxidation of red lead (Pb₃O₄) with chlorine in an alkaline slurry. Lead dioxide is electrically conductive and is formed in situ as the active material of the positive plates in lead–acid batteries. Since it is a vigorous oxidizing agent when heated, lead dioxide is used in the manufacture of chemicals, dyes, matches, pyrotechnics, and liquid polysulfide polymers [101]. Other applications of lead dioxide include antifriction compositions for plastic sliding bearings [102], ballistic modifiers in high-energy propellants [103], electrodes for seawater electrolysis [104], filters for desulfurization of waste gases [105], and vulcanizing agents for butyl rubber puncture-sealing layers inside tires [106].

Lead sesquioxide, lead trioxide, Pb_2O_3 , is an amorphous, orange-yellow powder. It is insoluble in cold water, it decomposes in hot water, and in acids it decomposes to the corresponding lead salts and lead dioxide. Lead sesquioxide can be prepared from lead dioxide by hydrothermal dissociation. It is used as a ballistic modifier for high-energy propellants [96], as a cathode material in lithium batteries [107], and as an additive to increase the shattering force of explosives [108].

Red lead, lead tetroxide, minium, Pb_3O_4 , is a brilliant orange-red pigment. It is insoluble in water and ethanol, but dissolves in acetic acid or hot hydrochloric acid. Red lead is manufactured by heating lead monoxide in a reverberatory furnace in the presence of air at 450–500 °C until the desired composition is obtained. It is used as a pigment in anticorrosion paints for steel surfaces and in 1984 accounted for U.S. shipments of 11 236 t [109]. It is also used in lead oxide pastes for tubular lead acid batteries [110], in ballistic modifiers for high-energy propellants [103], in ceramic glazes for porcelain [111], in lubricants for hot pressing metals [112], in radiation-shielding foam coatings in clinical X-ray exposures [113], and in rubber adhesives for roadway joints [114].

9.13.1.5 Silicates

Lead silicates are produced commercially to specific PbO/SiO_2 ratios required by the glass and ceramic, paint, rubber, and plastics industries. Some physical properties of lead silicates are given in Table 9.14.

Table 9.14: Physical properties of lead silicates [115].

Compound	mp , °C	ρ , g/cm ³	n_D^{20}
Lead monosilicate	700–784	6.50–6.65	2.00–2.02
Lead bisilicate	788–816	4.60–4.65	1.72–1.74
Tribasic lead silicate	705–733	7.52	2.20–2.24

Lead monosilicate, lead pyrosilicate, $3\text{PbO} \cdot \text{SiO}_2$, is a white, trigonal crystalline powder. It is insoluble in water and comprises 85% PbO and 15% SiO_2 . Commercial lead monosilicate is produced by dry roasting lead monoxide and silica in the mole ratio 3:2. It provides the most economical method of formulating lead-

bearing glazes for the ceramics industry and it is also used in the glass industry as a source of PbO .

Lead bisilicate, $\text{PbO} \cdot 0.03\text{Al}_2\text{O}_3 \cdot 1.95\text{SiO}_2$, is a pale yellow powder. It is insoluble in water and has the composition of 65% PbO , 1% Al_2O_3 , and 34% SiO_2 . It is available in granular form (10 mesh) and as a ground powder (325 mesh). Lead bisilicate was developed as a low-solubility source of lead in ceramic glazes for foodware, for which its low volatility and high viscosity are equally important.

Tribasic lead silicate, $3\text{PbO} \cdot \text{SiO}_2$, is a red-dish-yellow powder. It is sparingly soluble in water and has the composition of 92% PbO and 8% SiO_2 . It is available in granular form (10 mesh) and as a powder (325 mesh). Tribasic lead silicate has the lowest viscosity of the three commercial lead silicates and it is used primarily by glass and frit producers.

9.13.1.6 Sulfates

Lead forms a normal and several basic sulfates. The most important compound is tribasic lead sulfate because of its extensive use in the plastics industry.

Tribasic lead sulfate, $3\text{PbO} \cdot \text{PbSO}_4 \cdot \text{H}_2\text{O}$, ρ 6.9 g/cm³, refractive index 2.1, is a fine white powder. Its water solubility is 26.2 mg/L at 18 °C. Tribasic lead sulfate is made by boiling aqueous suspensions of lead oxide and lead sulfate. The anhydrous compound decomposes at 895 °C [116]. The addition of 2–7% tribasic lead sulfate to flexible and rigid poly(vinyl chloride) provides efficient, long-term, economical heat stability. The compound is easily dispersible, has excellent electrical insulation properties, and is an effective activator for azodicarbonamide blowing agents for vinyl foams.

9.13.1.7 Other Salts

Several salts of lead are used as heat stabilizers in the processing of poly(vinyl chloride), alone or in combination with a basic lead salt, such as tribasic lead sulfate. These

salts include dibasic lead phthalate, basic lead sulfate phthalate, and dibasic lead phosphite. In addition, dibasic lead stearate is sometimes employed as a combination internal lubricant and heat stabilizer in poly(vinyl chloride). Lead diamyl dithiocarbamate has been used as an antioxidant to retard the increase of viscosity and hardness of road asphalts at a loading of 2–6% in paving trials in the United States, Canada, and Australia [117]. Further field trials are underway to test the commercial feasibility and environmental acceptability of lead-stabilized paving asphalts.

9.13.2 Organolead Compounds

Organolead compounds are those containing one or more lead atoms covalently bonded to at least one carbon atom. Unlike the inorganic compounds of lead, nearly all organolead compounds are derived from tetravalent lead. Table 9.15 gives examples of organolead compounds in which from one to four carbon atoms are directly attached to a lead atom.

Table 9.15: Physical properties of lead silicates [115].

Compound	mp , °C	Uses
$\text{PhPb}(\text{OAc})_3$	102	Polyurethane foam catalyst [119]
$\text{Bu}_2\text{Pb}(\text{OAc})_2$	103	Anthelmintic for tapeworms [120]
$\text{Ph}_3\text{Pb}(\text{OAc})$	205	Toxicant for shipbottom paints [121]
Et_4Pb	–137	Antiknock agent in gasoline [122]

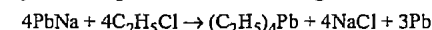
Properties. In general, organolead compounds are well-characterized substances that are quite stable at room temperature. However, they are thermally the least stable of the organometallic compounds of group 14. Most organolead compounds are liable to severe decomposition on heating to 100–200 °C, but they are not explosive. Stable organolead compounds are mostly derived from tetravalent lead and most fall within the four basic categories shown in Table 9.15, namely, RPbX_3 , R_2PbX_2 , R_3PbX , and R_4Pb (where R is an alkyl or aryl group; and X is a halogen, OH, or an acid radical). The R_2Pb species have limited stability and tend to form R_4Pb

upon heating. The tetraorganolead compounds range from the liquid, volatile tetramethyllead, $(\text{CH}_3)_4\text{Pb}$, to the crystalline, nonvolatile tetraaryllead compounds. Some physical properties of tetramethyllead and tetraethyllead are given in Table 9.16.

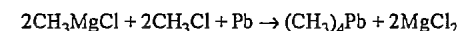
Table 9.16: Physical properties of tetramethyllead and tetraethyllead.

Compound	mp , °C	bp , °C (kPa)	ρ , g/cm ³	n_D
Tetramethyllead	–27.5	110 (101)	1.995 ^a	1.5120
Tetraethyllead	–137	91 (2.53)	1.659	1.5195

Production. The best known industrial process for producing tetramethyllead and tetraethyllead is the reaction of the sodium–lead alloy PbNa with methyl chloride and ethyl chloride, respectively. For example, tetraethyllead is produced according to the reaction:



Tetramethyllead (TML) is also manufactured by an electrolytic Grignard reaction:



In a third lead antiknock production process, a chemically redistributed mixture of tetraalkyllead compounds results. Thus, in the presence of selected Lewis acid catalysts (for example, aluminum halides or boron trifluoride), a mixture of TML and TEL undergoes a redistribution reaction in which an equilibrium mixture of the five possible tetraalkyllead compounds is produced.

Economic Aspects. There are three major industrial producers of TEL and lead alkyl antiknock additives for gasoline: Ethyl Corporation, du Pont, and Associated Octel. Data from the International Lead and Zinc Study Group in London indicate a decline of ca. 66% in the world consumption of refined lead for gasoline additives between 1970 and 1986. Thus, from a peak consumption of 365 200 t in 1970 (excluding Eastern-bloc countries), environmental regulations have resulted in a decline to 124 000 t of refined lead for gasoline additives in 1986 [122]. The limits in 1988 on lead content of gasoline in various countries are given in Table 9.17. These limits were imposed as a means of meeting automotive emission standards. For catalyst-

equipped cars, unleaded gasoline must be used to avoid poisoning of the catalytic converter.

Table 9.17: Limits on lead content of gasoline in 1988 [123].

Country	Maximum lead in gasoline, g/L
United States	0.026
Canada	0.291
Italy, France, Spain, Portugal	0.399
Other EEC countries	0.151
Australia	0.304–0.840
Austria, Sweden, Finland	0.151
Korea	0.301
Venezuela	0.840
Japan	0.000

Uses. Tetraethyllead is used worldwide in gasoline to prevent preignition knock in internal combustion engines prior to completion of the compression stroke. Accordingly, tetraethyllead is commonly called an antiknock agent. This application was for many years the single largest market for organometallic compounds. In addition to providing antiknock qualities to gasolines, organolead additives prevent valve seat wear in engines designed for leaded gasoline.

The preparation and properties of other organolead compounds are described in [118]. Thiomethyl triphenyllead is used as an antifungal agent [124], cotton preservative [125], and lubricant additive [126]; thiopropyl triphenyllead as a rodent repellent [127]; tributyllead acetate as a wood preservative [128] and cotton preservative [129]; tributyllead imidazole as a lubricant additive [130] and cotton preservative [129]; and tributyllead cyanamide and tributyllead cyanoguanidine as lubricant additives [131, 132].

9.13.3 Occupational Health

Lead is toxic in all forms, but to different degrees, depending upon the chemical nature and solubility of the lead compound. In general, organolead compounds are more toxic than inorganic lead salts if ingested, inhaled, or absorbed by humans. Children are more sensitive than adults to the effects of lead exposure. Such exposure may be acute (large

single dose) or chronic (repeated low doses). Prolonged absorption of lead should be avoided because the toxic effects are many, cumulative, and severe.

The most common indications of the onset of lead poisoning (plumbism) are gastrointestinal, including nausea, diarrhea, anorexia, and constipation followed by colic. Since these symptoms of plumbism may be similar to those of other ailments, blood and urine tests should be made on the basis of prior exposure to lead, clinical symptoms, evidence of increased lead absorption, and significant biochemical changes. Lead absorption can affect hemoglobin synthesis, red blood cell survival time, and neuromuscular function. In addition, the toxic effects of lead in women may include decreased fertility, increased abortion, and neonatal morbidity. Encephalopathy is the most serious result of lead poisoning. It occurs frequently in children, when they have very high blood lead levels, but seldom in adults.

Sources of lead in the environment include soils near smelters, lead-pigmented paints, automobile exhaust emissions, food and water, and industrial exposure. Each of these sources is being reduced or eliminated through environmental and occupational safety regulations. For example, in the United States, the ambient airborne lead limit is $1.5 \mu\text{g}/\text{m}^3$, measured over a calendar quarter, which applies to the exterior plant environment and emissions. Moreover, lead-based paints are banned for residential use; leaded gasoline is being phased out; lower limits of lead in drinking water have been proposed (below 20 parts lead per billion parts water).

As a result of exposure monitoring, respiratory protection, protective work clothing and equipment, isolated dining areas, and medical surveillance, there is a very low incidence today of lead poisoning from industrial exposure. Lead-exposed employees in the United States, for example, must be removed from work if the average of their last three blood lead determinations is at or above 50 micrograms lead/100 g whole blood and the airborne lead level is at or above $30 \mu\text{g}/\text{m}^3$ [133]. The permissible exposure limit (OSHA-PEL)

of lead for industrial workers is $50 \mu\text{g}/\text{m}^3$, averaged over an 8 h period. The TLV/TWA for lead is $0.15 \text{ mg}/\text{m}^3$, while the MAK value is $0.1 \text{ mg}/\text{m}^3$. Tetramethyl- and tetraethyllead have an MAK of $0.075 \text{ mg}/\text{m}^3$ ($0.01 \text{ mL}/\text{m}^3$).

9.14 Pigments

9.14.1 Lead Cyanamide

Lead cyanamide, PbCN_2 , is a lemon yellow powder which has the following properties [134]:

Density, g/cm^3	ca. 6.8
Apparent density, g/cm^3	550–750
Metal content, %	ca. 83
CN ₂ content, %	ca. 16
Specific surface area, m^2/g	2
pH	9–11
Conductivity, μS	< 300

9.14.2 Red Lead

Red lead, Pb_3O_4 , crystallizes in the tetragonal system and is a red powder with a density of $9.1 \text{ g}/\text{cm}^3$. It decomposes at ca. 500°C at atmospheric pressure.

Red lead should be regarded as the lead salt of orthoplumbic acid, H_4PbO_4 , i.e., it is lead(II) orthoplumbate, Pb_2PbO_4 , in which PbO_6 octahedra are linked by Pb(II) ions [135].

Red lead is produced industrially by oxidizing lead monoxide (PbO) at ca. $460\text{--}480^\circ\text{C}$ with agitation in a stream of air for 15–24 h. Most red lead is used in the glass, ceramic, and accumulator industries where an apparent density of $< 2 \text{ g}/\text{mL}$ is adequate. For the paint industry, however, highly dispersed red lead is normally necessary, with a sieve residue of $< 0.1\%$ on a 0.063 mm sieve (ISO 787, Part 18) and an apparent density of $1.3\text{--}2.0 \text{ g}/\text{mL}$ (ISO 510, DIN 55516).

The electrochemical action of red lead results from the fact that lead has valencies of 2 and 4 in lead orthoplumbate: Pb(IV) compounds are reduced to Pb(II) in the cathodic region [136]. The chemical anticorrosive effect is a result of lead soaps that are formed when fatty acids in the binder react with the

red lead. The lead soaps permeate the paint film as lamellae, and give good mechanical strength, water resistance, and adhesion to the steel surface. Furthermore, the corrosion-promoting chloride and sulfate ions are precipitated by lead(II) ions [137].

Red lead is still used for heavy-duty anti-corrosion applications, especially for surfaces bearing residual traces of rust. In waterborne paints, red lead has no advantages over zinc phosphate [138].

A trade name for red lead is Bleimennige, hochdispers (Heubach & Lindgens, Germany).

9.14.3 Calcium Plumbate

Calcium plumbate, Ca_2PbO_4 , density $5.7 \text{ g}/\text{cm}^3$, is a beige powder formed from lead monoxide and calcium oxide at ca. 750°C in a stream of air [139].

The anticorrosive properties of calcium plumbate are inferior to those of red lead [140]. Calcium hydroxide is formed as a hydrolysis product when water penetrates through a primer that contains calcium plumbate. The pH at the metal surface then increases to ca. 11–12 which inhibits corrosion.

The most important use is in primers for zinc-coated substrates. The pH change occurring on hydrolysis of the calcium plumbate etches the zinc surface which improves adhesion of primers, especially on hot-dip galvanized steel [141].

9.14.4 Lead Powder

Lead powder, mp 327.5°C , density $11 \text{ g}/\text{cm}^3$, is a dark gray powder containing 99% metallic lead and ca. 0.5% lead(II) oxide. It is produced by spraying molten lead at ca. 0.5 MPa and sifting. Owing to its high surface area (particle size $1\text{--}15 \mu\text{m}$), it is liable to oxidize, and is therefore supplied in airtight packages or as a paste.

Lead powder can be combined with many binders [142–143]. It does not affect the stability or viscosity of the paint. Binders that absorb only small amounts of water are

particularly suitable (e.g., epoxy resins, chlorinated rubber). When formulating paints based on lead powder, care must be taken not to dilute it with other pigments and extenders by more than 5 vol%.

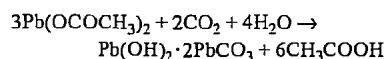
Lead powder coatings are mainly used for protecting against aggressive chemicals. They have a high UV reflection and extremely good elasticity. Lead powder pigments and pastes are also used in radiological protection.

9.14.5 Basic Lead Carbonate

[144–148]

Basic lead carbonate, $\text{Pb}(\text{OH})_2 \cdot 2\text{PbCO}_3$, is used for white pigments and for nacreous pigments. It is, besides natural pearl essence and bismuth oxychloride, one of the classic pearlescent pigments.

The first commercially successful synthetic nacreous pigments were hexagonal platelet crystals of lead salts: thiosulfate, hydrogenphosphate, hydrogenarsenate, and most important nowadays, basic carbonate. Basic lead carbonate is precipitated from aqueous lead acetate or lead propionate solutions with carbon dioxide:



Under appropriate reaction conditions regular hexagonal platelets (ca. 50 nm thick and 20 μm in diameter) can be obtained. The high refractive index ($n = 2.0$), high aspect ratio (> 200), and the extremely even surface of basic lead carbonate make it an optimal match to natural pearl essence.

The platelet thickness can be adjusted to produce interference colors by modifying reaction conditions. When aligned with its plane orthogonal to the incident light, the platelet crystal behaves as a thin, solid, optical film with two phase-shifted reflections from the upper and lower crystal planes (the phase boundaries).

The crystals are mechanically sensitive and their high density (6.4 g/cm³) results in fast sedimentation. In view of their agglomeration tendency and occupational health (toxic-

ity) risks they are not produced in powder form, but are flushed from the aqueous phase into suitable organic solvents or resins and handled as stabilized dispersions.

Currently, use of basic lead carbonate is limited to artificial pearls, buttons, and bijouterie. Due to the low chemical stability of this pigment and toxicity problems, it is being increasingly replaced by bismuth oxychloride and mica-based pigments. Worldwide production of basic lead carbonate pigment in 1995 was ca. 1000 t.

9.15 References

- W. Hoffman: *Lead and Lead Alloys, Properties and Technology*, 2nd ed., Engl. Transl., Springer Verlag, New York 1970.
- R. C. Weast (ed.): *Handbook of Chemistry and Physics*, 67th ed., CRC Press, Boca Raton, FL 1987.
- J. F. Smith, R. R. Kubalak (eds.): "Lead" in *Metals Handbook*, 9th ed., vol. 2, Metals Park, OH 1979.
- AIME World Symp. Min. Metall. Lead Zinc Proc. 1970, St. Louis, MO.
- J. M. Cigan, T. S. Mackey, T. J. O'Keefe (eds.): *Lead-Zinc-Tin '80* AIME, Warrendale, PA 1980.
- U.S. Bureau of Mines, Mineral Industry Survey Lead Reports, 1980–1988.
- H. H. Kellogg, S. K. Basu, *Trans. Metall. Soc. AIME* **218** (1960) 70–81.
- G. M. Willis: "The Physical Chemistry of Lead Extraction", in [5].
- G. W. Healey: "Sulfur Elimination in Updraft Lead Sintering — A Thermochemical Model", *J. Met.* **33** (1981) 30–37.
- J. T. Roy, J. R. Stone, *Trans. Metall. Soc. AIME* **227** (1963) 177–179.
- W. F. Caley, S. G. Whiteway, A. B. Neil, P. J. Dugdale: "Viscometer for Lead Blast Furnace Slags", 14th Annual Conference of Metallurgists, Canada, 1975 paper 113.
- H. Winterhager, R. Kammel, *Z. Erzgebau Metallhüttenwes.* **12** (1959) 479–486.
- G. W. Toop, presentation to 22nd Annual Conference of Metallurgists, Edmonton, Alta., Canada, 1983.
- H. Olaska, O. Notzold in [4].
- H. I. Elvander: "The Boliden Lead Process", *Pyrometallurgical Processes in Nonferrous Metallurgy*, AIME Metallurgical Society Conference, vol. 39, Pittsburgh 1965, p. 225.
- A. Perillo, A. Carminati, G. Carlini: "The Kivcet Lead Smelter at Portovesme, Commissioning and Operating Results", AIME Annual Meeting, Phoenix, AZ 1988, paper no. A88–2.
- S. Petersson: "Autogenous Smelting of Lead Concentrate in TBRC", paper presented at 106th AIME Annual Meeting, Atlanta, GA 1977, TMS-AIME paper no. A77–11.
- E. O. Nermes, T. T. Talonen: "Flash Smelting of Lead Concentrates", *Metall. (Berlin)* **36** (1982) no. 9, 1007–1009.
- A. I. Taskinen, L. M. Toivonen, T. T. Talonen: "Thermodynamics of Direct Lead Smelting", in H. A. Fine, D. R. Gaskell (eds.): *Int. Symp. Metallurgical Slags and Fluxes*, vol. 2, 1984.
- W. J. Errington, J. H. Fewings, V. P. Keran: "The Isasmelt Lead Smelting Process", Transactions of the Institute of Mining and Metallurgy, Section C, 870300, vol. 96, no. 3, pp. C1–C6.
- P. Fisher: "The QSL-Process: A New Lead Smelting Route Ready for Commercialization", Advances in Sulfide Smelting, AIME Conference Proceedings, San Francisco, Nov. 1983, vol. 2, Technology and Practice, pp. 513–527.
- M. Wong, F. Haver, R. Sandberg: "Ferric Chloride Leach-Electrolysis Process for Production of Lead", in [5].
- T. R. A. Davey: "The Physical Chemistry of Lead Refining", in [5].
- J. H. Fern, R. W. Shaw: "Copper Separation and Recovery at the BHAS Lead Smelter", MMIJ/Aus IMM Joint Sendai Symp., Port Pirie, S. Australia, 1983.
- J. A. DeKeyser, W. E. Jespers: "The Harris Refinery of S.A. Metallurgie Hoboken-Overpelt N.V.", AIME, TMS Paper Selection A81–10 1981.
- K. Emicke, G. Holzapfel, E. Kniptath: "Lead Refining at Norddeutsche Affinerie", *Erzmetall* **24** (1971) 205–215.
- BHASP Ltd., AU 502470, 1979 (D. H. Ward, J. D. Iley).
- D. L. Thomas, C. J. Krauss, R. C. Kerby, AIME, TMS Paper Selection A81–8, 1981.
- S. Bergsøe, N. Gram: "Lead Smelting, Refining, and Pollution", *Lead-Zinc-Tin '80 (Eighty) Proc. World Symp. Metall. Environ. Control* **1980**, 1023–1030.
- "CX Serap Battery Compounds Recovery Plant", Commercial Literature, Tecnologie Tonolli, Milano, 1986.
- J. D. Taylor, P. J. Moor: "Secondary Lead Smelting at Britannia Lead Company Limited", *Lead-Zinc-Tin '80 (Eighty) Proc. World Symp. Metall. Environ. Control* **1980**, 1003–1022.
- M. Koch, H. Niklas: "Processing of Lead-Acid Battery Scrap, the Varta Process", Productivity and Technology in the Metallurgical Industries, TMS Cologne, Sept. 1989, pp. 495–500.
- R. C. Egan, M. V. Rao, K. D. Libsch: "Rotary Kiln Smelting of Secondary Lead", *Lead-Zinc-Tin '80 (Eighty) Proc. World Symp. Metall. Environ. Control* **1980**, 935–973.
- J. Godfroi: "Five Years' Utilization of the Short Rotary Furnace in the Secondary Smelting of Lead", *Lead-Zinc-Tin '80 (Eighty) Proc. World Symp. Metall. Environ. Control* **1980**, 974–984.
- E. R. Cole, A. Y. Lee, D. L. Paulson: "Update on Recovering Lead from Scrap Batteries", *J. Met.* **37** (1985) 79–83.
- D. Hunter: *The Disease of Occupations*, The English University Press, London 1957.
- R. A. Kehoe, F. Thamann, J. Cholak: "On the Normal Absorption and Excretion of Lead", *J. Ind. Hyg.* **15** (1933).
- R. Amavis, J. Smeets, *Sci. Total Environ.* **18** (1981) 293–300.
- EPA: "Reducing Lead in Drinking Water: A Benefit Analysis", EPA Report no. EPA 230–09–86–019, 1986.
- D. Worth et al.: *Environmental Lead*, Academic Press, New York 1981.
- R. F. Lacey, M. R. Moore, W. N. Richards, *Sci. Total Environ.* **41** (1985) 235–257.
- B. E. Davies: *Lead in the Home Environment*, Science Reviews, Norchwood 1987.
- NHANES II — "Chronological Trend in Blood Lead Levels Between 1976 and 1980", *N. Engl. J. Med.* **308** (1983) 1373–1377.
- Air Quality Criteria for Lead*, Office of Research and Development, U.S. Environmental Protection Agency, Washington, DC, 1977.
- International Symposium on Environmental Lead Research, Dubrovnik, Yugoslavia, *Arch. Ind. Hyg. Tox.* **26** (1975) Supplement.
- N. Schmitt et al.: "Surface Soil as a Potential Source of Lead Exposure for Young Children", *CMAJ* **121** (1979) 1474–1478.
- Lead, Airborne Lead in Perspective, National Academy of Sciences, National Research Council, Washington, DC, 1972.
- R. A. Kehoe: "The Metabolism of Lead in Man in Health and Disease, The Normal Metabolism of Lead", *J. R. Inst. Pub. Health Hyg.* **24** (1961) 81–96.
- J. J. Chisolm: "The Continuing Hazard of Lead Exposure and Its Effects in Children", *Neurotoxicology* **5** (1984) 23–42.
- K. Horiuchi: "Lead in the Environment and Its Effect on Man in Japan", *Med. J. Osaka Univ.* **16** (1970) 1–28.
- K. Nozaki: "Method for Studies on Inhaled Particles in Human Respiratory System and Retention of Lead Fume", *Ind. Health* **4** (1966) 118–123.
- S. B. Gross: "Kehoe Balance Experiments, Oral and Inhalation Lead Exposures in Human Subjects", *J. Toxicol. Environ. Health* **8** (1979) 333–337.
- S. Hemberg, J. Kikkanen, G. Mellin, H. Lilius: "Delta-Aminolevulinic Acid Dehydrase as a Measure of Lead Exposure", *Arch. Environ. Health* **21** (1970) 140–145.
- H. L. Needleman et al.: "Deficits in Psychologic and Classroom Performance of Children with Elevated Dentine Lead Levels", *N. Engl. J. Med.* **300** (1979) 689–695.
- R. A. Goyer: *Current Topics in Pathology*, vol. 55, Springer Verlag, Heidelberg 1971.
- I. Lancranjan et al.: "Reproductive Ability of Workmen Occupationally Exposed to Lead", *Arch. Environ. Health* **30** (1975) 396–401.
- IARC Monographs on the Evaluation of Carcinogenic Risks to Humans, Overall Evaluation of Carcinogenicity: An Updating of IARC Monographs, vols. 1–42, Suppl. 7, 1987.
- A. C. Chamberlain et al.: "Uptake of Lead by Inhalation of Motor Exhaust", *Proc. R. Soc. London B* **192** (1975) 77–110.
- R. R. Lauwerys: "Industrial Chemical Exposure: Guidelines for Biological Monitoring", *Section 10* (1983) 29.
- A. A. Lamola, T. Yamane: "Zinc Protoporphyrin in the Erythrocytes of Patients with Lead Intoxication

- and Iron Deficiency Anemia", *Science (Washington, DC)* **186** (1974) 936.
60. H. E. Brown: *Lead Oxide - Properties and Applications*. Int. Lead Zinc Res. Organization, Research Triangle Park, NC, 1985.
 61. Greninger, V. Kollonitsch C. H. Kline: *Lead Chemicals*, International Lead Zinc Research Organization, Research Triangle Park, NC, 1975.
 62. *Gmelin*, Syst. No. 47.
 63. Kirk-Othmer, **14**, 160ff.
 64. H. Shapiro, F. W. Frey: *The Organic Compounds of Lead*. Interscience, New York 1968.
 65. L. C. Willemsens: *Organolead Chemistry*. International Lead Zinc Research Organization, Research Triangle Park, NC, 1964.
 66. L. C. Willemsens, G. J. M. van der Kerk: *Investigations in the Field of Organolead Chemistry*. International Lead Zinc Research Organization, Research Triangle Park, NC, 1965.
 67. R. C. Weast (ed.): *CRC Handbook of Chemistry and Physics*, 68th ed., CRC Press, Boca Raton, FL, 1987-1988.
 68. In [61] p. 296.
 69. Teijin Ltd., JP 18963, 1960 (S. Futami); *Chem. Abstr.* **62** (1965) 16413a.
 70. H. K. Porter Co., US 3112772, 1961 (R. E. Connor, J. C. Kitching); *Chem. Abstr.* **60** (1964) 4320g.
 71. Shell International Research, NL 6511631, 1965; *Chem. Abstr.* **65** (1966) 2046h.
 72. F. Kato, Y. Machino, JP 3910, 1960; *Chem. Abstr.* **60** (1964) 2781c.
 73. General Electric Company, US 3039989, 1959 (W. O. Eastman); *Chem. Abstr.* **57** (1962) 8746b.
 74. Tempil Corporation, FR 1335076, 1962; *Chem. Abstr.* **60** (1964) 4309a.
 75. Shell International Research, NL 6509144, 1964; *Chem. Abstr.* **64** (1966) 15661b.
 76. Rosendahl's Spinnerier A/S, NO 105799, 1962 (T. Ringvold); *Chem. Abstr.* **63** (1965) 4460a.
 77. Toshiba Corporation, JP-Kokai 60169155, 1984 (K. Kobayashi); *Chem. Abstr.* **104** (1986) 173110m.
 78. Daido Metal Co., Ltd., US 4312772, 1979 (S. Mori); *Chem. Abstr.* **96** (1982) 167214s.
 79. Riedel-de Haen AG, EP-A 167949, 1986 (E. Scholz, H. J. Luttmann); *Chem. Abstr.* **104** (1986) 114518w.
 80. Sumitomo Light Metal Industries, Ltd., JP-Kokai 6109995, 1984 (K. Ito et al.); *Chem. Abstr.* **104** (1986) 191348t.
 81. Nippon Sheet Glass Co., Ltd., JP-Kokai 60137852, 1983 (J. Nishii, T. Yamagishi); *Chem. Abstr.* **104** (1986) 55204r.
 82. Canon K.K., JP-Kokai 59189566, 1983; *Chem. Abstr.* **102** (1985) 175002d.
 83. In [61] p. 173.
 84. Chloride Group Ltd., GB 1601117, 1978 (S. Worrell, N. E. Bagshaw); *Chem. Abstr.* **96** (1982) 165647m.
 85. Mordavia State University, SU 969695, 1980 (V. P. Selyaev et al.); *Chem. Abstr.* **98** (1983) 180456h.
 86. Council of Scientific and Industrial Research (India), IN 153507, 1979 (S. Bhattacharya et al.); *Chem. Abstr.* **102** (1985) 118196w.
 87. Matsushita Electric Works, Ltd., JP-Kokai 57187379, 1981; *Chem. Abstr.* **98** (1983) 199981x.
 88. Agency of Industrial Sciences and Technology, JP-Kokai 57188663, 1981; *Chem. Abstr.* **98** (1983) 130513d.
 89. Nippon Sheet Glass Co., Ltd., JP-Kokai 60246242, 1984 (J. Nishii, T. Yamagishi); *Chem. Abstr.* **104** (1986) 154385g.
 90. Hooker Chemical Corporation, FR 2039700, 1969 (J. A. Peterson, H. W. Marciniak); *Chem. Abstr.* **75** (1971) 130482t.
 91. Nippon Sheet Glass Co. Ltd., JP-Kokai 6144734, 1984; *Chem. Abstr.* **104** (1986) 229306i.
 92. Mitsubishi Petrochemical Co. Ltd., JP 7499394, 1973 (Y. Fujita, C. Kaya); *Chem. Abstr.* **82** (1975) 113096x.
 93. L. Kacel, J. Pantoflick, L. Sramek, F. Anyz, CS 121444, 1965; *Chem. Abstr.* **67** (1967) 118693q.
 94. Fuji Photo Film Co., Ltd., DE-OS 2312675, 1973 (E. Inoue et al.); *Chem. Abstr.* **79** (1973) 151686k.
 95. Hitachi Maxell, Ltd., JP-Kokai 59141423, 1983; *Chem. Abstr.* **101** (1984) 233249g.
 96. Tomsk Polytechnic Institute, SU 956314, 1980 (M. A. Shustov, V. K. Zhuravlev, D. G. Kulagin); *Chem. Abstr.* **97** (1982) 205799s.
 97. G. Smoluk, *Mod. Plast.* **56** (1979) no. 9, 74.
 98. W. D. Woodbury, *Preprint from the 1985 Bureau of Mines Mineral Yearbook, Lead*, U.S. Department of the Interior, p. 19.
 99. In [61] pp. 59-60.
 100. H. E. Brown: *Lead Oxide Properties and Applications*, International Lead Zinc Research Organization, Research Triangle Park, NC, 1985.
 101. In [61] p. 69.
 102. N. M. Mamaev, S. M. Gubarev, V. G. Altynov, *Izv. Sev. Kavk. Nauchn. Tsentra Vyssh. Shk. Tekh. Nauki* (1980) no. 1, 49-52; *Chem. Abstr.* **93** (1980) 221426r.
 103. United States Dept. of the Army US 3996080, 1971 (J. S. Stack); *Chem. Abstr.* **86** (1977) 108814h.
 104. Mitsubishi Heavy Industries, Ltd., JP 7932435, 1973 (K. Ueda); *Chem. Abstr.* **92** (1980) 66846m.
 105. Mitsui Mining and Smelting Co., Ltd., JP 7628077, 1972 (A. Matsumoto, E. Isobe); *Chem. Abstr.* **87** (1977) 28337k.
 106. Toyo Rubber Industry Co., Ltd., JP 8030543, 1976; *Chem. Abstr.* **94** (1981) 31937f.
 107. Société des accumulateurs fixes et de traction (SAFT), US 4271244, 1978 (J. P. Gabano, M. Broussely); *Chem. Abstr.* **95** (1981) 105363k.
 108. V. Janda et al., CS 189225, 1976; *Chem. Abstr.* **97** (1982) 75012s.
 109. In [98] p. 18.
 110. Chloride Group Ltd., GB 1508991, 1974 (K. Peters); *Chem. Abstr.* **90** (1979) 8891v.
 111. H. Hayashi, JP-Kokai 8015969, 1978; *Chem. Abstr.* **93** (1980) 119147p.
 112. S. T. Basyuk, A. M. Zinder, A. A. Savatyugin, V. M. Kochetkov, SU 540907, 1974; *Chem. Abstr.* **87** (1977) 25819h.
 113. Nippon Akuriru Kagaku K.K., JP-Kokai 7796636, 1976 (S. Kawamura, S. Watanabe, Y. Shikimori); *Chem. Abstr.* **88** (1978) 39071r.
 114. Continental Gummi-Werke AG, BE 870811, 1977 (R. Sohnmann); *Chem. Abstr.* **91** (1979) 22198b.
 115. Kirk-Othmer, **14**, 173.
 116. In [61] p. 254.
 117. S. F. Radtke, D. S. Carr: "Lead Stabilized Asphalt", *Proc. Fifth Intl. Asphalt Conf.*, Australian Asphalt Pavement Association, Perth, Australia, Feb. 1983.
 118. L. C. Willemsens, G. J. M. van der Kerk: *Investigations in the Field of Organolead Chemistry*, International Lead Zinc Research Organization, Research Triangle Park, NC, 1965.
 119. International Lead Zinc Research Organization, US 3324054, 1967; US 3417113, 1968; US 3547481, 1970 (H. G. J. Overmars).
 120. International Lead Zinc Research Organization, US 3595964, 1971 (G. Gras).
 121. D. S. Carr: "Triphenyllead Acetate - Organolead Antifoulant Passes Tests", *Paint and Varn. Prod.* **64** (1974) no. 12, 19-23.
 122. H. Shapiro, F. W. Frey: *The Organic Compounds of Lead*, Interscience, New York 1968, pp. 399-403.
 123. D. R. Lynam: *The Past, Present and Future of Lead in Gasoline*, Ethyl Corporation, Baton Rouge, LA, 1988.
 124. International Lead Zinc Research Organization, US 3322779, 1967; US 3522352, 1970 (M. C. Henry, A. W. Krebs).
 125. International Lead Zinc Research Organization, US 3420700, 1969 (D. J. Donaldson, W. A. Guice, G. L. Drake, Jr., W. A. Reeves).
 126. International Lead Zinc Research Organization, US 3287265, 1966 (W. L. Pearlstein).
 127. International Lead Zinc Research Organization, US 3683090, 1972 (M. C. Henry, A. W. Krebs).
 128. G. J. M. van der Kerk: "New Developments in Organolead Chemistry", *Ind. Eng. Chem.* **58** (1966) no. 10, 29-35.
 129. International Lead Zinc Research Organization, US 3420701, 1969 (D. J. Donaldson, W. A. Guice, G. L. Drake, Jr., W. A. Reeves).
 130. International Lead Zinc Research Organization, US 3655683, 1972 (L. C. Willemsens).
 131. International Lead Zinc Research Organization, US 3527704, 1970 (W. L. Pearlstein, H. A. Beatty).
 132. International Lead Zinc Research Organization, US 3436414, 1969 (C. J. Worrell).
 133. Federal Register (U.S.), vol. 43, Nov. 14, 1978, pp. 52952-53014, as corrected in vol. 44, April 6, 1979, pp. 20680-20681.
 134. BASF AG, Ludwigshafen, company information, 1990.
 135. A. F. Wells: *Structural Inorganic Chemistry*, Clarendon Press, Oxford 1962.
 136. J. D'Ans, W. Breckheimer, H. J. Schuster, *Werkst. Korros.* **8** (1957) 677.
J. D'Ans, H. J. Schuster, *Farbe + Lack* **61** (1955) no. 10, 453.
J. E. O. Mayne, *Farbe + Lack* **76** (1970) no. 3, 243.
 137. G. Lincke, *Farbe + Lack* **77** (1971) no. 5, 443.
G. Lincke, *Congr. FATIPEC* **12th** 563.
 138. H. Berger, *Farbe + Lack* **88** (1982) no. 3 180-182.
 139. P. N. Martini, A. Bianchini, *J. Appl. Chem.* **19** (1969) 147.
 140. J. Ruf: *Korrosionsschutz durch Lacke und Pigmente*, A. W. Colomb, H. Heenemann GmbH, Stuttgart-Berlin 1972.
 141. J. F. H. van Eijnsbergen, *Farbe + Lack* **71** (1965) no. 10, 1005.
G. Meyer, *Dtsch. Farben-Z.* **16** (1962) 347.
 142. M. A. Newnham, *Paint Technol.* **42** (1968) 16.
 143. R. Hawner, *Farbe + Lack* **69** (1963) no. 6, 611.
 144. W. Bäumer, *Farbe + Lack* **79** (1973) p. 747.
 145. L. M. Greenstein in *Pigment Handbook*, 2nd ed., Vol. 1, J. P. Wiley & Sons, New York 1988, pp. 850-856.
 146. K. D. Franz, H. Härtner, R. Emmert, K. Nitta in *Ullmann's Encyclopedia of Industrial Chemistry*, Vol. A20, VCH Verlagsgesellschaft mbH, Weinheim 1992, p. 351.
 147. K. D. Franz, R. Emmert, K. Nitta, *Kontakte (Darmstadt)* **2** (1992) p. 3.
 148. R. Glausch, M. Kieser, R. Maisch, G. Pfaff, J. Weitzel in *Periglanzpigmente*, Curt R. Vincentz Verlag, Hannover 1996, pp. 26-29.

10 Zinc

GÜNTER G. GRAF (§§ 10.1–10.6); HEINRICH J. JOHNNEN (§ 10.7); DIETER M. M. ROHE (§§ 10.8.1–10.8.5); HANS UWE WOLF (§ 10.8.6); WOLF-DIETER GRIEBLER (§ 10.9.1); MARCEL DE LIEDEKERKE (§§ 10.9.2.1–10.9.2.7); GÜNTER ETZRODT (§§ 10.9.2.8, 10.9.3–10.9.7); HARALD GAEDCKE (§ 10.9.2.9); ROBERT BESOLD (§ 10.9.8)

10.1 History	641	10.8.1 Fluoride	663
10.2 Properties	643	10.8.2 Chloride	664
10.3 Starting Materials for Zinc		10.8.3 Bromide	665
Production	643	10.8.4 Iodide	665
10.3.1 Zinc Minerals	643	10.8.5 Sulfate	666
10.3.2 Zinc Reserves	645	10.8.6 Toxicology and Occupational Health	667
10.3.3 Secondary Raw Materials	645	10.9 Zinc Pigments	668
10.4 Pretreatment of Raw Materials for the		10.9.1 Zinc Sulfide Pigments	668
Production of Zinc Metal	646	10.9.1.1 Properties	669
10.4.1 Roasting	646	10.9.1.2 Production	670
10.4.2 Pyrometallurgical Concentration		10.9.1.3 Commercial Products	672
Processes	647	10.9.1.4 Uses	672
10.5 Production of Zinc Metal	648	10.9.1.5 Economic Aspects	673
10.5.1 Pyrometallurgical Zinc Production by the		10.9.1.6 Toxicology	673
Retort Process	649	10.9.2 Zinc Oxide (Zinc White)	673
10.5.2 Zinc Production in the Shaft Furnace	650	10.9.2.1 Introduction	673
10.5.3 Refining of Crude Zinc	652	10.9.2.2 Properties	674
10.5.4 Hydrometallurgical Zinc Production	652	10.9.2.3 Production	674
10.5.5 Treatment of Leaching Residues ...	657	10.9.2.4 Quality Specifications	676
10.5.6 Solution Purification	657	10.9.2.5 Uses	676
10.5.7 Electrolytic Production of Zinc	658	10.9.2.6 Economic Aspects	676
10.5.8 New Developments in Zinc		10.9.2.7 Toxicology and Occupational Health	677
Production	660	10.9.2.8 Anticorrosive Zinc Oxide	677
10.6 Uses and Economic Aspects	661	10.9.2.9 Transparent Zinc Oxide	677
10.6.1 Galvanizing	661	10.9.3 Zinc Phosphate	677
10.6.2 Zinc as a Construction Material ...	662	10.9.4 Zinc Hydroxyphosphite	678
10.6.3 Pressure Die Casting with Zinc	662	10.9.5 Zinc Cyanamide	678
10.6.4 Zinc as a Chemical	662	10.9.6 Zinc and Calcium Ferrites	678
10.6.5 Economic Aspects	663	10.9.7 Zinc Dust	679
10.7 Alloys	663	10.9.8 Flake Zinc Pigments	679
10.8 Compounds	663	10.10 References	679

10.1 History [1, 2, 4, 6–8]

Before 1500 A.D. the Chinese and Indians knew of zinc as a metal in its own right, and although it is not known precisely when zinc was first produced, coins containing 99% zinc were cast during the Ming Dynasty (1368–1644). In a book written in 1637, the Chinese describe zinc production by controlled smelting in stacked, hermetically sealed pots. In India, remains of zinc smelting operations found in Sawai Madhopur (Rajasthan) confirm that

zinc was produced prior to the 1300s. Although the Romans, the Greeks, and the entire western world knew how to produce brass, which was used as early as 8000 B.C. to make jewelry, metallic zinc was unknown. At that time, brass was produced by smelting copper ores or metallic copper with the zinc ore smithsonite. This method lasted until the 1800s. Brass smelting works were developed in the Middle Ages where localized deposits of smithsonite occurred in various places, e.g., near Lüttich and Aachen, and in Carinthia.

The efforts of the alchemists to convert base metals into gold led them to become interested in smithsonite, the ore that gave copper a golden color.

The first written sources to mention the word "zinc" appeared in the 1500s. However, the derivation is not entirely clear. The most likely assumption is that it is connected with the German word *Zinke* (the tooth of a comb), itself derived from *Zacke* (jagged peak), from the jagged appearance of the ore or of deposits in the furnace. A second possibility is that the word is derived from the Persian word *seng* meaning stone. GEORGIUS AGRICOLA (1494–1555), in his important *De re metallica*, describes how a material found in large quantities in the eastern Alps was called "zinc" by the local people. He gave the name "conterfey" to the white substance that was deposited at the front of the smelting furnaces during the treatment of Rammelsberg ores. This often consisted of metallic zinc, although he did not recognize it as such.

The metallurgical properties of zinc were first unambiguously described in Europe when zinc arrived there from India and China after the establishment of trade relations with the Far East.

In 1595, LIBAVIUS investigated a sample of this East Indian zinc imported from Holland and named "calaem". However, he confused it with silver and did not realize that it was the same material as that known as "cadmia" which was scraped off the walls of the furnace when Rammelsberg ore was smelted in the Harz Mountains to obtain lead and silver.

In 1617, LÖHNEYSS also described this process and clearly recognized this metal as "zinc" or the "conterfey" already described by Agricola, used to imitate gold. KUNKEL (1700) and STAHL (1718) considered that smithsonite added a metallic component to the copper during brass production. In 1721, HENKEL produced zinc from smithsonite in Upper Silesia using a process that he kept secret. In 1746, in Berlin, MARGGRAF produced zinc by distilling smithsonite in sealed vessels. He described his production principle in detail, thereby establishing the basic theory of zinc production.

The first industrial production of zinc was carried out in England, where it was produced on a large scale as early as 1720, probably based on knowledge of operating methods used in East Asia. CHAMPION patented a process adapted from brass production to produce zinc by distillation and built the first zinc smelting works in Bristol in 1743, with a capacity of > 200 t/a zinc. He also patented the process for producing zinc from sulfidic ores after preliminary roasting. The English zinc industry is concentrated in Bristol and Swansea even today.

The German zinc industry was founded by RUBERG. The first zinc smelting works, which used the horizontal retort process developed by him, was built in Wessola in Upper Silesia in 1798. The raw material initially used was zinc galmei, a by-product of lead and silver production. Later, it became possible to produce zinc directly from smithsonite, and easily smelted ore. This was shortly followed by the use of zinc blende, which had first to be converted into the oxidic form by roasting. After this development, other smelting works were soon erected in Silesia near the deposits, in the areas around Lüttich, Belgium and Aachen, Germany and in the Rhineland and Ruhr regions.

In the United States, the rich ore deposits led to rapid growth in zinc production in 1840, so that, by 1907, Germany, which had for long been the world's leading producer of zinc, was left behind.

The ores were often highly intergrown, and ore processing by sorting and flotation methods was started in the early 1920s.

At this time, the electrolytic production of high-purity zinc from sulfuric acid solutions was developed by the Consolidated Mining and Smelting Co. in Trail (Canada) and by the Anaconda Copper Co. in Anaconda, Montana (United States).

An important development in zinc production was achieved in 1930 at the New Jersey Co. in Palmerton (United States). Replacing the individual horizontal retorts by a single vertical retort enabled continuous operation

and also yielded relatively pure zinc (ca. 99.5%).

Statistical data on world production of zinc have been available since 1871. At this time, total production was 121 000 t/a, of which 58 000 t/a was produced in Germany and 45 000 t/a in Belgium. Total production at the turn of the century was 472 000 t/a and in 1913 10⁶ t/a. The earliest use for zinc was to produce brass for the manufacture of jewelry, domestic utensils, and coins.

Zinc castings were first produced on an industrial scale in the 1800s by GEISS (1805–1875). Backed by the building contracting SCHINKEL, the zinc foundry established by Geiss soon became of major importance.

The good resistance of zinc towards atmospheric corrosion soon led to its use in sheet steel production. The possibility of rolling zinc at 100–150 °C was discovered as early as 1805, and the first rolling mill was built in Belgium in 1812 by DONY. More such mills were built in Silesia from 1821 onwards.

Hot-dip galvanizing, the oldest anticorrosion process, was introduced in 1836 in France. This became possible on an industrial scale only after the development of effective processes for cleaning iron and steel surfaces. At first, only small workpieces were zinc coated. Continuous hot-dip galvanizing of semifinished products and wire came later.

10.2 Properties [1, 2, 7–11]

Physical Properties. Some physical properties of zinc are listed below.

Relative atomic mass	65.39
Crystal structure, α -Zn	fcc (diamond type)
β -Zn	tetragonal
Transformation temperature α -Zn \rightleftharpoons β -Zn	286.2 K
Heat of transformation	1966 J/mol
Density of β -Sn at 20 °C	7.286 g/cm ³
at 100 °C	7.32
at 230 °C	7.49
Density of α -Zn at 25 °C	7.265 g/cm ³
Density of liquid zinc at 240 °C	6.993 g/cm ³
at 400 °C	6.879
at 800 °C	6.611
at 1100 °C	6.484
mp	505.6 K
Heat of melting	7029 J/mol
bp	2876 K

Heat of vaporization	295.8 kJ/mol
Vapor pressure at 1100 K	9.8×10^{-6} mbar
at 1800 K	7.5
at 2100 K	83.9
at 2400 K	512.0
Thermal conductivity of β -Zn at 0 °C	0.63 Wcm ⁻¹ K ⁻¹
Electrical resistivity of α -Zn at 0 °C	5×10^{-6} Ω m
β -Zn at 25 °C	11.15×10^{-6}
Superconductivity critical temperature	3.70 K

The remarkably low boiling point of 906 °C (STP) is important in pyrometallurgical zinc production processes. Zinc can be worked at temperatures as low as 120 °C, and its good deformability is the basis for some of its uses.

In the electrochemical series, zinc is more negative than iron. The use of zinc in sacrificial anodes is based on this fact. The important use of zinc to coat iron to protect it from corrosion is based on the formation of passivating protective coatings of basic zinc carbonate by reaction with the atmosphere.

Chemical Properties. Zinc has an oxidation state of 2+ in all its compounds. It forms complexes with ammonia, amines, and cyanide and halide ions. Zinc dissolves in mineral acids, usually with evolution of hydrogen, but in nitric acid with evolution of NO_x. Zinc is used as a strong reducing agent in chemical processes, mainly in the form of powder or granules. Zinc is resistant to air because of the protective coating formed. It is also resistant to halogens, but is rapidly corroded by HCl gas. Because of its high surface area, zinc dust is much more reactive and can even be pyrophoric, e.g., reacting vigorously at elevated temperatures with the elements oxygen, chlorine, and sulfur.

Zinc chloride and sulfate are soluble in water, while the oxide, carbonate, phosphate, silicate, and organic complexes are insoluble or sparingly soluble.

10.3 Starting Materials for Zinc Production [1, 2, 4, 12–15]

10.3.1 Zinc Minerals

With an average concentration in the earth's crust of 65 g/t (0.0065%), zinc is the

24th element in order of abundance. It occurs only in the chemically combined state. Like copper and lead, zinc is a strongly chalcophilic element. It usually occurs as the sulfide, mostly deposited from hydrothermal solutions and simic and sialic magmas. Sedimentary deposits are of less importance. A series of deposits in carbonatic strata shows the characteristics of true marine sedimentary deposits. However, in these cases it can be assumed that the metal was introduced by hydrothermal transport from simic magmas. Zinc deposits, classified according to their origin, are listed here in order of their economic importance:

- Simic vulcanogenic-sedimentary deposits that sometimes occur as massive ore bodies and sometimes as impregnations, e.g., Kidd Creek (Canada), Mt. Isa and Broken Hill (Australia), Anvil Mine (Canada), Bleiberg (Austria), Reocin (Spain), and Rammelsberg and Meggen (Germany). Ores from these deposits represent 60% of total world reserves.
 - Simic-hydrothermal or marine sedimentary deposits, e.g., Kipishi (Zaire), Kabwe (Zambia), Tsumed (South-West Africa), and New Zinc Belt and Old and New Lead Belt (United States). Approximately 30% of all ore is produced from these deposits.
 - Sialic lodes (impregnation and replacement deposits), e.g., Bad Grund (Germany); western U.S. states such as Idaho, Colorado, and Utah; and Tepca (Yugoslavia). Only 10% of world ore production is from these deposits.
- Cadmium, silver, lead, and copper are important by-products of zinc ore extraction. Iso-morphous components of zinc blende such as cadmium, gallium, germanium, indium, and thallium do not form deposits of their own. Some of these metals are recovered during zinc ore processing.
- By far the most important zinc mineral today, and probably also the only primary ore, is zinc blende. The other minerals listed here are of only local importance. Native zinc is practically nonexistent.

Zinc blende, sphalerite, ZnS , theoretical composition 67.09% Zn, 32.91% S, is light yellow to black in color, usually black to brown depending on the iron content, crystallizes in the regular tetrahedral system, and has a Mohs hardness of 3–4 and a density of 3.9–4.1 g/cm³.

The most important impurity is FeS, which is always present at concentrations between 0.3 and > 20%. The grades with the highest iron contents are marmatite and christophite. Sulfides of Pb, Cd, Mn, and Cu are often present. Zinc blende also often contains small amounts of As, Sn, Bi, Co, Hg, In, Tl, Ga, and Ge, and nearly always contains Ag and often Au.

Wurzite is the hexagonal modification of ZnS . It often shows a conchoidal or radiating crystalline structure and is therefore also known as conchoidal or radiating blende. Its density is 3.98 g/cm³.

Smithsonite, zinc spar, or calamine, ZnCO_3 , has the theoretical composition 52.14% Zn, 35.10% CO_2 . Some of the ZnO can be replaced by FeO, MnO, CaO, or MgO, so that the ZnO content can be as low as 20%. Other typical impurities include SiO_2 , Fe_2O_3 , and Al_2O_3 .

The Mohs hardness is 5 and the density 4.30–4.45 g/cm³. The color is yellowish or reddish to brown, rarely colorless. Smithsonite crystallizes in the trigonal scalenohedral form and is usually amorphous or in amorphous mixtures with other carbonates. Minerals with higher impurity contents include manganese zinc spar (up to 15% MnCO_3), iron zinc spar (up to 53% FeCO_3), copper zinc spar (up to 6% CuCO_3), zinc lead spar (up to 1% PbO), and cadmium zinc spar (up to 7% CdCO_3).

Hemimorphite, $\text{Zn}_3\text{Si}_2\text{O}_7 \cdot \text{H}_2\text{O}$, has the theoretical composition 54.30% Zn, 24.94% SiO_2 , and 7.4% water of crystallization of which 50% is evolved on heating to 500 °C, the remainder at much higher temperatures.

The color is yellow to brown, more rarely colorless, green, or blue. It forms rhombic pyramidal crystals, but usually occurs in rough, massive, botryoidal, or earthy forms. Its Mohs

hardness is 4.5 and its density 3.4–3.5 g/cm³. It is often a component of “calamine” ores.

Willemite, Zn_2SiO_4 , has the theoretical composition 58.68% Zn, 26.95% SiO_2 . Its color can be white, yellow to reddish, greenish, or rarely blue. It forms rhombohedral crystals, has a Mohs hardness of 5–6 and a density of 4.0–4.2 g/cm³, and can contain FeO and MnO as impurities.

Franklinite, $(\text{Zn}, \text{Fe}, \text{Mn})\text{O} \cdot (\text{Fe}_2, \text{Mn}_2)\text{O}_3$, has the theoretical composition 21% ZnO , 59% Fe_2O_3 , 11% FeO, and 8% Mn_2O_3 , and can contain SiO_2 , Al_2O_3 , and MgO as impurities. Its color is black, it is weakly magnetic, and it forms cubic crystals, with Mohs hardness 6.0–6.5, and density 5.0–5.1 g/cm³.

Other zinc minerals of minor metallurgical importance include zinc bloom or hydrozincite, $\text{ZnCO}_3 \cdot n\text{Zn}(\text{OH})_2$; red zinc ore or zincite, ZnO ; and troostite or bairdite, $(\text{Zn}, \text{Mn})_2\text{SiO}_4$.

10.3.2 Zinc Reserves

The proven zinc mineral reserves worldwide are estimated at 185.3×10^6 t zinc. Potential reserves amount to 118.1×10^6 t. The undoubtedly considerable Chinese deposits are not included in this estimate, as no concrete information on these is available.

The proven and potential reserves are listed in Table 10.1. Canada, with 37.7×10^6 t (20.3%), has the largest reserves of any country, over 90% of which are in stratified vulcanogenic-sedimentary deposits. North and South America account for over 45.4% of known deposits. Western Europe has 16.7% of world zinc reserves, of which the most important are in Ireland, Sweden, and Yugoslavia (Kosovo). Australia accounts for over 9.5% of world reserves, the largest deposits being in Mt. Isa (Queensland) and Broken Hill (New South Wales).

The most important deposits in the GUS, accounting for 13.2% of the total, are in the central and eastern Kazakh, Uzbek, and Kirghiz. The reserves in Poland (Upper Silesia) are also important.

Table 10.1: The zinc reserves of the world [2, 3, 12, 13].

Country	Proven reserves		Potential reserves	
	10 ⁶ t	%	10 ⁶ t	%
Canada	37 560	20.3	6 620	5.6
United States	31 800	17.1	32 200	27.3
Mexico	3 600	1.9	1 000	0.8
Peru	7 150	3.8	1 500	1.3
Brazil	1 790	1.0	480	0.4
Rest of Latin America	2 360	1.3	2 820	2.4
Africa	5 930	3.2	9 580	8.1
Germany	1 850	1.0	1 500	1.3
Sweden	4 000	2.2	2 000	1.7
Finland	2 000	1.1	1 000	0.8
Ireland	8 820	4.8	350	0.3
Spain	5 060	2.7	1 200	1.0
Italy	2 200	1.2	1 100	0.9
Yugoslavia (Kosovo)	3 500	1.9	2 000	1.7
Rest of Western Europe	3 420	1.8	2 250	1.9
Australia	17 560	9.5	27 950	23.7
Iran	3 700	2.0	1 800	1.5
India	2 650	1.4	3 500	3.0
Japan	9 150	5.0	6 100	5.2
Rest of Asia	1 160	0.6	3 100	2.6
GUS and Eastern Europe	30 000	16.2	10 000	8.5
Total	185 260	100.0	118 050	100.0

10.3.3 Secondary Raw Materials [16, 17]

Typical secondary zinc raw materials include:

- Electric steel plant dusts containing 20–30% zinc (low grade) or 30–40% zinc (high grade)
- Liquor residues from zinc electrolysis containing 25–30% zinc
- Lead shaft furnace slags containing 10–15% zinc
- Residues from thermal zinc production containing 8–12% zinc

Thermal enrichment of such products in the Waelz kiln process gives a Waelz oxide containing 50–58% zinc and 8–12% lead. The lead content can be reduced by calcination. Other sources of secondary raw materials include zinc dross, which is produced in galvanizing plants and has a relatively high zinc content (50–85%); zinc-containing sludges (10–65% zinc), spent catalysts (50–60%

zinc), and dusts from the brass industry (60–75% zinc).

The increasing problems in disposing of zinc-containing materials are resulting in the continual extension of the range of zinc-containing secondary raw materials.

10.4 Pretreatment of Raw Materials for the Production of Zinc Metal [1–4, 10, 18–23]

Pyrometallurgical and electrolytic zinc production require an oxidic raw material. Sulfidic concentrates must be prepared for metal extraction by roasting, which removes the sulfur as SO_2 and converts ZnS to ZnO , but does not remove gangue material.

Low-zinc oxidic ores that are not suitable for mechanical beneficiation (e.g., by flotation), slag flue dusts, and other secondary raw materials are subjected to a thermal concentration stage, which usually consists of either slag fuming or roasting in a Waelz kiln.

10.4.1 Roasting

Both electrolytic and pyrometallurgical zinc production require oxidic raw materials. Sulfidic raw materials must therefore be converted to the oxidic form (known as calcine) before leaching or reduction.

Whereas early accounts of zinc metallurgy listed a large number of roasting processes, fluidized-bed and sinter roasting have now almost completely replaced older processes such as multiple-hearth and flash roasting. An essential requirement of any roasting process is that it must be possible to recover and use the SO_2 from the waste gas.

The various zinc production processes require feed materials with fundamentally different physical properties. A fine-grained calcine is necessary for leaching with dilute sulfuric acid. Flotation concentrates meet this requirement if oxidized by roasting in a fluidized bed. On the other hand, thermal processes require a porous feed material in lump form, as provided by sinter roasting [18].

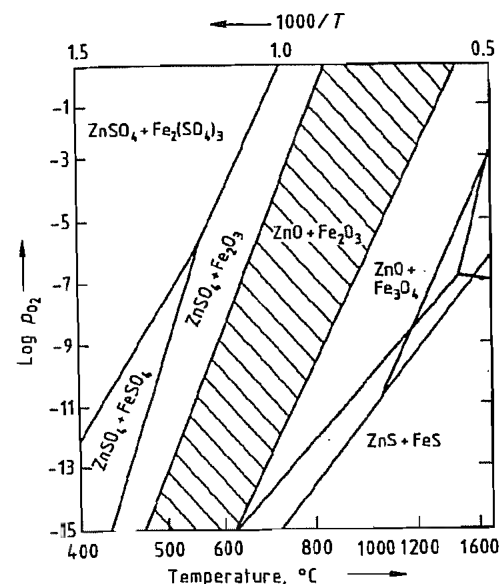


Figure 10.1: Phase diagram of the system Zn-Fe-S-O [23]. The conditions that exist in most fluidized-bed roasters are indicated by the hatched area.

Fluidized-Bed Roasting. Given a processed concentrate of suitable chemical constitution and particle size, the fluidized-bed reactor allows a calcine suitable for the leaching process to be produced. The parameters to be optimized are bed height, gas velocity, residence time, and temperature. In the fluidized-bed reactor, the reaction conditions are easily controlled and stabilized. The theoretical relationships, as shown in the phase diagram Zn-Fe-S-O (Figure 10.1), have been thoroughly investigated [19, 22, 23]. Fluidized-bed roasters generally operate at conditions in which ZnO and Fe_2O_3 are stable. Developments in electrolytic processing technology have enabled the presence of sulfates and ferrites in the calcine to be tolerated.

Fluidized-bed furnaces are often operated in two stages, in the first of which the roasted product contains 6–8% S. This overflows while hot into a second fluidized bed and is roasted with an excess of air to a residual sulfur content of 1.5% [3, p. 662].

Sinter Roasting. The first industrial application of sinter roasting was in the roasting of

lead ore in sintering pans. The crucial development in processing technology came from the sintering of iron ores, the results from which are transferable to the sinter roasting of sulfidic concentrates [21]. It is important that the temperature of the mixture should reach the sintering point. This is determined by the fuel content of the mixture (i.e., in single-stage sinter roasting, by the ratio of concentrate to roasted recycled material), the particle size distribution of the mixture, and the flow resistance (controllable by means of the particle size), which in turn determines the air pressure difference both in the induced-draft and pressure sintering processes. The moisture content of the mixture is an important factor here. It is important that all parameters affecting the process should be kept as constant as possible. Automatic control is not yet widely used.

In contrast to fluidized-bed roasting, where maximum reaction temperatures are in the range 900–950 °C and no volatilization occurs, maximum temperatures in the sintering zone reach 1450 °C, so that the cadmium and lead are volatilized to a considerable extent. For this reason, it is necessary to limit the maximum temperature in the sintering zone.

In principle, the temperatures in the reaction zone during sinter roasting are sufficient to ensure homogeneous sintering not only of concentrates but also of added flue dusts, dross, sludge, and other zinc-containing materials. An important advantage of sinter roasting is thus that it enables these materials to be prepared for shaft furnace treatment continuously and by the shortest route. The important characteristic parameters for sinter roasting, fluidized-bed roasting, and roasting in a multiple hearth furnace are compared in Table 10.2 [3, p. 662].

10.4.2 Pyrometallurgical Concentration Processes

The aim of pyrometallurgical concentration processes is usually the removal of zinc from flue dusts, slags, and low-grade, zinc-containing raw materials or raw materials of complex composition.

Table 10.2: Characteristic values for sinter and fluidized-bed roasting compared with multiple-hearth roasting [3, p. 662].

	Multiple-hearth roaster	Sintering belt	Fluidized-bed roaster
Roasting capacity, $\text{tSm}^{-2}\text{d}^{-1}$	0.08	0.7	7.5
Throughput, t/d	60	500	800
Grain size, mm	1.5	5	3
Dust content, %	13–15	2–3	50
SO_2 in exhaust gas, %	4–5	10	10
Steam output, t/t ore	0.4		1.0
Floor area, m^2td	7	10	3

The Waelz kiln process was originally used for the treatment of low-grade oxidic ores to obtain oxide suitable for smelting [24]. It is now mainly used as an enrichment process to treat secondary raw materials from zinc metallurgy, e.g., slags, flue dusts, and sludges.

In the Waelz kiln process, the zinc and lead from the raw materials appear in the oxide product, together with much of the sulfur, chlorine, and fluorine, both from the raw materials and from the carbonaceous reductant. The zinc metal is usually obtained from the oxide product by a thermal process. For this, the oxide can be compacted by sintering or forming it into briquettes. If oxide with a low lead content is required, it must be calcined, i.e., reheated to 1100–1350 °C without addition of reducing agents, to volatilize the Pb as PbO . The Waelz kiln process is carried out in a slightly inclined, slowly rotating, lined Waelz or rotary kiln through which air is passed at a controlled rate so that the mixture of raw material and coke breeze does not fuse together. The residues are discharged in a sintered but not molten state. Air from the furnace atmosphere diffuses to a limited extent into the reaction mixture which is carried up the walls of the rotating furnace, and a strongly reducing CO/CO_2 atmosphere is formed. This causes reduction not only of ZnO but also of zinc ferrites and silicates, and reoxidation to ZnO occurs after discharge. The following reactions take place in the rotating furnace:

Reaction in the solid charge: $\text{ZnO} + \text{C} \rightarrow \text{Zn}_{\text{g}} + \text{CO}$

Reaction in the gas space: $\text{Zn}_{\text{g}} + \text{CO} + \text{O}_2 \rightarrow \text{ZnO} + \text{CO}_2$

The heat liberated is due only to the overall reaction, i.e., the combustion of C to form CO_2 , as the reduction of ZnO to Zn is immediately reversed in the gas space above the charge. The zinc oxide leaving the furnace space is collected in bag filters. As the sulfur and halogens in the waste gases are bound to the zinc oxide, there are no environmental problems. The iron compounds in the charge are reduced to wuestite and to some extent to iron metal. In practical operation, the composition of the reaction mixture must be correctly formulated and an excess of coke breeze must be present to prevent the iron-containing components from fusing and forming incrustations in the furnace. The temperature regime of the process can be controlled by means of the filling height, residence time, and air flow rate in the upper part of the furnace. Overheating can cause incrustations to form and must be prevented [24–27].

Slag Fuming. In contrast to the Waelz kiln method, with which a range of raw materials can be treated, the slag fuming process is only used to remove zinc from molten slags from lead and copper smelting [28]. The zinc oxide so obtained can be used for zinc production. The molten slag is blown with reducing gases, so producing zinc vapor, which is burnt in the gas space above the molten slag by secondary air. The resulting high-grade oxide is cooled in a waste heat boiler in an EGR and collected [3, p. 65]. The composition of the reaction products from slag fuming in Port Pirie (Australia) is given in Table 10.3.

Table 10.3: Composition (in %) of reaction products from a slag fuming plant in Port Pirie, Australia.

	Zn	Pb	CaO	FeO	SiO_2	F	S
Slag before Zn removal	18.3	2.6	14.7	25.6	21.0	0.1	1.7
Slag after Zn removal	2.6	0.03					
Oxide	66.0	12.5				0.25	0.2

Oxide Calcination. The oxides obtained from Waelz kilns or slag fuming plants can be compacted in preparation for further processing by sintering or briquetting, without pretreatment. However, for electrolytic processing, for pig-

ment use, or for production of other zinc compounds, removal of harmful elements such as Pb, Cl, and F is required. This is carried out by calcination in rotary kilns at 1100–1150 °C. Not only are the harmful impurities removed, but the material is also densified [29, 30].

10.5 Production of Zinc Metal [1–5]

There are five industrial processes for the production of zinc: one electrolytic and four pyrometallurgical. Their relative importance during recent decades is illustrated in Figure 10.2 [3, p. 664]. Although the horizontal retort was the most important zinc production process at the turn of the century and still accounted for ca. 50% of total production capacity in 1950, the process is no longer of practical importance. The question of whether the energy-intensive electrolytic zinc production process can retain or even extend its lead depends on the development of the energy supply situation.

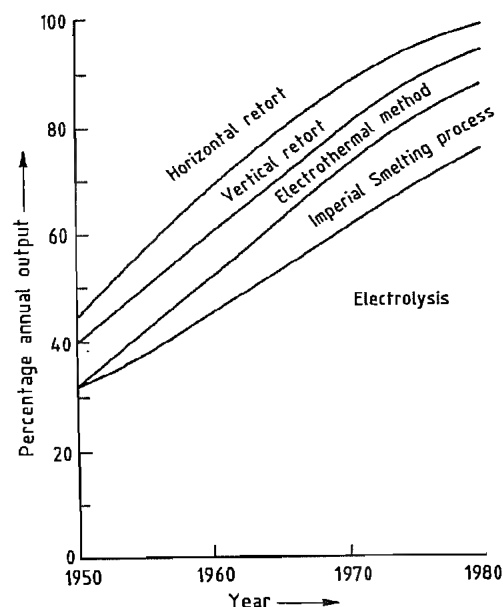
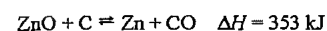


Figure 10.2: Annual outputs of the various zinc production processes expressed as a percentage of total annual output (idealized curves) [3, p. 664].

10.5.1 Pyrometallurgical Zinc Production by the Retort Process

Zinc oxide, produced by roasting, is reduced by carbon according to the equation



The reaction is so strongly endothermic that 5.4 MJ of heat is required to produce 1 kg of zinc. The reaction starts at ca. 1100 °C and is complete at 1300 °C, and the zinc (*bp* 920 °C) is therefore produced as a vapor. Zinc production by the retort process hence involves not only reduction of the oxide but also condensation of the zinc from the vapor to the liquid state. Care must be taken to prevent reoxidation, and the zinc vapor must not come into contact with the combustion gases. The reduction must therefore be carried out either in vessels with exterior heating (retorts) or by the electrothermal method. Horizontal, batch-operated retorts with circular or elliptical cross section can be used, or furnaces containing vertical, continuously operated retorts with a rectangular cross section. The quality of the furnace vessels is of great importance for the process, especially their stability at high temperature, resistance to large temperature fluctuations, good thermal conductivity, impermeability to reaction gases, and resistance towards chemical attack by the charge materials.

Reduction in Horizontal Retorts. Zinc has been produced in horizontal retorts since ca. 1800 in Belgium and Upper Silesia from smithsonite and later from roasted zinc blende. Retorts vary in their shape and arrangement in the furnace and in the fitting of receivers, in which the zinc vapor produced in the retort condenses as a liquid. Detachable devices made of sheet metal (so-called allongen) are fitted to the condensers to collect zinc escaping in the form of dust.

The retort furnaces are equipped with regenerators or recuperators which utilize the hot waste gases to preheat the combustion air and sometimes the fuel gas. The retorts used to be charged by hand, an extremely labor-intensive operation: one worker smelted ca. 0.5 t

ore per shift. Moreover, the yield was poor, only 60% of the zinc being obtained as molten castable metal, 10% remaining unreacted in the ash produced, and the rest reporting to the dross and dust in equal amounts. Although efforts were made to mechanize the process, especially the charging and discharging of the retorts, the main problem, i.e., the poor efficiency (ca. 20%), could not be solved. The horizontal retort is no longer an industrially important zinc production process.

Reduction in Vertical Retorts. The poor efficiency, batch operation, and above all labor intensity of zinc production in horizontal retorts provided the incentive to develop an improved process. The fact that the horizontal retort was inconsistent with the natural downward movement of the charge and upward movement of the zinc vapor suggested that a vertical arrangement would be better. Zinc reduction furnaces were therefore constructed with vertical retorts, but only after overcoming major difficulties. The system is known as the New Jersey process. The furnace, illustrated in Figure 10.3, consists of a retort 13.5 m high, 1.83 m long, and 0.3 m wide, constructed of silicon carbide. The retort is externally heated over a vertical length of 8 m (starting at 1.5 m from the lower end) to a temperature of 1250–1300 °C. Producer gas is fed from above into the heating chambers, and the exhaust gas phases out of the furnace at the bottom. The reaction air is fed through the sides of the furnace along its whole length. Above the heated part of the furnace is an unheated part 4 m in length which acts as a reflux condenser for the lead formed and is known as the lead collector. In the original design, the gas mixture passing out of the retort at 850 °C was cooled to 500 °C by a plate cooler, which also condensed and collected the zinc. This was tapped off from time to time. The zinc dust formed was collected by means of a water spray. The process was much improved by replacing the plate cooler by a spray condenser. A graphite disc, partially immersed in the pool of molten metal and spinning at ca. 400 rpm, atomizes the metal so that the waste gases from the re-

tort passes through a metal fog. The metal is collected at 500 °C in an exterior cooler. This prevents formation of dross, and the amount of zinc dust formed is reduced to 3% of the zinc product.

The charge material, containing 60–70% calcine and 30–40% coal, is formed into briquettes, which are then coked in a coke oven. The coked briquettes are charged into the top of the retort. After extraction of the zinc from the briquettes, they are discharged from the bottom of the retort through a water lute. The zinc-containing gases discharged from the top of the retort are cooled to ca. 500 °C in a condenser, in which the molten zinc collects at the bottom. The tail gases produced, which contain ca. 85% carbon monoxide, are scrubbed and recycled to the producer gas stream. Furnaces with vertical retorts are much more thermally efficient than those with horizontal retorts, and they have the further advantages of providing higher capacity, higher zinc purity, and longer working life of the retorts, and, above all, do not involve heavy manual labor or batch operation.

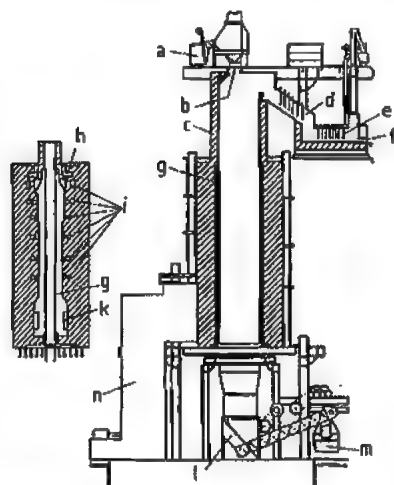


Figure 10.3: Schematic diagram of vertical retort [3, p. 666]: New Jersey retort with plate condenser for zinc recovery. The left- and right-hand sections are rotated 90° with respect to each other. a) Charging bucket; b) Cone; c) Lead collector; d) Inclined channel; e) Condenser; f) Tap hole; g) Retort; h) Fuel gas inlet; i) Air inlets; k) Exhaust gas exit openings; l) Ash removal equipment; m) Ash bucket; n) Recuperator.

10.5.2 Zinc Production in the Shaft Furnace [31]

Prolonged and extensive development work in the 1950s, aimed at utilizing the improved thermal efficiency and higher reaction temperatures of the coke shaft furnace, led to the lead-zinc shaft furnace of the Imperial Smelting Corp. Thus, a process became available that could be used with raw materials of complex composition, such as mixed ores and secondary raw materials containing impurities that would cause severe problems in electrolytic zinc production.

In the shaft furnace, the heat for the reduction is provided by the oxidation of C to CO₂ and CO. Under the reaction conditions normally used in a shaft furnace, the zinc vapor formed would be reoxidized to ZnO by the CO₂ in the furnace gas. Intensive research on the equilibria enabled conditions to be found under which this reoxidation does not occur.

In normal shaft furnace operation, the best possible heat utilization is achieved by using countercurrent flow to heat the charge material. The furnaces are relatively tall, and furnace gas exit temperatures of ca. 200 °C are aimed for. In accordance with the Boudouard equilibrium, this results in higher CO₂ contents in the furnace gas. The zinc shaft furnace requires gas temperatures of 1000 °C. In order not to lower the furnace gas exit temperature by the addition of the cold charge material, the coke is heated to > 800 °C and the calcine is added as hot sinter.

The shaft furnace obtains its heat of reaction from the combustion of coke in the reaction zone. This leads to large amounts of nitrogen in the furnace gas, lowering the partial pressure of the zinc. Therefore, the heat required is generated to a large extent outside the furnace. Thus, the combustion air is preheated to 700–950 °C, enabling the amount of furnace gas to be much reduced. The CO-rich furnace gas is cooled as it passes from the furnace to the condenser. To prevent reoxidation of zinc to ZnO, a small amount of atmospheric oxygen can be added to avoid a temperature

drop. This process step must be carefully controlled.

The zinc collects in a spray condenser. In contrast to the vertical retort process, lead is used as the condensing liquid instead of zinc. Dissolving zinc in lead greatly reduces its activity. As the solubility of zinc in lead is strongly temperature dependent, the zinc can be precipitated by cooling. In practice, a temperature of ca. 550 °C is maintained in the spray condenser. The metal flowing out of the condenser is cooled to 440 °C, causing the zinc to separate from the lead and float on the surface. It then flows over a weir and is collected. As the process does not take place under equilibrium conditions, the recovery of 1 t zinc does not require the theoretically calculated amount of lead (60 t), but ca. 400 t. The zinc is either cast as commercial grade ingots (98.5% Zn) or refined to higher grades.

The first full-scale industrial furnace went into operation in Swansea in 1960. The cross-sectional area of the shaft was 17.2 m², and this remains the standard size even today.

On licensing its ISO process, Imperial Smelting required that licensees should com-

pare their experiences of the process, and this has led to standardization of the major zinc-producing plants and to improvements in the plant performance. For example, the annual output of a furnace with a cross section of 17.2 m² has been increased from 35 000 t zinc and 17 000 t lead in 1963 to 80 000 t zinc and 40 000 t lead in 1990. At the same time the zinc yield was increased from 91.7 to 95.5%, and the lead yield from 94 to 95%. The Pb:Zn ratio in the charge material was increased from 0.49 to 0.6, further enhancing the main advantage of the process, i.e., its ability to treat ores of complex composition. In addition to Zn and Pb, many ores also contain Cu. Most of this is reduced to the metal and dissolved by the lead. Copper contents below 4% give few problems, as the copper separates as dross on cooling the lead and can be removed in the form of a solid crust. Higher concentrations can give problems due to the limited solubility of copper in lead. Special techniques are then required. A schematic diagram of a lead-zinc shaft furnace is given in Figure 10.4.

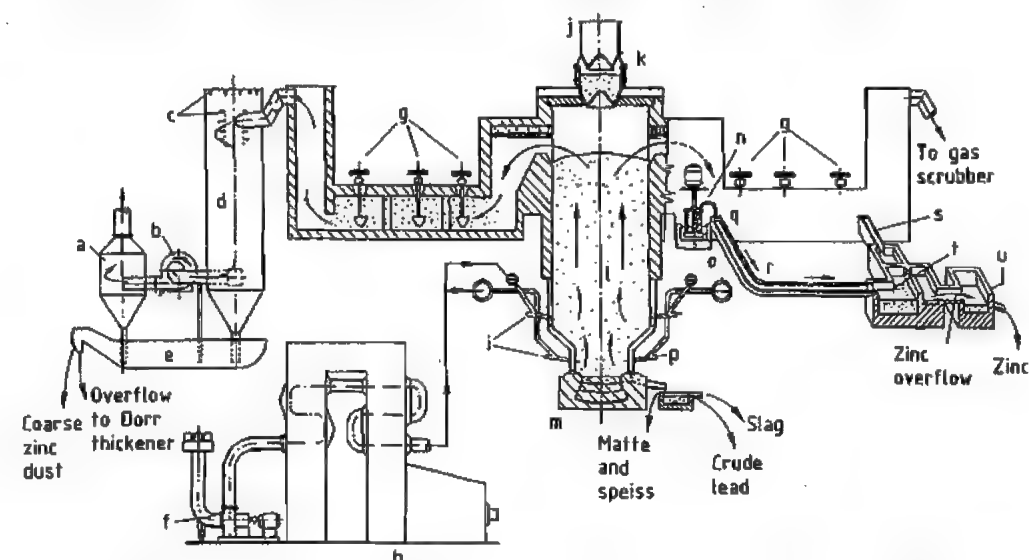


Figure 10.4: Zinc-lead shaft furnace: a) Moisture trap; b) Mechanical washer; c) Water jets; d) Gas scrubbing tower; e) Water seal for zinc dust removal; f) Blower; g) Stirrers; h) Air preheater; i) Jets; j) Feeding vessel for hot coke and calcine; k) Cone; l) Furnace; m) Hearth; n) Lead pump; o) Pump sump; p) Water jacket; q) Condenser; r) Water-cooled trough; s) Lead recycle trough; t) Separating wall; u) Zinc bath.

10.5.3 Refining of Crude Zinc

Zinc produced hydrometallurgically (see Section 10.5.4) does not need to be refined. However, crude zinc produced by pyrometallurgy contains 0.7–3% Pb, up to 0.2% Fe, up to 0.3% Cd, and sometimes small amounts of As, depending on the production method and the composition of the ore. The zinc used to produce pressure casting alloys should have a purity of 99.99–99.995%, and galvanizing processes require a purity of 98.5–99.95%, depending on the process used. Commercial grades of zinc cannot be produced simply by remelting and liquation or by treatment with fluxes. Simply cooling zinc melts until they approach the eutectics in the systems Zn–Pb or Zn–Fe does not produce the theoretical compositions 0.8% Pb and 0.02% Fe, respectively. The concentrations obtained in practice are 1.2% Pb and 0.03% Fe.

Hence, these processes are only suitable for producing zinc for the next stage of purification by distillation or for producing zinc dust. The refining of commercial zinc produced by a pyrometallurgical process (today usually the Imperial Smelting Shaft Furnace process) is carried out by distillation in high-temperature distillation columns constructed of ceramic-bonded SiC elements. The process was developed by the New Jersey Zinc Co., Palmerton (United States), and the first plant went into operation in 1932.

The distillation process makes use of the comparatively low boiling point of zinc (906 °C). However, as not only impurities with a high boiling point such as lead, copper, tin, and iron must be removed, but also cadmium, which boils at 762 °C, the refining process must be carried out in two stages. A plant based on the New Jersey process is illustrated in Figure 10.5. Molten crude zinc is fed into the top third of a distillation column, the lower part being heated to ca. 1100 °C. The upper part acts as a reflux cooler for the less volatile constituents, so that only Zn and Cd pass into the condenser. Because of the relatively small difference in boiling point between zinc and cadmium and the low cadmium content, a fur-

ther very careful fractional distillation must be carried out. The column for this is heated to ca. 950 °C, and the Cd which distills off is collected as a dust with a high zinc content. Depending on the composition of the initial materials and the quality of the process control, the zinc produced can have a purity of 99.996% and the concentration of the desired elements Pb, Cd, and Fe can be < 0.001%.

The “washing” zinc produced in the lead column contains Pb, Fe, Cu, and sometimes also In and Tl. The washing zinc is liquated, giving hard zinc and very impure lead. The hard zinc is recycled to the process, but the lead can be treated separately. In practice, this very impure lead is often added to crude lead from a smelter before it is refined.

The working life of the distillation columns is 2–3 years, and the energy consumption for 1 t of purified zinc is 6.5–7.3 GJ.

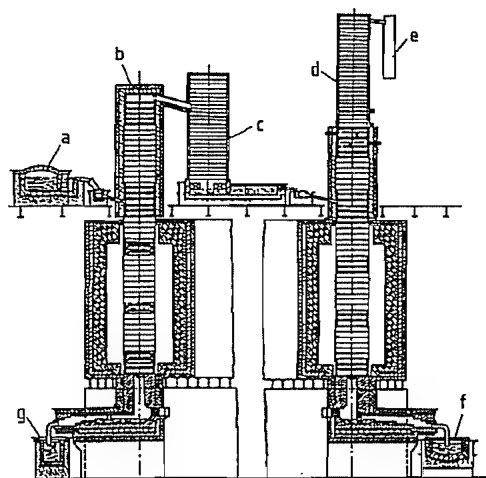


Figure 10.5: Zinc refining plant using the New Jersey process [3, vol. 1a, p. 116, Figure 34]: a) Melting furnace; b) Lead column; c) Condenser; d) Cadmium column; e) Cadmium canister; f) High-purity zinc furnace; g) Washed zinc furnace.

10.5.4 Hydrometallurgical Zinc Production [1–5, 10, 13]

Zinc can be deposited electrolytically both from aqueous solutions and molten salts. However, only aqueous electrolytes (i.e., solutions of zinc sulfate in dilute sulfuric acid)

have so far been used in industry. Other proposed processes such as the electrolytic production of zinc dust, amalgam electrolysis, and sulfate–chloride electrolysis have not attained industrial importance. Although a full-scale version of the electrolytic refining process, in which the impure zinc forms the anode, has been developed, it is not used, the reasons being mainly economic. The electrolytic production (electrowinning) of zinc from solutions of zinc sulfate in sulfuric acid has undergone unparalleled growth in recent decades. Approximately 80% of total world production comes from this process today, although a number of problems still need to be solved, principally in the preparation of pure electrolyte solutions.

Like the thermal processes of zinc production, the industrial electrolysis of zinc uses oxidic starting materials. The most important natural raw material, zinc blende, therefore still needs to be roasted to be converted to oxide. To ensure rapid dissolution of the calcine, the roasting processes used should therefore conserve the fine grained structure of the concentrate obtained by flotation. Commercial zinc oxide can usually be used directly and need only be treated if it contains impurities that have a harmful effect on the electrolytic process. Roasted oxide must be ground to improve its solubility. Using typical starting materials, the electrolytic process of zinc production consists of the following stages (Figure 10.6):

- Roasting
- Leaching
- Liquor purification
- Electrolysis
- Melting and casting.

The main problem in leaching and liquor purification is zinc–iron separation. In earlier processes, leaching was carried out such that a large excess of acid was avoided. Thus, the calcine and acid (exhausted electrolyte) were added simultaneously to the leaching tanks, the amount of acid being exactly that required to dissolve the zinc oxide. High yields of zinc could only be obtained with concentrates con-

taining ≤ 3% Fe. Iron in higher concentrations was dissolved to some extent. The solid residues contained ca. 20% Zn and 30% Fe. However, as a result of the roasting process, part of the zinc in the calcine is in the form of zinc ferrite (ZnFe_2O_4), which can only be dissolved at higher acid concentrations (50–150 g $\text{H}_2\text{SO}_4/\text{L}$). Maximum yields of zinc and also of other valuable impurities such as copper and cadmium require the use of higher acid concentrations in the leaching process. Hence, almost complete dissolution of the iron content of the zinc blende cannot be avoided. As the iron interferes with the electrolytic process even at low concentrations, it must be precipitated from the zinc sulfate solution obtained.

Precipitation of Iron Hydroxide. Precipitation of iron as its hydroxide has now been largely superseded owing to the poor zinc yield obtained (85–88%). The process is usually carried out in two stages.

The readily dissolved zinc oxide fraction is brought into solution by “neutral leaching” in a mixture of cell acid (150–200 g $\text{H}_2\text{SO}_4/\text{L}$) and the acidic solution (ca. 50 g $\text{H}_2\text{SO}_4/\text{L}$) produced during iron precipitation. At this stage of the process, it should be ensured that impurities such as iron, arsenic, antimony, and germanium are retained in the solid residues. A solid–liquid separation is carried out, giving an impure neutral liquor which is fed to the purification stage and a zinc-rich residue which is fed to the second, acid leaching stage, for which hot (ca. 95 °C) cell acid is used. A further solid–liquid separation produces a solid residue containing up to 5% zinc and any lead and silver present (which can be processed in a lead smelter) and a zinc solution containing ca. 80 g/L zinc together with the iron and other impurities, such as arsenic, antimony, germanium, nickel, and cobalt.

After oxidation of Fe(II) to Fe(III) in the solution obtained by “neutral leaching”, the iron is precipitated as its hydroxide by adding further calcine. The precipitation starts at pH 2.6 and continues up to pH 5.0. This gives solutions with residual iron contents of 10–20 mg/L. Because precipitation of iron causes ar-

senic, germanium, and zinc to be adsorptively coprecipitated, and the calcine used for neutralization cannot be subjected to hot acid leaching, this process gives unsatisfactory zinc yields. Higher zinc yields are only possible if the leaching residues can be more readily filtered. Three methods of achieving this are available, i.e., precipitation of the iron as jarosite, goethite, or hematite.

Sulfidic zinc concentrate

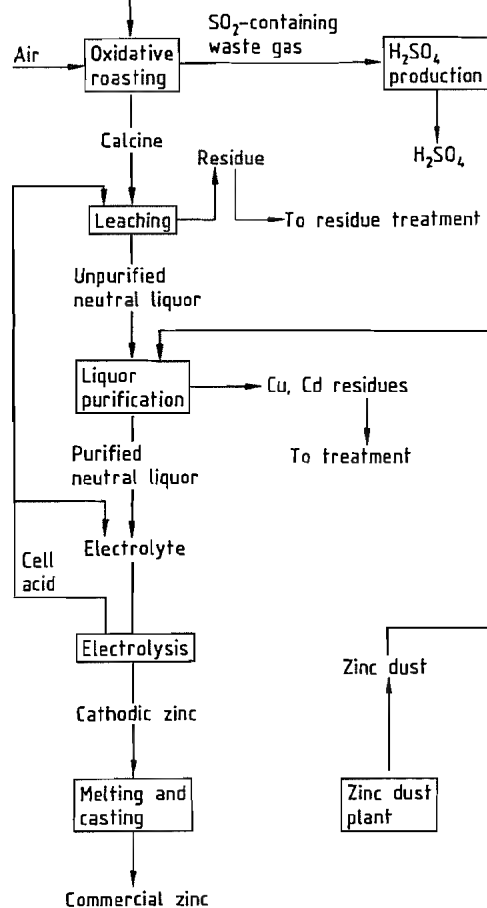


Figure 10.6: Flow diagram of the electrolytic zinc production process [2, p. 602].

Iron Removal by the Jarosite Process. In the jarosite process, an Fe(III) compound of the type $X[Fe_3(SO_4)_2(OH)_6]$, where X represents H_3O , Na, K, or NH_4 , is precipitated by adding alkali metal or ammonium ions. These com-

pounds correspond to the mineral jarosite. The process was independently developed between 1960 and 1965 in various zinc smelting plants around the world. It makes use of the fact that jarosite precipitates have the following advantages over iron hydroxide:

- They are almost insoluble in sulfuric acid
- They have a high iron content, so that the amount of precipitate formed is low
- They have good filtering properties

However, jarosite precipitates do not adsorb the harmful impurities as effectively, so that the purification effect of the process is inferior.

The additional cations needed for the precipitation are added to the liquor in the form of sulfates. In practice, ammonium sulfate, which forms an ammonium jarosite, is usually used.

A flow diagram of the process is given in Figure 10.7.

Precipitation of jarosite begins at pH < 1 and is complete at pH 1.5. Jarosite formation and precipitation being a temperature-dependent process, two alternative industrial processes exist, the first operating at temperatures up to 180 °C and with relatively high acid concentrations (60–90 g H_2SO_4/L) giving a high reaction rate, and the second at ca. 95 °C and considerably lower acid concentrations (5–10 g/L). The lower temperature method is more widely used, mainly because of the lower equipment costs.

Jarosite theoretically contains 37% iron and 13% sulfur as sulfate. In practice, these values are not reached, as the calcine added for pH control is not completely dissolved and hence adds impurities to the solid residue. For this reason, additional leaching processes are carried out, giving zinc contents of 4–6% in the residue. Zinc yields of 96–98% can be achieved by the jarosite process. As the jarosite contains sulfate, it helps regulate the sulfate balance of the plant.

Worldwide, the jarosite process has superseded the precipitation of iron hydroxide. However, problems are caused by the fact that the jarosite contains small amounts of soluble

zinc and so must be deposited in special waste disposal sites. New processes aimed at further increasing the zinc yield have therefore been developed.

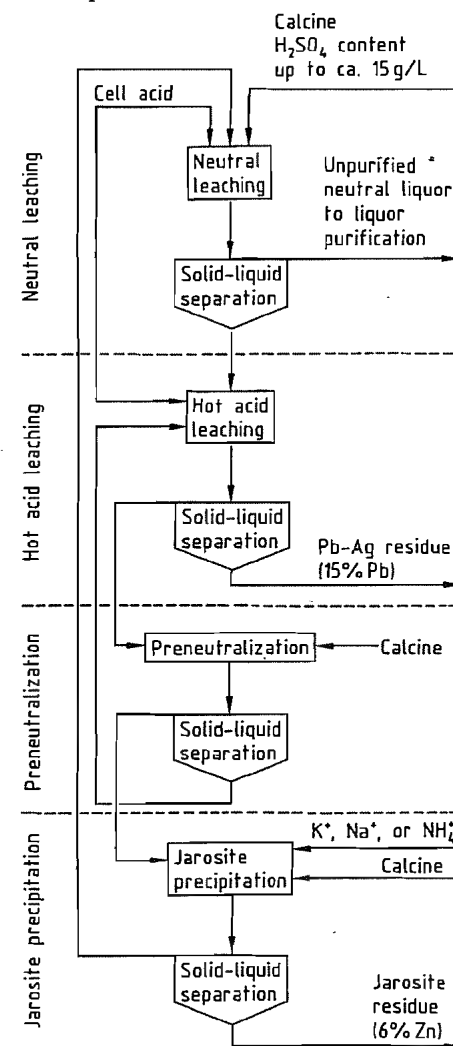


Figure 10.7: Flow diagram of the jarosite process with preneutralization [3, p. 678].

Iron Removal by the Goethite Process. As the flow diagram (Figure 10.8) shows, the first stages of the goethite process are the same as in the jarosite process. The solution from the first hot leach is then treated with zinc concentrate. The zinc dissolves, reducing the iron to the divalent state, and elemental sulfur is pre-

cipitated, so that compounds other than goethite (e.g., jarosite) are not precipitated in the final precipitation process. The excess zinc concentrate and the elemental sulfur are recycled to the roasting process. Oxygen is added in a controlled manner, precipitating goethite, $FeO(OH)$, at pH 2–3.5 and 70–90 °C.

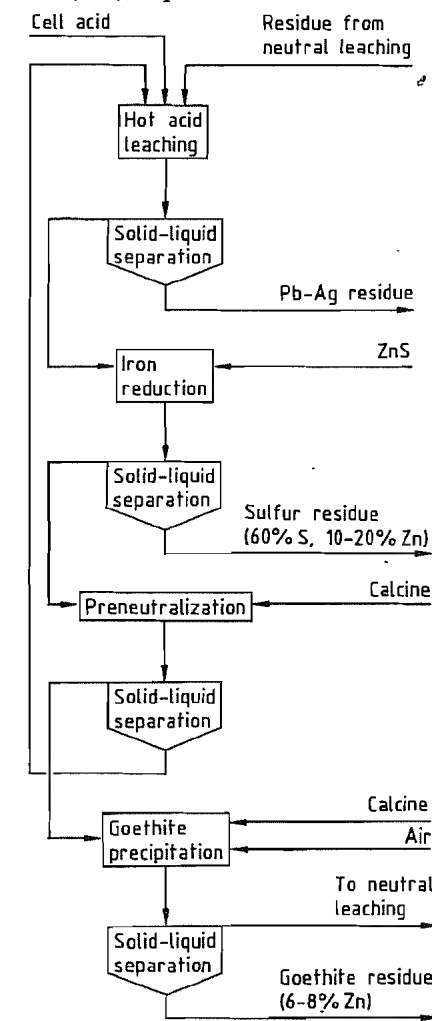


Figure 10.8: Flow diagram of the goethite process [3, p. 679].

The advantage of the goethite process is that the amount of residue that must be disposed of is considerably less than in the jarosite process. Whereas the zinc yield is comparable to the jarosite process, the yield of

copper is lower (80% instead of 90%) and that of silver is higher (96% instead of 90%). As the goethite produced, which contains 40–45% iron, always contains small amounts of basic sulfates, it cannot be used in blast furnaces.

Iron Removal by the Hematite Process. The hematite process (Figure 10.9) was developed to enable iron-containing residues from zinc production to be disposed of at moderate cost and without ecological problems. It differs from the other processes in that the residues are subjected to reductive leaching in which the reducing agent is an excess of zinc concentrate. The iron is reduced with formation of elemental sulfur. The insoluble solids and the liquor are heated in autoclaves, causing the sulfur to melt and wet the excess of zinc blende, forming small pellets. These are cooled, classified, and fed to the roasting plant. A lead–silver residue, which separates from the solution, is sent to a lead smelting plant. The liquor is preneutralized with calcine, and the resulting precipitate is recycled to the hot reductive leaching stage. The copper is precipitated from the zinc–iron solution by addition of zinc (cementation), and the solution is then neutralized with calcium carbonate. This is followed by the most important stage of the process, pressure treatment in an autoclave at 200 °C at an oxygen pressure of 10–15 bar. Under these conditions, iron is precipitated as Fe_2O_3 (hematite), which can be used in iron metallurgy. The zinc solution is recycled to the neutral leaching stage. The gypsum produced is dewatered and can then be used in the building materials industry. The yields of zinc and other valuable metals are comparable to those in the jarosite and goethite processes. As the iron can be produced in the form of a useful product, no landfill space is required. However, the costly and complex technology is restricting more widespread use of the process.

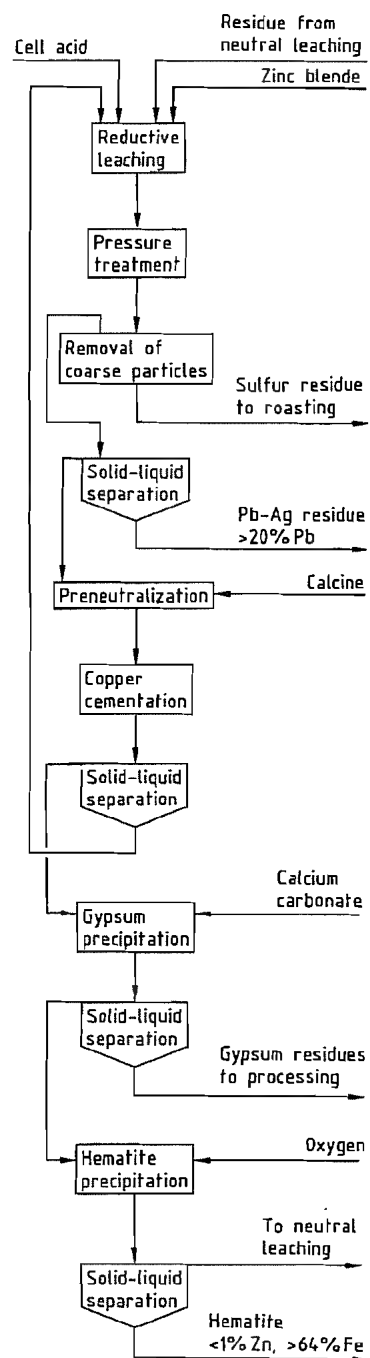


Figure 10.9: Flow diagram of the hematite process [3, p. 680].

10.5.5 Treatment of Leaching Residues

Residues from calcine leaching are primarily subjected to pyrometallurgical treatment. In some plants of older design, the residues from the neutral leaching stage are treated in a Waelz kiln. This removes the lead, and the resulting sinter oxide is ground and recycled to the leaching process. In a development of the classical Waelz kiln process, vaporization is carried out in a Waelz kiln fitted with an external burner. A rotary flame-fired furnace of the Dorschel type can also be used in a batch process.

A combination of flotation with pyrometallurgical and hydrometallurgical processes (sulfating roasting followed by leaching) enables the valuable metals to be recovered from the leaching residues.

10.5.6 Solution Purification

Impurities still present in the unpurified neutral liquors from the iron precipitation stage can lead to

- Lower current efficiency
- The presence of impurities in the cathodically deposited zinc
- Adverse effects on the anode and the cathode

If the critical impurity concentrations are exceeded and several impurities are present simultaneously, the electrolytic process may no longer be possible. The concentration limits of the harmful impurities cannot be precisely specified, but the following guidelines (in mg/L) can be used:

As	0.01–1
Sb	0.05–0.1
Ge	0.002–0.05
Ni	0.05–3.0
Co	0.1–1.0
Fe	20–30

In the formerly used iron hydroxide precipitation process, the adsorptive effect of the hydroxide precipitate caused most of the arsenic, antimony, and germanium to be removed along with the iron, so reducing their concentrations below the acceptable limits.

However, when the residues from the neutral leaching are subjected to hot acid leaching (mainly in the interest of higher zinc yields), the neutral liquors contain much higher levels of impurities. As these are not removed either in the iron precipitation or the leaching stage, careful purification of the liquor is necessary. In principle, there are the following possibilities:

- Chemical precipitation
- Electrochemical deposition
- Ion exchange (solvent extraction)
- Cementation with zinc

For high quality requirements, a combination of methods can be used. Chemical precipitation is mainly used for nickel and cobalt. For example, nickel can be precipitated by dimethylglyoxime and cobalt by α -nitroso- β -naphthol. However, as these reagents are expensive, their use can only be considered in exceptional cases for liquors with very low levels of impurities.

Processes involving the use of fluidized-bed electrolysis to remove impurities more noble than zinc and the use of solid and liquid ion exchangers are still at the development stage.

In most zinc electrolysis plants, the liquor is purified by cementation of harmful elements on zinc dust in a continuous, multistage process. An inert coating can form on the zinc particles or they may be chemically dissolved. Therefore, not all the zinc dust added can take part in the cementation process and a large excess of zinc dust (5–10 fold) is necessary to ensure effective purification.

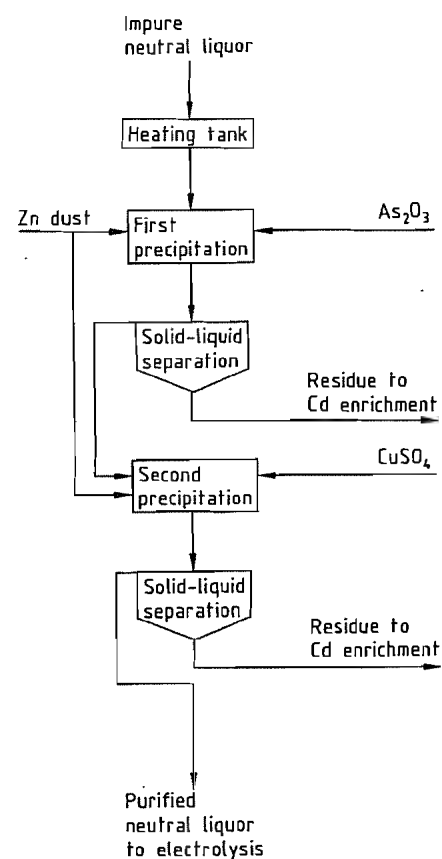


Figure 10.10: Hot-cold liquor purification [2, p. 607].

A typical process used in many plants is the hot-cold liquor purification process (Figure 10.10), which has two successive precipitation stages.

In the first stage, copper, nickel, and cobalt are precipitated by adding zinc dust in the presence of an added activator, usually As₂O₃. In the second stage, copper sulfate is the activator, and cadmium is removed. In many cases, a third fine purification stage is included.

The conventional hot-cold liquor purification process has a number of disadvantages:

- The necessity of adding copper if too little copper is present in the starting materials
- The possibility of releasing highly toxic arsenic

- The presence of the impurities arsenic and antimony in the precipitated copper
- The possibility that the precipitated metals may redissolve

These disadvantages have led to the development of the alternative reversed liquor purification process (Figure 10.11). Here, it is not necessary to add copper to remove cobalt and other impurities. The low concentrations of arsenic are sufficient to act as activator, the costly copper additions are avoided, and relatively pure cementates are obtained in both precipitation stages. This process can also be operated continuously, whereby the addition of zinc dust is controlled by measuring the electrode potential, which is a function of the copper and cadmium concentrations in the liquor.

10.5.7 Electrolytic Production of Zinc [1–5, 10, 13]

Principles of Zinc Electrolysis. As the standard electrode potential of Zn²⁺ is -0.763 v, a solution of zinc sulfate should not deposit zinc on electrolysis: hydrogen should be liberated instead. Zinc deposition is only possible because of the hydrogen overvoltage at the zinc electrode, which causes a voltage shift of magnitude approximately equivalent to the standard electrode potential of zinc. The overvoltage is influenced by a number of factors. For example, the effect of current density is expressed by the Tafel equation:

$$\eta = a + b \log i$$

It decreases with increasing temperature, but, as the conductivity decreases with decreasing temperature, the energy consumption increases. With these effects in mind, two typical methods of performing zinc electrolysis were used in industry for a long time. Either the electrolytes were slightly acidic and current densities were ca. 325 A/m² or they were strongly acidic and current densities were ca. 850 A/m². The process parameters widely used today give good current yields in zinc electrolysis using current densities in the

range 400–600 A/m² and a process temperature not exceeding 40 °C.

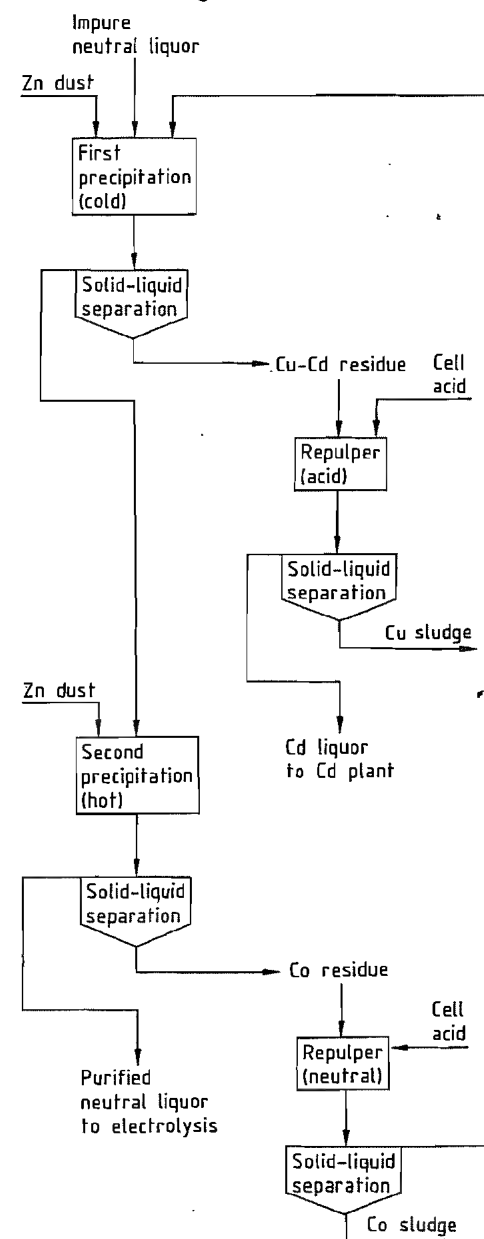


Figure 10.11: Reversed liquor purification [2, p. 608].

However, the hydrogen overvoltage is also influenced by the condition of the surface of the electrodes. Smooth surfaces lead to high

overvoltages. For this reason, the cathode plate must be stripped every other day in practical operation. Zinc electrolysis is extremely sensitive to impurities in the electrolyte. These fall into several groups:

- Impurities that are more electronegative than zinc, e.g., potassium, sodium, calcium, magnesium, aluminum, and manganese. These impurities do not directly interfere with the electrolytic process. If concentrations are too high, the viscosity of the electrolyte increases and the diffusion processes in the boundary layers are disturbed. A limit of 60 g/L is used as a guideline figure.
- Impurities whose electrode potential lies between those of Zn²⁺ and H⁺. In the case of lead, cadmium, thallium, and tin, the hydrogen overvoltage is higher than that of zinc. These metals are deposited and form impurities in the zinc. In the case of iron, cobalt, and nickel, the overvoltage is lower than of zinc. These are also deposited electrolytically but can be redissolved by the cell acid. Redox effects can lead to reduction in current yield. For this reason, the maximum tolerable concentrations are very low.
- Impurities that are more electropositive than zinc. These include copper, arsenic, antimony, indium, tellurium, and germanium. These lead to a reduction in the overvoltage. The deposition of copper, nickel, cobalt, arsenic, and antimony can have a strongly detrimental effect on current yield due to the formation of local elements on the cathode, leading to dissolution of the zinc. For this reason, the maximum tolerable concentrations of these impurities are also very low, and the zinc electrolytes must therefore be rigorously purified.

The Practice of Zinc Electrolysis. Zinc electrolysis is a complex system in which positive and negative factors, especially as they affect current yield, energy consumption, required purity of the liquor, and mechanization, must be balanced against each other.

The purification of the liquor is now so well controlled that lower current densities can be used, enabling the electrolysis time between

cathode changes to be extended from one to three days. Also, the cathode stripping operation, which involved heavy manual work, has been improved by the development of mechanical stripping equipment, and this has enabled cathodes with increased surface areas to be used.

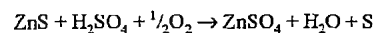
In general, the electrolytic cells are concrete baths cast in one piece and lined with polyethylene. Lead linings are no longer used in modern electrolysis plants. The cells are arranged in rows and connected in series. The electrolyte supply to each cell is usually individually controlled.

The cathode plates consist of sheet aluminum (99.5%), 5–7 mm thick, supported on carrier rods and provided with welded or plated copper contacts. The cathodes are polished at intervals of 4–6 weeks to prevent excessive adhesion of the cathode deposits. The latter problem can also be controlled by suspending the cathode plates in the bath and briefly running them as anodes.

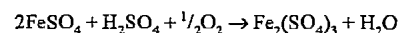
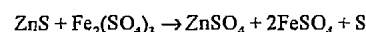
Anode materials are usually Pb–Ag alloys with a silver content of 0.25–0.75%. The anodes are usually made by casting the metal around a central copper carrier rod. Anodes that contain Sr and/or Ca and Ti in addition to Ag have higher strength and improved corrosion resistance.

10.5.8 New Developments in Zinc Production [2, 32]

Pressure Leaching of Sulfidic Zinc Concentrates. There have been many attempts to avoid the roasting process in the treatment of sulfidic zinc concentrates. For example, a process of pressure leaching of sulfidic concentrates has been developed by Sherritt Gordon Mines, Fort Saskatchewan, Alberta, Canada, and is used on an industrial scale. The process can be represented by the equation:



which consists of the partial reactions:



Dissolved iron originates either from marmatitic blende (Zn, Fe)S or pyrrhotite Fe_7S_8 , but not from pyrite, FeS_2 , which does not dissolve under these liquor conditions. This iron promotes the oxygen transfer reaction that converts the sulfide to sulfate.

The process is carried out in two stages, as shown schematically in Figure 10.12. The zinc concentrate is size reduced by wet grinding to $90\% < 44 \mu\text{m}$ and oxidatively leached in two stages at 150°C at an oxygen pressure of 1 bar. Exhausted electrolyte (cell acid) is used as solvent. In the first stage, 80% of the zinc present is dissolved, and in the second stage a further 18%.

The overflow from the thickener in the first stage, at a pH of 1.5–2.5, is treated with zinc oxide to neutralize the residual iron that was not precipitated in the autoclave, and the liquor so obtained is filtered and purified in the usual way. It is then fed to the zinc electrolysis stage.

The residue from the first stage is pumped together with cell acid into the autoclave of the second stage. After solid–liquid separation, the solution from the second stage is recycled to the first autoclave. The residue is washed in countercurrent flow to remove elemental sulfur if necessary, and the residual iron oxide is treated to recover lead and noble metals or disposed of, depending on its composition.

The process is used in two Canadian zinc smelting plants, one in Trail (Cominco), and the other in Timmins (Texas Gulf) in Ontario.

Direct Leaching of Oxidic Zinc Ores [2]. Some new methods of directly leaching oxidic ores (smithsonite, willemite, etc.) have been developed recently.

A willemite containing 40% zinc has been directly leached at the zinc smelting plant at Três Marias of the Companhia Mineira de Metais in Brazil. Smithsonite with a lower zinc content ($< 30\%$) is first enriched by treatment in a Waelz kiln, and the oxide obtained is then leached.

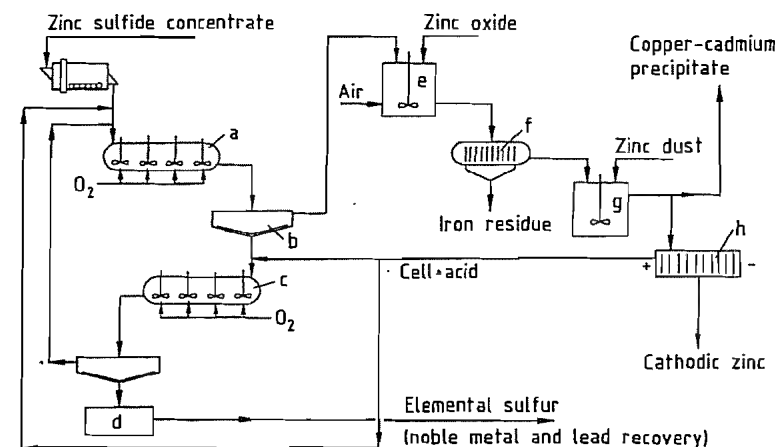


Figure 10.12: Pressure leaching of zinc concentrate [2, p. 610]: a) Pressure leaching, stage 1; b) Thickener; c) Pressure leaching, stage 2; d) Washing; e) Iron precipitation; f) Filtration; g) Cleaning tank; h) Electrolysis.

10.6 Uses and Economic Aspects

Two properties of zinc are of special relevance to its applications. Firstly, its standard electrode potential is considerably more positive than that of the construction material iron. Zinc coatings therefore provide very good corrosion protection for steel structures. Secondly, zinc has a relatively low melting point, which makes it suitable for use in pressure die casting of complex components.

10.6.1 Galvanizing [3, 33]

The ever-increasing need to make the best use of the world's raw material reserves means that corrosion prevention as a method of preserving the usefulness of commercial metals continues to increase in importance. Moreover, as the atmosphere becomes increasingly corrosive, standards of corrosion protection must continue to rise, especially in steel construction.

A zinc coating on steel ensures lasting protection against the corrosive effects of the weather by the following mechanisms:

- The effect on zinc of the carbon dioxide and moisture in the air is to form protective coat-

ings with a zinc carbonate basis, resulting in a low corrosion rate.

- Because of its electrochemical property of providing cathodic protection, zinc actively prevents the occurrence of corrosion in the region of small defects, damaged areas of coating, and cut edges of sheet.

In the industrialized countries, almost 50% of the zinc consumed is used for corrosion protection.

Commercial zinc (98.5–99.5%) is usually used for hot-dip galvanizing in production and jobbing plants, and high-purity zinc (99.95%) for the continuous galvanizing of steel strip or wire. The metallurgical processes used to produce the less pure grades of zinc mean that lead is the main impurity present. This is an advantage, as the presence of 1% lead reduces the surface tension of zinc by ca. 40% compared with that of the high-grade product. The components being galvanized are therefore more effectively wetted by the molten zinc.

During the process of immersion in the zinc bath, which takes only a few minutes, the component is heated to ca. 450°C . Diffusion processes cause layers of iron–zinc alloys to form on the steel surface, giving very good adhesion of the zinc coating.

Other galvanizing processes have been developed in addition to the hot-dip process. In

electrolytic galvanizing, a D.C. current causes the deposition of lustrous coating, 5–25 μm thick, from acidic, cyanide, or alkaline cyanide-free electrolytes. However, these only give protection against mildly corrosive media. In general, additional protection is provided by chromate passivation.

In the spray galvanizing process, zinc wire is melted in a fuel gas/oxygen flame or an electric arc at the jet of a spray pistol and is propelled by compressed air from a distance of 15 cm, giving a coating ca. 0.1 mm thick. The resulting purely mechanical adhesion of the zinc is inferior to that produced by alloy formation at the metal interface in hot-dip galvanizing.

10.6.2 Zinc as a Construction Material [2, 34]

Although zinc has fairly good strength properties, it was for a long time not used as a material of construction because of its very poor creep resistance. Low-alloy zinc grades based on Zn–Ti–Cu, which have very good ductility and creep resistance, were developed only ca. 40 years ago. This material can be rolled to form zinc plate or sheet which can be used in the manufacture of roof drainage components or for covering buildings. Recently, a wide range of shapes has been developed, enabling æsthetic appeal to be combined with protection of buildings from the rigors of nature.

10.6.3 Pressure Die Casting with Zinc [2, 35]

Pressure die casting is another major area of use and is dominated by alloys of the type ZnAl_4Cu_1 and modifications thereof. Some of the advantages of zinc for pressure die casting are:

- Production runs can be very large (60–1000 components), depending on the size and complexity of the components

- The dies are extremely durable, enabling up to 1×10^6 components to be produced from one die
- The low viscosities and low melting points of the alloys ensure a high definition product
- Dimensional accuracy is ensured as shrinkage of the zinc alloys is low and easily controlled
- Lustrous or matt surfaces can be obtained with various metallic coatings and effects
- Costs are low due to large production runs
- The products are durable because of their good mechanical and physical properties
- The energy requirements of manufacture are low

Approximately 50% of all zinc pressure die castings go to the automobile industry.

10.6.4 Zinc as a Chemical [2, 36]

Zinc-based chemicals, including zinc dust, account for ca. 12–15% of world's zinc consumption. Zinc oxide is quantitatively by far the most important zinc-based chemical product, followed by zinc dust, zinc sulfate, and zinc chloride in order of importance and quantity. All other zinc compounds are of minor importance.

World consumption figures for zinc oxide and zinc dust have remained constant for many years. However, the demand for zinc sulfate and chloride is decreasing. The rate of growth of the consumption of zinc thiocarbonate and zinc stearate matches that of rubber production, their main area of use. Zinc oxide, the compound most in demand, can be produced by various processes. Its purity and quality depend on the production method used. In the indirect (so-called French) process, pure zinc is heated and oxidized in a current of air. The very pure zinc oxide formed is collected as a powder in settling chambers where it separates into different particle sizes. This material is usually known as zinc white. In the direct (so-called American) process, the raw materials used are zinc ores or zinc by-products, which usually contain lead. A car-

bonaceous material is heated with the raw material, reducing it with formation of zinc vapor. This is oxidized with air and separated into particle size fractions.

The starting materials for wet chemical processes are solutions of purified zinc. Zinc carbonate or hydroxide is precipitated and is then filtered, washed, dried, and calcined at ca. 800 °C.

The various types of zinc oxide include an industrial grade, which is used as an intermediate product in the production of other chemicals; pigment grades, which include almost all the lead-containing grades; precipitated zinc oxides which have no pigment properties; and special grades such as the extremely finely-divided zinc oxide for photocopying paper.

The main consumer of zinc oxide is the rubber industry, in which it is used as a vulcanization activator and sometimes also as a filler.

Zinc oxide as a pigment in aqueous latex paints has lost a significant share of the market. Its use in agriculture as an additive to fertilizers to treat zinc deficiency in soils is of lesser importance. Zinc oxide is a component of formulations in the glass, enamel, and ceramic industries, where it influences the melting point and also the optical and elastic properties, color, and luster of the glaze. It is also a component of face powder, lipsticks, and creams used in the cosmetics industry. It is also used as an additive to lubricants, adhesives, drying agents, and delustering agents, and as a catalyst in methanol synthesis.

Zinc dust is produced by a similar process to that used for zinc oxide, but in a reducing atmosphere. There are two grades: pigment zinc dust and zinc dust for chemical use. Zinc dust is used as a pigment for anticorrosion paints and coatings whose primary function is to form an impermeable surface. The action of the environment leads to the formation of zinc carbonate and basic zinc compounds between the zinc particles, reinforcing this effect. These coatings also give cathodic protection, which is especially useful if there is slight damage to the coating layer.

10.6.5 Economic Aspects

The development of world zinc consumption in the important industrial countries and regions of the world is illustrated by the figures for the years 1980, 1985, and 1990, which are listed in Table 10.4.

10.7 Alloys

Zinc recrystallizes just above room temperature and has low creep resistance. It is therefore only suitable as a construction material when alloyed. The alloying elements, mainly Al, Cu, Ti, and Mg, cause grain refinement, mixed crystal formation, or precipitation hardening, thereby considerably improving the mechanical properties.

10.8 Compounds

10.8.1 Fluoride

Zinc fluoride, ZnF_2 , forms monoclinic tetragonal crystals with the rutile structure [37], mp 872 °C [38], ρ_{25} 4.95 g/cm³. The solubility of $\text{ZnF}_2 \cdot 4\text{H}_2\text{O}$ at 20 °C is only 1.62 g ZnF_2 in 1000 mL solution, but it is very soluble in aqueous ammonia. ZnF_2 reacts with sodium hydroxide solution to form flocculent precipitates of basic zinc fluorides.

Synthesis. $\text{ZnF}_2 \cdot 4\text{H}_2\text{O}$ is formed when zinc carbonate or zinc oxide reacts with aqueous hydrofluoric acid. The water of crystallization can be driven off by heating to > 200 °C and/or in a vacuum.

Analysis. Calcined commercial zinc fluoride has the typical analysis 61–63% Zn, and 33–36% F, with the following maximum impurity levels: Fe 500 ppm, Pb 100 ppm, and SO_4 100 ppm.

Uses. Zinc fluoride is used as an additive to electrolytic galvanizing baths, in glazes and enamels for porcelain, and special types of glass with a high refractive index. It is also used as a flux for welding and soldering and as a fluorinating agent in organic syntheses.

Table 10.4: Development of zinc consumption.

	1981	1985	1990
Germany	405.7	408.8	484.0
Belgium	151.8	169.1	177.6
France	330.0	246.9	284.0
United Kingdom	181.3	189.3	189.0
Italy	236.0	218.0	278.0
Netherlands	45.2	51.1	71.7
Greece	18.8	15.2	20.3
Portugal	19.0	8.3	16.0
Spain	91.1	95.3	118.7
Finland	24.4	26.0	29.1
Yugoslavia	87.8	105.6	108.9
Norway	20.2	21.0	15.9
Austria	26.9	31.9	39.0
Sweden	38.0	31.5	39.5
Switzerland	25.2	26.3	22.3
Denmark	16.1	12.2	13.0
Other Europe	1.4	1.3	1.4
Europe	1719.1	1657.8	1908.4
Hong Kong	22.6	21.5	17.3
India	95.3	134.0	135.0
Indonesia	51.4	50.6	53.2
Japan	752.3	780.1	814.3
Malaysia	14.5	14.6	22.6
Pakistan	9.7	11.6	25.0
Philippines	16.1	13.0	33.1
Singapore	11.8	6.4	13.0
South Korea	68.0	119.7	227.4
Taiwan	38.4	49.4	79.4
Thailand	33.3	39.6	66.0
Turkey	12.3	49.8	47.7
Other Asia	13.3	38.2	52.8
Asia	1139.0	1328.5	1586.6
Egypt	2.7	7.0	10.0
Algeria	11.0	11.0	15.0
Ivory Coast	4.0	4.6	2.0
Kenya	7.2	6.7	8.2
Morocco	3.0	2.7	3.0
Nigeria	12.7	7.9	6.0
South Africa	84.1	84.1	86.5
Tanzania	3.2	3.5	2.0
Other Africa	8.6	9.3	18.3
Africa	136.5	136.8	150.0
Argentina	30.9	25.8	19.1
Brazil	155.9	132.4	129.7
Canada	140.0	156.5	126.1
Colombia	14.6	18.3	8.6
Mexico	88.9	99.2	110.1
Peru	23.2	41.2	71.0
Venezuela	20.2	15.4	10.6
United States	878.6	961.4	996.8
Other America	28.0	22.7	14.1
America	1380.3	1472.9	1486.5
Australia	95.4	82.1	82.2
New Zealand	20.7	24.7	20.0
Other Oceania	0.1	0.1	0.1
Oceania	116.2	106.9	102.3
Western countries	4491.1	4702.9	5234.7

	1981	1985	1990
Bulgaria	75.0	70.0	46.6
East Germany	86.2	69.7	45.5
Poland	178.3	157.2	109.5
Romania	49.9	35.3	12.8
Czechoslovakia	67.0	58.0	51.8
Soviet Union	1030.0	1000.0	920.0
Hungary	25.0	24.5	12.0
China	259.0	349.0	500.0
Others	28.0	32.0	45.0
Cuba	1.5	1.8	1.2
Eastern countries	1799.9	1797.5	1744.4
World total	6291.0	6500.4	6979.1

10.8.2 Chloride

Zinc chloride, ZnCl_2 , forms hexagonal-rhombic crystals, usually in the form of a white powder, mp 283 °C, bp 732 °C, ρ 2.91 g/cm³ at 25 °C, which is very soluble in water (432 g ZnCl_2 in 100 g water at 25 °C, 615 g ZnCl_2 in 100 g water at 100 °C). It is also soluble in alcohols, ether, acetone, ethyl acetate, glycerine, pyridine, amines, and nitriles.

Zinc chloride is strongly hygroscopic and forms hydrates with 1–4 mol water. It has a strong affinity for water, and causes many organic compounds to undergo condensation reactions. Considerable heat is evolved when ZnCl_2 dissolves in water.

Zinc chloride reacts with NH_4Cl to form the compounds $(\text{NH}_4)_2[\text{ZnCl}_4]$, $(\text{NH}_4)_3[\text{ZnCl}_5]$, and $(\text{NH}_4)_4[\text{ZnCl}_6]$. Analogous compounds are formed with amine hydrochlorides. Ammonia forms complexes with the composition $[\text{Zn}(\text{NH}_3)_x\text{Cl}_2]$ ($x = 2, 4, 6$). Amines give analogous compounds. In water, zinc chloride behaves as an acid, forming aquoacids with the compositions $\text{H}[\text{ZnCl}_2\text{OH}]$ and $\text{H}_2[\text{ZnCl}_2(\text{OH})_2]$. With increasing dilution, the aquoacid anions take up water and lose Cl^- , eventually being converted into the aquocation complex $[\text{Zn}(\text{H}_2\text{O})_6]^{2+}$ and losing the strongly acid reaction.

Commercial zinc chloride often contains basic zinc salt which leads to cloudiness in aqueous media.

Production. High-purity zinc chloride is formed from zinc and HCl gas at 700 °C [39]. Spectroscopically pure zinc chloride can be

obtained by decomposing zinc amalgam with HCl [40]. Quality specifications are listed in Table 10.5.

Table 10.5: Quality specifications for zinc chloride.

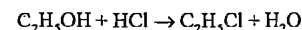
	Analytical-grade ZnCl_2 (ACS, ISO), %	High-purity ZnCl_2 (DAB, PhEur, BP, JP, USP), %
Assay (complexometric)	≥ 98	98–100.5
SO_4	≤ 0.002	< 0.01
Total N	≤ 0.001	< 0.01
As		< 0.0002
Ca	≤ 0.001	< 0.01
Fe	≤ 0.0005	< 0.001
K	≤ 0.001	0.001
NH_4	≤ 0.001	0.02
Na	≤ 0.001	
Oxychloride (as ZnO)	≤ 1.2	in accordance with test
pH (10% aq.)		4.6–5.5

Technical-grade zinc chloride is usually produced by leaching zinc oxides or zinc-containing waste such as zinc dross or ammonium chloride slags (unavoidable by-products of hot-dip galvanizing) with hydrochloric acid. Raw materials containing a high percentage of NH_3 must be subjected to an additional treatment stage, i.e., passing chlorine gas into the aqueous suspension to oxidize the ammonia to nitrogen.

The zinc-containing raw materials are dissolved in concentrated hydrochloric acid. The crude liquor contains varying amounts of the elements Fe, Mn, Pb, Cu, and Cd. Ferrous ion is oxidized to Fe^{3+} with H_2O_2 or KMnO_4 , and $\text{Fe}(\text{OH})_3$ is precipitated at pH 4.5. Also, the Mn is precipitated as MnO_2 by KMnO_4 . The remaining elements Cu, Pb, and Cd are removed by treatment with zinc dust (cementation). The solution is then evaporated to dryness. Aqueous solutions are sometimes subjected to further processing.

Uses

- Hydrochlorination of ethanol to monochloroethane



- Catalytic hydrolysis of benzotrichloride to benzoyl chloride

- Catalyst in the production of ammonium methylene-bis-dithiocarbamate from hydrogen peroxide, aqueous ammonia, carbon disulfide, and ethylenediamine

- Production of benzyl chloride from benzene, formaldehyde, and HCl/ZnCl_2
- Filling material for batteries, emulsion breaker in petrochemical processes, deodorizing agent
- Production of zinc compounds, e.g., zinc cyanide from potassium cyanide and a solution of zinc chloride (sometimes zinc sulfate)
- Production of zinc soaps from alkali metal soaps and zinc chloride

10.8.3 Bromide

Zinc bromide, ZnBr_2 , forms colorless rhombic crystals, mp 394 °C, bp 650 °C, ρ 4.29 g/cm³, which are strongly hygroscopic. The dihydrate, $\text{ZnBr}_2 \cdot 2\text{H}_2\text{O}$, melts at 35–47 °C with loss of water of crystallization. It is obtained by dissolving an aqueous suspension of ZnO or metallic zinc in aqueous HBr . Anhydrous ZnBr_2 is formed from its elements at ca. 600 °C or by thermal dehydration of the dihydrate in a stream of dry CO_2 . Its solubility in water at 25 °C is 820 g/L.

Uses

- A mild Lewis acid for alkylation reactions [41]
 - A catalyst for intramolecular reactions [42]
 - An activating agent in the production of activated carbon
 - An additive to photographic gelatins
 - An electrolyte for zinc bromide batteries
- High-purity ZnBr_2 contains $\geq 98\%$ ZnBr_2 , with the following maximum impurity contents: Ba 10 ppm, Ca 100 ppm, Fe 10 ppm, K 100 ppm, Mg 100 ppm, and Na 100 ppm.

10.8.4 Iodide

Zinc iodide, ZnI_2 , forms white to yellowish cubic crystals, mp 446 °C, bp 624 °C, ρ_{25} 4.73 g/cm³. It is produced by adding metallic zinc

to constant-boiling aqueous hydriodic acid until the yellow color disappears, by neutralizing aqueous HI with ZnO in the presence of a catalyst (precipitated silver), or by the reaction of I_2 vapor with molten zinc at 600 °C in a stream of N_2 [43]. Its solubility in water at 20 °C is 4500 g/L (hygroscopic).

Zinc iodide is used in medicine as a topical antiseptic astringent and in the preparation of iodide-zinc-starch solution.

10.8.5 Sulfate

Zinc sulfate, $ZnSO_4$, ρ 4.33 g/cm³, forms rhombic crystals. On heating to > 650 °C, zinc sulfate undergoes considerable decomposition with formation of basic sulfates. Above 800 °C, it decomposes completely into ZnO and SO_3 .

$ZnSO_4$ is very soluble in water, and forms hydrates with 1, 2, 4, 6, and 7 molecules of water of crystallization. The hepta-, hexa-, and monohydrates are produced on an industrial scale.

Zinc sulfate heptahydrate, $ZnSO_4 \cdot 7H_2O$, forms white, lustrous, columnar, rhombic crystals. It is transformed into the hexahydrate at 39 °C. It occurs in nature as goslarite. Mixed crystals are formed with the sulfates of Fe, Mg, Mn, Co, and Ni. It is very soluble in glycerine, but only sparingly soluble in other organic solvents.

Zinc sulfate is obtained by leaching zinc-containing materials with sulfuric acid in an aqueous medium. Suitable materials include zinc dross, slags, sweepings, oxides, sludges, metallic zinc, and zinc-containing flue dusts [44]. Used sulfuric acid can be utilized. It should be noted that arsine can be formed during the treatment of metallic dross and waste. Iron, manganese, and heavy metals are removed by the same process as that used to treat electrolyte liquors.

The purified solution of zinc sulfate is evaporated until its density reaches ca. 1.4 at 80 °C. On cooling, crystals of zinc sulfate heptahydrate form and are centrifuged off.

The crystals obtained are sometimes dried at ca. 30 °C to prevent efflorescence.

Pharmaceutical-grade $ZnSO_4 \cdot 7H_2O$ can be produced from sulfuric acid and pharmaceutical-grade zinc oxide. The impurity levels in the various grades of zinc sulfate are listed in Table 10.6.

Table 10.6: Commercial grades of $ZnSO_4 \cdot 7H_2O$.

	Analytical-grade	High-purity (DAB, USP, PhEur, FCC)	Pure
Assay	≤ 99.5%	99.5%	98%
As	0.5 ppm	2 ppm	10 ppm
Ca	10 ppm	50 ppm	
Cd	2 ppm	2 ppm	30 ppm
Cu	5 ppm	1 ppm	10 ppm
Fe	5 ppm	10 ppm	30 ppm
K	10 ppm	100 ppm	
Mg	10 ppm	50 ppm	
Mn	2 ppm	10 ppm	50 ppm
Na	50 ppm	1000 ppm	
Pb	5 ppm	5 ppm	50 ppm
Chloride	5 ppm	100 ppm	4000 ppm
Hg		1 ppm	
Se		5 ppm	
pH (5%, 20 °C)	4.4–5.6	4.4–5.6	

Zinc sulfate monohydrate, $ZnSO_4 \cdot H_2O$, is produced by thermal dehydration or by dehydrating with 95% ethanol. It crystallizes from a zinc sulfate mother liquor at temperatures above 70 °C [45]. It can be dried in a rotary, spray, or fluidized-bed driers.

Uses of zinc sulfate can be divided into direct and indirect uses.

Direct uses:

- Precipitating baths for viscose manufacture
- Electrolytes for galvanizing baths
- Additive (trace element) in fertilizers and animal feeds
- In medicine, as an emetic, astringent, or disinfectant
- Wood preservative, additive for paper bleaching, flocculent
- Water treatment

Indirect uses:

- Starting material for the production of other zinc compounds such as the fungicides Zineb and Mancozeb, zinc soaps, and the antidandruff agent zinc pyrithione

- Production of lithopone and zinc sulfide pigments
- Production of zinc cyanamide from potassium cyanamide
- Production of zinc phosphides

10.8.6 Toxicology and Occupational Health

Zinc metal and most of its compounds show very low toxicity compared to most other heavy metals. The toxicity of zinc salts varies to a certain extent, being dependent primarily on the toxicity of the anionic part of the compound. For example, the high toxicity and carcinogenicity of zinc chromate, $ZnCrO_4$, is not due to Zn^{2+} , but to the anionic CrO_4^{2-} component.

Intoxications with zinc and its compounds are comparatively rare. They can occur by ingestion of food contaminated with zinc leached from food containers or by inhalation of zinc or zinc oxide dust under occupational conditions (see below).

On the other hand, zinc is one of the most important essential elements for humans and all forms of plant and animal life. It is necessary for growth, skin integrity and function, testicular maturation, immunocompetence, wound healing, and for a variety of metabolic processes including carbohydrate, lipid, protein and nucleic acid synthesis or degradation. It is an essential, coenzyme-like component for the function of more than 70 metallo-enzymes, including alcohol dehydrogenase, carbonic anhydrase, and carboxypeptidase [46]. Physiological amounts of zinc have been shown to decrease the toxicity of other heavy metal ions such as Cd, Hg, Pb, and Sn [47].

Biological significance, biochemistry, toxicokinetics, human and animal toxicity, levels of tolerance, detoxification, evaluation of health risks to humans, and ecotoxicity of zinc and its compounds have been reviewed [47–50].

Toxicokinetics. As an essential element, zinc is absorbed in an active transport process, regulated by dietary zinc status and occurring pri-

marily in the ileum [51]. Zinc is bound to proteins to a large extent. Excretion occurs predominantly via the feces, and to a minor extent via urine and sweat. Excretion in the urine is up to 12.2 mmol/d; higher values indicate zinc intoxication [52].

Zinc is the most prevalent metal ion in human tissues other than blood. The body of a 70-kg man contains ca. 2.3 g of zinc [53], 64% of which is found in muscle and 28% in bone [54]. The highest zinc concentrations are found in reproductive organs, especially the prostate gland (87 µg/g wet weight), whereas the whole-body average is 33 µg/g wet weight [53]. Serum contains 10.7–22.9 mmol/L, plasma 17.4 ± 1.8 mmol/L, erythrocytes 184–198 mmol/L, and hair 3.30 ± 1.33 mmol/g [52].

Acute Toxicity. In contrast to numerous other heavy metals, zinc shows low acute toxicity. Zinc overload of the organism is rather unlikely and occurs almost exclusively by ingestion when food or drinks, especially acidic ones, are prepared or stored in galvanized containers [55, 56].

Symptoms of acute intoxication are gastrointestinal distress, diarrhea, nausea, and abdominal pain. Vomiting occurs almost universally. In elemental-zinc overdose, symptoms such as lethargy, slight ataxia, and difficulty in writing also appear. Abnormal laboratory parameters include increase of pancreatic enzyme activities, hypokalemia secondary to acute pancreatitis, and microhematuria [57, 58].

Zinc chloride, $ZnCl_2$, is caustic to the gastrointestinal tract, occasionally leading to hematemesis, beside the symptoms mentioned above. Furthermore, it is extremely detrimental to the lungs. An episode of pulmonary exposure to $ZnCl_2$ smoke resulted in ten fatalities due to pulmonary toxicity. Most survivors showed lachrymation, rhinitis, dyspnea, stridor, and retrosternal chest pain. In two autopsies, severe inflammation of the upper respiratory tract mucosa and pulmonary edema, but no changes in liver and kidneys, could be detected [59].

Zinc or zinc oxide fume is responsible for a syndrome which may occur in welding, galvanizing, or smelting operations, called "metal fume fever". Symptoms such as rapid breathing, dyspnea, cough, fever, shivering, sweating, chest and leg pain, myalgias, fatigue, metallic taste, salivation, thirst, and leukocytosis appear within 4–6 h after exposure and disappear after 24–48 h [60, 61]. The X ray of the chest is normally clear. A rapid tolerance (tachyphylaxis, "quick immunity" [62]) develops in workers within 48 h, but may be lost over the weekend ("monday morning fever"). Metal fume fever can also be caused by exposure to fumes of aluminum, antimony, copper, iron, magnesium, manganese, and nickel.

Zinc phosphide, Zn_3P_2 , is extremely toxic because of the formation of phosphine, PH_3 , on reaction with water or acids.

Chronic Toxicity. The development of a toxicosis has been reported in the case of a continuous uptake of drinking water contaminated with 40 ppm Zn from a galvanized pipe [63]. Dialysis patients are at risk of an elevation of the plasma concentration of zinc (and other heavy metal ions) [64, 65]. The symptoms are similar to those of acute toxicity, but are less pronounced.

Genotoxicity. Zinc apparently does not show any mutagenicity or carcinogenicity [47]. In human lymphocytes, 0.1–1000 $\mu\text{mol/L}$ of zinc acetate, alone or in combination with cadmium and lead acetates, failed to induce chromatid-type aberrations (deletions, acentric fragments) and gaps [66]. The carcinogenic effect of zinc chromate, ZnCrO_4 , is due to the chromate anion, not to the zinc cation.

Reproductive Toxicity. There are no indications for reproductive effects, especially for teratogenicity, of zinc [47].

Immunotoxicity. There are no reports concerning immunotoxic effects of zinc. However, zinc chromate, ZnCrO_4 , shows strong sensitizing effects and therefore is able to cause obstinate eczema under occupational conditions [67].

Toxicological Data. The lethal dose of ZnCl_2 in humans is 35 g. Since zinc sulfate, ZnSO_4 , is less caustic than the chloride, it has lower toxicity [68].

Treatment. Decontamination of the gastrointestinal tract after oral uptake of zinc compounds by syrup of ipecac, lavage, or cathartics is mostly unnecessary, since patients usually vomit sufficiently. For normalization of zinc levels, CaNa_2EDTA is the agent of choice [57, 59]. After oral uptake of ZnCl_2 , milk may be administered to decrease absorption of the metal [70].

After contact of the skin with ZnCl_2 , immediate removal is necessary using soap and plenty of water.

After contact of the eyes with ZnCl_2 , adequate measures are rinsing with plenty of water, use of Isogutt eye drops, and contacting an ophthalmologist as soon as possible [70, 71].

In cases of ZnCl_2 fume inhalation, cortisone preparations should be applied immediately (e.g., by inhalation of Auxiloson) to avoid development of lung edema [71]. In severe cases clinical observation for at least 24 h is necessary.

Occupational Health. The MAK value of zinc oxide, ZnO , is 5 mg ZnO/m^3 , measured as total fine dust [72]. The same TLV value has been set in Hungary, Japan, Poland, Sweden, and by the WHO, while it is 10 mg ZnO/m^3 in Bulgaria, Romania, and Pennsylvania (United States); it is 15 mg ZnO/m^3 in Finland. The United States has a TLV value of 1 $\text{mg ZnCl}_2/\text{m}^3$, and Massachusetts a 30-min limit of 0.2 mg/m^3 zinc chromate, ZnCrO_4 [53].

Zinc chromate, ZnCrO_4 is classified in group A1 (proven human carcinogens) of Appendix III of the MAK list [72].

10.9 Zinc Pigments

10.9.1 Zinc Sulfide Pigments [73–75]

White pigments based on zinc sulfide were first developed and patented in 1850 in

France. Although they are still of economic importance, they have continually lost market volume since the early 1950s when titanium dioxide was introduced. Only one modern production installation for zinc sulfide pigments still exists in the market-economy-oriented industrial nations (Sachtleben Chemie, Germany). There are other production plants in eastern Europe and in China.

The zinc-sulfide-containing white pigment with the largest sales volume is *lithopone*, which is produced by coprecipitation and subsequent calcination of a mixture of zinc sulfide, ZnS , and barium sulfate, BaSO_4 . Pure zinc sulfide is marketed as *Sachtolith*.

White zinc sulfide pigments maintain their market position in areas of use where not only their good light scattering ability but other properties such as low abrasion, low oil number, and low Mohs hardness are required. They are often produced from many types of industrial waste. This recycling relieves pressure on the environment, as these materials would otherwise have to be disposed of.

10.9.1.1 Properties

Some physical and chemical properties of ZnS and BaSO_4 are given in Table 10.7.

A white pigment must not absorb light in the visible region (wavelength 400–800 nm), but should disperse incident radiation in this region as completely as possible. The spectral reflectance curves of zinc sulfide and barium sulfate (Figure 10.13) fulfil these conditions to a large extent. The absorption maximum for ZnS at ca. 700 nm is a result of lattice stabilization with cobalt ions, whose function is explained in the next section. The absorption edge in the UV-A region is responsible for the bluish-white tinge of zinc sulfide. Depending on the production process, zinc sulfide has a sphalerite or wurtzite lattice type.

Table 10.7: Properties of the components of zinc sulfide pigments.

Property	Zinc sulfide	Barium sulfate ^a
<i>Physical properties</i>		
Refractive index n	2.37	1.64
Density, g/cm^3	4.08	4.48
Mohs hardness	3	3.5
Solubility in water (18 °C), %	1.8×10^{-4}	2.5×10^{-4}
<i>Chemical properties</i>		
Resistance to acids/bases	soluble in strong acids	insoluble
Resistance to organic solvents	insoluble	insoluble

^a Component of lithopone.

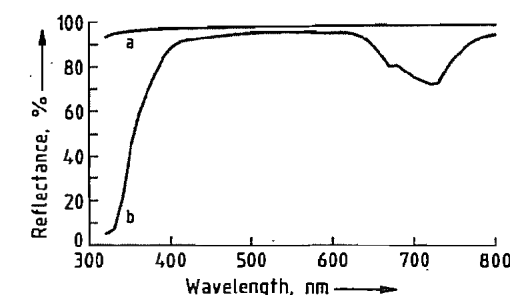


Figure 10.13: Spectral reflectance curves of barium sulfate and zinc sulfide: a) Barium sulfate; b) Zinc sulfide (Co-doped).

The refractive index n of ZnS , which determines its scattering properties, is 2.37 and is much greater than that of plastics and binders ($n = 1.5$ –1.6). Spheroidal ZnS particles have their maximum scattering power at a diameter of 294 nm. Barium sulfate does not directly contribute to the light scattering due to its relatively low refractive index ($n = 1.64$), but acts as an extender, and increases the scattering efficiency of the ZnS .

The barium sulfate in lithopone can be identified thermoanalytically by a reversible endothermic transformation at 1150 °C. Both Sachtolith and lithopone are thermally stable up to ca. 550 °C in the presence of air. Due to their low Mohs hardness, they are less abrasive than other white pigments. Barium sulfate is practically inert toward acids, bases, and organic solvents. Zinc sulfide is stable in aqueous media between pH 4 and 10, and is largely inert toward organic media. In the presence of

water and oxygen, it can be oxidatively decomposed by the action of UV radiation.

10.9.1.2 Production

Raw Materials. The source of zinc can be zinc oxide from a smelter, zinc dross or sweepings, ammonium chloride slag from hot dip galvanizing, or liquid waste such as pickle liquors from galvanizing plants. Variations in the price of zinc have a large effect on the economics of zinc sulfide pigments.

The starting material for water-soluble barium compounds is fused barium sulfide produced by coke reduction of naturally occurring barite with a low silica and strontium content. Suitable barite is readily available from many deposits worldwide.

Lithopone. The reaction of equimolar quantities of ZnSO_4 and BaS produces a white, water-insoluble coprecipitate with the theoretical composition 29.4% ZnS and 70.6% BaSO_4 :



By using a different molar ratio, this composition can be changed; for example, precipitation according to Equation (2) gives a product containing 62.5% ZnS and 37.5% BaSO_4 :



Figure 10.14 is a flow diagram of lithopone production. The solutions of zinc salts contain impurities (e.g., salts of iron, nickel, chromium, manganese, silver, cadmium) that depend on their origins. The main sources of zinc sulfate solutions are zinc electrolyses and the reprocessing of zinc scrap and zinc oxide. The first stage of purification consists of chlorination. Iron and manganese are precipitated as oxide-hydroxides, and cobalt, nickel, and cadmium as hydroxides. The solutions are then mixed with zinc dust at 80 °C. All the elements more noble than zinc (cadmium, indium, thallium, nickel, cobalt, lead, iron, copper, and silver) are almost completely precipitated, while zinc goes into solution. The metal slime is filtered off and taken to copper smelters for recovery of the noble metal components. A small quantity of a water-soluble

cobalt salt is added to the purified zinc salt solution. The cobalt (0.02–0.5%) becomes incorporated into the ZnS lattice during subsequent calcination to stabilize the final product against light. Zinc sulfide that is not treated in this way becomes gray in sunlight.

The barium sulfide solution is produced by dissolving fused barium sulfide in water. The barium sulfide is obtained by reducing an intimate mixture of crushed barite (ca. 1 cm lumps) with petroleum coke according to Equation (3) in a directly heated rotary kiln at 1200–1300 °C:

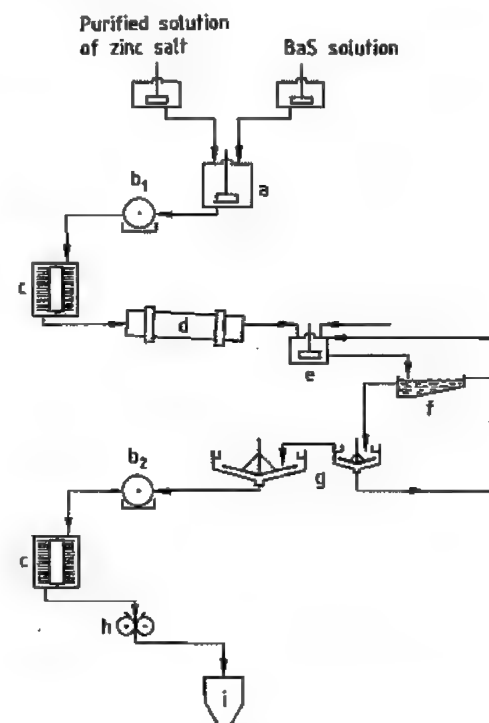


Figure 10.14: Flow diagram for lithopone production: a) Precipitation vessel; b) Rotary filter; c) Turbo dryer; d) Rotary kiln; e) Chilling vessel; f) Rake classifier; g) Thickener; h) Grinder; i) Silo.

The warm solution (60 °C) containing ca. 200 g/L barium sulfide is filtered and immediately pumped to the precipitation stage. Further purification is not necessary. Unreacted gangue and heavy metals are collected as insoluble sulfides in the filter cake. The almost clear so-

lution can be stored only for a short period. Longer storage leads to undesirable polysulfide formation.

The zinc salt and BaS solutions are mixed thoroughly under controlled conditions (vessel geometry, temperature, pH, salt concentration, and stirring speed, see (a) in Figure 10.14). The precipitated "raw lithopone" does not possess pigment properties. It is filtered off (b) and dried (c); ca. 2 cm lumps of the material are calcined in a rotary kiln (d) directly heated with natural gas at 650–700 °C. Crystal growth is controlled by adding 1–2% NaCl , 2% Na_2SO_4 and traces of Mg^{2+} (ca. 2000 ppm) and K^+ (ca. 100–200 ppm). The temperature profile and residence time in the kiln are controlled to obtain ZnS with an optimum particle size of ca. 300 nm.

The hot product from the kiln is quenched in water (e), passed via classifiers and hydroseparators (f) into thickeners (g), filtered on rotary filters (b₂), and washed until salt-free. The dried product is ground in high-intensity mills (g) and may undergo organic treatment (with a polyalcohol) depending on the application.

Figure 10.15 shows a scanning electron micrograph of lithopone. The ZnS and BaSO_4 particles can be distinguished by means of their size. The average particle diameter of BaSO_4 is 1 μm .

Sachtolith. Production is similar to that of lithopone. For process engineering reasons, a sodium sulfide solution is used as the sulfide component, and is formed according to Equation (4):



The BaSO_4 , which is produced as a by-product, is filtered, washed, dried, and ground. It is a high-quality extender (Blanc fixe) used in the paint industry.

Figure 10.15: Scanning electron micrograph of lithopone. The larger particles are barium sulfate (mean size 1.0 μm) and the smaller particles are zinc sulfide (mean size 0.3 μm).

The Na_2S solution is mixed with a cobalt-treated zinc salt solution under precisely controlled conditions. The resulting zinc sulfide precipitate is calcined and processed to give the finished product.

Hydrothermal Process. Crystal growth of ZnS can be achieved by a hydrothermal process instead of by calcination. The raw lithopone is precipitated with a slight excess of sulfide at pH 8.5. The pH is then adjusted to 12–13 with sodium hydroxide solution, and 0.5% sodium carbonate is added. The suspension is then autoclaved for ca. 15–20 min at 250–300 °C. In contrast to the wurtzite structure of the calcined product, the hydrothermal product has a sphalerite structure with a ca. 10% greater scattering power. Although the product is of better quality, the hydrothermal process is less economic due to the high cost of the materials required for lining the autoclave (e.g., tantalum or a zirconium alloy).

Environmental Protection. During the reduction of barite and the calcination of Sachtolith and lithopone, sulfur dioxide is liberated. This is removed from the waste gas in a purification stage which is based on the reversible, temperature-dependent solubility of sulfur dioxide in polyglycol. The absorbed sulfur dioxide can be recovered as a liquid product or as a raw material for sulfuric acid. Any soluble barium in the residue from the dissolution of the fused BaS is removed by

treatment with iron-containing waste hydrochloric acid. The gangue, in the form of a slime, is water-insoluble and can therefore be disposed of. The barium chloride solution is used as a raw material for the production of precipitated barium sulfate fillers.

10.9.1.3 Commercial Products

Commercial lithopone grades contain 30% ZnS (red seal) and 60% ZnS (silver seal). The ZnS content of Sachtolith is > 97%. Various chemical (e.g., polyalcohols, siloxanes, silanes) and mechanical treatments (e.g., jet milling) are used to obtain other products for special applications. The technical data for commercial red seal lithopone and Sachtolith are given in Table 10.8.

Table 10.8: Technical data for red seal lithopone and Sachtolith.

Parameter	Standard	Sachtolith	Red seal lithopone
ZnS, %	DIN 55910	≥ 97	ca. 29
ZnO, %	DIN 55910	0.2	0.1
BaSO ₄ , %	DIN 55910	≤ 3	ca. 70
Brightness ^a		98	98–99
Lightening power	DIN 53192	400	120
Water-soluble salts, %	DIN 53197	< 0.2	< 0.2
Sieve residue ^b , %		0.02	< 0.1
Oil number	DIN 53192	12	8
pH	DIN 53200	6–8	7
Specific surface area, m ² /g		8	3

^a BaSO₄ white standard = 100.

^b Test sieve 45 μm, DIN 4188, ISO DIS 3310/1.

10.9.1.4 Uses

Lithopone is mainly used in coating materials with relatively high pigment concentrations (Table 10.9). Examples are primers, plastic masses, putties and fillers, artists' colors, and emulsion paints. An important property of lithopone is its low binder requirement, giving paint products with good flow and application properties. It is suitable for almost all binder media, and has good wetting and dispersing properties. With optimum feed composition, good dispersion can be achieved

simply by the action of a dissolver. It can be economically advantageous to use lithopone in combination with TiO₂ pigments; the good hiding power of the TiO₂ pigments is combined with the economic and technical advantages of lithopone. Due to the strong shift of the absorption band towards the blue, lithopone is especially useful as a white pigment for UV-cured paint systems. Zinc compounds have a fungicidal and algicidal action, and inclusion of lithopone or Sachtolith in paint formulations for exterior use therefore prevents attack by algae or fungi.

Table 10.9: Uses of Sachtolith and lithopone (as percentage of total consumption).

Use	Sachtolith	Lithopone	
		Western Europe	World
Paints	20	79	94
Plastics	64	17	2
Lubricants	6		
Others	10	4	4

The material advantages of lithopone are used in plastics (e.g., good lightfastness and clear bluish-white shade). The product also imparts very good extruding properties to the plastic resulting in high throughput rates and economic extruder operation. In fire-resistant systems, ca. 50% of the flame retardant antimony trioxide can be replaced by nontoxic lithopone without any adverse effect.

Sachtolith is mainly used in plastics (Table 10.9). Functional properties such as lightening and hiding power are criteria for the use of Sachtolith. It has proved to be very useful for coloring many thermoplasts. During the dispersion process it does not cause abrasion of metallic production machinery or adversely effect the polymer, even at high operating temperatures or during multistage processing. Even ultrahigh molecular mass thermoplasts can be colored without problems. In glass-fiber-reinforced plastics, the soft texture of Sachtolith prevents mechanical fiber damage during extrusion. Sachtolith is also used as a dry lubricant during the fabrication of these materials.

The low abrasiveness of Sachtolith prolongs the operating life of stamping tools used in the manufacture of industrial rubber articles. The lightfastness and ageing resistance of many elastomers are improved by Sachtolith. It is also used as a dry lubricant for roller and plain bearings, and as a white pigment for greases and oils.

10.9.1.5 Economic Aspects

Total world production of lithopone in 1990 was 220×10^3 t. This was subdivided as follows (10^3 t):

Germany	30 (+ 7 Sachtolith)
Former Yugoslavia	5
Former Czechoslovakia	15
Former Soviet Union	50
China	120

Only estimated figures are available for the former Soviet Union and China.

A decrease in output is to be expected because replacement by TiO₂ is not yet at an end, especially in coating materials. In the long term, only the high-quality grades can maintain their place in the market, i.e., those in which technical properties are required in addition to light scattering.

10.9.1.6 Toxicology

The use of zinc sulfide and barium sulfate in contact with foods is permitted by the FDA (United States) and in most European countries. Some restrictions apply in France, Italy, the United Kingdom, and Czechoslovakia.

Soluble zinc is toxic in large amounts, but the human body requires small quantities (10–15 mg/d) for metabolism. Zinc sulfide is completely harmless in the human due to its low solubility. The acid concentration in the stomach and the rate of dissolution following ingestion are not sufficient to produce physiologically significant quantities of soluble zinc. LD₅₀ values in the rat exceed 20 g/kg. No cases of poisoning or chronic damage to health have been observed in the manufacture of zinc sulfide pigments despite exposure to dust that occurs mainly during grinding and packing.

10.9.2 Zinc Oxide (Zinc White)

[76–80]

10.9.2.1 Introduction

Zinc oxide, ZnO, was formerly used only as a white pigment, and was named zinc white (C.I. Pigment White 4), Chinese white, or flowers of zinc. The term zinc white now denotes zinc oxide produced by the combustion of zinc metal according to the indirect or French process.

Historical Aspects. Zinc oxide has long been known as a by-product of copper smelting. The Romans called it "cadmia" and used it as such in the production of brass. They also purified it for use in ointments by reduction followed by oxidation. In the Middle Ages, the alchemists thought that cadmia could be converted into gold.

In the mid-18th century, the German chemist CRAMER discovered that cadmia could be obtained by the combustion of metallic zinc. COURTOIS began to produce zinc white in 1781 in France, but it was not until 1840 that industrial production was started by LECLAIRE (indirect or French process). The use of this white pigment spread rapidly. Zinc oxide replaced white lead because it had the advantage of being nontoxic, of not darkening in the presence of sulfurous gases, and of having better hiding power.

Around 1850 S. WETHERILL of the New Jersey Zinc Company perfected a roasting furnace in which a grate was charged with coal and then covered with a mixture of zinc ore and coal. The zinc was reduced by the partial combustion of the coal and reoxidized at the furnace exit (direct or American process). These furnaces were subsequently improved but are now no longer used. During the second half of the nineteenth century, the use of ZnO in rubber was introduced to reduce the time needed for vulcanization. The discovery of the first organic accelerators for vulcanization in 1906 added to the importance of ZnO, which acts as an activator in these materials.

A third industrial production process exists but this wet process is less widely used.

10.9.2.2 Properties

Physical Properties. Zinc oxide is a fine white powder that turns yellow when heated above 300 °C. It absorbs UV light at wavelengths below 366 nm. Traces of monovalent or trivalent elements introduced into the crystal lattice impart semiconducting properties. The elementary particles of ZnO obtained by the thermal method may be granular or nodular (0.1–5 µm) or acicular (needle-shaped). Some physical properties are given below:

Density	5.65–5.68 g/cm ³
Refractive index	1.95–2.1
mp	1975 °C
Heat capacity	
25 °C	40.26 Jmol ⁻¹ K ⁻¹
100 °C	44.37 Jmol ⁻¹ K ⁻¹
1000 °C	54.95 Jmol ⁻¹ K ⁻¹
Thermal conductivity	25.2 Wm ⁻¹ K ⁻¹
Crystal structure	hexagonal, wurtzite
Mohs hardness	4–4.5

Chemical Properties. Zinc oxide is amphoteric; it reacts with organic and inorganic acids, and also dissolves in alkalis and ammonia solution to form zincates. It combines readily with acidic gases (e.g., CO₂, SO₂, and H₂S). It reacts at high temperatures with other oxides to form compounds such as zinc ferrites.

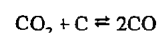
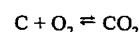
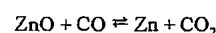
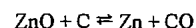
10.9.2.3 Production

About 1–2% of zinc oxide is produced by the wet process, 10–20% by the direct process, and the remainder by the indirect process.

Raw Materials. In the early days, the raw materials were mainly zinc ores or concentrates for the direct process, or metal from zinc producers for the indirect process. Nowadays, zinc oxide manufacturers mainly use residues and secondary zinc. This fact, combined with the demand for chemical purity imposed by the users, means that processes have had to be modified and a number of purification techniques are used.

Direct or American Process. The direct process is noted for its simplicity, low cost, and

excellent thermal efficiency. It consists of an initial high-temperature reduction (1000–1200 °C) of a zinc-containing material (as oxide), the reducing agent being coal. Reduction takes place according to Boudouard's equations:



The zinc vapor and the CO gas are then oxidized to zinc oxide and carbon dioxide above the reaction bed or at the furnace exit. Various zinc-containing materials are used, e.g., zinc concentrates, metallization residues, by-product zinc hydroxide, and above all zinc dross from casting furnaces or galvanizing. The dross must first be treated to remove chloride and lead by heating at ca. 1000 °C in rotary kilns.

Only rotary kilns are now used for the direct process; the use of static furnaces has been discontinued. The zinc content of raw materials is between 60 and 75%. There are two types of rotary kiln:

- One type is a long (ca. 30 m), fairly narrow (2.5 m diameter) kiln, heated by gas or oil. The raw material (a mixture of zinc-containing material and coal) is charged continuously either countercurrent or cocurrent to the combustion gases. The residues, which still contain some zinc and unburnt coal, leave the furnace continuously at the end opposite to the feed end. The excess coal is sieved out and recycled. The combustion gases, containing zinc vapor, ZnO, and CO, pass into a chamber where oxidation is completed and large particles of impurities settle out. The gases are then cooled in a heat exchanger or by dilution with air. The zinc oxide is collected in bag filters.
- The second type of rotary kiln is shorter (5 m) and has a larger diameter (ca. 3 m). Charging is continuous, but the dezincified residues are removed batchwise.

In both cases, operating conditions are controlled to obtain a high yield and to give the required particle shape and size. Provided no contamination is introduced, chemical purity is determined solely by the composition of the raw materials used.

Indirect or French Process. The zinc is boiled, and the resulting vapor is oxidized by combustion in air under defined conditions. The crystallographic and physical properties of the ZnO can be controlled by adjustment of the combustion conditions (e.g., flame turbulence and air excess). The chemical composition of the ZnO is solely a function of the composition of the zinc vapor.

Many types of furnace are available to produce vapor of the required purity from various raw materials and obtain a high yield of zinc. Pure zinc (super high grade, SHG; high grade, HG) or, to an increasing extent, metal residues (e.g., scrap zinc, die casting dross, or galvanizer's dross) are used as raw materials. Various liquid- or vapor-phase separation techniques are used for separating Cd, Pb, Fe, and Al from zinc metal before it is oxidized.

- **Muffle Furnaces or Retorts of Graphite or Silicon Carbide.** The metal is fed into the furnace either batchwise as a solid or continuously as a liquid. The heat of vaporization is supplied by heating the outside of the retort with a burner. The nonvolatile residues (iron and lead in the case of dross from smelting) accumulate in the retort and must be removed at intervals. This is facilitated by tipping the retorts.
- **Fractional Distillation.** The vapor containing Cd, Pb, Fe, Al, and Cu can be purified by fractional distillation in columns (New Jersey Zinc Co.) with silicon carbide plates. Oxidation takes place at the exit of the column.
- **Furnaces with Two Separate Chambers.** The metallic raw material, which can be in large pieces, is fed into the first chamber where it melts. This is connected to the second, electrically heated chamber where dis-

tillation takes place in the absence of air. The first version of this type of furnace was constructed by LUNDEVALL [81].

The nonmetallic residues are removed at the surface of the melting chamber. Impurities, such as Fe, Al, and some of the Pb, accumulate in the distillation chamber and are periodically removed in the liquid state. The last traces of lead are then removed by fractional distillation.

- **Smelting Process in a Rotary Kiln.** Indirect zinc oxide is also made by smelting in a rotary kiln, starting from the same raw materials. Melting, distillation, and part of the oxidation all take place in the same zone, allowing utilization of a large part of the heat of combustion of the zinc. By controlling the temperature and partial pressures of carbon dioxide and oxygen, the impurity content (Pb) can be limited and the shape and size of the ZnO particles can be adjusted, though to a lesser extent than in the other processes.

Wet Process. Zinc oxide is also produced industrially from purified solutions of zinc sulfate or chloride by precipitating the basic carbonate, which is then washed, filtered, and finally calcined. This method produces a grade of zinc oxide with a high specific surface area.

Products of this type are also obtained from waste hydroxides which are purified by a chemical route and then calcined.

Aftertreatment. Thermal treatment at temperatures up to 1000 °C improves the pigment properties of the ZnO and is mainly applied to oxide produced by the direct method. Controlled atmospheric calcination also improves the photoconducting properties of the high-purity oxide used in photocopying.

The ZnO surface is made more organophilic by coating it with oil and propionic acid. The ZnO is often deaerated and sometimes pelletized or granulated to improve handling properties.

10.9.2.4 Quality Specifications

Many standard specifications have been laid down for the more important uses of ZnO (rubber, paints, and the pharmaceutical industry). Various methods of classification are used, often based on the production process and the chemical composition. The most well-known are pharmacopeias, RAL 844 C3 (Reichs-Ausschuß für Lieferbedingungen), ASTM D79, BS 254, DAB 8 (Deutsches Arzneibuch), T 31006 NF (French standard), and ISO R 275. Table 10.10 shows the classification of commercially available zinc oxide grades.

Table 10.10: Classification of commercially available grades of zinc oxide.

Parameter	A	B	C	D
	Indirect process	Indirect process	Direct process	Wet process
ZnO (min.), %	99.5	99	98.5	93
Pb (max.), %	0.004	0.25	0.25	0.001
Cd (max.), %	0.001	0.05	0.03	0.001
Cu (max.), %	0.0005	0.003	0.005	0.00#
Mn (max.), %	0.0005	0.001	0.005	0.001
Water-soluble salts (max.), %	0.02	0.1	0.65	1
Loss on ignition (max.), %	0.3	0.3	0.3	4
Acidity, g H ₂ SO ₄ /100 g	0.01	0.1	0.3	0.2
Specific surface area, m ² /g	3–8	3–10	1–5	25 (min.)

Classification based on color codes is common in Europe, but is of limited value. Manufacturers have their own standards. In general, the terms silver seal and white seal indicate category A, and red seal category B.

10.9.2.5 Uses

Zinc oxide has many uses. By far the most important is in the *rubber industry*. Almost half the world's ZnO is used as an activator for vulcanization accelerators in natural and synthetic rubber. The reactivity of the ZnO is a function of its specific surface area, but is also influenced by the presence of impurities such as lead and sulfates. The ZnO also ensures good durability of the vulcanized rubber, and

increases its thermal conductivity. The ZnO content is usually 2–5%.

In *paints and coatings*, zinc oxide is no longer the principal white pigment, although its superb white color is used by artists. It is used as an additive in exterior paints for wood preservation. It is also utilized in antifouling and anticorrosion paints [82]. It improves film formation, durability, and resistance to mildew (having a synergistic effect with other fungicides) because it reacts with acidic products of oxidation and can absorb UV radiation.

The *pharmaceutical and cosmetic industries* use ZnO in powders and ointments because of its bactericidal properties. It is also used to form dental cements by its reaction with eugenol.

In the field of *glass, ceramics, and enamels*, ZnO is used for its ability to reduce thermal expansion, to lower the melting point, and to increase chemical resistance. It can also be used to modify gloss or to improve opacity.

Zinc oxide is used as a *raw material* for many products: stearates, phosphates, chromates, bromates, organic dithiophosphates, and ferrites (ZnO, MnO, Fe₂O₃). It is used as a source of zinc in animal feeds and in electro-galvanization. It is also used for desulfurizing gases.

Zinc oxide is used as a *catalyst* in organic syntheses (e.g., of methanol), often in conjunction with other oxides. It is present in some adhesive compositions.

The highest purity material is calcined with additives such as Bi₂O₃ and used in the manufacture of varistors [83]. The photoconducting properties of ZnO are used in photoreproduction processes. Doping with alumina causes a reduction in electrical resistance, hence, it can be used in the coatings on the master papers for offset reproduction [84].

10.9.2.6 Economic Aspects

The consumption of zinc oxide in Western Europe in 1990 was estimated to be 160 000 t. Annual world consumption is in the region of 500 000 t, representing ca. 10% of the total world zinc production. The rubber industry

consumes ca. 45% of the total and the remainder is divided among a large number of industries.

10.9.2.7 Toxicology and Occupational Health

Unlike other heavy metals, zinc is not considered to be toxic or dangerous. It is an essential element for humans, animals, and plants. The human body contains ca. 2 g, and it is recommended that 10–20 mg should be ingested per day [85]. The oral LD₅₀ value for rats is 630 mg/kg. The permitted concentration of the dust in air at the workplace is 5 mg/m³ (MAK), 10 mg/m³ (TLV-TWA). Values for zinc oxide fumes are 5 mg/m³ (TLV-TWA) and 10 mg/m³ (TLV-STEL).

If large quantities of ZnO are accidentally ingested or inhaled, fever, nausea, and irritation of the respiratory tract ensue after several hours. These symptoms rapidly disappear without long-term consequences.

10.9.2.8 Anticorrosive Zinc Oxide

Zinc oxide, ZnO, is a white powder that is usually used in combination with active anticorrosive pigments. It has the following physical properties:

Oil absorption value, g/100 g	20–24
Density, g/cm ³	5.6
Apparent density, cm ³ /100 g	100
Mean particle size, μm	0.11–0.22
BET surface area, m ² /g	3–10

The inhibiting action of zinc oxide is based on its ability to react with corrosive substances and to maintain an alkaline pH in the coating. It also reacts with acidic components of the binder to form soaps and absorbs UV light.

The lead content of commercial zinc oxide depends on the manufacturer and is in the range 0.002–1.5%. For a zinc oxide coating to be considered lead-free, the lead content must be less than 1.5%.

10.9.2.9 Transparent Zinc Oxide

Similar to transparent titanium dioxide, microparticles of zinc oxide are manufactured by using sol-gel processes or precipitation in the presence of protective colloids to limit particle growth [86].

An industrial process [87] operates with solutions of zinc sulfate and zinc chloride in the ratios 1:2. Basic zinc carbonate is precipitated by feeding simultaneously the zinc-salt solution and a mixed solution of sodium hydroxide and sodium carbonate into a reactor charged with water. The precipitated product is intensively washed several times and then spray-dried.

It is used for cosmetics and paints as a transparent UV-light shielding chemical.

Trade names include Sachtotec Micro-Zinkoxid (Sachtleben, Germany) and Z-cote HP1 (SunSmart Inc., USA).

10.9.3 Zinc Phosphate [88–92]

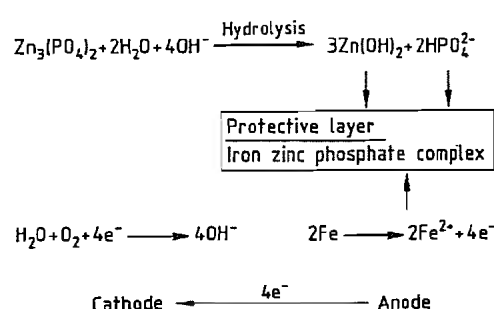
The most important phosphate-containing pigment is zinc phosphate, Zn₃(PO₄)₂·4H₂O. It can be used with a large number of binders and has a very wide range of uses [88, 89, 91–93].

Zinc phosphate is usually produced on an industrial scale from zinc oxide and phosphoric acid, or from zinc salts and phosphates [94]. Composition and properties are given in Table 10.11.

The mechanism of the action of zinc phosphate is shown in Figure 10.16. Zinc phosphate dihydrate pigment is hydrated to the tetrahydrate in an alkyd resin binder [95]. The tetrahydrate is then hydrolyzed to form zinc hydroxide and secondary phosphate ions which form a protective film of basic iron(III) phosphate on the iron surface [96]. The anticorrosive action of zinc phosphate depends on its particle size distribution. Micronization improves the anticorrosive properties [97–99].

Table 10.11: Composition and properties of zinc phosphate pigments.

Property (standard)	Zinc phosphate $\text{Zn}_3(\text{PO}_4)_2 \cdot 2-4\text{H}_2\text{O}$	Micronized zinc phosphate $\text{Zn}_3(\text{PO}_4)_2 \cdot 2-4\text{H}_2\text{O}$
Metal content, % (ISO 787, part 2)	51	51
Phosphate content, % (ISO 787, part 2)	49	< 49
Chloride content, % (ISO 787, part 13)	0.01	0.05
Sulfate content, % (ISO 787, part 13)	< 0.1	0.05
Water-soluble content, % (ISO 787, part 3)	< 0.1	0.1
Sieve residue, % (ISO 787, part 18)	0.01	0.01
Density, g/cm ³ (ISO 787, part 10)	3.2	3.4
Specific surface area, m ² /g (DIN 66131/66132)	1.0	4.3
Loss on ignition, % (ISO 787, part 2)	10–11	13
Oil absorption value, g/100 g (ISO 787, part 5)	20	24
Conductivity, μS (ISO 787, part 14)	100	300
pH (ISO 787, part 9)	6.2–7	7
Color	white-beige	white-beige

**Figure 10.16:** Passivation of iron by zinc phosphate [96].

The effect of corrosion-promoting ions on the anticorrosive properties of zinc phosphate is described in [100, 101].

Trade names are as follows:

Zinc phosphate: Sicor ZNP/M, ZNP/S (BASF, Germany); Heucophos ZP10 (Dr. H. Heubach, Germany); Halox Zinc Phosphate (Halox Pigments, USA); Phosphinox PZ20 (SNCZ, France); Hispafos N 2 (Colores Hispania, Spain).

Basic zinc phosphate: Heucophos ZPO (Dr. H. Heubach, Germany); HispafosSP (Colores Hispania, Spain).

10.9.4 Zinc Hydroxyphosphite

Commercial zinc hydroxyphosphite is a white, nontoxic pigment with basic character.

The pigment has the following physical properties [102]:

Oil absorption value, g/100 g	15–20
Density, g/cm ³	3.96
pH, 2% suspension	6.5–7.5
Mean particle size, μm	2–3

Water-soluble content, g/100 cm³ < 0.01
Specific conductivity, Ω/cm 9700

A trade name for zinc hydroxyphosphite is Nalcin 2 (National Lead Chemicals, USA; Kronos Titan, Germany).

10.9.5 Zinc Cyanamide

Zinc cyanamide, ZnCN_2 , is a white to beige powder which has the following properties [103]:

Density, g/cm ³	ca. 3.1
Apparent density, g/cm ³	ca. 250
Metal content, %	ca. 60
CN ₂ content, %	ca. 34
Specific surface area, m ² /g	ca. 50
pH	8.5
Conductivity, μS	< 1000

10.9.6 Zinc and Calcium Ferrites

Many paint formulations contain iron oxide as an extender. It is a physically protective anticorrosive pigment (only to a small extent). In order to obtain a chemically protective anticorrosive pigment with active constituents the iron oxide is heated with oxides or carbonates of alkaline earths (CaO , CaCO_3) or zinc (ZnO) to form pigments of the ferrite type [104, 105]. The following systems have been reported for alkyd resin primers: $2\text{CaO} \cdot \text{Fe}_2\text{O}_3$, $\text{CaO} \cdot \text{Fe}_2\text{O}_3$, and $\text{Zn}(\text{Mg})\text{O} \cdot \text{Fe}_2\text{O}_3$. In the coating these pigments are hydrolyzed with water to form alkaline-earth hydroxides or zinc hydroxide which prevent corrosion by increasing the pH. Alkaline-earth soaps are also formed in certain binder media [106]. However, the

pigment volume concentration must be high to ensure good results [107].

Only one zinc ferrite pigment has attained economic significance. Its properties are as follows [108]:

Water-soluble salts, %	max. 0.6
Oil absorption value, g/100 g	ca. 22
pH	9–11
Density g/cm ³	5.0

A trade name for zinc ferrite is Anticor 70 (Bayer, Germany; Mobay Chemical Corporation, USA).

10.9.7 Zinc Dust

Zinc dust, mp 419.4 °C, density 7.14 g/cm³, is a free-flowing blue-gray powder composed of spheroidal particles. It is produced by melting zinc in a crucible, vaporizing it at ca. 900–950 °C, and condensing and sifting the product. Alternatively, molten zinc is atomized with a nozzle to produce dust, which is then sifted. Properties of commercial zinc dust pigments are listed in Table 10.12 [109, 110].

Table 10.12: Properties of commercial zinc dust pigments.

Property	Zinc dust Ultra 25	Zinc dust Ultra 35
Total zinc content, %	> 99.0	> 99.0
Metallic zinc content ^a , %	94–96	94–96
Lead content, %	< 0.005	< 0.005
Cadmium content, %	< 0.005	< 0.005
Iron content, %	0.003	0.003
Copper content, %	0.001	0.001
Acid-insoluble material, %	< 0.1	< 0.1
Sieve residue ^b , %	< 0.01	< 0.01
Mean particle size ^c , μm	2.8–3.2	3.3–3.8

^a KMnO₄ method.

^b Sieve residue on 16 900 sieve (DIN 4188, aperture: 45 μm).

^c Air permeability method.

The action of zinc dust in primers with organic binders is based on sealing effects and electrochemical processes. The zinc reacts with water and atmospheric oxygen that diffuse into the binder, forming zinc hydroxide which is then neutralized by sulfuric acid (from SO₂ in the air) and hydrochloric acid (from Cl-containing substances in the air, e.g., NH₄Cl). This causes an increase in volume and decreases permeability. The corrosion products of zinc also have an anticorrosive ac-

tion [111]. Cathodic protection takes place when the zinc and iron come into contact; the zinc content in the primer must be at least 94–96% [112–115]. Zinc dust coatings are used in large quantities for structural steel, including underwater steel construction and shipbuilding. Zinc dust is also used in inorganic binder systems (alkali silicates or alkyl silicates) in the form of two-component systems [116].

A trade name is Zinc Dust Ultra 25' and 35 (Lindgens & Söhne, Germany).

10.9.8 Flake Zinc Pigments

Flake zinc pigments are used mainly as high-quality anticorrosive pigments in powder or paste form. Owing to their platelet structure they have a considerably higher surface area than spherical zinc dust particles. They can therefore take up much more binder which produces a more flexible coating film than that obtained with zinc dust. Other advantages include a lower settling tendency, good remixing, and problem-free application onto the precoated surface.

The flake zinc pigments give a considerably brighter, better metallic effect than zinc dust. Their appearance can be further improved by combining them with aluminum pigments or by applying a topcoat based on aluminum pigment.

Another widespread application for flake zinc pigments is the coating of small articles with complex shapes (e.g., screws, steel springs, bolts, rivets) and for special anticorrosive paints.

10.10 References

1. V. Tafel: *Lehrbuch der Metallhüttenkunde*, 2nd ed., vol. 2, Hürzel-Verlag, Leipzig 1953, pp. 357–655.
2. Ullmann, 4th ed., 24, 594–626.
3. F. Pawlek: *Metallhüttenkunde*, De Gruyter, Berlin-New York 1983, pp. 654–689.
4. Z. Horvath: *A Zinc Kohászata*, Akadémiai Kiadó, Budapest 1961.
5. N. N. Muratsch: *Handbuch des Metallhüttenmanns*, Verlag Technik, Berlin 1954, pp. 511–566.
6. J. Torka, R. Mewes: *Die Wunder der Technik*, Paul Oestergaard, Berlin.
7. Meyers *Neues Lexikon*, 2nd ed., vol. 15, Bibliographisches Institut, Leipzig 1977, pp. 444–445.

8. P. Klemm: *Der Weg aus der Wildnis*, vol. 3, Kinderbuchverlag, Berlin 1962.
9. Gmelin, System-no. 32, 1969, 21–26, 56–61.
10. R. Zimmermann, K. Günther: *Metallurgie und Werkstofftechnik*, vol. 1, pp. 216ff; vol. 2, pp. 117, Deutscher Verlag für Grundstoffindustrie, Leipzig 1977.
11. Römpp, 9th ed., vol. 6, Thieme Verlag, Stuttgart 1992, pp. 5136–5139.
12. Metallgesellschaft, *Metallstatistik 1980–1990*, vol. 78, Frankfurt 1990.
13. Zink, *der vielseitige Werkstoff*, vol. 22, Mitteilungen aus den Arbeitsbereichen der Metallgesellschaft, Frankfurt/Main 1980.
14. Brockhaus *Taschenbuch der Geologie*, Brockhaus Verlag, Leipzig 1955.
15. S. Jankovic: *Wirtschaftsgeologie der Erze*, Springer Verlag, Wien–New York 1974, Specific References.
16. R. Kola, *Erzmetall* 35 (1982) 130–137.
17. H. Maczek, R. Kola, *J. Met.* 32 (1980) 53–58.
18. *Sintering Symposium*, Port Pirie, South Australia, Sept. 1958.
19. N. B. Gray, M. R. Harvey, G. M. Willis: "Physical Chemistry of Process Metallurgy", *Inst. Min. Metall. Sect.* (1974) 19.
20. Y. Fukunaka et al., *Metall. Trans. B* 7B (1960) 307.
21. F. Cappel, H. Wendeborn: *Sintern von Eisenerzen*, Stahleisen, Düsseldorf 1973.
22. T. R. Ingraham, H. H. Kellogg, *Trans. Am. Inst. Min. Metall. Eng.* 227 (1963) 1419.
23. J. Krüger, R. Püllenberger, *Erzmetall* 33 (1980) 70; 34 (1981) 380.
24. F. Johannsen, *Z. Erzbergbau Metallhüttenwes.* 1 (1948) 235; *Erzmetall* 27 (1974) 313.
25. Ch. Friedrich et al., *Neue Hütte* 16 (1971) 457.
26. H. Maczek, R. Kola, *J. Met.* 32 (1980) 53.
27. G. Kossek et al., *Stahl Eisen* 96 (1976) 482.
28. J. Krüger, *Freiberg. Forschungsh. B* B228 (1981) 47.
29. O. Knacke, W. Neumann, *Erzmetall* 9 (1956) 261.
30. O. H. Schütze, *Erzmetall* 3 (1950) 69.
31. G. Hofmann: *Industrieöfen*, Deutscher Verlag für Grundstoffindustrie, Leipzig 1970.
32. H. Veltmann, D. R. Weir, *Erzmetall* 35 (1982) 76–77.
33. W. Thiele in: *Zink – der vielseitige Werkstoff*, Mitteilungen aus den Arbeitsbereichen der Metallgesellschaft, vol. 22, Frankfurt 1980, pp. 67–73.
34. W. Burggraef in [33], pp. 81–82.
35. J. Johnen in [33], pp. 83–84.
36. H. Kunze in [33], pp. 88–90.
37. W. Zachariasen, *Skr. Akad. Oslo* 1 (1926) 7.
38. *Handbook of Chemistry and Physics*, 54th ed., CRC Press, Cleveland, OH, 1973/1974, B-154, B-155.
39. O. Hönigschmid, M. von Mack, *Z. Anorg. Allg. Chem.* 246 (1941) 363.
40. R. T. Hamilton, J. A. von Butler, *J. Chem. Soc. (London)* 1932, 2283.
41. I. Paterson, *Tetrahedron Lett.* 1979, 1519.
42. L. F. Tietze, K. Biefuss, *Angew. Chem. Int. Ed. Engl.* 24 (1985) 1042.
43. M. Sato, M. Yosiyana, *Nippon Kagaku Kaishi* 60 (1939) 918.
44. F. Ensslin, *Met. Erz* 38 (1941) 196.
45. Gmelin, 8th ed., Zinc, p. 942.
46. B. L. Vallee, *BioFactors* 1 (1988) no. 1, 31–36.
47. A. Léonhard, C. B. Gerber, F. Léonhard, *Mutat. Res.* 168 (1986) 343–353.
48. R. L. Bertholf: "Zinc", in H. G. Seiler, H. Sigel, A. Sigel (eds.): *Handbook on Toxicity of Inorganic Compounds*, Marcel Dekker, New York 1988, pp. 787–800.
49. A. B. Abdel-Mageed, F. W. Oehme, *Vet. Hum. Toxicol.* 32 (1990) no. 1, 34–39.
50. R. S. Bedwal, N. Nair, R. S. Mathur, *Trace Elem. Med.* 8 (1991) no. 2, 89–100.
51. D. L. Antonson, A. J. Barak, J. A. Vanderhoof, *J. Nutr.* 109 (1979) 142–147.
52. N. S. Tietz in: *Clinical Guides to Laboratory Tests*, W. B. Saunders, Philadelphia 1983, pp. 516–519.
53. National Research Council, Subcommittee on Zinc: Zinc, University Park Press, Baltimore 1979, pp. 249–271.
54. H. Tipton, M. J. Cook, *Health Phys.* 9 (1963) 103–145.
55. G. R. Callendar, C. J. Genzkow, *Mil. Surg.* 80 (1937) 67–72.
56. M. A. Brown et al., *Arch. Environ. Health* 8 (1964) 657–660.
57. S. J. Chobanian, *Ann. Emerg. Med.* 10 (1981) 91–93.
58. J. V. Murphy, *J. Am. Med. Assoc.* 212 (1970) 2119–2120.
59. E. H. Evans, *Lancet* 2 (1945) 368–370.
60. M. J. Ellenhorn, D. G. Barceloux: *Medical Toxicology Diagnosis and Treatment of Human Poisoning*, Elsevier, New York 1988, pp. 1064–1065.
61. H. E. Stokinger: "The Metals. Zinc", in G. D. Clayton, F. E. Clayton (eds.): *Patty's Industrial Hygiene and Toxicology*, 3rd revised ed., vol. 2A, John Wiley & Sons, New York 1981.
62. C. P. McCord, *Ind. Med. Surg.* 29 (1960) 101–107.
63. G. Laurence, *Br. Med. J.* 1 (1958) 582–587.
64. J. Savory, R. L. Bertholf, M. R. Wills, *Clin. Endocrinol. Metab.* 14 (1985) 681–702.
65. E. D. M. Gallery, J. Blomfield, S. R. Dixon, *Br. Med. J.* 4 (1972) 331–333.
66. K. Gasiorsek, M. Bauchinger, *Environ. Mutagen.* 3 (1981) 513–518.
67. L. C. Robis, *New Engl. J. Med.* 260 (1969) 1091–1098.
68. W. Wirth, Chr. Gloxhuber: *Toxikologie*, 5th ed., Georg Thieme Verlag, Stuttgart 1994, pp. 126–128.
69. J. L. Potter, *Ann. Emerg. Med.* 10 (1981) 267–269.
70. R. Kühn, K. Birett: *Merkblätter Gefährliche Arbeitsstoffe*, 4th ed., ecomed verlag, Landsberg/Lech 1979, Datenblatt Z-004.
71. S. Risi, H. U. Wolf: "Zink", in H. U. Wolf (ed.): *HAGERs Handbuch der Pharmazeutischen Praxis*, vol. 3, Gifte, Springer Verlag, Berlin 1992, pp. 1257–1259.
72. Deutsche Forschungsgemeinschaft (ed.): *MAK- und BAT-Werte-Liste 1995*, Maximale Arbeitsplatzkonzentrationen und Biologische Arbeitsstofftoleranzwerte, Mitteilungen der Senatskommission zur Prüfung gesundheitsschädlicher Arbeitsstoffe, Mitteilung 31, VCH-Verlagsgesellschaft mbH, Weinheim 1995.
73. H. Clausen: "Zinc-Based Pigments", in P. A. Lewis (ed.): *Pigment Handbook*, 2nd ed., vol. 1, John Wiley & Sons, New York 1988.
74. M. Issel, *Modern Paint and Coatings* 9 (1991) 35–42.
75. M. Cremer: "Non-TiO₂ White Pigments with Special References to ZnS Pigments", *Industrial Minerals, Pigment & Extenders Supplement*, 1985.
76. H. Brown: *Zinc Oxide Rediscovered*, New Jersey Zinc Co., New York 1957.
77. H. Brown: *Zinc Oxide Properties and Applications*, International Lead Zinc Research Organ, New York 1976.
78. K. H. Ulbrich, W. Backhaus: *Zinkoxid in der Gummiindustrie Kautsch. Gummi, Kunstst.* 27 (1974) no. 7, 269–272.
79. G. Hänig, K. Ulbrich: "ZnO, Produkt zwischen Pigmentchemie und Hüttenwesen", *Erzmetall* 32 (1979) 140–146.
80. G. Heiland, E. Mollwo, F. Stockmann: *Electronic Processes in Zinc Oxide*, vol. 8, Solid State Physics, Academic Press, New York 1959.
81. Larvik, US 2939783, 1957 (G. Lundevall).
82. G. Meyer: *New Application for Zinc*, Zinc Inst. Inc., New York 1986.
83. E. Ziegler R. Helbig, *Physik Unserer Zeit* 17 (1986) no. 6, 171–177.
84. Matsushita, DE 3045591, 1980 (Sonoda).
85. Kieffer, in R. Henklin (ed.): *Metalle als Lebensnotwendige Spurenelemente für Pflanzen, Tiere und Menschen, Teil Zink*, Verlag Chemie, Weinheim 1984, pp. 117–123.
86. Nippon Shokubai Co., JP 07232919, 1994.
87. L. Brüggemann, DE 3900243, 1993 (G. Walde, A. Rudy).
88. BASF: *Sicor-Pigmente*, company brochure, Ludwigshafen 1987.
89. Dr. Hans Heubach GmbH & Co. KG: *Heucophos* company information, Langelsheim 1989.
90. Halox-Pigments: *Halox-Pigments*, company information, Pittsburgh 1973.
91. Société nouvelle des couleurs zinciques, company information, Beauchamp 1990.
92. Colores Hispania: *Anticorrosive Pigments*, company information, Barcelona 1990.
93. J. A. Burkill, J. E. O. Mayne, *J. Oil Colour Chem. Assoc.* 71 (1988) no. 9, 273–275.
94. G. Sziklai, J. Szucs, *Hung. J. Ind. Chem.* 10 (1982) 215–221.
95. P. J. Gardner, I. W. McArn, V. Barton, G. M. Seydt, *J. Oil Colour Chem. Assoc.* 73 (1990) no. 1–16.
96. G. Meyer, *Farbe + Lack* 68 (1962) no. 5, 315; *Dtsch. Farben-Z.* 20 (1966) 8; *Farbe + Lack* 79 (1967) no. 6, 529.
97. G. Rasack, *Farbe + Lack* 84 (1978) no. 7 497–500.
98. G. Adrian, A. Bittner, *J. Coat. Technol.* 58 (1986) 59–65.
99. P. Kresse, *Farbe + Lack* 83 (1977) no. 2, 85–95.
100. P. Reichle, W. Funke, *Farbe + Lack* 93 (1987) no. 7, 537–538.
101. M. Svoboda, *Farbe + Lack* 92 (1986) no. 8, 701–703.
102. NL Chemicals: *Nalcin 2*, company information, Hightstown, NJ 1983.
103. BASF AG, Ludwigshafen, company information, 1990.
104. Bayer AG, DE 2642049, 1976 (F. Hund et al.). Bayer AG, DE 2625401, 1976 (F. Hund et al.).
105. Tada Kogyo, US 3904421, 1975 (S. Shimizu et al.).
106. P. Kresse, *Farbe + Lack* 84 (1978) no. 3, 156–159.
107. M. Svoboda, *Farbe + Lack* 96 (1990) no. 7, 506–508.
108. Bayer: *Anticor 70*, product information, Leverkusen 1989.
109. Lindgens, Köln–Mülheim, company information, 1991.
110. M. Leclercq, *Farbe + Lack* 97 (1991) no. 3, 207–210.
111. T. Szauer, A. Miszczyk, *ACS Symp. Ser.* 322 (1986) 229–233.
112. K. M. Oesterle, R. Oberholzer, *Dtsch. Farben-Z.* 18 (1964) 151.
113. J. D'Ans, H. J. Schuster, *Farbe + Lack* 63 (1957) no. 9, 430.
114. G. Grillo, *Tech. Rundsch.* 60 (1968) 19.
115. A. Laberenz, *Farbe + Lack* 68 (1962) no. 7, 765.
116. E. V. Schmid, *Farbe + Lack* 84 (1978) no. 1, 16–19.

11 Tin

GÜNTER G. GRAF

11.1 History	683	11.5.1.3 Removal of Arsenic	703
11.2 Properties	684	11.5.1.4 Removal of Lead	704
11.3 Occurrence, Ore Extraction, and Beneficiation	685	11.5.1.5 Removal of Bismuth	704
11.3.1 Minerals	686	11.5.2 Electrorefining	704
11.3.2 Deposits	686	11.5.2.1 Electrorefining in Acid Medium	704
11.3.3 Mining	687	11.5.2.2 Electrorefining in an Alkaline Medium	705
11.3.4 Ore Beneficiation	688	11.5.2.3 Other Methods of Electrorefining	705
11.4 Smelting	689	11.6 Recovery of Tin from Scrap Materials and Residues	705
11.4.1 Fundamental Theory of Smelting ..	689	11.7 Analysis	706
11.4.2 Special Aspects of the Winning of Tin from its Ores	691	11.7.1 Analysis of Ores and Concentrates ..	706
11.4.3 Production of Crude Tin	692	11.7.2 Analysis of Metallic Tin	707
11.4.3.1 General Aspects	692	11.8 Economic Aspects	708
11.4.3.2 Ore Preparation prior to Reduction ..	692	11.9 Alloys and Coatings	708
11.4.3.3 Reduction	695	11.10 Compounds	709
11.4.3.4 Slag Processing	699	11.10.1 Tin(II) Compounds	709
11.5 Refining	702	11.10.2 Tin(IV) Compounds	710
11.5.1 Pyrometallurgical Refining	702	11.11 Toxicology	711
11.5.1.1 Removal of Iron	702	11.12 References	712
11.5.1.2 Removal of Copper	703		

11.1 History [1-4, 6, 11, 15]

Because of its luster and softness, tin was usually assigned to the planet Jupiter, more rarely to Venus. The name of the element is derived from the Old High German *zin* and the Norse *tin*. The symbol Sn from the Latin *stannum* was proposed by BERZELIUS. Historically tin is of major cultural importance, being an essential component of the copper alloy bronze which gave its name to the Bronze Age. The first bronze objects appeared in Egyptian tombs dating from the end of the 4th millennium B.C.

Pure tin was first produced in China and Japan around 1800 B.C. Around 600 B.C., the ancient Egyptians occasionally placed pure tin artifacts in mummies' tombs. Tin is not only an essential constituent of tin bronze, but is also a constituent of lead alloys for solders and tin plating. Tin and especially its alloys have shaped the development of many geographical

regions, e.g., China, Indochina, Indonesia, India, the Near East, North Africa, and Europe.

The cultural and historical importance of tin from the Middle Ages to early modern times lay in its use for sacred objects, articles of daily use, and jewelry.

There is no historical evidence concerning the oldest methods of tin extraction. It is fairly certain that in 100 B.C. in Cornwall, England, tin was smelted from very pure ore over wood fires in pits and later in small furnaces. Up to the 1200s, Cornwall provided most of Europe's tin. Today, these deposits are virtually exhausted. Tin was probably produced in Bohemia around 1150. Also, the first tin mines were opened in Saxony at this time, and these supplied European requirements until they were destroyed in the Thirty Years War. Then, as these various deposits gradually became exhausted and as ocean transport developed, tin from overseas became dominant.

The largest tin mines are in Asia, the most important ore-supplying countries in the world being Malaysia and Indonesia, followed by China. The second largest tin-producing region includes Brazil and Bolivia. The countries exporting the largest quantities of tin ores also produce the most tin metal. World annual production has developed as follows:

ca. 1800	9 100 t
ca. 1850	19 000 t
ca. 1900	91 900 t
ca. 1950	172 100 t
1980	243 600 t
1990	225 600 t

The principal consumer countries are the United States, Japan, China, and Russia.

11.2 Properties

Physical Properties [1, 2, 4, 16–19, 20]. Tin, Sn, exists in two crystalline modifications, the α - and β -forms. A third modification may also exist. Some physical properties of α - and β -tin are listed in the following:

Natural isotopes	10
Relative atomic mass	118.69
Crystal structure	
α -Sn (gray tin)	fcc (A_4) diamond type
β -Sn (white tin)	tetragonal (A_3)
Transformation temperature	
α -Sn \leftrightarrow β -Sn	286.2 K
Enthalpy of transformation	1966 J/mol
Lattice constants at 25 °C	
α -Sn	$a = 648.92$ pm
β -Sn	$a = 583.16$, $c = 318.13$
Density of β -tin at 20 °C	7.286 g/cm ³
100 °C	7.32
230 °C	7.40
Density of α -tin	5.765 g/cm ³
Density of liquid tin at 240 °C	6.992 g/cm ³
400 °C	6.879
800 °C	6.611
1000 °C	6.484
Molar heat capacity of β -tin	
25 °C	27.0 J/mol ⁻¹ K ⁻¹
230 °C	30.7
Liquid	28.5
Melting point	505.06 K
Enthalpy of fusion	7029 J/mol
Boiling point	2876 K
Enthalpy of vaporization	295 763 J/mol
Vapor pressure at 1000 K	9.8×10^{-4} Pa
1800 K	750
2100 K	8390
2400 K	51 200
Cubic coefficient of expansion	
α -tin at -130 °C to +10 °C	$(14.1 \text{ to } 4.7) \times 10^{-6}$ K ⁻¹
β -tin at 0 °C	59.8×10^{-6}
β -tin at 50 °C	69.2×10^{-6}

β -tin at 100 °C	71.4×10^{-6}
β -tin at 150 °C	80.2×10^{-6}
Molten tin at 700 °C	105.0×10^{-6}
Coefficient of thermal conductivity of β -tin at 0 °C	$0.63 \text{ W cm}^{-1} \text{ K}^{-1}$
Surface tension at 232 °C	0.53–0.62 N/m
400 °C	0.52–0.59
800 °C	0.51–0.52
1000 °C	0.49
Dynamic viscosity at 232 °C	$2.71 \times 10^{-3} \text{ Pa} \cdot \text{s}$
400 °C	1.32×10^{-3}
1000 °C	0.80×10^{-3}
Specific electrical resistivity	
α -tin at 0 °C	$5 \times 10^{-6} \Omega \text{ m}$
β -tin at 25 °C	11.15×10^{-6}
Transition temperature for superconductivity	3.70 K
Magnetic susceptibility of β -Sn	$2.6 \times 10^{-11} \text{ m}^3/\text{kg}$

In the periodic table, tin lies on the boundary between metals and nonmetals. The transformation of the α - to the β -modification is accompanied by a complete change of lattice structure, affecting the physical, chemical, and mechanical properties. Also, at 170 °C there is a second-order transformation accompanied by a discontinuous change in the lattice parameters and thermomechanical properties. A tetragonal high-pressure modification of tin, stable between 3500 and 11 000 MPa, is described in the literature the lattice constants being $a = 381$ pm and $b = 348$ pm.

The transformation of β -tin (white tin) into α -tin (gray tin) is of practical importance, as it involves a volume increase of 21%. The transformation process requires a high energy of activation, and can be very strongly hindered. White β -tin can therefore exist for many years at -30 °C. The presence of α -tin seed crystals is important for the transformation process, and these are formed by repeated phase transitions. Foreign “elements” also affect the transformation temperature and rate. These can consist of impurities and deformations. The effect of impurities on transformation behavior is described in [21]. Tin vapor consists of Sn_2 molecules.

Mechanical properties [1, 2, 4, 20–23] are not of great relevance to most applications of pure tin. The most important are listed in the following:

Yield strength at 25 °C	2.55 N/mm ²
Ultimate tensile strength at -120 °C	87.6 N/mm ²
15 °C	14.5
200 °C	4.5

Brinell hardness	
(10 mm, 3000 N, 10 s) at 0 °C	4.12
100 °C	2.26
200 °C	0.88
Modulus of elasticity E at -170 °C	65 000 N/mm ²
-20 °C	50 000
0 °C	52 000
40 °C	49 300
100 °C	44 700
200 °C	26 000

Chemical Properties [1, 2, 4, 20]. Tin has the atomic number 50 and is a member of group 14 of the periodic table. The electronic configuration is $1s^2 2s^2 p^6 3s^2 p^6 d^{10} 4s^2 p^4 d^{10} 5s^2 p^2$. Tin can be di- or tetravalent. It is stable in dry air, but is considerably more rapidly oxidized at a relative humidity of 80%. Bright metallic tin becomes dull within 100 d even in indoor atmospheres. Oxygen is rapidly and irreversibly chemisorbed, and the oxide layer formed grows at an exponentially increasing rate. Typical impurities present after metallurgical production (e.g., Sb, Tl, Bi, and Fe) promote oxidation. Treatment with carbonate or chromate solutions leads to passivation.

Molten tin at temperatures up to ca. 500 °C picks up oxygen from the air at a rate that obeys a parabolic law, a result of the compact layer of oxide formed.

Gaseous water and nitrogen do not dissolve in solid tin. Dissolution in molten tin only occurs at high temperatures (ca. > 1000 °C). Under the conditions of electrochemical reduction in hydrochloric acid solutions, atomic hydrogen forms SnH_4 , and elemental nitrogen forms Sn_3N_4 .

Tin is stable towards fluorine at room temperature, but SnF_2 or SnF_4 are formed at higher temperatures.

Rapid and vigorous reactions occur with chlorine, bromine, and iodine, these reactions being accelerated by moisture and elevated temperatures. The reaction products are SnCl_4 , SnBr_4 , SnI_2 , and SnI_4 .

Sulfur reacts rapidly with molten tin at > 600 °C to form the sulfides SnS , Sn_2S_3 , and SnS_2 . The reaction rate is lower above 900 °C, and only SnS is formed.

Reaction with hydrogen sulfide is slow and only occurs in the presence of oxygen and moisture. Sulfur dioxide reacts with molten tin

to form SnO_2 and S, and a molten solution of tin in copper reacts with SO_2 to form SnO_2 and Cu_2S (an important reaction in pyrometallurgy). Tin is stable towards pure hot water, steam, and dry ammonia. Nitrogen oxides only react with molten tin.

Tin is amphoteric, reacting with both strong bases and strong acids with evolution of hydrogen. Having a normal electrode potential of -0.136 V, tin lies between nickel and lead in the electrochemical series.

With sodium hydroxide solution, tin forms $\text{Na}_2[\text{Sn}(\text{OH})_4]$, and with potassium hydroxide solution $\text{K}_2[\text{Sn}(\text{OH})_4]$.

Tin reacts slowly with acids in the absence of oxygen. The high hydrogen overvoltage is caused by a layer of atomic hydrogen at the metal surface preventing further attack. Vigorous reactions occur with nitric acid, the rate depending on the acid concentration. The reactions are very vigorous with 35% acid, but complete passivation can occur at concentrations > 80%. Tin is stable towards fuming nitric acid. While hydrogen fluoride does not attack tin, hydrochloric acid reacts even at a concentration of 0.05% and temperatures below 0 °C. Tin is not attacked by sulfurous acid or by < 80% sulfuric acid.

The most important use of tin and tin-plated materials is in the preserved food industry. For this reason, the possibility of reactions of tin with certain organic acids is important. Lactic, malic, citric, tartaric, and acetic acids either do not react at all at normal temperatures or do so to a negligible extent, especially in the absence of atmospheric oxygen. This is also true of alcohols and hydrocarbons.

11.3 Occurrence, Ore Extraction, and Beneficiation

The average concentration of tin in the earth's crust is estimated to be 2–3 ppm, comparable to cerium and yttrium. Owing to the high atomic mass of tin and the high density of its important minerals, its volume concentration is very low. However, it occurs in only a small number of locations, where conse-



quently its relative abundance is high. In general, 1000-fold enrichment is necessary to give workable tin deposits, i.e., with a tin content of at least 0.2%. The question of whether a deposit can be economically extracted, for a given world market price level, depends on the mining conditions. For example, there are deposits in Bolivia containing 1% Sn which cannot be economically extracted, whereas in South East Asia placer deposits containing 0.02% Sn are successfully mined.

11.3.1 Minerals

Native tin occurs only very rarely and has only been identified with certainty in Canada.

Cassiterite, SnO_2 , is the most economically important tin mineral. It forms tetragonal crystals, has a Mohs hardness of 6–7, a density of 6.8–7.1 g/cm³, and a tin content of up to 79%. The color is usually brown to brownish black. The presence of Ti, Fe, Nb, Ta, or Mn can lead to colors varying from gray to white. Contact deposits of cassiterite can be combined with, e.g., magnetite, arsenical iron pyrites, or zinc blende. Placer deposits of cassiterite are of major importance. "Wood tin" consists of gel-like or very fine grained aggregates of cassiterite. Cassiterite is an oxidic mineral and is chemically very resistant, in particular towards weathering.

Stannite (bell metal ore), $\text{Cu}_2(\text{Fe}, \text{Zn})\text{SnS}_4$, forms tetragonal crystals, has a Mohs hardness of 4, a density of 4.4 g/cm³, and a tin content of up to 27.6%. Its color is steel gray with an olive green tinge. It is chemically less resistant than cassiterite, seldom occurs in hydrothermal deposits, and is of little economic importance.

Hydrocassiterite (varlamoffite), H_2SnO_3 , is a tetragonal gel-like stannic acid. It occurs in Bolivia, usually accompanying cassiterite.

Other tin minerals include teallite, $(\text{Sn}, \text{Sb})\text{S}$; herzenbergite, SnS ; franckeite, $\text{Pb}_5\text{Sn}_3\text{Sb}_2\text{S}_{14}$; cylindrite, $\text{Pb}_3\text{Sn}_4\text{Sb}_2\text{S}_{14}$; thoreaulite, SnTa_2O_7 ; hulsite, (iron tin borate); and stokesite, $\text{CaSn}(\text{Si}_3\text{O}_9) \cdot 2\text{H}_2\text{O}$. None are of economic importance.

Table 11.1: Tin ore reserves and mine outputs for various countries in 1990.

Country	Ore reserves (t metal content)	Output (t metal content)
Malaysia	1 200 000	28 500
Thailand	1 200 000	14 600
Indonesia	1 550 000	31 700
Bolivia	980 000	17 300
Russia	1 000 000	13 000
China	1 500 000	35 800
Australia	330 000	7 400
Brazil	400 000	35 100
Zaire	200 000	1 600
United Kingdom	260 000	3 200
South Africa	50 000	1 100
Nigeria	280 000	200
Others	765 000	17 000
World total	9 715 000	210 700

11.3.2 Deposits

The economically important tin deposits are closely associated with acidic to intermediate magmatic rocks which were formed in the orogenic phases of the earth's history. Tin, a volatile metal, was deposited primarily during the pegmatitic, pneumatolytic, or hydrothermal phase in the region of the exo- or endocontact of the intrusive bodies. The economically much more important secondary tin deposits exist as eluvial, alluvial, or marine placer deposits which can be near to or remote from these acidic magmatic rock complexes. An overview of the ore reserves and of the amounts extracted in 1990 is given in Table 11.1.

Primary deposits originate from the pegmatitic formation of cassiterite in contact with granites or their secondary rocks. Cassiterite occurs there in idiomorphic pyramidal crystals of > 2 mm diameter. These tin-bearing granites and pegmatites typically include the minerals quartz, albite, potassium feldspar, muscovite, and cassiterite. Columbite is an important accompanying mineral. Deposits of this type are found in central and southern Africa, Brazil, and Russia (Siberia). They account for < 5% of world production. Cassiterite quartzes of the pneumatolytic catathermal phase were formed in vein fissures of granites and their secondary rocks. Individual veins or lodes can have a tin content

of up to 3%. They can be 0.2–1 m thick and up to 200 m deep.

There are various types of paragenesis of the granites, leading to the greisen type (mica-feldspar-quartz formed by pneumatolysis with fluorspar, lepidolite, and tourmaline), the topaz-quartz type, the feldspar-quartz type, and the quartz type. Such deposits contain ca. 20% of the world's tin reserves, and are found in Malaysia, Russia (Siberia), and Germany (Erzgebirge in Saxony). Cassiterite-sulfide deposits of the hydrothermal phase are formed as vein ores associated with intrusions of granodioritic rocks, or are formed by remigration of the metal content of older pegmatitic tin deposits caused by younger acidic subvolcanoes. Characteristic of these types of deposit is the paragenesis of cassiterite with stannite, iron pyrites, arsenical iron pyrites, galena, zinc blende, magnetic iron pyrites, and copper sulfides. These deposits, which can be very large, are mined in Bolivia, Russia, southern China, Thailand, Burma, Australia, South Africa, and also England. They constitute ca. 15% of the world's tin reserves.

Because cassiterite is resistant to weathering and is hard and dense, the weathering of the primary tin-bearing rocks enables it to become concentrated as it is transported to form secondary deposits, i.e., eluvial, deluvial, or marine placers.

Alluvial placers are formed by intense weathering and breakdown of cassiterite-containing granites or granodiorites, especially under tropical climate conditions. The lighter minerals are washed out or carried away by wind, while the cassiterite and other heavy minerals remain behind and can become concentrated in deposits of considerable thickness, as in Malaysia and Zaire. Very coarse and deluvial placers are also formed by gravitational enrichment due to landslips and eluviation at the bottom of mountainsides.

Alluvial or fluvial placers are formed by the transport of weathered tin-bearing rocks by flowing water derived from atmospheric precipitation. The softer and lighter components of the rock are more extensively size reduced and therefore transported further than

the hard, resistant cassiterite minerals, which sink due to their high density and are deposited at points where flow rates are low. The most important alluvial placer deposits are in central Africa (Zaire, Rwanda), western Africa (Nigeria, Niger), and Brazil. Marine placers are formed where primary tin-bearing rock complexes have been directly transported by surf, or where rivers have carried the cassiterite-containing sediment into the sea, where it is then deposited in coastal strips. These are the most important deposits, and represent ca. 60% of the world's workable reserves. The largest of these deposits are in south-east Asia, the coast of Thailand, the Thai Island of Phuket, in Malaysia, and on the Indonesian Islands of Bangka and Billiton.

Secondary deposits usually have tin contents of 0.05–0.5%, reaching 3% in some cases. Marine placers have tin contents of 0.01–0.03%. At present, deposits containing 0.1% Sn are workable by the open-pit method. For underground mining, deposits should contain 0.3% Sn.

11.3.3 Mining

Primary tin ores are extracted by underground mining. Depths can reach 1000 m in exceptional cases. Most of the technologies used in nonferrous metal mining are used, the method in a given situation being determined by the thickness, shape, and orientation of the ore body, and geological factors.

In secondary deposits, the loosely packed weathered hard mineral rock which contains the cassiterite together with associated deposits of sand and gravel is extracted by high-production loading techniques which also perform preliminary classification. General local conditions, including the state of economic development in the region, have a great influence on the mining conditions. For example, in Zaire, surface eluvial deposits (weathered pegmatites) with tin contents of up to 0.15% are extracted by conventional open-pit methods. In Thailand, Malaysia, and Indonesia, loose alluvial and marine deposits in river valleys and in the undersea regions just off the

coast are extracted by dredging shovels, dragline excavators, chain and bucket excavators, and similar equipment specially designed for local conditions. The initial separation of gangue and other foreign materials (e.g., wood) is performed by this equipment. Cassiterite in thick deposits of loose sediments and coarse detritus in Southern China and Thailand is treated with powerful water jets operating at pressures of up to 1.5 MPa. These generate a mixture of water and heavy sand which is then fed to the treatment plant.

Off the coasts of Indonesia, Thailand, and Malaysia, chain and bucket excavators are used to extract cassiterite from alluvial deposits under water at depths of up to 40 m. This also gives a preliminary beneficiation.

11.3.4 Ore Beneficiation [11, 24–28]

The beneficiation of primary tin ores is difficult. The principal mineral, cassiterite, is nonmagnetic and is not suitable for flotation, so that mainly gravimetric sorting processes must be used. Furthermore, cassiterite is often strongly intergrown, and the accompanying minerals behave similarly to cassiterite during processing.

Current technologies are characterized by controlled multistage size reduction of the ores and separation of the cassiterite released after each size reduction stage using sorting methods based on density. Screen jigs and shaking tables of various designs are used. However, very small particles (< 30 μm) cannot be processed to give satisfactory yields and production rates. If the degree of intergrowth of the ores requires finer grinding, as is increasingly the case with ores from Russia, the United Kingdom, Bolivia, South Africa, and Portugal, the flotation method for sorting particles < 100 μm is sometimes used. This technique was also used for the tin ore from the Altenberg region of Saxony, whose mines were closed in 1990. The following stages of beneficiation of primary tin ores are used:

Ores with an average degree of intergrowth are concentrated mainly by processes based on density. Flotation is increasingly used to sort

fine-grained material and ground middlings obtained by the density-based sorting process, and has now become the preferred method for treating the most finely intergrown, complex tin ores. Flotation of cassiterite with particle sizes between 40 and 10 μm is mainly carried out with arsonic acids.

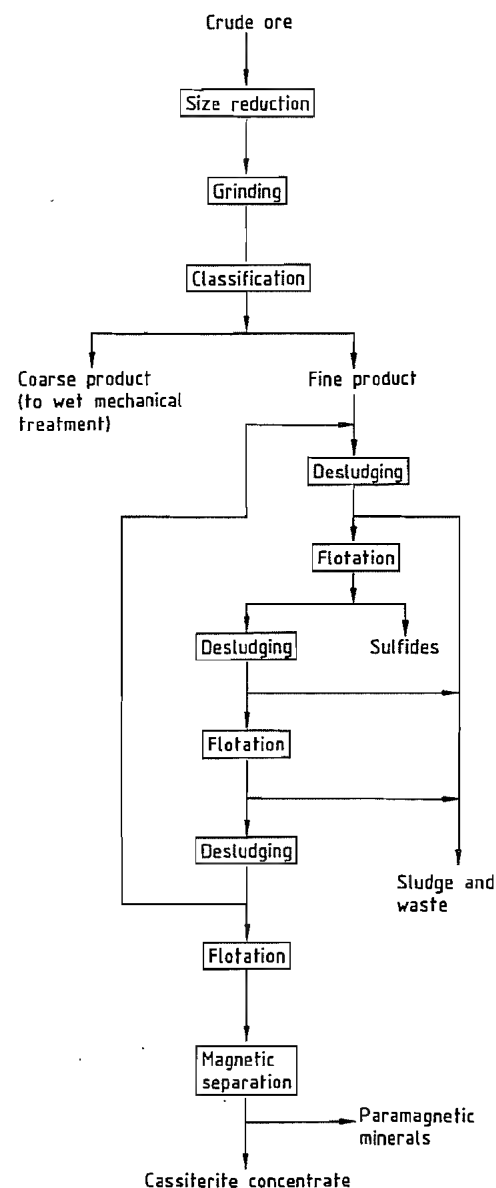


Figure 11.1: Flotation of primary tin ores.

The flow diagram (Figure 11.1) shows the flotation of primary tin concentrates to remove sulfides of similar paragenesis, followed by flotation of cassiterite from the preconcentrate, and magnetic separation of paramagnetic minerals from the flotation product.

Composition ranges for complex tin concentrates are:

Sn	5.6–60%
S	1.0–15%
As	0.1–3%
Sb	0.1–2%
Bi	0.1–0.5%
Cu	0.1–0.7%
Pb	0.1–3%
Zn	0.1–4%
Ag	up to 500 ppm
W	0.1–5% WO_3
Nb/Ta	1–3% $\text{Nb}_2\text{O}_5 + \text{Ta}_2\text{O}_5$

The ores from placer deposits are thoroughly broken down by natural weathering processes which separate the material roughly according to the rate at which it settles out of suspension. The fine-grained cassiterite is mixed with coarser sand or gravel. On board the floating dredges, which operate in artificial dredging ponds or natural surface waters, there is ore beneficiation equipment which produces a preconcentrate for further processing on shore (Figure 11.2). The ore passes through a drum screen which removes coarse gravel (10–20 mm), wood, and other foreign bodies. The material passing through the screen is deslugged in a hydrocyclone, and treatment on a three-stage screen jig then produces heavy metal concentrate for further processing on shore.

The ore obtained from placer deposits on land using water cannons or from the seabed using special ships with suction pumps is processed using conventional ore beneficiation methods such as screen jigs or screen troughs.

Concentrates from placer deposits are relatively pure; a typical analysis (in %) follows:

Sn	70	Ni	0.01
As	0.1	Ta_2O_5	0.2
Sb	0.05	Nb_2O_5	0.1
Pb	0.008	WO_3	0.05
Cu	0.005	SiO_2	5.0
Zn	0.01	CaO	0.1
Bi	0.015	TiO_2	0.1
Fe	0.3	Al_2O_3	1.0

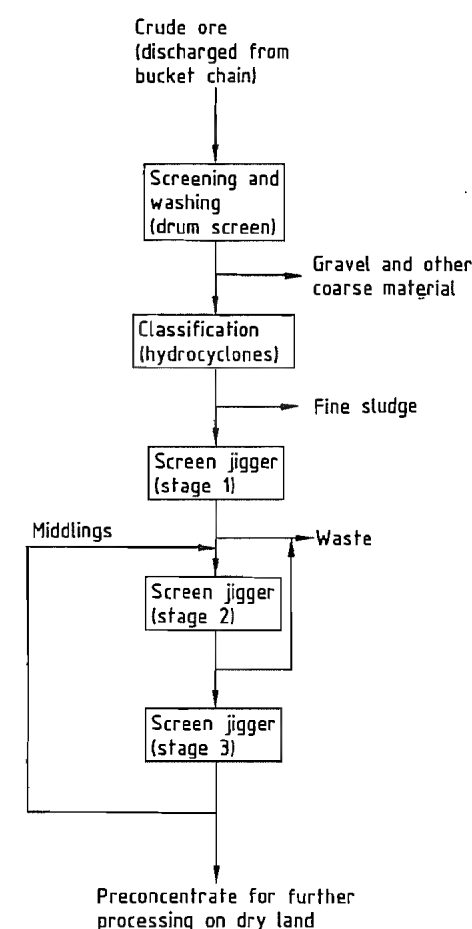
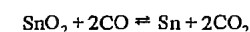


Figure 11.2: Preparation of secondary tin ores (placer deposits) on floating dredgers.

11.4 Smelting

11.4.1 Fundamental Theory of Smelting [1–3, 5, 29–34]

Because the most important tin-bearing mineral in tin ore is cassiterite (SnO_2), the carbothermic reaction



is of fundamental importance.

A theoretical consideration of tin smelting must include the temperature dependence of this equilibrium and the behavior of the im-

portant reactants (Sn, O, and C) and accompanying elements and impurities in the concentrate, e.g., Fe, Cu, Sb, Bi, Ag, Si, Ca, Al, Mg, Nb, Ta, etc., of which Fe is the most important. The equilibrium diagrams for Sn-O-C and Fe-O-C are of crucial importance in the reduction of tin. At temperatures above 1100 °C, not only the Sn but also the Fe present in the oxidic precursors is reduced, so that selective winning from industrial tin-containing raw materials, which always also contain iron, is impossible. Furthermore, in this temperature range, up to 20% tin dissolves in iron, and iron-tin compounds (known as hard head) are formed at lower temperatures, so that iron-free tin cannot be obtained under these conditions. This restricts the advantage of using a high process temperature to give a faster reaction rate in carbothermic cassiterite reduction. Also, the technique of stably binding iron in fayalite, to enable tin reduction to be carried out selectively, though realized on a laboratory scale by WRIGHT [29], could not be scaled up to production conditions.

The elements involved in tin reduction can be divided into the following groups:

- Elements more noble than tin are reduced at lower temperatures than tin, and dissolve in molten tin (e.g., Cu, Pb, and Sb)
- Elements that are much less noble than tin and which are not reduced under the reduction conditions, but which act as important slag formers, such as Ca, Al, and Si in the form of their oxides
- Iron, the most important accompanying element, which behaves similarly to tin
- Gaseous compounds produced in the reduction process
- Sulfur, which has an important role in the reduction and volatilization process of pyrometallurgical tin production

Both the iron and the slag formers must be removed in a liquid slag; this determines the minimum process temperature. The iron content of the metal product depends on the Fe/Sn ratio in the slag. This relationship, represented in Figure 11.3, illustrates the principal problem of tin production from oxidic raw materi-

als. If a high tin yield is to be obtained, i.e., small losses of tin in the slag (e.g., < 10%), high reduction temperatures must be used, giving an iron content in the tin of > 8%, so that subsequent refining is more difficult. If a purer metal is desired (e.g., 0.5% iron in the tin), there will be high losses of tin in the slag, whose tin content can be 10–25%. These slags are starting materials for a second process stage.

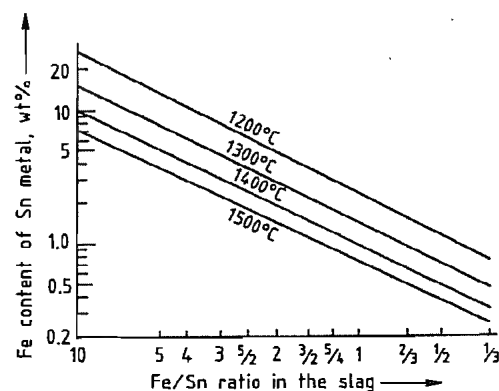
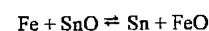


Figure 11.3: Calculated Fe/Sn ratios in the metal and slag at equilibrium as a function of temperature.

The reactions in the slag phase are of major importance for selective reduction, whereby SnO is an important component. Experiments on pure substances have shown that although SnO melts at 980 °C it is unstable below 1100 °C, decomposing into SnO₂ and Sn. The activity of SnO in SnO-SiO₂ melts obeys Raoult's law between 1000 and 1250 °C. The negative free energies of mixing SiO₂ with FeO, ZnO, PbO, MnO, and MgO increase in this order, and increase the SnO activities in the silicate melts. The position of the metal-slag equilibrium in the reaction



is expressed by the distribution coefficient

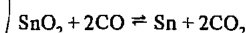
$$K = \left(\frac{\text{Sn}}{\text{Fe}} \right)_{\text{metal}} \cdot \left(\frac{\text{Fe}}{\text{Sn}} \right)_{\text{slag}}$$

K should be as large as possible, and at the usual reaction temperature of 1000–1100 °C used in tin metallurgy, should be ca. 300 to give an iron content of ca. 1% in the tin.

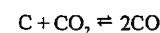
Binary and ternary slag systems containing tin oxides have been thoroughly investigated [33] and give useful guidance for carrying out the tin reduction. However, practical results depend very much on the viscosity of the molten products, the density differences, the surface tension, and colloidal dispersion and chemisorption of the slags. Thus, under production conditions stronger bases displace SnO bound in silicate, and FeO increases the fluidity of the slags.

The difference between the kinetics of tin oxide reduction and iron oxide reduction affects the selectivity of the reduction process and hence the iron content of the tin and the performance parameters of the furnace systems. Other important parameters are the pore structure and particle size of the raw materials, the partial pressures of the reduction gases, removal of the reaction gases, formation of seed crystals and coatings, and heat transfer. Thus, from the point of view of reaction rate, the reverberatory furnace is not the best equipment for carrying out reduction as it contains a large slow moving mass of material with a large bed thickness where heat is supplied only from above. The poor heat transfer leads to an extremely low smelting capacity, i.e., < 0.7 t metal per m³ furnace volume per day. Because slag formation is very slow, some of the tin reduced at the start of the process can be tapped off as a relatively pure, low-iron product before the entire charge is smelted.

In contrast, highly turbulent reaction systems lead to process rates orders of magnitude higher. Under practical reaction conditions above 900 °C, the reaction



is rapid, and the reaction



becomes rate determining. This is why oxygen has to be added to the mixture of solid charge and reducing carbon in the furnace.

World production of tin is two-thirds from oxidic and one-third from sulfidic raw materials. The main problem in treating sulfidic tin concentrates is their complex composition. As

many impurities as possible are vaporized in an initial roasting stage.

Arsenic requires special treatment, as it is oxidized to As₂O₃ and As₂O₅, which combines with Fe₂O₃, formed by roasting, to give non-volatile iron(III) arsenate. In practical operation, a somewhat reducing atmosphere is therefore produced by adding charcoal to the charge. Another possibility is to vaporize heavy metal chlorides by adding NaCl.

11.4.2 Special Aspects of the Winning of Tin from its Ores

Problems in ore beneficiation often lead to concentrates with low tin contents, as unacceptably high losses of material would occur if ore concentrates with higher tin contents were produced. Therefore, a pyrometallurgical "thermal ore beneficiation" stage is necessary prior to the actual reduction process. This is a volatilization process that exploits the fact that the iron compounds and other slag formers have low vapor pressures at 1000–1500 °C, while SnO and SnS volatilize very readily. This technique can also be used to treat tin-containing slags.

The vapor pressure of SnS is considerably higher than that of SnO. Therefore, in practice, SnS is vaporized and then oxidized to SnO and SO₂. Pyrite (FeS₂) added as sulfur source causes problems in later stages of the process, as the FeO formed must be slagged, and the SO₂ evolved makes waste-gas cleaning necessary. However, this is outweighed by the advantages of a high yield of tin at relatively low process temperatures.

Economic advantages can be achieved by using cheap sulfur-containing grades of heating oil as fuel in the roasting process.

The naturally occurring ore beneficiation process that takes place in cassiterite deposits in surface waters and the increasing use of ore concentration processes with finely intergrown ores lead to extremely fine grained materials. Processes of agglomeration or compaction would be very costly. For this reason, these types of raw material are usually treated in an ore reverberatory furnace.

The main problem in pyrometallurgical tin production processes is separating tin from iron. Under production conditions, simultaneous reduction of SnO and FeO cannot be prevented. Molten tin can dissolve large amounts of iron, and intermetallic compounds, which are very difficult to separate, can be formed on solidification. To minimize this problem, tin production is carried out in two stages. In the first stage, under mild reduction conditions, a relatively pure tin and a rich slag are produced. The latter is treated under strongly reducing conditions in the second stage, giving a discardable slag and a very impure tin-iron compound. The metallic phase is returned to the first stage, where the iron is re-oxidized. The two-stage process must be carried out such that the iron initially in the concentrate is eventually removed from the process in the waste slags.

11.4.3 Production of Crude Tin

11.4.3.1 General Aspects

The choice of a crude-tin production process involves consideration of factors associated with both raw materials and location, and the following questions must be posed:

- Whether the raw materials are highly enriched concentrates with low levels of impurities
- Whether the raw materials used are low-grade concentrates whose principal impurities are slag components
- Whether complex raw materials containing at least one other valuable element (e.g., W, Nb, or Ta) are used

Other important factors include the availability of raw materials, energy costs, environmental considerations, and personnel costs.

11.4.3.2 Ore Preparation prior to Reduction

As a result of the problems described in Section 11.3.4 and also of the efforts to recover as much of the tin from the ore as possi-

ble, the tin content of the ore concentrate can range from 8 to 60%. Hence in most cases, pretreatment is necessary, e.g., pyrometallurgical enrichment of low-grade raw materials, a roasting stage (sometimes with addition of fluxes), or a leaching operation.

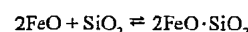
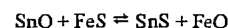
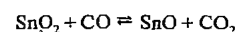
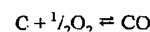
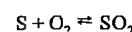
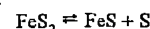
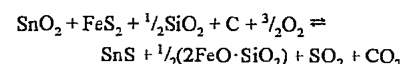
Pyrometallurgical Enrichment of Low-Grade Concentrates [1–5, 28–30, 34–41]

Low-grade tin concentrates are subjected to pyrometallurgical enrichment. The tin is vaporized as sulfide, and then oxidized in the gas phase by atmospheric oxygen to form SnO₂. The nonvolatile components of the raw material are selectively removed, and with careful process control, 90–95% of the tin can be recovered as an oxidized product containing 40–60% Sn.

Optimum results are only obtained if the reaction of the sulfide with oxygen takes place exclusively in the gas phase; therefore, reducing conditions must be maintained in the furnace. Although gaseous sulfur is the best sulfiding agent from a thermodynamic viewpoint, pyrites is used almost exclusively under production conditions. If calcium sulfate is used, the disadvantage that energy is required for its dissociation must be balanced against the advantage that the CaO produced is a useful slag former.

Although the vaporization of tin as SnS is used in all production plants, there is no generally accepted model of the reactions that take place. However, it is probable that in view of the S/Sn ratios required, the available polysulfidic sulfur in the pyrites does not take part in the formation of tin sulfide. Furthermore, it can be deduced from the importance of the added carbon to the reaction product obtained and from the CO content or oxygen demand of the reaction gases that SnO₂ is reduced first to SnO in an intermediate stage and SnS is then formed by the reaction of SnO with FeS. This is supported by the fact that the pyrites or the FeS formed therefrom forms SnS more readily than does sulfur vapor, contrary to what would be expected from thermodynamic considerations.

These results, especially when supported by practical experience, show that the overall equation and the individual reactions are probably as follows [28]:



Pyrometallurgical enrichment of low-grade tin concentrates can be carried out in various types of furnace.

Initially, rotary and shaft kilns were used for the vaporization process. Although the operation of both types of equipment was technically sophisticated, there were considerable disadvantages, which eventually led to their abandonment. Apart from the high energy and fuel requirements typical of both systems, the shaft kiln process led to a relatively low direct yield of tin in the flue dust, mainly due to the production of matte, which required separate processing. The rotary kiln method led to a low tin concentration in the flue dust, and, for raw material of high iron content, to the formation of matte, and hence to a drum clinker, which had then to be processed in a shaft kiln.

High-capacity thermal concentration processes, already established on a large scale in the nonferrous metal industry, were therefore adapted to tin enrichment. The fluidized bed and the cyclone smelting processes were not used. Also, the flash smelting (levitation smelting) process has severe limitations because of the raw materials used. Good results could be obtained with concentrates in which most of the material had a particle size of 200–300 μm. Using such concentrates containing 10–12% Sn, discardable slags containing 0.2–0.4% Sn and flue dusts containing 50–60% Sn could be obtained. On using low-grade concentrates that had not been desludged and

which contained significant amounts of material with a particle size of 50–60 μm, the amount of primary flue dust increases significantly, and the tin concentration in the flue dust sometimes decreases to < 40%. Also, the tin content of the slags is unacceptably high (1–2%).

The main disadvantage of the flash smelting process is that it imposes strict requirements on the physical form of the concentrate.

The slag blowing process, originally used for detinning the slags from the reduction process, has been increasingly used for enrichment of tin in low-grade concentrates and exploitable gangue from ore processing. These products were at first added to the initial smelting process, but they were later added in solid form directly to the blowing furnace. Smelting and blowing can be carried out in a single furnace, so that it is not necessary to build a special smelting plant. This enables capital and operating costs to be reduced.

An important part of the practical operation is the maintenance of the correct fuel-air mixture with uniform distribution of the fuel and air to the individual jets. Heating oil and natural gas are preferred because they are more easily metered than solid fuels. If pyrites is used as the sulfiding agent, an S/Sn ratio of 0.8 is necessary, which places high demands on the equipment for removing sulfur dioxide. When pyrites is used, only FeS is effective in the slag phase, so that only 50% of the sulfur is used for sulfiding. If pyrrhotite (magnetic pyrites) or calcium sulfide is used, the S/Sn ratio need only be 0.4, and the emission of sulfur dioxide decreases by 50%.

The good metallurgical results of the slag blowing process, in which flue dusts containing 65–70% Sn and final slags containing 0.1% Sn are obtained, must be balanced against the disadvantage of a batch process. This leads to nonuniform loading of the downstream plant, e.g., the waste heat recovery and gas cleaning equipment.

Roasting [1, 2, 4, 5, 11, 17, 32, 42–50]

The roasting process, not only converts sulfides to oxides, but also volatilizes major oxidic impurities (e.g., arsenic). Roasting can be an independent process, or a pretreatment prior to hydrometallurgical leaching. It is significant that the level of impurities As, Sb, Pb, and Bi in tin concentrates has increased in spite of great efforts to improve ore beneficiation technology. If the levels of As and Pb are > 0.1%, and of Bi and Sb > 0.03%, a roasting process, sometimes with the addition of a leaching stage, is both useful and necessary for the benefit of the final tin reduction and refining processes.

The important reactions in the roasting process are as follows (M = metallic impurity):

- Dissociation
 $\text{FeS}_2 \rightleftharpoons \text{FeS} + \frac{1}{2}\text{S}_2$
 $4\text{FeAsS} \rightleftharpoons 4\text{FeS} + \text{As}_4$
- Roasting reactions
 $\text{MS} + \frac{3}{2}\text{O}_2 \rightleftharpoons \text{MO} + \text{SO}_2$
- Oxidation
 $\text{MO} + \frac{1}{2}\text{O}_2 \rightleftharpoons \text{MO}_2$

Although the roasting reactions and especially the oxidation reactions are exothermic, addition of fuel is necessary in industrial-scale roasting processes. The pore structure of the material must be maintained to enable the gaseous metallic and nonmetallic impurities to be vaporized. The upper temperature limit for the roasting process is imposed by the melting point of the low-melting sulfide eutectic. However, the temperature should be kept as high as possible to prevent the formation of sulfates, e.g., lead and calcium sulfate.

A mildly reducing atmosphere is necessary to suppress sulfate formation and also prevent formation of higher nonvolatile oxides of the impurities (e.g., As_2O_5).

The roasting processes are carried out in multideck or rotary kilns. The use of fluidized-bed furnaces with carefully controlled operating parameters has been reported [48].

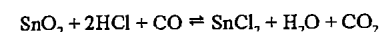
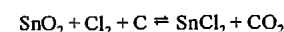
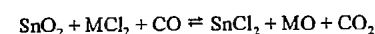
Chloridizing roasting is also suitable for the pretreatment of tin concentrates, owing to the high affinity of the main impurities for chlorine. However, problems can be caused by

chloridation of tin, which itself then volatilizes as SnCl_4 and SnCl_2 .

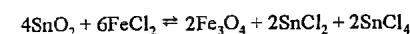
Chloridizing roasting of tin concentrates in rotary kilns is carried out in Thailand. The contents of lead and bismuth are lowered from 2.0% to 0.04%, and from 0.1% to 0.02%, respectively. The flue dust contains 10% As, 3% Sn, 20% Pb, and 4% Bi. Treatment of this product presents serious problems [2].

The processes for removing impurities by chloridation differ fundamentally from those for the volatilization of tin from concentrates, being based on the fact that a large phase field exists in the phase diagrams Sn-HCl-H_2 and Fe-HCl-H_2 between 900 and 1000 °C in which selective chloridation and volatilization of tin is possible without chloridizing iron.

The overall reactions are as follows (M = Mg, Ca, or Na):

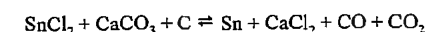
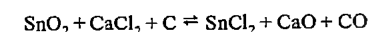


The presence of iron oxide increases yield and reaction rate, which can only be explained by intermediate formation of FeCl_2 :



Here, the instability of iron chloride in the presence of tin oxide is the reason for the good separation of tin from iron. In a reducing atmosphere, i.e., in the presence of C or CO, only SnCl_2 is formed.

In the Warren Spring process [50], CaCl_2 is used as chloridizing agent, and the CaO formed is used in the reductive smelting by adding limestone in accordance with the following equations:



The industrial-scale reaction is difficult to carry out, as moisture resulting from the hygroscopic properties of the tin chloride and the quicklime must be avoided. The corrosive properties of the reaction gases make very high demands on the construction materials used.

A special form of roasting is the heating of high-tungsten tin concentrates with NaOH or Na_2CO_3 to give soluble Na_2WO_4 , which can be leached out.

Leaching [1–4, 32, 47, 51–55]

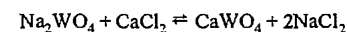
In tin metallurgy, the main use of leaching processes is to remove typical impurities from the concentrate. Tin, which is nearly always present in the raw materials as SnO_2 , can only be brought into aqueous solution if the SnO_2 is reduced to SnO in a precisely controlled CO/CO_2 atmosphere. It can then be extracted in acid or alkaline media. This procedure has not yet been operated on an industrial scale.

Only hydrochloric acid is used on an industrial scale to remove impurities by leaching, the typical impurities in the concentrate, Fe, Pb, Cu, Sb, or As, going into solution in the form of their chlorides. Best results are obtained using > 20% hydrochloric acid at 100–110 °C. Suitable reaction vessels are high-pressure, acid-resistant spherical autoclaves with a capacity of 20 t. This batch process must sometimes be repeated several times. The solids are removed by thickeners and vacuum filters, and the dissolved impurities are precipitated from the liquor by cementation on scrap iron.

The high costs of these special reactors, the batch mode of operation, and the expense of the process for recovering the hydrochloric acid have restricted the use of hydrochloric acid leaching to some special cases.

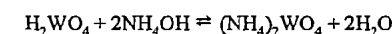
It is preferable to carry out chloridizing roasting before leaching out the impurities. This then only requires a dilute acid solution.

Leaching of tungsten-containing tin concentrates to recover tungsten is important. After digesting the ore with sodium carbonate in spherical boilers, the tungsten is converted to its hexavalent form, which is soluble in hot water. It is then precipitated from the neutral solution with CaCl_2 :



An easily filtered precipitate containing up to 60% WO_3 (on dry basis) is obtained.

Tungsten can also be extracted from tin concentrates by leaching with an aqueous solution of ammonia:



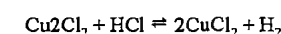
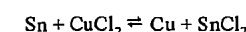
The concentration of WO_3 in the filtrate can reach 50 g/L, and this can be precipitated as artificial scheelite, $\text{Ca}(\text{WO}_4)$. The tungsten content of the tin concentrate can be reduced to 0.5%.

Most of the tin can be leached from a tin concentrate containing 2% bismuth with 5% hydrochloric acid at 80 °C [46].

Treatment with sulfuric acid is used to remove iron present as carbonate in Australian tin concentrates. By removing gangue material in this way, the tin content of the concentrate is increased from 37.2% to 47.1%.

A process for the removal of arsenic from tin concentrates by bacterial leaching with *Thiobacillus ferrooxidans* has been tested in Russian research institutes [54].

The tin can be leached out of ores that are difficult to treat if these are first reductively smelted with CuCl_2 and HCl, in accordance with the following series of reactions [42]:



Tin is precipitated from solution by adding zinc, and copper by adding iron.

11.4.3.3 Reduction

As explained, it is not possible to obtain high yield and high metal purity at the same time. Reduction is therefore carried out in two stages, the first stage giving a relatively pure metal (up to 97% Sn) and a rich slag (8–35% Sn). This slag is treated in a second stage, and sometimes in a third. Slag treatment processes are described later.

Various types of furnace are used for reduction. Very low grade ore in lump form can be treated in a shaft kiln. However, as most concentrates obtained in ore beneficiation are very finely divided, and agglomeration, e.g., by sintering, is impossible, other types of fur-

nace must be used in this case. Reverberatory or rotary air furnaces are often used for reduction, and electric furnaces are also employed. Each furnace type has its own advantages and disadvantages.

Reduction in a Shaft Kiln [1-3, 5, 30, 56, 57]

Shaft kilns are historically the oldest type used for tin reduction. They have their origin in the old Chinese natural draught furnaces made of rammed clay held together with wooden posts and operated on mountainsides. The hearth was usually sloped so that the molten product ran off continuously. Today, shaft kilns are water-jacketed, and have a melting capacity of $5.5-8 \text{ tm}^{-2}\text{d}^{-1}$. The good heat transfer and the continuous method of operation give a higher melting capacity than is obtained in comparable reverberatory furnaces. The air flow rate must be low to prevent volatilization. Shaft kilns require raw material in lump form. The iron content must be as low as possible in order to limit the formation of hard head in the reducing atmosphere.

Reduction in a Reverberatory Furnace [1-3, 5, 30, 32, 58-61]

The necessity for treating fine-grained concentrates from ore beneficiation has led to the replacement of the shaft furnace by the reverberatory furnace, and this is today the most important type of reduction equipment used in tin metallurgy. Modern reverberatory furnaces have internal dimensions of 3-4 m width, 10-13 m length, and 1-1.5 m height. In a freshly lined hearth the height available for the molten charge is no more than 0.5 m. This increases with increasing wear of the furnace bottom. The bath volume of modern tin ore reverberatory furnaces is 20-50 m^3 . As the tin is very fluid at the reaction temperatures (up to 1400 °C), high pressures can be produced at the bottom of the hearth. To prevent this, either holes must be provided in the steel sheet bottom to allow the tin to drip into a lower chamber where it can solidify in stalactite

form, or the reverberatory furnace must have a water-cooled bottom so that the tin solidifies in the gaps between the bricks.

The refractory bricks and mortar used to line the furnace must be made of high-grade chrome-magnesite. This must be very pure because of possible reactions of SnO or Sn with iron oxides or silica. Chamotte can only be used above the slag zone. To avoid disturbance of the brickwork in the melting zone, charging is carried out through the roof.

The burners, which use heavy fuel oil, are situated on the narrow sides of the furnace. The furnaces operate discontinuously using the regenerative principle, the duration of a heat being 16-20 h. Specific melting capacities are in the range $1.2-2.0 \text{ tm}^{-2}\text{d}^{-1}$. Charge batches consisting of concentrate, carbon, and fluxes weigh between 40 and 70 t. Optimum results can only be achieved by extremely careful operation.

Thus, at the start of a new heat, the amount of material charged to the furnace should be limited, e.g., by adding the charge in two portions, to prevent a large drop in temperature. The amount of carbon added in the form of coke, coal, petroleum coke, or charcoal is determined by the tin and iron contents and also by the incidence of hard head. The carbon addition is adjusted so that coreduction of the iron is prevented as far as possible.

The furnace draught must be kept low to prevent entry of cold air and to maintain the oxygen content in the waste gas below 5 vol%, thereby minimizing oxidation of the tin.

The first tin can be tapped off after 4-5 h of a 24 h cycle. As this is comparatively pure, it is preferable to treat it separately. The material tapped off later separates into metal and slag in a settler outside the smelting furnace. Some furnaces have facilities for tapping off the metal and the slag separately.

Up to 6% of the weight of charge material is converted to flue dust, which consists of entrained charge, SnO , and some SnS . Its tin content is therefore considerably higher than that in the charge material.

Compositions of products obtained when a relatively pure concentrate ($> 70\% \text{ Sn}$) is

treated in a reverberatory furnace are listed in Table 11.2. The amount of slag is relatively small (14% of the charge), but the slag must undergo a further stage of processing because of its high tin content.

A simplified flow diagram for the treatment of high-grade concentrates is shown in Figure 11.4.

The process flow diagram for low-grade, impure, and complex concentrates is considerably more complex. With high-grade concentrates, a tin yield, including that obtained from slag treatment, of 99.6% can be achieved, as actual losses of tin can only occur in the waste slag and by loss of airborne dust. In the treatment of low-grade concentrates, the yields of tin may only be 955%, and in exceptional cases 925%, because of the numerous tin-containing waste products.

Control of the CO partial pressure, which determines the reduction potential, is more

difficult in a stationary reverberatory furnace, which contains a slow-moving mass of charge, than in a shaft furnace, in which the coke and air move in countercurrent flow. This is also the reason for the poor heat transfer and hence the low rates of reduction and melting in a reverberatory furnace.

Table 11.2: Typical compositions of products from a reverberatory furnace (in %).

Component	Crude tin	Slag	Flue dust
Sn	97-99	8-25	40-70
Fe	0.02-2.0	15-40	0.8-4.0
As	0.01-2.0		0.1-0.7
Pb	0.01-0.1	0.1-0.5	0.2-1.6
Bi	0.003-0.02		0.01-0.1
Sb	0.005-0.2	0.01-0.02	0.1-0.4
Cu	0.001-0.1		0.02-0.05
Al_2O_3		7-12	≤ 1.0
SiO_2		10-30	≤ 2.0
CaO		4-14	≤ 0.6
MgO		1-4	≤ 0.6
S	0.01-0.05		≤ 1.0

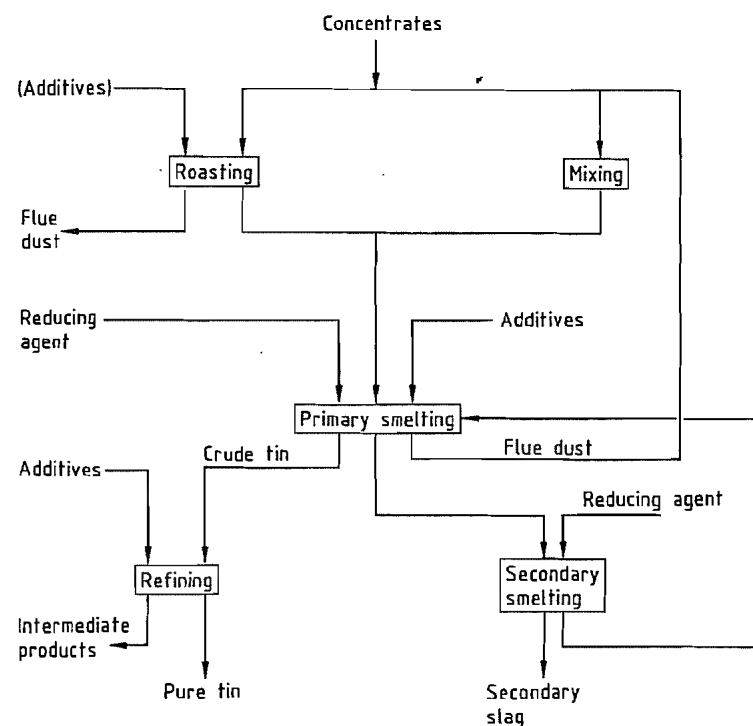


Figure 11.4: Process for treating high grade concentrates (simplified).

Under operating conditions, care must be taken that the slag formers do not melt too rapidly, as this impairs the contact between the furnace atmosphere and the unmelted charge. At the same time, the melting temperature of the slag must be as low as possible, so that the use of such slag formers as CaO and SiO₂ should be limited. Added lime is of special significance, because it displaces tin from silicate, can lead to calcium stannate formation if present in excess, and increases the melting point of the slag.

The effect of the slag constituents, especially on melting point and viscosity, is described in detail in [3]. In a process optimization/cost minimization exercise, it is always necessary to include the effect on costs of the amount of tin tied up in materials being recycled [59].

Reduction in Rotary Kilns [1–3, 5, 30, 32, 57–62]

Rotary kilns (rotary air kilns) are horizontal smelting units that operate batchwise. They have a higher melting capacity than stationary reverberatory furnaces, but lead to considerably more severe stress on the refractory lining. Operating procedures in two tin smelting works in Indonesia and Bolivia in which the reduction process is based on the rotary kiln principle are reported in the specialist literature [63]. The furnaces have a length of 8 m, a diameter of 3.6 m, a surface area of reacting material of ca. 22 m², and a specific melting capacity of 1.36–1.5 t m⁻² d⁻¹.

The furnace availability (300 d/a) is superior to that of reverberatory furnaces (260 d/a). Also, there is less requirement for mixing operations or agitation of the melt by stirring (rabbling). The metallurgical results of both types of furnace are very similar. However, the considerably poorer stability of the refractory lining, the higher energy requirement, and the significantly larger quantities of flue dust are all disadvantages. Separation of the tin from the slag has to be carried out outside the furnace in a settler.

Table 11.3: Typical compositions of products from rotary kiln at Mentok, Bangka (in %).

Component	Crude tin	Slag	Flue dust
Sn	99.78–99.83	14–25	60–72
Fe	0.089–0.144	15–26	1–4
Pb	0.010–0.031		
As	0.010–0.188		
Sb	0.005–0.010		
Bi	0.0025–0.003		
Cu	0.002–0.025		
SiO ₂		8–24	0.2–2.0
CaO		2–10	1–1.2
MgO		2–4	
S			0.2

Tin concentrate can also be reduced in short drum kilns in which the ratio of the length to the cross-section is 1. The metallurgical function is basically similar to that of the rotary kilns. The compositions of the smelting products in an Indonesian tin smelting works in which high-grade concentrates are reduced in a rotary kiln are given in Table 11.3.

Reduction in an Electric Furnace

[1–3, 5, 30, 32, 58, 64–68]

Electric resistance and arc furnaces used in metallurgy are characterized by high reaction temperatures and low waste-gas volumes. Disadvantages are the necessity for thorough pre-mixing of the raw materials and the batch operation. Tin smelting is often carried out in regions where electrical energy is less readily available than energy from other sources such as gas, coal, or oil. Wherever electric furnaces are used in tin metallurgy, the object is to utilize their advantages of high reaction temperature and the production of heat by the Joule effect directly in the smelting bath.

Because their reducing action is so effective, electric furnaces are particularly suitable for extracting tin from slag (see Section 11.4.3.4). In concentrates whose iron content is significantly less than 5%, it is even possible to produce crude tin in a single stage, with tin levels in the slag of < 0.7%. Electric furnaces are used in many tin smelting works for primary tin production from concentrates. These concentrates are often imported, e.g., in Germany, France, Italy, Canada, and Japan, al-

though tin concentrate producing countries, e.g., Brazil, Zaire, South Africa, Russia, Thailand, and China also use electric furnaces. The raw materials for the electric furnace process must be intensively mixed. Very fine-grained materials such as flue dust are pelletized. A moisture content of ca. 2% must not be exceeded. Typically, circular furnace vessels with an outside diameter of up to 4.5 m and a height of 1.5–3 m are used, or oval furnace vessels with dimensions 2.5 × 1.8 × 1.8 m. Heating is carried out with three-phase electric arcs using graphite electrodes. In single-phase furnaces, the furnace bottom acts as the counterelectrode for the immersed graphite electrodes.

Both stationary and tilting furnaces are used. Linings of carbon bricks give a service life of up to three years. Electric currents of 6–20 kA at 50–150 V are used. Depending on the characteristics of the raw materials, energy consumption is 750–1400 kWh/t concentrate (1300–1860 kWh/t tin). Precise control of the electrode immersion depth is essential for good control of the process.

Electric furnace technology enables a wide range of process parameters to be used. For example, when low-iron concentrates are treated, a tin quality suitable for normal refining can be produced. The high-tin slags produced (up to 30% tin) are treated in a second stage to recover the tin. If the iron contents are much greater than 3%, the tin obtained has a high iron content (3–10%).

It is also possible to operate at ca. 1400 °C by using strongly reducing conditions. A tin-containing slag is then obtained together with hard head containing ca. 40% tin and 50% iron. The iron can be removed by smelting with ferrosilicon in a second pass, and a crude tin containing ca. 1% iron is obtained.

Great efforts have been made to overcome the disadvantage of batch operation of the electric furnace. For example, a continuously operated lengthened double chamber electric furnace has been reported in Russia. Each chamber has a hearth area of 1 m² and two electrodes. The reduced tin flows out of the first chamber over an air-cooled overflow, and

the tin is extracted from the high-tin slag in a second chamber [68]. The process is still at the pilot stage. The furnace capacity is reported to be less than 10 t/d.

Other Reduction Processes [1–3, 5, 30, 58, 60, 69]

All the processes described above have disadvantages, and many other methods and types of equipment have therefore been suggested for the reductive treatment of tin concentrates, but few of these proposals have led to an industrial plant.

One of the few methods tested at full scale is the top blown rotary converter developed in the United States and based on the “Kaldo” converter used in ferrous metallurgy. Oxygen is blown onto the top of charge as the converter rotates about its axis, which is set at an angle. The volume of waste gas is very low as there is no ballast nitrogen. The favorable heat transfer to the charge leads to a high reaction rate. Disadvantages include batch operation, a high rate of wear of the refractory lining, and the complexity of the system for controlling the oxygen lance.

After completion of the reduction process, the tin is tapped off. The tin in the remaining slag is vaporized as chloride by adding calcium chloride, and a discardable slag is thereby produced.

The tin chloride is scrubbed out of the waste gases and then precipitated as SnO₂ by adding CaO, regenerating CaCl₂.

The potential for transferring proven processes used in nonferrous metallurgy to tin metallurgy is discussed in detail in [69].

Developments over recent years suggest that no completely new processes for reducing tin concentrates have become established in the industry because of the high capital investment required and the hidden risks involved.

11.4.3.4 Slag Processing [1, 2, 5, 32, 38, 47, 62, 63, 70–79]

The slags produced during the reduction of high-tin concentrates can contain 5–10% of

the tin. This can increase to 20% in the case of low-grade and complex ores. One- or two-stage treatment of the slag is then necessary. It is in principle possible to use strongly reductive smelting (e.g., in a reverberatory or rotary furnace) or blowing processes to volatilize the zinc from the slag.

On reductive smelting, the tin and iron form an alloy, the so-called hard head, which is recycled to the primary tin production process. The secondary slag has such a low tin content that it can be removed from the process.

In the blowing process, the tin is converted into a flue dust, which is recycled to the primary smelting process. The slag, which usually has a high iron content, can be discarded.

Table 11.4: Tin and iron balance for two-stage smelting of a concentrate containing 73% Sn and 0.7% Fe based on 1000 kg concentrate treated.

	kg Sn	kg Fe
Smelting of concentrate		
Charge:		
1000 kg concentrate	730	7
95 kg hard head	38	42
220 kg coke/coal		2
40 kg flue dust	18	
11 kg recycled material	6	3
Total	792	54
Product:		
733 kg crude tin	730	5
200 kg primary slag	47	51
30 kg flue dust	15	1
Total	792	54
Smelting of slag		
Charge:		
200 kg primary slag	47	51
40 kg coke/coal		
Total	47	51
Product:		
100 kg secondary slag	1	8
95 kg hard head	38	42
10 kg flue dust	5	
2 kg Fe alloy		1
Total	44	51

Under production conditions, the intermediate products, e.g., the tin-containing secondary slag, the hard head, and the flue dusts, contain considerable quantities of tin. These are important for the economic operation of the process because of the amount of capital tied up if they are not immediately treated.

The tin and iron balances in the treatment of a concentrate with a very high tin content and a low iron content are shown in simplified form in Table 11.4.

The balance shows that the iron introduced into the concentrate smelting process with the concentrate and reducing agent (7 + 2 kg) must be removed from the slag smelting process in the secondary slag and iron-tin alloy (8 + 1 kg). Of the tin in the concentrate, 6% is in circulation in the primary slag (47 kg out of 730 kg).

However, the concentrates treated usually contain considerably more iron, so that a larger amount of primary slag and hard head are produced, and the amount of tin contained therein can rise to 20% of the raw material used.

In practical slag smelting, the SnO in silica-rich slags is mainly present as $2\text{SnO} \cdot \text{SiO}_2$, and the high activity of the SnO in silica- and lime-containing slags decreases with increasing FeO contents, so that in practice simultaneous reduction of tin and iron occurs. Theoretically, it is only possible to produce crude tin and low-tin slag if the FeO activities are extremely low. However, the processes would proceed at high temperatures with large additions of reducing carbon.

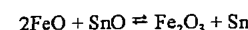
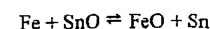
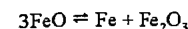
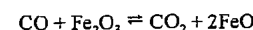
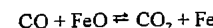
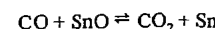
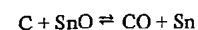
The binary Fe-Sn phase diagram shows a miscibility gap at $> 1100^\circ\text{C}$ between 20 and 50% Fe. On cooling to room temperature, separation of α -iron first takes place, followed by formation of FeSn and FeSn₂. At room temperature, the region of the composition of the hard head is always in the α -iron/FeSn two-phase region.

Wright has found by calculation of the distribution constant K at equilibrium

$$K = \left(\frac{\text{Fe}}{\text{Sn}} \right)_{\text{slag}} \cdot \left(\frac{\text{Sn}}{\text{Fe}} \right)_{\text{metal}}$$

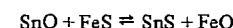
that the balance of the process is improved as the ratio in the first quotient increases, i.e., as the amount of iron removed in the slag increases. However, there must then be a higher iron concentration in the tin. If the tin in the

primary slag is present as $2\text{SnO} \cdot \text{SiO}_2$, the reaction mechanism is as follows:



Thus the reaction first occurs only at the surface of the carbon, and then via the iron oxides as intermediate phases. A high relative rate of reaction of carbon, slag, and reaction gas is therefore important for the reaction kinetics.

The reactions that occur in the detinning of slag are described in Section 11.4.3.2 (pyrometallurgical enrichment of low-grade concentrates), but here they start from SnO. As a matte phase must be present, the reaction will be:



As the slag is saturated with FeS, the amount of SnS formed is proportional to the activity of SnO in the slag, but indirectly proportional to the activity of FeO.

Reverberatory or electric furnaces are usually used in the reductive smelting process for the extraction of tin from primary reduction slags, though shaft kilns are occasionally used. The necessary intense reducing effect is achieved by adding 10–20% reduction carbon and by operating at temperatures up to 1500°C . In the electric furnace process, energy consumptions are 500–1000 kWh/t, and 1–10 kg electrode is consumed per tonne of slag. The reaction products, i.e., the final slag and the hard head alloy, are separated in settlers and then granulated in water.

As highly turbulent conditions are favorable to the process, reductive detinning can be carried out with a lance ("submerged combustion"), which produces a high reaction rate by agitation of the bath. Methane or natural gas

have been used as reducing gas, and experiments have also been carried out using hydrogen, carbon monoxide, and powdered solid fuels. Heat is produced by partial combustion of the injected gases and transferred to the molten slag. However, because SnO is volatile, 20% of the tin goes into airborne dust, a further undesired tin-containing reaction product in addition to the hard head.

An effective method of detinning primary tin reduction slags is by the blowing process, which can be carried out in reverberatory furnaces or true blowing furnaces. Gypsum or pyrite can be used as the sulfur source. The gypsum is first reduced to CaS, and then reacts with SnO to form SnS and CaO. If pyrite is used, impurities such as Pb, Zn, or As are introduced into the metallurgical process, adding to the difficulties of treating the tin-containing flue dusts. Blasting technology is also often used as the third stage of slag detinning. In the second stage, a thermal reduction, Sn contents of 2–5% and FeO contents of ca. 30% are obtained. The tin content of the molten slag in the furnace is reduced to ca. 0.5% by addition of sulfur sources. The addition of pyrite can be up to 400% of the theoretical amount calculated for the formation of SnS. Since smaller additions are possible in the case of acid slags, CaS is probably formed in basic slags. The treatment of primary slags in true blowing furnaces consists of blowing the pyrites into the molten slag. However, the process is discontinuous. The SnS vapor is oxidized in the furnace atmosphere, and recovered as SnO dust by filtration.

The slag blowing process can be carried out in furnaces of various designs, e.g., in a type of shaft kiln with a floor area of $0.5\text{--}6\text{ m}^2$ and a water-cooled shaft 7 m in height. The charge of primary slag can be 5–20 t. Cyclone and short drum kilns are also used. Process parameters, e.g., ratios of sulfur source to oxygen, fuel to atmospheric oxygen, and tin to sulfur must be carefully controlled to obtain optimum results.

Other proposed methods of detinning primary tin slags, such as vacuum-assisted volatilization of SnO (which has a considerably

lower vapor pressure than SnS), have not been used on an industrial scale [29].

11.5 Refining [1-3, 5, 32, 46, 47, 80-84]

The crude tin obtained by the reduction process is insufficiently pure for most applications.

Most national standards specify maximum contents of typical impurities. However, non-metallic impurities such as oxygen and sulfur and less common impurities such as noble metals are neglected, and the tin content is simply determined by subtracting the total amount of analytically determined impurities from 100.

The following three standard grades are accepted internationally: Sn 99.0%, Sn 99.75%, and Sn 99.9%.

There are some variations in these standards from country to country; the German standard is DIN 1704.

The level of impurities in the crude tin determines the extent of the refining operation. Treatment of very pure concentrates can give a tin content of up to 99.0% in the crude metal. The main impurity is iron (0.8%), the sum of all the other impurities being only 0.2%. In the case of low-grade and complex concentrates, the situation is very different, the tin content of the crude tin obtained sometimes being only 92%.

The impurities Fe, As, Sb, Cu, Ni, Pb, Bi, and the noble metals affect the amount of work involved in the refining process. The metals Zn, Cd, Mg, Si, Ca, Te, Se, and also sulfur and oxygen do not require special treatment, as they are present in the crude metal in only small concentrations, and are removed together with the other impurities during the various stages of purification. The phase diagrams for tin and its typical impurities lead to the following conclusions:

In the temperature range between 1000 and 1300 °C used in pyrometallurgical reduction, the impurities are completely soluble with the exception of Fe and Cr.

Only Sb, Cd, Bi, Zn, and Pb are significantly soluble in tin at room temperature. This is the basis for the removal of insoluble impurity elements by liquation. However, the liquation products have high tin contents, making costly recovery processes necessary.

In pyrometallurgical tin refining, the individual impurities are removed stepwise in batch processes. The use of the time-consuming operations is justified by their high selectivity.

Proposed continuous processes have not been operated on an industrial scale.

11.5.1 Pyrometallurgical Refining

11.5.1.1 Removal of Iron

The process for removing iron is based on the temperature dependence of the solubility of iron or Sn-Fe mixed crystals in tin. Accurate experiments have shown that the solubility of iron in tin at 250 °C is 0.0058% [81]. In industrial practice, even lower figures are achieved, which can only be explained by other impurities, such as Cu, As, or Sb, causing deviations from ideal solubility behavior. On cooling molten crude tin, α -Fe, γ -Fe, FeSn, and FeSn₂ precipitate successively. The density of the precipitated compounds is almost the same as that of the molten tin. In practice, "poling", i.e., passing steam or air into the melt, is used to coagulate the precipitated particles, which rise to the surface of the bath and are removed from the molten tin by filtration through graphite, slag wool, or a slab made of silica and limestone chippings. This should be carried out just above the melting point of tin, or in practice at a temperature not less than 260 °C. The process is sometimes carried out in two stages. Iron contents of 0.003-0.01% can be achieved.

As, Ni, Co, Cu, As, and Sb form intermetallic compounds with each other as well as with Fe, these impurities are also removed to some extent.

The treatment of the recovered intermetallic compounds is very complex, as these are in the form of a slurry with large amounts of ad-

hering molten tin. The iron content is only a few per cent, i.e., considerably less than that of the intermetallic compound FeSn₂.

The metal slurry is treated in small liquation furnaces. A controlled temperature increase over the range 230-300 °C enables pure tin to be removed, and a residue containing ca. 15% Fe suitable for use in the primary smelting stage to be obtained.

In high-capacity tin smelting works, high-temperature centrifuges are used. These enable a solid residue containing up to 25% Fe to be obtained [83].

11.5.1.2 Removal of Copper

After iron has been removed by liquation, the copper content is up to 0.01%. Elemental sulfur (2-5 kg/t) is stirred in at 250-300 °C, enabling copper contents as low as 0.001% to be attained. The resulting copper dross can be removed from the process after several stages of enrichment.

11.5.1.3 Removal of Arsenic

After removal of iron by liquation, the arsenic content is ca. 0.1%, significantly higher than permitted levels. For example, the commonly used Sn 99.75 grade should contain < 0.05% As according to DIN 1704.

Arsenic can be removed from the melts along with some Cu, Ni, and residual Fe by forming intermetallic compounds with aluminum. For this, the aluminum must be present as an ideal solution in the tin. For this reason, the melt must be heated to a temperature close to the melting point of aluminum before the aluminum is added. Special precautions are necessary, e.g., operation in a closed vessel so that the aluminum does not burn on the surface of the bath. The amount added must be approximately three times the stoichiometric amount. The use of Al-Sn master alloys enables the operation to be carried out at a lower temperature. Intense agitation if followed by a settling process with cooling to 350-400 °C, and the Al-As mixed crystals can then be re-

moved. Separation of the Al mixed crystals is assisted by poling.

With correct operation, As contents of < 0.02% can be achieved, i.e., below the permitted level for Sn 99.90%. This process enables Sb contents of 0.005%, Cu contents of 0.02%, and Ni contents of 0.005% to be attained, and any remaining Fe to be removed.

Any aluminum remaining in the molten tin can be removed by adding sodium, sodium hydroxide, chlorine, or steam, and residual sodium by adding sulfur.

The storage, transport, and treatment of the Al-As product presents problems. Contact with water must be avoided as this leads to the formation of highly toxic arsine and stibine. The material is stored in closed vessels and is converted into a safe product as soon as possible by oxidative roasting or by treating with alkali solution and collecting and burning the liberated arsine to form As₂O₃ and H₂O. The residues obtained both from the roasting and the leaching processes can be recycled to the process.

The large differences in vapor pressure between the impurities (arsenic, antimony, bismuth, and lead) and tin enable selective evaporation at reduced pressure to be used. However, numerous proposed processes have resulted in only two industrial applications.

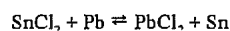
In a system tested in Russia, the impure tin flows from the top of a vertical reactor under a vacuum of 1 Pa into heated evaporating dishes. The evaporated impurities are collected in a separate chamber. Barometric valves are used to remove the purified tin and the condensate.

In the Bergsöe-Redlac system, a cylinder, cooled on the inside, rotates in a horizontal vacuum chamber above the melt, and the vaporized impurities are deposited on this in solid form. In the next stage of the process, they are scraped off and removed. The results of the vacuum distillation process depend on the reaction temperature and time. The high energy requirement for heating and for producing the vacuum, 400-700 kWh/t tin, is a disadvantage. Moreover, significant quantities of tin are vaporized. The use of selective evap-

oration of typical impurities in crude tin always involves a compromise between the purity and tin yield. Practical experiments are described in [85].

11.5.1.4 Removal of Lead

If the lead content is still not low enough after the first stages of the refining process, the lead can be converted into its dichloride by treatment with chlorine, tin dichloride, or tin tetrachloride:



The equilibrium is shifted to the right at low temperatures, so that the process must be carried out at a temperature only a little above the melting point of tin. The process also removes any remaining zinc and aluminum.

The best results are obtained by using two-stage operation, i.e., the product of the second stage, with a reduced lead content, is returned to the first stage. Precise control of the operation can lead to final lead contents of 0.008%.

11.5.1.5 Removal of Bismuth

In analogy to the thermal refining of lead, bismuth can be precipitated as an intermetallic compound by adding calcium or magnesium. The molar ratio Ca/Mg should be ca. 2 to obtain the best results [46]. A ternary compound is probably formed at this ratio. Under production conditions, scrap magnesium is used, as this is the most economic material.

Final bismuth contents of 0.06–0.003% have been reported for full-scale plant. In analogy to a technique used when removing arsenic from aluminum, the calcium and magnesium remaining in the tin can be converted to their chlorides and removed, e.g., by treatment with ammonium chloride.

11.5.2 Electrorefining

The theoretical conditions for the electrorefining of tin are favorable. The position of tin in the electrochemical series of the elements in aqueous solution show that Au, Ag, Cu, Bi, As, and Sb do not go into solution under elec-

trorefining conditions, but will appear in the anode slime. The elements Ni, Fe, Zn, and Al can be largely removed by a preliminary pyrometallurgical refining operation. Only lead lies close to tin in the electrochemical series. The high electrochemical equivalent weight of tin also favors the use of an electrometallurgical refining process. However, there are considerable problems in the practical realization of the process.

Simple and cheap electrolytes such as solutions of sulfate or chloride lead to spongy or needle-like deposits, and these effects are only slightly moderated by extremely large additions of colloidal materials. The process can only be operated at low current densities, leading to low process rates and inefficient utilization of energy (e.g., low current yields). Also, the presence of large amounts of expensive metal tied up in the process is undesirable economically.

These negative aspects mean that electrorefining is only worthwhile if the tin contains high concentrations of noble metals. Electrorefining can be carried out in acid or alkaline medium.

11.5.2.1 Electrorefining in Acid Medium

When sulfate electrolytes are used, additions of chloride, fluoride, crude cresol, glue, nicotine sulfide, α - and β -naphthol, diphenylamine, phenol, and/or cresolsulfonic acid are made. The sulfate ions cause the anodically dissolved lead to go into the anode slime in the form of lead sulfate. Also, sulfides such as nicotine sulfide can lead to the formation of lead sulfide, which is deposited in the anode slime. The organic sulfonic acids prevent the formation of basic tin salts on the anodes.

In spite of these precautions, the formation of coatings on the anode is the main problem in the electrolytic refining of tin in an acid medium. The main cause of coating formation is the lead content of the anodes, which must be removed mechanically when the bath voltage increases. The following operational data are quoted:

Anode mass:	100–200 kg
Anode thickness:	30 mm
Cell dimensions:	3.0–4.5 m long, 1.0–1.2 m wide, 1.0–1.5 m deep
Cell construction:	wooden cells with lead cladding or concrete
Cathode replacement:	after 6 d
Anode replacement:	after 10–12 d
Anode composition:	94–96% Sn, 0.01–0.03% Fe, 0.3–1.3% Pb, 0.1–0.6% Cu, 0.1–3.5% Bi, 0.02–0.35% As, 0.1–0.25% Sb, 100–300 g/t Ag, 0.3–0.7 g/t Au
Cathodes:	starter sheets of pure tin

The current yield is largely determined by the rate of removal of anode passivation. The energy consumption is 150–200 kWh/t tin. Because iron accumulates in the electrolyte, regeneration of the electrolyte is necessary.

11.5.2.2 Electrorefining in an Alkaline Medium

In alkaline medium, i.e., in NaOH or Na₂S electrolytes, less pure anodes (75% Sn) can be used than are used in an acid medium. A smooth deposit can be obtained without addition of colloids. However, current densities are very low, and the process must be carried out at 90 °C. Detailed information about the possibilities and limitations of electrorefining, deposition behavior, deposition mechanism, and effects of additives to the electrolyte, pH, and impurities are given in [4].

11.5.2.3 Other Methods of Electrorefining

Many attempts have been made to use molten salt electrorefining to overcome the disadvantages of electrorefining in aqueous solutions. The electrolyte was molten CaCl₂–KCl–NaCl. Various grades of crude tin were used. The electrodes consisted of graphite crucibles and graphite rods. The operating temperature was ca. 650 °C, and the current density 50–200 A/dm². Arsenic was effectively removed (reduced from 1.5% to 0.005%), and the antimony content was reduced from 0.32% to 0.01%. It proved impossible to scale up from pilot scale to full scale

operation, mainly because of problems in the control of the high-temperature process [77].

11.6 Recovery of Tin from Scrap Materials and Residues

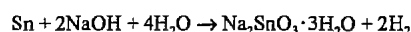
[1–3, 5, 11, 86, 87]

Scrap materials and residues which are produced during the processing of metals, to give semifinished and finished products are usually known as “new scrap”, while the returned old material from industry, trade, building construction, factories, and consumption is known as “old scrap”. The use of old and new scrap supplements primary production. It is collected by scrap merchants who work directly with the smelters. Also, in the neighborhood of metal smelting works there are often small scrap metal operations which sort, separate, refine and blend with primary metals to produce a primary metal that corresponds to the standard specification of an original metal [87].

The recovery of tin from tinplate is becoming increasingly difficult, as the change to electrolytic methods of tinning is leading to very thin coatings which sometimes diffuse into the steel sheet. The recycling of this material will continue to be a technically and economically difficult task. In principle, two processes are used today for recovering tin from tinplate: the alkaline electrolytic method and the alkaline chemical method.

In the alkaline electrolytic detinning of tinplate, baskets of cleaned scrap are immersed in hot 5–10% sodium hydroxide solution. The baskets form the anodes, and the tinned steel sheet forms the cathodes. The tin is deposited in the form of a sponge. As contact with atmospheric carbon dioxide cannot be prevented, sodium carbonate is formed, and the electrolyte bath must be frequently regenerated. The lacquer coating on the scrap tinplate is removed by adding solvents to the bath or by a special pretreatment process. The bath is operated at a temperature of 65–75 °C, a voltage of 1.5 V, and a cathode current density of 300 A/m².

In the alkaline chemical detinning of tinplate, the scrap material in perforated containers is immersed in sodium hydroxide solution. Hydrated sodium stannate is formed according to the equation



The hydrogen liberated must be reacted with an oxidizing agent; sodium nitrate is suitable. The dissolution process is accelerated by motion of the container in the liquor. The detinning time is 2–4 h, depending on the concentration and the temperature. If sodium nitrite is used instead of sodium nitrate, the tin goes into solution, the foreign metals, e.g., lead, iron, and antimony, can be precipitated, e.g., by hydrogen sulfide, and the tin can then be recovered by electrowinning.

Processing tin-containing alloys is easier than recovering tin from scrap tinplate. However, the tin content of many alloys has decreased over recent years, and alloys have in some cases been replaced by cheaper materials. Both these developments have tended to limit the potential for recovering secondary tin, and also explain why the amount of recovered tin in Europe has decreased from 15 800 t in 1980 to 13 300 t in 1990. In the United States, the amounts of recovered tin have remained almost constant at 16 900 t in 1980 and 17 100 t in 1990 [9].

The quantification of tin recovery from secondary raw materials is difficult because most of it is obtained from scrap alloy.

In addition to the tin concentrates treated in the primary smelting process, there are also other materials that must be treated, including the slags, oxidic flue dusts, ash, and sweepings containing very variable amounts of tin. Tin-containing processing scrap is also produced during casting, metal forming and cutting, tinning, and alloying. Considerable amounts of recycled scrap also come from the manufacture of cans, tinplate, tubes, foil, pure tin articles, and alloys such as solders, antifriction and bearing metals, type metal, etc.

In recycling it is essential to sort tin-containing materials into standard grades with ex-

act analytical specifications so that the metallurgical process can be optimized.

Short drum furnaces are suitable for processing oxidic materials, although shaft kilns and reverberatory furnaces are also used. The reduction is performed by coke/coal, with added sodium carbonate or fluorspar as flux. The process is operated in one or two stages, depending on the material. Scrap alloys containing high proportions of lead, antimony, or copper are remelted to form alloys. Scrap babbit (bearing metal) contains zinc, which is either removed in the slag or selectively volatilized. Scrap solder alloys are refined like crude tin.

11.7 Analysis [88]

11.7.1 Analysis of Ores and Concentrates

Determination of Sn. In the determination of tin in ore concentrates, the choice of method depends on the presence or absence of typical impurities.

Tungsten-Free Ores and Concentrates. After fusion with sodium peroxide and dissolution in water, the solution obtained is acidified with hydrochloric acid and partially evaporated to drive off arsenic. The antimony is then precipitated with iron powder (cementation). The tin in the filtrate can then be "cemented" by adding aluminum powder, and determined by iodometric titration.

Tungsten-Containing Ores and Concentrates. The tungsten can be precipitated from the acidified solution by adding cinchonine. The excess of this reagent in the filtrate is decomposed by fuming with sulfuric acid. The solution is then taken up in hydrochloric acid and treated as in the determination of tin in tungsten-free ores.

Silicate-Containing Ores and Concentrates. The material is boiled to dryness with nitric acid, and the residue is then strongly heated, fumed with $\text{HF}/\text{H}_2\text{SO}_4$, and fused with sodium peroxide. The tin determination can

then be carried out as for tungsten-free materials.

Determination of Other Elements. The determination of tungsten is carried out by precipitating with cinchonine after the fusion stage. The precipitate is strongly heated (ca. 750 °C) to form WO_3 , and tungsten is then determined gravimetrically.

Arsenic is determined by distilling it out of the acidified solution of fused product and then carrying out a bromatometric titration on the distillate.

Antimony is determined by adding iron powder to the acidified fusion product to precipitate antimony sponge. This is dissolved in Br_2/HCl , and any arsenic still present is driven off by evaporating with HCl . The antimony is purified by reprecipitation, and determined by bromatometric titration.

For the determination of other elements such as cadmium, iron, nickel, copper, bismuth, lead, zinc, and the noble metals, it is best to remove zinc, arsenic, and antimony from the dissolved product of a sodium peroxide fusion (acidified with HCl) by evaporating with Br_2/HBr . The elements can be determined in the solution by atomic absorption spectrometry.

To determine sulfur, the sample is heated in a stream of oxygen, the SO_2 formed is collected in a dilute solution of H_2O_2 , and the H_2SO_4 formed is determined by titration. The sulfur content of the tin is calculated from this.

11.7.2 Analysis of Metallic Tin

The preferred methods of analysis of pure and commercial-grade tin are detailed in DIN 1704 [88].

Arsenic is determined by dissolving the metal in a strongly acidic solution of FeCl_3 . The AsCl_3 formed is distilled off, and can be determined photometrically by the molybdenum blue method.

Antimony is determined by dissolving the metal in concentrated sulfuric acid. After adding hydrochloric acid, the antimony is oxidized with cerium(IV) to antimony(V). This is then extracted with isopropyl ether and can be

determined photometrically as yellow potassium tetraiodoantimonate.

Lead is determined by dissolving the metal in a mixture of Br_2 , HBr , and HClO_4 , fuming this to volatilize the zinc, removing any Tl that might still be present by extraction with isopropyl ether, and determining the lead by polarography.

In the determination of copper, the initial dissolution is similar to that used in the determination of lead. The copper in the solution then is determined photometrically as the diethyldithiocarbamate complex after extraction with CCl_4 .

The determination of zinc also requires a dissolution process similar to that for lead. The solution is acidified with hydrochloric acid, and heavy metals still present are precipitated as sulfides. The zinc in the filtrate obtained can be determined by polarography. Iron is determined by first carrying out the dissolution and precipitation of heavy metals as for zinc determination. The iron in the filtrate can be determined photometrically as the sulfosalicylic acid complex.

The determination of aluminum also requires dissolution and removal of heavy metals by precipitation of their sulfides as for iron determination. The aluminum in the filtrate can be determined photometrically as the eriochrome cyanine complex.

As well as the analytical methods recommended in DIN 1704, rapid and efficient methods such as atomic absorption spectrometry (AAS) and atomic emission spectrometry (ICP-AES) are also being used to an increasing extent [89]. These methods are specified in the German and international standards for the analysis of water, wastewater, and sewage sludge.

After dissolution of the tin in a mixture of Br_2 , HBr , and HClO_4 , the accompanying antimony, arsenic, bismuth, copper, iron, lead, aluminum, cadmium, and zinc can be determined with a high degree of accuracy in the presence of each other, without first separating them, by means of AAS and ICP-AES. In the determination of arsenic and antimony, other

dissolution processes must first be performed. The analysis of metallic tin and tin alloys is often carried out by spectral analysis with spark or arc excitation, and the analysis of tin slags and concentrates by X-ray fluorescence analysis.

Table 11.5: World production and consumption of tin (in 10^3 t).

Year	Mining output	Smelting output	Consumption
1980	235.5	243.6	221.4
1985	185.3	216.2	214.3
1990	210.7	225.6	232.7

Table 11.6: Mining output and consumption of tin in various countries in 1990 [9].

Country	Mining output		Consumption	
	in 10^3 t	as %	in 10^3 t	as %
Brazil	39.1	18.6	6.1	2.6
Indonesia	37.1	15.1	1.4	0.6
Malaysia	28.5	14.3	3.3	1.4
Bolivia	17.3	8.2	0.4	0.2
China	35.8	17.0	18.0	7.7
Russia	13.0	6.1	20.0	8.5
United States	0.1	0.04	37.3	16.0
Japan			33.8	14.5
Germany			19.3	8.2
United Kingdom	3.4	1.6	10.4	4.3

11.8 Economic Aspects [2, 9, 11]

There have been no large variations in the amounts of tin mined, smelted, and consumed in recent years. Figures for the years 1980–1990 are given in Table 11.5.

Even in 1938, smelting production amounted to 171 200 t [3], and this had increased by only 66 500 t or 38.8% in 1990. This is an average increase of 9.75% per annum.

Typically in the production and consumption of tin, the production processes of mining and smelting are geographically remote from the places where the metal is consumed.

The main producers, i.e., Brazil, Indonesia, Malaysia, Bolivia, and to some extent China, consume very little tin themselves (see Table 11.6). On the other hand, the United States, Japan, Germany, and the United Kingdom produce little or no primary tin themselves and are the main tin consumers. In the CIS, pro-

duction and consumption are approximately equal.

The continuous fall in the price of tin (> 30 000 DM/t in 1985, ca. 10 000 DM/t in 1990) has led to many casualties worldwide. The worst effects have been in Malaysia, where over 80 suppliers have been closed down. In 1980, Malaysia was the main producer of tin, with a mine output of 61 000 t. This fell to 28 500 t in 1990, and Malaysia now produces less tin than Brazil, China, or Indonesia. Even the well-known tin smelter Capper Pass in the United Kingdom has ceased production, as have the tin mines in the Altenberg region of Saxony.

11.9 Alloys and Coatings [1, 2, 11]

Tin is one of the most important constituents of low-melting nonferrous alloys. The following important properties of the metal are exploited

- Low melting point
- Low hardness
- Good wetting properties
- Effective incorporation of foreign particles
- Good compatibility with foodstuffs

Tin utensils have been produced for over 5000 years, and well-preserved examples exist from the various epochs.

Tin utensils are always made of tin alloys, as the pure metal is too soft. The most important alloying elements are antimony, copper, and lead. The tin is usually melted first, and it then readily forms alloys with pure metals, which have good solubility properties. To minimize burning, especially of antimony, master alloys are usually used.

Solders. Most solders are based on the tin lead binary system, which has a eutectic at ca. 63% tin and 183 °C. The solid solubility of 1–2% lead in tin and 13% tin in lead is not relevant to production conditions.

Although the copper–tin alloys are some of the oldest materials used by humans, their development is not yet exhausted even today.

The most important development aims are improvement of mechanical properties and corrosion resistance, and reduction of the tin content.

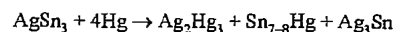
Sintering Metallurgy of Bronzes. An interesting new use for tin is as an addition in powder form when sintering bronze. Especially when this is for use as a bearing metal, economic advantages are obtained by the addition of 4% tin to the copper powder with or without lead addition.

Low-melting alloys are of great importance in several technical applications. Their melting points usually lie significantly below 150 °C. Bismuth is always an essential alloy constituent.

Their most important application areas are in mold making, safety systems for the prevention of fire and overheating, and stepwise soldering.

Amalgams. Tin has been used for dental fillings since the Middle Ages, and amalgams since the 1800s. Subsequent developments have led to the silver–tin amalgams used today. A typical amalgam has the following composition: 52% Hg, 33% Ag, 12.5% Sn, 2% Cu, 0.5% Zn.

When the mixture of metals is ground together, the following hardening reaction takes place:



The metallographic structure of a dental amalgam consists of islands of solid undissolved particles of alloy (Ag_3Sn) in a soft matrix of silver and tin amalgams.

11.10 Compounds

Consumption of inorganic tin compounds is lower than that of organic tin compounds, but they are often the starting materials used to produce the organic tin compounds.

In minerals, tin is nearly always tetravalent and bonded to oxygen or sulfur. The only exception is herzenbergite, SnS , in which it is divalent.

In industry, tin(II) and tin(IV) compounds are produced from metallic tin. Many tin(II) compounds which are sufficiently stable for practical purposes have a strong tendency to change into tin(IV) compounds and are therefore strongly reducing. For example, SnCl_2 precipitates gold and silver in metallic form from their salt solutions.

The salts in both valency states hydrolyze in aqueous solution to form insoluble salts. In alkaline media, stannites (divalent) and stannates (tetravalent) are formed.

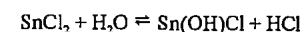
11.10.1 Tin(II) Compounds

Tin(II) chloride, SnCl_2 , is the most important inorganic tin(II) compound. It is produced on an industrial scale by reducing tin(IV) chloride with molten tin, or by direct chlorination of tin.

Solutions of tin(II) chloride are obtained by dissolving metallic tin in hydrochloric acid, or by reducing a solution of SnCl_4 with metallic tin.

The anhydrous substance is white, has a greasy luster, and dissolves readily in water alcohol, ethyl acetate, acetone, and ether. The clear, nondeliquescent, monoclinic dihydrate $\text{SnCl}_2 \cdot 2\text{H}_2\text{O}$, crystallizes from aqueous solution and is the commercial product.

On dilution, the aqueous solution becomes cloudy as hydrolysis causes precipitation of the basic salt:



The cloudiness can be prevented by small additions of hydrochloric acid, tartaric acid, or ammonium chloride. Because of its strong tendency to hydrolyze, the dihydrate can only be dehydrated over concentrated sulfuric acid or by heating in a stream of hydrogen chloride.

Tin(II) chloride is an important industrial reducing agent, being used to reduce aromatic nitro compounds to amines, aliphatic nitro compounds to oximes and hydroxylamines, and nitriles to aldehydes.

Tin electroplating can be carried out in a fused eutectic salt mixture of 20% SnCl_2 and 80% KCl at 200–400 °C [90, 91].

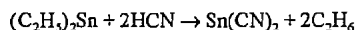
Tin(II) Oxide Hydrate and Tin(II) Oxide. If aqueous solutions of SnCl_2 or other tin(II) salts are reacted with alkali metal carbonate or ammonia, an amorphous white precipitate of tin(II) oxide hydrate, $5\text{SnO} \cdot 2\text{H}_2\text{O}$, is obtained [92]. $\text{Sn}(\text{OH})_2$ does not exist. Tin(II) oxide hydrate is amphoteric. Dehydration in a stream of carbon dioxide gives tin(II) oxide. Tin(II) oxide hydrate and tin(II) oxide are starting materials for the production of other tin(II) compounds.

Other Tin(II) Compounds. Tin(II) fluoride, SnF_2 , is formed from tin(II) oxide hydrate and hydrofluoric acid, and is added to toothpastes as an anticaries agent.

Tin(II) fluoroborate hydrate, $\text{Sn}(\text{BF}_4)_2 \cdot n\text{H}_2\text{O}$, is formed by dissolving the oxide hydrate or the oxide in aqueous fluoroboric acid. Sulfuric acid reacts with the oxide hydrate or the oxide to form tin(II) sulfate. Both tin(II) sulfate and tin(II) fluoroborate are important in the production of metallic tin coatings by electroplating.

Tin(II) bromide, SnBr_2 , and *tin(II) iodide*, SnI_2 , are produced by reacting metallic tin with the appropriate hydrogen halide.

Tin(II) cyanide, which is produced from bis(cyclopentadienyl)tin(II) and hydrogen cyanide, is the only known compound of tin with inorganic carbon:



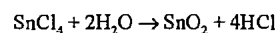
The tin(II) salt of ethylhexanoic acid is an effective catalyst in polyurethane production.

11.10.2 Tin(IV) Compounds

Tin(IV) Hydride. The toxic, colorless, flammable gas, tin(IV) hydride, is formed by the reduction of tin(IV) chloride by LiAlH_4 in diethyl ether at -30°C . It is stable for several days at room temperature, and decomposes into its elements at 150°C in the absence of air, forming a tin mirror.

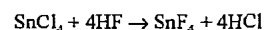
Tin(IV) Halides and Halostannates(IV). Anhydrous tin(IV) chloride is a colorless liquid which fumes strongly in air. It is a good solvent for sulfur, phosphorus, and iodine, and is miscible in all proportions with carbon di-

sulfide, alcohol, benzene, and other organic solvents. It hydrolyzes in water, evolving much heat and forming colloidal tin(IV) oxide and hydrochloric acid:

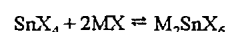


In moist air, the pentahydrate, $\text{SnCl}_4 \cdot 5\text{H}_2\text{O}$, is formed, the so-called butter of tin, a white deliquescent crystalline mass with a melting point of 60°C . In industry, SnCl_4 is produced by the reaction of chlorine with tin. The anhydrous product is obtained if the metal is covered with SnCl_4 . Anhydrous tin(IV) chloride is an important starting material for the production of organic tin compounds.

Tin(IV) bromide, SnBr_4 , and tin(IV) iodide, SnI_4 , are also obtained by the reaction of metallic tin with the halogens. Tin(IV) fluoride is produced by the reaction of tin(IV) chloride with anhydrous hydrogen fluoride:



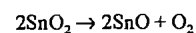
Tin(IV) halides react readily with metal halides to form the halostannates(IV), the coordination number of the tin increasing from four to six. The reaction proceeds as follows (X = halogen):



One of the best known compounds of this type is ammonium hexachlorostannate, $(\text{NH}_4)_2\text{SnCl}_6$, the so-called pink salt.

Hexachlorostannic acid, $\text{H}_2\text{SnCl}_6 \cdot 6\text{H}_2\text{O}$, is formed by passing HCl into a concentrated solution of SnCl_4 .

Tin(IV) Oxide, Tin(IV) Oxide Hydrate, and Stannates(IV). Tin(IV) oxide decomposes above 1500°C without melting to form tin(II) oxide:



Pure tin(IV) oxide can be obtained by the combustion of powdered tin or sprayed molten tin in a hot stream of air. It is insoluble in acids and alkalis. Specially prepared tin(IV) oxide has many uses, total world consumption of this material being > 4000 t/a. It is used in combination with other pigments to produce ceramic colorants. It has a rutile structure, and hence can absorb the colored ions of transition

metals. The products obtained form the basis of ceramic colors, and include tin vanadium yellow, tin antimony gray, and chrome tin pink. The thermal stability of the tin colors enables them to be used both in and under the glaze.

Electrodes made of SnO_2 are used in the production of lead glass [93]. They are resistant to corrosion by molten glass, and have good electrical conductivity when hot.

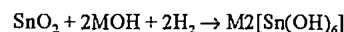
Coatings of tin(IV) oxide treated with indium oxide ($< 100 \mu\text{m}$ thick) give good transparency properties to aircraft window systems, increase their strength, and give protection from icing.

If tin(IV) oxide is reacted with a solution of alkali, or a solution of stannate is reacted with acid, a white, gel-like precipitate of tin(IV) oxide hydrates is formed which are very soluble in alkalis and acids. This precipitate was formerly known as " α -stannic acid", and the aged product, which is sparingly soluble, as " β -stannic acid" (metastannic acid). Today, this product is regarded as tin(IV) oxide hydrate with the formula $\text{SnO}_2 \cdot n\text{H}_2\text{O}$, where n decreases with aging.

The reaction of powdered or granulated tin with concentrated nitric acid leads to the formation of the reactive β -tin(IV) oxide hydrate. This can be used as a catalyst for aromatics.

The β -tin oxide hydrate gels precipitated from SnCl_4 by ammonia and then dried are stable towards nuclear radiation, and can be used in chromatographic columns for separating radioactive isotopes [94].

Fusion of tin(IV) oxide with alkali metal hydroxides leads to formation of alkali metal hexahydroxystannates according to the following reaction scheme (M = alkali metal):



The sodium and potassium complexes are used as alkaline electrolytes in electrolytic tin plating.

Tin(IV) sulfide, SnS_2 , is formed as golden yellow flakes with a hexagonal crystal structure by passing hydrogen sulfide through a weakly acidic solution of a tin(IV) salt. On

heating, the crystals become dark red to almost black, reverting to yellow on cooling.

The tin disulfide known as "mosaic gold" is produced industrially by heating tin amalgam with sulfur and ammonium chloride. It is used for gilding picture frames, and in painting to produce deep yellow to bronze color shades.

11.11 Toxicology

Metallic tin is generally considered to be nontoxic. As early as the Middle Ages, it was used in the form of plates, jugs, and drinking vessels. Even large amounts of tin salts in the digestive system cause negligible harm. Apparently, tin can migrate only very slowly through the intestinal walls into the blood. Orally ingested tin is poorly resorbed by animals and humans. The half-life in the kidneys and liver is 10–20 d, and in the bones 40–100 d. Cases of poisoning are almost unknown. Massive inhalation of tin or tin oxide dust by exposed industrial workers can lead to irritation of the respiratory tract. In extreme cases, metal fume fever with similar symptoms to those of "zinc fever" or "brass fever" also occurs. As the peroral ingestion of tin and its inorganic compounds is comparatively harmless because of the relatively low resorption, the limit value for the prevention of sickness and diarrhea for fruit preserves is ca. 250–500 mg/kg, and for fruit juices 500–1000 mg/kg. In current industrial practice, the tin cans are additionally lacquered, and the tin concentrations in preserved fruit and vegetables are < 250 ppm. The MAK value, calculated as tin and measured in total dust, has been 2 mg/m³ for many years [95, 96].

Hydrochloric acid formed by the hydrolysis of tin chloride can cause acid burns. Tin hydride is very toxic, having a similar effect on the human organism to arsine [97].

Organotin compounds are very toxic; the MAK value is 0.1 mg/m³ [96]. These compounds can differ widely in their effects, and can also be slowly converted to other compounds in the organism, so that toxic symptoms can change during the induction time.

The toxicity of alkyl and aryl tin compounds decreases in the series: trialkyl > dialkyl > tetraalkyl > monoalkyl compounds. Whereas tributyl- and triphenyltin compounds are almost as toxic as HCN, the monoalkyl compounds have a toxicity similar to that of the inorganic tin compounds.

The resorption of tin alkyl and tin aryl compounds can have harmful effects on the CNS, such as edema of the brain and spinal cord and damage to the respiratory center. The volatile organotin compounds cause persistent headaches, epileptiform convulsions, narcosis, and respiratory paralysis.

Dibutyltin dichloride, tributyltin chloride, and analogous alkyl tin halides, after a latent period, cause irritating and burning of the skin and especially the mucous membranes, and are intensely sternutatory and lachrymatory [98, 99].

In cases of poisoning by organotin compounds, long-term observation of the functioning of the liver and CNS is necessary.

11.12 References

- Ullmann, 3rd ed., 19, 145-170.
- Ullmann, 4th ed., 24, 641-679.
- V. Tafel: *Lehrbuch der Metallhüttenkunde*, 2nd ed., vol. 2, Hirzel-Verlag, Leipzig 1953, pp. 221-305.
- Gmelin, Teil B, pp. 205-214, 347-355.
- F. Pawlek: *Metallhüttenkunde*, De Gruyter, Berlin-New York 1983, pp. 482-500.
- Meyers Enzyklopädisches Lexikon, 9th ed., vol. 25, Bibliographisches Institut, Mannheim 1979, p. 730.
- F. Ahlfeld: *Zinn und Wolfram. Die metallischen Rohstoffe*, vol. 11, Enke Verlag, Stuttgart 1958.
- Landolt-Börnstein, New Series, Springer Verlag, Berlin 1971.
- Metallgesellschaft AG, *Metallstatistik*, vol. 78, Frankfurt, (1980-1990).
- Brockhaus Taschenbuch der Geologie, Brockhaus Verlag, Leipzig 1955.
- Zinn-Taschenbuch, 2nd ed., Metall-Verlag, Berlin 1981.
- A. Leube: "Zinn", in: *Lehrbuch der angewandten Geologie*, vol. 2, part 1, Enke Verlag, Stuttgart 1968.
- W. Gocht: *Handbuch der Metallmärkte*, Springer Verlag, Berlin-Heidelberg-New York 1974.
- S. Jankovic: *Wirtschaftsgeologie der Erze*, Springer Verlag, Wien-New York 1974.
- P. Klemm: *Der Weg aus der Wildnis*, vol. 3, KB Verlag, Berlin 1962.
- D'Ans-Lax: *Taschenbuch für Chemiker und Physiker*, 3rd ed., Springer Verlag, Berlin 1964.
- I. Barin et al.: *Thermochemical Properties of Inorganic Substances*, Suppl., Springer Verlag, Berlin-Heidelberg-New York 1977.
- R. Zimmermann, K. Günther: *Metallurgie und Werkstofftechnik*, vol. 1, Deutscher Verlag für Grundstoffindustrie, Leipzig 1977, p. 635.
- A. Eiling, J. S. Schilling, *J. Phys. F* 11 (1981) 623.
- Chemical Rubber Comp.: *Handbook of Chemistry and Physics*, 62nd ed., CRC Press, Boca Raton 1981.
- G. V. Raynow, R. W. Smith, *Proc. R. Soc. London Ser. A* 244 (1958), Nov. 27, 101.
- W. Köster, *Metallk.* 39 (1948) 1.
- E. G. Shidkovskii, A. A. Durgartan, *Nauchn. Dokl. Vyssh. Shk. Fiz. Mat. Nauki* 1958, no. 2, 211.
- H. Gundlach, W. Thormann, *Z. Disch. Geol. Ges.* 112 (1960) no. 1, 1.
- H. Breuer, *GlückaufForschungsh.* 42 (1981) 213.
- H. Breuer, A. Guzman, *Erzmetall* 32 (1979) 379.
- World Min.* 31 (1978) no. 5, 50.
- E. Müller, *Erzmetall* 30 (1977) 54.
- P. A. Wright: *Extractive Metallurgy of Tin*, Elsevier, Amsterdam 1966.
- J. M. Floyd, *Proc. Symp. Lead-Zinc-Tin '80*, AIME, Materials Park, OH, 1980.
- I. J. Bear, R. J. T. Canay, *Trans. Inst. Min. Metall. Sect. C* 85 (1976) no. 9, 139.
- N. N. Murach et al.: *Metallurgy of Tin*, vol. 2, National Lending Library for Science and Technology, Boston, Spa, England 1967.
- E. M. Llevin et al.: "Phase Diagrams for Ceramists", Am. Ceram. Soc., 1974.
- R. Zimmermann, K. Günther: *Metallurgie und Werkstofftechnik*, vol. 2, Deutscher Verlag für Grundstoffindustrie, Leipzig 1977, p. 116.
- P. Paschen, *Erzmetall* 27 (1974) 28.
- W. van Rijswijk de Jong, *Erzmetall* 27 (1974) 22.
- J. Barthel, *Freiberg. Forschungsh. B* B112 (1971) 13.
- K. Leipner, *Neue Hütte* 16 (1971) 395.
- L. Sivila, *Neue Hütte* 18 (1973) 395.
- W. T. Denholm, *Proc. Symp. Extr. Met.*, 1981.
- K. A. Foo, J. M. Floyd, *Proc. Symp. Lead-Zinc-Tin '80*, AIME, Materials Park, OH, 1980.
- V. I. Evdokimov, *Freiberg. Forschungsh. B* B113 (1976) 6.
- E. B. Kingl, L. W. Pommier, *5th Int. Conf. Tin*, La Paz 1977.
- G. Severin et al., *Neue Hütte* 20 (1975) 752.
- A. I. Evdokimov, I. S. Morosov, *Chim. Ind. (Paris)* 88 (1962) no. 2, 115.
- A. Lange, *Erzmetall* 15 (1962) 113.
- H. Weigel, D. Zetsche, *Erzmetall* 27 (1974) 237.
- Y. P. Zvonkov, A. A. Rozlovskii, *Tsvetn. Met. (N.Y.)* 10 (1969) no. 7, 35.
- G. Daradimos, U. Kuxmann, *Erzmetall* 24 (1971) 171.
- A. W. Fletscher et al., *Trans. Inst. Min. Metall. Sect. C* 76 (1967) 145.
- V. E. Dyakov, N. S. Saturin, *Tsvetn. Met. (N.Y.)* 9 (1968) no. 9, 55.
- L. W. Pommier, S. J. Escalera, *J. Met.* 31 (1979) no. 4, 10.
- H. Winterhager, U. Kleinert, *Erzmetall* 22 (1969) 310.
- G. I. Karaivko et al., *Orig. Izd. Nauka*, Moskau, engl. trans., Technikopy Ltd. London 1977.
- G. Holt, D. Pearson, *Trans. Inst. Min. Metall. Sect. C* 86 (1977) 77.
- T. R. A. Davey, *5th Int. Tin Conf.*, La Paz 1977.
- T. R. A. Davey, *Aust. Min.* 61 (1969) Aug., 62.
- T. R. A. Davey, *Proc. Symp. Lead-Zinc-Tin '80*, AIME, 1980.
- P. A. Wright: "Advances in Extractive Metallurgy and Refining", *Trans. Inst. Min. Metall.* 24 (1972) 467.
- T. R. A. Davey, G. M. Willis, *J. Met.* 29 (1977) 24.
- P. Paschen, *Erzmetall* 29 (1976) 14.
- T. R. A. Davey, F. J. Flossbach, *J. Met.* 24 (1972) 101.
- K. Batubara, *5th Int. Tin Conf.*, La Paz 1977.
- W. Gocht: "Der metallische Rohstoff Zinn", *Volks-wirtschaft. Schriften*, no. 131, Dunker & Humboldt, Berlin 1969.
- F. K. Oberbeckmann, M. Porten, *Proc. Symp. Lead-Zinc-Tin '80*, AIME, Febr. 1980.
- C. Ferrante in: *Handbuch der technischen Elektrochemie*, vol. 4: "Die Anwendung des elektrischen Ofens in der metallurgischen Industrie", Akad. Verlagsgesellschaft, Leipzig 1956.
- O. M. Katkov, *Tsvetn. Met. (N.Y.)* 17 (1976) 38.
- O. M. Katkov, *Tsvetn. Met. (N.Y.)* 12 (1971) 28.
- J. E. Joffe, *5th Int. Tin Conf.*, La Paz 1977.
- M. F. Barrett et al., *Trans. Inst. Min. Metall. Sect. C* 84 (1975) 231.
- J. Lema Patino, *4th Int. Tin Conf.*, Kuala Lumpur 1974.
- B. Möller, *Neue Hütte* 16 (1971) 400.
- D. N. Klushin, O. V. Nadinskaya, *J. Appl. Chem.* 29 (1956) no. 10, 1593.
- J. M. Floyd et al., *Aust. Min.* 64 (1972) Aug., 72.
- R. Kammel, H. Mirafzall, *Erzmetall* 30 (1977) 437.
- P. A. Wright, *Trans. Inst. Min. Metall. Sect. C* 80 (1971) 112.
- A. P. Samodelov, Y. K. Delimarskii, *Tsvetn. Met. (N.Y.)* 9 (1968) 41.
- K. Orlich, W. Dittrich, *Freiberg. Forschungsh. B* B156 (1970) 39.
- R. P. Elliott: *Constitution of Binary Alloys*, 1st Suppl., Mc Graw-Hill, New York 1965.
- J. D. Esdaile, *5th Int. Tin Conf.*, La Paz 1977.
- M. Hansen, K. Anderko: *Constitution of Binary Alloys*, Mc Graw-Hill New York 1958.
- S. Y. Shiratshi, H. B. Bell, *Trans. Inst. Min. Metall. Sect. C* 79 (1970) 120.
- E. Müller, P. Paschen: "Complex Metallurgy '78", *Proc. Inst. Min. Met.* 1978, 82; *Erzmetall* 31 (1978) 266.
- P. Paschen, *Metall (Berlin)* 33 (1979) 137.
- L. Marone, G. Lanfranco, *Metall Ital.* 63 (1971) no. 3, 121.
- Winnacker-Kühler 3rd ed., 6.
- L. Müller-Olsen in: *Die Weltwirtschaft im industriellen Entwicklungsprozeß*, J. C. B. Mohr, Tübingen 1981.
- O. Proske, G. Blumenthal: *Analyse der Metalle*, 3rd ed., vol. 1, Springer Verlag, Berlin-Heidelberg-New York 1986.
- K. Slickers: *Die automatische Atom-Emissions-Spektalanalyse*, 2nd ed., Buchvertrieb K. A. Slickers, Gießen 1992.
- A. I. Vitkin, K. Delimarskii, *Prot. Met. (Engl. Transl.)* 11 (1975) 245-246.
- T. Williamson, *Zinn Verw.* 124 (1980) 7-8.
- J. D. Donaldson, *Prog. Inorg. Chem.* 8 (1967) 287.
- C. J. Evans, *Zinn Verw.* 132 (1982) 5-8.
- W. B. Hampshire, C. J. Evans, *Zinn. Verw.* 118 (1979) 3-5.
- MAK-Werte 1982, Maximale Arbeitsplatzkonzentrationen, DFG, Verlag Chemie, Weinheim.
- Gefahrstoffe 1992*, Verlag Universum, Wiesbaden 1992.
- S. Moschlin: *Klinik und Therapie der Vergiftungen*, 5th ed., Thieme Verlag, Stuttgart 1972.
- R. Ludwig, K. Lohs: *Akute Vergiftungen*, G. Fischer Verlag, Jena 1988.
- Merkblätter für den Umgang mit gefährlichen Stoffen*, Verlag Tribüne, Berlin 1985.

12 Nickel

DEREK G. E. KERFOOT (§§ 12.1–12.15); F. WERNER STRASSBURG (§ 12.16); KEITH LASCELLES (§§ 12.17 EXCEPT 12.17.2 AND 12.17.5); DAVID NICHOLLS (§ 12.17.2); LINDSAY G. MORGAN (§ 12.17.5)

12.1 Introduction	716	12.6.3.1 Atmospheric Pressure Carbonyl Process.....	753
12.1.1 History	716	12.6.3.2 High-Pressure Carbonyl Process (BASF).....	753
12.1.2 Physical Properties	717	12.6.3.3 Inco Pressure Carbonyl Process ..	754
12.1.3 Chemical Properties	718	12.6.4 Hydrogen Reduction to Nickel Powder.....	757
12.2 Occurrence	718	12.7 Beneficiation of Oxide Ores.....	758
12.2.1 Minerals	719	12.7.1 Nippon Yakin Oheyama Process ..	758
12.2.2 Sulfide Ores	719	12.7.2 Segregation Processes	759
12.2.3 Oxide Ores	720	12.8 Pyrometallurgy of Oxide Ores.....	759
12.2.4 Economic Trends	721	12.8.1 Ore Pretreatment	760
12.3 Beneficiation of Nickel Sulfide Ores	722	12.8.2 Smelting to Nickel Matte.....	761
12.4 Pyrometallurgy of Nickel Concentrates.....	724	12.8.2.1 Blast Furnace Smelting	761
12.4.1 Roasting	724	12.8.2.2 Matte Production from Ferronickel	761
12.4.2 Smelting	726	12.8.2.3 Inco Selective Reduction Smelting Process.....	761
12.4.2.1 Primary Smelting	727	12.8.3 Energy Consumption in Laterite Smelting.....	762
12.4.2.2 Matte Converting	732	12.9 Hydrometallurgy of Oxide Ores ...	763
12.4.3 Environmental Aspects of Nickel Smelting	732	12.9.1 Caron Process	764
12.4.3.1 New Developments in Nickel Smelting	733	12.9.2 Pressure Leaching with Sulfuric Acid	767
12.4.4 Treatment of Converter Matte....	734	12.9.2.1 Moa Process	767
12.4.4.1 INCO Matte Separation Process..	735	12.9.2.2 Amax Acid Leach Process	769
12.4.4.2 Fluidized-Bed Roasting of Nickel Sulfide	736	12.10 By-Product Cobalt	770
12.5 Hydrometallurgy of Nickel Concentrates and Mattes.....	737	12.11 Recovery from Secondary Sources.....	771
12.5.1 Ammonia Pressure Leaching ...	738	12.12 Market Products.....	771
12.5.2 Atmospheric Acid Leaching	740	12.13 Uses.....	772
12.5.3 Acid Pressure Leaching	741	12.14 Economic Aspects.....	773
12.5.4 Chloride Leach Processes	743	12.15 Toxicology	775
12.5.5 Treatment of Nickeliferous Pyrrhotite	745	12.16 Alloys.....	775
12.6 Refining.....	745	12.17 Compounds.....	775
12.6.1 Electrowinning	746	12.17.1 Nickel Tetracarbonyl	780
12.6.1.1 Refining of Nickel Metal Anodes ..	746	12.17.2 Nickel Salts of Organic Acids	782
12.6.1.2 Refining of Nickel Matte Anodes ..	747	12.17.3 Analysis	782
12.6.1.3 Solution Purification	748	12.17.4 Economic Aspects	782
12.6.1.4 Electrowinning Operations	749	12.17.5 Toxicology.....	783
12.6.2 Electrowinning	750	12.17.5.1 Distribution in the Environment ..	783
12.6.2.1 Electrowinning from Sulfate Electrolytes	750	12.17.5.2 Ecotoxicity.....	783
12.6.2.2 Electrowinning from Chloride Electrolytes	751	12.17.5.3 Mammalian Toxicology	783
12.6.3 Carbonyl Refining.....	752	12.17.5.4 Nickel Carbonyl Poisoning	785
		12.17.5.5 Legislation.....	787
		12.18 References.....	788

12.1 Introduction

Nickel is a silver white metal with typical metallic properties. It occurs in the periodic table in the first triad of Group VIII (IUPAC Group 10), after iron and cobalt, to which it is closely related. The electronic configuration of nickel is $1s^2 2s^2 2p^6 3s^2 3p^6 3d^8 4s^2$.

Nickel occurs naturally as a mixture of five stable isotopes of mass number 58 (67.84%), 60 (26.23%), 61 (1.19%), 62 (3.66%), and 64 (1.08%). So far even artificial radioactive isotopes have been identified with mass numbers of 56, 57, 59, 63, 65, 66, and 67.

The great importance of nickel lies in its ability, when alloyed with other elements, to increase a metal's strength, toughness, and corrosion resistance over a wide temperature range. Nickel is essential to the iron and steel industry, and nickel-containing alloys have played a key role in the development of materials for the aerospace industry. World production of nickel increased from 20×10^3 t/a in 1920 to 750×10^3 t/a in 1976 at an average annual rate of increase of 3%. However, no significant increase in either consumption or production occurred between 1976 and 1986, with world nickel consumption falling as low as 650 000 t/a in 1981 and 1982. The known world reserves of nickel are more than adequate to maintain this level of production for many years.

12.1.1 History [1-4]

It is believed that the word "Nickel" or "Kupfer Nickel" is derived from a derogatory term applied by medieval miners in Saxony to a mineral which they mistakenly believed to be a copper ore, but from which they could extract no copper. It was in fact the nickel arsenide ore niccolite (NiAs). The Saxon miners not unnaturally assumed that evil spirits, or "Old Nick" himself, were responsible for their problems.

Nickel was first isolated by the Swedish mineralogist AXEL CRONSTEDT in 1751, when studying a gersdorffite (NiAsS) ore from Los in Sweden. Nickel's status as an independent

element was proved in 1775 by TORBERN BERGMAN and coworkers, but it was not until 1804 that JEREMIAS RICHTER produced a relatively pure sample of the metal and described its essential properties.

Nickel-containing alloys were in use long before CRONSTEDT's discovery. For centuries the Chinese had been making "pai thung" or "white copper" (40% Cu, 32% Ni, 25% Zn, and 3% Fe) which resembled silver in appearance. This material appeared in Europe in small quantities in the late 1700s. Since it costs only one quarter the price of silver, the alloy had obvious commercial potential as a silver substitute. By the 1830s, copper-nickel-zinc alloys, by then known as German Silver and later as nickel-silver, were being produced commercially in both Germany and England in significant amounts. In addition to its silver color, this alloy was easy to cast and fabricate, was resistant to tarnishing, and was economical to produce. The next significant development occurred in 1857 when the United States issued a cupronickel coin containing 12% nickel; other countries soon followed suit.

In the mid-1800s nickel was produced in small quantities from sulfide ores mined in Germany, Norway, Sweden, and Russia. Although refined metallic nickel was first produced in Germany in 1838, world production of nickel remained below 1000 t/a until 1876.

The demand for nickel increased abruptly in 1870-1880 when PARKES, MARBEAU, and RILEY demonstrated its use in alloy steels, as FLEITMANN succeeded in making malleable nickel, and as electrolytic nickel plating was successfully developed. The first nickel-steel armor plate was made in France in 1885 and soon afterwards in Italy, England, and the United States. In the early 1890s the adoption of nickel steels by the world's navies led to a steep rise in the demand for nickel.

In 1863, PIERRE GARNIER discovered the nickel oxide ores of New Caledonia, and from 1875 this French island became the world's main producer of nickel, which position it retained until displaced by Canada in 1905. Mining of the sulfide ores of the Sudbury Ba-

sin in Ontario, Canada, started in 1886, and these ore bodies were to remain the most important source of the world's nickel supply for most of the twentieth century. Even in 1950 the Sudbury area still supplied 95% of the nickel for the Western world. Since then Canada's preeminent position has been largely eroded, and by 1980 nickel was being mined, smelted, and refined in more than 20 countries.

Up to the end of World War I nickel was used almost exclusively for military purposes, but intensive research, between the world wars, into potential industrial uses soon led to a variety of new applications. In the 1990s there are thousands of nickel alloys in use with nickel contents ranging from 99% in wrought nickel to as little as 1% as hardening additives for various alloys.

12.1.2 Physical Properties

The physical properties of nickel [9-11] depend largely on its purity, on the physical state of the metal, and on its previous treatment. The wrought metal is highly malleable, moderately strong, tough, ductile, and highly resistant to corrosion in many media. Its good strength and ductility persist to subzero temperatures. Some important physical properties of nickel are as follows:

<i>mp</i>	1455 °C (1728 K)
<i>bp</i>	2730 °C (3003 K)
Relative density (25 °C)	8.9
Volume increase on melting	4.5%
Heat of fusion (<i>mp</i>)	302 J/g

Heat of sublimation (25 °C)	7317 J/g
Heat of vaporization (T_{m})	6375 J/g
Standard entropy	29.81 J/K
Thermal conductivity (0-100 °C)	88.5 W m ⁻¹ K ⁻¹
Heat capacity (0-100 °C)	0.452 J g ⁻¹ K ⁻¹
Electrical resistivity (20 °C)	6.9 μΩ/cm
Temperature coefficient of electrical resistivity (0-100 °C)	6.8×10^{-3} K ⁻¹
Thermal expansion coefficient (0-100 °C)	13.3×10^{-6} K ⁻¹
Modulus of elasticity	199.5 GPa _p
Brinell hardness	85

The density of molten nickel in g/cm³ is given by

$$\rho = \rho_0 - 1.16 \times 10^{-3} (t - t_0)$$

where

$$\rho_0 = 7.905, \quad t_0 = 1455;$$

the surface tension in mN/m, by

$$\sigma = \sigma_0 - 0.38 (t - t_0)$$

where

$$\sigma_0 = 1778, \quad t_0 = 1455;$$

and the viscosity in mPa·s, by

$$\eta = \eta_0 e^{E/RT}$$

where

$$\eta_0 = 0.1663, \quad E = 855 \text{ J/g}$$

Some mechanical properties of nickel are listed in Table 12.1.

Nickel normally forms a face-centered cubic crystal lattice, although a hexagonal modification is known, which changes to the cubic form at 250 °C. Cubic nickel is ferromagnetic below its Curie point of 357 °C, although less so than iron. The hexagonal form of nickel is not ferromagnetic.

Table 12.1: Mechanical properties of nickel (nominally 99.0% Ni).

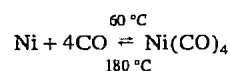
Property	Pretreatment							
	Tempered			Hot-rolled				
Temperature, °C	-200	-75	20	20	200	400	600	800
0.2% proof stress, MPa	230	170	160	170	150	140	110	
Tensile strength, MPa	710	560	500	490	540	540	250	170
Elongation, %	54	58	48	50	50	50	60	60
Impact value (Charpy)	230	230	230					

12.1.3 Chemical Properties

In its chemical properties [12] nickel resembles iron and cobalt, as well as copper. The +2 oxidation state is much the most important in nickel chemistry, although the +3 and +4 oxidation states are also known. The oxidation of nickel(II) salt solutions with chlorine, bromine, or persulfate in aqueous alkaline solution produces the insoluble nickel(III) oxide, β -NiO(OH). The nickel(IV) oxide $\text{NiO}_2 \cdot n\text{H}_2\text{O}$ is prepared by persulfate oxidation of nickel(II) hydroxide. In contrast to cobalt and iron, nickel is normally only stable in aqueous solution in the +2 oxidation state.

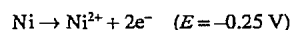
Nickel(II) ions form complexes very readily. The maximum coordination number is six. The green color of most hydrated nickel(II) salts and their aqueous solutions is due to the octahedral $\text{Ni}(\text{H}_2\text{O})_6^{2+}$ cation. The strong tendency of the nickel(II) ion to form complexes with ammonia, for example $\text{Ni}(\text{NH}_3)_6^{2+}$, or $\text{Ni}(\text{H}_2\text{O})_2(\text{NH}_3)_4^{2+}$, is utilized in a number of extraction processes.

The most unusual property of nickel is its ability to react directly with carbon monoxide to form a binary carbonyl complex. When carbon monoxide reacts with metallic nickel at 60 °C it forms the volatile nickel tetracarbonyl, $\text{Ni}(\text{CO})_4$. This reaction is reversible, with the carbonyl compound decomposing to carbon monoxide and nickel at higher temperatures (180 °C).



This reaction is the basis for the vapometallurgical refining of nickel. No other metal forms similar carbonyl compounds under such mild conditions at atmospheric pressure.

At moderate temperatures nickel has a high corrosion resistance against air, seawater, and nonoxidizing acids. Nickel is fairly electropositive with a standard electrode potential of -0.25 V, which is similar to cobalt (-0.28 V).



An outstanding property of nickel is its corrosion resistance to alkalis. The metal is therefore frequently used in the production and

handling of caustic soda. In contrast, nickel is attacked by aqueous ammonia solutions.

Nickel absorbs hydrogen, especially when finely divided; hydrogen absorption increases with increasing temperature. Defined hydride compounds have not been characterized. Nitrogen is not absorbed by nickel nor does it combine directly with it, although there is evidence for a nitride Ni_3N .

12.2 Occurrence

Nickel ranks twenty-fourth in the order of abundance of elements in the earth's crust with an estimated concentration of 0.008%. Although nickel is more abundant than copper, zinc, and lead there are relatively few nickel ore bodies of commercial significance.

The economically important ores can be divided into two types, sulfide and oxide (or silicate). Nickel does not occur as native metal. World reserves of nickel are currently (1988) estimated at about 50×10^6 t by the U.S. Bureau of Mines. This estimate includes only ores which are economically recoverable at prevailing metal prices. Identified world resources in deposits containing 1% Ni or more amount to over 130×10^6 t of nickel. About 80% of the nickel in these resources is in laterite ore bodies, with only 20% in sulfide deposits. The distribution of high-grade nickel reserves are detailed by country in Table 12.2, together with the corresponding 1988 mine production rates [13].

Nickel-containing manganese nodules, which occur in vast quantities on the seabed at depths between 3500 and 4000 m, typically contain 0.5–1.5% Ni. While not currently economically viable as a source of nickel, these deposits will undoubtedly become an increasingly important nickel resource in the future.

The United States has significant quantities of low-grade nickel resources such as the laterite ores of Oregon and northern California. However, none of these ores was considered as an economic nickel reserve by the Bureau of Mines at 1988 metal prices, and

consequently they are omitted from Table 12.2.

Table 12.2: World reserves of nickel [13].

Country	Reserves, 10^3 t	1988 Mine production, 10^3 t
Albania	180	10
Australia	1 270	74
Botswana	354	16
Brazil	666	15
Canada	8 130	190
China	726	25
Colombia	558	21
Cuba	18 140	34
Dominican Republic	517	23
Finland	80	11
Greece	454	12
Indonesia	3 200	58
New Caledonia	4 535	56
Philippines	408	8
South Africa	2 540	34
Former Soviet Union	6 620	186
Yugoslavia	158	4
Zimbabwe	77	11
World total	48 980	788

Table 12.3: Principal nickel minerals [1].

Mineral	Ideal formula	Nickel content, %
Sulfides		
Pentlandite	$(\text{Ni}, \text{Fe})_9\text{S}_8$	34.22 ^a
Millerite	NiS	64.67
Hazelwoodite	Ni_3S_2	73.30
Polydymite	Ni_3S_4	57.86
Siegenite	$(\text{Co}, \text{Ni})_3\text{S}_4$	28.89
Violarite	Ni_2FeS_4	38.94
Arsenides		
Niccolite	NiAs	43.92
Rammelsbergite	NiAs_2	28.15
Gersdorffite	NiAsS	35.42
Antimonides		
Breithauptite	NiSb	32.53
Silicates and oxides		
Garnierite	$(\text{Ni}, \text{Mg})_6\text{Si}_4\text{O}_{10}(\text{OH})_8$	≤ 47
Nickeliferous limonite	$(\text{Fe}, \text{Ni})\text{O}(\text{OH}) \cdot n\text{H}_2\text{O}$	low

12.2.1 Minerals

The most important nickel-containing minerals occurring in nickel deposits are listed in Table 12.3, together with their chemical compositions [1]. Some are relatively uncommon, and only pentlandite, garnierite, and nickeliferous limonite are of economic significance. The term garnierite is commonly used as a ge-

neric name for a series of mixed nickeliferous silicates with a wide range of nickel contents, and can include colloidal mixtures of silica and nickel hydroxide. Nickeliferous limonite is the term used to describe poorly crystalline nickel-bearing ferric oxides of which the main constituent is goethite (α - $\text{FeO} \cdot \text{OH}$).

Pyrrhotite ($\text{Fe}_{1-x}\text{S}_x$) is not included in the list of nickel minerals because it is an iron sulfide, and nickel is not essential to its composition. In pyrrhotites from different ore bodies the composition varies from FeS to Fe_7S_8 . Small amounts of nickel may substitute for the iron, making some pyrrhotite nickeliferous, independently of any particles of pentlandite they may contain.

12.2.2 Sulfide Ores

Sulfide nickel ores consist principally of nickeliferous pyrrhotite (Fe_7S_8), pentlandite ($(\text{Ni}, \text{Fe})_9\text{S}_8$), and chalcopyrite (CuFeS_2). Other minerals which occur in small but significant amounts include magnetite (Fe_3O_4), ilmenite (FeTiO_3), pyrite (FeS_2), cubanite (CuFe_2S_3), and violarite (Ni_2FeS_4). Sulfide ores typically grade 0.4–2.0% nickel, 0.2–2.0% copper, 10–30% iron, and 5–20% sulfur. The balance consists of silica, magnesia, alumina, and calcium oxide.

Pentlandite, the commonest of the sulfide minerals, probably accounts for 60% of world nickel production. Nickeliferous pyrrhotite is normally the most abundant phase in a nickel ore. It contains nickel in solid solution (0.2–0.5% Ni) in addition to very finely divided pentlandite inclusions. Chalcopyrite is the most important copper mineral, although cubanite is often present in lesser amounts.

Although the major minerals are the same in all large sulfide ore bodies, the relative amounts of pyrrhotite, pentlandite, and chalcopyrite vary widely. The relative amounts of the three minerals largely determine the choice of processing route.

In addition to nickel production, a large number of valuable by-products can be recovered from sulfide ores, including copper, cobalt, the platinum group metals, gold, silver,

selenium, tellurium, sulfur, and iron. Cobalt occurs principally in solid solution in pentlandite, at concentrations ranging from 1 to 5% of the nickel content. Discrete particles of gold, silver, and platinum group metals are very rare, and these metals are normally found in solid solution in the sulfide phases. The treatment processes are normally designed to yield optimum overall recovery of metal values.

Major sulfide ore bodies occur in Canada, the former Soviet Union, the Republic of South Africa, Australia, Zimbabwe, and Finland.

12.2.3 Oxide Ores

The oxidic ores of nickel are formed by a chemical concentration process that occurs as a result of the lateritic weathering of peridotite rock. Peridotite consists mainly of olivine, a

magnesium iron silicate containing up to 0.3% nickel. In many rocks the peridotite has been altered to serpentine, a hydrated magnesium silicate, prior to exposure to weathering. Olivine and serpentine are decomposed by groundwater containing carbon dioxide to form soluble magnesium, iron, and nickel, and colloidal silica. The iron rapidly oxidizes in contact with air and precipitates by hydrolysis to form goethite and hematite, which remain near the surface of the deposit. The dissolved nickel and magnesium, and the colloidal silica, percolate downwards in the laterite deposit, remaining in solution so long as the solution is acidic. When the solution is neutralized by reaction with rock and soil, nickel, silica, and some of the magnesium precipitate as hydrated silicates. This process is illustrated in Figure 12.1 [14].

Idealized laterite	Approximate analysis, %					Extractive procedure
	Ni	Co	Fe	Cr ₂ O ₃	MgO	
Hematitic cap	<0.8	<0.1	>50	>1	<0.5	Overburden to stockpile
Nickeliferous limonite	0.8 to 1.5	0.1 to 0.2	40 to 50	2 to 5	0.5 to 5	Hydrometallurgy
Altered peridotite	1.5 to 1.8	0.02 to 0.1	25 to 40	1 to 2	5 to 15	Hydrometallurgy or pyrometallurgy
Unaltered peridotite	1.8 to 3		10 to 25		15 to 35	Pyrometallurgy
	0.25 to 0.02	0.01 to 0.02	5	0.2 to 1	35 to 45	Left in situ

Figure 12.1: Typical section through a laterite deposit.

Complete separation of iron and nickel into distinct zones is never achieved. Some or even most of the nickel may in fact remain in the upper layer, which is thus enriched in iron and nickel, but depleted in magnesium and silica. Such material, consisting mainly of ferric oxide minerals, is described as limonitic. This type of ore is typically relatively rich in cobalt and chromium. By contrast, in the silicate minerals, the separation of iron and nickel is more complete, and the nickel is present in silicate minerals with a high magnesia content. Both types of material are almost always found in a laterite deposit, but in widely differing proportions.

The differences between limonitic and silicate minerals influence the methods by which they are treated for nickel recovery (Figure 12.1). The silicates, which are chemically and mineralogically heterogeneous and require a very flexible processing method, are normally treated by pyrometallurgical processes. The limonites on the other hand are relatively homogeneous in composition and mineralogy and are well suited to hydrometallurgical treatment.

The type of weathering which dissolves silica and metallic elements from rock to produce limonitic and silicate nickel ores occurs most frequently in tropical climates with high rainfall, and with decomposing vegetable matter to provide organic acids and carbon dioxide in the groundwater. Oxide nickel mineral deposits are currently exploited in Australia, Brazil, Cuba, the Dominican Republic, Greece, Indonesia, the Philippines, New Caledonia, Yugoslavia, the United States, and the former Soviet Union. The laterite deposits in Oregon and California were formed when the climate was subtropical in past geologic epochs.

12.2.4 Economic Trends

Although 80% of the world's known nickel resources on land are in oxide ore bodies, only 40% of nickel production comes from this source. The greater part of the nickel produced is recovered from sulfide ores. This situation

has arisen from the influence of political, geographic, technical, and economic factors. Sulfide ore deposits lie mostly in politically stable countries and close to the major nickel markets. The nickel content of sulfide ores can be concentrated relatively easily and cheaply by physical methods, while oxide ores must be treated in bulk. The potential for recovering the more numerous and valuable by-products also favors the exploitation of sulfide ore. However, the grades of sulfide ores are continually declining as the richer ores are consumed, and the cost of underground mining, particularly labor costs, is continually increasing. Inevitably therefore, oxide ore bodies, which are all relatively uniform in grade and can be surface mined, must in future support a larger share of nickel production.

Unfortunately, the production of nickel from oxide ores by the established processes consumes two to three times as much energy as the processing of sulfide ores. Nickel oxide ore treatment is therefore very sensitive to fuel oil and electrical power costs. A major expansion in the exploitation of oxide ores occurred in the decade prior to 1973 when fuel oil prices were low. Many of the new laterite treatment plants built in this period became uneconomic after the oil price increase in 1973, and as a result there was little or no increase in the proportion of nickel produced from oxide ores between 1975 and 1990.

Several international mining industry consortia evaluated the feasibility of recovering nickel from deep sea manganese nodules during the 1970s, and potential mining techniques were developed and tested. However, processing of the nodules to separate and recover the metals proved to be significantly more expensive than for land-based ores [15, 16]. The international legal aspects of ownership of these deep sea resources were the subject of the 11th Session of the Third U.N. Conference on the Law of the Sea, which ended in April 1982 with only a partial agreement which several major participants refused to sign [17]. These developments, in conjunction with low nickel prices, essentially killed any serious consideration of deep sea nodules as a source of nickel

during the 1980s. Development of this resource on a significant scale is therefore unlikely before the next century.

12.3 Beneficiation of Nickel Sulfide Ores [1, 18]

The low metal content of present-day nickel sulfide ores renders them unsuitable for either direct smelting or direct hydrometallurgical processing. Because the sulfide minerals usually occur as distinct grains in the rock matrix, these ores are amenable to a mechanical upgrading in which much of the rock content can be rejected. The metal content of the ore is concentrated by a physical treatment such as comminution to liberate the metal sulfide grains, followed by froth flotation or magnetic separation to recover a metal-rich concentrate [19].

In principle it is possible to produce separate nickel (pentlandite), copper (chalcopyrite), and iron (pyrrhotite) concentrates. However, a clean separation of pentlandite from pyrrhotite is difficult in practice since pyrrhotite typically contains intergrown inclusions of pentlandite as well as nickel in solid solution in the pyrrhotite. In fact pyrrhotite often contains 0.5–1 % Ni that cannot be separated by physical methods. The relatively high nickel content in pyrrhotite makes it difficult to achieve high yields of nickel from the ore unless the pyrrhotite is processed to recover its nickel content, and conversely the presence of nickel makes it difficult to obtain a marketable iron product from the pyrrhotite.

Most nickel producers, outside Canada, make no attempt to obtain separate nickel, copper, and iron concentrates and produce a bulk concentrate that contains pentlandite, pyrrhotite, and chalcopyrite as smelter feed. In Canada, both the major producers separate a large part of the pyrrhotite from pentlandite and chalcopyrite, and Inco further separates the pentlandite and chalcopyrite into separate nickel and copper concentrates. Even where the bulk of the pyrrhotite can be separated from pentlandite, residual pyrrhotite in the

nickel concentrate still contributes a major part of the sulfur content.

In response to ever tighter constraints on sulfur dioxide emissions from smelters during the 1970s and 1980s, the Canadian companies have made increased pyrrhotite rejection from smelter feed a major priority, and substantial improvements have been achieved. A pyrrhotite concentrate was treated by Inco for many years for nickel and iron oxide recovery. However, current environmental constraints on sulfur dioxide emissions have rendered the process obsolete, and pyrrhotite concentrates are now largely stockpiled, since none of the known treatment methods that avoid sulfur dioxide production is economic.

Pyrrhotite can be separated from pentlandite and chalcopyrite either by using its ferromagnetic properties or by flotation. Not all pyrrhotite is ferromagnetic, although in ores from the Sudbury, Ontario area the magnetic monoclinic form predominates over the paramagnetic or "nonmagnetic" hexagonal form [20]. In general, pyrrhotite containing less sulfur than $\text{Fe}_{0.87}\text{S}$ is nonmagnetic. This material can usually be separated from pentlandite by flotation.

Nickel or nickel copper concentrates typically range in grade from 5 to 15 % Ni + Cu, depending on the degree of pyrrhotite rejection achieved. An exceptionally high-grade concentrate, containing 28 % Ni and consisting largely of pentlandite, is produced in limited amounts at Inco's Thompson, Manitoba operation.

One of the more complex nickel concentration process flow sheets is that operated by Inco at its Sudbury operation [21]. In the two primary concentrators, the Clarabelle mill and the Frood-Stobie mill, 50 000 t/d of ore, grading 1.2 % Ni and 1.2 % Cu, is ground to a particle size of ca. 200 μm and treated by magnetic separation and flotation with a sodium amyl xanthate reagent to produce 5000 t/d of a bulk nickel copper concentrate and 8000 t/d of a pyrrhotite concentrate. Metallurgical data for the Clarabelle mill are given in Table 12.4.

Table 12.4: Metallurgical data for the magnetic separation and flotation of nickel ore (Clarabelle mill, Inco) [21].

	%	Analysis, %			Recovery, %		
		Cu	Ni	Pyrrhotite	Cu	Ni	Pyrrhotite
Ore	100	1.32	1.40	18.9	100	100	100
Magnetic concentrate	26	0.62	1.65	62.7	12	30	84
Flotation concentrate	8	14.4	11.6	15.9	84	64	7
Tails	66	0.07	0.13	2.5	4	6	9

Table 12.5: Metallurgical data for the upgrading of pyrrhotite and copper–nickel concentrate (Copper Cliff mill, Inco) [21].

	%	Analysis, %			Recovery, %		
		Cu	Ni	Pyrrhotite	Cu	Ni	Pyrrhotite
Feed	100	4.58	4.42	49.6	100	100	100
Copper concentrate	13	29.2	0.91	8.4	83	3	2
Nickel concentrate	29	2.28	12.8	43.0	14	85	25
Pyrrhotite concentrate	33	0.11	0.96	84.4	1	7	57
Tails	25	0.36	0.91	32.3	2	5	16

The two primary concentrates are further upgraded in the Copper Cliff mill. The bulk nickel copper concentrate is separated by flotation into separate nickel and copper concentrates by using lime and sodium cyanide at 30–35 °C to depress pentlandite and pyrrhotite. Under these conditions about 92 % of the copper is recovered to a concentrate grading 29 % Cu and 0.9 % Ni. About 98 % of the nickel and 92 % of the pyrrhotite are rejected to the separator tails, which grade 13 % Ni and 2 % Cu.

The Clarabelle rougher pyrrhotite concentrate is treated to separate residual chalcopyrite and pentlandite by grinding to ca. 74 μm followed by magnetic separation and flotation. A magnetic, cleaner pyrrhotite concentrate, a bulk nickel copper concentrate, and a nonmagnetic pyrrhotite tail are produced. The nonmagnetic tails stream (1 % Cu, 2 % Ni, and 30 % pyrrhotite) is further treated, by regrinding and flotation in the pyrrhotite rejection circuit, for final recovery of pentlandite and chalcopyrite before it is discharged to the tailings pond. Overall, about 80 % of the pyrrhotite content of the ore is rejected from smelter feed to the pyrrhotite concentrate and tails. Metallurgical data for the Copper Cliff mill are given in Table 12.5.

Falconbridge at its Strathcona mill in the Sudbury basin treats ore containing 1.5 % Ni and 1.1 % Cu by grinding and flotation to produce a nickel copper concentrate grading

6.7 % Ni and 5.6 % Cu at an average recovery of 83 % Ni and 93 % Cu [22–24]. A large part of the pyrrhotite content of the ore is rejected directly to the tailings pond. The separation of the nickel and copper in the bulk concentrate is carried out in the matte refining process after smelting.

The ore mined by Inco at Thompson, Manitoba consists of pentlandite and pyrrhotite with only a small amount of chalcopyrite (2.7 % Ni, 0.2 % Cu, 22 % pyrrhotite). Since the pyrrhotite contains 78 % of the sulfur but only 5.5 % of the nickel, a high degree of pyrrhotite rejection is feasible without seriously decreasing the nickel recovery [25]. The ore is ground and floated to recover a nickel copper concentrate and reject 90 % of the gangue and 60 % of the pyrrhotite to tails. The nickel copper concentrate is treated by flotation to separate first a copper concentrate, and then by magnetic separation and flotation to recover a high-grade (28 % Ni) pentlandite concentrate. The tailings stream from these steps forms the main nickel concentrate smelter feed (11 % Ni, 0.4 % Cu). The overall recovery of nickel to the nickel and pentlandite concentrates is about 87 %, while another 5 % of the nickel reports to the copper concentrate. Over 60 % of the pyrrhotite is rejected to tailings with only 8 % of the nickel.

At the BCL nickel–copper mine in Botswana the pyrrhotite/pentlandite ratio in

the ore averages about 13:1 and the pyrrhotite contains over 30% of the nickel either in solid solution or as small pentlandite inclusions. Consequently, high nickel recoveries can only be achieved by recovering the nickel from pyrrhotite. This is achieved by producing a bulk pentlandite-pyrrhotite-chalcopryrite concentrate, with a typical composition of 2.8% Ni and 3.2% Cu [26]. Modern nickel concentrators are largely automated and are equipped with process control systems based on on-line X-ray analysis of process streams [27].

12.4 Pyrometallurgy of Nickel Concentrates

Over 90% of the world's nickel sulfide concentrates are treated by pyrometallurgical processes to form nickel-containing mattes [1, 28–32]. Production capacities and composition of the feed concentrate and product matte are listed in Table 12.6 for several major nickel smelters.

The pyrometallurgical treatment of nickel concentrates includes three types of unit operation: roasting, smelting, and converting. In the roasting step sulfur is driven off as sulfur dioxide and part of the iron is oxidized. In smelting, the roaster product is melted with a siliceous flux which combines with the oxidized iron to produce two immiscible phases, a liquid silicate slag which can be discarded, and a solution of molten sulfides which contains the metal values. In the converting operation on the sulfide melt, more sulfur is driven off as sulfur dioxide, and the remaining iron is oxidized and fluxed for removal as silicate

slag, leaving a high-grade nickel copper sulfide matte.

In several modern operations the roasting step has been eliminated, and the nickel sulfide concentrate is treated directly in the smelter.

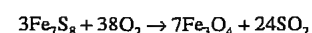
12.4.1 Roasting

Roasting [33] is basically a process in which the nickel sulfide concentrates are heated in an oxygen-containing gas, usually air, to a temperature (600–700 °C) at which oxygen oxidizes sulfide to sulfur dioxide and reacts with the metal values to form solid oxides, termed the calcine. The roasting step may also serve to preheat the charge for smelting.

The thermodynamic relationships between the metal sulfides and oxides provide the basis for the separation of iron from nickel, copper, and cobalt contained in the concentrate. The sulfides of iron, nickel, cobalt and copper are all in the same thermal stability range at the smelting temperatures (1200–1300 °C), but, in the presence of oxygen, each sulfide is unstable with respect to its corresponding oxide. Iron has the greatest affinity for oxygen, followed by cobalt, nickel, and copper. Consequently, if the nickel concentrate is roasted with a deficiency of oxygen the iron is oxidized preferentially, while virtually all of the nickel and copper remain as sulfides. Thus the degree of oxidation of the charge and the degree of elimination of sulfur can be controlled by regulating the supply of air to the roaster.

The degree of sulfur elimination achieved in the roasting step largely determines the grade of the matte produced as well as the losses of nickel and copper to the slag phase in the subsequent smelting operation. All the sulfur present in the calcine in excess of the amount needed to combine with the nickel, copper, and cobalt in the matte combines with iron, which therefore remains in the matte phase and lowers its nickel copper cobalt grade. The major constraint on achieving a high-matte grade in smelting is the increasing loss of nickel, copper, and cobalt to the slag phase. If all of the iron were to be oxidized in the roasting step so that it could be slagged off in the smelting stage and a high-grade matte produced directly, an increased amount of nickel, copper, and cobalt oxides would be formed in the roaster, and metal losses to the slag in smelting would increase substantially. Hence, each smelting operation seeks to operate at an optimum matte grade which gives the highest metal value recovery to the matte. The balance of the iron is removed in the converting step.

Normally only about 50% of the pyrrhotite content of the nickel concentrate is oxidized in roasting, and under these conditions less than 5% of the nickel and copper are oxidized, with the balance remaining as sulfides. The oxidation of pyrrhotite to magnetite can be represented by the following reaction:



This reaction is strongly exothermic, and autogenous roasting, without the use of an external heat source, is practiced whenever possible.

In order to achieve effective roasting the furnace must provide good contact between the sulfide particles and the oxygen-bearing gas. The furnace system must also be able to provide close control of the degree of sulfur elimination. Both multihearth roasters and fluidized-bed roasters are in current industrial use for nickel concentrate roasting. The use of traveling grate sintering machines, which were formerly widely used to prepare an agglomerated feed for blast furnace smelting, is

now practiced only in the former Soviet Union.

The multihearth roasting furnace consists of a series of vertically superimposed circular hearths. Wet concentrate and smelting flux are charged to the upper hearth. A central rotating shaft drives rabble arms that extend across the roaster hearths, turning over the concentrate charge and transferring it via dropholes to the next lower hearth. Air, preheated by the combustion of natural gas, passes upwards through the hearths, heating the concentrate to ignition temperature and providing the oxygen required to burn the concentrate. The temperature is controlled by regulating the flow of air into the roaster.

Since the area of contact between the furnace gas and concentrate particles on the hearths is very limited, the total time required for roasting in this type of furnace is long, resulting in low throughput rates. A further disadvantage of the multihearth roaster is that low oxygen utilization and high air infiltration rates produce an off-gas with a low concentration of sulfur dioxide which is unsuitable for sulfuric acid production.

Multihearth roasters are still used in the Copper Cliff smelter of Inco in Ontario, which was built in 1930. A battery of 24 roasters can each treat 300 t/d of wet concentrate mixed with 75–90 t/d of siliceous flux. About 40% of the sulfur content of the concentrate (13% Ni, 2–3% Cu, 30% S, and 40% Fe) is eliminated at a roasting temperature of 800 °C. Less than 5% of the nickel and copper are oxidized. This operation is not thermally self-sustaining, due to high heat losses from the roaster, and natural gas is used to provide supplementary heating. The off-gas is cleaned to recover dust and is vented to a stack. The roasted calcine discharge from the bottom of the furnaces is conveyed directly to the reverberatory smelting furnaces [34].

The fluidized-bed roaster is a more recent development and has an improved gas solids contact efficiency and a simpler construction (Figure 12.2). The roasting furnace is a vertical chamber of circular cross section with a grate hearth through which the oxygen-bearing

Table 12.6: Nickel sulfide smelters [30–32].

Smelter	Feed concentrate, %		Matte product, %		Nominal capacity, t/a Ni
	Ni	Cu	Ni	Cu	
Inco, Copper Cliff	13	2.7	63	15	110 000
Inco, Thompson	10.5	0.4	73	3	50 000
Western Mining	11.4	0.85	72	5	60 000
Falconbridge	6.7	5.6	40	34	45 400
Outokumpu	8–9	2–4	64	26	18 000
BCL, Botswana	2.8	3.2	38	40	20 000
Rustenburg	3.2	2.0	47	27	19 000
Bindura	10.6	3.4	70	20	14 400

ing gas is blown. As nickel concentrate and smelting flux are fed to the chamber, the particles are suspended in the vertical air flow. Since each sulfide particle is in constant turbulent motion in the oxidizing atmosphere, roasting is uniform and rapid, with efficient heat transfer and oxygen utilization. Solids are discharged from the furnace either by overflow through a side port or by entrainment in the off-gas stream. The dust-laden gas may be passed through waste-heat boilers to recover its sensible heat. The cleaned off-gas stream contains a high concentration of sulfur dioxide, which can be converted to sulfuric acid.

Fluidized-bed roasting of nickel concentrates is practiced by Inco at the Thompson smelter in Manitoba and at Copper Cliff, where 10% of the nickel concentrates are processed in fluidized-bed roasters, and by Falconbridge at its smelter in Ontario. The Thompson smelter operates five fluidized-bed roasters with a combined capacity of 3800 t/d of concentrate, while the Falconbridge smelter operates two roasters with a combined capacity of 2000 t/d of concentrate [22, 35].

In the Falconbridge smelter a slurry (75% solids) of nickel-copper concentrate (6.7% Ni, 5.6% Cu, 30% S, 40% Fe) in water is fed directly to the roaster. Siliceous flux is added separately. Sulfur elimination ranges from 50 to 60% at a roasting temperature of 600–650 °C. The operation is thermally autogenous, and the water contained in the feed slurry serves as a heat sink to control the bed temperature. Oxygen utilization is essentially 100%. About 85% of the calcine leaves the roaster in the off-gas stream which is treated in a series of cyclones, gas coolers, and electrostatic precipitators for solids recovery. The solids recovered from the gas cleaning system are combined with the coarser roaster bed overflow calcine, for charging to the electric smelting furnaces [24].

12.4.2 Smelting

In the treatment of nickel sulfide ores and concentrates the function of the smelting process is to eliminate the gangue minerals and

most of the iron sulfide and to concentrate the metal values into a high-grade nickel-copper matte containing 0.5–3.0% Fe and 6–22% S. Unlike copper, nickel metal cannot be produced by the oxidation of the sulfide at a practical smelting temperature (up to ca. 1400 °C).

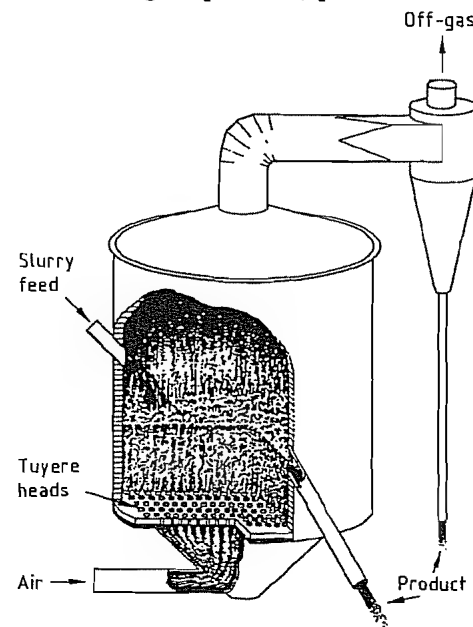


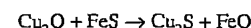
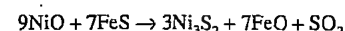
Figure 12.2: Cutaway view of a fluidized-bed roaster.

When a mixture of metal sulfides, iron oxide, gangue, and siliceous flux are melted together, the iron oxide, gangue, and silica form a slag layer that floats on the heavier, molten sulfide or matte phase. The two immiscible layers are separated and the slag is discarded.

The smelting process for nickel sulfide concentrates is normally carried out in two stages: primary smelting and converting. The oxidizing, slagging, and removal of iron in stages is critical to the efficiency and economics of smelting operations. If most of the iron were to be oxidized in the roaster and then slagged in a single smelting step, a matte high in nickel and low in iron would be produced. However, as noted above, significant amounts of the nickel and copper sulfides would also be oxidized in the roaster, and these oxides would be lost to the slag in the smelting step. Slag can also mechanically entrain droplets of

matte and these losses will also increase with matte grade. Thus if a high-grade matte were to be produced in one step, the overall recovery of nickel would be low.

Provided that only about half the iron is oxidized in the initial roasting step, only 5% of the nickel and copper sulfides are oxidized. In fact only a small amount of these oxidized metals will be lost to the slag because the oxides react with residual iron sulfides in the smelting process to produce the corresponding sulfides, which return to the matte phase.



Thus a low-grade, high-iron furnace matte is produced and only a small amount of nickel is lost to the slag as oxide when the nickel concentrate is treated in separate roasting and smelting steps.

The iron remaining in the furnace matte is oxidized and slagged in the secondary smelting step (converting). Since the slag produced in the converting stage, in which a high-grade, low-iron matte is produced, has a high nickel and copper content, it is returned to the primary smelting stage where the metal values are recovered by the reaction of the oxides with iron sulfide and by the settling of entrained droplets of matte. Thus the two-stage smelting process allows the production of a high-grade, low-iron nickel matte, and a high-iron slag of low metal grade which can be discarded without significant loss of metal values.

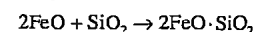
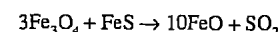
12.4.2.1 Primary Smelting

The primary smelting step is carried out in a variety of furnaces, including reverberatory, electric, and flash furnaces, which provide a wide variety of smelting conditions. Chemical losses of nickel and copper to the slag increase with the oxidation potential of the system. Thus metal losses to slag are much higher in the flash smelting furnace, in which the roasting step is combined with the primary smelting step, and smelting conditions are strongly oxidizing, than in the electric furnace, where

smelting is carried out under reducing conditions. Consequently, slag from the flash smelting process must be treated in a separate step to recover the contained metal values, while slag from the electric furnace or reverberatory furnace smelting processes can be discarded without further treatment.

A typical furnace matte containing 10% Ni, 65% Fe, and 25% S melts at ca. 950 °C, and nickel sulfide itself melts at ca. 790 °C. The melting point of a fayalite slag with an iron to silica ratio of about 7:3 is 1200 °C, although the slag melting point can be reduced to 1100 °C by the addition of a few percent of lime and alumina. With this type of slag, smelting is carried out at ca. 1200 °C. However, when significant levels of magnesia are present in the nickel concentrate or ore the melting point of the slag may be as high as 1260 °C, and smelting is then carried out at ca. 1400 °C [36–38].

Magnetite, which is formed in the partial roasting of the concentrates, reacts in the primary smelting step with the remaining iron sulfides and silica flux to form fayalite:



The presence of magnetite in slags and mattes not only affects the chemistry of the smelting operation, but has an important effect on the smelting furnace. Magnetite is formed under strongly oxidizing conditions and its formation is favored by low operating temperatures and by silica-deficient slags. The magnetite content of slags from the more oxidizing reverberatory and flash smelting furnaces is usually above 10%, with the content increasing with matte grade, while slags from reduction smelting electric furnaces typically contain less than 5% magnetite. Magnetite tends to settle out in the bottom of the smelting vessel and accretions can severely reduce the operating capacity of the furnace. Consequently it is always desirable to minimize the formation of magnetite in the smelting process.

Reverberatory Furnace Smelting. In the reverberatory furnace, fossil fuel (pulverized

coal, oil, or natural gas) is burned separately from the material being smelted. The furnace is a long rectangular structure with an arched roof and burners at one end and in the roof. A large part of the heat from the combustion gas radiates directly to the charge lying in the hearth below. A further substantial part of the heat is reflected from the walls and roof of the furnace into the charge. Solid charge is fed through vertical fettling pipes mounted in the roof along each side of the furnace. As the charge melts it flows towards the center of the furnace. Molten converter slag is introduced into the furnace at the firing end.

Slag is tapped from the end of the furnace opposite the burners, while matte is tapped from the side. This type of furnace has a low energy efficiency since the off-gas stream carries nearly 50% of the heating value of the fuel. Waste-heat boilers or heat exchangers are used to recover heat from the off-gases.

The reduction of the magnetite formed in the roaster to ferrous oxide is not complete in the reverberatory furnace, and slags contain up to 7% magnetite. Scrap iron or ferrosilicon is often added to control the formation of magnetite to minimize metal losses to the slag and to prevent magnetite buildup in the furnace hearth.

Inco uses two reverberatory furnaces equipped with roof-mounted oxyfuel burners for the primary smelting of nickel concentrates at its smelter in Copper Cliff, Ontario. Each furnace treats 1500 t/d of partially oxidized concentrate (13% Ni, 2.7% Cu) which is transferred at 700 °C from the multihearth roasters, together with 700 t/d of recycled molten converter slag. Oxygen enrichment of the combustion air supplied to the oxyfuel burners not only increases fuel utilization efficiency but also substantially increases the capacity of the furnace [34, 39–43].

The furnace matte contains 30–35% nickel plus copper, together with the precious metals content of the charge. The reverberatory slag, which normally analyzes 0.2% Ni, 0.1% Cu, 0.1% Co, 38% Fe, and 36% SiO₂, is discarded. The matte is tapped at 1150 °C and blown with oxygen-enriched air (30% O₂), in

one of 14 Peirce–Smith converters, to a high-grade, sulfur-deficient matte containing 78% Ni and Cu and 20% S. The converter slag, typically containing 2.3% Ni and Cu, 50% Fe, and 25% SiO₂, is recycled to the reverberatory furnace for recovery of the contained nickel and copper [42].

Electric Furnace Smelting. The energy required for smelting may be obtained from electrical power as an alternative to burning fossil fuels or sulfides in air or oxygen. The use of an electric furnace for nickel sulfide smelting is favored when the cost of electrical energy is low or when the required smelting temperature is high, for example, when the concentrate contains high levels of magnesia.

Heating of the bath is achieved by passing a three-phase electrical current through a circuit consisting of carbon electrodes immersed in the slag layer, which has a high electrical resistance (submerged arc technique). Electric furnaces used for nickel–copper matte smelting are either rectangular with six electrodes in line or circular with three electrodes in triangular configuration. The consumable electrodes are made of carbon and are either prebaked or are of the self-baking Söderberg type.

The charge of concentrate (or calcine) and flux is fed through the roof. Thus a layer of unsmelted charge covers the slag giving it a “cold top”. The concentrate or calcine gradually settles into the slag as it melts and then separates into slag and matte layers. The slag and matte are tapped intermittently, as required. Since there is no fuel combustion in an electric furnace the quantity of off-gas is much less than from a reverberatory furnace and heat and dust recovery from the off-gas is therefore easier.

Electric furnace smelting of nickel concentrates is practiced by Inco at its Thompson, Manitoba, operation; by Falconbridge at Sudbury, Ontario; by the Severonikel Combine in the former Soviet Union; by Rustenburg Platinum, Impala Platinum, and Western Platinum in the Republic of South Africa; and by Bindura Nickel in Zimbabwe. The Canadian oper-

ations treat partly roasted concentrate calcines, while Bindura and the platinum producers treat nickel–copper concentrates directly. The Severonikel electric furnace smelter treats high-grade ore from Norilsk (3.5% Ni, 3.5% Cu) directly [44]. Current industrial practice is illustrated by the following examples.

In the Rustenburg Refiners smelter [45] in the Republic of South Africa, pelletized nickel–copper concentrate, containing 3.2% Ni, 2% Cu, 15% Fe, 39% SiO₂, 15% MgO, 3% CuO, 6% Al₂O₃, 9% S, and ca. 130 g/t precious metals, is mixed with a lime flux and smelted directly in a 19.5 MVA electric furnace. About 98% of the nickel and 97% of the copper and most of the precious metals contained in the concentrate are recovered to a matte containing about 17% Ni, 10% Cu, 40% Fe, and 27% S. The electric furnace slag, containing 0.1% Ni and 0.06% Cu, is tapped at 1350 °C and discarded. The matte is tapped at 1180 °C and converted in Peirce–Smith converters to a product analyzing 48% Ni, 27% Cu, 1.5% Fe, and 20% S, again with high recovery of the precious metals to the matte.

The Falconbridge smelter in Sudbury, Ontario, which was built in 1978 on similar lines to Inco's Thompson smelter, is a good example of the modern large-scale application of fluidized-bed roasting and electric furnace smelting of nickel–copper concentrates (Figure 12.3). The smelter contains two roaster electric furnace lines, each of which was de-

signed to treat up to 1250 t/d of nickel–copper concentrate (6.7% Ni, 5.6% Cu). The electric furnaces are each rated at 33 MVA and have a six-in-line electrode configuration. The electrodes are of the Söderberg self-baking type. Typical furnace operating conditions are as follows [21, 46, 47]:

Concentrate feed rate	900 t/d
Power consumption	1.2 GJ/t solid charge
Slag temperature	1230 °C
Matte temperature	1130 °C
Off-gas temperature	700 °C
Calcine depth	500 mm
Slag depth	1500 mm
Matte depth	700 mm
Bottom buildup	150 mm
Electrode immersion	250 mm
Off-gas volume	28 300 m ³ /h (STP)

Roaster calcine together with the flux added prior to roasting, at about 600 °C, is conveyed directly to the furnace and added to the bath through fettling tubes mounted in the furnace roof. Recycle dusts and scrap together with reductants are added to the calcine conveyors. Converter slag is fed to the furnace through a launder above the matte-tapping end of the furnace.

Coke is added to the charge as a reductant, at a rate of 2.5% of the concentrate, to improve metal recoveries and to reduce magnetite formation. The use of coke reductant and operation of the furnace under “black top” conditions results in a significant power saving compared with open-bath operation under oxidizing conditions (1.2 GJ/t versus 1.5 GJ/t of solid charge).

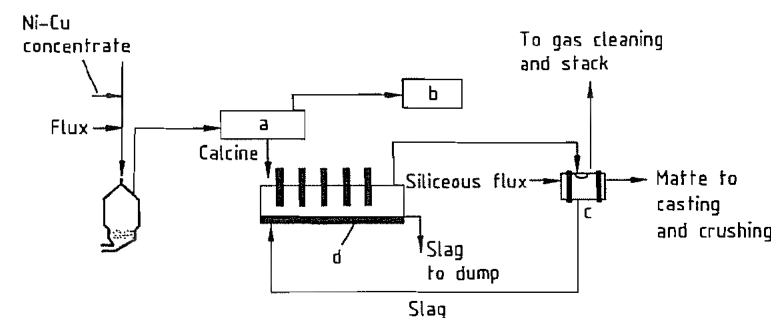


Figure 12.3: Flow sheet of the Falconbridge smelter: a) Gas-scrubbing and calcine recovery; b) Acid plant; c) Converter; d) Electric furnace.

The electric furnace slag, typically containing 0.12% Ni, 0.20% Cu, and ca. 4% magnetite, is tapped at 1230 °C and is transferred in slag pots to a disposal area. The furnace matte, which normally contains 24% Ni + Cu, is tapped at 1130 °C and is transferred to one of four Peirce-Smith converters where it is blown with air to produce a matte containing 74% Ni + Cu, 1% Co, 2.5% Fe, and 23% S. The converter matte is cast, crushed, and shipped to the Falconbridge refinery in Norway. The converter slag is recycled to the electric furnace, and the converter off-gases are cleaned in electrostatic precipitators and vented to a stack.

Flash Smelting. In flash smelting, a finely ground sulfide concentrate is smelted by burning some of its sulfur and iron content while the sulfide particles are suspended in the oxidizing atmosphere. The concentrate is roasted and smelted in a single process step. The predried concentrate and flux materials are injected with preheated oxygen-enriched air or commercial oxygen into the reaction shaft of a specially designed furnace. The exothermic heat of reaction of the iron sulfide with oxygen provides the energy to heat the particles to smelting temperature. The smelting temperature and the grade of matte formed are both controlled by adjusting the ratio of the amount of oxygen supplied to the furnace to the throughput rate of concentrate. In current practice, which uses oxygen-enriched air, the process can be thermally autogenous, and the addition of a fossil fuel is not generally required.

The flash smelting process was developed independently by Inco in Canada and Outokumpu in Finland, shortly after World War II. In both cases it was applied commercially to the treatment of copper concentrates. The Inco process uses commercial oxygen (95%) while the Outokumpu process initially used air, augmented by fuel oil, as the oxidant and energy sources. The Outokumpu process was first applied commercially to the treatment of nickel concentrates in 1959. Oxygen enrichment of the combustion air was introduced by Outo-

kumpu in 1971 and resulted in several major improvements in furnace performance. The Inco flash smelting process was successfully tested on a full production scale for the treatment of nickel concentrate in 1976, and will be utilized in the modernization of the Copper Cliff smelter scheduled for the early 1990s. In addition to its own installation at Harjavalta in Finland, the Outokumpu flash smelting process for nickel has been adopted by the Western Mining Corporation in Australia, by BCL in Botswana, and by the Norilsk Combine in Russia. The Outokumpu flash smelting process for copper has been adopted in about 30 operations worldwide [48, 49].

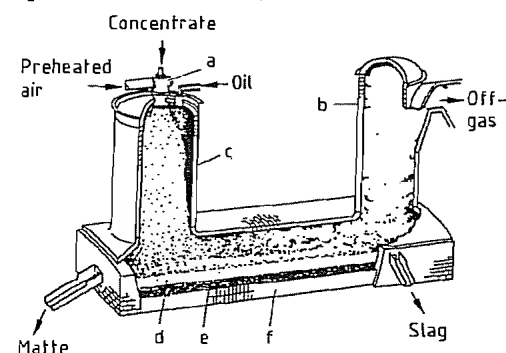
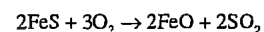


Figure 12.4: Cutaway view of an Outokumpu flash smelting furnace: a) Concentrate burner; b) Uptake; c) Reaction shaft; d) Slag; e) Matte; f) Settler.

The Outokumpu flash smelting furnace, essentially an upright U in shape, consists of a vertical reaction shaft, a horizontal reverberatory settler hearth, and a vertical gas uptake shaft (Figure 12.4). Predried nickel concentrates and fluxes are mixed with oxygen-enriched air and injected into the furnace by means of the concentrate burner mounted at the top of the reaction shaft. The resulting suspension spreads over the area of the reaction shaft. At operating temperatures, ignition of the iron sulfides occurs instantly, and the following exothermic reaction with oxygen provides all the heat required for smelting:



The nickel and copper sulfides melt to form a matte, while the iron oxide combines with silica flux to form a fayalite slag. Separation

of the molten particles from the combustion gases occurs as the gas stream leaves the reaction shaft. The melt collects in the settler, where the matte and slag form separate layers and are tapped at opposite ends of the furnace.

Nickel flash furnace mattes typically grade 50–55% Ni + Cu, and the grade is controlled by adjusting the ratio of oxygen to concentrate in the furnace. The furnace mattes are treated in Peirce-Smith converters with oxygen-enriched air to produce a high-grade matte product. The converter slag is either recycled to the flash furnace or treated directly in a slag cleaning furnace to recover the contained metal values. The composition of converter matte varies between smelters. The final sulfur content is adjusted in accordance with the requirements of the subsequent refining process. Thus at Harjavalta the matte is blown to a sulfur content of only 4–7%, while the other smelters produce matte containing about 20% S.

When oxygen-enriched air is used to produce a high-grade furnace matte, operating temperatures are sufficiently high to reduce magnetite formation and prevent significant magnetite accretions building up in the furnace. Inevitably, when a high-grade matte is produced under oxidizing conditions the slags contain too high a level of metal values to be discarded. Nickel flash furnace slags are generally cleaned by reduction and settling in an electric furnace, with coke as the reductant. The Western Mining flash furnace in Australia has been modified by the extension of the settler beyond the gas uptake shaft [50, 51]. This extension to the settler hearth contains two sets of electrodes and serves as a continuous slag cleaning furnace. The furnace slag tapped from the extension is sufficiently low in metal values to be discarded. At the BCL smelter in Botswana, which treats a very low-grade concentrate and consequently has a high slag to matte ratio, slag losses are controlled in the settler itself by the addition of lump coal, which floats on the surface of the slag and reduces the metal oxides [26, 52]. The slag is further cleaned in two electric furnaces connected in series before being discarded. Re-

cent metallurgical data for three flash smelting operations are presented in Table 12.7.

Off-gases leave the flash furnace through the uptake shaft and enter a waste-heat boiler where the heat content of the gas is recovered as high-pressure steam. The gas, which has a high sulfur dioxide content, is cleaned in electrostatic precipitators to recover entrained dust. The cleaned gas stream can be used as a feed to a sulfuric acid plant, for liquid sulfur dioxide recovery, or can be reduced to elemental sulfur with a fossil fuel.

The flash smelting process is particularly suited to the application of automated process control. The major control parameter is the ratio of oxygen in the combustion air to concentrate throughput. This parameter not only controls the degree of oxidation of the sulfides but also the grade of the matte and the operating temperature. The process is thus controlled by adjusting the flow rates of both combustion air and commercial oxygen, in relation to the concentrate feed rate. The slag composition is controlled by the rate of addition of flux materials to the concentrate in the furnace feed blend. Control of the process can thus be fully computerized [53].

Table 12.7: Metallurgical data for flash smelters [50–53].

Smelter		Outokumpu	Botswana	Western Mining
Capacity, t/a concentrate		190 000	800 000	600 000
Concentrate, %	Ni	8–9	2.8	11.4
	Cu	2–4	3.2	0.9
	Fe	24–27	43.5	38
	S	19–22	31.0	32
Furnace matte, %	Ni	33	15	44
	Cu	19	17	3
	Fe	18		27
	S	25		22
Converter matte, %	Ni	58	36	72
	Cu	32	40	5
	Fe	0.5	<1	<1
	S	6	20	21
Discard slag, %	Ni	0.15	0.15	0.28
	Cu	0.32	0.34	0.08
Smelter recovery, %		95	91.5	96

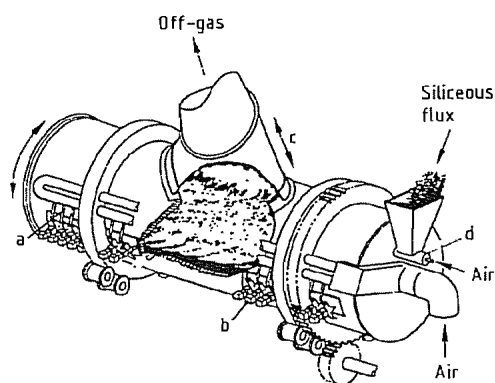
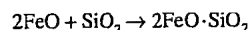
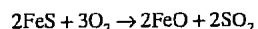


Figure 12.5: Cutaway view of a Peirce-Smith side blown converter: a) Tuyere pipes; b) Pneumatic punches; c) Hood; d) Flux gun.

12.4.2.2 Matte Converting

In the converting step [54–56], iron sulfide is removed from the molten, low-grade furnace matte by oxidation and slagging. The slag, which contains high levels of nickel and copper, is returned to the primary smelting furnace for recovery of metal values. The high-grade, low-iron nickel-copper matte, which typically contains 20% S, less than 1% Fe, and also any precious metals present in the original concentrates, is the final product of the smelting process.

Converting is a batch operation. The horizontal side blown converter, known as the Peirce-Smith converter (Figure 12.5), is normally used for the treatment of nickel furnace mattes, although top blown rotary converters are used in some modern plants, particularly for low production rates. Air or oxygen-enriched air is blown through the molten matte to form iron oxides and remove sulfur as sulfur dioxide. The iron oxides combine with added silica flux to form an iron silicate slag:



A substantial amount of magnetite is also formed in the conversion process.

Converter slags contain 20–35% silica, with the balance being iron oxides. Silica in the slag combines with iron(II) oxide, thus preventing further oxidation to magnetite.

Slags low in silica contain large amounts of magnetite. Typically, up to one-third of the iron may be in the iron(III) state in a 20% silica slag, while a slag with 35% silica contains less than 15% magnetite. Magnetite formation is useful in converting since it can be made to coat the inside of the brick-lined furnace and thus protects it from erosion and corrosion by the slag [57, 58].

The oxidation of iron sulfide is strongly exothermic and much of the heat generated in the conversion process can be utilized to melt additional ore or concentrate feed or recycled scrap materials. Since the throughput of a converter is almost directly proportional to the amount of oxygen blown through the charge, its capacity can be raised substantially by enriching the air with oxygen. In addition to increasing the converting rate, oxygen enrichment of the air permits the treatment of additional cold charge, and in fact the addition of cold charge is essential to control the bath temperature when oxygen-enriched air is used. Up to 3 t of cold charge materials can be smelted for each tonne of oxygen supplied.

12.4.3 Environmental Aspects of Nickel Smelting

During the 1970s and 1980s the nickel industry responded to increasing public concern over smelter emissions of sulfur dioxide to the environment by replacing outdated process equipment, such as multihearth roasters, sinter machines, blast furnaces, and reverberatory furnaces, by processes such as fluidized-bed roasting, electric furnace smelting, and flash furnace smelting, which are more energy efficient and environmentally cleaner.

However, while the technology is available to produce sulfuric acid economically from sulfur dioxide in the high-strength off-gas streams produced by the modern smelting techniques, there is not always a market for large amounts of acid within an economic shipping distance of the nickel smelter. Thus, although the Inco and Falconbridge smelters in the Sudbury area of Ontario do convert a substantial amount of their sulfur dioxide to

acid, more remote operations, including Inco's smelter at Thompson, Manitoba, Western Mining's smelter in Western Australia, and the BCL smelter in Botswana, vent SO_2 -containing off-gases to the atmosphere. In fact the BCL smelter was designed with the capability to convert sulfur dioxide to elemental sulfur by reduction with fuel oil. However, this process proved uneconomic when oil prices increased in the early 1970s and it has never been operated. A similar circuit that uses natural gas to reduce sulfur dioxide to sulfur is in operation at the Norilsk flash furnace smelter in the former Soviet Union, which was commissioned in 1981 [58].

A more cost-effective method of reducing sulfur dioxide emissions is to reject as much pyrrhotite as possible from the smelter feed by separating pyrrhotite from pentlandite in the concentrator. As much as 50–60% of the pyrrhotite content of the ore is now rejected in the major Canadian nickel operations at Sudbury and Thompson. At Thompson, Inco reduced SO_2 emissions by 45% between 1976 and 1986 simply by increasing pyrrhotite rejection, but incurred significant metallurgical penalties by doing so [25]. Not only was the overall recovery of nickel reduced but the absence of much of the pyrrhotite removed a major energy source for the smelting process. Since the roasting and converting steps were designed to be autogenous using the iron sulfide as fuel, when over 50% of the pyrrhotite is rejected prior to smelting insufficient iron is available to sustain the converting operation, and extra fuel must be supplied.

Maximum pyrrhotite rejection is practiced by both Inco and Falconbridge at their Sudbury operations. In these ores the nickel content of the pyrrhotite mineral is higher than in the Thompson ore and so pyrrhotite rejection results in significant losses in nickel recovery. A process to treat pyrrhotite concentrate separately to recover nickel, iron ore, and sulfuric acid, was operated by Inco for many years but the operation was abandoned in the mid 1980s when it became uneconomic due to increasingly stringent sulfur emission limits [32].

Falconbridge rejects over 55% of the pyrrhotite in its ore and recovers sulfuric acid from the sulfur dioxide in the fluidized-bed roaster off-gas stream. Electric furnace and converter off-gases are vented to the atmosphere as a low-strength sulfur dioxide stream. The distribution of sulfur in the Falconbridge operation in 1983 is detailed in Table 12.8 [24, 52].

Table 12.8: Sulfur distribution at Falconbridge, Sudbury, Ontario in 1983 [24].

	Sulfur, t/d	Distribution, %
Mill tailings, incl. pyrrhotite	540	58.5
Smelter slag	11	1.2
Nickel-copper matte	44	4.8
Sulfuric acid production	200	21.7
Stack emissions	104	11.3
Copper concentrate, etc.	23	2.5

Particulate emissions from the Falconbridge smelter were also reduced by 80% when the fluidized-bed roasting-electric furnace process replaced the old sintering blast furnace process in 1978.

The Outokumpu flash smelting process is probably the most environmentally compatible of the current commercial nickel smelting processes because it permits the capture of virtually all the sulfur dioxide produced prior to the conversion step. The recovery of sulfur dioxide from the off-gas stream from Peirce-Smith converters is not generally feasible due to the low sulfur content of the off-gas and intermittent nature of the operation.

12.4.3.1 New Developments in Nickel Smelting

In contrast to the copper industry, in which a number of continuous smelting processes have been commercialized, there has been little interest in developing a process for nickel concentrates in which the primary smelting and converting steps are combined into a single continuous operation. One such process was proposed by QUENEAU and SCHUMANN in 1976 hut has not been adopted commercially [59].

The major development in nickel smelting during the 1990s will be the modernization of

Inco's aging nickel-copper smelter at Copper Cliff, Ontario. Ontario Government regulatory measures to reduce acid rain require that Inco reduce its emissions of sulfur dioxide from 685×10^3 t/a in 1990 to 265×10^3 t/a by 1994, corresponding to an increase in the fixation of the sulfur in the ore from 70% to 90%. In the existing operation, 55% of the sulfur is rejected to tailings as pyrrhotite, and a further 15% is converted either to acid or to liquid sulfur dioxide. The remaining 30% is emitted to the environment as low sulfur dioxide content off-gases from the Herreschoff roasters, reverberatory furnaces, and the nickel matte and copper converters.

Several potential smelting options were examined by Inco, including the roast-reduction-smelting process, which was tested on a plant scale at Thompson in 1979 [32], and the oxygen flash smelting of nickel concentrate, which was tested with the copper flash furnace at Copper Cliff in 1976 [60]. However, none of these options was acceptable since they did not eliminate the copper converting operation, which itself produces more than the 1994 sulfur dioxide emission limit of 265 000 t/a [61].

The strategy eventually selected for the modernization is based on the oxygen flash smelting of bulk nickel copper concentrate followed by converting the high-grade furnace matte in the existing nickel converters. The converter matte will be separated into metallics, nickel sulfide, and copper sulfide fractions using the existing matte separation process, and the iron-free copper sulfide (Cu_2S) will be oxygen flash smelted to semi-blister copper. In this way the weak gas streams from the roasters, reverberatory furnaces, and copper converters will be totally eliminated, and the volume of gases from the nickel converters will be halved. All the sulfur dioxide in the high-strength (80% SO_2) off-gas streams from the flash furnaces will be fixed as sulfuric acid or liquid sulfur dioxide. The oxygen flash smelting process is very energy efficient, and energy consumption in the smelter will be halved.

Since the entire nickel-copper separation will in future be carried out in the matte separation plant, Inco's milling operations will be simplified. Operations will be consolidated in the Clarabelle mill, and the Copper Cliff and Froid-Stobie mills will be closed. The function of the modernized Clarabelle mill will be to reject pyrrhotite and produce a bulk nickel-copper concentrate. A large new semiautogenous grinding mill and new flotation cells, more than ten times larger than the existing cells, will be installed. These changes are projected to increase the rejection of sulfur from the ore as pyrrhotite to tailings to 67% [61].

In the smelter, two large new flash smelting furnaces, each capable of treating 1800 t/d of bulk concentrate, and a smaller flash furnace capable of treating 725 t/d of Cu_2S concentrate, will be constructed. A new oxygen plant will produce 450 t/d to supplement the 1300 t/d currently available.

A new sulfuric acid plant with a design rate of 2300 t/d will handle the off-gas from both large flash furnaces. Off-gas from the copper flash furnace will form the feed to the existing liquid sulfur dioxide plant. Installation of the new acid plant will permit the closing of the roaster operation and acid plant at the iron ore recovery plant.

The first large flash furnace together with the new oxygen plant and acid plant are scheduled for completion in 1992, while the second large flash furnace will be operating by the end of 1993.

12.4.4 Treatment of Converter Matte

Nickel-copper converter matte is essentially a melt of nickel, copper, and sulfur with small amounts of cobalt, iron, and oxygen, and traces of the noble metals and various undesirable impurities, including selenium, tellurium, and entrained slag. In the South African platinum industry, where nickel copper mattes containing over 1000 g/t platinum group metals are common, the noble metal content of the matte far exceeds the base metal content in value. The platinum group metal contents of

the Sudbury mattes, although much lower than in the South African mattes, are still of major economic significance.

Further processing of nickel copper converter mattes is carried out to separate and recover nickel, copper, cobalt, and the noble metals. Mattes may be treated by hydrometallurgy (the Sherritt, Outokumpu, and Falconbridge leach processes), by electrometallurgy if they are low in copper (Inco's direct electrorefining of matte anodes), or by pyrometallurgy (Inco's slow-cooling matte separation process).

12.4.4.1 INCO Matte Separation Process

The controlled slow-cooling matte separation process [1] was developed by Inco in the 1940s to replace the obsolete Orford Process which depended on the different solubilities of copper and nickel sulfides in molten sodium sulfide. Other operations which had used the Orford Process, Rustenburg Platinum in the Republic of South Africa and the major Soviet nickel producers, have subsequently adopted the slow-cooling technique.

This process is based on the fact that when molten nickel-copper mattes freeze slowly, the constituents segregate into grains that are separate and distinct chemical phases. The major phases are Cu_2S and Ni_3S_2 , but if the matte contains less sulfur than is required to form these compounds, the excess nickel forms a magnetic alloy phase with copper, which also preferentially collects the noble metals. The slow-cooled matte can then be comminuted and separated into nickel sulfide, copper sulfide, and nickel-copper alloy fractions by normal mineral beneficiation techniques. The nickel-copper alloy, which is separated magnetically, contains virtually all

the platinum group metal and gold values and a substantially increased grade compared to the converter matte.

In the Inco matte separation plant at Copper Cliff (Figure 12.6) [34] molten sulfur-deficient converter matte (50% Ni, 26% Cu, 0.5% Fe, 22% S) is poured into molds at 1000 °C and cooled slowly over a period of four days to about 200 °C. The solid matte is crushed and ground and is then separated into its components by magnetic separation and flotation. The copper sulfide concentrate (73% Cu, 5% Ni), which also contains most of the silver, selenium, and tellurium, is converted to blister copper in Inco's copper smelting circuit. The silver, selenium, and tellurium are recovered from the copper refinery anode slimes. The magnetic nickel copper alloy (65% Ni, 20% Cu) forms the major feedstock to Inco's Copper Cliff nickel refinery, where the nickel is refined by the pressure carbonyl process to high-grade nickel powder and pellets, and copper and the precious metals are recovered from the refining residue. The nickel sulfide concentrate (70% Ni, 0.6% Cu), which is essentially depleted in precious metals, forms the feed to the fluidized-bed roasting plant.

The three large sulfide nickel operations in the former Soviet Union at Pechenga, Monchegorsk, and Norilsk, all use similar slow-cooling matte separation processes, producing separate nickel and copper sulfide concentrates. Rustenburg Platinum in the Republic of South Africa uses the slow-cooling technique to separate a magnetic nickel-copper alloy with a high noble-metal content for processing to recover and refine the platinum group metals, but does not separate the nickel and copper sulfides. The bulk nickel-copper concentrate is treated by pressure hydrometallurgy to separate the nickel and copper.

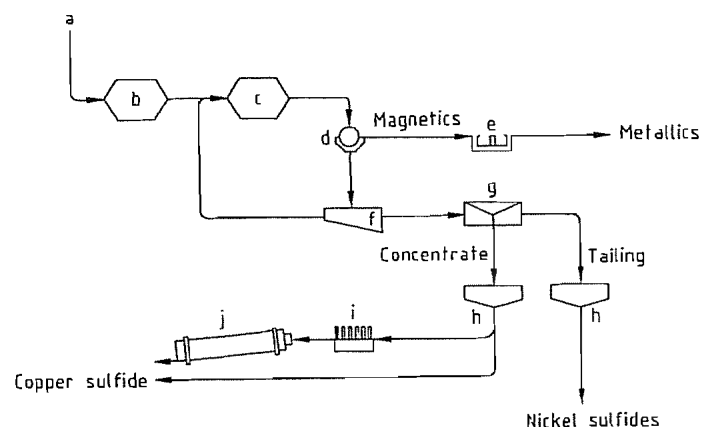


Figure 12.6: Flow sheet of the Inco matte separation process: a) Converter matte from Copper Cliff smelter; b) Rod mill; c) Ball mill; d) Magnetic separator; e) Centrifuge; f) Rake classifier; g) Flotation cell; h) Thickener; i) Disc filter; j) Dryer.

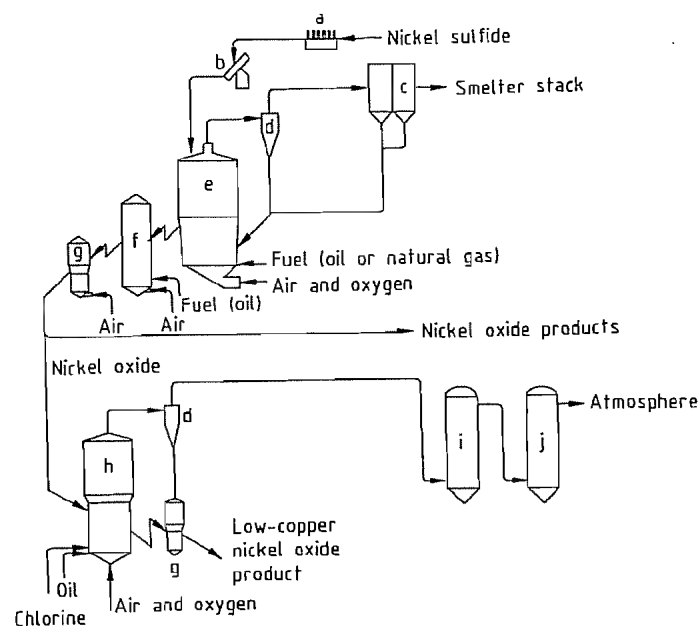


Figure 12.7: Flow sheet of the Inco nickel matte roasting process: a) Disc filter; b) Pelletizing disc; c) Electrostatic precipitator; d) Cyclone; e) Roaster; f) Reroaster; g) Cooler; h) Chlorination reactor; i) Splash tower; j) Packed tower.

12.4.4.2 Fluidized-Bed Roasting of Nickel Sulfide

Nickel sulfide concentrates are roasted in fluidized-bed roasters [62] to produce nickel oxide at Inco's matte treatment plant in Copper Cliff and at the major nickel operations in

the former Soviet Union. The dead roasting of finely ground nickel sulfide concentrates in a fluidized-bed roaster presents difficulties because nickel sulfide softens and becomes sticky at about 650 °C, while sulfur removal must be carried out at a temperature above 1100 °C, at which the sulfide is molten, to

achieve the required degree of sulfur elimination at an economic rate. A further problem is the very fine nature of the concentrates. Typically 99% of the particles are less than 75 µm, with about 20% in the 10 µm range. It is therefore difficult to feed such fine material into a fluidized-bed roaster without either incurring excessive dust carryover from the bed, or causing the bed to fuse with consequent loss of fluidization.

In Inco's practice (Figure 12.7) [34] the concentrate is pelletized in order to provide enough mass to carry the sulfide particles down through the rising gas stream into the bed. Agglomeration is carried out by adding recovered roaster dust (about 10% of the total) to the nickel sulfide concentrate slurry received from the matte flotation circuit. The green nickel sulfide pellets are charged into four fluidized-bed roasters which operate under optimum conditions at a superficial gas velocity of about 2 m/s with a bed expansion of about 150%. The average retention time of a particle in the bed is ca. 8 h. Roasting under these conditions is autogenous at 1100 °C, but the roaster air is enriched with oxygen to increase the elimination of sulfur and increase the concentrate throughput rate. A coarse granular nickel oxide (NiO) containing ca. 0.2% S is drawn off from the bed overflow. A single roaster can treat ca. 350 t/d of nickel concentrate.

The roaster calcine is either cooled in a fluidized cooler with water sprays from 1100 °C to 90 °C and shipped to one of Inco's nickel refineries (Copper Cliff or Port Colborne, Ontario; or Clydach, Wales), or is further desulfurized in a second fluidized-bed roaster. In this second roasting step the sulfur content is reduced to levels as low as 0.005%. This material is either marketed directly as 'Sinter 75' (75% Ni, 0.7% Cu, and 0.006% S), which is used in alloy steel making, or is treated by chlorination and reduction to lower its copper content. The removal of copper and other impurities is carried out by the injection of chlorine gas into a fluidized-bed reactor at 1200 °C, at a chlorine addition rate of about 3% of the reactor feed. The bed is heated by

light fuel oil and oxygen-enriched air. The reactor product typically contains 0.3% Cu and less than 0.01% S. It was formerly treated with a gas containing 75% hydrogen at 510 °C in another fluidized-bed reactor to yield Incomet, a metallic nickel product, which, however, is no longer made.

12.5 Hydrometallurgy of Nickel Concentrates and Mattes

Several hydrometallurgical processes [63] are in commercial operation for the treatment of nickel copper mattes to produce separate nickel and copper products. In addition, the hydrometallurgical process developed by Sherritt Gordon in the early 1950s for the direct treatment of nickel sulfide concentrates, as an alternative to smelting, is still commercially viable and competitive, despite very significant improvements in the economics and energy efficiency of nickel smelting technology [64].

In a typical hydrometallurgical process, the concentrate or matte is first leached in a sulfate or chloride solution to dissolve nickel, cobalt, and some of the copper, while the sulfide is oxidized to insoluble elemental sulfur or soluble sulfate. Frequently, leaching is carried out in a two-stage countercurrent system so that the matte can be used to partially purify the solution, for example, by precipitating copper by cementation. In this way a nickel copper matte can be treated in a two-stage leach process to produce a copper-free nickel sulfate or nickel chloride solution, and a leach residue enriched in copper. The copper-rich residue is treated by pressure leaching, or by roasting and leaching, to solubilize the copper as copper sulfate so that it can be recovered from solution electrolytically as cathode copper. Nickel is recovered from the purified nickel sulfate or chloride solution either electrolytically as a pure nickel cathode or by chemical reduction with hydrogen to give pure nickel powder.

Table 12.9: Hydrometallurgical nickel refineries [63].

Company/operation	Capacity, t/a Ni	Feed composition, %				
		Ni	Cu	Co	Fe	S
Falconbridge, Norway	54 000	35–40	30–35	1.0	2.5	22–24
Inco, Thompson	46 000	73	3	0.8	0.6	20
Western Mining	33 000	44–72	3–5	0.8	1–25	20–23
Sherritt Gordon	24 000	15–70	1–5	0.5	2–30	18–30
Sumitomo, Niihama	22 000	72	5	0.7	0.5	21
Rustenberg Refiners	20 000	47	27	0.5	3.0	21
Outokumpu, Harjavalta	17 000	55–65	25–35	0.6	0.2	6
SLN, Le Havre	16 000	75		1.5	2.5	20
Jianchuan, China	15 000	68	7	1.0	2.0	21
Bindura, Zimbabwe	14 400	66	25	0.6	0.2	6
Empress, Zimbabwe	5 000	40	52	0.2	0.2	6
Western Platinum	2 000	48	28	0.5	1.0	21

The range of compositions for mattes treated by hydrometallurgical processes is shown in Table 12.9 [63]. The nickel contents of the mattes treated hydrometallurgically are in the range 35–75%, while the copper content varies from 0 to 52%, and sulfur from 6 to 24%. Low-copper mattes (< 10% Cu) can be treated by ammoniacal pressure leaching, by ferric chloride leaching, or by direct electrorefining of the matte. High-copper mattes can be treated by high-pressure or atmospheric pressure sulfuric acid leaching or hydrochloric acid leaching.

The sulfur contents of the mattes are adjusted during the conversion process in the smelter to the optimal level for the subsequent leaching process. Sulfur levels are typically 20–23%, except when the matte is to be treated by the Outokumpu atmospheric pressure sulfuric acid leaching process, for which the sulfur content is reduced to about 6%.

12.5.1 Ammonia Pressure Leaching

The first successful commercialization of a hydrometallurgical process for the treatment of a nickel sulfide concentrate was realized by Sherritt Gordon Mines at Fort Saskatchewan, Alberta, Canada in 1954. This process was developed specifically to treat a pentlandite concentrate from Sherritt's Lynn Lake mine in northern Manitoba by ammonia pressure leaching [1, 65]. The original plant was de-

signed to produce 8000 t/a of nickel powder and briquettes by the chemical reduction of nickel in ammoniacal solution with hydrogen at high pressure. The same plant, with only minor process and equipment modifications, can now refine 24 000 t/a of nickel from a wide range of feed materials, including pentlandite concentrates, low-copper nickel mattes, and nickel sulfates and carbonates. The ammonia pressure leach process is also operated by Western Mining at Kwinana, Western Australia. Originally, this refinery processed nickel sulfide concentrates, but now treats a blend of converter and flash furnace nickel mattes to produce powder and briquettes at a rate of 33 000 t/a Ni. A block flow diagram of the ammonia pressure leach process as operated by Sherritt Gordon is shown in Figure 12.8.

The finely ground nickel sulfide concentrates and mattes are leached in ammoniacal ammonium sulfate solution at 80–95 °C under 850 kPa air pressure in a two-stage counter-current process in eight four-compartment horizontal autoclaves (Figure 12.9). Nickel, cobalt, and copper are dissolved as soluble ammonia complexes, while sulfide is oxidized to form a series of soluble thio salts. Reactive iron is oxidized and reports to the leach residue as a hydrated oxide together with pyrite which does not react in the leach:

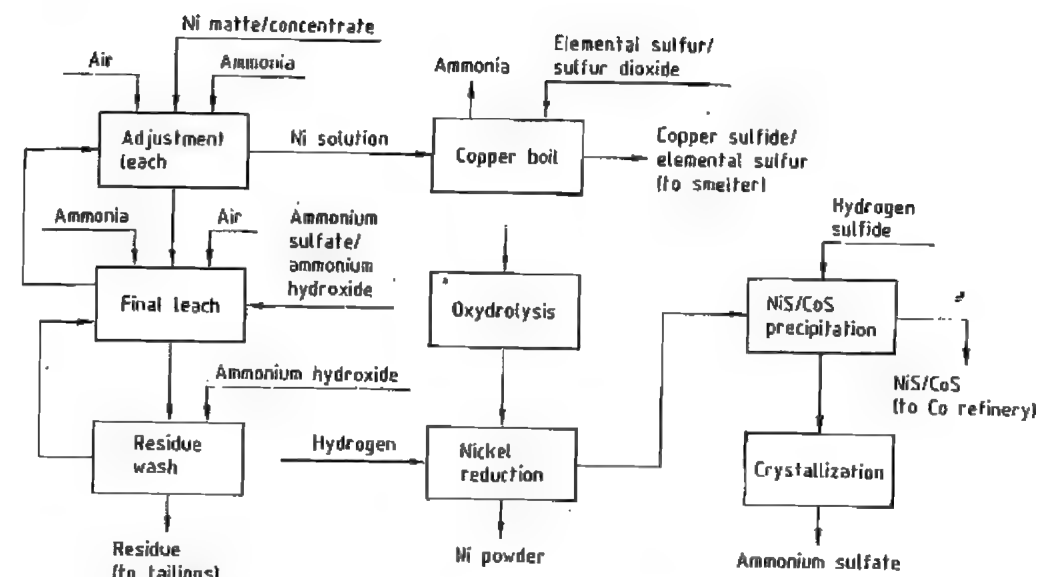
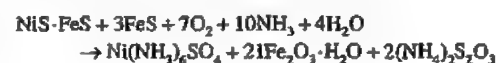


Figure 12.8: Flow sheet of the Sherritt ammonia pressure leach process.

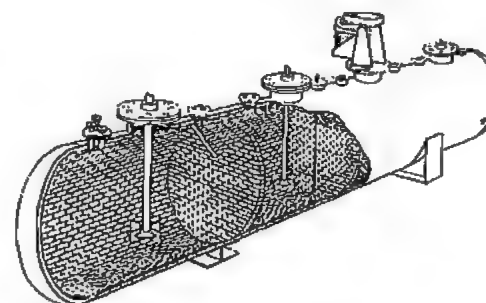
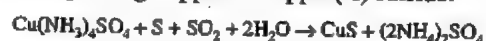


Figure 12.9: Cutaway view of a horizontal leaching autoclave.

The leach solution typically contains 50–60 g/L Ni, 1–2 g/L Co, 5–10 g/L Cu, 130 g/L NH_3 and varying amounts of thio salts, including thiosulfate and thionates, as well as ammonium sulfamate ($\text{H}_2\text{NSO}_3\text{NH}_4$), which is formed by the reaction of thionate with oxygen and ammonia.

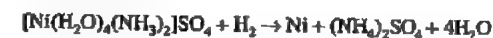
The leach solution is boiled to distil off the free ammonia, and elemental sulfur and sulfur dioxide are added to augment the thio salts in precipitating copper as copper(II) sulfide:



The copper sulfide is sold to a copper smelter. The ammonia to nickel molar ratio is

adjusted to 2:1 and the copper free ammoniacal nickel sulfate solution is oxidized at 235 °C under 4 MPa air pressure to convert the sulfur compounds to sulfate and to hydrolyze the sulfamate ion to sulfate. If these sulfur compounds were not fully converted to sulfate, the nickel powder product would contain unacceptably high levels of sulfur.

In the final step of the process, nickel is precipitated from solution as a metal powder by reduction with hydrogen under 3.6 MPa pressure at 200 °C in a four-agitator horizontal autoclave:

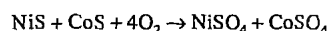


Details of the reduction technique are given in Section 12.6.4. The nickel powder is either compacted into briquettes for use in stainless steel production or is rolled into nickel strip for coinage production.

Under the specified process conditions cobalt is not precipitated during nickel reduction and the reduction end solution contains 1–2 g/L each of nickel and cobalt as well as about 400 g/L ammonium sulfate. This solution is treated with hydrogen sulfide to precipitate the nickel and cobalt as a mixed metal sulfide intermediate product, leaving a pure ammo-

mium sulfate solution which is evaporated to crystallize ammonium sulfate for sale as a fertilizer.

The mixed metal sulfides produced in both the Sherritt and the Western Mining nickel refineries are processed in Sherritt's cobalt refinery in Canada [65]. The sulfides are pressure leached in sulfuric acid under 1.15 MPa air pressure at 150 °C in a lead- and brick-lined, six-compartment horizontal autoclave to form a solution of nickel and cobalt sulfates:



Iron is removed from solution in a second autoclave by adjusting the pH to 2.5 with aqueous ammonia solution. At this stage the solution typically contains 40 g/L Ni, 30 g/L Co, and less than 10 mg/L Cu and Fe. The solution is then treated with aqueous ammonia solution under air pressure to oxidize the cobalt(II) ion to the cobalt(III) state which is stable as the soluble cobalt(III) pentammine complex ion $[\text{Co}(\text{NH}_3)_5 \cdot \text{H}_2\text{O}]^{3+}$. Nickel is removed in a two-stage process by adding sulfuric acid to selectively precipitate nickel(II) ammonium sulfate, which is recycled to the nickel refinery. The cobalt/nickel ratio in the purified solution is typically 3000:1.

The cobalt(III) ion is reduced to cobalt(II) by treating the purified solution with cobalt powder and sulfuric acid. Cobalt powder is precipitated from solution by reduction with hydrogen at 180 °C and 4.3 MPa.

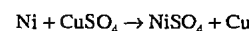
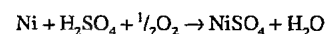
The pentammine cobalt refining process has also been operated by Outokumpu at Kokkola in Finland since 1968.

12.5.2 Atmospheric Acid Leaching

The atmospheric acid leach process for the treatment of high-copper, low-sulfur nickel matte was developed by Outokumpu [1] in 1960 to process material from its nickel mine in Finland, and was later adopted by the Bindura and Empress nickel refineries in Zimbabwe [66]. In this process the leaching operations are carried out in trains of air-agi-

tated pachuca tanks, in contrast to the mechanically-agitated horizontal autoclaves used in the pressure leaching process.

The Outokumpu process is outlined in Figure 12.10. Granulated matte, typically analyzing 55–65% Ni, 25–35% Cu, 0.6% Co, 0.2% Fe, and 6% S, is ground to 90% less than 54 µm and leached at 80 °C in acidic sulfate solution in a three-stage countercurrent leach circuit. Nickel, which is largely present in the low-sulfur matte as metallic nickel, dissolves in the first stage leach by reaction with sulfuric acid and with soluble copper, which is cemented from solution as copper metal. Copper sulfide in the matte does not react:



Most of the remaining nickel and some of the copper is leached in the second and third leach stages, which operate under increasingly oxidizing and acidic conditions. The solution from the first leach stage is a copper-free nickel sulfate solution, while the residue from the third stage is enriched in copper relative to nickel. Metal extractions in the atmospheric leach are typically about 90% Ni and 50% Cu.

The atmospheric leach residue, which contains about 15% Ni, 50% Cu, and 20% S, was originally recycled to the Outokumpu nickel smelter to recover the metal values. This residue is now treated in a fourth stage, a pressure leach under mildly oxidizing conditions at 160 °C, in which the nickel is extracted selectively, leaving a low-nickel, high-copper sulfide residue that can be treated directly in the copper smelter [67].

The Bindura and Empress refineries do not have a pressure leaching step and operate in the original Outokumpu mode, with copper recovery by electrowinning from the second-stage leach liquor, and recycle of the leach residue to a nickel smelter. At the Empress refinery, good quality copper cathode is produced, despite an unfavorable copper to nickel ratio in the solution, by using air-sparged cells at relatively low current density [66].

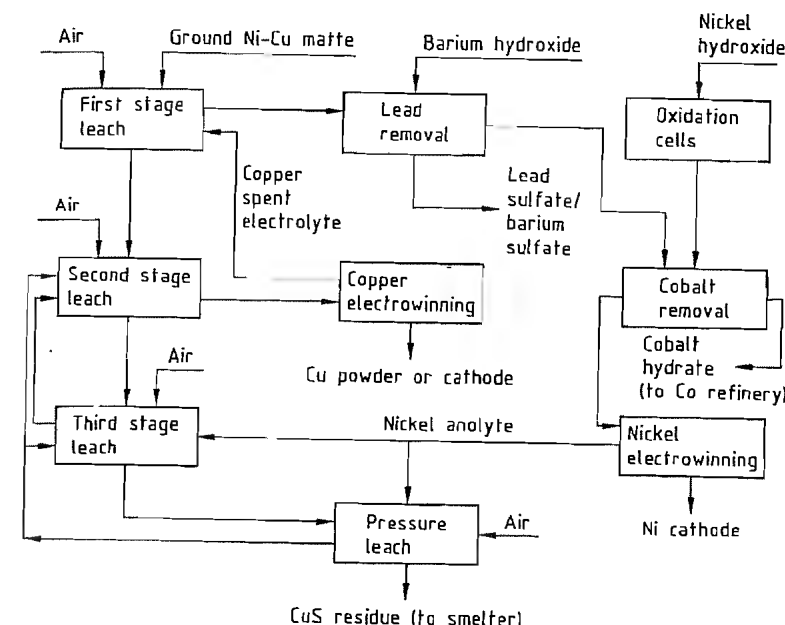
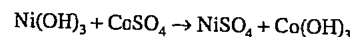


Figure 12.10: Flow sheet of the Outokumpu atmospheric acid leach process.

The first stage atmospheric leach step is primarily a solution purification step designed to produce a copper-free nickel sulfate solution. Air addition rates are reduced in the later pachuca leach tanks in the first stage to avoid redissolution of copper, and the pH is allowed to rise to 6.0 to ensure precipitation of iron by hydrolysis. Lead is precipitated by adding barium hydroxide or carbonate to the solution, either in the first stage leach or in a separate process step, to precipitate lead sulfate, which coprecipitates with barium sulfate. Cobalt is separated from the nickel sulfate solution in a later step, in which a slurry of nickel(III) hydroxide is added to precipitate cobalt as cobalt(III) hydroxide:



The nickel(III) hydroxide is produced by electrolytic oxidation of nickel(II) hydroxide, formed by neutralizing purified nickel sulfate solution with sodium hydroxide. The cobalt(III) hydroxide precipitate is refined to cobalt metal and cobalt salts by the pentammine process at Outokumpu's cobalt refinery at Kokkola, Finland.

Nickel is recovered from the purified nickel sulfate solution, which contains about 75 g/L Ni, as a high-grade cathode by direct electrowinning (see Section 12.6.2). Anolyte solution containing about 50 g/L Ni and 50 g/L H_2SO_4 , is recycled for use as a leachant in the leaching circuits.

12.5.3 Acid Pressure Leaching

The acid pressure leaching process for the treatment of high-copper nickel mattes was developed by Sherritt Gordon during the 1960s and is currently operated by all four platinum producers in the Republic of South Africa: Rustenburg Refiners, Impala Platinum, Western Platinum, and Barplats [68, 69]. A similar process was also operated by the Amax nickel refinery in Louisiana, United States, from 1974 to 1986 [70, 71].

Acid pressure leaching is normally carried out in brick- and lead-lined horizontal multi-compartment autoclaves at 135–160 °C and oxygen partial pressures of 140–350 kPa. The major advantage of this process for the platinum producers is that very high extractions of

nickel, copper, and sulfur can be achieved. Typically, the metal and sulfur extractions are greater than 99.9%, so that the leach residue is a high-grade platinum group metal concentrate that is virtually free from nickel, copper, and sulfur and can be treated directly in a platinum refinery. An upgrading factor for the platinum group metals of over 100 from the matte to the leach residue is readily attainable [69].

The process flow sheet differs significantly for the various operations. Rustenburg and Impala use two countercurrent stages of continuous pressure leaching at 135–150 °C, while the smaller Western Platinum and Barplats refineries operate an atmospheric leach at 85 °C followed by a single-stage continuous pressure leach at 160 °C. The nickel products also differ widely. Rustenburg Refiners recover nickel as a high-purity cathode by direct electrowinning, whereas Impala produces nickel powder and briquettes by hydrogen reduction, and Western Platinum and Barplats produce crystalline nickel sulfate, which is processed to metal or plating salts elsewhere.

The Impala Platinum flow sheet [72] is outlined in Figure 12.11. The nickel copper matte

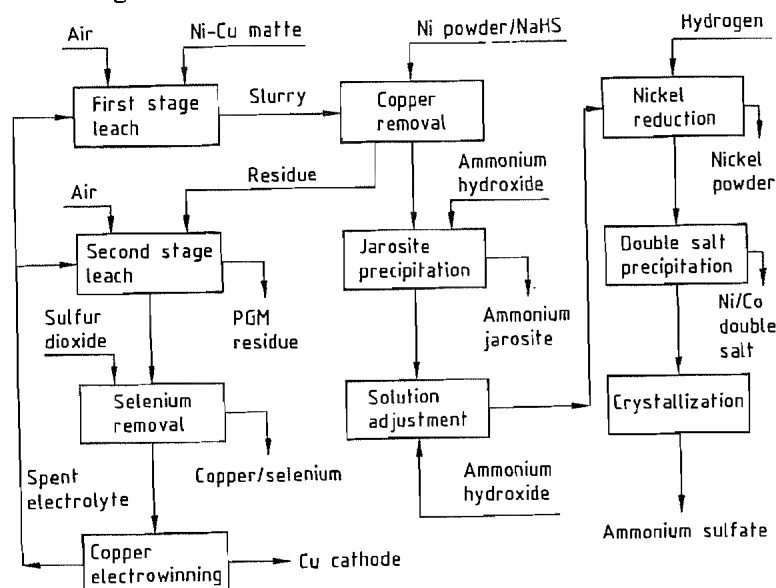
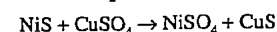
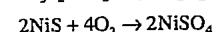
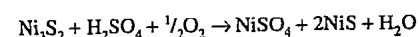
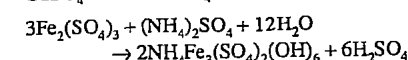
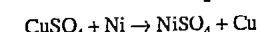


Figure 12.11: Flow sheet of Impala Platinum acid pressure leach process.

is leached in two stages at 135 °C under 1 MPa air pressure in spent copper electrolyte solution.



Solution from the first stage leach, which contains a high concentration of nickel (typically 100 g/L Ni) and low levels of copper and iron, is contacted with nickel powder and sodium hydrosulfide to precipitate copper, and iron is then removed as an ammonium jarosite precipitate using a horizontal multicompartiment autoclave operating at 150 °C:



The jarosite precipitation step also effectively removes lead and arsenic from the nickel sulfate solution. The purified nickel sulfate solution is adjusted with aqueous ammonia solution to form the nickel(II) diamine complex ion, and nickel is recovered as a powder by reduction with hydrogen under pressure:

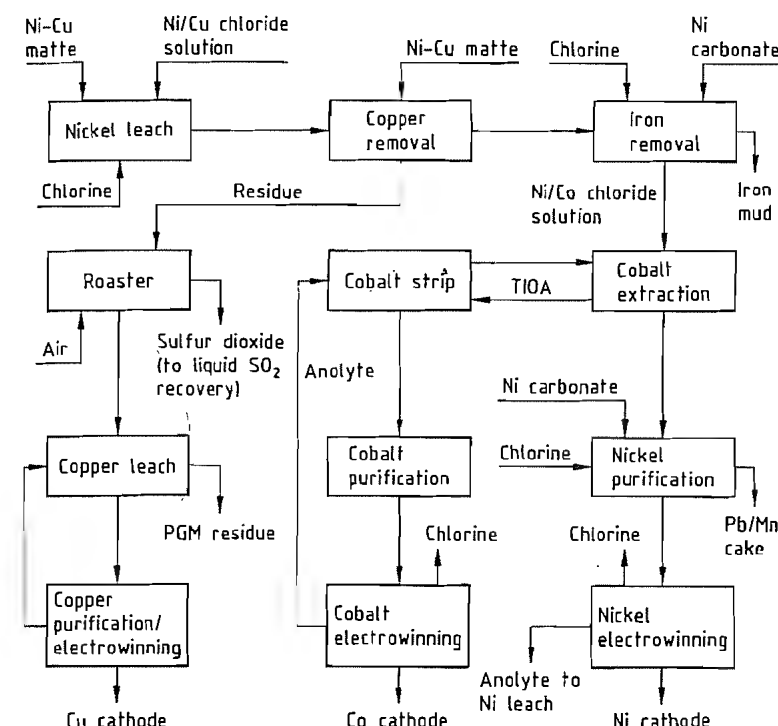
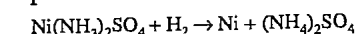
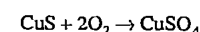
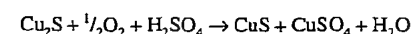
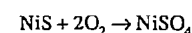


Figure 12.12: Flow sheet of the Falconbridge refinery process.

Cobalt and residual nickel are recovered from the reduction end solution as the nickel sulfate cobalt sulfate ammonium sulfate double salts, which are refined to produce cobalt metal powder by the Sherritt pentammine process and hydrogen reduction. The residue from the first stage leach is leached under more oxidizing and more acidic conditions in copper spent electrolyte in the second-stage pressure leach, which completes the extraction of nickel and copper sulfides:



The solution from the second-stage pressure leach, which contains both nickel and copper sulfate with traces of iron and selenium, is treated with sulfur dioxide to precipitate selenium as copper(I) selenide, and copper is recovered as cathode by electrowinning. The spent electrolyte, which contains

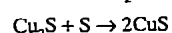
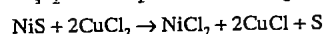
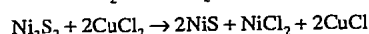
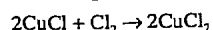
high levels of nickel as well as 20 g/L Cu and 50–70 g/L H_2SO_4 , is recycled to the pressure leach circuits. The second-stage leach residue contains the platinum group metals, with only minor levels of nickel, copper, and sulfur.

12.5.4 Chloride Leach Processes

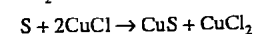
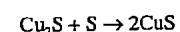
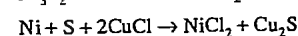
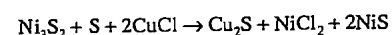
Nickel matte refining processes based on leaching in chloride solution in the presence of chlorine gas have been developed and successfully commercialized by Falconbridge at Kristiansand in Norway [73] and by Société Le Nickel (SLN) at Le Havre-Sandouville in France [74]. Leaching of the matte is carried out at atmospheric pressure at the boiling point of the leach solution (ca. 110 °C). Chlorine, which is recovered from the electrolysis cells, is sparged directly into the leach tanks. In the SLN process the leachant is the iron(III) chloride solution recovered from an iron removal step, whereas in the Falconbridge process the leachant is a solution of copper and

nickel chlorides recycled from the copper residue treatment circuit. The flow sheet of the Falconbridge process is shown in Figure 12.12.

Granulated nickel copper mattes from the Falconbridge smelter in Ontario, Canada and from BCL in Botswana, with an average composition of 40–45% Ni, 25–30% Cu, 20–22% S, 2–3% Fe, and 1–1.5% CO, are ground in a ball mill [73]. The ground matte is leached with chlorine in a nickel copper chloride solution in a train of agitated tanks. The leaching conditions are controlled by means of redox potential measurements to ensure selective leaching of nickel:



Essentially all the copper and sulfur present in the matte remain in the leach residue as CuS. The leach residue still contains about 8% Ni as unreacted NiS, and the leach solution still contains high concentrations of copper. The leach slurry is therefore heated to 140–145 °C in two vertical autoclaves, connected in series, to promote the precipitation of copper and the dissolution of nickel by a series of metathesis reactions:



The discharge from the autoclaves, which still contains about 7 g/L Cu in solution, is treated with fresh matte to reduce the copper concentration to less than 0.5 g/L. Overall nickel extraction is about 90%, and the final residue contains 6–8% Ni.

Iron, which is largely dissolved in the chlorine leach, is precipitated by oxidation with chlorine and hydrolysis with nickel carbonate. Cobalt is extracted from the nickel chloride solution by solvent extraction with triisooctylamine (TIOA) and, after purification of the strip solution, is recovered as high-purity cathode by electrowinning. The nickel

chloride raffinate is diluted and purified further by treatment with chlorine and nickel carbonate to remove the remaining traces of cobalt, iron, copper, arsenic, lead, and manganese. High-purity nickel is recovered by direct electrowinning as cathode, and as crowns by direct plating onto a suitably masked blank.

Copper is extracted from the chlorine leach residue by roasting it in a fluidized-bed roaster to convert the copper sulfide and elemental sulfur to copper oxide and sulfur dioxide, which is converted to sulfuric acid, and leaching the calcine in sulfuric acid to selectively leach the copper. The copper is recovered from the sulfate solution by conventional electrowinning.

The calcine leach residue, which contains 50% Ni and 18% Cu as well as the platinum group metals (PGM), undergoes further chloride leaching to recover the nickel and copper in solution for recycling to the leach circuit, leaving the platinum group metals in an upgraded concentrate. Typical process stream compositions for the Falconbridge operation are shown in Table 12.10.

Table 12.10: Process data for the Falconbridge chlorine leach process [73].

Stream	Ni	Co	Cu	Fe	S	Cl
Matte, %	45	1	28	2	22	
Feed solution, g/L	60		25	1		90
Sulfide leach residue, %	7	0.5	56	2	33	0.3
Pregnant solution, g/L	230	5	0.5	6		270
Ni electrolyte, g/L	60					60
Roaster calcine	9	0.5	63	2	0.5	
Cu electrolyte, g/L	60	6	60	2.5		
PGM concentrate, %	20	1	25	5	15	5

In the SLN process, in which the feed matte produced from laterite ore in New Caledonia contains virtually no copper, the pregnant leach liquor contains 200 g/L Ni with 5 g/L Co and 10 g/L Fe. Iron is removed as ferric chloride by solvent extraction with tributyl phosphate (TBP). Part of the ferric chloride strip solution is recycled to the chlorine leach, while the balance is concentrated and sold. Cobalt chloride is extracted with TIOA and sold as solution for cobalt recovery elsewhere.

Nickel is recovered from the purified solution as high-purity cathode by electrowinning [74].

12.5.5 Treatment of Nickeliferous Pyrrhotite [1]

Large tonnages of pyrrhotite concentrates containing up to 1% Ni are currently rejected in the milling and concentrating operations of the major Canadian nickel producers as a means of reducing the iron and sulfur inputs to their smelters, and hence reducing sulfur dioxide emissions. These pyrrhotite concentrates represent a major potential source of nickel and several attempts have been made to develop economically viable processes to exploit them. The primary requirement for a pyrrhotite treatment process is that it should produce an iron ore suitable for use in the steel industry and yield a good recovery of nickel. Such processes are typically based on roasting to eliminate all or part of the sulfur and hydrometallurgical treatment of the calcine to recover the nickel.

In 1956 Inco commissioned a plant at Copper Cliff, Ontario, to treat 1.2×10^6 t/a of pyrrhotite concentrate analyzing 0.9% Ni, 58% Fe, and 35% S. The iron sulfide concentrate was first oxidized to a low-sulfur calcine in fluidized-bed roasters, producing an off-gas containing sulfur dioxide from which sulfuric acid was produced. The calcine was then passed through a reducing kiln to reduce the nickel, cobalt, and copper oxides selectively to metallic form, so that they could be dissolved selectively in ammoniacal ammonium carbonate solution. The solution was purified to remove copper as the sulfide and nickel was precipitated as a basic nickel carbonate. The basic carbonate was calcined to a marketable oxide product containing 77% Ni. The leached iron oxide residue was pelletized and indurated for market. This plant operated until the early 1980s, when marginal economics and increasing constraints on sulfur emissions resulted in its closure.

From 1960 until the early 1970s, Falconbridge operated a process in which pyrrhotite concentrate, analyzing 1.1% Ni, 57% Fe, and

360% S, was sulfation roasted at 680 °C to convert the nickel, copper, and cobalt to their water-soluble sulfates. The calcine was then water-leached to extract the metals, and nickel, cobalt, and copper were precipitated from solution by cementation on iron turnings for recycling to the smelter. The iron oxide product analyzed 66% Fe, 0.13% Ni, and 0.5% S.

12.6 Refining [1, 63]

Nickel differs from copper in that it is largely used as an alloying element in stainless steel and alloy steel production. Thus, whereas most copper is used in electrical and thermal energy applications, which require a highly refined metal, a high-purity metal is not required for many of nickel's most important markets. Nickel products such as nickel oxide, metalized nickel oxide, and ferronickel, which are designated Class II products, are produced directly by smelting and roasting and are sufficiently pure, without refining, for many nickel applications such as stainless steel production. These Class II products may contain significant levels of cobalt and copper and a range of trace impurities.

In other applications, high-purity nickel is essential and Class I nickel products, which include electrolytic cathode, carbonyl powder, and hydrogen-reduced powder, are made by a variety of refining processes. In general nickel is refined to decrease to an acceptable level only those impurities which would have an adverse effect on subsequent processing or on the properties of the refined metal product. These elements include antimony, arsenic, bismuth, cobalt, copper, iron, lead, phosphorus, sulfur, tin, and zinc. Cobalt, which resembles nickel closely in physical and chemical properties, is difficult to remove completely and since it is not often a serious contaminant in most applications for nickel, many Class I products contain quite high levels of cobalt.

The object of the refining process is not only to remove the impurities from the nickel, but also to recover those that have an economic value. Obvious examples are the pre-

cious and platinum group metals (Pt, Pd, Os, Rh, Ir, and Ru), cobalt, and copper; sulfur, selenium, and tellurium can sometimes also be recovered economically. Historically the first successful nickel refining operation was established by the Mond Nickel Company (later absorbed by Inco) at Clydach, Wales, in 1902, using the carbonyl refining process invented by LUDWIG MOND and CARL LANGE in 1889. This refinery is still in operation using a modern version of the carbonyl process. A large refinery that uses a high-pressure version of the carbonyl process was established by Inco at Copper Cliff, Ontario in 1972 [75].

The first electrolytic nickel refinery, treating nickel metal anodes, was built by Hybinette in Kristiansand, Norway, in 1910, and this plant was acquired by Falconbridge in 1928. The Kristiansand Refinery was modernized in the late 1970s by replacing the Hybinette process with the present chlorine leach process [73]. Inco established its first nickel refinery in Canada at Port Colborne, Ontario, in 1926, using a version of the Hybinette refining process. This refinery operated until 1984. In 1989 the only electrolytic nickel in North America was produced by Inco's refinery at Thompson, Manitoba, which electrorefines matte anodes [76]. This process is also operated in Japan [77] and China. The electrorefining of nickel metal anodes, which is effectively obsolete in Western Europe and North America, is still practiced in the former Soviet Union [44].

Outokumpu, SLN, and Falconbridge in Europe and Bindura, Empress, and Rustenburg Refiners in Southern Africa all recover electrolytic nickel by direct electrowinning from purified solutions produced by the leaching of nickel or nickel copper mattes. Sherritt Gordon in Canada, Western Mining in Australia, and Impala Platinum in the Republic of South Africa recover refined nickel powder from purified ammoniacal solution by reduction with hydrogen.

12.6.1 Electrorefining

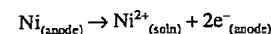
Nickel electrorefining [1] is carried out in a tank house containing a large number of electrolytic cells, each filled with a mixed nickel sulfate nickel chloride solution, and containing 30–40 anodes (slabs of metallic nickel or nickel matte), interspersed with cathodes that are thin sheets of pure nickel. The anodes and cathodes in each cell are connected electrically in parallel, and the cells are connected in series. When electrical current is passed through the cells the anodes dissolve, and pure nickel deposits on the cathodes. Cathodes and anodes are replaced periodically to maintain continuity of production.

Crude nickel anodes are made by reducing nickel oxide with coke at temperatures up to 1540 °C and casting the molten metal in molds. The pure nickel starting sheets are made in special electrolytic cells in which nickel is deposited onto permanent stainless steel or titanium cathode blanks, from which the thin sheet is stripped after 24 or 48 h of deposition. The sheets are fitted with suspension loops and placed in the production cells. The electrolytic cells are normally made of concrete and are lined with an acid-resistant membrane such as glass fiber reinforced plastic material.

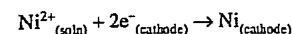
Nickel refining can be carried out with pure sulfate, mixed sulfate chloride, or pure chloride nickel electrolytes. In practice, the mixed sulfate chloride system is normally used for the electrorefining of either nickel metal or nickel matte. Sulfate and chloride electrolytes are used in the nickel electrowinning processes. The sulfate chloride electrolyte has two major advantages over the sulfate system, in having a higher conductivity which results in a lower cell voltage, and in permitting the use of chlorine for electrolyte purification.

12.6.1.1 Refining of Nickel Metal Anodes

In the refining of nickel metal anodes the principal reaction at the anode is the dissolution of nickel metal as nickel ions:



The principal cathodic reaction is the reduction of nickel ions from solution:



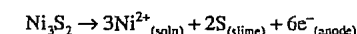
At the normal cell operating voltage (ca. 1.6 V for metal anodes) the principal impurities from the anode such as iron, cobalt, lead, arsenic, and copper go into solution with the nickel. Silver, gold, the platinum group metals, sulfur, selenium, and tellurium fall to the bottom of the cell as an insoluble slime. If the soluble impurities reach the cathode surface they will codeposit with the nickel. Consequently, to avoid contamination of the refined nickel cathodes, the impure anolyte solution is taken through a purification process. The purified solution is then returned to the cathode compartment of the cell, which is segregated from the anode by a porous diaphragm in the form of a bag or box enclosing the cathode. The purified solution is fed into the cathode compartment at a rate sufficient to maintain the rate of nickel deposition. The diaphragm cloth is tightly woven so that a hydrostatic head of solution builds up relative to the rest of the electrolyte. This hydrostatic head forces nickel-depleted electrolyte through the diaphragm, from the cathode compartment into the anolyte, at a rate sufficient to prevent the ingress of either anolyte itself, or impurity ions, by diffusion into the cathode compartment.

12.6.1.2 Refining of Nickel Matte Anodes

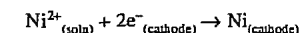
Nickel sulfide anodes can be electrorefined directly to pure nickel cathode without the intermediate process steps of roasting the sulfide to oxide and reducing the oxide to produce metallic nickel anodes. Nickel sulfide anodes can be cast directly from low-copper converter matte or from melted nickel sulfide concentrate produced by the matte separation process. Controlled cooling is necessary to produce anodes with the required mechanical properties. The anodes consist essentially of Ni_3S_2 and nickel alloy, but can contain up to

3 % copper as Cu_2S and other impurities such as iron, cobalt, lead, zinc, arsenic, selenium, and platinum group metals. Control of the sulfur content of the anodes is important because at sulfur contents of less than 15 %, the metallic nickel alloy phase dissolves preferentially, leaving nickel sulfide in the slime. At sulfur contents above 15 %, the matte anodes corrode uniformly to yield a slime containing elemental sulfur.

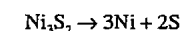
The principal anodic reactions are the oxidation of sulfide to elemental sulfur with simultaneous release of metal ions to the solution and of electrons to the anode:



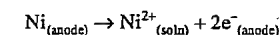
The cathodic reaction is the same as in the metal anode refining process:



The net cell reaction for the nickel sulfide phase is thus

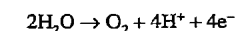


The metallic nickel phase dissolves electrolytically as in the refining of nickel metal anodes:



The actual cell voltage, including the potential drops across the contacts and through the electrolyte, is about 2.8 V for newly charged matte anodes. As the anodes corrode, the sludge, which consists mainly of elemental sulfur, forms a strongly adherent porous surface layer which causes an increase in volume and effectively doubles the bulk of the anode. As the sludge layer becomes thicker, the electrical resistance between the electrodes increases, and the cell voltage increases to about 4.0 V by the end of the anode cycle. The increase in cell resistance also results in increased heating of the electrolyte. The solution temperature rise in the cell increases from about 15 °C at the start of the anode cycle to about 25 °C at the end of the cycle.

The anode potential is sufficiently high that some water is decomposed:

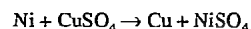


This unwanted reaction, together with the electrolytic dissolution of impurities from the anode, lowers the anode nickel dissolution efficiency so that nickel is removed from solution at the cathode faster than it dissolves at the anode. The imbalance is corrected during electrolyte purification by dissolving matte in the electrolyte to neutralize the free acid and replenish the nickel content.

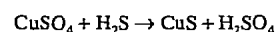
Operation of the nickel matte refining cell is similar to that of the metal anode cell except that the anodes are enclosed in bags to collect the voluminous sludge. The anode spacing in the matte refining cell is greater than in the metal refining cell, to allow for the increase in volume of the matte anode as it corrodes.

12.6.1.3 Solution Purification

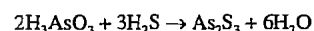
For the production of high-quality nickel cathode it is essential that the anolyte solution be purified before it is supplied to the cathode compartment. The purification methods used [1, 78] depend on the impurities present in the anode. Copper is often removed by cementation with activated metallic nickel powder, causing copper ions to precipitate as metallic copper while metallic nickel dissolves:



Alternatively copper may be precipitated as the sulfide with hydrogen sulfide:

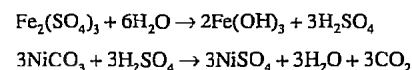


This procedure, which is used in the matte electrorefining process, also precipitates arsenic:



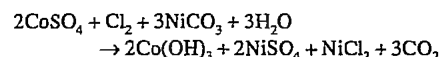
Careful control of the redox potential is necessary to ensure complete precipitation of copper and arsenic while minimizing the coprecipitation of nickel.

Iron is normally removed by treating the solution with chlorine and nickel carbonate to oxidize the iron to iron(III) and precipitate iron(III) hydroxide by hydrolysis:



Iron(III) hydroxide coprecipitates other impurities from the anolyte, particularly lead and arsenic. In the pure sulfate electrolyte systems, oxidation of iron is accomplished by using air instead of chlorine. Iron can be removed from pure chloride electrolytes by solvent extraction with tributyl phosphate.

Cobalt is precipitated as cobalt(III) hydroxide by treating the solution with chlorine or nickel(III) hydroxide to oxidize the cobalt(II) to cobalt(III). Nickel carbonate is added to control the pH.



Most of the cobalt precipitates at pH 4 at an oxidation potential of +1 V. Chlorine cannot be used in pure sulfate electrolyte, and in this system, nickel(III) hydroxide is normally used. Other oxidants which can be used to remove cobalt from the sulfate system include peroxide, persulfate, and ozone.

Cobalt is normally removed from pure chloride nickel electrolytes by solvent extraction with a tertiary amine such as triisooctylamine. Phosphine-based solvent extraction reagents such as di-(2-ethylhexyl) phosphoric acid (D2EHPA) are used to extract cobalt from nickel sulfate solutions.

In practice the purified solutions used in nickel electrorefining are not simple mixtures of nickel sulfate and nickel chloride. The electrolyte is a weakly acidic aqueous solution of nickel, sulfate, sodium, and chloride ions, and boric acid. The sodium and chloride ions carry about 30% of the current through the electrolyte. Most of the remaining current is carried by the slower moving divalent nickel and sulfate ions, since the concentration of hydrogen ions is negligible. The boric acid, which exists largely as undissociated molecules, acts as a buffer to maintain the pH of the solution below 6. The presence of boric acid thus prevents the precipitation of nickel(II) hydroxide at the surface of the cathode by the reaction between nickel ions and hydroxide produced in the minor cathodic reaction involving the electrolytic decomposition of water.

12.6.1.4 Electrorefining Operations

Although it is not currently operated in North America or Western Europe, the refining of metallic nickel anodes is still practiced in the former Soviet Union. The Severonikel complex at Monchegorsk in the Kola peninsula has the capacity to produce 142 000 t/a of electrolytic nickel [44]. The Monchegorsk smelter treats a blend of high-grade nickel copper ores, concentrates, mattes, and scrap from the nickel mining operations at Norilsk and Pechenga. Separate nickel and copper sulfide concentrates are produced by the slow-cooling matte separation process. The nickel sulfide is dead roasted at 1170 °C with oxygen-enriched air (25% O₂), and the oxide calcine is reduced with coke in a rotary kiln to form a metallized oxide, which is melted at 1550 °C in an electric arc furnace for anode casting. About 3% of the metallized oxide powder from the reduction kiln is retained for use in electrolyte purification. The anodes typically weigh 350 kg and analyze (%): 86–88 Ni, 2 Co, 4.5 Fe, 4 Cu, and 0.2 S.

The anodes are refined in an electrolyte containing 75–78 g/L Ni, 130–150 g/L SO₄²⁻, 14 g/L Cl, and 6 g/L H₃BO₃, at pH 2. Each electrolytic cell contains 43 anodes and 42 cathodes, and operates at a current density of 250 A/m². The cathodes are enclosed in a synthetic fiber bag supported on a polypropylene frame. Starting sheets are produced by plating nickel on to titanium blanks for 24 h. The sheets are stripped manually. The anode cycle is 30 d, while the cathode cycle is four or six days. Anode slimes are recovered by washing adhering material off the corroded anodes, and from the bottom of the electrolytic cells, at the end of each anode cycle, for subsequent processing to recover precious metal values.

Impure anolyte solution is treated to remove iron, copper, and cobalt, and to replenish the nickel content of the electrolyte, before the purified solution is returned to the cathode compartments. Iron is removed by controlled oxidation with chlorine and neutralization with nickel carbonate. Copper is precipitated

by cementation on nickel powder from the reduction kiln, and cobalt is precipitated by oxidation with chlorine and hydrolysis with nickel carbonate under highly oxidizing conditions. The nickel content of the solution is replenished by pressure leaching nickel sulfide concentrate (Ni₃S₂) in sulfuric acid solution under 1 MPa air pressure in vertical titanium autoclaves.

The electrorefining of nickel sulfide anodes is carried out by Inco at its Thompson operation in Canada, by Sumitomo Metal Mining Company at Niihama in Japan, and at Jianchuan in China.

The Thompson smelter [76] produces sulfide anodes by casting molten converter matte (73% Ni, 0.8% Co, 2.5–3.0% Cu, 0.5% Fe, and 20% S) directly into anodes weighing ca. 240 kg. The cast anodes are cooled slowly over about 36 h to improve their mechanical handling characteristics, but are nevertheless more brittle than metal anodes and require careful handling.

The sulfide anodes are electrolyzed in diaphragm cells in a sulfate chloride electrolyte. Nickel, cobalt, and copper dissolve from the anode, while sulfur, selenium, and the noble metals form an insoluble sludge or slime, from which they can be recovered. Nickel is plated on to pure nickel starting sheets, made by manually stripping 24-h deposits from stainless steel blanks. The anode cycle is 15 d and the cathode cycle is 10 d. Plating is carried out at a current density of 240 A/m². Details of the tankhouse operating parameters are as follows [76]:

Capacity	45 000 t/a Ni
Cells	608
Cell dimensions	1.6 m × 0.9 m × 5.8 m
Cell construction	fiber reinforced plastic lined precast concrete
Anode weight	238 kg
Anode dimensions	1.1 m × 0.7 m × 63 mm
Anode spacing	210 mm
Anodes/cell	27
Anode cycle	15 d
Cathode dimensions	1.0 m × 0.7 m × 13 mm
Cathode weight	88.5 kg
Cathodes/cell	26
Cathode cycle	10 d
Electrolyte flow	0.64 m ³ /h per cell
Electrolyte temperature	50 °C

Current density 240 A/m²
Cell voltage 3–6 V

The anolyte purification circuits at Thompson remove copper and arsenic by precipitation with hydrogen sulfide. The nickel content of the electrolyte is then replenished by reacting the solution with ground matte anode scrap under oxidizing conditions. For every 100 kg of nickel plated out in the tankhouse only 87 kg dissolves from the anode. This discrepancy is caused by the dissolution of 4 kg of copper, 1 kg of cobalt, 0.5 kg each of iron and arsenic, and by the formation of 0.2 kg of hydrogen ions. In the final stage of purification cobalt and iron are oxidized and hydrolyzed by the addition of chlorine and nickel carbonate. The cobalt(III) hydroxide precipitate is worked up for cobalt recovery. The purified electrolyte typically contains 75 g/L Ni, 120 g/L SO₄²⁻, 28 g/L Na, 50 g/L Cl⁻, and 8 g/L boric acid.

Until 1984, the principal products of the Thompson refinery were full nickel cathodes and cut shapes, made by shearing cathodes grown on nickel starting sheets. Now about 40% of the refinery's production is "S" and "R" Rounds for the plating industry, which are made by plating nickel directly on to stainless steel blanks, covered by a heat-set epoxy mask, with circular areas of steel exposed to plating. Metallurgical data for the Thompson refinery, including the cathode nickel analysis, are given in Table 12.11.

Table 12.11: Metallurgical data for the Inco Thompson refinery [76].

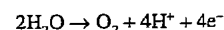
Element	Anode, %	Anolyte, g/L	Purified electrolyte, g/L	Electro-nickel, g/t
Ni	73		75	
Co	0.8	0.13	0.02	600
Cu	3.0	0.50	0.0007	25
As	0.2	0.03	0.0005	30
Fe	0.6	0.03		5
Pb	0.003			2
S	20			7

12.6.2 Electrowinning

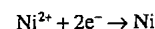
Electrowinning differs from electrorefining in that it is used to recover nickel from a leach liquor and can therefore be carried out with an

insoluble anode, since the only function of the anode is to transfer electrons from the electrolyte to the external circuit. The electrowinning of nickel is practiced commercially with both pure sulfate and pure chloride electrolytes. In the sulfate system the anodes are made of chemical lead or antimonial lead, which have a relatively long life in sulfate solution, although soluble in chloride solutions. In the highly corrosive chloride system, dimensionally stable anodes, made by coating a titanium substrate with a platinum group metal oxide, are used.

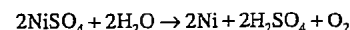
The principal anodic reaction in the sulfate system is the decomposition of water to produce gaseous oxygen:



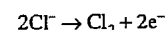
The main cathodic reaction, as in electrorefining, is the deposition of nickel ions to form nickel atoms on the cathode:



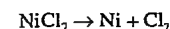
The overall cell reaction is:



The sulfuric acid generated at the anode is utilized by recirculating the anolyte to the leach circuits. In the chloride system the principal anodic reaction is the oxidation of chloride ion to chlorine gas:



The overall reaction is thus the decomposition of nickel(II) chloride to metallic nickel and chlorine gas:



The chlorine liberated at the anode is recycled for use in the leach circuits. In practice some decomposition of water also occurs to yield small quantities of hydrogen at the cathode and oxygen at the anode.

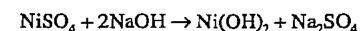
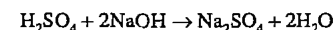
12.6.2.1 Electrowinning from Sulfate Electrolytes

In a sulfate electrowinning system the cathodes are suspended in bags, even though the nickel sulfate solution is purified before it enters the tankhouse. The cathode must still be

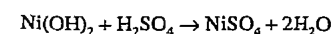
protected from the anolyte, which is strongly acidic due to anodic generation of hydrogen ions. A high concentration of hydrogen ions at the cathode would result in the formation of hydrogen gas which is formed in preference to nickel deposition, thus seriously reducing the current efficiency of the cell.

Details of the purification methods used to remove copper, iron, lead, and cobalt from nickel sulfate leach liquor prior to electrowinning are given in Section 12.5. Treatment of electrowinning anolyte or spent electrolyte varies depending on the type of leaching circuit used. In the Outokumpu atmospheric leach, in which very little sulfur is oxidized, almost all the anolyte can be recycled to the leaching circuits, where the acid is neutralized in leaching nickel from the matte, thus replenishing the nickel content of the solution. Only a small solution bleed is taken out of the circuit to control the concentration of sodium sulfate, which would otherwise build up to unacceptable levels.

In the Sherritt acid pressure leaching process, as practiced by Rustenburg Refiners, in which all the sulfur in the matte is oxidized to sulfate, a much larger bleed of solution is required to maintain a sulfur balance. Typically 25–35% of the anolyte stream must be removed from the circuit and treated to recover sodium sulfate. This bleed stream is reacted with sodium hydroxide or sodium carbonate to neutralize the acid and precipitate the remaining nickel as nickel(II) hydroxide or as basic nickel carbonate:



The nickel-free barren solution is evaporated to crystallize sodium sulfate. The precipitated nickel hydroxide or basic nickel carbonate is redissolved in a second portion of the anolyte stream to neutralize the acid content and replenish the nickel content:



This solution is recycled directly as feed solution to the electrowinning circuit. The balance of the anolyte is recycled for use in the

matte leach circuits, where the acid is neutralized and the nickel content replenished, and passes through the leach solution purification steps before returning to the tankhouse.

The Outokumpu nickel refinery at Harjavalta in Finland contains 126 electrowinning cells, each having 40 insoluble lead anodes and 39 cathodes [1, 48, 67]. The bagged cathodes are nickel starting sheets made by the deposition of nickel for 48 h onto a stainless steel mother blank. The deposits are stripped manually and automatically made up into starting sheets. The purified solution is fed to the cathode compartments at a rate sufficient to maintain a hydrostatic head of about 30 mm. The current density is 200 A/m², giving a cell voltage of about 3.6 V. The cathode cycle is seven days. The cells are hooded to collect and remove the oxygen and acid mist generated at the anode.

The feed solution at pH 3.2, containing 75 g/L Ni as well as sodium sulfate and boric acid, is heated to 60 °C and fed separately to each cathode compartment. The solution passes through the diaphragm cloth into the anolyte, which overflows from each end of the cell. The anolyte, which contains 50 g/L Ni and 40 g/L H₂SO₄, is recycled to the leaching circuits. The cathodes typically weigh ca. 75 kg and contain 99.95% Ni.

12.6.2.2 Electrowinning from Chloride Electrolytes

In the Falconbridge chloride electrowinning system [73], the dimensionally stable anodes are enclosed in a polyester diaphragm bag, to contain the chlorine gas generated in the anode reaction, and channel it to a vacuum hood fitted to the top of the anode. Ducts, connecting the top of the hood with a manifold that runs alongside the tank, allow the withdrawal of both chlorine and anolyte by suction. Purified solution is fed in at one end of the cell, and the solution level is held constant by maintaining a small overflow at the other end, while the greater portion of the electrolyte is withdrawn as anolyte with the chlorine gas.

The Falconbridge refinery at Kristiansand, Norway, which has a capacity of 54 000 t/a Ni, contains 326 electrolytic cells, of which 24 are devoted to starting sheet production. Each cell contains 46 anodes and 45 cathodes with an anode spacing of 145 mm. Typical operating parameters are as follows:

Inlet flow	4.0 m ³ /h per cell
Total current	24 000 A
Current density	220 A/m ²
Current efficiency	98–99%
Electrolyte temperature	60 °C
Catholyte Ni	60 g/L
Anolyte Ni	54 g/L

The refinery produces both regular nickel cathodes and Falconbridge crowns. The regular cathodes are produced by plating onto nickel starting sheets and are sheared to a variety of sizes for the nickel plating industry. Crowns weighing 30–60 g are produced by plating nickel onto specially designed cathode blanks, from which they are stripped and polished for market. The refinery produces a limited amount of exceptionally pure superelectro nickel, with less than 100 g/t of impurities including oxygen, and less than 5 g/t Co, by using a specially purified electrolyte.

12.6.3 Carbonyl Refining [1, 79, 80]

The reaction of carbon monoxide at atmospheric pressure with active nickel metal at 40–80 °C to form the gaseous nickel tetracarbonyl was discovered by LANGE and MOND in 1889 [75]. The reaction is readily reversible, with nickel tetracarbonyl decomposing to metallic nickel and carbon monoxide at 150–300 °C.

Nickel tetracarbonyl is a volatile liquid that melts at –19.3 °C and boils at 42.5 °C.

Under the mild conditions employed for reaction at atmospheric pressure, the carbonyl-forming impurities in crude nickel metal do not volatilize. Iron forms a volatile carbonyl, iron pentacarbonyl, Fe(CO)₅, with a freezing point of –20.5 °C and a boiling point of 103 °C, but the rate of formation is slow. Cobalt forms Co₂(CO)₈, which melts at 51 °C and decomposes at 52 °C to form Co₄(CO)₁₂, but both are solids with low volatility. Copper,

like most other elements, does not form carbonyls directly with carbon monoxide. Thus the extraction of nickel as a carbonyl from a crude metal feed is a highly selective process.

The formation of metal carbonyls by the interaction of carbon monoxide with reduced metals can be catalyzed. In fact if it were not for the large increase in reaction rate resulting from the addition of a controlled amount of catalyst, the tonnage extraction of nickel and iron as carbonyls from reduced metals would probably not be feasible. With the aid of catalysts or inhibitors it is possible to produce the carbonyls of nickel, cobalt, and iron either selectively or together.

Although catalysts such as ammonia, mercury, selenium, and tellurium have been used to increase the rate of nickel carbonyl formation, sulfide activation is normally used. Sulfur is a good, low cost catalyst which can be added in the form of hydrogen sulfide, carbonyl sulfide, or sulfur dioxide. It may be added during the reduction step or prior to volatilization. The carbonyl extraction process is notable not only for its selectivity in the volatilization of the metals as carbonyls but also for the relative ease with which the carbonyls can be separated and decomposed under mild conditions to produce high-purity metals. Nickel and iron carbonyls can be separated by simple fractional distillation as a result of the large difference in their boiling points.

The carbonyl process makes it possible to produce nickel of very high purity with an exceptionally low cobalt content, which makes it particularly useful for nuclear energy applications.

The thermal decomposition of nickel tetracarbonyl is carried out by two different methods. Very rapid heating of the gas phase produces a fine nickel powder. Alternatively if the carbonyl contacts a hot metal surface, nickel deposits on the surface. This effect is used to produce nickel granules by the successive deposition of layers of nickel onto a seed particle, until the required size is attained.

12.6.3.1 Atmospheric Pressure Carbonyl Process

The Inco nickel refinery at Clydach, Wales, began operation in 1902 using the Lange-Mond atmospheric pressure carbonyl process [1, 75]. Originally the plant treated nickel copper matte, but it now processes a granular nickel oxide, produced by fluidized-bed roasting of nickel sulfide at Inco's Copper Cliff smelter, which typically analyzes 74% Ni, 2.5% Cu, 1.0% CO, 0.3% Fe, and 0.1% S.

The refinery still uses the basic Lange-Mond process but the operation has been greatly increased in efficiency over the years. The first three steps in the process reduction, sulfide activation, and volatilization are now carried out in rotary kilns. The nickel oxide is first reduced to metal at 425 °C by countercurrent contact with preheated hydrogen gas. The metal is then sulfided in a smaller kiln to activate it, before being contacted countercurrently with carbon monoxide at 50–60 °C and atmospheric pressure in a third kiln. About 95% of the nickel volatilizes under these conditions but iron and cobalt are not carbonylated. The residue from the volatilizers is returned to Canada and forms part of the feed to the converters at the Copper Cliff nickel refinery.

The off-gas from the volatilizer kiln, which contains about 16 vol% nickel carbonyl, is fed to a pellet decomposer (Figure 12.13) where it is contacted with preheated nickel granules at 200 °C. The nickel carbonyl decomposes, releasing carbon monoxide and depositing a layer of metallic nickel on the granules, which steadily increase in size.

The decomposer is filled with about 30 t of pellets which flow downwards by gravity and are recirculated to the top of the vessel by an enclosed bucket elevator. As the pellets pass downwards they are heated to 200 °C before contacting the carbonyl-containing gas introduced at the bottom of the decomposer. The motion of the pellets prevents them from adhering together. Nickel powder is added periodically to nucleate new pellets, and market-size pellets (8 mm) are automatically segre-

gated from the smaller material and discharged. The off-gas from the decomposer contains ca. 93 vol% carbon monoxide and 0.1% nickel carbonyl, and is recycled to the volatilization kiln. Nickel pellets from the carbonyl process typically contain 99.97% Ni and less than 5 g/t Co. In addition to nickel pellets, carbonyl nickel powder is also produced at Clydach in electrically heated powder decomposers and accounts for ca. 20% of the refinery nickel output.

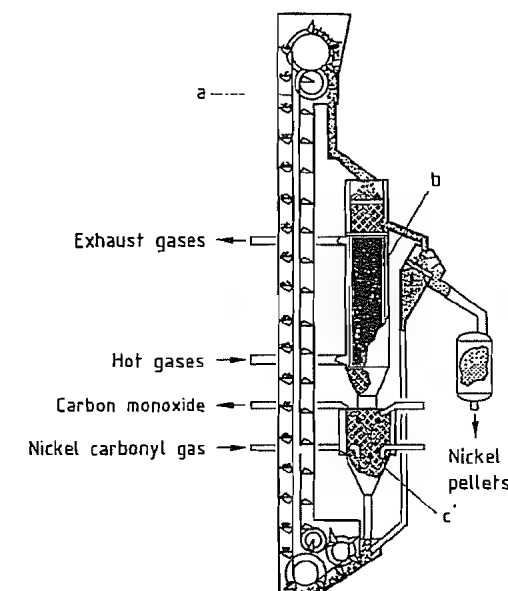
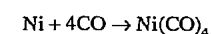


Figure 12.13: Cutaway view of a pellet decomposer: a) Bucket elevator; b) Preheater chamber; c) Reaction chamber.

12.6.3.2 High-Pressure Carbonyl Process (BASF)

Extraction of nickel with carbon monoxide is also used in processes that operate at high pressure and produce liquid nickel carbonyl. The volume change that occurs in the carbonyl reaction:



with four molecules of carbon monoxide forming one molecule of nickel carbonyl, means that an increase in pressure accelerates the formation of the carbonyl. The increased

pressure stabilizes the carbonyl and thus permits the process to be carried out at high temperature, which further increases the rate of reaction. As a result, activation of the nickel feed material is no longer necessary, and a wider range of feeds can be processed.

BASF in Germany operated a high-pressure carbonyl nickel refining process from 1932 until 1964. The feed materials were nickel copper matte or nickel scrap and residues. The feeds were melted and the composition was adjusted to provide just enough sulfur to combine with copper as Cu_2S and with part of the iron. The molten feed was granulated and reacted with carbon monoxide at 230 °C and 20 MPa. Over 95 % of the nickel was extracted as nickel carbonyl in a three-day batch treatment. Some iron was also carbonylated. Pure nickel powder was obtained by fractionation of the liquid carbonyls, and rapid heating of nickel carbonyl vapor to 280–300 °C.

12.6.3.3 Inco Pressure Carbonyl Process

The newest application of carbonyl refining to the treatment of a nickel-containing feed material is Inco's nickel refining complex in Copper Cliff, Ontario, which was commissioned in 1973 [80, 81]. This plant has a nominal capacity of 57 000 t/a of refined nickel.

The refinery consists of two operating plants: the converter plant and the pressure carbonyl plant. The converter plant produces granulated metallic nickel with a controlled sulfur content, using two top-blown rotary converters (TBRC's). The pressure carbonyl plant produces 45 000 t/a of nickel pellets, 9000 t/a of nickel powder, and 2200 t/a of ferromagnetic by-product from the granulated, sulfidized nickel feed.

The principal feed materials supplied to the refinery by the Copper Cliff smelter are the metallics fraction from the matte separation process and the less pure portions of the nickel oxide made by roasting the nickel sulfide concentrate as well as various other nickel-bearing residues and intermediates. The novel feature of this process is the preparation of a

nickel feed material which could be carbonylated at moderate pressure without the need for a separate activation step.

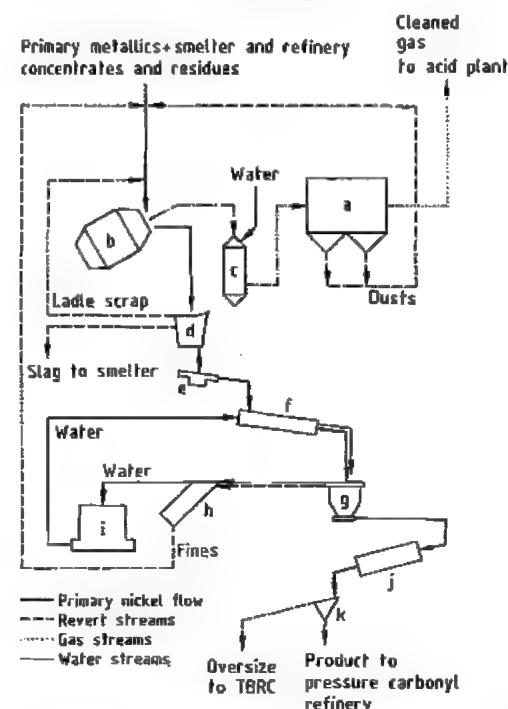


Figure 12.14: Flow sheet of the Inco pressure carbonyl converter plant: a) Electrostatic precipitator; b) Top-blown rotary converter (TBRC); c) Evaporation chamber; d) Bottom teeming ladle; e) Tundish; f) Granulating sluice; g) Dewatering bins; h) Lamella thickener; i) Cooling tower; j) Rotary dryer; k) Screen.

Figure 12.14 shows the process flow sheet for the preparation of the feed material in the converter plant. The feed materials are blended and smelted in two 50 t capacity top-blown rotary converters (Figure 12.15). Smelting is a batch operation carried out in three phases: charging/melting, blowing (sulfur removal), and reduction. In the charging/melting phase, blended feed materials are charged as the furnace rotates and is fired with a natural gas oxygen flame from a water-cooled lance. Coke is blended with the feed to reduce its oxide content, and the oxygen content of the flame is adjusted depending on the amount of sulfur to be removed. Charging is finished when the oxides have been reduced

and the temperature of the melt is about 1500 °C. During the charging and blowing phase the furnace is rotated to minimize dust emissions.

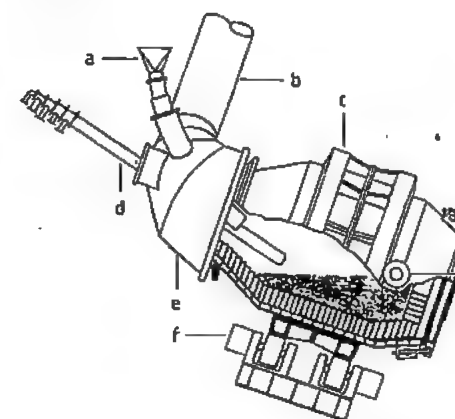


Figure 12.15: Cutaway view of a top-blown rotary converter: a) Water-cooled charging chute; b) Flue; c) Track ring; d) Water-cooled oxygen/natural gas lance; e) Hood; f) Rotar drive motor; g) Thrust roller.

In the blowing phase, a precalculated amount of high-pressure oxygen is blown at supersonic velocities into the converter charge to oxidize sufficient sulfur to produce a matte with a Cu/S ratio of about 4:1 (Cu_2S). In the reduction phase, oxides formed during blowing and oxygen dissolved in the bath are reduced with petroleum coke. Some sulfur removal also occurs when oxygen dissolved in the matte reacts with remaining sulfides. The converter is rotated at 15 rpm during reduction. Off-gases are drawn out through a movable hood and cleaned in electrostatic precipitators before being vented to a stack. The recovered dusts are recycled to a subsequent converter charge.

Molten matte at 1600 °C is granulated with high-pressure water jets at a rate of 1 t/min. The granulated matte is dried and transferred to the pressure carbonyl plant. The matte typically analyzes 75–80 % Ni, 12–17 % Cu, 2 % Co, 2 % Fe, and 3–4 % S, with a granule size of less than 9 mm.

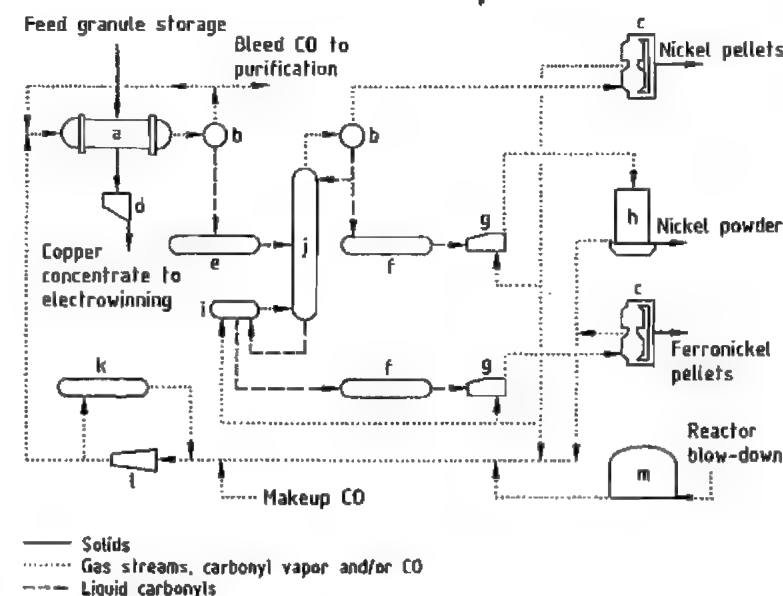


Figure 12.16: Flow sheet of the Inco pressure carbonyl refining process: a) Reactors; b) Condenser; c) Pellet decomposers; d) Slurry; e) Crude liquid storage; f) Storage; g) Vaporizer; h) Powder decomposers; i) Reboiler; j) Distillation columns; k) High-pressure CO storage; l) Main compressors; m) Low-pressure CO storage.

Figure 12.16 shows the process flow sheet for the pressure carbonyl refining operation. Matte granules are carbonylated in 150-t batches at temperatures up to 180 °C and pressures of 7 MPa in three horizontal cylindrical rotating reactors (Figure 12.17). Carbon monoxide is continually circulated through the reactor. Nickel carbonyl formation is very exothermic and the heat of reaction is removed by means of water-cooled heat exchanger tubes inside the reactors, which also serve as lifters to improve gas–solids contact as the vessel rotates. Micro-metallic filters at each end of the reactor prevent loss of solids entrained in the gas stream. The direction of gas flow is reversed periodically to prevent filter blinding.

Nickel and iron carbonyls are carried out of the reactor with the carbon monoxide stream, are liquefied by cooling, and stored as liquids at atmospheric pressure. The carbonylation reaction normally extracts about 97.5% of the nickel and 30% of the iron, leaving a residue typically containing 57% Cu, 8.5% Ni, 9% CO, 6% Fe, and 15% S, as well as the precious metals. The residue is treated hydrometallurgically to recover copper, cobalt, nickel, and the precious metals [82].

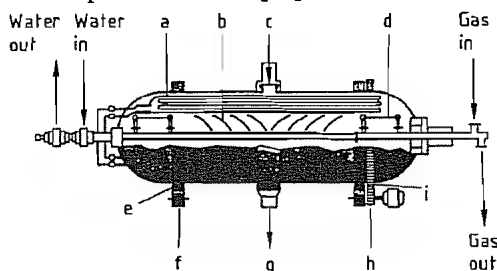


Figure 12.17: Cutaway view of a pressure carbonyl reactor: a) Coils; b) Flights; c) Feed chute; d) Metallic filters; e) Tires; f) Rollers; g) Discharge chute; h) Drive pinion; i) Spur gear.

The crude, liquid nickel–iron carbonyls typically contain 98.9% Ni and 1.1% Fe. This liquid is fractionated in two columns, each with twenty trays, to separate nickel carbonyl (*bp* 43 °C) from iron carbonyl (*bp* 103 °C). Distillation is carried out at below boiling temperatures with carbon monoxide as a carrier gas. Nickel carbonyl, which is obtained as

a mixture of vapor and liquid from the overhead partial condensers, is used to make extremely pure nickel powder and pellets. The bottoms from the reboilers, which contain 85% iron carbonyl and 15% nickel carbonyl liquids, are decomposed to form ferronickel pellets.

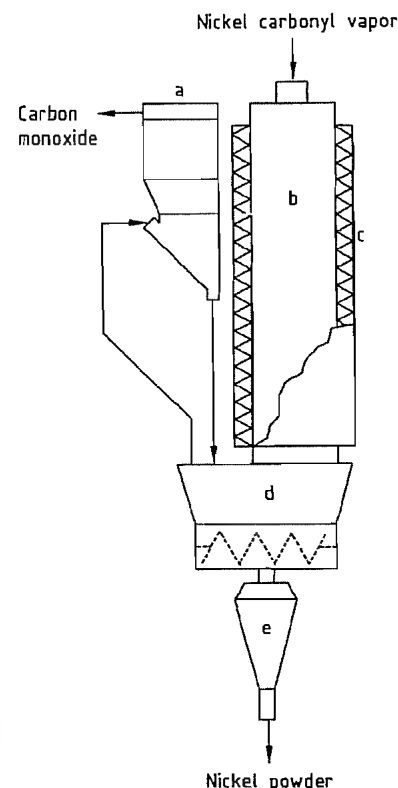
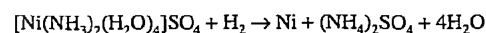


Figure 12.18: Cutaway view of a powder decomposer: a) Baghouse; b) Decomposer; c) Electric heaters; d) Connecting box; e) Discharge container.

The nickel carbonyl vapor from the distillation column passes directly to pellet decomposers (Figure 12.13) where it is contacted with preheated nickel pellets at 240–270 °C. The operation of the decomposers is essentially as described in Section 12.6.3.2 for the Inco refinery at Clydach. The condensed portion of the nickel carbonyl distillation overhead stream is revaporized with carbon monoxide carrier gas to avoid premature de-

composition and passed to electrically heated powder decomposers (Figure 12.18). Decomposition by thermal shock at 300 °C produces pure nickel powder, which can be varied in shape, size, morphology, and density by adjusting the operating conditions.

The iron carbonyl-containing bottoms product from distillation is treated by revaporizing the liquid at a sub-boiling temperature with carbon monoxide as carrier gas, and feeding it to a pellet decomposer to produce ferronickel pellets.

The pure nickel pellets, with a typical diameter of 10 mm, analyze over 99.97% Ni with 60 g/t C, 40 g/t O₂, and less than 0.2 g/t Co. The nickel powder, with a particle size in the range 3–7 μm, has significantly higher carbon and oxygen contents (650 g/t C and 570 g/t O₂).

12.6.4 Hydrogen Reduction to Nickel Powder

Nickel is recovered as a pure metal powder from nickel sulfate leach solutions by chemical reduction with hydrogen under pressure in several hydrometallurgical nickel refineries [1, 65]. Precipitation of the metal is carried out with an ammoniacal nickel sulfate solution having a molar ratio of ammonia to nickel of 2:1, so that the acid generated in the reduction reaction is neutralized by reaction with ammonia to form ammonium sulfate:

The reduction process is operated at 200 °C at a hydrogen pressure of 3 MPa in horizontal single-compartment autoclaves, each equipped with four agitators. The solution is processed batchwise, with the powder particles growing as successive layers of nickel are reduced, onto seed particles, from up to sixty batches of nickel-bearing feed solution. After each reduction or densification, which takes up to thirty minutes, the powder is allowed to settle, and the depleted solution is decanted off and replaced by fresh feed solution.

The nickel precipitation reaction can occur on any metal surface, and in the absence of suitable seed particles most of the metal deposition occurs on the vessel walls as a solid

plate. When suitable seed particles such as fine nickel powder are available, most of the nickel deposits on these particles, but even so, a minor but significant amount of nickel still plates on the walls, and must be released periodically. Normally this plating leach is carried out after each cycle of 50–60 densifications, and the leach liquor produced is used to prepare the seed particles for the subsequent densification cycle.

Seed particles are produced by adding an aqueous solution of iron(II) sulfate to the plating leach liquor to form a finely divided precipitate of ferrous hydroxide, and applying a hydrogen overpressure of 2.5 MPa at 115 °C. Under these conditions the nickel deposits onto the nuclei of ferrous hydroxide to form very fine particles of nickel metal, which provide the seed particles for densification. Once the nickel seed particles are formed, subsequent nickel deposition occurs autocatalytically on the surface of the particles, in preference to the vessel walls.

The reduction reaction is selective for nickel from a solution containing 50 g/L Ni and 1 g/L Co until the nickel content drops to about 1 g/L. Reduction is normally stopped at this point, leaving a solution containing about 1 g/L Ni and 1 g/L Co. This solution is reacted with hydrogen sulfide to precipitate a mixed nickel cobalt sulfide, which is treated hydrometallurgically to recover reformed cobalt, while the barren solution is evaporated to crystallize ammonium sulfate for sale as fertilizer.

At the end of a densification cycle when the powder has reached the desired particle size and density, the whole contents of the autoclave are discharged under pressure to a cone-bottomed flash tank. The solution is drawn off and the nickel powder is withdrawn from the bottom of the tank as a slurry containing 95% solids. The powder is washed with water and collected on a vacuum filter. The filter cake is dried in a rotary dryer fired with natural gas. The powder is either marketed as such or is converted to briquettes by mixing with an organic binder and pressing in briquetting rolls.

The "green" briquettes are sintered and desulfurized at 950 °C in a reducing atmosphere.

The powder typically analyzes 99.8% Ni, 0.08% Co, < 0.001% Cu, 0.002% Fe, 0.001% C, 0.025% S, and 0.02% O₂.

This process for recovering nickel powder from solution can be used in combination with the ammonia pressure leaching of nickel concentrates and mattes (as at Sherritt Gordon and Western Mining Corporation), with the acid pressure leaching of nickel-copper mattes (as at Impala Platinum and in the former Amax operation at Port Nickel), and with the Caron process for treating nickel laterites (as at Nonoc in the Philippines).

12.7 Beneficiation of Oxide Ores [1]

As described earlier, nickel oxide ores occur in two types: a limonitic type which occurs in the upper zone of a lateritic deposit, in which ferric oxide materials are predominant, and a silicate, or "garnierite" type, occurring at greater depth in the deposit, which has a lower iron content, but is usually richer in nickel than the limonite, and contains high levels of magnesia and silica. In nickeliferous limonite (Fe,Ni)O(OH)·*n*H₂O the nickel oxide is mainly present in solid solution with the iron oxides. In nickeliferous silicate, nickel, iron, and cobalt oxides occur in varying proportions, generally replacing part of the magnesium oxide in the serpentinite [Mg₆Si₄O₁₀(OH)₈].

Most deposits contain both types of ore. Usually it is possible to separate the ore by selective mining and screening into an iron-containing limonite fraction and a magnesium silicate fraction enriched in nickel. The metallurgy of nickel oxide ores differs from that of sulfides in that oxide ores are not amenable to most of the standard mineral beneficiation methods due to the chemical dissemination of the nickel in the oxide minerals. Screening may be used to reject the oversize, less weathered fragments that contain less nickel, but

this provides only a minor degree of upgrading.

In most cases the ore is treated directly by a pyrometallurgical or hydrometallurgical process. However, two processes have been developed in which the nickel is first converted by high-temperature treatment to a metallic phase, which can then be separated from the bulk of the ore by standard mineral beneficiation techniques. These processes are the Nippon Yakin Oheyama process (which was based on the Krupp-Renn process developed in Germany in the 1930s to produce iron from otherwise uneconomic low-grade iron ores) and the MINPRO-PAMCO segregation process.

12.7.1 Nippon Yakin Oheyama Process

Nippon Yakin Kogyo produces 12 000 t/a nickel as low-nickel ferronickel from silicate ores (2.3–2.6% Ni, 12–15% Fe), imported from New Caledonia, the Philippines, and Indonesia, at its Oheyama works in Japan [83]. The ore is ground and mixed with anthracite, coal, and flux, and briquetted. The briquettes are fed continuously through a rotary kiln, countercurrent to a flow of hot gas produced by the combustion of coal. As the temperature rises from 700 °C to 1300 °C, the charge is successively dried, dehydrated, and reduced. As the charge begins to melt, smelting occurs in the semifused state to form coalesced particles of spongy ferronickel (known as luppen, from the Krupp-Renn process) interspersed in a viscous slag phase. The kiln discharge is quenched in water and the luppen are separated from the slag by grinding, screening, jigging, and magnetic separation. Nickel recovery from ore is typically 95%.

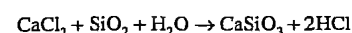
A major advantage of this process is that the ferronickel product is recovered in the form of 2–3 mm particles containing 22% Ni + Co, 0.45% S, 0.03% C, and 0.02% P which can be used directly in the AOD steel making process, without further upgrading or refining. Although the process is energy intensive, the major energy sources used are cheap anthra-

cite and coal, and no high cost electrical energy or oil is used for heating. Consequently, energy costs are relatively low.

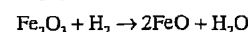
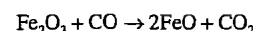
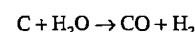
12.7.2 Segregation Processes

The segregation process [84, 85] was developed to recover copper from refractory minerals such as silicates, and has been applied with limited success on a commercial scale in Africa. Research has shown that the technique can be applied to the production of ferronickel from several types of nickel laterite ore, but the process has not yet been successfully applied on a commercial scale.

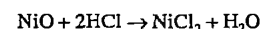
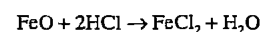
In the segregation process the ore is treated with a halide such as calcium chloride and a reductant such as coke at temperatures well below the melting range (950–1100 °C). Under these conditions the halide reacts with silicates and water vapor to form hydrogen chloride.



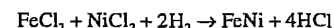
Iron(III) oxide is reduced to iron(II) oxide by hydrogen and carbon monoxide, which are formed in the reaction between coke and water.



The gaseous hydrogen chloride chloridizes both nickel oxide and iron(II) oxide to form the volatile metal chlorides.



The metal chlorides are reduced to metal by reaction with hydrogen at the surface of the coke particles,



releasing hydrogen chloride to react with further nickel and iron oxides. The ferronickel collects on the particles of coke and can be separated from the silicate phases by grinding and magnetic separation.

A major obstacle to the commercial development of this process has been the lack of a suitable reactor. The most promising ap-

proach, which was successfully tested at a rate of 1 t of ore per hour in 1981–1983, is the MINPRO-PAMCO segregation process. The reactor employed was a 850 kW former autogenous grinding mill, which was relined with two courses of refractory brick to permit operation at 950 °C.

In the pilot testwork, a nickel ore containing 2.3% Ni and 13.2% Fe was preheated in a rotary kiln to 950 °C, and treated in the segregation reactor with 40 kg calcium chloride and 20 kg coke per tonne of ore. The reactor discharge was cooled and ground prior to magnetic separation to yield a ferronickel product grading 59% Ni and 29% Fe, and a tailing with 0.45% Ni. Further upgrading to 68% Ni was shown to be possible with additional grinding and magnetic separation steps. Energy savings of 25–30% over the conventional smelting process have been projected by the developers of the process.

12.8 Pyrometallurgy of Oxide Ores

Nickel laterite ores have historically been treated almost exclusively by smelting processes, and except for Cuba, where nickel ore treatment is all essentially hydrometallurgical, the industry is still predominantly pyrometallurgical. The development of nickel oxide ore smelting has drawn heavily on iron and steel metallurgy for ferronickel production and on copper metallurgy for nickel matte production [1, 7, 8, 29].

The separation of nickel from the refractory oxides is relatively simple because there are large differences in the free energies of formation of nickel oxide and the gangue components such as silica and magnesia. Adjustment of the reduction conditions permits the complete reduction of nickel oxide while limiting the degree of reduction of iron oxide, but a total separation of nickel from iron by selective reduction is not possible. Two major process routes have been developed to overcome this problem.

In ferronickel production, the nickel oxide and part of the iron oxide are reduced to metal in an electric furnace. The fraction of iron reduced to metal is a function of the reduction potential of the system, so that ores with a low Ni/Fe ratio can be smelted to yield an acceptable ferronickel grade.

In nickel matte production, the ore is smelted with a reductant, a flux, and a source of sulfur, which may be gypsum, a sulfide mineral, or elemental sulfur. Most of the nickel and a large portion of the iron are reduced and sulfidized to form a low-sulfur matte phase. Iron removal can then be accomplished by fluxing and selective oxidation of the iron in a converter to produce a nickel matte containing over 75 % Ni, 20–22 % S, and less than 1 % Fe.

The smelting of nickel silicate ores in blast furnaces was developed by Société Le Nickel

(SLN) in New Caledonia in the 1870s [86]. Initially, attempts were made to produce ferronickel, but after encountering difficulties in eliminating sulfur from the product, the operation switched to the production of nickel iron sulfide matte. The furnace matte was blown to give a low-iron converter matte, which was shipped to Europe or North America where it was dead roasted to remove sulfur and reduced in briquette form with charcoal to metal rondelles. The SLN introduced electric furnace smelting of nickel silicate ores to ferronickel in 1958, using a furnace design developed by Elkem–Spigerverket of Norway, and most present-day ferronickel smelters use processes based on this technology [87].

Several of the world's major nickel laterite smelters are listed in Table 12.12 together with details of their ore and product nickel grades and production capacities.

Table 12.12: Nickel laterite smelters.

Smelter	Ore grade, % Ni	Product		1988 production, t/a Ni
		Type	Grade, % Ni	
SLN, New Caledonia	2.70	Fe–Ni matte	25 78	37 000 10 000
P.T. Inco Indonesia	1.97	matte	79	28 000
Pacific Metals, Japan	2.40	Fe–Ni	14–22	25 000 ^a
Falconbridge, Dominican Republic	1.75	Fe–Ni	38	29 300
Cerro Matoso, Colombia	2.90	Fe–Ni	45	19 000
LARCO, Greece	1.25	Fe–Ni	24–30	13 000
Hyuga Smelter, Japan	2.40	Fe–Ni	20–25	12 000 ^a
Orsk, former Soviet Union	1.02	matte	77	16 000
Nippon Mining, Japan	2.40	Fe–Ni	20	10 000 ^a
Glogovac, Yugoslavia	1.32	Fe–Ni	24	5 500
P.T. Aneka Tambang, Indonesia	2.25	Fe–Ni	25	4 800

^a 1985 production data.

12.8.1 Ore Pretreatment

Nickel laterite ores have high moisture contents (typically up to 45 %) as well as chemically bound water in the hydroxide form. All ore treatment plants use dryers, usually direct-fired rotary units operating at about 250 °C, which reduce the moisture content only to 15–20 % to minimize dusting during drying and subsequent smelting. Calcining to dehydrate the ore and prereduction prior to electric fur-

nace smelting are generally carried out in countercurrently fired rotary kilns. Chemically bound water is released above ca. 400 °C, and reduction of the oxides to metal starts at 500–600 °C. The maximum temperature reached in the kiln is generally limited to 800–900 °C because of the tendency of the ore to agglomerate and form accretions on the furnace walls. Dehydration and prereduction of the ore in the kiln prior to smelting, optimizes the utilization of energy available from the re-

ductants and fuel, thus reducing energy consumption in the smelting operation.

12.8.2 Smelting to Nickel Matte

Low-iron nickel sulfide matte has long been produced from oxide nickel ores by reduction and sulfidation in a blast furnace. This process is still practiced in Russia at three smelters in the Urals, but the blast furnace has given way to the electric furnace smelting process in New Caledonia and in the P. T. Inco operation in Indonesia.

12.8.2.1 Blast Furnace Smelting

The blast furnace production of nickel matte was practiced by SLN at its Doniambo smelter in New Caledonia from 1880 until 1972. The nickel silicate ore was blended with calcium sulfate and coke and reduced directly to matte in the blast furnace. The low-grade furnace matte was then blown to 78 % Ni and 20 % S in a converter [88].

At the Yuzhuralnikel Combine at Orsk^r in Russia, nickel silicate ores, averaging 1.02 % Ni, 15.4 % Fe, 10 % MgO, and 49 % SiO₂, are blended with ground coke, limestone, pyrite (0.1 % Cu content), and recycled converter slag and sintered at 1100–1200 °C in one of five 75 m² downdraft sinter machines. The resulting sinter is crushed and smelted in one of eleven low (5 m height) shaft furnaces using 24 % oxygen enriched air. The furnace matte, containing 17 % Ni, 54 % Fe, and 21 % S is tapped at 1200 °C and blown in Peirce–Smith converters to a high-grade matte (77 % Ni, 2.5 % Cu, 0.2 % Fe, 21 % S).

The converter slag is cleaned to reduce its nickel and cobalt contents in a two-stage contact with molten furnace matte, and the cleaned slag is recycled to the shaft furnaces. The converter matte is cast, ground, and roasted in fluidized-bed roasters to eliminate sulfur and is then treated in a chloridizing roast in a rotary kiln, followed by acid leaching to remove copper. The leached nickel ox-

ide is reduction smelted with coke and the metal is granulated. The Orsk combine produces 16 000 t/a of nickel granules analyzing 98.5 % Ni, 0.5 % Co, 0.55 % Cu, and 0.5 % Fe from its exceptionally low-grade nickel laterite ore feed [49].

12.8.2.2 Matte Production from Ferronickel

SLN now produces nickel matte from crude ferronickel (24 % Ni + Co, 69 % Fe, 2 % C, and 0.25 % S) by means of a sulfidizing treatment with elemental sulfur in a Peirce Smith converter [89]. After sulfidizing, the matte is blown with air to oxidize iron, which is slagged off with silica flux in two stages, to produce a matte containing 75–80 % Ni, 0.1 to 4 % Fe, and 20 % S. The cobalt content ranges from 0.4 % in matte containing 0.1 % Fe, to 1.2–1.7 % Co in matte containing 4 % Fe. This matte is shipped to the SLN nickel refinery at Le Havre-Sandouville in France, where it is refined to high-grade electrolytic nickel. Cobalt is recovered separately in the refilling process.

12.8.2.3 Inco Selective Reduction Smelting Process [90–94]

Inco's process for the production of nickel matte from laterite ores was developed for projects in Indonesia and Guatemala which started operation in 1977. The ore is dried and then calcined and partially reduced in a rotary kiln at 750–800 °C. Reduction is accomplished by adding coal to the kiln feed and by lancing high-sulfur oil into the ore bed. The hot calcine is smelted in an electric furnace. The bulk of the sulfur required to form a matte is added as molten elemental sulfur either to the kiln discharge, or directly to the electric furnace discharge. The resulting furnace matte is finally upgraded to the product matte in an air-blown converter.

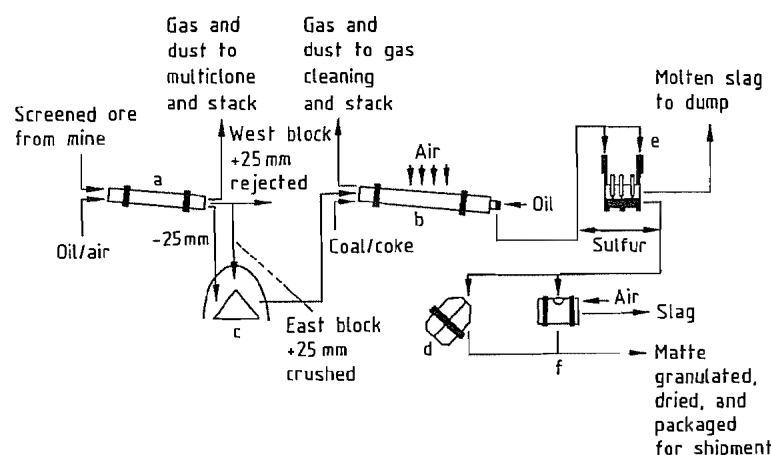


Figure 12.19: Flow sheet of the P.T. Inco Indonesia matte smelter: a) Drying kiln; b) Reduction kiln; c) Dried ore storage; d) Top-blown rotary converter; e) Electric furnace (melting); f) Peirce-Smith converter.

In the P.T. Inco Indonesia operation on the island of Sulawesi, two ore types are blended to maintain a SiO_2/MgO ratio of 1.9:1, and the moist ore is crushed and screened (Figure 12.19). The oversize ore is rejected and the fines, which typically contain 2.0% Ni, 19.3% Fe, 17% MgO , and 33.3% SiO_2 are dried to 20% moisture. The dried ore is fed to one of three 100-m long rotary kilns, each of which is divided into three zones, for calcining, sulfidizing, and reduction. Reduction is achieved by injecting high-sulfur oil into the hot calcine at the discharge end of the kiln. The combustible cracking products of the injected oil are burned gradually as they pass along the kiln, countercurrent to the ore, by injecting controlled amounts of combustion air. The calcine is discharged at 770 °C and is transferred to one of three 45 MVA electric smelting furnaces. Power for the smelting furnaces is supplied from a captive hydroelectric facility, which has proved a major economic advantage in comparison with most other nickel laterite operations, which are heavily dependent on the use of fossil fuels. Energy consumption in smelting is 2.1–2.2 GJ/t ore (580–600 kWh/t). Tapping temperatures are 1360 °C for the 32% Ni, 10% S matte and 1550 °C for the slag, which typically contains 0.16% Ni, 20% Fe, 45% SiO_2 , and 23.5% MgO .

The furnace matte is upgraded to converter matte (79% Ni, 19.5% S, 0.5% Fe) in one of two side-blown Peirce-Smith converters. These converters were installed to replace the top-blown rotary converters originally provided for this purpose, which had proved to be expensive to operate due to high refractory wear and high maintenance costs. The matte is granulated for shipment to the Japanese market.

The P.T. Inco Indonesia operation is to be expanded from its 1988 production rate of 34 000 t/a Ni to 47 000 t/a Ni in the early 1990s. A smaller Inco operation in Guatemala (Exmibal) which utilized the same process, but was dependent on fuel oil for power generation, closed in 1980 after three years of uneconomic operation.

12.8.3 Energy Consumption in Laterite Smelting

The pyrometallurgical production of ferronickel and nickel matte from oxide ores is extremely energy intensive and energy costs can account for 50% of the production cost of ferronickel. Energy is consumed in drying the moist ore, in calcining the dried ore to remove chemically bound water, in heating the charge to melting temperature, and in smelting. Typical fuel and electrical energy consumption

data collected in a 1986 survey [30] are presented in Table 12.13.

These figures reflect the trend to the use of coal in preference to oil in the decade following the increase in oil prices in 1973. The oil consumption reported for the Falcondo operation includes both the naphtha used in the metallurgical process and the heavy oil used for the production of electrical power in the on-site generating station. The distribution of energy consumption in a typical ferronickel smelter is illustrated by the following data (in GJ/t ore):

Drying	1.3–2.0
Preheating and prereduction	3.3–4.2
Electric smelting	1.4–2.2
Other electrical energy	0.22–0.29
Total	6.22–8.69

Electrical energy for the electric furnace actually accounts for only 25–30% of the total energy consumption in a smelter, while the rotary kiln operation consumes about 50% of the total energy required.

Total energy consumption at the P.T. Inco Indonesia operation was decreased from 620 GJ/t Ni in 1980 to 460 GJ/t Ni in 1985 by continuing process optimization [92]. During this period the percentage of energy provided by fuel oil was also decreased from 73% to 62% of the total by a partial substitution of oil by coal, which provided 8% of the energy used in 1985. Overall, therefore, these changes resulted in a 37% reduction in oil consumption per tonne of nickel produced. These economies in fuel oil usage, combined with a low cost source of hydroelectric power, have made the P. T. Inco operation in Indonesia one of the world's cheaper nickel producers [93].

12.9 Hydrometallurgy of Oxide Ores

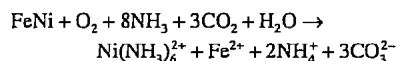
The chemical and mineralogical homogeneity of limonitic nickel ores, allied with the high value of potential by-products such as cobalt, chromium, and iron, make them ideal feed materials for hydrometallurgical treatment [1, 63]. Most of the nickel in iron-rich laterite ores is contained in goethite ($\alpha\text{-FeO}\cdot\text{OH}$), while the cobalt is almost always associated with manganese oxides. The recovery of nickel and cobalt thus essentially consists of separating them from iron and manganese.

A variety of potential hydrometallurgical or combined pyrometallurgical hydrometallurgical process routes have been proposed for laterite treatment. Approaches considered include sulfate or chloride roasting followed by water leaching to recover solubilized nickel and cobalt sulfates or chlorides, with soda roasting of the residue and water leaching to recover chromium, as well as the direct leaching of nickel and cobalt with sulfuric, nitric, or hydrochloric acid. Only two hydrometallurgical treatment processes have been commercialized, and although both recover cobalt and nickel, neither is currently operated for chromium or iron recovery. The two commercial processes, the Caron process, in which partially reduced ore is leached in ammoniacal solution, and the Moa Bay process, using direct sulfuric acid pressure leaching of ore, were both developed to treat the very large, high-iron laterite deposits of Cuba.

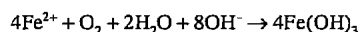
Table 12.13: Smelter fuel and power consumption data [30].

Operation	Ore grade, % Ni	Fe-Ni grade, % Ni	Coal, t/t Ni	Oil, 10^3 L/t Ni	Gas, $\text{m}^3(\text{STP})/\text{t Ni}$	Electricity, GJ/t Ni
Falcondo	1.75	38		15.7		
P.T. Inco	2.25	matte	1.1	6.9		140
Hyuga	2.4	20–25	7.5			115
Nippon	2.4	20	6.0	0.6		79
Aneka Tambang	2.25	25	2.3	3.8		108
Cerro Matoso	2.9	45	2.7		3.1	94

ammonium carbonate solution containing 7% NH_3 and 4% CO_2 . Leaching is carried out in three trains of four mechanically agitated, air-sparged leaching tanks at a pulp density of ca. 20% solids. The leaching reactions can be represented by the following equation:



The iron(II) is further oxidized and precipitates as iron(III) hydroxide:



However, significant losses of cobalt occur by coprecipitation with the iron hydroxide.

The pregnant liquor is separated from the leached ore in a seven-stage countercurrent decantation thickener circuit using ammoniacal solution as the washing medium. The washing efficiency is typically 99%. Ammonia is recovered from the washed leach residues by steam stripping, and the barren solids are discarded. The pregnant liquor recovered from the wash circuit, which contains 10 g/L Ni and 0.5 g/L Co, was formerly treated with ammonium hydrogen sulfide in a pipeline reactor to precipitate virtually all of the cobalt and about 10% of the nickel. The mixed sulfide product (15% Co, 40% Ni) was thickened, washed, and spray dried, and sold for cobalt and nickel recovery elsewhere. Ammonia and carbon dioxide were then stripped from the cobalt-free solution by direct stream injection to precipitate basic nickel carbonate.

Since 1988, the pregnant liquor has been treated by solvent extraction to separate nickel and cobalt [101]. An organic reagent (LIX 87 QN) is used to extract nickel selectively from the pregnant liquor. The nickel is recovered from the solvent by stripping with a more concentrated ammoniacal ammonium carbonate solution. Basic nickel carbonate can then be precipitated from the strip liquor by steam injection to remove ammonia and carbon dioxide. Copper sulfide is precipitated from the raffinate and refined elsewhere.

The basic nickel carbonate is recovered by thickening and filtration, and the wet filter cake, containing about 50% moisture, is dried

and calcined at 1300 °C in an oil-fired rotary kiln to yield nickel oxide. The nickel oxide calcine (77% Ni) is upgraded by partial hydrogen reduction to yield nickel oxides containing 85, 88, or 90% Ni, which are compacted to rondelles and sintered for market.

By the late 1980s the Greenvale nickel ore body, which had provided the sole feed to the Queensland Nickel refinery since 1974 was rapidly becoming depleted, and the operation started to treat laterite ores imported from New Caledonia and Indonesia.

The major difference between the process flow sheets used by Queensland Nickel and Marinduque/Nonoc was the production of refined nickel powder in the latter [99]. Basic nickel carbonate was redissolved in ammoniacal ammonium sulfate solution and metallic nickel powder was precipitated by reduction with hydrogen under pressure at 200 °C. The nickel powder typically analyzed 99.8% Ni, 0.08% Co, 0.01% Fe, 0.007% Cu, 0.006% C, and 0.004% S. By comparison the nickel oxide sinter produced prior to 1960 in the Nicaro plant, which had no cobalt separation step, analyzed 88% Ni, 0.7% Co, 0.04% Cu, 0.3% Fe, 0.05% C, 0.05% S, and 7.5% O_2 . In the Tocantins refinery a crude basic nickel-cobalt carbonate is redissolved in spent sulfuric acid electrolyte, and after purification by sulfide precipitation to remove cobalt and copper, the solution is treated by electrowinning to yield nickel cathode [63].

The Caron process is very energy intensive, and this factor proved a major economic handicap for the Queensland Nickel and Marinduque/Nonoc plants, which were both designed prior to 1973, with their heavy reliance on fuel oil for ore drying, reduction, and power generation. The fossil fuel energy requirements for the process for ore drying and reduction, and power and steam generation amount to ca. 6.7 GJ/t of dry ore, with an additional 200–250 MJ/t of electrical power. The Queensland Nickel plant originally consumed 900 t/d of fuel oil to treat 5700 t of ore. The distribution of oil consumption is as follows [102]:

Ore drying	14%
Steam and power generation	35%

Ore reduction roasting	47%
Nickel carbonate calcining	4%

Both Queensland Nickel and Marinduque/Nonoc converted their ore drying and steam and power generation facilities to use coal in place of oil in the early 1980s, with substantial economic benefit. However, conversion of the roasters to coal firing was not considered to be technically feasible. The Tocantins plant in Brazil makes extensive use of local eucalyptus wood as fuel in its ore treatment plant.

12.9.2 Pressure Leaching with Sulfuric Acid [1]

Because of the naturally high moisture content of limonite minerals (20–50% H_2O), it would be advantageous if the ore drying and reduction roasting steps, which together account for over 50% of the energy consumed in the Caron process, could be avoided, and the ore leached directly. However direct attack by the common mineral acids under ambient conditions is unselective and total dissolution of the ore results, with uneconomically high acid consumption. Fortunately, leaching of the ores in sulfuric acid at high temperature (> 250 °C) and pressure is highly selective since nickel and cobalt are stable as soluble sulfates, while iron(III) sulfate hydrolyzes and precipitates as a hydrated iron(III) oxide. Offsetting the energy savings in this type of process are the increased costs of construction materials capable of withstanding the highly corrosive environment of the high-temperature acid leach.

The applicability of the acid leach process is limited to those ores which do not contain substantial levels of other acid consuming minerals such as magnesia. It was for this reason that Freeport did not select an acid leaching process when seeking a process to treat the Nicaro ores (8% MgO). However when the same company subsequently developed the low-magnesia (1.7% MgO) limonitic ore body at Moa, Cuba, the sulfuric acid leach process was selected since it offered much higher (90% or more) recoveries for both

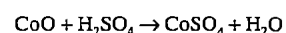
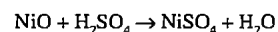
nickel and cobalt, with relatively low acid consumption. Although this process has been applied on a commercial scale only in the one plant at Moa, considerable process development effort was devoted during the 1970s to improving the economics and extending the applicability of the process to higher magnesia content ores, principally by Amax.

12.9.2.1 Moa Process

The plant at Moa was designed and built by Freeport in 1959 to produce 22 700 t/a Ni and 2000 t/a Co in the form of a mixed sulfide concentrate. The concentrate was to be refined to the pure metals in a separate plant which Freeport built at Port Nickel, Louisiana, where a cheap supply of natural gas was available. The Moa operation was nationalized in 1960 by the Cuban Government before construction was complete. It was recommissioned in mid-1961 with Soviet assistance, and since then the nickel-cobalt sulfide concentrate has been shipped to the former Soviet Union for further processing. The current production rate (1988) is believed to be 18 000 t/a Ni and 1600 t/a Co.

Although the original plant design is well documented, information on subsequent modifications is fragmentary. The following description is therefore based largely on accounts dating from 1960 [1, 95, 103–105]. The process flow sheet is shown in Figure 12.21. The ore, which consists mainly of goethite ($\alpha\text{-FeO}\cdot\text{OH}$), is slurried in water and screened to remove low-grade, oversize material, which is discarded. The fines fraction (< 1 mm) that forms the feed to the acid pressure leach averages 1.35% Ni, 0.15% Co, 48% Fe, 1.7% MgO, 9% Al_2O_3 , 3% Cr_2O_3 , and 4% SiO_2 in composition. It is leached at 45% solids pulp density with 98% sulfuric acid (240 kg H_2SO_4 /t dry ore) at about 245 °C and 4.3 MPa, with a retention time of 1–2 h. The acid is made on-site from elemental sulfur, and the waste heat from the acid plant is used in the leaching circuit. Leaching is carried out in four leaching trains each containing four large vertical autoclaves, which are lead- and brick-lined with titanium internal fittings. Agitation

is achieved by injecting high-pressure steam into a draft tube at the bottom of the vessel. Heat is recovered from the autoclave discharge slurry for use in preheating the cold feed slurry. Under these conditions, about 94 % of the nickel and cobalt dissolve, while iron solubility is limited to about 1 g/L.



The leach liquor typically contains 6 g/L Ni, 0.5 g/L Co, 2 g/L Mn, 0.8 g/L Fe, 0.4 g/L Cr, 2.5 g/L Mg, 2 g/L SiO_2 , 3 g/L Al, and 30 g/L H_2SO_4 . The liquor is separated from the leach residue (0.08 % Ni, 0.01 % Co, and 51 % Fe) by countercurrent decantation (CCD) washing with water in a six-stage thickener circuit. The washed residue is stockpiled for possible future use as iron ore.

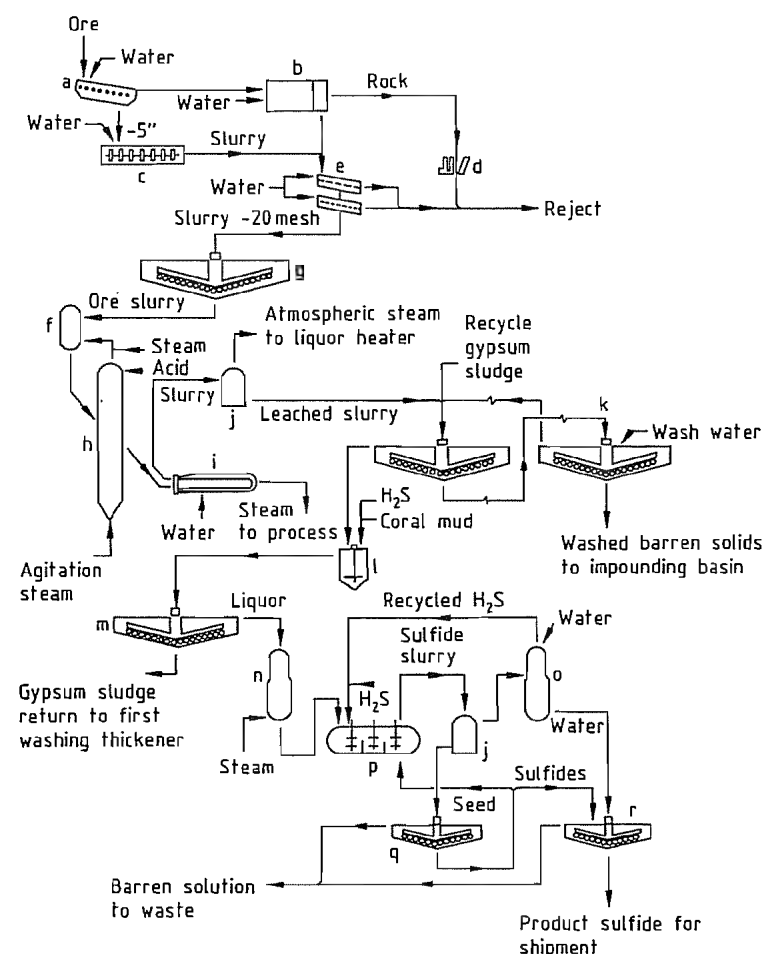
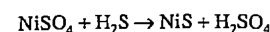


Figure 12.21: Flow sheet of the Moa nickel laterite plant: a) Shaking grizzly; b) Cylindrical scrubber; c) Log washer; d) Jaw crusher; e) Screens; f) Slurry heaters; g) Storage thickener; h) Leaching autoclaves (4 in series); i) Slurry cooler; j) Flash tank; k) Washing thickeners (6-stage CCD); l) Neutralizing tanks (4-stage cascade); m) Gypsum thickener; n) Heaters; o) Gas cooler; p) Precipitation autoclave; q) Sulfide thickener; r) Washing thickeners (2-stage CCD).

The pregnant solution is treated with coral mud (calcium carbonate) to neutralize the acid and precipitate most of the dissolved iron, aluminum, and manganese by hydrolysis. The precipitated sludge is recycled to the wash circuit and joins the leach residue for disposal. The neutralized solution typically contains (g/L): 3.5–4.0 Ni, 0.3–0.4 Co, 1.0 Mn, 0.3 Fe, 0.4 Cr, 2.5 Mg, 1.0 SiO_2 , and 3.0 Al at pH 2.5. Nickel and cobalt are recovered from solution in 98–99 % yield by precipitation at 120 °C with hydrogen sulfide at a pressure of 1.1 MPa in a three-compartment, brick-lined autoclave.



The barren solution typically contains (g/L): 0.05 Ni, 0.01 Co, 1.0 Mn, and 7 H_2SO_4 . The nickel cobalt concentrate contains 55 % Ni, 5 % Co, 0.7 % Fe, 0.2 % Cu, 1.0 % Zn, and 35 % S.

The refinery built by Freeport in Louisiana to treat the concentrate employed pressure hydrometallurgy and hydrogen reduction to separate and refine nickel and cobalt. This plant was being commissioned when the Cuban nickel industry was nationalized in 1960, and was never used for the purpose for which it was designed. Currently (1989) the total nickel–cobalt concentrate production from Moa Bay is shipped to the former Soviet Union, where it is treated at a smelter in the Urals to produce nickel–cobalt anodes analyzing 87 % Ni, 8 % Co, 2 % Fe, and 0.7 % Cu. The anodes are electrorefined at the Yuzhuralnikel Combine at Orsk in a conventional sulfate chloride electrolyte system. The nickel is recovered as high-grade electrolytic nickel, and cobalt is separated from anolyte by chlorine precipitation for subsequent processing to metal [49].

Energy consumption in the Moa acid leach process is relatively low because over half the steam requirement for the leach is provided by waste heat recovered from the sulfuric acid plant. The fuel oil requirement for the generation of power and steam has been estimated at about 40 kg/t of dry ore, which is only 20 % of the fuel requirement for the Caron process. However, this energy benefit is frequently out-

weighed by the high consumption of sulfuric acid which depends directly on the magnesia content of the ore [106].

12.9.2.2 Amax Acid Leach Process

The Amax acid leach process for the treatment of laterite ores [107–109] was developed, on the basis of the Moa process, with the object of increasing metal recoveries while decreasing acid and energy consumption. The process was tested extensively in pilot plant and prototype plant campaigns between 1975 and 1981, for a potential new project in New Caledonia which was subsequently abandoned.

In the Amax process (Figure 12.22) the ore is divided by selective mining or screening into a low-magnesia limonitic fraction and a smaller fraction of high-magnesia serpentinitic ore. The finer limonitic fraction is leached directly in the pressure leach at 270 °C, while the high-magnesia fraction is first calcined and then preleached at atmospheric pressure with the leach liquor from the countercurrent decantation wash circuit, before it goes to the pressure leach. Essentially stoichiometric utilization of the acid is achieved by this countercurrent leaching of the high-magnesia ore. The overall acid requirement is thus reduced substantially, and the need for a separate alkaline neutralizing agent (e.g., coral mud at Moa) is eliminated. Metal extractions of 94–97 % are normally achieved with a 20-min retention time in the pressure leach at 270 °C.

A major saving (up to 70 %) in energy consumption in the leaching step is achieved by using indirect heating of the feed slurry with flash steam recovered from the autoclave discharge slurry. By using this technique in place of direct steam sparging, the concentration of metals in solution is substantially increased, and the size and cost of subsequent processing steps is reduced. Overall the requirement for fossil fuel is estimated to be only 50 % of that for the Moa operation. A further simplification of the process was achieved by improving mass transfer in the sulfide precipitation step so that it could be operated at a lower pressure

of 0.2 MPa compared with 1.1 MPa at Moa Bay. The Amax acid leach process is claimed to be economically viable over a wide range of laterite ore compositions, with magnesia contents as high as 15% MgO.

12.10 By-Product Cobalt

All nickel ores, whether sulfide or oxide, contain significant amounts of cobalt that can potentially be recovered as a valuable by-product. Overall, however, the recovery of cobalt from nickel ores is very low, and the nickel industry provides less than 30% of world cobalt production. The greater part of world cobalt production arises from the copper operations in Zaire and Zambia.

No cobalt recovery at all is possible in ferronickel smelting, where the cobalt is distributed between the discard slags and the ferronickel product, in which it merely represents an impurity. The same comments apply to class II nickel products such as nickel oxide sinter, made by the smelting of sulfide concentrates or by the Caron process without a cobalt separation circuit.

Cobalt is normally recovered in high yield as a by-product of carbonyl, electrolytic, or hydrometallurgical refining of nickel metal or matte. However, even in these cases the over-

all recovery of cobalt from the ore is low, since most of the cobalt is lost to the slag phase in the prior smelting processes. Cobalt recovery in the converting operation depends critically on the final iron content of the matte. Typically if the matte is blown to less than 1% Fe, over 75% of the cobalt reports to the slag phase and is effectively lost. If the conversion process is stopped at 3–5% Fe, however, over 75% of the cobalt remains in the matte, and can be recovered during subsequent refining.

In practice few nickel smelters are operated to maximize the recovery of cobalt. The SLN in New Caledonia and the Soviet smelters producing matte from laterites are notable exceptions. Slags are cleaned by contact with a high-iron matte, which becomes enriched in cobalt. The cobalt is then recovered by hydrometallurgical treatment of the enriched material.

Even in the ammonia pressure leaching of nickel sulfide concentrates, where the smelting step is bypassed, cobalt recovery is much lower than that of nickel, due to a strong affinity of the iron oxide residue for soluble cobalt. Probably the highest overall recovery of cobalt from nickel ores is achieved in the sulfuric acid pressure leaching of laterite ores, in which a cobalt recovery of 90% is possible.

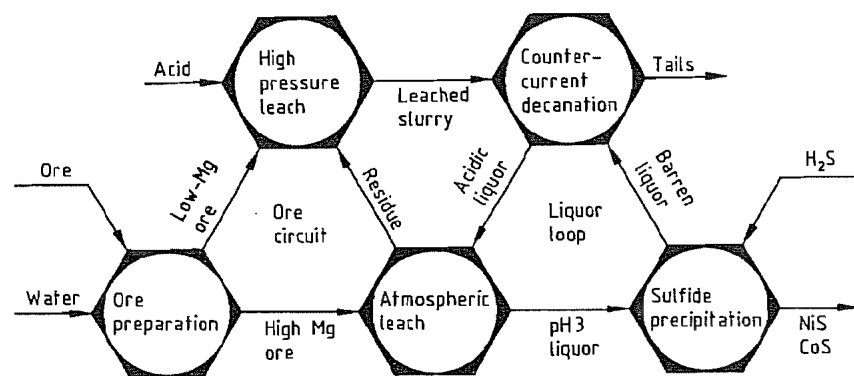


Figure 12.22: Flow sheet of the Amax nickel laterite process.

Table 12.15: Commercial forms of nickel [114].

Type	Composition, %						
	Ni	Co	Cu	Fe	C	S	O
Class I:							
Cathodes	> 99.90		0.005	0.002	0.01	0.001	
Pellets	> 99.97	5 ¥ 10–5	0.001	0.0015	< 0.10	0.0003	
Powder	99.74			< 0.10	< 0.10	< 0.010	< 0.15
Briquettes	99.90	0.03	0.001	0.01	0.01	0.0035	
Rondelles	99.25	0.37	0.046	0.022	0.022	0.004	0.042
Class II:							
Ferronickel	20–50	1–2		rest	1.5–1.8	< 0.3	
Nickel oxide	76.0	1.0	0.75	0.30		0.006	rest

12.11 Recovery from Secondary Sources

Nickel-containing scrap from forming processes in fabricating plants and machine shops is an important source of feed material for the production of nickel-containing stainless steel. Typically, in the United States about 40% of the nickel used for stainless steel production is provided in the form of stainless steel scrap from outside sources. Recycled in-house scrap is not included in this estimate [110, 111]. Nickel-containing scrap falls mainly into the categories of stainless steels, superalloys, copper nickel alloys, and nickel itself. Usually scrap is recycled to a plant which produces the same type of alloy.

Inco established The International Metals Reclamation Company (INMETCO) at Ellwood City, Pennsylvania in 1978, to collect and convert nickel-containing waste materials from specialty steel companies into a stainless steel remelt material. This 40 000 t/a capacity plant treats various grades of scrap materials including flue dusts, scale and turnings, as well as stainless steel scrap, to produce 23 kg remelt pigs containing ca. 18% Ni and 8% Cr [112]. Falconbridge also started to recycle nickel- and cobalt-containing alloys to its primary nickel smelter in 1985 [113].

12.12 Market Products

Unlike copper, nickel is rarely used without further processing and so the mechanical or physical properties of nickel products are of

no significance, and nickel is marketed solely on the basis of its chemical composition. Nickel is marketed according to its chemical purity as either a Class I or a Class II product. Class I includes the high-purity products, electrolytic cathode, carbonyl refined granules and powder, and hydrogen-reduced nickel in powder or briquette form. Commercial nickel of this class is normally 99.7% pure or better [114].

Class II includes the various grades of ferronickel, nickel oxide, and metallized nickel oxide. Typical compositions for Class I and II products are given in Table 12.15. Class II nickel products, which normally sell at a discount to Class I nickel, became more popular during the 1970s, since the new stainless steel making techniques such as the AOD process can tolerate higher impurity levels in the feed materials. However this trend was reversed during the 1980s, during the period of oversupply and low metal prices, particularly for alloy steel production where Class I nickel was preferred [111].

Some nickel products are designed for specific applications, such as the 0.02% S content “S Nickel Rounds” produced by Inco as “active” anode material for the plating industry, and the special powders used in Ni–Cd batteries. Traditionally, electrolytic nickel cathodes are cut into 2.5 cm squares for market. Both the major producers of electrolytic nickel, Inco and Falconbridge, now produce electrolytic nickel in the form of “rounds” (Inco) or “crowns” (Falconbridge), by plating nickel onto specially masked cathode blanks, to pro-

duce discrete round deposits. These deposits can be stripped from the blanks and drummed directly without shearing, and are easier for the consumer to handle than sheared cathode.

12.13 Uses [111, 115–117]

The major first uses of nickel are summarized in Table 12.16. Stainless steel production accounts for over 50 % of nickel consumption, followed by ferrous alloys, and nickel-base alloys. Electroplating takes only 11 % of nickel consumption [118].

Table 12.16: Western-world nickel consumption: distribution by first use in 1987 [118].

First use	Distribution, %
Stainless steel	51
Alloy steels	12
Nickel-base alloys	15
Copper-base alloys	3
Plating	11
Foundry	5
Other	3

Table 12.17: Western-world nickel consumption: distribution by end use in 1987 [118].

End use	Distribution, %
Consumer products	25
Construction and machinery	13
Automotive industry	11
Chemical industry	9
Building and construction	6
Process industry	6
Electronics	6
Power industry	5
Petroleum industry	5
Aerospace	3
Nickel chemicals	2
Marine applications	2
Coinage	2
Other	5

A more detailed breakdown of nickel consumption by end use is given in Table 12.17. The consumer product category, which includes the stainless steel used in kitchen sinks, laundry equipment, furniture and tableware, as well as nickel-plated parts for bicycles, motorcycles, jewelry, eyeglass frames, and musical instruments, accounts for one quarter of

nickel consumption. The high strength of nickel stainless steels combined with light weight and low maintenance have contributed to their growing use in railway cars and road tank trailers in the construction and machinery category [117].

Nickel consumption dropped significantly during the 1970s in the automotive industry with the amount of nickel used in the average U.S. car falling from about 2 kg in 1970 to only 0.5 kg by 1985 [111]. The chemical industry is the fourth largest market for nickel, mainly in stainless steels for a multitude of applications.

Building and construction, the process industries, and the electronics industries each accounted for about 6 % of nickel consumption in 1987. Stainless steel usage in architectural applications is increasing, as it is in environmental control equipment and food processing equipment. The growth rate of nickel usage in the electronics industry is greater than 10 % per annum. Alloy 42, a nickel-iron alloy, is widely used in lead frames, while a copper-nickel-tin alloy C72500, is used in springs, clips, and terminals.

In the power industry, nickel-containing stainless steels are widely used in nuclear power stations and are increasingly being applied in scrubber systems for the removal of sulfur dioxide from the flue gases of oil- and coal-fired power stations. Nickel-containing materials are used in the petroleum industry in applications ranging from drilling bits to piping and process vessels in petrochemical plants, and to the construction of off-shore production platforms. In the marine category, nickel-containing materials are used in ships and in desalination plants. In the aerospace industry nickel is a key element in superalloys that resist stress and corrosion at temperatures of 1000 °C and above. These materials are used in gas turbine engines.

Nickel chemicals are used in the production of nickel catalysts for use in the hydrogenation of vegetable oils, in heavy oil refining, as nickel salts in electroplating, and for color enhancement in ceramics. Coinage alloys con-

taining nickel have been used since ancient times [3]. Today the 75 Cu–25 Ni cupronickel alloy is the most widely used, although Canada, the Netherlands, and the Republic of South Africa use pure nickel coinage, which is particularly durable.

In 1984, after several years of decreasing world demand for nickel, sixteen of the major nickel producers cooperated to set up the Nickel Development Institute (NiDI) with headquarters in Toronto, Canada. The NiDI has a mandate to increase the use of nickel. In this function NiDI has taken over the market development role which was performed very effectively by Inco from the 1920s until the mid 1970s, when a much reduced share of world nickel production and the depressed nickel market forced Inco to cut its activity in this area. The NiDI, which is international in scope, has set up technical information offices in North America, Europe, Japan, India, and Central and South America, backed by a worldwide network of consultants. The organization publishes a periodical applications oriented magazine, "Nickel", which has wide circulation, as well as sponsoring technical papers and a series of reference books on selected topics. The NiDI has initiated a wide range of market development and research programs to promote the use of nickel, and provides expertise and advice to users of nickel and nickel-containing products [115, 117].

12.14 Economic Aspects

[115, 118]

Western-world nickel consumption increased by an average of 6.5 % per annum from 1945 to 1974, when it reached a level of 576 000 t (Figure 12.23). Consumption dropped sharply in 1975, and the demand for nickel remained flat for the next ten years, with annual rates fluctuating in the range 450 000–600 000 t/a. Although demand approached the 600 000 t/a consumption level in 1979 it was not exceeded until 1987 [119]. Western-world nickel consumption in 1987

and 1988 was 625 000 t and 640 000 t, respectively.

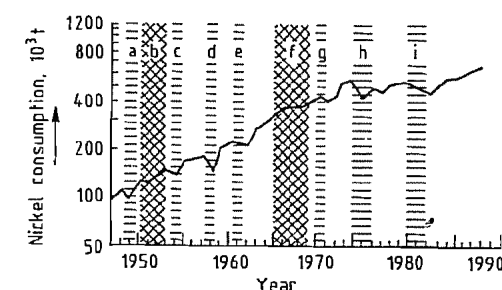


Figure 12.23: Western-world nickel consumption: a) 1949 recession; b) Korean war; c) 1954 recession; d) 1958 recession; e) 1961 recession; f) Vietnam war; g) 1971 recession; h) 1974–1976 recession; g) 1980–1982 recession.

The slowdown in the growth of nickel consumption in the mid 1970s coincided with a major increase in production capacity, when several laterite projects, which had been under development for five to ten years, came on stream. Many of these projects were heavily dependent on fuel oil and in consequence suffered a severe penalty when oil prices increased dramatically in 1973. During this period, nickel production by the Eastern-bloc countries also regularly exceeded consumption by 15 000 to 40 000 t/a, and substantial exports were made to Western markets.

By 1980 there were over forty nickel producers in 26 different countries, and the nickel price collapsed as the demand for nickel dropped in 1981 and 1982, and the producers fought for the shrinking market. Even the most cost efficient suffered heavy losses, and several higher cost producers were eventually forced to close permanently. The surviving operations sought to cut operating costs in every facet of nickel production, and as a result the nickel industry was much leaner and more cost efficient by the end of the 1980s.

When Western-world stainless steel production increased by 15 % in 1987, the demand for nickel increased by over 10 % from the relatively constant levels of 1984 to 1986. After more than ten years of depressed metal prices and production rates, the industry was unable to respond by increasing production

levels since producer inventories of metal had been run down to a minimum and most marginal capacity had been eliminated in the drive to reduce operating costs. The result was a two year period of inflated nickel prices, with the London Metal Exchange (LME) refined nickel cash price, which had averaged US \$1.60/lb in January 1987, peaking at \$10.84 in March 1988. The average price for the whole of 1988 was \$6.25/lb, and high prices continued through most of 1989 with an average price for the year of \$6.05. This development restored the financial health of the industry after many years of marginal or uneconomic operation.

The high nickel prices of 1988/89 raised concerns among both stainless steel and nickel producers that substitution of nickel-bearing materials by cheaper materials would be encouraged. Average industry operating costs in 1989 were estimated to be around US \$2/lb, while estimates of the capital expenditure required for a new integrated nickel project range upwards from US \$10/lb of annual capacity. A long-term nickel price of US \$4–5/lb, which would be needed to justify investment in new production capacity can be expected to depress demand and render new capacity unnecessary. Future increases in production thus appear more likely to come from the expansion of existing operations than from totally new projects.

Details of world nickel mine and smelter production by country for 1985 are given in Table 12.18 and the corresponding consumption breakdown is shown in Table 12.19. Table 12.20 provides a listing of the world's major nickel-producing operations.

For many years nickel was sold on the basis of posted producer prices, set to a large extent by Inco as the major producer. In 1979 the LME started trading in Class I nickel, and even though the LME handles only a relatively small percentage of total nickel production, it has since become the major factor in determining nickel price levels. Prices are quoted in US \$ per metric tonne of Class I metal.

Table 12.18: Production of nickel in 1993 [120].

Country	Production, 10 ³ t	
	Mine	Smelter/refinery ^a
Australia	64.7	50.4
Austria		3.5
Botswana	19.7	
Brazil	22.7	15.2
Canada	188.4	123.1
China	32.4	31.0
Colombia	20.2	20.2
Cuba	30.2	16.5
Dominican Republic	23.9	23.9
Finland	8.3	14.8
France		9.0
Greece	12.6	10.9
Indonesia	65.8	5.3
Japan		102.9
Korea		11.3
New Caledonia	98.1	36.9
Norway	3.6	56.8
Philippines	7.7	
Russia	180.0	190.0
South Africa	28.9	29.9
Taiwan		9.0
United Kingdom		28.0
United States	2.5	4.9
Yugoslavia	1.5	3.0
Zimbabwe	12.8	18.2
Total	824.0	814.7

^aIncluding ferronickel and nickel oxides as well as refined nickel.

Table 12.19: Consumption of nickel in 1989 [120].

Country	Consumption, 10 ³ t
Brazil	12.2
Canada	16.9
United States	132.2
<i>Other America</i>	5.0
China	45.0
India	13.0
Japan	156.7
Korea	33.2
Taiwan	21.0
<i>Other Asia</i>	8.1
Australasia	1.7
South Africa	11.0
Belgium	22.0
Germany	75.0
Finland	26.8
France	36.5
Italy	38.5
Russia	64.0
Spain	18.0
Sweden	22.8
United Kingdom	29.8
<i>Other Europe</i>	11.5
Total	825.0

12.15 Toxicology

The toxicology of nickel and its compounds and legislation pertaining to nickel and its compounds in the environment and workplace are discussed in detail in Section 12.17.5.

12.16 Alloys

Nickel forms mixed crystals over a wide range with copper, manganese, iron, chromium, and other metals. It is mainly used as an alloying element in many nonferrous materials and steels (approximately 2000) to improve their strength, toughness, corrosion resistance, and high-temperature properties. About 60 % of the primary nickel produced in the Western World is used in the production of stainless steels, and a further 13 % is used in the production of nickel-base alloys, including pure nickel semifinished products.

In 1988 primary nickel consumption by first use in the Western World broke down as follows (in %) [121]:

Alloy steels	6
Stainless steels	60
Nonferrous nickel-base alloys	13
Plating applications	10
Foundry industry	6
Other applications	5

12.17 Compounds

Of the worldwide production of nickel, only about 3 % is in the form of compounds if ferronickel, nickel oxide, and partially reduced nickel oxides used in the metallurgical industry are excluded.

The main uses of nickel compounds fall into four areas:

- **Electroplating.** This includes electroforming and electroless nickel plating as well as conventional nickel electroplating.
- **Catalysis.** Nickel, its alloys and compounds serve as catalysts for numerous chemical reactions. The main uses of nickel catalysts, prepared from nickel compounds, are in steam reforming, hydrocracking, and in hy-

drogenation reactions, including methanation.

- **Batteries.** There are various routes to the nickel hydroxide used as the active mass in nickel-cadmium batteries.
- **Pigments.** These include colorants in enamels, glassware, ceramics, and plastics.

Like all transition metals, nickel forms numerous complexes. These are of academic rather than industrial importance. Most nickel compounds are green; some are blue. Much information is available from the standard reference works [122–124] and a review [125]. There is an extensive review of the coordination chemistry of nickel in [126].

Nickel(II) amidosulfate, nickel sulfamate, $\text{Ni}(\text{NH}_2\text{SO}_3)_2 \cdot 4\text{H}_2\text{O}$, is a highly soluble salt which is used in solution in the electrolyte for nickel electroforming processes, giving low stress deposits.

Commercially, it is available not as a solid but as a solution containing about 11 % nickel. This is usually prepared by dissolving nickel powder in a hot solution of sulfamic acid ($\text{HSO}_3 \cdot \text{NH}_2$), but soluble nickel oxide, nickel hydroxide, or nickel carbonate can also be used. Short reaction times are necessary because of the hydrolysis of sulfamic acid to sulfuric acid.

Nickel(II) ammonium sulfate, $\text{NiSO}_4 \cdot (\text{NH}_4)_2\text{SO}_4 \cdot 6\text{H}_2\text{O}$, can be crystallized as blue-green crystals from a solution containing the two components in the appropriate ratio. It has low solubility in water, ca. 25 g/L at 20 °C. The salt was formerly used in electroplating, but now its uses are very limited.

Nickel(II) Carbonate. Although a hydrated carbonate $\text{NiCO}_3 \cdot 6\text{H}_2\text{O}$ and the anhydrous form NiCO_3 exist, the industrially important compound is the bright green, rhombic basic nickel carbonate approximating to $2\text{NiCO}_3 \cdot 3\text{Ni}(\text{OH})_2 \cdot 4\text{H}_2\text{O}$. It is virtually insoluble in water, but dissolves in acids with evolution of carbon dioxide. Heating to above ca. 450 °C in air gives a reactive nickel oxide with a high specific surface area.

Table 12.20: Major nickel producers (1990).

Country	Company or location	Operations ^a	Estimated capacity, t/a
Australia	Western Mining	M,S,R	80 000
	Queensland Nickel	M,R	27 000
Botswana	BCL Limited	M,S	22 000
Brazil	Cia. Niquel Tocantins	M,R	10 000
	Codemin SA	M,S	6 500
Canada	Inco Limited	M,S,R	163 900
	Falconbridge	M,S	45 000
	Sherritt Gordon	R	25 000
China	Jianchuan	M,S,R	25 000
Colombia	Cerro Matoso SA	M,S	20 000
Cuba	Cubaniquel	M,R	52 000
Dominican Republic	Falcondo	M,S	32 000
Finland	Outokumpu Oy	S,R	18 000
France	Société Le Nickel (SLN)	R	13 000
Greece	LARCO SA	M,S	25 000
Indonesia	PT Inco Indonesia	M,S	45 400
	PT Aneka Tambang	M,S	10 000
Japan	Pacific Metals	S	40 800
	Nippon Yakin Kogyo	S, R	12 700
	Sumitomo Metal Min.	S, R	46 000
	Tokyo Nickel Co.	R	36 000
Korea	Korea Nickel	R	12 000
New Caledonia	Société Le Nickel (SLN)	M,S	50 000
Norway	Falconbridge Nikkelverk	R	67 000
Russia	Norilsk	M, S, R	300 000
	Ural Nickel	M, S, R	70 000
South Africa	Rustenburg Platinum	M,S,R	19 000
	Impala Platinum	M,S,R	12 000
	Western Platinum	M, S, R	2 000
Ukraine	Pobugskoye	M, S	6 600
United Kingdom	Inco Europe, Clydach	R	36 000
United States	Glenbrook Nickel	M, S	26 000
Yugoslavia	Kavardarci	M,S	28 000
Zimbabwe	Bindura Nickel	M,S,R	15 000
	Rio Tinto, Empress	R	6 500

^a M = mine; S = smelter; R = refinery.

Commercial basic nickel carbonate is made by precipitation from a nickel solution, usually the sulfate, with sodium carbonate. The exact composition depends on the temperature and the concentrations of the components in solution.

Basic nickel carbonate is used for pH adjustment in nickel electroplating baths, in catalyst production, and in the manufacture of some nickel pigments and specialty nickel compounds.

Demand for basic nickel carbonate has recently increased due to the use of zinc-nickel

plating of steel by the automotive industry. In one electroplating method, the nickel in solution is replenished by basic nickel carbonate.

It is also possible to prepare nickel carbonate by dissolving nickel in ammonium carbonate solution in the presence of air and carbon dioxide. Boiling off the ammonia and carbon dioxide precipitates basic nickel carbonate. This method forms part of the Caron process for the refining of nickel. The carbonate is further processed to nickel oxide or nickel metal.

Nickel(II) Halides. Nickel forms dihalides with all four halogens, and each dihalide forms one or more hydrates. Only the chlorides are of industrial importance, particularly the hexahydrate $\text{NiCl}_2 \cdot 6\text{H}_2\text{O}$, which is available either as a solid or as a concentrated solution.

Table 12.21 lists some properties of the dihalides and the hydrate usually encountered. Known hydrates are $\text{NiF}_2 \cdot 4\text{H}_2\text{O}$, $\text{NiCl}_2 \cdot x\text{H}_2\text{O}$, ($x = 2, 4, 6, 7$). $\text{NiBr}_2 \cdot x\text{H}_2\text{O}$ ($x = 2, 3, 6, 9$), $\text{NiI}_2 \cdot x\text{H}_2\text{O}$ ($x = 4, 6$). Nickel dichloride hydrates are stable over the following temperature ranges:

$\text{NiCl}_2 \cdot 7\text{H}_2\text{O}$	low temperature
$\text{NiCl}_2 \cdot 6\text{H}_2\text{O}$	up to 36.25 °C
$\text{NiCl}_2 \cdot 4\text{H}_2\text{O}$	36.25 to 75 °C
$\text{NiCl}_2 \cdot 2\text{H}_2\text{O}$	above 75 °C

The difluoride is only slightly soluble in water, but the other halides are very soluble (e.g., 117 g $\text{NiCl}_2 \cdot 6\text{H}_2\text{O}$ per 100 mL solution at 20 °C).

Table 12.21: Nickel halides.

Compound	<i>d</i>	$-\Delta H^\circ$ (25 °C), kJ/mol	Color
NiF_2	4.63	651	light green
NiCl_2	3.55	305	pale yellow
NiBr_2	5.10	212	yellow
NiI_2	5.83	78	black
$\text{NiF}_2 \cdot 4\text{H}_2\text{O}$	2.22		light green
$\text{NiCl}_2 \cdot 6\text{H}_2\text{O}$	1.92	2103	green
$\text{NiBr}_2 \cdot 3\text{H}_2\text{O}$		1146	yellow-green
$\text{NiI}_2 \cdot 6\text{H}_2\text{O}$			blue-green

The difluoride has a tetragonal structure, and the other dihalides have hexagonal layer structures. They are relatively stable, and can be melted or sublimed in a vacuum or under an inert atmosphere.

Production. The anhydrous halides can be made by direct reaction of the elements at high temperature or in nonaqueous solution, although the fluoride is better made indirectly. They are also formed by dehydration of the hydrates in a stream of the hydrogen halide gas to prevent formation of nickel oxide.

The hydrates can be made by dissolving nickel metal, oxide, hydroxide, or carbonate in an aqueous solution of the halogen acid HX, followed by crystallization. Commercially, nickel dichloride hexahydrate is usually pro-

duced by dissolving nickel metal in hydrochloric acid, and then crystallizing. Nickel dichloride solutions are important in chloride-based processes for the extraction of nickel, but nickel metal is usually recovered by electrowinning.

Table 12.22: Specifications of nickel chloride hexahydrate for electroplating.

	BS 564 (1970), %	DIN 50970, %
Ni	24.0 (Ni + Co) min.	23.7 min.
Co	1 % of total metal, max.	0.5 max.
Cu	0.005 max.	0.002 max.
Fe	0.01 max.	0.01 max.
Pb	0.002 max.	0.002 max.
Zn	0.002 max.	0.006 max.
Insolubles	0.05 max.	0.05 max.
pH (40 % w/v)	2.0 min.	

Uses. Nickel dichloride hexahydrate is important in electroplating; it is used together with nickel sulfate in the Watts plating bath. Table 12.22 lists the purity specifications for its use in electroplating. It is also used in the production of some catalysts. Uses of the other dihalides are very minor.

Nickel(II) hydroxide, $\text{Ni}(\text{OH})_2$, *d* 4.15, ΔH° (25 °C) -514 kJ/mol. Treating a nickel salt solution with an alkali-metal hydroxide solution gives a green gelatinous precipitate of nickel hydroxide, also known as nickel hydrate. Filtering, washing, and drying give the pure compound. The precipitation conditions affect the physical characteristics of the nickel hydroxide produced.

Nickel hydroxide is virtually insoluble in water, but it is soluble in dilute acids, giving a nickel salt solution, and in ammoniacal solutions a blue ammine complex is formed. Heating to ca. 250 °C drives off water, leaving nickel oxide.

Nickel hydroxide has some use as an intermediate in catalyst production, but its main use is as the active mass in the positive electrode in nickel cadmium batteries. In pocket-plate electrodes, pellets of nickel hydroxide are used. In sintered electrodes, the nickel hydroxide is prepared within the electrode either by precipitation or electrochemically.

There are various hydrated oxides or hydroxides containing Ni(III) and possibly Ni(IV), some of which are not well characterized. The compounds are black and are referred to as nickel peroxide, nickelic hydroxide, or nickel black.

The β -NiO·OH, obtained by the oxidation of nickel salts in alkaline solution with an oxidizing agent such as sodium hypochlorite, is well characterized. It is also formed in batteries when Ni(II) hydroxide in a nickel electrode is charged.

Persulfate oxidation of nickel(II) hydroxide gives a substance formulated as NiO₂·xH₂O.

A commercial "nickel peroxide" corresponded to Ni₂O₃·2H₂O, and gave Ni₂O₃·H₂O (equivalent to NiO·OH) on partial dehydration [127].

Nickel(II) Nitrate. The commercially available compound is the green hexahydrate Ni(NO₃)₂·6H₂O, *d* 2.05, ΔH^0 (25 °C) -2212 kJ/mol. It is very soluble in water. On heating, the hexahydrate dissolves in its own water of crystallization at 56 °C. Progressive heating drives off the water of crystallization, giving basic nitrates and finally nickel(II) oxide.

The stability ranges of the hydrates are:

Ni(NO ₃) ₂ ·9H ₂ O	below -3 °C
Ni(NO ₃) ₂ ·6H ₂ O	-3 to 54 °C
Ni(NO ₃) ₂ ·4H ₂ O	54 to 85.4 °C
Ni(NO ₃) ₂ ·2H ₂ O	85.4 to ca. 105 °C

Nickel nitrate solution can be produced by dissolving nickel in nitric acid. The reaction is vigorous, and without careful control loss or breakdown of the nitric acid occurs, forming, among others, ammonium nitrate. The dissolution of nickel(II) oxide in nitric acid is easier to control; the hexahydrate is produced by crystallization of the resulting solution.

It is difficult to prepare the pale green, anhydrous nickel(II) nitrate by dehydration of the hexahydrate. It can be obtained by dehydration with dinitrogen pentoxide in fuming nitric acid, or from nickel tetracarbonyl and dinitrogen tetroxide.

Nickel(II) nitrate hexahydrate is widely used in the production of nickel catalysts, by impregnating an inert carrier and decomposing the nitrate. It is also used in the formation

of the nickel(II) hydroxide active mass in sintered nickel electrodes for nickel cadmium batteries.

Nickel(II) Oxide. Nickel oxide, NiO, *d* 6.8, ΔH^0 (25 °C) -240 kJ/mol, is green, with a cubic rock-salt structure. It occurs in nature as bunsenite. The exact color depends on factors such as purity and crystallite size. In general, the properties of nickel oxide depend on the method of preparation, especially temperature.

Nickel(II) oxide has a defect structure Ni_{1-y}O, which is responsible for its *p*-type semiconductor properties. In addition, nickel oxide can absorb surface oxygen to give higher O:Ni ratios. There is little evidence for Ni₂O₃ as a bulk compound, although it may exist as a surface compound on NiO.

World production of "nickel oxide" is ca. 40 000 t/a from INCO in Canada, Greenvale in Australia, and from Cuba, but only about 4000 t of this is chemical nickel oxide. The majority is metallurgical nickel oxide, or partially reduced nickel oxide containing 85–90% nickel, used mainly in the stainless steel industry. Chemical nickel oxide is available in two forms: green or black.

Production. Green nickel oxide can be made by calcining almost any nickel compound in air, for example, the nitrate, oxalate or hydroxide, at ca. 1000 °C. It can also be made by oxidation of carbonyl nickel powder, but some care is needed to ensure complete oxidation.

Black, or soluble, nickel oxide is made by calcining basic nickel carbonate at ca. 550 °C; it contains a slight excess of oxygen.

The green oxide is rather refractory, and dissolves only slowly in mineral acids. The black oxide is more reactive and dissolves readily. Both forms are insoluble in water and are easily reduced, for example by hydrogen, to nickel metal.

Uses. Nickel oxide is used in the production of catalysts, in the enamel industry for making frit, in the glass and ceramics industries, and in the manufacture of ferrites for the electronics industry.

Black nickel oxide is particularly suitable for dissolving in acids as a first step in the production of specialty nickel salts.

Higher oxides such as Ni₂O₃, and NiO₂ have been proposed but there is little evidence for their existence free of water.

Nickel(II) Sulfate. Two forms of nickel(II) sulfate are commercially available. The most common is the blue-green, tetragonal hexahydrate α -NiSO₄·6H₂O, *d* 2.07, ΔH^0 (25 °C) -2683 kJ/mol, nickel content 22.3%, which crystallizes from solution between 30.7 and 53.8 °C. The other form is the green, orthorhombic heptahydrate NiSO₄·7H₂O, *d* 1.95, nickel content 20.9%, which crystallizes from solution below 30.7 °C. Crystallization above 53.8 °C gives green β -NiSO₄·6H₂O.

The hydrates are readily soluble in water. The solubilities in grams per liter of solution are (the temperature in °C is given in parentheses):

NiSO ₄ ·7H ₂ O	578 (10)
NiSO ₄ ·7H ₂ O	775 (30)
α -NiSO ₄ ·6H ₂ O	770 (40)
α -NiSO ₄ ·6H ₂ O	851 (50)
β -NiSO ₄ ·6H ₂ O	959 (60)
β -NiSO ₄ ·6H ₂ O	1258 (100)

Data also exist for the solubility of nickel sulfate in sulfuric acid [128].

Heating the hydrates causes dehydration. Hydrates with 4 or 1 molecule of water are stable. The bright yellow, cubic, anhydrous salt NiSO₄, *d* 3.68, ΔH^0 (25 °C) -873 kJ/mol, is obtained above 330 °C. This decomposes above ca. 800 °C to give nickel oxide and sulfur trioxide. The lower hydrates can also be obtained by crystallization from nickel sulfate solutions containing excess sulfuric acid. They dissolve only slowly in water. Basic sulfates also exist.

Production. The worldwide production capacity is about 40 000 t/a, from producers in Europe, Japan, China, and the former Soviet Union. Most of the nickel sulfate is a by-product of electrolytic copper refining. A bleed stream is purified, finally giving a solution from which nickel sulfate is crystallized.

Nickel sulfate is also produced by dissolving nickel or nickel oxide in sulfuric acid and crystallizing. Several nickel refineries produce

nickel sulfate solution by leaching nickel mattes with sulfuric acid, but the nickel is usually recovered as nickel metal by electrowinning.

Uses. The main use of nickel sulfate is as the electrolyte in nickel electroplating baths. Table 12.23 lists the standards covering nickel sulfate for use in electroplating. It is also used in electroless nickel plating, in catalyst manufacture, and in the production of other nickel compounds.

Nickel Sulfides. Nickel(II) sulfide, NiS, *d* 5.65, ΔH^0 (25 °C) -82 kJ/mol, *mp* 797 °C.

Neutral nickel(II) salt solutions react with ammonium sulfide initially to give black α -NiS, a hydrous, amorphous precipitate of the type Ni(SH,OH)₂. At low pH, this crystallizes to give rhombohedral γ -NiS, whereas in more alkaline solution hexagonal β -NiS is formed.

Table 12.23: Specifications of nickel sulfate hexa- or heptahydrate for electroplating.

	BS 564 (1970) (6 or 7 hydrate), %	DIN 50970 (6 hydrate), %
Ni + Co	20.7 min.	22.0 min.
Co	1 % of total metal, max.	0.5 max.
Cu	0.002 max.	0.002 max.
Fe	0.005 max.	0.005 max.
Pb	0.002 max.	0.002 max.
Zn	0.002 max.	0.006 max.
Cd		0.005 max.
As		0.001 max.
Insolubles	0.005 max.	0.005 max.
pH (40 % w/v)	2 min.	

The γ -form occurs in nature as millerite. This shows little deviation from stoichiometry, but a high-temperature form has a stoichiometry range.

Other nickel sulfides exist, some of which occur in nature. These are Ni₃S₂, Ni₇S₆, Ni₃S₄, and NiS₂. All can be prepared by fusing the correct proportions of the elements.

Sulfide minerals are a major source of nickel, and nickel sulfide is an important intermediate in refining processes. The main use of nickel sulfides is as catalysts, for example, in the hydrogenation of sulfur compounds. The catalyst can be prepared in situ by sulfiding a supported nickel catalyst.

Nickel(II) tetrafluoroborate, $\text{Ni}(\text{BF}_4)_2 \cdot 6\text{H}_2\text{O}$, can be made as apple green needles by reacting fluoroboric acid with basic nickel carbonate, and crystallizing from solution. It has limited use in specialty high-speed nickel plating process, and other minor uses.

Nickel Complexes. In common with all transition metals nickel forms a vast number of inorganic complexes with different oxidation states and geometries. Only the ammine complexes, which are important in ammonia-based leaching processes, have industrial significance.

The structural, spectral, and magnetic properties of nickel complexes are important in studies of transition-metal complex chemistry. In particular, there are concentration and temperature dependent anomalies in properties due to polymerization and equilibria between different geometries.

The most common complex ion is octahedral $\text{Ni}(\text{II})$, for example, the green $\text{Ni}(\text{H}_2\text{O})_6^{2+}$ in aqueous solution. The electronic structure of these complexes is $[\text{Ar}]3d^8$ with two unpaired electrons, and hence they are paramagnetic. Other species can displace water molecules, for example, ammonia molecules in ammine complexes $[\text{Ni}(\text{H}_2\text{O})_x(\text{NH}_3)_{6-x}]^{2+}$, $x = 0-6$, which are blue or purple. The complex ion $[\text{Ni}(\text{H}_2\text{O})_4(\text{NH}_3)_2]^{2+}$ is the required ion in solution for the production of nickel powder by pressure reduction of solutions by hydrogen.

Four-coordinate $\text{Ni}(\text{II})$ complexes are quite common, either diamagnetic square planar complexes such as the yellow $\text{Ni}(\text{CN})_4^{2-}$ or paramagnetic tetrahedral complexes such as NiCl_4^{2-} . Five-coordinate $\text{Ni}(\text{II})$ complexes also exist, and are either trigonal bipyramidal or square pyramidal.

Complexes of nickel in lower oxidation states are mostly based on carbonyl ligands. An example of $\text{Ni}(\text{I})$ is $\text{Ni}(\text{PF}_3)_4$ and of $\text{Ni}(\text{I})$, $\text{Ni}(\text{PPh}_3)_3\text{X}$ ($\text{X} = \text{Cl}, \text{Br}, \text{I}$).

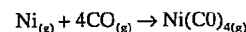
Higher oxidation states are stabilized by electronegative elements, e.g., $\text{Ni}(\text{III})$ in the violet K_3NiF_6 and $\text{Ni}(\text{IV})$ in red K_2NiF_6 , both of which are octahedral.

12.17.1 Nickel Tetracarbonyl

Nickel tetracarbonyl, $\text{Ni}(\text{CO})_4$, *bp* 42.2 °C, *mp* -19.3 °C, *d* 1.31, is a very toxic colorless liquid. It possesses a significant vapor pressure at ambient temperature (44 kPa at 20 °C; 65 kPa at 30 °C).

Nickel tetracarbonyl is virtually insoluble in water, but soluble in many organic solvents. It does not react with dilute mineral acids. It is thermally unstable, decomposing to nickel and carbon monoxide. It burns in air with a luminous flame, giving nickel oxide and carbon dioxide, and forms explosive mixtures with air (3–34 vol% $\text{Ni}(\text{CO})_4$). The molecule is tetrahedral, with linear $\text{Ni}-\text{C}-\text{O}$ bonds. The bonding consists of both a $\text{Ni}-\text{C}$ σ -bond and π bonding.

Production. Nickel tetracarbonyl is formed by direct reaction of carbon monoxide and finely divided nickel at relatively low temperatures:



$$\Delta G = -160\,410 + 418.27T \text{ J/mol} [129]$$

At atmospheric pressure, the maximum rate of formation of nickel tetracarbonyl is at 130 °C for pure nickel. The temperature at which the rate of formation is a maximum decreases in the presence of a catalyst such as sulfur, and increases with pressure. The reverse reaction begins above ca. 180 °C. This reversible reaction is the basis of the atmospheric-pressure Mond process and the INCO pressure process for the production of high-purity nickel pellet and powder. Nickel tetracarbonyl can also be prepared in solution by a variety of methods [130]. Users of nickel tetracarbonyl frequently produce their own supply, but it is commercially available in the United States.

The conditions under which nickel tetracarbonyl is formed are important because of the possibility of corrosion or transfer of nickel within a system, and in view of its high toxicity. The mere coexistence of carbon monoxide and nickel in some form does not mean that nickel tetracarbonyl will form. Other criteria must be met:

- A fully reduced nickel-containing surface,
- A reducing gas containing carbon monoxide,
- The formation must be thermodynamically possible, which generally means low temperature (ambient to 150 °C) and high carbon monoxide partial pressures.

In addition, the presence of a catalyst such as sulfur accelerates nickel tetracarbonyl formation.

One situation where a significant amount of nickel tetracarbonyl can form is from a finely divided reduced nickel catalyst and carbon monoxide at low temperature. This is well known to users of nickel catalysts, and such conditions are avoided. Other than this, it is rare that significant amounts of nickel tetracarbonyl are formed. Environmentally, precautions preventing contamination of the workplace by the carbon monoxide will also prevent contamination by any nickel tetracarbonyl.

The presence of nickel tetracarbonyl has been suggested but not demonstrated in cigarette smoke and in gases from the combustion of fossil fuels containing nickel. Attempts to detect it in welding fume failed [131].

Uses. Apart from being an intermediate in the carbonyl refining of nickel, nickel tetracarbonyl can be thermally decomposed to nickel plate other materials, for example, in mold production or in a fluidized bed. It is also used as a carbonylating agent or catalyst in organic chemistry.

Analysis. Nickel tetracarbonyl can be analyzed by decomposition and conventional analysis of the nickel, by gas chromatography, UV or IR spectroscopy. There is a highly sensitive method based on the chemiluminescent reaction of nickel tetracarbonyl with ozone [132]. Commercial instruments based on infrared or chemiluminescent analysis are available.

Reactions of Nickel Tetracarbonyl. Nickel tetracarbonyl undergoes oxidation, reduction, and substitution reactions [133, 134]. These are normally carried out in organic solvents

below ca. 50 °C to prevent thermal decomposition of the nickel tetracarbonyl.

Reaction with various oxidizing agents gives $\text{Ni}(\text{II})$ compounds. Concentrated nitric acid gives nickel nitrate. Solutions of nickel tetracarbonyl in organic solvents are oxidized by air to basic nickel carbonate and by halogens to the corresponding nickel dihalide. Decomposition of nickel tetracarbonyl with bromine water is useful as a means of disposal or for analysis.

Reduction reactions, generally with alkali metals, give polynuclear anions formulated as $[\text{Ni}_2(\text{CO})_6]^{2-}$, $[\text{Ni}_3(\text{CO})_8]^{2-}$, $[\text{Ni}_4(\text{CO})_9]^{2-}$, $[\text{Ni}_5(\text{CO})_9]^{2-}$, and $[\text{Ni}_6(\text{CO})_{12}]^{2-}$. Reduction of nickel tetracarbonyl by alkali metals in liquid ammonia gives a carbonyl hydride $[\text{NiH}(\text{CO})_3]_2$, isolated as a tetraammoniate.

Interest in substitution compounds of nickel tetracarbonyl blossomed following the publication in 1948 of work by REPPE and co-workers showing that an effective class of catalysts for the trimerization of acetylene compounds could be formed by substituting CO groups in $\text{Ni}(\text{CO})_4$ by donor ligands such as triphenylphosphine.

Thousands of substitution compounds of nickel tetracarbonyl have now been prepared. Most are with ligands containing the group 15 elements phosphorus, arsenic, or antimony as electron donor, but carbon, nitrogen, and unsaturated organic molecules can also serve as ligands.

Some of the simpler substitution compounds with phosphorus ligands are $\text{Ni}(\text{CO})_n(\text{PX}_3)_{4-n}$, $n = 0-3$, $\text{X} = \text{H}, \text{F}, \text{Cl}, \text{CH}_3, \text{C}_2\text{H}_5, \text{C}_6\text{H}_5$ (substituted phosphines) and $\text{X} = \text{OCH}_3, \text{OC}_2\text{H}_5, \text{OC}_6\text{H}_5$ (phosphites). The degree of substitution is controlled by steric and electronic effects. For example, with PF_3 and $\text{P}(\text{C}_6\text{H}_5)_3$, only mono- and disubstituted compounds are formed, whereas with PCl_3 and $\text{P}(\text{OC}_6\text{H}_5)_3$ the carbon monoxide molecules can be completely replaced. The tetrakis(ligand) compounds $\text{Ni}(\text{PF}_3)_4$ and $\text{Ni}[\text{P}(\text{C}_6\text{H}_5)_3]_4$ can be prepared by other means. Substitution by chelating ligands is also possible, e.g., $(\text{CO})_2\text{NiL}'$ and NiL'_2 , where $\text{L}' = o\text{-C}_6\text{H}_4[\text{P}(\text{C}_2\text{H}_5)_2]_2$.

Fewer substitution compounds based on arsenic and antimony have been prepared. Examples include $\text{Ni}(\text{CO})_3\text{AsX}_3$ ($\text{X} = \text{CH}_3, \text{C}_2\text{H}_5, \text{C}_6\text{H}_5, \text{OCH}_3, \text{OC}_2\text{H}_5, \text{OC}_6\text{H}_5$) and $\text{Ni}(\text{CO})_3\text{SbX}_3$ ($\text{X} = \text{Cl}, \text{C}_2\text{H}_5, \text{C}_6\text{H}_5, \text{OC}_6\text{H}_5$).

12.17.2 Nickel Salts of Organic Acids

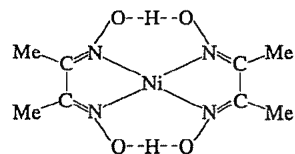
Nickel(II) acetate tetrahydrate $\text{Ni}(\text{CH}_3\text{COO})_2 \cdot 4\text{H}_2\text{O}$, d 1.744, can be obtained as green crystals when solutions of nickel(II) hydroxide or carbonate in acetic acid are evaporated at room temperature. It is readily soluble in water but is insoluble in ethanol.

Anhydrous nickel(II) acetate $\text{Ni}(\text{CH}_3\text{COO})_2$, d 1.798, can be prepared by dehydration of the tetrahydrate in vacuum or by heating the tetrahydrate under reflux with acetic anhydride. When heated in the absence of air these acetates decompose to give a residue of nickel and Ni_3C , evolving, among other products, carbon monoxide and carbon dioxide. Nickel acetate is a suspect carcinogen: the LD_{50} (rat) is 350 mg/kg [135].

Nickel(II) acetylacetonate $\text{Ni}(\text{CH}_3\text{COCHCOCH}_3)_2$, mp 230 °C (dec.), is obtained as emerald green crystals by dehydration of the dihydrate at 50 °C in vacuum; it has an unusual trimeric structure in the solid state [136]. The dihydrate $\text{Ni}(\text{CH}_3\text{COCH}_3)_2 \cdot 2\text{H}_2\text{O}$ is prepared by the addition of acetylacetone to solutions of nickel(II) salts in the presence of a weak base such as sodium acetate. Nickel(II) acetylacetonate is soluble in organic solvents and finds use in the synthesis of organometallic compounds such as nickelocene and bis(cyclooctadiene) nickel. It is also industrially important as a catalyst component in the oligomerization of alkenes and in the conversion of acetylene to cyclooctatetraene [137, 138].

Nickel(II) dimethylglyoximate bis(dimethylglyoximate) nickel(II), $\text{Ni}(\text{C}_4\text{H}_7\text{N}_2\text{O}_2)_2$, is obtained quantitatively as a bright red precipitate when an alcoholic solution of dimethylglyoxime is added to a neutral or slightly

alkaline solution of a nickel(II) salt. This reaction is used in the gravimetric estimation of nickel [139] and is also useful as a spot test for the presence of nickel ions. The structure of this diamagnetic solid [139] shows the nickel(II) ion to be in a square-planar environment; the dotted lines represent strong intramolecular hydrogen bonds.



Nickel(II) formate dihydrate $\text{Ni}(\text{HCOO})_2 \cdot 2\text{H}_2\text{O}$, d 2.154, is obtained as green crystals by evaporation of a solution of nickel carbonate in formic acid. The anhydrous salt is obtained when the dihydrate is heated to 140 °C; at 250 °C, finely divided nickel metal is produced. Hence, nickel(II) formate is used in the production of nickel catalysts.

Nickel(II) oxalate dihydrate $\text{Ni}(\text{COO})_2 \cdot 2\text{H}_2\text{O}$, precipitates as a green powder when oxalic acid or alkali-metal oxalate solutions are added to nickel(II) salt solutions. When heated in vacuum, it evolves water at 150 °C and decomposes completely at 300 °C, giving finely divided nickel suitable for use in catalysis or in the production of nickel carbonyl.

12.17.3 Analysis

The classical analytical method for nickel in solution is gravimetric, by precipitation of the red complex with butanedione dioxime (dimethylglyoxime). Other methods include electrodeposition, EDTA titration, and the standard spectroscopic methods of atomic absorption, flame emission, inductively coupled plasma optical emission, and X-ray fluorescence. There is a standard analytical method for nickel in biological tissue [140].

12.17.4 Economic Aspects

In general, nickel compounds cost the London Metal Exchange (LME) price for the contained nickel, plus a premium based on the

production cost. However, companies producing nickel compounds, particularly nickel sulfate, as a by-product of other processes are more flexible in their pricing.

The LME three-month nickel price decreased during the first part of the 1980s from about \$3 per pound in 1980 to below \$2 per pound in 1986. The price then rose to over \$5.50 per pound in 1988, but has since decreased.

12.17.5 Toxicology

12.17.5.1 Distribution in the Environment

Nickel is contained as a trace element in the soil in the lattices of iron and aluminum silicates, and the content is inversely proportional to the silicic acid content. At 40% or less of SiO_2 in the soil there is ca. 1600 g Ni/t while at 80% or more it is only 3 g Ni/t [141]. Nickel contents of 1–5 $\mu\text{g Ni/L}$ are generally found in surface waters, but values as high as 264 $\mu\text{g Ni/L}$ have been recorded. Plants generally contain 0.3–4 mg Ni/kg, and animals 0.1–3 mg Ni/kg (both dry weight). Atmospheric nickel in the United States averages 6 ng Ni/m^3 (nonurban) and 20 ng Ni/m^3 (urban), while 15.8 ng Ni/m^3 has been observed near primary sources [142]. The major part is in the form of sulfates and oxides and results from burning of fossil fuels and industrial activity [143].

Ingestion. The normal Western diet contains 150–600 $\mu\text{g Ni/d}$, derived primarily from its being a natural trace constituent of many food stuffs (e.g., cocoa contains 9800 $\mu\text{g Ni/kg}$) [144] and secondarily during food processing, which frequently involves nickel-containing equipment. Although no specific function for nickel has been established in animals, dietary induced nickel deficiency has been observed experimentally [145].

12.17.5.2 Ecotoxicity

Plant Life. Nickel is an essential element for certain types of plant, for example, legumes. Nickel-tolerant plants with nickel contents up to 1.35% dry weight occur in some serpentine soils, and hyperaccumulators indicate nickel-rich soils. Nickel is also toxic to plant life; the effective dose that produces a 50% reduction in normal growth depends upon the species (e.g., for rye grass it is 0.18 ppm and for alfalfa, 5 ppm) [146]. Sewage sludge containing a high level of nickel can be harmful when spread on soil because of the persistence of the metal and the difficulty of its removal.

Aquatic Toxicity. Results of acute toxicity tests depend upon the aquatic species, test conditions, and the solubility of the nickel compound under test. For example the LC_{50} for rainbow trout at a water hardness of 100 mg/L is 0.05 mg Ni/L [147].

12.17.5.3 Mammalian Toxicology

Human Carcinogenesis. The first suspicion that nickel might cause respiratory cancer followed the occurrence of a nasal cancer in a Welsh refinery worker in 1923 [148]. Subsequent observations of excess nasal and pulmonary cancers at this and other refineries (in Ontario, Canada; Kristiansand, Norway; and the former Soviet Union) resulted in suspicion falling on the high-temperature roasting of nickel-copper matte or impure nickel subsulfide or on nickel oxide, but there was no supporting evidence of any similar risk in other refining operations or in the nickel-using industries. This subject has been extensively reviewed by the International Committee on Nickel Carcinogenesis in Man, (ICNCM) [149], which updated the existing studies and evaluated the collective results. Exposures to high levels of sulfidic and oxidic nickel (especially nickel subsulfide and nickel copper oxide) were found to be implicated as well as impure soluble nickel compounds such as nickel sulfate in the Norwegian and Welsh refineries. However, at each facility where nickel sulfate exposure was associated with

excess cancer, there were also exposures to other substances. The ICNCM concluded that more than one form of nickel gave rise to respiratory cancer in men employed at the refineries considered in the study and "the respiratory cancer risks were primarily related to exposure to soluble nickel at concentrations in excess of 1 mg Ni/m³ and to less soluble forms at concentrations greater than 10 mg Ni/m³". The ICNCM found that:

- There was an absence of any evidence of hazard from metallic nickel,
- There was no substantial evidence that occupational exposure to nickel or any of its compounds was likely to produce cancer other than in the lung or nose,
- The few small excesses that were observed in cohorts with excess lung or nasal cancer could be attributed to misdiagnoses (bone and pharynx) or to chance (prostate).

The group also considered that the risk to the general population from exposure to < 1 µg Ni/m³, in the ambient air, is minute or non-existent.

Experimental Carcinogenesis. Experiments have been carried out in vivo and in vitro to establish the carcinogenicity of nickel and its compounds. A variety of routes of administration and animal species have been involved. The National Toxicological Programme in the United States is currently conducting a major inhalation bioassay on rodents, using nickel subsulfide, nickel oxide, and nickel sulfate [150]. Existing studies have been extensively reviewed [151–155]. An IARC review and assessment was published in 1990 [156]. SUNDERMAN [157] suggested that the ability of nickel to enter the target cell and release ions is the major determinant in carcinogenicity. This may occur by endocytosis, transmembrane diffusion, or the Ca²⁺ transport route. Having reached the target tissue the nickel ion may act by:

- Direct genotoxic mechanisms,
- Tumor promotion by blocking cell-to-cell communications,

- Enhancing tumor progression by inhibiting natural killer cell activity.

These processes can be modified by manganese and magnesium. Toxicity is related partly to the concentration of nickel reaching the intracellular tissues but also to the ability of cells to phagocytose less soluble particles.

Species Specific Carcinogenesis. Nickel subsulfide has been shown to be highly carcinogenic to rats by injection into a variety of tissues [158]. There is also a single positive inhalation study [159] and a dose-related positive intratracheal study in female rats [160]. The crystalline form was positive in in vitro tests [161]. There is some evidence of mutagenic potential of nickel sulfide in vitro but not in vivo [152].

The data for *nickel oxide* are less clear cut. The biological activity of nickel oxide is related to the temperature of its formation [154]; nevertheless, an inhalation study with high exposures (53.2 mg/m³) to the more reactive black form failed to produce a carcinogenic response [162]. Cell transformation studies with nickel oxide have given marginally weak positive results [152].

Metallic nickel dust has come under suspicion as an animal carcinogen but to date no adequate inhalation data have been produced [151]. Using intratracheal and intraperitoneal injections of metallic nickel powder, as well as a variety of nickel compounds and nickel alloys in female rats, POTT and coworkers [160, 163] obtained positive results, but intratracheal instillation of nickel metal and alloys in hamsters was negative [164].

The carcinogenicity of soluble nickel salts has also been studied and is currently of particular interest in view of the findings of the ICNCM [149]. In vitro studies involving nickel sulfate proved negative in the Syrian hamster embryo test but positive in cell transformation assays [165].

Allergenicity. Nickel contact dermatitis is a well recognized clinical entity [166]. In Denmark, 10% of women and 2% of men are known to be sensitized and similar results have come from elsewhere. Sensitization is

due to nickel-containing articles coming into contact with the skin. Persons who are sensitized can exhibit local or general cutaneous reactions. These can arise from external contact and may be exacerbated by internal exposure to nickel in food or prosthetic devices. Persistent hand eczema may occur. Recent studies have indicated that sensitization can be avoided by the use of alloys that are resistant to corrosion by sweat, and legislation has been effected in Denmark to eliminate the use of leachable alloys next to the skin (Decree 88/0088DK). Primary nonallergic skin irritation may occur from the handling of solutions of soluble nickel salts as in plating.

Pulmonary sensitization has occurred in a few workers exposed to aerosols of soluble nickel salts, generally the sulfate [132], which may also cause nasal irritation and epistaxis.

Acute Poisoning. Insoluble nickel is very poorly absorbed through the gastrointestinal tract and its toxicity is therefore low (Table 12.24) [167]. Human experience with soluble salts consists of death in a child who ate 5 g of nickel sulfate [152] and illness lasting a few days in workers who accidentally drank water contaminated with 1.63 g/L of soluble nickel (total dose of 0.5–2.5 g Ni) [168].

Table 12.24: Acute toxicity of nickel compounds in Sprague-Dawley rats, mg/kg [167].

Substance	LD ₅₀ , male	LD ₅₀ , female	Combined response	
			LD ₅₀	CI ^a
NiCl ₂ ·6H ₂ O	210	175	200	186–214
NiO, black, acid soluble	> 5000	> 5000	> 5000	
NiO, green, high temperature	> 5000	> 5000	> 5000	
Nickel powder	> 9000	> 9000	> 9000	
Ni ₃ S ₂	> 5000	> 5000	> 5000	
NiSO ₄ ·6H ₂ O	325	275	300	201–399
Ferronickel (30% Ni)	> 5000	> 5000	> 5000	
Ni(OH) ₂	1500	1700	1600	1176–2024
NiS, amorphous	> 5000	> 5000	> 5000	
NiCO ₃ ·xH ₂ O	1305	840	1044	822–1281
Ni(NH ₄) ₂ (SO ₄) ₂	440	400	420	340–1281
Ni ₃ As ₂	5840	6800	6300	5140–7470

^a CI = 95% Confidence interval.

Chronic Pulmonary Changes. Very high exposure to dust containing nickel oxide resulted in pneumoconiosis in hamsters. Lower exposures to soluble nickel and nickel metal powder caused injury to lung tissue at the macro- and microscopic levels. No clear evidence has been produced to suggest that pneumoconiosis or chronic bronchitis result from human exposure [132]. Nickel sulfate has also been shown to cause inflammatory reactions in lung tissue and olfactory epithelium in rats at concentrations of ca. 0.1 mg Ni/m³ [169].

12.17.5.4 Nickel Carbonyl Poisoning

Acute Poisoning. Exposure to nickel carbonyl gas is most likely to occur in accidental situations at refineries using the carbonyl process or in research laboratories. Accidents have occurred when carbon monoxide was passed over reduced, finely divided nickel at ambient temperature in catalyst manufacture and in some plating operations.

Poisoning by nickel carbonyl is characterized by a two-stage illness. The first consists of headaches, malaise, and pain in the chest lasting a few hours; this is generally followed by a short remission. The second phase starts after ca. 16 h. Symptoms of cough, breathlessness, and extreme fatigue characterize this chemical pneumonitis, which reaches its greatest severity in about four days. Death may result from cardiorespiratory or renal failure. Convalescence is often extremely protracted and is often complicated by depression, exhaustion, and dyspnea on exertion. Permanent respiratory damage is unusual. The severity of an exposure is established by the clinical findings and by monitoring urinary nickel [170]. Oxygen therapy in the early stages reduces the severity of any pulmonary edema. Sodium diethyldithiocarbamate chelates nickel and is used as a therapeutic agent. In practice its biological analogue, disulfiram (Antabuse) is more readily available and is an effective drug. Treatment (250 mg–1 g) should be started as soon as possible after exposure and accompanied by in-

haled and systemic steroids in order to minimize pulmonary toxic reactions [171]. Oxygen therapy may be indicated.

Carcinogenicity. There is debate about the carcinogenicity of nickel carbonyl gas [172]. However, since in modern refineries ambient levels are maintained below the local limit of detection (Section 12.17.5.5) in order to avoid acute effects, such debate is of no practical significance. Furthermore, epidemiological

data from the Clydach Refinery indicate that the cancer risk there was associated with the exposure to dust involved in the refining process rather than nickel carbonyl [173].

Teratogenicity. SUNDERMAN exposed rats to nickel carbonyl early in pregnancy and 28% were born with ocular abnormalities [174]. No similar effect has been noted with other nickel compounds.

Table 12.25: Labelling, limit values and legislation for nickel. Numbers within braces refer to notes following in the text.

	EC directives	EC member states (special rules)	United States	Canada
Occupational exposure limit	No figures yet; however, note directive 88/C34/03 ⁽¹¹⁾	Germany ⁽¹²⁾ 0.5 UK ⁽¹³⁾ 0.5 France 0.5 1 ⁽¹⁴⁾ 0.1 0.1 0.1 0.1 ⁽¹⁴⁾ 0.7 0.05 0.3 0.007 ^(14, 5)	Nil specific ⁽¹⁰⁾	e.g., Ontario ⁽⁵⁾ 1 0.1 0.35
General Atmospheric Emission	Air pollution from industrial plants; EC 84/360 ⁽⁷⁾	TALuft 1 mg/m ³ ⁽¹⁸⁾ UK 5 mg/m ³ ⁽¹⁹⁾	Nil specific ⁽¹⁰⁾	e.g., Ontario ⁽¹¹⁾ 5 µg/m ³
Level in drinking water ⁽¹²⁾	EC 80/778 ⁽¹³⁾ 50 µg/L	Applicable throughout EC ⁽¹⁴⁾	Guidance limit 0.15–1 mg/L SDWA 1986 ⁽¹⁵⁾	CWQG ⁽¹⁶⁾
Effluent discharge ⁽¹⁷⁾	EC 76/464 8–100 µg Ni/L ⁽¹⁸⁾ Sewage sludge EC 86/278 ⁽¹⁹⁾	UK The Red List, local consent 5.0 mg/L ⁽²⁰⁾ Germany 0.3 mg/L	Site consents daily max. 3.98 mg/L CWA ⁽²¹⁾	0.5 mg/L ⁽²²⁾ 1 mg/L ⁽²³⁾
Labelling requirements and subsequent amendments	EC 67/548 ⁽²⁴⁾ 79/831 83/467 90/C33/03	Germany Nickel powder and some insoluble Ni compounds require "cancer" label for inhalable forms ⁽²⁵⁾	Yes HCR 29CFR 7 ⁽²⁶⁾	Yes WHIMIS ⁽²⁷⁾
Importing and shipping rules	International rules IMDG Code 25A ⁽²⁸⁾ ADR (Road) ⁽²⁹⁾ Hazardous waste 86/279 ⁽³⁰⁾	Applicable throughout EC	TSCA Includes Ni ⁽³¹⁾ Dept. of Trade Regulations	Transport of Dangerous Goods Act IMDG Code
Industrial disease compensation	Commission recommendation 90/326/EC	UK Social Security Act Nickel refining 22a&b Nickel carbonyl C14 ⁽³²⁾ France = Matte roasting ⁽³³⁾	Workers Compensation & Common Law	Each province has specific Workers Compensation Acts
Emergency planning and right to know	Directive EC 82/501 amended; trigger at 1 t of Ni oxides, sulfides, and carbonates present as powders ⁽³⁴⁾	Applicable throughout EC	Superfund and right to know; nickel listed ⁽³⁵⁾ NIEHS 1989 report ⁽³⁶⁾	No right to know requirements

Notes for Table 12.25:

1. Directive 88/C34/03 (Carcinogens) relates to certain nickel refining processes.
2. MAK: Maximale Arbeitsplatzkonzentrationen 1989. In Germany preventive measures have to be taken at action levels below these limits.
3. EH 40/90 of the Health & Safety Executive. These are maximum values and it is necessary to get as far below them as it is reasonably practicable. For Ni(CO)₄ this is a 10 min short-term exposure limit.

4. OSHA Permissible Exposure Limits 29CFR (1910.1000).
5. ACGIH (American Conference of Governmental Industrial Hygienists) propose reduction of Threshold Limit Values (TLVs) to 0.05 mg/m³.
6. ACGIH figures generally used in Canada, the provinces make own rules.
7. Directive 84/360 (Air Pollution from Industrial Plants).

8. German regulations Technische Anleitung zur Reinhaltung der Luft (TA Luft of 27. February 1986) applicable to Belgium and Holland.
9. Notice on best practical means; Jan. 1988.
10. Environmental Protection Agency — nil specific for Nickel, some states have specific levels.
11. Ontario Environmental Pollution Act. Regulation 308 Schedule I (half hour average).
12. Sayre I. M. International Standards for Drinking Water J. American Water Works Association 80(1):53–60 January 1988.
13. Directive 80/778 Drinking Water Directive.
14. United Kingdom Control of Pollution Act 1974 Part II.
15. Safe drinking water regulations 1986 Amendments. No standard set yet — guidance only.
16. Canadian water quality guidelines. Canadian Council of Resource & Environment March 1987.
17. Technical Report of Environmental Aspects of the Metal Finishing Industry, p. 53–57.
18. Nickel is a Class II material requiring legislation. Member states to make their own rules. Directive 76/464 (Pollution to the Aquatic Environment).
19. Directive 86/278 (environment, soil, sewage sludge) limits nickel in soil to 30–75 mg/kg and in sewage sludge to 300–400 mg/kg.
20. Water and the Environment DOE circular 7/89 of 30.3.1989.
21. Clean Water Act (Public Law 92-217) 1977.
22. Canadian Fisheries Act: Metal mining liquid effluent regulations.
23. Control of Industrial Water Discharge; Ontario.
24. Directive 67/548 (Classification packaging and labelling) has many amendments: the 7th is near adoption.
25. UK Classification, Packaging and Labelling of Dangerous Substances Regulations 1978. Similar rules in all European states. FRG Gefahrstoffverordnung: Inhalable nickel powder "may cause cancer".
26. Hazard Communication rule 29CFR7. Title 49 Transportation — Rules for packaging of Ni Powder.
27. Workplace Hazardous Materials Information System (WHIMIS).
28. International Marine Dangerous Goods Code.
29. European Agreement of International Carriage of Dangerous Goods by Road. HMSO 1985.21.
30. Directive 86/279. Transfrontier shipment of hazardous waste — amended 89/C9/01.
31. Toxic Substances Control Act TSCA. Nickel and many of its compounds are subject to TSCA and Section 5 requires the importer to comply with special rules and orders.

32. UK Social Security Act 1945. Industrial Diseases.
33. France: Tableaux de maladies professionnelles 37, 37 bis et 37 ter — 1987.
34. Directive 82/501 (Major Accident Hazards) amended as 88/C119/02. One tonne of nickel etc. in the form capable of causing a major accident hazard.
35. Title III Superfund amendments and reauthorisation Act (SARA); nickel listed in Section 3.13.
36. National Institute of Environmental Health Sciences 5th Annual Report on Carcinogens Summary 1989 NTP 89-239 Nickel pp. 187–192 (Legislation p. 192).
XX Others relevant EEC Directives with bearing upon nickel included are Major Accident Hazard and Amendments 88/610.
Protection of Water from Dusts related to Chemicals, Physical and Biological Agents at Work 88/842.

12.17.5.5 Legislation

Prevention of cancer in nickel workers is directed at maintaining occupational exposure as low as is reasonably practicable. This is achieved by the standard hierarchy of control measures: enclosure, wet methods of handling, exhaust ventilation, respiratory protection, and atmospheric monitoring. Biological monitoring is considered to be of little value [175].

Table 12.25 lists various legislative controls and where appropriate the relevant limit values. The notes attached to this table give the relevant authority.

Nickel is currently the subject of legislative activity in the EC and member states and also in the United States and considerable revision of these rules and limit values is likely to take place within the foreseeable future. The Directorate General XI (DGXI) of the EC is currently deciding on classification of pure substances. DGIII has responsibility for mixtures including alloys while DGV is involved in workplace safety and occupational exposure limits. In the United States the EPA is setting standards for nickel in the general atmosphere and water, and the ACGIH has proposed reduction of the TLV to 50 µg Ni/m³.

12.18 References

1. J. K. Boldt, P. E. Queneau: *The Winning of Nickel*, Longmans Canada, Toronto 1967.
2. *Gmelin*, system no. 57, part A11, p. 1.
3. F. B. Howard-White: *Nickel, An Historical Review*, Methuen, London 1963.
4. Gesellschaft Deutscher Metallhütten und Bergleute e.V.: *Symposium über Nickel*, Wiesbaden 1970.
5. G. P. Tyroler, C. A. Landolt (eds.): *Extractive Metallurgy of Nickel and Cobalt*, The Metallurgical Society of AIME, Warrendale, PA, 1988.
6. E. Ozberk, S. W. Marcuson (eds.): *Nickel Metallurgy*, vol. 1: "Extraction and Refining of Nickel", The Metallurgical Society of CIM, Montréal, Québec, 1986.
7. D. J. I. Evans, R. S. Shoemaker, H. Veltman (eds.): *International Laterite Symposium*, SME-AIME, New York 1979.
8. Y. Ogura, I. Doi (eds.): "Proceedings of International Symposium on Laterite", *Int. J. Miner. Process.* **19** (1987) 1-4.
9. K. E. Volk: *Nickel und Nickellegierungen*, Springer Verlag, Berlin 1970.
10. W. Betteridge: *Nickel and its Alloys*, MacDonald and Evans Ltd., Plymouth, United Kingdom 1977.
11. C. J. Smithells: *Metals Reference Book*, 5th ed., Butterworths, London 1976.
12. D. Nicholls: *The Chemistry of Iron, Cobalt, and Nickel*, Pergamon Texts in Inorganic Chemistry, vol. 24, Pergamon Press, Oxford 1975.
13. W. S. Kirk: "Mineral Commodity Summaries 1989: Nickel", *U.S. Bur. Mines, Miner. Inf. Office*, Washington, D.C., 1989.
14. H. J. Roorda, P. E. Queneau, *Trans. Inst. Min. Metall. Sect. C* **82** (1973) 79-87.
15. R. A. Alcock in [5, pp. 67-89].
16. Inco Ltd., *First Quarter Report*, Toronto 1978.
17. T. D. Ellison: *Mining Annual Review - 1983*, London 1984, p. 68.
18. H. J. Roorda in [4, pp. 41-48].
19. H. S. Mashanyare, M. J. Storey in [6, pp. 13-36].
20. J. M. Toguri, *Can. Metall. Q.* **14** (1975) no. 4, 323-338.
21. A. N. Kerr, W. B. Kipkie: "Recent Developments at Inco's Copper Cliff Milling Complex", *TMS-AIME Extractive and Process Metallurgy Meeting*, San Diego, CA, 1985.
22. R. Fish, *Can. Min. J.* **99** (1979) no. 5, 25-69.
23. Falconbridge Ltd., *Annual Report*, Toronto 1983.
24. R. R. Hoffman, G. H. Kaiura: "Smelting Process Update at Falconbridge Limited - Sudbury Operations", *114th TMS-AIME Annual Meeting*, New York 1985.
25. T. J. Bruce, R. G. Orr in [6, pp. 57-94].
26. B. J. Elliot, K. Robinson, B. V. Stewart in H. Y. Sohn, D. E. George, A. D. Zunkel (eds.): "Advances in Sulfide Smelting", vol. 2, *TMS-AIME*, Warrendale, PA 1983, p. 875.
27. S. Heimala, M. Himmi, S. Jounela, M. Saari in [6, pp. 37-56].
28. C. S. Simolls, *J. Met.* **23** (1971) no. 11, 48-58.
29. C. M. Diaz et al. in [5, pp. 211-239].
30. C. M. Diaz et al., *J. Met.* **40** (1988) no. 9, 28-33.
30. E. Ozberk, S. A. Gendron, G. H. Kaiura in [6, pp. 304-319].
31. C. A. Landolt, J. C. Taylor in J. C. Taylor, H. R. Traulsen (eds.): "World Survey of Non-Ferrous Smelters", *TMS-AIME*, Warrendale, PA 1987.
32. Canada's Non Ferrous Metals Industry: *Nickel and Copper*, Energy Mines and Resources Canada, Ottawa 1984.
33. T. R. Ingraham, R. Kerby, *Can. Metall. Q.* **6** (1967) no. 2, 89.
34. W. Schabas, *Can. Min. J.* **98** (1977) no. 5, 10-81.
35. R. G. Orr, A. E. M. Warner: "Fluid Bed Roasting in the Thompson Smelter", *13th CIM Annual Conference of Metallurgists*, Toronto, Ontario 1974.
36. B. R. Conard et al. in [6, pp. 222-246].
37. Y. Austin Chang, Ker Chang Hsieh in [6, pp. 248-276].
38. S. L. Lee, J. M. Larrain, H. H. Kellogg, *Metall. Trans. B* **11B** (1980) June, 251-255.
39. J. A. Blanco, T. N. Antonioni, C. A. Landolt, G. J. Danyliw: "Oxyfuel Smelting in Reverberatory Furnaces at Inco's Copper Cliff Smelter", *50th Congress of the Chilean Inst. Min. Metall. Eng.* Santiago, Chile 1980.
40. T. N. Antonioni, J. A. Blanco, C. A. Landolt, W. J. Middleton: "Energy Conservation at Inco's Copper Cliff Smelter", *114th TMS-AIME Annual Meeting*, New York 1985.
41. J. A. Blanco, T. N. Antonioni, C. A. Landolt, C. M. Mitchell: "Productivity Improvements at Inco's Copper Cliff Smelter", *115th TMS-AIME Annual Meeting*, New Orleans, LA 1986.
42. T. N. Antonioni, A. Dutton, C. A. Landolt, A. Vahed: "Recent Developments in the Operation of Nickel Converters at Inco's Copper Cliff Smelter", *23rd CIM Annual Conference of Metallurgists*, Québec City, Québec 1984.
43. J. W. Matousek, *CIM Bull.* **76** (1983) no. 856, 86-90.
44. R. G. Telewiak: "Canadian Nickel Mission to the U.S.S.R.", (Sept. 1988), *Energy Mines and Resources Canada*, Ottawa 1990.
45. J. C. Mostert, P. N. Roberts, *TMS-AIME Pap.* **A73-48** (1973).
46. A. L. McKague, G. E. Norman, *CIM Bull.* **77** (1984) no. 866, 86-92.
47. G. E. Norman, R. E. Michelutti, *CIM Bull.* **77** (1984) no. 866, 93-98.
48. *Outokumpu News* **15** (1978) no. 3, 3-6.
49. "Outokumpu's Nickel Technology", *Met. Monthly* **157** (1984) Jan, 53-60.
50. C. J. D. Williams in *Extraction Metallurgy '81*, Inst. Min. Metall. London 1981, p. 214.
51. C. W. Hastie, D. R. Hall, C. A. Hohnen, J. M. Limerick: "Kalgoorlie Nickel Smelter: Integration of Flash Smelting and Slag Cleaning within one Process Unit", *Aust. IMM Symposium on Extractive Metallurgy*, Melbourne 1984.
52. T. M. Young, W. P. Imrie: "Energy Developments in Nickel-Copper Smelting for Minimum Dependence on Oil Fuel", *109th TMS AIME Annual Meeting*, Las Vegas, NV 1980.
53. J. Asteljoki, J. Sulanto, T. T. Talonen in M. J. Jones, P. Gill (eds.): *Mineral Processing and Extractive Metallurgy*, Inst. Min. Metall., London 1984, pp. 171-185.
54. J. S. Diakow, Y. F. Mak, R. G. Orr: "Metallurgy of the Converting Process in the Thompson Smelter", *14th CIM Annual Conference of Metallurgists*, Edmonton, Alberta 1975.
55. R. J. Neal, R. A. Reyburn in R. E. Johnson (ed.): "Copper and Nickel Converters", *TMS-AIME*, New York 1979, pp. 167-184.
56. A. A. Bustos et al. in [5, pp. 335-354].
57. S. S. Wang, N. H. Santander, J. M. Toguri, *Metall. Trans. B* **5** (1974) Jan., 261-265.
58. H. H. Kellogg in [6, pp. 95-128].
59. P. E. Queneau, R. Schumann, Jr, US 3941587, 1976.
60. M. Y. Solar, R. J. Neal, T. N. Antonioni, M. C. Bell, *J. Met.* **31** (1979) no. 1, 26-31.
61. M. C. Bell, J. A. Blanco, H. Davies, P. Garritsen, *CIM Bull.* **83** (1990) no. 933, 47-50.
62. W. Curlock: "Fluid Bed Roasting of Nickel Sulfide", *62nd CIM Annual Central Meeting*, Toronto, Ontario 1960.
63. D. G. E. Kerfoot, D. R. Weir in [5, pp. 241-270].
64. F. A. Forward, US 2576314, 1951.
65. V. N. Mackiw, H. Veltman: "Recovery of Metals by Pressure Hydrometallurgy - The Sherritt Technology", *Int. Min. Exhibition and Conference*, Calgary, Alberta 1980.
66. R. J. E. Stewart, J. L. Nixon, J. D. G. Groom: "Recovery of Nickel in Zimbabwe from Mixed Nickel Copper Sulfides by Outokumpu Technology", in *Mining and Metallurgical Operations in Zimbabwe*, Harare, Zimbabwe 1983, vol. IV, 457-485.
67. P. Koskinen, M. Virtanen, H. Eerola in [5, pp. 355-372].
68. R. P. Plasket, S. Romanchuk, *Hydrometallurgy* **3** (1978) 135-151.
69. C. F. Brugman, D. G. Kerfoot in [6, pp. 512-531].
70. J. L. Blanco, *World Min.* **31** (1978) March, 80-82.
71. Z. R. Llanos, P. E. Queneau, R. S. Rickard, *CIM Bull.* **67** (1974) no. 742, 75-81.
72. R. P. Plasket, G. M. Dunn in J. E. Dutrizac, A. J. Monhemius (eds.): *Iron Control in Hydrometallurgy*, Ellis Harwood, Chichester, United Kingdom 1986, pp. 695-718.
73. E. O. Stensholt, H. Zachariasen, J. H. Lund, P. G. Thornhill in [5, pp. 403-412].
74. P. Lenoir, A. van Peteghem, C. Feneau, *Proc. Int. Conf. Cobalt: Metall. Uses* **1981** 51-62.
75. S. Walker, *Int. Min.* **6** (1989, Nov.) 18-21.
76. M. L. Goble, J. A. Chapman in [6, pp. 464-480].
77. T. Inami, Y. Ishikawa, N. Tsuchida, T. Sugiura in [5, pp. 413-427].
78. D. G. E. Kerfoot in [6, pp. 426-441].
79. P. E. Queneau, C. E. O'Neill, A. Illis, J. S. Warner, *J. Met.* **21** (1969) no. 7, 35-45.
80. M. D. Head, V. A. Englesakis, B. C. Pearson, D. H. Wilkinson: "Nickel Refining by the TBRC Smelting and Pressure Carbonyl Route", *105th TMS-AIME Annual Meeting*, Las Vegas, NV 1976.
81. L. G. Wiseman, R. A. Bale, E. T. Chapman, B. Martin in [5, pp. 373-390].
82. P. M. Tyroler, T. S. Sanmiya, E. W. Hodkin in [5, pp. 391-402].
83. T. Watanabe, S. Ono, H. Arai, T. Matsumori in [8, pp. 173-187].
84. A. A. Dor (ed.): *Nickel Segregation*, TMS-AIME, New York 1972.
85. A. S. Ericksen, J. Svensson, K. Ishii in [8, pp. 223-236].
86. C. S. Simons in [5, pp. 91-134].
87. A. A. Dor, H. Skretting in [7, pp. 459-490].
88. M. de Vernon in J. N. Anderson, P. E. Queneau (eds.): *Pyrometallurgical Processes in Non-Ferrous Metallurgy*, TMS, vol. 39, Gordon and Breach, New York 1967.
89. *SLN Bull.* **1** (1976) 1.
90. T. T. Toomver in [7, pp. 252-271].
91. R. Musu, J. A. E. Bell in [7, pp. 300-322].
92. J. D. Guiry, A. D. Dalvi in [8, pp. 199-214].
93. M. C. Bell, W. P. Clement, *CIM Bull.* **83** (1990) no. 933, 57-59.
94. M. D. Sopko in [7, pp. 272-291].
95. R. Hoppe, *Eng. Min. J.* **178** (1977) no. 11, 123-126.
96. J. G. Reid in [7, pp. 368-381].
97. *Min. J. (London)* **313** (1989) July 7, 3.
98. D. R. Weir, V. B. Sefton in [7, pp. 325-345].
99. N. Colvin, J. W. Gulyas in [7, pp. 346-356].
100. *Met. Week* **58** (1987) August 31, 2.
101. Henkel Corp., *Tech/News* **1** (1988) 1.
102. J. G. Reid in [5, pp. 325-334].
103. L. C. Rodriguez, *Min. Cuba* **2** (1976) no. 3, 42-49.
104. S. L. Sobol et al., *Min. Cuba* **3** (1977) no. 2, 2-18.
105. M. C. Pestana, G. G. Lahens, *Revista Tecnológica* **19** (1989) no. 1, 52-56.
106. P. T. O' Kane in [7, pp. 503-523].
107. W. P. C. Duyvesteyn, G. R. Wicker, R. E. Doane in [7, pp. 553-570].
108. G. R. Wicker, M. C. Jha in [6, pp. 566-577].
109. D. Urbain, J. P. Dutierque, P. Palanque, P. Rey in [6, pp. 578-596].
110. E. Ozberk, S. W. Marcuson (eds.): *Nickel Metallurgy*, vol. II: "Industrial Applications of Nickel", The Metallurgical Society of CIM, Montréal, Québec 1986.
111. P. G. Chamberlain in [110, pp. 193-215].
112. Inco Ltd., *Annual Reports*, Toronto 1977 and 1978.
113. Falconbridge Ltd., *Annual Report*, Toronto 1986.
114. I. D. Corrick: *Nickel Mineral Commodity Profiles* (May 1979), U.S. Bureau of Mines, Washington, D.C., 1979.
115. M. O. Pearce in [8, pp. 5-14].
116. J. P. Schade in [110, pp. 1-16].
117. E. A. Thiers in [5, pp. 21-31].
118. J. P. Schade, M. O. Pearce in [5, pp. 53-63].
119. *Mining Annual Review*, 1989, C 73.
120. Metal Statistics 1995, Nonferrous Edition, 87th Edition, American Metal Market, Chilton Publications, New York, NY, 1995, pp. 297-310.
121. J. P. Schade, *Stahl Eisen* **109** (1989) 539-542.
122. J. Mellor: *A Comprehensive Treatise on Inorganic and Theoretical Chemistry*, vol. 15, Longmans, Greens and Co., London 1936, pp. 1-497.
123. *Gmelin*, system no. 57, part B 2.
124. D. Nicholls in J. C. Bailar, H. J. Emeleus, R. Nyholm, A. F. Trotman-Dickenson (eds.): *Comprehensive Inorganic Chemistry*, vol. 3, Pergamon Press, Oxford 1973, pp. 1109-1162.

125. E. R. Braithwaite in R. Thompson (ed.): *Speciality Inorganic Chemicals*, RSC special publication 40, 1981, pp. 375–402.
126. L. Sacconi, F. Mani, A. Bencini in G. Wilkinson, R. D. Gillard, J. A. McCleverty (eds.): *Comprehensive Coordination Chemistry*, vol. 5, Pergamon Press, Oxford 1987, pp. 1–347.
127. G. C. Bond, J. B. P. Tripathi, *J. Chem. Soc. Faraday Trans. 73* (1977) 545–552.
128. T. E. Girich, A. K. Buchinskii, *Zh. Prikl. Khim. (Leningrad)* 59 (1986) 884–886.
T. E. Girich et al., *Zh. Neorg. Khim.* 31 (1986) 1575–1577.
T. E. Girich et al., *Vopr. Khim. Khim. Tekhnol.* 82 (1986) 60–63.
129. Y. Monteil, P. Raffin, J. Bouix, *Thermochim. Acta* 125 (1988) 327–346.
130. F. Boix et al., *Synth. Commun.* 17 (1987) 1149–1153.
131. L. G. Wiseman, *Weld. J. (Miami)* 68 (1989) 192–197.
132. P. M. Hout, A. Van der Waal, F. Langeweg, *Anal. Chim. Acta* 136 (1982) 421–424.
133. P. W. Jolly, G. Wilke: *The Organic Chemistry of Nickel*, vol. 1, Academic Press, New York 1974.
134. P. W. Jolly in G. Wilkinson, F. G. A. Stone, E. W. Abel (eds.): *Comprehensive organometallic Chemistry*, vol. 6, Pergamon Press, Oxford 1982, pp. 1–36.
135. *The Sigma-Aldrich Library of Chemical Safety Data*, ed. 11, vol. 11, Sigma Aldrich Corporation, 1988.
136. D. Nicholls in: *Comprehensive Inorganic Chemistry*, vol. 4, Pergamon Press, Oxford 1973, p. 1149.
137. P. W. Jolly in: *Comprehensive Organometallic Chemistry*, vol. 8, Pergamon Press, Oxford 1982.
138. P. W. Jolly, G. Wilke in: *The Organic Chemistry of Nickel*, vol. 2, Academic Press, New York 1975, p. 6.
139. A. I. Vogel: *A Textbook of Quantitative Inorganic Analysis*, 4th ed., Longman, 1978, p. 447.
140. F. W. Sunderman, Jr.: "Selected Methods of Analysis", *IARC Monogr. Environ. Carcinog.*, (1986) pp. 79–92.
141. J. O. Nriagu: *Nickel in the Environment*, Wiley Interscience, New York 1980.
142. National Institute of Environmental Health Sciences, 5th Annual Report on Carcinogens, Survey, NTP89-239 (1989) 187–192.
143. Health Assessment Document for Nickel and Nickel Compounds, EPA/600/883/012FF (1986).
144. G. Ellen, G. van den Bosch-Tibbesma, F. F. Douma, *Z. Lebensm. Unters. Forsch.* 166 (1978) 145–147.
145. T. P. Coogan, D. M. Latta, E. T. Snow, M. Costa: "Toxicity and Carcinogenicity of Nickel Compounds", *CRC Crit. Rev. Toxicol.* 19 (1989) 341–394.
146. M. E. Farago, M. M. Cole in H. Sigel, A. Sigel (eds.): *Nickel – its Role in Biology*, vol. 23, Marcel Dekker, New York 1988, p. 47.
147. P. Stokes in H. Sigel, A. Sigel (eds.): *Nickel – its Role in Biology*, vol. 23, Marcel Dekker, New York 1988, p. 31.
148. R. Doll in F. W. Sunderman, Jr. (ed.): "Nickel in the Human Environment", *IARC Sci. Pub.* 53 (1984) 3–22.
149. R. Doll: "Report of the International Committee on Nickel Carcinogens in Man", *Scand. J. Work Environ. Health* 16 (1990) no. 1.
150. J. K. Dunnick, C. W. Jameson, J. M. Benson in S. S. Brown, F. W. Sunderman, Jr. (eds.): *Progress in Nickel Toxicology*, IUPAC Blackwell Scientific Publications 1984, p. 49.
151. S. Fairhurst, H. P. A. Illing: "The Toxicity of Nickel and its Inorganic Compounds", *Toxic. Rev. HMSO* (1987).
152. ECETOC Technical Report No. 33, *Nickel and Nickel Compounds*. Review of toxicological epidemiology with special reference to carcinogens, European Chemical Industry Ecology, Toxicology Centre, Brussels 1989.
153. R. Maximilien: *Critical Review of Animal Carcinogens by Nickel and its Inorganic Compounds*, EURATOM Report No. EUR 12456 (1989).
154. F. W. Sunderman, Jr.: Final Report to the NIPERA concerning phase III of research on biological activities of nickel oxides, Farmington, CT, 1987.
155. A. Berlin, M. Draper, E. Krug, R. Roi, M. Th. Van der Venne: *The Toxicology of Chemicals*, 1st Carcinogenicity Summary of Reviews of the Scientific Evidence, vol. 2, EUR 12481 EN 199c.
156. IARC Monographs on the Evaluation of Carcinogenic Risks to Humans, vol. 49, Chromium, Nickel and Welding, IARC, Lyon 1990.
157. F. W. Sunderman, Jr.: "Mechanism of Nickel Carcinogenesis", *Scand. J. Work Environ. Health* 15 (1989) 1–12.
158. F. W. Sunderman, Jr. et al.: "Carcinogenicity of Nickel Subsulfide in Fischer Rats and Syrian Hamsters after Administration by Various Routes", *Adv. Exp. Med. Biol.* 91 (1978) 57–67.
159. D. Ottolenghi et al.: "Inhalation Studies of Nickel Sulfide in Pulmonary Carcinogenesis of Rats", *J. Nat. Cancer Inst.* 54 (1974) no. 5, 1165–1172.
160. F. Pott et al.: "Carcinogenicity Studies on Fibres, Metal Compounds and Some Other Dusts in Rats", *Exp. Pathol.* 32 (1987) 129–152.
161. M. Costa, J. D. Heek: "Specific Nickel Compounds as Carcinogens", *Trends Pharmacol. Sci.* 3 (1982) 408–410.
162. A. P. Wehner, D. K. Craig: "Toxicology of Inhaled Nickel Monoxide and Cobalt Monoxide in Syrian Golden Hamsters", *Am. Ind. Hyg. Assoc. J.* 33 (1972) 146–155.
163. F. Pott et al. in E. Nieboer, A. Aitio (eds.): *Advances in Environmental Science and Technology, Nickel and Human Health Current Perspectives*, Wiley and Sons, New York 1991 (in press).
164. H. Muhle et al. in E. Nieboer, A. Aitio (eds.): *Advances in Environmental Science and Technology, Nickel and Human Health Current Perspectives*, John Wiley and Sons, New York 1991 (in press).
165. E. Riverdal, T. Sanner: "Synergistic Effect on Morphological Transformation of Hamster Embryo Cells by Nickel Sulfate and Benzo(a)pyrene", *Cancer Lett. (Shannon, Ire.)* 8 (1980) 203–208.
166. H. I. Maibach, T. Menne: *Nickel and the Skin, Immunology and Toxicology*, CRC Press, Boca Raton, FL, 1989.
167. E. Mastromatteo: "Nickel", *Am. Ind. Hyg. Assoc. J.* 47 (1986) 589–601.
168. F. W. Sunderman, Jr., B. Dingle, S. M. Hopfer, T. Swift: "Acute Nickel Toxicity in Electroplating Workers who Accidentally Ingested a Solution of Nickel Sulfate and Nickel Chloride", *Am. J. Ind. Med.* 14 (1988) 257–266.
169. J. M. Benson et al.: "Subchronic Inhalation Toxicity of Nickel Sulfate to Rats and Mice" (abstract), *The Toxicologist* 8 (1988) 68.
170. J. G. Morgan: "A Simplified Method for the Estimation of Nickel in Urine", *Br. J. Ind. Med.* 17 (1960) 209–212.
171. S. Zincheng: "Acute Nickel Carbonyl Poisoning. A Report of 179 Cases", *Br. J. Ind. Med.* 63 (1986) 422–424.
172. *IARC Monogr. Eval. of Carcinog. Risk Chem. Man* 11 (1976) 75–112.
173. J. G. Morgan: "Some Observations on the Incidence of Respiratory Cancer in Nickel Workers", *Br. J. Ind. Med.* 15 (1958) 224–234.
174. F. W. Sunderman, Jr., K. S. K. Shen, M. C. Reid P. R. Allpass: "Teratogenicity and Embryotoxicity of Nickel Carbonyl in Syrian Hamsters", *Teratog. Carcinog. Mutagen.* 1 (1980) 223–233.
175. F. W. Sunderman, Jr., A. Aitio, L. G. Morgan, T. Norseth: "Biological Monitoring of Nickel", *Toxicol. Ind. Health* 2 (1986) 17–78.

Part Four

Secondary Metals

																		H	He
Li	Be											B	C	N	O	F	Ne		
Na	Mg	Al												Si	P	S	Cl	Ar	
K	Ca	Sc	Ti	V	Cr	Mn	Fe	Co	Ni	Cu	Zn	Ga	Ge	As	Se	Br	Kr		
Rb	Sr	Y	Zr	Nb	Mo	Tc	Ru	Rh	Pd	Ag	Cd	In	Sn	Sb	Te	I	Xe		
Cs	Ba	La [†]	Hf	Ta	W	Re	Os	Ir	Pt	Au	Hg	Tl	Pb	Bi	Po	At	Rn		
Fr	Ra	Ac [†]																	

†	Ce	Pr	Nd	Pm	Sm	Eu	Gd	Tb	Dy	Ho	Er	Tm	Yb	Lu
---	----	----	----	----	----	----	----	----	----	----	----	----	----	----

‡	Th	Pa	U	Np	Pu	Am	Cm	Bk	Cf	Es	Fm	Md	No	Lr
---	----	----	---	----	----	----	----	----	----	----	----	----	----	----

13 Arsenic

HORST GROSSMAN, KUNIBERT HANUSCH, KARL-ALBERT HERBST, GERHARD ROSE (§§ 13.1–13.9); HANS UWE WOLF (§ 13.10)

13.1 Introduction	795	13.7 Compounds	809
13.2 History	795	13.7.1 Arsenic Trioxide	809
13.3 Physical and Chemical Properties ..	796	13.7.2 Arsenous Acid	810
13.4 Occurrence	796	13.7.3 Arsenic Pentoxide	811
13.5 Production	797	13.7.4 Arsenic Acid	811
13.5.1 Production of Arsenic Trioxide	797	13.7.5 Arsenic Sulfides	813
13.5.1.1 Beneficiation	797	13.7.6 Arsenic Halides	814
13.5.1.2 Roasting of Arsenical Materials ...	799	13.7.7 Arsenic Hydride and Arsenides	814
13.5.1.3 Production of Refined As_2O_3	803	13.8 Uses and Economic Aspects.	815
13.5.2 Production of the Metal	804	13.9 Safety Measures.	816
13.6 Treatment of Arsenic-Containing By-products	807	13.10 Toxicology	817
		13.11 References	820

13.1 Introduction

Arsenic belongs to main group V of the periodic table and has an atomic number of 33. In compounds, it has oxidation states of 3+, 5+, and 3–.

Arsenic is a bright silver-gray metal. Its surface tarnishes in humid air. Arsenic forms trigonal crystals, which are brittle and of average hardness (3–4 on the Mohs scale).

In addition to the metallic modification, there are other modifications, namely, yellow arsenic and three amorphous forms (β , γ , δ) [1]. Of these, black arsenic (the β form) is the best known. Black arsenic is formed as a coating (arsenic mirror) when arsenic hydride is passed through an incandescent glass tube and also, together with other modifications, when the vapor is rapidly cooled. Yellow arsenic is formed by the sudden cooling of arsenic vapor and consists of transparent, waxy, regular crystals. It is unstable and changes into metallic arsenic on exposure to light or on gentle heating. All amorphous modifications change into the metallic form above 270 °C. Another form, brown arsenic (ρ 3.7–4.1 g/cm³), is either a special modification or simply a more finely divided form. This brown modification is obtained in the reduction of solutions of ar-

senic trioxide in hydrochloric acid with tin(II) chloride or hypophosphorous acid.

13.2 History

The natural sulfides, realgar and orpiment, were known in pre-Christian times and had already been named by ARISTOTLES and his pupil THEOPHRAST. In the first century A.D., PLINIUS mentioned sandarac (realgar) as occurring in gold and silver mines. The color of the yellow sulfide gave it the name orpiment. The Greek name $\alpha\rho\sigma\epsilon\nu\iota\kappa\omicron\nu$ (fearless, brave, manly), which was given to the sulfides on account of their reactivity with metals, derived from the custom prevailing at the time of classifying the metals as male or female. Subsequently, the name was applied to the metal itself. Many early authors described medicinal applications. DIOSKORIDES (first century A.D.) reported on the roasting of the sulfides and that they were used as remedies and artist's colors. In the fifth century A.D., OLYMPIODORUS described the production of the arsenic oxide As_2O_3 . An incomplete description of metallic arsenic dating from the fourth century has also been found. The alchemists were more closely concerned with the sulfides of arsenic. They generally called the roasted product "white arsenic". Many considered the arsenic oxide,

like sulfur, to be a basic constituent of metals. ALBERTUS MAGNUS apparently obtained the element in 1250; SCHRÖDER described two methods of preparation in 1649. In 1733, BRANDT showed that white arsenic is the oxide of the metal. The alchemists were aware of the poisonousness of white arsenic (As_2O_3). Records show that the compounds of arsenic were extensively used by the poison brewers of the Middle Ages. In the Renaissance it was PARACELSUS who pioneered the use of arsenic compounds in medicine. Arsenic acid and arsenic hydride were discovered by SCHEELÉ in 1775.

13.3 Physical and Chemical Properties

Densities: metallic arsenic 5.72 g/cm³ at 20 °C, yellow arsenic 2.03 g/cm³

Melting point: 1090 K (817 °C) at 3.7 MPa

Sublimation point: 886 K (613 °C) at 0.1 MPa

Linear coefficient of thermal expansion: ca. $5 \times 10^{-6} \text{ K}^{-1}$

Specific heat capacity: 0.329 Jg⁻¹K⁻¹ at 291 K (18 °C), 0.344 Jg⁻¹K⁻¹ on average between 273 K (0 °C) and 373 K (100 °C)

Electrical resistivity: $24 \times 10^{-6} \Omega \cdot \text{cm}$ at 273 K (0 °C)

The normal potential of arsenic with respect to the normal hydrogen electrode is ca. 0.24 V. Arsenic therefore comes between bismuth and copper in the electrochemical series.

The various forms of arsenic have different behaviors in air. Whereas the amorphous forms remain unchanged for months in dry air, the crystallized α form turns black in a few days, as originally observed by BERZELIUS. Powdered, moist arsenic is oxidized to arsenic trioxide with evolution of heat. When heated in air, it burns with a bluish-white flame, forming dense vapors of arsenic trioxide. When heated, arsenic metal gives off a characteristic garlic-like odor.

Concentrated nitric acid and aqua regia oxidize arsenic to arsenic acid; arsenic is oxidized to the 3+ state by dilute nitric acid or concentrated sulfuric acid and by boiling alkali hydroxides in air. Hydrochloric acid has little effect on arsenic. Chlorine combines fierily with arsenic to form arsenic trichloride. When the metal is heated with sulfur, AsS , As_2S_3 , or

As_2S_5 is obtained, depending on the ratios used. A mixture of fine arsenic and potassium chlorate explodes on impact.

Arsenic combines with metals to form arsenides. When subjected to oxidizing roasting, arsenides give partly metal oxide and arsenous acid and partly basic arsenates. When subjected to chloridizing roasting, they give arsenic trichloride. On heating in the absence of air, a sublimate of arsenic metal is formed from the heavy metal arsenides, although the arsenic can only be partly removed even at very high temperatures.

With oxygen, arsenic forms three oxides, namely arsenic trioxide, As_2O_3 ; arsenic pentoxide, As_2O_5 ; and As_2O_4 , which apparently contains trivalent and pentavalent arsenic alongside. The first two oxides may be regarded as acid anhydrides. Arsenous acid is derived from arsenic trioxide and can only exist in aqueous solution. Its well-known salts are the arsenates(III) (formerly arsenites). Arsenic acid is derived from arsenic pentoxide. Its salts, the arsenates, generally correspond to the phosphates in their stoichiometry. However, solid arsenic acids that correspond to the phosphorus acids are not known; instead, $\text{H}_3\text{AsO}_4 \cdot \frac{1}{2}\text{H}_2\text{O}$ or $\text{As}_2\text{O}_5 \cdot 4\text{H}_2\text{O}$ crystallizes from arsenic acid solutions.

The highly poisonous arsenic hydride, AsH_3 , is formed from arsenic compounds in acidic solution in the presence of strong reducing agents (e.g., Zn) or from suitable arsenides (e.g., As_2Zn_3) and acids.

13.4 Occurrence

Arsenic is widespread and can be detected in traces everywhere. Its abundance in the earth's crust is ca. $6 \times 10^{-4}\%$, i.e., it is roughly as abundant as molybdenum or tin, although the arsenic content of minerals is usually too low for them to have any economic significance.

Native arsenic is found in many places, but only in small quantities, usually in ores containing gold, silver, cobalt, nickel, and antimony. Although many arsenic-bearing

minerals are known, only a few occur in such quantities that they can be worked economically. The most important arsenic minerals are shown in Table 13.1. Other arsenides are chloanthite, NiAs_2 ; niccolite, NiAs ; smaltite, CoAs_2 ; cobaltite, CoAsS ; gersdorffite, NiAsS . Arsenic-bearing fahlores include inter alia tennantite, $4\text{Cu}_2\text{S} \cdot \text{As}_2\text{S}_3$; proustite, $3\text{Ag}_2\text{S} \cdot \text{As}_2\text{S}_3$. These minerals may be regarded as thioarsenites. Enargite, $3\text{Cu}_2\text{S} \cdot \text{As}_2\text{S}_5 = \text{Cu}_3\text{AsS}_4$, is a thioarsenate.

Table 13.1: Most important arsenic-bearing minerals.

	Mohs hardness	ρ , g/cm ³	Crystal system	Arsenic content, %
Arsenopyrite (FeAsS)	5.5–6	5.9–6.2	orthorh.	46
Löllingite (FeAs_2)	5–5.5	7.1–7.3	orthorh.	73
Orpiment (As_2S_3)	1.5–2	3.4–3.5	mon.	61
Realgar (AsS)	1.5–2	3.4–3.6	mon.	70
Native arsenic	3–4	5.6–5.8	trig.	90–100

13.5 Production

Most of the arsenic produced commercially accumulates as a by-product in the smelting of nonferrous metal ores containing gold, silver, lead, nickel, and cobalt.

Arsenopyrite often contains primary gold deposits. Fahlores and proustites always contain silver. Gersdorffite can accompany copper ores. Arsenopyrite and löllingite accompany pyrites [2].

Arsenic is mainly obtained from complex ores, such as enargite-containing copper, lead, and zinc ores and pyritic copper ores rich in arsenic. The arsenic content varies considerably.

Because of the volatility of arsenic sulfides and arsenic oxides, arsenic is concentrated in the gas phase. A crude oxide is produced from the intermediate products, and, after refining, is reduced to the metal or is sold as is to the chemical industry for further treatment.

The falling world demand for arsenic oxide, the increasingly elaborate treatment of complex ores, the high toxicity, and new environmental requirements have made arsenic-containing by-products a problem for many

producers. Recently, new methods have been sought to concentrate arsenic into more stable compounds or to avoid intermediate products altogether. Today arsenic is almost always an unwanted accompanying element in metallurgy.

13.5.1 Production of Arsenic Trioxide

History. Arsenic trioxide has been produced in China for 500 years in extremely simple plants, consisting of retorts with condensation chambers, from an ore containing 15% As. However, it was not until the beginning of the 18th century that a smelter for native arsenic was set up in Germany at the instigation of J. v. SCHARFENBERG in Reichenstein, Silesia. Because the demand for As_2O_3 was relatively low, it was not until the 19th century that a second country, Great Britain, began producing As_2O_3 . Thereafter, from the middle of the 19th century to 1901, Great Britain was the leading As_2O_3 producer. Production figures up to 1945 are only estimates. When legislation was introduced in various countries to avoid damage caused by release of As_2O_3 -containing fumes, world production of As_2O_3 increased considerably. The production of native arsenic was given a fresh impetus by the appearance of the boll weevil in Mexico and the United States – damage from 1909 to 1923 was estimated at \$3 billion. Calcium arsenate was used to combat the boll weevil. The demand for arsenic became so great that it exceeded supply. New plants were established, particularly in the United States and Mexico. The largest plant was operated between 1932 and 1962 by Boliden AB in Rönnskär, Sweden.

13.5.1.1 Beneficiation

The mining and dressing of ores with the primary object of recovering arsenic minerals are of little if any importance. Most arsenic raw materials are by-products from the dressing and smelting of arsenical ores. The raw materials differ widely in character: mostly

they are sulfides, often with pyrites as the principal constituent. For dressing, mixed arsenide-sulfide concentrates of very high metal content are floated, whereas the concentration of pure arsenic minerals is of secondary importance and should be avoided altogether.

The NF-metal concentrates used for the recovery of arsenic have arsenic contents from < 1% to, in exceptional cases, 10%. Table 13.2 shows As distributions in the concentrates and in the waste products, based on the As initial concentration in the ore.

In the concentration of complex ores, most of the arsenic remains in the tailings. In dressing tin ore, only 7.8% of the arsenic passes into the tin concentrate. In the case of copper and copper-zinc ores, the arsenic is concentrated in the copper concentrate to a level of around 30% of the quantity originally present in the starting ore. The copper concentrate therefore contains 0.5–1% As, and concentrates of the complex ores up to 5–8% As [3].

One example of copper ore in which a large part of the copper is bound to arsenic, as enargite or luzonite, $3\text{Cu}_2\text{S} \cdot \text{As}_2\text{S}_5$, is the Lepanto ore from the Philippines. The flotation product contains approximately 28% Cu, 32% S, and 9% As. In most ores, however, only a small proportion of the copper is bound chemically to arsenic, and the copper concentrates have a considerably lower arsenic content. Enargite-containing copper concentrates are produced in Cerro de Pasco (Peru) and Butte, Montana (USA).

In many precious metal ores, gold and silver occur together with arsenopyrite (FeAsS), löllingite (FeAs_2), and pyrites or other sulfides. Although the metals are not chemically bound to the arsenic, instead occurring as native gold and in the form of non arsenical minerals, separation by selective flotation is not satisfactory on account of a partially extensive intergrowth of the minerals. In such a case, a combined concentrate of the sulfides and arsenides – the arsenic content can vary from a few percent to more than 30% – is floated. One example is the ore from Salsigne, France, an arsenopyrite-pyrites ore containing precious metals in large quantities, some copper, and a little bismuth. The metal concentrate obtained contains ca. 23% As, 27% S, 34% Fe, 0.7% Cu, 0.6% Bi, 55 ppm Au, and 115 ppm Ag.

Arsenopyrite often occurs in pyritic copper ores, for example, on the Iberian Peninsula, in the Balkan countries, in Sweden, and in New Brunswick, Canada. The arsenopyrite can be recovered by selective flotation. Copper pyrites are removed by flotation with higher xanthates, the other sulfide minerals being held back by lime. After acidifying and heating the pulp, the pyrites and lastly, after further acidification and activation with copper sulfate, the arsenopyrite are floated. Alternatively, after flotation of the copper pyrites, the arsenopyrite may be selectively floated from the pyrites pulp after heating and activation with copper sulfate.

Table 13.2: Distribution of arsenic in the production of the concentrated raw materials (% of arsenic content in starting ore) [3].

	Complex ores	Copper and copper-zinc ores	Tin ore	Gold-bearing ore	Nickel-cobalt-bearing ore
Starting ore	100.0	100.0	100.0	100.0	100.0
Concentrates, total	15.3	41.0	17.4	35.0	1.9
Lead	7.8	—	—	—	—
Zinc	3.8	1.8	—	—	—
Copper	3.3	30.1	9.6	—	—
Pyritic	0.4	9.1	—	—	—
Tin	—	—	7.8	—	—
Gold-containing	—	—	—	35.0	—
Others	—	—	—	—	1.9
Waste products	84.7	59.0	82.6	65.0	98.1

Lead and copper concentrates rich in arsenic are produced in Mexico, South America, and South West Africa; cobalt concentrates in North Africa; and precious metal concentrates in Canada, South America, and other regions. Arsenic ores worth extracting and usable in concentrated or unconcentrated form as starting material for the production of arsenic occur in the former USSR and China.

13.5.1.2 Roasting of Arsenical Materials

Arsenic should be separated off as early as possible in the metallurgical process. Its presence in relatively large quantities complicates both pyrometallurgical and hydrometallurgical processes. Phases rich in arsenic, so-called speisses, can be formed in the reducing smelting of raw materials rich in arsenic. Because of the variety of different compositions of these speiss phases and their different solubilities in sulfide and metal melts, the speisses always lead to losses of valuable metal. Arsenic is usually unwanted in the end product metals because it adversely affects their physical properties, e.g., conductivity, and their mechanical properties, e.g., deformability [2, 4].

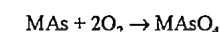
The removal of arsenic by refining is extremely difficult. Industrial safety regulations also dictate that arsenic be removed from metallurgical processes as early as possible.

The separation of arsenic by roasting is one possibility. The multivalency of arsenic, i.e., its ability to form more than one compound or complex with one and the same element, complicates separation. The final product should contain so little arsenic that it may be further processed as a quasi-arsenic-free material. To obtain a high arsenic removal rate and, hence, a high concentration of arsenic in as few processing steps as possible, the roasting processes must be conducted in such a way that only volatile arsenic compounds or volatile As_4 form. The formation of nonvolatile arsenates, i.e., arsenic remaining in the roasted material, must be avoided. The valuable metals remain in the roasted material as sulfite or ox-

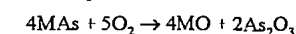
ide, depending on the starting material and the process conditions.

A relatively high oxygen partial pressure during roasting promotes the formation of metal arsenates and a poor yield of As in the flue dust. Metal arsenates are considerably more stable than the sulfates and decompose only at high temperatures.

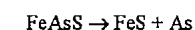
The overall course of the reaction may be written as:



At a high SO_2 partial pressure, i.e., at a low O_2 partial pressure in the roasting zone, mainly volatile arsenic oxides are formed:



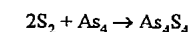
As_2S_2 and As_2S_3 are volatile at low temperatures. Arsenopyrite and similar compounds decompose:

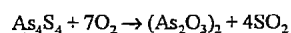


If the roasting is correctly controlled, arsenic can be separated in high yields from the most important arsenic minerals, namely, arsenopyrite, FeAsS ; löllingite, FeAs_2 ; and enargite, $3\text{Cu}_2\text{S} \cdot \text{As}_2\text{S}_5$. Nickel and cobalt arsenide minerals are much more stable and therefore more difficult to roast. Fahlores and proustite are also very stable.

Another roasting process makes use of the fact that at certain oxygen partial pressures magnetite is formed. Magnetite, in contrast to hematite, does not react with arsenic oxides to form arsenates [2]. In this process the oxygen partial pressure is adjusted by the introduction of steam and recycled roasting gases. For two roasting gases, containing 16.7% and 11.5% SO_2 , the amount of recycled gas required is calculated to be ca. 5.5% of the total quantity. The amount of air is regulated to exactly 5%. In this way an arsenic content in the roasted material of 0.01–0.05% is obtained for starting material containing 0.4% As [2].

At a low oxygen partial pressure, particularly in the case of pyrites-containing materials, the sulfur partial pressure reaches such high levels that reactions of the following type assume practical significance in the gas phase:





In the dearsenicating roasting of a raw material containing arsenopyrite or other dissociable substances, the dissociation reaction and secondary reactions are important factors. The best results are obtained by roasting at a low oxygen partial pressure. To convert all the arsenic into the trioxide, the oxidation of the dissociation products has to be completed at a relatively high oxygen partial pressure. Before cooling and purification, therefore, the roasting furnace gases are burnt under controlled conditions. If only partial desulfurization is necessary, a single-stage process is generally sufficient. For substantially complete desulfurization, however, a two-stage process may be necessary.

Roasting Plants. In principle, any standard roasting furnaces (multiple-bed and fluidized-bed furnaces, sintering apparatus and cyclones) may be used for roasting arsenical raw materials. The waste gases from the roasting reactors may also be burnt. They are then freed from dust in a hot cyclone and a hot electrostatic precipitator above the condensation temperature of As_2O_3 and subsequently cooled to 100 °C. The As_2O_3 is deposited relatively pure in a bag filter. Multiple-bed furnaces are the most suitable for dearsenicating roasting.

Multiple-Bed Furnaces. Where roasting is carried out in a multiple-bed furnace (e.g., a Wedge furnace), the atmosphere in the material bed during the first part of the roasting process should be sufficiently low in oxygen to prevent formation of arsenates. In this region most of the arsenic compounds are released from the material being roasted and are then oxidized in the atmosphere richer in oxygen over the bed of material being roasted before dust separation and cooling. Before it is discharged, the roasted material encounters the oxygen-rich fresh gas through the quantity of which the sulfur content can be adjusted to the required level. On account of the long residence time, mass diffusion is not a problem, even in relatively large particles. However, the maximum temperatures have to be limited to avoid melting and contamination. Multiple-

bed furnaces operate under reduced pressure. The flue dust content of the off-gases is relatively low.

Fluidized-Bed Furnaces. By virtue of their high roasting capacity, their low maintenance costs, and the high content of SO_2 in the off-gas, fluidized beds are being used increasingly to roast sulfidic raw materials. Raw materials rich in arsenic are roasted in fluidized beds, but to a minor extent compared with multiple-bed roasting in the production of arsenic. In contrast, the fluidized-bed roasting of pyrites poor in arsenic, with the object of separating arsenic from the ferrous raw material, has acquired considerable significance.

In fluidized-bed roasting, temperature and gas composition are easily kept constant at a level favoring separation of arsenic and subsequent complete desulfurization. The composition of the mineral, the arsenic content, and the grain size of the raw material are critical factors affecting the efficiency of arsenic separation during roasting. The roasted material is completely or partly transported with the off-gases to the gas-cleaning system, which makes gas cleaning difficult. During cooling of the gas, the arsenic trioxide can react with the metal oxides, so that the roasted material must be mechanically separated at elevated temperature. Even after this has been done, the gas still has a high flue dust content, which affects the separation of As_2O_3 and necessitates the installation of equipment for selective gas cleaning if the highest possible As_2O_3 content is to be obtained in the product.

Arsenopyrite. The roasting plant run by Boliden AB at Rönnskär and the technique it uses for roasting arsenopyrite and arsenic-containing copper pyrites concentrates are a good example of a commercial operation [5]. The multiple-bed furnace contains 9–11 hearths with a total hearth area of 230 m². The maximum roasting temperature is 500–800 °C. Most of the arsenic is actually removed in the upper hearths. Arsenic and arsenic sulfides are then allowed to burn in the roasting gas. After passing through a cyclone and a flue-dust filter, the roasted material is

cooled in a metal air cooler below the condensation temperature of As_2O_3 and purified in a hot precipitator with an exit temperature of 120–140 °C. Sulfuric acid is recovered from the gas containing 3–5% SO_2 in a fine purification plant (washing tower or wet electric precipitator). In the roasting of concentrates containing 12% As, the crude oxide accumulating in the air cooler and the hot precipitator has an As_2O_3 content of 80–95%. It is difficult to reduce the arsenic content of the roasted material below 0.5%. For roasting copper concentrates of low arsenic content, see below.

The arsenopyrite concentrates from Canadian gold mines are roasted by various methods. The end product required is a roasted material low in arsenic that is suitable for the cyanide leaching plant. For example, in the Giant Yellowknife Gold Mines, roasting is carried out in a two-stage fluidized-bed installation. The concentrate is fed directly to the first fluidized-bed reactor as a pulp for pre-roasting and is roasted to completion in a second stage. A 10–66% oxide is obtained in the electric precipitator, and the roasted material contains ca. 0.5% As for an arsenic content in the concentrate of ca. 11% [6].

In the former USSR an arsenopyrite pyrites concentrate from Darasunskii containing 9–13% As and 32–40% S is partially roasted at around 575 °C in a fluidized-bed furnace. After the roasting gas has been cleaned in a hot cyclone and a hot electric precipitator (400 °C), the oxide is separated in a condensation chamber. The roasted material contains ca. 0.5% As and 12–20% S; the oxide is 92–97% pure [7].

Arsenic-Containing Copper Concentrate. Copper smelters are the biggest producers of arsenic-containing intermediate products. The bulk accumulates in the roasting of copper concentrates containing enargite and arsenopyrite. The arsenic content of those concentrates varies within wide limits, in many cases reaching 10%. Normally the copper concentrate is roasted in multiple-bed furnaces. The process is controlled in such a way that opti-

mal conditions for removal of the arsenic prevail in the upper hearths, whereas in the lower hearths the sulfur content of the material being roasted is reduced to the level required for the subsequent smelting of low-grade matte, e.g., to 15–20%.

The processes and plants used are much like those used for the roasting of arsenopyrite (see above). Roasting is exothermic, and the maximum roasting temperature can reach 500–800 °C, depending on the composition of the batch. The yield of arsenic also depends on the composition of the batch, the type and quantity of the arsenic minerals, the roasting temperature, and other factors. For high arsenic contents or when arsenopyrite or enargite are present, the yield can be more than 80%. For lower arsenic contents the yield can be much lower because a few tenths of a percent of arsenic always remain in the roasted material.

After the hot roasting gas has been cleaned in cyclones and dust-settling chambers, relatively small quantities of a crude arsenic heavily contaminated by flue dust and volatile substances are obtained by cooling the off-gas. The As_2O_3 content of the product is generally between 10 and 50%. However, far higher contents can be obtained by using electric precipitators to remove dust from the hot gas. The dust left after cleaning of the hot gas is returned to the process.

The cleaned SO_2 -containing gas still contains traces of arsenic and other impurities that have to be removed by washing with water or a circulating washing liquid containing sulfuric acid and by final cleaning in a wet electric precipitator. The sulfur is used to produce sulfuric acid. The arsenic-containing slurries that accumulate during wet cleaning and effluent treatment are collected and neutralized to recover valuable materials.

Arsenic-Containing Pyrite Concentrates. The stocks of arsenopyrite-containing pyritic ore with < 1% As are quite large and make up a significant percentage of the raw material reserves for arsenic. Pyrites of this type are widely used as raw material for sulfur and

iron. They are also roasted to produce sulfur dioxide and iron oxides. The iron oxide must have the lowest possible arsenic content, in any case below 0.1%, and best below 0.05%. The roasting process must be conducted in such a way that as much arsenic as possible is removed. In addition, the gas must be freed completely from arsenic before it is delivered to the sulfuric acid factory or otherwise used. The products resulting from cleaning the arsenic-containing gas are being worked up to an increasing extent in the interest of protecting the environment. The most economical way is by working them up to arsenic compounds. Other constituents, such as selenium, mercury, and lead, may be obtained at the same time. In the past this way of obtaining arsenic has played a minor role. In the future, however, significant quantities of arsenic will be obtained by this method.

The traditional process for the dearsenicating roasting of pyrites is multiple-bed roasting controlled so that the arsenic is released in the low-oxygen atmosphere of the upper beds whereas the sulfur is released in the oxygen-rich atmosphere of the lower beds. The gases formed have a relatively low SO_2 content and such a high oxygen content that arsenic, sulfur, and the arsenic sulfides are completely oxidized. The As_2O_3 formed reacts further with Fe_2O_3 and oxygen to form iron arsenate. Therefore, most of the arsenic in the dust is in bound form and, in addition, because of the low total content, is an unsuitable starting material for arsenic. In recent years the multiple-bed roasting of pyrites has largely been replaced by fluidized-bed roasting.

The standard process for roasting pyrites in a fluidized bed forms Fe_2O_3 with excess air. This is unsuitable for roasting arsenic-bearing ores because the arsenic then is bound as iron arsenate in the roasted material. Two fundamentally different processes have been developed for the fluidized-bed roasting of arsenic-bearing pyrites: the two-stage BASF process and the single-stage Boliden process.

In the two-stage process developed by BASF, about one half of the sulfur present is roasted off in the first reactor at around 900 °C

at a low oxygen partial pressure. After solids and gas have been separated in a cyclone, roasting is completed in a second reactor around 800 °C in excess air. Air is added to the gas stream of the first reactor to burn the sulfides and other volatile substances still present. The gas is then cooled in a waste-heat boiler and cleaned in a hot precipitator and by washing. Some of the arsenic is present as iron arsenate in the dust precipitated, and some is washed out as As_2O_3 during wet cleaning [8, 9].

In the single-stage fluidized-bed roasting process developed by Boliden AB at Reymerholm, the pyrites are roasted in such a way that magnetite, Fe_3O_4 , is formed from the iron in the ore at a low oxygen partial pressure. In contrast to Fe_2O_3 , magnetite does not react with the As_2O_3 to form arsenate. A small amount of iron arsenate is separated with the flue dust. The gas freed from the flue dust is mixed with air to burn the dissociation products. Then it is cooled in a waste-heat boiler, freed from dust in a hot precipitator, and subjected to wet gas cleaning which separates most of the arsenic as As_2O_3 [10, 11].

In the wet cleaning of the roasting gases, the gases are washed with water or circulating sulfuric acid solutions in washing towers, Venturi scrubbers, or other apparatus and finally are cleaned in wet precipitators. Separation of the arsenic by the wash liquid is almost complete, although neutralization, utilization, or storage of the arsenic removed presents problems. Normally the process water is circulated so that a high concentration of dissolved substances builds up; a side stream is purified. For example, the arsenic may be precipitated with lime, possibly after neutralization with alkalis. Because the wash liquids are strongly acidic and contain many impurities, the consumption of chemicals is high and the product impure. Selective precipitation may be carried out. At the Reymerholm works of Boliden AB, the As_2O_3 is continuously recovered from the circulating sulfuric acid wash solution by crystallization. The product obtained serves as raw material for the production of refined As_2O_3 .

The bulk of world production of arsenic trioxide comes from the intermediate products of the roasting of arsenic-bearing ores, above all copper ores, lead ores, and arsenopyrite ores. Therefore the level of arsenic production is limited by the amount of metals production. The raw material base will likely increase through the exploitation of low-grade by-products.

13.5.1.3 Production of Refined As_2O_3

Preliminary Concentration. The starting material for the industrial production of refined As_2O_3 is the arsenic-rich dust or slurry that accumulates as an intermediate product in the roasting and smelting of arsenic-bearing ores and concentrates. The bulk of this arsenic raw material comes from copper smelters, although some also comes from lead, cobalt, and other smelters. Occasionally, in the former USSR and possibly China, arsenic-rich ore is roasted with the primary object of recovering arsenic. All these raw materials of various origins and arsenic contents have in common that they are obtained as products of gas cleaning and also contain other condensation products and flue dusts. Arsenic is mainly present as As_2O_3 , although some may also be bound as arsenite or arsenate. The arsenic content can vary enormously, depending on the ore used and the way in which roasting and gas cleaning are carried out. The gas-cleaning products often contain other valuable constituents and, because of this, must be worked up even if the arsenic content is very low. In such cases the materials are circulated until the arsenic content exceeds 10%. Low-grade gas-cleaning products of low As_2O_3 content from copper and lead roasting plants contain flue dust from the furnace charge as their principal impurity, whereas the high-grade products mainly contain volatile impurities, such as lead, antimony, bismuth, and selenium. Most of the impurities are present as oxide or sulfate.

Low-grade starting materials are treated in a multistage process. In the first stage the material is roasted to produce $\geq 80\%$ As_2O_3 . This

is sublimed and separated from the roasting gases. The bulk of the impurities remains in the roasted material, which is returned to the original process or treated separately to recover valuable secondary products. To increase the yield of arsenic and to facilitate the movement of material through the roasting furnace, sulfides or charcoal are added as reducing agents to the furnace charge. The reducing atmosphere thus established in the material decomposes the metal arsenates and no more arsenate is formed. For example, dust from the gas-cleaning process is mixed with a few percent of iron pyrites concentrate, and the resulting mixture heated at 300–500 °C in oil-fired multiple-bed furnaces. The arsenic-containing gas is cooled in a long brick pipe, passes through a flue-dust chamber, and then through several chambers in which the temperature falls from 220 °C to below 100 °C to separate the arsenic. Finally the gas is cleaned in bag filters. In this system the flue dust and gaseous impurities of low vapor pressure are separated preferably in the first part of the system, so that the gas-cleaning process is fractionated. In a critical temperature range above 200 °C, a relatively small quantity of impure, amorphous glassy arsenic trioxide accumulates. However, most of the arsenic trioxide obtained is crystalline. A product containing the high vapor pressure impurities is separated in the bag filter.

Some of the crude arsenic from the separating chambers containing more than 95% As_2O_3 is sold, but most of it is refined further. The less pure products are returned to the process.

Refining. High-purity crude oxide, obtained either directly or via concentration processes, can be dry refined by sublimation or wet refined by dissolution and crystallization.

The widely used sublimation process is carried out by heating the crude arsenic in a reverberatory furnace. The gases are passed through a dust-settling chamber to a ca. 70-m-long system of, e.g., 39 brick arsenic separation chambers called kitchens. The kitchens are followed by a bag filter. The temperature

in the dust-settling chamber is kept at ca. 295 °C, which is considerably above the condensation temperature of arsenic trioxide. The temperature of the bag filter is kept at 90–100 °C. A black, amorphous arsenic trioxide containing ca. 95% As_2O_3 accumulates in the first kitchens. In the following kitchens, in the temperature range from 180 to 120 °C, most of the arsenic trioxide accumulates in a crystalline form analyzing more than 99%. The product separated in the last kitchens below 120 °C and in the bag filters assays ca. 90% As_2O_3 . The low-purity products are returned to the process or, if they assay more than 95% As_2O_3 , are sold as crude arsenic. The high-purity products from the middle kitchens are marketed as white arsenic.

Several versions of the dry refining process, e.g., with repeated sublimation, have been described in the literature. The Rönnskär works have developed a process for the production of nondusting white arsenic by shock cooling of hot-cleaned sublimation gas.

The wet refining of crude oxide was introduced at the Rönnskär works back in the 1930s and is now the only refining process practiced here. The process is based on the large temperature coefficient of the solubility of As_2O_3 in water (12.1 g/L at 0 °C, 18.1 g/L at 20 °C, 81.8 g/L at 98.5 °C), on the low solubility of the impurities, and on the purification accompanying crystallization of the As_2O_3 .

The crude oxide, assaying from 80 to 95% As_2O_3 , is brought in a closed system to the refining plant and pressure leached in steam-heated autoclaves with water or circulating solution. The As_2O_3 dissolves, whereas the impurities, such as oxides, sulfides, sulfates, and arsenates of lead, bismuth, antimony, iron, and other metals, as well as silica, selenium, and other substances, form a slightly soluble sludge, which is separated from the hot leaching solution. The solution is vacuum cooled, and the crystallization is controlled to give a relatively coarse product, which is separated by centrifuging from the solution, washed, dried, and packaged in a closed system. The mother liquor is recycled. The process is fully continuous and also satisfies stringent indus-

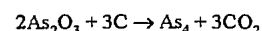
trial hygiene requirements. The wet-refined arsenic contains more than 99% As_2O_3 and is marketed as white arsenic, either in metal casks or in lined wooden casks.

13.5.2 Production of the Metal

Metallic arsenic is produced on a fairly wide scale as commercial arsenic metal, primarily as an additive for alloys, and to a lesser extent as high-purity arsenic for electronic applications.

Commercial Arsenic Metal. The starting material for the production of a metal of commercial quality is usually white arsenic. However, the metal can also be produced from arsenopyrite or löllingite.

In the processing of As_2O_3 the oxide is normally reduced with carbon:



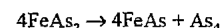
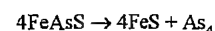
The reaction is endothermic and is carried out at 500–800 °C. The elemental arsenic sublimates and is condensed out of the reaction gas by cooling.

There are several versions of the carbon reduction process. In one version a mixture of As_2O_3 with 25% charcoal is placed in a horizontal steel retort jacketed with firebrick and heated to 650–700 °C in a gas-fired furnace. The reaction gas is collected in water-cooled condensers, in which the metal separates as crystals. After about 10 h, the heating is stopped, and, after the furnace has cooled, the metal can be removed from the condensers.

Similar processes are thought to have been used by several producers. For example, at the Rönnskär works of Boliden AB, steel retorts are provided with demountable air-cooled condensers. After the cold retorts have been charged, they are closed and heated to 700–800 °C in an electric furnace. The metal is separated in the condenser, while the off-gases are cleaned in a scrubber system. Most of the metal is coarsely crystalline. After size reduction and grading, the arsenic is packaged in metal casks. In the process used at the Reichenstein works in Silesia, As_2O_3 was vaporized by indirect heating in a gas-heated retort

furnace, and the vapor was passed through a 3-m-tall incandescent coke layer into a tower reactor in which it was reduced to gaseous arsenic. The metal was separated in large condensers arranged in series.

Carbon monoxide [12] or ammonia [13] may also be used as reducing agents. Metallic arsenic may be obtained from arsenopyrite or löllingite by thermal dissociation:



V. G. RCHILADZE [14] described the theory of this process in detail and suggested how it may be carried out in practice. Arsenopyrite is placed in steel retorts lined with diabase or basalt and heated electrically in two stages to 700–900 °C. This causes the arsenic and a small quantity of sulfur compounds to volatilize. The metal vapor is condensed at 450–500 °C in an electrically heated steel condenser. The metal is scraped off the condenser walls and cooled in a closed system. The volatile sulfur compounds are separated from the off-gas at a lower temperature. The purity of the metal depends on the ore, specifically on the content of volatile impurities that condense under the same conditions as the arsenic. Some sulfur content is always present. In an experiment, metal containing more than 99% As was obtained from arsenopyrite assaying from 25 to 45% As. The principal impurities were sulfur and bismuth.

Practical experience in the production of metallic arsenic by reduction with carbon has shown that there are many difficulties. The danger to personnel and the risk of explosion are the two most important. In addition, As vapor is highly corrosive, so that the useful life of the plant is shortened significantly [15]. To overcome these problems, attempts are being made to produce metallic arsenic in other ways. Crystallized As can be obtained from AsCl_3 , As_2S_3 , or As_2O_3 by gas-phase reduction with hydrogen. The hydrogen required for reduction is produced in situ by the thermal dissociation of ammonia. The reduction is highly exothermic. This process is said to give an arsenic yield of 93–98%. The off-gas contains

70% N_2 and 30% hydrogen. An advantage lies in a certain degree of refining that takes place. Table 13.3 shows one example of how impurities present in As_2O_3 affect the purity of the metallic arsenic. Figure 13.1 shows a schematic diagram for one such plant.

Table 13.3: Refining effect in the reduction of As_2O_3 with H_2 .

	As_2O_3 , ppm	As, ppm
Ag	<1	<0.1
Al	7	1
Bi	2	2
Ca	9	3
Cd	<1	<1
Co	<1	<1
Cu	5	2
Mg	3	<1
Mn	<1	<1
Na	20	<10
Ni	<1	0.3
Pb	10	0.5
Sb	1000	0.2
Zn	3	3
Cr	<1	<1
Fe	20	8
Si	50	10
Sn	<1	<0.3
Te	<30	<10

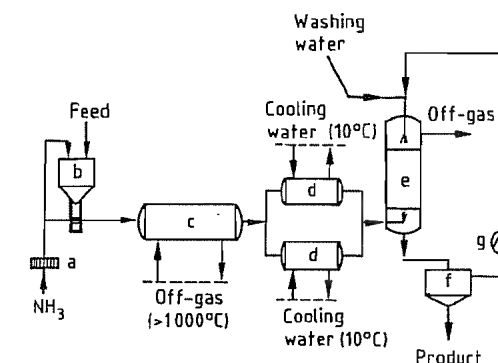


Figure 13.1: Plant for producing crystalline arsenic metal: a) Roots blower; b) Reservoir; c) Reactor; d) Condensers in parallel; e) Washing tower; f) Decanter; g) Pump.

Another way of obtaining metallic arsenic is to sublime a Pb–As–Sb alloy to give 99% pure arsenic metal. Flue dust containing antimony and arsenic and a lead-containing residue from the electrolytic refining of Pb are reduced with carbon to a lead alloy containing 7–12% As and 18–30% Sb. A 90% As con-

taining 10% Sb and 0.05% Cd is produced in a first vacuum distillation stage carried out at 480–590 °C (Figure 13.2).

A 99% As suitable for the commercial market is obtained in a second vacuum distillation stage carried out after removal of the cadmium from the residue [16].

Commercial arsenic produced from As₂O₃ contains > 99% As and as its main impurities antimony and oxygen. This quality is used primarily for the production of alloys.

High-Purity Arsenic. Arsenic is produced in various high-purity grades for special applications. A limited refining effect can be obtained by resubliming commercial metal in a stream of hydrogen. In general, however, various purification stages are combined in the production of high-purity metal.

Commercial arsenic is sublimed, reacted with oxygen to produce As₂O₃ which is recrystallized from aqueous hydrochloric acid, sublimed in a stream of hydrogen, and then reduced to the metal with hydrogen at 800–850 °C. The arsenic obtained has a purity > 99.999% [17]. The process most often reported in the literature uses white arsenic as its starting material. This is reacted with hydrochloric acid to form arsenic trichloride [18]. The arsenic trichloride is purified by fractional distillation, possibly in combination with chemical methods, and is reduced by reaction with hydrogen in a tube heated to 500–900 °C. The metal vapor is condensed at 300–500 °C to crystalline form. After sublimation, the metal is packaged in glass ampoules. An arsenic content of > 99.999(9)% can be obtained by this method. The number in parenthesis indicates the limits of analytical accuracy.

Table 13.4: Content of impurities (% by weight) in two samples of pure arsenic (Content of Ni, Bi, Pb, Cr, and Mn in all samples, < 5 × 10⁻⁶%; Sb, In, Sn, and Cd, < 5 × 10⁻³%).

	Sample no.	Cu × 10 ⁶	Al × 10 ⁵	Fe × 10 ⁵	Si × 10 ⁵	Mg × 10 ⁵	S × 10 ⁵
After reduction	1	1	1	0.5	10	4	7
	2	1	0.5	1	5	2	20
After distillation in hydrogen	1	1	0.5	1	1	1	5
	2	1	2	1	2	2	2
After vacuum distillation	1	1	0.5	1	2	1	2
	2	1	1	1	1	1	2

Figure 13.3 shows the distribution of arsenic in the production of semiconductor-purity arsenic. The yield is 62%. Table 13.4 shows the impurities present in the high-purity arsenic after the individual process steps [19].

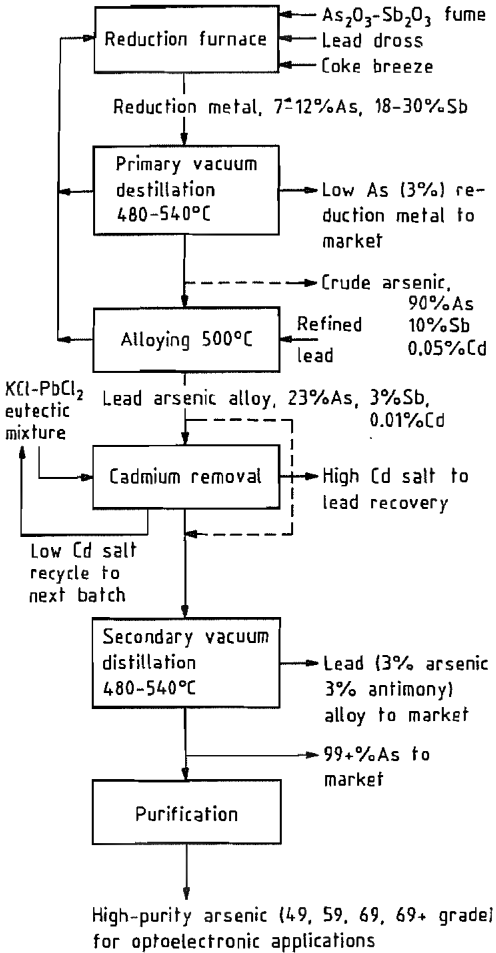


Figure 13.2: Flow sheet of the Cominco recovery process.

Table 13.5: Circulation of arsenic in lead and copper smelters (% of total arsenic in circulation).

	Lead processing						Copper processing		
	1 ^a	2	3	4	5	6	7	8	9
Arsenic in circulation	100.0	100.0	100.0	100.0	100.0	100.0	100.0	100.0	100.0
Dusts	33.0	24.5	32.8	19.4	12.3	68.6	77.2	34.7	—
Slags	0.3	0.3	0.9	2.0	3.4	2.9	21.4	65.3	100.0
Dross	65.3	73.8	49.1	41.0	69.1	15.4	—	—	—
Unconditioned matte	0.7	—	8.2	—	15.2	—	—	—	—
Melt	—	—	—	31.8	—	8.2	—	—	—
Others	0.7	1.4	9.0	5.8	—	4.9	1.4	—	—
Arsenic in circulation in %, based on the total used	52.1	5.8	14.0	11.1	3.3	2.9	3.6	4.3	2.9

^a The numbers 1 to 9 stand for different lead resp. copper producers.

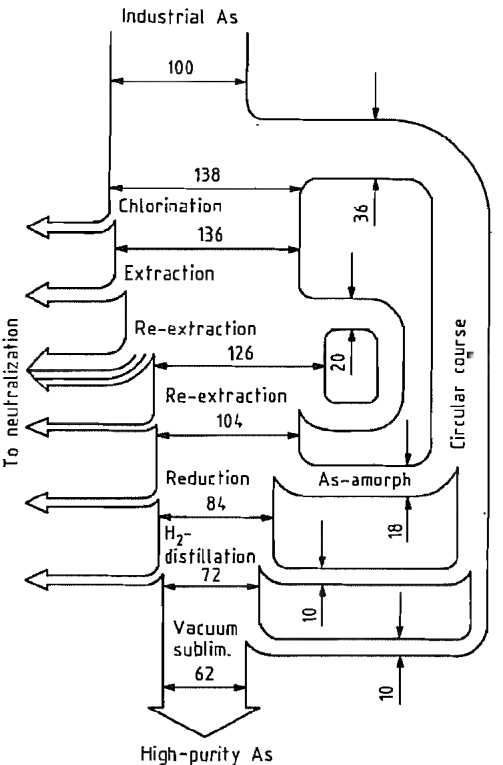
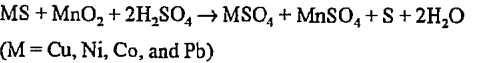


Figure 13.3: Material flow in the production of semiconductor-purity arsenic by the chloride method.

significant drop in demand. On the other hand, increasing quantities of arsenic-containing by-products are accumulating as the production of heavy metals increases. These products build up in the material circuits of the individual factories [20]. Ultimately, arsenic-containing materials have to be removed from those circuits. The processes involved are very cost intensive. In addition, if the demand for As is inadequate, special measures must be taken to dispose or store those materials [21]. In lead smelters, for example, considerable amounts of As forerun come from circulating materials.

Table 13.5 shows the distribution in flue dusts, slags, dross, and matte in copper and lead smelters. Most of the arsenic in lead processing circulates in the form of flue dusts and copper dross. In copper processing the main arsenic carriers are flue dust and slags [3].

In recent years various methods of removing the As have been examined. For example, a lead-copper matte containing 25.7% Cu, 18.2% Ni, 1.65% Co, 27.2% Pb, and 4.14% As is leached with concentrated H₂SO₄ at 85–100 °C in the presence of MnO₂:



The metals Ni, Co, Fe, and As dissolve, leaving a residue of elemental sulfur and PbSO₄. The residue is separated. As is precipitated as FeAsO₄ by addition of NaOH or Ca(OH)₂ at pH 4. The FeAsO₄ takes up 88–92% of the arsenic. It consists of 24% As, 22% Fe, and 3–5% Cu and is in a suitable form for safe disposal [22, 23]. As shown in

13.6 Treatment of Arsenic-Containing By-products

Arsenic and products containing arsenic are under an increasing barrage of criticism, because of their toxicity. This has produced a

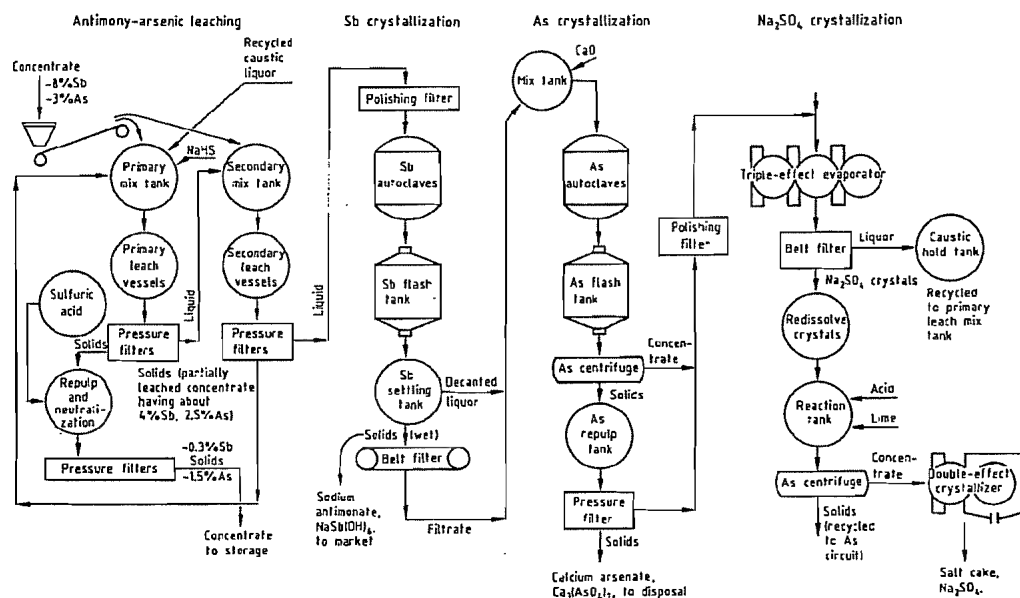


Figure 13.7: Simplified schematic flow sheet of leach plant at Equity Silver Mines Ltd.

This modification is directly formed when condensation is carried out at temperatures above 221 °C. Condensation above 250 °C results generally in the formation of the amorphous, glassy phase, ρ 3.70 g/cm³, which devitrifies into the octahedral modification at room temperature.

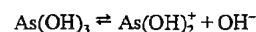
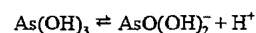
In an open vessel, arsenic trioxide sublimes without melting above 135 °C. The monoclinic form melts at 312.3 °C under its own vapor pressure. Up to about 800 °C the vapor density corresponds to the formula As_4O_6 ; at 1800 °C, dissociation into As_2O_3 molecules is complete. The As_4O_6 molecules were also detected in nitrobenzene solutions.

Arsenic trioxide is moderately soluble in water. The glassy-amorphous As_2O_3 dissolves much more easily than the crystalline form; its solubility is 12 g/L at 2 °C and 114.6 g/L at 100 °C [34]. The solution has a sweetish taste with an unpleasant metallic tang. As little as 0.1 g can be fatal, if As_2O_3 enters the stomach.

13.7.2 Arsenous Acid

Arsenous acid cannot be obtained from aqueous solutions of As_2O_3 ; instead, As_2O_3 is

reprecipitated. However, in aqueous solution it exists in equilibrium with its dissociation products. It is still not clear what formula should be assigned to dissolved arsenous acid. In addition to the formulation as orthoacid, H_3AsO_3 or $\text{As}(\text{OH})_3$, which is used here, the dissolved acid may also be formulated as metaacid, HAsO_2 or $\text{AsO}(\text{OH})$, or as hexahydroxoacid, $\text{H}_3[\text{As}(\text{OH})_6]$. Arsenous acid is amphoteric, dissociating in two ways:



The dissociation constants are 6×10^{-10} and 1×10^{-14} , respectively. Accordingly, arsenous acid is a very weak acid, approximately equal in strength to boric acid, but it is a much weaker base. The As^{3+} ions occur in significant quantities only in very strongly acidic solutions.

Arsenates(III). The salts of arsenous acid are called arsenates(III). Formerly they were called arsenites. Some salts exist in the forms MH_2AsO_3 , M_2HAsO_3 , and M_3AsO_3 , although most salts of arsenous acid are derived from

the metaacid, HAsO_2 , i.e., have the formula MASO_2 .

The alkali-metal arsenates(III) dissolve easily in water, whereas the alkaline-earth arsenates(III) are slightly soluble to insoluble. The compounds of arsenous acid with heavy metals are insoluble in water. Arsenous acid can be retained in considerable quantities by slimy metal oxide hydrates, such as iron oxide hydrate by adsorption.

The arsenates(III) are decomposed by strong acids because they are salts of a very weak acid.

Sodium arsenate(III), NaAsO_2 , does not exist in crystallized form. Solutions of the salt are obtained by dissolving arsenic trioxide in sodium hydroxide. For manufacture, arsenic trioxide is mixed with caustic soda. After the addition of a little water, a vigorous reaction begins, spreading quickly through the mixture. Soda may also be mixed with the oxide and a little water, and the resulting mixture dried at elevated temperature in a furnace. In both cases, a water-soluble product is obtained after grinding. It is used in the manufacture of insecticides, herbicides, etc.

Other arsenates(III) are known. Many complex metal arsenates(III) are known. They include *Scheele's green*, formerly used as an artist's color. It is a mixture of copper arsenates(III) to which formulas such as $\text{Cu}_3(\text{AsO}_3)_2$, CuHAsO_3 , and $\text{Cu}(\text{AsO}_2)_2$ have been assigned. The double salt of copper arsenate(III) and copper acetate, $\text{Cu}(\text{CH}_3\text{COO})_2 \cdot 3\text{Cu}(\text{AsO}_2)_2$, is *Schweinfurth green*, another artist's color. This use has declined enormously because of the poisonousness. Calcium and copper arsenates(III) were formerly used as "*copper-arsenic liquor*", to control pests in viniculture.

13.7.3 Arsenic Pentoxide

Arsenic pentoxide, As_2O_5 , is a white glassy mass (ρ 4.32 g/cm³), which deliquesces in air to form arsenic acid. On heating, arsenic pentoxide begins to decompose near its melting point, ca. 300 °C. The vapor consists of arsenic trioxide and oxygen. The pentoxide can

be prepared by reaction of arsenic trioxide with oxygen under pressure or by dehydration of crystalline arsenic acid at temperatures above 200 °C [35]. The crystal structure was unknown until recently. The monocrystals were grown under oxygen excess pressure: space group $\text{P}2_12_12_1$ [36, 37].

13.7.4 Arsenic Acid

Arsenic acid, H_3AsO_4 , is known in the solid state only as the hemihydrate $\text{H}_3\text{AsO}_4 \cdot 0.5\text{H}_2\text{O}$ in the form of rhombic, deliquescent crystals. Solutions in water behave as a tribasic acid with the dissociation constants $K_1 = 5.6 \times 10^{-3}$, $K_2 = 1.7 \times 10^{-7}$, and $K_3 = 3 \times 10^{-12}$. Arsenic acid loses water when heated to 120 °C with the formation of pyroarsenic acid, $\text{H}_4\text{As}_2\text{O}_7$. At higher temperatures, more water is lost and metaarsenic acid, HAsO_3 , forms [35]. If the protons of the acids are completely or partly replaced by metals, the arsenates(V), which generally correspond to the phosphates, are formed. In acidic solution, arsenic acid and its salts are strong oxidizing agents.

Production. Arsenic acid is produced solely by the oxidation of As_2O_3 . Various processes for its production based mostly on oxidation with nitric acid, which gives a high yield, are described in the patent literature. Originally the apparatus used for those processes were usually made of stoneware but they are now made of alloys resistant to nitric acid.

The plant usually consists of so-called developers and a regenerator for nitric acid. The developers are ca. 4-m³ vessels equipped with a high-speed stirrer, a steam coil, and a mechanical feeder for oxide. About 2000 L of 38% HNO_3 is introduced initially, and the oxide is run in with strong heating until the nitric acid has been consumed. The oxides of nitrogen formed pass from the developer into the regenerator, where they are worked up to nitric acid in the presence of air and water. Up to 90% of the NO and NO_2 formed are converted back into nitric acid. One developer can process 2000 kg of As_2O_3 into arsenic acid in 24 h.

Oxidation with sodium or calcium chlorate also enables a relatively large quantity of oxide to be oxidized in a short time. The oxide is suspended in water and a little arsenic acid is added to the resulting suspension. An aqueous solution of the chlorate is run in at boiling temperature. The reaction takes place smoothly while chlorate is uniformly run in. The input of chlorine must be reduced towards the end of the reaction because otherwise chlorine readily escapes. The arsenic acid obtained by the chlorate process always contains chloride, which causes problems in the production of lead arsenate.

Arsenic acid is used as a defoliant and as a starting material for important inorganic and organic arsenic compounds.

Arsenates(V). Arsenic acid gives three series of salts. They correspond generally to the phosphates in their compositions and solubilities. Many of them are also isomorphous with the phosphates, e.g., ammonium magnesium arsenate(V), $\text{MgNH}_4\text{AsO}_4 \cdot 6\text{H}_2\text{O}$, which changes on calcination into magnesium pyroarsenate(V), $\text{Mg}_2\text{As}_2\text{O}_7$, a form suitable for the quantitative determination of arsenic acid. Unlike silver phosphate, which is yellow, the silver salt Ag_3AsO_4 is brown.

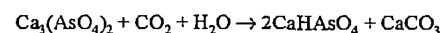
Of the numerous salts of arsenic acid, the salts of potassium, sodium, calcium, and lead are important commercially. Even today they are used on a wide scale in pest control, although modern synthetic organic compositions have reduced the use of arsenates. In some countries, the use of arsenic compounds in plant protection agents has been banned. The same applies to metal arsenates(V) as active constituents of arsenic-containing wood preservatives [38, 49].

Monopotassium arsenate(V), KH_2AsO_4 , $\text{mp } 288^\circ\text{C}$, $\rho \text{ } 2.867 \text{ g/cm}^3$, was used in the manufacture of insecticides and in the preservation of skins. It is prepared by calcining a mixture of equal parts of arsenic oxide and potassium nitrate in cast-iron cylinders, leaching the melt with water, and concentrating the solution with arsenic acid. It forms white crystal crusts.

Trisodium arsenate(V), $\rho \text{ } 1.759 \text{ g/cm}^3$, $\text{mp } 86.3^\circ\text{C}$, is obtained most easily by neutralizing arsenic acid with sodium carbonate or sodium hydroxide. Concentration by evaporation gives a marketable product having the formula $\text{Na}_3\text{AsO}_4 \cdot 12\text{H}_2\text{O}$.

Disodium arsenate(V), Na_2HASO_4 , $\rho \text{ } 1.72 \text{ g/cm}^3$, is obtained by roasting a mixture of arsenic oxide with sodium carbonate and sodium nitrate in the presence of air. In addition, this compound can be easily obtained by calcining sodium arsenate(III) in the presence of air. Sodium arsenate(V) is used in the production of other arsenates, such as calcium and lead arsenates.

Calcium arsenates(V). There are three known calcium salts of arsenic acid, $\text{Ca}(\text{H}_2\text{AsO}_4)_2 \cdot \text{H}_2\text{O}$, $\text{CaHASO}_4 \cdot \text{H}_2\text{O}$, and $\text{Ca}_3(\text{AsO}_4)_2 \cdot 3\text{H}_2\text{O}$. In addition, there are basic salts, for example, $\text{Ca}_5\text{OH}(\text{AsO}_4)_3$, which corresponds to apatite. Commercial preparations are based on the neutral salt. However, different manufacturers use different methods and do not always guarantee the production of a strictly neutral salt. Because of the risk of damage to plants that acid arsenic salts involve, a basic character is given to the commercial product during its production by using excess lime. Elevated temperature, abundant moisture, and atmospheric carbon dioxide cause calcium arsenate to convert into the plant-damaging acid arsenate:



The reason the acid salt is harmful is its greater solubility in water, 0.31% As_2O_5 vs. 0.013% for the neutral salt. The neutral salt begins to turn acid only after the excess lime added has been converted completely into carbonate. For the solubility in the presence of atmospheric carbon dioxide, see [33].

Calcium arsenate(V) is generally prepared by reacting milk of lime with arsenic acid. Maintaining a certain temperature and an experimentally determined feed rate and stirring speed, the arsenic acid can be run as a fine distribution into the milk of lime. The precipitate obtained is filtered, washed, and dried.

Calcium arsenate(V) is also obtained by heating calcium arsenate(III) in a stream of dry air.

Lead arsenate(V), PbHASO_4 , is a white water-insoluble powder of density $\rho \text{ } 5.79 \text{ g/cm}^3$. It was marketed as a plant protection agent in the form of powders and pastes. It is produced mainly from lead acetate, lead nitrate, and lead oxide and disodium arsenate. The direct reaction of arsenic acid with litharge in the presence of nitric acid gives a dilead arsenate. Commercial lead arsenates contain mostly PbHASO_4 along with varying amounts of $\text{Pb}_3(\text{AsO}_4)_2$. Accordingly, their lead content is higher and their As_2O_3 content lower than the levels calculated for PbHASO_4 .

Arsenic-containing plant protection agents have been banned in Europe. However, they are still used in East Asia [38, 49].

13.7.5 Arsenic Sulfides

Table 13.7 shows some physical data of the arsenic sulfides [34, 39].

Table 13.7: Physical data of arsenic sulfides.

		Color	mp, °C	bp, °C
Arsenic disulfide (re-algar)	As_4S_4	red	307	565
Arsenic(III) sulfide (orpiment)	As_4S_6	yellow	320	707
Arsenic(V) sulfide	As_4S_{10}	yellow	> 95 decomp.	—

Arsenic disulfide, As_4S_4 (realgar, red arsenic glass, red glass, ruby arsenic, arsenic blend), occurs in ruby-red crystals or as an amorphous reddish mass. Its commercial value is determined less by the chemical composition than by its purity and fineness. Industrially produced red arsenic glass varies in its composition. Whereas the red glasses previously contained 70% As and 30% S, substantially corresponding to the formula AsS , they now contain around 61–64% As and 39–36% S. The red glass is marketed in finely divided form.

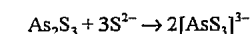
Red glass has long been produced on a large scale from arsenic ores and sulfur ores or from arsenopyrite containing iron pyrites. Another industrial process based on production

from arsenous acid and sulfur has recently been perfected. Prolonged development problems were presented by discolored products that had to be converted into an attractive, marketable red glass. The red glass is produced in two separate steps. A red glass that does not yet have the desired composition and that needs refining in appearance is obtained in the first step by melting and sublimation. The intermediate product is therefore refined and is given the required color.

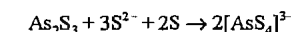
Production by melting a mixture of elemental arsenic and sulfur gives a red glass particularly fine in appearance but too expensive on account of the high price of the elemental arsenic. The processing of arsenopyrite and sulfur, although possible, is not usual.

Most red glass is used in tanneries as a depilatory in the manufacture of fine leather.

Arsenic(III) sulfide, As_4S_6 , occurs as a yellow mineral known as orpiment. It can be produced by precipitation of compounds of trivalent arsenic with hydrogen sulfide. The colloidal solution of the arsenic trisulfide can be flocculated by hydrochloric acid, in which it is insoluble. However, it dissolves readily in basic reagents, above all in alkali-metal sulfide solutions, including ammonium sulfide, to form thioarsenites:



If yellow ammonium hydrogen sulfide is allowed to act on arsenic trisulfide, the dissolved sulfur promotes oxidation to thioarsenate:



Arsenic trisulfide is a lemon-yellow compound, which begins to sublime before melting, melts at 310°C to form a red liquid, and boils at 707°C without decomposing. It is used as an artist's color, marketed in pure form as king's yellow. The impure product obtained by fusing arsenic trioxide with sulfur is marketed as orpiment. Orpiment always contains unchanged arsenic trioxide and, unlike the pure sulfide, is poisonous.

Orpiment was once used for cosmetic purposes. It is now used in the semiconductor in-

dustry, for the production of IR-permeable windows, and as a pigment.

Arsenic(V) sulfide, As_4S_{10} , is produced by fusing stoichiometric quantities of As and S powder or by precipitation from highly acidic arsenate(V) solution with H_2S . At relatively high temperatures As_4S_{10} decomposes into arsenic(III) sulfide and sulfur.

13.7.6 Arsenic Halides

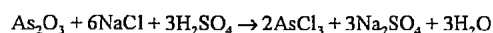
The known arsenic halides are listed in Table 13.8 [34, 39, 40].

Table 13.8: Physical data of arsenic halides.

	Form	mp, °C	bp, °C
Arsenic(V) fluoride	colorless gas	-88.7	-58.2
Arsenic(V) chloride		-50 (decomp.)	—
Arsenic(V) oxychloride	colorless liquid	-78	—
Arsenic(III) fluoride	colorless liquid	-8.5	60.4
Arsenic(III) chloride	colorless liquid	-13	130.2
Arsenic(III) bromide	yellow liquid	31	221
Arsenic(III) iodide	red solid	140.7	ca. 400

All arsenic halides can be produced by direct combination of the components. They can also be obtained by halogenation of the oxides or sulfides. The bonds are hydrolyzed by water. Only arsenic(III) chloride is commercially significant.

Arsenic trichloride, AsCl_3 , is a colorless oily liquid that fumes in air, ρ 2.17 g/cm³. By virtue of its low boiling point, AsCl_3 is easy to separate from SbCl_3 and the chlorides of other metals. $\text{As}(\text{OH})_3$ forms during hydrolysis. The direct synthesis of AsCl_3 is uneconomical. An old commercial production method is the Glauber process using arsenic trioxide:



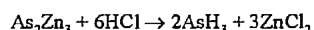
However, AsCl_3 is easier to produce by reacting As_2O_3 with gaseous hydrogen chloride at 180–200 °C.

Arsenic(III) chloride is a starting material for numerous organoarsenic compounds and for the preparation of chlorine derivatives of the arsines. It is used as a dopant in the manufacture of semiconductors and in the production of high-purity arsenic metal [41].

13.7.7 Arsenic Hydride and Arsenides

Arsenic hydride, AsH_3 , arsine, bp -55 °C, mp -116.3 °C, is the only known hydrogen compound of arsenic; it is a colorless gas with an unpleasant, garlic-like odor. It is extremely toxic: in many cases the inhalation of small amounts has caused death. Arsine does not ignite spontaneously but burns with a grayish-blue flame to form arsenic trioxide. If the flame is extinguished, for example, by holding a cold porcelain dish in it, arsenic is deposited as a black patch. The pure gas is stable at normal temperature. If arsenic hydride is passed through a red-hot glass tube, it decomposes into hydrogen and arsenic (arsenic mirror), 185.1 kJ being released per mole of arsenic. The arsenic is deposited just behind the heated area as a bright, metallic black mirror (Marsh test). When treated with hypochlorite solution or with alkaline hydrogen peroxide solution, the patch changes into soluble arsenate. Arsenic hydride has a strong reducing action. It precipitates metallic silver from silver nitrate solution. It reacts with solid silver nitrate to form the yellow compound $\text{AsAg}_3 \cdot 3\text{AgNO}_3$ (Gutzeit arsenic test).

Arsine cannot be prepared by direct synthesis. The most convenient method of production is the reaction between sodium arsenide and water or zinc arsenide and dilute hydrochloric acid:



These reactions are fast and complete and have the advantage that the product is not contaminated with hydrogen. Arsenic hydride can also be produced by cathodic reduction or by reduction of arsenic compounds in acidic solution with zinc or magnesium. The last reaction is not quantitative because elemental arsenic, which does not react, precipitates. The product also has a high hydrogen content. Because arsenic is present as a common impurity in numerous metals suitable for the production of hydrogen, hydrogen produced by acid-metal reduction must be passed through a potassium permanganate solution to destroy any arsenic

hydride present. Particular practical significance is attributed to the formation of arsenic hydride in the pickling of metals when arsenic-containing sulfuric acid is used.

Arsenic hydride is so poisonous that a few inhalations of air containing arsenic hydride can result in death. The MAK is 0.2 mg/m³.

Arsenic hydride is used as a dopant in the semiconductor industry [41].

Arsenides. A number of arsenides occur in nature. Some have a defined composition, others are probably mixtures. Naturally occurring arsenides include Cu_3As (domeykite), FeAs_2 (löllingite), NiAs_2 (chloanthite), NiAs (niccolite), and CoAs_2 (smaltite). There are many minerals in which sulfur is partially replaced by arsenic.

The arsenides themselves have little commercial significance. Those produced are obtained by direct synthesis. The alkali-metal arsenides are also obtained by reaction in liquid ammonia. However, in this case polyarsenides can form in addition to the simple arsenides. The arsenides of the alkali metals, alkaline-earth metals, zinc, etc., are rapidly decomposed by water and acids with the formation of arsine. They may be regarded as derivatives of arsenic hydride. Most of the heavy metal arsenides, whose composition often does not reflect any simple relationship to arsenic hydride, are intermetallic phases and are highly resistant to acids. Gallium and indium arsenides are important in the semiconductor industry.

13.8 Uses and Economic Aspects

The demand for metallic arsenic is limited. It is used in nonferrous alloys, and high-purity arsenic is used in electronic and semiconductor devices. The addition of ca. 0.5% As to the lead grid in lead-acid storage batteries increases endurance and corrosion resistance. Additions of the same order to copper alloys improve high-temperature stability, recrystallization temperature, and corrosion resis-

tance. The addition of up to 2% As to lead used in shot improves its sphericity.

High-purity arsenic (at least 99.999%) is used in electronics in conjunction with gallium or indium for the production of diodes (LED), infrared detectors, and lasers. Solar cells based on gallium arsenide have an efficiency of 20% [42]. Commercial arsenic metal has a purity of 99%. Most arsenic is used in the form of compounds, arsenic trioxide being the sole starting material. Arsenic compounds are used in the following fields:

- Agriculture and forestry: herbicides and insecticides in cotton, coffee, and rice growing; wood preservatives; feed additives to aid in fattening and prevent infection
- Industrial chemicals: electrolyte purification in the electrolysis of zinc; metal pickles containing phosphoric acid
- Glass industry: fining agents and decolorizers [43]

Internationally, these fields of applications are all of importance; the regional differences are shown in Table 13.9 [44, 45], which also shows consumption figures for 1979.

The major producing countries for arsenic trioxide in order of capacity are Sweden, Mexico, France, the United States, the former Soviet Union, South-West Africa, and Peru. The principal manufacturers are:

Country	Manufacturer
France	Société minière et métallurgique de Pennaroya; Mines et Produits chimiques de Salsigne
Mexico	Industrial Minera Mexico SA (IMM)
Peru	Centromin-Peru (Empresa minera del centro de Perú)
South-West Africa	Tsumeb Corporation Ltd.
Sweden	Boliden Metall AB
USA	ASARCO Inc.
Former USSR	State-run companies

Production information is limited. The report of the Bundesumweltamt (Federal Department of the Environment, Germany) [45] based on a Bureau of Mines report [46] quotes a world production of 60 000 t for 1974. FRIEDENSBURG [47], in a world production

analysis (Table 13.10), arrives at only half that figure; however, that table only covers the ores smelted in the producing country.

Table 13.9: Arsenic consumption in tons of As_2O_3 content per year in 1979.

	United States		Former Fed. Rep. of Germany	
	t/a	%	t/a	%
Agriculture and forestry	13 500	70	0	0
Industrial chemicals	4 000	20	290	37
Glass industry	960	5	300	38
Alloys and electronics	600	3	171	22
Others (pharmaceuticals, catalysts, feed additives)	360	2	30	4
Total	19 420		791	

The world production of arsenic trioxide has been falling steadily since 1974. Production in Sweden and South-West Africa has declined to less than half. Because arsenic trioxide is a by-product, production is determined not by the demand for arsenic but by the demand for copper, lead, etc.

The biggest consumers of arsenic trioxide are the United States, Malaysia, and the United Kingdom, in that order. Malaysia uses arsenic-based herbicides in its rubber plantations; the United Kingdom imports As_2O_3 and

exports arsenic-containing pesticides and wood preservatives [44].

Storage. Arsenic trioxide is marketed as a bulk product packed in casks. Since arsenic compounds are classified as dangerous goods, all containers and shipments must be identified [48].

13.9 Safety Measures

Although pure metallic arsenic is not poisonous, the occurrence of toxic arsenic oxides formed by oxidation in air is unavoidable. In handling or manufacture of arsenical materials, inhalation of dust and skin contact with arsenic-containing gases must be prevented. In the absence of adequate safety measures the following jobs involve a risk:

- Metal recovery/contamination by arsenic
- Roasting of iron pyrites
- Cleaning of lead chambers in the manufacture of sulfuric acid
- Processing of arsenical minerals
- Production of arsenic-containing pharmaceuticals
- Use in pyrotechnics
- Burnishing of metal surfaces

Table 13.10: Arsenic production in tons of As_2O_3 content per year.

	1968	1969	1970	1971	1972	1973	1974	1975	1976	1977	1978 ^a	1979
Europe	42 780	38 127	19 868	16 344	16 659	16 790	16 770				22 189	
Germany	800	588	370	36	445	470	450				563	
France	13 600	13 600	10 191	8 022	9 000	9 000	9 000				7 280	
Portugal	200	247	190	186	14	20	20				—	
Sweden	21 050	16 500	2 000	1 000	—	16 525	—				6 706	
Spain	130	92	17	—	—	—	—				—	
USSR ^b	7 000	7 100	7 100	7 100	7 200	7 300	7 300				7 640	
Asia (Japan)	686	580	883	956	427	500	500				551	
SW Africa	484	2 217	4 062	3 700	2 370	8 140	8 000				2 407	
America (except USA)	15 380	8 934	10 272	12 330	6 306	5 548	5 050				—	
Brazil	312	300	298	148	164	69	50				—	
Canada	314	154	64	45	27	—	—				72	
Mexico	13 528	8 000	9 138	11 481	5 096	4 379	4 000				6 263	
Peru	1 226	480	772	656	1 019	1 100	1 000				1 257	
Total	59 330	49 858	35 085	33 330	25 762	30 978	30 320	—	—	—	32 739	
World (Bureau of Mines, [44])		63 945	65 263	62 029	58 557	59 994	59 395	51 971	42 989	38 918	40 283	40 475

^a From [44].

^b Estimated.

- Use of arsenic-containing raw materials in the glass industry
- Repair or cleaning of flue-dust plants, filters, etc.
- Use in wood preservatives.

All working involving arsenic or its compounds should be carried out in sealed containers. In filling and emptying of apparatus, adequate measures must be taken to ensure that the maximum allowable concentrations (MAK values) are not exceeded. A dust-free working environment should be ensured by maintaining reduced pressure in the apparatus or by an adequate exhaust system.

Sampling must be carried out only with the aid of suitable equipment, e.g., air locks, vacuum injectors, and sealed sampling vessels. Rooms used for work involving arsenical materials should be adequately ventilated and dust free. If there is a general danger of inhaling arsenical materials, e.g., during open sampling, respirators must be worn. In relatively heavily dust-laden atmospheres, special protective clothing should be worn to prevent any skin contact with arsenic. The arsenic content in the air of the working environment should be monitored continuously.

The MAK for AsH_3 in air is 0.2 mg/m^3 [50]. In Germany, arsenic trioxide, arsenic pentoxide, arsenous acid, arsenic acid, and their salts are included in the list of carcinogenic working materials. As a result a standard concentration of 0.2 mg/m^3 is stipulated for all arsenical compounds in Germany [49].

In Germany, all work involving arsenic and its compounds is governed by the regulations for dangerous materials (TRGA) [49]. Emphasis should be placed on personal hygiene, e.g., on the banning of eating and smoking in workrooms, on the need to wash before eating, and on the need to shower after finishing work. Adopting these measures can ensure a high level of occupational hygiene, even where work involving arsenic is carried out on an industrial scale.

In every country there are special provisions for packaging, identification, storage, and transportation of arsenical products. The

dangers involved in the use of arsenical preparations are not treated as seriously in the United States as in the EEC, where generally speaking such preparations are completely banned.

13.10 Toxicology

Nearly all arsenic compounds are considerably toxic, especially the inorganic ones.

The trivalent arsenic compounds, such as arsenic trioxide, As_2O_3 , arsenic trifluoride, AsF_3 , arsenic trichloride, $AsCl_3$, and arsine, AsH_3 , are markedly more toxic than the pentavalent compounds. Elemental arsenic itself is not appreciably toxic, but it is converted readily to toxic compounds in the organism. Pure arsenic(III) sulfide, As_2S_3 , also seems to have a comparatively low toxicity, but often the crude sulfide is contaminated by arsenic trioxide. In contrast, some pentavalent organic compounds have been used as therapeutics; these benzenearsonic derivatives contain a stable carbon-arsenic bond and are practically not converted to inorganic arsenicals [51].

Absorption. Arsenicals can be absorbed mainly by ingestion and inhalation, and also through the skin. They are widely distributed within 24 h into different tissues, mainly the liver, kidney, lung, spleen, bone marrow, skin, and, to a lesser extent, brain, heart, and uterus. Small quantities can be detected in hair and nails several months after the main portion of the arsenic has been eliminated from the body [52]. Inorganic arsenicals do not cross the blood-brain barrier but can pass across the mammalian placental membrane [53].

Excretion of arsenicals occurs mainly via urine, to a smaller extent via the feces [54], and by loss of hair and skin shedding. After the administration of a single dose, the concentration of arsenic in liver and kidney starts to decrease only after 24 h [54]. The concentration of arsenic in urine of unexposed persons is between zero and 0.22 mg/L , after industrial exposure between 0.04 and 0.9 mg/L [55]. After inhalation of arsenic dust, the excretion of methylated arsenic could be ob-

served [56]; traces of arsenic can be exhaled as trimethylarsine [57].

Metabolism. Most arsenic compounds – trivalent or pentavalent, inorganic or organic – are transformed to an arsenic oxide form, which can react readily with proteins, especially with those containing two vicinal mercapto groups, thus forming stable cyclic structures. The inhibition of essential enzymes is considered to be the first step of cell damage [51]. The high affinity of the arsenoxide moiety to the vicinal mercapto groups of 2,3-dimercapto-1-propanol (BAL, British Anti Lewisite) and of 2,3-dimercapto-1-propane-sulfonic acid is used successfully in arsenic poisoning therapy.

Arsenicals can cause acute, subacute, and chronic poisoning. However, acute poisoning is currently rare in comparison to subacute or chronic poisoning.

Acute Toxicity. Arsenic poisoning mostly occurs by ingestion of inorganic trivalent compounds such as arsenic trioxide. The smallest doses of As_2O_3 reported to be fatal after ingestion are 70–180 mg [52]. Symptoms which can occur within a few minutes or after a delay of several hours are vomiting, diarrhea, damage of the intestinal tract, muscular cramps, facial edema, cardiac abnormalities, dehydration, and – as a consequence – shock. The inhalation of irritant arsenic compounds, such as arsenic trichloride or arsenical war gases, causes cough, dyspnea, pain in the chest, severe damage to the respiratory tract, headache, general weakness, nausea, vomiting, and colic diarrhea. Airborne dusts often result in irritation of exposed skin and mucous membranes such as bronchitis, conjunctivitis, laryngitis, and dermatitis [58]. Arsenic trichloride may be absorbed through the skin with fatal consequences [59].

Chronic Toxicity. Chronic arsenic poisoning can be caused by intake of food and water contaminated with arsenicals or by inhalation of air-borne dusts during long-term occupational exposure, mainly in smelting plants of ores containing arsenic, insecticide factories, and

among vineyard workers, even many years after termination of exposure. Symptoms of these chronic poisonings were symmetrical palmar and plantar hyperkeratosis, white striæ of the finger nails, cardiovascular manifestations, myocardial ischemia, hypertension, liver dysfunctions, hematological changes, and vascular disorders resulting in gangrenes of the lower extremities (blackfoot disease). A variety of severe symptoms is treated below.

Skin lesions are frequently observed, e.g., in the production of insecticides [60] and in copper ore smelting plants [61]. Typical symptoms are hyperkeratosis, warts, melanosis, contact dermatitis, eczematoid features of varying degrees of severity, and vascular lesions. Hyperkeratosis often is characterized by thickening, drying, and cracking of the skin [62]. Arsenical melanosis is also a common sign after long-term exposure and can occur on the chest, abdomen, scrotum, and back. Further characteristic symptoms are depigmentation (leukoderma) of pigmented areas and white striæ of the fingernails [63].

Effects on mucous membranes are conjunctivitis with swelling and pain, keratoconjunctivitis (resulting from exposure to the insecticide calcium arsenate, $Ca_3(AsO_4)_2$), irritation of the pharynx and bronchial passages, and irritation of the nose resulting in acute and chronic rhinitis. Among copper smelter workers, perforation of the nasal septum has been commonly observed [64].

Peripheral neuritis, with such symptoms as pain, difficulties in walking, burning and tenderness in the affected limbs, and later on severe weakness in both legs and feet, has been described after long-term exposure to arsenate dusts [62]. In contrast to the peripheral neuritis caused by lead, the arsenic-caused neuritis is painful; the nerves of these patients show neuronal degeneration [52]. Further symptoms, observed especially in cases of severe chronic intoxications, are headache, aphasia, drowsiness, disorientation, and changes in the personality.

Liver damages, especially liver cirrhosis, have been observed, e.g., in vintagers who used arsenical herbicides [65] and after long-

term consumption of arsenic-contaminated homemade wine [66]. These liver disturbances, which often are complicated by the additional occurrence of chronic hepatitis, ascites, and enlarged liver, are probably not due to skin contact with or inhalation of arsenicals, but to ingestion of contaminated wine. The occurrence of liver damage among industrial workers is reported to be less frequent [58].

Circulatory system symptoms after chronic arsenical poisoning are abnormalities in the electrocardiogram [67] indicating a toxic myocardial effect, peripheral vascular disturbances, gangrene of the extremities, atrophic acrodermatitis, endoangitis [68], and the so-called blackfoot disease [69].

Gastrointestinal disturbances are less common among workers with long-term exposure to arsenicals [70]. During chronic intoxication by ingestion, digestive disturbances, nausea, vomiting, and loss of appetite are occasionally reported.

Hematological changes are also less common in chronic poisoning after industrial airborne exposure. Symptoms like moderate anemia, leucopenia, and thrombocytopenia have been observed after long-term ingestion of inorganic arsenicals. However, these symptoms disappeared 2–3 weeks after termination of the arsenic ingestion [71].

Cancer. Workers in smelters or in insecticide factories exposed to arsenic trioxide have a significantly higher risk of lung cancer in comparison to persons not exposed [72, 73]. A significant excess of oral and pharyngeal cancer could be noticed among male textile workers in England and Wales engaged in fiber preparation [74]; this excess could be traced to arsenic-containing disinfectants used on sheep. Skin cancer as a result of ingesting of contaminated water, with multifocal lesions over the entire body, occurred in Cordoba, Argentina [75], Antofagasta, Chile [76], and in Taiwan [77]. The development of other types of tumors related to long-term exposure by ingestion, inhalation, or dermal contact has been observed frequently; however, in these cases the relationship between arsenic exposure and

development of tumors could not be confirmed as yet unequivocally [55].

Mutagenicity. The mutagenic action of inorganic and organic arsenicals has been tested on microorganisms (DNA damage in *Bacillus subtilis*) [78], *Drosophila* (increase in crossing-over frequencies) [79], and mammalian cells in vivo and in vitro. A significant increase of chromosomal aberrations could be demonstrated as a result of contact with arsenicals in lymphocytes from peripheral blood [80] and in fibroblast cultures of humans [81].

Teratogenicity. Teratogenic effects of disodium arsenate, such as exencephaly [82], cleft palate and lip, microanophthalmia, genitourinary abnormalities, ear deformities, and renal agenesis, were observed in hamster fetuses [83–85]. In the case of a 17-year-old girl, the ingestion of arsenic during the third trimester of her pregnancy caused the death of her baby (1100 g!) 11 h after birth; liver, kidney, and brain of the baby contained high concentrations of arsenic [86]. Among employees and persons living near a smelter, a significant decrease of the birth weight of the offspring, an increased frequency of spontaneous abortions, and a higher rate of malformations of the children born were observed [87, 88].

Arsine. Acute poisoning with arsine, AsH_3 , which is rather frequent among industrial workers as compared to poisoning with other arsenicals, results in general malaise, nausea, vomiting, abdominal cramps, coppery skin pigmentation, red staining of the conjunctiva [89], and leucocytosis [90]. A most characteristic symptom of acute arsine poisoning is rapid hemolytic anemia, which results in hemoglobinuria, decreased hemoglobin level, jaundice, and after 2–24 h, shock, oliguria, and anuria due to blockade of renal tubuli [91] by membrane residues of red blood cells. Other symptoms are pyrexia, edema of the lungs, delirium, and coma. Death after few days is mostly due to myocardial failure. In all cases of arsine poisoning an elevation of the T-wave in the electrocardiogram can be noticed. Depending on the severity of the intoxi-

cation, the time of the appearance of symptoms may vary between a few minutes and 24 h.

Chronic arsine poisoning shows a delayed onset of symptoms mentioned above, and in some cases peripheral neuritis [92], hemoglobin levels as low as 32 g/L, and basophilic stippling of red blood cells [93] have been observed.

Toxicological Data and Exposure Limits. Toxicological data of commonly used arsenicals are summarized in Table 13.11. The MAK values for arsenicals such as oxides, arsenic acids, and their salts are not established because these compounds have been proved to cause malignant tumors in humans [107]. The MAK value of arsine is 0.2 mg/m³ (0.05 ppm) [107]. The TRK values (Technical Guideline in Germany) for all compounds with the exception of arsine is 0.2 mg/m³ (as As) [108]. In the USA, the permissible exposure limit at work for calcium arsenate is 1 mg/m³, for arsine 0.2 mg/m³, for all other inorganic arsenic compounds 0.01 mg/m³, and for organic arsenicals 0.5 mg/m³ (as As) [109]. In Japan, the maximum allowable workplace air concentration for arsenic trioxide is 0.5 mg/m³, and for arsine 0.2 mg/m³ [110]. In Sweden, this value

is 0.05 mg/m³ (as As) for all arsenic compounds [111].

13.11 References

1. H. Stöhr, *Z. Anorg. Allg. Chem.* **242** (1939) 138.
2. F. Pawlek: *Metallhüttenkunde*, De Gruyter, Berlin 1982, pp. 530–533.
3. L. K. Chuchalin, G. L. Pashkov, *Cvetnye Metally* **1980**, no. 9, 16–18.
4. *Ullmann*, 4th ed., vol. 8, 46–66.
5. K. Hanusch: Private information of Boliden AB.
6. K. C. Grogan, *Can. Min. Metall. Bull.* **46** (1953) 214–218.
7. B. M. Reingold et al., *Cvetnye Metally* **42** (1969) no. 6, 42–45.
8. *Sulphur* **1968**, no. 78, 20–24.
9. H. Wolf et al., *Chem. Ing. Tech.* **40** (1968) 441.
10. *Sulphur* **1969**, no. 84, 30–32.
11. K. G. Görling et al., *Z. Erzbergbau Metallhüttenwesen* **12** (1959) 553–557.
12. Patentaktiebolaget Gröndal-Ramén, DE 628554, 1937.
13. Boliden AB, DE-OS 1806647, 1968.
14. V. G. Rchiladze: *Arsen*, Moscow 1969.
15. Boliden AB, CA 863857, 1971 (S. T. Henriksson).
16. H. E. Hirsch: "The recovery of metallic arsenic in COMINCO's lead operations", Proceedings of Lead-Zinc-Tin 80, committee at the 109th AIME Annual Meeting, Las Vegas, NV, Febr. 1980, pp. 24–28.
17. D. Lezal et al., *Chem. Zvesti* **19** (1968) 620–627.
18. Siemens-Schuckert-Werke AG, DE 1181919, 1964.
19. A. S. Girenko, O. N. Kalashnik, V. A. Kirichenko, I. I. Skakovskii, A. M. Tuzovskii: "Producing arsenic of semiconductor purity by the chloride method", *Cvetnye Metally* **1972**, no. 1, 59–62.

Table 13.11: Toxicological data of arsenic and some arsenic compounds.

Compound	Toxicological parameter	Dose	Species	Route	Reference
Arsenic	LDLo	20 mg/kg	rat	intramuscular	[94]
Arsenic acid, hemihydrate	LD ₅₀	6 mg/kg	rabbit	i.v.	[95]
Arsenic pentoxide	LD ₅₀	55 mg/kg	mouse	oral	[96]
Arsenic trichloride	LDLo	100 mg/m ³ , 1 h	cat	inhal.	[97]
Arsenic trifluoride	LDLo	2000 mg/m ³ , 10 min	mouse	inhal.	[98]
Arsenic trioxide	LD ₅₀	45 mg/kg	mouse	oral	[96]
	LD ₅₀	20 mg/kg	rat	oral	[99]
	LDLo	4 mg/kg (as As)	rabbit	i.v.	[95]
Arsine	TCLo	3 mL/m ³	human	inhal.	[52]
	LCLo	25 mL/m ³ , 30 min	human	inhal.	[100]
	TCLo	93 µL/m ³	human	inhal.	[101]
Calcium arsenate	LDLo	50 mg/kg	rabbit	oral	[102]
Disodium arsenate	LDLo	30 mg/kg	rat	i.p.	[103]
Disodium arsenate, heptahydrate	TDL ₀	43 mg/kg	mouse	i.p.	[104]
Lead arsenate	LD ₅₀	100 mg/kg	rat	oral	[105]
	LDLo	75 mg/kg	rabbit	oral	[102]
Sodium metaarsenite	TDL ₀	40 mg/kg	mouse	oral	[106]

20. E. I. Ponomarewa, W. D. Solowiewa, *Vestn. Akad. Nauk Kaz. SSR* **1974**, no. 6, 52–55.
21. J. Roger Loebenstein: "Arsenic", *Bull. U.S. Bur. Mines* **1980**, no. 671, 47–54.
22. G. Sandberg, T. L. Hebble, D. L. Paulson: "Oxidative sulfuric acid leaching of lead smelter mattes", *Rep. Invest. U.S. Bur. Mines*, RI 8371 (1979) 1–16.
23. "New USBM methods boost metals recovery in leaching processes in this month in mining", *Eng. Min. J.* **181** March 1980, 43.
24. P. A. Bloom, J. H. Maysilles, H. Dolezal: "Hydrometallurgical treatment of arsenic-containing lead-smelter flue dust", *Rep. Invest. U.S. Bur. Mines*, RI 8679 (1982) 1–12.
25. A. Metha: "A research investigation of new techniques for control of smelter arsenic flue dust wastes", EPA Grant R 804 595 010, Min. Res. Center Montana, Techn. Alumin. Foundation, Butte, MT, 1977, sec. 4, pp. 1–43.
26. Hazen Research, US 4244734, 1981 (J. E. Rupolds, E. L. Coltrinari).
27. St. Dayton: "Equity silver on line with leach plant. How purged from a high-silver copper concentrate before smelting", *Eng. Min. J.* **183** (Jan. 1982), 78–83.
28. L. S. Celochsaev, R. A. Isakowa, B. C. Tarasenko, I. K. Chaschimov, Ju. A. Seleznev, *Cvetnye Metally*, **1980**, no. 9, 25–27.
29. Klöckner-Humboldt-Deutz, DE 3003635 A 1, 1981 (I. Barin, G. Michael, R. Hesse, S. Wirosiedirio).
30. E. A. Woolson: "Arsenical Pesticides", *ACS Symp. Ser.* **1975**, no. 7, 108–124.
31. R. S. Braman: "No Arsenical Pesticides", *ACS Symp. Ser.* **1974**, no. 7, 1–13.
32. H. Berg, H. Sperlich: "Nachweis und Bestimmung von Organoarsenverbindungen auf Früchten", *Mitteilungsbl. GDCh Fachgruppe Lebensmittelchem. Gerichl. Chem.* **28** (1974) 298.
33. R. G. Robins: "The Solubility of Metal Arsenates", *Met. Trans.* **12B** (1981) 103.
34. *Handbook of Chemistry and Physics*, 63rd ed., 1982–1983, The Chemical Rubber Co., Cleveland.
35. Kirk Othmer, 3rd ed., vol. 3, p. 243–266.
36. M. Jansen, *Angew. Chem.* **89** (1977) 326.
37. M. Jansen, *Z. Anorg. Allg. Chem.* **411** (1978) 5.
38. R. Wegler: *Chemie der Pflanzenschutz- und Schädlingsbekämpfungsmittel*, vol. 4 + 5, Springer Verlag, Berlin-Göttingen-Heidelberg-New York 1977.
39. D. D. Wagman et al., *NBS Tech. Note U.S.* **1968**, no. 270-3, 95–98.
40. K. Seppelt, *Z. Anorg. Allg. Chem.* **434** (1977) 5; 439 (1978) 5.
41. *Winnacker-Küchler*, 4th ed., vol. 3 (1983), p. 422.
42. CAEN, 9 May 1977, 5.
43. K. P. Hanke: "Blasenbildung in Glasschmelzen", *Umschau Wiss. Tech.* **72** (1972) 436.
44. U.S. Bureau of Mines, Bulletin 671, Mineral Facts and Problems, 1980.
45. Umweltbundesamt: *Umwelt- und Gesundheitskriterien für Arsen*, Berichte 4/83, E. Schmidt Verlag, Berlin 1983.
46. U.S. Bureau of Mines (1975) Metals, Minerals, and Fuels. In: *Minerals Yearbook*, Washington, DC, U.S. Dep. of Interior, Vol. 1.
47. F. Friedensburg, G. Dorstewitz: *Die Bergwirtschaft der Erde*, 7th ed., Enke Verlag, Stuttgart 1976.
48. Gesetz über die Beförderung gefährlicher Güter v. 6.8.1975, BGBl. I, p. 2121 and 18.9.1980, BGBl. I, p. 1729.
49. Arbeitsstoffverordnung v. 29.7.1980, BGBl. I, p. 1071, 1536, 2159 and v. 11.2.1982, BGBl. I, p. 144.
50. Maximale Arbeitsplatzkonzentration, Mitteilungen der XVII. Senatskommission zur Prüfung gesundheitsschädlicher Arbeitsstoffe 1981, Verlag H. Boldt, Boppard (mit Nachlieferungen).
51. L. S. Goodman, A. Gilman: *The Pharmacological Basis of Therapeutics*, 5th ed., MacMillan Publ. Co. New York 1975, p. 925.
52. B. L. Vallee, D. D. Ulmer, W. E. C. Wacker, *AMA Arch. Ind. Health* **21** (1960) 132.
53. H. P. Morris, E. P. Laug, H. J. Morris, R. L. Grant, *J. Pharmacol. Exp. Ther.* **64** (1938) 420.
54. F. T. Hunter, A. F. Kip, J. W. Irvine, *J. Pharmacol. Exp. Ther.* **76** (1942) 207.
55. IARC Monographs on the Evaluation of the Carcinogenic Risk of Chemicals to Humans, vol. 23, *Internat. Agency for Research on Cancer*, Lyon 1980, p. 39.
56. T. J. Smith, E. A. Crecelius, J. C. Reading, *EHP Environ. Health Perspect.* **19** (1977) 89.
57. H. A. Satterlee, *AMA Arch. Ind. Health* **17** (1958) 218.
58. K. Tsuchiya, N. Ishinishi, B. J. Fowler in: "Toxicology of Metals", EPA-600/1-77-022, *Environ. Health Effects Ser.* **2** (1977) 30.
59. S. Delepine, *J. Ind. Hyg.* **4** (1923) 346, 410.
60. P. Vigne, *Ann. Dermatol. Syphiligr.*, VII^e Sér., **1** (1930) 1150.
61. I. Holmqvist, *Acta Derm. Venereol.* **31**, Suppl. 26, (1951) 1.
62. R. M. Watrous, M. B. McCaughey, *Ind. Med.* **14** (1945) 639.
63. R. A. Mees, *JAMA J. Am. Med. Assoc.* **72** (1919) 1337.
64. S. S. Pinto, C. M. McGill, *Ind. Med. Surg.* **22** (1953) 281.
65. H. Luchtrath, *Dtsch. Med. Wochenschr.* **97** (1972) 21.
66. K. H. Butzengeiger, *Klin. Wochenschr.* **19** (1940) 523.
67. F. S. Glazener, J. G. Ellis, P. K. Johnson, *Calif. Med.* **109** (1968) 158.
68. K. H. Butzengeiger, *Dtsch. Arch. Klin. Med.* **194** (1949) 1.
69. S. Yeh, *Natl. Cancer Inst. Monogr.* **10** (1963) 81.
70. W. D. Buchanan: *Toxicity of Arsenic Compounds*, Elsevier, Amsterdam 1962.
71. R. A. Kyle, G. L. Pease, *New Engl. J. Med.* **273** (1965) 18.
72. M. G. Ott, B. B. Holder, H. L. Gordon, *Arch. Environ. Health* **29** (1974) 250.
73. S. S. Pinto, V. Henderson, P. E. Enterline, *Arch. Environ. Health* **33** (1978) 325.
74. E. Moss, W. R. Lee, *Br. J. Ind. Med.* **31** (1974) 224.
75. L. Manzano, E. E. Tello, *Rev. Fac. Cienc. Med. Cordoba* **13** (1955) 133.
76. J. M. Borgeño, P. Vicent, H. Venturino, A. Infante, *EHP Environ. Health Perspect.* **19** (1977) 103.

77. W. P. Tseng, *EHP Environ. Health Perspect.* **19** (1977) 109.
78. H. Nishioka, *Mutat. Res.* **31** (1975) 185.
79. G. W. R. Walker, A. M. Bradley, *Can. J. Gen. Cytol.* **11** (1969) 677.
80. J. K. Petres, K. Schmid-Ulrich, V. Wolf, *Dtsch. Med. Wochenschr.* **95** (1970) 79.
81. R. Happle, H. Hoehn, *Clin. Genet.* **4** (1973) 17.
82. V. H. Ferm, S. Carpenter, *J. Reprod. Fertil.* **17** (1968) 199.
83. V. H. Ferm, A. Saxon, *Experientia* **27** (1971) 1066.
84. V. H. Ferm, A. Saxon, B. W. Smith, *Arch. Environ. Health* **22** (1971) 557.
85. V. H. Ferm, *Rev. Environ. Health* **1** (1974) 238.
86. G. Luego, G. Cassady, P. Palmisano, *Am. J. Dis. Child* **117** (1969) 328.
87. S. Nordström, L. Beckman, I. Nordensen, *Hereditas* **90** (1979) 291.
88. S. Nordström, L. Beckman, I. Nordensen, *Hereditas* **90** (1979) 297.
89. D. Macaway, D. A. Stanley, *Br. J. Ind. Med.* **13** (1956) 217.
90. S. S. Pinto, S. J. Petronella, D. R. Johns, M. F. Arnold, *Arch. Ind. Hyg. Occup. Med.* **1** (1950) 437.
91. W. J. Levinsky, R. V. Smalley, P. N. Hillyer, R. L. Shindler, *Arch. Environ. Health* **20** (1970) 436.
92. S. F. Dudley, *J. Ind. Hyg.* **1** (1919) 215.
93. F. M. R. Bulmer, H. E. Rothwell, S. S. Polack, D. W. Stewart, *J. Ind. Hyg. Toxicol.* **22** (1940) 111.
94. Progress Report for Contract No. PH-43-64-886, National Cancer Institute, Institute of Chemical Biology, Univ. of San Francisco, Sept. 1970.
95. G. Joachimoglu, *Biochem. Z.* **70** (1915) 144.
96. G. Bünemann, W. Klosterkötter, *Int. Arch. Gewerbepathol. Gewerbehyg.* **20** (1963) 21.
97. F. Flury, *Z. Gesamte Exp. Med.* **13** (1921) 523.
98. National Defense Research Committee, Office of Scientific Research and Development, Progress Rep. NDCrc-132, Aug. 1942.
99. J. W. E. Harrison, E. W. Packman, D. D. Abbott, *AMA Arch. Ind. Health* **17** (1958) 118.
100. D. T. Teitelbaum, L. C. Kier, *Arch. Environ. Health* **19** (1969) 133.
101. G. G. Parish, R. Glass, R. Kimbrough, *Arch. Environ. Health* **34** (1979) 224.
102. C. W. Muehlberger, *J. Pharmacol. Exp. Ther.* **39** (1930) 246.
103. K. W. Franke, A. L. Moxon, *J. Pharmacol. Exp. Ther.* **58** (1936) 454.
104. R. D. Hood, S. L. Bishop, *Arch. Environ. Health* **24** (1972) 62.
105. *Assoc. Food Drug Off. U.S. Q. Bull.* **15** (1951) 122.
106. M. N. Baxley, R. D. Hood, G. C. Vedel, W. P. Harrison, G. M. Szczech, *Bull. Environ. Contam. Toxicol.* **26** (1981) 749.
107. Deutsche Forschungsgemeinschaft (eds.): *Maximale Arbeitsplatzkonzentrationen (MAK)* 1982, Verlag Chemie, Weinheim 1982.
108. R. Kühn, K. Birett: *Merkblätter Gefährliche Arbeitsstoffe*, vol. 2: "TRK-Liste", Verlag Moderne Industrie, München 1981.
109. US Occupational Safety and Health Administration, *Occup. Saf. Health Rep.* **7** (1978) 1842, 1881.
110. Japanese Society for Industrial Hygiene, *Sangyo Igaku* **20** (1978) 290.
111. M. Winell, *Ambio* **4** (1975) 34.

14 Antimony

KUNIBERT HANUSCH, KARL-ALBERT HERBST, GERHARD ROSE (§§ 14.1–14.10, 14.12–14.13); HANS UWE WOLF (§ 14.14)

14.1 Introduction	823	14.9 Alloys and Intermetallic Compounds.....	837
14.2 History.....	823	14.10 Compounds.....	837
14.3 Properties	824	14.10.1 Antimony Chlorides.....	837
14.4 Occurrence.....	825	14.10.2 Antimony Fluorides.....	838
14.5 Beneficiation	825	14.10.3 Antimony Tribromide.....	838
14.6 Recovery of the Metal	826	14.10.4 Antimony Triiodide	838
14.6.1 Roasting.....	826	14.10.5 Antimony Oxides.....	838
14.6.2 Reduction of Oxide to the Metal ...	828	14.10.6 Antimonic Acid and Antimonates ..	839
14.6.3 Direct Reduction to the Metal	829	14.10.7 Antimony Sulfides	839
14.6.4 Other Direct Processes.....	830	14.10.8 Antimony Sulfate	840
14.6.5 Hydrometallurgical and Electrolytic Methods.....	830	14.10.9 Stibine	840
14.6.6 Recovery from By-products, Complex Ores, and Recycled Material	832	14.11 Chemical Analysis	840
14.7 Refining.....	833	14.12 Uses.....	840
14.8 Fine Purification	835	14.13 Economic Aspects.....	841
		14.14 Toxicology	841
		14.15 References.....	843

14.1 Introduction

Antimony is an element of main group V having atomic number 51 and atomic mass M_r 121.75. Two isotopes occur in nature, mass numbers 121 and 123. The configuration in the outer electron shell is $5s^25p^3$. If these electrons are donated, antimony is electropositive and trivalent, as in SbCl_3 , or pentavalent, as in SbCl_5 ; if three electrons are added to the outer shell, the antimony is electronegative and trivalent, as in SbH_3 .

Usually antimony is a white lustrous metal of average hardness, 3.0 on the Mohs scale. It is brittle and easy to pulverize. If it solidifies slowly, pure antimony has a foliated structure; if rapidly, a granular structure. It forms rhombohedral crystals.

Metallic antimony is the only stable allotope. There are unstable forms: yellow antimony, black amorphous antimony, and what is known as explosive antimony. Yellow antimony is formed when air or oxygen is passed through liquid stibine. Black amorphous antimony is obtained by rapidly cooling antimony

vapors and is also formed from yellow antimony at -90°C . At room temperature black antimony slowly reverts to metallic antimony, and at 400°C reversion is spontaneous. Black amorphous antimony ignites spontaneously in air. Explosive antimony is obtained by electrolysis of antimony(III) chloride solution in hydrochloric acid at a high current density with an antimony anode and a platinum cathode. It consists of black amorphous antimony contaminated with antimony trichloride.

14.2 History

Antimony was known to the Chinese 5000 years ago. The ancient Egyptians were also acquainted with it, but they considered it to be a variety of lead, a belief that persisted until the 16th century. The first instructions on processing the Latin *stibium* or the Egyptian *stim* (antimony glance or stibnite) appeared at the beginning of our era. PEDANIOS DIOSKORIDES and PLINY THE ELDER referred to antimony glance as platyophthalmion (eye dilator), callibphary (eyelid cosmetic), and gynaikeios

(feminine), because antimony(III) sulfide powder was then an ophthalmic ointment and a coveted cosmetic.

The word *Antimonium* seems to have been first used for antimony(III) sulfide in 1050 by CONSTANTINUS AFRICANUS. Light was gradually shed on the chemistry of antimony and on antimony therapy by PARACELUS (1526–1541), ANDREAS LIBAVIUS (*Alchemia*, 1597, and the *Syntagmatis Arcanorum* volumes, 1613–1615), the Benedictine monk BASILIUS VALENTINUS (*Triumphwagen Antimonii*, 1604), N. LEMERY (*Traité de l'antimoine*, 1707), and other works of the iatrochemical epoch. At an early stage, alchemists understood the significance of antimony for separating gold from silver. The recovery of *antimonium crudum* from its ores was described in detail by LAZARUS ERCKER (1574) and GEORGIUS AGRICOLA (*De re metallica*, 1556).

14.3 Properties

Density	
solid at 20 °C	6.688 g/cm ³
liquid at 630.5 °C	6.55 g/cm ³
Melting point	630.5 °C
Heat of fusion	10.49 kJ/mol
Boiling point at 101.3 kPa	1325 °C
Tensile strength	10.8 N/mm ²
Modulus of elasticity	566 N/mm ²
Surface tension	
solid at 432 °C	317.2 mN/m
liquid at 630 °C	349 mN/m
liquid at 1200 °C	255 mN/m
The surface tension of the solid decreases nearly linearly with temperature. The slope at the melting point is $-0.07 \text{ mNm}^{-1}\text{K}^{-1}$	
Molar heat capacity at 630.5 °C	
solid	30.446 Jmol ⁻¹ K ⁻¹
liquid	31.401
Coefficient of linear expansion	
between 0 and 100 °C	$10.8 \times 10^{-6} \text{ °C}^{-1}$
Thermal conductivity	
at 0 °C	18.51 Wm ⁻¹ K ⁻¹
at 100 °C	16.58

Roughly 1/20th of the thermal conductivity of copper. The thermal conductivity of antimony depends on the grain size and the direction in the crystal.

Electrical resistivity at 0 °C	$30.0 \times 10^{-6} \Omega \text{cm}$
Molar susceptibility at 20 °C	-99.0×10^{-6}

Polycrystalline antimony is diamagnetic.

Pure antimony does not change in air at room temperature, and it is not tarnished in humid air or pure water. If antimony is heated to redness in air, the molten metal ignites. Above 750 °C, steam oxidizes liquid antimony to antimony trioxide, and hydrogen is evolved. Antimony can be removed from lead–antimony alloys with steam. Antimony cannot be ignited in a current of hydrogen. If it is heated to redness in a current of nitrogen, gray vapors are given off, which condense to amorphous antimony.

Neither solid nor liquid antimony dissolves nitrogen. Fluorine, chlorine, bromine, and iodine react violently with antimony, even at room temperature, to form trihalides. The reaction with chlorine yields either SbCl₃ or a mixture of SbCl₃ and SbCl₅. Antimony(III) sulfide is the product of the reaction with sulfur, hydrogen sulfide, or dry sulfur dioxide. In the presence of an oxidizing agent or sulfur, aqueous sodium sulfide dissolves antimony to yield sodium thioantimonite. Yellow ammonium sulfide and sulfur-containing potassium sulfide solutions also readily dissolve antimony.

Molten antimony reacts with phosphorus, arsenic, selenium, and tellurium but not with boron, carbon, and silicon. The eutectic with lead contains 13% antimony and melts at 246 °C.

Antimony is resistant to concentrated hydrofluoric, dilute hydrochloric, and dilute nitric acids. It is readily soluble in a mixture of nitric and tartaric acids and in aqua regia. Phosphoric acid and a few organic acids also dissolve the metal, although acetic acid hardly belongs to this category. At room temperature it is not attacked by dilute or concentrated sulfuric acid. It is attacked at 90–95 °C by concentrated sulfuric acid, and sulfur dioxide is evolved.

Pure antimony is resistant to solutions of ammonium and alkali-metal hydroxides and to molten sodium carbonate. If heated to redness, it reacts with molten sodium or potassium hydroxide to form hydrogen gas and antimonites.

In the electrochemical series antimony falls between hydrogen and bismuth: H, Sb, Bi, As, Cu.

14.4 Occurrence

The average antimony content of the earth's crust has been estimated at $3 \times 10^{-5}\%$. Most antimony lodes occur in areas of volcanic activity and frequently in volcanic rocks themselves. They are found predominantly in ancient formations ranging up to the Carboniferous. Antimony deposits are seldom of sedimentary or epigenetic origin.

The most important antimony ore is rhombic *antimony glance* (gray antimony, antimonite, or stibnite), Sb₂S₃. It contains 71.7% antimony and occurs as characteristic black acicular crystals. Other ores include antimony oxides (valentinite, Sb₂O₃, rhombohedral; senarmontite, Sb₂O₃, cubic; cervantite, Sb₂O₄, orthorhombic), antimony hydroxides (stibiconite, Sb₂O₄·H₂O), antimony oxide sulfides (kermesite, pyrostibite, red antimony, 2Sb₂S₃·Sb₂O₃), native antimony, and double sulfides (jamesonite, Sb₂S₃·2PbS, which may contain silver, tetrahedrite, Sb₂S₃·4Cu₂S₂; and livingstonite, 2Sb₂S₃·HgS). More than 100 minerals containing antimony are known: there are eight antimonides, one sulfide (stibnite), 59 mixed antimonides and sulfides, and 46 oxide minerals.

Other sources of antimony besides ores are the intermediates in the processing of lead ores and the copper ore tetrahedrite, including the dross and slags from lead refining (particularly in the Harris process), speiss, flue dust, and anode slime.

Until about 1930, *deposits* in China supplied 70% of the world production of antimony ores. These were mined in Ksikwangschan (Hunan) and the provinces of Kwangsi Chuang, Kwangtung, and Yunnan. Now China's contribution has dropped to 16%, and China is only the third largest producer. Since the mid-1970s, Bolivia has been the largest producer of antimony ores, accounting for about 25% of the world total. The

production figures were 13 019 t in 1979, 17 092 t in 1980, and 15 296 t in 1981. The regions in which the ores are mined are San Juan, Tubiza (near Atocha), Huari, and Uncia. The second largest producer is South Africa (Murchison Range), accounting for an average of 18% of the total.

The fourth largest is the former USSR (Chajdarkan and Kadam-Dzai in Central Asia and the Ural and Caucasus Mountains), accounting for about 10% of the world production. Significant amounts are produced in Mexico, Thailand, Canada, Yugoslavia, Australia, Turkey, Greece, Italy, Spain, Austria, the United States, Morocco, Guatemala, former Czechoslovakia, and Brazil. Today, about two thirds of the world production of antimony ores is mined in Western countries, the American continents alone accounting for 30–40%. Frequently, the recovery of lead, silver, and gold is the primary mining goal, with the antimony only a by-product. An exception is the Murchison Mine in South Africa.

14.5 Beneficiation

The beneficiation process used depends chiefly on the content of antimony and other substances in the ore. Another important factor is how the ores are dispersed in the rock. If an antimony ore is not closely interlaced with the gangue, hand-picking techniques or jigs suffice for separation.

If stibnite (Sb₂S₃) ore contains more than 90% stibnite, it can be sold directly as Sb₂S₃ (crude antimony). Stibnite has a low melting point, and it can be extracted by melting if the ore contains 45–60% antimony and is free from lead and arsenic. This technique is called liquation. If the antimony content lies between 5 and 25%, the antimony is concentrated in a flue dust by volatilizing roasting. Antimony ores may contain auriferous antimony sulfides and arsenopyrites. Beneficiating such ores may become profitable again because of their precious metal content.

As a rule, low-grade and complex ores or ores in which the minerals are finely dispersed

throughout the gangue are beneficiated by flotation, particularly if they contain precious metals [15–18].

Flotation. A run-of-mine ore containing about 0.5% arsenic in the form of auriferous arsenopyrites and 5–20% antimony in the form of antimonite can be floated in a pulp made strongly alkaline by potassium hydroxide or water glass. The flotation agent is often potassium xanthate, and a high selectivity is ensured by frothing agents, such as the synthetic foaming agent Flotol for arsenopyrites and dicesyl dithiophosphoric acid (Phosokreslo and Aerofloat) for antimonite [15].

Liquation. Ores with more than 40–60% Sb_2S_3 and free from lead and arsenic often are beneficiated by heating. Because stibnite, Sb_2S_3 , has an unusually low melting point, 546–548 °C, it can be separated from the gangue by melting (liquation). Stibnite more than 90% pure is obtained and is referred to as *crude antimony*. It can be sold as such for producing antimony compounds, or it can be converted to antimony metal.

The commercial product should have a striated crystalline structure and a metallic gloss, and its color should be that of graphite. These properties are attained only if the molten antimony(III) sulfide is cooled very slowly. Ores with less than 40–45% Sb_2S_3 are unsuitable for liquation because the large amount of gangue interferes and too much antimony is retained in the residue. The ore is best fed in the form of walnut-sized lumps (1–4 cm). If the ore is too fine, the molten Sb_2S_3 does not flow. The most suitable temperature range is 550–660 °C because the volatilization of the Sb_2S_3 (*bp* 1000 °C) is prevented, and liquation is successful. Liquation is carried out in a reducing atmosphere in crucibles or in reverberatory furnaces. The main impurities in crude antimony are arsenic, lead, and iron sulfide.

14.6 Recovery of the Metal

Antimony metal is recovered from ore primarily by pyrometallurgical techniques. Either antimony(III) sulfide is converted into the

oxide, which is then reduced, or the ore is partially roasted and allowed to react with sulfide to form the metal and sulfur dioxide.

Sulfide ores with antimony contents between 5 and 25% are roasted to give volatile Sb_2O_3 , which is reduced directly to the metal. In many smelters mixed oxide–sulfide ores are processed in water-jacketed furnaces together with recycled material and by-products containing antimony. Reverberatory furnaces are used mostly for reducing rich oxide materials. The most suitable processes are listed in Table 14.1 for the various oxide and sulfide ores.

Table 14.1: Suitable processes for various antimony ores or concentrates.

Nature of the ore	Antimony content, %	Process
Sulfide	< 20	volatilizing roasting
Sulfide	< 35	smelting in shaft furnaces
Sulfide	> 60	liquation and cyclone volatilizing
Oxide	< 30	smelting in reverberatory furnaces and shaft furnaces
Oxide	< 50	direct reduction
Mixed sulfide and oxide	—	smelting in shaft furnaces

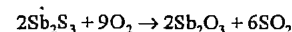
Special processes are used if the ore is rich in precious metals. Hydrometallurgical techniques can be used to minimize losses of precious metals. For example, crude metal is obtained at the cathode in a hydrometallurgical process used by the Sunshine Mining Co. (Cœur d'Alene district). Because rich ores are becoming rare, greater recourse is being taken to intermediates in processing and metal industries. Also, more and more complex ores are being processed.

14.6.1 Roasting

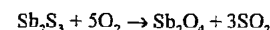
The sulfide can be oxidized to antimony(III) oxide (volatilizing roasting) or to antimony(IV) oxide (nonvolatilizing or dead roasting). Furnace control in the production of the nonvolatile antimony(IV) oxide is comparatively simple, but the oxide is not separated from the residue. If the ore contains a high proportion of gangue, difficulties are en-

countered in reduction. As a result this process is used rarely today.

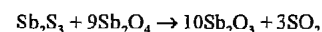
Volatilizing roasting has the advantage that volatile Sb_2O_3 is produced selectively in a 98% yield and is separated from the residue, which contains the precious metals in a recoverable form. However, temperature and draft control in the furnace is difficult. The oxide forms between 290 and 340 °C in an oxidizing atmosphere, and the rate of reaction attains its maximum at 500 °C, where antimony(IV) oxide begins to form. The basic reaction is



If too much oxygen is available, antimony(IV) oxide is formed:



Above 560 °C the rate of reaction drops considerably. During roasting, antimony(IV) oxide can react with antimony(III) sulfide to give antimony(III) oxide:



Therefore, the process must be engineered so that Sb_2O_3 is formed rapidly and preferentially. The temperature must be high enough to ensure adequate volatilization, and the oxygen supply must be kept low to inhibit the formation of antimony(IV) oxide. However, if the temperature is too high, part of the charge will melt, envelope the sulfide grains, and prevent their oxidation. During condensation of antimony(III) oxide, the oxygen content in the gas phase must be kept low enough to prevent oxidation to antimony(IV) oxide.

The temperature level is governed by the sulfide content of the ore. Low-grade ores can be roasted between 850 and 1000 °C. If rich ores are roasted, the upper limit is the melting point of the sulfide (546 °C). In practice, the temperature should not exceed 400 °C. The oxygen supply is controlled by mixing wood charcoal or coke breeze with the charge and by admitting only the amount of air required to form carbon monoxide and antimony(III) oxide. The carbon monoxide suppresses oxidation to antimony(IV) oxide. Despite everything, however, formation of antimony(IV) oxide cannot be entirely sup-

pressed. Antimony(IV) oxide, lead(II) oxide, and flue dust are obtained in the first condenser. The antimony(III) oxide condenses in the second, and the very volatile arsenic(III) oxide condenses in the last. If the oxygen concentration in the roaster is too low, partial oxidation can occur and give a mixture of oxide and sulfide melting at 485 °C. If the concentration of oxygen is too high, arsenates and antimonates of lead, copper, and other metals can form and pass into the slag.

A grain size of 5–10 cm suffices in conventional processes because fresh surface is always exposed for reaction owing to volatilization of the trioxide. Very low grade ores must be ground more finely to separate the sulfide from the gangue. The yield depends on the process and the sulfide content of the ore, varying between 60 and 90% or more.

Commercial antimony(III) oxide should be at least 99.5% Sb_2O_3 . If it is finely crystalline, adheres firmly to the fingers, and does not cake, it is considered of good quality. The oxide must be white; a reddish tinge indicates the presence of antimony(III) sulfide. The yellowish shade of selenium and lead(II) oxide is also undesirable. The arsenic content should be on the order of 0.1%. Typical specifications and grain size distribution [19] are listed below (in %).

Assay	99.5
Sb_2O_3	0.209
As_2O_3	0.11
PbO	0.15
Fe_2O_3	0.03
SeO	0.001
S	0.18
Solubility in tartaric acid	> 99.5
Solubility in water	< 0.4
Whiteness measured by reflectometry	> 90
Size distribution	
0–1.5 μm	60
1.5–3 μm	38
> 3 μm	2
> 44 μm	0.1
Apparent density	0.8 kg/L

The *roasting furnaces* most commonly encountered today are rotary kilns. If the throughput is high, antimony(III) oxide yields of 95–98% are attainable. The yield does not depend on the nature of the ore. The antimony content of sulfide ores does not affect the

kiln's efficiency; therefore, sorting and flotation of low-grade sulfide ores are unnecessary. Rotary kilns are also suitable for oxide sulfide ores, reducing the antimony initially to the metal. The metal volatilizes and is oxidized to antimony(III) oxide that is free of nonvolatile impurities and the off-gases produced on reduction. Some rotary kilns are heated not by burners but by hot air blown into them. The gas flow rate is significantly less than that in the old burner-heated furnaces, and less gangue is entrained in the gas stream. Nevertheless, hot-air heating does not entirely avoid temperature peaks, with melting of the charge.

Cyclone smelting entirely eliminates melting of the charge. The antimony smelter at Vinto, Bolivia, was the first in the Western Hemisphere to use the cyclone furnace smelting process. Conventional antimony roasting consumes large amounts of coal, and the lack of domestic coal has favored the cyclone furnace. The feed contains at least 60% antimony and less than 0.5% lead plus arsenic. Antimony is volatilized as antimony sulfide, burned, and separated in a baghouse as antimony(III) oxide. The impure oxide is pelletized and melted in a rotary furnace. The cyclone slag contains about 1% antimony [20].

14.6.2 Reduction of Oxide to the Metal

The oxides from volatilizing roasting, as well as other oxidized antimony materials, are reduced to the metal with carbonaceous materials. Occasionally oxide ores containing more than 50% antimony are finely ground and also reduced. Sometimes the oxide must be treated beforehand to remove arsenic, but improved roasting techniques frequently make this unnecessary. The amount of carbon required for reduction depends on the composition of the oxide, ranging between 8 and 12%. Pulverized charcoal, anthracite dust, or lean coal dust are used. To prevent the loss of volatile Sb_2O_3 , a sodium salt, such as soda (Na_2CO_3) or Glauber's salt (Na_2SO_4), is added to give a slag of low viscosity. Impurities such as cop-

per and iron are converted to matte by adding sulfur, usually in the form of crude antimony. The slags can contain 5–20% antimony, which must be recovered. The oxides are reduced in shaft, reverberatory, or short rotary furnaces. All types of furnaces require efficient precipitators and off-gas filters to remove volatilized antimony(III) oxide.

The pronounced reducing action in shaft furnaces does not produce pure metal but does yield slags containing a maximum of only 2.5% antimony and usually less than 1%. These slags can be used in glass manufacture. The furnaces have large height to diameter ratios, e.g., 6:1. The charge must be in the form of lumps or briquets. The yield is between 95 and 98%; the impure product contains 90–92% antimony, 5–7% iron, and arsenic and lead.

Reverberatory furnaces produce metal of comparatively high purity, but the slag is rich in antimony and requires further treatment. These furnaces are fed with high-grade ores that yield fairly small quantities of slag and with antimony-laden flue dust.

Stationary reverberatory furnaces have been largely replaced by *short rotary furnaces* in which the charge is very thoroughly mixed and rapidly melted. The rotary movement efficiently transfers heat to the charge. Tapholes are arranged at various heights in the furnace to allow molten metal, liquefied slag, and solid residues to be withdrawn. The great advantage of this process is that reduction in the furnace can be controlled so that the accompanying metals, such as lead, iron, and arsenic, are not reduced or are volatilized. This makes the refining simpler. At the antimony smelter at Vinto, Bolivia, the oxide melt passes from the rotary furnace to reverberatory furnaces for reduction and final refining at 800 °C. Coal and sodium hydroxide are added. The final product contains 99.6% antimony. If less pure, it can be alloyed with copper, nickel, or lead. The total antimony recovery rate for the smelter is 92% [20].

The complete flowsheet is shown in Figure 14.1.

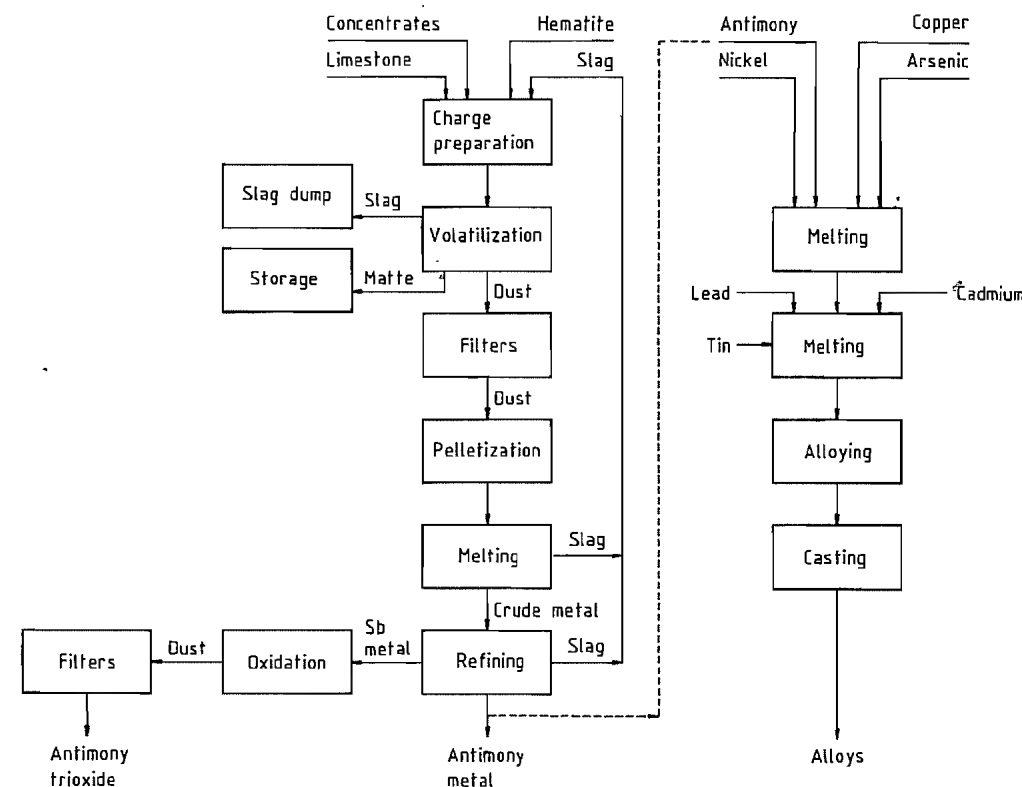
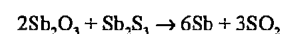


Figure 14.1: Antimony flowsheet for the smelter at Vinto, Bolivia [20].

14.6.3 Direct Reduction to the Metal

In blast furnace smelting the charge is antimony(III) sulfide, either alone or mixed with antimony oxides. The molten sulfide is first oxidized by the air blast. The oxide formed reacts with unconverted sulfide to yield metallic antimony.



In view of the many oxidation states through which the antimony must pass, this process is undoubtedly more complex than the equivalent lead and copper processes. It has been successfully practiced for many years in Mexico, Belgium, Great Britain, and former Czechoslovakia. Best results are obtained with sulfide ores containing 25–30% antimony. The main disadvantage of the direct process is

that antimony compounds are volatilized; this has been offset by using high, slender smelting columns.

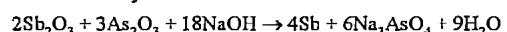
Standard practice favors low air pressures, e.g., 5.5 kPa at a flow rate of 1200 m³/s. The antimony content of the mixed charge should be less than 20%. Suitable fluxes are limestone, pyrite cinders, and ferrous slags. The required proportion of coke is about 15%. The slag and the metal usually are separated in a heated forehearth.

The yield of antimony can be as high as 98%, but not all of this is metal. Some leaves the shaft furnace as oxide, which must be trapped in filters. The metal is contaminated by iron, lead, and some copper and arsenic and must be refined.

14.6.4 Other Direct Processes

Reduction smelting of sulfidic antimony ores together with alkaline slags is a standard, long-established practice. A charge containing 8% sodium carbonate, 4% sodium sulfate, and 8–12% coal, for example, is smelted in a short rotary kiln. The alkaline melt absorbs the sulfur, so the metallic antimony produced must be refined.

Smelting antimony oxide flue dust containing arsenic, such as is obtained in roasting ores, with sodium hydroxide produces metallic antimony.



The arsenic dissolves in the alkaline slag [21–23].

14.6.5 Hydrometallurgical and Electrolytic Methods

Hydrometallurgical processing is suitable for some ores, particularly those containing gold, silver, and copper, and especially tetrahedrite, $\text{Sb}_2\text{S}_3 \cdot 4\text{Cu}_2\text{S}$ [24–27]. The high antimony content makes extracting the precious metals with cyanide difficult.

A number of methods have been proposed; however, most are plagued by unresolved problems. If sulfidic antimony ores are digested with acids, hydrogen sulfide is given off. Sulfuric acid does not digest the ores completely at 300 °C. Although hydrochloric acid is a better solvent and the antimony(III) chloride is adequately soluble, the problems involved in further processing have not been resolved. Cementation with iron, precipitation as the sulfide, and electrolysis have been investigated as means of separating the antimony. Explosive antimony is likely to form if electrolysis is used on antimony chlorides.

Antimony ores can be digested by *alkalies*. The antimony then can be reduced from the solutions electrolytically or by cementation with aluminum or zinc. Very pure rhombohedral antimony is obtained by electrolysis.

Any raw materials that are soluble in sodium sulfide, e.g., antimony glance or foundry products containing antimony sulfide, are suit-

able starting materials for antimony recovery by electrolysis. The solution is purified and then electrolyzed in diaphragm cells with iron or lead anodes and iron cathodes. The purity of the antimony is 96–99%.

The source of all the valuable metals in the Sunshine Mine ore is an argentiferous tetrahedrite (a silver copper–antimony sulfide), which cannot be broken down physically into its constituents. The tetrahedrite occurs reasonably free, and about 85% can be floated into a high-grade concentrate after grinding to a relatively coarse size.

The high antimony content precludes adoption of large-scale copper smelting for the concentrate, and lead smelting is just as unsuccessful because of the high antimony and copper contents and the presence of bismuth. Instead, the antimony is extracted from the argentiferous tetrahedrite by an alkaline sulfide solution. The residue consists of insoluble silver and copper sulfides. The antimony is recovered from the alkaline solution by electrolysis.

The steps are as follows:

- The antimony is batch leached with hot concentrated sodium sulfide solution from milled tetrahedrite concentrate to give a solution containing about 250 g Na_2S and 50 g Sb per liter. The leaching time is 8–10 h at 100–103 °C.
- After the residue settles, the supernatant solution is decanted. The residue is recovered by two-stage filtration with a repulping step between the stages. The pregnant solution is fed to the electrolytic section through two anolyte and two catholyte tanks.
- The solution is batch electrolyzed in banks of diaphragm cells. The antimony is deposited at mild-steel cathodes. The electrolytic section consists of 96 cells in series, arranged in cascades of six.

During electrolysis, the antimony is deposited at the cathodes, and sulfur is concentrated in the anolyte, with the result that sodium polysulfide (Na_2S_3), sodium sulfite (Na_2SO_3), sodium thiosulfate ($\text{Na}_2\text{S}_2\text{O}_3$), and sodium sulfate (Na_2SO_4) form. The alkalinity of the

anolyte decreases, whereas that of the catholyte increases.

Fresh anolyte is made up from a mixture of caustic soda solution and barren catholyte to be equivalent to 225 g NaOH per liter. It is discharged into the anolyte feed tanks in 7.5-t batches, and the same volume, having an alkalinity of about 175 g/L, is withdrawn to the regeneration section.

The fresh catholyte, also handled in batches, carries about 50 g of antimony and the equivalent of 250 g of NaOH per liter.

Catholyte is introduced near the bottom of each cell and withdrawn at the top. Because antimony depletion lowers the specific gravity, the weakest solution is drawn off and fed to the following cascade. The solution leaving the final cell in a cascade is pumped back to the catholyte feed tank, unless its antimony content has been reduced to the barren solution level of 8–10 g/L. The barren solution has an alkalinity equivalent of ≈ 250 g NaOH per

liter. About 30 t of barren solution is withdrawn during each cycle, and the same amount of fresh pregnant solution is added to the feed tank.

The busbar current is 1500 A, producing a current density of 300 A/m². There is no gasing at the cathodes until the antimony content of the solution falls below 8 g/L. The voltage drop varies slowly between 2.5 and 3 V per cell, depending on the alkalinity of the anolyte, averaging about 2.65 V. The cathodes are stripped every three days.

The spent solution from both the catholyte and anolyte cell banks are led to the regeneration circuit for treatment with barium sulfide solution. After the precipitated barium salts have been separated, the solutions are returned to the leaching circuit. The precipitated barium salts are mixed with coal and passed through a rotary kiln for reduction to a black ash containing barium sulfide.

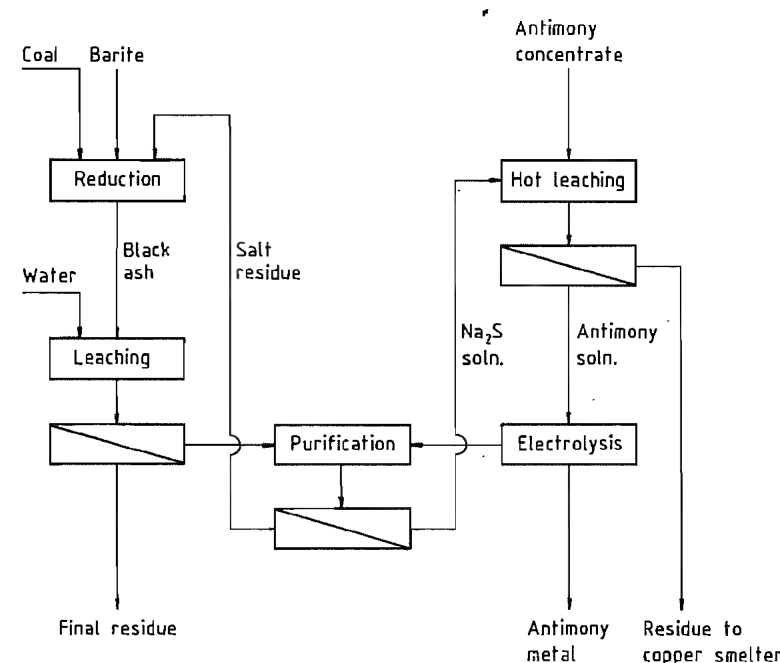


Figure 14.2: Flowsheet for the Sunshine electrolytic antimony plant.

The process is cyclic and regenerative, except that some barite must be supplied, and some caustic soda must be added to the anolyte to replace sodium lost with the copper residue. The antimony is sold as unrefined granular cathode antimony containing 96–97% antimony and 2–3% arsenic. Copper, lead, iron, bismuth, and other elements make up less than 0.4%. The small remainder is probably sodium sulfate. The flowsheet for the Sunshine Mining Co. electrolytic process is shown in Figure 14.2 [28].

In a method devised by the U.S. Bureau of Mines [29], the concentrate containing precious metals is smelted together with some iron. The metal obtained is deposited electrolytically at the cathode and refined. As much as 80–90% of the antimony is recovered as metal; 80–94% of the gold and 30–48% of the silver pass into the anode mud (Figure 14.3).

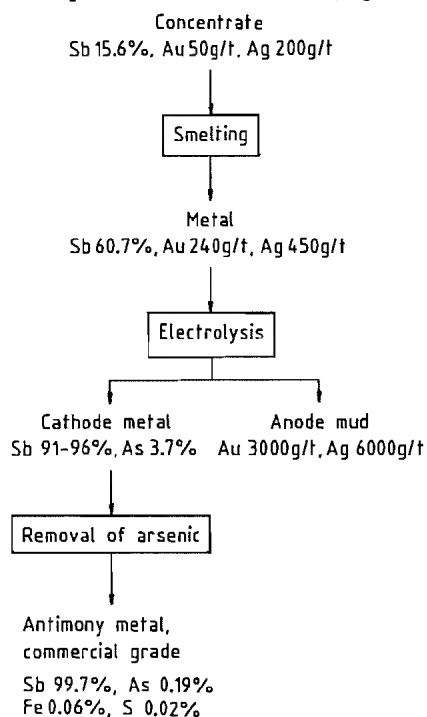


Figure 14.3: Beneficiation of a concentrate containing precious metals [29].

In another process the ore is smelted with soda and tetrahydrate and leached with lime.

The antimony passes into solution as sodium thioantimonate, Na_3SbS_4 . The arsenic is precipitated. If the ratio of sodium to sulfur in the electrolyte is 2:1 and the current density on the order of 1000 A/m², no diaphragms are needed; the current efficiency is 60% [30].

14.6.6 Recovery from By-products, Complex Ores, and Recycled Material

Lead and copper ores often contain antimony, which is concentrated and removed during the recovery of the main metal.

In the pyrometallurgical processing of *antimony-containing lead ores* about 90% of the antimony is recovered in the lead. During refining, the antimony is oxidized, usually in reverberatory furnaces, into an oxide slag, called antimony skimmings. After the entrained lead has been liquated, skimmings are smelted together with coal and fluxes, frequently in short rotary kilns, to yield a crude antimonial lead.

In the Harris process, lead bullion is treated at 400 °C with a melt of sodium chloride, sodium monoxide, and sodium nitrate. Arsenic, tin, and antimony are converted into a slag containing the antimony as sodium antimonate. Hydrometallurgical processing of the slag separates arsenic, tin, and antimony. The residue contains 45–50% antimony and can be reduced to antimony metal or used to produce antimony compounds.

In some cases electrolytic refining is used, particularly for lead rich in bismuth. The antimony is retained in the anode mud, together with the other undissolved metals—copper, arsenic, bismuth, and precious metals [31, 32]. The anode mud is smelted under reducing conditions to give a lead alloy. The arsenic and antimony are removed by selective oxidation at 900–1000 °C and converted into a slag in a procedure similar to that used in lead refining. The slag is smelted under reducing conditions to yield antimony containing arsenic.

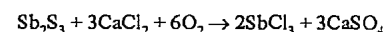
About 85–95% of the antimony in lead ores is recovered in the form of antimony–lead alloys, which are usually diluted with refined

lead and sold as is. These alloys are used mainly in lead–acid storage batteries.

In smelting *antimonial copper ores*, about 85% of the antimony enters the flue dust. The dust from the converter stage contains about 50% of the antimony, the arsenic, and frequently lead as well. The particular composition determines how these flue dusts are processed; there are no standard procedures. If iron, nickel, cobalt, arsenic, and antimony are present in sufficient amounts, they accumulate, together with the precious metals, in the copper matte during smelting. This speiss is difficult to process, and there is no satisfactory method that can be adopted generally.

Before *mercury-containing antimony ores* are processed, they generally must be roasted below 400 °C to volatilize the mercury. The temperature must be controlled accurately by regulating the admission of air to avoid overheating the charge and thus volatilizing antimony compounds. The roasted ore still contains antimony sulfide. The ore is removed from the furnace special bunkers. The antimony is recovered by reduction or iron precipitation in open-hearth furnaces.

Another way to process *complex antimony sulfide ores* is reaction with calcium chloride. The reaction takes place in an oxidizing atmosphere at about 500 °C:



More than 90% of the antimony volatilizes as SbCl_3 , which can be purified by distillation and hydrolyzed to Sb_2O_3 . The flow sheet is shown in Figure 14.4 [19].

The main forms of *antimony scrap* are type metal, Babbitt metal, lead and tin waste, antimonial lead, and especially waste lead–acid batteries: the recycling of antimony is closely connected to lead recycling. The extent to which antimony is recycled has increased steadily over the last few decades, in proportion to the worldwide production of automobiles.

Antimony accounts for about 1.8–2% of the total weight of an automobile battery, although the trend is towards using less. Today,

waste batteries are separated mechanically into a plastics fraction, a metal fraction, and an oxide–sulfate sludge. The grid metal contains 87–88% lead and 3–3.5% antimony; the sludge, 70–76% lead and 0.5–1% antimony. Most refineries process these materials separately from ore or concentrate. The waste grid metal can be smelted in rotating reverberatory or rotary kilns to yield antimony–lead alloy. The sludge is treated with reagents that bind sulfur, e.g., iron filings and soda, and smelted under reducing conditions to antimonial lead in rotating reverberatory furnaces, short rotating furnaces, or in some cases rotating tube furnaces. The antimonial lead produced can be remelted together with lead containing a higher proportion of antimony to produce commercial alloy. Frequently, the antimony in the crude antimonial lead is converted by oxidation into an antimonial slag or skimmings, as in the refining of lead bullion. These oxidized products, essentially lead and antimony, are treated with fluxes and coal and smelted in short rotating or rotating reverberatory furnaces to yield lead containing a high proportion of antimony. Because battery alloys now contain less antimony, the proportion of antimony in recycled lead will be lower in the years to come.

14.7 Refining

Antimony from the smelter usually contains iron, arsenic, tin, zinc, copper, lead, and bismuth. Several processes are used to produce a commercial grade containing $\geq 99\%$ antimony and $\leq 0.3\%$ arsenic. Iron, arsenic, and tin are removed by melting with caustic soda. A slow current of air is passed over the metal–caustic soda bath. Generally the caustic soda is renewed once during purification. At a bath temperature of 950 °C and a total air flow of 500 m³/kg arsenic is reduced in two hours to a residual 0.05% and iron is reduced to a residual 0.005%. Sodium nitrate can be used instead of the combination of caustic soda and air.

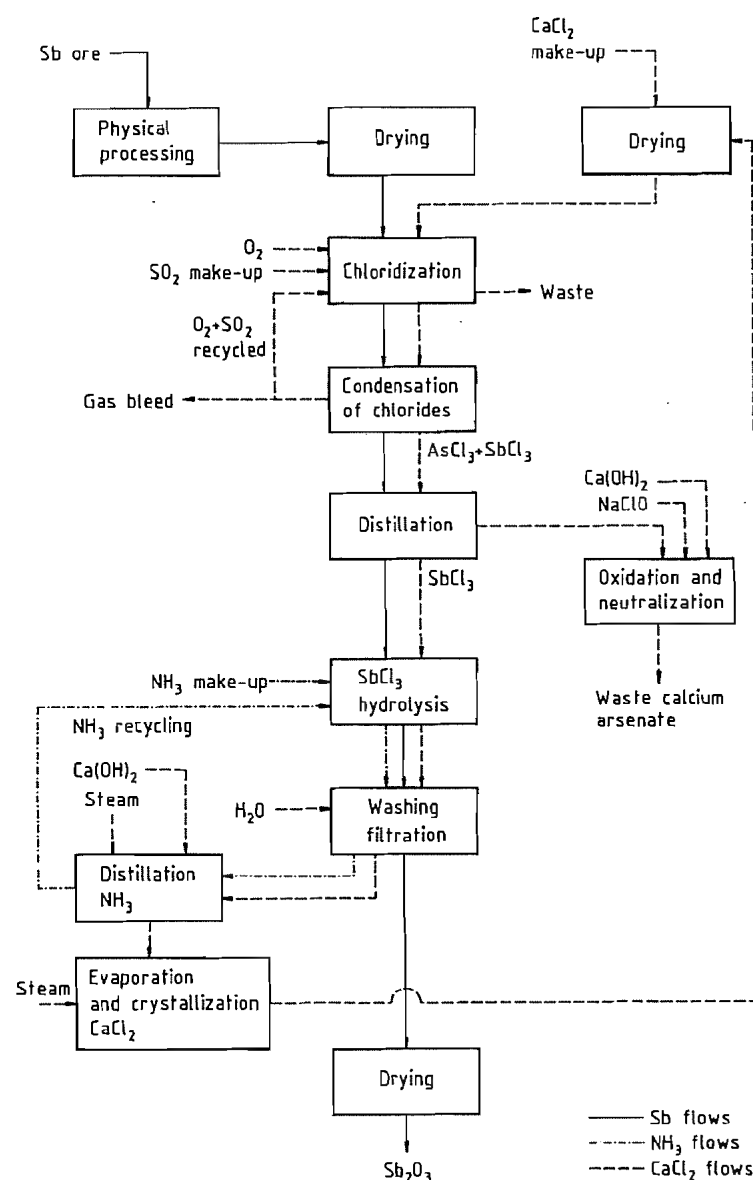


Figure 14.4: Chloridization process.

Although the maximum permissible arsenic content is 0.3%, a maximum of 0.1% is often specified. The measures taken to ensure such a low content must begin in the earliest beneficiation stages. The methods are well known, and some of them are standard practice [4, pp. 38–45].

To a great extent arsenic can be prevented by selective flotation from entering the concentrate [15, 33, 34]. About 88% of the arsenic can be volatilized from concentrates and antimony oxide flue dust by roasting in the presence of steam at 475–500 °C. The associated antimony losses are limited to 10–45%. If

arsenic antimony oxides are treated with hot caustic soda, the arsenic trioxide passes into solution as arsenite, whereas the antimony oxide is not changed. One to six kilograms of caustic soda is required for each kilogram of arsenic. The arsenic is completely separated from the antimony [4, p. 44].

Electrostatic precipitators offer means of separating arsenic from antimony at elevated temperature because gaseous arsenic trioxide can pass through them, whereas solid antimony trioxide precipitates. The best results, only 0.66–0.79% arsenic in the antimony trioxide, are obtained for a gas-inlet temperature of 620–650 °C and an outlet temperature of 430–470 °C.

The removal of lead from crude antimony is of less importance because most antimony produced is used in lead alloys. In any case, separation is difficult owing to the affinity between the two metals. Suitable methods are electrolysis, chloridization, and sulfidization.

A number of methods have been proposed, and occasionally used, for electrolytic separation of lead from antimony on an industrial scale [4, 24]. Although pure antimony is obtained from alkaline thioantimonite solutions, the current efficiency is low, and there are difficulties, including the formation of an insoluble film at the anode. Under some circumstances, electrolysis of antimony chloride gives rise to explosive antimony.

However, the only electrolysis that gives better results involves antimony trifluoride. The crude metal can be refined in a sulfate-fluoride solution. Even if the percentage of lead is quite high, lead-free antimony is obtained at the cathode. The excess sulfuric acid in the electrolyte precipitates the lead as lead sulfate, which passes into the anode mud. The energy consumed is 320 kWh/t. Arsenic must be removed beforehand; otherwise, it also deposits on the cathode. Operational details are given in [25].

It is claimed [4, pp. 46, 47; 35] that antimony of 99.2% purity is produced if 96.5% antimony with lead as the main impurity is treated with chloride at 1100 °C. If antimony rich in lead is fused with a sulfur flux, the lead,

as well as zinc, copper, and bismuth, is removed almost completely [4, p. 48]. This method is simpler and cheaper than electrolysis.

Electrolytic refining in molten sodium and potassium chloride at 750–800 °C is said to yield pure antimony. Iron can be reduced rapidly to a residual 50–90 ppm. Lead and copper are difficult to remove; therefore, the antimony should be purified pyrometallurgically beforehand.

14.8 Fine Purification

The antimony used as a solvent for extremely pure silicon must also be extremely pure. Silver, aluminum, chromium, copper, iron, magnesium, manganese, and nickel can be removed almost completely by subliming commercial antimony (99.5–99.9% Sb). However, almost all of the arsenic, lead, tin, and sulfur enters the sublimate, and the product is often contaminated with carbon and silicon. If commercial antimony is alloyed with 0.5–4% manganese, the sublimate is free from tin and largely free from sulfur. If 2% aluminum is used in addition to the manganese, the lead and arsenic contents are also reduced substantially. However, this procedure is not effective unless the rate of sublimation is reduced, to one third in the first case or one tenth in the second. This refining by sublimation is shown schematically in Figure 14.5.

There is growing demand for extremely pure antimony. It is derived from previously purified metal or from antimony(III) oxide. (Table 14.2 shows typical compositions of the starting materials.) The impurities remaining are removed by physical, chemical, and metallurgical methods, including distillation [37], ion exchange [38], liquid–liquid extraction [39], precipitation of intermetallic compounds [9], and zone melting [40–46].

A method described by M. TANENBAUM involves dissolving antimony of 99.8% purity in hydrochloric acid, repeatedly distilling the antimony trichloride obtained to remove the arsenic, and reducing the purified antimony

trichloride with iron pentacarbonyl. Zone melting then gives a product of 99.999% purity [45].

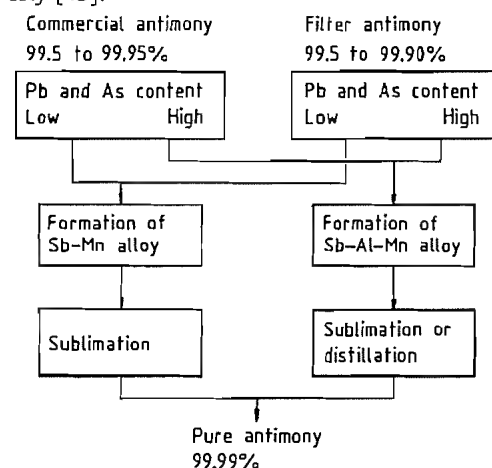


Figure 14.5: Sublimation refining.

Table 14.2: Spectrographic analysis of antimony regulus and of the antimony trioxide obtained by oxidation [36].

Element	Contents, ppm unless otherwise indicated	
	Antimony regulus	Antimony trioxide
As	210	192
Pb	3600	380
Fe	206	158
Ni	85	15
Cu	90	10
Sn	22	12
Bi	17	7
Ag	12	< 1
S	230	106
Sb	99.5%	> 83.38%
Sb as Sb ₂ O ₃	—	> 99.8%

A process patented by M. WILHELM uses hydrogen to reduce antimony pentachloride that has been purified by repeated distillation at 700–900 °C in an atmosphere of argon. The yield is ≤ 70% [46].

Antimony can be separated from numerous impurities by fractional distillation of the anhydrous trichloride or pentachloride [37]. Platinum, gold, silver, manganese, nickel, cobalt, and copper remain behind in the residue. If the heating is carried out carefully, the lead, bismuth, zinc, thallium, and cadmium also remain in the residue. Aluminum chloride, arsenic trichloride, and tin(IV) chloride pass completely into the first fractions, whereas

tin(II) chloride remains behind. Currently only hydrochloric acid solutions are distilled. Under these circumstances, arsenic trichloride distills at temperatures below 110 °C. Because distillation above 110 °C results in considerable loss of antimony, the temperature must be kept slightly under 110 °C.

LEVA and VIGDOROVICH stressed the effectiveness of chemical methods in separating arsenic from antimony and in lowering antimony's heavy metal content. Antimony trichloride is prepared by dissolving technical-grade antimony in hydrochloric acid and is hydrolyzed to give antimony trioxide, which is reduced with pure sucrose. The metal is then purified by zone melting to give a product with 99.995% antimony in 51–53% yield [47].

One rather complex procedure consists of the following: (1) dissolving technical-grade antimony in hydrochloric acid, (2) purifying the antimony trichloride obtained by fractional distillation, (3) converting the purified antimony trichloride into antimony trisulfide, (4) dissolving the sulfide in pure hydrochloric acid, (5) distilling the antimony trichloride, (6) hydrolyzing the trichloride into antimony trioxide, and (7) reducing the oxide with hydrogen. The purity of the antimony exceeds 99.998%, but the yield is low because of the large number of operations.

Very pure antimony trichloride can be purified further by hydrolysis to antimony trioxide with extremely pure water. The trioxide is reduced with purified hydrogen, first at about 600 °C and then at a somewhat higher temperature [9].

The recrystallization of chloroantimonic acid (H₂SbCl₆) efficiently removes final traces of iron [37].

Ion exchange removes cobalt, nickel, zinc, and lead [48, 49]. However, hydrolysis can result in less than quantitative elution.

Liquid-liquid extraction offers a means for refining antimony [39], e.g., by purifying acidic solutions of antimony with alkylphosphoric acid or separating copper, iron, and lead from hydrochloric acid solutions by extraction with ethyl acetate. Pentavalent anti-

mony dissolved in hydrochloric acid can be extracted by dibutyl ether, amyl alcohol, hexyl alcohol, *n*-octyl alcohol, and diisooamyl ether. However, liquid-liquid extraction is seldom used in practice.

The effectiveness of zone melting, usually the last stage in fine purification, depends on the impurities present. Arsenic, tin, and bismuth have unfavorable distribution coefficients (Table 14.3) and are difficult to remove by zone melting. Arsenic must be removed completely in the preceding purification steps. Lead and germanium are easier to remove. In one case, seven passages of the melted zone dropped the nickel, lead, silver, and copper contents to one tenth their original values [44, 45]. The impurity levels, in ppm, are reduced to < 0.5 Ag, < 5 As, < 1 Bi, 0.5 Cu, < 1 Fe, < 5 Ni, 2 Pb, and < 2 Sn [36].

Very pure antimony is produced in three grades: > 99.99% (four 9s), > 99.999% (five 9s), and > 99.9999% (six 9s).

Table 14.3: Distribution coefficients in antimony [36].

As	0.64	Pb	0.06
Sn	0.3	Ge	< 0.06
Bi	0.2		

14.9 Alloys and Intermetallic Compounds

Antimony is a component of many lead and tin alloys. These alloys are important materials for making bearings and solders.

The intermetallic compounds AlSb, GaSb, and InSb are important. Zinc antimonide, ZnSb, has interesting semiconductor and thermoelectric properties; cadmium antimonide, CdSb, has interesting semiconductor properties. Antimony is used to dope very pure germanium, silicon, and gallium arsenide to produce *n*-type semiconductors.

14.10 Compounds

Antimony can be trivalent or pentavalent in compounds. Both exist in antimony(IV) oxide, Sb₂O₄, and presumably in the deep violet haloantimonates(IV), such as Cs₂(SbCl₆). The

pentavalent compounds, as well as most of the trivalent ones, are hydrolyzed by water to form antimony salts, e.g., SbOCl, and hydrated oxides. The only halides of antimony that have any industrial significance are the chlorides and fluorides.

Mixed antimony(V) chloride fluorides and bromide fluorides exist, but antimony pentabromide does not. The tribromide, SbBr₃, is chemically similar to the trichloride. Stable complex halides are known, mainly hexahaloantimony anions of the types [SbX₆]³⁻ and [SbX₆]⁻.

14.10.1 Antimony Chlorides

Antimony trichloride (antimony chloride, butter of antimony, caustic antimony), SbCl₃, *mp* 73 °C, *bp* 223 °C, *p* 3.064 g/cm³ at 26 °C, is soft, crystalline, colorless, and very hygroscopic. It is soluble in the usual organic solvents, including benzene, carbon disulfide, carbon tetrachloride, acetone, and ethanol. Only highly concentrated aqueous solutions are stable. Dilution causes antimony(III) chloride oxide, SbOCl, to precipitate. The addition of more water causes further hydrolysis to take place, forming hydrated antimony(III) oxide. Antimony trichloride forms complexes with numerous compounds, some having a striking deep color.

Antimony trichloride is an intermediate in the production of other antimony compounds, a catalyst in organic chlorination and polymerization reactions, and a vitamin A reagent. Large quantities are consumed in rendering textiles, plastics, and other combustible substances flame retardant or self-extinguishing.

Although manufacture from antimony metal and chlorine is expensive, it is feasible on a small scale. The best procedure is to react chlorine with antimony metal in liquid antimony trichloride or concentrated hydrochloric acid. In the first case the temperature can be as high as 200 °C. Equally good results are obtained by dissolving antimony oxides in hot, concentrated hydrochloric acid. Distillation of the crude product or its solution in strong hydrochloric acid in the presence of some me-

tallic antimony or iron (to reduce antimony(V) and iron(III) compounds) then yields pure antimony trichloride.

Stibnite is usually digested in concentrated hydrochloric acid. The antimony passes into solution, whereas the arsenic largely remains in the residue. Disadvantages are the noxious hydrogen sulfide given off and difficulties in heating the strongly acidic solutions.

Antimony chloride oxide (oxychloride), SbOCl , is a white crystalline powder. It is precipitated by hydrolysis when concentrated solutions of antimony trichloride in water or hydrochloric acid are diluted. Because other chloride oxides, e.g., $\text{Sb}_4\text{O}_5\text{Cl}_2$, also form, reaction conditions must be controlled carefully. Antimony chloride oxide is an intermediate in the production of antimony salts and is used in smoke-producing agents.

Antimony pentachloride, SbCl_5 , *mp* 4 °C, *bp* 140 °C, ρ 2.34 g/cm³ at 20 °C, is a pale yellow fuming liquid of unpleasant odor. It can be produced by saturating molten antimony trichloride with chlorine, followed by vacuum distillation. Other methods are the direct chlorination of antimony and the chlorination of antimony oxides or sulfides.

Antimony pentachloride, which easily dissociates and tends to chelate, acts as a chlorine donor in the chlorination of organic compounds. It is also used as a polymerization catalyst.

14.10.2 Antimony Fluorides

Antimony trifluoride, SbF_3 , *mp* 292 °C, *bp* 319 °C, ρ 4.39 g/cm³, is a colorless compound that crystallizes readily and volatilizes at room temperature. If it is exposed to atmospheric moisture, hydrogen fluoride is given off. In organic solvents it is less soluble than the chloride, but both dilute and concentrated aqueous solutions are stable. Antimony trifluoride forms complexes with inorganic compounds. It is an important fluorinating agent, replacing chlorine or bromine by fluorine in both inorganic and organic compounds. It is especially useful for converting acid chlorides to the fluorides. However, if the halogen group in or-

ganic compounds is not very reactive, fluorination is quite sluggish. The rate of reaction can be increased considerably by adding some antimony pentachloride or bromine, in order to form antimony(V) bromide fluorides. Antimony trifluoride is used in the production of pottery and porcelain, and potassium fluoroantimonate(III) is a mordant in dyeing.

Antimony pentafluoride, SbF_5 , ρ 2.99 g/cm³, is a colorless oily liquid at room temperature. Under atmospheric pressure at 7 °C it solidifies to a crystalline mass; it boils at 150 °C. The solid dissolves in water with a violent reaction. The pentafluoride carbonizes and fluorinates organic substances. The chlorine in chlorinated hydrocarbons is replaced by fluorine. Many inorganic substances form complexes with antimony pentafluoride.

Antimony pentafluoride is prepared by treating antimony pentachloride with excess anhydrous hydrogen fluoride. The antimony pentafluoride is separated from the volatile by-products by fractional distillation. It can also be prepared by allowing fluorine to react with antimony powder or molten antimony trifluoride.

The main use of antimony pentafluoride is as a fluorinating agent.

14.10.3 Antimony Tribromide

Antimony tribromide, SbBr_3 , *mp* 96.6 °C, *bp* 280 °C, ρ 4.15 g/cm³, is a white solid. It is used as a mordant.

14.10.4 Antimony Triiodide

Antimony triiodide, SbI_3 , *mp* 167 °C, *bp* 401 °C, ρ 4.78 g/cm³, is a red solid that hydrolyzes readily and forms complex ions. It adds to ethers, aldehydes, and thiols. Antimony triiodide is prepared by reacting iodine with antimony or antimony sulfide in an organic solvent. The triiodide is used in medicine.

14.10.5 Antimony Oxides

Antimony trioxide, Sb_2O_3 , has two modifications: senarmonite below 570 °C, ρ 5.25 g/cm³, and valentinite (white antimony, anti-

mony bloom) above 570 °C, ρ 5.7 g/cm³. The melting point is 656 °C. The commercial product is a white crystalline powder with a density of 5.2–5.8 g/cm³. On heating, it becomes yellow but turns white again on cooling. Antimony trioxide dissolves in acids and alkalis.

Antimony trioxide can be produced by roasting antimony trisulfide, by burning antimony in air or oxygen, by alkaline hydrolysis of antimony halides (trichloride, tribromide, or triiodide), and by hydrolysis of antimony trisulfide with superheated steam. The production of antimony trioxide from antimony trisulfide during ore processing is described in Section 14.6.1.

Antimony tetraoxide, Sb_2O_4 , is a white nonvolatile powder that is soluble in alkalis but not in acids. Its density can differ considerably according to the duration of heating during preparation: 4.07–7.5 g/cm³. Cervantite has a density of 4.07 g/cm³. Antimony tetraoxide is obtained by roasting antimony trisulfide in a current of air or by heating antimony trioxide at 300–400 °C in air. The tetraoxide is used in ceramics.

Antimony pentoxide, Sb_2O_5 , is a whitish yellow powder. On heating, it first turns deep yellow; above 300 °C it turns from brownish yellow to brown but becomes paler above 380 °C. Its density ranges from 3.78 to 7.86 g/cm³. Antimony pentoxide is sparingly soluble in water but readily soluble in alkalis.

The pentoxide can be produced by the action of strong oxidizing agents on mechanized antimony or antimony trioxide. Hydrated antimony pentoxide can be produced by the hydrolysis of antimony pentachloride. The hydrate can be dried without difficulty.

14.10.6 Antimonic Acid and Antimonates

Many years ago antimonic acid was thought to have ortho, pyro, and meta forms, but these have all turned out to be only hydrated antimony oxide, primarily colloidal and differing in water content and solubility in acids and bases.

Potassium antimonate, $\text{K}[\text{Sb}(\text{OH})_6]$. Heating antimony pentoxide with excess potassium hydroxide produces rubbery, granular, or crystalline products. If the substance is recrystallized from a little water, deliquescent mammilated crystals form. Treated with copious cold water or boiled together with a small quantity of water, they are converted into potassium hexahydroxyantimonate, $\text{K}[\text{Sb}(\text{OH})_6]$, which is sparingly soluble in cold water but somewhat more soluble in warm water. Solutions precipitate sodium as the sparingly soluble sodium hexahydroxyantimonate, $\text{Na}[\text{Sb}(\text{OH})_6]$. This reaction is used for the detection of sodium.

Sodium hexahydroxyantimonate was formerly thought to be sodium pyroantimonate, $\text{Na}_2\text{H}_2\text{Sb}_2\text{O}_7 \cdot 5\text{H}_2\text{O}$. The hexahydroxyantimonate is prepared by melting antimony or antimony oxides with excess sodium nitrate. It is used as an opacifier for glass and enamel.

According to X-ray diffraction analysis, the hydrated antimonates(V) of magnesium, cobalt, and nickel are hexahydroxyantimonates, $[\text{M}(\text{H}_2\text{O})_6][\text{Sb}(\text{OH})_6]_2$, $\text{M} = \text{Mg}, \text{Co}, \text{or Ni}$.

14.10.7 Antimony Sulfides

Antimony trisulfide (stibnite). Sb_2S_3 , *mp* 550 °C, ρ 4.64 g/cm³, has a black crystalline modification and an unstable red-orange modification. If both occur together, the mixture can be carmine or brownish red.

Antimony trisulfide is soluble in alkalis and in concentrated, but not dilute, hydrochloric acid. It also goes into solution if it is boiled in alkali carbonate solutions. However, it precipitates as a reddish-brown powder, of non-definite oxygen content (kermesite), when the solution is cooled. It forms thioantimonates if it is dissolved in alkali-metal sulfides. Antimony trisulfide is a starting material for the production of antimony and antimony compounds.

Antimony pentasulfide, Sb_2S_5 , is an orange to dark red powder. It is doubtful whether stoichiometric Sb_2S_5 exists, because the preparations contain free sulfur and have variable composition. Antimony pentasulfide is insoluble.

ble in water but soluble in alkalies and alkali-metal carbonates. Thioantimonates are formed if the pentasulfide is dissolved in alkali sulfides; the most important of these is Schlippe's salt, sodium tetrathioantimonate, $\text{Na}_3\text{SbS}_4 \cdot 9\text{H}_2\text{O}$, which is produced on a commercial scale by melting stibnite, sodium sulfide, and sulfur together. Antimony pentasulfide can be obtained from Schlippe's salt by reaction with hydrochloric acid.

14.10.8 Antimony Sulfate

Antimony sulfate, $\text{Sb}_2(\text{SO}_4)_3$, ρ 3.62 g/cm³, is a hygroscopic compound in the form of needles with a silken sheen. When antimony or antimony trioxide, trisulfide, or oxychloride is dissolved in hot sulfuric acid, antimony sulfate or antimony salts are recovered. Antimony sulfate is used in the manufacture of explosives and in fireworks.

14.10.9 Stibine

Stibine, antimony hydride, SbH_3 , is a poisonous, foul-smelling gas of density 5.685 g/L (STP). The liquid boils at -88.5 °C. The gas is slightly soluble in water, soluble in alcohol, and very soluble in CS_2 . Its formation is endothermic, $\Delta H_f = 140$ kJ/mol, and it easily decomposes to hydrogen gas and antimony metal. Stibine is used to prepare *n*-type silicon semiconductors.

14.11 Chemical Analysis

The presence of antimony can be demonstrated by the Marsh test. There are a number of classical gravimetric and volumetric methods for determining antimony. A popular colorimetric method is based on a complex between rhodamine B and antimony. Instrumental methods for traces of antimony include polarography, emission spectrography, neutron activation, and atomic absorption [50].

14.12 Uses

Antimony metal is used mainly in alloys with lead or other metals. Nearly 50% of the total demand is accounted for by storage batteries, power transmission devices, communications equipment, type metal, solder, and ammunition. The compounds of antimony have a wide range of industrial uses, including uses in flame retardants, industrial chemicals, rubber, plastics, ceramics, and glass. The uses of antimony alloys, oxides, and sulfides are given in this section, whereas the special uses of the less important compounds are described with the compounds themselves in Section 14.10.

Secondary antimony is consumed chiefly as antimonial lead. These antimony-lead alloys find use in battery grids, pumps and pipes for chemicals, tank linings, roofing, and cable sheaths. The antimony increases their strength and inhibits chemical corrosion. Hard tin-antimony crystals lengthen the life of anti-friction bearings. Antimony increases hardness, minimizes shrinkage, gives sharp definition, and lowers the melting point of type metal. Precision in duplication, durability, the metallic luster, and economy are characteristics of antimonial alloys such as pewter. The amount of antimony used to harden the lead alloys for car battery grids has been reduced over the years. Antimony has been replaced by other metals in batteries for starting, lighting, and ignition, although it is still used in some replacement batteries.

High-purity antimony metal is being used in increasing amounts in intermetallic compounds for electronic semiconductors and thermoelectric devices.

The decline in the use for batteries is being offset by increased consumption of *antimony oxide* as a flame retardant, now the dominant market for primary antimony. In fact at present the main use for antimony(III) oxide is as a flame retardant in plastics. Large quantities of both antimony trioxide and trichloride are consumed in rendering textiles, plastics, and other combustible substances flame retardant or self-extinguishing. Textile finishes consist-

ing of antimony trioxide, chlorinated paraffin wax, and lime protect the fibers from damage by ultraviolet radiation. Further, antimony trioxide is used extensively in plastics, metalware, and ceramic enamels. It is used as a white pigment in paints. Its unusual light-transmission characteristics make it useful in glass manufacture.

The crude commercial *antimony sulfide* can be used directly in the manufacture of matches or Bengal lights. For the production of high-quality pyrotechnics, e.g., electrically ignited detonators, the crude antimony must be remelted in a reducing atmosphere at as low a temperature as possible. Under these circumstances, a well-crystallized, readily ground product is obtained. For several years, synthetic antimony(III) sulfide that satisfies the severe requirements imposed in pyrotechnics has been prepared from sulfur and antimony.

Antimony compounds yield black, vermilion, yellow, and orange pigments. Antimony trisulfide, which reflects infrared radiation much like vegetation, is a constituent of camouflage paints. Antimony pentasulfide is used as a vulcanizing agent in rubber.

Antimony finds a number of uses in ammunition. In alloys it hardens lead small-arms bullets and shot. Tracer bullets have a basal recess containing a light-emitting antimony sulfide mixture. A small annual tonnage of antimony trisulfide goes into the production of percussion primers, in which it acts as a friction composition and heat-transfer medium.

Burning antimony trisulfide emits a dense white smoke, which is used in visual fire control, marine markers, and visual signaling.

14.13 Economic Aspects

Antimony is produced from its ores and as a smelter by-product in about 20 countries, on all continents. Most of the 1979 production is attributed to Bolivia, South Africa, China, and the former Soviet Union, which together contributed 67 of the estimated total (also see Section 14.4). Table 14.4 shows the mine and smelter production by country in 1978.

The total 1978 world production of primary and secondary antimony was approximately 145 600 short tons; therefore, 50% is produced from scrap.

The U.S. consumption by end use is shown in Table 14.5.

Table 14.4: World production of primary antimony in 1978, tons of metal.

Country	Mine	Smelter
North America		
United States	1 213	12 800
Others	5 780	1 270
Total	6 993	14 070
South America		
Bolivia	12 671	2 903
Others	1 148	453
Total	13 819	3 356
Europe		
Belgium	—	7 711
France	—	7 983
Germany	—	2 268
Former USSR	7 892	6 350
Yugoslavia	2 758	544
Others	2 210	5 217
Total	12 860	30 073
Africa		
South Africa	9 093	—
Others	2 465	—
Total	11 558	—
Asia and Australia		
Japan	—	7 257
China	12 700	10 433
Thailand	2 873	272
Other Asian countries	3 597	453
Australia	1 514	—
Total	20 684	18 415
World total	65 914	65 914

Table 14.5: U.S. antimony consumption, tons.

	1970	1974	1979 ^a
Transportation, including batteries	18757	17782	18506
Flame retardants	2358	6063	8890
Chemicals	5652	6871	5806
Miscellaneous	2377	1077	3068
Rubber products	2540	3638	2721
Machinery	1451	2020	2268
Ceramics and glass	1633	2425	2086

14.14 Toxicology

Antimony, which is considered a nonessential element, is comparable in its toxicological

behavior to arsenic and bismuth [51]. In analogy to arsenic, trivalent antimony compounds generally are more toxic than the pentavalent compounds [52]. Poisoning with antimony and its compounds can result from acute and chronic exposure, especially from exposure to airborne particles in the workplace; to a minor extent, exposure occurs through treatment of tropical diseases with antimony compounds.

Most antimony compounds, mainly those with poor water solubility, are absorbed only slowly from the gastrointestinal tract. Trivalent compounds especially tend to accumulate in the human body, because they are excreted very slowly via urine and feces [52]. Antimony and its compounds react readily with mercapto groups in various cellular constituents, especially in enzymes, blocking their activity. After acute and chronic exposure highest concentrations are found in liver, kidney, adrenals, and thyroid.

Acute Toxicity. Acute oral poisoning by antimony compounds after ingestion of contaminated drinks was observed in 150 children; the symptoms were nausea, diarrhea, and vomiting [53]. Acute respiratory exposure of seven workers to 70–80 mg/m³ of antimony trichloride, SbCl₃, resulted in irritation of the upper respiratory tract [54]. Antimony pentachloride, SbCl₅, caused severe pulmonary edema in three cases, two of them being lethal [55]. Stibine, SbH₃, a highly toxic, relatively unstable gas with an unpleasant odor, causes symptoms of the central nervous and circulatory systems, such as nausea, vomiting, headache, slow breathing, weak pulse, hemolysis, hematuria, abdominal pain, and death [56, 57]. Stibine is generated if nascent hydrogen can react with antimony in acid, e.g., in lead acid batteries, where antimony may be a component of the battery plates [58].

People who are exposed to antimony and its compounds often show transient pustular skin eruption [59]. These "antimony spots" mainly occur in those regions of the skin that are exposed to heat and sweat.

Antimony trifluoride and pentafluoride are highly toxic and irritant to the skin; they cause

eczematous eruptions and inflammation of mucous membranes of nose and throat.

Chronic Toxicity. Chronic poisoning after oral ingestion of antimony compounds has been observed in many cases of clinical treatment with antimony compounds. These chronic intoxications resulted in nausea and vomiting [60]; liver damage, with increased plasma values of aspartate-aminotransferase and alanine-aminotransferase [61]; changes in the electrocardiogram, indicating a cardiotoxic effect of these compounds [62]; and even sudden death [63].

Most cases of chronic respiratory intoxications result from exposure to airborne particles in the workplace. In a study involving 78 workers in antimony smelters, symptoms such as soreness, nosebleeds, rhinitis, pharyngitis, pneumonitis, and tracheitis could be observed after exposure times of up to five months, the air containing antimony trioxide, Sb₂O₃, in a concentration of 4.7–11.8 mg/m³ [59]. Long-term exposures often result in lung X-rays that are similar to those seen in pneumoconiosis [64]. Workers who had been exposed to Sb₂O₃ for up to 28 years had pneumoconiosis (21%) and symptoms of emphysema (42%) [65]. Brieger et al. [66] extensively examined 125 workers who had inhaled antimony trisulfide, Sb₂S₃, in air at concentrations of 0.6–5.5 mg/m³ for 8–24 months. An increased morbidity and mortality were observed among these workers. Changes in the electrocardiogram were seen in 37 cases out of 75. In addition, a significantly higher incidence (6%) of peptic ulcers occurred within the group of workers exposed to antimony compared to the incidence within the total plant population (1.5%). During the period of this study, six workmen died suddenly, and two others died from chronic heart diseases. After extensive exposure to antimony fumes, workers showed gastrointestinal symptoms, such as diarrhea, vomiting, and abdominal convulsions [59].

Mutagenicity, Carcinogenicity. Antimony has been demonstrated to be mutagenic in bacteria and phages, and to induce chromosomal aberrations and abnormal cell divisions in ani-

mal and plant cells [67]. Antimony trioxide is a suspected carcinogen in humans [68].

Toxicological Data. Antimony, Sb, MAK 0.5 mg/m³, LDLo 100 mg/kg (rat, intraperit.) [69].

Antimony hydride, stibine, SbH₃, MAK 0.1 ppm (0.5 mg/m³), LCLo 92 ppm (guinea pig, inhalation, 1 h) [70].

Antimony trifluoride, SbF₃, MAK 0.5 mg/m³ (as Sb), TLV 0.5 mg/m³ (as Sb), LDLo 100 mg/kg (guinea pig, oral) [71].

Antimony pentafluoride, SbF₅, MAK 0.5 mg/m³ (as Sb).

Antimony trichloride, SbCl₃, MAK 0.5 mg/m³ (as Sb), TLV 0.5 mg/m³ (as Sb), TDLo 73 mg/m³ (human, inhalation) [54].

Antimony pentachloride, SbCl₅, MAK 0.5 mg/m³ (as Sb), TLV 0.5 mg/m³ (as Sb), LD₅₀ 1115 mg/kg (rat, oral) [72], causes mutation in *Bacillus subtilis* at 30 µL/disk [73].

Antimony trioxide, Sb₂O₃, carcinogenic potential suspected for humans, TLV 0.5 mg/m³ (as Sb), TCLo 4.2 mg/m³ during 52 weeks, carcinogenic (rat, inhalation) [74].

Antimony pentoxide, Sb₂O₅, LDLo 4000 mg/kg (rat, intraperit.) [69].

Antimony trisulfide, Sb₂S₃, TLV 0.5 mg/m³ (as Sb), TCLo 580 µg/m³ during 35 weeks (humans, inhalation) [66], LDLo 1000 mg/kg (rat, intraperit.) [69].

Antimony pentasulfide, Sb₂S₅, TLV 0.5 mg/m³ (as Sb), LD₅₀ 1500 mg/kg (rat, intraperit.) [69].

14.15 References

- Gmelin, Sb (system no. 18), Main A3 (1950) 303–351.
- V. Tafel: *Lehrbuch der Metallhüttenkunde*, vol. 2, Hirzel, Leipzig 1951.
- C. Y. Wang: *Antimony*, C. Griffin & Co., London 1952.
- W. Wendt: *Antimon und seine Verhüttung*, Deuticke, Vienna 1950.
- R. C. Weast (ed.): *Handbook of Chemistry and Physics*, 56th ed., CRC Press, Cleveland, OH, 1975.
- H. Quiring: *Die metallischen Rohstoffe*, vol. 7, Enke Verlag, Stuttgart 1945.
- W. J. Maack: *The Radiochemistry of Antimony*, U.S. At. Energy Comm. 1961.
- F. Pawlek: *Metallhüttenkunde*, De Gruyter, Berlin-New York 1983.
- Ullmann, 4th ed., vol. 8, pp. 1–18.
- Kirk-Othmer, 2nd ed. vol. 2, pp. 562–588.
- B. Tougarinoff: "Nouveaux métaux et matériaux", *Rev. Soc. R. Belge Ing. Ind.* 1966, no. 9, 10.
- E. Bonnier, M. Charveriat: "Purification de l'antimoine par sublimation", *ATB Metall.* 5 (1965) 319.
- Ullmann, 3rd ed., vol. 3, pp. 806–827.
- A. F. Taggart: *Handbook of Mineral Dressings, Ores and Industrial Minerals*, J. Wiley & Sons, New York-London-Sidney 1976.
- E. W. Mayer in H. Schranz (ed.): *Flotation*, Hirzel, Leipzig 1931, p. 375.
- U. S. Popova, R. L. Popov, V. G. Nesterov: "The Effect of Non-metalliferous Components in Antimony Ores on the Flotation of Antimonite", *Sb. Nauchn. Tr. Sredneaziat. Nauchno Issled. Proektn. Inst. Tsvet. Metall.* 1972, no. 5, 75–80.
- K. Kijayakumar, K. K. Majumdar, *J. Mines Met. Fuels* 20 (1972) no. 11, 342–346.
- H. Grothe, L. Engel, H. Hock, K. Löhberg, K. Schönert: *Hüttentechnik*, vol. 1, Rowohlt, Hamburg-Reinbek 1972, p. 36.
- G. Morizot, J. M. Winter, G. Barbery: *Volatilization Chloridization with Calcium Chloride of Complex Sulphide Minerals and Concentrates*, published in *Complex Sulphide Ores*, papers presented at Complex Sulphide Ores Conference by the Inst. Min. Metall, Rome 1980, pp. 151–158.
- D. A. Pazour, *World Min.* 33 (1980) no. 6, 42–47.
- Min. Mag. 134 (1976) no. 5, 369–374.
- H. W. Burkley, US 1654527, 1926; US 1654528, 1926.
- AB Metallreduction, NO 48804, 1929.
- G. N. Kirsebom, GB 315811, 1929.
- N. P. Shashin in N. Muratsch (ed.): *Handbuch des Metallhüttenmannes*, vol. 1, VEB Verlag Technik, Berlin 1954.
- C. L. Mantell: *Electrochemical Engineering*, 4th ed., McGraw-Hill, New York 1960, pp. 232–234, 238.
- Chung Yu Wang, G. C. Riddell in O. M. Liddell (ed.): *Handbook of Nonferrous Metallurgy*, McGraw-Hill, New York 1945.
- W. Schopper in G. Eger (ed.): *Handbuch der technischen Elektrochemie. Die technische Elektrolyse wässriger Lösungen*, vol. 1, part 1, Akademische Verlags GmbH, Leipzig 1961.
- W. C. Holmes, *Eng. Min. J.* 145 (1944) no. 3, 54–58.
- J. Koster, M. B. Roger: "Electrolyte Recovery of Antimony from Antimonial Gold Ores", *Rep. Invest. U.S. Bur. Mines* RI 3491 (1946).
- A. E. Albrethsen, M. L. Hollander: "The ASARCO Antimony Electrowinning Process", *TMS Pap. Sel. A* 79-64 (1979) 9.
- W. G. Agejenko: *Elektrometallurgie wässriger Lösungen*, Verlag Technik, Berlin 1952.
- E. Freni, *Erzmetall* 23 (1970) 128–132.
- W. G. Clark, B. H. Moore, *Min. Mag.* 43 (1930) 58.
- N. J. Tschumarow, G. M. Goutscharowa, *Tsvetn. Met.* 16 (1941) 43–45.
- T. Rondelli, IT 380529, 1940.
- D. Jevtić, D. Vitorović, *Ind. Eng. Chem. Prod. Res. Dev.* 13 (1974) no. 4, 275–279.
- E. Groschuff, *Z. Anorg. Allg. Chem.* 103 (1918) 164–188.
- Y. Y. Lure, N. A. Filparu, *Zavod. Lab.* 14 (1948) 159.

39. G. R. Smithson et al., *J. Met.* 17 (1966) 1037–1046.
40. W. G. Pfann: *Zone Melting*, 2nd ed., J. Wiley & Sons, New York 1966.
41. H. Schildknecht: *Zonenschmelzen*, Verlag Chemie, Weinheim 1964.
42. Z. Trousil, *Chemie (Prag)* 9 (1957) 633.
43. H. Schell, *Z. Metallkd.* 46 (1955) 58.
44. M. Tanenbaum, A. J. Goss, W. G. Pfann, *J. Met.* 7 (1955) 297–303.
45. M. Tanenbaum, A. J. Goss, W. G. Pfann, *J. Met.* 6 (1954) 762–763.
46. M. Wilhelm, DE 1155914, 1964.
47. V. N. Vigdorovich, V. S. Ileva, L. Y. Krol, *Izv. Akad. Nauk SSSR Otd. Tekh. Nauk Metall. Topl.* 1960, no. 1, 44.
48. W. A. Kusnetzow: "Ion Exchange in Hydrometallurgy", (Russ.) in *Metallurgy of Alloys and Rare Metals 1967*, Natl. Inst. for Text Books and Tech. Information, Moscow 1968, pp. 81–105.
49. E. Scheffler, S. Ziegenbalg, *Freiberg. Forschungsh.* B99 (1964) 43–63.
50. E. Merian: *Metalle in der Umwelt*, Verlag Chemie, Weinheim 1984, p. 310.
C. Veillon in J. D. Wineforder (ed.): *Trace Analysis: Spectroscopic Methods for Elements*, J. Wiley & Sons, New York 1976, pp. 164–165.
51. *Ullmann* 4th. ed., vol. 8, pp. 16–18.
52. L. S. Godman, A. Gilman: *The Pharmacological Basis of Therapeutics*, 5th ed., Macmillan, New York 1975, pp. 929–930.
53. N. Werrin, Hussock, *Food Drug Off. U.S. Quart. Bull.* 27 (1963) 38–45.
54. P. J. Taylor, *Br. J. Ind. Med.* 23 (1966) 318–321.
55. E. M. Cordasco, F. D. Stone, *Chest* 64 (1973) 182–185.
56. H. E. Stokinger, in G. D. Clayton, F. E. Clayton (eds.): *Patty's Industrial Hygiene and Toxicology*, 3rd ed., vol. 2A, Wiley-Interscience, New York 1981, pp. 1505–1517.
57. *Merck Index*, 9th ed., Merck and Co., Inc., Rahway, NJ, 1976, p. 95.
58. E. Browning: *Toxicity of Industrial Metals*, 2nd ed., Appleton-Century Crofts, New York 1969, pp. 23–38.
59. L. E. Renes, *Arch. Ind. Hyg. Occup. Med.* 7 (1953) 99–108.
60. M. R. Pedrique, S. Barbera, N. Ercoli, *Ann. Trop. Med. Parasitol.* 64 (1970) 225–261.
61. A. W. Woodruff, *Ann. N. Y. Acad. Sci.* 160 (1969) 650–655.
62. D. W. Sapire, N. H. Silverman, *South African Med. J.* 44 (1970) 948–950.
63. A. A. El Halawani, *Bull. Endemic Dis.* 10 (1968) 123–133.
64. R. C. Browne, *Br. J. Ind. Med.* 25 (1968) 187–193.
65. I. Klucik, A. Juck, J. Gruberová, *Pracovní Lékarství* 14 (1962) 363–368 (in Czech; information from Scientific Reports of Industrial Hygiene and Occupational Diseases in Czechoslovakia 7, 56; English summaries only).
66. H. Brieger, C. W. Semisch, J. Stasney, M. A. Piatnek, *Ind. Med. Surg.* 23 (1954) 521–523.
67. C. P. Flessel, *Adv. Exp. Med. Biol.* 91 (1977) 117–128.
68. Deutsche Forschungsgemeinschaft (ed.): *Maximale Arbeitsplatzkonzentrationen (MAK) 1984*, part III B, Verlag Chemie, Weinheim 1984.
69. W. R. Bradley, W. G. Frederick, *Ind. Med.* 10, Ind. Hyg. Sect. 2 (1941) 15.
70. E. Browning: *Toxicity of Industrial Metals*, Butterworths, London 1961, p. 30.
71. Registry of Toxic Effects of Chemical Substances, NIOSH (ed.), Cincinnati, OH, 1976.
72. Registry of Toxic Effects of Chemical Substances, NIOSH (ed.), Cincinnati, OH, 1977.
73. N. Kanematsu, M. Hara, T. Kada, *Mutation Res.* 77 (1980) 109–116.
74. *Ann. Meet. Am. Ind. Hyg. Assoc.* 20 (1980) 1.

15 Bismuth

JOACHIM KROGER, MANFRED LOCK, EBERHARD LUDERITZ, PETER WINKLER (§§ 15.1–15.10); HANS UWE WOLF (§ 15.11); JÖRG ADEL, HENNING WIENAND (§§ 15.12.1–15.12.4); RALF EMMERT, KLAUS-DIETER FRANZ, HARTMUT HARTNER, KATSUHISA NITTA, GERHARD PFAFF (§ 15.12.5)

15.1 Introduction	845	15.6 Refining	855
15.2 History	845	15.7 Alloys	857
15.3 Properties	845	15.8 Compounds	859
15.4 Occurrence	846	15.9 Chemical Analysis	861
15.5 Production	847	15.10 Economic Aspects	861
15.5.1 Crude Bismuth from Bismuth-Rich Mixed Concentrates	847	15.11 Toxicology of Bismuth and Bismuth Compounds	862
15.5.2 Crude Bismuth from Lead Concentrates	849	15.12 Pigments	863
15.5.2.1 Pyrometallurgical Separation of Bismuth from Metallic Lead	850	15.12.1 Properties	864
15.5.2.2 Processing of Bismuth-Containing Drosses	851	15.12.2 Production	864
15.5.2.3 Electrolytic Separation of Lead and Bismuth. Bismuth Production	852	15.12.3 Uses	865
15.5.3 Crude Bismuth from Copper and Tin Concentrates	854	15.12.4 Toxicology	865
		15.12.5 Bismuth Oxychloride	865
		15.13 References	866

15.1 Introduction

Bismuth belongs to the fifth main group of the periodic table. Its chemical behavior is similar to that of the other group VB elements arsenic and antimony.

The electron configuration is $[\text{Xe}] 4f^{14} 5d^{10} 6s^2 6p^3$. Only one stable isotope, ^{209}Bi , is known, but there are several unstable isotopes (^{199}Bi – ^{215}Bi). Isotopes with mass number > 210 are found in the natural decay chains of radioactive elements. Isotopes with mass number < 208 have been formed in nuclear transformations.

Bismuth is used as an alloying component in fusible alloys, but no commercial use of pure bismuth metal is known. Consumption seems to be declining; the current world production is only about 4000 t/a.

15.2 History

The name of the metalloid is to be found in all western languages. It is probably of Ger-

manic origin and was mentioned first by ALBERTUS MAGNUS (1193–1250). Around 1450 BASILIUS VALENTINUS calls it *bismutum* and PARACELSUS (1493–1541) named the metal *wismut*. GEORGIUS AGRICOLA thought it to be a special kind of lead and describes the winning of *plumbum cinerum*. In 1739, POTT finally distinguished pure bismuth from other metals. Bismuth was known as a low-melting alloying element in the 16th and 17th centuries, and it was also used in the form of the subnitrate – in cosmetics and medicine. Industrial production began around 1830 in Saxony and increased after the first bismuth ores were shipped to Europe in 1867. The discovery of fusible alloys caused production to increase in the 1930s [1–4].

15.3 Properties [1–6]

Physical Properties. Bismuth is a heavy, lustrous, silver-white metal with a slight pink cast. If solidification is slow, large brittle crystals form. For a metal, bismuth has some unusual properties:

- Like germanium and gallium, its volume increases on solidification. The increase is 3.32%.
- Bismuth is the most diamagnetic metal. Its specific susceptibility is $-16 \times 10^{-9} \text{ m}^3/\text{kg}$ at 293 K.
- Only liquid mercury has a lower thermal conductivity.
- The electrical resistance of solid bismuth is greater than that of liquid bismuth. Superconductivity has not been detected. The increase in resistivity in a magnetic field (the Hall effect) is the largest of all metals.
- Bismuth alloys show large thermoelectric effects.
- With the exception of beryllium, bismuth has the lowest absorption cross section for thermal neutrons.

Atomic radius	0.18 nm
Melting point	271.40 °C
Boiling point	1564 °C
Crystal system	rhombohedral
Lattice constant	$a = 0.47457 \text{ nm}$ $\alpha = 57.24^\circ$
Latent heat of fusion	11 280 J/mol
Latent heat of vaporization	178 632 J/mol
Volume expansion on solidification	3.32%
Coefficient of linear expansion	$13.5 \times 10^{-6} \text{ K}^{-1}$
Density at 20 °C	9790 kg/m ³
Electrical resistivity	
at 0 °C	106.8 $\mu\Omega\text{cm}$
at 1000 °C	160.2
Specific heat at 25 °C	25.5 Jmol ⁻¹ K ⁻¹
Thermal conductivity	
at 0 °C	8.2 Js ⁻¹ m ⁻¹ K ⁻¹
at 300 °C	11.3
at 400 °C	12.3
Vapor pressure	
at 893 °C	$1.013 \times 10^{-3} \text{ bar}$
at 1053 °C	1.013×10^{-2}
at 1266 °C	1.013×10^{-1}
Surface tension	
at 300 °C	376 mN/m
at 400 °C	370
at 500 °C	363
Absorption cross section for thermal neutrons	$(3.4 \pm 0.2) \times 10^{-30} \text{ m}^2/\text{atom}$
Hardness, Brinell	184 N/mm ²
Hardness, Mohs	2.5
Poisson's ratio	0.33
Shear modulus	12 400 MPa
Modulus of elasticity	338 GPa
Tensile strength at 20 °C	
soft	5 MPa
hard	20
Diffusion coefficient of Bi in dilute Bi-Sn alloys [7]	$(2.33 \pm 0.18 \text{ cm}^2/\text{s}) \times$

Viscosity [8]

at 300 °C	1.65 MPa·s
at 350 °C	1.49
at 400 °C	1.37
at 500 °C	1.19
at 600 °C	1.06
Hall coefficient at 18 °C	$-6.33 \times 10^{-7} \text{ m}^3\text{A}^{-1}\text{s}^{-1}$
Magnetic induction	0.393 T

Thermal expansion, compressibility, heat conduction, self-diffusion, electrical resistivity, and mass susceptibility depend on crystal orientation [8].

Chemical Properties. Bismuth is not very reactive; generally, it is less reactive than lead and more reactive than silver. It shows annealing colors when heated but otherwise does not oxidize in dry air. Liquid bismuth is covered by an oxide film of Bi_2O_3 that protects it from further oxidation. At 817–821 °C the oxide melts, and then the metal oxidizes rapidly. Therefore it is possible to separate bismuth from the noble metals by cupellation. Moisture is slightly oxidizing at high temperatures. Other possible oxides are Bi_2O_4 and Bi_2O_5 . In most compounds, bismuth has a 3+ oxidation state, although in some compounds, such as Bi_2O_5 , bismuth pentahalides, and a number of organobismuth compounds, it has oxidation state 5+. Stable compounds with selenium and tellurium have interesting semiconductivity and thermoelectric properties. Bismuth has a standard electrode potential of +0.28 V, placing it between antimony and copper in the electrochemical series. It can be separated from lead by electrolysis [2].

15.4 Occurrence [2, 3]

Bismuth ranks 64th in abundance in the earth's crust; like antimony and cadmium, its abundance is estimated to be 0.17 to 0.2 ppm. Most bismuth sulfides occur associated with lead, copper, and silver. A few deposits in which bismuth is a major mineral are also known. The most important pure bismuth minerals are native bismuth and bismuth glance, Bi_2S_3 . Other bismuth minerals are bis-

$$10^{-4} e^{-Q/RT} \text{ where} \\ Q = 10.6719 \pm 0.365 \text{ kJ/mol}$$

mite, Bi_2O_3 ; bismuth ochre, $\text{Bi}_2\text{O}_3 \cdot 3\text{H}_2\text{O}$; and bismutite and bismutosphaerite, $\text{Bi}_2(\text{O}_2/\text{CO}_3)$.

Deposits from magmatic granite nearly always contain bismuth in low concentration. Bismuth is mainly found surrounding intrusive rocks, thus it is perimagmatic. Together with complex minerals of silver, copper, and lead, it can end up in deposits far from igneous bodies. If the other elements are carried further, the bismuth ochre left may be worth working.

Significant European deposits are situated in Spain and Saxony (Germany). In China bismuth occurs together with tungsten, molybdenum, and tin ores, which may be dressed up to 60–63% Bi. Bismuth minerals are found together with tungsten ores in South Korea. Important ex-USSR deposits are in Adrasman, Tajikistan. The most important bismuth deposits are in South America. The Cu, Pb, and Zn concentrates from Peru (Junin and Oroya) contain bismuth; in Bolivia, bismuth is found together with tin and sometimes with tungsten. Mines are found in Tasua and Chorolque, Department Potosi, and Caracoles, Cimsa Cruz Cordillere, where oxide and sulfide concentrates with 35–45% Bi are produced.

15.5 Production

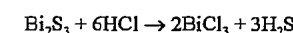
Bismuth is produced in small amounts from so-called bismuth ores or concentrates. The largest amounts are recovered as by-products from lead and copper production, mostly during processing complex copper concentrates. Bismuth is also won from molybdenum, tungsten, and tin concentrates.

15.5.1 Crude Bismuth from Bismuth-Rich Mixed Concentrates

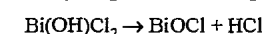
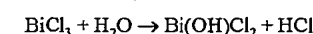
Only in rare cases are as-mined ores rich enough to be treated directly to produce metal. Usually the ores have to be enriched before processing. Because of the large variety of ore compositions there is no standard procedure for upgrading. A special process has to be developed for each deposit: mechanical enrichment and flotation are usually the preferred

methods. Often these methods do not produce the desired results, and the bismuth concentrates must be enriched further, either by leaching or by volatilization, or some combination of both.

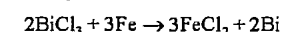
For the selective separation of bismuth from complex nonferrous metal concentrates that contain up to several percent bismuth, leaching with hydrochloric acid has proved effective:



If weak acid is used, the reaction must be supported with H_2O_2 . The bismuth is precipitated by hydrolysis on dilution or partial neutralization,



or by cementation with iron turnings,



Neither procedure leads to a pure precipitate. The hydrolysis precipitates slightly soluble chlorides along with the bismuth compound. These chlorides can be precipitated only partially in advance. The cementation also precipitates the more noble metals. Such precipitates are usually smelted with soda or Na_2S to separate bismuth metal from copper and lead, which go into a matte low in bismuth.

Processing of Complex Molybdenum-Bismuth Preconcentrates. The bismuth in a preconcentrate containing 4.8% Bi, 14.5% Mo, 17.9% Fe, 8.0% Pb, 2.5% Cu, and 7.4% SiO_2 can be dissolved with concentrated hydrochloric acid; molybdenum does not dissolve. The dissolved bismuth is then cemented with iron turnings.

	Composition, %		
	Mo	Bi	Cu
Concentrates before leaching	14.5	4.8	2.5
Concentrates after leaching	16.3	0.02	— ^a
Cementate	<0.1	86–95	<0.1

^aNot usually given.

The enriched product is refined. The bismuth-free molybdenum preconcentrates may

be upgraded further by flotation [9]. The flow diagram of this process is shown in Figure 15.1. The Molybdenite Corporation of Canada floats bismuth-containing molybdenum ores: 70–80% of the Bi and 93–95% of the Mo are recovered. This process produces a highly enriched Mo–Bi concentrate and an Mo concentrate (Table 15.1). In the first stage the Mo–Bi concentrate is leached with hydrochloric acid at 90–100 °C and finally with nitric acid. BiOCl precipitates from the bismuth-containing solution upon dilution to pH 2–3. Silver and lead chlorides also precipitate. Copper may be cemented afterwards with iron scrap. The crude bismuth has to be refined further [10].

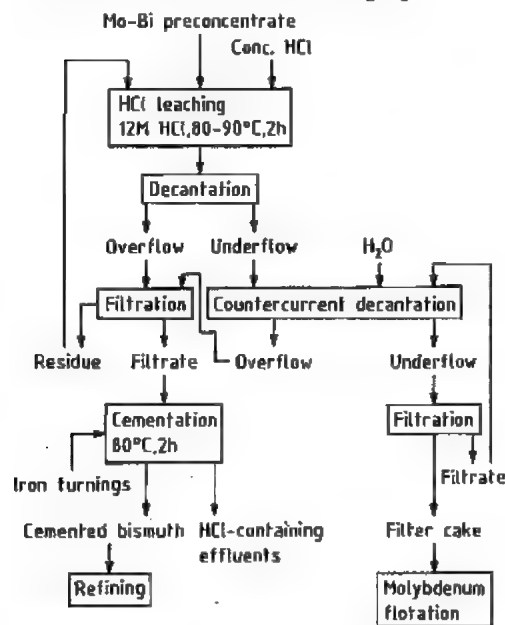


Figure 15.1: Hydrometallurgical separation of bismuth from Mo–Bi preconcentrate [9].

Processing of Sulfidic Copper–Bismuth Concentrates. The recovery of crude bismuth from sulfidic Cu–Bi concentrates is best illustrated by two examples.

The bismuth can be dissolved selectively with HCl in the presence of an oxidizing agent and precipitated as BiOCl by hydrolysis on

neutralization of the solution. Figure 15.2 shows the flow diagram, and Table 15.2 shows the distribution of elements in the intermediate products. The wash water is recycled, which increases the recovery of Cu, Bi, and Pb. Altogether 95% of the bismuth (and ≈ 1% of the copper) is found in the BiOCl precipitate, and 98% of the copper (and ≈ 4% of the bismuth) is found with the copper concentrate and cement copper.

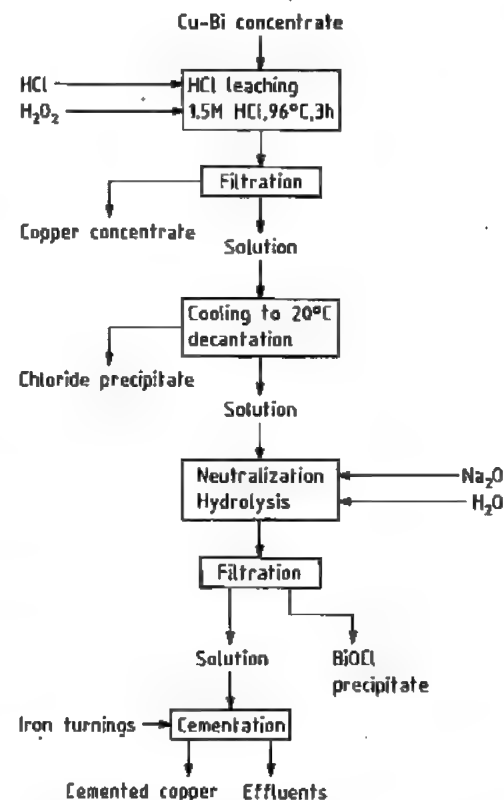


Figure 15.2: Hydrometallurgical separation of Bi from Cu–Bi concentrates [11].

Table 15.1: Bismuth separation from bismuth-containing molybdenum ores [10].

Substance	Concentration, %			
	MoS ₂	Bi	Cu	Fe
Ore, as mined	0.32	0.042	≤ 0.1	0.5–2.0
Mo–Bi concentrate	75–80	6–9	1P2	—
BiOCl	—	75	0.3 Ag	4 Pb
Crude bismuth	—	96	0.3 Ag	3 Pb

Table 15.2: Distribution of elements (%) in various intermediates of the oxidizing leaching process for Cu–Bi concentrates [11].

Substance ^a	Bi	Cu	Pb	Ag	Au
Cu concentrate	4	76	80	82	100
Chloride precipitate	< 1	—	9	8	—
BiOCl	74	< 1	< 2	< 3	—
Cemented copper	—	14	< 1	—	—
Wash water	21	8	3	—	—
Effluents	—	< 1	—	—	—

^aPercentage of the initial concentrations in the Cu–Bi concentrate. These initial concentrations are 1.7% Bi, 10.8% Cu, 8.0% Pb, and 0.34% Ag. Also present are 26.0% Fe, 29.4% S, 12.0% SiO₂, and 2.8% Zn.

Table 15.3: Bismuth contents and distribution during conventional lead smelting [13].

Substance	Bi content, %	Bi distribution, %
Sinter roasting input		
Lead concentrates	0.03	66.3
Lead flue dusts	0.06	13.9
Copper flue dusts	0.07	15.1
Sinter roasting output		
Sinter	0.04	97.5
Flue dust	0.08	2.5
Blast furnace input		
Sinter	0.04	75.0
Drosses	0.07	14.4
Pb–Ag residue	0.02	3.1
Recycled slag	0.08	5.9
Blast furnace output		
Pig lead	0.08	77.3
Flue dust	0.04	12.8
Slag	0.001	1.1

The Cu–B concentrate is leached first with hydrochloric acid (90–100 °C) and then with nitric acid. BiOCl precipitates from the solution after dilution to a pH of 2–3. Silver and lead chlorides coprecipitate. Copper may be cemented afterwards with iron scrap [11].

Bismuth copper concentrates are smelted in Telamayu, Bolivia, under reducing conditions after addition of soda to produce crude bismuth (> 92% Bi), a lean alkaline copper matte (< 10% Cu, < 0.3% Bi, < 20% Na), and a slag waste. The soda makes the slag low melting (< 1000 °C) and keeps the Bi content of the copper matte as low as possible. The flow sheet is shown in Figure 15.3. The crude bismuth is refined by conventional pyrometallurgical methods, the prerefining in Bolivia, the final refining in Belgium [12].

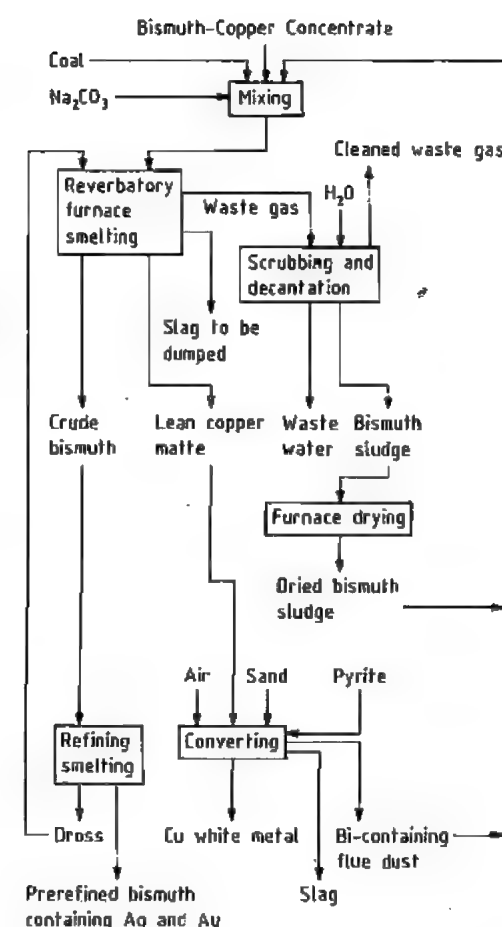


Figure 15.3: Processing of Bi–Cu concentrates in Telamayu, Bolivia [12].

15.5.2 Crude Bismuth from Lead Concentrates

Lead concentrates can contain significant quantities of bismuth. The average bismuth contents (g/t) are given below for several such concentrates [2]:

Kassandra, Greece	1800–2400
La Oroya, Peru	2300
Trepča, Yugoslavia	1600
Saxberget, Sweden	1100–1200
Milpo, Peru	1050
Aouli, Morocco	900
Atacocha, Peru	850
Raura, Peru	300–500
Bathurst, New Brunswick	450

Kimberley, British Columbia	350
Renström, Sweden	350
Garpenberg, Sweden	140–240
Rammelsberg, Germany	130–150

Lead production is usually carried out in two steps: (1) sintering and (2) reduction in a blast furnace. During this process the bismuth follows the lead without major losses, despite the volatility of bismuth (Table 15.3). In any case, the flue dusts are usually recycled. The loss of bismuth in the slag is low, since bismuth is reduced before lead [14].

Usually, bismuth is only a trace element throughout lead processing: only during lead refining is it enriched up to a few percent. The clean separation of bismuth from lead and the other elements present cannot be done by pyrometallurgical or electrolytic refining. Bismuth has less tendency than lead to form oxides, sulfides, or halides. Therefore, normal pyrometallurgical refining is not possible. Also, it is less electropositive:

$\text{Sn}^{2+} + 2\text{e}^- \rightarrow \text{Sn}_{(s)}$	-0.14 V
$\text{Pb}^{2+} + 2\text{e}^- \rightarrow \text{Pb}_{(s)}$	-0.13 V
$\text{Sb}^{3+} + 3\text{e}^- \rightarrow \text{Sb}_{(s)}$	+0.2 V
$\text{Bi}^{3+} + 3\text{e}^- \rightarrow \text{Bi}_{(s)}$	+0.28 V
$\text{As}^{3+} + 3\text{e}^- \rightarrow \text{As}_{(s)}$	+0.3 V
$\text{Cu}^{2+} + 2\text{e}^- \rightarrow \text{Cu}_{(s)}$	+0.345 V

Electrolytic refining can separate lead and bismuth, but Sb, As, Bi, and Cu remain together.

15.5.2.1 Pyrometallurgical Separation of Bismuth from Metallic Lead

One method has been found to separate bismuth from lead: precipitation of the intermetallic compound CaMg_2Bi_2 . The CaMg_2Bi_2 forms after addition of calcium–magnesium alloy to bismuth-containing lead melt (Kroll–Betterton process). The calcium and magnesium are added at 420 °C to the lead bath. The temperature is allowed to fall at a rate of 20 K/h until it is close to the melting point

(330 °C). Then the intermetallic compounds rich in bismuth solidify, and, having a lower density than lead, float to the top, where they can be removed in the dross by skimming. The simultaneous solubilities of Ca, Bi, and Mg in lead close to its melting point can be calculated from the solubility product [15].

$$[\text{Mg}, \%]_{\text{Pb}}^2 \times [\text{Ca}, \%]_{\text{Pb}} \times [\text{Bi}, \%]_{\text{Pb}}^2 = 4.3 \times 10^{-8}$$

Figure 15.4 shows these equilibrium solubilities of bismuth in the lead corner of the Pb–Ca–Mg system. In practice, the bismuth concentrations in refined lead are slightly higher than the calculated values: usually $\approx 0.01\%$. This is shown in Table 15.4 for two reported cases. The final bismuth concentration can be reduced below 0.01% if antimony is added to a melt already treated with Ca and Mg [18].

The Ca–Mg consumption can be calculated. Because the residual concentrations of Ca and Mg are greater for lower bismuth contents, the specific consumption is much greater for low Bi contents, as can be seen in Table 15.5 [16, 17].

Earlier, a mixture of K and Mg was used to separate the bismuth (Jollivet–Penarroya process), but the process is no longer in use. The reactions are analogous [15].

Table 15.4: Concentrations (%) in molten lead after bismuth separation and calculated solubility product.

Smelter	Bi	Mg	Ca	$\frac{[\text{Mg}]_{\text{Pb}}^2 \times [\text{Ca}]_{\text{Pb}}}{[\text{Bi}]_{\text{Pb}}^2}$	Ref.
Chimkent	0.009	0.145	0.066	1.1×10^{-7}	[16]
Norddeutsche Affinerie	0.014	0.1	0.03	0.6×10^{-7}	[17]

Table 15.5: Specific Ca and Mg consumptions for Bi removal from lead melts.

[Bi]Pb, %		Specific consumption, kg metal per kg Bi content	
before	after	Ca	Mg
0.05	0.009	1.06	3.5 calculated
0.09	0.009	0.62	2.05 calculated [16]
0.18	0.009	0.36	1.06 calculated [16]
0.2	0.020	0.25	0.60 ^a
0.68	0.014	0.15	0.39 [17]

^aCalculated from data in *Ullmann*, 3rd ed., vol. 18, p. 635.

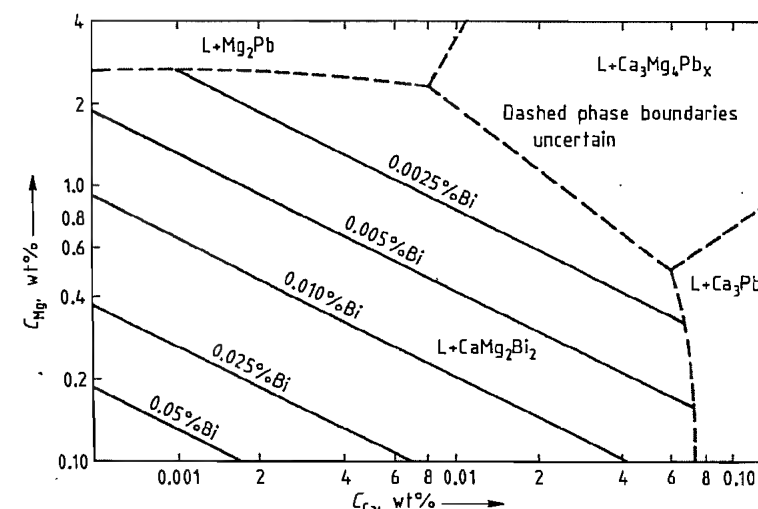


Figure 15.4: The Pb–Bi–Ca–Mg system, the liquidus surface in the lead corner [15].

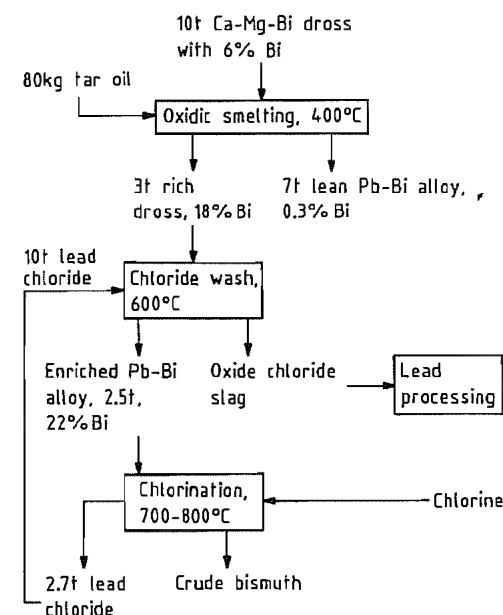


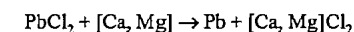
Figure 15.5: Conventional treatment of bismuth dross [19].

15.5.2.2 Processing of Bismuth-Containing Drosses

The dross resulting from the Kroll–Betterton process contains only a few percent bismuth. A typical composition is 6% Bi, 0.8%

Ca, and 1.3% Mg. The rest is Pb. If possible, the dross is enriched before bismuth recovery.

Several methods are available: liquation, pressing with a Howard press, partial oxidation, or partial chlorination. Usually one-stage enrichment is insufficient, so a multistage procedure is chosen. Often tar oil is mixed with the hot dross, which then burns immediately, oxidizing part of the Mg and Ca. At the same time the lead melts and separates from the dross. The flow sheet is shown in Figure 15.5. The solid dross remaining can be smelted to a lead–bismuth alloy. Calcium and magnesium can be removed from the dross by adding lead chloride.



The resulting Pb–Bi alloy containing 20–30% bismuth is chlorinated at 700–800 °C. The lead is converted to PbCl_2 . The crude bismuth contains less than 0.5% lead.

A process proposed by ASARCO (Figure 15.6) minimizes the costs. Vacuum filtration at 450 °C separates most of the lead without oxidation. The filter cake is heated slightly higher and burns, mostly by self-sustaining combustion. Washing with PbCl_2 separates the oxide residue into a Pb–Bi alloy and an oxide chloride slag. The alloy is refined in the usual way [19].

Although chlorine can be used to separate lead and bismuth, chlorine consumption is high and PbCl_2 , not Pb, is produced. Both the Norddeutsche Affinerie, Hamburg, and the Vieille Montagne, Belgium, have chosen another method. The Bi-Cu-Mg dross is soaked in a Pb-Bi melt. The Ca and Mg are oxidized in the presence of small amounts of NaOH, < 20 kg per tonne dross. The bismuth-rich lead is cast into anodes and electrolyzed to pure lead and anode slime, which can be melted to give crude bismuth. Only the lead remaining in the crude bismuth is chlorinated. In this way the largest portion of the lead is obtained directly as metal [17, 20].

15.5.2.3 Electrolytic Separation of Lead and Bismuth. Bismuth Production

Some lead producers use electrolytic lead refining, usually with $\text{PbSiF}_6\text{-H}_2\text{SiF}_6$ electrolyte, which allows an almost complete lead bismuth separation, independent of the bismuth content. Final bismuth contents ≤ 10 ppm can be achieved [17, 19, 21]. Almost all the bismuth goes into the anode slimes, which can contain between 2 and 25% Bi, depending on the bismuth content of the anodes (Trail, 2–4%; Oroya, 18–22%; Kamioka, 22% [2]).

At Centromin (formerly Cerro de Pasco Corp.) in La Oroya, Peru, dried anode slimes (35% Sb, 22% Bi, 14% Pb, 9% Ag, 0.03% Au) are smelted in a reverberatory furnace to partially evaporate the antimony. The metal then is 22.9% Sb, 30.8% Bi, 21% Pb, 19.6% Ag, and 0.069% Au. This metal is air-oxidized in a converter in two stages. In the first stage, at 900–1000 °C, a metal with $\approx 45\%$ Bi is produced. In the second stage, at 1100–1200 °C, a high-grade lead silver-bismuth alloy, 50–55% Ag and 30% Bi, and a slag with 40% Bi, 11% Pb, 4% Cu, and 2.5% Sb are obtained. This slag can be reduced at 1000–1100 °C to crude bismuth (73% Bi, 17% Pb, 3.6% Ag, 3% Cu) [2, 22]. The flow sheet is shown in Figure 15.7.

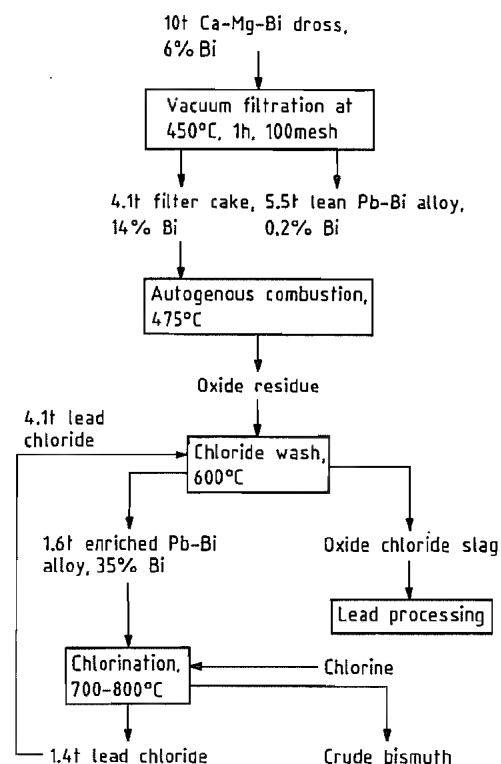


Figure 15.6: Bismuth treatment at ASARCO [19].

The anode slimes of the electrolytic lead refinery of Consolidated Mining and Smelting Corp., Trail, Canada, contain only 2–4% Bi. These anode slimes are smelted in a reverberatory Furnace at 900–950 °C, and the resulting alloy is oxidized in two stages, at 800–850 °C for arsenic and antimony oxidation and at 1000–1100 °C for oxidation of bismuth, lead, and copper. The slag of the second stage is the raw material for bismuth recovery. It is reduced to give a Pb-Bi alloy with 25–30% Bi, which is desilvered and again electrolyzed. The secondary anode slime consists mostly of bismuth. It contains 2% Pb and only traces of other elements. The slime is reduced to crude bismuth. After treatment with chlorine to remove lead, final treatment with caustic soda yields bismuth of 99.994% purity (20 ppm Pb, 14 ppm Cu, 33 ppm Ag). Figure 15.8 shows the flow sheet [2].

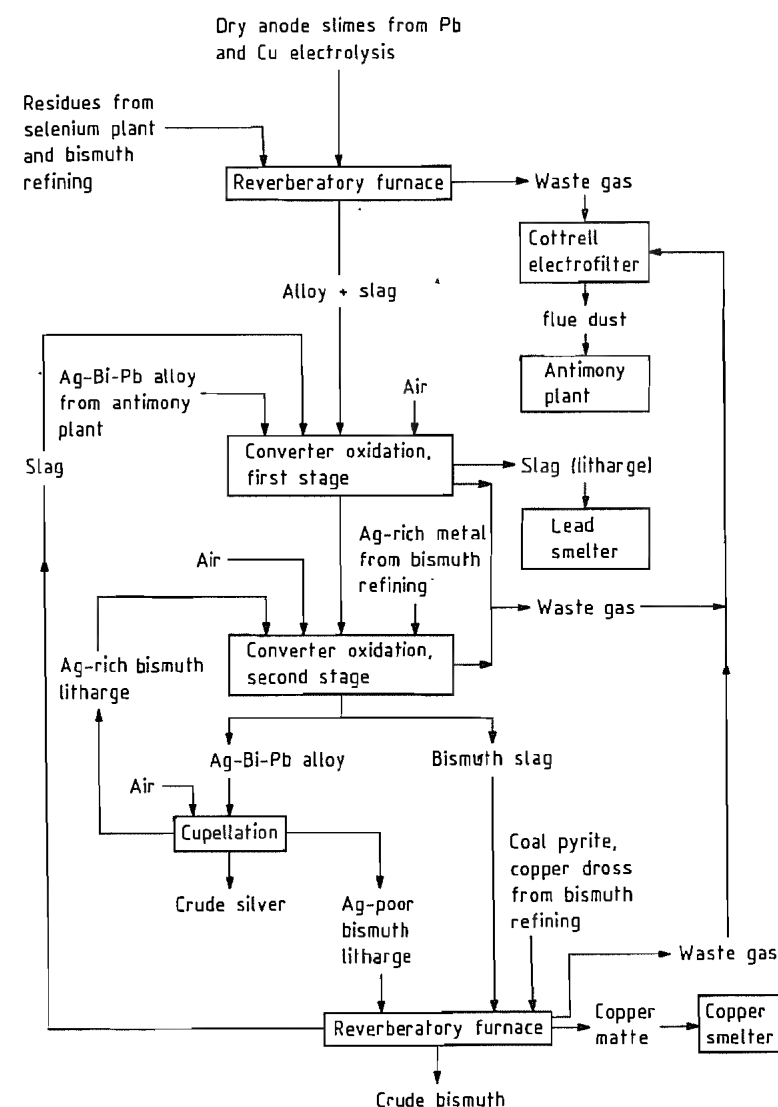


Figure 15.7: Recovery of crude bismuth from anode slimes at La Oroya, Peru [23].

The lead anode slime in San Gavino Monreale is treated to produce antimonial lead and bismuth.

Norddeutsche Affinerie has a special status among bismuth producers. The Kroll-Betterton procedure gives a Bi-Ca-Mg dross, which is separated from lead (0.05–3.5% Bi) and melted to a Pb-Bi alloy. This alloy is refined along with prerefined bismuth-rich lead in an electrolytic lead refinery. The anode slimes,

which are rich in bismuth, are smelted directly to crude bismuth [17]. The flow sheet is shown in Figure 15.9. The intermediate products have the following compositions (%):

	Pb	Cu	Bi
Anodes	90–95 ^a	< 0.01	4–8
Cathodes	99.99	0.0003	0.001
Anode slimes	2–4	0.06	88–90

^aOr more.

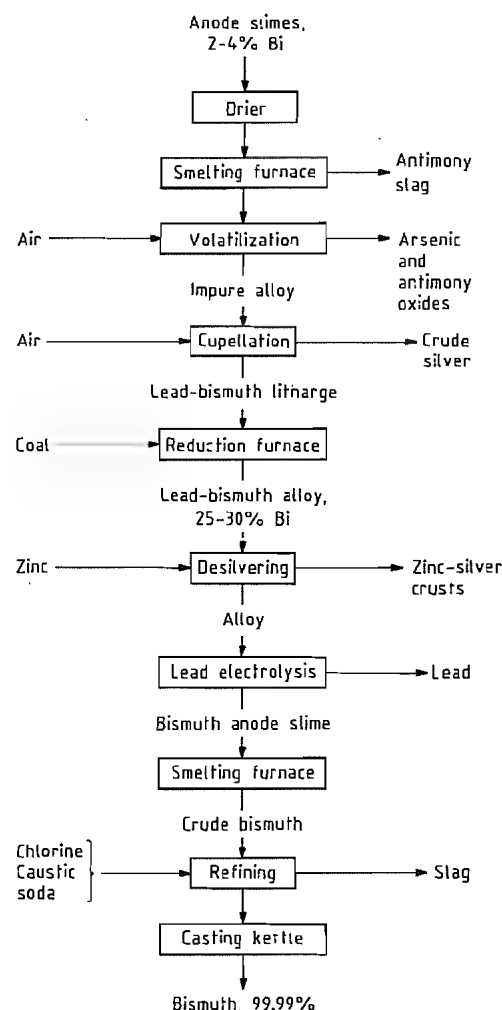


Figure 15.8: Bismuth recovery from lead anode slimes, Consolidated Mining and Smelting Co. of Canada [2].

15.5.3 Crude Bismuth from Copper and Tin Concentrates

Bismuth Separation from Copper Concentrates. Copper concentrates contain various amounts of bismuth. In g/t,

Gaspé, Québec	250
Skelefteå district, Sweden	700
Bathurst, New Brunswick [14]	200
Adrasman, Turkestan	several percent
La Oroya, Peru	400
Rokana, Sambia	200
Mufulira, Sambia	300

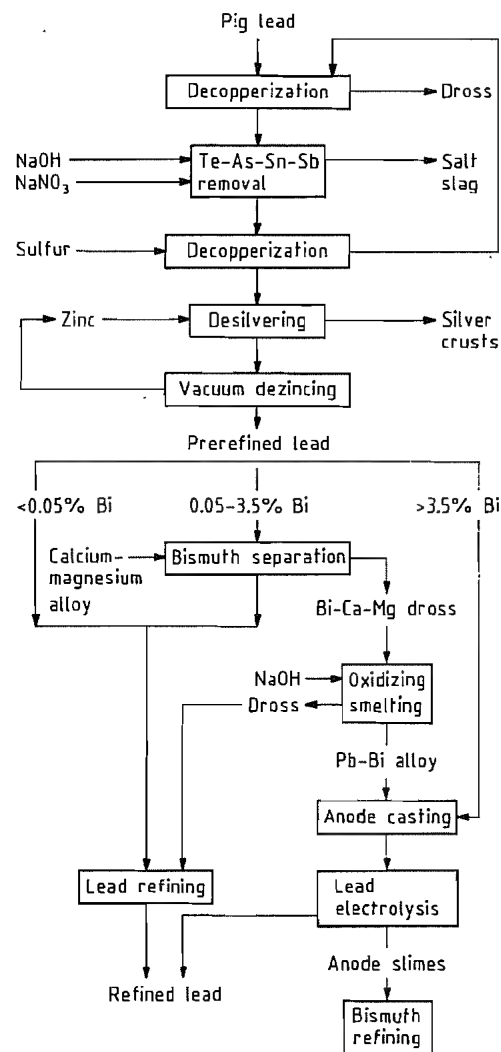


Figure 15.9: Simplified flow sheet of lead refining and bismuth separation at Norddeutsche Affinerie, Hamburg [17].

Åkulla and Kristineberg, Sweden 100-150
Rammelsberg, Harz 160

Most of the bismuth is volatilized during smelting of the concentrates, but the flue dusts are recycled to the smelting furnaces, at least in flash smelters, so that separation at this stage is not possible. In the following converter step the bismuth (more than 50%), along with Pb, Sb, and As, can be separated and enriched in the flue dust, which contains

several percent bismuth. After decopperization by leaching with sulfuric acid, these flue dusts are sent to lead smelters for further metal recovery. The bismuth distribution in various steps is shown in Table 15.6.

Separate treatment of the converter flue dusts is also possible. After decopperization, bismuth can be leached out selectively with $\text{H}_2\text{SO}_4\text{-NaCl}$. It is precipitated as BiOCl [25].

The bismuth remaining in the blister copper is difficult to remove by distillation [26] or during copper electrolysis. The anode slimes contain considerable amounts of bismuth (Table 15.7), and treatment of these copper anode slimes enriches bismuth in the lead-bismuth litharge, which can be processed pyrometallurgically (Figures 15.7 and 15.8).

Table 15.6: Bismuth distribution (%) during copper smelting and converting.

		Sn	Pb	Bi	Ref.
Matte melting	matte	97	<2	<0.3	
	slag	50-60	10-40	3-30	[24]
	flue dust	2	80-90	<20	[25]
Converting	blister copper	>99.97	<0.02	<0.01	
	slag				
	flue dust				
Electrolysis	cathodes				
	anode slimes				
	electrolyte				

Bismuth Separation from Tin Concentrates. Tin concentrates often contain bismuth. The bismuth can be leached with HCl and then precipitated as BiOCl , a process similar to the treatment of molybdenum concentrates [6].

In Vinto, Bolivia, the 0.5-5% bismuth is separated from the rich tin concentrates (55-63% Sn) by volatilization during a chloridiz-

Table 15.7: Average content of copper anode slimes, % [19].

	Element							
	Se	Te	Ag	Cu	Pb	Sb	As	Bi
Rönnskär, Sweden	20	1	10	40	5	1	2	0.5
Rokana NCCM, Sambia	13	1	4.5	44	1	0.1	0.3	1.1
Kennecott Copper Corp., Garfield, UT	11-12	5	14	26	8.6	0.5	1.4	0.14
Mufulira RCM, Sambia	5	0.3	11-12	35-43	2-3	—	—	0.3
Port Kembla, New South Wales	3	2.5	6	18	10-25	8	7	0.4
Centromin, La Oroya, Peru	2.5	3	26	—	26	12	1.5	0.9
Anaconda Co., Great Falls, MT	1.5	6	28	14-20	4-5	2-4	4-5	0.2

ing roasting process in a multiple hearth furnace. Optimum volatilization occurs at 800-850 °C for an NaCl excess of only 25-50%. A retention time of ≈ 1 h leads to a volatilization exceeding 97%. The volatilized chlorides are absorbed in water and precipitated as BiOCl [27, 28].

If the bismuth is removed only partially or not at all from tin ores before reduction, it is reduced together with tin and can be separated with lead by vacuum distillation at ≈ 1150 °C and 10 Pa (0.1 mbar). The primary condensate is distilled again to give a secondary condensate. In this way the tin codistilled in the first distillation is recovered [29-32]. The rate-limiting step is evaporation at 1200 °C and diffusion at 1000 °C [29]. The extent of bismuth separation is shown in the following, all quantities in % [31, 32]:

15.6 Refining

Crude bismuth is always refined by pyrometallurgical methods, even though electrolytic refining is possible. The pyrometallurgical refining is almost identical with conventional lead refining consisting of the following steps:

- Decopperization by liquation and sulfuring
- Te, As, and Sb removal by addition of NaOH-NaNO₃, the Harris process

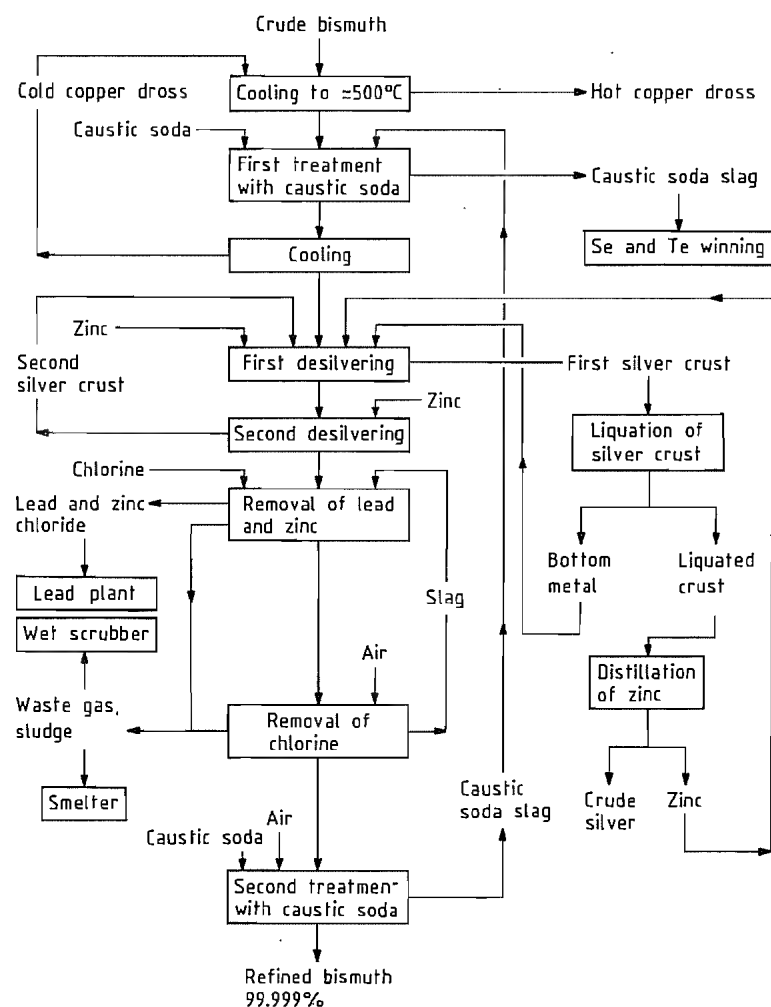


Figure 15.10: Refining of bismuth at Centromin, La Oroya, Peru [23].

- Removal of precious metals by Zn addition (Parkes process)
- Lead and zinc removal by chlorination
- Final oxidation with air in the presence of NaOH

With this procedure Norddeutsche Affinerie and Centromin produce 99.999% Bi. The residual impurities are 2 ppm Cu, 3 ppm Zn, and 2 ppm Fe. Figure 15.10 shows a typical flow sheet.

Liquation slightly above the melting point of bismuth removes copper and other impurities. Copper can be removed more effectively

if sulfur, soda, and charcoal are added. At 400–500 °C metal sulfides form, reducing the copper concentration to 10 ppm. The elements Se, Te, As, Sb, Sn, and Zn can be oxidized with NaNO_3 at 400 °C and dissolved in NaOH melt. Precious metals are removed by the addition of zinc, which forms an insoluble silver–zinc alloy. Just as in lead refining, removal takes place in two stages: liquation of rich and poor silver crusts. Approximately 12.5 kg Zn per tonne of Bi plus 2 kg Zn per kg of Ag are required, much greater amounts than in lead refining. The residual contents of Cu,

Ni, and Co are removed during desilvering, also by formation of insoluble alloys. After desilvering, bismuth contains more than 1% Zn and residual contents of lead, both of which can be reduced to a few ppm by chlorination at 400–500 °C. Excess chlorine can be blown out with air, or the bismuth can be washed with NaOH. Also copper, nickel, and cobalt can be removed from bismuth with chlorine [33]. The chlorination can be supported electrochemically: the bismuth melt, which is covered with a chloride melt, is the anode. Generally NaCl – CaCl_2 or KCl – ZnCl_2 melt is used. Lead and copper are converted into chlorides. Current densities can reach 0.4–0.8 A/cm^2 [34]. This multiple-step refining can be shortened considerably if the starting material is crust and dross from bismuth separation or anode slime from electrolytic lead refining. The quality of refinery bismuth is shown in Table 15.8.

Bismuth of *very high purity* is produced by vacuum distillation or zone melting. The starting material is always prerefined metal. Highest purities can be achieved by a combination of vacuum distillation and multiple zone melting. Vacuum evaporation at 800–850 °C and condensation at 650–750 °C refine bismuth almost completely. Al, Au, Ba, Be, Ca, Co, Cr, Fe, Ga, In, Ir, Li, Mo, Ni, Pd, Pt, Rh, Sn, Sr, Ti, and V stay in the residue. Cd, K, Na, Sc, and Zn evaporate but do not condense. Only a few elements cannot be removed: Ag, As, Mg, Pb, and Sb are insufficiently separated. Ce, Mn, and Tl follow the bismuth. At 800 °C the distillation rate is only 3.5 $\text{kgm}^{-2}\text{h}^{-1}$ and at 850 °C it is only 14 $\text{kgm}^{-2}\text{h}^{-1}$; 75–80% of the feed bismuth can be evaporated [35, 36].

Table 15.8: Composition of refinery bismuth [4].

	Bi, %	Contents, ppm				
		Cu	Ag	Zn	Pb	Fe
Centromin, La Oroya	99.999	2	—	3	—	2
Norddeutsche Affinerie, Hamburg	99.999	—	—	—	—	—
Cominco, Trail, Canada	99.999	—	—	—	—	—
Mitsui, Kamioka	99.99	6	9	—	10	—
San Gavino, Sardinia	99.99	10	15	—	10	—

Multiple zone melting of distilled bismuth produces very pure bismuth. Only 1 ppm of Ca, Pb, and Si and a total of 1.5 ppm of Al, Ca, Fe, and Mg are found.

Smelting bismuth with NaOH at 400 °C completely removes As, Sb, Sn, and Zn and almost completely slags Te and Pb. Careful chlorination before distillation and zone melting is recommended [37]. Treatment with chlorine removes Cu, Pb, Sn, and Zn completely. Zone melting then enriches Ag, Cu, Ni, Pb, Se, Sn, Tl, and Zn in the end piece of the rod.

15.7 Alloys

The binary systems of alkali metals or alkaline-earth metals with bismuth show intermetallic compounds with high melting points. In the system Bi–Li, for example, the compound Li_3Bi melts at 1145 °C. Some intermetallic compounds, especially those with K, Ca, and Mg, are or were used to separate bismuth from lead (see Section 15.5.2.1). The systems with Zn, Al, Ga, Co, or Si show limited solubility in the liquid phase. Bismuth and iron are insoluble in one another; therefore, iron equipment can be used for melting and refining the metal. The rare case of complete solubility in both the liquid phase and the solid phase appears in the system Bi–Sb. Some binary alloys, particularly those with Cd, In, Pb, Sn, and Tl, as well as some multicomponent alloys, form low-melting eutectics (Table 15.9). The most common ones, called fusible alloys, are offered under the trade names Asarco, Cerrolow, Cerrobend, Belmont, and Ostalloy.

Some multicomponent and some noneutectic compositions have both low melting points and the unusual characteristic of not contracting or even expanding on solidification. The alloy with 56% Bi, 20% Sn, and 24% Pb is said to have the largest volume expansion of any alloy [6]. Some alloys show effectively no volume change: 50% Bi–50% Pb and 70% Bi–30% Pb, for example.

Table 15.9: Fusible alloys [6, 38].

System	Eutectic composition, %	Eutectic temperature, °C
Cd-Bi	Cd 40, Bi 60	144
In-Bi	In 66.3, Bi 33.7	72
	In 33	109
	Bi 67	
Pb-Bi	Pb 43.5, Bi 56.5	125
Sn-Bi	Sn 43, Bi 57	139
Tl-Bi	Tl 23.5, Bi 76.5	198
	Tl 52.5, Bi 47.5	188
Pb-Cd-Bi	Pb 40, Cd 8, Bi 52	92
Sn-Cd-Bi	Sn 26, Cd 20, Bi 54	102
In-Sn-Bi	In 16, Sn 26, Bi 58	79
Tl-Pb-Bi	Tl 11.5, Pb 33.3, Bi 55.2	91
	Tl 48, Pb 9.8, Bi 42.2	186
Tl-Sn-Bi	Tl 14.3, Sn 35.7, Bi 50	124
	Tl 25, Sn 31, Bi 44	167
Pb-Sn-Cd-Bi	Pb 26.7, Sn 13.3, Cd 10, Bi 50	70
In-Cd-Pb-Sn-Bi	In 19.1, Cd 5.3, Pb 22.6, Sn 8.3, Bi 44.7	47
	In 4.0, Cd 9.6, Pb 25.6, Sn 12.8, Bi 48.0	64

Bismuth forms with alkali metals and alkaline-earth metals alloys that superconduct at low temperatures. Examples are LiBi, NaBi, CsBi₂, and BaBi₃. Their transition temperatures are 2.47 K, 2.22 K, 4.75 K, and 4.69 K, respectively.

Bismuth alloys are usually prepared by melting the components together, but prealloyed metals are used for the exact adjustment of the composition.

Bismuth is used as an alloy addition in steel and aluminum. The fabrication of low-carbon steel and stainless steel is improved by addition of 0.15% Bi and 2.2% Pb. To aluminum alloys 0.2–0.7% each of bismuth and lead are added [6].

Uses. The versatility of bismuth alloys results from their extremely low melting points and their volume changes on solidification combined with low viscosity and low surface tension. The composition can be chosen so that the alloy contracts, remains the same, or expands as a result of solidification. The last two cases, because they are unusual, are the most important.

The eutectic alloy Bi–Cd–In–Pb–Sn, melting at 47 °C, and some alloys melting higher

are used for the automatic release of fire alarm systems, automatic sprinkler systems, electric fuses, and safety plugs for storage tanks.

Thin-walled tubes and parts for the automobile and aviation industries are covered or filled up with bismuth alloy melting below 100 °C before bending or deforming to prevent collapse. After forming, the alloy can be melted out by dipping the part into boiling water. Especially suitable is the eutectic alloy Bi–Cd–Pb–Sn, which melts at 70 °C. It is very ductile and expands on solidification and during the first hour thereafter; therefore, it keeps the worked part under tension during bending or forming.

The noneutectic alloy with 48% Bi, 28.5% Pb, 9% Sb, and 14.5% Sn, which melts over the range 103–227 °C, expands greatly during the first hours after casting, reaching its final volume after ≈ 500 h. It can be used to grip tubes, tools, punches, and parts to be machined. Because it is diamagnetic, it is suited for embedding magnets in equipment or filling the space between magnets.

The noneutectic Bi–Sn alloy with 40% Bi and 60% Sn, which melts over the range 138–169 °C, contracts only 0.01% during solidification and aging. Such an alloy exactly reproduces the shape and dimensions of the casting mold. In sprayed parts it reproduces the base in every detail. This alloy is used for test casts, copies of irregular parts, molds for thermoplastic material in the rubber and plastic industry, and for meltable casting cores. The eutectic Bi–Sn alloy with 57% Bi, melting at 138 °C, expands 0.07% on solidification but contracts during the next 5 h. The final net expansion is only 0.02%. This alloy is used in dentistry for the production of models and molds [39].

Some bismuth alloys wet glass, mica, and enamelled ceramics. They are used to seal such substances to each other and to metals, as well as to produce high-vacuum seals for glass equipment. A so-called bismuth cement consists of 35% Bi, 37% Pb, and 25% Sn. Such alloys are used in holding devices for grinding and polishing glass and plastic lenses. Low-melting bismuth solders are used for the sol-

dering of temperature-sensitive electronic parts [40].

Cs–Bi alloys are used in photocathodes. The low conductivity of bismuth results in a good quantum yield. Bismuth tellurides and a bismuth–antimony alloy with 11% Sb are used in photoelectric infrared detectors. The compound Bi₂Te₃, especially its solid solutions with Bi₂Se₃ and Sb₂Te₃, is a useful thermoelectric material. The system AgSbTe₂–AgBiTe₂ also has interesting thermoelectric properties [41]. Mn–Bi alloys are permanent magnets [34].

In nuclear technology, bismuth and its alloys may be useful for cooling and as heat-exchange mediums because bismuth has an extremely low absorption cross section for thermal neutrons. However, nothing specific has been reported about use in modern reactors.

15.8 Compounds

In its inorganic compounds bismuth usually has 3+ or 5+ oxidation state. The 5+ oxidation state is a strong oxidation agent, e.g., NaBiO₆ or BiF₅. Bismuth has an oxidation state of 3– in a few intermetallic compounds, e.g., Li₃Bi and CaMg₂Bi₂. In gases, such as BiCl or BiO, in Bi(AlCl₄), and in alloy-like compounds, such as BiS or BiSe, bismuth can have 1+ or 2+ oxidation state, and 1+, 0, and 1– are present in polynuclear ionic species. However, the 1+ and 2+ states are rare, and compounds

with 4+ probably do exist also. On dissolution, bismuth compounds hydrolyze easily, yielding nearly insoluble basic salts of the type BiOX. In the presence of strong acids or in complexing agents, bismuth remains in solution. Table 15.10 shows some physical properties of the most important inorganic bismuth compounds.

Only a few inorganic bismuth compounds are produced commercially. Bismuth oxychloride is used in cosmetics. It is the basic ingredient of a pearly pigment found in eye shadow, hair sprays, powders, nail polishes, and other cosmetic products. Bismuth oxide can substitute for lead oxide in glass or porcelain.

Today the use of bismuth compounds in medicine is decreasing and the use of bismuth in pharmaceutical products is being viewed more and more as a questionable practice [42]. France, which in 1972 consumed more than 1000 t of bismuth, making it the largest bismuth consumer, has restricted the use of bismuth in pharmaceuticals, resulting in a sharp drop in bismuth consumption [43]. Bismuth compounds have been used because of their astringent, antiphlogistic, bacteriostatic, and disinfecting actions. In dermatology bismuth subgallate is still used in vulnerary salves and powders as well as in antimycotics. Medicines for depigmentation can no longer contain bismuth. Even bismuth subcarbonate, bismuth subnitrate, or the recently developed complex bismuth citrates ought not be used for the treatment of gastric disturbances.

Table 15.10: Physical properties of inorganic bismuth compounds.

Compound	Formula	Gibbs free energy of formation, kJ/mol	Density, g/cm ³	mp, °C	bp, °C
Bismuth tribromide	BiBr ₃	–263.8	5.72	219	461
Bismuthyl carbonate	(BiO) ₂ CO ₃	—	8.15	decomp.	—
Bismuth trichloride	BiCl ₃	–379.3	4.76	233.5	440.1
Bismuth chloride oxide	BiOCl	–374.3	7.72	232.5	447
Bismuth trifluoride	BiF ₃	–883.4	7.90	227	405
Bismuth pentafluoride	BiF ₅	—	5.40	151.4	230
Bismuth triiodide	BiI ₃	–333.5	5.80	408.5	542
Bismuth trinitrate pentahydrate	Bi(NO ₃) ₃ · 5H ₂ O	—	2.80	75	decomp.
Bismuth trioxide	Bi ₂ O ₃	–575.7	9.32	824	1890
Bismuth trisulfide	Bi ₂ S ₃	–176.7	6.81	747	—

Bismuth Tribromide, BiBr_3 . Golden-yellow crystals, cubic, hygroscopic. Prepared by reaction of the elements at 250 °C [44] or in methanol [45], by reaction of bismuth with molten iodine bromide and extraction with CCl_4 [46], or by dissolving Bi_2O_3 in concentrated hydrobromic acid, drying, and distillation in a stream of nitrogen. Bismuth tribromide is soluble in acetone, ether, acetic acetate, glacial acetic acid, and aqueous solutions of HCl, KCl, KBr, and KI. In water it hydrolyzes to BiOBr . It is insoluble in alcohol and carbon disulfide.

Bismuthyl Carbonate, $(\text{BiO})_2\text{CO}_3$. Naturally occurring as bismutite. White powder, sensitive to light, decomposition during heating. Preparation by precipitation with sodium or ammonium carbonate from nitrate solutions [47, 48].

Bismuth Trichloride, BiCl_3 . White powder, cubic, very hygroscopic. Prepared by chlorination of the molten metal [44] or by dissolution of the metal in aqua regia, boiling down, and distillation. *Bismuth chloride oxide*, bismuth oxychloride, BiOCl , is formed by heating BiCl_3 in air or by hydrolysis of BiCl_3 . The oxychloride is a white, lustrous, crystalline powder, ρ 7.72 g/cm³, that is practically insoluble in water, ethanol, acids, and bases. Hot concentrated alkali solutions convert it into the trioxide.

Bismuthine, BiH_3 . Bismuthine is a colorless gas unstable at room temperature. Prepared by treating Mg_3Bi_2 with dilute acids [49], decomposition of methylbismuthine or dimethylbismuthine [50], or reaction of bismuth halides with LiAlH_4 in a vacuum [3].

Bismuth Trifluoride, BiF_3 . White, fine powder, rhombic. Prepared by dissolving Bi_2O_3 in hydrofluoric acid [51] or by precipitation from an aqueous solution of bismuth trinitrate with aqueous KF or NaF [52]. Soluble only in acetone and liquid organic acids, insoluble in water. *Bismuth fluoride oxides*, $\text{BiO}_x\text{F}_{3-2x}$, form when BiF_3 is heated in air at 670–850 °C.

Bismuth Pentafluoride, BiF_5 . White needles, formed by fluorination of bismuth metal or

BiF_3 at 500 °C [53]; strong oxidant, violent reaction with water.

Bismuth Triiodide, BiI_3 . Greenish-black crystalline powder. Prepared by heating stoichiometric quantities of the elements in a sealed vessel at 150–180 °C [54] or by reaction of concentrated hydriodic acid with a solution of BiCl_3 in hydrochloric acid [55]. Insoluble in cold water. Boiling BiI_3 with water produces BiOI . Bismuth triiodide is soluble in alcohol, natural gasoline, xylene, and toluene. Red triammine complexes are formed in aqueous ammonia. The yellowish-orange Dragendorff reagent, KBiI_4 , for precipitating alkaloids, is formed by dissolving BiI_3 in potassium iodide solution.

Bismuth Trinitrate Pentahydrate, $\text{Bi}(\text{NO}_3)_3 \cdot 5\text{H}_2\text{O}$. Colorless, columnar crystals. Prepared by dissolving bismuth metal, Bi_2O_3 , or $(\text{BiO})_2\text{CO}_3$ in nitric acid [56]. Hydrolyzes in water to basic salts. The nitrate is soluble in strong inorganic acids, glacial acetic acid, and glycerol. It is the starting material for basic bismuth nitrates of composition $x\text{Bi}_2\text{O}_3 \cdot y\text{N}_2\text{O}_5 \cdot z\text{H}_2\text{O}$. Bismutum subnitricum, approximate composition $6\text{Bi}_2\text{O}_3 \cdot 5\text{N}_2\text{O}_5 \cdot 9\text{H}_2\text{O}$, was commonly used for medical purposes.

Bismuth Oxides. Bismuth trioxide, Bi_2O_3 , is the only bismuth oxide which has been isolated in a pure state. There is also a Bi_2O_5 , but its characteristics are not yet well defined. Information about other oxides and related compounds is scarce.

Bismuth trioxide, Bi_2O_3 , is prepared by oxidation of bismuth metal at 750–800 °C, by thermal decomposition of carbonates, or by addition of alkali-metal hydroxides to a bismuth salt solution. In the last case hydrated bismuth trioxide precipitates. This gelatinous compound is usually represented by the formula $\text{Bi}(\text{OH})_3$; calcining it yields Bi_2O_3 .

Monoclinic $\alpha\text{-Bi}_2\text{O}_3$ converts in an endothermic transition at 710–740 °C to the high-temperature cubic modification $\delta\text{-Bi}_2\text{O}_3$, which is stable between 710 °C and the melting point. The transition is reversible, and δ -

Bi_2O_3 is not stable at room temperature. Quenching thin layers of molten Bi_2O_3 forms metastable tetragonal $\beta\text{-Bi}_2\text{O}_3$, which converts back to $\alpha\text{-Bi}_2\text{O}_3$ when heated. This metastable $\beta\text{-Bi}_2\text{O}_3$ dissolves oxygen in its lattice without a structure change, the composition can range from $\text{BiO}_{1.50}$ to $\text{BiO}_{1.75}$. Heating $\beta\text{-Bi}_2\text{O}_3$ to 750 °C and quenching at a moderate rate forms metastable cubic $\gamma\text{-Bi}_2\text{O}_3$, which contains more oxygen than the stoichiometric formula Bi_2O_3 expresses. The preparation of all these modifications is described in detail in [3]. Quenching molten mixtures of Bi_2O_3 and other metal oxides from 800–1000 °C to 0 °C produces stabilized δ - and β -modifications; tempering for 24 h at 600 °C yields a γ -modification contaminated with other oxides.

Bismuth trioxide is soluble in strong inorganic acids and concentrated alkaline solutions containing glycerol. Above 710 °C it attacks metal oxides; in fact, molten bismuth trioxide dissolves every metal oxide and even corrodes platinum.

Bismuth trioxide monohydrate, $\text{Bi}_2\text{O}_3 \cdot \text{H}_2\text{O}$, is a white powder. Its composition and constitution are not completely elucidated. $\text{Bi}(\text{OH})_3$ and BiOOH probably do exist. A hydrated oxide precipitate is formed by reaction of an acidic bismuth nitrate solution with ammonia or caustic soda solution [57].

Bismuth pentoxide, Bi_2O_5 , is prepared by oxidizing suspended Bi_2O_3 with Cl_2 , Br_2 , or H_2O_2 in an aqueous alkaline solution. Each of these reactions goes almost to completion. Molten mixtures of Bi_2O_3 and alkali-metal oxides can be oxidized by air or oxygen. The reaction is favored by excess alkali. The excess alkali can be stripped with methanol at 0 °C to form yellowish-orange sodium metabismuthate, NaBiO_3 . Addition of nitric or perchloric acid leads to a compound whose composition varies from $\text{Bi}_2\text{O}_4 \cdot x\text{H}_2\text{O}$ to $\text{Bi}_2\text{O}_5 \cdot x\text{H}_2\text{O}$. Both compounds are strong oxidants.

Bismuth Trisulfide, Bi_2S_3 . Naturally occurring as bismuth glance. Dark brown to grayish black, metallic luster, rhombic. Prepared by heating bismuth with sulfur or bismuth trioxide with sulfur compounds or by precipitation

from aqueous bismuth(III) solutions with H_2S . It is insoluble in water and alkaline solutions but soluble in hot aqueous salt solution or concentrated nitric acid. Concentrated alkaline metal sulfide solutions or melts dissolve Bi_2S_3 to form compounds of the type KBiS_2 . Similar compounds naturally occur with copper, silver, and lead.

15.9 Chemical Analysis

For qualitative determination bismuth [58] is precipitated as Bi_2S_3 from slightly acidic solution with H_2S . The precipitate is brown black and soluble in strong acids and hot dilute nitric acid. Yellow-green Bi_2S_3 precipitates from alkaline solution on addition of Na_2S . Bismuth can be precipitated by hydrolysis from hot dilute hydrochloric acid as bismuth oxychloride, provided excess chloride ions are absent. Aqueous ammonia precipitates bismuth as white bismuth oxide hydrate, which can be reduced to bismuth metal with alkaline stannate(II) solution.

Bismuth phosphate, BiPO_4 , can be precipitated quantitatively from very dilute nitric acid solution. Bismuth in medicinal preparations is determined by precipitation as basic bismuth carbonate. Calcining at 550 °C yields Bi_2O_3 . A thiourea–bismuth mixture is of yellow color in nitric acid solution, and this is the basis for a photometric method. If ions such as Fe, Hg, Zr, etc., are absent, titration with EDTA is a selective, quantitative, and fast method of bismuth analysis. This method has become very popular [59]. Emission, mass, or atomic absorption spectrometry allow detection of less than 1 ppm Bi.

15.10 Economic Aspects

Bismuth concentrates are a by-product of nonferrous metal ore dressing. The metal available from concentrates has remained nearly the same, between 3600 and 4600 t/a since the 1960s. The world's one and only bismuth mine, Telamayu in Bolivia, which had produced about 15% of the worldwide supply,

stopped production in 1980 because of either declining demand or perhaps total exhaustion of the site. Also Australia and Peru are reducing their production. Only a part of bismuth refining is carried out in the mining countries. Table 15.11 shows the metal content of bismuth ores and concentrates, corresponding closely to the world production of 3795 t in 1980. The main producer of bismuth metal is the United States, producing ≈ 950 t/a [61]. Bismuth suppliers are listed in [63].

Bismuth (99.99%) is quoted in London and New York in \$/lb (1 lb = 0.454 kg). After rising to \$9/lb in 1974 the price of bismuth fell steadily for years. The price was \$1.67 per pound in December, 1983. However, since then the price has increased, to \$6.60 in February, 1985. The prices are much higher for high-purity bismuth (99.999%). Table 15.12 shows actual U.S. bismuth consumption. No consumption data for the European market have been published for several years. Because of substitution and regulatory restrictions bismuth consumption has decreased more in Europe than in the United States.

Table 15.11: Bismuth in ores and concentrates, t [60–62].

	1970	1973	1977	1980
Australia	363	500	912	907
Bolivia	567	690	680	11
Canada	272	300	165	171
China	200 ^a	250	249	259
France	59	65	66	59
Germany	18	20	10	9
Italy	23	25	15	10 ^a
Japan	68	75	80 ^a	80 ^a
Mexico	453	600	729	748
Peru	816	690	590	522
Romania	9	10	80	80 ^a
South Korea	136	150	134	90 ^a
Sweden	32	35	15	15 ^a
Former USSR	50 ^a	50	66	73
United States	363	400	400	400 ^a
Former Yugoslavia	108	120	74	73
Others	204	320	399 ^b	215 ^b
Total	3741	4300	4664	3722

^a Estimated.

^b Calculated.

Table 15.12: Bismuth consumption in the United States, t [61].

	1970	1973	1978	1980
Chemical industry ^a	567	543	521	556
Fusible alloys	292	423	379	291
Metallurgical additions	236	376	210	211
Other alloys	6	7	10	11
Others	5	5	8	7
Total	1106	1354	1128	1076

^a Including pharmaceutical products and cosmetics.

15.11 Toxicology of Bismuth and Bismuth Compounds

Poisoning by bismuth and bismuth compounds has occurred more frequently during medical therapy than by exposure at the workplace [64]. It resembles poisoning caused by lead and mercury and their compounds. After oral administration, water-insoluble bismuth compounds, such as bismuth nitrate oxide, $\text{BiO}(\text{NO}_3)$, are hardly absorbed, and acute poisoning is seldom. Increased absorption was observed, however, when large quantities of such compounds were applied to skin lesions, resulting in serious poisoning, sometimes fatal. Water-soluble bismuth compounds are absorbed quickly, and acute poisoning is likely to occur. However, the relatively high toxicity of bismuth nitrate oxide, which was observed especially in children, is most likely not caused by bismuth but by reduction of nitrate to nitrite and subsequent methemoglobin formation by intestinal bacteria.

The main hazard of bismuth is the chronic exposure that took place during long-term therapy (up to 30 years in some cases) practiced earlier. Such exposure can have serious consequences for humans and animals. First symptoms of chronic intoxication by bismuth are hypersalivation, stomatitis, and a grayish black seam surrounding the gums (symptoms similar to those caused by lead).

According to many investigations, e.g., [65] and [66], long-term oral administration caused encephalopathies accompanied by distractions, ataxia, myoclonic spasms, insomnia, and headache in many cases and less frequently epileptic attacks. Some cases ended in

death, the brains of the deceased containing large quantities of lipid-soluble bismuth compounds [67]. This crossing of the blood-brain barrier by bismuth compounds was demonstrated in other experiments, e.g., for trivinylbismuth in pigs [68]. In another epidemiological study, a group of patients with manifest bismuth poisoning was compared to a control group that had been exposed to the same amount of bismuth but that did not show any symptoms of poisoning [69]. The investigators concluded that bismuth poisoning is caused by the transformation of bismuth compounds of low toxicity into those of high toxicity by intestinal bacteria.

The occurrence of osteolytic and osteonecrotic arthropathies of the shoulder was pointed out in [70]. In over 59 cases of bismuth poisoning, bone lesions accompanied by encephalopathies were described [71]. Caused by the elimination of bismuth compounds in the urine, albuminuria and nephritis were observed also [64]. Bismuth also causes eye defects [72], which was confirmed by experiments with mice [73]. Inhalation of trimethylbismuth, $\text{Bi}(\text{CH}_3)_3$, by humans causes irritations of the respiratory tract and conjunctivas. Cats and dogs that inhaled trimethylbismuth for 10–20 min showed ataxia, restlessness, and convulsions; after 24 h severe encephalitis was observed [74].

In a long-term carcinogenicity test bismuth chloride oxide, BiOCl , was fed to rats over a period of two years (1, 2, and 5% in the feed) [75]: neither carcinogenic nor other toxic effects that were caused by bismuth chloride oxide could be found. So far there is no evidence for carcinogenicity, mutagenicity, and teratogenicity of bismuth compounds [76].

The following toxicological data are available for bismuth and bismuth compounds: lowest published lethal dose for bismuth, 221 mg/kg (humans, presumably oral) [77]; bismuth chloride oxide, BiOCl , LD_{50} 22 g/kg (rat, oral); trimethylbismuth, $\text{Bi}(\text{CH}_3)_3$, LD_{50} 484 mg/kg (rabbit, oral), LD_{50} 182 mg/kg (rabbit, subcutaneous), LDLo 11 mg/kg (rabbit, intravenous) [74]. In the Swiss list of toxic substances bismuth nitrate oxide, BiONO_3 ,

and triphenyl bismuth, $\text{Bi}(\text{C}_6\text{H}_5)_3$, are in class 3; bismuth titanate, $\text{Bi}_2(\text{TiO}_4)_3$, is in class 5.

15.12 Pigments

Bismuth-containing special effect pigments based on platelet-shaped crystals of bismuth oxide chloride (bismuth oxychloride, BiOCl) have been known for a long time (see Section 15.12.5). More recently, greenish yellow pigments based on bismuth orthovanadate, BiVO_4 , have attracted increasing interest. They represent a new class of pigments with interesting coloristic properties, extending the familiar range of yellow inorganic pigments (iron yellow, chrome yellow, cadmium yellow, nickel titanium yellow, and chromium titan yellow). In particular they are able to substitute the greenish yellow shades of the lead chromate and cadmium sulfide pigments.

Historical Aspects. Bismuth vanadate occurs naturally as the brown mineral pucherite (orthorhombic), as Clinobisvanite (monoclinic) and as Deyerite (tetragonal). Its synthesis was first reported in 1924 in a patent for pharmaceutical uses [78]. The development of pigments based on BiVO_4 began in the mid 1970s. In 1976, Du Pont described the preparation and properties of “brilliant primrose yellow” monoclinic bismuth vanadate [79]. Montedison developed numerous pigment combinations based on BiVO_4 [80]. Pigments containing other phases besides BiVO_4 , e.g., Bi_2XO_6 ($\text{X} = \text{Mo}$ or W), have been reported by BASF [81] and became the first commercial product (trade name Sicopal® Yellow L1110). Since then Bayer [82], Ciba-Geigy [83], BASF [84], and others have published further methods for the manufacture of pigments based on BiVO_4 . On the market are now pigments for the use in paints and plastics of the following suppliers: BASF, Ciba-Geigy, Bayer, Capelle, Bruchsaler Farbenfabrik, and Heubach.

Recently, BASF placed a new reddish yellow bismuth vanadate pigment on the market (trade name Sicopal® Yellow L 1600).

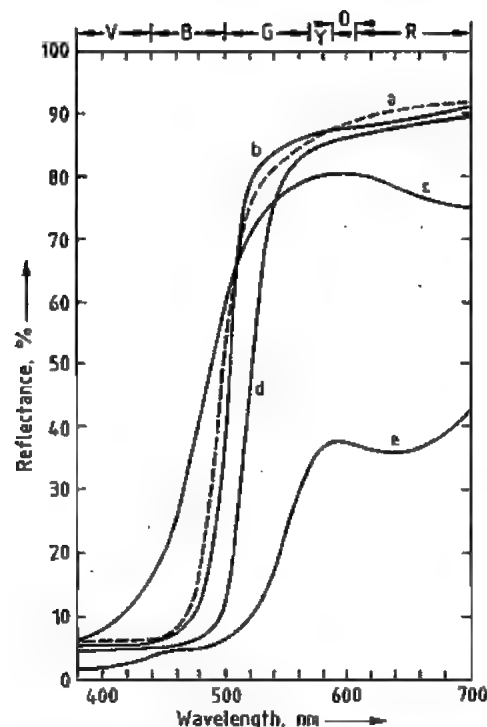


Figure 15.11: Reflectance curves of yellow pigments: a) BiVO_4 ; b) CdS ; c) $(\text{Ti, Ni, Sb})\text{O}_2$; d) $\text{PbCrO}_4\text{-PbSO}_4$; e) FeOOH .

15.12.1 Properties

Most of the commercial bismuth vanadate pigments are now based on pure bismuth vanadate with monoclinic structure, though there are still pigments based on the two-phase system bismuth vanadate molybdate, $4\text{BiVO}_4 \cdot 3\text{Bi}_2\text{MoO}_6$. The pure bismuth vanadate pigments show a higher chroma than the two phase systems. In the following the physical and coloristic properties of a pure bismuth vanadate pigment are given (Sicopal® Yellow L1100, BASF):

Density	6.1 g/cm ³
Refractive index <i>n</i>	2.45
Specific surface area (BET)	13 m ² /g
Oil absorption	33 g/100 g of pigment
Composition: Bi	64.51%
V	15.73%
O	19.76%

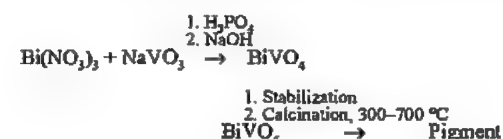
Bismuth vanadate, C. I. Pigment Yellow 184, is a pigment with a greenish yellow co-

lour, having high tinting strength, high chroma, and very good hiding power. When compared with other yellow inorganic pigments, it most closely resembles cadmium yellow and chrome yellow in its colouristic properties (Figure 15.11). Bismuth vanadate shows a sharp increase in reflection at 450 nm and considerably higher chroma than iron yellow or nickel titanium yellow. It has very good weather resistance both in full shade and in combination with TiO_2 . Pigment properties follow:

Hue angle H° (HGD, hue grade; CIELAB)	93.7
Chroma C^*ab (CIELAB)	95.5
Hiding power	at 42.5% by weight in dry film about 70 µm over black/white
Weather resistance (DIN 54002)	alkyd/melamine
Full shade	4-5
Mixed with TiO_2 , 1:10	4-5
Chemical resistance in crosslinked paint films	
acid	5 (2% HCl)
alkali	5 (2% NaOH)
Heat stability	> 200 °C

15.12.2 Production

The production process for bismuth vanadate pigments consists usually of a precipitation reaction followed by a calcination step. The calcination step is different from producer to producer and can be completely absent depending on the precipitation process and the desired product properties.



In this process first, a fine precipitate is formed by adding an alkaline solution of sodium or ammonium vanadate to an acidic bismuth nitrate solution in presence of a considerable amount of phosphate or, in the inverse process, by adding the bismuth nitrate solution to a sodium or ammonium vanadate solution. Thereafter, the pH is set between 5 and 8 with sodium hydroxide and the precipitate crystallizes to monoclinic bismuth orthovanadate usually by heating to reflux. After

this crystallization, the pigment is often coated with calcium or zinc phosphate or aluminum oxide to improve the lightfastness and weather-resistance. The final process is usually the calcination followed by wet milling and spray drying. The spray drying process produces a fine granulated dust-free pigment.

For the use in plastics, the pigment is additionally coated with silica and other components to increase the heat stability in certain polymers, like polyamide, up to 320 °C.

(A)

(B)

Figure 15.12: Particle size after precipitation (A) and subsequent heating (B) (magnification $\times 6000$).

15.12.3 Uses

Bismuth vanadate pigments are used in the manufacture of lead-free, weather-resistant, brilliant yellow colors for automobile finishes and industrial paints. They are suitable for the pigmentation of solvent-containing paints, water-based paints, powder coatings, and coil-coating systems. It can be mixed with other pigments especially to produce brilliant colours in the orange, red, and green regions like the german standard colors RAL 1021, 1028, 2004, 3020, 6018, and 6029.

Recently, different producers have developed bismuth vanadate pigments for the use in plastics. These pigments are used in every type of polymer, especially in polyethylene and technical plastics.

The annual production of bismuth vanadate pigments is now about 500 t. In the near future an increasing market of 1000 to 2000 t/a is expected.

15.12.4 Toxicology

Bismuth vanadate pigments are acute toxic neither on inhalative nor oral incorporation. They show chronic toxicity on inhalation due to the vanadium content. The "no-effect level" for rats is 0.1 mg/m³ (exposure: 3 months, 6 hours/day, 5 days/week). The critical factor for the inhalation toxicity is the real amount of pigment in the lungs, and not just the concentration in air. Because of the high density of the pigment and because the supply form is a fine granulate the risk of inhalation is very low. Therefore the dust-free pigments can be handled under usual hygienic working conditions [85].

15.12.5 Bismuth Oxychloride

[86-96]

Bismuth oxychloride, BiOCl , is, besides natural pearl essence and basic lead carbonate, one of the classic pearlescent pigments.

Powders containing bismuth compounds have long been used for decorative purposes to generate a shiny luster or lustrous colors (e.g., facial cosmetic powders in ancient Egypt, imitation pearls made by coating glass and ceramic beads). Bismuth oxychloride was the first synthetic nontoxic nacreous pigment. It is produced by hydrolysis of acidic bismuth solutions in the presence of chloride ions. Precipitation conditions may be varied (concentration, temperature, pH, pressure) or surfactants added to obtain the desired crystal quality. The virtually tetragonal bipyramidal structure is thereby "squashed" into a flat platelet.

Pure BiOCl is available in three grades with different nacreous effects that depend on the aspect ratios and crystal size:

- Low- or medium-luster powder (aspect ratio 1:10 to 1:15), mainly used as a highly compressible, white, lustrous filler with excellent skin feel
- Dispersion of high luster quality (aspect ratio 1:20 to 1:40) consisting of square or octagonal platelets in nitrocellulose lacquers (nail polish) or castor oil (lipsticks)

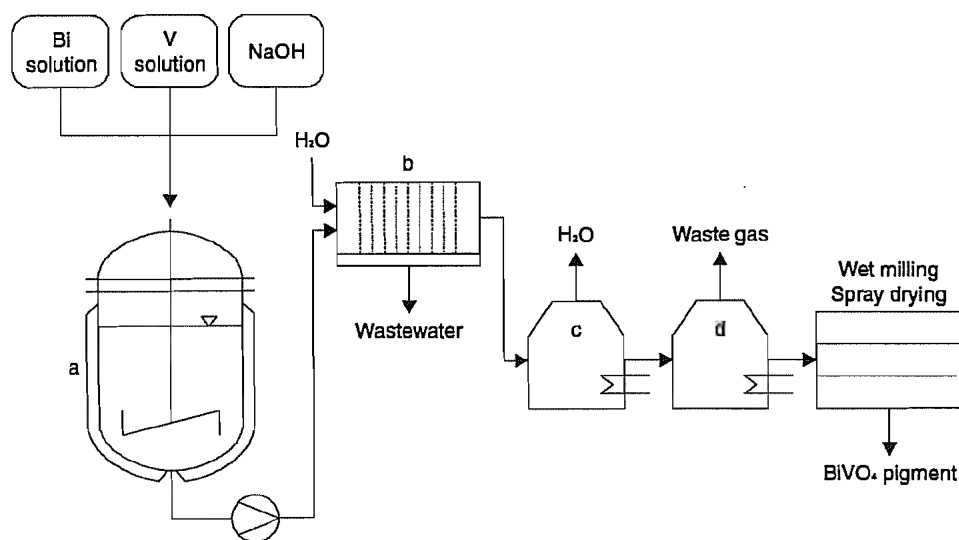


Figure 15.13: Flow diagram for the production of bismuth vanadate pigment: a) Reaction vessel; b) Filter; c) Dryer; d) Furnace treatment.

- Dispersion of very high luster quality (aspect ratio > 1:50) consisting of lens-shaped platelets in nitrocellulose lacquer, castor oil, or butyl acetate

Pigments consisting of BiOCl-coated mica or talc and blends of BiOCl with other organic or inorganic colorants are also available.

The dominant market for BiOCl is still the cosmetic industry. Its low light stability (it turns from silver white to metallic grey in sunlight), relatively high price, fast settling (high density, 7.73 g/cm³), and mechanical sensitivity limit its use in technical applications. Although the darkening reaction is not yet understood, low-luster grades with improved light stability are available. Some manufacturers promote the combination with UV stabilizers for technical purposes. Uses are in the button industry, bijouterie, printing, and for X-ray contrast in catheters. The current world market is ca. 500 t/a.

15.13 References

1. V. Tafel: *Lehrbuch der Metallhüttenkunde*, Hirzel Verlag, Leipzig 1951.
2. J. Feiser in: *Die metallischen Rohstoffe*, vol. 17: *Nebenmetalle*, Enke Verlag, Stuttgart 1966.

3. Gmelin, System No. 19, Main Volume (1927, reprinted 1971), Supplement Volume (1964), organobismuth Compounds (1977).
4. C. A. Hampel: *Rare Metals Handbook*, 2nd ed., Reinhold Publ. Co., London 1961.
5. Winnacker-Küchler, 3rd ed., vol. 6, pp. 350–354.
6. Kirk-Othmer, vol. 3, pp. 912–937.
7. J. D. Verhoeven, E. D. Gibson, M. B. Beardsley, *Metall. Trans. B* 6B (1975) no. 2, 349.
8. D'Ans-Lax: *Taschenbuch für Chemiker und Physiker*, Springer Verlag, Berlin-Göttingen-Heidelberg-New York 1967.
9. I. I. Mekler, V. M. Yashchenkova, A. A. Egizarov, E. A. Simkin, M. I. Gorodi, N. F. Plaksa, *Sov. J. Non Ferrous Met. (Engl. Transl.)* 12 (1971) no. 7, 51–53.
10. L. Borbasch, *Can. Min. J.* 82 (1961) no. 8, 66.
11. L. A. Chazova, E. N. Glazkov, S. A. Ovintseva, S. M. Barakov, A. V. Levchenko, *Sov. J. Non Ferrous Met. (Engl. Transl.)* 7 (1966) no. 1, 36–38.
12. Z. Tapia, *Perfil. Minero Metalurgico* 1979 no. 14, 13–20.
13. K. Z. Kuanysheva, S. T. Takeshanov, G. L. Pashkov, *Sov. J. Non Ferrous Met. (Engl. Transl.)* 14 (1973) no. 2, 31–32.
14. D. O. Rausch, B. O. Mariacher: *Lead & Zinc Mining and Concentrating of Lead and Zinc*, AIME, New York 1970.
15. J. M. Cigan, T. S. Mackey, T. J. O'Keefe: *Lead-Zinc-Tin '80*, AIME, Warrendale 1979.
16. R. Z. Khobdabergenov, M. P. Smirnov, U. B. Kolosov, *Sov. J. Non Ferrous Met. (Engl. Transl.)* 8 (1967) no. 2, 54–55.
17. K. Eimcke, G. Holzapfel, E. Kniprath, *Erzmetall* 24 (1971) 205–215.
18. Am. Smelt. Ref. Co, US 2056164, 1935.

19. C. H. Cotterill, J. M. Cigan: *Lead & Zinc, Extractive Metallurgy of Lead and Zinc*, AIME, New York 1970.
20. L. Marck, *Z. Erzbau Metallhüttenwes.* 14 (1961) 113–123.
21. E. R. Freni: "Symposium Hydrometallurgie", *Erzmetall* 22 (1969) B128–B132.
22. D. A. Pazour, *WorldMin.* 32 (1979) no. 8, 40–45.
23. I. L. Barker, *J. Met.* 8 (1956) 1058.
24. W. C. Smith, P. J. Hickey, *Trans. Metall. Soc. AIME* 224 (1962) 224.
25. A. K. Biswas, W. G. Davenport: *Extractive Metallurgy of Copper*, Pergamon Press, Oxford 1976.
26. R. Hanks, J. van der Zel, P. Chesney, G. B. Harris, *Trans. Inst. Min. Metall. Sect. C* 88 (1979) C99–C106.
27. K. G. Lombeck, J. Krüger, H. Winterhager, *Metall (Berlin)* 36 (1982) 1192–1196.
28. J. E. Joffe, F. R. Padilla, *Rev. Metall. (Bolivia)* 1975, no. 2, 10–13.
29. *Min. Mag.* 1976 (May) 369–374.
30. R. Kammel, H. Mirafzali, *Erzmetall* 30 (1977) 437.
31. J. A. Villaroel, *Rev. Metall. (Bolivia)* 1977, no. 3, 35.
32. P. Paschen, *Metall (Berlin)* 33 (1979) no. 2, 137.
33. E. Müller, P. Paschen, *Erzmetall* 32 (1979) no. 6, 266–272.
34. M. Marone, R. Tarrico, *Metall. Ital.* 62 (1970) 482–484.
35. V. A. Shavga, V. N. Vigdorovich, J. U. Samson, *Izv. Akad. Nauk SSSR Met.* 1970, no. 5, 101–109.
36. Yu. K. Delimarskii, A. A. Omel'schuk, O. G. Zarubitskii, *Ukr. Khim. Zh. (Russ. Ed.)* 42 (1976) no. 11, 1202–1204.
37. B. N. Aleksandrov, V. I. Udovikov, *Izv. Akad. Nauk SSSR Met.* 1973, no. 1, 57–62.
38. B. N. Aleksandrov, V. I. Udovikov, L. E. Usenko, *Russ. Metall. (Engl. Transl.)* 1969, no. 6, 57–63.
39. V. V. Malyshev, A. P. Kolesnev, V. I. Panomarenko, V. N. Vigdovich, *Tsvetn. Met.* 1973, no. 9, 9–11.
40. *Alloy Digest*, Feb. 1978, Bi 3; Sept. 1978, Bi 7; Oct. 1978, Bi 8; Nov. 1980, Bi 20.
41. *Metals Handbook*, Am. Soc. of Metals, Cleveland, OH, 1948, p. 744.
42. M. Hansen: *Constitution of Binary Alloys*, McGraw-Hill, New York 1958.
43. F. A. Eich, *J. Prosthet. Dent.* 1 (1951) 594.
44. D. A. Bancel, *Eng. Min. J.* 172 (1971) no. 3, 115–116.
45. W. C. Cooper: *Tellurium*, Van Nostrand-Reinhold, New York 1971, pp. 333–353.
46. T. Durst, H. J. Goldsmid, L. B. Harns, *Sol. Energy Mater.* 5 (1981) no. 2, 181–186.
47. S. C. Harvey in L. S. Goodman, A. Gilman (eds.): *The Pharmacological Basis of Therapeutics*, MacMillan, New York 1975, p. 930.
48. D. Fitzgerald, *Eng. Min. J.* 183 (1982) no. 3, 104.
49. H. A. Skinner, L. E. Sutton, *Trans. Faraday Soc.* 36 (1940) 681.
50. H. M. Haendler, E. A. Johnson, D. S. Crockett, *J. Am. Chem. Soc.* 80 (1958) 2662.
51. V. Gutmann, *Monatsh. Chem.* 82 (1951) 280.
52. C. Frondel, *Am. Mineral.* 28 (1943) 521.
53. H. Hecht, R. Reißner, *Z. Anal. Chem.* 103 (1935) 186.

49. F. Paneth, *Ber. Dtsch. Chem. Ges.* 51 (1918) 1704, 1728; 55 (1922) 769; 58 (1925) 1138.
50. E. Amberger, *Chem. Ber.* 94 (1961) 1447.
51. B. Aurivillius, *Acta Chem. Scand.* 9 (1955) 1206.
52. F. Hund, *Z. Anorg. Allg. Chem.* 258 (1949) 198.
53. J. Fischer, E. Rudzitis, *J. Am. Chem. Soc.* 81 (1959) 6375.
54. S. Y. Yosim et al., *J. Phys. Chem.* 66 (1962) 28.
55. E. Dönges, *Z. Anorg. Allg. Chem.* 263 (1950) 112.
56. G. Gatlow, G. Kiel, *Z. Anorg. Allg. Chem.* 335 (1965) 61.
57. P. Kirkov, *Ber. Chem. Ges. Belgrad* 22 (1957) 431.
58. *Analyse der Metalle*, vol. II/2, Springer Verlag, Berlin-Göttingen-Heidelberg 1961.
59. G. Schwarzenbach, H. Flaschka: *Die komplexometrische Titration*, Enke Verlag, Stuttgart 1965.
60. P. Zilveti, *Eng. Min. J.* 175 (1974) no. 2, 122.
61. *Metal Bull. Handbook*, 14th ed., Metal Bulletin Books, London 1981.
62. *Metallstatistik* 69, Metallgesellschaft AG, Frankfurt/Main 1982.
63. R. Serjeantson, R. Cordero (eds.): *Nonferrous Metal Works of the World*, 3rd ed., Metal Bulletin Books, London 1982.
64. W. Wirth, C. Gloxhuber: *Toxikologie*, Thieme Verlag, Stuttgart-New York 1981, p. 140.
65. A. Buge, G. Rancurel, H. Dechy, *Rev. Neurol.* 133 (1977) 401.
66. V. S. Viterbo, C. Sicard, H. P. Cathala, *Rev. Electroencephalogr. Neurophysiol. Clin.* 7 (1977) no. 2, 139.
67. J. L. Ribadeau Dumas, B. Lechevalier, M. Breteau, Y. Allain, *Nouv. presse méd.* 7 (1978) 4021.
68. S. Pollet, S. Albouze, F. Le Saux, N. Baumann, R. Bourdon, *Toxicol. Eur. Res.* 2 (1979) 123.
69. G. Martin-Bouyer, G. Foulon, H. Guerbois, C. Barin, *Clin. Toxicol.* 18 (1981) 1277.
70. A. Buge, A. Hubault, G. Rancurel, *Rev. rhum. mal. ostéo-articulaires* 42 (1975) 721.
71. J. Émile, J. M. de Bray, M. Bernat, T. Morer, P. Al-lain, *Clin. Toxicol.* 18 (1981) 1285.
72. A. Neetens, J. Martin, Y. Hendrata, M. C. Rubbens, *Bull. soc. belge ophtalmol.* 178 (1975) 51.
73. P. Lechat, J. Fontagne, N. Letteron, *Ann. Pharm. Fr.* 34 (1976) 173.
74. T. Sollmann, J. Seifter, *J. Pharmacol. Exp. Ther.* 67 (1939) 17.
75. R. Preußmann, S. Ivankovic, *Food Cosmet. Toxicol.* 13 (1975) 543.
76. B. A. Fowler, V. B. Vouk, U.S. Environ. Prot. Agency, Off. Res. Dev., Rep. EPA/ISS EPA-600/1-77-022, Toxicol. Met. vol. 2; Pb-268324, 1977, p. 110.
77. J. M. Arena: *Poisoning: Toxicology, Symptoms, Treatments*, 2nd ed., C. C. Thomas, Springfield, IL, 1970, p. 73.
78. DE 422947, 1924 (E. Zintl, L. Vanino).
79. Du Pont, US 4026722, 1976 (R. W. Hess); DE 2727864, 1977 (D. H. Piltingsrud); DE 2727863, 1977 (R. W. Hess); US 4063956, 1976 (J. F. Higgins).
80. Montedison, DE 2933778, 1979 (L. Balducci, M. Rustioni); DE 2940185, 1979 (L. Balducci, M. Rustioni); DE 3004083, 1980 (L. Balducci, M. Rustioni).

- tion); DE 3106625, 1981 (L. Balducci, M. Rustioni).
81. BASF, EP 74049, 1982 (H. Wienand, W. Ostertag, K. Bittler); EP 271813, 1986 (H. Wienand, W. Ostertag, C. Schwidetzky, H. Knittel); DE 3926870, 1989 (H. Wienand, W. Ostertag, C. Schwidetzky).
82. Bayer, DE 3315850, 1983 (P. Köhler, P. Ringe); DE 3315851, 1983 (P. Köhler, P. Ringe, H. Heine); EP 492244, 1991 (F. Schwochow); DE 4119668, 1991 (F. Schwochow, R. Hill); EP 723998, 1996 (H. Schittenhelm, R. Hill).
83. Ciba-Geigy, EP 239526, 1987 (F. Herren); EP 304399, 1988 (R. Sullivan); EP 430888, 1990 (L. Erkens, G. Schmitt, H. Geurts, W. Corvers); DE 4037878, 1990 (F. Herren, L. Erkens); US 5399335, 1993 (R. Sullivan).
84. BASF, EP 551637, 1992 (E. Liedek, H. Knittel, H. Reisacher, N. Mronga, H. Ochmann, H. Wienand); EP 640566, 1994 (G. Etzrodt, H. Knittel, H. Reisacher).
85. H. Endriß, *Farbe + Lack* 100 (1994) no. 6, 397-398; H. Endriß, M. Haid, *Kunststoffe* 86 (1996) no. 4, 538-540.
86. W. Bäumer, *Farbe + Lack* 79 (1973) p. 747.
87. S. Hachisu, *Prog. Org. Coat.* 3 (1975) p. 191.
88. W. Bäumer, *Metal Finishing* 10 (1977) p. 17.
89. W. Bäumer, *Paint Manuf.* 47 (1977) p. 31.
90. G. J. Rhee, B. S. Yu, *Bull. Bismuth Inst. (Brussels)* 28 (1980) p. 1.
91. Y. Morita, *J. Chem. Educ.* 62 (1985) p. 1072.
92. H. A. Miller, *Bull. Bismuth Inst. (Brussels)* 52 (1987) p. 1.
93. L. M. Greenstein in *Pigment Handbook*, 2nd ed., Vol. 1, J. P. Wiley & Sons, New York, 1988, pp. 843-855.
94. K. D. Franz, H. Härtner, R. Emmert, K. Nitta in *Ullmann's Encyclopedia of Industrial Chemistry*, Vol. A20, VCH Verlagsgesellschaft mbH, Weinheim 1992, pp. 351-352.
95. K. D. Franz, R. Emmert, K. Nitta, *Kontakte (Darmstadt)* 2 (1992) p. 3.
96. R. Glausch, M. Kieser, R. Maisch, G. Pfaff, J. Weitzel in *Periglantzpigmente*, Curt R. Vincentz Verlag, Hannover 1996, p. 29-31.

16 Cadmium

KARL-HEINZ SCHULTE-SCHREPPING (§§ 16.1-16.10); MAGNUS PISCATOR (§ 16.11); GERHARD BERGER, HARTMUT ENDRIS, STEFANIE SCHWARZ (§ 16.12)

16.1 Introduction	869	16.9.2 Waste Water	878
16.2 Properties	869	16.9.3 Air	879
16.3 Occurrence, Raw Materials	870	16.9.4 Soil	879
16.4 Refining	870	16.10 Economic Aspects	879
16.4.1 The Starting Materials	870	16.11 Toxicology and Occupational Health	880
16.4.2 Leaching of the Starting Materials and Cementation	871	16.12 Cadmium Pigments	884
16.4.3 Electrolytic Recovery	872	16.12.1 Cadmium Sulfide	884
16.4.4 Distillation	872	16.12.2 Cadmium Yellow	885
16.4.5 Other Processes	873	16.12.3 Cadmium Sulfoselenide (Cadmium Red)	885
16.4.6 Recycling	873	16.12.4 Cadmium Mercury Sulfide	886
16.5 Quality Specifications and Analysis	873	16.12.5 Properties and Uses	886
16.6 Uses	874	16.12.6 Quality Specifications	887
16.7 Alloys	875	16.12.7 Economic Aspects	887
16.8 Compounds	875	16.12.8 Toxicology and Environmental Protection	887
16.9 Environmental Protection	878	16.13 References	889
16.9.1 Emission	878		

16.1 Introduction

Cadmium, atomic number 48, belongs to the zinc subgroup of the periodic table along with mercury. In its compounds it has an oxidation state of 2+. There are eight natural isotopes, with mass numbers ranging from 106-116. The most abundant are ¹¹⁴Cd (29%) and ¹¹²Cd (24%). There are also a number of meta-stable isotopes.

STROHMEYER discovered cadmium in 1817 in the course of investigating zinc carbonate. He recognized that the yellow color of a sample of zinc oxide produced by roasting was due to the presence of an unknown metal oxide. Because this new element also occurred in the zinc ore calamine, a name derived from the Latin word "cadmia", he named the new element cadmium.

Unlike some other heavy metals, such as lead or mercury, which have been used since ancient times, cadmium has been refined and utilized only relatively recently. After its discovery more than a century elapsed before the

metal or its compounds were employed to any significant extent. Only in the last 40-50 years have production and consumption risen distinctly. The primary uses today are electroplated cadmium coatings, nickel-cadmium storage batteries, pigments, and stabilizers for plastics. Publicity about the toxicity of cadmium has affected the consumption.

16.2 Properties

Cadmium is a soft, ductile, silver-white metal. Like tin, it makes a grating sound when bent. The most important physical properties are given below.

mp	320.9 °C
bp	767 ± 2 °C
Vapor pressure at	
218 °C	0.133 Pa
302 °C	6.666 Pa
392 °C	133.32 Pa
485 °C	1333.2 Pa
611 °C	13.332 kPa
727 °C	66.660 kPa
765 °C	101.33 kPa
Density	8.64 g/cm ³
Specific heat at 20 °C	0.230 Jg ⁻¹ K ⁻¹

Heat of fusion	55 J/g
Heat of vaporization at 767 °C	890 J/g
Thermal conductivity at 18 °C	$92 \text{ J m}^{-1} \text{ s}^{-1} \text{ K}^{-1}$
Electrical resistivity at 18 °C	$7.5 \times 10^{-6} \Omega \text{ cm}$
Brinell hardness	22–24
Coefficient of linear expansion at 20 °C	$31 \times 10^{-6} \text{ K}^{-1}$
Ionization potential	8.96 V
Electrochemical potential	–0.40 V
Cross section for thermal neutrons	$2450 \times 10^{-28} \text{ m}^2$

The crystal structure is distorted closest packed hexagonal.

Cadmium is stable in air; only a slight loss in luster occurs after an extended period of time in air. When it is heated, initially yellow to brown colors develop as a thin oxide layer forms. If the metal is heated to volatilization, it burns with a red-yellow flame to form brown cadmium oxide, which is poisonous. Cadmium dissolves readily in nitric acid but only slowly in hydrochloric or sulfuric acid and not at all in bases. Zinc displaces it from solution.

16.3 Occurrence, Raw Materials

Cadmium is widely distributed. It occurs in the earth's crust with a content estimated to be between 0.08 and 0.5 ppm. In top soil cadmium content usually lies between 0.1 and 1 ppm.

The best known cadmium mineral is greenockite, cadmium sulfide (77.6% Cd). One mineral form of cadmium carbonate (61.5% Cd) was named otavite after its discovery site, the Tsumeb Mine, in the Otavi deposit of South-West Africa. In Sardinia, pure cadmium oxide (87.5% Cd) was found in a zinc deposit. However, none of these cadmium minerals is of industrial importance because the deposits are too small.

Only zinc minerals in which cadmium is found as an isomorphic component, with concentrations ranging from 0.05 to 0.8%, averaging about 0.2%, have economic significance for cadmium recovery [2]. In addition, lead and copper ores contain small amounts of cadmium, which can be separated during the roasting and smelting processes.

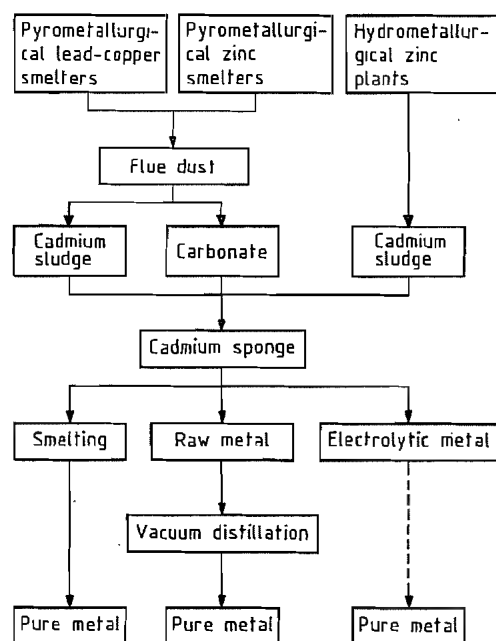


Figure 16.1: Processes for the production of cadmium metal.

16.4 Refining

Figure 16.1 summarizes the individual process steps and their combination. Detailed description, with emphasis on the distillation process, can be found in [3].

16.4.1 The Starting Materials

The flue dust on which the volatile cadmium collects when zinc, copper, and lead ores are heated in air are the primary starting material for cadmium recovery and refining. In many cases it is necessary to recirculate this dust to obtain higher cadmium concentrations [4].

In the Outokumpu Zinc Works in Finland, roasting material contains 0.19–0.24% Cd. The cadmium content is extracted in the third step of the zinc process and results in a cake consisting of 90% cadmium and 10% zinc. This is the starting material for further processing [5].

If the primary flue dust is reduced in a rotary oven, lead and zinc remain in the oven, while the cadmium is volatilized and enriched in the secondary flue dust.

In the Berzelius Metal Works, Duisburg, Germany, complex lead–zinc ores are refined by the Imperial smelting process. When the concentrate is roasted in the sintering furnaces, cadmium-containing flue dust is produced. This is leached in an acid solution, and the cadmium is subsequently precipitated as cadmium carbonate. The cadmium in secondary raw materials, such as steel mill dust, leaching sediments, and sludge from water treatment, can be processed at the same time. However, before they are mixed with the concentrates they are enriched in a rotating tube furnace (Waelz process).

In hydrometallurgical zinc refining, the cadmium-containing zinc concentrate is leached with sulfuric acid. The cadmium is removed from the solution together with copper by reduction with zinc dust to give a metallic sludge. Similar cadmium sludges form in the purification of zinc solutions used in the production of zinc sulfide pigments or zinc carbonate. These cadmium sludges are the most important starting materials for cadmium refining today. The secondary starting materials mentioned above can be added to the primary raw materials without causing large alterations in the refining process.

Also of economic significance is the recycling of used nickel–cadmium storage batteries; cadmium-containing alloys, such as Sn–Cd metallizing alloys from the manufacture of rectifiers; defective industrial batches; residues from the production of cadmium pigments; and cadmium-containing fluorescent materials. Special processes are usually necessary to convert the cadmium content into a form that can be processed normally. The most important processes of this type are discussed in Section 16.4.6.

16.4.2 Leaching of the Starting Materials and Cementation

Cadmium is extracted from the enriched starting materials by oxidizing solutions. The extraction must be carried out in such a way that all the cadmium as well as the zinc dissolves. The procedure of Ruhr Zinc, Datteln, Germany, is described here as an example. The liquid from electrolytic baths, which has a sulfuric acid concentration of 25–30 g/L, is conveyed into 50-m³ tanks. In order to oxidize the cadmium, either air is blown in or manganese dioxide is added. Fresh cadmium sludge or cadmium carbonate is added to decrease the acidity of the solution, and a copper-containing precipitate is removed with a filter press. Zinc, cadmium, and thallium are almost completely dissolved in the solution along with almost no copper, cobalt, nickel, and arsenic [6].

Copper chloride mixed with other metal chlorides or iron(III) chloride can be used as an oxidant instead of air [7, 8]. Dust from the sintering process can also be roasted to give sulfates and then be extracted in a similar fashion with water [9].

Independent of the further processing of the cadmium, it is precipitated from the solution as a metal sponge by reduction with zinc. It is necessary the solution is purified first.

The cadmium raw solution resulting from the leaching step at Ruhr Zinc contains about 30 g/L of zinc and small amounts of cobalt, nickel, thallium, and copper in addition to the 30–40 g/L of cadmium. The cadmium is precipitated in a 50-m³ tank at a temperature of 60 ° in order to avoid excess zinc in the cadmium sponge, only 80% of the stoichiometric amount of the zinc is added initially. The remaining zinc dust is added in small portions until the cadmium concentration of the solution is below 0.1 g/L. After decanting, the cadmium sponge is left in the reaction container. The precipitation is carried out three times, principally to reduce the amount of zinc. After the final precipitation, the sponge is washed, and the wash water is recycled to the zinc plant. The precipitated sponge contains 90% cadmium and only 2–5% zinc [6].

The procedure of the Outokumpu Zinc Works starts with a purified cadmium solution because of the nature of the succeeding metal recovery (see Section 16.4.5). Copper is removed with zinc powder, and lead is removed with barium carbonate. The separation of the cadmium sponge from the solution, however, scarcely deviates from the Ruhr Zinc processes. The greatest difference is that the cementation is interrupted at cadmium concentrations of 3–5 g/L, and the solution recirculated. Together with a very careful wash, this reduces the residual content of zinc in the compacted cadmium-sponge briquettes to 0.5–2.0% [5].

16.4.3 Electrolytic Recovery

Today, the largest amounts of cadmium are recovered electrolytically. It is customary to extract the cadmium sponge in the same tank with the cadmium-containing electrolytic acid. Air is supplied at a temperature of 80 °C for 6–10 h. Concentrated sulfuric acid is added to keep the concentration of free sulfuric acid at 100 g/L. Manganese dioxide can also be used as oxidant [6].

The time required to dissolve the cadmium sponge at room temperature can be reduced by blowing air through special reactors. The relationship between solid and liquid, the amount of air, and the pH are carefully controlled to reduce the time and temperature required for the dissolution [10].

The electrolytic deposition of cadmium requires that the impurities that cause problems during the electrolysis or that are deposited as impurity with cadmium be removed prior to electrolysis. Traces of copper can be removed by addition of small quantities of sodium sulfide in the form of copper sulfide or by cementation with zinc dust. Thallium is removed as thallium dichromate by addition of potassium dichromate. Thallium can also be removed as thallium(III) hydroxide by addition of potassium permanganate. Any arsenic is eliminated as iron arsenate by oxidation with the potassium permanganate. The lead remaining

in solution is removed by adding strontium carbonate to occlude lead carbonate [6].

The anode consists of lead, which does not dissolve, and the cathode is sheet aluminum. Today rotating cathodes, which allowed high current density, have disappeared because current densities of 100 A/m², permitting economic electrolysis, can also be attained with fixed cathodes. However, the cathode deposit must be stripped after 12-h intervals to avoid low yields caused by short circuits between cathode and anode. The current yield is ≈ 93%; the energy consumption is 1250 kWh per tonne of cadmium cathode sheet deposited. Careful operation and the use of hide glue and sodium silicate allow cadmium of high purity to be produced. Typical impurity levels in electrolytic cadmium sheet are 5–10 ppm Cu, 15–20 ppm Pb, 5–10 ppm Tl, and 5 ppm Zn.

Some sheet is used as is. Otherwise, it is melted under a cover of sodium hydroxide to prevent oxidation and to reduce the amount of zinc. The molten metal is poured into molds to produce marketable shapes.

16.4.4 Distillation

After mixing with a reducing agent such as pulverized coke, the cadmium sponge can be briquetted. The briquettes can be distilled under atmospheric pressure to a raw metal still containing thallium and zinc. These impurities can be separated from the fused metal by addition of ammonium chloride and caustic soda. Distillation under reduced pressure avoids a number of disadvantages of distillation at atmospheric pressure. The differences between the vapor pressure of cadmium and those of the most important accompanying elements allows Preussag (Germany) to produce a 99.99% pure metal in a single step. The raw cadmium can contain up to 3% lead and thallium as well as 1% copper [11]. Every hour, 100 kg of pure cadmium is produced at a distillation pressure of 0.7–2.7 kPa and a temperature of 420–485 °C. The presence of thallium, the most volatile impurity, at a concentration exceeding 10 ppm in the distillate

indicates that the distillation is not functioning properly.

The cadmium distillation process of Hoboken Overpelt, Belgium, allows the processing of cadmium–zinc alloys containing 15–20% Zn. In a two-step distillation procedure, both zinc and cadmium are obtained highly pure (99.995%) [12].

16.4.5 Other Processes

The cadmium sponge of the Outokumpu Zinc Works contains 0.5–2% zinc, 13 ppm lead, and 15 ppm copper. The briquettes pressed out of this material are smelted with sodium hydroxide. In seven hours 2.2 t of cadmium is obtained using a 110-kW furnace. The refined metal is drawn in a continual casting machine to a cadmium wire, which is then cut to rod. These cadmium rods have a purity of at least 99.95%; the impurities (max.) consisting of 20 ppm Cu, 10 ppm Zn, 5 ppm Tl, 5 ppm Fe, and 15 ppm Pb [5].

The removal of cadmium from solution by ion exchange has been described [13]. After stripping, the cadmium is processed further by cementation and smelting. Complexation of the cations to give anionic cadmium species allows selective separation of the cadmium even from copper and iron [14]. Aliphatic carboxylic acids [15] and *o*-aminomethylphenols [16] selectively extract cadmium from aqueous solution.

16.4.6 Recycling

The purpose of the recycling procedures described here is the production of intermediate products by special procedures that can then be fed into the normal cadmium production processes.

The recovery of *cadmium–tin alloys*, about 65% Sn and 35% Cd, usually begins by dissolving the scrap in nitric acid. The tin stays in the residue as stannic acid. An impure carbonate is precipitated from the cadmium nitrate solution with soda.

The residue and the rejected batches from the production of *cadmium pigments* contain-

ing cadmium sulfide and selenide are dissolved in strongly oxidizing acid. The cadmium is recovered by cementation or as the carbonate. A variation of this process is described in [17].

In order to recycle the cadmium from *nickel–cadmium batteries* and similar production scrap, the parts are dissolved in agitated 2% sulfuric acid. A reasonably good separation from the dissolved nickel can be attained by taking advantage of the lower stability of the ammine complexes of cadmium: cadmium can be precipitated from ammonium hydroxide solution as carbonate, whereas nickel remains in solution [18]. Alternatively, nickel can be extracted from the ammonia solution with chelating reagents before cadmium carbonate is precipitated [19].

Sludge from the treatment of cadmium-containing waste water can often be injected directly into the refinery process (Section 16.4.1). Preliminary, conventional wet chemical enrichment is possible but is usually omitted for economic reasons [20]. Several methods for conversion of electroplating waste water to sludge not requiring special handling can be found in [21].

A plant was constructed by Sab-Nife in Sweden for recycling used batteries and scrap at the same location where nickel–cadmium batteries are produced. Cadmium-containing waste and filter dust are leached with acid, and the cadmium is deposited by electrolysis. Used batteries are dismantled in a semiautomatic process. From the iron- and cadmium-containing plates, the cadmium is distilled under a reducing atmosphere at 850 °C and returned to the production department. Even sealed cells can be processed by distillation after the plastic is destroyed by pyrolytic pretreatment in a slightly oxidizing atmosphere [22].

16.5 Quality Specifications and Analysis

The quality of the cadmium depends on the production process. However, for 99.99%

cadmium, the following maximum impurity levels are generally accepted [11]: 1 ppm Cu, 5 ppm Pb, 5 ppm Tl, and 2 ppm Zn. For special purposes > 99.9998% cadmium is available.

The maximum amounts of impurities and the analysis procedures are given in ASTM C-752. Although the classical analytical methods for impurities are still used, today atomic absorption spectroscopy is the most common method [23].

16.6 Uses

Cadmium metal is used for cadmium coatings, nickel-cadmium batteries, and to a limited extent for reactor construction.

Electrodeposited Cadmium Coatings. Cadmium coatings are superior to other metallic coatings because of their optimal combination of properties: corrosion protection, ductility, frictional behavior, and soldering potential. Cadmium coatings have considerable significance in *automotive construction*, where disk brake calipers, bearing races, screws, nuts, bolts, springs, tubing connectors, contacts, and steering parts are all cadmium plated. In *machine construction and factory construction*, the surface of fastening elements, especially screws, is coated. Although the corrosion protection is most important, the frictional properties are also important. For example, even screws that are extremely tight must last for years and then be removable without difficulty. Precision screws and other connecting elements are subject to similar requirements. In the machines of chemical plants they are subjected to corrosion in addition. Aircraft parts not made from stainless steel are usually cadmium coated.

For the often necessary *attachment of different metals*, such as copper alloys, stainless steel, and titanium alloys to aluminum or magnesium alloys, cadmium coating is an absolute prerequisite to avoid corrosion. Cadmium plating is often required in military procurement contracts to ensure that the weapons and equipment function reliably over many years.

Nickel-Cadmium Accumulators. The second most widely used storage battery is based on cadmium and nickel. In the charged state the negative electrode consists of cadmium powder, and the positive electrode consists of nickel(III) hydroxide. As the battery discharges, cadmium hydroxide and nickel(II) hydroxide form. Charging reestablishes the original composition. The starting material for the production of the negative electrode is usually cadmium metal, which is dissolved in nitric acid and then precipitated as cadmium hydroxide. In another technique, cadmium hydroxide is repeatedly precipitated into the pores of sintered bodies, which become the negative electrode. A further variation uses electrodeposited cadmium powder, which is mixed with an electrical conductor such as graphite. A properly designed accumulating system does not release gas, even when overcharged, and can be sealed gastight. This development opened the way for new applications, such as rechargeable accumulators not larger than a single primary cell for use in portable electronic products.

In addition to the general advantages of accumulators, nickel-cadmium cells have a long life and are insensitive to low temperature and storage in the uncharged condition. Nonsealed nickel-cadmium accumulators are used in airplanes; telephone, telegraph, and radar stations; computer installations; and emergency power stations. Gastight cells are used in transportable pocket computers, razors, flashlights, etc.

Other Uses. Cadmium compounds, stabilizers for plastics, and pigments are generally produced from cadmium metal. The metal is dissolved in a mineral acid, usually sulfuric acid. Dissolution requires considerable time even at high temperatures. Increasingly, cadmium sheets from electrodeposition are used because they, unlike metal blocks, have a larger surface area and dissolve more quickly. Because they do not have to be melted, production costs are lower. In many cases, the high purity of the sheet allows direct use of the cadmium solution without additional purification,

especially as the noble impurities remain as residue.

Today a small amount of cadmium is converted into cadmium sulfide-copper sulfide *solar cells*, which directly convert light into electrical energy. The yield at present is $\approx 10\%$. A yield of 15% is thought to be attainable. It is expected that these cells can be produced inexpensively. Other cadmium compounds - cadmium telluride, cadmium selenide, and the combination cadmium sulfide-indium phosphide - have also been tested successfully. The amounts of cadmium consumed for the most important uses are given in Table 16.2.

16.7 Alloys

Numerous binary and tertiary cadmium alloys, often with complicated phase diagrams, are known. For practical purposes, cadmium does not dissolve in molten iron or aluminum. A tabular summary of cadmium alloys is available [24], and there is special literature about cadmium alloys [25]. A number of cadmium alloys, as a rule produced simply by melting, are used industrially. They can be divided by their principal use: solder, electrical conductors, and other.

Solder. Cadmium forms alloys with silver, copper, and zinc that have low melting points and are widely applicable for the hard soldering of metals. The cadmium lowers the melting point. More than 80% of the cadmium used in alloys is used for this purpose.

Aluminum or aluminum alloys can be soldered to copper, brass, or stainless steel by lead alloys that contain antimony, tin, and 2.6-17%, cadmium [26, 27]. Similar alloys that contain between 0.6 and 60% cadmium join glass and ceramics at temperatures under 180 °C [28]. For soldered connections on gold-plated electrical conductors, cadmium-containing zinc-lead-indium alloys are recommended [29, 30]. Occupational-medicine aspects of cadmium-containing soldering are treated in [31].

Electrical Contacts and Conducting Wire.

The addition of cadmium or cadmium oxide to silver, often the contact material in electrical switches, reduces the metal loss due to sparking. In addition, the welding tendency is decreased. Cadmium (0.8-1%) improves the mechanical properties of copper wire without reducing its electrical conductivity. This is especially useful in the case of the overhead wires supplying power to electrically powered locomotives [32, 33].

Other Alloys. Cadmium is a component of a few bearing alloys based on tin, copper, and aluminum, usually in amounts under 1%. Wood's alloy and Lipowitz's alloy, which contain between 6 and 14% Cd, are used as fusible alloys in automatic fire-protection sprinklers and other devices. Cadmium in the form of a 5% alloy with silver and indium is put to use in the control rods of nuclear reactors because ^{113}Cd has a particularly large neutron capture cross section. A cadmium-selenium-indium alloy is an important component of a white-light laser for optical data processing systems [25].

16.8 Compounds

Generally water-soluble cadmium compounds are colorless. Aluminum and zinc can be used to precipitate cadmium metal from solutions of cadmium salts. From weakly acid or neutral solutions, cadmium sulfide is precipitated by hydrogen sulfide, sodium sulfide, and sodium hydrogensulfides. The temperature, concentration, and presence or absence of Cl^- determine the color of the precipitate: lemon yellow, orange, or even red. Sodium selenide precipitates black cadmium selenide. Mixed precipitates of cadmium sulfide and cadmium selenide are brown. Sodium hydroxide gives white cadmium hydroxide, which is insoluble in excess hydroxide. The precipitate formed by ammonia redissolves in excess reagent to form the complex $[\text{Cd}(\text{NH}_3)_6]^{2+}$. This complex also forms when ammonia is added to precipitates such as the hydroxide or oxalate. Sodium carbonate produces insoluble cadmium car-

bonate. Sodium cyanide reacts with aqueous cadmium solutions to give cadmium cyanide, which redissolves in excess reagent to form $[\text{Cd}(\text{CN})_4]^{2-}$. This complex is weak enough that the cadmium can be completely precipitated with hydrogen sulfide. Cadmium solutions react with hexacyanoferrate(II) to give a white precipitate, whereas they react with hexacyanoferrate(III) to give a yellow precipitate. Cadmium sulfite is only slightly soluble and can be precipitated from cadmium solution with sodium sulfite. All insoluble cadmium compounds can be dissolved in mineral acids. A few cadmium compounds fluoresce or phosphoresce, the silicate yellow to rose, the borate rose. Silver- or copper-activated cadmium-zinc sulfide gives colors spread over the entire spectrum.

The properties and uses of numerous cadmium compounds are described in [24]. The following text is limited to the most important industrial cadmium compounds.

Cadmium oxide, CdO . The amorphous form is yellow red, brown red, or brown black, the color depending on the particle size and the stoichiometry. It has a density of 6.95 g/cm^3 . The amorphous oxide is insoluble in water and bases but is readily soluble in dilute acids, ammonia, ammonium salt solutions, and sodium cyanide solutions.

The lustrous black cubic crystals of cadmium oxide have a density of 8.15 g/cm^3 . They sublime at $\approx 700^\circ\text{C}$. The low specific resistance at 0°C , $5.5 \times 10^{-3} \Omega\text{cm}$, is caused by an excess of Cd^{2+} ions, which makes CdO a semiconductor.

Cadmium oxide is produced by evaporation of cadmium metal and oxidation of the vapor. It can also be obtained by thermal decomposition of cadmium nitrate or carbonate or by oxidation of molten cadmium by an oxidizing agent. Commercial cadmium oxide should be completely soluble in sodium cyanide solution and contain no heavy-metal or sulfur impurities.

Cadmium oxide is used as a catalyst in oxidation-reduction reactions, dehydrogenation, cleavage, polymerization, the production of

multiply unsaturated alcohols, hydrogenation of unsaturated fatty acids, and as a mixed catalyst component to produce methanol from carbon monoxide and water. Further uses include resistant enamels, metal coatings for plastics, heat-resistant plastics, selenium ruby glass, starting material for other cadmium compounds, and stabilizers for poly(vinyl chloride). Cadmium oxide combined with an alkali-metal cyanide is the salt mixture used in the baths for cadmium electroplating. Cadmium oxide is a component of batteries. It is temperature resistant and together with silver useful in heavy-duty electrical contacts. Cadmium oxide improves the behavior of some high-temperature plastics.

Cadmium hydroxide, $\text{Cd}(\text{OH})_2$, is a colorless powder with a hexagonal, layered lattice. The precipitation of fine-grained cadmium hydroxide is only possible from nitric acid solution, basic salts often resulting from precipitation from other solutions. In the presence of halogenide ions, X^- , the complex $[\text{CdX}_4]^{2-}$ forms. In fact, precipitation of $\text{Cd}(\text{OH})_2$ can be prevented by a high concentration of alkali-metal chloride. Cadmium hydroxide is a component of cadmium nickel accumulators and silver-cadmium batteries. Cadmium hydroxide often replaces the oxide as the starting material for other cadmium compounds.

Cadmium carbonate, CdCO_3 , has a density of 5.3 g/cm^3 . (The density of $\text{CdCO}_3 \cdot \text{H}_2\text{O}$ is 4.3 g/cm^3 .) The white crystalline powder with an orthorhombic lattice of the calcite type decomposes above 360°C . Often precipitation with sodium carbonate produces hydroxy products, which contain water difficult to remove. Cadmium carbonate is a starting material for the production of cadmium pigments and other cadmium salts.

Cadmium chloride, CdCl_2 , has a density of 4.05 g/cm^3 . The colorless, lustrous orthorhombic crystals, which melt at 568°C to a liquid that boils at 967°C , are slightly soluble in water. The hydrates are $\text{CdCl}_2 \cdot \text{H}_2\text{O}$, $\text{CdCl}_2 \cdot \frac{1}{2}\text{H}_2\text{O}$, and $\text{CdCl}_2 \cdot 4\text{H}_2\text{O}$. Cadmium chloride

is produced by reaction of molten cadmium and chlorine gas at 600°C or by dissolving cadmium metal or the oxide in hydrochloric acid, subsequently vaporizing the solution. The salt is used in electroplating. An aqueous solution absorbs hydrogen sulfide. Molten cadmium chloride dissolves cadmium metal. Upon cooling, the metal precipitates.

The significance of cadmium chloride as a commercial product is declining. It occurs, however, as an intermediate in the production of cadmium-containing stabilizers and pigments, which are often obtained from a cadmium chloride solution itself obtained from cadmium metal, oxide, hydroxide, or carbonate.

Cadmium nitrate tetrahydrate, $\text{Cd}(\text{NO}_3)_2 \cdot 4\text{H}_2\text{O}$, has a density of 2.46 g/cm^3 . The small colorless deliquescent crystals readily dissolve in water. They have a *mp* of 59.9°C , and the liquid has a *bp* of 132°C . There are three hydrates, including the tetrahydrate, and the anhydrous salt (stability ranges):

$\text{Cd}(\text{NO}_3)_2 \cdot 9\text{H}_2\text{O}$	(-16 to 3.5°C)
$\text{Cd}(\text{NO}_3)_2 \cdot 4\text{H}_2\text{O}$	(3.5 to 48.7°C)
$\text{Cd}(\text{NO}_3)_2 \cdot 2\text{H}_2\text{O}$	(48.7 to 56.8°C)
$\text{Cd}(\text{NO}_3)_2$	(> 56.8°C)

Cadmium nitrate is produced by dissolving cadmium metal in nitric acid, purifying if necessary, concentrating, and crystallizing. It is used for the production of red lusters in glass and porcelain and in cadmium-nickel sinter plates of storage batteries.

Cadmium sulfate, CdSO_4 , 4.7 g/cm^3 . The melting point of the anhydrous salt is 1000°C . Anhydrous cadmium sulfate is produced by melting cadmium with ammonium or sodium peroxodisulfate. A saturated aqueous solution contains 76 g CdSO_4 per 100 g of water at 0°C , 77.2 g at 20°C , 69.4 g at 74.5°C , and 58.0 g at 100°C .

$\text{CdSO}_4 \cdot \frac{8}{3}\text{H}_2\text{O}$, $\rho 3.09 \text{ g/cm}^3$. The colorless monoclinic crystals, which effloresce in air, are soluble in water (see above). This hydrate melts at 41.5°C in its own water of crystallization, converting to the monohydrate.

Calcium sulfate monohydrate, $\text{CdSO}_4 \cdot \text{H}_2\text{O}$, $\rho 3.79 \text{ g/cm}^3$, which is the form usually marketed, is produced by evaporating a cadmium sulfate solution above 41.5°C .

Cadmium sulfate is used in electroplating and as a starting material for pigments, stabilizers, and other cadmium compounds that can be precipitated from aqueous solution. It is used to produce fluorescent materials and in analysis. A cadmium sulfate solution is a component of the Weston cell, which has an almost constant voltage of 1.0186 V .

Cadmium cyanide, $\text{Cd}(\text{CN})_2$, $\rho 2.226 \text{ g/cm}^3$, is cubic and isostructural with $\text{Zn}(\text{CN})_2$. The solubility in water is 17 g per liter at 15°C . The solubility in sodium cyanide solution is greater because tricyanocadmium ions, $\text{Cd}(\text{CN})_3^-$ form. Cadmium cyanide is produced from dilute cyanic acid and cadmium hydroxide by evaporation or by precipitation from a concentrated solution of cadmium salt and alkali-metal cyanide. Cadmium cyanide and its mixtures with an alkali-metal cyanide are used in electroplating. Cadmium cyanide baths for the electroplating of cadmium metal coatings have the advantage that they are easy to work with. Metal removed from the solution as electroplate is replaced by dissolution of the cadmium anode. These cadmium anodes should be at least 99.95% pure.

Storage and Transportation. The labeling for transport of cadmium compounds in Germany and the European Economic Community are similar [34, 35]. The rules specify the use of certain symbols and directions for safety precautions. The international provisions for sea and air transport have recently been made compatible [36, 37], although special regulations for individual lands are often still very different. Frequently there are even different provisions for the various types of transportation or routes.

Table 16.1: Cadmium emission in Germany.

Source (Year)	Emission, t/a			
	Air	Soil	Water	Total ^a
Production of Cd metal and recycling (1980)	5-7	—	62	69
Pigments (1980)	0.17	—	1.2	1.4
Stabilizers (1980)	0.05	—	0.18	0.23
Electroplating (1981)	—	—	0.7	0.7
Batteries (1982)	0.31	—	0.9	1.2
Alloys (1982)	0.5	—	—	0.5
Glass (1982)	3	—	—	3
Fossil fuels (1982)	<5	—	—	5
Iron and steel (1982)	5	—	—	5
Cement (1982)	0.3	—	—	0.3
Fertilizer (1982)	—	35	0.5	35
Waste-water sludge (1982)	0.1	3.6-14.4 ^b	—	14
Man-made deposits (1982)	—	—	—	—
Waste burning (1982)	2.9-3.8	—	—	3.8
Automobile exhaust (1982)	<0.5	—	<0.5	1.0
Total, max.	26	49	66	140

^aMaximum.

^b Forty percent of the 1.8×10^{-6} t of waste-water sludge produced each year, or 0.72×10^{-6} t, is used agriculturally. If the sludge contains, on the average, 5 ppm Cd, this corresponds to the minimum estimate, 3.6 t Cd. Twenty ppm corresponds to the maximum estimate, 14.4 t Cd.

16.9 Environmental Protection

Cadmium has been ubiquitously distributed in the natural environment for millions of years, and information about this natural distribution in soil and water can be found in general literature, e.g., [24]. Industrial production of cadmium has affected the total distribution in soil and water only insignificantly, although in some restricted areas environmental problems have developed.

More than 90% of the total nonsmoker intake of cadmium is reported to be through food (see Section 16.11). All sources of cadmium that contaminate cultivated soil, whether by air, fertilizer, or water, should be reduced as much as possible.

Cases of cadmium poisoning caused by the contamination of the environment are described in Section 16.11.

16.9.1 Emission

Cadmium emission in Germany is given in Table 16.1. Summaries for the United Kingdom [38], the European Economic Community [39], and the United States [40] are difficult to compare because different parameters have been selected. However, this literature cites its sources, so comparison based on tabulations in these sources is possible. Data about industrial emission in the European Economic Community and extensive discussion of the technologies to reduce emissions have been collected [41].

16.9.2 Waste Water

Cadmium ions are normally separated from sewage by precipitation with an alkali-metal hydroxide or carbonate, with subsequent separation of the sediment. The required limit of 1 mg/L, however, is only attainable when the pH is adjusted to 9.5 or higher, and the precipitate is thoroughly separated from the solution. New regulations go even further and the "Cadmium Guidelines" for the European Economic Community require concentration limits of 0.3-0.5 mg/L after 1986 and <0.2 mg/L after 1989 [42]. These limits can only be met by manufacturers and consumers with special methods [41]. Especially useful for producers of cadmium and cadmium compounds are the coprecipitation of cadmium in so-called collectors and subsequent filtration or special treatment during production and before combination with cadmium-free waste water. In special cases, ion exchange, precipitation, for example, with a sulfide compound, or electrolytic separation is used. Clearly the most important factor is the reduction of the amount of cadmium carried into the waste water. Consequently the guidelines of the European Community concentrate on reduction of the amount of cadmium in waste water.

The constant tightening of the standards for waste water purification is intended to prevent excessive concentrations of cadmium in the sludge produced in biological waste-water treatment. When the concentration of heavy

metals is too high, the sludge can no longer be used in agriculture. In Germany, maximum cadmium content in sludge is restricted to 20 mg per kilogram of dry waste, along with a limitation on the total amount of waste [43]. Similar requirements are in preparation for the European Economic Community.

16.9.3 Air

Practically all cadmium emission sources are in the form of the oxide because this compound is formed in pyrometallurgical production, high-temperature processing, and combustion, either directly or via the metal. Initially the oxide is finely divided, but these fine particles can be made to agglomerate into coarse grains in suitable apparatus. However, this specialized apparatus is often not practical, and other methods, which also work well enough with fine particles, must be used. The laws vary from land to land. In *TA-Luft* (Technical Regulations for Air), a new proposal, Germany requires that not more than 0.2 mg Cd per m³ of air be released.

Larger gas effluents are usually subject to an electrostatic purification, for example, the removal of particles from gas exhausts of power plants and garbage disposal plants. For low cadmium contents this separation suffices. For high cadmium concentrations filtration is used. The filters can be made from metal screen, ceramic, or a variety of textiles. Regulations and gas release must be carefully adapted to conditions. Washing, especially with Demisters, has proved useful for removal of water-soluble aerosols [44].

16.9.4 Soil

Cadmium reaches agricultural soil via airborne particles; wastes, particularly sludge; and phosphate fertilizers. The importance of these three has been summarized and described for Germany [45].

The normal content of an agricultural field lies between 0.1 and 1 mg Cd per kilogram of soil (0.1-1 ppm). Maximum 3 ppm in a 30-cm layer of top soil is thought allowable, corre-

sponding to 13.5 kg/ha. The contribution to this reservoir per year is 7 g/ha from the air and 6 g/ha from phosphate fertilizer. The removal by harvest is about 4 g/ha. The annual increase is then 9 g/ha. This means that a soil with a content of 4.5 kg/ha, corresponding to 1 ppm, would reach the upper limit after 1000 years.

A number of studies deal with the disposal of sludge [46]. Even then there are still 265 years until the upper limit is reached; therefore, there is time to solve the problem of cadmium emissions. The national regulations for the production of waste-water sediment are tabulated in [47].

However, there are already problems associated with excessive cadmium contents in soil on the grounds of old mining and smelting plants. In the immediate vicinity of the sources of emission, the amount of cadmium in the soil exceeds that thought allowable. Here the use of the adjacent agricultural land must be limited, but there is no large-scale danger. Apparently man-made waste deposits do not create a cadmium source for plants since transfer of cadmium to the soil does not take place.

In addition to concern about the amounts of cadmium [48], the complicated mechanism of transfer from the soil to the plant must be considered. A transport model, from soil into the plant, has been proposed [39].

16.10 Economic Aspects

Since 1970 the production of the non-Communist countries has remained rather constant, 12-15 kt/a. The increase in European production was balanced by the decrease in North America. Consumption has remained in equilibrium with production. The amounts of cadmium for various uses have varied since 1970, affected by technical, economic, and environmental factors [49]. The cadmium price from 1970 to the beginning of the 1980s varied strongly, from \$0.50 to \$4 per pound. The consumption in the Western world between 1970 and 1982 is tabulated in Table 16.2. The figures are totals of the published statistics for

Germany, Japan, the United Kingdom, and the United States, which together account for about two thirds of non-Communist consumption.

Table 16.2: Consumption of cadmium, t.

Use	1970	1973	1976	1979	1982
Plating	3096	3273	3578	3326	2205
Batteries	680	1580	2106	2202	2180
Pigments	2021	3231	2466	2578	1819
Stabilizers	1947	1892	1195	1184	947
Alloys	642	877	519	400	488
Total	8386	10853	9864	9690	7639

16.11 Toxicology and Occupational Health

For more than a century there have been many reports on acute poisoning caused by cadmium compounds. Cadmium uptake occurred either via inhalation during occupational exposures or by oral poisoning due to ingestion of contaminated food or beverages [50]. About 35 years ago it was established [51] that long-term inhalation of cadmium oxide dust could cause a syndrome characterized by damage to the pulmonary and renal systems. Since then many studies have been made in various countries, establishing that occupational exposure to cadmium compounds can cause adverse effects, especially in the kidneys.

During the last decades it was also recognized that cadmium can cause renal effects in the general population. In Japan, a large population is exposed to cadmium via food, especially rice; in one area this resulted in an epidemic of chronic cadmium poisoning with severe bone damage, called *Itai-Itai disease*.

Whereas the exposure levels were reduced considerably in many industries, there is a growing concern about risks for the general population around the world. This is not only caused by emissions from industry. Waste disposal, especially by incineration, the increasing use of phosphate fertilizers, and pH changes in soil and water caused by acid rain are other factors of concern. For more detailed information on different aspects of occur-

rence, metabolism, and effects of cadmium, see [50, 52–56].

Exposure Levels. The average normal daily intake via food is 10–20 µg in most countries; considerably higher values, from 30 to above 200 µg/d, have been reported from certain areas in Japan [50, 52, 54, 55]. The highest cadmium concentrations are found in some basic foodstuffs such as wheat and rice and in liver, kidney, and certain seafoods. Drinking water generally is a minor source. Atmospheric levels of cadmium in rural areas are less than 1 ng/m³, in urban areas 1–10 ng/m³, and in certain industrialized areas a yearly average of up to 50 ng/m³ has been found [50]. Atmospheric exposure to cadmium therefore is of minor importance.

Tobacco may contain 1–2 µg Cd per gram, and smoking twenty cigarettes a day has been estimated to result in an inhalation of about 3 µg. Because a large part of that dose will be absorbed, exposure via cigarette smoking may contribute to the internal dose as much as that absorbed from food [50, 52, 55].

Metabolism. In order to understand the toxicity of cadmium some basic facts about the metabolism of this metal must be known.

The fate of inhaled cadmium compounds depends on particle size and solubility. Finely divided cadmium oxides, especially fumes, deposit in the lower respiratory tract, because of their relatively high solubility about 30% of the inhaled amount is absorbed. Cadmium sulfide and sulfoselenide are relatively slightly soluble, and they are not absorbed to the same extent. (Mucociliary transport to the gut occurs, but the absorption from the gut probably is only a few percent.)

Ingested cadmium generally is absorbed to a few percent [50, 57]. Nutritional deficiencies, e.g., in iron and calcium, will cause higher absorption. Women with severe iron depletion absorbed up to 20% of the cadmium ingested orally [57].

Cadmium absorbed from the lungs or the gut initially is stored mainly in the liver. Exposure to cadmium induces the synthesis of metallothionein, a low molecular mass, cysteine-

rich protein, which strongly binds cadmium but also zinc and copper [58]. The liver has a high capacity to synthesize this protein, and even at very high exposures most of the cadmium in the liver will be bound to metallothionein. The protein breaks down relatively fast, but continuous synthesis ensures that cadmium does not escape to bind to other structures.

In the blood, cadmium is found in the cells and plasma, the concentrations being approximately equal. However, with increasing cadmium levels in the body more cadmium will be found in the cells. In the red blood cells cadmium is bound to several proteins, a major part to metallothionein. In plasma only a minor part is bound to metallothionein. Plasma metallothionein easily passes the glomeruli, and as a protein it will be reabsorbed in the proximal tubules. In the kidneys the protein then breaks down, and cadmium is released. The kidney can also synthesize metallothionein, which ensures that cadmium is trapped in an inert form. However, when the synthesizing capacity is exceeded, cadmium ions will be released and toxic effects may occur.

The cadmium excretion from the kidney is very small. Long retention times in liver and kidney, as well as in other tissue, lead to an accumulation of cadmium in the kidneys from birth to middle age. The newborn is virtually free from cadmium because the placenta is an efficient barrier. The gross biological half-life of cadmium in the body has been estimated to be about twenty years [50].

The average cadmium concentration in the liver of adults is about 1 mg/kg wet weight; the concentration in the renal cortex is about 20 mg/kg in most European countries and in North America [55, 56, 59]. In Belgium higher concentrations, on the average 40 mg/kg in renal cortex, have been reported [60]. The highest concentrations in members of the general population have been found in Japan [55, 58, 59, 60].

Smokers generally have about twice as high cadmium concentrations in the renal cortex (about 25 mg/kg wet weight) as compared with nonsmokers [59, 60].

In the blood the cadmium concentrations in nonsmokers are generally less than 1 µg/L, whereas smokers have up to 5 µg/L [60]. The difference between smokers and nonsmokers is also obvious in the urine. Nonsmokers in Europe and North America excrete about 0.4 µg/g creatinine, whereas smokers excrete about twice as much [59, 61]. This urinary excretion is related to the level of cadmium in the body and is useful for monitoring general populations as well as most persons that are occupationally exposed to cadmium. The total body burden in adult nonsmokers generally is less than 10 mg [59], whereas that of the newborn is only a few micrograms.

Acute Toxicity. Acute cadmium poisoning by inhalation has mainly been caused by accidental exposure to cadmium fumes. The highest risk is in welding, cutting, or soldering operations when cadmium-containing materials are treated, especially if the worker is unaware cadmium is present. There may be a latent period of up to 24 h after exposure before symptoms occur. Chemical pneumonitis occurs, which may lead to lung edema and general symptoms, in some cases with lethal outcome [50, 55, 62, 63].

The concentration of cadmium in the air has not been measured at the time of accidents. Based on cadmium analysis of lung tissue from people dying after acute exposure it has been estimated that the lethal dose corresponds to 1 mg/m³ as cadmium fume for eight hours. Concentrations of 0.5–1 mg Cd/m³ for a couple of hours may cause pneumonitis [53]. A short-term exposure limit for cadmium oxide fumes and respirable dust of 0.25 mg Cd/m³ has been recommended to prevent acute lung reactions [53].

Single *oral* doses of about 10–15 mg may cause gastrointestinal disturbances, but the lethal dose is probably several hundreds of milligrams [53, 55].

Chronic Toxicity. The chronic effects after long-term inhalation are mainly seen in lungs and kidneys [50, 51, 55]. In earlier times anemia, anosmia, and yellow lines on the teeth were common among cadmium workers but

are uncommon today. Emphysema was a major finding in some earlier studies involving exposure to cadmium oxide fume and dust [50]. Because of the decrease in exposure, lung dysfunction is nowadays rare, and if it occurs the symptoms are mild. Figure 16.2 shows how air concentrations of cadmium have decreased during the years in a Swedish factory, where emphysema was seen in the 1940s [51, 64]. It has been concluded that to prevent any pulmonary effect of cadmium the time-weighted average concentration of respirable dust in air should not exceed $20 \mu\text{g}/\text{m}^3$ [53].

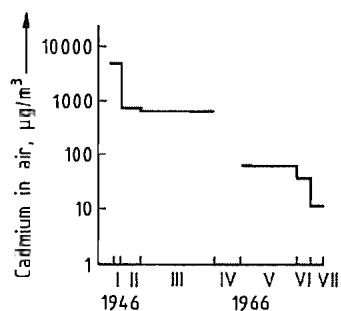


Figure 16.2: Concentration of cadmium in workroom air from 1946 to 1977. Arithmetic means of personal and stationary samples were obtained within seven subperiods. Data covering period IV, 1961–1964, are not available.

The critical effect of cadmium is *renal tubular dysfunction*. In 1950 it was discovered that workers exposed to cadmium oxide dust in an alkaline battery factory had an unusual type of proteinuria [51]. The majority of the proteins were of low molecular mass. Studies of renal function showed that the glomerular filtration rate and the concentrating capacity were decreased. The proteinuria in chronic cadmium poisoning is a tubular proteinuria, caused by a decrease in the reabsorption of filtered plasma proteins in the proximal tubules [50].

The urinary excretion of protein was found to be related to exposure time [65]. The critical cadmium concentration in renal cortex was estimated to be 200 mg/kg wet weight [50]. This value was confirmed by further studies [66–68] and is to be compared with the normal concentrations reported in the previous sec-

tion. A critical urine concentration of about $10 \mu\text{g}$ of cadmium per gram of creatinine has also been established, which generally is a good indicator of the body burden [50, 67–69].

The best dose-response relationship seems to be between cadmium concentration in the liver, determined by in vivo neutron activation, and the degree of tubular dysfunction [67]. At liver concentrations above 30 mg/kg wet weight proteinuria appeared; this corresponds to a cadmium concentration in renal cortex of about 200 mg/kg .

At present, the increased excretion of low molecular mass proteins is regarded as the first sign of renal tubular effects caused by cadmium. This is also consistent with the fact that cadmium primarily is deposited in the proximal tubules, because the cadmium-containing metallothionein is reabsorbed.

At this early stage there are no measurable changes in the excretion of other substances. However, if exposure goes on and the renal levels increase, other functions may be disturbed. In advanced cases of chronic cadmium poisoning the excretion of glucose, amino acids, and phosphate is increased (Fanconi syndrome). Disturbances in mineral metabolism may cause the formation of renal stones. For detailed discussion, see [70, 71].

The *diagnosis* of chronic cadmium poisoning must be based on occupational history, exposure levels in air, levels of cadmium in blood and urine, and protein analysis in urine.

The tubular damage is irreversible, and *prevention* is thus more important than diagnosis. The determination of cadmium in whole blood gives information about recent exposure, but is not always a good indicator of the body burden or risk for renal dysfunction, especially in smokers. Cadmium in urine should be used to monitor this risk. As long as the urinary excretion of cadmium is below $5 \mu\text{g}$ per gram of creatinine there should be no risk for the kidneys. At concentrations of $5\text{--}10 \mu\text{g}$ per gram of creatinine, exposure should be minimized to prevent further accumulation in the kidneys.

Monitoring is also necessary after exposure has ceased. Intensive exposure during rela-

tively short periods may lead to a high cadmium concentration in the liver. Cadmium will then be released from the liver and transported to the kidneys for a long time. The renal concentrations may reach a critical level many years after the last exposure.

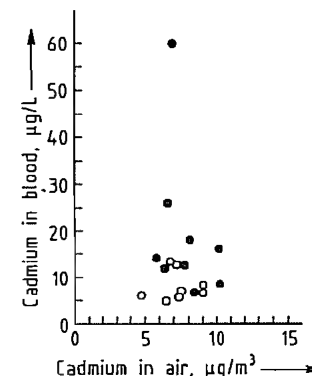


Figure 16.3: Cadmium in blood vs. cadmium in air. Arithmetic means of 4–5 samples of blood cadmium and 9–11 personal samples of airborne cadmium dust for 17 alkaline battery workers. Smokers are represented by the solid circles; nonsmokers, by open circles.

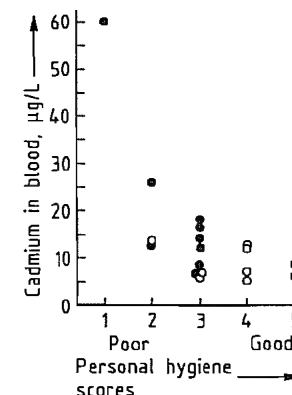


Figure 16.4: Cadmium in blood in relation to the personal hygiene score. Arithmetic means of five samples of cadmium in blood from nine smokers (solid circles) and of 4–5 samples from nine nonsmokers (open circles).

The concentration of cadmium in air is seldom of help in evaluating risks. The long biological half-life of cadmium will lead to a continuous increase in renal levels over many years, and past exposure often is more important than present exposure. Changes in workplace exposure during several decades are shown in Figure 16.2. Figure 16.3 demon-

strates that cadmium blood levels vary greatly even at the current low exposure levels. This is most obvious with smokers. The natural cadmium content of cigarettes does not explain this finding, which is caused instead by contamination of cigarettes or pipe tobacco during work and poor personal hygiene, as illustrated in Figure 16.4 [63].

Therefore, it is imperative to prevent smoking in the workshops and the carrying of tobacco in work clothes; such measures will have much more impact than small reductions of cadmium concentrations in air. Dust accumulation must be prevented in the workshop to minimize exposure caused by contamination of work clothes and hand-to-mouth transfer. The latter may lead to considerable gastrointestinal exposure [72].

The present threshold limits for cadmium in air differ among countries, varying from $10 \mu\text{g Cd}/\text{m}^3$ in Finland to $100 \mu\text{g}/\text{m}^3$ (total dust) in East European countries. The low values, $10\text{--}20 \mu\text{g}/\text{m}^3$, should prevent renal damage, but as indicated above, smoking and poor personal hygiene may increase the internal exposure.

Carcinogenicity. Cadmium has been implicated as a carcinogenic agent, especially with regard to cancer of the prostate. The evidence is weak and based on deaths from cancer of the prostate. However, this cancer is extremely common among elderly men, and it often does not give any symptoms [73, 74]. There is therefore no evidence that cadmium induces this cancer; diet and hormonal factors are more important determinants. However, it cannot be excluded that in heavily exposed workers cadmium might have affected zinc metabolism in the prostate or caused hormonal changes. It is extremely unlikely that low exposures will have any effect on the prostatic function.

According to animal experiments long-term exposure to cadmium chloride aerosols causes lung cancer in rats [75]. The concentrations of cadmium in air were relatively low, $12.5\text{--}50 \mu\text{g}/\text{m}^3$, but exposures were for 23 h a day. Humans are generally not exposed to cad-

mium chloride. In Germany cadmium chloride has been listed as a carcinogen. There have been a number of studies on the occurrence of lung cancer among workers exposed to cadmium oxide dust, but there are no conclusive results indicating that cadmium oxide causes lung cancer in humans [73].

Poisoning from Contamination of the General Environment. Contamination of the general environment has caused cadmium poisoning in certain areas of Japan [64]. Cadmium levels in rice caused daily intakes of several hundreds of micrograms, which should be compared to the "normal" intake of 10–20 μg in most countries in Europe and North America. The exposure in Japan has caused renal tubular dysfunction of the same type as described in the section on chronic toxicity. In one area in the Toyama prefecture the cadmium exposure resulted in the development of severe bone damage, Itai-Itai disease. Mainly multiparous women above 40 years of age were affected. The males in the area had tubular dysfunction but generally did not develop the bone disease. The women had poor nutritional status with deficient intakes of calcium, vitamin D, and protein, probably also of iron. Cadmium alone can hardly cause such severe bone changes, but combined with severe calcium deficiency the result became disastrous. It is not likely that Itai-Itai disease will occur again, but as mentioned tubular dysfunction is common in several other areas of Japan.

There are some contaminated areas in Europe, where signs of renal disease have been sought [76, 77]. No definite conclusions can yet be drawn, but the investigated populations had higher cadmium levels than generally found in Europe [77, 78].

Most domestic animals are not at risk for cadmium poisoning. An exception is the horse. Adult horses generally have about five times higher cadmium concentrations in the renal cortex than adult humans in the same area [79].

16.12 Cadmium Pigments

Among the inorganic pigments, cadmium pigments have particularly brilliant red and yellow colors, as well as a high durability. All cadmium pigments are based on cadmium sulfide and crystallize with a hexagonal wurtzite lattice (Figure 16.5). The sulfur atoms have a hexagonal, tightly packed arrangement, in which the cadmium atoms occupy half of the tetrahedral holes. In this wurtzite lattice the cations and anions can be replaced within certain limits by chemically similar elements; nevertheless, the only substitutions which are used in practice are zinc and mercury for the cations and selenium for the anions.

The use of zinc yields greenish yellow pigments due to the lower lattice constants; mercury and selenium lead to expansion of the lattice. With an increasing content of selenium, or especially mercury, the shades of the pigments change to orange, red, and ultimately to deep red (bordeaux). The brilliant colors of cadmium pigments are primarily due to their almost ideal reflectance curves with a steep ascent (Figure 16.6).

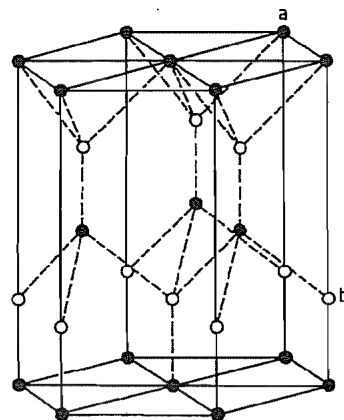


Figure 16.5: Crystal lattice of cadmium pigments (wurtzite structure): a) Sulfur (selenium); b) Cadmium (zinc, mercury).

16.12.1 Cadmium Sulfide

Cadmium sulfide, CdS , occurs as greenockite or cadmiumblende in several natural deposits, which are, however, of no importance

as pigments. The mineral crystallizes hexagonally in the wurtzite lattice (α -form).

When hydrogen sulfide is passed into cadmium salt solutions, cadmium sulfide is formed as a yellow precipitate with a zinc blende structure (cubic, β -form). The β -form can be converted into the α -form (e.g., by heating). α -Cadmium sulfide shows photoconductivity due to defects in the crystal lattice (usage in photovoltaic cells) [80]. The solubility in water at 25 $^{\circ}\text{C}$ is 1.46×10^{-10} mol/L [81]. Cadmium sulfide forms the basis for all cadmium pigments.

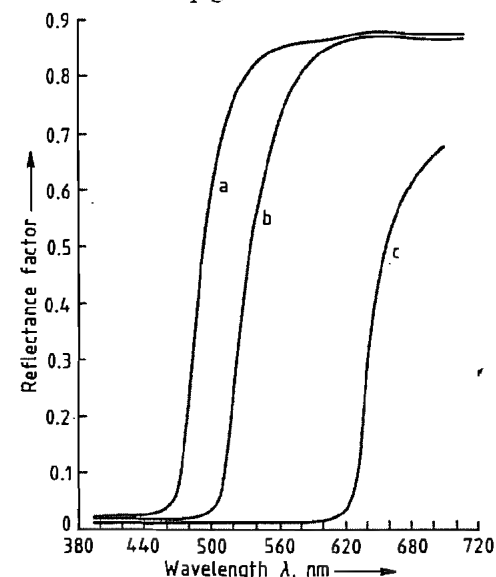


Figure 16.6: Reflectance curves of cadmium pigments (pigment volume concentration 10%): a) Cadmium yellow; b) Cadmium golden yellow; c) Cadmium red (bordeaux).

16.12.2 Cadmium Yellow

Cadmium yellow consists of pure cadmium sulfide (golden yellow color) or mixed crystals of zinc and cadmium sulfide, $(\text{Cd}, \text{Zn})\text{S}$, in which up to one-third of the cadmium can be replaced by zinc. The density of this pigment is 4.5–4.8 g/cm^3 and its refractive index is 2.4–2.5. The prevalent particle size is ca. 0.2 μm with cubic to spheroidal habits. Cadmium yellow is practically insoluble in water and alkali, and of low solubility in dilute mineral

acid. It dissolves in concentrated mineral acid with generation of hydrogen sulfide.

Production. The raw material for the production of cadmium yellow pigments is high-purity cadmium metal (99.99%), cadmium oxide, or cadmium carbonate. If the metal is used it is first dissolved in mineral acid. A zinc salt is then added to the solution; the amount added depends on the desired shade. The zinc salt is followed by addition of sodium sulfide solution. An extremely finely divided cadmium sulfide or cadmium zinc sulfide precipitate is formed, which does not possess any pigment properties. This intermediate product can also be obtained by mixing the cadmium or cadmium–zinc salt solution with sodium carbonate solution. An alkaline cadmium carbonate or cadmium zinc carbonate precipitate is formed which reacts in suspension with added sodium sulfide solution.

The crude precipitated cadmium yellow is washed and then calcined at ca. 600 $^{\circ}\text{C}$, at which temperature the cubic crystal form changes to the hexagonal form. This process determines the particle size distribution, which is essential for the pigment properties.

If the starting material is cadmium oxide or cadmium carbonate, it is mixed with sulfur and calcined at ca. 600 $^{\circ}\text{C}$. After calcination, the pigment product is washed with dilute mineral acid to remove any remaining soluble salts, dried, and ground.

16.12.3 Cadmium Sulfoselenide (Cadmium Red)

Pure cadmium selenide, CdSe , is brownish black and has no pigment properties. Like cadmium sulfide, it is dimorphous and occurs in hexagonal and cubic modifications. Cadmium selenide is insoluble in dilute acid. It readily liberates hydrogen selenide in concentrated hydrochloric acid. It dissolves completely in fuming nitric acid, the Se^{2-} ions being converted to SeO_4^{2-} ions. Cadmium selenide is an n-type semiconductor.

Cadmium red consists of cadmium sulfoselenide, $\text{Cd}(\text{S}, \text{Se})$, and is formed when sulfur

is replaced by selenium in the cadmium sulfide lattice. With increasing selenium content, the color changes to orange, red, and finally dark red. The density of these pigments increases correspondingly from 4.6 to 5.6 g/cm³ and the refractive index from 2.5 to 2.8. The crystals have cubic or spheroidal habits, the prevalent particle size is 0.3–0.4 µm.

Production. Cadmium red pigments are produced in a similar way to the cadmium yellow pigments. The cadmium salt solution is prepared by dissolving the metal in mineral acid and then sodium sulfide is added. A certain amount of selenium powder is dissolved in the sodium sulfide solution to obtain the desired color shade. In an alternative procedure, the cadmium solution is mixed with sodium carbonate solution to precipitate cadmium carbonate which is reacted with the selenium-containing sodium sulfide solution.

The cadmium red pigment intermediate is obtained as a precipitate which is filtered off, washed, and calcined at ca. 600 °C. As with cadmium yellow, calcination yields the red pigment and determines the particle size, particle size distribution, and color shade. Analogously to the cadmium yellow process, cadmium red can be produced by direct reaction of cadmium oxide or cadmium carbonate with sulfur and the required amount of selenium at ca. 600 °C.

Products in which selenium is totally or partially replaced by tellurium [82, 83] have not had any commercial application owing to their poor coloristic properties.

16.12.4 Cadmium Mercury Sulfide

The cadmium in the wurtzite lattice of cadmium sulfide can be replaced by divalent mercury to give cadmium mercury sulfide (cadmium cinnabar). As the quantity of mercury increases, the lattice expands, and the color deepens, changing from yellow to orange and finally dark red. The coloring properties of cadmium cinnabar resemble those of the selenium-containing cadmium red pig-

ments. Use of these mercury-containing pigments can be justified for economic reasons. However, their use is no longer justifiable from the ecological point of view because adequate nontoxic substitutes are available.

16.12.5 Properties and Uses

Cadmium pigments are mainly used to color plastics. They have brilliant, pure shades (yellow, orange, red, and bordeaux), good hiding power, and moderate tinting strength.

Their process-relevant properties are determined by their high thermal stability and chemical resistance to aggressive additives or to molten plastics that have a reducing action (e.g., polyamides). Other advantages for use in plastics are good lightfastness, weather resistance, and migration resistance. The cadmium pigments also protect polyalkenes against aging because they absorb UV light. Premature embrittlement is prevented and the polymer can be recycled [84].

A very useful feature of plastics colored with cadmium pigments is the dimensional stability of injection-molded parts with a large surface area. The combination of these properties is not matched by any other class of colorant.

For economic reasons, cadmium pigments are no longer used for coloring plastics where the pigment property requirements are less stringent. In poly(vinyl chloride) and to a large extent in low-density polyethylene, they have been replaced by less expensive inorganic and organic pigments.

For ecological reasons, cadmium pigments are increasingly being replaced in plastics where high demands are made on the colorants, sometimes with concessions as regards product quality. Plastics processed at high temperature are now colored with high-quality organic pigments (e.g., perylene, quinacridone, and high-quality azo pigments). On account of the color stability of the cadmium pigments at high temperatures, there are very few alternatives for the following applications in the plastic industry:

- Processing temperatures above 300 °C

- Aggressive plastic melts
- Outdoor uses

A further use of cadmium pigments is in paints and coatings (powder paints, silicone resins, and automotive topcoats) but this is declining.

Cadmium pigments are irreplaceable for coloring enamels, ceramic glazes, and glass. Brilliant transparent glasses are obtained by adding a small amount of cadmium red, while 10% cadmium red with a cadmium oxide stabilizer produces dark decorative glasses. Other areas of application are ceramics (wall and floor tiles, household and decorative ceramic ware). Very small amounts of cadmium pigments are used for artists' colors. The terms cadmium yellow and cadmium red have become synonyms for very brilliant red and yellow shades.

Cadmium pigments, especially cadmium red, are very sensitive to intensive grinding, which causes loss of brilliance due to an increase in the number of irregular lattice defects. A brilliant red shade may become a dirty brownish red.

The cadmium pigments are lightfast but, like all sulfide pigments, are slowly oxidized to soluble sulfates by UV light, air, and water. This photooxidation is more pronounced with cadmium yellow than with cadmium red and can still be detected in the powder pigment which normally contains 0.1% moisture.

16.12.6 Quality Specifications

The quality requirements and conditions for the supply of cadmium pigments given in ISO 4620 have lost their significance in practice. According to this standard, cadmium pigments must be free from organic colorants, inorganic colored pigments, and other additives. The acid-soluble components (0.1 mol/L HCl) should not exceed 0.2% Cd (determined according to ISO 4620 and ISO 3856/4); in practice, they are usually < 0.01% Cd.

Cadmium pigments are sold as homogeneous powders and as preparations mixed with barium sulfate to give the required tinting

strength. To reduce the risk of inhalation, they are supplied as low-dust powders and fine granules.

In dust-free and dispersed form, they are supplied as concentrated plastic granules (master-batch pellets), as concentrated pastes, and as liquid colors. These products are added at different stages in the processing of plastics.

16.12.7 Economic Aspects

The output of cadmium pigments in the industrialized countries in 1990 was ca. 5800 t, of which 2800 t were produced in Europe and 2000 t in the United States. Consumption is distributed approximately as follows: plastics 90%, ceramics 5%, and others 5%.

Manufacturers and trade names of cadmium pigments include BASF Lacke + Farben, Stuttgart, Germany (Sicotherm Pigments); Degussa, Frankfurt, Germany; Orkem, Narbonne, France (Langdopec Pigments); Blythe Colours, Stoke on Trent, UK; Brown, London, UK; Reckitts, Hull, UK; Ferro Corporation, Color Division, Cleveland, USA; and Harshaw Chemical Co., Cleveland, USA.

16.12.8 Toxicology and Environmental Protection

Production. Since soluble cadmium compounds have a toxic effect on humans and the environment, all wastewater originating from the production of cadmium pigments must be treated to remove cadmium. This is carried out by methods outlined elsewhere. In the EC, the following limits for the pigment production must be observed: 0.2 mg Cd/L in wastewater and 0.3 kg Cd per tonne of used cadmium compounds calculated as metal [85].

The exhaust air from the production plants and the ventilation equipment must be cleaned. Tubular filters and, more recently, absolute filters have been used to remove cadmium compounds in dust form. With these high-performance filters, it is possible to comply with the limits specified in Germany (0.2 mg Cd/m³ air, 1 g Cd/h, emission limit; 5 µg

Cd/m² per day, immission limit). During pigment production, occupational hygiene and safety measures for toxic materials must be observed. Exposure to cadmium can be determined by measurements of the workplace concentration and by examination of the cadmium levels in blood and urine. In Germany, the following maximum biological tolerance levels are allowed at the workplace (BAT values): 15 µg Cd/L urine and 1.5 µg Cd/100 mL blood. In the future, a TRK value will apply which is below the earlier MAK value of 50 µg Cd/m³. In the United States, the TLV value for cadmium fumes and salts is 50 µg Cd/m³. Lower values have been recommended by OSHA, but they are still being discussed.

Toxicity. The toxicity of soluble cadmium compounds is described elsewhere. Cadmium pigments are cadmium compounds with a low solubility, however, small quantities of cadmium dissolve in dilute hydrochloric acid (concentration equivalent to stomach acid), and in cases of long-term oral intake of cadmium pigments, they can accumulate in the human body. On inhalation of subchronic amounts of cadmium pigments, a small proportion of cadmium is biologically available [86, 87].

Cadmium pigments have no acute toxic effect (oral LD₅₀, rat, > 10 g/kg). The pigments do not have any adverse effects on the skin and mucous membranes.

Genotoxic Effects and Carcinogenicity. Tests for damages of the DNA [88] and cell transformation caused by crystalline cadmium sulfide were positive [89]. Cadmium sulfide also proved to be carcinogenic by intraperitoneal and after intratracheal administration [90]. The significance of such animal studies is being controversially discussed by toxicologists.

Long-term animal feeding studies with various cadmium compounds show no carcinogenic risks. However inhalation studies with rats, mice, and hamsters (with cadmium chloride, cadmium sulfate, cadmium chloride, and cadmium sulfide) showed that all four compounds produced a significant increase of lung

cancer in rats [91]. The results for mice were inconclusive and no carcinogenicity in hamsters was observed [92]. Reinvestigation of the inhalation studies has shown that the test was not applicable to cadmium sulfide. The inhaled liquid cadmium sulfide suspension contained ≤ 40% cadmium sulfate formed by light-induced oxidation.

In 1989 the German Senate Commission for the Assessment of Dangerous Substances classified cadmium and its compounds (including cadmium sulfide) as substances that have carcinogenic properties as found in animal studies. Cadmium pigments and preparations which contain cadmium pigments in concentrations above 0.1%, must therefore be regarded as carcinogenic if they occur in an inhalable form.

In the United States, the National Toxicology Program (NTP) has shown that cadmium and different cadmium compounds (including cadmium sulfide) have a carcinogenic effect in animal experiments.

In 1991 the EC reported the above-mentioned fault in the inhalation studies and classified cadmium sulfide in the EC Cancer List in Category III (suspected carcinogen).

Limitations of Use. In 1981 Sweden prohibited the use of cadmium pigments (with some exceptions) for ecological reasons. In 1987 Switzerland prohibited the use of cadmium pigments in plastics. Exceptions are possible if valid reasons can be given.

In 1991 the EC passed a directive to prohibit the use of cadmium pigments as colorants for certain plastics that can easily be colored with other pigments [93]. For further series of plastics, use of substitution pigments will be compulsory in 1996. Plastics that require high processing temperatures or that are mainly for outdoor use are not affected by this prohibition owing to the poor performance of possible substitution pigments.

In 1996 the use in coating media will be prohibited. Use in artists' colors and ceramic products is still permitted.

Regulations Affecting Foods. The cadmium pigments fulfill the legal requirements of the

EC countries for colorants used in plastics which come in contact with food. Except for polyamide 6, only microgram quantities of cadmium can be extracted from colored plastics into simulants [94, 95].

To prevent even minimal intake of cadmium, the European Commission has passed a resolution which states that cadmium pigments should only be used for these purposes if adequate substitutes are not available [96].

The use of cadmium pigments in ceramics is controlled in the EC Guideline No. 84/500/EC. International standards [Part I (Methods) and Part II (Limit Values)] are as follows: ceramic surfaces ISO 6486, enamel ISO 4531, and glass ISO 7086.

16.13 References

1. Bundesverband der Deutschen Industrie e.V. (ed.): *Cadmium - Eine Dokumentation*, No. 154, Köln 1982.
2. A. v. Röpenack, *Erzmetall* 35 (1982) 534.
3. *Raffinationsverfahren in der Metallurgie '83*, Section D4, pp. 139-156, Verlag Chemie, Weinheim 1983.
4. D. Blana, *Erzmetall* 32 (1979) 262-266.
5. V. Sipilä, *Erzmetall* 32 (1979) 527-529.
6. *Metal Bulletin Monthly*, April 1983, 115-117.
7. Soc. minière et métallurg. de Penarroya, US 4230487, 1979.
8. Cyprus Metallurg. Proc. Corp., GB 1511323, 1974.
9. R. E. Sheppard, A. O. Martel, *Min. Eng. (Littleton, CO)* 24 (1972) 80.
10. I. Pajak et al., *Pr. Inst. Met. Niezelaz.* 8 (1979) no. 4, 185-191.
11. G. Schenker, *Erzmetall* 32 (1979) 524-526.
12. C. A. Lemaître, *Erzmetall* 32 (1979) 530-531.
13. A. Cornea et al., *Rev. Chim. (Bucharest)* 29 (1978) no. 11, 1031-1034.
14. Nederlandse Centrale Organisatie Voor Toegepast Natuurwetenschappelijk Onderzoek, GB 2014122A, 1978.
15. M. Verhaege, *Bull. Soc. chim. Belg.* 87 (1978) no. 9, 651-657.
16. Berol Kemi AB, GB 2001618A, 1977.
17. K. Hanusch, *Metall (Berlin)* 35 (1981) 911-912.
18. Degussa, DE 2001985, 1970.
19. Nife Jungner AB, GB 1475863, 1975.
20. T. B. Lloyd, K. J. Wise, *Ed. Proc. Int. Cadmium Conf. 3rd*, Miami 3-5 Feb. 1981, Cadmium Association, London.
21. R. Kammel, H.-W. Lieber, *Galvanotechnik* 68 (1977) 710-715.
22. N.-E. Barring, *Ed. Proc. Int. Cadmium Conf. 4th*, Munich 1-4 March 1983, Cadmium Association, London.
23. E. Jackwerth, S. Salewski, *Fresenius Z. Anal. Chem.* 310 (1982) 108-110.
24. M. Farnsworth: *Cadmium Chemicals*, Int. Lead Zinc Research Organisation, New York 1980.
25. J. F. Cole, D. S. Carr, *Ed. Proc. Int. Cadmium Conf. 4th*, Munich 1-4 March 1983, Cadmium Association, London.
26. Soc. anonyme des usines Chausson, US 3969110, 1974.
27. Soc. anonyme des usines Chausson, GB 2019440A, 1978.
28. Asahi Glass Co., US 4106930, 1972.
29. V. Prakash et al., *Proceedings, Solder Seminar*, Bangalore, India, 5-6 Nov. 1979, Lead Development Association, London.
30. H. Heinzel, K. E. Saeger, *DVS Ber.* 1976. no. 40, 55-58.
31. M. Mahler, K. F. Zimmermann, *Schweißen + Schneiden* 34 (1982) 277-281.
32. A. K. Woollaston, M. S. Stamford, *Metall. Met. Form.* 44 (1977) 100-101, 103-104.
33. S. T. Udeshi, A. A. Sahay, *Proceedings, Cadmium Seminar*, Udaipur, India, 26 Feb. 1980, Cadmium Association, London.
34. *Arbeitsstoffverordnung*, Bundesgesetzblatt 1982, part 1, p. 144.
35. Guideline 79/831/EEC, 18 Sept. 1979, Official Journal of the European Community no. L 259/10, 15 Oct. 1979.
36. International Maritime Organisation London: *International Maritime Dangerous Goods - Code (IMDG-Code) Amendment 20-82*.
37. International Civil Aviation Organisation (ICAO): *Technical Instructions for the Safe Transport of Dangerous Goods by Air*. Addition 1984.
38. Department of the Environment: *Cadmium in the Environment and its Significance to Man*, Pollution Paper no. 17, Her Majesty's Stationery Office, London 1980.
39. M. Hutton: *Cadmium in the European Community*, contract no. 333, ENV U.K., London 1982.
40. R. Coleman et al., *Sources of Atmospheric Cadmium*, contract no. 68-02-2836, prepared for U.S. Environmental Protection Agency, 1979.
41. A. Raubut, *Industrial Emissions of Cadmium in the European Community*, European Community Study contract no. ENV/223/74E, Oct. 1978.
42. Guideline 83/514/EEC, 26 Sept. 1983, Official Journal of the European Community no. L 291/1, 24 Oct. 1983.
43. *Klärschlammverordnung AbfKlärV*, 25 June 1982, Bundesgesetzblatt 1982, part 1, 26 June 1982, p. 734.
44. K. H. Schulte-Schlepping, *Cadmium, Ed. Proc. Int. Cadmium Conf. 2nd*, Cannes 6-8 Feb. 1979, Metal Bulletin, London.
45. K. H. Schulte-Schlepping, *Ed. Proc. Int. Cadmium Conf. 4th*, Munich 1-4 March 1983, Cadmium Association, London.
46. A. Klope: *Landwirtschaftliche Forschung*, Sonderheft 39, Kongressband 1982, I. D. Sauerländer's Verlag, Frankfurt, p. 302.
47. D. Purves: *International Conference Heavy Metals in the Environment*, Amsterdam Sept. 1981, CEP Consultants Edinburgh U.K.

48. A. Cottenie: *International Conference Heavy Metals in the Environment*, Amsterdam Sept. 1981, CEP Consultants Edinburgh U.K.
49. D. A. Temple, D. N. Wilson: *Ed. Proc. Int. Cadmium Conf. 4th*, Munich 1–4 March 1983, Cadmium Association, London.
50. L. Friberg, M. Piscator, G. F. Nordberg, T. Kjellström: *Cadmium in the Environment*, 2nd ed., Chemical Rubber Co., Cleveland 1974.
51. L. Friberg, *Acta Med. Scand. Suppl.* **138** (1950) 240.
52. Commission of the European Communities: *Evaluation of the Impact of Cadmium on the Health of Man*, Luxembourg 1977.
53. World Health Organization: "Recommended Health-based Limits in Occupational Exposure to Heavy Metals", *Tech. Rep. Ser.* **647** (1980).
54. K. Tsuchiya (ed.): *Cadmium Studies in Japan – A Review*, Elsevier – North Holland Biomedical Press, Amsterdam 1978.
55. L. Friberg, I. Kjellström, G. Nordberg, M. Piscator in L. Friberg, G. Nordberg, V. Vouk (eds.): *Handbook of the Toxicology of Metals*, Elsevier – North Holland Biomedical Press, Amsterdam 1979, pp. 355–381.
56. M. Piscator in A. S. Prasad (ed.): *Clinical, Biomedical, and Nutritional Aspects of Trace Elements*, A. R. Liss, Inc., New York 1982, pp. 521–536.
57. P. R. Flanagan, J. S. McLellan, J. Haist, G. Cherian, et al., *Gastroenterology* **71** (1978) 841–846.
58. J. H. R. Kägi, M. Nordberg (eds.): *Metallothionein*, Birkhäuser, Basel 1979.
59. T. Kjellström, *EHP Environ. Health Perspect.* **28** (1979) 169–197.
60. L. Friberg, M. Vahter, *Environ. Res.* **30** (1983) 95–128.
61. C.-G. Elinder, T. Kjellström, L. Linnman, G. Pershagen, *Environ. Res.* **15** (1978) 473–484.
62. P. A. Lucas, A. G. Jariwalla, J. H. Jones, J. Gough et al., *Lancet* 1980, vol. II, 205.
63. J. R. Patwardhan, E. S. Finch, *Med. J. Aust.* **1** (1976) 962–966.
64. F. Hassler "Exposure to Cadmium and Nickel", Dissertation, Karolinska Institute, Stockholm 1983.
65. M. Piscator, *Arch. Environ. Health* **4** (1962) 607–621.
66. K. J. Ellis, W. D. Morgan, I. Zanzi, S. Yasamura et al., *J. Toxicol. Environ. Health* **7** (1981) 691–703.
67. H. Roels, R. R. Lauwerys, J. P. Buchet, A. Bernhard et al., *Environ. Res.* **26** (1981) 217–240.
68. H. Roels, R. Lauwerys, A. N. Dardenne, *Toxicol. Lett.* **15** (1983) 357–360.
69. R. Lauwerys, H. Roels, M. Regniers, J. P. Buchet et al., *Environ. Res.* **20** (1979) 375–391.
70. A. Bernhard, J. P. Buchet, H. Roels, P. Masson et al., *Eur. J. Clin. Invest.* **9** (1979) 11–22.
71. M. Piscator in H. Zumkley (ed.): *Spurenelemente*, Thieme Verlag, Stuttgart 1983, pp. 81–97.
72. E. Adamsson, M. Piscator, K. Nogawa, *EHP Environ. Health Perspect.* **28** (1979) 219–222.
73. M. Piscator, *EHP Environ. Health Perspect.* **40** (1981) 107–120.
74. M. Piscator in D. Wilson, R. A. Volpe (eds.): *Ed. Proc. Int. Cadmium Conf. 3rd*, Miami 3–5 Feb. 1981, Cadmium Association, London 1982, pp. 135–137.
75. S. Takenaka, H. Oldiges, H. König, D. Hochrainer et al., *J. Natl. Cancer Inst.* **70** (1983) 367–371.
76. M. Caruthers, B. Smith, *Lancet* 1979, vol. 1, 845–847.
77. H. R. Roels, R. K. Lauwerys, J.-P. Buchet, A. Bernhard, *Environ. Res.* **24** (1981) 117–130.
78. T. C. Harvey, D. R. Chettle, J. H. Fremlin, I. K. Al Haddad et al., *Lancet* 1979, vol. 1, 551.
79. C.-G. Elinder, L. Jönsson, M. Piscator, B. Rahnster, *Environ. Res.* **26** (1981) 121.
80. K. Weiss, Z. Naturforsch. A Astrophys. Phys. Phys. Chem. **2A** (1947) 650–652.
81. S. F. Ravik, *J. Phys. Chem.* **40** (1936) 69.
82. Siegle & Co., DE 1007907, 1955.
83. Bayer, DE-OS 2151234, 1971.
84. H. Endriß, *Kunststoffe* **75** (1985) 10, 758–761.
85. EEC Council Directive, FEC 83/514, Sept. 26, 1983, on the limits for cadmium in waste water.
86. G. Rusch, J. S. O'Grodnick, W. E. Rinehart, *Am. Ind. Hyg. Assoc. J.* **47** (1986) no. 12, 754.
87. H.-J. Klimisch, C. Gembardt, H. P. Gelbke: *Lung Deposition and Clearance, Lung Pathology and Renal Accumulation of Inhaled Cadmium Chloride and Cadmium Sulfide in Rat*, BASF, Ludwigshafen 1991.
88. S. A. Robinson, O. Cantoni, M. Costa, *Carcinogenesis (London)* **3** (1982) no. 6, 657.
89. M. Costa, J. D. Heck, S. H. Robinson, *Cancer Res.* **42** (1982) 2757.
90. F. Pott et al., *Exp. Pathol.* **32** (1987) 129.
91. H. Oldiges, D. Hochrainer, M. Glaser, *Toxicol. Environ. Chem.* **19** (1988) 217.
92. U. Heinrich et al.: Investigation of the Carcinogenic Effects of Various Cadmium Compounds after Inhalation Exposure in Hamsters and Mice", *Exp. Pathol.* **38**, in press.
93. EEC Council Directive, EEC 91/338, 1991.
94. D. Råde, A. Dornemann, *Proceedings of the Third International Cadmium Conference Miami, 1981*, Cadmium Association, London, pp. 37–40.
95. H. Endriß, *Kunststoffe* **69** (1979) 39–43.
96. European Commission: "On the Use of Colourants in Plastic Materials Coming in Contact with Food", Resolution AP (89) 1., Sept. 13, 1989.

17 Mercury

MATTHIAS SIMON (§§ 17.1–17.10, 17.13–17.14); PETER JÖNK (RETIRED) (§ 17.11); GABRIELE WÜHL-COUTURIER (§ 17.12); MAX DAUNDERER (§ 17.14)

17.1 Introduction	891	17.5.2.2 Water Purification	905
17.2 Properties	891	17.6 Quality Specifications	906
17.2.1 Physical Properties	891	17.7 Chemical Analysis	906
17.2.2 Chemical Properties	892	17.8 Storage and Transportation	907
17.3 Resources and Raw Materials	893	17.9 Uses	907
17.3.1 Deposits	893	17.10 Mercury Alloys	908
17.3.2 Secondary Sources	895	17.11 Compounds	910
17.4 Production	895	17.11.1 Mercury Chalconides	910
17.4.1 Extraction from Primary Sources ..	895	17.11.2 Mercury Halides	911
17.4.1.1 Beneficiation	895	17.11.3 Mercury Pseudohalides	913
17.4.1.2 Processing to Metallic Mercury ...	895	17.11.4 Acetates, Nitrates, Sulfates	913
17.4.1.3 Furnace Systems	896	17.11.5 Mercury–Nitrogen Compounds	914
17.4.2 Extraction from Secondary Sources	897	17.11.6 Analysis, Storage, and Transportation; Protective Measures	914
17.4.3 Condensation of Mercury from Furnace Off-Gas	898	17.12 Selected Organic Compounds	915
17.4.4 Treatment of the Sludge	900	17.13 Economic Aspects	915
17.5 Environmental Protection	901	17.14 Toxicology and Occupational Health	917
17.5.1 Natural Distribution of Mercury ...	901	17.15 References	920
17.5.1.1 Mercury in Soil, Plants, and Animals	901		
17.5.1.2 Mercury in Food	902		
17.5.2 Mercury Emissions	904		
17.5.2.1 Gas Purification	904		

17.1 Introduction

Mercury (also called quicksilver), symbol Hg from the Greek υδραρ = water and αργυρος = silver, was known as early as 1000 B.C. because of its liquid state at room temperature ($mp -38.89^\circ\text{C}$). The discovery in 1938 of 1 kg of the metal in 2500-year-old sand layers on the eastern coast of Greece indicates that mercury was used in the extraction of gold at an early date [1]. Mercury was mentioned about 200 B.C. in India as well as in China (Han dynasty).

As early as 1556, GEORGES BAUER, known as AGRICOLA, reported five different methods for extracting mercury from its ores [2]. He also realized that mercury vapors are heavier than air and that they could therefore conveniently be trapped in condensers beneath the reaction vessel.

Because of the considerable vapor pressure of mercury even at room temperature and the toxicity of its vapors, particularly safe and reliable methods must be used in the extraction of mercury to avoid releasing even the slightest trace of the metal into the environment. The problem of gas and water purification is therefore particularly important.

17.2 Properties

17.2.1 Physical Properties

Mercury is a silvery-white, shiny metal, which is liquid at room temperature. The most important physical properties are listed below:

Isotope masses (ordered according to decreasing abundance)	202, 200, 199, 201 198 204, 196
mp	-38.89°C
bp (101.3 kPa)	357.3°C
Density (0°C)	13.5956 g/cm^3
Specific heat capacity c_p (0°C)	$0.1397\text{ J g}^{-1}\text{K}^{-1}$

Heat of fusion	11.807 J/g
Heat of evaporation (357.3 °C)	59.453 kJ/mol
Thermal conductivity (17 °C)	0.082 Wcm ⁻¹ K ⁻¹
Thermal expansion coefficient β (0–100 °C)	1.826 × 10 ⁻⁴ K ⁻¹
Electrical conductivity (0 °C)	1.063 × 10 ⁻⁴ mΩ ⁻¹ mm ⁻²
Crystal structure	rhombohedral
Viscosity (0 °C)	1.685 mPa·s
Surface tension	480.3 × 10 ⁻⁵ N/cm
<i>t</i> _{crit}	1450 °C
<i>P</i> _{crit}	105.5 MPa
Critical density	5 g/cm ³
Evaporation number (25 °C)	0.085 mgK ⁻¹ cm ⁻²

Mercury has a relatively high vapor pressure, even at room temperature. Saturation vapor pressures at 0–100 °C are listed in Table 17.1 (corresponding to a specified mercury content in air). The temperature dependence of the density of mercury is given in Table 17.2.

Mercury vapor is excited to a state of luminescence by electrical discharge (mercury vapor lamps). Ultraviolet radiation is released primarily, it can be used to start and to promote chemical reactions.

Table 17.1: Saturation vapor pressure of mercury at different temperatures.

<i>t</i> , °C	<i>p</i> , Pa	Hg content in air, g/m ³
0	0.026	0.00238
10	0.070	0.00604
20	0.170	0.01406
30	0.390	0.03144
100	36.841	2.40400

Table 17.2: Density of mercury as a function of temperature.

<i>t</i> , °C	Density, g/cm ³	<i>t</i> , °C	Density, g/cm ³
-38.89	13.6902	200	13.1139
0	13.5956	250	12.9957
50	13.4733	300	12.8778
100	13.3524	350	12.7640
150	13.2327		

Table 17.3: Temperature dependence of the dynamic viscosity of mercury.

<i>t</i> , °C	Density, g/cm ³	<i>t</i> , °C	Density, g/cm ³
-20	1.855	60	1.367
-10	1.764	80	1.298
0	1.685	100	1.240
10	1.615	200	1.052
20	1.554	300	0.950
30	1.499	340	0.921
40	1.450		

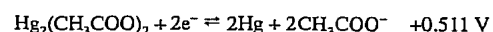
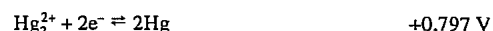
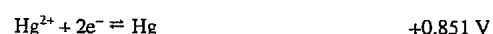
The surface tension of mercury is ca. six times greater than that of water, which is the reason for its poor wettability by water.

The dynamic viscosity η of mercury (Table 17.3) is of the same order of magnitude as that of water [3].

Some other metals, such as gold, silver, and zinc, dissolve readily in mercury to form amalgams. The solubility of mercury in water is strongly temperature dependent [4]. At room temperature, the solubility is ca. 60 µg/L; at 50 °C, ca. 250 µg/L; and at 90 °C, ca. 1100 µg/L. At low temperature, the addition of sodium chloride reduces the water solubility.

17.2.2 Chemical Properties

Mercury exists in the oxidation states 0, 1+, and 2+; monovalent mercury is found only in Hg–Hg bonds. The redox potentials E^0 at 298.15 K and 101.325 kPa relative to the standard hydrogen electrode are as follows [3]:



The standard potentials show that mercury is a relatively noble metal. Metallic mercury dissolves in nitric acid, aqua regia, warm concentrated hydrochloric acid and sulfuric acid. It is sparingly soluble in dilute HCl, HBr, and HI as well as in cold sulfuric acid. Most of its chemical compounds have densities of 5–9 g/cm³. The oxide of mercury (HgO) decomposes at 400–500 °C. This effect is utilized in the extraction of mercury from oxidic sources. Mercury forms monovalent and divalent compounds with the halogens fluorine, chlorine, bromine, and iodine. It also forms monovalent and divalent compounds with sulfur.

17.3 Resources and Raw Materials

17.3.1 Deposits

All known mercury ores are relatively low-grade ores, the average mercury content being ca. 1 %. Because mercury ores lie close to the earth's surface, the mining depth is ca. 800 m at most. The overwhelming proportion of mercury has always been produced in Europe; some of the most important deposits are listed below. Over the last ten years, the former Soviet Union, Spain, China, Algeria, Turkey, and the United States have accounted for ca. 90 % of world mining production.

Spain. The deposits at Almadén have been mined for more than 2000 years. Almadén is situated in the southwest of the province of Ciudad Real in New Castile, about 200 km from Madrid, on the northern edge of the Sierra Morena. The ore-bearing deposits are porous sedimentary rocks (sandstone, bituminous shale, Silurian quartzite) that contain mercury sulfide (cinnabar). Needles of coarsely crystalline cinnabar as well as metallic mercury in lenticular ore-bearing bodies are also found over a roughly 20-km stretch in the valley of the Valdeazogues river. The ore is extracted in several mines (San Pedro y San Diego, San Francisco, San Nicolas). The richest strata contained 12–14 % mercury at a depth of 170–200 m. Mining is carried out today at a depth of 500 m; 1 t of ore yields about one flask of mercury (= 34.473 kg of mercury, corresponding to a 3.5 % mercury content in the ore).

This deposit was probably known to the Celts and Phoenicians, and was mined by the Romans from 150 B.C. These mines were subsequently worked by the Moors, then by the orders of knights, by the Spanish royal house, and from 1525–1645 by the Fuggers. Since then the mines have been under state management. From 1449 (when production records start) to the present, ca. 300 000 t of mercury has been mined.

In 1988 Almadén produced ca. 1380 t of mercury. The ore-bearing body has an average mercury content of 5%. Because of the low price of mercury the plant operates for only a few months of the year. The operating company, Minas de Almadén y Arrayanes SA, is state-owned [5, 6].

Italy. A roughly 25-km-wide, 50-km-long belt running from Monte Amiata to the coast in southern Tuscany contains many closed mines as well as some that are still operating. Although these deposits had been mined by the Etruscans, they were not intensively worked by the Romans, to the benefit of the Spanish mines at Almadén. The Siele mine recommenced operation only in 1846, and the Abbazia San Salvatore mine, at present still the largest, in 1898.

Mercury occurs as cinnabar and metacinnabarite in pyrites, marcasite, antimonite, and realgar, mainly in Eocene sediments (shale, sandstone, marl, limestone) under a covering layer of trachyte. The gangue consists largely of clay or dolomite. The ores contain on average 0.2–0.8 % mercury. Mercury extraction is organized by the Monte Amiata works, its latent production capacity being up to 2000 t/a. No mercury has been mined since 1983.

Former Yugoslavia. The third largest mercury deposits in Europe are situated in Idrija in Slovenia, about 40 km west of Ljubljana. These deposits have been worked since 1497. The mines were under Austrian ownership from 1580 to 1918, then under Italian ownership, and finally reverted to Yugoslavia after World War II.

The tectonics of this region are complicated. Shell marl and shale are impregnated with cinnabar and native mercury, and typically contain admixtures of pyrites, gypsum, and bitumen. The ore contains ca. 0.5 % mercury. Idrija has a capacity of about 600 t/a. About 60 t mercury was mined in 1986. Additional deposits in Yugoslavia are located at Maškara in Croatia, Berg Avala to the south of Beograd in Serbia, Neumarkt in the Karavanen, and Montenegro.

Algeria. Algeria has become the second largest mercury producer in the western hemisphere after Spain, and in 1986 ca. 690 t of mercury was produced.

Germany. In 1936 a modern mercury works was built at Landsberg near Obermoschel in the northern Pfalz (Palatinate), which had to be closed in 1942 because working the very low-grade ore, containing only 0.1 % Hg, was uneconomical.

Austria. Fahl ore containing 1.8 % mercury is mined in small amounts at Schwaz in the Tyrol. Other deposits at Dollach on the Drava are no longer mined.

Finland. Outokumpu obtains about 100 t of mercury per year from the processing of zinc concentrates.

Former Czechoslovakia. Three important deposits exist: at Kotrbachy, mercury is obtained as a by-product of a fahl ore. Cinnabar is found southwest of Gelnica in a workable ore containing 0.25 % mercury. Finally, mercury has been obtained in the region between Mernik and Vranov since the end of the 17th century. This production ceased in 1937.

Romania. Romania has mercury ores at Zlatna and Baboia in Transylvania.

Turkey. In Turkey about 220 t of mercury is obtained annually from mining operations. At present, because of its low price, mercury is extracted from only two mines, which belong to the state-owned Etibank. The deposits are at Izmir-Ödemiş-Haliköy (1×10^6 t of ore containing 0.25 % mercury), Konya-Ladik, and Konya-Sizma (1.15×10^6 t of ore containing 0.23 % mercury). These deposits alone account for ca. 40 % of the Turkish reserves of mercury [7].

Former Soviet Union. The most important deposits in the former Soviet Union are at Nikotovka in the Ukraine. Per year about 400 t of mercury is produced there from an antimonite ore containing 0.4 % mercury. Cinnabar deposits have recently been discovered in the Crimea, although no further details are available. Additional ore deposits are mined in the

Northern Caucasus, Urals, Altai Mountains, and in Turkestan and Dagestan.

China. China has important deposits in the provinces of Yunnan, Hunan, and Kweichow. The mines at Wanshanchang and Patschai are well known. Mined production was ca. 760 t of mercury in 1987.

Japan. In Japan, mercury is extracted on the island of Hokkaido.

Canada. Mercury ore deposits are situated in the west of Canada in British Columbia at Pinchi Lake and in the vicinity of Vancouver (Kamloops, Bridge River).

United States. The number of mines in the United States has decreased considerably in the last 20 years. Whereas 149 mines were operating in 1965, only 3 mines were still operating by 1981. The principal mining regions are California and Nevada. Placer, Inc., a subsidiary of the Canadian company Placer Development, accounts for ca. 99 % of production. The average mercury content in the ore is 0.3–0.5 %. Mining production in 1986 was ca. 400 t and falling.

Mexico. The 200 known mercury ore deposits are distributed over 20 states. The most important mines are in the provinces of Zacatecas, Guerro, Durango, Chihuahua, Guanajuato, San Luis Potosi Aguascalientes, and Quere-taro; total mercury production is some 500 t/a.

South America. South America is of only minor importance as a mercury producer. Chile occupies first place among the mercury-producing countries. The Santa Barbara mine at Huancavelica in Peru is now exhausted, although it supplied substantial amounts of mercury in the 17th and 18th centuries: some 50 000 t was used for precious-metal extraction. Small amounts of mercury are mined in Venezuela and Bolivia.

A U.S. estimate made in 1983 gave the following amounts of mercury extracted by mining operations [8]:

Spain	50 000 t
China	17 200 t
Soviet Union	17 200 t
Yugoslavia	17 200 t

Italy	12 100 t
United States	12 100 t
Other countries	29 000 t
World total	154 800 t

Mining activities and exploitation of deposits are, as with most base metals, greatly dependent on current world market prices. Too low returns have led in recent years to a number of mines being closed, which has resulted in a concentration of plants (less plants with increased production).

17.3.2 Secondary Sources

Like primary ores, industrial waste containing mercury also contributes to its production. The majority of plants used in chlor-alkali electrolysis employ liquid mercury cathodes, resulting in residues containing 10 % mercury or more. In addition to this major secondary source, mercury batteries, mercury fluorescent tubes, electrical switches, thermometer breakage, and obsolete rectifiers should be regarded as mercury sources.

Although the overall production of mercury has decreased over the last 20 years, sufficient potential uses and thus secondary sources remain for the foreseeable future, thanks to the unique properties of this metal.

17.4 Production

17.4.1 Extraction from Primary Sources

17.4.1.1 Beneficiation

Preliminary concentration is desirable, especially for working low-grade ores. This is often performed in the mine by classification. Because of the brittleness of cinnabar, pieces of ore break easily at the mercury sulfide veins. Crystalline mercury sulfide in brittle ore can be concentrated by using settling tables.

Another method of concentration is the use of a flotation stage to increase the mercury content. Separation of the antimony and arsenic fractions is particularly important, and

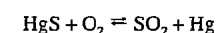
the ores are comminuted to grain sizes of ≤ 0.075 mm (200 mesh) in the case of antimony and ≤ 0.5 mm (25 mesh) in the case of arsenic. After comminution, lead(II) nitrate [$\text{Pb}(\text{NO}_3)_2$], butyl xanthate, and pine oil are added to the first flotation stage. Flotation is performed at pH 7.1. After purification, mercury is selectively floated, and a concentrate of ca. 50 % antimony is obtained. Potassium dichromate ($\text{K}_2\text{Cr}_2\text{O}_7$) is added as reactant. The end concentrate has a mercury content of ca. 70 % [9]. Another way of concentrating mercury by flotation is to add potassium oleate as collector [10].

Only a coarse preliminary grinding to ca. 50-mm grain size is necessary for high-concentration mercury sulfide ores. During subsequent thermal treatment, the ore particles burst because of the high vapor pressure, resulting in further comminution.

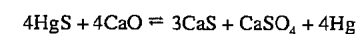
17.4.1.2 Processing to Metallic Mercury [11, 12]

The most important starting material for mercury extraction is mercury sulfide (cinnabar, cinnabarite); it is nonpoisonous and can be stored and transported without any problem.

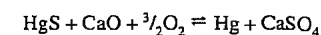
The coarsely ground ore is processed in directly or indirectly heated furnaces, retorts, or muffles. Reaction with oxygen begins at 300 °C, according to



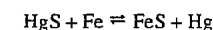
Quicklime can be added as flux to bind the sulfur in solid form. The overall reaction in the absence of oxygen is as follows:



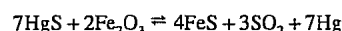
In the *presence of oxygen*, the reaction is



Addition of metallic iron in the form of iron filings enables the following reaction to occur:



Instead of metallic iron, iron oxides can also be used:



For this reason, sulfur-resistant steel should be used as construction material. Processing is normally performed with the addition of air, and the sulfur dioxide formed can be converted in a downstream wet scrubber.

17.4.1.3 Furnace Systems

Mercury sulfide-containing ores are processed pyrometallurgically. Distinction is made between *directly* and *indirectly* heated furnaces. This is important because the formation of *stupp* cannot be avoided in pyrometallurgical processing (the word *stupp* is an Austrian expression that simply means powder; in the case of mercury, a mercury-containing powder). The greater the formation of dust in the furnace, the greater is the occurrence of *stupp*. Because of the presence of combustion air in the furnace, directly heated furnaces generally create more dust than indirectly heated ones. Mercury in vapor form condenses to some extent on the small dust particles which act as condensation nuclei.

Another difference between directly and indirectly heated furnaces is that mercury vapor in indirectly heated systems is more highly concentrated because it is not diluted by combustion gases.

Directly Heated Furnaces. Cylindrical Bustamente furnaces, multiple-hearth furnaces, and rotary kilns are used.

The *Bustamente furnace* is still used in Spain (Almadén) [5]. The cylindrical vessel is heated outside the shaft, only the combustion gases come into contact with the ore. A historical feature is that mercury vapors are condensed in air-cooled terracotta pipes.

The *multiple-hearth furnace* is advantageous for working up rich concentrates, mercury waste of a similar type, or *stupp*. This kind of furnace has been used for many decades in various mercury mines in North America, and in Almadén most of the ore extracted since 1961 has been processed in multiple-hearth furnaces. The hearths and outer walls of the furnaces are built of shaped fire-

clay bricks. The furnaces are lined with sheet steel. Cast steels with additions of titanium, chromium, and nickel have proved suitable for internal structural elements (stirrer shaft, raking arm). A modern furnace is up to 10 m high, has a diameter of ca. 5 m, and contains up to 16 hearths that are heated with wood, gas, or oil (mainly the upper and lower hearths). An attempt is made to keep the flow velocities for the reaction gas low (maximally 3 m/s) by skillful feeding of the material (if possible by special sliding surfaces at the throats in the case of small hearth interspacings) and by separately installed gas passageways. The amount of flue dust is thereby lowered (0.2–3% of the feedstock), and the formation of *stupp* is minimized. Addition of combustion air through the insulated hollow shaft and raking arm and, if necessary, preheating of the fuel oil both reduce fuel consumption. By accurate metering of the inlet air, a lower amount of gas can be passed through the furnace, and the capacity of the subsequent condensation unit can be reduced. Table 17.4 shows some operational examples of multiple-hearth furnaces.

With regard to environmental protection, multiple-hearth furnaces are relatively difficult to make gastight and, in some cases, have had to be shut down.

Rotary kilns have been used since 1913 to extract mercury. Rotary kilns and rotary drum furnaces provide a high mercury yield with a good throughput rate of the ore because the reaction temperature can be controlled accurately; the ore does not have to be specially preheated; and material throughput can be regulated.

Table 17.4: Operational data for multiple-hearth furnaces for mercury extraction.

	New Almadén	Pershing	Quicksilver Mines
Furnace diameter, m	4.9	4.9	5.5
Number of hearths	6	8	6
Worked material	ore	ore	ore
Throughput, t/d	38	77	50
Fuel consumption per tonne of material	47 L oil	21 L oil	0.15 m ³ wood

The ore is ground to about 65-mm particle size before it is charged. Lime, charcoal, or low-temperature coke may be added as fluxes, and the furnaces are heated directly by oil or gas. The furnaces are operated at 320–400 °C at the charging head and 700–800 °C at the discharge end. For normal furnace sizes and ores, heat consumption is $(1 \text{ to } 1.25) \times 10^6$ kJ per tonne of throughput. Without the addition of coal as flux, this corresponds to up to 30 L of oil or 250 m³ (STP) of fuel gas per tonne of ore throughput. A disadvantage of rotary kilns is the dust formed by the intense material movement, which leads to increased *stupp* formation in subsequent condensation and can cause stoppage in the waste-gas line. Flue dust amounting to 0.75–6% of the ore feedstock by weight is observed. In many cases, dust formation can be reduced by fluxes having a sintering effect. Some operating examples of older rotary kilns are listed in Table 17.5.

Indirectly Heated Furnaces. The basic advantage of indirect heating is the lower gas velocity in the reactor and the higher mercury concentration of the process gas. The furnaces are heated by gas, coal, or by electricity and consist in some cases of clay muffles, vessels lined with fireclay or ceramics, or iron vessels lined with silicon carbide.

F. Krupp-Grusonwerk AG has arranged several tubular individual muffles in a rotary kiln around a thermally insulated, centrally

aligned shaft. A rotary kiln constructed from two concentric tubes was developed several years later. The ore passes continuously through the inner tube; the outer tube is heated. A highly thermally conducting, gastight silicon carbide is used as cladding. Several proposals for processing mercury-containing material in indirectly heated furnaces have been made, and patents have been issued [13–15].

The subsequent condensation of mercury from the furnace off-gas is treated later.

17.4.2 Extraction from Secondary Sources

Because of the relatively high toxicity of metallic mercury and some of its compounds, spent products must be reprocessed to a large extent. Storage of slurry-like residues is complicated and expensive, and is governed by the limited storage capacity of the closed mines. Active carbon slurries from the effluent concentration resulting from chlor-alkali electrolysis constitute the major proportion of mercury residues that must be reprocessed.

In addition to these residues, the processing of fluorescent bulbs, which contain about 15–50 mg of metallic mercury per lamp, is becoming increasingly important. Several plants dealing specifically with the disposal of these lamps already exist in Germany [16].

Table 17.5: Operational data for rotary kilns for mercury extraction.

	Gelnica	Abbadia San Salvatore	New Indria	Nevada, Quick-silver Mines	Pershing, Quick-silver Mines	Mercury Mining Company
Furnace length, m	14	16	17	12.2	18.3	21
Internal diameter, m	1.5	1.25	1.22	0.92	1.22	1.22
Thickness for lining, mm	250	200	150			
Gradient, %	4	5	4			
Time for one revolution, s	72		42	45	50	
Moisture content of ore, %	5–10					
Hg content of ore, %	0.2	0.6–0.8				
Grain size of ore, mm	50	5		64	40	50
Ore throughput, t/d	40	100	125	40	45	45
Fuel consumption per tonne of ore	100 m ³ (STP) gas + 0.3 m ³ wood	100 kg wood	19 L oil	26.5 L oil	30 L oil	29 L oil

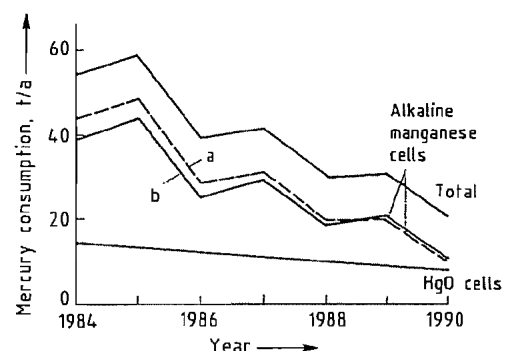


Figure 17.1: Reduction of mercury in primary batteries in Germany [17]: a) Mercury in sold primary batteries; b) Mercury in domestic refuse.

The mercury content of normal zinc-manganese dioxide batteries has been reduced considerably over the last few years (addition of mercury inhibits the formation of gas by zinc). In Germany, the mercury content of batteries will be reduced to 0.15% by 1990 (Figure 17.1), starting from a level of 1% [17].

In addition to zinc-manganese dioxide batteries, zinc-mercury(II) oxide batteries are also widely used as round cells. These contain ca. 30% mercury, which must be recovered. Mercury in concentrations of ca. 1% is also found in zinc-silver(II) oxide and zinc-oxygen batteries. A particular problem in reprocessing batteries is grading and sorting the various types, which are inadequately identified and, in some cases, have the same external dimensions for different electrochemical systems. Treatment processes have been developed in Japan [18], Germany [19, 20], and other countries [21], which can remove mercury by treatment in rotary kilns or in a distillation chamber. The individual types of batteries do not have to be sorted beforehand, and a mixture of batteries can be processed.

Because batteries also include a large number of plastics (e.g., as sealants), waste gases must be treated and burned if necessary.

Because a proportion of spent batteries end up in domestic refuse, high mercury concentrations can be found in waste gas from domestic refuse combustion. Mercury-containing older printing inks are another source. Because mercury can be precipitated

from waste gas most efficiently by adsorption on activated carbon or similar substances, mercury-containing charcoal from waste gas purification will also require reprocessing in the future.

The mercury-selenium residue formed in the primary smelting of mercury-containing sulfidic ores requires special reprocessing. This substance, which occurs as a slurry, has been reprocessed in a multiple-hearth furnace in which the mercury fraction is evaporated [22]. Another company converts the residue to metallic mercury in a rotary kiln by adding lime fluxes, with a relatively inert residue remaining behind [23]. A hydrometallurgical reprocessing treatment has been investigated on a pilot scale in a research project [24]. Mercury is extracted in the form of mercury(II) oxide and sulfide, and can be added to the conventional extraction processes. The method does not appear to be economically practical at present because of the relatively expensive reactants involved.

Additional secondary sources, such as thermometer breakage, electric switches, and amalgams, can generally be worked up by conventional distillation methods [25, 26]. A comprehensive monograph on the topic of evaporation and thermal dissociation of mercury sulfide is available [27]. Electrolysis has been proposed for the removal of mercury from gold-containing solutions: 90–95% mercury and < 10% gold are deposited at 1.0–1.5 V [28].

17.4.3 Condensation of Mercury from Furnace Off-Gas

The vapor pressure p (mbar of mercury) can be calculated according to a relationship given by BARIN and KNACKE [29]:

$$\log p = -\frac{3305}{T} - 0.795 \log T + 10.47893$$

where T is measured in kelvin.

The degree of saturation s (kg of mercury per cubic meter) of the gas at t (°C) or T (K) and $p = 101.3$ kPa can be determined from the

pressure and density of mercury vapor (3.9091 kg/m³ at 357 °C) ($\alpha = 1/273$):

$$s = 3.9091 \frac{1 + 357\alpha}{1 + \alpha t} \frac{p}{101.3} = 3.9091 \frac{630}{T} \frac{p}{101.3}$$

The degree of saturation s of mercury vapor calculated according to this formula for different temperatures is summarized in Table 17.6. Figure 17.2 shows p and s plotted as a function of $1/T$ on a semilogarithmic scale.

Mercury losses during condensation can be calculated as follows: 1 m³ of saturated vapor at 140 °C (413 K) enters the condensation unit laden with 14.464 g of mercury. There it is cooled to 20 °C (293 K) ($s = 0.0141$ g/m³), and a volume contraction to $293/413 = 0.71$ m³ occurs. The saturated vapor leaving the unit therefore contains $0.71 \times 0.0141 = 0.01$ g of mercury. The loss of uncondensed mercury removed with the waste gas is thus 0.07% of the initial amount. With a condensation end temperature of 40 °C and otherwise identical conditions, the loss increases to 0.35% Hg.

Table 17.6: Saturation content of mercury vapor at various temperatures.

p , kPa	T , K	Saturation content, s	
		g/m ³	g/m ³ (STP)
7.03×10^{-5}	283	0.00604	0.00626
1.71×10^{-4}	293	0.01406	0.01508
3.919×10^{-4}	303	0.03144	0.03489
8.514×10^{-4}	313	0.06612	0.07588
1.761×10^{-3}	323	0.1325	0.1568
3.486×10^{-3}	333	0.2545	0.3104
6.625×10^{-3}	343	0.4695	0.5893
0.012138	353	0.8359	1.081
0.02150	363	1.440	1.915
0.03690	373	2.404	3.284
0.06154	383	3.906	5.478
0.100	393	6.187	8.906
0.1585	403	9.558	14.110
0.2457	413	14.464	21.385
0.3727	423	21.417	33.175
2.2894	473	117.65	203.65
3.8743	523	458.97	879.25
32.808	573	1391.5	2921.0
101.3	630	3909.1	9021.1

In practical operation the mercury content in the hot reaction waste gases is always far below the saturation limit because the theoretical vapor-liquid equilibrium is not reached. Directly heated mechanical roasting furnaces

require a heat input of ca. 1.2×10^6 kJ per tonne of ore. The following amounts of waste gas [in m³ (STP)] are produced per 1000 kJ for the different fuels with 20% excess of air:

Wood	0.387
Generator gas	0.42
Oil	0.32

Per tonne of ore, this corresponds to about 470 m³ (STP) with wood or generator gas firing and 375 m³ (STP) with oil firing. With 5% water content in the ore, 70 m³ (STP) of steam is produced in addition. If an ore containing 0.3% Hg is worked up, the mercury content with wood or gas firing is 5.56 g/m³ (STP), and with oil firing 6.75 g/m³ (STP), at 140 °C.

With a condensation end temperature of 20 °C at which the gas still contains 0.0141 g of mercury per cubic meter corresponding to the saturation limit a loss of 0.21–0.25% mercury occurs, and at a condensation end temperature of 40 °C, a loss of 1.1–1.3% mercury from the waste gas occurs.

In general, the mercury residual content in waste gas, compared to the amount at 20 °C, increases with a temperature increase of 10 °C by a factor of 2.2
20 °C by a factor of 4.7

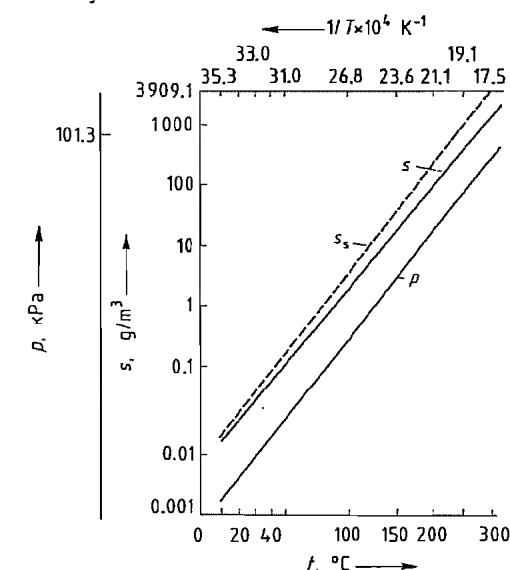


Figure 17.2: Vapor pressure p and saturation content s (g/m³) as a function of temperature; s_s saturation content under standard conditions [g/m³ (STP)].

30 °C by a factor of 9.4
 40 °C by a factor of 18.1
 50 °C by a factor of 33.4

Thus efficient cooling of the waste gas is necessary. In a plant that processes an ore with 5% moisture content, as much as 50% of the cooler capacity is used for condensation of evaporated moisture alone, without the steam originating from fuel combustion being taken into account.

Several practical requirements must be met for satisfactory operation: (1) The ore should be as dry as possible. (2) The amount of waste gas produced by the fuel should be low. (3) When the gas enters the condenser, its temperature should be only 10–20 °C above the mercury dew point. (4) The outlet temperature should be as low as possible. (5) Before entering the stack, the reaction gas should pass through an afterpurification section, if possible. Stupp formation can be kept low by (1) indirect heating, (2) separate processing of fine-grain classes of ore, (3) predrying of ore that is too wet, or (4) wetting of ore that is too dry. The flue dust should be separated as completely as possible from the still hot reaction gas before it enters the mercury condensation unit.

A conveniently arranged condensation system for a *directly heated* mercury smelting plant operating with mechanical roasting furnaces consists of the following parts:

- Dust separator in the form of a cyclone, an electrostatic precipitator, or a combination of both
- Fan (e.g., of Monel Metal)
- Cooling unit for mercury condensation
- Afterpurification chamber for separating mercury residues
- Injection chamber for separating traces of mercury
- Fan (e.g., of Monel Metal)

The cooling unit is itself in many cases also constructed of monel metal, and consists of tubular condensers (CERMAK type) formed from six to ten trains arranged in parallel, each with eight inverted U-tubes of elliptical cross section whose arms terminate in acutely taper-

ing, water-filled deflection boxes. The tubes are sprinkled with water. The mutually corresponding tubes of all the individual trains in each case end in a common box, and in this way the stupp can be classified. Gate valves in each train enable the draft to be regulated or even permit the train to be separately disengaged.

The ratio of tube cross section to fan output must be matched so that the gas flow velocity is maximally 0.75 m/s in narrow parts of the tubular condenser. The overall unit must be designed so that half of the tube trains can be decommissioned for cleaning and repair, whereas the remaining tube trains ensure satisfactory cooling of the reaction gas while maintaining draft conditions in the furnace.

Gases from *indirectly heated furnaces* that contain only a small amount of flue dust can be condensed by spraying water directly into the mercury-containing waste-gas stream. To ensure sufficient mercury condensation, the gas must pass through a succession of water curtains. Fewer parallel tubes of larger diameter are used in the cooling unit for directly heated furnaces. The last stage operates with fresh water; for the other cooling stages, water is circulated and recycled through suitably dimensioned settling tanks.

All setting tanks within the condensation unit have sloping floors and connecting pipes through which mercury metal flows to the lowest part of the system. The tanks stand on feet on a smooth cement floor, which slopes so that any leakage can be detected and escaping mercury collected. The material for these tanks is wood or cast iron; stupp-collecting tanks are also constructed of concrete. When the plant is operating continuously, all places prone to thick deposits must be mechanically cleaned once a week; the remaining areas can be cleaned at longer intervals.

17.4.4 Treatment of the Stupp

The amount of mercury contained in the stupp may represent a substantial proportion of production. In Idrija, when processing high-bituminous ore, for example, 78–91% of the

mercury is extracted from the stupp and only 9–22% is extracted directly. To extract mercury from the stupp, individual mercury droplets must be coagulated, which can generally be achieved by kneading and pressing the mass. Stirring the stupp with sievelike perforated rakes in iron vessels also gives good results. Addition of quicklime to the stupp neutralizes any acids contained in the condensate, saponifies any fats present, absorbs a large proportion of the water, and chemically reduces mercury sulfate.

Mercury and dust can also be mechanically separated by simple wash treatment with water. A tenfold mercury enrichment from the stupp by *flotation* was described in 1929 [30]. This very effective method of separating mercury enables the waste material to be dumped directly onto the waste tip in certain cases. Generally, however, extraction of mercury from the stupp is not so effective, with the result that the low-mercury fraction must be returned to the smelting process. For regularly occurring large amounts of stupp, a special furnace unit is worthwhile (retorts or multiple-hearth furnace).

17.5 Environmental Protection

17.5.1 Natural Distribution of Mercury

Because of its high vapor pressure, metallic mercury disperses relatively quickly into the atmosphere and, with suitable air movement, is taken up by plants and animals. The average concentration in the earth's crust is 0.08 ppm and in seawater 3×10^{-5} ppm. Mercury is thus one of earth's relatively rare elements. The natural mercury content of the atmosphere is 0.005–0.06 ng/m³ [31]; in plants, 0.001–0.3 µg/g (generally < 0.01 µg/g); and in meat, 0.001–0.05 µg/g [32]. A comprehensive list of mercury in the environment appears in [33].

A quantitative summary of the occurrence, distribution, and utilization of mercury is given in the following material [34]:

Mercury content of the oceans	70 000 000 t
Mercury content of the earth's crust (1-m-thick layer)	100 000 000 t
Natural atmospheric mercury emission (volcanoes, wind erosion, degassing)	25–100 000 t/a
Natural mercury emission in water (weathering in rivers)	5000 t/a
Use of fossil fuels (minerals, deposits)	8–10 000 t/a
Use of mercury and its compounds	6000 t/a

Natural air emissions from mechanical activity, wind erosion, and degassing constitute the largest proportion of emitted mercury. By contrast, the utilization of mercury is relatively small, although this should not minimize or obscure the danger of mercury at high concentration.

17.5.1.1 Mercury in Soil, Plants, and Animals

Relatively large amounts of mercury are circulated due to the constant exchange of mercury among water, soil, and the atmosphere. Some of this migrating mercury is retained in the soil in the form of humus compounds and, in certain cases, is also concentrated [35]. The mercury content of various soils in Austria unless otherwise stated (mg per kilogram of soil) is as follows [36, 37]:

Meadowland in Niederösterreich	0.039
Arable land in Niederösterreich	0.180
Vineyards in the Burgenland	0.080
Reed belt on the Neusiedlersee	0.340
Arable land (3% humus) in Kremsmünster	0.065
Meadowland (4.8% humus) in Kremsmünster	0.070
Woodland (10.2% humus) in Kremsmünster	0.170
Garden soil in England	0.25–15.0
Rice field slurry in Japan	0.40–1.8
Fields for agricultural use in Niedersachsen, Germany	0.055–0.104
Woodland in Niedersachsen, Germany	0.249–1.672
Mean mercury value for Europe (10-cm-thick humus layer)	120 g/ha
Organically bound mercury is also added to the soil with seeds as a seed treatment agent (fungicide). Amounts of mercury used for seed treatment or soil disinfection are as follows:	
Grain (wheat) added as seed treatment agent to the soil per 150 kg of seed material/ha	ca. 7 g/ha
Sugar beet (seed material in pill form) added as seed treatment agent to the soil per 200 000 pills/ha	ca. 1 g/ha
Cotton (seed treatment and disinfection)	ca. 20 g/ha

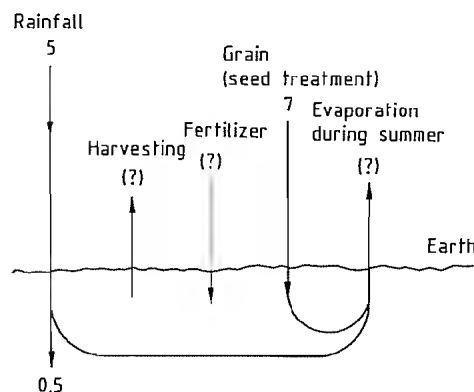


Figure 17.3: Microcirculation of mercury (in gha-1a-1) in the soil [36].

However, neither soils that have received mercury-treated seeds for many years, nor plants grown on such soils, exhibit a high mercury content [35]. As pot tests have shown, the mercury is partly retained in the humus and partly evaporates from the soil [38, 39]. The amount of residue passing into groundwater is insignificant [40] (Figure 17.3).

According to investigations carried out in Norway, the mercury content of soil varies between 0.022 and 0.55 ppm (mean value 0.19), without any "recognizable" effect due to human activity [41]. The mercury content in soil is higher in geothermal or ore-containing regions and can be as high as several parts per million. Thus, mercury is often used as a tracer metal in geological exploration [42].

Mercury content has been investigated in soil and lichen in the mercury mining region around Monte Amiata (Italy). The mercury content in the soil and in the lichen decreases sharply with increasing distance from the mine. Mine waste gases and worked ore are the main sources of emission [43].

Mercury in Fungi and Mushrooms. The fleshy parts of fungi and mushrooms can contain unexpectedly high concentrations of mercury [44, 45]. Because of the affinity of mercury for the sulfur-containing constituents of fungi, the latter can absorb and concentrate mercury from the local soil. Mercury-rich fungi and mushrooms are found everywhere,

regardless of whether the soil has been anthropogenically contaminated [46]. With more serious contamination, especially atmospheric, the mercury content of fungi and mushrooms increases considerably [47].

Mercury in Fish and Seals. The mercury content in fish varies depending on type and habitat [48]. The assumption that fish concentrate mercury to 2000 times its concentration in the ambient medium is neither valid nor statistically relevant and has no significance as a rule of thumb [48]. Mercury uptake in warm, tropical waters is higher than in cold northern waters [49]. Because of the concentration of mercury in sediment, dabbling fish, which collect their food from the bottom of the water, absorb more mercury than nondabbling fish. Predatory fish (e.g., pike) contain higher than normal levels of mercury only if they preferentially feed on dabbling fish.

The controversy surrounding canned tuna in the United States has revealed that tuna preparations in the Smithsonian Institute from ca. 1880 have the same mercury concentration as present-day fish. Under the assumption that the values found in museum preparations constitute a lower limit—some of the mercury might well have evaporated over the course of time—the fact that present-day values are the same as previous values means that no concentration has occurred.

Data from the Danube upstream of large cities and industrial regions, where trout have been found with a mercury content of > 1 mg of mercury per kilogram of fish, point to factors other than industrialization. The high mercury concentration in the liver of seals in the northern section of the east coast of North America (Labrador), where no large cities or industrial regions are to be found, is attributed to underwater volcanic emissions.

17.5.1.2 Mercury in Food

Many investigations were carried out on foods from the 1920s and 1930s onward [50]. In Germany, the Zentrale Erfassungs- und Bewertungsstelle für Umweltchemikalien (central office for collecting and evaluating data on

environmental chemicals; ZEBS) of the Federal Ministry of Health in Berlin in particular, has collected data from 1975, 1979, and 1982. According to these data, if average consumption patterns are assumed, mercury uptake in 1979 was about 0.052 mg per week for the "average" inhabitant of Germany (i.e., only about one-sixth of the upper limit recommended by WHO). The major proportion of mercury is absorbed from animal foods [51]. The legal limits are given in Table 17.7.

The most recent ZEBS investigations [52], covering 1978–1982, are presented in Tables 17.8 and 17.9. The 1982 values essentially confirm the analytical data of 1979. The values for milk, condensed milk, cheese, and eggs; veal, beef, pork, calves liver, calves kidneys, poultry, sausages, and meat products; vegetable oils and fats; rice, rye, and potatoes;

leafy, sprouting, fruit, or root vegetables and canned vegetables; pomaceous, stone, berry, citrus, shell, or canned fruit; fruit and vegetable juices; and beverages such as wine, beer, and chocolate are all < 0.020 mg of mercury per kilogram of fresh substance and, in most cases, < 0.010 mg/kg.

The average amounts of mercury actually absorbed per week are compared in Table 17.9 with the limiting values specified by WHO. Foods contain the major proportion as follows: drinking water (14.8%), wheat (12.9%), milk (10.2%), mineral water (8.1%), canned fish (8.0%), coffee (7.2%), potatoes (6.0%), and fish (5.6%). Another detailed investigation carried out by ZEBS is concerned with the mercury, magnesium, and zinc content of breast milk, blood serum, and the fatty tissue of nursing mothers [53].

Table 17.7: Legal limiting values for total uptake of mercury (1980).

	Fish, mg/kg	Total uptake, mg/week
Switzerland	0.5	
Japan	0.4 (Hg) 0.3 (Hg methyl)	0.17 mg of Hg per 50 kg of body weight
United States	1.0	0.005 mg/kg of body weight (Hg) 0.0033 mg/kg of body weight (Hg methyl)
Sweden	no limit (lakes that contain fish with more than 1 ppm Hg are placed on a blacklist); fish with a high Hg content may be legally rejected.	
Germany	1.0	
WHO recommendation		0.3 (max.)

Table 17.8: Mercury in food.

Food	Content, kg/kg of fresh substance	
	1982	1979
Cow's liver	0.021	0.015
Pig's liver	0.047	0.058
Cow's kidneys	0.077	0.066
Pig's kidneys	0.246	0.260
Freshwater fish	0.271	0.257
Saltwater fish, except Hg-susceptible fish	0.196	0.127
Hg-susceptible fish ^a	1.070	0.859
Fish products	0.208	
Canned fish	0.206	0.188
Wheat	0.026	0.003
Coffee	0.041	

^a Hg-susceptible fish include: mackerel shark, dogfish, blue ling, halibut, black halibut, turbot, and Greenland shark.

Table 17.9: Uptake amounts of mercury in absolute figures and as a proportion of WHO values.

	Hg
WHO value	
mg/week (70 kg)	0.35
mg/week (58 kg)	(0.290)
Men (70 kg)	
mg/week ^a	0.1229
Proportion of WHO figure, %	35.11
Women (58 kg)	
mg/week ^a	0.0933
Proportion of WGO figure, %	32.17

^a The median values of toxic substance levels were taken into account.

17.5.2 Mercury Emissions

17.5.2.1 Gas Purification

In a large number of combustion processes, mercury is transferred to the gaseous phase and must be removed again by subsequent treatment. The largest amounts of secondary mercury occur in the smelting of sulfidic ores. Mercury which is present as mercury sulfide is released during roasting. At present, two methods are primarily used for waste-gas purification.

In the first method, the gas is treated with sulfuric acid (90%) at 200 °C. The mercury(I) sulfate formed is deposited in wash towers. Fine purification is performed by afterpurification with sodium sulfide [54].

In the second method, the cooled and dusted roast gas is treated with a mercury(II) chloride solution, and mercury precipitates as mercury(I) chloride (Hg_2Cl_2). Mercury is removed from the wash liquid by treatment with sodium sulfide. Part of the mercury(I) chloride produced is oxidized to mercury(II) chloride with gaseous chlorine and returned to the process. The final level of mercury in the waste gas is 0.05–0.1 mg/m³ [55, 56].

In a third method, waste gas containing mercury and sulfur dioxide is treated with a wash solution containing Cu^{2+} and Hg^{2+} ions in addition to H_2SO_4 (200–300 g/L) and HCl (5 g/L). Mercury in the vapor is thereby oxidized to Hg^+ , and the Hg^0 values of the waste gas are 0.02–0.05 mg/m³ [57].

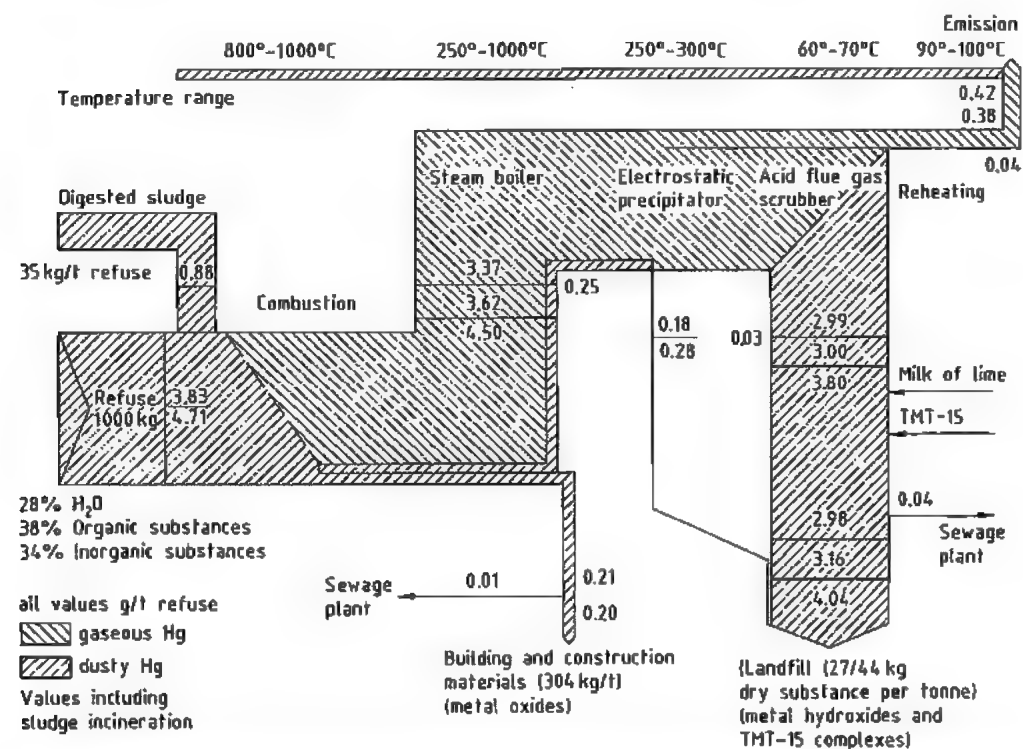


Figure 17.4: Specific mercury load distribution in the Bamberg refuse heating and power station with TMT-15 precipitation, with and without sludge combustion [63].

Another source of mercury emission is refuse combustion. Mercury occurs in the form of thermometer breakage, fluorescent tubes, switches, and batteries in domestic refuse. Investigations have shown that mercury in flue gases is present as mercury(II) chloride [58]. Below ca. 150 °C, the flue ash contained in flue gases adsorbs mercury(II) chloride and reduces it to mercury(I) chloride. Active carbon or active carbon impregnated with iodine compounds can also be used as a mercury adsorbent [59–62]. The mercury content of domestic refuse is 3–5 g/t [63]. The percentage distribution of mercury in a typical refuse combustion plant is shown schematically in Figure 17.4. Most of the mercury passes into the residue to be dumped.

17.5.2.2 Water Purification

The solubility of mercury in water depends strongly on the temperature. It decreases with decreasing temperature and can be reduced further by addition of salts (e.g., sodium chloride).

A whole range of equipment and devices can be used in purification methods to remove mercury from water. Examples are activated carbon filters, ion exchangers, and electrolysis systems. Mercury can also be removed from solution by addition of suitable reagents.

The level of 10–30 mg of mercury per liter in wastewater from chlor-alkali electrolysis can be reduced to 0.1 mg/L by using *activated carbon* and graphite powder. The carbon has a grain size of 5–100 µm [64, 65]. In principle, all types of activated carbon can be used for the fine purification of mercury-containing water. Carbon is dispersed in the water and then filtered.

For *ion exchangers*, a distinction can be made between reusable and disposable ones [65–67]. In some cases, sulfur-containing substances are used as active groups, which remove mercury from the solution in the form of a mercury sulfide compound.

Copper fluidized-bed electrolysis provides another method for mercury separation. The copper powder cathode is held in suspension

by the flowing solution, and mercury is deposited as an amalgam. The copper amalgam is purified by distillation [68].

By adding *small amounts of oil* which are dispersed in the aqueous solution, mercury can be concentrated in the oil phase. The mercury content of the purified aqueous solution is in some cases < 10 µg/L. The oil is separated by centrifugation, and line purification is carried out by using a conventional oil–water emulsion splitting unit. The initial mercury concentration should be between 0.5 and 2.0 mg/L [4]. Tin(II) chloride dissolved in dilute hydrochloric acid has been proposed for treating mercury ion-containing wash water from combustion units. The reducing agent tin(II) chloride is added in above-stoichiometric quantities. Reduced mercury is added together with the wash water to an evaporation device and is expelled by passage of stripping gas at elevated temperature. Condensation is effected by cooling the gas stream. The mercury content is thus reduced from 5 mg/L to < 0.1 mg/L, depending on the concentration of tin(II) chloride [69].

To purify flue gas wash water from *refuse combined heating and power stations*, the additive TMT-15 developed by Degussa is used in some cases on an industrial scale (Figure 17.4). The active substance of the additive consists of trimercapto-s-triazine in the form of a sodium salt. Mercury is bound as $\text{C}_6\text{N}_6\text{S}_6\text{Hg}_3$. The compound is stable up to 210 °C and is only sparingly soluble in the elution test (a test to determine the soluble components of a solid material). The mercury content is reduced from ca. 4 mg/L to < 0.05 mg/L [70, 71]. The additional costs involved in TMT-15 precipitation amount to ca. 0.25 DM per tonne of refuse.

Mercury can be removed from *concentrated sodium hydroxide solution* by the use of ultrasound when the solution is filtered. The initial mercury content of ca. 20 mg/kg of aqueous sodium hydroxide is reduced to ca. 0.4 mg/kg after filtration [72].

The fine purification of crude phosphoric acid can be performed at pH 0.5–1.5 by using a diorganodithiophosphorus compound in

conjunction with activated carbon as adsorbent. The final mercury concentration is < 0.02 µg/g of solution [73]. At present, no standard methods exist for removing mercury from sulfuric acid [74].

17.6 Quality Specifications

Fine Purification of Metallic Mercury [75]. Most of the mercury on the market is 4N material (99.99 % mercury). Higher purity is seldom required. Impurities in the form of gold (> 10 ppm) are manifested as dark particles after dissolution in nitric acid. Only a few purification methods exist.

- **Dry Oxidation.** In this method, readily oxidizable constituents such as magnesium, zinc, copper, aluminum, calcium, silicon, and sodium can be removed by passing air or oxygen through the liquid metal. The oxides formed have a lower density than mercury and float on its surface. They can be removed by filtration, scooping, or withdrawing the mercury through an opening in the bottom.
- **Wet Oxidation.** In an aqueous medium, mercury is dissolved by adding nitric, hydrochloric, or sulfuric acid with dichromate, permanganate, or peroxide, to oxidize impurities. Good dispersion of the mercury is extremely important in this method. The aqueous solution can be separated from the mercury by decanting, and traces of water can be removed with calcium oxide. A plant for the wet purification of mercury has been described [76].
- **Electrolytic Refining.** Perchloric acid containing mercury oxide serves as the electrolyte.
- **Distillation.** Mercury can be evaporated under atmospheric pressure or in vacuo. Distillation can be carried out in normal steel vessels or in a glass apparatus. Elements with a lower vapor pressure than mercury can be separated in this way. In many cases, mercury must be distilled repeatedly to achieve the desired purity, particularly if it is

to be used to produce cadmium-mercury telluride.

Additional methods, adapted to the relevant processes, are available for purifying and working up larger amounts of mercury [77, 78].

17.7 Chemical Analysis

The oldest and simplest method for determining mercury in minerals is described by Eschka; it involves a gravimetric method in which mercury is precipitated as an amalgam [79]. The ore sample is weighed in a porcelain crucible, intimately mixed with iron filings, and then covered with a layer of zinc oxide, magnesium oxide, or calcium oxide. The crucible is closed with a tightly fitting cover of gold foil having a cup-shaped depression in the middle, which is sprayed from above with cooling water. On careful heating of the sample, mercury is distilled and deposits on the underside of the cover. When a constant weight is reached at the gold foil, all the mercury has been collected. Measurements can be affected by cadmium and arsenic, which also condense on the gold foil. This method of mercury determination requires a high level of experimental skill and care on the part of the analyst, whose technique greatly affects the accuracy and reproducibility of the results. The reliably detectable minimum mercury content is between 10 and 50 ppm. Theoretically, the accuracy could be improved by increasing the amount of sample, although this would give rise to difficulties with regard to the apparatus.

A method for precipitating *monovalent* mercury as an iodate from a neutral or weakly acidic solution (nitric acid) is described in [80]. Mercury can be determined gravimetrically after the mercury(I) iodate precipitate is washed with ethanol and diethyl ether. Parallel gravimetric determination of the excess of potassium iodate precipitation agent is possible with thiosulfate after the mother liquor has been acidified with sulfuric acid and potas-

sium iodide has been added. Both methods give good results.

A quick method for determining mercury(II) is based on the fact that a complex is formed when an excess of potassium iodide is added to a neutral or weakly ammoniacal mercury solution. This complexes with copper diethylenediamine sulfate to form violet crystals of the complex double salt copper diethylenediamine mercury iodide, which is practically insoluble in ethyl alcohol or diethyl ether [81].

In a rapid classical qualitative method for detecting mercury, ca. 1 g of the substance to be tested is digested with acid; the resultant solution is oxidized with a drop of bromine (the solution must not turn yellow) and then boiled with a few milliliters of the reagent (10 g of KI and 100 g of NaOH in 100 mL of H₂O) and filtered. In the filtrate, mercury is determined by the black precipitate formed on dropwise addition of a Sn²⁺ solution [82].

Modern operational monitoring employs physical analytical methods and test tube methods suitable for quick detection. Both *X-ray fluorescence spectroscopy* and *atomic absorption spectroscopy* (AAS) have proved suitable for quantitative and qualitative mercury determination. The detection limit for these methods is so low that the maximum workplace concentration values can be monitored precisely [83].

Portable atomic absorption spectrometers, for example, are available, which indicate the atmospheric mercury concentration as an analog or digital display after a short warm-up time of the spectrometer. The result of the analysis is available immediately and simplifies the monitoring of a production plant. The measurement value can also be recorded continuously at stationary measurement sites with a recorder. The influence of interfering factors in AAS determination is discussed in [84].

Differential pulse anodic stripping voltammetry in conjunction with a gold electrode can be used to detect copper and mercury in natural water and wine [85, 86]. A mercury concentration of 0.02 µg/L can be measured.

Mercury in the air can be detected down to 0.1 ng/m³ with the *Coleman mercury analyzer* system (based on a very selective cold vapor atomic absorption), to an accuracy of 10%. One analysis takes about 3 min [83].

17.8 Storage and Transportation

A classification for the transportation of mercury, mercury oxide, mercury(I) chloride, and mercury(II) chloride is given in [87] (specification sheets 831, 863, 865, 868). DORIS presents a detailed description of the properties, handling, storage, and transportation of dangerous substances [88], as well as a list of addresses of the relevant authorities (throughout Europe) for information purposes. The provisions differ from country to country and must be ascertained from the relevant authorities.

In general, containers of stainless steel, normal-quality steel, iron, glass, ceramics, and a range of plastics are suitable for storing mercury. When storing liquids that contain extremely low levels of mercury (µg/g–ng/g range) in plastic containers, mercury losses occur with a large number of plastics. When water containing 5 ng/g of mercury was stored in polyethylene bottles, only 5 % of the mercury was present after 21 d. Approximately 77 % of the mercury had been adsorbed on the side walls, and 18 % had evaporated. The Hg²⁺ ions are assumed to be reduced to Hg⁺ ions, which in turn disproportionate to Hg⁰ and Hg²⁺ [89]. Addition of Au³⁺ ions in trace amounts is sometimes recommended [90]. Further investigations on the storage of mercury in dilute solution are discussed in [91–95].

17.9 Uses

Because of its special properties, mercury has had a number of uses for a long time. The conventional application is the thermometer. Mercury is frequently used in pressure gauges and for thermal content measurements.

Table 17.10: Uses of mercury and its compounds [96].

Area of use	Form	Approximate amount, t/a	Emissions	Other sectors, waste elimination	Remarks
Chemicals, reagents	compound	40	laboratories		largely impossible to find suitable replacement; environmental damage can be reduced by other measures
Alkali-manganese batteries	chloride/metal	37		refuse combustion	reduced emission by separate collection possible
Mercury oxide batteries	oxide	20		refuse combustion	alternatives still too expensive; separate collection declining
Pesticides		27	distribution		now only for seed treatment; substitutes are available
Medicinal sector		26		refuse combustion	separate collection possible
Dental amalgams	metal compound				
Disinfection					
Fungicides for paints	compound	10	weathering	exploitation; removal of old paint coats	declining; in some cases restrictions on use
Catalysts	compound	8		chemical industry	declining
Thermometers, barometers, manometers	metal	8	instrument and apparatus breakage	refuse combustion	replacement by other methods and processes possible (e.g., electronics)
Electrical engineering components	metal	6		refuse combustion	declining; substitution possible largely through electronic components
interval switches				exploitation of scrap	
Fluorescent tubes	metal	3	lamp breakage	refuse combustion	demand for fluorescent tubes increasing, despite reduction in mercury use per tube; total use increasing
Pigments	sulfide	1		refuse combustion	declining

In mechanical engineering, mercury is used in mercury vapor diffusion pumps for producing a high vacuum.

One important area of use is the lighting industry, where mercury is added to various types of bulbs. Among electrical components, mercury switches, rectifiers, oscillators, and primary batteries can be mentioned, which contain up to 30 % mercury.

Mercury is used as a liquid cathode in the production of chlorine and sodium hydroxide by chlor-alkali electrolysis. Because mercury forms alloys with a large number of metals, mercury alloys have a wide range of applications. Table 17.10 summarizes the areas of use of mercury and its compounds.

17.10 Mercury Alloys

The alloys of mercury (amalgams) occupy a special position among metal alloys because they can be solid, plastic, or liquid at room temperature.

Liquid amalgams are true solutions of the alloying elements in mercury, whereas plastic amalgams are suspensions of solid particles of the alloying partners in mercury or a saturated mercury solution. Solid amalgams are intermediary phases, often mixed with alloying partners or their primary mixed crystals. Solid amalgams may contain liquid-phase inclusions. An amalgam is sometimes difficult to identify experimentally. JANGG has suggested a suitable apparatus for synthesizing and analyzing amalgams [97].

The solubility of many metals in mercury depends strongly on temperature (Figure 17.5). The solubility of some metals in mercury at room temperature is given in Table 17.11. Amalgam formation may be exothermic (e.g., sodium) or endothermic (e.g., gold).

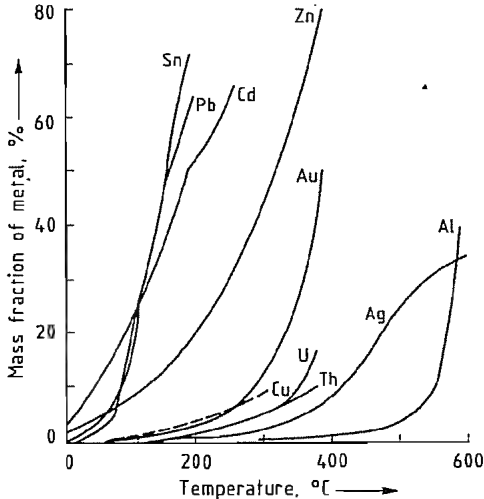


Figure 17.5: Solubility of some metals in mercury as a function of temperature [99].

Table 17.11: Solubility of some metals in mercury at 20 °C [97].

Metal	Solubility, %	Metal	Solubility, %
Tl	42.5	Mg	ca. 0.3
Cd	5.0	Au	0.131
Zn	1.99	Ag	0.035
Pb	147	Cu	ca. 0.002
Sn	ca. 0.9	Al	0.002
Na	0.62	Fe	ca. 10 ⁻⁵
K	ca. 0.4	Si	virtually insoluble

Ammonium amalgam, which has been known for a long time, is an interesting case of the NH₄ group acting as a metal-like alloying constituent. The synthesis of tetramethylammonium amalgam is described in [98].

Technically important amalgams are those of tin-copper precious metals used in conservative dental treatment.

Gold, silver, or tin amalgams are still used for much gold- and silver-plating work, as well as for production of certain types of mirrors. The measurement range of mercury thermometers can be extended to -58 °C by addition of thallium to mercury.

Alkali amalgam is an important intermediate in chlor alkali electrolysis by the amalgam method. Amalgams also play a role in the extraction of cadmium or aluminum [99].

A comprehensive list of thermodynamic data on amalgam formation has been collected by GUMINSKI [100]. After surveying the literature, he is of the opinion that liquid mercury greatly influences intermetallic compound formation. The reactions are comparable to the solid-state formation of ionic and nonionic substances in liquids.

Production of Amalgams. Three methods are used for the industrial production of amalgams:

- **Powder Metallurgy Method.** The powdered alloying components are mixed with mercury. The reaction rate of spontaneously occurring amalgam formation is determined by the degree of dispersion of the powder, the rate at which reactants diffuse into one another, and the wettability of the powder by liquid mercury. If other components besides mercury are added simultaneously, they are preferably pulverized as master alloy in the desired weight ratio. In many cases, the powder reacts with mercury more quickly in the presence of a salt of the element to be amalgamated.
- **Galvanic Method.** Many metals can be deposited from their aqueous solutions or from salt melts on mercury cathodes, with simultaneous formation of an amalgam. Because of the high overvoltage of hydrogen on mercury or amalgam cathodes, even nonprecious metals (Zn, Fe, Mn) can be deposited from acid solutions. Nonaqueous solutions may also be used (with Mg, Ti).
- **Reaction with Sodium Amalgam.** Metal exchange can occur in a fast and stoichiometric reaction through the phase boundary by reaction of sodium amalgam with the salt solution of a precious metal (or, generally, by reacting a nonprecious amalgam with a noble-metal salt solution).

17.11 Compounds

Mercury occupies a special position in group 12 of the periodic table. In contrast to the two other members of this group (zinc and cadmium), it forms compounds in two valence states.

Compounds of *monovalent* mercury contain ions in the unusual form Hg^{2+} . These compounds are not very stable and disproportionate easily to form elemental mercury and the corresponding divalent mercury derivative. Most of the monovalent compounds are sparingly soluble in water. The more soluble salts, e.g., the nitrate, are partially hydrolyzed in aqueous solution: after acidification of these solutions, the poorly soluble compounds can be obtained by precipitation. In addition, compounds of monovalent mercury can be prepared from those of the divalent element by reduction with metallic mercury.

The compounds of *divalent* mercury can be divided into those that are strongly dissociated and those that are weakly dissociated. The former, such as the sulfate and the nitrate, undergo considerable hydrolytic cleavage in water. The weakly dissociated compounds, e.g., the chloride and the cyanide, are less prone to hydrolysis by water. With excess anions they form complexes that are more soluble than the salts themselves.

The starting material for all of these compounds is elemental mercury: the metal is treated initially with a suitable oxidizing agent, e.g., chlorine or nitric acid. The other compounds can be obtained from the resulting oxidation product by further reaction. Multi-step processes are often necessary.

17.11.1 Mercury Chalconides

Chalconides of monovalent mercury are unknown: precipitation from a solution of mercury(I) nitrate with sodium hydroxide does not lead to the expected mercury(I) oxide, but rather to a mixture of finely divided elemental mercury and mercury(II) oxide. The chalconides of divalent mercury exist in na-

ture as minerals: the oxide HgO as montroydite, the sulfide HgS as cinnabar and metacinnabar, the selenide HgSe as tiemannite, and the telluride HgTe as coloradoite. They can also be produced synthetically. Only the oxide and the sulfide are of practical importance.

Mercury(II) oxide, HgO , ρ 11.1 g/cm³, is a red or yellow powder. The color depends on the size of the crystals: the yellow oxide consists of crystals < 2 μm ; the red one of crystals > 8 μm in diameter. Samples with particle sizes between these two values appear yellow-to red-orange. Increasing the temperature leads to an intensification of the color: the yellow oxide becomes yellow-orange; the red one, dark red. The crystal lattice is rhombic and identical for both forms. Under certain preparative conditions a hexagonal form exists. This modification has no practical importance and can be converted to the more stable rhombic form by heating above 200 °C.

Heating above 450 °C causes the oxide to decompose into elemental mercury and oxygen. Mercury(II) oxide is sparingly soluble in water and in ethanol. With dilute mineral acids, solutions of the corresponding salts are formed, a method that can be used to prepare these salts.

Production. Mercury(II) oxide can be prepared via the *anhydrous route* by reaction of the elements at 350–420 °C under oxygen pressure or by thermal decomposition of mercury nitrates at ca. 320 °C. Production via the *wet route* by precipitation is more important: the oxide is precipitated from solutions of mercury(II) salts by addition of caustic alkali [usually mercury(II) chloride solutions with sodium hydroxide]. Whether the yellow or the red form is obtained depends on reaction conditions: slow crystal growth during heating of mercury with oxygen or during thermal decomposition of mercury(I) nitrate leads to relatively large crystals (i.e., the red form). Rapid precipitation from solution gives finer particles (i.e., the yellow form). Nevertheless, depending on the conditions during precipitation such as stirring speed, pH, temperature, and

method of mixing the components, large crystals can be obtained by the wet route and, therefore, the red form is produced [101].

Uses. Red mercury(II) oxide in particular has become increasingly important for the production of galvanic cells with mercury oxide anodes in combination with zinc or cadmium cathodes. These cells are distinguished from other systems in that their voltage remains very constant during discharge; they are used mainly as small button-shaped batteries, e.g., for hearing devices, digital watches, exposure meters, pocket calculators, and security installations. Additional uses of mercury(II) oxide include the following: for the production of mercury(II) salts by treatment with the corresponding acids, and as a reagent in analytical chemistry. Its importance as an additive to antifouling paint for ships and in medicine (e.g., for eye ointment) has decreased.

Mercury(II) sulfide, HgS , is the most important starting material for mercury extraction; it can exist in two forms: α - HgS (*cinnabar*, cinnabarite) has a density of 8.1 g/cm³, and β - HgS (*metacinnabar*) has a density of 7.7 g/cm³. The β -form slowly changes to α - HgS on heating. The latter sublimes at 583 °C. Of the two sulfide minerals, cinnabar is the most important ore for the production of mercury (see Section 17.4.1.2). When pure, the compound is bright red and forms hexagonal crystals. *Metacinnabar* is black and forms cubic crystals (zinc blende lattice). Both have extremely low water solubility; they are also insoluble in mineral acids and in caustic alkali. They dissolve only in aqua regia, to release sulfur, and in alkali sulfide solutions, to form thio complex-salt ions, such as $[\text{HgS}_2]^{2-}$.

Production by either the dry or the wet route is possible. In the former, a mixture of mercury and sulfur is heated. The elements react slowly together even on mixing. Production from aqueous solutions is more important. The sulfide is precipitated from solutions of mercury(II) salts by treatment with hydrogen sulfide, alkali, or ammonium sulfide solutions. Initially, the black sulfide is formed.

It can be converted to the more stable red form by heating in the presence of the mother liquor or with ammonium polysulfide solutions. The reaction of mercury and sulfur by heating with a solution of sodium polysulfide has been described [102].

17.11.2 Mercury Halides

Halides of both mono- and divalent mercury are known. Of these, only the fluorides are ionic compounds: they undergo hydrolysis with water; mercury(I) fluoride simultaneously undergoes disproportionation. The other halides either are already composed of molecules in the crystal lattice or form these by dissolution or evaporation. Accordingly, their melting and boiling points are low. The halides of monovalent mercury are sparingly soluble in water: the solubility of divalent mercury halides decreases with increasing molecular mass. Mercury halides form numerous basic compounds.

Mercury(II) fluoride, HgF_2 , *mp* 645 °C, ρ 9.0 g/cm³, forms colorless octahedral crystals with a cubic ionic lattice (fluorite type). It is unstable in humid air; hydrolysis yields a yellow color. Mercury(II) fluoride is insoluble in organic solvents.

The compound is *produced* from mercury and fluorine at elevated temperature or from mercury(II) oxide and hydrogen fluoride under oxygen pressure at 450 °C [103]. Synthesis from mercury(II) oxide and sulfur tetrafluoride has been suggested [104]. The compound is used in organic synthesis as a fluorinating agent.

Mercury(I) chloride, calomel, Hg_2Cl_2 , ρ 7.15 g/cm³, is rarely found as a mineral in nature. When pure, it exists as a heavy white powder or as colorless crystals with a silvery luster, having a tetragonal molecular lattice. It sublimes at 385 °C; above 400 °C the molecules decompose into a vapor composed of mercury and mercury(II) chloride. The substance is sparingly soluble in water, ethanol, diethyl ether, and acetone. A black color occurs in ammonia solution, whereby a mixture of

finely divided elemental mercury and mercury(II) ammonium chloride is formed by disproportionation—hence, the name *calomel*, from the Greek word meaning beautiful black.

Production. An intimate mixture of mercury and mercury(II) chloride is heated at 525 °C in closed iron or fused silica tubes, attached to cooled receivers in which calomel vapor condenses [105, 106]. Synthesis from the elements is also possible [101]. Very finely divided mercury(I) chloride can be obtained by precipitation from a dilute nitric acid solution of mercury(I) nitrate and sodium chloride [105].

Mercury(I) chloride finds *application* in calomel electrodes, which serve as standard electrodes for the measurement of electrochemical potential; it is also employed as a fungicide and insecticide in agriculture, and as a catalyst in organic synthesis. Mercury(I) chloride is mixed with gold for painting on porcelain.

Mercury(II) chloride, corrosive sublimate, HgCl_2 , *mp* 280 °C, *bp* 303 °C, ρ 5.43 g/cm³, is a white, heavy, crystalline powder with a rhombic crystal lattice. At the melting point the vapor pressure is 560 kPa; the substance can, therefore, sublime under reduced pressure. The sublimate is moderately soluble in cold water. Its solubility increases sharply with increasing temperature: the saturation limit is 6.2% at 20 °C and 36.0% at 100 °C; the compound may therefore be purified by recrystallization from water. The sublimate is readily soluble in organic solvents, in contrast to mercury(I) chloride, so that a clear solution, for example, in ether, is an indication of the absence of calomel. Molecules of mercury(II) chloride exist as such in all solvents; mixing Hg^{2+} ions with Cl^- in aqueous solution leads immediately to undissociated mercury(II) chloride molecules; this process is used analytically to bind chloride ions in determining the COD of effluents. Aqueous solutions of sublimate are weakly acidic, resulting from hydrolysis of a small amount of the chloride. The sublimate is much more soluble in alkali chloride solution than in pure water, because

of the formation of chloro complex ions, e.g., $[\text{HgCl}_4]^{2-}$.

Production. For the formation of mercury(II) chloride from the elements, mercury is oxidized with chlorine in heated retorts; the reaction is carried out with the appearance of flame at > 300 °C. The escaping sublimate vapor is condensed in cooled receivers, where it settles as fine crystals. Formation of mercury(I) chloride is avoided by the use of excess chlorine [101]. Mercury and chlorine also react in the presence of water; in this case, intensive stirring is necessary. The chloride formed precipitates as crystals after the solubility limit has been exceeded. If an alkali chloride solution is used in place of water, solutions of chloro complex salts are formed, which are used mainly for the production of other compounds of divalent mercury [107].

Mercury(II) chloride can also be prepared from other mercury compounds. Mercury(II) sulfate, for example, is heated in the dry state with sodium chloride, and the evolving mercury(II) chloride vapor is condensed to a solid in receivers. A warm sublimate solution is obtained from the reaction of mercury(II) oxide and a stoichiometric amount of hydrochloric acid; the chloride separates as crystals on cooling.

Uses. Mercury(II) chloride is an important intermediate in the production of other mercury compounds, e.g., mercury(I) chloride, mercury(II) oxide, mercury(II) iodide, mercury(II) ammonium chloride, and organic mercury compounds. The compound is used as a catalyst in the synthesis of vinyl chloride, as a depolarizer in dry batteries, and as a reagent in analytical chemistry. It has minor importance as a wood preservative and retains some importance as a fungicide. Other uses (e.g., as a pesticide or in seed treatment) have declined considerably.

Mercury(II) bromide, HgBr_2 , *mp* 236 °C, *bp* 320 °C, ρ 6.05 g/cm³, forms colorless crystals with a rhombic layered lattice. Its water solubility is highly temperature dependent: the concentration limit is 0.6% at 25 °C and 18% at 100 °C. Mercury(II) bromide is readily sol-

uble in diethyl ether and ethanol. The compound is *produced* from mercury and bromine in the presence of water; by dissolution of mercury(II) oxide in hydrobromic acid; or by precipitation from a nitric acid solution of mercury(II) nitrate with addition of sodium bromide [108]. It is used as a reagent for arsenic and antimony, as an intermediate in the production of bromine-containing organomercury compounds (see Section 17.12), and as a catalyst in organic synthesis. The melt is used as a nonaqueous solvent.

Mercury(II) iodide, HgI_2 , exists in a red and a yellow form. Red mercury(II) iodide is soluble in diethyl ether, chloroform, and methanol. The compound is produced by adding an aqueous solution of potassium iodide to an aqueous solution of mercury(II) chloride with stirring; the precipitate is then filtered off, washed, and dried at 70 °C. A yellow product is formed by sublimation; on cooling, it turns red.

Yellow mercury(II) iodide, *mp* 259 °C, *bp* 354 °C, is unstable at room temperature and is converted to the red form at the slightest touch or upon heating. The transition temperature is 127 °C. Yellow mercury(II) iodide is prepared by pouring an alcoholic solution of the red form into cold water, whereby a pale yellow emulsion is formed, from which the mercury(II) iodide crystallizes after a few hours.

Potassium mercury iodide, K_2HgI_4 , readily soluble in water, is prepared by dissolving mercury(II) iodide in a concentrated potassium iodide solution.

17.11.3 Mercury Pseudohalides

The *cyanides* and *thiocyanates* of divalent mercury resemble the halides, in that they also exist in solution as undissociated molecules and form highly soluble complexes with an excess of the anion; moreover, numerous basic compounds are derived from them. Mercury(I) cyanide is unknown; the poorly soluble mercury(I) thiocyanate, which can be obtained by precipitation from mercury(I) nitrate solution, has no practical importance.

Mercury(II) thiocyanate, $\text{Hg}(\text{SCN})_2$, ρ 3.71 g/cm³, is a white powder which is thermally unstable. Decomposition begins at 110 °C and becomes spontaneous at 165 °C, with the compound swelling to many times its normal volume. In air a blue flame appears, and a dark-colored, voluminous residue is left. The thiocyanate is sparingly soluble in cold water. It is produced by precipitation from mercury(II) nitrate solution with a stoichiometric amount of potassium thiocyanate solution and is used as an analytical reagent and as an intensifier in photography.

17.11.4 Acetates, Nitrates, Sulfates

The acetates, nitrates, and sulfates of mercury are composed of ions and undergo hydrolysis with water. The acetate and the sulfate of monovalent mercury are sparingly soluble and the nitrate is quite soluble in dilute acid. Compounds of divalent mercury are readily soluble in dilute acid.

Mercury(II) acetate, $(\text{CH}_3\text{COO})_2\text{Hg}$, ρ 3.27 g/cm³, *mp* 178 °C, exists as a fine white powder or colorless shiny crystal flakes. It is soluble in diethyl ether and ethanol. It is produced by dissolution of mercury(II) oxide in dilute acetic acid and concentration of the resulting solution. Mercury(II) acetate is used for the synthesis of organomercury compounds, as a catalyst in organic polymerization reactions, and as a reagent in analytical chemistry.

Mercury(I) nitrate, $\text{Hg}_2(\text{NO}_3)_2 \cdot 2\text{H}_2\text{O}$, ρ 4.68 g/cm³, *mp* 70 °C, which forms colorless crystals (monoclinic ionic lattice), is produced by dissolving mercury in cold dilute nitric acid and crystallizing the compound from the resulting solution.

Uses. Mercury(I) nitrate is the most readily available soluble salt of monovalent mercury and is, therefore, an important intermediate for other mercury(I) derivatives; sparingly soluble compounds can easily be prepared from it by precipitation from aqueous solution. Thermal decomposition leads to red mercury(II) oxide. "Millons reagent", a solution of mercury nitrate and nitrous acid in dilute nitric

acid, is used as an analytical reagent for the indication of tyrosine-containing proteins.

Mercury(II) nitrate, $\text{Hg}(\text{NO}_3)_2$ or $\text{Hg}(\text{NO}_3)_2 \cdot \text{H}_2\text{O}$, forms colorless, hygroscopic crystals. Apart from the anhydrous salt and the monohydrate, several other hydrates and basic compounds are known. Mercury(II) nitrate is produced by dissolving mercury in hot concentrated nitric acid; the resulting solution is concentrated and the nitrate crystallized by cooling. Uses include the production of other divalent mercury derivatives, as a nitrating agent in organic synthesis, and as an analytical reagent.

Mercury(I) sulfate, Hg_2SO_4 , ρ 7.56 g/cm³, is a colorless microcrystalline powder (monoclinic crystal system) that is very sensitive to light. The compound is prepared by precipitation from a solution of mercury(I) nitrate with sulfuric acid or sodium sulfate solution, or by electrochemical oxidation of mercury in dilute sulfuric acid. It is used as a depolarizer in standard cells after Clark and Weston.

Mercury(II) sulfate, HgSO_4 , ρ 6.49 g/cm³, is a white powder (rhombic crystal type). It is prepared by fuming mercury with concentrated sulfuric acid or by dissolving mercury(II) oxide in dilute sulfuric acid and evaporating the resulting solution until the compound crystallizes. Mercury(II) sulfate is used in analytical chemistry to bind chloride ions in the determination of the COD of wastewater [109]; as a catalyst in the production of acetaldehyde from acetylene and of anthraquinonesulfonic acids; and as a depolarizer in galvanic elements.

17.11.5 Mercury-Nitrogen Compounds

Reaction of mercury(II) compounds with ammonia solution leads, depending on reaction conditions, to amine complexes or mercury(II) nitrogen compounds. Of the numerous compounds known, only mercury(II) amidochloride has any practical importance.

Mercury(II) amidochloride, HgNH_2Cl , ρ 5.38 g/cm³, is a fine, white crystalline powder with a rhombic crystal lattice. It is insoluble in water and in ethanol, and soluble in warm acid, ammonium carbonate solution, and sodium thiosulfate solution. On heating it decomposes without melting. The compound can be precipitated from mercury(II) chloride solution with an ammonia solution. Mercury(II) amidochloride is used in the treatment of severe skin disease, as an eye ointment, and as a veterinary preparation; its importance is declining because of the development of mercury-free products.

17.11.6 Analysis, Storage, and Transportation; Protective Measures

Analysis. Determination of the purity of mercury compounds, which consists of the determination of trace amounts of foreign cations and anions, involves specific reactions of these ions [110]. conventional methods for the trace analysis of cations have been supplemented or replaced by methods involving the simultaneous determination of several elements by means of plasma emission spectroscopy [111].

Storage and Transportation. Plastic-lined steel drums are normally employed for packing. Small amounts (e.g., for chemical laboratories) are usually placed in plastic or glass bottles. Many compounds are light-sensitive and must, therefore, be adequately protected from light sources. Proper consideration must be given to the chemical and toxic properties of mercury compounds and the necessary protective measures; this is particularly true in container labeling.

Protective Measures. Most mercury compounds, because of their toxicity, require the same protective measures during production and processing as metallic mercury. Furthermore, environmental protection necessitates appropriate precautions (see Section 17.5).

17.12 Selected Organic Compounds

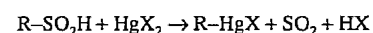
Organic mercury derivatives [112, 113] are among the oldest known organometallic compounds. Organometallic compounds of *divalent mercury* are stable toward air, oxygen, and water. In contrast, organic derivatives of monovalent mercury are unstable and can be prepared only at low temperature. After 1990, use of organic mercury derivatives in Germany will be difficult because mercury will not be allowed in industrial effluent or wastewater.

Organomercury compounds can be divided into two major groups: compounds of the type $\text{R}^1\text{-Hg-R}^2$, where R^1 and R^2 are aliphatic or aromatic groups, and compounds of the type R-Hg-X , where R is aliphatic or aromatic and X is a halogen or an acid group.

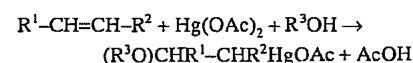
Synthesis of organic mercury compounds can be carried out by reaction of Grignard reagents with mercury halides [114, 115]. To obtain pure products, the mercury salt and the Grignard reagent must contain the same anion

$$\text{RMgX} + \text{HgX}_2 \rightarrow \text{RHgX} + \text{MgX}_2$$

Furthermore, organic mercury compounds can be produced by the reaction of sulfinic acids or their sodium salts with mercury(II) halides [116]:



Hydroxy- or alkoxymercury derivatives can be obtained via the solvomercuration reaction (Hofmann-Sand reaction) by addition of mercury(II) compounds to alkenes in aqueous, alkaline, or alcoholic solutions [114, 117]:



Organic mercury compounds can be converted to other organometallic derivatives by electrolysis or transmetallization [118].

Dialkyl- or Alkoxyalkylmercury Compounds. Dimethylmercury, $\text{CH}_3\text{-Hg-CH}_3$, a colorless, sweet-smelling liquid, is very toxic; it has a density of 3.069 g/cm³, *bp* 96 °C, and is soluble in ethanol and diethyl ether. In acidic aqueous solution, dialkylmercury compounds are hydrolyzed to monoalkylmercury deriva-

tives. Dimethylmercury is formed in organisms by enzymatic methylation of elementary mercury or a mercury compound. In an organism it is easily converted to methylmercury ($\text{CH}_3\text{-Hg}^+$) or methylmercury(II) chloride ($\text{CH}_3\text{-Hg-Cl}$). These species can react with free S-H groups of biologically important molecules, leading to the diseases that have been caused by mercury and its derivatives.

Mixed dialkylmercury compounds (e.g., methylpropylmercury compounds) are less volatile than symmetrical dialkylmercury compounds (e.g., diethylmercury). Dialkylmercury derivatives are generally very reactive and can also undergo transalkylation with simple alkyl halides (e.g., ethyl iodide).

Diarylmercury Derivatives. The best known diarylmercury derivative is diphenylmercury, $(\text{C}_6\text{H}_5)_2\text{Hg}$, which is produced by direct mercuriation.

Analysis. Organic mercury compounds may be analyzed in the following ways: they can be determined *qualitatively* (1) by digestion with concentrated sulfuric acid and 30% hydrogen peroxide or (2) by digestion with 10% sulfuric acid and subsequent addition of dithizone (diphenylthiocarbazone) in carbon tetrachloride solution. In the presence of mercury the green solution turns orange. Organic mercury compounds can be determined *quantitatively* by atomic absorption spectroscopy.

17.13 Economic Aspects

A detailed description of the development of production is given in the metal statistics of Metallgesellschaft AG, Frankfurt [119] (Table 17.12). Over the last ten years, production figures have changed only slightly. According to U.S. estimates, current production is ca. 53% of the potential capacity. Because of reduced demand many mines and smelting plants are no longer operating or have greatly cut back production. Intervention by the former Soviet Union has seriously depressed the price of mercury to dumping price levels, although this has been resisted by Spain and Algeria. The change in the price of mercury

since 1979 is shown in Table 17.13 [119]. A survey of previous mercury prices is included in [120].

The main producers of mercury extracted by mining are as follows [121] (figures refer to flasks):

Algeria	23 000
China	20 000
Finland	2 300
Yugoslavia	2 000
Mexico	10 000
Spain	42 000
Former Czechoslovakia	4 400
Turkey	6 000
Former Soviet Union	66 000
United States	14 000 ¹

The Algerian mercury producer, Entreprise nationale des non-ferreux et substances utiles (ENOF), quotes production prices of \$300 per flask. Most of the Chinese production is exported to the United States. China claims to have the largest mercury resources in the world. Guizhou Province contains five mines, accounting for ca. 90% of Chinese production. Italy, once a large mercury producer, now imports mercury from Algeria, the Netherlands, and former Yugoslavia. In Mexico, ca.

¹ The sole producer in the United States discontinued mining operations from the middle of 1987 to February 1988. The production for 1988 is 14 000 flasks.

Table 17.12: Production of mercury in tonnes [119].

	1984	1985	1986	1987	1988	1989	1990	1991	1992	1993	1994
Europe ^a	1672	1757	1693	1764	1704	1178	1140	135	128	734	475
Spain	1520	1539	1471	1553	1499	967	962	52	36	636	386
Finland	80	130	147	144	135	160	141	74	85	98	89
Yugoslavia	72	88	75	67	70	51	37	9 ^b	7		
Asia ^a (Turkey)	182	226	262	211	97	202	60	25	5		
Africa (Algeria)	586	801	764	756	662	587	639	431	476	459	400
America	1043	965	695	264	724	1065	1195	398	85	82	80
Dominican Republic	2	1									
Mexico	384	394	185	124	345	651	735	340 ^b	21 ^b	12	10
United States	657	570	510 ^b	140 ^b	379 ^b	414 ^b	460 ^b	58 ^b	64 ^b	70	70
Total Western countries	3483	3749	3414	2995	3187	3032	3034	989	694	1275	955
Czechoslovakia	152	158	168	164	168	131	126	75	60 ^b	50	50
USSR ^b	1220	1200	1200	1200	1180	1180	2100	1900	1900	1700	1500
China ^b	800	800	850	900	900	1200	800	780	392	468	408
Total Eastern countries	2172	2158	2218	2264	2248	2511	3026	2755	2352	2218	1958
Total world	5655	5907	5632	5259	5435	5543	6060	3744	3046	3493	2913

^a Excluding Eastern-Bloc countries.

^b Estimates.

350 t of mercury (ca. 10 000 flasks) was extracted from mines in 1986, a large part of the production being exported to Brazil and Argentina. Spanish mercury production is ca. 40 000 fl. The main importers are the United States, Belgium, Luxemburg, and France. The former Soviet Union produces ca. 67 000 fl of mercury; in contrast to the high export level in 1986, almost the entire production is now reserved for domestic use. The capacity of production plants at the Anzob antimony mercury complex in Tajikistan has been doubled. The major proportion of former Yugoslav production of ca. 2000 fl of mercury is exported.

The development of prices and production figures will certainly be influenced substantially by acceptance of the metal mercury, and in large sectors no foreseeable substitute exists. The utilization of mercury in a highly industrialized country such as Germany is shown in Table 17.14 [122]. The purchase of mercury by individual sectors has decreased sharply since 1980. The main user of mercury is the electrical engineering industry, followed by the alkali chloride industry. The use of mercury in paints, pigments, and pesticides has fallen sharply.

Table 17.13: Quoted prices for mercury in London and New York.

Year	European price		U.S. Price	
	£ per flask (34.473 kg)	£/kg	\$ per flask (34.473 kg)	\$/kg
1985	284.02–293.24	8.24–8.51	310.957	9.02
1986	187.49–200.36	5.44–5.81	232.785	6.75
1987	245.64–255.23	7.13–7.40	295.503	8.57
1988	297.17–310.49	8.62–9.01	335.517	9.73
1989	246.43–261.63	7.15–7.59	287.722	8.35
1990	200.91–218.79	5.83–7.22	249.218	7.23
1991	103.33–119.44	3.00–3.46	122.424	3.55
1992	126.85–173.35	3.68–5.03	201.390	5.84
1993	107.02–125.05	3.10–3.63	186.510	5.41
1994	103.23–119.32	2.99–3.46	194.453	5.64

17.14 Toxicology and Occupational Health [123]

Uptake, Mode of Action, Metabolism. The toxicity of mercury depends, among other things, on its state of aggregation and degree of dispersion. Both fine particulate dust containing mercury and mercury vapors are very toxic in comparison to the liquid metal. Various mercury compounds are very potent poisons. Compounds containing divalent mercury are generally more poisonous than monovalent ones. The toxicity of *inorganic* mercury compounds increases with increasing solubility. Still, in most cases, they are less toxic than *organic* mercury compounds.

The toxicity of mercury is based upon its action as a general cell and protoplasmic poison, i.e., bonding to the sulfhydryl groups of proteins; denaturing proteins; damaging membranes; and reducing the RNA content of cells. This leads to blocking of many enzyme systems. The kidneys and nervous system are especially vulnerable. In animal experiments, methyl mercury and mercury(II) chloride cause a dose-dependent suppression of spermatogenesis.

Acute poisoning occurs when mercury ion concentrations reach 0.2 mg per 100 mL of blood. Daily 5-h exposure to inhaled mercury vapor concentrations of 0.1 mg/m³ leads to severe chronic mercury poisoning.

In foods, different mercury concentrations are tolerated: e.g., in the United States, 0.05 ppm; in Germany, 0.1 ppm. Environmental contamination with mercury leads to a critical concentration effect in animals that occupy higher positions in the food chain (large fish and fish-eating sea fowl). In certain fish, concentrations of 10 ppm of mercury and more have been found: fish and clams originating in Japan's Minamata Bay contained up to 9.6 mg of mercury per kilogram. Eggs of wild birds on the Finnish coast contained up to 3.5 mg of mercury per kilogram. Up to 270 mg of mercury per kilogram of organ tissue was found in dead seed-eating birds.

Table 17.14: Breakdown of mercury use (in tonnes) in former West Germany according to sector [122].

	1973	1974	1975	1976	1977	1978	1979	1980	1981	1982	1983	1984	1985
Alkali chloride industry (without changes in stock levels)	128.0	127.0	99.0	103.0	78.0	87.5	87.5	72.0	50.4	46.3	40.7	31.6	41.8
Catalysis	45.0	29.0	9.0	10.0	11.6	4.8	27.5	18.1	14.1	17.9	6.0	4.5	3.9
Paints, dyes	19.5	18.9	5.6	12.4	12.6	12.6	9.1	3.8	3.5	3.8	1.0	0.6	0.3
Pesticides	30.5	33.7	26.6	27.6	28.7	28.5	33.0	31.8	26.7	4.1	19.0	14.0	9.0
Electrical engineering	26.2	42.1	40.6	43.4	40.4	43.5	45.4	51.5	55.0	54.2	53.1	56.2	65.8
Control instruments and apparatus construction	14.8	17.3	8.7	10.3	14.6	13.4	13.3	16.5	15.7	17.1	7.0	6.1	7.2
Chemicals and reagents	25.3	7.0	33.1	45.8	22.0	31.4	43.2	35.5	27.1	53.9	36.2	24.7	
Medicine	24.2	25.2	25.0	26.0	23.9	24.3	24.2	24.2	22.9	23.6	23.5	24.3	24.1
Miscellaneous	32.8	31.1	44.2	46.7	30.0	30.0	30.0	42.1	32.5	35.7	30.1	30.2	30.2
Total	346.3	331.3	291.8	325.2	261.8	276.0	313.2	295.5	247.9	256.6	216.6	192.2	182.3
Total, % (1980 = 100%)	117	112	99	110	89	94	106	100	84	86	73	65	62

Humans are estimated to consume 0.2 mg of mercury weekly in their diet. Mercury uptake with food leads to concentrations in the kidney of < 0.1–3 mg/kg; the corresponding concentrations with intoxication are 10–70 mg/kg.

Amalgam fillings are the most frequent cause of chronic mercury and tin intoxication. The metal is transformed to highly toxic organic compounds by oral microorganisms. During chewing (gum) up to 26 mg/L of mercury and 0.3 mg/L tin may be set free.

After 15 min, the mercury content of the respiratory air increased eightfold.

Toxicity of Metallic Mercury and Inorganic Mercury Compounds. The toxicity of mercury and its compounds depends predominantly on their solubility, which determines absorption and distribution in the organism. Thus metallic mercury and all mercury compounds are toxic, with the exception of red mercury sulfide, which is practically insoluble in the body. Mercury vapor causes acute damage to the lungs and chronic damage to the central nervous system. Mercury salts are caustic to the mucous membranes of the gastrointestinal tract and nephrotoxic when absorbed.

Metallic Mercury. Liquid mercury is not highly toxic; in earlier times, it was used as a treatment for ileus. Thermometers that break in the rectum lead to mercury intoxication only if a wound is created and mercury is pressed into the tissues from which it is slowly absorbed. Granulomas develop when mercury is injected into subcutaneous fat tissue; this can occur in suicide attempts or injuries to the hand caused by broken thermometers. Absorption occurs when the mercury depot is broken up into minuscule droplets, for example, after surgical excision. Occasionally liquid mercury has been injected intravenously, either suicidally [124, 125] or accidentally during intracardiac catheter studies when blood was drawn for blood gas analysis by using mercury-filled syringes. Mercury embolisms resulted, and some of the patients showed symptoms of intoxication. One of

nine patients died after five months as a result of the intoxication. Blindness as a result of occlusion of the central artery also occurred. Antisyphilitic treatment with gray mercury ointment caused numerous intoxications, with all grades of severity being encountered. They resulted from skin absorption and from inhalation of the mercury that vaporized on the skin.

Acute *inhalant poisoning* is very dangerous. In four cases, after several hour's exposure to mercury vapor concentrations of 1–3 mg/m³, acute pneumonitis resulted. Chronic inhalant intoxication can be expected with mercury vapor concentrations of 0.1–1 mg/m³. With < 0.1 mg of mercury per cubic meter, even mild intoxication is improbable. In sensitive persons, an increase in subjective signs (micromercurialism) has been observed at 0.02–0.1 mg/m³ [125].

Mercury Salts. Salts of divalent mercury are more toxic than monovalent ones, regardless of the route of administration. In animal experiments the LD₅₀ after parenteral injection for divalent salts is ca. 5 mg of mercury per kilogram. As a result of their poor absorption, they are much less toxic if administered orally, the LD₅₀ in this case being of the order of 100 mg of mercury per kilogram [126]. Strongly dissociated salts are more caustic and generally more toxic than less dissociated ones. An exception to this is mercury oxycyanide [Hg(CN)₂·HgO], which is highly poisonous even though it hardly dissociates. Cyanide ions may enhance the toxicity.

Acute Poisoning in Humans. Mercury(II) chloride (corrosive sublimate) is one of the strongest corrosive poisons; for adults, oral doses of 0.50–1.0 g (in several cases even 0.2 g) are fatal, even though people have survived after ingesting 5 g. A total of 0.2 g introduced into the vagina can be fatal. Administration of 1.5 g of *mercury oxycyanide* was lethal. The toxicity of *mercury(I) chloride* (calomel) depends on its retention time in the gastrointestinal tract. The lethal dosage for adults is generally 2–3 g; for children, 0.4 g [125]. However, in former times, therapeutically administered doses of 0.1 g of mercury(I) chloride have led to death, especially when the

laxative effect did not occur. Chronic intoxication with mercury salts is unusual; in industrial poisonings, exposition to mercury vapors generally exists concomitantly. Mercury salts act as direct skin irritants. Furthermore, they are sensitizing, especially mercury fulminate.

Toxicity of Organic Mercury Compounds. Most organic mercury compounds are lipid soluble. Some of them vaporize easily and thus also act in the gaseous phase. Organic mercury compounds can cause toxic dermatitis and, as a result of their lipid solubility, can severely damage the central nervous system. Hypersensitivity reactions, as well as kidney damage, also occur.

In the organism, *phenylmercury* and *alkoxyalkylmercury* compounds are metabolized to inorganic mercury compounds and act like mercury salts. The stable alkylmercury compounds are neurotoxic and embryotoxic.

Alkylmercury Compounds. Numerous toxicity studies on animals have been reported. The LD₅₀ in rats and mice of most methyl- and ethylmercury compounds is 10–30 mg of mercury per kilogram. This holds true for parenteral and oral administration [126]. In humans, almost all alkylmercury poisoning has been caused by contaminated food, almost all involved chronic poisoning, the dose ingested is unknown, and estimated values are questionable. Mass poisoning in Iraq was caused by pita bread baked with flour made from seed grain; the grain contained ca. 15 mg of mercury per kilogram of alkylmercury (mainly methylmercury) salt.

The bread weighed 220 g and had a water content of 31 %. Affected adults are estimated to have eaten six to eight loaves per day; the first fatalities occurred six to eight weeks after distribution of the seed grain [126, 127].

Minamata disease developed in fishermen and their family members who ate fish daily or at least several times a week, consuming 250–500 g of fish with each meal. The average methylmercury concentration of the fish eaten is not known (estimates: 5–20 mg of mercury per kilogram of fish). Thus, a daily uptake of 1.5–4 mg of mercury would have resulted, re-

spectively [4]. Affected patients had mercury concentrations of 200–2000 µg/L in their blood and 50–500 mg/kg in their hair [128]; the brain of patients who died contained > 5 mg of mercury per kilogram [126]. Mild symptoms are assumed to occur with concentrations of 100 µg of mercury per liter of blood and 30 mg of mercury per kilogram of hair. Daily ingestion of 5 µg of mercury per kilogram of body weight in the form of methylmercury compounds is considered the minimal toxic dose [128].

Mercury is *mutagenic*, *teratogenic*, and *embryotoxic*, especially in the form of alkylmercury compounds [129, 130]. The fetus is three to four times more sensitive to methylmercury than the pregnant woman [128]. Congenital brain damage occurred in 5–6% of the children from Minamata Bay, where the rate expected was 0.1–0.6%. The mothers belonged to the group of people heavily exposed to methylmercury but did not show any clear symptoms of intoxication [126].

Arylmercury Compounds. In animal experiments, arylmercury compounds are as toxic as alkylmercury compounds when administered parenterally; administered orally, however, they are less toxic. As a result of their instability they act like a combination of organically bound mercury and mercury vapor. In adults, ingestion of 100 mg of mercury in the form of phenylmercury nitrate led to abdominal pain and mild diarrhea; however, 120 mg was also tolerated without symptoms. Even after ingestion of 1.25 g of mercury, clinical chemistry values and kidney biopsy results were normal. Concentrations > 0.6 g/L are locally caustic [126].

Antagonism. Mercury and selenium are antagonists; within certain limits, selenium can reduce the toxicity of inorganic and methylmercury. In animal experiments, selenium predominantly delays the appearance of intoxication symptoms but reduces the lethality only slightly. Whether a high dietary selenium content can protect against methylmercury poisoning is still open to question: the fish that caused Minamata disease

contained, in addition to large amounts of mercury, a high proportion of selenium [128, 131].

Occupational Health. The MAK value for metallic mercury in Germany is presently 0.1 mg/m³ (0.01 ppm); for mercury vapor the MAK value is 0.05 mg/m³ [123]. The TWA of mercury is 0.05 mg/m³. The theoretically possible vapor pressure concentration can, however, far exceed this value. The odor threshold for mercury is 13 mg/m³.

The legal requirements covering industrial safety and hygiene when working with mercury and its compounds depend on the laws of individual countries. The measures adopted by a highly industrialized country such as Germany are described below.

The special safety measures for handling and working with mercury-containing materials are given in the TRgA (Technische Regeln für gefährliche Arbeitsstoffe; technical regulations for dangerous substances). They do not cover mercury(II) sulfide, inorganic compounds containing < 0.1 % mercury, or organic compounds containing < 0.05 % mercury. The working methods and procedures must basically be designed so that employees are not exposed to mercury vapor, mist, or dust. Further details are given in [132].

A series of specification sheets for handling mercury has been published, which describes the technical and personal safety measures to be adopted [133]. Explanatory information and instructions for work and health safety are summarized in a comprehensive poisons list [134].

Persons working with mercury should be monitored regularly. With metallic mercury, inorganic mercury compounds, and organic nonalkyl mercury compounds, mercury values in urine should not exceed 150 µg/L. The blood levels should be < 35 µg/L. With organic alkylmercury compounds, the limiting blood level is 75 µg/L.

17.15 References

1. P. T. Craddock, *Bull. Metals Museum* 10 (1985) no. 10, 3–25.
2. G. Agricola: *12 Bücher des Bergbaus und des Hüttenwesens*, pp. 370–375.
3. R. C. Weast, M. J. Astle (eds.): *Handbook of Chemistry and Physics*, 64th ed., CRC Press Boca Raton, FL, 1983.
4. Hüls, DE 3709570, 1987 (S. Sridhar).
5. K. R. Suttill, *Eng. Min. J.* (1989) 24–27.
6. W. Peters, *Erzmetall* 35 (1982) no. 7/8, 389–395.
7. H. Köse, M. Kemal, F. Şimşir, *Erzmetall* 42 (1989) no. 6, 276–278.
8. SRI International, *Chemical Economics Handbook*, Menlo Park 1984.
9. X. Wang, Z. Wu: *Mineral Processing and Extractive Metallurgy*, The Institution of Mining and Metallurgy, Portland Place, London 1984, p. 44.
10. L. D. Skrylio, L. M. Lopatenko, L. A. Sin'kova, *Sov. Non-Ferrous Met. Res. (Engl. Transl.)* 13 (1985) no. 3, 186–187.
11. V. Tafel: *Lehrbuch der Metallhüttenkunde* 2nd ed., vol. 1, Hirzel, Leipzig 1951, p. 590 ff.
12. F. Pawlek: *Metallhüttenkunde*, Berlin, Waller de Gruyter, 1983.
13. Lumalampan, DE 3243813, 1982 (A. Sikander).
14. Linden Chemical & Plastics, EP 0042509, 1982 (R. J. Burkett).
15. Elektro-Ofenbau Matthias Marcus, DE 3609517, 1986.
16. H. Kulander, *Sprechsaal* 119 (1986) no. 11, 1016–1018.
17. F. Hiller: *Entsorgung von Gerätebatterien*, lecture held at the Technische Akademie Eßlingen, März 1988.
18. N. Hirayama: *Behandlung von Sonderabfall 1*, EF-Verlag, Berlin 1987.
19. H. Pietsch, Bundesministerium für Forschung und Technologie, Forschungsprojekt FKZ: 143 03 553, Lurgi, Frankfurt 1986.
20. H. Laig-Hoerstebroek, Bundesministerium für Forschung und Technologie, Forschungsprojekt FKZ: 143 0273/0, Varta, Kelkheim 1986.
21. H. Kulander: *Behandlung von Sonderabfall 1*, EF-Verlag, Berlin 1987.
22. Preussag AG Metall, internal report, 1989, Goslar, Germany.
23. Outokumpu O.Y., DE 2406119, 1973.
24. Preussag AG Metall, DE 2558115, 1975 (G. Heyer).
25. K. Hanusch, BMFT-Forschungsbericht NTS 0103/0, Nov. 1973, Harlingerode.
26. J. L. Gallant, *World Conf. Int. Nucl. Targ. Development Soc.*, Boston, MA, 13 Oct. 1979, Plenum Press 8 (181), pp. 213–216.
27. F. Desmet, L. Lemaître, A. P. van Petegham, *Mater. Chem. Phys.* 11 (1984) 305–309.
28. A. D. Pogorelyi, G. M. Tysh, *Tsvetn. Met.* 1979, no. 5, 10–18.
29. S. A. N. Sheya, J. H. Maysilles, R. G. Sandberg, *Rep. Invest. U.S. Bur. Mines* 9191 (1988) 1–12.
30. I. Barin, O. Knacke: *Thermochemical Properties of Inorganic Substances*, Springer Verlag, Berlin, Verlag Stahleisen, Düsseldorf 1973, p. 339.
31. Ch. G. Maier, *Am. Inst. Min. Metall. Eng. Techn. Publ.* no. 264 (1929).
32. R. Heindryckx et al., "Mercury and Cadmium in Belgian Aerosols", in: *CEC 1974 Problems of the Contamination of Man and his Environment by Mercury and Cadmium*, Commission of the European Communities, Luxemburg, pp. 135–148.
33. NAS, *An Assessment of Mercury in the Environment*, National Academy of Sciences, Washington, DC, 1978.
34. J. K. Piotrowski, D. O. Coleman: *MARC-Report 20, Environmental Hazards of Heavy Metals: Summary Evaluation of Lead, Cadmium, and Mercury*, MARC-Monitoring and Assessment Research Center, GEMS Global Environmental Monitoring System, Genève, London 1980.
35. H. J. Rösler, H. Lange: *Geochemische Tabellen*, 2nd ed., Enke Verlag, Stuttgart 1976.
36. *Schwermetalle in Lebewesen und Böden* ANS-Mitteilungen, Sonderheft 2, p. 18 ff.
37. P. Koronowski: *Nebenwirkung von Quecksilberverbindungen auf Mensch und Tier*, Berlin 1973.
38. S. Bombach, L. Peters, *Naturwissenschaften* 62 (1975) 575–576.
39. E. Heinrich, H. Paucke, H.-D. Nagel, D. Hansen: *Agrochemikalien in der Umwelt*, VEB Fischer Verlag, Jena 1976, p. 57.
40. R. D. Rogers, J. C. McFarlane, *J. Environ. Qual.* 8 (1979) no. 2, 255–260.
41. R. Taylor, T. Bogacka, M. Balcerska, *Environ. Prot. Eng.* 4 (1978) no. 2, 179–182.
42. J. Lag, E. Steiners, *Acta Agric. Scand.* 28 (1978) 393–396.
43. R. W. Klusman, R. A. Landers, *J. Volcanol. Geotherm. Res.* 5 (1979) 49–65.
44. R. Bargagli, F. P. Iosco, C. Barghigiani, *Water Air Soil Pollut.* 36 (1987) 219–225.
45. T. Stijve, R. Roschnik, *Mitt. Geb. Lebensmittelunters. Hyg.* 65 (1974) 208–220.
46. R. Seegers, *Z. Lebensm. Unters. Forsch.* 160 (1976) 303–312.
47. K. Aichberger, O. Horak, *Bodenkultur* 26 (1975) no. 1, 8–14.
48. W. Rauter, *Z. Lebensm. Unters. Forsch.* 159 (1975) 149–151.
49. E. Hauser, M. Mohadjerani, *Mitt. Geb. Lebensmittelunters. Hyg.* 67 (1976) 389–401.
50. M. Cember, M. Curtis, B. G. Blaylock, *Environ. Pollut.* 17 (1978) no. 4, 311–319.
51. A. Stock, *Z. Angew. Chem.* 41 (1928) 663.
52. Blei-, Cadmium- und Quecksilbergehalte von Lebensmitteln in der Bundesrepublik Deutschland, Bericht der Zentralen Erfassungs- und Bewertungsstelle für Umweltchemikalien im Bundesgesundheitsamt Berlin (ZEBS), Stand 1975, und ZEBS-Berichte 1/79.
53. *Arsen, Blei, Cadmium und Quecksilber in und auf Lebensmitteln*, ZEBS-Bericht, Berlin, 1/1984.
54. *Quecksilber-, Magnesium- und Zinkgehalte in der Frauenmilch, im Blutserum und Fettgewebe der Mütter*, ZEBS-Hefte, Berlin, 1/1986.
55. A. Kuivala, J. Poijärvi, *Erzmetall* 30 (1977) 556.
56. Boliden AB, EP 179040, 1985 (F. Dyvik).
57. F. Dyvik: "Extraction Metallurgy 85", *Proc. Conf.* London 1985, The Institution of Mining and Metallurgy, London, pp. 189–198.
58. Norddeutsche Affinerie AG, EP 278537, 1988 (H. Winkler, C. Reppenhagen).
59. H. Braun, M. Metzger, H. Vogg, *Müll. Abfall* 18 (1986) no. 2, 62–71, 89–95.
60. Kernforschungszentrum Karlsruhe, DE 3715046, 1987 (H. Vogg, H. Braun, M. Metzger, A. Merz).
61. Kernforschungszentrum Karlsruhe, EP 0289810, 1988 (H. Vogg, H. Braun, M. Metzger, A. Merz).
62. Kernforschungszentrum Karlsruhe, EP 0289809, 1988 (H. Vogg, H. Braun).
63. Bergwerksverband, DE 3715526, 1987 (K. Knoblauch, K. Wybrands, K.-D. Henning, J. Degel, H. Ruppert).
64. D. Reimann, *Umweltmagazin*, Oct. 1984, 48–54.
65. VEB Chemieanlagenbau- und Montagekombinat Leizig, DD 139068, 1976 (H. Tischendorf, R. Boege, G. Kreutzberger).
66. M. D. Rosenzweig, *Chem. Eng. (London)* 82 (1975, Jan. 20) 60–61; *Chem. Eng. (London)* 82 (1975, Feb. 3) 36–37.
67. Chlorine Inst.: *Water Pollution Aspects*, 5. 3. 1971.
68. K.-H. Bergk, F. Wolf, S. Eckert, *Z. Chem.* 17 (1977) 85–89.
69. G. van der Heiden, C. M. S. Raats, M. F. Boon, *Chem. Ing. Tech.* 51 (1979) 631–653.
70. Kernforschungszentrum Karlsruhe, DE 3721141, 1987 (M. Metzger, H. Braun).
71. D. O. Reimann, *VGB Kraftwerkstechnik* 64 (1984) no. 3, 230–235.
72. "Umwelt und Degussa, TMT-15 für die Abtrennung von Schwermetallen aus Abwässern", *Degussa Broschüre*, 1982.
73. Wacker-Chemie, DE 3335127, 1983 (J.-H. Janssen, B. Bangler, K.-H. Fahrmeier).
74. Hoechst AG, EP 0091043, 1983 (H. von Plessen, R. Gradl, G. Schimmel).
75. R. Kola, *Erzmetall* 30 (1977) no. 12, 559–561.
76. R. K. Willardson, A. C. Beer, *Semicond. Semimetals* 18 (1981) 21–45.
77. Montedison S.p.A., EP 0148023, 1984 (M. Gramondo, G. Donati, G. Fatta, G. L. Marziano).
78. *Chem. Eng. (London)* 82 (1975) no. 2, 60.
79. *Chem. Eng. (London)* 82 (1975) no. 3, 36.
80. Chemikerausschuß der Ges. Dtsch. Metallhütten- und Bergleute: *Analyse der Metalle*, vol. 2, Springer Verlag, Berlin-Göttingen-Heidelberg 1953, p. 590.
81. *Z. Anal. Chem.* 96 (1934) 30.
82. *Z. Anal. Chem.* 89 (1932) 187.
83. *Z. Anal. Chem.* 98 (1934) 331.
84. R. Dumarey, R. Heindryckx, R. Dams, J. Hoste, *Anal. Chim. Acta* 107 (1979) 159–167.
85. G. R. Garrick, W. Barnett, W. Slavin, *Spectrochim. Acta Part B*, 41 B (1986) no. 9, 991–997.
86. L. Sipos, J. Golimowski, P. Valenta, H. W. Nürnberg, *Fresenius Z. Anal. Chem.* 298 (1979) no. 1, 1–8.
87. H. Bloom, B. Noller: *Trends in Electrochemistry*, Badford, Australia 1976, 241–252.
88. H. Dorias: *Gefährliche Güter, Eigenschaften, Handhabung, Lagerung und Beförderung*, Springer Verlag, Berlin 1984.
89. G. Hommel: *Handbuch der gefährlichen Güter*, Springer Verlag, Berlin 1985.
90. J. M. Lo, C. M. Wai, *Anal. Chem.* 47 (1975) no. 11, 1869–1870.
91. S. Dogan, W. Herdi, *Anal. Chim. Acta* 101 (1978) no. 2, 433–436.
92. T. Suzuki, M. Fujita, K. Iwashima, *Eisei Kagaku* 26 (1980) no. 5, 229–235.

92. J. C. Meranger, B. R. Hollebone, G. A. Blanchette, *J. Anal. Toxicol.* **5** (1981) no. 1, 33–41.
93. J. R. Kechtel, *Analyst (London)* **105** (1980) 826–829.
94. R. W. Heiden, D. A. Aikens, *Anal. Chem.* **51** (1979) no. 1, 151–156.
95. P. R. Ludlam, J. G. King, *Analyst (London)* **106** (1981) 488–489.
96. R. Schaaf, *Müll Abfall* **11** (1983) 277–283.
97. G. Jangg, H. Palman, *Z. Metallk.* **54** (1963) 364.
98. G. Brauer, G. Düsing, *Z. Anorg. Allg. Chemie* **328** (1964) 154.
99. G. Jangg, *Metall (Berlin)* **13** (1959) 407.
100. C. Guminski, *Z. Metallk.* **77** (1986) no. 2, 87–96.
101. N. P. Chohey, *Chem. Eng. (N.Y.)* **68** (1961) no. 25, 120.
102. A. Giordano, US 3061412, 1960.
103. Du Pont, US 2757070, 1956.
104. Du Pont, US 2904398, 1959.
105. R. A. Feldhoff, *Pharm. Ztg.* **75** (1930) 11.
106. R. Hirayama, JP 174101, 1946.
107. Wood-Ridge Chem. Co., US 3424552, 1967.
108. Y. V. Karyankin, J. J. Angelov: Chisty Klimicheskije Reativy (pure chemical reagents), state-owned scientific-technical publisher for chemical literature, Moskva 1955, p. 457.
109. W. Leithe, *Vom Wasser* **37** (1970) 106.
110. Merck-Standards, pp. 807–830, 1971, Darmstadt, Germany.
111. J. Dahmen, *Proc. 6th Indo-Ger. Semin. on Trace Element Analysis – Methods and Selected Applications*, Oct. 1978 (Maria Laach).
112. L. G. Makarova, A. N. Nesemeyanow: *The Organic Compounds of Mercury*, North-Holland Publ. Co., Amsterdam 1967.
113. *Beilstein*, E IV (4), 4426–4463; E IV (16), 1701–1718.
114. C. Larock, *Angew. Chem.* **90** (1978) 28–38.
115. C. Larock: *Organo Mercury Compounds in Organic Synthesis*, Springer Verlag, Berlin 1985.
116. W. Peters, *Ber. Dtsch. Chem. Ges.* **38** (1905) 2567. Bayer, DE 1003733, 1955.
117. J. B. Johnson, J. P. Fletcher, *Anal. Chem.* **31** (1959) 1563.
118. D. Steinborn, U. Sedlak, *Z. Chem.* **25** (1985) 376 ff.
119. Metallstatistik 1987 der Metallgesellschaft AG, Frankfurt/Main 1987.
120. *Ullmann*, 4th ed., 19, 654.
121. United States Department of the Interior: *Minerals Yearbook 1986*, vol. 1, Bureau of Mines, US Government Printing Office, Washington 1988, p. 659 ff.
122. A. Rauhut, *Metall (Berlin)* **42** (1988) no. 11, 1137–1141.
123. D. Henschler (ed.): *Gesundheitsschädliche Arbeitsstoffe. Toxikologisch-arbeitsmedizinische Begründung von MAK-Werten, Quecksilber*, Verlag Chemie, Weinheim 1981.
124. H. E. Stockinger: "The Metals, Mercury, Hg", in: G. D. Clayton, F. E. Clayton (eds.): *Patty's Industrial Hygiene and Toxicology*, vol. 2A, John Wiley & Sons, New York–Chichester–Brisbane–Toronto 1981, 1769–1792.
125. E. W. Baader: "Quecksilbervergiftung", *Handbuch der gesamten Arbeitsmedizin*, vol. II/1, Urban & Schwarzenberg, München 1961.
126. L. Friberg: "Aspects of Chronic Poisoning with Mercury", *Nord. Hyg. Tidskr.* **32** (1951) 240–249, *Arch. Ind. Hyg.* **5** (1952) 596–597.
127. L. Friberg, J. Vostal (eds.): *Mercury in the Environment*, CRC Press, Cleveland, OH 1974.
128. M. R. Greenwood: "Methylmercury Poisoning in Iraq. An Epidemiological Study in the 1971–1972 Outbreak", *J. Appl. Toxicol.* **5** (1985) 148–159.
129. M. J. Inskip, J. K. Piotrowski: "Review of the Health Effects of Methylmercury", *J. Appl. Toxicol.* **5** (1985) 113–133.
130. J. O. Nriagu (ed.): *The Biogeochemistry of Mercury in the Environment*, Elsevier-North Holland Biomedical Press, Amsterdam–New York–Oxford 1979.
131. M. R. Greenwood: "Quecksilber", in E. Merian (ed.): *Metalle in der Umwelt*, Verlag Chemie, Weinheim 1984, 511–539.
132. E. J. Underwood: *Trace Elements in Human and Animal Nutrition*, Academic Press, New York–San Francisco–London 1977, 375–387.
133. Technische Regeln für gefährliche Arbeitsstoffe (TRGA), Berufsgenossenschaftliches Institut für Arbeitssicherheit 1983.
134. Berufsgenossenschaft der chemischen Industrie: *Quecksilber und seine Verbindungen*, Merkblatt M 0247/80, Jedermann-Verlag, Heidelberg 1980.
135. L. Roth, M. Daunderer: "Giftliste, Gifte, Krebs-zeugende, gesundheitsschädliche und reizende Stoffe", *Toxikologische Enzyklopädie*, Ecomed, 36, supplement 3/89.

18 Cobalt

JOHN DALLAS DONALDSON (§§ 18.1–18.11); HARALD GAEDCKE (§ 18.12)

18.1 Introduction	923	18.8 Compounds	936
18.2 History	924	18.8.1 Chemical Properties of Cobalt	936
18.3 Physical Properties	925	18.8.2 Commercially Important Cobalt Compounds	940
18.4 Occurrence	927	18.8.3 Industrial Applications of Cobalt Compounds	943
18.5 Production	929	18.8.3.1 Glasses, Ceramics, and Refractories	943
18.5.1 Concentration of the Ores	929	18.8.3.2 Driers, Paints, Varnishes, and Dressings	944
18.5.2 Extraction	930	18.8.3.3 Catalysts	945
18.5.2.1 Leaching of Cobalt Ores and Concentrates	930	18.8.3.4 Electroplating	947
18.5.2.2 Separation of Cobalt from Other Metal Ions in Leach Solutions	933	18.8.3.5 Electronics and Solid-State Devices	948
18.5.2.3 Electrowinning	934	18.8.3.6 Agriculture, Nutrition, and Medicine	948
18.6 Cobalt Powders	934	18.9 Analysis	948
18.6.1 Production	934	18.10 Economic Aspects	949
18.6.2 Uses	936	18.11 Physiology and Toxicology	949
18.6.2.1 Cemented Carbides	936	18.12 Pigments	950
18.6.2.2 Cobalt Powders in Powder Metallurgy and Cobalt-containing Metal	936	18.13 References	950
18.7 Alloys	936		

18.1 Introduction [1–3]

Cobalt is a metallic element whose electronic configuration is $3d^7 4s^2$ beyond the argon core, giving it an atomic number of 27. The relative atomic mass of cobalt is 58.9332. Only one of its isotopes, ^{59}Co , is stable and occurs naturally; the other 12 known isotopes are radioactive and have the following mass numbers (half-lives in parentheses): 54 (0.2 s), 55 (18.2 h), 56 (80 d), 57 (270 d), 58 (9 h), 58 (72 d), 60 (10.1 months), 60 (5.3 a), 61 (99 months), 62 (1.6 months), 62 (13.9 months), and 64 (< 28 s).

The γ -rays emitted in the decay of ^{60}Co have energies of 1.17 and 1.33 MeV, and these taken with the 5.3-a half-life of the isotope provide a widely used source of radioactivity for use in food sterilization, radiography, and radiotherapy as an external source. The isotope is also used in chemical and metallurgical analysis and in biological studies as a radioactive tracer. The ^{57}Co isotope decays by electron capture to give ^{57}Fe , the most widely used

isotope in γ -resonance (Mössbauer) spectroscopy [4].

Pure metallic cobalt has few applications, but its use as an alloying element and as a source of chemicals makes it a strategically important metal. End uses of cobalt-containing alloys include superalloys for aircraft engines, magnetic alloys for powerful permanent magnets, hard metal alloys for cutting-tool materials, cemented carbides, wear-resistant alloys, corrosion-resistant alloys, and electrodeposited alloys to provide wear and corrosion-resistant metal coatings. Cobalt chemicals, among their many applications, are used as pigments in the glass, ceramics, and paint industries; as catalysts in the petroleum industry; as paint driers; and as trace metal additives for agricultural and medical use. About 36% of the worldwide annual production of cobalt is converted to chemicals, whereas high-temperature and magnetic alloys account for 41% and 14% of the consumption, respectively. Detail on all aspects of the science and technology of cobalt in general reviews [1–3]

can be supplemented by reference to journals of abstracts published between 1975 and 1985 [5] and restarted in 1984 [6, 7].

18.2 History

Although very little cobalt metal was used until the 20th century, its ores have been used for thousands of years as blue coloring agents for glass and pottery. Blue glazed pottery found in Egyptian tombs and dated at ca. 2600 B.C. has been found to contain cobalt, as have Persian glass beads dating from 2250 B.C. The Portland vase in the British Museum provides evidence that cobalt pigments were used by Greek glassworkers around the beginning of the Christian era. Cobalt-containing materials were also used to impart blue coloration to Chinese pottery during the Tang (600–900 A.D.) and Ming (1350–1650 A.D.) dynasties and to Venetian glass produced in the first part of the 15th century. The brilliant blue pigment used for these purposes can be produced by fusing an ore containing cobalt oxide with potash and silica to produce a vitreous material called smalt, which is powdered to produce the pigment. The secret of making the pigment was apparently lost during the Middle Ages and rediscovered during the 15th century. LEONARDO DA VINCI was one of the first artists to use the rediscovered blue pigment when painting "The Madonna of the Rocks". In the 16th century, P. WEIDENHAMMER produced a blue pigment, which he called zaffre, from the silver-cobalt-bismuth-nickel-arsenate ores found in Saxony. The next development in the use of cobalt-containing materials was the discovery, early in the 18th century, that solutions containing bismuth and cobalt could be used as sympathetic inks. The invisible writing obtained by using the inks became green when heated, with the color change apparently due to the presence of cobalt. It was not until 1735 that G. BRANDT, a Swedish scientist, first isolated cobalt metal as an impure sample by reducing an ore; in 1780 T. O. BERGMAN showed that the metal was in fact an element. The use of cobalt as a metal dates from 1907, when E.

HAYNES patented a series of cobalt-chromium alloys named Stellites that were the forerunners of modern superalloys. In 1930 it was shown that addition of cobalt to certain alloys of iron, nickel, and aluminum enhanced their properties as permanent magnets.

From the 16th to the 19th century, the world's supply of cobalt — mainly as smalt and zaffre — was produced in Norway, Sweden, Hungary, and Saxony. Outside of Europe cobalt-containing ores were worked in Burma from 1651 and in New Caledonia from 1864. Major developments in cobalt recovery in the 20th century have stemmed from the discovery of new ore bodies and improvements in the methods of winning the metal from ores. Cobalt-containing copper ores were discovered in Zaire in 1914, and extraction of cobalt from the ores began in 1924, whereas recovery of cobalt from pyrite roasting residues was started in Germany in 1926. Mining of cobalt-nickel-gold-silver ores began in Morocco in 1932, and production of cobalt from copper-cobalt ores began in Zambia in 1933. The Outokumpu copper-cobalt-zinc deposit was discovered in 1913 and has been exploited on a large scale since 1928. In 1940 the International Nickel Co. (INCO) introduced a method of recovering cobalt from nickel ores, and from 1952 to 1955 the production of cobalt by the Canadian companies, Falconbridge Nickel Mines and the Sherritt Gordon Mining Co., began. Recent developments include the commissioning in 1975 of a cobalt refining plant based on a combination of pressure leaching, solvent extraction, and electrowinning by the Sumitomo Metal Mining Co. in Japan.

Worldwide production of cobalt ores in 1980 was 32 700 t of contained cobalt, of which 14 700 t was from Zaire, about 3000 t each from Australia, New Caledonia, and Zambia, about 2000 t from the former Soviet Union, and about 1600 t from Canada.

The production of cobalt is usually subsidiary to that of other metals, such as copper and nickel, and its output cannot be significantly increased without a corresponding increase in the markets of the primary metals. Another

important factor in the economics of the supply of cobalt is the fact that a large proportion of the world's ore comes from one country, Zaire, and is therefore dependent on the political stability of that country. Cobalt is regarded as a strategic metal and is stockpiled in some countries.

The name cobalt is derived from the Greek word κόβαλος or the German word Kobold for goblin or evil spirit. The term Kobold was applied by miners in the Harz mountains of Germany to an ore that gave no metal when smelted and that also produced highly toxic fumes of arsenic oxide.

18.3 Physical Properties

The physical and mechanical properties [1–3] of cobalt metal are susceptible to variations because of variations in the structures of metal samples arising from a slow cubic to hexagonal phase transformation. The data quoted in this section are for the highest purity metal available; details of the effects of impurities on the properties of cobalt are to be found in a review by W. BETTERIDGE [8].

Cobalt exists in two allotropic modifications, a close-packed hexagonal ϵ -form stable below ca. 400 °C and a face-centered cubic α -form stable at high temperature.

The transformation temperature is 421.5 °C. The free energy change associated with the transformation is low, being ca. 500 J/mol for the $\epsilon \rightarrow \alpha$ change and ca. 360 J/mol for the $\alpha \rightarrow \epsilon$ change; this accounts for the slowness of the transformation. The mechanism of the phase change is martensitic and involves dislocation movements on the octahedral planes of the cubic lattice. Grain size affects the stability of the two allotropes, with finer grain size favoring the cubic high-temperature form. For this reason the fine grain sizes found in cobalt powders, sponge, thin films, and fibers are responsible for the retention of essentially cubic structures down to ambient temperature. The cubic form is also favored by the presence of a few percent of iron in the lattice. Table 18.1 shows the cell

parameters and other properties of the allotropes. The density of the metal decreases with increasing temperature and shows an anomalous fall of ca. 0.15% at the transformation temperature. The liquid density just above the melting point is 7.73 g/cm³, and at 2000 °C it is 7.26 g/cm³.

Table 18.1: Properties of the allotropic forms of cobalt.

Hexagonal ϵ -form	
Cell dimensions (ambient temperature)	$a = 0.25071$ nm
	$c/a = 1.6233$
(417 °C)	$a = 0.2541$ nm
	$c/a = 1.631$
Density (20 °C)	8.832 g/cm ³
Co-Co interatomic distances	0.294–0.251 nm
Stacking fault energy (20 °C)	31×10^{-7} J/cm ²
(370 °C)	20.5×10^{-7} J/cm ²
Cubic α -form	
Cell dimension (ambient temperature)	$a = 0.35441$ nm
(520 °C)	$a = 0.35688$ nm
(1398 °C)	$a = 0.36214$ nm
Density (ambient temperature)	8.80 g/cm ³
(1495 °C)	8.18 g/cm ³
Co-Co interatomic distance	0.251 nm
Stacking fault energy (500 °C)	13.5×10^{-7} J/cm ²
(710 °C)	18.5×10^{-7} J/cm ²

Thermal Properties. The melting point of cobalt is 1495 ± 2 °C, and its boiling point at normal pressure is 2800 ± 50 °C. The vapor pressure of cobalt varies from less than 10^{-5} Pa (at 1250 °C) to greater than 10^5 Pa (at 3200 °C). The heats of fusion and vaporization of cobalt are 17.2 and 425 kJ/mol, respectively. The thermal conductivity (λ) of the metal falls steadily with increasing temperature; there is no marked change in conductivity at the transformation temperature, but the data show a minimum in the region of the Curie temperature at 1121 °C. The values of λ at 0, 100, and 800 °C are 102, 85, and 50 Wm⁻¹, respectively. The heat capacity of cobalt rises steadily with increasing temperature. There is only a slight inflection in the c_p vs. T curve at the transformation temperature, but a large change does occur at the magnetic transformation. The thermal expansion coefficient of hexagonal cobalt depends on the orientation of the crystals being, for example, 14.62×10^{-6} K⁻¹ along the $\langle 0001 \rangle$ and 10.96×10^{-6} K⁻¹ along the $\langle 1120 \rangle$ direction (at 20 °C). The av-

erage value for polycrystalline cobalt is $12.14 \times 10^{-6} \text{ K}^{-1}$. The curve of the coefficient vs. temperature shows a sharp change at the transformation temperature because of the volume expansion of ca. 0.36% associated with the phase change from hexagonal to cubic crystals. Cubic cobalt has a higher mean thermal expansion coefficient with values of (14.2, 15.7, 16.0, and 16.8) $\times 10^{-6} \text{ K}^{-1}$ at 200, 400, 600, and 750 °C, respectively.

Mechanical Properties. The mechanical properties of cobalt are critically dependent on the purity of the metal and its thermal history. For well-annealed samples of high-purity cobalt, the *Vickers hardness* at normal temperature has values between 140 and 160 N/mm². The Vickers hardness of annealed cobalt decreases with increasing temperature to values of under 50 N/mm² at 750 °C with no marked change at the phase transformation. Microhardness studies on zone-refined single crystals of the metal show variations with crystal orientation and give values between 81 and 250 N/mm². Electrodeposited cobalt has high hardness (270–310 N/mm²), presumably because of its fine grain size.

Table 18.2: Elastic moduli at 20 °C for cobalt along different crystal directions.

Crystal direction	Young's modulus, 10 ³ MN/m ²	Shear modulus, 10 ³ MN/m ²
1120	174	62.2
1010	175	62.2
1012	169	74.1
0001	213	62.4

Measurements of elastic properties on polycrystalline bars of high-purity sintered metal annealed at 1000 °C give a *Young's modulus* of $211 \times 10^3 \text{ MN/m}$ and a *shear modulus* of $82 \times 10^3 \text{ MN/m}$ at room temperature. The moduli decrease with increasing temperature, with the shear modulus showing an inflection and the Young's modulus a hysteresis at the phase change. For single crystals the moduli do vary with crystal direction, as shown in Table 18.2. Values of *Poisson's ratio* for cobalt are found to be in the range of 0.29–0.32.

Vacuum-melted, hot-worked cobalt annealed at 800–1000 °C has *tensile strengths* of 800–875 MN/m² and an elongation of 15–30%. Air-melted samples are much less ductile. Cobalt has a maximum *ductility* at 500 °C, and this is the best working temperature for the metal, although the vacuum-degassed metal free from lead, sulfur, and zinc, can be hot-rolled in the temperature range of 600–1000 °C. Both elongation and tensile strength values show changes at the phase transformation.

The activation energy for *creep* is higher for hexagonal cobalt than for the cubic form; the values near the phase change temperature are 540 and 190 kJ/mol, respectively. The hexagonal crystals have lower values of friction and wear than the cubic crystals. The *friction coefficient* of cobalt rises steeply at temperatures above 300 °C to values of ca. 1.6 at 400 °C. The low coefficient associated with the hexagonal form is due to easy slip on the basal plane accompanied by the formation of a surface layer with the basal planes oriented parallel to the surface. In actual applications, however, the frictional and wear behavior of the metal will be determined by surface oxide films.

Magnetic Properties. Pure cobalt has the highest known Curie temperature. Hexagonal cobalt is ferromagnetic at all temperatures, but the cubic form becomes paramagnetic at $1121 \pm 3 \text{ °C}$. The magnetic properties of single crystals show marked anisotropy. For hexagonal crystals at ambient temperature, the *c*-axis is the direction of easiest magnetization, but with increasing temperature magnetization becomes easier in a direction perpendicular to the *c*-axis; however, at ca. 250 °C the metal is magnetically isotropic. At even higher temperature, the *c*-axis becomes the most difficult to magnetize. Near the phase change temperature, the direction of easiest magnetization of the cubic form is along the $\langle 111 \rangle$ cube diagonal. Differences between this and other directions diminish with increasing temperatures until, at 1000 °C, the cubic form is magnetically isotropic.

The magnetic properties of polycrystalline samples of cobalt depend on the purity of the metal and its thermal history; this applies particularly to the development of preferred orientation. Magnetic anisotropy can, for example, be developed by slowly cooling the metal over the phase transformation temperature range in a strong magnetic field. Typical values for magnetic property parameters are listed in Table 18.3. The magnetostrictive behavior of cobalt is also strongly anisotropic and reaches a maximum value for hexagonal crystals of $\Delta l/l = -27 \times 10^{-6}$ in a magnetic field of 560 kA/m along the $\langle 1120 \rangle$ direction. The volume magnetostriction shows a maximum contraction of 10^{-6} in a field of 480 kA/m and a magnetostrictive expansion when the fields are above 760 kA/m.

Table 18.3: Magnetic properties of cobalt.

Curie temperature	1121 °C
Maximum permeability	$3.1 \times 10^{-4} \text{ H/m}$
Coercive force	707 A/m
Remanence	0.49 T
Saturation magnetization	1.79 T

Table 18.4: Electrical resistivity and temperature coefficient of resistivity for cobalt.

Temperature, °C	Resistivity, $\times 10^{-8} \Omega \text{ m}$	Temperature coefficient, $\times 10^{-11} \Omega \text{ m/K}$
–100	2.65	—
–50	3.84	—
0	5.25	30
50	6.81	34
100	8.52	39
200	12.80	50
300	18.38	60
400	24.72	71
500	30.65	75
600	39.1	87
800	57.9	105
1000	78.5	100
1200	92.7	41
1400	100.0	34

Electrical Properties. The electrical resistivity and the temperature coefficient of the resistivity of high-purity (99.999%) polycrystalline cobalt are given in Table 18.4. The cubic form has a lower resistivity than the hexagonal modification whenever the forms coexist. The resistivity of single crystals of co-

balt shows a marked dependence on orientation.

Other Properties. The self-diffusion of cobalt in the temperature range between 1057 and 1306 °C follows an Arrhenius-type law, the *diffusion coefficient* being given by the formula $2.2 \times e^{-295/RT}$. The rate of diffusion is very dependent on grain size, being about 10 times faster for powder-metal samples than for bulk samples prepared by melting.

The *optical reflectance* of polished cobalt at ambient temperature and near normal incidence increases with wavelength from 60% (at 1 μm) to 97% (at 12 μm). The reflectance is much less at high angles of incidence. The optical emission spectrum of cobalt is complex and has over 330 lines in the range of 974–201 nm. The most important lines for analytical purposes are listed in Table 18.5. The characteristic $K\alpha_1$, $K\alpha_2$, and $K\beta_1$ X radiation from a cobalt target occur at 0.1789, 0.1793, and 0.1621 nm, respectively; the K absorption edge is at 0.1608 nm.

Table 18.5: Optical emission lines of cobalt used in atomic emission analysis.

Wavelength, nm	Relative intensity	
	Arc source	Spark source
352.9813	1000	30
346.5800	2000	25
345.3505	3000	200
340.5120	2000	150
251.9822	40	200
238.8918	10	35
237.8622	25	50
236.3787	25	50
230.7857	25	50
228.6156	40	300

18.4 Occurrence [1, 2, 9]

Cobalt occurs in nature in a widespread but dispersed form in trace quantities in many rocks, soils, and plants. It is also found in sea water and in manganese-rich marine nodules. The cobalt content of the earth's crust is about 20 mg/kg, whereas its concentration in sea water has been reported as being 0.1–1 part in 10^9 . The concentration of the element in marine nodules is usually 0.1–1%. The largest concentrations of cobalt are found in mafic

and ultramafic igneous rocks; the concentration of the element and the nickel cobalt ratio decreases from ultramafic to acidic rocks, as shown in Table 18.6. The nickel cobalt ratio changes because cobalt enters the lattice of early crystallizing magnesium silicates less readily than nickel. Sedimentary rocks contain varying amounts of cobalt, with average values of 4, 6, and 40 mg/kg being reported for sandstone, carbonate rocks, and clays or shales, respectively. During the formation of metamorphic rocks, very little movement or concentration of cobalt took place; thus, the levels of cobalt found in metamorphic rocks depend essentially on the amount of the element in the original igneous or sedimentary source. Those formed from ultramafic or mafic sources contain an average cobalt content of ca. 100 mg/kg, whereas gneissic granites and metasedimentary rocks contain an average of 16 and 8 mg/kg, respectively.

Table 18.6: Average cobalt content of igneous rocks.

Rock type	Cobalt content, mg/kg	Ni-Co ratio
Ultramafic	270	7
Gabbro	51	2.6
Basalt	41	2.5
Diabase	31	2.3
Intermediate igneous	14	1.9
Felsic	5	1.1

Under oxidizing conditions, cobalt shows a strong tendency to concentrate with manganese oxides. In the weathering process of mafic and ultramafic rocks to form laterites, nickel tended to be leached downward with magnesia and silica, whereas cobalt with manganese oxides was residually enriched near the surface of the deposit. The concentration of cobalt and other metals in marine nodules has been attributed to the strong ion-exchange properties of the submicroscopic particles of colloidal manganese dioxide from which the nodules were formed.

Cobalt is a major constituent of about 70 minerals [10] and is a minor or trace constituent of several hundred more, particularly those containing nickel, iron, and manganese. The minerals that have been mined or concentrated for their cobalt content and those that are rela-

tively high in cobalt are listed in Table 18.7. The sulfide minerals include the copper-containing carrollite, which is one of the main sources of cobalt in Zaire, linnæite found in Zaire, Zambia, and the United States, and cattierite, which is also present in ores from Zaire. The arsenide ores include smaltite, which is found in the silver-copper ores from Cobalt, Ontario and in Morocco, and skutterudite, the main cobalt mineral in Canadian and Moroccan deposits. The sulfoarsenide, cobaltite, is found in ore bodies in Zaire, Canada, and the United States. The oxide mineral heterogenite is a hydrated metal oxide containing varying amounts of cobalt and copper and is one of the main cobalt-bearing components of the Zaire deposits. The hydrated manganese-cobalt mineral, asbolite, is the source of most of the cobalt in ores from New Caledonia.

Table 18.7: Cobalt minerals.

Mineral	Cobalt content, %
Cattierite, CoS_2 (pure)	47.8
Linnærite, Co_3S_4 (pure)	58.0
Siegenite, $(\text{Co},\text{Ni})_3\text{S}_4$	20.4–26.0
Carrollite, $(\text{Co}_2\text{Cu})\text{S}_4$	35.2–36.0
Cobaltite, $(\text{Co},\text{Fe})\text{AsS}$	26.0–32.4
Safflorite, $(\text{Co},\text{Fe})\text{As}_2$	13.0–18.6
Smaltite, $(\text{Ca},\text{Ni})\text{As}_2$	ca. 21
Glauco-dot, $(\text{Co},\text{Fe})\text{AsS}$	12.0–31.6
Skutterudite, $(\text{Co},\text{Fe})\text{As}_3$	10.9–20.9
Heterogenite, $\text{CoO}(\text{OH})$ (pure)	64.1
Asbolite	0.5–5.0
Erythrite, $(\text{CoNi})_3(\text{AsO}_4)_2 \cdot 8\text{H}_2\text{O}$	18.7–26.3
Gersdorffite, $(\text{Ni},\text{Co})\text{AsS}$	(low)
Pyrrhotite, $(\text{Fe},\text{Ni},\text{Co})_{x-1}\text{S}_x$	up to 1.00
Pentlandite, $(\text{Fe},\text{Ni},\text{Co})_9\text{S}_8$	up to 1.50
Pyrite, $(\text{Fe},\text{Ni},\text{Co})\text{S}_2$	up to 13.00
Sphalerite, $\text{Zn}(\text{Co})\text{S}$	up to 0.30
Arsenopyrite, $\text{Fe}(\text{Co})\text{AsS}$	up to 0.38
Manganese oxide minerals	0.10–1.0

Ore Deposits. Cobalt is produced mainly as a by-product of the mining and processing of the ores of other metals, particularly those of copper, nickel, and silver, but also those of gold, lead, and zinc.

The deposits of cobalt can be classified under the following headings:

- **Hypogene deposits** associated with mafic intrusive igneous rocks. The massive and disseminated iron-nickel-copper sulfides containing cobalt are important examples

of this type of deposit. They include the ore from the Sudbury district of Ontario, which has an average cobalt content of 0.07%. The suite of ore minerals consists of pyrrhotite, pentlandite, pyrite, marcasite, cobaltite, and gersdorffite in veins stringers and disseminated grains within an igneous host rock of Precambrian age.

- **Contact metamorphic deposits** associated with mafic rocks. Deposits of magnetite, chalcopyrite, and cobalt-containing pyrite, formed by contact metamorphism of carbonate rock by sills and dikes of diabase, gave the ore deposits at Cornwall and Morgantown in the United States.
- **Lateritic Deposits.** The weathering of peridotite and serpentine generally gives laterite that is rich in iron, nickel, cobalt, and chromium. Commercially valuable deposits contain 40–50% iron, 1–2% nickel, and 0.01–0.1% cobalt. Major lateritic deposits occur in Cuba, New Caledonia, Australia, the United States, and Russia.
- **Massive sulfide deposits** in metamorphic rocks, largely of volcanic sedimentary origin. These deposits consist mainly of pyrite and pyrrhotite and are mined in the United States.
- **Hydrothermal deposits** are subdivided into two classes: vein deposits and replacement deposits. Some of these deposits are the only ones that have been mined specifically as sources of cobalt. In Canada, veins that contain as much as 10% cobalt occur in the Cobalt-Gowganda region of Ontario, whereas veins in the Bou-Azzer area of Morocco contain an average of 1.2% cobalt. Hydrothermal replacement deposits containing 0.5% cobalt as gersdorffite are found in Burma and at Outokumpu in Finland; a copper-rich sulfide deposit contains 0.2% cobalt mainly in linnæite.
- **Strata-bound deposits:** the copper-cobalt deposits of Zaire and Zambia are of this type. They occur in folded shale and dolomite and contain a number of minerals, including chalcopyrite, bornite, chalcocite, linnæite, and carrollite. The ore bed is 6–24

m thick and currently provides the world's major source of cobalt.

- **Deposits formed as chemical precipitates** usually contain chemically precipitated cobalt in associated marine manganese nodules.

Reserves. As generally accepted, there are $3\text{--}5 \times 10^6$ t of minable cobalt reserves and a further $4\text{--}5 \times 10^6$ t of potential reserves, Table 18.8 lists the reported reserves in a number of countries. However, the minable reserves do not have the same degree of profitability. Cuba has minable resources of cobalt, but provides only 5% of the world production because its ore bodies are laterites with only small quantities of nickel and cobalt that are costly to refine. Zaire produces more than half of the world's cobalt because its ores can be treated more profitably.

In addition to the land-based reserves listed in Table 18.8, almost 6×10^9 t of copper is available in marine nodules if it can be recovered and worked economically.

Table 18.8: Cobalt reserves.

Country	Reserves, $\times 10^3$ t	Country	Reserves, $\times 10^3$ t
Australia	295	New Caledonia	385
Brazil	> 9	New Guinea	18
Burma	16	Philippines	159
Canada	250	Puerto Rico	68
Colombia	22.5	Solomon Islands	22.5
Cuba	1 048.5	Soviet Union	181.5
Dominican Republic	89	Uganda	8
Finland	22.5	United States	> 764
Guatemala	45.5	Venezuela	60
Japan	2.5	Zaire	1 920
		Zambia	370

18.5 Production

18.5.1 Concentration of the Ores

[1, 2, 9]

The first stages of the production of cobalt from its ores involve the separation of cobalt-bearing minerals from the gangue and from minerals containing other desirable metals but not cobalt. The concentrates obtained by applying physical separation methods such as gravity separation or froth flotation to ores can

increase the cobalt content to 10–15% from cobalt-rich ores. However, in general, these processes only increase the level of cobalt from 0.1–0.6% in ores to a few percent. The concentration procedures for the main types of ores are described in this section.

Arsenide Ores. Cobalt arsenide minerals have specific gravities of 6.5–7.2 g/cm³ and can be separated at relatively large grain size by gravity methods. Concentrates containing 13–14% cobalt have been produced by these methods from Moroccan ores at Bou-Azzer containing 2% cobalt.

Sulfoarsenide Ores. The main mineral in this type of ore, cobaltite, can be effectively separated by froth flotation with xanthate at pH 4–5, although iron sulfide minerals are also floated under similar conditions and must be separated from the cobalt concentrate.

Sulfide Ores. The chalcocite and carrollite fractions of the ores of the Shaba province in Zaire are floated together at pH 9.2 by using lime, xanthates as collectors, and triethoxybutane as the frothing agent to give a concentrate containing 43–53% copper and 0.5–3% cobalt. The copper cobalt sulfide ores of Zambia are first treated to float the copper minerals selectively at pH 10.5–11; at this stage the presence of sodium cyanide depresses the cobalt minerals. These are subsequently activated by sulfuric acid and floated at pH 8.5–9 with sodium isopropyl xanthate; the concentrates contain up to 3.5% cobalt. The flotation process at the Outokumpu Keretti Mill first separates the copper minerals with xanthates at pH 11–11.5 in the presence of lime and sodium cyanide. The cobalt minerals are then floated at pH 9 to recover 65–75% of the cobalt from an ore containing 0.23–0.31% cobalt; the concentrate contains 0.7–0.82% cobalt. The nickel–copper–cobalt sulfide ores of Ontario are first treated to separate the sulfide minerals from gangue, and the cobalt minerals are then contained in the nickel sulfide concentrate.

Oxide Ores. Two methods have been used on a commercial scale to float oxide ores. The *palm oil process* collects the concentrate in a

3:1 mixture of hydrolyzed palm oil and gas oil emulsified in carbonated hot water; this process can give concentrates containing 23–25% copper and 2–3% cobalt, representing a cobalt recovery of 50–70% from the ore. The *sulfidization process* is used for mixed oxide–sulfide ores to float sulfide ores first and to concentrate oxide minerals subsequently in a xanthate flotation.

18.5.2 Extraction [1, 2, 9]

Cobalt can be extracted from concentrates and occasionally directly from the ore itself by hydrometallurgical, pyrometallurgical, and electrometallurgical processes. Although most methods of extraction are based on hydrometallurgy, cobalt concentrates, mattes, and alloys have been reduced to metal by pyrometallurgical methods. Most arsenic-free cobalt concentrates can, for example, be mixed with lime and coal and melted in a reducing atmosphere to give cobalt–copper–iron alloys. Two types of alloys are obtained, a *white alloy* containing ca. 40% cobalt that is processed for cobalt and a *red alloy* containing ca. 4% cobalt that is processed for copper. Recovery of copper from the red alloy produces a cobalt-rich slag that can be recycled with the ores. The hydrometallurgical processes involve (1) leaching of concentrates to give a cobalt-containing solution, (2) separation of cobalt from the other metal ions in solution, and (3) reduction of cobalt ions to metal. Electrometallurgical processes are used in the electrowinning of the metal from leach solutions and in refining the cobalt that has been extracted by hydrometallurgical or pyrometallurgical methods.

18.5.2.1 Leaching of Cobalt Ores and Concentrates

Cobalt can be leached from its ores and concentrates in both acidic and alkaline media. Processes involving acid–sulfate leaching include (1) treatment of oxide ore concentrates with sulfuric acid containing a reducing agent, (2) extraction of cobalt sulfate from sulfide ores following an oxidizing roast, (3) extrac-

tion following a sulfatizing roast, and (4) extraction by pressure leaching with sulfuric acid, often in the presence of oxygen; the *Chemico process* for the treatment of arsenic-containing ores is, for example, based on an acid pressure leach. Acid leaching processes based on hydrochloric acid extraction and chloridation roasting have also been used.

Processes that involve the extraction of cobalt into alkaline solutions depend on the formation of the hexamminocobalt(II) species $[\text{Co}(\text{NH}_3)_6]^{2+}$, which remains in solution for long periods because of its kinetic stability, even though it has low thermodynamic stability. Ammoniacal leaching has been successfully applied to ores after a reducing roast, and the Sherritt Gordon process depends on ammonia solution pressure leaching.

Cobalt from Copper–Cobalt Concentrates. The copper–cobalt ores of Zaire and Zambia are treated by a sulfatizing roast in a fluidized-bed furnace to convert copper and cobalt sulfides into soluble oxides and iron into insoluble hematite. The calcine is subsequently leached with sulfuric acid from the spent copper recovery electrolyte. Oxide concentrates are introduced at this leaching step to maintain the acid balance in the circuit. Iron and aluminum are removed from the leach solution, and copper is electrowon on copper cathodes. A part of the spent electrolyte enters the cobalt recovery circuit and is purified by removal of iron, copper, nickel, and zinc prior to precipitation of cobalt as its hydroxide. In the final stages, this cobalt hydroxide is redissolved and the metal is refined by electrolysis and by degassing to remove any traces of hydrogen. Figure 18.1 shows the flow diagram of the process used at the Générale des carrières et des mines (Gécamines) plant in Luilu.

Cobalt from Nickel Sulfide Concentrates. Nickel sulfide concentrates can be treated by either roasting or flash smelting to give a matte from which nickel and cobalt can be recovered hydrometallurgically, or they may be treated directly by an ammonia solution pressure leach. In the *Sherritt Gordon process* used at Fort Saskatchewan in Canada, which is

illustrated as a flow diagram in Figure 18.2, a feed of matte and sulfide concentrate, containing about 10% nickel, 2% copper, 0.4% cobalt, 33% iron, and 30% sulfur, is pressure leached in autoclaves at 83 °C and 0.7 MPa (7 bar) with an ammoniacal medium. This converts most of the sulfide via thiosulfate and polythionate to sulfate and solubilizes nickel, copper, and cobalt as ammine complexes. Most of the copper in the leach solution is precipitated as copper sulfides when the solution is distilled to recycle ammonia. The solution is treated with hydrogen sulfide to remove any residual copper, and any sulfide or sulfamate remaining at this stage is converted to sulfate by a pressure oxidation hydrolysis reaction at 6.5 MPa (65 bar). The solution then enters reduction autoclaves, where nickel powder is precipitated by reduction with hydrogen at 3.6 MPa (36 bar). The remaining solution, which contains 1–1.5 g/L of both cobalt and nickel, is treated in an autoclave with hydrogen sulfide to precipitate cobalt and nickel sulfides, which are subsequently leached with sulfuric acid at 140 °C and 6.4 MPa (64 bar). Iron is removed from this leach liquid at pH 2.5–3.0 by addition of ammonia solution. The cobalt(II) in solution is oxidized in air to give a very soluble cobalt(III) pentammine complex. Nickel is subsequently precipitated from the solution in two steps as a nickel ammonium sulfate. Cobalt powder is then added along with sulfuric acid to reduce the cobalt(III) pentammine complex to cobalt(II), which is finally reduced to cobalt powder by treatment with hydrogen at 120 °C and 4.6 MPa (46 bar).

Cobalt-containing mattes and mixed sulfide concentrates have also been treated by pressure leaching with sulfuric acid, for example, at Amax at Port Nickel in the United States, MRR in South Africa, Nippon Mining and Sumitomo Metals Mining Co. in Japan, and Outokumpu Oy in Finland. The flow diagram for the Outokumpu Kukkola plant (Figure 18.3) is used to illustrate this type of cobalt recovery process. Two companies, Falconbridge in Canada and Norway and Société le Nickel in France, leach nickel mattes and sulfide con-

concentrates in chloride media at ambient pressure.

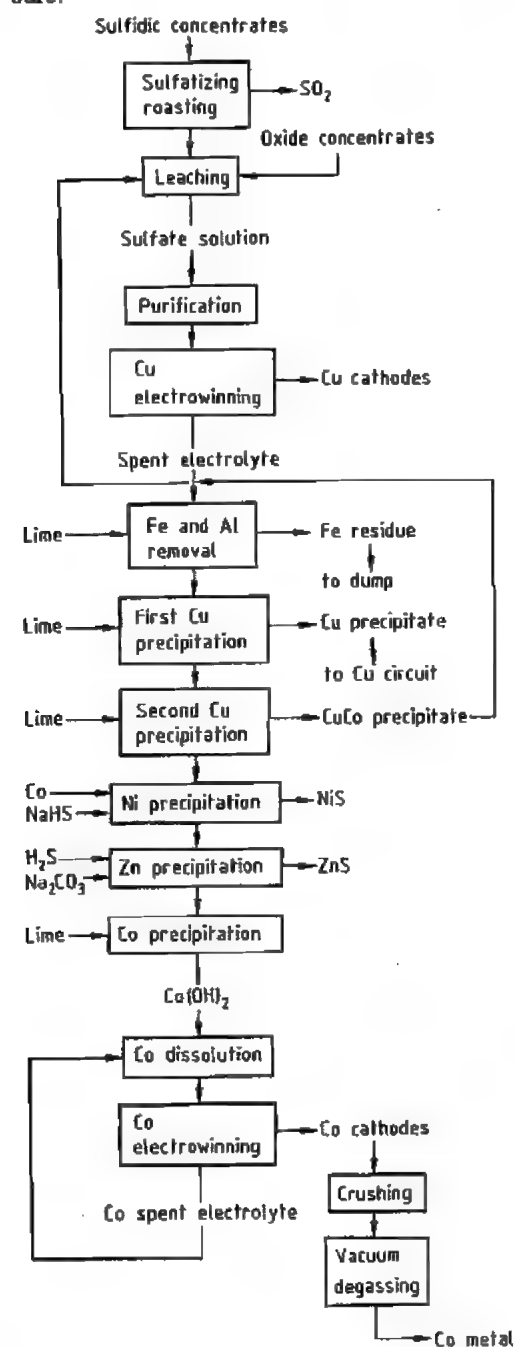


Figure 18.1: Flow diagram of the Gécamines process.

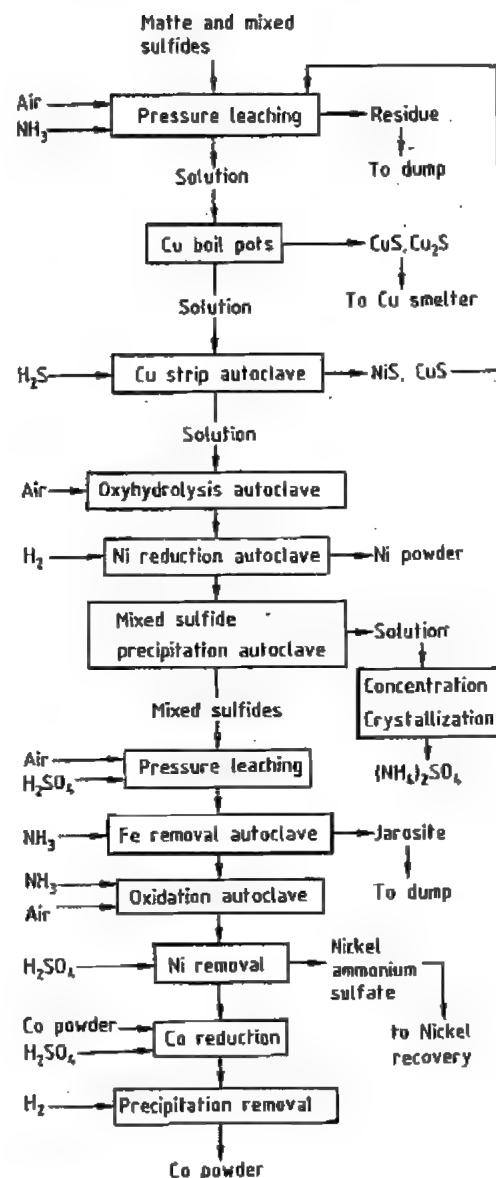


Figure 18.2: Flow diagram of the Sherritt Gordon process.

Falconbridge use a hydrochloric acid leach at 70 °C for about 15% of their feed and a direct chlorine leach for the remainder. The leach medium used by Société le Nickel is chlorine in iron(III) chloride. At the INCO Copper Cliff plant nickel-copper mattes are

cooled slowly and crushed prior to magnetic separation, which isolates a nickel-copper-cobalt alloy. The alloy is smelted in a top-blown rotary converter, desulfurized by oxygen lancing, and granulated. Nickel is volatilized from the granules as Ni(CO)_4 by the INCO carbonyl process to give a residue from which cobalt can be leached; the solution obtained allows cobalt to be electrowon after some purification steps.

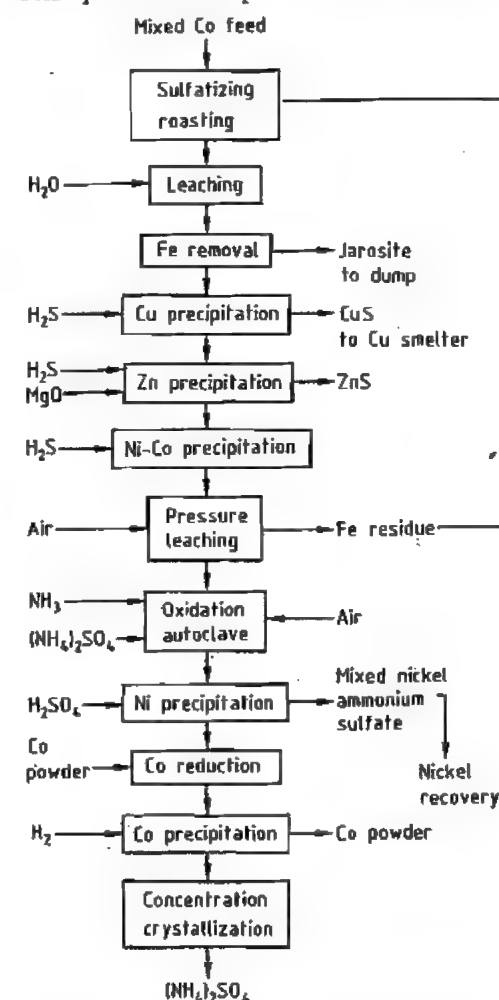


Figure 18.3: Flow diagram of the Outokumpu process.

Cobalt from Laterite Ores. Laterite ores can be treated by the methods described above for nickel mattes after a calcining preroast.

Greenvale Mines in Queensland (Australia) have developed a new process for laterite ore treatment. The ground ore is mixed with 40% of fuel oil and roasted in Herreshoff furnaces with 17 overlapping heating elements. As the ore falls down the furnace through increasingly hotter zones in a reducing atmosphere, the ore is finally reduced to metal at 750 °C in an oxygen-free atmosphere. The roasted ore is leached with an ammonia-ammonium carbonate solution to solubilize the nickel and cobalt as ammine complexes. The leach solution is then purified by removing iron as the hydroxide prior to precipitation of cobalt and part of the nickel as sulfides with hydrogen sulfide. The cobalt-rich sulfide is calcined to provide a material from which cobalt can be extracted.

Cobalt from Arsenide Ores. Arsenic-containing concentrates are roasted in a fluidized bed at 600–700 °C to remove 60–70% of the arsenic present as arsenic(III) oxide. The roasted ores can be treated with hydrochloric acid and chlorine or with sulfuric acid to give a leach solution that can be purified by hydrometallurgical methods and from which cobalt can be recovered by electrolysis or by carbonate precipitation.

18.5.2.2 Separation of Cobalt from Other Metal Ions in Leach Solutions

A major part of cobalt recovery from leach solutions is concerned with its separation from other elements. Because of the similarities in chemical behavior of cobalt and nickel, the separation of these two elements has been studied extensively and is well-known. This section deals with chemical methods of separation of cobalt from nickel and with physico-chemical methods of separation of cobalt from other elements.

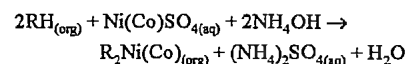
Chemical Methods of Separation. The chemical methods of separating cobalt from other metals use the different solubilities and kinetic or thermodynamic stabilities of their compounds. The most important compounds that have been used in separation are hydroxides, carbonates, ammine complexes, double

ammonium sulfates, sulfides, chlorides, and carbonyls; the cementation to metal is also utilized. For examples, see Section 18.5.2.1. The relative solubilities of cobalt(III) and nickel(II) hydroxides in the presence and absence of complexing agents and of cobalt(II) and nickel(II) carbonates in solutions containing NH_3 and CO_2 have also been used to separate these elements. Fractional crystallization of chloride-containing media can be used to concentrate cobalt in solution and nickel in solid nickel chloride dihydrate.

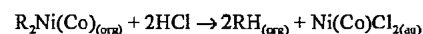
Physical Methods of Separation. Many physical methods have been used to separate cobalt from other elements, but the three most important are electrolysis, solvent extraction, and ion exchange.

In most solvent extraction processes, cobalt is extracted with a tertiary amine from chloride solutions although cobalt and nickel can be separated from each other with phosphate or carboxylic acid reagents from ammoniacal sulfate solutions. In the sulfuric acid leach process of Nippon Mining at Hitachi, solvent extraction is used to extract zinc from the leach solution with di-(2-ethylhexyl) phosphonic acid (DEHPA) at pH 2–3 prior to solvent extraction of cobalt with an alkylphosphonic acid. The Falconbridge and Société le Nickel processes both involve solvent extraction of cobalt from chloride solution with trioctylamine. The Sumitomo Metals Mining Co. uses a solvent extraction process to coextract cobalt and nickel with versatic acid. The extract is then stripped with hydrochloric acid and cobalt is reextracted from the chloride solution with tri-*n*-octylamine to give an extract from which cobalt is stripped and electrowon. The flow diagram for this process is shown in Figure 18.4, and the solvent extraction process can be expressed in terms of the following chemical equations:

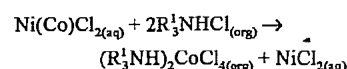
Extraction:



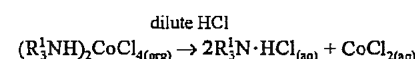
Stripping:



Extraction:



Stripping:



where RH is versatic acid in kerosene and R_3N is tri-*n*-octylamine in xylene; (org) and (aq) are organic and aqueous phases, respectively.

18.5.2.3 Electrowinning [9]

Cobalt can be extracted and obtained as high-purity metal by electrolysis of sulfate or chloride solutions. Solutions of pH 1–4 are necessary for the electrowinning of cobalt, and the pH is often maintained by suspending cobalt hydroxide or cobalt carbonate in the electrolyte to use up the acid produced at the anode. Current densities of 5 A/dm² are used with current consumptions of ca. 6.5 kWh per kilogram of cobalt. Electrolytically refined cobalt is usually purer than 99.5%.

18.6 Cobalt Powders [11–13]

18.6.1 Production

Cobalt powder can be produced by a number of methods, but those of industrial importance involve the reduction of oxides, the pyrolysis of carboxylates, and the reduction of cobalt ions in aqueous solution with hydrogen under pressure. Very pure cobalt powder is prepared by the decomposition of cobalt carbonyls.

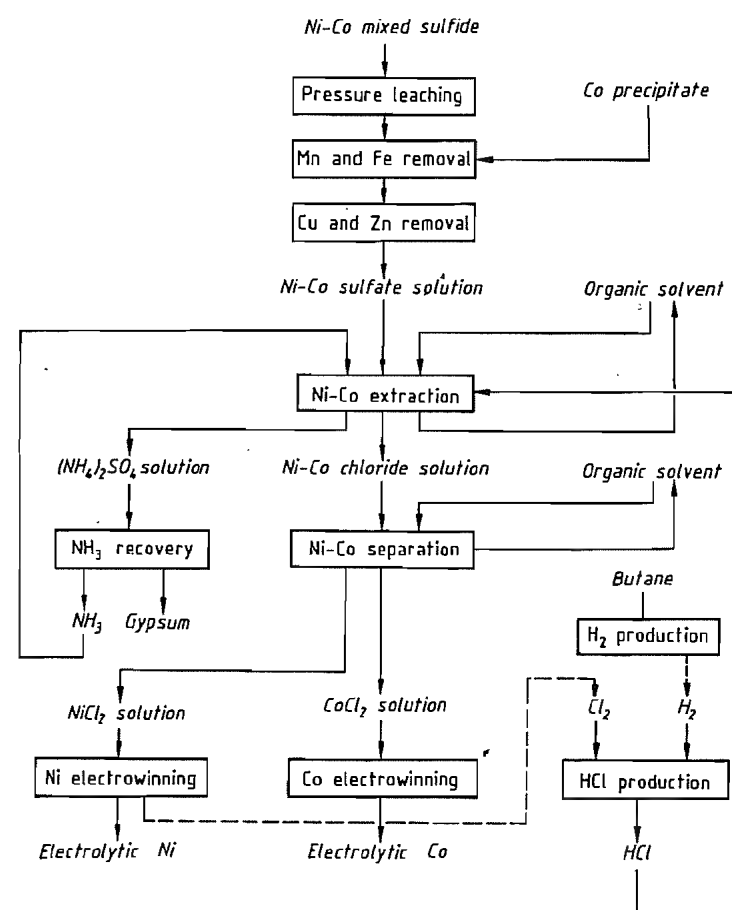


Figure 18.4: Flow diagram of the Sumitomo process.

Reduction of Oxides. Grey cobalt(II) oxide (CoO) or black cobalt(II) cobalt(III) oxide (Co_3O_4) is reduced to metal powder with carbon monoxide or hydrogen. The reactions occur under conditions well below the melting point of the oxides or the metal. The purity of the powder obtained is 99.5% with a particle size of ca. 4 μm , although the density and the particle size of the final product depend on the reduction conditions and on the particle size of the parent oxide. The finely powdered metal is stored at very low temperature.

Pyrolysis of Carboxylates. The thermal decomposition of such cobalt carboxylates as formate or oxalate in a controlled reducing or neutral atmosphere produces a high-purity

(about 99.9%), light, malleable cobalt powder with a particle size of ca. 1 μm that is particularly suitable for the manufacture of cemented carbides. The particle size, form, and porosity of the powder grains can be changed by altering the pyrolysis conditions.

Reduction of Cobalt Ions in Solution. Purified leach solutions containing cobalt pentammine complex ions can be treated in autoclaves with hydrogen under pressure and at high temperature to give an irregular chain-like form of the powder that is suitable for consolidation by direct strip rolling.

18.6.2 Uses

18.6.2.1 Cemented Carbides

One of the most important uses of metallic cobalt is as a bonding agent in cemented carbides [14, 15] that are used extensively as cutting tools for metals, rocks, and other high-strength materials. No suitable substitute has been found for cobalt as a cementing agent for carbides. The most commonly used cemented carbide, tungsten carbide containing 2–30% cobalt, is manufactured as follows: pure cobalt powder is added to tungsten carbide (particle size ca. 1 μm), and the mixture is ball-milled for a long period by using hard metal balls. The mixed powders are then consolidated by cold pressing, by hot pressing at ca. 1300–1400 °C, by cold extension, or by slip casting to produce small artifacts, large artifacts, constant-section rods, and complex-shaped articles, respectively. The consolidated parts are sintered in a reducing atmosphere at 1300–1600 °C. The sintering process involves the formation of a liquid phase; the cobalt liquefies at ca. 1320 °C and dissolves tungsten and carbon from the carbide. When the mixture is cooled, most of the tungsten and carbon reprecipitates, but the binder phase is much stronger than pure cobalt because enough tungsten and carbon are present to stabilize the metal in its cubic form. During the sintering process, the consolidated powders shrink by 20%. The binding mechanism depends on (1) the liquid metal phase to wet the carbide particles so that surface tension forces help densify the sintered phases and (2) on the ability of the liquid to dissolve and retain traces of carbide impurities.

The properties of cemented carbides are controlled by the amount of cobalt present and the particle size of the carbide used. The hardness of the cemented carbides increases with decreasing particle size and with increasing cobalt content. The impact strength of cemented carbides is directly proportional to the cobalt content it rises from less than 1 kgm for a sample with 6% cobalt to ca. 2.5 kgm for a sample with 25% cobalt in tungsten carbide

with a particle size of 1.4–3.1 μm . The properties of cemented tungsten carbides can be improved by the addition of other carbides such as those of niobium, tantalum, or titanium.

18.6.2.2 Cobalt Powders in Powder Metallurgy and Cobalt-containing Metal [15]

Cobalt powders have been used in the formation of a number of alloy phases including maraging steel by hot extension of prealloyed powders, cobalt-based superalloys by consolidation of powders involving liquid phase sintering, fine-particle magnetic alloys, and bearing materials impregnated with low-friction substances such as graphite, lead, nylon, and molybdenum disulfide.

18.7 Alloys [1–3, 9]

About 64% of the cobalt is consumed in alloy compositions. The most important cobalt alloys are discussed in this article under the following headings:

- High-temperature alloys
- Magnetic alloys
- Hard metal alloys
- Cobalt-containing high-strength steels
- Electrodeposited alloys
- Alloys with special properties

18.8 Compounds [17]

18.8.1 Chemical Properties of Cobalt

Cobalt is much less reactive than iron. It is stable to atmospheric oxygen unless heated. When heated, it is first oxidized to Co_3O_4 and then, above 900 °C, to CoO , which is also the product of the reaction between the red-hot metal and steam. The activation energy of the oxidation above 900 °C has been calculated as 155–160 kJ/mol. The metal does not combine directly with hydrogen or nitrogen, but it combines with carbon, phosphorus, and sulfur on

heating. The reaction with sulfur is influenced by the formation of a low melting eutectic (877 °C) between the metal and the Co_4S_3 phase; the reaction between cobalt and sulfur is rapid above this temperature. Below 877 °C, a protective layer of sulfide scale is formed. In an atmosphere of hydrogen sulfide, cobalt also forms a scale of sulfide, but in air containing sulfur dioxide, a mixed oxide sulfide scale is formed.

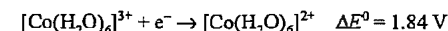
In bulk form, cobalt is resistant to many mild corrosive agents, but it is more readily attacked when it is finely divided. Table 18.9 gives the corrosion rates of cobalt in some aqueous media. Cobalt is strongly attacked by concentrated nitric acid at ambient temperature. The metal dissolves slowly in dilute mineral acids, the Co^{2+}/Co potential being -0.277 V .

Table 18.9: Corrosion of cobalt in aqueous media at 25 °C.

Corrosive medium	Rate of cobalt corrosion, $\text{mg dm}^{-2}\text{d}^{-1}$
Distilled water	1.1
5 vol% Ammonia	5.3
10 vol% Sodium hydroxide	5.6
Conc. phosphoric acid	7.4
50% Phosphoric acid (aqueous)	65.1
5 vol% Acetic acid	12.5
5 vol% Sulfuric acid	56.8
50% Hydrofluoric acid (aqueous)	178.6

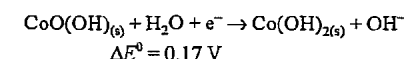
The solubility of oxygen in cobalt is 0.006, 0.013, 0.125, and 0.4% (at 600, 1200, 1510, and 1700 °C, respectively). Nitrogen is only slightly soluble (40 mg/kg) in cobalt at its melting point; the solubility rises to 60–70 mg/kg at 1750 °C. The solubility of hydrogen in cobalt increases with temperature from 1 mg/kg at 700 °C to ca. 8 mg/kg at the melting point. The solubility of hydrogen in the liquid metal increases to ca. 20 mg/kg at 1500 °C and to ca. 27 mg/kg at 1750 °C.

The main oxidation states of cobalt are Co^{2+} and Co^{3+} . In acid solution and in the absence of complexing agents, Co^{2+} is the stable oxidation state, with oxidation to Co^{3+} being difficult.



The oxidation can be achieved by electrolysis or ozone, but the Co^{3+} is very unstable and rapidly reduced to Co^{2+} , even at room temperature, with evolution of oxygen from the water. The solution chemistry of cobalt in acid solution in the absence of complexing agents is dominated by Co^{2+} . The most common species present is $[\text{Co}(\text{H}_2\text{O})_6]^{2+}$, although the ions $[\text{CoX}_3]^-$, $[\text{CoX}_4]^{2-}$, and $[\text{CoX}_6]^{4-}$ ($\text{X} = \text{halide}$) are also found in solutions of hydrogen halides. Cobalt is often removed from solution as its sulfide, and it is interesting to note that although the precipitates of cobalt sulfide obtained by using H_2S are not readily soluble in dilute acids, those obtained by using Na_2S or $(\text{NH}_4)_2\text{S}$ are soluble. All sulfide precipitates become less soluble as they age in the atmosphere to form $\text{Co}(\text{OH})\text{S}$. The cobalt dihalides (except fluoride) are also readily soluble in some organic solvents such as alcohol, acetone, and methyl acetate.

In alkali, Co^{2+} is more readily oxidized to Co^{3+} :



In the presence of complexing agents, oxidation is very easy in any solution because Co^{3+} has a particularly high affinity for complex formation. With N-donor ligands the redox reaction in the presence of ammonia is:



Table 18.10: ΔE^0 for some $\text{Co}^{3+}/\text{Co}^{2+}$ couples in acid solution.

Redox reaction	ΔE^0
$[\text{Co}(\text{C}_2\text{O}_4)_3]^{3-} + \text{e}^- \rightleftharpoons [\text{Co}(\text{C}_2\text{O}_4)_3]^{4-}$	0.57
$[\text{Co}(\text{EDTA})]^- + \text{e}^- \rightleftharpoons [\text{Co}(\text{EDTA})]^{2-}$	0.37
$[\text{Co}(\text{bipy})_3]^{3+} + \text{e}^- \rightleftharpoons [\text{Co}(\text{bipy})_3]^{2+}$	0.31
$[\text{Co}(\text{en})_3]^{3+} + \text{e}^- \rightleftharpoons [\text{Co}(\text{en})_3]^{2+}$	0.18
$[\text{Co}(\text{CN})_6]^{3-} + \text{H}_2\text{O} + \text{e}^- \rightleftharpoons [\text{Co}(\text{CN})_5(\text{H}_2\text{O})]^{2-} + \text{CN}^-$	-0.8

Oxidation of Co^{2+} solutions containing complexing agents can be achieved with air or hydrogen peroxide. Thus, the solution chemistry of cobalt in the presence of complexing agents is dominated by the complex chemistry of Co^{3+} . The sensitivity of the reduction potential of the $\text{Co}^{3+}/\text{Co}^{2+}$ couple to different ligands whose presence renders Co^{2+} unstable

to air oxidation is shown by the data in Table 18.10.

Cobalt(II) Compounds. Cobalt combines with oxygen to form cobalt(II) oxide, CoO , which is stable above 900 °C. This oxide has the sodium chloride structure and is antiferromagnetic at ordinary temperature. When cobalt(II) oxide is heated at 400–500 °C in an atmosphere of oxygen, the cobalt(II,III) oxide, Co_2O_3 , is formed. This mixed-valence oxide has the spinel structure with cobalt(II) in tetrahedral sites and cobalt(III) in octahedral sites. Cobalt hydroxide, $\text{Co}(\text{OH})_2$, is a product of the hydrolysis of solutions containing Co^{2+} ions. The hydroxide is amphoteric, dissolving both in alkali, to give blue solutions containing the $[\text{Co}(\text{OH})_4]^{2-}$ ion, and in acids. Cobalt(II) forms an extensive range of simple and hydrated salts with all of the common anions including acetate, bromide, carbonate, chloride, fluoride, nitrate, perchlorate, and sulfate. Many of the hydrated salts and their solutions contain the pink octahedral $[\text{Co}(\text{H}_2\text{O})_6]^{2+}$ ion. Although complexes of cobalt(II) are generally unstable to oxidation, a number of octahedral species are formed, including (1) a series of $[\text{Co}(\text{N}-\text{N})_3]^{2+}$ complexes with neutral bidentate donor ligands, such as ethylenediamine and bipyridyl, and (2) the acetylacetonates $[\text{Co}(\text{acac})_2 \cdot 2\text{H}_2\text{O}]$ and $\text{Co}(\text{acac})_2$. Tetrahedral complexes $[\text{CoX}_4]^{2-}$ are usually formed with monodentate anionic ligands, such as chloride, bromide, iodide, thiocyanate, azide, and hydroxyl. Tetrahedral $[\text{CoX}_2\text{L}_2]$ complexes are formed by a combination of two such ligands with two neutral ligands (L). Addition of cyanide to a solution of Co^{2+} produces a dark green color attributed to the $[\text{Co}(\text{CN})_5]^{3-}$ ion.

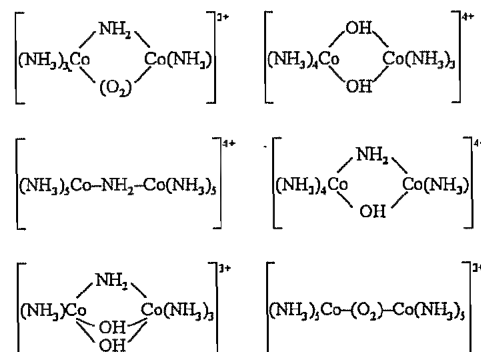
The colors produced by cobalt(II) complexes in aqueous media have been used to distinguish between octahedral and tetrahedral coordination in the complexes. In general, octahedral species are pink to violet, whereas tetrahedral species are blue. This is not an infallible distinction, but it does provide a use-

ful guide that can be improved by analyzing the electronic spectra of the complexes.

Cobalt(III) Compounds. In addition to the mixed-valence oxide Co_2O_3 , impure forms of the unstable cobalt(III) oxide, Co_2O_3 , have been prepared. Very few simple cobalt(III) salts are known. The blue sulfate, $\text{Co}_2(\text{SO}_4)_3 \cdot 18\text{H}_2\text{O}$, which contains the $[\text{Co}(\text{H}_2\text{O})_6]^{3+}$ species, can be obtained by the electrolytic oxidation of cobalt(II) in 4 M sulfuric acid solution. It is stable when dry, but decomposes in the presence of moisture. The alums $\text{MCo}(\text{III})(\text{SO}_4)_2 \cdot 2\text{H}_2\text{O}$ (M = K, Rb, Cs, NH_4) are also known, and a hydrated fluoride $2\text{CoF}_3 \cdot 7\text{H}_2\text{O}$ has been reported.

The chemistry of cobalt(III) is dominated by complex formation. Cobalt(III) complexes are kinetically inert, and for this reason, indirect methods of syntheses are used to obtain them. Usually the ligand is added to a solution of Co^{2+} , which is then oxidized with some convenient oxidant, often in the presence of a catalyst such as activated charcoal. A wide range of cobaltamines have been prepared and studied; the species identified in solution or as solid derivatives include $[\text{Co}(\text{NH}_3)_6]^{3+}$, $[\text{Co}(\text{NH}_3)_5\text{H}_2\text{O}]^{3+}$, $[\text{Co}(\text{NH}_3)_5\text{X}]^{2+}$ (X = Cl, Br, NO_2 , NO_3), and *cis*- and *trans*- $[\text{Co}(\text{NH}_3)_4\text{X}_2]^{+}$ (X = Cl, NO_2).

In addition to these simple cobaltamines, a number of polynuclear species containing bridging groups such as NH_2^- , NH_2^{2-} , NO_2^- , OH^- , and O_2 have been prepared. Polynuclear cobaltamines that have been identified include:



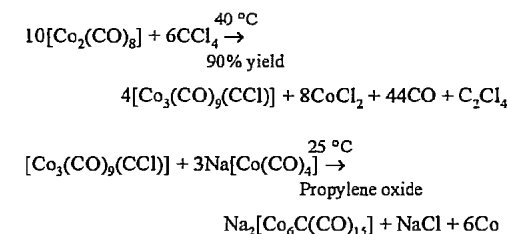
Complexes of cobalt(III) with O-donor ligands are generally less stable than those with N-donor species, although $[\text{Co}(\text{acac})_3]$ and $[\text{Co}(\text{C}_2\text{O}_4)_3]^{3-}$ are known. Apart from the O_2 -bridged compounds mentioned above, the octahedral fluoro complexes $[\text{CoF}_6]^{3-}$ and $[\text{CoF}_3(\text{H}_2\text{O})_3]$ are the only known high-spin cobalt(III) complexes, the paramagnetic moment of $[\text{CoF}_6]^{3-}$ at room temperature being about 5.8 BM. All other cobalt(III) complexes are low-spin and diamagnetic, including the hexacyanocobaltates(III), $[\text{Co}(\text{CN})_6]^{3-}$, and the hexanitritocobaltates(III), $[\text{Co}(\text{NO}_2)_6]^{3-}$.

In addition to the two most stable oxidation states, 2+ and 3+, cobalt also forms compounds in the 1-, 0, 1+, and 4+ oxidation states. There are only a few reported examples of Co(IV) compounds, mainly fluoro complexes, CoF_6^{2-} , and mixed-metal oxides (the purity of compounds in this oxidation state is questionable).

The formation of cobalt compounds in oxidation states lower than 2+ requires the presence of stabilizing π -acceptor ligands. The 1+ state is not common for cobalt, and most of the known examples are pentacoordinated complexes of the type $[\text{Co}(\text{NCR})_5]^+$ (NCR = organic nitrile). Cobalt forms a wide range of complexes in which its formal oxidation state is 0 or 1-. Many of these contain ligands such as CO, CN^- , NO^+ , and RNC , but other ligands such as tertiary phosphanes also stabilize lower oxidation states to give compounds like $[\text{Co}(\text{P}(\text{CH}_3)_3)_4]^+$, which is prepared by reducing an ethereal solution of cobalt(II) chloride with sodium or magnesium amalgam in the presence of trimethylphosphane.

Cobalt Carbonyls [17, 18]. The carbonyl complexes of cobalt are important because of their uses as hydroformylation catalysts. Because cobalt has an odd number of valence electrons, it can satisfy only the eighteen-electron rule in its carbonyls if Co-Co bonds are formed. For this reason, the principal binary carbonyls of the element are octacarbonyldicobalt, $[\text{Co}_2(\text{CO})_8]$, dodecacarbonyltetracobalt, $[\text{Co}_4(\text{CO})_{12}]$, and hexadecacarbonylhexas-cobalt, $[\text{Co}_6(\text{CO})_{16}]$.

Octacarbonyldicobalt is prepared by heating the metal to 250–300 °C at 200–300 bar of carbon monoxide or by heating cobalt carbonate under similar conditions in the presence of hydrogen. It is an air-sensitive orange-red solid with a melting point of 51 °C. The compound can be reduced with sodium amalgam in benzene to give the tetrahedral monomeric ion $[\text{Co}(\text{CO})_4]^-$, acidification of which leads to tetracarbonylhydridocobalt, $[\text{HCo}(\text{CO})_4]$. This hydride is a yellow liquid that forms a colorless vapor. It melts at -26 °C and decomposes above this temperature to H_2 and $[\text{Co}_2(\text{CO})_8]$. It is partly soluble in water to give a strong acid solution containing $[\text{Co}(\text{CO})_4]^-$ ions. The hydrogen atom in $[\text{HCo}(\text{CO})_4]$ is bound directly to the cobalt, giving a Co-H infrared stretching frequency of ca. 1934 cm^{-1} . The $[\text{Co}(\text{CO})_4]^-$ ion is reoxidized to $[\text{Co}_2(\text{CO})_8]$ by carbon tetrachloride, and further reaction with this reagent leads to a triply bridged chloromethynyl derivative, from which a carbidocarbonyl compound, disodium carbidopentadecacarbonylhexas-cobaltate, $\text{Na}_2[\text{Co}_6\text{C}(\text{CO})_{15}]$, can be obtained:



Other carbidocarbonyls are obtained by similar routes, including $[\text{Co}_6\text{C}(\text{CO})_{14}]^-$, $[\text{Co}_8\text{C}(\text{CO})_{18}]^{2-}$, and $[\text{Co}_{13}\text{C}(\text{CO})_{24}\text{H}]^{4-}$. Dodecacarbonyltetracobalt is obtained as a green black solid by heating $[\text{Co}_2(\text{CO})_8]$ in an inert atmosphere at 50 °C.

The structure of $[\text{Co}_2(\text{CO})_8]$ in the solid state is different from that in solution. The solid-state structure shown in Figure 18.5A involves two bridging carbonyl groups and can be best rationalized in terms of the formation of a bent Co-Co bond. In solution, however, this structure is in equilibrium with the form shown in Figure 18.5B, in which the dimer is held together by a Co-Co bond. The structure

of $[\text{Co}_4(\text{CO})_{12}]$ is shown in Figure 18.5C. The structure of the carbidocarbonyl (Figure 18.5D) shows the presence of a carbon atom at the center of a distorted square antiprismatic cobalt cluster.

In addition to the carbonyls, cobalt also forms complexes with N_2 and NO^+ , which are isoelectronic with CO. Examples of this type of complex are $[\text{CoH}(\text{PR}_3)_3(\text{N}_2)]$ and $[\text{Co}(\text{CO})_3\text{NO}]$, where R is an alkyl group.

18.8.2 Commercially Important Cobalt Compounds [19]

Table 18.11 lists the known applications of cobalt compounds. The most important commercially available compounds are the oxides, as well as hydroxide, chloride, sulfate, nitrate, phosphate, carbonate, acetate, oxalate, and other carboxylic acid derivatives.

Cobalt Oxides. Two main types of cobalt oxide distinguishable by their colors are available: *grey* cobalt(II) oxide, containing 75–

78% cobalt, and *black* cobalt(II) dicobalt(III) oxide, containing 70–74% cobalt.

Cobalt(II) oxide, CoO (78.66% Co), is usually prepared by the controlled oxidation of the metal above 900 °C followed by cooling in a protective atmosphere to prevent partial oxidation to Co_3O_4 . Cobalt(II) oxide has a cubic unit cell with $a = 0.425$ nm. It is insoluble in water, ammonium hydroxide, and alcohol, but dissolves in strong acids in the cold and in weak acids on heating. Cobalt oxide (CoO) absorbs a large amount of oxygen at room temperature. Cobalt(II) dicobalt(III) tetroxide, Co_3O_4 (73.44% Co), can be prepared by the controlled oxidation of cobalt metal or CoO or by the thermal decomposition of cobalt(II) salts at temperatures below 900 °C. The cubic spinel lattice has $a = 0.807$ nm; the solid material readily absorbs oxygen at room temperature, but never transforms into cobalt(III) trioxide, Co_2O_3 . The mixed-valence oxide is insoluble in water and only slightly soluble in acids.

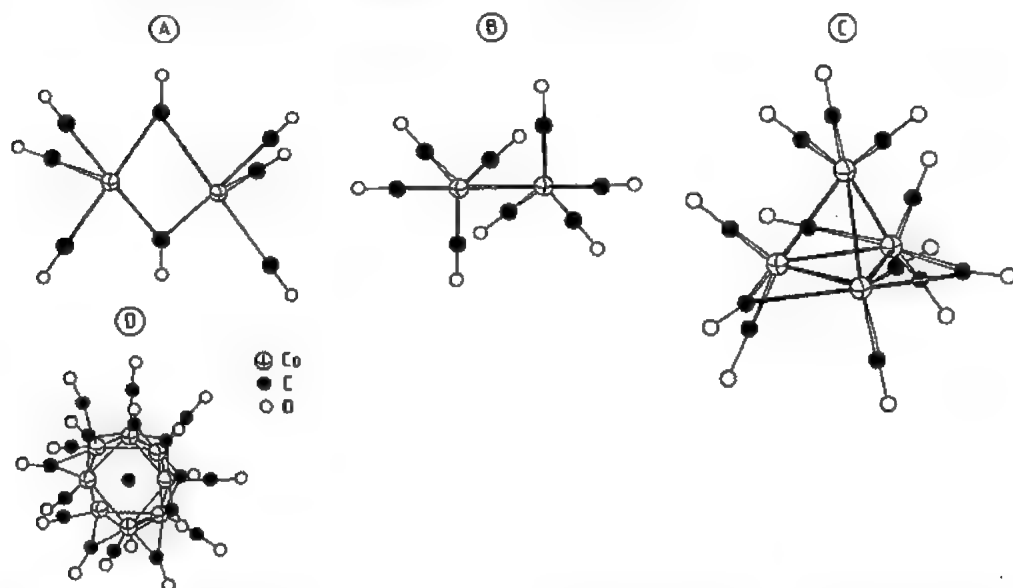


Figure 18.5: Structures of carbonyl complexes of cobalt. A) $[\text{Co}_2(\text{CO})_8]$ (solid state); B) $[\text{Co}_2(\text{CO})_8]$ (solution); C) $[\text{Co}_4(\text{CO})_{12}]$; D) $[\text{Co}_8\text{C}(\text{CO})_{18}]$.

Table 18.11: Industrial uses of cobalt compounds.

Compound	Formula	Uses
Acetate(III)	$\text{Co}(\text{CH}_3\text{COO})_3$	catalyst
Acetate(II)	$\text{Co}(\text{CH}_3\text{COO})_2 \cdot 4\text{H}_2\text{O}$	driers for lacquers and varnishes, sympathetic inks, catalysts, pigment for oil cloth, mineral supplement, anodizing, stabilizer for malt beverages
Acetylacetonate	$\text{Co}(\text{C}_5\text{H}_7\text{O}_2)_3$	vapor plating of cobalt
Aluminate	CoAl_2O_4	pigment, catalysts, grain refining
Ammonium sulfate	$\text{CoSO}_4(\text{NH}_4)_2\text{SO}_4 \cdot 6\text{H}_2\text{O}$	catalysts, plating solutions
Arsenate	$\text{Co}_3(\text{AsO}_4)_2 \cdot 8\text{H}_2\text{O}$	pigment for paint, glass, and porcelain
Bromide(II)	CoBr_2	catalyst, hydrometers
Carbonate	CoCO_3	pigment, ceramics, feed supplements, catalyst
Carbonate (basic)	$2\text{CoCO}_3 \cdot \text{Co}(\text{OH})_2 \cdot \text{H}_2\text{O}$	chemicals
Carbonyl	$\text{Co}_2(\text{CO})_8$	catalyst
Chloride	$\text{CoCl}_2 \cdot 6\text{H}_2\text{O}$	chemicals, sympathetic inks, hydrometers, plating baths, metal refining, pigment, catalyst
Chromate	CoCrO_4	pigment
Citrate	$\text{Co}_3(\text{C}_6\text{H}_5\text{O}_7)_2 \cdot 2\text{H}_2\text{O}$	therapeutic agents, vitamin preparations
Ferrate	CoFe_2O_4	catalyst, pigment
Fluoride	$\text{CoF}_2, \text{CoF}_3$	fluorinating agents
Fluoride	$\text{CoF}_2 \cdot 4\text{H}_2\text{O}$	catalyst
Fluorosilicate	$\text{CoSiF}_6 \cdot 6\text{H}_2\text{O}$	ceramics
Formate	$\text{Co}(\text{CHO})_2 \cdot 2\text{H}_2\text{O}$	catalyst
Hydroxide	$\text{Co}(\text{OH})_2$	paints, chemicals, catalysts, printing inks
Iodide	CoI_2	moisture indicator
Linoleate	$\text{Co}(\text{C}_{18}\text{H}_{31}\text{O}_2)_2$	paint and varnish drier
Manganate	CoMn_2O_4	catalyst, electrocatalyst
Naphthenate	$\text{Co}(\text{C}_{11}\text{H}_{19}\text{O}_2)_2$	catalyst, paint and varnish drier
Nitrate	$\text{Co}(\text{NO}_3)_2 \cdot 6\text{H}_2\text{O}$	pigments, chemicals, ceramics, feed supplements, catalyst
2-Ethylhexanoate	$\text{Co}(\text{C}_8\text{H}_{15}\text{O}_2)_2$	paint and varnish drier
Oleate	$\text{Co}(\text{C}_{18}\text{H}_{31}\text{O}_2)_2$	paint and varnish drier
Oxalate	CoC_2O_4	catalysts, cobalt powders
Oxide	CoO	chemicals, catalysts, pigments
Oxide	Co_3O_4	enamels, semiconductors
Oxides	(mixed metal)	pigments
Dilanthanum tetroxide	La_2CoO_4	catalyst, anode
Tricobalt tetralanthanum decaoxide	$\text{La}_4\text{Co}_3\text{O}_{10}$	catalyst
Lithium oxide	LiCoO_2	battery electrode
Sodium oxide	NaCoO_2	battery electrode
Dicobalt manganese tetroxide	MnCo_2O_4	catalyst
Dicobalt nickel tetroxide	NiCo_2O_4	catalyst, anode
Lanthanum trioxide	LaCoO_3	oxygen, electrode
Phosphate	$\text{Co}_3(\text{PO}_4)_2 \cdot 8\text{H}_2\text{O}$	glazes, enamels, pigments, steel pretreatment
Potassium nitrite	$\text{K}_3\text{Co}(\text{NO}_2)_6 \cdot 1.5\text{H}_2\text{O}$	pigment
Resinate	$\text{Co}(\text{C}_{24}\text{H}_{47}\text{O}_3)_2$	paint and varnish drier, catalyst
Succinate	$\text{Co}(\text{C}_4\text{H}_4\text{O}_4)_2 \cdot 4\text{H}_2\text{O}$	therapeutic agents, vitamin preparations
Sulfamate	$\text{Co}(\text{NH}_2\text{SO}_3)_2 \cdot 3\text{H}_2\text{O}$	plating baths
Sulfate	$\text{CoSO}_4 \cdot x\text{H}_2\text{O}$	chemicals, ceramics, pigments
Sulfide	CoS	catalysts
Tungstate	CoWO_4	drier for paints and varnishes

Cobalt(II) Hydroxide. $\text{Co}(\text{OH})_2$ (63.43% Co) is prepared commercially as a pink solid by precipitation from a cobalt(II) salt solution with sodium hydroxide. It has a hexagonal crystal structure with $a = 0.317$ nm and $c/a =$

1.46. It is insoluble in water and alkaline solutions, but dissolves readily in most inorganic and organic acids; for this reason, it is commonly used as a starting material in the synthesis of cobalt chemicals. $\text{Co}(\text{OH})_2$

decomposes thermally by loss of water, starting at 150 °C, to give the anhydrous oxide at 300 °C. Care must be taken to store the hydroxide in the absence of air because slow air oxidation leads to a product that is poorly soluble in weak acids.

Cobalt(II) Chloride. Cobalt(II) chloride hexahydrate, $\text{CoCl}_2 \cdot 6\text{H}_2\text{O}$ (24.79% Co), is a dark red deliquescent crystalline compound with a monoclinic unit cell ($a = 0.886 \text{ nm}$, $b = 0.707 \text{ nm}$, $c = 1.312 \text{ nm}$, $\beta = 97^\circ 17'$). It is prepared by concentrating a hydrochloric acid solution of cobalt oxide or carbonate. The chloride is very soluble in water, alcohols, and a number of other organic solvents. The solubility of the chloride in aqueous media does, however decrease with increasing hydrochloric acid content. The hexahydrate dehydrates thermally in three stages, giving the dihydrate at 50 °C, the monohydrate at 90 °C, and the anhydrous chloride at 130–140 °C.

The anhydrous chloride and the lower hydrates are very hygroscopic and transform to the hexahydrate in a moist atmosphere. The fact that the anhydrous chloride is blue and the hexahydrate red is used as a humidity indicator in silica gel desiccants. The chloride is also used in the electroplating, ceramics, glass, chemical, agricultural, and pharmaceutical industries.

Cobalt(II) Sulfate. Cobalt(II) sulfate hexahydrate, $\text{CoSO}_4 \cdot 6\text{H}_2\text{O}$ (20.98% Co), is a brownish-red crystalline compound with a monoclinic unit cell ($a = 1.545 \text{ nm}$, $b = 1.308 \text{ nm}$, $c = 2.004 \text{ nm}$, $b = 104^\circ 40'$). It is prepared by concentrating a sulfuric acid solution of cobalt oxide or carbonate. It is an efflorescent substance and loses one molecule of water when exposed to dry air or when heated gently. The hexahydrate obtained loses water in two stages to give the monohydrate at 100 °C and the anhydrous sulfate above 250 °C. The monohydrate, $\text{CoSO}_4 \cdot \text{H}_2\text{O}$ (34.08% Co), has been manufactured and sold commercially. Cobalt sulfates are very soluble in water and are generally more stable than cobalt(II) chlorides or nitrates; for this reason they have been widely used as sources of cobalt(II) in solution

for the manufacture of chemicals and for the electroplating industries. The sulfates are also used in the ceramics, linoleum, and agricultural industries.

Cobalt(II) Nitrate. Cobalt(II) nitrate hexahydrate, $\text{Co}(\text{NO}_3)_2 \cdot 6\text{H}_2\text{O}$ (20.26% Co), is a red-brown crystalline compound with a monoclinic unit cell ($a = 1.509 \text{ nm}$, $b = 0.612 \text{ nm}$, $c = 1.269 \text{ nm}$, $\beta = 119^\circ$). It is prepared by concentrating a nitric acid solution of cobalt oxide or carbonate. The hexahydrate loses water rapidly at 55 °C to give the trihydrate; the monohydrate can also be prepared. The nitrates are very soluble in water, alcohols, and acetone. Cobalt nitrate is an important source of high-purity cobalt for use in the electronics and related industries, and the compound has also found uses in the chemical and ceramics industries.

Cobalt(II) Phosphate. Cobalt(II) phosphate octahydrate, $\text{Co}_3(\text{PO}_4)_2 \cdot 8\text{H}_2\text{O}$ (34.63% Co), is obtained as a purple flocculent precipitate when an alkali-metal phosphate is added to the solution of a cobalt(II) salt. The phosphate is soluble in inorganic acids and particularly in phosphoric acid, but is insoluble in water or alkaline solutions. It is used in the paints and ceramics industries and is a component of some steel phosphating formulations.

Cobalt(II) Carbonate. Although pure CoCO_3 has a cobalt content of 49.57% and a pseudohexagonal unit cell, the material available commercially is a mauve basic carbonate, $[\text{CoCO}_3]_x \cdot [\text{Co}(\text{OH})_2]_y \cdot z\text{H}_2\text{O}$, of indeterminate composition and a cobalt content of 45–47%. The basic carbonate is insoluble in water, but dissolves easily in most inorganic and organic acids. for this reason it is often used as a starting material for the manufacture of other chemicals. The basic carbonate is also used in the ceramics and agricultural industries.

Cobalt(II) Acetate. Cobalt(II) acetate tetrahydrate, $\text{Co}(\text{CH}_3\text{CO}_2)_2 \cdot 4\text{H}_2\text{O}$ (23.68% Co), is a deliquescent mauve-pink crystalline compound with a monoclinic unit cell ($a = 0.847 \text{ nm}$, $b = 1.190 \text{ nm}$, $c = 0.482 \text{ nm}$, $\beta = 94^\circ 18'$). It is prepared by concentrating solutions of co-

balt hydroxide or carbonate in acetic acid. The tetrahydrate is soluble in water, alcohols, inorganic, and organic acids including acetic acid. The compound loses its water of crystallization at ca. 140 °C. It is used in the manufacture of drying agents for inks and varnishes, fabrics dressings, catalysts, and pigments, as well as in the anodizing and agricultural industries.

Cobalt(II) Oxalate. Cobalt(II) oxalate dihydrate, $\text{Co}(\text{C}_2\text{O}_4) \cdot 2\text{H}_2\text{O}$ (32.23% Co), is obtained as a pink precipitate when oxalic acid or an alkali-metal oxalate is added to the solution of a cobalt(II) salt. The dihydrate loses water when it is heated gently in air, and at 200 °C it decomposes to cobalt(II) oxide. The oxalate is insoluble in water, slightly soluble in acids, but soluble in solutions containing ammonia or an ammonium salt. The main use of cobalt oxalate is as a starting material for the preparation of cobalt metal powders.

Cobalt(II) Carboxylates. The cobalt salts of carboxylic acids can be made by the direct reaction of cobalt powder, oxide, or hydroxide with the organic acid or by precipitation reactions involving the addition of the sodium salt of the acid to an aqueous solution of a cobalt salt, such as the sulfate. Cobalt(II) resinate, oleate, linoleate, soyate, naphthenate, ethylhexanoate, formate, acetylacetonate, and citrate have been produced for use in a variety of applications including catalysts, drying agents, metal from production, and medical uses.

18.8.3 Industrial Applications of Cobalt Compounds [19]

The more important applications of cobalt chemicals listed in Table 18.12 can be considered under the following headings: glasses, ceramics, and refractories; driers, paints, varnishes, and dressings; catalysts; electroplating; electronics and solid-state devices; and agricultural, nutritional, and medical uses.

Table 18.12: Effects of several elements in cobalt superalloys.

Element	Effect (M = metal)
Chromium	improves oxidation and hot-corrosion resistance; produces strengthening by formation of M_7C_3 and M_{23}C_6 carbides
Molybdenum Tungsten	solid-solution strengtheners; produce strengthening by formation of intermetallic compound Co_3M ; formation of M_6C carbide
Tantalum Niobium	solid-solution strengtheners; produce strengthening by formation of intermetallic compound Co_3M and MC carbide; formation of M_6C carbide
Aluminum	improves oxidation resistance; formation of intermetallic compound CoAl
Titanium	produces strengthening by formation of MC carbide and intermetallic compound Co_3Ti ; with sufficient nickel produces strengthening by formation of intermetallic compound Ni_3Ti
Nickel	stabilizes the face-centered cubic form of matrix; produces strengthening by formation of intermetallic compound Ni_3Ti ; improves forgeability
Boron Zirconium	produce strengthening by effect on grain boundaries and by precipitate formation; zirconium produces strengthening by formation of MC carbide
Carbon	produces strengthening by formation of MC, M_7C_3 , M_{23}C_6 , and possibly M_6C carbides
Yttrium Lanthanum	increase oxidation resistance

18.8.3.1 Glasses, Ceramics, and Refractories

The addition of cobalt oxides to provide a blue pigment for glass, ceramics, and enamels has been used for many centuries. The level of cobalt in the final product depends on the color intensity required, but is typically 0.4–0.5% for colored ceramic bodies, 0.5% for the blue glass used in welder's goggles, and a few mg/kg in camera lens glass. A range of cobalt-containing mixed-metal oxides and cobalt tripotassium hexanitrite (a yellow pigment) is also available for use as pigments. An indication of the colors obtained from mixed-metal oxide pigments is given in Table 18.13. The shades of the colors also depend on the exact composition of the oxide and on the method of preparing the pigment. The compositions of

some ceramic pigments are given in Table 18.14.

Table 18.13: Colors of cobalt-containing pigments.

Metals in mixed-metal oxide	Color
Co Al	blue
Co P	violet
Co Zn	green
Co Sn Si	light blue
Co Cr Al	turquoise
Co Mg	pink
Co Fe	brown

Table 18.14: Compositions of cobalt-containing pigments.

Color	Content of Co ₃ O ₄ , %	Content of other components (% in parentheses)
Mazarine blue	68.0	SiO ₂ (12), cornish stone (16), CaCO ₃ (4)
Willow blue	33.3	CaCO ₃ (50), SiO ₂ (16.7)
Dark blue	44.6	Al ₂ O ₃ (55.4)
Matt blue	20.0	Al ₂ O ₃ (60), ZnO (20)
Blue-green	41.8	Al ₂ O ₃ (39), Cr ₂ O ₃ (19.2)
Black	20.6	Fe ₂ O ₃ (41.1), Cr ₂ O ₃ (32.4), MnO ₂ (5.9)

The pigments are normally prepared by mixing the ingredients as oxides or as readily decomposable salts and then calcining the mixture at 1100–1300 °C prior to milling the product to obtain the pigment as a fine powder. In ceramic applications, the pigments can be added to the ceramic base materials to give a body color or, after being mixed with suitable fluxes, applied as an underglaze (as on Delft china), or overglaze decoration. The final shade after the ceramic has been fired may be modified by reaction between the pigment and the clay base.

Cobalt pigments are used for decolorizing both glass and pottery articles that contain iron oxide, which would give a yellow coloration to the products in the absence of a decolorizer. The yellow color is masked by the complementary blue color of the cobalt pigment added. The levels of cobalt required for the compensation of iron oxide colorations in typical pottery bodies, enamels, and glasses are 0.003–0.02%, 0.002–0.01%, and 1–2 mg/kg, respectively.

The color of the pigments and of the compounds used for decolorizing arise from the

optical absorption spectra of cobalt atoms modified by lattice effects in the pigments and in the final products.

In the vitreous enameling of steel sheet, a small amount of cobalt oxide (0.15–1.0%) is included in the ground coat mixture of feldspar, sand, borax, and soda ash to improve the adhesion of the enamel to the steel. As generally accepted, the cobalt does not contribute directly to the adhesion process, but it is involved in creating suitable conditions for the development of good adhesion.

Ceramic coatings for low-carbon and low-alloy steels for high-temperature use can consist of a mixture of aluminum oxide and two cobalt coats, one of which is high-firing and the other low-firing. The purpose of the latter is to seal off oxygen at low temperatures to protect the base metal from oxidation from the start of the firing. These coatings are claimed to withstand combustion products and corrosive vapors up to 750 °C and have been used to protect flue gas and gas turbine exhaust pipes.

The metal–glass coatings used to protect plain carbon steels typically contain 80% powdered chromium and 20% of a borosilicate glass containing 5% cobalt oxide. Superalloys have also been coated with a ceramic consisting of high-firing cobalt ground coats with high aluminum oxide content or with boron nitride containing a lithium cobalt oxide binding agent.

18.8.3.2 Driers, Paints, Varnishes, and Dressings

A number of cobalt pigments have been used in oil paintings, including Cobalt blue smalt (a silicate), Thenard's blue (an aluminate), Cerulean blue (a stannate), Cobalt violet (a phosphate), and Aureolin yellow (potassium cobalt(III) nitrite). Some of the pigments have also been used for inks, for printing on fabrics and paper, and for coloring plastics.

Cobalt acetate is used for coloring the oxide layers in anodized aluminum to give shades varying from bronze to black. The anodized metal is immersed in a 20% solution of cobalt

acetate and then either in a solution of ammonium sulfide to produce cobalt sulfide (black) or in a solution of potassium permanganate (bronze). The different depths of bronze shades are achieved by different numbers of alternate immersions in the cobalt acetate and permanganate solutions. In addition to its use as a coloring agent, cobalt acetate is also used to improve the lightfastness of anodized aluminum dyed with organic pigments.

The cobalt(II) salts of a number of organic acids have been used as drying agents for non-saturated oils in paints, varnishes, and inks. The salts used for this purpose include the oleate, ethylhexanoate, naphthenate, soyate, linoleate, resinates, and tallate. These cobalt salts are either soluble in the non-saturated oils or they react with them to form soluble compounds that then act both as oxidation accelerators of the oil and as polymerization catalysts, forming a film with increased stability, resistance, and flexibility. The drying action is due entirely to the redox behavior of the cobalt species present, the carboxylate moieties simply act as oleophilic groups to solubilize the cobalt compounds in the oils. The amounts of cobalt added to the oils as drying agents are in the range 0.01–0.6%; the salts can be added as solutions in organic solvents or as dispersions of ultrafine powders. Cobalt-containing drying agents are also used in low-temperature curing processes for silicone resins. The cobalt species promote drying at the surface of the film in contact with atmospheric oxygen. Its action is so fast that a hard polymeric film can be formed that prevents deep drying; for this reason cobalt is often used in conjunction with other metals such as zinc and calcium that do not have a drying action but slow down and control the effects of cobalt.

18.8.3.3 Catalysts [9]

Cobalt compounds are versatile catalysts. Cobalt-containing materials have been used to catalyze the following types of reactions: hydrogenation; dehydrogenation; hydrogenolysis including hydrodenitritification and hydrodesulfurization; hydrotreatment of pe-

troleum products; selective oxidation; ammoxidation; oxidation; hydroformylation; polymerization; selective decomposition; and ammonia synthesis. In addition to these more general reactions, there are a number of reactions for which cobalt chemicals are among the best catalysts. These include their uses as driers, in the oxidation of ammonia to nitric acid, and the syntheses of fluorocarbons.

The effectiveness of cobalt as a catalyst is related to the ease with which the element forms complexes and particularly to the large variety of ligands in these complexes.

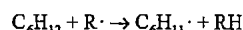
The main industrial processes using cobalt catalysts are the removal of sulfur from various petroleum-based feedstocks (hydrodesulfurization), selective liquid-phase oxidation, and hydroformylation. The catalysts used in the hydropurification reactions including *hydrodesulfurization* consist of cobalt and molybdenum oxides supported on an inert material such as alumina and contain 2.5–3.7% cobalt. The homogeneous catalysts used in the *liquid-phase oxidation* processes are soluble cobalt(II) carboxylates such as acetate, naphthenate, and oleate. Relatively large concentrations of cobalt (0.1–1%) are used as cobalt salts in the catalysis of *hydroformylation* reactions in which HCo(CO)₄ is the active material. The amounts of cobalt catalysts used in hydrodesulfurization, oxidation, and hydroformylation have been estimated at 800–1800, 200, and 800 t/a, respectively.

In *hydrotreating*, the cobalt–molybdenum catalysts function in the sulfide form and catalyze two reactions, hydrogenation and hydrogenolysis of carbon heteroatom bonds. Two theories have been used to explain the enhanced catalytic activity obtained by having both cobalt and molybdenum oxides in the catalysts: the *pseudointercalation model* and the *remote control model*. The first model assumes an association between molybdenum sulfide (MoS₂) and cobalt to produce active sites for the catalysis. The remote control model, on the other hand, assumes that active centers are created in the MoS₂ lattice by a mobile species of hydrogen produced at a cobalt sulfide component. The cobalt in the cata-

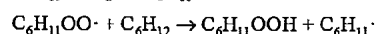
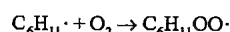
lyst thus controls the nature and the number of catalytically active sites formed.

The types of *oxidations* catalyzed by cobalt salt solutions include *p*-xylene to terephthalic acid, cyclohexane to adipic acid, and hydrocarbons or acetaldehyde to acetic acid. All of these liquid phase oxidations follow classical radical chain mechanisms. The following reaction mechanism for cyclohexane oxidation shows the role of cobalt in decomposing the hydroperoxides formed in the reaction and thus avoiding unwanted side reactions:

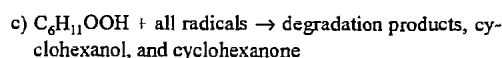
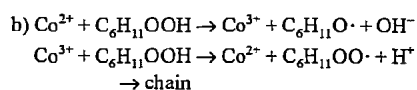
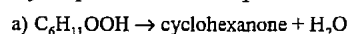
Initiation:



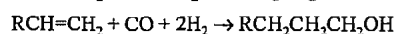
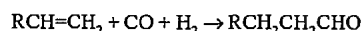
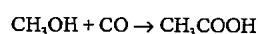
Chain reaction:



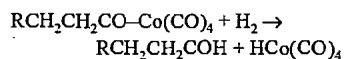
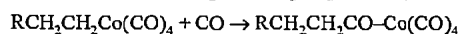
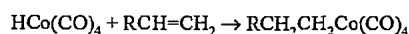
Hydroperoxide decomposition:



In *hydroformylation* and *hydroesterification*, oxo reactions such as those listed below occur:



The cobalt salts added to the reaction mixture are converted into $HCo(CO)_4$, which catalyzes the oxo reaction by the following types of mechanism:



In addition to the main types of reactions catalyzed by cobalt species, cobalt compounds have also been used as catalysts for automobile exhaust gas purification, for the manufacture of nitric acid, for heterogeneous oxidation reactions, and for the oxidation of toluene to

benzoic acid. Cobalt(II) dicobalt(III) tetroxide is one of the most effective catalysts for the oxidation of carbon monoxide and also has a high activity in oxidizing nitrogen monoxide; these properties have led to the use of Co_3O_4 and the $LaCoO_3$ (perovskite phase) as components of exhaust gas purification catalysts. The oxide Co_3O_4 is also a highly selective catalyst in the oxidation of ammonia to nitric acid, although it loses activity due to sintering after repeated use and due to poisoning by sulfur dioxide.

Cobalt is often cited in the patent literature as an additive in nearly all heterogeneous oxidation catalyses, including the oxidations of propene, butane, butenes, and methanol. New systems containing cobalt can also be used to catalyze the conversion of thiols to disulfides in gasoline sweetening.

Cobalt compounds have considerable potential in *homogeneous catalytic systems* and are used with copper in the oxidation of toluene to benzoic acid; good selectivities for the conversion of methanol to ethanol have been achieved by using cobalt cluster catalysts.

Cobalt fluoride can be used as a catalyst in the *fluorination* of hydrocarbons. These reactions utilize the cobalt fluoride as a fluorine carrier and take place in two steps – oxidation of CoF_2 to CoF_3 at 150–200 °C followed by fluorination of the hydrocarbon at 250–350 °C. Both stages of the reaction are exothermic, and careful control of the reaction is needed to obtain optimum yields.

Cobalt has been a component of the catalysts used in the *Fischer-Tropsch synthesis* of hydrocarbons from synthesis gas. The mixed cobalt–thorium oxide–magnesium oxide–kieselguhr catalyst (100:5:8:200), for example, is generally prepared by boiling solutions of sodium carbonate containing cobalt and thorium nitrates to precipitate the metals as carbonates prior to adding magnesium oxide and kieselguhr. The mixture of metal carbonates and support materials is then filtered off, washed, dried, milled, and reduced in a hydrogen atmosphere to produce the Fischer-Tropsch catalyst.

Table 18.15: Compositions of cobalt-containing plating baths.

Electrolyte composition			Content, g/L	Metal deposited
Metal salts	Content, g/L	Additives		
$CoSO_4 \cdot 7H_2O$	332	H_3BO_3	30	Co
$CoCl_2 \cdot 6H_2O$	300	H_3BO_3	30	Co
$CoSO_4(NH_4)_2SO_4 \cdot 6H_2O$	200	H_3BO_3	25	Co
$Co(SO_3NH_2)_2 \cdot 4H_2O$	450	$HCoNH_2$	30 ^a	Co
$Co(BF_4)_2$	116–154	H_3BO_3	15	Co
$NiSO_4 \cdot 7H_2O$	240	H_3BO_3	30	Co–Ni
$NiCl_2 \cdot 6H_2O$	45	$NaHCO_2$	35	
$CoSO_4 \cdot 7H_2O$	3–15			Co–W
$CoSO_4 \cdot 7H_2O$	150	NaCl	28	
$NaWO_3$	15–50	H_3BO_3	40	
		Na heptanoate	100	

^amL/L.

Raney cobalt can be prepared by leaching a finely powdered aluminum–cobalt alloy containing 40–50% cobalt with sodium hydroxide at 15–20 °C, which dissolves the aluminum to leave a very active porous cobalt residue. The properties of Raney cobalt are similar to those of Raney nickel, and the materials can be used to catalyze the same types of reaction.

18.8.3.4 Electroplating [16]

Cobalt is readily electrodeposited from a number of electrolyte solutions. Pure plated layers of cobalt are of little commercial value, but cobalt is an important component of a number of alloy electrodeposits. The electrochemical equivalent of cobalt is $1.099 \text{ g A}^{-1} \text{ h}^{-1}$ and, with cathode efficiencies of 90–100% for most electrolytes, the deposition rates are ca. $1 \text{ g A}^{-1} \text{ h}^{-1}$. Solutions of cobalt sulfate, chloride, sulfamate, or fluoroborate have been used as electrolytes. The compositions of typical plating baths are listed in Table 18.15. To obtain a smooth metal deposit at a cathode efficiency of 90–100% and a current density of 5 A/dm^2 , the bath should have a high cobalt ion concentration (65–100 g/L) and should be operated at a temperature of 25–50 °C and a pH of 4–5.

Additions of cobalt sulfate to nickel plating baths have been used to produce bright nickel plates consisting of nickel–cobalt alloys. The proportion of cobalt in the electrolyte controls the composition of the alloy deposited. Since

the deposition potential of cobalt is less than that of nickel, the cobalt–nickel ratio is higher in the deposit than in the electrolyte. A typical bath composition is given in Table 18.15. If this bath is operated at 55–60 °C, pH 4–4.3, and with a current density of $2.5\text{--}4 \text{ A/dm}^2$, an alloy deposit containing 18% cobalt is produced. The cobalt content of the bath must be maintained by the addition of the cobalt salt when nickel anodes are used. Cobalt sulfamate is used as an alternative to cobalt sulfate in some chloride sulfate nickel plating baths.

Cobalt–tungsten alloys with tungsten contents of up to 10% can be deposited from baths containing cobalt sulfate and sodium tungstate (typical electrolyte composition given in Table 18.15). A temperature of 70–90 °C and a pH of 7–9 are used to obtain smooth crack-free cobalt–tungsten deposits. Cobalt–molybdenum alloys can be obtained under similar conditions when sodium molybdate replaces the sodium tungstate in the electrolyte. A number of other cobalt-containing alloys can be obtained as electrodeposits, including cobalt–iron, cobalt–platinum, cobalt–gold, and cobalt–phosphorus.

Electrodeposited cobalt and cobalt alloys have been used as matrices for composite wear-resistant coatings in systems that codeposit suspended particles of materials such as alumina and silicon carbide with the plating metal.

18.8.3.5 Electronics and Solid-State Devices

There has been recent interest in black cobalt oxide, Co_3O_4 , as a selective coating material for high-temperature solar collectors [20]. The cobalt oxide coatings are superior to the black chrome coatings often used. The function of cobalt oxide as a coating intended to operate up to 1000 °C is to concentrate the solar radiation on the collector surface by a factor of up to 2000 times. For this purpose, a high solar absorbance with low infrared emittance is required. Cobalt oxide coatings can be prepared by plating, pyrolysis of cobalt salts on heated substrates, vacuum deposition, and by use of Co_3O_4 -based paints. Table 18.16 gives absorbance and emittance data for cobalt oxide coated solar panels prepared in a variety of ways on different substrates.

Cobalt(II) oxide has been used in thermistors to improve both the resistivity and the temperature coefficient of the resistivity of the device. A number of mixed-metal cobalt oxides have been used in devices, including NiCoO_4 and La_2CoO_4 as anodic materials in water electrolysis, LiCoO_2 as an electrode in lithium batteries, NaCoO_2 as cathodes in sodium batteries, and CoMoO_4 as a fuel cell electrode. Iron oxides doped with cobalt are used extensively in thin-film coatings for magnetic recording tapes.

18.8.3.6 Agriculture, Nutrition, and Medicine

Cobalt chemicals are used to correct cobalt deficiencies in soils and in animals. Soil treatments usually involve top dressings containing cobalt sulfates, whereas treatment of ruminant animals involves the use of either salt licks containing ca. 0.1% of cobalt as sulfate, or concentrated feeds, or pellets of cobalt oxide bound in an inert material such as china clay.

The medicinal uses of cobalt are dominated by the use of vitamin B_{12} . The vitamin is obtained from the mother liquors of the microbial formation of antibiotics such as

streptomycin, aureomycin, and terramycin after the removal of the antibiotic. Vitamin B_{12} and cobalt treatments are used as remedies in certain types of anemia. Cobalt salts, administered intravenously, have been used as an antidote in cyanide poisoning.

The mechanisms of the agricultural and medicinal uses of cobalt chemicals are discussed in Section 18.10.

Table 18.16: Properties of cobalt oxide coated solar panels.

Coating method	Substrate	Absorbance, %	Emittance, %
Plated	Cu, Ni	93	28
Plated	Ni-plated steel	90	7
Plated/thermal decomposition	Ag-coated steel	> 90	20
Plated	Ni	95	—
Plated	Cu-coated steel	96	13
Oxidized paint	Al	91	30
Paint	Ni alloy	85	10
Spray pyrolysis	Al, galvanized Fe	91, 92	13, 12
Spray pyrolysis	Stainless steel	93	14

18.9 Analysis [21, 22]

Cobalt can be determined gravimetrically as anthranilate, as Co_2O_3 or Co after precipitation of the 1-nitroso-2-naphthol complex and subsequent decomposition, and as a pyridine thiocyanate. Volumetric methods include the use of 8-hydroxyquinoline, ethylenediamine tetraacetic acid (EDTA), and iron(III) cyanide solutions as titrants. In the case of complexometric methods, cobalt is often back-titrated with magnesium or zinc solutions after an excess of EDTA has been added. The metal can also be determined by electrodeposition on perforated platinum electrodes.

Trace levels of cobalt in most materials can be determined by a number of instrumental techniques, including X-ray fluorescence, activation analysis, atomic absorption, atomic emission, and polarography. The reagents that can be used to measure cobalt by colorimetry include dimethylglyoxime, dithizone, 8-hydroxyquinoline, nitrosonaphthols, diethyldithiocarbamate, and tripyridyl.

Table 18.17: Average annual production of refined cobalt in the Western World, t.

Country	Number of producers	1970–1974	1975–1979	1980–1984	1985	
					Production	Capacity
Zaire	1	14 800	12 300	9 250	10 680	17 600
Zambia	1	2 000	2 000	2 850	4 300	5 100
Canada	3	1 900	2 000	3 100	3 710	4 600
Finland	1	900	960	1 400	1 430	1 600
Japan	2	—	1 200	1 900	1 240	2 600
Others	6	1 800	1 700	1 000	520	3 100
Total production		21 400	20 200	19 500	21 880	—
Total utilization		25 500	28 300	31 800	34 600	34 600

Table 18.18: Average annual consumption of cobalt in the Western World, t.

Country	1970–1974	1975–1979	1980–1984	1985
Western World	21 500	19 550	15 900	16 750
North America	8 800	8 400	6 900	7 350
Europe	7 600	6 800	5 400	5 500
Japan	3 700	3 000	2 000	2 400
Others	1 150	1 350	1 400	1 500

18.10 Economic Aspects [23]

Cobalt production and marketing depend very much on the situation in African countries. In May 1978, the economic balance was upset by an invasion of the Shaba province in Zaire by a Katangan army. The result was a drop in cobalt production and a very sharp increase in its price. The dependence of the world's cobalt supply on African producers is shown by the production data in Table 18.17. Western world cobalt production has been increasing at an average rate of 2.8% per year since 1950. Table 18.18 contains the consumption data for cobalt. In addition to primary production, the recovery and recycling of cobalt has become important [24]. During the period 1960–1977, the cobalt price showed a moderate growth pattern of 2.8% in real terms. The 1960 and 1977 average producer prices of the metal were \$3.3 and \$13 per kilogram, respectively. In the period 1978–1979, the price of the metal rose to a maximum of \$108 per kilogram and has since fallen; in early 1985, it was \$24–27 per kilogram.

Cobalt is regarded as a strategic metal in many countries, and a stockpile is held by the

General Services Administration in the United States.

Estimates of cobalt production suggest that in 1990 40 000 t of the metal will be produced in the Western World with a large fraction (68%) still originating in Africa. The outlook for cobalt supplies to the world market is reasonably satisfactory; reserves are large, but the production of cobalt depends on the working of cobalt-containing ores for other metals such as copper and nickel, which will have important economic effects in determining the ores from which cobalt will be produced in the future.

18.11 Physiology and Toxicology [25–29]

The wasting disease in sheep and cattle known as pine in Britain, bush sickness in New Zealand, coast disease in Australia, and salt sick in the United States is treated with vitamin B_{12} . This vitamin is a coenzyme in a number of biochemical processes, the most important of which is the formation of red blood cells.

The acute rat toxicity LD_{50} for cobalt powder is 1500 mg/kg and the TLV is 0.1 mg/m³. Prolonged exposure to the powder may produce allergic sensitization and chronic bronchitis. In 1977 NIOSH recommended that when the cobalt content of cemented carbide dusts exceeds 2%, the dust level should not exceed 0.1 mg/m³ in air. Occupational cobalt poisoning is caused primarily by inhalation of dust containing cobalt particles and by skin contact with cobalt salts. Very few people have been affected by cobalt dust, but those li-

able to be affected must be protected adequately. Skin irritation and diseases caused by cobalt are extremely rare, but it is possible to distinguish two types: one appears as erythema, which is normally found on the hands shortly after contact with cobalt especially during warm weather; the other appears as eczema. However, this form of allergy does not appear until after many years of contact with cobalt compounds.

Toxic effects have been observed from cobalt therapy for certain types of anemia. A single oral dose of up to 500 mg of cobalt chloride has resulted in severe toxic effects, but milder symptoms have been caused by daily intravenous injection of 5–10 mg. In some patients, cobalt has been shown to have a toxic effect on thyroid function.

Over 100 cases of serious heart ailments appeared between 1966 and 1969 in Canada, the United States, and Belgium. They were finally traced to cobalt sulfate that several brewers added to beer (0.075–1 mg/kg) to stabilize the froth. Apparently, chronic alcoholism combined with a lack of nourishment sensitized the hearts of those affected. The acute oral toxicities (LD_{50} , rats) for cobalt oxides, cobalt carbonate, cobalt chloride hexahydrate, cobalt nitrate hexahydrate, and cobalt acetate tetrahydrate are 1750, 630, 766, 691, and 821 mg/kg, respectively [29].

18.12 Pigments

Transparent Cobalt Blue. Cobalt blue, C.I. Pigment Blue 28:77346, is also produced as a transparent pigment by precipitating cobalt and then aluminum as hydroxides or carbonates from salt solutions using alkali. The hydroxides or carbonates are then filtered, washed, dried, and calcined at 1000 °C [30]. It is important to carry out the precipitation with high dilution and to distribute the alkali uniformly throughout the entire reaction volume.

Transparent cobalt blue pigments have the form of small tiles (primary particle size 20–100 nm, thickness ca. 5 nm, specific surface area (BET) ca. 100 m²/g). They are resistant to

light and weather and are used in metallic paint, but are of little importance.

Transparent Cobalt Green. Analogous to cobalt blue, a transparent cobalt green spinel, C.I. Pigment Green 19:77335, can be manufactured.

The green, as well as the blue transparent cobalt pigment, are used as filter materials for cathode ray tubes (CRT) [31].

18.13 References

1. *Cobalt Monograph*, Centre d'information du cobalt, Brussels 1960.
2. R. S. Young: "Cobalt", *ACS Monogr. Ser.* 149, New York 1960.
3. W. Betteridge: *Cobalt and its Alloys*, Ellis Horwood, Chichester 1982.
4. N. N. Greenwood, T. C. Gibb: *Mössbauer Spectroscopy*, Chapman Hall, London 1971.
5. *Cobalt and Cobalt Abstracts*, Centre d'information du cobalt, Brussels 1958–1975.
6. S. M. Grimes (ed.): "Cobalt Abstracts", *ATB Metall.* 24 (1984).
7. S. M. Grimes (ed.): *Cobalt Abstracts*, Cobalt Development Institute, London 1985.
8. W. Betteridge, *Prog. Mater. Sci.* 24 (1979) 2.
9. *Proceedings International Conference on Cobalt: Metallurgy and Uses*, Brussels Nov. 10–13 1981, vol. I and II, *ATB Metall.* (1981).
10. R. W. Andrews: *Cobalt: Overseas Geol. Surveys*, Mineral Resources Div., H. M. Stationary Office, London 1962.
11. H. Hagon, *Metall (Berlin)* 29 (1975) no. 11, 1157–1158.
12. H. Hagon, *Met. Powder Rep.* 31 (1976) no. 1.
13. P. Doyen, H. Hagon, *Rev. Univ. Mines* 115 (1972) 205.
14. H. E. Exner, *Int. Met. Rev.* 24 (1979) no. 4, 137–176.
15. J. D. Donaldson, S. J. Clark: "Cobalt in Superalloys", The Monograph Series, Cobalt Development Institute, London 1985.
16. F. R. Morral, W. H. Safrawek in F. A. Lowenheim (ed.): *Modern Electroplating*, 3rd ed., Wiley, New York 1974, pp. 152–164.
17. *Gmelin*, vol. 58.
18. B. F. G. Johnson, R. E. Benfield in G. L. Geoffroy (ed.): *Topics in Inorganic Stereochemistry*, Wiley, New York 1981, pp. 253–335.
19. E. DeBie, P. Doyen, *Cobalt* 1962, no. 15, 3–13; no. 16, 3–15.
20. S. J. Clark, J. D. Donaldson, S. M. Grimes, *Cobalt News* 1983, no. 4, 6.
21. C. Tombu, *Cobalt* 1963, no. 20, 103–110; no. 21, 185–189.
22. M. Pinta: *Modern Methods for Trace Element Analysis*, Publ. Ann Arbor Science, Ann Arbor, Michigan, 1978.
23. M. Junes, *Cobalt News* 1986, no. 1, 6.
24. J. D. Donaldson, S. M. Grimes, *Cobalt News* 1984, no. 1, 6–7.
25. R. S. Young: *Cobalt in Biology and Biochemistry*, Academic Press, London 1979.
26. E. Browning: *Toxicity of Industrial Metals*, Butterworths, London 1969.
27. F. Caudrolle, D. Meynier, *Rev. Pathol. Cen. Physiol. Clin.* 55 (1959) 245.
28. H. E. Harding, *J. Ind. Med.* 7 (1950) 76.
29. J. D. Donaldson, S. J. Clark, S. M. Grimes: "Cobalt in Medicine, Agriculture and the Environment", The Monograph Series, Cobalt Development Institute, London 1986.
30. BASF, DE 2840870, 1978 (A. Seitz).
31. Tokyo Shibaura Denikbushiki Kaisha, EP 0019710, 1980 (Wakatsuki).

Part Five

Light Metals

																		H		He			
Li	Be																	B	C	N	O	F	Ne
Na	Mg	Al																	Si	P	S	Cl	Ar
K	Ca	Sc	Ti	V	Cr	Mn	Fe	Co	Ni	Cu	Zn	Ga	Ge	As	Se	Br	Kr						
Rb	Sr	Y	Zr	Nb	Mo	Tc	Ru	Rh	Pd	Ag	Cd	In	Sn	Sb	Te	I	Xe						
Cs	Ba	La†	Hf	Ta	W	Re	Os	Ir	Pt	Au	Hg	Tl	Pb	Bi	Po	At	Rn						
Fr	Ra	Ac†																					

†	Ce	Pr	Nd	Pm	Sm	Eu	Gd	Tb	Dy	Ho	Er	Tm	Yb	Lu
---	----	----	----	----	----	----	----	----	----	----	----	----	----	----

‡	Th	Pa	U	Np	Pu	Am	Cm	Bk	Cf	Es	Fm	Md	No	Lr
---	----	----	---	----	----	----	----	----	----	----	----	----	----	----

19 Beryllium

FRITZ ALDINGER, SIGURD JONSSON, GÜNTHER PETZOW, OTTO P. PREUSS (§ 19.16)

19.1 Introduction	955	19.8 Environmental Protection	969
19.2 History	955	19.9 Quality Specifications	969
19.3 Physical Properties	956	19.10 Alloys	971
19.4 Mechanical Properties	957	19.11 Compounds	972
19.5 Chemical Properties	959	19.12 Chemical Analysis	974
19.6 Resources, Raw Material	960	19.13 Storage, Transportation, Legal Aspects	974
19.7 Production	961	19.14 Uses of the Metal	974
19.7.1 Processing of Beryl	961	19.15 Economic Aspects	975
19.7.2 Processing of Bertrandite	963	19.16 Toxicology and Occupational Health	975
19.7.3 Production of Reducible Compounds	964	19.17 References	977
19.7.4 Metal Production	965		
19.7.5 Refining and Further Processing	966		

19.1 Introduction

Beryllium is the first element in the second main group of the periodic table. It is a light metal with hexagonal-closest-packed (hcp) structure. Both finely divided metal and the compounds have serious toxic effects on the lungs. In addition to the name beryllium, derived from the mineral beryl, this element with atomic number 4 was formerly called glucinium, chiefly in France, because of the pronounced sweetish taste of its salts.

19.2 History

In 1797 VAUQUELIN [1] discovered beryllium oxide while analyzing varieties of beryl including emerald and aquamarine. WÖHLER [2] and BUSSY [3], working independently, prepared elemental beryllium in 1828 by reduction of beryllium chloride with potassium. In 1899 LEBEAU [4] obtained beryllium crystals by electrolysis of molten sodium beryllium fluoride. Industrial production of beryllium began in 1916 in several countries. The publication in 1916 by ØSTERHELD [5] of the phase diagrams of beryllium with iron, nickel, and copper led to the first important use of beryllium in 1931, namely, as an addi-

tive, about 2%, in age-hardenable copper alloys [6].

The demand for beryllium increased around 1950 with the development of nuclear reactors because the nuclear properties and low density of beryllium seemed to indicate that the metal would be especially suitable for nonstationary nuclear reactors of the types used in airplanes, space craft, ships, and submarines [7, 8]. However, beryllium was a disappointment because it swells and becomes brittle when exposed to the simultaneous action of radioactivity and heat [9]. However, the increased research activity in beryllium technology associated with this period produced significant advances in the chemistry, physics, and processing technology of beryllium [7, 10–14].

Since the end of the 1950s, there has been increased interest in beryllium as a structural material, especially in aeronautical and astronautical uses because its mechanical and thermal properties relative to weight are superior to those of all other materials [15–19]. Most of the beryllium produced today is used for military purposes. Greater use in the civilian sector is hindered mainly by the high price, the toxicity, and the room-temperature susceptibility to brittle fracture of the metal. On the

other hand, beryllium oxide is finding increasing use in electrical engineering as an electrical insulator [20]. Beryllium properties, production methods, and applications have been comprehensively reviewed recently [21].

19.3 Physical Properties

The properties listed here were measured, for the most part, on commercial grades of beryllium. These contain various impurities and have various grain structures. Many grades currently available show little similarity to the grades commonly used only a few years ago. The most reliable values of the important physical properties of beryllium [10, p. 320; 18, p. 201; 22–36] are compiled below. On first glance the most outstanding characteristics of the metal are low density and high melting point.

Atomic number	4
Atomic weight	9.0122
Electronic structure	1s ² 2s ²
Atomic radius	112.50 pm
Atomic volume at 298 K	4.877 cm ³ /mol
Crystal structures	
hexagonal closest packed at 293 K	
<i>a</i>	228.56 pm
<i>c</i>	358.22 pm
<i>c/a</i>	1.5677
body-centered cubic at 1523 K	
<i>a</i>	255.0 pm
Melting point	1560 K or 1287 °C
Boiling point	2745 K or 2472 °C
Transformation point	1527 K or 1254 °C
Density at	
298 K	1.8477 g/cm ³
1773 K	1.42
Standard enthalpy	216 J/g
Standard entropy	1.054 J g ⁻¹ K ⁻¹
Heat of fusion	1357 J/g
Entropy of fusion	0.87 J g ⁻¹ K ⁻¹
Heat of transformation	837 J/g
Entropy of transformation	0.186 J g ⁻¹ K ⁻¹
Vapor pressure at	
500 K	5.7 × 10 ⁻²⁹ MPa
1000 K	4.73 × 10 ⁻¹²
1560 K	4.84 × 10 ⁻⁶
Specific heat, at	
298 K	1.830 J g ⁻¹ K ⁻¹
700 K	2.740
Thermal conductivity at 298 K	165 ± 15 W m ⁻¹ K ⁻¹
Linear coefficient of thermal expansion, 298–373 K	11.5 × 10 ⁻⁶ K ⁻¹
Electrical resistivity at 298 K	4.31 × 10 ⁻⁸ Ωm
Magnetic susceptibility at	
93 K	-0.75 × 10 ⁻⁹ m ³ /kg
293 K	-1.00 × 10 ⁻⁹

573 K	-1.20 × 10 ⁻⁹
Hall coefficient	2.4 × 10 ⁻⁹ m ³ A ⁻¹ s ⁻¹
Thermoelectric voltage at 298 K	≈ 5 × 10 ⁻⁶ V/K
Photoelectric work function	3.92 eV
Compressibility	
isothermal	0.0883 × 10 ⁻¹⁰ m ² /N
adiabatic	0.103 × 10 ⁻¹⁰
Speed of sound	12 600 m/s
Surface tension at	
1557 K	1.960 J/m ²
1773 K	1.100
Volume contraction on solidification 3%	

The *c*-to-*a* ratio of hexagonal-closest-packed beryllium is very small and decreases with temperature [26]. The existence of the body-centered-cubic high-temperature modification was disputed for many years but has now been demonstrated conclusively [24, 27]. The transformation point is slightly below the melting point [24–28]. The sum of the heats of fusion and transformation is given as 1641 J/g, which allows a heat of transformation of 284 J/g to be estimated [28]. However, a much higher value, 837 J/g, was determined directly [18, p. 201].

The *vapor pressure* values in the literature show considerable variation, probably due to the variable formation of oxide and nitride coatings [37]. They were compiled by HULTGREN [28]. The high *specific heat* [28] and *thermal conductivity* [7; 10, p. 320; 31] are noteworthy. Low-temperature measurements show that the thermal conductivity perpendicular to the basal plane is greater than that parallel to the basal plane [38].

The coefficient of *linear expansion* is comparatively low. The values given in the literature vary widely, a fact that can be attributed to differences in grain structure of the samples. This is shown by measurements on single crystals parallel and perpendicular to the basal plane [39] and on highly textured material perpendicular and parallel to the pressing direction [40].

The *electrical resistivity* between 40 and 200 K is significantly lower than that of copper or aluminum [41]. Of course, the differences among the reported values are particularly great for electrical properties [11, 22, 31, 36, 42–45] because impurities are especially important here, as has been clearly

shown by measurements of residual resistance in materials of different degrees of purity [46, 47]. The information on the superconductivity of beryllium is contradictory. Some investigators [22, 48] have found *superconductivity* at temperatures below 11 K, others [49] have found superconductivity only in thin films below transition temperatures between 7 and 9 K, and still others [45, 50, 51] have been unable to find superconductivity at all.

Beryllium is *diamagnetic*, little work [33, 34] has been reported on the magnetic properties. The available measurements on the thermoelectric force show considerable variation, probably a result of the experimental conditions and sample characteristics [7, 38, 52].

The reflexivity of beryllium is high, particularly in the infrared region [53]. Beryllium transmits X-rays well because of its low atomic number. Even relatively long-wave gamma rays cause beryllium to emit neutrons, on account of a (γ,n) reaction. Other nuclear reactions of beryllium and its most important nuclear properties [10, pp. 14, 328; 22; 53; 54] are given below and in Table 19.1:

Magnetic dipole moment	5.9468 Am ²
Electric quadrupole moment	0.02 × 10 ⁻²⁴ cm ²
Binding energy of the last neutron	1.664 MeV
Absorption cross section for thermal neutrons (0.025 eV)	
microscopic (σ _a)	0.9 fm ²
macroscopic (Σ _a)	0.0011 cm ⁻¹
Scattering cross section for epithermal neutrons	
microscopic (σ _s)	610 fm ²
macroscopic (Σ _s)	0.76 cm ⁻¹

The nuclear reactions of beryllium with fast neutrons and hard γ rays do not result in long-lived radioactivity. However, additional neutrons and gaseous reaction products may be produced. For example, bombardment with 10²² fast neutrons per cm² generated a total of 23 cm³ of gas per cm³ of beryllium: 5% of this gas was tritium, the remainder was helium [56]. The gas was initially located at interstitial sites or at dislocations. Heating at 1170 K caused the formation of gas-filled pores at the grain boundaries and within the grains, which resulted in a decrease in density of 20%. The volume increase due to pore formation begins at about 870 K. In addition to the formation of noble gases and tritium, normal radiation damage also occurs as a result of elastic colli-

sions of fast neutrons with beryllium atoms [7], but the effect of this radiation damage can hardly be separated from the effect of the gas formation.

The moderator and reflector properties of beryllium for thermal and epithermal neutrons are also favorable [8, 9].

Table 19.1: Properties of beryllium isotopes.

Isotope	Half-life	Radiation, MeV	Source
⁶ Be	0.4 s	—	—
⁷ Be	53.5 d	γ 0.453–0.485	⁶ Li(d,n) ⁷ Li(p,n) ¹⁰ B(p,d) ¹⁰ B(p,α) ¹⁰ B(d,α,n)
⁸ Be	1.4 × 10 ⁻¹⁶ s	α 0.055	⁹ Be(γ,n) ⁹ Be(n,2n)
⁹ Be	stable	—	—
¹⁰ Be	2.7 × 10 ⁶ a	β 0.56–0.65	⁹ Be(α,p) ⁹ Be(d,p) ⁹ Be(n,γ) ¹⁰ Be(n,p) ¹³ C(n,α)
¹¹ Be	—	—	—

Nuclear reactions of the stable isotope ⁹Be:
 Gamma-ray bombardment ⁹Be(γ,n)⁸Be
 Neutron bombardment ⁹Be(n,α)⁶He
⁹Be(n,γ)¹⁰Be
⁹Be(n,2n)⁸Be

19.4 Mechanical Properties

As in the case of other metals and alloys, e.g., aluminum or brass, the term beryllium is understood to mean a large group of different beryllium grades, whose properties differ to a greater or lesser extent as a result of differences in recovery and processing. This is also the reason for the more or less large ranges for many properties. Nevertheless, the principles of the deformation modes are known, which is the bridge to an understanding of the mechanical behavior of polycrystalline beryllium.

Beryllium *deforms* primarily on basal planes and secondarily on first-order prismatic planes. Slip systems with a nonbasal Burgers vector, e.g., second-order pyramidal slip, are difficult to activate, especially at room temperature. The strong anisotropy of flow stresses on the active slip systems is illustrated in Figure 19.1. The basal plane has a very low

surface energy and hence acts as a cleavage plane. One main reason for the *brittleness* of beryllium is the fact that the basal plane acts both as the cleavage plane and the slip plane [21, vol. I, pp. 7–114]. Twinning, which is a very important deformation mechanism in several hexagonal closed-packed metals, e.g., zinc, titanium, zirconium, does not play a similar role in beryllium. In beryllium, twinning acts more as a crack inducer or enhances crack propagation, rather than to increase the deformability.

In polycrystalline beryllium brittle fracture occurs even after comparatively low strain at room temperature [11, 15, 57–59].

The reason for this tendency toward brittle fracture is the preferred occurrence of basal slip due to the described strong deformational anisotropy, which induces microcracks [10, p. 372; 60–62]. The brittleness can be reduced by purification of the material (e.g., to reduce oxide content) and special thermomechanical treatment (upset forging), which results in a microstructure with a very small grain size [63].

The average *modulus of elasticity* of beryllium is unusually high, 320 000 MPa, and is strongly anisotropic [64, 65]: 269 000 MPa in the basal plane and 365 000 MPa perpendicu-

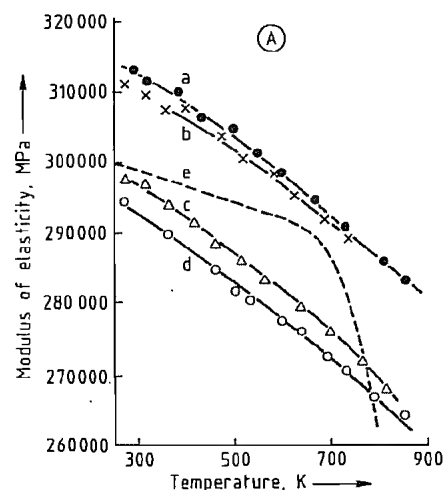


Figure 19.2: Mechanical properties of beryllium as a function of temperature. A) Modulus of elasticity of various grades of beryllium: a) Pressure sintered [66]; b) Cross-rolled cast material [66]; c) Extruded cast material [66]; d) Extruded P/M (powder-metallurgy) material [66]; e) Pressure sintered, 1% BeO [67]. B) Shear modulus and Poisson ratio of cross-rolled cast beryllium [66].

lar to the basal plane [28]. As a result the modulus of elasticity of individual polycrystalline specimens shows considerable variation depending on the type of working, and thus on differences in microstructure (Figure 19.2A). The shear modulus decreases somewhat more rapidly than does the modulus of elasticity as the temperature increases. The Poisson ratio shows a corresponding increase with temperature (Figure 19.2B).

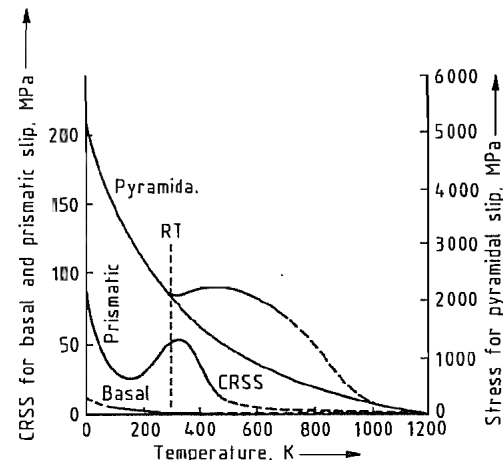
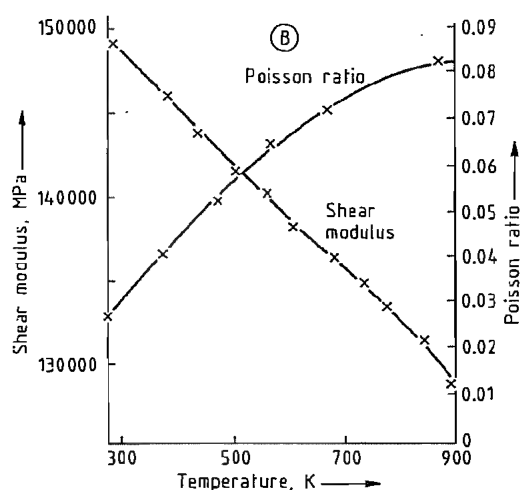


Figure 19.1: Flow stress for basal, prismatic, and pyramidal c + a slip versus temperature [21, vol. I, pp. 7–114]. CRSS stands for critical resolved shear stress.



The deformational anisotropy and susceptibility to brittle fracture become lower as the temperature is increased [10, p. 372] so that beryllium is readily workable above 450 K [57]. However, the *elongation* of some commercial grades of beryllium decreases sharply in the temperature range 650–900 K, then increasing again [15, p. 3; 57; 58] (Figure 19.3, Curves a, b, and c). This decrease in elongation at intermediate temperatures is caused by impurities. However, when the concentrations of aluminum, iron, and beryllium oxide are adjusted in a well-defined manner, the hot-working characteristics can be greatly improved by effective heat treatment [15, p. 112; 68; 69] (Figure 19.3, Curve e). The preferred occurrence of basal slip during warm working, which is usually performed in the temperature range 670–1360 K, also results in a pronounced microstructure. This consists of a preferential orientation of the basal planes, e.g., parallel to the direction of extrusion or parallel to the rolling plane [12, p. 240; 15]. The microstructure strongly limits the basal slip at room temperature in the case of deformation parallel to this preferential direction so that the susceptibility to brittle fracture in this direction of deformation is reduced. Considerable elongation can be attained because of the preferred occurrence of prismatic slip. Perpendicular to the preferred direction of the basal plane the potential elongation is almost equal to zero because the direction of prismatic slip lies in the basal plane.

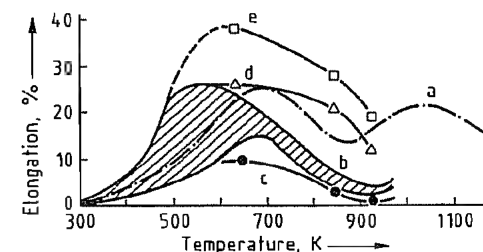


Figure 19.3: Elongation of various beryllium grades as a function of temperature: a) Cast, extruded [57]; b) Pressure sintered [15, p. 3]; c) Pressure sintered, impurities uncontrolled; d) Pressure sintered, Fe and Al content controlled; e) Pressure sintered, BeO, Al, and Fe content controlled [69].

Improvement of the *forming characteristics* by grain refining during melting and casting is possible only to a limited extent [10, p. 136; 12, p. 55; 15, pp. 193, 237, 246; 58; 70–72]. The mechanical properties after powder-metallurgical processing are significantly better than those after casting, and material produced by powder metallurgy is now used almost exclusively.

The susceptibility of beryllium to cleavage fracture is significantly reduced under compressive load so that the deformation values of cast or pressure-sintered material are usually greater than 20%. The buckling strength is comparable to the yield strength; however, the compressive strength is significantly higher than the tensile strength (Table 19.2).

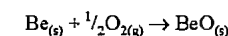
Table 19.2: Strength values, MPa, of extruded beryllium measured in compression test [73].

	Cast		Pressure sintered	
	Room temperature	670 K	Room temperature	670 K
Two-tenths buckling strength	210	179	240	178
Compressive strength	657	460	635	460

19.5 Chemical Properties

The two 2s electrons of beryllium are valence electrons. The first ionization potential ($\text{Be}^0 \rightarrow \text{Be}^+ + e^-$) is 9.32 eV, and the second ($\text{Be}^+ \rightarrow \text{Be}^{2+} + e^-$) is 18.21 eV [74]. Although beryllium is almost always divalent in its compounds, it is far more similar to aluminum than to magnesium or calcium [7, 10, 11, 37, 74, 75]. For example, like aluminum, it is amphoteric, and in humid air and water vapor forms a strongly adhering surface layer of oxide that prevents further oxidation up to about 600 °C [37, 76]. Above 600 °C the oxide layer thickens, but oxidation that destroys the metal by break away does not occur below 700 °C.

The affinity of beryllium for oxygen is very great



$$\Delta G_f^\circ (\text{J/g}) = -66469 + 10.5T \pm 4.7$$

and beryllium is an excellent reducing agent. At temperatures $> 900^{\circ}\text{C}$ it reacts violently with nitrogen or ammonia to form beryllium nitride, Be_3N_2 . However, beryllium does not react with hydrogen, even at high temperatures, because the formations of the hydrides BeH_2 and BeH , which are difficult to prepare, are endothermic, and the hydrides rapidly decompose at only slightly elevated temperatures. Below $500\text{--}600^{\circ}\text{C}$ beryllium is not attacked by dry carbon dioxide and is attacked only very slowly by moist carbon dioxide. Beryllium powder reacts with fluorine at room temperature, and at elevated temperatures it reacts with chlorine, bromine, and iodine and with sulfur, selenium, and tellurium vapor; in each case, beryllium burns with a flame.

The adhering oxide film protects beryllium from attack by both cold and hot water. It also protects cold beryllium from attack by oxidizing acids [76]. The stability of the film can be increased by addition of dichromate to the water to form a protective chromate layer as in the case of aluminum. Beryllium dissolves in dilute nonoxidizing mineral acids, accompanied by hydrogen evolution and salt formation. In accord with its amphoteric nature it is also attacked by aqueous hydroxide accompanied by hydrogen evolution and beryllate formation. Since most beryllium compounds have a highly exothermic heat of formation, beryllium reduces the salts and the borates and silicates of many metals. For example, the only halides that are stable towards beryllium are those of the alkali metals and magnesium; all others are reduced by beryllium. Molten alkali-metal hydroxides react explosively with beryllium.

Beryllium forms several intermetallic phases with carbon; all transition metals; the alkaline-earth metals magnesium, calcium, and strontium; and the metalloids boron, arsenic, tellurium, etc. [25]. Some of these phases have extensive homogeneity ranges and high melting points [77–79]. With very few exceptions, the solubility of metals in solid beryllium and vice versa is very low, even at high temperatures. The binary and ter-

nary beryllium systems were reviewed [21, vol. 1, pp. 235–305].

Beryllium is very stable towards liquid lithium, sodium, potassium, zinc, magnesium, cadmium, mercury, gallium, indium, tin, lead, antimony, and bismuth. Some of these metals do not dissolve beryllium at all, even at high temperatures, so long as oxygen is not present. If the melts contain metal oxides, the metal oxides are reduced by beryllium with the formation of beryllium oxide. The layer of BeO formed in this way is not adherent and is removed by the melt, so that a fresh surface of beryllium is always available for reduction.

Beryllium is very reactive in the liquid state, reacting with most oxides, nitrides, sulfides, and carbides, including those of magnesium, calcium, aluminum, titanium, and zirconium.

19.6 Resources, Raw Material

Beryllium is a rare element; its abundance in the earth's crust is about 6 ppm. However, it occurs in concentrated form in various minerals. The total exploitable world reserves of beryllium are estimated at 200 000 tons.

The first beryllium mineral commercially exploited was *beryl*, $3\text{BeO}\cdot\text{Al}_2\text{O}_3\cdot 6\text{SiO}_2$, *mp* 1650°C , ρ $2.67\text{--}2.76\text{ g/cm}^3$, hardness of 7.5–8 on the Mohs' scale, optically negative with weak double refraction, $n = 1.57\text{--}1.60$. It crystallizes in hexagonal prisms, which are often very large in size; indeed, crystals weighing several tons have been discovered. It is found in mica schist, granite, pegmatite, and argillite. The crystals often show signs of weathering, and only rarely do they have the ideal composition. Beryl contains about 11% beryllium oxide (4% Be) and is often obtained as a by-product of feldspar quarrying. The largest deposits are found in Brazil, Argentina, India, Mozambique, Madagascar, Uganda, Zimbabwe, South Africa, and the USSR. In addition to the aluminum oxide and silicon dioxide, principal impurities in the ores include alkali

metals, alkaline-earth metals, iron, manganese, and phosphorus.

Until the late 1960s, beryl was the only beryllium mineral having industrial importance. In 1969 Brush Wellmann Inc. began the processing of *bertrandite* ores in Utah. This is presently the most important commercial beryllium mineral. Its formula is $4\text{BeO}\cdot\text{SiO}_2\cdot\text{H}_2\text{O}$, but ores contain only 0.2–0.35% Be [19, p. 21]. Chrysoberyl, $\text{BeO}\cdot\text{Al}_2\text{O}_3$; phenakite, $2\text{BeO}\cdot\text{SiO}_2$; euclase, $\text{BeAlSiO}_4(\text{OH})$; and the precious varieties of beryl, emerald and aquamarine, are highly prized as gemstones. About 40 other beryllium-bearing minerals are known.

19.7 Production

Since the density of beryl is close to that of quartz, concentration by density is not possible. Hand sorting has been the chief means of separation. Flotation is successful only for a few ores [80]. An automatic machine, the Beryl Picker, has been used recently [81]; the ore is first γ -irradiated to render the beryllium atoms radioactive, $^9\text{Be}(\gamma, n)^8\text{Be}$. The beryl crystals are then selected out by a sorter guided by a neutron counter [82].

The recovery of beryllium from both beryl and bertrandite includes several stages. The ores are first converted to an acid-soluble form by fusion. Complex chemical processes are then used to obtain comparatively pure beryllium hydroxide or oxide and then beryllium chloride or fluoride. These halogenides are reduced to metallic beryllium with other metals or by melt electrolysis. The beryllium metal obtained is subjected to one or more refining processes and then to further treatment by powder metallurgy or in some cases fusion metallurgy [7, 10–12].

19.7.1 Processing of Beryl

Beryl is treated mainly by the sulfate and fluoride processes. The chloride process is a direct, inexpensive process for recovering beryllium chloride for electrolysis [10, p. 102].

Other processes are not used because of problems with reactions and apparatus [11, 83].

Sulfate Process. First the beryl, which is only slightly soluble in sulfuric acid even under such extreme conditions as heating for several hours in an autoclave at 400°C , is subjected to either an alkali or a heat treatment.

The *alkali treatment* corresponds to the usual silicate treatment of analytical chemistry: finely ground beryl is heated until fusion or sintered below the melting point with a sufficient quantity of alkaline flux. Suitable alkalis include hydroxides or carbonates of sodium, potassium, and calcium; mixtures of these carbonates; calcium oxide; borax; lead chloride; and sodium sulfate and charcoal. The mechanism of the fusion is still not fully understood [84]. The ratio of flux to beryl depends on the operating conditions, especially the temperature: the higher the temperature the less flux. For alkali treatments involving molten material, gas-heated or oil-heated rotary furnaces or blast furnaces are suitable. Rotary kilns, muffle furnaces, or tunnel kilns are used for sintering.

In the *heat treatment* the beryl is melted (*mp* 1650°C) without additives and then quenched in water. After this treatment about 50–60% of the beryl has a greater solubility in sulfuric acid. The rest of the beryllium oxide forms a solid solution with silicon dioxide that is not attacked by sulfuric acid. At 900°C this solid solution separates into its components, and a heat treatment at this temperature produces a free beryllium oxide that is soluble in sulfuric acid. Such a two-stage heat treatment renders a total of 90–95% of the beryl soluble.

The heat-treated beryl is extracted with hot concentrated sulfuric acid, whereas alkali-treated beryl is extracted with cold sulfuric acid. In the second case there is no heating cost, but the total consumption of acid is greater because of the alkali added. The liquor is diluted with water, and the insoluble silicon dioxide separated by filtration. At this point the filtrate contains not only beryllium and aluminum sulfate but also considerable quantities of iron sulfate and smaller amounts of

other impurities, all of which must be removed before precipitation of beryllium hydroxide. Examples of the many separation methods [11] include the alum separation, the ammonium carbonate separation, and the chelate separation.

In the *alum separation* excess ammonium or potassium sulfate is added to the hot sulfate solution. Upon cooling, all the aluminum precipitates as alum and can be separated from the beryllium sulfate solution in a centrifuge. The filtrate is diluted and then oxidized with potassium permanganate. It is then heated to the boiling point, and calcium carbonate slurry is added until a pH of 3.8–4.2 is reached. This causes iron and manganese to precipitate as the hydroxides and calcium to precipitate as calcium sulfate dihydrate. The beryllium hydroxide is then precipitated by addition of ammonia.

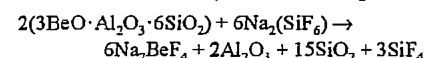
In the *ammonium carbonate separation* the liquor obtained from the fusion treatment is treated with saturated ammonium carbonate solution to precipitate aluminum, iron, and other heavy metals as hydroxides, which are then separated by filtration. The filtrate, which contains the soluble beryllium hydroxide, is concentrated by boiling to precipitate readily filterable sparingly soluble basic beryllium carbonate, which is converted to low-density beryllium oxide by calcining at low temperatures.

In the *chelate separation* iron and aluminum are chelated, e.g., with ethylenediamine-tetraacetic acid. The beryllium can be precipitated as hydroxide, while these complexes remain in solution.

If the separation process does not lead directly to fine-grained, readily filterable beryllium hydroxide or oxide, the fusion liquor is adjusted to pH 7.5 with ammonia or sodium hydroxide and then heated to 95–98 °C. A crystalline, readily filterable beryllium hydroxide is obtained under these conditions. At lower pH gelatinous hydroxide is obtained; at higher pH, amorphous hydroxide is obtained [11]. If the temperature is too low, the crystalline hydroxide forms too slowly.

Brush Wellman Inc., the world's largest beryllium producer, has fully automated its process, called the caustic process. This process uses a heat fusion treatment and is characterized by low consumption of sulfuric acid, reliable separation of iron and other heavy metal impurities by combined alum and chelate separation, and recovery of an easily filterable beryllium hydroxide by hydrolysis of the sodium beryllate [10, p. 71].

Fluoride Process. In the fluoride process beryl is melted or sintered at ≈ 700 °C with sodium hexafluorosilicate. Only the beryllium oxide is converted to a water-soluble salt; aluminum oxide, silicon dioxide, and other impurities are essentially unattacked [83, 85]:



The formation of other beryllium salts (NaBeF_3 , BeF_2) is not observed. Water-soluble Na_3AlF_6 may also be formed in small amounts.

Other suitable extracting agents are hydrogen fluoride at 630 °C, molten fluorides, other fluorosilicates, or silicon tetrafluoride [86]. Rotary kilns are used for reaction with the gases; the solid mixtures are briquetted and sintered in muffle furnaces or tunnel kilns.

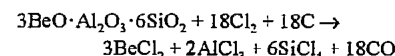
The sodium hexafluorosilicate needed for the fluoride process is relatively expensive. However, consumption can be greatly reduced by adding sodium fluoride [87] or sodium carbonate [88], which traps and thus "recycles" the liberated silicon tetrafluoride.

The sodium fluoride remaining in solution after precipitation of the beryllium hydroxide can also be recovered. Sodium hexafluoroferate(III) is obtained by precipitation with iron(III) sulfate [89] and can be used instead of sodium hexafluorosilicate.

The reaction product must be leached with water at room temperature because silicon dioxide is attacked by fluoride solutions at elevated temperatures. On the other hand, the leaching must be performed as rapidly as possible because otherwise the beryllium salt that is already dissolved will precipitate [11] and in this form it is sparingly soluble, unlike the

form which is present in the original fusion product. In order to obtain beryllium hydroxide the solution is made alkaline with NaOH. Beryllium hydroxide precipitates when the solution is diluted with water and then boiled. The fluoride process is being tested in a pilot plant by Bhabha Atomic Research Centre, India [90].

Chloride Process. At temperatures above 630 °C the components of beryl can be extracted in a stream of chlorine; reducing conditions greatly enhance the yield:



In practice a mixture of pulverized beryl and carbon is either heated near 800 °C in a stream of chlorine [91, 92] or melted in an electric-arc furnace. In the second case the carbides that form are chlorinated [93, 94]. The reaction can also be carried out with gases that contain chlorine, such as hydrogen chloride [83], carbon tetrachloride [95], sulfur chloride [83], or phosgene [96, 97]. The volatile chlorides are separated by fractional condensation or liquid–liquid extraction with sulfur dichloride, sulfuryl chloride, phosphorus trichloride, phosphorus oxychloride, boron chloride, carbon tetrachloride, or phosgene [83].

Reducing chlorination of the beryllium hydroxide or oxide obtained in the sulfate or fluoride process gives beryllium chloride, the starting material for the electrolytic production of beryllium.

19.7.2 Processing of Bertrandite

The beryllium-poor bertrandite ores (≤ 0.5 – 0.8% BeO) discovered in the United States in 1960 cannot be economically smelted by conventional methods. A new process was therefore developed by Brush Wellman Inc., called the *SX-Carbonate process* (Figure 19.4) [98, 99]. This process produces a very pure beryllium hydroxide (Table 19.3) by liquid–liquid extraction with organic phases [74].

Table 19.3: Typical analyses of beryllium hydroxide obtained by two processes, ppm, with respect to BeO [98, 99].

Element	SX-Carbonate process	Caustic process
Al	200	3000
Fe	200	1300
Cr	50	125
Li	70	300
Mg	100	6000
Mn	10	900
Ni	10	30
Na	500	10000
Ca	200	800
Cu	5	25
Si	100	1500
Zn	20	700

Unlike beryl, bertrandite is soluble in sulfuric acid without pretreatment. The insoluble residue (SiO_2 , etc.) and the aluminum content, which precipitates as an aluminum alum, are removed. The sulfate solution, pH = 0.5, then contains the beryllium and also aluminum, calcium, iron, sodium, and traces of other elements.

The sulfate solution is extracted with a 0.3 M solution of ammonium di-2-ethylhexyl phosphate/di-2-ethylhexyl phosphoric acid/kerosene (DAP) in a five-stage mixer at ≈ 50 °C. In the first mixer the pH is about 2, and after the last stage it is about 5.5. The acid strength is adjusted in a well-defined manner in each stage by means of the ratio of the ammoniacal to the acid component of the organic phase. Beryllium, aluminum, and iron enter the organic phase almost quantitatively, while the other impurities remain in the sulfate solution. Following separation of the two liquid phases, the metal ions are removed from the organic compounds by a 3.0–3.5 m ammonium carbonate solution in a two-stage mixer. This results in the formation of a basic beryllium carbonate solution, which is actually a slurry since it contains precipitated aluminum hydroxide (the ABC slurry). The organic phase, which is now free of metal ions, is returned to the process after purification. Iron is precipitated from the ABC slurry by heat treatment, 45 min at 85 °C, and filtered off with the aluminum hydroxide. The beryllium remains in solution as basic carbonate.

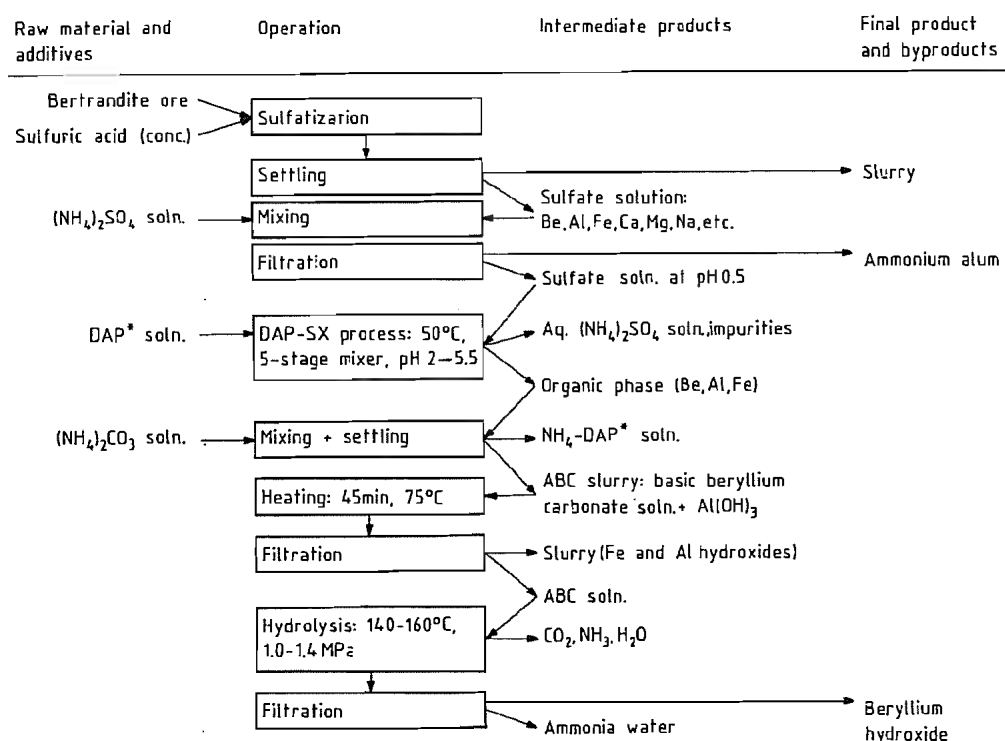


Figure 19.4: Flow diagram of the SX-Carbonate process (Brush Wellman Inc., USA) [98–99]. DAP is the abbreviation for the solution ammonium di-2-ethylhexyl phosphate-di-(2-ethylhexyl) phosphoric acid-kerosene.

The specified time must be observed as closely as possible: if the heat treatment is too short, iron is only partially precipitated. If it is too long, the beryllium loss will be too great. Even so, about 2% of the beryllium is coprecipitated and about 4–6% is contained in the hydroxide filter cake. Half of the beryllium can be separated by careful washing. The remainder is recovered by dissolving the precipitate in sulfuric acid, extracting the iron with an organic phase, and recycling the beryllium- and aluminum-containing sulfate solution to the process before the alum precipitation.

The basic beryllium carbonate solution separated from the ABC slurry by filtration is decomposed in an autoclave (140–160 °C, 1.0–1.4 MPa) into ammonia, carbon dioxide, and a beryllium hydroxide that is easily filtered off and that is quite pure (Table 19.3). The ammonia and carbon dioxide are used to produce ammonium carbonate, which is returned to the

process. The ABC slurry can be treated additionally to further reduce the concentration of impurities, e.g., to reduce the iron content to less than 50 ppm. For this reason beryl ores are today also treated by the SX-Carbonate process, following the usual heat treatment.

19.7.3 Production of Reducible Compounds

The most important metal production processes are based on reduction of beryllium fluoride by magnesium and beryllium chloride by melt electrolysis. Therefore, the beryllium hydroxide or oxide obtained from the fusion process must be converted into one of these halides.

Beryllium Fluoride. First beryllium hydroxide is dissolved in an ammonium hydrogen fluoride solution. The resulting ammonium tetrafluoroberyllate is dissociated to such a

small extent in the solution that the pH can be varied over a wide range without beryllium hydroxide precipitating. Impurities can thus be precipitated relatively easily as hydroxides. Aluminum is precipitated as hydroxide by increasing the pH to 8.3. Chromium and manganese are precipitated by oxidation with lead dioxide, and manganese is precipitated by oxidation with lead dioxide and manganese dioxide. Copper, nickel, and lead are precipitated as sulfides.

Ammonium tetrafluoroberyllate is freely soluble in water. When concentrated by evaporation, it crystallizes without water of hydration. Above 130 °C it dissociates into ammonium fluoride and beryllium fluoride. Between 900 and 1100 °C ammonium tetrafluoroberyllate dissociates into gaseous beryllium fluoride and gaseous ammonium fluoride. The latter can be recycled to the process as ammonium hydrogen fluoride by dissolution in aqueous hydrogen fluoride. Cooling produces beryllium fluoride as vitreous grains [10, p. 71; 100].

Beryllium Chloride. Beryllium chloride can be prepared either directly from beryl by the chloride process or by chlorination of beryllium oxide under reducing conditions [101].

Beryllium chloride is especially well suited for purification by distillation in a stream of hydrogen [10, p. 102] and fractional condensation [102]. The significantly lower-boiling chlorides of aluminum, silicon, and iron(III) can be separated by careful temperature control. Iron(II) chloride, which is reduced by hydrogen, stays in the residue.

19.7.4 Metal Production

The chief difficulties involved in the production of beryllium metal are the reactivity and high melting point of the metal and the extreme stability of the oxide. Of the many possible methods of producing beryllium [10, 11, 84] two are used in industry presently: fusion electrolysis and reduction of halides by metals.

Only calcium is able to reduce the extremely stable beryllium oxide directly under

standard conditions. However, calcium forms the very stable intermetallic compound CaBe [103]. Reduction of BeO with titanium, zirconium [104], or carbon [105] at high temperatures is theoretically possible: the volatile beryllium would have to be distilled off from the reaction zone immediately. However, this method is not used.

Reduction with Metals. The most important industrial process is the reduction of beryllium fluoride with magnesium [10, p. 71; 106–109], the process presently used by Brush Wellman Inc.

The reaction is started by heating a mixture of relatively coarse-grained beryllium fluoride and magnesium in a graphite crucible. At a temperature of about 1300 °C the reaction produces a mixture of beryllium pebbles and magnesium fluoride. The reaction cannot be performed without external heating because the heat of reaction is not great and because the beryllium fluoride must be processed in the form of relatively large particles due to its toxicity and hygroscopicity. Normally about 70% of the stoichiometric quantity of magnesium is used. In this way a readily water-soluble beryllium magnesium fluoride slag, easily separated from the coarse-grained beryllium, is produced. The unreacted beryllium fluoride is separated from the magnesium fluoride and returned to the process.

The reaction of beryllium chloride with magnesium or sodium or the reaction of beryllium fluoride with sodium cannot be carried out in the same way. Sodium is more difficult to work with because of its low boiling point and its reaction with graphite. Beryllium chloride (*bp* 520 °C) is too volatile. The reduction of beryllium chloride with sodium in the vapor phase at 250 °C is the only process developed to the production stage [110–112]. However, this process does not currently have any economic importance.

Fusion Electrolysis. All practical electrolytic methods of production are based on the decomposition of beryllium fluoride, beryllium oxide, or beryllium chloride mixed with halides of the alkali metals or alkaline-earth met-

als [83]. These main group I and II halides are necessary to form a stable melt electrolyte with good conducting properties — the molten beryllium halides are covalently bonded and thus poor electrical conductors. In addition, only beryllium fluoride has a sufficiently large interval between melting point and boiling point at atmospheric pressure.

The electrolysis of the fluoride was developed by A. STOCK, H. GOLDSCHMIDT [113], Siemens & Halske [114], and the Beryllium Research Society. The electrolysis was carried out above the melting point of beryllium, at 1290–1400 °C. These methods and the similar methods of J. DICKINSON [115] and A. C. VRYLAN [116] are now obsolete.

The electrolysis of beryllium chloride [117] can be carried out at temperatures so low that the metal neither melts nor oxidizes. The beryllium is obtained as solid flakes, which are separated by washing out the electrolyte.

Mixtures of approximately equal parts of beryllium chloride and sodium chloride are electrolyzed at ≈ 350 –400 °C. The composition of the electrolyte is held as constant as possible. The apparatus consists of two identical nickel vessels hanging in electric furnaces. The crucible covers are fitted with the connections. One of the covers contains the anode and can be placed alternately on each crucible, the crucibles themselves serve as cathodes. During electrolysis (4–6 V, 0.08 A per cm² of cathode surface area) the metal is deposited as flakes on the cathode wall. When the beryllium chloride concentration in the melt has fallen to 45%, the melt is siphoned into the second crucible, in which beryllium chloride and sodium chloride have previously been melted down in quantities corresponding to the quantities consumed by the electrolysis in the first crucible. In this way the bath is again given its original composition. The crucible covers are then exchanged, and electrolysis is started in the second crucible. The chlorine generated at the anode during electrolysis is collected and used in the production of beryllium chloride.

The equipment for this process was developed by Degussa. Since the Second World

War this process has been used by Pechiney Cie. Chloride electrolysis was also used in France by Tréfinétaux G.P., a joint subsidiary of Pechiney Cie. and Kawecki Berylco Ind. Inc., and by NGK Insulators in Japan. It was used in slightly modified form by Murex Ltd., England [10]. It is also used in the former Soviet Union [118].

19.7.5 Refining and Further Processing

The as-reduced beryllium pebbles or flakes still contain many impurities and have to be refined before they are used to fabricate structural pieces. The main impurities in electrolytic beryllium are sodium and chlorine. The main impurities in beryllium from the magnesium reduction process are magnesium and magnesium fluoride. Other impurities include beryllium oxide, carbon, and metals, the most important being aluminum, iron, and silicon. Typical analyses of magnesium-reduced beryllium and electrolytic beryllium (CR flakes, Pechiney Cie.) are given in Table 19.4. Some of the impurities have adverse effects on the mechanical properties and corrosion of beryllium or are reactor poisons. Commercial grades of beryllium are refined exclusively by vacuum melting in beryllium oxide or magnesium oxide crucibles and casting in graphite ingot molds. The ingots weigh ≈ 200 kg. Their surfaces are machined (skinned) to remove the high carbon content material adjacent to the mold wall.

The melting of magnesium-reduced beryllium in a high vacuum produces a degree of purity comparable to that of electrolytic beryllium. Melting the electrolytic flakes in a vacuum further reduces the content of halides and low-boiling metals. A very pure grade of beryllium, particularly with respect to the content of oxide, aluminum, iron, silicon, carbon, and halides, can be produced by electrolytic purification (SR flakes, Pechiney Cie.). Other methods, such as vacuum distillation [10, 11, 18, 119–123], zone melting [18, 47, 124, 125], or liquid-metal extraction [18] have been used in the laboratory only.

Table 19.4: Composition of beryllium produced by various methods, ppm [12].

Element	Mg-reduced, coarse-grained	Electrolysis	
		CR flakes	SR flakes
O	—	2300	500–800
Al	400	< 200	60
Fe	500	300	50
Ni	100	150	30
Si	50	75	30
B	—	2	2
Cr	100	20	5
Mn	100	60	30
Ca	—	200	30
Mg	15 000	50	30
Na	—	300	—
C	300	300	150
F	20 000	—	—
Cl	—	1000	700
Be, %	96.0	96.5	99.87

Melting and Casting. The main purpose of melting and casting of beryllium is purification (see above); the production of semifinished goods is of secondary importance [12, p. 55]. The reason for this is that parts produced from castings have significantly poorer properties, even after working, than parts made by powder metallurgy. Cast flaws due to gas evolution during solidification and transcrystalline microcracks [10, p. 136; 15, p. 677] caused by cooling stresses cannot be prevented, even though they can be greatly reduced by mold design and construction [126]. Another significant disadvantage is the coarse-grained texture that develops during solidification, resulting in poor mechanical properties not improvable by thermomechanical treatment [10, p. 136; 12, p. 55; 15, pp. 193, 237, 246; 71, 72]. Fairly often crystals several centimeters in length are observed after induction melting [12, p. 55], and often crystals several millimeters in length are observed after electric-arc melting [15, pp. 677, 687; 126]. No effective grain-reducing agent is known [126].

Powder Manufacture. Beryllium was first worked by powder metallurgy in 1946. Since then many methods of powder production and compaction capable of producing ductile beryllium parts with good high-temperature strength have been studied and tested [12; 21,

vol. 2, pp. 13–29; 127]. However, the concentration of impurities is increased during powder-metallurgical working. Atmospheric oxygen and nitrogen, as well as iron and carbon from the mechanical working of the material into powders, are especially important. Above all, there is an increase in the oxide content as the grain size is decreased, i.e., as the specific surface increases. On the other hand, the oxide is desirable in certain circumstances because it increases strength and inhibits grain growth.

Powder manufacturing starts with cast ingots of inherently coarse grain size characterized by low ductility and resistance to fracture. These ingots are chipped with a lathe. The equipment is heavy duty: a multipoint tool can chip a 65-kg ingot in a single pass. These relatively coarse chips must be ground, or otherwise comminuted to finer particle sizes.

The first milling method commercially employed was *rotary grinding* between one stationary water-cooled and one rotating beryllium disk. The coarse chips were fed through a central hole in the stationary disk, and the fine powder emerged peripherally. The mill was enclosed into a sealed system to minimize contamination of the powder and to protect the environment from the toxic beryllium dust. This method was the standard for many years. Almost everywhere it has now been replaced by the impact attrition mill.

Within the *impact attrition mill* the coarse powder is fed into a gas stream, accelerated through a nozzle and impacted against a beryllium target. The morphology of the powder particles comminuted by this process is more spherical and less flat than disk-milled powder. Therefore, the mechanical properties of impact-ground powder compacts are more uniform. Because of the improved isotropy and a lower amount of inclusions and impurities the elongations of beryllium grades produced from impact-attrition material are higher.

Another commercial production process is *ball-milling*. It is used for high-oxide ultrafine powder (≈ 5 μ m), which is made especially for instrumentation uses. The high microyield

strength specified for such qualities is provided by the fine particle size and the high oxide content that strengthen the grain boundaries within the unpacked material. Because ball-milled powders are flat, like the particles produced by rotary grinding, they are difficult to handle and cause anisotropic physical and mechanical properties in the compacted beryllium billets.

Other powder production methods, like fluid-energy milling, disintegration of beryllium melts by gas atomization, rotating electrode process, or centrifuged shot-casting, have been used only in the laboratory [21, vol. 2, pp. 13–29]. Nevertheless, some of these processes may be used to produce commercial beryllium powder within the foreseeable future.

Powder Consolidation. *Vacuum hot pressing* of beryllium powder in graphite or steel dies is by far the most important commercial consolidation process. The powder is either dynamically compacted in the die or prepressed under cold isostatic conditions. After the die has been heated to 1000–1200 °C, a pressure of 1.4–10 MPa is applied. In this way billets up to 1.80 m in diameter and 6 t in weight, with relative density of nearly 100%, have been manufactured.

Hot isostatic pressing is used to produce more complicated parts with improved isotropic properties. The powders are either directly consolidated in a one-step process or preconsolidated. In preconsolidation the powder is prepressed at 210–700 MPa under cold isostatic conditions in rubber containers, the cold compact degassed at 650 °C, and the compact pressed isostatically for 2–3 h at 70 MPa and 760 °C in evacuated stainless steel containers [128].

The combination of *cold pressing and sintering* has been applied in the production of special parts, e.g., aircraft brake segments. Preforms may be sintered using mandrels to limit distortion and give better shape control. Sintering is usually carried out in a vacuum, which ensures better consolidation and higher densities than those achieved in argon.

The hot-pressed ingots are worked into semifinished goods or finished parts by machining, rolling (760–870 °C), extrusion (900–1090 °C), drawing (400–430 °C), deep-drawing (710–760 °C), forging, and compression (400–430 °C) [13, 14].

During hot deformation the beryllium is usually enclosed in a steel container. Working with such “canned” material greatly simplifies the operation because the workpieces need not be in a vacuum and need to be heated only slightly or not at all. The steel cover reduces oxidation and surface damage, improves lubrication, and produces a uniform temperature distribution in the workpiece. Although hot-deformed parts are usually less expensive than machined parts, they have highly anisotropic properties, with the favorable values in the direction of material flow during deformation and the less favorable values perpendicular to this direction. Cross-rolling produces uniform properties, e.g., in the sheet plane. Other processes used only in special cases are slip casting [21, vol. 2, pp. 13–29; 127; 129; 130], spark sintering [131], sinter forging [12, p. 102; 132], plasma injection [133], and isostatic hot-pressing [128].

Production of Single Crystals. The first comprehensive work on beryllium single crystals was done in the early 1950s [10, p. 372; 134–137]. These crystals were used mainly for investigations of the mechanical and cleavage fracture behavior of beryllium and were produced only in the laboratory. They were grown by slow solidification from the melt in a crucible [10, p. 372; 137], direct crystallization from vapor [138], and crucibleless zone melting [134, 139–145]. Efforts to produce beryllium single crystals using the Bridgman method were unsuccessful [146].

During the late 1970s it was recognized that beryllium would be the most efficient material for neutron monochromators, both because of its excellent nuclear properties and its excellent crystallographic properties [147, 148]. Many attempts to obtain beryllium single crystals with monochromator qualities failed [146, 149–152], but recent improvements in

equipment and technique have opened a new field that will likely lead to single-crystal manufacturing on an industrial scale.

Crystals with a diameter of 15 mm having a proper substructure can be grown by crucibleless zone melting at a rate of 1 mm/min. The application of the necking technique is inevitable. A modified double-ellipsoid mirror furnace, originally developed for crystal growth experiments during spacelab missions, is used [153]. The mosaic spread of the as-grown beryllium crystals can be increased from a few minutes to any desired value by plastic deformation on prismatic planes [154].

19.8 Environmental Protection

Because of the toxicity of beryllium vapor and dust, all operations should be carried out in properly ventilated rooms, and with vented equipment. Source exhaust has been found to be most effective [155–157]. In the presence of poorly controlled high workplace concentrations, fine-dust masks with filters of the specific safety level must be worn. The following limits have been recommended by the U.S. Atomic Energy Commission and the American Conference of Governmental Industrial Hygienists as a guideline for controlling beryllium hazards:

- In-plant atmospheric concentration should not exceed 2 µg/m³ throughout an 8-h working day.
- A brief exposure should not exceed 25 µg/m³.
- In the neighborhood of a plant handling beryllium the average monthly concentration should not exceed 0.01 µg/m³.

In order to meet these safety regulations the plant exhaust air has to be efficiently filtered before it is discharged into the atmosphere. All persons employed in processing areas with high risk potential for beryllium dust exposure are advised to wear shop-laundered work clothes to prevent neighborhood contamination. Care must also be exercised in disposal

of wastes from beryllium facilities: securely packed solid wastes are disposed by ground burial in concrete trenches. Liquid wastes are chemically treated to remove the toxic substances and to bring down the beryllium concentration to a safe level of approximately 1 ppm before discharge into public sewers.

In order to monitor the workplace concentration of 2 µg/m³, dust collectors must have suction speeds between 0.02 and 2 m³/min, depending on the type of sampling [155]. Presently a sufficiently sensitive analytical method for detecting the comparatively low beryllium concentrations is spectral analysis. Metallic beryllium in powder form can burn when ignited by sparks or an external heat source but does not self-ignite or explode. Beryllium oxide and alloys are not combustible. The naturally occurring isotope ⁹Be is not radioactive.

19.9 Quality Specifications

To date there is only one company — Brush Wellman Inc. — in the Western world that produces beryllium, beryllium-rich alloys, and beryllium compounds commercially. Brush Wellman Inc. produces beryllium from bertrandite by the SX-Carbonate process, reduces beryllium fluoride with magnesium, and refines it by vacuum melting and casting. Different grades are produced by different powder-metallurgy processes and metallurgical treatments, e.g., forging, extruding, rolling, and annealing. A high-purity grade, as obtained by electrolytic refining, is not available currently.

The composition, yield strength $\sigma_{0.2}$, tensile strength σ_F , and failure strain δ of several typical, commercial types of beryllium are compiled in Tables 19.5 and 19.6. However, these values guaranteed by the manufacturers are generally exceeded. The vacuum hot-pressed materials of Table 19.5 are used in nuclear technology, aeronautics, astronautics, and wherever high strength is required. The table shows that the yield strength and tensile strength increase with oxide content, while the elongation is not significantly affected. The

brake grade (BG-170) is characterized by greatly reduced hot brittleness (Curve c in Figure 19.3) [68, 69]. In the case of the instrument grades 1-220A and 1-400, the concentration of impurities is used to give a high precision elastic limit (PEL), below which the plastic strain is smaller than 10^{-6} or one microstrain.

The development of texture in extruded parts and plates results in failure strain values of 5 and 10% in the direction of extrusion and in the rolling plane, respectively (Table 19.6); perpendicular to this direction the failure strain is < 1%. Forged parts have elongations of 3%, and high-strength wire ($\phi < 0.25$ mm) has an elongation of 1%.

As an example of the effect of temperature on tensile strength, yield strength, elongation, and necking at failure, the values measured for plate material parallel to the plane of the plate are plotted in Figure 19.5. The plate material was produced by cross-rolling high-purity isostatically hot-pressed ingot material.

The creep rupture strength is usually high [67, 161, 162]. In the case of cross-rolled plates the ten-hour creep rupture strength is equal to the tensile strength up to 800 K and can be significantly increased by carbon or beryllium oxide [37]. The little information that is available on the fatigue strength [161–165] (Figure 19.6) indicates that beryllium has high fatigue strength and that the dynamic crack propagation is much less critical under alternating stress than under normal stress.

Table 19.5: Manufacturer-guaranteed composition and mechanical properties of various grades of beryllium [158].

	S-65B	S-100E	S-200E	I-70A	I-220A	I-400	BG-170
Chemical composition							
Be, min. %	99.0	98.5	98.0	99.0	98.0	94.0	98.0
BeO, max. %	1.0	1.2	2.0	0.7	2.2	4.2 ^a	1.2
Al, max. ppm	600	1400	1600	700	1000	1600	500
C, max. ppm	1000	1500	1500	700	1500	2500	1500
Fe, max. ppm	800	1500	1800	1000	1500	2500	1500
Mg, max. ppm	600	800	800	700	800	800	800
Si, max. ppm	600	800	800	700	800	800	500
Others, each, max. ppm	400	400	400	400	400	1000	—
Tensile properties							
σ_F , min. MPa	290	241	276	241	310	344	345
$\sigma_{0.2}$, min. MPa (0.2% offset)	207	186	207	172	241	—	207
Elongation, min. %	3	1	1	2	2	—	1
Microyield, min. MPa	—	—	—	—	34	55	—

^aBeO specified is minimum in this instance.

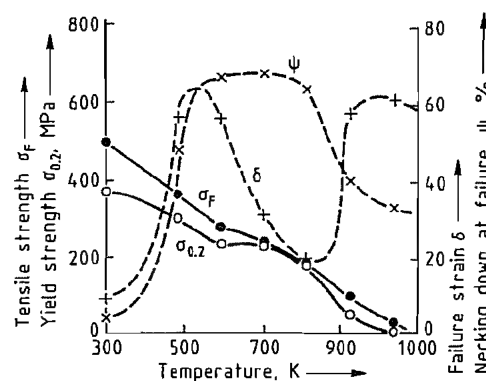


Figure 19.5: Mechanical properties of high-purity beryllium [160].

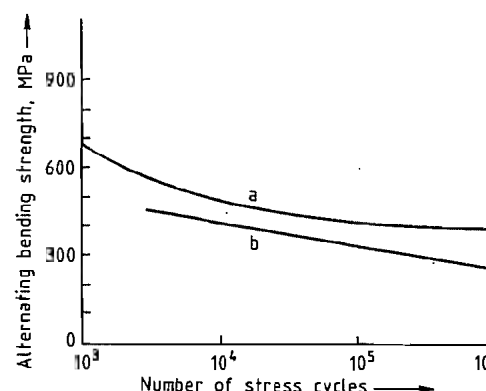


Figure 19.6: Fatigue strength of pressure-sintered, hot-worked beryllium [161]: a) Extruded and forged; b) Cross rolled.

Table 19.6: Mechanical properties of various semifinished beryllium products [158, 159].

	Plates ^a	Extruded parts ^a	Forged parts ^a	Wire, $\phi < 0.25$ mm
BeO content, % max.	2.0	2.0	2.0	0.02
$\sigma_{0.2}$, MPa	350	280	280	760
σ_F , MPa	480	480	450	900
δ , %	10	5	3	1

^aProperties parallel to the direction of extrusion or to the rolling plane.

A compilation [163, 164] of the K_{IC} (a measure of the toughness) values published so far shows that there is a great deal of variation. Most values lie between 10 and 20 $\text{MPa}/\text{m}^{1/2}$, but values up to 40 $\text{MPa}/\text{m}^{1/2}$ have been reported. However, the impact strength of notched and unnotched specimens is very low and depends on the type of working (Table 19.7).

Table 19.7: Impact strength (Charpy test), 10^{-2} MPa, of beryllium produced in various ways [58].

	Unnotched	Notched
Cast and extruded	0.16	—
Pressure sintered	1.1–3.4	0.68–1.3
Pressure sintered and extruded	5.6–6.1	—
Pressure sintered and rolled	2.7–4.1	—

The hardness of high-purity beryllium (Pechiney SR) is plotted in Figure 19.7 as a function of the mean grain size. The Brinell hardness of commercial pressure-sintered beryllium varies between 100 and 200, depending on the composition of the tested material [52].

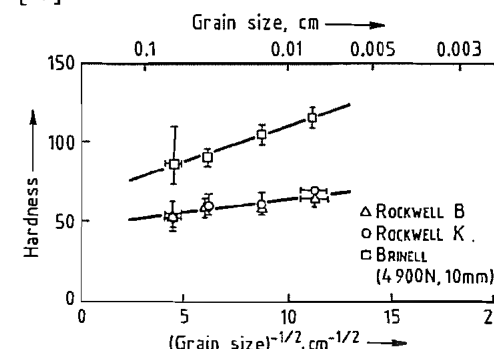


Figure 19.7: Brinell and Rockwell hardnesses of high-purity beryllium (Pechiney SR) as a function of the mean grain size [74].

19.10 Alloys

Beryllium-rich alloys have little industrial importance. The motivation for industrial research on beryllium alloys [10, p. 555; 12, p. 179; 15, pp. 601, 634; 17, p. 103; 132; 166–174] is not great because the solubility of most elements in solid beryllium is low (< 1 mol%), and only copper, nickel, cobalt, iron, silver, and platinum have solubilities between 1 and 10 mol%, even at elevated temperatures. In addition, most metals form intermetallic compounds with beryllium [25, 77–79], and these intermetallics are usually quite brittle.

The only alloy containing large amounts of beryllium is Lockalloy [169], which is produced by powder metallurgy and contains 38% Al. Aluminum does not form any beryllides. Therefore, this alloy contains beryllium grains embedded in the ductile aluminum phase with a more or less uniform distribution. This combination has a comparatively high modulus of elasticity (E), low density, and comparatively useful deformation behavior at room temperature. In addition, the notch sensitivity is lower than that of commercial beryllium (Table 19.8) [17, p. 103; 173]. However, Lockalloy has found only limited commercial use.

Table 19.8: Mechanical properties of powder-metallurgy Lockalloy [169] and beryllium-titanium composite materials (extruded powder mixtures [174]).

	ρ , g/cm ³	σ_F , MPa	E , MPa	δ , %	$\sigma_{0.2}$, MPa
Lockalloy	2.09	386	200 000	≈ 10	255
60 vol% Ti	3.4	1100	175 000	5	≈ 770
40 vol% Ti	2.85	829	215 000	2.5	≈ 580

Composite materials made of beryllium and titanium have been developed for use, e.g., as compressor blades in gas turbines [174]. At present, these materials are the only composite materials that allow definite plastic deformation, are impact resistant, and offer the choice of secondary cold or hot working (Table 19.8). Furthermore they can be used to a limited extent even at 400–500 °C.

Beryllium is used as an alloying component in a number of age-hardening alloys [6] based

on copper, nickel, cobalt, and/or iron [10, pp. 24, 49; 175–179]. Small amounts of beryllium improve the castability and oxidation resistance of aluminum and magnesium alloys [180–187]. These alloys are described under the principal component.

Table 19.9: Physical properties of beryllium oxide and carbide [7; 8; 10, p. 599; 11; 12, p. 267; 37; 189, 190].

	BeO	Be ₂ C
Structural type	ZnS	CaF ₂
Melting point, °C	2300–2570	≈ 2400
Density, g/cm ³	3.01	≈ 2.3
Modulus of elasticity, MPa	370 000	320 000
Linear coefficient of thermal expansion, K ⁻¹	5 × 10 ⁻⁶	5.8 × 10 ⁻⁶
Specific heat, Jg ⁻¹ K ⁻¹		
60 K	0.029	
292 K	1.00	1.4
1173 K	2.04	
Thermal conductivity, Wm ⁻¹ K ⁻¹		
room temperature	264	24
673 K	92	
1073 K	29	
Electrical resistance, Wm		
room temperature	10 ¹⁶	1.1 × 10 ⁻²
1273 K	8 × 10 ¹¹	0.45 × 10 ⁻²
2373 K	8 × 10 ⁶	
Compressive strength, MPa	800	720
Bending strength, MPa	285–380	91–98
σ ₂ , fm ²	0.9	2.3
Σ ₂ , cm ⁻¹	0.00066	0.0011
σ ₃ , fm ²	990	1690
Σ ₃ , cm ⁻¹	0.72	0.81

19.11 Compounds

Most beryllium compounds are important only in the production of beryllium metal, and these aspects are described earlier in this article.

Beryllium oxide, BeO, is obtained directly from beryllium hydroxide by calcination or from the basic carbonate, acetate, or sulfate by ignition [11]. The white, reactive powders differ in grain size, morphology, and impurity content [188]. They are used in the production of beryllium oxide ceramics, some of which have most unusual properties (Table 19.9). These ceramics are being used to an ever increasing extent [20].

Beryllium oxide is extremely stable [37]. However, its stability depends on its structure and is determined by the content of bound water. The higher the calcination temperature the more inert the beryllium oxide.

Beryllium nitride, Be₃N₂, is formed by heating beryllium in dry nitrogen in the presence of 2–6% hydrogen (700–1400 °C) or ammonia (1000 °C) [10, p. 570]. Moldings are produced by nitration of beryllium powder in porous molds by hot pressing the nitride at 1800–1900 °C. Relative densities up to almost 100% are achieved in this way. Beryllium nitride is stable in dry oxygen up to 500 °C, but in the presence of water vapor it reacts at lower temperatures. Beryllium nitride is cubic at room temperature, converting to hexagonal at 1400 °C. Two other nitrides, Be(N₃)₂ and BeN, and two beryllium silicon nitrides, Be₄SiN₄ and BeSiN₄, are known. These ternary nitrides are very hard, extremely inert, and stable up to 1850 °C [191].

Beryllium carbide, Be₂C, cubic, is obtained by direct reaction of solid or liquid beryllium with carbon or by reaction of beryllium oxide with finely divided carbon at 2080 °C [7; 10, p. 570]. Moldings are produced by hot pressing the carbide powder in graphite molds at 1800–1950 °C and 7–35 MPa. Beryllium carbide hydrolyzes very readily, even at room temperature, to form beryllium oxide and methane. At high temperatures it is not stable in air. Beryllium carbide vaporizes and decomposes in a vacuum above 2100 °C. The properties given in Table 19.10 are reference values because the beryllium carbide grades which were tested had indefinite structure. The nuclear properties of beryllium carbide are favorable. Beryllium borocarbide is extremely hard and is formed by melting mixtures of beryllium oxide, boron, and carbon in an electric arc.

Beryllium hydride, BeH₂, is a very light (ρ 0.58 g/cm³), white powder at room temperature that is difficult to prepare. It dissociates into beryllium and hydrogen at ≈ 130 °C [37]. Beryllium hydride is of interest as a high-energy solid fuel.

Beryllium hydroxide, Be(OH)₂, is obtained as a white voluminous precipitate on addition of bases to beryllium salt solutions. The fresh precipitate dissolves in sodium and potassium hydroxide and ammonium carbonate solution, but it ages quickly and becomes less and less soluble. The hydroxide also dissolves in aqueous BeSO₄ to form basic sulfates.

Basic beryllium carbonate, BeCO₃·nBe(OH)₂, n = 2–5, is formed in the reaction of beryllium salt solutions with alkali-metal or ammonium carbonate solutions. If excess ammonium carbonate is used, then a readily filtered precipitate of variable composition is formed on boiling. This salt is a suitable starting material for the preparation of beryllium salts of all types. Gentle calcining causes ammonia to escape, leaving beryllium oxide.

Beryllium nitrate, Be(NO₃)₂·4H₂O, is obtained by dissolving pure hydroxide or gently calcined, pure basic carbonate in nitric acid and concentrating the solution until crystallization takes place. Concentrated solutions are also commercially available. The nitrate is sometimes used in the incandescent gas mantle industry for stiffening mantles.

Beryllium sulfate, BeSO₄·4H₂O, is obtained by heating beryllium oxide with sulfuric acid. The tetrahydrate crystallizes from the aqueous solution in well-developed crystals. It can be obtained in very pure form by this method. The tetrahydrate is stable in air, can be dehydrated at about 400 °C, and decomposes above 600 °C to sulfur trioxide. The aqueous solution can dissolve considerable quantities of BeO to form basic sulfate. The sulfate is important chiefly for the recovery of beryllium.

Beryllium fluoride, BeF₂, is a white, freely soluble, low-melting salt. Molten beryllium fluoride is a poor electrical conductor due to the its covalent character. (See Section 19.7.3 for production of BeF₂.) In addition to its use as an intermediate in the preparation of beryllium, it is also sometimes used as an additive to welding and soldering fluxes because it dissolves metal oxides readily.

Beryllium chloride, BeCl₂, crystallizes in asbestos-like matted needles. It is extremely hygroscopic, forming a tetrahydrate. Its reaction with water is intensely exothermic and is accompanied by the release of HCl vapor. Beryllium chloride melts at 416 °C, boils at 520 °C, and, like the fluoride, is a poor electrical conductor in the molten state. (See Section 19.7.3 for production of BeCl₂.) Its principal uses are as the raw material for the electrolytic production of beryllium and as the starting material for syntheses of organoberyllium compounds.

Beryllium bromide, BeBr₂, melts at 490 °C. It is obtained as white needles by the reaction of bromine with a mixture of beryllium oxide and carbon. It is used in organic syntheses.

Beryllium orthophosphate, Be₃(PO₄)₂·6H₂O, is obtained by reaction of beryllium salts with disodium phosphate or diammonium phosphate in acetic acid solution. Its solubility is very low at room temperature but increases sharply with temperature.

Beryllium ammonium phosphate, NH₄BePO₄, whose composition varies greatly due to partial separation of beryllium hydrogen phosphate, is sparingly soluble. Freshly precipitated NH₄BePO₄ is amorphous.

Aqueous beryllium perchlorate, Be(ClO₄)₂, is a solvent for cellulose.

Basic beryllium acetate, a hexaacetato complex, Be₂O(CH₃COO)₆, like the acetylacetonate and a few other organic beryllium compounds can be distilled without decomposition. Insoluble in water, it melts at 280 °C and boils at 331 °C. The organic beryllium compounds are being used to an increasing extent as intermediates in the purification of beryllium.

Beryllides of some transition metals are promising structural materials or protective coating materials for high-temperature applications because of their low density, high melting point, good mechanical properties, and resistance to oxidation, even up to high temperatures (Table 19.10) [192–197].

Table 19.10: Properties of some beryllides [193] (RT = room temperature).

Beryllide m_p , K	Oxidation in air, 10^{-3} mm in 100 h		Coefficient of thermal expansion, 10^{-6} K $^{-1}$		Thermal conductivity, W m $^{-1}$ K $^{-1}$	Bending strength, MPa		Modulus of elasticity, 10^4 MPa		Strain at failure, %		Compressive strength, MPa	
	1640 K	1750 K	RT-1790 K	1750 K		RT	1640 K	RT	1640 K	RT	1640 K	RT	1640 K
NbBe ₁₂	1960	22	50	16.8	107.5	152	276	31.4	17.2	0.1	1.0	2.4	1380
Nb ₂ Be ₁₇	1980	15	47.5	15.9	112	214	434	29.6	17.2	0.1	2.0	≈ 7	—
Nb ₂ Be ₁₉	≈ 1980	—	—	—	—	206	448	—	—	0.1	2.0	3.0	—
TaBe ₁₂	2130	12.5	22	15.1	123	214	296	31.0	13.8	0.1	1.1	2.6	1030
Ta ₂ Be ₁₇	2265	7.5	22	15.7	—	206	386	31.0	13.8	0.1	2.6	≈ 5	—
ZrBe ₁₃	2200	12.5	32.5	17.7	119	172	255	32.4	13.8	0.05	0.25	0.6	1310
Zr ₂ Be ₁₇	2260	12.5	30	15.1	—	172	276	31.0	13.8	0.1	0.3	0.1	482

19.12 Chemical Analysis

The quantitative determination of beryllium, even in very small amounts, is especially important because of the toxicity of beryllium [155, 198]. The best method is atomic absorption spectrometry. When an acetylene/nitrous oxide flame is used, even beryllium oxide is excited, and it is possible to analyze any solution or dispersion without preliminary treatment [155, 199, 200]. Other methods [201–205] have also been described.

19.13 Storage, Transportation, Legal Aspects

Solid parts and structures made from beryllium metal, alloys, and ceramic beryllium can be stored and transported safely without special precautions as long as neither vapor nor dust is generated. Beryllium and beryllium oxide powder have to be handled with care, as is described in Section 19.8. For storage and transportation of the powders, sealed, unbreakable containers and proper instructions are a necessity.

Because beryllium is used mainly in military, nuclear, aeronautical, and rocket technologies, its trade is restricted. A special license is necessary for export from the United States.

19.14 Uses of the Metal

The properties of beryllium, especially the mechanical properties, are strongly affected by even small amounts of additives, e.g., 1000 ppm or less, and in this sense even commercial grades of beryllium (Table 19.5) represent alloys. The crucial advantage of beryllium over other materials is its combinations of favorable properties. Detailed discussions of the relationship between properties and uses have been published [19, 41].

Table 19.11: World production of beryl (t).

	1975	1976	1977	1978	1979 ^a	1980 ^a	1981 ^b	1982 ^b	1984	1989 ^c	1990	1991 ^a	1992 ^a	1993 ^c
Argentina	303	123	182	24	13	34	33	29	NA ^d	32	34	34	34	35
Brazil	770	406	547	815	498	606	894	882	878	900	850	850	850	850
China ^{e, f}	—	—	—	—	—	—	—	—	—	54	55	55	—	—
Kazakhstan	—	—	—	—	—	—	—	—	—	—	—	—	100	100
Madagascar	—	—	17 ^c	12	11	11	10	11	NA	32	—	—	—	—
Mozambique	9	—	NA	NA	31	22	20	17	—	—	—	—	—	—
Portugal	—	—	—	—	6	21	20	21	—	—	—	—	—	—
Rwanda	20	51	60 ^c	64	51	119	100	110	—	—	—	—	—	—
South Africa	3	3	3	4	1	—	134	66	—	—	—	—	—	—
Uganda ^c	—	60	50	—	—	—	—	—	—	—	—	—	—	—
USA ^f	—	—	—	—	—	—	—	—	—	4566	4548	4339	4826	4939
USSR ^c	1760	1820	1870	1930	2000	2000	2000	2000	NA	1770	1600 ^g	1300 ^g	1100 ^h	800 ^h
Zimbabwe	70	70	114	39	31	10	46	22	NA	28	28	29	23	23
Others	135	20	1	—	6	21	20	NA	—	—	36 ⁱ	15 ⁱ	19 ⁱ	19 ⁱ
Total	3070	2553	2844	2888	2642	2823	3254	3158	878	7382	7151	6622	6952	6766

^aRevised.

^bPreliminary.

^cEstimated.

^dNA = not available.

^eWorld mined beryllium production ($\times 10^3$ t containing Be).

^fMine shipments, incl. bertrandite ore, calculated as equivalent to beryl containing 11% BeO.

^gUSSR/CIS.

^hRussia.

ⁱIncl. Madagascar, Namibia, Nepal, Portugal, South Africa.

The low density of beryllium combined with its high strength, high melting point, and resistance to oxidation is the basis for its use in structural parts that must be light and are exposed to inertial or centrifugal forces. In addition, it has a high modulus of elasticity, which gives light-weight components a high degree of rigidity [19]. Another area of use is in so-called dimensionally stable parts, in which high microyield strength and good thermal conductivity and reflexivity are exploited. It is an excellent heat sink, and therefore used especially for brake systems of airplanes. Applications in civilian nuclear reactors as reflectors and moderators have not met expectations because of radiation damage. However, its favorable nuclear properties have been exploited in weapons systems and in various physical instruments. Beryllium single crystals are the most efficient material for neutron monochromators. Beryllium foil is widely used as windows in energy-dispersive X-ray analyzers.

19.15 Economic Aspects

Data on production and consumption of beryllium is scanty and incomplete, in most cases because beryllium is used mainly for military and similar purposes. The most complete summary is published annually by the U.S. Bureau of Mines (Table 19.11), but the data mainly concerns mined beryl.

19.16 Toxicology and Occupational Health

Beryllium and its compounds when inhaled in finely divided form dust, fume, or vapor may affect the upper airways and lungs. Contact with water-soluble beryllium salts may cause inflammatory reactions of the skin. Beryllium metal, alloys, and ceramic beryllium can be handled safely without special precautions as long as the fabrication process does not require high temperatures or produce particles smaller than 10 μ m.

Prior to 1950, many cases of acute chemical bronchitis, pneumonitis, and contact dermatitis had occurred from high exposures to

water-soluble beryllium salts because the potentially harmful effects of beryllium were insufficiently known. During the same period, numerous cases of *chronic beryllium disease* from exposures to beryllium oxide and metal dusts were reported among production workers, members of their family, and others living close to the plants. Strict exposure control introduced in 1950 succeeded promptly in eliminating neighborhood cases and all forms of the acute disease [206, 207].

However, chronic beryllium disease must still be kept in mind as a potential hazard associated with the basic production and fabrication of beryllium materials. *Metallic beryllium* and *beryllium oxide*, when inhaled as dust, represent the greatest risk; chronic cases have also been reported from inhalation of *beryllium-copper particles* in the form of fine dusts or fumes.

In contrast with other pneumoconioses, chronic beryllium disease is highly selective, because even under the most severe exposure conditions never more than 2% of all workers were affected. The reason for this epidemiological peculiarity is an allergy-like immune reaction that occurs only in a very small portion of the population. The actual cause of this predisposition is not yet fully understood, nor can it be predetermined. Therefore, strict exposure control is needed for all individuals at risk. Any process likely to generate respirable particles of beryllium, such as grinding, polishing, and buffing of metallic beryllium, beryllium oxide, or beryllium alloys, must be considered as potentially harmful and requires adequate venting. Special attention is indicated for beryllium copper because the vapor pressure of beryllium is greater than that of copper.

Cold rolling, drawing, stamping, and slitting generally produce no or very few fine particles and are unlikely to cause atmospheric beryllium concentrations in excess of the exposure limits. The same is true for drilling and sawing with the use of liquid coolants, if the appropriate precautions are taken. Dry sawing and drilling with fine tools usually generates

fairly large amounts of respirable dusts, and proper venting equipment must be installed.

Beryllium in the Body [208]. Upon ingestion, beryllium metal, oxide, or alloys do not exert harmful effects on the intestinal mucosa and are not absorbed to any significant degree. Absorption through the skin is also minimal and without clinical consequences. Beryllium-containing particulates, if inhaled in low concentrations, will be removed from the alveolar spaces by macrophages and eliminated from the airways via mucociliary escalation. Amounts exceeding the capacity of this mechanism will be transported into the lung tissue and from there gradually into bone, liver, and kidney tissues. Because of a very slow elimination from the body, the biological half-life is long. In most individuals beryllium is removed from these storage organs and excreted via the kidneys without any harmful effect.

Clinical Symptoms [208, 209]. Only in individuals predisposed to sensitization can the inhalation of excessive beryllium lead to *chronic beryllium disease* (also known as *berylliosis*), an inflammatory process involving the connective tissues of the lungs. However, latent periods of 5–25 years may precede the manifestation of the disease — shortness of breath on exertion; chronic, dry cough; and burning substernal pain. A gradual reduction in lung volume caused by replacement of the normal lung structures by scar tissue and interference with gas exchange between alveolar air and blood are the primary causes of these symptoms. Their extent may show great variations. Approximately one third of all affected individuals have relatively little incapacitation and a normal life expectancy. At the other end of the spectrum, marked scarring and shrinkage of the lung tissue may cause a severe chronic strain on the right heart chamber and serious physical impairment.

Because it shares many features with other lung diseases, the accurate diagnosis of chronic beryllium disease is difficult. It requires a reliable exposure history and, in addition to chest X-rays and pulmonary function evaluation, a lymphoblast transformation test,

really the only specific proof of the disease [207, 208].

Corticosteroids are helpful in therapy. Although they do not cure the disease, they may bring it to a standstill and relieve symptoms. Further exposure to beryllium must be avoided.

Carcinogenicity. Beryllium compounds have produced tumors in several animal species [210, 211]. *Mutagenicity* tests were negative in bacteria and yeasts, but they were positive in cultures of mammalian cells [212, 213]. Regarding *teratogenic* and *reproductive* effects, the presently available information is insufficient for any conclusions. No convincing evidence exists, in spite of forty years of close observation, that beryllium is carcinogenic for humans.

Prevention [207, 209, 211]. In the United States the TLV is $2 \mu\text{g}/\text{m}^3$ as a daily weighted average with a 30-min peak of $25 \mu\text{g}/\text{m}^3$. Beryllium is classified in group A2 (suspected of carcinogenic potential in humans) by ACGIH. In Germany, beryllium is also classified as an A2 material and a TRK of $5 \mu\text{g}/\text{m}^3$ for grinding of beryllium metal and alloys and $2 \mu\text{g}/\text{m}^3$ for all other compounds was established (1983).

No new cases of chronic beryllium disease have developed whenever atmospheric beryllium levels were kept consistently at or below these levels. However, inhalation of high concentrations of beryllium during very short periods has also resulted in chronic beryllium disease. For that reason duration and concentrations of the short-term exposure limit of $25 \mu\text{g}/\text{m}^3$ must not be exceeded.

Ore extraction and production of beryllium metal, oxide, and alloys present the greatest risk for excessive exposures: here the most efficient venting equipment and shop-laundered work clothes are required. Melting and welding of beryllium alloys also belong to this category.

Cutting, milling, or turning of beryllium metal or alloys produce significantly less respirable particles, and the concentration in the shop air can be readily kept at or below 1

$\mu\text{g}/\text{m}^3$ with the help of source exhaust systems. Many fabricating operations for beryllium alloys and ceramic oxide generate such low breathing zone and ambient air concentrations that special venting may not be needed. In those instances ordinary shop coats are sufficient.

Medical surveillance [207, 208] should include chest X-rays and spirometry prior to employment, annually, and on termination. For minimum exposure risks, less frequent intervals may be satisfactory.

19.17 References

The following abbreviations are used in the citations.

- | | |
|-------|---|
| AERE | Atomic Energy Research Establishment |
| AIME | American Institute of Mining, Metallurgical, and Petroleum Engineers |
| AMC | American Motor Co. |
| ASD | Avco Systems Division |
| AWRE | United Kingdom Atomic Research Authority, Atomic Weapons Research Establishment |
| BBC | Brush Beryllium Co. |
| DMIC | Defense Metals Information Center, Battelle Memorial Institute |
| FIRL | Franklin Institute Research Laboratories |
| GEC | General Electric Co. |
| NASA | National Aeronautics and Space Administration |
| NMAB | National Materials Advisory Board |
| NMI | Nuclear Metals Inc. |
| RFP | The Dow Chemical Co., Rocky Flats Division |
| SAE | Society of Automotive Engineers |
| UCRL | University of California, Lawrence Radiation Laboratory |
| USAEC | United States Atomic Energy Commission |
| WADC | Wright Air Development Center |
1. L. N. Vauquelin, *Ann. Chim. (Paris)* **26** (1798) 155, 170, 259; **30** (1799) 82.
 2. F. Wöhler, *Pogg. Ann.* **13** (1828) 577.
 3. A. A. B. Bussy, *J. Chim. Med. Pharm. Toxicol.* **4** (1828) 453.
 4. P. Lebeau, *Ann. Chim. Phys.* **57** **16** (1899) 457.
 5. G. Esterheld, *Z. Anorg. Allg. Chem.* **97** (1916) 14.
 6. G. Masing, O. Dahl, *Wiss. Veröff. Siemens Werke* **8** (1929) 126.
 7. W. W. Beaver, D. W. Lillie in C. R. Tipton, Jr. (ed.): *Reactor Handbook*, Interscience, New York 1960, p. 897.
 8. H. H. Hausner: "Beryllium as a Moderator and a Reflector for Nuclear Reactor", *At. Energy Rev.* **1** (1963) no. 2, 99.
 9. J. B. Rich C. B. Redding R. S. Barnes, *J. Nucl. Mater.* **1** (1959) 96.
 10. D. W. White, J. F. Burke: *The Metal Beryllium*, The American Society for Metals, Cleveland 1955.
 11. G. E. Darwin, J. H. Buddery: *Beryllium*, Butterworths, London 1960.

12. H. H. Hausner, *Beryllium, Its Metallurgy and Properties*, University of California Press, Berkeley-Los Angeles 1965.
13. R. F. Williams S. E. Ingels, *NASA Tech. Rep. TM-X-53453* vol. 1-6 (1966).
14. G. E. Meyer, J. H. Henning, *DMIC Rep. S-29* (1970).
15. *The Metallurgy of Beryllium*, Proc. Int. Conf., London 1961, Institute of Metals, Monograph and Report Series no. 28, Chapman & Hall, London 1963.
16. *Proc. Int. Conf. Beryllium 1st*, AIME, Gatlinburg, PA, 1963.
17. *Proc. Int. Conf. Beryllium 2nd*, AIME, Philadelphia 1964.
18. *Conf. Int. Metall. Beryllium Commun. 3rd* 1965.
19. *Proc. Beryllium Conf.*, Arlington, VA, 1970, NMAB Rep. 272 (1970).
20. F. E. Buresch: *Berylliumoxidkeramik unter besonderer Berücksichtigung moderner Anwendungen; Appl. Mineralogy - Technische Mineralogie*, Springer Verlag, Berlin 1974/75.
21. D. Webster, G. J. London (eds.): *Beryllium Science and Technology*, vol. I.
D. R. Floyd, J. N. Lowe (eds.): *Beryllium Science and Technology*, vol. II, Plenum Press, New York 1979.
22. M. C. Udy, H. L. Shaw, F. W. Boulger, *Nucleonics* 11 (1953) 52.
23. C. J. Smithells: *Metals Reference Book*, Interscience, New York 1955.
24. A. J. Martin, A. Moore in: *Symposium on the Study of Metals and Alloys above 1200 °C*, Oxford Univ. Press, England 1958.
25. W. B. Pearson: *Lattice Spacings and Structure of Metals and Alloys*, vol. 2, Pergamon Press, London 1967.
26. P. Gordon, *J. Appl. Phys.* 31 (1960) 1221.
27. A. J. Martin, A. Moore, *J. Less-Common Metals* 1 (1959) 85.
28. R. Hultgren et al.: *Selected Values of Thermodynamic Properties of Metals and Alloys*, J Wiley & Sons, New York 1963.
29. R. W. Hill, P. L. Smith, *Philos. Mag.* 44 (1953) 636.
30. V. N. Eremenko, V. I. Nizhenko, Shou Wei Tai, *Izv. Akad. Nauk SSSR Otd. Tekh. Nauk Metall. Topl.* 3 (1960) 116.
31. R. L. Powell, *Philos. Mag.* 44 (1953) 645.
32. K. M. Treco, *Trans.* 188 (1950) 1274.
33. M. Owens, *Ann. Phys.* 37 (1912) 657.
34. A. Ciccione, *Nature (London)* 130 (1932) 315.
35. M. M. Mann, Jr., L. A. du Bridge, *Phys. Rev.* 51 (1937) 120.
36. C. B. Sawyer, B. R. F. Kjellgren, *Met. Alloys* 11 (1940) 163.
37. F. Aldinger, *Metall (Berlin)* 26 (1972) 711.
38. R. L. Powell, *Philos. Mag.* 31 (1960) 1221.
39. R. W. Meyerhoff, J. F. Smith, *J. Appl. Phys.* 33 (1962) 223.
40. A. R. Kaufmann, *USAEC MIT-1113* (1953).
41. F. Aldinger, G. Petzow, *Radex Rundsch.* 3/4 (1972) 275.
42. E. J. Lewis, *Phys. Rev.* 34 (1929) 1575.
43. L. Losana, *Aluminio* 8 (1939) 67.
44. P. Gordon, *USAEC MDDC-1370, CT-3315* (1945).
45. F. K. Lampson, *USAEC NEPA-186* (1951).
46. S. H. Gelles, *NMI Q. Prog. Rep.* (Jan.-March 1962).
47. M. Wilhelm, *Dissertation*, University of Stuttgart, 1974.
48. *Extracts on Soviet Beryllium and Beryllium Alloys*, DMIC Tech. Note (June 1969).
49. B. G. Lazarev, A. I. Sudovtsev, E. E. Semenenko, *Zh. Eksp. Teor. Fiz.* 37 (1959) 1461.
50. A. E. Cruzon, A. J. Mascall, *J. Phys. C* 2 (1969) 383.
51. G. K. White, S. B. Woods, *Can. J. Phys.* 33 (1955) 58.
52. M. C. Udy, H. L. Shaw, F. W. Boulger, *USAEC AECD-3382* (1949).
53. J. E. Janssen et al., *Honeywell Center Rep. ASD-TR-61-147* (1961).
54. D. E. Gray: *Am. Inst. of Phys. Handbook*, McGraw-Hill, New York 1957.
55. D. Strominger, J. M. Hollander, G. T. Seaborg, *Rev. Mod. Phys.* 30 (1958) 585.
56. C. E. Ellis, E. C. Perryman, *J. Nucl. Mater.* 1 (1959) 96.
57. A. R. Kaufmann, P. Gordon, D. W. Lillie, *Trans. Am. Soc. Met.* 42 (1950) 785.
58. W. W. Beaver, K. G. Wikle, *Trans. Am. Min. Metall. Pet. Eng.* 200 (1954) 559.
59. H. D. Hanes, S. W. Porembka, J. B. Melehan, P. J. Gripshover, *DMIC Rep.* (1965).
60. H. Comad, G. London, V. V. Damiano in F. W. Vahl-diek, S. A. Mersol (eds.): *Anisotropy in Single Crystal Refractory Compounds*, vol. 2, Plenum Press, New York 1968.
61. A. N. Stroh, *Philos. Mag.* 3 (1958) 397.
62. J. J. Gilman, *Trans. Am. Inst. Min. Metall. Pet. Eng.* 200 (1954) 621.
63. D. Webster, *Conf. Strength Met. Alloys Conf. Proc. 4th* 2 (1976) 669.
64. J. F. Smith C. L. Arbogast, *J. Appl. Phys.* 31 (1960) 99.
65. W. D. Rowland, J. S. White, *J. Phys. F* 2 (1972) 231.
66. M. P. Baldwin, *AWRE Rep. O-49/70* (1970).
67. D. R. G. O'Rourke et al., *USAEC COO-312* (1956).
68. R. A. Foos, A. J. Stonehouse, K. A. Walsh, *BBC Rep. TR-456* (1970).
69. K. W. Walsh, A. J. Stonehouse, A. J. Sandor, *BBC Rep. TR-465* (1971).
70. J. Greenspan, *USAEC NMI-1174* (1957).
71. N. Maropis, J. B. Jones, *USAEC NYO-7788* (1957).
72. V. V. Damiano et al., *FIRL Rep. F-B2373* (1966), *F-C1820* (1967), *F-C2031* (1968), *F-C2233* (1969), *F-C2521* (1970).
73. R. Syre, *Met. Corros. Ind.* 33 (1958) 406.
74. A. V. Novoselova, L. R. Batsanova: *Analytical Chemistry of Beryllium*, Ann Arbor-Humphrey Science Publ., Ann Arbor-London 1969.
75. *Gmelin*, system no. 26, Beryllium (1930).
76. P. D. Miller, W. K. Boyd, *DMIC Rep.* 242 (1967).
77. M. Hansen, K. Anderko: *Constitution of Binary Alloys*, McGraw-Hill, New York 1958.
78. R. P. Elliott: *Constitution of Binary Alloys*, 1st Suppl., McGraw-Hill, New York 1965.
79. F. A. Shunk: *Constitution of Binary Alloys*, 2nd Suppl., McGraw-Hill, New York 1969.
80. B. H. Clemmons, J. S. Browning, *Min. Eng. (Littleton, CO)* 5 (1953) 786.
81. A. M. Gaudin et al., *Min. Eng. (Littleton, CO)* 2 (1950) 495.
82. R. G. Bellamy, N. A. Hill: *Extraction and Metallurgy of Uranium, Thorium and Beryllium*, Pergamon Press, Oxford 1963.
83. G. Jäger, *Metall (Berlin)* 4 (1950) 183.
84. K. C. Chen, *Dissertation*, London 1950.
85. W. L. W. Ludekens *Dissertation*, London 1950.
86. *Ullmann*, 3rd ed., vol. 4, p. 322.
87. H. Claffin US 1929014, 1933.
88. R. A. Opatowski, US 2209131, 1941.
89. H. C. Kaweck, US 2312297, 1943; *Trans. Electrochem. Soc.* 89 (1946) 229.
90. C. V. Sundaram, C. M. Paul, B. P. Sharma, *Trans. Indian Inst. Met.* 35 (1982) no. 2, 171.
91. R. W. Winters, L. F. Yntema, *Trans. Electrochem. Soc.* 55 (1929) 205.
92. F. K. McTaggart, *J. Counc. Sci. Ind. Res. (Aust.)* 20 (1947) 564.
93. L. Burgess, *Am. Electrochem. Soc.* 47 (1925) 317.
94. J. Kielland, L. Tronstad, *K. Nor. Vidensk. Selsk. Arsbetn.* 8 (1935) 147.
95. J. Besson, C. R. Hebd. Séances Acad. Sci. 214 (1942) 861.
96. C. Matignon, J. Cathala, C. R. Hebd. Séances Acad. Sci. 181 (1925) 1066.
97. J. M. Schmidt, *Sci. Ind. (Paris)* 13 (1929) 110.
98. R. A. Foos: *Applications of Solvent Extraction to Beryllium Oxide Manufacturing*, AIME Conference, New York 1968.
99. Brush Beryllium Co., US 3259456, 1964.
100. C. W. Schwenzfeier et al., US 2660515, 1953.
101. G. Jeager, DE 752729, 1938.
102. *Industrial Challenge of Nuclear Energy III*, part 3, Stresa Conference 1959, OEEC 1960.
103. R. W. Buddery, R. W. Thackray, *J. Inorg. Nucl. Chem.* 3 (1956) 1901.
104. W. Kroll, *Z. Anorg. Allg. Chem.* 240 (1939) 332.
105. O. Kruh, AT 147634, 1934.
106. H. v. Zeppelin, DE 705645, 1937.
107. B. Wempe, US 2091087, 1933.
108. B. R. F. Kjellgren, *Trans. Electrochem. Soc.* 93 (1948) 122.
109. L. J. Derham, D. A. Temple: *Extraction and Refining of the Rarer Metals*, Inst. Min. Metall, London 1957.
110. J. M. Tien, *Trans. Electrochem. Soc.* 89 (1946) 237.
111. Brush Beryllium Co., *Progr. Rep.* 12-17 (1947).
112. T. T. Campbell, R. E. Mussler, F. E. Block, *Metall. Trans.* 1 (1970) 2881.
113. A. Stock, H. Goldschmidt, DE 375824, 1924.
114. K. Illig et al., *Wiss. Veröff. Siemens Werke* 8 (1929) no. 1, 47.
115. J. Dickinson, US 1511829, 1921.
116. A. C. Vivian, *Trans. Faraday Soc.* 22 (1926) 211.
117. Degussa, DE 646088, 1937.
118. G. A. Meyerson, *Proc. U.N. Int. Conf. Peaceful Uses At. Energy, 1st* 1955, 633.
119. R. B. Holden et al., *J. Am. Chem. Soc.* 70 (1948) 3897.
120. F. A. Gulbranssen, K. F. Andrew, *J. Electrochem. Soc.* 97 (1950) 383.
121. N. D. Erway, R. I. Seifert, *J. Electrochem. Soc.* 93 (1951) 83.
122. J. P. Pemsler et al., *NMI Rep. TJ-38* (1961).
123. S. H. Gelles et al., *ASD Rep. TDR-62-509* (1962).
124. G. W. Pfann, *J. Met.* 4 (1952) 747.
125. C. S. Pearshall, *USAEC MIT-1103* (1952).
126. J. P. Denny, B. H. Hessler, *ASD Rep. TDR-62-390* (1962).
127. S. W. Porembka, H. D. Hanes, P. J. Gripshover, *DMIC Rep.* 239 (1967).
128. F. T. Zurey, H. D. Hanes, P. J. Gripshover: *Hot Iso-static Pressing of Beryllium*, vol. 1, Batelle Mem. Inst., Columbus, OH, 1968.
129. G. W. Fischer et al., *GEC Rep. IR-8-12* (1965).
130. C. A. Bielowski, J. G. Theodore, W. W. Beaver, *NASA Tech. Rep.* 334-241 (1963).
131. *Spark Sintering of Parts and Preforms*, Lockheed Missiles & Space Comp., Sunnyvale, CA, 1969.
132. M. Hirschvogel, F. Aldinger, *Proc. Int. Powder Met. Conf. 4th*, Toronto 1973.
133. M. L. Headmann, T. J. Roseberry, F. L. Parkinson, *West. Gear Corp. Rep.* 649-229 (1964).
134. H. T. Lee, R. M. Brick: "Slip and Twinning in Single Crystals of Beryllium", *J. Met.* 4 (1952) 147-148.
135. H. T. Lee, R. M. Brick: "Deformation of Beryllium Single Crystals at 25 to 500 °C", *Trans. Am. Soc. Met.* 48 (1956) 103-107.
136. C. S. Pearshall, *Nucl. Sci. Abstr.* 7 (1953) 1434.
137. L. Gold, *USAEC AECD-2643* (1949).
138. I. I. Papirov, G. F. Tikhinskij, *Kristallografiya* 9 (1964) 310.
139. M. Wilhelm, F. Aldinger, *Z. Metallkd.* 66 (1975) 323.
140. G. J. London, J. D. Meakins, *FIRL Rep. P-C1870-3-1*, Philadelphia 1970.
141. G. E. Spangler, M. W. Herman, E. J. Arndt, *FIRL Rep. F-A2476*, Philadelphia 1961.
142. M. Herman, G. E. Spangler in: *The Metallurgy of Beryllium*, Institute of Metals, Monograph and Report Series no. 28, Chapman & Hall, London 1963, p. 75.
143. L. M. McDonald-Schetky, H. A. Johnson (eds.): *Beryllium Technology*, vol. 1, Gordon & Breach, New York 1964.
144. D. F. Kaufman, E. D. Levine, J. J. Pickett, L. R. Aro-nin in: *Proc. Conf. Phys. Metall. Beryllium, AEC-CONF-170* (1963) 69.
145. D. Beasley, *Conf. Int. Metall. Beryllium Commun. 3rd* 1965, 129.
146. J. D. Meakin, *FIRL Rep. F-C1870*, Philadelphia 1971.
147. A. Freund, J. O. Forsyth in: *Treatise on Materials Science and Technology*, vol. 15, Neutron Scattering, Academic Press, New York 1979, chap. 10.
148. S. Jönsson, *Naturwissenschaften* 69 (1982) 483.
149. F. Aldinger, A. Freund in: "Beryllium 1977", *Proc. 4th Int. Conf. Beryllium*, Royal Society, London 1977, p. 55/1.
150. J. Faure-Deloché, *Thesis*, University of Grenoble 1973.
151. A. S. Kapcherin, I. I. Papirov, G. F. Tikhinskij, A. S. Avotin in: "Beryllium 1977", *Proc. 4th Int. Conf. Beryllium*, Royal Society, London 1977, p. 5/1.
152. S. Jönsson, A. Freund, F. Aldinger, *Metall (Berlin)* 33 (1979) 1257.
153. S. Stilz, S. Jönsson, *Metall (Berlin)* 38 (1984) 748.
154. A. K. Freund, S. Jönsson, S. Stilz, G. Petzow, *J. Nucl. Mat.* 124 (1984) 215.
155. S. Mönch, *Metall (Berlin)* 23 (1969) 238.

156. H. Zorn, H. Diem, *Zentralbl. Arbeitsmed. Arbeitsschutz* 24 (1974) 3.
157. G. Petzow, H. Zorn, *Chem. Ztg.* 98 (1974) no. 5, 236.
158. Brush Wellman Inc., Cleveland, OH, *Specification Sheets* (1972).
159. Kawecki Berylo Ind., Hazleton, PA, *Product Specifications* (1971).
160. Kawecki Berylo Ind., Hazleton, PA, *Product Specification*, File no. 302-PD10 (1972).
161. G. G. Winkle et al., *AMC Rep.* 60-7-631 (1960).
162. E. Crawford et al., *ASD Rep.* TR 61-692 (1962).
163. P. C. Paris, D. O. Harris, *UCRL Rep.* 72442 (1970).
164. R. E. Cooper, *AWRE Rep.* 0-17172 (1972).
165. J. G. Klein, L. M. Perelman, W. W. Beaver, *WADC Rep.* TR-58-478 (1958).
166. R. E. Evans, D. Beasley, J. N. Lowe, "Alloy Strengthened Beryllium Sheet", *AWRE Rep.* 0-12/67 (1967).
167. J. G. Klein, L. M. Perelman, W. W. Beaver, *WADC Rep.* 58-478, I (1959), II (1960).
168. W. W. Beaver, *BBC Rep.* TR-242 (1968).
169. Lockheed Missiles & Space Comp., US 3337334, 1963.
170. C. Carson, J. P. Denny: *Solid Solution Strengthened Beryllium Alloy Ingot Sheet*, Beryllium Corp., Reading, PA, 1966/67.
171. W. Taylor, C. Carson: *Solid Solution Strengthened Beryllium Alloy Ingot Sheet*, Beryllium Corp., Reading, PA, 1967/68.
172. W. Fischer, F. Aldinger, *Tagung Verbundwerkstoffe*, Konstanz 1974.
173. R. W. Fenn et al., *SAE Rep.* 660652 (1966).
174. D. B. King, A. J. Stonehouse, *Ordinance*, in press.
175. D. Böhme, *Z. Metallkd.* 56 (1965) 487.
176. Vakuumschmelze Hanau, *Tech. Informationsblätter F 3* (1967).
177. Vakuumschmelze Hanau, *F 004* (1967).
178. Deutsche Beryllium GmbH, *Tech. Inf.* no. 1006 G (1982).
179. I. Pfeiffer, *Z. Metallkd.* 57 (1966) 635.
180. J. R. Burns, *Trans. Am. Soc. Met.* 40 (1948) 143.
181. S. Balicki, *Pr. Inst. Hutn.* 10 (1958) 208.
182. *Tech. Rundsch.* 51 (1959) no. 35, 5.
183. K. E. Mann, *Z. Metallkd.* 46 (1955) 17.
184. E. Nachtigall, H. Landerl, *Alum. Ranshofen Mitt.* 4 (1956) 15.
185. L. David, *Light Met. (London)* 18 (1955) 15.
186. V. de Pierre, H. Bernstein, *Trans. Am. Soc. Met.* 43 (1951) 635.
187. A. L. Mincher, *Met. Ind. (London)* 76 (1950) 435.
188. F. E. Buresch, *Jahresber. Kernforschungsanlage Jülich JÜL-552-RW* (1968).
189. E. Ryshkewitch: *Oxide Ceramics*, Academic Press, New York-London 1960, p. 318.
190. A. Boltax, J. H. Handwerk, *Proc. Conf. Nucl. Appl. Nonfissionable Ceram.* 1966, 169.
191. A. Rabenau, P. Eckerlin in P. Popper (ed.): *Special Ceramics*, Heywood & Co., London 1960, p. 136.
192. J. R. Lewis, *J. Met.* 13 (1961) 357.
193. A. J. Stonehouse, *Mater. Des. Eng.* 55 (1962) no. 2, 84.
194. G. Ervin, Jr., M. M. Nakata, *J. Electrochem. Soc.* 110 (1963) 1103.
195. R. M. Paine, A. J. Stonehouse, W. W. Beaver, *Corrosion (Houston)* 20 (1964) 307.
196. W. W. Beaver, A. J. Stonehouse, R. M. Paine, *Met. Space Age: Plansee Proc. Pap. Plansee Semin. "De Re Met."* 5th 1964, 682.
197. G. Petzow, M. Stümke, *Keram. Z.* 20 (1968) no. 12, 795.
198. H. E. Stockinger: *Beryllium, Its Industrial Hygiene Aspects*, Academic Press, New York 1964.
199. D. L. Bokowski, *RFP Rep.* 787 (1966).
200. J. D. Taylor, T. W. Steele, *Rep. Nat. Inst. Metall. (S. Afr.)* 173 (1967).
201. G. Kimmerle: *Handbuch der experimentellen Pharmakologie XXI: Beryllium*, Springer Verlag, Berlin 1966.
202. D. A. Everest: *The Chemistry of Beryllium*, Elsevier, Amsterdam 1964.
203. J. S. Pollok, I. S. Jones, *AERE Rep.* R-5106 (1966).
204. P. Iredale, *AERE Rep.* EL/M 108 (1960).
205. W. D. Ross, R. E. Sievers, *Talanta* 15 (1968) 87.
206. NIOSH Criteria Document TR-003-72: *Recommendations for an Occupational Exposure Standard for Beryllium*, PB-2-0806, National Technical Information Service, U.S. Department of Commerce (1972).
207. O. Preuss, H. Oster: *Zur Gesundheitsgefährdung durch Beryllium aus heutiger Sicht*, *Arbeitsmed. Sozialmed. Präventivmed.* 1980, no. 11, 270-275.
208. W. R. Parkes: *Occupational Lung Disorders*, Butterworth, London 1982, pp. 333-358.
209. O. P. Preuss in C. Zenz (ed.): *1975 Occupational Medicine*, Yearbook Publ., Chicago, pp. 619-636.
210. A. L. Reeves: "Beryllium Carcinogenesis", in G. N. Schrauzer (ed.): *Inorganic and Nutritional Aspects of Cancer*, Plenum Publishing, New York 1978, pp. 13-27.
211. H. E. Stockinger in G. D. Clayton, E. F. Clayton (eds.): *Patty's Industrial Hygiene and Toxicology*, 3rd ed., vol. 2A, Wiley-Interscience, New York 1981, pp. 1537-1558.
212. A. W. Hsieh, J. P. O'Neill, J. R. San Sebastian, D. B. Couch et al.: "Quantitative Mammalian Cell Genetic Mutagenicity of Seventy Individual Environmental Agents Related to Energy Technology and Three Subfractions of Crude Synthetic Oil in the CHO/HGPRT System", *Environ. Sci. Res.* 15 (1979) 291-315.
213. V. F. Simmon, H. S. Rosenkranz, E. Zeiger, L. A. Polrler: "Mutagenic Activity of Chemical Carcinogens and Related Compounds in the Intraperitoneal Host-Mediated Assay", *JNCI J. Natl. Cancer Inst.* 62 (1979) 911-918.

20 Magnesium

KNUT ANDREASSEN, TERJE KR. AUNE, TURID HAUGERØD, NILS OVE HØY-PETERSEN †, DAG ØYMO, OLE SKANE, TORE VRALSTAD (§§ 20.1-20.10); MARGARETE SEEGER (§§ 20.11 INTRODUCTION, 20.11.1, 20.11.3.1-20.11.3.4); WALTER OTTO (RETIRED) (§§ 20.11.2, 20.11.4); WILHELM FLICK (§ 20.11.3.5)

20.1 Introduction	981	20.11.2.5 Quality Specifications and Analysis	1011
20.2 History	981	20.11.2.6 Transportation and Storage	1011
20.3 Properties	982	20.11.2.7 Uses	1011
20.4 Raw Materials	983	20.11.2.8 Economic Aspects	1012
20.5 Production	983	20.11.2.9 Toxicology and Occupational Health	1012
20.5.1 Extraction by Electrolysis	984	20.11.3 Magnesium Oxide and Hydroxide	1013
20.5.1.1 Preparation of Magnesium Chloride Cell Feed	984	20.11.3.1 Properties	1013
20.5.1.2 Electrolysis	988	20.11.3.2 Production of Magnesium Oxide	1014
20.5.2 Metallothermic Reduction	993	20.11.3.3 Uses	1022
20.5.3 Refining and Casting	996	20.11.3.4 Economic Aspects	1025
20.5.4 Particulate Magnesium	998	20.11.3.5 Fused Magnesium Oxide	1026
20.6 Environmental Aspects	998	20.11.4 Magnesium Sulfate	1029
20.7 Quality Specifications	999	20.11.4.1 Properties	1029
20.8 Uses	999	20.11.4.2 Occurrence and Raw Materials	1030
20.9 Economic Aspects	1000	20.11.4.3 Production	1030
20.10 Toxicity and Occupational Health	1002	20.11.4.4 Quality Specifications and Analysis	1032
20.11 Compounds	1003	20.11.4.5 Transportation and Storage	1033
20.11.1 Magnesium Carbonate	1003	20.11.4.6 Uses	1033
20.11.2 Magnesium Chloride	1004	20.11.4.7 Economic Aspects	1034
20.11.2.1 Properties	1004	20.11.4.8 Toxicology and Occupational Health	1034
20.11.2.2 Raw Materials	1005		
20.11.2.3 Production	1005	20.12 References	1034
20.11.2.4 Environmental and Legal Aspects	1010		

20.1 Introduction

Magnesium is a silvery white metal; it has a valence of two, and its configuration is $1s^2 2s^2 2p^6 3s^2$. The crystal structure is dense hexagonal; lattice constants at 20 °C are $a = 0.32$ nm, $c = 0.52$ nm. The element has an atomic number of 12 and belongs to group 2A of the periodic table. It occurs as three isotopes: ^{24}Mg (78.70%), ^{25}Mg (10.13%), and ^{26}Mg (11.17%).

20.2 History

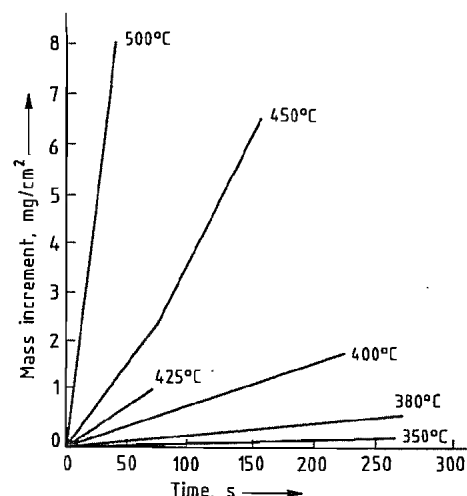
Metallic magnesium was first isolated by DAVY in 1808, via electrolysis of anhydrous

magnesium chloride with a mercury cathode. Bussy extracted the metal in 1828 by reducing fused magnesium chloride with metallic potassium vapor. In 1833 FARADAY electrolyzed dehydrated liquid magnesium chloride to form liquid magnesium and chlorine gas. The first industrial production of magnesium by electrolysis of molten carnallite began in 1886 in Hemelingen (Germany).

In 1940 L. M. PIDGEON pioneered the first industrial metallothermic magnesium extraction plant in Canada; it was based on early German patents in which dolomite was reduced with ferrosilicon under vacuum [1].

Table 20.1: Mechanical properties of magnesium at 20 °C.

	Tensile strength, MPa	Tensile yield strength (0.2%), MPa	Compressing yield strength (0.2%), MPa	Elongation ^a , %	Brinell hardness ^b
Sand cast, thickness 13 mm	90	21	21	2–6	30
Extrusion, thickness 13 mm	165–205	69–105	34–55	5–8	35
Hard rolled sheet	180–220	115–140	105–115	2–10	45–47
Annealed sheet	160–195	90–105	69–83	3–15	40–41

^aIn 50 mm.^bWith 500-kg load, 10-mm diameter ball.**Figure 20.1:** Rate of oxidation of magnesium in moist air [22].

20.3 Properties

Physical properties of magnesium follow (see also [2]):

<i>mp</i> [3]	650 ± 2 °C
<i>bp</i> [3]	1107 ± 10 °C
Latent heat of fusion [4]	0.37 MJ/kg
Latent heat of evaporation [5]	5.25 MJ/kg
Heat of combustion [4]	25.1 MJ/kg
Specific heat [3]	
at 20 °C	1030 J kg ⁻¹ K ⁻¹
at 600 °C	1178
Electrical resistivity at 20 °C [3]	4.45 μΩ·cm
Thermal conductivity at 25 °C [4]	155 W m ⁻¹ K ⁻¹
Linear coefficient of thermal expansion [3]	
at 20 °C	25.2 × 10 ⁻⁶ K ⁻¹
at 20–300 °C [5]	27–28 × 10 ⁻⁶
Density (solid) [4]	
at 20 °C	1738 g/cm ³
at 600 °C	1622
Density above 650 °C (liquid) [6]	1.834 – 2.647 × 10 ⁻⁴ T g/cm ³
Standard redox potential [6]	–2.372 V

Mechanical properties of magnesium are listed in Table 20.1. Its dynamic modulus of elasticity is 45 GPa, and its static modulus of elasticity 43 GPa. Pure magnesium is not used for commercial structural applications although the metal has a high damping capacity and is easily machined and formed into shapes by casting or hot forming processes [3].

Chemical Properties. Magnesium burns in air with an intense white flame. The ignition temperature is 645 °C in dry air but decreases with increasing moisture content [5]. The rate of oxidation in moist air at different temperatures is illustrated in Figure 20.1 [7]. Burning magnesium reacts violently with water. Fire is extinguished with magnesium chloride, alkali chlorides, dry sand, or dry iron sponge. Magnesium reacts with gaseous chlorine to form magnesium chloride and with nitrogen at ca. 500 °C to form Mg₃N₂.

Pure magnesium has a high resistance to corrosion because its galvanic activity is low. Contamination with heavy metals (usually copper, iron, and nickel), chlorides, and oxide or nitride inclusions combined with exposure to chloride-containing solutions on untreated surfaces, strongly promote corrosion due to enhanced galvanic activity. The metal is readily dissolved by most organic and inorganic acids. A protective layer of water-insoluble magnesium hydroxide is formed when magnesium is exposed to moist air or clean water at room temperature. Magnesium is resistant to alkali hydroxide solutions, hydrofluoric acid, fluorine, and fluorine compounds (including ammonium hydrogen difluoride) due to the formation of protective hydroxide and fluoride films.

The ability of magnesium to form stable protective oxide, chromate, phosphate, sulfate, and fluoride films is employed commercially in protective coating systems used as primers for paints or as final coatings. The behavior of magnesium against various chemicals is listed in [8, p. 575].

20.4 Raw Materials [9, 10]

Magnesium is the eighth most abundant element in the earth's crust (average magnesium content, 2.1%). Magnesium does not occur in nature in elemental form but in the form of compounds in seawater, minerals, brines, and rocks. The element is enriched in ultrabasic rocks.

The prime raw material sources for magnesium extraction are the minerals dolomite (CaCO₃·MgCO₃), magnesite (MgCO₃), and brucite [Mg(OH)₂]; magnesium-rich salts such as carnallite (MgCl₂·KCl·xH₂O), kieserite (MgSO₄·H₂O), bischofite (MgCl₂·6H₂O), kainite (KCl·MgSO₄·3H₂O), and langbeinite (K₂SO₄·MgSO₄); and magnesium-rich brines and seawater. High-quality magnesites contain: MgO 45–47%, CaO 0.5–1.2%, SiO₂ 0.1–0.15%, Al₂O₃ and Fe₂O₃ 0.1–0.6%, Mn 20–500 ppm, Ni 2–300 ppm, B 10–60 ppm. Magnesium-rich brines are obtained as by-products from potash production or from surfacial or underground brine deposits. Analyses of dolomites and brines used for magnesium extraction are given in Tables 20.2 and 20.3, respectively.

Magnesium silicates such as olivine [Mg·Fe(SiO₄)₂] and forsterite (Mg₂SiO₄) have not been used so far for magnesium extraction.

Table 20.2: Composition of dolomites (%).

Deposit	MgO	CaO	Fe ₂ O ₃ + Al ₂ O ₃	SiO ₂
Serfold, Norway	21.2	30.4	0.1	1.3
Tochigi, Japan	17.4	35.1	0.5	0.15
Addy, Washington	20–21.8	30–31.5		1.5
Marignac, France	19–20	32–34	0.3–0.5	0.2–0.4
Haley, Canada	21.3	30.7	0.1	0.15

Table 20.3: Composition of brines (%).

Brine	Mg ²⁺	Na ⁺	Ca ²⁺	Cl ⁻	SO ₄ ²⁻
Great Salt Lake ^a	1.1	7.6	0.02	14.1	2.0
Dead Sea	3.4	3.3	1.4	17.5	0.7
Seawater	0.13	1.08	0.04	1.94	0.27
"Edelsole", Kali und Salz AG	8.5	0.2		25	0.24

^aComposition is subject to seasonal and long-term variations.

Total world production of magnesium in 1988 was ca. 240 × 10³ t, of which 42% came from dolomite, 36% from salt or brine deposits, 18% from seawater, and 4% from magnesite. Recent plants in Canada increased the share of magnesite.

20.5 Production

Magnesium is produced commercially by electrolysis of magnesium chloride melts and by metallothermic reduction of magnesium oxide with silicon. A wide variety of processes are used. The extraction of magnesium by electrolysis consists of two steps: (1) preparation of the magnesium chloride cell feed and (2) electrolysis. All extraction processes are followed by refining and casting.

Electrolysis of magnesium oxide dissolved in fused fluorides has also been considered. However, the solubility of magnesium oxide in the electrolyte is low, and practical solutions for metal collection have not been found. For further details, see [11]. Composite MgO–C anodes have been tested in fluoride, fluoride-chloride, and chloride electrolytes on a laboratory scale [12].

Electrolysis of magnesium chloride in aqueous solution liberates hydrogen, not magnesium, at the cathode. Attempts to electrolyze magnesium salts in organic solvents have not been successful.

Carbothermic reduction of magnesium oxide is not used industrially. The main problems are high reaction temperature (1800–2000 °C) and rapid cooling of reaction gases to suppress magnesium oxide formation [13]. Recent experimental studies have been based on rapid adiabatic expansion of the gases or cooling in liquid metal [14]. Attempts to en-

hance selectivity of the reduction step in the carbothermic reduction of magnesium oxide in molten $\text{CaO} \cdot \text{Al}_2\text{O}_3 \cdot \text{MgO}$ slag have been reported [15].

20.5.1 Extraction by Electrolysis

20.5.1.1 Preparation of Magnesium Chloride Cell Feed

Magnesium chloride cell feeds in industrial use consist of dehydrated $\text{MgCl}_{2(s)}$ or $\text{MgCl}_{2(l)}$; dehydrated carnallite $\text{MgCl}_2 \cdot \text{KCl}_{(s)}$; or $\text{MgCl}_2 \cdot 1.5\text{H}_2\text{O}_{(s)}$. Cell feeds contain 3–8% alkali chlorides and minor impurities of C, SiO_2 , MgO , SO_4^{2-} , B, and heavy-metal compounds. Alkali chlorides accumulate in the electrolytic cell as major constituents of the electrolyte. Metallic and nonmetallic impurities are undesirable because they adversely affect cell performance and the corrosion resistance of magnesium.

The use of pure dehydrated magnesium chloride allows coproduction of highly concentrated chlorine gas and electrolysis at high current efficiencies. Dehydrated carnallite (which contains only 50% MgCl_2) leads to accumulation of significant tonnages of potassium-rich electrolyte in the electrolysis. The impurity level of Russian carnallite, the only carnallite cell feed in use, is high and increases power consumption in electrolysis. The chlorine concentration is high. The water content of $\text{MgCl}_2 \cdot 1.5\text{H}_2\text{O}$ results in high consumption of anode carbon and formation of sludge in the cell; power consumption is high.

Dehydration of Magnesium Chloride

The two main routes to the production of dehydrated magnesium chloride cell feed are: (1) chlorination of magnesia (MgO) or magnesite (MgCO_3) in the presence of carbon or carbon monoxide and (2) dehydration of aqueous magnesium chloride solutions (brines) or hydrous carnallite ($\text{MgCl}_2 \cdot \text{KCl} \cdot 6\text{H}_2\text{O}$).

Dissolution of magnesium chloride in ethylene glycol with subsequent dehydration and

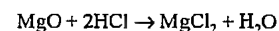
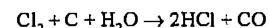
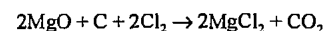
regeneration of the alcohol via a complex magnesium chloride ammonia compound has been suggested [16]. The process has not, however, been used industrially.

Chlorination of Magnesia and Magnesite

Two principal processes are used industrially to chlorinate magnesia and magnesite: (1) the IG Farben process presently in operation at Norsk Hydro's Porsgrunn plant and (2) the MagCan process under installation in Alberta, Canada.

IG Farben Process (Figure 20.2). In the process used by Norsk Hydro, caustic magnesium oxide (lightly burned) extracted from seawater, is mixed with charcoal and magnesium chloride brine on a rotating disk to form pellets with a diameter of 5–10 mm. Hydrated magnesium oxide and magnesium oxychlorides act as binders. After slight drying, pellets containing ca. 50% magnesium oxide, 15–20% magnesium chloride, 15–20% water, 10% carbon, and a balance of alkali chlorides are conveyed to the chlorinators (Figure 20.3).

The lower third of the brick-lined cylindrical shaft furnace is filled with carbon blocks (c) that act as resistors and are heated by carbon electrodes (e). Chlorine produced during subsequent electrolysis of magnesium chloride is introduced in the resistor-filled zone. The charge (b) resting on the resistor bed reacts with chlorine at 1000–1200 °C. The main reactions are:



The reaction mechanism is complex and involves further side reactions. Chlorinator-grade magnesium oxide is processed for minimum impurities and high surface area. Molten magnesium chloride collects in the bottom of the furnace from where it is tapped and transported to the electrolytic cells in sealed containers.

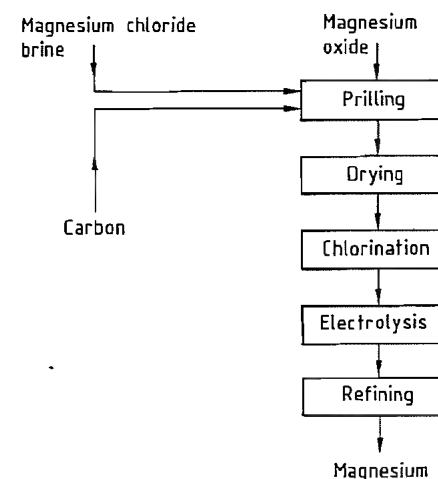


Figure 20.2: Flow sheet for production of magnesium via chlorination of magnesia (Norsk Hydro).

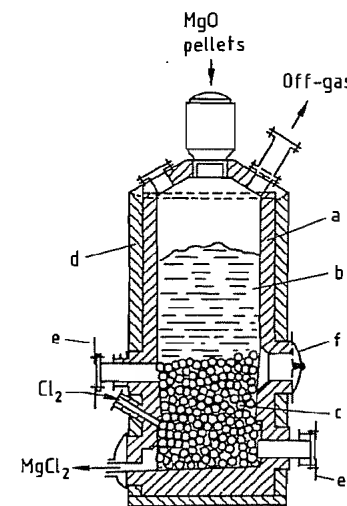


Figure 20.3: The IG chlorinator: a) Refractory material; b) Charge; c) Carbon resistors; d) Steel mantle; e) Carbon electrodes; f) Door for slag removal.

Off-gases at 100–200 °C containing air, CO , CO_2 , traces of HCl , Cl_2 , SO_2 , H_2S , and chlorinated hydrocarbons are scrubbed; the wash water is then filtered and chemically treated in several stages before release to stack and sewers. Slag rich in magnesium silicate formed due to the presence of silica in the magnesia is removed at intervals.

The magnesium yield is ca. 90%, and the carbon consumption is 0.45 t per tonne of

magnesium. Magnesium chloride solution added to the charge compensates for chlorine losses. The anhydrous MgCl_2 product typically contains less than 0.1% MgO , 0.1% C, 0.1% SiO_2 , and 20 ppm B. Each chlorinator has an equivalent annual magnesium production capacity of 1800–2000 t.

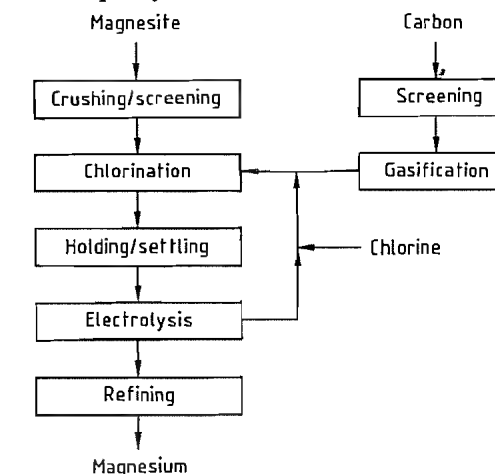
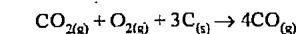
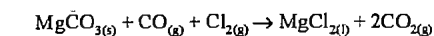


Figure 20.4: Flow sheet for production of magnesium via chlorination of magnesite (MagCan).

MagCan Process (Figure 20.4). Natural magnesite from British Columbia is crushed and screened. Magnesite fines with a particle size < 6 mm are disposed as solid waste. The coarse material is charged at intervals to a reactor of the same general description as the IG shaft furnace (Figure 20.3). Chlorine from the electrolysis is mixed with fresh makeup chlorine and carbon monoxide from a gas generator. It is then fed into the lower section of the reactor where it reacts with preheated magnesite resting on a bed of carbon resistors. The main reactions are



The magnesite is present in lump form. During the reaction, chlorine and carbon monoxide must penetrate the lumps while magnesium chloride simultaneously drains from the surface [17].

The process is in thermal balance at 1010 °C which is also the temperature in the

reaction zone. Off-gases leaving the top of the reactor at 250–650 °C contain primarily carbon dioxide; small amounts of carbon monoxide; and unreacted chlorine, hydrogen chloride, sulfur dioxide, phosgene, chlorides of aluminum, iron and silicon, and traces of chlorinated hydrocarbons. The off-gases are passed through multistage absorption towers and activated carbon columns to remove residual chlorinated hydrocarbons, sulfur dioxide, chlorine, and phosgene before release to the stack. Part of the cleaned off-gas is mixed with oxygen and recirculated to the gas generator after compression. The gas generators operate on calcined petroleum coke with a particle size > 6 mm. Residual tar and volatile oils in the fresh coke are driven off by the heat of reaction and leave via a separate upper gas off-take.

Liquid process effluents are injected in deep wells after chemical treatment and removal of inert solid material. The latter is deposited as landfill. Off-gases are washed with sodium carbonate and sodium hydroxide. Sodium chloride is removed from the liquid purge streams by passing the solutions over a catalyst. Acidic and alkaline streams are combined to adjust the pH. The resulting liquid is used to dissolve soluble components (mostly chlorides) from liquid wastes and is then filtered and disposed of in an injection well.

Molten magnesium chloride is tapped from the reactors at 800 °C at frequent intervals. During operation, silica-rich slag gradually builds up at the bottom of the magnesite bed, which must eventually be cleaned out. Each reactor is reported to have an equivalent annual production capacity of 1500 t of magnesium. Magnesium chloride containing < 0.2% magnesium oxide is conveyed to melt cells where granular sodium chloride and potassium chloride are added to obtain the desired electrolyte composition. The temperature in the melt cells is adjusted to 700 °C. The cells act as intermediate storage tanks for magnesium chloride and as settling tanks for magnesium oxide and other particulate matter.

The process requires nondecrepitating, high-purity magnesite and consumes ca. 1 t of

chlorine, 0.55 t of coke, 0.5 t of oxygen, and 4.3 t of magnesite per tonne of magnesium. The MagCan process is proprietary and protected by patents [18].

Dehydration of Aqueous Magnesium Chloride Solutions

Brines containing 33–34% of magnesium chloride may be derived as by-product from the potassium industry or produced by dissolving magnesium-bearing minerals in hydrochloric acid (Norsk Hydro process). Naturally occurring dilute brines are concentrated by solar evaporation (National Lead process) or conventional dehydration processes (Dow Chemical process). Unwanted impurities in the brines (e.g., Fe, Ni, SO_4^{2-} , B, Br_2) are removed prior to dehydration. To avoid hydrolysis above 200 °C, the final dehydration is performed in an atmosphere of dry hydrogen chloride.

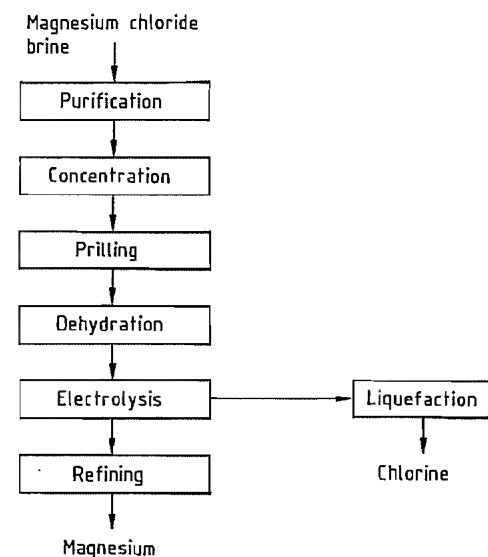


Figure 20.5: Flow sheet for production of magnesium via dehydration of magnesium brine (Norsk Hydro).

Norsk Hydro Process (Figure 20.5). The raw material for magnesium production in Norway is brine from the German potash industry with the following average composition: 33% MgCl_2 , 1.08% MgSO_4 , 0.5% NaCl , and 0.2%

KCl. Feedstock for the Norsk Hydro magnesium plant in Quebec is obtained by dissolving magnesite in hydrochloric acid.

The brine is treated with sodium sulfide, calcium chloride, and barium chloride to remove heavy metals and sulfates by precipitation and filtration. Purified 34% magnesium chloride solution is preheated by process waste heat and concentrated to 45–50% magnesium chloride by steam heat exchangers before prilling. Sizes of the prills are kept within close tolerances, and their shape is controlled to optimize the subsequent dehydration step in fluidized beds employing hot air at 150–180 °C and finally hydrogen chloride gas at 300–400 °C. Water and magnesium chloride dust in off-gases from the hydrogen chloride dehydration step are absorbed in concentrated magnesium chloride solution by extractive distillation. Essentially dry hydrogen chloride gas is preheated and returned to the hydrogen chloride dehydration step. Magnesium chloride prills containing < 0.1% magnesium oxide are transported pneumatically to the electrolysis cells. Magnesium and chlorine recoveries in this continuous, high-volume, closed process are ≥ 97%. The process is proprietary and covered by patents [19].

National Lead Industries Process (Figure 20.6). The National Lead Industries magnesium plant at the Great Salt Lake, Utah, was started in 1972 and is owned and operated by Amax. Seawater containing 0.5–1% Mg, 0.8% SO_4^{2-} , 3% Na, and 0.25% K is concentrated in solar evaporation ponds to precipitate potassium chloride, sodium chloride, and some carnallite ($\text{MgCl}_2 \cdot \text{KCl} \cdot 6\text{H}_2\text{O}$). The resulting crude brine contains 7.5% Mg, 4% SO_4^{2-} , and < 1% K and Na, and is desulfated with calcium chloride solution generated in the process. The boron content is decreased from 500 to 3 ppm by liquid extraction with kerosene. The brine is preheated before spray drying by direct contact with hot off-gases from the spray dryers. Each spray dryer is connected to a turbine fired with natural gas. Exhaust gases enter the top of the spray dryers at

515 °C. The energy efficiency of this system is ca. 80%.

The resulting spray-dried powder contains ca. 4% water and 4% magnesium oxide. It is melted in an electrically heated, brick-lined melt cell and treated with carbon and chlorine gas to lower the content of magnesium oxide, water, bromine, sulfate, aluminum, and heavy metals. In a second reactor vessel, impurities are further reduced with chlorine gas in the presence of carbon at 830 °C to an average magnesium oxide level of 0.05%. Iron(III) chloride acts as a catalyst in these reactions, forming a complex with magnesium chloride.

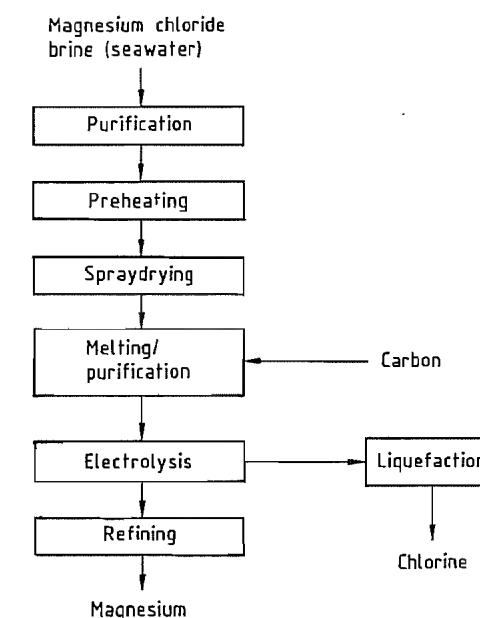


Figure 20.6: Flow sheet for production of magnesium via dehydration of seawater (National Lead Industries).

Off-gases containing chlorine, hydrogen chloride, sulfur dioxide, magnesium chloride dust, and chlorinated hydrocarbons are scrubbed with milk of lime [$\text{Ca}(\text{OH})_2$] to form the calcium chloride used in the desulfation stage. The molten magnesium chloride product is transported to the electrolytic cells in trucks and contains 95% MgCl_2 , < 0.1% MgO , and 0.01% SO_4^{2-} , the balance being alkali chlorides. The process is a net producer of

chlorine (0.5–0.8 t per tonne of magnesium) [20].

Dow Chemical Process (Figure 20.7). Hydrous magnesium chloride ($\text{MgCl}_2 \cdot 1.5\text{H}_2\text{O}$) is used as cell feed by Dow Chemical. Magnesium hydroxide slurry precipitated from seawater with calcined dolomite is dewatered on rotary filters to 8–12% magnesium, dispersed in magnesium chloride solution, and neutralized with hydrogen chloride. Sulfuric acid is added to precipitate excess calcium, which is then removed by filtration. Sulfate ions are adjusted by a proprietary process. The brine is further concentrated to 35% magnesium chloride with waste heat. The purified brine is fed to a dryer where it is concentrated further to 70% magnesium chloride, which is a dry granular solid [21]. Alternatively, the 35% brine can be concentrated directly to 70% solid particles in a spouting bed where the brine is sprayed on solidified particles in an airstream at 180 °C. Undersized particles are separated in cyclones and returned to the dryer.

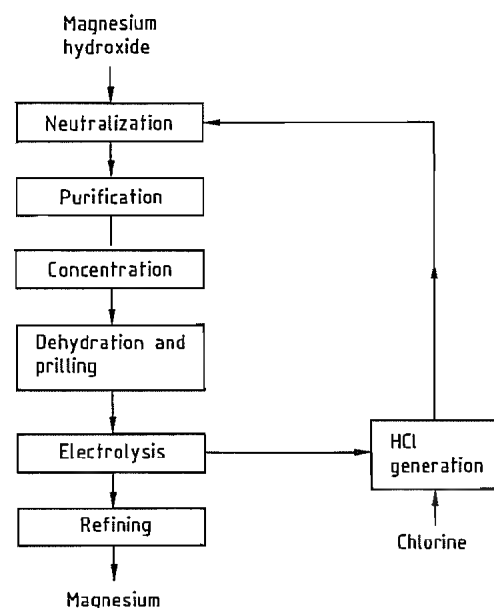


Figure 20.7: Flow sheet for production of magnesium via dehydration of seawater (Dow Chemical).

The hydrogen chloride used for neutralization is partly recovered from the anode gases and partly added to the hydrogen chloride furnaces as makeup chloride in various forms. The Dow process has the potential to produce saleable liquid chlorine when magnesium chloride solutions are used as feedstock.

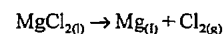
Dehydration of Carnallite

Carnallite cell feed for magnesium production is used only in the former Soviet Union. Carnallite ($\text{MgCl}_2 \cdot \text{KCl} \cdot 6\text{H}_2\text{O}$) is obtained as a natural mineral or as a by-product in the processing of potassium chloride from complex salt deposits. Dehydration of carnallite is simpler than that of aqueous magnesium chloride because hydrolysis is weaker. According to [22], impurities in the carnallite must not exceed the following levels: CaSO_4 0.06%, B 0.001%, Fe 0.01%, and SiO_2 0.01%. The sodium chloride content may be 5–7%.

Carnallite is dehydrated in two stages. The first stage is performed in a fluidized bed at 160–200 °C to give a water content of 3.7–4.8%. The second stage, which yields molten dehydrated carnallite, is performed in a chlorinator at 700–750 °C. The chlorinator combines melting, chlorination, and settling mixing in a single unit. The final product contains 49–51% magnesium chloride and 0.6–1% magnesium oxide. Efforts are being made to reduce the degree of hydrolysis during dehydration and to replace the chlorination stage by hydrogen chloride treatment in a fluidized bed.

20.5.1.2 Electrolysis [7]

Magnesium chloride is electrolyzed in a molten mixture with alkali chlorides at 700–800 °C, the main reaction being



The electrolyte is contained in brick-lined vessels or a steel shell. The magnesium rises to the surface because it is lighter than the electrolyte.

Table 20.4: Composition and properties of electrolytes.

Electrolyte	Composition, %	mp, °C	Properties at 700 °C			
			Density, kg/m ³	Conductivity, S/m	Viscosity, mPa·s	Surface tension, mN/m
Potassium	5–12 MgCl_2 70–78 KCl 12–16 NaCl	650	1600	183	1.35	104
Sodium–potassium	10 MgCl_2 50 NaCl 40 KCl	625	1625	200	1.58	108
Sodium–calcium	8–16 MgCl_2 30–40 CaCl_2 35–45 NaCl 0–10 KCl	575	1780	200	2.22	110
Lithium–potassium	10 MgCl_2 70 LiCl 20 KCl	550	1500	420	1.20	
Lithium–sodium	10 MgCl_2 70 LiCl 20 NaCl	560	1521	488		
Sodium–barium	10 MgCl_2 20 BaCl_2 50 NaCl 20 KCl	686	1800	217	1.70	110
Magnesium		649	1580			

Technical Data

Industrial electrolytic cells differ in electrode configuration, flow pattern of the electrolyte, and collection system for reaction products. Steel cathodes and graphite anodes are arranged vertically or at an angle. Electrodes may be monopolar, bipolar, or a combination of both, with interpolar gaps ranging from 3 to 12 cm and current densities from 2000 to 8000 A/m².

Electrolyte filled with chlorine gas adjacent to the anodes has a lower density than the bulk electrolyte, which results in circulation. The circulating electrolyte carries magnesium globules to the collecting area. Small bubbles of chlorine may follow the flow and escape into the ventilation system [23].

Under operating conditions (10% MgCl_2 and 1000 K) the energy of formation of magnesium is 520.9 kJ/mol, and the enthalpy 597.3 kJ/mol. Consequently, the reversible decomposition voltage is 2.70 V. The thermoneutral voltage ($\Delta H/2F$) is 3.095 V. According to Faraday's law, 4.534×10^{-4} kg of magnesium is formed per ampere per hour.

Under thermoneutral conditions energy consumption is 6.8 kWh/kg. In industrial cells, however, power consumption may range from 10 to 20 kWh/kg; 40–65% of the energy input generates heat as a result of ohmic resistance of the electrolyte and recombination of magnesium and chlorine. Heat generation is necessary to compensate for heat losses from the electrodes and the cell surface. Heat balances for IG cells are reported in [3, 7]. Current efficiencies normally range from 0.75 to 0.95. The main cause of reduced current efficiency is the recombination of dissolved chlorine and magnesium in the electrolyte.

The composition and primary characteristics of electrolytes used in the electrolysis are listed in Table 20.4; they normally contain 8–20% magnesium chloride. Other chlorides (BaCl_2 or LiCl) may be added to influence the density; lithium chloride also increases the conductivity of the melt. The density of the lithium potassium chloride electrolyte is lower than that of liquid magnesium, permitting magnesium to collect at the bottom of the cell. The solubilities of magnesium and chlorine in commercial electrolytes at 730 °C are 0.005%

and $6.27 \times 10^7 \text{ mol/cm}^3$, respectively. Solubilities increase with increasing temperature [24].

Comprehensive measurements of the characteristics of electrolyte compositions and the pure salts are reported in [25]. Excess electrolyte components brought to the cell with the cell feed are removed by pumping into molds or by closed, vacuum-operated containers mounted on trucks. At 750°C the standard decomposition voltages of the electrolyte components are: MgCl_2 2.51 V, NaCl 3.22 V, KCl 3.27 V, LiCl 3.30 V, CaCl_2 3.33 V, and BaCl_2 3.40 V. With magnesium chloride contents below ca. 5%, sodium is deposited; this lowers current efficiency and causes a temperature rise due to recombination of sodium and chlorine.

Impurities in the cell feed disturb cell performance by passivating the cathode surface and hindering the coalescence of metal globules or their free rise to the surface. The upper permissible limits for common electrolyte impurities, in parts per million, follow [26]:

MgO	2000
C	1500
H ₂ O	1000
Mn	600
Fe	200
S	100
Si	100
P	50
B	10

Small additions of calcium fluoride, sodium fluoride, amorphous carbon, and alkaline-earth metals to the electrolyte counteract these undesired effects.

Magnesium chloride and magnesium react with oxygen in air or with oxygen-containing compounds to form magnesium oxide, which has a low solubility in the melt. The oxide can form a layer on the cathode surface, resulting in higher electrical resistance. Magnesium oxide with entrapped electrolyte and magnesium globules form a sludge at the bottom of the cell which must be removed at intervals. The amount of sludge is significantly lower in sealed as opposed to open cell designs.

Theoretically, 2.918 t of chlorine is produced per tonne of magnesium; commercial cells operating with dehydrated magnesium chloride may yield 2.7–2.8 t of chlorine with a

concentration of $\geq 95\%$. The chlorine gas from cells operated on dehydrated cell feed contains small amounts of air, dust from the electrolyte components, and minor amounts of chlorinated hydrocarbons requiring efficient systems for collection and destruction. Electrolytic magnesium contains typically $\geq 99.8\%$ magnesium.

Electrolytic Cells

IG Cell. The cell concept first developed by IG Farben Industrie in Germany in the 1930s is now in operation in the former Soviet Union, China, and the United States. Figure 20.8 illustrates the electrode configuration and the circulation of the electrolyte [26].

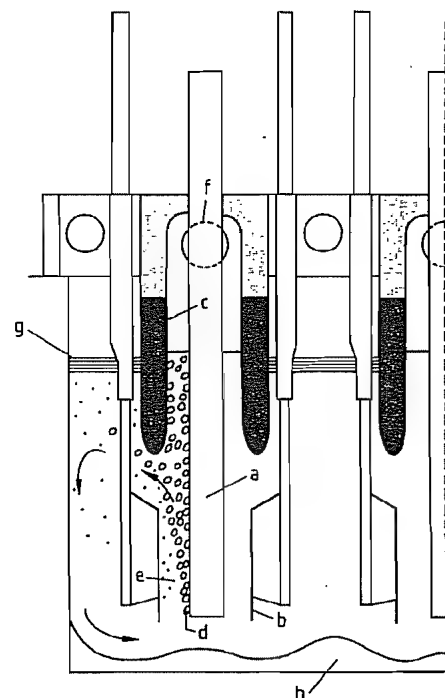


Figure 20.8: Electrode configuration in the IG cell: a) Graphite cathode; b) Steel cathode; c) Semi wall; d) Chlorine bubbles; e) Magnesium globules; f) Chlorine outlet; g) Magnesium; h) Sludge.

The brick-lined cell is divided into four to six compartments by semisubmerged refractory partition walls termed semi walls (c). Three to five water- or air-cooled graphite an-

ode plates (a) are installed and tightly sealed in the refractory cover of the cell. The semi walls on each side of the anodes separate the magnesium metal and the chlorine gas. Steel cathodes (b) are installed in the cathode compartments from above or through the side walls. Cells operated at $750\text{--}780^\circ\text{C}$ have a life of ca. one year, limited by the deterioration of the semi walls. The metal is collected from each of several cathode compartments and chlorine from each anode compartment. Extensive cathode chamber ventilation causes oxygen and water in the ventilation gases to react with metal and electrolyte to form sludge. The current efficiency is typically 0.80–0.85, and the amperage is in the range 60–120 kA. The chlorine concentration may reach 90–95% and is limited by air leaks through the semi walls. Anode consumption is 15–20 kg per tonne of magnesium. Cell regularity (days in operation divided by total days available) is 95–98% of available time, and the power consumption per tonne of magnesium is 16–18 MWh when operated on molten magnesium chloride. For further details of the IG cell, see [27].

Norsk Hydro Cell. This cell has been in operation since 1978 and consists of a sealed, bricklined apparatus that is divided into two separate chambers for electrolysis and metal collection, respectively (Figure 20.9). Densely packed, cooled graphite anode plates (b) are installed through the roof and double-acting steel plate cathodes (c) through the back wall. Chlorine (98%) is collected from a central pipe in the anode compartment. Circulation of the electrolyte (h) is parallel to the electrodes bringing the magnesium metal to the collecting chamber from where it is extracted by vacuum and transported to the foundry. This cell operates on solid or liquid cell feed conveyed continuously or at intervals to the cell at $700\text{--}720^\circ\text{C}$ with a current load of 350–400 kA. Energy consumption is 12–14 kWh per kilogram of magnesium and cell life exceeds five years.

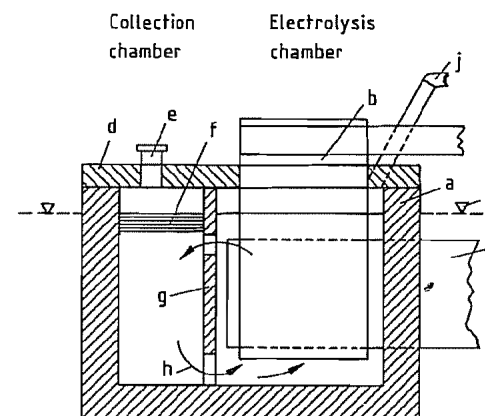


Figure 20.9: Norsk Hydro cell: a) Refractory material; b) Graphite anode; c) Steel cathode; d) Refractory cover; e) Metal outlet; f) Metal; g) Partition wall; h) Electrolyte flow; i) Electrolyte level; j) Chlorine outlet.

VAMI Cell. The cell developed by VAMI, St. Petersburg, is based on the same principles as the Norsk Hydro cell but operates at 150–180 kA and $700\text{--}740^\circ\text{C}$. Various electrode arrangements are reported. Current density varies between 1000 and 5000 A/m^2 , with a preferred optimum at 2000 A/m^2 . The low-carbon steel used for the cathodes is claimed to undergo transformation during operation from 0.2–0.3% carbon to 0.02% carbon, thus coarsening the ferritic grains 100-fold and improving current efficiency. When operated on dehydrated molten magnesium chloride obtained after reduction of titanium(IV) chloride with magnesium (Kroll process), the current efficiency is ca. 0.80, with an electric energy consumption of 13.5 kWh per kilogram of magnesium [22].

Alcan Cell. Magnesium cells developed by Alcan, Canada, for the electrolysis of anhydrous magnesium chloride have been operating since 1961 in Japan and the United States. They are used in titanium plants where magnesium is employed in the reduction of titanium(IV) chloride (Kroll process). The cells are divided by a curtain wall into a front compartment where the metal accumulates on the heavier chloride bath and an electrolysis compartment where chlorine ($\geq 97\%$) is collected.

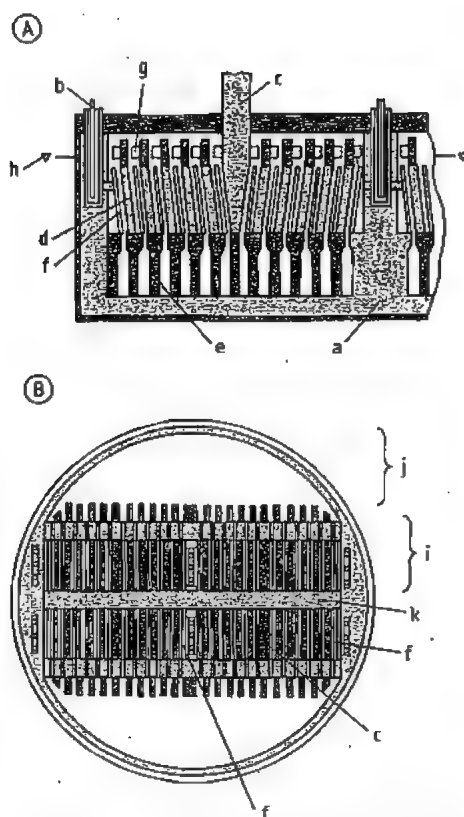


Figure 20.10: Vertical section (A) and top view (B) of Ishizuka cell: a) Refractory material; b) Steel cathode; c) Graphite anode; d) Bipolar electrode (steel-graphite); e) Bipolar support; f) End cathode; g) Electrolyte ports; h) Electrolyte level; i) Electrolysis chamber; j) Metal-collecting chamber; k) Refractory wall.

The two compartments have insulating covers through which water-cooled graphite anodes are installed. The cathodes are parallel to the anodes and are installed through the refractory back wall below the bath level. The operating temperature (660–680 °C) is controlled just above the melting point of the metal.

A new multipolar cell design has been in operation since 1982 in which electrodes are added between the anode and the cathode surfaces. The energy consumption of this cell when operating on high-purity molten magnesium chloride from Kroll titanium production is claimed to be 9.5–10 kWh per kilogram of magnesium. Cell productivity has reached

1000 t/a. The cell operates at 100 kA with a life of up to two years [28].

Ishizuka Cell. The Ishizuka Research Institute, Japan, has developed a bipolar cell that has been used since 1983 for industrial magnesium production by Showa Titanium, Toyama (Figure 20.10).

The outer, brick-lined, cylindrical, water- or air-cooled shell is divided in half by a refractory wall (k). Each half is subdivided with a refractory partition wall into a metal-collecting chamber (j) and an electrode chamber (i) where electrolysis is performed. The electrode chambers have three steel cathodes, one at each end and one in the center (b); a graphite anode (c) is located between each pair of cathodes. Five bipolar electrodes (d) are located between each set of anodes and cathodes. The bipolar electrodes are made of graphite with steel plates attached to the cathode side. The current load is connected to the cathodes and graphite anodes penetrating through the refractory-lined cover of the cell. The bipolar electrodes are submerged in the electrolyte. The electrolyte flow induced by gas production carries the metal into the collecting chamber through openings in the partition wall. The electrolyte returns to the electrode chamber in the bottom part of the cell. The cell operates at 670 °C and carries 50 kA, corresponding to 300 kA in a monopolar cell. Current density is 5600 A/m², and the interpolar gap is 4 cm. At a current efficiency of 0.76, the power consumption is 11 kWh per kilogram of magnesium when operated on molten magnesium chloride from Kroll titanium production. The furnace cell life is ca. three years.

The prime advantage of the bipolar cells is reduction of heat losses. Special provisions are made to prevent current leaks from bypassing the bipolar electrode system. Ishizuka states a preferred electrolyte composition of 50% NaCl, 30% KCl, and 20% MgCl₂. The cell maintained at a pressure of 0–1.33 kPa yields ≥ 96% chlorine [29].

Dow Cell. Electrolysis of hydrous cell feed (MgCl₂·1.5H₂O) in the Dow cell (Figure 20.11) requires graphite anodes which can be

lowered into the cells to compensate for consumed graphite. Densely packed cylindrical anodes (c) are led through openings in the refractory cell hood (d) and sealed to reduce air leaks. They are centered by insulating ceramic spacers. The development of efficient anode seals to withstand severe corrosive environment and high temperature has been a challenge. Conical cathodes (b) are welded to the steel shell (a) holding the electrolyte. Magnesium metal is conducted by the electrolyte flow to a collecting chamber (e) at the front of the cell. Water in the cell feed is partly flashed off, and partly reacts with chlorine (to form HCl) and with oxygen in the graphite (to form CO and CO₂). Graphite consumption is probably 60–70 kg per tonne of magnesium. The Dow cell is operated at 700 °C with an estimated current load of 180 kA and current efficiency of ca. 0.8.

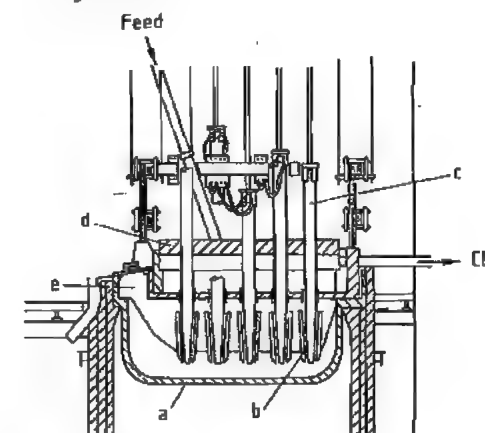


Figure 20.11: Dow cell: a) Steel mantle; b) Steel cathode; c) Graphite anode; d) Refractory cover; e) Magnesium collection compartment.

In comparison with an anhydrous cell feed, the hydrous cell feed increases electric power consumption as well as the formation of sludge and dilute anode gases. The presence of hydrogen, chlorine, and carbon in the cell at high temperature promotes formation of chlorinated hydrocarbons in off-gases.

Dow has patented an inert anode that is protected by a ceramic cover of doped and sintered Ti⁴⁺ and Ti³⁺ compounds [30], which could improve the performance of the cell. Ef-

forts to reduce the overall energy consumption in Dow's operations from 325 MJ per kilogram of magnesium in 1978 by 15–20% over ten years have been reported [8, 21].

20.5.2 Metallothermic Reduction

Industrial metallothermic processes for magnesium production are based on the reduction of magnesium oxide with ferrosilicon (FeSi). Magnesium oxide is provided in the form of calcined dolomite (MgO·CaO), sometimes enriched with calcined magnesite (MgO). The basic reaction is:



This reaction is highly endothermic ($\Delta G \approx 210$ kJ/mol). The vapor pressure at 1800 °C is 0.1 MPa. Industrial processes operate under vacuum at a lower temperature (1200–1500 °C) to limit wear on construction materials and to suppress undesirable side reactions in the gas systems. Reduction is carried out in the batch mode. Various reactor designs have been suggested [31]; determining factors are transfer of heat to the charge and attempts to develop a continuous process. Active developmental work aims at increasing reactor capacity and improving metal yield [32].

Three principles are applied for the reaction chamber:

- Externally heated retorts producing 70 kg/d (Pidgeon)
- Internally heated reactors producing 2 t/d (Bolzano)
- Internally heated reactors with molten slag producing ca. 12 t/d (Magnetherm)

Pidgeon Process. The process developed by Pidgeon in the early 1940s is presently used by Timminco in Canada and Ube Industries in Japan (Figure 20.12). Briquettes of crushed calcined dolomite and ferrosilicon fines in a stoichiometric ratio of 2:1 are loaded into tubular refractory steel retorts, heated externally to a reaction temperature of 1200 °C, and evacuated to 13.3 Pa. Magnesium vapor condenses at the cooled end of the retorts.

Reaction kinetics depend on the thermal conductivity of the briquettes, the shrinking

core pattern of the reaction zone, and the diffusion rate of magnesium vapor. Heat transfer to the charge limits the diameter of the retorts. Timminco operates retorts that are 3 m long and have a bore diameter of 275 mm, each retort yields 70 kg of magnesium per day. Ferrosilicon grades containing 65–90%, but preferably 75–90% silicon, have been used. Metal recoveries up to 90% are attainable if a slight excess of silicon above stoichiometric requirements is used. Recovery increases with increasing ferrosilicon concentrations. Handling of the charge and removal of slag and condensate have been highly automated reducing down time to 1 h per day. The productivity of the Pidgeon process is now 25 t/a per employee with a total energy requirement of 30 kWh/kg. The high-purity dolomite from Haley (99.5% $\text{CaCO}_3 \cdot \text{MgCO}_3$) enables Timminco to produce 99.95%, and even 99.98%, magnesium in commercial quantities. The company has recently introduced to the market ultrapure AZ 91 alloys with improved corrosion resistance [33].

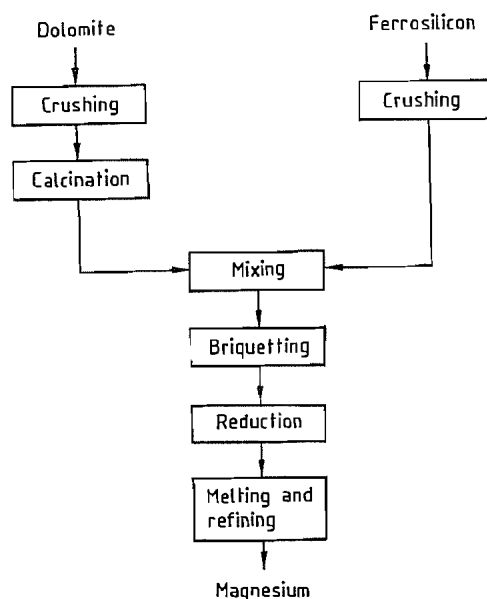


Figure 20.12: Flow sheet for the production of metallothermic magnesium (Pidgeon and Bolzano processes).

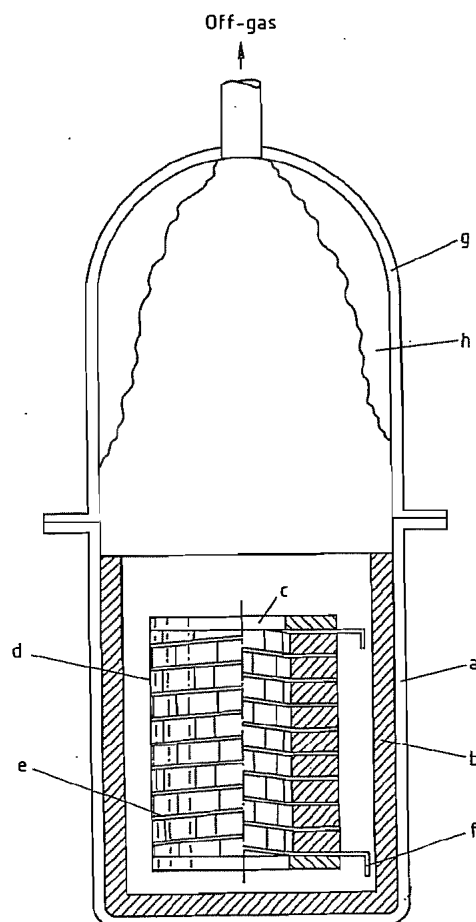
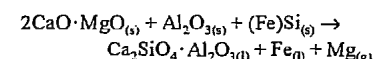


Figure 20.13: Bolzano reactor: a) Steel mantle; b) Refractory; c) Removable charge pack; d) Charge briquettes; e) Charge support; f) Electric heating connection; g) Removable condenser; h) Condensed magnesium.

Bolzano Process. The Bolzano process is operated in Italy by Società Italiana per il Leghe di Magnesio (SAIM) and in Brazil by Brasmag. It employs an internally heated, brick-lined cylindrical reactor (Figure 20.13). The briquetted charge of homogeneously mixed calcined dolomite and ferrosilicon lines (d) is loaded on a charge support system (e). Internal electrical heating (f) is conducted to the charge through the charge support system. The process operates at 1200 °C and < 400 Pa. Magnesium vapor condenses inside the condensers that are water-cooled to 400–500 °C. Each re-

actor has a production capacity of ca. 2 t of magnesium per 20–24 h reaction cycle, with a shutdown time of 0.5–0.75 h per cycle. Production of 1 t of magnesium consumes 7–7.3 MWh, 5–5.2 t calcined dolomite, and 0.7 t of silicon contained in 78% ferrosilicon, with 81% silicon recovery; 5–5.2 t of slag is produced per tonne of magnesium and sold for use in plaster and building bricks. Mechanization of charge handling and slag removal is a challenge in this process. Magnesium with a purity of 99.98–99.99% is obtained [34].

Magnetherm Process. The magnetherm process was developed by Pechiney Électrometallurgie in 1963 and is still in use at the company's magnesium extraction plant in Marignac, France. The process is now also operated by North West Alloys (United States), Japan Metals and Chemicals (Japan), and Magnohrom (former Yugoslavia). The total installed production capacity worldwide is 65 000 t/a. The overall equation for the process is



The dicalcium silicate slag formed in the reaction of calcined dolomite with ferrosilicon (Pidgeon and Bolzano processes) has a melting point of 2000 °C and is solid at the reaction temperature (1200 °C). The Magnetherm process, however, operates with a partly molten slag of the general composition $2\text{CaO} \cdot \text{SiO}_2 \cdot n\text{Al}_2\text{O}_3$ at 1550–1600 °C. The slag contains 50% Ca_2SiO_4 , 18% Al_2O_3 , 14% MgO , and 18% CaO and is kept in an electrically heated, cylindrical, brick- and carbon-lined steel vessel (Figure 20.14). The power input (4500 kW) is conveyed through a water-cooled copper electrode (a) from the top through the slag (g) to the bottom graphite lining (b) of the reactor, which acts as a power outlet. Coarse calcined dolomite and alumina screened to 3–30 mm, as well as ferrosilicon containing a minimum amount of fines, are added continuously to the slag under a vacuum of 0.40–0.67 kPa through charge holes in the water-cooled furnace roof. Magnesium vapor condenses in a separate condenser system.

The main impurities of the metal produced at Marignac (France) are manganese 0.04%, silicon 0.03%, iron 0.01%, zinc 0.007%, and copper 0.005%.

The slag is not homogeneous and contains about 40% solid Ca_2SiO_4 . The main endothermic reaction takes place close to the surface of the slag. Deeper in the molten slag, the higher pressure slows down and finally stops the reaction at a ferrosilicon content in the bottom layer of ca. 20%. Slag and 20% ferrosilicon are tapped twice during a cycle of ca. 18 h, having produced more than 10 t of magnesium. Adjustment of the slag composition to higher magnesium oxide content and heating the surface of the slag with arc or plasma burners to 1900–1950 °C have been suggested to allow reduction to occur at atmospheric pressure [35].

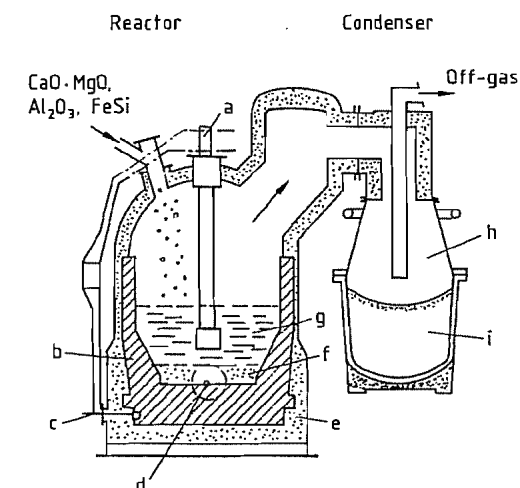


Figure 20.14: Magnetherm reactor: a) Copper electrode; b) Graphite lining; c) Bottom electrode; d) Taphole; e) Refractory; f) Low-grade FeSi; g) Slag; h) Condenser; i) Condenser crucible.

Production of 1 t of magnesium requires 5.7 t calcined dolomite, 0.75 t bauxite, 0.65 t of silicon contained in 77% ferrosilicon (88% Si recovery), and < 9 MWh of power. About 6 t of slag is produced per tonne of magnesium and is used in the cement industry for road building and as a source of magnesium and silicon in agricultural soil. The 20% ferrosilicon by-product (yield 0.15 t per tonne of magne-

sium) is used in the metallurgical industry, in the production of heavy liquid media for the separation of metals, or in drilling mud. The productivity of the process is estimated to be ca. 50 t per manyear [36].

20.5.3 Refining and Casting

All magnesium extraction processes are followed by refining to remove impurities and casting to convert the metal to ingots, billets, slabs, or granules [5].

Refining. Nonmetallic impurities in the form of particulate oxides, nitrides, carbides, and chloride inclusions impair corrosion resistance as well as mechanical and surface properties. Most alkali chloride and magnesium chloride fluxes wet and coat the surface of the impurity particles. The higher density of the chlorides causes the impurities to sink to the bottom of the melt as a sludge. Fluxes are composed to maintain a minimum difference in density compared to that of the metal of 0.15–0.20 g/cm³.

Inspissating (thickening) agents such as magnesium oxide and calcium fluoride reduce the fluidity of the sludge to prevent it from contaminating the metal after settling. Inspissated fluxes are also used to protect the metal surface during holding and casting because of their viscosity and stability (Table 20.5).

Table 20.5: Composition of fluxes used in melting and refining (%).

Purpose	CaCl ₂	NaCl	KCl	MgCl ₂	CaF ₂	MgO
Melting	40	30	20	10		
Melting and refining	20	10	10	35	15	10
Refining	15	10	10	35	20	10

Metallic impurities are normally controlled by the choice of raw materials and extraction process parameters. The most common metal impurities in pure magnesium are iron, copper, nickel, manganese, zinc, aluminum, silicon, calcium, and sodium. Intermetallic particles of aluminum, manganese, iron, and silicon have also been identified.

Heavy metals reduce the corrosion resistance of magnesium while acting as cathodes

in galvanic cells in the metal. Metallic impurities are also undesirable for certain applications in which magnesium is used as a reductant (Ti, Zr, U) or as a canning material for the fuel elements in nuclear reactors where the metal's neutron absorption properties are important.

The solubility of iron in magnesium increases with temperature (Figure 20.15). Iron levels can be kept low by operating at low temperature (660–680 °C) under clean conditions [37]. The iron content can be reduced further by adding manganese, zinc, beryllium, or titanium(IV) chloride. Silicon can be removed by adding zinc chloride or cobalt(II) chloride. In these processes, complex iron and silicon compounds precipitate. Sodium and calcium are efficiently reduced and converted to their chlorides by stirring magnesium chloride into the melt [5].

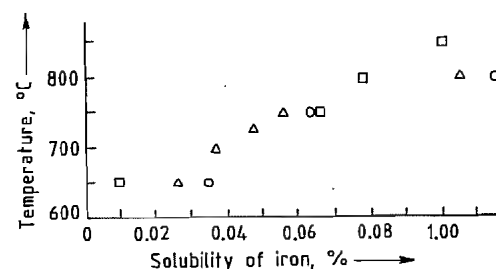


Figure 20.15: Solubility of iron in magnesium [36]. Symbols indicate results obtained from different sources.

Hydrogen is formed when magnesium reacts with moisture contained in the air or in materials used in the process. The normal level of hydrogen in pure magnesium is 1–7 cm³ per 100 g, which is acceptable for most purposes. Higher levels cause porosity on solidification; this is especially important in magnesium alloys. The level of dissolved hydrogen can be reduced by treatment with chlorine at 725–750 °C, nitrogen at 650–680 °C, argon, or helium.

Equipment. The standard equipment in magnesium refineries consists of large, stationary, brick-lined furnaces or externally heated steel crucibles containing 10–25 t or 2–6 t of molten magnesium, respectively. The stationary furnaces can be heated electrically,

with gas or oil burners from the roof, or by submerged electrical heating systems.

Electrolytic magnesium recovered and processed in the molten state can be refined in continuous stationary furnaces. Proprietary installations are in use with metal yield > 99.5% and negligible flux consumption (Figure 20.16) [38].

Metallurgical magnesium crowns (condensed magnesium crystals) or condensates are recovered in the solid state. Standard practice involves batchwise melting and refining in steel crucibles that are transported by crane to the casting area. The melting process and the high content of nonmetallic impurities require a flux consumption that is 5–10% of the metal volume; metal recoveries are in the range 95–98%.

Casting. Highly automated casting by pumping or static pressure is state of the art. Magnesium contracting 4.2% during solidification and 5% during cooling to 20 °C is sensitive to surface cracks and shrink holes. Turbulent flow favors the formation of nonmetallic inclusions. Consequently, care is taken to control the solidification process and to reduce turbulence. At elevated temperature or in the case of turbulent metal flow, sulfur dust may be sprayed on the metal surface to suppress oxidation.

The level of impurities in standard 99.8% magnesium does not influence the solidification pattern. Pure magnesium solidifies at its

melting point (649 °C). During holding and casting, the metal surface is protected against oxidation by a cushion of protective gas. Air may be completely replaced by helium or argon; low concentrations of sulfur hexafluoride or sulfur dioxide in air form protective layers on the metal surface. Blends of air, sulfur hexafluoride, and carbon dioxide are being used increasingly because of their nontoxic character and low cost [39].

Billets are cast in multi-strand continuous or semicontinuous direct-chill casting machines. The number of parallel strands is limited to four to six because of practical problems associated with the metal's low heat content and tendency to skin formation. Hot top and airslip systems are state of the art.

Single-crystal magnesium may be continuously cast by the Ohno horizontal continuous casting process. The metal is cooled directly with a water spray immediately outside the mold maintained at a temperature above the melting point (64 °C). The rapid cooling produces metal with unidirectional solid structure, which is reported to exhibit excellent workability and superior anticorrosion properties [40].

To avoid discoloration and surface corrosion during transportation and handling under severe climatic conditions, the metal is protected by suitable ventilated plastic or paper wrappings. Magnesium ingots are sometimes protected by a thin layer of mineral oil.

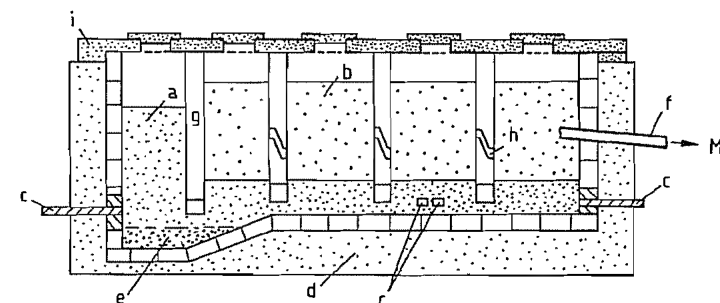


Figure 20.16: Norsk Hydro refining furnace [38]: a) Salt melt; b) Magnesium metal; c) Electrodes; d) Refractory; e) Sludge; f) Tapping spout; g) Partition wall; h) Metal port; i) Refractory cover.

20.5.4 Particulate Magnesium

Particulate magnesium comprises powders, granules, turnings, and raspings; particle sizes range from 0.04 to 5 mm, and particle shapes vary. Particulate products are used in chemical and metallurgical processes in which magnesium acts as a reagent, catalyst, or alloying element. Fine powders are used in pyrotechnics.

Particulate magnesium is considered inflammable and subject to specific labeling and packing regulations according to IMDG codes classes 4.1 and 4.3; UN No. 1869 and 1418; CFR 49: 172.01, flammable solid; RID/ADR class 4.1, number 13b, class 4.3 number 1d.

Flowability, uniformity of grain size, and defined area volume ratios are important for injection into molten metal (steel, aluminum). Particulate magnesium is frequently blended with inert and active components (e.g., lime or alumina) or coated with salt or refractories. These products are used for desulfurization of iron. Blending and coating reduce the reactivity and increase the magnesium yield. Turnings and raspings commonly used for Grignard syntheses and pharmaceuticals are adjusted for reactivity (surface-to-weight ratio) and form of the particles according to customer specifications. Finely divided powder for pyrotechnics is subject to narrow tolerance limits, including the content of organic material.

Particulate magnesium is produced directly from the molten state by shotting, atomization, or granulation or by machining ingots, slabs, or billets, with subsequent grinding and screening. Airborne dust with a particle size < 0.15 mm is explosive. Safety precautions for machining and atomizing operations include prevention of explosion hazards in the processing and handling of fine dust, as well as design of the general plant layout to limit the consequences of accidental blowouts. Clean operation and personal hygiene are important.

Nearly spherical magnesium shots in the 0.2–2-mm size range are produced by nozzle spraying in a cooling tower with an inert atmosphere [41]. Atomizing is performed in a pro-

TECTIVE atmosphere of argon, helium, or methane. Magnesium may be atomized on a rotating disk or in a gas stream. During shotting and atomizing, precautions are taken to avoid the formation of layers of highly ignitable, pyrophoric substances.

Salt-coated granules were originally developed in the former Soviet Union and are produced by mixing alkali chloride salts and molten magnesium in a rotating perforated cup; the metal is disintegrated by centrifugal force with subsequent air cooling. Spheroidal particle sizes range from 0.2 to 2.5 mm, with a salt content of 10% [22, 42]. Other methods include mixing molten mixtures of magnesium and alkali chlorides and adding a stabilizing boron compound [43]. Various proprietary processes employ eutectic salt compounds with low hygroscopicity to produce particles with high flowability [44]. The salt and metal are separated by gentle crushing and screening, leaving granules with 5–10% salt as coating. The production of salt-coated granules is safer than that of pure magnesium powder and can be integrated in normal foundry operations.

20.6 Environmental Aspects

All magnesium extraction processes require installations for cleaning off-gases and treating wastewater. Significant amounts of solid waste are deposited as landfill. All processes involve calcination of carbonaceous minerals or dehydration of hydroxides in which dust is removed by conventional methods. Gases emitted to the atmosphere contain carbon dioxide, nitrogen oxides, and sulfur dioxide from the combustion and calcination processes. The content is frequently lowered by scrubbing the gases with seawater to comply with local emission regulations.

In *electrolytic processes*, carbon is used as a reductant in the preparation of anhydrous magnesium chloride and as anode material in electrolysis. The presence of carbon, water, chloride, or hydrogen chloride, even in low concentrations, at elevated temperature leads

to formation of chlorinated hydrocarbons and other organic compounds. Chloromethanes, chlorobenzenes, polychlorinated biphenyls, chlorodibenzofurans, and chlorodibenzo-*p*-dioxins are highly toxic and are only slowly degraded in nature. Although such compounds only occur in liquid effluents from scrubber systems at low concentrations (a few micrograms per liter), collection and destruction are mandatory.

Chlorinated organic compounds can be either in solution or present as small particles in the liquid effluents. Particles may be flocculated with appropriate cationic or nonionic agents. The agglomerates adhere to solid inorganic particles that are often present in the effluents (carbon and hydroxides or oxides of iron, aluminum, silicon, etc.). The particles are removed by filtration or centrifugation. Liquids may be treated with activated carbon. Traces of chlorine or hydrochloric acid in off-gases are scrubbed, recycled, or neutralized by conventional methods.

By-products from *metallothermic processes* are either used for industrial purposes or deposited as landfill.

Sludge from *foundry operations* contains entrapped metallic magnesium globules. When deposited as landfill, precautions must be taken to control hydrogen emission from the reaction of entrapped magnesium with water. Off-gases from foundry operations containing hydrogen chloride, sulfur dioxide, and magnesium oxide are scrubbed by conventional methods to comply with local regulations.

20.7 Quality Specifications

The ASTM designation B 92M-83 covers pure magnesium in the form of ingot or stick for remelting in the following grades: 9980, 9990, 9995, and 9998 (Table 20.6). Examples of other standards for pure magnesium corresponding to those of the ASTM are ISO 8287 and DTN 17800.

Table 20.6: Magnesium grades according to ASTM B 92M-83. Figures refer to maximum content in weight percent except otherwise specified.

Component	9980 A	9980 B	9990 A	9995 A	9998 A
Aluminum			0.003	0.01	0.005
Copper	0.02	0.02			0.0005
Iron			0.04	0.003	0.002
Lead	0.01	0.01			0.001
Manganese	0.10	0.10	0.004	0.004	0.002
Nickel	0.001	0.005	0.001	0.001	0.0005
Silicon			0.005	0.005	0.003
Tin	0.01	0.01			
Titanium				0.01	0.001
Other impurities (each) ^a	0.05	0.05	0.01 ^b	0.005 ^b	0.005 ^b
Magnesium (by difference, min.)	99.80	99.80	99.90	99.95	99.98

^aFor specific applications, other minor impurities may be limited by agreement.

^bFor nuclear applications, cadmium and boron concentrations are specified as follows: Cd (min. 0.00005; max. 0.0001%); B (min. 0.00003; max. 0.00007%).

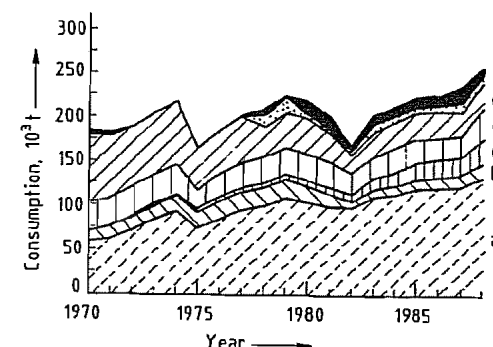


Figure 20.17: Consumption by end uses. Pure magnesium: a) Aluminum alloys; b) Iron nodularization; c) Desulfurization; d) Chemical applications. Magnesium alloys: e) Pressurized die casting; f) Structural applications. Pure magnesium and alloys: g) Other uses.

Grade 9980A is adequate for most uses and can be obtained by electrolysis by using controlled standard operations. Grades 9995A and 9998A are normally produced only by metallothermic processes. High-purity magnesium can also be produced by distillation of lower grades, but this is expensive [5, p. 178; 22, p. 313].

20.8 Uses

The uses and consumption of magnesium are summarized in Figure 20.17. The overall growth rate in the use of magnesium is esti-

mated as of 1989 to be 3–4% for the next few years.

Aluminum Alloys. The largest single use of magnesium is as an alloying element in aluminum alloys. Aluminum–magnesium alloys have improved ductility, enhanced resistance to saltwater corrosion, and improved cryogenic properties. User forms are ingots weighing 1–25 kg or sows weighing 250–500 kg. The market growth of this application depends on the growth of aluminum and the recycling efficiency of aluminum scrap, particularly beverage cans.

Desulfurization and Nodularization. In the iron and steel industry magnesium is used for desulfurization and nodularization. Particulate magnesium alone or blended with other ingredients is injected into crude iron melts. The typical magnesium consumption for desulfurization of low-iron steel is 0.5 kg per tonne of steel. Magnesium also triggers the transformation of laminar carbon to globules in nodular iron. For this purpose the metal is either added with ferrosilicon as an alloying element or directly in the form of lumps, impregnated coke, or granules. Magnesium has a modifying effect on nonmetallic inclusions in steel. Effect and user forms are currently being studied [45].

Magnesium-based alloys are normally delivered as alloyed ingots from the primary producers. Magnesium alloys are used for pressure die casting, structural applications, numerous lightweight applications (automotive, hand tools, computers, etc.), and where the metal's damping capacity is of importance. The magnesium-based magnox alloys are used in extruded form as canning materials in gas-cooled nuclear reactors (Calder Hall) because of their low neutron absorption area. Uses of magnesium for uranium and nuclear application account for less than 1% of the market in the Western world [46].

Chemical applications include the use of magnesium as a reagent in the production of titanium and zirconium by the Kroll process, the reduction of uranium fluoride to uranium

metal, and the production of beryllium and hafnium. Titanium constitutes by far the largest user segment in this group, the magnesium being added in ingot form. Magnesium chloride from the Kroll process is electrolyzed to recover magnesium and chlorine. The normal magnesium requirement to compensate for losses is 0.1 t per tonne of titanium.

Magnesium raspings for the production of metallic uranium have a specified limited content of boron, cadmium, and rare-earth elements including gadolinium, samarium, europium, and dysprosium.

The use of particulate magnesium, raspings, or turnings in Grignard syntheses has been declining, due primarily to restricted use of tetraethyllead.

Other Uses. The electronegative character of magnesium is used for corrosion abatement as sacrificial soil and hot-water tank anodes. European restrictions on aluminum in drinking water have encouraged the use of magnesium anodes for hot-water tanks. Magnesium batteries for military purposes and rescue systems combine light weight and high energy content.

Pure magnesium (preferably atomized powder) combines readily with hydrogen to form magnesium hydride which can be released in a reversible process. Magnesium hydride has a higher concentration of hydrogen per unit volume than liquid hydrogen. The reversibility of the process is dependent on the surface activity of the powder. Magnesium as a carrier for hydrogen could represent a future use [47].

20.9 Economic Aspects

Considered a strategic material for military applications during and shortly after World War II, magnesium is now used predominantly for nonmilitary purposes. Since the oil crises in the early 1970s, magnesium consumption has fluctuated in line with other commodity materials dependent on changes in the industrial growth in major consumer countries. The capacities are given in Table 20.7.

Table 20.7: Main magnesium producers.

Company	Installed production capacity, 10 ³ t	Production process
Norsk Hydro a.s., Norway	1	electrolytic
Norsk Hydro Canada, Canada	(40)	electrolytic ^a
Dow Chemical, USA	90	electrolytic
Amax, USA	35	electrolytic
Northwest Alloys, USA	35	thermic
Pechiney Électrometallurgie, France	15	thermic
MagCan, Canada	(12)	electrolytic ^b
Timminco, Canada	12	thermic
Magnesio (SAM), Italy	10	thermic
Ube Industries, Japan	7	thermic
Furukawa Magnesium Co., Japan	(6)	thermic ^c
Brasmag, Brazil	5	thermic
Magnohrom, Yugoslavia	5	thermic
Japan Metals and Chemical Co., Japan	3	thermic
Former Soviet Union	86	electrolytic
China	9	electrolytic

^a Capacity under installation; start-up planned mid-1989.

^b Capacity under installation; start-up planned early 1990.

^c Facility closed in 1988.

Total production of magnesium in the Western world in 1988 was 241×10^3 t, and consumption was 255×10^3 t, including 13.2×10^3 t exported to Eastern countries. Approximately 75% of the total world magnesium production (1989) is electrolytic and 25% metallothermic. The main Western consumer regions were North America (125×10^3 t) Latin America (11.7×10^3 t), Europe (73.3×10^3 t), Africa and the Middle East (3.8×10^3 t), and Asia-Oceania (37.2×10^3 t) (source: International Magnesium Association). The per capita consumption was 0.51 kg in the United States, 0.18 kg in Japan, 0.17 kg in Western Europe, and 0.04 kg in South America.

World production of primary magnesium in the five-year periods 1963–1967 and 1983–1987 is summarized in Table 20.8. Growth in the interval between these periods occurred primarily in Norway, the former Soviet Union, and the United States. In 1983–1987 the United States was the largest producer (ca. 40% of the world total), followed by the former Soviet Union (28%) and Norway (15%). Significant growth is anticipated in Canada, with an additional capacity of more

than 50 000 t annually expected to come on stream in 1989.

The per capita consumption of magnesium in selected countries is summarized in Table 20.9. In 1983–1987 the United States had the highest consumption, followed by the Soviet Union and Japan.

The metal is not traded on the London Metal Exchange, and the major producers control their own distribution network. Price fluctuations have been less cyclical than for other metals in world trade (Figure 20.18).

Table 20.8: Average annual world primary magnesium production (10³ t), as reported by the U.S. Bureau of Mines, Department of the Interior.

Country	1963–1967	1983–1987
Brazil		3.4
Canada	8.0	7.0
China	0.9	7.0
France	2.6	13.2
Italy	6.2	9.3
Japan	4.2	7.6
Norway	24.7	48.2
Former Soviet Union	34.7	87.0
United Kingdom	4.7	
United States	7.5	127.2
Yugoslavia		4.5
World total	161.3	314.4

Table 20.9: Average annual per capita primary magnesium consumption (kg) in selected countries.

Country	1963–1967	1983–1987
Australia	0.054	0.255
Brazil	0.233	0.417
Canada	0.220	0.243
China	0.001	0.012
France	0.085	0.175
West Germany	0.632	0.458
Italy	0.025	0.076
Japan	0.050	1.633
Norway	0.270	0.967
Soviet Union	1.243	2.629
Sweden	0.069	0.188
Switzerland	0.119	0.298
United Kingdom ^a	0.164	0.084
United States	3.258	2.986

^a Includes secondary magnesium.

Magnesium duty tariffs are regulated by the General Agreement on Tariff and Trade (GATT). In 1989 the following export tariffs were applied on pure magnesium: to the United States from Europe 8%, Canada 7.2%, and Brazil 0%; to Canada from the United

States 3.6% (declining to 2.8% by 1991) and Europe 4%; and to Europe from the United States, Canada, and Brazil 5.3%.

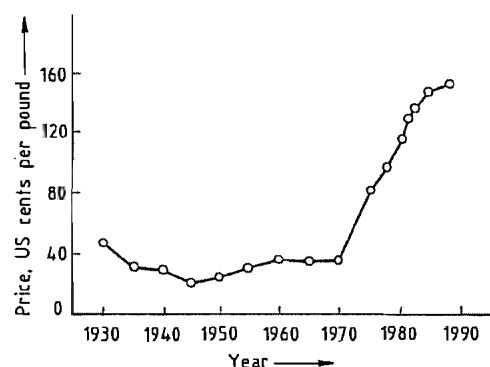


Figure 20.18: Magnesium prices.

20.10 Toxicity and Occupational Health

Magnesium and magnesium compounds are regarded as having low toxicity. No reports of serious poisoning in industry have appeared in the literature. Industrial exposure of humans resulting in magnesium serum values twice the normal level did not cause any ill effects [48]. In humans the only sign of acute toxicity is metal fume fever resulting from inhalation of freshly generated magnesium oxide. This is in contrast to animals, where magnesium cause both systemic and cutaneous responses. No evidence is available that inhalation of magnesium dust can cause lung injury. However, fine magnesium dust is generated in the printing trade, and complaints have been made about discolored sputum [49].

The acute oral toxicity of magnesium compounds in animals is low: LD₅₀ values (rat, oral) for magnesium nitrate and chloride are 5440 and 2800 mg/kg, respectively. However, oral intake can impair kidney function; toxic symptoms include a sudden drop in blood pressure and respiratory paralysis due to depression of the central nervous system (CNS) [48]. Intravenously administered magnesium compounds have been shown to be more toxic to animals than orally administered com-

pounds. Toxic response includes general anesthesia and narcosis. Intravenous administration of calcium counteracts the reaction.

Magnesium is essential for metabolic reactions involving ATP. It is a cofactor for enzymes that participate in transfer of phosphate from ATP and other nucleotide triphosphates. However, the activity of a large number of enzymes is also magnesium dependent (e.g., phosphatases and pyrophosphatases).

Some effects of magnesium on the nervous system are similar to those of calcium. An increased concentration of magnesium in the extracellular fluid causes CNS depression. Hypomagnesemia causes increased CNS irritability, disorientation, and convulsions.

In the cardiovascular system some of the effects of excess magnesium are similar to those of potassium. Magnesium has a direct depressant effect on skeletal muscle.

Magnesium salts are poorly absorbed from the alimentary tract, and primarily from the small intestine. Net magnesium absorption is 35–40% with a normal dietary intake and increases to ca. 80% at low magnesium intake. Nutritional requirements have been calculated to be approximately 150 mg/d for maintaining a normal plasma level [50]. Normal adult dietary intake is 300–400 mg/d. Drastic reduction of dietary intake of magnesium is needed to induce a negative balance because of extremely effective renal retention and increasing intestinal absorption. The effect of magnesium (as well as of zinc) supplementation and depletion on carcinogenesis has been reviewed comprehensively [51]. Magnesium (or zinc) supplementation tends to inhibit carcinogenesis, and magnesium deficiency increases the incidence of neoplasia in humans and animals.

Various magnesium compounds such as magnesium hydroxide (milk of magnesia) are used as gastric antacids and can also be components of poison antidotes. Magnesium sulfate acts as a purgative because it is poorly absorbed from the gut and causes osmotic withdrawal of water from the gut wall. Fatal intoxication can occur with very high dietary

levels (15 000–25 000 ppm) or under circumstances that increase magnesium absorption [52].

Particles of metallic magnesium that perforate the skin or gain entry through cuts and scratches may produce a severe local lesion characterized by evolution of gas and an acute inflammatory reaction, frequently with necrosis (chemical gas gangrene). Gaseous blebs may develop within 24 h of injury and are very slow to heal. However, the most serious hazard presented by magnesium is the danger of burns from molten metal.

20.11 Compounds

Magnesium occurs in divalent form in all of its compounds. The bromide, iodide, sulfate, and nitrate salts are water soluble. Some of the water-soluble salts are highly hygroscopic and form crystals with a high water content. Magnesium fluoride, oxide, hydroxide, phosphate, and carbonate are sparingly soluble or insoluble in water.

The water-soluble magnesium salts tend to undergo hydrolysis and form basic salts due to the weakly basic character of magnesium hydroxide. This is responsible for the highly corrosive action of magnesium salt solutions; dehydration of magnesium salts containing water of crystallization without hydrolytic decomposition is also difficult to achieve.

The most important magnesium compounds are magnesium oxide, which is used for refractory magnesia bricks and as a heat-storage medium, and magnesium chloride which is electrolyzed to produce magnesium metal. Naturally occurring magnesium carbonate (magnesite) is mainly burned to give sintered magnesia for the production of magnesia bricks. Seawater is an important source of magnesium oxide and magnesium chloride. Calcined dolomite (CaCO₃·MgCO₃) is used as a raw material for the silicothermic production of magnesium metal. Basic magnesium carbonate is used for thermal insulation.

Anhydrous magnesium nitrate is difficult to produce (*mp* of the hexahydrate 89 °C). Con-

centrated magnesium nitrate solutions (e.g., from MgCO₃ and 60% nitric acid) are used for the production of highly concentrated nitric acid.

Naturally occurring magnesium silicates include asbestos and talc. Materials for electrical insulation are also based on magnesium silicates. A series of refractory ceramics are based on magnesium.

Organomagnesium compounds are also known, the most important of these being the Grignard reagents which play an important role in synthetic organic chemistry.

20.11.1 Magnesium Carbonate

Properties. *Anhydrous magnesium carbonate*, MgCO₃, occurs naturally as magnesite which is the starting material for the production of magnesia, MgO. Magnesium carbonate is also synthesized by reacting Mg(OH)₂ with carbon dioxide at high pressure [53]. Magnesium carbonate begins to decompose at ca. 400 °C, the reaction proceeds rapidly above 550 °C. The compound forms colorless or white to gray, trigonal crystals: lattice constant $a = 0.585$ nm, $\alpha = 103^\circ 20'$, $Z = 4$, cleavage parallel to (10 $\bar{1}$ 1).

Density	2.96 g/cm ³
Mohs hardness	4–4.5
Refractive index	$n_D 1.700$, $n_E 1.509$
Enthalpy of formation (298 K)	−1096 kJ/mol
Dissociation energy (298 K)	+1190 kJ/kg
Solubility in cold water	0.0106%

Barringtonite, MgCO₃·2H₂O, forms colorless triclinic crystals, lattice constants $a = 0.9115$ nm, $b = 0.6202$ nm, $c = 0.6092$ nm; $\alpha = 94.00^\circ$, $\beta = 95.53^\circ$, $\gamma = 108.87^\circ$; $Z = 4$; refractive index 1.458, 1.473, 1.501; density 2.83 g/cm³.

The mineral *nesquehonite*, MgCO₃·3H₂O, occurs as colorless to white crystals. This carbonate can also be synthesized by carbonation of Mg(OH)₂ at atmospheric pressure. Density 1.84 g/cm³, *mp* 165 °C (decomp.), solubility in cold water 0.129%.

Lansfordite, MgCO₃·5H₂O, forms white monoclinic crystals, density 1.73 g/cm³. The natural mineral hydromagnesite, 4MgCO₃·Mg(OH)₂·4H₂O, forms white monoclinic

crystals, density 2.25 g/cm³ [54]. The synthetic product is known as magnesita alba.

Other MgCO₃-containing minerals include *huntite*, CaCO₃·3MgCO₃ [54] and *dolomite*, CaCO₃·MgCO₃. Dolomite is a rock-forming mineral and is much more common than magnesite. It is burned to form sintered dolomite (for refractory bricks) and light-burned dolomite (used as a fluxing agent).

Uses. The main use of magnesite is the production of magnesita. Small quantities are used as a filler. Plans have been proposed for producing magnesium metal from naturally occurring (cheap) magnesite [55]. The synthetic carbonates are used as fillers for paper, plastics, and rubber and as thickening agents for printing inks. Pharmaceutical-grade magnesium carbonate (magnesita alba) is also used in toothpaste and as an antacid. High-purity magnesium carbonate is employed in cosmetics.

20.11.2 Magnesium Chloride

Magnesium chloride, MgCl₂, is the commonest naturally occurring, water-soluble magnesium compound. It is a constituent of many salt lakes and natural brines [56, 57]; sea salt contains 17% MgCl₂. Mineral salt deposits contain the important minerals carnallite KCl·MgCl₂·6H₂O, bischofite MgCl₂·6H₂O, and occasionally the double salt tachhydrite in which the magnesium chloride is combined with calcium chloride (CaCl₂·2MgCl₂·12H₂O). Tachhydrite is found in salt deposits in Brazil and the Congo region.

Magnesium chloride is obtained from mineral salt deposits by processing the spent liquors remaining after extraction of potassium chloride and also by direct solution mining; it is also recovered from salt lakes and seawater.

20.11.2.1 Properties

Anhydrous Magnesium Chloride. Anhydrous magnesium chloride forms hexagonal crystals, its physical properties are as follows:

M_r	95.23
mp	713 °C

Refractive index (n)	1.675, 1.59
d_4^{20}	2.41 g/cm ³
Specific heat (c_p) between 0 and 713 °C (mp): $c_p = 0.78011 + 0.20607 \times 10^{-3}(t-20)$ $- 0.10853 \times 10^{-6}(t-20)^2$ kJkg ⁻¹ K ⁻¹	
Specific electrical conductivity at	
700 °C	1.00 Ω ⁻¹ cm ⁻¹
750 °C	1.09
800 °C	1.17
Solubility in water at	
20 °C	35.3%, 54.6 g/100 g
40 °C	36.5%, 57.5
60 °C	37.9%, 61.0
80 °C	39.8%, 66.1
100 °C	42.2%, 73.0
Solubility in methanol at	
0 °C	15.5 g/100 g
60 °C	20.4
Solubility in ethanol at	
0 °C	3.61 g/100 g
60 °C	5.89

Properties of the Hydrates. Magnesium chloride forms five hydrates whose transformation temperatures and solubilities are given in Table 20.10 (see also Figure 20.19). The most important is the hexahydrate, MgCl₂·6H₂O, which forms monoclinic crystals and is present in mineral salt deposits:

M_r	203.31
mp	117 °C
Heat of fusion	34.3 kJ/mol
Density	1.57 g/cm ³
Refractive index (n)	1.495, 1.507, 1.528
Specific heat at	
48.6 °C	1.415 kJkg ⁻¹ K ⁻¹
100 °C	1.537

The penta- and hexahydrates can be dehydrated to the tetrahydrate stage almost without decomposition. On dehydration to the dihydrate, however, hydrolytic decomposition starts. Dehydration of the dihydrate at 240 °C leads to extensive decomposition forming magnesium oxychlorides or oxide. To obtain anhydrous MgCl₂, the dihydrate must be dehydrated in an atmosphere of hydrogen chloride.

Table 20.10: Transformation temperatures and corresponding solubilities of magnesium chloride hydrates.

Hydrate transformation	Temperature, °C	Solubility, g MgCl ₂ /100 g H ₂ O
MgCl ₂ solution → MgCl ₂ ·12H ₂ O	-33.6	27.2
MgCl ₂ ·12H ₂ O → MgCl ₂ ·8H ₂ O	-17.4	47.6
MgCl ₂ ·8H ₂ O → MgCl ₂ ·6H ₂ O	-3.4	52.3
MgCl ₂ ·6H ₂ O → MgCl ₂ ·4H ₂ O	116.8	85.6
MgCl ₂ ·4H ₂ O → MgCl ₂ ·2H ₂ O	181.5	125.7

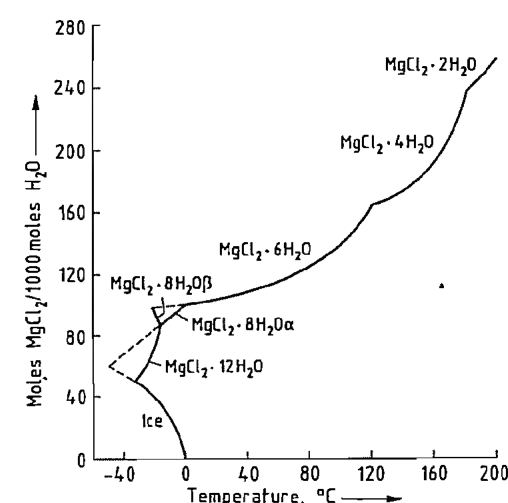


Figure 20.19: State diagram of the system MgCl₂·nH₂O.

Chemical Properties. Magnesium chloride can be decomposed by oxygen to form magnesium oxide and chlorine [58]—the converse of the reaction between magnesium oxide and chlorine to form MgCl₂. With ammonia, MgCl₂ forms ammines that are analogous to the hydrates: MgCl₂·NH₃, MgCl₂·2NH₃, and MgCl₂·6NH₃. Corresponding addition compounds are formed with alcohols and with other organic compounds such as ethers, acetic acid, amines, ethyl acetate, pyridine, hexamethylenetetramine, and dioxane (e.g., MgCl₂·6CH₃COOH).

A series of basic chlorides (magnesium oxychlorides) are formed with magnesium oxide and are of commercial importance as Sorel cement. The following oxychlorides are known: MgCl₂·MgO, MgCl₂·MgO·H₂O, 2MgCl₂·MgO·H₂O, MgCl₂·3MgO·11H₂O, and MgCl₂·3MgO·7H₂O. The compounds MgCl₂·MgO and 2MgCl₂·MgO·H₂O are formed on dehydration of MgCl₂·H₂O at 280–495 °C. Aqueous MgCl₂ solutions are acidic due to hydrolysis. The electrolysis of aqueous MgCl₂ solutions produces magnesium hydroxide and chlorine, whereas electrolysis of anhydrous MgCl₂ yields magnesium metal and chlorine.

20.11.2.2 Raw Materials

Of the three main sources of raw materials for magnesium chloride production, the most important is *seawater*. Magnesium can be directly precipitated from seawater as magnesium hydroxide and converted to magnesium chloride by treatment with chlorine. The residues (bitterns) obtained after production of drinking water or sea salt from seawater can also be used. A second large source is the *spent liquor from the potash industry* arising from the processing of hard salts and carnallite-bearing raw materials. A third source is provided by the *salt lakes* in many parts of the world, the Dead Sea and the Great Salt Lake being particularly important.

20.11.2.3 Production

Precipitation of Magnesium Hydroxide from Seawater

If seawater cannot be preconcentrated by solar energy, magnesium chloride salts or solutions can only be produced on a large scale by precipitation as the hydroxide, followed by conversion to the chloride with hydrogen chloride.

The Dow Chemical process is described elsewhere. This process has been used to manufacture magnesium chloride from seawater in large quantities since 1941 in Freeport (Texas). It is an intermediate step in the production of magnesium metal.

Recovery from Spent Liquors from the Potash Industry

The spent liquors obtained after recovery of potassium chloride from carnallite-containing raw salts typically contain (in grams per liter): MgCl₂ 293, MgSO₄ 48, KCl 39, NaCl 26, and H₂O 890. They are used as a raw material for the recovery of magnesium chloride by the Norsk Hydro process.

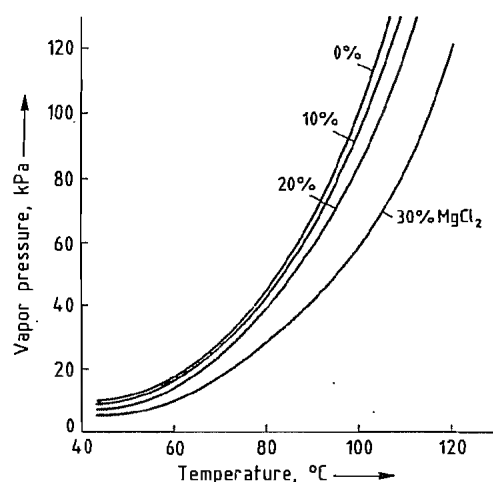


Figure 20.20: Vapor pressure of MgCl_2 solutions as a function of temperature.

Production of Concentrated MgCl_2 Solutions by Kali und Salz AG (Western Germany). The spent liquor contains ca. 280–300 g/L MgCl_2 and is concentrated in a two-stage vacuum evaporator to ca. 460 g/L MgCl_2 . (Vapor pressures of MgCl_2 solutions as a function of concentration and temperature are shown in Figure 20.20).

The solution in the first evaporator stage is heated by the vapor from the second stage to a steady temperature of ca. 55 °C. The second-stage liquor is maintained at 95 °C by heating with steam at 0.1 MPa and the hot, cloudy solution is clarified by removing the salts [carnallite, NaCl , $\text{MgSO}_4 \cdot \frac{5}{4}\text{H}_2\text{O}$, and impurities such as $\text{Fe}(\text{OH})_3$ and clay] by means of a rotary filter and centrifuge. On cooling carnallite crystallizes out from the solution. The crystallized salts and sludge are sent to the potassium chloride plant where carnallite is decomposed together with carnallite containing crude potash salt. The carnallite is mixed with water or a low- MgCl_2 brine to produce a spent liquor containing 280–300 g/L of MgCl_2 and solid potassium chloride contaminated with sodium chloride and $\text{MgSO}_4 \cdot \frac{5}{4}\text{H}_2\text{O}$. The cooled MgCl_2 solution is purified by reheating and removing bromine with chlorine. The debrominated solution is neutralized with lime, partly precipitating the sulfate ions in the form of

gypsum. The precipitated sediment is removed. The highly concentrated 32–33% MgCl_2 solution is sold as such or can be processed further to obtain magnesium chloride hydrates.

Production of Concentrated MgCl_2 Solution by the VEB Kombinat Kali (Eastern Germany). The spent liquor from the manufacture of potassium salts has a MgCl_2 content of ca. 260 g/L. The solution is first mixed with synthetic carnallite from the vacuum cooling stage; the MgCl_2 from the carnallite dissolves leaving the undissolved potassium chloride behind. The increased MgCl_2 content (ca. 320 g/L) of the solution lowers the solubility of the alkali-metal salts causing the precipitation of potassium and sodium chlorides. After removal of these salts, the solution is pumped to the second of the two evaporation stages. The preconcentrated solution from the second evaporation stage is pumped to the first evaporation stage where $\text{MgSO}_4 \cdot \frac{5}{4}\text{H}_2\text{O}$ precipitates together with some langbeinite, carnallite, and sodium chloride. On cooling this solution, (after removal of the salts) in multistage vacuum coolers, synthetic carnallite precipitates. The carnallite is filtered off and recycled to the first step of the process. All the evaporators are of the forced circulation type [59]. The first evaporator stage is operated at 120 °C and heated with steam. The second stage is heated at 80 °C by the vapor from the first stage. The vapors from the second stage are cooled with water.

In a variation of the process, the solution containing 320 g/L MgCl_2 is mixed with part of the product solution (containing 460 g/L MgCl_2). The increase in the MgCl_2 content causes more sodium chloride and carnallite to be precipitated. Evaporation of the solution from the first stages then does not precipitate carnallite or langbeinite ($\text{K}_2\text{SO}_4 \cdot \text{MgSO}_4$). Only synthetic kieserite ($\text{MgSO}_4 \cdot \frac{5}{4}\text{H}_2\text{O}$) and sodium chloride are precipitated and these are removed. The solution produced has a density of 1.340 g/cm³ and contains 460 g/L MgCl_2 , 25 g/L MgSO_4 , 2 g/L KCl , 6 g/L NaCl , 2 g/L CaSO_4 , and 4 g/L Br^- . If this solution is to be

used for the production of magnesium metal, it is debrominated with chlorine. If it is used for production of high-quality sintered magnesia, boron is also removed by boron-selective resins. The boron content decreases from 30 to 5–10 mg/L [60].

Recovery from Raw Salts Containing Carnallite. Patents have been applied for in which pure carnallite or raw salts containing carnallite are decomposed with C_1 – C_4 alcohols, causing the MgCl_2 to pass into the alcohol phase [61]. The alcoholic solution is concentrated by evaporation to an alcohol content of 10% and the hexahydrate is precipitated by addition of water. Alternatively, evaporation is continued until the solution contains 1–2 mol of alcohol per mole of MgCl_2 ; the alcoholate is then thermally decomposed in a hydrogen chloride atmosphere at 400–500 °C.

Evaporation of Seawater and Natural Brines

The direct production of MgCl_2 from seawater or brines by evaporation is only economical where the dilute solutions can be preconcentrated by solar evaporation.

Recovery from the Dead Sea. Magnesium chloride-containing solutions are produced in large quantities by solar evaporation of brine from the Dead Sea. At the Dead Sea Works, carnallite precipitates out and solutions are obtained containing 360 g/L MgCl_2 , 110 g/L CaCl_2 , 7 g/L NaCl , and 5 g/L KCl . Owing to the low vapor pressure of water, solar evaporation only occurs at very low atmospheric humidity levels. After two or three months of evaporation, a density of 1365 g/L is achieved and bischofite separates out [62]. Large quantities of MgCl_2 -containing liquors of this type are now used by Dead Sea Periclase solely for the production of magnesium oxide by thermal decomposition.

In a process patented by the Dead Sea Works for the manufacture of magnesium chloride hexahydrate (bischofite), carnallite or a natural mixture of carnallite and sodium chloride is decomposed in its own water of

crystallization in closed vessels under pressure at 167.5 °C. The potassium chloride remains together with the sodium chloride as a sediment and is removed. The residual solution contains up to 8.2% potassium chloride and 42.3% magnesium chloride. On cooling to 115 °C by flash evaporation, carnallite is precipitated and is fed back into the circulating system. The residual solution contains 1% potassium chloride and consists essentially of bischofite [63].

Recovery from the Kara-Bogaz Gulf, former Soviet Union. Following the isolation of the Kara-Bogaz Gulf from the rest of the Caspian Sea by a dam in 1979, the MgCl_2 content increased to 250 g/L. Research was carried out to find a new method of processing this brine [64]. The brines evaporated in summer contain 25–30% MgCl_2 . When they are cooled in winter, epsomite ($\text{MgSO}_4 \cdot 7\text{H}_2\text{O}$) precipitates and is used for producing schönite ($\text{K}_2\text{SO}_4 \cdot \text{MgSO}_4 \cdot 6\text{H}_2\text{O}$). The liquid phase is used for MgCl_2 production.

Recovery from Spent Liquors after Extraction of NaCl from Seawater. The spent liquors (sea bitters) obtained after extraction of salt from seawater are evaporated in crystallizing pans by solar energy to a density of 1290 g/L. After removing the sodium chloride, the solution is cooled to 5 °C, which can be achieved in winter without energy consumption. Magnesium sulfate (epsomite) crystallizes out with a few impurities and is removed. The bitters are cooled to 0 °C; sodium sulfate (Glauber's salt) crystallizes out and is removed. The solution is then debrominated with chlorine to exclude crystallization of magnesium bromide in subsequent processing. After neutralizing with potassium hydroxide, the liquor is heated to 125 °C. On cooling to 100 °C, a crude potassium-containing salt mixture separates out that consists of langbeinite ($\text{K}_2\text{SO}_4 \cdot 2\text{MgSO}_4$) and kainite ($\text{KCl} \cdot \text{MgSO}_4 \cdot 3\text{H}_2\text{O}$), with some kieserite ($\text{MgSO}_4 \cdot \frac{5}{4}\text{H}_2\text{O}$) and sodium chloride. On further cooling to 20 °C, carnallite crystallizes out which can be treated with water to form a MgCl_2 -con-

taining solution and solid potassium chloride [65].

Recovery from the Great Salt Lake. For the National Lead Industries process, see Section 20.5.1.1. In the process operated by the Great Salt Lake Minerals Chemical Corporation, a 35% MgCl_2 solution is first produced by solar evaporation, and this is then subjected to vacuum evaporation until bischofite ($\text{MgCl}_2 \cdot 6\text{H}_2\text{O}$) and hydrated MgSO_4 are precipitated. Proposed further treatment consists of heating the crystals to 120–150 °C to redissolve the bischofite and allow removal of magnesium sulfate. The bischofite can then be crystallized out [66]. Alternatively, the solution can be maintained at 120 °C until the magnesium sulfate content decreases to < 20 g/L as a result of crystallization of kieserite. The bischofite is then crystallized by vacuum evaporation at 90 °C [67].

Recovery from Naturally Occurring Brines with High CaCl_2 Contents. Up to the end of World War II, the Dow Chemical Company used underground brines from Midland (Michigan) and Marysville for bromine production and also for the production of MgCl_2 which was electrolyzed to obtain magnesium. The alkali-metal salts were removed by evaporation and crystallization. In an older process the calcium was then separated together with the magnesium as tachhydrite ($2\text{MgCl}_2 \cdot \text{CaCl}_2 \cdot 12\text{H}_2\text{O}$) which was converted into $\text{MgCl}_2 \cdot 6\text{H}_2\text{O}$. In a later process, the solution is reacted with an amount of magnesium hydroxide (produced from magnesite) equivalent to the calcium chloride content. The calcium is then removed as calcium carbonate by treating the solution with the carbon dioxide from the magnesite calcination, and the MgCl_2 is then obtained from the solution.

Today, Dow obtains magnesium chloride for magnesium production only from seawater. The production of bischofite from Michigan brines has been discontinued.

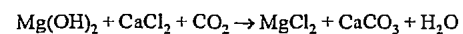
Solution Mining

A 20% MgCl_2 solution is produced in large quantities in the Netherlands from a carnallite salt deposit. It is not used to produce concentrated MgCl_2 solutions, but is almost exclusively converted to magnesium hydroxide [68].

Solution Mining of Carnallite. Carnallite ($\text{KCl} \cdot \text{MgCl}_2 \cdot 6\text{H}_2\text{O}$) deposits contain large amounts of magnesium sulfate as well as MgCl_2 . Evaporation of solutions with high magnesium sulfate contents leads to precipitation of double salts containing sodium chloride and magnesium sulfate. In the processing of these solutions, most of the magnesium sulfate is precipitated as langbeinite ($\text{K}_2\text{SO}_4 \cdot 2\text{MgSO}_4$) [69], or as schönite ($\text{K}_2\text{SO}_4 \cdot \text{MgSO}_4 \cdot 6\text{H}_2\text{O}$) by precipitation with methanol [70]. In a process developed by the Mines de potasse d'Alsace, a solution containing 320 g/L MgCl_2 can be obtained together with solid potassium chloride by solution mining. The solution used to extract the carnallite from the deposit contains a flotation agent for potassium chloride (C_{12} – C_{20} fatty amines or their salts) and a gas-producing agent such as hydrogen peroxide. The potassium chloride floats and can be pumped out along with the MgCl_2 solution [71]. This production method appears promising, but it is not known whether large-scale development is planned.

Other Methods

Magnesium chloride can be produced from dolomite in combination with soda by the Solvay process. In the early part of World War II at a plant belonging to the Diamond Alkali Corporation in Painesville, Ohio, the dolomite was calcined in rotary furnaces, hydrated, and used to regenerate ammonia from the ammonium chloride solution produced in soda manufacture. Only the calcium hydroxide took part in the reaction. On treatment of the remaining solution with carbon dioxide, a magnesium chloride solution was obtained:



This process is, however, no longer used.

In the Mathison Alkali Works, the calcium chloride solution from the soda process was reacted with calcined dolomite while carbon dioxide was introduced. This process also produced a MgCl_2 solution but has been discontinued. Calcined magnesite or magnesium hydroxide can also be used in the soda process to produce a MgCl_2 solution.

Production of Magnesium Chloride Hydrates

Production of $\text{MgCl}_2 \cdot 6\text{H}_2\text{O}$ (Bischofite). In a process used by Kali und Salz AG, end bittern from potash production is treated in a single-stage vacuum evaporator to produce a ca. 42% MgCl_2 solution, and is further evaporated in pans with steam at 1.1 MPa. After neutralization with lime and removal of calcium sulfate, synthetic kieserite, and other impurities, the melt is fed onto rotating drum coolers or cooling bands to form a slab which is broken up and marketed. Alternatively, after the initial single-stage evaporation, the solution can be prilled in a prilling tower or spray dried in a fluidized bed [72].

A very pure MgCl_2 hydrate with 4–6 molecules of water can be prepared in 99.9% purity according to a patent of the VEB Kombinat Kali [73]. Carnallite is dehydrated at 180–200 °C and then cooled. The cooled salt is then treated with acetone in which the MgCl_2 dissolves. After removal of the undissolved salt, the hydrate is precipitated from the acetone solution by adding the correct amount of water [73].

In a patent of the Mines de potasse d'Alsace, MgCl_2 is precipitated from solution by addition of 10–25% 1,4-dioxane at room temperature. At lower temperatures the yield of MgCl_2 is increased. The MgCl_2 -dioxane complex separates as a voluminous precipitate that is easy to filter or centrifuge. It can be purified by washing with a little dioxane. The dioxane can be distilled off from the filtrate as an 80% azeotrope and can then be directly reused. The MgCl_2 hydrate can be obtained by washing with water. During drying the remaining diox-

ane (ca. 20–25% of the total) is evaporated off and can also be reused [74].

Production of $\text{MgCl}_2 \cdot (2-3)\text{H}_2\text{O}$. In a process used by Kali und Salz AG, a ca. 33% MgCl_2 solution is heated to 110–130 °C and sprayed into a fluidized bed of magnesium chloride granules at 130 °C. The heating gas is at 400–600 °C. The average residence time of the granules is ca. 30 min. Fines and pulverized oversize granules are recirculated to the fluidized bed. The final product has a water content of ca. 30% [72].

Production of Anhydrous Magnesium Chloride

The Nalco Chemical Company at its plant in Freeport, Texas, produces tetramethyl and tetraethyllead. The Grignard reagents needed as intermediates for the process require a very pure source of magnesium. This is produced by the electrolysis of pure, anhydrous magnesium chloride, for which the following process has been developed.

Ethylene glycol is added with stirring to a 30–35% MgCl_2 solution, the quantity added being sufficient to produce a 10–20% MgCl_2 solution. All the water, including water of crystallization, is then removed by vacuum distillation. The distillate contains < 50 ppm ethylene glycol, and the residual solution contains < 25 ppm water together with all the other salts. Gaseous ammonia is then bubbled through the solution under slight pressure. The mixture is cooled to remove the evolved heat; in practice the temperature is allowed to rise to ca. 70 °C. When the glycol is saturated with ammonia, the hexaammine compound $\text{MgCl}_2 \cdot 6\text{NH}_3$ is formed. Towards the end of the reaction, the mixture is cooled to 15–30 °C, the $\text{MgCl}_2 \cdot 6\text{NH}_3$ precipitates and is filtered off. Any adhering solution is removed by washing with methanol. The ammonia and methanol are then removed in two stages: the methanol and some ammonia are first driven off at 74 °C. The rest of the ammonia is then removed in a calcination furnace at 400 °C [75].

As with the dehydration of carnallite, ammonium carnallite can be dehydrated almost without decomposition at 90–180 °C. It can then be decomposed at 180–400 °C to give ammonium chloride and anhydrous MgCl_2 [76, 77].

In the process developed by Esso Research, a 20–50% solution of magnesium chloride reacts with ammonium chloride in a three-stage fluidized bed. Anhydrous magnesium chloride is produced at 350–550 °C [78].

In another process [79], ammonium carnallite containing $n \text{ NH}_3$ or $n \text{ H}_2\text{O}$ is decomposed at 800 °C. A product with a low magnesium oxide content is obtained. If the starting material contains water of crystallization, some is removed in a first stage, and further dehydration takes place after adding ammonia. After the dehydration, the $\text{MgCl}_2 \cdot 6\text{NH}_3$ is thermally decomposed [80].

A process for the dehydration of magnesium chloride hydrates in a hydrogen chloride atmosphere is described in Section 20.5.1.1.

Purification of Magnesium Chloride Solutions

Calcium ions can be removed from magnesium chloride solutions by adding the stoichiometric amount of sulfate ions [81]. Conversely, sulfate ions can be removed by adding calcium chloride solutions. Calcium and other metallic ions can be extracted with dialkylphosphoric acid in a water-immiscible solvent. This process is used in the production of pure sintered magnesia from solutions of impure magnesites in hydrochloric acid [82]. These solutions can be treated with substances such as MgO , CaO , or $\text{Mg}(\text{OH})_2$ to increase the pH, while simultaneously purging with air or oxygen at 80–90 °C. This removes impurities such as iron, aluminum, and manganese as hydrated oxides or hydroxides. This process is also used in the manufacture of pure sintered magnesia [83].

Materials of Construction for the Evaporation of Magnesium Chloride Solutions

At temperatures up to 110 °C, corrosion is usually prevented by the use of coatings, rubber linings, or plastic reinforced with glass fibers. Heater tubes and distillation trays are usually made of aluminum bronze (AlB_{5-7}) as used in the potash industry, with a composition of 4–8% Al, 89–96% Cu, and small amounts of Fe, Ni, Mn, As, Si, or Zn. Pumps are made of Ni-Resist D2.

Above 110 °C, and especially in the presence of chlorine and bromine (during debromination), glass and Teflon are suitable, with titanium being used for preheaters and pipework. According to [84] brick-lined steel vessels are used for evaporating MgCl_2 solutions and steam-heated tubes are made of Inconel alloy or stainless steel 347. Monel metal is also used for > 50% MgCl_2 solutions.

20.11.2.4 Environmental and Legal Aspects

Magnesium chloride is a constituent of seawater. In the EEC Regulations (May 4th, 1976) concerning disposal of hazardous substances in lakes and rivers, this substance is not mentioned. However, if large quantities are discharged into lakes or rivers, the concentration can be high enough to injure aquatic organisms and immediate dilution must be carried out. The WHO international standard for drinking water for magnesium is 30 mg/L Mg, or 125 mg/L if the sulfate concentration is < 250 mg/L and the chloride concentration is < 200 mg/L. In the EEC regulation 80/778 EWG the limit for drinking water is 50 mg/L Mg and 25 mg/L Cl^- . In the dehydration of magnesium chloride hydrates, hydrogen chloride occurs in the waste gases due to partial decomposition to magnesium oxide and the concentration must be kept below the permitted limit by use of gas purification equipment. The German TA Luft Regulations specify a maximum of 30 mg/m³ HCl in air. Limits in

Australia are 200–400, in the United Kingdom 150, and in Japan 80–700 mg/m³.

20.11.2.5 Quality Specifications and Analysis

Quality Specifications. Magnesium chloride is available commercially in the form of solutions or solid hydrates. Solutions usually have a MgCl_2 content of 32–33%. A typical solution with a MgCl_2 content of 32–33% has the following approximate composition (in grams per liter):

MgCl_2	430–440
MgSO_4	12–25
KCl	2–3
NaCl	4–6
H_2O	ca. 870

For many applications, however, solutions produced by decomposition of carnallite are used directly; due to transport costs this only applies when the user is close to the supplier.

The most important hydrate sold commercially is the hexahydrate (bischofite) which contains 43–47% MgCl_2 , ca. 51.5% water, ca. 2% alkali-metal chlorides, and, depending on its origin, some MgSO_4 , CaSO_4 , or CaCl_2 . It is supplied in the form of broken pieces or flakes, or as blocks produced by melting and pouring into drums. Another hydrate in granular form contains ca 2–3 mol of water per mole of MgCl_2 and corresponds to 67% MgCl_2 . Anhydrous magnesium chloride is mostly used directly by the producer for electrolytic magnesium production.

Analysis. For quality control the MgCl_2 solutions and the solid hydrates must be analyzed for the following ions Mg^{2+} , Ca^{2+} , K^+ , Na^+ , Cl^- , SO_4^{2-} , and Br^- . In special cases, determination of boron, iron, and other ions may be required.

Magnesium and calcium are titrated complexometrically with ethylenediaminetetraacetic acid (EDTA) [85, 86]. Potassium and sodium are determined by flame photometry [87, 88]. For the determination of sulfate ions, a titration with barium perchlorate solution in a 2-propanol water mixture is carried out with thorin as the indicator [89]. Bromide is deter-

mined gravimetrically by the method of D'ANS and HÖFER [90].

The water content of the hydrates is determined by heating to 450–600 °C or by the lead oxide method [91]. Boron can be determined photometrically with azomethine-H or dianthrimide-1-amine [92, 93] and iron with bathophenanthroline (4,7-diphenyl-1,10-phenanthroline) [94]. Iron can also be determined by atomic absorption spectrophotometry [95].

20.11.2.6 Transportation and Storage

Magnesium chloride solutions can be transported in tank wagons. Owing to their corrosive properties, they should be stored in plastic containers reinforced with glass fiber, but iron vessels can also be used. When a 32–33% MgCl_2 solution is cooled, MgCl_2 hydrates precipitate, gradually forming a sludge. At –33.6 °C the residual solution containing 21.4% MgCl_2 freezes as a eutectic mixture. The hexahydrate is transported in polyethylene sacks or “Big Bags” capable of holding > 50 kg. It is also supplied in the form of broken pieces or solid blocks produced by pouring molten salt in single-journey steel drums. Sealed vessels can be stored almost indefinitely, but, after opening, the material must be used immediately because of its hygroscopicity. All containers must be stored under dry conditions.

20.11.2.7 Uses

Anhydrous magnesium chloride is used chiefly for the electrolytic production of magnesium metal. Large quantities of magnesium chloride solutions are used to produce anhydrous magnesium chloride for this purpose.

An important area of application for the hexahydrate and the hydrate containing 67% MgCl_2 is in the production of Sorel cement. This is made by mixing magnesium oxide with MgCl_2 solutions, and is mainly used as a binder for industrial floorings on account of its high elasticity and bending tensile strength

properties [96]. This binder is also used in the manufacture of abrasive materials and grindstones, and for cementing rock faces during coal mining operations [97]. In combination with wood chippings, it can be used to make lightweight building slabs. Sorel cement mixtures are also used in water- and fire-resistant building materials [98]. They also serve as a binder for granulated fertilizers and in the production of salt licks for animals, where the magnesium also acts as a feed additive, preventing diseases such as grass tetany in cattle that are caused by magnesium deficiency [99].

Another application for MgCl_2 solutions and the hexahydrate is the manufacture of sintered magnesia. A high proportion of the solutions produced in Germany and Israel are used for this purpose. The brines obtained by solution mining in the Netherlands are also used to make sintered magnesia. Magnesium chloride hexahydrate and potassium chloride are used to produce artificial carnallite which is used as a covering flux in the melting of light metal alloys. In the Quentin process used in the sugar industry, the alkali-metal ions in the dilute sugar syrup are replaced by magnesium ions by treating it with an anion-exchange resin, thus reducing sugar losses in the molasses by improving sugar crystallization [100]. The resin is regenerated by adding MgCl_2 solution. In the mineral oil industry, MgCl_2 solutions are used for the drilling fluid in rocks with a high salt content. The low freezing point of the 21% MgCl_2 solution ($< -30^\circ\text{C}$) is utilized to prevent wet bulk materials from freezing to a solid mass, as a de-icing agent in winter, as a ballast liquid for the tires of construction machinery and agricultural vehicles, for fire extinguishing foams at low temperatures, and as brine for refrigeration. It is also used as a heat storage medium in solar heating installations, as an additive in the steel industry, as a coagulant in wastewater treatment, and in the treatment of combustion gases (MgCl_2 solution absorbs HCl and improves the removal of SO_2 by limestone). In the plastics industry it is used in the manufacture of polymerization catalysts. Addition of MgCl_2 also reduces losses of ammonia that is used as a fertilizer [101].

20.11.2.8 Economic Aspects

The total worldwide production of MgCl_2 in 1988 was 1.3×10^6 t. In the world export markets ca. 300 000 t MgCl_2 was handled: ca. 200 000 t in the form of 33% MgCl_2 solutions, and 100 000 t in the form of the hexahydrate. About half of the MgCl_2 solution was used for production of magnesium metal. In addition, approximately 180 000 t MgCl_2 from solution mining brines and 150 000 t MgCl_2 as 33% solution were converted to magnesium oxide; these quantities were reported as material produced but not marketed. A further ca. 700 000 t magnesium chloride was not recorded in any statistics because it was used solely as an intermediate for the production of magnesium by electrolysis.

The most important countries for the production of MgCl_2 solutions and the hexahydrate are given below (excluding magnesium metal producers):

Germany (Kali und Salz AG and VEB Kali)	by-product solutions from the potash industry
Israel	Dead Sea brines
Netherlands	solution mining brines
Japan	sea bitterns from salt production
France	sea bitterns
United States	Great Salt Lake brines
Italy	sea bitterns
China	brines from various salt lakes

Two thirds of the material appearing on the market originates from Germany.

20.11.2.9 Toxicology and Occupational Health

The handling of MgCl_2 hydrates, anhydrous MgCl_2 , or MgCl_2 solutions on a laboratory scale does not present any personal hazards. German chemical regulations do not require any special marking. The LD_{50} (rat, oral) for $\text{MgCl}_2 \cdot 6\text{H}_2\text{O}$ is 8100 mg/kg. Eye protection and rubber gloves should be worn for handling anhydrous MgCl_2 , MgCl_2 hydrates, or solutions. Prolonged contact with concentrated (ca. 35%) solutions or with MgCl_2 dust can cause skin irritation, and possibly allergic skin reactions. In the event of skin problems, the affected area should be

washed with copious amounts of soap and water, followed by treatment with a fat-containing skin cream. In case of contact with the eye, the eye should be washed with water and medical assistance should be obtained.

20.11.3 Magnesium Oxide and Hydroxide [102]

Magnesium oxide seldom occurs as a natural mineral; it is found in contact metamorphic limestone and dolomite, in volcanic ejecta, and in serpentine rocks. It does not form rocks or salt deposits because it is converted to magnesium hydroxide by the water vapor in the atmosphere. The primary sources of industrially produced magnesia are natural magnesite (MgCO_3), seawater, and natural and synthetic brines. Magnesium hydroxide is formed as an intermediate in the production of magnesia from seawater and brines. Magnesia is used in technical applications on account of its high melting point, chemical resistance, high thermal conductivity, low electrical conductivity, and biological activity.

Technical-grade magnesia is mainly sintered to form sintered magnesia (also known as magnesia sinter, dead-burned magnesia, or sintered magnesite) which is used primarily as a refractory material and in the steel industry. Large quantities of calcined (decarbonated) material known as caustic magnesia or caustic-calcined magnesia, are produced for use in agriculture and the building industry. Fused magnesia is normally produced by melting caustic magnesia.

Magnesium hydroxide is produced by precipitation of seawater and brines with calcium hydroxide or by precipitation of soluble magnesium salts. Natural deposits are rare and are not currently being mined.

20.11.3.1 Properties

Magnesium oxide, MgO (magnesia, periclase [103]), is stable in an oxidizing atmosphere up

to ca. 2300°C and up to ca. 1700°C in a reducing atmosphere.

Crystal Structure. Magnesia forms colorless, green, or brown, cubic hexoctahedral crystals, space group $O_h^5 - Fm \bar{3}m$, ionic radius of Mg^{2+} 0.078 nm, $a = 0.421$ nm, $Z = 4$, cleavage parallel to $\{100\}$.

Physical Properties

mp	ca. 2800°C
Mohs hardness	5.5–6
Density	3.58 g/cm^3
Refractive index at 589 nm	1.736
Enthalpy of formation (298 K)	$-14\,900 \text{ kJ/kg}$
Specific heat c_p	
20–200 $^\circ\text{C}$	$1.0 \text{ kJ kg}^{-1} \text{K}^{-1}$
20–1000 $^\circ\text{C}$	1.2
Thermal conductivity	
pure crystals 300 $^\circ\text{C}$	$22 \text{ W m}^{-1} \text{K}^{-1}$
1000 $^\circ\text{C}$	7
technical-grade 300 $^\circ\text{C}$	12
1000 $^\circ\text{C}$	5
Linear thermal expansion coefficient	
room temperature	$6.7 \times 10^{-6} \text{ K}^{-1}$
1000 $^\circ\text{C}$	14×10^{-6}
1800 $^\circ\text{C}$	16×10^{-6}
Modulus of elasticity (sintered magnesia, bulk density 3.51 g/cm^3)	
25 $^\circ\text{C}$	$3 \times 10^4 \text{ MPa}$
1000 $^\circ\text{C}$	2.5×10^4
Dielectric constant (30 Hz–1 MHz)	11
Electrical resistivity	
room temperature	$1 \times 10^{14} \Omega \cdot \text{cm}$
500 $^\circ\text{C}$	1×10^{11}
1000 $^\circ\text{C}$	1×10^7
1300 $^\circ\text{C}$	1×10^3

Magnesium hydroxide, $\text{Mg}(\text{OH})_2$ (brucite), starts to decompose at 380°C .

Crystal Structure. Magnesium hydroxide forms ditrigonal scalenohedral crystals with a typical layer structure, space group $D_{3d}^3 - P \bar{3}m$, $a = 0.313$ nm, $c = 0.474$ nm, $Z = 1$, cleavage parallel to $\{0001\}$.

Physical Properties

Mohs hardness	2.5
Density	2.38 g/cm^3
Refractive index	$n_e 1.566, n_o 1.581$
Enthalpy of formation (298 K)	$-15\,800 \text{ kJ/kg}$
Dissociation energy (298 K)	$+570 \text{ kJ/kg}$
Hydration energy	-386 kJ/kg
Solubility in cold water	0.0009%

Toxicity. Magnesium oxide and hydroxide are not toxic. Precautions for handling dust must be observed when products with a small particle size are used.

20.11.3.2 Production of Magnesium Oxide

Caustic and sintered magnesia are generally obtained from magnesium carbonate or magnesium hydroxide. The production of the latter starting materials is described in the four next subsections. The burning and sintering processes are dealt with in the fifth subsection. The production, properties, and uses of fused magnesia are described in Section 20.11.3.5.

Production from Magnesite [104]

The production of magnesium oxide from magnesite began over 100 years ago in Austria, after the development of processes for the manufacture of steel from high-phosphorus pig iron in crucibles lined with sintered dolomite ($\text{CaO} \cdot \text{MgO}$).

Occurrence of Magnesite. Magnesite is produced from macro- and cryptocrystalline magnesite. Metamorphic *macrocrystalline magnesite* occurs in two Alpine mountain chains in varying degrees of purity. The rocks mainly consist of the isomorphous carbonate mineral (Mg,Fe) CO_3 (breunnerite), whose calcination results in the inclusion of 1–10% Fe_2O_3 in the periclase lattice. In addition, they contain small amounts of dolomite ($\text{CaCO}_3 \cdot \text{MgCO}_3$), calcite (CaCO_3), phyllosilicates (e.g., talc, mica, chlorites, or clay minerals), graphitic particles, and sometimes quartz. Similar magnesite deposits are exploited in Czechoslovakia, in the Pyrenees, in Ural (Satka), South Manchuria (Liaoning), East Brazil, and Canada, both by open-cast and underground mining. The macrocrystalline rocks are always subjected to some form of processing before calcination.

In contrast to the macrocrystalline magnesites, which form extensive or lenticular deposits, *cryptocrystalline magnesite* deposits are irregular and often veined. The rocks are mostly snow white, even if they are not com-

posed of high-purity MgCO_3 . They are regarded as being formed by the alteration of ultrabasic rocks (e.g., serpentines) through the action of water containing carbon dioxide. Deposits of this type occur in former Yugoslavia, Greece (Chalkidike and Euboa), Turkey, India, Nepal, and South Africa. They contain chalcedony (finely divided SiO_2), various magnesium silicates, and dolomite as accompanying minerals. The deposits are exploited mainly by open-cast mining, but also by underground mining.

Sedimentary deposits of cryptocrystalline magnesite have been identified in the last 20 years. They are often associated with deposits of hydromagnesite and huntite. The sedimentary deposits are formed in semi-arid basins associated with strongly weathered ultrabasic rocks. The material washed into the basin dissolved and then recrystallized on the basin rim, mostly in the form of porous concretions. A more recent formation of this type has been found in Southwest Turkey [105], while an older deposit has been reported in North Greece [106, 107]. A large deposit of this type was discovered in Australia (Kunwarara) in 1985. The Queensland magnesia project has been planned for the production of sintered and fused magnesia [108, 109].

Magnesite Beneficiation. The insufficient purity of the magnesite and the stringent specifications for the uniformity of sintered magnesia mean that beneficiation of the magnesite is usually necessary. The steps used in the beneficiation process depend on the ore being processed and the required carbonate purity.

The highest quality magnesites, particularly those for refractory applications, are needed for a magnesia product with a high MgO content, a $\text{CaO}:\text{SiO}_2$ mass ratio of 2–3, and low contents of Fe_2O_3 and Al_2O_3 . The presence of accompanying, low-melting minerals can adversely affect the properties of the sintered magnesia (Table 20.11).

Table 20.11: Minerals accompanying periclase in sintered magnesia.

Mineral	Formula	Abbreviation ^a	C:S ^b	mp, °C
Forsterite	$2\text{MgO} \cdot \text{SiO}_2$	M_2S	0	1890
Monticellite	$\text{CaO} \cdot \text{MgO} \cdot \text{SiO}_2$	CMS	0.94	1495
Merwinite	$3\text{CaO} \cdot \text{MgO} \cdot 2\text{SiO}_2$	C_3MS_2	1.40	1575 (decomp.)
Dicalcium silicate ^c	$2\text{CaO} \cdot \text{SiO}_2$	C_2S	1.87	2130
Tricalcium silicate	$3\text{CaO} \cdot \text{SiO}_2$	C_3S	> 1.87	1900 (decomp.)
Magnesioferrite	$\text{MgO} \cdot \text{Fe}_2\text{O}_3$	MF		1750
Dicalcium ferrite	$2\text{CaO} \cdot \text{Fe}_2\text{O}_3$	C_2F	> 1.87	1435

^a Abbreviations as used in the cement industry: M = MgO , C = CaO , S = SiO_2 , F = Fe_2O_3 .

^b Mass ratio of CaO to SiO_2 (dissolution of small amounts of CaO in the MgO is neglected).

^c Several modifications.

Preliminary sorting of the ore can be achieved by *selective mining*. The ore is then subjected to *selective coarse grinding* in impact crushers. The tailings can be separated from the ore by taking advantage of the difference in hardness; the ore is selectively crushed and removed by screening. Crushing is usually performed in several stages. The final particle size for calcination in shaft kilns is 20–200 mm, while a particle size of 2–60 mm is required for the more commonly used rotary kilns.

The difference in color between the cryptocrystalline magnesite ore and the tailings is usually so pronounced that sorting can be carried out by hand on a conveyor belt or with an automatic optical system.

The coarsely ground material is often washed and subjected to wet desliming to remove fine particles. Ore that is intended for direct caustic calcination is separated from fine material (often lamellar silicate particles) by screening.

When the magnesite is not intimately intergrown with its accompanying minerals, lump material for rotary kilns can be sorted by gravity separation. This is carried out in one or two stages in a dense-medium separator or cyclone to give particles of sizes of 10–40 or 4–60 mm respectively. Since the differences in density are small (magnesite 2.95–3.05, dolomite 2.90, calcite 2.70, lamellar silicates 2.5–2.95, quartz 2.65, graphite 2.1–2.2 g/cm³), separation depends on exact control of the density. Finely divided ferrosilicon is generally used as the dense medium; the impurities are removed as floats. The throughput in modern plants is 50–150 t/h.

If the degree of intergrowth of the magnesite with its accessories lies in the range 0.03–1 mm, separation can only be achieved after thorough grinding of the ore (particle size below ca. 0.2 mm) to expose the accompanying minerals. The currently most effective separation and enrichment process for this material is *flotation* which exploits the differing wettabilities of the various minerals. The process must be optimized for each deposit.

The magnesite is finely ground in rod or ball mills and should have as narrow a particle size distribution as possible (ca. 0.09 mm for coarsely crystalline magnesite). This is achieved by combining milling with gravity classification and classification cyclones. Flotation is usually preceded by desliming to remove the finest particles, which would otherwise cause problems in the flotation step.

The removal of talc, $\text{Mg}_3(\text{OH})_2\text{Si}_4\text{O}_{10}$, is straightforward. Upon mixing with air in the presence of weak collectors–frothers (e.g., pine oil and primary aliphatic fatty amines), the talc particles float to the surface on bubbles and are removed by skimming.

The main problem in flotation is the separation of magnesite from dolomite, calcite, and silicates other than talc. Separation is achieved by *direct magnesite flotation* which entails the use of nonspecific, anionic collecting agents (that also act as frothers) and selective depressing agents for dolomite, calcite, and silicates. The flotation cells have a capacity of 0.5–3 m³. The operational conditions in the flotation cells must be optimized (temperature, pH value, reagent dosing). In large-scale flotation plants, several series of cells are run in parallel. The typical throughput of a series

is 20 t/h of magnesite, corresponding to 60 m³ of suspension with a density of 1.25 g/cm³.

The magnesite concentrate is removed as a foam, then thickened, and brought to a residual water content of 8–12% in centrifuges or filters. The product is then briquetted and burned. The waste slurries from the desliming and flotation stages are treated in thickeners, filters, and settling basins.

An important sorting process for high-iron sintered magnesite is *magnetic separation*. The isomorphous inclusions of iron in the magnesite crystal cannot be removed by mechanical separation. After sintering and subsequent cooling, they are converted to magnetic magnesioferrite (MgO·Fe₂O₃), either in the periclase lattice or at its crystal boundaries (Figure 20.21B). Calcite and dolomite usually do not contain iron in the carbonate lattice; the calcination of large crystals gives large pieces of very pure, usually only lightly sintered, nonmagnetic CaO or CaO and MgO. These oxides can be separated, together with nonmagnetic silicates, from the sintered iron-rich magnesite in magnetic drum separators.

Recently developed magnets are reported to be able to remove pieces of sintered magnesite.

Table 20.12: Typical analyses of sintered magnesite.

Type of magnesite ^a	Composition, %						Bulk density ^b , g/cm ³	Theoretical density, g/cm ³
	MgO	CaO	SiO ₂	Fe ₂ O ₃	Al ₂ O ₃	B ₂ O ₃		
1	91.5	1.5	4.5	1.1	1.4	0.14	3.27	3.57
2	89.0	2.4	0.5	7.8	0.3		3.26	3.64
3	88.0	2.5	0.6	8.6	0.3	< 0.01	3.38	3.65
4	91.3	1.9	0.5	6.0	0.3	< 0.01	3.40	3.63
5	98.0	0.7	0.7	0.2	< 0.2	0.30	3.28	3.57
6	97.2	1.9	0.5	≤ 0.2	0.2	0.05	3.43	3.57
7	96.4	2.0	1.1	0.4	< 0.1	< 0.01	3.43	3.57
8	97.2	2.0	0.4	0.3	≤ 0.1	< 0.01	3.42	3.57
9	98.5	0.7	0.15	0.5	< 0.1	0.015	3.45	3.58
10	99.0	0.7	0.1	< 0.1	< 0.1	< 0.01	3.43	3.58

^a 1) Lump sintered magnesite with a high silicate (and iron) content.

^a 2) High-iron sintered magnesite produced from flotation concentrate.

^a 3, 4) Lump high-iron sintered magnesite.

^a 5) Sintered magnesite produced from seawater type 11 (C:S = 1:1).

^a 6) Sintered magnesite produced from seawater type 31 (C:S = 3:1).

^a 7) Lump low-iron sintered magnesite.

^a 8) Low-iron sintered magnesite with large crystals (LC) produced from flotation concentrate.

^a 9) Sintered magnesite produced from MgCl₂ brine.

^a 10) Sintered magnesite produced from pyrohydrolyzed MgCl₂.

^b According to DIN 51065, part 2.

sia with a somewhat higher iron content from low-iron sinter [108].

Table 20.12 lists typical analyses of sintered magnesite produced from natural magnesite (types 1–4, 7).

Production from Seawater [110, 111]

Few deposits of pure or easily accessible magnesite were known up to the mid-1980s. In the 1960s the increasing demand for sintered magnesite as a refractory lining material in the steel industry stimulated new developments in methods for production of magnesite from seawater. This method was first introduced on a small scale in 1865 on the French Mediterranean coast. Since the 1930s it has been employed on a large scale in the United States and England (Hartlepool).

The composition of seawater is given in Table 20.13 [112]. Calculations show that 470 m³ of seawater are required to produce 1 t of MgO, in practice 600 m³ are needed. The process is based on the precipitation of magnesium hydroxide (solubility in water 0.0009%) by addition of calcium hydroxide (solubility 0.185%):

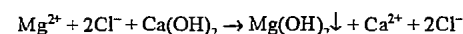


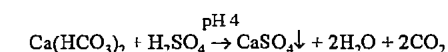
Table 20.13: Composition of seawater [112].

Cation	Concentration		Anion	Concentration	
	g/kg	mmol/kg		g/kg	mmol/kg
Sodium	10.47	455.0	chloride	18.97	535.1
Potassium	0.38	9.7	bromide	0.065	0.81
Magnesium	1.28	52.5	sulfate	2.65	27.6
Calcium	0.41	10.2	bicarbonate	0.14	2.35
Strontium	0.013	0.15	borate	0.027	0.44

Freshwater from rivers contaminated with suspended material must not flow into the seawater used for magnesite production. Furthermore, the seawater to be extracted should not be mixed with already extracted seawater, this requires a suitable topography and tidal currents that run parallel to the coast. A supply of freshwater (> 40 m³ per tonne MgO) is required to wash the Mg(OH)₂ and to produce the milk of lime. High-purity limestone or dolomite deposits should be available in the vicinity; they are calcined and slaked to provide Ca(OH)₂ as the precipitating agent and should therefore contain minimal quantities of elements that form insoluble carbonates, sulfates, etc. The MgCO₃ in dolomite is converted to Mg(OH)₂, and thus provides a further source of magnesite.

Production of Precipitating Agent. The limestone or dolomite is thoroughly washed, crushed, and calcined at > 1400 °C in a rotary or shaft kiln. The CaCO₃ must be completely decarbonated to CaO (< 0.2% CO₂), but should be lightly burned, and should contain minimal amounts of sulfur and other contaminants. In order to achieve rapid, complete reaction of the seawater, the calcined lime (quicklime) or dolomite (dolime) is ground, slaked to form Ca(OH)₂ and then converted into milk of lime or dolomitic slaked lime (containing ca. 20% solids).

The seawater is pumped to the plant and suspended material is removed. Seawater contains dissolved carbon dioxide and must therefore be treated with sulfuric acid to prevent the subsequent formation of insoluble calcium carbonate on addition of Ca(OH)₂:



The freshwater is also partially decarbonated.

To ensure maximum removal of carbon dioxide, the water is pumped through a trickling installation into the reactor containing the milk of lime. The water leaving the reactor is pumped back into the sea; it has a low magnesium content, a high calcium content, and a pH of 10.5. In modern plants using the overlime process (see below) the extracted water is first pumped into settling basins where the excess lime is diluted with fresh seawater to precipitate more Mg(OH)₂ and to lower the pH to more ecologically acceptable values.

Precipitation. The aqueous suspension of finely precipitated Mg(OH)₂ is seeded with larger Mg(OH)₂ crystals in large, flat settling tanks to convert it into a thick, dense slurry for filtering. The slurry is removed from the bottom of the tank and fed into tanks where it is washed with decarbonated seawater and decarbonated fresh water to remove most of the alkali metal, chloride, and other ions. The water content of the Mg(OH)₂ slurry is then reduced to < 50% by filtration (vacuum disk or drum filter). The product is used as a starting material for caustic and sintered magnesite.

Unless specially treated, caustic and sintered magnesite produced from seawater usually contain ca. 0.2% B₂O₃ and small amounts of CaO, SiO₂, Al₂O₃, and Fe₂O₃ derived from the limestone or wastes in the seawater. The contaminants and the CaO:SiO₂ (C:S) ratio have a pronounced effect on the behavior of the magnesite during sintering and in its subsequent applications. The C:S ratio is therefore adjusted to the desired value (3–4 or more for the high-quality sinters used in oxygen metallurgy). The B₂O₃ content of the magnesite is also generally lowered to ca. 0.05% by using a 5–12% excess of lime for precipitation (overliming); this increases the pH to 12 and minimizes the adsorption of boron. Addition of small quantities of Na₂CO₃ prior to sintering further decreases the B₂O₃ content to 0.03% due to the formation of volatile sodium borate during sintering. Prolonged sintering at the maximum temperature decreases the B₂O₃ content. Ion exchange can also be used to

lower the boron content of the seawater and thus of the sintered product.

Typical compositions of the two most common types of magnesia sinter derived from seawater are given in Table 20.12 (types 5 and 6).

Production from Brines

Precipitation of Magnesium Hydroxide. Large marine and terrestrial salt deposits were formed in various geological periods. Fossil mineral salt deposits have been mainly mined for their potassium salts: magnesium salts or magnesium brines are obtained as waste or as a by-product.

Magnesium salts are formed in arid areas by evaporation of brines in flat basins, their composition often differs from those obtained from seawater. Magnesia is obtained from magnesium (potassium) brines of varying origin:

- Synthetic brines produced during solution mining (e.g., Veendam, Netherlands)
- Spent liquors obtained in salt production from natural brines (e.g., Dead Sea potash production; Laguma de Rey, Mexico, sodium sulfate production)
- Spent liquors obtained in salt production from salt deposits (e.g., Teutschenthal, Germany)

In the Netherlands (Veendam Ost-Groningen), purified freshwater is forced into an anticline at a depth of 1500 m to dissolve the bischofite ($\text{MgCl}_2 \cdot 6\text{H}_2\text{O}$) and carnallite ($\text{KCl} \cdot \text{MgCl}_2 \cdot 6\text{H}_2\text{O}$) [113]. The brine is then pumped to the surface and contains 20% MgCl_2 and small amounts of alkali chlorides and MgSO_4 . After removal of the sulfate, the magnesium is precipitated as $\text{Mg}(\text{OH})_2$ with dolomitic slaked lime, thickened, and then sintered. The advantage of this deposit is that the bicarbonate and boron contents of the resulting brines are much lower than those of seawater and do not have to be removed by complex methods.

Pyrohydrolysis of Magnesium Chloride [114, 115]. In pyrohydrolysis, metal (M) ha-

lides (especially chlorides) are thermally decomposed in the presence of superheated steam at 300–1000 °C to give a pure, fine metal oxide precipitate:



Pyrohydrolysis was originally used to recover hydrochloric acid in the pickling of steel but it can also be employed for the large-scale production of metal oxides. Magnesium oxide is produced from natural or synthetic MgCl_2 brines. Complete hydrolysis of MgCl_2 by conventional methods is not possible because evaporation leads to precipitation of bischofite ($\text{MgCl}_2 \cdot 6\text{H}_2\text{O}$) which, on further heating, melts or dissolves in its own water of crystallization. Complete pyrohydrolysis of MgCl_2 is achieved in a spray reactor without hydrolysis of CaCl_2 and alkali chlorides (Aman process).

Table 20.14: Composition (in grams per liter) of brines used in the production of magnesia by the spray roasting method.

Component	Natural brine	Brine for pyrohydrolysis after KCl extraction
Mg^{2+}	41	102
Na^+	40	2
Ca^{2+}	17	9
K^+	7.5	2
Cl^-	215	319
Br^-	5	6
SO_4^{2-}	0.7	
Total	326	440
MgCl_2	163	400

The *Aman process* has been used since 1973 in an industrial plant with a current capacity of 70 000 t/a near the Dead Sea. The starting material for this process is the spent liquor (brine) obtained after extraction of KCl from a magnesium- and alkali-chloride-rich natural brine. The compositions of these brines are given in Table 20.14.

The brine is purified to remove bromide and traces of boron and then fed via steel pipes into the spray nozzles of the reactor. It is sprayed into the cylindrical, externally insulated reactor at ca. 600 t. The reactor is lined with refractories, it also has a conical base and tangentially positioned burners which ensure rotating circulation of the reactants. The exhaust gases leave the top of the reactor at

450 °C. The water evaporates from the atomized brine droplets leaving a perforated chloride crust which reacts with the steam to form MgO and HCl . The hollow spherical MgO agglomerates are removed from the bottom of the reactor via a gas lock, together with non-pyrolyzed, water-soluble potassium, sodium, and calcium salts.

The crude product is washed with water and hydrated in a stirred tank, and then concentrated in a thickener. The resulting slurry is difficult to filter and is washed and dewatered in a two-stage vacuum drum filter. The calcined product typically contains $\geq 99.5\%$ MgO , $< 1\%$ CaO , $\leq 0.05\%$ SiO_2 , $\leq 0.05\%$ Fe_2O_3 , $\leq 0.005\%$ Al_2O_3 , and $\leq 0.01\%$ B_2O_3 ; its specific surface area is 2–50 m^2/g , the loose bulk density ranges from 0.8 to 0.2 g/cm^3 .

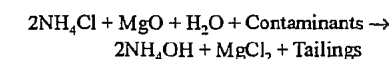
Most of the MgO dust in the hydrogen chloride exhaust gas is removed with a cyclone. The hot gas is then used to heat the fresh MgCl_2 solution in a wash recuperator where any remaining MgO dust is collected. The HCl gas is scrubbed with water in an absorption column. After removal of the combustion gases and steam, 20% hydrochloric acid is obtained which is used to dissolve local phosphate deposits; this makes the process economically viable.

Pyrohydrolysis of Magnesium-Containing Waste. The principle of the above method can also be used for the pyrohydrolysis of chloride solutions obtained from impure magnesium minerals such as magnesite, tailings, dust, asbestos, talc, and other magnesium silicate waste [116]. The hydrochloric acid by-product is recycled within the process (former Yugoslavia, Nepal, Austria, and Germany).

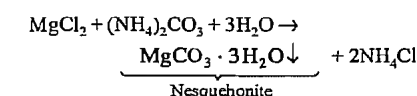
The magnesium is dissolved with hydrochloric acid in a two-stage process. Neutralizing agents (filter dust or crude MgO), oxidizing agents (air, chlorine gas), and sulfate ions are then added. Heavy-metal hydroxides, calcium sulfate, and other contaminants precipitate out and are filtered off to leave a MgCl_2 solution that is concentrated in a vacuum evaporator and sprayed into the reactor.

Miscellaneous Processes

Sulmag II Process [117]. The Sulmag II process was developed by Sulzer for producing light-burned caustic magnesia in a gas suspension kiln from low-magnesite ores. Dissolved magnesium chloride is obtained by selective extraction with recycled NH_4Cl solution:



After filtration and washing, needle-shaped crystals of nesquehonite are precipitated out in the reactor and filtered off:



Caustic magnesia with a high specific surface area is obtained by directly heating the nesquehonite with oil or gas and briquetting while still hot. The product is then sintered. This process is reported to produce significant energy savings and is environmentally favorable due to the almost complete recycling. A pilot plant has been in operation in Switzerland for several years and a plant designed to produce 30 000 t/a of sintered magnesia is under construction for Tamilnadu Magnesite in India.

Other Processes. Processes have been described in which dolomite is decarbonated to form a mixture of CaO and MgO and the CaO is then chemically extracted. Patents also describe the partial decarbonation of dolomite, slaking of the MgO , and recarbonation. The product consists of large nesquehonite crystals ($\text{MgCO}_3 \cdot 3\text{H}_2\text{O}$) which are separated from the microcrystalline CaCO_3 by flotation. The accessory calcite and dolomite can also be extracted from magnesite rocks because they are readily soluble in acid.

Magnesia can also be prepared from Epsom salt ($\text{MgSO}_4 \cdot 7\text{H}_2\text{O}$) or kieserite ($\text{MgSO}_4 \cdot \text{H}_2\text{O}$) but this technique is not used industrially at present.

MgO and CaO Production by Sintering of Dolomite. Complete decarbonation of dolo-

mite theoretically leaves a finely crystalline mixture of MgO (42%) and CaO (58%).

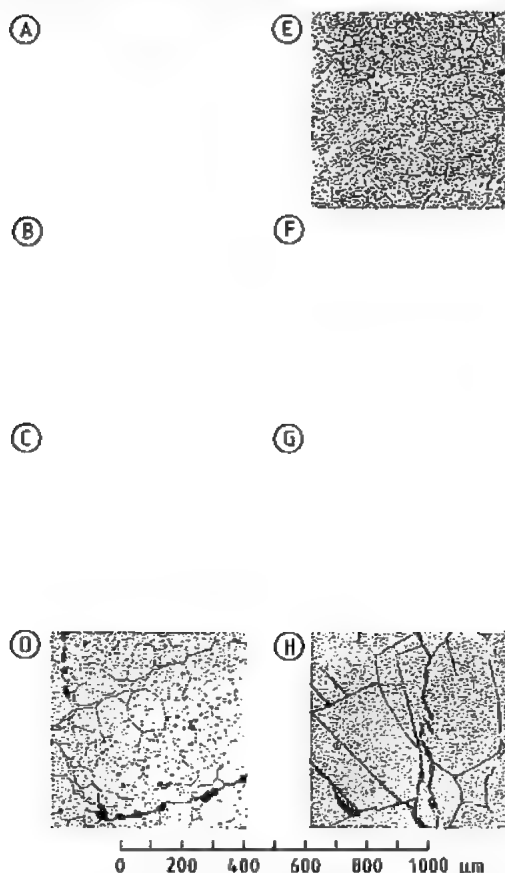


Figure 20.21: Polished sections of sintered dolomite (A), sintered magnesite (B-G), and fused magnesite (H). A) Sintered dolomite: white areas are MgO, gray areas CaO, and black areas pores; B) High-iron magnesite sintered in lumps: white domains are $2\text{CaO}\cdot\text{Fe}_2\text{O}_3$ and $\text{MgO}\cdot\text{Fe}_2\text{O}_3$, dark gray areas are pores that run parallel to the carbonate cleavage planes (type 4 in Table 20.12); C) Briquetted high-iron sintered magnesite with a high porosity (type 2 in Table 20.12); D) Low iron magnesite sintered in lumps (type 7 in Table 20.12); E) Seawater magnesite "31" (type 6 in Table 20.12); F) Sintered magnesite from brine (type 9 in Table 20.12); G) Low-iron C sintered magnesite (type 8 in Table 20.12); H) Fused magnesite with periclase cleavage planes.

Since large supplies of natural, high-purity dolomitic rocks are available, removal of contaminants by beneficiation is not economical. The high-purity lump dolomite is calcined, and sintered in a rotary or shaft kiln. In a spe-

cial procedure the dolomite is decarbonated, briquetted, and sintered at a lower temperature than the lump material to give a high-density product. The CaO and MgO crystals in sintered dolomite lie directly adjacent to one another (Figure 20.21A); despite the intense burning they are much smaller than those of sintered magnesite because they mutually hinder one another's crystal growth.

Calcination of Caustic and Sintered Magnesia

Caustic magnesia is a very reactive, finely crystalline material that is produced by calcining MgCO_3 or $\text{Mg}(\text{OH})_2$ slightly above the decomposition temperature. The decomposition curves for $\text{Mg}(\text{OH})_2$, MgCO_3 , and $\text{MgCO}_3\cdot 3\text{H}_2\text{O}$ are shown in Figure 20.22. Caustic magnesia may be the end product of magnesite production or may be further burned to give sintered magnesia.

Caustic magnesia is produced industrially by calcining lump MgCO_3 (up to 50 mm) or liner material at 600–1000 °C in shaft, rotary, or multiple-hearth (Herreshoff) kilns. Heat-exchange kilns are also employed. In the case of $\text{Mg}(\text{OH})_2$, dewatered filter cakes are usually calcined in lump form at ca 950 °C in multiple-hearth kilns. These kilns generally contain ten shelves (hearth), one above the other; each hearth is provided with four burners in the vertical cylindrical kiln wall. The material is fed continuously into the top of the kiln and its residence time can be adjusted via the rake that rotates above each hearth. The calcining conditions must be carefully adapted to the contaminants in the feed, otherwise overburning results in excessive growth of the reactive MgO crystallites which lowers their activity. In modern gas suspension furnaces, $\text{Mg}(\text{OH})_2$ or flotation concentrate can be converted into homogeneous caustic magnesia; energy consumption is low [118].

Caustic magnesia was formerly produced exclusively from cryptocrystalline magnesite with a low iron content but is now also obtained from all types of magnesite and $\text{Mg}(\text{OH})_2$. Its MgO content ranges from ca 65

to 99%, and may even reach 99.9%. The magnesia is often ground prior to use. Extremely reactive caustic magnesia may have a surface area of up to 160 m²/g.

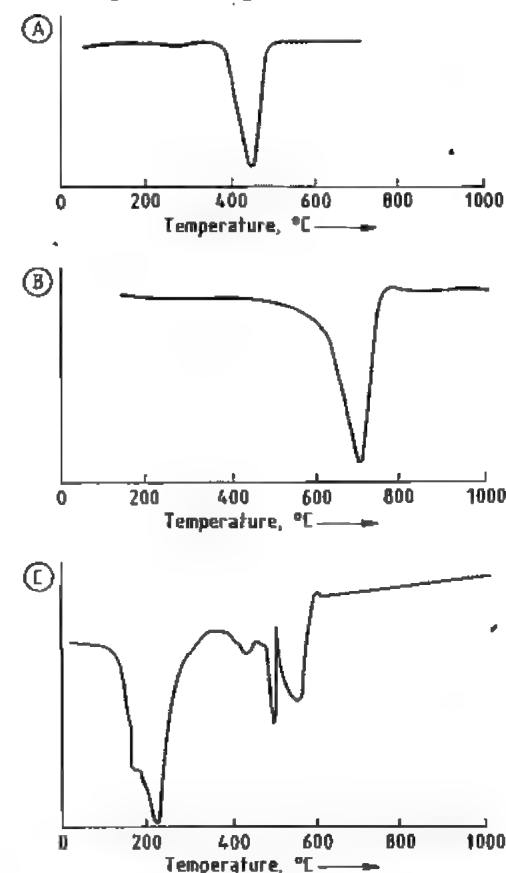


Figure 20.22: Differential thermal curves for $\text{Mg}(\text{OH})_2$ (A), MgCO_3 (B), and $\text{MgCO}_3\cdot 3\text{H}_2\text{O}$ (C) [133].

Depending on the calcining temperature, the product is termed *light burned* (870–1000 °C) or *hard burned* (1550–1650 °C). Light-burned caustic magnesia becomes hydrated in cold water and is soluble in dilute acid. It has a loose bulk density of 0.3–0.5 g/cm³ and a specific surface area (BET) of 10–65 m²/g. Hard-burned caustic magnesia has a loose bulk density of 1.2 g/cm³ (bulk density 2 g/cm³).

Sintered Magnesia. Most (ca. 85%) MgCO_3 and $\text{Mg}(\text{OH})_2$ is converted into sintered mag-

nesia (also known as magnesia clinker or dead-burned magnesia, Figure 20.21B–G). Typical analyses and densities of sintered magnesia are given in Table 20.12. Uses are described in Section 20.11.3.3. Sinter quality depends not only on chemical composition but also on the bulk density or porosity; a high density gives a better product. Sintering capability decreases considerably with increasing purity, making a high density difficult to achieve. In the early 1960s lump magnesite with a low iron content could not even be sintered to a density of 3.40 g/cm³ (porosity ca. 5 vol%). Although some briquetted, low-iron, C₂S-containing sinters have densities of up to 3.46 g/cm³ (porosity ca. 3.5 vol%), the density is usually in the range 3.35–3.40 g/cm³. The final bulk density of the sinter depends on chemical composition, sintering temperature and time, and the degree of compression of the material prior to sintering (briquetting is therefore used and not pelletizing or granulation). The material is usually sintered in lump form.

Caustic magnesia (preferably hot, 200–500 °C) is compressed into briquettes on high-pressure roller presses (pressure 4–15 t/cm²). The briquettes are then screened and dried or hardened. The screened fines are mixed with fresh caustic magnesia and briquetted.

Binding and adhesive agents are added to fine magnesite flotation concentrates prior to briquetting; magnesium sulfate solution, sulfuric acid, lignin sulfonates, and reactive MgO flue dust are usually used. Magnesite concentrates are also used to produce double-burned sinter. Here the concentrates are first calcined to reduce the mass and the resulting gas pressure; they are then briquetted and sintered.

In some cases dewatering of *magnesium hydroxide* slurries is so efficient (high-performance filter presses) that pieces of the hard filter cake can be fed directly into a rotary kiln. This saves a considerable amount of energy and the sintered magnesia product usually has a sufficiently high bulk density. In most modern plants, however, the hydroxide slurry is first calcined and then briquetted.

Shaft kilns are heated with coke, gas, or oil (with or without oxygen) and must be fed with

large pieces of material due to the pattern of gas circulation and movement of material within the shaft. Today, shaft furnaces can be better controlled than was the case a few years ago [119]. Smaller lumps (0.5–60 mm, product 0–30 mm) are used in rotary kilns to minimize abrasion and guarantee even movement of the material from the rotating kiln wall. Rotary kilns are generally oil- or gas-fired, sometimes with addition of coal dust or petroleum coke. Depending on the content of fluxing agents, sintering is performed at 1700 to > 2000 °C for 2–15 h (rotary kiln) or ca. 20 h (shaft kiln). The sinter from rotary kilns is generally homogeneous but has a smaller particle size and contains more dust than that from shaft kilns; this can lead to undesirable, round particles and an excess of fines during brick production. Cryptocrystalline magnesite with a low content of fluxing agents gives a sinter with a needle-like structure also after sintering in a rotary kiln.

Energy consumption for the burning of high-quality sintered magnesite from various starting materials depends on kiln design and the water content of the $\text{Mg}(\text{OH})_2$ slurry; typical values are as follows (MJ/kg MgO):

Magnesite: single-stage burning (magnesite → sinter)	4.5–12
Magnesite: double-stage burning (magnesite → caustic magnesite → sinter)	8–16
Seawater magnesite [$\text{Mg}(\text{OH})_2$ → caustic magnesite → sinter, value includes energy required for production of precipitation agent]	22–32
Sulmag II process	23
Magnesite produced by pyrohydrolysis	40

In an effort to improve sinter quality, manufacturers first turned their attention to increasing the size of the periclase crystallites by adding sinter-promoting agents, such as ZrO_2 . Burning conditions were subsequently modified. In larger crystallites the MgO is less easily reduced by carbon at high temperatures (e.g., in magnesite graphite bricks; see also Figure 20.21G).

Modification of Sinter Composition. In the case of concentrates, slurries, or caustic magnesite, the final composition of the sinter can be modified by mixing in small amounts of additives such as CaO , SiO_2 , and Fe_2O_3 prior to briquetting. Magnesite concentrates obtained

by flotation and fine $\text{Mg}(\text{OH})_2$ or MgO can also be mixed with large quantities of other fine substances (primarily chromium ores, calcined lime or dolomite), briquetted, and sintered to form coclinker. In refractory bricks made from pure sintered magnesite and low-silicate chromium ores, the chromium ore only becomes fully integrated with the periclase at high temperature (≥ 1700 °C) and in a suitable atmosphere. In briquettes made from magnesite and fine chromium ore, however, sintering results in complete dissolution of the mixed spinels of the ore in the periclase. On cooling, fine crystalline spinels or skeleton crystals precipitate in the periclase; some idiomorphic spinels ($\text{Mg,Fe}^{2+}\text{O}(\text{Cr,Fe}^{3+},\text{Al})_2\text{O}_3$) are evenly deposited between the periclase crystallites.

20.11.3.3 Uses

The use of magnesium oxide and hydroxide as intermediates in the production of magnesium metal is described elsewhere.

Use of Sintered Magnesite as a Refractory

Oxides are best suited as “vessel linings” for most industrial high-temperature processes. Magnesium oxide has the highest melting point of the moderately priced oxides and is therefore an important raw material for refractory bricks and other materials. It is the only material apart from ZrO_2 that can withstand long-term heating above 2000 °C. Refractory construction materials based on magnesite (with chromium ore or CaO) are also resistant to neutral and basic slags and gases.

The boom in the production of low-iron sintered magnesite occurred after it was discovered that the use of refractory magnesite linings in steelmaking vessels (open-hearth furnace, electric arc furnace, and basic oxygen furnaces) allowed phosphorus and sulfur to be removed in the basic slag.

Sintered magnesite is converted into fired bricks by techniques used for traditional ce-

ramics. It is first broken up, ground, and classified. Batches (1 to > 2 t) of individual fractions are mixed with a temporary aqueous binder (e.g., lignin sulfonates) and pressed into bricks of the desired shape weighing up to ca. 35 kg. After drying, the bricks are usually fired at 1500–1800 °C in a tunnel kiln. They have a final porosity of 12–20 vol%.

Bricks (especially those that are to be used in basic oxygen furnaces) may then be *impregnated with pitch* to prevent the slag from infiltrating them and dissolving their surface. Fired magnesite bricks have a high thermal expansion coefficient and a relatively low thermal shock resistance, especially during periodic operation. Fired bricks made from sintered magnesite and chromium ore (or alumina or spinel) are more resistant to thermal shock.

A large proportion of the magnesite bricks are not fired (i.e., do not form a ceramic bond) but are *bonded with pitch or resin*. The individual particle fractions are mixed with hot pitch, compressed into bricks, and tempered at 200–500 °C. When the bricks are used, a coke structure is formed which makes them more elastic than the ceramic-bonded bricks. Addition of 5–20% flake graphite increases heat transfer, lowers thermal expansion and attack by the slag, and improves thermal shock resistance. This development is applied in electric arc furnaces, converters, and metal ladles for secondary steelmaking processes. The low-oxygen atmosphere formed in these bricks during use can cause significant reduction of the magnesite. To prevent this, manufacturers have recently developed high-quality magnesite with larger periclase crystals and a low internal sinter surface area [120].

Chemically bonded bricks with chrome ore contain chemical bonding agents (e.g., Epsom salt, $\text{MgSO}_4 \cdot 7\text{H}_2\text{O}$) and are produced in the same way as fired magnesite bricks up until the drying stage. The bonding agents decompose and form a ceramic when the bricks are used at high temperature.

Pig iron mixers, transport vessels, and secondary refining ladles used in the steel industry are lined with magnesite bricks. Sliding

gates and nozzles are also made from sintered magnesite.

On account of their high refractoriness (refractoriness under load and low creep in compression), resistance to alkali, and high heat storage capacity, magnesite bricks are used in the crowns, port linings, and the hot parts of the checkerwork in glass-melting tanks. Magnesite chrome or magnesite spinel bricks are more suitable for the sintering zones of rotary cement kilns due to their good stress deformation behavior. Magnesite bricks are preferred for lime shaft kilns. Large quantities of sintered magnesite are used for unshaped repair materials.

The increased demands made on refractory materials as a result of higher operating temperatures and shorter tap to tap times in metallurgical furnaces and reactors can only be met by pure, high-density magnesite sinters. Small quantities of “contaminants” are disadvantageous if they form low-melting eutectics with MgO (e.g., with CMS at 1485 °C or with C_2F at 1200 °C, Table 20.11) because this leads to deterioration of mechanical properties (e.g., strength and volume stability) at high temperatures. High-quality sinters therefore have a low content of high-melting silicate phases (such as C_2S), a low B_2O_3 content, and a high degree of direct periclase–periclase contact (without intermediate silicate phases).

Use of Sintered Magnesite as a Heat-Storage Medium

Magnesite bricks have a high heat storage capacity (about 160% that of chamotte) and a high thermal conductivity [121]. They are used in efficient off-peak storage heaters. The heat generated by a heating element is transferred to the magnesite brick and increases its temperature.

The most suitable bricks are fired and have the following properties: a high bulk density (up to 3.10 g/cm³) and thus a high degree of sintering, a high thermal conductivity (up to 9 $\text{W m}^{-1}\text{K}^{-1}$ at 600 °C), and a high specific heat (1.1 $\text{kJ kg}^{-1}\text{K}^{-1}$ at 600 °C). The influence of

large pieces of material due to the pattern of gas circulation and movement of material within the shaft. Today, shaft furnaces can be better controlled than was the case a few years ago [119]. Smaller lumps (0.5–60 mm, product 0–30 mm) are used in rotary kilns to minimize abrasion and guarantee even movement of the material from the rotating kiln wall. Rotary kilns are generally oil- or gas-fired, sometimes with addition of coal dust or petroleum coke. Depending on the content of fluxing agents, sintering is performed at 1700 to > 2000 °C for 2–15 h (rotary kiln) or ca. 20 h (shaft kiln). The sinter from rotary kilns is generally homogeneous but has a smaller particle size and contains more dust than that from shaft kilns; this can lead to undesirable, round particles and an excess of fines during brick production. Cryptocrystalline magnesite with a low content of fluxing agents gives a sinter with a needle-like structure also after sintering in a rotary kiln.

Energy consumption for the burning of high-quality sintered magnesite from various starting materials depends on kiln design and the water content of the $\text{Mg}(\text{OH})_2$ slurry; typical values are as follows (MJ/kg MgO):

Magnesite: single-stage burning (magnesite \rightarrow sinter)	4.5–12
Magnesite: double-stage burning (magnesite \rightarrow caustic magnesite \rightarrow sinter)	8–16
Seawater magnesite [$\text{Mg}(\text{OH})_2 \rightarrow$ caustic magnesite \rightarrow sinter, value includes energy required for production of precipitation agent]	22–32
Sulmag II process	23
Magnesite produced by pyrohydrolysis	40

In an effort to improve sinter quality, manufacturers first turned their attention to increasing the size of the periclase crystallites by adding sinter-promoting agents, such as ZrO_2 . Burning conditions were subsequently modified. In larger crystallites the MgO is less easily reduced by carbon at high temperatures (e.g., in magnesite graphite bricks; see also Figure 20.21G).

Modification of Sinter Composition. In the case of concentrates, slurries, or caustic magnesite, the final composition of the sinter can be modified by mixing in small amounts of additives such as CaO , SiO_2 , and Fe_2O_3 prior to briquetting. Magnesite concentrates obtained

by flotation and fine $\text{Mg}(\text{OH})_2$ or MgO can also be mixed with large quantities of other fine substances (primarily chromium ores, calcined lime or dolomite), briquetted, and sintered to form coclinker. In refractory bricks made from pure sintered magnesite and low-silicate chromium ores, the chromium ore only becomes fully integrated with the periclase at high temperature (≥ 1700 °C) and in a suitable atmosphere. In briquettes made from magnesite and fine chromium ore, however, sintering results in complete dissolution of the mixed spinels of the ore in the periclase. On cooling, fine crystalline spinels or skeleton crystals precipitate in the periclase; some idiomorphic spinels ($\text{Mg,Fe}^{2+}\text{O}(\text{Cr,Fe}^{3+},\text{Al})_2\text{O}_3$) are evenly deposited between the periclase crystallites.

20.11.3.3 Uses

The use of magnesium oxide and hydroxide as intermediates in the production of magnesium metal is described elsewhere.

Use of Sintered Magnesite as a Refractory

Oxides are best suited as “vessel linings” for most industrial high-temperature processes. Magnesium oxide has the highest melting point of the moderately priced oxides and is therefore an important raw material for refractory bricks and other materials. It is the only material apart from ZrO_2 that can withstand long-term heating above 2000 °C. Refractory construction materials based on magnesite (with chromium ore or CaO) are also resistant to neutral and basic slags and gases.

The boom in the production of low-iron sintered magnesite occurred after it was discovered that the use of refractory magnesite linings in steelmaking vessels (open-hearth furnace, electric arc furnace, and basic oxygen furnaces) allowed phosphorus and sulfur to be removed in the basic slag.

Sintered magnesite is converted into fired bricks by techniques used for traditional ce-

ramics. It is first broken up, ground, and classified. Batches (1 to > 2 t) of individual fractions are mixed with a temporary aqueous binder (e.g., lignin sulfonates) and pressed into bricks of the desired shape weighing up to ca. 35 kg. After drying, the bricks are usually fired at 1500–1800 °C in a tunnel kiln. They have a final porosity of 12–20 vol%.

Bricks (especially those that are to be used in basic oxygen furnaces) may then be *impregnated with pitch* to prevent the slag from infiltrating them and dissolving their surface. Fired magnesite bricks have a high thermal expansion coefficient and a relatively low thermal shock resistance, especially during periodic operation. Fired bricks made from sintered magnesite and chromium ore (or alumina or spinel) are more resistant to thermal shock.

A large proportion of the magnesite bricks are not fired (i.e., do not form a ceramic bond) but are *bonded with pitch or resin*. The individual particle fractions are mixed with hot pitch, compressed into bricks, and tempered at 200–500 °C. When the bricks are used, a coke structure is formed which makes them more elastic than the ceramic-bonded bricks. Addition of 5–20% flake graphite increases heat transfer, lowers thermal expansion and attack by the slag, and improves thermal shock resistance. This development is applied in electric arc furnaces, converters, and metal ladles for secondary steelmaking processes. The low-oxygen atmosphere formed in these bricks during use can cause significant reduction of the magnesite. To prevent this, manufacturers have recently developed high-quality magnesite with larger periclase crystals and a low internal sinter surface area [120].

Chemically bonded bricks with chrome ore contain chemical bonding agents (e.g., Epsom salt, $\text{MgSO}_4 \cdot 7\text{H}_2\text{O}$) and are produced in the same way as fired magnesite bricks up until the drying stage. The bonding agents decompose and form a ceramic when the bricks are used at high temperature.

Pig iron mixers, transport vessels, and secondary refining ladles used in the steel industry are lined with magnesite bricks. Sliding

gates and nozzles are also made from sintered magnesite.

On account of their high refractoriness (refractoriness under load and low creep in compression), resistance to alkali, and high heat storage capacity, magnesite bricks are used in the crowns, port linings, and the hot parts of the checkerwork in glass-melting tanks. Magnesite chrome or magnesite spinel bricks are more suitable for the sintering zones of rotary cement kilns due to their good stress deformation behavior. Magnesite bricks are preferred for lime shaft kilns. Large quantities of sintered magnesite are used for unshaped repair materials.

The increased demands made on refractory materials as a result of higher operating temperatures and shorter tap to tap times in metallurgical furnaces and reactors can only be met by pure, high-density magnesite sinters. Small quantities of “contaminants” are disadvantageous if they form low-melting eutectics with MgO (e.g., with CMS at 1485 °C or with C_2F at 1200 °C, Table 20.11) because this leads to deterioration of mechanical properties (e.g., strength and volume stability) at high temperatures. High-quality sinters therefore have a low content of high-melting silicate phases (such as C_2S), a low B_2O_3 content, and a high degree of direct periclase–periclase contact (without intermediate silicate phases).

Use of Sintered Magnesite as a Heat-Storage Medium

Magnesite bricks have a high heat storage capacity (about 160% that of chamotte) and a high thermal conductivity [121]. They are used in efficient off-peak storage heaters. The heat generated by a heating element is transferred to the magnesite brick and increases its temperature.

The most suitable bricks are fired and have the following properties: a high bulk density (up to 3.10 g/cm³) and thus a high degree of sintering, a high thermal conductivity (up to 9 $\text{Wm}^{-1}\text{K}^{-1}$ at 600 °C), and a high specific heat (1.1 $\text{kJkg}^{-1}\text{K}^{-1}$ at 600 °C). The influence of

impurities on these factors is not as critical as in refractories.

The bulk density depends on the chemical composition, the sinter porosity and the method used to produce the bricks. Thermal conductivity is increased by a high periclase content and a low porosity. The specific heat is only slightly lowered by SiO_2 and Al_2O_3 , but is significantly lowered by CaO , Cr_2O_3 , and Fe_2O_3 . The bricks should not contain free CaO (risk of hydration) or crystal phases with different modifications.

Uses of Caustic Magnesia

Agriculture. In the 1970s and 1980s the use of caustic magnesia increased the most in fertilizers and animal feeds [122–125]. Magnesium is a constituent of plant-chlorophyll and also plays a role in enzyme activity. It is regarded as an essential plant nutrient and is used in fertilizers. Magnesium deficiency (symptoms: chlorosis, necrosis) became especially common after fertilizers containing a high percentage of potassium replaced potassium-magnesium fertilizers based on kainite ($\text{KCl} \cdot \text{MgSO}_4 \cdot 3\text{H}_2\text{O}$). In countries with salt deposits (e.g., Germany), magnesium is supplied in the form of kieserite, magnesia lime ($> 10\%$ MgO), and calcined dolomite. In all other countries (e.g., Netherlands, UK, USA), caustic magnesia (particle size 4 mm, $\geq 70\%$ MgO) and magnesite are used.

Ground caustic magnesia (particle size ≤ 2 mm, $\geq 85\%$ MgO) is used as a supplement for animal feeds. Magnesium is usually present in green fodder, but cattle and sheep feeding on fodder from slightly acid soils may suffer from "grass staggers" in spring which is caused by magnesium deficiency.

Building Industry. Caustic magnesia mixed with concentrated solutions of magnesium salts and a small amount of sodium phosphate becomes extremely hard and sets in air (e.g., with MgCl_2 solutions it forms $3\text{MgO} \cdot \text{MgCl}_2 \cdot 11\text{H}_2\text{O}$). However, the hardened material is not stable in water and is therefore not a true cement (which must set in air and water) but a

magnesia binder. These binders were originally referred to as Sorel cement or as stone-wood (xylolith) when mixed with sawdust as a filler. Since their high chloride content can corrode metals and other construction materials, magnesia binders must never be reinforced. They can be used as mastics or protective coatings at room temperature. Large quantities of caustic magnesia derived from carbonate are used for stonewood or plaster flooring in the Eastern Bloc. The low-iron caustic magnesia generally used for this purpose contains 75–87% MgO and is ground ($40\text{--}45\% < 10 \mu\text{m}$).

An important use of caustic magnesia is in *lightweight construction boards* (Heraklith) for thermal and acoustic insulation (thickness 5–100 μm). The boards are produced on fully automatic lines at ca. 60 °C from finely ground caustic magnesia (MgO content 65–80%, starting material magnesite containing silicates and dolomite), MgSO_4 solution as a binder, and impregnated pinewood chips. Mineral wool is also used as a filler. Subsequent hardening results in highly nonflammable boards which can be made fire-retardant and resistant to moisture and microorganisms by coating one side with plaster. The prefabricated boards are used to make formworks for concrete, and large quantities are used in combination with polystyrene in laminated boards.

Other Uses. Caustic magnesia containing ca. 70–99% MgO is used in wastewater treatment in prevention of corrosion, as a buffer, in preparative chemistry, and in the pharmaceutical industry.

Caustic magnesia can be used to remove heavy metals and silicate from wastewater. Ammonia can be precipitated and removed in the form of $\text{Mg} \cdot \text{NH}_4 \cdot \text{PO}_4 \cdot 6\text{H}_2\text{O}$ following addition of phosphoric acid and caustic magnesia [126]. The magnesium ammonium phosphate can be used as a fertilizer. This principle is also used to remove phosphate. Caustic magnesia is a mild base and neutralizes acids and acidic water, it also acts as a weak buffer.

Low-iron caustic magnesia is used as a filler in the plastics and rubber industries and

allows adjustment of viscosity and stiffness. It also acts as a chlorine acceptor in chlorinated hydrocarbon polymers and stabilizes them.

Large quantities of pure magnesium oxide are used in the chemical industry for the synthesis of magnesium compounds. Basic magnesium sulfonates and finely dispersed MgO are used as lubricant and motor fuel additives to neutralize combustion residues. Magnesium oxide in fuels binds sulfur and other compounds and prevents formation of acidic exhaust gases.

Large quantities of caustic magnesia are used in the paper and cellulose industries (magnesium bisulfite digestion). Caustic magnesia with graded particle size is also used as a polishing agent.

Caustic magnesia, magnesium carbonate (precipitated from caustic magnesia), and high-purity magnesia are utilized in preparative chemistry and cosmetics. In the pharmaceutical industry magnesium oxide ($\geq 98\%$ MgO) is used as an antacid, as a powder base, and for magnesium substitution therapy.

A potential use of caustic magnesia is as a slag additive to reduce the dissolution of MgO from refractory bricks in the steel industry. Treatment of the surface of grain-oriented steel transformer sheets decreases magnetic losses. A suspension of caustic magnesia is applied to the sheet and annealed.

Uses of Magnesium Hydroxide

The most important use of magnesium hydroxide is as an intermediate in the production of magnesia. In Japan it is used to replace polyhalogenated diphenyl ether as a flame retardant in thermoplasts processed at 200–350 °C. Hydrated alumina cannot be used at these temperatures because of its low decomposition temperature. This application is being tested in Germany [127]. Well-dispersed single $\text{Mg}(\text{OH})_2$ crystals seem to be more suitable than agglomerates.

Table 20.15: Production capacities for sintered and caustic magnesia in 1988/1989 (10^6 t/a) [108].

Country	Sintered magnesia		Caustic magnesia	
	Natural magnesite	Seawater and brines	Natural magnesite	Seawater and brines
EEC	0.6	0.5	0.3	0.1
Western Europe (not EEC) and Asia Minor	0.9	0.14	0.2	< 0.1
Eastern Bloc	2.8			
North and South America	0.4	0.7	0.2	> 0.1
Asia	2.0	0.6	0.3	< 0.1
Australia	« 0.1		« 0.1	
Africa	« 0.1		« 0.1	
World total	6.8	1.9	1.0	0.4

20.11.3.4 Economic Aspects

Developments in the production capacities, production, and consumption of magnesia can be briefly summarized as:

- 1974 World magnesia shortage [128]
- 1977 From shortage to surplus [129]
- 1981 Agricultural oversupply and industrial underdemand for caustic magnesia [123]
- 1982 Contraction of refractory magnesia and stagnation of caustic magnesia [130]
- 1984 China, the magnesite giant [131]
- 1987 The world magnesia industry, smaller but fitter and purer [132]
- 1989 Magnesia markets – fit for optimism [108]

These changes reflect the dependence of economics on the economic and technological developments in the steel industry. The discovery of highly pure magnesite deposits in Australia in 1985, which will allow magnesia to be obtained directly from the carbonate, has led not only to optimism for producers there, but also to concern among those using the energy-intensive process via magnesium hydroxide.

Recent developments are aimed at reducing energy consumption by improving the filterability of precipitated products, optimizing kiln design, and increasing the size of the periclase crystallites and the bulk density of sintered magnesia. The estimated production capacities for caustic and sintered magnesia are given in Table 20.15. The estimated production of crude magnesite ore increased from 16×10^6 t/a in 1981 to 20×10^6 t/a in 1988.

20.11.3.5 Fused Magnesium Oxide

Properties

Fused magnesia is crystalline magnesium oxide (*mp* 2800 °C) that has been melted in an electric arc. It has the same crystal structure as sodium chloride (i.e., face-centered cubic) and occurs naturally as periclase. No phase changes take place on heating up to the melting point.

Pure fused magnesia is white, although the presence of iron impurities impart a greenish color due to the presence of the mixed crystal compound magnesioferrite (Mg,Fe)O. When the pale green fused magnesia is heated in air, the color changes to brown owing to the formation of magnesioferrite (MgFe₂O₄) [134].

Fused magnesium oxide has a much lower tendency to undergo hydration than sintered magnesium oxide or caustic calcined magnesite [135], and is essentially stable towards the atmosphere. Thus, polished crystal faces of periclase only begin to lose their luster after several weeks, depending on atmospheric moisture content and temperature. Reaction with atmospheric carbon dioxide to form basic carbonates is also noticeable only after several weeks or months. Fused magnesia is stable in an oxidizing atmosphere up to ca 2200 °C, above which vaporization and partial dissociation take place. Theoretical vapor pressures of magnesium oxide and partial pressures of its dissociation products in the temperature range 1227–2727 °C are given in [136].

In a reducing atmosphere (e.g., in the presence of carbon), fused magnesia is stable only up to ca 1700 °C. This temperature is also the limit for vacuum use because of the resultant vapor pressure [137].

The most important physical properties of fused magnesia (e.g., thermal conductivity and electrical resistivity) depend on the density, purity, particle size distribution, type, and distribution of the foreign mineralogical phases present. Consequently, data obtained from measurements on single magnesium oxide crystals [138] or pure, polycrystalline magnesium oxide (> 99%) cannot be regarded

as characteristic of commercial fused magnesia.

The following data (see also Section 20.11.3.1) are therefore partly based on information from manufacturers of fused magnesia and include the grades most commonly available today (MgO content > 92%, particle size 0–400 µm):

Density of pure periclase (theoretical)	3.56–3.58 g/cm ³
Knoop hardness	370
Mohs hardness	6
Linear thermal expansion coefficient (1000 °C)	14 × 10 ⁻⁶ K ⁻¹
Specific heat (<i>c_p</i>)	
100 °C	0.96 kJ kg ⁻¹ K ⁻¹
1800 °C	1.21
Thermal conductivity (1000 °C) for densities of 3.0–3.58 g/cm ³	ca. 2.9–8.4 W m ⁻¹ K ⁻¹
Dielectric constant, ϵ (30 Hz–1 MHz)	11
Electrical resistivity (technical grades, manufacturers' data)	
600 °C	2 × 10 ⁹ –10 ¹¹ Ω·cm
800 °C	3 × 10 ⁸ –2 × 10 ⁹
1000 °C	10 ⁷ –9 × 10 ⁷
Electrical resistivity of MgO single crystals (for comparison)	
500 °C	2 × 10 ¹³ Ω·cm
1000 °C	6 × 10 ⁸

Production

Fused magnesia is mainly produced from naturally occurring magnesite (MgCO₃) that has been calcined at 1200–1400 °C ("dead burned"). The calcined product usually contains > 92% MgO, 1–4% SiO₂, 0.5–2% CaO, 0.1–2% Al₂O₃, up to 0.2% Fe₂O₃, and traces of ZrO₂, NiO, Na₂O, K₂O, B₂O₃, and S. Magnesite from seawater, containing > 97% MgO, is also used as a raw material.

When fused magnesia is used as an electrical insulator for heating applications (tubular elements), the amount of conductive impurities in the raw material must be minimal. Therefore magnesites that contain, for example, iron oxides or sulfur in appreciable amounts cannot be used. Contamination with sulfur is avoided by calcining the magnesite in wood-fired furnaces.

Fused magnesia is usually produced in a batch process by melting the raw material at 2800–3000 °C in electric arc furnaces [139].

The furnaces are heated by either single-phase or, more usually, three-phase a.c. current (Higgins furnace, block-making process). They have a moving base and a conical, water-cooled steel cover. The raw material is added batchwise and acts as a refractory lining for the furnace walls, and the furnace base is usually lined with magnesite bricks or a rammed graphitic material bonded with bitumen. The furnaces are heated by either two or three graphite electrodes. The arcs are struck onto a layer of coke and the electrodes can be vertically adjusted to suit the height of the molten bath.

The current in, for example, a 1000-kW a.c. electric arc furnace (Higgins furnace) is 6000–9000 A at 90–150 V. The electric power required to produce the fused blocks is ca. 2000–4000 kWh/t [139].

In addition to the traditional block-making process (Higgins furnace), tilting furnace technology is also used for the industrial production of fused magnesia [140]. The melting process is continuous, and the molten product is poured intermittently into water-cooled or refractory-lined molds. Manufacture of fused magnesia by an electric arc trough melting process [141] and in a high-frequency plasma [142] has also been described.

On completion of melting, the electrodes are withdrawn and, after a cooling period, the furnace cover is removed. The fused magnesia blocks can weigh as much as 20 t. After cooling to room temperature, preliminary size reduction is carried out. This is followed by further size reduction of the large broken pieces. The blocks are not homogeneous with respect to structure or chemical composition, and their surface is covered with a coating or crust of agglomerated sintered magnesia.

The impurities in the raw product consist of compounds formed from the quaternary system MgO–CaO–SiO₂–Fe₂O₃, e.g., magnesium silicates such as forsterite (2MgO·SiO₂, *mp* 1890 °C) and monticellite (CaO·MgO·SiO₂, *mp* 1500 °C, incongruent melting) whose melting points lie far below that of pure magnesium oxide. The foreign phases are mainly concentrated locally in the surface zone of the

fused block and constitute the "melt residues" along with imperfectly melted magnesium oxide (the sintered crust). They are hand separated from the fused product which is a white to pale green crystalline periclase with crystallite sizes from several hundred micrometers up to several centimeters. Hand sorting is the normal industrial method of impurity removal, no better method has yet been found. However, some of the silicate impurities associated with the raw material form inclusions of foreign phases in the crystals of the pulverized magnesium oxide end product. This is because the rate of growth of the magnesium oxide crystals in certain regions of the solidifying melt is greater than the migration rate of the melt residues. Thus, magnesium oxide blocks from a Higgins furnace contain foreign phases (monticellite and forsterite) deposited at the grain boundaries, while magnesium oxide produced by casting from a tilting furnace usually exhibits an intracrystalline distribution of these phases (Figure 20.23). Further treatment of the hand-sorted, size-reduced, fused product includes several size reductions with jaw crushers, roller crushers, and gyratory crushers. Iron particles produced by abrasion and other magnetic impurities are removed by high power magnetic separators. Finally, the finely grained material is classified into particle size ranges using a series of sieves. Fused magnesia intended for electrical heating applications is heated in an oxidizing, neutral, or reducing (although not carbon-forming) atmosphere at 1100–1400 °C [143] to remove moisture and carbon (originating from breakdown of the electrodes) and to reduce surface and lattice defects of the magnesium oxide particles.

Uses

Fused magnesia is mainly used as an *insulating material* in the electrical heating industry. The particulate material is packed into the space between the heating coil and the outer tube in a heating element for air or liquids [144]. Such elements are used in IR heaters, grill elements, tubular hot plates, and tubular

heating elements for ovens, storage heaters, radiators, continuous-flow heaters, washing machines, coffee machines, electric irons, and industrial liquid heating equipment.

by modifying the particle shape by treatment in a fluidized bed [145].

The electrical and thermal properties of fused magnesia can be improved by adding synthetic or natural minerals (e.g., pyrophyllites [146], fused zircon sand [147], enstatite [148], cordierite [149], or magnesium aluminum silicates [150]) to the prepared mixture of magnesia particles. The mechanism of action of these additives has not yet been explained.

The chemical composition of some of the industrial grades of fused magnesia (electrical grade) are given in Table 20.16. The important properties of the mixture of fused magnesia particles (as used for electrical heating, i.e., thermal conductivity, long life time, sinter index, specific electrical impedance, leakage current, tap density, flow rate, grain size distribution) are tested by standard methods (ASTM D2858, D2900, D3026, D3215, D3347; DIN 44872).

Fused magnesia has a further application as a *refractory material*, especially as a lining for induction furnaces and crucibles. Induction furnace linings based on fused magnesia do not shrink (unlike those based on sintered magnesia) owing to the low porosity of the fused material. Magnesia graphite bricks with an addition of fused magnesia [151] are used in ultrahigh-power furnaces for steel production. The low porosity of the fused magnesia and the size of the periclase crystals considerably improve the corrosion resistance of the refractory lining. The refractory-grade material has a lower SiO₂ content and a higher CaO:SiO₂ ratio than the electrical-grade fused magnesia (i.e., for electrical heating, see Table 20.16). In special applications, fused magnesia is also used as a molding material for precision casting, as a raw material for magnesium oxide ceramics and as single crystals [152] for optical windows and lenses.

Economic Aspects

The most important countries and companies producing fused magnesia are:

France	Pechiney Électrometallurgie
Germany	Höls AG

Table 20.16: Chemical composition (typical) of some commercially available fused magnesia grades.

Producer	Grade	MgO, %	SiO ₂ , %	CaO, %	Fe ₂ O ₃ , %	CaO:SiO ₂ ratio	Density, g/cm ³
Pechiney, France	Ca 250 ^a	95.5 (min.)	2.2	1.5	0.008	0.68	2.39 ^b
Höls, Germany	Dynatherm ^a 1246 CS	96.3	2.0	1.5	0.10 (max.)	0.75	2.36–2.40 ^b
Thermal Syndicate, UK	Maglox ^a 1GNI	96.8	2.3	0.8	0.10	0.35	2.35–2.40 ^b
Universal Abrasives, UK	M 70 ^a	93.1	3.7	1.6	0.16	0.43	2.36–2.40 ^b
Muscle Shoals Minerals, USA	22SR ^a	96.0	3.1	0.8	0.07	0.26	2.38–2.41 ^b
Pechiney, France	UR1 AT ^a	98.0	0.5	1.1	0.15	2.2	2.50 ^d
Baymag, Canada	Electromag ^a	96.7	0.2	2.2	0.5	11	3.50 ^d
Tateho, Japan	KMA ^a	98.5	0.35	0.9	0.15	2.6	3.57 ^d

^aElectrical grades for high-duty tubular heating elements.

^bTap density according to ASTM D3347, grain size 40–325 mesh.

^cRefractory grades.

^dApparent density.

United Kingdom	Universal Abrasives, Thermal Syndicate
Austria	Österreichisch Amerikanische Magnesit AG (refractory grades)
United States	Muscle Shoals Minerals, Tateho America (formerly CE-Minerals), Insultherm
Canada	Baymag (refractory grades)
Japan	Tateho Chemical Ind.

Further information on these manufacturers (e.g., production capacities) is given in [153].

The world consumption of fused magnesia for electrical heating (electrical grade) is estimated to be ca. 35 000–40 000 t/a. There are no figures available for refractory grade material because the grades of fused magnesia are not listed separately in the statistics.

20.11.4 Magnesium Sulfate

Magnesium sulfate does not occur in nature in anhydrous form. It is found in the form of hydrates and double salts in salt and potash deposits (e.g., in the United States, Germany, and the former Soviet Union). Magnesium sulfate also occurs in dissolved form in salt lakes.

20.11.4.1 Properties

The transformation temperatures of the stable magnesium sulfate hydrates and their solubilities in water are given in Table 20.17. Table 20.18 lists the molecular masses, the specific heats, refractive indices, and crystal classes of the anhydrous salt and some of the hydrates [154, 155]. Anhydrous magnesium sulfate can be obtained without decomposition

by dehydrating the hydrates at 400–500 °C. At 700 °C, however, the compound decomposes to give magnesium oxide, sulfur dioxide, and oxygen. This accounts for the fact that the melting point of magnesium sulfate cannot be accurately determined, it is between 1120 and 1150 °C.

Table 20.17: Stable magnesium sulfate hydrates.

Hydrates	Transformation temperature, °C	Solubility, g MgSO ₄ /100 g H ₂ O
Ice–MgSO ₄ ·12H ₂ O	–3.9	22.0
MgSO ₄ ·12H ₂ O–MgSO ₄ ·7H ₂ O	1.8	27.2
MgSO ₄ ·7H ₂ O–MgSO ₄ ·6H ₂ O	48.1	49.5
MgSO ₄ ·6H ₂ O–MgSO ₄ ·H ₂ O	67.5	56.6

Table 20.18: Properties of magnesium sulfate and its hydrates.

Compound	Specific heat, kJ kg ^{–1} K ^{–1}	Density, g/cm ³	Crystal class	Refractive index
MgSO ₄	0.800	2.66	orthorhombic	
MgSO ₄ ·H ₂ O	1.047	2.57	monoclinic	1.523, 1.535, 1.586
MgSO ₄ ·2H ₂ O	1.124			
MgSO ₄ ·4H ₂ O	1.305	2.01	monoclinic	1.490, 1.491, 1.497
MgSO ₄ ·6H ₂ O	1.525	1.75		1.456, 1.453, 1.426
MgSO ₄ ·7H ₂ O	1.546	1.68	orthorhombic	1.432, 4.4554, 1.4609

Magnesium sulfate is hygroscopic and absorbs water to form hydrates, finally the heptahydrate. Various hydrates can be obtained by

A ↑ 100 μm
B ↓ 40 μm

Figure 20.23: Photomicrograph of polished sections of fused magnesia (dark areas: MgO; light areas: foreign phases monticellite and forsterite). A) Magnesia produced in a Higgins furnace: foreign phases deposited at the grain boundaries; B) Magnesia produced by casting in a tilting furnace: foreign phases occur mainly as intracrystalline material.

The most important factor in this application of fused magnesia is its combination of high electrical resistance with high thermal conductivity. This is superior to that of other refractory oxides or other materials.

The grade of magnesium oxide recommended depends on the application for which the heating element is used (surface temperature of the tube) and the electrical insulation requirements. The grades usually have a size range of 0–400 μm and a tap density of 2.2–2.7 g/cm³. The product must have well-defined flow properties, which can be influenced

stepwise dehydration of higher hydrates or by crystallization from aqueous solution. Hydrates of analogous composition can be produced by these two methods, but X-ray crystallography shows that their structures differ due to destruction of the crystal lattice during dehydration.

Five stable hydrates can be crystallized from aqueous solutions: $\text{MgSO}_4 \cdot 12\text{H}_2\text{O}$, $\text{MgSO}_4 \cdot 7\text{H}_2\text{O}$ (Epsom salt, epsomite, Bittersalz), $\text{MgSO}_4 \cdot 6\text{H}_2\text{O}$ (hexahydrate), $\text{MgSO}_4 \cdot \frac{5}{4}\text{H}_2\text{O}$ ($\frac{5}{4}$ hydrate or synthetic kieserite) and $\text{MgSO}_4 \cdot \text{H}_2\text{O}$ (kieserite). Three metastable forms also occur: a second form of the heptahydrate, $\text{MgSO}_4 \cdot 5\text{H}_2\text{O}$ (allenite), and $\text{MgSO}_4 \cdot 4\text{H}_2\text{O}$ (leonardite). Stepwise dehydration yields hydrates with 1, $\frac{3}{4}$, 2, 3, 4, and 6 molecules of water. The solubility of kieserite decreases with increasing temperature due to its negative heat of dissolution. Its dissolution rate increases with increasing temperature and decreasing pH.

The acid sulfates $\text{MgSO}_4 \cdot \text{H}_2\text{SO}_4$ and $\text{MgSO}_4 \cdot 3\text{H}_2\text{SO}_4$ crystallize when MgSO_4 is dissolved in sulfuric acid. Magnesium sulfate-ammine hydrates ($\text{MgSO}_4 \cdot 3\text{NH}_3 \cdot 3\text{H}_2\text{O}$, $\text{MgSO}_4 \cdot 2\text{NH}_3 \cdot 4\text{H}_2\text{O}$, and $\text{MgSO}_4 \cdot 2\text{NH}_3 \cdot 2\text{H}_2\text{O}$) are produced when Epsom salt reacts with gaseous ammonia. On reaction with alkali, magnesium hydroxide precipitates out; a precipitate of nesquehonite ($\text{MgCO}_3 \cdot 3\text{H}_2\text{O}$) is formed with sodium carbonate. After addition of sulfite, phosphate, or stearate solutions, insoluble magnesium sulfite, magnesium phosphate, or magnesium stearate precipitates out. Magnesium chloride reacts with magnesium oxide to form oxychlorides, magnesium sulfate reacts in the same way to form oxysulfates ($\text{MgSO}_4 \cdot 3\text{MgO} \cdot 11\text{H}_2\text{O}$ and $\text{MgSO}_4 \cdot 5\text{MgO} \cdot 8\text{H}_2\text{O}$): it can therefore be used as a slower type of sulfate Sorel cement binder. Magnesium sulfate forms double salts with other salts, most of which also occur in nature:

$\text{KCl} \cdot \text{MgSO}_4 \cdot 3\text{H}_2\text{O}$ kainite

$\text{K}_2\text{SO}_4 \cdot 2\text{MgSO}_4$ langbeinite

$\text{K}_2\text{SO}_4 \cdot \text{MgSO}_4 \cdot 4\text{H}_2\text{O}$ leonite

$\text{K}_2\text{SO}_4 \cdot \text{MgSO}_4 \cdot 6\text{H}_2\text{O}$ schönite (picromerite)

$\text{Na}_2\text{SO}_4 \cdot \text{MgSO}_4 \cdot 4\text{H}_2\text{O}$ astrakanite (bloedite)

$6\text{Na}_2\text{SO}_4 \cdot 7\text{MgSO}_4 \cdot 15\text{H}_2\text{O}$ loeweite

$\text{K}_2\text{SO}_4 \cdot \text{MgSO}_4 \cdot 2\text{CaSO}_4 \cdot 2\text{H}_2\text{O}$ polyhalite

20.11.4.2 Occurrence and Raw Materials

The most important source of MgSO_4 in Germany is kieserite, which is a constituent of raw potash salt. In the United States, MgSO_4 is obtained from langbeinite and in Italy from kainite. The raw salts used by the potash industry in the former Soviet Union (Stebnik, Kalush) contain magnesium sulfate salts. Magnesium sulfate is also found in the brines of the Great Salt Lake and the Kara-Bogaz Gulf of the Caspian Sea. Seawater bitterns provide a further source (Epsom salt), the MgSO_4 is obtained by cooling. In many countries MgSO_4 is also produced from magnesite, dolomite, seawater magnesia, or other magnesium minerals.

20.11.4.3 Production

Production of Kieserite ($\text{MgSO}_4 \cdot \text{H}_2\text{O}$)

Production of Kieserite by Selective Dissolution of Residues from Potash Salt Production. The raw material for this process is a crude salt that contains kieserite (hard salt, carnallite). The sodium chloride is selectively dissolved from residues of potash salt production. The filtered or centrifuged residues obtained during the production of potassium chloride are first washed with a partially saturated NaCl solution from a subsequent washing step. The NaCl in the residues is readily soluble and dissolves in the NaCl solution until it becomes saturated; the kieserite, however, remains largely undissolved due to its slow dissolution rate. Kieserite and residual NaCl are separated from the washing medium with a bucket conveyor or elevator. The kieserite-NaCl mixture is then washed with water in a second stage to dissolve any residual NaCl. Washing is performed in pipes lined with fused basalt that are several hundred meters long. The quantity of NaCl solution

produced can be minimized by using the electrostatic production process (see below).

Ecological Aspects. The saturated NaCl solution contains 280–300 g NaCl per liter. Its disposal entails considerable ecological problems. Large quantities have been stored in jointed rock formations (platy dolomite) that are filled with slightly salted groundwater, but with only limited capacity [156].

Production of Kieserite by Flotation. Kieserite can be separated from rock salt by flotation. Prestaminol, oleic acid, fatty alcohol sulfates, or oxystearic acid are used as flotation agents for kieserite and anhydrite (CaSO_4) [157]. The kieserite can be further purified by separating it from the anhydrite and/or langbeinite. This is achieved by using oleic acid or a fatty acid amine as a flotation agent for the kieserite [158–160].

Electrostatic Separation of Kieserite. The electrostatic production process (ESTA process) developed by Kali und Salz AG (Germany) eliminates the formation of the large quantities of NaCl solution produced in the selective dissolution process (see above) [161, 162].

Kieserite can be electrostatically separated in one or two stages. In the one-stage process the raw salt is treated with aliphatic or a mixture of aliphatic and aromatic monocarboxylic acids that are combined with ammonium salts of aliphatic carboxylic acids, usually ammonium acetate. The salt is then heated at a defined relative humidity and electrostatically charged [163]. The kieserite becomes positively charged with respect to the potassium chloride and sodium chloride. Repeated separation of the kieserite deposited at the negative electrode yields MgSO_4 in an extremely pure, marketable form.

In the two-stage process rock salt is first separated and then the highly pure kieserite. The raw salt is first treated with aromatic monocarboxylic acids, heated at a defined relative humidity, and then charged [164]. The rock salt becomes positively charged with respect to the potassium chloride and the

kieserite. The rock salt is removed and the KCl-kieserite mixture separated at the positive electrode. The mixture is treated with aliphatic monocarboxylic acids, heated once again at a defined relative humidity, and charged [163]. The kieserite now becomes positive with respect to the potassium chloride. Repeated separation of the kieserite deposited at the negative electrode gives an extremely pure, marketable product.

The potassium chloride fraction is still contaminated with kieserite and sodium chloride; it is used for the production of potassium salts [165, 166].

Production of Granulated Kieserite. After addition of 3 parts of a solution containing preferably 18% Na_2SO_4 or 20% Na_3PO_4 to 47 parts of kieserite, the product can be pressed in a moist state and then ground [167]. After addition of ammonium sulfate and hot magnesium sulfate solution, kieserite can also be granulated with a dish granulator [168]. Mono-, di-, or polysaccharides (usually lactose) are highly suitable additives for preparing these rolled granulates. The kieserite should have a broad particle size range; at least 20% of the particles must be less than 0.09 mm in diameter [169]. Addition of phosphate allows production of a rolled granulate of high strength even without drying [170].

Production of Epsom Salt

Production of Epsom Salt from Kieserite. Kieserite is dissolved in hot water (90 °C) to give a clear solution. Dissolution is performed in single large vats with capacities of up to 500 m³ that have a sieve base covered with coconut mats. The process has the disadvantage that the throughput is very low and the sieve plate gradually becomes encrusted with anhydrite and double salts. Kali und Salz AG therefore uses a multichamber cascade with slow stirring; the slurry density in the chambers is 70%. Hot water is added from below and kieserite from above. The solution produced at the top of the cascade contains 400 g/L

MgSO₄. At the bottom the residue containing anhydrite can be removed at intervals [171].

The hot concentrated solution is cooled in multistage vacuum coolers in which large crystals of Epsom salt are formed. After thickening, the Epsom salt is either filtered or centrifuged. The moist salt is dried in drum driers with air at ca. 50 °C.

Production of Epsom Salt from Magnesite, Magnesite, and Other Materials. Magnesium sulfate solution can be produced by treating seawater magnesite (MgO) or magnesite (MgCO₃) with sulfuric acid. Waste sulfuric acid contaminated with organic compounds may be used [172]. The resulting solution is clarified, evaporated to a density of 1.35–1.36 kg/L, and processed as described above. The product can be spray dried at 150 °C. Dolomite, olivine, serpentine, or peridotite can also be reacted with sulfuric acid. Magnesium sulfate can also be obtained by adding MgO to pyrite during roasting and subsequent extraction [173].

Waste serpentine from asbestos production can be reacted with ammonium sulfate above 250 °C and the reaction mixture extracted with water [174, 175]. The resulting solution is evaporated and the Epsom salt crystallizes out.

Production of Epsom Salt from Seawater Bitterns or Salt Lakes Brines. Pure Epsom salt can be obtained directly from seawater bitterns and from brines from salt lakes with a high MgSO₄ content (e.g., Kara-Bogaz Bay) by diluting with water and cooling to –10 °C [176, 177].

Production of Epsom Salt from Langbeinite. Langbeinite (K₂SO₄·2MgSO₄) is decomposed by treating with water for 6 h at 50–60 °C to produce MgSO₄·6H₂O. On cooling the mother liquor to 20–35 °C the Epsom salt crystallizes out [178].

Production of Epsom Salt from Magnesite or Dolomite and Gypsum. A mixture of ground dolomite and gypsum is treated with steam at 1.5–3.0 MPa and filtered to remove

the CaCO₃ from the MgSO₄ solution [179]. Magnesite is calcined at 760–835 °C, hydrated in the presence of gypsum at 56–60 °C, and carbonized with carbon dioxide. The MgSO₄ solution is filtered to remove the CaCO₃ [180] and processed to obtain Epsom salt.

Production of Anhydrous Magnesium Sulfate

Anhydrous MgSO₄ does not occur in nature and can only be produced by dehydrating MgSO₄ hydrates. Kieserite is purified by removing anhydrite and langbeinite in a special electrostatic procedure. It is subsequently washed with water to remove residual chloride [181]; langbeinite and anhydrite may also be removed by flotation. It is then dehydrated by heating at ca. 500 °C in a gas-heated calcination drum and finally cooled [182]. If Epsom salt is used as starting material instead of kieserite, six molecules of water of crystallization can be removed at < 70 °C and the remaining molecule at 500 °C.

20.11.4.4 Quality Specifications and Analysis

Magnesium sulfate is sold as kieserite (73–83% MgSO₄), 99.9%-pure Epsom salt (48.8% MgSO₄), and anhydrous MgSO₄ (> 98% MgSO₄). Epsom salt is marketed as a chemically pure product, as a clinical product that complies with pharmacopeia specifications, and as an analytical grade reagent. Maximum contamination limits for clinical grades vary according to the pharmacopeia: chloride 100–300 mg/kg, iron 20 mg/kg, and heavy metals 10 mg/kg. Maximum limits for arsenic, selenium, and other substances may also be specified.

The analytical procedures used for quality control are the same as those employed for magnesium chloride. Sulfate, however, is determined by a gravimetric method [183].

20.11.4.5 Transportation and Storage

Depending on the atmospheric humidity, Epsom salt can lose or absorb water during storage and thus tends to harden. It is therefore preferably supplied in Clupack valve sacks. Kieserite is transported in railroad cars and trucks, both in bulk and in valve paper sacks. Anhydrous MgSO₄ is also supplied in bulk and in sacks.

20.11.4.6 Uses

Large quantities of kieserite and Epsom salt are used in Germany for the production of potassium sulfate. Kieserite is used in fertilizers, either as an additive in multinutrient fertilizers or directly to combat magnesium deficiency. In multinutrient fertilizers kieserite aids granulation and improves granulate properties. In cases of acute magnesium deficiency, Epsom salt is an especially effective foliar fertilizer.

Magnesium sulfate is a component of magnesium binders (Sorel cement) and can also be used as a binding agent in the production of magnesite bricks. Addition of MgSO₄ and Al₂(SO₄)₃ leads to the formation of spinels during firing of refractory products. Decomposition of MgSO₄ in refractory products at > 1100 °C results in the formation of sulfur dioxide and thus gives a light product. Magnesium sulfate is also used in the production of Portland cement from blast furnace slag and as an additive in gypsum-containing building materials.

Magnesium sulfate is employed in the sugar industry for refining the sugar liquor and for improving the sugar yield from molasses (Quentin procedure) [184]. It is utilized in fermentations for the production of amino acids, antibiotics, bakers' yeast, biomass, and citric acid. It increases the activity of glucose isomerase, the enzyme which converts glucose to fructose.

In the aluminum industry, a mixture of kieserite and calcium oxide or hydroxide is used to precipitate contaminants from alumi-

nate solutions. Magnesium sulfate is also employed in fixative baths used to color aluminum surfaces by means of anodic oxidation. It is a component of the electrolytic baths used for chrome plating, zinc plating, copper plating, nickel plating, and the electroplating of tungsten, manganese, vanadium, cobalt, and cobalt alloys. It is also used in the phosphating of iron.

In the glass industry, sinters with a defined porosity can be obtained by incorporating MgSO₄ of a defined particle size and then leaching it. Magnesium sulfate is used as an additive in enamels and pigments. In the detergent industry it prevents gel formation during spray drying; magnesium silicate synthesized from MgSO₄ stabilizes peroxides and thus improves bleaching. Magnesium sulfate is also used as a make-up chemical in the sulfite pulping process and as a stabilizer for cellulose during oxygen bleaching of pulp. In the paper industry it is used in the preparation of paper for coating and in the deinking of recycled printed paper.

Other uses include treatment of waste and wastewater and soil stabilization. The compound is also used as an additive in drilling fluids, lead acid batteries, oil and coal fuels, ore preparation, "electrolyte" beverages, low-NaCl salt mixtures, cosmetics, bath salts, infusions, photographic developers, dye baths, and animal feeds.

In the plastics industry MgSO₄ is employed as a coagulant, polymerization catalyst, stabilizer, and flame retardant. In the petrochemical industry it is employed together with manganese chloride for cracking petroleum. Use of MgSO₄ in the leather industry makes the leather more supple, increases its weight, and removes calcium carbonate. Magnesium sulfate is also used as a heat storage medium and as a raw material for the production of magnesium aluminate, magnesium aluminosilicate, and other magnesium compounds. One of the important applications of Epsom salt is as a laxative.

20.11.4.7 Economic Aspects

Epsom salt is produced in many countries, the most important being Germany, Japan, and the United States. It is usually consumed in the country in which it is produced. Only Germany and China export the compound. Other commercially available products are kieserite, anhydrous MgSO_4 , and fertilizers containing kieserite (Germany) and langbeinite (USA). Estimated production figures are given in Table 20.19.

20.11.4.8 Toxicology and Occupational Health

Magnesium sulfate and its hydrates are not dangerous to human health when handled in accordance with the appropriate regulations. The LDL_0 (mouse, oral) for MgSO_4 is 5000 mg/kg. Magnesium sulfate is not listed in the EEC directive of May 5th, 1976 concerning the discharge of hazardous substances into water; it is classified as a nonhazardous substance in the EEC directive of June 12th, 1987 (WGK:O).

Table 20.19: Estimated production and consumption of magnesium sulfate products in 1988 (10^3 t).

Product	Production	Consumption in fertilizers	Consumption in other areas
Anhydrous	110	40	70
Kieserite ($\text{MgSO}_4 \cdot \text{H}_2\text{O}$)	2300	2250	50
Epsom salt ($\text{MgSO}_4 \cdot 7\text{H}_2\text{O}$)	280	180	100
Sulfate of potash magnesia	1000	1000	
Total	3690	3470	220

20.12 References

- C. J. P. Ball: "The History of Magnesium", *J. Inst. Met.* **84** (1955/56) 399.
- R. S. Busk: *Magnesium Products Design*, Marcel Dekker, New York 1987.
- Metals Handbook*, American Society for Metals, Ohio 1985.
- Comprehensive Inorganic Chemistry*, 1st ed, Pergamon Press, Oxford 1973.
- E. F. Emley: *Principles of Magnesium Technology*, Pergamon Press, London 1966.
- P. J. McGonigal et al., *J. Phys. Chem.* **66** (1962) 737-740.

- Kh. L. Strelets: *Electrolytic Production of Magnesium*, Israel Program for Scientific Translations, Jerusalem 1977.
- Kirk-Othmer*, 3rd ed., vol. 14, pp. 570-615.
- Utah Deposits of Natural Resources, Bull 116, 1980.
- A. N. Strahler: *Principles of Physical Geology*, Harper and Row Publ., New York 1977.
- A. P. Lysenko et al., *Tsvetn. Met.* **1987**, no. 8, 53-55.
- J. C. Withers, R. O. Loufy, *Light Met. (Warrendale, PA)* 1986, no. 2, 1013-1017.
- A. P. Ratvik et al., *J. Electrochem. Soc.* **134** (1987) no. 2, 321-327.
- D. A. Elkins et al.: *An Economic and Technical Evaluation of Magnesium Production Methods*, Part 2; Carbothermic, US Bureau of Mines RI 6946, 1967.
- F. Hori, US 4200264-A, 1980.
- Shell Int. Res., US 4572736-A, 1986.
- A. M. Cameron et al.: "Carbothermic Production of Magnesium", *Pyrometallurg* **87**, Institutions of Mining and Metallurgy, London 1987, pp 195-222.
- R. J. Allain et al.: *Proc. Annu. Meet. Int. Magnesium Assoc.* **34th**, 1979.
- D. V. Prutskov et al., *Tsvetn. Met.* **1986**, no. 5, 52-56.
- MPLC, US 4269816, 1981 (C. E. E. Shackleton).
- Norsk Hydro a.s., US 3272550, 1970; US 3742100, 1969; US 3779870, 1970.
- R. D. Toomey, *Proc. Annu. Meet. Int. Magnesium Assoc.* **35th**, 1980.
- M. P. Neipert, *Proc. Annu. Meet. Int. Magnesium Assoc.* **35th**, 1980.
- A. N. Petrunko et al., *Proc. Annu. Meet. Int. Magnesium Assoc.* **32nd**, 1977.
- D. R. Sadoway, Report 1983, DOE/CE/90033-6, Order No. 84006436.
- E. Aarebrot et al., *Light Met. (Warrendale, PA)* 1977, no. 1, 491-512.
- T. Østfold, H. A. Øye, *Light Met. (Warrendale, PA)* 1980, 937-947.
- K. Grjotheim et al., *Acta Chem. Scand.* **24** (1970) 489-509.
- K. Grjotheim et al., *Trans. Faraday Soc.* **57** (1971) 640-648.
- K. Grjotheim et al., *Acta Chem. Scand.* **26** (1972) 2050-2062.
- D. Dumas et al., *Acta Chem. Scand.* **27** (1973) 319-328.
- E. I. Savinkova, A. I. Orekhova, *Izv. Vyssh. Uchebn. Zaved., Tsvetn. Metall.* **1978**, no. 3, 76-80.
- J. B. Belavadi et al., *J. Appl. Electrochem.* **12** (1982) no. 5, 501-503.
- J. B. Belavadi et al., *Adv. Electrometall. Proc. Symp.* **1983**, 2/27-2/43.
- K. Andreassen, *Erzmetall* **31** (1978) no. 7/8, 301-309.
- N. Hey-Petersen, *J. Met.* **21** (1969) no. 4, 43-49.
- O. G. Sivilotti, *Light Met. (Warrendale, PA)* **1988**, 817-822.
- H. Ishizuka, US 4495037, 1985; US 4647355, 1987.
- Dow Chemical Co., US 4448654, 1984 (S. F. Spangenberg et al.).
- K. S. Dean et al.: *An Economic and Technical Evaluation of Magnesium Production Methods*, Part 1: Silicothermic, US Bureau of Mines RI 6656, 1965.

- Knapsack-Griesheim, DE 1023233, 1954 (W. Moschel, O. Brettschneider).
- Soc. Ital. Magnesio, US 4238224, 1980 (C. Bettanini et al.).
- L. M. Pidgeon et al., *Trans. Metall. Soc. AIME* **159** (1944) 315.
- J. R. Wynnkyj et al., *Metall. Soc. CIM Annu. Vol.* **1978**, 73-81.
- A. Froats, *Light Met. (Warrendale, PA)* **1980**, 969-979.
- Soc. Ital. Magnesio, US 4238224, 1980 (C. Bettanini et al.); US 4238223, 1980 (C. Bettanini et al.); US 4264778, 1981 (S. E. Ravelli et al.).
- University of Manchester, WO 89/00 613, 1988 (A. M. Cameron).
- C. Faure, J. Marchal, *Metals* **16** (1964) 721.
- M. P. Lugagne, *Erzmetall* **31** (1978) 310-313.
- R. A. Christini, *Light Met. (Warrendale, PA)* **1980**, 981-995.
- A. E. Vol: *Handbook of Binary Metallic Systems*, vol. 2, Moscow 1962, pp. 483-484; transl. Jerusalem 1967.
- Norsk Hydro a.s., US 4385931, 1983 (O. Wallevik, J. B. Ronhang).
- R. S. Busk, R. B. Jackson, *Proc. Annu. Meet. Int. Magnesium Assoc.* **35th**, 1980.
- S. L. Couling, *Proc. Annu. Meet. Int. Magnesium Assoc.* **34th**, 1979.
- A. Ohno, *Proc. Annu. Meet. Int. Magnesium Assoc.* **42nd**, 1987.
- Extramet, CA 1175618, 1984 (G. Bienvenue, B. Chaleat).
- J. A. Barannik et al., SU 384423, 1971.
- Dow Chemical Co., US 4186000, 1980 (E. J. Shačk, G. B. Cobel).
- Norsk Hydro a.s., US 4421551, 1983 (U. Mueller).
- N. A. Voronova: *Desulfurization of Hot Metal by Magnesium*, The International Magnesium Association and The Iron and Steel Society of the AIME, Dayton, OH, 1983.
- J. C. Agarwal: *Economic Benefits of Hot Metal Desulfurization with Magnesium*, Charles River Associates, Boston, MA.
- S. K. Saxena, *Second. Steelmaking, Proc. Conf.* **1989**.
- S. K. Saxena, *Clean Steel, Proc. Engl. Int. Conf.* **3rd** (1986).
- K. G. Summer, *Proc. Annu. Meet. Int. Magnesium Assoc.* **42nd**, 1987.
- B. Vigeholm, *Proc. Annu. Meet. Int. Magnesium Assoc.* **39th**, 1984.
- E. Browning: *Toxicity of Industrial Metals*, 2nd ed., Butterworths, London 1969.
- M. A. Jochimsen, *JAMA J. Am. Med. Assoc.* **155** (1943) 534.
- B. E. C. Nordin: *Calcium, Phosphate and Magnesium Metabolism*, Churchill Livingstone, Edinburgh 1976.
- K. S. Kasprzak, M. P. Waalkes, *Adv. Exp. Med. Biol.* **206** (1986) 497-515.
- G. D. Clayton, F. E. Clayton (eds.): *Patty's Industrial Hygiene and Toxicology*, Wiley Interscience, 3rd ed., vol. 2A, New York 1981, p. 1745.
- H. L. Pattinson, GB 9102 1841.
- W. Wetzstein: "Limnische Huntit-Hydromagnesit-Magnesitlagerstätten in Macedonien/Nordgriechenland", *Miner. Deposita* **10** (1975) 129-140.
- B. M. Coope: "Magnesia Markets. Fit for optimism", *Ind. Miner. (London)*, Sept. 1989, 45-57.
- Gmelin* **27 A**, 57ff.
- H. Ginsberg, K. Wefers, *Die Metallischen Rohstoffe*, vol. 15: Aluminium und Magnesium, F. Enke Verlag, Stuttgart 1971.
- Dead Sea Works, DE-OS 2532022, 1975 (J. A. Epstein et al.).
- B. Breiter J. Steuöloff, *Neue Bergbautech.* **16** (1986) no. 1, 23-27.
- Standard-Messo Verfahrenstechnik GmbH, DD 229678, 1984 (R. Schmitz, K. Wamser, H. Zahalka).
- C. Dähne B. Maurer, *Neue Bergbautech.* **15** (1985) no. 8, 291-294.
- Bechtel Internat. Corp. US 230986 1972; US 347222, 1973.
- Kaliforschungsinstitut Sondershausen DE-OS 1467293, 1964 (H. Hoppe); DE-AS 1198802, 1964 (H. Hoppe).
- J. Kenat, *Symp. Salt (Proc.)* **2nd**, vol. 2, 1965, 195-203.
- Israel Chemicals Ltd., DE-OS 2746503, 1977 (A. Sadan, H. Pitnach).
- E. E. Frolovskii, N. A. Alekseeva, L. B. Anikina, L. E. Bosiyak, *Khim. Promst. Ser. Kaliinaya Promst.* **1979**, no. 3, 21-24; *Chem. Abstr.* **92** (1980) 78938 f.
- S. F. Estefan, *Hydrometallurgy* **10** (1983) 39-45.
- Great Salt Lake Minerals and Chem. Corp., US 3690844, 1972 (U. Neitzel, H. G. Flint); P. Behrens, *Bull. Utah Geol. Miner. Surv.* **116** (1980) 223-228.
- Salzdetfurth AG, US 3642455, 1972 (B. J. Hahn, R. M. E. Reise, W. R. Raschka).
- L. van den Assen, D. Buyze, H. P. Rogaar, *Rev. Metall. CIT*, April 1985, 295-305.
- Kali und Salz, DE 2513947, 1975 (G. Budan, D. Kunze, W. Otto, I. Steingart).
- H. Schnabel et al., DD 71758, 1968.
- Mines de potasse d'Alsace, FR 8104391, 1981 (M. Bichara, M. Bodu, J. P. Koensgen, M. Meriaux J.-P. Zimmermann).
- Kali und Salz, BASF, DE 3119968, 1981 (K. Wintermantel, D. Stockburger, A. Hollstein, D. Kunze, F. Werdelmann).
- VEB Kombinat Kali, DD 211105, 1982 (H. Scherzberg, W. Ulrich, R. Tober, W. Staufenbiel, M. Matern).
- Mines de potasse d'Alsace, DE 2751420, 1977 (A. Aubry, M. Bichara).
- Nalco Chemical Company, DE-OS 3010755, 1980 (R. Allain, D. Braithwaite, J. P. Maniscalco).
- R. J. Allain, D. Braithwaite, *Proc. Annu. World Conf., Magnesium*, June 1979, 24-28.
- Dow Chemical, US 3282642, 1966 (R. D. Goode-nough, R. A. Gaska).
- Kaiser Aluminium & Chem. Corp., US 3181930, 1931 (O. C. Olsen).
- ISSO Res. & Eng. Co., US 3347625, 1965 (C. N. Kimberlin, Jr., W. F. Arey, Jr., F. J. Buchmann).
- M. Nakayasu, Y. Suzukawa, W. Kobayashi: "Thermal Decomposition of $\text{MgCl}_2 \cdot \text{NH}_4\text{Cl} \cdot n\text{NH}_3$ ", *Denki Kagaku oyobi Kogyo Butsuri Kagaku* **51**

- (1983) no. 4, 396–402.
Chem. Abstr. 99 (1983) 81676 m.
80. J. T. May, V. E. Edlund, D. C. Seidel: "Dehydrating Magnesium Chloride by Double-Salt Decomposition", *Rep. Invest. U.S. Bur. Mines*, RI 3277 (1978); *Chem. Abstr.* 89 (1978) 45748 d.
 81. Ruthner Engineering GmbH, DE-OS 2638123, 1976 (J. Jeney).
 82. Ustav pro vyzkum rud, DE-OS 3415784, 1984 (V. Horák, V. Bumbálek, K. Matouš, F. Sehnálek).
 83. Veitscher Magnesitwerke-AG, DE-OS 3045796, 1980 (M. Grill, H. Grohmann, E. Klein, A. Kullig).
 84. *Kirk-Othmer*, 2nd ed., vol. 12, p. 672.
 85. EEC Directive L213/81–84, Method 5.1, Association of Official Analytical Chemists—Methods, 1984, no. 2.168, p. 30.
 86. Association of Official Analytical Chemists—Methods (AOAC), 14th ed., 1984, no. 2.126–2.130 (AAS) and 2.141.
 87. Association of Official Analytical Chemists—Methods (AOAC), 1984, Method no. 2.108–2.113.
 88. Association of Official Analytical Chemists—Methods (AOAC), 1984, Method no. 2.173–2.176; Verband Deutscher Landwirtschaftlicher Untersuchungs- und Forschungsanstalten (Lufa): *Handbuch der landwirtschaftlichen Versuchs- und Untersuchungsmethodik (Methodenbuch)*, vol. 2: Die Untersuchung von Düngemitteln, Verlag J. Neumann-Neudamm, Melsungen 1973, 9₆₅–9₆₆, Method 9.18.2.
 89. J. Fries, H. Getrost: *Organische Reagenzien für die Spurenanalyse*, 3rd ed., F. Merck, Darmstadt, Verlag Chemie, Weinheim 1966, p. 331 ff.
 90. Lufa-Methodenbuch 9₂₃, Method 9.8.1.
 91. Lufa-Methodenbuch 9₉₁–9₉₃, Method 9.28.2.
 92. DIN 38405, part 17; H. Baron, *Fresenius Z. Anal. Chem.* 143 (1954) 339.
 93. M. Zimmermann: *Fotometrische Metall- und Wasseranalysen*, Wiss. Verlagsanstalt, Stuttgart 1954.
 94. E. Merck: *Organische Reagenzien für die Spurenanalyse*, 3rd ed., Verlag Chemie, Weinheim 1966, pp. 69–72.
 95. Association of Official Analytical Chemists—Methods, Method no. 2.157–2.160, pp. 29/30.
 96. R. Mathur, A. K. Misra, M. P. S. Chandrawa, *Res. Ind.* 31 (1986) June, 181–184.
Kali und Salz, DE 3230962, 1982 (A. Singewald, K.-R. Löblich, H. Duyster).
Kali und Salz, DE-OS 3031086, 1980 (H. Duyster, W. Prinzler, G. Nürnberger, K. Springer).
 97. Saarbergwerke, DE-OS 2204281, 1972 (W. Schuhknecht, H. Kunz, H. G. Klinkner, G. Culmann); DE-OS 2405223, 1974 (H. G. Klinkner, G. Culmann).
 98. Norsk Proco A/S, EP-A 0241103, 1987 (J. G. Berg, R. E. Smith-Johannsen).
 99. M. C. Bell, *Feedstuffs* 50 (1978) no. 6, 24–25.
 100. W. Pannekeet, *Chem. Ind. (London)* 21 (1983) 821–824.
 101. G. Gascho, *J. Fert. Issues* 3 (1986) no. 2, 62–65.
Kali und Salz, DE-OS 3432327, 1984 (R. Wotschke, G. Budan, G. Kemmler).
 102. L. R. Duncan: "Today's Magnesia Industry", paper given at International Symposium on Refractories, Hangzhou, 1988.
 - E. Naujokat, D. v. Mallinckrodt, C. Zografou, *Keram. Zeitschr.* 35 (1983) 440–442.
 103. W. Zednicek: "Periklas. Ein bemerkenswertes und wesentliches Mineral in der Feuerfest-Keramik", *Radex Rundsch.* 1985, no. 4, 651–695.
 104. V. Weiß: "Die Aufbereitung von Magnesit" in: *Handbuch der Keramik*, Verlag Schmid, Freiburg 1968.
 105. H. Schmid: "Turkey's Salda Lake. A Genetic Model for Australia's Newly Discovered Magnesite Deposits", *Ind. Miner. (London)* August 1987, 19–31.
 106. W. Wetzstein: "Limnische Huntit-Hydromagnesit-Magnesitlagerstätten in Mazedonien/Nordgriechenland", *Miner. Deposita* 10 (1975) 129–140.
 107. W. Wetzstein, D. Zachmann: "Sedimentäre magnesium-karbonatische Bildungen im Servia-Bekken/Nordgriechenland", *Radex Rundsch.* 1977, no. 1, 29–49.
 108. M. Coope: "Magnesia Markets. Fit for Optimism", *Ind. Miner. (London)* Sept. 1989, 45–57.
 109. I. H. Howard-Smith: "Kunwarara Magnesite Deposit, Australia", Information Memorandum, Queensland Metals Corp., Toowoong (Brisbane), Queensland, Australia, June 1989.
 110. W. C. Gilpin, N. Heasman, *Chem. Ind. (London)* 1977, 567–572.
 111. J. C. Drum, S. Tangney, *Trans. J. Br. Ceramic Soc.* 77 (1978) no. 4, 10–14.
 112. T. F. W. Barth, C. W. Correns, P. Eskola: *Die Entstehung der Gesteine*, Springer Verlag, Berlin 1960.
 113. L. van den Assem: "Planning for New Industrial Minerals Projects – Magnesium Oxide from Brine in the Netherlands", *Ind. Miner. (London)*, January 1982, 35–42.
 114. I. A. Epstein: "Utilization of the Dead Sea Minerals (a review)", *Hydrometallurgy* 2 (1976) 1–10.
 115. H. Jedlicka: "Neue Anwendungen des Sprührösterverfahrens in der Chlorid-Naßmetallurgie", Schriftenreihe über Entwicklungen und Verfahren der Ruthner Industrieanlagen AG, Wien 1977, lecture Leningrad 1976.
 116. H. K. Krivanec, W. F. Kladnig: "Herstellung von Oxidrohstoffen nach dem Andritz-Ruthner-Sprührösterverfahren", *TIZ* 112 (1988) no. 11, 762–769.
 117. W. S. Ainscow: "Aufbereitung von Magnesit zu hochwertiger Sintermagnesia", *TIZ* 110 (1986) no. 6, 363–368. Sulmag II the Sinter Magazine Process, Sulzer Brothers Ltd., Winterthur, Switzerland.
 118. H. G. Schulte: "Polcal – An Economical Process for Calcining Magnesium Hydrate", *Ind. Miner. (London)*, November 1982, 37–47.
 119. H. Priemer, G. Mörl: "High Temperature Shaft Kiln for Large Crystal Periclase Materials", *Proceedings of International Symposium on Refractories*, Hangzhou 1988, 167–178.
 120. Z. Foroglou et al.: "Refractory Raw Materials of Natural Origin and High Performance Refractories Based on such Products", *Proceedings of International Symposium on Refractories*, Hangzhou 1988, 204–213.
 121. A. Eschner: "Die wärmetechnischen Eigenschaften von Magnesitesteinen für Niedertarifspeicherungen", Dissertation Fakultät für Bergbau, Hüttenwesen und Maschinenwesen der Techn. Universität Clausthal 1978.

122. "Magnesium Oxide Makes a Comeback", *Chem. Week*, January 1981, 43.
123. B. M. Coope: "Caustic Magnesia Markets – Agricultural Oversupply and Industrial Underdemand", *Ind. Miner. (London)* February 1981, 43–51.
124. I. Watson: "Minerals in Animal Feedstuffs – Plenty of Food for Thought", *Ind. Miner. (London)* April 1982, 71–91.
125. "Why Apply Magnesium with Potash?", *Phosphorus Potassium* 161 (1989) May–June, 20–28.
126. R. Schulze-Rettmer, T. Yawari: "Versuche mit dem Verfahren der Fällung von Magnesium-Ammonium-Phosphat (MAP) aus verschiedenen Abwässern", *Vom Wasser* 71 (1988) 41–54.
127. "Flammenschutzmittel und Füllstoffe auf Basis hochreiner Magnesiumverbindungen", *Kunststoffe*, June 1988.
Japan Chemical Week, 26th March 1987.
128. "World Magnesia Shortage, Particularly in High Purity Grades", *Ind. Miner. (London)* May 1974, 23–32.
129. "Magnesia – from Shortage to Surplus", *Ind. Miner. (London)* Sept. 1977, 31–55.
130. B. M. Coope: "Magnesia Markets – Refractory Contraction and Caustic Stagnation", *Ind. Miner. (London)* August 1983, 57–87.
131. H. Schmid: "China – the Magnesite Giant", *Ind. Miner. (London)* August 1984, 27–45.
132. B. M. Coope: "The World Magnesia Industry, Smaller but Fitter and Purer", *Ind. Miner. (London)* February 1987, 21–48.
133. R. C. Mackenzie: *The Differential Thermal Investigation of Clays*, Mineralogical Society (Clay Minerals Group), London 1957.
134. B. Brezny, *Ber. Dtsch. Keram. Ges.* 42 (1965) 308–310.
135. I. S. Raeva, *Ogneupory* 24 (1983) no. 4, 31–34.
136. G. V. Samsonov (ed.): *The Oxide Handbook*, IFI/Plenum, Data Corporation, New York–Washington–London 1973, p. 185.
137. P. D. Johnson, *J. Am. Ceram. Soc.* 33 (1950) no. 5, 168–171.
138. S. P. Mitoff, *J. Chem. Phys.* 31 (1959) 1261–1269.
139. A. Cermak, *Silikatechnik* 18 (1967) no. 7, 219–223.
140. G. Schönfelder, *Elektrowärme Int. Ed.* B 41 (1983) B5 214–221.
Norton Co., DE-OS 2333601, 1973 (J. J. Scott).
141. Norton Co., US 3410666, 1968 (J. J. Scott, N. C. Turnbull).
142. General Electric, DE-OS 1592116, 1966 (J. W. Rutler, E. M. Clausen).
143. Norton Co., US 2280515, 1939 (R. R. Ridgeway); Dynamit Nobel, DE 1249145, 1965 (H. R. Müller).
144. R. Czepek, *Elektrowärme Int.* 27 (1969) no. 12, 473–481.
145. Dynamit Nobel, DE-OS 1592089, 1967 (P. Hack, M. Neidhardt, H. Warmann).
146. General Electric, US 3592771, 1968 (W. Vedder, J. Schultz).
147. Norton Co., US 3457092, 1966 (R. O. Tervo).
148. Dynamit Nobel, DE 1921789, 1969 (M. Neidhardt, J. Schneider).
149. Dynamit Nobel, DE 2363790, 1973 (H. Clasen, K. Deneke).
150. Dynamit Nobel, DE 2525441, 1975 (G. E. Bockstiegel, M. Neidhardt, G. Rehfeld).
151. P. Bartha, F. Metz, K. H. Nitsch, *Stahl Eisen* 107 (1987) no. 13, 639–643.
152. A. Rabenau, *Chem. Ind. Techn.* 36 (1964) 542–545.
153. T. Power in E. M. Dickson (ed.): *Raw Materials for the Refractories Industry*, 2nd ed., Industrial Minerals, London 1986, pp. 163–177.
154. D'Ans-Lax: *Taschenbuch für Chemiker und Physiker*, vol. 1, Springer Verlag, Berlin–Heidelberg–New York 1967, pp. 417–418.
155. *Kirk-Othmer*, 14, pp. 636–639.
156. Kali und Salz, DE 3223366, 1982 (U. Neitzel, H. Schroth, A. Hollstein, A. Singewald).
157. DD 25546, 1958 (S. Mildner, L. Döhler).
158. VEB Kombinat Kali, DD 220237, 1983 (L. Herrmann, H. Baldauf, W. Kramer, H. Schubert, F. Aurich).
159. Wintershall, DE 1064891, 1957 (G. Budan).
160. Duval Corp., US 4045335, 1977 (B. F. Adams, J. Jr. Edward).
161. Kali und Salz, DE 3637226, 1986 (A. Singewald, U. Neitzel, G. Fricke).
162. Kali und Salz, DE 3637227, 1986 (A. Singewald, G. Fricke, H. Schroth).
163. Kali und Salz, DE 1667814, 1968 (G. Fricke, A. Singewald).
164. Kali und Salz, DE 1792120 (A. Singewald, G. Fricke).
165. G. Fricke, *Kali Steinsalz* 7 (1979) no. 12, 492.
166. A. Singewald, U. Neitzel, *Potash Technol. Min. Process. Maint. Transp. Occup. Health Saf. Environ. [Int. Potash Technol. Conf. 1st]* (1983) 589–595.
167. Kali und Salz, DE 3148404, 1981 (H. Zentgraf, H. Fetzer, A. Hollstein, G. Fricke).
168. Kali und Salz, DE 2748152, 1977 (G. Bruns).
169. Kali und Salz, DE 3618058, 1986 (K.-R. Löblich, G. Bruns, G. Peuschel).
170. Kali und Salz, DE 3707785, 1987 (K.-R. Löblich, G. Bruns, H. Zentgraf, E. Czaplinsky).
171. Kali und Salz, DE 2512246, 1975 (E. Höfling, H. Eberle, A. Hollstein, B. Hahn).
172. Wigton-Abbot Corp., US 2754175, 1956 (F. J. Hendel); *Chem. Abstr.* 77 (1972) 22391 v, JP 7116245, 1971.
Chem. Abstr. 89 (1978) 77069 z; B. Mikhailov et al., *Khim. Ind. (Sofia)* 1978, 50(3) 105–106.
173. Gypsum Industries Ltd., ZA 6700450, 1968 (N. Rudolph).
174. Société nationale de l'amiante, Thetford Mines, DE-OS 3006050, 1980 (J.-M. Lalancette); US 4277449, 1979.
175. *Chem. Abstr.* 95 (1989) 222201 s; P. Bozadzhev et al., *God. Viss. Khim-Tekhnol. Inst., Sofia* 24 (1978) no. 2, 19–24.
176. J. A. Fernandez-Lozano: "Recovery of Epsomite and Sylvite from Seawater Bittern by Crystallisation", *Fourth International Symposium on Salt*, Northern Ohio Geological Society, vol. 2, 1974, pp. 501–510.
177. *Chem. Abstr.* 85 (1976) 162612 h.
178. IMCC, US 2733132, 1956.
Sincat, FR 1363066, 1964.

179. *Chem. Abstr.* **89** (1978) 26924 s; RO 59695, 1971 (S. Kiss et al.).
180. SU 1127846, 1983 (N. P. Balandin); *Chem. Abstr.* **102** (1985) 134380 g.
181. Kali und Salz, DE 3334665, 1983 (G. Fricke, I. Geisler).
182. R. Burmeister, *Bergakademie* **16** (1964) no. 9, 558-559.
183. Association of Official Analytical Chemists—Methods (AOAC), Method no. 2.182-2.183, 1984, p.32.
184. J. F. T. Oldfield et al., *Int. Sugar J.* **82** (1979) 138-143.

21 Aluminum

WILLIAM B. FRANK, WARREN E. HAUPIN (§§ 21.1-21.9); ROBERT K. DAWLESS (§ 21.5); DOUGLAS A. GRANGER (§ 21.6); MORGAN KOMMER, MAURICE W. WEI (§ 21.7); THOMAS B. BONNEY (§ 21.8); ROBERT JAMES (§ 21.9); J. PAUL LYLE (§ 21.10); L. KEITH HUDSON (RETIRED), CHANAKYA MISRA, KARL WEFERS (§§ 21.10.1, 21.10.3.1); OTTO HELMBOLDT (§§ 21.10.2-21.10.3); HANS STARK (§§ 21.10.5.1, 21.10.6); MAX DANNER (§§ 21.10.5.2-21.10.5.3, 21.10.6); TAKAO MAKI (§ 21.10.7); WILLIAM BRIAN CORK (§ 21.11.1); GÜNTER ETZRODT (§ 21.11.2); ROBERT BESOLD (§ 21.11.3)

21.1 Introduction	1039	21.10 Compounds	1062
21.2 Properties of Pure Aluminum	1040	21.10.1 Aluminum Oxide	1062
21.2.1 Mechanical Properties	1041	21.10.1.1 General Aspects	1062
21.2.2 Physical Properties	1041	21.10.1.2 Bauxite, the Principal Raw Material	1068
21.3 Chemical Properties	1042	21.10.1.3 Bayer Process	1072
21.3.1 Oxidation of Aluminum	1042	21.10.1.4 Other Processes for Alumina Production	1091
21.3.2 Reactions with Aqueous Solutions	1043	21.10.1.5 Metallurgical Alumina	1094
21.3.3 Reactions at High Temperatures	1043	21.10.1.6 Industrial Alumina Chemicals	1095
21.3.4 Corrosion	1043	21.10.1.7 Ceramic Uses of Alumina	1101
21.3.5 Gases and Aluminum	1044	21.10.2 Aluminum Sulfate and Alums	1102
21.4 Production	1044	21.10.2.1 Aluminum Sulfate	1102
21.4.1 History of the Electrolytic Reduction of Alumina	1044	21.10.2.2 Alums	1105
21.4.2 Raw Materials	1045	21.10.3 Aluminates	1109
21.4.3 Hall-Héroult Cell	1046	21.10.3.1 Sodium Aluminate	1109
21.4.3.1 Electrolyte	1047	21.10.3.2 Barium Aluminates	1110
21.4.3.2 Electrode Reactions	1048	21.10.4 Aluminum Alkoxides	1110
21.4.3.3 Current Efficiency	1050	21.10.5 Aluminum Chloride	1111
21.4.3.4 Cell Voltage	1051	21.10.5.1 Anhydrous Aluminum Chloride	1111
21.4.3.5 Heat Balance	1051	21.10.5.2 Aluminum Chloride Hexahydrate	1114
21.4.3.6 Fluid Dynamics	1052	21.10.5.3 Basic Aluminum Chlorides	1114
21.4.4 Thermodynamic Considerations	1052	21.10.6 Toxicology	1116
21.4.5 Alternate Processes	1053	21.10.7 Aluminum Benzoate	1116
21.5 High-Purity Aluminum	1054	21.11 Pigments	1116
21.6 Aluminum Casting: Remelt Ingot	1055	21.11.1 Ultramarine Pigments	1116
21.7 Environmental Protection	1056	21.11.1.1 Chemical Structure	1116
21.7.1 Air Emission	1056	21.11.1.2 Properties	1118
21.7.2 Wastewater Discharge	1057	21.11.1.3 Production	1119
21.7.3 Solid Waste	1058	21.11.1.4 Uses	1120
21.7.4 Regulatory Requirements	1058	21.11.1.5 Toxicity and Environmental Aspects	1121
21.8 Toxicology and Occupational Health	1059	21.11.1.6 Economic Aspects	1121
21.9 Major Markets	1061	21.11.2 Aluminum Phosphate	1121
		21.11.3 Production	1122
		21.12 References	1122

21.1 Introduction

Aluminum is the most abundant metallic element in the earth's crust. It is normally found combined with other elements, and occurs rarely, if at all, in its pure state. However elemental aluminum particles have been dis-

covered in lunar soil and small amounts of native aluminum have been reported in Russia and China. Aluminum appears in a wide variety of minerals combined with oxygen, silicon, the alkali and alkaline-earth metals, and fluorine, and as hydroxides, sulfates, and phosphates. Aluminum has become the pre-

dominant nonferrous metal in use, yet it is one of the newest of the common metals. Aluminous minerals are quite stable; large amounts of energy and high temperatures are required to reduce these compounds to metal. This explains why the metal has been isolated and produced commercially only in relatively recent times.

In the late 18th and early 19th centuries many famous scientists worked at isolating aluminum, including LAVOISIER, DALTON, BERZELIUS, DAVY, and ØRSTED. In 1825 HANS CHRISTIAN ØRSTED discovered a method to prepare anhydrous aluminum chloride, a compound that was to play an important role in the production of the metal. ØRSTED is sometimes credited with the discovery of aluminum but often that honor is accorded to FRIEDRICH WÖHLER. His isolation of aluminum in 1827 was based on the reaction in a porcelain crucible of anhydrous aluminum chloride with potassium.

In 1854, H. SAINTE-CLAIRE DEVILLE improved the method of preparing aluminum by substituting sodium for potassium as the reductant for aluminum chloride. He was the first to record that fused cryolite serves as a solvent for aluminum oxide. DEVILLE emerges as the outstanding figure in aluminum technology in the period after its discovery and before commercialization of the Hall-Héroult process. His development of the chemical reduction process raised aluminum from a laboratory curiosity to a useful metal.

The chemical production process was further refined throughout the second half of the 19th century and the aluminum industry grew significantly during this period. Chemical production of aluminum by reduction of cryolite or aluminum fluoride with sodium or potassium was also under development in the late 19th century. The metal exhibited at the Paris Exposition of 1889 was produced at Alliance Aluminium of London, probably by sodiothermic reduction of cryolite. Reduction methods were used into the 1890s, when electrolyte production became dominant.

In the late 19th century many unsuccessful attempts were made to electrolyze aluminum

from aqueous solutions. Aluminum was first prepared electrolytically by a method discovered independently in 1854 by DEVILLE in France and BUNSEN in Germany. A sodium chloride-aluminum chloride fusion was electrolyzed in a porcelain crucible using carbon electrodes. Production based on this electrolysis of aluminum chloride was begun in 1975 by the Aluminum Company of America but operation was abandoned in 1982 for economic reasons.

For a discussion of the Hall-Héroult process, see Section 21.4.1.

21.2 Properties of Pure Aluminum

Certain physical and chemical properties of aluminum depend primarily on purity. There is no generally accepted nomenclature for the degrees of purity of aluminum. The following classification is suggested:

% Aluminum	Designation
< 99.0	Low grade
99.0-99.9	Commercial purity
99.90-99.95	High purity
99.95-99.996	Super purity
> 99.996	Extreme purity

The aluminum produced by the Hall-Héroult process is of commercial purity. Iron and silicon are the predominant impurities. Aluminum of super purity, produced by the three-layer electrolytic process, first became available in 1920 (see Section 21.5). The properties of this grade of metal have been studied extensively. Methods for preparing aluminum of even higher purity include zone refining, fractional crystallization, and preparation from aluminum alkyls. Electrical resistivity at low temperatures is employed as a measure of purity for high purity and super purity aluminum. Newer methods for analysis of trace impurities, including activation analysis, have improved the sensitivity and scope of analyses for very pure materials. Aluminum purer than 99.9999% has been prepared and characterized [14].

Many applications of aluminum and its alloys are based upon its inherent properties of low density, high electrical and thermal conductivities, high reflexivity, and great resistance to corrosion. Pure aluminum is soft and lacks strength, but it can be alloyed with many other elements to increase strength and impart a number of useful properties. Alloys of aluminum are light, strong, and readily formable by many metal-working processes; they can be cast, joined, or machined easily and accept a wide variety of finishes.

21.2.1 Mechanical Properties

Some mechanical properties of aluminum of several purities are given in Table 21.1 [15]. The data are from different sources and caution should be exercised in any direct comparison. Difficulties occur because of problems in analysis, temper of the specimen, and test methods. However, even small amounts of impurities present in commercial aluminum raise the tensile strength and hardness over that of the purest aluminum in the table.

Table 21.1: Mechanical properties of pure aluminum at room temperature.

Purity, %	Tensile strength		Elongation in 50 mm, %
	MPa	ksi ^a	
99.99	45	6.5	50
99.8	60	8.7	45
99.6	70	10.2	43

^akips (1000 pounds) per square inch.

21.2.2 Physical Properties

The physical properties of pure aluminum are summarized as follows [15]:

<i>mp</i>	660.5 °C
<i>bp</i>	2494 °C
Heat of fusion	397 J/g
Heat of vaporization	10.8 kJ/g
Heat capacity	0.90 J g ⁻¹ K ⁻¹
Density (solid)	
theoretical, based on lattice spacing	2699 kg/m ³
polycrystalline material	2697-2699
Density (liquid)	
at 700 °C	2357 kg/m ³
at 900 °C	2304
Thermal neutron cross section	(2.32 ± 0.03) × 10 ⁻²⁵ cm ² (0.232 ± 0.003 barn)

Lattice constant (length of unit cube) at 25 °C	4.0496 × 10 ⁻¹⁰ m
Coefficient of expansion at 20 °C	23 × 10 ⁻⁶ K ⁻¹
Thermal conductivity at 25 °C	2.37 W cm ⁻¹ K ⁻¹
Volume resistivity	2.655 × 10 ⁻⁸ Ω m
Magnetic susceptibility at 25 °C	16 × 10 ⁻³ mm ³ mol ⁻¹
Surface tension at <i>mp</i>	8.68 × 10 ⁻³ N/cm
Viscosity at <i>mp</i>	0.0012 Pa·s

Atomic Structure, Nuclear Properties [15]. Aluminum has an atomic number of 13 and atomic mass of 26.98154 based on ¹²C. The only abundant isotope, ²⁷Al, is stable and consists of 14 neutrons and 13 protons. Except for a single isotope, ²⁶Al, which has a half-life of 10⁶ years, all isotopes have half-lives of less than 8 s and are of negligible abundance. The naturally occurring isotope has a low cross section for thermal neutrons of 2.3 × 10⁻²⁵ cm², increasing in an irregular manner to 6 × 10⁻²⁵ cm² at 700-800 MeV. The nuclear magnetic moment is 1.84 × 10⁻²⁶ A·m².

Crystal Structure. Aluminum crystallizes in a face-centered cubic lattice that is stable from -269 °C to the melting point. The coordination number is 12 with four atoms to the unit cell. The edge length of the unit lattice cube for pure aluminum is 4.049596 × 10⁻¹⁰ m at 25 °C. Hence, the atomic diameter of aluminum is 2.86 × 10⁻¹⁰ m and its atomic volume 9.999 × 10⁻⁶ m³/mol. The lattice parameter is affected only slightly by impurities.

Thermal Expansion. Values for the coefficient of thermal expansion are given in Table 21.2 [15]. The coefficient of thermal expansion is probably isotropic, meaning it is the same in all directions.

Table 21.2: Thermal expansion coefficient of pure aluminum.

Temperature, K	α (× 10 ⁻⁶ K ⁻¹)	Temperature, K	α (× 10 ⁻⁶ K ⁻¹)
25	0.5	400	24.9
50	3.5	500	26.5
75	8.1	600	28.2
100	12.0	700	30.4
150	17.1	800	33.5
200	20.2	900	37.3
293	23		

Thermal Conductivity. Above 100 K the thermal conductivity of well-annealed 99.99% aluminum is relatively insensitive to

the impurity level. Below 100 K thermal conductivity becomes highly sensitive to the level of impurities. Values for thermal conductivity are given in Table 21.3 [15].

Table 21.3: Thermal conductivity of aluminum.

Temperature, K	Thermal conductivity, Wcm ⁻¹ K ⁻¹	Temperature, K	Thermal conductivity, Wcm ⁻¹ K ⁻¹
Solid		298.2	2.37
0	0	300	2.37
1	41.1	400	2.40
2	81.8	500	2.36
3	121	600	2.31
4	157	700	2.25
5	188	800	2.18
9	239	900	2.10
10	235	933.52	2.08
20	117	Liquid	
30	49.5	933.52	0.907
40	24.0	1000	0.930
50	13.5	1100	0.964
100	3.02	1200	0.994
150	2.48	1300	1.02
200	2.37	1400	1.02
250	2.35	1500	1.07
273.2	2.36		

Electrical Resistivity. The application of aluminum as an electrical conductor depends upon the low electrical resistivity of unalloyed aluminum. The electrical conductivity of pure aluminum at room temperature is 64.94% of that specified for copper in the International Annealed Copper Standard (IACS). At temperatures below 50 K, the electrical resistivity of aluminum is less than that of copper and silver of very high purity. Aluminum becomes superconducting below 1.2 K.

The resistivity of aluminum below 100 K is highly sensitive to purity. The *residual resistivity ratio* (RRR), or the ratio of electrical resistivity at room temperature to that at 4.2 K (boiling point of helium), is sometimes used as a measure of purity. Resistivity ratios of more than 3×10^4 have been reported for 99.999% aluminum.

Values for the electrical resistivity of aluminum are given in tabular form (Table 21.4) and schematically (Figure 21.1).

21.3 Chemical Properties

The 13 electrons in the aluminum atom are distributed: $1s^2 2s^2 2p^6 3s^2 3p^1$. With few excep-

tions the valence of aluminum in chemical compounds is 3+. At elevated temperatures aluminum is monovalent in gaseous molecules, such as AlCl, AlF, and Al₂O. Such species disproportionate at lower temperatures into the normal trivalent condensed compounds and elemental aluminum.

Table 21.4: Electrical resistivity of pure aluminum.

Symbol	Temperature, K	Resistivity, $\mu\Omega \cdot \text{cm}$	Sample
Δ	1.65	9.25×10^{-5}	99.9998% aluminum, single crystal, large diameter (≈ 10 mm)
	4.22	9.25×10^{-5}	
	14	2.61×10^{-4}	
	20.4	7.53×10^{-4}	
	58	8.70×10^{-2}	
	63.5	0.117	
	77.4	0.210	
	90.31	0.351	
	111.6	0.614	
\bullet	273	2.50	99.9% aluminum, 0.05% silicon, 127- μm diameter wire
	373	3.62	
	473	4.78	
	573	6.00	
	673	7.29	
	773	8.63	
	873	10.10	
	923	10.90	
\circ	933	10.95 (s)	99.99% aluminum
	933	24.2 (l)	
	1173	27.75	
	1273	29.2	
	1473	32.15	
---	4.2	5.7×10^{-3}	99.999% aluminum annealed at 150 °C for 4 h
	77	0.22	
	4.2	2.3×10^{-3}	99.9999% aluminum annealed at 150 °C for 4 h
	77	0.22	

21.3.1 Oxidation of Aluminum

Although aluminum is one of the most reactive of the common commercial metals, it is remarkably stable in many oxidizing environments. It owes its stability to the continuous film of aluminum oxide that rapidly grows on a nascent aluminum surface exposed to oxygen, water, or other oxidants. The molecular volume of the oxide is about 1.3 times greater than that of the aluminum consumed in the oxidation reaction. The surface layer, therefore, is under compressive stress and rapidly heals when damaged. In dry oxygen, the surface layer attains a limiting thickness that is a func-

tion of temperature. At room temperature this thickness is about 2.5–3.0 nm.

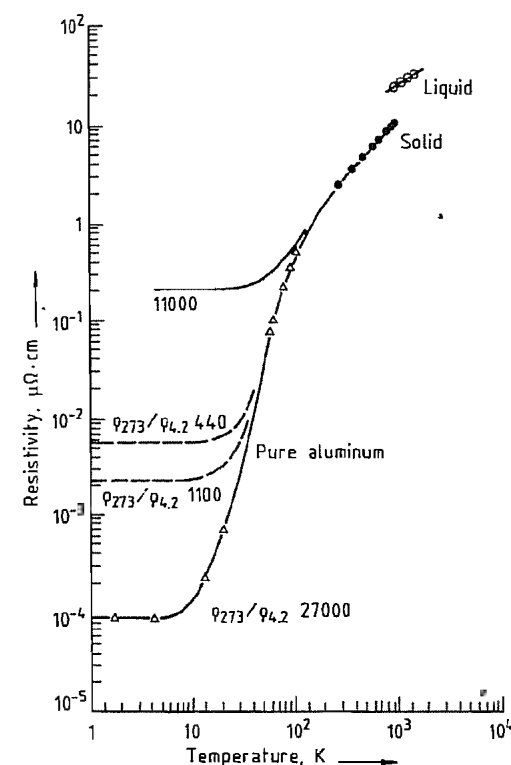
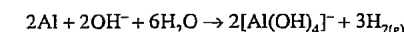


Figure 21.1: Electrical resistivity of aluminum [15].

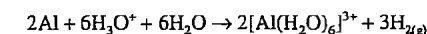
Film thickness is also a function of the amount of water vapor present. At room temperature and 100% relative humidity, about twice as much oxide is formed as in dry oxygen. In both cases, however, the same rate laws apply. Two film layers generally form in wet environments; the continuous oxide layer closest to the metal surface changes to a hydroxylated film at the solid-gas interface. At higher temperatures and on aluminum alloys, especially those containing magnesium and copper, more complex film structures develop, and oxide growth no longer can be described by simple time laws [16].

21.3.2 Reactions with Aqueous Solutions

Large pieces of aluminum of purity greater than 99.95% resist attack by most acids but dissolve in aqua regia. Therefore, aluminum is used to store nitric acid, concentrated sulfuric acid, organic acids, and many other reagents. However, its oxide film dissolves in alkaline solutions; corrosion is rapid, producing soluble alkali-metal aluminate and hydrogen:



Aluminum is amphoteric and can react with mineral acids to form soluble salts and evolve hydrogen:



Molten aluminum can react explosively with water. The mechanism of the reaction is not well understood. Molten aluminum should not be allowed in contact with moist tools or containers.

21.3.3 Reactions at High Temperatures

Molten aluminum reduces many compounds containing oxygen. These reactions are used in the manufacture of certain metals and alloys by the thermite reaction, which is the reaction of a metal oxide with aluminum to produce aluminum oxide (Al₂O₃) and the free metal. Aluminum reduces silicates, particularly glasses. The reaction can start well below the melting point of aluminum.

21.3.4 Corrosion

Atmospheric corrosion is generally electrochemical in nature, depending on current flow between anodic and cathodic areas. Attack is often nonuniform and limited to specific areas of the surface. The corrosion resistance of some alloy sheet can be improved by cladding the sheet with a thin layer of unalloyed aluminum; however, the aluminum must be anodic to the base metal. Aluminum performs poorly in direct contact with more noble metals in the presence of an electrolyte; galvanic attack of

aluminum may take place near the contact area.

21.3.5 Gases and Aluminum

Hydrogen is appreciably soluble in both solid and molten aluminum. Other gases reported to be present occur when nonmetallics in the metal react with the environment. Molten aluminum reacts readily with carbon monoxide and carbon dioxide; it also reacts with water vapor in the atmosphere, adsorbed water, water present in hydrated oxide films on scrap, and water adsorbed on or combined in refractories. Solid aluminum reacts with moisture in the atmosphere of a furnace to form oxides and hydrogen. Hydrogen is considerably less soluble in solid than in molten aluminum. The gas diffuses out of the metal at a rate determined by the temperature. However, when the reaction of aluminum with water vapor leads to a high activity of hydrogen at the solid-gas interface, the concentration gradient can be reversed. As a result, the rate of outgassing is decreased and a higher level of hydrogen is retained in the metal. In solid aluminum, hydrogen in excess of the solution limit can precipitate as H_2 at grain boundaries, thus lowering the hydrogen ion concentration and in turn further facilitating the diffusion of hydrogen ions from the interface into the metal.

21.4 Production

The only method now used industrially to produce primary aluminum is the Hall-Héroult process. Production of aluminum before its development was discussed previously in this article. Alternate means of producing aluminum are treated in Section 21.4.5.

21.4.1 History of the Electrolytic Reduction of Alumina

The technological elements of the process—electrolysis of fused salts to produce metals (including aluminum), the use of cryolite as a flux to dissolve alumina, and the use of carbon

electrodes—had been exploited for some time prior to 1886. The workable electrolytic process was discovered independently, and almost simultaneously, in early 1886 by CHARLES MARTIN HALL in Oberlin, Ohio, and PAUL L. T. HÉROULT in Gentilly, France. Both these young scientists were familiar with the work of SAINT-CLAIRE DEVILLE.

In less than three years, the invention had been implemented industrially in North America and in Europe. In November 1888 aluminum was first produced commercially by the electrolytic reduction of alumina by HALL and others in a company that later was to become the Aluminum Company of America. At about the same time, HÉROULT was associated with a company (later to be known as Alusuisse) that operated aluminum electrowinning cells at Neuhausen, Switzerland.

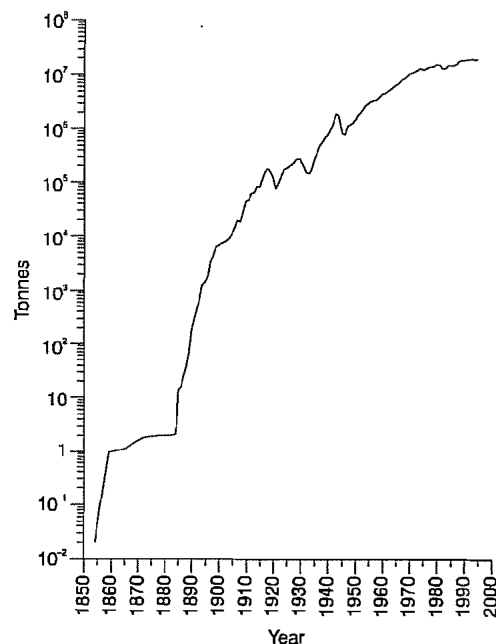


Figure 21.2: Annual world production of primary aluminum 1854–1996.

KARL JOSEF BAYER, an Austrian chemist, was issued a patent, DE 43977, in July 1887 for an improved method of producing alumina from bauxite. Bauxite, discovered by P. BERTHIER in 1821, is named for Les Baux, the village in the south of France near which it was

first found. With the development of a process to produce pure aluminum oxide from this abundant ore, the technology was then complete to spur rapid growth of the aluminum industry in Europe and North America in the last decade of the 19th century. The increase in the production of primary aluminum during the past hundred years is shown in Figure 21.2.

21.4.2 Raw Materials

Carbon. In the industrial electrowinning (separation by electrolysis) of aluminum, part of the energy for reducing alumina is supplied as electricity and part comes from consumption of the carbon *anode*. Carbon is also used as the cathode lining. Because 0.4–0.5 kg of anode is consumed for each kilogram of aluminum produced, this represents the major carbon requirement. Because the ash from the carbon will contaminate either the aluminum produced or the electrolyte, high-purity carbon is desirable. Certain impurities, such as vanadium, are particularly harmful in that they catalyze air burning of the carbon. Other impurities, such as phosphorus, accumulate in the electrolyte and undergo cyclic redox reactions (partial reduction followed by reoxidation), consuming electric current without producing product. The coke residue from petroleum refining is quite pure and, therefore, has been the major source of carbon for anodes. The structure of petroleum coke varies depending on the nature of the petroleum feedstocks used at the refinery, the refinery flowstream, and the coking conditions used. This coke produced at about 500 °C requires calcining at about 1200 °C to remove volatile constituents and increase its density before it is blended into the anode mix. After calcination, the coke is ground and mixed with crushed spent anodes and sufficient coal-tar pitch to allow molding into anode blocks by pressing or by vibrating. They are baked at 1000–1200 °C, causing the pitch to carbonize, forming strong carbon blocks. These blocks are made with one or more sockets into each of which is fastened a steel stub by pouring cast iron around it. These stubs both conduct

electric current into the anode and support the anodes in the cell. The cost of petroleum coke for prebaked carbon anodes in the United States was about \$0.20/kg (\$0.09/pound) in 1996.

Anthracite has been the major constituent in the cell *cathode* blocks, although graphite and metallurgical coke have been used to some extent. The anthracite is calcined at 1200 °C or higher, crushed and sized, mixed with coal-tar pitch, molded into blocks, and baked. These blocks, mortared together with a carbonaceous seam mix, form the pot lining, which is the container for both the aluminum and the electrolyte. High purity is not as important for the cathode blocks because leaching of impurities is very slow. Consumption of cathode carbon amounts to 0.02–0.04 kg of carbon per kilogram of aluminum produced. The life of a pot (typically 2–6 years) generally is terminated by failure of the carbon pot lining.

Aluminum Oxide. Depending on its purity and losses in handling, 1.90–1.95 kg of alumina are consumed in producing 1 kg of aluminum. The cost of alumina at United States smelting facilities was \$0.16–0.20/kg (\$0.07–0.09/pound) in 1996. The preparation of metallurgical alumina and its required physical and chemical properties are discussed in Section 21.10.1.

Electrolyte Materials. The electrolyte for electrowinning aluminum is basically a solution of aluminum oxide in cryolite. The presence of cryolite is essential for dissolution of alumina. Cryolite usually comprises more than 75% of the electrolyte which typically also contains calcium fluoride (4–8%), excess aluminum fluoride (5–15%), alumina (1–6%), and sometimes lithium fluoride (0–5%) and magnesium fluoride (0–5%). These additives lower operating temperature and increase current efficiency.

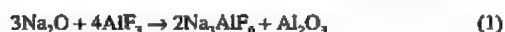
The mineral cryolite is the double fluoride of sodium and aluminum and has a stoichiometry very near the formula Na_3AlF_6 and a melting point of about 1010 °C. It has been found in substantial quantities only in Green-

land, and was mined extensively there in the early 20th century but now is essentially exhausted. Synthetic cryolite can be produced by reacting hydrofluoric acid with an alkaline sodium aluminate solution:



Cryolite also can be recovered from used pot linings. The lining is crushed and treated with dilute sodium hydroxide solution to dissolve fluorides. After being filtered, the solution is neutralized with carbon dioxide to precipitate the cryolite.

Cryolite is produced directly in reduction cells by reaction of the soda impurity in the feed alumina with added aluminum fluoride:



Electrolyte generated by the above reaction must be tapped from the cells periodically. In modern smelters with dry scrubbing equipment for fume treatment and cell lives greater than 3 years, cryolite is a by-product rather than a raw material in producing aluminum. Synthetic cryolite could be purchased in the United States for \$500–600/t in 1983.

Aluminum fluoride, AlF_3 , may comprise as much as 15% of the electrolyte in excess of the amount represented by the cryolite composition. Aluminum fluoride is consumed during normal operation by three major mechanisms. First, losses of aluminum fluoride by vaporization are appreciable; the most volatile species present in the electrolyte is sodium tetrafluoroaluminate, NaAlF_4 , having a partial pressure of 200–600 Pa over the operating melt, depending on composition and temperature. Second, aluminum fluoride is depleted by hydrolysis:



Aluminum fluoride is also consumed by the evolution of carbon tetrachloride during anode effects.

And finally, aluminum fluoride is consumed by reaction with the soda present in feed alumina (Equation 1).

Fume capture and scrubbing efficiencies have improved in recent years at aluminum smelters. Fluoride previously lost by vaporiza-

tion of NaAlF_4 and hydrolysis of bath is now almost completely recycled to the cells. Nevertheless, aluminum fluoride consumption amounts to 0.01–0.04 kg AlF_3 per kilogram of aluminum product. In 1996 technical anhydrous aluminum fluoride could be purchased in the United States for about \$350/t.

21.4.3 Hall-Héroult Cell

All commercial production of aluminum today is done in Hall-Héroult cells. Two major types of cells are currently in use: those employing prebaked carbon anodes and those employing self-baking Söderberg anodes. The Hall-Héroult cell with *prebaked anodes* is shown in Figure 21.3. Essentially pure alumina is fed into the previously discussed cryolite base electrolyte. Electric current deposits aluminum into a pool of molten aluminum held under the electrolyte in the carbon lined cavity of the cell. Oxygen from the alumina deposits electrolytically onto the carbon anode (burns) the anode. Cells typically range from 9 to 14 m long, 3 to 5 m wide, and 1 to 1.2 m high. Thermal insulation surrounds the carbon lining of the cell to control heat losses. Although carbon is the material known to withstand best the combined corrosive action of molten fluorides and molten aluminum, even carbon would have a very limited life in contact with the electrolyte at the sides of the cell were it not protected by a layer of frozen electrolyte. The thermal insulation is adjusted carefully to maintain a protective coating on the walls but not on the bottom, which must remain substantially bare for good electrical contact. Steel collector bars in the carbon cathode conduct electric current from the cell. These bars are inserted into holes that have been sized carefully so that thermal expansion forms a tight electrical contact, or cemented in place with a carbonaceous cement containing metal particles, or bonded in place with cast iron.

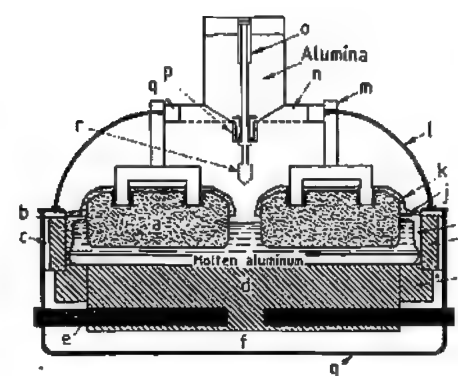


Figure 21.3: Hall-Héroult cell with prebaked anodes: a) Carbon anode; b) Electrolyte; c) Insulation; d) Carbon lining; e) Current collector bar; f) Thermal insulation; g) Steel shell; h) Carbon block; i) Ledge; j) Crust; k) Alumina cover; l) Removable covers; m) Anode rods; n) Fume collection; o) Air cylinder; p) Feeder; q) Current supply; r) Crust breaker.

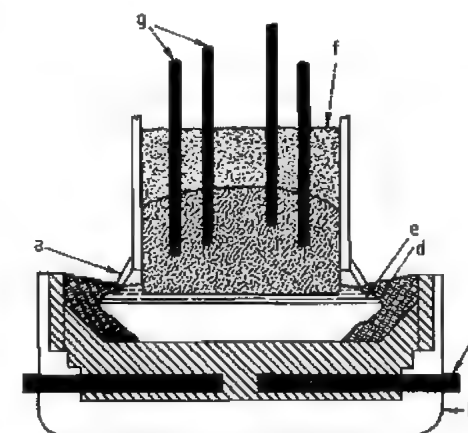


Figure 21.4: Aluminum electrolyzing cell with Söderberg anode: a) Manifold gas; b) Steel shell; c) Current collector bars; d) Frozen ledge; e) Molten electrolyte; f) Coke and tar paste; g) Current supplying pins.

The electrical resistivity of prebaked anodes ranges from 0.005 to 0.006 Ωcm . Current density at the anode race is 0.6–1.3 A/cm^2 .

The *Söderberg anode* (Figure 21.4) uses a premixed “paste” of petroleum coke and coal-tar pitch. This mixture is added at the top of a rectangular steel casing that is typically 6–8 m long, 2 m wide, and 1 m high. Heat from the electrolyte and heat from the electric current

passing through the anode bakes the carbonaceous mix as it progresses through the casing.

The baked portion extends past the casing and into the molten electrolyte. Baked mix replaces anode being consumed at the bottom surface. Electric current enters the anode through either vertical or sloping steel spikes. These spikes are pulled and reset to a higher level as they approach the lower surface. Söderberg anodes have an electrical resistivity about 30% higher than that of prebaked anodes. Because of the resulting lower power efficiency and the greater difficulty in collecting and disposing of baking fumes, Söderberg anodes are being replaced by prebaked anodes, even though the former save the capital, labor, and energy required to manufacture the latter.

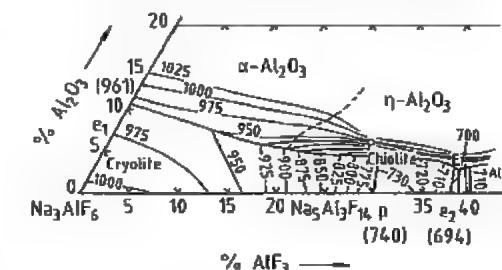


Figure 21.5: The Na_3AlF_6 - AlF_3 - Al_2O_3 system [17].

21.4.3.1 Electrolyte

Pure cryolite melts at about 1010 °C. Alumina and other additives lower the melting point, allowing operation at 940–980 °C. The cryolite-aluminum fluoride-alumina system (Figure 21.5) [17] has binary eutectic points at 961 °C and 694 °C and a ternary one at 684 °C. Calcium fluoride and lithium fluoride further reduce the liquidus temperature (Figures 21.6 [18] and 21.7 [19]). Calcium fluoride is seldom added intentionally. Because of a small amount of calcium oxide impurity in the alumina, it attains a steady-state concentration of 3–8% in the melt. At this level calcium is codeposited into the aluminum and emitted in the off-gas at a rate equal to its introduction. Magnesium fluoride accumulates to 0.1–0.3%, in the electrolyte by the same mechanism as calcium fluoride. Some opera-

tors add up to 5% MgF_2 because it expels carbon dust from the electrolyte by decreasing the electrolyte's ability to wet carbon.

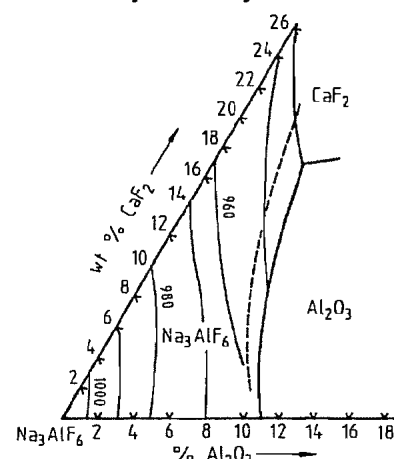


Figure 21.6: The Na_3AlF_6 - Al_2O_3 - CaF_2 system [18].

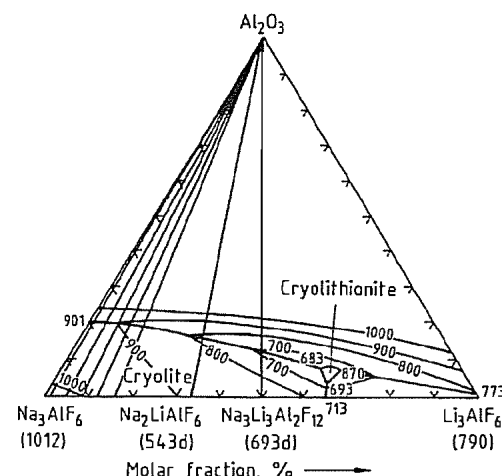
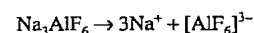


Figure 21.7: The Na_3AlF_6 - Li_3AlF_6 - Al_2O_3 system [19].

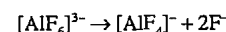
Calcium fluoride, in addition to lowering the liquidus temperature, decreases the vapor pressure and solubility of reduced species in the electrolyte for better current efficiency. Detrimentally, it lowers alumina solubility and electrical conductivity and increases density, viscosity, and surface tension of the electrolyte. Lithium fluoride in addition to lowering the melting point, decreases the vapor pressure, density, reduced species solubility, and viscosity; it also increases electrical conduc-

tivity. The only negative effect appears to be lowered alumina solubility. Its high cost, however, requires that its benefits be weighed against the price. Aluminum fluoride decreases solubility of reduced species and lowers surface tension, viscosity, and density. It has the undesirable effects of decreasing alumina solubility and electrical conductivity and increasing vapor pressure. Aluminum fluoride acts as a Lewis acid with sodium fluoride acting as a Lewis base. Neutrality has been defined arbitrarily as a molar ratio of sodium fluoride to aluminum fluoride of 3:1. Control of electrolyte acidity or the $\text{NaF}:\text{AlF}_3$ molar ratio, referred to as the *cryolite ratio* (R_c) is of importance to cell operation. Lithium fluoride is a slightly weaker Lewis base than sodium fluoride. Magnesium fluoride is a weak Lewis acid.

Ionic Structure of the Melt. There is general agreement that molten cryolite is completely ionized to sodium ions and hexafluoroaluminate ions:

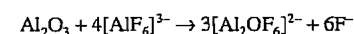
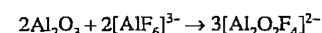


Also it is well established that the hexafluoroaluminate ion dissociates further:



At 100 °C, $[\text{AlF}_6]^{3-}$ is about 25% dissociated [20]. Dissociation increases with decreasing cryolite ratio [20].

The nature of the species formed when alumina is added is not so well established. Combination of the results of cryoscopic measurements, Raman spectrographic data, and equilibrium studies and vapor pressure measurements (reviewed in [20]) leads to the conclusion that $[\text{Al}_2\text{O}_2\text{F}_4]^{2-}$ and $[\text{Al}_2\text{OF}_6]^{2-}$ are the two major oxygen-containing ions in the melt. Possible reactions for their formation are:



21.4.3.2 Electrode Reactions

Cathode Reaction. Even though Na^+ is the principal current carrier, it does not discharge

at the cathode. The reversible electromotive force for the formation of liquid aluminum is about 0.24 V lower than that for the formation of sodium gas at 101.3 kPa (1 atm) for the range of compositions and temperatures used industrially. Aluminum-containing ions, mainly AlF_4^- , must diffuse to the cathode interface where they are reduced, leaving behind fluoride ions. Electrical neutrality is maintained by the electrical transport to the cathode of sodium ions (and lithium ions when LiF is present). This results in a diffusional flux of NaF away from the cathode and an increase in the $\text{NaF}:\text{AlF}_3$ ratio at the cathode interface.

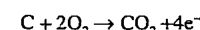
The cathode overvoltage can be represented by [21]:

$$\eta_{cc} = \frac{RT(1.375 - 0.125R_c)}{1.5F} \ln \frac{i}{0.257} \quad (2)$$

where R is the gas constant, T is the temperature (K), R_c is the mole ratio $\text{NaF}:\text{AlF}_3$, F is the Faraday constant, and i is the electrode's current density (in A/cm^2).

Although this relationship mathematically looks like activation overvoltage, actually the cathode overvoltage is caused by an increase in the $\text{NaF}:\text{AlF}_3$ ratio at the aluminum surface [22]. Using Fick's first law, the resulting concentration gradients were calculated and good agreement was found between the measured overvoltages and the electromotive forces between the two aluminum half-cells, one containing electrolyte of the bulk composition and the other, electrolyte corresponding to the calculated interfacial composition.

Anode Reactions. The primary anode reaction can be written:



However, O_2 ion is not present in the bulk electrolyte; instead, oxygen is present as structurally large complexes, i.e., $[\text{Al}_2\text{OF}_6]^{2-}$ and $[\text{Al}_2\text{O}_2\text{F}_4]^{2-}$. Thermodynamically, oxygen depositing onto carbon at 950–1000 °C should equilibrate to about 99% CO and 1% CO_2 . However, based on either net carbon consumption or the volume of gas produced, the primary anode product is essentially all CO_2 . The high anodic overvoltage implies that reac-

tion kinetics cause this surprising displacement from thermodynamic equilibrium. Rotating disk [23] and impedance [24] measurements indicate that there is a small diffusional overvoltage, probably caused by reaction within the pores of the electrode. Using the general treatment for heterogeneous reaction control [25], overvoltage data can be expressed by the relationship:

$$\eta_{sa} = \frac{vRT}{pnF} \ln \frac{i}{i^0} \quad (3)$$

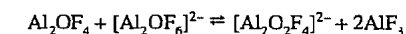
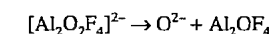
where v is the number of executions of rate-controlling steps to produce one overall step, p is the reaction order, n is the number of electrons transferred in one overall step, and i^0 is the reaction-limiting current density.

The reaction order, $p = 0.57$, was found from measurements of overvoltage versus current density [26]. In industrial practice, the reaction order ranges from 0.4 to 0.6, varying with carbon reactivity and porosity. The reaction-limiting current density i^0 goes from 0.0039 to 0.0085 A/cm^2 as alumina concentration varies from 2 to 8%. The reaction order also has been determined [26] from the rate of change of the limiting current with reactive species concentration and a similar value obtained:

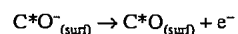
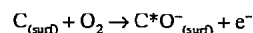
$$p = \frac{d \ln i^0}{d \ln c_{\text{Al}_2\text{O}_3}} = 0.56$$

Measurements [27] of the ordinary combustion of graphite have shown that when oxygen reacts both in pores and on the surface, a chemical reaction of approximately half-order results. Linear sweep voltammograms showed voltage peaks with increasing current density corresponding to discharge of CO_2 , COF_2 , and CF_4 [28].

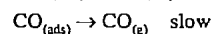
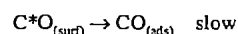
The following anode reaction mechanism is consistent with these observations. Oxyfluoride ions dissociate within the double layer to oxygen ions:



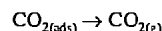
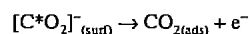
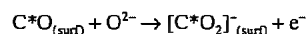
Oxygen ions discharge upon the carbon surface (surf) forming an activated complex, CO:



The activated complex converts very slowly to CO_(g) through an adsorbed (ads) intermediate:



Carbon burning in pure oxygen at 940–970 °C has a combustion rate equivalent to between 0.1 and 0.2 mA/cm². One would expect this reaction to proceed at a similarly slow rate. As available surface sites become covered with C*O, oxygen is deposited at higher energy (overvoltage) onto a carbon site already bonded to oxygen, producing unstable [C*O₂]⁻, which breaks carbon to carbon bonds almost immediately as it is formed:



The adsorbed CO₂ quickly desorbs as CO_{2(g)}. This mechanism explains both the high anodic overvoltage and the primary production of CO₂ instead of the thermodynamically favored CO.

When there is insufficient alumina dissolved in the electrolyte, the cell experiences a phenomenon called *anode effect*. Bubbles grow larger and larger on the anode until the electrolyte no longer wets the anode. With a constant potential the current falls to a low value; but with the constant current source used industrially, the cell potential rises to ≥ 30 V. Current then penetrates the gas film by a multitude of small electric arcs or sparks. The gas produced at the anode changes from CO₂ to CO, with significant quantities (3–25%) of CF₄ and minor amounts of C₂F₆ generated. Fluorocarbon compounds most likely deposit on the surface of the anode and trigger the anode effect. As alumina is depleted, anode overvoltage increases. At about 1.2 V anode overpotential, sufficient thermodynamic ac-

tivity of fluorine is produced to cause fluorine to bond to the carbon. Even though these low-surface-energy carbon–fluorine compounds decompose on the surface to CF₄ and C₂F₆ at cell temperature, their rate of formation can exceed the rate of thermal decomposition, producing high coverage. Once the cell is on anode effect, restoring the alumina concentration is not sufficient to return it to normal operation. The gas film must be broken by splashing aluminum, by interrupting the current momentarily, or by lowering the anodes to expose new areas not contaminated with fluorine.

21.4.3.3 Current Efficiency

According to Faraday's law, 1 kA·h of electric current should produce 0.3356 kg of aluminum, but only 85–96% of this amount is obtained. The principal loss mechanism is recombination of anodic and cathodic products. Reduced species go into solution in the electrolyte at the aluminum–electrolyte interface (Figure 21.8). The equilibrium (Equation 4) produces a thermodynamic activity of sodium in the melt, whereas Equation (5) produces an activity of aluminum monofluoride.

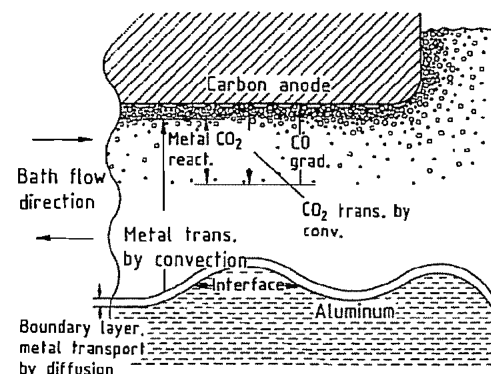
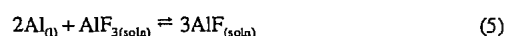
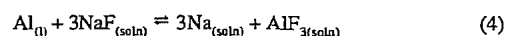


Figure 21.8: Current efficiency loss by metal reoxidation.

Metal going into solution must first diffuse through the metal–electrolyte boundary layer (Figure 21.8). The metal is then transported by convection to the vicinity of the anode. Here it

reacts with carbon dioxide. Chemical reactions appear to be fast compared to mass transport. The rate-controlling step is usually assumed to be diffusion of dissolved metal through the boundary layer at the metal–electrolyte interface. However, mixed control, with diffusion at both the aluminum–electrolyte interface and the bubble–electrolyte interface being important, has been reported [29].

There are several mechanisms accounting for additional minor losses in current efficiency. New cell linings absorb sodium, with Equation (4) maintaining an equilibrium activity of sodium. Fortunately, the lining saturates early in the cell's life but until this occurs, current efficiency is low. The sodium metal dissolved in the electrolyte imparts electronic conductivity to the electrolyte [30]. This may cause between 1 and 3% loss in current efficiency, the higher value being associated with higher ratios of NaF:AlF₃. Such elements as phosphorus and vanadium, which can be reduced partially at the cathode and then reoxidized at the anode, may lower efficiency.

21.4.3.4 Cell Voltage

The voltage of a Hall–Héroult cell is made up of a number of components:

$$E_{cell} = E^0 + \eta_{CA} + \eta_{CC} + \eta_{SA} + \eta_{SC} - I(R_A + R_B + R_C + R_X)$$

where E^0 is the thermodynamic equilibrium voltage described in Section 21.4.4; η_{CA} is the concentration overpotential at the anode; η_{SA} is the surface overpotential at the anode described by Equation (3); η_{CC} is the concentration overpotential at the cathode described by Equation (2); η_{SC} is the surface overpotential at the cathode, generally negligible; I is the total cell current; R_A is the electrical resistance of the anodes or anode; R_B is the effective resistance of the bath, allowing for fanning out of current as it flows from anode to cathode and the increased bath resistivity caused by gas bubbles; R_C is the cathode resistance; and R_X is the resistance external to the cell but included in calculating power consumption.

The anode concentration overpotential can be calculated by:

$$\eta_{CA} = \frac{RT}{2F} \ln \frac{i_c}{i_c - i}$$

The quantity i_c is the concentration-limited current density and it varies between 1.0 ± 0.5 A/cm² at 1% Al₂O₃ and 15 A/cm² at 8% Al₂O₃. The specific power consumption in kilowatt-hours per kilogram of aluminum can be calculated:

$$\text{kWh/kg} = 298.06 \frac{E_{cell}}{\% \text{ CE}}$$

where % CE is the percentage current efficiency or Faraday efficiency and E_{cell} is the cell voltage.

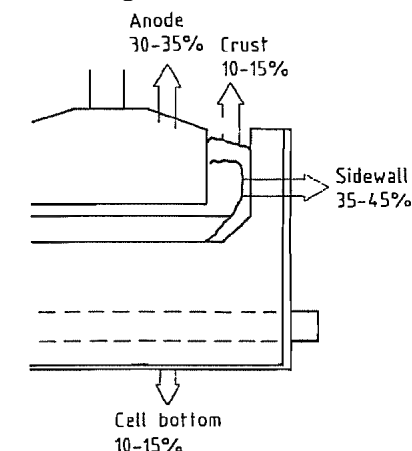


Figure 21.9: Cell heat loss distribution [33].

21.4.3.5 Heat Balance

Heat balance considerations are important in designing and operating a cell at the optimum temperature. Calculation is complicated by simultaneous heat flow and heat generation in conductors that carry electric current into and out of the cell. More than 50% of the heat loss may occur through the anodes and tap crust. The sidewalls must be protected from erosion by a ledge of frozen electrolyte maintained by extracting the exact amount of heat required for the desired ledge thickness. These calculations have been described [31, 32]. The complex geometry and the interaction be-

tween heat flow and electrical flow generally require a computer using either a finite element or finite difference technique for heat balances. Figure 21.9 [33] shows a typical heat loss distribution for a center-fed cell and Figure 21.10 [33], the typical temperature distribution.

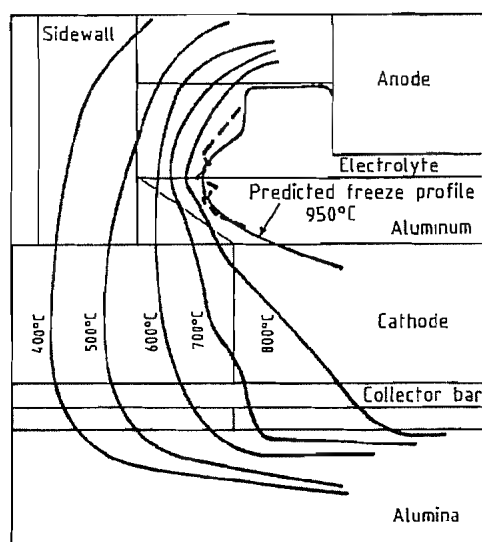


Figure 21.10: Cell lining isotherms [33]. Dashed line: measured profile.

21.4.3.6 Fluid Dynamics

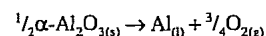
The large electric currents used in modern cells generate relatively strong magnetic fields within the cell. These magnetic fields interact with electric currents and exert Lorentz forces, producing movement of liquid conductors. Three types of magnetic disturbances have been observed: a vertical or static displacement of the metal pad, a circulating flow within the metal pad with velocities as high as 20 cm/s, and finally a wave motion in the metal pad. The last is probably the most harmful because waves may lead to electrical short circuiting. Calculation of the magnetic fields and electric current flow patterns is complicated. Computer programs have been designed to make these calculations and describe the fluid-dynamic consequences. These calculations have been refined to the point where

today, cells of over 3.0×10^5 A have been designed and operated with high efficiency. Natural convection caused by temperature gradients or composition differences in the electrolyte are insignificant compared with the movement induced by magnetic forces and gas bubbles. Gas bubbles produce significant stirring in the electrolyte and are the dominant force in bath movement, whereas electromagnetic forces predominate in metal pad movement.

21.4.4 Thermodynamic Considerations

Thermodynamic data used in the following section are from the *JANAF Thermochemical Tables* [34].

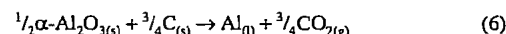
For pure α -alumina, reduction to aluminum can be represented:



At 960 °C (1233 K), $\Delta G_{1233}^0 = +642.1$ kJ and

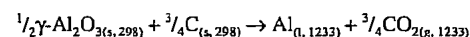
$\Delta H_{1233}^0 = +845.6$ kJ

In the industrial production of aluminum, a portion of the energy is supplied by the combustion of carbon anodes to carbon dioxide. The overall cell reaction can be represented:



At 960 °C, $\Delta H_{1233}^0 = +549$ kJ

Additional energy is required to heat alumina and carbon from room temperature to operating temperature. The alumina fed to the cell usually is not pure α -alumina. For γ -alumina, the overall process can be represented:



The enthalpy requirement for transformation of the reactants at 25 °C (298 K) to products at 960 °C (1233 K) is:

$$\Delta H_{(35)} = \Delta H_{1233}^0 + \frac{1}{2}(H_{1233}^0 - H_{298}^0)\gamma\text{-Al}_2\text{O}_3 + \frac{3}{4}(H_{1233}^0 - H_{298}^0)\text{C}_{(s)} = 606.4 \text{ kJ}$$

This value corresponds to a theoretical energy requirement of 6.25 kWh per kilogram of aluminum produced.

The reversible cell potential (decomposition voltage) for Reaction (6) can be calculated from the relation:

$$\Delta G_{1233}^0 = -nFE_{\text{sat}, 1233}^0 \quad (7)$$

where ΔG_{1233}^0 is the Gibbs free energy change for reaction (6), 3.448×10^5 J; n is the number of electrons per unit cell reaction, i.e., 3; F is the Faraday constant, 96,487 kJ V⁻¹ mol⁻¹; and $E_{\text{sat}, 1233}^0$ is the standard electrode potential, in volts, at 960 °C for the reaction with all reactants and products at unit activity. Substituting the appropriate values into Equation (7) and solving for the cell potential:

$$E_{\text{sat}, 1233}^0 = 1.191 \text{ V}$$

The above decomposition potential applies to electrolyte saturated with alumina at 950 °C. The decomposition potential from melts with alumina activity less than unity can be calculated [21] from the equation:

$$E^0 = E_{\text{sat}}^0 + \frac{RT}{6F} \ln a_{\text{Al}_2\text{O}_3}$$

The activity of alumina in cryolite-base melts can be approximated [21] from the equation:

$$a_{\text{Al}_2\text{O}_3} = (c_{\text{Al}_2\text{O}_3}/c_{\text{Al}_2\text{O}_3}^*)^n$$

where $c_{\text{Al}_2\text{O}_3}$ is the concentration of alumina in the electrolyte, in %, $c_{\text{Al}_2\text{O}_3}^*$ is the saturation concentration of alumina, in %, and $n = 1.5$ for $c_{\text{Al}_2\text{O}_3} > 0.45 c_{\text{Al}_2\text{O}_3}^*$ and $n = 3$ for dilute solutions.

21.4.5 Alternate Processes

Although the Hall-Héroult process has gained industrial dominance, it has several inherent disadvantages. The most serious are the large capital investment required and the high consumption of costly electrical power. There are also the costs of the Bayer alumina refining plant and of the carbon anode plant. Many of the aluminum-producing countries must import alumina or bauxite. The supply of petroleum coke is limited. These deficiencies have spurred research to find alternate processes.

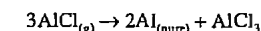
The earliest commercial process for producing aluminum was sodiothermic reduction of aluminum halides. Reduction of aluminum chloride by manganese has been studied and

reviewed [35]. However, neither can compete with the Bayer/Hall-Héroult process. Many attempts have been made at direct carbothermic reduction of alumina but these have resulted in very low yields, owing to the formation of solid aluminum carbide, aluminum suboxide vapor, and aluminum vapor that reacts with carbon monoxide as the temperature drops on the way from the furnace. Yields as high as 67% can be obtained by staging the reactions to produce aluminum carbide at 1930–2030 °C, which then reacts with alumina to produce aluminum and carbon monoxide at 2030–2130 °C [35].

Better yields result from adding to the furnace a metal (or a metal oxide that is subsequently reduced to a metal), such as iron, silicon, or copper, to alloy with the aluminum and lower its vapor pressure. Of course it is then necessary to extract the aluminum from the alloy. In principle this can be accomplished by electrolytic refining, by fractional crystallization, or by monohalide distillation. In the latter process the aluminum extraction takes place at 1000–1400 °C:



The AlCl gas is transported to a cooler zone, 600–800 °C, where pure aluminum is formed:



These combined processes to date have proved noncompetitive. Selective solution of aluminum from the alloy by using a volatile metal, such as mercury, lead, bismuth, cadmium, magnesium, or zinc, has been investigated. Following extraction, the volatile metal is distilled, leaving pure aluminum. If FeAl₃, TiAl₃, or Al₄C₃ is formed, neither electrolysis nor volatile metal extraction will remove the aluminum from the compound.

The aluminum vapor pressure can be lowered also by alloying the aluminum with aluminum carbide. Over 40% aluminum carbide is soluble in aluminum at 2200 °C [35]. This observation led to a process in which an alloy of aluminum and aluminum carbide was produced at 2400 °C. When this alloy was tapped from the furnace and allowed to cool slowly,

the aluminum carbide crystallized into an open lattice, the interstices of which were filled with pure aluminum. Pure aluminum was then removed either by leaching with molten chloride fluxes or by vacuum distillation. The aluminum carbide residue was recycled to the arc furnace. Alternately, the aluminum carbide could be distilled destructively above 2200 °C to produce aluminum and a residue of pure graphite.

In a joint project with the U.S. Department of Energy concluded in 1983, Alcoa investigated producing aluminum-silicon alloy in a blast furnace. The required high temperature was obtained by using a pure oxygen blast. Using a low-pressure blast furnace to produce an aluminum-silicon alloy was found to be infeasible because of severe bridging and interruption of the burden movement caused by total reflux of Al, Al₂O₃, and SiO vapors. Addition of iron improved operation but required an improved technique for extracting the aluminum from the dilute aluminum alloy. An alloy having higher aluminum content could be obtained if a significant portion of the process energy was supplied by electrical power. The aluminum blast furnace concept aims for a low-silicon, high-iron alloy. This improves the blast furnace efficiency but complicates extraction of pure aluminum from the alloy.

In 1976 Alcoa described a smelting process wherein aluminum chloride, dissolved in a molten sodium chloride-lithium chloride electrolyte, was electrolyzed in a bipolar electrode cell to produce aluminum and chlorine. The chlorine was recycled to a fluid-bed chemical reactor, where it reacted with alumina, pyrolytically coated with carbon from fuel oil, to produce aluminum chloride, carbon dioxide, and carbon monoxide. This reaction was highly exothermic. The aluminum chloride was desublimed to separate it from the gas and recycled to the cell to produce more aluminum and chlorine. This process required 30% less electrical power than their best Hall-Héroult cells. Because the entire process is a closed system, it was also environmentally more attractive than the Hall-Héroult process. Problems with the chemical plant and high

maintenance caused the demonstration plant to be shut down in 1982.

21.5 High-Purity Aluminum

The Hall-Héroult process has produced aluminum with a purity as great as 99.95%. Other techniques, such as electrolytic refining or fractional crystallization, are required to produce purer metal. Alcoa developed a three-layer electrolytic aluminum-refining cell in the 1920s. Copper was added to the bottom layer of impure aluminum to increase its density above that of the fused salt electrolyte. The electrolyte contained 25–30% sodium fluoride, 30–38% aluminum fluoride, and 30–38% barium fluoride to increase the electrolyte's density so that pure aluminum would float to the top. Electric current entered the anode alloy through carbon or graphite blocks at the bottom of the cell and left through graphite electrodes dipping into the high-purity aluminum on top. Aluminum was transported preferentially. Metals more difficult to oxidize than aluminum remained in the anode or alloy layer, and metals more difficult to reduce than aluminum remained in the electrolyte. A ledge of frozen electrolyte on the carbon sidewalls prevented electrical short circuiting between the floating pure aluminum layer and the carbon wall. The cell operated at 950–1000 °C and produced 99.98% pure metal.

In 1932 the Pechiney Company in France operated a cell using a fluoride-chloride electrolyte and nonconducting magnesia brick sidewalls. The electrolyte consisted of 17% sodium fluoride, 23% aluminum fluoride, and 60% barium chloride. The cell operated at 750 °C and produced 99.995% pure aluminum. An all-fluoride electrolyte (18% sodium fluoride, 48% aluminum fluoride, 16% calcium fluoride, 18% barium fluoride) also can be used in magnesia-lined cells. Modern electrolytic refining cells (Figure 21.11) add a segregation sump [36]. The sump, normally operated at least 30 °C cooler than the aluminum alloy anode, serves as a charging port for aluminum and permits impurity removal. As

impurities concentrate in the bottom layer, saturation is reached and crystals form in the cooler sump area, where they can be removed. This procedure greatly extends the operating life of the cell.

Fractional crystallization also is used commercially to refine aluminum. As aluminum freezes most impurities preferentially concentrate in either the liquid or the solid. A molten zone is moved along an aluminum bar in zone refining. Impurities that lower the melting point of aluminum concentrate at one end of the bar, whereas impurities that raise the melting point concentrate at the other end. After several passes the ends are removed, leaving a middle portion of high-purity aluminum.

Super-purity aluminum is produced by another fractional crystallization process [37]. In the first step, peritectic elements are removed from molten aluminum by reacting them with boron to form borides, which are precipitated and settled before the metal is transferred to a second furnace. Here the surface of molten aluminum is cooled with forced air, causing metal to crystallize. When the furnace is nearly filled with crystals, the remaining impure aluminum is drained. Then the crystals are remelted to yield very pure metal. Aluminum of purity higher than 99.995% has been produced from 99.9% pure smelting-grade aluminum by this process.

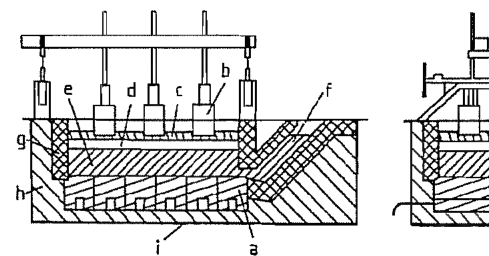


Figure 21.11: Longitudinal and cross sections of 15 000-ampere aluminum refining cell: a) Anode (carbon blocks); b) Cathode (graphite electrodes); c) Refined aluminum; d) Electrolyte; e) Alloy serving as anode; f) Segregation sump; g) Magnesia brick; h) Refractory block; i) Iron shell.

21.6 Aluminum Casting: Remelt Ingot

Metal tapped from the Hall-Héroult cell may be treated in one of several ways. First, it may be transported in the molten state to a holding furnace, where, along with solid scrap, it is alloyed, fluxed, filtered, and cast into a form suitable for fabrication by rolling, forging, etc., or for remelting by a foundry. It may be transported further (over distances up to 200 km) on trucks, equipped with well-insulated containers to prevent freezing, to a foundry where it is alloyed and used to make shaped castings. Both these methods of utilizing the molten metal are favored because energy required for remelting is conserved.

Alternatively, where ingot casting facilities or foundries are not nearby, metal is cast using cast iron molds into "primary" ingots for remelting. Generally, these unalloyed remelt ingots come as stackable 22-, 340-, or 680-kg ingots. Casting machines, such as the one illustrated in Figure 21.12, are often fully automated, with production rates of up to 20 000 kg/h. An important consideration is metal transfer from the ladle to the mold, which must be as quiescent as possible in order to minimize oxide contamination. Unalloyed ingot is sold in various purity grades, such as P0506 or P1520, depending on the maximum Si and Fe levels; e.g., P0506 is aluminum with 0.05% Si and 0.06% Fe maximum.

The larger sizes of unalloyed remelt ingot may be cast on semicontinuous DC (direct chill) casting equipment with a "T" cross section for ease of handling and stacking. This ingot usually is cut into lengths weighing approximately 340 kg.

Primary metal producers also make remelt ingot, which is prealloyed for the foundry industry. This is known as foundry ingot and generally is alloyed so that its composition lies within the limits of the alloy desired in the final shaped casting. Foundry ingot may be cast into open molds or continuously cast, cut to length, and stacked (Figure 21.13). The most common masses for this ingot, which is re-

melted in furnaces smaller than those used by wrought alloy producers, are approximately 14 kg and 22 kg. The general practice, where applicable, is to premodify and grain refine this foundry ingot. Also the molten metal is filtered and fluxed in a manner similar to that employed for wrought alloy ingot in order to insure optimum metal quality for the foundry user.

tal concern: air emissions, wastewater discharges, and solid waste. In the early years of the aluminum industry, most of the effort was directed toward controlling fluoride emission from the cells. The technology for fluoride control is now well established throughout the industry. Other significant air emissions from the anode production process have been controlled in recent years, or will be controlled through the Primary Maximum Achievable Control Technology (MACT) rule.

Wastewater effluent usually is not a major problem, except in those plants where wet processes are still used to scrub the air emissions from the cells and anode baking furnaces.

Cathode linings in aluminum cells are removed when lining failure occurs and large amounts of this material, called spent pot lining, must be discarded. Historically, spent pot-liner has been reclaimed for fluoride value, stockpiled, or landfilled. One company is now offering incineration treatment for potliner and many others are investigating incineration or fluoride recovery methods.

21.7.1 Air Emission

Cell Room Emission. Atmospheric emissions produced by an aluminum cell consist of particulate and gaseous fluoride (predominately HF), alumina, carbon dust, sulfur dioxide, carbon dioxide, and carbon monoxide. Typical values for total fluorides generated by the cell related to aluminum production range from 20 to 30 kg/t. Approximately the same amounts of alumina and carbon dusts also are produced. Sulfur dioxide varies according to the sulfur content of the coke used to prepare the anodes, whereas carbon monoxide emissions generally are less than 30×10^{-6} parts by volume.

Control of Cell Emissions. To control cell emissions, each cell is equipped with a closely fitted hood to collect the evolved gases, which are then ducted to pollution-control equipment. After air dilution the cell gas temperature ranges from 85 to 125 °C, depending on the ambient temperature. Both wet and dry

systems are employed to treat cell gas. Some of the older smelters use a combination of electrostatic precipitators for solids removal following by spray towers for removing hydrogen fluoride gas and some sulfur dioxide. Wet precipitators also are quite effective for collecting both gaseous and particulate fluorides; some sulfur dioxide also may be collected by wet precipitators.

Because of inherent disadvantages in wet systems, not the least of which is potential water pollution, new smelters employ *dry scrubbers* for controlling cell emission. A dry scrubber uses either a fluidized bed or direct injection of metal-grade alumina into the gas stream to remove the hydrogen fluoride gas by sorption. The larger the specific surface area of the alumina, the greater is its sorptive capacity for hydrogen fluoride.

The alumina usually is recovered from the gas stream by a fabric filter, which also removes the other entrained particulate species. Dry scrubber efficiencies are generally greater than 98 % for both the gaseous fluoride and the particulate matter. Dry scrubbers are considered to be state of the art control technology. The aluminum fluoride that is recycled to the cells represents a significant material recovery value.

Emissions from Anode Preparation. In the production of anodes, coke dust and pitch fumes are generated at the mixers and at the anode forming equipment. These emissions have historically been collected and exhausted from the area for worker protection. Current regulatory requirements in the US will require that these emissions be scrubbed using fluid coke or injected coke fines and baghouses. The collected pitch volatiles and coke will be recycled into the anode mix.

Pitch fumes, coke dusts, and fluorides are the chief pollutants in the waste gases from the anode baking furnaces. In most countries, limits are established for aluminum fluorides (0.05 kg per ton of aluminum) and particulate (dust) emissions, or opacity limits are set in lieu of particulate limitations.

Control Systems for Anode Baking Furnaces. The control systems for the baking furnace emissions are similar to those described for the cell, with both wet and dry systems being utilized. Fluidized alumina beds and alumina injection systems are used to control gaseous fluorides and hydrocarbons from most new furnaces. A major difference, however, is the need to cool the baking furnace gas in order to condense the hydrocarbons so that they can be extracted by the dusts on the bag filter.

21.7.2 Wastewater Discharge

Fume Collection Systems. Wastewater generation has been reduced drastically in recent years with the development of dry systems for controlling emissions. Some older facilities still rely on wet collection devices, which result in a wastewater stream contaminated with acid, fluoride, and organic material. Conventional treatment involves addition of lime and prolonged retention times (12 h to several days) for neutralization and removal of the calcium fluoride precipitate and a significant portion of the dissolved organic compounds, e.g., benz[a]anthracene, benzo[fluoranthene], benzo[a]pyrene, chrysene, and phenanthrene. At least 98 % of these can be removed by biologic treatment in a facultative lagoon that employs aerobic as well as anaerobic bacteria. Partial decomposition of the organic material occurs in the anaerobic bottom layer, whereas the aerobic bacteria present in the upper levels complete the degradation process. Other organic removal mechanisms in the facultative lagoon include skimming, adsorption, and sedimentation.

Sodium hydroxide and alum are used in place of lime for fluoride removal at some plants. This treatment creates a fluoride sludge that, after drying, can be used as a cryolite replacement in the aluminum cell.

Pot Wash Water. After failure of a cathode lining, most of the metal and bath are tapped from the cell and materials remaining within the shell are removed. This "pot digging" op-

Figure 21.12: Casting machine for the production of open-mold remelt ingot (courtesy Gautschi Electrofour SA).

Figure 21.13: Different types of aluminum castings: a) Continuously cast "T" section bar-look; b) Open-mold foundry ingot.

21.7 Environmental Protection

In the primary production of aluminum there are three principal areas of environmen-

eration can be done either "wet" or "dry". In "wet digging", water is applied to the pot to shock thermally and to fracture the bath, metal, and lining material that remain in the pot.

The best approach to handling pot wash water is to minimize the amount of wastewater generated through good management practices during the soaking operation. Excess water is collected in a sump and used as makeup to the next pot brought in for relining. Under no circumstances is this water discharged to a receiving stream because it may contain cyanide (10–200 mg/L total CN⁻) and fluoride (100–600 mg/L).

Plant Runoff. Although aluminum smelting is a dry process, some water is required for services, such as boiler makeup, various equipment cooling needs, and area wash water. A major source of wastewater at a smelting plant is stormwater runoff. Although intermittent, the contaminant loading is significant if efforts are not made to keep courtyards relatively free of dust and to protect spent pot linings from the elements. To minimize the environmental impact of storm water and the other miscellaneous flows, many primary aluminum plants direct their storm sewers through an equalization/holding basin before discharge. This basin is designed to remove suspended solids and floating matter (oil and grease) and also to equalize the fluoride concentration.

21.7.3 Solid Waste

Eventually, the lining of an operating aluminum smelting pot, due to physical deterioration and both impregnation, either falls or needs to be replaced because of poor performance or metal quality. This lining, once removed from the pot, is known as "spent potlining" or SPL. SPL is the largest-volume solid waste generated by aluminum smelters, roughly 2% to 4% by weight of aluminum produced.

SPL consists of mostly carbon, sodium aluminum fluoride, and various compounds of aluminum, sodium, fluorides, and less than

1% cyanides. The heat value of SPL ranges from 5000 to 8000 BTU per pound. Grey to black in appearance, SPL is very hard and its size distribution is extreme: large chunks to very fine powder. It often has an ammonia odor.

The United States Environmental Protection Agency has listed SPL as a hazardous waste due to cyanide content. As of early 1997, U.S. regulations require treatment of SPL prior to land disposal. Other countries of the world regulate SPL or are considering such regulation.

After removal from the pot, SPL is temporarily stored in containers or piles inside buildings, protected from wind dispersal and precipitation. Typical treatment for SPL destroys the cyanides using thermal technology and renders the fluorides less soluble with chemical fixation or stabilization. Recycling options for SPL generally recover or use its heat or fluoride value. SPL has been used to manufacture cement, mineral wool, bricks, asphalt materials, and as flux in the steel industry. Research is continuing with goals to minimize SPL generation and further develop recycling options that are economical, technologically sound, and protective of the environment and health.

21.7.4 Regulatory Requirements

Regulatory limits throughout the world have been summarized in an International Primary Aluminum Institute publication [38]. In the United States new carbon bake furnace emissions are limited to 20% opacity and the total fluoride as a function of aluminum produced is set at 0.05 kg/t. New potroom emissions are limited to 10% opacity and 0.95 kg/t Al of Total Fluoride in the US by New Source Performance Standards. MACT (Maximum Achievable Control Technology) standards for existing sources regulate Total Fluoride for various sources from 0.95 to 1.5 kg/t Al (depending on source type) and also limit POM emissions from Söderberg reduction plants. MACT standards are also being set for new

and existing carbon baking furnaces and anode mixing and forming processes.

In the United States, effluent limitation guidelines have been promulgated for aluminum smelting that control toxic and other pollutants. These regulations are found in the Code of Federal Regulation, Title 40 — Protection of the Environment, Part 421, Subpart B — Primary Aluminum Smelting (40 CFR 421). Limitations are based on the level of production at each facility discharging wastewater. The pollutants regulated under the guidelines are benzo(a)pyrene, antimony, nickel, aluminum, fluoride, oil and grease, total suspended solids, and pH. The wastewater sources for which these limitations are applicable include:

- Anode and cathode paste plant wet air pollution control;
- Anode bake plant wet air pollution control;
- Cathode reprocessing;
- Anode and briquette contact cooling;
- Potline wet air pollution control;
- Potline SO₂ wet air pollution control;
- Potroom wet air pollution control;
- Pot repair and pot soaking.

21.8 Toxicology and Occupational Health

The American Conference of Governmental Industrial Hygienists continues to recommend a 10-mg/m³ TLV for aluminum metal and alumina dust, the same as for nuisance or biologically inert materials [39]. They also have established a lower limit applicable to aluminum pyro powder and aluminum welding fumes, 5 mg/m³. This concentration is consistent with limits for nuisance materials with particle sizes in the respirable range. Health regulatory agencies in Australia, Germany, the Netherlands, Sweden, and many other countries consider aluminum oxide dusts to be nuisance particulates [40]. No MAK values have been set.

The bulk of the epidemiologic literature confirms that, in humans, aluminum and its

compounds exhibit a very low order of toxicity [41–44]. Whether taken into the body by ingestion or by inhalation, very little aluminum finds its way into body tissues. The aluminum content of the adult human body is 50–150 mg [45, 46]. Because of its ubiquitous nature, aluminum also is found in many foods that make up our normal diets. The amount ingested ranges from as little as 1 to > 100 mg/d [47]. The use of aluminum cooking utensils and food packaging does not contribute significantly to the amount that is ingested normally [48, 49]. Regardless of the route of intake, most of the aluminum absorbed systemically is excreted in the urine.

For many years aluminum, in the form of Al(OH)₃, was used widely at high dosages as an antacid, with no apparent ill effects. Although aluminum is known to have neurotoxic properties [50–53], it does not exhibit these properties in normal human beings because it is eliminated readily from the body. On the other hand, for those who have impaired renal function, it can be neurotoxic. There are strong implications that aluminum is a major factor in dialysis encephalopathy, an ultimately fatal condition that sometimes occurs in those with renal failure who undergo dialysis. The major symptoms are speech difficulties, dementia, and seizures. Traces of aluminum in the water used for the preparation of dialysis fluid can accumulate in the patient because the impaired kidneys are unable to eliminate it.

Aluminum toxicity with neurologic effects has been reported in patients with renal insufficiency not receiving dialysis who chronically ingested aluminum-containing phosphate-binding gels [54]. Likewise, premature infants with immature renal systems have developed Al toxicity as a result of Al-rich IV infusions, formula, and medications [55, 56].

Those with renal failure, whose aluminum serum levels are elevated as a result of dialysis or the oral administration of aluminum compounds, are also at special risk of developing osteomalacia, a softening of the bone that re-

sults in pain and an increased incidence of bone fractures.

Although aluminum has been implicated as being associated with Alzheimer's disease, a condition of premature senility [57, 58], the evidence to date suggests that it is not causal. Aluminum's role, if it plays a part at all, appears to be secondary to some unknown primary agent [59, 60].

With a few exceptions, most of the literature dealing with inhalation exposures of humans and experimental animals to aluminum and its compounds shows these materials to be relatively innocuous. However, there are reports contending that aluminum and aluminum oxide dusts are fibrogenic. Critical examination of the original references reveals that the evidence for this contention is inconsistent and mitigated by compounding variables.

Cases of pulmonary fibrosis attributed to aluminum powder exposures have been reported in the literature [61–66]. In most of these instances, environmental conditions were poor, dust exposures were extremely high, materials other than aluminum were known or suspected to be present, smoking and work histories of those affected were not given, and the types of fibrosis seen were not always consistent. Of these cases, 47 in all, one was reported from Japan and the remainder from Europe. No case has been reported from North America, even though similar production operations were conducted there over the same period of time.

An unusual form of pulmonary fibrosis has been reported in workers exposed during the manufacture of fine aluminum dust ("pyropowder") used in explosives and pyrotechnics. First reported in Germany during and after World War II, it was later described in England [67–69] but has never been described in North America.

That disorder has been related to manufacturing methods in which aluminum powder is coated with a lubricant to prevent its spontaneous oxidation [70]. The traditional lubricant used for this purpose was stearic acid, a fatty acid which reacts with aluminum to form sta-

ble aluminum stearate. Less often, mineral oil was used.

Fibrosis developed only in those exposed to metallic aluminum coated with mineral oil [71, 72]. Unlike stearic acid, mineral oil does not react with aluminum and can be readily removed. Following inhalation, mineral oil-coated particles are ingested by alveolar macrophages which remove the mineral oil coating, allowing the aluminum to oxidize and cause pulmonary injury leading to pulmonary fibrosis [73, 74]. This particular lung disease has not been reported since methods of production changed more than 20 years ago.

A study of 125 employees involved in a powder stamping operation in the United States failed to show any evidence of fibrosis [75]. Their exposure times ranged from 6 to 23 years (mean average of 12). Furthermore, a therapeutic administration of heavy doses of aluminum powder, by inhalation, to silicotics over a period of 30–50 weeks showed no detrimental effects to the patients [75]. A report in 1973 indicated that the failure of inhaled metallic aluminum powder to cause pulmonary fibrosis in experimental animals "parallels the clinical experience in the United States but it leaves unexplained the occurrence of fatal pulmonary fibrosis in England from the inhalation of pyro aluminum powder" [76]. Worldwide, no case has been reported since 1962.

In 1947 cases of pulmonary fibrosis were attributed to aluminum oxide fume exposure [77]. Subsequent investigations demonstrated the presence of silica in these fumes [78]. Silica generally is accepted today as the principal cause.

Pulmonary exposure to nearly all forms of aluminum oxide (alumina) are without adverse effects [70, 79]. However, one specific transitional gamma form of alumina caused pulmonary fibrosis in animals after intratracheal injection, but not after inhalation [80–82]. That alumina is rarely encountered in aluminum production and has little relevance to occupational health concerns.

In humans, there is no systematic evidence that bauxite or alumina cause pulmonary fi-

brosis. Review of mortality experience for nearly 6000 aluminum smelter workers found no deaths due to fibrosis, although deaths from other respiratory diseases were increased [83]. Bauxite refinery workers had increased risk of obstructive pulmonary changes, consistent with industrial bronchitis from dust exposure, but the effect was less than that attributable to smoking [84, 85]. Moreover, none of the cross-sectional studies of aluminum smelter workers has found evidence of significant restrictive ventilatory defects, decreased pulmonary compliance or pneumoconiosis on chest x-ray [72].

21.9 Major Markets [86, 87]

By far the greatest part of aluminum shipments is in the form of aluminum alloys, and production of primary aluminum and consumption of aluminum are the best indicators of the importance of aluminum alloys.

World production of primary aluminum is summarized in Table 21.5, which shows average annual production for two five-year periods. In the interval between these periods, production increased in almost every country: the world increase exceeded 280%. In the latest period, the United States was the largest producer, with about 30% of the world total, followed by the former Soviet Union (12%), Canada (7%), Japan (6%), and West Germany (5%).

Per capita consumption of aluminum in selected countries is summarized in Table 21.6, which shows average annual per capita consumption for two five-year periods. Where data are available for both periods, consumption increased 1.3–7.0 times. For the latest period, the United States had the highest consumption, followed by Norway, West Germany, Japan, and Australia.

The major markets for aluminum products are shown in terms of use by major industries in the United States in Table 21.15. To eliminate duplication, the figures exclude intra-industry shipments for further fabrication.

Table 21.5: Average annual world primary aluminum production in kilotons.

Country	1978–1982	1960–1964
Argentina	116	—
Australia	316	33
Austria	93	73
Bahrain	135	—
Brazil	248	20
Cameroon	42	50
Canada	1034	667
China ^a	365	96
Czechoslovakia ^{ab}	37	53
Egypt	116	—
West Germany	732	189
France	409	285
East Germany ^a	61	48
Ghana	166	—
Greece	145	—
Hungary	73	53
Iceland	74	—
India	206	37
Iran	12	—
Italy	270	91
Japan	856	190
North Korea ^a	10	—
South Korea	19	—
Mexico	43	—
Netherlands	260	—
New Zealand	156	—
Norway	644	206
Poland ^c	80	43
Romania ^b	226	—
South Africa	85	—
Spain	324	41
Suriname	52	—
Sweden	82	19
Switzerland	83	51
Turkey	35	—
Taiwan	42	12
United Kingdom	332	32
United States	4266	1978
USSR ^a	1771	801
Venezuela	237	—
Yugoslavia	177	30

^a Estimated by the U.S. Bureau of Mines, Dept. of the Interior.

^b Includes secondary unalloyed ingot.

^c Includes primary alloyed ingot.

The weight shipped to the containers and packaging industry increased almost eightfold between the two periods, compared with increases of 1.5–2 for other industries. This is a striking shift in market distribution: containers and packaging moved from 7% to 24% of the market and is now the major market for aluminum products. This rapid growth reflects

the growth of the metal-can market, with aluminum capturing an ever-increasing share of that market. The impressive growth in shipments of aluminum sheet for cans is shown in Figure 21.14.

Table 21.6: Average annual per capita aluminum consumption (kg per person) in selected countries.

Country	1978-1982	1960-1964
Argentina	2.4	—
Australia	17.0	5.5
Austria	11.5	—
Bahrain	7.9	—
Belgium	8.7	3.4
Brazil	2.7	0.6
Cameroon	2.0	—
Canada	15.9	6.6
Denmark	14.5	—
El Salvador	0.3	—
Finland	7.4	—
West Germany	20.7	7.4
France	12.4	5.2
Greece	7.1	—
Iceland	9.9	2.5
Ireland	4.4	—
Italy	12.7	3.4
Japan	19.5	2.8
Mexico	2.4	—
Netherlands	11.0	2.7
New Zealand	8.1	—
Norway	21.8	6.7
Panama	0.9	0.3
Philippines	0.5	—
Saudi Arabia	8.7	—
Singapore	9.4	—
South Africa	3.6	—
Spain	5.6	1.3
Sweden	16.0	6.9
Switzerland	15.1	8.6
Taiwan	6.3	0.7
Turkey	1.1	—
United Kingdom	10.1	7.8
United States	26.9	13.8
Venezuela	5.8	1.2

21.10 Compounds

21.10.1 Aluminum Oxide

21.10.1.1 General Aspects

The first reference to an aluminum compound dates back to the fifth century B.C., when HERODOTUS mentioned alum. PLINY de-

scribed the use of "alumen" as a mordant around 80 A.D. The term alumina is probably derived from the word alumen. In 1754 MARGGRAF showed that a distinct compound existed in both alum and clays. GREVILLE (1798) described a mineral from India that had the composition Al_2O_3 and named it corundum, believing that this was the native name for this stone. HAÜY (1801) called a mineral "diaspore", whose composition, $\text{Al}_2\text{O}_3 \cdot \text{H}_2\text{O}$, was determined by VAUQUELIN in 1802. Gibbsite was found by DEWEY in 1820; TORNEY (1822) showed this mineral to be $\text{Al}_2\text{O}_3 \cdot 3\text{H}_2\text{O}$. The name hydrargillite was given to a similar mineral found later in the Ural Mountains. The latter term is used more widely outside the United States.

By X-ray diffraction, BÖHM and NICLASSEN [97] identified $\gamma\text{-AlO}(\text{OH})$, later named böhmite (boehmite). BÖHM discovered a second type of $\text{Al}(\text{OH})_3$ a year later. FRICKE [98] suggested the name bayerite for this material. Only a few, uncertain finds of natural bayerite have been mentioned in the literature [99]. VAN NORDSTRAND et al. [100] reported a third form of trihydroxide, which was later named nordstrandite in his honor.

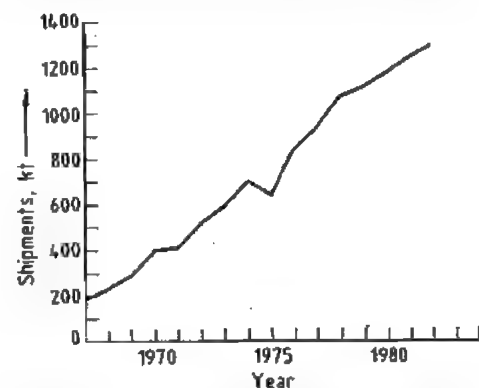


Figure 21.14: Shipments of aluminum sheet for cans.

Aluminum Hydroxides

A general classification of the various modifications of aluminum hydroxides is shown in Figure 21.15. The best defined *crystalline forms* are the three trihydroxides, $\text{Al}(\text{OH})_3$: gibbsite, bayerite, and nordstrandite. In addi-

tion two modifications of aluminum oxide hydroxide, $\text{AlO}(\text{OH})$, exist: boehmite and diaspore. Besides these well-defined crystalline phases, several other forms have been described in the literature [89, 90]. However,

there is controversy as to whether they are truly new phases or simply forms with distorted lattices containing adsorbed or interlamellar water and impurities.

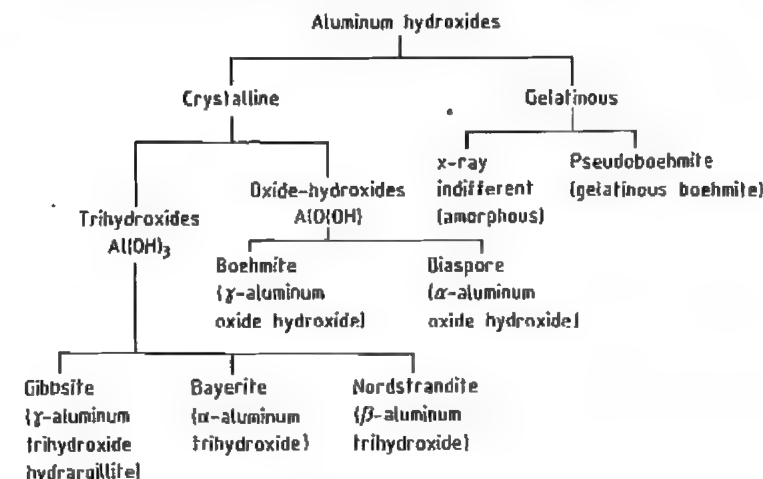


Figure 21.15: Classification of aluminum hydroxides (All figures courtesy of Aluminum Company of America).

Table 21.7: Mineralogical properties of oxides and hydroxides [90].

Phase	Refractive index n_D^{20}				Cleavage	Brittleness	Mohs hardness	Luster
	α	β	γ	Average				
Gibbsite	1.568	1.568	1.587	—	(001) perfect	tough	2.5 to 3.5	pearly vitreous
Bayerite	—	—	—	1.583	—	—	—	—
Boehmite	1.649	1.659	1.665	—	(010)	—	3.5 to 4	—
Diaspore	1.702	1.722	1.750	—	(010) perfect	brittle	6.5 to 7	brilliant pearly
Corundum	1.7604	1.7686	—	—	none	tough when compact	9	pearly adamantine

Table 21.8: Structural properties of oxides and hydroxides [90].

Phase	Formula	Crystal system	Space group	Molecules per unit cell	Unit axis length, $\times 10^{-1}$ nm			Angle	Density, g/cm^3
					a	b	c		
Gibbsite	$\text{Al}(\text{OH})_3$	monoclinic	C_{2h}^2	4	8.68	5.07	9.72	$94^\circ 34'$	2.42
Gibbsite	$\text{Al}(\text{OH})_3$	triclinic	—	16	17.33	10.08	9.73	$94^\circ 10'$ $92^\circ 08'$ $90^\circ 0'$	—
Bayerite	$\text{Al}(\text{OH})_3$	monoclinic	C_{2h}^2	2	5.06	8.67	4.71	$90^\circ 16'$	2.53
Nordstrandite	$\text{Al}(\text{OH})_3$	triclinic	C_1^1	4	98.75	5.07	10.24	$109^\circ 20'$ $97^\circ 40'$ $88^\circ 20'$	—
Boehmite	$\text{AlO}(\text{OH})$	orthorhombic	D_{2h}^{17}	2	2.868	12.227	3.700	—	3.01
Diaspore	$\text{AlO}(\text{OH})$	orthorhombic	D_{2h}^{16}	2	4.396	9.426	2.844	—	3.44
Corundum	Al_2O_3	hexagonal (rhomb.)	D_{3d}^4	2	4.758	—	12.991	—	3.98

Gelatinous hydroxides may consist of predominantly X-ray indifferent aluminum hydroxide or pseudoboehmite. The X-ray diffraction pattern of the latter shows broad bands that coincide with strong reflections of the well-crystallized oxide hydroxide boehmite.

Identification of the different hydroxides and oxides is best carried out by X-ray diffraction methods [90]. Mineralogical and structural data are listed in Tables 21.7 and 21.8.

The aluminum hydroxides found abundantly in nature are gibbsite, boehmite, and diaspore. *Gibbsite* and *bayerite* have similar structures. Their lattices are built of layers of anion octahedra in which aluminum occupies two thirds of the octahedral interstices. In the gibbsite structure, the layers are somewhat displaced relative to one another in the direction of the *a* axis. The hexagonal symmetry of this lattice type (brucite type) is lowered to monoclinic. Triclinic symmetry was found in larger gibbsite single crystals from the Ural Mountains [101]. This investigation revealed that the layer packets were slightly shifted in the direction of the *b* axis as well.

In bayerite the layers are arranged in approximately hexagonally close packing. Because of shorter distances between the layers, the density is higher than in the case of gibbsite. The crystal class and space group of bayerite have not yet been established clearly.

The individual layers of hydroxyl ion octahedra in both the gibbsite and the bayerite structure are linked to one another through weak hydrogen bonds only. Bayerite does not form large single crystals. The most commonly observed growth forms are spindle- or hourglass-shaped somatoids. The long axis of these somatoids stands normal to the basal plane, i.e., the somatoids consist of stacks of $\text{Al}(\text{OH})_3$ layers (Figure 21.16). The effect of alkali ions on the structures of $\text{Al}(\text{OH})_3$ types was investigated by several workers [90, 102, 103].

Gibbsite crystals of appreciable size are not uncommon. Clear pseudo-hexagonal platelets about 1 mm in diameter are known from Aro in Norway. Prismatic crystals of 0.5–1 mm

length are occasionally produced in the Bayer process.

Figure 21.16: Somatoids of bayerite.

Nordstrandite, the third form of $\text{Al}(\text{OH})_3$, was described by VAN NORDSTRAND [100] and others [104]. The structures of nordstrandite and bayerite were investigated [105] and compared with those of the monoclinic and triclinic gibbsite, which had been determined previously [101].

The lattice of nordstrandite is built of the same, electrically neutral $\text{Al}(\text{OH})_3$ octahedral layers that form the structural elements of gibbsite and bayerite [98]. The lattice period amounts to 1.911 nm in the direction of the normal to the layer. This corresponds to the sum of identical layer distances of bayerite plus gibbsite. The ideal nordstrandite structure consists of alternating double layers, in which the OH octahedra are arranged once in the packing sequence of bayerite, and then in that of gibbsite. Material containing continuous transitions from bayerite via nordstrandite to gibbsite has been prepared through the proper selection of precipitation conditions [102].

Tucanite, which contains about 0.5% SiO_2 , has the composition $\text{Al}_2\text{O}_3 \cdot 3.5\text{H}_2\text{O}$ [106]. Preliminary X-ray diffraction data show a resemblance of the tucanite structure to triclinic gibbsite. Yet, the layer spacing seems to be somewhat larger than in triclinic and monoclinic $\gamma\text{-Al}(\text{OH})_3$. Incorporated water molecules may be the cause of this.

A similar influence of water molecules on layer spacing has been observed in the oxide hydroxide boehmite [105].

Pseudoboehmite is formed during aging of X-ray indifferent hydroxide gels as a precursor of trihydroxide. The reflexes of pseudoboehmite are broadened not only because of the very small particle size, but also because of variable distances of the $\text{AlO}(\text{OH})$ double chains, which form the structural element of pseudoboehmite as well as of well-crystallized $\gamma\text{-AlO}(\text{OH})$. The lattice spacing in the direction of the *c* axis increases by 0.117 nm for each mole of excess water [105].

Aluminum Oxide Hydroxides

The $\text{Al}_2\text{O}_3\text{-H}_2\text{O}$ System. Under the equilibrium vapor pressure of water, crystalline $\text{Al}(\text{OH})_3$ converts to $\text{AlO}(\text{OH})$ at about 375 K. The conversion temperature appears to be the same for all three forms of $\text{Al}(\text{OH})_3$. At temperatures lower than 575 K, boehmite is the prevailing $\text{AlO}(\text{OH})$ modification, unless diaspore seed is present. Spontaneous nucleation of diaspore requires temperatures in excess of 575 K and pressures higher than 20 MPa. In the older literature, therefore, diaspore was considered the high-temperature form of $\text{AlO}(\text{OH})$. The first reaction diagram of the phase transitions in the $\text{Al}_2\text{O}_3\text{-H}_2\text{O}$ system was published in 1943 [107]. These workers determined the gibbsite \rightarrow boehmite conversion temperature to be 428 K. Boehmite transformed to diaspore above 550 K; diaspore converted to corundum, $\alpha\text{-Al}_2\text{O}_3$, at 725 K. Similar results were reported in 1951 [108].

The system was reinvestigated in 1959 [109] and in 1965 [110]. A phase diagram based on these data is shown in Figure 21.17. Diaspore is the stable modification of $\text{AlO}(\text{OH})$; boehmite is considered metastable, although it is kinetically favored at lower temperatures and pressures. This is because the nucleation energy is lower for boehmite than for the considerably more dense diaspore. In addition, $\gamma\text{-Al}(\text{OH})_3$ and $\gamma\text{-AlO}(\text{OH})$ have similar structures. Nucleation is, therefore, additionally facilitated by the possibility that boehmite can grow epitaxially on $\text{Al}(\text{OH})_3$. In the $\text{Al}_2\text{O}_3\text{-Fe}_2\text{O}_3\text{-H}_2\text{O}$ system, the presence of

the isostructural goethite, $\alpha\text{-FeO}(\text{OH})$, lowers the nucleation energy for diaspore so that this $\text{AlO}(\text{OH})$ modification crystallizes at temperatures near 373 K [111]. This observation explains the occurrence of diaspore in clays and bauxite deposits that have never been subjected to high temperatures or pressures.

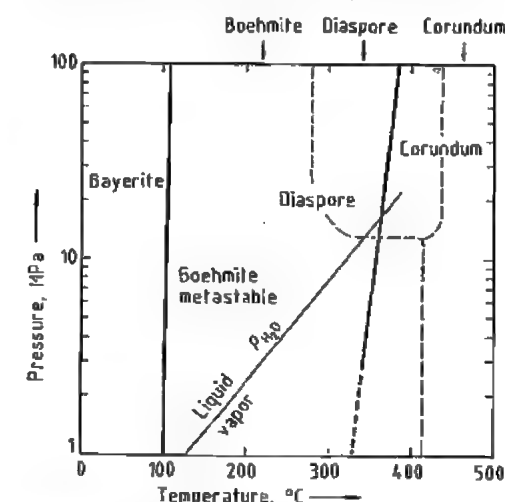


Figure 21.17: The $\text{Al}_2\text{O}_3\text{-H}_2\text{O}$ system. Dashed lines [108], solid lines [109, 110].

Structure. Boehmite consists of O, OH double layers in which the anions are in cubic packing. The aluminum ions are octahedrally coordinated. These layers are composed of chains of $[\text{AlO}(\text{OH})]_2$ extending in the direction of the *a* axis [112]. The double layers are linked by hydrogen bonds between hydroxyl ions in adjacent planes. Boehmite crystals exhibit perfect cleavage parallel to the (010) plane.

In the diaspore structure the oxygen ions are nearly equivalent, each being joined to another oxygen through a hydrogen ion. The anions are hexagonally close packed [113]. The position of the hydrogen ion has been established by neutron diffraction [114]. The O-H...O distance is 0.265 nm.

By infrared studies, the bond energy for the hydrogen bridges in diaspore was determined to be 28.7 kJ/mol, compared with 20.1 kJ/mol for boehmite [115].

Nomenclature. Although there is fairly good agreement in the more recent literature on phase fields and structures of the crystalline phases in the $\text{Al}_2\text{O}_3\text{--H}_2\text{O}$ system, the nomenclature is still rather unsystematic.

Bayerite, gibbsite (hydrargillite), and nordstrandite are trihydroxides of aluminum, and not oxide hydrates. The designation "aluminum oxide monohydrate" for boehmite and diasporite is also incorrect. Both are true oxide hydroxides. Molecular water has been determined in poorly crystallized, non-stoichiometric pseudoboehmite only.

The sodium ions have been removed from the lattice of the so-called β -alumina, $\text{Na}_2\text{O} \cdot 11\text{Al}_2\text{O}_3$, by leaching with H_2SO_4 , and the ions replaced with H_2O molecules [117]. This is to date the only case in which the existence and structure of an alumina hydrate have been confirmed. As an intercalation compound, however, this hydrate has no phase field in the $\text{Al}_2\text{O}_3\text{--H}_2\text{O}$ system.

The designation of the modifications of aluminum hydroxides and oxides lacks uniformity just as much as does the nomenclature of the compounds. According to the general usage in crystallography, the most densely packed structures are designated as α -modifications [90]. Bayerite, diasporite, and corundum fall within this class. The compounds with cubic packing sequence, gibbsite and boehmite, have been designated by the symbol γ . Nordstrandite can be classified as β - $\text{Al}(\text{OH})_3$ when regarding this compound not as an intergrowth of bayerite and gibbsite, but as an independent modification.

Aluminum Oxide, Corundum

The hexagonally closest packed α - Al_2O_3 modification is the only stable oxide in the $\text{Al}_2\text{O}_3\text{--H}_2\text{O}$ system. Corundum is a common mineral in igneous and metamorphic rocks. Red and blue varieties of gem quality are called ruby and sapphire, respectively. The lattice of corundum is composed of hexagonally closest packed oxygen ions forming layers parallel to the $\langle 0001 \rangle$ plane. Only two thirds of the octahedral interstices are occupied by alu-

minum ions. The structure may be described roughly as consisting of alternating layers of Al and O ions. The corundum structure was determined in the early 1920s [118]; numerous workers later confirmed and refined these data [90]. Properties of corundum are listed in Tables 21.7 and 21.8.

Thermal Decomposition of Aluminum Hydroxides

When aluminum hydroxides or oxide hydroxides are heated in air at atmospheric pressure, they undergo a series of compositional and structural changes before ultimately being converted to α - Al_2O_3 . These thermal transformations are topotactic. Despite a loss of 34 or 15% of mass for the trihydroxides or oxide hydroxides, respectively, the habit of the primary crystals and crystal aggregates changes very little. This leads to considerable internal porosity, which may increase the specific surface area of the material to several hundred m^2/g . Structural forms develop that, although not thermodynamically stable, are well reproducible and characteristic for a given temperature range and starting material. These transition aluminas have been the subject of numerous investigations because of their surface activity, sorptive capacity, and usefulness in heterogeneous catalysis. The literature in this field of physical chemistry has been reviewed up to 1972 [90].

The simplest transformation is that of diasporite to corundum. As the structures of these two compounds are very similar, the nucleation of α - Al_2O_3 requires only minor rearrangement of the oxygen lattice after the hydrogen bonds are broken. A temperature below 860–870 K is sufficient for complete conversion. The newly formed corundum grows epitaxially on the decomposing diasporite, with the $\langle 0001 \rangle$ plane of Al_2O_3 parallel to the $\langle 010 \rangle$ plane of $\text{AlO}(\text{OH})$ [119].

The thermal transformation, at ambient pressure, of α - $\text{AlO}(\text{OH})$ and the trihydroxides to α - Al_2O_3 requires considerably more structural rearrangements and is generally not completed until the temperature reaches at least

1375–1400 K. The first step in the reaction sequence is the diffusion of protons to adjacent OH groups and the subsequent formation of water [120, 121]. This process begins at a temperature near 475 K. If this water cannot diffuse rapidly out of larger trihydroxide particles, hydrothermal conditions may develop locally, resulting in the formation of γ - $\text{AlO}(\text{OH})$. With increasing loss of water, a large internal porosity develops. The lattice voids left by the escaping water are not readily healed because of the slow diffusion in this low temperature range. The voids are oriented parallel and perpendicular to the basal plane of the trihydroxide crystals (Figure 21.18).

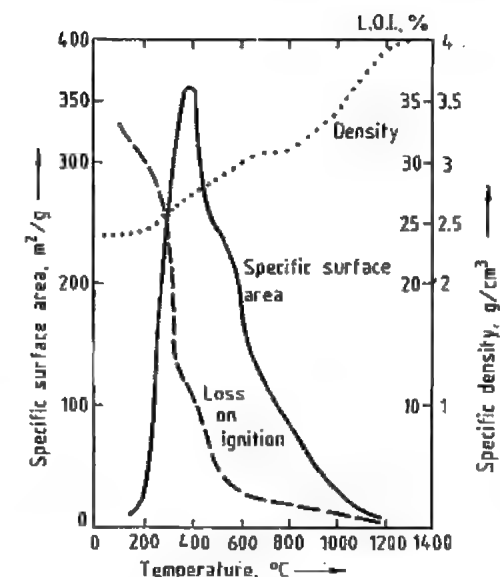


Figure 21.19: Specific surface area, loss on ignition (L.O.I.), and density of heated $\text{Al}(\text{OH})_3$.

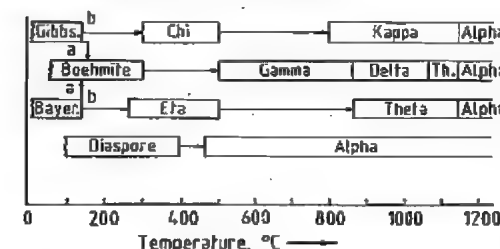


Figure 21.18: Gibbsite heated to 573 K.

The highest surface area and lowest crystalline order of the solid (not counting newly formed boehmite) is obtained at a temperature around 675 K. With increasing temperature the surface area decreases, while the density of the solid shows progressively higher values (Figure 21.19). This trend is the result of progressive reordering and consolidation of the solid.

During the thermally activated consolidation and reordering, the solid goes through structural stages that are influenced by the nature of the starting material as well as by heating rates, furnace atmosphere, and impurities. The general reaction paths are illustrated in Figure 21.20.

Figure 21.20: Decomposition sequence of aluminum hydroxide.

Transition oxides formed at lower temperatures are mostly two-dimensionally, short-range ordered domains within the texture of the decomposed hydroxides. Extensive three-dimensional ordering begins at about 1050 K. Until completely converted to corundum, the solid retains considerable amounts of OH^- ions. Most likely protons are retained to maintain electroneutrality in areas deficient of cations. The presence of protons therefore may retard the reordering of the cation sublattice. Addition of fluorine to the furnace atmosphere removes protons. As a result, rapid transition to α - Al_2O_3 occurs at temperatures as low as 1150 K. Markedly tabular corundum crystals form, possibly because the preceding transi-

tion alumina is mostly two-dimensionally ordered [122].

Transition forms other than the ones shown in Figure 21.20 can be obtained by hydrothermal treatment [90]. The structures of various transition forms have been investigated [123, 101, 105].

Aluminates and Related Compounds

Sodium oxide forms several compounds with aluminum oxide. These so-called β -aluminas represent a group of aluminates having the same, or very similar, structures but variable chemical composition. Their molar ratios ($\text{Na}_2\text{O}:\text{Al}_2\text{O}_3$) can vary between 1:1 and 1:11. The 1:1 sodium aluminate, NaAlO_2 , exists in at least two allotropic modifications. Orthorhombic β - NaAlO_2 is stable below 750 K; the higher-temperature γ modification is tetragonal. For preparation and properties of technical sodium aluminate, see Section 21.10.3.1.

The 1:11 β - Al_2O_3 crystallizes from melts containing aluminum oxide and sodium oxide or other sodium compounds. A 1:5 β -alumina has been prepared by heating α - Al_2O_3 with NaAlO_2 or Na_2CO_3 at about 1325 K.

Several other β -aluminas containing CaO , BaO , or SrO in 1:6 ratio also have been reported [90].

Recent interest in β -alumina is related to its use as a solid electrolyte in sodium sulfur secondary batteries.

21.10.1.2 Bauxite, the Principal Raw Material

Definition and Geology

The term bauxite is used for sedimentary rocks that contain economically recoverable quantities of the aluminum minerals gibbsite, boehmite, and diaspore. The name derives from the description by BERTHIER, in 1821, of a sediment that occurred near the village of Les Baux in the Provence, France. Originally assumed to be a dihydrate of aluminum oxide, bauxite was later recognized to be composed of aluminum hydroxide, iron oxide and hy-

droxide, titanium dioxide, and aluminosilicate minerals [89].

Early in this century, major bauxite deposits were found in various parts of the Tertiary and Cretaceous limestone formations of the European Alpidic mountains; also in several locations on the North American continent, e.g., in Arkansas, Alabama, and Georgia. Since the 1920s, extensive deposits have been discovered in the tropical and subtropical climate belts.

The oldest known bauxites developed in the Precambrian; the youngest are of recent origin. Deposits may occur as extensive, flat bodies blanketing areas of many square miles; they may form irregularly shaped fillings of dolinas in old karst surfaces, or lenses several hundred meters in diameter and tens of meters thick. Allochthonous, i.e., displaced bauxites, are also common; erosion of primary deposits and redeposition of the detritus in valleys or along mountain slopes has frequently led to mineable accumulations of ore.

Many of the geologically younger bauxites are covered only by thin layers of soil; others are buried by coastal or alluvial sediments. Older deposits, especially in the Balkans or the Ural Mountains, often are overlain by carbonate rocks hundreds of meters thick. Regardless of their geologic age, all bauxites were formed during continental periods [124].

Composition and Properties

The chemical composition of bauxites of various origin is given in Table 21.9 [89]. Aluminum oxide, iron oxide, and titanium and silicon dioxides are the major chemical components of all bauxites. Alkali and alkaline earth compounds are rarely found.

Gibbsite, γ - $\text{Al}(\text{OH})_3$, is the predominant aluminum mineral in the geologically young bauxites of the tropical climate belt. Mesozoic and older bauxite contain mostly boehmite (γ - $\text{AlO}(\text{OH})$) or diaspore (α - $\text{AlO}(\text{OH})$). Since their formation, many of the older bauxites have been buried under considerable layers of younger sediments and often were subjected to tectonic stress. Boehmite and diaspore for-

mation appears to be related to an increasing degree of metamorphism. However both minerals also occur in young deposits, although in minor quantities. The chemical environment obviously plays as important a role in the formation of boehmite and diaspore as do pressure and stress [124].

Table 21.9: Principal chemical constituents of various bauxites, %.

Country and location	Al_2O_3	SiO_2	Fe_2O_3	TiO_2	Loss on ignition
Australia					
Darling Range	37	26.5	16.4	1.1	19.3
Weipa	58	4.5	6.9	2.5	26.8
Brazil					
Trombetas	52	5.1	13.9	1.2	28.1
France					
Southern districts	57	4.6	22.6	2.9	15.1
Guyana					
Mackenzie	59	4.9	2.9	2.4	30.4
Guinea					
Friguia	49	6.1	14.2	1.6	28.1
Boké	56	1.5	7.9	3.7	30.1
Hungary					
Halimba	52	6.6	23.5	2.9	18.1
India					
Orissa	46	2.7	22.4	1.1	24.2
Indonesia					
Bintan	53.5	3.9	12.1	1.6	29.2
Jamaica					
Clarendon	47.8	2.6	17.6	2.3	27.3
Suriname					
Onverdacht	59	4.3	3.1	2.5	30.9
Moengo	54	4.2	10.4	2.8	28.9
United States					
Arkansas	51	11.2	6.6	2.2	28.4
Former USSR					
Severouralsk	54	6.2	14.8	2.4	15.7
Former Yugoslavia					
Mostar	52	3.9	21.2	2.7	16.2

Dissolution of gibbsite requires the mildest conditions in the Bayer process. Higher temperatures and alkali concentrations are necessary for the digestion of boehmite and diaspore. Technically, both oxide hydroxides can be processed without difficulties. The current abundance of high-grade gibbsitic bauxites, however, has made boehmite- and diaspore-rich ores economically less attractive.

Goethite, α - $\text{FeO}(\text{OH})$, and hematite, α - Fe_2O_3 , are the most prevalent iron minerals in

bauxites. They are practically inert under the conditions of the Bayer process. In both minerals, some of the iron may be replaced isomorphically by aluminum ions. This amount of aluminum is included in the chemical analysis of the bauxite but is normally not extracted in the digest. Magnetite (Fe_3O_4) is found in some European bauxites; pyrite (FeS_2) and siderite (FeCO_3) also may occur. Decomposition of pyrite may lead to high sulfur levels in the process solutions.

Anatase, TiO_2 , is the titanium mineral found most frequently in bauxites. Rutile, TiO_2 , occurs in some European deposits; FeTiO_3 is also present in minor quantities, especially in titanium-rich bauxites. Titanium dioxide minerals are attacked under only the most severe conditions of the Bayer process.

Silicon dioxide may occur as quartz, as in the bauxites of the Darling Range in Western Australia. Most commonly, however, SiO_2 is associated with the clay minerals kaolinite, halloysite, or montmorillonite. These aluminosilicates react with sodium aluminate solutions to form insoluble sodium aluminum silicates during digest, causing loss of sodium hydroxide and extractable alumina. The amount of the so-called reactive silica is one of the major factors determining quality and price of the ore.

Minor constituents, such as chromium, vanadium, zinc, and gallium, have little effect on the Bayer process or on the quality of the final product. Some tend to accumulate in the recirculated process solutions (e.g., gallium and vanadium) and must be removed periodically by appropriate treatments.

The physical properties of bauxites, i.e., texture, hardness, and density, can vary widely. Geologically old diaspore bauxites, especially those high in iron oxide, are very hard and can reach densities of 3.6 g/cm^3 . Young tropical deposits, in contrast, may have an earthy, soft texture and a density around $2.0\text{--}2.5 \text{ g/cm}^3$. Allochthonous bauxite often consists of hard nodules embedded in a soft, usually clayey matrix. Porous textures also occur. The color of bauxites is largely determined by the type and particle size of the

prevalent iron mineral. Highly dispersed goethite tends to be yellow to orange, whereas dark brown tones usually are associated with coarser hematite. Colors can vary greatly within a single ore body.

Hardness, texture, and the amount of overburden determine the methods applied for bauxite mining. Deposits in Greece, former Yugoslavia, Hungary, and former USSR require deep mining to depths of several hundred meters, often complicated by the difficulties of controlling water levels in the porous limestone formations. Tropical bauxites frequently are located so close to the surface that they can be recovered with normal earth-moving equipment.

Genesis of Bauxites

Many of the geologically young bauxite deposits are located in the savannah region, which extends north and south of the tropical rain forest belt. The climate of this region is characterized by a high mean annual temperature and abundant precipitation during the rainy season. Deposits occur on gently sloping hills or on peneplains. The stratigraphic evidence shows that these bauxites have formed in situ. Parent rocks may be coarse-grained, igneous rocks such as syenite, phonolite, basalt, or gabbro. However, large deposits also developed on kaolinitic sandstones, on phyllites, and on schists. A layer of kaolinitic clay is frequently found between the ore body and the parent rock.

Bauxite probably forms during long periods of low geologic activity when the combination of high temperature, abundant precipitation, and good vertical drainage favors intensive chemical weathering. The sequence of leaching begins with removal of alkali followed by the removal of alkaline earths. Oxides of iron, aluminum, titanium, and silicon are mobilized and reprecipitated as hydroxides and oxides. Aluminum hydroxide and silica form kaolinite, $\text{Al}_4(\text{OH})_8\text{Si}_4\text{O}_{10}$. This sequence first leads to the formation of tropical soils (laterites). Bauxitization follows when the climatic, chemical, and topographic

conditions prevail long enough to allow the removal of silicon dioxide as well.

The bauxite deposits of the Mediterranean region, the Caribbean Islands, and many other locations that are associated with tertiary and older limestone formations (karst bauxites) were formed by a similar weathering process. Parent materials were lateritic soils and clays transported into the karst region and deposited in depressions. During extended terrestrial periods, high mean temperatures, copious precipitation, and good vertical draining through the porous limestone bedrock facilitated a thorough desilification. In the older literature, the parent material for karst bauxitization was reported to be clayey residue left after weathering of substantial layers of carbonate rocks [125]. Researchers have shown conclusively that igneous rocks were the source of this material [126–128].

Comprehensive reviews of the geology, mineralogy, and genesis of bauxites have been given [124, 129].

Table 21.10: World bauxite reserves and production, $\times 10^3$ t [130].

Country	Mine production		Reserve base
	1982	1983	
Australia	23 621	23 000	4 600 000
Brazil	4 186	3 900	2 300 000
Greece	2 853	3 100	650 000
Guinea	10 908	9 000	5 900 000
Guyana	953	800	900 000
Hungary	2 627	2 800	300 000
India	1 854	2 000	1 200 000
Jamaica	8 380	7 400	2 000 000
Suriname	3 059	2 700	600 000
United States	732	700	40 000
Former USSR	4 600	4 600	300 000
Former Yugoslavia	3 668	3 600	400 000
Other market economy countries	4 820	5 000	3 100 000
Other centrally planned countries	2 180	2 300	200 000
<i>World total (rounded)</i>	<i>74 441</i>	<i>71 000</i>	<i>22 500 000</i>

Major Bauxite Deposits

Until the 1950s, the European aluminum industry was supplied from the karst bauxite deposits of France, Hungary, Yugoslavia, and Greece. United States sources (Arkansas) and ore from Suriname provided the raw material

for North American production. Since then, the picture has changed drastically. The four largest bauxite producers of 1982, namely, Australia, Guinea, Jamaica, and Brazil (Table 4) [130], hardly would have been mentioned in 1950. Today, they provide more than half of the world's total bauxite output (even at the depressed levels shown for 1982, which are more than 10^7 t lower than the production in 1981).

Africa. The savannah region covers an area of the African continent that has experienced low geologic activity for a long time. In this belt, which stretches from the Ivory Coast to Madagascar, very large bauxite deposits were found. The major production is currently concentrated in Guinea and Ghana. Cameroon, Sierra Leone, Mali, and the Congo region, among other areas, have substantial reserves.

Australia. Major deposits are located in the Darling Range in Western Australia, on the Gove Peninsula in the Northern Territory, and on the Cape York Peninsula in Queensland. Bauxite also occurs in New South Wales, in Victoria, and on the island of Tasmania. The Australian deposits developed between the Eocene and Pliocene epochs on substrates ranging from Precambrian sandstones to Tertiary basalts. Gibbsite is the predominant aluminum mineral, although some boehmite occurs in all but the Western Australian deposits.

South America. On the outer slopes of the old Guyana Shield, many economically important deposits have been found. They are located in the Amazon Basin of Brazil, in Colombia, Venezuela, Suriname, Guyana, and French Guyana. Suriname and Guyana have been producing for more than 60 years, whereas the Brazilian Amazon deposits have been mined only recently. Bauxite also is produced in the Pocos de Caldas area in Southern Brazil, state of Minas Gerais. The South American bauxites generally are geologically young, gibbsitic ores.

Caribbean. Jamaica and the Dominican Republic have major reserves of karst bauxites that occur on Tertiary limestones under generally very thin overburden. Although gibbsite

is the main aluminum mineral, some boehmite also is present. Jamaica has been one of the world's leading bauxite producers for the past 20 years.

North America. The only economically important deposit is located in Arkansas, where gibbsitic bauxite developed on nepheline syenite during the Eocene. Less than 5×10^7 t of bauxite remain, and the grade is declining.

Europe. Except for a few commercially insignificant occurrences, all European bauxites are of the karst type. The oldest deposits (Devonian/Mississippian) are those of the Tikhvin area in the USSR; the youngest are the Eocene bauxites of Yugoslavia. Most European deposits developed during the Lower and Upper Cretaceous, e.g., the diaspore and boehmite bauxites of France, Greece, and Romania, and the gibbsite and boehmite bauxites found in Hungary, Yugoslavia, and Italy. Today, all European mines combined contribute only about 17% of world production.

Asia. Major deposits of gibbsite bauxites occur in India; the island of Kilimantan (Indonesia) has large potential reserves. Numerous bauxite deposits, most of them containing geologically old, diaspore-rich ore, were found in China. Substantial deposits also are located in Western Siberia.

Economic Aspects

The proved reserves of bauxite shown in Table 21.10 are sufficient to supply the world aluminum industry for a few centuries. Total resources are estimated by the U.S. Geological Survey at 40 to 50×10^9 t. Because of the worldwide distribution of significant ore deposits, a disruption of bauxite supply for political reasons appears highly unlikely. In 1974 several major bauxite-producing nations formed the International Bauxite Association (IBA) with the intent of increasing control over the exploitation of their bauxite deposits. Although levies were increased substantially, competition from countries not associated with the IBA helped maintain a reasonable price structure.

Economic and political considerations currently favor refining of bauxite near the deposit and shipment of either alumina or aluminum ingot. Brazil, Suriname, and Australia have smelters, although their refining capacity by far exceeds the demands of domestic metal production. Jamaica and Guinea refine a substantial portion of their own bauxite production.

About 25% of all bauxite mined is used for producing abrasives, catalysts, adsorbents, and other industrial chemicals.

21.10.1.3 Bayer Process

History and Procedure

Pure Al_2O_3 became the raw material for aluminum production upon development of the Hall-Héroult cell. The first alumina was prepared by thermal decomposition of aluminum salts and by sintering bauxite with soda (LE CHÂTELIER). This changed when in 1887 the Austrian chemist, KARL JOSEF BAYER, developed the process that bears his name. His first work was done in an experimental plant in Russia. Construction of the first large commercial Bayer plant was begun in 1901 in East St. Louis, Illinois. Since that beginning, plants have been built in at least 25 countries, and the present world capacity is over 4×10^7 t/a [88-93].

The important features exploited in the Bayer process are that boehmite, gibbsite, and diasporite can be dissolved in NaOH solutions under moderate conditions; the solubility of Al_2O_3 in NaOH is temperature dependent; most other components of the bauxite are quite inert in the process; and the silica that does dissolve subsequently forms a nearly insoluble compound. These features permit formation of a sodium aluminate solution, physical separation of the impurities, and precipitation of pure $\text{Al}(\text{OH})_3$ from the cooled solution.

Figure 21.21 shows the flow sheet of the process as it is now practiced.

Each operation in the process is carried out in a variety of ways. The process begins with

preparation of the bauxite by blending for uniform composition followed by grinding. In most plants the bauxite is ground while suspended in a portion of the process solution. This slurry is mixed with the balance of the heated NaOH solution, then treated in a digester vessel at well above atmospheric pressure. The digest reaction is:



Additional reactions convert impurities such as SiO_2 , P_2O_5 , and CO_2 to relatively insoluble compounds. The other bauxite constituents remain as solids. The slurry leaves the digester at a temperature above its atmospheric boiling point and is cooled by flashing off steam as the pressure is reduced in several stages. The flashed steam is used to heat the slurry and the solution going to the digester. The bauxite residue solids are separated from the sodium aluminate solution in two steps so that the coarse fraction is processed separately from the fine. Both residue fractions are washed and discarded. The solution, being free of solids, is cooled and seeded with fine crystals of $\text{Al}(\text{OH})_3$; this causes the $\text{Al}(\text{OH})_4^-$ ions to decompose to $\text{Al}(\text{OH})_3$, thereby reversing the reaction that previously had taken place in the digester. Again, the heat removed in cooling the solution is used to heat a colder stream in the process. After the precipitation reaction has proceeded to the point that about half of the Al_2O_3 in the solution has been removed, the mixture of solids and solution is sent to classifiers. The fine $\text{Al}(\text{OH})_3$ particles are returned to the process to serve as seed. The coarse particles are washed and calcined to Al_2O_3 . Excess solution introduced in washing the product and the residue must be removed by evaporation. In some cases the solution is treated to remove both organic and inorganic impurities before the solution is recycled through the plant.

Bauxite Preparation

The bauxite entering the refinery must be uniform and sufficiently fine that extraction of the Al_2O_3 and that the other operations are successful. The chemical composition of

bauxite varies. Uniformity is improved by blending material mined from several pits and, if necessary, by adding bauxite from storage piles. A more recent development is to store ground bauxite slurry in surge tanks before it is pumped to digestion. These agitated tanks are operated so that plant feed is uniformly blended for several hours. Sometimes bauxites are dried to improve handling or washed to remove clay.

Hard bauxite is reduced to particles finer than 2 cm in roll or cone crushers and hammermills. Before it enters the process it is ground further to less than 0.15 cm.

Previously, fine grinding was done in dry mills operating in closed circuit with vibrating screens. Such operation required very dry bauxite to avoid blinding the screens. This resulted in a dusty working environment. In most modern plants, the bauxite is mixed with a portion of the process solution and is ground as a slurry. Rod mills and ball mills are used most frequently. The ground slurry may be passed over screens or through cyclones, with the fine particles progressing and the coarse ones being returned to the mills.

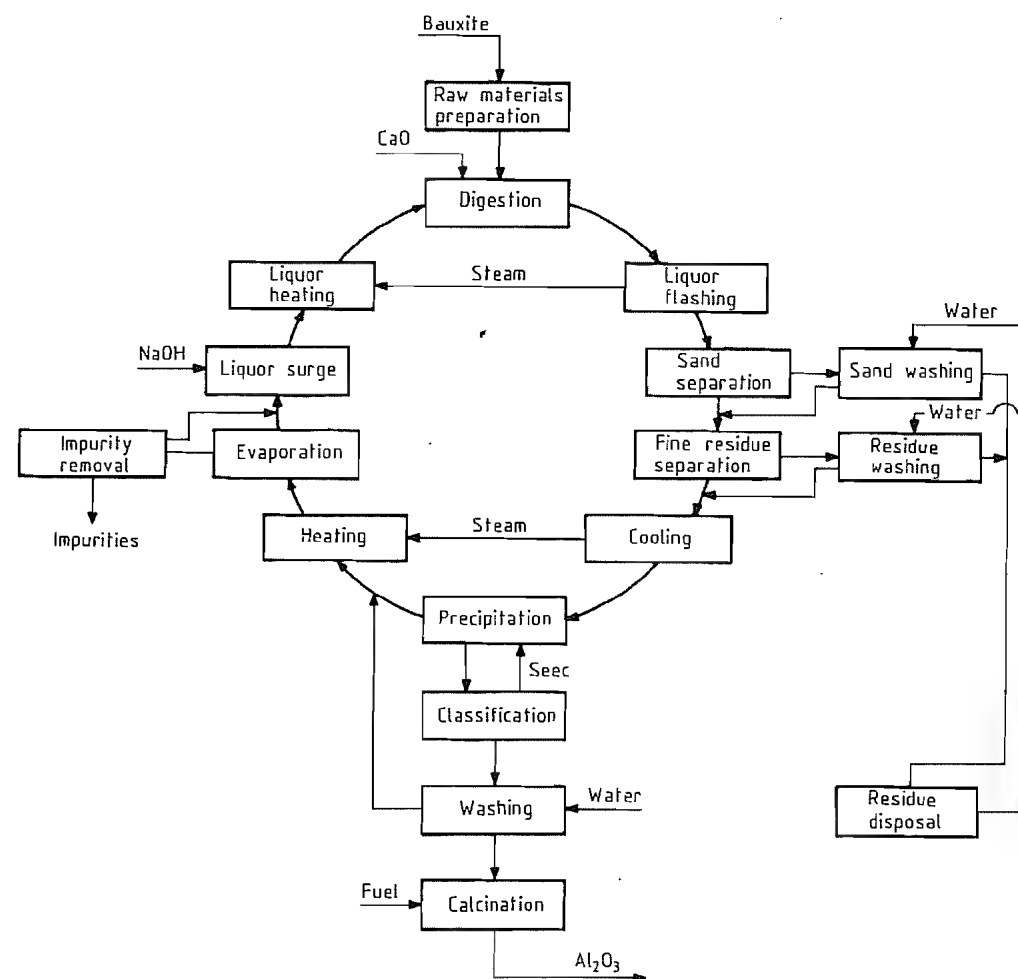


Figure 21.21: Bayer process flow sheet.

In all-wet grinding the bauxite feed and the flow of solution are controlled to keep the solids content of the slurry between 45 and 55%. The power consumed by the mill drive is an indicator of the amount of grinding being done and may be used to control the feed to the mill. On a longer time scale the particle size of the product can be used to make changes in the grinding operation.

Digestion

In digestion, all of the Al_2O_3 in the bauxite must be extracted. A solution is produced that contains the maximum Al_2O_3 concentration that can remain stable through the rest of the process. This must be accomplished while using a minimum amount of energy.

The conditions for digestion can and do vary widely. The first consideration is whether the available Al_2O_3 is present as gibbsite, boehmite, diaspor, or a mixture of these minerals. The dissolution rates of the three are quite different. Generally, if the bauxite contains mixed phases, the digestion conditions will be chosen on the basis of the least soluble compound. Any $\text{Al}(\text{OH})_3$ or AlOOH left undissolved can act as seed in the clarification step, causing precipitation of $\text{Al}(\text{OH})_3$ while the residue is still in contact with the solution. In the sweetening process, boehmitic bauxite is digested under relatively mild conditions, producing an intermediate Al_2O_3 concentration. In a separate vessel, gibbsitic bauxite is added to the flow from the first digest to raise the Al_2O_3 concentration to the desired level. Another approach is to digest only the gibbsite in a mixed bauxite. The residue is separated from the solution and redigested under more severe conditions to recover the boehmite. This method reduces the flow to the high-temperature digest and so requires lower capital and operating costs.

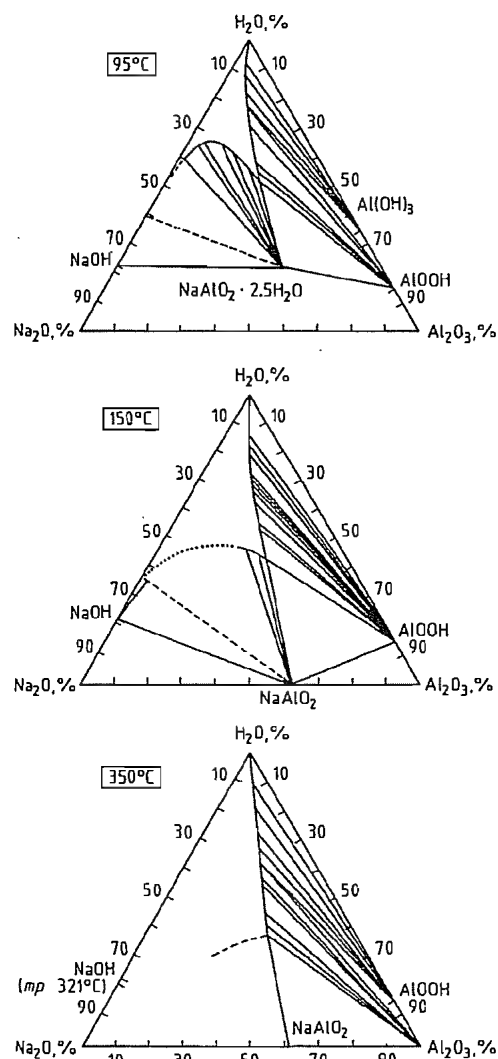


Figure 21.22: Phase diagram $\text{Na}_2\text{O}-\text{Al}_2\text{O}_3-\text{H}_2\text{O}$.

The solubility data (Figure 21.22) show that the Al_2O_3 concentration in the process solution can be increased by increasing either the temperature, the NaOH concentration, or both [88–91]. As a result, operating conditions in plants vary widely. Higher digest temperatures result in higher pressures, making the equipment more expensive. There also is the need for more heat-exchange equipment, which further increases capital costs. High concentrations, on the other hand, permit in-

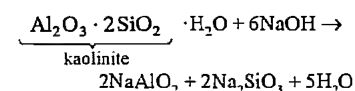
creased production from a given flow rate and, hence, from a given plant installation. Precipitation is thought to occur better at lower concentrations, but use of low precipitation concentrations while digesting at high concentrations requires dilution and additional operating costs for subsequent evaporation. Choosing digester conditions involves balancing these physical factors with local economics, together with the designer's experience. This has resulted in the spectrum of operating conditions given in Table 21.11.

Table 21.11: Commercial digestion conditions.

Bauxite type	Temperature, K	c_{NaOH} , g/L	Final $c_{\text{Al}_2\text{O}_3}$, g/L
gibbsitic	380	260	165
	415	105–145	90–130
boehmite	470	150–250	120–160
	510	105–145	90–130
diaspor ^a	535	150–250	100–150

^aCaO is added to digests to accelerate dissolution of diaspor.

The conditions listed in the first line of Table 21.11 are those for digesting bauxite at the atmospheric boiling point. Quite high alkali concentrations are required and the evaporation requirement is an extraordinary 5.3 t of water for a ton of Al_2O_3 . Most plants digesting gibbsitic bauxite use the conditions on the second line of Table 21.8. Boehmitic bauxite is digested using one of two general sets of conditions. The first is European practice, in which higher concentrations and dilution prior to precipitation are preferred to higher digest temperatures. When American companies began processing boehmitic bauxite from the Caribbean area, most chose the same concentrations used for gibbsitic bauxites; therefore, a higher temperature was required. The second important reaction in digestion is desilication. In the equation below, kaolinite is used to illustrate the reaction of siliceous minerals with the process solution:



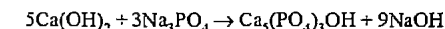
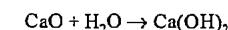
The soluble products react to form a series of precipitates with zeolite structure, having a

composition of approximately $\text{Na}_8\text{Al}_6\text{Si}_6\text{O}_{24}(\text{OH})_2$.

Depending on temperature and concentration, the ratio of $\text{Al}_2\text{O}_3:\text{SiO}_2$ in the zeolite (tectosilicate) structure can vary. For each Al^{3+} replacing Si^{4+} in the lattice, one Na^+ is taken up to maintain charge neutrality. Anions, such as SO_4^{2-} or CO_3^{2-} may substitute for OH^- in the structure. The formation of the zeolitic desilication product (DSP) therefore leads to costly loss of sodium hydroxide. This reaction, however, is necessary for lowering the level of dissolved SiO_2 to less than 0.6 g/L, the maximum acceptable concentration.

The rate-determining step in the desilication reaction is the nucleation and crystallization of the desilication product. Therefore, the presence of seed particles is important; without seeds, solutions containing 0.75 g/L SiO_2 will not react in 40 min at 415 K. This has led to the paradoxical situation that some bauxites contain too little reactive SiO_2 for good desilication. The slurry blending and storage operation discussed earlier can be an important part of the desilication process. If the storage temperature is above 355 K, about 80% of the reaction takes place in 8 h. More important, seed is formed so the desilication reaction in the digester is not delayed. Very low SiO_2 concentrations can be achieved if an excess of CaO is charged. At high temperatures, and with the lime additions, a less soluble desilication compound (cancrinite) is formed. European plants use longer holding times during or after digestion to facilitate desilication.

Some CaO is added to the digest even when extreme desilication is not required. The calcium reacts with the carbonate and phosphate compounds as follows:



The last reaction controls the level of phosphates in the process solution; this impurity can affect clarification adversely. Causticization in the digest was more important when prices were such that the sodium required by the process was supplied more cheaply as

Na_2CO_3 . Its current importance is in control of the CO_3^{2-} concentration, which, at high levels, can affect precipitation. In modern practice, the causticization reaction is carried out on dilute process solutions outside the digester. Maintaining low concentrations and having much of the NaOH combined as NaAlO_2 are favorable to more complete reaction of CO_3^{2-} with Ca^{2+} .

Equipment

The equipment for digestion includes the reactor vessel, heat-exchange equipment, and pumps. The first reactors were horizontal vessels with crude agitators mounted on axial shafts. These were filled with a slurry of bauxite, lime, and process solution. They were closed and heated individually by injecting high-pressure steam. At the end of the designated holding time, a discharge valve was opened and the slurry was forced into another vessel at atmospheric pressure. Only a small portion of the steam flashing from the slurry as the pressure was reduced could be recovered. Continuous operation was introduced in the 1930s in which heat could be exchanged between the hot stream leaving the digester and the cooler, incoming stream. This greatly reduces the energy requirements.

Reactors. Digester vessels, whether batch or continuous, provide intimate contact between the bauxite and the solution for a period long enough to complete the extraction and desili-

cation processes. The equipment designed for this purpose is quite diverse. Agitated horizontal vessels have been replaced by vertical units to avoid the mechanical problems with sealing the agitator shaft. Both designs have used a series of vessels to minimize short-circuiting of the flow. European practice includes use of a series of vertical agitated vessels, each operating at a higher temperature than the preceding one. These units are heated by flashed steam in internal steam coils. A German digester design uses concentric pipes; the liquid being heated flows through the inner pipe while the hot slurry from the digester is returned through the outer pipe. This tube digester has been modified by placing several tubes for the cold slurry in parallel inside a larger outer tube. This reduces the length of the unit. The variety of digester design is illustrated in Figures 21.23 and 21.24. The flow through single-digester units may be as high as $12 \text{ m}^3/\text{min}$.

The usual *construction material* for digesters is mild (low-carbon) steel, despite data showing that, at the temperatures and NaOH concentrations involved, there may be stress corrosion cracking resulting from alkali embrittlement. The presence of the $\text{Al}(\text{OH})_4^-$ ions reduces the activity of OH^- in the solution. Finely divided Fe_2O_3 in the bauxite quickly saturates the solution with Fe^{3+} , suppressing corrosion of the metal. Some digestion equipment has been nickel plated for safety.

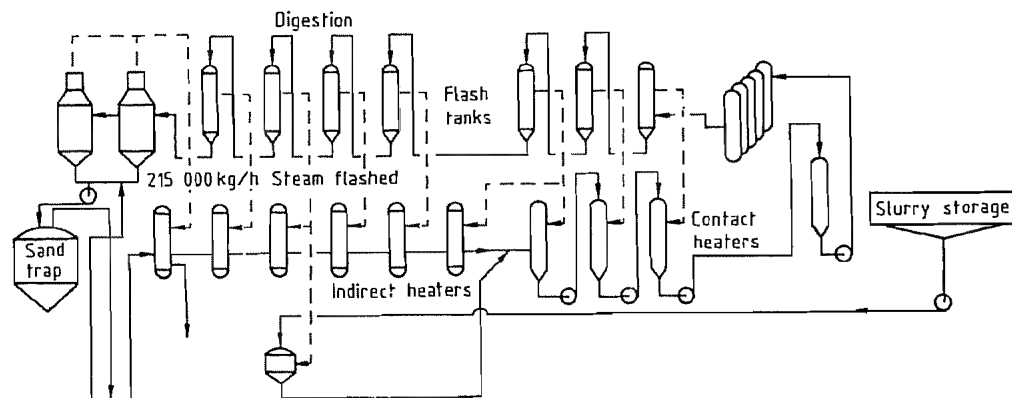


Figure 21.23: High-temperature digestion and heat recovery.

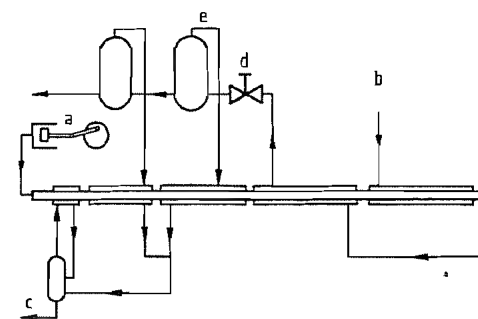


Figure 21.24: Tube digester: a) Piston pump; b) Heat; c) Condensate; d) Flow control valve; e) Steam.

Flashing. In most plants the hot slurry from the digester is flashed in a series of pressure vessels until it reaches the atmospheric boiling point. The steam generated in flashing is used in heat exchangers to heat the flow of liquor and bauxite coming to the digester. Flashing also removes water from the process stream, thereby accomplishing a significant portion of the evaporation needed. Normally, heaters are tubular, but coils of tubing also are used. As few as three stages of flashing may be needed when the digestion temperature is 418 K, and this may be increased to ten stages for a unit operated at 515 K. Figure 21.23 is a schematic diagram of a high-temperature digestion unit.

Heat Exchangers. Operating practice has been divided as to whether the bauxite slurry should be heated separately or whether it should be mixed with the rest of the solution and then heated. These two modes of operation have been designated the single- and the double-stream processes. Those favoring separate heating of the bauxite slurry, the double-stream option, feared rapid deposition of desilication product on the heat-transfer surfaces. Experience has shown that, particularly if the bauxite slurry is stored for blending, those fears are unfounded. The rate of fouling is no higher than for heating clean liquor. In both options there is slow deposition of desilication product on the heat-exchanger surface because the desilication reaction does not reach equilibrium in the digester and continues at a slow rate wherever the solution temperature is raised. The encrustation must be

removed periodically by washing with dilute HCl or H_2SO_4 , or by mechanical means to maintain a high heat-transfer rate.

In some plants using the double-stream system, the bauxite slurry is heated in contact heaters. These heaters are designed much like barometric condensers. The liquid is forced to fall through the steam in the heater in droplets or in thin films. The large surface area exposed results in high heat-transfer rates, and because there is no metallic surface, there is no fouling. The penalty is higher dilution.

The heat needed to raise the temperature above that achieved in the flashing system can be introduced by direct injection of steam. More often the final heating to the digest temperature is done in a separate heat exchanger, with the energy coming from steam, hot oil, or molten salts.

Pumps. *Centrifugal pumps* are used in most digester systems. Those used for pumping slurries are built of wear-resisting alloys. A great deal of maintenance is required to keep the shaft seals operating well. In some plants, concern about pump wear has led to the use of *diaphragm pumps*. In such pumps a check valve admits the slurry to a chamber on one side of a flexible diaphragm. When that chamber is full, oil at high pressure is forced into a chamber on the other side of the diaphragm. This moves the slurry through another check valve into the digester. Therefore, no rapidly moving parts are in contact with the slurry. In a Japanese modification, called the *Hydrohoist*, the diaphragm is replaced by a sphere that is free to move the length of a cylinder. Slurry is kept in one end of the cylinder and the drive fluid, which is clean process solution, is in the other end. Because of this choice of drive fluid, leakage past the sphere is of no consequence and tight clearances are not required.

Measurement and Control. Operating variables that must be controlled are temperature, solution concentration, and degree of desilication. The holding time is fixed by the design of the digester vessels. As noncondensable gases are formed by the reaction of the solution with

organic materials in the digest, it is necessary to vent these gases so that the digester remains full. Venting can be controlled by sensing the liquid level with a float or a radioactive sensor. Temperature measurement and control are relatively simple because only the temperature from the final heater is critical. Concentration control comes from blending the bauxite and careful proportioning of the slurry and clean solution flows. Originally, feedforward control was used in which the composition of the incoming materials was used to set the rates at which they were added. In modern practice feedback control is based on the composition of the exiting solution. Chemical analyses of the solution can be used, but the time lag involved makes this control imprecise. Nearly real-time control has been achieved by using the fact that the conductivity of the solution at a given temperature is a linear function of the mass ratio of Al_2O_3 and NaOH . This is the variable of interest. In modern plants the output of the sensor goes to a computer, which in turn controls the amount of bauxite slurry pumped. Such control has reduced the variance in concentrations to about a third of the values experienced earlier. This permits operation closer to the maximum safe concentration with less risk of premature precipitation of Al_2O_3 in clarification.

Clarification

The next step in the process is the separation of bauxite residue solids from the solution. There is a wide variety of equipment and procedures used in this operation. The methods chosen depend on the quantity and properties of the residue.

The particle size distribution of the residue solids is usually bimodal. The coarse fraction over 100 μm in diameter is termed *sand*, whereas the rest of the solids are finer than 10 μm . The sand fraction may range from 5 to nearly 50% of the total. The lowest amounts are in the Caribbean bauxites and the highest are in the residue from Western Australian bauxite. In the plant the sand fraction is separated from the process stream in liquid-solids

cyclones or in more primitive settling devices. A variety of equipment, including Dorr, Hardinge, and Aikens classifiers, have been used to wash the sand free of process solution before it is discarded. In all of these units the sand moves countercurrently to the wash water so that a maximum of washing is done with a minimum of water. The wash solution is added to the balance of the process flow and proceeds to further clarification steps for removal of the fine solids.

In most plants the fine residue fraction is settled in raking thickeners of the type illustrated in Figure 21.25. These vessels may exceed 49 m in diameter. Some older plants used multideck thickeners. Difficulties in keeping the multideck units in balanced operation have led to almost exclusive use of single-deck units in new construction.

The desanded slurry is fed at the center of the thickener and clarified solution overflows at the perimeter. As the solution flows radially across the thickener both the horizontal and vertical velocities become very low. The solids, having a higher specific gravity than the solution, sink to the bottom of the thickener. A settling rate of 1.5 m/h is sufficient for commercial operation. The solution overflowing the thickener usually contains less than 0.3 g/L solids, whereas the underflow ranges from 15 to 35% solids. The rotating mechanism has plows mounted at an angle to the arm. These slowly move the settled pulp across the bottom of the thickener to a discharge port. A few units have been designed with the discharge at the perimeter rather than at the center.

The objective was to avoid the need to elevate the units to provide access to a center discharge.

The fine solids behave as a relatively stable colloidal suspension, so they settle slowly if not treated further. The addition of *flocclulants* improves the clarity of the thickener overflow, the settling rate of the solids, and the solids content of the underflow pulp. Flocclulants act by binding the very fine particles into flocs that may be several millimeters in diameter. The ratio of mass to drag forces is increased so the flocs settle more rapidly.

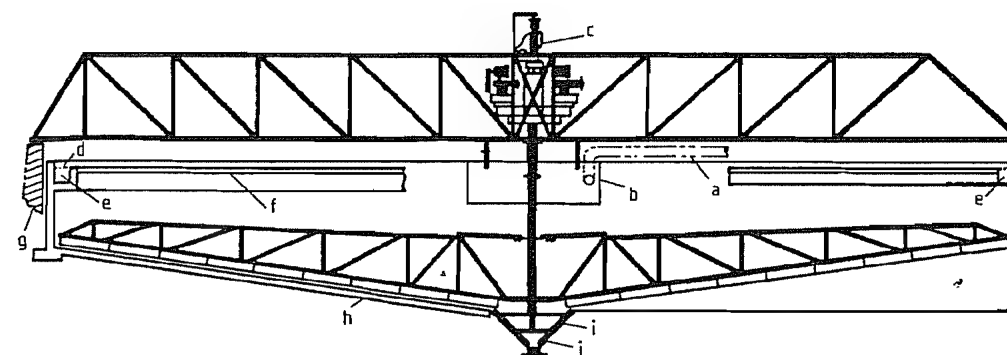


Figure 21.25: Residue thickener: a) Feedpipe; b) Feedwell; c) Motorized lifting device; d) Liquid level; e) Overflow launder; f) Weir; g) Off-tank support; h) Tank; i) Cone scraper; j) Discharge cone.

Starch from either grains or roots was the first flocculant; the dosage varied from 0.5 to 3 kg per ton of bauxite. The amount required increases as the surface of the residue increases and is affected by the mineral composition of the residue. Starch has the advantages of being inexpensive and ubiquitous. It does react with the NaOH in the solution to add organic compounds to the solution. In the 1950s water-dispersible polymers were proposed as flocculants. The first compounds were effective when added at 10% of the starch charge, but they were expensive so they offered no economic advantage. More recently, flocculants based on acrylate-acrylamide copolymers have begun to replace starch. The functional groups of these anionic flocculants can be modified to suit specific operating conditions. Different materials may be used in the thickeners and in the washing operation. In some cases a small amount of starch is added to the synthetic flocculant to improve overflow clarity. These synthetic materials now offer an economic advantage because they have been made less expensive and more effective.

With the residue concentrated in the thickener underflow, the next task is to wash it free of process solution so that it can be discarded. This is usually done in countercurrent decantation systems using washing thickeners that are similar in design to those used for settling. The washing operation is done in as many as seven stages with the solids moving countercurrent to the wash stream. This is illustrated

in Figure 21.26. An equation can be written for each stage expressing a material balance between soluble materials and dilution. Computer models of the washing system allow accurate prediction of performance.

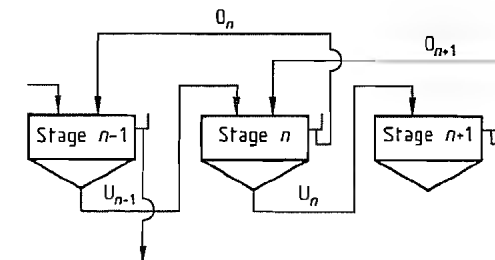


Figure 21.26: Flows at stage n in countercurrent decantation (O = overflow; U = underflow).

In *residue washing*, the objective is to minimize both the value of the soluble salts lost and the cost of evaporating the added wash water. The solubles in the discarded pulp can be reduced by increasing the solids content of the underflow. This reduces the amount of solubles carried from one stage to the next so that dilution is more effective and can be accomplished by using more flocculant or by increasing the holding time in the thickener. There is some risk in the latter change. If some undissolved gibbsite or boehmite remains in the residue, it may induce precipitation with a resulting loss of Al_2O_3 .

In some plants vacuum drum-type washing filters are used to replace some or all of the washing thickener stages. The solids content of the residue may be increased to 50–60% by

filtration. Therefore only about 33% as much solution is needed compared to plants using thickeners and this results in a great increase in the effectiveness of washing. Calculations for countercurrent washing show that two stages discharging at 55% solids are more effective than six stages operating at 20% solids.

Another approach only recently introduced into plant practice is called the deep thickener. This equipment was developed in the British coal industry to concentrate the slimes from coal washing. In the deep thickener, increased quantities of flocculant are used and a column of residue pulp up to 10 m deep is maintained. The hydraulic pressure of the deep column appears to densify the pulp so that underflow solids approaching the concentration of filter cake are obtained. The overflow from these units contains more solids than the flow from standard thickeners, but the units are finding use in concentrating residue for washing and for disposal. The simplicity of the equipment adds to its appeal.

The final stage of clarification is *polish filtration* of the solution, sometimes called clear pressing. Most of the residue solids have been removed from the process solution in the previous steps, but product purity must be protected by removing the few particles of solids remaining. Filter presses are used most widely.

Another approach to polish filtration is use of a stationary filter in which the medium is uniform, fine sand a meter deep. Gravity provides the force to move the solution through the sand bed. During operation, the fine solids are mixed with the sand, from which they are elutriated at the end of the cycle. Such filters can be automated and are especially effective with residues that are difficult to process.

Close attention is required to keep the solids content of the filtrate down to 0.5 mg/L to protect product purity. Light transmission of the filtrate is used as an index of clarity. Purity originally was determined visually, but nephelometers are used now. If evidence of solids is found, the filtrate from each filter is scanned to locate the source. Some solids may

pass through the filter cloth before a layer of solids forms to serve as a barrier, so it is common practice to recycle the first portion of filtrate.

Control in clarification has two major objectives; the solids must be removed and the washed residue must be prepared for discard, using a minimum of wash water. The first objective is achieved by measuring the cloudiness of the filtrate. High solids in the underflow are dependent in part on the retention time in the thickener, so measurements must be made of the pulp level in the unit. Automatic determination of the interface between clarified liquid and pulp has been done by ultrasonic and by optical scanning. The density of the underflow pulp is monitored by a device measuring absorption of radiation or by gravimetric measurement. If the pulp is too dilute the rate of withdrawal is decreased. This control can be overridden if the pulp level in the unit rises too high so that there is concern that the solids in the filter feed may become excessive. The flows of solids and wash water also must be measured and proportioned for efficient operation.

Precipitation

The filtered solution is at a temperature of 375 K and it must be cooled to 335–345 K before precipitation. This *cooling* is usually done in a flashing system analogous to that used in recovering heat in digestion. Because the temperatures are below the atmospheric boiling point, the flash vessels and the heat exchangers must operate under vacuum. This requires a method for removing noncondensable gases from the system. Usually a steam jet pump is used. Most heat removed by flashing is transferred to the colder solution returning from precipitation. Heat from the final cooling stage is ejected to the atmosphere or, preferably, to wash water entering the plant. Barometric condensers can be used for this final cooling. A recent development is to cool the solution further midway through the precipitation operation. This allows higher recovery of

Al_2O_3 without using conditions that lead to excessive nucleation of product.

Recovery of the $\text{Al}(\text{OH})_3$ from the process solution is known as precipitation, decomposition, or Ausrührung. The reaction is the reverse of the digester reaction given earlier. The cooling done after digestion and filtration has moved the solution into an area of the solubility diagram known as the metastable region. The concentration and temperature are such that the solution is supersaturated with $\text{Al}(\text{OH})_3$ but is not saturated enough for spontaneous crystallization. This is illustrated by Figure 21.27. At the digest temperature, T_1 , the Al_2O_3 concentration is increased to point P on the diagram. Cooling to temperature T_2 results in crossing the solubility curve into the metastable region. Addition of $\text{Al}(\text{OH})_3$ seed at this point causes precipitation and the concentration of Al_2O_3 approaches the solubility curve at T_2 . The additional cooling recently adopted moves the solution conditions further to the left in the diagram above a lower point on the solubility curve.

The kinetics of the precipitation reaction are represented by the equation:

$$-\frac{dc}{dt} = ke^{-\frac{E}{RT}}A(c_i - c_\infty)^2$$

where: $c = \text{Al}_2\text{O}_3$ concentration in g/L, $k =$ constant, $E =$ activation energy, about 59 000 J/mol, $R = 8.31441 \text{ J/mol}^\circ\text{K}^{-1}$, $T =$ temperature in K, $A =$ seed area in m^2/L , $c_\infty =$ concentration at equilibrium.

The reaction is second order, i.e., the rate is affected by the square of the difference between the actual Al_2O_3 concentration and the equilibrium concentration. The operating temperature affects the equilibrium concentration and the reaction rate. Because seed area is important, the seed charge must be as high as can be maintained while meeting other operating objectives.

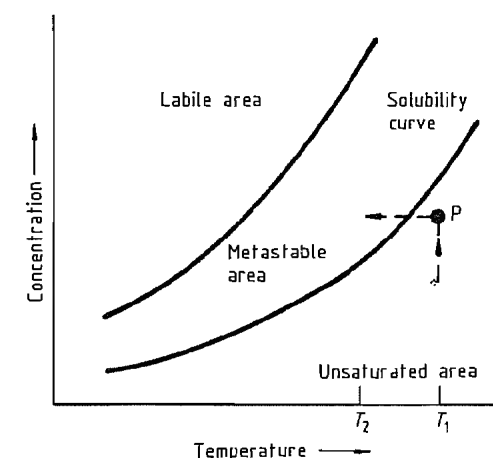


Figure 21.27: Generalized solubility curve.

The first objective in precipitation is to produce $\text{Al}(\text{OH})_3$ that, when calcined, meets the specifications for metallurgical alumina. These specifications are discussed in Section 21.10.1.5. The second objective is to obtain a high yield from each volume of solution. This increases the plant capacity and reduces the amount of energy spent in heating and pumping the solution. At the same time, the processes serving to create new $\text{Al}(\text{OH})_3$ particles must be controlled so that the number of seed particles created equals the number of particles leaving the system as product. This requires balancing nucleation, agglomeration, growth, and particle breakage, so a combination of science and art has developed.

About 2×10^{10} nuclei must be formed in each liter of solution to balance the process. The rate of *nucleation* is a strong function of both the degree of supersaturation and of temperature. Very few nuclei are formed if the temperature is above 350 K. A change in the operating temperature of only five degrees will change a system from a net producer to a net consumer of nuclei. Temperature changes of two to three degrees are the most frequently used control measures.

The nuclei *grow* slowly by accumulation of $\text{Al}(\text{OH})_3$ on their surface if they become large enough to be viable seeds. The rate of growth can be as high as 9 $\mu\text{m}/\text{h}$, but it is generally much lower. The growth rate is independent of

the particle diameter. Particles also increase in size by *agglomeration*. By a process that is not well understood, the nuclei form clusters in the first few hours of the cycle in batch precipitation. When the supersaturation is low, this agglomeration does not occur. Some speculate that when the rate of precipitation is high, the $\text{Al}(\text{OH})_3$ is not well crystallized when it is first deposited on the seed. This later may serve as the bond for agglomeration. At low supersaturation the deposited material is better ordered. The action of mechanical equipment in precipitation can *break* fragments off crystals or break up agglomerates, creating secondary nuclei, but this is not a major factor in most plants.

Figure 21.28 is an electron micrograph of some $\text{Al}(\text{OH})_3$ produced in a plant operation. The particles are obviously the result of agglomeration. Those agglomerates having fewer particles can be shown by thin-section micrographs to have grown radially from an agglomerate of relatively few nuclei.

Figure 21.28: Technical aluminum hydroxide (gibbsite), 200 \times .

In Figure 21.29, the Al_2O_3 concentrations in experimental precipitations is shown as a function of time and temperature. The slopes of these curves indicate the rates at which precipitation is progressing. All curves show a high rate at the start and appear to be approaching a final value asymptotically. The final concentrations were well above the saturation level, but in these as in plant opera-

tion the rate became unusually low, so the process was terminated.

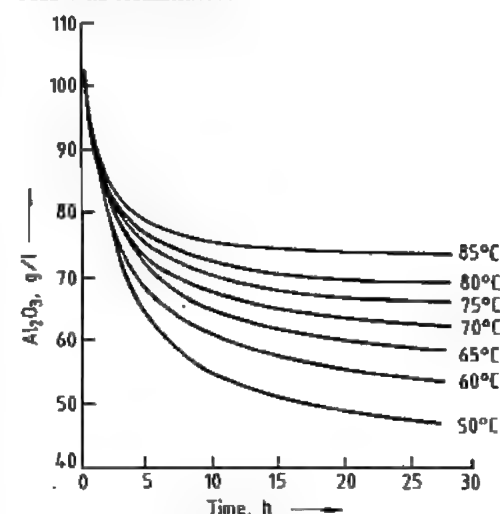


Figure 21.29: Effect of temperature on precipitation.

Precipitators are vertical cylinders; the height, which may be 30 m, is usually 2.5–3.0 times the diameter. The seeded slurry is circulated to maintain intimate contact between solids and solution. Early precipitators circulated the material by means of a central air lift pipe. Air introduced at the bottom of the pipe reduced the apparent density of the slurry within the pipe. This caused slurry to flow into the bottom of the pipe to establish circulation. Modern precipitators are circulated mechanically by impellers up to 3 m in diameter operating in a draft tube. In these units the flow is downward through the tube, so the tank bottoms are nearly flat to reverse the flow and cause upward motion of the slurry. Tanks with air lifts have conical bottoms to direct the flow to the central air lift.

Originally, precipitators were filled individually in *batch operation*. This method had several disadvantages, chief of which was the need for many operators because the operating cycle of a single precipitator required at least 15 separate operations. Control was difficult and batch operation left equipment out of service part of the time.

Nearly all plants built in the last 30 years have used the *continuous system*. Up to 13

tanks are placed in series so that the flow of seed and solution moves by gravity through channels connecting the tank tops. Continuous flows are much easier to measure and to automate. The number of flows is reduced, so control is better and the labor requirement is reduced. There are some operating problems. One is to avoid passage of the slurry across the tank tops, thereby reducing the retention time. Movement of solids from tank to tank is also a problem. An ideal system would retain fine particles in the tanks and move only the coarse material to the discharge. This is not possible, so a compromise method of operation must be found. Precipitation takes place at constant conditions in each tank instead of following a continuous curve, as in Figure 21.30. This tends to decrease production per tank, but the loss is more than recovered because the tanks are always in use.

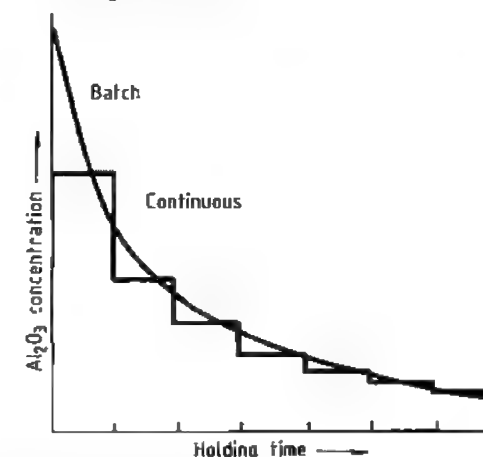


Figure 21.30: Al_2O_3 concentration profiles in batch and continuous precipitation.

Several patterns have been used to supply the *seed for precipitation*. The earliest was to neutralize a portion of the solution. An $\text{Al}(\text{OH})_3$ gel was precipitated that changed into fine crystallites on aging. This very fine material was grown through at least one cycle to provide an active seed for product precipitation. The more common approach is to use fine particles, produced in the operation, as seed. The slurry leaving precipitation is classified into a coarse product fraction and one or

more fine fractions. The fines are returned to the process to grow to product size. Classification is done by controlling the flow rate through tanks so that the fines are elutriated. Liquid solid cyclones are coming into use because they provide more accurate separations. The seeding and classification systems have become increasingly complex. In modern plants at least three fractions are separated. In some plants the agglomerates formed from fine seed must pass through the system once more before becoming product. This reflects the belief that the agglomerates must be made tougher by deposition of additional $\text{Al}(\text{OH})_3$ so that they do not disintegrate in calcination and subsequent handling.

In a recently disclosed modification [131], a relatively small charge of fine seed is added to the first tank in a series. This promotes agglomeration. Then, additional coarser seed is added to the second or third tank to provide the large seed area needed for high production. As indicated previously, cooling may be done between units in a series to increase the supersaturation in the final tanks, thereby increasing the production rate. A further change in modern plants is to filter the seed slurry being recycled. This decreases the amount of spent solution returning to the system and increases both the Al_2O_3 concentration in the first tank of the series and the overall production.

The control variables available to the precipitation operator are the temperatures in the system; the flow per unit, which translates into holding time; the amount of seed; and the particle size of the seed. Some of these variables are difficult to control, so the system usually cycles slowly from coarser than desired to finer. There is enough inventory in the process so that minor cycles can be tolerated without affecting plant output.

Impurities

The impurities in the product Al_2O_3 are affected by all of the foregoing operations, including selection of the bauxite. There are at least three classes of impurities. The first is residue solids that are not removed in clarifi-

cation. The large surface area of $\text{Al}(\text{OH})_3$ in precipitation effectively sweeps up these solids into the product. The preventive measure is increased vigilance in filter maintenance and operating. The second class is materials that are in true solution, such as sodium and gallium. The third group includes materials that are in solute form at the temperatures of digestion but precipitate later in the process. Their solubilities may be only milligrams per liter and return of the solution to equilibrium at lower temperatures may be slow. If precipitation is not completed before filtration, the remaining impurities appear in the product. There are also other impurities that do not fall neatly into these categories.

Sodium is the main component of the process solution and is also the largest contaminant of the product. The Na_2O content of alumina can be decreased by increasing the seed charge and by increasing the precipitation temperatures. The real variable that these operating changes help control is the rate of crystal growth. Higher temperatures, greater seed area, and lower Al_2O_3 concentrations all slow growth and give impurities more time to diffuse from the surface. By proper control of these variables an order of magnitude decrease in the Na_2O content of a commercial product has been achieved. Some sodium is lost in the Hall-Héroult cells during smelting by absorption into the cell lining and by conversion to sodium metal, so complete absence of sodium in metallurgical alumina is not necessary. The target is to balance the input to the cells with the losses. This requires Al_2O_3 containing about 0.4–0.5% Na_2O .

Gallium is a ubiquitous component of aluminous ores. Its chemistry is similar to that of aluminum, so it accumulates in Bayer process solutions until an equilibrium is reached at about 0.2 g/L. The gallium content of Al_2O_3 is a linear function of the gallium concentration in the solution. Therefore, the amount leaving in the product equals the input. Because gallium is in true solution, the same changes that lower the Na_2O content of the product lower the gallium content. Only in the production of high-purity metal has there been concern

about the gallium content of alumina. About 10 t/a of gallium is recovered from Bayer process solutions. This is the best source for the production of gallium.

Silicon is a component of many aluminum alloys, yet the specification for Al_2O_3 is less than 0.02% SiO_2 . This value is only 25% of that specified 50 years ago. The SiO_2 is in solution, but it appears to be added to the product through a slow continuation of the desilication reaction. There is also evidence that if the rate of Al_2O_3 deposition on seed is not high, the seed surface becomes at least partially covered with desilication product, thereby becoming less active as a seed for $\text{Al}(\text{OH})_3$ precipitation and more active toward SiO_2 . This impurity is controlled by driving the desilication reaction nearer to completion. Lowering the SiO_2 concentration of the solution below 0.1 g/L gives a product containing less than 0.003% SiO_2 .

Potassium is undesirable in the Al_2O_3 because it may destroy the graphite in Hall-Héroult cells by intercalation, i.e., it diffuses between the layers of the graphite structure, thus expanding its volume. Although it is soluble in Bayer solutions, there has not been a recorded instance of K_2O concentrations becoming high enough to affect the Al_2O_3 quality.

Iron(III) oxide (Fe_2O_3) as an impurity in Al_2O_3 has been the subject of much investigation. It is soluble up to ≈ 1 g/L in the solutions at digest temperatures (400–500 K), but only to ≈ 0.001 g/L at 333 K [132]. This reconciles the observations that Fe_2O_3 behaved at times as if it were in solution and as a colloid at others. There are several iron minerals that can serve as sources for the impurity. Hematite ($\alpha\text{-Fe}_2\text{O}_3$) and goethite ($\alpha\text{-FeO}(\text{OH})$) are present in most bauxites. Goethite is slowly converted to hematite in high-temperature digests, particularly if CaO is present. This conversion improves clarification because hematite settles better than goethite. The mineral siderite (FeCO_3) present in some bauxites not only is a source of iron but also reacts with NaOH to increase the amount of causticization needed. Pyrite (FeS_2) is almost insoluble in Bayer so-

lutions; its adverse effects occur when the sulfur is oxidized to sulfate in the presence of air and water. The sulfate will react with NaOH to form Na_2SO_4 which has to be removed periodically.

Paradoxically, there is less difficulty with Fe_2O_3 as an impurity in processing bauxites containing a large amount of iron oxides. This is probably because the iron oxides serve as seed and hasten hydrolysis of the NaFeO_2 formed in the digest. Running the solution over iron oxide particles before filtration has been effective in controlling this impurity. Another process for lowering the iron content of Al_2O_3 is termed step precipitation. The filtered Bayer solution is lightly seeded with $\text{Al}(\text{OH})_3$ for a short time to precipitate up to 3 g/L Al_2O_3 . The seed and the small amount of precipitation effectively sweep the colloidal iron hydroxide particles from the solution, leaving an Fe_2O_3 concentration of less than 0.005 g/L.

Calcium also is a common impurity. The presence of increasing amounts of Na_2CO_3 in the Bayer solution seems to increase the CaO in the product. The CaO is not harmful to the aluminum produced; there is calcium in the Hall-Héroult cell bath. As with sodium, additions to the cells should not exceed the losses to avoid buildup in the electrolyte. Calcium can be controlled by step precipitation or by lowering the carbonate content of the solution. Another alkaline metal, *lithium*, also is acceptable in Hall-Héroult cells. It can be removed by step precipitation.

The *other metallic impurities* that appear in many bauxites in small amounts are chromium, copper, manganese, titanium, vanadium, and zinc. Generally, these impurities are not so concentrated that removal processes are required. Sulfide salts have been added to precipitate copper and zinc. The chromium is a problem only if it is oxidized; the organic salts in the solution are usually a sufficient reductant. The addition of manganese compounds as oxidants for organic material has been reported.

Anions, such as carbonate, chloride, fluoride, and sulfate, are known to interfere with $\text{Al}(\text{OH})_3$ precipitation. The carbonate ion is

controlled by addition of lime, although processes have been reported in which Na_2CO_3 is removed by evaporative crystallization or by cooling the solution to 260 K. The sulfate and chloride ions usually are controlled naturally, as their salts are incorporated in the desilication product in sufficient quantities to maintain an equilibrium. There are commercial operations in which the sulfate salt is removed by evaporation and crystallization. The least soluble salt is schairerite ($\text{Na}_2\text{SO}_4 \cdot \text{NaF}$), and when the fluoride ion is depleted, burkeite ($2\text{Na}_2\text{SO}_4 \cdot \text{Na}_2\text{CO}_3$) appears. The fluoride ion is almost never present in quantities large enough to be harmful.

Many bauxites contain *phosphate minerals*. Apatite ($3\text{Ca}_2\text{P}_2\text{O}_8 \cdot \text{CaF}_2$) does not react in the process; indeed, this compound or its hydroxy counterpart is formed when soluble phosphates react with calcium in the digest. Aluminum phosphates, such as wavellite ($4\text{AlPO}_4 \cdot \text{Al}(\text{OH})_3 \cdot 9\text{H}_2\text{O}$) do react, forming Na_3PO_4 as the soluble phosphate. The phosphate ion interferes with flocculation of bauxite residues containing goethite, probably by competing for attachment sites [133]. The concentration of phosphates never is high enough to interfere with Al_2O_3 purity. Addition of CaO to the digest is the control measure.

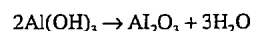
The *organic matter* in bauxite, whether it be roots and twigs from plants or humic acids from decayed matter, reacts in the digest to form a wide variety of organic compounds. Some operation process streams have exceeded 15 g/L organic carbon in solution. There is evidence that larger molecules are oxidized in the process all the way to Na_2CO_3 and sodium oxalate ($\text{Na}_2\text{C}_2\text{O}_4$). In addition some, but not all, of the organic compounds may interfere with precipitation [91].

The effect of sodium oxalate on processing has not been quantitatively determined, yet many plants incorporate equipment for crystallization of the oxalate salt from the solution. Others wash this salt from the $\text{Al}(\text{OH})_3$ seed and recover it from the wash water. The evidence is overwhelming that operations are improved by the oxalate removal techniques. Early removal processes included evapora-

tion to high concentrations followed by centrifugal separation of the gelatinous salt mass. In other plants, a portion of the solution was mixed with bauxite or $\text{Al}(\text{OH})_3$ and heated to 1280 K. This destroyed the organic compounds and formed NaAlO_2 , which could be recovered in the process. A German process adds magnesium salts to the digest to remove the deleterious organic compounds. Still others are investigating methods of oxidizing the organic material in the solution [134].

Calcination

The final operation in production of alumina is calcination. The temperature of the $\text{Al}(\text{OH})_3$ is raised above 1380 K resulting in the reaction:



As discussed in Section 21.10.1.2, this reaction can take several pathways and several transition forms may appear. The end of all pathways is α -alumina. In older European practice, a major portion of the alumina was converted to the α -phase, sometimes by the addition of a fluoride salt to lower the temperature of transformation. In American practice,

calcination always has been less severe; so, normally, $\leq 20\%$ of the alumina is in the α -phase.

Before calcination, it is necessary to wash the process solution from the coarse $\text{Al}(\text{OH})_3$. This is done countercurrently, using storage tanks and filters. As in residue washing, increasing the number of washing stages and the concentration of solids leaving each stage improves the effectiveness of washing. Vacuum filters of several designs have been used for the final separation. The early Oliver and Dorr drum filters have been replaced by horizontal rotary filters because better washing can be achieved. The quality of the wash water is of some concern because such impurities as calcium and magnesium can be adsorbed on the surface of the $\text{Al}(\text{OH})_3$.

Previously, calcination was done in reverberatory furnaces. These had neither the capacity nor the thermal efficiency required, so they were soon replaced by *rotary kilns*. These kilns are cylinders that may be 3.5 m in diameter and over 80 m long. They are mounted on bearings and rotate about an axis inclined at a small angle to the horizontal.

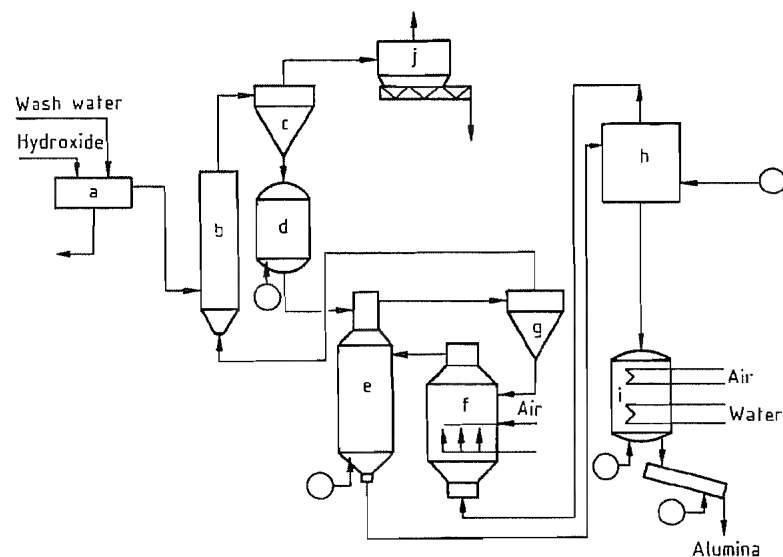


Figure 21.31: Alcoa flash calciner: a) Filter; b) Flash dryer; c) Cyclone; d) Fluidized-bed dryer; e) Holding vessel; f) Furnace; g) Cyclone; h) Multistage cyclone cooler; i) Fluidized-bed cooler; j) Electrostatic precipitator.

Damp $\text{Al}(\text{OH})_3$ from the filters enters the upper end and slowly tumbles toward the lower end, traveling against a stream of hot gas formed by combustion of natural gas or oil at the discharge end. Early kilns were less than 40 m long, but longer units have better thermal efficiency and higher capacity.

Product coolers were added to kilns so that part of the heat in the incandescent product could be transferred to the combustion air. Early coolers followed designs developed in the cement industry and were themselves rotary units much like, although smaller than, the kilns. Improved coolers fluidize the product Al_2O_3 around heat-exchange surfaces, often in several stages. In such coolers, the heat can be recovered in combustion air or in wash water and the product can be cooled readily to 425 K. The best rotary kilns require about 4800 MJ per ton of product.

Rotary kilns are being replaced by *stationary calciners*. In stationary calciners, a combination of fluid beds and stages in which the solids are transported in suspension is used. Figure 21.31 is a schematic diagram of a commercial unit capable of calcining 1500 t/d.

The $\text{Al}(\text{OH})_3$ is washed and dewatered on the filter (a) and is conveyed into the flash dryer (b), where it encounters hot gas from cyclone (g). The gas evaporates the free water from the particle surfaces. Because the temperature exceeds 480 K, a portion of the water of hydration also is driven from the crystals. Cyclone (c) separates the solids from the gas. The gas, cooled almost to its dew point, leaves the unit through the electrostatic precipitator (j), where dust is recovered. Vessel (d) serves as a surge buffer to smooth the flow of solids through the unit. The solids are separated in cyclone (g) to enter the vessel (f) where combustion of fuel is taking place. Vessel (e) allows a holding time at the calcination temperature so that the water content of the product is low. A small amount of fuel can be burned in this vessel if a higher temperature is desired. In this design the flow of solids is counter to the flow of the gas.

The solids are cooled, also in counterflow, by the combustion air in unit (h). Final cooling

is in a fluidized-bed unit (i). In the fluidized unit a small amount of air is introduced through a membrane at the bottom. This lifts but does not entrain the solids, so they behave much like a fluid. Heat is transferred at high rate to air or water flowing through tubes submerged in the bed. The product Al_2O_3 can be cooled below 400 K with all of the recovered energy being used in the process.

The great advantage of the stationary units is that the heat required for calcination is 3250 MJ/t. The capital costs are lower than for rotary kilns of equal capacity and the maintenance costs are lower primarily because the refractories are not subjected to rotational stresses. Because the capacity per unit is high and automation is quite easy, the labor requirements are low. The stationary units are being installed in retrofitting older plants as well as in new construction.

Alumina calcined in stationary kilns has a lower α -alumina content and a higher surface area than alumina calcined at the same temperature in a rotary kiln. This reflects the shorter residence time and the absence of a high-temperature flame in the static units. Photomicrographs show that the rapid temperature rise creates vapor pressure within the particles that tends to fracture large crystals.

The characteristics of the metallurgical alumina are controlled mostly by the time and temperature of calcination. The important control is the relation between the $\text{Al}(\text{OH})_3$ feed and the flow of fuel. The fuel must be free of impurities that can contaminate the alumina. Sulfur and vanadium in fuel oil are limited by concern for product purity. The amount of combustion air must be sufficient to burn the fuel completely without the use of a great excess that increases the gas flow and thereby reduces the thermal efficiency.

Evaporation

As is shown on the flow sheet for the Bayer process (Figure 21.21), the solution continuously cycles through the plant. Consequently, any wash water used must be evaporated so that the solution volume can be controlled.

About 10% of the flow is evaporated in the two cooling areas by being flashed into steam. In high-temperature digesters, the amount of flash evaporation is even larger. At least one plant processing high-grade bauxite was designed without any additional evaporation capacity. In most cases, the economics require installation and operation of evaporators. The objective is to minimize the summed costs of evaporation and the value of the soluble salts lost by incomplete washing. The minimum is usually attained with a net dilution of the residue of 1.5–2.0 kg/kg.

Table 21.12 lists the input and exit streams that compromise the dilution balance in an operating plant. Efficiency demands that all of these flows be monitored.

Table 21.12: Dilution balance.

Inputs	Losses
residue wash	evaporation
sand wash	—
Al(OH) ₃ wash	heat interchange flash
free moisture in bauxite	Al(OH) ₃ to calcination
water in gibbsite and boehmite	free water with Al(OH) ₃
injected steam	water with residue
purge water	vapor from solution surfaces
sodium hydroxide	
cleanup water (maintenance)	
uncontrolled dilutions	

Several evaporator designs are used in Bayer plants, but nearly all designs are used in *multiple-effect configurations*. In such units each stage operates at a lower pressure than the preceding one. Therefore, the vapor evaporated from the solution in the first stage is at a temperature high enough to heat the solution in the second stage, causing it to boil. This continues to the final stage, where the vapor is condensed. The condenser operates under vacuum so a jet pump is necessary to remove non-condensable gases from it. The more times the latent heat is used, i.e., the more stages that are present, the more water can be evaporated by the fuel steam used in the first effect. With Bayer solutions the maximum number of effects is six. This is because the boiling point of the solution is elevated 5–8 K by the dissolved solids. This reduces the steam temperature in each effect; with many effects there is little

temperature difference available to cause evaporation.

An unconventional design called *continuous regenerative evaporators* has been used in some plants. These units are similar to the heating and flashing equipment used in digestion in that the feed is heated through up to ten stages without evaporation; the hot solution is then flashed through an equal number of stages and the steam is used for heating the feed. These units are not as efficient as most multiple-effect evaporators. The design choice is based on economics. Special evaporator designs may be used when it is necessary to crystallize organic or inorganic salts from the solution. In such designs pumps are used to increase the thermally induced flow through the tubes in the heaters. The heat-transfer surfaces in evaporators must be cleaned periodically to remove encrustations of desilication product and soluble salts.

Evaporators are controlled primarily by changing the amount of steam used. The flow of feed solution is regulated so that crystallization of soluble salts is either induced or avoided, depending on the operating mode. Temperature readings at each effect are compared to design values to indicate operating difficulties.

Residue Disposal

The most important environmental problem in the Bayer process is disposal of the bauxite residue. The solution left with the residue after an economical amount of washing is still very alkaline and cannot be allowed to contaminate ground water. Furthermore, the desilication product in the residue which is in contact with water has the capacity to exchange sodium for hydrogen. An aqueous slurry of the residue that had been washed with 1000 times its mass of distilled water still reached a pH value of 10.5 on standing. The undrained fine residue, even after years of consolidation, does not have enough strength to support buildings or equipment. These properties make disposal a difficult problem.

Previously, disposal was to a marine environment where the alkalinity was diluted by large quantities of water. This method has been used in the seas off Europe and Japan and in a river in the United States. Studies by environmentalists have indicated little damage to flora or fauna by the residue in a disposal area [135]. Today, however, environmental concern is so great that any new refinery is unlikely to be permitted to use marine disposal.

Early inland refineries simply dammed a convenient valley or built retaining dikes on flat land to form residue disposal areas. In some cases, the sandy portion of the residue was used to build the dikes. This method can be effective and cheap if care is taken to protect the surroundings by proper sealing techniques. The compacted residue has a lower permeability than many clays; yet, there have been isolated leaks into aquifers from such impoundments. Improved designs have been developed.

In Germany, retaining dikes are built with a portion of the structure designed to be porous. The dilute solution draining from the residue is channeled by the porous sections into water-treatment facilities before being discarded. In some cases, the dike material exchanged ions with the solution so that little treatment was needed. The draining allowed consolidation of the residue so that it could support equipment. An American firm used a drained lake in which the bottom of the disposal area was covered with sand in which draining pipes were laid. The residue was pumped to these areas in the traditional manner as a dilute slurry. Most of the conveying water was decanted, while some percolated through the deposit to the drains. This design has two advantages: the residue consolidates better, so the storage capacity of an area is increased, and the hydraulic head on the bottom is reduced to zero, so that leakage is unlikely. Recent lakes have been built using the sand drains on top of seals of clay and plastic film for additional environmental safety.

Another modern disposal method, called *dry stacking*, takes advantage of the thixotropic nature of the residue. By some method,

usually vacuum filtration, the residue is concentrated to 35–50% solids. The slurry is agitated to reduce its viscosity by as much as two orders of magnitude and pumped to a disposal area. There it flows in lava-like fashion over the surface, establishing a slope away from the discharge point. In the absence of shear, the viscosity of the slurry increases and flow stops. Water does not separate from the slurry and the slope causes rain to run off rapidly, so the surface usually is losing water to the atmosphere. The surface becomes deeply fissured, further assisting drying. In about 90 days the residue may dry to 75% solids, far drier than in any of the other disposal methods. In this state, it can support heavy earth-moving equipment and can be recovered or used for increasing the height of retaining dikes. This method maximizes the storage capacity of a given area and seems to pose the minimum threat to the environment. It does require construction of a permanent lake area for water storage and for cooling water. If any use is to be made of the residue, recovery is relatively easy.

In some countries there is a requirement that the area devoted to residue disposal be returned to productive use. Some Australian residue areas have been covered with the sandy fraction of the residue. By the addition of organic matter and fertilizer, the area has been returned to agriculture. At the University of Georgia, microorganisms given the proper nutrients grew in the residue and produced simple organic acids that neutralized the alkalinity of the residue. Draining was needed so that high concentrations of sodium were washed away, then the residue could support plant and simple animal life. The addition of gypsum hastened the neutralization process, probably by forming the neutral Na₂SO₄. Agricultural use of residue areas is therefore possible after some effort and expense. The bearing strength of dry-stacked residue is sufficient to support homes and light industrial buildings.

Many investigations have been directed toward finding a commercial use for bauxite residue. The high iron content of some residues suggested production of pig iron. The quality

of the iron was poor and the amount of slag formed exceeded the original amount of residue. Similarly, chemical processes have been developed for recovery of Al_2O_3 , Na_2O , and TiO_2 from residue. Although all are technically possible, none has been feasible economically. Small quantities of residue have been used in making Portland cement, and smaller quantities have been used as a mold wash, as an insulating material, and, after reaction with H_2SO_4 , as a water treatment. No chemical use is likely to consume a significant part of the residue [88, 92].

The residue is claylike and can be used in ceramic materials. The sodium causes formation of glasses at 1450 K, giving a vitreous bond. Bricks have been made commercially, but economic factors and other shortcomings of the brick have eliminated this use. Sintering the residue into aggregate for concrete may be economical where natural aggregate is not available.

In Texas, agronomists have shown that the residue can be used to neutralize acidic soil, replacing limestone. The cost of preparing the material for application and the logistics argue against extensive use. The conclusion is that large-scale use of bauxite residue is unlikely, so efforts should be directed toward reclamation of disposal areas.

Energy in the Process

Approximately 16 MJ are required to produce a kilogram of Al_2O_3 . The worldwide range is 7.4–32.6 MJ/kg [136]. Variations in the quality of bauxite, plant design, and the size of the plants are the reasons for the wide differences. Even with existing plants, large improvement in energy usage can be made. The Aluminum Association (USA) reports that the energy used per unit of alumina production in 1980 was 68% of the energy used in 1972 [137]. The energy used in mining is less than 5% of the total and is difficult to change. The energy for transporting bauxite is double that for mining it, because the average ton of bauxite used in the United States is transported 4700 km. The situation worldwide is

different because much of the bauxite is refined close to the mines.

Within the refinery, more than half of the energy is used for pumping and heating the solution and for evaporation. The previous discussion has shown that plant design can affect heat recovery and minimize energy use. Emphasis is being placed on increasing the amount of Al_2O_3 recovered from less than 50 g/L to over 65 g/L; some claim yields as high as 80 g/L. Because energy is more closely related to the flow of solution than to yield, the energy savings are large. The static calciners are nearly as efficient as they can be made because the temperatures of the gas and of the product leaving the units are very low. The change from rotary kilns has made up a large portion of the savings. There are still opportunities to improve operating practice and design to reduce energy consumption [138].

Economic Aspects

The largest cost elements in alumina production are raw materials, energy, and capital-related costs for the production equipment. Labor, operating supplies, and miscellaneous costs are much smaller than these three.

Bauxite is the most important raw material. Its cost includes those for mining, transport, levies, and taxes. In addition, the relative quality of the bauxite ore influences the expenditures for necessary reagents. Mining is relatively inexpensive because most deposits are covered with only a shallow overburden and can be mined with efficient equipment. Since the formation of the International Bauxite Association (IBA), levies and taxes have become a large part of the cost of bauxite. These costs have become relatively stable because most are related to the selling price of aluminum. The availability of bauxite from outside the IBA countries has allowed the effect of supply and demand to influence this cost. Where levies are not imposed, some system of taxation provides income to the producing nation. Transportation costs vary from very small to as much as half the delivered cost of the bauxite. Some bauxite travels less

than 5 km by truck or conveyor belt to the refinery. Other bauxite may travel more than halfway around the world. The characteristics of bauxite most important in influencing its value are the available alumina and the reactive silica contents. The latter quantity has a great effect on the amount of sodium hydroxide and lime required in processing. Bonuses are given for high available alumina values, and penalties are charged for excessive silica.

In the previous section, values were given showing the fourfold range in energy used to produce alumina. The most important variables are the plant design and the quality of the bauxite being processed. The most energy-efficient bauxites are gibbsitic, with very low residue content.

The capital costs also show wide variation. In 1980 U.S. dollars, new installations may cost from \$400 to \$800 per annual ton of capacity. The variables are design factors, location, capacity, and the properties of the bauxite to be processed. Much of the world capacity was constructed before construction costs were inflated and so has lower capital costs. The effect of capacity is also large, and plants producing 2×10^6 t/a have costs well below those of plants producing less than 10^5 t/a.

There is more capacity for producing metallurgical alumina than there is smelting capacity. Not all smelters have alumina capacity dedicated to them; they buy alumina on contract. Long-term contracts are common. In other instances, alumina is bought when needed at spot market prices. Since 1980, alumina has sold on the spot market for less than \$150/t to over \$280, reflecting a change in the relationship between supply and demand. Economics do not always control production because many corporations own refineries to supply their smelters. In other instances, national governments own a significant portion of a refinery and for political reasons may choose to operate in a noncompetitive situation. Costs per ton of alumina can, under unfavorable conditions, exceed \$200, although efficient plants may produce at roughly half this figure.

21.10.1.4 Other Processes for Alumina Production

Raw Materials

Many investigators have sought processes to replace the Bayer process using raw materials other than bauxite [89]. Clay, primarily kaolinite, has been most considered because it can contain up to 39% Al_2O_3 . Other materials, including anorthosite, nepheline, coal wastes, and fly ash, have been candidate raw materials. Yet, less than 2% of the world supply of alumina is not made by the Bayer process. This happens only where use of a domestic raw material and production of a desirable by-product change the economic picture. Alumina from ores other than bauxite normally costs 1.5–2.5 times that from the Bayer process.

Because aluminum is amphoteric, both acid and alkaline processes have been developed. Most of the processes in each class follow the same general flow sheets.

Alkaline Processes

Sodium compounds, such as Na_2CO_3 , react at 1280 K with the Al_2O_3 in aluminous ores to produce water-soluble NaAlO_2 . This compound can be leached from the sinter with water and the solution treated to remove impurities; the purified solution is neutralized with CO_2 to recover $\text{Al}(\text{OH})_3$. The last step regenerates the Na_2CO_3 for recycle. Difficulty arises because the aluminous ores contain SiO_2 , which also reacts in the sinter to form soluble Na_2SiO_3 . In processing, the desilication reaction discussed earlier takes place, so the net recovery of Al_2O_3 is small or zero. If 2 mol of CaO , usually as limestone, is charged for every mole of SiO_2 in the raw material, insoluble calcium silicate compounds are formed. Under proper leaching conditions the NaAlO_2 can be recovered from such sinters with only slight loss.

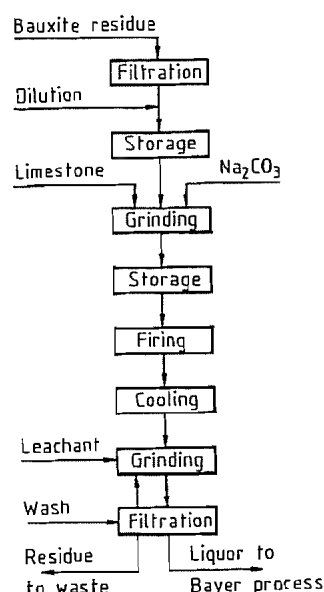
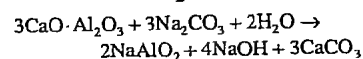


Figure 21.32: Lime/soda sinter process flow sheet.

This process has been used commercially in two American plants to recover most of the Na_2O and Al_2O_3 lost in the desilication product formed while treating high-silica native bauxite. A schematic flow sheet is given in Figure 21.32. The same process was investigated by the U.S. Bureau of Mines in a large pilot plant using anorthosite as the raw feed [139]. [Anorthosite is a mixture of the minerals anorthite ($\text{CaAl}_2\text{Si}_2\text{O}_8$) and albite ($\text{NaAlSi}_3\text{O}_8$).] Unless the composition, sintering, and leaching were closely controlled, the residue formed a gel in leaching and became very difficult to filter.

In a variation of the sintering approach, calcium replaces the sodium so that calcium aluminate ($3\text{CaO} \cdot \text{Al}_2\text{O}_3$) is formed as well as calcium silicate (CaSiO_3). The calcium aluminate reacts with Na_2CO_3 in an aqueous leach to form NaAlO_2 .



In carbonation, $\text{Al}(\text{OH})_3$ is formed and the Na_2CO_3 solution is regenerated. Nepheline, $(\text{Na},\text{K})\text{AlSi}_3\text{O}_8$, is treated by this process in former USSR. The calcium silicate residue is processed to make about 10 t of cement per

ton of alumina. The two products make the process viable here.

In the Pedersen process, the sinter is replaced with a reducing fusion so that ferric ions in the ore were reduced to metal. Iron and the calcium slag were separated by decantation. During cooling, the CaSiO_3 passes through a crystalline phase change and the resulting stresses reduce the slag to powder [88, 89].

The sinter processes suffer economically for several reasons. The energy for sintering and for evaporation of the leach solution must be added to the energy required from operations analogous to those in Bayer processing. The capital investment is increased by the need for sintering equipment, and although limestone is inexpensive, the quantity required is so large that the expense is considerable.

Acid Processes

All of the acid processes follow the general flow sheet given in Figure 21.33. The clay is prepared by grinding and by roasting it to about 1000 K. The roasting changes the kaolinite to meta-kaolin, from which the aluminum can be dissolved as the acid salt. The roasted clay is leached in an acid solution, usually at the atmospheric boiling point. Some investigators have chosen to leach at elevated temperatures for processing advantages even though corrosion problems become more severe [88]. The siliceous residue is separated using sedimentation and filtration as in the Bayer process. Small amounts of iron salts remain in the clarified solution. These salts are removed by extraction with an organic compound that forms a complex with the iron but not with the aluminum salts. The organic solution is decanted from the aqueous phase and is treated to separate the iron salt and to regenerate the organic extractant.

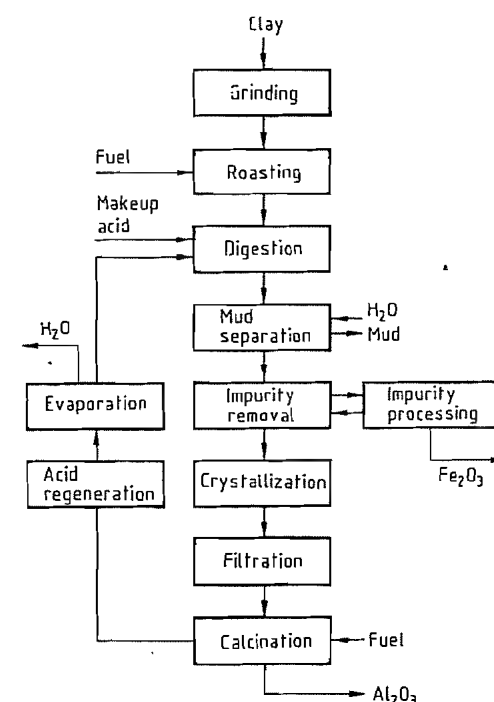


Figure 21.33: Generalized acid process flow sheet.

A hydrated aluminum salt is recovered from the aqueous solution, usually by evaporation and cooling to cause crystallization. In the *hydrogen chloride process*, advantage is taken of the low solubility of AlCl_3 in HCl . The HCl gas is absorbed in the solution both to regenerate the acid for leaching and to precipitate $\text{AlCl}_3 \cdot 6\text{H}_2\text{O}$. In all acid processes the hydrated salt is decomposed to Al_2O_3 by heating to 1300 K. Both water and the acid radical are driven off, and the acid is absorbed for recycling.

The U.S. Bureau of Mines sponsored a cooperative effort with several aluminum companies to investigate acid processes for recovery of alumina from clay [139]. For several reasons the HCl process was preferred: the reagent is inexpensive, processing conditions are not severe, the salt can be recovered without evaporation. The HCl is not decomposed in calcination, and the water content of the acid salt is half that of other acid salts. Despite these features the process is not competi-

tive economically with the Bayer process. A major fault is the amount of energy used to roast the clay, to evaporate the solution, and to decompose the acid salt. The investment is increased because of the corrosive solutions. A process disadvantage is that the Al_2O_3 is physically different from Bayer alumina, so smelting practice has to be changed for this aluminum source.

Pechiney and Alcan jointly operated a pilot plant using the H^+ process, a modification of the HCl process in which H_2SO_4 is added to the digest [140]. The combination of acids eliminated the need to roast the clay. Other processes use H_2SO_4 , H_2SO_3 , HNO_3 , or NH_4HSO_4 as reagents to attack the clay, but no commercial use has been made of any of them.

Clay is a major impurity of coal, so the ash from coal may be considered an overroasted clay. The acid processes, with minor modifications, will extract alumina from ash [140]. Anorthosite that is high in anorthite reacts with boiling HCl ; this approach has been investigated in Norway and Canada [141]. So far, all of these methods have served only to enrich the technical literature.

Two aluminous minerals that do not contain silica have attracted attention and, because of their composition, require different technology. Alunite, $\text{K}_2\text{SO}_4 \cdot \text{Al}_2(\text{SO}_4)_3 \cdot 2\text{Al}_2\text{O}_3 \cdot 6\text{H}_2\text{O}$ has been used commercially in Russia. Both H_2SO_4 and K_2SO_4 are useful by-products of alumina production by this method. The alunite is heated to drive off the hydrated water; additional heating under reducing conditions decomposes the aluminum sulfate without adversely affecting alumina recovery. The solid residue from the roast is a mixture of K_2SO_4 , Al_2O_3 , and gangue. The K_2SO_4 is dissolved in water and recovered. Alumina is extracted from the gangue in a modification of the Bayer process. In other approaches using alunite, the solutions are kept acidic so the alumina is recovered as a salt [142].

Dawsonite, $\text{Na}_2\text{O} \cdot \text{Al}_2\text{O}_3 \cdot 2\text{CO}_2 \cdot 2\text{H}_2\text{O}$, is found in some oil shales. The temperatures used to recover the oil from the shale decompose the dawsonite to NaAlO_2 , which is soluble in dilute NaOH . The $\text{Al}(\text{OH})_3$ and Na_2CO_3

can be recovered from the solution by carbonation. The economics are such that recovery of the oil must be competitive before mining and by-product recovery can be considered.

21.10.1.5 Metallurgical Alumina

Aluminum production is the principal application for alumina; more than 92 % of world alumina production is used for this purpose. The property requirements for commercial metallurgical alumina therefore are of considerable importance to the alumina industry. Specifications have responded to changes in energy costs, aluminum cell design, cell gas scrubbing techniques, environmental regulations, working conditions in smelters, and the technology for alumina calcination. In general, there has been a shift away from relatively small-particle-size, highly calcined, "floury" alumina to a coarse, free flowing, dust-free, less calcined, "sandy" alumina of narrower particle sizing and higher chemical purity.

Alumina Properties Required for Electrolysis

Five developments have had a significant impact on alumina properties.

Cell Design. New, high current efficiency, prebaked anode cells with automatic center-feed systems require that the alumina be consistent, with trouble-free handling properties to insure proper conveying and volumetric metering from the feeder. These criteria are best met by a free-flowing, moderate- to low-calcined alumina with relatively coarse and narrow particle size distribution.

Cell Gas Dry Scrubbing. The use of dry scrubber systems employing cell-feed alumina as adsorbent for fluorides in effluent gas from the cells dictates other requirements for metallurgical alumina:

- High adsorption capacity for hydrogen fluoride. This property is closely related to the specific surface area of the alumina, which is higher for the lower calcined aluminas.

- Attrition resistance.
- Free flowability.
- Higher chemical purity to compensate for capture in the dry scrubber of impurities which are recycled to the cell.

Pot Room Working Conditions. Use of low-calcined, high surface area alumina as a cover for the cell bath reduces fluoride evolution within the pot room. Working conditions in the smelter are degraded by dust caused by fine particles of alumina. Reduction of the fines fraction ($< 44 \mu\text{m}$) in the alumina and high attrition resistance are important for reducing dust.

Use of Stationary Calciners and Pneumatic Handling Systems for Alumina. The replacement of rotary alumina kilns by the energy-efficient stationary calciners has resulted in producing a different type of calcined alumina for smelter feed. This difference is reflected in the interrelationship between degree of calcination (measured by the mass loss on ignition), specific surface area, and the $\alpha\text{-Al}_2\text{O}_3$ content [143].

The strength of the alumina particles has become of concern not only because of relatively higher breakdown in the stationary calciners, but also because of attrition occurring in pneumatic unloading and conveying equipment and in fluid-bed dry-scrubbing systems. The generation of fine particles in such equipment, apart from causing unacceptable dusting conditions in the smelters, often results in troublesome segregation problems in alumina storage bins and bunkers.

Electrolyte Composition and Temperature. The trend to operating cells at lower temperatures with electrolyte having a lower bath ratio ($\text{NaF}:\text{AlF}_3$) has decreased the solubility and rate of dissolution of alumina in the electrolyte. The rate of dissolution is greater for aluminas having higher surface areas and low content of $\alpha\text{-Al}_2\text{O}_3$. Both properties can be achieved by a low degree of calcination.

Typical Specifications for Metallurgical Alumina

The considerations discussed above have contributed to the evolution of the general specifications used in production and international trading (Table 21.13). These values are only representative and considerable variation exists in actual practice depending on price, availability, smelting practices, and many other factors.

Table 21.13: Typical properties of metallurgical alumina.

Physical property	
Particle size distribution, %	
+ 100 mesh (Tyler)	< 5
+ 325 ($44 \mu\text{m}$)	> 92
- 325	> 8
Bulk density, kg/L	
loose	0.95–1.00
packed	1.05–1.10
Specific surface area, m^2/g	50–80
Moisture (to 573 K), %	< 1.0
Loss on ignition (573–1473 K), %	< 1.0
Attrition index (modified Forsythe–Hertwig method)	increase in $< 44 \mu\text{m}$ particles 4–15 %
$\alpha\text{-Al}_2\text{O}_3$ content (by optical or X-ray method), %	< 20
Chemical analysis, %	
Fe_2O_3	< 0.020
SiO_2	< 0.020
TiO_2	< 0.004
CaO	< 0.040
Na_2O	< 0.500

21.10.1.6 Industrial Alumina Chemicals

Alumina, in various forms, is one of the inorganic chemicals produced in greatest volume today. Although production of aluminum metal currently consumes $\approx 90\%$ of all alumina, an increasing amount is being applied in the chemical industry for fillers, adsorbents, catalysts, ceramics, abrasives, and refractories. With the development and growth of applications and markets for alumina chemicals, all the major alumina producers have, over the years, converted a part of their capacity to produce various alumina chemicals. In fact, some of the older, smaller alumina refining plants have been totally converted to alumina chemi-

cals production in order to be economically viable. Chemical uses account for nearly 8 % of the world production.

Aluminum Hydroxides

Aluminum hydroxides constitute a versatile group of industrial chemicals. Important uses requiring large quantities are as fillers in plastic and polymer systems and for the production of aluminum chemicals. A moderate amount is used for the production of alumina-based adsorbents and catalysts.

Aluminum hydroxide meets most of the requirements for an effective filler: white or near-white color; large volume production base, resulting in price and supply stability; consistency of physical and chemical properties; a wide range of particle size distributions chemical inertness; and nontoxicity. However, its increasing popularity as a plastics filler is strongly related to its fire-retardant and smoke-suppressant properties, which justify the somewhat higher price compared with calcium carbonate and other mineral fillers. Aluminum hydroxide acts as a fire retardant by adsorbing heat through endothermic dehydration and dilution of pyrolytically produced combustion gas by the released steam. Dehydration and water release processes become significant at temperatures above 500 K. The smoke-inhibiting activity of aluminum hydroxide filler has been attributed to promotion of solid-phase charring in place of soot formation. Although offering these desirable features, aluminum hydroxide has certain disadvantages that impose some limitations on its uses as a filler. Like other nonreinforcing mineral fillers, it generally lowers strength. Because it undergoes thermal decomposition, it is not suitable for processing above 500 K. These factors are responsible for the larger use of aluminum hydroxide in latex carpet backings and in glass-reinforced polyesters, where processing temperatures below about 480 K generally are used. These are also chemically cross-linked or fiber-reinforced systems, in which loss of strength caused by a nonreinforcing filler may not be very important. Alu-

minum hydroxide filler has been used less extensively in thermoplastics, e.g., poly(vinyl chloride) and polyethylene, and elastomeric materials. For use as a filler, the crystalline aluminum hydroxide from the Bayer process is dried and ground to particles $\leq 10\text{ }\mu\text{m}$ size. Special grades with increased whiteness and a variety of both particle size ranges and chemical purity also are available commercially.

Fine, precipitated aluminum hydroxide having a uniform particle size ($\approx 1\text{ }\mu\text{m}$) is used in paper making as a filler pigment and as a coating. As a filler, it disperses rapidly with low sedimentation. Improved printing properties are reported for the hydroxide-filled paper. The application of fine, platy aluminum hydroxide as a paper coating is well established in the paper industry. It gives a coating of high brightness, opacity, and gloss.

Technical aluminum hydroxide obtained from the Bayer process is 99.5% pure. It dissolves readily in strong acids and bases. For these reasons, aluminum hydroxide is the preferred raw material for the production of a large number of aluminum compounds. These include pure, iron-free aluminum sulfate (used in the paper industry and for water purification), aluminum fluoride, synthetic zeolites, and sodium aluminate. Aluminum hydroxide also is used in the glass industry and in cosmetic and pharmaceutical preparations. An important cosmetic use of aluminum hydroxide is in toothpaste. The mildly abrasive hydroxide cleans and polishes teeth.

The price of aluminum hydroxides ranged from \$0.20 to \$0.60 per kg in 1982, the price range reflecting the cost of additional processing of the usual Bayer process product to suit application requirements. These include grinding, higher purity, classification, surface treatment, etc. Pharmaceutical-grade gel hydroxides were at the top of the price range.

Adsorbent and Catalytic Aluminas

Activated aluminas represent another group of technically important alumina chemicals. Principal uses are as drying agents, adsorbents, catalysts, and catalyst carriers. These

products are obtained by thermal dehydration of different aluminum hydroxides in the 250–800 °C temperature range.

Preparation of Activated Aluminas

Bayer aluminum hydroxide is the chief source of commercial activated alumina products. Powder forms of activated alumina are produced by heating the hydroxide directly at 575–1825 K in ovens or in rotary or fluidized-bed calciners. The products have surface areas of 200–350 m²/g and losses on ignition of 3–12% (at 300–1200 °C). Such products are used as decolorizing agents for organic chemicals and as starting material for the production of aluminum fluoride. Other uses include chromatographic and catalytic applications in organic chemistry.

Granular activated alumina produced from Bayer plant crust is one of the oldest commercial forms of this product and still is used widely. A flow sheet of the production process is shown in Figure 21.34. The activated material is a hard, nondusting product. Table 21.14 lists some properties of a commercial product of this type (Alcoa F-1). A similar granular product has been produced by compacting Bayer hydroxide by mechanical pressure (Martinswerk GmbH, Germany). The process utilizes a roll-type compactor. The product from the compactor is broken up and sieved to the required size fractions and activated at 450–600 °C in a rotary calciner.

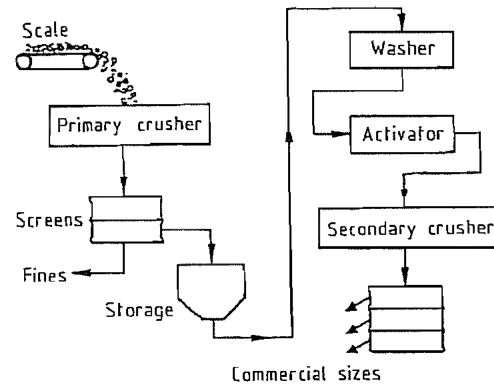


Figure 21.34: Flow sheet for production of activated alumina from Bayer plant crust.

Table 21.14: Typical properties of Alcoa activated aluminas.

	F-1	H-151	S-100
% Al ₂ O ₃	92	30	95
% Na ₂ O	0.58	1.6	0.35
% SiO ₂	0.12	2.0	0.03
% Fe ₂ O ₃	0.06	0.03	0.05
% LOI	7	6	5
Loose bulk density			
g/cm ³	0.83	0.82	0.80
lb/ft ³	52	51	50
Packed bulk density			
g/cm ³	0.85	0.85	0.75
lb/ft ³	55	53	47
Pore characteristics and surface area of typical Alcoa activated aluminas			
Helium (true) density, g/cm ³	3.25	3.40	3.15
Mercury (particle) density, g/cm ³	1.42	1.38	1.24
Micro pore volume (pores < 3.5 nm), cm ³ /g	0.017	0.023	0.012
Macro pore volume (> 3.5 nm), cm ³ /g	0.023	0.020	0.037
Total pore volume, cm ³ /g	0.40	0.43	0.49
Total porosity, %	56.3	59.4	60.6
Pore diameter at 50% total pore volume, nm	17.7	3.5	4.7
Primary pore size range, nm	0–10 000	0–40	0–500
BET surface area, m ² /g	250	360	260
Pore diameter, nm			
10 ⁶ –10 ⁷ Pore volume, cm ³ /g	0.0031	0.0003	0.0000
10 ⁵ –10 ⁶	0.0045	0.0001	0.0001
10 ⁴ –10 ⁵	0.0059	0.0001	0.0004
10 ³ –10 ⁴	0.0029	0.0004	0.0033
10 ² –10 ³	0.0045	0.0093	0.0047
35–10 ²	0.0021	0.0099	0.0289
2–35	0.0165	0.0232	0.0115
	0.095	0.0433	0.0489

Fast dehydration of Bayer aluminum hydroxide, either by vacuum or by exposure to high-temperature gas (780–1000 °C) for a few seconds, has been used for the production of ball-shaped, activated alumina having properties superior to the granular product. This process results in the formation of nearly amorphous ρ -Al₂O₃. The product is finely ground and using water as binder, formed into spherical agglomerates in a rotating pan agglomerator. Rehydration of ρ -Al₂O₃ with water leads to crystallization of bayerite, causing the agglomerates to harden. Reactivation of the hard balls at 400–500 °C produces the activated product (5–20 mm in diameter) having a surface area of 320–380 m²/g.

Alumina gels also have been used for the manufacture of activated aluminas. These gels are produced by neutralization of aluminum sulfate or ammonium alum by NH₄OH, or from sodium aluminate by neutralization with acids, CO₂, NaHCO₃, and Al₂(SO₄)₃. The ge-

latinous aluminum hydroxide precipitate is filtered and thoroughly washed and dried. The dried product is activated, milled, and agglomerated to a spherical product. Other forming processes, such as extrusion, pelletizing, and tableting, also can be used. The product is finally activated at 400–600 °C to a loss on ignition value of about 6%. Although gels of various textures can be prepared, the usual industrial adsorbent products have very small pores (less than 4 nm in diameter) and surface areas in the range of 300–400 m²/g. A flow sheet of a manufacturing process is shown in Figure 21.35. Table 21.14 reports data on a commercial, gel-based product (Alcoa H-151).

Aluminum oxide hydroxide (boehmite), a by-product from the Ziegler process for linear alcohol production, is another source of activated alumina. The high purity of this material favors its use in catalytic applications. The fine particle boehmite is normally extruded to

various shapes. The material is claimed to serve as its own binder when peptized with glacial acetic acid. The extrudate is cut to the required size, dried, and activated at 500–600 °C. The surface area of the activated product is 185–250 m²/g. Commercial bayerite also has been used to produce activated alumina; the product is preferred in some catalytic applications.

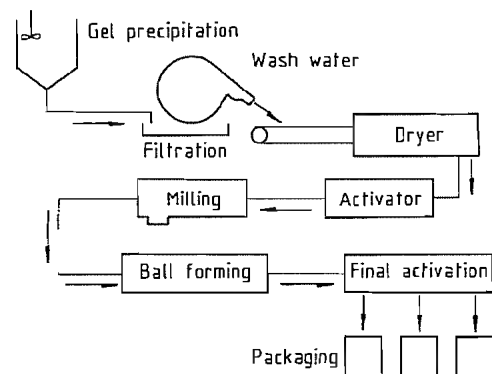


Figure 21.35: Production of gel-based activated alumina.

Adsorbent Applications

A major application of activated alumina is in the field of adsorption, where its high surface area, pore structure, strength, and chemical inertness favor its use. The alumina performs important technical functions, such as gas and liquid drying, water purification, and selective adsorption in the petroleum industry.

Gases that have been dried successfully by alumina desiccants are:

acetylene	ethylene	natural gas
air	freon	nitrogen
ammonia	furnace gas	oxygen
argon	helium	propane
carbon dioxide	hydrogen	propene
chlorine	hydrogen chloride	sulfur dioxide
cracked gas	hydrogen sulfide	
ethane	methane	

In many applications an alumina desiccant can dry gas to a lower dew point than any other commercially available desiccant. The static water adsorption capacities of two typical activated aluminas (Alcoa F-1 and H-151) in con-

tact with air at different relative humidity conditions are shown in Figure 21.36.

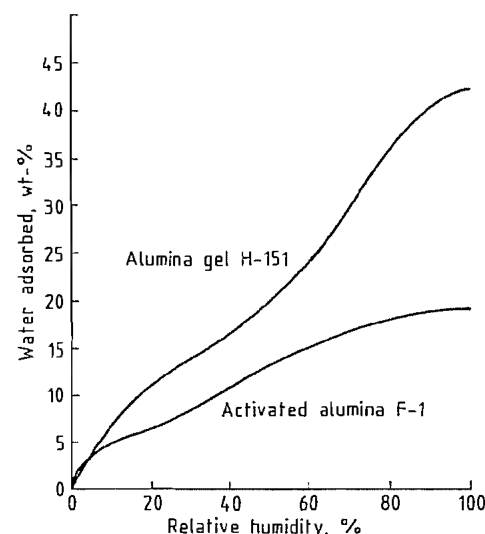


Figure 21.36: Static water adsorption capacity of typical commercial activated alumina at 25 °C.

Moist gas usually is dried by passing it through a column (or tower) packed with the adsorbent. Adsorption of water on activated alumina is strongly exothermic, releasing between 45 and 55 kJ of heat per mole of water adsorbed. This factor must be considered in the design of the drying tower. Both granular and spherical forms of activated alumina can be used in desiccant beds. Sizes from 2 to 20 mm are available commercially. The granular products have lower surface areas and their application is based on low cost per kilogram, low water load, and low stream pressure. Spherical products, produced by either the gel or the fast dehydration processes, have larger surface areas, a narrower pore structure, and a high adsorption capacity, and they are relatively more expensive than the granular variety. The spherical kind usually is specified for high-pressure, high-moisture removal duties. The alumina desiccant is regenerated by passing a current of hot, dry gas (200 °C) through the bed, usually countercurrent to the main gas flow.

Liquids that can be dried with activated alumina include aromatic hydrocarbons, higher

molecular mass alkanes, gasoline, kerosene, cyclohexane, power system coolants, lubricants, and many halogenated hydrocarbons. Liquids that are highly adsorbed on alumina (e.g., ethyl or methyl alcohol), react or polymerize in contact with activated alumina. Those containing components that tend to deposit on the alumina surface cannot be dried by activated alumina. Regeneration schemes for liquid dehydration units are varied and depend on the liquid being dried. In some applications the liquid being dried is vaporized, heated, and passed through the desiccant bed to desorb water. Hot, dry gases also are used for regeneration.

An evolving application of activated alumina is in water purification. Several important contaminants have been removed from water successfully and economically in pilot-plants as well as in large-scale treatment plants. These include reduction of fluoride concentration in drinking water and in some industrial effluents, and removal of color and odor from effluent water from dye works and paper plants. Removal of phosphate and arsenic also has been investigated.

Activated alumina can be used to separate one or more components from a gas or liquid stream by taking advantage of differences in adsorption or desorption kinetics. For example, a short cycle process has been used to recover heavy hydrocarbons from a stream of lighter hydrocarbons. Often a regeneration scheme can be devised that permits cyclic use of the alumina. In other instances, such as removal of catalyst in polyethylene and hydrogen peroxide production, it is more economical not to recycle the alumina.

Catalytic Applications

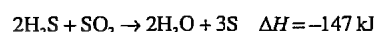
Alumina is used in many industrial catalytic processes, both as the catalyst and as a support for catalytically active components. In many instances, the alumina support contributes to catalytic activity and so assumes an essential role in the catalyst system. Other catalytic uses of alumina take advantage of its strength, heat resistance, and inertness.

Although the common adsorbent aluminas derived from Bayer hydroxide have many catalytic applications, high-purity materials (e.g., boehmite from the Ziegler process for linear alcohol production) are sometimes preferred. Because of the lower cost of Bayer process-based products, such techniques as water and acid washing of the activated product have been employed to reduce the alkali (Na₂O) content of the Bayer material. The sodium oxide is known to have a negative influence in many catalytic processes. Catalyst-forming methods include tableting, pelletizing, compacting, ball forming (agglomeration), and extrusion. Such factors as purity, surface area, pore volume, and size distribution, and rate of deactivation influence catalyst performance and selectivity. In addition, crushing strength and resistance to attrition of the catalyst pellets are important considerations in practical operation of catalytic reactors. Although these physical aspects of alumina catalysts are well characterized, the surface structure and chemistry responsible for catalytic activity still remains unclear. Many investigators have attributed catalytic activity to the intrinsic acidity of the surface of activated alumina. First, the combination of two neighboring OH⁻ groups to form water during the dehydration process leaves behind an exposed Al³⁺ ion, which, because of its electron deficiency, behaves as a Lewis acid site. In addition, hydroxyl groups are retained during thermal decomposition of aluminum hydroxide. These OH⁻ ions on the surface may act as proton-donors (Brønsted acids). These Lewis and Brønsted acid sites have been looked upon as the active catalytic centers. Further "defect" structures are formed with increasing degree of dehydration [144]. Of the types of defects created during dehydration, those assumed to have the greatest catalytic importance are the triplet vacancies. They provide unusual exposure of the aluminum ions in the underlying layer and constitute strong acid sites.

Catalytic applications of alumina are extensive. Important industrial processes employing alumina as a catalyst by itself include alcohol dehydration and the Claus process for

sulfur recovery. Dehydration of alcohols over activated alumina is one of the oldest catalytic processes. The products are olefins and/or ethers. Typical reaction conditions for olefin production are 300–400 °C and atmospheric pressure. Lower temperatures favor the formation of ethers. The most suitable aluminas for alcohol dehydration catalysis are those that have large surface areas (150–200 m²/g) and possess good thermal and hydrothermal stability. Coke formation occurs over a period of several hundred operating hours and the catalyst must be regenerated by burning off the carbon with hot air at 500–600 °C.

The largest present-day catalytic application of activated alumina itself is in the Claus process, which is used to recover sulfur from hydrogen sulfide (H₂S).



The reaction is carried out catalytically in two or more conversion stages using alumina catalysts. Reaction temperature in the first stage is around 350 °C. At this temperature, the conversion of H₂S is only about 65%. Subsequent lower temperature catalytic stages are used to further reduce the H₂S concentration. Spherical, high-strength activated alumina catalysts are used in the Claus converters. Service life as high as 5 years has been reported. Deactivation of the alumina catalyst occurs by sulfation, thermal aging, and carbon and/or sulfur deposition. Regeneration of Claus catalyst involves removal of sulfur and burning off of carbon deposits.

Alumina-supported catalysts are used extensively in the petroleum and chemical industries. In general, the petroleum industry catalysts have high surface area and high porosity; the support is mostly activated alumina. On the other hand, many typical chemical process catalysts (e.g., ammonia synthesis, steam reforming) are characterized by lower surface area (< 20 m²/g) and are non-porous or have very large diameter pores. The carrier in this case is inert and consists mostly of calcined or sintered alumina products.

Two different methods have been used commonly for preparation of alumina-supported catalysts: impregnation and coprecipitation. The alumina support used in the *impregnation process* generally has been formed into its final shape (extrudates, tablets) prior to the impregnation step. Impregnation with a salt solution of the active species is then carried out, followed by drying and thermal decomposition of the salt. In the *coprecipitation procedure*, hydroxides of aluminum together with the active component are precipitated from a salt solution by neutralization with ammonia or alkali. The washed precipitate is dried, powdered, and processed (e.g., by extrusion) to the desired shape and finally activated by thermal dehydration. The coprecipitation method is used when the active species must be present in high concentrations or when more uniform distribution of the active component is desired.

The technical and patent literature contains innumerable examples of the use of alumina as a catalyst support. Some important examples are the catalytic dehydration of *n*-butane to butadiene (used in synthetic rubber), using a chromia-impregnated alumina catalyst, cobalt molybdenum–alumina catalysts, used in hydrorefining operations (e.g., desulfurization) in petroleum refining; and pelleted catalysts containing platinum, palladium, and rhodium on an alumina base, used in automobile exhaust catalytic converters.

United States production of adsorbent-grade activated aluminas, both granular and spherical, amounted to nearly 250 000 t in 1980. Price of the cheaper, granular product was quoted around \$0.40–0.50 per kg. Price of the spherical product ranged from \$0.55 to \$0.65 per kg. Total catalytic applications of alumina in the United States were estimated to be around 400 000 t in 1980. Price of pre-formed alumina for catalytic applications ranges from \$0.60 to \$4.00 per kg, depending on source and purity. Alumina-based Claus catalyst was priced between \$3.00 and \$3.50 per kg.

21.10.1.7 Ceramic Uses of Alumina

Alumina is used extensively as a ceramic material. Products range from relatively low-calcined grades of polishing aluminas to the extremely hard, fused alumina and synthetically produced sapphire. The characteristics that make alumina valuable in ceramic applications are high melting point (2050 °C), hardness (9 on the Mohs scale), strength, dimensional stability, chemical inertness, and electrical insulating ability. These, together with availability in large quantities at moderate prices, have led to extensive and varied uses of alumina as a ceramic material.

Calcined Alumina

Ceramic aluminas are generally produced by calcining Bayer aluminum hydroxide at temperatures high enough for the formation of α-Al₂O₃. By control of calcination time and temperature and by the addition of mineralizers, such as fluorine and boron, the crystallite size in the calcined product can be varied from 0.2 to 100 μm. These calcined aluminas can be categorized broadly according to their sodium

content. There are two general types: those having about 0.5% Na₂O and low-soda grades with a content < 0.1%.

Reactive alumina is a material manufactured by dry grinding calcined alumina to particle sizes smaller than 1 μm. The large surface area associated with very fine particles and the high packing densities obtainable considerably lower the temperatures required for sintering.

Tabular aluminas are manufactured by grinding, shaping, and sintering calcined alumina. The thermal treatment at 1630–1880 °C causes the oxide to recrystallize into large, tabular crystals of 0.2–0.3 mm.

Fused Alumina

For ceramic applications and for the production of abrasives, fused aluminas are manufactured by melting a suitable raw material in an electric arc furnace. Calcined alumina from the Bayer process is used as a starting material for the highest quality fused alumina. Bauxites with varying levels of iron oxide, silicates, and titanium minerals are melted to produce the brown or less pure black qualities.

Table 21.15: Average annual net shipments by major markets in the United States.

Industry	Average annual net shipments, kt		Market distribution, %	
	1978–1982	1960–1964	1978–1982	1960–1964
Containers and packaging	1522	192	24.3	7.3
Building and construction	1241	666	19.8	25.3
Transportation	1115	549	17.8	20.8
Electrical	627	305	10.0	11.6
Consumer durables	436	284	6.9	10.8
Machinery and equipment	387	190	6.2	7.2
Other	277	229	4.4	8.7
Statistical adjustment	65	—	1.0	—
<i>Domestic total</i>	5670	2415	90.4	81.9
Exports	601	218	9.6	9.2
<i>Total</i>	6271	2633	100.0	100.9

Table 21.16: Solubility of aluminum sulfate as a function of temperature (grams of anhydrous salt per 100 g water).

t, °C											Reference
0	10	20	30	40	50	60	70	80	90	100	
31.3	33.5	36.15	40.36	45.73	52.13	59.10	66.23	73.14	80.83	89.11	[145]
31.2	33.5	36.4	40.4	46.1	52.2	59.2	66.1	73.0	80.0	89.0	[146]
27.5	27.6		28.0	28.8	29.9	31.0	21.8	36.6	38.74	46.85	[147]
23.9	25.0	26.9		31.5		36.4		41.7		47.0	[148]

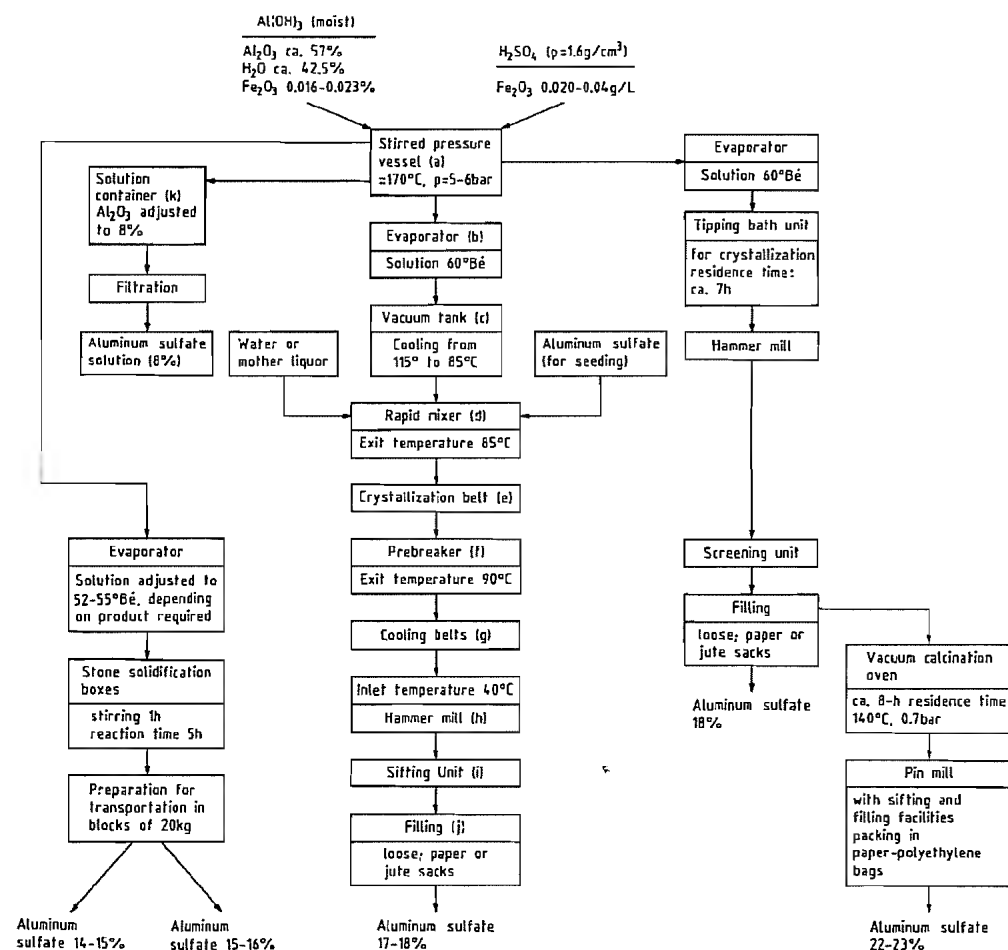


Figure 21.37: Production of aluminum sulfate by the Giulini process [154].

21.10.2 Aluminum Sulfate and Alums

21.10.2.1 Aluminum Sulfate

Aluminum sulfate is the second most important industrial compound of aluminum, after aluminum oxide. Aluminum sulfate was first used in Paris in 1844 to replace potassium alum. Today, it has taken over almost all areas of application that potassium alum originally had.

Properties

Aluminum sulfate is almost insoluble in anhydrous alcohol but readily soluble in water; aqueous solutions are acidic. Literature data on solubility and the structure of the precipitate in water differ markedly and should be used with caution (Table 21.16). Previously, $\text{Al}_2(\text{SO}_4)_3 \cdot 18\text{H}_2\text{O}$ was thought to crystallize from aqueous solution under normal conditions (20 °C, 1 bar). This is now doubted, because such factors as hydrolysis, oversaturation, shifts in equilibrium, and, particularly, poor crystal formation make definitive characterization difficult [149]. The

common form of aluminum sulfate, generally considered to be $\text{Al}_2(\text{SO}_4)_3 \cdot 18\text{H}_2\text{O}$, occurs in nature as alunogen (hair salt) and can be crystallized from hydrochloric acid solution as microscopically small, white needles. However, some researchers ascribe a hydrate water content of 17 mol to this form of aluminum sulfate [150]. A hydrate containing 27 mol of water can be prepared readily and in high purity [145]. Other well-defined aluminum sulfates contain 16, 10, and 6 mol of water. A total of 39 basic and 3 acidic aluminum sulfates, as well as 13 different hydrates of the neutral salt, are described in the literature [151]. The existence of aluminum sulfates with 14, 13, 12, 9, 7, 4, 2, and 1 mol of water can be concluded from the vapor-pressure curves and the dehydration curves of the $\text{Al}_2(\text{SO}_4)_3\text{-H}_2\text{O}$ and $\text{Al}_2(\text{SO}_4)_3\text{-Al(OH)}_3\text{-H}_2\text{O}$ systems [152, 153].

In industrial practice, the hydrate water content is unimportant because "crystalline" aluminum sulfate is a ground, microcrystalline solid with variable water content, which is obtained from a melt. The desired Al_2O_3 content is adjusted within certain limits by heating. At a temperature above 340 °C, anhydrous aluminum sulfate is formed, a white powder, ρ 2.71 g/cm³, that decomposes above 770 °C to aluminum oxide [153].

Production

In Germany and most European countries today, aluminum sulfate is produced on a large scale only from aluminum hydroxide and sulfuric acid by the Giulini process. In this process, aluminum sulfate is obtained relatively easily with high purity. Production by the action of sulfuric acid on aluminum-containing ores (clays and bauxite with high silicon and low iron content, e.g., bauxite with $\text{SiO}_2 > 5\%$, Fe_2O_3 ca. 1%) is still important in some countries (Sweden, Spain, UK, USA, former USSR, Turkey, Venezuela) but to differing degrees.

Giulini Process [154]. The Giulini method for producing various grades of aluminum sulfate, containing between 8 and 23% Al_2O_3 , is shown schematically in Figure 21.37.

A pressure-resistant, stirred vessel (a) is filled with aluminum hydroxide (moist or dry). The calculated quantity of warm sulfuric acid is added from a preheater, and the mixture is stirred. In calculating the sulfuric acid concentration required to obtain an SO_3 content of ca. 1% below stoichiometric, all process steps involving the introduction or the removal of water must be accounted for. Generally, acid of density 1.6 g/cm³ is used. The reaction starts after 60–300 s and is complete after 10–12 min. The heat of reaction causes the temperature to rise to ca. 170 °C, while the pressure rises to 5–6 bar. The mixture must not be stirred for more than 1 h because otherwise the aluminum sulfate can hydrolyze to give insoluble basic aluminum sulfate and strongly acidic sulfate melt. An autoclave unit allowing batches of 2.5 t can produce ca. 50 t of aluminum sulfate in a 10-h shift.

The melt is led into a copper container where it is concentrated by flash evaporation (b). From the evaporator, the melt is sucked into a well-isolated vacuum tank (c), which is evacuated to the vapor pressure of the aluminum sulfate melt. This vacuum cooling avoids incrustation of the heat exchanger surfaces.

The melt falls from the vacuum container into the mixer, where it is seeded at 85 °C with 1–2% aluminum sulfate powder. The pulplike product reaches the "crystallization belt", a smooth heat-resistant trough-form rubber conveyor belt (e), and crystallizes there in ca. 30 min. Because of the high heat of crystallization, the material has a temperature of ca. 90 °C and cannot be broken to fine size in one step (f). It passes over aircooled conveyor belts until it has cooled to 40 °C after which it is ground (h) and sieved (i). The goods are filled (j) into paper or jute sacks or transported loose in silo cars. Aluminum sulfate with 17.2% Al_2O_3 produced in this way contains only 0.01% insoluble material; therefore, digestion of the aluminum hydroxide is almost complete. For transportation as a solution the Al_2O_3 content is adjusted to ca. 8% to avoid crystallization during transport.

Production from Bauxite. Finely ground bauxite (for example, 60% Al_2O_3 , 1.5% Fe_2O_3 , 1.6% TiO_2 , 3.0% SiO_2 , 32% H_2O) also can be used as starting material. In this case, 3 mol H_2SO_4 are charged onto 1 mol Al_2O_3 . The Fe_2O_3 component in bauxite is disregarded because the Al_2O_3 is only 97–98% digested and therefore sufficient sulfuric acid is available for production of aluminum sulfate containing 17.5% Al_2O_3 . The aluminum sulfate obtained by digestion of bauxite contains ca. 0.5% Fe_2O_3 and ca. 2.2% insoluble residue.

Production from Less Pure Starting Materials. Acid digestion of predominately silicon-rich raw materials gives a solution of aluminum sulfate. The purity depends on the process and starting materials. Iron, which strongly interferes, is precipitated with calcium hexacyanoferrate(II) as Berlin blue (iron hexacyanoferrate(II)), with calcium sulfide as iron sulfide, or by hydrolysis as basic iron sulfate. For details, see [155]. The clear solution is decanted and sold as a liquid or concentrated to 61.5°Bé, allowed to solidify, and milled. The final product, which contains ca. 0.5% Fe_2O_3 and 0.1% insoluble material, is the technical grade. In addition, there is an iron-free grade having an Fe_2O_3 content of ca. 0.005%.

The Kretschmar process is used to produce very pure, iron-free aluminum sulfate by digestion of clay (for example, 40–43% Al_2O_3 , 53–56% SiO_2 , 2–4% Fe_2O_3) with sulfuric acid. The greater part of the impurities is removed and crystals are separated from the solution by stirring. The formation of colloids is avoided by using vacuum apparatus. Pure, large crystals of $\text{Al}_2(\text{SO}_4)_3 \cdot 18\text{H}_2\text{O}$ (15.3% Al_2O_3) can be separated easily from the impure mother liquor by centrifuging [156]. The residue from the digestion process (SiO_2) can be converted with lime to calcium hydrosilicate, which increases the hardness of and also plasticizes lime mortar.

In a process developed by the U.S. Bureau of Mines, alcohol is used to reduce the viscosity of the oversaturated aluminum sulfate mother liquor [157].

Olin Mathieson Chemical Corp. developed an economical process for producing high-quality aluminum sulfate from the clay or waste shale of coal mines. Large crystals (1.5–3 mm) with iron contents of less than 0.03% are produced in a patented crystallizer [158]. A process for producing aluminum sulfate from alum-containing ores is given in [159].

Aluminum sulfate is produced from waste “red mud” (from the aluminum oxide industry) by suspending the mud in water and passing sulfur dioxide through the suspension until pH 2 is reached. After filtration and removal of the sulfur dioxide in vacuo to give a pH of 4.5–5.0, $\text{Al}(\text{OH})\text{SO}_3$ and $\text{SiO}_2 \cdot n\text{H}_2\text{O}$ precipitate. The precipitate is filtered and treated with sulfuric acid, whereby aluminum sulfate dissolves. [160].

Commercial Grades. Whereas $\text{Al}_2(\text{SO}_4)_3 \cdot 18\text{H}_2\text{O}$ theoretically contains 15.3% Al_2O_3 , commercial grades of aluminum sulfate contain 14–15%, 15–16%, 17–18%, 18%, or 22–23% Al_2O_3 (Table 21.17). Generally, the aluminum sulfate containing 17–18% Al_2O_3 (water-soluble aluminum content, calculated as Al_2O_3) is used most frequently. The calculated hydrate water content of this aluminum sulfate is 13 mol. The commercial grade containing 17–18% Al_2O_3 is delivered also with various special qualities, such as low arsenic or low iron content.

Table 21.17: Commercial grades of aluminum sulfate.

Grade	Al_2O_3 , %	Fe_2O_3 , %	Insoluble material, %	Basicity ^a , %
8% (solution)	8	0.004	—	1
14–15%	14–15	0.006–0.008	0.04	0.1–1.0
15–16%	15.1–16.0	0.006–0.008	0.04	0.1–1.0
17–18%	ca. 17.2	< 0.01	0.03	0.1–1.0
18%	ca. 18.0	< 0.01	< 0.03	0.8–1.5
22–23%	ca. 22.8	< 0.02	ca. 0.03	1.0–1.8

^a Defined in text.

The *basicity* of the product is defined as the excess in Al_2O_3 over the stoichiometric $\text{SO}_3:\text{Al}_2\text{O}_3$ ratio. The 17–18% Al_2O_3 grade has a basicity of 0.11%, i.e., the Al_2O_3 content exceeds the stoichiometric amount by 0.1–1%. Occasionally, the term “basicity” is de-

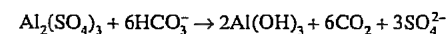
fined as the ratio % SO_3 to % Al_2O_3 . For commercial aluminum sulfate, this ratio is ca. 2.30, whereas the theoretical value is 2.35. This weakly basic aluminum sulfate has the advantage that it is less hygroscopic and therefore hardly affects either the metal parts of the apparatus during use or paper sacks during transport. Also, free acid damages cellulose fibers in the paper industry.

Uses

About two thirds of the total aluminum sulfate production is used for treating water. About one half of the total production goes into the paper industry (paper sizing, pH adjustment wastewater purification) [161, p. 246].

Paper Industry. Aluminum sulfate is used for precipitating and fixing sizing agents, wet-strength agents, and basic dyes; for improving retention; for dispersing resin particles that stick together and block sieves; as the starting material of a high-quality slip for coating glossy paper (satin white); and for the production of lake dyes and wallpaper. For an overview of uses in newspaper factories, see [162]; for a detailed discussion on the importance of aluminum sulfate in paper production, see [149]. Aluminum sulfate with more than 0.2% Fe_2O_3 gives paper a yellow tinge and cannot be used for good-quality white paper.

Water Purification. Aluminum sulfate is an important flocculating agent for purifying water [163]. The mechanism is as follows: Positively charged aluminum ions, which are hydrated or hydroxylated with water via numerous intermediate stages, neutralize the negative charge on the colloidal material in the water. As a result of mutual adsorption, the material flocculates, sediments at various rates, and finally settles as sludge after 15–150 min. To neutralize the hydrogen atoms formed on hydrolysis of aluminum sulfate, some carbonate hardness is consumed:



For 50 mg/L of the 17–18% Al_2O_3 grade 0.25 mmol/L of carbonate hardness (based on

alkaline-earth ions) is consumed. Generally, 5–50 g aluminum sulfate is sufficient to purify 1 m³ of water. An advantage of using aluminum sulfate is the lack of postflocculation, provided the correct amount is added. Disadvantages are the formation of free carbon dioxide, the increase of noncarbonate hardness, such as calcium sulfate, and the pH remaining between 5 and 7. If no natural bicarbonate hardness is present, an alkaline substance that also has a dispersing effect, such as lime or sodium aluminate, must be added. Aluminum sulfate, used in combination with calcined leached clay, is suitable for binding mercury ions, for example, in sea water [164].

Other Uses. Aluminum sulfate with a very low iron content (below 0.01%) is used as a mordant in dyeing; a higher iron content is unacceptable because this leads to color changes. Further uses are for pickling of seeds, deodorizing of mineral oils, tawing, and producing aluminum hydroxide gel employed, for example, as a filler for synthetic rubber. Aluminum sulfate has some importance also as a catalyst support. Finally, it is the starting material for almost all other aluminum compounds.

Production and Capacity Data. Aluminum sulfate production in the United States was 1 168 000 t in 1980 and 1 075 000 t in 1982 [165]; that in Japan was 757 000 t in 1980 [166]. The main U.S. producer of aluminum sulfate is Allied Corp. The main Japanese producers are Nikkei Kako Co. and Scintoma Aluminum Smelting Co.

21.10.2.2 Alums

Historical Aspects. *Alumen*, from which the word alum is derived, was known to the ancient Greeks and Romans as an astringent and also as a mordant in dyeing wool. Alum was employed in processing skins, for embalming animal and human corpses, and for fireproofing wood. However, what was known at first as alum was not a defined substance but referred to both alum-containing minerals and mixtures of alum with iron vitriol. PARACELSUS was the first to distinguish true alum from iron

vitriol. In the years 1776–1798, CHAPTAL and VAUQUELIN established that alum was a double salt of potassium and aluminum sulfates and that the potassium ions could be replaced by ammonium ions. The raw material of the ancient alum industry was alum stone (alunite) or alum shale. Alum stone contains all components of the alum in the correct ratios and is processed by roasting and leaching. Roasting, aging for several years, and leaching of alum shale gave an aluminum solution from which the alum was precipitated with alkali. The alum industry played an important role during the whole of the Middle Ages.

The industrial production of the alums ceased to have particular importance when it became possible to produce aluminum sulfate economically in high purity, because only the aluminum content is of practical importance. Most of the alum production methods now have only limited, partly only historical, interest. Clay and other alkali-containing silicates, particularly bauxite, were used as raw materials and were digested using alkali or acid. Today, alums are produced only from aluminum hydroxide, which is obtained by the Bayer process from bauxite.

General Properties. Alums are crystalline double salts of the general formula (cation 1)⁺ (cation 2)³⁺(anion²⁻)₂·12H₂O. The most useful alums are those with trivalent aluminum cations and sulfate anions, M⁺Al³⁺(SO₄)₂·12H₂O. The individual components of the alum can be replaced, retaining both the regular crystalline form and the hydrate water. Alums with the following trivalent metals are known: iron, chromium, cobalt, manganese, titanium, vanadium, gallium, indium, scan-

dium, rhodium, and iridium. The monovalent component can be an alkali metal, or it can be ammonium, alkylammonium, arylammonium, or thallium. The existence of a lithium alum is uncertain. Known combinations include potassium–aluminum, cesium–aluminum, potassium–chromium, and hydroxyammonium–aluminum. A selenate alum also is known: KAl(SeO₄)₂·12H₂O.

All alums crystallize in strongly refracting octahedra or cubes [145]. They have an astringent taste and rot-proofing, protein-precipitating properties.

In *aqueous solution*, alums show all the chemical properties that their components show separately. Physical properties, such as color, electrical conductivity, and freezing-point lowering, are the sum of the properties of the components, provided the solutions are very dilute. At higher concentrations, complexes, such as [Al(SO₄)₂·(H₂O)₂]⁻, are formed. The solubilities of the alums in water decrease from sodium to cesium (see Table 21.18). On heating, the alums lose their water of crystallization either partially or completely. However, part of the water is taken up again at normal temperature and humidity.

Potassium Aluminum Sulfate

Potassium aluminum sulfate, known as potassium alum, KAl(SO₄)₂·12H₂O, ρ 1.75 g/cm³, and ammonium aluminum sulfate are the aluminum compounds known longest. Potassium alum occurs in nature as efflorescence on alum shale and in volcanic areas on trachyte and lava as feather alum.

Table 21.18: Solubility of some aluminum alums as a function of temperature (grams of anhydrous salt per 100 g water).

t, °C	0	10	20	30	40	50	60	70	80	90	100
Sodium	56.2	60.5	61.5	66.7							
Potassium	3.0	4.0	5.9	7.9	11.7	17	25	40	71	109	154
Ammonium	2.6	4.5	6.6	9.0	12.4	15.9	21.1	26.9	35.2	50.3	70.8
Rubidium	0.71	1.09	1.40		3.1	4.98			21.6		
Cesium	0.2	0.3	0.4		0.8	1.24			5.3		22.8
Thallium	3.05	4.4	6.2		12.6		26.0				

Potassium alum crystallizes in large, colorless, transparent octahedra, which melt at 92.5 °C in their own water of crystallization. The hardness of the crystals on the Mohs scale is 2. The octahedra absorb long-wavelength IR radiation almost completely, but are transparent to visible light. Certain substances (hydroxides, carbonates, borates, carbamides, also metals and organic dyes) promote the formation of basic aluminum sulfate by binding free sulfuric acid in the mother liquor. Under these conditions, the cubic form is favored (cubic or Roman alum).

Potassium alum is stable in air of normal humidity. Dehydration does not begin below 30 °C, but at 65 °C nine moles of water are lost. Literature data on the dehydration are contradictory. Recent investigations on thermal decomposition are given in [167]. According to these results, K₂SO₄, γ-Al₂O₃, and 3K₂SO₄·Al₂(SO₄)₃ form at 780 °C, whereas K₂SO₄, α-Al₂O₃, and K₂O·12Al₂O₃ are produced at 1400 °C. When heated above its melting point, potassium alum dehydrates, forming calcined alum (alum ustum), KAl(SO₄)₂. At red heat, SO₃ is released.

Potassium alum is soluble in dilute acid but almost insoluble in anhydrous alcohol, acetone, and methyl acetate. Because of the marked increase in solubility in water with temperature, potassium alum can be purified more easily than other aluminum salts by recrystallization and, in particular, can be freed from iron sulfate. Mixed crystals form readily with ammonium sulfate.

Basic potassium aluminum sulfate, K[Al(OH)₃](SO₄)₂·³/₂H₂O, occurs in nature as löwigite. The compound is made synthetically as a rather insoluble, amorphous powder by heating aluminum sulfate, water, and an excess of potassium sulfate or by heating potassium alum with water in the ratio 1:4 to 200 °C [168]. Another basic potassium aluminum sulfate, K[Al₃(OH)₆(SO₄)₂], containing less water, is the alum stone (alunite) occurring in nature.

Production. Aluminum hydroxide (wet hydrate; Al₂O₃ ca. 57%, Fe₂O₃ 0.016–0.023%,

H₂O 42.5%) and sulfuric acid (ρ ≈ 1.6 g/cm³; Fe₂O₃ 0.020–0.040 g/L) react in a stirred, corrosion-resistant pressure boiler at 5–6 bar to form aluminum sulfate as shown in Figure 21.37. The aluminum sulfate melt is then led, with release of pressure, into a copper container. Here, a stoichiometric quantity of potassium sulfate (as chloride-free as possible) is added. The solution is heated to ca. 100 °C for 2–3 h and adjusted to 40–44 °Bé with mother liquor. After filtration from insoluble material, the alum melt is left in crystallization boxes for 10 days, after which the alum is removed in blocks. The product obtained in this way contains < 0.001% Fe₂O₃, 0.001–0.004% chloride, and < 0.01% insoluble material.

For the production of *alum crystals*, the alum melt is brought into a stirred crystallization bath, where it is cooled to ca. 40 °C by air bubbles. The pulp is then separated from the mother liquor by centrifuging and washed. The mother liquor is collected and returned to the copper container. The potassium alum is dried at 50–60 °C. The salt, which forms lustrous crystals, is sieved and packed in paper bags that are lined with polyethylene.

A process for obtaining potassium alum from alum-containing ores is given in [159], and the production of basic potassium and sodium alums from synthetic alum is described in [169].

Uses. As already mentioned, the industrial importance of potassium alum has declined considerably. However, it is still employed in tawing skins, as a mordant in dyeing, and as a coagulating agent for latex. Because of its astringent and protein-precipitating properties, potassium alum is used in the pharmaceutical and cosmetics industries. The use of potassium alum as a styptic pencil, because of its blood-stanching property, is very widespread and popular. The most important application today is in the gypsum industry, which employs potassium alum as hardening agent and setting accelerator for the production of marble cement and alabaster plaster. However, for purifying water and sizing paper, potassium alum has been replaced completely by alumi-

num sulfate. In the paper industry, aluminum sulfate is designated traditionally, although incorrectly, as an alum.

Ammonium Aluminum Sulfate

Ammonium aluminum sulfate, also called ammonium alum, $\text{NH}_4\text{Al}(\text{SO}_4)_2 \cdot 12\text{H}_2\text{O}$, ρ 1.64 g/cm³, mp 93.5 °C, occurs in nature as shermigite. Crystals doped with other alums show birefringence. The solubility of ammonium alum in water is similar to that of potassium alum, with which it forms a continuous series of mixed crystals. Ammonium alum is slightly soluble in dilute acids and glycerol but insoluble in absolute alcohol. In aqueous solution, ammonium alum is neutral.

Data on loss of water on heating are in disagreement. GEL'PERIN and CHEROTKEVICH [170] have reported that water of crystallization is released in three stages: first to give the hydrate with 21 mol water, then to that with 3 mol water and finally to the anhydrous product, so that it is in fact more correct to formulate ammonium alum with 24 mol water. Above 193 °C, decomposition with the release of ammonia begins. On glowing above 1000 °C, sulfur trioxide is lost, leaving an aluminum oxide residue.

Production. Ammonium alum is made today mainly by dissolving aluminum hydroxide in sulfuric acid and adding ammonium sulfate but sometimes by the reaction of ammonia gas with aluminum sulfate and sulfuric acid. The procedure is analogous to the potassium alum process. To obtain a quality particularly low in iron oxide or other metal oxides (< 0.0001 % Fe_2O_3 ; normal quality ca. 0.001 % Fe_2O_3), as is required for production of synthetic gems, very pure starting materials must be used. Ammonium alum occurs as an intermediate in the "aloton" process, which operates in a sulfuric acid medium. This process had some importance prior to 1945 in Germany and the United States for aluminum hydroxide and aluminum oxide production.

Uses. In Europe, ammonium alum is not used in large quantities. Applications include those

in dressing furs in tanning, in the production of very fine aluminum oxide particles for polishing metallographic surfaces, and, in some countries outside Europe, as a disinfectant. In the United States, ammonium alum is important as an additive in baking powder; ca. 500 t/a are produced for this purpose. More recently, ammonium alum has gained considerable importance as starting material for the production of the finely powdered, loose aluminum oxide of high purity that is required for synthesizing corundum gems, such as rubies and sapphires. This quality of aluminum oxide is made by heating ammonium alum (or ammonium aluminum selenate alum) to 1000 °C.

Sodium Aluminum Sulfate

Sodium aluminum sulfate, sodium alum, $\text{NaAl}(\text{SO}_4)_2 \cdot 12\text{H}_2\text{O}$, melts at 61 °C in its water of crystallization. In nature, it occurs as the mineral mendozite. Again, the data on thermal dehydration disagree. Sodium alum is insoluble in absolute alcohol but is much more soluble in water than all other alums. Alum powder (very fine crystalline form) is not available commercially. These two facts make it difficult to obtain sodium alum free from iron. Because of this and also because of its strong tendency to age, sodium alum has never gained the same importance as the other alums. In Europe, its use has been abandoned. In the United States, however, sodium alum is still utilized in relatively large quantities (ca. 3000 t/a) in baking powder.

Production. In the United States, sodium alum is produced by adding a clear solution of sodium sulfate to aluminum sulfate. After dilution to 30 °Bé and subsequent heating, a sludge of potassium sulfate, sodium silicate, and caustic soda is added to improve the purity of the product. The mixture is pumped into a stirred vessel, where it is mixed for several hours. During this stage, the ratio of aluminum sulfate to sodium sulfate is adjusted to the stoichiometric amount. Afterwards, the melt is pumped into an evaporator and concentrated to such an extent that it solidifies to a hard cake on pouring into a cooling tank. This so-

dium alum cake is then heated and finally ground to the desired size (99% through a sieve of 100 mesh) [161, p. 250].

21.10.3 Aluminates

Only the aluminates of barium and sodium have importance in industry. Aluminates occur also in cement and in spinels.

21.10.3.1 Sodium Aluminate

Sodium aluminate is an important commercial inorganic chemical. It functions as an effective source of aluminum hydroxide for many industrial and technical applications. Commercial grades of sodium aluminate are available in solid and liquid forms. Pure sodium aluminate (anhydrous) is a white crystalline solid having a formula variously given as NaAlO_2 , $\text{Na}_2\text{O} \cdot \text{Al}_2\text{O}_3$, or $\text{Na}_2\text{Al}_2\text{O}_4$. Commercial grades, however, always contain more than the stoichiometric amount of Na_2O , the excess being on the order of 1.05 to 1.50 times the formula requirement. Hydrated forms of sodium aluminate are crystallized from concentrated solutions.

Sodium aluminate has no defined melting point; it softens above 1700 °C when sodium begins to evaporate slowly, leaving aluminum oxide.

Production. The chief commercial process for the manufacture of sodium aluminate is the dissolution of aluminum hydroxides in sodium hydroxide solution. Aluminum trihydroxide (gibbsite) from the Bayer process can be dissolved in 10–30% aqueous NaOH solution at a temperature near the boiling point.

The use of more concentrated NaOH solutions leads to a semisolid product. The process is carried out in steam-heated vessels of nickel or steel, and the aluminum hydroxide is boiled with ca. 50 % aqueous sodium hydroxide until a pulp forms. After this is poured into a tank and cooled, a solid mass containing about 70 % NaAlO_2 is formed. After being crushed, this product is dehydrated in a rotary oven heated either directly or indirectly by burning hydrogen. The resulting product contains ca.

90% NaAlO_2 and 1 % water together with 1 % free NaOH. The solubility of the salt produced in this way depends strongly on how much excess sodium hydroxide is used.

Alternatively, bauxite can be used directly as the alumina source. Bauxites containing gibbsite are extracted at 150 °C and 5 bar, whereas boehmite containing bauxite requires higher temperatures (230 °C) and pressures. The sodium aluminate solution obtained from the digestion process is separated from any impurities and then concentrated to the commercial liquid grade by evaporation. The solid product is obtained by drying the liquid.

The sinter method also has been used to produce sodium aluminate. By sintering sodium carbonate directly with Bayer aluminum trihydroxide in rotary sintering kilns at 1000 °C, an essentially anhydrous product can be obtained. When sintering bauxite, it is essential to leach the sinter mass with water and separate the impurities.

Uses. The major use of sodium aluminate is for water treatment, including both potable and industrial waters. Sodium aluminate is used as an adjunct to water softening systems, as a coagulant aid to improve flocculation, and for removing dissolved silica. Sodium aluminate dissolves in water to give a solution that has a pH value of 8. The aluminum hydroxide that precipitates from this solution has excellent flocculation properties and coagulates other impurities present in the water. Depending on the impurities, the conditions of precipitation can be improved by adding aluminum sulfate [171].

In *construction technology*, sodium aluminate is employed to accelerate the solidification of concrete, mainly when working during frost, under water, and in humid soil (Table 21.19). Compared to calcium chloride, which acts in a similar manner, sodium aluminate has the advantage of greater setting acceleration at low water-to-cement ratios [172]. Because it does not attack the reinforcing metals, it can be used for work with steel-reinforced concrete. Too rapid setting can cause cracks in the concrete, affecting the final strength of the

building. By adding substances such as oxoacids [173], sugar, naphthene [174], K_2CO_3 , or Na_2SO_4 [175] the final strength increases without affecting the setting rate significantly. Sodium aluminate increases the resistance of mortar to water, alkali, and acid. For the production of expanded concrete, sodium aluminate serves to activate nitrogen-releasing substances [176]. To stabilize foam formation in the production of light refractory bricks, up to 5% (relative to the total dry mass) sodium aluminate is added.

Table 21.19: Acceleration of setting by sodium aluminate in a mixture of 6 parts sand, 2 parts concrete, and 1 part water.

% $NaAlO_2$ in concrete	Setting started	Setting completed
0	4 h 30 min	6 h
1	30 min	1 h 40 min
1.5	15 min	30 min
2	10 min	15 min
10	instantly	

Increasingly, sodium aluminate is being used for the production of *synthetic zeolites*, used as catalyst supports or as catalysts [177–180] and as adsorbents. Sodium aluminate is one of the principal sources of *alumina* of the preparation of alumina adsorbents and catalysts.

In the *paper industry*, sodium aluminate increases the opacity [181], retention of fibers and filling materials [182], and the paper strength [183]. Also, it stabilizes the pH value of the water circulation [184] and increases the dispersion stability of titanium dioxide [185].

Another application of sodium aluminate is as a *pickle* to protect metallic surfaces (copper [186], aluminum [187], among others). This effect is based on the formation of a thin, very firmly adhering layer of aluminum hydroxide or, after heat treatment, of aluminum oxide on the surface, which does not affect the metallic luster. In the *enamel industry*, sodium aluminate is added to enamel mixtures to achieve low-melting covers [188].

Further applications of sodium aluminate are in lithography for the production of printing inks [189] and print forms [190], in the de-

tergent and varnish industries, in the production of water-insoluble floor waxes [191], as a dispersion agent for production of high-purity asbestos [192], as an additive to drilling fluids [193], and in the textile industry as a mordant in dyeing and in printing cloth. Many other uses of sodium aluminate have been reported. These include inhibition of glass etching by alkaline solutions; protection of steel surface during galvanizing; improving dyeing, antipiling, and antistatic properties of polyester synthetic fibers; as an additive to foundry sand molds and cores; and as a binder in the ceramics industry.

21.10.3.2 Barium Aluminates

The industrially important barium aluminates are $BaO \cdot 6Al_2O_3$, *mp* 1915 °C; $BaO \cdot Al_2O_3$, *mp* 1815 °C; and $3BaO \cdot Al_2O_3$, *mp* 1425 °C [194]. The first two crystallize hexagonally.

Barium aluminates are produced by melting bauxite with coal and barite. Leaching the melt gives a solution of barium aluminate, from which the salt is obtained by evaporation. Very pure barium aluminates can be produced by sintering mixtures of aluminum oxide with barium carbonate. All barium aluminates, including such hydrated compounds as $BaO \cdot Al_2O_3 \cdot 4H_2O$, $2BaO \cdot Al_2O_3 \cdot 5H_2O$, $BaO \cdot Al_2O_3 \cdot 7H_2O$, and $7BaO \cdot 6Al_2O_3 \cdot 36H_2O$, hydrolyze in water, forming hydrargillite (gibbsite), $Al(OH)_3$, and relatively soluble barium hydroxide.

Barium aluminate is used for purifying water because the Ba^{2+} ion precipitates both the sulfates and the carbonates, whereas the aluminate ions form insoluble calcium aluminate. A further use of barium aluminates is as a special cement, for example, as binding agent for the production of high-temperature refractories, and in the production of radiation shields [195].

21.10.4 Aluminum Alkoxides

Aluminum alkoxides (alcoholates) are solid or liquid compounds of covalent character.

They are readily soluble in hydrocarbons, but sparingly soluble in alcohols. Hydrolysis with water occurs readily, giving aluminum hydroxide and the corresponding alcohol. For a general review of aluminum alkoxides, see [196]. Industrially, only the isopropoxide (isopropylate) and *sec*-butoxide (*sec*-butylate) are important. These compounds are used to adjust the viscosity of varnishes, to impregnate textiles, as intermediates in the production of pharmaceuticals, and as antitranspirants in cosmetics. In the industrial production of ketones and aldehydes, aluminum alkoxides are employed as reducing agents (Meerwein-Ponndorf reaction).

Aluminum iso-propoxide, $Al(OCH(CH_3)_2)_3$, is a white solid, *mp* 118 °C, *bp* 125–130 °C at 533 Pa, d_4^{20} 1.0346, flash point 26 °C. It is usually produced by direct reaction of aluminum and isopropyl alcohol in the presence of mercury(II) chloride catalyst. In a later version of the process [197], the alcohol was heated under reflux in a column filled with aluminum chips; no catalyst was required and nearly quantitative conversion was obtained. The alkoxide can be purified by distillation. In an alternative production method, excess isopropyl alcohol is added to a solution of aluminum chloride in benzene; the hydrogen chloride formed is removed by introducing dry ammonia into the reactor and filtering off the ammonium chloride that precipitates.

Aluminum sec-butoxide, $Al(OC_4H_9)_3$, is a colorless liquid, *bp* 180 °C at 533 Pa, d_4^{20} 0.9671, flash point 26 °C, and is produced in a manner similar to aluminum isopropoxide.

21.10.5 Aluminum Chloride

21.10.5.1 Anhydrous Aluminum Chloride

ØRSTED first prepared anhydrous aluminum chloride in 1825 by the reaction of chlorine gas with a mixture of alumina and carbon. This compound has acquired great significance in organic chemistry as a catalyst, particularly for Friedel–Crafts syntheses and

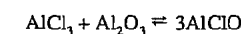
allied reactions for the production of alkylated aromatics, dyestuffs, pharmaceuticals, and perfumery chemicals. For general literature, see [145] and [198].

Properties

Physical Properties. In the solid and gas phases at temperatures up to 400 °C, aluminum chloride is present as the dimer, Al_2Cl_6 . Dissociation of the dimer progresses with rising temperature and is quantitative above 800 °C. Solid aluminum chloride crystallizes to form a monoclinic layer lattice. Pure aluminum chloride is white, but the commercial product usually has a yellowish or grayish tinge because of small amounts of iron chloride or aluminum impurities. Physical properties of anhydrous aluminum chloride [199]:

ρ at 25 °C	2.44 g/cm ³
Sublimation temperature at 101.3 kPa	181.2 °C
Triple point, at 233 kPa	192.5 °C
Heat of formation at 25 °C	−705.63 ± 0.84 kJ/mol
Heat of sublimation of dimer at 25 °C	115.73 ± 2.30 kJ/mol
Heat of fusion	35.35 ± 0.84 kJ/mol
Heat of solution at 20 °C	−325.1 kJ/mol

Chemical Properties. Anhydrous aluminum chloride reacts extremely violently with water, evolving hydrogen chloride. The hexahydrate, $AlCl_3 \cdot 6H_2O$, is formed in this reaction. In aqueous solution, aluminum chloride is partially hydrolyzed to hydrochloric acid and aluminum oxychloride, $AlClO$. For this reason, anhydrous aluminum chloride cannot be obtained by concentrating the solution and calcining the hydrate. When aluminum chloride is heated with γ -alumina, aluminum oxychloride, $AlClO$, forms, but this reaction goes in the reverse direction at temperatures above 700 °C:



If aluminum chloride vapor is passed at 1000 °C under reduced pressure over molten aluminum, volatile aluminum monochloride, $AlCl_3$, is formed, but this decomposes immedi-

ately into the elements in cooler zones of the reactor. This method has been adopted for purifying aluminum.

Reaction between aluminum chloride and other metal halides, such as CaCl_2 , CrCl_3 , and FeCl_3 , gives mixed halides. Eutectic melts with other metal chlorides are of industrial significance, for example, that with sodium chloride is used as a solvent in chlorination reactions.

Anhydrous aluminum chloride dissolves readily in polar organic solvents. As a Lewis acid it forms addition compounds with numerous electron donors, such as hydrogen chloride, hydrogen sulfide, sulfur dioxide, sulfur tetrachloride, phosphorus trichloride, ethers, esters, amines, and alcohols.

Production

The starting materials are either aluminum or pure aluminum oxide. Bauxite now has no economic significance as a raw material because of the iron chloride always present in the product.

Chlorination of Aluminum [200]. Today, most anhydrous aluminum chloride is made by chlorinating aluminum.

Chlorine is passed through molten aluminum in ceramic-lined, tube-shaped reactors. The reaction is highly exothermic:



The temperature in the reactor is maintained at 670–850 °C by controlling the admission rates of chlorine and aluminum and by cooling the reactor walls with water. The aluminum usually is replenished in the form of lumps. The difficulty of controlling the large heat of reaction can be overcome also by dividing the process into a number of small units.

The aluminum chloride vapor leaving the reactors is passed through ceramic-lined tubes into large air-cooled iron chambers. Solid aluminum chloride is withdrawn from the condenser walls at regular intervals, ground (insuring exclusion of moisture), and classified by sieving. Chlorine in the off-gas is re-

moved by conventional methods such as absorption in caustic soda solution.

Chlorination of Pure Aluminum Oxide. Chlorination of alumina is advantageous over the formerly widely used bauxite process (less reactor corrosion and higher-purity product), and at the same time it avoids the high raw material costs involved in metal chlorination [201].

Carbon monoxide and chlorine are partially converted to phosgene over an activated charcoal catalyst. The gaseous reaction mixture enters a brick-lined, fluidized-bed reactor, where it reacts with finely divided γ -alumina to yield aluminum chloride. The reaction is exothermic enough (ca. 300 kJ/mol, based on AlCl_3) to maintain the temperature at 500–600 °C without external heat. Consequently, the process permits large units, and the low reaction temperature insures that the brick lining has a long life.

The aluminum chloride vapor is filtered through a bed of coarse pumice chips, condensed, and further processed described above. The off-gas contains chlorine, phosgene, and large amounts of carbon dioxide. The chlorine is removed by scrubbing, and the phosgene is hydrolyzed with water. Extremely pure aluminum chloride is obtained by resublimation from molten sodium aluminum chloride.

Quality Specifications and Analysis

Anhydrous aluminum chloride is ground and marketed as powder or granules. Aluminum usually is determined by complexometry; the chloride, by argentometry. The assay is 98–99% AlCl_3 . The main impurity is iron (0.05% max. or 0.01% for resublimed product). Sampling and analysis of anhydrous aluminum chloride must be carried out in an atmosphere of dry air or nitrogen.

Handling, Storage, and Transportation

Because of its corrosive and irritant action, anhydrous aluminum chloride is classified as a

dangerous substance. National and international regulations must be observed, such as 67/548/EEC, the key European Economic Community directive dealing with the classification, packaging, and labeling of dangerous substances.

Handling. Goggles, gloves, and protective clothing must be worn when handling aluminum chloride. A fume cupboard or a respirator with filter type B/St against acid gases should be used. Because hydrogen chloride is evolved when aluminum chloride is exposed to water, any spills must be taken up dry, and only small, residual amounts can be washed away with plenty of water. Sodium bicarbonate or slaked lime should be used for neutralization.

Storage and Transportation. Aluminum chloride is dispatched in vented steel drums or in tank trucks or rail tankcars that can be emptied pneumatically with dry air or nitrogen (dew point below –40 °C). Because the product tends to cake, it should not be stored for more than six months. International marine transportation is governed by the IMDG code, class 8, UN no. 1726. RID, ADR, ADN: Class 8, no. 11b, Rn 801, 2801, 6801, respectively. EEC: Yellow Book 78/79, EG no. 013-003-00-7. United Kingdom: Blue Book, Corrosives & IMDG code E 8031. United States: DOT regulations, corrosive solid, CFR 49, 172.101.

Uses

Anhydrous aluminum chloride is an important *Friedel–Crafts catalyst* in the chemical and petrochemical industries [202, 203]. A principal application is the alkylation of benzene by alkyl halides to form alkylbenzenes that are consumed in the production of synthetic detergents, such as alkylbenzene-sulfonates. Aluminum chloride also catalyzes the liquid-phase ethylation of benzene with ethylene to yield ethylbenzene, most of which is used in the production of styrene.

Ethyl chloride is produced mainly by the reaction of hydrochloric acid and ethylene in

the presence of aluminum chloride; the consumption has significantly decreased because of the declining demand for tetraethyl lead as an antiknock additive.

In the dyestuffs industry, aluminum chloride is widely used as catalyst in the production of anthraquinone and its derivatives and of pigments, such as phthalocyanine green. A further application of aluminum chloride is as a finish for titanium dioxide pigments, which are in this way protected from oxidation by an oxide layer.

Until 1960, aluminum chloride was used extensively in petroleum refining for cracking and isomerization, but it has now been replaced by zeolite catalysts. It is still employed in reforming hydrocarbons, as a polymerization catalyst in the production of hydrocarbon resins, and for the production of butyl rubber.

It is a catalyst also in the production of compounds, such as aromatic aldehydes, ketones, and 2-phenyl-ethanol, used in fragrances. Other applications for anhydrous aluminum chloride include the production of aluminum borohydride, lithium aluminum hydride, as well as compounds of phosphorus and sulfur.

Most of these reactions with aluminum chloride produce a solution that is often used as a flocculating agent in the treatment of waste water.

Aluminum chloride also is an intermediate in the production of aluminum by the Alcoa smelting process [204].

Data on the consumption of anhydrous aluminum chloride in the United States are given in Table 21.20.

Table 21.20: United States anhydrous aluminum chloride consumption in 1993 (not including the amounts consumed in the production of aluminum) [205].

Alkylate detergents	2 200 t
Ethylbenzene	4 000 t
Hydrocarbon resins	3 900 t
Pharmaceuticals	4 000 t
Titanium dioxide	2 200 t
Miscellaneous	4 900 t
Total	21 200 t

21.10.5.2 Aluminum Chloride Hexahydrate

Properties. The white hydrate $\text{AlCl}_3 \cdot 6\text{H}_2\text{O}$ crystallizes hexagonally and dissolves exothermally in water (133 g hexahydrate per 100 g water at 20 °C) [206]. The solubility increases only slightly with temperature. The aqueous solutions are strongly acidic because the salt hydrolyzes. Hydrogen chloride is evolved on heating concentrated solutions. The structure of aqueous solutions of $\text{AlCl}_3 \cdot 6\text{H}_2\text{O}$ is discussed in [207].

Production and Uses. Aqueous solutions of $\text{AlCl}_3 \cdot 6\text{H}_2\text{O}$ can be obtained by dissolving aluminum hydroxide in hydrochloric acid: the hexahydrate crystallizes when hydrogen chloride passes into cold (about 20 °C) saturated solution. In this way, impurities, particularly iron(III) chloride, can be removed [206]. Aluminum chloride hexahydrate has only minor importance as such; for example, it is used for hardening photographic layers. However, it is of industrial importance as an intermediate in the production of aluminum oxide [208, 209].

21.10.5.3 Basic Aluminum Chlorides

Properties. Basic aluminum chlorides, aluminum hydroxychlorides, aluminum chloride hydroxides, poly(aluminum hydroxychlorides), have the general formula $\text{Al}_2(\text{OH})_{6-n}\text{Cl}_n \cdot x\text{H}_2\text{O}$. The individual compounds are best defined either by the molar ratio of aluminum to chloride ($^{2/}_n$) or by their basicity, defined as $(1 - \frac{n}{6}) \times 100\%$. Below a minimum water content, which depends on n , the compounds are unstable; they decompose to aluminum hydroxide and aluminum oxide on heating to above 80 °C, releasing water and hydrogen chloride. All basic aluminum chlorides with $n = 1-5$ can be isolated, and all are white, in some cases crystalline substances, partially soluble in the lower alcohols [210, 211], but readily soluble in water. For example, 170 g of the compound $\text{Al}_2(\text{OH})_5\text{Cl} \cdot 2.5\text{H}_2\text{O}$ dissolves in 100 g water at 20 °C. However, the viscos-

ity of the solution prevents further amounts from dissolving. The *electrical conductivities* of the aqueous solutions, shown in Figure 21.38, are characteristic of the basic aluminum chlorides.

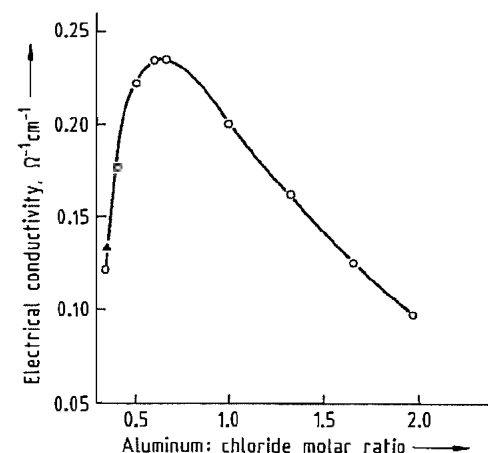


Figure 21.38: Electrical conductivity of freshly prepared basic aluminum chloride solutions: ○ from Locron L (ca. 50 % aqueous solution of $\text{Al}_2(\text{OH})_5\text{Cl} \cdot 2.5\text{H}_2\text{O}$) and hydrochloric acid at constant aluminum oxide concentration (11.5 %) and 20 °C; ▲ prepared directly from $\text{AlCl}_3 \cdot 6\text{H}_2\text{O}$.

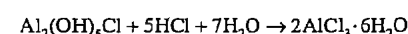
Table 21.21: pH values of aqueous solutions of $\text{Al}_2(\text{OH})_5\text{Cl} \cdot 2.5\text{H}_2\text{O}$ at 20 °C (mass fractions, w , in %).

w	pH
60	3.4
30	4.0
15	4.2
10	4.3
5	4.4
3	4.4

Aqueous solutions of basic aluminum chlorides are acidic because the compounds hydrolyze (Table 21.21). The stability of the solutions depends on the basicity: compounds with aluminum to chloride molar ratios of ca. 0.5:1 to about 1.6:1, corresponding to basicities of ca. 30–75 %, decompose to give insoluble basic aluminum chloride at a rate that depends on the temperature and concentration of the solution [212]. On the other hand, compounds of basicity greater than 75 % are very stable in aqueous solution. For example, compounds with the approximate composition $\text{Al}_2(\text{OH})_5\text{Cl} \cdot 2-3\text{H}_2\text{O}$ are so stable at concen-

trations > 50 % that no decomposition occurs, even on boiling for days.

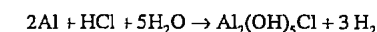
In contrast to the aluminum chlorides of low basicity (below 65 %), the compounds of high basicity (above 65 %) do not crystallize from their aqueous solutions, but form glassy masses. When solutions in the basicity range 30–65 % are evaporated, the compound $\text{Al}_2(\text{OH})_{3.7}\text{Cl}_{2.3} \cdot 6.05\text{H}_2\text{O}$ (basicity 62 %) always crystallizes [213]. On addition of alkali to basic aluminum chlorides, aluminum hydroxide precipitates. Hydrochloric acid converts all basic aluminum chlorides to the hexahydrate:



Chemical Structure. Basic aluminum chlorides have been known for a long time [145, p. 205], but only recently have investigations given significant insight into their chemical structures [214–217]. Basic aluminum chlorides are mixtures of complex compounds of various degrees of polymerization. Spectroscopic and kinetic investigations of the basic aluminum chlorides and of their solutions [214–218] lead to the conclusion that the complex ion $[\text{Al}_{13}\text{O}_4(\text{OH})_{24}(\text{H}_2\text{O})_{12}]^{7+}$ is present and is in equilibrium with its polymeric forms. Variations observed in the properties of these aqueous solutions such as viscosity and pH are caused by polymerization and depolymerization [219, 220].

Analysis. Basic aluminum chlorides are so stable that the aluminum content can be determined only after decomposition of the complex ion [221, 222]. The usual procedure is to mix the solution containing aluminum with 60 % sulfuric acid and 0.1 M disodium ethylenediaminetetraacetate, followed by ca. 20 % sodium hydroxide. The pH is adjusted to 4.7–4.9 at 60–70 °C. After the solution is cooled to about 25 °C and buffer solution (acetic acid, ammonium acetate), acetone, and indicator (dithizone in ethanol) are added, the solution is back-titrated with 0.1 M zinc sulfate. One milliliter of 0.1 M disodium ethylenediaminetetraacetate is equivalent to 2.698 mg of aluminum.

Production. Basic aluminum chlorides are made by dissolving either aluminum hydroxide or metallic aluminum in hydrochloric acid. Aged aluminum hydroxide leads only to compounds of basicity up to 65 % [212]. To obtain aluminum chlorides of high basicity, freshly precipitated aluminum hydroxide [223] must be used. However, the preferred method is to dissolve aluminum in hydrochloric acid either thermally or electrochemically:



This method is exemplified by the following process [224]:

Aluminum electrodes are set up at distances of 40 mm in a corrosion-resistant electrolysis cell. Hydrochloric acid (ρ 1.04 g/cm³) is poured into the cell at a rate such that the reaction temperature remains at ca. 80 °C. After all the hydrochloric acid has been added, the voltage between the first and last electrodes is set so that an average voltage of 0.6 V per electrode pair is obtained at a current density of ca. 170 A/m². The formation of explosive gas mixtures must be avoided throughout the reaction by diluting the hydrogen with air or nitrogen to below the explosion limit. After about 70 h, the density of the electrolyte increases to about 1.2–1.3 g/cm³, and the pH value to about 3.5. At the same time the cell voltage fails. The electrolyte then consists of a solution containing aluminum and chloride in the molar ratio 2:1, corresponding to a basicity of 83%. The corresponding bromides as well as iodides are obtained by the same method. The solid halides are obtained from the solutions by careful evaporation or by spray drying [225]. Recently, another method may be of interest: controlled thermic decomposition of $\text{AlCl}_3 \cdot 6\text{H}_2\text{O}$ [226].

Uses and Quality. The scope of applications for basic aluminum chlorides has increased considerably in recent years. The most important basic aluminum chloride has the composition $\text{Al}_2(\text{OH})_5\text{Cl} \cdot 2-3\text{H}_2\text{O}$. Very stringent purity specifications apply to this substance. The maximum levels permitted are Fe 100 ppm, SO_4 500 ppm, Pb 20 ppm, As 3 ppm. These are required for its chief application,

namely, that in the cosmetics industry as the effective component of antiperspirants [227, 228]; trade names are Chlorhydrol (Reheis, USA), Locron (Hoechst, Germany), and Wickenol (Wickhen, USA). Other areas of application for this aluminum chloride are in the production of catalysts and highly temperature-resistant fibers based on Al_2O_3 , as a hydrophobic agent for impregnation of cotton textiles, for tanning leather, as a retention agent in paper production, as a binding agent for fire-resistant ceramic products, and as a hardening agent for rapid fixing baths in the photographic industry. Aluminum chlorides of low and moderate basicities, often known collectively as poly(aluminum chloride), are used particularly in flocculation chemicals for the treatment of water [229, 230]. For example, trade name of one of such a substance is Povimal (Hoechst).

21.10.6 Toxicology

Aluminum sulfate is classified as nontoxic; an LD_{50} value of 6207 mg/kg (mouse, oral) is reported [231]. Alum solutions are known for their astringent (tissue-contracting) effects. A TLV of 2 mg/m³ was established for water-soluble aluminum salts [232].

Anhydrous aluminum chloride has a corrosive and irritant effect on the skin, respiratory tract, and eyes. The toxic effect is caused by the evolution of hydrochloric acid when the product is exposed to moist air. The resulting respiratory difficulties vary from mild irritation to coughing. The MAK value (1995) and TLV (1983) for hydrochloric acid are both 7 mg/m³ [232, 233].

The extensive use of the *basic aluminum chloride* $\text{Al}_2(\text{OH})_5\text{Cl} \cdot 2\text{--}3\text{H}_2\text{O}$ in the cosmetic industry worldwide over more than 30 years has shown that this compound is not irritating to the skin in the concentrations used commercially. Although intermittent application of 150 mg $\text{Al}_2(\text{OH})_5\text{Cl} \cdot 2\text{--}3\text{H}_2\text{O}$ over a period of 3 days was found to cause mild skin irritation in humans, a dose of only 7.5 mg of $\text{AlCl}_3 \cdot 6\text{H}_2\text{O}$ caused the same degree of irritation [234].

21.10.7 Aluminum Benzoate

$\text{Al}(\text{C}_6\text{H}_5\text{O}_2)_3$, a crystalline powder, is slightly soluble in water. Aluminum benzoate is used as a stabilizer in poly(vinyl chloride).

21.11 Pigments

21.11.1 Ultramarine Pigments

Blue ultramarine (blue from over the sea) is the name which European artists of the Middle Ages gave to the pigment derived from lapis lazuli a semiprecious stone imported mainly from Afghanistan. Ultramarine was the supreme blue of medieval times, but eventually it became scarce and very expensive.

In 1828, J. B. GUIMET in France and CHRISTIAN GMELIN in Germany independently devised similar processes for synthetic preparation. Relatively abundant supplies soon became available, the price fell dramatically, and ultramarine was adopted as a general-purpose color.

Synthetic ultramarines are inorganic powder pigments, commercially available in three colors:

- Reddish blue, C.I. Pigment Blue 29:77007
- Violet, C.I. Pigment Violet 15:77007
- Pink, C.I. Pigment Red 259:77007

A green variety, once produced in small quantities, is no longer available.

Within limits set by stability considerations, the proportions of the chemical constituents can vary. The typical lattice repeat unit of a blue ultramarine is $\text{Na}_{6.9}\text{Al}_{5.6}\text{Si}_{6.4}\text{O}_{24}\text{S}_{4.2}$. The violet and pink variants differ from the blue mainly in the oxidation state of the sulfur groups. This is reflected in somewhat lower sodium and sulfur contents.

21.11.1.1 Chemical Structure

Reviews of work on the structure of ultramarine are given in [235, 236].

Ultramarine is essentially a three-dimensional aluminosilicate lattice with entrapped sodium ions and ionic sulfur groups (Figure 21.39). The lattice has the sodalite structure,

with a cubic unit cell dimension of ca. 0.9 nm. In synthetic ultramarine derived from China clay by calcination, the lattice distribution of silicon and aluminum ions is disordered. This contrasts with the ordered array in natural ultramarines.

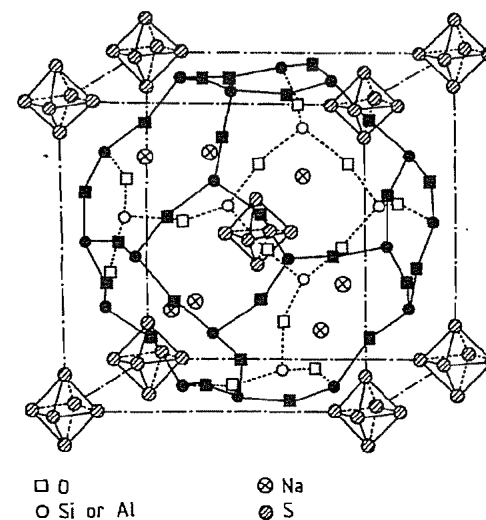


Figure 21.39: Schematic drawing of the basic structure of standard ultramarine showing the available sites for sulfur and sodium.

In the simplest ultramarine structure, equal numbers of silicon and aluminum ions are present and the basic lattice unit is $\text{Na}_6\text{Al}_6\text{Si}_6\text{O}_{24}$ or $(\text{Na}^+)_6(\text{Al}^{3+})_6(\text{Si}^{4+})_6(\text{O}^{2-})_{24}$ with a net ionic charge of zero as required for structural stability.

The nature of the sulfur groups responsible for the color is reviewed in [237–239]. There are two types of sulfur group in blue ultramarine, S_3^- and S_2^- , both being free radicals stabilized by lattice entrapment. In the predominant S_3^- species, the spacing between the three sulfurs is 0.2 nm and the angle between them is 103°. S_3^- absorbs a broad energy band in the visible green-yellow orange region centered at 600 nm, while S_2^- absorbs in the violet-ultraviolet region at 380 nm (Figure 21.40).

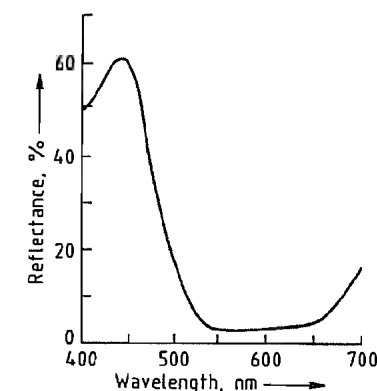


Figure 21.40: Spectral reflectance distribution of blue ultramarine.

The basic lattice $(\text{Na}^+)_6(\text{Al}^{3+})_6(\text{Si}^{4+})_6(\text{O}^{2-})_{24}$ is derived from $\text{Si}_{12}\text{O}_{24}$ by substituting six of the silicon ions by aluminum. Every Al^{3+} must be accompanied by a Na^+ so that the overall ionic charge for the structure is zero. Hence, six of the eight sodium sites are always filled by sodiums required for lattice stability and the remaining two sites are filled with sodiums associated with ionic sulfur groups. This means that only one S_3^{2-} polysulfide ion can be inserted into the lattice (as Na_2S_3) even though subsequent oxidation to S_3^- leads to loss of one of the accompanying sodium ions. This gives a basic ultramarine lattice formula of $\text{Na}_7\text{Al}_6\text{Si}_6\text{O}_{24}\text{S}_3$.

To increase the sulfur content and thereby improve color quality, the lattice aluminum content can be decreased by including a high-silicon feldspar in the manufacturing recipe. This reduces the number of sodium ions needed for lattice stabilization and leaves more for sulfur group equivalence. A typical product would be $\text{Na}_{6.9}\text{Al}_{5.6}\text{Si}_{6.4}\text{O}_{24}\text{S}_{4.2}$ with a stronger, redder shade of blue than the simpler type.

In violet (Figure 21.41) and pink (Figure 21.42) ultramarines, the lattice structure is little changed, but the sulfur chromophores are further oxidized, possibly to S_3Cl^- , S_4 , or S_4^- .

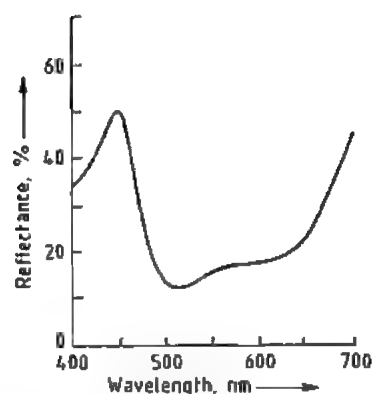


Figure 21.41: Spectral reflectance distribution of violet ultramarine.

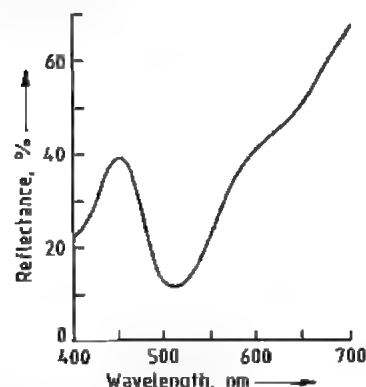


Figure 21.42: Spectral reflectance distribution of pink ultramarine.

Ultramarines are zeolites, though lattice paths are restricted by 0.4 nm diameter channels. The sodium ions can be exchanged for other metal ions (e.g., silver, potassium, lithium, copper). Although this produces marked color change, none of the products have commercial value.

21.11.1.2 Properties

The basic ultramarine color is a rich, bright reddish blue, the red-green tone varying with chemical composition. The violet and pink derivatives have weaker, less saturated colors (see Figures 21.40–21.42, for reflectance spectra).

The color quality of commercial pigments is developed by grinding to reduce particle

size and thus enhance tinting strength. Mean particle size ranges typically from 0.7 to 5.0 μm . Figure 21.43 shows an electron micrograph of a 1.0 μm grade. Fine pigments are lighter in shade and rather greener than coarser grades, but when reduced with white, their color is brighter and more saturated.

Figure 21.43: Electron micrograph of blue ultramarine with a mean particle size of 1.0 μm (magnification $\times 5800$).

With a refractive index close to 1.5, similar to that of paint and plastics media, ultramarine gives a transparent blue in gloss paints and clear plastics. Opacity is obtained by adding a small quantity of a white pigment. Increasing quantities of white give paler shades, and a trace of ultramarine added to a white enhances the whiteness and acceptability.

In many applications ultramarine blue is stable to around 400 °C, violet to 250 °C, and pink to 200 °C. All have excellent lightfastness with a 7–8 rating (full and reduced shades) on the International Blue Wool Scale. Color fade attributed to light exposure or moderate heat is almost always caused by acid attack. Ultramarines react with all acids, and if there is sufficient acid, the pigment is completely decomposed losing all color to form silica, sodium and aluminum salts, sulfur, and hydrogen sulfide. Evolution of hydrogen sulfide with acids is a useful test for ultramarine.

Grades resistant to transient acidity are available, in which the pigment particles are protected by a coating of impervious silica. Blue and violet grades are stable in mildly alkaline conditions, but pink tends to revert to a violet shade.

Ultramarines are insoluble in water and organic solvents, so the color does not bleed or migrate from paints or polymers.

Being macromolecular, the fine ultramarine particles have a high surface energy and are cohesive. The finer grades, with their greater surface area, are therefore less easy to disperse than the coarser types, and some are available with pigment surfaces treated to reduce energy and improve dispersibility.

Ultramarines adsorb moisture on the external particle surfaces and at the internal surfaces of the zeolite structure. External surface moisture (1–2% according to particle size) is driven off at 100–105 °C, but the additional 1% of internal moisture needs 235 °C for complete removal.

Ultramarine particles are hard and can cause abrasion in equipment handling either dry or slurried pigment.

Specific gravity is 2.35, but bulk density of the pigment powder is much lower, varying with particle size between 0.5 and 0.9 g/cm³.

Oil absorption also varies with particle size (usually 30–40 g%). The pH lies between 6 and 9. Ultramarine pigments are largely odorless, nonflammable, and do not support combustion.

21.11.1.3 Production

Ultramarine is made from simple, relatively cheap materials, typically china clay, feldspar, anhydrous sodium carbonate, sulfur, and a reducing agent (oil, pitch, coal etc.). Use of a synthetic zeolite has been proposed [240, 241], but this method is not known to be in commercial use.

Clay Activation. The clay is heated to about 700 °C to destabilize the kaolinite structure by removing hydroxyl ions as water. This can be either a batch process with the clay in crucibles in a directly fired kiln, or a continuous

process in a tunnel kiln, rotary kiln, or other furnace.

Blending and Heating Raw Materials. The activated clay is blended with the other raw materials and dry-ground, usually in batch or continuous ball mills, to a mean size approaching 15 μm . Typical recipes (in %) are:

	Green-tone	Red tone
Calcined clay	32.0	30.0
Feldspar		7.0
Sodium carbonate	29.0	27.0
Sulfur	34.5	33.0
Reducing agent	4.5	3.0

The ground mixture is heated to about 750 °C under reducing conditions, normally in a batch process. This can be done in directly fired kilns with the blend in lidded crucibles of controlled porosity, or muffle kilns. The heating medium can be solid fuel, oil, or gas. The sodium carbonate reacts with the sulfur and reducing agent at 300 °C to form sodium polysulfide. At higher temperatures the clay lattice reforms into a three-dimensional framework, which at 700 °C is transformed to the sodalite structure, with entrapped sodium and polysulfide ions.

Oxidation. The furnace is allowed to cool to ca. 500 °C when air is admitted in controlled amounts. The oxygen reacts with excess sulfur to form sulfur dioxide, which exothermically oxidizes the di- and triatomic polysulfide ions to S₂ and S₃ free radicals, leaving sodium sulfoxides and sulfur as by-products. When oxidation is complete, the furnace cools and is unloaded a full kiln cycle can take several weeks. The "raw" ultramarine product typically contains 75% blue ultramarine, 23% sodium sulfoxides, and 2% free (uncombined) sulfur with some iron sulfide.

Purification and Refinement. The purification and refinement operations can be batch or continuous. The raw blue is crushed and ground, slurried in warm water, then filtered and washed to remove the sulfoxides. Reslurrying and wet grinding release the sulfurous impurities and reduce the ultramarine particle size, often to 0.1–10.0 μm . The impurities are floated off by boiling or cold froth flotation.

The liquor is then separated into discrete particle size fractions by gravity or centrifugal separation; residual fine particles are reclaimed by flocculation and filtration. The separated fractions are dried and disintegrated to give pigment grades differentiated by particle size. These are blended to sales-grade standard, adjusting hue, brightness, and strength to achieve specified color tolerance.

Violet ultramarine can be prepared by heating a mid-range blue grade with ammonium chloride at ca. 240 °C in the presence of air. Treating the violet with hydrogen chloride gas at 140 °C gives the pink derivative.

A good ultramarine pigment would meet the following specification:

Tinting strength/standard	± 2 % max.
Reduced shade/standard	1 CIELAB unit max.
Free sulfur	0.05 % max.
Water-soluble matter	1.0 % max.
Sieve residue (45 µm)	0.1 % max.
Moisture	
coarse grade	1.0 % max.
fine grade	2.0 % max.
Heavy metals	traces

21.11.1.4 Uses

The stability and safety of ultramarine pigments are the basis of their wide range of applications which include the following:

Plastics
 Paints and powder coatings
 Printing inks
 Paper and paper coating
 Rubber and thermoplastic elastomers
 Latex products
 Detergents
 Cosmetics and soaps
 Artists colors
 Toys and educational equipment
 Leather finishes
 Powder markers
 Roofing granules
 Synthetic fibers
 Theatrical paints and blue mattes
 Cattle salt licks
 White enhancement

Plastics. Blue ultramarine can be used in any polymer; violet ultramarine has a maximum processing temperature of 250 °C, and pink ultramarine has a maximum processing temperature of 200 °C. With PVC, acid-resistant grades must be used if color fades during pro-

cessing. Surface-treated grades are available for enhanced dispersibility. Ultramarines do not cause shrinkage or warping in polyolefins. Ultramarine pigments are permitted worldwide for coloring food-contact plastics.

Paints. Ultramarine pigments are used in decorative paints, stoving finishes, transparent lacquers, industrial paints, and powder coatings. They are not recommended for colored, air-drying paints for outdoor use in urban atmospheres.

Printing Inks. Ultramarine pigments can be used in inks for most printing processes including hot-foil stamping. Letterpress, flexography, and gravure need high-strength grades; lithography needs water-repellent grades; any grade is suitable for screen inks, fabric printing, and hot-foil stamping.

Paper and Paper Coating. Ultramarine pigments are used to enhance the hue of white paper or for colored paper. They can be added directly to the paper pulp, or used in applied coatings. When added to the pulp, acid-resistant grades must be used if acid-sizing is employed. They are particularly suitable for colored paper for children's use.

Detergents. Ultramarine pigments are widely used to enhance the effects of optical brightening agents in improving whiteness of laundered fabrics [242]. They do not stain or build up with repeated use.

Cosmetics and Soaps. Ultramarine pigments are widely used in cosmetics. Pink is not recommended for toilet soaps because of the color shift to violet. Advantages are complete safety, nonstaining, and conformance to all major regulations.

Artists' Colors. This traditional use for ultramarine in all types of media is still an important application. Unique color properties, stability, and safety are highly prized.

Toys and other Articles/Materials for Children's Use. Ultramarine pigments are widely used in plastics and surface coatings for toys, children's paints and finger paints, modeling compositions, colored paper, crayons, etc.

They comply with major regulations and standards.

21.11.1.5 Toxicity and Environmental Aspects

Ultramarines are safe in both manufacture and use. Their only known hazard is the evolution of hydrogen sulfide on contact with acid. Massive exposure of workers in well over a century of manufacture, worldwide use for whitening clothes, and use in a number of countries for whitening sugar have all been without reported ill-effects.

Tests sponsored by Reckitt's Colours confirm that acute oral toxicity in rats and mice (LD₅₀) is greater than 10 000 mg/kg. Fish toxicity (LC₅₀ in rainbow trout) exceeds 32 000 mg/L. Ultramarine is nonmutagenic, nonirritant, and nonsensitizing to skin.

There is no listed threshold limit value or maximum exposure limit for the pigment. Normal practice is to consider it a nuisance dust with TLV 10 mg/m³. The pigment is not listed as a dangerous substance in the EC nor in any similar national or international classification; neither is it classified as hazardous for disposal.

The production process evolves close to 1 t of gaseous sulfur dioxide and 0.3 t of water-soluble sodium sulfoxides for every tonne of pigment produced. These must be disposed of in an environmentally acceptable manner. If the soluble salts are fully oxidized, they can be discharged safely into tidal waters. Future legislation in all producing countries may require removal of sulfur dioxide from the effluent gases before discharge to the atmosphere.

21.11.1.6 Economic Aspects

Ultramarines can be categorized as either laundry grades, which are low-strength and

sometimes low-purity materials, or as industrial grades, which are high-strength, high-purity pigments.

Factories in several countries produce laundry-grade materials, including several in China, India, Eastern European countries, and one in Pakistan. Neither the numbers of these units nor their outputs are accurately known.

There are only three major producers of high-grade ultramarine pigments – Dainichi Seika (Japan), Nubiola (Spain), and Reckitt's Colours (France, United Kingdom) – with two smaller producers in Austria and Colombia. In 1990 total worldwide production was ca. 20 000 t/a.

21.11.2 Aluminum Phosphate

Commercial aluminum phosphate anticorrosive pigments consist of aluminum zinc phosphate hydrates [243, 244], or zinc-containing aluminum triphosphate [245]. Their compositions and properties are listed in Table 21.22. Aluminum zinc phosphate hydrate pigments are produced by reacting acid solutions of aluminum hydrogen phosphate with zinc oxide and alkali aluminate. The precipitated pigment is filtered off from the mother liquor, washed, dried, and ground [246]. Commercial aluminum triphosphate pigments contain ions of trimeric phosphoric acid which form stable aluminum-containing iron phosphate complexes [245].

The aluminum phosphate pigments give good adhesion of the paint film to the metallic substrate.

Trade names are as follows:

Zinc aluminum phosphate: K-White 105 (Teikoku Kako, Japan); Heucophos ZPA (Dr. H. Heubach, Germany); Phosphinal PZ04 (SNCZ, France).

Aluminum triphosphate: K-White 82, -84 (Teikoku Kako, Japan).

Table 21.22: Composition and properties of aluminum phosphate anticorrosive pigments.

Property	Aluminum triphosphate (commercial product 1; K-White 82) [245]	Aluminum triphosphate (commercial product 2; K-White 84) [245]	Aluminum zinc phosphate hydrate (commercial product 3; Heucophos ZPA, Phosphinal PZ 04) [243, 244]
Al content, %	5.5–7.7	4.7–6.9	4–5
Zn content, %	11.6–14.9	21.3–24.5	35–39
P ₂ O ₅ content, %	42.0–46.0	36.0–40.0	30/37
SiO ₂ content, %	13.0–17.0	11.0–15.0	
Loss on ignition (600 °C), %	ca. 10	ca. 8	10–16
Density, g/cm ³	3.0	3.1	3.2
Oil absorption value, g/100 g	35	30	30/35
Particle size, µm	0.5–10	0.5–10	0.5–10
pH value	6–7	6–7	6.5
Water-soluble content, %	max. 1.0	max. 1.0	0.1
Color	white	white	white

21.11.3 Production

Aluminum pigments are produced by grinding aluminum powder, usually obtained by atomizing molten aluminum. The starting material is mainly aluminum ingots with a purity of 99.5% (DIN 1712), or pure aluminum (> 99.95%) for special outdoor applications (acid-resistant grades).

Aluminum powder forms explosive mixtures with air; the lower explosive limit being ca. 35–50 g/cm³. Dust-free aluminum paste is therefore used in most applications.

Aluminum pigments are mainly produced by wet milling in white spirit. The resulting pigment suspension is usually fractionated, sieved, and filtered on a filter press. The filter cake is mixed with solvents to give the usual commercial consistency with 65% solids. Other solvents may be used instead of white spirit, the choice being governed by the intended application. The white spirit can be removed by vacuum drying and replaced by another solvent if necessary (e.g., for printing inks or coloring plastics).

Aluminum behaves as an amphoteric metal, liberating hydrogen from both alkaline and acid aqueous media. In waterborne paints and coloring systems, special stabilized aluminum pigments are therefore required [247]. Aluminum pigments must not be used with halogen-containing solvents because they re-

act very violently to release hydrogen halides (Friedel–Crafts reaction).

The leafing properties of aluminum pigments can be adversely affected by polar solvents or binders. "Leafing-stabilized" aluminum pigments are available for these applications.

Along with special pigments for modern environmentally-friendly coating systems (e.g., waterborne paints and powder coatings) described above, aluminum pigments coated with colored metal oxides (e.g., iron oxide) have appeared on the market which produce not only reflection but also interference effects [248]. Novel color effects are obtained by combining the metal-oxide-coated pigments with transparent colored pigments.

Aluminum has a very low toxicity and is permitted as a coloring agent (EEC no. E173, C.I. 77000). It is also approved by the FDA, § 175300 (USA).

21.12 References

1. *Aluminum Industry Abstracts*, ASM International and Institute of Materials. (This abstract bulletin is useful for keeping abreast of technical and economic developments in aluminum production. Published literature, government reports, theses, and patent literature are covered in this monthly journal.)
2. R. Beck, H. Lax, W. Prast, J. Scott in J. Keefe (ed.): *Aluminum: Profile of the Industry*, McGraw-Hill, New York 1982.

3. R. Sergeantson (ed.): *World Aluminum: A Metal Bulletin Data Book*, Metal Bulletin Books Ltd., Surrey, England, 1990.
4. L. F. Mondolfo: *Aluminum Alloys: Structure and Properties*, Butterworths, Boston 1976.
5. J. E. Hatch (ed.): *Aluminum, Its Properties and Physical Metallurgy*, American Society for Metals, Metals Park, OH, 1984.
6. *Aluminum Statistical Review*, Annual Publication of the Aluminum Association, 900 19th Street, NW, Washington, DC 20006.
7. M. Conserva, G. Donzelli, R. Tripodda, *Aluminium and Its Applications*, Edimet Spa Brescia, Italy, 1992.
8. M. Rolin: *L'électrolyse de l'aluminium (Le procédé Hall-Héroult)*, Institut national des sciences appliquées de Lyon, Villeurbanne, France, 1981.
9. K. Grjotheim, C. Krohn, M. Malinovsky, K. Matiasovsky, J. Thonstad: *Aluminium Electrolysis. Fundamentals of the Hall-Héroult Process*, Aluminium Verlag GmbH, Düsseldorf 1982.
10. K. Grjotheim, B. J. Welch: *Aluminium Smelter Technology*, 2nd edition, Aluminium Verlag GmbH, Düsseldorf 1988.
11. K. Grjotheim, H. Kvande (eds.): *Introduction to Aluminium Electrolysis. Understanding the Hall-Héroult Process*, 2nd edition, Aluminium Verlag, 1993.
12. A. R. Burkin (ed.): *Production of Aluminium and Alumina*, Society of Chemical Industry, 1987.
13. H. J. Gitelman (ed.): *Aluminum and Health: A Critical Review*, Marcel Dekker Inc., New York 1989.
14. G. Ibe: "High-purity Aluminum for Electrotechnical Applications", *ETZ Elektrotech. Z.* **101** (1980) no. 6, 366–368.
15. J. E. Hatch (ed.): *Aluminum: Its Properties and Physical Metallurgy*, American Society for Metals, Metals Park, OH, 1984, Chap. 1.
16. K. Wefers: "Properties and Characterization of Surface Oxides on Aluminum Alloys", *Aluminium* **57** (1981) 722–726.
17. P. A. Foster, Jr.: "Phase diagram of a Portion of the System NaAlF₆–AlF₃–Al₂O₃", *J. Am. Ceram. Soc.* **58** (1975) no. 7–8, 288–291.
18. A. Fenerty, E. A. Hollingshead: "Liquidus Curves for Aluminum Cell Electrolyte III. Systems Cryolite and Cryolite–Alumina with Aluminum Fluoride and Calcium Fluoride", *J. Electrochem. Soc.* **107** (1960) no. 12, 993–997.
19. D. F. Craig, R. T. Cassidy, J. J. Brown, Jr.: "A Review of Phase Equilibria in the NaAlF₆–LiF–CaF₂–AlF₃–Al₂O₃ System", *Applications of Phase Diagrams in Metallurgy and Ceramics*, vol. 1, National Bureau of Standards SP-496, Washington, DC, March 1978, p. 272–345.
20. In [11], pp. 41–43.
21. W. E. Haupin, W. B. Frank: "Electrometallurgy of Aluminum", *Comprehensive Treatise of Electrochemistry*, vol. 2, Plenum Publishing, New York 1981, p. 122.
22. J. Thonstad, S. Rolseth, *Proceedings at 3rd ICSOBA Conference*, Nice, France, September 1973, p. 657.
23. J. P. Millet, M. Rolin: "Electrolysis of Alumina in Molten Cryolite. Study of the Anodic Discharge Mechanism with Rotating Disk Electrode", *Fourth International Congress for the Study of Bauxite, Alumina, and Aluminum*, vol. 3, Athens, Greece, October 9–12, 1978, p. 265–286.
24. J. Thonstad, *Electrochim. Acta* **15** (1970) 1569.
25. K. Vetter: *Electrochemical Kinetics*, Academic Press, New York 1967.
26. J. Thonstad, *Electrochim. Acta* **15** (1970) 1581.
27. G. Blyholder, J. Eyring, *J. Phys. Chem.* **61** (1957) 682.
28. A. J. Calandra, C. E. Castellano, C. M. Ferro, *Electrochim. Acta* **24** (1979) 425.
29. S. Rolseth, J. Thonstad, *Light Met. (N.Y.)* **1981**, 289–301; *Proc. AIME Annual Meeting*, Chicago, IL, Feb. 1981.
30. G. M. Haarberg, K. S. Olsen, J. Thonstad, R. J. Heus, J. J. Egan, *Metall. Trans. B* **24B** (1993) 729–735.
31. W. E. Haupin, *J. Met.* **42** (1971) no. 7, 41.
32. J. Thonstad, S. Rolseth, *Light Met.* **1983**, 415–435; *Proc. AIME Annual Meeting*, Atlanta, GA, March 1983.
33. N. Jarrett, W. B. Frank, R. Keller: "Advances in the Smelting of Aluminum", *Metallurgical Treatises*, The Metallurgical Society of AIME, Warrendale, PA, 1981, p. 137–158.
34. *JANAF Thermochemical Tables*, 3rd ed., National Standards Reference Data Service, National Bureau of Standards, New York 1986.
35. K. Motzfeldt, H. Kvande, R. Schei, K. Grjotheim, *Carbothermal Production of Aluminium*, Aluminium Verlag, Düsseldorf 1989.
36. H. Ginsberg, *Aluminium* **23** (1941) 131.
37. S. C. Jacobs, US 3303019, 1967.
38. International Primary Aluminum Institute, *Environmental Legislation Survey*, London, UK, 1981.
39. American Conference of Governmental Industrial Hygienists (ACGIH) (ed.): *Threshold Limit Values (TLV)* 1983–1984, Cincinnati, OH, 1983, p. 10, 35, 52.
40. *The Measurement of Employee Exposures in Aluminium Reduction Plants*, International Primary Aluminium Institute, London 1982, p. 47.
41. I. R. Campbell, J. S. Cass, J. Cholak, R. A. Kehoe: "Aluminum in the Environment of Man", *Arch. Ind. Hyg.* **15** (1957) 359.
42. J. R. J. Sorenson, I. R. Campbell, L. B. Tepper, R. D. Lingg: "Aluminum in the Environment and Human Health", *Environ. Health Perspect.* **8** (1974) 3.
43. G. L. Krueger, T. K. Morris, R. R. Suskind, E. M. Widner: "The Health Effects of Aluminum Compounds in Mammals", *CRC Critical Reviews in Toxicology*, to be published in 1984.
44. Hygienic Guide "Aluminum and Aluminum Oxide", *Amer. Ind. Hyg. Ass.* revised (1978).
45. W. Huepke, "Die Spurenstoffe", *Münch. Med. Wochenschr.* **92** (1950) 351.
46. *Report of the Task Group on Reference Man*, International Commission on Radiation Protection, ICRP Publication No. 23, Pergamon Press, Oxford 1975.
47. J. R. J. Sorenson, I. R. Campbell, L. B. Tepper, R. D. Lingg: "Aluminum in the Environment and Human Health", *Environ. Health Perspect.* **8** (1974) 3.
48. A. J. Lehman, W. I. Patterson: "F and DA Acceptance Criteria: Basic Considerations in Determina-

- tions Safety of Chemicals Used in Food-Packaging Materials", *Mod. Packag.* 28 (1955) 115, 172.
49. *Safety of Cooking Utensils*, FDA Fact Sheet, U.S. Food and Drug Administration, Washington, DC, July 1971.
 50. L. Kopeloff, S. Barrera, N. Kopeloff: "Recurrent Convulsive Seizures in Animals Produced by Immunologic and Chemical Means", *Am. J. Psych.* 98 (1942) 881-902.
 51. H. M. Wisniewski, R. D. Terry, C. Pena, E. Streicher, et al.: "Experimental Production of Neurofibrillary Degeneration", *J. Neuropath. Exp. Neurol.* 24 (1965) 139.
 52. I. Klatzo, H. M. Wisniewski, E. Streicher: "Experimental Production of Neurofibrillary Degeneration: I. Light Microscopic Observations", *J. Neuropath. Exp. Neurol.* 24 (1965) 187-199.
 53. D. R. Crapper, A. J. Dalton: "Alterations in Short-Term Retention, Conditioned Avoidance Response Acquisition and Motivation Following Aluminum Induced Neurofibrillary Degeneration", *Physiol. and Behav.* 10 (1973) 925-933.
 54. A. C. Alfrey, "Aluminum toxicity in humans", in H. Tomita (ed.): *Trace Elements in Clinical Medicine*, Springer Verlag, New York 1990, pp. 459-464.
 55. A. B. Sedman, G. L. Klein, R. J. Merritt et al., "Evidence of aluminum loading in infants receiving intravenous therapy", *N. Engl. J. Med.* 312 (1985) 1339-1343.
 56. M. Freundlich, G. Zilleruelo, C. Abitbol et al., "Infant formula as a cause of aluminium toxicity in neonatal uraemia", *Lancet* II (1985) 527-529.
 57. D. R. Crapper, S. S. Krishnan, S. Quittkat: "Aluminum, Neurofibrillary Degeneration and Alzheimer's Disease", *Brain* 99 (1976) 67-80.
 58. G. A. Trapp, G. D. Miner, R. L. Zimmerman, A. R. Mastri et al.: "Aluminum Levels in Brain in Alzheimer's Disease", *Biol. Psych.* 13 (1978) 709-718.
 59. W. R. Markesbery, W. D. Ehmann, T. I. M. Hossain, M. Alauddin et al.: "Instrumental Neutron Activation Analysis of Brain Aluminum in Alzheimer Disease and Aging", *Ann. Neurol.* 10 (1981) 511-516.
 60. G. P. Cooper, G. L. Krueger, E. M. Widner: *Neurotoxicity of Aluminum*, University of Cincinnati, Cincinnati 1981, p. 27.
 61. G. Goralewski: "Die Aluminiumlunge - eine neue Gewerbeerkrankung", *Zschr. Ges. inn. Med.* 2 (1947) 665-673.
 62. M. Ueda, Y. Mizoi, Z. Maki, R. Maeda et al., *J. Med. Sci.* 4 (1958) 91.
 63. J. W. Jordan: "Pulmonary Fibrosis in a Worker Using an Aluminum Powder", *Br. J. Ind. Med.* 18 (1961) 21.
 64. J. Mitchell, G. B. Manning, M. Molyneux, R. E. Lane: "Pulmonary Fibrosis in Workers Exposed to Finely Powdered Aluminum", *Br. J. Ind. Med.* 18 (1961) 10.
 65. N. P. Edling, *Acta Radiol.* 56 (1961) 170.
 66. A. I. G. McLaughlin, G. Kazantzis, E. King, D. Teare et al.: "Pulmonary Fibrosis and Encephalopathy Associated with the Inhalation of Aluminum Dust", *Br. J. Ind. Med.* 19 (1962) 253-263.
 67. G. Goralewski, "Die Aluminiumlunge: Eine neue Gewerbeerkrankung", *Z. Gesamte Inn. Med.* 2 (1947) 665-673.
 68. J. Mitchell, G. B. Manning, M. Molyneux et al., "Pulmonary fibrosis in workers exposed to finely powdered aluminium", *Br. J. Ind. Med.* 18 (1961) 10-20.
 69. J. W. Jordan, "Pulmonary fibrosis in a worker using an aluminum powder", *Br. J. Ind. Med.* 18 (1961) 21-23.
 70. B. D. Dinman, "Aluminum in the lung: the pyropowder conundrum", *J. Occup. Med.* 29 (1987) 869-876.
 71. H. A. Waldron, "Non-neoplastic disorders due to metallic, chemical and physical agents", in W. R. Parkes (ed.): *Occupational Lung Disorders*, Butterworths-Heinemann, Oxford 1994, pp. 593-643.
 72. M. I. Abramson, J. H. Włodarczyk, N. A. Saunders et al., "Does aluminum smelting cause lung disease?", *Am. Rev. Respir. Dis.* 139 (1989) 1042-1057.
 73. B. Corrin, "Aluminium pneumoconiosis I. In vitro comparison of stamped aluminium powders containing different lubricating agents and a granular aluminium powder", *Br. J. Ind. Med.* 20 (1963) 264-267.
 74. B. Corrin, "Aluminium pneumoconiosis II. Effect on the rat lung of intratracheal injections of stamped aluminium powders containing different lubricating agents and of a granular aluminium powder", *Br. J. Ind. Med.* 20 (1963) 268-276.
 75. D. W. Crombie, J. L. Blaisdell, G. MacPherson, *Can. Med. Assoc. J.* 50 (1944) 318.
 76. P. Gross, R. A. Harley, Jr., R. T. P. de Treville: "Pulmonary Reaction to Metallic Aluminum Powders", *Arch. Environ. Health* 26 (1973) 227.
 77. C. Shaver, A. R. Riddell: "Lung Changes Associated with the Manufacture of Alumina Abrasives", *J. Ind. Hyg.* 29 (1947) 145.
 78. C. M. Jephcott, *J. Occup. Med.* 5 (1948) 701.
 79. W. K. C. Morgan, B. D. Dinman, "Pulmonary Effects of Aluminum", in H. J. Gitelman (ed.): *Aluminum and Health: A Critical Review*, Marcel Dekker, New York 1989, pp. 203-234.
 80. E. J. King, C. V. Harrison, G. P. Mohanty et al., "The effect of various forms of alumina on the lungs of rats", *J. Pathol. Bacteriol.* 69 (1955) 81-93.
 81. B. D. Stacy, E. J. King, C. V. Harrison, "Tissue changes in rats' lungs caused by hydroxides, oxides and phosphates of aluminum and iron", *J. Pathol. Bacteriol.* 77 (1959) 417-426.
 82. W. Klosterkötter, "Effects of ultramicroscopic gamma-aluminium oxide on rats and mice", *AMA Arch. Ind. Health* 21 (1960) 458-472.
 83. G. W. Gibbs, "Mortality of aluminum reduction plant workers, 1950 through 1977", *J. Occup. Med.* 27 (1985) 761-770.
 84. M. C. Townsend, P. E. Enterline, N. B. Sussman et al., "Pulmonary function in relation to total dust exposure at a bauxite refinery and alumina-based chemical products plant", *Am. Rev. Respir. Dis.* 132 (1985) 1174-1180.
 85. M. C. Townsend, N. B. Sussman, P. E. Enterline et al., "Radiographic abnormalities in relation to total dust exposure at a bauxite refinery and alumina-based chemical products plant", *Am. Rev. Respir. Dis.* 138 (1988) 90-95.
 86. *Aluminum Statistical Review for 1982*, The Aluminum Association, Washington, DC.
 87. *Aluminum Statistical Review - Historical Supplement*, The Aluminum Association, Washington, DC, 1982.
 88. H. Ginsberg, F. W. Wrigge: *Tonerde und Aluminium, Teil I, Die Tonerde*, W. De Gruyter, Berlin 1964.
 89. H. Ginsberg, K. Wefers: *Aluminium und Magnesium*, vol. 15, *Die metallischen Rohstoffe*, Enke Verlag, Stuttgart 1971.
 90. K. Wefers, G. M. Bell: *Oxides and Hydroxides of Aluminum*, Alcoa T.P. 19, Pittsburgh 1972.
 91. T. G. Parson: *The Chemical Background of the Aluminum Industry: Lectures, Monographs, and Reports*, no. 3, The Royal Institute of Chemistry, London 1955.
 92. P. Barrand, R. Gadeau: *L'aluminium*, part 1, Éditions Eyrolles, Paris 1964.
 93. A. N. Adamson, E. J. Bloore, A. R. Carr: *Basic Principles of Bayer Process Design, Extractive Metallurgy of Aluminum*, vol. 1, Interscience Publishers, New York 1963.
 94. A. N. Adamson: "Aluminum Production Principles and Practice", *The Chemical Eng. (London)*, June 1970, 156-171.
 95. S. I. Kuznetsov, V. A. Derevyankin: *The Physical Chemistry of Alumina Production by the Bayer Process*, Moscow 1964.
 96. W. H. Gitzen: *Alumina as a Ceramic Material*, The Amer. Cer. Society, Columbus, OH, 1970.
 97. J. Böhm, H. Niclassen, *Z. Anorg. Allg. Chem.* 132 (1923) 1.
 98. R. Fricke, *Z. Anorg. Allg. Chem.* 175 (1928) 249; 179 (1929) 287.
 99. T. G. Gedeon, *Acta Geol. Acad. Sci. Hung.* 4 (1956) 95.
 100. R. A. Van Nordstrand, W. P. Hettinger, C. Keith, *Nature (London)* 177 (1956) 713.
 101. H. Saalfeld, *Neues Jahrb. Mineral. Abh.* 95 (1960) 1.
 102. H. Ginsberg, W. Hüttig, H. Stiehl, *Z. Anorg. Allg. Chem.* 309 (1961) 233; 318 (1962) 238.
 103. K. Wefers, *Naturwissenschaften* 49 (1962) 204.
 104. U. Hauschild, *Z. Anorg. Allg. Chem.* 324 (1963) 15.
 105. B. C. Lippens, Ph. D. Dissertation, University Delft (1961).
 106. M. Karsulin, *Symposium sur les bauxites*, Zagreb 1963, p. 37.
 107. A. W. Laubengayer, R. S. Weiß, *J. Am. Chem. Soc.* 65 (1943) 247.
 108. G. Ervin, E. F. Osborn, *J. Geol.* 59 (1951) 381.
 109. G. C. Kennedy, *Am. J. Sci.* 257 (1959) 563.
 110. A. Neuhaus, H. Heide, *Ber. Dtsch. Keram. Ges.* 42 (1965) 167.
 111. K. Wefers, *Erzmetall* 20 (1967) 13, 71.
 112. H. D. Megaw, *Z. Kristallogr.* 87 (1934) 185.
 113. F. J. Ewing, *J. Chem. Phys.* 3 (1935) 203.
 114. W. R. Busing, H. A. Levy, *Acta Crystallogr.* 11 (1958) 798.
 115. O. Glemser, E. Hartert, *Z. Anorg. Allg. Chem.* 283 (1956) 111.
 116. N. P. Pentscheff, A. Z. Zaprianova, C. R. Séances Acad. Sci. Sér. C 268 (1969) 54.
 117. H. Saalfeld, M. Matthies, S. K. Datta, *Ber. Keram. Ges.* 45 (1968) 212.
 118. W. H. Bragg, *J. Chem. Soc.* 121 (1922) 2766.
 119. H. Schwiensch, *Chem. Erde* 8 (1933) 252.
 120. W. Feitknecht, A. Wittenbach, W. Buser: *4th Symposium on Reactivity of Solids*, Elsevier, Amsterdam 1961, p. 234.
 121. F. Freund, *Ber. Dtsch. Keram. Ges.* 42 (1965) 23; 44 (1967) 141.
 122. K. Wefers, *Erzmetall* 17 (1964) 583.
 123. H. C. Stumpf, A. S. Russell, J. W. Newsome, C. M. Tucker, *Ind. Eng. Chem.* 42 (1950) 1398.
 124. I. Valetton: "Bauxites", *Dev. Soil Sci.* 1 (1972).
 125. J. G. deWeisse: *Les bauxites de l'Europe centrale*, Univ. Lausanne 1948.
 126. V. Z. Zans, *Geonotes* 5 (1959) 123.
 127. M. E. Roch: "Les bauxites du Midi de la France", *Rev. Gen. Sci. Pures Appl. Bull. Assoc. Fr. Av. Sci.* 66 (1958) no. 5/6, 151-156.
 128. H. Erhart: "La genèse des sols", *Évolution des sciences*, Masson, Paris 1956.
 129. G. Bardossy: *Bibliographie des travaux concernant les bauxites*, ICSOBA, Paris 1966.
 130. *Mineral Commodity Summaries*, U.S. Bureau of Mines, 1984.
 131. Nippon Light Metal Col., DE 2807245, 1977 (M. Kanehara, A. Kainuma, M. Fujiike).
 132. P. Basu, "Reactions of Iron Minerals in Sodium Aluminate Solutions", *Light Met. (N.Y.)* 1983, 83-98.
 133. D. K. Gribbs, S. C. Libby, J. K. Rodenburg, K. Wefers, *J. Geol. Soc. Jam.* 4 (1980) 176-186.
 134. K. Yamada, T. Harato, H. Kato, *Light Met. (N.Y.)* 1981, 117-128.
 135. *UNEP/UNIDO Workshop Envir. Asp. Alumina Prod.*, Paris 1981.
 136. K. Bielfeldt, K. Kämpf, G. Winkhaus, *Erzmetall* 29 (1976) 120-125.
 137. The Aluminum Association, Inc., N.Y., Report no. 4, Sept. 15, 1981.
 138. G. Lang, K. Solymar, J. Steincr, *Light Met. (N.Y.)* 1981, 201-214.
 139. H. W. St. Clair, D. A. Elkins, W. M. Mahan, R. C. Merritt, M. R. Howcroft, M. Hayashi, Bulletin 577, U.S. Bureau of Mines, 1959.
 140. K. B. Bergston, *Light Met. (N.Y.)* 1979, 217-282.
 141. N. Gjelsvik, *Light Met. (N.Y.)* 1980, 133-148.
 142. V. S. Sazlin, A. K. Zapolskii, *Tsvetn. Metall. UDK* 669.712.2 (1968) 64.
 143. E. Barrilon, *Erzmetall* 31 (1978) 519-522.
 144. H. Knözinger, P. Ratnasamy, *Catal. Rev. Sci. Eng.* 17 (1978) 31-70.
 145. *Gmelin*, System No. 35 "Aluminium", part B.
 146. N. A. Lange: *Handbook of Chemistry*, 10th ed., McGraw-Hill, New York 1961.
 147. A. Seidell, W. F. Linke: *Solubilities of Inorganic and Metal Organic Compounds*, 4th ed., vol. 1, Van Nostrand, Princeton, NJ, 1958.
 148. D'Ans-Lax: *Taschenbuch für Chemiker und Physiker*, 3rd. ed., vol. 1, Springer Verlag, Berlin 1967.
 149. J. Kaltenbach, *Papier (Darmstadt)* 17 (1963) 14.
 150. N. O. Smith, P. N. Walsh, *J. Am. Chem. Soc.* 76 (1954) 2054.
 151. J. L. Henry, G. B. King, *J. Am. Chem. Soc.* 72 (1950) 1282.
 152. P. Barret, R. Thiard, C. R. Heb. Séances Acad. Sci. 260 (1965) 2823.
 153. H. A. Papazian, P. J. Pizzolato, R. R. Orrell, *Thermochim. Acta* 4 (1972) 97.

154. Giulini, DE 1125894, 1960 (J. Rüter, H. Cherdron); DE 1146042, 1960 (J. Rüter, F. Fäßle).
155. Ullmann, 3rd ed., vol. 3, p. 425.
156. H. Kretschmar, *Aluminium (Düsseldorf)* 39 (1963) 624; US 2951743, 1957.
157. E. A. Gee, W. K. Cunningham, R. A. Heindl, *Ind. Eng. Chem.* 39 (1947) 1178.
158. *Chem. Eng. (N.Y.)* 68 (1961) 36.
159. G. B. Skakhtakhinskii, A. N. Khalilov, *Mater. Konf. Molodykh Uch. Inst. Neorg. Fiz. Khim. Akad. Nauk Az. SSR* 1968, 34; *Chem. Abstr.* 74 (1971) 101-183.
160. Jui-Hsiung Tsai, US 3574537, 1967.
161. Kirk-Othmer, 3rd ed., vol. 2.
162. R. G. Lebel, *Pulp Pap. Mag. Can.* 71 (1970) 23.
163. K. E. Oehler: "Technologie des Wassers", in *Handbuch der Lebensmittelchemie*, vol. VIII, part 1: Wasser und Luft, Springer Verlag, Berlin 1969.
164. Boliden, SE 341381, 1971.
165. *Chem. Eng. News* 61 (1983) 32.
166. Chemfacts Japan, Chemical Data Series, IPC Industrial Press, Sutton, Surrey UK 1981.
167. M. M. Kazakov et al., *Uzb. Khim. Zh.* 16 (1972) no. 2, 10; *Chem. Abstr.* 77 (1972) 50847.
168. A. Mitscherlich, *J. Prakt. Chem.* 83 (1861) 477.
169. G. L. Akhmetova et al., *Tr. Khim. Metall. Inst. Akad. Nauk Kaz. SSR* 15 (1970) 110.
170. N. I. Gel'Perin, G. V. Chebotkevich, *Zh. Prikl. Khim. (Leningrad)* 44 (1971) 420.
171. I. Kh. Kovarskaya, *Nauch. Issled. Inst. Akad. Kommunal Khoz* 3 (1967) 77-87.
172. M. Venuat, *Mater. Constr. Trav. Publics* 1967, no. 626-672, 394-446. Ind. liants hydrauliques, Paris.
173. Progil, US 3433657, 1964; FR 6941443, 1969.
174. P. P. Stupaschenko, E. P. Kholoshin, *Izv. Vyssh. Uchebn. Zaved. Stroit. Arkhit.* 11 (1968) no. 7, 105-108.
175. Promstroiniiproekt Inst. Rostov, SU 229889 1967.
176. Winkler, Kaspar & Co. ZA 6801274, 1968.
177. FMC Corp., GB 1136688, 1967.
178. Esso Research & Eng. Co., US 3380915, 1965.
179. Eastman Kodak US 3285863, 1964.
180. Office national industriel de l'azote, FR 1433595, 1965.
181. E. Hechler, *Wochenbl. Papierfabr.* 96 (1968) no. 23/24, 868-872.
182. *Abstr. Bull. Inst. Pap. Chem.* 37 (1967) no. 7, 415-416.
183. Nalco Chemical Co., US 3264174, 1962.
184. W. Vogel: *Einsatz von Natriumaluminat im Wasserkreislauf von Papierfabriken*, PTS-WAF-Seminar, München, 4-6 Nov. 1980.
185. Cabot Corp., US 3212911, 1961.
186. Imperial Metal Ind. (Kynoch), FR 1507547, 1967.
187. Compagnie générale du duralumin et du cuivre, FR 1470389, 1966.
188. T. Chmiel et al. PL 55018 1966.
189. Eastman Kodak, FR 1516507, 1968.
190. Aluminum Co. of America, US 3290151, 1963; CS 126439, 1963.
191. American Cyanamid, US 3328328, 1964.
192. Union Carbide, US 3297516, 1963.
193. VEB Cerital-Werk Mieste, NL 6503849, 1965.
194. G. Puri: "Binary System BaO·Al₂O₃", *Radex Rundsch.* 4 (1960) 201.
195. A. Branski: "Refractory Barium Aluminate Cements", *Tonind. Ztg. Keram. Rundsch.* 85 (1961) no. 6, 125-129.
196. D. C. Bradley: "Metal Alkoxides", in F. A. Cotton (ed.): *Prox. Inorg. Chem.* 2 (1960) 303.
197. Anderson Chemical Corp., US 2965663, 1960 (W. E. Smith, A. R. Anderson).
198. J. Andrioly, J. Enezian, *Ind. Chim. (Paris)* 55 (1968) 203-213.
199. JANEF Thermochemical Tables, NSRDS-NBS 37, 2nd ed., National Bureau of Standards, Gaithersburg, MD, 1971.
200. R. L. de Beauchamp: "Preparation of Anhydrous Aluminum Chloride", *Inf. Circ. U.S. Bur. Mines*, no. 8412, 1969.
201. J. Hille, W. Dürrwächter, *Angew. Chem.* 72 (1960) 850-855.
202. C. A. Thomas: *Anhydrous Aluminum Chloride in Organic Chemistry*, ACS Monograph Series, Reinhold Publ. Co., New York 1941.
203. G. A. Olah: *Friedel-Crafts and Related Reactions*, Wiley-Interscience, New York 1963.
204. H. J. Gardener, K. Grjotheim, B. J. Welch: *Alumina Production Until 2000*, ICSOBA-Hungary, Hungary, Budapest 1981.
205. *Chemical Economics Handbook*, SRI International, Oct. 1994.
206. R. R. Brown, G. E. Daut, R. v. Mrazek, N. A. Gokcen, *Rep. Invest. U.S. Bur. Mines*, no. 8379, 1979, p. 1.
207. J. F. McIntyre R. T. Foley, B. F. Brown, *Inorg. Chem.* 21 (1982) 1167.
208. K. B. Bengtson, 108th Annual Meeting, American Institute of Mining, Metallurgical and Petroleum Engineers, New Orleans 1979; *Light Met. (N.Y.)* 1979, vol. 1 p. 217.
209. J. Cohen, J. Mercier: Proceedings, 105th Annual Meeting, American Institute of Mining Engineering, Las Vegas 1976: *Light Met. (N.Y.)* 1976, vol. 2, p. 3.
210. Hoechst, DE 2408751, 1974 (M. Danner, K. Zeisberger).
211. Hoechst DE 2704850, 1977 (M. Danner, K. Zeisberger).
212. Hoechst, DE 2309610, 1973 (M. Danner, M. Krieg).
213. Hoechst, DE 2907671, 1979 (M. Danner R. Schlosser).
214. S. Schönherr, H.-P. Frey, *Z. Anorg. Allg. Chem.* 452 (1979) 167.
215. S. Schönherr, H. Götz, W. Geßner, M. Winzer, D. Müller, *Z. Anorg. Allg. Chem.* 476 (1981) 195.
216. F. v. Lampe, D. Müller W. Geßner A.-R. Grimmer, G. Scheler, *Z. Anorg. Allg. Chem.* 489 (1982) 16.
217. S. Schönherr, H. Götz, R. Bertram D. Müller, W. Geßner, *Z. Anorg. Allg. Chem.* 502 (1983) 113.
218. Bertram, W. Geßner, D. Müller, H. Götz, S. Schönherr, *Z. anorg. allg. Chem.* 525 (1985) 14-22.
219. Chr. Dobrev P. Dobrev, *Rheol. Acta* 22 (1983) 237.
220. B. Clauss, *Die angewandte makromolekulare Chemie* 217 (1994) 139.
221. E. Wänninen, A. Ringbom, *Anal. Chim. Acta* 12 (1955) 308.
222. M. Danner, R. Schlosser, E. Hambsch (Hoechst), unpublished results, 1981.
223. C. F. Asche & Co., DE 1041933, 1957 (K. Langer).

224. Hoechst DE 1174751, 1961 (J. König, H.-K. Platzer).
225. Hoechst DE 2263333, 1972 (M. Danner, M. Krieg, K. Matschke).
226. A.I.R. Lippewerk, DE 4202937, 1995 (G. Kuder-mann, K. H. Blaufuß, B. Simbach, R. Thome, H. Bings).
227. S. Plechner, "Antiperspirants and Deodorants", in M. S. Balsam, E. Sagarin (eds.): *Cosmetics, Science and Technology*. 2nd ed., vol. 2, Wiley-Interscience, New York 1972, p. 373.
228. Cosmetic, Toiletry and Fragrance Association (CTFA), Washington DC, 1971.
229. J. C. Ginocchio, *Techn. Rundsch. Sulzer* 65 (1983) no. 3, 12.
230. R. Bertram, W. Geßner, D. Müller, M. Danner, *Acta hydrochim. hydrobiol.* 22 (1994) 265-269.
231. *Br. J. Ind. Med.* 23 (1966) 305.
232. American Conference of Governmental Industrial Hygienists (ACGIH) (ed.): *Threshold Limit Values 1982*, Cincinnati, OH, 1982.
233. Deutsche Forschungsgemeinschaft (ed.): *Maximale Arbeitsplatzkonzentrationen (MAK) 1995*, Verlag Chemie, Weinheim 1995.
234. V. A. Drill, P. Lazar (eds.): *Cutaneous Toxicity*, Academic Press, New York 1977, p. 127.
235. S. E. Tarling, P. Barnes, A. L. Mackay, *J. Appl. Cryst.* 17 (1984) 96-99.
236. S. E. Tarling, P. Barnes, J. Klinowsky, *Acta Cryst.* B44 (1988) 128-135.
237. R. J. H. Clark, M. L. Franks, *Chem. Phys. Lett.* 34 (1975) 69-72.
238. R. J. H. Clark, D. G. Cobbold, *Inorg. Chem.* 17 (1978) 3169-3174.
239. R. J. H. Clark, T. J. Dines, M. Kummo, *Inorg. Chem.* 22 (1983) 2766-2772.
240. Interchemical Corp., US 2535057, 1950 (A. E. Gessler, C. A. Kummis).
241. Toyo Soda, JP-KK 81045513, 1978.
242. Reckitt's Colours Ltd., *The Cost of Whiteness*, Hull, United Kingdom.
243. Dr. Hans Heubach GmbH & Co. KG: Heucophos company information, Langelsheim 1989.
244. Société nouvelle des couleurs zinciques, company information, Beauchamp 1990.
245. Teikoku Kako Co. Ltd.: *K-White*, company information, Osaka 1987.
246. Goslarer Farbenwerke Dr. Hans Heubach, DE 3046698, 1980 (W. Haacke et al.).
247. R. Besold, R. Reißer, E. Roth, *Farbe + Lack* 97 (1991) 311.
248. W. Ostertag, *Congr. FATIPEC XIX*, vol II/103, 1988.

22 Titanium

HEINZ SIBUM (§§ 22.1–22.6, 22.8–22.12); AXEL WESTERHAUS, PETER WODITSCH (§§ 22.7.1–22.7.9); MANFRED MANSMANN, DIETER RADE, VOLKER WILHELM (§ 22.7.10); RALF EMMERT, KLAUS-DIETER FRANZ, HARTMUT HARTNER, KATSUHISA NITTA, GERHARD PFAFF (§ 22.7.11); HARALD GAEDCKE (§ 22.7.12); FATHI HABASHI (§ 22.13); HANS UWE WOLF (§ 22.14)

22.1 Introduction	1129	22.9 Production of Titanium Sponge.....	1161
22.2 History.....	1129	22.9.1 Reduction of Titanium Dioxide ...	1162
22.3 Physical Properties.....	1130	22.9.2 Reduction of Titanium Halides.....	1162
22.4 Mechanical Properties.....	1131	22.9.3 Thermal Decomposition of Titanium Halides	1164
22.5 Corrosion Behavior	1132	22.9.4 Electrowinning of Titanium	1165
22.6 Occurrence	1133	22.10 Processing and Reuse of Scrap Metal.....	1166
22.7 Titanium Dioxide	1134	22.11 Processing of Titanium Sponge.....	1166
22.7.1 Properties.....	1135	22.12 Production and Processing of Semifinished Products	1168
22.7.2 Raw Materials	1136	22.13 Compounds.....	1169
22.7.2.1 Natural Raw Materials	1136	22.13.1 Titanium(II) Compounds	1170
22.7.2.2 Synthetic Raw Materials	1139	22.13.2 Titanium(III) Compounds	1170
22.7.3 Production	1140	22.13.2.1 Titanium(III) Sulfate and Double Sulfates.....	1171
22.7.3.1 Sulfate Method.....	1141	22.13.2.2 Titanium(III) Hydroxide.....	1171
22.7.3.2 The Chloride Process.....	1143	22.13.2.3 Titanium(III) Oxide	1171
22.7.3.3 Pigment Quality.....	1145	22.13.2.4 Titanium Nitride, TiN	1171
22.7.3.4 Aftertreatment	1146	22.13.3 Titanium(IV) Compounds	1171
22.7.3.5 Problems with Aqueous and Gaseous Waste.....	1147	22.13.3.1 Titanates.....	1172
22.7.4 Economic Aspects	1150	22.13.3.2 Peroxytitanic Acid and Peroxytitanates.....	1173
22.7.5 Pigment Properties.....	1150	22.13.3.3 Titanium Sulfides	1173
22.7.6 Analysis	1153	22.13.3.4 Titanium Carbides and Carbonitrides	1173
22.7.7 Uses of Pigmentary TiO ₂	1153	22.13.3.5 Titanium Borides	1173
22.7.8 Uses of Nonpigmentary TiO ₂	1154	22.14 Toxicology and Occupational Health.....	1174
22.7.9 Toxicology.....	1155	22.15 References.....	1176
22.7.10 Rutile Mixed Metal Oxide Pigments	1155		
22.7.11 Titanium Dioxide-Mica Pigment ..	1156		
22.7.12 Transparent Titanium Dioxide....	1159		
22.8 Production of Titanium Tetrachloride	1160		

22.1 Introduction

Titanium, is a member of group 4 of the periodic table. It has two 4s and two 3d valence electrons and is a transition element. The electronic configuration is $1s^2 2s^2 2p^6 3s^2 3p^6 4s^2$. Natural titanium is a mixture of five stable isotopes [7]:

Mass number:	46	47	48	49	50
Abundance, %:	7.95	7.75	73.43	5.51	5.34

The following unstable isotopes also exist:

Mass number:	43	44	45	51
Half-life:	0.58 ± 0.004 s [8]	1000 a	3.08 ± 0.06 h [9], 72 d [10]	6 min [11], ± 2 d [12]

22.2 History

In 1791, GREGOR isolated a metal oxide from the black, magnetic iron-containing sand found at Manaccan in Cornwall, and conjectured that it contained a hitherto unknown

metal, which he named manaccanite. In 1795, KLAPROTH investigated the red schorl rock from Boinik in Hungary, and he also decided that this mineral must contain an as yet unknown metal, which he named titanium after the Titans, the sons of the primeval Earth Mother. After detecting the new metal, also in oxidic form, in other minerals such as titanite and ilmenite, KLAPROTH showed that it was identical with the metal in manaccanite.

Although the fundamental reactions of modern titanium production (digestion with sulfuric acid, hydrolysis of the resulting liquor, and reduction in acidic solution) were already known before 1800, the first preparation of pure titanium oxide was carried out only in 1908, while full-scale production began in 1916 in Norway.

In 1910, HUNTER prepared 98–99% pure titanium metal by reduction with sodium. The strong affinity of titanium for oxygen, nitrogen, and carbon made preparation of the pure, ductile metal difficult, and this was first achieved by VAN ARKEL in 1922 by reducing potassium hexafluorotitanate with sodium in an inert atmosphere. The foundations for large-scale industrial production were laid by KROLL's discovery of the reduction of titanium tetrachloride by magnesium. WARTMAN of the Bureau of Mines then developed a method of treating the titanium sponge so obtained and melting it in an electric arc furnace.

22.3 Physical Properties

Pure titanium is a silvery white, ductile metal, *mp* 1668–3500 °C [15]. The atomic radius is 0.145 nm for coordination number six in the crystal lattice [16].

α -Ti has hexagonal structure of the Mg type, almost close-packed and somewhat compressed along the *c*-axis. The lattice constants of α -Ti at room temperature are *c* = 0.4679 nm, *a* = 0.2951 nm, *c/a* = 1.585 for twice-refined iodide titanium [17].

At 882.5 °C [18], titanium transforms into the body-centered cubic β -phase, the heat of transformation being 3.685 kJ/mol [19]. Ex-

trapolation of the lattice constants of titanium alloys whose β -phase can be quenched to room temperature, gives a lattice constant *a* = 0.3269 nm at room temperature [20] and 0.328 nm above 620 °C. Increasing contents of oxygen, nitrogen, and carbon, which are incorporated interstitially, slightly elongate the *a*-axis of α -Ti and considerably elongate its *c*-axis. These effects are most marked with carbon, and are very slight with hydrogen. The effect on the lattice constants of titanium of elements that form substitution mixed crystals is variable. Some important physical data of titanium are as follows:

Density at 25 °C	
high purity	4.5 g/cm ³
commercial purity	4.51
at 870 °C (α -Ti)	4.35
at 900 °C (β -Ti)	4.33
Coefficient of linear expansion at 25 °C	$8.5 \times 10^{-6} \text{ K}^{-1}$
Mean coefficient of linear expansion, 20–700 °C	$(9.0\text{--}10.1) \times 10^{-6} \text{ K}^{-1}$
Latent heat of fusion	20.9 kJ/mol
Latent heat of sublimation	464.7 kJ/mol
Latent heat of vaporization	397.8 kJ/mol
Specific heat capacity at 25 °C	$0.523 \text{ J g}^{-1} \text{ K}^{-1}$
at 200 °C	0.569
at 400 °C	0.628
Thermal conductivity at 20–25 °C	
high purity	$0.221 \text{ W cm}^{-1} \text{ K}^{-1}$
commercial purity	0.226–0.201
Surface tension at 1600 °C	1.7 N/m
Diffusion coefficient (self diffusion)	
at 750 °C (α -Ti)	$4 \times 10^{-13} \text{ cm}^2/\text{s}$
(β -Ti)	2.4×10^{-9}
Modulus of elasticity at 25 °C	100–110 GPa
Temperature coefficient	–0.687 GPa/K
Modulus of rigidity at 25 °C	411.8–431.5 GPa
Temperature coefficient	0.265 GPa/K
Bulk modulus at 25 °C	122.6 GPa
Transverse contraction number at 25 °C	0.30
Electrical resistivity at 25 °C	42 $\mu\Omega\text{cm}$
at 600 °C	140–150
Superconductivity (iodide titanium), transition temperature	$0.40 \pm 0.04 \text{ K}$
Magnetic susceptibility of α -Ti at 25 °C	$3.2 \times 10^{-6} \text{ cm}^3/\text{g}$
Temperature coefficient for –200 to 800 °C	$1.2 \times 10^{-9} \text{ cm}^3 \text{ g}^{-1} \text{ K}^{-1}$
Magnetic permeability at 25 °C	1.00005

Further details can be found in [13–15, 21–37]. Many properties of titanium at a given temperature show variations that depend on the composition and condition of the metal (purity, alloying elements, thermal and mechanical pretreatment).

Variation in properties such as electrical and thermal conductivity and plastic behavior are caused by lattice defects. Cold working increases hardness and strength by producing dislocations, and reduces modulus of elasticity and electrical conductivity, e.g., by producing holes in the lattice. Annealing in the recovery range (300–500 °C) and in the recrystallization range (500–800 °C) restores the original values. The moduli of elasticity and shear elasticity also depend on heat treatment. The presence of foreign elements, even at low concentrations, often has a marked effect. In general, electrical resistivity, hardness, and strength increase with decreasing purity.

22.4 Mechanical Properties

High-purity titanium (iodide and electrolytic titanium) still contains traces of other elements due to the high affinity of the metal for atmospheric gases. Above room temperature, the strength decreases, by 50% at 200 °C, whereas the fracture strain remains virtually unchanged. Increasing the grain size decreases tensile strength and yield strength but increases elongation and reduction in area at fracture. Compositions and mechanical properties of high-purity titanium grades are listed in Table 22.1.

Table 22.1: Percentage chemical compositions and strength properties of high-purity grades of titanium.

	Iodide titanium [38]	Electrolytic titanium ^a [39]
O	0.021	0.020
N	0.004	0.002
C	0.015	0.009
H		0.003
Fe	0.005	0.001
Al	0.04	
Tensile strength, MPa	230	229
Yield strength, MPa	121.5	103.0
Fracture strain ^b , %	55	55
Reduction in area, %	60	

^a Typical figures for Brinell hardness 60–65.

^b Measured length 25.4 mm (1 inch).

Titanium of Commercial Purity. As oxygen, nitrogen, and hydrogen contents increase, strength increases and toughness decreases. Whereas oxygen is the only element deliber-

ately added to give increased strength, the others, together with iron and carbon, are impurities introduced during production.

The chemical compositions and strength properties of commercial grades of titanium in the recrystallized-annealed state are listed in Table 22.2. The Grade 1 material is the softest grade of titanium, and has excellent cold working properties. It is used for deep drawing, cladding of steel reactors, as a coating applied by explosive cladding, for components that must have good corrosion resistance but need not have high strength, and in electrical technology. Titanium Grade 2 is the most widely used commercially pure titanium. It has good cold working properties, and may also be used for load-bearing components at temperatures up to ca. 250 °C. Titanium Grade 3 is used almost exclusively for pressure vessels. This material has adequate cold-working properties and can be used at lower wall thicknesses than softer grades of titanium. Titanium Grade 4 has the highest strength and is used for the manufacture of fittings and in aircraft construction. Complex components made of this grade of titanium have to be formed at ca. 300 °C.

Table 22.2: Chemical compositions (maximum contents, %) and strength properties (minimum values) of commercially pure grades of titanium.

Grade number ^a	3.7025 (Ti 1)	3.7035 (Ti 2)	3.7055 (Ti 3)	3.7065 (Ti 4)
O	0.12	0.18	0.25	0.35
N	0.05	0.05	0.05	0.05
C	0.06	0.06	0.06	0.06
H	0.013	0.013	0.013	0.013
Tensile strength, MPa	290–410	390–540	460–590	540–740
0.2% Yield strength, MPa	180	250	320	390
1% Yield strength, MPa	200	270	350	410
Fracture strain, %	24	22	18	16

^a DIN 17850, Nov. 1990, and DIN 17860, Nov. 1990.

As shown in Figure 22.1, the high-temperature tensile strength of all industrial grades of titanium decreases rapidly with increasing temperature. As titanium creeps under prolonged stress even at room temperature, the characteristic high-temperature strength val-

ues used in calculations based on 100 000 h periods, as required for chemical pressure vessels, are considerably lower than those for short periods [40]. The use of titanium Grade 1 for pressure vessels is not recommended.

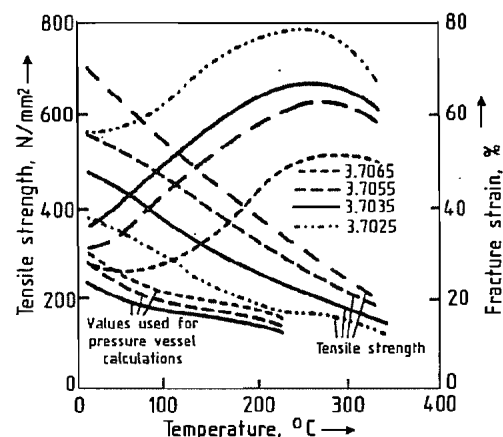


Figure 22.1: High-temperature tensile strength and fracture strain of titanium pressure vessel calculations (105 h). Titanium grade numbers are explained in Table 22.2.

In addition to the fundamental strength properties determined by destructive testing and the creep strength values determined by long-term static load tests, fatigue strength (resistance to oscillatory stress) is also important. In the case of titanium, it is between 50 and 75% of the ultimate tensile strength.

Cold working (80–90% deformation) doubles the tensile strength of titanium, and both the elongation and reduction in area at fracture decrease by ca. 50%.

22.5 Corrosion Behavior

The standard electrode potential of the reaction $\text{Ti} \rightleftharpoons \text{Ti}^{2+} + 2e^-$ is -1.75 V. The corrosion resistance of titanium metal is due to the formation of a thin, dense, stable, adherent surface film of oxide, which immediately reforms after mechanical damage if oxygen is present in the surrounding medium. Titanium is less resistant to corrosion in strongly reducing media.

The corrosion-resistant oxide layer is destroyed in completely water-free environ-

ments such as dry chlorine, dry oxygen, and red-fuming nitric acid, and in reducing corrosive media. In neutral aqueous solutions, especially in the presence of chloride ions, localized penetration of the passive layer can lead to pitting and crevice corrosion.

Passivation. In a corrosive medium, the electrode potential of a titanium surface decreases with time [41]. The passivation potential usually lies between -0.2 and -0.5 V. With increasing concentration and temperature, the passivation current density increases in the passive range, while the passivation potential remains constant [42]. The corrosion loss in the passive range therefore increases [43]. Small additions of oxidizing metal ions such as Cu^{2+} , Fe^{3+} , Cr^{4+} , Au^{3+} , and Pt^{4+} cause passivation of titanium in reducing media. With increasing temperature and acid concentration, the concentration of inhibitor necessary to give passivation increases. Anodic treatment strengthens the coatings and can delay their degradation under reducing conditions.

Additions. The corrosion behavior of titanium-based materials can often be improved by the addition of at least 0.15% palladium to the alloy, without affecting its strength properties [44, 45].

Likewise, small additions ($< 1\%$) of other noble metals improve the corrosion behavior of titanium [46]. Improvement of corrosion resistance as well as strength properties is achieved by addition of, e.g., 0.8% nickel with 0.3% molybdenum [47].

Crevice Corrosion, Stress Corrosion Cracking, and Pitting. Titanium is not very susceptible to crevice corrosion except at elevated temperatures in the presence of high concentrations of halide and sulfate ions or in moist chlorine gas. Additions of palladium to the alloy have a beneficial effect. Titanium is very resistant to pitting in the presence of chlorides, except in high concentrations of chlorides of calcium, aluminum, or zinc at elevated temperatures [48]. Titanium is not susceptible to stress corrosion cracking, except by red-fuming nitric acid containing $< 1.5\%$

water, by uranyl sulfate, or by anhydrous methanol.

Reaction with Hydrogen, Oxygen, Nitrogen, and Air. The presence of hydrogen (produced in a chemical process or as a corrosion product) or of hydrogen-containing compounds leads to local hydrogen pickup by titanium, with consequent embrittlement and impairment of corrosion resistance. The rate of hydrogen pickup depends on temperature, time, and the condition of the metal surface [49]. Oxide coatings reduce or prevent hydrogen pickup [50].

The oxide film that forms on the surface of activated titanium metal at room temperature reaches a thickness of 1.7 nm in 2 h, 3.5 nm in 40 d, and 25 nm in 4 years [51]. The color of the oxide film varies with its thickness and temperature of formation, and also with the alloy content of the parent metal. As the temperature increases from 200 to ca. 500 °C, the film thickness increases, and its color changes from golden yellow to brown, dark blue, violet, and light blue, showing iridescent effects, while at higher temperatures a gray haze forms followed by a silvery-white and then a dirty gray scale layer, after which a yellowish white to brown scale layer of variable thickness appears, depending on the alloy composition [52]. With increasing heating time and temperature, the depth of penetration of oxygen, and hence the hardness, increases [53].

Up to ca. 500 °C, the weight increase of titanium due to oxidation is small. Higher temperatures lead to a rapid weight increase associated with dissolution of oxygen in the metal.

In a nitrogen atmosphere, a titanium nitride layer with metallic character is formed. Above 700 °C, the titanium nitride increasingly reacts with oxygen to form titanium oxide. Titanium reacts with nitrogen considerably more slowly than with oxygen, so that the reaction with nitrogen makes little contribution to scale formation in air. In the presence of water vapor, hydrogen is also taken up.

Behavior in Salts, Bases, Acids, and Molten Materials. The corrosion behavior of com-

mercially pure titanium is summarized in Table 22.3. Oxidizing conditions and the presence of oxidizing agents under reducing conditions improve corrosion resistance, whereas strongly reducing conditions or increases in concentration and temperature impair it [52].

Table 22.3: Corrosion behavior of commercially pure titanium.

Resistant	Limited resistance	Nonresistant
Nitric acid	Sulfuric acid	Fluorine
Chromic acid	Hydrochloric acid	Dry chlorine gas
Sulfurous acid	Phosphoric acid	Red-fuming nitric acid
Alkali lyes	Oxalic acid	
Ammonia	Formic acid	
Aqueous chlorides		
Brine		
Seawater		
Wet chlorine gas		
Acetic acid		
Maleic acid		
Acetaldehyde		
Carbamate		
Dimethylhydrazine		
Liquid hydrogen		

Titanium is stable in molten alkali metals up to 600 °C, in magnesium up to 650 °C, in gallium, tin, lead, and lead–bismuth–tin alloys up to 300 °C, and in mercury up to 150 °C [54]. Titanium is corroded by molten mixtures of chlorides and fluorides.

22.6 Occurrence

Titanium is relatively widely distributed and abundant. With an estimated average concentration in the earth's crust of 0.6%, it is ninth in order of abundance after oxygen, silicon, aluminum, iron, magnesium, calcium, sodium, and potassium. Its concentration is ca. 1/20 that of aluminum, and 1/10 that of iron. It is 5–10 times as abundant as chlorine, sulfur, or phosphorus, and more abundant than the rest of the metals put together. Thus, for example it is 60 times as abundant as copper or nickel and 300 times as abundant as molybdenum.

As the ionic radius of titanium is similar to that of some of the most common elements (Al^{3+} , Fe^{3+} , Mg^{2+}), most minerals, rocks, and soils contain small amounts of titanium, al-

though true titanium minerals, containing > 1% titanium, of which there are at least 87, are found in only a few locations.

Primary titanium occurs in igneous rocks, where it forms the acidic component of basic magmas and the basic component of acidic magmas. In the first case, titanates are present, the most important of which are ilmenite (FeTiO_3) and perovskite (CaTiO_3). In the second case, oxidic compounds of titanium are formed. Intermediate forms also exist, e.g., in silicates, in which titanium is present mainly as a basic element (e.g., in zircon minerals and aluminosilicates), but also as a replacement for silicon. These transitional forms include titanite (sphene), $\text{CaTi}(\text{SiO}_4)\text{O}$, a common component of magmatic rocks. All these forms also occur in metamorphic titanium-containing rocks. The two TiO_2 modifications anatase and brookite occur exclusively in metamorphic deposits.

Secondary deposits of titanium include the widely distributed ilmenite placer deposits and ilmenite sands, which mostly occur in coastal regions, and the TiO_2 deposits in clays. Ilmenite is the main starting material for titanium dioxide pigments.

The most important titanium minerals are anatase (TiO_2); ilmenite (FeTiO_3), which contains up to 53% TiO_2 , and its low-iron weathering product leucoxene; perovskite (CaTiO_3); rutile (TiO_2); and sphene [$\text{CaTi}(\text{SiO}_4)\text{O}$]. Of these, only ilmenite, leucoxene, and rutile are of economic importance due to the ease with which they can be processed. The anatase deposits in Brazil and the perovskite deposits of Colorado (United States) may achieve economic importance in the future.

The most useful mineral for the extraction of titanium and titanium compounds is rutile (TiO_2). Although it is rarer than ilmenite, its TiO_2 content is higher. Naturally occurring enriched rutile is brown to black, and contains 90–97% TiO_2 together with impurities including up to 10% silica, iron oxides, vanadium, niobium, and tantalum, and traces of tin, chromium, and molybdenum compounds.

Primary rutile deposits occur at Kragero in south east Norway (albite with 25% rutile)

and in Virginia (United States). However, more important are the secondary placer deposits, e.g., in Brazil, Cameroon, and Arkansas (United States), and the beach sands, of which the most important are on the east coasts of Australia and Florida (United States) and in northern Transvaal (South Africa). All rutile and two-thirds of ilmenite are extracted from placer deposits and sands, the rest of the ilmenite being obtained from titanomagnetites and titanohematites.

Rutile-bearing beach and dune deposits can be mined if TiO_2 contents exceed 0.3%. The TiO_2 content of the ilmenite sands depends on the degree of weathering. In the South African deposits it is 10–48%, in Australian sands 54%, and in ilmenite from Kerala (India) and the east coast of Sri Lanka up to 80%. The ilmenite-bearing titanomagnetites and titanohematites contain 35% TiO_2 in Canada, ca. 20% in the United States, 18% in Norway, and 13% in Finland [55].

Titanium occurs in many stars. It is less abundant in meteorites than in the earth's crust, and is mainly associated with the silicate phase [56].

Reserves. Proven world reserves of rutile and ilmenite, calculated as TiO_2 , content have been estimated at 423×10^6 to 600×10^6 t. The largest reserves of ilmenite are in South Africa, India, the United States, Canada, Norway, Australia, Ukraine, Russia, and Kazakhstan, and of rutile in Brazil [57]. The existence of other reserves, e.g., in Bangladesh, Chile, Italy, Mexico, and New Zealand, makes it likely that the actual mineable world reserves considerably exceed the accepted figures.

22.7 Titanium Dioxide

Titanium dioxide, TiO_2 , occurs in nature in the modifications rutile, anatase, and brookite. Rutile and anatase are produced industrially in large quantities and are used as pigments and catalysts, and in the production of ceramic materials.

Titanium dioxide is of outstanding importance as a white pigment because of its scattering properties (which are superior to those of all other white pigments), its chemical stability, and lack of toxicity. Titanium dioxide is the most important inorganic pigment in terms of quantity, 3×10^6 t were produced in 1989. World production of titanium dioxide pigment is shown in Table 22.4 [58].

Table 22.4: World production of TiO_2 pigment.

Year	Sulfate process		Chloride process		Total 10^3 t/a
	10^3 t/a	%	10^3 t/a	%	
1965	1254	90.3	135	9.7	1389
1970	1499	77.4	437	22.6	1936
1977	1873	72.3	716	27.7	2589
1988	1781	60.2	1178	39.8	2959
1995*	2000	ca. 49	2100	51.0	4100

* Estimated.

22.7.1 Properties [59, 60]

Physical Properties. Of the three modifications of TiO_2 , rutile is the most thermodynamically stable. Nevertheless, the lattice energies of the other phases are similar and hence are stable over long periods. Above 700 °C, the monotropic conversion of anatase to rutile takes place rapidly. Brookite is difficult to produce, and therefore has no value in the TiO_2 pigment industry.

In all three TiO_2 modifications one titanium atom in the lattice is surrounded octahedrally by six oxygen atoms, and each oxygen atom is surrounded by three titanium atoms in a trigonal arrangement. The three modifications correspond to different ways of linking the octahedra at their corners and edges. Crystal lattice constants and densities are given in Table 22.5.

Table 22.5: Crystallographic data for TiO_2 modifications.

Phase	Crystal system	Lattice constants, nm			Density, g/cm^3
		a	b	c	
Rutile	tetragonal	0.4594		0.2958	4.21
Anatase	tetragonal	0.3785		0.9514	4.06
Brookite	rhombic	0.9184	0.5447	0.5145	4.13

Rutile and anatase crystallize in the tetragonal system, brookite in the rhombic system. The melting point of TiO_2 is ca. 1800 °C.

Above 1000 °C, the oxygen partial pressure increases continuously as oxygen is liberated and lower oxides of titanium are formed. This is accompanied by changes in color and electrical conductivity. Above 400 °C, a significant yellow color develops, caused by thermal expansion of the lattice; this is reversible. Rutile has the highest density and the most compact atomic structure, and is thus the hardest modification (Mohs hardness 6.5–7.0). Anatase is considerably softer (Mohs hardness 5.5).

Titanium dioxide is a light-sensitive semiconductor, and absorbs electromagnetic radiation in the near UV region. The energy difference between the valence and the conductivity bands in the solid state is 3.05 eV for rutile and 3.29 eV for anatase, corresponding to an absorption band at < 415 nm for rutile and < 385 nm for anatase.

Absorption of light energy causes an electron to be excited from the valence band to the conductivity band. This electron and the electron hole are mobile, and can move on the surface of the solid where they take part in redox reactions.

Chemical Properties. Titanium dioxide is amphoteric with very weak acidic and basic character. Accordingly, alkali-metal titanates and free titanate acids are unstable in water, forming amorphous titanium oxide hydroxides on hydrolysis.

Titanium dioxide is chemically very stable, and is not attacked by most organic and inorganic reagents. It dissolves in concentrated sulfuric acid and in hydrofluoric acid, and is attacked and dissolved by alkaline and acidic molten materials.

At high temperature, TiO_2 reacts with reducing agents such as carbon monoxide, hydrogen, and ammonia to form titanium oxides of lower valency; metallic titanium is not formed. Titanium dioxide reacts with chlorine in the presence of carbon above 500 °C to form titanium tetrachloride.

Surface Properties of TiO_2 Pigments. The specific surface area of TiO_2 pigments can vary between 0.5 and 300 m^2/g depending on

its use. The surface of TiO_2 is saturated by coordinatively bonded water, which then forms hydroxyl ions. Depending on the type of bonding of the hydroxyl groups to the titanium, these groups possess acidic or basic character [61, 62]. The surface of TiO_2 is thus always polar. The surface covering of hydroxyl groups has a decisive influence on pigment properties such as dispersibility and weather resistance.

The presence of the hydroxyl groups makes photochemically induced reactions possible, e.g., the decomposition of water into hydrogen and oxygen and the reduction of nitrogen to ammonia and hydrazine [63].

22.7.2 Raw Materials [64]

The raw materials for TiO_2 production include natural products such as ilmenite, leucoxene, and rutile, and some very important synthetic materials such as titanium slag and synthetic rutile. Production capacities for the most important titanium-containing raw materials are listed in Table 22.6 [65].

Table 22.6: Production capacities of titanium-containing raw materials (1987).

Raw material	Location	Capacity, 10^3 t/a
Ilmenite	Australia	1550
	India	240
	Malaysia	130
	Sri Lanka	150
	Brazil	80
	United States	260
	Norway	650
	Total	3060
Natural rutile	Australia	250
	Sierra Leone	125
	South Africa	55
	United States	27
	Others	33
	Total	490
Titanium slag	Canada	1000
	South Africa	650
	Norway	200
	Total	1850
Synthetic rutile	Australia	272
	India	50
	Japan	48
	United States	100
	Total	470

22.7.2.1 Natural Raw Materials

Titanium is the ninth most abundant element in the earth's crust, and always occurs in combination with oxygen. The more important titanium minerals are shown in Table 22.7. Of the natural titanium minerals, only ilmenite (leucoxene) and rutile are of economic importance. Leucoxene is a weathering product of ilmenite.

Table 22.7: Titanium minerals.

Mineral	Formula	TiO_2 , %
Rutile	TiO_2	92–98
Anatase	TiO_2	90–95
Brookite	TiO_2	90–100
Ilmenite	FeTiO_3	35–60
Leucoxene	$\text{Fe}_2\text{O}_3\cdot\text{TiO}_2$	60–90
Perovskite	CaTiO_3	40–60
Sphene (titanite)	CaTiSiO_5	30–42
Titanomagnetite	$\text{Fe}(\text{Ti})\text{Fe}_2\text{O}_4$	2–20

The largest titanium reserves in the world are in the form of anatase and titanomagnetite, but these cannot be worked economically at the present time. About 95% of the world's production of ilmenite and rutile is used to produce TiO_2 pigments, the remainder for the manufacture of titanium metal and in welding electrodes.

Ilmenite and Leucoxene. Ilmenite is found worldwide in primary massive ore deposits or as secondary alluvial deposits (sands) that contain heavy minerals. In the massive ores, the ilmenite is frequently associated with intermediary intrusions (Tellnes in Norway and Lake Allard in Canada). The concentrates obtained from these massive ores often have high iron contents in the form of segregated hematite or magnetite in the ilmenite. These reduce the TiO_2 content of the concentrates (Table 22.8). Direct use of these ilmenites has decreased owing to their high iron content. A digestion process is employed to produce iron sulfate heptahydrate. In cases where iron sulfate is not required as a product, metallurgical recovery of iron from the iron-rich ilmenites and production of a titanium-rich slag are being increasingly used.

The enrichment of ilmenite in beach sand in existing or fossil coastlines is important for

TiO_2 production. The action of surf, currents, and/or wind results in concentration of the ilmenite and other heavy minerals such as rutile, zircon, monazite, and other silicates in the dunes or beaches. This concentration process frequently leads to layering of the minerals. Attack by seawater and air over geological periods of time leads to corrosion of the ilmenite. Iron is removed from the ilmenite lattice, resulting in enrichment of the TiO_2 in the remaining material. The lattice is stable with TiO_2 contents up to ca. 65%, but further removal of iron leads to the formation of a sub-microscopic mixture of minerals which may include anatase, rutile, and amorphous phases. Mixtures with TiO_2 contents as high as 90% are referred to as leucoxene. Leucoxene is present in corroded ilmenite and in some deposits is recovered and treated separately. However, the quantities produced are small in comparison to those of ilmenite.

The concentrates obtained from ilmenite sand, being depleted in iron, are generally richer in TiO_2 than those from the massive deposits. Other elements in these concentrates include magnesium, manganese, and vanadium (present in the ilmenite) and aluminum, calcium, chromium, and silicon which originate from mineral intrusions.

Table 22.8: Composition of ilmenite deposits (%).

Component	Tellnes (Norway)	Richard's Bay (South Africa)	Capel (Western Australia)	Quilon (India)
TiO_2	43.8	46.5	54.8	60.3
Fe_2O_3	14.0	11.4	16.0	24.8
FeO	34.4	34.2	23.8	9.7
Al_2O_3	0.6	1.3	1.0	1.0
SiO_2	2.2	1.6	0.8	1.4
MnO	0.3		1.5	0.4
Cr_2O_3		0.1	0.1	0.1
V_2O_5	0.3	0.3	0.2	0.2
MgO	3.7	0.9	0.15	0.9

Two-thirds of the known ilmenite reserves that could be economically worked are in China, Norway (both massive deposits), and the former Soviet Union (sands and massive deposits). On the basis of current production capacities, these countries could cover all requirements for ca. 150 years. However, the countries with the largest outputs are Australia

(sands), Canada (massive ore), South Africa (sands), and the former Soviet Union (sands, massive ore). Other producers are the United States (sands, Florida), India (sands, Quilon), Sri Lanka (sands), and Brazil (rutile e ilmenita do Brasil). Important deposits have been found in Madagascar.

Rutile is formed primarily by the crystallization of magma with high titanium and low iron contents, or by the metamorphosis of titanium-bearing sediments or magmatites. The rutile concentrations in primary rocks are not workable. Therefore, only sands in which rutile is accompanied by zircon and/or ilmenite and other heavy minerals can be regarded as reserves. The world reserves of rutile are estimated to be 28×10^6 t, including the massive Piampaludo ore reserves in Italy, whose workability is in dispute.

As in the case of ilmenite, the largest producers are in Australia, South Africa, the United States, and India. There is not enough natural rutile to meet demand, and it is therefore gradually being replaced by the synthetic variety. Compositions of typical rutile concentrates are given in Table 22.9.

Table 22.9: Composition of rutile deposits [66].

Rutile component	Content, %		
	Eastern Australia	Sierra Leone	South Africa
TiO_2	96.00	95.70	95.40
Fe_2O_3	0.70	0.90	0.70
Cr_2O_3	0.27	0.23	0.10
MnO	0.02		
Nb_2O_5	0.45	0.21	0.32
V_2O_5	0.50	1.00	0.65
ZrO_2	0.50	0.67	0.46
Al_2O_3	0.15	0.20	0.65
CaO	0.02		0.05
P_2O_5	0.02	0.04	0.02
SiO_2	1.00	0.70	1.75

Anatase, like rutile, is a modification of TiO_2 . The largest reserves of this mineral are found in carboniferous intrusions in Brazil. Ore preparation techniques allow production of concentrates containing 80% TiO_2 , with possible further concentration to 90% TiO_2 by treatment with hydrochloric acid [67]. Attempts to use these substantial mineral depos-

its ($< 100 \times 10^6$ t TiO_2) as a pigment raw material are at the pilot-plant stage.

Ore Preparation. Most of the world's titanium ore production starts from heavy mineral sands. Figure 22.2 shows a schematic of the production process. The ilmenite is usually associated with rutile and zircon, so that ilmenite production is linked to the recovery of these minerals. Geological and hydrological conditions permitting, the raw sand (usually containing 3–10% heavy minerals) is obtained by wet dredging (a). After a sieve test (b), the raw sand is subjected to gravity concentration in several stages with Reichert cones (d) and/or spirals (e) to give a product containing 90–98% heavy minerals. This equipment separates the heavy from the light minerals (densities: $4.2\text{--}4.8$ g/cm³ and < 3 g/cm³ respectively) [68].

The magnetic minerals (ilmenite) are then separated from the nonmagnetic (rutile, zircon, and silicates) by dry or wet magnetic separation (f). If the ores are from unweathered deposits, the magnetite must first be removed. An electrostatic separation stage (h) allows separation of harmful nonconducting mineral impurities such as granite, silicates, and phosphates from the ilmenite, which is a good conductor. The nonmagnetic fraction (leucoxene, rutile, and zircon) then undergoes further hydromechanical processing (i) (shaking table, spirals) to remove the remaining low-density minerals (mostly quartz). Recovery of the weakly magnetic weathered ilmenites and leucoxenes is by high-intensity magnetic separation (j) in a final dry stage. The conducting rutile is then separated from the nonconducting zircon electrostatically in several stages (l). Residual quartz is removed by an air blast.

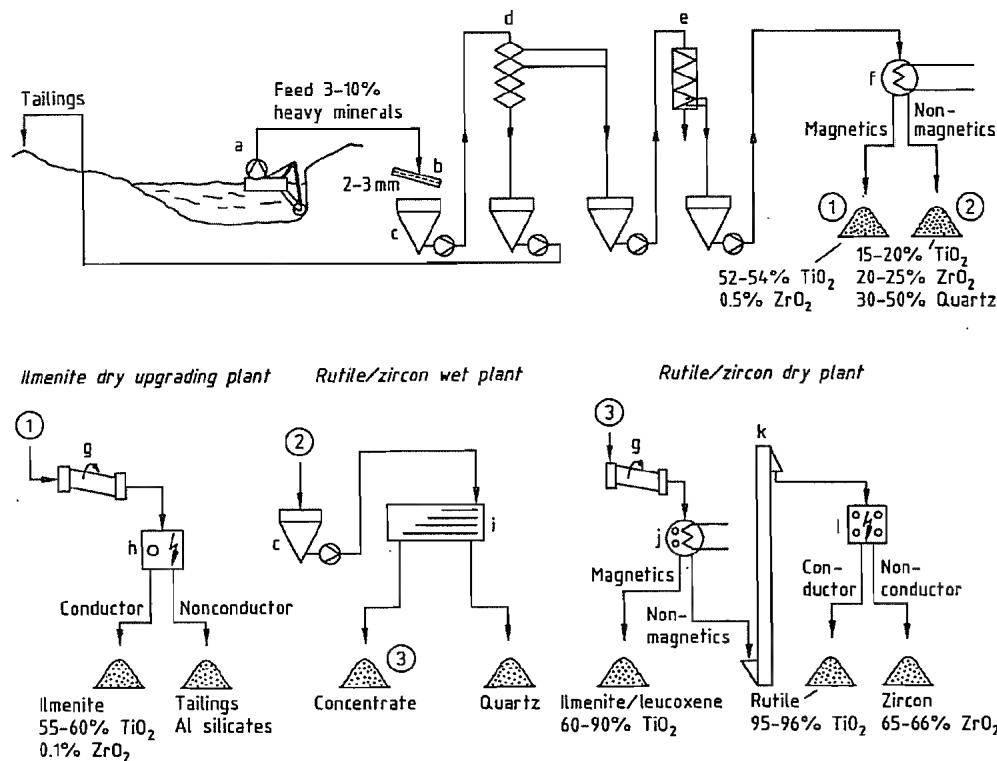


Figure 22.2: The processing of heavy mineral sands: a) Dredger; b) Sieve; c) Bunker; d) Reichert cones; e) Spirals; f) Magnetic separator; g) Dryer; h) Electrostatic separator; i) Shaking table; j) Dry magnetic separator; k) Vertical belt conveyor; l) Electrostatic separator.

Table 22.10: Production plants for synthetic rutiles in 1987 [80].

Process development	Process steps	By-products	Producer and location ^a
Benilite Corporation of America (BCA)	partial reduction to Fe(II), digestion with HCl solution, calcination	20–23% FeCl_3 , pyrolyzed to Fe_2O_3 and HCl	Kerr McGee, Mobile, USA (100); Kerala Minerals and Metals Ltd., Chavara, Kerala (25); Indian Rare Earths, Orissa, India (100)
Western Titanium	oxidation to Fe(III), reduction to Fe(0), digestion with FeCl_3 , with air oxidation	iron hydroxides	Associated Minerals Consolidated, Casl, Australia (60); AMC, Narmgulu, Australia (112)
Lurgi	reduction to Fe(0), digestion with air blowing, hydrocyclone separation, calcination	iron hydroxides	Westralian Sand Ltd., Capel, Australia (100)
Ishibara Sangyo Kaisha	reduction to Fe(II), digestion with H_2SO_4 , calcination	FeSO_4 solution reacted with NH_3 to form ammonium sulfate and iron hydroxide	Ishibara, Yokkaichi, Japan (48)
Dhrangadhra Chemical Works	reduction to Fe(II)/Fe(0), digestion with HCl solution, calcination	iron(II) chloride solution	Dhrangadhra Chemical Works Ltd., Suhupuram, Tamil Nadu, India (25)

^aCapacity in 10^3 t is given in parentheses.

22.7.2.2 Synthetic Raw Materials

Increasing demand for raw materials with high TiO_2 contents has led to the development of synthetic TiO_2 raw materials. In all production processes, iron is removed from ilmenites or titanomagnetites.

Titanium Slag. The metallurgical process for removing iron from ilmenite is based on slag formation in which the iron is reduced by anthracite or coke to metal at $1200\text{--}1600^\circ\text{C}$ in an electric arc furnace, and then separated. Titanium-free pig iron is produced together with slags containing 70–85% TiO_2 (depending on the ore used) that can be digested with sulfuric acid because they are high in Ti^{3+} and low in carbon. Raw materials of this type are produced in Canada by the Québec Iron and Titanium Corporation (QIT), in South Africa by Richard's Bay Iron and Titanium Ltd. (RBM), and to a smaller extent in Japan by Hokuetro Metal and Tinfos Titan and Iron K.S. (Tyssedal, Norway).

Synthetic Rutile. In contrast to ilmenite, only a small number of rutile deposits can be mined economically, and the price of natural rutile is therefore high. Consequently, many different processes have been developed to remove the iron from ilmenite concentrates without changing the grain size of the mineral because

this is highly suitable for the subsequent fluidized-bed chlorination process. All industrial processes involve reduction of Fe^{3+} with carbon or hydrogen, sometimes after preliminary activation of the ilmenite by oxidation. Depending on the reducing conditions, either Fe^{2+} is formed in an activated ilmenite lattice, or metallic iron is produced.

The activated Fe^{2+} -containing ilmenite can be treated with hydrochloric or dilute sulfuric acid (preferably under pressure), and a "synthetic rutile" with a TiO_2 content of 85–96% is obtained [69]. The solutions containing iron(II) salts are concentrated and then thermally decomposed to form iron oxide and the free acid, which can be used again in the digestion process [70].

Metallic iron can be removed in various ways. The following processes are described in the patent literature:

- Size reduction followed by physical processes such as magnetic separation of flotation.
- Dissolution in iron(III) chloride solutions [71], the resulting iron(II) salt is oxidized with air to give iron oxide hydroxides and iron(III) salts.
- Dissolution in acid.

- Oxidation with air in the presence of electrolytes. Various iron oxide or iron oxide hydroxide phases are formed depending on the electrolyte used. Possible electrolytes include iron(II) chloride solutions [72], ammonium chloride [73], or ammonium carbonate carbonic acid [74].
- Oxidation with the iron(III) sulfate from ilmenite digestion [75], followed by crystallization of the iron(II) sulfate.
- Chlorination to form iron(III) chloride [76].
- Reaction with carbon monoxide to form iron carbonyls [77] which can be decomposed to give high-purity iron.

Another possible method of increasing the TiO_2 content of ilmenite is by partial chlorination of the iron in the presence of carbon. This is operated on a large scale by several compa-

nies [78, 79]. Table 22.10 summarizes plants producing synthetic rutile in 1987.

22.7.3 Production

Titanium dioxide pigments are produced by two different processes. The older *sulfate process* depends on the breakdown of the titanium-containing raw material ilmenite or titanium slag with concentrated sulfuric acid at 150–220 °C. Relatively pure TiO_2 dihydrate is precipitated by hydrolysis of the sulfate solution, which contains colored heavy metal sulfates, sometimes in high concentration. The impurities are largely removed in further purification stages. The hydrate is then calcined, ground, and further treated.

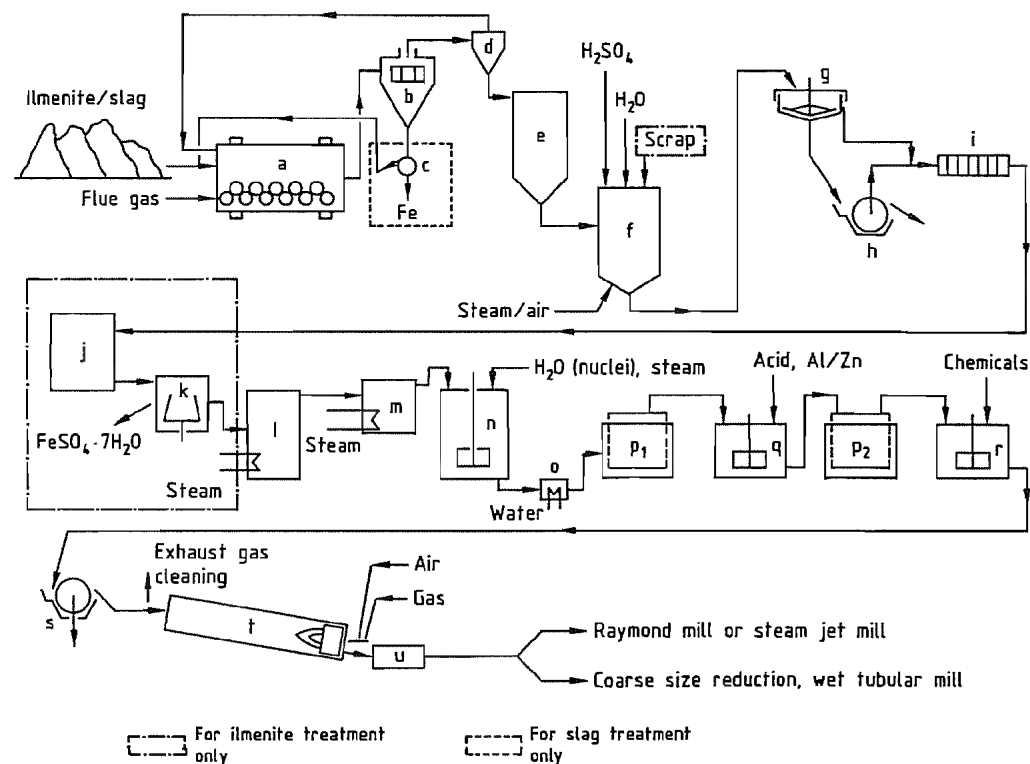


Figure 22.3: Production of TiO_2 by the sulfate process: a) Ball mill/dryer; b) Screen; c) Magnetic separator; d) Cyclone; e) Silo; f) Digestion vessel; g) Thickener; h) Rotary filter; i) Filter press; j) Crystallizer; k) Centrifuge; l) Vacuum evaporator; m) Preheater; n) Stirred tank for hydrolysis; o) Cooler; p) Moore filters; q) Stirred tank for bleaching; r) Stirred tank for doping; s) Rotary filter for dewatering; t) Rotary kiln; u) Cooler.

In the *chloride process*, the titanium-containing raw materials ilmenite, leucoxene, natural and synthetic rutile, titanium slag, and anatase are chlorinated at 700–1200 °C. Titanium tetrachloride is separated from other chlorides by distillation. Vanadium tetrachloride (VCl_4) and vanadium oxychloride (VOCl_3) must, however, first be reduced to solid chlorides. The TiCl_4 is burnt at temperatures of 900–1400 °C to form TiO_2 . This extremely pure pigment undergoes further treatment depending on the type of application.

22.7.3.1 Sulfate Method

The sulfate method is summarized in Figure 22.3.

Grinding. The titanium-bearing raw materials are dried to a moisture content of < 0.1%. Drying is mainly intended to prevent heating and premature reaction on mixing with sulfuric acid. The raw materials are ground in ball mills to give a mean particle size of ca. 40 μm . The combination of grinding and drying shown in Figure 22.3 (a) is recommended. The small amount of metallic iron present in titanium slag is removed magnetically (c), which almost completely eliminates hydrogen evolution during subsequent digestion.

Digestion. Batch digestion is usually employed. The ground raw materials (ilmenite, titanium slag, or mixtures of the two) are mixed with 80–98% H_2SO_4 . The ratio of H_2SO_4 to raw material is chosen so that the weight ratio of free H_2SO_4 to TiO_2 in the suspension produced by the hydrolysis is between 1.8 and 2.2 (the so-called “acid number”). The reaction in the digestion vessel (f) is started by adding water, dilute sulfuric acid, oleum, or sometimes steam. The temperature initially increases to 50–70 °C due to the heat of hydration of the acid. The exothermic sulfate formation then increases the temperature to 170–220 °C. If dilute acid or sparingly soluble raw materials are used, external heating is required.

After the maximum temperature has been reached, the reaction mixture must be left to mature for 1–12 h, depending on the raw material, so that the titanium-containing components become as soluble as possible. Digestion can be accelerated by blowing air through the mass while the temperature is increasing, and also during the maturing period.

Several *continuous digestion processes* have been proposed [81]. A proven method is to continuously feed a mixture of ilmenite and water together with the acid into a double-paddle screw conveyor. After a relatively short dwell time (< 1 h), a crumbly cake is produced [82]. This process utilizes a more limited range of raw materials than the batch process because they need to be very reactive.

Dissolution and Reduction. The cake obtained by digestion is dissolved in cold water or in dilute acid recycled from the process. A low temperature must be maintained (< 85 °C) to avoid premature hydrolysis, especially with the product from ilmenite. Air is blown in to agitate the mixture during dissolution. With the ilmenite product, the TiO_2 concentration of the solution is 8–12%, and with the slag product between 13 and 18%.

The trivalent iron is hydrolyzed together with the titanium compounds, and adheres to the titanium oxide hydrate. All the Fe^{3+} is reduced to Fe^{2+} by scrap iron during dissolution of the ilmenite product, or immediately afterwards. Reoxidation of the iron during subsequent processing is prevented with Ti^{3+} which is obtained by reducing a small part of the Ti^{4+} . Alternatively, reduction of Ti^{4+} to Ti^{3+} can be carried out in part of the solution under optimized conditions; this concentrated Ti^{3+} solution is then added in a controlled manner to the reaction solution [83]. In solutions obtained from titanium slag, the Ti^{3+} content of the solution must be decreased by oxidation with atmospheric oxygen so that no loss of yield occurs during hydrolysis.

With both ilmenite and titanium slag, mixed digestion can be carried out in which the Ti^{3+} content of the slag reduces all the Fe^{3+} to Fe^{2+} . The dissolved products obtained from

the separate digestion of ilmenite and titanium slag can also be mixed [84, 85].

Clarification. All undissolved solid material must be removed as completely as possible from the solution. The most economical method is to employ preliminary settling in a thickener (g), followed by filtration of the sediment with a rotary vacuum filter (h). The filtrate and the supernatant from the thickener are passed through filter presses (i) to remove fines. Owing to the poor filtering properties of the solution, the rotary filter must be operated as a precoat filter. Preliminary separation in the thickener must be assisted by adding chemicals to promote sedimentation. Attempts to carry out the entire clarification process in a single stage using automated filter presses have been reported [86].

Crystallization. The solutions from slag digestion contain 5–6% FeSO_4 , and those from ilmenite digestion 16–20% FeSO_4 after reduction of the Fe^{3+} . The solution is cooled under vacuum to crystallize out $\text{FeSO}_4 \cdot 7\text{H}_2\text{O}$ (j) and reduce the quantity of FeSO_4 discharged with the waste acid. The concentration of the TiO_2 in the solution is thereby increased by ca. 25%. The salt is separated by filtration or centrifugation (k).

The iron sulfate is used in water purification, and as a raw material for the production of iron oxide pigments. Alternatively, it can be dehydrated and thermally decomposed to give iron(III) oxide and sulfur dioxide.

Hydrolysis. Titanium oxide hydrate is precipitated by hydrolysis at 94–110 °C. Other sulfuric-acid-soluble components of the raw material are precipitated simultaneously, mainly niobium as its oxide hydrate.

Hydrolysis is carried out in brick-lined, stirred tanks (n) into which steam is passed. The hydrolysate does not have any pigment properties, but these are strongly influenced by the particle size and degree of flocculation of the hydrolysate (mean particle size of hydrolysate is ca. 5 nm, and of TiO_2 pigments 200–300 nm).

The properties of the hydrolysate depend on several factors:

- The hydrolysis of concentrated solutions of titanium sulfate (170–230 g TiO_2/L) proceeds very sluggishly and incompletely (even if boiled) unless suitable nuclei are added or formed to accelerate hydrolysis. The nuclei are usually produced by two methods. In the Mecklenburg method, colloidal titanium oxide hydrate is precipitated with sodium hydroxide at 100 °C; 1% of this hydrate is sufficient. In the Blumenfeld method a small part of the sulfate solution is hydrolyzed in boiling water and then added to the bulk solution [87]. The particle size of the hydrolysate depends on the number of nuclei.
- The particle size and degree of flocculation of the hydrolysate depend on the intensity of agitation during the nuclei formation by the Blumenfeld method and also during the initial stage of the hydrolysis.
- The titanium sulfate concentration has a great influence on the flocculation of the hydrolysate. It is adjusted, if necessary by vacuum evaporation, to give a TiO_2 content of 170–230 g/L during hydrolysis. Lower concentrations result in a coarser particle size.
- The acid number should be between 1.8 and 2.2. It has a considerable effect on the TiO_2 yield and on the particle size of the hydrolysate. For a normal hydrolysis period (3–6 h) the TiO_2 yield is 93–96%.
- The properties of the hydrolysate are affected by the concentrations of other salts present, especially FeSO_4 . High concentrations lead to finely divided hydrolysates.
- The temperature regime mainly affects the volume–time yield and hence the purity of the hydrolysate.

Purification of the Hydrolysate. After hydrolysis, the liquid phase of the titanium oxide hydrate suspension contains 20–28% H_2SO_4 and various amounts of dissolved sulfates, depending on the raw material. The hydrate is filtered off from the solution (p₁) (weak acid), and washed with water or dilute acid. Even

with acid washing, too many heavy metal ions are adsorbed on the hydrate for it to be directly usable in the production of white pigment. Most of the impurities can be removed by reduction (bleaching), whereby the filter cake is slurried with dilute acid (3–10%) at 50–90 °C and mixed with zinc or aluminum powder (q). Bleaching can also be carried out with powerful nonmetallic reducing agents (e.g., $\text{HOCH}_2\text{SO}_2\text{Na}$). After a second filtration and washing process (p₂), the hydrate only has low concentrations (ppm) of colored impurities but still contains chemisorbed 5–10% H_2SO_4 . This cannot be removed by washing and is driven off by heating to a high temperature.

Doping of the Hydrate. When producing titanium dioxide of maximum purity, the hydrate is heated (calcined) without any further additions. This gives a fairly coarse grade of TiO_2 with a rutile content that depends on the heating temperature. However, to produce specific pigment grades, the hydrate must be treated with alkali-metal compounds and phosphoric acid as mineralizers (< 1%) prior to calcination (r). Anatase pigments contain more phosphoric acid than rutile pigments. To produce rutile pigments, rutile nuclei (< 10%) must be added; ZnO , Al_2O_3 , and/or Sb_2O_3 (< 3%) are sometimes also added to stabilize the crystal structure.

Nuclei are produced by converting the purified titanium oxide hydrate to sodium titanate, which is washed free of sulfate and then treated with hydrochloric acid to produce the rutile nuclei. Rutile nuclei can also be prepared by precipitation from titanium tetrachloride solutions with sodium hydroxide solution.

Calcination. The doped hydrate is filtered with rotary vacuum filters (s) to remove water until a TiO_2 content of ca. 30–40% is reached. Pressure rotary filters or automatic filter presses can also be used to obtain a TiO_2 content of ca. 50%. Some of the water-soluble dopants are lost in the filtrate and can be replaced by adding them to the filter cake before it is charged into the kiln. Calcination is performed in rotary kilns (t) directly heated with gas or oil in countercurrent flow. Approxi-

mately two-thirds of the residence time (7–20 h in total) is needed to dry the material. Above ca. 500 °C, sulfur trioxide is driven off which partially decomposes to sulfur dioxide and oxygen at higher temperatures. The product reaches a maximum temperature of 800–1100 °C depending on pigment type, throughput, and temperature profile of the kiln. Rutile content, particle size, size distribution, and aggregate formation are extremely dependent on the operating regime of the kiln. After leaving the kiln, the clinker can be indirectly cooled or directly air-cooled in drum coolers (u).

The exhaust gas must have a temperature of > 300 °C at the exit of the kiln to prevent condensation of sulfuric acid in the ducting. Energy can be saved by recirculating some of the gas to the combustion chamber of the kiln and mixing it with the fuel gases as a partial replacement for air. Alternatively, it can be used for concentrating the dilute acid. The gas then goes to the waste-gas purification system.

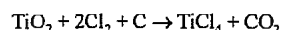
Grinding. The agglomerates and aggregates in the clinker can be reduced to pigment fineness by wet or dry grinding. Coarse size reduction should be carried out in hammer mills prior to wet grinding in tube mills (with addition of wetting agents). The coarse fraction can be removed from the suspension by centrifugation, and recycled to the mills. Hammer mills, cross-beater mills, and particularly pendular and steam-jet mills are suitable for dry grinding. Special grinding additives can be used that act as wetting agents during subsequent pigment treatment or improve the dispersibility of untreated pigments.

22.7.3.2 The Chloride Process

The chloride process is summarized in Figure 22.4.

Chlorination. The titanium in the raw material is converted to titanium tetrachloride in a reducing atmosphere. Calcined petroleum coke is used as the reducing agent because it has an extremely low ash content and, due to its low volatiles content, very little HCl is

formed. The titanium dioxide reacts exothermically as follows:



As the temperature rises, an endothermic reaction also occurs to an increasing extent in which carbon monoxide is formed from the carbon dioxide and carbon. Therefore, oxygen must be blown in with the chlorine to maintain the reaction temperature between 800 and 1200 °C. The coke consumption per tonne of TiO_2 is 250–300 kg. If CO_2 -containing chlorine from the combustion of TiCl_4 is used, the coke consumption increases to 350–450 kg.

The older *fixed-bed chlorination method* is hardly used today. In this process, the ground titanium-containing raw material is mixed with petroleum coke and a binder, and formed into briquettes. Chlorination is carried out at 700–900 °C in brick-lined reactors.

Fluidized-bed chlorination was started in 1950. The titanium raw material (with a particle size similar to that of sand) and petroleum coke (with a mean particle size ca. five times that of the TiO_2) are reacted with chlorine and oxygen in a brick-lined fluidized-bed reactor (Figure 22.4, c) at 800–1200 °C. The raw materials must be as dry as possible to avoid HCl formation. Since the only losses are those due to dust entrainment the chlorine is 98–100% reacted, and the titanium in the raw material is 95–100% reacted, depending on the reactor design and the gas velocity. Magnesium chloride and calcium chloride can accumulate in the fluidized-bed reactor due to their low volatility. Zirconium silicate also accumulates because it is chlorinated only very slowly at the temperatures used. All the other constituents of the raw materials are volatilized as chlorides in the reaction gases.

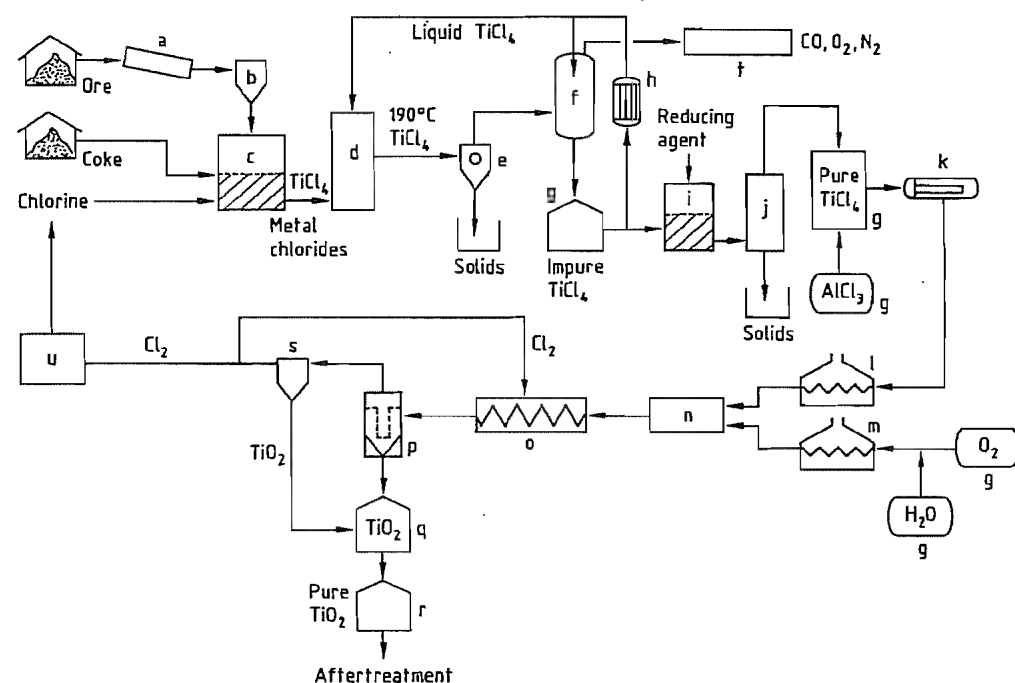


Figure 22.4: Flow diagram of TiO_2 production by the chloride process: a) Mill; b) Silo; c) Fluidized-bed reactor; d) Cooling tower; e) Separation of metal chlorides; f) TiCl_4 condensation; g) Tank; h) Cooler; i) Vanadium reduction; j) Distillation; k) Evaporator; l) TiCl_4 superheater; m) O_2 superheater; n) Burner; o) Cooling coil; p) Filter; q) TiO_2 purification; r) Silo; s) Gas purification; t) Waste-gas cleaning; u) Cl_2 liquefaction.

The ceramic cladding of the fluidized-bed reactor is rather rapidly destroyed by abrasion and corrosion. If chlorination is interrupted, there is a further danger that the raw materials may sinter and eventually cannot be fluidized.

Gas Cooling. The reaction gases are cooled with liquid TiCl_4 either indirectly or directly (d). Crystallization of the chlorides of the other components causes problems because they tend to build up on the cooling surfaces, especially the large quantities of iron(II) and iron(III) chlorides formed on chlorination of ilmenite [88]. In this first stage, the reaction gases are cooled only down to a temperature (< 300 °C) at which the accompanying chlorides can be satisfactorily separated from the TiCl_4 by condensation or sublimation (e).

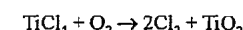
The gas then consists mainly of TiCl_4 and is cooled below 0 °C, causing most of the TiCl_4 to condense (f). The small amounts of TiCl_4 and Cl_2 remaining in the exhaust gas (CO_2 , CO and N_2) are removed by scrubbing with alkali (t).

Purification of TiCl_4 . The chlorides that are solid at room temperature and the entrained dust can be separated from the TiCl_4 by simply evaporating (distilling) this off (j). Dissolved chlorine can be removed by heating or reduction with metal powders (Fe, Cu, or Sn).

Removal of vanadium tetrachloride (VCl_4) and vanadium oxychloride (VOCl_3) from the TiCl_4 by distillation is very difficult owing to the closeness of their boiling points. They are therefore reduced to form solid, low-value vanadium chlorides (i). An enormous number of reducing agents have been recommended; important examples are copper, titanium trichloride, hydrogen sulfide, hydrocarbons, soaps, fatty acids, and amines. After subsequent evaporation (j) the titanium chloride should contain < 5 ppm vanadium. If organic reducing agents are used, the residues may cause problems by baking onto the surfaces of the heat exchanger.

Phosgene and SiCl_4 can be removed by fractional distillation.

Oxidation of TiCl_4 and Recovery of TiO_2 . Titanium tetrachloride is combusted with oxygen at 900–1400 °C to form TiO_2 pigment and chlorine (n). The purified TiCl_4 is vaporized (k) and the vapor is indirectly heated to ca. 500–1000 °C (l). The reaction



is weakly exothermic, and requires a high reaction temperature, so that the oxygen must also be heated to > 1000 °C (m). This can be achieved with an electric plasma flame, by reacting part of the oxygen with carbon monoxide, or by indirect heating. Hot TiCl_4 and oxygen (110–150% of the stoichiometric amount) are fed separately into a reaction chamber where they must be mixed as rapidly and completely as possible to give a high reaction rate. For this reason, and also because the TiO_2 has a strong tendency to cake onto the walls [89–91], many different reactor designs have been proposed and used. The same considerations apply to the cooling unit (o) where the pigment is very rapidly cooled to below 600 °C. Cooling zones of various geometries are used. If caking occurs, the material can be removed by introducing abrasive particles [92].

The mixture of gases (Cl_2 , O_2 , CO_2) and pigment can be further cooled during dry separation of the pigment either indirectly or directly by solid particles, e.g., sand. The pigment-containing gas is then filtered (p). The gas stream is recycled to the cooling zone (o) of the combustion furnace and to the chlorination process as oxygen-containing chlorine via the liquefaction unit (u). The chlorine adsorbed on the pigment can be removed by heating or by flushing with nitrogen or air.

The wet separation process, in which the pigment-containing gas mixture (Cl_2 , O_2 , and CO_2) is quenched in water, has not become established.

22.7.3.3 Pigment Quality

The quality of the TiO_2 pigment is influenced by various factors. Reaction temperature, excess oxygen, and flow conditions in

the reactor affect particle size and size distribution. Therefore, optimum conditions must be established for every reactor design. Caking of the TiO_2 on the walls of the reactor leads to impairment of quality.

The presence of water during combustion of the TiCl_4 gives rise to nuclei which promote the formation of finely divided pigment particles. It can be added directly to the oxygen or can be produced by the combustion of hydrogen-containing materials.

The presence of AlCl_3 promotes the formation of rutile and a more finely divided pigment. It is added in amounts of up to 5 mol%. Many methods have been proposed for rapidly generating and directly introducing the AlCl_3 vapor into the TiCl_4 vapor. Addition of PCl_3 and SiCl_4 suppresses rutile formation, so that anatase pigment is obtained [93]. However, pigments of this type have not appeared on the market.

Pigments produced by the chloride process (chloride pigments) have better lightness and a more neutral hue than pigments produced by the sulfate process (sulfate pigments). Pigments used in demanding applications are almost always subjected to inorganic aftertreatment.

22.7.3.4 Aftertreatment

Aftertreatment of the pigment particles improves the weather resistance and lightfastness of the pigmented organic matrix, and dispersibility in this matrix. The treatment consists of coating the individual pigment particles with colorless inorganic compounds of low solubility by precipitating them onto the surface. However, this reduces the optical performance of the pigment approximately in proportion to the decrease in the TiO_2 content. The surface coatings prevent direct contact between the binder matrix and the reactive surface of the TiO_2 . The effectiveness of these coatings largely depends on their composition and method of application, which may give too porous or too dense a coating. The treatment process also affects the dispersibility of the pigment, and therefore a compromise of-

ten has to be made. High weather resistance and good dispersibility of the pigment in the binder or matrix are usually desired. These effects are controlled by using different coating densities and porosities. Other organic substances can be added during the final milling of the dried pigment.

Several types of treatment are used:

- Deposition from the gas phase by hydrolysis or decomposition of volatile substances such as chlorides or organometallic compounds. Precipitation onto the pigment surface is brought about by adding water vapor. This method is especially applicable to chloride pigments, which are formed under dry conditions.
- Addition of oxides hydroxides or substances that can be adsorbed onto the surface during pigment grinding. This can produce partial coating of the pigment surface.
- Precipitation of the coating from aqueous solutions onto the suspended TiO_2 particles. Batch processes in stirred tanks are preferred; various compounds are deposited one after the other under optimum conditions. There is a very extensive patent literature on this subject. Continuous precipitation is sometimes used in mixing lines or cascades of stirred tanks. Coatings of widely differing compounds are produced in a variety of sequences. The most common are oxides, oxide hydrates, silicates, and/or phosphates of titanium, zirconium, silicon, and aluminum. For special applications, boron, tin, zinc, cerium, manganese, antimony, or vanadium compounds can be used [94, 95].

Three groups of pigments have very good lightfastness or weather resistance:

- Pigments with dense surface coatings for paints or plastics formed by:
 - Homogeneous precipitation of SiO_2 with precise control of temperature, pH, and precipitation rate [96]: ca. 88% TiO_2
 - Two complete aftertreatments, calcination is performed at 500–800 °C after the first

or second aftertreatment [97]: ca. 91% TiO_2

– Aftertreatment with Zr, Ti, Al, and Si compounds, sometimes followed by calcination at 700–800 °C [98]: ca. 95% TiO_2

- Pigments with porous coatings for use in emulsion paints obtained by simple treatment with Ti, Al, and Si compounds, giving a silica content of 10% and a TiO_2 content of 80–85%
- Lightfast pigments with dense surface coatings for the paper industry that have a stabilized lattice and a surface coating based on silicates or phosphates of titanium, zirconium, and aluminum: ca. 90% TiO_2

Coprecipitation of special cations such as antimony or cerium can improve lightfastness further [99]. After treatment in aqueous media, the pigments are washed on a rotary vacuum filter until they are free of salt, and then dried using, e.g., belt, spray, or fluidized-bed dryers.

Before micronizing the pigment in air-jet or steam-jet mills, and sometimes also before drying, the pigment surface is improved by adding substances to improve dispersibility and facilitate further processing. The choice of compounds used, which are mostly organic, depends on the intended use of the pigment. The final surface can be made either hydrophobic (e.g., using silicones, organophosphates, and alkyl phthalates) or hydrophilic (e.g., using alcohols, esters, ethers and their polymers, amines, organic acids). Combinations of hydrophobic and hydrophilic substances have proved especially useful for obtaining surface properties that give better dispersibility and longer shelf life [100].

22.7.3.5 Problems with Aqueous and Gaseous Waste

Aqueous Waste. In the *sulfate process*, 2.4–3.5 t concentrated H_2SO_4 are used per tonne of

TiO_2 produced, depending on the raw material. During processing, some of this sulfuric acid is converted to sulfate, primarily iron(II) sulfate, the rest is obtained as free sulfuric acid (weak acid). Filtration of the hydrolysate suspension can be carried out to give 70–95% of the SO_4^{2-} in a weak acid fraction containing ca. 20–25% free acid, the remaining sulfate (5–30%) is highly diluted with wash-water.

It has so far been common practice to discharge the waste acid directly into the open sea or coastal waters. If required by law, the acid is conveyed by ship to the open sea and discharged under supervision. The weak acid problem has been the subject of public discussion and criticism. As a result the discharge of weak acid into open waters will decline and eventually stop. Precipitation of the waste sulfuric acid as gypsum does not eliminate the wastewater problem because it is then necessary to dispose of large quantities of solid waste (gypsum) for which there is insufficient demand.

A process has been demonstrated in which both the free and the bound sulfuric acid (as metal sulfates) can be recovered from the weak acid in the calcination furnace (k, Figure 22.5) and in metal sulfate calcination (Figure 22.6). The process consists of two stages:

- Concentration and recovery of the free acid by evaporation
- Thermal decomposition of the metal sulfates and production of sulfuric acid from the resulting sulfur dioxide

As a result of energy requirements only acid containing > 20% H_2SO_4 can be economically recovered by evaporation. The weak acid is concentrated from ca. 20–25% to ca. 28% with minimum heat (i.e., energy) consumption, e.g., by using waste heat from sulfuric acid produced by the contact process [101], or from the waste gases from the calcination kilns used in TiO_2 production [102] (Figure 22.6).

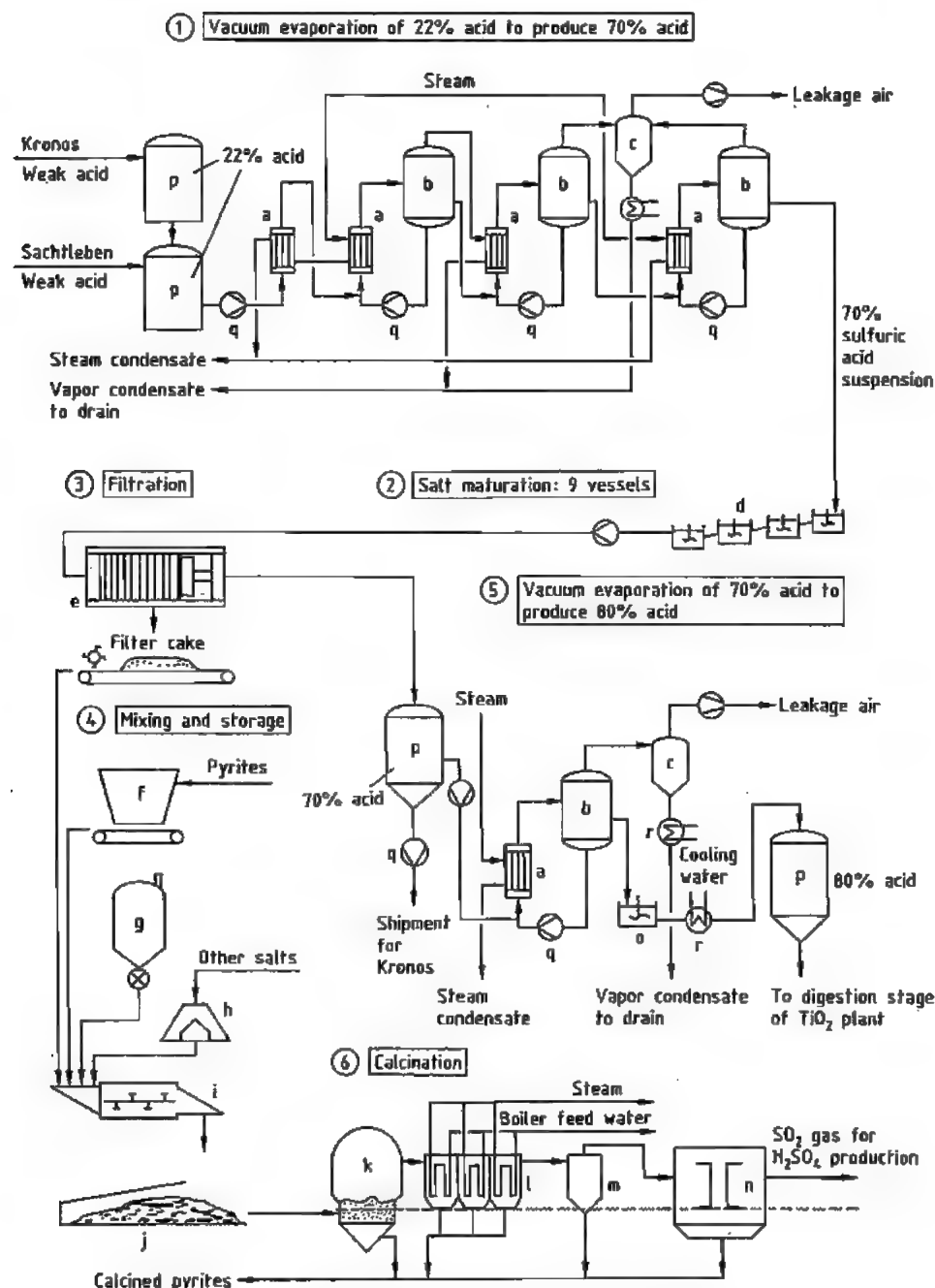


Figure 22.5: Weak acid recovery plant used by Sachtleben Chemie (based on know-how of Bayer AG): a) Heat exchanger; b) Evaporator; c) Injection condenser; d) Stirred salt maturing vessels; e) Filter press; f) Bunker for pyrites; g) Coal silo; h) Bunker; i) Mixing screw unit; j) Covered store for mixed filter cake; k) Calcination furnace; l) Waste-heat boiler; m) Cyclone; n) Electrostatic precipitator; o) Stirred tank; p) Storage tank; q) Pump; r) Cooler.

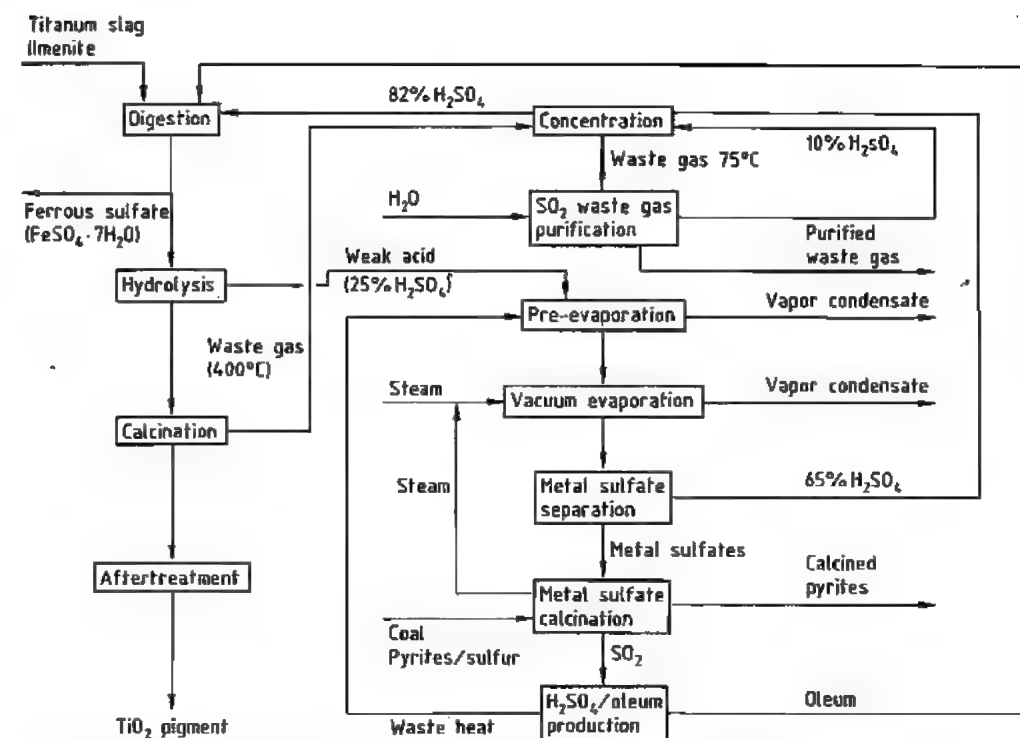


Figure 22.6: Waste heat recovery and sulfuric acid recycling during weak acid treatment (Bayer AG).

Following preliminary evaporation, further concentration is carried out in multi-effect vacuum evaporators. Since the water vapor pressure decreases strongly as the H_2SO_4 concentration increases, in general only two-stage evaporation can effectively exploit the water vapor as a heating medium. Evaporation produces a suspension of metal sulfates in 60–70% sulfuric acid (stage 1 in Figure 22.5). The suspension is cooled to 40–60 °C in a series of stirred tanks (stage 2, d) [103], giving a product with good filtering properties and an acid of suitable quality for recycling to the digestion process. Filtration (stage 3, e) is usually carried out with pressure filters [104] because they give a filter cake with an extremely low residual liquid content.

The concentration of the acid recycled to the digestion process depends on the quality of the titanium-containing raw material. For raw materials with a high titanium content, the 65–70% sulfuric acid separated from the metal

sulfates must be further concentrated to give 80–87% acid (stage 5).

Concentration can be carried out in steam-heated vacuum evaporators, or by using the heat from the TiO_2 calcination kilns [105]. Cooling the acid obtained after this concentration process yields a suspension of metal sulfates that can be directly used for digestion of the raw material. The metal sulfates recovered from the sulfuric acid in stage 3 are moist because they contain 65–70% sulfuric acid; they therefore have no direct use. They can be converted to a disposable material by reaction with calcium compounds [106]. Thermal decomposition of the metal sulfates to form the metal oxides, sulfur dioxide, water, and oxygen is energy intensive, but is advantageous from the ecological point of view. The energy requirement is ca. 4×10^9 J per tonne of filter cake. Thermal decomposition is carried out at 850–1100 °C in a fluidized-bed furnace (stage 6). The energy is supplied by coal, pyrites, or

sulfur. The sulfur dioxide produced by the thermal decomposition is purified by the usual methods, dried, and converted into sulfuric acid or oleum. This pure acid or oleum is mixed with the recovered sulfuric acid and used in the digestion process.

The metal oxides produced by thermal decomposition contain all the elements initially present in the raw material apart from the titanium which has been converted into pigment. The mixture of metal oxides, mainly iron oxide, can be used as an additive in the cement industry if demand exists.

The continually increasing demand for environmentally friendly industrial processes has also led to the development of techniques for recycling of the acidic wash water. In the *chloride process*, wastewater problems arise if the raw material contains < 90% TiO₂. The metal chloride by-products are sometimes disposed of in solution by the "deep well" method (e.g., at Du Pont). The metal chloride solutions are pumped via deep boreholes into porous geological strata. Special geological formations are necessary to avoid contamination of the groundwater by impurities.

Increasing restrictions also apply to the chloride process, so that efforts are continually being made to use the iron chloride by-product, e.g., in water treatment and as a flocculation agent.

Waste Gas Problems. The gases produced in the calcination kiln are cooled in a heat exchanger, and entrained pigment is removed, washed, and recycled to the process. The SO₂ and SO₃ formed during calcination are then scrubbed from the gases to form dilute sulfuric acid which is recycled.

22.7.4 Economic Aspects

The burning of TiCl₄ with oxygen or the calcination of TiO₂ hydrolysates produces either anatase or rutile pigments, depending on the doping and lattice stabilization. They are marketed directly or after being coated with oxides or hydroxides of various elements. Different treatments are necessary depending on the field of application, and all major pigment

producers have a large number of pigment grades. Product groups are listed in Table 22.11. Pigments of all grades are available with or without organic treatment. Over 400 different TiO₂ pigment grades are currently on the market. Table 22.12 gives the capacities and processes of the most important pigment producers.

Table 22.11: Classification of TiO₂ pigments according to composition (DIN draft specification E 55912, sheet 2, issue 4075).

Pigment	Class	TiO ₂ (min.), %	Water-solu- ble salts, %	Volatiles (max.), %
Anatase (Type A)	A1	98	0.6	0.5
	A2	92	0.5	0.8
Rutile R1 (Type R)		97	0.6	0.5
	R2	90	0.5	1.5
	R3	80	0.7	2.5

There have been few increases in production capacity since the early 1980s resulting in a titanium dioxide shortage. A considerable increase of capacity is planned by debottlenecking and building new plants. The proposed expansions reported in the literature indicate that capacity will increase to 4×10^6 t by 1995 [58].

Powdered TiO₂ pigments are usually supplied in 25 kg sacks (50 lbs, USA) or in large bags containing 0.5–1 t pigment. Aqueous suspensions with solids contents of 68–75% are also available and have great advantages as regards the distribution and metering of the pigment in aqueous systems. The dust formation that occurs with dry pigment is also avoided. With the development of products with improved flow properties and modern pneumatic delivery technology, supply in silo wagons is becoming increasingly important.

22.7.5 Pigment Properties

The pigment properties are extremely important when TiO₂ is used as a white pigment; they include lightening power, hiding power, lightness, hue, gloss formation, gloss haze, dispersibility, lightfastness, and weather resistance. These properties are a function of chemical purity, lattice stabilization, particle size and size distribution, and the coating pro-

duced by aftertreatment. They also depend on the medium and cannot generally be accurately described in scientific terms. Some of the important properties of TiO₂ pigments are described below.

Scattering Power. The refractive indices of rutile and anatase are very high (2.70 and 2.55, respectively). Even after incorporation in a wide range of binders, they lie in the range between 1.33 (water) and 1.73 (polyester fibers). The scattering power depends on the particle size, and for TiO₂ is at its maximum at a particle size of 0.2 μm (Mie's theory) [107]. The scattering power also depends on the wavelength; TiO₂ pigment particles with a size < 0.2 μm scatter light of shorter wavelengths more strongly and therefore show a slight blue tinge, while larger particles have a yellow tone.

Hue. The whiteness (lightness and hue) of TiO₂ pigments depends primarily on the crystalline modification, the purity, and the particle size of the TiO₂ (see above). As the absorption band (385 nm) of anatase pigments is shifted into the UV region, compared with rutile pigments they have less yellow undertone. Any transition elements present in the crystal structure have an adverse effect on the whiteness, so manufacturing conditions are of the greatest importance. Thus, pigments produced by the chloride process (which includes distillative purification of TiCl₄ before the combustion stage) have a higher color purity and very high lightness values.

Dispersion. Good disintegration and dispersion of the TiO₂ pigments in the medium are necessary to obtain high gloss and low gloss haze. These requirements are satisfied by intensive grinding and by coating the pigment surface with organic compounds. The compounds used for this surface treatment depend on the field of application.

Lightfastness and Weather Resistance. Weathering of paints and coatings containing TiO₂ leads to pigment chalking [108]. If weathering occurs in the absence of oxygen,

or in binders with low permeability to oxygen (e.g., in melamine formaldehyde resins), no chalking is observed, but graying takes place, which decreases on exposure to air. Graying is greatly reduced in the absence of water. Both effects are more severe with anatase pigments. Empirical stabilization processes have been developed by pigment producers, e.g., doping with zinc or aluminum prior to calcination.

According to modern theories, impairment of the lightfastness and weather resistance of TiO₂ pigments proceeds according to the following cycle [109]:

1. Molecules of water are bound to the TiO₂ surface forming hydroxyl groups on the surface.
2. Absorption of light of short wavelength (anatase < 385 nm, rutile < 415 nm) occurs, producing an electron and an electron defect or "hole" (exciton) in the crystal lattice which migrate to the surface of the pigment.
3. At the surface of the pigment, an OH⁻ ion is oxidized to an OH[•] radical by an electron "hole". The OH⁻ ion is then desorbed and can oxidatively break down the binder. A Ti³⁺ ion is simultaneously produced by reduction of Ti⁴⁺ with the remaining electron of the exciton.
4. The Ti³⁺ ion can be oxidized by adsorbed oxygen with formation of an O₂⁻ ion. The latter reacts with H⁺ and is converted into an HO₂[•] radical.
5. The cycle ends with the binding of water to the regenerated TiO₂ surface.

The chalking process can be regarded as the reaction of water and oxygen to form OH[•] and HO₂[•] radicals under the influence of shortwave radiation and the catalytic activity of the TiO₂ surface:

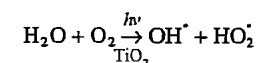


Table 22.12: World TiO₂ pigment producers (1988).

Country	Company	Location	Capacity, 10 ³ t/a		
			Chloride	Sulfate	Total
United States	Du Pont	New Johnsonville	250		545
		De Lisle	141		
		Edge Moore	119		
		Antioch	36		
	SCM Corporation	Baltimore	45	60	196
		Ashtabula	47	44	
		Savannah	52	48	100
	Kemira Oy	Hamilton	78		78
		Kerr McGhee Corporation	Varennes	40	36
NL Chemicals Incorporated		Tracy		42	42
Canada	Tioxide Canada				
Brazil	Titanio do Brasil/Bayer	Salvador		54	54
Mexico	Du Pont	Tampico	60		60
<i>Total, America</i>					1151
Germany	Kronos Titan	Leverkusen	80	35	175
	NL Chemicals	Nordenham			
	Bayer	Krefeld-Urdigen			
	Sachtleben Chemie, Metallgesellschaft	Duisburg-Homberg			
United Kingdom	Tioxide UK	Grimsby	50	105	155
	SCM Chemicals	Stallingborough	78	31	109
	Thann et Mulhouse (Rhône-Poulenc)	Le Havre		95	125
France	Tioxide France	Thann		30	
		Calais		80	80
Finland	Kemira Oy	Pori		80	80
Italy	Tioxide Italia	Scarlino		75	75
Belgium	Kronos Titan	Langebrügge		1 40	40
	Bayer	Antwerpen		30	30
Spain	Tioxide Españ.	Huelva		65	65
Netherlands	TDF Tiofine	Botlek		39	39
Norway	Kronos Titan	Fredrikstad		27	27
<i>Total, Western Europe</i>					1145
Soviet Union	state-owned	numerous plants		100	100
Poland	ZPN	Police		36	36
Yugoslavia	Cinkarne Celje	Celje		28	28
Czechoslovakia	Prerovske Chemiske	Prerov		22	22
<i>Total, Eastern Europe</i>					186
South Africa	SA Tioxide	Umbogwintwini		35	35
<i>Total Africa</i>					35
Australia	SCM Chemical	Australind		36	36
	Tioxide Australia	Burnie		35	35
<i>Total, Australia</i>					71
Japan	Ishibara Sangyo Kaisha	Yokkaichi	38	92	130
		Teikoku Kako		42	42
		Sakai Chemical		37	37
		Furukawa Mining		18	18
		Fuji Titanium		16	16
		Titan Kogyo		16	16
		Hakusai Chemical		15	15
		Tohoku Chemical		11	11
		Akita			
<i>Total, Japan</i>					285
India	Kerala Minerals & Metals	Kerala	22		22
	Travancore Titanium	Trivandrum		13	13
China	state-owned	numerous plants		25	25
South Korea	Hankuk Titanium	Young Dung Po		18	18
Taiwan	China Metal & Chemicals	Chin Shin		(6)	(6)
	Chung Tai	Chin Shin			
	ISK Taiwan, Ishibara	Kaohsing (only aftertreatment)			
<i>Total, Far East (excluding Japan)</i>					88
<i>Total world capacity</i>			1135	1826	2961

The enthalpy requirement for this reaction (312 kJ/mol) is provided by radiation of wavelength 385 nm. The cycle (1)–(5) is broken by excluding air or water. If oxygen is excluded or a binder is chosen in which the diffusion of oxygen is rate determining, a concentration of Ti³⁺ ions builds up. Graying then takes place, but this decreases with gradual exposure to oxygen. If water is excluded, rehydration and formation of surface hydroxyl groups do not take place; breakdown of the binder therefore ceases. Despite this photochemical breakdown of the binder, treated rutile pigments are used to stabilize many binders. This is because non-pigmented coatings are degraded by exposure to light and weathering; the added TiO₂ pigments prevent light from penetrating the deeper layers of the coating film and thus inhibit breakdown of the binder. High-quality TiO₂ pigments must satisfy stringent requirements with respect to weather resistance. They must withstand the severe climatic conditions of the Florida test, resisting a two-year exposure without appreciable chalking or deterioration of gloss.

22.7.6 Analysis

The crystal structure of the pigments is determined by X-ray analysis which is sensitive enough to determine 0.3–0.5% anatase in the presence of 99.7–99.5% rutile.

A qualitative test for TiO₂ is a blue violet coloration of beads of microcosmic salt (NaNH₄HPO₄·4H₂O), or a yellow orange coloration produced when hydrogen peroxide is added to a test solution in hot, concentrated sulfuric acid containing ammonium sulfate. For quantitative determination, the pigment is dissolved or digested in sulfuric acid and the solution is reduced to Ti³⁺ with cadmium, zinc, or aluminum. The Ti³⁺ ions are then usually titrated with a standard solution of iron(III) ammonium sulfate solution, with potassium rhodanide as an indicator, or using potentiometric end point determination.

Impurities can be determined by wet analysis, X-ray fluorescence, or spectrographic analysis (e.g., atomic absorption).

Typical analysis figures for an untreated rutile pigment are TiO₂ 99.4%, K₂O 0.24%, P₂O₅ 0.21%, Fe₂O₃ 40 ppm, Sb₂O₃ 24 ppm, Al₂O₃ 20 ppm, Mg 5 ppm, Zn 3 ppm, Cr 2 ppm, Mn, Cu, Hg, Cd, Co, Ni, Se, Sn, Ag < 1 ppm.

Table 22.13: Consumption of TiO₂ pigments in 1987 (10³ t) [58].

Use	United States	Western Europe	Asia and Pacific	Rest of world	World total
Coatings	466	453	285	361	1565
Paper	259	91	24	49	423
Plastics	172	154	65	77	479
Other	54	82	109	60	305
Total	951	780	494	547	2772
Use per capita, kg	4.2	2.3	0.2	0.2	0.5

Table 22.14: Predicted percentage annual growth rates for use of TiO₂ (1986–1992) [103].

End use	United States	Western Europe	Asia and Pacific	Rest of world	World total
Coatings	1.0	1.0	4.5	2.0	1.5
Paper	2.5	2.0	2.0	1.5	2.5
Plastics	4.0	3.5	6.0	4.0	4.0
Other	0.5	1.0	1.0	2.0	1.0
Total	2.0	1.7	4.3	2.1	2.3

22.7.7 Uses of Pigmentary TiO₂

Titanium dioxide is used universally, having almost completely replaced other white pigments. Consumption figures for 1987 are given in Table 22.13 [58]. The greatest annual increase in use has been for coloring plastics (> 4%), followed by the coloring of paper (ca. 2.5%). Geographically, the increase in consumption of TiO₂ has been the greatest in Asia (Table 22.14).

Paints and coatings amount for the largest volume of TiO₂ production. The presence of the pigment enables the protective potential of the coating material to be fully exploited. As a result of continuing developments in TiO₂ pigments, coatings only a few micrometers thick fully cover the substrate. Commercially available pigments permit paint manufacture with simple dispersion equipment, such as disk dispersers. Organic treatment prior to steam jet micronization yields pigments with improved gloss properties and reduced gloss haze for

use in stoving enamels. Sedimentation does not occur when these products are stored, and they possess good lightfastness and weather resistance.

Printing Inks. Modern printing processes operate at coating thicknesses of $< 10 \mu\text{m}$, and therefore require the finest possible TiO_2 pigments. These very low film thicknesses are only possible with TiO_2 pigments that have a lightening (reducing) power seven times that of lithopone. Because of its neutral hue, TiO_2 is especially suitable for lightening (reducing) colored pigments.

Plastics. Titanium dioxide is used to color plastic packaging films $< 100 \mu\text{m}$ thick. This coloring is required by the customer to hide the packaged goods from view, and to allow the film to be printed for advertising and information purposes. Furthermore, TiO_2 pigments absorb UV radiation with a wavelength $< 415 \text{ nm}$ and thus protect the packaged goods from these harmful rays which could, for example, reduce the storage life of fat-containing food.

Fibers. Titanium dioxide pigments give a matt appearance to synthetic fibers, eliminating the greasy appearance caused by their translucent properties. Anatase pigments are used for this because their abrasive effect on the spinning operation is about one quarter that of the rutile pigments. The poor lightfastness of anatase pigments in polyamide fibers can be improved by treatment with manganese or vanadium phosphate.

Paper. In Europe, fillers such as kaolin, chalk, or talc are preferred as brightening agents and opacifiers in paper manufacture. Titanium dioxide pigments are suitable for very white paper that has to be opaque even when very thin (air mail or thin printing paper). The TiO_2 can be incorporated into the body of the paper or applied as a coating to give a superior quality ("art" paper).

Laminated papers are usually colored with extremely lightfast rutile pigments before being impregnated with melamine urea resin for use as decorative layers or films.

Other areas of application for TiO_2 pigments include the enamel and ceramic industries, the manufacture of white cement, and the coloring of rubber and linoleum.

Titanium dioxide pigments are also used as UV absorbers in sunscreen products, soaps, cosmetic powders, creams, toothpaste, cigar wrappers, and in the cosmetics industry. Their most important properties are their lack of toxicity, compatibility with skin and mucous membranes, and good dispersibility in organic and inorganic solutions and binders.

Electrically conducting TiO_2 pigments have been produced by an aftertreatment to give a coating of mixed oxides of indium and tin, or antimony and tin [110]. These pigments are applied to fibers used in photosensitive papers for electrophotography, and for the production of antistatic plastics.

22.7.8 Uses of Nonpigmentary TiO_2

A number of industrial products require TiO_2 starting materials with well-defined properties for a specific application. Some of the most important of these grades of titanium dioxide are those with a high specific surface area, a small particle size, and very high reactivity. Stringent requirements often exist regarding purity and property consistency. The world consumption of this nonpigmentary TiO_2 in 1990 was ca. 110 000 t and was broken down as follows:

Enamels ceramics	28 000 t
Glass, glass ceramics	26 000 t
Electroceramics	14 000 t
Catalysts and catalyst supports	10 000 t
Welding fluxes	10 000 t
Colored pigments (lightfast pigments)	9 000 t
Electrical conductors	5 000 t
Titanium boride and carbide	300 t
Potassium hexafluorotitanate	2 000 t
Optical glasses	1 000 t
Potassium titanate	1 000 t
Standard ceramics	500 t
Refractory coatings	200 t
UV-screening	100 t

The annual growth rate in these markets is expected to be a few per cent. Growth could be higher if catalysts for environmental protection become mandatory, or if rutile mixed-

phase pigments seem likely to replace other pigments thought to have toxic properties

Electroceramics. Titanates prepared from finely divided, high-purity TiO_2 hydrolysates are used in capacitors and piezoelectric materials. The specifications of the TiO_2 starting materials with respect to purity, reactivity, and sintering properties are expected to become more stringent.

Catalysts. The main area of application for TiO_2 is in catalysts for the removal of nitrogen oxides from waste gases from power stations and industry. The nitrogen oxides in the waste gas are reacted with ammonia in the presence of oxygen on the catalyst to form nitrogen and water (Selective Catalytic Reduction) [111]. The first equipment of this type is now in operation in Germany and Japan. Increasing demand is expected following reductions in permitted levels of emission, the spread of these ideas to other countries, and maintenance requirements during operation. In addition to TiO_2 the catalysts usually contain ca. 10% tungsten oxide and ca. 1% V_2O_5 , and are extruded into a honeycomb shape. The TiO_2 has high specifications with respect to purity, particle size, and porosity to ensure that the desired catalytic activity is obtained.

Mixed Metal Oxide Pigments. The starting material is a TiO_2 hydrolysate, which is calcined with oxides of transition metals to form chromium rutile or nickel rutile pigments. Depending on the particle size, pigments with various shades of yellow are produced. These pigments should have considerable growth potential on account of their quality and environmental safety.

UV Absorption. Finely divided TiO_2 pigments are used as sunscreens in the cosmetic industry. Intensive research work is in progress worldwide aimed at utilizing the photoactivity of TiO_2 . Titanium dioxide catalyzes the decomposition of organic compounds in wastewater; water is decomposed into hydrogen and oxygen in the presence of sunlight.

22.7.9 Toxicology

Titanium dioxide is highly stable and is regarded as completely nontoxic. Investigations on animals which have been fed TiO_2 over a long period give no indication of titanium uptake [112]. Absorption of finely divided TiO_2 pigments in the lungs does not have any carcinogenic effect [113].

22.7.10 Rutile Mixed Metal Oxide Pigments

The rutile (TiO_2) lattice offers considerable scope for variation [114]. In this lattice, titanium ions are surrounded by six neighboring oxygen atoms at the corners of a regular, but slightly distorted octahedron. Colored pigments may be obtained by substituting transition-metal ions for the titanium ions [115]. If the colored cation substituent is not tetravalent, another cation of appropriate valency must be substituted into the rutile lattice to maintain an average cation valency of four.

H. II. SCHAUMANN prepared the first mixed-phase rutile pigments by incorporating nickel oxide and antimony oxide into rutile to give a yellow pigment, and cobalt and antimony oxides to give an ochre pigment [116]. Other rutile mixed metal oxide phases were first used as ceramic colorants (e.g., with chromium-tungsten, brown [117]) or for coloring porcelain enamels (e.g., with copper-antimony, lemon yellow; manganese-antimony, dark brown; iron antimony, gray [118]; and vanadium-antimony, dark gray). In commercial mixed-phase rutile pigments, between 10 and 20 mol% of the titanium ions are replaced by substituent metal ions.

Nickel and chromium mixed-phase rutile pigments are industrially important. When nickel and chromium are substituted into the rutile lattice, higher valency metals (e.g., antimony, niobium, or tungsten) must also be substituted to maintain an average valency of four.

Nickel rutile yellow, C.I. Pigment Yellow 53:77788, is a light lemon yellow pigment with the approximate composition

($\text{Ti}_{0.85}\text{Sb}_{0.10}\text{Ni}_{0.05}\text{O}_2$). Antimony can be replaced by niobium without any appreciable change in color [119].

Chromium rutile yellow pigments, C.I. Pigment Brown 24:77310, usually contain antimony to balance the valency. Their composition is approximately ($\text{Ti}_{0.90}\text{Sb}_{0.05}\text{Cr}_{0.05}\text{O}_2$). Depending on particle size, the color varies from light to medium ochre (buff). Stability towards plastics at high temperature is considerably improved by the incorporation of small quantities of lithium [120] or magnesium [121]. If antimony is replaced by tungsten, the products become darker in color, whereas replacement by niobium leaves the color unchanged.

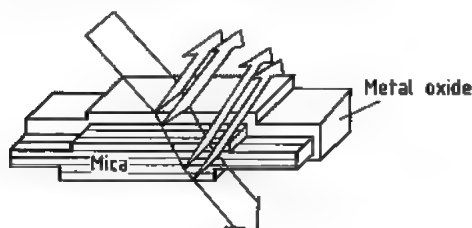


Figure 22.7: Simplified scheme of light reflection at the phase boundaries of a metal oxide-mica pigment.

22.7.11 Titanium Dioxide-Mica Pigment [122-127]

The dominant class of nacreous pigments is based on platelets of natural mica coated with thin films of transparent metal oxides (Figure 22.7). Mica minerals are sheet layer silicates. Nacreous pigments are usually based on transparent muscovite but some are based on dark brown phlogopite. Although muscovite occurs worldwide, few deposits are suitable for pigments; it is biologically inert and approved for use as a filler and colorant.

Selection and workup of the mica substrate are two of the key factors which determine the quality and appearance of nacreous pigments [124-127]. The aspect ratio of the final pigment depends on the particle size distribution of the mica platelets which have a thickness of 300-600 nm and various diameter ranges (e.g., 5-25, 10-50, 30-110 nes of the metal oxide-coated mica and scattered from the

edges, brilliance and hiding power are inversely related to each other.

A mica pigment coated with a metal oxide has three layers with different refractive indices and four phase boundaries P_1 - P_4 : (P_1) TiO_2 (P_2) mica (P_3) TiO_2 (P_4) (Figure 22.8). Interference of light is generated by reflections of all six combinations of phase boundaries, some of which are equal: $P_1P_2 = P_3P_4$, $P_1P_3 = P_2P_4$, P_1P_4 and P_2P_3 . The thickness of the mica platelets varies in accordance with a statistical distribution. Consequently, interference effects involving the phase boundaries between the mica substrate and the oxide coating add together to give a white background reflectance. The interference color of a large number of particles therefore depends only on the thickness of the upper and lower metal oxide coating layers [122-127].

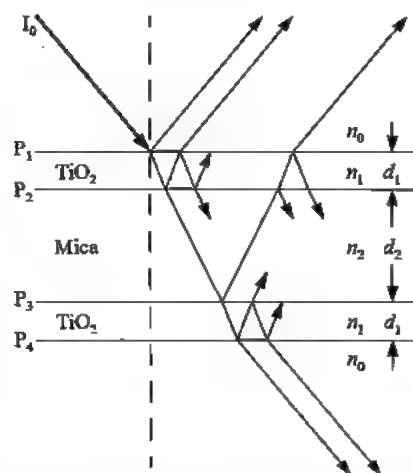


Figure 22.8: Multilayer, thin-film pigment consisting of a TiO_2 coating (high n_1) surrounding a mica platelet (low n_2). The four phase boundaries (P_1 - P_4) are indicated.

The development of the mica-based pigments started with pearlescent colors (Figure 22.9A, TiO_2 -mica). It was followed by brilliant, mass-tone-colored combination pigments (i.e., mica, TiO_2 , and another metal oxide) with one color (interference color same as mass tone) or two colors (interference and mass tone different) that depend on composition and viewing angle (Figure 22.9B). In the 1980s further development was made by coat-

ing mica particles with transparent layers of iron(III) oxide (Figure 22.9C).

The first multilayer pigments were marketed in the 1960s as TiO_2 -coated muscovite

micas [122-127]. Two different processes are used for coating mica in aqueous suspension on a commercial basis:

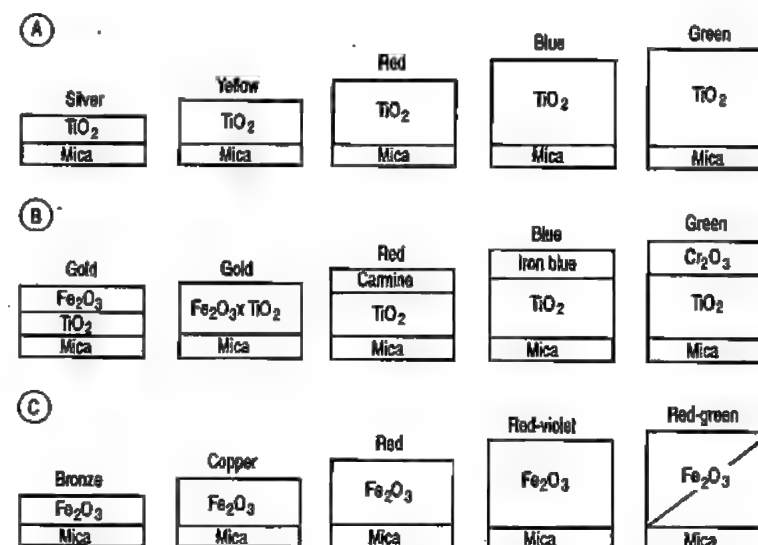


Figure 22.9: Upper half of metal oxide-mica pigments. Increasing layer thickness of metal oxide causes different interference colors in reflection. Combination with absorption colorants (e.g., Fe_2O_3) produces metallic effects. A) Interference colors; B) Combination pigments; C) Metallic colors.

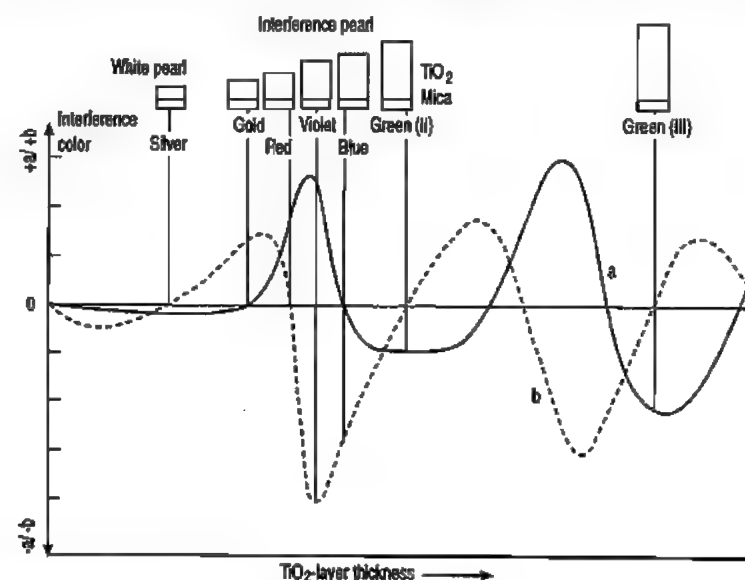
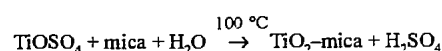
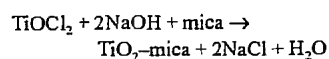


Figure 22.10: Experimental dependence of interference colors on the TiO_2 layer thickness on mica expressed in the Hunter $L a b$ scale (a, b only).

● Homogeneous hydrolysis (sulfate process)

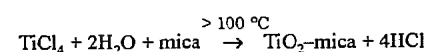


● Titration (chloride process)



The pigments are then dried and calcined at 700–900 °C. The titration process is preferred for interference pigments with thick TiO₂ layers because it is easier to control.

Chemical vapor deposition in a fluidized bed has also been proposed [128, 129]:



Only the TiO₂ anatase crystal modification is formed on the mica surface. Small amounts of SnO₂ are therefore used to catalyze conversion to the rutile structure with its higher refractive index, brilliance, color intensity, and superior weather resistance.

The sequence of interference colors obtained with increasing TiO₂ layer thickness agrees with theoretical calculations in the color space. An experimental development of *L a b* values is given in Figure 22.10.

TiO₂-mica pigments are used in all color formulations of conventional pigments where brilliance and luster are required in addition to color, i.e., in plastics, coatings, printing, and cosmetics. The major market for silver white pigments (pearl pigments, “white metallic”) is the plastics industry.

One possibility for attractive combination pigments is the coating of TiO₂-mica pigments with an additional layer of an inorganic or organic colorant. The thickness of the TiO₂ layer is decisive for the brilliance or interference effect under regular viewing conditions whereas the transparent colorant dominates at all other viewing angles. A deep, rich color with a luster flop at all angles is attained for the case that colorant and interference color are matched. If interference color and masstone of the colorant are different, a color flop (two-tone pigments) is seen in addition to the luster flop.

Iron(III) oxide is the most important metal oxide for combination with titanium dioxide on mica flakes. Brilliant golden pigments result which can be applied for several purposes. Two routes are used to synthesize these pigments, and different structures are formed [122, 124, 125, 127]. In the first case, a thin layer of Fe₂O₃ is coated on the surface of a TiO₂-mica pigment. The overall interference color is the result of both metal oxide layers. The masstone is determined by the Fe₂O₃ layer, and interesting gold pigments (e.g., reddish gold) are possible. In the second case, coprecipitation of iron and titanium oxide hydroxides on mica particles and calcination leads to greenish gold pigments.

Coating of TiO₂-mica pigments with an organic colorant for a masstone or two-tone pigment is done by precipitation or deposition on the pigment surface in aqueous suspension, assisted by complexation or surfactants. A second route is fixing the colorants as a mechanically stable layer using suitable additives.

Solid state reactions and CVD process enlarge the possibilities for the synthesis of modified TiO₂-mica pigments. In addition, the calcination of the materials in the presence of inert (e.g., N₂, Ar) or reactive gases (e.g., NH₃, H₂, hydrocarbons) allows the formation of phases which are not producible by working in air. Table 22.15 contains examples for TiO₂-mica-based pearlescent pigments with special coloristic properties.

Titanium dioxide-mica pigments have been developed at first only because of their excellent coloristical properties. Meanwhile, they are also interesting for functional uses. In coatings with a high content of platelet fillers, an advantageous overlapping roof-tile type arrangement is possible that provides close interparticle contact, barrier effects, and dense covering. The composition of the oxide layer on the mica surface and its thickness are always responsible for the physical properties like IR-reflexivity or laser markability. So TiO₂-mica pigments can be used for IR-reflecting plastic sheets [135] (e.g. for domed

and continuous rooflights) or for laser marking of plastics and coatings [133].

Table 22.15: Examples for mica-based pearlescent pigments with special coloristic properties.

Pigment composition	Preparation	Remarks	Ref.
TiO _{2-x} /TiO ₂ /mica	TiO ₂ /mica + H ₂ (Ti, Si) grey, <i>T</i> > 900 °C (solid-state reaction)	blue-grey	[130]
TiO ₂ N ₂ /TiO ₂ /mica	TiO ₂ /mica + NH ₃ , <i>T</i> > 900 °C (solid-state reaction)	grey, blue-grey	[131]
FeTiO ₃ /TiO ₂ /mica	Fe ₂ O ₃ /mica + H ₂ , <i>T</i> > 600 °C (solid-state reaction)	grey (ilmenite pigments)	[132]
TiO ₂ /C/mica	TiOCl ₂ + C + mica (precipitation) calcination under N ₂	silver-grey, interference colors (carbon inclusion pigments)	[133]
BaSO ₄ /TiO ₂ /mica	Ba ²⁺ + SO ₄ ²⁻ + TiOCl ₂ + mica (precipitation)	low luster pigments	[134]

22.7.12 Transparent Titanium Dioxide

Titanium dioxide can also be produced with a primary particle size of 10–30 nm, and hence shows transparent properties. Microcrystalline titanium dioxide was first mentioned in Japanese patents in 1978.

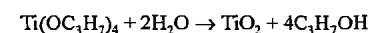
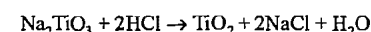
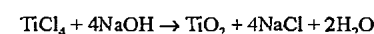
The use of micro titanium dioxide as a white pigment is limited because its light scattering is very low due to the very fine crystal size, which means that the coloring effect of conventional TiO₂ is lost. The physical properties changed significantly; there is strong UV light absorption. Consequently, such fine-particle TiO₂ is used as an UV light absorbing additive:

- for cosmetics, mainly for sunscreen formulations because of its effective UV protection over the UVC, UVB, and UVA spectrum [136];
- for automotive paints, especially in combination with aluminum flakes giving a pearlescent-like appearance; the color flop depends on the concentration of the micro

titanium dioxide in the formulation [137, 138];

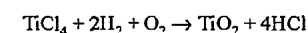
- for clear coats and wood varnishes to protect the base due to its transparency and its property to absorb UV light;
- for plastics to improve the UV durability of the polymer films itself as well as to protect UV-sensible foodstuff in plastic wrapping [139];
- as heat stabilizers in silicon rubber, as catalysts for hydrogenation [140] and oxidation [141] as well as for surface protective films for furniture and optical material [142].

Microfine TiO₂ can be obtained mainly with rutile structure by different manufacturing routes which depend on starting materials used:



The process steps include precipitation, neutralisation, filtration and washing, drying, and micronisation. Due to its small particle size the transparent titanium dioxide has a high photoactivity. To reduce this and in order to get a better weatherfastness the fine particles are coated with various combinations of inorganic oxides (e.g., silica, alumina, zirconia, iron) before drying in a similar way as that used for the conventional titanium dioxide.

Microfine TiO₂ with predominant anatase structure can also be manufactured by reductive flame hydrolysis of TiCl₄ at < 700 °C [143]:



Worldwide consumption is increasing and estimated at 1300 t/a.

Trade names include Titanium Dioxide P25 (Degussa, Germany), Hombitec RM Series (Sachtleben Chemie, Germany), and Micro Titanium Dioxide MT-Series (Tayca, Japan). Transparent titanium dioxide is also produced by Ishihara (Japan) and Kemira Oy (Finland).

22.8 Production of Titanium Tetrachloride

Titanium metal is produced exclusively by reduction of titanium tetrachloride, which is manufactured from natural rutile or from the so-called synthetic rutile obtained from ilmenite or from the TiO_2 -rich slag produced by metallurgical treatment of ilmenite (ore preparation, production of TiO_2 -rich slags, and production of synthetic rutile are described in Section 22.7.2).

The TiO_2 produced for the pigment industry by treatment of ilmenite with sulfuric acid is unsuitable as a starting material for production of the metal because of the impurities present. Also, titanium white (TiO_2) is increasingly produced from TiCl_4 . At the present time, approximately one-third of TiO_2 world production (2.1×10^6 t/a) is produced by the chloride process. Over 95% of the total quantity of titanium minerals extracted worldwide is used to produce TiO_2 pigment, and only ca. 4% for titanium metal.

In spite of the wide distribution of titanium minerals, the mining of rutile-containing ores is mainly concentrated on Australia, from which 90% of world production comes. Other important producing countries are Sierra Leone and South Africa. The most important ilmenite-producing countries are Australia (one-third of total world production) and Norway, the United States, and the Ukraine, while the leading producers of titanium slag from ilmenite are Canada and South Africa.

Chlorination of titanium dioxide is now carried out almost exclusively by the fluidized-bed process. In the discontinuous fixed-bed process, which is now hardly used, rutile concentrate (> 96%) is mixed with 20–25% petroleum coke and a binder (wood tar, asphalt, etc.), sometimes with added catalysts (e.g., MnO_2), and briquetted [144]. The briquettes are stacked in the lower part of a brick-lined chlorination tower over a layer of carbon which acts as an electrode, and are reacted with chlorine at 500–850 °C. The chlorine gas is heated to ca. 1000 °C by the resistance-

heated carbon bed and then reacts exothermically with the rutile and carbon in the briquettes.

The process can also be carried out in two stages, in the first of which rutile is reduced by carbon at 1200–1400 °C to give titanium carbide and titanium monoxide. The latter reacts with chlorine more readily than rutile.

Since ca. 1950, chlorination has been carried out almost exclusively by the fluidized-bed process because of its higher reaction rate and improved heat transfer, and also because of the shortage of briquetting facilities. Also, higher temperatures (ca. 1000 °C) can be achieved. After the reaction has started at ca. 600 °C no further external heat supply is necessary. Apart from the benefit of continuous operation, fluidized-bed chlorination has the further advantage of being less sensitive to impurities in the rutile or the carbon. The conversion of chlorine is 95–100%, of rutile titanium 90–95%, and of carbon 95%.

Ilmenite is now less often used as starting material, because of excessive chlorine consumption due to formation of iron(III) chloride for which there is little demand and from which chlorine can only be recovered at high cost. Furthermore, in spite of its higher boiling point, FeCl_3 is entrained by the TiCl_4 vapor and is deposited in the coolers as a powder, its solubility in liquid TiCl_4 being only 0.03% [145].

In contrast to the ilmenite-treatment process, the treatment of TiO_2 -rich slags containing < 10% iron is increasing in importance: As these materials contain lower oxides of titanium, they react with chlorine at lower temperatures and require less carbon than rutile [146]. However, compared with rutile, problems are caused by the higher iron content of these slags and their alkaline earth metal content. Calcium and magnesium are converted to their chlorides, which are molten at the reaction temperature and coat the surface of the briquettes in the fixed-bed process, preventing chlorine from penetrating. In the fluidized-bed process, the continuous addition of an inert bed (sand) can give good gas distribution and dilution of the chlorides, so that with continu-

ous removal of residues, slags containing up to 6% calcium or magnesium can be treated.

The use of other reducing or chlorinating agents (CO , COCl_2 , CCl_4 , sulfur chlorides) and other methods of producing TiCl_4 has not achieved industrial importance. For example, the electrolysis of a chloride melt using titanium carbide anodes has been proposed [147]. The most promising process seems to be to digest ilmenite with sulfuric acid and precipitate potassium hexachlorotitanate from the sulfate solution after removal of iron. On heating, this decomposes to form TiCl_4 vapor and KCl , which is returned to the process [148].

Separation and Purification of Titanium Tetrachloride. In the chlorination of rutile, the reaction products are gaseous, consisting of TiCl_4 and CO , with small amounts of CO_2 , phosgene (COCl_2), and other metal chlorides.

The gases leaving the chlorination reactor are cooled by heat exchangers and by spraying with titanium tetrachloride, and the iron(III) chloride that precipitates at 150 °C is scrubbed out by the TiCl_4 [149]. Further cooling causes the titanium tetrachloride to condense. The yellow filtered product contains 94% TiCl_4 , ca. 4% solid constituents such as rutile, carbon, sulfur, and insoluble metallic chlorides, and 2% soluble metal oxide chlorides. The chlorides include SiCl_4 and SnCl_4 (low-boiling substances), VOCl_3 which has a similar boiling point (127 °C) to TiCl_4 (136 °C), and FeCl_3 and AlCl_3 , which have higher boiling points. Other high-boiling chlorides, e.g., of calcium, manganese, magnesium, and sodium, produce unwanted deposits in the equipment.

To purify TiCl_4 (Section 22.7.3.2 and Figure 22.11), the solid constituents are first allowed to settle out. Small amounts of water are added to precipitate aluminum as its oxide chloride. SiCl_4 and SnCl_4 are removed by distillation at < 136 °C. H_2S is passed in and copper powder is added at 90 °C to reduce VOCl_3 to VOCl_2 , which precipitates. FeCl_3 and AlCl_3 distil at > 136 °C. Unsaturated organic compounds, especially oleic acid, promote good

separation of chromium and vanadium oxychlorides [150].

Dissolved chlorine can be removed by simply heating or by heating with metal powders (iron, copper, or tin). Purification with H_2S can also be carried out continuously in a fluidized bed of silica sand or iron sulfide at 140–300 °C. The impurities then form solid products which can be continuously removed from the fluidized bed.

The purified titanium tetrachloride contains only 0.002% V_2O_5 , and is fractionally distilled to remove residual phosgene and SiCl_4 . The purity of the TiCl_4 is 99.9% min.

22.9 Production of Titanium Sponge

The large heat of formation of titanium dioxide (945.4 kJ/mol) combined with the high solubility of oxygen in titanium at high temperatures has so far made it impossible to develop an economic process for the direct reduction of titanium dioxide to low-oxygen titanium metal. The standard industrial processes for the production of titanium metal are therefore based on titanium halides.

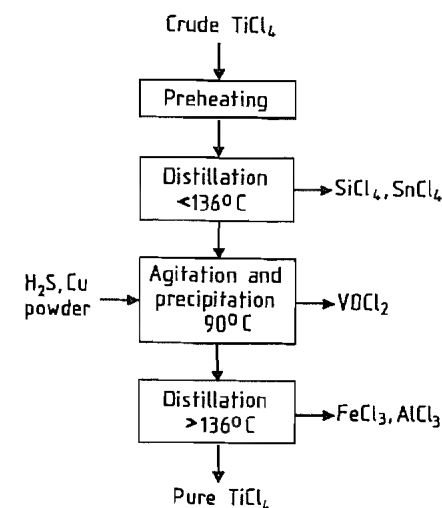


Figure 22.11: Purification of crude titanium tetrachloride.

22.9.1 Reduction of Titanium Dioxide

The reduction of titanium dioxide by carbon is only possible above 6000 °C. Using carbon-containing reducing agents, some titanium carbide is formed, even in high vacuum [151, 152]. Reduction by hydrogen in the presence of inert gases leads to mixtures of lower oxides [153]. A more complete reduction of titanium dioxide is only possible with alkaline earth metals, whereby reduction with calcium gives the lowest oxygen content [154]. Using reactions at temperatures of 600–1200 °C in a vacuum followed by dissolution of excess calcium and calcium oxide in hydrochloric acid, an oxygen content of 0.1–0.3% in the titanium is obtained [155]. Reduction with calcium hydride at 600–700 °C gives titanium hydride, which decomposes at 900 °C into titanium (containing 0.2% oxygen) and hydrogen [156].

22.9.2 Reduction of Titanium Halides

When TiCl_4 is reduced with hydrogen in an electric arc, subchlorides are formed in side reactions, and this reaction is consequently uneconomic on an industrial scale [157]. The reduction of TiCl_4 with calcium is strongly exothermic [158], but this reaction also has not been used commercially.

Reduction of Titanium Tetrachloride with Sodium. In 1910, HUNTER succeeded in producing larger quantities of pure titanium by reacting titanium tetrachloride with sodium in an evacuated steel bomb [159].

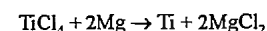
The Degussa process uses a mixture of oxide-free sodium and potassium at 700–800 °C. To prevent overheating (sodium chloride *mp* 797 °C, sodium *bp* 877 °C), molten sodium chloride is first placed in the reactor [160]. Finely powdered sodium chloride at 200–620 °C can also be used. Molten sodium is then fed into the reactor from above, and TiCl_4 is blown in from below, together with the inert gas [161].

In industrial plant molten sodium and TiCl_4 are fed simultaneously into a steel reactor filled with argon, heated to 650 °C. After the reaction has begun, the temperature can rise to 900 °C. When reaction is complete, more sodium is added and the temperature is raised to 950 °C.

In the two-stage process, TiCl_4 is first converted at 235 °C into low-melting sodium titanium chloride compounds and titanium(II) chloride, and is then reduced to titanium and sodium chloride in a second reactor after further addition of sodium. This technique distributes the heat of reaction, and the process is therefore more easily controlled. After size reduction of the reaction product, the NaCl is dissolved in water, and the titanium sponge left behind is centrifuged off and dried.

The Hunter process has been almost completely superseded by the Kroll process. Industrial scale plants are currently only operated in China [162].

Reduction of Titanium Tetrachloride with Magnesium (Kroll Process). The reduction of titanium tetrachloride with magnesium



was discovered by KROLL [158, 163], and was developed into an industrial process by the Bureau of Mines in Boulder City, Nevada [164]. Magnesium boils at 1120 °C, and magnesium chloride melts at 711 °C. The resulting temperature range and the high purity of magnesium are advantageous for the industrial production of titanium sponge from TiCl_4 .

The reactor is constructed of plain carbon steel, chromium–nickel steel, and the interior walls are cleaned by brushing, or are titanium coated. The reactor is charged with oxide-free lumps of magnesium and filled with argon, and the magnesium is melted at 651 °C (Figure 22.12). When the temperature reaches 700 °C, purified TiCl_4 is run in slowly from above or blown in as a vapor, such that a reaction temperature of 850–950 °C is established. The titanium sponge is deposited on the reactor walls and forms a solid cake above the molten magnesium. The molten MgCl_2 collects beneath the magnesium and is drawn off.

The magnesium rises through the porous cake to its surface by capillary action, and reacts there with the gaseous TiCl_4 .

The temperature must not exceed 1025 °C, to prevent reaction between the titanium and the iron of the reactor, although titanium can pick up iron even below 950 °C. The amounts of TiCl_4 reacted are 10–15% substoichiometric amount, as some of magnesium and MgCl_2 remain in the titanium sponge. However, an excess of TiCl_4 leads to the formation of lower titanium chlorides and iron chlorides, which increases the iron content of the titanium sponge.

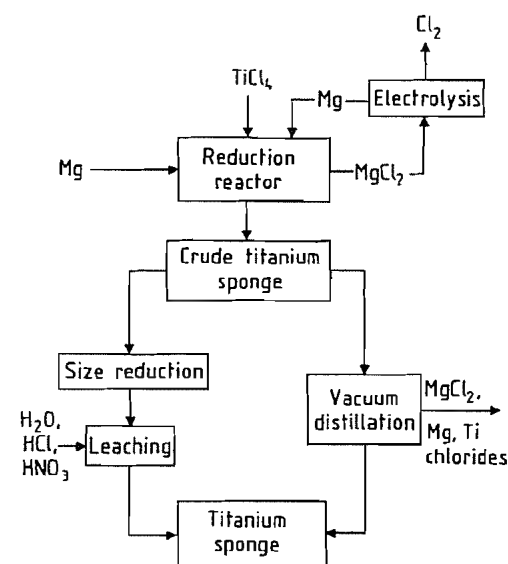


Figure 22.12: Reduction of titanium tetrachloride to titanium sponge by the Kroll process (reduction with magnesium).

The temperature range that can be used in practice is 850–950 °C, the lower temperatures giving longer reaction times but purer titanium sponge. After the molten MgCl_2 has been removed and the temperature of the reactor contents has fallen below 200 °C, the reaction vessel is opened in a dry room (MgCl_2 and titanium chloride are hygroscopic).

The crude titanium sponge is generally purified by vacuum distillation; leaching is now rarely used. Around 98% of titanium sponge produced is vacuum distilled. Immediately af-

ter completion of the reaction a vacuum hood usually is attached to the reduction reactor. At ca. 0.1 Pa (10^{-3} mbar) and 900–1000 °C, the metal chloride impurities, mainly magnesium and titanium chlorides, are distilled off together with magnesium metal while the titanium sponge remains behind.

In the leaching process, the size-reduced sponge is treated with a hot mixture of hydrochloric and nitric acids (8% HCl, 3% HNO₃) in tanks or in an inclined rotating titanium drum containing an Archimedean screw. Because of the heat of solution of the MgCl_2 , cooling must be provided to prevent the temperature from exceeding 25 °C. During leaching, the titanium sponge picks up hydrogen, which can be removed by melting in a vacuum electric-arc furnace with a high-performance vacuum pump.

The process of drilling out the crude sponge from the reactor can be avoided by using a perforated crucible if the level of the molten magnesium is maintained above the perforated base [165]. Removal of the sponge from the perforated crucible can be facilitated by facing it with stainless steel or high-carbon steel sheet.

The reduction reactors, usually gas heated, have titanium sponge capacities between 1.5 and 10 t. Production of 1 kg titanium sponge theoretically requires 3.96 kg TiCl_4 and 1.015 kg magnesium, 3.975 kg MgCl_2 being formed. However, in practice, only 65–70% of the magnesium takes part in the reduction process. Most of the remainder is recovered in vacuum distillation, whereas it is lost in the leaching process. The magnesium is recovered from MgCl_2 electrolytically. The proportion of the titanium sponge that can be used for the production of titanium metal is 75–85%, and the total titanium yield is ca. 98%. The energy consumption is 30 kWh/kg titanium sponge. The reduction process takes ca. 95 h, and the distillation ca. 85 h.

Variants of the Kroll process, so far not used industrially, are aimed at giving better separation of the sponge from the MgCl_2 and at achieving continuous operation. For example, in a ram reactor the sponge is compressed

by a ram and is ejected as compact metal from the magnesium chloride bath [166].

The reduction can be carried out under vacuum instead of in an argon atmosphere, and the magnesium chloride can be distilled off immediately after completion of the reaction [167].

The simultaneous injection of TiCl_4 vapor and magnesium vapor into a reactor packed with titanium netting at 800–1100 °C and ca. 10^{-2} Pa produces pure titanium, which grows as crystals on the netting, while the by-products (Mg vapor and MgCl_2 vapor) distil off [168].

In Japan, a quasi-continuous process is being developed in which the distillation of TiCl_4 , Mg, and MgCl_2 and the melting of a titanium block are performed simultaneously [169]. A production of ≥ 500 t titanium sponge per furnace per month is expected.

Comparison of the Sodium and Magnesium Reduction Processes. Both methods are used industrially and produce titanium sponge of sufficiently high purity. Their advantages and disadvantages are as follows:

Sodium has a lower melting point than magnesium and can therefore be transported in the molten state. Reduction with sodium requires only the theoretical quantity, whereas ca. 130% of the stoichiometric quantity of magnesium is required. With sodium reduction, the titanium sponge is more easily removed from the reactor, as NaCl collects on the reactor walls, while in the Kroll process the sponge builds up on the reactor walls. Sodium chloride is soluble in water and is therefore easily removed from the titanium sponge. This is a more economic method than vacuum purification of the titanium sponge produced by magnesium reduction. The density of magnesium-reduced sponge is 1.0–1.2 g/cm³, (sodium-reduced sponge 0.7–0.9 g/cm³) and it has larger particles than sodium-reduced sponge, which contains a high proportion of fines. Typical figures for the chemical composition of various types of sponge produced by both processes are listed in Table 22.16. This titanium from the Kroll process has a lower

average oxygen content and that from the sodium reduction process, a lower average iron content. The highest purity achieved in the Kroll process so far is reported to be 99.999% [169].

The costs of reduction with sodium are usually ca. 10% lower than reduction with magnesium, although the economics of the Kroll process can be improved by using larger reduction reactors, improved vacuum distillation, and higher capacity electrolysis cells for recovery of magnesium. In both cases, batch operation is a disadvantage.

The sponges produced by different processes of chemical reduction, size reduction, and purification differ in hardness, lump size, density, and compressibility, but all are equally suitable for melting into ingots. Therefore, the reasons for selecting a particular reduction process are mainly economic, e.g., availability and reprocessing of reduction metals, energy costs, and capital costs.

In 1995, ca. 98% of world titanium-sponge production was by the Kroll process.

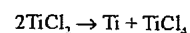
Reduction of Titanium Tetrafluoride. Titanium tetrafluoride is easily produced from titanium dioxide and hydrogen fluoride, can be readily purified by sublimation, and, in contrast to titanium tetrachloride, titanium tetrafluoride can also be reduced by silicon. The high-purity titanium so produced contains only 0.009% silicon [170].

22.9.3 Thermal Decomposition of Titanium Halides

The oldest process of this type is that of VAN ARKEL and DE BOER in which titanium tetraiodide is decomposed on electrically heated tungsten wires at 1000 °C. If wires or single crystal fibers of titanium are used, tungsten-free titanium of the highest purity can be obtained (as a single crystal in the latter case). The iodine liberated is reacted with crude titanium to regenerate titanium tetraiodide in the same vessel below 200 °C or above 500 °C. Above 200 °C lower titanium iodides (TiI_2 , TiI_3) are formed, which only act as titanium

carriers above 500 °C because of their low volatility [171]. The process enables titanium of the highest purity to be produced from crude titanium or titanium scrap.

Very high purity titanium can also be obtained by thermal disproportionation of titanium(II) chloride or bromide. By passing TiCl_4 vapor over titanium-containing material (titanium scrap, crude titanium, or titanium alloys) at 950–1500 °C, TiCl_2 vapor is formed, which condenses and is decomposed at ca. 1000 °C



The TiCl_4 is fed back to the process [172].

22.9.4 Electrowinning of Titanium

The high affinity of titanium for oxygen and hydrogen together with its electrode potential ($\text{Ti}/\text{Ti}^{2+} = -1.75$ V) prevents its deposition from aqueous solution [173]. Hence only molten salt electrolysis can be used.

Titanium dioxide is almost insoluble (0.07–0.02%) in molten chlorides of alkali metals and alkaline earth metals. It is soluble (ca. 8%) in sodium and potassium fluorides and in potassium hexafluorotitanate (ca. 14%) [174]. However, attempts to electrolyze the oxide in halide melts (in analogy to aluminum production) only produced lower titanium oxides [175]. Thus only titanium halides are suitable starting materials for molten salt electrolysis.

Titanium tetrafluoride combines with alkali metal and alkaline earth metal fluorides to form complex hexafluorotitanates. These compounds decompose below their melting

points with vaporization of titanium tetrafluoride. They can only be used in molten salt electrolysis as components of a low-melting molten salt bath containing other diluent salts [176]. Special problems arise in molten salt electrolysis with graphite electrodes due to the anode effect. Although this can be counteracted by controlled addition of oxides to the salt bath, oxygen pickup by the titanium metal produced must be prevented by using low temperatures, by separating the anode space from the cathode space, and by avoiding turbulence in the electrolyte [177].

Although **titanium tetrachloride** is insoluble in molten alkali and alkaline earth metal chlorides, stable molten electrolytes can be obtained by using lower titanium chlorides. These can be produced directly from titanium tetrachloride in the electrolytic cell, but they react with the chlorine liberated at the anode to reform titanium tetrachloride, which then evaporates. This can be avoided by using a porous, basket-shaped cathode into which the titanium tetrachloride is fed, as the electrolyte (e.g., an NaCl–SrCl₂ eutectic) can then be kept free of lower titanium chlorides [178, 179].

The problems of electrolyte composition and the anode effect can be completely solved by using soluble anodes, as in this case no changes to the electrolyte occur and no gas is emitted at the anode, at least at low current densities [180]. Soluble anodes can be made of crude titanium, titanium scrap, and titanium compounds such as titanium carbide, sometimes mixed with titanium monoxide [181, 182] and titanium nitride [183], which can be produced directly from titanium ores.

Table 22.16: Chemical composition (in %) of titanium sponge.

Reduction process	Maximum hardness (Brinell)	C	N	O	H	Fe	Mg	Na	Cl
Magnesium	95	0.006	0.003	0.045	0.002	0.02	0.03		0.10
	100	0.08	0.05	0.5	0.002	0.04			0.09
	110	0.08	0.05	0.6	0.002	0.05	0.03		0.08
	120	0.08	0.05	0.7	0.002	0.06	0.03		0.09
Sodium	120	0.009	0.004	0.07	0.01	0.016		0.08	0.13
Electrolysis	60	0.003	0.002	0.01	0.003	0.001			0.08
	75	0.013	0.004	0.03	0.004	0.0040.0			0.09
	90	0.018	0.004	0.04	0.004	20			0.16

Semitechnical plants using processes analogous to the production of magnesium from magnesium chloride can operate at 900 °C under argon, using TiCl_4 and NaCl as starting materials. The NaCl fed into the cathode space is decomposed, and the sodium liberated reduces the TiCl_4 (which is fed in later) stepwise via TiCl_3 , TiCl_2 , and TiCl to give titanium. The energy consumption is only 40% of that required for the reduction of TiCl_4 with magnesium (ca. 43 kWh/kg) [184].

All electrolytic processes yield a very pure metal (> 99% titanium), but have the disadvantage that the titanium is produced at the cathode in the form of poorly adhering dendritic crystals. The cathodes must be lifted out of the molten electrolyte and cooled in an inert atmosphere. The titanium metal is then scraped off and removed from the electrolytic cell through an air lock.

A production plant, now shut down, to produce titanium sponge electrolytically operated at 520–650 °C with an electrolyte consisting of a mixture of LiCl and KCl of approximately eutectic composition and with TiCl_4 as the raw material. The titanium concentration in the electrolyte is ca. 1.5%. The TiCl_4 is fed through a steel tube into the molten electrolyte in a metal crucible. The graphite anode is surrounded by a wire mesh coated with cobalt or nickel. Metallic titanium is deposited on steel cathodes. After size reduction, dissolution of the salt in 0.5% hydrochloric acid, washing, and drying, the titanium yield is ca. 98% [185].

A number of attempts have been made to produce titanium by electrolytic processes on an industrial scale but none have led to permanent application [162].

22.10 Processing and Reuse of Scrap Metal

With increasing titanium production, the use of titanium scrap as a raw material instead of titanium sponge has become increasingly important. Titanium scrap is produced during the production of semifinished products, their

processing to finished products, and the scraping of used equipment. Before remelting, titanium scrap must be pretreated. Adhering scale and other residues must be removed from the surface by abrasive blasting, pickling, or surface grinding. The various alloys must be sorted so that the alloy added to the melt is of consistent quality. Depending on the melting process, the scrap may be mixed with the sponge and compressed, or may be welded together for addition in the form of a consumable electrode. Alternatively, it can be directly added to the melt in small pieces. In another process, ground, hydrogenated titanium scrap is used instead of titanium sponge for melting to obtain titanium.

Untreated titanium scrap is used as an additive to steel, nickel, aluminum, copper, and zinc alloys, and in the production of master alloys such as ferrotitanium.

In the United States, ca. 40% of titanium consumption is from processed titanium scrap. In Europe, due to the low price of titanium sponge only 10–30% is accounted for by scrap [186, 187].

22.11 Processing of Titanium Sponge

Melting Processes. Titanium reacts in the molten state with air and with all the conventional crucible materials. Melting is therefore only possible under vacuum or in an inert gas atmosphere in cooled metal crucibles of high thermal conductivity, usually copper. The crucible walls are cooled with water or molten sodium–potassium alloy. The energy source is chiefly an electric arc, although to an increasing extent the metal is melted by a plasma, by electron beams, or, on the laboratory scale, by induction.

On the industrial scale, vacuum arc furnaces are generally used, with consumable electrodes made of titanium sponge, titanium scrap, and alloy components. Vacuum arc furnaces with rotating water-cooled copper electrodes are only used for first stage melting.

To produce consumable electrodes, titanium sponge, sometimes mixed with scrap and alloying components, is compressed to form electrode pieces, which are welded into electrodes, by plasma or MIG welding. Large pieces of scrap can also be welded together to form electrodes.

The melting of the electrode (negative pole) takes place when the arc is formed with the bottom of the crucible under argon or a vacuum of ca. 1 Pa (10^{-2} mbar), with currents of 15–40 kA and an average melting capacity of 1 kg/kWh. The solidified titanium is remelted in a similar manner, as this gives improved homogeneity. For special applications involving critical service conditions, the titanium is melted three times.

Vacuum arc with solid negative electrodes [188] and cold-hearth melting furnaces with electron-beam (EBCHM) [189] or plasma heating (PCHM) [190] do not require consumable electrodes. The sponge and scrap in lump form are melted by feeding them continuously into the molten metal. These furnaces have so far only been used for the first melt. In cold-hearth melting, sponge and processed scrap are melted in a pre-crucible. The melt is fed into the mold through a channel, whereby impurities can be retained in the skull—the solidified surface forming on the melt in the channel. This method is expected to give better retention of impurities from the scrap. The mold can be designed for producing ingots or slabs. Multiple burners are employed to obtain a continuous ingot or slab. The crucible is equipped with a withdrawable bottom, and the crude ingot is melted to form a strand which is lowered at a rate corresponding to the melting process.

The commercial crude ingots produced by melting can have a mass of 1–13 t, but are usually in the range 3–8 t. Diameters are in the range 500–1100 mm.

Casting. When arc furnaces with consumable or solid electrodes are used [191], the titanium

drains into water-cooled tilting copper crucibles, or the melt is superheated by electric current under an inert gas. The metal is cast in graphite, ceramic, or metallic molds, or by centrifugal casting. Electron-beam furnaces can also be used [192]. Depending on the process, the mass of a casting can range from 750 kg to a few grams in the case of high precision castings with small wall thicknesses produced by the lost wax process. The output of titanium castings is barely 1% of the total output of semifinished products. In a new melting process a combination of cold-wall crucible and plasma burner is used.

Powder Metallurgy. The production of components from titanium and titanium alloys by powder metallurgy has so far not achieved industrial importance. Production of powder by sieving the fine material from titanium sponge or by supersaturating the sponge with hydrogen, milling under inert gas, and dehydrogenation [193] are not widely used because of the poor flow properties of the powder obtained. These properties can be improved by partial melting of the powder to give spheroidal particles.

Spheroidal powder with good flow properties and good densification behavior can also be produced by an atomization process in which titanium rods are rotated at high speed in an electric arc or plasma [194].

Advances in cold-wall crucible technology have now made possible inert gas atomization with argon or helium in a ceramic-free process [195]. Fine, spheroidal titanium powder can be produced by the induction drip-melting atomization process and by the electrode-induction-melting, gas-atomization process.

In the calciothermic production of titanium alloys in powder form, the starting materials are the metal oxides, CaO , Ca , and KClO_4 . Fine powders with good densification properties (60%) and with oxygen contents of 0.14–0.18% and carbon contents of 0.03–0.06% [196] are obtained.

22.12 Production and Processing of Semifinished Products

Semifinished products are chiefly produced by pressing, forging, rolling, or drawing.

Hot Forming. In hot forming, the temperature of the metal is above its recrystallization temperature. A slightly oxidizing atmosphere and a uniform temperature are maintained in the reheating furnace to prevent hydrogen pickup and consequent embrittlement. In hot rolling, temperatures are usually 20–100 °C below those used for forging.

For pressing or forging heavy section components, a preforming stage is carried out in the β -range, and the final is then carried out, usually in the $(\alpha + \beta)$ -range sufficiently below the $(\alpha + \beta)/\beta$ -interphase, with deformations of at least 60–75% to produce the desired structure and properties of the material.

Cold Forming. In cold forming to produce wire, thin sheet, and foil, the high yield strength of titanium, which increases with increasing tensile strength, and the low elongation without necking must be taken into consideration. Commercially pure titanium should be work annealed after 30–40% deformation.

Heat Treatment after Deformation. Low-strength titanium (Grade 1, DIN designation 3.7025) generally does not require stress-relief annealing, but annealing is necessary for higher strength and especially complex components.

Recrystallization annealing to give a ductile product is required after hot forming of semifinished and drop forged products, and for work annealing after forming of sheet.

Descaling and Pickling. Titanium is descaled by abrasive blasting followed by pickling in aqueous mixtures of 20–40% HNO_3 and 1–3% HF , in sodium hydroxide-based salt baths with added oxidizing agents such as sodium nitrate and borax at 450–510 °C, or in sodium

hydride baths at 380 °C. Hydrogen pickup can occur if the pickling time is too long.

Processing of Semifinished Products. Of the noncutting forming processes, deep drawing can be used with titanium-based materials, but stretch-forming is less suitable. In cutting, stamping, pressing, and hole punching, titanium behaves like steel. To give crack-free bending, folding, and edging, radii should be large and deformation rates small. The use of load-bearing lubricants and plastic coatings gives improved drawing behavior [197].

In machining, the low thermal conductivity, low specific heat capacity, low modulus of elasticity, and high toughness lead to considerably higher temperatures in the contact zone than with steel under similar cutting conditions. Also, because of the small extent of chip compression, the contact zone is restricted, leading to additional thermal stress on the tip of the tool. For low heat generation at the tool a high cutting speed, a low chip removed rate, and sufficient cooling should be provided.

Chemical and electrochemical machining of mechanically machined surfaces are widely used processes, and give high accuracy. Hydrofluoric acid, usually with additions of nitric or chromic acid, is used for chemical machining, while electrochemical machining is carried out with direct current in a solution of NaCl .

Welding. In principle, titanium of all strength grades is weldable. However, it can only be welded with exclusion of air or in an inert gas atmosphere because hot solid or molten titanium reacts readily with the atmosphere, reducing toughness and causing embrittlement, even with low levels of pickup. Electron-beam welding is limited to special applications, particularly the aerospace industries, but MIG, TIG, plasma, and laser-beam welding are widely used. Friction and diffusion welding can also be employed with titanium.

Soldering is only possible if a solderable coating is first applied to titanium. For brazing, the dense passive layer on the titanium must first be removed by a flux, which usually consists

of alkali metal halides with addition of AgCl . Suitable solders include silver, titanium–silver, and aluminum–silver alloys. It is preferable to solder in a vacuum or in an inert gas atmosphere to minimize diffusion of atmospheric gases into the metal [198]. Soldered joints can have a tensile strength of $> 800 \text{ N/mm}^2$ and a shear strength of ca. 150 N/mm^2 .

Adhesives. Adhesive bonds with shear strengths of $> 200 \text{ N/mm}^2$ can be produced if the titanium surface is pretreated and anodically oxidized or coated with metals by spraying or vapor deposition [199, 200].

Explosive Cladding. Industrial low-strength grades of titanium can be applied to metallic substrates, usually steel, by explosive cladding at ca. 5000 MPa, giving shear strengths of ca. 300 N/mm^2 . To prevent diffusion between the parent metal and the coating leading to embrittlement of the bonding zone, the upper limit of the usage temperature should be 550 °C [201]. Other substrate metals such as aluminum, copper, and zirconium can also be explosively clad.

Super Plastic Forming (SPF). Alloyed titanium with a two-phase fine structure often exhibits ductility properties that allow ca. 1000% elongation. In combination with diffusion welding, highly complex structural components can be produced in a single operation [202].

Tribology. In general, the surface of titanium components is not very resistant against wear. Therefore, wear resistant films are formed by ion implantation or by PVD or CVD. In-situ formation of titanium nitride, carbide, or boride films of varying thickness is achieved by annealing under the corresponding atmosphere or by laser melting [203–207].

22.13 Compounds [208, 209]

Titanium is usually quadrivalent in its compounds, but may also function as trivalent and,

in a few compounds as bivalent; the compounds of bivalent titanium are prepared only with difficulty, and are unstable in aqueous solution. The existence of titanium(I) compounds has not been established, although certain observations point to their formation, e.g., the observation that there is a maximum volatility in the Ti–S system at a composition corresponding roughly to the formula Ti_2S .

Quadrivalent titanium has a strong tendency to form anions such as $[\text{TiO}_3]^{2-}$ (titanate ion), $[\text{TiF}_6]^{2-}$ (fluorotitanate ion), $[\text{TiCl}_6]^{2-}$ (chlorotitanate ion), and $[\text{Ti}(\text{SO}_4)_3]^{2-}$ (sulfatotitanate ion). The soluble titanium(IV) compounds have a strong tendency to undergo hydrolytic decomposition. Incomplete hydrolysis may give rise to compounds of the type TiOx_2 . Compounds containing the radical $[\text{TiO}]^{2+}$ are called titanyl compounds.

The oxidation potential $\text{Ti}^{3+}/\text{Ti}^{4+}$ (referred to the normal hydrogen electrode at 0 °C) is +0.04 V. If a platinum foil is dipped in a solution containing equal concentrations of Ti^{3+} and Ti^{4+} ions, and combined with a normal hydrogen electrode to form a galvanic cell, the current flows through the wire joining the two electrodes from the normal hydrogen electrode to the platinum foil dipping in the titanium salt solution. Hydrogen is evolved at the former, while Ti^{3+} ions are oxidized to Ti^{4+} ions at the latter. Titanium(III) ions have so strong a reducing action, that in some circumstances they can evolve hydrogen from acid solutions. For the couple $\text{Ti}^{2+}/\text{Ti}^{3+}$ the oxidation potential $E^0 = +0.37 \text{ V}$, for the couple $\text{Ti}^{2+}/\text{Ti}^{4+}$, $E^0 = +0.20 \text{ V}$. The normal potential of Ti in contact with a Ti(II) salt solution is +1.75 V.

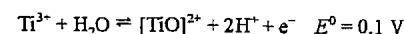
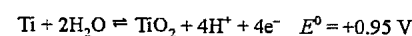
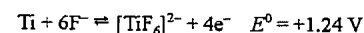


Table 22.17 gives a summary of the most important titanium compounds.

Table 22.17: Titanium compounds.

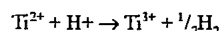
Type	Compounds	Color
Fluorides	TiF ₃	violet
	TiF ₄	white
Chlorides	TiCl ₂	black
	TiCl ₃	violet
	TiCl ₄	violet
Bromides	TiBr ₂	black
	TiBr ₃	black
	TiBr ₄	amber
Iodides	TiI ₂	black-brown
	TiI ₃	dark violet
	TiI ₄	red-brown
Oxides	TiO	gold
	Ti ₂ O ₃	violet
	Ti ₄ O ₇ (?)	dark blue
	TiO ₂	white
Sulfides	TiS _{<1}	grey
	TiS	dark brown
	Ti ₂ S ₃	green-black
	TiS ₂	brassy
	TiS ₃	graphite-like
Phosphides	Ti ₃ P (?)	
	TiP	
Carbides	Ti ₂ C (?)	
	TiC	black
Nitrides	TiN	gold

22.13.1 Titanium(II) Compounds

Compounds of bivalent titanium can be prepared by reduction of titanium(IV) or titanium(III) compounds. Thus titanium(II) chloride, TiCl₂, is produced from titanium tetrachloride by means of sodium amalgam, as a black powder which is slowly decomposed by water with the evolution of hydrogen. Aqueous solutions which contain titanium(II) chloride (together with titanium(III) chloride) can be prepared by dissolving TiO in cold dilute hydrochloric acid. Ti²⁺ ions are rapidly oxidized to Ti³⁺ ions by water at ordinary temperature; the solutions are more stable at lower temperatures. In the pure state, TiCl₂ (*d* 3.13) is best obtained, by thermal decomposition of TiCl₃, or by heating TiCl₄ with Ti shavings. TiBr₂ (*d* 4.31) and TiI₂ (*d* 4.99) can be prepared by direct union of their components.

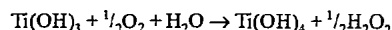
TiO (*d* 4.94, *mp* 175 °C) can be obtained by heating a mixture of TiO₂ and Ti. It has the NaCl type crystal structure, but a certain proportion of the lattice sites (distributed at ran-

dom) is vacant. At the one end of the homogeneity range, these vacant sites represent missing Ti atoms, and at the other extreme O atoms. When TiO is dissolved in dilute hydrochloric acid, partial oxidation occurs:



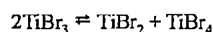
22.13.2 Titanium(III) Compounds

Titanium(III) compounds are obtained by reducing soluble titanium(IV) compounds with zinc and acid, or electrolytically. The solutions contain violet colored titanium(III) ions; these have a strong tendency to revert to titanium(IV) ions. The ability of trivalent titanium to bring about indirect oxidation by means of oxygen is so great that even water can play the part of an acceptor in the presence of titanium(III) compounds in alkaline solution, and is thereby converted to hydrogen peroxide:



Anhydrous titanium(III) chloride is obtained as a violet powder by passing the vapor of titanium tetrachloride, mixed with excess hydrogen, through a red hot tube. When it is heated in hydrogen to about 700 °C it decomposes into TiCl₂ and TiCl₄. Titanium(III) chloride is obtained in solution by reducing a solution of titanium(IV) salt in hydrochloric acid by means of zinc, or by dissolving metallic titanium in hydrochloric acid. A violet hexahydrate, TiCl₃·6H₂O, crystallizes from the solution.

TiBr₃·6H₂O forms reddish violet crystals (*mp* 115 °C) which are readily soluble in alcohol and acetone, as well as in water. Anhydrous TiBr₃ exists in two modifications. It decomposes reversibly at 400 °C, according to:



TiF₃ may be obtained as a dark blue powder by treating Ti or TiCl₃ with HF. It is very unreactive chemically, and begins to sublime at 900 °C in a vacuum.

22.13.2.1 Titanium(III) Sulfate and Double Sulfates

In the electrolytic reduction of a sulfuric acid solution of titanium(IV) sulfate, a black-violet colored solution is first obtained. The solution becomes lighter with continued reduction, and when practically all the titanium is converted to the trivalent state, it has a transparent pure violet color. An acid titanium(III) sulfate, with the composition 3Ti₂(SO₄)₃·H₂SO₄·25H₂O can be isolated from the solution in the form of a crystalline violet powder. This may be converted to anhydrous neutral titanium(III) sulfate, Ti₂(SO₄)₃, by fuming with sulfuric acid.

Neutral titanium(III) sulfate is a green crystalline powder, insoluble in water but soluble in dilute acid giving violet solutions. Exchange of hydrogen in acid titanium(III) sulfate by metal ions gives rise to double or complex salts, with the composition 3Ti₂(SO₄)₃·M₂SO₄, or M^ITi₃(SO₄)₅, (with variable water content), e.g., an ammonium salt NH₄Ti₃(SO₄)₅·9H₂O, forming blue crystals, sparingly soluble in water. Another type of double sulfate of trivalent titanium corresponds to the alums in composition and crystalline form. The only known titanium alums are the rubidium and cesium compounds, e.g., RbTi(SO₄)₂·12H₂O (red-violet). These salts can be recrystallized without decomposition from dilute sulfuric acid, but not from water. Yet another type is represented by the sodium double sulfate, a violet crystalline mass with the composition NaTi(SO₄)₂·2.5H₂O.

22.13.2.2 Titanium(III) Hydroxide

Formed by reaction of titanium(III) salt solutions with alkali hydroxides, as a deeply colored precipitate which acts as a vigorous reducing agent, and is therefore difficult to obtain pure.

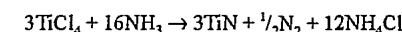
22.13.2.3 Titanium(III) Oxide

Dititanium trioxide, Ti₂O₃ (*d* 4.49, *mp* about 1900 °C), may be obtained crystalline

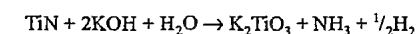
by heating titanium dioxide at 1000 °C in a stream of hydrogen and titanium tetrachloride. It has the same crystal structure as corundum.

22.13.2.4 Titanium Nitride, TiN

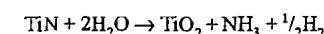
If titanium compounds are reduced at high temperature in the presence of nitrogen, titanium nitride is readily formed in an impure state. Pure titanium nitride TiN is obtainable in the form of a bronze colored powder by strongly heating titanium tetrachloride in a current of ammonia:



It has a structure of rock salt type, decomposed by hot caustic potash:

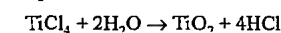


and by superheated steam:



22.13.3 Titanium(IV) Compounds

Titanium tetrachloride, TiCl₄, may be obtained by passing chlorine over heated titanium, titanium carbide, or over a mixture of titanium dioxide and carbon. In the pure state, it forms a colorless liquid, boiling at 136.5 °C, solidifying at -23 °C, and having a density of 1.76 at 0 °C. It has a pungent smell, fumes strongly in moist air, and rapidly hydrolyzed by water:

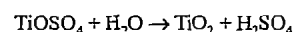


If the hydrolysis is repressed by addition of acid, or if only a little water enters into reaction, oxychlorides can appear as intermediate products. Titanium tetrachloride adds on chloride ions, forming the complex chlorotitanate ion [TiCl₆]²⁻, e.g., the ammonium salt (NH₄)₂[TiCl₆]·2H₂O (yellow crystals). The corresponding free acid can only exist in aqueous solution; its formation therein is demonstrated by the yellow coloration produced by the addition of concentrated hydrochloric acid to titanium tetrachloride.

Titanium fluoride, TiF₄, is prepared by reaction of TiCl₄ with HF, forms a white, powder of density 2.80. It displays a much stronger

tendency than does the chloride to form acid salts. These correspond to the type $M_2^{II}[TiF_6]$ fluorotitanates. All the alkali and alkaline earth salts of this type, and numerous salts of the heavy metals have been prepared. Titanium tetrabromide, $TiBr_4$, obtained in a similar manner to $TiCl_4$ (as yellow octahedral crystals, d 3.25, mp 40 °C, bp 230 °C), is similar to the chloride in its chemical behavior. It is extremely hygroscopic, soluble in alcohol and moderately soluble in ether. Titanium tetraiodide, TiI_4 , is prepared by double decomposition of $TiCl_4$ with HI . It crystallizes in red-brown octahedra (mp 150 °C, bp 365 °C).

When titanium dioxide is fumed with concentrated sulfuric acid, titanyl sulfate, $TiOSO_4$, is formed, as a white powder, soluble in cold water. It is decomposed by hot water, with the deposition of gelatinous titanium dioxide:



In addition to titanyl sulfate, there are other titanium sulfates, both with greater and with smaller SO_3 contents. The neutral titanium sulfate, $Ti(SO_4)_2$, is not known with certainty in the free state. Double salts derived from it are known; in particular the sulfatotitanates of the type $M_2^{II}[Ti(SO_4)_3]$. Titanyl sulfate also forms double salts, e.g., $(NH_4)_2[TiO(SO_4)_2] \cdot H_2O$.

22.13.3.1 Titanates

Neglecting their water of crystallization, the alkali titanates correspond mostly to the formulas $M_2^{II}TiO_3$ and $M_2^{II}Ti_2O_5$. They may be obtained in the wet way, by evaporating solutions of α -titanic acid in concentrated alkali hydroxide solutions (β -titanic acid is insoluble). They can be prepared in the anhydrous state by fusing titanium dioxide with alkali carbonates. The titanates of other metals can also be prepared by high temperature methods. Compounds of the type $M_4^{II}TiO_4$ (orthotitanates) are formed in this way by a few metals, as well as those of the type $M_4^{II}TiO_3$ (metatitanates). Numerous polytitanates (compounds with more than one TiO_2 per one

$M_2^{II}O$) have been obtained by fusion methods. Alkaline earth titanates are known corresponding to the types $M^{II}TiO_3$, $M^{II}Ti_2O_5$, and $M^{II}TiO_5$. Calcium titanate, $CaTiO_3$, occurs in nature as perovskite. The compound Li_2TiO_3 is not a titanate, but is a double oxide with the rock salt structure.

The more commonly occurring mineral ilmenite, iron(II) titanate, $FeTiO_3$, usually contains more iron than is required by this formula. It is isomorphous with hematite, Fe_2O_3 ; in consequence hematite ores often contain considerable amounts of titanium dioxide. The crystal structure of ilmenite is derived from that of corundum, with which hematite is isomorphous, in such a way that the aluminum atoms are replaced alternately by titanium and iron atoms. The metatitanates of Co^{II} , Ni^{II} , Mn^{II} , Cd , and Mg likewise crystallize with the ilmenite structure. $CaTiO_3$, $SrTiO_3$, and $BaTiO_3$, on the other hand, crystallize in the perovskite structure. In the ilmenite structure, as also in the perovskite structure, Ti has the coordination number 6 towards oxygen. The same is true for the structure of the compound Fe_2TiO_5 (crystallizing rhombic), which occurs in nature as pseudobrookite. It is built up of (somewhat distorted) TiO_6 octahedra, which are linked together by two opposite corners, so as to form chains running parallel to the c axis. The iron atoms are inserted into the spaces of the crystal lattice in such a way that every iron atom is surrounded, roughly tetrahedrally, by 4 O atoms. Those titanates of the formula $M^{II}TiO_4$ for which the structures are known ($M^{II} = Mg, Zn, Mn, Co$), crystallize with the spinel structure.

Titanite or sphene, a monoclinic mineral of the composition $CaO \cdot TiO_2 \cdot SiO_2$, is best represented by the formula $Ca(Ti^{IV}, Fe^{III})(O, OH)[SiO_4]$. X-ray structure analysis has shown that titanite is a silicate built up of isolated, somewhat distorted $[SiO_4]$ tetrahedra, in the structure of which the Ti atoms are arranged in such a way that each of them is surrounded by the vertices of 4 $[SiO_4]$ tetrahedra, and also by 20 atoms which link pairs of neighboring Ti atoms together. The Ti atoms can be partially replaced by Fe^{III} . A corresponding proportion

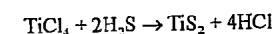
of the O atoms linking them together are then exchanged for OH groups.

22.13.3.2 Peroxytitanic Acid and Peroxytitanates

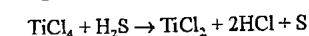
Titanium salts, in neutral or acid solution, are colored an intense orange red by hydrogen peroxide. From sufficiently concentrated solutions, peroxytitanic acid, H_4TiO_5 , can be precipitated by ammonia as a brownish yellow precipitate. Like titanate acid, peroxytitanic acid forms a gel with a variable water content. The compound contains one peroxy group $-O-O-$. It was shown to be a true peroxyacid, and not an H_2O_2 -addition product. Peroxytitanate ions are formed when any dilute, strongly acidified titanium or titanyl salt solutions are treated with hydrogen peroxide. This is made use of for the analytical detection of titanium.

22.13.3.3 Titanium Sulfides

Titanium disulfide, TiS_2 , is formed by passing a mixture of titanium tetrachloride and hydrogen sulfide through a red-hot porcelain tube:



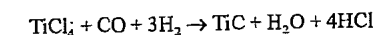
A different reaction takes place between titanium tetrachloride and hydrogen sulfide in the cold, since the latter then acts as a reducing agent, according to:



Titanium disulfide forms brassy-yellow scales, with a metallic luster. It is stable in air at ordinary temperature. When heated it is converted into TiO_2 , and on heating in a stream of hydrogen or of nitrogen it yields lower sulfides, Ti_2S_3 and TiS . It is not decomposed by water even on boiling and is likewise stable towards dilute sulfuric acid, hydrochloric acid, and ammonia. It is decomposed by nitric acid, as well as by hot concentrated sulfuric acid, with the deposition of sulfur. The disulfide is dissolved by boiling caustic potash, with the formation of potassium titanate and potassium sulfide.

22.13.3.4 Titanium Carbides and Carbonitrides

Titanium carbide, TiC , is present in titanium-ferrous cast iron. It was first prepared pure in an electric furnace by Moissan. Small amounts can be obtained by the reaction



taking place on a heated wire, or on the heating of a carbon filament in $TiCl_4$ vapor. For the preparation of larger quantities of the pure carbide in the compact form, an intimate mixture of finely powdered Ti or TiO_2 and carbon black is first heated in a graphite tube furnace, in an atmosphere of hydrogen, to about 2000 °C. The carbide so formed, after powdering, is compressed under high pressures (2000 kg/cm²) into rods (pellets) and fired in a graphite tube furnace at 2500–3000 °C. The firing process is repeated, after fresh powdering and pressing, until the rod is sufficiently compacted and solidified. This is followed by a high temperature sintering process, in which a powerful electric current is passed through the rod, i.e., it is heated up almost to the melting point of the carbide, whereby the impurities evaporate.

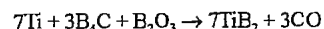
Titanium carbide is similar to titanium metal in appearance and behavior, although less readily attacked by acids, melting point 3450 °C. One g mole of TiC is capable of taking up to about 0.1 g atom of Ti in solid solution. The possible existence of a second carbide, Ti_2C , is uncertain. On account of its great hardness, TiC finds application for the preparation of sintered "hard metals".

Two compounds of titanium with carbon and nitrogen are known: titanium dicyanide (titanium carbonitride, cochranite), $Ti(CN)_2$, blue crystals, harder than steel, and titanium cyanonitride, $Ti_{10}C_2N_8$ or $Ti(CN)_2 \cdot 3Ti_3N_2$, red crystals.

22.13.3.5 Titanium Borides

Titanium can take considerable amounts of boron into solid solution. It also forms two compounds with boron: TiB (cubic) crystallizes with the zinc blende structure, and TiB_2

(hexagonal) is isotypic with AlB_2 . TiB_2 is harder than any other known metallic boride. It is prepared technically from boron carbide, B_4C , which is manufactured on a considerable scale as an abrasive. This is mixed with B_2O_3 , and treated with metallic Ti:



22.14 Toxicology and Occupational Health

Ti metal generally shows relatively low toxicity as compared to most other heavy metals. The toxicity of its compounds varies to a large extent, being dependent on their physicochemical properties (e.g., water solubility) and chemical reactivity. Ti apparently is not an essential element for humans [210].

The most important compound of Ti industrially is titanium dioxide, TiO_2 . Titanium tetrachloride is a starting material for other Ti compounds.

In medicine, Ti metal is used in surgical implants and is mostly tolerated by tissue. Other Ti compounds, such as the dioxide, salicylate, and tannate, are widely used in pharmaceutical and cosmetic products. They have been reported to show practically no adverse effects. Ionic cyclopentadienyltitanium(IV) derivatives (titanocene complexes), a new type of antitumor agent, have shown antitumor activities against certain experimental animal tumors [211, 212].

Intoxications with Ti and its compounds are comparatively rare; they occur almost exclusively by occupational exposure.

Biochemistry, toxicokinetics, human and animal toxicity, levels of tolerance, evaluation of health risks to humans, and ecotoxicity of Ti and its compounds have been reviewed [210, 213].

Toxicokinetics. The average intake of TiO_2 in humans is 0.3–0.5 mg/d. Approximately the same amount is excreted daily: at least 0.29 mg/d via the feces and 0.01 mg/d via the urine [210, 214, 215]. The rate of gastrointestinal absorption is about 3% of the ingested mate-

rial, i.e., most of the ingested Ti is excreted unabsorbed. The mean Ti concentration in blood is 0.07 mg/L [216].

The lungs and the lymph nodes are the predominant target organs for the accumulation of TiO_2 [216, 217]. About 0.4 μg Ti is stored in the lungs per day. In experimental studies in rats, after a single exposure to TiO_2 , 40–45% of the deposited material is removed by pulmonary clearance after 25 d. Storage of Ti in the lung is a dose-dependent process [218].

The biological half-life of Ti is between 320 and 640 d. Excretion by other routes than via urine is unknown [210].

Acute Toxicity. Generally TiO_2 behaves as an inert substance which is practically free of acute toxicity. After short-term exposure of guinea pigs to TiO_2 aerosols, an inflammatory response could not be detected; the number of leukocytes and macrophages did not change [219]. In addition, TiO_2 did not lead to the production of hydroxyproline by fibroblasts, which indicates a lack of fibrogenicity [220].

In contrast, TiCl_4 represents a considerable toxic hazard to humans [221]. Contact with the skin, the mucous membranes, and the conjunctiva leads to severe irritation and necrosis due to the hydrochloric acid formed by immediate hydrolysis. Contact with the eyes can cause blindness. The vapor leads to lachrymation and to irritation of the lower respiratory tract, with the danger of lung edema. In animal experiments the development of lung edema was more rapid and the death rate after exposure to TiCl_4 was higher than with an equivalent concentration of HCl alone, since HCl adsorbed on the particles of hydrolyzed TiCl_4 is transported to deeper parts of the respiratory tract which usually are not reached by the highly water soluble HCl [222].

Chronic Toxicity. In a long-term study of up to 390 d with various species, but very low numbers of test animals (two guinea pigs, two rabbits, four cats, one dog), the animals received between 0.6 and 9 g technical grade TiO_2 per day. There were no adverse effects and no histological abnormalities in any of these animals [223]. In a long-term study with

mice from weaning to natural death, the addition of 5 mg of titanium potassium oxalate per liter of drinking water led to a decrease of the survival rate after 18 months, which was slight in female mice and more pronounced in male mice [224]. The titanium-fed mice generally showed a higher body weight.

Inhalation of TiO_2 dust by rats for a period of up to 13 months (4 times per day, 5 d per week), followed by a 7-month period of fresh air, did not lead to any pathological effect on the lungs; the weight of the rats remained unchanged [225]. In another inhalation study (10–250 mg/m³ for 6 h/d, 5 d/week) performed for 2 years with rats, exposed groups showed an increase in the incidence of pneumonia, tracheitis, and rhinitis with squamous metaplasia of the anterior nasal cavity. Rats exposed to 50 and 250 mg/m³ showed various signs of disturbance of respiratory tract function and dust deposition in the tracheobronchial lymph nodes [226] (see also "Genotoxicity"). These findings were confirmed in detail by an analogous study in which an accumulation of TiO_2 was observed in the upper respiratory tract, lungs, gastrointestinal tract, lymphatic system, liver, and spleen [227].

Similar results concerning effects on respiratory tract function were obtained in a long-term study with rats exposed to TiCl_4 (0–10 mg/m³, 6 h/d, 5 d/week) for two years [228].

Ti compounds such as the hydride, carbide, and boride as well as potassium octatitanate and titanium phosphate fibers apparently are fibrinogenic in animal tests [210].

In humans, the most pronounced effects of a chronic occupational TiO_2 exposure appear in the respiratory system [decreased FEV₁ (Forced Expiration Volume during the first second) and FVC (Forced Vital Capacity)], resulting from deposition of TiO_2 in the lung [229].

A case of TiO_2 pneumoconiosis accompanied by lung cancer and slight fibrosis of the interstitium around bronchioles and vessels has been observed with a fifty-three-year-old man who had been employed for about thirteen years with packing of TiO_2 [230].

Genotoxicity. In an inhalation study with TiO_2 dust (10–250 mg/m³ for 6 h/d, 5 d/week) performed for two years with rats, there was an increased incidence of bronchioalveolar adenomas and cystic keratinizing squamous cell carcinomas as well as excessive dust loading in the lung of the 250 mg/m³ exposure group [226, 227]. These tumors were different from common human lung cancers with respect to tumor type, anatomic location, and tumorigenesis, and were devoid of tumor metastasis [226]. In a ³²P postlabeling assay for the detection of DNA adducts, TiO_2 formed one of the two DNA adducts that could be quantitated separately [228]. In contrast, up to 5% TiO_2 in the diet during 130 weeks did not cause carcinogenic effects in rats [231].

According to the IARC [232], there is inadequate evidence for the carcinogenicity of TiO_2 in humans, and limited evidence for the carcinogenicity of TiO_2 in experimental animals. TiO_2 is not classifiable as to its carcinogenicity to humans (Group 3).

Intratracheal administration of TiO_2 combined with benzo[a]pyrene to hamsters causes an increase in the incidence of benign and malignant tumors of the larynx, trachea, and lungs over that in benzo[a]pyrene-treated controls.

A two-year inhalation study with rats exposed to TiCl_4 (0–10 mg/m³, 6 h/d, 5 d/week) revealed an increased incidence of cystic keratinizing squamous cell carcinomas in high-dose groups [233].

The inhalation of fibrous potassium octatitanate by rats, hamsters, and guinea pigs has basically the same effects on the lungs as asbestos, although the effects are considerably less pronounced [234]. These findings were confirmed by an in-vivo test system [235].

Synthetic titanium phosphate mineral fiber shows a fibrinogenic potential in rats and hamsters after intratracheal injection, similar to that of asbestos; however, in contrast to the results with asbestos, no abnormal increase of the abdominal tumor rate after intraperitoneal injection of 2–10 mg/kg was observed [236].

Reproductive Toxicity. In a three-generation study with rats, the addition of titanium potassium oxalate to the drinking water (5 mg/L) led to a marked decrease in the number of animals surviving to the third generation [210]. In pregnant mice, the application of 30 or 60 mg/kg of the antitumor agent titanocene dichloride on day 10 and 12 resulted in the appearance of cleft palate in numerous fetuses and of costal malformations in some fetuses [237].

Immunotoxicity. In a group of dermatitis patients, no evidence of a skin sensitizing potential of TiO_2 could be observed [238].

Toxicological Data. Titanium dioxide, TiO_2 : TDLo (rat, intramuscular) 360 mg/kg [239]; titanium tetrachloride, TiCl_4 : LDLo (mouse, 2 h, inhalation) 10 mg/m³ [240]; LC₅₀ (rat, 4 h, inhalation) 460 mg/m³ [241]; calcium titanate, CaTiO_3 : LD₅₀ (rat, i.p.) 5300 mg/kg; barium titanate, BaTiO_3 : LD₅₀ (rat, i.p.) 3000 mg/kg; lead titanate, PbTiO_3 : LD₅₀ (rat, i.p.) 2000 mg/kg [210]; tetrabutyl titanate: LD₅₀ (mouse, i.v.) 180 mg/kg [242]; dicyclopentadienyltitanium: LDLo (rat, intramuscular) 50 mg/kg, LDLo (hamster, intramuscular) 83 mg/kg [239].

Treatment. After contact of the skin with TiCl_4 immediate dry removal (without use of water) is necessary. Thereafter, remaining traces of TiCl_4 should be removed with soap and plenty of water. After contact of the eyes with TiCl_4 , adequate measures are rinsing with plenty of water, use of Isogutt eye drops, and contacting an ophthalmologist as soon as possible. In cases of TiCl_4 vapor inhalation, cortisone preparations should be applied immediately (e.g., inhalation of Auxiloson) to avoid the development of lung edema. In severe cases clinical observation for at least 24 h is necessary.

Occupational Health. The MAK value is 6 mg TiO_2 /m³, measured as total fine dust [243]. In the United States the ACGIH set a TLV value of 10–20 mg TiO_2 /m³ in 1980 [244].

Lung fibrosis caused by titanium and some of its compounds (carbide, hydride) is in-

cluded in the list of the German Berufskrankheitenverordnung (Occupational Disease Regulations) [245].

Since TiO_2 tends to accumulate, persons heavily exposed at the workplace should undergo periodical medical examinations, including chest X rays and ventilatory function tests.

22.15 References

1. M. Hansen, K. Anderko: *Constitution of Binary Alloys*, McGraw-Hill, New York 1958.
2. U. Zwicker: *Titan und Titanlegierungen*, Springer-Verlag, Berlin 1974.
3. *The Economics of Titanium*, 3rd. ed., Roskill Information Service Ltd., London 1980.
4. K. Rüdinger: "Titan", in C. Rohrbach (ed.): *Werkstoffe, erforscht, geprüft, verarbeitet*, Technische-wissenschaftliche Vorträge auf der Industrieausstellung, Colloquium-Vlg., Berlin 1971, pp. 129–172.
5. H. H. Weigand: "Titan und Titanlegierungen", *Stahl Eisen* 80 (1960) 174–182, 301–309.
6. K. Rüdinger: "Titan und Titanlegierungen – Moderne Werkstoffe – Auswahl – Prüfung – Anwendung – Übersichten über Sondergebiete der Werkstofftechnik für Studium und Praxis", *Z. Werkstofftech.* 9 (1978) 181–189, 214–218.
7. Atomic Energy Commission (ed.): *The Reactor Handbook*, vol. I, AECD 3645, 1955, p. 352.
8. A. D. Schelberg, M. B. Sampson, A. C. G. Mitchell, *Phys. Rev.* 74 (1948) 1239.
9. J. S. V. Allen, M. I. Pool, J. D. Kurbatov, L. L. Quill, *Phys. Rev.* 60 (1941) 425–429.
10. G. T. Seaborg, I. Pearlman, *Rev. Mod. Phys.* 20 (1948) 585–667.
11. L. Seren, H. N. Friedlander, S. H. Turkel, *Phys. Rev.* 72 (1947) 888–901.
12. H. Walke, E. J. Williams, G. R. Evans, *Proc. Soc. London Ser. A* 171 (1939) 360–382.
13. T. H. Schofield, *Proc. Phys. Soc. London Sect. B* 67 (1954) 845–847.
14. K. D. Deardorff, E. T. Hayes, *J. Met.* 8 (1956) 509–511.
15. A. D. McQuillan, M. K. McQuillan: *Titanium*, Butterworth, London 1956.
16. G. Hägg, *Z. Phys. Chem. Abt. B* 11 (1931) 433–454.
17. S. Koncz, S. Szanto, H. Waldhauser, *Naturwissenschaften* 42 (1955) 368–369.
18. A. D. McQuillan, *Proc. Soc. London Ser. A* 204 (1950) 309–323.
19. I. Backhurst, *J. Iron Steel Inst. London* 198 (1968) 124–134.
20. B. W. Levinger, *Trans. Am. Inst. Min. Metall. Pet. Eng.* 197 (1953) 195.
21. H. T. Clark, *Trans. Am. Inst. Min. Metall. Pet. Eng.* 185 (1949) 588–589.
22. J. M. Blocher, I. E. Campbell, *J. Am. Chem. Soc.* 71 (1949) 4040–4042.
23. P. Schüler, *DEW-Tech. Ber.* 7 (1967) 5–12.
24. K. Bungardt, K. Rüdinger, *Z. Metallkd.* 52 (1961) 120–135.
25. K. Bungardt, K. Rüdinger, *Metall (Berlin)* 14 (1960) 988–994.
26. K. Rüdinger: "Titan", in E. Rabald, D. Behrens (eds.): *DECHEMA-Werkstoff-Tabelle, Physikalische Eigenschaften*, Deutsche Gesellschaft für Apparatewesen, Frankfurt/M. 1966.
27. R. G. Netzel, J. R. Dillinger, *Proc. Int. Conf. Low Temp. Phys. 7th* 1961, 389–391.
28. W. Spyra, *DEW-Tech. Ber.* 5 (1965) 20–24.
29. F. R. Brotzen, E. L. Harmon, Jr., A. R. Troiano, *Trans. Am. Inst. Min. Metall. Pet. Eng.* 203 (1955) 414.
30. R. W. Powell, R. P. Tye, *J. Less Common Met.* 3 (1961) 226–233.
31. W. Spyra, *DWE-Tech. Ber.* 1 (1961) 156–161.
32. D. L. Burk, I. Estermann, S. A. Friedberg, *Z. Phys. Chem. (Munich)* 16 (1958) 183–193.
33. L. G. Carpenter, F. R. Reavell, *Nature (London)* 163 (1949) 527.
34. C. M. Libanati, S. F. Dymont, *Acta Metall.* 11 (1963) 1263–1268.
35. R. N. Jeffery, *Urbana Scientific and Techn. Aerospace Report* 9 (1971) no. 6, W71–16 778.
36. Lepkowski, Holladay, TML Report No. 73, Battelle Memorial Inst., Columbus, OH, 1957.
37. B. W. Roberts: "Properties of Selected Superconducting Materials", NBS Techn. Note 983, Suppl., 1978.
38. F. B. Litton, B. W. Gonser, *Met. Prog.* 55 (1949) 346–347.
39. J. D. Ramsdell, D. R. Matthews, *Bur. Mines Rep. Invest.* 5701 (1960).
40. W. Knorr, L. Kopp, C. M. v. Meysenbug, K. Rüdinger, *Z. Werkstofftech.* 7 (1976) 437–451.
41. D. Schlain, *Bur. Mines Rep. Invest.* 4965 (1953).
42. R. Otsuka, *Sci. Pap. Inst. Phys. Chem. Res. (Jpn.)* 54 (1960) 97–23.
43. M. Stern, H. Wissemberg, *J. Electrochem. Soc.* 106 (1959) 755–759.
44. M. Stern, C. R. Bishop, *ASM Trans. Q.* 52 (1960) 239–256.
45. K. Rüdinger, *Werkst. Korros.* 16 (1965) 109–115.
46. M. Stern, H. Wissemberg, *J. Electrochem. Soc.* 106 (1959) 759–764.
47. R. Boyer, G. Welsch, E. W. Collings (eds.): "Titanium Alloys", *Materials Properties Handbook*, ASM, Materials Park, OH, 1994, pp. 175–176.
48. K. Rüdinger, *Werkst. Korros.* 13 (1962) 401–405.
49. E. A. Gulbransen, K. F. Andrew, *J. Elektrochem. Soc.* 96 (1949) 363–376.
50. D. N. Williams et al., *WADC Techn. Rep.*, Battelle Memorial Inst., Columbus, OH, 1957, pp. 54–661.
51. U. Zwicker, *Z. Metallkd.* 49 (1958) 179–184; 50 (1959) 261–268.
52. K. Rüdinger: "Sonderwerkstoffe für den Korrosionsschutz", in H. Gräfen (ed.): *Die Praxis des Korrosionsschutzes*, vol. 64, "Kontakt u. Studium Werkstoffe", Expert-Verlag, Grafenau/Württ. 1981, pp. 111–144; 345–347.
53. K. Rüdinger, H. H. Weigand, *Metall (Berlin)* 27 (1973) 241–245.
54. R. N. Lyon: *Liquid Metals Handbook*, vol. 733 (Rev.) Atomic Energy Commission, Dept. of the Navy, Washington, D.C., Navexos 1952, pp. 144–183.
55. P. Eggert et al., *Metall (Berlin)* 35 (1981) 340–342.
56. G. P. Merrill, *Mem. Nat. Acad. Sci. Washington* 14 (1916) 28.
57. Titanium, Mineral Commodity Profiles MCP-18, U.S. Bureau of Mines, Washington, DC (Aug. 1978).
58. G. Clarke, *Ind. Min. (London)* 251 (1988) Aug., 17–31.
59. R. Wyckoff: *Crystal Structure*, J. Wiley & Sons, New York 1965.
60. Gmelin, 41 p. 242.
61. H. P. Boehm, *Chem. Ing. Tech.* 46 (1974) 716.
62. A. R. v. Veen, *Z. Phys. Chem. Suppl.* 162 (1989) 215–219.
63. G. N. Schrauzer, T. D. Guth, *Am. Chem. Soc. Div. Org.* 99 (1977) 7189.
64. R. R. Townner, J. M. Gray, K. M. Porter, US-Geological Survey Circular 930-G, United States Government Printing Office, Supt. of Docs. no.: 1 19.4/2: 930-G (1988).
65. B. A. Ellis, *Mining Annual Review* 1988, p. 53.
66. R. Adams, Environment Matters (GB), February 1990, EM 6/6 (1990).
67. Companhia Vale do Rio Doce, Projecto Titanio, CURO-revista, vol. 7, no. 23, Mar. 86 (1986).
68. R. Leutz, *Erzmetall* 42 (1989) no. 9, 383.
69. British Titanium Products DE-OS 2038244, 2038246–248, 1970 (F. R. Williams et al.); 2038245, 1970 (J. Whitehead et al.).
70. Ruthner, DE-OS 1533123, 1966.
71. Oceanic Process Corp., US 3252787, 1966 (C. D. Shiam).
72. Anglo American Corp. of South Africa, DE-AS 1948742, 1969 (T. J. Coyle, H. J. Bovey).
73. Laporte, DE-AS 1184292, 1961.
74. Du Pont, DE-AS 1218734, 1965 (J. W. Reeves).
75. American Cyanamid, DE-OS 2744805, 1977 (P. J. Preston et al.).
76. W. Dunn, DE-OS 2528894, 1975 (W. E. Dunn, Jr.).
77. Cochran, GB 1368564, 1974 (A. G. Starlipper, A. A. Cochran).
78. Du Pont, US 3926614, 1974 (H. H. Glaeser).
79. Mitsubishi Chemical, US 3950489, 1974 (S. Fukushima).
80. G. Clarke, *Ind. Min. (London)* 225 (1986) June, 47–55.
81. J. Barksdale: *Titanium*, 2nd ed., Ronald Press Comp., New York 1966, p. 240 ff.
82. Du Pont, US 2098025, 1935, US 2098055, 1935 (J. E. Booge, J. J. Krichma, R. H. McKinney).
83. Bayer, DE 2015155, 1970 (G. Kienast, H. Stütgens, H. G. Zander).
84. FS Ishihara Sangyo Kaisha, Ltd., 30-5166, 1955.
85. Bayer, DE-OS 2951799, 1979 (P. Panek, W. Gutsche, P. Woditsch).
86. Bayer, DE 2454220, 1974 (R. Leiber, J. Leuriclan, J. Renier).
87. J. Barksdale in [64], pp. 264, 276, 278.
88. Du Pont, US 2446181, 1946 (R. B. Kraus); DE 1467357, 1964 (F. L. Larins, O. Kleinfelder); US 3628913, 1969 (K. L. Uhland).
89. Kronos Titan, EP 0265551, 1990 (A. Hartmann, H. Thumm).

90. PPG Industries Inc., DE 1592960, 1967 (H. W. Rahn, K. W. Richardson).
91. Du Pont, DE 1767798, 1968 (J. R. Auld).
92. Cabot Corp., DE 1908747, 1969 (H. Weaver, R. B. Roaper II, Jr.); US 3607049, 1970 (H. Weaver, R. B. Roaper II, Jr.).
93. Du Pont, DE 2342889, 1973 (A. H. Angerman, C. G. Moore).
94. Du Pont, US 4781761, 1987 (H. W. Jacobson).
95. Ishihara Sangyo Kaisha, J 58134-158A 1982.
96. Du Pont, US 2885366, 1956 (R. K. Jeer).
97. Tioxide Group Ltd., GB 1008652, 1961 (A. W. Evans, C. Shon).
98. Kronos Titangesellschaft mbH, DE 1208438, 1960 (H. Rechmann, F. Vial, H. Weber). British Titanium Products, DE 1467412, 1965 (J. R. Moody, G. Lederer).
99. Du Pont, US 4461810, 1984 (H. G. Jacobson).
100. Bayer, DE 2946549, 1977 (K. Köhler, P. Woditsch, H. Rieck, F. Rodi).
101. Metallgesellschaft AG, Bayer, DE 2529708, 1977 (K. H. Dörr et al.).
102. Kronos, EP 313715, 1989 (A. Kulling, A. Schinkitz, J. Mauer, J. Steinhausen).
103. Bayer, EP 133505, 1985 (R. Gerken, G. Lailach, E. Bayer, W. Gutsche).
104. Bayer, EP 194544, 1986 (R. Gerken, G. Lailach, A. van Fürden).
105. Bayer, EP 97259, 1984 (R. Gerken, G. Lailach, K. H. Schultz).
106. Bayer, EP 132820, 1985 (G. Lailach, R. Gerken, W. D. Müller, K. Brändle).
107. G. Mie, *Ann. Phys.* **25** (1908) 377.
108. G. Kämpf et al., *Farbe + Lack* **79** (1973) 9 ff.
109. H. G. Volz et al., *Farbe + Lack* **82** (1976) no. 9, 805 ff.
110. K. K. Ricoh, J 58025-363, 1981.
111. M. Kotter, H.-G. Lintz, F. Weyland, *Chem.-Ing.-Tech.* **58** (8), (1986), 617.
112. P. Fournier, *C. R. Hebd. Seances Acad. Sci.* **231** (1950) 1343.
113. H. Mühle, *Am. J. Ind. Med.* **15** (1989) 343-346.
114. F. Hund, *Angew. Chem.* **74** (1962) 23-27.
115. F. Hund, *Farbe + Lack* **73** (1967) 111-120.
116. Bayer, US 3022186, 1959 (F. Hund).
117. Du Pont, US 2257278, 1939 (H. H. Schaumann).
118. The Harshaw Chemical Comp., US 2251829, 1939 (C. J. Harbert).
119. Bayer, DE-AS 1195913, 1959 (H. Kyri, H. Weber).
120. Ferro Corp., US 3832205, 1973 (H. E. Lowery).
121. Bayer, DE-OS 3740635, 1987 (V. Wilhelm, M. Mansmann).
122. BASF Lacke + Farben AG, EP-A 0233601, 1987 (H. Knittel, R. Bauer, E. Liedek, G. Etzrodt).
123. W. Bäumer, *Farbe + Lack* **79** (1973) p. 747.
124. L. M. Greenstein, in *Pigment Handbook*, 2nd. ed., Vol. 1, J. P. Wiley & Sons, New York 1988, p. 842-846.
125. K. D. Franz, H. Härtner, R. Emmert, K. Nitta in *Ullmann's Encyclopedia of Industrial Chemistry*, Vol. A20, VCH Verlagsgesellschaft mbH, Weinheim 1992, p. 352-355.
126. K. D. Franz, R. Emmert, K. Nitta, *Kontakte (Darmstadt)* **2** (1992) p. 3.
127. G. Pfaff, R. Maisch, *Farbe + Lack* **101** (1995) p. 89.
128. R. Glausch, M. Kieser, R. Maisch, G. Pfaff, J. Weitzel in *Perlganzpigmente*, Curt R. Vincentz Verlag, Hannover 1996, p. 31-42.
129. BASF, US 4552593, 1985 (W. Ostertag).
130. W. Ostertag, *Nachr. Chem. Techn. Lab.* **42** (1994) p. 849.
131. Merck KGaA, WO 93/19131 (K. D. Franz, K. Ambrosius, S. Wilhelm, K. Nitta).
132. W. Ostertag, N. Mronga, P. Hauser, *Farbe + Lack* **93** (1987) p. 973.
133. Merck KGaA, EP 354374, 1990 (K. D. Franz, K. Ambrosius, C. Prengel).
134. G. Pfaff, P. Reynders, *Chem. Rundschau Jahrbuch* **1993**, p. 31.
135. Merck KGaA, US 4603047, 1986 (T. Watanabe, T. Noguchi).
136. Merck KGaA/Hyplast, WO 94/05727 (T. Daponte, P. Verschieren, M. Kieser, G. Edler).
137. V. P. S. Judin, V. T. Salonen, *Seifen Öle Fette Wachs* **119** (August 1993) no. 8, 491.
138. W. H. Kettler, G. Richter, *Farbe + Lack* **98** (February 1992) 93.
139. BASF, US 932741, 1986 (S. Punush).
140. D. R. Robertson, F. Gaw, *Congr. Add '95*, Paper 12.
141. M. A. Vannice, R. L. Garten, *J. Catal.* **63** (1980) 255.
142. Huels, DE-OS 3010710, 1984 (K. Neubold, K.-D. Gollner).
143. Mitsubishi Materials Corp., JP 07062326.
144. Degussa, EP 609533, 1994 (W. Hartmann, D. Kerner).
145. O. Priess, DE 334249, 1921.
146. D. Y. Toptygin, I. S. Morozov, *Zh. Prikl. Khim. (Leningrad)* **34** (1961) 691.
147. E. C. Perkins, H. Dolezal, D. M. Taylor, R. S. Lang, *Bur. Mines Rep. Invest.* **6317** (1963).
148. British Titanium Prod. Co., EP 745931, 1952.
149. Illinois Inst. of Techn. Res. Inst., *Chem. Eng. News* **42** (1964) March 23, 47.
150. Pittsburgh Plate Glass Co., US 2245358, 1939.
151. C. K. Stoddard, E. Pietz, *Bur. Mines Rep. Invest.* **4153** (1947).
152. E. Junker, *Z. Anorg. Chem.* **228** (1936) 97-111.
153. R. Kieffer, E. Lihl, E. Effenberger, *Z. Metallkd.* **60** (1969) 94-100.
154. Z. Wyss, *Ann. Chim. (Paris)* **3** (1948) 215-219.
155. O. Kubaschewski, W. A. Dench, *Trans. Inst. Min. Metall.* **66** (81956/57) 1-6.
156. Südd. Kalkstickstoffwerke, DE 1111403, 1958.
157. Bayer, DE 974210, 1954.
158. L. D. Jaffe, R. K. Pitler, *Trans. Am. Inst. Min. Metall. Pet. Eng.* **188** (1950) 1396.
159. W. J. Kroll, *Trans. Electrochem. Soc.* **78** (1940) 35-47.
160. M. A. Hunter, *J. Am. Chem. Soc.* **32** (1910) 330-336.
161. H. Freudenberg, DE 658995, 1936.
162. J. P. Quin, GB 717930, 1952; GB 720517, 1954.
163. T. Ikeshima: "Recent Development in Titanium Sponge Production in Titanium Science and Technology", in G. Lütjering, U. Zwicker, W. Bunk (eds.): *Proc. 5th Int. Conf. Titanium*, München 1984, DGM, Oberursel 1985, pp. 3ff.
164. W. J. Kroll, US 2205854, 1940.

165. F. S. Wartman et al., *Bur. Mines Rep. Invest.* **4519** (1949).
166. P. J. Maddex, US 2556763, 1948.
167. Titangesellschaft, DE 1045720, 1954; DE 1107942, 1957.
168. R. Holst, *Angew. Chem.* **68** (1956) 154.
169. Kinzoku Zairyo Kenkyusoku, EP 837905, 1957.
170. Y. Okura: "Titanium Sponge Production Technology", *Proc. 8th World Conf. Titanium*, Birmingham 22-26 Oct. 1995, The Institute of Materials, London 1996.
171. Barium Steel Corp., DE 1103033, 1957.
172. O. J. C. Runnals, L. M. Pidgeon, *J. Met.* **4** (1952) 843.
173. Fulmer Res. Inst., DE 974695, 1952.
174. W. E. Reid, J. M. Bisch, A. Brenner, *J. Electrochem. Soc.* **104** (1957) 21-29.
175. V. G. Gopenko, I. A. Ivanov, *Russ. Metall. Fuels* **1960**, 21-23.
176. M. E. Sibert, O. H. McKenna, M. A. Steinberg, E. Wainer, *J. Electrochem. Soc.* **102** (1955) 252-262.
177. Horizons Titanium Corp., DE 1060605, 1953.
178. W. J. Kroll, *Metall (Berlin)* **9** (1955) 370-376.
179. W. R. Opie, O. W. Moles, *Trans. Met. Soc. AIME* **218** (1960) 646-649.
180. Titangesellschaft, DE 975587, 1951; DE 1045667, 1955; DE 1093562, 1957; DE 1103600, 1952.
181. P. Ehrlich, H. Kühnl, *Z. Anorg. Allg. Chem.* **298** (1959) 176-192.
182. Deutsche Norton-Ges. mbH, DE 1072393, 1953.
183. Horizons Titanium Corp., DE 1063814, 1953.
184. ICI, DE 1115032, 1956.
185. R. I. Jaffee: *Titanium '80, Science and Technology*, The Metallurgical Society of AIME, Warrendale, PA, 1980, pp. 53-74.
186. G. Cobel, J. Fisher, L. E. Snyder: *Titanium '80, Science and Technology*, The Metallurgical Society of AIME, Warrendale, PA, 1980, pp. 1969-1976.
187. K. Rüdinger, *Metall (Berlin)* **35** (1981) 778-779.
188. S. Tamamoto: "Present Features in Production of Titanium Sponge and Ingot", in F. H. Froes, I. L. Caplan: *Titanium '92, Science and Technology*, TMS Publication, Warrendale, PA, 1993, pp. 53-63.
189. K. Rüdinger et al.: "Investigation of Heat Exchange in the Electrode Tip of the Non-Consumable Electrode Vacuum Arc Furnace for Melting Titanium", in F. H. Froes, I. L. Caplan: *Titanium '92, Science and Technology*, TMS Publication, Warrendale, PA, 1993, pp. 2355-2362.
190. C. H. Entekin, H. R. Harter: "State of the Art in Electron Beam Melting of Titanium", in F. H. Froes, I. L. Caplan: *Titanium '92, Science and Technology*, TMS Publication, Warrendale, PA, 1993, pp. 2339-2346.
191. W. R. Chinnis, W. H. Buttrill: "Production Titanium Plasma Cold Hearth Melting", in F. H. Froes, I. L. Caplan: *Titanium '92, Science and Technology*, TMS Publication, Warrendale, PA, 1993, pp. 2363-2370.
192. A. R. Vaia, R. R. Akers: *Titanium Science and Technology*, Plenum Press, New York 1973, pp. 331-341.
193. H. Stephan: *Titanium Science and Technology*, Plenum Press, New York 1973, pp. 343-352.
194. J. Greenspan, F. J. Rizzitano, E. Scala: *Titanium Science and Technology*, Plenum Press, New York 1973, pp. 365-379.
195. R. F. Geisendorfer, R. J. Saidak: *Titanium Science and Technology*, Plenum Press, New York 1973, pp. 399-418.
196. M. Hohmann, S. Jönsson: "New Concepts of Inert Gas Atomization Plants", *Metall Powder Report* (1990) Jan.
197. H. G. Domazer, G. Büttner, H. Eggert, DE 3017782 A1, 1980.
198. K. Rüdinger, *Blech Rohre Profile* **28** (1981) 234-237.
199. K. Rüdinger, A. Ismer, *Schweißen Schneiden* **19** (1967) 71-73.
200. A. Matting, K. Ulmer, *Metall (Berlin)* **16** (1962) 2-6.
201. F. Hesselt, *DGLR-Jahrestagung*, Report no. 56, Bremen 1969.
202. K. Rüdinger, *Z. Werkstofftech.* **2** (1971) 169-174.
203. P.-J. Winkler: "Recent Advances in Superplasticity and Superplastic Forming of Titanium Alloys", in P. Lacombe, R. Tricot, G. Béranger (eds.): *Proc. 6th World Conf. Titanium*, Société française de métallurgie, Cannes, 6-9 June 1988.
204. F. Pfeiffer, P. Minarski, F. Hoffmann: "Hochdrucknitrieren von Titanwerkstoffen", *HTM* **46** (1991) 361-366.
205. D. Muster (ed.): "Comparison of Surface Modifications", *Brite-Euram Final Report*, Contr. BREU-0477, CHRU BP 426, Strasbourg 1995.
206. A. Weisheit: *Lasergaslegierung von Titanwerkstoffen*, Ph.D. Thesis TU Clausthal, 1993.
207. A. Lang, H. Waldmann, H. W. Bergmann: "Cladding of Metallic Substrates with Diamonds and Cubic Boron Nitride", *ECLAT '94*, Bremen, DVS-Verlag, Düsseldorf 1994, pp. 456-461.
208. B. L. Mordike, R. Haude: "Titanwerkstoffe in Präzisionsbearbeitung mit Festkörperlaser", *Laser in der Materialbearbeitung*, vol. 4, VDI-Verlag, Düsseldorf 1995, pp. 173-184.
209. Gmelin *Handbook of Inorganic Chemistry*, System No. 41: Titanium, Springer Verlag, Berlin 1951.
210. H. Remy, *Lehrbuch der anorganischen Chemie*, volume 2, Akademische Verlagsgesellschaft, Leipzig 1961, pp. 72-84.
211. World Health Organization: *Titanium, Environmental Health Criteria* **24**, Geneva 1982, pp. 1-68.
212. P. Koepf-Maier, T. Klapotke, *Arzneim. Forsch.* **39** (1989) no. 4, 488-490.
213. P. Koepf-Maier et al., *Cancer Chemother. Pharmacol.* **24** (1989) no. 1, 23-27.
214. R. Wennig, N. Kirsch in H. G. Seiler, H. Sigel, A. Sigel (eds.): *Handbook on Toxicity of Inorganic Compounds*, Marcel Dekker, New York 1988, pp. 705-714.
215. H. Valentin, K. H. Schaller, Titanium, in L. Alessio et al. (eds.): *Human Biological Monitoring of Industrial Chemical Series*, Commission of the EC, Publication EUR 8476 EN, Luxembourg 1983, pp. 15-157.
216. H. A. Schroeder, J. J. Balassa, I. H. Tripton, *J. Chron. Dis.* **16** (1963) 55-69.
217. E. I. Hamilton, M. J. Minski, J. J. Cleary, *Sci. Total Environ.* **1** (1972) 341-347.
218. W. Röthig, J. H. Wehran, *Dtsch. Gesundheitswes.* **27** (1972) 1555-1559.

218. J. Ferin, M. L. Feldstein, *Environ. Res.* 16 (1978) 342-352.
219. R. Rylander, M. Sjöstrand, R. Bergström, *Toxicology* 12 (1979) 211-220.
220. A. G. Heppleston in W. H. Walton (ed.): *Inhaled Particles and Vapors*, vol. III, Unwin Brothers Ltd., pp. 357-369.
221. R. Kühn, K. Birett: *Merkblätter Gefährliche Arbeitsstoffe*, 4th ed., ecomed verlag, Landsberg/Lech 1979, Datenblatt T050.
222. E. A. Mel'nikova, *Gig. Sanit.* 5 (1958) 27-31.
223. K. B. Lehmann, L. Herget, *Chem. Ztg.* 51 (1927) 793-794.
224. H. A. Schroeder, J. J. Balassa, W. H. Vinton, Jr., *J. Nutr.* 83 (1964) 239-250.
225. H. Christie, R. J. MacKay, A. M. Fisher, *Am. Ind. Hyg. Assoc. J.* 24 (1963) 42-46.
226. K. P. Lee, H. J. Trochimowicz, C. F. Reinhardt, *Toxicol. Appl. Pharmacol.* 79 (1985) 179-192.
227. DuPont Corp., EPA/OTS 88-85008005 1986.
228. J. Gallagher et al., *Carcinogenesis* 15 (1994) 1291-1299.
229. *Arbete och Halsa* 32 (1989) 44-54.
230. I. Yamadori, S. Ohsumi, K. Taguchi, *Acta Pathol. Jpn.* 36 (1986) 783-790.
231. B. K. Bernard, M. R. Osberhoff, A. Hofmann, J. H. Mennear, *J. Toxicol. Environ. Health* 29 (1990) 417-429.
232. IARC International Agency on Cancer Research, *Monographs on the Evaluation of the Carcinogenic Risk of Chemicals to Humans* 47 (1989) 307-326.
233. Haskell Labs., EPA/OTS 88-9680208, 1986.
234. K. P. Lee et al., *Environ. Res.* 24 (1981) 176-191.
235. A. Poole, R. C. Brown, A. P. Rood, *Br. J. Exp. Pathol.* 67 (1986) 289-296.
236. P. Gross, R. J. Kociba, G. L. Sparschu, J. M. Norris, *Arch. Pathol. Lab. Med.* 101 (1977) 550.
237. P. Koepf-Maier, P. Erkenwick, *Toxicology* 33 (1984) 171-181.
238. BIBRA Working group, The British Industrial Biological Research Association: *Titanium Dioxide, Toxicity Profile*, Carshalton/London, 1990, p. 7.
239. Natl. Cancer Inst. (US), Progress Report for Contract No. PH-43-64-886, July 1968.
240. National Technical Information Service, AEC-TR-6710.
241. D. P. Kelly, K. P. Lee, B. A. Burgess, *The Toxicologist* 1 (1981) 76-77.
242. CSLNX, U.S. Army Armament Research and Development Command, Chemical Systems Laboratory, NX 01650.
243. Deutsche Forschungsgemeinschaft (ed.): *MAK- und BAT-Werte-Liste 1995*, Maximale Arbeitsplatzkonzentrationen und Biologische Arbeitsstofftoleranzwerte, Mitteilungen der Senatskommission zur Prüfung gesundheitsschädlicher Arbeitsstoffe, Mitteilung 31, VCH Verlagsgesellschaft, Weinheim 1995.
244. J. Whitehead, "Titan", in E. Merian (ed.): *Metalle in der Umwelt*, Verlag Chemie, Weinheim 1984, pp. 585-588.
245. Berufskrankheitenverordnung, BK Nr. 4107: Erkrankungen durch Lungenfibrose durch Metallstäube bei der Herstellung oder Verarbeitung von Hartmetallen.

Handbook of Extractive Metallurgy

Edited by Fathi Habashi

**Volume III: Precious Metals
Refractory Metals
Scattered Metals
Radioactive Metals
Rare Earth Metals**

 **WILEY-VCH**

Weinheim • Chichester • New York • Toronto • Brisbane • Singapore

Professor Fathi Habashi
Université Laval
Département de Mines et de Métallurgie
Québec G1K 7P4
Canada

This book was carefully produced. Nevertheless, the editor, the authors and publisher do not warrant the information contained therein to be free of errors. Readers are advised to keep in mind that statements, data, illustrations, procedural details or other items may inadvertently be inaccurate.

Editorial Directors: Karin Sora, Ilse Bedrich
Production Manager: Peter J. Biel
Cover Illustration: Michel Meyer/mmada

Library of Congress Card No. applied for
A CIP catalogue record for this book is available from the British Library

Die Deutsche Bibliothek – CIP-Einheitsaufnahme
Handbook of extractive metallurgy / ed. by Fathi Habashi. –
Weinheim ; New York ; Chichester ; Brisbane ; Singapore ; Toronto :
WILEY-VCH ISBN 3-527-28792-2

Vol. 1. The metal industry, ferrous metals. – 1997

Vol. 2. Primary metals, secondary metals, light metals. – 1997

Vol. 3. Precious metals, refractory metals, scattered metals, radioactive metals, rare earth metals. – 1997

Vol. 4. Ferrous alloy metals, alkali metals, alkaline earth metals; Name index; Subject index. – 1997

© VCH Verlagsgesellschaft mbH – A Wiley company,
D-69451 Weinheim, Federal Republic of Germany, 1997

Printed on acid-free and low-chlorine paper

All rights reserved (including those of translation into other languages). No part of this book may be reproduced in any form – by photoprinting, microfilm, or any other means – nor transmitted or translated into a machine language without written permission from the publishers. Registered names, trademarks, etc. used in this book, even when not specifically marked as such, are not to be considered unprotected by law.

Composition: Jean François Morin, Québec, Canada
Printing: Strauss Offsetdruck GmbH, D-69509 Mörlenbach
Bookbinding: Wilhelm Oswald & Co., D-67433 Neustadt/Weinstraße

Printed in the Federal Republic of Germany

Preface

Extractive metallurgy is that branch of metallurgy that deals with ores as raw material and metals as finished products. It is an ancient art that has been transformed into a modern science as a result of developments in chemistry and chemical engineering. The present volume is a collective work of a number of authors in which metals, their history, properties, extraction technology, and most important inorganic compounds and toxicology are systematically described.

Metals are neither arranged by alphabetical order as in an encyclopedia, nor according to the Periodic Table as in chemistry textbooks. The system used here is according to an economic classification which reflects mainly the uses, the occurrence, and the economic value of metals. First, the ferrous metals, i.e., the production of iron, steel, and ferroalloys are outlined. Then, nonferrous metals are subdivided into primary, secondary, light, precious, refractory, scattered, radioactive, rare earths, ferroalloy metals, the alkali, and the alkaline earth metals.

Although the general tendency today in teaching extractive metallurgy is based on the fundamental aspects rather than on a systematic description of metal extraction processes, it has been found by experience that the two approaches are complementary. The student must have a basic knowledge of metal extraction processes: hydro-, pyro-, and electrometallurgy, and at the same time he must have at his disposal a description of how a particular metal is extracted industrially from different raw materials and know what are its important compounds. It is for this reason, that this *Handbook* has been conceived.

The *Handbook* is the first of its type for extractive metallurgy. Chemical engineers have already had their Perry's *Chemical Engineers' Handbook* for over fifty years, and physical metallurgists have an impressive 18-volume *ASM Metals Handbook*. It is hoped that the

present four volumes will fill the gap for modern extractive metallurgy.

The *Handbook* is an updated collection of more than a hundred entries in *Ullmann's Encyclopedia of Industrial Chemistry* written by over 200 specialists. Some articles were written specifically for the *Handbook*. Some problems are certainly faced when preparing such a vast amount of material. The following may be mentioned:

- Although arsenic, antimony, bismuth, boron, germanium, silicon, selenium, and tellurium are metalloids because they have covalent and not metallic bonds, they are included here because most of them are produced in metallurgical plants, either in the elemental form or as ferroalloys.
- Each chapter contains the articles on the metal in question and its most important inorganic compounds. However, there are certain compounds that are conveniently described together and not under the metals in question for a variety of reasons. These are: the hydrides, carbides, nitrides, cyano compounds, peroxo compounds, nitrates, nitrites, silicates, fluorine compounds, bromides, iodides, sulfites, thiosulfates, dithionites, and phosphates. These are collected together in a special supplement entitled *Special Topics*, under preparation.
- Because of limitation of space, it was not possible to include the alloys of metals in the present work. Another supplement entitled *Alloys* is under preparation.
- Since the largest amount of coke is consumed in iron production as compared to other metals, the articles "Coal" and "Coal Pyrolysis" are included in the chapter dealing with iron.

I am grateful to the editors at VCH Verlagsgesellschaft for their excellent cooperation, in particular Mrs. Karin Sora who followed the project since its conception in 1994, and to

Jean-François Morin at Laval University for his expertise in word processing.

The present work should be useful as a reference work for the practising engineers and the students of metallurgy, chemistry, chemical engineering, geology, mining, and mineral beneficiation. Extractive metallurgy and the chemical industry are closely related; this *Handbook* will

therefore be useful to industrial chemists as well. It can also be useful to engineers and scientists from other disciplines, but it is an essential aid for the extractive metallurgist.

Fathi Habashi

Table of Contents

Volume I		Part Seven	Refractory Metals
Part One	The Metal Industry		26 Tungsten.....1329
	1 The Economic Classification of Metals.....1		27 Molybdenum.....1361
	2 Metal Production.....15		28 Niobium.....1403
	3 Recycling of Metals.....21		29 Tantalum.....1417
	4 By-Product Metals.....23		30 Zirconium.....1431
Part Two	Ferrous Metals		31 Hafnium.....1459
	5 Iron.....29		32 Vanadium.....1471
	6 Steel.....269	Part Eight	Scattered Metals
	7 Ferroalloys.....403		33 Rhenium.....1491
Volume II			34 Germanium.....1505
Part Three	Primary Metals		35 Gallium.....1523
	8 Copper.....491		36 Indium.....1531
	9 Lead.....581		37 Thallium.....1543
	10 Zinc.....641		38 Selenium.....1557
	11 Tin.....683	Part Nine	Radioactive Metals
	12 Nickel.....715		39 Tellurium.....1571
Part Four	Secondary Metals		40 General.....1585
	13 Arsenic.....795		41 Uranium.....1599
	14 Antimony.....823		42 Thorium.....1649
	15 Bismuth.....845		43 Plutonium.....1685
	16 Cadmium.....869	Part Ten	Rare Earth Metals
	17 Mercury.....891		44 General.....1695
	18 Cobalt.....923		45 Cerium.....1743
Part Five	Light Metals	Volume IV	
	19 Beryllium.....955	Part Eleven	Ferroalloy Metals
	20 Magnesium.....981		46 Chromium.....1761
	21 Aluminum.....1039		47 Manganese.....1813
	22 Titanium.....1129		48 Silicon.....1861
Volume III			49 Boron.....1985
Part Six	Precious Metals	Part Twelve	Alkali Metals
	23 Gold.....1183		50 Lithium.....2029
	24 Silver.....1215		51 Sodium.....2053
	25 Platinum Group Metals.....1269		52 Potassium.....2141
			53 Rubidium.....2211
			54 Cesium.....2215

	55 Alkali Sulfur Compounds.....	2221
<i>Part</i>	Alkaline Earth Metals	
<i>Thirteen</i>	56 Calcium.....	2249
	57 Strontium.....	2329
	58 Barium.....	2337
	Authors.....	2355
	Name Index.....	2375
	Subject Index.....	2379

Part Six

Precious Metals

																H	He
Li	Be											B	C	N	O	F	Ne
Na	Mg	Al											Si	P	S	Cl	Ar
K	Ca	Sc	Ti	V	Cr	Mn	Fe	Co	Ni	Cu	Zn	Ga	Ge	As	Se	Br	Kr
Rb	Sr	Y	Zr	Nb	Mo	Tc	Ru	Rh	Pd	Ag	Cd	In	Sn	Sb	Te	I	Xe
Cs	Ba	La [†]	Hf	Ta	W	Re	Os	Ir	Pt	Au	Hg	Tl	Pb	Bi	Po	At	Rn
Fr	Ra	Ac [‡]															
			†	Ce	Pr	Nd	Pm	Sm	Eu	Gd	Tb	Dy	Ho	Er	Tm	Yb	Lu
			‡	Th	Pa	U	Np	Pu	Am	Cm	Bk	Cf	Es	Fm	Md	No	Lr

23 Gold

HERMANN RENNER (WHOLE CHAPTER EXCEPT § 23.4.3); MARK W. JOHNS (§ 23.4.3)

23.1 History	1183	23.7.3 Sodium Disulfiteaurate(I)	1201
23.2 Properties	1186	23.7.4 Miscellaneous Gold Compounds ..	1202
23.2.1 Physical	1186	23.8 Alloys	1202
23.2.2 Chemical	1186	23.9 Quality Specifications and	
23.3 Occurrence	1188	Analysis	1202
23.3.1 Abundance	1188	23.9.1 Quality Specifications	1202
23.3.2 Gold Deposits	1188	23.9.2 Sampling	1203
23.3.3 Gold Reserves and Resources ..	1189	23.9.3 Quantitative Analysis	1203
23.4 Production	1189	23.9.4 Purity Analysis	1203
23.4.1 Ore Treatment	1189	23.9.5 Trace Analysis	1204
23.4.2 Cyanidation	1190	23.10 Uses of Gold and Gold Alloys	1204
23.4.3 Recovery of Gold with Carbon ..	1190	23.10.1 Coins, Medals, Bars	1204
23.4.3.1 Adsorption of Gold by Carbon ..	1191	23.10.2 Jewelry	1204
23.4.3.2 Carbon-in-Pulp Process	1192	23.10.3 Electronics and Electrical	
23.4.3.3 Carbon-in-Leach Process	1194	Engineering	1207
23.5 Gold Refining	1194	23.10.4 Solders	1207
23.5.1 Chemical	1194	23.10.5 Pen Nibs	1207
23.5.2 Electrolytic	1196	23.10.6 Chemical Technology	1208
23.6 Recovery of Gold from Secondary		23.10.7 Dental Materials	1208
Materials	1197	23.10.8 Coatings	1208
23.6.1 Recovery from Gold Alloys	1197	23.10.9 Gold Leaf	1209
23.6.2 Recovery from Sweeps	1197	23.10.10 Catalysts	1209
23.6.3 Recovery from Surface-Coated		23.11 Economic Aspects	1209
Materials	1198	23.12 Toxicology and Occupational	
23.7 Compounds	1199	Health	1211
23.7.1 Potassium Dicyanoaurate(I)	1199	23.13 References	1211
23.7.2 Tetrachloroauric(III) Acid	1201		

23.1 History

Gold is the first element that humans recognized as a metal. Towards the end of the Middle Stone Age and the onset of the Neolithic Age (ca. 8000 B.C.), the world's climate changed greatly. Large areas became arid, necessitating the establishment of permanent settlements in river valleys such as the Euphrates, the Tigris, and the Nile. The earliest archeological finds that can be reliably dated were made in predynastic Egypt (ca. 4000 B.C.) and Mesopotamia, which the Sumerians settled in 3000 B.C. Outstanding finds (ca. 3000 B.C.) were made close to modern Varna, on the Bulgarian shores of the Black Sea. Gold was first mentioned in literature in the Indian

Vedanta (before 1000 B.C.), the writings of Herodotus (484–425 B.C.), and the Old Testament (1000 B.C.).

Egypt was the principal gold country in the pre-Christian era and maintained that status until ca. 1500 B.C. Gold production reached its peak about 1300 B.C. when the first legal foundations for the production of gold were laid, awarding the Pharaoh the absolute monopoly. In ca. 2700 B.C. gold rings were introduced as means of payment; the first gold coins appeared around 600 B.C.

The origin of the gold used by the Egyptians is unclear. Substantial portions appear to have come from Nubia in Upper Egypt (nub = gold), but considerable quantities were proba-

bly imported following the frequently mentioned expeditions to "Punt".

The special status enjoyed by gold in Egypt also exerted an influence in neighbouring countries. The country of Ophir mentioned by Solomon as the origin of his gold may be identical with Punt, but India may also have been the supplier. The Egyptian gold trade expanded particularly under the impetus of the seafaring Phoenicians and Greeks.

Although Egypt was the principal gold country until about 1 B.C., gold was also found and utilized in other regions including India, Ireland, Bohemia, the Carpathian Mountains, Gaul, on the Iberian peninsula, and in the Caucasus.

Even in ancient times the ownership of gold shifted from one ruler to the other through conquests and the collection of tributes. Alexander the Great obtained possession of Indian gold as well as considerable portions of the Pharaohs' treasure. The Romans had little of the metal in their own regions but their military expeditions netted them major amounts in the form of booty; they also exploited the mineral wealth of the countries they had conquered, especially Spain, where up to 40 000 slaves were employed in mining. The state's accumulation of gold bars and coins was immense. Later, however, more and more gold was used in luxury goods and towards the end of the Roman empire a gold shortage was experienced.

The advent of Christianity in Europe in the Middle Ages reduced the general striving for gold. Moreover, until the beginning of the Middle Ages no dominant political power existed for organizing large-scale gold production. In Europe, only the deposits in the Sudeten mountains, the Carpathians, and the Alps were of any significance. Outside Europe, gold was produced in India, Japan, and Siberia.

Following the discovery of America at the end of the fifteenth century, the Spaniards transferred considerable amounts of gold from the New World to Europe. Although the conquistadors found a highly developed mining industry in Central America, their efforts to in-

crease gold production were largely unsuccessful; most of the finds consisted of silver. It was not until the discovery of deposits in Brazil that there was a noticeable increase in world gold production. These deposits were exploited from 1725 to about 1800.

Since about 1750 gold has been mined on a major scale on the eastern slopes of the Ural mountains. In 1840, alluvial gold was discovered in Siberia. The Russian deposits were exploited by the Czars and the land owners, who had to pay their taxes in gold. Russia produced about one fifth of the world's gold production, a proportion maintained until the present day.

The discovery of gold in California in 1848 increased gold production greatly. The special laws issued in the Western parts of the United States allowed private mining thanks to the right to stake claims. This type of working continued when gold deposits were found in Eastern Australia (1851), Nevada (1859), Colorado (1875), Alaska (1886), New Zealand and Western Australia (1892), and Western Canada (1896). However, these deposits soon lost much of their importance.

The strongest impetus was given to gold production through the discovery of the gold-fields of the Witwatersrand in South Africa in 1885. This extremely rich deposit appeared to guarantee steady exploitation far into the future. South African gold soon occupied a commanding position in the world market. Production grew continuously except for a short interruption by the Boer War (1899–1902). In the 1970s, gold production largely stabilized in South Africa and in the rest of the world. In South Africa, more than 300 000 people are now employed in the production of gold.

The discovery of large deposits of gold in Brazil in the 1970s stimulated prospecting activities. New production centers have been established in the Sierra Pelada of Brazil, Canada, Australia, Venezuela, and New Guinea (Ok Tedi), causing a pronounced shift in the geographic distribution of world gold production.

Gold mining in Ghana (Gold Coast) only began to play a role, if a modest one, in the

twentieth century, although the deposits were already known in the Middle Ages. Gold production in Zimbabwe and the neighboring eastern part of the South African bush veld form a moderate but not insignificant part in the overall production of southern Africa.

Total gold production in antiquity can only be assessed approximately. Up to the fall of the Roman Empire, production may have amounted to 10 000 t.

A total production figure of 2000–3000 t has been quoted for the Middle Ages. By the time of the discovery of America, annual world production had reached about 5 t.

An annual production of ca. 10 t was reached in ca. 1700, rising to ca. 15 t in 1800 and to 40 t by 1848, the year the Californian deposits were discovered. As early as 1852, more than 200 t/a were mined, but production subsequently decreased until 1890. Thereafter, the increased output of the South African mines raised annual world production to 500 t in 1904, 700 t in 1907, and 1000 t in 1936. At present that figure has reached 1700 t, of which Eastern-bloc countries contribute ca. 300 t.

The total world production of gold to date exceeds 10^5 t. More than a third of the present-day gold inventory is held by the central banks of the Western industrialized nations as currency backing. An even larger proportion is in private hands, much of it in the form of jewelry. Krugerrands alone account for 2000 t, and smaller quantities are circulating in industry.

The shares of individual states in the overall production until now are divided among South Africa (40%), the United States (15%), the ancient empires (ca. 10%), the former Soviet Union (ca. 10%), Australia (ca. 10%), and Canada (ca. 5%).

In antiquity, gold grains obtained by washing river sands were cold-worked into the desired objects. From ca. 3900 B.C., alluvial gold could be fused into larger lumps. The ancient Egyptians were the first to quarry gold-bearing rocks. Comminution of the rocks and washing were often preceded by heat treatment.

Analyses of archeological finds show that, in Egypt, the separation of gold from silver and copper was feasible, possibly as early as 2000 B.C. Silver was removed by annealing with common salt to give silver chloride [8]. The naturally occurring gold-silver alloy, electrum magicum, was separated into its constituents. The slagging of copper by adding lead followed by cupellation was also known.

In Spain, the Romans developed the technique of flush mining, by which vast masses of rock were dropped from a height, comminuted, and moved by currents of water. Amalgamation presumably originated at that time, although it was first mentioned in the literature in the 11th century A.D.

In the Middle Ages, fusion with lead and cupellation were developed further. Water-powered crushing machines were also introduced for pulverizing ore, and miners learned to process arsenic-containing gold ores by roasting.

The alchemists endeavored to manufacture gold by transmutation of base metals. It was not until the end of the 18th century that the entire concept was finally rejected as false. However, these endeavors led to a better understanding of chemical processes and to the birth of the true natural sciences.

The 17th century saw the discovery of separation by inquartation, i.e., the separation of gold and silver by nitric acid, and of affination, i.e., separation by sulfuric acid. With advancing industrialization in the 19th century new methods replaced the old, but some of the latter have retained some importance to this day. Production of gold as a by-product of other metallurgical processes, (e.g., the refining of copper, zinc, and lead), played an increasingly important role in Germany (Rammelsberg/Harz). In 1863, Plattner's method of chlorination was introduced in the United States and shortly afterwards in Australia. In 1867, MILLER succeeded in refining gold with chlorine. Refining by electrolysis according to WOHLWILL was introduced in 1878 and is still used for all fine gold of 9995 and 9999 purity. Since 1888, cyanide leaching has permitted economical beneficiation of the

Witwatersrand ores, which were less amenable to other methods due to the extremely fine distribution of the gold. Since 1970, conventional cyanide leaching has been superseded by the carbon-in-pulp process, which dispenses with filtration of the leached rock powder. More recently, the ecological problems caused by cyanide leaching have been overcome by treating the cyanide in the wastewater with hydrogen peroxide.

The recent expansion of gold production is also due to the mechanization of ore transportation and beneficiation. In South America, however, manual mining of ores is once again being resorted to. This politically motivated measure, taken with a view to creating jobs, made employment possible for 500 000 people.

Solvent extraction is being investigated as a new method for the rapid and effective refining of fine gold.

23.2 Properties [1, 20, 24–31]

The distinction between noble and base metals is in many ways arbitrary, and is generally determined by practical considerations and tradition. Gold is the classic noble metal and complies with all the criteria for this group of elements: resistance to air, humidity, and to normal wear. Gold is also remarkable among the metals in that it occurs in nature almost exclusively in its elementary state.

23.2.1 Physical

Gold, atomic number 79, atomic mass 196.96654, has only one naturally occurring isotope, ^{197}Au . Its most important radioisotope, which is used in medicine, is ^{195}Au ; it emits ϵ and γ rays and has a half-life of 183 d. The electronic configuration of gold is $[\text{Xe}] 4f^{14}5d^{10}6s^1$. Its atomic radius is 0.1439 nm. The ionic radius for coordination number 6 is 0.1379 nm for Au^+ , and 0.085 nm for Au^{3+} .

Some physical properties of gold are as follows:

mp	1064.43 °C
bp	2808 °C
Density at 20 °C	19.32 g/cm ³

at 900 °C	18.32
at 1000 °C	18.32
at 1065 °C	17.32
at 1200 °C	17.12
at 1300 °C	17.00
Vapor pressure at 1064 °C	0.002 Pa
at 1319 °C	0.1
at 1616 °C	10
at 1810 °C	100
at 2360 °C	10 000
Atomic volume at 20 °C	10.21 cm ³ /mol
Electrical resistivity at 0 °C	$2.06 \times 10^{-6} \Omega\text{cm}$
Thermal conductivity at 0 °C	$3.14 \text{ W cm}^{-1}\text{K}^{-1}$
Specific heat	$0.138 \text{ J g}^{-1}\text{K}^{-1}$
Enthalpy of fusion	12.77 kJ/mol
Enthalpy of vaporization	324.4 kJ/mol
Tensile strength	127.5 N/mm ²

The melting point of gold has been a fixed point on the temperature scale since 1968.

The unit cell of gold is face-centered cubic (type A1), with a lattice constant (a_0) of 0.40781 nm. Gold as it occurs in nature usually does not have a very crystalline appearance. It exhibits threadlike, leaf-shaped, and spherical forms, on which cubic, octahedral, and dodecahedral surfaces can sometimes be seen. When large amounts of molten gold solidify, a characteristic pattern of concentric rings appears on the surface.

Pure gold that has not been mechanically pretreated is very soft. Its hardness on the Mohs' scale is 2.5, and its Brinell hardness is 18 HB. Gold is the most ductile of all metals. It can be cold drawn to give wires of less than 10 μm diameter, and beaten into gold foil with a thickness of 0.2 μm . Because of its softness, gold can be highly polished; this, together with its noble characteristics and brilliant color, gives it its yellow luster. The color of utility gold is less rich and varies considerably according to its alloy composition. Very thin gold foil is translucent; transmitted light appears blue-green.

The physical properties of gold and its alloys have been thoroughly investigated because of their significance for modern technology. For detailed information see [24].

23.2.2 Chemical [32]

Gold does not react with water, dry or humid air, oxygen (even at high temperature), ozone, nitrogen, hydrogen, fluorine, iodine,

sulfur, and hydrogen sulfide under normal conditions.

Sulfuric acid, hydrochloric acid, hydrofluoric acid, phosphoric acid, halide-free nitric acid (except in very high concentrations), and practically all organic acids have no effect on gold, either in concentrated or dilute solutions and at temperatures up to the boiling point. If a hydrohalic acid is combined with an oxidizing agent, such as nitric acid, a halogen, hydrogen peroxide, or chromic acid, gold will dissolve. Gold can also be dissolved in a combination of water and a halogen (the Plattner process) and in selenic acid. Figure 23.1 shows the dissolution rates of gold in the most important industrial agents used for its dissolution.

Aqueous solutions of alkali metal hydroxides, alkali metal salts of the mineral acids, and alkali metal sulfides do not attack gold. However, gold dissolves in solutions of alkali metal cyanides in the presence of oxygen (Figure 23.1) or other oxidizing agents, such as cyanogen bromide (the Diehl process), 4-nitrobenzoic acid (Figure 23.1) and 3-nitrobenzenesulfonic acid, provided they do not rapidly destroy the cyanide. Gold is also attacked by sodium thiosulfate solutions in the presence of oxygen, and by alkali metal polysulfide solutions.

Fused caustic alkalis do not attack gold, provided air and other oxidizing agents are excluded. Gold reacts vigorously with alkali metal peroxides to form aurates. It is inert to the alkali metal phosphates and borates, and to the alkali metal salts of the mineral acids, which can therefore be used as slagging agents for removing metallic impurities from gold.

Gold reacts readily with dry chlorine. The maximum reactivity occurs at 250 °C, and the minimum at 475 °C. Above 475 °C the reactivity increases with increasing temperature up to and beyond the melting point.

Gold can be recovered from solution by electrolytic deposition or by chemical reduction. If the tetrachloroaurate(III) complex is present, then iron(II) salts, tin(II) salts, sulfur dioxide, hydrazine, hydrazonium salts, oxalic acid, or ascorbic acid can be used as reducing agents.

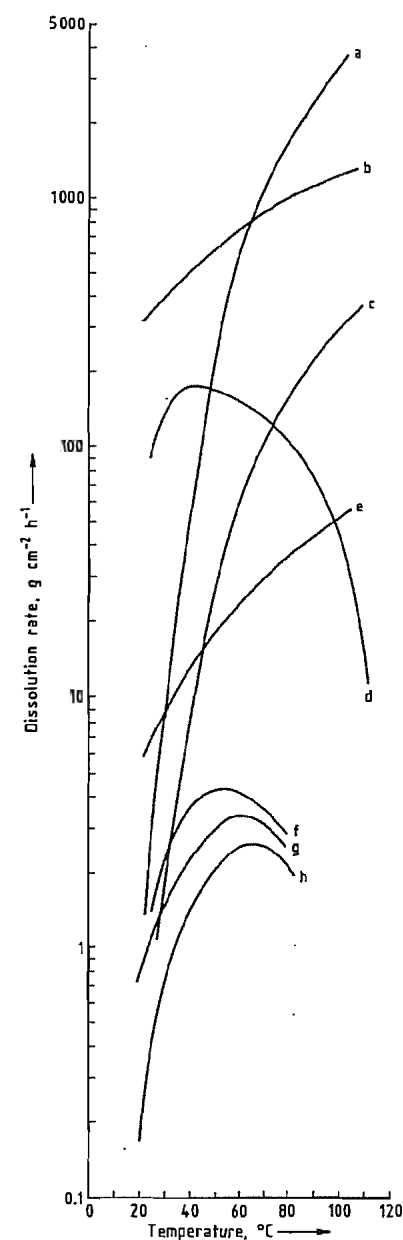


Figure 23.1: Rate of dissolution of fine gold sheet metal in various oxidizing agents: a) Aqua regia, 6 mol/L; b) HCl , 6 mol/L + Br_2 , 0.2 mol/L; c) NaCN , 0.45 mol/L + 4-nitrobenzoic acid, 0.1 mol/L + NaOH , 0.2 mol/L; d) HCl , 6 mol/L + Cl_2 (saturated); e) HCl , 6 mol/L + H_2O_2 , 0.22 mol/L; f) NaCN , 1 mol/L + air; g) NaCN , 0.45 mol/L + NaOH , 0.2 mol/L + air; h) NaCN , 0.006 mol/L + $\text{Ca}(\text{OH})_2$, 0.04 mol/L + air.

The very stable dicyanoaurate complex requires stronger reducing agents such as zinc. Anion exchangers, which are used for the recovery of gold from solutions, sometimes reduce this complex to metallic gold. Similar results are achieved with activated carbon.

The standard potential of Au/Au^{3+} is +1.498 V, of Au/Au^+ +1.68 V, and of $\text{Au}^+/\text{Au}^{3+}$ +1.29 V.

Gold can be alloyed with many other metals. In classic metallurgical processes (e.g., the lead blast furnace process and the reverberatory furnace process for copper ore), gold and silver follow the same route. Zinc, lead, and copper act as collecting agents for gold through the formation of alloys. Gold exhibits the greatest affinity for zinc, followed by lead, and then copper. Zinc is used to remove gold from molten lead in the Parkes process. The readiness with which gold takes up lead, tellurium, selenium, antimony, and bismuth is a disadvantage, particularly with regard to subsequent mechanical processing. Gold alloys readily with mercury at room temperature to form an amalgam. The mercury can be distilled out by heating. This property is utilized in the amalgamation process, and in fire gilding.

Colloidal gold forms hydrosols of an intense red or violet color, which are relatively resistant even without protective colloids.

23.3 Occurrence [1, 2, 6, 20, 34–39]

23.3.1 Abundance

Gold is distributed very unevenly in the Earth's crust, mainly due to enriching processes that have taken place near the surface. Its average abundance is very low and is estimated at ca. 0.005 ppm, although widely varying figures are given.

The gold content of ocean water also varies greatly, depending on the location. Gold contents of 0.008–4 mg/m³ (ppb) have been reported.

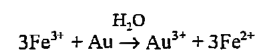
23.3.2 Gold Deposits [7, 11, 38]

The gold deposits which are most easily recognized, and which were the earliest to be discovered, are enriched veins and deposits of gold particles. These particles were originally present in primary rock that was worn down by weathering. Enrichment then followed with partial consolidation due to flowing water. Such deposits are known as *placer* or *secondary deposits*. Typical examples are the relatively small gold deposits in the Rhine Valley, California, and Alaska. The abundance of gold in placer deposits fluctuates greatly especially as the gold particles may be concentrated in very small areas, e.g., a stream bed. Under favorable conditions, placer deposits containing as little as 1 ppm gold may be successfully exploited.

Quartz veins containing gold are often found along the fault plane of rock fractures. As the gold particles have remained at their place of origin, these are termed *primary deposits*. In general, it can be assumed that this gold has been formed hydrothermally, i.e., it has been through an intermediate stage in aqueous solution. Such deposits are found in East Africa, Australia, Canada, and the former Soviet Union. Their gold content varies greatly.

The Witwatersrand goldfields in South Africa (Transvaal and Orange Free State) were also formed by sedimentation. These are sand and shingle deposits that have been compacted to form massive rock, in which the gold is distributed as very fine particles. This type of gold deposit is known as a *conglomerate deposit*. The average gold content of the ore when separated from the gangue is ca. 12 ppm. Mining reaches a depth of 4000 m. To date about 30 000 t of gold, i.e., about one-third of the total world gold production, have come from this ore. The waste extracted sand which is found, for example, around Johannesburg, contains about 1500 t gold (0.5 ppm), mainly contained in pyrites (FeS_2) which is not dissolved by cyanide treatment. This material can also be processed economically.

Sulfidic copper ores may have gold inclusions which can become highly concentrated as a result of weathering. In the outer oxidation zone, hydrothermal reactions take place, such as



while in the underlying cementation zones, the corresponding back reaction occurs. Such deposits are found in Papua New Guinea (Ok Tedi) and in Brazil. The Ok Tedi deposit contains about 4 ppm of gold in the cementation zone.

Copper sulfide ores normally contain only a small proportion of gold (< 1 ppm); however, they can be a significant gold source. During smelting, gold accompanies silver and can be separated in the copper anode slimes. Practically all silver ores also contain some gold.

23.3.3 Gold Reserves and Resources

The term reserves denotes those resources whose existence has been established by prospecting and for which mining is economically viable. Today, world gold ore reserves are assessed at 70 000 t, or more than 40 times the world annual primary production. In 1970, gold reserves were calculated to be one-fifth of this amount. At that time, the extensive Brazilian deposits had not been discovered.

Of the reserves known today, 40% are found in South Africa, 35% in Brazil, and 15% in the Soviet Union. These are followed by the United States, Canada, Australia, Zimbabwe, and Ghana, with 1–3% each.

23.4 Production [1, 2, 20, 23, 31, 33, 39–49, 115]

23.4.1 Ore Treatment

In many places, gold is still mined by individuals and converted on the spot into marketable raw gold using simple manual and mechanical processes, such as panning (grav-

ity separation), milling, and amalgamation. Amalgamation is carried out by allowing a slurry of ground gold-containing ore to flow over mercury-coated copper plates. The resulting gold amalgam is periodically removed by scraping. Very fine gold particles cannot be recovered by these methods, and in many cases, especially in Brazil, the use of cyanidation to extract the residual gold has been proposed.

Where gold is found in river sands covering a large area, the ore is often mined and processed in floating dredgers. This type of mining is found, for example, in Siberia, and in the north of the American continent.

In the conglomerate gold deposits in Witwatersrand, South Africa, most of the gold occurs as very fine particles. This means that mechanical enrichment and amalgamation are impossible, and the gold must be converted to a soluble form by reaction with sodium cyanide. For this purpose, the gold particles are first released from the rock material by means of breakers, wet ball mills, and classifiers. In newer plants, this milling process takes place underground.

Ground gold ore that contains large gold particles or sulfides may be unsuitable for cyanidation. Pretreatment, consisting of gravity concentration, generally followed by amalgamation, is therefore nearly always necessary; this also allows up to 50% of the gold to be extracted faster than by the cyanidation process.

Gravity concentration was formerly carried out using a cord cloth. The cloth was laid on a suitable support, and a water slurry of ground ore was passed over it, the grooves in the cloth being arranged at right angles to the direction of flow. The denser particles were retained in the grooves while the lighter quartz particles flowed away with the water.

The cord cloth has now been replaced by corrugated rubber (thickness 10 mm, groove depth 3 mm, distance between grooves 6 mm). Modern mechanical equipment has endless belts (width 1.5 m, length 7.2 m), tilted at an angle of 11°. These advance at a speed of 0.4 m/min against the direction of flow of the ore

slurry. The concentrate is sprayed off with water and sent to the amalgamation plant. In place of endless belts, slowly rotating cylinders lined with corrugated rubber are sometimes used (length 3.6 m, diameter 0.9 m, inclination 3.75°).

Concentrates from gravity separation processes cannot be directly melted down into gold bars, because they contain considerable amounts of iron pyrites and metallic iron. Gold and silver are therefore generally separated from these components by *amalgamation*. The concentrate, which has a water content of about 70%, is filled into a cast iron drum (length 0.9 m, diameter 0.6 m) containing steel balls (diameter 50 mm). The drum is rotated for 12 h, after which the gold particles are free from all impurities. Mercury is then added, and the drum is rotated for a further 2 h. The resulting amalgam is separated from the other components in a hydrocyclone (diameter 200 mm, inclination 20°); water and excess mercury are removed in a filter press. Remaining mercury is removed by distillation, leaving an impure mass of spongy gold, which is melted down into gold bars.

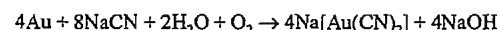
A *flotation process* is often used before gravity concentration in cases where the gold is closely associated with pyritiferous materials.

Roasting of ores in air is a secondary process which is sometimes used after gravity separation or flotation. The resulting oxides are then washed and treated by cyanidation. Gold ores containing sulfidic minerals can also be treated in a *bioleaching* process, which dissolves the sulfides, exposing the gold particles for subsequent cyanidation.

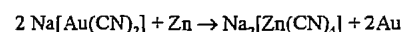
23.4.2 Cyanidation [42]

The cyanidation process has been used in South Africa since 1890. In this process, the powdered mineral slurry, which contains ca. 10 ppm gold in the solid matter, is treated with an aerated 0.03% sodium cyanide solution. Black cyanide ($\text{Ca}(\text{CN})_2$ containing carbon and sodium chloride as impurities), a product of American Cyanamid, is often used instead

of the more expensive sodium cyanide. The addition of calcium oxide ensures that the solution remains slightly alkaline. Dissolution takes place according to the following reaction:



The dead powdered mineral is filtered off in large rotary vacuum filters. The filter cake contains less than a tenth of the original gold content of the ore. The filtrate is treated with zinc chips, which are preactivated in lead acetate solution, to precipitate the gold:



The raw gold is treated with sulfuric acid to remove excess zinc, dried, and then roasted in air at 800 °C to oxidize lead, zinc, and iron. A flux, usually borax, is added, and the material is melted down to raw gold, with a gold content of 80–90%.

An ecological problem is caused by the presence of sodium cyanide in the cake of dead rock material and in the wastewater. However, when exposed to air and sunlight, the cyanide is converted to nontoxic cyanate, and subsequently carbonate.

23.4.3 Recovery of Gold with Carbon [50–62]

The first mention of the ability of carbon to adsorb precious metals was made in 1847. In 1880, it was found that gold can be recovered from chlorinated leach liquors by wood charcoal. McARTHUR and the FOREST brothers discovered that cyanide was a good lixiviant for gold in 1890 and, in 1894, charcoal was used to recover gold from cyanide solutions. The charcoal was prepared from wood and did not possess the high surface area and porosity of carbon today. As no elution procedure was known, the gold was recovered from the carbon by smelting. The use of carbon reached a high point of efficiency in Australia in 1917 when fine carbon was used to recover gold from pregnant cyanide solution, but, as the zinc cementation process advanced, so interest in the use of carbon dropped off.

In the 1940s, a carbon of higher activity and greater abrasion resistance was developed from fruit pips and, in 1952, an elution procedure involving the use of sodium hydroxide and cyanide (the caustic–cyanide procedure) was developed. In 1960, a plant using carbon was erected in Canada, and the first major carbon-in-pulp (CIP) plant to treat the fraction from which the coarse material has been removed (slimes) was built in the United States at Homestake in 1973 to treat 2200 t/d.

Major developments in CIP continued in South Africa, for treatment of the total cyanided pulp. By 1976, a small pilot plant was in operation and, by 1978, a plant processing 250 t/d was on line. The CIP process is now the preferred method worldwide for the recovery of gold from cyanided pulp. The only exception appears to be the former Soviet Union, where the resin-in-pulp process is used. The CIP process is used for the treatment of a variety of feed materials ranging from run-of-mine ore to dump materials and roaster-bed products.

The advantages of the CIP process over zinc cementation are:

- Capital costs are lower.
- Operating costs are lower.
- The ability of carbon to adsorb gold is not affected by any of the common constituents of leach liquors.
- Carbon is added directly to the cyanided pulp, and therefore the need for the expensive filtration and clarification stage is avoided.
- The losses of soluble gold are usually lower than in the zinc cementation process.
- Ores that contain carbonaceous material can be processed without loss of gold to the carbonaceous fraction.
- Materials that are difficult to filter or thicken can be treated successfully.

23.4.3.1 Adsorption of Gold by Carbon

Activated carbon has a porous structure. The following theories have been proposed for the mechanism by which activated carbon loads gold cyanide:

- Complete reduction to metal
- A chemical precipitation mechanism involving gold, carbon monoxide, and cyanide
- Physical adsorption of sodium dicyanoaurate(I)
- Adsorption of the dicyanoaurate(I) ion
- Ion-exchange adsorption of the dicyanoaurate(I) ion
- Adsorption of a neutral complex whose nature is pH dependent
- Electrostatic interaction between the dicyanoaurate(I) ion and positively charged sites
- A physisorption process
- A two-step process in which an ion pair is adsorbed onto carbon and then reduced to an unidentified species.

The last-mentioned theory is now generally accepted.

The adsorption of gold cyanide onto activated carbon is reversible. Thus, an equilibrium exists between the gold in solution and the gold loaded on the carbon. Factors which affect the rate of gold adsorption and those which affect the equilibrium loading of gold are listed in Table 23.1.

Table 23.1: Factors influencing the adsorption of gold by carbon.

Factor	Effect of increasing the factor	
	on rate	on equilibrium loading of gold
pH	slight decrease	decrease
Ionic strength	slight decrease	increase
Free cyanide	slight decrease	decrease
Temperature	slight increase	decrease
Base metals	decrease	decrease
Carbon particle size	decrease	none
Mixing intensity	increase	none
Pulp density	decrease	none

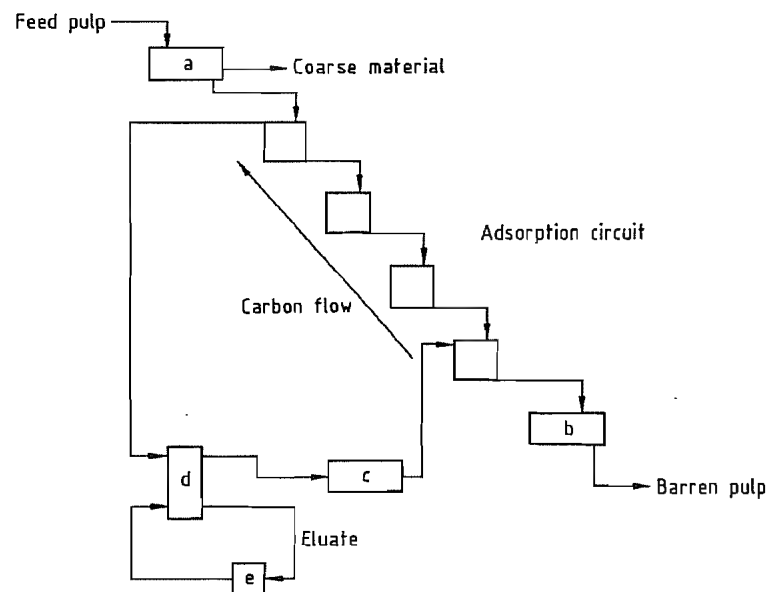


Figure 23.2: Schematic of the carbon-in-pulp circuit: a) Prescreening; b) Final screening; c) Regeneration; d) Elution; e) Electrowinning.

Certain materials poison activated carbon for gold adsorption. Calcium carbonate can form in the pores and is detrimental to adsorption, but is removed by acid-washing. Organic materials (e.g., machine lubricants, detergents, flotation reagents) also poison carbon to some extent, but are removed during reactivation. Lower adsorption efficiencies are attained when a pulp containing calcine, shale, or clay is used, since these finely divided minerals can block the pores. Copper can decrease efficiency of adsorption by competing with gold for adsorption sites, particularly at low concentrations of cyanide.

23.4.3.2 Carbon-in-Pulp Process

Ores containing 0.25–100 g/t gold are processed in CIP plants at tonnages from 100–10⁶ t per month. The density of the pulp varies from 1.3 to 1.45 g/cm³, depending on its viscosity.

A schematic of a CIP plant is shown in Figure 23.2. The cyanided pulp is prescreened to remove coarse material that would otherwise move with the carbon granules, and might

later block the screens in the CIP circuit. The pulp then flows through a series of six or eight flat-bottomed, cylindrical, agitated tanks. The residence time of the pulp in each stage is ca. 1 h. Reactivated carbon is added to the last stage, and is moved countercurrent to the flow of pulp. The carbon is held in each stage by interstage screens. The residence time of the carbon in each stage is 2 d. The carbon concentration in a CIP circuit is 15–30 g per liter of pulp. The barren pulp leaving the circuit is screened to remove fine carbon.

The loaded carbon, which contains 200–20 000 g of gold per ton, is removed periodically from the first stage and eluted with a caustic-cyanide solution. The carbon is washed with acid to remove calcium carbonate, and then reactivated at high temperature in a kiln. The gold in the eluate is generally recovered by electrowinning.

Screening. The total pulp fraction has to be *prescreened* at a smaller aperture (0.6 mm, 28 mesh) than that of the interstage screens. Prescreening removes coarse material to avoid blocking of the screens further downstream. Two types of screen are used: (1) vibrating

screens with woven wire or polyurethane mesh, and (2) linear moving-belt screens.

Wood chips constitute a small fraction of the incoming pulp, and cause problems further downstream when vibrating screens are used. Another prescreening device, such as a dummy tank, is then required. A dummy-tank is a closed circuit tank in which the pulp passes through submerged air-cleaned screens to remove wood chips.

Interstage screens are used to retain carbon while allowing the finer pulp to flow down through the train.

The two types of screen that are used are external and submerged. With *external screens*, the pulp is air lifted onto the screens (normally vibrating decks), and transferred to the next stage, while the carbon is returned to the stage from which it came. A number of *submerged screens* have been developed. Air-cleaned screens normally use square metal mesh, while mechanically cleaned screens use wedge-wire. Duties on these screens vary from 50 to 200 m³ of pulp per square metre of screen per hour. The aperture of the screens is 0.8 mm (20 mesh). The size of the carbon particles used in CIP is 1–2 mm (8 to 16 mesh), although larger particles are used when problems are encountered with screening.

Abraded carbon resulting from breakage of the carbon in the CIP circuit is recovered from the barren pulp by a final screen. The units and apertures of this screen are similar to those used for prescreening.

Interstage movement of carbon is achieved using airlift pumps, vertical spindle pumps, centrifugal pumps, or peristaltic pumps. Factors that affect the choice of pump are controllability, carbon wear, and operating costs. In most plants, carbon is transferred intermittently, but may also be transferred continuously. The following methods are used:

- Loaded carbon is removed from stage one, the carbon in stage two is then transferred to stage one, and so on down the train.
- Regenerated carbon is added to the last stage, the carbon in the last stage is then

transferred to the second-last stage, and so on up the train.

- All the pumps are turned on to transfer the carbon in each stage to the next stage up the train.

Agitation. The optimum agitation system provides a high pulp flow and low shear to avoid carbon breakage. Mechanical agitation is favored over air agitation because it consumes less power, provides better 'live' vessel volume, and has acceptable carbon-attrition rates. Draft tubes and open-impeller agitators are used. Power inputs vary from 0.015 to 0.2 kW/m³ of pulp.

Elution. The gold capacity of carbon decreases with increasing temperature. Increasing the concentration of cyanide and hydroxide ions also decreases the capacity of the carbon for gold.

These two facts were exploited by ZADRA in 1952 to develop the first efficient elution technique to remove gold from carbon. Other elution procedures have since been developed.

The *Zadra process* involves the recycling of a solution containing 1–2% sodium cyanide and 1–2% sodium hydroxide through a bed of carbon. The temperature is over 85 °C, and the flowrate is about one bed volume per hour. The elution takes 48 h to complete. An electrowinning cell is used to recover the gold from the eluate. The advantages of this system are that the capital costs are low, the process is simple, and the reagent consumption is low. Its major disadvantage is that the rate of stripping is slow.

The *AARL process*, which was developed by the Anglo American Research Laboratories, has two stages. In the first stage, the carbon is pre-soaked under pressure at a temperature above 115 °C, in a solution containing 1–5% sodium cyanide and 1–5% sodium hydroxide for several hours. In the second stage, the carbon is eluted with five to seven bed volumes of water at 50–100 kPa and above 110 °C for 5 h at a flowrate of three bed volumes per hour. The advantages of this procedure are that elution is fast and the gold concentration in the eluate is high, which leads to

efficient electrolysis. Its disadvantages include the need for high-quality water, more expensive equipment than that used by the Zadra process, and higher reagent consumption.

Elution with Organic Solvents. The addition of, for example, a 20% solution of ethanol to a caustic-cyanide eluant increases the rate of elution, which takes ca. 6 h at atmospheric pressure and 80 °C. Disadvantages include higher reagent costs and handling problems associated with organic solvents.

The *high-pressure stripping process* is similar to the Zadra process, except that elution is carried out at up to 160 °C and at ca. 350 kPa. It has the advantages of lower reagent consumption, smaller elution inventory, and a smaller elution circuit. Disadvantages are more costly equipment, and that effluent solutions have to be cooled to avoid flashing.

Gold Recovery. The gold is recovered from the eluate either by zinc precipitation or by electrowinning. A number of electrowinning cells have been developed.

The *Zadra cylindrical cell* consists of a cylindrical core (polypropylene basket), which contains steel wool and acts as the cathode. The anode (stainless steel) surrounds the cathode in the cell, and the eluate is pumped into the center.

The most commonly used cell is the *Mintek cell*. It has a rectangular configuration with alternating anodes and cathodes in parallel, similar to those in copper-electrowinning cells. The cathodes are removable plastic baskets with perforated sides, packed with steel wool. The anodes are perforated stainless-steel plates. The flow of eluate is parallel to the flow of current.

Regeneration of carbon is carried out in two stages: (1) washing with acid to remove calcium carbonate and some base metals, and (2) thermal reactivation to remove organic materials and reexpose the pore structure.

The loaded carbon is washed with a 5% solution of hydrochloric acid for 6 h at 75 °C in a column constructed of Hastelloy or rubber-lined mild steel. The carbon is then neutralized

with sodium hydroxide. Acid-washing can be carried out before or after elution, but is generally done first because this increases the efficiency of elution.

In thermal reactivation, the degree of activation increases with increasing temperature and residence time, but micropores are destroyed if the conditions are too harsh. Reactivation is typically carried out at 700 °C for 10 min. Air should be excluded during regeneration. The steam generated from the carbon is normally sufficient to exclude air. The regenerated carbon is normally cooled by quenching in water.

Regeneration is usually carried out in a *rotary kiln*, which is heated externally by electrical resistive windings. In the *Rintoul furnace*, heating is achieved by passing an electric current through a bed of predried carbon in the presence of steam.

23.4.3.3 Carbon-in-Leach Process

Some ores contain carbonaceous material that is slightly active and can adsorb dissolved gold. These carbonaceous materials are termed *preg-robbers*. When a *preg-ropper* is present in an ore, the carbon-in-leach (CIL) process is used, in which cyanidation and carbon adsorption occur in the same reactor.

The CIL circuit is similar to a CIP circuit, the main difference being the residence time of the pulp, since in CIL this is determined by the rate of gold dissolution and not by the rate of gold adsorption as in CIP. Hence, residence times of 4 h per stage are used. The presence of activated carbon prevents the *preg-ropper* from adsorbing gold.

23.5 Gold Refining [1, 20, 23, 31, 33, 40, 41, 45, 47, 49]

23.5.1 Chemical [2, 63]

The historical methods for separating gold from silver depended on dissolving silver and any accompanying base metals from solid solutions containing gold, using either nitric acid (inpartation) or sulfuric acid (affination).

They were accepted up to the second half of the nineteenth century as the best way of manufacturing relatively pure gold. However, these methods are now considered inefficient, both with regard to the purity of the gold recovered and process management.

A method which allows recovery of relatively pure gold is to dissolve the raw gold in hydrochloric acid in the presence of an oxidizing agent. Silver chloride precipitates and can be removed, while gold is precipitated by reduction with oxalic acid. However, a single reductive precipitation process is usually insufficient, as part of any palladium present is entrained by the gold. If sulfur dioxide is used instead, the same applies to copper, nickel, zinc, and lead. Precipitation and separation normally have to be repeated several times before fine gold of sufficient purity is obtained. This method has therefore only found acceptance in cases where the commoner processes have not been established, either because the amounts involved are too small, or because the need arises only sporadically. However, acid dissolution has several advantages: the metal is tied up for a short time only; a high yield of gold can be obtained in a single process step; and conventional equipment can be used.

The Miller process [64] has been of commercial significance since the 1870s. Probably more than two thirds of all gold produced to date has been through this process. It is extremely economical, and the gold quality obtained (99.5–99.6%) meets the requirements of the gold trade. The largest plant in the world is the Rand Refinery in Gerniston, South Africa, which refines all the gold from South African mines, as well as that from neighboring countries. The Miller process is used not only by the mining companies of almost all gold-producing countries, but also in recycling processes.

The Miller process is based on the fact that gold chlorides are unstable above 400 °C and thus do not form at a reaction temperature of ca. 1100 °C, whereas silver and base metals react with chlorine to form stable chlorides. At this temperature, AgCl (*bp* 1554 °C) and CuCl (*bp* 1490 °C) are molten and therefore collect

in a slag layer, which is considerably less dense than molten gold. The chlorides of the other metals volatilize at the reaction temperature, for example, PbCl₂ (*bp* 954 °C), FeCl₂ (*bp* 1023 °C), FeCl₃ (*bp* 319 °C), ZnCl₂ (*bp* 732 °C), and CuCl₂ (*bp* 655 °C). As the process is effective when only a slight excess of chlorine is used, the amount of CuCl and FeCl₂ formed is greater than that of CuCl₂ and FeCl₃.

The raw gold delivered to the Rand refinery is weighed to an accuracy of 0.01 oz and then melted in an induction furnace. Four samples are taken and analyzed for gold content. The gold is cast into bars and reweighed. The gold content of the whole load is then determined. The bars are remelted in an induction furnace in batches of 500 kg, and chlorine gas is passed into the molten metal through quartz pipes at a pressure of 0.2 kPa. First, the chlorine reacts selectively with iron, zinc, and lead (Figure 23.3), whose chlorides are volatile at the reaction temperature and are thus removed as vapors. Finally, silver and copper chlorides form (Figure 23.3). These are molten at the reaction temperature and thus form a slag which floats on the molten gold. Borax is added to the slag as a flux. The end point of the reaction is indicated by the appearance of red gold chloride vapor, and is confirmed by taking a sample for analysis. The silver content, which is determined by X-ray fluorescence analysis, must be below 0.4%. After pouring off the slag, the gold is poured into tared molds.

The chloride slag is ground and screened. Entrained gold is separated and returned to the process. Copper(I) chloride is oxidized to copper(II) chloride using sodium chlorate solution containing hydrochloric acid, and brought into solution. The solution is filtered and copper is cemented. Silver chloride is reduced with zinc in aqueous solution, and sent to a silver-refining electrolysis process.

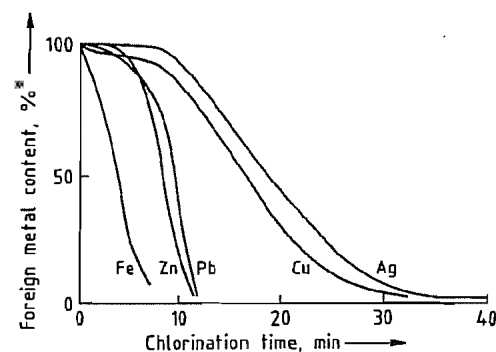


Figure 23.3: Decrease in the concentration of impurities in gold as a function of chlorination time. * Expressed as a percentage of the initial metal content. Typical starting concentrations, %: Ag 9.0, Cu 1.4, Pb 0.35, Fe 0.18, Zn 0.06.

Platinum-group metals cannot be separated by the Miller process, as their chlorides, like those of gold, do not exist at the reaction temperature. However, this is not a disadvantage for gold from the Witwatersrand deposits, as this is free from platinum-group metals.

The great economic advantage of the Miller process, in addition to low production costs, lies in the fact that the gold leaves the refinery in a marketable form, thus minimizing the financial losses due to tying up of the metal.

Tetrachloroauric(III) acid can be extracted from aqueous solution by many organic solvents [66]. Solvents which can form metal complexes (e.g., ethers and esters) are most effective. Total separation from the usual accompanying elements cannot, however, be achieved.

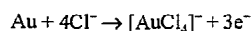
With the exception of dibutyl carbitol, no systems have yet been discovered which can be applied commercially. Yet a system with a high degree of separation efficiency and simple process management, including stripping the pure gold, could offer considerable advantages over currently used methods.

23.5.2 Electrolytic [23, 65]

The Wohlwill electrolytic refining process for gold was developed in 1878 at the Nord-deutsche Affinerie in Hamburg. It is still indispensable for the industrial production of fine

gold of quality $\geq 99.9\%$ (in practice usually 99.95% and 99.99%).

The Wohlwill process uses an electrolyte containing 2.5 mol/L of hydrochloric acid and 2 mol/L of tetrachloroauric acid. Electrolysis is carried out with agitation at 65–75 °C. The raw gold is introduced as cast anode plates. The cathodes, on which the pure gold is deposited, were for many years made of fine gold of thickness 0.25 mm. These have now largely been replaced by sheet titanium cathodes, from which the thick layer of fine gold can be peeled off. In a typical electrolysis cell (Figure 23.4), gold anodes weighing 12 kg and having dimensions 280 × 230 × 12 mm are used. Opposite them are conductively connected cathode plates, arranged two or three on a support rail. One cell normally contains five or six cathode units and four or five anodes. The maximum cell voltage is 1.5 V and the maximum anodic current density 1500 A/m². At the anode, the reaction



takes place, and at the cathode the reverse reaction. Anodes and cathodes are normally replaced every two days. About 10% of the anode gold, especially parts located above the electrolyte, is remelted to form new anodes. The anode slime is collected in a trough in the bath. In addition to silver chloride, it contains rhodium, iridium, ruthenium, and osmium, which can be recovered. Platinum and palladium can be recovered from the electrolyte, which also contains copper, iron, and nickel.

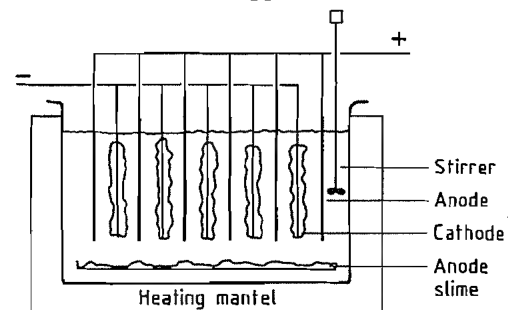


Figure 23.4: Wohlwill electrolysis cell.

The accumulation of metallic impurities in the electrolyte, and of anode slime in the cell,

means that the electrolyte can only be used for a limited period of time. Therefore, the material to be refined should have a high gold content (generally > 95%) and it is often best to use gold which has already been through the Miller process. The gold quality of the cathode deposits depends on the condition of the electrolyte, and on the amount of anode slime that has collected in the cell. A purity of 99.9% is considered to be a minimum, which is the quality of Russian commercial gold. Today, 99.99% can be considered as the norm, rather than 99.95%.

The great advantage of the Wohlwill electrolysis process is the high purity of the gold produced. In addition, the by-products, especially platinum-group metals, are also relatively easy to isolate. A disadvantage is the fairly long period during which the noble metal is tied up, leading to considerable financial losses.

World capacities for Wohlwill electrolysis are very large. In South Africa, approximately a quarter of all gold from primary production, after it has gone through the Miller process, undergoes final purification to fine gold by Wohlwill electrolysis. In the former Soviet Union, all gold is treated by electrolysis, as it normally contains platinum-group metals. Practically all noble-metal parting works which recover gold from secondary materials are dependent on electrolytic refining, again because platinum-group metals are normally present. Today, almost exclusively fine gold (99.99%) is used, both for industrial purposes, and for investment; trading countries such as Switzerland therefore have large refining capacities, mainly producing gold of a quality between "good delivery" (99.5%) and 99.9%.

23.6 Recovery of Gold from Secondary Materials [1, 3, 20, 23, 31, 40, 41, 67–72]

23.6.1 Recovery from Gold Alloys

For the recovery of gold from alloys with a gold content of more than 30%, the Miller

process is the most economical method. This also applies to the treatment of anode slimes from the electrolytic refining of silver, providing these have a high gold content and can be melted.

For small quantities of *gold-rich alloys*, a useful treatment is dissolution in hot aqua regia, or in hydrochloric acid (usually at 20–50 °C) containing a halogen or hydrogen peroxide. Silver precipitates as sparingly soluble silver chloride. Relatively pure gold is recovered from the solution by selective reduction. If copper and lead ions are present, the best reducing agents are sulfur dioxide or hydrazine; if platinum-group metals are present, oxalic acid is used.

In the case of *gold-copper alloys*, which also may contain silver and nickel, treatment with aerated dilute sulfuric acid allows the separation of noble metals from base metals. Gold can only be separated from base metals in this way if the gold content of the alloy is less than ca. 65%, and the material has been finely milled or powdered.

Two historically important processes for treating *gold-silver alloys* are rarely used today. The silver may be dissolved with nitric acid, preferably after realloying to a silver-gold ratio of 3:1 (inquartation); or hot concentrated sulfuric acid can be used (affination). Silver-copper alloys with a low gold content are not suited to the above process, but can be treated in noble-metal works by the lead cupellation process. Lead is removed as litharge, PbO, which also takes up copper as CuO, and other metal and metalloid oxides, leaving behind dore silver. This is subjected to electrolytic refining; gold collects in the anode slime.

23.6.2 Recovery from Sweeps

The noble-metal processing industry produces large amounts of waste dust and debris, known as sweeps (e.g., slag, ash, soot, precipitation and emulsion residues, and sweepings). The gold content of these materials is mostly in the range 0.5–10%. Usually they are first carefully ground, screened, and, if necessary, dried or burned. The fine nonmetallic fraction

and the coarse metallic fraction, which can usually be melted, are analyzed separately.

The usual method for treating gold-containing sweeps is to melt the material down, together with silver-containing sweeps, in a lead shaft furnace. Depending on the composition of the sweeps, calcium carbonate, silicic acid, lead oxide, carbon, and materials containing sulfur are added. The mixture of powdered components is normally briquetted, pelletized, or sintered before being fed into the shaft furnace. The metallic phase (alloy) produced in the furnace contains lead and almost all of the noble metal. This alloy is then converted to dore silver (a few percent Au; < 0.1% Pb; the rest Ag) in a cupel furnace by oxidizing lead to lead(II) oxide. The silicate slag from the shaft furnace contains a negligible quantity of noble metal, and can usually be discarded. The slagging process may have to be repeated, for example if the noble-metal content exceeds 300 ppm. In the sulfidic phase, which forms between the metallic phase and the slag, almost all the copper collects with the nickel to form copper matte. The relatively high content of silver and valuable nonferrous heavy metals in the copper matte makes special treatment necessary; this is usually carried out at copper smelting works.

When raw gold is refined, the resulting residues contain more gold than silver. These substances are treated in a shaft furnace and then in a refining furnace, together with raw silver from the Miller process. Unlike other pyrometallurgical recycling methods for silver and gold, a copper matte phase is not formed in the shaft furnace. The Au:Ag ratio is normally 1:4.

23.6.3 Recovery from Surface-Coated Materials

Surface coatings containing gold come mainly from the electronics industry, plus a small proportion from the jewelry industry and electrical engineering. The base material is essentially metallic; the gold coatings are often only a few micrometers thick, but may

account for a gold content between a few tenths percent and a few percent.

The most economic solution is usually to remove only the gold coating, and to send the underlying base material directly to a recycling process. Mechanical pretreatment is often required to expose the gold surface. Depending on the particular combination of materials and the degree and type of finishing employed, this can be carried out with a shredder, jaw crusher, or edge runner. Frequently, this is followed by air separation, gravity separation, or magnetic separation to remove the ballast materials. It is normally not advisable to burn off plastic materials because the gold diffuses into the metallic base, and it is then impossible to remove it all. For this reason it is preferable to decompose the plastic material by pyrolysis.

To remove the gold from the metallic base, the material is usually agitated in alkaline cyanide solutions (10–20 g/L NaCN). Air is only rarely used as an oxidizing agent, because of the relatively low rate of dissolution. Instead, water-soluble aromatic nitro compounds (e.g., nitrobenzoic acid or nitrobenzenesulfonic acid) are normally employed. Potassium peroxodisulfate and hydrogen peroxide are also suitable, but they have a greater tendency to oxidize the cyanide ion. The base materials (e.g., iron, nickel, and cobalt) are attacked only to a limited extent during the dissolution process. When the base material is composed of copper, or a copper-rich alloy, zinc cyanide or lead salts are usually added as inhibitors to keep them from being attacked.

The gold is recovered from cyanide solution by adding zinc powder, after any excess oxidizing agent has been reduced with hydrazine or formaldehyde. The gold can also be recovered by electrolysis, using insoluble graphite or magnetite anodes (100 A/m² cathode, 3–4 V), or platinized titanium anodes. Excess oxidizing agent should also be reduced to obtain optimum current efficiency and speed of deposition. In addition to the reductive deposition of gold, thermal decomposition of the dicyanoaurate(I) complex is also possible.

Gold-plated metallic wastes can also be directly depleted by electrolysis, preferably in electroplating drums used as anodes. The gold is recovered in metallic form from the cathode in a single step. The method is, however, not very well suited to the recovery of gold from bulk material in anode baskets, because the electric field is screened off from the material at the center of the load, and as a result not all the gold is removed.

Gold can be extracted from solutions with a very low gold content (≤ 0.1 g/L) by anion-exchange resins (e.g., Lewatit M 500) [71] or activated charcoal [72]. However, elution is costly and usually incomplete; the gold-loaded carriers are therefore most frequently ashed, and the gold recovered from the ash. The solutions are not returned to the deplating process because they contain degradation products, especially from organic nitro compounds, which would interfere with the process.

The methods described above can also be used to treat other cyanide gold solutions, e.g., unusable electroplating baths.

Gold-plated materials are occasionally smelted together with copper ores in large copper-smelting works. In addition to silver, these ores always contain some gold. A disadvantage of this method is the long time the gold has to stay in the process. Gold collects in the anode slimes during electrolytic refining of the copper and can be recovered from these. All gold concentrates recovered using the processes described here still require refining.

23.7 Compounds [1, 12, 20, 32, 39, 63, 73–77]

Almost all gold compounds occur in the oxidation states 1+ and 3+. The oxidation states 2+ and 5+ are also known. Bimetallic compounds of gold(II) are usually mixed valence compounds containing gold(I) and gold(III).

The generally very low stability of binary gold(I) and gold(III) compounds based on ionic bonding can be ascribed to the structure of the two outer electron shells. The ten electrons of the 5d level and the single electron of

the 6s level differ only slightly in energy. Therefore, ionization of the 6s¹ electron to leave a 5s²6d¹⁰ valence shell, i.e., the reaction $\text{Au} \rightarrow \text{Au}^+$, is energetically not particularly favorable. Gold(III) compounds with the 5s²6d⁸ valence shell exhibit a tendency to fill the 5d level. Thus, the electron-acceptor effect is strong, and the compounds are strong oxidizing agents. The simultaneous participation of both outer electron shells gives rise to properties characteristic of the transition metals, such as variable oxidation state, colored compounds, and the tendency to form complexes.

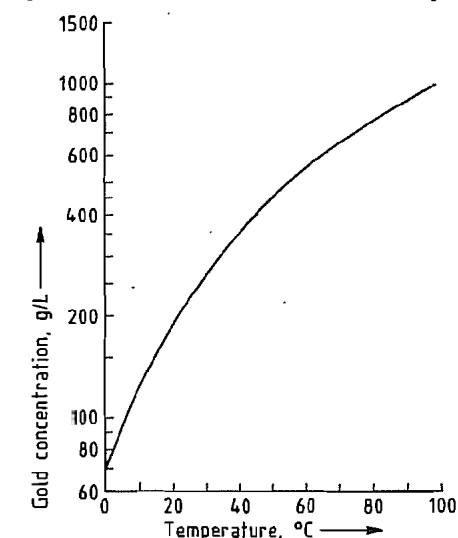


Figure 23.5: Solubility of potassium dicyanoaurate(I) in water as a function of temperature.

23.7.1 Potassium Dicyanoaurate(I)

Properties. Potassium dicyanoaurate(I), $\text{K}[\text{Au}(\text{CN})_2]$, ρ 3.452 g/cm³, forms colorless crystals which are readily soluble in water and alcohol, but insoluble in acetone and ether. The solubility in water is strongly dependent on the temperature (Figure 23.5). The effect of potassium cyanide concentration on the solubility of potassium dicyanoaurate is shown in Figure 23.6. The complex is neither air nor light sensitive and is stable in aqueous solution above pH 3.

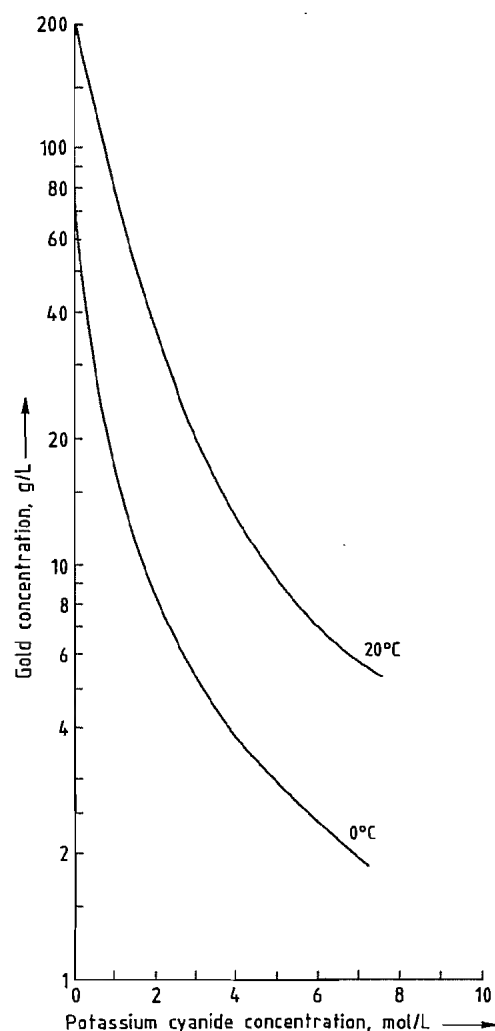


Figure 23.6: Dependence of the solubility of potassium dicyanoaurate(I) in water upon the concentration of potassium cyanide at 20 °C and at 0 °C.

Preparation [63, 78]. Potassium dicyanoaurate is prepared from fulminating gold, from gold(III) hydroxide, and by electrolysis.

From Fulminating Gold. Fulminating gold is precipitated from a solution of tetrachloroauric(III) acid by addition of excess aqueous ammonia; the precise composition of the precipitate is not known. The chloride content of the precipitate decreases with increasing excess of ammonia.

Fulminating gold must not be allowed to dry, since it is highly explosive in this state. The fulminating gold must be thoroughly washed with deionized water to remove chloride, since chloride ions interfere in electroplating processes. After washing, the precipitate is dissolved in a small excess of potassium cyanide solution. This is followed by filtration, concentration, and crystallization. The mother liquor is repeatedly reused in the process.

Electrolysis. When a gold anode is dissolved in aqueous potassium cyanide, potassium dicyanoaurate(I) is formed with hydrogen being liberated at the cathode. To prevent the dicyanoaurate(I) ion from being electrolyzed at the cathode with deposition of gold, a diaphragm is used. Fluoropolymer-based ion-exchange membranes are used for this purpose. The mother liquor is reused or worked up following crystallization of the potassium dicyanoaurate(I). This can be carried out under particularly mild conditions by using the continuously-cooled crystallization process. Cyanide and chloride are the major impurities. Electrolysis produces potassium dicyanoaurate(I) with a particularly low chloride content, which depends solely on the quality of the potassium cyanide and of the water.

From Gold(III) Hydroxide. Instead of fulminating gold, gold(III) hydroxide may be reacted with potassium cyanide solution. Precipitation of gold(III) hydroxide from tetrachloroauric(III) acid by addition of an alkali metal hydroxide does not always go to completion. Aging of the gold(III) hydroxide considerably reduces its rate of dissolution in potassium cyanide solution.

Uses and Economic Aspects. Potassium dicyanoaurate(I) serves as the gold component in the baths commonly used for electroplating and to a lesser extent in electroless plating.

With increasing utilization of gold-plated electronic components, the demand for gold plating baths, and hence for potassium dicyanoaurate(I), has grown considerably. In 1987, a little under one tenth of the 1300 t of gold

processed annually in the world was used by the electronics industry. In the jewelry industry, too, that demand has increased as a result of rolled gold being superseded by electroplating with hard gold.

23.7.2 Tetrachloroauric(III) Acid

Properties. Tetrachloroauric(III) acid, $H[AuCl_4]$, crystallizes as a tetrahydrate in the form of light yellow, deliquescent crystals. It is readily soluble in water, soluble in alcohol and ether, and is corrosive.

Preparation [63]. Tetrachloroauric acid is prepared by dissolving gold in warm aqua regia. In order to remove residual nitric acid, the solution is concentrated by evaporation with repeated addition of hydrochloric acid, and the resulting melt is poured into porcelain dishes. Moisture must be excluded while the melt cools, solidifies, and is finally powdered. Crystallization from the aqueous mother liquor produces an extremely hygroscopic material. Instead of nitric acid, other oxidants (e.g., chlorine) may be added to the hydrochloric acid. The high rate of dissolution of aqua regia is only rarely attained (Figure 23.1), but the pollution caused by it is lower and control of the reaction is simpler, especially under industrial conditions. Care must be taken to assure removal of any excess oxidants and their reaction products. Tetrachloroauric(III) acid can also be prepared by anodic dissolution of gold in hydrochloric acid, but this requires the use of a diaphragm.

Uses [1]. Tetrachloroauric(III) acid is used to prepare other gold compounds. It is also used to make gold ruby glass, gold purple (Purple of Cassius), and purple colorants for enameling of ceramics.

23.7.3 Sodium Disulfitoaurate(I)

Properties. Sodium disulfitoaurate(I), $Na_3Au(SO_3)_2$, is relatively unstable in the solid state, and is therefore not isolated as crystals for industrial use. It is stable in

weakly alkaline solutions above pH 8.5, even upon heating and when exposed to light.

Preparation. Sodium disulfitoaurate(I) is prepared from fulminating gold or from gold(III) hydroxide.

From Fulminating Gold. Fulminating gold is dissolved with stirring in a dilute solution of sodium hydrogen carbonate, sodium sulfite is then added. The reaction mixture is stirred at 70 °C until it clears. The pH must be maintained above 9. This is achieved by addition of sodium hydrogen carbonate solution. In order to remove ammonia, the solution is heated to about 90 °C with the simultaneous introduction of air. The gold content of the solution is kept at ca. 100 g/L by evaporation or by dilution with deionized water. This concentration is desirable for electroplating purposes. Instead of sodium sulfite, gaseous sulfur dioxide and a correspondingly higher quantity of sodium hydroxide solution may be used; the pH is controlled as described above.

From Gold(III) Hydroxide. Instead of fulminating gold, gold(III) hydroxide may be used. The reaction takes place under approximately the same conditions as with fulminating gold. The disadvantages are the same as in the preparation of potassium dicyanoaurate(I) from gold(III) hydroxide.

Uses. Sodium disulfitoaurate(I) is sometimes used in preference to potassium dicyanoaurate(I) in electroplating baths. These baths are especially advantageous for the production of ductile and wear-resistant coatings and in white-gold and rose-gold electroplating. Their drawbacks are difficult handling, shorter service life, and higher price. Their low toxicity is counterbalanced by problems in waste water disposal, e.g., those caused by the ethylenediaminetetraacetic acid (EDTA) complexes of the alloying elements.

Sodium disulfitoaurate(I) is increasingly being replaced by the corresponding ammonium salt, which provides special advantages with Au-Pd-Cu baths, such as the facility to produce very dense coatings.

23.7.4 Miscellaneous Gold

Compounds [1, 20, 63]

Bright gold preparations (gold sulfosulfates) are used for gilding ceramics and glass. Other compounds, some of which have applications in preparative and analytical chemistry, include gold(III) chloride AuCl_3 , gold(I) chloride AuCl , gold(III) hydroxide $\text{Au}(\text{OH})_3$ or $\text{AuO}(\text{OH})$, gold(III) oxide Au_2O_3 , the gold sulfides Au_2S , AuS , and Au_2S_3 , gold(I) cyanide AuCN , and gold(I) acetylide Au_2C_2 . Sodium dithiosulfatoaurate(I), $\text{Na}_3[\text{Au}(\text{S}_2\text{O}_3)_2] \cdot 2\text{H}_2\text{O}$, is used as a photographic sensitizer, and gold(III) selenate, $\text{Au}_2(\text{SeO}_4)_3$, for staining glass.

Gold compounds, particularly gold thiosulfate, gold mercaptides, and gold malate, have long been used for the treatment of rheumatic disease. The triethylphosphine gold complex of thioglucose tetraacetate, Auranofin, is very effective against chronic inflammation of joints. Gold(I) complexes of diphosphines may be beneficial in tumor therapy.

23.8 Alloys [1, 12, 20, 24, 31, 39, 79–90]

Gold forms alloys with many metals and metalloids. The most important alloys are composed of elements from the same group in the periodic table (Ag, Cu) and from the neighboring groups (Ni, Pd, Pt, less often Zn, Cd, Hg). The most frequently used elements, i.e., Ag, Cu, Ni, Pd, and Pt crystallize like gold with face-centered cubic unit cells, and coordination number 12. Thus, they readily form continuous solid solutions with gold, especially as their metallic atomic radii (Au 144.2 pm; Ag 144.5 pm; Cu 127.8 pm; Ni 124.6 pm; Pd 137.6 pm; Pt 137.3 pm) in certain cases are very similar. Zinc, cadmium, and mercury have metallic atomic radii of 133.5 pm, 148.9 pm and 150.3 pm, respectively. These metals all have hexagonal unit cells, which renders the formation of alloys with gold more complex.

The practical uses of gold alloys and of fine gold are mainly determined by their color,

hardness, corrosion resistance, melting point, and relative value. The degree of hardness can be controlled by heat treatment. The melting point plays a significant role during manufacture and processing.

For centuries, the color (Figure 23.7), hardness, and corrosion resistance of gold were modified by variations in the Au–Ag–Cu system. When white gold, with its resemblance to platinum, became fashionable at the beginning of this century, Ni and Pd were added; these were soon followed by Zn, and later by platinum. The gold alloys used for modern dental materials are complex because they must have specific properties.

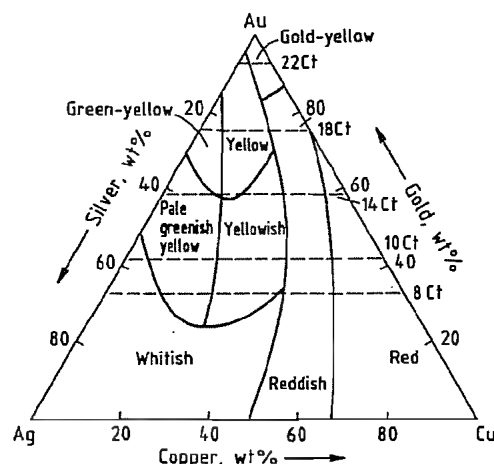


Figure 23.7: Gradation of color of gold-silver-copper alloys.

23.9 Quality Specifications and Analysis [20, 91, 92]

23.9.1 Quality Specifications [33]

The gold content of fine gold and gold alloys is usually expressed in fineness (parts per thousand) or in carat, where 24 carat represent 1000/000 fine, 18 carat thus being equal to 750/000. For ores, intermediate products, and older materials, the gold content is usually given in grams per metric tonne (g/t) (ppm), ounces per metric tonne (oz/t), and ounces per short ton, where 1 oz = 1 troy ounce = 31.1035

g and 1 short ton = 907.184 kg. Other units are 1 dwt = 1 pennyweight = 0.05 oz = 1.555 g and 1 troy grain = 1/24 dwt = 0.0648 g. 1 tola = 0.375 oz is an Indian measure for gold.

In general, marketable grades of gold are subject to the purity standards given in Table 23.2.

Table 23.2: Marketable gold qualities.

Designation	Gold content, %	Content of other metals, ppm
"Good delivery" gold	≥ 99.5	Any metals (total) ≤ 5000
Fine gold	≥ 99.99	Ag ≤ 100 Cu ≤ 20 others ≤ 30 total ≤ 100
Fine gold, chemically pure	≥ 99.995	Ag ≤ 25 others ≤ 25 total ≤ 50
Fine gold, high purity	≥ 99.999	Ag ≤ 3 Fe ≤ 3 Bi ≤ 2 Al ≤ 0.5 Cu ≤ 0.5 Ni ≤ 0.5 Pd + Pt ≤ 5.0 total ≤ 10

23.9.2 Sampling [93]

Accurate determination of gold depends on the use of correct sampling methods.

Exact procedures have been laid down for taking samples from ingots of raw gold, or from material separated in recycling processes. The samples may be taken by drilling, cutting, or sawing. As a rule, they are taken from several places in an ingot, which helps to avoid errors arising through possible segregation effects.

Powdered material is usually first screened to separate the fine from the coarse material. These are then subjected separately to a mechanical or manual sampling process.

Recycled electronic material usually contains only a few percent gold together with plastic and base metal components. Mechanical size reduction, e.g., in a shredder, or by cold grinding using liquid nitrogen, often produces material from which samples can be taken.

23.9.3 Quantitative Analysis

Quantitative analysis forms the basis for calculating the gold content of end products, intermediate products, gold ores, and recycling materials. The most important method for gold, as for silver, is still the centuries-old docimastic analysis, or docimasy (Greek: testing, assay), more commonly known as the fire assay. In this process, noble metals are taken up by molten lead, while base metals are removed by slagging. Two methods are used. In the *crucible assay*, a mixture of lead oxide, a reducing agent (e.g., carbon), and a flux is melted at ca. 1250 °C. In the *scorification assay*, the sample is subjected to oxidative smelting with grain lead and borax at ca. 1000 °C. In each case, a bead of lead containing gold and other noble metals is formed. The lead is then oxidized at ca. 800 °C to litharge (PbO) on a magnesia bed (cupellation process). The PbO melt is absorbed by the porous magnesia and a drop of noble metal, which later solidifies to a grain, remains behind. If the grain contains platinum-group metals in addition to gold, then a chemical or physical analysis follows. Reductive precipitation followed by weighing the gold is the most common method. X-Ray fluorescence analysis of the grain has the advantage of greater speed and economy [94, 95].

In the gold trade, docimasy is the generally accepted method for determining gold. Annual mercantile transactions worth ca. DM 40×10^9 are based on the results of docimastic analyses. Determination of the gold content of high-percentage alloys using physical methods has not been accepted, because it is not sufficiently accurate. The gold content of fine gold can be determined far more accurately from the sum of the impurities than by direct determination of the noble metal content.

23.9.4 Purity Analysis

Purity tests for commercial gold are today almost exclusively carried out by physical methods, the most important being emission spectrography, plasma emission spectrogra-

phy, and atomic absorption spectroscopy. In special cases, mainly for ultrapure materials, mass spectroscopy, glow discharge, and neutron activation are used. Physical methods have largely replaced chemical and colorimetric methods in the determination of trace impurities for reasons of economy and speed.

23.9.5 Trace Analysis

The determination of trace amounts of gold is important in ore prospecting and in the evaluation of residues and waste materials from the metallurgical industry. The gold content of these materials may be very low (ca. 1–1000 ppm). The solids can be dissolved and the resulting solution analyzed by atomic absorption spectroscopy. The solution can be enriched prior to the determination, if required, by solvent extraction. Alternatively, metallic gold can be collected in molten copper or lead. The resulting alloy can then be dissolved and the solution analyzed by atomic absorption spectroscopy. The solid alloy can be analyzed by neutron activation, total reflection X-ray fluorescence, and inductively coupled plasma mass spectroscopy. Fire assaying is also still significant in this field.

23.10 Uses of Gold and Gold Alloys [6, 12, 19, 20, 24, 31, 33, 39, 41, 96]

23.10.1 Coins, Medals, Bars [97]

In antiquity, gold was considered an object of value and used as a means of exchange, at first in the form of nuggets or flattened disks, and from 650 B.C. as minted coins. The composition of the metal used varied from alloys containing a high proportion of gold, to electrum which had a relatively high silver content. The confusing variety of gold coins, and the great variation in fine gold content, was first limited in the 19th century, when legal regulations were introduced for coinage, which specified nominal values of gold coins, their weight, and gold content. After World War I, gold coins were no longer legal tender.

They are now traded as collectors' items and as a form of investment. With the liberalization of private gold trading in the 1950s, the demand for gold increased. A successful new enterprise in this market was the minting and marketing of the krugerrand (gold content of 1 oz troy) by South Africa. Between 1967 and 1985, a total of 2000 t (ca. 65×10^6 oz) were sold. Following the repressive measures which have been inflicted on the krugerrand, new coins were introduced by other countries (Table 23.3).

Gold was already stored in the form of bars in antiquity, especially in Rome. Today, gold bars weighing ca. 400 oz (ca. 12 kg) of good delivery quality (99.5%) are the main form used in public and institutional investment. Gross weight, gold content, the manufacturing firm and reference number are stamped on the bars, and provide direct and binding information as to their value. Smaller gold bars are manufactured for private investors.

The difference between the buying and selling price in banks (broker's commission) is normally ca. 3–4% plus value added tax.

23.10.2 Jewelry [98]

Fine Content of Jewelry Gold. The gold value of jewelry alloys is determined by their gold content (fineness). In most countries, laws govern the terms used in designating the fineness of gold jewelry for manufacturers, processors, and dealers.

Only alloys with a minimum gold content of 585/000 are sufficiently tarnish resistant for jewelry. Better quality jewelry customarily has a gold content of 750/000. These alloys offer optimum color and mechanical properties. For less expensive jewelry, alloys with a low gold content are often used. In Germany, 333/000 fine is common, and in the United States 417/000. These alloys tarnish under unfavorable conditions, and cracks may form as a result of stress corrosion. The highest grade alloys are used only occasionally in the manufacture of jewelry, due to their low strength. However, no alloy can match the fine color of pure gold.

Table 23.3: Coinage alloys.

Coin	Country	Mintage period	Fineness	Carat	Gross weight, g	Gold content
20 mark	German Reich	1871–1915	900	21.6	7.964	7.168
10 mark			900	21.6	3.982	3.584
5 mark			900	21.6	1.991	1.792
1 ducat	German Confederation	up to 1871	986.1	23.7	3.490	3.441 g
Krugerrand ^a	South Africa	since 1967	916.6	22	33.931	1 oz
Maple Leaf ^a	Canada	since 1979	999.9	24	31.103	1 oz
American Eagle ^a	United States	since 1986	916.6	22	33.931	1 oz
Britannia ^a	Great Britain	since 1987	916.6	22	33.931	1 oz
Nugget ^a	Australia	since 1987	999.9	24	31.103	1 oz
Tscherwonez	Former USSR	since 1975	900	21.6	8.60	7.74 g

^a Also in $\frac{1}{2}$, $\frac{1}{4}$, and $\frac{1}{10}$ oz gold.

Table 23.4: Composition of gold alloys for jewelry.

	Gold content, %	Content of alloy components, %
<i>Colored gold</i>		
20 carat	88.3	Ag 0–16.7, Cu 0–16.7
18 carat	75	Ag 0–20, Cu 5–25
14 carat	58.5	Ag 8–34, Cu 7.5–33.5
8 carat	33.3	Ag 8qP35, Cu 30–55, Zn 0–20
<i>White gold</i>		
18 carat	76	Cu 4–8, Ni 10–18, Zn 3–6
18 carat	75	Pd 10–20, Cu + Zn 5, rest Ag
14 carat	59	Cu 15–25, Ni 10–16, Zn 5–8

Colored gold alloys used in the jewelry industry are mostly based on the ternary alloy system Au–Ag–Cu, allowing a wide variety of colors. The workability and resistance to wear of an alloy depend on its mechanical properties; these, and its resistance to corrosion, can be controlled by adding zinc. The classification ranges for colored gold alloys used in the jewelry sector are shown in Table 23.4. To designate the different qualities, special codes are used, most of which are specific to particular firms. The properties cover a broad range of values to meet all practical requirements (Table 23.5). In 1966 in Germany, an industrial standard, DIN 8238 "Gold colors" (including white gold), was created to standardize colors in gold alloys and to provide manufacturers with a better means of mutual understanding. This standard closely reflects similar specifications in Switzerland

and France. A combination of values representing tone (T), saturation level (S), and darkness (D), measured using spectrophotometric methods, is attributed to each color (Table 23.6).

Gold Solders. The most frequently used method of making joins in the manufacture of jewelry from gold alloys is hard soldering. In addition to fine gold, colored gold solders also contain silver, cadmium, copper, and zinc. Their melting temperature is always lower than that of the material to be soldered. The additives are adjusted so that the solders have graduated working temperatures. Three solders are generally sufficient, with graduations of ca. 50 °C in their working temperatures. Some examples of colored gold solders are given in Table 23.7.

White gold alloys were first developed in the early 1900s, in an effort to replace platinum by a cheaper material with identical properties. White gold also differs from colored gold in having a higher melting range and is usually harder. Nickel and palladium are the only suitable additives to give gold a color approaching whitish-gray. The demand for white gold has fallen in the last few years in favor of colored gold and platinum. Information about white gold alloys is given in Table 23.4.

Table 23.5: Properties and applications of jewelry gold alloys.

Carat	Designation	Color	Melting range, °C	Density, g/cm ³	Brinell hardness (after soft annealing), kg/mm ²	Rings, brooches	Deep pulling work	Pressing work	Enamelling	Castings	Chains, lattice work	Blanks for minting	Bracelets	Wedding ring blanks	Pipes, seamless
Colored gold															
18 ct	750/2	red	880–865	15.0	140 hard	•			•				•		
	750/4½	reddish	875–850	15.3	125 medium hard	•				•					
	750 150	pale yellow	900–850	15.5	120 medium hard	•	•	•		•	•		•	•	•
	750 130	yellow	890–850	15.5	125 medium hard	•	•	•		•	•		•	•	•
	750/10	pale yellow	970–900	15.8	85 soft		•		•			•			
14 ct	585/2	red	920–880	13.0	105 soft	•	•	•	•	•	•			•	
	585/4	reddish	905–860	13.1	125 medium hard	•									
	585/5 M	reddish yellow	860–790	13.2	120 medium hard	•				•			•	•	
	585/10	deep yellow	845–825	13.6	160 very hard									•	
	585/13	pale yellow	840–800	13.7	140 hard									•	
	585/15	pale yellow	890–820	13.7	125 medium hard	•	•	•	•	•	•		•	•	•
	585/17	green yellow	980–940	13.8	100 soft		•	•	•		•	•			
8 ct	333/4½	reddish	930–890	11.0	100 soft	•					•	•	•		
	333/6	pale yellow	845–770	10.9	90 soft	•	•	•		•	•	•			
	333/9	yellow	860–750	11.1	120 medium hard								•	•	•
	333/16	pale yellow	810–750	11.5	125 medium hard				•						
White gold															
18 ct	760 H	white contains Ni	950–875	14.8	185 very hard or hard	•				•					
	750 M	white contains Pd	1170–1040	16.0	110 medium hard or hard	•									
	750 S	white contains Pd	1170–1040	15.6	95 soft	•	•	•		•	•			•	
14 ct	590 H	white contains Ni	1000–870	12.8	150 hard	•				•			•		
	590 M	white contains Pd	1120–1060	14.1	130 medium hard or hard	•									
	590 S	white contains Pd	1150–1050	14.0	95 soft	•	•	•		•	•			•	

Table 23.6: Gold colors according to DIN 8238.

Symbol	German classification	Swiss and French classification	Colorimetric measures according to DIN 6164			Examples of approximately corresponding gold alloys
			T	S	D	
N	weiß		1.2	0.9	1.6	590 H
8 N	grün gelb		24.8	1.6	1.2	585/17
1 N	blau gelb	jaune pâle	1.7	1.7	1.2	585/15
2 N	hell gelb	jaune pâle	1.8	1.8	1.3	750/150
3 N	gelb	jaune	2.0	1.8	1.3	750/130
4 N	rosé	rosé	2.4	1.6	1.4	750/4½
5 N	rot	rouge	2.6	1.5	1.4	750/2

Table 23.7: Working temperatures of colored gold solders.

Gold content, carat	Solder designation (Degussa)	Working temperature, °C
18	L 750/3	820
	L 750/1:	750
	L 750/1	700
14	L 585/7	780
	L 585/8	720
	L 585/3½	670
8	L 333/15	700
	L 333/10½	640

23.10.3 Electronics and Electrical Engineering [99, 100]

Modern electronics require the use of noble metals, especially gold, particularly in the areas of information processing, telecommunications, and military and space electronics. It is used in active components (diodes, transistors, integrated circuits, semiconductor memories), assembly and connection engineering (packages, thick-film circuits, printed boards, and plugs) and, to a lesser extent, for passive components (capacitors and resistors).

The great advantage of gold is its high resistance to oxidation and corrosion, and its high conductivity which give it excellent contact properties. Gold plating is usually carried out by electrochemical deposition. Thin gold coatings can also be produced by firing of gold-containing pastes, usually coated on ceramics. Gold is very malleable, so that it can be worked into very thin bonding wires, usually with a diameter of ca. 25 µm. Fine gold wires can easily be welded to each other, or to other metals, by pressure or by a combination of heat and pressure. These microwelded joints can easily be made on microelectronic circuits at high speed.

Modern methods used in bonding chips require bumps on the contact surfaces of the crystal; these bumps are made from gold.

The gold used in electronics, with the exception of gold solders, is practically always fine gold of purity 99.99 or 99.999%. Very few parts are made of massive gold for reasons of economy.

Because of its high price, gold is not used a great deal in electrical engineering. Roll-bonded gold claddings, or gold coatings made by electrodeposition, are occasionally used for special contact problems. Gold–nickel and gold–silver alloys are used in weak-current engineering, as contact materials for very low voltage switches, and where the contact forces are low (relays, plugs, measuring instruments). Micromigration of these alloys is very low, and there is little tendency for insulating layers to form.

Gold–manganese alloys are used for wire-wound resistance thermometers. The thermocouples Cu + Au 99.4/Co 0.6 and Pt 90/Ir 10 + Au 60/Pd 40 are suitable for the temperature ranges 0 to –240 °C and 0 to 700 °C, respectively; the gold alloys form the negative leg.

23.10.4 Solders [101]

The eutectics of the following systems are used as solders for joining materials in transistor production technology: gold–tin (25% Sn, *mp* 280 °C), gold–silicon (30% Si, *mp* 370 °C), and gold–germanium (26% Ge, *mp* 350 °C).

Alloys of gold with tin or silicon are used to make hard solders with a low melting point, high corrosion resistance, good thermal and electrical conductivity, and high mechanical strength. Heat-sensitive components are soldered using these materials.

Certain types of apparatus have components made of iron and nickel alloys which have to withstand high vacuums and high temperatures. To join these materials, vacuum hard solders are used, made of either fine gold, or gold–copper, gold–silver–copper, gold–nickel, gold–copper–nickel, and gold–palladium alloys. Soldering is carried out in a vacuum furnace or in a protective gas (hydrogen, cracked gas).

Hard silver solder is normally used to join stainless steels. However, if these joints do not exhibit sufficient corrosion resistance, gold–nickel–zinc alloys similar to white gold, with ca. 80% gold, 15% nickel, and 5% zinc, are occasionally used.

23.10.5 Pen Nibs

Nibs for fountain pens are usually made from Au–Ag–Cu yellow gold alloys which are relatively hard; occasionally white gold alloys are also used. The alloys must be able to withstand the very corrosive ferro-gallic inks; only 14 or 18 carat alloys are suitable. The nib points must be made of hard metal alloys, which usually contain Ru, Os, Ir, W, or Co.

Nibs made of stainless, ink-resistant nickel chromium steel are sometimes coated with a thin layer of gold; however, this does not improve their ink resistance.

23.10.6 Chemical Technology [102]

Gold-platinum alloys containing 50–70% gold, which can be age-hardened, are used to make spinnerets used in the production of man-made fibers. Their fine-grained structure is of great advantage in making the necessary fine holes (diameter 25–120 μm).

Gold alloys are sometimes used for seals and rupture disks that come into contact with corrosive substances. A gold-silver-palladium alloy (Pallacid) containing 30% gold and 30% palladium is resistant to strong mineral acids, is considerably cheaper than gold, and also has greater high-temperature strength.

A gold alloy containing 10% platinum is used to make crucibles for analytical laboratories, e.g., for ash determination of flour and other phosphorus-containing foods. Unlike platinum crucibles, it is resistant to corrosion by phosphorus compounds when red-hot.

23.10.7 Dental Materials

Gold alloys are of great importance in prosthetic dentistry, for solid parts such as gold fillings, crowns, bridges, cast dentures, clasps, anchorage pins, and metal bases for dental ceramics. These materials have to meet a number of requirements. They must be resistant to normal conditions in the mouth, of a suitable color, of different strengths, and be easy to work. Today almost all alloys used are of a complex composition, containing high proportions of gold, palladium, and platinum. The advantage of these alloys mainly lies in their very fine-grained and homogeneous structure.

23.10.8 Coatings [103–105]

The technical and decorative properties of gold can be combined with a variety of cheap

base materials, by applying a thin layer of gold to base metals, ceramics, glass, or plastics.

Electroplating is by far the most frequently used method. In most cases, gold is separated from an electrolyte containing potassium dicyanoaurate. Occasionally, electroplating baths containing sodium disulfiteaurate or cyanide complexes of trivalent gold are used.

Electroforming is used to manufacture cheap hollow jewelry. Gold up to a thickness of 0.2 mm is deposited on a mandrel. The mandrel is then removed; wax mandrels can be melted out. A self-supporting gold layer is left, which can be reinforced by a filler material.

Bright Gold. Ceramic materials, especially high-quality porcelain and glass, are often gilded by firing on preparations of bright gold and burnished gold. The essential components of these lacquer-like paints are gold sulfosinates, mixed with natural oils and resins. The colors are applied either by hand, or by screen or offset printing processes. Firing is carried out at 500–1250 °C. Gold coatings for technological applications also may be applied by this method.

Rolled gold is still used for spectacle frames and gold-plated watches. However, it has lost its former significance in favor of electroplating. Rolled gold is fabricated by soldering gold sheets, usually 14 carat, to blocks made of copper alloy or stainless steel. These are then rolled or drawn to the desired shape, producing strips and wires with a largely non-porous gold coating, usually 510 μm thick.

Fire Gilding. In this process, the part to be gilded is painted with gold amalgam. The mercury is evaporated by heating, leaving a relatively thick gold layer. The process is very problematical with regard to industrial hygiene.

Vapor Deposition of Gold. Glass panes can be insulated against loss of heat, through reflection of infrared rays, by applying very thin layers of gold in a sputtering process (cathode evaporation). Plastic components can be thinly gilded by sputtering in a vacuum.

Gilded films are also used in space technology, e.g., in space suits, to produce reflective coatings and thus protect against heat.

23.10.9 Gold Leaf

Gold leaf is usually made of fine gold or Au-Ag-Cu alloys with a very high gold content. The crystal plane {100} in beaten gold leaf lies in the plane of the leaf. Gold leaf is used to gild wooden statues, book edges, and fabric prints. In certain beverages (Danziger Goldwasser), and recently also in some foods, it is used to achieve visual effects.

In former times, small rolls of gold leaf were used to fill cavities in teeth.

23.10.10 Catalysts

Gold is of almost no significance as a catalytically active metal. It is occasionally used as an additive in platinum-group metal or silver-based catalysts.

Platinum vapor, which forms from platinum-rhodium catalysts during the oxidation of ammonia to nitric acid can be retained by a gold or gold-palladium gauze. This process has long been in industrial use.

23.11 Economic Aspects [2, 4, 18–20, 33, 34, 41, 106–111]

Production. Gold represents a significant portion of the total world economy. In South Africa, it occupies in terms of value the highest position among all industrial goods. Over 500 000 people are employed worldwide in gold production. The value of the gold from primary production in 1987 was DM 32×10^9 . Thus it occupies third place in the metal trade, after pig iron (DM 200×10^9) and aluminum (DM 45×10^9), and before copper (DM 22×10^9).

At present, almost half of the gold obtained from ores is produced in South Africa. Brazil, the United States, Canada, and Australia are currently expanding production. Since the dis-

covery of the large Brazilian deposits around 1970 and the new activities of other producer countries, the supply is more balanced and less dependent on political constellations than it used to be. Table 23.8 shows the primary production of gold in the various producer countries.

Supply and Demand. As a consequence of the free market, the supply and demand for gold are on the whole quite well balanced. High prices are regulated by reduced consumption, especially in the jewelry sector, and in investment purchases, as well as through the replacement of noble metals used in technology by other materials. The price is also reduced by the expansion of primary production and recycling, as well as by reductions in stocks. Low prices then cause an increase in demand, renewed reductions in primary and secondary production (often because profitability sinks too low), and accumulation of reserves.

The supply of gold on the market in 1987 was about 2000 t/a (Figure 23.8). Most of this (65%) came from Western mine production, 20% came from recycling processes, and 15% was sold by Eastern-bloc countries. Buying and selling on the part of government monetary authorities can have a strong effect on the market; at the present time, however, this effect is insignificant. The same applies to the sale of private stocks.

Figure 23.9 shows the demand for gold according to applications.

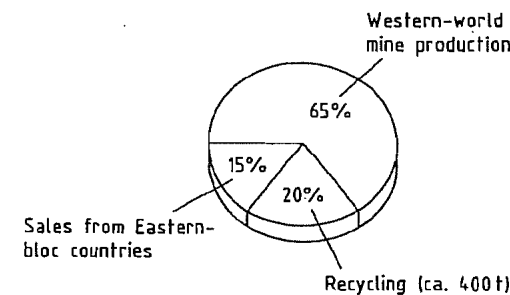


Figure 23.8: Gold supply in 1987 (ca. 2000 t).

Table 23.8: Primary gold production in various producer countries, t.

Country	1900	1930	1940	1950	1960	1970	1975	1980	1985	1986	1987
South Africa	10	333	437	363	665	1000	713	675	672	640	607
United States	119	69	150	74	46	54	32	31	80	118	155
Canada	4	65	165	138	143	75	52	52	52	106	120
Australia	110	19	66	29	35	20	16	17	59	75	108
Brazil	4	a	a	a	a	9	12	35	72	67	84
Philippine Islands	a	a	a	a	a	19	16	22	37	40	40
Papua/New Guinea	0	a	a	a	a	1	18	14	31	36	34
Colombia	3	a	20	13	14	7	11	17	26	27	26
Chile	a	a	a	a	a	a	4	7	18	19	19
Venezuela	a	a	a	a	a	a	a	1	12	15	16
Zimbabwe (Rhodesia)	3	17	25	16	18	15	11	11	15	15	14
Japan	2	11	26	0	11	8	5	7	9	14	14
Zaire (Congo)	0	4	15	11	10	6	4	3	8	8	12
Ghana (Gold Coast)	1	8	28	21	27	22	16	11	12	12	12
Peru	a	a	a	a	a	3	3	5	11	11	11
Mexico	14	21	28	12	9	6	5	6	8	8	8
Dominican Republic	a	a	a	a	a	0	3	12	10	9	8
Bolivia	a	a	a	a	a	a	a	2	6	6	6
India	16	10	9	6	5	3	3	3	2	2	2
Others	64	43	151	67	71	22	19	30	55	48	78
Former Soviet Union	30 ^b	27	140	138	143	336	407	c	c	c	c
Other Eastern-bloc countries				c	c	18	20	c	c	c	c
Total	390	627	1260	900	1200	1624	1370	1400	1600	1600	1700

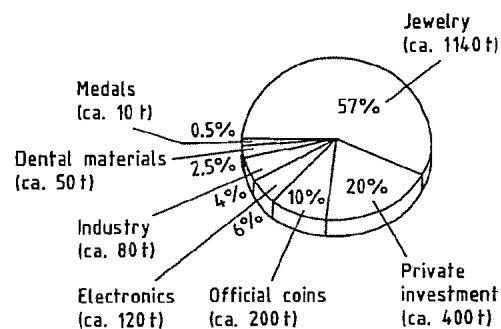
^aIncluded in others.^bImperial Russia.^cData withheld.

Figure 23.9: Gold demand in the western world in 1987 (ca. 2000 t).

Gold Trade. London is the most important market for gold in terms of the quantity traded. The London gold market has a fixing system, whereby the price of gold is determined twice daily, according to supply and demand, by representatives from five firms of brokers. This is then published as the "fixed price". The United States futures markets have a strong influence on the calculation of this price. The fixed price serves as an orientation point for gold traders all over the world.

Zürich is also an important center of the gold trade, and is comparable to London in terms of quantity. A considerable part of the gold from South African primary production, which up to 1968 all went to London, is now sold to Zurich, as well as most of the gold from the former Soviet Union.

Other important centers are New York and Chicago. Other metal exchanges, such as Hong-Kong, Frankfurt, Paris, Singapore, and Tokyo, are of more regional importance.

Gold is traded internationally in the form of gold bars of various weights, and with a gold content of 99.50–99.99%. In London, gold bullion must contain gold weighing between 350 and 430 oz; the commonest figure is about 400 oz (ca. 12 kg).

Important factors which influence the price of gold are assessment of political circumstances, inflation rates, and the rate of interest of the US dollar as a key world currency. The huge gold holdings of the issuing banks (ca. 30 000 t) could have a great effect on the price of gold, if anything were to change in the

present role of gold in the monetary system. Today its role is limited to providing backing for credits and partially for the current money, and to the procurement of foreign exchange through sales.

On July 19th, 1989, the price of gold was \$370 per ounce (DM 23.20 per gram).

23.12 Toxicology and Occupational Health [112, 113]

Gold, even if finely divided, has no effect on living organisms. Like most soluble heavy metal salts, compounds of trivalent gold, especially the complexes, have a toxic effect when they enter into the metabolism. In the case of gold, however, only the side-effects of clinical gold therapy for arthritis are known in this connection. The side effects include kidney and liver damage, stomatitis, and hematopoietic disorders [114].

Tetrachloroauric acid, $H[AuCl_4]$ in aqueous solution is a strong acid, and can thus have a caustic effect. In contact with the skin, the compound is reduced to elemental gold and becomes red. The complex $K[Au(CN)_2]$ is toxic due to its cyanide content. Neither MAK, TLV, nor ADI values have been established for gold and its compounds.

23.13 References

- Gmelin, System no. 62.
- H. Quiring: *Die metallischen Rohstoffe*, 2nd ed., vol. 3 "Gold", Enke Verlag, Stuttgart 1953.
- Degussa, *Sol & Luna – auf den Spuren von Gold und Silber*, Frankfurt 1973.
- B Neumann: *Die Metalle – Geschichte, Vorkommen und Gewinnung nebst ausführlicher Produktionsstatistik*, Verlag Wilhelm Knapp, Halle 1904.
- H. Moesta: *Erze und Metalle – ihre Kulturgeschichte im Experiment*, Springer Verlag, Berlin 1983.
- H. Römpf: *Chemie der Metalle*, Franckh'sche Verlagshandlung, Stuttgart 1941.
- H. W. A. Sommerlatte: *Gold und Ruinen in Zimbabwe – aus Tagebüchern und Berichten des Schwaben Karl Mauch (1837–1875)*, Verlag Bertelsmann Fachzeitschriften GmbH, Gütersloh 1987.
- A. Hartmann, E. Sangmeister: "Zur Erforschung urchgeschichtlicher Metallurgie", *Angew. Chem.* 84 (1972) 668–678.
- K. Löhberg: "Beiträge der Metallkunde zur Archäologie", *Jahrbuch 1979 der Berliner Wissenschaftlichen Gesellschaft e. V.*, p. 48.
- G. Biegel (ed.): *Das erste Gold der Menschheit*, Verlag Karl Schillinger, Freiburg 1986.
- F. Kirchheimer: "Über das Rheingold", *Jahreshefte des geologischen Landesamts Baden Württemb.* 7 (1965) 77.
- World Gold Council, *Gold Bulletin – Quarterly review of research on gold and its applications in industry*, vol. 1 (1968)–vol. 22 (1989), Geneva.
- A. Binz: *Edelmetalle – ihr Fluch und Segen*, Limpert-Verlag, Berlin 1943.
- H. Pohl: *Gold – seine Macht und Magie in der Geschichte*, W. Heyne Verlag, München 1958.
- C. H. V. Sutherland: *Gold – Macht, Schönheit und Magie*, Verlag A. Schroll & Co., Wien–München 1970.
- G. Breitling et al.: *Das Buch vom Gold*, Verlag C. J. Bucher, Luzern–Frankfurt 1975.
- H. G. Fuchs: *Gold*, Fritz Knapp Verlag, Frankfurt 1981.
- P. Vilar: *Gold und Geld in der Geschichte*, Verlag H. C. Beck, München 1984.
- H. J. Funk (ed.): *Gold*, Edition Deutsche Bank, Battenberg Verlag, München 1986.
- Fonds der Chemischen Industrie, *Edelmetalle – Gewinnung, Verarbeitung, Anwendung*, Folienserie, Frankfurt 1989.
- A. Neuburger: *Die Technik des Altertums*, Voigtländer Verlag, Leipzig 1920, Prisma-Verlag, Gütersloh 1983.
- J. H. F. Notton, "Ancient Egyptian Gold Refining", *Gold Bulletin* 7 (1974) 50–56.
- V. Tafel: *Lehrbuch der Metallhüttenkunde*, vol. 1, S. Hirzel Verlag, Leipzig 1951.
- Degussa, *Edelmetall-Taschenbuch*, Frankfurt 1967.
- Doduco, *Datenbuch*, Pforzheim 1974.
- R. C. Weast: *Handbook of Chemistry and Physics*, 69th ed., CRC-Press, Cleveland 1989.
- D'Ans-Lax: *Taschenbuch für Chemiker und Physiker*, Springer Verlag, Berlin 1967.
- D. G. Cooper: *Das Periodensystem der Elemente*, Taschentext Nr. 6, Verlag Chemie, Weinheim 1972.
- G. H. Aylward, T. J. V. Findlay: *Datensammlung Chemie*, Taschentext Nr. 27, Verlag Chemie, Weinheim 1975.
- F. Fluck, K. G. Heumann: *Periodic Table of the Elements*, VCH Verlagsgesellschaft, Weinheim 1986.
- E. M. Wise: *Gold—Recovery, Properties and Application*, Van Nostrand, New York 1964.
- C. E. Wicks, F. E. Block: *Thermodynamic Properties of 65 Elements – their Oxides, Halides, Carbides, and Nitrides*, Bureau of Mines Rep. No. 605, Washington, DC, 1963.
- W. Gocht: *Handbuch der Metallmärkte*, 2nd ed., Springer Verlag, Berlin 1985.
- R. Saager: *Metallische Rohstoffe von Antimon bis Zirkonium*, Bank Vontobel, Zürich 1984.
- J. Lurie: *South African Geology for Mining, Metallurgical, Hydrological and Civil Engineering*, McGraw-Hill, Johannesburg 1981.
- C. B. Coetzee: *Mineral Resources of the Republic of South Africa*, Pretoria, Department of Mines, 1976.

37. H. Schneiderhöhn: *Erzlagerstätten*, G. Fischer Verlag, Stuttgart 1962.
38. R. Jackson: *Ok Tedi – The Pot of Gold*, World Publishing Co., Boroko, Papua-New Guinea, 1982.
39. *Kirk-Othmer*, 3rd ed., 11, pp. 972–995.
40. F. Pawlek: *Metallhüttenkunde*, de Gruyter, Berlin 1983.
41. Wilmacher-Küchler, 3rd ed., 4, 544–547.
42. *Ullmann*, 3rd ed., 8, pp. 269–284.
43. G. Agricola, *Vom Berg- und Hüttenwesen*, DTV-Verlag, München 1980.
44. D. Meadows, E. Zahn, P. Milling: *Die Grenzen des Wachstums*, Deutsche Verlagsanstalt, Stuttgart 1972.
45. R. J. Adamson (ed.): *Gold Metallurgy in South Africa*, Chamber of Mines, Johannesburg 1972.
46. J. V. N. Dorr, F. L. Bosqui: *Cyanidation and Concentration of Gold and Silver Ores*, McGraw-Hill, New York 1950.
47. A. King: *Gold Metallurgy on the Witwatersrand*, Chamber of Mines, Johannesburg 1949.
48. D. M. Liddell: *Handbook of Nonferrous Metallurgy*, McGraw-Hill, New York 1945.
49. T. K. Rose, W. A. C. Newman: *The Metallurgy of Gold*, Griffin, London 1937.
50. E. A. Cho, S. N. Dixon, C. H. Pitt: "The Kinetics of Gold Cyanide Adsorption onto Activated Charcoal", *Metall. Trans. B* 10B (1979), 185–189.
51. A. S. Dahya, D. J. King: "Developments in Carbon-in-Pulp Technology for Gold Recovery", *CIM Bull.* 76 (1983) no. 857, 55–61.
52. C. A. Fleming: "Some Aspects of the Chemistry of Carbon-in-Pulp and Resin-in-Pulp Processes", in *papers presented at The Australasian Institute of Mining and Metallurgy, Seminar on Carbon-in-Pulp Technology for the Extraction of Gold*, Kalgoorlie (Australia), July 1982.
53. C. A. Fleming in K. Osseo-Assare, J. D. Miller (eds.): *Hydrometallurgy: Research, Development and Plant Practice*, "Recent Developments in Carbon-in-Pulp Technology in South Africa", The Metallurgical Society of AIME, Warrendale, PA, 1983, pp. 839–858.
54. C. A. Fleming, M. J. Nicol: "The Adsorption of Gold Cyanide onto Activated Carbon III. Factors Influencing the Rate of Loading and the Equilibrium Capacity", *J. S. Afr. Inst. Min. Metall.* 84 (1984) no. 4, 85–93.
55. C. A. Fleming, M. J. Nicol, D. J. Nicol: "The Optimization of a Carbon-in-Pulp Adsorption Circuit Based on the Kinetics of Extraction of Aurocyanide by Activated Carbon", *paper presented at the Symposium: Ion Exchange and Solvent Extraction in Mineral Processing held at Mintek, Randburg, Feb. 1980*.
56. P. A. Laxen, G. S. M. Becker, R. Rubin: "Developments in the Application of Carbon-in-Pulp for Gold Recovery from South African Ores", *J. S. Afr. Inst. Min. Metall.* 79 (1979) no. 11, 315–326.
57. P. A. Laxen, T. D. Brown in L. F. Haughton (ed.): *Mintek 50: Proceedings of the International Conference on Mineral Science and Technology*, "The Carbon-in-Pulp Plant at Rand Mines Mining and Mining Company Limited: Problems and Development", vol. 2, Council for Mineral Technology, Randburg 1985, pp. 695–706.
58. P. A. Laxen, C. A. Fleming, D. A. Holtum, R. Rubin in H. W. Glen (ed.): *Proceedings, Twelfth Congress of the Council of Mining and Metallurgical Institutions*, "A Review of Pilot-Plant Testwork Conducted on the Carbon-in-Pulp Process for the Recovery of Gold", vol. 2, The South African Institute of Mining and Metallurgy, Johannesburg 1982, pp. 551–561.
59. G. J. McDougall, R. D. Hancock: "Gold Complexes and Activated Carbon. A Literature Review", *Gold Bull.* 14 (1981) no. 4, 138–153.
60. M. J. Nicol, C. A. Fleming, G. Cromberge: "The Adsorption of Gold Cyanide onto Activated Carbon. I. The Kinetics of Adsorption from Pulp", *J. S. Afr. Inst. Min. Metall.* 84 (1984) no. 2, 50–54.
61. M. J. Nicol, C. A. Fleming, G. Cromberge: "The Adsorption of Gold Cyanide onto Activated Carbon. II. Application of the Kinetic Model to Multistage Absorption Circuits", *J. S. Afr. Inst. Min. Metall.* 84 (1984) no. 3, 70–78.
62. D. F. Williams, D. Glasser: "The Modelling and Simulation of Processes for the Absorption of Gold by Activated Charcoal", *J. S. Afr. Inst. Min. Metall.* 85 (1985) no. 8, 237–243.
63. G. Brauer: *Handbuch der Präparativen Anorganischen Chemie*, vol. 2, 3rd ed., Enke Verlag, Stuttgart 1978.
64. Chamber of Mines (ed.): *Rand Refinery*, P.R.D. Series No. 149, Johannesburg 1970.
65. G. Eger: *Das Scheiden der Edelmetalle durch Elektrolyse*, W. Knapp Verlag, Halle 1929.
66. M. Fiberg, I. R. Edwards: *The Extraction of Gold from Chloride Solutions*, Report No. 1996, National Institute for Metallurgy, Randburg 1978.
67. W. W. Behning, *Metall (Berlin)* 24 (1970) 794.
68. E. Krone, W. Dähne, *Chem. Ztg.* 101 (1977) 421.
69. G. Cornelius, *Erzmetall* 32 (1979) 467.
70. *Recycling – Rohstoffsicherung und Umweltschutz*, Degussa, Frankfurt (M) 1981.
71. F. H. Burstall, P. J. Forrest, R. A. Wells, *Ind. Eng. Chem.* 45 (1953) 1648–1658.
72. K. B. Ball, *World Min.* 27 (1974) no. 11, 44–45.
73. R. J. Puddephatt: *The Chemistry of Gold*, Elsevier, Amsterdam 1978.
74. G. Wilkinson, R. D. Gillard, J. A. McCleverty: *Comprehensive Coordination Chemistry*, vol 5, Pergamon Press, Oxford 1987.
75. G. Wilkinson, F. G. A. Stone, E. Abel: *Comprehensive Organometallic Chemistry*, vol. 2, Pergamon Press, Oxford 1982.
76. N. N. Greenwood, A. Earnshaw, *Chemistry of the Elements*, Pergamon Press, Oxford 1984; German: *Chemie der Elemente*, VCH-Verlagsgesellschaft, Weinheim 1988.
77. N. P. Finkelstein, R. D. Hancock: "A New Approach to the Chemistry of Gold", *Gold Bull.* 7 (1974) 72–77.
78. A. Prior: "Possibilities of Using Ion Exchange Membrane in the Recovery and Processing of Precious Metals", *Proceedings of the 11th International Precious Metals Institute Conference*, Brussels 1987.
79. E. Raub: *Die Edelmetalle und ihre Legierungen*, Springer Verlag, Berlin 1940.

80. E. Jäneke: *Kurzgefaßtes Handbuch aller Legierungen*, C. Winter Verlag, Heidelberg 1949.
81. J. L. Haughton, A. Prince: *The Constitution, Diagrams of Alloys. A Bibliography*, Institute of Metals, London 1956.
82. A. Prince: *Multicomponent Alloy Constitution, Bibliography 1955–1973*, Metals Society, London 1978.
83. A. Prince: *Multicomponent Alloy Constitution, Bibliography 1974–1977*, Metals Society, London 1981.
84. W. Home-Rothery, G. V. Raynor: *The Structure of Metals and Alloys*, Institute of Metals, London 1954.
85. M. Hansen: *Der Aufbau der Zweistoff-Legierungen*, Springer Verlag, Berlin 1936.
86. M. Hansen, K. Anderko: *Constitution of Binary Alloys*, 2nd ed., McGraw-Hill, New York 1958.
87. R. P. Elliott: *Constitution of Binary Alloys*, 1st Suppl., McGraw-Hill, New York 1965.
88. E. A. Shunk: *Constitution of Binary Alloys*, 2nd Suppl., McGraw-Hill, New York 1969.
89. W. G. Moffatt: *The Handbook of Binary Phase Diagrams*, General Electric Company, Schenectady, NY, 1976/77 (halbjährliche Nachträge).
90. G. Petzow, G. Effenberg: *Ternary Alloys*, vol. 1, 2, VCH-Verlagsgesellschaft, Weinheim 1988.
91. F. Ensslin: *Edelmetall-Analyse*, Springer Verlag, Berlin 1964.
92. Chemikerausschuß der GDMB (ed.): *Analyse der Metalle*, 2nd ed., Springer Verlag, Berlin 1961.
93. H. M. Lüscho: *Probenahme, Theorie und Praxis*, "Schriftenreihe d. GDMB", Verlag Chemie, Weinheim 1980.
94. H. M. Lüscho: "Zur Probenahme von Edelmetallen. Teil 1: Probenahme von metallischen Materialien", *Erzmetall* 42 (1989) 153–159.
95. J. Suchomel, *Fresenius' Z. Anal. Chem.* 300 (1980) 257–266.
96. W. S. Rapson, T. Groenewald: *Gold Usage*, Academic Press, London 1978.
97. A. Luschin v. Ebengreuth: *Allgemeine Münzkunde und Goldgeschichte*, Oldenburg, München 1971.
98. World Gold Council, *Aurum – quarterly magazine for manufacturers, designers and retailers of gold jewelry*, no. 1 (1980), no. 31 (1987) Geneva.
99. E. Roser, *Handelsblatt-Magazin*, 1983, no. 12, 32–36.
100. A. Keil: *Werkstoffe für elektrische Kontakte*, Springer Verlag, Berlin 1960.
101. Degussa: "Technik die verbindet", *Berichte aus Forschung und Praxis*.
102. W. Funk, G. Reinacher: "Gold Alloy Spinnerets for the Production of Viscose Rayon", *Gold Bull.* 7 (1974) 2–9.
103. A. von Krusenstjern: *Edelmetall-Galvanotechnik*, Verlag Leuze, Saulgau 1970.
104. H.-D. Lachmann, H. G. Simanowski: *Gold als Oberfläche*, Leuze Verlag, Saulgau 1982.
105. Degussa: *Glanzgolddübel*, Eigenverlag, Frankfurt 1979.
106. W. Knies, *Metall* 43 (1989) 651–653.
107. International Gold Corp, *Krügerrand Bulletin*, up to 1985, Geneva.
108. International Gold Corp., *Gold Letter*, since 1985, Geneva.
109. B. Bandulet: *Gold Guide*, Fortuna Finanz-Verlag, Niederglatt/Zürich 1984.
110. K. Bolz, U. Harms, P. Pissulla, H. Schmidt: *Gold, Platinmetalle und Diamanten in der sowjetischen Handelspolitik*, Verlag Weltarchiv, Hamburg 1985.
111. H. Kutzer: *Metalle – zwischen Mangel und Überfluß*, Handelsblatt-Schriftenreihe, Düsseldorf 1981.
112. E. Merian: *Metalle in der Umwelt – Verteilung, Analytik und biologische Relevanz*, Verlag Chemie, Weinheim 1984.
113. E. Merian: *Metals and their Compounds in the Environment – Occurrence, Analysis, and Biological Relevance*, 2nd ed., VCH-Verlagsgesellschaft, Weinheim 1989.
114. N. O. Rothermich, V. K. Phillips, W. Berger, M. H. Thomas, *Arthritis Rheum.* 19 (1976) 1321.
115. G. G. Stanley (ed.): *The Extractive Metallurgy of Gold in South Africa*, The South African Institute of Mining and Metallurgy, Johannesburg 1987.
116. E. Krone, "Probleme der Primärgoldlaugung", *Erzmetall* 42 (1989) 253–258.

24 Silver

HERMANN RENNER

24.1 History	1216	24.5.5 Via Scrap Metal Electrolysis	1236
24.1.1 Production	1217	24.5.6 Processing of Flue Dust	1236
24.1.2 Monetary Significance and Price Structure	1218	24.5.7 Processing of Copper Matte	1237
24.2 Properties	1219	24.5.8 Processing of Photographic Materials	1237
24.2.1 Atomic Properties	1219	24.5.9 Surface Desilvering	1239
24.2.2 Physical Properties	1219	24.5.10 Processing of Special Scrap	1240
24.2.3 Chemical Properties	1219	24.6 Silver Refining	1240
24.3 Occurrence and Raw Materials	1220	24.6.1 Fine Smelting	1240
24.3.1 Formation, Abundance, and Distribution of Ores	1220	24.6.2 Refining with Nitric Acid (Inquartation)	1240
24.3.2 Silver Minerals	1221	24.6.3 Refining with Sulfuric Acid (Affination)	1241
24.3.3 Deposits	1222	24.6.4 Möbius Electrolysis	1241
24.3.4 Secondary Silver	1223	24.6.5 Balbach-Thum Electrolysis	1242
24.3.5 Resources and Reserves	1224	24.7 Inorganic Compounds	1242
24.4 Extraction from Ores	1224	24.7.1 Silver Nitrate	1242
24.4.1 Extraction from Silver Ores	1224	24.7.2 Silver Halides	1244
24.4.1.1 Smelting	1224	24.7.3 Silver Oxides	1245
24.4.1.2 Amalgamation	1224	24.7.4 Other Soluble Silver Compounds	1246
24.4.1.3 Cyanidation	1225	24.7.5 Other Insoluble Silver Compounds	1246
24.4.1.4 Thiosulfate Leaching (Patera Process)	1225	24.7.6 Silver Complexes	1247
24.4.1.5 Metallurgical Processes	1226	24.7.7 Explosive Silver Compounds	1247
24.4.2 Extraction from Lead and Lead-Zinc Ores	1226	24.8 Disperse Silver	1248
24.4.2.1 Production of Lead Bullion	1226	24.8.1 Silver Powder	1248
24.4.2.2 Cupellation without Prior Silver Enrichment	1226	24.8.2 Colloidal Silver	1250
24.4.2.3 Silver Enrichment by the Pattinson Process	1226	24.9 Uses	1251
24.4.2.4 Silver Enrichment by the Parkes Process	1227	24.9.1 Coins	1251
24.4.2.5 Cupellation of Enriched Lead	1227	24.9.2 Jewelry	1252
24.4.2.6 Silver Extraction from Electrolytic Lead Refining	1228	24.9.3 Medicine	1252
24.4.3 Extraction from Copper and Copper- Nickel Ores	1228	24.9.4 Dentistry	1253
24.4.3.1 Formation of Silver-Containing Copper Anode Slimes	1228	24.9.5 Silver Plating	1253
24.4.3.2 Pretreatment of Copper Anode Slimes	1228	24.9.6 Electrical Technology	1255
24.4.3.3 Processing of Copper Anode Slimes	1229	24.9.7 Chemical Equipment	1257
24.4.3.4 Silver Extraction from Copper Matte	1231	24.9.8 Catalysts	1257
24.4.4 Extraction from Gold Ores	1232	24.9.9 Photography	1258
24.4.5 Extraction from Tin Ores	1232	24.9.10 Other Uses	1258
24.5 Recovery from Secondary Silver	1232	24.10 Quality Specifications and Analysis	1259
24.5.1 Via Copper Smelters	1233	24.10.1 Qualitative Analysis	1260
24.5.2 Via Lead Smelters	1233	24.10.2 Quantitative Analysis and Accountancy Analysis	1260
24.5.3 Via the Lead-Silver Smelting Process	1233	24.10.3 Purity Analysis	1261
24.5.4 Via Scrap Metal Leaching	1235	24.10.4 Trace Analysis	1262
		24.10.5 Argentometry	1262
		24.11 Economic Aspects	1262
		24.11.1 Production	1262
		24.11.2 Supply and Demand	1262
		24.11.3 Silver Market and Trading	1263

24.12 Health and Safety	1263	24.12.3 Explosion Hazards	1264
24.12.1 Toxicology	1263	24.13 References	1265
24.12.2 Bactericidal (Oligodynamic) Effect	1264		

24.1 History

Ancient Times [1–6]. Like gold, silver occurs in native form and therefore has been known to humans since prehistoric times. The oldest finds of silver whose age can be determined date from around 4157 B.C. in Egypt. In the following years, silver appeared in the entire cultural region of the eastern Mediterranean. In the second millennium B.C., the Phoenicians obtained large quantities of silver from deposits on the Iberian Peninsula, which were distributed by their companies of traveling merchants.

The first upsurge in the production of silver took place when the Greeks exploited the mines of Laurion, which reached their peak productivity in ca. 500 B.C. The Greeks also worked silver mines in Thrace, Asia Minor, and the entire Aegean region. The Athenian empire and its claim to power were based to a large extent on the role of silver for coinage. Modern methods of trace analysis have elucidated the relationship between the extraction and processing of the Greek silver deposits and their effects on the political developments at that time [7–11].

Rome was initially poor in silver. However, considerable quantities were soon obtained in the provinces that fell to the Roman Empire (i.e., southern Spain, the Balkans, the Carpathians, etc.). In many Roman expeditions of conquest (e.g., the Punic wars and those in the period of the civil wars), the seizing of silver mines was often a cause of war-like disputes. The introduction of the silver denarius as the common currency in ca. 300 B.C. elevated the political importance of the national metal.

Undoubtedly, silver was also extracted in pre-Christian times in middle and northern Europe, although this only became known through the Romans' written records. Likewise in India, China, and Japan the production of silver probably dates back to ancient times.

When the migration of the Germanic people began and the political dissolution of the Roman Empire occurred, silver production practically ceased. This situation changed with the reorganization of the western lands by the Carolingians.

Middle Ages. During the Middle Ages, the extraction of silver became widespread in central Europe. Some of the production locations are listed here, with their starting dates: Bohemia (Pribram: 753; Miss: 1137; Kuttenberg: 1240), Sweden (Sala: 8th century), Saxony (Freiberg: 1103; Mittweida and Frankenberg: 922), Erzgebirge (Joachimsthal: 1510; Annaberg, Schneeberg), Alsace (Markirch: 7th century), the Lahn region, Siegerland (ca. 860), Silesia (Beuthen, Tarnowitz), Hungary (Schemnitz), Norway (Kongsberg), Tyrol, Steiermark, Salzburg, the southern Black Forest (Freiburg im Breisgau), Harz Rammelsberg, which provided much of Europe's silver in the 11th and 12th centuries: 968; St. Andreasberg; Mansfeld, which was the source of most of the silver produced in Germany at that time: 1450).

Many of these deposits were exhausted by the end of the Middle Ages and often long before this. However, the mines in the Harz, Siebenbürgen, Freiberg, Norway, and Alsace retained some of their importance up to the industrial revolution.

The deposits in India, Japan, China, and pre-Columbian America, were also mined during the Middle Ages.

Modern Times. After the discovery of America, silver was plundered by the Spanish and brought to Europe in large quantities. Also, new deposits were developed. Soon, America was producing more silver than Europe, and prices collapsed. Up to ca. 1700, world production was dominated by Central and South America (Peru, Bolivia, Chile, and Argentina).

In the 1800s, the main center of production moved to North America, i.e., Mexico, Canada, and the United States (Nevada). Also, significant quantities of silver were produced in Russia and Australia, and the output from Europe increased, although by then this was almost entirely associated with lead and zinc ores.

After World War II, Poland became an important producer following the exploitation of newly discovered silver-containing copper deposits.

24.1.1 Production [1–13]

By the beginning of the Middle Ages (ca. 800 A.D.), a total of ca 75 000 t of silver is estimated to have been extracted. By then the silver deposits of the European Mediterranean region, almost the only regions to be mined in ancient times were effectively exhausted.

At the end of the Middle Ages, world production had almost dropped to 50 t/a. During the whole of the Middle Ages, ca. 250 000 t silver was extracted, most of which came from Europe, mainly the German-speaking area.

By 1975, average world primary silver production ca. > 10 000 t/a, and by 1991, it reached a peak of 11 500 t/a. The countries of North and South America today account for more than two-thirds of world production. In 1975, Poland was by far the largest producer in Europe. For primary production figures, see Table 24.1.

In total, $(1-1.2) \times 10^6$ t silver has been extracted worldwide. This is about 10 times the figure for gold production and 100 times the total world production of platinum.

Table 24.1: Western world silver production (t/a).

Region	1989	1990	1991	1992
Mining production	11481	11833	11560	11480
Mexico	2306	2360	2250	2400
United States	2007	2080	1850	1820
Peru	1840	1725	1770	1500
Canada	1306	1535	1290	1150
Australia	1168	1321	1180	1080
Others	2854	2812	3220	3530
Secondary silver	3344	3700	3380	3450
Total	14825	15533	14940	14930

Very little has been written about the techniques of silver extraction in ancient times. The Egyptians are thought to have separated gold from silver by heating with salt. They must therefore have known how to convert the silver chloride produced into metallic silver.

The main source of silver in ancient times was silver-containing lead ores. In the Middle Ages, deposits of native silver were also important, especially in Central Europe. The rich ores could be smelted simply after hand separation (i.e., after crushing and separating from the worthless rock). Large pieces weighing more than 100 kg, or large blocks weighing many tons and containing native metal, were found and processed in this way.

The Greeks, the Romans, and the miners of the Middle Ages knew how to process silver-containing lead ores by smelting to produce lead. In the Middle Ages, the lead was removed by oxidation in cupellation furnaces to produce silver with a fineness of 650/1000–875/1000. This could then be oxidized further to give a fineness of 990/1000.

When the silver was accompanied by copper in the deposit, the liquation process [14] was used. The silver-containing copper was melted with lead, and the silver-rich liquid phase recovered by liquation was blown with air.

Introduction of the amalgamation process in 1566 improved silver productivity and production rates in Mexican and South American mines. This process later became dominant and was used in the United States and, from 1800, in Europe in a modified form suitable for a wide range of raw materials.

After the mid-1800s several new techniques were developed that replaced the old processes or improved economics. For example, the lead cupellation process was made more efficient by introduction of the Pattinson process (1833) which for a time was very widely used. This was based on the segregation of solid lead from the lead silver melt by cooling. This increased the silver content to 2.5% and thereby decreased the load on the cupellation process. The Parkes process (1850) soon replaced the Pattinson process be-

cause of its superior economics. In this process, silver was transferred from the lead to zinc floating on the surface of the lead; this formed a crust that could be removed. The Parkes process is still virtually the only process used today for extracting silver from lead ores. It is also used to extract silver from lead-zinc and zinc ores.

The chloridizing roasting of copper ores followed by leaching with brine to dissolve the silver chloride formed was introduced in 1843 by Augustin; it was soon replaced by sulfation roasting, at temperatures below the decomposition temperature of silver sulfate and above that of copper sulfate, followed by leaching with water. This was known as the Ziervogel process, and for almost 100 years most of the silver in German ores was extracted in this way. The sulfuric acid extraction of dead-burnt copper ore in a stream of air, to form a silver-containing slime, was used for only a short period. After 1856, thiosulfate leaching of chloridized roasted ore was used primarily in Mexico and California. In the Paterson process, sodium thiosulfate was used; in the Kiss process, calcium thiosulfate; and in the Russel process, sodium copper thiosulfate. Since ca. 1900, cyanide leaching, which is still used for silver ores that are not smelted, has been the most important aqueous treatment process.

Since ca. 1876, almost all the silver associated with copper has been obtained from the electrolytic refining of copper. The silver appears in the copper anode slimes, which are generally treated by pyrometallurgical processes.

To separate silver from the gold in auriferous silver (the end product of nearly all smelting and hydrometallurgical extraction processes), the nitric acid process (developed in 1433) and the sulfuric acid process (dating from 1802) have been completely replaced by electrolytic refining.

24.1.2 Monetary Significance and Price Structure [1, 15, 16]

From ancient times to the Middle Ages and later, even into the present century, silver was the classic metal for currency. In comparison, gold played an almost insignificant role.

In the 6th century B.C., King Croesus ordered the minting of silver coins. In ancient Greece, silver currency was the basis of the economic system. In 296 B.C. the Romans introduced the silver denarius as the general method of payment, and gold ceased being used in coins from 217 B.C. Silver was the basis of the coinage reform by the Byzantine Empire in A.D. 310, and was recognized throughout the Mediterranean region, so that silver maintained its importance as a coinage metal for many centuries. Charlemagne made silver the basis of the currency system of his empire.

During the last two centuries, gold began to displace silver, mainly due to the reduction in the price of silver caused by the surplus from new production, as well as the demonetization of silver.

Between the two world wars, strong moves, triggered by inflation and the world economic crisis, were made to remonetize silver, but these largely came to naught.

After World War II, because of the increasing demand and the shortage of supply, the price of silver rose so much that by 1970 the value of the silver in the most important silver coins still in circulation (U.S. dollars and Swiss francs) exceeded the face value of the coins. Silver was therefore virtually completely demonetized.

After the 17th century, the ratio of the prices of silver and gold remained fairly constant at ca. 1:15 for a long period. However, free price movements have continually tended to shift this ratio, and it has often been kept constant by state intervention. A fairly gradual increase in the price of gold began ca. 120 years ago. At the beginning of World War I, the ratio reached 1:40. During the World War II it rose to 1:100, and during the following

three decades it fluctuated around 1:40. In 1981 it was 1:50, and in 1992 it was 1:95.

Silver prices have been freely determined by supply and demand from 1970, after which the price rose steadily from ca. 180 DM/kg to 300–500 DM/kg. In late 1979 and early 1980, speculative dealings of a hitherto unimagined volume occurred, and the price of silver briefly reached nearly 2750 DM/kg [17]. In the following decade, and up to the present, a rapid and fairly continuous decline in price has taken place, reaching a low of 15 DM/kg in 1992. The price of silver now reflects its status as an industrial metal and depends on the current economic situation. In parallel with this, silver has lost its importance as an investment metal. The high stock levels and sales of these stocks from time to time also affect price reductions.

24.2 Properties [18–23]

Silver, like gold and the platinum-group metals, is a noble metal. Silver, gold, and copper are known as the coinage metals.

24.2.1 Atomic Properties [24]

Silver has an atomic number of 47 and a relative atomic mass of 107.8682. Natural silver consists of the stable isotopes ^{107}Ag (51.8%) and ^{109}Ag (48.2%). Many artificial isotopes with relative atomic masses between 102 and 117 are known.

The electronic configuration of silver is $[\text{Kr}] 4d^{10}5s^1$. The $5s^1$ shell is the principal valence orbital, which accounts for the preference for oxidation state 1. The $4d$ shell can also act as a valence orbital, resulting in oxidation states 2 and 3. Thus, silver behaves as a transition metal due to the contribution from the inner valence orbital. Since the differences between the energies of the valence electrons are small, silver has a tendency to form complexes with covalent bonds and to exhibit other properties such as catalytic activity typical of transition metals.

The atomic radius of silver (with 12-fold metallic coordination) is 0.144 nm; the ionic

radius of Ag^+ (six-coordinate) is 0.137 nm, and of Ag^{3+} (six-coordinate) 0.075 nm.

24.2.2 Physical Properties

The physical properties of silver are generally intermediate between those of copper and gold. These three elements have strong similarities, although silver has some anomalous properties, which are directly related to the $d^{10}s^1$ electronic configuration and the irregularity of the atomic radii. Some physical data are given below:

Lattice constant at 20 °C	0.40774 nm
Atomic radius (in metal)	0.144 nm
Melting point	961.9 °C
Boiling point	2210 °C
Specific heat capacity at 25 °C	0.23 J kg ⁻¹ K ⁻¹
Thermal conductivity	418 W m ⁻¹ K ⁻¹
Vapor pressure at 1030 °C	1.33 Pa
1190 °C	13.3
1360 °C	133
1580 °C	1330
1870 °C	13 300
Density at 20 °C	10.49 g/cm ³
Density of liquid at mp	9.30 g/cm ³
Density of liquid at 1250 °C	9.05 g/cm ³
Brinell hardness	26
Modulus of elasticity	82 000 MPa
Tensile strength	140 MPa
Resistivity at 0 °C	1.50 Ω cm

Like copper and gold, silver crystallizes in a face-centered cubic structure in which each metal atom is surrounded by 12 neighbors. This high degree of symmetry results in a structure with many slip planes and is the reason for its good mechanical formability. Silver is only slightly less ductile than gold. It can be given a high polish and has a warm, white luster. Very thin films are blue or green by transmitted light, thicker films being yellow to brown.

Silver has the highest electrical conductivity, the highest thermal conductivity, and the lowest electrical contact resistance of all metals.

24.2.3 Chemical Properties

Molten silver absorbs oxygen and releases it during solidification, with bubbling of the metal surface. At 1000 °C, 1 cm³ of molten silver dissolves a maximum of ca. 20 cm³ of oxygen, corresponding to a stoichiometric

composition of $\text{AgO}_{0.01}$. The solubility of oxygen in silver just below its melting point is only ca. 1/40 of that at 1000 °C. Hydrogen is very slightly soluble in molten silver, whereas nitrogen, carbon monoxide, carbon dioxide, and the noble gases are insoluble.

Halogens react violently with silver at red heat. Moist chlorine gas corrodes silver even at low temperature. Ozone blackens the surface of silver due to oxide formation.

Hydrogen sulfide (gaseous or in solution) and aqueous solutions of sulfides immediately form a black coating of silver sulfide on the surface of the metal. At high temperature, the reaction with hydrogen sulfide gas or sodium polysulfide solution can lead to complete conversion of silver to silver sulfide.

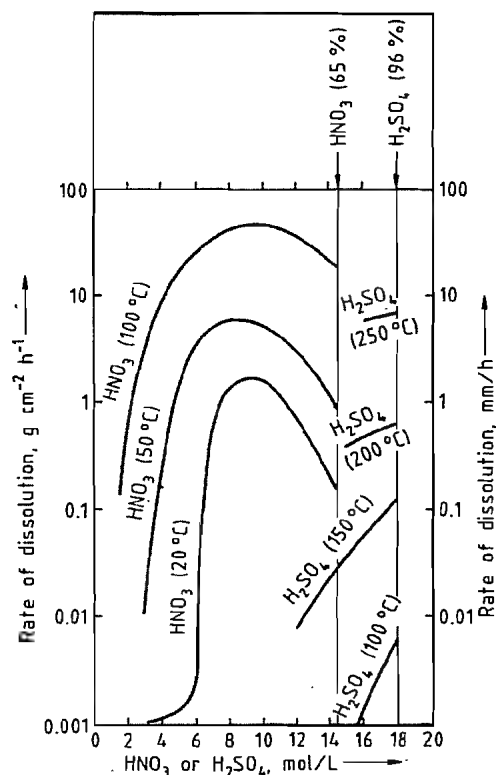


Figure 24.1: Rate of dissolution of silver in nitric acid and sulfuric acid as a function of concentration and temperature.

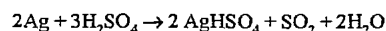
The solubility of metallic silver in water is very low, but it is sufficient to exhibit an oligo-

dynamic (bactericidal) effect (see Section 24.12.2).

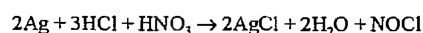
The preferred medium for dissolution of silver is hot, concentrated nitric acid (Figure 24.1):



Silver also dissolves rapidly in hot concentrated sulfuric acid (Figure 24.1):



Rates of dissolution in dilute sulfuric acid are appreciable if oxygen or hydrogen peroxide are present. The initially vigorous reaction with aqua regia



is rapidly slowed by the formation of a coating of silver chloride. Most common oxidizing aqueous media attack silver, including chromic acid, permanganate solutions, persulfuric acid, selenic acid, and aqueous solutions of free halogens. The following also attack silver: hydrochloric acid, phosphoric acid, bromine water, solutions of alkali-metal chlorides, copper chloride, and iron chloride. The reactions are often strongly dependent on temperature and in some cases on the formation of protective coatings. Silver is resistant to aqueous solutions of organic acids and aqueous alkali.

Silver is fairly resistant toward fused sodium hydroxide at ca. 550 °C in the absence of atmospheric oxygen and moisture. Potassium hydroxide is more aggressive. Silver is attacked by fused salts such as sodium peroxide, potassium nitrate, sodium carbonate, potassium hydrogensulfate, and potassium cyanide.

24.3 Occurrence and Raw Materials [1–3, 25–27]

24.3.1 Formation, Abundance, and Distribution of Ores

Because of its chalcophilic character, silver became concentrated in oxidic sulfidic materials during the formation of the Earth's mantle, which has a silver content of ca. 10 ppm. The

metallic core of the Earth should have a much lower silver content because silver does not alloy with iron or nickel. This is confirmed by investigation of iron meteorites. In the region accessible to mining (i.e., to a depth of 5 km), the Earth's crust has an average silver content of 0.05–0.1 ppm. Thus, silver is 100 to 1000 times more abundant than gold or platinum. The average silver content of the oceans is ca. 0.001 ppm [28], but it often reaches much higher values at the mouths of rivers. This enormous reserve of silver (10^9 t) cannot, however, be extracted economically.

Silver became concentrated at particular sites in the Earth's crust by the recrystallization of silicate magmas caused by volcanic action in impregnation zones. Most sulfidic, arsenic, and antimonidic formations were originated in this way. Hydrothermal processes caused conversion to metallic deposits. Also, the action of the atmosphere and hydrosphere was involved (e.g., in the formation of caps over magmatic deposits). Unlike gold and the platinum metals, silver has not formed sedimentary deposits to any extent, since it is dissolved much more readily than gold or platinum by the action of the hydrosphere. However, silver-containing sedimentary deposits of other elements are known (e.g., Mansfeld copper slate).

24.3.2 Silver Minerals [3]

Nearly all silver minerals are compounds of silver with sulfur, its homologues selenium and tellurium, and their neighbors in the periodic table, arsenic, antimony, and bismuth. These ores generally have a metallic luster and are semiconductors. Other silver minerals include the halides and the free metal. The major mineralogical groups—oxides, silicates, spinels, phosphates, gypsum, and carbonates—are not represented.

Native silver occurs in the form of nuggets, dendrites, sand-like material, or sometimes as large lumps or blocks. It often forms mixed crystals with gold, and can also contain copper and other metals and metalloids.

Argentite, Ag_2S , is the most common silver compound found in the sulfidic ores of other metals, especially galena, PbS , in which it is present with other sulfidic minerals in the form of very fine inclusions. In the Middle Ages, argentite was often found in high concentrations and was a mineral in its own right with a high silver content.

Pyrargyrite, antimony silver blende, Ag_3SbS_3 , is an important mineral occurring in true silver ores, which are now found and mined mainly in Central America.

Proustite, arsenic silver ore, Ag_3AsS_3 , is of similar occurrence to the corresponding antimony-containing sulfur compound Ag_3SbS_3 .

Stephanite, Ag_5SbS_4 , is very characteristic of the silver ores familiar to miners from early times.

Cerargyrite, horn silver, AgCl , does not occur in large quantities. It has extremely low hardness and crystallizes with the NaCl lattice type.

Apart from the compounds mentioned above, many other well-defined silver minerals exist. Some of them, particularly the sulfur compounds, still make a significant contribution to silver production.

Some examples are given below:

Miargyrite	AgSbS_2
Polybasite (Eugenite)	Ag_9SbS_6
Freibergite	$(\text{Cu}, \text{Ag})_{12}\text{Sb}_4\text{S}_{13}$
Freieslebenite	$\text{Ag}_3\text{Pb}_2\text{Sb}_3\text{S}_8$
Andorite	AgPbSbS_6
Stromeyerite	$\text{Ag}_2\text{Cu}_2\text{S}_2$
Schapbachite	AgBiS_2
Argyrodite	Ag_8GeS_6
Sternbergite	AgFe_2S_3
Argentopyrite	AgFe_3S_5
Argyropyrite	$\text{Ag}_2\text{Fe}_7\text{S}_{11}$
Sundite	AgFeSbS_9
Hessite	Ag_2Te
Petzite	Ag_3AuTe_2
Silvanite	AgAuTe_4
Bromyrite (Bromargyrite)	AgBr
Embolite	$\text{Ag}(\text{Cl}, \text{Br})$
Iodite (Iodargyrite)	AgI

Silver is a component of most sulfidic minerals, at least at the parts-per-million level. The silver compounds are present as mixed crystals or as microscopic inclusions with a crystal structure that deviates from that of the matrix.

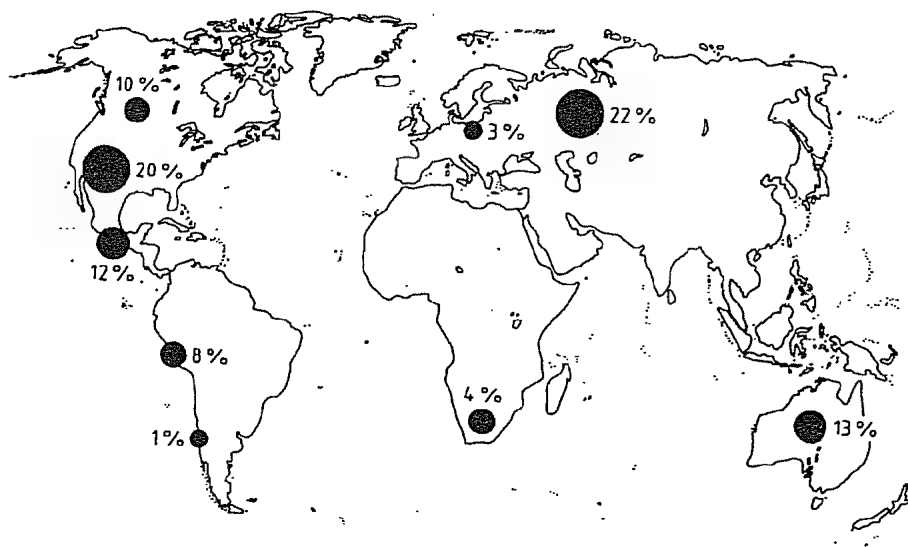


Figure 24.2: Reserves of silver by region.

24.3.3 Deposits [3, 29–34]

The known silver deposits are associated mainly with vulcanism in the Tertiary period running, for example, in a continuous line along the entire west coast of the American continent (Figure 24.2).

True silver ores, in which silver is practically the only valuable metal, are mined mainly in Mexico (Pachuca, Frenillo, and San Fernando de l'Oro) and to a small extent in the United States (Utah). In Europe, such deposits are almost completely exhausted. Worldwide, they still account for more than one-tenth of the silver mined. Depending on the price of silver, it can be economic to process materials containing 0.01% (100 ppm) silver, or even less. The deposits in Ontario, which contain native silver associated with cobalt sulfide and arsenide, can also be regarded as true silver ores, since only the silver is extracted.

Argentiferous lead and lead–zinc ores, which often occur in association, are distributed widely. In almost all silver-producing countries, they constitute an important fraction of the silver produced by mining and account for ca. 50% of world silver production. The separation and recovery of silver during

lead production is profitable even for a silver content of a few parts per million. The important reserves in Europe include those in Spain (Lineares, Sierra Morena), Germany (Rammelsberg/Harz), former Yugoslavia (Trepca), and to a lesser extent Italy (Montevocchio, Monteponi), Greece (Laurion), and France (Savoy). Argentiferous lead and lead–zinc ores are mined in large quantities in the United States (Helena, Montana; Denver, Colorado; Coeur d'Alene, Idaho), Mexico, Peru, Bolivia, and Argentina. In Australia and Tasmania, lead and lead–zinc ores are the primary source of silver. In North Africa (Djebel Hallouf, Tunisia; BeniSat, Algeria), Nigeria, and Namibia (Otavi), these are of some importance. In South Africa, other silver ores are more important. In India, the extraction of silver from lead and lead–zinc ores is extremely important, and this appears to also be true of the Commonwealth of Independent States (CIS).

Argentiferous copper ores, which sometimes also contain nickel and cobalt, satisfy ca. 30% of the world silver demand. Even very low contents of silver can be recovered profitably from copper ores, since almost all the copper is electrowon, and the silver remains in the anode slimes. In Europe, the large-

est reserves of argentiferous copper ore are in Poland (Katowice), Yugoslavia (Bor), and Sweden. Smaller reserves can be found in Finland. The CIS, from which little information is available, is also believed to have reserves of this type. The largest argentiferous copper reserves in the world are in Canada (Sudbury, Ontario, Rouyn–Noranda, Québec). Silver is also recovered during copper smelting in Chile, Bolivia, Peru, Katanga, Namibia, Zimbabwe, and South Africa.

Extraction of silver from gold ores is carried out mainly in South Africa, and also in Canada, Alaska, and Sweden (Boliden). The quantity obtained in this way is < 10% of world silver production. Silver-containing tin deposits are concentrated in Bolivia (Cerro de Pasco, Potosi) but also occur in Burma and Argentina. Silver produced from tin ores amounts to only 2% of world production.

24.3.4 Secondary Silver [35–40]

The demand for silver that cannot be met by mining must be made up by recycling and by release from stocks. However, stocks of silver are often in a condition (e.g., type of alloy or low purity) that is not accepted directly by the market. Hence, these materials must generally be refined.

Silver coins have been almost entirely withdrawn from circulation. Some were refined immediately, but a smaller number were saved. From time to time, large stocks of these coins are released unpredictably, usually in association with speculative dealings on the silver market.

Even when the coins are of uniform composition, the alloy generally cannot be reused directly because, for example, the quantity is too large or the alloy is too complex. The silver content of coinage alloys is 40–90%. Copper is the other main alloy component, and nickel, zinc, or traces of other metals are generally present.

The old Indian silver reserves come onto the market in the form of fittings and similar articles; the silver content is 90–95%.

Photographic slimes, produced during the manufacture of films and photographic paper, have a silver content of 5–30%. The silver is present as a halide, the remainder being mainly gelatin and water.

Approximately 50% of the silver used in the photographic industry ends up in fixing baths. The silver-containing fixing bath solutions are rarely supplied directly to refineries. Instead, silver is usually extracted from them where they were produced, either by electrolysis to yield compact crude silver of fairly high purity or by chemical reduction to give slime concentrates (10–60% Ag).

The archives of X-ray films and motion pictures, which are stored for a limited period only, are a continuing source of recycled silver. In developed X-ray film the silver content is 1–2%; in developed black-and-white film it is 0.2%, but in developed color film the amount is negligible. The films are converted to ashes or slimes with silver contents up to 90%.

Offcuts of X-ray and graphic film from the photographic industry and film material stored too long (e.g., from military stocks) have a silver content up to 3%.

Photographic printing paper offcuts from the photographic industry have a silver content of ca. 0.4%. These papers used to contain up to 50% barium sulfate filler, but modern papers are mainly polymer coated and have a low filler content.

Scrap silver from tableware and ornaments usually with silver content of 80 or 92.5%, is important during periods of high silver prices. The treatment of silver-plated utensils (e.g., cutlery with ca. 4–5% Ag) is usually profitable only in large quantities.

The electrical industry and its suppliers generate waste materials during the manufacture of electrical contacts at various stages of the production processes. Waste also arises from the production of small batteries for domestic electronic use and larger units for the military and air transport areas [41]. These cells often contain mercury. Silver-plated switching elements are produced in the electronics industry.

The chemical industry provides spent silver-containing catalysts [36]. These include silver wire mesh or silver crystals used in the oxidation of methanol to formaldehyde and Ag- α -Al₂O₃ catalysts for the oxidation of ethylene to ethylene oxide.

A regular, though small, quantity of silver comes from equipment and silver-plated vessels or pipework used in the chemical industry. Finally, the amount of silver waste from the production of dental amalgams is not inconsiderable. It consists of granules of Ag-Sn-Hg alloys and is usually contaminated with other materials, including organic substances.

24.3.5 Resources and Reserves

[15, 23, 25, 34]

Mineral "resources" include all the principal known deposits, including those that have not yet been proved, but are only assumed. They also include deposits that are known for certain to exist, but cannot be extracted for economic or ecological reasons [42].

Mineral "reserves" include only those deposits that are already economically exploitable, or whose existence, based on prospecting work, is certain or probable [42]. These mineral reserves amount to ca. 250 000 t of silver at the present time. With a demand of ca. 10 000 t/a, silver is one of those metals whose known raw material reserves can supply the demand only for a limited period. By far the largest proportion of the silver is contained in lead, zinc, and copper ores, so silver production is linked primarily to the demand for these metals. This is probably not a good situation from viewpoint of future supplies. However, the advantage is that silver reserves are much more widely distributed than those of gold and the platinum metals, so the supply of silver to industrialized nations would be much less threatened by possible political crises than the supplies of other important raw materials.

24.4 Extraction from Ores

[1, 3, 12, 19, 42-44]

24.4.1 Extraction from Silver Ores

24.4.1.1 Smelting

In the early days, considerable quantities of silver were extracted simply by smelting high-percentage silver ores under oxidizing or reducing conditions with conversion of accompanying materials into slag. The starting materials were almost exclusively ores containing elemental silver, silver sulfide, or silver halides.

24.4.1.2 Amalgamation

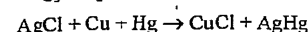
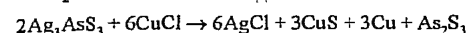
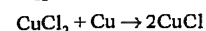
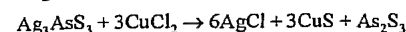
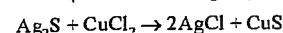
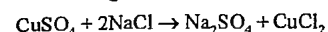
For many centuries, amalgamation was the most important process for the treatment of true silver ores. Today, it is rarely used because of high costs, poor yields, and the toxicity of mercury. It is now carried on in privately owned small mines. The amalgamation process can be used directly only if the silver is native or is present as the chloride. In this form it will amalgamate on contact with mercury without any other treatment.

Amalgam formation does not take place as rapidly as with gold, but the reaction velocity and rate of dissolution of silver in mercury are nevertheless fairly high. The copper-plate amalgamation process used with gold cannot be used with silver because reaction times are too short to give a useful yield. To ensure problem-free amalgam formation, the silver or silver halide particles should first be liberated, preferably by wet grinding. However, an extremely fine particle size is detrimental to the process.

Sulfidic, arsenidic, and antimonidic silver minerals do not react directly to form an amalgam and therefore require pretreatment. This can consist of a simple oxidative roasting process or roasting accompanied by chloridization or sulfation.

The reaction is accelerated and the yield improved by the addition of base metals (e.g.,

iron and copper), sodium chloride, copper(I) or copper(II) chloride, or copper sulfate. The following are some of the reactions that occur:



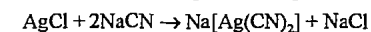
The operating techniques and the choice of reaction conditions have undergone many changes. In the Patio process, a paste of finely ground ore, sodium chloride, mercury, and water was kneaded. Other processes employ copper or iron pans, stirring apparatus, or rotating vessels, either with or without heating. The resulting metallic phase is washed to remove accompanying materials, and the residual liquid mercury is separated from the solid amalgam. The latter is heated in retorts to distill off the mercury and yield impure silver. The overall yields of silver obtained in the amalgamation process reach 95% under favorable circumstances. The loss of mercury amounts to 0.2-2 kg for each kilogram of silver.

24.4.1.3 Cyanidation

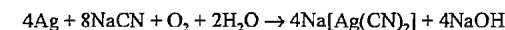
Because of its favorable economics, the aqueous cyanide process is the dominant process for extraction of silver from true silver ores. The conditions are essentially the same as those for the gold cyanide process.

The ore is crushed, wet milled, and treated with an aqueous solution of sodium cyanide (5-10 g/L) for several days in a Pachuca tank [3]. Solids are removed by a thickener and filter, and silver is precipitated from solution by cementation on zinc dust. Other possible methods of recovering silver are ion exchange or electrolytic reduction [4]. Another process involves adsorption of the silver cyanide complex onto active carbon [45, 46], analogous to the carbon-in-pulp process for gold. This process has been fully developed, but has not achieved the same importance or productivity as in the case of gold.

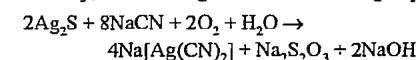
Silver chloride, either naturally occurring or produced by a chloridizing roast, is dissolved according to the equation



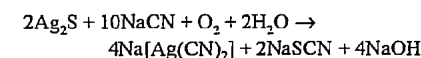
Elemental silver is dissolved by passing air into the solution:



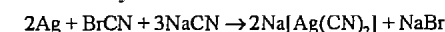
Silver sulfide is also attacked, but more slowly, according to the following equations:



and



If the ores contain cyanide-insoluble silver compounds such as proustite (Ag₃AsS₃) and pyrargite (Ag₃SbS₃), cyanide extraction must be preceded by chloridization roasting. The dissolution of selenidic and telluridic compounds of silver by cyanide is also difficult, but is improved by fine grinding and roasting, as well as by the use of cyanogen bromide, which also increases the solvent action of the sodium cyanide on metallic silver:



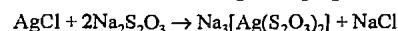
Coarse metallic silver particles and manganese-containing silver ores can also lead to complications.

In general, the leaching of silver ores proceeds more slowly than with gold ores. Also, the yield with gold is higher than that with silver. If only metallic silver and silver chloride are present the yield can reach 98%, but with other ores it is sometimes only 80%. The final silver content of the powdered ore after the extraction of silver can be as low as 0.5 ppm in favorable cases.

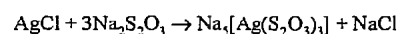
24.4.1.4 Thiosulfate Leaching (Patera Process)

The process of leaching silver ores with thiosulfate solution was developed originally in Europe under the name of the Patera process. In the 1800s its importance increased in Central and South America, and later in North America as well. It replaced the amalgamation

process, mainly because of its higher yield and lower cost. However, in a few decades it was replaced by the more economical cyanide leaching process and is now seldom used. Halide-containing silver ores or chloridized roasted ores undergo the same reactions that form the basis of the photographic fixing:



and



An excess of sodium thiosulfate should be present to prevent formation of the sparingly soluble complex $\text{Na}[\text{Ag}(\text{S}_2\text{O}_3)]$. The sodium thiosulfate concentration is usually 2.5–25 g/L. In variations of the process, sodium copper thiosulfate or calcium thiosulfate is used. Silver is precipitated from solutions by the addition of sodium sulfide. Yields of silver in the thiosulfate process are lower than in the cyanide process. Processing techniques are similar. A disadvantage of the thiosulfate process is that gold is insoluble and therefore not recovered.

24.4.1.5 Metallurgical Processes

True silver ores are often added directly to copper or lead smelting operations. This is especially true if the accompanying gangue minerals are of use in the smelting process (e.g., quartz, which benefits the copper shaft furnace process).

24.4.2 Extraction from Lead and Lead-Zinc Ores [32]

24.4.2.1 Production of Lead Bullion

In all process stages in the extraction of lead from lead and lead zinc ores, silver follows lead. This applies to ore flotation; ore sintering; reductive smelting in the blast furnace; removal of copper by sulfur, and removal of arsenic, antimony, and tin by selective oxidation (see Chapter 9).

The next stage is the extraction of silver and other noble metals. Historically, several

processes have been used in succession, each one replacing its predecessor, namely, cupellation (oxidation), cupellation after the silver has been concentrated by the Pattinson process, and concentration by the Parkes process followed by zinc removal and cupellation.

24.4.2.2 Cupellation without Prior Silver Enrichment

Before processes for concentrating the silver in lead bullion were developed (i.e., up to the 1800s), all the lead had to be converted to litharge (PbO) by oxidation (cupellation), and then the litharge removed from the silver-enriched metallic phase. This yielded an impure product that was converted to contemporary commercial-grade silver by a refining operation, which consisted essentially of further oxidation in a small furnace. Here, the elements copper, selenium, and tellurium were removed by repeated addition of pure lead, and subsequent addition of silver sulfate removed bismuth and lead. Oxidizing agents such as sodium nitrate and sodium carbonate were also added, and removal of the last traces of litharge formed was assisted by the addition of fluxes (e.g., glass).

24.4.2.3 Silver Enrichment by the Pattinson Process

A significant technical advance in the process of silver concentration was achieved by PATTINSON (1833). After this discovery, silver-containing lead no longer had to be treated by the costly cupellation process because the crude lead could be separated into two fractions, one with a low silver content and the other containing 2% Ag. The process was based on the fact that when molten silver-containing lead is cooled (e.g., 0.2% silver), pure lead separates until the silver content in the liquid phase reaches 2.5%. However, because of the difficulty of separating lead crystals from the silver-containing molten metal, complete separation cannot be achieved in a single operation. If the process is repeated, a grade of lead with a low silver and bismuth content (\leq

10 ppm silver), and a grade of lead with a high silver content ($\leq 2\%$ silver) that is suitable for cupellation, can be produced, at an acceptable cost.

The fraction that contains silver and bismuth also contains gold. The theoretical silver content of 2.5% is not achieved in practice, since the small temperature difference between the melting point of pure lead (327 °C) and that of the eutectic mixture (304 °C) means that separation becomes more difficult as the eutectic point is approached. The presence of copper, nickel, arsenic, antimony, and bismuth can also interfere with the removal of silver. Larger amounts of these elements therefore have to be removed first. Some copper goes into the Pb-Ag alloy, and some into the lead crystals, so that purified lead from the Pattinson process always contains some copper. Arsenic is found mainly in the lead crystals, whereas nickel and antimony follow bismuth into the silver-containing melt. In the usual operating procedure, either the lead crystals were removed by hand sieving, or the silver-containing melt was siphoned or tapped off. The fractions obtained were then treated again by crystallization. A series of cast iron vessels of 10–15 t capacity was employed, using countercurrent flow from the center to both sides. About 15 units were needed. Two-thirds of the contents of the vessel were recovered as crystals, and one-third remained as melt.

24.4.2.4 Silver Enrichment by the Parkes Process

Today, the silver in bullion lead, together with gold and platinum metals, is concentrated by the Parkes process. The process involves the production of a solid alloy of lead, zinc, and silver by stirring zinc into molten impure lead. This so-called zinc crust floats on the surface of the molten metal (450 °C). It is skimmed off; the adhering liquid lead is removed by hot pressing, and the zinc is distilled in a retort or vacuum furnace. The residue consists of a lead noble-metal alloy with up to 50% silver, ca. 1% zinc, and some copper, ar-

senic, antimony, and bismuth. It is oxidized by cupellation to obtain crude silver or, if appreciable amounts of gold are present, auriferous silver.

24.4.2.5 Cupellation of Enriched Lead

The cupellation process removes lead and small amounts of other base elements from the silver and accompanying noble metals by selective oxidation.

In the cupellation process, the lead melt is blown with air to produce molten lead oxide (litharge, PbO), while the silver, gold, and platinum-group metals do not react. The liquid layer of lead oxide produced covers the molten metal completely, but the oxidation reaction is not seriously impeded since the hot litharge takes up oxygen and then releases it to the molten metal. Copper, which is usually present, also assists the transport of oxygen. During cupellation, the temperature must be sufficiently high for the litharge (mp 886 °C) to form a low-viscosity melt that does not incorporate metallic and noble-metal components. At the end of the process, when the melt has a higher silver content and therefore a higher melting point, the operating temperature must be significantly greater than the melting point of silver (963 °C). In practice, the process is operated at 900–1100 °C. If the temperature is too high, volatilization can occur, which leads to losses of silver. The molten litharge formed must be removed continuously to prevent the layer from becoming too thick. The end of the smelting process is recognized when the litharge layer becomes thin and finally breaks up. The bright surface of the silver can then be seen. The last traces of litharge are mixed with marl (calcium carbonate) to facilitate its complete removal. Molten silver is usually cast into anodes for electrorefining. The copper and lead contents of the crude silver should preferably not exceed 1.0 and 0.1%, respectively. Of the normal impurities, zinc, arsenic, antimony, and copper go mainly into the litharge that is first produced, although some go into the slag that can be re-

moved after the initial melting operation. Bismuth becomes concentrated in the end fraction of the litharge.

The so-called English cupellation furnace (cupel) is now nearly always used for the cupellation process in lead smelting plants. The hearth, which is replaceable, is lined with magnesite bricks, and can be tilted to pour off the litharge and molten silver. It is fired under a flat hood. Air is blown through nozzles over the surface of the melt, freeing part of the metal surface of molten litharge. The litharge layer is removed when it reaches a thickness of ca. 1 cm. About 100 kg of lead is oxidized per hour per square meter of furnace area; the capacity is ca. 1000–2000 kg silver. The so-called German cupel is larger and has a fixed hearth with a launder at the front that can be lowered continuously, so that as the volume of molten metal decreases, the litharge is continually removed. Molten silver must be skimmed off. The greatest advantage of the smaller English smelting furnace is that less silver is required for its operation. The lining of the hearth of the cupel picks up a certain amount of silver, so that after dismantling, the broken lining with litharge attached must be treated in a lead shaft furnace.

24.4.2.6 Silver Extraction from Electrolytic Lead Refining

The aqueous electrorefining of lead bullion usually produces anode slimes that are difficult to process, whose composition is similar to that of the anode slimes from the electrorefining of copper [Cox] (Table 24.3). They contain all the noble metals and other impurities associated with crude lead. They are treated by pyrometallurgical processes to obtain auriferous silver and other valuable metals. Copper anode slimes and lead anode slimes are sometimes mixed and treated together.

24.4.3 Extraction from Copper and Copper-Nickel Ores [31, 45–51]

24.4.3.1 Formation of Silver-Containing Copper Anode Slimes

In silver-bearing ores of copper, copper-nickel, and copper-nickel-cobalt, the silver stays with the copper-rich fractions during all concentration stages, including mechanical processing and smelting (see Chapters 8 and 12). It is transferred from the copper matte into the crude copper. Gold also follows the copper and silver, but only a small fraction of the platinum metals go to the crude copper, the majority accompanying the nickel. Today, all crude copper is electrorefined. The copper anode slimes formed contain almost all the silver and noble metals, and large amounts of copper, lead, nickel, selenium, tellurium, arsenic, antimony, and sulfur. Because of their composition, the economic and ecologically acceptable treatment of copper anode slimes is one of the most difficult tasks in the metallurgy of noble metals. Before the introduction of electrorefining, silver had to be extracted from copper matte produced by the copper shaft furnace.

24.4.3.2 Pretreatment of Copper Anode Slimes

Coarse copper particles that become detached from the anodes or appear as growths on the cathodes are removed first by sieving which eliminates ca. 30% of the weight of the slime. In the following pretreatment process, elemental copper (formed by disproportionation of Cu^+ in the electrolyte), copper telluride, and copper selenide are dissolved by treatment with 4–5 mol/L sulfuric acid, with addition of air or oxygen at 60–95 °C. The effectiveness of this technique is limited, especially if the selenium content is high.

Table 24.2: Typical compositions (%) of untreated and pretreated copper anode slimes and untreated lead anode slime.

Source	Ag	Au	Se	Te	As	Sb	Bi	Cu	Pb	Fe	Ni	SiO ₂	Al ₂ O ₃	S
Untreated copper anode slime														
Asarco, USA	18	1	9	1	4	4		21	10					5
Boliden, Sweden	11	2	21	1	1	1	1	40	10		1			3
Nordd. Affinerie, Hamburg	10	0.3	5			7		17	15					
Outokumpu, Finland	10	0.5	4		0.7	0.1		11	3	0.6	45	2		2
Mt. Lyell, Australia	1	0.2	3		0.7	0.1	0.01	67	1		0.1	1		10
El. Ref. Smelt. Co., Australia	8	2	3	3	4	8	0.1	14	24	0.4	0.5	10		8
Can. Copper Ref., Montréal	19	1	20	3	0.6	0.5		37		0.6	0.2			
Noranda, Québec	13	2	28	4	0.3	0.3		46		0.4	0.2			
Rio Tinto, Spain	8	0.7	8	0.5	2	3	0.5	25	10	0.3	0.1	20		
Pelabora, South Africa	15	0.6	5	0.5				15	5		4	30	10	
Cerro, Oroya, Peru	28	0.1	2	2	2	11	1	2	24					
Pretreated copper anode slime														
Impex	49	4	3	6				3	1		0.1	12	20	
Codelco, Chile	24	1	16	0.3	0.3	5		2	1					
Nordd. Affinerie, Hamburg	13	0.3	5	1	3	8	0.6	3	15	0.2	3	7		6
Outokumpu, Finland	37	2	13		0.3	0.2		0.5	12	0.3	1	13		
El. Ref. Smelt. Co., Australia	12	3	0.7	4	1	10	0.1	2	28		0.4			5
Can. Copper Ref., Montréal	41	4	7	3				4						
Boliden, Sweden	29	5	20			4	2	2	30		0.7	2		
Enami, Chile	50	0.9	6	2	1	10	0.4	0.4	7			6		
Untreated lead anode slime														
Cerro, Oroya, Peru	10	0.01	0.1	0.7	5	33	21	2	16					

Examples of the composition of untreated and pretreated copper anode slimes are given in Table 24.2. The wide variation in the compositions of the slimes both before and after treatment results in many process steps being carried out under very specific conditions that the processing industries often do not disclose.

24.4.3.3 Processing of Copper Anode Slimes [52, 53]

Processing of Copper Anode Slimes by Roasting. *Oxidizing Roasting at 300–400 °C.* Roasting is performed on a thin layer of material or in an air-blown rotary furnace. Metallic copper is oxidized fairly easily. The selenides and tellurides of copper and silver are converted to selenites and tellurites. Only a small fraction of selenium dioxide is volatilized. The product is treated with dilute sodium hydroxide solution, which dissolves mainly the selenium. Treatment with dilute sulfuric acid dissolves tellurium preferentially, and some silver as well. Most of the selenium and tellurium (75–90%) can be brought into solution.

Oxidizing Roasting at 600–800 °C. The material is mixed with bentonite as a binder

and with copper(II) oxide and iron(III) oxide as reaction accelerators, pelletized, and reacted with air blowing. Up to 98% of the selenium can be recovered as SeO_2 sublimate. The product is then leached with dilute sulfuric acid, which dissolves copper, tellurium, and some silver.

Roasting with Sodium Carbonate. A mixture of anode slime with sodium carbonate (sometimes with the addition of sodium hydroxide or sodium nitrate) is generally pelletized and heated at ca. 400 °C in air, so that selenium and tellurium are converted into water-soluble compounds. Copper, which is also oxidized, and most of the tellurium can be dissolved with dilute sulfuric acid. The resulting solution also contains some silver in the form of its sulfate.

Processing of Copper Anode Slimes by Sulfation. Dried anode slime is mixed with concentrated sulfuric acid and heated, first to 300 °C, and then to 400–500 °C, causing sulfation and oxidation. Most of the selenium sublimes as selenium dioxide. Most of the copper, silver, and nickel can be dissolved

with hot water, whereas the tellurium oxide formed remains undissolved in the residue.

Hydrometallurgical Treatment of Copper Anode Slimes [54]. Copper anode slimes can be dissolved in oxidizing acids. Treatment with HCl-Cl_2 [55] gives a residue that contains silver chloride, silica, and lead chloride. Gold, platinum, selenium, and tellurium must be recovered from solution, and other accompanying elements are eliminated by wastewater treatment.

Copper anode slime is reportedly digested in a high-pressure process, either after the removal of copper or after one of the roasting processes [56]. Temperatures between 160 and 180 °C are recommended. If 10–40% sodium hydroxide solution is used, selenium and tellurium go into solution, while silver and most of the copper remain undissolved. If dilute sulfuric acid is used in the presence of air, selenium, tellurium, silver, and copper dissolve. Problems arise if selenium and tellurium exceed an oxidation state of 4. Solutions of selenate(VI) and tellurate(VI) cannot be readily reduced to the elements. The favorable economics of the pressure process are mainly a consequence of the improved sharpness of separation compared to other processes and of the short reaction times.

Processing of Copper Anode Slimes in a Cupellation Furnace. If pretreated anode slimes contain only moderate amounts of copper, selenium, tellurium, antimony, and arsenic, the noble metals can be recovered in a cupellation process. However, a two-stage process in separate furnaces is necessary for treating the low-grade and high-grade materials.

Processing of Copper Anode Slimes in the Doré Furnace. In the Doré process, pretreated anode slimes (i.e., with copper removed) are treated with slag-forming and oxidizing materials for a long period in the molten state. In addition to the crude silver fraction, three

types of slag are usually produced and removed separately. Flue dust is also obtained.

Sodium carbonate, lime, cullet (broken glass), and sand are added to form a silicate slag that takes up primarily iron, arsenic, antimony, lead, nickel, and tin. Selenium matte, which consists mainly of selenides and tellurides of copper and silver, forms an intermediate layer between the silicate slag and the molten metal if the starting material has a high selenium and tellurium content. After removal of the silicate layer, selenium matte is blown with air and treated with sodium carbonate and sodium nitrate. This produces a slag that contains sodium selenite, sodium selenate, sodium tellurite, sodium tellurate, and only ca. 1% silver. This slag is tapped off, and the molten metal is reacted with additional sodium nitrate to remove the remaining copper, lead, selenium, and tellurium. The doré silver produced has a noble-metal content of 99.0–99.5% and is sent to the silver electrorefining process. Its main impurity is copper, but it also contains some lead, bismuth, selenium, and (depending on the starting material) tellurium. Doré furnaces are usually oil fired along their length, and are similar to German fixed hearth or English tilting hearth cupels. For hearth sizes between 3 and 6 m², a charge of 8–15 t anode slime is treated in 100–200-kg lots. The reaction time is 3–6 d or longer. Waste gases are passed through dedusting chambers, coolers, scrubbers, and electrostatic gas purifying equipment.

Slags produced by oxidation of selenium matte, and flue dust and slimes from the scrubbers are major sources of selenium and tellurium. The most valuable material in the wash liquor is selenium. All other drosses, including residues from selenium and tellurium production, which contain noble metals, are recycled to the copper shaft furnace or to the doré process.

Typical compositions of intermediate products are given in Table 24.3. These can, however, vary over a wide range.

Table 24.3: Percentage composition of intermediate products from copper anode slimes and copper matte.

	Ag	Au	Se	Te	As	Sb	Bi	Cu	Pb	Ni	SiO ₂
Cupellation											
After melting	1		1		3	10		4	40	5	10
Tapped off selenium matte	20	0.1	20						25		
Tapped off litharge	1		0.5			2	3	10	60		
Argentiferous lead	40	0.5	1					5			
Auriferous silver	97	2									
Doré Process											
Selenium matte	55	0.1	25	4				13	1		
Selenite-tellurite slag	1		18	6				2			
Potassium nitrate slag	4		6	1				16			
Flue dust	4	0.3	30	3		10		5			
Gas scrubber sediment	10	0.2	35	2				0.5			
Crude metal (before treatment with NaNO ₃)	79	4	4	1				4	1		
Doré metal	95	4	<0.1				<0.1	1	0.1		
Ziervogel Process											
Mansfeld copper matte (before Ziervogel process)	0.5							75			
Mansfeld copper matte (after Ziervogel process)	0.02										

Treatment of Copper Anode Slimes with Molten Salts. Powdered anode slimes can be digested below their melting point, without forming molten metal by fusing with Na_2CO_3 and NaNO_3 or similar mixtures. The reaction is also possible at sintering temperature. After leaching with water, a separation process must be used similar to that used after acidic hydrometallurgical digestion of copper anode slimes.

Other Methods of Processing Copper Anode Slimes. Dried, decopperized anode slimes can be treated with chlorine at ca. 700 °C. Silver chloride remains in the residue, and the chlorides of selenium, tellurium, copper, tin, arsenic, etc., are sublimed or distilled.

If the decopperized anode slimes are heated to 700 °C in a vacuum, silver selenide decomposes and selenium sublimes.

24.4.3.4 Silver Extraction from Copper Matte

Before electrolytic technology became available for refining copper, copper-silver separation had to be performed on copper matte from the copper shaft furnace. Two main processes were used.

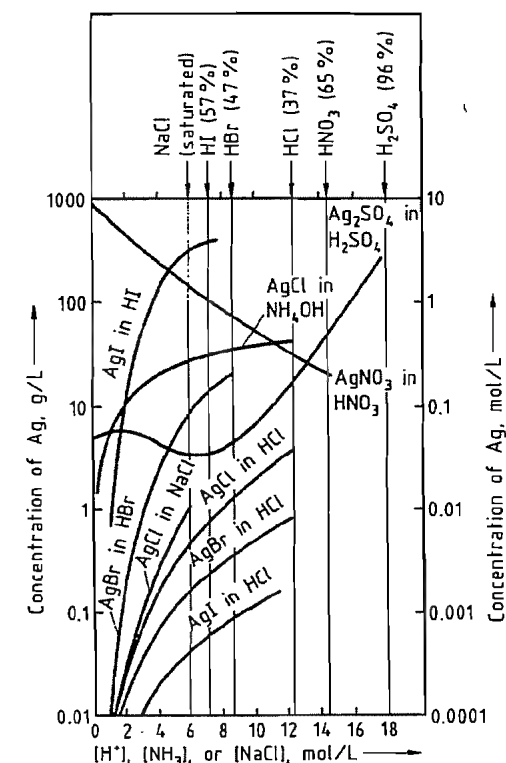


Figure 24.3: Solubilities of silver compounds in aqueous electrolytes at 20 °C.

- In the Augustin process, copper matte was roasted under chloridizing conditions, and the silver chloride formed was leached out with hot brine, leaving behind the unchanged copper sulfide (Figure 24.3).
- In the mid-1800s, the Augustin process was replaced by the Ziervogel process, which involved sulfation roasting of powdered copper matte with a precisely controlled temperature program. This first decomposes silver sulfide to silver and sulfur. The silver reacts with sulfur trioxide liberated from iron sulfate and copper sulfate, forming the more stable silver sulfate, which is water soluble. The copper is then in the form of copper(II) oxide. Treatment with water acidified with a little sulfuric acid dissolves silver sulfate, leaving copper(II) oxide in the residue. More than 90% of the silver goes into solution, 5% is in the flue dust, and the rest stays in the copper oxide (Table 24.3). Gold is undissolved and remains in the copper. Thus, the gold content of copper matte cannot be recovered by the Ziervogel process.

24.4.4 Extraction from Gold Ores

The silver present in most gold ores follows the gold in all pretreatment processes, as well as in the aqueous cyanide process. Crude gold as mined usually contains 10–12% silver. In the commonly used Miller process, silver and base metals are separated from gold by conversion to their chlorides (AgCl, CuCl, etc.). The reaction is carried out by passing chlorine through the molten metal. Silver chloride and the base-metal chlorides form a slag on the molten gold to which borax is added as a flux. Solidified slag is leached with a solution of sodium chlorate in hydrochloric acid, which dissolves the base-metal chlorides and leaves silver chloride as residue. The silver chloride is reduced with zinc dust in suspension to precipitate crude silver, which is then electrorefined.

Small amounts of silver and gold are also recovered from sodium carbonate-containing slag and broken crucible fragments from the

melting of precipitated gold in the cyanidation process. These materials are treated by the lead–silver blast furnace process and the cupellation process.

24.4.5 Extraction from Tin Ores

Silver-containing concentrates from the treatment of Bolivian tin ores usually contain a few hundred parts per million of silver, present mainly as sulfidic compounds. The ore is roasted under oxidizing conditions in the presence of sodium chloride, to convert silver to silver chloride, which can then be leached out. Alternatively, the concentrates can be treated by an amalgamation process, with or without a preliminary roasting operation. A more economical solution is often to add these materials to the feed for the copper smelting process. Silver then ends up in anode slimes from the electrorefining of copper.

Leaching with Hydrochloric Acid or Aqueous Sodium Chloride. Leaching with HCl is carried out at ca. 100 °C. Tin dioxide is not dissolved, but most of the other materials are, including silver. Silver can be cemented with scrap iron. The cementate produced is treated in copper or lead smelting processes.

Leaching with Aqueous Thiosulfate. When the silver content is high, aqueous thiosulfate is often used because of the high and selective solubility of silver chloride in thiosulfate. The process was formerly used widely to treat true silver ores.

24.5 Recovery from Secondary Silver [3, 19, 35–40, 54, 55]

The collection and treatment of silver-containing scrap and residues is of major economic importance. These materials can be divided into metallic products that can be melted to form a homogeneous material and nonmetallic concentrates (drosses, see Section 24.3.4). As in the production of silver from ores, the aim is to obtain a crude silver that can be treated in the refining process. Only seldom

is good-delivery silver obtained that does not need refining.

24.5.1 Via Copper Smelters

In principle, all silver-containing recycled materials can be treated in the usual copper production processes. Since the silver is tied up in the process for a long period, only a few types of silver-containing scrap are treated in this way. Copper must be the principal base metal present. This category of scrap includes fabrication waste and recycled material from the electronics industry. Usually, they would be fed to the copper shaft furnace or the cupel. Flue dust and copper matte from the lead silver blast furnace are also treated in copper smelters.

24.5.2 Via Lead Smelters

The only use of lead smelters in silver recycling is in treating the silver-containing flue dusts from lead silver blast furnaces. These smelters are very suitable for dealing with the high lead and zinc content of flue dusts.

24.5.3 Via the Lead–Silver Smelting Process [22, 23, 56]

Some companies that recover noble metals from scrap use a special lead-based smelting process. The pyrometallurgical reactions are the same as those used for noble-metal extraction in ancient times and correspond in principle to those of the modern lead smelting process. There are two main stages of the pro-

cess: the blast furnace stage and the oxidation stage. In the blast furnace, silver and the other noble metals are taken up by lead bullion formed in the process. In the oxidation furnace (converter), the lead is then oxidized to lead oxide (PbO, litharge). The main product is a metal with a high percentage of silver (auriferous silver). Lead oxide is recycled to the blast furnace blast. The accompanying elements that enter the system in the raw material are eliminated via three by-products of the blast furnace: copper matte, slag, and flue dust. Slag, which contains the oxide and silicate components, is worthless and can be discarded. Copper matte, which contains the chalcophilic elements copper and nickel, and flue dust, which contains zinc and cadmium, must be treated separately.

Nonmetallic concentrates (drosses) containing noble metals are generally smelted in the lead–silver blast furnace. Metallic scrap materials are often treated directly in the converter. In this case, base metals go into the litharge, though some are in the flue dust. The choice of treatment process is often determined by the cost of tying up the value of the noble metal, thereby incurring loss of interest, rather than by actual operating costs.

Typical compositions of materials involved in the lead–silver smelting process are given in Table 24.4.

The Blast Furnace. In the blast furnace (Figure 24.4), the following reactions take place:

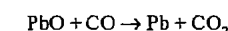
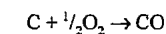


Table 24.4: Typical compositions of materials produced during noble-metal smelting.

Source	Material	Ag	Au	Nonnoble impurities, %												Relative quantities, t
				Cu	Pb	S	Halo-gen	Fe	Ni	Zn	Cd	Sn	SiO ₂	Al ₂ O ₃	CaO	
Blast furnace process	slag	100 ppm	2 ppm	0.5	1			15		2			35	20	15	30
	copper matte	3%	100 ppm	40	10	25		15	1							3
	lead bullion	20%	1%	15	60	1		2	2	4		3				6
Cupellation process	litharge	4%	100 ppm	15	60		2	2				3				6
	auriferous silver	97%	1%	1	0.1											1
Gas purification	flue dust	1%	100 ppm	3	20	2	25	2	1	8	3					1

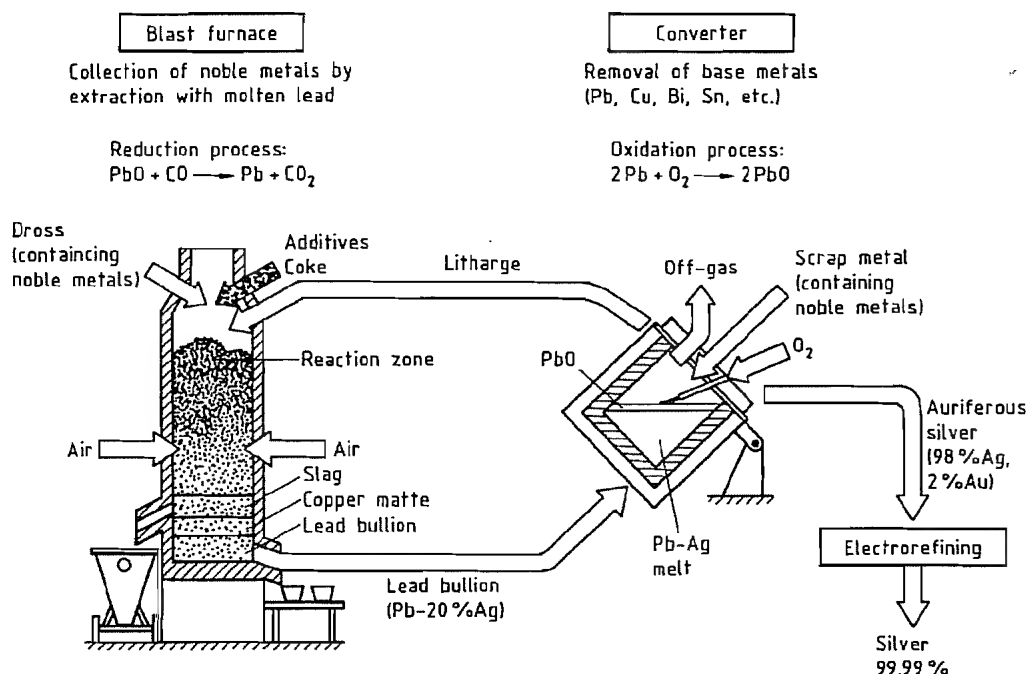


Figure 24.4: Silver recovery in a blast furnace and converter.

Here, lead is formed from the litharge produced in the converter and acts as a collector for noble metals. The chemical reactions, which also form the copper matte and slag phases, take place at 1100–1300 °C.

In the operation of the lead–silver blast furnace a large number of parameters must be controlled and various boundary conditions observed. The widely varying composition of the raw materials and of the recycled litharge, must be compensated by varying the amount of quartz, limestone, sulfur, iron oxide, pyrites, and coke added. This ensures the formation of a low-viscosity slag that does not incorporate droplets of metal. The amount of sulfur added is calculated from the amount of nonferrous metal. The ability of the slag to take up aluminum oxide is limited. If the Al_2O_3 content reaches 20%, the slag viscosity increases. This must be taken into account when catalysts supported on γ - or α -aluminum oxide are processed.

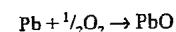
The ability of lead and auriferous silver to alloy with gold, platinum, and palladium is

unlimited. However, rhodium, iridium, ruthenium, and osmium, together with other refractory metals such as tungsten and molybdenum, collect at the bottom of the blast furnace or at the bottom of the converter. For this reason, as well as the volatility of ruthenium and osmium compounds in the blast furnace, the presence of these metals is undesirable. Halides in the raw materials end up almost completely in the flue dust in the form of lead and silver halides. Zinc and cadmium take the same route.

The elements arsenic, selenium, and tellurium are kept out of noble-metal smelters as much as possible because they form compounds with noble metals (speisses) that are difficult to process.

Instead of using a blast furnace, the lead smelting stage can be operated in a flame-fired furnace. This, too, is followed by an oxidation stage.

Oxidation in the Top-Blown Rotary Converter. The following reaction takes place in a converter:



The molten lead oxide (litharge) produced is removed continuously from the surface of the liquid metal and recycled to the blast furnace. Silver and other noble metals remain in the elemental state and are concentrated from ca. 20% in the starting material (lead bullion) to ca. 99% in auriferous silver (Table 24.4). The lead oxide contains silver particle inclusions, appreciable quantities of copper, and small amounts of other accompanying base metals as their oxides (Table 24.4).

The oxidation of argentiferous lead was carried out for a long time exclusively in shallow flame-fired furnaces (cupels) like those used in the lead smelting process. Lead was oxidized by applying a flame and a stream of air to the surface of the melt. The reaction temperatures during cupellation were ca. 900 °C at the start and ca. 1100 °C at the end of the process. The lower limit is determined by the melting temperature of PbO (890 °C), silver (961 °C), and auriferous silver (ca. 1050 °C).

Since ca. 1975, top-blown rotary converters have been used instead of cupels. The oxidizing agent is gaseous oxygen [57]. Such converters contain several tonnes of metal, and the litharge is poured off through a spout. A natural gas oxygen burner produces very intense heating. The great economic advantages compared to conventional cupellation hearths result from the much higher rate of reaction due to convection in the melt, low energy requirements, improved working conditions, longer lifetime of the furnace lining and the potential for automation.

If scrap alloys are processed directly in the converter and not in the shaft furnace, to speed up noble-metal throughput, the litharge picks up more base metal, mainly copper. The copper can be removed in copper matte only after the litharge has been transferred to the blast furnace. Therefore the noble metal is sometimes concentrated by a preliminary treatment of the raw material.

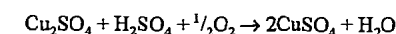
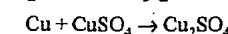
Both the oxidation process with direct feeding of scrap metal and the shaft furnace process can be carried out with copper instead of

silver. This is appropriate if the raw material has a high content of platinum-group metals that do not readily form alloys with silver (e.g., rhodium). The copper oxide formed is then usually processed by leaching with sulfuric acid.

24.5.4 Via Scrap Metal Leaching [58]

Alloys based on silver–copper, which can also contain nickel, zinc, other base metals, gold, and platinum-group metals, can be treated hydrometallurgically to recover the noble and base metals.

The basis for this is the very wide miscibility gap between silver and copper in the alloy system. Copper can be selectively dissolved by dilute sulfuric acid, with addition of air, gaseous oxygen, or hydrogen peroxide:



Copper can also be oxidized in a prior roasting stage. Dissolution by sulfuric acid is then possible without addition of oxidizing agents. The preferred reaction temperature is ca. 90 °C. In the concentration range Ag 30 Cu 70 to Ag 70 Cu 30, the silver in the alloy retains its structure during the process. The reaction rate decreases nonlinearly with increasing depth of attack due to the restriction of diffusion through the silver skeleton. For acceptable times of solution, the thickness of the alloy pieces should not exceed 0.1–0.2 mm. This can be achieved by machining the alloy to form chippings or by spraying the molten metal to form a powder. In both cases, a material is obtained that can easily be kept in suspension by stirring. If the solidified metal is slowly cooled to ca. 200 °C, formation of mixed crystals on the silver-rich side of the system can be inhibited, which increases the rate of copper dissolution. The silver that remains behind is generally electrorefined. Copper sulfate or electrolytic copper can be recovered from solution.

Silver-containing alloys can be dissolved in nitric acid or hydrochloric acid, and

silver can be precipitated as silver chloride. However, this is not economical on an industrial scale. Copper nitrate can be converted to copper oxide or copper(I) chloride. Copper cementation processes are seldom carried out because of environmental problems.

24.5.5 Via Scrap Metal Electrolysis [59]

Dietzel Electrolysis (Figure 24.5) [60]. A recycled alloy, usually of silver, gold, and copper, is anodically dissolved in an electrolyte of slightly acidified copper nitrate. The anode and cathode spaces are separated by a textile diaphragm. The anolyte is removed continuously via an overflow, and silver is precipitated from it by cementation with copper. The desilvered anolyte is fed continuously into the cathode space, where copper is deposited on rotating roller-shaped cathodes and is removed in sheet form from time to time. The flow of desilvered solution into the cathode space, and the outflow of silver-containing solution from the anode space, which is caused hydrostatically, produce a flow of solution through the diaphragm in the direction of the anode. Very little dissolved silver reaches the cathode space. Copper with a low silver content is recovered at the cathode. This copper is electrorefined, whereby a gold-containing anode is produced.

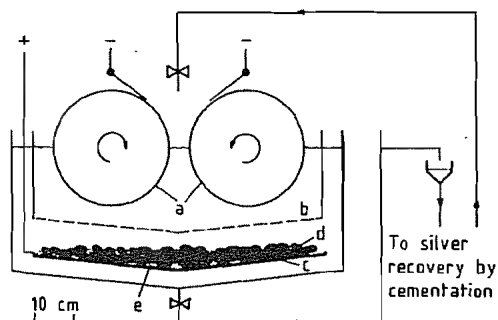


Figure 24.5: Dietzel electrolysis (front view): a) Roller-shaped cathodes; b) Diaphragm; c) Anode; d) Pieces of scrap silver; e) Anode slime.

The process is still used industrially. One disadvantage is the high cost of equipment.

Several variations of the process have been described [61].

Demag Electrolysis [61]. Copper can be dissolved from silver copper anodes by a dilute sulfuric acid electrolyte and deposited on the cathode, while silver remains undissolved. If the metal has an average silver content, as is necessary for the sulfuric acid leaching of scrap silver, a felt-like mass of silver is produced that retains the shape of the original anode. With increasing depth of penetration into the anode, the dissolution reaction is inhibited by the silver structure, which presents diffusion. Therefore, the thickness of the anode sheet must not exceed ca. 5 mm. If anode baskets are used, avoiding the production of zones from which the copper has not been completely removed is even more difficult.

As dissolution proceeds, the current voltage characteristic of the electrolytic cell changes. Potentiostatic control of electrolysis is therefore essential to prevent excessive voltage, which would cause silver to dissolve and be deposited with copper on the cathode. As in the sulfuric acid dissolution process, preliminary thermal treatment must be carried out to prevent excessive amounts of copper from appearing in the silver crystals due to the formation of silver-copper mixed crystals. Also, the copper-containing electrolyte must be carefully washed out of the silver felt, which contains very fine pores.

Electrolysis in sulfuric acid also removes the other metals that usually accompany copper and silver, but nickel accumulates in the electrolyte where it causes problems. If zinc, cadmium, lead, and tin are present in the recycled alloy, it should be oxidized first in a converter. Tin, especially, can interfere with electrolysis by precipitation of stannic acid.

24.5.6 Processing of Flue Dust

Flue dust from the waste gases of the lead-silver smelting process nearly always contains silver. Flue dust can be recovered quantitatively by means of settling chambers, electrostatic processes, wet and dry filtration, and scrubbing towers.

Dust from the lead-silver shaft furnace and the cupel generally contains the following: lead(II) oxide, lead sulfide, silver sulfide, elementary silver, copper oxide, copper sulfide, slag components, etc. It can normally be recycled to the shaft furnace.

If halides, mainly from photographic materials, are introduced into the smelting process, they are essentially bound as halides of lead and silver, which because of their low boiling points (b_p of $PbCl_2 = 916^\circ C$), are found almost entirely in the flue dusts. If the flue dust is recycled to the shaft furnace the halides revolatilize, and only the other components form slags or are reduced. The halide content of flue dust increases due to the recirculating system, and when it exceeds a certain figure, the dust is treated with sodium carbonate solution or milk of lime. Soluble halides are disposed with wastewater. All heavy metals, nonferrous metals, and noble metals remain as oxides, carbonates, or metals in the residue, which is fed back to the shaft furnace process.

Like the halides, the elements zinc and cadmium become concentrated in the flue dust, passing unchanged through the reducing shaft furnace due to their vapor pressure if they have not already been removed in the slag during cupellation or by distillation from the feed material. After sufficient concentration, they are dissolved as sulfates by treatment with sulfuric acid. The main component of the residue, which is fed back to the shaft furnace, is lead sulfate. The distribution of silver between the solution and the residue must be monitored.

The arsenic, antimony, selenium, and tellurium in flue dusts are especially troublesome. Noble-metal smelters attempt to remove these elements, which are readily sublimable in the elemental state, before the flue dust is introduced into the recycling system. Recycling of dusts of this type is usually confined to copper and lead smelters, where the elements can be picked up in the slag, either in the shaft furnace or the dore furnace.

24.5.7 Processing of Copper Matte [62]

Because of its high silver content, copper matte (see also Section 24.4.3.4) from the lead-silver shaft furnace used in noble-metal smelting must be treated without delay to minimize interest losses. Silver can be recovered quickly by the lead shaft furnace process, followed by isolation of silver by the Parkes process. Treatment in the shaft furnace of a copper refinery is possible, but silver is bound for a long time in the copper electrorefining stage and then in the copper anode slimes. In principle, copper matte can be ground, roasted in air, and leached with dilute sulfuric acid to dissolve the copper and leave a silver-containing residue. The same result is obtained by directly leaching ground copper matte with dilute sulfuric acid at ca. $160^\circ C$ in autoclaves, with introduction of air. Direct electrolysis of copper matte anodes has also been proposed. Copper is deposited on the cathode, whereas silver remains in the anode slime. However, mechanically stable anodes are difficult to produce.

24.5.8 Processing of Photographic Materials [38, 40, 62]

Films. Film material in which the film base is nonuniform, and therefore difficult to reuse, is best treated by incineration, generally after size reduction in a cutting mill. The combustion temperature must be controlled carefully to minimize volatilization of the silver, which can lead to high losses in the combustion gases, and consequent high recycling costs. The durability of the furnace lining is also strongly dependent on temperature. Usual incineration temperatures are in the range of $1000\text{--}1200^\circ C$. The temperature can be lowered by water spraying [63].

If pyrolysis [64] is used rather than incineration, flue dust problems are largely avoided. The end products of incineration of pyrolysis can be treated by smelting or electrorefining, depending on the silver content. In pyrolysis, temperatures of $600\text{--}700^\circ C$ are used. If the

film substrate is to be reused, a washing process is employed that destroys the gelatin coating and liberates silver or silver halide. Suitable washing solutions include hot dilute sulfuric acid, hot dilute sodium hydroxide solution, sodium hypochlorite solution, or enzyme solutions [65]. If developed films are to be treated, the grains of silver can be oxidized with a solution of iron(III) chloride, and the silver halide formed can be washed off with a solution of sodium thiosulfate. The silver concentrates, which must be reduced to silver if silver halides are present, generally have a sufficiently high silver content to be treated by electrorefining.

Older films, such as those from archives, must be tested carefully to determine whether they are made of extremely flammable nitrocellulose film material. The storage of such materials requires elaborate safety precautions.

Photographic Paper. Washing processes are uneconomic because the silver content of photographic papers is low and the substrate materials cannot be reused after washing. Instead, silver is usually recovered by incineration or pyrolysis.

Photographic Emulsions. The photographic industry produces unusable, usually pasty or lumpy residues of photographic emulsions, which are supplied to recovery plants for treatment. Apart from silver halides, they contain water and considerable amounts of gelatin. Treatment can be by combustion, pyrolysis, or chemical breakdown of the gelatin in solution or suspension. The silver halides can be reduced at the same time or in a subsequent operation. The isolated silver halides can be converted into metallic silver by fusion with sodium carbonate or by hydrometallurgical reduction.

Fixing Baths [66–73]. Silver-containing fixing baths from photographic plants and laboratories, hospital X-ray departments, and doctors' surgeries are rarely sent directly to recovery plants. They are generally treated chemically or electrochemically in situ to pre-

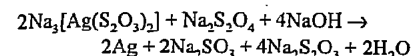
cipitate the silver. Alternatively, they may be purchased by specialist companies that convert them to concentrates and detoxify the highly contaminated wastewater.

In times of high silver prices, ca. 75% of all fixing baths are treated to recover the silver in spite of their wide dispersal. In addition to the economic value of the silver recovered from fixing baths, ecological considerations are important.

In concentrations of > 0.04 ppm, silver ions have harmful effects on biological systems. However, these effects are much reduced if the silver in photographic wastewater is in the form of a complex. The potentially harmful effects on biological wastewater treatment systems are prevented by rapid reaction of dissolved silver with the sulfide that is always present in such systems to forming insoluble and, therefore nontoxic, silver sulfide. Although no harmful effects on biological sewage treatment plants have been observed in practice, the silver concentration in wastewater passing into the main drainage system is usually limited to 1–2 ppm.

Many processes have been used to treat silver-containing fixing baths. Chemical precipitation processes have largely been displaced by electrolytic processes for ecological reasons. The original method of precipitating silver sulfide from the fixing bath by adding sodium sulfide is obsolete and unacceptable for reasons of industrial hygiene. Precipitated silver sulfide was often reacted with iron powder above the melting point of silver to form metallic silver and iron sulfide. Later, silver sulfide was precipitated by adding trimercapto-s-triazine [71]. This reaction takes place without liberation of hydrogen sulfide and can be followed potentiometrically. The method is also suitable for treating the much more dilute fixing and bleaching baths from color photography, for rinsing solutions, and for wastewater that contains copper, cadmium, mercury, nickel, and lead. Final concentrations of ca. 1 mg/L silver are obtained. The cementation of silver with zinc powder is dangerous due to the hydrogen evolved and has led to severe accidents. It also produces

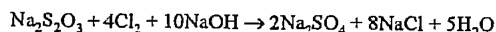
zinc-containing wastewater. The use of sodium borohydride as reducing agent has been suggested, although this also results in evolution of hydrogen. The use of sodium dithionite as a reducing agent is recommended in the photographic industry:



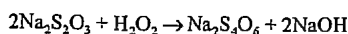
Most fixing bath treatment companies now use a process in which silver is recovered quantitatively by electrolysis. Fairly pure silver is removed from the stainless steel cathodes in the form of sheets and budlike growths. In large laboratories and hospital X-ray departments, part of the silver is recovered continuously in electrolytic cells, so that the fixing bath can be used for a longer period and no longer need be discarded so frequently and replaced with new material. For smaller laboratories and doctors' surgeries, the recovery of silver from fixing baths is carried out by using containers packed with steel wool [72]. The spent fixing bath solution is run through slowly, whereby silver is reduced and precipitates on the steel wool. The suppliers take back the containers with the silver and send them to recovery plants.

Electrolysis equipment [73, 74] of various sizes is also rented out by many business establishments who undertake the refining and purchase of the silver produced. This system has become important mainly in European countries except Germany [75].

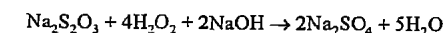
The complex-forming thiosulfate in the fixing bath can be decomposed by sodium hypochlorite or chlorine and neutralized with sodium hydroxide solution:



The silver chloride formed can be filtered off and reduced. In practice, oxidation with hydrogen peroxide is often preferred [76]. The advantages are ease and safety in handling, and the avoidance of contamination with toxic chlorinated organic substances. The reactions are



which can be summarized as



This can be taken to either the tetrathionate or the sulfate stage, depending on the desired BOD value of the wastewater produced. The silver precipitates as a mixture of Ag_2O , AgBr , and Ag_2S .

In low-silver fixing baths (e.g., washing baths or fixing baths from which silver has been removed electrolytically) the small amounts of residual silver can be removed by ion exchange [77–79].

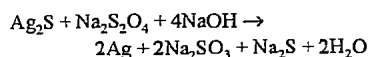
24.5.9 Surface Desilvering

In silver-plated material for jewelry, the base metal is usually German silver, a copper–nickel–zinc alloy. The base materials of silver-plated electronic components are generally copper–iron, iron–nickel–cobalt alloys, or brass. In addition they contain tin as a brazing alloy component and gold as a contact material. In electrical low-current contacts, carrier materials for the silver coating can be copper, copper–tin, copper–beryllium, brass, German silver, or copper–nickel–tin.

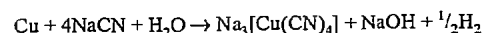
The processing of these materials in the lead–silver smelting process (see Section 24.4.2) is uneconomical. The large amounts of copper result in formation of additional copper matte, which can often incorporate more silver than is introduced in the scrap material. Nickel and iron lead to the formation of undesired furnace bottoms. Silver-plated materials are better treated by the copper-smelting route (see Section 24.4.3), which allows recovery of copper, nickel, silver, and gold in high yield. A disadvantage is that the noble metal is tied up for a long period.

In the dissolution of silver coatings from metallic substrates by acid treatment, both silver and the base metal are attacked, especially in the reaction of nitric acid with German silver. A mixture of concentrated sulfuric acid and concentrated nitric acid gives better results. Silver-plated items may also be reacted with hot sodium polysulfide solution, which rapidly and selectively converts the silver to

silver sulfide. The sulfide coating can then be removed by mechanical or thermal shock, or by reduction with aluminum or reducing agents, e.g.:



The dissolution of silver coatings in sodium cyanide solution in the presence of oxygen is slow and therefore suitable only for very thin films (a few micrometers), such as those on electronic products. As with gold, higher rates of dissolution are achieved if water-soluble aromatic nitro compounds (e.g., nitrobenzene-sulfonic acid or nitrobenzoic acid) are used as oxidizing agent instead of air [80]. When the base material consists of copper or copper alloys, unwanted side reactions of the type



are difficult to avoid. Silver can be obtained from the resulting solution by electrolysis or by decomposition of the cyanide with chlorine.

24.5.10 Processing of Special Scrap

Silver residues for recovery often arise in combination with other valuable materials. In these cases, conventional processes may fail, either because the accompanying substances cause problems, or because they cannot be recovered. In many cases (e.g., Ag- α -Al₂O₃, Ag-W, Ag-Ta), silver can be dissolved by nitric acid without attacking the accompanying material. More reactive metals such as aluminum, nickel, tin, cadmium, or indium can generally be dissolved even if they are alloyed with silver by using acid, acid mixtures, or alkali, or by anodic dissolution, leaving silver as the residue.

Before dental amalgam wastes are treated chemically to recover silver, they are usually heated to > 500 °C in closed equipment with strict control of the surrounding atmosphere to distill the mercury.

24.6 Silver Refining [2, 3, 19, 54, 59, 81]

Crude silver, from ores in primary production and from recycling operations generally has a purity of 98–99.5%, which may include gold and platinum-group metals because these processes only separate noble metals from base metals.

The main task of silver refining (world output: 10 000 t/a) is the production of silver with a purity of > 99.9% and > 99.97%. A purity of > 99.99% is increasingly being specified for industrial applications. The first and most important task is the recovery of gold and platinum metals from crude silver. The value of the gold in doré silver and auriferous silver often exceeds that of the silver itself. The refining of silver therefore generally includes a gold-silver separation process. Before refining, the noble metals are in very concentrated form, so the process must involve the shortest possible tying-up of the noble metal.

24.6.1 Fine Smelting

If the crude silver contains hardly any gold or platinum-group metals, silver of fineness 999/1000 can be obtained by an oxidation process, generally carried out in a separate refining furnace. The purification process is improved by adding alkali-metal nitrates, alkali-metal carbonates, or silver sulfate, and by blowing with oxygen.

24.6.2 Refining with Nitric Acid (Inquartation) [3]

The long-known process of dissolving a silver-gold alloy in nitric acid is still used today, although to a minor extent. Silver dissolves according to the equation

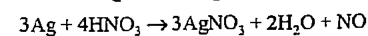
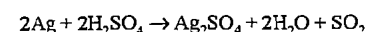


(Figure 24.1), and the gold remains undissolved. The separation becomes increasingly efficient as the composition of the alloy approaches Ag 75 Au 25. Ag-Cu-Au alloys can also be treated by this process. In addition to silver, the base-metal components and most of

the platinum metals are dissolved. Silver nitrate can be isolated from the solution; metallic silver can be obtained by cementation or electrolytic reduction; or silver chloride can be precipitated. Historically, the process was temporarily replaced by the sulfuric acid separation process, because of the high consumption of nitric acid and the large amount of recycled noble metal. Its advantage is rapid recovery of the 'gold'. Hence alloys with high gold content (e.g., 10–20%) are treated by this process.

24.6.3 Refining with Sulfuric Acid (Affination) [3]

Silver-gold alloys are treated with ca. 86% sulfuric acid at 240 °C, whereby the silver is oxidized according to the equation



and remains in solution as the more soluble silver hydrogensulfate. The solution is diluted with water to precipitate silver sulfate, which is filtered off and treated with iron in a cementation process. The silver sulfate still in solution is treated by cementation with copper to produce copper sulfate. This refining process can deal with a wider range of alloy compositions than the nitric acid process (Section 24.6.2). The alloys treated may contain appreciable amounts of copper. Also, the consumption of acid is much lower than in the nitric acid process. On the other hand, this refining process requires more costly equipment and results in considerable off-gas problems. The sulfuric acid process has not been used since World War II.

24.6.4 Möbius Electrolysis [22, 23]

The Möbius electrolysis process for refining silver is used mainly in Europe (Figure 24.6). A silver nitrate-sodium nitrate-nitric acid electrolyte is employed. Silver and the accompanying base metals are dissolved by anodic oxidation, and the concentration and current-voltage ratios are controlled so that only silver is deposited at the cathode. Cast

crude silver anodes are suspended and surrounded by anode bags in which anode slime collects. This contains all the gold in the form of metal, selenide, or telluride, as well as platinum-group metals, silver particles that become detached, lead dioxide, and oxidic copper compounds. Dendritic silver crystals are deposited on the stainless steel cathode sheet and removed continuously by automatic scrapers to prevent short circuits. Copper accumulates in the electrolyte. If the concentration of copper becomes too high, it can deposit with the silver, and the purity specification may not be met. The same is true of selenium. Palladium goes partly into solution but separates on the cathode to a very minor extent.

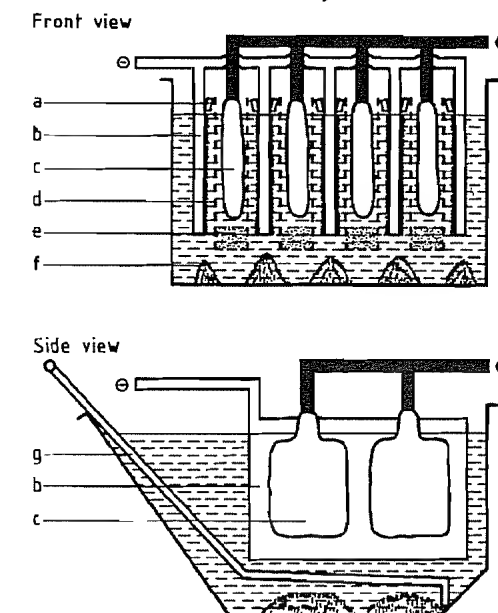


Figure 24.6: Silver electrorefining by the Möbius process: a) Scraper; b) Cathode (stainless steel); c) Anode (crude silver); d) Anode bag; e) Anode slime (gold, platinum-group metals); f) Silver crystals; g) Scraper.

The silver concentration in the electrolyte is ca. 50 g/L, with 10 g/L of free HNO₃, and the anodic current density is 400–500 A/m². The cell voltage is 2.0–2.5 V. The anodes and cathodes are usually arranged in parallel in the cell, and the energy consumption is ca. 0.6 kWh/kg of pure silver. To compensate for the anodically dissolved base metals that are not

removed at the cathode (mainly copper), silver nitrate solution is fed into the electrolyte to prevent depletion of silver.

At one time, the Möbius process had to be interrupted to remove crystals of fine silver. The anode and cathode carrying device was lifted from the bath, and the perforated false bottom was raised to enable the silver crystals to be collected. Today, cells are usually constructed so that the silver crystals can be scraped manually over the edge of the vessel without interrupting electrolysis (Figure 24.6). The spent anodes are replaced continually by new anodes, so that interruption of electrolysis is necessary only if the electrolyte must be replaced due to excessive copper concentration, or if the anode bags have to be emptied. The electrolyte is usually treated with copper to recover the silver by cementation, and the copper is then recovered by cementation with iron. The electrolyte can also be treated by chemical precipitation methods or by the "black melt" process in which a mixture of silver nitrate and copper nitrate is obtained by evaporating to dryness (see Section 24.7.1). The main accompanying metal, copper, is reported to be removed by liquid-liquid extraction, in which case the remaining silver-containing solution could then be returned to the system [82, 83].

The Möbius electrolysis process is most suitable for crude silver containing > 90% Ag. With high copper content, the electrolyte must be regenerated too often, and with high gold content, the anode bags require frequent emptying. Both are costly operations. A single electrolysis gives a purity of 99.95–99.99% Ag and a double electrolysis gives a purity of 99.995–99.999%.

24.6.5 Balbach–Thum Electrolysis [22, 23]

The Balbach–Thum electrolysis process uses virtually the same electrochemical conditions as the Möbius process. Only the geometrical arrangement is different (Figure 24.7). The anodes and cathodes are arranged horizontally. Each cell is provided with only one

anode and one cathode. The cathode is a stainless steel plate covering the entire floor area. Above this, at a distance of 10 cm, is a slightly smaller framework of nonconducting material, covered with fabric and containing the anodes. The anode and cathode are supplied with electric current via silver contacts. The crude silver anodes are completely covered by electrolyte, and therefore completely dissolved, unlike the anodes of the Möbius process, which leave behind some unconsumed metal. Another advantage of Balbach–Thum electrolysis is that the anode slime is recovered more easily, which is especially important when the crude silver has a high gold content. Disadvantages include the large space requirement and high energy consumption. The Balbach–Thum process is used mainly in the United States.

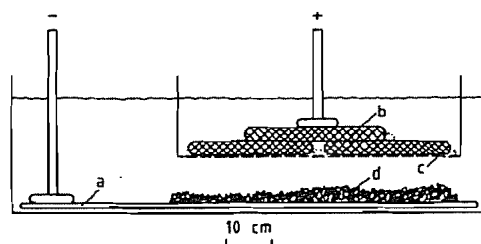


Figure 24.7: Balbach–Thum electrorefining: a) Cathode; b) Silver anode; c) Diaphragm; d) Silver crystals.

24.7 Inorganic Compounds

[19, 84–86]

24.7.1 Silver Nitrate [2]

Properties. Silver nitrate, theoretical silver content 63.50%, colorless rhombic crystals, *mp* 209 °C, temperature of transformation to the trigonal form 160 °C, decomposition temperature 444 °C, density 4.352 g/cm³ (Table 24.5), is very soluble in water, the solubility being strongly dependent on temperature (Figure 24.8), with complete miscibility in the AgNO₃–H₂O system at > 159 °C. Its solubility in water is decreased considerably by the presence of nitric acid (Figure 24.1). The solubility in ethanol is 20.8 g/L, in methanol 35 g/L, and in benzene 2.2 g/L.

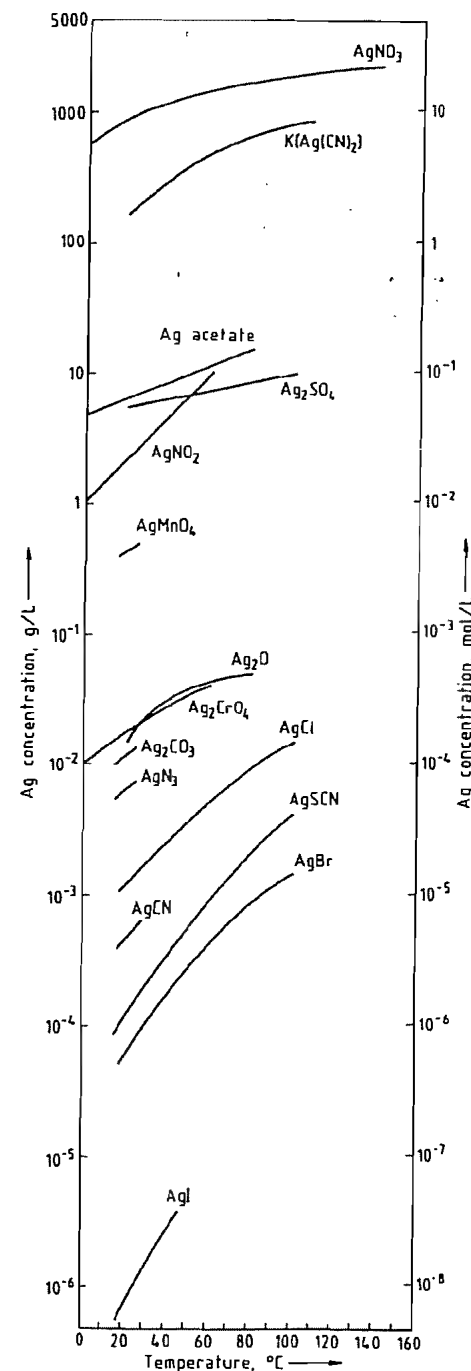


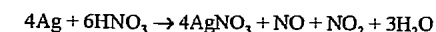
Figure 24.8: Solubilities of silver compounds in water as a function of temperature.

Table 24.5: Saturated solutions of silver nitrate in water.

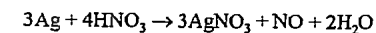
Temperature	AgNO ₃				Density, g/cm ³
	g per 100 mL H ₂ O	g/L of solution	molarity	%	
-7	94	773	4.6	48.5	1.60
0	115	909	5.4	53.5	1.70
10	160	1170	6.9	61.5	1.90
20	215	1438	8.5	68.2	2.11
25	241	1551	9.1	70.7	2.19
30	282	1710	10.0	73.8	2.32
40	335	1892	11.1	77.0	2.46
50	400	2083	12.3	80.0	2.60
60	471	2261	13.3	82.5	2.74
80	652	2608	15.4	86.7	3.01
90	762	2768	16.3	88.4	3.13
100	1024	3052	18.0	91.1	3.35
110	1105	3120	18.4	91.7	3.40
125	1624	3430	20.2	94.2	3.64
133	1941	3552	20.9	95.1	3.74
> 159	∞				

Silver nitrate has an oxidizing action on organic materials, which can lead to ignition and combustion, sometimes with explosion. Silver nitrate is decomposed even by traces of dust, with formation of finely divided, black silver. The reaction is accelerated by light. Silver nitrate and its solutions are unstable toward light over long periods.

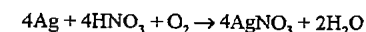
Production. Silver nitrate is generally produced by dissolving pure silver in hot 32% nitric acid:



If all the nitrogen dioxide is recycled by reaction with the water in the system to form nitric acid (see below), the overall reaction is

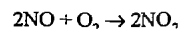


In practice, the mass balance lies somewhere between these two equations. A slight excess of nitric acid is required, which can be recovered when the product is crystallized by evaporation. Many producers pass oxygen or air through the reaction mixture, giving improved recovery of nitric acid:

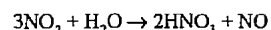


However, the formation of nitrogen oxides can be largely suppressed by using a closed vessel, so that off-gas treatment can be avoided. The nitrogen oxides produced were formerly thermally decomposed at > 600 °C in a flame, to

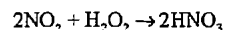
produce nitrogen and oxygen, but energy costs are high. An alternative method is to use the reactions



and



or the direct reaction



These processes are best carried out in countercurrent gas scrubbing equipment. The nitric acid formed is recycled to the process.

Since silver nitrate for the photographic industry is of a purity higher than that of refined silver (Table 24.11), a purification stage is required. The classical crystallization process is in principle very effective, but due to the high solubility of silver nitrate even in the cold (Table 24.5) and in the presence of HNO_3 (Figure 24.1), the amount recycled is high. Precipitation and adsorption of copper, iron, lead, tin, etc., as their oxide-hydrates by the addition of silver(I) oxide are recommended. This is added to the weakly acid aqueous solution until the pH reaches 6. Chromatographic purification methods based on $\gamma\text{-Al}_2\text{O}_3$ have also been described [87, 88]. Small traces of compounds of the platinum-group metals can lead to undesirable photochemical sensitization and can be converted into the inactive elemental form by irradiation with UV light [89]. Final purification can be carried out by heating molten anhydrous silver nitrate to ca. 350 °C, which mainly removes copper [19, 34]. At this temperature, silver nitrate does not decompose to the nitrite, but the decomposition temperature of most other heavy-metal nitrates to their oxides is exceeded. The copper oxide formed gives a dark-colored melt (black melt process). Precipitated impurities are removed by dissolving the product in water and filtering. The purified solution is then concentrated, and the silver nitrate is crystallized, washed carefully, and dried.

In the production of silver nitrate on an industrial scale, the equipment must be closed so that no loss of silver nitrate solution, aerosols, or dusts occurs. All operations can be carried out in stainless steel equipment.

The silver may be recovered from the mother liquor by cementation on copper, or the mixed nitrates can be treated by the black melt process to separate silver and copper. Alternatively, silver may be precipitated as silver chloride.

Uses. Most of the silver nitrate produced commercially is used in the photographic industry. Therefore, the quality specification for this application is the one in general use. Silver nitrate is also the starting material for the production of most other silver compounds and preparations, e.g., potassium dicyanoargentate(I), silver oxide, and supported catalysts. The process of electroless silver plating is also based on silver nitrate. Approximately 45% of the worldwide annual consumption of industrial silver (ca. 15 000 t) is in the form of silver nitrate.

24.7.2 Silver Halides

Silver chloride, AgCl ; **silver bromide**, AgBr ; and **silver iodide**, AgI (Table 24.6 and Figure 24.8) resemble one another in properties. Silver astatide (AgAt) is a member of this series, although it is likely to be sensitive to oxidation, even by atmospheric oxygen [90].

Silver halides become increasingly insoluble in the series AgCl , AgBr , AgI . Their solubility can be reduced further by addition of the respective common ion in low concentration. Higher concentrations of the common ion cause a marked increase in solubility due to the formation of complexes of the type $[\text{AgX}_2]^-$ (Figure 24.3). Soluble complexes are also formed with thiosulfate, cyanide, and ammonia (see Section 24.7.6). Solubility in organic solvents increases with increasingly nonpolar character of the chemical bond from chloride to iodide.

Table 24.6: Properties of the sparingly soluble halides and pseudohalides of silver.

Property	AgCl	AgBr	AgI	AgCN^a	Silver isocyanate Ag-N=C=O^a	Silver thiocyanate $\text{Ag-S-C}\equiv\text{N}^a$	Silver fulminate $\text{Ag-C}\equiv\text{N-O}^a$	Silver azide Ag-N_3
Ag content, %	79.26	57.44	45.95	80.56	71.97	60.91	71.97	71.97
Crystal system ^b	cubic	cubic	hexagonal (< 150 °C) cubic (> 150 °C)	hexagonal	monoclinic	monoclinic	rhombic	rhombic
Density, g/cm ³	5.56	6.473	5.683 6.010	3.95	4.00	3.746	4.09	4.09
mp, °C	455	430	557	350 (decomp.)	335 (decomp.)	224 (decomp.)	explosive	explosive
bp, °C	1547	1533	1506					
Solubility at 20 °C, mg Ag/L								
Water	1.3	0.08	0.001	0.2		0.1	500	60
HMPT ^c	0.12	0.08				20		10
Methanol	0.03	0.003	0.0001			0.01		0.3
Liquid SO_2	3300	25	100	200		130		

^aThe isomeric compounds corresponding to the tautomeric formulas $\text{H-N}\equiv\text{C}$, $\text{H-O-C}\equiv\text{N}$, $\text{H-N-C}\equiv\text{S}$, and $\text{H-O-N}\equiv\text{C}$, are not known in all cases, or the isomerism is not well defined in the solid state; the nomenclature used in the literature is contradictory [19, 95, 97].

^bHigh-temperature and high-pressure modifications also generally exist.

^cHexamethylphosphoric triamide.

All three compounds are sensitive to light and are used in photographic coatings on film and paper. Other industrial applications of silver halides are much less important.

Silver halides are produced almost exclusively by precipitation from aqueous silver nitrate solution by the addition of solutions of alkali-metal halides. Synthesis from the elements is also possible [91–93]. In the temperature range between the melting points of the metal and the halide, silver chloride, in particular, can be produced readily and economically.

24.7.3 Silver Oxides [2]

Silver(I) oxide, Ag_2O , theoretical silver content 93.10%, silver content of commercial product 93.0%, ρ 7.143 g/cm³, is a dark brown powder with cubic crystal structure. It decomposes slowly at ca. 150 °C and rapidly at 300 °C.

Silver(I) oxide is formed when alkali-metal hydroxides are added to solutions of silver salts such as silver nitrate. Silver hydroxide cannot be isolated as an intermediate product, although an aqueous suspension of the sparingly soluble silver(I) oxide in water has a marked alkaline reaction. In electrolytes containing sodium hydroxide or in neutral electrolytes that do not produce sparingly soluble silver salts, silver(I) oxide can be produced by anodic oxidation of metallic silver.

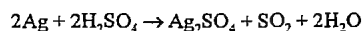
Silver(I) oxide is used in considerable quantities (i.e., several hundred tons per year) in batteries (see Section 24.9.5). In organic synthesis, it is used to replace halogen atoms with OH groups.

Silver(II) oxide, AgO , theoretical silver content 87.08%, AgO content of commercial product 97.5%, is now known to have the formula $\text{Ag}^{\text{I}}\text{Ag}^{\text{II}}\text{O}_2$. It is a gray-black powder, with a monoclinic crystal structure, which decomposes slowly to the elements above ca. 85 °C and rapidly above 100 °C. Silver(I) oxide has not been detected as an intermediate of this reaction.

Silver(II) oxide is usually prepared by the oxidation of monovalent or elemental silver by peroxodisulfate [94]. Other suitable oxidizing agents are potassium permanganate, ozone, sodium hypochlorite, or an electric current. Silver(II) oxide is a strong oxidizing agent. In contact with organic compounds, including solvents, spontaneous reaction can occur. It is increasingly used in voltaic cells, where the amount of electricity produced per mole of silver(II) oxide reacted is twice that produced per mole of silver(I) oxide, leading to economies in weight and space. The lower silver consumption means it is often more economical to use silver(II) oxide than silver(I) oxide, despite higher production costs.

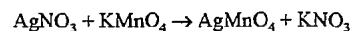
24.7.4 Other Soluble Silver Compounds

Silver sulfate, Ag_2SO_4 , silver content 34.60%, mp 657 °C, p 5.45 g/cm³, is a white, crystalline salt with rhombic structure. It is fairly soluble in water (Figure 24.8) and more soluble in sulfuric acid (Figure 24.1), forming AgHSO_4 , which can be isolated. Silver sulfate is produced by the reaction of silver with hot, concentrated sulfuric acid.



It can also be prepared by precipitation with sulfuric acid from AgNO_3 solution, followed by recrystallization from dilute sulfuric acid.

Silver permanganate, AgMnO_4 , silver content 47.60%, is a black-violet salt that is moderately soluble in water (Figure 24.8). It can be used as a disinfectant and oxidizing agent. It is produced as the least soluble component in the system



or by the reaction of silver(I) oxide or silver carbonate with a solution of permanganic acid.

Silver(I) fluoride, AgF , silver content 87.79%, mp 434 °C, p 5.852 g/cm³, is a white, flaky, crystalline solid with cubic crystal structure. It is hygroscopic and soluble in water. With increasing temperature, the solid

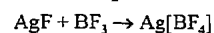
phases $\text{AgF} \cdot 4\text{H}_2\text{O}$ and $\text{AgF} \cdot 2\text{H}_2\text{O}$ exist in equilibrium with the saturated solutions.

Silver fluoride is prepared by the reaction of silver(I) oxide or silver carbonate with hydrofluoric acid, or by dissolving finely divided precipitated silver powder in hydrofluoric acid and hydrogen peroxide.

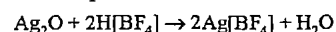
Silver fluoride is of minor industrial importance but is used in preparative fluorine chemistry.

Disilver fluoride, Ag_2F , is water sensitive, and silver(II) fluoride, AgF_2 , is highly reactive.

Silver tetrafluoroborate, $\text{Ag}[\text{BF}_4]$, is used in aqueous solution as an absorbent for ethylene. It can be produced in benzene



or in aqueous solution



The compound is very hygroscopic and unstable to light.

Oxy Salts of Halogens. Silver chlorate, AgClO_3 , is moderately soluble in water, and silver perchlorate, AgClO_4 , is very soluble.

Soluble Organic Silver Compounds. Silver(I) acetate (Figure 24.8), silver(I) propionate, and silver(I) lactate are fairly soluble in water.

24.7.5 Other Insoluble Silver Compounds

Silver sulfide, Ag_2S , mp 845 °C, p 7.326 g/cm³, silver content 87.06%, forms black crystals or powders with monoclinic crystal structure (as argentite, cubic), and is the least soluble silver compound (7×10^{-14} g/L at 20 °C). It is not dissolved by the ligands ammonia and thiosulfate, but is dissolved by cyanide. Silver sulfide can be dissolved by oxidative reactions (e.g., in hot, concentrated nitric acid). It can be reduced by base metals or by dithionite in alkaline solution. The latter is used to remove the dark coating from tarnished silver. Silver sulfide is prepared from the elements at 250–400 °C or by precipitation of silver by sulfide ions.

Silver carbonate, Ag_2CO_3 , p 6.077 g/cm³, is a white powder that rapidly turns yellow. It has a monoclinic crystal structure and decomposes at 218 °C, liberating carbon dioxide. It is prepared from soluble silver compounds by precipitation with alkali-metal carbonate.

Silver isocyanate, AgNCO , can be precipitated from aqueous solution. A mainly covalent Ag–N bond is present in AgNCO . Silver cyanate, AgOCN , apparently does not exist. Unlike the isomeric silver fulminate, AgCNO (see Section 24.7.7), silver isocyanate is thermally stable. The nomenclature for cyanates and isocyanates is, however, not yet uniform [19, 95–97].

Silver cyanide, AgCN , mp 350 °C, p 4.62 g/cm³, is a white powder with a trigonal crystal structure. It is prepared from soluble silver salts by precipitation with cyanide anions. This compound is the precursor in the production of potassium dicyanoargentate(I). Silver cyanide used to be important in analytical chemistry because of its low solubility in water, and the ease and rapidity with which it can be converted into the dicyanoargentate complex.

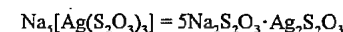
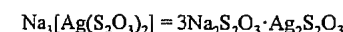
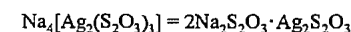
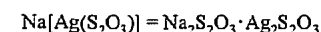
Silver thiocyanate, AgSCN , p 3.746 g/cm³, is a white powder with a monoclinic crystal structure that decomposes on melting. It is produced by precipitation from aqueous solution, a reaction that is also used in quantitative analysis.

24.7.6 Silver Complexes

Potassium dicyanoargentate(I), $\text{K}[\text{Ag}(\text{CN})_2]$, silver content 54.20%, p 2.364 g/cm³, forms white crystals with trigonal structure, which are very soluble in water (Figure 24.8) and fairly soluble in ethanol. It is prepared by dissolving silver cyanide in an aqueous solution of KCN, concentrating by evaporation, and crystallizing. It can also be obtained electrolytically by the anodic oxidation of silver in aqueous potassium cyanide solution. This method is analogous to that for the preparation of $\text{K}[\text{Au}(\text{CN})_2]$. Potassium dicyanoargentate is the basis of cyanide plating baths and is

used extensively in the jewelry industry. The corresponding sodium salt has similar properties and is an intermediate in the extraction of silver from ores by the cyanide process.

Thiosulfate Complexes. Several complexes are known, for example,



All these take part in the photographic fixing process (see Section 24.9.9) but have no technical importance in their own right. Their solubility in water increases as the ratio of $\text{S}_2\text{O}_3^{2-}$ to silver in the complex increases.

Diammine Complexes. The cationic complex $[\text{Ag}(\text{NH}_3)_2]^+$ is formed when most silver compounds are dissolved in aqueous ammonia. The solution is unstable and can precipitate highly explosive fulminating silver.

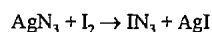
24.7.7 Explosive Silver Compounds [98]

Many unstable silver compounds are known whose decomposition can occur spontaneously and explosively. This reaction is usually initiated by heat, pressure, impact, or abrasion. These unstable silver compounds are all light sensitive. Hence, high-energy flashes of light can also occasionally cause explosive decomposition. Such compounds are no longer used to any extent, or are used only for very special preparative work, partly because of the near impossibility of storing them safely. Nevertheless, they can be formed in many chemical reactions and processes and, if their existence and properties are unrecognized, can result in accidents.

Silver azide, AgN_3 , silver content 71.97%, has colorless, needle-like crystals (mp 252 °C). It is an extremely explosive compound, sensitive to heat, impact, and pressure.

Silver azide is insoluble in water and can be obtained by precipitation from solutions of sodium azide and silver nitrate. It can be used to

prepare the equally explosive iodine azide (IN_3):



It is less stable than lead azide and has therefore not been used as a detonator.

Fulminating silver forms black crystals that consist of a mixture of silver nitride, Ag_3N , and silver imide, Ag_2NH . It is formed when aqueous ammoniacal solutions of silver compounds are stored, and by the action of ammonia on silver oxide or silver carbonate.

An explosion can be caused by slight movement of a vessel containing an aqueous solution in which a small amount of fulminating silver has precipitated and collected at the bottom. Aqueous solutions containing $[\text{Ag}(\text{NH}_3)_2]^+$ should therefore never be stored.

Silver amide, AgNH_2 , is highly explosive. It is formed mainly by the reaction of silver compounds with liquid ammonia. Silver fittings or equipment should therefore not be used in contact with liquid ammonia.

Silver fulminate, AgCNO , is the silver salt of fulminic acid, HCNO [95, 99], and is sometimes also referred to as fulminating silver (see above). It forms white needles that explode under mechanical or thermal stress, and is considerably less stable than mercury fulminate.

Silver acetylide, Ag_2C_2 , is an amorphous compound that decomposes explosively on impact or heating. On treatment with alkali-metal hydroxides, hydrolytic decomposition takes place.

Silver acetylide is prepared by passing acetylene into an ammoniacal solution of silver salts. If acetylene is passed into a neutral solution of silver nitrate, crystalline addition compounds, such as $\text{Ag}_2\text{C}_2 \cdot \text{AgNO}_3$ or $\text{Ag}_2\text{C}_2 \cdot 6\text{AgNO}_3$, are precipitated. Explosive silver acetylide is also formed when silver compounds come in contact with an acetylene flame. The existence of this hazard is the reason acetylene flames are not used for the exci-

tation of silver in solution for spectral analysis. Apparatus and containers for acetylene should not include fittings or components made of silver or high-silver alloys. Conventional silver brazing alloys are safe.

Silver oxalate, $(\text{COOAg})_2$, is a white compound that is insoluble in water and can be prepared by precipitation. It is temperature sensitive and decomposes on gradual heating, but detonates if heated rapidly.

24.8 Disperse Silver [18, 19, 56, 99]

24.8.1 Silver Powder

Silver powder is classified as microcrystalline, spheroidal, or lamellar (flakes and bronzes), according to its particle shape. All three types, which differ in method of manufacture, have specific areas of use. The basic material is pure silver or combinations of silver and palladium.

For various applications, the following properties are important: bulk density, tapped density, and tamped density (Table 24.7), sinterability, flow properties, densities achievable by compression and sintering, specific surface area, and content of impurities such as Na^+ , K^+ , and Cu^{2+} . These properties depend ultimately on particle shape and size, and on particle-size distribution. The size of the primary particles is not identical to the particle size measured by particle-size analysis, especially for dendritic powders in which agglomerates often occur. Earlier quality specifications were based mainly on sieve analysis, which has now largely been replaced by laser granulometry. The latter gives a value for particle size such that a defined fraction of the material (e.g., 90%) is finer than the quoted particle size. Methods for particle-size analysis are being supplemented more and more by optical and scanning electron microscopy.

Table 24.7: Silver powder (physical properties, old system).

Origin	Production method	Particle shape	Bulk density, g/cm	Specific surface area (BET), m ² /g	Sinterability	Flow properties	Sieve analysis
Degussa	chemical precipitation	crystalline (isometric)	ca. 12	ca. 10	good	poor	< 32 μm ca. 90% 32–40 μm ca. 10% 40–60 μm ca. 1% 60–75 μm 0.1% 75–100 μm ca. 0.1% > 100 μm ca. 0.1%
	electrolysis of acidic electrolytes	crystalline (isometric dendritic)	ca. 1.6	ca. 0.8	good	fair	< 32 μm ca. 70% 32–40 μm ca. 20% 40–60 μm ca. 10% 60–75 μm 1% 75–100 μm ca. 0% > 100 μm ca. 0%
	cementation	crystalline (dendritic)	ca. 1.5	ca. 0.3	good	fair	< 32 μm ca. 50% 32–40 μm ca. 20% 40–60 μm ca. 20% 60–75 μm 5% 75–100 μm ca. 5% > 100 μm ca. 3%
	atomization	spheroidal	ca. 4.2	ca. 0.06	poor	good	< 32 μm ca. 50% 32–40 μm ca. 30% 40–60 μm ca. 20% 60–75 μm 1% 75–100 μm ca. 1% > 100 μm ca. 0%

Table 24.8: Silver powder and flakes (physical properties, new system).

Producer	Product no.	Particle shape	Tapped density, g/cm ³ ^a	BET surface, m ² /g	Particle size ^b , μm	Impurities, ppm		
						Na ⁺	K ⁺	Cu ⁺
Demetron	309	microcrystalline	1.2–1.6	0.5–0.9	< 19	< 100	< 10	< 500
	328	microcrystalline	1.0–1.6	1.2–1.7	< 19	< 100	< 10	< 10
	331	microcrystalline	2.8–3.8	0.7–1.2	< 10	< 10	< 10	< 10
	F 14	flakes	2.1–3.2	0.7–1.1	< 32	< 20	< 10	< 500
	D 12	flakes	2.5–3.1	1.0–1.5	< 20	< 30	< 10	< 500
	D 25	flakes	3.0–4.0	1.2–1.8	< 16	< 150	< 10	< 10
	D 27	flakes	3.3–4.3	1.0–1.8	< 16	< 100	< 10	< 10
Metz	D 35	flakes	3.0–4.0	1.0–1.5	< 18	< 10	< 10	< 10
	Q-100	microcrystalline	0.9–2.0	0.55–1.05	< 18	< 25	< 10	0.20
	C-200 ED	microcrystalline	2.6–4.2	0.5–0.9	< 8	< 50	< 30	< 30
	EG 200	microcrystalline	1.5–3.0	0.15–0.4	< 13	< 125	< 10	< 30
	9	flakes	2.6–3.5	0.9–1.2	< 11	< 150	< 200	< 350
	15	flakes	2.8–4.0	0.6–1.2	< 10	< 50	< 10	< 30
	25	flakes	3.35–4.3	0.35–0.75	< 22	< 30	< 30	< 30
	52	flakes	3.6–4.65	0.4–0.7	< 14	< 30	< 30	< 30

^a ASTM 527-85.

^b Typical particle size distribution by laser granulometry; Demetron, 84% smaller than stated particle size; Metz, 90% smaller than stated particle size.

Microcrystalline Silver Powder. Several basic types of microcrystalline silver powder are available, differing in method of preparation, type of particle, and properties (Table 24.8). They were used almost entirely in sintering technology for a long time. Today, they are also used in stoving preparations (e.g., metal-

lization of ceramics) and in pastes for repairing heated rear windows of motor vehicles.

The most important method of production is precipitation by reducing agents, such as formaldehyde, potassium sodium tartrate, and hydrazine, from solutions of silver nitrate in dilute sodium hydroxide solution. Alterna-

tively, Ag_2O or Ag_2CO_3 suspensions are sometimes reduced with these reducing agents.

Cementation with less noble metals is no longer of practical importance because of contamination of silver with the precipitating metal and wastewater problems.

Electrolytic reduction of silver nitrate solutions under conditions used in Möbius electrolysis leads to a coarsely crystalline product that is not generally regarded as a silver powder and is marketed as "crystal silver". However, by using special methods of scraping or washing the cathode and varying the conditions, the electrolysis of silver nitrate can be made to yield a finely powdered material suitable for sintering applications. Electrolysis of an acidic medium has the advantage that base metals are not usually deposited with the silver. This allows less pure starting materials to be used [100]. Cathodic reduction of semiconducting silver(I) oxide in a medium containing sodium hydroxide leads to finely divided silver powder that is very similar to the chemically precipitated product. Silver oxide can be obtained by precipitation or by oxidation of a silver anode and deposition of the oxide on the cathode. Also, thermal decomposition of silver(I) oxide or silver carbonate gives a silver powder with a relatively small specific surface area.

Spheroidal Silver Powder. Atomization of molten silver by compressed air, inert gas, a water jet, or a rapidly rotating knife produces spheroidal silver powder, which is used mainly in sintering technology. It is character-

ized by relatively high bulk density, low specific surface area, and good flow properties.

Flakes and Bronzes. Lamellar particles are obtained by ball milling microcrystalline silver powder. Flakes and bronzes are incorporated into paints and adhesives, where they impart electrical conductivity to the polymer matrix due to the good particle-to-particle electrical contact.

Silver-palladium powder is used in the production of conducting electrodes in ceramic multilayer capacitors. Palladium improves the migration resistance. Several types of powder are produced by different methods, including mixtures of silver and palladium powders (composite blends), simultaneously precipitated Ag-Pd powders (coprecipitates), and alloy powders (solid solutions). Examples of these stoving powders are given in Table 24.9.

24.8.2 Colloidal Silver [2, 19, 84, 101]

Like most noble metals, silver forms very stable colloidal solutions in water.

Properties typical of colloids are observed mainly for the particle-size range 0.001–0.1 μm . Fine-grained photographic emulsions can also consist of dispersions of colloidal dimensions. Most commercial silver colloids have an average particle size between 0.01 and 0.05 μm , corresponding to specific surface areas between 50 and 250 m^2/g silver. The use of silver sols in medicine and for the disinfection of water on the high reactivity of silver resulting from its large surface area.

As with all colloidal solutions of metals in water, the stability of the solution is maintained by the negative charge on the metal particles and their consequent mutual repulsion. The negative charge is caused by the adsorption of anions. If it is disturbed by aging or by the adsorption of electrolytes until the isoelectric point is reached, partial or complete coagulation and flocculation occur.

Aging and the effects of electrolytes can be inhibited by adding protective colloids, generally naturally occurring polymers. These can still be effective after the dispersant has evaporated, allowing the powder left behind to produce a colloidal solution on rewetting. Such reversible colloids are often preferred to colloidal solutions because of ease of handling.

Colloidal silver is generally produced by reduction of a dilute solution of silver nitrate by the usual reducing agents (e.g., formaldehyde, hydrazine) at elevated temperature. Polymers that behave both as protective colloids and contain reducing groups can also be used [102]. A silver sol can also be produced by the electrical dispersion of compact metallic silver immersed in water. Commercial silver sols usually have concentrations of ca. 1% silver. Their color by transmitted light varies between yellow and brown, and they show green to blue fluorescence effects by reflected light. Colloidal silver powder, which is black and granular, has a silver content varying between 75 and 97%. On redispersion in water, dark brown to black colors are obtained.

24.9 Uses [103]

24.9.1 Coins [1, 2, 6, 104]

The amount of coinage in circulation has undergone with fluctuations throughout the course of history. The interchange between the monetary and functional use of silver has often been influenced by the political situation. In times of war, silver was monetized to a greater extent to pay the costs, and when prosperity was restored, the metal returned to private possession in the form of silver articles.

Since the growth of the industrial demand for silver, it has become demonetized. Nevertheless, large quantities of silver coins, withdrawn from circulation, are still used as national reserves. Even today, in some countries, small coins and banknotes are backed up by actual quantities of silver. In Germany, the circulation of silver coins reached a high point in 1880 before the introduction of paper money.

In ancient times, silver coins were minted from refined silver (980/1000 to 990/1000), especially in Athens and Rome. The coins of the Middle Ages usually have a fineness between 900/1000 and 990/1000. The actual value of these coins matched their face value. However, in periods of coinage debasement, so-called token coins also existed, whose metal value was less than their face value, and in which the silver content was reduced to ca. 500/1000. In the 1900s, token coins were minted generally. The silver content fluctuates between 945/1000 and 400/1000.

The technique of minting silver coins has undergone many changes over time. At first, silver coins were produced partly by casting and partly by means of a hammered die. Various designs of press were then used. Today, rods or ingots are first produced by continuous casting. The ingots or rods are rolled to form plates of the exact thickness for coinage production. These plates are then heat treated to remove the effects of cold work hardening. Blanks are then cut or punched out from the plates, which are then blanched (whitened) by dipping in dilute sulfuric acid to dissolve both the thin oxide layer and the copper near the surface of the metal. This gives a lighter surface color and a pure silver appearance. After being washed, the coin blanks are dried in centrifuges, the edges are knurled in milling or crimping machines, and the edge lettering is added, this is followed by minting in a coining press or coining machine. Modern minting machines produce 8000 coins per hour.

Table 24.9: Silver-palladium powders for multilayer capacitors.

Producer	Product no.	Composition, %	Particle shape	Tapped density, g/cm^3	Particle size, μm	Specific surface area, m^2/g
Demetron	6427 1202	Ag 70 Pd 30	spheroidal	1.4	< 30	3.0
	6427 1102	Ag 80 Pd 20	spheroidal	0.6	< 12	3.6
	6437 0401	Ag 80 Pd 20	flakes	3.2	< 8	2.2
	6437 2401	Ag 70 Pd 30	flakes	3.4	< 7	3.6
	6437 0501	Ag 60 Pd 40	flakes	2.6	< 8	1.6
Metz	5030-1	Ag 70 Pd 30	spheroidal	1.2–2.2	< 5	1.5–2.4
	5070	Ag 30 Pd 70	spheroidal	1.5–3.0	< 5	1.5–4.0
	3030-1	Ag 70 Pd 30	spheroidal	2.1–3.2	< 2.6	1.2–2.4
	3030 flake	Ag 70 Pd 30	flakes	2.7–4.6	< 6.5	1.5–2.2
	3070	Ag 30 Pd 70	spheroidal	1.5–2.3	< 3.5	1.9–3.0

24.9.2 Jewelry [18, 23]

In earlier times, the manufacture of silver articles for jewelry and general use was the main outlet for silver, apart from coinage manufacture, and it is still very important. The category includes table silver such as cutlery, jugs, dishes, plates, and cups, as well as goblets, trophies, cases, church silverware, vases, lamps, and articles of jewelry such as necklaces, bracelets, broaches, pendants, and rings. Silver is also used in the fabrication of musical instruments, especially flutes. Apart from its investment and display aspects, the bactericidal action of silver has always been an important aspect of the purchase and use of silver tableware articles (see Section 24.12.2).

Today, silver-copper alloys with finenesses of 925/1000, 835/1000, and 800/1000 are used in all forms of jewelry because of their favorable properties for both manufacture and use [105, 106]. Whereas fineness is now marked in thousandths, the earlier system used "Lot" units. Fineness was also expressed in the Russian solotnik system.

The standard materials, Ag925, Ag835, and Ag800 are supplied in the form of sheets, bands, wires, rods, and profiles. The industrial process of alloy production in a vacuum oven followed by casting and cold forming has now been replaced almost entirely by continuous casting. The quality of the alloys has thereby been improved, especially with respect to homogeneity, shrinkage, gas cavities, and formability.

Tarnishing of silver is a result of the formation of silver sulfide caused by the action of hydrogen sulfide and its organic or inorganic derivatives. Incorporation of gold, platinum, or palladium into the alloy improves tarnish resistance but is expensive. Base-metal alloy components such as zinc and cadmium change the color and luster without preventing tarnishing completely. Electrolytic pure silver coatings are more resistant to tarnishing than the usual silver copper alloys. Rhodium coatings, which were sometimes used in the past, are expensive and alter the appearance, albeit only slightly. Colorless coatings (e.g., lac-

quers) also spoil the appearance of the silver surface.

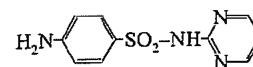
Dipping baths for removing the tarnished layer reduce silver sulfide to fine silver, which washes off without affecting appearance. Pastes are also used that contain extremely fine abrasives and reducing agents such as sodium dithionite. Surface-active additives, usually silicone based, give some extended protection. The tarnishing of cutlery, in particular, can be prevented by wrapping it in a cloth impregnated with finely divided elemental silver. These cloths absorb sulfidic compounds from the air so that they cannot react with the compact metal surface. The most effective method of treatment, however, is still the laborious process of cleaning with a paste, which removes not only the surface layer of silver sulfide but also small surface imperfections, giving a smooth polish and restoring the original luster and warm color of the silver.

Coloring. The only important coloring processes are blanching with sulfuric acid and forming oxidized silver, which is a type of partial tarnishing.

24.9.3 Medicine [1, 2, 18, 22, 23]

Silver compounds are used only sporadically in internal medical therapy, although they were more widely used in earlier times for the treatment of epilepsy and gastric ulcers. Today, their main use is for their bactericidal action on certain pathogens. Here, they behave similarly to mercury compounds but are less toxic. Several complex compounds of silver that can be absorbed through the mucous membranes are used, mainly for disinfection of the throat. The use of very dilute solutions of silver nitrate was for a long time a legally prescribed prophylactic treatment against possible streptococcal infection of the mucous membrane of the eyes of newborn babies in Germany. Silver nitrate is a component of Fisan silver powder for the treatment of surface wounds. The local caustic effect of silver nitrate can be used to destroy proliferating tissue. A protective layer of silver chloride and silver albuminate is formed by reaction with

the skin, limiting the extent of the caustic effect which is also associated with an antiseptic and astringent action. Sulfadiazine silver(I) [AgSD, 2-sulfanilamidopyrimidine silver(I)]



is used as a bacteriostatic compound in the treatment of life-threatening burns [103, 107].

Colloidal silver sols have similar bactericidal properties due to the oligodynamic action of silver. They are used in the form of stabilized solutions for disinfecting wounds, as are colloidal sols of sparingly soluble silver compounds.

Silver and silver alloys have long been used as bone replacements, mainly in cranial surgery. Also, silver wire is used in suturing connective tissue, and fine silver gauze is used as an implant. Here, too, the oligodynamic properties of silver are beneficial. It was once common to place silver foil or even silver coins on wounds for the same reason.

24.9.4 Dentistry [18, 22, 23, 56]

Silver-tin amalgams are used in dentistry to fill tooth cavities. The preferred alloys contain $\geq 40\%$ silver, $\leq 32\%$ tin, 30% copper, 2% zinc, and 3% mercury. They are produced initially in the form of cast blocks, which are then powdered by machining or converted to small spherical particles by atomization. The dentist mixes this alloy powder with an approximately equal weight of mercury to give a stiff paste. This paste is pressed carefully into the tooth cavity, the liquid mercury acting as a lubricant. Hardening is complete after a few hours and is accompanied by a small volume increase. In the older types of alloy, the important metallic phases present before hardening started were Ag_3Sn , Sn, and Hg. During hardening, the Ag_3Sn γ -phase, which is the main component of the powdered amalgam, reacts with mercury to form a solid phase Ag_3Hg_4 (γ_1), and a solid Sn-Hg mixed-crystal phase Sn_8Hg (γ_2). The reactions are incomplete be-

cause the amount of mercury is insufficient. Some Ag_3Sn (γ) always remains in excess.

Because of the presence of the relatively base metal tin, the γ_2 -phase is the weakest component of a filling with respect to both corrosion and mechanical properties. Formation of the γ_2 -phase can be suppressed by increasing the copper content and decreasing tin. Such formulations are known as non-gamma-2 amalgams. Despite advances in polymer-based filling materials whose color matches that of the tooth, non-gamma-2 amalgams have continued to fulfill an important function in the treatment of back teeth where biting forces are greater.

Silver-containing alloys are also used in dental prostheses. The gold-colored (gold-based) noble-metal alloys contain some palladium or platinum and ca. 10–15% silver, and the white noble-metal alloys based on silver palladium contain up to 65% silver.

24.9.5 Silver Plating [18, 23, 108, 109]

Silver Electroplating [110, 111]. Electrolytic deposition is the most important process for producing silver coatings. The electrolytes used are alkaline baths of potassium dicyanoargentate(I) containing an excess of potassium cyanide, with potassium carbonate as the conducting salt. Soluble pure silver anodes replace the metal deposited from the electrolyte onto the cathode. For plating articles in daily use, the preferred substrate is German silver (45–70% Cu, 5–30% Ni, 8–45% Zn), which combines good mechanical properties with good adhesion to the silver coating. Copper and nickel can also be electroplated directly. A thin initial silver coating (strike), produced in a special bath, often increases adhesion considerably. When electroplating iron, an intermediate coating of copper or nickel is necessary. Articles made of plastic (mainly acrylonitrile-butadiene-styrene and polyurethane) or ceramic can be electroplated with silver if the surface is first provided with an electrically conducting coating by the electrodeless deposition of copper or nickel.

The luster of silver coatings can be improved by additions of xanthates or thiourea to the plating bath. Their hardness can be influenced by doping the bath with antimony, bismuth, arsenic, selenium, or lead [112]. Highly abrasion-resistant coatings, so-called dispersion coatings, are produced by dispersing ceramic materials in the electrolyte during deposition.

Coatings having different thicknesses at different parts of a workpiece can be produced by using special anodes that match the geometric shape of the workpiece and by controlling the electric field in the electrolyte with the aid of masks. This technique can be used, for example, to produce thicker deposits on cutlery at places where increased wear is expected.

Silver electroplating is used mainly in the cutlery, jewelry, and electronics industries. In total, considerably more silver is used in the manufacture of electroplated cutlery than for solid silver cutlery. The potassium dicyanoargentate(I) used in the process is the silver compound produced in greatest quantity after silver nitrate and silver(I) oxide. The quality of silver plating on cutlery is quoted in grams of silver per dozen table settings consisting of three items per setting. For the usual qualities, 60, 90, or 100 minimum coating thicknesses are specified (e.g., 36 μm for a 90-g silver plating) [109, 113]. For jewelry, coatings are considerably thinner (e.g., 5–10 μm). In electronics, thicknesses of a few micrometers are often sufficient.

The deposition of silver alloys usually leads to heterogeneous coatings with inferior technical properties, although significant improvements have been obtained using gold-colored Au–Cu–Ag alloy coatings, in which silver is used in place of cadmium to lighten the color [56].

Silver electroplating is carried out in batch or continuous equipment and by barrel plating. Wire-plating plants are also operated. In some cases, partial silver plating is carried by brush plating, in which the anode and cathode are linked by a pad soaked in electrolyte.

In bulk production, continuous-flow plating plants are widely used, especially in the production of electronic components [56]. As with electroforming, their importance for gold is greater than for silver.

Silver Plating by Chemical Reactions [2, 18, 108]. Deposition of silver from aqueous solutions of silver salts onto workpieces of base metals normally leads to silver coatings of inadequate quality. However, by using a solution of $\text{K}[\text{Ag}(\text{CN})_2]$, a fairly adherent—although very thin ($< 1 \mu\text{m}$) and somewhat porous—coating can be deposited on copper by this simple method. The process is known as cementation plating.

The deposition of silver can be accelerated by contacting the metal to be plated with aluminum or zinc (contact silver plating). This plating process gives thicker, pore-free silver coatings. Contact silver plating is carried out in hot cyanide electrolytes. It is very economical for mass-produced articles, but has declined in importance.

Instead of base metals, chemical reducing agents can be added to the cyanide electrolytes [e.g., sodium hypophosphite (NaH_2PO_2), sodium borohydride, hydroquinone, or hydrazine hydrate]. The cementation reaction with the substrate metal also takes place to some extent. This plating process is improved by the addition of complexing agents such as ethylenediaminetetraacetic acid. Plastics and ceramics can also be plated by an electroless method after activating pretreatment with tin(II) chloride and palladium(II) chloride solution.

Silvering of glass, mainly for mirrors, Christmas tree decorations, and vacuum flasks, is performed with an ammoniacal silver nitrate solution to which a solution of formaldehyde and sodium hydroxide is added as reducing agent [2, 114]. Silver is deposited on the surface of the glass, usually on warming. This reduction reaction is also used in spray silvering, in which the two solutions are applied through the separate nozzles of a spray gun.

Friction plating consists of rubbing a workpiece with a moist mixture of very fine silver powder, silver chloride, and a reducing agent. This process was formerly used for silvering clock faces.

Titanium articles can be silver plated by dipping into molten silver chloride. This produces a coating of silver that adheres well but is not entirely free of pores [115].

Mechanical and Thermomechanical Plating [18]. Mechanical plating processes are often used to produce thick silver coatings, mainly for chemical apparatus, heavy-current contacts, and coating composite semifinished products.

In roll cladding, silver is bonded to the base metal at a very thin boundary region where the two metallic crystal lattices become interlocked. Cold and hot roll cladding can be carried out.

In solder plating, a silver brazing alloy is introduced between the two surfaces to be joined, and the melting point is exceeded by a definite amount on compressing the heated metal sheets. In some systems (e.g., silver-copper), a solder-like bond is produced if the melting point of the eutectic mixture of the two metals is exceeded in the boundary region. This process is known as hot press welding or eutectic welding.

Other plating processes that can be used with silver include cold press welding, atomic hydrogen arc welding, and explosive cladding.

Vapor-Phase Processes. As with the other noble metals, vacuum vaporization of silver can be achieved by cathodic sputtering or ion plating. These processes are used mainly to produce very thin films (e.g., for microelectronics).

Firing Processes [18]. Ceramic articles (e.g., porcelain tableware and industrial porcelain components) and glass can be silvered by melting pasty silver-containing preparations. The resulting coatings can be soldered, polished if they are sufficiently thick (1–10 μm), or used as a basis for further electroplating.

The pastes consist of suspensions of very fine silver powder or organic silver compounds with powdered glass in essential oils. Heating must be carried out with addition of air to burn off the organic components completely, preferably at 550–800 °C. Electronic components are often selectively silver plated by screen printing. In the mass production of glasses and porcelain tableware, decorative patterns are applied by transfer processes.

24.9.6 Electrical Technology

See references [2, 18, 22, 23, 116]. Silver is used in electrical technology because of its good oxidation resistance and high electrical and thermal conductivity. Pure silver; silver-copper and silver-nickel alloys; the composite metals Ag–Ni, Ag–W, Ag–Mo; and the composite materials Ag–CdO, Ag–SnO₂, Ag-graphite, and Ag–WC are used (Table 24.10).

In heavy-current technology, silver is used mainly as the contact material in switches [117–120]. The loss of metal due to arcing is considerably less with pure silver than with copper contacts. Even better results are obtained with silver alloys or composite materials based on silver. These materials cause the interruption arc to be extinguished more rapidly. Their high-temperature stability under pressure is greater, which also reduces the danger of welding. Electrical conductivities and often frictional properties are important in selecting the most suitable material. Some of the materials used are listed in Table 24.10. In preference to alloys, composite metals are used, which consist of sintered bodies made of two metals that do not form alloys to an appreciable extent. Composites that include nonmetallic components are also employed. Today, ecological as well as purely technological considerations are important, so that, for example, the Ag–CdO system has been replaced by Ag–SnO₂, which is nontoxic and has better resistance to burning off. The composite materials are usually produced from mixtures of the components by powder metallurgy or they can sometimes be obtained by coprecipitation followed by thermal treatment.

Table 24.10: Silver-based materials for electrical contacts.

Compositions, %										Electrical conductivity ^a	Characteristic properties	Uses
Ag	Cu	Cd	Ni	CdO	C	SnO ₂	W	Mo	WC			
Alloys												
99.9										104	tendency to weld	low-current contacts (wide use)
92.5 705										88	higher mechanical strength	relay contacts
90 10										88	and lower welding tendency than fine silver	
72 28										84		
85 15										35	reduced welding tendency	fuses (early type)
77 22.6										31		
Composite metals												
95 5										95	resistant to electrode burning; formable and claddable	mechanically and thermally stressed (domestic equipment)
90 10										87		
85 15										80		
70 30										55		
60 40										44		
40 60										25		
90 10										92	resistant to electrode burning; large contacting forces needed	heavy-current switching
50 50										62		
35 65										51		
50 50										52	similar to Ag-W; somewhat less resistant to electrode burning	heavy-current switching
40 60										47		
Composite materials												
97.5 2.5										88	very resistant to welding; intermediate coating needed for soldering	fuses
95 5										84		
90 10										75		
85 15										65		
99.5 0.5										102	extremely resistant to welding; brittle; severe electrode burning	low-voltage, heavy-current switching; sliding contacts
99 1										99		
98 2										77		
95 5										55		
90 10										35		
95 5											slightly susceptible to welding	open fuses (air break contactors)
92 8												
88 12												
65 35										57	resistant to electrode burning; very resistant to welding; difficult to work	heavy-current fuses
50 50										47		
40 60										37		

*Copper = 100.

For example, the composite system Ag-CdO can be produced by internal oxidation of the cadmium in an Ag-Cd alloy. In the case of molybdenum and tungsten, silver can be absorbed into a matrix of these refractory metals.

The important components in low-current technology are contact breakers (relays), sliding contacts, plug and socket connectors, soldered joints, and screw connectors. The requirements for these contact materials are different from those for heavy-current technology. These include low contact resistance,

resistance to effects of the atmosphere, and good abrasion resistance. A good connection must be obtained even after a large number of switching operations. In low-current technology, silver alloys are generally used in preference to expensive composite materials. These are deposited on the contacts as very thin films. In telephone relays, so-called reed contacts, based on Ag-Pd, are used.

In microelectronics, silver coatings on system carriers often facilitate both good contacting behavior and good solderability. Silver,

silver-palladium, and silver-platinum pastes are deposited as thick films on Al₂O₃ substrates to provide the conducting paths in switching circuits. Conductive adhesives with silver powder as the filler are used increasingly to give good electrical contact with semiconductor crystals and other electronic components and circuits.

For fuses, silver-coated copper wires are preferred because they do not oxidize even after prolonged heating, and their resistance therefore remains constant. So-called superquick-acting fuses for protecting semiconductor components are made of silver wires with a defined reduction in cross section at certain points.

Silver compounds are used in the construction of electric batteries. Silver(I) oxide is used in button cells for general electronic equipment. Silver(II) oxide, which has a higher capacity owing to divalent silver, is increasingly being used in button cells in both space and military applications. The AgCl-Zn combination is employed in emergency batteries used at sea. These start to operate automatically on contact with seawater.

24.9.7 Chemical Equipment [18, 121-124]

Silver is a very useful, although expensive, material of construction in the chemical industry, having good chemical resistance, high thermal conductivity, and good mechanical and working properties.

In the chemical laboratory, silver crucibles are used mainly for alkaline fusion [123]. The presence of ca. 0.15% nickel in the alloy prevents recrystallization on heating to red heat, which can lead to a coarse and brittle metal structure. In preparative fluorine chemistry, silver, as well as copper, is often used for equipment parts [84].

Silver-plated articles are used in chemical process technology. These include vessels, autoclaves, pipework, heat exchangers, and sometimes small fittings. Equipment made of massive silver is uncommon, but is used for concentrating strongly alkaline solutions, for

solutions of hydrochloric acid, and for fruit juices. For cost reasons, the load-bearing material is usually copper or steel, with silver cladding a few millimeters thick. In most cases, the two sheets of metal are bonded together by a combination of mechanical treatment and fusion, and the equipment is fabricated from the resulting composite. Alternatively, silver cladding can be applied to a finished steel construction. Vessels to withstand several hundred degrees Celsius are sometimes provided with a loosely fitting silver lining. Although this does not give optimum heat transfer, the difference in the expansion of the two metals does not constitute a risk of damage to the vessel. Vessels can also be plated internally by electrodeposition. Coatings > 50 µm thick are generally nonporous.

Silver fittings are often machined from castings. In chemical equipment, the metal can be pure silver, fine-grained silver, or oxide dispersion-hardened silver, which has better high-temperature strength.

Filter elements of sintered spheroidal silver powder are used in the food industry, principally in fruit presses. Membranes for bursting disks to protect equipment against excess pressure can be made of 0.1-0.5-mm-thick silver disks. They can be used in the range of 0.1-40 MPa at < 120 °C. Small tubes of palladium or Pd 77 Ag 23 are used in diffusion cells for the production of pure hydrogen. Pure silver and gold-silver alloys in wire or ring form are used in the manufacture of sealing materials for oxygen compressors and ultra-high-vacuum equipment.

24.9.8 Catalysts [124]

Metallic silver is an excellent oxidation catalyst. Without doubt, the specific activation of oxygen at the metallic silver surface, forming an intermediate state, plays a part in catalytic activity. Usually, fairly coarse-grained metallic silver is used, because a finely divided product with very large specific surface area would in many cases cause total oxidation of

the organic substance to carbon dioxide and water.

Ethylene oxide is produced by direct oxidation of ethylene on silver catalysts at 230–270 °C [125]. These are supported on α - Al_2O_3 or silicates and have a silver content of ca. 15%. The specific surface area of the metal is fairly low. These catalysts usually have a lifetime of several years.

Skeletal silver catalysts have also been proposed for the oxidation of ethylene to ethylene oxide [126, 127]. They are best prepared by decomposing the alloy Ag–Ca with water. However, they have not yet been used industrially.

Catalytic dehydrogenation of methanol to formaldehyde is carried out at 600–720 °C over silver gauze or crystals. Catalytic oxidative dehydrogenation of isopropanol to acetone also takes place on silver catalysts. In gas-phase reactions over silver catalysts, glyoxal is produced from glycol, and acetaldehyde from ethanol. Likewise, organic amines can be dehydrated to nitriles on silver catalysts.

24.9.9 Photography [128]

Almost all modern photographic technology is based on the light sensitivity of silver halides. This is true of black-and-white, X-ray, infrared, color, and instant photography.

In black-and-white photography, the light-sensitive emulsion coating consists of a gelatin layer in which silver halide crystals are suspended (two gelatin layers in X-ray films). The bromide ion is used more than chloride or iodide. The method of precipitation determines the structure of the particles in the silver halide mixture, and hence the photographic properties of the emulsion. The distribution of individual halides in the emulsion particles, the grain size, and the grain shape can be varied over a wide range, as can the bromide:chloride:iodide ratio. Properties are also influenced by physical and chemical maturing processes. In the development of black-and-white film and paper, the grains that come in contact with photons are reduced by chemi-

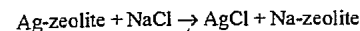
cals to elemental silver, to produce the black color. Silver halide grains that have not come in contact with light do not react and are dissolved by sodium thiosulfate during fixing.

In color photography, three primary colors, corresponding to the sensitivity of the human eye, must be produced. For each of the three colors, a photographically sensitive layer is required, which contains special dye components, sensitizers, and light-sensitive silver halide. On illumination, the silver halide is reduced to one of the primary colors in the layer that has been sensitized. On development, a silver image is first produced in each layer, as in black-and-white photography. An oxidation product of the developing substance is formed at the same time as elemental silver, and this couples with the dye component in each layer to form a dye, thus giving the three colored images. The three silver images are then dissolved oxidatively (bleaching), and the silver halide that has been illuminated is removed with sodium thiosulfate solution. Thus, the remaining colored image does not contain silver. Silver consumption for color photography is lower than that for black-and-white photography per unit of surface area. In all cases, high-purity silver nitrate is the starting material. Recovery of silver in color photography is a complex operation but is nevertheless economical because of the large size of most color processing laboratories.

24.9.10 Other Uses

Silver halides are incorporated in photochromic glasses [129, 130]. The UV component in daylight liberates elemental silver, so that the glass darkens in sunlight. As the light intensity decreases, colorless silver halide is re-formed, and the coloration decreases. The effect is used mainly in sunglasses. The change in light absorption can vary (e.g., from 10 to 50% or from 15 to 75%). Silver chloride in the form of colorless glass-clear films is used in special radiation detectors.

Molecular sieves charged with Ag^+ ions are used in sea rescue for producing drinking water from seawater by the reaction



In standard sea rescue equipment, 80 g of zeolite charged with ca. 25 g of silver provides 0.4 L of drinking water.

In an increasingly used alternative to the conventional methods of removing bacteria from drinking water [131], filters containing ion exchangers or activated carbon charged with silver are used. The extent of application of this method will depend mainly on limits to the allowable silver content of drinking water in the future. The proposed maximum of 0.01 mg/L Ag is exceeded in this process.

Colloidal silver, mostly in the form of a 1% solution, is used for disinfection of swimming baths. Effective silver concentrations are ca. 0.1 mg/L. The advantage of the method over hypochlorite treatment consists mainly in the lack of odor. With more highly contaminated water (e.g., in open swimming baths) the effectiveness is generally inadequate.

Silver iodide, generally mixed with sodium chloride, can cause the precipitation of rain or hail if it is dispersed in the form of very small crystals with a particle size of ca. 0.1 μm . These provide the necessary condensation nuclei. To produce early precipitation of hail, condensation nuclei are distributed in clouds in such numbers ($> 100\,000\text{ m}^{-3}$) that the hailstones formed are small and not dangerous [132]. Of more importance is the precipitation of rain in barren regions of the Earth.

24.10 Quality Specifications and Analysis [133–135]

Silver is handled in various purity grades (Table 24.11). The silver market is usually supplied with good-delivery silver. For most industrial uses, silver with a fineness of 999.7 (e.g., for alloying) or 999.9 (e.g., for electrical contacts and electroplating) is required.

Silver is supplied mainly in ingot form. For good-delivery quality, the ingot weight is generally ca. 31 kg (ca. 1000 oz). Small investors usually prefer 1000-g fine silver ingots, although many other weights are available, as required by the market (e.g., cast ingots

weighing 5000, 500, and 250 g; stamped plates weighing 100, 50, and 20 g; patterned plates normally 1 ounce in weight, or medallions). Craft workers and industrial users sometimes prefer granules, which are sold in sacks up to 20 kg content. Ingots are marked with their net weight in kilograms or troy ounces (1 troy ounce = 31.103486 g) and their fineness. Up to World War II, ingots of sterling silver were also available.

Table 24.11: Marketable silver qualities.

Name	Silver content, %	Impurities, ppm	
Good-delivery silver	≥ 99.9	copper	≤ 900
		others	≤ 100
Fine silver	≥ 99.97	copper	≤ 300
		others	≤ 50
		including lead	≤ 10
		bismuth	≤ 10
		total	≤ 300
Fine silver 999.9	≥ 99.99	copper	≤ 50
		others	≤ 50
		including lead	≤ 10
		bismuth	≤ 10
Fine silver, chemically pure	≥ 99.995	copper	≤ 15
		others	≤ 35
		including lead	≤ 5
		iron	≤ 5
		gold	≤ 1
		bismuth	≤ 1
Fine silver, high purity	≥ 99.999	aluminum	≤ 2
		iron	≤ 2
		silicon	≤ 2
		tin	≤ 2
		lead	≤ 1
		gold	≤ 1
		cadmium	≤ 0.5
		bismuth	≤ 0.5
		copper	≤ 0.4
		manganese	≤ 0.4
		total	≤ 10
Silver nitrate DAB 7, for photographic use	63.5	copper	≤ 2
		iron	≤ 2
		lead	≤ 10
		sulfate	≤ 10
		nitrate	≤ 10
		water insoluble	≤ 10
		not precipitated by HCl	≤ 10
		moisture	≤ 200

Correct sampling methods are essential for the accurate determination of silver [136–138].

Samples are taken from ingots by means of holes drilled diagonally, or by producing

metal cuttings by sawing across the entire cross section at various parts of the ingot. Similar methods are used for semifinished products. If possible, nonhomogeneous materials are melted and cast into ingots that can be sampled.

Silver-containing waste liquids may contain sediments and deposits on the vessel walls that can be removed by filtration or dissolution, or samples can be taken after stirring.

Products in lump or powder form that cannot be melted, such as dross, are ground and sieved. The fine and coarse fractions are analyzed separately. If a metallic coarse fraction is obtained, this can be melted.

Special methods have been developed for sampling large amounts of ore, after which the above procedures are carried out.

24.10.1 Qualitative Analysis

The qualitative analysis of silver [134] is in practice usually a preliminary to quantitative analysis.

Chemical Methods. Silver in solution is generally determined by precipitating white silver chloride by addition of chloride. It is dissolved as $[\text{Ag}(\text{NH}_3)_2]^+$ by the addition of ammonia and reprecipitated on acidifying with nitric acid. For low silver content, chloride addition produces only a characteristic cloudiness. If the solution contains cyanide, thiosulfate, ammonia, or hydrochloric acid, silver chloride cannot be precipitated because soluble silver complexes are formed. If necessary, the complex formers can be decomposed by oxidation or change of pH.

Photometric methods of determination also exist [139], but these are seldom used because of possible interference from other metallic ions and the reliability of the AgCl precipitation method.

Physical Methods. Atomic absorption spectroscopy [140] is useful for qualitative determination of silver in solution (e.g., in wastewater). However, silver concentrations in the solutions must be known not to be too high; otherwise, the acetylene-air flame gen-

erally used to excite silver ions can lead to the formation of highly explosive silver acetylide. In the past, this has caused explosions in analytical equipment.

Emission spectroscopy, X-ray fluorescence spectroscopy, and other physical methods of qualitative analysis are also suitable.

Docimasy [134, 135] can, in principle, be used for qualitative analysis. Here, all the base metals in a sample are converted to slag, leaving a bead of silver. Products of cementation or residues from the evaporation of solutions can also be analyzed by this method.

24.10.2 Quantitative Analysis and Accountancy Analysis [22, 133, 135, 136]

A large proportion of the 15 000 t silver used annually by industry, with a total value of $(3-4) \times 10^9$ DM, is converted by the users into alloys or into many varied forms suitable for recycling. The silver analyses of these materials must therefore be highly accurate, since the results are used to calculate the sales value of the products.

Docimasy [134, 136], which has been used for hundreds of years to determine the value of silver and gold, is the most important method of quantitative analysis. Here, noble metals in the samples are taken up by molten lead, and base materials are converted to slag. In the crucible assay, a mixture of lead oxide, reducing agent, and fluxes is melted at ca. 1250 °C in a crucible. In the scorification assay, the sample is melted with granular lead and borax at ca. 1000 °C under oxidized conditions. The lead is finally oxidized at ca. 800 °C to litharge (cupellation), and a bead of noble metal is left behind while PbO is absorbed into the porous magnesite base (cupel). If the bead contains several noble metals, a wet chemical or physical analysis is carried out. Direct X-ray fluorescence analysis of the bead is also possible, and has the advantage of greater speed and lower cost.

Docimastic techniques have recently been improved to give even greater accuracy.

Volumetric Determination of Silver [134-136, 141, 142]. The volumetric titration of GAY-LUSSAC is still used today. In this method, a solution acidified with nitric acid is titrated with NaCl solution, to precipitate silver chloride. The so-called clear point or end point of the nitration is determined by visual observation. A high degree of accuracy can be obtained by precise control of titration conditions, which are established in a previous determination of the approximate silver content of the sample to be analyzed. Hardly any interference results from the usual elements that accompany silver (Cu , Zn , Ni , etc.), but lead, mercury, and tin can cause problems. This method is still used for umpire assays.

Potentiometric titration also depends on the precipitation of silver chloride by the controlled addition of NaCl solution acidified with nitric acid. In some cases, because of the even lower solubility of the other silver halides, sodium bromide or sodium iodide is also used as precipitation agent. Automation of the potentiometric titration process enables this method to be used for routine determinations. Modern automated titration equipment with potentiometric endpoint indication, can analyze up to 30 sample solutions per hour. The potentiometric determination of silver is even less subject to interference than Gay-Lussac titration. In recent decades, it has become the principal method of silver determination.

The determination of silver in solutions acidified with nitric acid by Volhard titration is based on the precipitation of insoluble silver thiocyanate in the presence of Fe^{3+} ions. The end point is detected by the brown coloration of the solution by iron(III) rhodanide. The method is not very accurate and is used mainly for internal plant control analysis.

Other gravimetric methods have decreased in importance. These include the precipitation of silver iodide by I^- ions, followed by iodometric titration of excess iodide; the Fajans titration with adsorption indicators; and titration with dithizone. The Mohr titration is rarely used for silver determination but was formerly used for halide determination.

A volumetric method that has recently become important is the precipitation of Ag_2S , in which the end point is detected by voltametry [143] or by determining the EMF of a silver-sensitive electrode [142, 144].

Gravimetric Determination of Silver. The most important gravimetric method is the precipitation of silver chloride in hot solution acidified with hydrochloric acid. Silver chloride can be weighed directly or reduced with hydrazine in ammoniacal solution to obtain the metal. Gravimetric determination with organic precipitants is described in [139, 145].

Physical Methods. In systems of known constitution (e.g., silver brazing alloys or jewelry alloys), X-ray fluorescence analysis can be carried out [146-148] with an accuracy comparable to that of wet chemical methods and hence adequate for accountancy purposes. The silver button produced by docimasy can also be analyzed by X-ray fluorescence.

Atomic emission spectroscopy with glow discharge, spark or plasma excitation is being used increasingly for the quantitative determination of silver in its alloys.

Atomic absorption spectroscopy (AAS) is less accurate and therefore more often used for process control analysis than for accounting purposes. If the solutions used have high concentrations of silver, a danger exists of Ag_2C_2 formation in the acetylene flame, so the solutions analyzed must be very dilute.

24.10.3 Purity Analysis

In purity control of silver, the fineness is calculated from the sum of the impurities. The fineness of metal or the purity of compounds was formerly determined by docimasy, supplemented by wet chemical determination of the main impurities. Today, metal samples, pressings, or solutions are analyzed by emission spectroscopy [149, 150]. For this, plasma excitation is increasingly used due to the better limits of detection, and the possibility of rapid simultaneous analysis and lower costs. Atomic absorption analysis and polarography are also used for analysis of trace impurities.

High-performance liquid chromatography is less important. In some cases, especially for ultrapure materials, mass spectrometry is used, more recently with glow discharge excitation and neutron activation.

The fineness of noble metals can be determined much more accurately from the sum of the impurities than by direct analysis of the noble-metal matrix. Physical methods of trace analysis have largely replaced wet chemical and colorimetric methods for reasons of economy and speed.

24.10.4 Trace Analysis

Apart from docimasy, which is used mainly for oxidic drosses, silver-containing ores, and precipitates from solutions, all other methods of silver determination are also used for trace analysis. For extremely low levels of impurities, other methods are used, including graphite-tube AAS, neutron activation analysis, total reflection X-ray fluorescence analysis, and inductively coupled plasma spectrometry. Photometric methods are rarely used, but AgCl formation is measured by nephelometry [151].

The maximum allowed concentration of silver in wastewater is very important now because of the widespread use of biological wastewater treatment. Silver(I) ions interfere with the biological equilibrium at a concentration of > 0.04 ppm. Atomic absorption spectroscopy is widely used for wastewater analysis.

Trace analysis of noble metals in waste materials from the noble-metal industry, especially scrap recovery plants, is of great importance for checking the economic efficiency of the process.

24.10.5 Argentometry [141, 142]

The precipitation reactions used for volumetric determination of silver can also be used for determination of ions that form insoluble precipitates with Ag⁺. Techniques for determining chloride, bromide, iodide, cyanide, thiocyanate, etc., which are derived from the

methods described for silver are generally known as argentometry and include the following:

- Potentiometric titration of halides by the controlled addition of AgNO₃ solution
- Reverse GAY-LUSSAC titration for determination of halides and cyanides
- Reverse Volhard titration for determination of halides, cyanide, or thiocyanate

Argentometric methods employing chemical indicators are rarely used.

24.11 Economic Aspects

[15, 16, 22]

24.11.1 Production

Of all the noble metals, silver comes first in terms of annual production. In terms of value, however gold exceeds silver by a factor of 15 (Table 24.12).

In 1992, the amount of silver produced worldwide by mining was 11 400 t, and the amount recovered from scrap materials was 3600 t. The largest producers of silver are Mexico, the United States, Peru, Canada, and Australia in that order. This has been true since the end of World War II.

Table 24.12: Value of noble-metal production in 1992.

Metal	Primary production, t/a	Price, DM/g	Total value, 10 ⁶ DM
Au	1800	18	32 400
Ag	11 500	0.2	2200
Pt	120	19	2300
Pd	115	5	600
Rh	12	128	1500
Ru	12	2	20
Ir	1	11	10
Os	0.5	26	13

24.11.2 Supply and Demand

The supply of silver to the world market (Figure 24.9) is mainly determined by production from mines. The amount produced is relatively insensitive to price movements, which are sometimes large and generally of a speculative nature, because silver is mainly a side

product of the extraction of base metals. Also, market price fluctuations are reflected to only a limited extent in production from recycled materials. However, government sales, and sometimes purchases, are strongly dependent on price changes. Sales of silver from the CIS have a relatively small influence on the total supply situation in the Western world in spite of the considerable production in this region. Also, in comparison to gold and the platinum-group metals, large amounts of silver are frequently released to the world market from the old stocks in India, estimated at around 120 000 t. This material was accumulated many years ago from domestic production and commercial transactions. The total stocks of the Western world (excluding India) amount to ca. 80 000 t, of which approximately 50% is owned by the U.S. government.

The demand for silver (Figure 24.10) is fairly well matched by the supply. The relatively even distribution of demand over various sectors is not expected to change fundamentally in the foreseeable future. However, the relatively small extent of known silver reserves in ores, compared to other metals, could in the future lead to a change in stockpiling practice. The greatly increasing status of silver as an industrial metal could also have major effects. In technology, an important factor in the future is likely to be a decrease in the importance of classical silver-based photography, to the benefit of electronic image-making techniques.

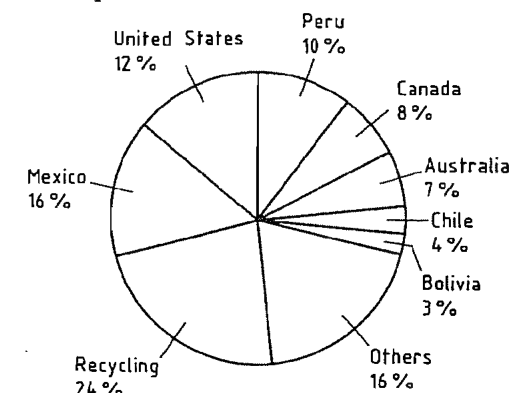


Figure 24.9: Western world silver supplies, 1992.

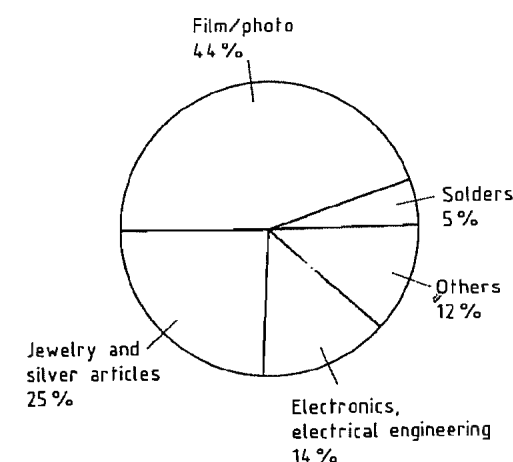


Figure 24.10: Western world silver consumption, 1992.

24.11.3 Silver Market and Trading

The most important silver exchanges are the New York Commodity Exchange; Chicago Board of Trade; West Coast Commodity Exchange Los Angeles; and Broker's Market London, which provides daily price information. Bargains are struck in London for delivery promptly or after 3, 6, or 12 months. The amounts of silver transferred yearly are often more than two orders of magnitude greater than the world's demand for silver.

On June 22, 1992, the price of silver was \$4.30 per ounce (DM 227/kg), having remained around this low level for many years. The low point of \$3.65 per ounce (DM 180/kg) reached in 1972 was again reached in 1992.

24.12 Health and Safety [2, 44, 152, 153]

24.12.1 Toxicology [152, 154, 155]

The acute and chronic toxicity of silver compounds in humans is much lower than that of other heavy metals such as mercury, thallium, or cadmium. This is due mainly to their rapid conversion into insoluble silver compounds, especially silver chloride and silver albuminate, in the body. The LD₅₀ for soluble

silver compounds is 50–500 mg/kg as Ag. Almost the only cause of acute silver poisoning is accidental overdosing with silver-containing pharmaceuticals. The main hazard of the water-soluble compounds silver nitrate and silver fluoride is a caustic effect of fluoride toxicity, respectively.

Prolonged contact with silver compounds or finely divided elemental silver leads to absorption of the metal by the human body. This can cause argyria, which has no pathological effects but can lead to a disfiguring darkening of the skin, beginning with mirror effects on the pupils of the eyes and coloration of the skin exposed to light. This effect is irreversible and cannot be treated medically. In addition to the deposition of elemental silver, silver sulfide may be formed. In cases of severe argyria, a person can absorb up to 20 g of silver. The silver is usually taken up from respired air, although excessive doses of silver-containing drugs (e.g., colloidal silver) can also lead to argyria. Workers involved in the production of silver nitrate and in silver-plating processes face the greatest risk.

The MAK value for elemental silver and soluble silver compounds is 0.01 mg/m³ as Ag. This is intended mainly to prevent argyria and is not a true toxicity limit. For drinking water, the limit is 0.05 mg/L.

24.12.2 Bactericidal (Oligodynamic) Effect

The use of silver preparations in medicine and in water purification depends on the sensitivity of bacterial metabolism to silver ions. Their advantage compared to other bactericidal metallic ions such as Hg²⁺ lies in the fact that the effective Ag⁺ concentrations lie well below the danger level for the human organism (i.e., at 0.01–1 mg/L). Hence, even sparingly soluble compounds such as silver chloride have a bactericidal effect, but the extremely insoluble compound silver sulfide does not.

In the presence of atmospheric oxygen, metallic silver also has a bactericidal effect due to the formation of silver oxide, which is soluble

enough to cause it. Bactericidal concentrations are produced extremely rapidly by adding colloidal silver, which has a high surface area, but even objects with a solid silver surface (e.g., table silver, silver coins, or silver foil) have a bactericidal effect in the absence of sulfide, which would otherwise combine with the Ag⁺ ions.

The death of microorganisms such as bacteria, molds, spores, and fungi on contact with silver articles was discovered by VON NÄGELI (1817–1891), although he did not identify the cause. The effect was certainly used in antiquity, and silver drinking vessels were carried by military commanders on expeditions for protection against disease. NÄGELI named the effect that he discovered the oligodynamic effect. This is now generally understood to mean the damaging effect of very small amounts of metallic cations on living cells.

24.12.3 Explosion Hazards

Silver forms many unstable compounds (see Section 24.7.7) that can explode or detonate on thermal or mechanical stress, on drying, under the influence of light, or sometimes spontaneously without any known cause. This group includes several nitrogen compounds of silver, organic compounds (especially silver acetylide and its derivatives), and silver(II) oxide in contact with finely divided organic materials.

Since some of these compounds can be formed by reaction with elemental silver, acetylene and ammonia in the gaseous or liquid state should not be allowed to come in contact with items of equipment made of silver or its alloys. Also, silver and its compounds must be kept away from acetylene flames.

Silver salts of strongly oxidizing acids (e.g., silver chlorate and nitrate) can lead to dangerous explosions on contact with oxidizable materials (e.g., organic substances, sulfur, soot). Contact of silver nitrate with alcohol leads to immediate formation of explosive silver fulminate. Many explosions have resulted from formation of nitride in ammoniacal solutions of silver. Silver oxalate is reported to de-

compose at 140 °C, but explosions have occurred on drying at 80 °C.

24.13 References

1. R. Kerschagl: *Silber, Metallische Rohstoffe*, vol. 13, Enke, Stuttgart 1961.
2. A. Butts, C. D. Cox: *Silver—Economics, Metallurgy, and Use*, R. E. Krieger Publ. Co., Huntington 1975.
3. V. Tafel: *Lehrbuch der Metallhüttenkunde*, Hirzel, Leipzig 1951.
4. D. Büttner, *Naturwiss. Unterr. Phys/Chem.* **28** (1980) 129–140.
5. A. Binz: *Edelmetalle, ihr Fluch und ihr Segen*, W. Limpert, Berlin 1943.
6. H. Römpf: *Chemie der Metalle*, Franckh'sche Verlagshandlung, Stuttgart 1941.
7. N. H. Gale, W. Gentner, G. A. Wagner, *Metall. Numis.* **1** (1980) 3–49.
8. W. Gentner, H. Gropengießer, G. A. Wagner, *Mannheimer Forum* 1979/80, Boehringer Mannheim.
9. W. Gentner, O. Müller, G. A. Wagner, N. H. Gale, *Naturwissenschaften* **65** (1978) 273–284.
10. E. Pernicka, *Erzmetall* **34** (1981) 396–400.
11. H.-G. Bachmann, *Erzmetall* **35** (1982) no. 5, 246.
12. C. Schnabel: *Lehrbuch der allgemeinen Hüttenkunde*, Springer, Berlin 1913.
13. G. Agricola: *Vom Berg- und Hüttenwesen*, Deutscher Taschenbuchverlag, München 1980.
14. L. Suhling: *Der Seigerhüttenprozeß*, Riederer Verlag, Stuttgart 1976.
15. W. Gocht: *Handbuch der Metallmärkte*, 2nd ed., Springer Verlag, Berlin 1985.
16. E. Schmidt, *Metall* **47** (1993) 644–667.
17. S. D. Dial, *Metall (Berlin)* **35** (1981) 580–590.
18. Degussa: *Edelmetall-Taschenbuch*, Frankfurt 1967.
19. Gmelin, Silber, System no. 61, 1970/76.
20. G. H. Aylward, T. J. Findlay: *Datensammlung Chemie*, Verlag Chemie, Weinheim 1975.
21. E. Fluck, K. G. Heumann: *Periodic Table of the Elements*, VCH Verlagsgesellschaft, Weinheim 1986.
22. Fonds der Chemischen Industrie: *Edelmetalle—Gewinnung, Verarbeitung, Anwendung*, Folienserie no. 12, Frankfurt/Main 1989.
23. Degussa: *Edelmetall-Taschenbuch*, 2nd ed., Metallverlag, Berlin 1994, in press.
24. D. G. Cooper: *Das Periodensystem der Elemente*, Verlag Chemie, Weinheim 1972.
25. D. Mehadows, E. Zahn, P. Milling: *Die Grenzen des Wachstums*, Deutsche Verlagsanstalt, Stuttgart 1972/1979.
26. N. N. Grennwood, A. Earnshaw: *Chemie der Elemente*, VCH Verlagsgesellschaft, Weinheim 1988.
27. F. Pawlek: *Metallhüttenkunde*, Walter de Gruyter, Berlin 1983.
28. D. F. Schutz, K. K. Turekian, *Geochim. Cosmochim. Acta* **29** (1965) 259–313.
29. H. Schneiderhöhn: *Erzlagerstätten*, G. Fischer Verlag, Stuttgart 1962.
30. A. Cissarz: *Einführung in die allgemeine und systematische Lagerstättenlehre*, E. Schweizerbart'sche Verlagsbuchhandlung, Stuttgart 1965.
31. Metallgesellschaft: *Die Welt der Metalle—Kupfer (Kupferatlas), The World of Metals—Copper*, Frankfurt 1993.
32. Metallgesellschaft: *Die Welt der Metalle—Blei, Zink*, Frankfurt 1994, in press.
33. L. van Zyl, C. P. Schreuder (eds.): *South Africa's Mineral Industry*, Department of Mineral and Energy Affairs, Bramfontein 1991/92.
34. R. Saager: *Metallische Rohstoffe von Antimon bis Zirkonium*, Bank Vontobel, Zürich 1984.
35. Degussa: *Recycling—Rohstoffsicherung und Umweltschutz*, Frankfurt 1981.
36. National Association of Recycling Industries: *Precious Metals*, New York 1980.
37. E. Krone, W. Dähne, *Chem. Ztg.* **1977**, 421–425.
38. W. Kumpf, K. Maas, H. Straub, G. Hösel, W. Schenkel: *Müll- und Abfallbeseitigung (Müll-Handbuch)*, Kennzahl 8572 (C. Knorr: Rückgewinnung von Silber aus photographischen Rückständen), Kennzahl 8595 (H. Renner: Behandlung und Verwertung von verbrauchten edelmetallhaltigen Katalysatoren), Erich Schmidt Verlag, Berlin 1980/81.
39. W. W. Behning, *Metall (Berlin)* **24** (1970) 794–796.
40. W. Dähne: *Recycling von Silber aus Fotomaterialien*, GDMB Gesellschaft Deutscher Metallhütten- und Bergleute, no. 3, lecture of 10/23, Nov. 1991 in Würzburg, Clausthal-Zellerfeld 1991.
41. D. H. Chambers, B. W. Dunning: *Silver Recovery from Aircraft Scrap*, Report no. 8477, Bureau of Mines, Washington 1980.
42. Ullmann, 3rd ed., **15**, 630.
43. K. Winnacker, L. Küchler: *Chemische Technologie*, 4th ed., vol. 6, Carl Hanser Verlag, München 1986.
44. Kirk-Othmer, 3rd ed. **21**, 1–31.
45. H. J. Bovey, S. Marks, *S. Afr. Chem. Process* **4** (1969) no. 2, 28–34.
46. M. Toyoda, A. Ohta, T. Shimizu: *Slime Treatment at Niihama Copper Refinery*, Metallurgical Society of AIME, New York 1976.
47. F. Habashi, *Chem. Ztg.* **86** (1962) 483–487.
48. R. A. Zingaro, W. C. Cooper: *Selenium*, Van Nostrand Reinhold, New York 1974.
49. W. C. Cooper: *Tellurium*, Van Nostrand Reinhold, New York 1971.
50. J. Feiser: *Nebenmetalle. Die metallischen Rohstoffe*, vol. 17, Enke, Stuttgart 1966.
51. W. Schreiter: *Seltene Metalle*, vols. II and III, Deutscher Verlag f. Grundstoffindustrie, Leipzig 1961.
52. Inko, DE-OS 2914439, 1979.
53. American Metal Climax, DE 2117513, 1971.
54. W. Truthe: *Hundert Jahre Gold- und Silberscheidung nebst Gewinnung der Platinmetalle*, Degussa, Frankfurt 1943, unpublished.
55. G. A. Walker: "Recovery and Refining of Secondary Silver", 9th Commonwealth Mining and Metallurgical Congress, London 1969.
56. Degussa: *Metall—Forschung und Entwicklung*, Frankfurt/M. 1991.
57. Degussa, DE 2059235, 1970.
58. Outokumpu Oy, DE 2543027, 1975.
59. G. Eger: *Das Scheiden der Edelmetalle durch Elektrolyse*, W. Knapp, Halle 1929.
60. Dietzel, DE 68990, 1892; DE 82390, 1895.
61. H. Walden, *Chem. Ing. Tech.* **36** (1964) 647–651.

62. Kodak: *Die Silberrückgewinnung in der Fotografie*, Stuttgart 1972.
63. Kodak, US 2944886, 1958.
64. Cendres & Métaux, CH 613787, 1976.
65. Röhm GmbH: Ablösen der silberhaltigen Gelatineschicht von Filmabfällen, Company brochure, Darmstadt 1977.
66. B. Krauß, *Moderne Fototechnik* 1979, 125–127, 237–240, 433–437.
67. E. Mutter, *Röntgen-Laboratoriumsprax.* 13 (1960) 158–165, 175–191.
68. H. Aisenberg, U. Fritz, *Röntgenpraxis (Stuttgart)* 19 (1966) 284–307.
69. G. Kolb, *Chem. Lab. Betr.* 32 (1981) 43–48.
70. W. Großmann, *Moderne Fototechnik* 1980, 557–558.
71. Degussa: TMT 15 für die Abtrennung von Schwermetallen aus Abwässern (Reihe Umwelt und Degussa), Frankfurt 1980.
72. Minesota Mining, US 4110109, 1978.
73. Siemens, DE-AS 2543600, 1975.
74. Ciba-Geigy, US 4186067, 1978.
75. Comptoir Lyon-Alemand, Louyot & Co.: Procédé Purhypo, Company brochure, Paris 1979.
76. Degussa: Behandlung photochemischer Abwässer mit Wasserstoffperoxid (Reihe Umwelt und Degussa), Frankfurt 1980.
77. R. Mina: "Silver Recovery from Photographic Effluents by Ion Exchange Methods", SPSE-Symposium, Las Vegas 1980.
78. D. J. Degenkolb, F. J. Scobey, *J. Soc. Motion Pict. Telev. Eng.* 86 (1977) 66–68.
79. C. Ramsey: Ion Exchange for Silver Removal from Effluents, PMA Fall Seminar, 1979.
80. MacDermid Inc., US 3242090, 1964.
81. J. W. Hunter: "Electrochemical Principles and Refining", IPMI-Seminar, Skytop Lodge 1980.
82. Brookside Metal Comp., CH 614238, 1974; US 3975244, 1976.
83. A. Prior, R. Marr, H. J. Bart in: *Raffinationsverfahren in der Metallurgie*, Verlag Chemie, Weinheim 1983, pp. 243–252.
84. G. Brauer: *Handbuch der präparativen anorganischen Chemie*, vol. 2, Enke, Stuttgart 1978.
85. L. Vanino: *Präparative Chemie*, vol. 1, Ferdinand Enke Verlag, Stuttgart 1925.
86. N. R. Thompson: *Comprehensive Inorganic Chemistry*, vol. 17, Pergamon Press, Oxford 1973.
87. Du Pont, US 2614029, 1951.
88. Du Pont, US 2543792, 1949.
89. Du Pont, US 2940828, 1957.
90. W. A. Chalkin, E. Herrmann, J. W. Norseev, I. Dreyer, *Chem. Ztg.* 101 (1977) 470–481.
91. JANAF, Thermochemical Tables, NSRDS-NBS 37, 1971; Supplements 1974, 1975, 1976, 1978.
92. O. Kubaschewski, C. B. Alcock: *Metallurgical Thermochemistry*, Pergamon Press, New York 1978.
93. I. Barin, O. Knacke, O. Kubaschewski: *Thermodynamical Properties Inorganic Substances*, Springer, New York 1977.
94. Varta, DT 2430910, 1974.
95. A. M. Golub et al.: *Chemie der Pseudohalogenide*, Hüthig Verlag, Heidelberg 1979.
96. IUPAC: *Regeln für die Nomenklatur der Anorganischen Chemie*, Verlag Chemie, Weinheim 1970.
97. A. F. Holleman, E. Wiberg: *Lehrbuch der Anorganischen Chemie*, de Gruyter, Berlin 1976.
98. A. Stettbacher, *Explosivstoffe* 2 (1954) 1.
99. W. Romanowski, S. Engels: *Hochdisperse Metalle*, VCH Verlagsgesellschaft, Weinheim, in press.
100. H. Stegemann, DE-AS P 31196357, 1981.
101. W. Ostwald: *Die Welt der vernachlässigten Dimensionen*, Th. Steinkopff, Dresden 1927.
102. Degussa, DE 2302277, 1973.
103. A. A. Boraiko, *National Geographic* 160 (1981) 280–313.
104. A. Luschin v. Ebengreuth: *Allgemeine Münzkunde und Goldgeschichte*, R. Oldenbourg, München 1971.
105. W. Londershausen, *Metall (Berlin)* 35 (1981) 465–466.
106. M. Rosenberg: *Goldmerkmale*, Frankfurter Verlagsanstalt, Frankfurt 1922.
107. A. Bult, *Pharm. Weekbl. Sci. Ed.* 3 (1981) 213–223.
108. E. v. Angerer, H. Ebert: *Technische Kunstgriffe bei physikalischen Untersuchungen*, Vieweg u. Sohn, Braunschweig 1964.
109. J. Fischer: *Galvanische Edelmetallüberzüge*, Leuze Verlag, Saulgau 1960.
110. H. W. Dettner, J. Elze, E. Raub: *Handbuch der Galvanotechnik*, C. Hanser, München 1966.
111. A. v. Krusenstjern: *Edelmetallgalvanotechnik*, Leuze Verlag, Saulgau 1970.
112. A. Keil, *Metalloberfläche* 9 (1955) A81.
113. Deutscher Normenausschuß (ed.): *Versilberte Be-stecke*, RAL 691 B 3, Beuth-Vertrieb, Berlin 1969.
114. G. Brauer: *Handbuch der präparativen anorganischen Chemie*, 1st ed., Enke, Stuttgart 1954.
115. Degussa, DE-OS 2803060, 1978.
116. A. Keil: *Werkstoffe für elektrische Kontakte*, Springer Verlag, Berlin 1960.
117. W. Böhm, N. Behrens, M. Clasing, *Metall (Berlin)* 35 (1981) 539–543.
118. K.-W. Jäger, B. Gegenbach, *Metall (Berlin)* 35 (1981) 534–539.
119. M. Poniatowski, K.-H. Schröder, F. D. Schulz, *Metall (Berlin)* 31 (1977) 1338–1342.
120. M. Lindmayer, *Metall (Berlin)* 34 (1980) 621–625.
121. G. Reinacher, *Chem. Anlagen + Verfahren* 1972, no. 5, 44–46.
122. Degussa: *Silberhalbzeug*, Hanau 1980.
123. R. Bock: *Aufschlußmethoden der anorganischen Chemie*, Verlag Chemie, Weinheim 1972.
124. K. Weißermel, H.-J. Arpe: *Industrielle organische Chemie*, Verlag Chemie, Weinheim 1978.
125. S. Rebsdatt, S. Mayer, J. Alfranseder, *Chem. Ing. Tech.* 53 (1981) 850–854.
126. A. Camborn, D. Alexander, *Can. J. Chem.* 34 (1956) 665.
127. B. M. Bogolowski, S. Kasakowa: *Skelettkatalysatoren in der organischen Chemie*, Dt. Verlag der Wissenschaften, Ostberlin 1960.
128. Fonds der Chemischen Industrie: *Silber-Fotographie*, Folienserie no. 23, Frankfurt/Main 1989.
129. B. J. L. Kratzer, *DOZ Dtsch. Optikerztg.* 33 (1978) 153–156.
130. W. Grimm, *DOZ Dtsch. Optikerztg.* 34 (1979) 173–180.
131. F. Krusche: *Die Trinkwassersilberung*, Verlag R. Oldenbourg, München 1957.
132. B. Federer, *Umsch. Wiss. Tech.* 79 (1979) 463–468.
133. H. Pohl: Studie über Problem der chemischen Edelmetallanalyse, Forschungsbericht Nr. 15 der Bundesanstalt für Materialprüfung (BAM), Berlin 1972.
134. *Edelmetall-Analyse*, Springer Verlag, Berlin 1964.
135. *Handbuch der analytischen Chemie*, 3rd part, vol. 1, Springer Verlag, Berlin 1967.
136. *Analyse der Metalle*, Springer Verlag, Berlin 1961–1975.
137. H.-M. Lüschoff in Ges. Dt. Metallhütten- und Bergleute (eds.): *Probenahme, Theorie und Praxis*, Verlag Chemie, Weinheim 1980.
138. P. M. Gy: *Sampling of Particulate Materials*, Elsevier, Amsterdam 1979.
139. J. Fries, H. Getrost: *Organische Reagentien für die anorganische Spurenanalyse*, E. Merck, Darmstadt 1975.
140. B. Welz: *Atomabsorptionsspektroskopie*, 2nd ed., Verlag Chemie, Weinheim 1975.
141. G. Jander, K. F. Jahr, H. Knoll: *Maßanalyse*, vol. II, Sammlung Göschen vol. 1002, Walter de Gruyter, Berlin 1973.
142. *Metrohm-Information*, Jahrgang 1 (1971); Jahrgang 11 (1981).
143. K. Lenhardt, *Erzmetall* 28 (1975) 172–177.
144. A. M. Bond: *Modern Polarographic Methods in Analytical Chemistry*, Marcel Dekker, New York 1980.
145. W. Prodinger: *Organische Fällungsmittel in der quantitativen Analyse*, Enke, Stuttgart 1954.
146. H. G. Bachmann, E. Koberstein, R. Straub, *Chem. Tech. (Heidelberg)* 7 (1978) 441–446.
147. J. Suchomel, *Fresenius' Z. Anal. Chem.* 300 (1980) 257–266.
148. J. Suchomel, *Fresenius' Z. Anal. Chem.* 307 (1981) 14–18.
149. H. M. Lüschoff in K.-H. Koch, H. Maßmann (eds.): *Tagungsband der 13. Spektrometertagung 1980*, de Gruyter, Berlin 1981.
150. W. Diehl, *Metall (Berlin)* 23 (1967) 587–589.
151. B. Lange: *Kolorimetrische Analyse*, Verlag Chemie, Weinheim 1962.
152. E. Merian (ed.): *Metals and their Compounds in the Environments—Occurrence, Analysis and Biological Relevance*, 2nd ed., VCH Verlagsgesellschaft, Weinheim 1989.
153. L. Friberg, G. F. Nordberg, V. B. Vouk: *Handbook on the Toxicology of Metals*, Elsevier, Amsterdam 1979.
154. W. Dähne: MAK-Wert für Silber, Bericht über das Geschäftsjahr 1978 der Fachvereinigung Edelmetalle e.V., Düsseldorf 1979.
155. D. Henschler in Deutsche Forschungsgemeinschaft (eds.): *Gesundheitsschädliche Arbeitsstoffe*, Verlag Chemie, Weinheim 1979.

25 Platinum Group Metals

HERMANN RENNER

25.1 History	1269	25.6.9 Construction Materials	1301
25.2 Properties	1272	25.7 Compounds	1301
25.3 Occurrence	1275	25.7.1 Platinum Compounds	1301
25.3.1 Abundance	1275	25.7.2 Palladium Compounds	1303
25.3.2 Ores and Their Origin	1275	25.7.3 Rhodium Compounds	1303
25.3.3 Primary Deposits	1276	25.7.4 Iridium Compounds	1304
25.3.4 Secondary Deposits	1278	25.7.5 Ruthenium Compounds	1304
25.3.5 Recovery of Secondary Platinum Group Metals	1278	25.7.6 Osmium Compounds	1304
25.3.6 Reserves and Resources	1279	25.8 Quality Specifications and Analysis	1304
25.4 Mineral Dressing	1281	25.9 Uses	1307
25.4.1 Alluvial Platinum Deposits	1281	25.9.1 Jewelry, Coinage, Investment	1307
25.4.2 Primary Deposits	1281	25.9.2 Apparatus	1307
25.4.3 Nickel Ores	1282	25.9.3 Heterogeneous Catalysts	1308
25.4.4 Metal Scrap	1283	25.9.4 Homogeneous Catalysts	1310
25.4.5 Dross	1283	25.9.5 Automobile Exhaust Catalysts	1310
25.4.6 Supported Catalysts	1284	25.9.6 Sensors	1311
25.4.7 Treatment of Solutions	1285	25.9.7 Electrical Technology	1312
25.5 Dissolution Methods	1285	25.9.8 Electronics	1312
25.5.1 Dissolution in Aqua Regia	1285	25.9.9 Coatings	1313
25.5.2 Dissolution in Hydrochloric Acid- Chlorine	1286	25.9.9.1 Coatings Produced by Aqueous Electrolysis	1313
25.5.3 Dissolution in Hydrochloric Acid- Bromine	1286	25.9.9.2 Coatings Produced by Chemical Reaction	1314
25.5.4 Other Dissolution Processes	1286	25.9.9.3 Coatings Produced by Physical Methods	1314
25.5.5 Salt Fusion	1287	25.9.10 Dental Materials	1314
25.6 Separation of Platinum Group Metals	1287	25.10 Economic Aspects	1315
25.6.1 Chemistry of Platinum Group Metal Separation	1288	25.10.1 Supply	1315
25.6.2 Old Separation Processes	1290	25.10.2 Demand	1316
25.6.3 Current Separation Processes	1293	25.10.3 Prices	1317
25.6.4 Processes Used in Coarse Separation	1293	25.10.4 Producers	1317
25.6.5 Purification	1297	25.10.5 Commercial Aspects	1318
25.6.6 Conversion of Salts into Metals	1298	25.11 Health and Safety	1319
25.6.7 Partial Purification	1300	25.11.1 Toxicology	1319
25.6.8 Treatment of Internally Recycled Material	1300	25.11.2 Explosion Hazards	1320
		25.12 References	1321

25.1 History [1-10]

Early Times. The earliest evidence of platinum is provided by a gold etui covered with hieroglyphic inscriptions, dating from the 7th century B.C. Around 1900, BERTHELOT (1827-1907) investigated the etui, which was kept in

the Louvre, and found that some of the inlays hitherto thought to be silver were in fact platinum.

In ca. 1900, Jewelry made of native platinum was discovered in Ecuador, which was part of the Inca empire in pre-Columbian

times. This probably dates from the first five centuries A.D.

In ancient times, the technique of washing river sands and fusing together the grains of platinum was undoubtedly known, as was the making of alloys by heating alluvial platinum and gold with a blowpipe, these methods being similar to those used in gold extraction and working. Pre-Columbian Indians were familiar with a powder metallurgy technique.

16th–18th Century [11, 12]. In their search for gold in the New World, particularly in the area of present-day Colombia, the Spanish often found alluvial ("placer") platinum. The earliest written report of the metal was made in 1557 by J. C. SCALIGER (1484–1558). However, platinum was worked to produce jewelry and utensils only after man had learned that the metal, initially believed to be infusible, could be melted and cast by first adding other metals to lower its melting point. Platinum was essentially regarded as a troublesome material, accompanying gold and silver, which lowered their workability. The Spanish named the metal *platina*, the diminutive form of *plata* (silver), as a derogatory term because it was found only in small quantities or as small granules. The terms "white gold" and "heavy silver" were also sometimes used. When the metal became well known in Europe in 1748, thanks to the Spanish mathematician A. DE ULLOA (1716–1795), the demand for platinum increased. Its high density enabled it to be used to adulterate gold, and its introduction into Europe was therefore prohibited. Until 1908, the price of platinum was lower than that of gold. Around 1750, the scientific investigation of platinum began, initiated largely by C. WOOD (1702–1774), who learned of the metal in Jamaica in 1741. He can be regarded as the true discoverer of platinum, having presented a paper in 1750 to the Royal Society entitled "The New Semi-Metal Called Platina". In this initial period, fundamental investigations into the chemistry of platinum (solubility in aqua regia, precipitation by addition of ammonium chloride, fusion by addition of arsenic, lead cupellation, etc.) were

carried out by W. WATSON (1715–1787), W. LEWIS (1708–1781), and others. These workers, including WOOD often collaborated. Research at this time had as its primary aim, distinguishing and separating platinum and gold, although platinum was at first widely believed to consist of gold contaminated with other elements.

An important development in platinum technology was the technique of converting the alluvial (placer) deposits into platinum sponge, which could be satisfactorily formed by heat into compact platinum or platinum artifacts. F. C. ACHARD (1753–1821) discovered the method of oxidizing an easily fusible platinum–arsenic alloy to remove arsenic. As early as 1784, he produced the first platinum crucible from platinum sponge made in this way.

19th Century. Around 1800, the accompanying metals in native platinum, which generally contains up to 80% Pt, were discovered. W. H. WOLLASTON (1766–1828) discovered palladium (initially also known as "new silver") and rhodium; S. TENNANT (1761–1815) discovered iridium and osmium. At the same time, the existence of platinum as a true element was established. C. CLAUS (1796–1864) discovered ruthenium in 1844.

In 1823, J. W. DOEBEREINER (1780–1849) first used the catalytic action of platinum in the gas lighter named after him. In about 1810, the process invented by W. H. WOLLASTON became established: dissolving the raw material in aqua regia, purifying it by precipitation of ammonium hexachloroplatinate, $(\text{NH}_4)_2[\text{PtCl}_6]$, and heating this strongly to form platinum sponge. In 1817, this led to the formation of Johnson, Matthey & Co., London [13], which laid the foundation of modern platinum technology.

Until the beginning of the 19th century, almost all platinum was obtained from the area now known as Colombia, which from 1739 to 1819 belonged to the Spanish Crown Dependency of New Granada. At this time, ca. 1 t/a of platinum was extracted. ALEXANDER VON HUMBOLDT was the most accomplished prospector and developer of noble-metal deposits

in New Granada (1819) and of the newly discovered platinum deposit in the Urals. In 1819, platinum was extracted from alluvial gold, but soon after this, the main production was switched to platinum placers with low gold content. In 1825, Russia became the primary producer of platinum. The minting of platinum coins in Russia in 1828–1845 necessitated an increase in production, which reached 3.5 t in 1843 [14–16]. Almost all Russian platinum ore was used for coinage (15 t total). Technology for the extraction and treatment of placer deposits had reached a high standard by this time.

After the closing of the refinery in St. Petersburg, which was associated with the local mint and produced a metal of ca. 97% platinum, 1.2% iridium, 0.5% ruthenium, 0.25% palladium, 1.5% iron, and 0.4% copper, the refining and working of Russian platinum ore were carried out almost exclusively in Western Europe. New companies for the refining and working of platinum were founded, including Desmoutis, Paris (1822); Baker & Co., New York (from 1904: Engelhard, Newark, New Jersey); Heræus, Hanau (1851); Siebert, Hanau (1881; from 1930 part of Degussa, Frankfurt); J. Bishop & Co., Malverne, Pennsylvania and others.

20th Century [17–20]. The platinum industry grew vigorously after 1880 due to increasing demands of the electrical industry, dentistry, and chemical technology. The primary consumer was the United States. In 1913, annual production of crude platinum reached 7 t. At this time, Russia began to make itself less dependent on other countries by constructing a modern platinum refinery and smelting point at Ekaterinburg (formerly Sverdlovsk). However, at the result of an ideologically negative attitude toward noble metals and a false estimate of their economic importance, platinum production was abandoned after the Russian Revolution.

The result was that, after World War I, Colombia once again became the largest platinum producer. The raw materials were exclusively alluvial deposits, which were ex-

tracted by panning, as they are even today. Almost all of the Colombian crude platinum was refined in the United States.

In 1925, production in the Urals was restarted. New alluvial deposits were discovered in Siberia. Also, mining of primary platinum became important. Today, a large proportion of the platinum group metals supplied by the CIS comes from sulfidic nickel deposits. For some decades, the Soviet Union has been one of the largest producers of platinum and especially palladium. Production figures are not available thus far. Estimates are approximate and are based on export figures.

During World War I, the demand for nickel increased, and Canada became an important producer of palladium and platinum, because nickel ores also contained platinum group metals. Since 1890, these ores have been extracted by the Mond Nickel Co. (since 1961, INCO, London), later allied with the International Nickel Co. of Canada. From 1925, platinum metals were produced in their own refinery in Acton in London. Another important producer of platinum is Falconbridge Nickel Mines in Toronto.

After World War I, worldwide demand could no longer be satisfied by Russia and other producers, and new sources were developed. In South Africa, the search was particularly well rewarded. Platinum and osmium were discovered at Black Reef (1888), Witwatersrand (1892), Great Dyk (Rhodesia, 1918), and later at Waterberg. The award of prospecting rights to private persons led to prospecting on a wide scale. A systematic geological survey of the Bushveld by J. MERENSKY was highly successful, leading to the discovery of platinum in the dunite pipes (1924) and subsequently in the stratiform platinum deposits known as the Merensky Reef (1925), the largest platinum deposit in the world.

This discovery brought about the greatest upheaval yet seen in the platinum market. It occurred during a period of both high demand (mainly for catalysts for ammonia oxidation) and high prices, the result being the foundation of about 50 producing companies. The primary platinum-bearing rock typical of

South African deposits presented the ore treatment and smelting technologies with completely new problems. Technical difficulties combined with a fall in the price of platinum led to a slump. The largest of the surviving companies formed Rustenburg Platinum Mines Ltd. in 1931, whose output reached 3 t/a during World War II.

After World War II, the Union of South Africa (Republic of South Africa) became the main producer of platinum. From 1969, all of the crude platinum produced by South Africa was refined by Johnson Matthey in England, although Matthey Rustenburg Refiners now refines considerable quantities of material produced in Rustenburg. Recently, some new producers have appeared in South Africa [e.g., Impala Platinum, Western Platinum (a subsidiary of Lonrho and Falconbridge), and Anglo-Transvaal Consolidated Investment (Anglovaal) and its subsidiary Atok Platinum Mines].

Figure 25.1 shows the history of world platinum output, and Table 25.1 lists the development of PGM production according to region.

25.2 Properties

Atomic Properties [21, 22]. The electronic structures of platinum group metals start from the inert gas structures of krypton and xenon:

Ru	[Kr] 4d ⁷ 5s ¹
Os	[Xe] 4f ¹⁴ 5s ² 5p ⁶ 5d ⁶ 6s ²
Rh	[Kr] 4d ⁸ 5s ¹
Ir	[Xe] 4f ¹⁴ 5s ² 5p ⁶ 5d ⁷ 6s ²
Pd	[Kr] 4d ¹⁰
Pt	[Xe] 4f ¹⁴ 5s ² 5p ⁶ 5d ⁹ 6s ¹

Table 25.1: Historical development of the production of platinum group metals according to region (other countries account for only 1–2% of world production) (in t/a).

	1800	1850	1900	1910	1920	1930	1940	1950	1960	1970	1975	1980	1985	1990
Colombia	1	<1	<1	<1	2	2	2	1	1	<1	<1	<1	<1	<1
Russia*	1	2	12	11	1	3	10	6	12	30	70	70	70	70
Canada			«1	«1	1	2	6	7	12	12	12	12	12	12
South Africa						2	2	4	20	50	90	120	120	130
United States			«1	«1	«1	<1	2	2	1	1	1	1	1	10
World	1	2	12	12	4	10	22	20	45	93	173	203	203	222

* Estimated.

Two valence orbitals exist: an *s* shell and an inner *d* shell. The small energy difference between them means that the electron shells are filled in inconsistently, so that with some elements, one or both electrons from the outer 5*s* or 6*s* shells are taken up by the 4*d* or 5*d* shells.

Because of the small energy differences between the valence shells, a number of oxidation states occur. The following oxidation states are known in the compounds of platinum group metals (principal oxidation states in bold print):

Ru:	-2,	0,	+2,	+3,	+4,	+5,	+6,	+7,	+8
Rh:	-1,	0,	+1,	+2,	+3,	+4,	+5,	+6	
Pd:			0,	+2,	+3,	+4			
Os:	-2,	0,	+1,	+2,	+3,	+4,	+5,	+6,	+8
Ir:	-1,	0,	+1,	+2,	+3,	+4,	+5,	+6	
Pt:			0,	+2,	+4,	+5			

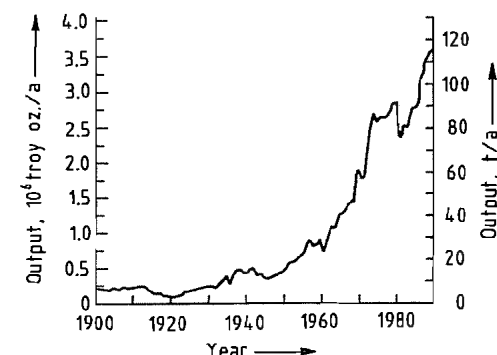


Figure 25.1: History of world platinum output (including Soviet sales to Western World).

The other properties typical of transition metals are very marked; for example, catalytic activity due to their readiness to change valence, formation of intermediate compounds with different reagents, color, paramagnetism due to unpaired electrons, and strong tendency to form complexes.

Table 25.2: Atomic and physical properties of the platinum group metals.

Property	Ru	Rh	Pd	Os	Ir	Pt
Atomic number	44	45	46	76	77	78
Relative atomic mass	101.07	102.90550	106.42	190.2	192.22	195.08
Abundance of major natural isotopes	101 (17.0%) 102 (31.6%) 104 (18.7%)	103 (100%)	105 (22.3%) 106 (27.3%) 108 (26.5%)	189 (16.1%) 190 (26.4%) 192 (41.0%)	191 (37.3%) 193 (62.7%)	194 (32.9%) 195 (33.8%) 196 (25.3%)
Crystal structure	hcp	fcc	fcc	hcp	fcc	fcc
Lattice constants at 20 °C						
<i>a</i> , nm	0.27058	0.38031	0.38898	0.27341	0.38394	0.3923
<i>c</i> , nm	0.42819			0.43197		σ
Atomic radius, nm	0.133	0.134	0.138	0.134	0.136	0.139
<i>mp</i> , °C	2310	1966	1554	3045	2410	1772
<i>bp</i> , °C	4050	3760	2940	5025	4550	4170
Specific heat at 25 °C <i>c_p</i> , J g ⁻¹ K ⁻¹	0.25	0.24	0.23	0.13	0.13	0.13
Thermal conductivity <i>λ</i> , W m ⁻¹ K ⁻¹	106	89	75	87	59	73
Density at 20 °C, g/cm ³	12.45	12.41	12.02	22.61	22.63	21.45
Brinell hardness	200	101	52	250	172	50
Young's modulus <i>E</i> , N/mm ²	475 785	379 058	121 251	559 170	528 072	169 909
Tensile strength <i>σ_B</i> , N/mm ²	490.5	412	196.2		490.5	137.3
Specific electrical resistance at 0 °C, μΩ cm	6.71	4.33	9.92	8.12	4.71	9.85
Temperature coefficient of electrical resistance (0–100 °C), K ⁻¹	0.004	0.0046	0.0038	0.0042	0.0043	0.0039
Thermoelectric voltage versus Pt at 100 °C <i>E_T</i> , V	+0.68	+0.70	-0.57		+0.66	

Comparisons within the group of platinum metals, also including neighboring elements, often give an insight into the relationship between electronic configuration and chemical properties.

Many properties show marked similarities along the two horizontal rows:

Ru ↔ Rh ↔ Pd ↔ (Ag)

Os ↔ Ir ↔ Pt ↔ (Au)

Also, the tendency toward complex formation and higher oxidation states is more marked in the row of heavy elements than in the row of light elements.

Vertical similarities between the elements also occur (e.g., in their behavior toward acids; (see Table 25.3):

Ru Rh Pd (Ag)

↑ ↓ ↑ ↓

Os Ir Pt (Au)

Similarities also exist in the following diagonal sequence, sometimes with ruthenium and iridium changing places:

Ru Rh Pd (Ag)

↑ ↓ ↑ ↓ ↑ ↓

Os Ir Pt (Au)

The chemical properties of the platinum group metals and the chemistry of their compounds fit less well into such a scheme than their physical properties.

All platinum group metals have several naturally occurring stable isotopes, with the exception of rhodium, which has only one.

Physical Properties [22–27]. Apart from their chemical inertness (Table 25.1), the platinum metals have a number of physical properties of great value for their industrial use. These include high melting point, low vapor pressure, high temperature coefficient of electrical resistivity, and low coefficient of thermal expansion. Table 25.2 lists atomic and crystal data and a physical properties of the platinum group metals.

Chemical Properties [28–33]. Table 25.3 shows the chemical behavior of platinum group metals toward various reagents. Resem-

blances are most clear within the two groups of elements. The aim is to quantify the reactions, so as to provide useful information when choosing construction materials or dis-

solving platinum group metals. Some combinations of reagents that can be used to dissolve these metals are also detailed later.

Table 25.3: Chemical resistance of the platinum group metals.

Reagent	Conditions	Temperature, °C	Pd	Pt	Rh	Ir	Ru	Os
Hydrochloric acid	36%	20	—	—	—	—	—	—
		100	•	—	—	—	—	•
Nitric acid	65%	20	•	—	—	—	—	•
		100	•	—	—	—	—	•
Sulfuric acid	96%	20	—	—	—	—	—	—
		100	•	—	•	—	—	—
		300	•	•	•	—	—	—
Hydrobromic acid	60%	20	•	•	•	—	—	—
		100	•	•	•	—	—	•
Hydroiodic acid	57%	20	•	—	—	—	—	•
		100	•	•	—	—	—	•
Hydrofluoric acid	40%	20	—	—	—	—	—	—
Phosphoric acid		100	•	•	—	—	—	•
Acetic acid	99%	100	—	—	—	—	—	—
Hydrochloric acid/chlorine	20%/saturated	20	•	•	—	—	—	—
		80	•	•	—	—	—	—
		100	•	•	•	•	—	—
Hydrochloric acid/bromine		20	•	•	•	—	—	—
		100	•	•	•	—	—	•
Aqua regia		20	•	•	—	—	—	•
		100	•	•	—	—	—	•
		150	•	•	—	•	—	—
Hydrochloric acid/H ₂ O ₂		20	•	•	—	—	—	—
		100	•	•	—	—	—	—
Hydrobromic acid/bromine	60%	100	•	—	•	—	—	—
Water/bromine		20	•	—	—	—	—	—
Ethanol/iodine		20	•	—	•	—	—	—
Sodium hypochlorite solution		20	•	—	•	—	•	•
		100	•	—	•	—	•	•
Sodium cyanide solution		20	•	—	—	—	—	—
		100	•	•	—	—	—	—
Copper(II) chloride solution		100	•	—	—	—	—	—
NaOH melt	+ air	500	•	•	•	—	•	•
KOH melt	+ air	500	•	•	•	—	•	•
NaOH melt	+ air	800	•	•	•	—	•	•
KOH melt	+ air	800	•	•	•	—	•	•
KHSO ₄ melt	+ air	440	•	—	•	—	•	•
NaCN melt	+ air	700	•	•	•	•	•	•
KCN melt	+ air	700	•	•	•	•	•	•
NaCN/KCN melt (2:1)	+ air	550	•	•	•	•	•	•
Chlorine, gaseous	dry	20	•	•	—	—	—	—
	moist	20	•	•	—	—	—	•
Bromine liquid	dry	20	•	•	—	—	—	•
	moist	20	•	•	—	—	—	•
Iodine, solid	dry	20	—	—	—	—	—	•
	moist	20	•	•	—	—	—	—
Fluorine, gaseous		20	—	•	—	—	—	—
Hydrogen sulfide, gaseous	moist	20	—	—	—	—	—	—

— Mass loss < 0.01 mgcm⁻²h⁻¹; ideal as construction material
 • Mass loss ca. 0.1 mgcm⁻²h⁻¹; limited use as construction material
 • Mass loss ca. 1 mgcm⁻²h⁻¹; limited use for dissolution processes
 • #Mass loss 10 mgcm⁻²h⁻¹; suitable for dissolution processes

25.3 Occurrence

25.3.1 Abundance [10, 30, 34–37]

The abundance of platinum group metals (PGMs), which occupy an intermediate position based on their atomic number and atomic weight, would be expected to be 10⁻⁴ ppm, based on the mode of formation of atomic nuclei [38]. They are concentrated in planetary regions, reaching ca. 30 ppm in the earth. Considerable fractionation has taken place in the earth's interior, due mainly to the siderophilic chemical character of PGMs, so that virtually the entire mass of PGMs is in the earth's metallic core. The siliceous lithosphere is estimated to contain 0.05–0.5 ppm.

On theoretical grounds, the PGMs in the earth are assumed to contain ca. 20% each of platinum, palladium, ruthenium, and osmium, and ca. 6% each of rhodium, and iridium. In the case of ruthenium and especially osmium, these values are not reflected in the deposits mined to date.

25.3.2 Ores and Their Origin

[10, 30, 31, 34, 39–46]

The PGMs in the lithosphere have been transferred from the earth's interior. Tectonic movements of the earth's crust, followed by the eruption of magma, have led to their presence in regions close to the surface. Solidification processes, differences in melting point and density, gas emissions, convection due to heat, and the flow and eruption of magma, have all produced concentration and separation effects, mainly in marginal zones. Chemical interaction with high-temperature silicate layers, especially their sulfide, arsenide, antimonide, selenide, and telluride components, has also played a major role. Almost invariably, the platinum group elements have separated from ultrabasic magmas. Norite (Mg–Fe–Ca–Al silicate) contains mainly sulfidic intrusions, whereas those in dunite (Mg–Fe silicate) are mainly sulfide free. Platinum and palladium (often with nickel, copper, chro-

mium, etc.) sometimes undergo hydrothermal reactions with chlorides in the earth's interior. All of these processes have led to the formation of the primary deposits of platinum-bearing rock. Workability depends on many factors: concentration of platinum metals, accessibility, size of deposit, value and potential uses of accompanying materials—and is economical in only a few cases.

When primary deposits are altered and transported by the natural action of the hydrosphere and atmosphere, secondary deposits, also known as placers or alluvial deposits, are formed. Mechanical concentration of the heavy constituents by flowing water takes place, together with chemical dissolution and reprecipitation of the platinum metals. Recently, hydrothermal processes have been shown to be considerably more important than was at first thought. Alluvial deposits usually originate from dunite.

The platinum metals occur in a large number of minerals. Workable ore deposits contain mainly sperrylite (PtAs₂), cooperite (PtS), stibopalladinite (Pd₃Sb), laurite (RuS₂), ferroplatinum (Fe–Pt), polyxene (Fe–Pt–other platinum metals), osmiridium (Os–Ir), and iridium platinum (Ir–Pt). These minerals are associated with particular carrier materials, which are often valuable themselves (e.g., iron pyrites, nickel iron pyrites, or chrome iron ore).

The minerals are seldom present in an exact stoichiometric ratio. This is true of the platinum group metals themselves, which are nearly always present in varying ratios, and of the accompanying elements with which they form compounds or alloys. Isomorphism opens up the possibility of further variations. Isomorphic intercalations make up a larger part of the economically workable reserves. Electron probe microanalysis (EPMA) has enabled a large number of definite compounds and intermetallic phases to be identified where mixtures or homogeneous solid solutions had formerly been assumed to be present.

Outside of true deposits, platinum group metals are widely distributed in very high dilution as isomorphous combinations with vari-

ous metals such as nickel, cobalt, and copper, mainly in their sulfides.

25.3.3 Primary Deposits [47-63]

The dunite bodies in the Urals are the most important of the old Russian platinum deposits, either as primary deposits or as material for the formation of secondary deposits. The only important primary deposit is at Nishnij-Tagil, which is mined in many locations. It is a projectile-like intrusion of dunite through the earth's crust, which appears to reach a depth of more than 100 km and has an area on the earth's surface of 25 km². Platinum metals are concentrated in dunite in the form of striae, lenses, nests, and pillars. They are present mainly as polyxene (Fe-Pt), iridium-rich platinum, and osmiridium, and are often associated with serpentine or chromite. Most of the platinum has been obtained from ores with a platinum metal content of 10-20 ppm. However, ores containing 400 ppm are found in some places. In the total dunite body, the average platinum content is ca. 0.1 ppm. Other dunite bodies in this region are not economically important either for their metal content or for the extent of the deposit.

The dunite pipes at the eastern border of the South African Bushveld have a similar origin to the Russian dunite bodies and are of the same base material. The platinum-bearing core of this narrow intrusion often has a diameter of 20 m or less. Veins are rarely present. The excavations at Driekop and Onverwacht are the most well known. Mining is difficult. Since the exploitation of the Merensky Reef, they can be mined economically only in certain cases. Platinum group metals are sometimes present in the metallic state and sometimes as sperrylite in association with chromite. Platinum concentrations are 1-200 ppm, and locally higher.

The richest and scientifically most interesting deposits, although small in extent, are the quartz lodes of Rietfontein on the Waterberg in the Western Cape Province. Owing to their hydrothermal origin, the platinum metals are present in native form, accompanied by hema-

tite. The PGM content of the ore often reaches almost 5000 ppm. Deposits of similar structure have not been found elsewhere.

The largest known primary deposit of PGMs is the South African Bushveld Complex, with a total extent of ca. 250 km from north to south and 480 km from east to west. This oval-shaped zone was apparently produced by an outflow of PGM-bearing norite magma into a flat basin. At the bottom of this, the minerals sperrylite (PtAs₂) and cooperite (PtS) have separated along with iron pyrites, nickel pyrites, copper pyrites, and chromite. The relatively thin PGM-bearing layers at the edges of the outflow near the earth's surface are mined. These are in both the oxidation and the sulfidic zones, and begin at a depth of < 100 m. The working depth extends to almost 1000 m. The platinum content of the mined ore is 320 ppm. Palladium is less important than platinum; all the platinum group metals are present. The deposit has great economic importance owing to its consistent quality, ease of extraction, and large extent. The Bushveld is mined at the western and southwestern edges (Rustenburg region) and the eastern and northeastern edges (Lydenburg region) (Figure 25.2) in two wide areas. The Bushveld is also the world's largest chromium and vanadium deposit, and has large deposits of nickel, cobalt, copper, iron, tin, fluor spar, and alusite, magnesite, and asbestos.

These deposits were discovered in 1925 by the geologist HANS MERENSKY (1871-1952) [17]. He laid the foundations for the most important phase in the development of platinum extraction by his wide-ranging prospecting work and fundamental observations on the geology of the Bushveld. The most important areas of PGM deposits in the western and eastern part of the Bushveld are known as the Merensky Reef. Not far from these deposits lie the less important Platreef and the UG 2 Reef (Upper Group Reef), which has recently increased in importance due to its very high rhodium content in many places. This metal is in great demand and therefore very expensive.

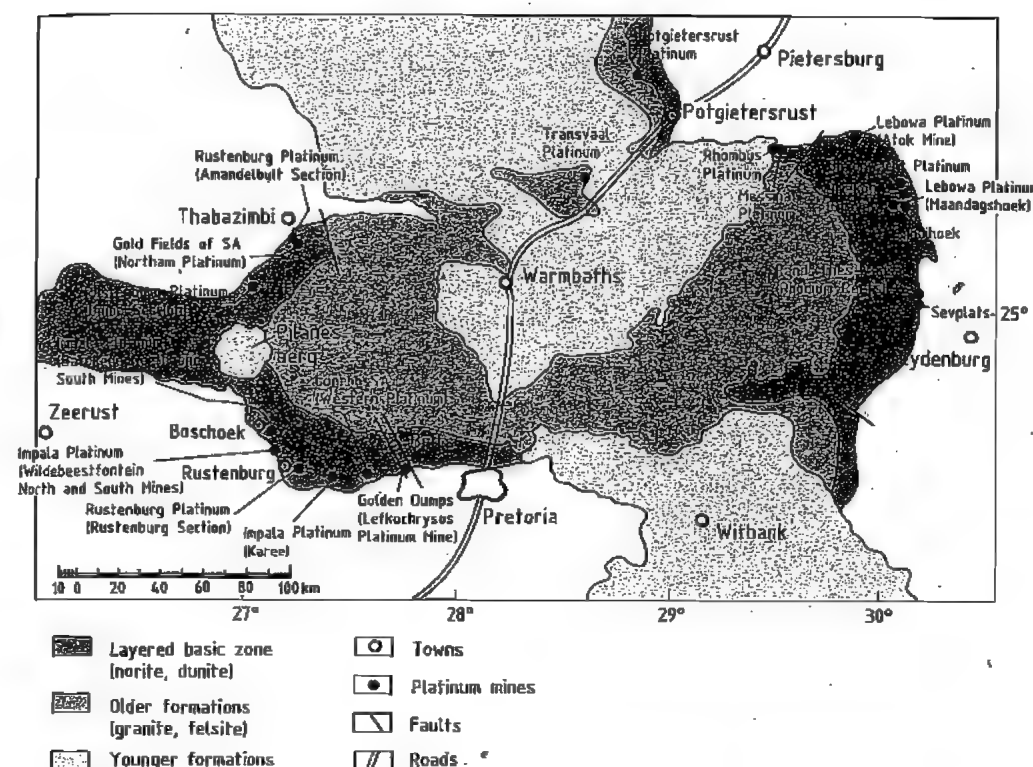


Figure 25.2: Geology and platinum mines of the Bushveld Complex.

The UG 2 reef is a chromite layer running parallel to the Merensky Reef, but somewhat deeper [64, 65].

Some examples of small deposits include the Black Reef in the Bushveld and, a few hundred kilometers north, the Great Dyk Mine in Zimbabwe.

The Stillwater deposit in Montana, United States is similar in origin and structure to the Bushveld deposit. However, PGM separation occurred at the boundary zone of a subterranean magma intrusion resembling a sloping lens. This deposit extends for a length of ca. 80 km. The total PGM content, with high levels of palladium and rhodium, is higher than that of the Merensky Reef deposit.

The nickel sulfide deposits of the Sudbury, Ontario district of Canada, yielding iron pyrite, FeS₂, pentlandite, (Fe, Ni)₉S₈, and chalcopyrite, CuFeS₂, are today important sources of platinum, and more especially of palladium.

These deposits are associated with noritic magma. The average platinum metal content of the untreated ore is only ca. 0.3 ppm, with a nickel content of ca. 2%. However, the treatment process for the nickel ore concentrates the platinum metals to > 50 ppm without extra cost.

Palladium-containing sperrylite (Pt-PdAs₂) and stibiopalladinite (Pd₂Sb) are present in the ores, and the platinum group metals also form isomorphic mixtures with the heavy-metal sulfides. During formation of these deposits, the sulfides of nickel and copper acted as collectors. The large reserves in Noril'sk in Central Siberia, which have a high palladium content, are similar to the Canadian deposits with regard to composition and ore treatment methods. Some lead-zinc ores [e.g., in the Rammelsberg (Harz) mountains], contain small amounts of platinum and palladium.

Comparisons with other metals indicate that PGM reserves may exist in the Antarctic [66]. The magma flow in the South African Bushveld occurred in an early geological epoch (Cambrian—more than 2×10^9 years ago), when the African and Antarctic continents were still part of Gondwanaland.

25.3.4 Secondary Deposits

Alluvial deposits are typical reserves of this type. They were produced in recent geological epochs (Quaternary Holocene) by weathering and washing of primary deposits, mainly dunitic, which resulted in concentration of the more resistant and heavier components (i.e., the metallic and arsenidic platinum minerals, gold, magnetite, chromite, cassiterite, zircon, and granite) in clay and sand. These oxidation zones are often located above the primary deposits. River placers are formed from the alluvial deposits by the erosive action of water, to yield so-called black sands. However, typical nuggets (mainly small granules but also sizable metallic lumps weighing up to several kilograms) seem to have been formed mainly by mechanical agglomeration, usually involving chloridic dissolution and reprecipitation. Very old deposits that formed conglomerates by adhesive action are termed fossil placers. The platinum metal content of secondary deposits varies over a wide range. Deep alluvium and river headwater placers are the most productive.

For easily washable sand, a PGM content of 0.05 ppm is economic. Before World War I, the PGM content of economic deposits was ca. 2 ppm, but today it is much lower. More platinum metals are recovered from river placers than from alluvial deposits.

Secondary deposits occur mainly in the Urals, Siberia, Colombia, and Ethiopia. Often, the recovery of gold and platinum metals from such deposits is so interdependent that sometimes one metal, and sometimes the other, is the main product. Osmiridium is obtained mainly in Alaska and in the Witwatersrand of South Africa, along with secondary deposits of gold.

25.3.5 Recovery of Secondary Platinum Group Metals [67–70]

Platinum metals not only are extracted from ore but, due to their high value, are also recovered from a wide range of industrial residues. These residues are of variable composition and quality, and recovery plants must be very flexible.

Often, the recovery operation is included in the sales contract for semifinished and finished goods, so materials are sent directly for recovery and do not appear on the raw materials market. For regular customers, accounts are kept of the weights of noble metals involved. The supply of material is facilitated, and risks due to price variation are minimized.

Metallic Materials. Large quantities of metallic materials in the form of used platinum rhodium gauze catalysts result from the oxidation of ammonia. These catalysts must be reprocessed chemically after 3–18 months of use. At present, ca. 50 t of Pt–Rh is bound up in these gauzes. The Pd–Au gauzes used to recover Pt–Rh vaporized in ammonia oxidation plants are also recycled.

The glass industry generates large quantities of defective components for chemical recovery (e.g., from melting vessels and other equipment).

Spinnerets from textile fiber manufacture must normally be replaced after about one year of operation owing to erosion of the holes.

Defective laboratory equipment, mainly crucibles and dishes, makes a considerable contribution, but chemical apparatus components are of little significance.

Considerable quantities of platinum-rhodium scrap are provided by the electrical measurement industry, mainly in thermocouple components. Other residues from the electrical and electronic sectors include electrical contacts, heater elements, and electronic components.

Manufacture of fountain pen nibs yields residues in the form of small spheres or dust that can contain ruthenium, osmium, iridium,

rhenium, tungsten, molybdenum, tantalum, nickel, and cobalt as alloy components. Treatment of these materials is among the most difficult of all separation techniques.

Dross. Waste materials include slag, ash, furnace residue, corrosion residue from equipment, and precipitation residue. Catalyst residues of poorly defined composition are also included. The PGM content of these materials is usually low; they are extremely variable and usually nonmetallic.

Supported Catalysts [68]. Large quantities of platinum group metals must be recovered from spent catalysts. The most important of these, both in quantity and in value, are the heterogeneous catalysts used in the petroleum industry, especially in reforming processes, where > 50 t of platinum is bound up worldwide. The lifetime of these catalysts is 4–8 years. Residues usually contain 0.3–0.7% platinum on γ - Al_2O_3 , and usually also include palladium, rhodium, iridium, and rhenium, which must also be recovered. The other large-scale processes in the petroleum industry—hydrofining and hydrocracking—yield palladium and platinum catalysts on aluminum silicate carriers.

Another source of material for recovery of platinum metals is spent automobile catalytic converters [67–69]. However, the PGM content is low (2 g per unit), and the units are enclosed in steel sheet and widely scattered. Collection and treatment are therefore difficult. A satisfactory and economical solution to this problem has yet to be found. In Germany, collection logistics are coupled to the recycling of automobiles.

The chemical industry produces considerable amounts of palladium catalysts on carbon carriers, often in a moist state that presents sampling problems. Similar residues come from platinum-carbon, rhodium-carbon, and PtO_2 catalysts, although these are sometimes unsupported. Platinum asbestos, which was formerly used widely in sulfuric acid production, is now of very little importance.

Solutions [67]. Amounts of liquid residues from homogeneous catalysts used in the oxo process (hydroformylation) have increased relatively rapidly. The rhodium content of the organic solvents or oily process residues is between 50 and 1000 ppm. Sometimes, these organic solutions contain iridium, ruthenium, or palladium. Aqueous residues, especially homogeneous catalysts containing rhodium, are currently being produced in increasing quantities.

The electroplating industry yields exhausted electrolytes that cannot be regenerated. The most important of these contain tetranitroplatinate(II), rhodium(III) sulfate, and rhodium(III) phosphate.

Finally, the processes used for separating the platinum group metals also produce waste solutions that must be reclaimed (e.g., mother liquor from crystallization). These operations form part of the separation process.

Radioactive Residues. An as-yet unsolved problem is the treatment of radioactively contaminated platinum equipment from chemical laboratories and processes.

Fission of ^{235}U in nuclear power stations produces considerable amounts of platinum group metals; one tonne of spent reactor fuel contains 1.2 kg of palladium, 0.5 kg of rhodium, and 2.3 kg of ruthenium [70].

However, the radioactivity of the material has not permitted the commercial use of this PGM source until now [71]. The most important PGM isotopes in spent reactor fuel are: ^{107}Pd ($t_{1/2} 7 \times 10^6$ a), ^{102}Rh ($t_{1/2}$ 3 a), and ^{106}Ru ($t_{1/2}$ 1 a). ^{107}Pd is a very low-energy β -emitter, which would not exclude its use in many major applications; alternatively, it may be removed by isotope separation. The active isotopes of rhodium and ruthenium will have decayed to background levels after intermediate storage of ca. 30 years.

25.3.6 Reserves and Resources

Natural Reserves. Data concerning reserves (discovered by prospecting and having assessable economic value) and resources (which in-

clude additional supposed deposits and those with no current economic value) are very dependent on the time prospecting was carried out, and also on technical and economic parameters.

For platinum group metals, the current estimate of workable deposits is 70 000 t [44, 72, 73], 20 years ago, a figure of about one-third of this was assumed [74].

World reserves of the individual metals can best be estimated from the observed compositions of the deposits (Table 25.4) and the total amounts of PGMs that they contain (Figure 25.3). This does not include osmiridium, which usually occurs with gold.

Industrial Residues. Industrial residues have considerable potential for the supply of platinum group metals, in addition to their extrac-

tion from ore. In most sectors, the possibilities are now fully exploited. In others, recovery is difficult because of the low PGM contents of the waste materials (e.g., certain catalysts). Economic recovery is also difficult when small PGM-containing components are widely distributed (e.g., in electronics).

In particular, no satisfactory solution has been found to the problem of collecting used automobile exhaust catalysts. In 1991, more than 7 t of platinum was recovered from this source in the United States and Europe and about 0.5 t of rhodium in the United States [224].

A total of ca. 1 t/a of rhodium is currently produced worldwide in nuclear power stations. Some of this is placed in intermediate storage, and some in final repositories.

Table 25.4: Relative proportions of platinum group metals in selected deposits, and their grades.

	Bushveld complex		South Africa Plat Reef	Sudbury, Canada	Noril'sk, CIS	Colombia	Stillwater, United States	Average
	Merensky Reef	UG 2 Reef						
Platinum, %	59	42	42	38	25	93	19	45
Palladium, %	25	35	46	40	71	1	66.5	30
Ruthenium, %	8	12	4	2.9	1		4.0	5
Rhodium, %	3	8	3	3.3	3	2	7.6	4
Iridium, %	1	2.3	0.8	1.2		3	2.4	1
Osmium, %	0.8		0.6	1.2		1		<1
Gold, %	3.2	0.7	3.4	13.5			0.5	
Grade, g/t	8.1	8.71	7-27	0.9	3.8		22.3	

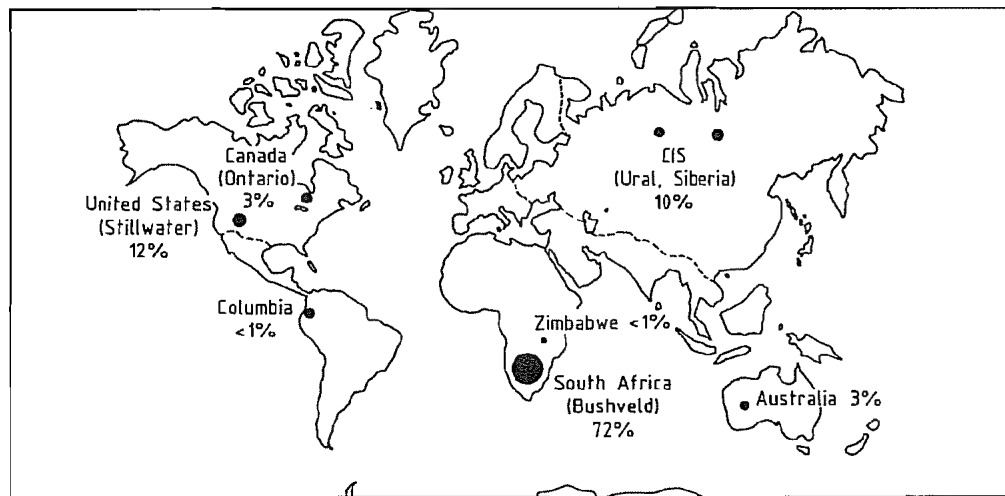


Figure 25.3: World platinum group metal reserves (total 70 000 t).

25.4 Mineral Dressing

25.4.1 Alluvial Platinum Deposits

[5, 10, 19, 29-31, 34, 39, 41-46, 75-83]

Gangue materials must normally be removed from the platinum-bearing placer deposits. Some deposits are extracted by subsurface mining.

Hydraulic classification can be carried out by hand washing with simple equipment, such as shovels, sieves, and troughs. This was the most common method of treating the Colombian deposits and is still used today. More modern methods involve rotary sieves, troughs, and perforated boxes with running water or water jets.

The most economical process is dredging river placers. This is a simple earth-moving technique linked with a natural inexhaustible water supply. Large installations have capacities of several thousand tonnes of sedimentary material per day, with a water consumption of ca. 10 times this figure. Aboard the dredger, deposits are treated mainly by gravity concentration with sieves and sedimentation equipment, using stirrers, thickeners, washing boxes, etc.

The last stage of concentration is often magnetic separation, with various field strengths used to separate magnetite, ferroplatinum-containing minerals such as chromite, and nonmagnetic components into fractions. Often, a final hand washing is carried out. In some types of deposit, gold particles or gold-containing platinum particles can be separated as amalgam from the platinum concentrate. Another process involves concentrating the platinum metals chemically by dissolving the other components in nitric acid. The concentrates so produced can contain up to 90% platinum group metals. These can be used directly by refineries.

A problem may occur with high losses of platinum carried out as very fine metal from the gravity separation process, often exceeding the amount of the product itself. Losses can be reduced to some extent by recycling the

lighter fraction during hydraulic classification of the platinum deposits.

25.4.2 Primary Deposits [44, 54, 64, 65, 83, 84]

The treatment of platinum-bearing rock, which is always supplied in lump form from primary deposits, consists of an initial size reduction by crushing and grinding, usually wet grinding.

After discovery of the South African primary deposits in the Merensky Reef, attempts were initially made to treat this platinum-bearing rock by the methods used for alluvial deposits. Many processes were investigated including gravity concentration, flotation, and metallurgical and chemical processes, such as chloride formation by calcining the powdered ore at 500-600 °C in the presence of sodium chloride. The results were unsatisfactory.

The modern process for the winning of PGMs from sulfide ores is shown in Figure 25.4. Ground ores from the workable oxidation zone, which contain the platinum metals in native form, are first subjected to gravity concentration on cordyroy and James tables or by hydrocyclones, to separate the metallic particles from the platinum-bearing minerals and give a concentrate with a high PGM content that can be processed quickly with low losses.

Flotation is then carried out to remove the gangue from the sulfidic minerals, which are also associated with arsenidic and sulfidic platinum metal compounds and very finely divided elemental platinum metals. This concentrates the platinum group elements by a factor of 10-50. After filtration with a rotary filter, the platinum metals in the flotation concentrate are present at a total concentration of several hundred parts per million, along with a small percentage of sulfur, copper, nickel, and iron.

This sequence of process steps is not suitable for all types of deposits and production equipment. Magnetic or electrostatic separation can sometimes be carried out before the smelting operations.

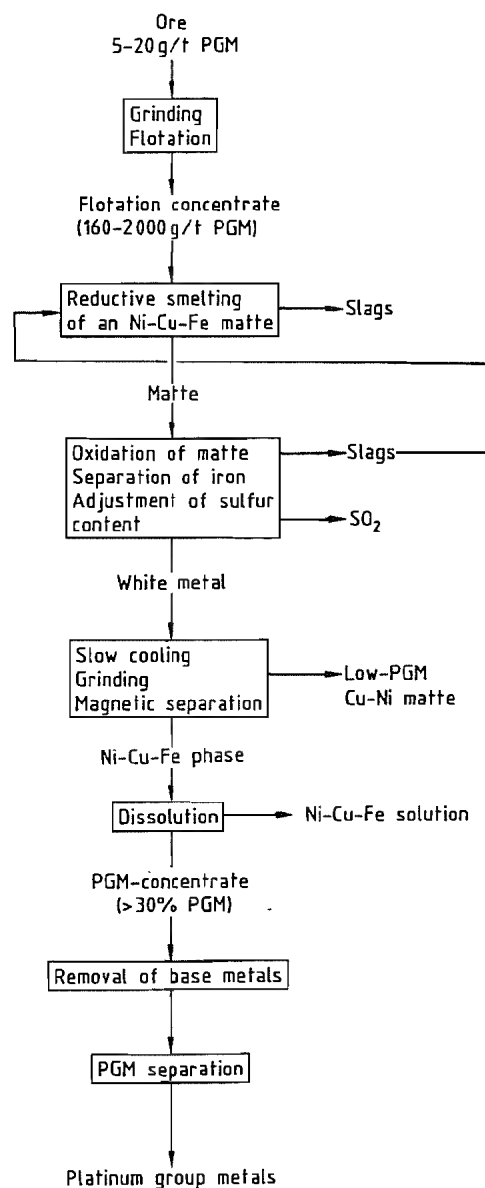


Figure 25.4: Winning of platinum group metals from sulfide ores.

The pelletized material is smelted in a shaft furnace to form a copper-nickel matte. Oxygen is then blown into the converter to oxidize the iron sulfide selectively to iron oxide, which forms a slag. These two processes concentrate the platinum metals in the copper

nickel matte to > 0.1%. The blowing operation is controlled so as to give the correct sulfur content for the next concentration stage. In this recently developed, slow-cooling matte separation process, a finely crystalline, homogeneously distributed Ni-Cu-Fe phase, in which the PGMs are concentrated in high yield, is formed in the almost iron-free copper sulfide matte phase (see Section 12.4.4). The product is ground, and the PGM-containing magnetic Ni-Cu-Fe phase is recovered from the PGM-free matte by magnetic separation. Base metals are then removed by treatment with sulfuric acid and oxygen. The concentrate obtained contains 50–90% PGMs. The next stage is to separate the platinum group metals from one another.

The older pyrometallurgical process is time consuming and does not give such good separation. After air blowing the iron, the converter matte produced is smelted with sodium sulfide and separated into copper-containing and nickel-containing layers (tops and bottoms process). The nickel-containing material is roasted and then reduced in a reverberatory furnace to give PGM-containing impure nickel. The platinum group metals are recovered from the anode slime produced during electrorefining. A method of this kind is apparently still used to treat sulfidic PGM deposits in the Urals.

Problems arise during treatment of the high-chromite ores of the UG 2 reef by the sulfidic route; these are therefore often mixed with ore from the Merensky deposit. A process that shows great economic promise for the future is to smelt a metallic concentrate directly from the ore in a plasma furnace [64]. Both types of ore are suitable, although the chromite-containing ore is better.

25.4.3 Nickel Ores [61, 62]

In the processing of sulfide nickel ores, which always contain copper, the platinum group metals follow the nickel in the smelting process. When the crude copper is electrorefined, the amount of PGMs obtained in the anode slime is very small.

When nickel is electrorefined, the platinum group metals remain behind in the slime formed at the nickel anode. The base metals and the silver are dissolved by acid treatment, giving a concentrate that contains ca. 70% platinum group metals and differs from the nickel anode slime obtained from platinum ores of the Merensky reef in having an appreciably higher palladium content. Also, the concentration of platinum group elements in the unrefined nickel is about 100 times lower than that in the nickel obtained from platinum ore from the Merensky or UG 2 reef.

When crude nickel is refined by the carbonyl process (see Section 12.6.3) residues with a lower PGM content are obtained. These are suitable for concentration by smelting under reducing conditions with lead(II) oxide and sodium carbonate. The lead is driven off, and the silver is dissolved and removed. These concentrates are of high enough quality for separation into individual metals.

The treatment of PGM-containing copper anode slime obtained from nickeliferous pyrrhotite is a long and costly process. The metals copper, selenium, tellurium, arsenic and antimony must first be removed (e.g., by forming their sulfates in a high-temperature process), followed by dissolution or by producing slags via smelting in the presence of potassium nitrate with an air blast. This yields so-called Doré metal. The platinum group metals are then concentrated in the anode slime produced in the subsequent silver electrorefining process.

Copper ores can also contain very small amounts of platinum group metals. These appear in the copper anode slime during copper electrorefining.

25.4.4 Metal Scrap

A high proportion of the metallic waste from used equipment and from semifinished products can simply be dissolved without any prior treatment. These types of material include crucibles, dishes, thermocouple elements, gauze catalysts, and fiber spinneret nozzles.

Massive materials such as heavy-gauge sheets or bars should be size reduced by crushing or machining to produce swarf. For the highly refractory metals of the platinum group (Rh, Ir, Ru, and Os) and their alloys, mechanical methods are usually not sufficient to produce a surface susceptible to dissolution. This is also true of platinum alloys with > 30% rhodium or 20% iridium. In these cases, alloys of platinum or palladium, which can be dissolved more easily, are preferable.

Very highly dispersed noble-metal black, which is often more soluble, is obtained by alloying the highly refractory platinum metals with base metals and then dissolving the latter out. The noble-metal black must not be heated, or the optimum surface properties for the solution process would be adversely affected. Suitable alloying elements include copper, lead, nickel, zinc, aluminum, bismuth, and silver.

Commercial powdered rhodium and iridium also cannot be dissolved by direct chemical means, but they can be treated with chlorine at ca. 500–600 °C to form chlorides (also insoluble), and these can be reduced at low temperature (e.g., by hydrogen or by hydrazine in aqueous suspension) to produce finely divided blacks that can be dissolved in hydrochloric acid-chlorine.

Concentrates of platinum metals often contain oxides that are less soluble in oxidizing acid mixtures than the metals. In these cases, the material must first be reduced by heating in a hydrogen atmosphere or by treating with aqueous hydrazine hydrate at ca. 80 °C. For rhodium oxides, solutions must be highly alkaline and at their boiling point.

25.4.5 Dross [85–89]

If platinum metals cannot be separated by chemical or mechanical methods from accompanying nonmetallic materials, as is usually the case with low-grade waste, pyrometallurgical processes must be used (as in ore treatment).

The most convenient and long-established pyrometallurgical process for low-grade waste

is smelting with lead in a shaft furnace to produce slag. Materials containing silver and gold are treated in this way. The lead acts as a collector for the platinum group metals. The presence of gold and silver also considerably affects the distribution equilibrium of the platinum group metals in the melt. In the lead shaft furnace, some of the high-melting noble metals rhodium, iridium, and ruthenium separate as so-called furnace shows. When the lead is oxidized and removed as litharge, most of the Rh, Ir, and Ru (so-called bottom metals) precipitates from the increasingly silver-rich alloys. Considerable amounts of rhodium and iridium pass into the shaft furnace slag and are lost. Ruthenium and particularly osmium are lost in large amounts in flue dust and waste gases.

When the gold-silver alloy from the above process is electrefined to obtain silver, gold and the platinum group metals remain in the anode slime. If this consists mainly of gold, it is converted to pure gold by Wohlwill electrolysis, in which platinum and palladium are concentrated in the electrolyte, and silver chloride and the remaining platinum group metals in the anode slime. Alternatively, the silver can be dissolved from the gold-silver alloy by nitric acid to form silver nitrate, which is purified by thermal decomposition of the accompanying nitrates; the platinum group metals remain in the water-insoluble oxide residue.

All the concentrates mentioned above can be dissolved, and the individual platinum group metals obtained from these solutions.

25.4.6 Supported Catalysts [68, 69, 90-93]

Spent, inactive catalysts consisting of platinum metals supported on active carbon, or carrier-free noble-metal catalysts that have become coated with organic residues, are concentrated by combustion. These materials are sometimes spontaneously flammable. When they are being burned, strong air currents are suppressed to prevent dust losses. If the result-

ing ash contains platinum metal oxides, these are reduced to the metal.

Catalysts with incombustible carriers insoluble in acid and alkali (e.g., γ - Al_2O_3 , silica gel, asbestos, and zeolites) can often be treated with oxidizing acid, but the noble metals dissolve completely only in the absence of organic residues (especially tarry matter) and if the carriers are very porous. Otherwise, the platinum metals must be concentrated by the lead shaft furnace process (see Section 25.4.5).

Reforming catalysts consist of γ - Al_2O_3 impregnated with platinum, platinum-rhodium, platinum-iridium, or platinum-rhenium. This carrier material is soluble in acid and alkali, and is dissolved (e.g., in hot sulfuric acid or hot caustic soda solution) leaving the noble metal as an insoluble residue. However, small, but not negligible, amounts of noble metal also go into solution. Moreover, sulfidic impurities in the catalyst can lead to the release of toxic hydrogen sulfide. Other practical processes are dissolving the catalyst in sodium carbonate solution (usually at 220 °C in a pressurized reactor), or sintering with sodium hydroxide or sodium carbonate. Carbon and other products of the breakdown of mineral oil in the spent catalyst must be burned off before treatment with acid or alkali, because these materials interfere with the filtering of the platinum metal concentrate.

Spent automobile exhaust catalysts can be processed at high temperature in a plasma or a submerged arc furnace. In the former, a plasma is produced between an electrode and the molten feed material. The energy of recombination of the plasma is released into the melt. In the resistance furnace, slag serves as the electrical resistance in which heat is produced. In both processes, the oxide carrier is melted with or without addition of a flux of lower the melting point. Iron or copper is added as a collector, forming a metallic melt that takes up the platinum group metals. The concentration of PGMs can reach 20%.

25.4.7 Treatment of Solutions [67, 94, 95]

In homogeneous catalysis, high-boiling distillation residues are usually produced that contain no valuable materials apart from rhodium and sometimes ruthenium. These residues can be carefully burned, and the ash treated by wet chemical processes. Other techniques for recovering rhodium have been suggested (i.e., liquid-liquid extraction, reductive precipitation of the metal, and pyrolytic hydrogenation). A process used in industry, especially for the treatment of rhodium-containing oily residues from oxo synthesis, is precipitation of acid-soluble rhodium telluride by reacting the organically bound rhodium with tellurium. This process is notable for the high efficiency of rhodium recovery.

The methods used to produce concentrates from a variety of aqueous wastes are to a large extent the same as those used for the internal recycling of platinum metals in the solutions produced in metal winning processes (see Section 25.6.8).

25.5 Dissolution Methods

[34, 46]

Whether separating platinum group metals or producing compounds and catalysts, the usual starting point is an aqueous solution.

Most raw materials can be dissolved in oxidizing acids. Dissolution can be carried out at atmospheric pressure, or at elevated pressure to obtain higher temperature. Convective or microwave heating can be used.

Highly refractory raw materials, such as rhodium and iridium powder, can be converted into a highly dispersed form, by chlorination at ca. 500 °C, followed by reduction with hydrogen at 100-200 °C or hydrazine in aqueous suspension. Alternatively, rhodium can be oxidized to Rh_2O_3 and then reduced.

In some cases, melt processes at higher reaction temperature must be used. A review of the dissolution properties of platinum group metals is given in Figure 25.5 and Table 25.3.

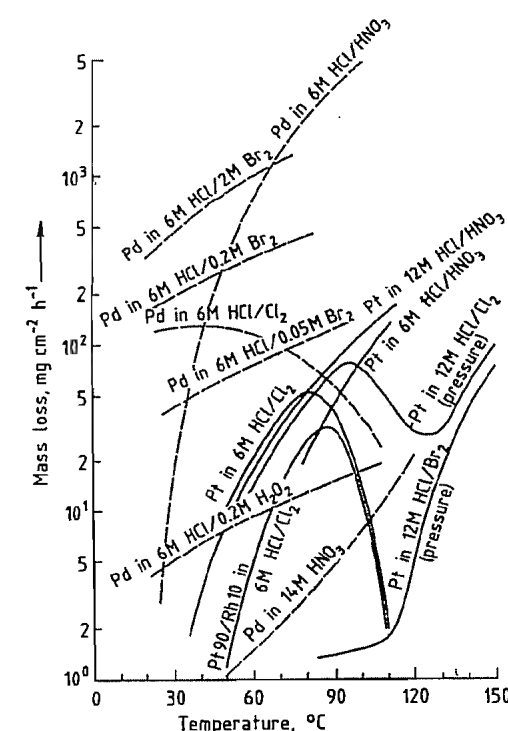
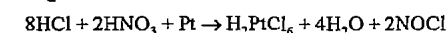


Figure 25.5: Rate of dissolution of platinum and palladium in oxidizing acids.

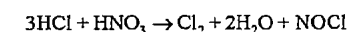
The cost of the dissolution step is an appreciable fraction of the cost of the entire process if many small amounts must be dissolved individually for the determination of value; therefore, the choice of method is important.

25.5.1 Dissolution in Aqua Regia

The following reaction takes place in aqua regia:



as does the following decomposition:



The highest rates of dissolution occur at the boiling point of aqua regia. The rate depends only slightly on acid concentration between 6 and 12 M, and is virtually unaffected by the presence of dissolved platinum group metals.

The aqua regia method is preferred for compact metallic platinum and high-platinum alloys (sheet, wire, turnings, etc.). The reac-

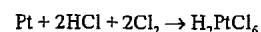
tions must be carried out in a sealed apparatus to prevent loss of material by splashing and mist formation. Before the next stage of treatment, nitric acid must usually be removed by concentration with the addition of hydrochloric acid.

To suppress side reactions, the reactants must not be allowed to boil too violently, although maintaining them at the boiling point and use of 6 M acid offers the most convenient method of sustaining consistent reaction conditions. To avoid boiling over, especially during heating, the initial charge of nitric acid should be added slowly and evenly to boiling hydrochloric acid. This method should also be used when aqua regia is added to replace spent acid.

Finely powdered material also tends to cause boiling over. To avoid a violent reaction when dissolving palladium-rich alloys, dilute acids should be used.

25.5.2 Dissolution in Hydrochloric Acid-Chlorine

In the reaction between platinum and a solution of chlorine in hydrochloric acid



the dissolution rates for platinum and platinum-rich alloys have a maximum in the range 8090 °C (Figure 25.5). As the boiling point of hydrochloric acid (110 °C) is approached, the rate of reaction decreases rapidly, increasing again at higher temperature. For palladium, the rate of dissolution is considerably higher.

For these dissolution reactions, 6–8 M hydrochloric acid is preferred since, in this concentration range, both the amount of acid consumed and the amount of hydrogen chloride in the waste gas are lower than if more concentrated hydrochloric acid is used. The presence of dissolved platinum metals does not decrease the rate of dissolution. By careful control of addition rates, a very slight excess of chlorine can be used, so that this method leads to lower levels of waste gas contamination than the aqua regia method. However, the rates of dissolution decrease considerably in

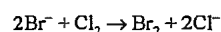
the absence of agitation, and the process is most suitable for easily stirred powders, slurries, or concentrates and unsuitable for bulk material.

Metal dissolves more slowly in the vapor phase or in refluxing hydrochloric acid containing dissolved chlorine (Figure 25.5).

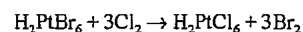
Hydrogen peroxide can be used in place of chlorine as oxidizing agent. Optimum concentrations are difficult to maintain owing to the decomposition of hydrogen peroxide into oxygen and water; therefore, reaction rates are very low compared with those for HCl–Cl₂. The HCl–H₂O₂ system has some limited use for palladium.

25.5.3 Dissolution in Hydrochloric Acid-Bromine

Palladium dissolves more rapidly in hydrochloric acid-bromine mixtures than in hydrochloric acid-chlorine (Figure 25.5). Bromine is more soluble than chlorine in hydrochloric acid, enabling high halogen concentrations to be used. If the temperature is kept well below the boiling point of bromine (59 °C), losses in the waste gases become very small. Bromide formed in the dissolution reaction can be oxidized to bromine by chlorine in an easily controllable reaction, recovered by distillation, and recycled. Since the conversion of bromide to bromine



or



can take place in parallel with the dissolution process, bromine can be present in substoichiometric amounts.

Platinum and its alloys with rhodium or iridium are more resistant to hydrochloric acid-bromine than to hydrochloric acid-chlorine.

25.5.4 Other Dissolution Processes

Concentrated nitric acid is suitable for dissolving palladium (Figure 25.5).

Concentrated sulfuric acid dissolves finely divided rhodium at ca. 300 °C, but strongly

heated rhodium powder is largely insoluble in sulfuric acid.

Concentrated hydrobromic acid is the only reagent that can directly dissolve oxides of the platinum group metals such as PdO, PtO₂, Rh₂O₃, and IrO₂. Platinum can be dissolved in a mixture of hydrobromic acid and bromine above 100 °C in a pressurized reactor. Metallic rhodium is quite soluble in concentrated hydrobromic acid near its boiling point.

Powdered ruthenium or osmium can be treated with an alkaline solution of potassium peroxodisulfate (K₂S₂O₈) to form solutions of ruthenate or osmate. In acidic media, osmium is oxidized by peroxodisulfate or chromic acid to form OsO₄.

Perchloric acid has been reported to be a solvent for platinum and its alloys, ruthenium, and osmium.

25.5.5 Salt Fusion [33]

Aqueous dissolution processes are not successful for all types of concentrates and raw materials. Often, reactions in molten salts are more effective. For many raw materials, molten salt methods are selective and therefore also suitable for separation.

Rhodium can be converted into water-soluble rhodium(III) sulfate at ca. 600 °C by melting with potassium or sodium hydrogensulfate, which is converted to the pyrosulfate with loss of water. Platinum, iridium, and ruthenium are not attacked.

Ruthenium is converted into water-soluble K₂[RuO₄] when reacted with KOH–KNO₃. Osmium reacts similarly. This reaction can be used to treat finely divided osmiridium, especially after preliminary treatment with molten zinc, in which the iridium remains undissolved (see also Section 25.4.4). Potassium salts are more effective than sodium salts. Alkali-metal carbonates can be used instead of alkali-metal hydroxides.

Ruthenium and osmium are very readily attacked by molten Na₂O₂. The reaction can be prevented from becoming too violent by addition of NaOH or Na₂CO₃ to reduce the melt

temperature. Iridium can be oxidized to acid-soluble iridate by fusion with Na₂O₂.

Iridium can also be converted to acid-soluble iridate by treatment with fused BaO₂ or BaO₂–Ba(NO₃)₂. This has the advantage of enabling the cation to subsequently be removed simply by precipitation as BaSO₄. The process is also used to treat osmiridium, although osmium is converted to OsO₄ and must be recovered from the waste gas.

When mixtures of powdered platinum group metals are heated at 700 °C in a chlorine atmosphere, acid-soluble chlorides of palladium and platinum, and acid-insoluble RhCl₃, are formed. Chlorination of iridium and ruthenium produces substoichiometric acid-insoluble products.

All of the platinum group metals form water-soluble complex chlorides when treated with sodium chloride in a chlorine atmosphere.

25.6 Separation of Platinum Group Metals [30, 96]

After the platinum group metals have been dissolved, the individual metals must be recovered. Depending on the raw material, the solution may contain all or some of the PGMs, together with gold, silver, and base metals.

Over the past 200 years, numerous separation processes have been developed and used [30, 31, 34, 39]. Many of the individual steps are still very important in modern processes. Others are of historical interest, but may be used in special cases to treat very small quantities. In addition to the large-scale separations carried out by mining companies and refineries a number of small companies exist, mainly in the United States.

In general, coarse separation is followed by a purification stage. The process used for coarse separation is determined largely by the composition of the starting solution, and the purification process depends on the particular PGM. The purification stage is necessary because, with few exceptions, an individual platinum group metal of commercially acceptable

Reduction to Metal. Since the PGMs are all electrochemically noble metals, selective reduction and cementation by base metals are not possible. In the past, collective cementation from aqueous solution by zinc was often an important step, both for separation and for the recovery of PGMs from recycled solutions. However, the use of zinc as a cementation agent is now ruled out for environmental reasons. Where cementation cannot be avoided, iron, aluminum, or Fe-Al alloys can be used instead. In aqueous media, hydrazine, formate, or borate can be used to reductively precipitate elemental PGMs.

Solvent Extraction [117–126]. Many liquid-liquid extraction systems have been described that can be used for solvent extraction of metals. Much research into the platinum group metals has been carried out, mainly aimed at their separation. The extraction processes do not usually involve a true Nernst distribution of the extractable compounds between the organic and the aqueous phases. More often, the extractable compounds (generally organometallic) are formed in the extraction system itself. The reactants are dissolved in an inert organic phase or, if they are themselves liquids, can be used as such. The system is generally diluted with an inert solvent to lower the viscosity.

The extractants and extraction mechanisms are classified in the following groups:

- Compound formation
- Anion exchange
- Cation exchange
- Solvation
- Solvent extraction without reaction

Of the many systems investigated, very few are of practical use.

The organic phase often increases significantly in viscosity as metal content increases and is usually diluted by a hydrocarbon mixture in the 150–200 °C *bp* range.

The extracted metal is stripped from the organic phase by an aqueous phase.

25.6.2 Old Separation Processes

[30]

Some separation methods, shown in Figure 25.8, were commonly used for separating PGMs in earlier times. Modifications of these may still be used today or included with more modern individual stages in an integrated process. In special cases, they can contribute to the solution of separation problems.

Separation Process A [34, 41]. The process used by INCO in the Acton refinery in England has been known for a long time. It is especially suitable for treatment of the anode slime from the electrolysis of nickel. Here, selective dissolution of Pt–Pd can be achieved since the refractory PGMs are concentrated in separate particles. Some special process steps are used, including alloying with lead, and selective dissolution of rhodium, ruthenium and iridium by salt fusion.

Separation Process B. A process formerly used by the platinum smelting company Siebert/Degussa is characterized by the recycling of unacceptably large amounts of platinum due to the relatively high solubility of sodium chloroplatinate. Recovery of the rarer platinum group metals by cementation led to serious pollution of the wastewater. The cemented metals were usually dissolved with NaCl–Cl₂. An advantage of the process was the efficient separation of iridium.

Separation Process C [34, 127, 128] is suitable only for raw materials with low palladium, rhodium, and iridium content, because of the difficulty of handling their hydroxide precipitates, which have adsorptive properties. It has been used only in small separation plants for secondary metal and yields very pure platinum.

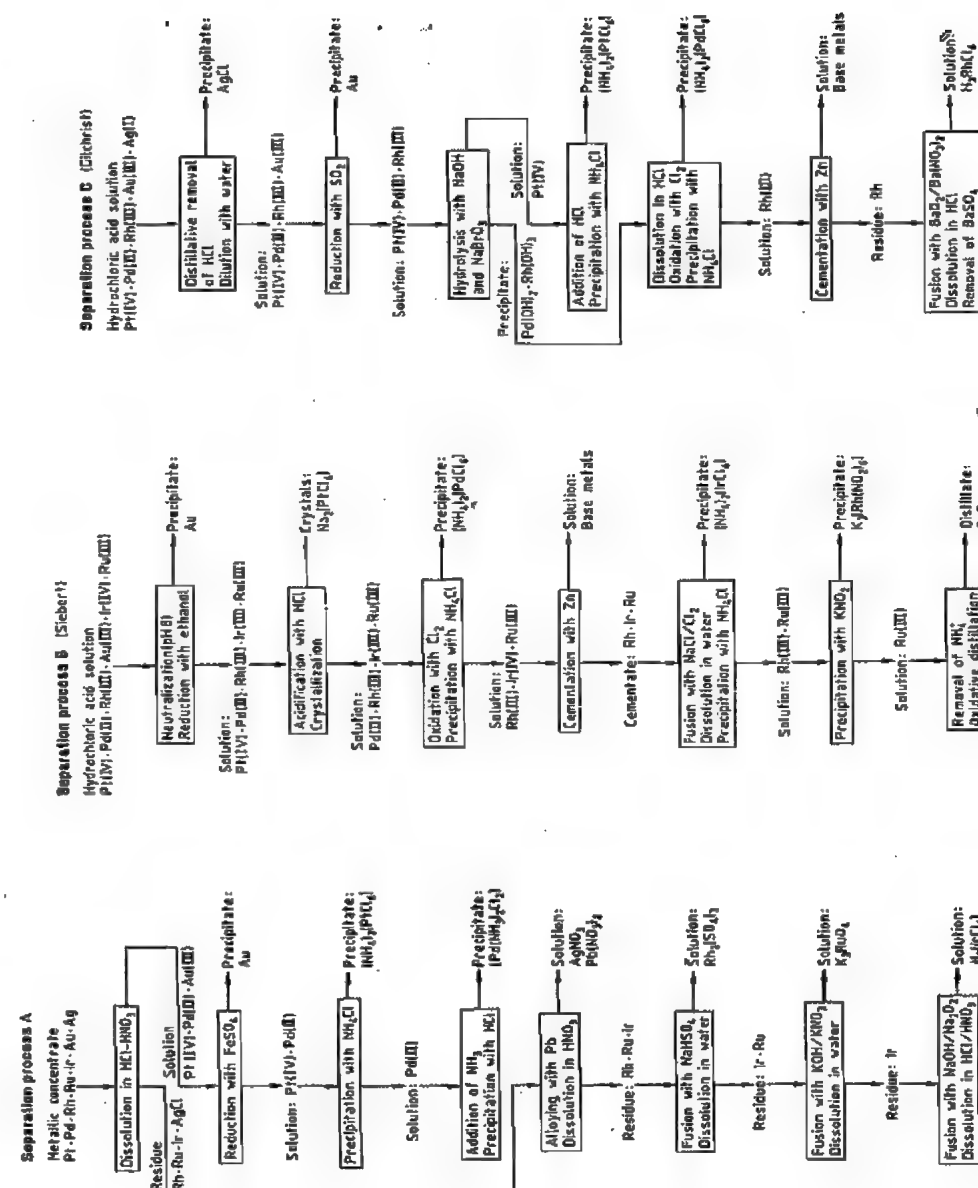


Figure 25.8: Older separation processes.

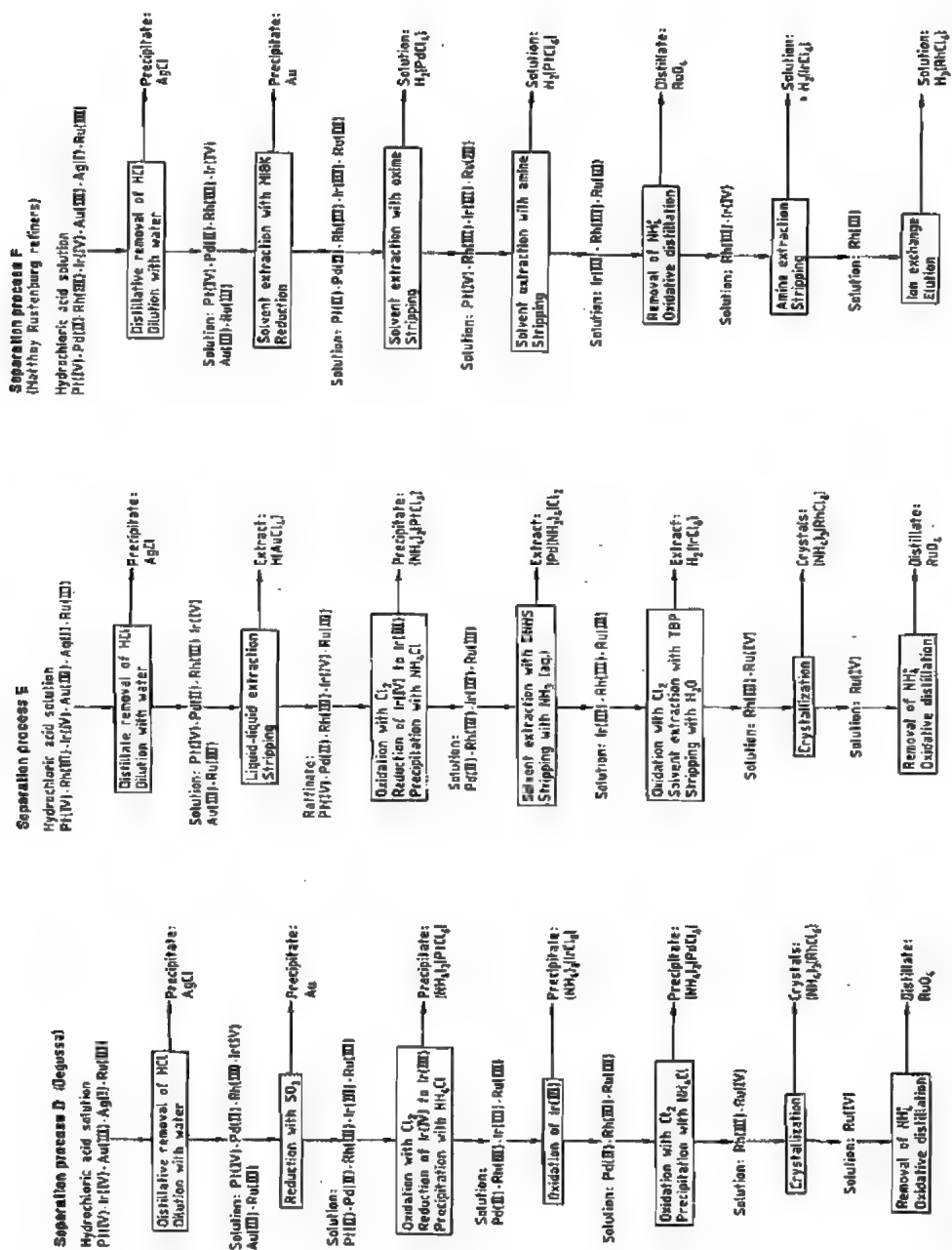


Figure 25.9: Modern separation processes.

25.6.3 Current Separation Processes

Modern separation processes (Figure 25.9) are designed for high separation efficiency, minimum recycle, reduced holdup times of expensive PGMs, and minimization of losses of noble metals. Ecological considerations are often crucial, even when costs must be kept low. Thus, cementation on zinc, an extremely expensive process even if the cost of necessary wastewater treatment is excluded, has to a very large extent been eliminated from PGM separation processes for environmental reasons.

Separation Process D [30, 85]. All process steps can be carried out on the same solution by using simple, similar process operations, which is economically beneficial. The process is very flexible, which is an advantage, particularly for the recovery of secondary metal when the ratio of PGMs changes continuously. If the ruthenium content is high, RuO_4 should be removed by distillation as the first step of the separation process.

Separation Process E. Solvent extraction with dialkyl sulfide is used. Unlike process D, this provides a practically quantitative and sharp separation of palladium, which yields favorable conditions for the purification of palladium and platinum. Solvent extraction of iridium can be carried out almost quantitatively and is very useful when iridium content is low. Under these conditions, use of precipitation crystallization would result in excessive amounts of iridium remaining as soluble $(\text{NH}_4)_2[\text{IrCl}_6]$ in the mother liquor.

Separation Process F [129]. A process used mainly in mining operations (i.e., with primary raw materials) has, as its most notable feature, solvent extraction of platinum, which is the metal present in highest concentration. Oximes are better than thioethers for solvent extraction; the higher rate of complex formation enables column technology to be used. Also, the separation process can be set up as an integrated unit. Ion exchange, which is also carried out on columns, results only in separa-

tion of base metals. Similar separation processes based on solvent extraction are in industrial use or development [122–126, 130–136].

25.6.4 Processes Used in Coarse Separation [30]

Separation of Silver. Insoluble silver chloride is formed in the dissolution process and is removed by careful filtration from the starting solution in concentrated hydrochloric acid. However, this acid at its usual concentration leads to unacceptably high levels of silver remaining in solution due to $\text{H}[\text{AgCl}_2]$ formation. Lowering the free hydrochloric acid concentration, preferably by evaporation and dilution, considerably reduces the solubility of silver chloride. The settling rate and ease of filtration are improved by flocculating agents.

Traces of silver (usually together with Cu and Pd) can be extracted from chloride solutions of platinum group metals at pH 5.5 by dithizone in chloroform.

Separation of Gold. The usual process for gold separation involves reducing Au(III) to elemental gold in acid solution. Reducing agents that can be used include iron(II) salts, oxalic acid, sulfur dioxide, and ascorbic acid. Sodium nitrite, hydrogen peroxide, sodium formate, and ethyl alcohol are also used [126]. The separation process is improved if reducing agents and reaction conditions are chosen such that Pt(IV) is not reduced to Pt(II). Otherwise, Pt(II) must be reoxidized to Pt(IV). The separation of gold from PGMs is becoming increasingly important [136].

Selective Dissolution Reactions and Melt Reactions. Dissolution processes usually do not give very sharp separation of platinum group metals.

Problems with salt fusion lead to poor diffusion conditions. In dry chlorination of platinum group metals, the chlorides are thermodynamically stable over only a small range. Also, in reaction of the metals with sodium chloride and chlorine, temperatures must be chosen such that unreacted metal particles

are not blocked by molten salt. In practice, achieving complete reaction in a single stage is usually impossible.

Separation of Platinum, Iridium, and Palladium by Precipitation Crystallization [137–139]. The same basic process has been used for the separation of the largest quantities of platinum group metals since the beginning of separation technology—precipitation crystallization of ammonium hexachloro complexes $(\text{NH}_4)_2[\text{MCl}_6]$. This process can be optimized in many ways by influencing solubilities (e.g., by valence changes, addition of a common ion, or changing the temperature and rate of precipitation).

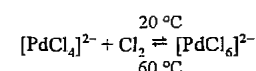
The first step in separation is usually to precipitate platinum as $(\text{NH}_4)_2[\text{PtCl}_6]$. If the dissolved platinum is present as Pt^{II} , it must first be oxidized to Pt^{IV} (e.g., by chlorine). Excess dissolved chlorine is driven off by boiling, which also causes the palladium that had been oxidized to palladium(IV) to be reduced to palladium(II). Any iridium(IV) present must be selectively reduced to iridium(III), for example, with iron(II) salts or ascorbic acid. The ammonium hexachloroplatinate(IV) is precipitated preferably by slow addition of concentrated ammonium chloride solution at room temperature with stirring. The hydrochloric acid concentration should be 1 M, and the platinum content should be 50–200 g/L. After precipitation, the excess of NH_4Cl in the solution should be at least 0.5 mol/L. The mother liquor is removed from the salt by washing with semisaturated cold ammonium chloride solution. The deep-yellow ammonium hexachloroplatinate(IV) is recovered with a purity of 99.0–99.5% in > 99% yield.

Attempts have been made to precipitate the $(\text{NH}_4)_2[\text{PtCl}_6]$ slowly by gradual formation of NH_4^+ ions in the reaction medium (e.g., by hydrolysis of urea or hexamethylenetetramine). In this way, an almost ideally homogeneous precipitation medium is produced. However, the purities and yields achieved do not justify the cost.

To precipitate iridium as $(\text{NH}_4)_2[\text{IrCl}_6]$, iridium(III) is converted to iridium(IV) by treat-

ment with an oxidizing agent at ca. 100 °C, while palladium remains in the divalent state at this temperature. Black $(\text{NH}_4)_2[\text{IrCl}_6]$ is filtered off from the cold solution. It is more readily soluble than the corresponding platinum salt, and therefore sufficient excess of NH_4Cl (0.5–1.0 mol/L) and good cooling (20 °C) must be used, and the minimum amount of concentrated NH_4Cl solution must be used for washing. Chlorine is then passed into the solution at room temperature, the excess NH_4Cl in solution being > 1 mol/L, and palladium is precipitated in the pure state in the form of the sparingly soluble, brick-red ammonium hexachloropalladate(IV), $(\text{NH}_4)_2[\text{PdCl}_6]$. The separation from rhodium(III) is, however, not sharp.

The main problem encountered in this precipitation is the difficulty of producing sufficiently large crystals for filtration, which can be favored by adding the palladium solution to the NH_4Cl solution. High temperature favors crystal growth but must be avoided to prevent the following reaction from occurring:



A virtually quantitative yield is obtained if the crystals are isolated quickly and washed with a cold concentration NH_4Cl solution saturated with Cl_2 .

Separation of Rhodium. Ammonium hexachlororhodate, $(\text{NH}_4)_3[\text{RhCl}_6]$, can be isolated from rhodium solutions in hydrochloric acid such as those obtained after removal of the other platinum group metals. Ammonium chloride is added, followed by concentration and crystallization. Much of the remaining $(\text{NH}_4)_2[\text{PtCl}_6]$ and $(\text{NH}_4)_2[\text{IrCl}_6]$ is precipitated at the same time. Chlorides of the base metals mostly remain in solution. The $(\text{NH}_4)_3[\text{RhCl}_6]$ can be selectively redissolved in water at room temperature to form an almost saturated solution. This gives a purified solution of rhodium. Both $(\text{NH}_4)_2[\text{PtCl}_6]$ and $(\text{NH}_4)_2[\text{IrCl}_6]$ are recovered by filtration.

The rhodium can also be isolated as chloropentamminerhodium(III) chloride, $[\text{RhCl}$

$(\text{NH}_3)_5]\text{Cl}_2$, or potassium hexanitrorhodate(III), $\text{K}_3[\text{Rh}(\text{NO}_2)_6]$, but the precipitations must be carried out in weakly alkaline solution. These methods are unsuitable for solutions that contain large quantities of base metals because, under reaction conditions, these form insoluble hydroxides that are difficult to filter.

Cementation of rhodium by other metals (see Section 25.6.3) can also be carried out. However, all of the noble metals and the copper remain with the rhodium. An advantage is that precipitation of rhodium is complete in this process.

Distillation of Ruthenium(VIII) Oxide. The most important industrial process for the isolation of ruthenium is distillation of the very volatile ruthenium(VIII) oxide, RuO_4 , from aqueous solution. This compound is formed in solutions of potassium ruthenate(VI), $\text{K}_2[\text{RuO}_4]$, and hexachlororuthenate(III), $\text{K}_3[\text{RuCl}_6]$, by oxidation with chlorine at around neutral pH. Oxidation can also be carried out in dilute sulfuric acid solution with potassium permanganate, or with potassium chlorate in sulfuric acid solution, but these methods are less satisfactory for safety reasons. The volatile RuO_4 is absorbed by dilute hydrochloric acid, and is converted into water-soluble chlororuthenate complexes.

Even in the absence of potassium permanganate, chlorate, or their reaction products, the distillation of RuO_4 is hazardous. The presence of NH_4^+ salts can lead to the formation of explosive chlorides of nitrogen. Therefore, removing ruthenium at the start of a separation process is often preferable. The formation of chlorine dioxide, chlorate, and perchlorate is also possible. Moreover, RuO_4 can explode by spontaneous decomposition, especially at > 100 °C and on contact with organic substances. To improve safety, work should be carried out under an inert gas and by avoiding the presence of large quantities (e.g., using a continuous process).

Distillation of Osmium(VIII) Oxide. As a rule, osmium is present in only a few primary and secondary raw materials. osmium should,

if possible, be isolated as the first step of a separation process, so that later operations will not lead to loss of volatile OsO_4 .

Solutions obtained from digestion of ores normally contain osmates. Treatment of solutions in dilute sulfuric acid with oxidizing agents such as CrO_3 , $\text{K}_2\text{S}_2\text{O}_8$, or HNO_3 causes osmium(VIII) oxide to be formed and to distill off. From this distillate, OsO_4 can be isolated directly as a water-insoluble oil (mp 40 °C). Alternatively, it can be absorbed in potassium hydroxide solution, forming K_2OsO_4 , or can be converted to metallic osmium by reaction with formaldehyde solution. Owing to the toxicity of OsO_4 , its escape into the atmosphere must be prevented by use of the best possible absorption equipment. No danger of explosion exists.

Also, OsO_4 can be formed and distilled off by heating fine osmium powder in a stream of oxygen.

Solvent Extraction. Liquid–liquid extraction is often characterized by distribution coefficients that vary greatly from element to element. These can usually be modified by chemical methods to give conditions favorable for the separation of PGMs. However, the separation factors resulting from the ratios of the distribution coefficients rarely enable a single separation stage to provide purities that fulfill modern requirements for metal quality. Although separations are generally better than those effected by precipitation crystallization, coarse separation by solvent extraction must be followed by purification.

In practical industrial separation processes, mainly four extractants are used [102, 123–126, 136–139]. The most long-standing process is the separation of Pt(IV) and Ir(IV) from Rh(III) with tributyl phosphate (TBP) [140, 141]. The extraction of $\text{H}_2[\text{PtCl}_6]$ and $\text{H}_2[\text{IrCl}_6]$ must be carried out in 4–6 M HCl (Figure 25.10). If the usual mixture of 1 part TBP with 3 parts petroleum ether is used, the capacity of the organic phase is limited in practice to ca. 10 g of Pt–Ir and it is therefore less suitable for extraction treatment of solu-

tions whose main constituent is platinum (e.g., normal refinery feed solutions).

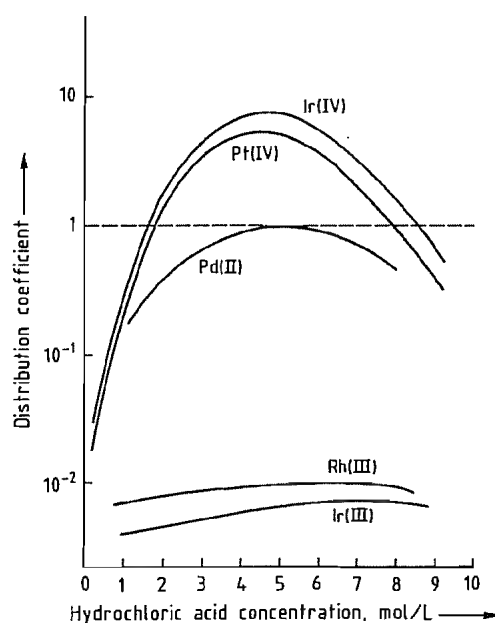


Figure 25.10: Extraction of platinum group metal chloro complexes by tributyl phosphate.

Trioctylamine is used widely for the solvent extraction of large amounts of platinum from refinery solutions [142–144]. It is also used for the solvent extraction of Ir(IV) (Figure 25.11). Stripping can be facilitated by changing the stripping solution or the valence of the metal. Diluent solvents are also employed when carrying out solvent extraction with amines.

For the solvent extraction of palladium, thioesters are currently used (e.g., di-*n*-hexyl sulfide or di-*n*-octyl sulfide) [103, 143–147]. They produce good separation from other PGMs and have a high capacity for the metal. A disadvantage is the poor kinetics of complex formation, the reaction times required being 30 mins or more. Hence, mixer settler equipment must be used rather than column equipment. Stripping with aqueous ammonia produces $[\text{Pd}(\text{NH}_3)_4]\text{Cl}_2$; this can be converted easily to $[\text{Pd}(\text{NH}_3)_2\text{Cl}_2]$, which is then purified.

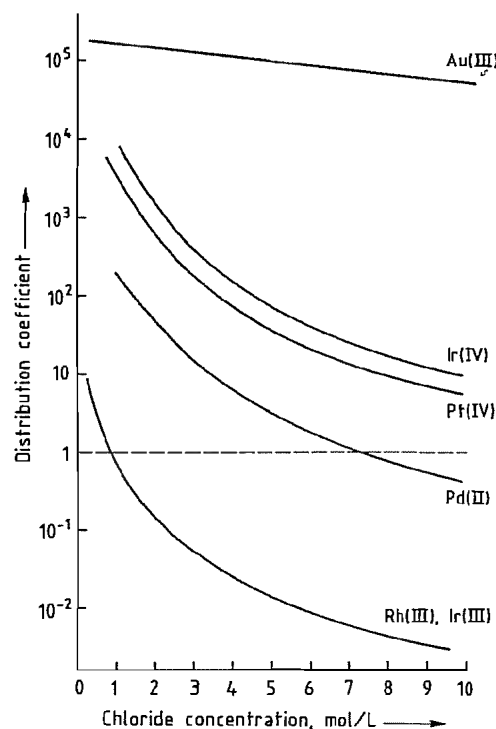


Figure 25.11: Extraction of platinum group metal and gold chloro complexes by trioctylamine.

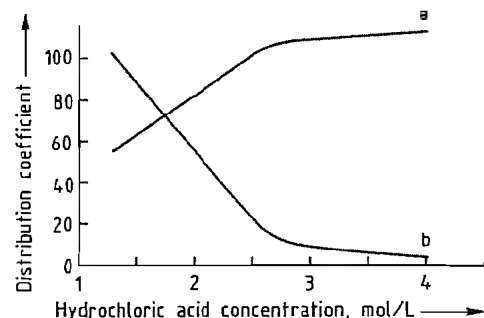


Figure 25.12: Extraction of palladium(II) and platinum(IV) chloro complexes by an aldoxime (LIX TN 1911): a) Platinum(IV); b) Palladium(II).

The method used for high-tonnage production of copper by solvent extraction with oximes is also successfully used for palladium (Figure 25.12). However, high concentrations of palladium in the organic phase cannot be achieved.

Numerous other solvent extraction systems have been investigated, some of which are un-

dergoing industrial development [107, 108, 141, 148–151].

25.6.5 Purification

Methods used for purification of the products from the separation process employ the same principles (i.e., valence change, temperature change, addition of common ions, and modification of complexes by chemical reaction).

Purification of Platinum. Recrystallization of sodium hexachloroplatinate(IV), $\text{Na}_2[\text{PtCl}_6]$, from hot water is effective, but large amounts of platinum must be recycled.

Very effective purification is achieved by the oxidative hydrolysis of the metallic impurities palladium, rhodium, iridium, ruthenium, and base heavy metals, which are removed as insoluble hydroxides (Figure 25.8, Separation Process C). Precipitation from hot aqueous solution is carried out by addition of sodium bromate at pH 6.5 or by passing through chlorine at slightly alkaline pH. The oxide hydrates adsorb considerable amounts of platinum. The yield of platinum therefore depends on the purity of the feed material.

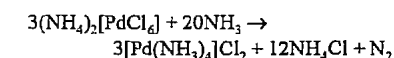
The classical method of purification is by repeated precipitation of $(\text{NH}_4)_2[\text{PtCl}_6]$. The crude salt is converted into metallic platinum, dissolved to form $\text{H}_2[\text{PtCl}_6]$ (see Section 25.5), and reprecipitated. By repeating this many times, very high purities are obtained, although the cost is also high. Also, $(\text{NH}_4)_2[\text{PtCl}_6]$ can be converted directly to H_2PtCl_6 by oxidation of the NH_4^+ or by cation exchange. In the oxidative decomposition of NH_4^+ (e.g., by heating the aqueous solution with addition of Cl_2 or HNO_3), care must be taken to use a carrier gas or distillative conditions to prevent accumulation of explosive nitrogen-halogen compounds.

Conventional crystallizations from water are possible, but the solubility of $(\text{NH}_4)_2[\text{PtCl}_6]$ is relatively low, so that despite favorable temperature coefficients (Figure 25.6), large volumes must be used. Modified crystallization methods are more economic (e.g., utilization of the considerably higher

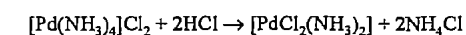
solubilities in water above 100 °C at higher pressure). The purification effected by crystallization is enhanced by hydrolysis. In neutral or very slightly acidic media above 90 °C, the conversion of the chloro complexes of the platinum group metals (especially metals other than platinum) into hydroxo complexes and oxide hydrates begins. These cannot form mixed crystals with $(\text{NH}_4)_2[\text{PtCl}_6]$. The extent of hydrolysis of hexachloroplatinate(IV) increases with increasing temperature and reaction time. Therefore, high temperature and long reaction time lead to a lower yield of crystalline product. The reaction is reversible in the presence of hydrochloric acid.

When the products of solvent extraction by substituted amines are stripped, solutions of platinum compounds in hydrochloric acid are obtained. From these, pure $(\text{NH}_4)_2[\text{PtCl}_6]$ is precipitated by addition of NH_4Cl .

Purification of Palladium [152]. Impure ammonium hexachloropalladate(IV), $(\text{NH}_4)_2[\text{PdCl}_6]$, can be dissolved directly for purification. This is achieved by the following reaction:



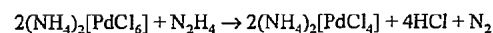
Acidification of a solution of $[\text{Pd}(\text{NH}_3)_4]\text{Cl}_2$ precipitates the sparingly soluble, pale yellow *trans*-diamminedichloropalladium(II):



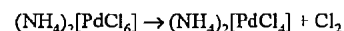
The impure salt should be dissolved quickly at room temperature with agitation to prevent appreciable quantities of the $(\text{NH}_4)_2[\text{PtCl}_6]$ present as an impurity from dissolving. Undissolved material, mainly hydroxides and $(\text{NH}_4)_2[\text{PdCl}_6]$, is filtered off. Hydrochloric acid is added to the solution until a pH of 1 is reached, causing $[\text{PdCl}_2(\text{NH}_3)_2]$ to precipitate as easily filterable crystals. Possible causes of poor purification are too high a concentration of $(\text{NH}_4)_2[\text{PdCl}_6]$ in the impure material, too prolonged a reaction with ammonia, too high a concentration of ammonia, or problems with filtration of the hydroxidic precipitate before precipitating $[\text{PdCl}_2(\text{NH}_3)_2]$. High temperature is also detrimental. If the acid concentration is

too high, the yield is reduced due to further reaction to form soluble $(\text{NH}_4)_2[\text{PdCl}_4]$.

Other possible methods for dissolving $(\text{NH}_4)_2[\text{PdCl}_6]$ are



or



Pure $(\text{NH}_4)_2[\text{PdCl}_6]$ can be obtained in almost quantitative yield by passing chlorine through the solution and adding NH_4Cl .

The purification of $(\text{NH}_4)_2[\text{PdCl}_6]$ by reprecipitation is useful in the presence of silver and most base metals. In the presence of rhodium, platinum, iridium, and copper, however, better purification is achieved by precipitating $[\text{PdCl}_2(\text{NH}_3)_2]$, although higher losses of palladium to the mother liquor must be tolerated.

Dichlorodiamminepalladium(II), $[\text{PdCl}_2(\text{NH}_3)_2]$, can be produced by direct precipitation from an impure solution of palladium resulting from crude separation or inadequate purification. It is dissolved in aqueous ammonia solution to form $[\text{Pd}(\text{NH}_3)_4]\text{Cl}_2$ and reprecipitated by hydrochloric acid.

An ammoniacal stripping solution is used after solvent extraction of palladium by dialkyl sulfide. Palladium can be precipitated from this by acidifying to pH 1, thus producing $[\text{Pd}(\text{NH}_3)_2\text{Cl}_2]$ directly in a highly pure form.

Purification of Iridium. The purification of crude ammonium hexachloroiridate(IV), $(\text{NH}_4)_2[\text{IrCl}_6]$, is carried out by precipitation of the unwanted elements as sulfides; these consist mainly of other platinum group metals and heavy base metals. This converts hexachloroiridate(IV) to hexachloroiridate(III), which must be reoxidized to precipitate $(\text{NH}_4)_2[\text{IrCl}_6]$. The sulfides are precipitated from slightly acidic solution by hydrogen sulfide. To ensure optimum precipitation conditions for all elements present, the sulfide precipitation must usually be carried out repeatedly. Iridium can be purified by liquid-liquid extraction [153]. It is extracted relatively easily in the tetravalent state, but not in the trivalent state (cf. Figure 25.10). Reduc-

tion by Fe^{2+} , As^{3+} , or ascorbic acid at room temperature causes selective reduction of Ir(IV) or Ir(III); Pt(IV) is unaffected.

Purification of Rhodium [154]. Ammonium hexachlororhodate(III), $(\text{NH}_4)_3[\text{RhCl}_6]$, can be crystallized from water or hydrochloric acid. However, the yields are poor, as is the degree of separation from platinum and iridium. Precipitation of $[\text{Rh}(\text{NH}_3)_5\text{Cl}]\text{Cl}_2$ or $(\text{NH}_4)_3[\text{Rh}(\text{NO}_2)_6]$ is more effective, although yields are not good, and treatment of the mother liquor is problematical.

Good results are obtained when $\text{H}_2[\text{PtCl}_6]$ and $\text{H}_2[\text{IrCl}_6]$ are removed by liquid-liquid extraction, and base metal cations by strongly acidic ion-exchange resins. At one time, treatment of crude rhodium with chlorine at 700 °C was an important process. The reaction product consisted mainly of insoluble RhCl_3 from which the chlorides of platinum, palladium, and base metals were dissolved by treatment with hydrochloric acid. Satisfactory purification could usually be obtained only by repeating the process.

Crude potassium hexanitritorhodate(III), $\text{K}_3[\text{Rh}(\text{NO}_2)_6]$, can be converted to hexachlororhodate(III) by heating with hydrochloric acid. This can be followed by reprecipitating $\text{K}_3[\text{Rh}(\text{NO}_2)_6]$ or precipitating $[\text{RhCl}(\text{NH}_3)_5]\text{Cl}_2$.

25.6.6 Conversion of Salts into Metals [30, 34, 39, 101, 111]

The end products of PGM separation are metal compounds, but all platinum group metals are marketed almost exclusively in the form of metallic sponge or powder.

Conversion to the metals is carried out mainly by thermal decomposition of the ammonium chloro complexes (calcination). These compounds have decomposition temperatures (Figure 25.13), of 200–500 °C. The size and geometry of the charge affect the reaction course. The low thermal conductivity of the charge means that the reaction proceeds slowly, but smooth production of the desired decomposition products is ensured. Also, the

negative heat of reaction of the decomposition tends to slow down the process. In practice, favorable conditions are achieved by external heating at 900–1000 °C.

In earlier days, the thermal decomposition of PGM compounds was carried out in gas-heated muffle furnaces that were not very leaktight. The best of these were provided with a collection chamber for NH_4Cl (sublimation temperature 340 °C) and included a waste gas system [41]. Today, tubular fused silica reactors, enclosed in an electrically heated furnace, are used. A stream of inert gas can be passed through at a controlled rate, and absorption equipment is present for NH_4Cl and HCl . Automated plants are in operation [155, 156].

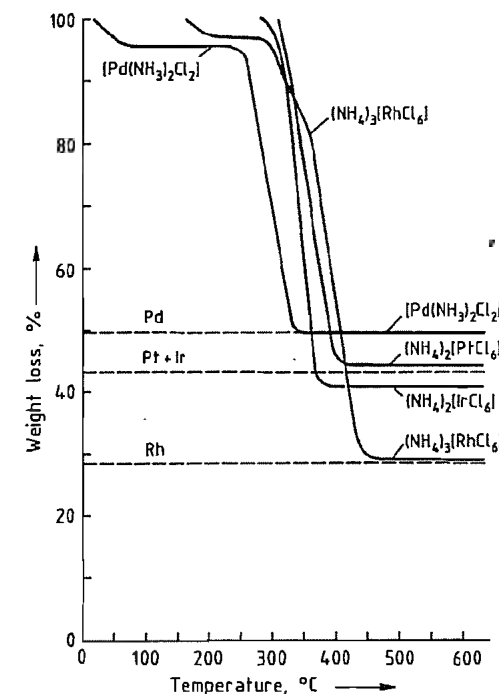
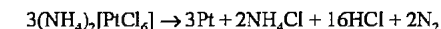


Figure 25.13: Thermal decomposition of platinum group metal complexes.

Thermal treatment of PGM compounds can also be carried out in the presence of hydrogen. For safety reasons, a mixture of hydrogen and nitrogen below the ignition temperature is preferable.

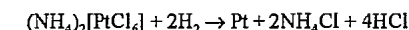
Chemical reduction of PGM compounds in aqueous medium (e.g., by hydrazine) has not proven to be economical in large refineries.

Platinum. The compound $(\text{NH}_4)_2\text{PtCl}_6$ can be converted to platinum sponge by thermal decomposition at 800 °C, according to



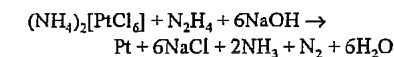
Excessive carryover of platinum can be avoided by introducing ammonium hexachloroplatinate(IV) into the reaction zone at ca. 300 °C and heating it rapidly. Waste gas is washed with water to extract ammonium chloride, both for environmental reasons and to prevent the loss of traces of platinum.

If the reaction is carried out in a hydrogen atmosphere, elemental platinum is formed below the sublimation temperature of NH_4Cl (ca. 350 °C). Platinum carryover is then appreciably less, and more ammonium chloride is formed:



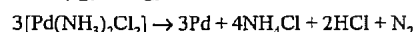
If NH_4Cl is not sublimed but is removed by dissolving in water, finely divided platinum powder can be produced by this process. Calcination of the hexachloroplatinate(IV) of an alkali metal is not recommended, because the alkali metal chloride produced is difficult to remove by aqueous dissolution from the platinum sponge.

Hexachloroplatinates can usually be reduced in aqueous solution or suspension according to



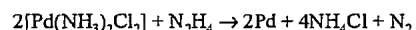
The reaction proceeds best above 80 °C, with excess NaOH maintained at 2 M and the reaction controlled by adjusting the rate of addition of N_2H_4 . The reaction must be flushed with nitrogen, because hydrogen can be formed in a side reaction. The platinum black formed is washed to remove salts, and either dried to produce powder or heated strongly to produce sponge. Overall, wet chemical reduction is more expensive than calcination but should be used if alkali metal hexachlorometallates are present, because their decomposition products cannot be sublimed.

Palladium. The thermal decomposition of dichlorodiamminepalladium(II), $[\text{Pd}(\text{NH}_3)_2\text{Cl}_2]$, begins at ca. 290 °C in an inert atmosphere. Process conditions are the same as for $(\text{NH}_4)_2[\text{PtCl}_6]$. The reaction is



For the calcination of ammonium hexachloropalladate(IV), which loses chlorine at ca. 280 °C, the temperature should be increased extremely slowly over the range 100–300 °C. If calcination is carried out in air, the palladium sponge formed contains large amounts of PdO , which must be reduced by strong heating in a hydrogen atmosphere.

The wet chemical reduction

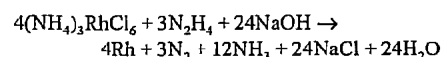


and the reduction of $(\text{NH}_4)_2[\text{PdCl}_6]$ proceed quantitatively in strongly ammoniacal solution above 50 °C. Sodium formate in alkaline solution can also be used as reducing agent. A nitrogen atmosphere must be used in both cases to prevent formation of explosive gas mixtures. Chemical reduction often produces pyrophoric palladium black, which must be dried in an inert gas atmosphere.

Iridium. The best method of producing iridium is to reduce ammonium hexachloroiridate(IV), $(\text{NH}_4)_2[\text{IrCl}_6]$, in a hydrogen atmosphere ca. 800 °C, yielding the metal powder. Calcination in air gives an oxide-containing material. Wet chemical reduction with hydrazine is possible only in strongly alkaline sodium hydroxide solution and does not always go to completion.

Rhodium. Ammonium hexachlororhodate(III) is subjected to the same process of thermal reduction as used for $(\text{NH}_4)_2[\text{IrCl}_6]$.

Wet chemical reduction with hydrazine according to



must be carried out with a large excess of hydrazine and NaOH at ca. 100 °C to ensure complete reaction.

Ruthenium. Ammonium hexachlororuthenate(III–IV) is reduced, preferably in a hydro-

gen atmosphere, at ca. 800 °C. Aqueous solutions of ruthenates(IV) (e.g., produced by adding RuO_4 to an alkali-metal hydroxide solution) are treated with ethanol to precipitate hydrated RuO_2 , which is reduced in a hydrogen atmosphere at 800 °C.

Osmium. Osmium tetroxide that has been absorbed in potassium hydroxide solution is precipitated as potassium osmate(IV) by adding ethanol. This is reduced by strong heating in a hydrogen atmosphere or reacted with NaBH_4 in aqueous solution [157]. The product must be washed with water in both cases.

25.6.7 Partial Purification

Platinum–Rhodium Mixtures. For industrial use, platinum and rhodium are often alloyed together, and separating these elements during the recovery process may be unnecessary. The solutions obtained by dissolving metallic platinum rhodium scrap can be used. The neutral solutions are treated with a sodium-loaded ion exchanger to replace all unwanted cations with sodium. Sometimes, Na^+ is replaced by H^+ , giving a solution of $\text{H}_2[\text{PtCl}_6]$ and $\text{H}_3[\text{RhCl}_6]$ suitable for further treatment (e.g., reduction by hydrazine to give Pt–Rh powder).

Similar processes can be used for treating some single metal catalysts (e.g., material from the calcination of carbon palladium).

Surface Cleaning. Some returned metallic materials with only surface contamination require merely surface cleaning, thereby avoiding a wet separation process. They can be treated with acids, such as hydrofluoric acid, or with fused salt (e.g., NaHSO_4), although some of the outer layer of platinum dissolves.

25.6.8 Treatment of Internally Recycled Material

A buildup of base metals occurs in recycled material such as mother liquor from precipitation and crystallization. These base metals originate from the raw materials and from salts formed in the reactions, and also include

small quantities of platinum group metals from the separation process. The quantity or recycled noble metals should normally not exceed 1% of the metal in the starting material. The extent of recycle must be limited, because losses are relatively high when noble metals are recovered from this type of material.

Solutions containing platinum metals with only small amounts of other materials should be concentrated by evaporation in the presence of hydrochloric acid. They can be combined with fresh raw material for separation.

If the solutions contain only ammonium chloride and platinum group metals, they can often be reused directly as a precipitating agent after concentration in acid conditions.

If the solutions contain large amounts of salts of alkali metals, alkaline earths, or other metals along with platinum and palladium residues, it is advantageous to separate the ions $[\text{PtCl}_6]^{2-}$ and $[\text{PdCl}_4]^{2-}$ from the other materials by using strongly basic ion exchangers. Good separation is achieved if only the two chloro complexes are present. For rhodium and iridium this condition is often not achieved, because of hydrolysis to give hydroxo complexes, so this method cannot be used unless special precautions are taken.

In earlier times, noble metals were recovered from such solutions by cementation with zinc in a hydrochloric acid solution. Aluminum is now the preferred reducing agent because of the high cost of zinc, which must be present in large excess, and the resultant environmental problems. Noble metals can also be recovered with sodium borohydride. Alternatively, they can be reduced by hydrazine in alkaline solution. If no precautions are taken, hydroxides of base metals are also precipitated, but these can easily be redissolved. Copper is also precipitated in this reduction process. After redissolving the metals, the latter can be reprecipitated as copper(II) oxalate or another copper(I) or copper(II) salt that is sparingly soluble in slightly acidic solution.

All materials from which noble metals have been recovered must be monitored carefully for possible noble-metal content before disposal, so that no irrevocable losses occur.

25.6.9 Construction Materials

Many of the operations described above pose special problems in the choice of materials for equipment and vessels.

Plastics resistant to mineral acids can often be used. Vessels and reactors lined with hard rubber are resistant to acids and saturated chlorine solutions at 90 °C. Unsuitable metals for commonly occurring solutions of platinum and other platinum group metals include stainless steel, titanium, zirconium, the Hastelloys, and silver, because these materials cause cementation of platinum group metals. Tantalum is an exception. It is resistant to dissolved halogens and does not cement platinum group metals from solution. It is a suitable material for steam-heated heat exchangers. Equipment constructed of borosilicate glass and glass-lined steel reactors are chemically resistant to all of these materials. For solutions containing large amounts of ruthenium or osmium, other construction materials are recommended, including graphite for some items.

For treating raw materials with acidic molten salts or salts that have a chlorinating action, and for calcination, the use of fused silica equipment is best. Treatment with molten oxidizing alkaline salts is carried out in silver or nickel crucibles.

25.7 Compounds [5, 6, 29, 31, 34, 39, 85, 98–100, 158]

Because of the many possible oxidation states of platinum group metals and their tendency to form complexes, the range of compounds is extremely wide. Only a few of these are of industrial importance.

25.7.1 Platinum Compounds

Hexachloroplatinic(IV) acid, $\text{H}_2[\text{PtCl}_6] \cdot 6\text{H}_2\text{O}$, theoretical platinum content 37.68%, platinum content of commercial product ca. 40% [commercial names: chloroplatinic acid, hydrogen hexachloroplatinate(IV)], forms reddish brown crystals (*mp* ca. 150 °C), which deliquesce in moist air and are readily soluble

in water or alcohol. The usual commercial product is an aqueous solution with a platinum content of 25%.

Production. Platinum sponge is treated with moderately concentrated hydrochloric acid saturated with chlorine in a stirred vessel at ca. 80 °C. The solution obtained is evaporated until it reaches 150 °C. When cooled, it changes into solid $\text{H}_2\text{PtCl}_6 \cdot 4.5\text{H}_2\text{O}$, which contains ca. 40% platinum, no mother liquor is produced. If the platinum is dissolved in aqua regia instead of hydrochloric acid chlorine, the nitric acid and NOCl formed must be removed completely, preferably by repeated evaporation to a syrupy consistency and redissolution in hydrochloric acid.

Uses. Hexachloroplatinic(IV) acid is the most industrially important platinum compound. It is used in the production of most other platinum compounds and preparations. It is used primarily to make catalysts by impregnating support materials.

Hexachloroplatinates(IV). Ammonium hexachloroplatinate(IV), $(\text{NH}_4)_2[\text{PtCl}_6]$, and, to a limited extent, the orange-red salt sodium hexachloroplatinate(IV), $\text{Na}_2[\text{PtCl}_6]$, are important in platinum separation processes (see Section 25.6).

Platinum Chlorides. Platinum(IV) chloride, PtCl_4 , is produced by careful dehydration of $\text{H}_2\text{PtCl}_6 \cdot 6\text{H}_2\text{O}$ at ca. 300 °C in a stream of chlorine. It is a red-brown, crystalline, hygroscopic powder with a relatively narrow range of thermal stability.

Above 380 °C, PtCl_4 liberates chlorine and forms platinum(II) chloride, PtCl_2 , which is stable between 435 and 580 °C. Platinum(III) chloride, PtCl_3 , is probably formed as an intermediate in this reaction. Above 580 °C, further decomposition occurs to yield metallic platinum. Platinum(IV) chloride is the only chloride of platinum that is soluble in water.

Platinum(II) chloride can also be obtained from a solution of $\text{H}_2[\text{PtCl}_4]$ by careful evaporation under vacuum. Chlorides of platinum can be produced by reacting chlorine with finely divided platinum. The chloride obtained

will be the one that is stable at the reaction temperature.

Platinum Oxides. The most industrially important oxide of platinum is platinum(IV) oxide hydrate, $\text{PtO}_2 \cdot \text{H}_2\text{O}$, a hydrogenation catalyst. To prepare this substance, a solution of 9 parts sodium nitrate and 1 part platinum as $\text{H}_2[\text{PtCl}_6]$ is evaporated to dryness. The product mixture is finely powdered and added to molten NaNO_3 (10 parts) at 520 °C with agitation. The product is dissolved in water, washed, and carefully dried to give a brown powder, insoluble in aqua regia, with poorly defined stoichiometry.

Platinum(II) oxide, PtO , and platinum(II) oxide hydrate, $\text{PtO} \cdot \text{H}_2\text{O}$, are also known, but have little or no industrial importance.

Other Platinum Compounds. The following compounds are used in aqueous electrochemistry: potassium tetranitroplatinate(II), $\text{K}_2[\text{Pt}(\text{NO}_2)_4]$; dinitro-diammineplatinum(II), $[\text{Pt}(\text{NH}_3)_2(\text{NO}_2)_2]$; and sodium hexahydroxyplatinate(IV), $\text{Na}_2[\text{Pt}(\text{OH})_6]$.

Potassium tetracyanoplatinate(II), $\text{K}_2[\text{Pt}(\text{CN})_4]$, can be used in electroplating by molten salt electrolysis. Barium tetracyanoplatinate(II), $\text{Ba}[\text{Pt}(\text{CN})_4]$, is used in the manufacture of fluorescent screens. Many other cyano complexes are known. Simple cyanides such as $\text{Pt}(\text{CN})_2$ and $\text{Pd}(\text{CN})_2$ also exist.

Potassium tetrachloroplatinate(II), $\text{K}_2[\text{PtCl}_4]$, is a starting material for the synthesis of most Pt(II) compounds. Platinum(II) acetylacetonate is used in the pyrolytic production of platinum surface coatings (see Section 25.9.9.2) and is superior to other platinum compounds in this application.

Dichlorodiammineplatinum(II), $[\text{PtCl}_2(\text{NH}_3)_2]$, is of historical interest and was known in two forms: "Peyrone's chloride" and "Reiset's second chloride". In 1893, WERNER recognized that these were *cis* and *trans* isomers. The compound *cis*- $[\text{PtCl}_2(\text{NH}_3)_2]$ (*cis*-platin) is expected to grow in importance because of its cytostatic properties.

25.7.2 Palladium Compounds [159]

Tetrachloropalladic(II) acid, $\text{H}_2[\text{PdCl}_4]$, is stable only in solution. Commercial solutions in hydrochloric acid contain 20% palladium and are dark brown.

Production. The method of producing $\text{H}_2[\text{PdCl}_4]$ solution is similar to that for $\text{H}_2[\text{PtCl}_4]$ solution. The metal is dissolved in $\text{HCl}-\text{Cl}_2$ or $\text{HCl}-\text{HNO}_3$, the rate of dissolution being higher than with platinum (Figure 25.5). If dissolution occurs below ca. 50 °C, hexachloropalladic(IV) acid is formed first.

Uses. The solution of tetrachloropalladic(II) acid is the most industrially important palladium preparation. It is the starting material for almost all other palladium compounds, particularly catalysts.

Palladium(II) chloride, PdCl_2 , theoretical palladium content 60.0%, palladium content of commercial product 59.9%, is a brown to brownish violet powder, insoluble in water, but readily soluble in hydrochloric acid and solutions of alkali-metal chlorides. It sublimes at 590 °C. Decomposition begins at 600 °C and is complete at 740 °C.

Production. The best method of production of PdCl_2 is careful evaporation of a solution of $\text{H}_2[\text{PdCl}_4]$ in hydrochloric acid, preferably in a rotary evaporator.

Uses. Anhydrous PdCl_2 is the starting material for a number of palladium compounds.

Palladium Oxides. Poorly defined oxide hydrates are obtained by adding alkali to aqueous solutions of Pd(II) compounds. The Pd(IV) oxide hydrates obtained from Pd(IV) solutions release oxygen. A catalytically active palladium preparation analogous to $\text{PtO}_2 \cdot x\text{H}_2\text{O}$ can be obtained by evaporating a solution of $\text{H}_2[\text{PdCl}_4]$ and NaNO_3 , and fusing the product.

Stoichiometric palladium(II) oxide, PdO , which is crystallographically well defined, is obtained by reaction of palladium black with oxygen or air at 750 °C. Decomposition occurs at 850 °C.

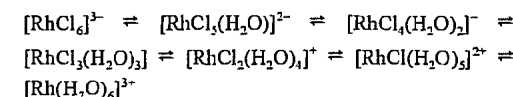
Palladium Ammine Complexes. The addition of ammonia to solutions of palladium

chloride first causes the formation of a pink precipitate of the binuclear complex $[\text{Pd}(\text{NH}_3)_4\text{PdCl}_4]$, known as Vauquelin's salt, which is converted to soluble tetramminepalladium(II) chloride, $[\text{Pd}(\text{NH}_3)_4]\text{Cl}_2$, by further addition of NH_3 . Acidification of this solution yields the sparingly soluble light-yellow *trans*-diamminedichloropalladium(II), $[\text{PdCl}_2(\text{NH}_3)_2]$. These compounds and reactions are important in the industrial separation of palladium (see Section 25.6).

Other Palladium Compounds. Ammonium hexachloropalladate(IV), $(\text{NH}_4)_2[\text{PdCl}_6]$, is important in separation technology. It is an oxidation product of tetrachloropalladate(II) (see Section 25.6). Palladium(II) sulfate, palladium(II) nitrate, and palladium(II) acetate are of some importance in preparative chemistry. The ready formation of palladium hydride is exploited industrially for example for the purification of hydrogen.

25.7.3 Rhodium Compounds [160]

Hexachlororhodic(III) Acid, H_3RhCl_6 . Wet separation processes and molten salt dissolution usually produce $(\text{NH}_4)_3[\text{RhCl}_6]$ or $\text{Na}_3[\text{RhCl}_6] \cdot 12\text{H}_2\text{O}$ in crystalline form. Both compounds form deep-red crystals, which are very soluble in water. Free hexachlororhodic(III) acid, $\text{H}_3[\text{RhCl}_6]$, can be obtained by cation exchange or by oxidative decomposition of the cation in the case of the NH_4^+ salt (see Section 25.6.2). The composition of the chloro complexes of rhodium depends strongly on the concentration of hydrochloric acid, the temperature, the duration of reaction, and the previous treatment of the solution. By starting with a strongly acidic medium, the following transformations are possible:



The color varies from raspberry red to brown.

Rhodium Chlorides. Anhydrous, brownish red rhodium(III) chloride, RhCl_3 , which is insoluble in water and mineral acids, is obtained

by heating rhodium powder to 700 °C in a chlorine atmosphere.

So-called soluble rhodium chloride, with the approximate composition $\text{RhCl}_3 \cdot 2.5\text{H}_2\text{O}$, is obtained by evaporating a solution of $\text{H}_2[\text{RhCl}_6]$ in hydrochloric acid, preferably in a rotary evaporator. This compound is the most important commercial rhodium product, and is used as the starting material for other rhodium compounds and catalysts.

Rhodium Sulfate. Rhodium(III) sulfate, $\text{Rh}_2(\text{SO}_4)_3$, can crystallize with varying amounts of water; it can be obtained by dissolving $\text{Rh}(\text{OH})_3 \cdot x\text{H}_2\text{O}$ in sulfuric acid or by the action of hot sulfuric acid on freshly precipitated rhodium black. It is used in rhodium plating.

Chloro-tris-(triphenylphosphine)rhodium(I), $\text{RhCl}[\text{P}(\text{C}_6\text{H}_5)_3]_3$, is formed by the reaction of triphenylphosphine with soluble rhodium(III) chloride in ethanol solution under reflux. It separates as deep-red crystals.

This complex, and rhodium compounds with similar structures, are important homogeneous catalysts.

25.7.4 Iridium Compounds

Hexachloroiridic(IV) acid, $\text{H}_2[\text{IrCl}_6]$, is produced in aqueous solution by the methods used to obtain $\text{H}_3[\text{RhCl}_6]$ (i.e., from the ammonium or sodium salts). It is by far the most important iridium compound. The oxidation state is relatively easily changed (in either direction), the very intense dark brown $[\text{Ir}^{\text{IV}}\text{Cl}_6]_2$ changing to the lighter colored $[\text{Ir}^{\text{III}}\text{Cl}_6]_3$ or vice versa. The ammonium salts of both anions are important in separation technology (see Section 25.6).

Iridium(III) Chloride, IrCl_3 . A product stoichiometrically deficient in chlorine is obtained by heating iridium powder in a stream of chlorine at 650 °C. The chlorination reaction is assisted by the presence of carbon monoxide.

25.7.5 Ruthenium Compounds

Ruthenium(VIII) oxide, RuO_4 is formed by the oxidation of aqueous solutions of ruthenates. It has a melting point of 25.5 °C and is therefore a liquid at room temperature. It is both toxic and explosive (see Section 25.9.1).

Soluble Ruthenium(IV) Chloride. So-called soluble ruthenium chloride consists mainly of $\text{Ru}(\text{OH})\text{Cl}_3$ with some $\text{RuCl}_3 \cdot \text{H}_2\text{O}$, and is prepared by reacting RuO_4 with hydrochloric acid and evaporating the solution. The compound $(\text{NH}_4)_2[\text{RuCl}_6]$ can be precipitated by adding NH_4Cl .

Potassium ruthenate(VI), $\text{K}_2[\text{RuO}_4]$, is formed by fusing ruthenium with KOH-KNO_3 or by dissolving RuO_4 in potassium hydroxide solution.

25.7.6 Osmium Compounds

Osmium(VIII) oxide, OsO_4 , is the most important osmium compound. It is formed even at room temperature by the oxidation of osmium powder by air. It is prepared by strongly heating osmium in a stream of oxygen at 500–800 °C. The melting point is 40.6 °C, and the boiling point 131.2 °C. Sublimation takes place even at room temperature.

Potassium osmate(VI), $\text{K}_2[\text{OsO}_2(\text{OH})_4]$, is formed by the reaction of OsO_4 with potassium hydroxide solution and alcohol.

25.8 Quality Specifications and Analysis [5, 34, 161–177]

In industry, the purity and fineness of platinum and platinum metals are even today often described by the classifications “technically pure” (99%), “chemically pure” (99.9%), “physically pure” (99.99%), and “spectroscopically pure” (99.999%). These are taken from the recommendations of the Physikalisch-Technischen Reichsanstalt [28].

Present practice is to use the following qualities:

99% (now hardly used)
99.9%

99.95%
99.98%
99.99%
99.999%
99.9999% (only in exceptional cases)

Other specifications are used for particular applications (e.g., physical properties if used in sensors or microelectronics [178, 179]).

Most commercially available platinum and palladium from primary and secondary production have purities of 99.95–99.98%. Higher purities usually sell at higher prices. Platinum and palladium are generally supplied as ingots or plates (stamped with the purity). Other platinum metals are supplied mainly as powder.

Platinum and palladium ingots of 500–1000 g are preferred for investment purposes in Japan [1].

Determination of Purity. The purity of commercial platinum group metals is determined by physical methods. The most important of these are emission spectroscopy, with glow discharge or spark excitation of the solid; plasma emission spectroscopy with inductively coupled plasma (ICP) or direct current plasma; and atomic absorption spectroscopy (AAS) for solutions. High-performance liquid chromatography is of minor importance for the analysis of PGMs. Mass spectrometry is used in special cases, especially for ultrapure material, recently with glow discharge excitation, ICP excitation (ICP-MS), or neutron activation.

The noble-metal content can be determined more precisely by measuring the total content of impurities than by direct determination. Physical methods for the determination of trace impurities have replaced wet chemical and colorimetric analytical methods for reasons of economy and speed.

Trace Analysis of Platinum Group Metals. The determination of traces of noble metals is of great importance in mineral prospecting. Since metal contents of only a few parts per million are of interest, sensitivity requirements are higher than in purity analysis. Methods such as graphite tube AAS, neutron activation analysis, total reflection X-ray fluo-

rescence analysis, and ICP mass spectrometry are used after appropriate enrichment procedures (e.g., with a nickel sulfide melt).

The analysis for traces of noble metals in waste materials from the noble-metal processing industry, especially refineries, has always been very important in monitoring the economic effectiveness of the process.

Trace analysis for platinum has become even more important in recent years. Whereas both the occurrence and the use of platinum group metals have hitherto been localized, automobile exhaust-gas catalysis now constitutes a widespread use. Although no toxic effects on the environment have thus far been reported, methods of analysis must be continually improved as permitted levels in the soil and the atmosphere become increasingly strict. The collection of the PGMs in a nickel sulfide phase, followed by spark AAS is suitable for analysis in the ppb range.

Qualitative Analysis. Qualitative analysis for platinum metals is used in checking the progress of industrial processes, and is a useful decision-making tool during wet chemical separation for analytical purposes.

The older wet chemical qualitative reactions have not entirely lost their usefulness.

Platinum in solution in dilute hydrochloric acid can be detected by adding tin(II) chloride. A yellow to red coloration is produced, depending on platinum concentration. The detection limit is ca. 1 mg/L (Pd, Rh, and Au can interfere).

Palladium in weakly acid solution reacts with dimethylglyoxime to give a characteristic yellow, voluminous precipitate.

Rhodium can be detected by the orange-red precipitate formed with thionalide [2-mercapto-*N*-(2-naphthyl)acetamide].

Iridium can be detected by fuming the solution with sulfuric acid and adding ammonium nitrate, which gives an intense blue color.

Ruthenium reacts with thiourea in hydrochloric acid solution to give a blue color. The blue color obtained on heating with dithiooxamide in hydrochloric acid solution is very specific.

Osmium reacts with thiourea to give a red color. The odor of osmium tetroxide is also characteristic.

In the PGM industry, physical methods are used almost exclusively for qualitative analysis. These include UV emission spectrophotometry, X-ray fluorescence analysis, inductively coupled plasma (ICP) emission spectroscopy, and atomic absorption spectroscopy.

Chemical Assay Methods. The methods of analysis used when buying and selling crude products, alloys, compounds, etc., must be of a very high standard because of the high value of platinum group metals. For commonly occurring combinations of elements, mandatory methods of analysis and sampling have been developed. The following methods of separation are standard and are still used today to a considerable extent. Platinum group metals are often subjected to preliminary docimastic concentration prior to assaying and are always brought into solution.

Platinum Metals-Base Metals. Platinum is precipitated as $(\text{NH}_4)_2[\text{PtCl}_6]$ from a nitrate-free solution of $\text{H}_2[\text{PtCl}_6]$ by addition of NH_4Cl , and the precipitate is heated strongly, which converts it to platinum, and then weighed. Platinum remaining in the mother liquor is precipitated as the sulfide with H_2S and carefully roasted. The heavy-metal sulfides are dissolved in 10% HNO_3 , and the residue is treated with H_2SO_4 -HF and weighed as platinum. For Pt- α - Al_2O_3 catalysts used in the petroleum industry, the mandatory method of determining platinum is by the coloration produced with tin(II) chloride, which is determined photometrically after extraction with ethyl acetate.

Platinum-Rhodium. A finely divided metal black is obtained by fusion with zinc followed by treatment with hydrochloric acid. Platinum is dissolved in aqua regia, and $(\text{NH}_4)_2[\text{PtCl}_6]$ is precipitated and heated strongly to yield platinum. The remaining noble metal is cemented from the mother liquor, combined with the residue remaining after aqua regia treatment, and treated with chlorine

at 650–700 °C. The RhCl_3 obtained, which is insoluble in aqua regia, is heated strongly in a hydrogen atmosphere to produce the metal, which is weighed. Base metals remain in solution with some residual platinum. The latter is isolated by precipitation as sulfide, and the figure obtained is included with the main amount.

Platinum-Palladium. Palladium is quantitatively precipitated by dimethylglyoxime from a dilute solution in aqua regia. It is filtered off, washed thoroughly, calcined carefully, reduced to the metal by hydrogen, and weighed. The dimethylglyoxime in solution is decomposed by aqua regia, and platinum is converted to $(\text{NH}_4)_2[\text{PtCl}_6]$, precipitated as sulfide, isolated as the metal, and weighed.

Platinum-Iridium. Platinum-iridium is converted into a finely divided state by fusion with zinc, and the platinum is dissolved with aqua regia. Iridium remains undissolved and, after reduction with hydrogen, is weighed.

Pt-Pd-Rh-Ir-Ru-Os-Au Ore Concentrates. After being melted with zinc in a stream of hydrogen, the alloy is dissolved in hydrochloric acid, and the metal black is isolated. The OsO_4 is driven off by heating to 1000 °C in a stream of oxygen. The metal that remains after removal of osmium is reduced in a stream of H_2 and rendered soluble by fusion with KOH-KNO_3 .

The fusion product is dissolved in water; RuO_4 is distilled from the solution in the presence of an oxidizing agent (e.g., Cl_2) collected in a receiver containing an alcoholic solution of hydrogen chloride, and finally weighed as metal. The distillation residue is reduced to the noble metals by treatment with NaOH and ethanol, filtered off, and heated gently in a stream of H_2 . It is then dissolved in aqua regia, and the insoluble residue is filtered. Gold is then determined with oxalic acid and palladium with dimethylglyoxime. The remaining noble metal is obtained by cementation with zinc and combined with the insoluble aqua regia residue. A further fusion with zinc is carried out, followed by final treatment with hydrochloric acid. Dry chlorination at 650 °C produces platinum chloride, which is dissolved in

33% aqua regia. The residue is treated with NaCl and Cl_2 at 650 °C; the product is dissolved in water and acidified, precipitating $(\text{NH}_4)_2[\text{IrCl}_6]$, and rhodium is cemented from the solution with zinc. The product is then chlorinated at 650 °C. This again extracts platinum, and the solution is combined with the other solution, which contains most of the platinum. Platinum is determined by precipitating $(\text{NH}_4)_2[\text{PtCl}_6]$, and rhodium by reduction of the RhCl_3 residue.

The platinum content of commercial compounds and preparations is usually determined reduction with hydrazine. Cementation from solution in strong hydrochloric acid by treatment with zinc turnings is an exact method if carefully carried out.

Physical Methods. Physical methods—especially spectroscopic ones—are increasingly being used, because they are inexpensive and, with improvements in the equipment, have sufficient accuracy for accounting purposes. If the PGMs are brought into solution by suitable fusion and separation methods, all the metals can be determined in the presence of each other by X-ray fluorescence or ICP analysis, for example. The former can also be used for direct analysis of metallic materials with sufficient accuracy for production control in the manufacture of defined alloys. Calibration of this method, when used on higher alloys, is, however, difficult.

25.9 Uses [3, 5, 29, 30, 180]

25.9.1 Jewelry, Coinage, Investment [158]

In recent decades, platinum has been in such demand for jewelry and high-quality watchmaking that more than one-third of all the platinum consumed has been used for this purpose. Of this amount, Japan uses about 90%, with the United States taking the next largest share. Most of the alloys employed contain 95% platinum and are stamped PLAT 950. The mechanically more stable alloys Pt95-Cu5, Pt96-Pd4, and Pt90-Ir10 are used

for mounting precious stones. Forming costs for platinum are considerably higher than those for gold because the metal is more difficult to work, and recycling costs are high. These factors markedly affect total cost.

Very good resistance to corrosion and erosion is required of alloys used for the nib tips of high-quality fountain pens [158]. These alloys are based on ruthenium, iridium, and osmium.

In the Russian Empire in 1828–1845, a total of 15 t of platinum was formed into 3-, 6-, and 12-ruble pieces by sintering, minted, and brought into circulation.

The fineness was 99% platinum or 99.2% PGM [15]. Between 1977 and 1980, platinum coins were again minted for the Moscow Olympic Games. These were 150-ruble pieces, fineness: 9999, $\frac{1}{2}$ ounce, in five designs. Since then, platinum coins have been officially minted in other states (e.g., a Platinum Noble in the UK, a Platinum Maple Leaf in Canada, and a Platinum Koala in Australia). The standard issue of all these coins contained one troy ounce (31.1035 g) of fine platinum. Small ingots, usually containing 99.995% platinum, are also minted, intended mainly for small investors. The use of palladium for this purpose has recently begun on a small scale.

25.9.2 Apparatus [181–184]

Laboratory Technology. Platinum crucibles, dishes, boats, and electrodes (for electrogravimetry) have long been basic items of equipment in chemical laboratories. In earlier times, the purity of platinum was variable. Moreover, equipment made of pure platinum is not dimensionally stable, so today the more stable alloys Pt97-Ir3, Pt95-Au5, and occasionally Pt99.7-Ir0.3, are mainly used [185].

Another type of dimensionally stable platinum is dispersion-hardened platinum, which contains ca. 100 ppm of high-melting oxide (e.g., ZrO_2) in finely divided form [85]. The presence of this material reduces the mobility of crystal imperfections. It is produced by coprecipitation followed by sintering of the powder. The metal can be unalloyed platinum, or

alloys of platinum with rhodium or gold. Rhodium and iridium crucibles can resist extremely aggressive conditions in nonoxidizing atmospheres.

Chemical and Electrochemical Apparatus [186]. The platinum metals and their compounds are of limited use in chemical process technology owing to their high cost. However, platinum components are essential in fluorine chemistry. Bursting disks for protection against excessive pressure are occasionally made of platinum or palladium. Single crystals for the optical industry and for laser technology are grown in crucibles of platinum, rhodium, or (most commonly) iridium. For the electrochemical production of peroxo compounds, such as hydrogen peroxide and peroxosulfate, massive platinum anodes or hollow platinum wires are used, although such use has decreased.

Glass Technology [186–189]. The corrosion and erosion resistance of platinum metals toward molten glass is not matched by any other material [85]. High-purity optical glass is best melted in crucibles of unalloyed platinum. Special iron-free glass for sodium vapor lamps, X-ray windows, and cathode-ray tubes is melted in Pt–Rh vessels.

In the automated production of bottles by large holding furnaces, the use of platinum components ensures problem-free operation over long periods. These components include skimmers, pouring funnels, thermocouple protection tubes, and level-measuring devices. Dispersion-hardened platinum has also recently been used in glassmaking technology.

In the manufacture of glass fibers and glass wool, the spinnerets are made of Pt–Rh. Rock wool and slag wool are made by a centrifugal spinning process with platinum centrifuges.

Textile Technology. Nozzles made of platinum alloys such as Au70–Pt30 and Pt92–Ir8 are used for spinning viscose fibers [190].

Soldering Materials. Gold and palladium have been used in some special solders.

Nuclear Technology. In recently published research, a deuterium-saturated Pd–Ag target was claimed to catalyze a controlled deuterium–deuterium fusion reaction.

25.9.3 Heterogeneous Catalysts

[191–196]

All platinum group metals have strong catalytic activity, especially for hydrogenation reactions. These heterogeneous catalysts, including supported catalysts, are of major importance in chemical technology. As of 1992, ca. 200 t of platinum group metals are in use worldwide in the form of supported catalysts. Next in order of importance are bulk metallic catalysts in the form of wire gauzes, highly dispersed carrier-free metals, and oxides. Platinum and palladium are much more important than rhodium, ruthenium, iridium, and osmium. Often, two or more platinum group metals are combined (Table 25.6).

Supported Catalysts. The properties of supported catalysts are very dependent on the interaction between noble-metal catalysts and support material. Classical support materials were asbestos and pumice stone. Important support materials today include aluminum oxides, activated carbon, silicates (e.g., zeolites), and silicic acid.

Powdered support materials are used as suspension catalysts; porous pressed shapes or pellets are used for fixed-bed catalyst.

The largest demand for platinum catalysts comes from the petroleum industry [197, 198]. These are used in reforming high-boiling fractions from the distillation of crude oil at atmospheric pressure. The most important reactions are the dehydrogenation of alkylcyclohexanes, the isomerization and dehydrogenation of alkylcyclopentanes, and the dehydrogenation and cyclization of alkanes, all of which form aromatics, as well as hydrogenative cleavage of alkanes and naphthenes, and dealkylation of alkylaromatics. The resulting product mixtures are gasolines with high antiknock properties. The most important catalysts are Pt– γ -Al₂O₃.

Table 25.6: Modification of the catalytic activity of the platinum group metals by additional metals.

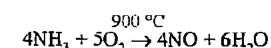
Base metal	Additional metal	Reaction	Effect of additive
Pt	5–20% Rh	ammonia oxidation	increased NO yield lower Pt losses
Pt	Ge, Sn, In, Ga	dehydration and hydrocracking of alkanes	longer catalyst life due to fewer deposits
Pt	Sn + Re	dehydrocyclization and aromatization of alkanes	increased catalyst activity and stability
Pt	Pb, Cu	dehydrocyclization and aromatization of alkanes	effective aromatization
Pt, Pd, Ir	Au	oxidative dehydrogenation of alkanes, <i>n</i> -butene to butadiene	better selectivity
Ru, Os	Cu(Ag)	reforming	less hydrogenation relative to isomerization
Ir	Au(Ag, Cu)	hydroforming of paraffins and cycloalkanes	high yield of aromatics above 500 °C
Pd	Sn, Zn, Pb	selective hydrogenation of alkynes to alkenes	
Pd	Ni, Rh, Ag	alkane dehydrogenation and dehydrocyclization	hinders coking

Combinations of metals such as platinum–rhenium, platinum–iridium, platinum–palladium, and platinum–germanium are also used.

Another use for PGM catalysts in the petroleum industry is in hydrotreating processes. In addition to base-metal catalysts, platinum and palladium catalysts supported on γ -Al₂O₃ or aluminum silicates (zeolites) are used. In the pharmaceutical industry, palladium active carbon hydrogenation catalysts are widely used, mainly with a palladium content of 5%. Other catalysts used include rhodium–active carbon, platinum–active carbon, and palladium–platinum–active carbon.

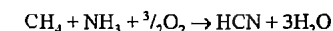
Solid Metal Catalysts [199–202]. Platinum–rhodium gauzes are used as catalysts for the large-scale oxidation of ammonia to nitric oxide (Ostwald and Brauer process) in the manufacture of nitric acid.

The oxidation reaction



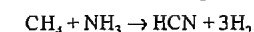
takes place in reactors in which many fine-mesh gauzes are stacked above one another. The rate of loss of noble metal varies between 0.2 and 2.0 g per tonne of nitrogen reacted, depending on process conditions. If a rhodium–platinum alloy is used, the rate of loss of noble metal is reduced; powdering of the gauze takes place more slowly, and its lifetime is increased.

In the production of hydrogen cyanide (Andrussow process),



platinum–rhodium or platinum–iridium gauzes are used as catalysts.

The Degussa process



uses α -Al₂O₃ tubes coated on the inside with platinum film.

Finely Divided Metallic Catalysts. The so-called platinum metal blacks are well-established catalysts for hydrogenation, dehydrogenation, and oxidation, mainly on a laboratory scale. Their high degree of dispersion is shown by their large specific surface (> 100 m²/g). These catalysts are very active even at low temperature, so reactions with labile molecules are possible. In the production of hydrogen peroxide by the anthraquinone process, palladium black is used to a considerable extent in suspension in a nonaqueous medium or as a fixed bed to catalyze the reduction of alkylanthraquinone to the corresponding hydroquinone. The platinum oxide PtO·2H₂O (Adam's catalyst) is used widely as an unsupported catalyst in the pharmaceutical industry for the hydrogenation of alkenes and carbonyl groups. Nishimura's catalyst contains rhodium oxide in addition to platinum oxide. Platinum on electrically conducting carbon black is used as a catalyst in fuel cells.

Catalyst Poisoning and Regeneration [203]. All catalysts are liable to be deactivated (poisoned) by chemical, mechanical, and thermal means. Typical contact poisons for platinum group metals include sulfur, phosphorus, carbon monoxide, hydrogen cyanide, lead, and mercury.

Reactivation is often possible, especially with supported catalysts, by heating, steam treatment, reaction with oxidizing or reducing gases, or washing.

25.9.4 Homogeneous Catalysts

[29, 85, 204–206]

Homogeneous catalysis by platinum group metals, especially rhodium, has made a major impact in industrial chemistry. Important characteristics of these catalysts include high activity and, therefore, low concentration; high selectivity leading to absence of side products; and mild reaction conditions, enabling the use of low temperature and pressure and facilitating the control of reaction conditions. These factors are of great importance and allow expensive PGMs to be used economically. The discovery of chloro-*tris*-(triphenylphosphine)rhodium(I), $[\text{RhCl}(\text{P}(\text{C}_6\text{H}_5)_3)_3]$, a highly effective hydrogenation catalyst, by WILKINSON [207] opened a new chapter in homogeneous catalysis and in the complex chemistry of rhodium. Today, a number of modified complexes of this and similar types are known.

Homogeneous catalysis by rhodium complexes in oxo synthesis (hydroformylation) has attained great importance and made possible the synthesis of industrially important aldehydes from alkenes. This process was formerly carried out with homogeneous cobalt catalysts. Initially, $[\text{RhCl}(\text{P}(\text{C}_6\text{H}_5)_3)_3]$ was used as catalyst; subsequently, halogen-free catalysts were introduced. Some of these can be used at room temperature, whereas cobalt complexes require temperatures up to 200 °C, necessitating the use of high-pressure reactors. Generally, the catalytically active compound is not manufactured. Instead, other compounds are used as precursors from which the

actual catalyst is formed during the reaction. These include $[\text{Rh}(\text{CO})_2 \text{ acac}]$, $[\text{Rh}\{\text{P}(\text{C}_6\text{H}_5)_3\}(\text{CO}) \text{ acac}]$, and $[\text{Rh}(\text{CO})_2 \text{ Cl}]_2$, which form the catalyst $[\text{RhH}(\text{CO})\{\text{P}(\text{C}_6\text{H}_5)_3\}_3]$.

The Monsanto acetic acid process uses Rh(III) iodide as the catalyst precursor.

In silicone chemistry, hydrosilylation is carried out with homogeneous PGM catalysts [208].

Enantiomerically pure products are prepared by stereospecific hydrogenation with chiral noble-metal complexes as homogeneous catalysts [208]. The substrates are usually steroids or amino acid derivatives. Asymmetrically catalyzed reactions are used mainly in the production of pharmaceuticals. For example, asymmetric hydrogenation is used in the synthesis of L-dopa, a drug for the treatment of Parkinson's disease. These catalysts are modified Wilkinson catalysts in which PPh_3 is replaced by an optically active diphosphine ligand. The catalyst was previously formed in situ by reacting the readily obtainable $\text{Rh}(\text{diene})\text{Cl}_2$ complex with the required chiral phosphine. Cationic complexes with a chiral phosphine are also used. These have extremely high activity.

Osmium(VIII) oxide and ruthenium(VIII) oxide have long been used as homogeneous catalysts for hydroxylation, oxidation, and epoxidation. Palladium(II) chloride and tetrachloropalladic(II) acid are important homogeneous catalysts used in the large-scale oxidation of ethylene to acetaldehyde in the Wacker process.

25.9.5 Automobile Exhaust Catalysts

[31, 209–212]

The use of supported noble-metal catalysts for the treatment of exhaust gases from automobiles has been introduced in recent years in all industrialized countries. Regulations controlling the quality of exhaust gases can be complied with only by the use of such catalysts. In particular, carbon monoxide (CO), hydrocarbons (CH_x), and nitrogen oxides (NO_x) must be reduced to one-tenth of their

initial concentrations. Combinations of metals that have a catalytic action on exhaust gases include Pt–Rh, Pt–Pd, and Pt–Pd–Rh.

Combinations that can reduce all three harmful components are known as three-way catalysts. The three-way technique also includes control of the air–fuel ratio by means of a λ -probe (see Section 25.9.6). Exhaust-gas catalysts have their optimum activity only if the engine and the catalytic unit are matched. Two principal types are used. In one of these, the exhaust gas passes through catalyst pellets, and in the other “monolithic” or ceramic type, the gases pass through numerous parallel channels through extruded bodies that are coated with a catalytically active layer of PGM– $\gamma\text{-Al}_2\text{O}_3$. The ceramic support material is cordierite. Recently, sheet steel labyrinths have been used with improved heat-transfer characteristics, especially on starting; their main advantage is the lower pressure drop across the catalyst. An improvement in exhaust-gas specifications is currently under consideration, so exhaust-gas catalyst systems will have an even more important role to play in the future.

Each catalytic converter contains ca. 2 g Pt–Rh or Pt–Pd (i.e., 0.05% of the pellets, or 0.5% if the support consists of cordierite). The demand for these materials worldwide amounts to more than one-third of the annual production of platinum and more than four-fifths of the annual production of rhodium. The PGM catalysts are at present the only practical materials for this purpose.

The required lifetime of an exhaust-gas catalyst, as laid down by the widely accepted U.S. standard, corresponds to 80 000 km.

Three-way catalysts, used in conjunction with λ -probes, are also employed in thermal power stations. Here, lifetimes are considerably longer because of the steady loads and the absence of mechanical disturbance.

Catalysts similar to those used for the treatment of automobile exhaust gases are also used to treat industrial waste gases contaminated with harmful organic materials.

25.9.6 Sensors

[29, 85, 158]

Platinum metals and their alloys are widely used in thermocouples (Table 25.7), because these have longer lifetimes than those made of base metals and can be used at higher temperature. The most important thermocouple element pair used in industry is Pt90/Rh10–Pt (wire thickness: ca. 0.5 mm), which gives accurate temperature measurements over the range 800–1600 °C.

Table 25.7: Commonly used noble metal thermocouple pairs.

Positive leg	Negative leg	Operating temperature
Cu	Au99.4 Co0.6	–240 to 0 °C
Pt90 Ir10	Au60 Pd40	0 to 700 °C
Pt90 Rh10	Pt	850 to 1600 °C
Pt70 Rh30	Pt94 Rh6	1000 to 2800 °C
Rh40 Ir60	Ir	1000 to 2200 °C

Resistance Thermometry. The electrical resistance of metals increases with increasing temperature. Because of this, pure, chemically stable metals that undergo no aging over a wide temperature range can be used to construct temperature-sensitive devices that are stable for long periods. Platinum is very suitable for this application. The changes in its resistance over certain temperature ranges (e.g., between –200 and +850 °C) have been specified in standards.

Platinum wire-wound resistors, whose resistance is determined by the length and cross section of the wire, have been almost completely displaced by so-called thin-film resistors, manufactured by thin-film technology. A film of platinum ca. 1 μm thick is deposited on an insulating ceramic substrate by vacuum deposition or cathodic sputtering. A meandering resistance path is formed in the film of noble metal by cutting with a laser beam or by ionic etching through a masking coating produced by photolithography. The thickness of the film and the total path length determine the resistance at 0 °C. Path widths are in the region of 20 μm . The connecting leads, which are joined to the thin film by special bonding processes, also consist of noble metals or their compounds. Modern resistance thermometers

based on thin-film technology have the advantage over wire-wound resistance thermometers because they can be manufactured by highly automated methods and require only small amounts of PGM (< 1 mg per device).

Resistance thermometers are used today in a wide range of technologies, from household appliances to chemical equipment, and from road transportation to air and space travel.

Gas Sensors (Lambda Probes). Oxygen sensors utilize the high electrical conductivity imparted to solid electrolytes (e.g., ZrO_2) by the presence of oxygen ions, compared to their normal conductivity due to electrons. If this ionic conductor acts as a separator between two gas spaces, and if it is provided with platinum electrodes on both sides, a difference in the oxygen partial pressure causes a so-called Nernst emf to be produced between the electrodes. These probes are used to control the fuel-air mixture in conjunction with automobile exhaust-gas catalysts in Otto engines.

Noble-metal catalysts are also used in sensors for detecting combustible gases in air or explosive gas mixtures. Heat evolution is normally detected by sensors known as Pellistors, which consist of platinum wire in a small sphere of Al_2O_3 (diameter: 1.5 mm). The sphere is saturated with a noble-metal catalyst. If a chemical reaction takes place on the catalyst, a temperature increase occurs that can be measured by the change in resistance of the platinum wire. These heat evolution sensors are used in explosion protection equipment.

25.9.7 Electrical Technology

[181, 213]

In low-current technology, electrical contacts of gold, silver, palladium, rhodium, platinum, and their alloys are used. Contacts made of bulk noble metals are becoming less common than those coated by electrolytic and mechanical processes.

For a long time, large numbers of so-called reed contacts have been used in telephone relays. These are Ag-Pd-, rhodium-, or ruthenium-coated contacts operating under a

protective gas. Such contacts must be resistant to sparking, corrosion, and erosion, and must not become welded together. During a lifetime of 30 years, they must carry out millions of switching operations without damage. Furthermore, their contact resistance must be low, and their nominal resistance must be constant.

Platinum sealing wires are also now used only for specialty light bulbs and transmitter tubes. Heating elements made of platinum metals or their compounds are used in resistance-heated furnaces above 1200 °C. Windings of Pt70-Rh30 can be used up to 1500 °C, and ribbon windings of rhodium up to 1800 °C. Furnace elements made of platinum metals can be used without a protective gas. Platinum, rhodium, iridium, and ruthenium are used as susceptor materials in induction furnaces.

Platinum-iridium alloys are useful for spark plug contacts for high-power aeroplane and automobile engines.

25.9.8 Electronics [29, 85, 158]

In modern electronics, noble-metal pastes, including those of the platinum group metals and their alloys, are key products in the production of many important components. They are used in active components such as diodes, transistors, integrated circuits, thick-film hybrid circuits, and semiconductor memories, and are also used in passive electronic components such as very small multilayer capacitors, thick-film resistors, and conductors. The metallization process is generally carried out with Ag-Pd paste, and occasionally with Ag-Pt paste. Printed resistors use RuO_2 as the conducting pigment.

The metal powder pastes can be used in the form of drying preparations, baking preparations, or soldering pastes, depending on the application. All types contain an organic binder that melts during baking. The baking preparations usually also contain powdered glass as an adhesive. The pastes are generally applied to the substrate by screen printing, although soldering pastes have recently been applied via a stencil. The edge regions of

multilayer capacitors are prepared for metallization by a dipping process.

The powders used in the pastes are generally produced by reduction. Bimetallic powders are produced by mechanical mixing to give composite blends or by coprecipitation. Their specific surface area is usually ca. 1 m^2/g . The particle shape can be spheroidal, microcrystalline, or laminar. The substrate is usually $\alpha\text{-Al}_2\text{O}_3$.

Thin-film technology is used in microelectronics (see Section 25.9.9), although noble metals are not used to the same extent here as in thick-film technology.

25.9.9 Coatings [29, 30, 86, 158]

Coatings of platinum metals may be applied to a substrate by various methods.

25.9.9.1 Coatings Produced by Aqueous Electrolysis [214]

Platinum. Lustrous thin films for decorative purposes are deposited from an electrolyte obtained by reacting potassium tetranitroplatinate(II), $\text{K}_2[\text{Pt}(\text{NO}_2)_4]$, with sulfuric acid. The active complex is $\text{H}_2[\text{Pt}(\text{NO}_2)_2\text{SO}_4]$. This is more stable than other platinum plating baths.

Relatively thick coatings can be deposited from alkaline solutions of sodium hexahydroxyplatinate(IV), $\text{Na}_2[\text{Pt}(\text{OH})_6]$, although this electrolyte is unstable.

Platinum(II) diamminedinitrite, $[\text{Pt}(\text{NH}_3)_2(\text{NO}_2)_2]$, was formerly very widely used and today along with $\text{Na}_2[\text{Pt}(\text{OH})_6]$, is used for coating titanium by aqueous electrolysis. These coatings are of lower quality than those produced by high-temperature electrolysis. Also, extensive pretreatment of the substrate metal is necessary, mainly to prevent cathodic absorption of hydrogen.

Rhodium [160]. Rhodium coatings are superior to all other PGM coatings, having better hardness, mechanical and chemical stability, and reflexivity. For these reasons, rhodium is more widely used than the other platinum group metals.

Electrolytes consisting of rhodium sulfate (10–20 g/L Rh) in sulfuric acid can give comparatively thick coatings (10–12 μm). Crack formation can be countered by addition of sulfite, selenic acid, magnesium sulfate, or magnesium sulfamate. These baths are used to produce rhodium coatings for heavy-duty slip ring contacts and optical reflectors, and were at one time used for reed contacts in telephone technology.

Rhodium sulfate or phosphate baths containing 2 g/L of rhodium are used for decorative purposes and give strongly reflective thin films (0.1–0.5 μm) that prevent silver or white gold from tarnishing. They are also used for plating eyeglass frames.

Palladium [159]. Palladium can sometimes replace gold in coatings for electronics. The plating batches contain palladium(II) diamminedinitrite, $[\text{Pd}(\text{NH}_3)_2(\text{NO}_2)_2]$ (palladium P-salt), with additions of sodium and ammonium nitrates, or sulfamates.

Successful results have recently been obtained with plating baths based on organopalladium complexes. Concentrated hydrochloric acid plating baths with dissolving palladium anodes are rarely used now.

Ruthenium is deposited electrolytically from solutions of ruthenium complexes with a bridging nitrido ligand, for example, nitridooctachlorodiaquodiruthenate(IV), $\text{H}_2\text{O} \cdot [\text{H}_2\text{O}(\text{Cl}_4\text{Ru})-\text{N}-(\text{RuCl}_4)\text{H}_2\text{O}]^{3-}$, the basis of the so-called RuNC baths. The corresponding complex with hydroxo ligands instead of chloro ligands can also be used.

Platinum baths based on ruthenium nitrosylsulfamate are also used.

High-Temperature Electrolysis (HTE) [29, 85, 215–217]. Platinum group metals can be deposited electrolytically from cyanide-containing melts in which a soluble anode provides the noble metal that is deposited on the cathode. The metal most widely used in this process is platinum, although iridium is sometimes used.

The molten salt, an eutectic mixture of KCN and NaCN, is maintained at 500–600 °C

in an electrically heated crucible. The platinum is deposited from the melt onto the substrate, which forms the cathode in the electric circuit.

Process parameters are as follows:

Electrolyte	$K_2[Pt(CN)_4]$ in KCN-NaCN
Operating temperature	500–600 °C
Deposition voltage	0.1–2 V
Cathodic current density	1–5 A/m ²
Cathodic current yield	> 60%
Mean rate of deposition	10–20 µm/h

Oxidation of the melt and of the metal is prevented by a protective atmosphere of high-purity argon. Suitable substrate materials for HTE platinum deposition include refractory metals such as titanium, niobium, tantalum, molybdenum, tungsten, zirconium; steels; and other metals such as copper. They must generally be pretreated by sandblasting and degreasing.

Advantages of HTE platinum coatings, compared with those produced by aqueous electrolysis, include low porosity; a wide range of film thicknesses (1–400 µm), excellent adhesion; good resistance to mechanical impact, thermal shock, and sliding wear; high thermal conductivity; and high ductility.

The largest use is in producing anodes for cathodic corrosion protection [218] (often in the form of expanded metal) or insoluble anodes for electrolytic technology. Platinum-coated molybdenum wire is used in the construction of thermionic tubes and for fusion with glass. High-temperature electrolysis is also used for electroforming.

25.9.9.2 Coatings Produced by Chemical Reaction [30]

Surface coatings of platinum metals can be deposited onto metallic or nonmetallic substrates by chemical reduction or thermal decomposition of PGM compounds.

Platinum acetylacetonate is used for platinization of titanium. The titanium articles are painted with a solution of this compound, dried, and heated. Repeated application is necessary. The process is not widely used due to allergic reaction and the low quality of the coatings.

Platinum coatings are produced on ceramic tubes by saturating them with hexachloroplatinic acid and heating to 600–800 °C [219]. Such tubes are used as catalysts for the synthesis of hydrogen cyanide.

Platinum metal resins are used as ceramic colorants [220, 221]. These can be employed to produce conductive platinum coatings on ceramic substrates, onto which further layers can be deposited electrolytically. Platinum coatings are also used for decorative purposes.

Hexachlororuthenic(III) acid, $H_3[RuCl_6]$, dissolved in alcohol, is painted onto the substrate, dried, and heated strongly in air to produce an extremely adherent coating of RuO_2 [222, 223]. Titanium sheet, coated in this way, has outstanding electrochemical properties and is being used in chloralkali electrolysis as dimensionally stable anodes. The RuO_2 coatings are also used in the production of circuit boards by screen printing.

25.9.9.3 Coatings Produced by Physical Methods [85]

Platinum can be deposited as a thin film on substrates by evaporating the metal in a high vacuum. Modern thin-film technology is based mainly on the generation of fine particles from a cathode (cathodic sputtering). Due to the high kinetic energy of these metal particles, extremely good adhesion is obtained. In the case of platinum group metals, sputtering targets are used only for microelectronics. Ion plating is also used to produce high-quality coatings.

Roll-bonded PGM coatings are no longer important.

25.9.10 Dental Materials [85]

Platinum and palladium have major importance in dentistry.

Up to ca. 1900, dental prostheses such as gold fillings, crowns, and bridges were made mainly of alloys with the same composition as those used in coinage and jewelry, and later of

22-carat gold (83.3%). Platinum was used only to make fixing pins.

Important quality requirements such as oral stability, biological compatibility, color, strength, and good functional properties are achieved only by modern dental alloys. These complex alloys, unlike the earlier gold-containing ones, have a very fine-grained, homogeneous crystalline structure, giving much better corrosion resistance. Also, their hardness is controllable over a wide range and can be adapted to particular requirements.

Standard Alloys. Modern alloys for making dentures or prostheses have compositions mainly in the range 65–85% gold, 1–10% platinum, 1–4% palladium, 10–15% silver, 0–10% copper, and 0–1% zinc.

In low-gold alloys, which are cheaper, the gold is replaced partially by silver or palladium. These alloys contain 40–60% gold, 0–2% platinum, 3–10% palladium, 23–35% silver, 0–12% copper, and 0–5% tin, indium, and zinc.

Silver-base alloys have very low gold content. Adequate oral stability can be achieved by including at least 25% platinum group metals or gold. Inexpensive alloys in this category contain at least 20–25% palladium, 0–3% gold, ca. 55–70% silver, and copper and zinc, and are therefore no longer yellow, but white.

Alloys with ceramic veneers are used in the production of ceramic-metal systems. This technique, in which a dental ceramic is fused onto a metal casting, has been used in dentistry for ca. 25 years. A durable and strong bond can then be produced between the tooth stump and the porcelain-metal system. The advantages of this are a natural appearance combined with compatibility with human tissue. To obtain a good bond between the metal and the ceramic, alloys must contain components that form so-called adhesive oxides when the ceramic is fired. Because firing is carried out at ca. 980 °C, the alloys must have a minimum solidus temperature of ca. 1050 °C.

Alloys with a high gold content have compositions in the range 75–90% gold, 5–10%

platinum, 1–10% palladium, 0–3% silver, with small additions of iron, indium, tin, zinc, and other elements.

Attempts have been made to reduce the cost of these alloys by replacing gold by palladium and silver. Typical Au-Pd-Ag alloys have compositions in the following range: 42–62% gold, 25–43% palladium, 5–20% silver, and 4–10% base metals such as copper, tin, indium, gallium, and zinc. Typical silver-free Au-Pd alloys have the following composition: 45–60% gold, 32–40% palladium, and 0–14% of the base metals tin, indium, zinc, or gallium.

Palladium-base dental alloys were introduced in Germany in the early 1980s. These were developed to reduce cost. Silver-free and silver-containing alloys are available. Both contain very small amounts, if any, of gold and platinum. The range of compositions for the silver-containing palladium-based alloys is 53–61% palladium, 28–38% silver, 0–12% tin, indium, zinc, and gallium. For the silver-free palladium-based alloys, the composition range is 73–88% palladium, 0–2% gold, and 12–26% of the base metals copper, cobalt, tin, indium, and gallium.

25.10 Economic Aspects

See references [5, 10, 23, 29, 44, 46, 55–61, 73, 211, 224–231].

25.10.1 Supply

The platinum group metals as a whole are of moderate importance in the world metal market as measured by the total value of the raw product obtained from the ore. This total value fluctuates according to prices, generally equaling the figure for silver, and is ca. 20% of the value of gold production. The latter amounted to ca. 32×10^6 DM/a, and is the third most important metal in terms of value after iron and aluminum.

The primary production of platinum, palladium, and rhodium for various producing countries is listed in Table 25.8. Production figures for the former Soviet Union have

never been published: the figures indicate sales to the West.

In addition to PGMs obtained from ores, a considerable amount of secondary material exists. The extent of this is very variable and fluctuates with time.

Averaged over all the PGMs, it amounts at present to ca. 20% of primary production, with the greatest emphasis on platinum and especially palladium. The present effort directed toward recovery from spent automobile catalysts will considerably increase the proportional secondary production of platinum and rhodium.

A high proportion of the PGMs is recycled by the users or, in the case of contract suppliers of semifinished products (e.g., catalysts),

by the producers. These materials do not appear on the market either on the supply or on the demand side, so supply figures essentially reflect only mined products and sales from the former Soviet Union.

25.10.2 Demand

The demands of individual countries or regions, excluding the former Eastern bloc countries, for platinum, palladium, and rhodium in 1990 are indicated in Figure 25.14. This shows that, in value terms, rhodium has moved into first place for the first time (see Table 25.9 for prices).

Figure 25.15 depicts how various PGMs are divided among areas of use.

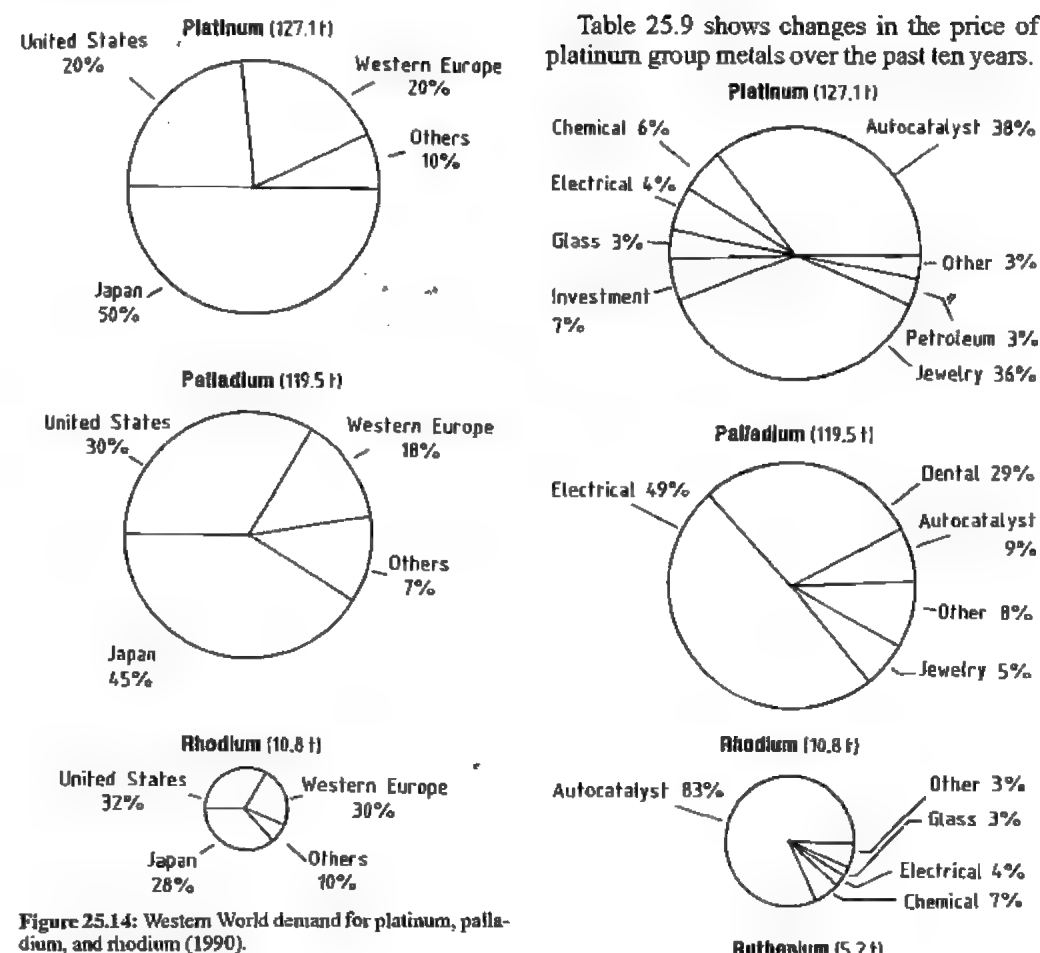
Table 25.8: Platinum, palladium, and rhodium output by regions (10³ troy oz).

	1980	1981	1982	1983	1984	1985	1986	1987	1988	1989	1990
Platinum											
South Africa	2320	1800	1960	2070	2280	2340	2350	2520	2580	2590	2780
Soviet Union (sales)	340	370	380	290	250	230	290	400	440	550	700
Canada	130	130	120	80	150	150	150	140	145	150	185*
Others	30	30	30	40	40	40	40	40	95*	85*	65
Total	2820	2330	2490	2480	2720	2760	2830	3100	3260	3375	3730
Total, t	80	73	77	77	85	86	88	96	101	105	116
Palladium											
South Africa	1400				1690	1440	1600	1790	1770	1650	1850
Soviet Union (sales)	870				950	1010	1040	1090	1105	1135	1235
Canada	200				190	190	190	190	170	205	370*
Others	60				90	90	90	90	270*	215	70
Total	2340				2920	2730	2920	3160	3315	3205	3525
Total, t	73				91	85	91	98	103	100	110
Rhodium											
South Africa					165	175	195	195	185	185	205
Soviet Union (sales)					45	85	100	100	130	130	155
Canada					15	15	18	20	15	15	17
Others					0	0	0	0	0	0	0
Total					200	225	275	313	315	330	377
Total, t					6	7	9	10	10	12	12

* Including United States.

Table 25.9: Prices of the platinum group metals and gold (rounded, DM/g).

	1st July 1983	1st Sept. 1984	15th August 1985	1st May 1986	1st Oct. 1988	1st June 1990	15th June 1991
Osmium	14	54	98	51	40	34	31
Platinum	37	34	29	28	30	28	22
Palladium	13	15	11	7	8	7	5
Rhodium	30	77	83	78	70	143	285
Iridium	31	51	42	28	20	18	16
Ruthenium	6	17	9	5	5	4	4
Gold	34	33	31	24	25	20	21



25.10.3 Prices

Variations in the price of platinum group metals mostly tend to be linked to the price of gold. However, the demand for platinum group metals sometimes changes rapidly, even suddenly, usually following technical innovations, and therefore extremely rapid price changes are not uncommon. This is especially true of metals other than platinum, because the availability of a given metal cannot be increased by increasing the production of that metal alone. The demand for platinum, the most abundant platinum group metal, is the most important factor in deciding whether to increase the capacity of a mine.

25.10.4 Producers

For a long time, the largest producer of platinum in South Africa and the world has been Rustenburg Platinum Holdings (RPH), which was founded in 1931. Its capacity in

1992 was 46.4 t (1.5×10^6 troy ounces). Until 1972, only the first stages of the production of a 50–70% PGM concentrate were carried out in South Africa, while the production of pure metals was carried out by Johnson Matthey & Co., London, in their refinery in Royston, England. In 1972, Rustenburg and Johnson Matthey founded the joint subsidiary company Matthey Rustenburg Refiners, which since that time has converted all the concentrate produced in Rustenburg to pure metals. In 1989 the new SAREF refinery of RPH began operation in Bophuthatswana and is now the only Refinery in the RPH group.

In 1969, Impala Platinum became a new producer of platinum. From the beginning, this company concentrated on the complete process of production of pure metal in South Africa. The production capacity is ca. 32 t/a.

Another newcomer among South African platinum producers is Western Platinum, a company managed jointly by Lonrho and the Canadian company Falconbridge, and almost completely owned by Lonrho, which took over Falconbridge in 1987. The production capacity, which started at 85 000 troy ounces (2.7 t) of PGMs per year, is now estimated to have increased to 500 000 troy ounces (15 t).

More recently, Gold Fields South Africa (located mainly at the head office of the Anglo-American Corp. of South Africa) has become a major PGM producer, with a planned annual capacity of 10.6 t PGM.

Many small firms, mostly in Southern Africa, extract PGM more or less independently, sometimes carrying out only part of the process. In the meantime, most of these, such as Anglo-Transvaal Consolidated Investment (Anglovaal), and their subsidiaries Atok Platinum Mines, Messina, and Lebowa Platinum have been taken over by the major producers. The Barplats Crocodile River Mine (formerly Lefkochrysos) was closed down soon after being taken over by Impala in 1991 because it was not profitable.

Since 19827 the Stillwater Mining Company in Stillwater (United States), the most recent producer, has established 19 production plants, with an annual capacity estimated at

50 000 troy ounces (1.6 t) of platinum, and ca. 180 000 troy ounces (6 t) of palladium.

Canadian PGM-bearing nickel ores have been worked since 18907 mainly by Mond Nickel Co. (from 1961) and International Nickel Co. (Mond) Ltd. (INCO), London, later in association with INCO (Canada). Since 1925, platinum group metals have been produced in the refinery in Acton, London.

Another important producer of platinum is Falconbridge Nickel Mines, Toronto, which formerly owned a refinery in Kristiansund, Norway, although this produces only platinum and palladium as pure metals.

No reliable information is available about the capacity of Russian platinum production, which is mainly a by-product of nickel production, with the main production center in Norilsk and smaller production centers in the Urals.

25.10.5 Commercial Aspects

The more important PGM producers sell their product through agents (i.e., not via the commodity exchange). The agent for Rustenburg material is Johnson Matthey VCC, London. Impala uses Ayrton Metals Ltd., London, and INCO uses Engelhard, New York. The other producers sell the PGMs themselves.

For platinum, and to a limited extent other PGMs, so-called producer prices have existed alongside free market prices for large industrial consumers for some decades. These prices are established by contract and are normally well below those of the free market. The main aim was to maintain a cautious pricing policy to discourage any active search for substitute materials. Around 1980, the largest South African PGM producer, Rustenburg Platinum Mines, abandoned this pricing policy, which had been in force for a long time. Its selling agents now publish daily prices that are closely linked to the market.

Since 1975, the so-called London free market price for platinum is calculated and published twice daily. Since 1976, a London palladium quotation has also been available. Both of these were only price indications, not

to be compared with the fixed quotations for gold and silver. The London Platinum and Palladium Market has since been established and publishes fixed quotations twice daily.

Platinum and palladium are also traded on the New York Mercantile exchange; platinum is also traded on the TOCM in Tokyo.

Trading in platinum on the New York exchange is in the form of contracts for units of 50 troy ounces. The purity of platinum supplied in fulfillment of such a contract must be at least 99.9%, and the platinum must originate from a producer or assayer registered with the exchange. For palladium, the contract amount is 100 troy ounces, and the purity must be 99.9%.

Spot transactions (immediate delivery and payment) are guided by the London quotation and the New York exchange quotation.

25.11 Health and Safety

25.11.1 Toxicology [35, 36]

The physiological effects of platinum group metals on the human body have been extensively investigated (Figure 25.16), particularly due to the use of PGMs in automobile catalytic converters, which leads to widespread exposure of the general public.

Platinum Allergy [232, 233]. Contact with platinum compounds, mainly of the hexachloroplatinate type, has long been known to lead to strong allergic reactions.

Approximately half of the people exposed experience symptoms. These range from irritation of the skin to rhinitis, and sometimes severe asthma attacks. Allergic reaction seldom occurs immediately. It usually becomes noticeable after weeks, months or, sometimes years. People suffering from other allergies are more rapidly and seriously affected, and existence of a platinum allergy often results in increased sensitivity toward other allergens. Once sensitivity has been acquired, it can remain for life. In general, if a platinum allergy is present, the only effective countermeasure is a change of workplace. Sensitivity can be

detected in advance by allergen tests (smearing the skin with a solution of hexachloroplatinate). Protective measures taken at the workplace include the installation of effective waste-gas extraction systems, and hermetic sealing of all containers and apparatus. All processes that produce dust or aerosols must be contained. This applies to every operation involving hot solutions of hexachloroplatinic(IV) acid or its salts, pyrolytic decomposition reactions, and pouring of fine crystals and solutions.

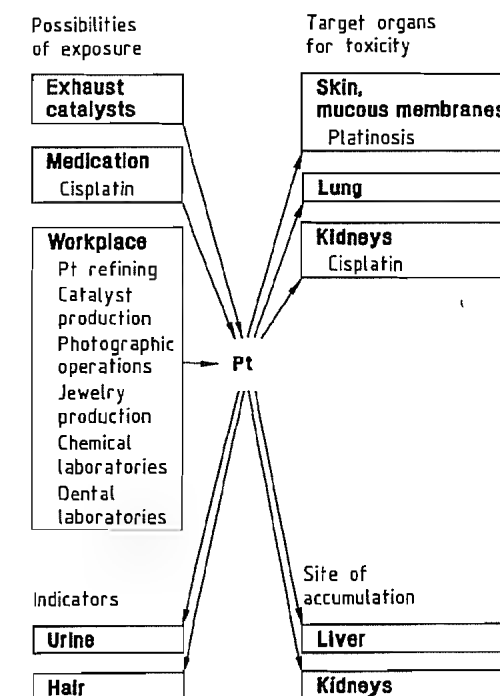


Figure 25.16: Schematic representation of the toxic effects of platinum.

Other platinum compounds have not been found to have definite allergenic properties, probably because they are not handled to a comparable extent. Metallic platinum is regarded as harmless, even in finely divided form. Compounds of other elements of the platinum group do not cause health problems of this type.

Toxicity. Soluble platinum compounds cause symptoms similar to those produced by other

heavy metals when taken orally. The main symptoms are violent vomiting and impairment of kidney function. Acute toxic symptoms of this kind, which often severely distress the patient, are frequently observed during the treatment of tumors by *cis* platinum. Here, the maximum dose rate is ca. 120 mg of platinum per square meter body surface per day [234].

Osmium(VIII) oxide, which is very volatile, is very toxic, has a strong irritant effect on the mucous membranes, and causes headaches [235]. Ruthenium(VIII) oxide produces similar symptoms. When OsO_4 is present in the atmosphere, it affects the mucous membrane of the eye, producing a characteristic symptom (i.e., the appearance of haloes around lights) caused by cloudiness of the cornea. Considerable deterioration of vision can occur, which may lead to serious hazard when driving at night.

The MAK values for platinum compounds are 0.002 mg/m^3 (calculated as Pt); for rhodium compounds: 0.001 mg/m^3 (calculated as Rh); and for OsO_4 : 0.002 mg/m^3 (0.0002 ppm).

Automobile Exhaust Catalysts [236, 237]. When automobile exhaust catalysts are used, some emission of platinum group metals, especially platinum, must take place. Rhodium and palladium can also be emitted. The noble metals present are 90% in the elemental state, 20% of which is respirable. Studies are yielding consistent results and give no indication of a health hazard from automobile catalysts. Some published theories that conflict with this are not borne out by the facts. Undoubted health benefits can be gained by preventing the emission of nitrogen oxides, hydrocarbons, and carbon monoxide through use of automobile exhaust catalysts.

25.11.2 Explosion Hazards [238]

Alloy Formation. The formation of some intermetallic phases is accompanied by considerable heat evolution. Violent reactions may occur between platinum or ruthenium, and

lithium, titanium, or arsenic, for example, especially when finely powdered, sometimes with explosive effect. Initiation can take place by ignition of exposed surfaces of compacted material.

Spontaneous Decomposition. Some complexes of platinum group metals, like explosives, contain both oxidizing and oxidizable groups. These include all PGM complexes containing ammonium and nitrate [e.g., $[\text{Pt}(\text{NH}_3)_4](\text{NO}_3)_2$], ammonium and nitro ligands (e.g., $(\text{NH}_4)_2[\text{Pt}(\text{NO}_2)_4]$), and mixed-ligand complexes such as $[\text{Pt}(\text{NH}_3)_2(\text{NO}_2)_2]$.

In standard BAM explosion tests, some of these compounds give higher values than the well-known explosive ammonium nitrate. They are sensitive to impact and decompose at impact energies of more than 10 J (corresponding to a 5-kg weight falling through 20 cm in the falling hammer test).

They can explode on impact or even on grinding of crystal agglomerates. These compounds should therefore be handled in the form of aqueous solutions. Some PGM-containing homogeneous catalysts may ignite as a result of friction.

Ruthenium(VIII) oxide, RuO_4 , is produced during the separation of platinum group metals and is removed by distillation. It can undergo spontaneous explosive decomposition near its boiling point or at 100°C . Quantities of several gram should only be steam distilled. Ruthenium(VIII) oxide should not be stored in either the solid or the liquid state (*mp* 25°C) owing to its explosive potential. The compound OsO_4 is much more stable than RuO_4 .

Oxidative Properties. The oxides of the platinum group metals are generally exothermic compounds. Therefore, most of them are strong oxidizing agents that can react explosively with organic substances or other reducible materials. Ruthenium(VIII) oxide is a very strong oxidizing agent. It reacts, for example, with organic materials such as filter paper, alcohol, ammonium compounds, grease for glass stoppers, or residues in dirty containers, sometimes with explosive violence.

Hydrogen Explosions. The greatest danger of explosion involving platinum group metals arises from their hydrogen content, which is often high, especially when the metals are in the form of highly dispersed powders. Hydrogen is present in the form of metallic hydrides, which are usually nonstoichiometric. Upon minor external influences (e.g., shock), free hydrogen can be released suddenly, mix with atmospheric oxygen, and lead to a violent explosion catalyzed by the noble metal. The capacity of all PGMs to absorb hydrogen is very high (Table 25.10).

Table 25.10: Binding and release of hydrogen by platinum group metals.

Element	mL H_2 bound per g metal	Stoichiometry	Resulting H_2 - O_2 mixture, L/g metal
Ru	123	$\text{RuH}_{1.1}$	3.1
Rh	24	$\text{RhH}_{0.2}$	0.6
Pd	75	$\text{PdH}_{0.7}$	1.8
Os	7.5	$\text{OsH}_{1.2}$	1.8
Ir	35	$\text{IrH}_{0.6}$	0.9
Pt	2.4	$\text{PtH}_{0.04}$	0.06

Platinum metals produced by reduction of their compounds at low temperature have a high capacity to absorb hydrogen formed as a by-product. The formation of ruthenium by reduction with sodium borohydride is especially critical. Ruthenium black is common cause of accidents. Detonation can occur on contact with water or stirring with a spatula, even with material that has been stored for a long time. Many accidents have occurred after alloying iridium, platinum, or rhodium with zinc, followed by dissolution of the zinc with acid.

Spent platinum oxide catalysts often contain hydrogen and sometimes explode on mechanical handling. Hydrogen oxygen, hydrogen chlorine, and some gas air mixtures explode immediately in the presence of noble metals without any ignition source.

Flammability. Platinum, palladium, and iridium are pyrophoric when sufficiently finely divided because oxide formation by reaction with air is strongly exothermic. Organic solvents, paper, and active carbon can ignite on contact with pyrophoric platinum metals. Great care must be taken when drying spent

noble metal carbon catalysts, especially palladium black.

Almost all organic compounds of the platinum group metals are combustible, and many can ignite spontaneously on exposure to air.

Catalytic Decomposition. Sufficiently concentrated hydrogen peroxide can decompose explosively on addition of PGM catalysts. The violence of this reaction decreases in the order $\text{Os} > \text{Pd} > \text{Pt} > \text{Ir} > \text{Au} > \text{Ag} > \text{base metals}$

Peroxides, ozonides, hydrazine, and concentrated peroxo acids such as peroxosulfuric acid explode even on contact with massive platinum.

Concentrated formic acid can also explode in the presence of noble-metal catalysts.

25.12 References

1. D. McDonald: *A History of Platinum*, J. Matthey Co., London 1960.
2. D. McDonald, L. B. Hunt: *A History of Platinum and its Allied Metals*, J. Matthey Co., London 1982.
3. *Platinum Metals Review*, vol. 1 (1957)–vol. 36 (1992), J. Matthey Co., London.
4. A. Binz: *Edelmetalle – Ihr Fluch und Segen*, W. Limpert-Verlag, Berlin 1943.
5. Fonds der Chemischen Industrie: "Edelmetalle Gewinnung, Verarbeitung, Anwendung", *Folienserie*, no. 12, Frankfurt 1989.
6. J. Falbe, M. Regitz (eds.): *Römppe Chemie Lexikon*, 9th ed., Thieme, Stuttgart 1989–1992.
7. H. Römppe: *Chemie der Metalle*, Franckh'sche Verlagshandlung, Stuttgart 1941.
8. P. Walden: *Chronologische Übersichtstabellen zur Geschichte der Chemie (Altertum bis 1950)*, Springer-Verlag, Berlin 1952.
9. S. Neufeld: *Chronologie Chemie 1800–1980*, VCH-Verlagsgesellschaft, Weinheim 1987.
10. H. Quiring: "Platinmetalle". *Die metallischen Rohstoffe*, vol 16, Enke Verlag, Stuttgart 1962.
11. J. Morin: *La platine, l'or blanc ou le huitième métal*, Paris 1758.
12. A. Galán, R. Moreno: "Platinum in Eighteenth Century – A Further Spanish Contribution to an Understanding of Its Discovery and early Metallurgy", *Platinum Met. Rev.* 36 (1992) 40–47.
13. D. McDonald: "One Hundred and Fifty Years – An Anniversary Review of Johnson Matthey's Role in the Economic History of Platinum", *Plat. Met. Rev.* 11 (1967) 18–29.
14. H. M. Severin: *Gold and Platinum Coinage of Imperial Russia from 1701–1911*, Crown and Taler Publ. Co., New York 1958.
15. H.-G. Bachmann, H. Renner: "Nineteenth Century Platinum Coins", *Platinum Met. Rev.* 28 (1984) 126–131.

16. A. L. von Erenkreuth: *Allgemeine Münzkunde und Geldgeschichte des Mittelalters und der neueren Zeit*, R. Oldenbourg, München 1971.
17. L. B. Hunt: "Dr. Hans Merensky - Centenary of the Discoverer of the Platinum Reef", *Platinum Met. Rev.* 15 (1971) 102-107.
18. J. Levin: *The Story of Mintek 1934-1984*, Council for Mineral Technology (Mintek), Randburg 1985.
19. A. M. Edwards, M. H. Silk: *Platinum in South Africa*, Council for Mineral Technology (Mintek), Randburg 1987.
20. H. Houben: *Festschrift zum fünfzigjährigen Bestehen der Platinschmelze G. Siebert GmbH, Hanau*, Alberti's Hofbuchhandlung, Hanau 1931.
21. D. G. Cooper: *Das Periodensystem der Elemente*, Vlg. Chemie, Weinheim 1972.
22. E. Fluck, K. G. Heumann, *Periodensystem der Elemente*, IUPAC-Empfehlungen, VCH-Verlagsges., Weinheim 1985.
23. H. P. Münster, *Taschenbuch des Metallhandels*, 8th ed., Metallverlag, Berlin 1989.
24. G. H. Aylward, I. J. Findlay: *Datensammlung Chemie*, Verlag Chemie Weinheim 1975.
25. National Bureau of Standards Circulars.
26. R. W. Douglass, F. C. Holden, R. J. Jaffee: *High-Temperature Properties and Alloying Behavior of the Refractory Platinum-group Metals*, Battelle Memorial Institute, Columbus 1959.
27. E. M. Savitskii, V. P. Polyakova, M. A. Tylkina: *Palladium Alloys*, Primary Sources/Publ., New York 1968.
28. Doduco: *Datenbuch - Handbuch für Techniker und Kaufleute*, 2nd ed., Pforzheim 1977.
29. The Platinum Association: *Platinum, Production Properties and Applications, a Short Course*, Hill & Knowlton, Frankfurt 1989.
30. Ullmann, 4th ed., 18, 700 ff.
31. Kirk-Othmer, 3rd ed., 18, 230.
32. Degussa: *Platingerte - Beständigkeit und Handhabung*, Hanau 1976.
33. R. Bock: *Aufschlußmethoden der anorganischen und organischen Chemie*, Vlg. Chemie, Weinheim 1972.
34. Gmelin, 8th ed, System no. 68 (Platin), 65 (Palladium), 64 (Rhodium), 67 (Iridium), 63 (Ruthenium), 66 (Osmium).
35. F. Merian: *Metals and their Compounds in the Environment - Occurrence, Analysis, and Biological Relevance*, 2nd ed., VCH-Verlagsgesellschaft, Weinheim 1991.
36. E. Merian (ed.): *Metalle in der Umwelt*, Verlag Chemie, Weinheim 1984.
37. R. G. Schwab, "Was wissen wir über die tieferen Schichten der Erde?", *Angew. Chem.* 86 (1974) 612-624.
38. C. Bresch, *Zwischenstufe Leben*, Piper-Verlag, München 1977.
39. W. Schreiter: *Seltene Metalle*, vol. 2, Dtsch. Verlag f. Grundstoffind., Leipzig 1961.
40. H. Scheiderhöhn: *Erzlagertstätten*, Fischer Verlag, Stuttgart 1962.
41. V. Tafel: *Lehrbuch der Metallhüttenkunde*, vol. 1, Hirzel Vlg., Leipzig 1951.
42. A. Cissarz: "Verbreitung der Platinmetalle, ihre Lagerstättenkundliche Stellung und ihre Anteile an der Weltproduktion", *Erzmetall* 25 (1972) 7-16.
43. Gesellschaft Deutscher Metallhütten- und Bergleute (ed.): "Edelmetalle Exploration und Gewinnung", *Schriftreihe der GDMB*, no. 44, VCH-Verlagsgesellschaft, Weinheim 1986.
44. W. Gocht: *Handbuch der Metallmärkte-Erzvorkommen, Metallgewinnung, Metallverwendung, Preisbildung, Handelsregelungen*, 2nd ed., Springer-Verlag, Berlin 1985.
45. F. Pawlek, *Metallhüttenkunde*, Walter de Gruyter Verlag, Berlin 1983.
46. Winnacker-Küchler, 4th ed., 4, pp. 541-572.
47. R. L. Bates, J. A. Jackson (eds.): *Glossary of Geology*, 2nd ed., American Geological Institute, 1980.
48. J. R. Loebenstein: *Mineral Commodity Profiles, 1984*, Bureau of Mines, US Department of the Interior, Washington, annually.
49. V. I. Smimov (ed.): *Ore Deposits of the USSR*, vol. II, Pitman Publishing, 1977.
50. C. B. Coetzee: *Mineral Resources of the Republic of South Africa*, Department of Mines, Pretoria 1976.
51. J. Lurie: *South African Geology for Mining, Metallurgical, Hydrological and Civil Engineering*, McGraw-Hill, Johannesburg 1981.
52. W. Herzberg: "Der Bergbau Südafrikas", *Metall* 37 (1984) 407-411.
53. R. C. Hochreiter, D. C. Kennedy, W. Muir, A. I. Woods: "Platinum in South Africa", *J. S. Afr. Inst. Min. & Metall.* 85 (1985) no. 6, 165.
54. A. M. Edwards, M. H. Silk: "Platinum in South Africa", *Mintek Special Publication*, no. 12, Randburg 1987.
55. H. Renner, U. Tröbs: "Rohstoffprofil Ruthenium", *Metall* 42 (1988) 714-716.
56. H. Renner, U. Tröbs: "Rohstoffprofil Osmium", *Metall* 44 (1990) 687-690.
57. H. Renner, U. Tröbs: "Rohstoffprofil Iridium", *Metall* 40 (1986) 726-730.
58. H. Renner, U. Tröbs: "Rohstoffprofil Rhodium", *Metall* 38 (1984) 1002-1005.
59. O. Stoppinski: *Platinum Group Metals*, National Research Council, Washington 1977.
60. Hargreaves, Williamson (eds.): *The Platinum Industry. Prospects in Recovery*, Shearson/American Express, London 1984.
61. L. B. Cabril: *Platinum-Group Elements*, The Canadian Institute of Mining and Metallurgy, Ottawa 1981.
62. "Metalle aus dem Meteoritenkrater-Nickel, Kupfer, und Platin in Sudbury", *Neue Zürcher Zeitung* 1990, no. 258, Nov. 7.
63. T. P. Mohide: *Platinum Group Metals - Ontario and the World*, Ministry of Natural Resources, Ontario 1979.
64. Mintek: "The Successful Development of an Industrial Process for the Recovery of Platinum-group Metals from the UG-2 Reef", *Application Report*, no. 1, Randburg 1987.
65. Mintek: "Recovery of PGMs from the UG-2 Reef", *Research Digest*, no. 29, Randburg 1988.
66. G. Hempel: "Wozu Polarforschung?", *Erzmetall* 37 (1984) 577-584.
67. H. Renner: *Behandlung und Verwertung von verbrauchten edelmetallhaltigen Katalysatoren, Müll- und Abfallbeseitigung (Müllhandbuch)*, 2nd ed., no. 8595, E. Schmidt-Verlag, Berlin 1987.
68. W. Hasenpusch: "Aufarbeitung von Autoabgaskatalysatoren—Die oberirdische Platin-Mine", *EFCE Publ. Ser.* 10 (1989) no. 79.
69. H. Giegerich, C. Hensel: "Autokat-Recycling - ein Beitrag zur künftigen Edelmetallversorgung", *Metall* 44 (1990) 684-687.
70. G. A. Jensen: "Platinum-group Metals as a Possible By-product of Nuclear Reactions", *Precious Met. Proc. Int. Precious Met. Inst. Conf., 9th Meeting*, Allentown, PA, 1985, 235-252.
71. G. Buckow et al.: *Verwertung von Reststoffen aus einer Wiederaufbereitungsanlage*, Gesellschaft für Reaktorsicherheit (GRS), Köln 1986.
72. H. Röthemeyer: *Endlagerung radioaktiver Abfälle*, VCH-Verlagsges., Weinheim 1991.
73. R. Saager: *Metallische Rohstoffe von Antimon bis Zirkonium*, Bank Vontobel, Zürich 1984.
74. V. E. McKelvey, E. N. Cameron: *The Mineral Potential of United States 1975-2000*, University Wisconsin Press, Madison 1973.
75. D. Meadows, E. Zahn, P. Milling: *Die Grenzen des Wachstums*, 15th ed., Deutsche Verlagsanstalt, Stuttgart 1990.
76. L. Trueb: "Das Platin und seine fünf Geschwister einer Geschichte der Platinmetalle", *Neue Zürcher Zeitung* 1989, no. 298 (Dec. 21).
77. L. Trueb: "Platinmetalle - Vom Bergwerk zum Katalysator", *Neue Zürcher Zeitung* 1989 no. 194 (Jun. 14).
78. O. S. North: *Mineral Exploration, Mining and Processing Patents*, McGraw-Hill, New York, annually.
79. E. Henglein: *Lexikon Chemische Technik*, VCH-Verlagsgesellschaft, Weinheim 1988.
80. G. Agricola: *Vom Berg- und Hüttenwesen*, DTV-Verlag, München 1980.
81. W. Truthe: *Hundert Jahre Gold- und Silber-Scheidung nebst Gewinnung der Platinmetalle*, Degussa 1943, unpublished.
82. E. Jackson: *Hydrometallurgical Extraction and Refining*, Ellis Horwood, Chichester 1986.
83. E. M. Savitskii: *Handbook of Precious Metals*, Hemisphere Publishing Corp., New York 1989.
84. J. C. Mostert, P. N. Roberts: "Electric Smelting at Rustenburg Platinum Mines Ltd. of Nickel-Copper Concentrates containing Platinum Group Metals", *J. S. Afr. Inst. Min. Metall.* 73 (1973) no. 9, 290.
85. C. F. Brugman, D. G. Kerfoot: "Treatment of Nickel-Copper Matte at Western Platinum by the Sherritt Acid Leach Process", *International Nickel Conference*, Toronto, Canada, 1985.
86. Degussa: *Metall Forschung und Entwicklung im Degussa-Forschungszentrum Wolfgang*, Frankfurt 1991.
87. J. E. Hoffmann, *J. Met.* 40 (1988) no. 6, 40-44.
88. E. J. Kohlmeier, K. von Sprenger, *Z. Anorg. Chem.* 257 (1948) 199-214.
89. V. Jung, *J. Met.* 33 (1981) no. 10, 42-44.
90. Degussa, DE 2059235, 1970 (V. Jung).
91. V. Jung: "The Treatment of Automotive Exhaust Catalysts", *TMS/GDMB-Conference*, Productivity and Technology in the Metallurgical Industries, Köln, Sept. 1989.
92. D. Meredith et al., *Stahl + Eisen* 17 (1988) 796-800.
93. S. E. Stenkvist, *Steel Times*, 1985, no. 10, 480-483.
94. Iron and Steel Society, *Plasma Technology in Metallurgical Processing*, Grand Junction, CO/USA, 1987.
95. Degussa, DE 3223501, 1983 (H. Renner, K. Kleis, R. Schlodder).
96. W. C. Heræus GmbH, DE 2911193, 1979.
97. International Precious Metals Institute (ed.): *Current Publications and Proceedings of Conferences and Seminars*, Dave Schneller, Boulder 1979, pp. 92 ff.
98. F. A. Cotton, G. Wilkinson: *Advanced Inorganic Chemistry*, 4th ed., John Wiley & Sons, New York 1980, pp. 950-966.
99. F. A. Cotton, G. Wilkinson: *Anorganische Chemie*, Vlg. Chemie, Weinheim 1970.
100. G. Wilkinson, R. D. Gillard, J. A. McCleverty: *Comprehensive Coordination Chemistry*, vol. 5, Pergamon Press, Oxford 1987.
101. F. R. Hartley: *The Chemistry of Platinum and Palladium*, John Wiley & Sons, New York 1973.
102. S. E. Livingstone, in J. C. Bailar et al. (eds.): *Comprehensive Inorganic Chemistry*, vol. III, Pergamon Press, New York 1973, pp. 163-1370.
103. N. N. Greenwood, A. Eamshaw: *Chemie der Elemente*, VCH-Verlagsgesellschaft, Weinheim 1988.
104. S. Daamach, G. Cote, D. Bauer: "Separation of Platinum-group Metals in Hydrochloric media: Solvent Extraction of Palladium(II) with Dialkyl Sulfides", *IPMI* 1977, No. 22.
105. D. W. Agers, E. R. de Ment: "The Evaluation of New LIX Reagents for the Extraction of Copper and Suggestions for the Design of Commercial Mixer-Settler Plants", *The Metallurgical Society of AIME*, Paper no. A 72-82, 1972.
106. Matthey Rustenburg Ref., GB 2013644, 1978/1979 (K. J. Shanton, R. A. Grant).
107. Matthey Rustenburg Ref., DE-OS 2459099, 1973/1975 (J. B. Payne).
108. L. Manziak (ed.): "Precious Metals Recovery and Refining", *Proceedings of the Precious Metals Recovery and Refining Seminar*, Nov. 12-14, 1989, Scottsdale, Arizona.
109. V. H. Apprahamian, G. P. Demopoulos, G. B. Harris: "The Behavior of Impurities during the Solvent Extraction of Platinum Metals with TN 1911 Extractants" in *Precious Metals 1991*, IPMI, Allentown, PA, 1991, p. 143.
110. W. Hasenpusch: "Die Trennung der Platinmetalle", *CLB, Chem. Labor Betr.* 38 (1987) 454.
111. Ch. Baes, R. E. Mesmer: *The Hydrolysis of Cations*, J. Wiley and Sons, New York 1976.
112. M. Knothe: "Untersuchungen zum Verhalten des Rh, Pd, Ir und Pt im Chloridmedium an Anionen-austauschern", *Z. Anorg. Allgem. Chem.* 463 (1980) 204-212.
113. R. J. Evers, R. J. Edwards, M. Fieberg, DE 2726558 B2, 1976/1981.
114. G. Schmuckler, US 4885143, 1989.
115. W. Proding: *Organische Fällungsmittel in der quantitativen Analyse*, Enke Verlag, Stuttgart 1954.

115. J. Fries, H. Getrost: *Organische Reagentien für die Spurenanalyse*, E. Merck, Darmstadt 1977.
116. D. A. Boyd: *A Novel Approach to PCM Refining*, IPMI, 1992.
117. R. Marr, H.-J. Bart: "Metallsalz-Extraktion", *Chem.-Ing.-Tech.* **54** (1979) 119–129.
118. L. Alders: *Liquid-Liquid Extraction—Theory and Laboratory Practice*, Elsevier Publishing, Amsterdam 1959.
119. G. M. Ritcey, A. W. Ashbrook: *Solvent Extraction: Principles and Application to Process Metallurgy*, Elsevier, New York 1984.
120. F. Habashi: "Hydrometallurgy", *Principles of Extractive Metallurgy*, vol. 2, Gordon and Breach, New York 1970.
121. G. H. Morrison, H. Freiser: *Solvent Extraction in Analytical Chemistry*, J. Wiley & Sons, New York 1957.
122. E. J. Barnes, J. D. Edwards: "Solvent Extractions at Inco's Acton Precious Metal Refinery", *Chem. & Ind. (London)* **1982** no. 3, 151–164.
123. R. J. Edwards: "Refining of the Platinum-group Metals", *J. Met.* **28** (1976) no. 8, 49.
124. R. J. Edwards: "Selective Solvent Extractants for the Refining of Platinum Metals", *Proceedings of the International Solvent Extraction Conference ISEC 7*, Vol. 1, CIM, Special Vol. 21, 24 (1979).
125. D. S. Flett: "Solvent Extraction in Precious Metal Refining", *IMPT Seminar*, London 1982.
126. E. M. Elkin, P. W. Bennett: "A new Technique for the Recovery of Palladium and Platinum from Gold Electrolyte", *J. Met.* **17** (1965) no. 3, 252–254.
127. G. Brauer: *Handbuch der präparativen anorganischen Chemie*, vol. 3, Enke, Stuttgart 1980.
128. R. Gilchrist: "The Platinum Metals", *Chem. Rev.* **32** (1943) 277–372.
129. Matthey Rustenburg Ref., GB 2065092, 1980 (R. A. Grant).
130. Matthey Rustenburg Ref.: "The Separation Chemistry of Rhodium and Iridium", *Proceedings of a Seminar of the International Precious Metals Institute*, IMPI, Scottsdale, AZ, 1989.
131. P. Charlesworth: "Separating the Platinum Group Metals by Liquid-Liquid Extraction", *Platinum Met. Rev.* **25** (1981) 106–112.
132. L. R. P. Reavill, P. Charlesworth: "The Application of Solvent Extraction to Platinum Group Metals Refining", *Proceedings of the International Solvent Extraction Conference, ISEC '80* vol. 3, Liège 1980.
133. M. J. Cleary, P. Charlesworth, D. J. Bryson: "Solvent Extraction in Platinum Group Metal Processing", *J. Chem. Technol. Biotechnol.* **29** (1979) 210–214.
134. Matthey Rustenburg Ref., US 3979207, 1974 (J. J. McGregor).
135. INCO, US 4390366, 1983 (R. K. Lea, J. D. Edwards, D. F. Colton).
136. M. Fieberg, R. J. Edwards: "The Extraction of Gold from Chloride Solutions", *Rep. Natl. Inst. Metall. (S. Afr.)* **1978**, no. 1996.
137. A. S. Myerson, K. Toyokura (eds.): "Crystallisation as a Separations Process", *ACS Symp. Ser.* **438** (1990).
138. W. Gösele et al.: "Feststoffbildung durch Kristallisation und Fällung", *Chem.-Ing.-Tech.* **62** (1990) 544–552.
139. W. Hasenpusch, K. Bonin: "Kristallisation von Ammonium-Hexachloroplatinat(IV)", *Chem.-Ztg.* **1991**, no. 5, 129–133.
140. R. B. Wilson, W. D. Jacobs: "Separation of Iridium from Rhodium by Extraction with Tributyl Phosphate", *Anal. Chem.* **33** (1961) 1650–1652.
141. S. J. Tanaka: "The Recovery and Purification of Rhodium using Superlig™ Technology from a Platinum-group Metals Stream", IPMI 1992.
142. Matthey Rustenburg Ref., US 4382067, 1982/1983 (R. A. Grant).
143. Matthey Rustenburg Ref., DE-OS 2457672, GB 5682673, 1973/1979 (J. J. McGregor).
144. PGM Industries, DE-OS 2726390, 1977/1979 (J. Baltz, E. Coltrinari).
145. National Institute for Metallurgy (NIM), GB 1490815, 1974/1977 (R. J. Edwards).
146. AT & T Technologies, US 4479922, 1983 (R. Haynes, A. Jackson).
147. H. Renner: "The Selective Solvent Extraction of Palladium by the Use of Di-Normal-Hexylsulfide", *Rep.-MINTÉK*, 1985, no. 217.
148. G. P. Demopoulos: "Solvent Extraction in Precious Metals Refining", *J. Met.* **1986** no. 6, 13–17.
149. G. P. Demopoulos: "A Radically New Solvent Extraction Process for Rhodium Recovery", in *Precious Metals 1992*, IPMI, 1992.
150. M. Grote, U. Hüppe, A. Kettrop: "Solvent Extraction of Noble Metals by Formazons(II)", *Hydrometallurgy* **19** (1987) 51–68.
151. K.-H. König: "Zur Solventextraktion von Platinmetallen", *Achema*, Frankfurt 1985.
152. M. Knothe: "Die Fällung des Pd^{II} als Pd(NH₃)₂Cl₂ sowie des Verhaltens verschiedener Begleitelemente", *Z. Anorg. Allg. Chem.* **503** (1983) 213–223.
153. A. P. Evers, R. J. Edwards, M. M. Fieberg, SA 763681, 1976.
154. R. F. Edwards, M. M. Fieberg, W. te Riele, B. C. Want, US 4155750, 1979.
155. A. Prior, K. H. Ohrbach, A. Kettrop, G. Matuschek: "Calcination of Platinum Group Metal Complexes to Form Pure Metals", *IPMI Seminar*, 1988.
156. A. Prior, B. Lerwill: "Cost Management Strategies in Refineries in the 1990s", *IPMI Seminar*, Tempe, AZ, 1991.
157. V. S. Khain, E. V. Fomina: "Reduction of OsO₄ by Sodium Tetrahydroborate in Acidic Medium", *Russ. J. Inorg. Chem. (Engl. Transl.)* **25** (1980) 307–308.
158. Degussa: *Edelmetall-Taschenbuch*, Frankfurt 1967.
159. E. M. Wise: *Palladium*, Academic Press, New York 1968.
160. J. A. Federov: *Rhodium*, Nauka Vlg., Moskau 1966.
161. J. C. Chaston: "The Purity of Platinum", *Platinum Met. Rev.* **15** (1971) 122–128.
162. A. Wogrinz: *Analytische Chemie der Edelmetalle*, Enke Verlag, Stuttgart 1936.
163. F. Ensslin: *Edelmetall-Analyse*, Springer-Verlag, Berlin 1964.
164. Chemikerausschuß der GDMB (ed.): *Analyse der Metalle*, 2nd ed., Springer-Verlag, Berlin 1961.
165. F. E. Beamish, J. C. van Loon: *Analysis of Noble Metals*, Academic Press, New York 1977.

166. S. Kallmann: "A Survey of the Determination of the Platinum Group Elements", *Talanta* **34** (1987) no. 8, 677–698.
167. H. G. Sigel, A. Sigel (eds.): *Handbook on Toxicity of Inorganic Compounds*, Marcel Dekker, New York 1988.
168. E. D. Goldberg et al.: "Determination of Platinum Sediments", *Anal. Chem.* **58** (1986) 616–620.
169. H.-M. Lüscho: "Probenahme, Theorie und Praxis", *Schriftenreihe der GDMB*, Verlag Chemie, Weinheim 1980.
170. H.-M. Lüscho: "Zur Probenahme von Edelmetallen", *Erzmetall* **42** (1989) 153–159.
171. H.-G. Bachmann, E. Koberstein, R. Straub: *Chemie-Technik* **7** (1978) 441–446.
172. J. Suchomel, Fresenius' *Z. Anal. Chem.* **300** (1980) 257–266; *Fresenius' Z. Anal. Chem.* **307** (1981) 14–18.
173. B. Welz: *Atomic Absorption Spectrometry*, VCH-Verlagsgesellschaft, Weinheim 1985.
174. G. Jäger: *Über die Platinbestimmung in Platinierung-Katalysatoren*, Dissertation, Mainz 1957.
175. W. Diehl: "Die quantitative Bestimmung der Verunreinigungen der Ag, Au, Pt und Rh mit einem 3,4-m-Gitterspektrographen", *Metall (Berlin)* **23** (1969) 587–589.
176. F. Mylius: "Reinheitsgrade von Metallen des Handels", *Z. Anorg. Chem.* **74** (1912) 407.
177. F. Mylius, A. Mazzuchelli: "Über die Platinanalyse", *Z. Anorg. Allg. Chem.* **89** (1914) 1–38.
178. DIN 43760, 1968.
179. DIN 43710, 1977.
180. *Gmelin, Platin*, suppl. vol. A1, 8.
181. H. Wolf: "Die Edelmetalle in Forschung und Industrie", *Metall* **12** (1958) no. 7, 3–16.
182. J. Sagochen: "Platin-Laborgeräte", *Chem. Ztg.* **88** (1964) 420–429.
183. G. Reinacher: "Platin-Geräte im Labor", *Chem. Anlagen + Verfahren* **1970**, no. 1/2, 61–63.
184. Degussa: *Platin-Geräte für Labor und Praxis*, no. 1 ff., Frankfurt 1977 ff.
185. G. Reinacher: "Über die Gewichtskonstanz von Geräten aus der Legierung Platin/3% Iridium bei analytischen Operationen", *Werkst. Korros.* **1964**, no. 1, 84–88.
186. G. Reinacher, H. Roters: "Neuere Anwendungen von Platinwerkstoffen in Chemie und Glasindustrie", *Metall* **23** (1969), 570–575.
187. G. Reinacher: "Anwendung von Platin-Werkstoffen in Glashütten", *Chem. Anlagen + Verfahren* **1975**, no. 10, 27–34.
188. D. Böttger: "The Use of Platinum in the Glass Industry", *Glass* **62** (1985) no. 5, 177–178; *Metall* **39** (1985) 748–750.
189. M. Rove: "Noble Metals in the Glass Industry", *Ceram. Eng. Sci. Proc.* **6** (1985) 256–268.
190. W. Funk, R. Schumm: "Spinddüsen – Bauteile für die Chemiefaserindustrie", *Chemiefasern + Text. Anwendungstech./Text.-Ind.* **22** (1972) 518–521.
191. J. R. Anderson, M. Baudart: *Catalysis, Science and Technology*, vols. 12, Springer-Verlag, Berlin 1981.
192. Fonds der Chemischen Industrie: "Katalyse", *Fo-lienserie*, no. 19, Frankfurt 1986.
193. K. Weissmermel, H. J. Arpe: *Industrial Organic Chemistry*, Verlag Chemie, Weinheim 1978.
194. P. N. Rylander: *Catalysis Hydrogenation over Platinum Metals*, Academic Press, New York, 1967.
195. W. Hölderich, M. Scheerzmann, W. D. Mross: "Heterogene Katalysatoren in der chemischen Industrie", *Erzmetall* **39** (1986) 292–298.
196. A. J. Bird, A. B. Stiles: *Catalyst Supports and Supported Catalysts*, Butterworth, London 1987.
197. J. Falbe, U. Haserodt: *Katalysatoren, Tenside und Mineralöladditive*, Thieme Verlag, Stuttgart 1978.
198. D. M. Little: *Catalytic Reforming*, Pennwall Pub., Tulsa 1985.
199. W. Ostwald, E. Brauer, in H. Huben (ed.): *Festschrift zum fünfzigjährigen Bestehen der Platin-schmelze G. Siebert GmbH*, Hanau, Hanau 1931, pp. 240–256.
200. H. Holzmann: "Über die katalytische Oxidation von Ammoniak bei der industriellen Salpetersäure-Herstellung", *Chem.-Ing.-Tech.* **39** (1967) 89–95.
201. F. Sperner, W. Hohmann: "Rhodium-Platinum Gauzes for Ammonia Oxidation", *Platinum Met. Rev.* **20** (1976) 12–20.
202. H. Connor: "The Role of Platinum Alloys Gauzes in the Ammonia Oxidation Process", *Platinum Met. Rev.* **11** (1967) 2–9, 60–69.
203. E. G. Schlosser: "Die Katalysator-Desaktivierung und -Vergiftung in verfahrenstechnischer Sicht", *Chem.-Ing.-Tech.* **47** (1975) 997–1005.
204. R. Ugo: "Aspects of Homogeneous Catalysis", D. Reibel Publ., Dordrecht 1970.
205. F. J. Smith: "New Technology for Industrial Hydroformulation", *Platinum Met. Rev.* **19** (1975) 93–95.
206. K.-H. Schmidt: "Neuentwicklungen in der homogenen Katalyse", *Chem. Ind.* **37** (1985) 762–765.
207. J. Osborn, G. Wilkinson, *Chem. Commun.* **1965**, 131.
208. H. Brunner: "Rhodium-Katalysatoren für die enantioselektive Hydrosylierung – ein neues Konzept zur Entwicklung asymmetrischer Katalysatoren", *Angew. Chem.* **95** (1985) 921–931.
209. G. J. K. Acres, B. J. Cooper: "Automobil Emission Control Systems", *Platinum Met. Rev.* **16** (1972) 74–86.
210. W. Weigert, E. Koberstein, E. Lakatos: "Katalysatoren zur Reinigung von Autoabgasen", *Chem.-Ztg.* **97** (1973) 469–478.
211. O. Stopinski: *Platinum-group Metals*, National Research Council, Washington 1977.
212. E. Koberstein: "Katalysatoren zur Reinigung von Autoabgasen", *Chemie in unserer Zeit* **18** (1984) no. 2, 37–45.
213. A. Keil: *Werkstoffe für elektrische Kontakte*, Springer, Berlin 1960.
214. A. von Krusenstjern: *Edelmetall-Galvanotechnik*, Leuze-Vlg., Saulgau 1970.
215. D. Schlain et al.: "Electrodisposition of Platinum Metals from Molten Cyanides", *Platinum Met. Rev.* **21** (1977) 38–42.
216. J. H. Notton: "Fused Salt Platinum Plating for Industrial Applications", *Platinum Met. Rev.* **21** (1977) 122–128.
217. H.-H. Beyer, F. Simon, *Metall* **34** (1980) 1016–1018.

26 Tungsten

ERIK LASSNER, WOLF-DIETER SCHUBERT (§§ 26.1, 26.2.2, 26.3–26.11); HANS UWE WOLF (§ 26.12)

26.1 Introduction	1329	26.5 Uses	1345
26.2 Properties	1330	26.6 Analysis	1347
26.2.1 Physical Properties	1330	26.6.1 Raw Materials	1347
26.2.2 Chemical Properties	1332	26.6.2 High-Purity Intermediate Products, Tungsten Powder, and Compact Tungsten Metal	1347
26.3 Raw Materials	1333	26.6.3 Trace Elements in High-Purity Tungsten Metal	1348
26.3.1 Natural Resources	1333	26.7 Compounds and Intermetallic Compounds	1348
26.3.2 Tungsten Scrap	1335	26.7.1 Tungsten Chemistry	1348
26.4 Production	1335	26.7.2 Tungsten–Boron Compounds	1349
26.4.1 Ore Beneficiation	1335	26.7.3 Tungsten–Carbon Compounds	1349
26.4.2 Pretreatment of Ore Concentrates and Scrap	1336	26.7.4 Tungsten–Silicon Compounds	1349
26.4.3 Hydrometallurgy	1336	26.7.5 Tungsten–Nitrogen Compounds	1349
26.4.3.1 Digestion	1336	26.7.6 Tungsten–Phosphorus Compounds	1350
26.4.3.2 Purification	1337	26.7.7 Tungsten–Arsenic Compounds	1350
26.4.3.3 Conversion of Sodium Tungstate Solution to Ammonium Tungstate Solution ..	1339	26.7.8 Tungsten–Oxygen Compounds	1350
26.4.3.4 Crystallization of Ammonium Paratungstate (APT)	1340	26.7.9 Tungsten–Chalcogenide Compounds	1352
26.4.4 Calcination of Ammonium Paratungstate	1340	26.7.10 Tungsten–Halogenide Compounds	1352
26.4.5 Reduction by Hydrogen to Tungsten Metal Powder	1340	26.8 Tungsten in Catalysis	1353
26.4.6 Production of Compact Metal	1342	26.9 Economic Aspects	1353
26.4.7 Processing of Sintered Parts	1342	26.10 Tungsten Recycling	1355
26.4.7.1 Shaping	1342	26.11 Beneficial Effects on Human Health	1356
26.4.7.2 Mechanical Bonding of Tungsten to Tungsten and Other Metals	1343	26.12 Toxicology and Occupational Health	1356
26.4.8 Surface Treatment	1344	26.13 References	1358
26.4.9 Tungsten Coatings	1344		
26.4.10 Production of High-Purity Tungsten Metal (99.999–99.9999%)	1345		

26.1 Introduction

Tungsten (wolfram, W), is a transition metal in the third long period and group 6 of the periodic table. Its electron configuration is $[\text{Xe}] 6s^2 4f^{14} 5d^4$ but can also be interpreted as $[\text{Xe}] 6s^1 4f^{14} 5d^5$. The naturally occurring isotopes (abundances in parentheses) have relative atomic mass 180 (0.14%), 182 (26.42%), 183 (14.40%), 184 (30.64%), and 186 (28.41%). There are also 17 known artificial isotopes and isomers from ^{137}W to ^{189}W , with half-lives between 14 μs and 140 d. In nature, tungsten occurs only in a chemically com-

bined state (mainly as tungstate). The metal, which has a silvery white luster, has a very high density (19.3 g/cm^3 at 20°C), and the highest melting point (3410°C) of all the metallic elements.

History. Long before elemental tungsten was discovered (1783), the mineral wolframite was known, e.g., in the tin mines of Saxony and Bohemia. It was first described in 1574 by LAZARUS ERCKER, and thought to be a tin mineral that contained arsenic and iron.

The name wolfram is derived from the word wolf, i.e., the wolf that devoured tin. A foam (Latin: *lupi spuma*, wolf's foam) was

formed on the molten tin during the smelting of tin ore, reducing the yield of tin.

In 1757, a new mineral with density 6 (scheelite) was described by A. F. CRONSTEDT. He named this "tungsten" (Swedish: *tung sten*, heavy stone) and considered it to be a calcium-containing iron mineral. In 1781, C. W. SCHEEL analyzed the ore and announced that it contained calcium with a hitherto unknown acid. He described digesting the mineral with K_2CO_3 , precipitating the unknown acid with nitric acid, decomposing the mineral with mineral acids, and dissolving the precipitated acid in ammonia. In the same year, T. BERGMAN suggested that the metal might be obtained by reduction of the acid with carbon.

In 1783, the element was produced by the brothers J. J. and F. DE ELHUYAR from wolframite by reduction of the oxide with carbon. They named it wolfram. In 1786, the hardening of steel was described by H. I. DU MONCEAU. In 1821, K. C. VON LEONHARD proposed the name scheelite for the mineral $CaWO_4$.

The real chemistry of tungsten originated with R. OXLAND (1874), who patented a method for producing sodium tungstate, tungsten oxide, and metallic tungsten. He was also the first to propose a method for the production of ferrotungsten. The possibility of using tungsten as an alloying element to increase the hardness of steel could not initially be realized because of the high price of the metal.

The developments that led to the industrial use of tungsten began in 1890 with the production of WC by H. MOISSAN. They may be summarized as follows:

- In 1900, the Bethlehem Steel Company announced the first high-speed, high-temperature steel at the Paris Exhibition.
- In 1903, the first tungsten filaments for incandescent lamps were produced in Hungary by the method patented by JUST and HANAMANN.
- In his patent of 1909, W. D. COOLIDGE described the production of ductile tungsten wire by powder metallurgy, a process that has not changed in its essential features even

today. This process represents the first industrial use of powder metallurgy.

- In 1922, the Osram Research Association obtained a patent for the production of tungsten carbide-cobalt hard metals.
- Four years later, the Krupp organization introduced the first hard metal cutting tool at the Leipzig Exhibition.

The increasing use of hard metals in the machining of steel and in the mining industry (energy production) led to a great increase in the demand for tungsten. As a result of the uncertain availability of raw materials in crisis situations and the increased use of tungsten materials in the armaments industry (hard metals, tungsten-containing heavy metals), the metal has become of strategic importance.

All later materials developments are essentially only a broadening and diversification of the early work on the production of the metal and its alloys. Tungsten compounds are becoming increasingly important, e.g., as the active components in catalysts.

Continuously increasing demand up to the 1980s led to the constant exploration of tungsten deposits and the opening of mines and processing plants. However, owing to a fall in price and demand, a large number of mines have been closed since 1985, especially in the industrialized countries.

In terms of quantity, tungsten is the second most important high-melting metal, after molybdenum; however, it is the most important refractory metal used in powder metallurgy.

General information on tungsten and its alloys and compounds can be found in [1-7]. A summary of the early history can be found in [8].

26.2 Properties

26.2.1 Physical Properties

Tungsten has the highest melting point of all metals, exceeded only by elemental carbon and the metallic monocarbides of niobium, zirconium, tantalum, and hafnium. The extremely high bonding energy (due to the half-

filled 5d shell) leads to extreme values of other properties. For example, tungsten has the lowest vapor pressure of all metals, the lowest compressibility, an extremely high density, a high modulus of elasticity, low thermal expansion, and high thermal conductivity.

Some physical properties of tungsten follow [1, 3, 9]:

Lattice type	A2, bcc
Lattice parameter	0.31648 nm
Atomic radius	0.139 nm
Ionic radius (4-valent)	0.064 nm
(6-valent)	0.068
Absorption cross section for thermal neutrons	19.2 barn
1st ionization potential	8.0 eV
mp	3410 °C
bp	5900 °C
Heat of fusion	35.17 kJ/mol
Heat of sublimation	850.8 kJ/mol
Molar heat capacity at 20 °C	24.28 J mol ⁻¹ K ⁻¹
Specific heat capacity at 25 °C	0.135 kJ kg ⁻¹ K ⁻¹
at 1000 °C	0.17
at 2000 °C	0.20
Coefficient of thermal expansion at 500 °C	2.3 mm/m
at 1500 °C	7.6
at 3000 °C	19.2
Thermal conductivity at 0 °C	129.5 W m ⁻¹ K ⁻¹
at 1000 °C	112.5
at 2000 °C	96.0
Vapor pressure at 1700 °C	1 × 10 ⁻¹⁰ Pa
at 2300 °C	4 × 10 ⁻¹
at 3000 °C	2 × 10 ⁻³
Standard entropy S_{25}^0 at 101 kPa	32.76 J mol ⁻¹ K ⁻¹
Standard enthalpy H_{25-273}^0	5.09 kJ/mol
Specific electrical resistivity at 20 °C	0.055 μΩ m
at 1000 °C	0.330
at 2000 °C	0.655
at 3000 °C	1.40
Magnetic susceptibility at 25 °C	0.32 × 10 ⁻⁶ cm ³ /g
Black body temperature at 727 °C (λ = 665 nm)	693 °C
Spectral emission at 25 °C (λ = 665 nm)	0.47
Total radiation at 527 °C	0.173
at 1127 °C	3.82
at 2327 °C	80.60
Electron emission at 727 °C	1.07 × 10 ⁻¹⁵ A/cm ²
at 1627 °C	2.28 × 10 ⁻⁴
at 2227 °C	2.98 × 10 ⁻¹
Electron yield at 727 °C	1.77 × 10 ⁻⁵ A/W
at 1627 °C	1.22 × 10 ⁻⁵
at 2227 °C	4.26 × 10 ⁻⁵
Density at 20 °C	19.3 g/cm ³
Hardness (Vickers) HV 30 at 0 °C	450
recrystallized	300
deformed	≤ 650
at 400 °C	240
at 800 °C	190
Modulus of elasticity at 0 °C	407 kN/mm ²

at 1000 °C	365
at 2000 °C	285
Velocity of sound longitudinal	5320 m/s
transverse	2840
Minimum compression strength (sintered)	1150 N/mm ²
Shear modulus at 20 °C	177 kN/mm ²

Mechanical and Metallurgical Properties.

Pure metallic tungsten has a body-centered cubic structure, is brittle at room temperature, and is therefore not suitable for cold forming. At elevated temperatures (ca. 100–500 °C) it is transformed into the ductile state. The temperature of this sharply defined transformation is mainly dependent on the purity and the history of deformation and heat treatment of the material. The transformation temperature is increased by the presence of extremely small amounts of interstitially soluble elements, e.g., oxygen, carbon, and nitrogen, which lead to intergranular precipitation. The transformation temperature decreases with increasing deformation; highly deformed products such as thin sheet and wire are ductile at room temperature. This is mainly due to the distribution of the precipitated impurities over a larger intergranular area, and the formation of a fine-grained fibrous structure which tends to prevent intergranular failure perpendicular to the fiber direction. In the fiber direction, the tendency toward intergranular failure is more or less constant.

Addition of rhenium can cause the transformation temperature to fall below room temperature, even for only slightly deformed products. With extremely pure single crystals, brittle-ductile transformation temperatures as low as -190 °C are observed.

The grain size and grain structure have a great influence on the mechanical properties of tungsten. These can be controlled by sintering conditions, type of deformation, degree of deformation, and annealing processes during and after machining (intermediate annealing, stress-relieving annealing, soft annealing, recrystallization annealing).

Consequences of the high bonding energy of tungsten include its high ultimate strength

and yield strength, high modulus of elasticity, and high recrystallization temperature.

The hot strength of tungsten, like its elongation, depends on its deformation and annealed condition, and can vary widely at a given temperature (Figure 26.1). The hot strength of tungsten is exceeded only by that of rhenium. The upper limit for the hot tensile strength corresponds to a stress-relieved sheet, and the lower limit to a recrystallized sheet. At ca. 1500 °C, both limiting curves coincide, i.e., at this temperature the tungsten completely recrystallizes as it is heated to the tensile testing temperature (and therefore at temperatures above this) independently of the starting condition of the tungsten, so that is always has the hot strength of recrystallized tungsten. The results of hot tensile testing are to some extent influenced by the strain rate.

The relation between temperature and fracture strain of recrystallized tungsten sheets is shown in Figure 26.2.

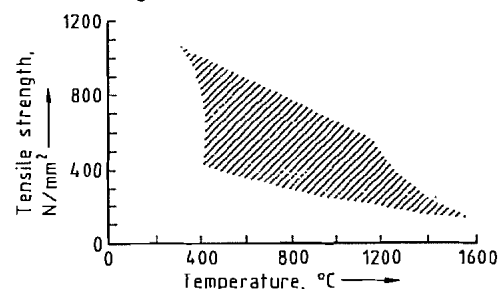


Figure 26.1: Hot tensile strength of tungsten sheet, thickness 1 mm, strain rate $15\% \text{ min}^{-1}$ [3].

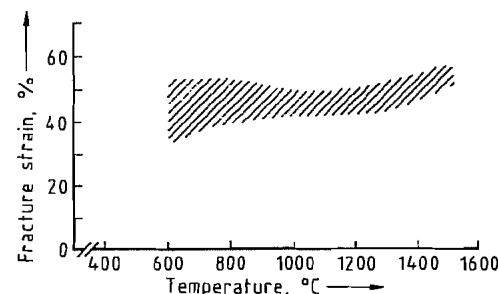


Figure 26.2: Effect of temperature on fracture strain of recrystallized tungsten sheet [3].

No allotropic transformations of group 6 metals are known which could lead to changes

in their properties. The solubility of the non-metals carbon, silicon, oxygen, nitrogen, and water in these metals is very small. Therefore, impurities in the form of interstitially dissolved nonmetals have a smaller effect on the mechanical properties than is the case with other transition metals, but have a very significant effect if the solubility limits are exceeded. Carbides, silicides, nitrides, and oxides are then formed [9], and the inclusions have a marked effect on grain shape and size.

As the solubility of interstitial impurities (O, N, C) at room temperature is well below 0.1 µg/g, and the solubilities, even at the eutectic temperature, are only 0.01–0.1% [10], the insoluble excess segregates at the grain boundaries on cooling. Oxide impurities, in particular, considerably reduce intergranular strength. With carbide impurities, a beneficial effect on ductility is apparent, depending on the form of the carbides. The effect of nitrides is not yet fully understood. In deformed tungsten, it leads to marked anisotropy of the mechanical properties in the direction of deformation, so that sheet and bar tend to split. In recrystallized tungsten, the intergranular impurities enable plastic deformation to take place above the transformation temperature, as already mentioned [9].

26.2.2 Chemical Properties

Tungsten is stable in air up to 350 °C, but begins to oxidize above 400 °C. A thin film of blue tungsten oxides forms on the surface, and this at first prevents further attack. As the temperature increases, cracks develop in the oxide film, and these favor oxidative attack. Above 800 °C, rapid oxidation takes place with formation of WO_3 , which sublimates. In oxygen, tungsten burns at 500–600 °C. Tungsten is stable to mineral acids in the cold, and is only slightly attacked at higher temperatures. Its stability to cold and hot hydrofluoric acid is of practical importance. Mixtures of hydrofluoric and nitric acids dissolve tungsten very readily, the tungsten remaining in solution because of the complexing effect of the fluoride ions. Hydrogen peroxide is a good solvent for finely

divided tungsten; the peroxo complexes so formed keep the tungsten in solution. Alkaline solutions do not attack tungsten, which is also very stable to molten alkalis. In the presence of oxidizing agents (Na_2O_2 , NaNO_2 , or NaNO_3), rapid dissolution takes place.

Tungsten is stable to molten glass and silica up to 1400 °C. At higher temperatures, it reacts with many elements, e.g., B, C, Si, P, As, S, Se, Te, and the halogens. It reacts with fluorine at lower temperatures. It is stable to chlorine up to 250 °C, and to bromine and iodine up to 500 °C. It is very stable to gaseous nitrogen and ammonia up to 1400 °C. There is no reaction with hydrogen. With carbon monoxide, the hexacarbonyl is formed at low temperatures, and the carbide above 800 °C.

26.3 Raw Materials

26.3.1 Natural Resources

The average concentration of tungsten in the earth's crust is 1.5 g/t. It is thus a rare element.

Minerals. Tungsten occurs only in combined form. The most important tungsten minerals are [4]:

Anthoinite	$\text{Al}(\text{WO}_4)(\text{OH}) \cdot \text{H}_2\text{O}$
Cuprotungstite	$\text{Cu}_2(\text{WO}_4)(\text{OH})_2$
Ferritungstite	$\text{Ca}_2\text{Fe}_2^{2+}\text{Fe}_2^{3+}(\text{WO}_4)_7 \cdot 9\text{H}_2\text{O}$
Raspite	PbWO_4
Russellite	Bi_2WO_6
Sanmartinite	ZnWO_4
Scheelite	CaWO_4
Stolzite	PbWO_4
Tungstenite	WS_2
Tungstite	$\text{WO}_3 \cdot \text{H}_2\text{O}$
Ferberite	FeWO_4 with up to 20% MnWO_4
Hübnerite	MnWO_4 with up to 20% FeWO_4
Wolframite	$(\text{Fe}, \text{Mn})\text{WO}_4$

With the exception of tungstenite, all the minerals are tungstates, but only scheelite and the wolframite group are of industrial importance. The most important properties of scheelite and the wolframites are listed in Table 26.1 [4].

Scheelite is often associated with the isomorphous calcium molybdate (powellite).

Pure scheelite has a blue fluorescence in ultraviolet light, becoming white with a molybdenum content of ca. 1%, and yellow above this concentration. This property is utilized in prospecting for scheelite.

Wolframite is a general term for a mixed crystal series (with no miscibility gap) of Fe(II) and Mn(II) tungstates. The minerals between pure iron tungstate and 20% MnWO_4 are known as ferberite. Manganese tungstate and mixed crystals containing up to 20% FeWO_4 are known as hübnerite.

The minerals tungstite and cuprotungstite have achieved a small degree of industrial importance.

Deposits. All tungsten deposits are of magmatic-hydrothermal origin. During cooling of the magma, differential crystallization occurs, first of basic and later of slightly acidic rocks, and enrichment of tungstate and other ions takes place, accompanied by an increase in the concentration of silica in the remaining magma and the hydrothermal solution. Tungsten cannot replace the main elements such as Fe, Mg, Ca, Al, and Si in the basic and slightly acidic rocks, and is not incorporated in the first material to crystallize. Therefore, scheelite and wolframite are often to be found in the last crystallization stage of a magma, i.e., the pegmatites and the material crystallized from hydrothermal solutions.

There are many types of deposit:

- Pegmatite deposits are relatively rare and can contain wolframite and scheelite. The tungsten minerals are crystallized together with the pegmatitic minerals.
- Greisen deposits contain wolframite, and are formed by the mineralization of intrusive rock (and of the rock it penetrates) by hydrothermal solution processes.
- Contact-metasomatic deposits are the commonest type and are of pure scheelite. They are formed by the reaction between limestone and residual magma or hydrothermal solutions that penetrate into it.

Table 26.1: Physical and chemical properties of ferberite, wolframite, hübnerite, and scheelite.

	Ferberite	Wolframite	Hübnerite	Scheelite
Formula	FeWO ₄	(Fe, Mn)WO ₄	MnWO ₄	CaWO ₄
WO ₃ content, %	76.3	76.5	76.6	80.6
Crystal structure	monoclinic	monoclinic	monoclinic	tetragonal
Lattice parameters				0.5257
a, nm	0.471	0.479	a 0.485	1.1373
b, nm	0.570	0.574	c 0.577	a/c 1:2.165
c, nm	0.574	0.499	a/c 0.498	
β	90°	90°26'	90°53'	
Density, g/cm ³	7.5	7.1–7.5	7.2–7.3	5.4–6.1
Color	black	dark gray–black	red–brown–black	brown, yellowish, white
Hardness (Mohs)	5	5–5.5	5	4.5–5
Common form	well-formed crystals or crystal masses	irregular crystal masses or radiating crystal groups	radiating groups or lamellar crystals	crystals, mainly fine grained

- Vein deposits can contain wolframite and scheelite. Hot magma causes cracks and faults in the surrounding rock, into which hydrothermal solution is injected. It then crystallizes.
- Pneumatolytic deposits are rare, and are formed by the transport of volatile tungsten compounds in the gas phase.
- Secondary enriched deposits are very rare and contain tungstite formed by weathering of wolframite.
- Placer deposits, in which high density materials become concentrated in river sediments, are also very rare.

The gangue minerals differ not only among the various deposits, but can also vary greatly within a single mine. This is easily understood, as the various types of deposits can often occur together in one mine. The commonest types of gangue minerals are: quartzite, various silicates, limestone, magnesite, fluor spar, apatite, and various sulfide ores.

The concentration of workable ores is 0.1–2.5% WO₃, contents of ca. 2% being rare. The average content is ca. 0.5% WO₃. The lower limit of workability depends on the ore type, gangue composition, and world market price. It fluctuates between 0.1 and 0.3% WO₃.

Reserves. Tungsten deposits occur throughout the younger mountain ranges, e.g., the Alps, the Himalayas, and the circum-Pacific belt. The most recent figures for world tungsten re-

serves (in 10³ t) date from 1985, and are listed here [11]:

North America	985
United States	290
Canada	670
Mexico	20
Others	5
South America	110
Bolivia	70
Brazil	20
Others	20
Europe	665
Austria	20
France	20
Portugal	40
Former Soviet Union	490
United Kingdom	70
Others	25
Africa	20
Rwanda	5
Zimbabwe	5
Others	10
Asia	1535
Burma	15
China	1230
North Korea	100
South Korea	60
Malaysia	20
Thailand	30
Turkey	70
Others	10
Oceania	10
Australia	140

These figures include reserves that are known, but have so far not been found to be economically workable. This type of information is partly based on estimates, as countries such as China and the former Soviet countries have not published any accurate information. By far the largest reserves are in China (35%, but may exceed 50%), followed by Canada (19%), and the former Soviet Union (14%). At the current world annual consumption rate

of 30 000 t, these known reserves of ore are likely to last for ca. 120 years. Of the ore deposits, 75% are of scheelite and 25% wolframite, with a few in which both minerals occur together [12]. Over half the reserves of ore are in developing countries.

26.3.2 Tungsten Scrap

Tungsten scrap has been used as a raw material for production of pure tungsten for more than 50 years. There are several reasons for this:

- The low concentration in the earth's crust results in a consistently high cost of the metal; recycling has always been economic.
- The concentration of tungsten in the various types of scrap is always considerably higher (30–99%) than in any ore, so there are no concentration costs.
- The accompanying elements in scrap do not cause serious problems during chemical processing.

High demand and consequent high prices from 1975 to 1985 led to an increase in scrap processing, and made lower-grade scrap (grinding wheel swarf and dusts) more attractive for reuse [13]. Since then, the amount of scrap used as a percentage of the total tungsten raw materials has increased still further in spite of falling price and demand. This is largely because environmental regulations have become increasingly strict, making it impossible to dispose of scrap with even a low tungsten content, e.g., wheel swarf or similar materials. Consequently, scrap is classified as a primary tungsten raw material. This is shown in Figure 26.3, which also shows that approximately one-third of demand is supplied from scrap [14].

The processing of scrap is environmentally beneficial. No energy is required for mining and preparation, and no chemicals for concentration processes. This reduces both atmospheric pollution and chemical waste. Especially important for the future is the fact that scrap recycling conserves reserves of ore.

Scrap is classified as either "hard" or "soft". Soft scrap is finely divided material, e.g., powder, dust, grindings, and turnings, with tungsten content 10–98%. Hard scrap is in lump form (sintered material, scrap bar and sheet, wire, etc.) with tungsten content 40–99.9%.

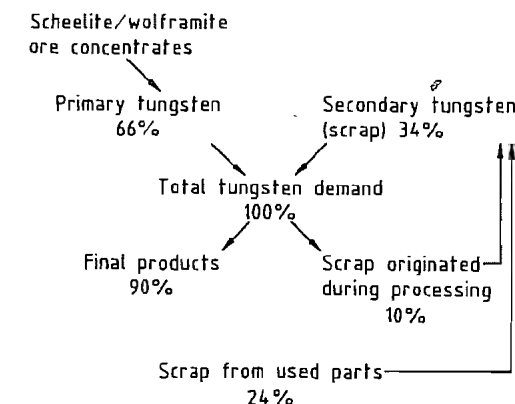


Figure 26.3: Tungsten flowchart.

26.4 Production

26.4.1 Ore Beneficiation

Most tungsten ores contain less than 1.5% WO₃. Therefore, ore-dressing plants are always in close proximity to the mine to keep transport costs low. The first steps in the procedure are crushing and milling to liberate the tungsten mineral crystals from the gangue materials. The final grain size to which the ore must be reduced depends on the size of mineralization present in the tungsten ore body. This can be quite different from deposit to deposit. The finer the mineralization, the more costly the pretreatment and the lower the recovery. No more crushing and milling should be applied than is absolutely required, to minimize losses.

Scheelite Ore. After crushing, coarsely crystallized scheelite can be concentrated by gravimetric methods (hydrocyclones, tables, spirals, etc.). Finely mineralized scheelite, however, has to undergo froth flotation. A very high purity may be obtained by gravity

methods (sometimes > 90% scheelite in the concentrate). The yield is normally 60–70% and sometimes 80–90%. The flotation process allows recoveries of 80–90%. Modern plants combine gravimetric and flotation methods because on disintegration some of the scheelite crystals are broken into fine particles which are lost if only gravity methods are used (scheelite is very brittle). The fine particles can be recovered in a subsequent flotation step. Typical commercial concentrates contain > 70% WO_3 . Fully downstream integrated plants that process their concentrates themselves keep the final WO_3 concentration in the flotation process low (5–40%) to minimize losses, giving overall yields of > 90%.

Wolframite Ore. Gravity methods are used for wolframite ore, sometimes in combination with magnetic separation. The weakly magnetic wolframite properties enable a further concentration. Commercial concentrates should assay > 65%.

26.4.2 Pretreatment of Ore Concentrates and Scrap

Hydrochloric acid leaching of scheelite concentrates at room temperature is used to reduce phosphorus, arsenic, and sulfur content [4].

Calcination in air (500–600 °C) is used to oxidize organic flotation agents which could have a detrimental effect on subsequent processing [15, 16]. Also, in mixtures of concentrates with high sulfide and calcium carbonate contents, gypsum is formed [16], and arsenic and sulfur are removed if they are present in high concentrations in wolframites.

Grinding is necessary for scheelite concentrates produced by gravity methods, and with all wolframite concentrates.

Oxidation of soft scrap by heating in air at 700–800 °C allows the tungsten to be dissolved in subsequent pressure leaching processes [17].

26.4.3 Hydrometallurgy

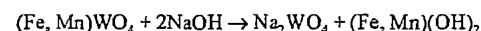
This section deals with the production of high-purity ammonium paratungstate (APT), which is now the most important raw material for all other tungsten products. Only the modern process is described; a comparison with classical methods [7] is given in Figure 26.4. The most important differences are:

- The use of solvent extraction instead of precipitation of CaWO_4 to convert the sodium tungstate solution to ammonium tungstate solution, followed by decomposition to H_2WO_4 .
 - Conversion of the tungsten in aqueous solution to a solid compound by crystallization rather than precipitation. Each crystallization is a slower process than immediate precipitation, and therefore leads to a purer product.
- The advantages of the modern process are:
- The possibility of using various raw materials (wolframite, scheelite, scrap)
 - Better energy efficiency
 - Less labor required
 - Ease of automation
 - Higher yields
 - Uniformity and higher purity of the product

A flow diagram of a modern APT production plant based on various raw materials is shown in Figure 26.5.

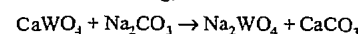
26.4.3.1 Digestion

Wolframite concentrates can be dissolved either at atmospheric pressure with concentrated NaOH solution (40–50%, 15 mol/L) at 100–145 °C followed by dilution [18], or by high-pressure digestion with dilute NaOH solution [19].



Scheelite concentrates are always leached with Na_2CO_3 solution under pressure [4]. The process requires a large excess of reagent, but gives a milder reaction with respect to dissolution of gangue, and can be carried out in mild

steel autoclaves (NaOH treatment requires Inconel cladding).



Mixtures of concentrates of wolframite and scheelite can be dissolved by Na_2CO_3 solutions with addition of NaOH under pressure [20]. Oxidized soft scrap is digested with NaOH solution, as in the treatment of wolframite [15].

Information on the parameters and yields for various chemical leaching processes is given in Table 26.2.

26.4.3.2 Purification

The sodium tungstate solution obtained by leaching the ore contains amounts of dissolved impurity elements depending on the composition of the raw material. If the concentration of

these elements is too high, subsequent processing may be disturbed or the end product may have too high an impurity level. Purification is carried out by precipitation and filtration.

Silicate Precipitation. Silicates are common gangue minerals which dissolve on pressure leaching, at least partially. Dissolved silicate can be precipitated by the addition of an aluminum sulfate or magnesium sulfate solution, or a mixture of the two at pH 8–11 [21]. The chemistry of the precipitation is complex and has not been investigated in detail. With higher silicate content, a two-stage precipitation with a mixture of aluminum and magnesium sulfates is preferable, enabling the SiO_2 content to be reduced to 3060 mg/L [4].

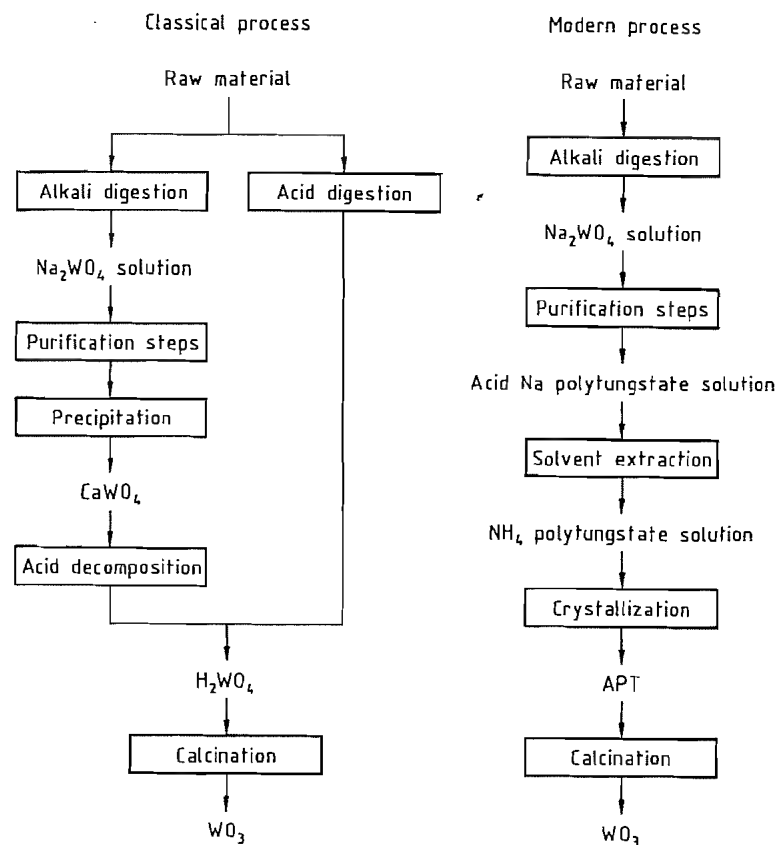


Figure 26.4: Comparison of classical and modern WO_3 production.

Table 26.2: Typical parameters for pressure leaching of tungsten raw materials.

	Scheelite concentrate	Wolframite concentrate	Oxidized scrap
Particle size, μm	<44 to <90	<44	<100
Temperature, $^{\circ}\text{C}$	190–225	175–190	150–200
Pressure, MPa	1.2–2.6	0.8–1.2	0.5–1.2
Time, h	1.5–4	4	2–4
Reagent concentration, %	10–18 (Na_2CO_3)	7–10 (NaOH)	20 (NaOH)
Molar ratio WO_3 :reagent	1:2.5–4.5	1:1.05	1:1.4

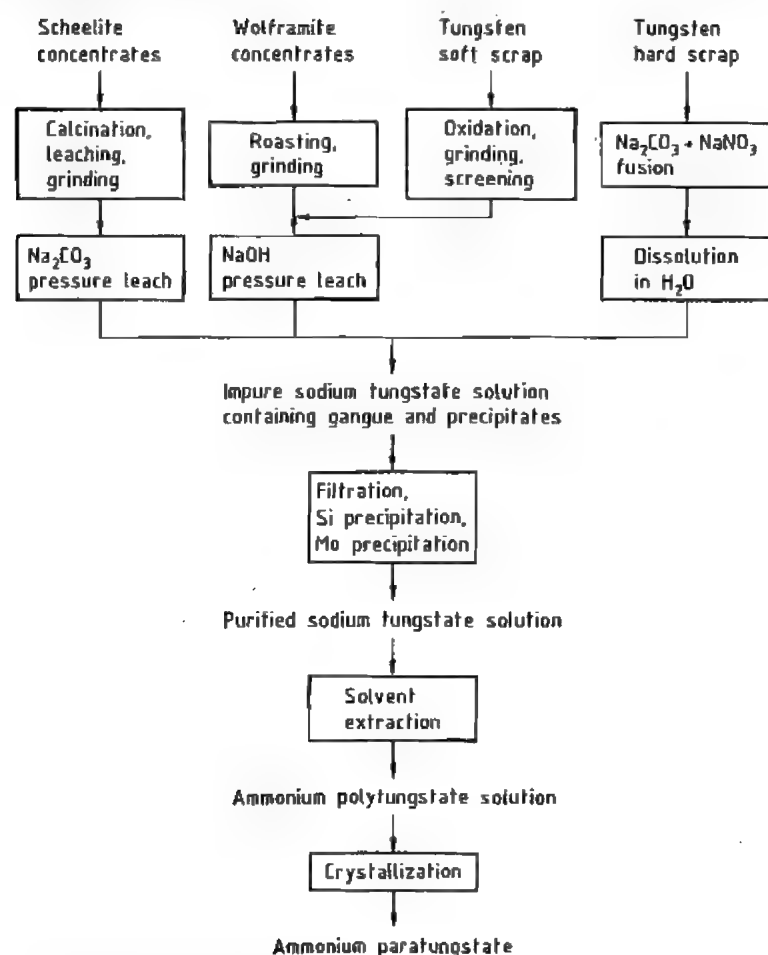


Figure 26.5: The modern APT process.

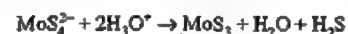
This precipitation technique reduces not only the silicate content, but also the phosphate and fluoride concentration. Precipitation is first performed with magnesium sulfate at pH 10–11, and then with aluminum sulfate at pH 7–8 [22].

Molybdenum Precipitation. Molybdenum is a very common companion element in tungsten ores. It remains in the concentrate and goes into solution on chemical digestion, either completely or partially. Precipitation is carried out by adding excess sodium sulfide to

the neutral or mildly alkaline solution, forming thiomolybdate:



The solution is then acidified with sulfuric acid to pH 2.5–3.0. This causes the molybdenum to be precipitated as the trisulfide [20]:



This purification stage is not only effective for Mo, but also removes a number of other elements that form insoluble sulfides, e.g., As, Sb, Bi, Pb, and Co.

Solvent Extraction [4, 23], (Figure 26.6)

The sodium tungstate solution (pH 2–3) is contacted with the organic phase, which extracts the isopolytungstate ions as an ion associate complex. Mixtures of tertiary or secondary aliphatic amines (e.g., trioctylamine) with isodecanol and kerosene form the organic phase. The amine is the reagent that forms the ion associate complex, the isodecanol increases the solubility of the complex (modifier), and kerosene is the solvent.



Table 26.3: Maximum impurity concentrations in APT crystallization.

Element	Feed solution, mg/L	Mother liquor, mg/L	APT, ppm
Al	<10	<100 ^a <3000 ^b	<10
As	<50	<2000	<20
F	<250	<3000	<10
Fe	<10	<200	<10
Mo	<10	<60	<20
Na	<10	<100	<10
P	<50	<400	<20
Si	<10	<200	<20
V	<100	<1200	<20

^aIn absence of fluoride.

^bFor fluoride concentration of ca. 4000 mg/L.

26.4.3.3 Conversion of Sodium Tungstate Solution to Ammonium Tungstate Solution

In modern plants, this reaction is now carried out exclusively by solvent extraction or ion exchange resins. The sodium ion concentration must be reduced from ca. 70 g/L to <10 mg/L, as sodium levels >10 ppm in the APT cause problems during the reduction to metal powder.

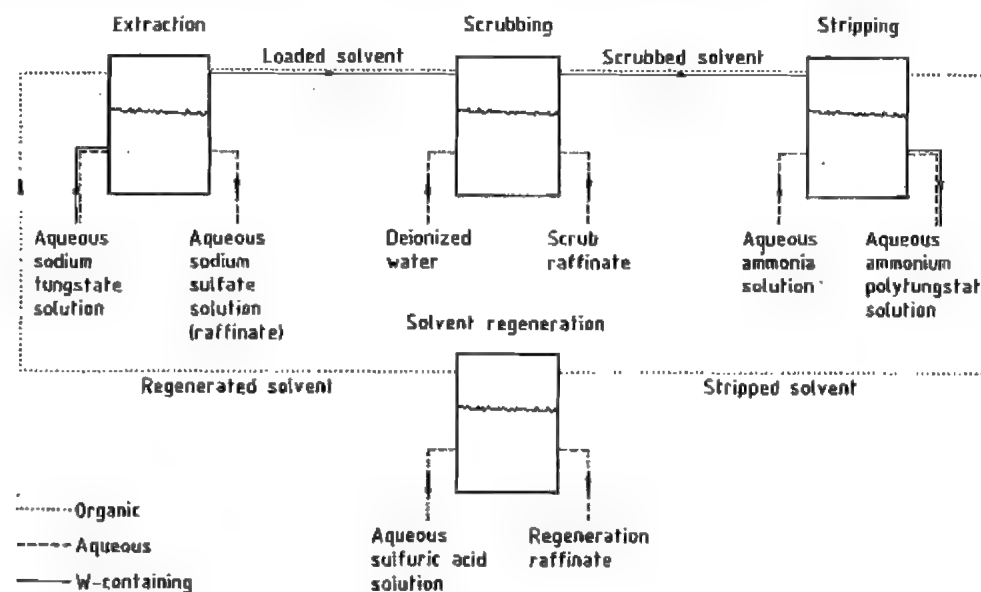
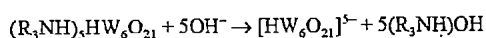


Figure 26.6: Tungsten solvent extraction.

The extract is washed with deionized water, and the isopolytungstate is then reextracted with dilute ammonia solution into an aqueous phase:



The solvent goes through a regeneration stage and is then returned to the extraction process.

Ion Exchange Process [24, 25]

This process is now used only in small plants in China. A strongly alkaline ion exchange resin in the chloride form is used. On contact with the sodium tungstate solution, the tungstate is adsorbed. Desorption is carried out with ammonium chloride solution. Elements that form heteropolytungstates, e.g., Si, P, As, and Mo, can be removed.

26.4.3.4 Crystallization of Ammonium Paratungstate (APT) [26]

This compound has the formula $(NH_4)_{10}(H_2W_{12}O_{42}) \cdot 4H_2O$.

On evaporation of the isopolytungstate solution, water and ammonia are distilled, the pH of the solution decreases, and the sparingly soluble APT crystallizes [27, 28]. The ammonia-water mixture is condensed and recycled to the solvent extraction process. The crystallization conditions are used to control the physical properties that influence the subsequent processing to give tungsten powder. The process is carried out batchwise or continuously in recirculating crystallizers with partial recycling of mother liquor (to maintain the concentration of impurities in the mother liquor and hence in the crystals formed). Owing to the low solubility of APT compared with the impurities in the mother liquor, this process step represents not only a conversion from the dissolved form to a solid, but also a very important purification (Table 26.3).

26.4.4 Calcination of Ammonium Paratungstate [4, 21]

On heating APT to 400–800 °C, ammonia and water are evolved. This decomposition becomes more complete as the temperature and duration of heating are increased. The form of the solid phase is determined by the decomposition temperature, the retention time in the reactor, and the reduction potential of the decomposition atmosphere. If heating takes place with air addition, yellow WO_3 is obtained; with exclusion of air, blue oxide. In the blue oxide, some tungsten atoms are pentavalent, owing to H_2 reduction (NH_3 decomposition). Unlike the yellow oxide, blue oxide is not a single, well-defined chemical compound. It contains WO_3 together with the oxides $W_{20}O_{58}$ and $W_{18}O_{47}$, depending on the decomposition conditions, and also ammonium and hydrogen tungsten oxide bronzes (residual NH_3 and H_2O content). Nevertheless, it is currently used more than the yellow oxide.

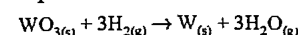
On an industrial scale, calcination is usually carried out in rotary furnaces, more rarely in pusher furnaces. The former yield a more uniform product. The chemical composition and micromorphology of the oxide particles are determined by the duration and temperature of heating. The micromorphology is very important in the production of submicron tungsten powders.

26.4.5 Reduction by Hydrogen to Tungsten Metal Powder [29–31]

The production of tungsten metal powder is today carried out almost exclusively by the hydrogen reduction of high-purity tungsten oxides (WO_3 , WO_{3-x}). Reduction of the oxide by carbon is now used only for the production of tungsten carbide (direct carburization). The reduction of tungsten halides (Axel Johnson process) has not become established on a large scale.

The reduction of tungsten trioxide or blue oxide can be controlled by the temperature and the water vapor partial pressure.

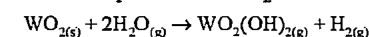
At lower temperatures (600 °C) and lower moisture contents, the reduction proceeds by solid-state diffusion of the oxygen out of the oxide, and can be represented by the following equation:



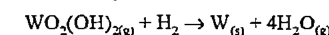
On complete reduction, an oxide-pseudomorphic metal sponge is formed.

At higher temperatures and moisture contents, the reaction proceeds stepwise via the oxides $W_{20}O_{58}$, $W_{18}O_{47}$ and WO_2 to tungsten metal. Only the first transformation to $W_{20}O_{58}$ and each nucleation of a newly formed phase on further reduction are solid-state reactions. All other transformations are linked with gas-phase transport of tungsten as the volatile oxide hydrate $WO_2(OH)_2$, and are associated with a significant change in shape of the crystal faces. The formation of the vapor-phase oxide hydrate takes place by reaction of the corresponding suboxide with water formed in the reduction. The vapor pressure of the oxide-hydrate in equilibrium with a stable compound formed under the reaction conditions is lower than that in equilibrium with the continually decreasing amount of the unstable compound. As a result of these gradients, chemical vapor transport (CVT) takes place, so that the higher oxide decreases in quantity, and the lower oxide increases. The interphase reaction can plausibly be divided into three steps:

- Formation of $WO_2(OH)_2$ from the oxygen-rich compound with H_2O



- Transport of $WO_2(OH)_2$ to the compound of lower oxygen content
- Reduction of $WO_2(OH)_2$ by hydrogen at the surface of the compound of lower oxygen content (or the metal)



Formation of a new phase must be preceded by nucleation. This takes place on the surface of the reacting oxide if the water vapor pressure is lower than the equilibrium water vapor pressure for the phase transformation concerned. The nucleus then continues to grow as described above.

Reduction on an industrial scale is carried out in pusher furnaces, in which the powder passes through the furnace in boats, or in rotary furnaces. Walking beam furnaces or furnaces with internal band conveyors are less often used. Furnaces are provided with several temperature zones controllable between 600 and 1100 °C. The flow of hydrogen is usually in a countercurrent direction, more rarely cocurrent, and a drying stage is always included in the circuit, as a large excess is used. The hydrogen acts not only as a reducing agent, but also carries away the water formed. The flow rate is therefore one of the parameters for controlling the water vapor partial pressure. Other control parameters are:

- The amount of oxide charged to the furnace per unit time
- The depth of the oxide bed
- The porosity of the oxide bed (particle size and particle size distribution)
- The moisture content of the hydrogen entering the furnace

The porosity and depth of the bed, in conjunction with the H_2 flow rate, determine the rate of diffusion of water vapor from the bed.

In practice, the average grain size of the tungsten powder (0.1–60 μm) is controlled empirically by setting the temperature, oxide quantity, heating time, and H_2 flow rate. In general, these have the following effects:

- Fine Powder: lower temperature, low bed depth, long dwell time, and high H_2 flow rate. These conditions correspond to a low water vapor partial pressure (and hence a more rapid nucleation rate), low crystal growth rate via the gas phase and short transport distances of $WO_2(OH)_2$. The furnace capacity is low.
- Coarse Powder: high temperature, greater bed depth, lower heating time, lower H_2 flow rate. These conditions correspond to a high water vapor partial pressure, a lower rate of nucleation, and more rapid transport via the gas phase over longer distances. The furnace capacity is high.

In the powder bed, there is a water vapor concentration gradient, as diffusion from the interior takes longer than from the outer parts. This leads to a grain size distribution in the tungsten powder; the powder in the interior of the bed is coarser than that in the outer zones and at the surface.

Doping with low concentrations of alkali metals (Na or Li salts) catalyzes crystal growth during the reduction process, and enables coarser tungsten powders (100–200 μm) to be produced [32].

26.4.6 Production of Compact Metal

Conversion of tungsten metal powder to compact metal is carried out exclusively by powder metallurgy, i.e., by a heat treatment (sintering) of a compacted preform.

Compaction. In the first step, the powder is compacted hydraulically or mechanically by a polydirectional pressure of 200 MPa (2000 bar) to produce preforms—rods or plates that have edge stability and are of the correct dimensions. Circular blanks with a low height/diameter ratio and small items such as pins are produced in automatic presses at high outputs. The raw material for this must consist of free-flowing granules similar to the granulated hard metals produced in spray drying equipment [33].

Sintering. Pure tungsten is today sintered almost exclusively by the economic indirect sintering process. Furnaces for this consist of tungsten heating elements surrounded by radiation shielding made of tungsten sheets on the inside and molybdenum on the outside, and are purged with hydrogen as a protective gas. At maximum sintering temperature (2800 °C), sintering times of several hours are required. In the production of so-called non-sag tungsten for incandescent lamp manufacture, direct sintering, i.e., by passage of an electric current, is usual. In both processes, the sintered densities achieved are ca. 95% of theoretical.

The weight of individual sintered tungsten components is usually 1–100 kg. The choice of optimum sintering parameters greatly influences the structure and hence the strength and ductility of sintered tungsten.

In the direct sintering process, very high sintering temperatures, and hence short sintering times can be used. However, the practical limits on rod dimensions and production rates are a considerable disadvantage, and electricity costs per kilogram are significantly higher than with indirect sintering. Also, the fixing points, which are poorly sintered, must be knocked off the rod, causing further loss. Disadvantages of the indirect sintering process include the high cost of the plant and heating elements. Nevertheless, overall this process is considerably more economic, and it is the only process that allows the sintering of preforms.

Another important aspect is that sintering is an extremely effective purification process, removing a high proportion of impurities from the material. The hydrogen flow rate during sintering should therefore be high enough to transport the impurities away.

Melting. Approximately since the 1950s, i.e., after the development of electric arc melting plants and high-capacity vacuum equipment, it has been possible to melt highly refractory metals on an industrial scale. Some time later, trials on plasma melting and electron beam melting of tungsten showed that these processes led to a product with extremely coarse crystals and hence poor working properties, so these melting processes are of no technical value for tungsten (unlike molybdenum and its alloys). Electron beam zone melting is in fact used in the production of single crystals of tungsten [5], but these products have only a few special uses as production costs are high.

26.4.7 Processing of Sintered Parts

26.4.7.1 Shaping

Completely dense, pore-free bodies cannot be obtained by sintering, the residual porosity being 3–10%. To obtain a completely dense

material, a complex multi-stage forming process is required. Tungsten can be shaped by all the usual forming processes, e.g., forging, rolling, extruding, and wire drawing. The first forming step is usually carried out at 1500–1700 °C. Many reheating stages are necessary in the first stages of shaping, as the heat is rapidly lost at these temperatures and a stress-relieving operation below the recrystallization temperature is often advantageous. Intermediate heating operations are necessary for recrystallization. The forming temperature is progressively reduced, since the recrystallization temperature decreases as forming proceeds. To give a well-defined fiber structure (high degree of deformation), a final cold forming can be carried out, as already stated.

Chipless Forming, Including Stamping and Cutting. The temperature range for the forming of tungsten has a lower limit, set by the transformation temperature, and an upper limit, set by the recrystallization temperature. Thin, strongly deformed sheet and foil have a pronounced structure in the longitudinal direction due to elongation of the grains during rolling. The bending properties along the direction of rolling are therefore different from those across it. Tungsten sheet should therefore always be bent perpendicular to the rolling or longitudinal direction. If bending in the longitudinal direction cannot be avoided, owing to the design, a much higher temperature is required.

Tungsten can also be formed at high temperatures by pressing, flow-turning (spinning), or forging.

Die stamping of tungsten sheet is possible if the working temperatures of the sheet and the tool are kept high.

Tungsten can be punched and forged at high temperatures. Blunt edges on punching tools and shears, or low punching or cutting temperatures can cause cracking and splitting.

Machining. Tungsten can be drilled, turned, milled, planed, and ground. However, machining operations require great experience and close adherence to optimum conditions [3]. Complex shapes and holes can be produced by

spark erosion; the tungsten workpiece forms the anode and the working electrode the cathode. Suitable electrode materials can be based on tungsten–copper.

26.4.7.2 Mechanical Bonding of Tungsten to Tungsten and Other Metals

Rivets. Tungsten components can be bonded together or to components made of other metals by means of rivets, provided the joint need not be impermeable to liquids and/or gases. Tungsten rivets and round-head and countersunk molybdenum rivets can be used.

Brazing. The parts to be joined must be free from grease, oils, oxides, or other impurities, and should preferably be etched immediately before brazing. As tungsten is very sensitive to oxidation, it is preferable to carry out the operation under a protective gas, hydrogen, or vacuum. Parts with a large surface area or of complex geometric shape should be brazed in a furnace with the aid of a special jig. If brazing temperatures exceed 1150 °C, there is a possibility of recrystallization. Typical brazing metals and temperatures are: Rh (1970 °C), Pd (1550 °C), CuNi45 (1300 °C), etc. [3].

Welding. Tungsten has only moderate welding properties. The weld seams have a coarse-grained structure in the hot fusion zone, owing to recrystallization, and can therefore withstand only low mechanical stresses. If welding is unavoidable, weld seams should if possible be located in regions of low internal and mechanical stress. It is preferable to locate weld seams as far as possible from the edges or ends of fabricated articles.

Tungsten inert gas (TIG) welding can be performed in protective gas chambers. However, in electron beam welding, the melting and hot fusion zones are much more limited in size, so this technique is preferable for welding tungsten. It is advantageous to preheat the parts to be joined to ca. 700–800 °C by a defocused electron beam immediately before welding. Welded components should be

cooled as slowly as possible. Tungsten can be electron beam welded to tungsten-rhenium and molybdenum-rhenium alloys, copper, and stainless steel. Tungsten-rhenium alloys are recommended as filler metal for welding tungsten.

As fusion welding can be used only under certain circumstances, diffusion welding of tungsten to tungsten and to other metals is important. Despite the high melting point of tungsten, temperatures of 1300–2000 °C and pressures of 2–20 N/mm² give satisfactory joints. The diffusion welding of tungsten is carried out in either vacuum or pure hydrogen.

Thin intermediate layers in the form of films of nickel, platinum, rhodium, ruthenium, and especially palladium, considerably accelerate the diffusion processes.

Tungsten wires and small tungsten components can be bonded to fusible alloys based on iron-nickel-cobalt and to other metals by spot welding under a protective gas blanket. The use of small pieces of foil made of platinum, niobium, tantalum, or zirconium is recommended. Laser beam welding of tungsten is likely to become very important in the future.

26.4.8 Surface Treatment

Tungsten components can be degreased with trichloroethylene, perchloroethylene, and similar solvents.

Tungsten can be etched with alkaline and acid media. Whereas oxidized tungsten is more easily cleaned with alkaline etchants, grinding residues and metallic contamination are more easily removed by acids; very clean tungsten surfaces can be obtained by alkaline etching followed by acid etching.

An alkaline etchant can consist of molten NaOH containing 10% NaNO₂. The melt temperature is 400–450 °C. Thin oxide films can also be removed by dipping tungsten in alkaline solutions of K₃[Fe(CN)₆]. Other common alkaline etchants are 10% solutions of NaOH or NH₃/H₂O₂. Acid etchants usually consist of HNO₃/HF/H₂O mixtures. Other commonly used mixtures are HNO₃/HF/CH₃COOH and HClO₄/H₃PO₄/H₂O.

Electropolishing. Tungsten can be anodically electropolished in a K₂CO₃/KClO₃/NaOH/H₂O mixture. Another possible electrolyte is CH₃OH/H₂SO₄/HF.

26.4.9 Tungsten Coatings

Tungsten coatings are applied to metals, glass, ceramics, semiconductors, inorganic woven products, uranium carbide nuclear fuel granules, etc., for a large number of reasons, including the improvement of wear resistance, corrosion resistance, emissivity, and high-temperature properties [5]. The most important processes used today are:

Plasma Spraying. This process is often used to apply very thick tungsten coatings (e.g., in the construction of engines and rockets), as the flame spraying process (used successfully with molybdenum) cannot be used with tungsten. The cathode material in the plasma burner is also tungsten.

Vacuum Vapor Deposition, Ion Sputtering, and Physical Vapor Deposition (PVD). In most of the usual coating processes, the substrate material must be raised to a high temperature, which usually has a detrimental effect on its mechanical properties. When tungsten is deposited by vacuum vapor deposition or ion sputtering onto a relatively cool substrate, these problems can be largely avoided. These coating methods are therefore very useful for metallizing semiconductors, ceramics, glasses, and also metals. The coatings are comparatively thin, but adhere well [34].

Deposition from the Vapor Phase, Chemical Vapor Deposition (CVD). Suitable readily vaporizable tungsten compounds include chlorides, fluorides [35], carbonyl compounds, and organometallic tungsten compounds. The carrier gas is hydrogen or a noble gas. Tungsten and tungsten alloys are applied in this way to, e.g., nuclear fuels (UC, UO₂), metallic substrates, and semiconductors. Small tungsten components are today manufactured by CVD.

Electrolytic Methods. Although there is an extensive patent literature [5] on the electrolytic deposition of tungsten coatings on metallic substrates, the method is not of practical significance. The production of tungsten coatings by diffusion, metallization, or cladding (including explosion cladding), has often been proposed, but has not become established as an alternative to other methods.

26.4.10 Production of High-Purity Tungsten Metal (99.999–99.9999 %)

The starting material is ammonium paratungstate (APT) of normal purity, but with uranium and thorium contents as low as possible. Important steps to high purity include:

- Selective extraction of uranium and thorium [36]
- Multiple crystallization of APT (giving a general reduction in the various trace impurities)
- Working under clean-room conditions [38]
- Electron beam zone melting [37, 39]

26.5 Uses

The uses of tungsten, its alloys, and compounds are extremely diverse. They can be divided into the following large groups (by consumption):

Hard metals	50–60%
Steel	20–30%
Tungsten metal and its alloys	6–20%
Tungsten chemicals (for uses, see Section 26.7)	4–8%

Hard Metals. These products represent by far the largest consumption of tungsten worldwide. With few exceptions, their main component is tungsten carbide (WC). Carbides, nitrides, or carbonitrides of Ti, Nb, Ta, and Hf can also be present as mixed crystal formers. The hard material phases are bonded together by a ductile metallic phase that surrounds them (cemented carbides), usually Co, more rarely Ni or Fe alloys.

The outstanding properties of the hard metals are their high hardness and wear resistance, especially at high temperatures, combined

with good toughness properties. This unusual combination of properties is achieved by combining the hard and brittle carbide phase(s) with the ductile and deformable binder. By varying the carbide/binder ratio, and by suitable choice of the carbide composition, the properties can be varied within wide limits. A further control parameter for certain properties is the microstructure, i.e., the grain size of the carbide phase(s), which can be controlled via the particle size of the powder used, the powder milling, and the sintering conditions.

The most important groups of applications of hard metals are:

- Metal cutting tools (drilling, turning, milling)
- Tools for processing wood and plastics
- Drilling tools in mining and mineral oil and water drilling technology
- Wear-resistant components in a wide range of machinery (a continuously increasing group with the widest diversification)
- Elastically bonded abrasive materials

Steel. Tungsten is added to a very wide range of steels in a concentration of 1–18%. It increases the hardness and wear resistance at high temperatures (carbide formation), resistance to thermal shock, and high-temperature properties. The main areas of use are in high-speed steels, high-temperature steels, and tool steels. The use of tungsten in steel is significantly greater in China and the former Eastern Bloc countries, as high-speed steel is still used for many applications rather than hard metals, as in the West. In the United States, tungsten has mainly been replaced by molybdenum in high-speed steels.

Tungsten and Tungsten Alloys. This group represents the widest range of uses. It extends from everyday uses, e.g., the coil of an incandescent lamp or the contact tip of an automobile horn, to components of nuclear fusion reactors or ion drive motors in space probes. The reason for this range of uses lies in the many outstanding properties of tungsten:

- High melting point
- Low vapor pressure

- High atomic number
 - Good electrical and thermal conductivity
 - High density and modulus of elasticity
 - Wide radiation band in visible light and good light yield
 - Good X-ray yield
 - Expansion coefficient comparable to those of glass and silica
- The following list shows this versatility very clearly.

● *Lighting Technology*

- Incandescent lamps (NS-W)
- Halogen lamps (NS-W)
- Gas discharge lamps: Hg, Na vapor lamps (W)
- Fluorescent tubes (W)
- Xe short arc lamps (W, W-ThO₂, W-Re)

● *Electrical and Electronic Technology*

- Sputter targets in VLSI technology (W-Ti, high-purity W)
- Transistors (W)
- Diodes (W)
- Electronic tubes (W, W-ThO₂, porous W with Ba or ThO₂)
- Thyristors (W)
- Switch contacts [W, W-Cu, W-Ag, W-Fe-Ni-(Cu)]
- Heat sinks (W-Cu)

● *High-Temperature Technology* (furnace construction, nuclear energy, thermal power stations)

- Structural components (W)
- Walls of fusion reactors (W, W-Re-ThO₂, W-Re-HfC)
- Construction components in the plasma space in magnetohydrodynamic electricity production (W, W-Cu)
- Thermocouple elements (W/WRe, W/Mo, W/Ir, W/graphite)
- Heating elements (W)

● *Vacuum and Plasma Metallization, Welding, Spark Erosion*

- Nozzles (W-ThO₂)

- Electrodes [W-ThO₂, W-Ag, W-Fe-Ni(Mo)]

- Welding electrodes (W-ThO₂, W-LaO₂, W-CeO₂, W-ZrO₂, W-Y₂O₃)

● *X-Ray and Radiation Technology, Medical Technology*

- Anodes (W)
- Rotating anodes (W-Re)
- Containers for radioactive materials (W-Fe-Ni)
- Components for radiation shielding, e.g., collimators in computer tomography scanners [W-Fe-Ni-(Cu)]

● *Machinery and Motor Construction*

- Governor balance weights, counterbalance weights, flywheel weights and other weights, e.g., in Formula 1 racing cars [W-Fe-Ni-(Cu)]

● *Chemical Industry*

- Electrodes, nozzles, crucibles (W)
- Construction materials (W-Mo)

● *Space Travel*

- Rocket nozzles (W, W-Ag)
- Space nuclear reactors (W-Re)
- Thermionic converters (porous W, CVD-W, W-Re)
- Ionic reactive thrust motors (porous W)
- Structural components (tungsten fiber-reinforced niobium matrix composites, superalloys, Al, Ti)

● *Armaments*

- Armor piercing shells, armor plating, scatter grenades, shaped charge liners, counterweights in tanks, nozzles for air-to-air rockets, gas rudders (W-Fe-Ni, W-Cu, W-ThO₂)

● *Aircraft*

- Aircraft nose counterweights (W-Fe-Ni)
- Turbine blades of fiber-reinforced nickel-based superalloys (W-Re-ThO₂ and W-Re-HfC fibers)

● *Laser Technology*

- Cathodes (porous W/barium aluminate)
- Components of gas lasers (W-Cu)

26.6 Analysis

26.6.1 Raw Materials

The determination of the tungsten content of ore concentrates and scrap is very important, as the price is calculated from this. Sampling procedures are also extremely important, as the high density of tungsten can easily lead to segregation [40]. Determination of tungsten itself is almost exclusively carried out by X-ray fluorescence analysis [41]. Thus, matrix effects are compensated for by dissolution and dilution, and by the addition of an internal standard. Molten lithium tetraborate is widely used as a solvent, with tantalum pentoxide as an internal standard. Matrix corrections are carried out with computer programs.

26.6.2 High-Purity Intermediate Products, Tungsten Powder, and Compact Tungsten Metal

In these materials, it is not sufficient to determine the tungsten. In any case, especially in the metallic state (99.97–99.98% W) this would be far too inaccurate. Here, it is important to measure trace impurity contents. In all these products, the specifications applicable are very rigorous, setting maximum acceptable upper limits for concentrations of individual elements. For industrial tungsten and its high-purity precursor materials, these are all in the µg/g range, the maximum tolerable level for most elements being 10 µg/g. Exceptions include Mo (50 µg/g), Si (20 µg/g), and H (1 µg/g).

Routine determination of trace elements is mainly carried out by the following methods:

- Flame atomic absorption spectrometry
- Graphite tube atomic absorption spectrometry
- Inductively coupled plasma optical spectrometry
- Photometry
- Vacuum fusion hot extraction (H, N)
- Carrier gas hot extraction (O)

- Ignition in oxygen combined with IR spectrometry (C)

Up-to-date literature on this topic is rare, as improved and refined analytical methods are increasingly regarded as industrial secrets. The determination of metallic trace impurities is described in [42, 43], and of nonmetallic trace impurities in [44–46].

Large samples are always used. The result therefore always represents a mean value. Also, these analyses give no information on the distribution of a trace element and its state of bonding in the compact metal [47, 48]. It is well known that impurities can exist in various forms and states of combination in metals (dissolved interstitially or as mixed crystals, as precipitates in the crystal or at grain boundaries, etc.). This knowledge is often important for subsequent treatment processes or for the final properties. Topochemical analytical methods are also used:

- Scanning electron microscopy coupled with energy or wavelength dispersive X-ray spectrometry
- Auger electron spectroscopy
- Auger microprobes
- Ion beam microprobes UV and X-ray photoelectron spectrometry, etc.

These techniques are not used routinely, mainly because of their cost, but for special applications and in research.

Heterogeneous impurities represent a special case (though often widely occurring) of particular importance in powder metallurgy. These impurities are small foreign particles present in a certain statistical distribution alongside the matrix particles. In most cases, they are due to mechanical abrasion or corrosion of production equipment. They can become concentrated in furnaces by vaporization, and can then end up in the material. Organic materials can also be present in the powders, e.g., fibers from filter cloths, packing materials, or plastic films. The various types of heterogeneous impurities, their effects, and their analytical determination are described in [49–52].

The presence of this type of heterogeneous impurity can lead to very serious material defects on powder metallurgical processing. Unlike molten metallurgical processes, where small foreign particles can dissolve in the homogeneous melt or slag, and hence cause very little change to the composition, the sintering of a compact can still leave locally high concentrations of a foreign element. Consequently, many kinds of defects can occur, e.g., empty or filled pores, porous zones, zones with completely changed material properties, etc., leading to fractures and cracks on subsequent processing. Fine wires and thin sheets are therefore extremely sensitive to heterogeneous impurities.

In the characterization of tungsten powder, physical analysis is important as well as chemical analysis [53]. Typical powder characteristics include:

- Mean grain size (Fisher sub-sieve sizer, ASTM No. 430-1970)
- Morphology, heterogeneity (scanning electron microscopy, SEM)
- Particle size distribution (sedimentation, laser scattering, ultracentrifuge)
- Bulk, tapped, and pressed density
- Specific surface area (BET method)
- Degree of agglomeration

26.6.3 Trace Elements in High-Purity Tungsten Metal

In high-purity tungsten metal, levels of trace elements are in the ng/g range. There are therefore special analytical requirements:

- Working in a clean-room laboratory
- Prevention of any other contamination
- Correct calibration, etc.

Comparisons between various methods and laboratories show clearly that in trace analysis of this kind the results can have considerable scatter [54, 55]. The analytical techniques are always very complex and expensive, the most important being:

- Glow discharge mass spectrometry
- Secondary ion mass spectrometry

- Isotope dilution mass spectrometry
- Trace matrix separation combined with inductively coupled plasma mass spectrometry

Very significant improvements in this type of analysis have been achieved, especially in recent years [38].

26.7 Compounds and Intermetallic Compounds

26.7.1 Tungsten Chemistry

Tungsten occurs in all oxidation states from 2+ to 6+ inclusive, the most important being 6+. Valencies between 2- and 1+ exist only in organometallic compounds and compounds with π -acceptor ligands. In the lower valencies, tungsten forms bases (sometimes unstable), but in the higher valencies it forms very stable acids.

Tungsten combines with most elements and with a large number of inorganic and organic ligands. The highest coordination number is 8, and the most important donor atoms are O, N, S, and the halogens. Tungsten has a very marked tendency to form polymeric compounds.

This chemistry is extremely complex [58, 59], as the tungstate anion exists in monomeric form only in strongly alkaline solutions. In mildly alkaline solution, the tungstate anions begin to polymerize, and this progresses with decreasing pH. Below pH 1, sparingly soluble tungsten oxide hydrate (tungstic acid) precipitates. Various degrees of polymerization (isopolytungstates, metatungstates, paratungstates, etc.) are favored as the pH changes [60]. Other parameters influencing the polymerization include concentration, temperature, and time. Time plays an important role in reactions that proceed slowly. Thus, the properties of mildly acid or almost neutral solutions of tungsten change markedly after long periods of storage (a process often referred to as aging). Foreign ions also influence various polymerization reactions. Ammonium ions favor polymerization, even at higher pH values.

This is why $(\text{NH}_4)_2\text{WO}_4$ cannot be crystallized from aqueous solution (it always forms APT), but only from tungstic acid and liquid ammonia. Anions such as phosphate, silicate, arsenate, etc., copolymerize with tungstates to form heteropolytungstates which usually have a higher degree of polymerization than the isopolytungstates stable at the same pH. Several isopolytungstates group around the central heteropolyanion.

Fluoride, sulfide, and peroxo anions have a depolymerizing effect, as these replace O atoms on the W [58]. The substitution of several O atoms by organic compounds with two or more donor atoms leads to the formation of numerous chelate complexes, and hence to depolymerization [58].

There are a number of compounds of tungsten with the elements Al, Be, Co, Ni, Fe, Zr, Hf, Ir, Os, Re, Ru, and Tc which can play a positive or negative role in the metallurgy of tungsten alloys. A comprehensive review of the literature on this subject can be found in [4].

26.7.2 Tungsten-Boron Compounds [4, 61]

The following compounds are known: W_2B , WB , W_3B_5 , and WB_4 . They are prepared by sintering the elements, from the oxides in an aluminothermic reaction, or by deposition from the gas phase. They are hard, brittle, crystalline, and electrically conducting, and are of no industrial importance.

26.7.3 Tungsten-Carbon Compounds [4]

There are three carbides (Table 26.4): W_2C , WC, and the cubic high-temperature phase $\alpha\text{-WC}_{1-x}$.

Table 26.4: Physical properties of tungsten carbides.

	mp, °C	Crystal system	Density, g/cm ³
W_2C	2770	hexagonal	17.2
WC	> 2600 (decomp.)	hexagonal	15.6
$\alpha\text{-WC}_{1-x}$	ca. 2750	cubic	

Production. The carbides are formed from tungsten or its compounds by reaction with carbon or carbon compounds. The most important industrial process is the reaction of tungsten metal powder with carbon black or graphite at 900–2200 °C. The reaction of WO_3 with carbon is of less importance, as it is difficult to control the carbon balance.

Industrial Importance. WC is quantitatively the most important tungsten compound because of its hardness. It is also used as a reforming catalyst.

W_2C , like WC, is present in the carbide melt used for "hard facing".

Mixed-crystal carbides such as WC–TiC (50:50) and WC–TiC–Ta(Nb)C (very variable composition) are widely used in hard metal production.

The η -carbides, of composition $\text{Co}_6\text{W}_6\text{C}$ and $\text{Co}_2\text{W}_4\text{C}$ to $\text{Co}_3\text{W}_3\text{C}$, and analogous compounds with Fe occur as intermediates in tungsten-containing steels and in special grades of hard metal.

Tungsten Hexacarbonyl $\text{W}(\text{CO})_6$ [62]. This can be produced from $\text{W} + \text{CO}$ or from $\text{WCl}_6 + \text{CO} + \text{Al}$. It is a white, crystalline substance that decomposes at 150 °C and is soluble in organic solvents, e.g., CCl_4 . It is used as a catalyst in organic syntheses.

26.7.4 Tungsten-Silicon Compounds [4, 61–63]

The following compounds are known: WSi_2 , W_5Si , W_3Si_2 , W_2Si_3 , and W_5Si_2 . They are produced by heating the elements together. They are hard and stable to 900 °C. Tungsten silicide sputter targets are used in microelectronics to produce WSi_x films because of their exceptional characteristics and their thermal and chemical stability.

26.7.5 Tungsten-Nitrogen Compounds [62]

The following compounds are known: W_2N and WN. They are not formed by reaction of the elements, but by heating tungsten in am-

monia gas. They are of no industrial importance.

26.7.6 Tungsten-Phosphorus Compounds [4, 63]

The following compounds are known: WP_2 , WP , W_2P . These can be synthesized from the elements. They are of no industrial importance.

26.7.7 Tungsten-Arsenic Compounds [4]

The following compounds are known: WAs_2 , W_2As_3 . Synthesis is from the elements. They have no industrial importance.

26.7.8 Tungsten-Oxygen Compounds

Oxides [62, 64]. In the W-O system, there are not only the stoichiometric oxides WO_3 , $WO_{2.9}$, $WO_{2.72}$, WO_2 , but also nonstoichiometric structures that represent the ordered or partially ordered defect structures of the oxygen-rich oxides, in which the central W atom is octahedrally surrounded by six oxygen atoms. In WO_3 , neighboring octahedra are in contact only at the corners. With increasing oxygen deficiency (reduction, conversion to lower oxides), common edges and surfaces are progressively formed.

Tungsten trioxide, WO_3 , is formed on strongly heating tungstic acid or APT in air. It is yellow, but even a small oxygen deficiency leads to greenish colorations. There are several crystallographic modifications which differ structurally from each other (variable distortion of the WO_6 octahedra). Commercial WO_3 (density 7.29 g/cm³) is monoclinic at room temperature. Heating to just below 700 °C leads to orthorhombic WO_3 , and above this temperature to the tetragonal form. It begins to vaporize appreciably below its melting point (1473 °C). It is much more volatile in the presence of water vapor. WO_3 is soluble in alkaline solutions and melts.

$WO_{2.9}$ ($W_{20}O_{58}$) is bluish-violet, and occurs as an intermediate product during the reduction of WO_3 with hydrogen. It can be prepared by the reduction of WO_3 by moist hydrogen (e.g., 500–550 °C, water vapor pressure 60 kPa). It is a component of commercial blue oxide.

$WO_{2.72}$ ($W_{18}O_{49}$) is reddish-violet, and above 570 °C occurs as a characteristic needle-shaped intermediate product of WO_3 reduction. It is prepared in the pure state by reducing WO_3 with moist hydrogen (e.g., 800 °C, water vapor pressure 80 kPa). It can be present at low concentrations in industrial blue oxide.

Tungsten dioxide, WO_2 , is chocolate brown in color, and is also an intermediate product of the reduction of tungsten compounds. It forms monoclinic crystals with a distorted rutile structure, and is therefore structurally very different from the higher oxides. The pure material is produced by reduction of WO_3 with moist hydrogen (e.g., 900 °C, water vapor pressure 50 kPa).

β -Tungsten, W_3O , [65, 66], is a gray or black substance produced at low reduction temperatures, usually during the reduction of doped tungsten oxides. It has a cubic A_{15} structure, and was first described as an allotropic modification of the metal, later as the suboxide W_3O . It is now thought that it is a metastable metallic phase stabilized by oxygen. It is stabilized by a series of other foreign elements, e.g., K, Be, P, B, As, and Al. It occurs as a characteristic intermediate product in the reduction of tungsten oxides doped with K, Al, and Si. Pure β -tungsten (by X-ray analysis) can be prepared by reduction of a thin layer of $W_{20}O_{58}$ powder in dry hydrogen at 500–600 °C.

Oxide Hydrates. $WO_3 \cdot H_2O$ or $WO_2(OH)_2$ [67] occurs as a monomeric gaseous compound during the industrial reduction of tungsten oxides with hydrogen at > 600 °C. It is formed by the reaction of the oxides with the water vapor formed during the reduction, and is the substance on which the chemical vapor transport of tungsten depends.

Tungstic Acids [4, 62, 68]. H_2WO_4 is formed when a hot alkali metal tungstate solution is acidified with a strong acid. It is a yellow powder, very sparingly soluble in water and acids, but very soluble in alkaline media.

White tungstic acid is obtained by precipitating in the cold and reversing the order of addition. It corresponds to the composition $WO_3 \cdot xH_2O$, where $x \approx 2$.

If tungstic acids are dried at < 300 °C, the orange-yellow hemihydrate $2WO_3 \cdot H_2O$ is obtained.

Tungstic acid was formerly the most important high-purity intermediate product used in tungsten production, but has now been replaced by APT.

Tungstic acid in a highly pure form is today produced from APT by treatment with strong acids, and is used in the production of very fine tungsten powder and various tungsten-based chemicals.

Tungstates [4, 62, 69]. These are formed by most metal cations (e.g., Na_2WO_4 , $NiWO_4$, Cr_2WO_6 , ZrW_2O_8). The structure of the tungstates is mainly determined by the size of the metal cation. Tungstates with large bivalent cations (> 0.1 nm) have the scheelite structure, and those with smaller ions (< 0.1 nm) the wolframite structure. Apart from the alkali metal and magnesium tungstates, these are all sparingly soluble in water. All the most important ores are tungstates.

Sodium tungstate crystallizes with two molecules of water of crystallization. Aqueous solutions are used as heavy liquids, in fuel cells, for flame-resistant and antistatic textiles, in cigarette filters, and as corrosion inhibitors for steel. Anhydrous sodium tungstate is obtained by melting WO_3 with sodium hydroxide or carbonate.

Calcium tungstate fluoresces under ultraviolet light, a phenomenon which is utilized when prospecting for scheelite deposits. Calcium tungstate is used in the production of phosphors for lasers, fluorescent lamps, oscilloscopes, luminescent dyes, scintillation counters, X-ray screens, etc.

A wide range of tungstates are used in the ceramic industry, in catalysts, and in pigments.

Polytungstates. The tendency of tungstate ions to polymerize in aqueous solution has already been referred to. The degree of polymerization increases with decreasing pH until tungstic acid is precipitated at pH 1. Other anions, e.g., arsenate, phosphate, silicate, can be incorporated into these highly polymeric ions. According to whether the polyanions are composed only of tungstate or also include foreign ions, they are referred to as isopolytungstates or heteropolytungstates.

Isopolytungstates can have various preferred degrees of polymerization, as mentioned above [60]. The most industrially important compound in this class is APT, the most widely used high-purity raw material in the tungsten industry.

Ammonium metatungstate is produced either with the aid of ion exchangers or by electrodialysis, and, owing to its high solubility in water, is used for impregnating carriers (e.g., aluminum oxide) in the production of catalysts.

Sodium metatungstate is used as a heavy liquid when drilling for oil.

Amine Tungstates [60, 70, 71]. Organic amines form water-insoluble ion associate complexes with isopolytungstates. Complex long-chain amines (C_8 – C_{10}) are used as reagents in the industrial solvent extraction of tungsten. Complexes with short-chain amines (ethylenediamine, propylamine, etc.) show autoreductive and autocarburizing properties on heating. This is of interest for the production of finely powdered W or WC, which can be obtained from the precursor in a single-step process.

Heteropolytungstates. There are over 30 elements known to form the central anion in these compounds. Typical properties independent of the central heteroatom include high relative molecular mass (> 3000), high degree of hydration, and high solubility in water and organic solvents. A summary of possible

structures and compositions can be found in [62].

One of the most industrially important compounds in this group is $\text{Na}_3\text{PW}_{12}\text{O}_{40} \cdot x\text{H}_2\text{O}$ [72, 73]. This has many uses: for fixing and oxidizing in photographic processes; as an additive in electroplating; for waterproofing plastics, adhesives, and cement; in the production of organic pigments; for the surface treatment of skins; as an antistatic agent for textiles; for printing and paper dyes; for coatings; wax pigments; steel passivation; and as a catalyst in the organic chemical industry.

Tungsten Bronzes [4, 62, 69]. These are well-defined though nonstoichiometric compounds with the general formula M_xWO_3 , in which x is between 0 and 1; M represents a metal cation, H^+ , or NH_4^+ . The name is derived from the metallic luster and intense colors (golden yellow to blue-black) of these compounds. The bronze character is determined by the amount of metal in the structure. With high values of x , interaction between the metal ions leads to the formation of metallic bonds. The stability of the bronzes is determined by the size of the metal ions. Stability decreases as the ionic radius decreases. Small metal ions, e.g., Si and Ge, do not form bronzes. Owing to the oxygen deficit, these compounds are electrical semiconductors or conductors. The sodium bronzes for which the Na/WO_3 ratio is > 0.3 have a positive temperature-resistance coefficient, and vice versa.

The bronzes are produced:

- By partial reduction of the corresponding tungstates
- By electrolytic reduction
- By the reaction in the fused or solid state of WO_3 - WO_2 mixtures with metal compounds

Tungsten bronzes are used as colored pigments, catalysts, e.g., for the oxidation of CO, and in fuel cells. Electrodes made of La_xWO_3 are used in sensors for the potentiometric determination of dissolved oxygen.

Hydrogen and alkali metal bronzes are used as electrochromic coatings for so-called dynamic glasses. Application of an electrical potential causes migration of the ions (H^+ , Na^+)

into or out of the coating, thereby changing the properties of the glass from transparent (oxidic) to reflecting (metallic due to bronze formation). The only practical application of this so far is in electrochromic sunglasses.

26.7.9 Tungsten-Chalcogenide Compounds

Tungsten-Sulfur Compounds [4, 62, 74, 75]. The following compounds are known: WS_2 , WS_3 . Tungsten disulfide is of industrial importance. It is black, forms hexagonal or rhombic crystals, and can be synthesized from the elements. It is used as a catalyst for the desulfurization of mineral oil, and as an oil-soluble lubricant under extreme conditions (pressure, temperature, vacuum).

Tungsten-Selenium Compounds [4, 75]. The following compounds are known: WSe_2 , WSe_3 . The diselenide can be synthesized from the elements, and is used as an oil-soluble lubricant.

Tungsten-Tellurium Compounds [4]. WTe_2 is known, but is of no industrial importance.

26.7.10 Tungsten-Halogenide Compounds

Tungsten-Fluorine Compounds [4, 62]. The following compounds are known: WF_6 , WF_5 , WF_4 , WOF_4 , WO_2F_2 , WOF_2 . Only the hexafluoride is of industrial importance, being used to produce CVD tungsten. It can be produced by the reaction of tungsten hexachloride with hydrogen fluoride, or by direct combination of the elements at 350–400 °C. The boiling point is 17.5 °C. The colorless gas is soluble in organic solvents, and is sensitive to moisture (hydrolysis).

Tungsten-Chlorine Compounds [4, 62]. The following compounds are known: WCl_6 , WCl_5 , WCl_4 , WCl_2 , WOCl_4 , WO_2Cl_2 , WOCl_3 , WOCl_2 . Two of these are of industrial importance:

Tungsten hexachloride is a crystalline blue-black compound (mp 275 °C, bp 346 °C). It is

obtained by direct combination of the elements at 600 °C. It is soluble in carbon disulfide and organic solvents, and is hydrolyzed by water. It has a wide range of uses in catalysis.

Tungsten oxytetrachloride forms red crystals (mp 211 °C, bp 327 °C), and is soluble in carbon disulfide and benzene. It is produced by the reaction of sulfuryl chloride with WO_3 . It too has a wide range of uses in catalysis.

Tungsten-Bromine Compounds [4, 62]. The known compounds, which are of no industrial importance, are: WBr_6 , WBr_5 , WBr_4 , WBr_3 , WOBr_4 , WO_2Br_2 , WOBr_2 , WOBr_3 .

Tungsten-Iodine Compounds [4, 62]. The known compounds, which are of no industrial importance, are: WI_6 , WI_5 , WI_4 , WO_2I_2 , WOI_2 , WO_2I , WOI_4 .

26.8 Tungsten in Catalysis [57, 76–78]

Tungsten, both in metallic form and in a wide range of compounds, is used as a catalyst or catalyst component in a large number of chemical processes.

In the form of a metallic alloy with Ni, Co, or Rh, sometimes in the form of a sulfide, and sometimes on aluminum oxide carriers, it can catalyze the reaction of CO with H_2 , and also hydrotreating, hydrocracking, reforming, and hydrosulfurization reactions.

The following oxides are used as catalysts:

WO_3 is used in colloidal form for the photocatalytic reduction of organic compounds.

$\text{W}_{20}\text{O}_{58}$ catalyzes hydrogenation, dehydrogenation, hydroxylation, epoxidation, etc.

Mixed oxides of WO_3 with TiO_2 and/or V_2O_5 , Al_2O_3 , or SiO_2 have a wide range of uses, e.g., as DENOX catalysts for exhaust gas cleaning in thermal power stations, hydrogenation, aldol condensation, ring opening reactions, dimethyl sulfoxide synthesis, etc.

Of the halides, the compounds WCl_6 and WOCl_4 play a very important role in organic chemistry as catalyst components, e.g., in association with organometallic compounds such as $\text{AlCl}_3(\text{C}_2\text{H}_5)_3$, $\text{Sn}(\text{C}_6\text{H}_5)_4$, $\text{Sn}(\text{CH}_3)_4$,

$\text{Sn}(\text{C}_4\text{H}_9)_4$, triaryl- or trialkyltin hydroxides, or the analogous lead compounds. Typical uses include: diene polymerizations, ring opening polymerizations, alkylations, etc.

WC is used for reforming *n*-heptane, as a redox catalyst for the oxidation of hydrogen in fuel cells, and for the formation of hydrogen from water.

$\text{W}(\text{CO})_6$ catalyzes a wide range of organic reactions, e.g., the metathesis of alkenes.

Sodium tungsten bronze catalyzes the oxidation of CO.

The sodium salt of 12-tungstophosphoric acid is used as a catalyst for isomerization, polymerization, nitrile synthesis, dehydrochlorination, dehydrogenation, ketone syntheses, and ring closure syntheses.

WS_2 and WSe_2 in the form of colloidal coatings have been tested for photocatalysis.

26.9 Economic Aspects [79]

The price of tungsten in ore concentrate depends on supply and demand, and is therefore subject to fluctuations (Figure 26.7). It is expressed either as \$/STU (short ton unit = 20 lb WO_3 = 7.19 kg W) or in \$/MTU (metric ton unit = 10 kg WO_3 = 7.93 kg W). In times of warlike confrontation, the strategic importance and consequently increased demand for tungsten have led to high prices. On average, prices increased until 1977, although this was partly caused by inflation. The price maximum reached in 1977 was a consequence of increased consumption. Hand in hand with this development, the mining of tungsten shifted from the developing countries to the highly industrialized countries. This was mainly to secure supplies in times of crisis. In 1970, 49% of tungsten came from western industrialized countries. In 1980, this figure was 58%, and 69% was predicted for 1990. However, this figure was never reached, as the market share of China had continuously increased (Figure 26.8).

In 1977, world tungsten demand was still < 40 000 t. As shown in Figure 26.8, demand continued to increase until 1989, reaching ca. 52 000 t, but the price fell from 1977 onward.

Thus, the price control mechanism that had been operating well until then was obviously no longer effective.

Several circumstances were responsible for this:

Up to 1977, China, for long the most important exporter of tungsten ore concentrates, had been price conscious in its trading, as this was only carried out by state officials. Following the liberalization of trading in China, producers attempted to obtain foreign currency directly by quoting low prices. Internal competition and pressure from dealers led to continued price reductions.

This fall in prices was exacerbated by the fact that high-purity intermediate products, e.g., APT, blue tungsten oxide, tungstic acid, and ferrotungsten, were offered at the same price per unit of tungsten as ore concentrates. At the end of 1993, the price of high-purity APT was so low that even the Chinese producers were no longer able to sell at a profit.

The drastic fall in demand that started in 1990 and which was caused by the general recession, the breakdown of the communist world, and the associated decline in the armaments industry led to stabilization of the lower prices.

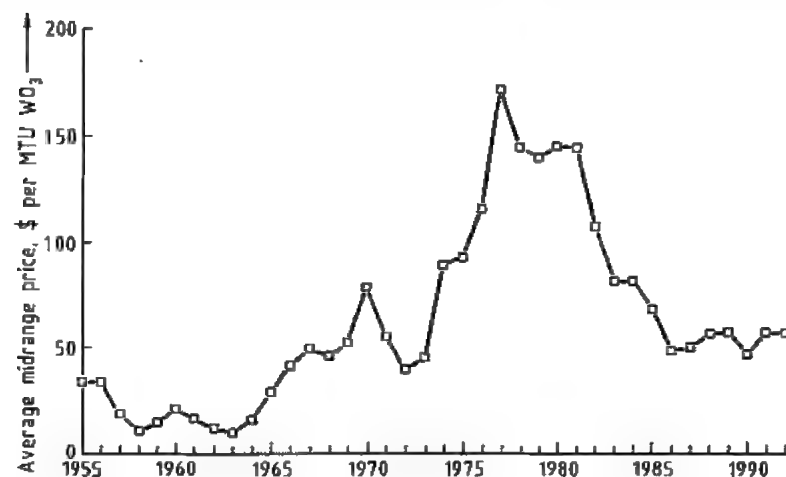


Figure 26.7: Average mid-range price of wolframite 1955–1992 (from *Metall Bulletin*).

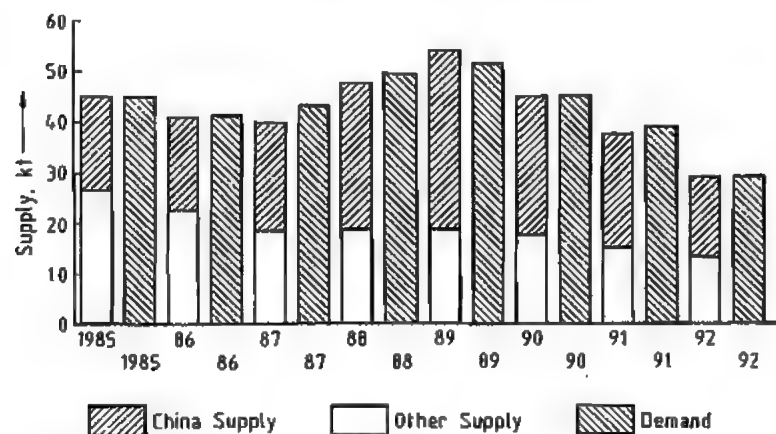


Figure 26.8: Tungsten supply and demand 1985–1992.

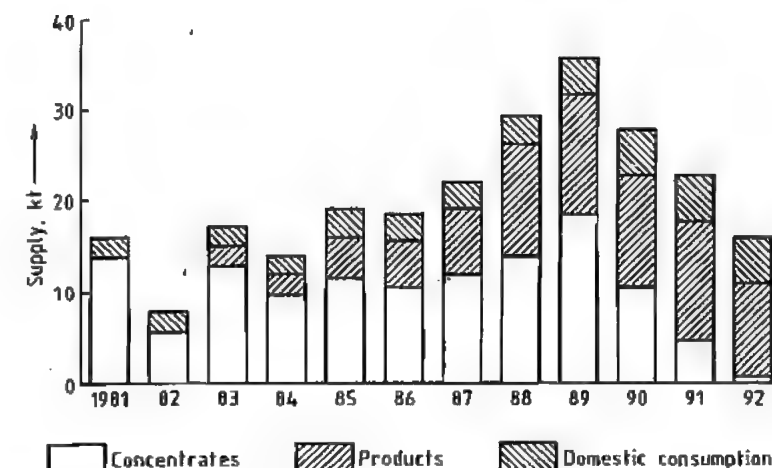


Figure 26.9: Tungsten supply in China 1981–1992.

Quite simply, the low tungsten price and the fact that there was no price difference between ore concentrate and intermediate product led to the enforced closure of almost all the larger mines in North America, Europe, South Korea, and Australia, and the suspension of many associated industries based on the treatment of ore concentrates.

In consequence, not only has the proportion of tungsten supplied from China increased (Figure 26.8), but also the makeup of the products has changed (Figure 26.9). Whereas China was still an exporter exclusively of tungsten ore concentrate in the early 1980s, today it is the largest supplier of high-purity tungsten intermediate products.

Thus, none of the predictions, e.g., 4% annual growth, opening of new mines, further shifting of mine production to the industrialized countries, self-sufficiency, etc., has been fulfilled. World demand for tungsten has decreased drastically; China is the main supplier.

26.10 Tungsten Recycling

As stated in Section 26.3, large amounts of tungsten scrap have been used as a raw material for several decades. This is because of:

- The value of the tungsten content

- The value of other metals in the alloys, e.g., Ta and Co in hard metals and Ni in heavy metals

- Environmental aspects

- Economic aspects

Methods for the treatment of scrap and utilization of the recovered materials are optimized where possible in the light of these factors.

Both direct and indirect recycling processes are used. In direct recycling, scrap is converted from the compact form to a powder which is then recycled only to the process that produced the material from which the scrap originated. For this, the scrap must consist of one grade only, and must not contain heterogeneous impurities.

In the indirect process, scrap is chemically converted to materials from which the impurities and other components are removed, and is then converted to APT as described in Section 26.4.

The direct method is preferable for economic and environmental reasons, but it can be used only for certain types of scrap, and the demand for the recycled product is not always certain. For this reason, the proportion of scrap tungsten treated by conversion to APT is continually increasing.

Table 26.5: Tungsten recycling (B = best; G = good; L = least economic use) [13, 14].

Treatment	Hard metal scrap	Heavy metal		W-Cu	W-Ag	Pure tungsten
		Hard	Soft			
Zinc process	B					
Coldstream	B		G			L
Bloating/crushing	B					
Oxidation/reduction			B			L
Hydrometallurgy		L	L	B	B	L
Electrolytic		L	L	B	G	L
Chlorination	L	L	L	L	L	L
Melting (ferrotungsten, stellite)	G	G	G			G

Combined processes are also used, e.g., the selective separation and recovery of one alloying component. Examples include the leach milling of hard metal scrap to liberate the cobalt binder metal, leaving behind the carbide phase(s), which can be recycled to the hard metal production process.

A proportion of tungsten scrap goes to smelting metallurgy for the production of stellites, melting base alloys, menstruum WC, and steel.

The economics of various treatment processes for the important types of scrap are compared in Table 26.5.

26.11 Beneficial Effects on Human Health [80, 81]

In contrast to certain toxic effects of metallic tungsten and its compounds and alloys, some very beneficial effects on human health have recently been described. An aqueous solution of sodium tungstate (ca. 2%) was taken orally, applied to the skin, used as a gargle or an eye lotion, or injected subcutaneously. Experiments on 100 people in Japan showed remarkably successful results with a wide range of illnesses, e.g., cataract, stomach ulcers, duodenal ulcers, cancer, diabetes, herpes, migraine, gout, cardiac arrhythmia, and many others. Tungstate is also beneficial in cases of mercury or selenium poisoning, burns, and sunburn, and it can counteract the unpleasant aftereffects of excessive alcohol consumption, as is also reported for molybdate. It has furthermore been established that the natural aging process is significantly retarded. It is to be hoped that funded scientific investigations

into the action of tungstate will be undertaken as soon as possible.

26.12 Toxicology and Occupational Health

Tungsten and most of its compounds generally show relatively low toxicity compared to most other heavy metals and their compounds. However, some tungsten compounds are more toxic than they were originally considered to be.

Intoxications with tungsten and its compounds are comparatively rare; they occur almost exclusively by occupational exposure.

Physiological responses, toxicokinetics, toxic effects, levels of tolerance, and ecotoxicity of tungsten and its compounds have been reviewed [82–84].

Toxicokinetics. In animal models, nearly one-half of ingested soluble tungsten compounds and roughly one-third of deposited inhaled tungsten trioxide aerosol is readily absorbed. Most of the absorbed tungsten is rapidly excreted in the urine. The remainder is distributed among the red blood cells, spleen, kidney, and bone. About 3 months after ingestion and 6 months after inhalation, most of the complete tungsten body burden has been transferred into bone. However, this amount is very small as compared to the administered dose [83]. The biological half-life of tungsten in bone is calculated at 1100 d for the slowest component of a three-component elimination kinetics [85].

Tungsten seems to have an influence on molybdenum homeostasis. In rats, the addi-

tion of 100 ppm tungsten to a diet containing 30 ppm molybdenum caused a decrease in the activities of sulfite oxidase and xanthine oxidase, which led to a significant increase in the susceptibility of these animals to sulfur dioxide [86].

Acute Toxicity. Acute intoxications are caused especially by tungsten hexafluoride, WF_6 . Liquid or gaseous WF_6 reacts readily with water, generating highly toxic hydrogen fluoride. Consequently, the mucous membranes of the respiratory tract and the eyes are damaged severely after contact with WF_6 . Acute intoxication causes a strong irritation of the upper respiratory tract, laryngitis, and bronchitis; after a period of less severe symptoms the development of cyanosis and lung edema is possible [87].

In contrast, 25–80 g of powdered tungsten metal did not cause adverse effects when administered orally as a substitute for barium sulfate in radiological examinations [88].

Chronic Toxicity. Cemented tungsten carbide, WC, is suspected of causing respiratory diseases in humans. However, these effects are possibly not due to WC itself, but rather to its content of cobalt metal. In workers processing WC the development of interstitial pulmonary fibrosis has been reported [89, 90]; the clinical picture includes cough, exertional dyspnea, and weight loss. Abnormal gas transfer was detected in respiratory function tests.

In the case of a 33-year-old woman who was exposed to cemented WC for several years and who died after development of pneumoconiosis, an increased content of cobalt ions in bones and lung was demonstrated after autopsy [91]. In various test series with rats there were strong indications that cobalt was the main reason for the development of the lung diseases [92].

In long-term studies with rats and mice, 5 ppm tungsten (as sodium tungstate) was added to the drinking water during the life span of the test animals. In rats, growth development increased slightly, whereas the life span decreased significantly [93]. Mice did not show these effects [94].

Genotoxicity. In a long-term study with mice, in which 5 ppm tungsten (as sodium tungstate) was added to the drinking water during their life span, no tumorigenic effect was seen [94].

Reproductive Toxicity. In rats, tungsten causes an increased embryo lethality and decreased ossification of bones in a dose range with no toxic effects to the maternal organism [95]. Tungsten accumulates in the fetus without being retained significantly by the placenta.

In another study on the embryonic and fetal development in mice [96], tungsten was injected as sodium tungstate before implantation or at early organogenesis (on day 3 or 8 of pregnancy, injection of 0.1 mL of 25 mmol/L sodium tungstate). The treatment did not show any effect on implantation, but increased the frequency of resorption.

Immunotoxicity. In a patch test, no allergic reactions to Na_2WO_4 were seen on the skin of 853 hard-metal workers [97]. However, irritant pustular reactions appeared in 2% of the test persons.

Toxicological Data. Tungsten: LD_{50} (rat, i.p.) 5000 mg/kg [98]; sodium tungstate, Na_2WO_4 (rat, s.c.) 223–255 mg/kg [99]; phosphotungstic acid, $H_3P(W_3O_{10})_4$: LD_{50} (rat, oral) 3300 mg/kg [100]; tungsten carbide, WC (containing 8% cobalt): $LDLo$ (rat, intratracheal) 75 mg/kg [101]; tungsten carbide, WC (containing 15% cobalt): $LDLo$ (rat, intratracheal) 50 mg/kg [101].

In humans normal mean blood levels are considered to be $5.8 (\pm 3.5) \mu g/W/L$ [82].

Treatment. Dimercaprol (British Anti-Lewisite) may be useful in the treatment of acute tungsten poisoning [102]. Cortisone preparations have been proposed for decreasing the development of lung fibrosis [103].

Occupational Health. The MAK value is $1 mg/m^3$ for tungsten and soluble tungsten compounds, and $5 mg/m^3$ for tungsten carbide and other insoluble tungsten compounds, measured as total dust [104]. In the United States, NIOSH has set exposure limits (TLV-TWA)

of 1 mg/m³ for soluble and 5 mg/m³ for insoluble tungsten compounds [105].

Lung fibrosis caused by tungsten or tungsten carbide is included in the list of the German Berufskrankheitenverordnung (Occupation Disease Regulations) [106].

Since tungsten tends to accumulate, persons exposed at the workplace should undergo periodical medical checks including chest X rays and ventilatory function tests for insoluble tungsten compounds, as well as examinations of the digestive tract and the central nervous system for soluble tungsten compounds [107].

26.13 References

1. R. Kieffer, G. Jangg, P. Ettmayer: *Sondermetalle*, Springer Verlag, Wien-New York 1971.
2. A. G. Quarrell (ed.): *Niobium, Tantalum, Molybdenum and Tungsten*, Elsevier, Amsterdam 1971.
3. Metallwerk Plansee, Wolfram, company brochure, Reutte, Austria, 1980.
4. S. W. H. Yih, C. T. Wang: *Tungsten: Sources, Metallurgy, Properties and Applications*, Plenum Press, New York-London 1979.
5. Gmelin, system no. 54, Suppl. vol. A1.
6. Gmelin, system no. 54, part B2; part B3; part B4.
7. Ullmann, 4th ed., 24, 457.
8. B. Aronsson: "Some Notes about the History of Tungsten and Scheelite", booklet printed by AB Sandvik Coromant, R & D Materials and Processing Library, Stockholm 1978.
9. R. Eck, E. Lugscheider: "Molybdän, Wolfram und ihre Legierungen", Lecture on Sondermetalle at Technischen Akademie Esslingen, Esslingen 1980.
10. E. Fromm, E. Gebhardt: *Gase und Kohlenstoff in Metallen*, Springer Verlag, Berlin-Heidelberg-New York 1976.
11. Roskill Information Services: *The Economics of Tungsten*, London, Feb. 1990.
12. R. F. Stevens, Jr., *Bull. U.S. Bur. Mines* **667** (1975) 1161.
13. B. F. Kieffer, E. F. Baroch in H. Y. Sohn, O. N. Carlson, J. T. Smith (eds.): "Extractive Metallurgy of Refractory Metals", *Proc. TMS-AIME Annu. Meeting*, **1981**, 273.
14. B. F. Kieffer, E. Lassner, *Tungsten Proc. Int. Tungsten Symp.* **4th**, 1987, 59.
15. E. Lassner in H. Y. Sohn, O. N. Carlson, J. T. Smith (eds.): "Extractive Metallurgy of Refractory Metals", *Proc. TMS-AIME Annu. Meeting*, **1981**, 269.
16. AMAX, US 4338287, 1983 (R. F. Hogsett, D. K. Huggins, L. B. Beckstead).
17. E. Lassner, B. F. Kieffer, *Conf. Proc. Adv. in Hard Materials Production*, London 1988, Contr. 5.
18. GTE Prod., US 4353878, 1982 (L. R. Quatrini, M. B. Terlizzi, B. E. Martin).
19. Engelhard Minerals and Chem., US 4092400, 1978 (V. Zbraneck, D. A. Burnham).
20. AMAX, US 4320096, 1982 (P. B. Queneau, D. K. Huggins, L. W. Beckstead).
21. E. Lassner, *Österr. Chem. Ztg.* **80** (1979) 111.
22. AMAX, US 4311679, 1982 (P. B. Queneau, L. W. Beckstead, D. K. Huggins).
23. M. B. Macinnis, T. K. Kim, *Int. J. Refr. Hard Met.* **5** (1986) 78.
24. T. Zuo, Q. Zhao, S. Li, J. Wang, *Proc. 1st Int. Conf. Metall. Sci. W, Ti, Re and Sb* **1** (1988) 11.
25. J. Zhou, J. Xue, *Proc. 5th Int. Tungsten Symp.*, Budapest 1990, pp. 73-86.
26. E. Lassner in B. Lux, L. Bartha, E. Lassner, W. D. Schubert (eds.): *Chemistry of Doped Non Sag Tungsten* (in press).
27. J. W. van Put, T. W. Zegers, A. van Sandwijk, P. J. M. van der Straten in C. S. Baird, C. Vijayan (eds.): *Proc. 2nd Int. Conf. Separation Sci. Technol.*, Hamilton, Canada, 1989, p. 387.
28. J. W. van Put, D. M. de Konig, A. van Sandwijk, G. J. Witkamp in GVC.VDI/E.F.C.A. Mersman (ed.): *Proc. 11th Symp. Ind. Crystallization*, Garmisch Partenkirchen 1990, p. 647.
29. R. Haubner et al., *Int. J. Refr. Hard Met.* **2** (1983) 108, 156.
30. W. D. Schubert, *Int. J. Refr. Met. Hard Mat.* **9** (1991) 178.
31. W. D. Schubert, E. Lassner, *Int. J. Refr. Met. Hard Mat.* **10** (1991) 133, 171.
32. R. Haubner, W. D. Schubert, B. Lux, E. Lassner in H. M. Ortner (ed.): *Proc. 11th Plansee-Seminar* **2** (1985) 69.
33. F. Benesovsky (ed.): *Pulvermetallurgie und Sinterwerkstoffe*, 3rd ed., Metallwerk Plansee GmbH, Reutte, Austria, 1982.
34. W. Schintelmeyer, O. Pacher, K. Kailer, W. Wallgram in H. M. Ortner (ed.): *Proc. 10th Plansee-Seminar* **2** (1981) 635.
35. Y. M. Korolev, V. A. Sorkin in H. Bildstein, H. M. Ortner (eds.): *Proc. 12th Plansee-Seminar* **1** (1989) 247.
36. J. P. Wittenauer, T. G. Niemi, J. Wadsworth, *Adv. Mater. Process.* **9** (1992) 28.
37. H. S. Yu et al., *Int. J. Refr. Met. Hard Mat.* **11** (1992) 317.
38. R. Huenert, G. Winter, W. Kiliani, D. Greifendorf, *Int. J. Refr. Met. Hard Mat.* **11** (1992) 331.
39. V. G. Glebovsky in H. Bildstein, H. M. Ortner (eds.): *Proc. 12th Plansee-Seminar* **3** (1989) 379.
40. O. Grau: "Sampling in the Non-Ferrous Industry", in G. Kraft (ed.): *Series of Bulk Material Handling*, vol. 6, Trans Tech Publ., Clausthal-Zellerfeld 1993, p. 131.
41. Gesellschaft deutscher Metallhütten- und Bergleute e.V. (eds.): *Analyse der Metalle*, Suppl. vol. 1, Springer Verlag, Berlin-Heidelberg-New York 1980, p. 213.
42. V. Scherer, D. Hirschfeld, *Erzmetall* **39** (1986) 251.
43. Gesellschaft Deutscher Metallhütten- und Bergleute e.V. (eds.): *Analyse der Metalle*, Suppl. vol. 1, Springer Verlag, Berlin-Heidelberg-New York 1980, p. 229.
44. H. M. Ortner, *Talanta* **26** (1979) 629.
45. D. Hirschfeld, H. M. Ortner, *Metall (Berlin)* **35** (1981) 434.
46. C. Vandecasteele, K. Strijckmans, C. Engelmann, H. M. Ortner, *Talanta* **28** (1981) 19.
47. H. M. Ortner in O. van der Biest (ed.): *Analysis of High Temperature Materials*, Applied Science Publ., London-New York 1983.
48. H. M. Ortner, *Erzmetall* **35** (1982) 555, 612.
49. E. Lassner, F. Benesovsky, *Mikrochim. Acta Suppl.* **5** (1974) 291.
50. H. M. Ortner, *Erzmetall* **32** (1979) 507.
51. E. Lassner, H. Petter, *Mikrochim. Acta Suppl.* **6** (1975) 133.
52. V. Scherer in H. M. Ortner (ed.): *Proc. 10th Plansee-Seminar* **2** (1981) 269.
53. W. D. Schubert, E. Lassner, *Int. J. Refr. Met. Hard Mat.* **10** (1991) 133.
54. P. Wilhartiz, H. M. Ortner, R. Krismer in H. Bildstein, H. M. Ortner (eds.): *Proc. 12th Plansee-Seminar* **3** (1989) 575.
55. K. G. Heumann, P. Herzer, H. E. Gabler in H. Bildstein, H. M. Ortner (eds.): *Proc. 12th Plansee-Seminar* **4** (1989) 191.
56. Treibacher Chemische Werke, Lieferprogramm Wolfram-Melting Base, Treibach 1991.
57. Gesellschaft für Elektrometallurgie, Lieferprogramm, Nürnberg 1989.
58. R. Püschel, E. Lassner: "Chelates and Chelating Agents in the Analytical Chemistry of Mo and W", in H. Flaschka, A. J. Barnard (eds.): *Chelates in Analytical Chemistry*, Marcel Dekker, New York 1967.
59. K. H. Tytko, O. Glemser, *Adv. Inorg. Chem. Radiochem.* **19** (1976) 239.
60. T. K. Kim, R. W. Mooney, V. Chiola, *Sep. Sci.* **3** (1968) 467.
61. H. J. Goldschmidt: *Interstitial Alloys*, Plenum Publ., New York 1967.
62. Kirk-Othmer, **23**, 426-438.
63. W. B. Pearson: *Handbook of Lattice Spacings and Structure of Metals*, Pergamon Press, New York 1967.
64. J. Booth, T. Eckström, E. Iguchi, R. J. D. Tilley, *J. Solid State Chem.* **41** (1982) 293.
65. A. J. Hegedüs, T. Millner, J. Neugebauer, *Z. Anorg. Allg. Chem.* **281** (1955) 64-82.
66. W. R. Morcom, W. L. Worrell, H. G. Sell, *Met. Trans.* (1974) 155-161.
67. O. Glemser, H. Ackermann, *Z. Anorg. Allg. Chem.* **325** (1963) 281-286.
68. G. Yidong, *Proc. 1st Int. Conf. Metall. Mat. Sci. W, Ti, Re and Sb*, **1** (1988) 213.
69. T. Eckström, R. J. D. Tilley, *Chem. Sci.* **16** (1980) 1.
70. GTE Sylvania, US 4175109, 1979 (T. K. Kim).
71. Tang Xinhua, Ph.D. Thesis, Technical University Vienna 1994.
72. Sylvania, Technical Information Bull. CM-9003, no. 9, Towanda, PA, 1980.
73. Misono Makoto: "Catalysis Review", *Sci. Eng.* **29** (1987) 269.
74. J. C. Wildervanck, F. Jelinek, *Z. Anorg. Chem.* **328** (1964) 309.
75. O. Glemser, H. Sauer, B. König, *Z. Anorg. Allg. Chem.* **257** (1948) 241.
76. J. Desilvestro, M. Neumann-Spallart, *J. Phys. Chem.* **89** (1985) 3684.
77. I. Bedja, S. Hotchandani, P. Kamat, *J. Phys. Chem.* **97** (1993) 11064.
78. M. Neumann-Spallart, *Hydrogen Energy Prog.* **VI** **12** (1986) 577.
79. International Tungsten Industry Association (eds.): *Newsletter*, 280 Earls Court Road, London SW5 9AS, June 1993.
80. K. Kase: *Tungsten Sui Soda*, Tokyo 1991.
81. E. Lassner, W. Aschenbrenner, *Proceedings of the 6th Tungsten Symposium*, Guangzhou 1993.
82. H. E. Stokinger in G. D. Clayton, F. E. Clayton (eds.): *Patty's Industrial Hygiene and Toxicology*, 3rd ed., Wiley-Interscience, New York 1981, pp. 1981-1995.
83. G. Kazantzis in L. Friberg, G. F. Nordberg, V. Vouk (eds.): *Handbook on the Toxicology of Metals*, 2nd ed., Elsevier Science Publisher, Amsterdam 1986, pp. 610-622.
84. R. Wennig, N. Kirsch in H. G. Seiler, H. Sigel, A. Sigel (eds.): *Handbook on Toxicity of Inorganic Compounds*, Marcel Dekker, New York 1988, pp. 731-738.
85. S. V. Kaye, *Health Phys.* **15** (1968) 398-417.
86. H. J. Cohen, R. T. Drews, J. L. Johnson, K. V. Rajagopalan, *Proc. Natl. Sci. USA* **70** (1973) 3655-3659.
87. R. Kühn, K. Birett: *Merckblätter gefährliche Arbeitsstoffe*, 4th ed., ecocom Verlag, Landsberg/Lech, Datenblatt W-004.
88. R. Krüger, *Muench. Med. Wochenschr.* **35** (1912) 1910.
89. E. O. Coates, J. H. L. Watson, *Ann. Intern. Med.* **75** (1971) 709-716.
90. N. L. Sprince, R. I. Chabern, C. A. Hales, A. L. Weber, H. Kazemi, *Chest* **86** (1984) 549-557.
91. H. Kitamura, *Yokohama Med. Bull.* **31** (1980) 103-126.
92. H. Kitamura, Y. Yoshimura, I. Tozawa, K. Koshi, *Acta Pathol. Jpn.* **30** (1980) 241-254.
93. H. A. Schroeder, M. Mitchener, *J. Nutr.* **105** (1975) 421-427.
94. H. A. Schroeder, M. Mitchener, *J. Nutr.* **105** (1975) 452-458.
95. V. G. Nadeenko, V. G. Lenchenko, S. B. Genkina, T. A. Arkhipenko, *Farmakol. Toksikol. (Moscow)* **41** (1978) 620-623.
96. M. Wide, *Environm. Res.* **33** (1984) 47-53.
97. I. Rystedt, T. Fischer, B. Lagerholm, *Contact Dermatitis* **9** (1983) 69-73.
98. American Conference of Governmental Industrial Hygienists (eds.): *Documentation of Threshold Limit Values for Substances in Workroom Air*, Cincinnati, OH, 1980, p. 273.
99. F. W. Kinard, J. van de Erve, *Am. J. Med. Sci.* **199** (1940) 668-670.
100. E. H. Vernot, J. D. MacEwen, C. C. Haun, E. R. Kinkead, *Toxicol. Appl. Pharmacol.* **42** (1977) 417-423.
101. National Technical Information Service, AEC-TR-6710. English translation of: Z. E. Izraelson: *Toxicology of the Rare Metals*, Moscow 1963.
102. M. J. Ellenhom, D. G. Barceloux: *Medical Toxicology: Diagnosis and Treatment of Human Poisoning*, Elsevier, New York 1988, p. 77.
103. S. Moeschlin: *Klinik und Therapie der Vergiftungen*, 7th ed., Georg Thieme, Stuttgart 1986, p. 201.

104. Deutsche Forschungsgemeinschaft (ed.): *MAK- und BAT-Werte-Liste 1993*, Maximale Arbeitsplatzkonzentrationen und Biologische Arbeitsstofftoleranzwerte, Mitteilungen der Senatskommission zur Prüfung gesundheitsschädlicher Arbeitsstoffe, Mitteilung 29, VCH Verlagsgesellschaft, Weinheim 1993.
105. American Conference of Governmental Industrial Hygienists (eds.): *Threshold Limit Values (TLV)* 1982, Cincinnati, OH, 1982.
106. Berufskrankheitenverordnung, BK Nr. 4107: Erkrankungen durch Lungenfibrose durch Metallstäube bei der Herstellung oder Verarbeitung von Hartmetallen.
107. R. Roi, W. G. Town, W. G. Hunter, L. Alessio (eds.): *Occupational Health Guidelines for Chemical Risks*, CEC Publ. Eur 8513, Luxembourg 1983, pp. 128-129.

27 Molybdenum

ROGER F. SEBENIK (§§ 27.1, 27.4.1-27.4.4); ALFRED RICHARD BURKIN (§§ 27.2-27.3, 27.8); ROBERT R. DORFLER, JOHN M. LAFERTY (RETIRED) (§§ 27.4.1-27.4.4); GERHARD LEICHTFRIED (§§ 27.4.5-27.4.8, 27.5); PHILIP C. H. MITCHELL (§ 27.6); MARK S. VUKASOVICH (RETIRED) (§ 27.7 EXCEPT §§ 27.7.4.1-27.7.4.2); GERHARD ADRIAN (RETIRED); KARL BRANDT (§ 27.7.4.1); GÜNTER ETZRODT (§ 27.7.4.2); DOUGLAS A. CHURCH (§ 27.9); GARY G. VAN RIVER (§ 27.10); JAMES C. GILLILAND (RETIRED) (§§ 27.10-27.11); STANLEY A. THIELKE (§ 27.11)

27.1 History	1361	27.6.3 Halides	1381
27.2 Properties	1362	27.6.4 Molybdates, Isopolymolybdates, and Heteropolymolybdates	1382
27.3 Occurrence	1363	27.6.5 Other Compounds	1383
27.3.1 Minerals	1363	27.7 Uses of Molybdenum Compounds	1384
27.3.2 Deposits	1363	27.7.1 Lubrication	1386
27.4 Production	1365	27.7.2 Corrosion Inhibition	1387
27.4.1 Concentration	1365	27.7.3 Flame Retardancy and Smoke Suppression	1388
27.4.2 Processing of Concentrate	1367	27.7.4 Pigments	1388
27.4.3 Recovery from Spent Petroleum Catalysts	1369	27.7.4.1 Molybdate Red and Molybdate Orange	1389
27.4.4 Recovery during Production of Tungsten Ores	1371	27.7.4.2 Molybdate Pigments	1390
27.4.5 Production of Molybdenum Metal Powder	1371	27.7.5 Agriculture	1391
27.4.6 Production of Compact Molybdenum Metal	1372	27.8 Analysis	1391
27.4.7 Processing of Molybdenum	1373	27.9 Economic Aspects	1393
27.4.8 Alloys	1374	27.10 Environmental Aspects	1394
27.5 Uses	1375	27.11 Toxicology and Occupational Health	1396
27.6 Compounds	1376	27.12 References	1399
27.6.1 Oxides	1378		
27.6.2 Chalcogenides	1379		

27.1 History [1-4]

Molybdenum commonly occurs in nature as the mineral molybdenite, MoS_2 , and is found as veins in quartz rock. It was discovered by SCHEEL in 1778, but for the next hundred years, molybdenite was merely a laboratory curiosity. The first major use came during World War I when additions of molybdenum produced steels with excellent toughness and strength at high temperatures for use as tank armor and in aircraft engines.

The main source of molybdenite throughout the 19th century was the Knaben mine in Norway in which the molybdenite was concentrated by hand. The World War I demand for molybdenum, however, spurred development of the Climax Mine (Colorado), which

was put on stream in 1918 by the Climax Molybdenum Company. By that time the froth flotation process had replaced hand sorting for concentrating ores.

Although the Climax Mine was closed after the war because of the suddenly decreased demand, it was reopened in 1924 as new peacetime uses of molybdenum, largely in the automotive industry, were developed. Demand for molybdenum steadily grew as new chemical and metallurgical applications continued to be developed, largely stimulated by the research efforts of the Climax Molybdenum Company.

In 1933 a process for the selective flotation of molybdenite from copper porphyry ores was developed by the Anaconda Company at its Cananea subsidiary in Mexico. The Ken-

necott Copper Company soon followed at its Utah mines. The technology was later extended to Chile at Kennecott's El Teniente Mine and Anaconda's Chuquicamata mine. Thus began the age of molybdenum production as a by-product of copper.

During World War II, the United States supplied about 90% of the world molybdenum demand, most coming from Climax with the balance from Kennecott's Utah mines and MolyCorp's Questa mine. The largest of the other Western-world producing countries were Chile, Mexico, and Norway.

Climax Molybdenum Company continued to be the largest Western-World producer into the 1980s, doubling its capacity when it opened the massive Henderson mine (near Empire, Colorado) in 1976. Production from Mexico and Norway remained small, but less expensive by-product molybdenum production from Chile and the United States continued to grow, and the Endako and other mines in Canada began molybdenum production. In 1977, total world production exceeded 200 $\times 10^6$ pounds (ca. 90 000 t) for the first time.

During the late 1970s the high price of molybdenum stimulated the opening of several new primary mines and the expansion of many by-product molybdenum facilities. When the price declined in the early 1980s, by-product molybdenum became the dominant economic force in the marketplace. Climax Molybdenum Company closed the underground mine at Climax, but was still a major producer with the Henderson mine and the open pit at Climax Cyprus Minerals, with four operating mines, became a major producer. Other important Western-world producers at the end of the 1980s were Codelco's Chuquicamata mine in Chile, Placer's Endako mine in Canada, the La Caridad mine in Mexico, and the Cuajone and Toquepala mines in Peru. Annual world production and consumption averaged (180–200) $\times 10^6$ pounds (80 000–90 000 t) of molybdenum during the late 1980s.

27.2 Properties

Physical Properties. Molybdenum, electronic configuration [Kr] $4d^5 5s^1$, is the second member of group 6 of the periodic table. As a transition element it may have a valency of 2, 3, 4, 5, or 6. In the massive state molybdenum is a lustrous silver-white solid with typically metallic properties. When produced as a powder it is dull grey. It has a body-centred cubic lattice with $a_0 = 0.31472$ nm. The physical properties of molybdenum depend to a large degree on the method used to produce it and on its subsequent treatment. For example, its relative density calculated from a_0 is 10.22 whereas an earlier measurement gave 9.01 and later work showed that the lower value increases with the amount of mechanical working to which the metal is subjected. The accepted values of the main physical properties of the metal are given below. A more extensive compilation is available giving, in particular, data of importance to metallurgists [5].

mp	2617 °C
bp (101.3 kPa)	4612 °C
Latent heat of fusion at mp	35.6 kJ/mol
Mean specific heat (0–100 °C)	251 J kg ⁻¹ K ⁻¹
Density (20 °C)	10.22 g/cm ³
Thermal conductivity (0–100 °C)	137 W m ⁻¹ K ⁻¹
Electrical resistivity (20 °C)	5.7 $\mu\Omega \cdot cm$
Temperature coefficient (0–100 °C)	4.35×10^{-3} K ⁻¹
Elastic constants of polycrystalline metal (20 °C)	
Young's modulus	324.8 GPa
Rigidity modulus	125.6 GPa
Bulk modulus	261.2 GPa
Poisson's ratio	0.293
Linear coefficient of thermal expansion (0–100 °C)	5.1×10^{-6} K ⁻¹
Standard electrode potential $E^0_{Mo^{3+}, Mo}$	-0.200 V

Chemical Properties. Molybdenum retains its luster almost indefinitely in air, particularly when it has been drawn to fine wire. It can be passivated by oxidation, especially by electrolytic oxidation, becoming chemically unreactive. On prolonged heating in air below 600 °C, the metal becomes covered with its trioxide; at 600 °C the oxide sublimates and rapid oxidation occurs. Molybdenum burns in oxygen at 500–600 °C. It is slowly oxidized by steam, is attacked by fluorine when cold and by chlorine and bromine when hot. Dilute

acids and concentrated hydrochloric acid have very little effect on the metal. Moderately concentrated nitric acid dissolves it but concentrated nitric acid soon passivates the surface and reaction ceases. Molybdenum is dissolved by a mixture of concentrated nitric and concentrated hydrofluoric acids. It is practically unaffected by alkaline solutions and very nearly so by fused alkali-metal hydroxides. However fused oxidizing salts such as sodium peroxide, sodium or potassium nitrate or perchlorate dissolve the metal rapidly. It reacts on heating with carbon, boron, nitrogen, and silicon and forms many alloys. It is used in a variety of catalysts, especially combined with cobalt in the desulfurization of petroleum. Molybdenum is a biologically active metal which is involved in the functioning of enzymes causing reduction of nitrogen to ammonia, and of nitrates.

27.3 Occurrence

27.3.1 Minerals

Molybdenum occurs in the earth's crust in an abundance of about $10^{-4}\%$, mainly as molybdenite, MoS_2 . Small quantities are also associated with other metals having similar chemical properties. Thus wulfenite ($PbMoO_4$) is found in oxidized parts of sulfidic lead deposits in many regions of the world; powellite [$Ca(Mo,W)O_4$] is a calcium molybdate usually formed from the modification of molybdenite in deposits containing tungsten as scheelite ($CaWO_4$) and tungsten substitutes for molybdenum up to about 10%. Ferrimolybdate ($Fe_2Mo_3O_{12} \cdot 8H_2O$) is the product of oxidation of molybdenite in the presence of iron(III) compounds. Molybdenite is the primary source of molybdenum. Should demand for molybdenum rise so that additional sources become necessary, wulfenite, powellite, and ferrimolybdate may become commercially significant. Other molybdenum minerals include achrematite, belonesite, chialagite, eosite, ilsemanite, jordisite, koechlin-

ite, lindgrenite, and paterite. These are of no commercial importance however.

27.3.2 Deposits

There are five genetic types of molybdenum deposits:

- Porphyry deposits in which metallic sulfides are disseminated throughout large volumes of altered and fractured rock
- Contact-metamorphic zones and bodies in which silicated limestone is adjacent to intrusive granites
- Quartz veins
- Pegmatites
- Deposits bedded in sedimentary rocks.

The first three types are of hydrothermal origin and provide almost all of the molybdenum ore currently mined. The last two are of no economic importance at present. Average molybdenite concentrations in primary porphyry deposits range from 0.05 to 0.25%; in secondary copper molybdenum porphyry deposits molybdenite concentrations are much lower (0.01–0.05%) so that the mineral can only be recovered as a by-product.

In hydrothermal deposits, the cracks and interstices of the intrusive rock forming the matrix were originally penetrated by aqueous metal-containing solutions. Such solutions are often formed close to magma and so are at a high temperature and pressure and contain sulfide species. As the solution cools, minerals are deposited within the intrusive matrix and also commonly in the surrounding country rock. Thus the famous deposit at Climax, Colorado (USA) was formed by an intrusion of a quartz-monzonite magma into a granitic country rock. The hydrothermal solution deposited quartz and molybdenite in even the smallest fractures so that the host rock appears to consist of angular fragments separated by narrow bands of the minerals. In many porphyry deposits small amounts of molybdenite are disseminated with copper sulfide minerals throughout large volumes of granitic rock. The chief mineral values are chalcocite (Cu_2S) and chalcocite (Cu_2S), associated

with pyrite (FeS_2), and small amounts of other sulfides, including molybdenite. Where secondary enrichment of the copper ore has occurred, chalcocite has replaced pyrite and chalcopyrite. In limestone silicate sedimentary rocks containing intrusions of granitic rocks, small amounts of molybdenite are occasionally widely distributed along the interfaces between the rocks and are often associated with scheelite (CaWO_4), bismuthinite (Bi_2S_3), or copper sulfides. These deposits may contain up to 0.6% molybdenite.

Pegmatites are the result of igneous activity and subsequent solidification of the magma. The slow cooling of the mass results in the formation of coarse crystals, almost exclusively of quartz and feldspar. Molybdenite occurs in small amounts as an accessory mineral, usually as large crystals; pegmatites are not an important source of molybdenum. Nevertheless, a pegmatite deposit containing molybdenite together with bismuth was mined until recently at Val d'Or and Preissac (Québec, Canada). Sedimentary rocks in which molybdenum minerals may occur include coals, shales, phosphorites, and sandstones. They are not used as sources of molybdenum and the technology to recover it from them has not been developed.

Molybdenum is obtained commercially almost exclusively from molybdenite, which is either mined and concentrated as the primary product of the mine or open pit, or recovered as a concentrate during the processing of ore from a copper mine. In the latter case the molybdenite can be either a by- or a coproduct, depending on its economic importance to the output of the mine. Molybdenum is also recovered from solutions obtained by leaching scheelite ores in the production of tungsten. Molybdenum supply in the Western world can be broken down into four production segments [6]:

- Primary mine production (ca. 40%)
- By- or coproduction output from copper and scheelite mines (ca. 55%)
- Imports from China (3%)

- Molybdenum recovered from the processing of spent petroleum catalyst (2%).

Reserves of molybdenite in the market economy countries have been estimated by evaluating identified ore bodies [7], i.e., those which have been explored as well as those which have been exploited. The results indicate the following amounts of recoverable molybdenum (10^3 t): United States, 4100; Chile, 1770; Canada, 928; Mexico, 306; Peru, 288; other countries, 356. Ore bodies producing primarily molybdenum contain 55% of the reserves identified; only 29% of these ore bodies were being exploited at the time of the survey (January 1985). Properties producing molybdenum as a by-product contained the remaining 45% of reserves and 67% of them were producing molybdenite. The total recoverable molybdenum from primary and by-product reserves has been estimated as follows (10^3 t molybdenum in concentrate) [8]:

Primary producing properties	1265
Primary nonproducing properties	3036
By-product producing properties	2316
By-product nonproducing properties	1142

Molybdenum occurs widely in all continents but usually in small quantities. The large-scale mining, milling, and processing facilities now required for economic production of molybdenum compounds are only justified where large reserves of ore exist. Where these are exploited they are the primary molybdenum producing mines. In Canada, Endako (Placer Dome) is the only primary molybdenum mine and is in British Columbia. The Cu-mobabi mine (Empresso Frisco SA de CV) is in Mexico; the Jinduicheng mine is the largest molybdenum producer in China and all of the others, except perhaps for some in the former Soviet Union, are in the United States. In Alaska, Quartz Hill is under long-term development. The famous, very large Climax and Henderson mines (both Amax) are in Colorado; Thompson Creek (Cyprus Minerals) is in Idaho; Tonopah (Cyprus Minerals) is in Nevada; and Questa (Molycorp) is in New Mexico. A detailed list of major molybdenum-producing companies is given in [8].

Molybdenum is extracted as a by-product or coproduct of copper production in Canada, Chile, Iran, Mexico, Papua New Guinea, Peru, Philippines and, in the United States (Arizona, Nevada, New Mexico, and Utah). It is extracted from the scheelite mine at Sang-dong, Gangwondo, Korea (Korea Tungsten Mining) as a by-product of tungsten recovery.

27.4 Production

27.4.1 Concentration [9]

Molybdenum ore is mined by underground and open-pit methods. A typical primary molybdenum ore body contains 0.05–0.25% Mo, and secondary ore bodies (copper porphyry ores) average 0.3–1.6% Cu and 0.01–0.05% Mo. Flotation remains the preferred and almost exclusive method of upgrading the molybdenite mineral to an industrial-grade molybdenite concentrate containing 90–95% MoS_2 , the balance being gangue.

The flotation process [10, 11] starts by pulverizing the ore to liberate the molybdenite (either alone or in association with copper sulfide minerals) from the host rock (mainly quartz monzonite), and then agitating the pulverized ore with water, a collector oil, and other special chemicals to cause preferential wetting of the host rock particles. The unwetted copper and molybdenum mineral particles are carried to the surface by air bubbles as the wetted host rock particles settle or remain suspended. A frothing agent is used to stabilize the bubbles, which contain the sulfide minerals, for easy skimming from the surface.

Molybdenite flotation is so spontaneous that it is termed a natural floaters. Other minerals, such as clay and covellite (CuS), that are commonly associated with molybdenite-containing ores are, however, also natural floaters. For this reason the flotation process for molybdenum production from primary ore bodies differs from that of secondary ore bodies. Factors such as the grinding method, particle size, alkalinity, slurry density, and reagent usage dictate the recoveries and process economics.

Recovery from Primary Ore Bodies. Figure 27.1 illustrates a basic recovery flowsheet from a primary molybdenum ore body. Although the methods of comminution vary, the objectives are to break down the ore to liberate the molybdenite. For example, Climax uses primary, secondary, and tertiary crushing with screening and rougher ball mills in closed circuit with spiral and hydrocyclone classification to produce a flotation feed [12]. Henderson [13] and Thompson Creek [14] use primary crushing and semi-autogenous grinding in closed circuit with hydrocyclone classification.

An initial primary grind [ca. 48%–200 mesh (74 μm)] is usually acceptable to produce a 2.5–5.0% Mo concentrate in the first “rougher” flotation stage. This concentrate is then upgraded by further grinding and “cleaner” floating. This concept of upgrading progressively smaller volumes of concentrate has proved to be the most cost effective means of handling large tonnages of low-grade molybdenum ores.

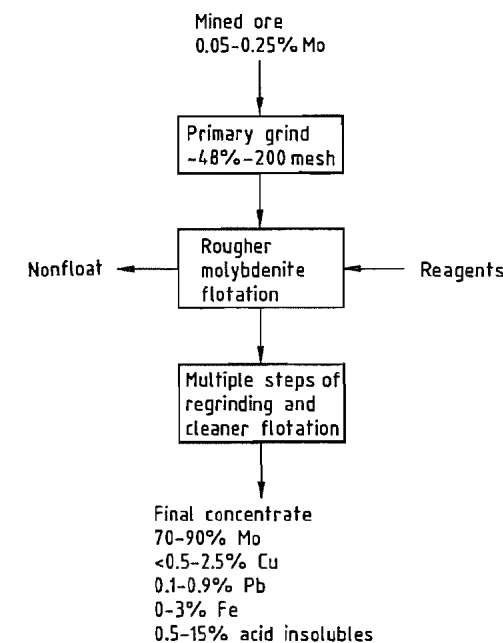


Figure 27.1: Primary molybdenite recovery process [9].

Sufficient regrind and cleaner steps follow to obtain the degree of liberation required for a final concentrate grade. For example, six cleaner flotation steps are used at Thompson Creek [14], five at Climax [12], and four at Henderson [13]. The nonfloat from the last stage of cleaner flotation is circulated counter-currently through the previous cleaner stages. Overall recovery is generally about 85%.

At each flotation step molybdenite particles are floated and collected, and contaminants are depressed and rejected by adding reagents. Different reagent programs are used depending on the properties of the mined ore [15]. Simple hydrocarbon collectors can be used such as kerosene, stove oil, or light oil. Pine oils and Syntex VB (sulfated monoglyceride of coconut oil), which also have emulsifying and collecting properties, are used as frothers; lime or soda ash is used to control alkalinity, usually at pH 8.5. Contaminants are rejected by controlling the pH at an optimum level and by adding depressing reagents such as Noke's reagent (a product formed by reaction between stoichiometric quantities of sodium hydroxide and phosphorus pentasulfide) and sodium cyanide. Sodium silicate is used to disperse slimes.

Recovery from Secondary Ores. The generally accepted practice for secondary molybdenum recovery (Figure 27.2) is to float a copper-molybdenum sulfide concentrate and then extract the molybdenum from the combined concentrate by methods governed by the type of copper mineralization present.

In practice, fine grinding [50–70%–200 mesh (74 μm)] is usually performed to maximize copper recovery [16]. Then bulk flotation of the molybdenum-copper sulfide concentrate generally employs strong alkyl xanthates (e.g., potassium amyl xanthate or sodium isopropyl xanthate) and nonselective frothers (e.g., methylisobutylcarbinol) to float as much of the total copper-molybdenum product as possible.

The bulk copper-molybdenum flotation stream is thickened by settling the solids and decanting the clear process water to obtain a

copper-molybdenum slurry with a higher solids content. The slurry is conditioned by adding reagents during the thickening step as a method of premixing the reagents that will be used in the rougher flotation step.

On a worldwide basis, molybdenum losses in the copper molybdenum bulk flotation process amount to about 48% of the total molybdenum feed, but this level is gradually being reduced. Most of the molybdenum losses are incurred because the circuits are designed and operated for optimum copper recovery.

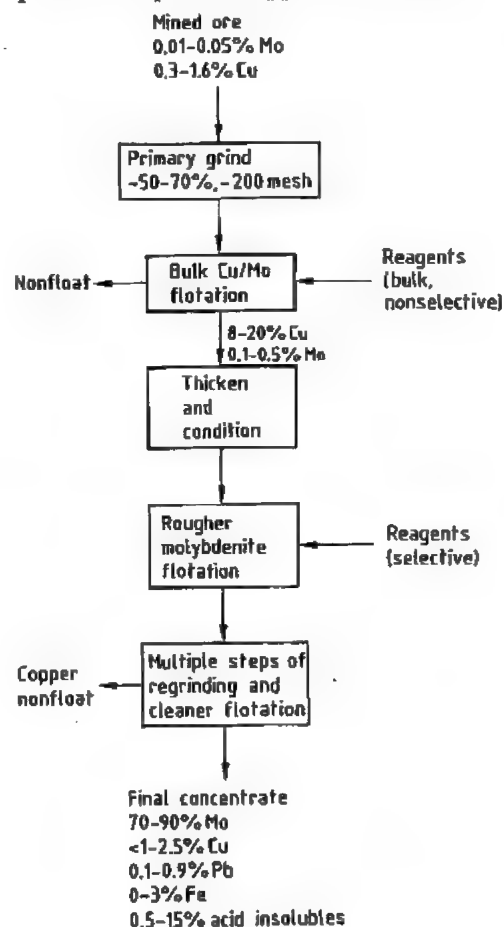


Figure 27.2: By-product copper-molybdenite recovery process [9].

Selective collectors [17] are then used for separating molybdenum from the bulk copper molybdenum concentrate beginning in the

rougher flotation stages. For example, chalcocopyrite (CuFeS_2), the most common type of copper mineralization, is particularly amenable to sodium hydrosulfide treatment. It is depressed with a 40% solution of sodium sulfide or hydrosulfide. The hydrosulfide ion in the solution preferentially desorbs the bulk collector from the copper sulfide mineral, leaving it in the water-wetting nonfloating condition.

Hypochlorides, peroxides, permanganates, and dichromates can also oxidize the adsorbed collectors giving an initial depressing effect to copper sulfides; cyanides will further depress copper to yield a high-grade molybdenite concentrate. When using these oxidants and depressants, chalcocite (Cu_2S) ores require more circuit design, i.e., additional flotation stages and more reagent addition points.

Covellite (CuS) ores float naturally and have been removed from flotation (depressed) with lignin sulfonate but now the simpler process of adding excess collector is used. Clays have been depressed with aluminum sulfate. Noke's reagent is a strong but short-lived depressant of copper sulfides. Lime is used for pH control at 9.5–11.5 to diminish pyrite flotation.

Sufficient grind and cleaner steps follow to obtain the desired degree of separation of the copper ore and molybdenite. Common reagents used for cleaner flotation are diesel oil and other light hydrocarbons. The nonfloat copper ore is filtered and dried before being converted to copper metal by smelting. The floated MoS_2 is filtered to remove bulk water. The wet, oily MoS_2 is not treated any further before roasting to MoO_3 .

A careful balance of all reagent combinations must be determined in actual plant practice. The scarcity of collector oils has initiated intensive studies of collector substitutes, and environmental considerations are causing concentrators to move away from cyanides, arsenates, chromates, and other hazardous reagents.

27.4.2 Processing of Concentrate

Direct Use. Some commercial-grade molybdenite concentrate is subjected to additional

grinding and flotation to produce lubricant-grade molybdenum disulfide (99% MoS_2). Residual flotation oils and water are then volatilized by passing the upgraded concentrate through an inert-gas-swept kiln. This high-purity product is added to grease and oils as a solid lubricant.

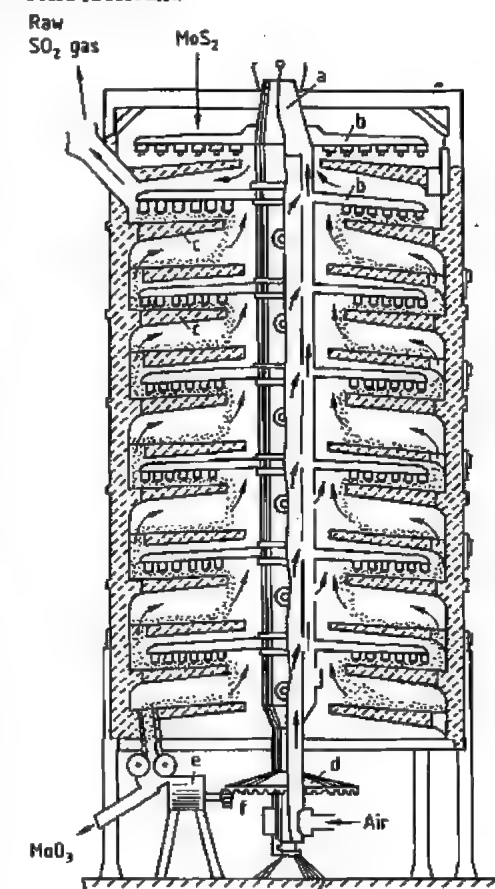


Figure 27.3: Multiple-hearth roasting furnace of the Nichols-Herreshoff type [20]: a) Rotating hollow shaft for passage of air to hearth; b) Rabble arms connected to shaft; c) Multilevel hearths; d) Beveled gear; e) Motor; f) Drive gear.

Production of Molybdenum Trioxide. The principal commercial molybdenum product is technical-grade molybdenum trioxide (MoO_3). In addition to being the major compound for adding molybdenum to steel, it is also the starting compound for all other molybdenum products including ammonium di-

molybdate, pure molybdenum trioxide, sodium molybdate, molybdenum metal, and ferromolybdenum.

Molybdenite is converted to technical-grade MoO_3 by roasting it in air in a multiple-hearth furnace of the Nichols–Herreshoff or Lurgi design [16, 17], (Figure 27.3). The roasted MoO_3 product typically contains < 0.1% sulfur. The multiple-hearth furnace is used because the hearths can be segmented to accomplish specific and different conversion operations within a single unit. Figure 27.4 shows the hearth-by-hearth composition of the molybdenum during roasting [18].

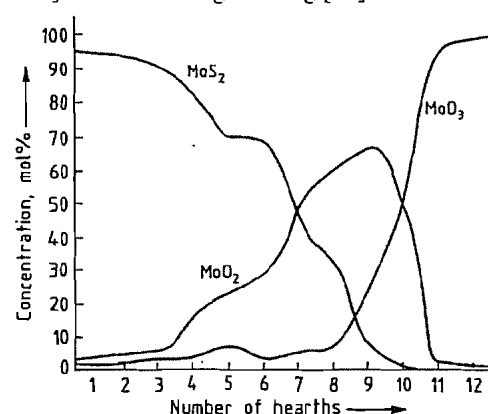
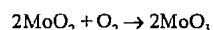
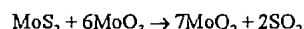
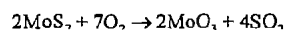


Figure 27.4: Composition of molybdenum sulfide and oxide in multiple-hearth roasting [18].

The upper hearths of the furnace are mainly used to burn off flotation oils and evaporate water. This part of the process is usually augmented by burning fossil fuels to ensure consistent temperature control and uniform roasting throughout the remainder of the unit. Upper hearth temperatures range between 600 and 700 °C.

The bulk of the sulfur is removed by oxidation in the intermediate hearths:



Since the sulfur oxidation reactions are highly exothermic, additional heating is not needed in this section. The hearth temperatures are controlled between 600 and 650 °C by the ad-

dition of excess air and/or with water spray cooling.

As sulfur burning nears completion, the composition of the roaster hearth is mostly MoO_2 with < 20% MoO_3 and MoS_2 . The reaction of MoO_3 with MoS_2 to form MoO_2 is driven by the strong oxidizing power of MoO_3 , so that the production of MoO_3 is limited until most of the MoS_2 is gone.

Once the availability of MoS_2 is less than the availability of MoO_3 , MoO_2 is rapidly converted to MoO_3 . Although this reaction is exothermic, it is not sufficient to maintain the temperatures above 525 °C which are required to complete sulfur removal and conversion to MoO_3 . Hence supplementary heating is required in these lower hearths. The oxide product is discharged from the roaster, cooled, and milled to form technical-grade MoO_3 . Technical-grade MoO_3 typically contains 85–90% MoO_3 , the balance being silica with some Fe_2O_3 and Al_2O_3 .

Sulfur dioxide and sulfur trioxide leave the roaster in the flue-gas stream. This gas stream is handled by methods which comply with emission regulations. The most common are contacting the off-gas with lime to produce disposable $\text{CaSO}_4 \cdot 2\text{H}_2\text{O}$ and the production of sulfuric acid. Sulfuric acid is produced by catalytically oxidizing the sulfur dioxide to sulfur trioxide which is absorbed by a H_2SO_4 solution.

In addition to sulfur removal, certain metal contaminants tend to vaporize during the roasting process. Any rhenium oxide, Re_2O_7 , in the concentrate can be scrubbed from the off-gas stream and recovered by solvent extraction or ion-exchange processes. Selenium oxide, SeO_2 , is also preferentially vaporized and can be collected to avoid creating an environmental hazard.

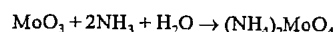
In many cases chemical leaching of the concentrate is required prior to roasting to preferentially remove nonferrous impurities detrimental to steel production. Three leaching processes are practiced:

- Sodium cyanide leachate is used for copper and gold removal

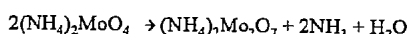
- Iron(III) chloride for copper, lead, and calcium removal
- Hydrochloric acid for lead and bismuth removal.

Pure molybdenum trioxide can be produced from technical-grade MoO_3 via calcination of ammonium dimolybdate (ADM) or by sublimation.

Ammonium dimolybdate is obtained by first leaching the technical-grade oxide with water at ca. 75 °C to remove soluble alkali impurities, primarily potassium [20, 21]. The oxide is then filtered and dissolved in a 10–20% ammonium hydroxide solution at 40–80 °C to form ammonium molybdate:



The ammonium molybdate solution is separated from the insoluble gangue minerals (primarily silica and some iron) by filtration and then further purified by precipitation of the heavy metals (e.g., copper) with sulfide. The filtered solution is then fed to an evaporative crystallizer operating at atmospheric pressure to produce ADM crystals:



Varying degrees of rejection for sodium, calcium, magnesium, and aluminum occur during crystallization and these impurities build up in the mother liquor. They are eliminated by periodic purging of the crystallizer. The ADM crystals are recovered by centrifugation and then dried. Calcining the ammonium dimolybdate in an indirectly fired rotary kiln at temperatures in excess of 420 °C produces pure MoO_3 .

Pure MoO_3 is also produced by sublimation of technical-grade MoO_3 [22]. The oxide is heated to 1100–1200 °C as a thin layer on a doughnut-shaped furnace hearth that rotates under electrical resistance heating elements. Air is drawn over the heated surface and sweeps away the vaporized MoO_3 , leaving the nonvolatile gangue and other metallic impurity elements behind. The charge on the hearth makes one pass under the heating elements. The residue, still rich in molybdenum, is discharged for use as a steel additive. The subli-

mation yield is about 60–70%. The sublimed vapor is then cooled, condensed, and collected in baghouses prior to densifying, screening, and packaging.

The molybdenum oxides produced by the ADM and sublimation processes are both of high purity (99.9% MoO_3). Compared to calcined ADM, sublimed pure oxide has a significantly lower alkali content, but higher silica, iron, lead, and tin levels. Sublimed pure oxide also tends to be finer in size and acicular (needle-like) in shape.

Sodium molybdate (and other similar molybdates) may also be produced from technical-grade MoO_3 [23], although pure MoO_3 is a common, but more expensive, starting material. Technical-grade MoO_3 is leached as in the ADM process and then dissolved in sodium hydroxide at 50–70 °C to produce an almost saturated solution of sodium molybdate. A minimum excess of caustic (NaOH) is maintained to inhibit silica dissolution; a small quantity of sulfide ion is added to precipitate heavy metals. If pure oxide is used, the initial leaching step is eliminated.

After filtration, the solution is fed to an evaporative crystallizer to produce sodium molybdate dihydrate ($\text{Na}_2\text{MoO}_4 \cdot 2\text{H}_2\text{O}$). If crystallization is performed below 10 °C, the decahydrate is formed ($\text{Na}_2\text{MoO}_4 \cdot 10\text{H}_2\text{O}$). The crystals are recovered by centrifugation and dried at 70 °C. Anhydrous sodium molybdate (Na_2MoO_4) is produced by drying at > 100 °C.

27.4.3 Recovery from Spent Petroleum Catalysts

Molybdenum-containing catalysts are widely used in the petroleum refining industry for mild hydrogenation and removal of heteroatoms such as sulfur (hydrodesulfurization), nitrogen, and oxygen, as well as metals like nickel and vanadium. A typical catalyst uses molybdenum in combination with cobalt or nickel on a porous alumina (Al_2O_3) support. The composition range of such a catalyst when spent is 2–10% Mo, 0–12% V, 0.5–4%

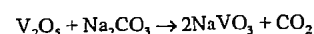
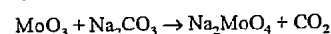
Co, 0.5–10% Ni, 10% S, 10% C, with the balance being Al_2O_3 .

Numerous approaches have been explored to recover the metal values from spent catalysts. The fundamental strategy involves:

- Initial heat treatment in air to remove the residual sulfur, carbon, and hydrocarbons, and to oxidize the metals to soluble molybdate and vanadate.
- A leaching step resulting in preferential solubilization of molybdate and vanadate, leaving the Ni–Co–alumina as a solid.
- Separation of the Mo and V.
- Treatment of the Ni–Co–alumina residue to recover Ni and Co.

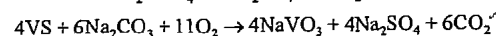
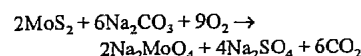
Production of Molybdate and Vanadate.

One basic process is to roast the ground (100 mesh, $< 149 \mu\text{m}$), spent catalyst in air at 600°C and then mix the roasted material thoroughly with soda ash (Na_2CO_3) [24]. The Na_2CO_3 –spent catalyst mix is roasted again in air at 600 – 800°C to convert the molybdenum and vanadium oxides to soluble sodium molybdate and sodium vanadate, respectively:



The roasted mix is leached with water at up to 100°C to dissolve the soluble molybdenum and vanadium compounds. The molybdenum- and vanadium-containing solution is recovered by filtration for subsequent separation; the insoluble Ni–Co–alumina filter cake is treated separately to recover the respective metal values. A similar process uses sodium chloride instead of soda ash and results in the same sodium molybdate–sodium vanadate solution [25].

An alternative process uses wet-air oxidation to combine the first two oxidation steps [26]. The as-received and ground (100 mesh, $< 149 \mu\text{m}$) spent catalyst is slurried with water and soda ash at temperatures up to 300°C and air pressures up to ca. 17 MPa (2500 psi). The molybdenum and vanadium sulfides are directly converted to soluble sodium molybdate and vanadate, respectively:



In addition all the carbon and hydrocarbons are oxidized (burned off). The nickel and cobalt sulfides are also oxidized and the sulfur is converted to sodium sulfate. The Ni–Co–alumina remains insoluble as in the previous processes.

Recovery of Molybdenum and Vanadium.

A number of technologies are available for recovering the metal values from the molybdenum- and vanadium-containing solution [26]. For example, addition of ammonium chloride or ammonium sulfate precipitates the vanadium as ammonium vanadate, NH_4VO_3 , which is removed by filtration [24]. The molybdenum can then be precipitated as calcium molybdate by adding lime.

In another method, treating the solution with hydrogen sulfide under very acidic conditions (1–2 mol/L H_2SO_4) preferentially precipitates molybdenum trisulfide. The vanadium remaining in solution can be precipitated as the hydrated oxide, $\text{V}(\text{OH})_4 \cdot 1.5\text{H}_2\text{O}$, by neutralization of the solution with sodium hydroxide, or as red cake ($\text{Na}_2\text{H}_2\text{V}_6\text{O}_{17}$) by first oxidizing the vanadium in solution with NaClO_3 and adjusting the pH to about 6 with NaOH or Na_2CO_3 . In a final solvent extraction method the vanadium is preferentially extracted from the solution with a quaternary ammonium compound such as Aliquat 336 (tricapryl monomethyl ammonium chloride). The molybdenum can then be extracted with a secondary amine such as Adogen 283, a ditridecylamine.

Recovery of Nickel and Cobalt. A number of technologies are also available to recover the nickel and cobalt from the alumina. They can be leached from the alumina with 5% HCl or H_2SO_4 solution at 75°C [27]. They can also be recovered by caustic digestion of a slurry of the Ni–Co–alumina residue in a 25% caustic (NaOH) solution at 250°C for 2 h [26]. The dissolved nickel and cobalt are recovered and separated by other methods standard in the nickel industry.

27.4.4 Recovery during Production of Tungsten Ores

The occurrence of tungsten ores, such as scheelite (CaWO_4), is commonly associated with trace amounts of powellite (CaMoO_4). Most of the powellite stays with the scheelite during its processing to a sodium tungstate solution by soda ash digestion in an autoclave. The powellite forms sodium molybdate and is solubilized. This is not a significant source of molybdenum and the recovered molybdenum is usually discarded because it is contaminated with tungsten. However the molybdate is routinely removed from the tungstate solution to purify the tungsten.

The most common method of removing molybdenum from a sodium tungstate solution is to treat the solution with sodium sulfhydrylate, $\text{NaSH} \cdot 2\text{H}_2\text{O}$ [28]. This compound reacts with the sodium molybdate and some of the sodium tungstate to precipitate the trisulfides, MoS_3 and WS_3 , respectively. The precipitate generally contains two to three parts of molybdenum to one part of tungsten; it can be calcined to give the relevant oxides and then leached with strong hydrochloric acid to dissolve the molybdenum, leaving the tungsten.

27.4.5 Production of Molybdenum Metal Powder

Molybdenum metal powder is produced industrially [30] by reducing high-purity molybdenum compounds with hydrogen. The following compounds are used:

- Molybdenum trioxide, MoO_3 (grey-green powder).
- Ammonium hexamolybdate, $(\text{NH}_4)_6\text{Mo}_6\text{O}_{19}$ (yellow powder).
- Ammonium dimolybdate, $(\text{NH}_4)_2\text{Mo}_2\text{O}_7$ (white powder).

To allow further processing by powder metallurgy, reduction conditions should result in a powder that can be pressed and sintered. Reduction is usually performed in two stages:

- Reduction to MoO_2 (molybdenum red).

- Reduction of MoO_2 to molybdenum metal powder.

This gives satisfactory yields of a completely reduced powder with the desired particle size distribution and a sufficiently high specific surface area in a reasonable length of time. Since reduction to MoO_2 is exothermic, this step is performed at 600°C to prevent caking due to the melting of MoO_3 ($m.p. 800^\circ\text{C}$). The MoO_2 is reduced to molybdenum powder at ca. 1050°C . The powder has a particle size of 2–10 μm , a specific surface area of 0.1–1 m^2/g , and an oxygen content of 100–500 mg/kg (partly adsorbed and partly as oxide).

Reduction is usually performed in an electrically heated continuous furnace (e.g., a pusher furnace, a walking beam furnace, or a rotary kiln) with a counterflowing stream of hydrogen. Reduction in fluidized-bed reactors is also known. Introduction of impurities should be avoided at all stages. Molybdenum powder SN5 with an impurity content of ≤ 5 mg/kg can be produced; this figure does not, however, take into consideration gases and refractory metals. Special purification procedures such as multiple recrystallization, ion exchange, solvent extraction and adsorption are used to remove undesirable impurities such as alkali metals, ferrous metals, and radioactive elements from molybdenum to be used in the semiconductor industry. Special mixer linings, furnace linings, and sintering boats prevent contamination with iron and ceramic particles.

Good flow properties and a constant apparent density are critical for satisfactory processing of molybdenum powder in automatic presses. Molybdenum powder is typically mixed with an organic binder, e.g., poly(vinyl alcohol), and a volatile agent, e.g., water. The slurry is sprayed into a heated free-fall chamber where spherical agglomerates are formed due to surface tension. Heating causes vaporization of the volatile agent, giving a hard, densely packed agglomerate (spray-drying process).

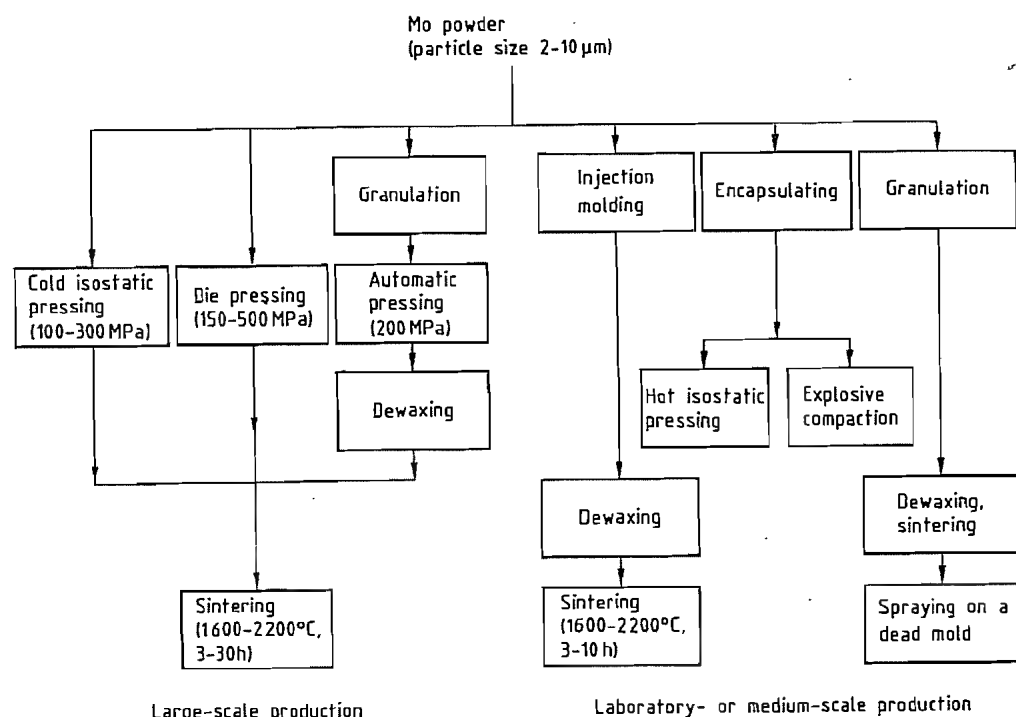


Figure 27.5: Production of molybdenum by powder metallurgy.

27.4.6 Production of Compact Molybdenum Metal [30, 31]

More than 95% of the total world production of molybdenum and molybdenum alloys high in molybdenum is produced by powder metallurgy, the remainder is obtained by vacuum arc remelting and electron beam melting.

Molybdenum produced initially by melting has to be worked by extrusion due to its coarse-grained, columnar microstructure; metal produced by powder metallurgy can, however, be worked by almost all standard hot metalworking techniques.

Production by Powder Metallurgy. More than 99% of industrially produced molybdenum is prepared by the method shown on the left-hand side of Figure 27.5. In the case of large workpieces and round bars, the molybdenum powder is filled into rubber containers that are sealed and then compressed isostatically at 100–300 MPa. Due to frictional

losses, a somewhat higher pressure (150–500 MPa) is used with die presses.

Sintering with resistance heating according to the Coolidge method is still used but indirect heating with tungsten heating elements is now the most common method. This procedure has a lower specific energy consumption, produces a homogeneous structure, and can be used to sinter large and complex components. Large items weighing up to 5 t (such as are used in isothermal forging dies) can only be produced by this method.

Depending on furnace design and the molybdenum alloy, sintering is performed at 1600–2200 °C for 3–30 h in a hydrogen atmosphere. Minimum sinter densities of 90%, but preferably 95%, are required to avoid subsequent processing difficulties. Neck formation between the particles starts at ca. 1200 °C and shrinkage at ca. 1600 °C. Addition of small quantities of platinum, palladium, or nickel allows the sintering temperature to be reduced

to 1300–C. These dopants have a low solubility in molybdenum and accumulate at the grain boundaries where they accelerate diffusion but have an adverse effect on ductility.

Production by Melting. Vacuum arc furnaces are used for large-scale melting of molybdenum. Electron beam devices are, however, used for special applications, particularly for the production of sputtering targets. Presintered molybdenum rods are fed into the electric arc furnace as electrodes and melted. In electron beam devices, sintered or hot isostatically compressed molybdenum rods are used. The resulting molybdenum billets are extruded by the Séjournet process. In this process the heated billet is rolled over a bed of glass powder, which softens during contact, insulates the tooling from the hot billet, and lowers oxidation.

Recent efforts have been directed at producing a fine-grained as-cast structure by vacuum double-electrode remelting or cold hearth electron beam melting. This should give molten molybdenum which can be processed immediately without intermediate hot extrusion.

27.4.7 Processing of Molybdenum

Manufacture of Semifinished Products. Molybdenum produced by powder metallurgy can be processed into semifinished articles by almost all classical forming techniques. High temperatures are, however, necessary and special equipment and tools are required. In molybdenum produced by melting the initial forming steps are important for obtaining a fine-grained structure.

The sintered starting material first has to be preheated to 1200–1400 °C to prevent any damage occurring during the first deformation steps. In this temperature range the tensile strengths of some molybdenum alloys correspond to those of hot-work tool steels at 700 °C. Preheating can be performed in electrical or gas-fired furnaces in a neutral or reducing atmosphere. Processing is carried out in air even though considerable oxidation occurs at this temperature. Embrittlement does

not occur because oxygen and nitrogen are almost completely insoluble in molybdenum.

As forming proceeds, ductility increases and the temperature can gradually be reduced to room temperature. After hot and cold working, the molybdenum is subjected to stress-relief annealing at ca. 800 °C.

Large items are produced by press forging. Round products (diameter 10 μm to ca. 200 mm) are manufactured by extruding (Séjournet method), forging, swagging, rolling, or drawing. Sheets are available in thicknesses of 10 μm to 50 mm.

Manufacture of Finished Products. Molybdenum can be worked by most of the customary techniques (e.g., deep drawing, flow turning). The working temperature should be higher than the ductile-to-brittle transition temperature but lower than the recrystallization temperature (1100 °C).

Molybdenum can readily be machined by chip removal and by electrical discharge. Tools used for milling, turning, and planing should comply with ISO hardmetal K specifications and have a highly positive cutting geometry. Since the cutting edges of the tools must be extremely sharp, coated indexable inserts are unsuitable. Commercially available emulsions or, in special cases, highly chlorinated hydrocarbons are used as coolants and lubricants.

When ceramic silicon carbide disks are used for grinding, low speeds must be used (< 33 m/s) to avoid buildup of heat. Molybdenum is machined by electrical discharge with zinc-coated brass wires and behaves similarly to hard metals. Graphite or tungsten copper electrodes are recommended for cavity sinking by electrical discharge machining.

Joining [32]. Molybdenum and molybdenum alloys can be welded and brazed but mechanical joining methods are widely used to avoid embrittlement.

Welding. Tungsten inert-gas welding (in gastight chambers filled with argon) and electron-beam welding are usually employed. The oxygen partial pressure must be extremely low

(< 0.5 Pa) because molten molybdenum rapidly takes up oxygen which leads to the precipitation of MoO_3 on cooling and thus to pore formation.

Diffusion welding at a welding temperature slightly below the recrystallization temperature (1100 °C) is particularly suitable for workpieces that are to be subjected to high mechanical loading. Resistance welding is primarily used in the electron tube and lamp industries for joining thin wires, ribbons, and foils.

Brazing is a suitable alternative to welding for operating temperatures below 1400 °C. Since the thermal expansion coefficient of molybdenum is about the same as that of graphite, molybdenum-graphite composites with advantageous properties can be produced, particularly for applications in nuclear fusion research and aerospace. Amongst others AgCu, PdCu, PdAg, Zr, and Ti are used as brazing filler materials.

Oxidation-Resistant Coatings [33]. Molybdenum alloys that can withstand oxidizing conditions at high temperature are still not available. Oxidation resistance decreases drastically above 500 °C and above 600 °C significant loss of material occurs due to formation of volatile MoO_3 . Owing to the increasing demand for high-temperature materials (e.g., in aerospace, turbine construction, and chemical reactors), oxidation-resistant coatings are being developed to permit the use of molybdenum materials in these applications.

Coatings based on aluminides, silicides, ceramics (e.g., Al_2O_3 , ZrO_2), and metals (chromium, noble metals) have been studied. Coating processes such as dip alloying, electroplating, but primarily pack cementation and slurry techniques, as well as plasma spraying, physical vapor deposition, and chemical vapor deposition have all been used.

Coatings based on silicides (e.g., MoSi_2 , maximum use temperature 1600 °C) and complex silicides (e.g., SiCrFe , maximum use temperature 1500 °C) provide the best protection against oxidation but are only effective for a limited period.

Surface Hardening. Nitriding, carburizing, and boriding have been increasingly used to increase the surface hardness and abrasion resistance of molybdenum materials. These thermochemical processes harden the surface to a depth of ca. 0.2 mm. Plasma-assisted processes are also becoming more important.

27.4.8 Alloys [34–36]

Alloying with rhenium increases the strength and ductility, the latter effect is especially pronounced in alloys containing 40–50% rhenium. These alloys also have excellent welding properties.

Molybdenum-tungsten alloys are extremely resistant to molten zinc and are therefore used in zinc metallurgy for tanks, pipes, pumps, and stirrers.

Table 27.1: Uses of molybdenum and molybdenum alloys.

Area of application	Examples of uses
Lamp and lighting industries	support wires, sealing ribbons, dimming caps
Electronic and semiconductor industries	semiconductor base plates, heat sinks, contact pins, sputtering targets, control grids, klystron and travelling-wave tube components
High-temperature and vacuum furnace construction	heating elements, thermal radiation shields, furnace ware
Glass and ceramic industries	glass-melting electrodes, installations in glass production tanks, drawing dies, crucibles for producing sapphire single crystals
Casting technology and metalworking	forging dies for isothermal forging, extrusion dies, die-casting molds, hot-galvanizing equipment
Coating	spray wire, spray powder, evaporation boats, sputtering targets, components of chemical vapor deposition equipment
Nuclear technology	furnace parts and charging equipment for sintering UO_2 ; first wall, divertor, and limiter components for experimental fusion reactors
Medicine	rotating X-ray anodes, collimators

27.5 Uses

Molybdenum is mainly used as an alloying element in steel, cast iron, and superalloys to increase hardenability, strength, toughness, and corrosion resistance. However, only the use of elemental molybdenum and molybdenum-base alloys is discussed in this section.

Initially, molybdenum was primarily used in the lamp industry. It is, however, now an increasingly important material in a wide range of applications (Table 27.1). In high-temperature applications, molybdenum competes with iron-, nickel-, and cobalt-base superalloys, ceramics, and other high-melting metals (tungsten, tantalum, and niobium). Superalloys can be used up to 1200 °C; molybdenum materials, especially the carbide-hardened alloys and molybdenum doped with potassium silicate, show adequate heat resistance (Figure 27.6) and creep properties up to 1800 °C. The lack of resistance to oxidation should, however, always be borne in mind. Molybdenum materials have a higher failure tolerance and ductility than ceramics and are less expensive than tantalum and niobium. Heating elements, thermal radiation shields, and furnace ware made of molybdenum are used, for example, in hot isostatic presses, sintering furnaces for the ceramic industry, and heat treatment furnaces.

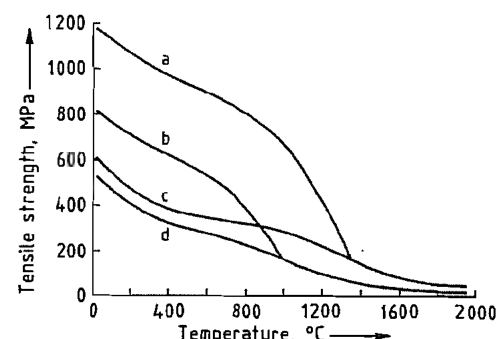


Figure 27.6: Tensile strengths of 1-mm thick molybdenum and TBM sheets as a function of temperature: a) TBM subjected to stress-relieving annealing; b) Molybdenum subjected to stress-relieving annealing; c) Recrystallized TBM; d) Recrystallized molybdenum.

Molybdenum is resistant to corrosion by most glasses and is therefore used as an electrode material in electric glass-melting furnaces. Glass produced in such furnaces is of better quality than that produced in fuel-fired furnaces and the process is more acceptable environmentally.

Crucibles and mandrels used to draw quartz glass or crucibles used for making single sapphire crystals have to withstand temperatures up to ca. 2100 °C. Molybdenum ribbon is used for electrical lead-in (e.g., in halogen lamps). In this application a vacuum-tight seal is formed by squeezing the quartz tubing around the ribbon at high temperature (ca. 2100 °C) and pressure. The high heat resistance of molybdenum and its low coefficient of thermal expansion are important prerequisites for these applications.

Electronic applications have and will continue to be a high-growth market for molybdenum parts. Molybdenum disks are used as base plates and heat sinks for power transistors and silicon rectifiers.

Molybdenum is also an important sputtering target material for electronic applications, mainly for codeposition of MoSi_3 films from ultra-high-purity molybdenum and silicon targets. Integrated circuits employing these films have low parasitic capacitances and also low gate and interconnection propagation delays.

Molybdenum layers produced by thermal spraying possess exceptionally good sliding properties and high abrasion resistance. They are deposited on machine components, especially car engine parts such as piston rings, synchronizers, and selector forks.

More than 80% of the rotating X-ray anodes currently used in clinical diagnostics are made of molybdenum alloys. Loading can be increased by a thin tungsten rhenium layer on the molybdenum body. Rhenium in tungsten has the same effect on ductility as rhenium in molybdenum and decreases the susceptibility to cracking initiated by thermal stress. Brazing a thick graphite disk onto the back of a target increases its heat and emission capacity.

27.6 Compounds

As a transition element, molybdenum shows variable valency and forms many complexes and colored compounds. The outstanding feature of molybdenum is its chemical versatility: oxidation states from 2- to 6+; coordination numbers from 4 to 8 and, accordingly, a very varied stereochemistry; the ability to form compounds with most inorganic and organic ligands, with a particular preference for oxygen, sulfur, fluorine, and chlorine donor atoms; the formation of bi- and polynuclear compounds containing bridging oxide and chloride ligands and/or Mo-Mo bonds.

Molybdenum is very similar to tungsten, the third member of Group 6, but different from the first member, chromium. Molybdates(VI), unlike chromates(VI), are not strong oxidizing agents: much of the familiar chemistry of molybdenum is that of the 6+ and 5+ oxidation states.

In recent years research on molybdenum compounds has greatly increased because of their academic interest and their developing technical applications as lubricant additives (molybdenum disulfide and sulfur complexes), corrosion inhibitors, pigments, smoke suppressants, and heterogeneous catalysts (molybdenum trioxide and molybdates).

Recognition of the central role of molybdenum in a number of metalloenzymes (nitrogenase, nitrate reductase, xanthine oxidase) and the problem of molybdenum toxicity in ruminants have stimulated research in both molybdenum biochemistry and inorganic chemistry. The fact that molybdenum compounds are nontoxic to humans has led to interest in the possibility of replacing compounds of toxic metals with safer molybdenum compounds, e.g., chromium in corrosion inhibitors, anti-mony in flame and smoke suppressants.

For more background information on molybdenum chemistry, see [37-42].

Compound Types. Typical compounds of molybdenum(VI) are the trioxide, MoO_3 ; sodium molybdate, Na_2MoO_4 ; and ammonium

heptamolybdate, $(\text{NH}_4)_6\text{Mo}_7\text{O}_{24} \cdot 4\text{H}_2\text{O}$ and $(\text{NH}_4)_6\text{Mo}_7\text{O}_{24} \cdot 2\text{H}_2\text{O}$. These compounds are the starting points for the preparation of many other molybdenum compounds. The chemistry of the higher oxidation states (4+ to 6+) is dominated by oxomolybdenum cations, e.g., MoO^{2+} , $\text{Mo}_2\text{O}_4^{2+}$, $\text{Mo}_2\text{O}_3^{4+}$, MoO_3^{3+} , MoO_2^{2+} . The oxide ligands may be bound to just one molybdenum (terminal oxide) or to two or more molybdenum atoms (bridging) [43]. Replacement of one or more oxide ligands by sulfide has produced many molybdenum-sulfur complexes and clusters [44, 45].

The higher halides are covalent, e.g., molybdenum hexafluoride, MoF_6 , and molybdenum pentachloride, MoCl_5 .

Compounds of molybdenum(II) and lower oxidation states are stabilized by unsaturated ligands such as carbon monoxide, e.g., in molybdenum hexacarbonyl, $\text{Mo}(\text{CO})_6$, and by molybdenum-molybdenum bonds, and so are bi- or polynuclear, e.g., molybdenum(II) acetate, $\text{Mo}_2(\text{CH}_3\text{COO})_4$, and molybdenum(II) chloride, Mo_2Cl_2 .

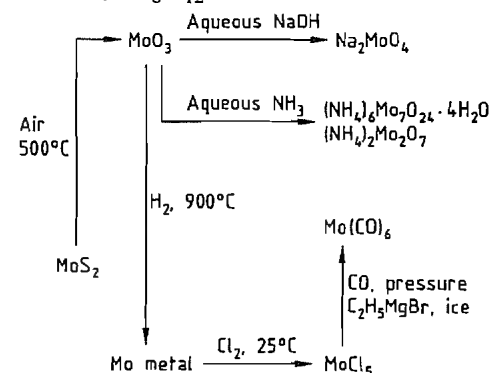


Figure 27.7: Relationship between some molybdenum compounds.

Preparative Chemistry. The starting point in preparative molybdenum chemistry is molybdenum(VI) oxide, MoO_3 (Figure 27.7). Molybdenum disulfide, the naturally occurring form of molybdenum, is unreactive.

Aqueous Solution Chemistry. The aqueous chemistry of molybdenum is complicated [38]. It is dominated by oxo species which are prone to dimerize or polymerize. Hydrated

cations (i.e., cations having only water bound to molybdenum) are known only for oxidation states 2+ and 3+; they are powerful reducing agents which oxidize in air. The aqueous chemistry of molybdenum is summarized in Figure 27.8. The aqueous ion of molybdenum(IV) (not shown in Figure 27.8) is the red trimer, $[\text{Mo}_3\text{O}_4(\text{H}_2\text{O})_9]^{4+}$.

Redox Chemistry. Molybdenum exemplifies the general trend of a transition metal group; the higher oxidation states of the heavier elements (molybdenum and tungsten) are more stable (resistant to reduction) and the lower oxidation states less stable (more prone to oxidation) than those of the first element (chromium). Reduction potentials are summarized in Figure 27.9 [46]. Note that reduction in water bypasses molybdenum(IV).

For the reduction of molybdate in neutral or alkaline solution, sodium dithionite is useful, e.g., in the preparation of the molybdenum(V) cysteine complex, $\text{Na}_2[\text{Mo}_2\text{O}_4\{\text{SCH}_2\text{CH}(\text{NH}_2)\text{COO}\}_2] \cdot 5\text{H}_2\text{O}$ [47].

Molybdenum(III) solutions oxidize rapidly in air and must be handled under nitrogen or argon. With molybdenum(V), aerial oxidation is slow. Titration of reduced molybdenum solutions with cerium(IV) sulfate or permangan-

ate is a volumetric method of determining molybdenum [48].

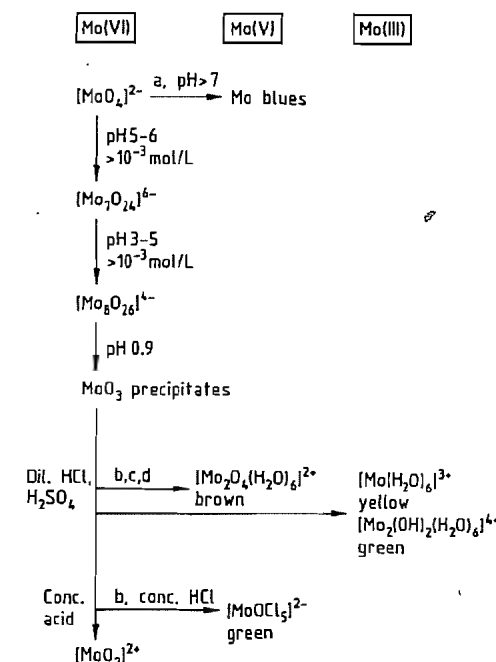


Figure 27.8: Aqueous chemistry of molybdenum showing species [38], reducing agents, and conditions. Reducing agents: a) Sodium dithionite, $\text{Na}_2\text{S}_2\text{O}_4$; b) Hydrazinium hydrate, $\text{N}_2\text{H}_4 \cdot \text{H}_2\text{O}$; c) Tin(II) chloride; d) Liquid mercury.

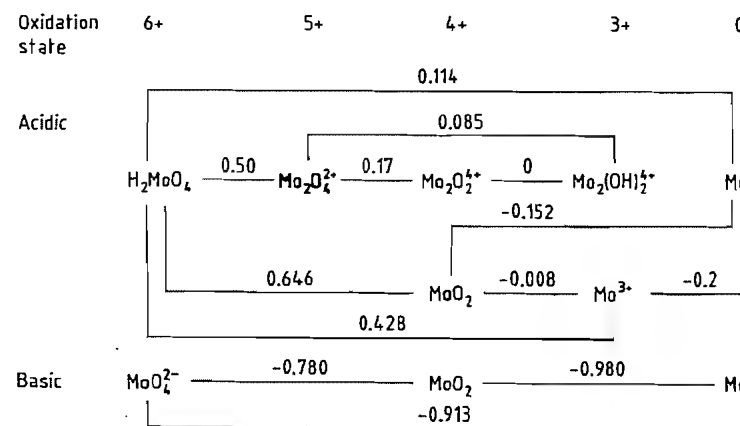


Figure 27.9: Reduction potentials (in volts) of molybdenum couples in acidic and alkaline aqueous solutions [46]. The more negative the potential, the more reducing is the couple, i.e., the more stable is the higher oxidation state.

Table 27.2: Properties of molybdenum trioxide and dioxide.

Property	MoO ₃	MoO ₂
Crystal structure	orthorhombic	monoclinic
Space group	<i>Pbnm</i>	<i>P2₁c</i>
<i>Z</i>	4	4
<i>a</i> , nm	0.39628	0.56109
<i>b</i> , nm	1.3855	0.48562
<i>c</i> , nm	0.36964	0.56285
α, β, γ	90°, 90°, 90°	90°, 120.95°, 90°
Mo coordination	octahedral, distorted	octahedral, distorted rutile
ΔH_f° , kJ/mol ^a	-745.2	-588.7
ΔG_f° , kJ/mol ^a	-667.9	-533.1
<i>S</i> ^o , J/K ^a	77.7	47.2
Density, g/cm ³ (21 °C)	4.692	6.29
<i>mp</i> , °C	801	
<i>bp</i> , °C	1155	
Sublimation, °C	ca. 700	ca. 1100
Solubility, g/L		
Water 28 °C	0.49	insoluble
100 °C	1.5	insoluble
HNO ₃ (4 mol/L, 20 °C)	ca. 14	insoluble
Aqueous ammonia and alkali	soluble	insoluble
Organic solvents	insoluble	insoluble

^a Standard enthalpy and free energy of formation from the elements and entropy at 298.15 K [49, 50].

27.6.1 Oxides

Well characterized oxides are molybdenum trioxide, MoO₃, and molybdenum dioxide, MoO₂. Mixed-valency oxides and molybdenum blues are also important.

Molybdenum Trioxide. Molybdenum trioxide, molybdenum(VI) oxide, MoO₃, is the ultimate product of the oxidation of molybdenum compounds. It forms white orthorhombic crystals that are photosensitive, i.e., turn blue in light. The compound is weakly paramagnetic and an *n*-type semiconductor.

Other properties are listed in Table 27.2. It is produced by roasting molybdenum disulfide in air at 600 °C and may be purified by sublimation (see Section 27.4.2). It can also be prepared by reacting ammonium molybdate at 550 °C with oxygen or by precipitation from an aqueous ammonium molybdate solution treated with concentrated nitric acid [51].

The structure of molybdenum trioxide comprises layers built from linked, distorted MoO₆ octahedra. Crystal morphology depends on the method of preparation: needles occur after vapor condensation, platelets after crystal growth on silica or graphite [52]. Molybdenum trioxide has a characteristic IR spectrum showing Mo–O vibrations (996, 870, 821, and 570 cm⁻¹).

Molybdenum trioxide is an acidic oxide soluble in aqueous alkali and ammonia. Freshly precipitated MoO₃, which is much more reactive than the aged oxide, dissolves in aqueous solutions of citric, malic, and other hydroxycarboxylic acids [53], and in solutions of ethylene glycol, glycerol, and other polyols to form molybdenum(VI) complexes [54]. Molybdenum trioxide also reacts with β -diketones (e.g., acetylacetone) to form complexes such as MoO₂(CH₃COCHCOCH₃)₂ which is a useful starting compound for preparing other molybdenum(VI) complexes by ligand exchange reactions. It is reduced by hydrogen at 500–600 °C to MoO₂ and at 900–1000 °C to molybdenum metal.

Molybdenum trioxide in combination with more basic metal oxides finds application in heterogeneous catalysis. Studies of MoO₃ specimens with different crystal habits have demonstrated structure sensitivity of MoO₃ selective oxidation catalysts; the type of reaction catalyzed depends on the predominant crystal face. Platelike crystallites predominantly expose the {010} face which is responsible for insertion of oxygen into allylic compounds; activation of, for example, propene occurs at the {100} and {101} faces, and total oxidation at all faces [52].

Hydrates of MoO₃. The monohydrate, MoO₃·H₂O, precipitates when a concentrated solution of sodium molybdate is acidified with hydrochloric acid. The dihydrate, MoO₃·2H₂O, precipitates when a solution of ammonium heptamolybdate is acidified with nitric acid [51]; it is commonly referred to as molybdic acid (H₂MoO₄·H₂O). Both hydrates are yellow.

Molybdenum Dioxide. Molybdenum dioxide, molybdenum(IV) oxide, MoO₂, is a dark blue crystalline solid and consists of chains of distorted MoO₆ octahedra. The distortions arise from Mo–Mo bonding leading to alternate long (0.31118 nm) and short (0.25106 nm) Mo–Mo distances [55, 56]. Properties are listed in Table 27.2. Molybdenum dioxide is a metallic conductor and is weakly paramagnetic. It is produced by reducing MoO₃ with hydrogen, ammonia, and carbon monoxide at 600 °C.

Molybdenum dioxide is a neutral oxide that is insoluble in acid and alkali. It reacts with chlorine giving dichlorodioxomolybdenum(IV), MoO₂Cl₂, and with carbon tetrachloride giving molybdenum tetrachloride, MoCl₄.

Molybdenum Blues. Molybdenum blues, so called because of their blue color, are mixed oxide hydroxides of molybdenum(VI) and molybdenum(V) (Figure 27.8) [57]. They are amorphous solids that are soluble in water and alcohols. A typical species is (Mo₃⁶⁺Mo₃⁵⁺O₁₈H)⁻ which has an absorption maximum at 450 nm.

The formation of molybdenum blues is the basis of a colorimetric method for determining phosphorus [58]. Molybdate and orthophosphate ions condense in acidic solution to give molybdophosphoric acid which is reduced by hydrazinium sulfate to a molybdenum blue with maximum light absorbance at 820–830 nm. The color intensity is proportional to the amount of phosphate incorporated. The reduced molybdophosphate is an example of a heteropoly blue [57].

Mixed Valency Oxides. The mixed Mo(VI)–Mo(V) oxides (molybdenum oxide bronzes) have an intense color and metallic luster [59].

The binary bronzes MoO_x (*x* between 2 and 3), constitute a series of deep blue or purple compounds. They are prepared by heating MoO₃ in vacuo or with molybdenum metal. The structures are built from edge- and corner-sharing [MoO₆] octahedra, or [MoO₆] octahe-

dra and [MoO₄] tetrahedra. The Magneli phases, Mo₄O₁₁, and Mo₈O₂₃, have metallic properties at room temperature.

The ternary oxides include the red bronzes, A_{0.33}MoO₃ (*A* = Li, K, Rb, Cs, Tl), which are semiconductors, the blue bronzes A_{0.3}MoO₃ (*A* = K, Rb, Tl), purple bronzes A_{0.9}Mo₈O₁₇ (*A* = Li, Na, K, Tl), and a rare-earth bronze La₂Mo₂O₇; they behave like metals at room temperature. Interest in these compounds is focused on their electrical and optical properties.

27.6.2 Chalcogenides

The most important chalcogenide of molybdenum is molybdenum disulfide, which is the principal source of molybdenum, in the form of the mineral molybdenite. Molybdenum selenide, MoSe₂, and telluride, MoTe₂, are also known.

Molybdenum Disulfide. Molybdenum disulfide, molybdenum(IV) sulfide, MoS₂, is a black crystalline solid that occurs in two forms: hexagonal, which is found in the mineral molybdenite and rhombohedral (Table 27.3). The solid is diamagnetic and a semiconductor. It is built of S–Mo–S layers whose sulfur atoms are in contact (Figure 27.10). Within each layer molybdenum is at the centre of a trigonal prism of sulfur atoms. Since the forces operating between the layers are weak van der Waals attractions, the layers can slide over one another giving molybdenum disulfide a slippery texture and solid-state lubrication properties like graphite.

The hexagonal form is produced by heating molybdenum with sulfur, ammonium tetrathiomolybdate [(NH₄)₂MoS₄], or molybdenum trisulfide at 1100 °C. The compound is amorphous at 250–400 °C; crystallization requires prolonged heating at 1100 °C. The rhombic form is obtained by heating the hexagonal form in vacuo at 7.5 GPa and 1200 °C, or by reacting MoO₃ with sulfur and potassium carbonate at 1100 °C.

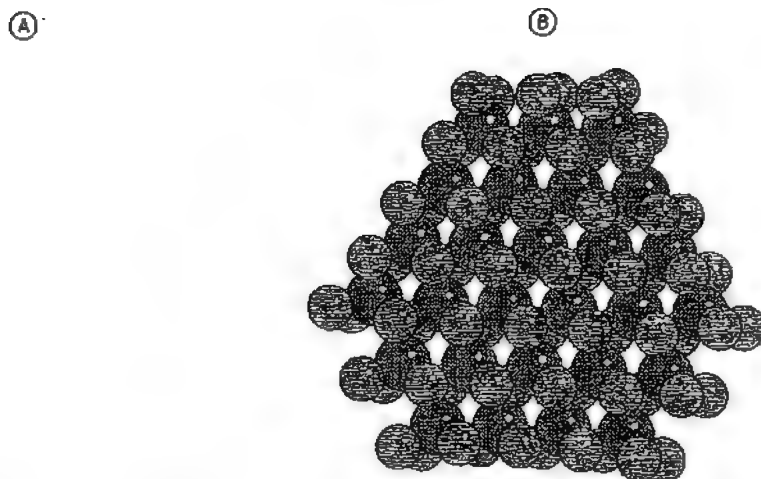


Figure 27.10: Structure of molybdenum disulfide. A) Side view showing the S-Mo-S layers; B) Top view of a hexagonal fragment of one layer.

Table 27.3: Properties of molybdenum disulfide.

Property	Hexagonal crystal structure	Trigonal prismatic crystal structure
Space group	$P6_3/mmc, D_{6h}^{20}$	$R\bar{3}m, C_{3v}^{21}$
Z	2	3
a, b, c, nm	0.316, 0.316, 1.229	0.317, 0.317, 1.838
α, β, γ	90°, 90°, 120°	90°, 90°, 90°
Density, g/cm ³	5.05	5.02
Mo coordination	trigonal prismatic	
Interatomic distances, nm		
Mo-S	0.242	
Mo-Mo	0.316	
S-S	0.349	
ΔH_f° , kJ/mol*	-234.1	
ΔG_f° , kJ/mol	-225.7	
S° , J/K	62.8	
mp, °C	> 1600	

* Standard enthalpy and free energy of formation from the elements and entropy at 298.15 K [49, 50, 60].

Molybdenum disulfide dissolves only in strongly oxidizing acids (e.g., aqua regia) to give molybdenum(VI) compounds. When heated in vacuo at 1200 °C it decomposes to Mo₂S₃ and metallic molybdenum. Heating in air at 500 °C produces MoO₃. Reduction with hydrogen at 1100 °C or > 1500 °C yields Mo₂S₃ or molybdenum metal, respectively.

Molybdenum Sesquisulfide. Molybdenum sesquisulfide, dimolybdenum trisulfide, mo-

lybdenum(III) sulfide, Mo₂S₃, has a different structure from MoS₂; the molybdenum is at the center of a distorted octahedron of sulfur atoms. Molybdenum sesquisulfide is a grey solid and is prepared by heating molybdenum and sulfur (2:3) in vacuo at 1400 °C. It dissolves in, and is oxidized to molybdenum(VI), by aqua regia. In air at 350 °C it oxidizes to molybdenum trioxide. Hydrogen at 1500 °C reduces it to molybdenum metal.

Molybdenum Trisulfide. Molybdenum trisulfide, molybdenum(VI) sulfide, MoS₃, is the sulfide precipitated in conventional inorganic analysis when hydrogen sulfide is passed through an acidified molybdate solution. Molybdenum trisulfide, like the sulfides of tin, arsenic and antimony, dissolves in yellow ammonium sulfide giving a tetrathio salt, MoS₄²⁻.

According to X-ray absorption spectroscopy, the composition MoS₃ corresponds to Mo(S²⁻)₂(S₂²⁻)_{0.5}, one third of the sulfur is disulfide (S₂²⁻); the formal oxidation state of the molybdenum is 5+ [61].

When heated in nitrogen at ca. 350 °C molybdenum trisulfide decomposes to amorphous molybdenum disulfide. Heated in air, it begins to oxidize to molybdenum trioxide at 200 °C.

Chevreil Phases. The Chevrel phases are ternary molybdenum chalcogenides, M_xMo₆X₈ (where M is a metal and X a chalcogenide), for example, PbMo₆S₈ [62]. They are black powders prepared by heating the constituent elements in vacuo at 1000 °C. They consist of linked [Mo₆S₈] clusters having sulfur atoms at the corners of a cube and molybdenum atoms at the face centers (the same structure as the [Mo₆Cl₈] structure. These compounds have attracted great interest as superconductors with critical temperatures as high as 15 K and as battery materials.

Ammonium Tetrathiomolybdate. Ammonium tetrathiomolybdate, (NH₄)₂[MoS₄], crystallizes from a solution of ammonium molybdate saturated with hydrogen sulfide to form deep red crystals. The [MoS₄]²⁻ ion is tetrahedral and is the thio analogue of molybdate. Ammonium tetrathiomolybdate has an extensive chemistry and is an entry point to much molybdenum sulfur chemistry. The sulfur atoms form bridges to metal ions so forming clusters, e.g., the species [S₂MoS₂CoS₂MoS₂]²⁻ with Co²⁺ [38].

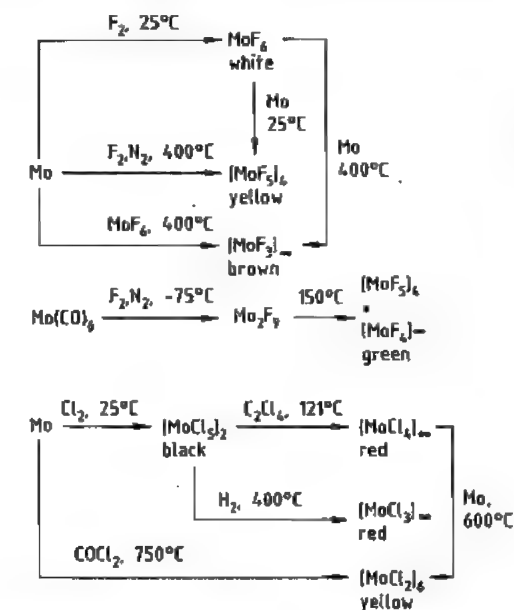


Figure 27.11: Preparation of molybdenum fluorides and chlorides.

27.6.3 Halides

Binary halides are known for molybdenum in oxidation states (II) to (VI). The preparation of molybdenum fluorides and chlorides is summarized in Figure 27.11. The only molecular halide is molybdenum hexafluoride, MoF₆, which is a volatile liquid. The coordination number of molybdenum is six in the halides of Mo(V), (IV), and (III), the molybdenum atoms being linked by bridging halogens.

Molybdenum(II) chloride is an extended solid containing [Mo₆Cl₈]⁴⁺ clusters linked by bridging chlorines so giving the formula Mo₆Cl₁₂. In the cluster eight chlorine atoms are at the corners of a cube. Molybdenum atoms, linked by Mo-Mo bonds, are at the face centers of the cube and so constitute an octahedral Mo₆ cluster. The cluster is very stable both to hydrolysis and oxidation and persists through many reactions.

A feature of the halides of Mo(IV), (III), and (II) is the formation of bonds between molybdenum atoms. Consequently, there is pairing of electron spins on adjacent molybdenum atoms and so the magnetic moments of the halides are less than the spin-only values.

Molybdenum Pentachloride. Molybdenum pentachloride, molybdenum(V) chloride, MoCl₅, is the most important molybdenum halide. The dark green black crystals (mp 194 °C) consist of Mo₂Cl₁₀ dimers; the vapor and solutions contain MoCl₅ monomers.

Molybdenum pentachloride is soluble in carbon tetrachloride, benzene, and many other organic solvents. It is very reactive, undergoing hydrolysis in air, water, and damp organic solvents to form brown oxomolybdenum(V) chlorides. It is supplied and stored in sealed ampoules and must be handled under argon or nitrogen or in vacuo.

The outstanding property of molybdenum pentachloride is its ability to abstract an oxygen atom from water, sulfur dioxide, triphenylphosphine oxide (Ph₃PO), dimethyl sulfoxide (Me₂SO), and other oxygen-containing compounds to form oxomolybdenum complexes, MoOCl₃A₂, (e.g., A = Ph₃PO,

Me₂SO). In concentrated hydrochloric acid molybdenum pentachloride forms the deep green complex ion [MoOCl₃]²⁻.

Molybdenum pentachloride is the starting point for much nonaqueous and organomolybdenum chemistry.

Oxomolybdenum Halides. In oxidation states 5+ and 6+ molybdenum has a strong tendency to form multiple bonds to oxygen. The oxomolybdenum halides are volatile solids which may be sublimed in vacuo. They are more stable than the binary halides and are formed when the binary halides are exposed to air and water.

Oxomolybdenum(VI) compounds are of two types: MoOX₄ (X = F, Cl), and MoO₂X₂ (X = F, Cl, Br). Oxomolybdenum(V) compounds are generally monoxo, e.g., MoOCl₃.

Trichlorooxomolybdenum(V). Trichlorooxomolybdenum(V), MoOCl₃, is a green solid consisting of octahedral [MoOCl₃] units linked through cis-chlorine atoms. It forms adducts with many organic ligands, e.g., MoOCl₃·L (L = ligand) with acetylacetone and

2,2'-bipyridyl, and MoOCl₃·2L with diethyl ether and pyridine.

27.6.4 Molybdates, Isopolymolybdates, and Heteropolymolybdates

Sodium molybdate and other simple molybdates contain the tetrahedral [MoO₄]²⁻ ion. Ammonium heptamolybdate (an isopolymolybdate), (NH₄)₆Mo₇O₂₄·4H₂O, is composed of linked, distorted [MoO₆] octahedra. In the heteropolymolybdates, molybdenum and another element are present in the same structure. The properties of some of the more important molybdates are summarized in Table 27.4.

Ammonium and Alkali-Metal Molybdates. Ammonium and alkali-metal molybdates are soluble in water (Table 27.4). They are made by crystallizing or evaporating solutions of molybdenum trioxide dissolved in aqueous alkali. Ammonium dimolybdate is used as an intermediate for purifying technical-grade MoO₃.

Table 27.4: Properties of some molybdates [39, 63].

Molybdate	<i>M_r</i>	Structure ^a	Color	Solubility in water, % ^b	Δ <i>H_f</i> ⁰ , kJ/mol ^c
(NH ₄) ₂ MoO ₄	196.01	4	white	39	
(NH ₄) ₂ Mo ₂ O ₇	339.95	4 or 6		30	
(NH ₄) ₆ Mo ₇ O ₂₄ ·4H ₂ O	1235.8	6	white	30	
Na ₂ MoO ₄	205.92	6 + 4	white	40	-1466
MgMoO ₄	184.24	6 + 6	white	16	-1248
CaMoO ₄	200.01	8 + 4	white	0.005	-1548
SrMoO ₄	247.56	8 + 4	white	0.003	-1449
BaMoO ₄	297.26	8 + 4	white	0.005	-562
CoMo ₄ ^d	218.87				-1032
a		6 + 4	violet		
b		6 + 6	rose		
NiMoO ₄ ^d	218.63				-947.7
a		6 + 4	green		
b		6 + 6	green		
PbMoO ₄	367.14	8 + 4	white	10 ⁻⁵	-1076
ZnMoO ₄	225.33	5 or 6 + 4	white	0.5	-1140
Fe ₂ (MoO ₄) ₃	591.50	6 + 4	yellow		-2963

^a Coordination of the counteraction (except ammonium) by oxide and coordination of molybdenum (4 = tetrahedral; 6 = octahedral).

^b Weight percent of anhydrous salt in 100 g saturated solution at 25 °C.

^c Standard heat of formation from the elements at 298.15 K.

^d Two polymorphs: low-temperature form, b, transforms to the high-temperature form, a, at 400 °C [64].

Ammonium molybdates are made by dissolving MoO₃ in aqueous ammonia solution; (NH₄)₂MoO₄ then crystallizes from aqueous ammonia, (NH₄)₆Mo₇O₂₄·4H₂O from a solution kept at the boiling point for 1 h, and (NH₄)₂Mo₈O₂₆·5H₂O from an acidified aqueous solution of (NH₄)₆Mo₇O₂₄·4H₂O. The dimolybdate, (NH₄)₂Mo₂O₇, may be crystallized from hot ammoniacal molybdate solutions.

The structures of the isopolymolybdates are based on linked, distorted [MoO₆] octahedra. The structure of ammonium dimolybdate consists of infinite chains of pairs of edge-shared [MoO₆] octahedra with adjacent pairs linked by [MoO₄] tetrahedra [65].

Ammonium di- and heptamolybdates are used as sources of water-soluble molybdenum, for example, in the preparation of catalysts. When the catalyst is calcined, the molybdate decomposes to molybdenum trioxide and ammonia.

Molybdates of Di- and Trivalent Cations. Molybdates of divalent cations (except Mg²⁺) are insoluble in water (Table 27.4). They are prepared by precipitation from a sodium or ammonium molybdate solution or by heating mixed solid oxides. The coordination environment of the molybdenum may be tetrahedral or octahedral.

Molybdates of trivalent cations have the formula A₂(MoO₄)₃ or A₂Mo₃O₁₂, with A = Al, Cr, Fe, Bi, lanthanide. Coordination of the molybdenum is tetrahedral; the other cation is usually octahedral.

A number of these molybdates have important uses. Cobalt, iron, and bismuth molybdates are catalysts for the selective oxidation of organic compounds: olefins are oxidized to unsaturated aldehydes and ketones, e.g., propene to acrolein (cobalt and bismuth), propene and ammonia to acrylonitrile (bismuth), methanol to formaldehyde (iron). Molybdenum is the source of selectivity in these reactions. The first step is generally activation of a C-H bond over the more basic (nonmolybdenum) oxide and the molybdenum then controls oxygen insertion. The well known Co-Mo/alumina hy-

drodesulfurization catalyst does not, however, strictly contain cobalt molybdate.

Other actual or proposed applications are: calcium and strontium molybdates doped with neodymium as lasers; lanthanide molybdates for optical and optoelectric applications; zinc molybdate as a white pigment and corrosion inhibitor.

Heteropolymolybdates. The heteropolymolybdates consist of [MoO₆] octahedra incorporating atoms of a different element, the heteroatom [38, 66]. The heteroatoms are completely surrounded by the oxygen atoms of the [MoO₆] octahedra. The resulting coordination of the heteroatom may be tetra- or octahedral. The 12-molybdo species, [Xⁿ⁺Mo₁₂O₄₀]⁽⁸⁻ⁿ⁾⁻, is an important group with tetrahedrally coordinated heteroatoms (X). An example is 12-molybdophosphoric acid, H₃[PMo₁₂O₄₀]₂₈H₂O, prepared by dissolving molybdenum trioxide in phosphoric acid; it is yellow and readily soluble in water. Ammonium 12-molybdophosphate, which precipitates when ammonium molybdate is added to a solution of disodium hydrogen phosphate, is used for the gravimetric determination of phosphate [62]. The phosphomolybdates are selective oxidation catalysts, e.g., in the conversion of acrolein to acrylic acid [67].

27.6.5 Other Compounds

Molybdenum forms a large number of coordination compounds or complexes [38]. Complexes with organosulfur ligands attract a great deal of current interest because of their significance in molybdenum biochemistry and applications as oil-soluble antiwear and friction-reducing additives [68]. Examples of the latter are phosphorodithioates (dithiophosphates) and dithiocarbamates, [Mo₂O₃L₄] and [Mo₂O₂S₂L₂] where L is (RO)₂PS₂, R₂NCS₂⁻.

Molybdenum hexacarbonyl, Mo(CO)₆, *mp* 150 °C, *bp* 156.4 °C (sublimes), is a white, air-stable solid that is insoluble in water but soluble in organic solvents. It is made from molybdenum pentachloride (Figure 27.7) and is commercially available. It is a starting point for the synthesis of low-valent and organomo-

lybdenum compounds [69]. The structure consists of CO groups octahedrally disposed around molybdenum and bound through carbon.

27.7 Uses of Molybdenum Compounds

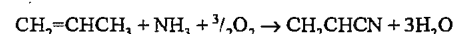
Molybdenum-containing catalysts are used for a broad range of reactions [76]. In some cases, the catalyst is a single molybdenum compound, and either soluble (homogeneous) or insoluble (heterogeneous) in the reaction medium. In other cases, the catalyst is a binary mixture of the oxides and/or sulfides of molybdenum and of another element (usually Co, Ni, Fe, W, or Bi). The catalytic properties of these binary compositions differ greatly from those of the individual compounds. The heterogeneous catalysts are often formed and supported on a substrate such as activated alumina, silica, carbon, or zeolite. The support can greatly improve catalyst activity, selectivity, and mechanical strength. In industrial practice other elements or compounds (e.g., potassium, phosphorus, tungsten, or silica) are often added to the binary compositions as additives to further enhance activity, selectivity, and strength.

The scope and versatility of molybdenum catalysts are illustrated in Table 27.5 [77]. The activity and selectivity of catalysts based on MoO₃ and MoS₂ are summarized for redox reactions; isomerization, polymerization, addition, and decomposition (usually classified as acid base reactions).

One of the largest uses for molybdenum catalysts is in the desulfurization of petroleum, petrochemicals, and coal-derived liquids, in which organosulfur compounds react with hydrogen at the catalyst surface and sulfide ions are removed as hydrogen sulfide. Desulfurization is used to improve product color, smell, and stability, to eliminate sulfur dioxide emission on fuel combustion, and to make possible subsequent reforming processes which may use sulfur-sensitive cata-

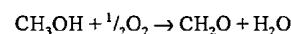
lysts. Today, environmental air quality is a major reason for desulfurization.

The most common desulfurization catalyst is a binary mixture of cobalt oxide and an excess of molybdenum trioxide on an activated alumina substrate. After being charged into the industrial reactor, the catalyst reacts with the sulfur-containing reducing atmosphere to form molybdenum and cobalt sulfides as the working catalyst. A major development in the history of hydrocarbon oxidation was the discovery of bismuth molybdate catalysts for the partial oxidation and ammoxidation of propene to acrylonitrile in one step [78].



The original catalyst was reported to have a composition of 50% Bi₂PbMo₁₂O₃₂ and 50% SiO₂, with the silica gel support preventing catalyst disintegration in the fluidized bed operation. This catalyst and its modifications account for virtually all of the acrylonitrile production in the world.

Another major catalyst based on ferric molybdate (5MoO₃·Fe₂O₃) is used to selectively oxidize methanol to formaldehyde [79]:



Molybdenum catalysts are also important in commercial coal liquefaction processes where coal is converted into upgraded liquid fuels. Coal liquefaction processes commonly utilize either alumina-supported cobalt molybdate or molybdenum trioxide as catalyst to effect desulfurization, denitrogenation, deoxygenation, cracking, and hydrogenation.

Phosphomolybdate compounds are acidic oxidants and are used in both homogeneously and heterogeneously catalyzed processes such as the hydration of propene in liquid phase and the oxidation of isobutyric acid to methacrylic acid.

Molybdenum hexacarbonyl is a versatile homogeneous and heterogeneous catalyst. It is widely used in the production of methanol from carbon monoxide, to effect olefin metathesis, desulfurization, aqueous coal liquefaction, and epoxidation.

Table 27.5: Reactions catalyzed by molybdenum oxides and sulfides [77].

Type of reaction	Example	Catalyst	Temperature range, °C	Conversion, %	Selectivity, %
Reactions with molecular hydrogen					
Isotropic exchange	H ₂ + D ₂ → 2HD	MoO ₃ /Al ₂ O ₃ -SiO ₂	80		very high
Hydrogenation	benzene → cyclohexane	MoO ₃	420-450	60	
	acetylene → ethylene	MoO ₃ -CoCl ₂ /SiO ₂	260-300		100
	naphthalene → decalene	MoS ₂	340		yield 77
	sulfur → hydrogen sulfide	MoS ₂	200	100	
	selenium → hydrogen selenide	MoS ₂	330-350	100	
	maleic anhydride → succinic anhydride	CuMoO ₄ /SiO ₂	120-160	100	
Hydrogenolysis	α- and β-methyl naphthalene → naphthalene + methane	CoO-MoO ₃ /Al ₂ O ₃			yield 40
	ethylcyclohexane → products	MoO ₃ /Al ₂ O ₃	510		
	phenol → benzene + H ₂ O	MoS ₂	350		yield 88-98
Reduction	thiophenol → benzene + H ₂ S	MoS ₂	200	100	
	thiophene → C ₄ H ₁₀ + H ₂ S	MoS ₂	300	98	
	C ₄ H ₆ C ₄ H ₈ C ₄ H ₁₀ organic sulfur compounds → hydrocarbons	CoO-MoO ₃ /Al ₂ O ₃	225-425		
Reactions with molecular oxygen					
Selective oxidation	propene → acrolein	Bi ₂ O ₃ -MoO ₃	450	95	95
	butene → maleic anhydride	CoO-MoO ₃ -P ₂ O ₅ /Al ₂ O ₃	450	76	50
	benzene → maleic anhydride	V ₂ O ₅ -MoO ₃ -P ₂ O ₅ /Al ₂ O ₃	425-450		85
	o-xylene → phthalic anhydride	V ₂ O ₅ -MoO ₃	400		48
	methanol → formaldehyde	Fe ₂ (MoO ₄) ₃	300-400	92	92
	acrolein → acrylic acid	CoO-MoO ₃ -TeO ₂	383	85	65
Oxidation of functional groups	propene + NH ₃ → acrylonitrile	Bi ₂ O ₃ -MoO ₃	400-500		yield 80
Oxidative condensation	toluene + NH ₃ → benzonitrile	V ₂ O ₅ -MoO ₃ /Al ₂ O ₃	415		yield 94
	butene → butadiene	Bi ₂ O ₃ -MoO ₃	370-550		90
Oxidative dehydrogenation	ethylbenzene → styrene	MoO ₃ -MgO	420-450		82-84
Oxyhydration	propene → acetone	SnO ₂ -MoO ₃	135		85
Oxidative dehydrocondensation	n-butane + SO ₂ → thiophene	MoO ₃ /Al ₂ O ₃	595	70	44
	butene + H ₂ S → thiophene	CoO-MoO ₃ /Al ₂ O ₃	570		yield 37
Oxidation with other oxidants					
Epoxidation	propene + H ₂ O ₂ → propylene oxide	MoO ₃ in H ₂ O ₂ and pyridine	60	80	100
Isomerization					
Structural isomerization	n-pentane → isopentanes	MoO ₃ /Al ₂ O ₃	425-450	50	95
Ring concentration	cyclohexane → methylcyclopentane	MoO ₃ /Al ₂ O ₃	455-495		yield 37
Disproportionation					
Olefin metathesis	propene → butene + ethylene	MoO ₃ /Al ₂ O ₃	66-288	43	94
Polymerization	ethylene → polyethylene	MoO ₃ /Al ₂ O ₃	200-260	50	
	acetylene → benzene	CoO-MoO ₃ /Al ₂ O ₃	62	98	100
Etherification					
Formation of complex ethers	succinic acid + hexanol → ether	MoS ₂ /carbon	130-220	45-97	100
Addition to C=C					
allylic alcohol + H ₂ O ₂ → glycerol		MoO ₃ in acetic acid	70-100		
Decomposition					
Dehydration	2-propanol → propene	MoO ₃	191-224		100
	ammonium benzoate → benzonitrile	MoO ₃	225-245		
Dehydrogenation	ethylbenzene → styrene	MoS ₂	414		yield 94
	cyclohexane → benzene	MoO ₃ /Al ₂ O ₃	500		yield 63
Dehydrocyclization	n-heptane → toluene	MoO ₃ /Al ₂ O ₃	450-500		yield 75
Dehydrocondensation	isobutene → xylenes	MoO ₃ /Al ₂ O ₃	200		yield 90

27.7.1 Lubrication

Molybdenum disulfide is an important solid lubricant, being used primarily to reduce wear, friction, and sustain lubrication under boundary sliding conditions. It is a black powder that is insoluble in ordinary aqueous and organic solvents but dissolves by complex formation in potassium cyanide, and reacts with strong oxidizing agents such as aqua regia or hot concentrated sulfuric acid to give hexavalent molybdenum species. It is an excellent high-temperature lubricant which is stable in vacuo or an inert atmosphere to 1200 °C, and to about 350 °C in air.

The primary commercial source for MoS₂ is the mineral molybdenite, from which > 98% pure powder is recovered and purified using oil flotation and other techniques with carbon being the major impurity. The lubricating powder is available in several grades based on its median particle size which may range from ca. 1 to 40 µm.

The crystal structure of natural MoS₂ is hexagonal (Figure 27.10). Its excellent intrinsic lubricating properties are attributed to the wide spacing and weak van der Waals bonding between the S-Mo-S sandwich layers, and to the net positive charge on the surface which promotes easy shear by means of electrostatic repulsion [80]. This intrinsic lubricating quality contrasts with graphite, which requires the presence of condensable vapors (e.g., from water or hydrocarbons) to promote crystal cleavage and low friction [81].

The fundamental and practical aspects of MoS₂ lubrication are reviewed in [73, 82, 83]. Molybdenum disulfide is sometimes simply rubbed on surfaces as a thin film to provide short-term lubrication. As an additive, it enhances the performance of other lubricants like grease or oil. It can also be incorporated into paint-like coatings for longer service life. Finally, it can be incorporated into plastics, rubber, and powder metal matrices as an alternative to conventional lubricants to impart lifetime self-lubrication.

Summaries have been published describing the use of MoS₂ in greases [84], rubber

[85], bonded coatings [86], and motor oils [87].

The largest consumption of MoS₂ is in greases used in mining, manufacturing, and transportation [84]. In greases, 1–20% molybdenum disulfide gives added protection from wear and galling, and provides back-up lubrication should the grease deplete or thermally degrade. Pastes composed of grease and containing 20–60% MoS₂ are used with open gears, universal joints, spline drives, and in metal forming, press-fitting and various wear-in operations. They have outstanding boundary lubrication behavior which prevents fretting, galling, and seizing.

As an extra-fine powder, MoS₂ (0.5–1%) is suspended in *industrial oils, motor oils, and synthetic fluids*, with the aid of chemical dispersants such as polyethylene where it behaves as an extreme-pressure and antiwear additive. In motor oils, it also improves vehicular fuel economy.

Paint-like coatings containing 30–85 vol% MoS₂ in either an organic or inorganic silicate binder are used on fasteners, machine tools, forklift chains, door locks, chutes, and sliding parts of office equipment to reduce friction and wear. Temporary coatings of MoS₂ in water-soluble binders (e.g., poly(vinyl alcohol) and polyacrylates) are used in die casting as a mold release, and in metal forming operations such as ironing, wire drawing, and extrusion.

In *plastic, rubber, and powdered metal compositions*, 0.5–4% MoS₂ imparts self-lubricating behavior obviating the requirement for externally applied lubrication. These materials are used in articles such as cams, thrust washers, ball bearing retainers, compressor piston rings, sheaves, gears, conveyor belting, and dynamic seals.

Molybdenum disulfide is not the only molybdenum compound used in lubrication. *Oil-soluble molybdenum-sulfur compounds* have also long been used as antiwear and extreme-pressure additives in lubricating oils and greases [88]. Commercial oil-soluble additives are compositions based on tetrathiomolybdates and complexes of molybdenum with xanthates, dithiocarbamates, dithiophos-

phates, diketones, dithiols, and dimercaptothiadiazoles [88].

27.7.2 Corrosion Inhibition

In 1939, two patents first described the use of readily soluble sodium, potassium, and ammonium molybdates as corrosion inhibitors for motor vehicle engine coolants [89, 90]. These and other inorganic molybdates are now among the most popular corrosion inhibitors because of their favorable properties and behavior. Molybdate is an anodic inhibitor, i.e., it inhibits by increasing the polarization of the anode component of the metal corrosion cell. It does this by precipitating escaping metal cations as molybdate species to block anodic sites and strengthen developing metal oxide films. Molybdate inhibits the corrosion of more ferrous and nonferrous metals over a wider pH range than any other inhibitor apart from chromate. Unlike chromate, however, the simple molybdate anion is not an oxidant and thus can be used with chemicals and systems that do not tolerate the strongly oxidizing chromate. Of even greater importance, molybdate has a very low toxicity. The toxicity, environmental aspects, behavior, mechanistic studies, and many applications of the molybdates are reviewed in [91, 92].

Molybdates are seldom used alone—as with other anodically active inhibitors, molybdate efficacy is improved and its concentration requirement significantly reduced when it is combined with other inhibitors. The most widely employed synergists of molybdate inhibition are the cathodically active compounds, especially zinc salts (e.g., zinc sulfate). Other synergists are the oxidizing inhibitors (e.g., nitrite) and the filming inhibitors (e.g., amine phosphonates and hydroxyfatty acids) [92]. Filming inhibitors strongly adsorb to the metal surface and protect it from attack.

Sodium molybdate is a component of many of the factory-fill and after-market engine coolants used in the United States, Europe, and Japan. A modern engine coolant concentrate formulation containing molybdate and

other inhibitors is as follows [93] (concentrations in weight percent):

Ethylene glycol	95.56
Sodium nitrate	0.10
Sodium molybdate dihydrate	0.20
Sodium tetraborate pentahydrate	0.40
Sodium silicate solution N ¹	0.30
Phosphoric acid 85%	0.15
Sodium mercaptobenzothiazole, 50% solution	0.50
Sodium tolyltriazole, 50% solution	0.20
Sodium hydroxide	0.235
Water	2.30
Polyglycol	0.05
Dye	0.005

The largest consumption of molybdates for corrosion inhibition is in the treatment of cooling water in open and closed recirculating cooling systems. Open systems include cooling tower waters associated with power generation, manufacturing operations, and with metals production and chemicals processing. A formulation of a corrosion inhibition treatment in an open cooling tower system (milligrams per liter) follows:

1-hydroxyethylidene-1,1-diphosphonic acid, 60% solution	10
Sodium molybdate dihydrate	10
Zinc sulfate monohydrate	2
Sodium tolyltriazole, 50% solution	2

Closed loop waters are used in stationary power engines, in refrigeration and humidity control, and in chilled-water air conditioning; a formulation of a corrosion inhibition treatment for a closed chilled-water air conditioning system (milligrams per liter) follows:

Sodium molybdate dihydrate	150
Sodium nitrite	150
Sodium tolyltriazole, 50% solution	4

Not only the highly soluble sodium, potassium, lithium, and ammonium molybdate salts are used in corrosion inhibition; the very slightly soluble zinc, strontium, and calcium molybdates are effective corrosion-inhibiting pigments in primer paints for steel and aluminum [94]. The pure compounds are no longer used; they have been replaced by equally and, in some cases, more effective pigments made by precipitating the pure compounds on less expensive, synergistic core materials such as zinc oxide, calcium carbonate, talc, or zinc phosphate [95–97].

¹ Registered trademark of PQ Corp., Valley Forge, PA.

Other products and processes which utilize molybdates as corrosion inhibitors include water-based hydraulic and metalworking fluids, lithium halide refrigerating brines, boiler waters, hot forging lubricants, aluminum anodizing processes, coal water slurries, temporary rust-preventive coatings, rinses for phosphate conversion coating, oil field drilling muds, brake linings, water used for quenching after heat treatment, paint-spray water curtains, wet ball milling of ores, salt brines for ice-making, passivation treatments for galvanized zinc and tin plate, packaging paper and board used for metal parts, temporary coating of aluminum to prevent staining by water during storage and transport, and as a pitting inhibitor for stainless steels in mineral acids. These and other applications are reviewed in [92].

27.7.3 Flame Retardancy and Smoke Suppression

Treatments based on molybdenum compounds exhibit both flame retardancy and smoke suppression; they are particularly effective smoke suppressants for synthetic polymers.

In the early 1930s, heteropolymolybdates were found to act as flame retardants for wood [98]. Some 15 years later, ammonium heptamolybdate and sodium molybdate were shown to retard the flammability of cotton fabric, although the treatment was not durable to laundering [99]. Other molybdenum compounds were subsequently used as additives to suppress the flammability and smoke output of plastics [nylon, poly(vinyl chloride), poly(vinylidene chloride), polyesters, and epoxy resins] [100].

The following molybdenum compounds are effective flame retardants and smoke suppressants for both rigid and plasticized poly(vinyl chloride) and halogenated polyester systems [101]:

Molybdenum disulfide, MoS_2
Molybdenum(VI) oxide, MoO_3
Ammonium dimolybdate(VI)(2), $(\text{NH}_4)_2\text{Mo}_2\text{O}_7$
Ammonium heptamolybdate(VI)(6)-4-water,
 $(\text{NH}_4)_6\text{Mo}_7\text{O}_{24} \cdot 4\text{H}_2\text{O}$

Ammonium octamolybdate(VI)(4), $(\text{NH}_4)_4\text{Mo}_8\text{O}_{26}$
Sodium molybdate(VI), Na_2MoO_4
Calcium molybdate(VI), CaMoO_4
Zinc molybdate(VI), ZnMoO_4
Copper molybdate(VI), CuMoO_4
Nickel molybdate(VI), NiMoO_4
Iron(III) molybdate(VI), $\text{Fe}_2(\text{MoO}_4)_3$

Flame retardancy in these compounds is linked to the accelerated loss of halogen; their smoke retardancy depends on increased char formation [102].

Molybdenum trioxide and extended proprietary zinc and calcium molybdate compositions are employed as flame retardants in the above-mentioned plastics that are used in the building, transportation, and wire and cable industries.

27.7.4 Pigments

Sodium molybdate is the usual starting material for the production of inorganic molybdate chrome pigments and a number of organic pigments (toners) based on cationic or basic dyes. Small amounts of sodium molybdate are also used as a condensation catalyst for phthalocyanine pigments as well as to fix and shade the coloring of furs and hair with azines and the amino- and hydroxy-substituted aromatic compounds used for red brown shades.

Inorganic Pigments. Molybdate chrome pigments (molybdenum orange) are generally considered to be modified lead chrome pigments, i.e., compounds of lead chromate and mixed lead chromate and sulfate whose hues range from lemon yellow to primrose. Molybdate chrome pigments exhibit bright red-orange to bright yellow-red hues with the redder hues containing more molybdenum. Molybdate orange pigments are mixed tetragonal crystals whereas the lead chrome pigments form monoclinic and rhombic crystals.

Molybdate chrome pigments are made by coprecipitating lead chromate, molybdate, and sulfate from lead nitrate solutions with sodium chromate, molybdate, and sulfate solutions. The stoichiometry and conditions of precipitation are adjusted to determine the hue. Lead molybdate is itself white, but in the coprecipi-

tated product it distorts the monoclinic lead chromate crystals sufficiently to produce the tetragonal form.

The molybdate chrome pigments exhibit clean colors, good tinctorial and hiding properties; are nonbleeding and soft-grinding; have high heat resistance, and better film gloss and light fastness than lead chrome. They are often used with organic pigments to supply needed hiding power.

Molybdate chrome pigments are more expensive than the lead chromes, but are preferred in many applications for their reddish hue, cleanliness and brightness of color. They are employed in paints, plastics, rubber, and often in printing inks where their opacity, low cost, and heat stability are advantages over organic red pigments.

Organic Pigments. Sodium molybdate is also used in the production of organic pigments. Organic pigments have a higher tinctorial strength and brightness than inorganic pigments, but their thermo- and photochemical stabilities are lower and they are more transparent and expensive. Their biggest single use is in the coloring of plastics.

Molybdenum compounds are used in the production of toners derived from cationic or basic dyes that have free or substituted amino groups. The most important dyes are:

Diphenylmethane	Auramine	C.I. 655
Triaryl methane	Malachite Green	C.I. 657
	Brilliant Green	C.I. 662
	Rhoduline Blue 6G	C.I. 658
	Acronol Brilliant Blue	C.I. 664
	Methyl Violet B	C.I. 680
	Victoria Pure Blue BO	C.I. Pr198
Xanthene	Rhodamine B	C.I. 749
	Rhodamine 6G	

The dyes are made into pigments (i.e., insolubilized) by replacing the simple anions (chloride and sulfate) with a heteropolymolybdate acid salt, such as 12-molybdophosphate, $[\text{PMo}_{12}\text{O}_{40}]^{3-}$. This acid salt is formed from disodium phosphate and sodium molybdate in the presence of a strong mineral acid (e.g., HCl). The commercial phosphomolybdate pigments or toners are collectively known as PMA colors. The heteropolymolybdate complexes with the basic dye may contain 1 mol

P_2O_5 with from 12 to 24 mol MoO_3 as either the free acids or acid sodium salts. Pigments made with combinations of both phosphotungstate (PTA) and phosphomolybdate are known as PTMA colors. The PTMA colors show better fastness than either the PMA or PTA colors, but are also generally costlier.

27.7.4.1 Molybdate Red and Molybdate Orange

Molybdate red and molybdate orange, C.I. Pigment Red 104:77605, are mixed-phase pigments with the general formula $\text{Pb}(\text{Cr}, \text{Mo}, \text{S})\text{O}_4$ [103]. Most commercial products have a MoO_3 content of 4–6% (refractive index 2.3–2.65, density 5.4–6.3 g/cm³). Their hue depends on the proportion of molybdate, crystal form, and particle size.

Pure tetragonal lead molybdate, which is colorless, forms orange to red tetragonal mixed-phase pigments with lead sulfochromate. The composition of molybdate red and molybdate orange pigments can be varied to give the required coloristic properties; commercial products usually contain ca. 10% lead molybdate. Lead molybdate pigments have a thermodynamically unstable tetragonal crystal modification that can be transformed into the undesirable stable yellow modification merely by dispersing [104]. This is especially true of the bluish varieties of molybdate red which have larger particles whose color can be changed to yellow by shear forces. The tetragonal modification of the lead molybdate pigments must therefore be stabilized after precipitation [105, 106].

The fastness properties of the molybdate orange and molybdate red pigments are comparable with those of the chrome yellows. As with the chrome yellows, the pigment particles can be coated with metal oxides, metal phosphates, silicates, etc., to give stabilized pigments with high color brilliance and good fastness properties, as well as highly stabilized grades with very good resistance to light, weathering, sulfur dioxide, and temperature, and with a very low content of acid-soluble

lead (DIN 55770, 1986 or DIN/ISO 6713, 1985).

The colors of lead molybdate pigments vary from red with a yellow hue to red with a blue hue. Since chrome orange is no longer available, molybdate orange has become much more important.

Production. In the Sherwin-Williams process, a lead nitrate solution is reacted with a solution of sodium dichromate, ammonium molybdate, and sulfuric acid [107]. Instead of ammonium molybdate, the corresponding tungsten salt can be used, giving a pigment based on lead tungstate. The pigment is stabilized by adding sodium silicate (25% SiO₂) and aluminum sulfate (Al₂(SO₄)₃·18H₂O) to the suspension, which is then neutralized with sodium hydroxide or sodium carbonate. The pigment is filtered off, washed until free of electrolyte, dried, and ground. Treatment with silicate increases the oil absorption; it also improves light fastness and working properties.

In the Bayer process molybdate red is formed from lead nitrate, potassium chromate, sodium sulfate, and ammonium molybdate [111]. The pigment is then stabilized by adding water glass (28% SiO₂, 8.3% Na₂O) to the suspension with stirring, followed by solid antimony trifluoride, stirring for 10 min, and further addition of water glass. The pH is adjusted to 7 with dilute sulfuric acid and the pigment is filtered off, washed free of electrolyte, dried, and ground.

To give the lead molybdate pigments very good stability to light, weathering, chemical attack, and temperature, the same methods are used as those for the stabilization of chrome yellow pigments [108–116].

Uses. Molybdate orange and molybdate red are mainly used in paints, coil coatings, and for coloring plastics (e.g., polyethylene, polyesters polystyrene). The temperature-stable grades are the most suitable for coil coatings and plastics.

Molybdate orange and molybdate red have a low binder demand; good dispersibility, hiding power, and tinting strength; and very high light-fastness and weather resistance. Stabili-

zation also gives high-grade pigments with good resistance to sulfur dioxide and high temperature.

Like the chrome yellows, the molybdate reds are used to produce mixed pigments. Combinations with organic red pigments give a considerably extended color range. Such combinations have very good stability properties because the lightfastness and weather resistance of many organic red pigments are not adversely affected by molybdate pigments.

Total world production of molybdate orange and molybdate red in 1996 was ca. 13 000 t.

27.7.4.2 Molybdate Pigments

Molybdenum-based anticorrosive pigments offer a nontoxic alternative to the zinc chromate pigments [117]. They all have a neutral color (white) but the pure compounds are very expensive. To produce economically competitive pigments molybdate and phosphate pigments are combined, or molybdate compounds are applied to inorganic fillers (e.g., zinc oxide, alkaline-earth carbonates, or talc) [118–121].

Commercially important pigments include basic zinc molybdates (ZnMoO₄, ZnO), sodium zinc molybdates [Na₂Zn(MoO₄)₂], basic zinc calcium carbonate molybdate, and basic calcium zinc carbonate phosphate molybdate pigments (CaMoO₄, CaCO₃, ZnO, Zn₃(PO₄)₂). Properties are given in Table 27.6.

Phosphate-containing molybdate pigments are especially suitable for water-thinnable or latex-based binders, because they improve adhesion to iron substrates. The other molybdate pigments are mainly used in solventborne binder systems.

Unlike chromate ions in chromate pigments, the MoO₄²⁻ ions in molybdate pigments are not chemically reduced in most coatings. Hence, they are ineffective for cathodic protection. Their protective action is assumed to be due to activity in the anodic region, similar to that of phosphate ions. As with the protective phosphate films, molybdate films are very resistant to chloride and sulfate [122]. The du-

ration of maximum activity depends on the metal ions used in the pigment and is probably due to differences in solubility.

Trade names are as follows:

Molybdenum-based: Moly-White 101, 212, 331 (The Sherwin-Williams Company, USA).

Zinc molybdenum phosphate: Actirox 102, -106 (Colores Hispania, Spain); Moly-White ZNP, -MZA (The Sherwin-Williams Company, USA); Heucophos ZMP (Dr. H. Heubach, Germany).

27.7.5 Agriculture

Molybdenum is an essential trace element for enzymes which fix nitrogen in leguminous crops. Sodium molybdate is used as a soil additive in areas where natural molybdenum is deficient and plant growth suffers. It is usually applied as part of fertilizer or seed treatments.

Table 27.6: Properties of molybdenum-containing pigments.

Property	Zinc molybdate pigment	Cadmium zinc molybdate pigment	Basic sodium zinc molybdate pigment	Basic calcium zinc phosphomolybdate pigment
Density, g/cm ³	5.06	3.00	4.00	3.00
Oil absorption value, g/100 g	14	18	14	16
Mean particle size, μm (Fisher subsieve sizer)	0.65	1.88	1.02	2.2
pH	6.5	8.5		8

Table 27.7: Atomic absorption spectroscopic analysis for molybdenum.

Absorption line, nm	Sensitivity, ppm/1% abs ^a	Reference
313.26	0.8	[124, 125]
313.26 ^b	0.4	[126]
317.03	1.1	[124]
379.83	1.3	[124]
319.40	1.4	[124]
386.41	1.7	[124]
390.30	2.4	[124]
315.82	2.8	[124]
320.88	5.9	[124]

^a Defined as the concentration in parts per million (μg/mL) in aqueous solution which produces a 1% absorption signal (0.0044 absorbance) under optimum conditions.

^b Nitrous oxide-acetylene flame, in all other cases air-acetylene flames, were used.

About 0.25 kg molybdenum per acre (0.62 kg/ha) may be used.

27.8 Analysis

Molybdenum can be determined by gravimetric, volumetric, and colorimetric methods [123]. As long as great accuracy is not required, the most satisfactory method is, however, atomic absorption spectroscopy.

Atomic Absorption Spectroscopy. The absorption lines used and the achievable sensitivities in atomic absorption spectroscopy are shown in Table 27.7. Sensitivity may be increased by using a three-slot burner or by inert gas separation of the flame. Interference due to the presence of calcium, strontium, manganese, iron, and sulfate is reported to be eliminated in the presence of large amounts of aluminum [127] or 2% ammonium chloride [124].

In the first report of the use of atomic absorption for molybdenum analysis [127], stainless steel samples were employed with an air-acetylene flame and ammonium chloride as a releasing agent. If the composition in the molybdenum standard solutions is matched with that of the sample solution by addition of appropriate quantities of the other metal salts present in the samples [128], a releasing agent is not necessary. An alternative is to separate the molybdenum from other metals in the sample solution by liquid-liquid (or solvent) extraction. This technique can also be used to concentrate the molybdenum solution before analyzing it. For example, quantities as low as 10⁻⁴% have been determined in silicate rocks by extracting molybdenum from the aqueous sample with 8-hydroxyquinoline [129]; tolu-

ene-3,4-dithiol and ammonium pyrrolidine dithiocarbamate can also be used as extraction agents. Rock samples can be fused with sodium hydroxide and baked at ca. 650 °C for 30 min.; after cooling the residue is treated with sulfuric acid and filtered. Alternatively, the sample can be treated directly with acid and filtered. Molybdenum in the filtrate has been extracted with α -benzoinoxime into chloroform [130].

Volumetric Methods. In the volumetric procedure, molybdenum in solution is reduced by zinc in a Jones reductor, the emerging solution is led under the surface of a ferric sulfate solution and titrated with potassium permanganate [123].

Gravimetric Methods. The older of the two main gravimetric methods is the precipitation of lead molybdate by slow addition of a lead acetate solution to a hot dilute acetic acid–ammonium acetate buffer solution containing the molybdenum. Free mineral acids prevent complete precipitation of the molybdenum. Cobalt, copper, magnesium, manganese, mercury, nickel and zinc do not interfere. Sulfate must be absent if alkaline-earth metals are present. If chloride is present, addition of a large excess of the lead acetate solution must be avoided. Since many metals interfere with the determination (antimony, arsenic, chromium, iron, phosphorus, silicon, tin, titanium, tungsten, and vanadium), it is not suitable for the determination of molybdenum in steels.

The other important gravimetric method is fairly satisfactory for steels and involves precipitation of molybdenum with α -benzoinoxime and ignition of the precipitated complex to molybdenum trioxide, which is weighed.

The sample is dissolved in dilute (1:6) sulfuric acid and the solution is treated with a minimum amount (ca. 2 mL) of concentrated nitric acid to decompose carbides and oxidize the iron and molybdenum. The solution is boiled to expel nitrogen oxides and filtered if necessary. To the cool solution sufficient iron(II) ammonium sulfate solution is added to reduce vanadium(V) and chromium(VI) acids.

An excess of a 2% solution of α -benzoinoxime in ethanol is added at 5 °C, followed by bromine water until the solution is pale yellow, and then more α -benzoinoxime. The precipitate on the filter paper is washed with a freshly prepared solution containing 10 mL of the 2% reagent solution and 2 mL of concentrated sulfuric acid diluted to 200 mL. After charring, ignition at 500–525 °C, and weighing, the residue is treated with 5 mL of concentrated ammonia to remove the molybdenum and tungsten trioxides and the residual solid is ignited and weighed. If tungsten is present the ammoniacal extract is acidified with sulfuric acid and evaporated to dense white fumes. After diluting, the tungsten is precipitated using cinchonine and weighed as the trioxide after ignition at 750–850 °C.

Another gravimetric method often described involves precipitation of molybdenum as sulfide and ignition to oxide. This is not satisfactory because loss due to volatilization is likely to occur. The complex of molybdenum with 8-hydroxyquinoline, $\text{MoO}_2(\text{C}_9\text{H}_6\text{ON})_2$, is precipitated within the pH range 3.3–7.6. It differs from complexes of the reagent with other metals in being insoluble in organic solvents and in many concentrated inorganic acids. The freshly precipitated compound dissolves only in concentrated sulfuric acid and in hot solutions of alkali-metal hydroxides. This determination allows complete separation of molybdenum and rhenium.

Colorimetric Methods. Molybdenum(VI) in acidic solution can be reduced to give mainly molybdenum(V), which forms a red complex with thiocyanate. This complex can be extracted from water with organic solvents, particularly oxygenated compounds, providing a very sensitive spectrophotometric method. Tin(II) chloride is a suitable reducing agent, preferably used in the presence of a little iron(II). The method can be used to determine molybdenum in steels.

The steel sample is dissolved in mixed hydrochloric perchloric acids, heated until dense white fumes are evolved and finally heated for a further 6–7 min. After cooling the solution is

diluted with water and made up to a known volume. An aliquot is reduced with tin(II) chloride in the presence of iron(II) and potassium thiocyanate is added. The color depends on the acid concentration (optimum value 1 mol/L) and the thiocyanate concentration (should not be less than 1%). The red complex is extracted into 3-methyl-1-butanol and the optical density measured at 465 nm. When the quantity of Mo in a 1-cm cell is 10 μg the following elements cause an error greater than 3% when present in the amount specified: vanadium > 0.4 mg (interference is prevented by washing the organic extract with tin(II) chloride solution); chromium(VI) > 2 mg; tungsten(VI) > 0.15 mg; cobalt > 12 mg; copper > 5 mg; lead > 10 mg; titanium(III) in the presence of fluoride > 30 mg. The method is also recommended for the determination of molybdenum present as a trace element in fertilizers and animal feeds, the complex being extracted from the aqueous solution using a 1:1 mixture of carbon tetrachloride and 3-methyl-1-butanol [131]. The sample solution is prepared by dry ashing the feed at ≤ 450 °C, treating the ash with hydrochloric acid, and evaporating to dryness. The residue is successively extracted with hot hydrochloric acid, the penultimate treatment being to take to dryness with a little nitric acid. The combined extracts are diluted to give an approximately 1 mol/L solution of acid. Inorganic fertilizers are extracted directly with hydrochloric acid. After evaporation to dryness the residue is treated in the same way as the ash from feeds.

27.9 Economic Aspects

Three factors form the basic economic character of the molybdenum industry:

- Molybdenum consumption
- Molybdenum supply
- Excess production capacity

The iron and steel industry accounts for ca. 80% of all *molybdenum consumption* in the Western world. The balance of consumption is split between nonferrous metallurgical uses and chemical applications. Estimated con-

sumption of molybdenum in the Western world in 1989 according to end use is as follows (exports to Eastern-Bloc countries are not included):

Alloy steel	35%
Stainless steel	27%
Mo-base and superalloys	12%
Chemicals	11%
Tool steel	9%
Cast irons	6%

The metallurgical uses of molybdenum are primarily for the fabrication of plant and equipment; its consumption follows the capital goods cycle. The chemical uses for molybdenum involve chiefly catalyst, lubricant, aqueous corrosion inhibition, and color applications whose demand adheres to general industrial activity.

Sources of *molybdenum supply* in the Western world in 1989 were estimated to be as follows:

Primary mines	41%
By- and coproducts of copper mining	54%
Imports from China	3%
Recovery from spent petroleum catalysts	2%

In general, the cash cost of nonprimary production is significantly lower than the cost of primary mine production. This cost advantage enables nonprimary producers to sell at lower prices than their primary counterparts. Primary production is the first supply segment to react to changes in market conditions.

The molybdenum industry has significant *excess capacity*. Encouraged by unrealistic demand expectations, nearly 50 000 t of primary mine capacity was installed during the late 1970s and early 1980s. This, in combination with the continued growth of by-product production and the emergence of China as a supplier, has resulted in a Western world supply capacity of over 125 000 t. Western world demand in 1989, including exports to the Eastern-Bloc countries, though at record levels, was only 95 700 t.

Tables 27.8 and 27.9 contain estimates for molybdenum supply and demand which show that production exceeded demand during most of the past decade. Tables 27.10 and 27.11 list the major molybdenum mines and conversion operations (molybdenum roasting and ferromolybdenum conversion).

Table 27.8: Estimated Western world molybdenum demand (10^3 t contained Mo).

	1980	1981	1982	1983	1984	1985	1986	1987	1988	1989
United States	27.2	26.3	15.4	14.1	17.7	16.8	17.2	18.6	23.1	24.5
Western Europe	29.5	26.8	25.0	24.0	29.5	29.5	29.5	30.4	37.2	37.2
Japan	12.7	12.7	11.8	10.9	11.8	12.2	11.8	11.8	15.4	15.0
Other Western Countries	5.9	6.4	5.9	6.4	6.8	7.3	7.7	7.7	8.2	8.2
Exports to Eastern Bloc	11.3	11.3	11.3	10.4	11.3	11.8	10.5	10.4	10.0	10.8
Total demand	86.6	83.5	69.4	65.8	77.1	77.6	76.7	78.9	93.9	95.7

Table 27.9: Estimated Western world molybdenum production (10^3 t) (includes both mine production and recovery from spent petroleum catalyst).

	1980	1981	1982	1983	1984	1985	1986	1987	1988	1989
United States	68.3	63.3	38.5	15.2	46.3	49.6	42.5	35.0	43.8	64.0
Chile	13.7	15.4	20.0	15.3	16.9	18.4	16.6	16.9	15.5	17.0
Canada	15.4	17.5	14.4	9.3	8.9	7.4	11.9	12.4	12.5	14.4
Other ^a	3.4	3.9	8.2	8.4	9.3	9.8	12.5	13.4	11.4	11.5
Total production	100.8	100.1	81.1	48.2	81.4	85.2	83.5	77.7	83.2	106.9
Metal loss	1.5	1.5	1.2	0.7	1.2	1.3	1.3	1.2	1.0	1.5
Net production	99.3	98.6	79.9	47.5	80.2	83.9	82.2	76.5	82.2	105.4

^aIncludes Western world imports from China.**Table 27.10:** Major molybdenum sites (Source: Climax Metals Company).

Parent company	Mine ^a	Location
AMAX-Climax	Henderson (P)	Colorado, USA
AMAX-Climax	Climax (P)	Colorado, USA
Cyprus	Thompson Creek (P)	Idaho, USA
Cyprus	Tonopah (P)	Nevada, USA
UNOCAL-Molycorp	Questa (P)	New Mexico, USA
Placer	Endako (P)	B.C., Canada
BHP	Island Copper	B.C., Canada
Codelco	Andina	Chile
Codelco	Chuquibambilla	Chile
Codelco	El Salvador	Chile
Codelco	El Teniente	Chile
Cyprus	Bagdad	Arizona, USA
Cyprus	Sierrita	Arizona, USA
Highland Valley Copper	Highland Valley	B.C., Canada
Magma Copper	San Manuel/Pinto Valley	Arizona, USA
Mexicana de Cobre	La Caridad	Mexico
Montana Resources	Butte	Montana, USA
National Iranian Copper	Sar Cheshmeh	Iran
Noranda ^b	Brenda	B.C., Canada
Phelps Dodge	Chino/Morenci	Arizona, USA
RTZ-Kennecott	Bingham Canyon	Arizona, USA
Southern Peru Copper	Cuajone	Peru
Southern Peru Copper	Toquepala	Peru

^aP = primary mine.^bClosed June 1990 with depletion of mining reserves.**Table 27.11:** Major molybdenum converters (Source: Climax Metals Company).

Parent company	Location
AMAX-Climax	USA, UK, Netherlands
Anglo Blackwells	UK
Codelco	Chile
Cyprus	USA
Eldorado Gold Mines	Canada
Empresas Frisco	Mexico
Ferro Alloys	UK
H. C. Starck	Germany
Japan Metals & Chemicals	Japan
Molycorp	USA
Molymet	Chile
M. P. Trollhattan	Sweden
Murex	UK
Nippon Denko	Japan
Pechiney	France
Placer	Canada
RTZ-Kennecott	USA
Sadacem	Belgium
Showa Denko	Japan
Treibacher C. W.	Austria

27.10 Environmental Aspects

The regulation of chemical discharges into the environment is increasing dramatically and will continue to do so in the 1990s. Existing restrictions on molybdenum discharges

will likely be enforced at the state or local level in the United States and at the national level in Europe.

General aspects of molybdenum in the environment are reviewed in [132]. Additional studies and reviews further explore the impact of molybdenum in the environment [133, 134]. Although molybdenum can cause problems in the environment when discharged in excessive quantities, the problems are well defined and are easily corrected in most instances.

Wastewater. Soluble molybdenum compounds exhibit medium to low levels of toxicity when discharged into either fresh water, salt water, or sewage treatment facilities. Table 27.12 summarizes relevant ecotoxicity data.

In the United States, effluent guidelines for molybdenum have been established for some industrial categories. These guidelines are technology-based and not toxicity-related. Calculation of individual discharge limitations is based on process production rates. The EPA^a has not established generic molybdenum lim-

its for industrial discharges nor has it established stream or drinking water standards for molybdenum.

Exhaust Gas. Molybdenum compounds are not specifically regulated as a component of process exhaust gases. Control of molybdenum compounds in exhaust gases is accomplished by use of standard equipment such as bag houses, cyclones, and scrubbers. Efficiency of removal is typically monitored by noting total suspended particulate discharge rates. Work place exposure for insoluble molybdenum compounds in the United States is currently controlled at 10 mg/m^3 [144] which is the same as the TLV-TWA for nuisance dusts. Soluble molybdenum compounds in the work place are controlled at 5 mg/m^3 [144]. Exposure limits in other countries may differ slightly from the U.S. values and should be consulted accordingly. Under the United States Emergency Planning and Community Right-To-Know Act, molybdenum trioxide is considered a toxic chemical and is subject to annual chemical release reporting [145].

Table 27.12: Ecotoxicity of molybdenum compounds.

Species or medium	Molybdenum compound	Toxicity	Reference
Freshwater fish	sodium molybdate dihydrate	LC ₅₀ (96 h) fathead minnow, 7630 mg/L	[135]
	ammonium dimolybdate	LC ₅₀ (96 h) bluegill, 6790 mg/L	[136]
	molybdenum trioxide (pure)	LC ₅₀ (96 h) rainbow trout, 7340 mg/L	[136]
		LC ₅₀ (96 h) channel catfish, > 10 000 mg/L	
		LC ₅₀ (48 h) bluegill, 157 mg/L	
		LC ₅₀ (48 h) rainbow trout, 135 mg/L	
		LC ₅₀ (48 h) bluegill, 65 < LC ₅₀ < 87 mg/L	
Daphnia	sodium molybdate dihydrate	LC ₅₀ (96 h), 3940 mg/L	[135]
Saltwater species	sodium molybdate dihydrate	LC ₅₀ (96 h) mysid shrimp, 3997 mg/L	[137]
	ammonium molybdate	LC ₅₀ (96 h) sheepshead minnow, 6590 mg/L	[138]
		LC ₅₀ (96 h) pink shrimp, 3997 mg/L	
		EC ₅₀ American oyster, 3526 mg/L	
		LC ₅₀ (48 h) marine shore crab, 1018 mg/L as Mo	
Activated sludge	sodium molybdate dihydrate	no effect level > 2522 mg/L (slug dose)	[139]
Anaerobic sludge	sodium molybdate dihydrate	no effect level > 2522 mg/L (slug dose)	[139]
Mammals	molybdenum trioxide (pure)	LD ₅₀ oral-SD rat 2.73 g/kg	[140]
	molybdenum trioxide (technical)	LD ₅₀ oral-SD rat 6.66 g/kg	[141]
	sodium molybdate	LD ₅₀ ipr-mus 344 mg/kg	[142]
	molybdenum disulfide	no effect level, oral-SD rat > 15 g/kg	[143]

Solid Waste. Within the European Economic Community (EEC) and some other European countries (e.g., Switzerland), the molybdenum content of sewage sludge used for agricultural purposes is subject to regulation. In the United States, the EPA is developing guidelines for use of sewage sludge in agriculture, and will set acceptable limits for metals. Industrial waste in the United States and the EEC is not specifically regulated as to molybdenum content.

The Netherlands has adopted soil and groundwater contamination guidelines for molybdenum [146]. The pollutants regulated are classified in the "Black" and "Grey" lists, and are derived from a 1976 EEC Directive [147]. Chemicals on the Black list are considered very toxic and are persistent and/or bioaccumulate. Chemicals on the Grey list, which includes molybdenum, are of general concern in the environment.

The most widely studied environmental problem with molybdenum is its impact on ruminants that graze on forage with a high molybdenum content [148]. Environmental protection must therefore first identify the probable land use and then develop the control strategy necessary to mitigate the impact. For example, treatment of soil with sewage sludge has to be controlled so that the soil molybdenum content does not exceed 10 mg/kg [149]. Liming of soil lowers the accumulation of molybdenum in the surface plow layer because of the increased solubility at alkaline pH [149]. Due to the biological antagonism of copper toward molybdenum, dietary supplementation of ruminants with copper mitigates the effects of molybdenosis [149]. Sewage sludge with a high molybdenum content usually has a high copper content too which reduces the probability of molybdenosis in ruminants foraging on sludge-treated pasture. Sludge with less than 50 mg/kg molybdenum on a dry weight basis should therefore be acceptable for long-term land application at an annual addition rate of 10 000 kg/ha.

27.11 Toxicology and Occupational Health

"Molybdenum compounds in general are of a low order of toxicity, both from the point of view of observed clinical effects as well as from the histopathologic point of view" [150]. Toxicity is primarily associated with soluble molybdenum compounds. For example, both inhalation and ingestion of insoluble molybdenum disulfide and calcium molybdate failed to produce significant histopathological findings in either rat or guinea pigs [150].

Human Nutrition. Molybdenum is an essential trace element. Leguminous plants require molybdenum for bacterial fixation of nitrogen. In animals and humans it serves as a cofactor for the enzymes xanthine oxidase (which oxidizes xanthine to uric acid [151]) and aldehyde oxidase. Probably 25–75% of molybdenum in the diet is absorbed through the gastrointestinal tract and is rapidly eliminated, primarily via the urine. The biological half-life is not well established for humans, but most of the absorbed molybdenum is eliminated within a few days or weeks. Animal data indicate that the metabolism of molybdenum is closely related to the metabolism of copper and sulfur compounds [152].

The normal daily human dietary intake of molybdenum in the United States is estimated to be 100–500 µg. High molybdenum concentrations are generally found in leafy vegetables (up to 5 µg/g wet weight); legumes with edible roots have a low molybdenum content (< 1 µg/g wet weight). There are no human or animal studies implying accumulation of molybdenum in the body during the life cycle [153].

The relationship of molybdenum deficiency and esophageal cancer in humans was first reported in 1966 [154]. The high incidence of this cancer was attributed to the consumption of food locally grown in soil low in molybdenum. As reported in 1981, a study in China demonstrated an inverse relationship between the mortality rate of esophageal cancer and the content of Mo, Zn, Mn, Si, Ni, Fe,

Bi, and I in cereal and drinking water samples [155]. Levels of molybdenum in the serum, hair, and urine of the inhabitants of the high-risk area were lower than those in the low-risk areas. Utilizing animal models, this inhibitory effect of molybdenum on esophageal, fore stomach, and mammary carcinogenesis has been demonstrated in laboratory studies [156, 157, 158].

Human Toxicity. Information on the toxic effects of molybdenum in humans is scarce. A 1961 study reported a high incidence of gout in an area of Armenia in which the soil contained 77 mg/kg of molybdenum and 39 mg/kg of copper [153]. Daily dietary intake of molybdenum was calculated to be 10–15 mg and that of copper 5–10 mg; corresponding values in the control area were 1–2 mg Mo and 10–15 mg Cu. The study showed an increased prevalence of goutlike joint disorders, elevated blood levels of uric acid, and an increase in the urinary excretion of uric acid [153]. The results are difficult to evaluate since no details are given concerning the study population and the selection of subjects. Furthermore the control group consisted of only five subjects.

A study in another high-molybdenum province in the former Soviet Union failed to detect biological changes in the study population. A tentative explanation is that a higher intake of natural copper may have protected the population against the molybdenum exposure [153]. Animal studies have demonstrated a biological antagonism of copper toward molybdenum.

A study of four humans in India, detected a significant increase in copper metabolism with dietary intakes of molybdenum ranging from 160 to 2540 µg/d. However, the study failed to detect any effect on the urinary excretion of uric acid [159].

On the basis of the above studies, MERTZ suggests that a dietary intake of more than 10 mg/d of molybdenum is dangerous to human health, but that intakes of up to 1.5 mg/d do not appear to have an effect except for an increase in urinary copper excretion [160]. With a daily molybdenum intake of 540 µg, copper

excretion was elevated but was still within normal range. In adult humans with a normal copper intake (1.5–2.5 mg/d), MERTZ proposes that a dietary molybdenum intake of 0.5–1.0 mg/d can be assumed to be safe. Based on balance studies conducted in areas where the diet is generally adequate in molybdenum and no molybdenum disease has been observed in humans, the U.S. National Academy of Sciences has estimated an adequate and safe intake of molybdenum for humans as being 0.15–0.5 mg/d [161].

Animal Toxicity. Most observations on the toxicity of molybdenum are based on animal data. Excessive exposure to molybdenum via food can cause severe disease in ruminants which involves diarrhea, anemia, and emaciation, and may progress to death. The disease was first identified in 1938 as the cause of a long-recognized problem in cattle grazing in areas called "teart" pastures in Somerset, England. By 1943 large doses of copper sulfate were shown to prevent or cure "teart" disease. The clinical signs of molybdenum toxicity in animals are primarily due to copper deficiency. After long exposure, the hair loses its color and lameness with a characteristic stiff gait may develop. The latter symptoms may be associated with disturbance of phosphorous metabolism resulting in osteoporosis and joint abnormalities [162].

Young lambs grazing on high-molybdenum pastures suffer from a bone or joint disorder known as swayback. Sheep also develop steely wool, but not the severe diarrhea seen in cattle [163]. Copper deficiency in lambs also lowers their resistance to infections, such as pneumonia [164].

Evidence indicates that cattle are the most susceptible to molybdenum toxicity of any species, followed by sheep. Horses grazed the "teart" pastures of Somerset without showing any clinical signs of toxicity. Rabbits [165], guinea pigs, rats, pigs, and chickens [164] are comparatively tolerant to molybdenum.

Due to the great variability in results, the data available for cattle and sheep provide little assurance about safe levels of molybde-

num; a level of 5–10 ppm in pasture forage is usually considered a conservatively safe molybdenum level. The clinical symptoms of molybdenum toxicity or molybdenosis are primarily due to a conditioned or secondary copper deficiency. The most reliable indication of molybdenosis or copper deficiency is alteration of the symptoms by copper supplementation. In some areas where animal forage is deficient in copper, pastures with molybdenum levels normally considered to be in the safe range could trigger signs of molybdenosis. At the other extreme, forage that is naturally high in copper produces copper toxicity and supplemental dietary molybdenum may be necessary.

The results of acute toxicity tests (LD_{50} and LC_{50} values) are given in Table 27.12. In literature citing acute testing, low LD_{50} values (i.e., high toxicity) are sometimes given for molybdenum compounds. Some of these low levels are the result of long-term feeding studies but are interpreted as single-dose acute studies. For example, the acute oral LD_{50} in rats for molybdenum trioxide is frequently listed in the literature as 125 mg/kg, indicating that it is highly toxic. This LD_{50} was, however, determined by a 44-day feeding study [150], not by a single dose. The acute oral LD_{50} of molybdenum trioxide, pure grade, when determined by a single dose in rats, ranges from 2960 mg/kg to 3520 mg/kg [166].

Occupational Health. Several studies on the industrial exposure of humans to molybdenum have been reported from the former Soviet Union. A 1963 study reported 3 cases of pneumoconiosis out of 19 workers exposed to metallic molybdenum and its oxide. Early signs of pneumoconiosis were identified by X-ray in a 44-year old woman exposed for 5 years to molybdenum concentrations ranging from 1–3 mg/m³ and in a 44-year old man exposed for 4 years to concentrations between 6 and 19 mg/m³. A 34-year old man exposed for 7 years to concentrations between 6 and 19 mg/m³ showed fully developed pneumoconiosis [167].

In another Russian study 73 workers in a copper molybdenum plant complex and 10 control subjects were studied [168]. Workers with the highest exposure had the highest blood level of uric acid, and increased blood uric acid was found in 34 out of the 37 workers who complained of arthralgia. The actual values of uric acid in blood were not reported in this study, nor was the exposure defined.

Hyperuricemia was also described in another study on 85 workers in a copper molybdenum plant in Kadzaran, former Soviet Union [169]. An increase in blood concentrations of bilirubin, globulins, and cholesterol was observed but no values or exposure data were provided. In a study on 500 workers from a Russian molybdenum and copper mine, nonspecific symptoms and changes in the central nervous system were reported. Molybdenum dust levels in the mines were in some cases 10–100 times higher than the Soviet maximum permissible level of 6 mg Mo/m³ [170].

The effects of molybdenum exposure was studied in 25 male workers [mean age 28.3 years (19–44 years), mean duration of employment 4.0 years (0.5–20 years)] from a roasting plant in Denver, Colorado, where molybdenum sulfide was converted to molybdenum oxides [171]. Total dust samples were collected in the roaster area and the 8-h time weighted average (TWA) molybdenum exposure was calculated to be 9.47 mg/m³. The respirable (< 10 μ m) molybdenum concentration in the dust at the base of the roaster was 1.02 mg/m³ and the minimum daily body burden of molybdenum was calculated to be 10.2 mg. Urinary and plasma molybdenum levels were higher for the worker group than for the control group. Except for some generalized medical complaints, the only adverse biochemical findings were elevated serum ceruloplasmin levels and a small increase in serum uric acid the mean value of which was within the normal range of the control group. No gout-like symptoms were reported. Urinary copper excretion was normal in 13 of the 14 workers.

In the United States, health and safety regulations have established permissible exposure limits (PELs) in the occupational environment at 5 mg/m³ for soluble molybdenum compounds. The Threshold Limit Values (TLVs) have also been established by the ACGIH for soluble and insoluble molybdenum at 5 and 10 mg/m³, respectively. Both the PELs and TLVs are time-weighted averages (TWAs) for 8 h/d. Although the study of the 25 workers [171] may be considered limited because of the small population and high employment turnover, the absence of any adverse health effects at an exposure level approximately twice the soluble molybdenum PEL is of considerable value in assessing the potential worker risk to molybdenum exposure.

27.12 References

1. A. Sutulov: *Molybdenum Extractive Metallurgy*, University of Concepción, Chile 1965.
2. A. Sutulov: *International Molybdenum Encyclopedia 1778–1978*, vol II. Internet Publications, Santiago, Chile 1979.
3. J. W. Blossom: *Minerals Yearbook*, vol I, Metals and Minerals, U.S. Bureau of Mines, U.S. Government Printing Office, Washington, D.C. 1987, pp. 633–640.
4. J. W. Blossom: *Mineral Facts and Problems*, U.S. Bureau of Mines, Bulletin 675, U.S. Government Printing Office, Washington, D.C. 1985, pp. 521–534.
5. L. Northcott: *Molybdenum*, Butterworths Scientific Publications, London 1956.
6. S. M. Johnson in: *Mining Annual Review 1989*, Mining Journal, London 1989, p. C72.
7. Bureau of Mines: *An Appraisal of Minerals Availability for 34 Commodities*, Bulletin 692, U.S. Department of the Interior, Washington, D.C. 1987, p. 191.
8. J. Banfield (ed.): *Financial Times International Year Book 1989*, Longman Group UK Ltd., Harlow, Essex, United Kingdom; St. James Press, Chicago, Illinois 1988.
9. R. R. Dorfler, J. M. Laferty: "Review of Molybdenum Recovery Processes", *J. Met.* 31 (1981) no. 7, 48–54.
10. "50 Years of Flotation... It's Men, Ideas, and Machines", *Eng. Min. J.* 162 (1961) 83–91, 116, 120, 123, 125, 127.
11. V. A. Glemholtskii: *Flotation*, Primary Sources, New York 1963.
12. C. A. Born, F. N. Bender, O. A. Kiehn: "Molybdenite Flotation Reagent Development at Climax, Colorado", in D. W. Fürstenau (ed.) *A. M. Gaudin Memorial Vol. II*, AIME, New York 1976, pp. 1147–1184.
13. R. E. Cuthbertson: "Unusual Reagent Combination Improves Flotation at Climax", *Min. Elec. Mech. Eng.* 24 (1944) no. 292 1675–1680.
14. K. P. Neumann, W. A. Gibson: "Amoco Develops Thompson Creek Molybdenum Mine", *Min. Eng. Littleton. Color.* 36 (1984) 27–30.
15. D. Malhotra, R. M. Rowe, A. K. Bhasin: "Evaluation of Collectors for Molybdenite Flotation", *Minerals and Metallurgical Processing*, V3, m3, Aug. 1986, pp. 184–186.
16. J. F. Shirley: "By-product Molybdenite Plant Design", *Can. Min. J.* 102 (1981) no. 3, 27–28.
17. R. D. Crozier: "Flotation Reagent Practice in Primary and By-product Molybdenum Recovery", *Min. Mag.* 7 (1979) 174–178.
18. L. F. McHugh, J. Godshalk, M. Kuzlor: "Climax Conversion Practice III (for Molybdenite)", *Conference of the Metallurgical Society of CIM*, 1977, Canadian Institute of Mining and Metallurgy, Montréal 1978.
19. D. G. Lindsay: "Endako Roasting Practice", *Conference of the Metallurgical Society of CIM*, 1977, Canadian Institute of Mining and Metallurgy, Montréal 1978.
20. Amax, Inc., US 4207296, 1980 (H. H. K. Nauta, J. W. Kok, J. Harte).
21. Herman C. Starck, US 3860419, 1975 (T. A. Weber, R. F. Borrmann).
22. L. F. McHugh, P. L. Sallade: "Molybdenum Conversion Practice", Paper no. 86–154, presented at SME Annual Meeting, New Orleans, LA, March 2–6, 1986.
23. Engelhard Min. & Chem. Corp., US 4296077, 1981 (S. R. Heuer, Z. Zbranek).
24. Akzona, Inc., US 4087510, 1978 (G. F. Steenken).
25. Union Carbide Corp., US 3773890, 1973 (J. S. Fox, J. E. Litz).
26. Amax, Inc., US 4495157, 1985 (R. F. Sebenik, P. P. LaValle, J. M. Laferty, W. A. May).
27. Marubeni Corp. and Fuji Fine Chemical Co., US 4145397, 1979 (S. Toida, A. Ohno, K. Higuchi).
28. Individual, US 3256058, 1966 (B. Burwell, Sr.).
29. *Gmelin*, System no. 53, Molybdän; suppl., part A1.
30. G. Dowson, *Met. Powder Rep.* 44 (1989) no. 4, 272–275.
31. W. C. Hagel, J. A. Shields, S. M. Tuominen, CONF-8308130, US Department of Energy, Oak Ridge, USA 1984.
32. A. J. Bryhan, *Weld. Res. Council Bull.* 312 (1986) 1–20.
33. C. A. Krier, DMIC, Battelle Information Center, Rep. 263 (1961) Columbus, Ohio.
34. R. Eck, J. Tinzl, *12th International Plansee Seminar, Proc.* 1 (1989) 829–843.
35. J. Wadsworth, T. G. Nieh, J. J. Stephens, *Int. Mat. Rev.* 33 (1988) no. 3, 131–150.
36. T. J. Patrician, V. P. Sylvester: "Physical Metallurgy and Technology of Molybdenum and its Alloys", *Proc. of Symp. AMAX Material Research Center*, Ann Arbor, Michigan 1985, pp. 1–11.
37. *Gmelin*, Molybdenum Suppl., vols. B1, B2.
38. F. A. Cotton, G. Wilkinson: *Advanced Inorganic Chemistry*, 5th ed., Wiley, New York 1988, pp. 804–847.

39. J. Aubry, D. Burnel, C. Gleitzer in P. Pascal (ed.): *Compléments au Nouveau Traité de chimie minérale*, vol. 5, Masson, Paris 1976.
40. C. L. Rollinson in A. F. Trotman-Dickenson (ed.): *Comprehensive Inorganic Chemistry*, vol. 3, Pergamon Press, Oxford 1973, pp 632-770.
41. G. Brauer (ed.): *Handbook of Preparative Inorganic Chemistry*, 2nd ed., vol. 2, Academic Press, New York 1965, pp 1401-1417.
42. Chem. Uses Molybdenum, *Proc. Int. Conf.* 1st, 1973 (*J. Less-Common Met.* 36 (1974) 1-542); 2nd, 1976 (*J. Less-Common Met.* 54 (1977) 1-564); 3rd, 1979; 4th, 1982; 5th, 1985 (*Polyhedron* 5 (1986) 1-606).
43. P. C. H. Mitchell, *Q. Rev. Chem. Soc.* 20 (1966) 103-118; E. I. Stiefel, *Prog. Inorg. Chem.* 22 (1977) 1; Z. Dori, *Prog. Inorg. Chem.* 28 (1981) 239.
44. F. A. Cotton, *Polyhedron* 5 (1986) 3.
45. A. Muller, *Polyhedron* 5 (1986) 323.
46. A. J. Bard, R. Parson, J. Jordan: *Standard Potentials in Aqueous Solutions*, Marcel Dekker, New York 1985, p. 480; J. Emsley: *The Elements*, Clarendon Press, Oxford 1989, p. 116.
47. A. Kay, P. C. H. Mitchell, *Nature (London)* 219 (1968) 267; *J. Chem. Soc. A* 1970, 2421.
48. J. Bassett, R. C. Denney, G. H. Jeffery, J. Mendham: *Vogel's Textbook of Quantitative Inorganic Analysis*, 4th ed., Longman, London 1978, p. 367.
49. T. L. Woods, R. M. Garrels: *Thermodynamic Values at Low Temperatures for Natural Inorganic Materials* (mean values), Oxford University Press, Oxford 1987.
50. Climax Molybdenum Company: *Thermodynamic Properties of Molybdenum Compounds*, Bulletin Cdb-2, Climax Molybdenum Company, Ann Arbor, Michigan 1954 (some values have been superseded, see [49, 60]).
51. See [41] p. 1412.
52. J. E. Germain in M. Che and G. C. Bond (eds.): *Adsorption and Catalysis on Oxide Surfaces*, Elsevier, Amsterdam 1985, p. 355; K. Bruckman, J. Haber, T. Wiltowski, *J. Catal.* 106 (1987) 188; J. Haber, E. Serwicka, *Polyhedron* 5 (1986) 107; K. Bruckman et al., *J. Catal.* 104 (1987) 71.
53. C. B. Knobler et al., *J. Chem. Soc. Dalton Trans.* 1983, 1299.
54. F. A. Schroder, J. Scherle, *Z. Naturforsch. B: Anorg. Chem. Org. Chem.* 28B (1973) 46; see also C. B. Knobler, B. R. Penfold, G. T. Wilkins, *J. Chem. Soc. Dalton Trans.* 1980, 248.
55. A. Magneli, *Acta Chem. Scand.* 9 (1955) 1378.
56. B. G. Brandt, A. C. Skapski, *Acta Chem. Scand.* 21 (1967) 661; *Acta Crystallogr. Sect. A Cryst. Phys. Diff. Theor. Gen. Crystallogr.* A24 (1968) 699.
57. V. K. Rudenko, *Koord. Khim.* 5 (1979) 307; (*Sov. J. Coord. Chem. — Engl. Transl.*) 5 (1979) 231.
58. See ref. [48] p. 756.
59. M. Greenblat, *Chem. Rev.* 88 (1988) 31.
60. K. C. Mills: *Thermodynamic Data for Inorganic Sulphides, Selenides, and Tellurides*, Butterworths, London 1974.
61. K. S. Liang et al., *J. Non-Cryst. Solids* 42 (1980) 345.
62. R. Chevreil, M. Hirrien, M. Sergent, *Polyhedron* 5 (1986) 87.
63. Climax Molybdenum Company: *Properties of the Simple Molybdates*, Bulletin Cdb-4, Climax Molybdenum Company, Ann Arbor, Michigan 1962.
64. F. Corbet, C. Eyraud, *Bull. Soc. Chim. Fr.* 1961, 571; J. Chojnacki, R. Kozłowski, J. Haber, *J. Solid State Chem.* 11 (1974) 106; J. Haber in P. C. H. Mitchell (ed.): *Climax First International Conference on the Chemistry and Uses of Molybdenum*, Climax Molybdenum Co. Ltd., London 1973, p. 146.
65. A. W. Armour, M. G. B. Drew, P. C. H. Mitchell, *J. Chem. Soc. Dalton Transactions* 1975, 1493.
66. M. T. Pope: *Heteropoly and Isopoly Oxometalates*, Springer Verlag, Berlin 1983.
67. J. B. Black et al., *Polyhedron* 5 (1986) 141.
68. P. C. H. Mitchell, *Wear* 100 (1984) 281.
69. See ref. [38] p. 1046.
70. D. H. Killefer, A. Linz: *Molybdenum Compounds, Their Chemistry and Technology*, Interscience, New York 1952.
71. O. Weisser, S. Landa: *Sulfide Catalysts, Their Properties and Applications*, Pergamon Press, New York 1973.
72. F. J. Clauss: *Solid Lubricants and Self-Lubricating Solids*, Academic Press, New York 1972.
73. T. J. Risdon: *Properties of Molybdenum Disulfide*, Bulletin C-5c, AMAX Mineral Sales, AMAX Inc., Greenwich, Connecticut, February 1987.
74. J. W. Lyons: *The Chemistry and Uses of Fire Retardants*, Wiley Interscience, New York 1970.
75. R. J. Cole, P. C. H. Mitchell: *Molybdenum Compounds in the Paint and Allied Industries*, Bulletin of Climax Molybdenum Co., AMAX Inc., Greenwich, Connecticut 1971.
76. *Molybdenum Catalyst Bibliography*, Bulletins C-40, C-54, C-73, C-77, C-96, C-111, C-119, C-130, C-135, C-139, Climax Molybdenum Co., AMAX Inc., Greenwich, Connecticut 1950-1983.
77. J. Haber: *The Role of Molybdenum in Catalysis*, Bulletin of Climax Molybdenum Co. Ltd., London, AMAX Inc., Greenwich, Connecticut 1981, pp 3-4.
78. F. Veatch, J. L. Callahan, J. D. Idol, Jr., E. C. Milberger, *Chem. Eng. Prog.* 56 (1960) no. 10, 65-67.
79. H. Adkins, W. Peterson, *J. Am. Chem. Soc.* 53 (1931) 1512-1516.
80. W. F. Jamison, *ASLE Trans.* 15 (1972) 296-305.
81. E. R. Braithwaite, *Sci. Lubr.* 18 (1966) 13-18.
82. W. O. Winer, *Wear* 10 (1967) 422-452.
83. J. P. G. Farr, *Wear* 35 (1975) 1-22.
84. R. S. Barnett: *Molybdenum Disulfide as an Additive for Lubricating Greases*, Bulletin of Climax Molybdenum Co., AMAX Inc., Greenwich, Connecticut 1981.
85. R. D. Loban, D. A. Gresty: *Molybdenum Disulfide in Rubber*, Bulletin of Climax Molybdenum Co., AMAX Inc., Greenwich, Connecticut 1976.
86. R. L. Johnson: *Bonded Lubricant Coatings — A Status Report*, Bulletin of Climax Molybdenum Co., AMAX Inc., Greenwich, Connecticut 1979.
87. T. J. Risdon, D. A. Gresty: *An Historical Review of Reductions in Fuel Consumption of United States and European Engines with MoS₂*, SAE Paper No. 750674, Houston, Texas, June 1975.
88. P. C. H. Mitchell, *Wear* 100 (1984) 281-300.

89. Carbide and Carbon Chemicals Corp., US 2147395, 1939 (A. L. Bayes).
90. Carbide and Carbon Chemicals Corp., US 2147409, 1939 (H. Lamprey).
91. M. S. Vukasovich, J. P. G. Farr, *Mater. Perform.* 25 (1986) no. 5, 9-18.
92. M. S. Vukasovich: *Molybdate — The Versatile Inhibitor*, NACE Paper No. 444, NACE, New Orleans, LA, April 1989.
93. L. C. Rowe, R. L. Chance, M. S. Walker, *Mater. Perform.* 22 (1983) no. 6, 17-23.
94. H. O. Schoen, B. G. Brand, *Off. Dig. Fed. Soc. Paint Technol.* 32 (1960) 1522-1543.
95. The Sherwin Williams Co., US 3353979, 1967 (J. V. Hunn).
96. The Sherwin Williams Co., US 3677783, 1972 (T. Kirkpatrick, J. J. Nilles).
97. American Metal Climax Inc., US 3726694, 1973 (F. W. Moore, D. R. Robitaille, H. F. Barry).
98. T. R. Truax, C. A. Harrison, R. H. Baechler, *Proc. Annu. Meet. Am. Wood Preserv. Assoc.* 231 (1933) 107-123.
99. J. E. Ramsbottom: *The Fireproofing of Fabrics*, His Majesty's Stationery Office, London 1947.
100. F. W. Moore, G. A. Tsigdinos: "The Role of Molybdenum in Flame Retardancy and Smoke Retardation", in P. C. H. Mitchell, A. Seaman (eds.): *Proc. 2nd Intl. Conf. Chemistry and Uses of Molybdenum*, Climax Molybdenum Co., AMAX Inc., Greenwich, Connecticut 1976, pp. 145-149.
101. F. W. Moore, G. A. Tsigdinos: "Advances in the Use of Molybdenum Additives as Smoke Suppressants and Flame Retardants for Polyvinyl Chloride", *Proc. Intl. Symp. Flammability and Fire Retardants*, Technomic Press, Westport, Connecticut 1978, pp. 160-172.
102. M. Das, P. J. Haines, T. J. Lever, G. A. Skinner: "The Role of Molybdenum Trioxide as a Flame Retardant and Smoke Suppressant in Halogenated Polyester Thermosets", in H. F. Barry, P. C. H. Mitchell (eds.): *Proc. 4th Intl. Conf. Chemistry and Uses of Molybdenum*, Climax Molybdenum Co., AMAX Inc., Greenwich, Connecticut 1982, pp. 218-223.
103. F. Hund, *Farbe + Lack* 73 (1967) 111-120.
104. H. Schäfer, *Farbe + Lack* 77 (1971) no. 11, 1081-1089.
105. Hoechst, DE-OS 2127279, 1971 (R. Kohlhaas et al.).
106. Hoechst, DE-OS 2062775, 1970 (R. Kohlhaas et al.).
107. Sherwin-Williams, US 2237104, 1938 (N. F. Livingston).
108. J. F. Clay & Cromford Color, GB 730176, 1951; H. Lesche, *Farbe + Lack* 65 (1959) 79, 80.
109. Du Pont, US 2808339, 1957 (J. J. Jackson).
110. Du Pont, DE-OS 1807891, 1969 (H. R. Linton).
111. Bayer, DE-OS 1952538, 1969 (C. H. Elstermann, F. Hund).
112. ICI, DE-OS 2049519, 1970 (Ch. H. Buckley, G. L. Collier, J. B. Mitchell).
113. Ten Horn Pigment, DE-OS 2600365, 1976 (J. J. Einerhand et al.).
114. BASF, DE 3323247 A1, 1983 (E. Liedek et al.).
115. Heubach, DE 3806214 A1, 1988 (I. Ressler, W. Horn, G. Adrian).
116. Heubach, DE 3906670 A1, 1989 (I. Ressler, W. Horn, G. Adrian).
117. G. Meyer, *DEFAZET Dtsch. Farben Z.* 5 (1963) 201-205.
118. Sherwin-Williams Chemicals: *Moly White*, company information, Coffeyville, KS 1986.
119. W. J. Banke, *Mod. Paint Coat.* 70 (1980) Febr., 45-47.
120. American Metal Climax, CH 602899, 1973 (D. R. Robitaille et al.); DE 2334541, 1973 (D. R. Robitaille et al.).
121. Noranda Miners Ltd., US 4132667, 1977 (D. Kerfoot); DE 2814454, 1978 (D. Kerfoot).
122. J. Ruf, *Farbe + Lack* 79 (1973) no. 1, 22-27.
123. A. I. Vogel: *Quantitative Inorganic Analysis*, 5th ed., Longman, London 1989.
124. R. A. Mostyn, A. F. Cunningham, *Anal. Chem.* 38 (1966) 121.
125. *Analytical Methods in Atomic Absorption Spectrophotometry*, Perkin Elmer Corp., Norwalk, Connecticut 1971.
126. M. D. Amos, J. B. Willis, *Spectrochim. Acta* 22 (1966) 1325.
127. D. J. David, *Analyst (London)* 86 (1961) 730.
128. D. M. Knight, M. K. Pyzyna, *Atomic Absorption Newsletter* 8 (1969) 129.
129. L. R. P. Butler, P. M. Mathews, *Anal. Chim. Acta* 36 (1966) 319.
130. D. Hutchinson, *Analyst (London)* 97 (1972) 118.
131. *Official Methods of Analysis*, 10th ed., Association of Official Agricultural Chemists, Washington, D.C. 1965.
132. W. R. Chappell, K. K. Peterson: *Molybdenum in the Environment*, vols. 1 and 2, Marcel Dekker, New York-Basel 1976.
133. C. F. Mills, I. Bremner, J. K. Chesters (eds.): "Trace Elements in Man and Animals", *Proc. Int. Symp. Trace Elem. Man Animals* 5th, Commonwealth Agricultural Bureaux, Farnham, United Kingdom 1985.
134. L. S. Hurley, C. L. Keen, B. Lonnardal, R. B. Rucker (eds.): *Trace Elements in Man and Animals* 6, Plenum Press, New York-London 1988.
135. *Acute Toxicity of Sodium Molybdate to Bluegill (Lepomis macrochirus), Rainbow Trout (Salmo gairdneri), Fathead Minnow (Pimephales promelas), Channel Catfish (Ictalurus punctatus), Water Flea (Daphnia magna) and Scud (Gammarus fasciatus)*, Bioassay Report Submitted to Climax Molybdenum Company of Michigan, Bionomics, Inc., Wareham, MA, December 1973.
136. *Acute Toxicity of Ammonium Molybdate and Molybdic Trioxide to Bluegill (Lepomis macrochirus) and Rainbow Trout (Salmo gairdneri)*, Bioassay Report Submitted to AMAX, Inc., Bionomics, Inc., Wareham, MA, January 1975.
137. D. W. Knothe, Dr. G. G. Van Riper: "Acute Toxicity of Sodium Molybdate Dihydrate (Molyhibil 100) to Selected Saltwater Organisms", *Bull. of Environ. Contam. and Toxicol.* 40 (1988) 785.
138. O. J. Abbott: "The Toxicity of Ammonium Molybdate to Marine Invertebrates", *Marine Poll. Bull.* 8 (1977) no. 9, 204-205.

139. *Evaluation of Acute Effects of Sodium Molybdate on the Activated Sludge Process and on the Batch Anaerobic Sludge Digestion Process*, Laboratory Report for AMAX Inc., Stearns Catalytic Corp., January 1985.
140. *Acute Oral LD₅₀ Assay in Rats*, FDRL ID: 81-0393 for AMAX Inc., Aug. 1981.
141. *Acute Oral LD₅₀ Assay in Rats*, FDRL ID: 81-0394 for AMAX Inc., Aug. 1981.
142. N. Irving Sax: *Dangerous Properties of Industrial Materials*, 6th ed., Van Nostrand Reinhold Co., New York 1984, p. 1953.
143. *Acute Oral Toxicity in Rats of MoS₃*, FDRL ID: 9589A for AMAX Inc., Nov. 29, 1987.
144. *Threshold Limit Values and Biological Exposure Indices for 1989-1990*, American Conference of Governmental Industrial Hygienists, Cincinnati, Ohio 1990.
145. *Emergency Planning and Community Right-to-Know Act of 1986*, enacted by Public Law 99-499, October 17, 1986.
146. Wet Bodembescherming (Wbb), Soil Protection Act, The Netherlands 1988.
147. Council of the European Communities Directive, 76/464/EEC, May 4, 1976.
148. W. S. Ferguson, A. H. Lewis, S. J. Watson, *Nature (London)* **141** (1938) 553.
149. S. B. Hornick, D. E. Baker, S. B. Guss: "Crop Production and Animal Health Problems Associated with High Soil Molybdenum", *Molybdenum in the Environment*, vol. 2, Marcel Dekker, New York-Basel 1977.
150. L. Fairhall, R. Dunn, N. Sharpless, E. Pritchard: "The Toxicity of Molybdenum", *U.S. Public Health Bull.*, no. 293, 1945.
151. J. Johnson, K. Rajagopalan: "Molecular Basis of the Biological Function of Molybdenum", *J. Biol. Chem.* **249** (1974) 859-866.
152. L. Friberg, P. Boston, G. Nordberg, M. Piscator, K. Robert: *Molybdenum - A Toxicological Appraisal*, EPA 600/1-75-004, U S Environmental Protection Agency, Research Triangle Park, North Carolina 1975.
153. V. Kovalskii, G. Yarovaya, D. Schmayovyan: "Changes in Purine Metabolism in Humans and Animals Living in Biogeochemical Areas with High Molybdenum Concentrations", *Z. Obsc. Biol.* **22** (1961) 179.
154. R. Burrell, W. Roach, A. Shadwell: "Esophageal Cancer in the Bantu of the Transkei Associated with Mineral Deficiency in Garden Plants", *J. Natl. Cancer Inst.* **35** (1966) 201-209.
155. S. Yang et al.: "Molybdenum Deficiency and Esophageal Cancer in China", *Fed. Proc. Fed. Am. Soc. Exp. Biol.* **40** (1981) 918.
156. S. Yang, H. Wei, X. Luo, H. Sproat: "Effect of Molybdenum on N-Nitrososarcosine Ethyl Ester-Induced Carcinogenesis in Rats", *Fed. Proc. Fed. Am. Soc. Exp. Biol.* **41** (1982) 280.
157. S. Yang, X. Luo, H. Wei: "Inhibitory Effects of Molybdenum on Esophageal and Forestomach Carcinogenesis in Rats", *JNCI J. Natl. Cancer Inst.* **17** (1980) 75-80.
158. S. Yang, H. Wei, X. Luo: "Effects of Molybdenum and Tungsten on Mammary Carcinogenesis in S. D. Rats", *JNCI J. Natl. Cancer Inst.* **74** (1985) 469-473.
159. Y. Doesthale, C. Gopalan: "The Effect of Molybdenum Levels in Sorghum (Sorghum Vulgare Pers) on Uric Acid and Copper Excretion in Man", *Br. J. Nutr.* **31** (1974) 351-353.
160. W. Mertz: "Defining Trace Element Deficiencies and Toxicities in Man", *Molybdenum in the Environment*, vol. 1, Chap. 18, Marcel Dekker, New York 1976.
161. National Academy of Sciences: *Mineral Tolerance of Domestic Animals*, Washington, D.C. 1980.
162. G. Nordheim, G. Frostlie: "Copper Molybdenum Interactions in Relation to Chronic Copper Poisoning in Sheep in Norway", *Nutr. Rev. Suppl.* **1985**, 535-538.
163. A. Lesperance, G. Cook, V. Bohman, E. Jensen: "Interrelationship of Molybdenum and Certain Factors to the Development of the Molybdenum Toxicity Syndrome", *J. Animal Sci.* **25** (1966) 96-101.
164. N. Suttle: "Copper Deficiency in Ruminants; Recent Developments", *Vet. Rec.* **119** (1986) 519-522.
165. L. Arlington, G. Davis: "Molybdenum Toxicity in the Rabbit", *J. Nutr.* **51** (1953) 295.
166. Food and Drug Research Laboratories, Inc.: *Acute Oral LD₅₀ Assay in Rats for Molybdenum Trioxide Pure Grade*, Waverly, New York 1981.
167. O. Mogilevskaia: "Experimental Studies on the Effect on the organism of Rare, Dispersed and Other Metals and Their Compounds Used in Industry", in Z. I. Izraelson (ed.): *Toxicology of the Rare Metals*, Israel Program for Scientific Translations Ltd., Jerusalem 1967.
168. O. Akopajan: "Some Biological Shifts in the Bodies of Workers in Contact with Molybdenum Dust", *Second Scientific Conference on The Institute of Labor of Hygiene and Occupational Diseases on Problems of Labor Hygiene and Occupational Pathology*, Erevan 1963, pp. 103-106.
169. M. Avakjan: "A Dynamic Study of the Experimental Effect of Molybdenum on Some Metabolic Processes", *Scientific Session on Problems of Labor Hygiene and Occupational Pathology in the Chemical and Mining Industries*, Alastan, 1966.
170. S. Eolajan: "The Effects of Molybdenum on the Nervous System", *Z. Exp. Klin. Med.* **5** (1965) 70-73.
171. P. S. Walravens et al.: "Biochemical Abnormalities in Workers Exposed to Molybdenum Dust", *Arch. Environ. Health* **34** (1979) 302-308.

28 Niobium

JOACHIM ECKERT

28.1 Introduction	1403	28.6.1 Oxides	1408
28.2 History	1403	28.6.2 Halides	1409
28.3 Properties	1403	28.6.3 Carbides and Hard Materials	1409
28.4 Occurrence	1404	28.7 Niobium Metal	1411
28.5 Processing of Niobium Ores	1405	28.7.1 Reduction of Niobium Pentoxide	1411
28.5.1 Pyrochlore Concentrates	1405	28.7.2 Reduction of Halides	1411
28.5.2 Production of Niobium Oxide from Columbites and Tantalites	1405	28.7.3 Refining	1412
28.5.2.1 Extraction Processes	1405	28.7.4 Uses	1412
28.5.2.2 Chlorination	1406	28.8 Analysis	1413
28.6 Compounds	1408	28.9 Economic Aspects	1413
		28.10 References	1414

28.1 Introduction

Niobium, Nb, atomic number 41, A_r 92.91, is also known as columbium, Cb, in the United States. There are many artificial radionuclides, but only one known natural nonradioactive isotope, ^{93}Nb . The electronic configuration of the ground state is $4s^2p^6d^35s^2$, which explains the existence of the oxidation states +2 to +5.

28.2 History

Niobium was discovered by HATCHETT in 1801 in the mineral columbite and was named columbium. In 1844 the name niobium was proposed by ROSE.

28.3 Properties

Some important physical properties of niobium metal are listed in Table 28.1 [1-3].

The mechanical properties like those of most refractory metals are influenced by the purity of the metal, the production method, and the mechanical treatment. Even small amounts of interstitial impurities increase the hardness and strength but reduce the ductility. Some important mechanical properties of commercial niobium are listed in Table 28.2 [4].

Table 28.1: Physical properties of niobium.

Density at 20 °C (g/cm ³)	8.57
Crystal structure	body-centered cubic ($a = 3.3 \times 10^{-10}$ m)
m_p (°C)	2468 ± 10
b_p (°C)	4927
Linear coefficient of thermal expansion (K ⁻¹)	6.892×10^{-6}
Specific heat (kJ kg ⁻¹ K ⁻¹)	0.26
Latent heat of fusion (kJ/kg)	290
Latent heat of vaporization (kJ/kg)	7490
Thermal conductivity at 0 °C (W cm ⁻¹ K ⁻¹)	0.533
Electrical resistivity (μΩ·cm)	15.22
Temperature coefficient (0-600 °C) (K ⁻¹)	0.0396
Electrochemical equivalent (mg/C)	0.19256
Standard electrode potential E^0 Nb/Nb ⁵⁺ (V)	-0.96
Magnetic susceptibility at 25 °C	2.28×10^{-6}
Superconductivity T_c (K)	9.13
Spectral emissivity at 650×10^{-10} m (at 2003 K)	2.28×10^{-6}
Ionization potential (eV)	6.67
Work function (eV)	4.01

Niobium is very resistant to most organic and inorganic acids, with the exception of HF, at temperatures up to 100 °C [1]. Concentrated sulfuric acid above 150 °C causes embrittlement. The resistance towards alkaline solutions is lower. Because niobium has a marked tendency to form oxides, hydrides, nitrides, and carbides, its use in air is limited to temperatures up to ca. 200 °C.

Table 28.2: Mechanical properties of niobium.

<i>Annealed niobium</i>	
Ultimate tensile strength	195 MPa
Yield strength	105 MPa
Elongation	30% +
Reduction in area	80% +
Hardness	60 HV
Poisson's ratio	0.38
Strain hardening exponent	0.24
Elastic modulus	
tension	103 GPa
shear	17.5 GPa
Ductile-brittle transition temperature	< 147 K
Recrystallization temperature	800–1000 °C
<i>Cold worked niobium</i>	
Ultimate tensile strength	585 MPa
Elongation	5%
Hardness	150 HV

28.4 Occurrence

Niobium occupies the 33rd place in order of natural abundance, being present in the earth's crust at 24 µg/g. It is thus more common than cobalt, molybdenum, or tantalum. The most important niobium mineral is pyrochlore, a compound with the general formula $(\text{Ca}, \text{Na})_2 - n \text{Nb}_2\text{O}_6 (\text{O}, \text{OH}, \text{F})_{1-n} \cdot x\text{H}_2\text{O}$. The lattice positions of Na and Ca can also be occupied by Ba, Sr, rare earths, Th, and U. The latter two elements are responsible for the radioactivity of some pyrochlore concentrates.

Two types of niobium ore deposits are known. In primary deposits, the pyrochlore is always interstratified in carbonatites. This is so in the Canadian deposits at Niobec and

Oka, in which calciopyrochlore is interstratified in dolomite. The ore contains 0.5–0.7% niobium pentoxide. In the important secondary Brazilian deposits at Araxa and Catalao, the niobium content of the carbonate minerals has been considerably enriched by weathering. Here, the ore is present in combination with apatite, iron oxide, and barite and contains about 3% Nb_2O_5 , 46% Fe_2O_3 , 17–18% BaO , and 1.5% P as apatite [5]. Table 28.3 shows the average Nb_2O_5 capacity, the production, and the reserves of various deposits [6]. In addition to the sources listed in Table 28.3, other, potential sources exist in Canada, Africa, Brazil, China, the United States, and the former Soviet Union.

The most commercially important deposits are in Brazil, Canada, Nigeria, and Zaire. World reserves are estimated to be 4.1×10^6 t Nb, of which 78% are in Brazil. The Canadian reserves are estimated at 0.12×10^6 t.

The second most important niobium mineral is columbite, $(\text{Fe}, \text{Mn})(\text{Nb}, \text{Ta})_2\text{O}_6$, in which niobium is nearly always present with tantalum. These ores are referred to as columbites if the Nb_2O_5 content is greater than that of Ta_2O_5 , otherwise as tantalites. Columbites and tantalites contain at least 60% combined pentoxides. These minerals occur as primary deposits in granites and pegmatites, or in alluvial secondary deposits. Table 28.4 lists the chemical compositions of various niobium and tantalum minerals [7].

Table 28.3: Niobium deposits [6].

Location	Capacity, 10^6 kg Nb_2O_5	Ore grade	Reserves, 10^6 t Nb_2O_5	Production, 10^6 kg Nb_2O_5
Araxa, Brazil	24.75	3.0	500 +	9.45
St. Honoré, Québec	3.15	0.7	11	3.15
Catalao, Brazil	2.48	1.5	50	2.48
Nigeria	0.9			
Thailand	0.45–0.9			
Zaire	pilot scale	2–3	extensive	0.23

Table 28.4: Chemical composition of the principal niobium-bearing materials, % [7].

Mineral	Nb_2O_5	Ta_2O_5	TiO_2	Fe	MnO	SnO ₂
Pyrochlore, $\text{NaCaNb}_2\text{O}_6\text{F}$	40–65	2	1–6	2		
Columbite, $(\text{Fe}, \text{Mn})(\text{Nb}, \text{Ta})_2\text{O}_6$	40–75	1–40	0.5–3	10–20	2.6	2
Tantalocolumbite, $(\text{Fe}, \text{Mn})(\text{Nb}, \text{Ta})_2\text{O}_6$	25–60	20–50	0.5–3	10–20	2.6	2
Tantalite, $(\text{Fe}, \text{Mn})(\text{Ta}, \text{Nb})_2\text{O}_6$	2–40	42–84	0.5–3	10–20	2.6	2
Microlite, $\text{Ca}_2(\text{Ta}, \text{Nb})_2\text{O}_6(\text{OH}, \text{F})$		60–70				

Columbites are mined in Australia, Brazil, Nigeria, Malaysia, and Zaire. Since the discovery of the enormous deposits of pyrochlore in Brazil, world production of columbite has decreased considerably. This trend could change when the extraction of columbite as a by-product of tin extraction is started with the Pitinga deposits in Brazil [8]. The discovery of large deposits of pyrochlore in South Greenland (Motzfeld Center) was reported in 1986.

A further source of niobium is provided by tantalum–niobium slags from tin production, since columbites and tantalites are often associated with cassiterite; niobium and tantalum concentrate in the slags as oxides. The niobium and tantalum pentoxide content of various tin slags is given in Table 28.5 [9]. Niobium and tantalum are also found in rare minerals such as stibiocolumbites $(\text{Sb}, \text{Nb})\text{TaO}_4$, fergusonites $(\text{Re}^{3+})\text{NbO}_4$, and euxenite $\text{Y}(\text{Nb}, \text{Ti})_2\text{O}_6$. The last two of these, however, are of no commercial significance.

Table 28.5: Niobium and tantalum pentoxide content of various tin slags, % [9].

Country	Nb_2O_5	Ta_2O_5
Malaysia	4	4
Nigeria	14	4
Portugal	7	7
Singapore	3	2
Thailand	8	12
Zaire	5	9

28.5 Processing of Niobium Ores

28.5.1 Pyrochlore Concentrates

Concentrates containing 50–60% Nb_2O_5 are obtained from pyrochlore-containing carbonatites or weathered ores by conventional beneficiation processes such as crushing, grinding, magnetic separation, and flotation. Brazilian concentrates (Araxa) are also treated chemically to remove lead, phosphorus, and sulfur. The raw concentrate is roasted in the presence of calcium chloride and calcium oxide in a rotary furnace at 800–900 °C, and the product is leached with hydrochloric acid. In

the case of Brazilian pyrochlore, this procedure also leads to replacement of barium by calcium [10].

Whereas pyrochlore from Araxa can be converted directly to ferroniobium, pyrochlore concentrates from other sources must first be chemically pretreated before niobium can be obtained. Some well-known processes are treatment with concentrated sulfuric acid or with molten soda. Reductive chlorination of pyrochlore at ca. 1000 °C produces volatile chlorides of niobium and other metals. These processes are, however, generally regarded as uneconomical. This is also true of the process in which digestion of pyrochlore with mixtures of hydrofluoric and sulfuric acids is followed by solvent extraction [11].

28.5.2 Production of Niobium Oxide from Columbites and Tantalites

28.5.2.1 Extraction Processes

Niobium and tantalum always occur together in columbites and tantalites and must be separated not only from the other elements present but also from each other. The industrial separation of tantalum from niobium has long been carried out by the Marignac process of fractional crystallization of potassium heptafluorotantalate and potassium heptafluoroniobate [12]. This expensive process of precipitation and crystallization, which is also environmentally unacceptable, has been abandoned, together with the long established Fansteel process [12], in favor of processes based on solvent extraction.

Tantalite and columbite, either naturally occurring or synthetically produced as concentrates from tin slags [13, 14], are digested with hydrofluoric and sulfuric acids at elevated temperature. The accompanying elements are dissolved along with the tantalum and niobium, which form the complex heptafluorides H_2TaF_7 and H_2NbOF_5 or H_2NbF_7 . After filtering off the insoluble residue (fluorides of alkaline earth and rare earth metals), the aqueous

solution of Ta–Nb in hydrofluoric acid is extracted in several continuously operated mixer-settlers with an organic solvent, e.g., methyl isobutyl ketone (MIBK) [15–17]. The complex fluorides of niobium and tantalum are extracted by the organic phase, whereas most of the impurities and other elements, such as iron, manganese, titanium, etc., remain in the aqueous phase. In practice, Nb_2O_5 + Ta_2O_5 concentrations of 150–200 g/L in the organic phase are used. The organic phase is washed with 6–15 N sulfuric acid and then reextracted with water or dilute sulfuric acid to obtain the niobium. The aqueous phase takes up the complex fluoroniobate and free hydrofluoric acid, while the complex fluorotantalate remains dissolved in the organic phase. The aqueous niobium solution is reextracted with a small amount of MIBK to remove traces of tantalum. The resulting organic phase is returned to the combined tantalum niobium extraction stage. Gaseous or aqueous ammonia is added to the aqueous niobium solution to precipitate niobium oxide hydrate. Crystallization of K_2NbF_7 can only be achieved in strong hydrofluoric acid solution; therefore, it is only carried out on a small scale because of the high costs arising from the increased consumption of hydrofluoric acid.

The tantalum is reextracted from the organic phase with water or dilute ammonia solution, and tantalum oxide hydrate is precipitated by ammonia, or potassium salts are added to produce K_2TaF_7 , which is used in the production of tantalum metal.

The oxide hydrates are collected by filtration, dried, and calcined at up to 1100 °C. Variation of the conditions of precipitation, drying and calcination produces different particle sizes, giving oxides suitable for various applications. Depending on the quality requirements, the calcination is carried out in directly or indirectly heated chamber or rotary furnaces. The nature of the furnace lining has considerable influence on purity.

Sophisticated process control and optimization enable niobium and tantalum to be produced with high yield (> 95%) and purity (> 99.9%).

A number of alternative extraction media have been reported in the literature, most of which have never been used in industry, except for tributyl phosphate (TBP) [18] and tri-*n*-octylphosphine oxide (TOPO) [19].

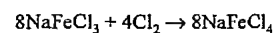
Figure 28.1 shows the flow diagram of an industrial installation for the processing of tantalum niobium raw materials [20].

28.5.2.2 Chlorination

The chlorination process is a modern alternative to the extraction process. There are two versions: reductive chlorination of natural and synthetic raw materials, and chlorination of tantalum–niobium ferroalloys.

In reductive chlorination, the ore or concentrate is pelletized with coal/coke and pitch, dried, and reacted in a stream of chlorine at 900 °C. The nonvolatile alkaline earth metal chlorides remain behind, while the readily volatilized tetrachlorides of silicon, tin, titanium, the pentachlorides NbCl_5 and TaCl_5 , and WOCl_4 are distilled off and fractionated. The waste gas, which contains large amounts of phosgene and chlorine, must be rigorously purified.

The chlorination of ferroalloys is much simpler and more economical [21, 22]. Ferro-niobium or ferroniobium tantalum are produced by the aluminothermic or electrothermic process, size reduced, and fed together with sodium chloride into a NaCl FeCl_3 melt. The chlorinating agent is NaFeCl_4 . Chlorine is passed into the melt, continuously regenerating NaFeCl_4 . The following overall reactions take place:



The reaction temperature of 500–600 °C is much lower than that required for reductive chlorination. The volatile chlorides are evolved from the molten salt bath. The boiling points of NbCl_5 , TaCl_5 , and WOCl_4 lie between 228 and 248 °C, and these compounds must therefore be separated by means of a distillation column.

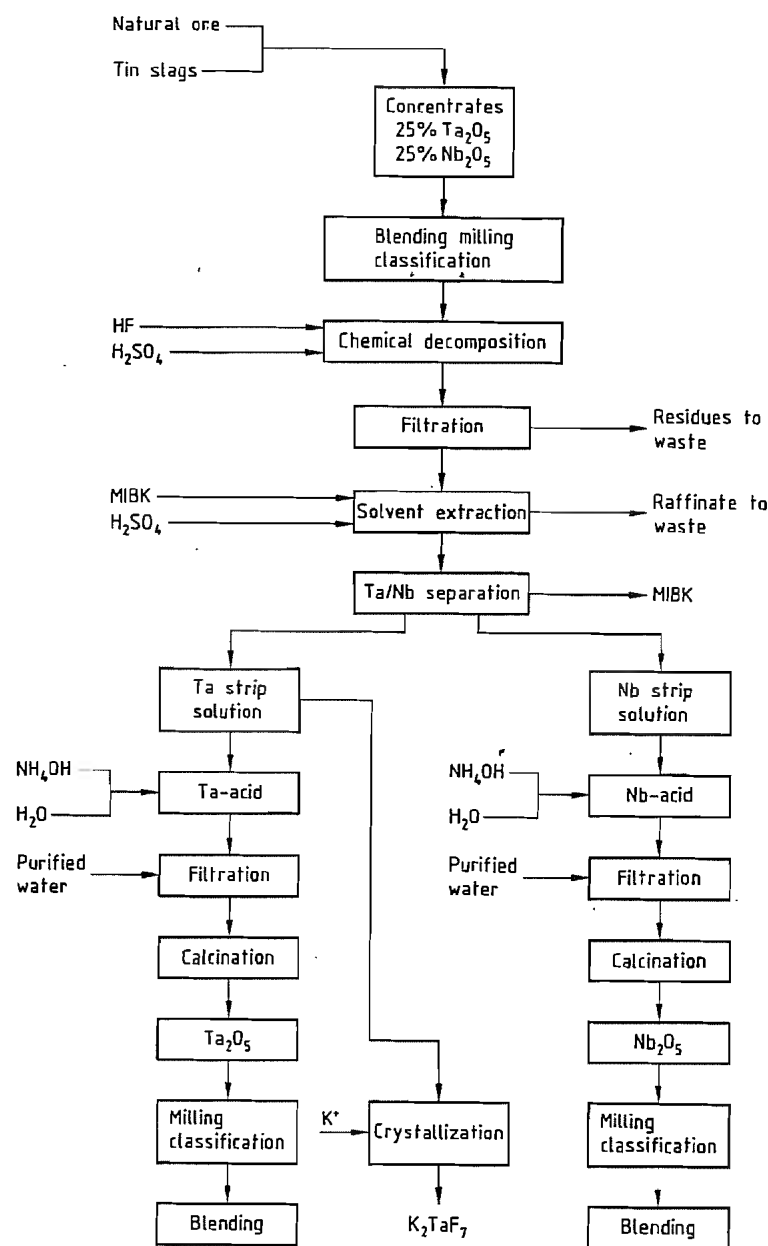


Figure 28.1: Flow diagram for the processing of tantalum–niobium raw materials [20].

The chlorination of ferroalloys produces very pure niobium pentachloride and tantalum pentachloride in tonnage quantities. The NbCl_5 contains less than 30 µg/g Ta, and other metallic impurities only amount to 1–2 µg/g.

Niobium pentachloride is an intermediate in the production of oxides and organometallic compounds, and is the starting material for production of niobium powder and for chemical vapor deposition of niobium coatings.

Table 28.6: Commercially available niobium oxides [20].

Specification	Technically pure grade	Chemically pure grade	Ceramic grade	Grade HPO (high purity optical)	Grade UP (ultra pure)
Composition Nb ₂ O ₅	min. 99%	min. 99.7%	min. 99.8%	min. 99.95%	min. 99.997%
Ta	max. 1600 ppm	max. 800 ppm	max. 500 ppm	max. 100 ppm	max. 8 ppm
Al				max. 2 ppm	max. 0.5 ppm
B					max. 0.2 ppm
Bi					max. 0.5 ppm
Ca	max. 700 ppm	max. 200 ppm		max. 10 ppm	max. 1 ppm
Cl					max. 10 ppm
Co				max. 2 ppm	max. 0.2 ppm
Cr				max. 2 ppm	max. 0.2 ppm
Cu				max. 2 ppm	max. 0.2 ppm
F					max. 1 ppm
Fe	max. 1000 ppm	max. 200 ppm	max. 100 ppm	max. 10 ppm	max. 1 ppm
K					max. 1 ppm
Mg					max. 0.5 ppm
Mn				max. 2 ppm	max. 0.2 ppm
Mo					max. 2 ppm
Na	max. 400 ppm	max. 200 ppm			max. 1 ppm
Ni			max. 100 ppm	max. 2 ppm	max. 0.2 ppm
Pb					max. 0.5 ppm
Rare earths					max. 1 ppm
S			max. 30 ppm		max. 1 ppm
Si	max. 1000 ppm	max. 250 ppm	max. 50 ppm	max. 50 ppm	max. 1 ppm
Sn					max. 0.5 ppm
Ti	max. 300 ppm	max. 100 ppm	max. 100 ppm		max. 1 ppm
V				max. 2 ppm	max. 0.5 ppm
W			max. 50 ppm		max. 1 ppm
Zr			max. 50 ppm		max. 1 ppm
Alkali			max. 200 ppm		
Loss on ignition	max. 1%	max. 0.5%	max. 0.4%	max. 0.2%	max. 0.005%
Average particle size (FSSS)	1–10 μm	0.5–10 μm	0.7–0.8 μm	max. 5 μm	1–3 μm
Tap density			0.8–1 g/cm ³		0.8–1.25 g/cm ³
Apparent density (Scott)			0.5–0.7 g/cm ³		
Microtac analysis			90% < 1.2 μm 50% 0.7–0.8 μm 10% < 0.5 μm		
Grain size				1. < 600 μm HPO 600 2. < 400 μm HPO 400 3. < 150 μm HPO 150	< 255 μm
Crystal structure			orthorhombic (T-phase)	monoclinic (H-phase)	monoclinic (H-phase) + orthorhombic (T-phase)

28.6 Compounds

28.6.1 Oxides

Niobium pentoxide, niobic acid, Nb₂O₅, *mp* 265 °C, *bp* 1495 °C, is a colorless powder that can only be dissolved by fusion with acidic or alkaline fluxes such as NaOH or KHSO₄, or in hydrofluoric acid. It is prepared by hydrolyz-

ing solutions of alkali-metal niobates, niobium alkoxides (e.g., Nb(OC₂H₅)₅), or niobium pentachloride, or by precipitation from hydrofluoric acid solutions with alkali-metal hydroxides or ammonia. Depending on the method used, the oxide hydrate formed is either a gel that is difficult to filter or is flocculent. The oxide hydrate is filtered, washed, and calcined at 800–1100 °C. The temperature and treatment time

determine which of the various crystalline modifications is formed. Nearly all the phase changes are irreversible [23–25].

Uses. Niobium pentoxide is used in metallurgy, for the production of hard materials, in optics, and in electronics. Hydrated Nb₂O₅, which can be regarded as an isopolyacid, has a high surface acidity, and catalyzes the polymerization of alkenes, e.g., propylene [26].

Various applications require different qualities of Nb₂O₅. For the electrothermic and metallothermic manufacture of niobium metal or its alloys, technical quality niobium pentoxide (> 98–99%) is suitable. For higher quality requirements, chemically pure niobium pentoxide (> 99.7%) is used.

In optics, niobium pentoxide is used as an additive to molten glass to prevent devitrification and to control properties such as refractive index and light absorption [27]. Optical-grade niobium pentoxide, with a purity of > 99.9%, must be free from colored impurities such as chromium, nickel, iron, manganese, etc.

Extremely stringent purity requirements apply to Nb₂O₅ used in the manufacture of LiNbO₃ or KNbO₃ single crystals (Nb₂O₅ ultra pure grade, > 99.995%). These compounds are used for electroacoustic and electrooptical components such as modulators, frequency doublers, and wave filters [28, 29].

Ceramic-grade niobium pentoxide, used for making dielectric materials, must be manufactured with a special particle size distribution. This market sector will demand greatly increased quantities of niobium pentoxide if the development of the new class of ferroelectric perovskites (relaxers) is successful, e.g., Pb(Mg_{1/3}Nb_{2/3})O₃ for the manufacture of ceramic capacitors [30–32].

Details of the various commercial qualities of niobium pentoxide are given in Table 28.6 [20].

28.6.2 Halides

Niobium pentachloride, NbCl₅, *M_r* 270.2, *mp* 209.5 °C, *bp* 249 °C, is now produced ex-

clusively by chlorination of ferri niobium, niobium metal, or niobium scrap (see Section 28.5.2.2.).

Niobium pentachloride forms strongly hygroscopic yellow crystals that react with water to form NbOCl₃ or Nb₂O₅·xH₂O. The pentachloride is very soluble in dry ethanol, tetrahydrofuran, and benzene. Alcoholic solutions of niobium pentachloride are used in the production of niobium alkoxides such as the pentaethoxide, Nb(OC₂H₅)₅, from which micronized niobium pentoxide is produced [33]. Pure niobium pentachloride is used for large scale production of niobium pentoxide and niobium metal.

Niobium tetrachloride, NbCl₄, sublims between 350 and 400 °C. Niobium trichloride, NbCl₃, disproportionates between 900 and 1000 °C. Niobium trichloride and niobium dichloride, NbCl₂, are formed by reduction of NbCl₅ with hydrogen, but are of no industrial importance.

Niobium oxychloride, NbOCl₃, *M_r* 215.28, is a colorless, crystalline compound that sublims at 400 °C and partly decomposes into niobium pentoxide and niobium pentachloride on further heating.

Niobium pentafluoride NbF₅, *M_r* 187.91, *mp* 72 °C, *bp* 236 °C, can be prepared by fluorination of niobium pentachloride or niobium metal with fluorine or anhydrous HF. The reaction of Nb₂O₅ with aqueous HF yields fluoroniobic acids of various compositions (e.g., H₂NbF₇ or H₂NbOF₃), depending on the acid concentration. They are soluble in organic solvents and consequently play an important part in the separation of tantalum from niobium by solvent extraction.

28.6.3 Carbides and Hard Materials

The carbides, borides, silicides, and nitrides of niobium are metallic hard materials [34]. Some of their physical properties are listed in Table 28.7. Only the carbides are commercially important.

Table 28.7: Physical properties of borides, carbides, nitrides, and silicides of niobium [34].

	Nb ₃ B ₂	NbB	Nb ₃ B ₄	NbB ₂	Nb ₂ C	NbC	Nb ₂ N	NbN	Nb ₃ Si	Nb ₃ Si ₃	NbSi ₂
Crystal structure	hexagonal, U ₃ Si ₂ type	orthorhombic, CrB type	orthorhombic, Ta ₃ B ₄ type	hexagonal, AlB ₂ type	hexagonal	face-centered cubic, NaCl type	hexagonal, W ₂ C type	face-centered cubic, NaCl type	hexagonal, ZrSi ₂ type	α-tetragonal, β-tetragonal	hexagonal, CrSi ₂ type
Density, g/cm ³	8.0			6.6	7.83	7.78	8.33	8.2	7.74	6.26	5.45
Hardness ^a	2060	2200	2290	2600	2123	2400	2123	8 ^b	550	600	700
<i>m.p.</i> , °C	1860 (decomp.)	2280	2700 (decomp.)	3000	3100 (decomp.)	3600			1950	2480	1950
Electrical resistivity, μΩ·cm		64.5		12/34		35		60	10	40	50.4
Superconductivity transition temperature, K		8.25	1.27	1.27	9.18	6		9.5	15.2	1.27	1.2

^a Vickers hardness at 0.5 N loading.
^b Mohs hardness.

Niobium Carbides. The niobium-carbon phase diagram [35] indicates the existence of a face-centered cubic compound, NbC, which melts without decomposition at 3600 °C with a broad region of homogeneity, and of Nb₂C, which has a peritectic melting point. Only NbC has practical applications. In addition to its original use as a grain growth inhibitor in tungsten carbide cobalt hard materials, it is now used mainly as solid solutions with titanium carbide, tantalum carbide, and tungsten carbide for cutting tools. The precise effect of niobium on the composition, microstructure, and properties of these hard materials is not yet fully understood [36]. In practice, up to 50% of the more expensive TaC can be replaced by NbC without appreciably affecting the hardness or fracture strength [37].

Production, like that of TaC, is by carburizing the oxide, hydride, or metal at 1500 °C in a carbon tube furnace, vacuum furnace, or in the presence of a molten metallic menstruum such as iron or aluminum. Some of the physical properties of niobium carbides are given in Table 28.7.

Niobium Borides. The niobium-boron phase diagram [38] shows the existence of Nb₃B₂, NbB, Nb₃B₄, and NbB₂. However, these high-melting, very hard materials, have no industrial uses. Table 28.7 lists their physical properties.

Niobium silicides, Nb₄Si, Nb₅Si₃, and NbSi₂, are produced by the silicothermic reduction of Nb₂O₅ or from the elements by sintering, pressure sintering, or fusion in an electric arc furnace. Some physical data are given in Table 28.7. These compounds are not used industrially.

Niobium Nitrides. Various nitride phases, with regions of homogeneity varying in distinctness, are obtained by heating niobium metal or mixtures of niobium oxide and carbon in a stream of ammonia or nitrogen [39]. Niobium metal can be produced by thermal decomposition of NbN in high vacuum. The pure nitrides have not as yet found any indus-

trial application. Table 28.7 lists some of the physical properties of niobium nitrides.

Niobium Hydrides. On heating niobium in a pure hydrogen atmosphere to 350–500 °C, hydrogen (ca. 44 atom%) is absorbed, causing expansion of the lattice and embrittlement. Apart from the NbH_{0.9} thus formed, the hydride Nb₄H₃ [40, 41] and the unstable dihydride NbH [42] are also known.

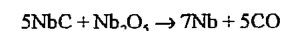
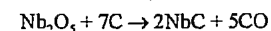
The reversible uptake and release of hydrogen by NbH is used in industry as a means of producing niobium powder from compact niobium, e.g., scrap or ingots. The metal is first hydrogenated, then ground, and finally dehydrogenated in a vacuum furnace or under an inert gas.

28.7 Niobium Metal

The industrial production of niobium is usually carried out by the reduction of the pentoxide or halides. The crude metal is then refined electrothermally.

28.7.1 Reduction of Niobium Pentoxide

Niobium pentoxide is reacted with carbon, aluminum, or silicon at high temperature. In the carbothermic process, niobium pentoxide is mixed with carbon black, and the mixture is pelletized and reduced in a vacuum furnace in a two-stage process at 1950 °C:

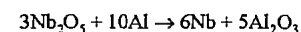


The reaction takes place with the formation of NbC, Nb₂C, NbO₂ and NbO [43, 44]. A crude product containing oxygen and carbon is produced, which must be refined in further high-temperature processes.

The following one-stage carbonitrothermic reduction of niobium pentoxide has been successfully carried out on the pilot-plant scale. A pelletized mixture of niobium pentoxide and carbon black is reacted in a stream of ammonia in an induction furnace at 1570 ± 20 °C to form niobium nitride, NbN, which is then thermally decomposed in high vacuum at

2000–2100 °C. However, the process does not yet appear to have been used on an industrial scale [45, 46].

Over 90% of niobium metal is produced by aluminothermic reduction:



Niobium metal produced by this process is designated ATR niobium. In general, an excess of aluminum is used, producing a niobium-aluminum alloy which is melted in a vacuum, electric arc, or electron beam furnace to produce low-oxygen, carbon-free niobium [47, 48]. The amount of excess aluminum determines the yield of niobium and its oxygen content [49].

The silicothermic reduction of niobium pentoxide can lead to silicide formation, and the thermodynamics of this reaction are less favorable. This process is therefore not in regular use.

28.7.2 Reduction of Halides

The reduction of niobium pentachloride can be achieved with hydrogen at 600–650 °C [50]. Alternatively, niobium pentachloride vapor is reduced with hydrogen in a fluidized bed furnace at 750–1050 °C [51] or in a hydrogen plasma above 2000 °C [52]. Metallothermic reduction with sodium or magnesium has also been reported [53]. The company TOHO Titanium Corporation has commissioned a plant with a capacity of 30 t/a niobium in which niobium pentachloride is reduced by magnesium [54]. A reduction process with zinc using the auxiliary metal bath technique is also known [55]. In contrast to the production of tantalum, the reduction of the fluoroniobates K₂NbF₇ and K₂NbOF₅ has not become industrially significant.

Very pure niobium can be obtained by electrowinning from oxygen-free molten salt systems with double fluorides or chlorides as the source of metal [56]. These molten salts are very corrosive and the current efficiencies are low. For these reasons, molten salt electrowinning of metallic niobium is not carried out commercially.

28.7.3 Refining

Crude niobium must be refined in order to remove impurities introduced either from the raw materials or during the treatment stages.

Purification can be achieved by high-temperature treatment because the melting point of niobium (2497 °C) is so high that most other elements can be removed by vaporization. Niobium is extremely reactive towards all but the inert gases [57], and melting must therefore always be carried out in a high or ultra-high vacuum or under a pure inert gas to minimize the concentration of harmful interstitial foreign atoms.

In comparison to the classical sintering and electric arc melting processes, electron beam melting (EBM) has considerable technical advantages for the production of pure metal.

The vaporization of the impurities can be controlled in each melting cycle [58, 59]:

- by optimizing the melting rate,
- by maintaining the bath in a liquid state for a long period, and
- by controlled superheating of the molten metal.

Sufficient refinement cannot be achieved with one melting cycle only, so that in practice the solid ingot produced must be remelted. The melting rate (kg/h Nb) for the first melt (main refining step) depends on the raw material and is lower for ATR niobium because of the high content of aluminum and NbO that must be evaporated compared with compacted granular niobium. Further development of the plasma melting technique would enable a simple plasma furnace to be used for the first melting operation [60, 61]. In the second and third melting cycles, the melting rate can be increased by a factor of 3–4, depending on the specification of the material.

Optimization of the equipment used in the electron beam melting process, leading to reduction in residual gas pressure and leakage rate, has enabled standard quality niobium to be produced from ATR niobium on a large scale with only two melting cycles [62].

The electron beam melting and remelting technique enables niobium metal with less than 50 µg/g interstitial impurities to be produced for high-frequency superconductors. Figure 28.2 shows the concentration of interstitial impurities (O, N, and C) as a function of the number of melting cycles [63].

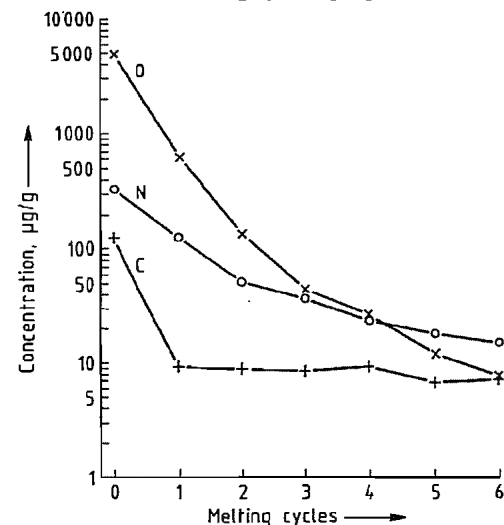


Figure 28.2: Contents of interstitial impurities (O, N, and C) of an electron beam melted niobium ingot as a function of the number of melting cycles [63].

Ultra-high-purity niobium can be obtained from metal melted by the EBM method by a series of additional sophisticated process steps, including electrorefining and electron beam zone melting, followed by high-temperature treatment in high vacuum. By these methods, niobium metal can be prepared with metallic impurities in the parts per billion range and with interstitial impurities < 1 ppm [64].

28.7.4 Uses

Niobium has good resistance towards corrosive chemicals [4, 65] even at high temperatures, and is therefore used in the construction of chemical equipment, though it is not quite so resistant as tantalum. The process of oxide dispersion hardening of niobium with titanium dioxide gives a material which can be used both for chemical equipment and for medical

implants subjected to high mechanical loading [66]. High-niobium alloys such as KBI 40/41 [67] can also be used under these conditions, for which formerly the more expensive metal tantalum had to be used.

Because niobium has a low neutron capture cross section and is unusually resistant towards corrosion by liquid sodium, it is used in the pure state or as the alloy NbZr1 in the nuclear industry for the production of fuel element cans. This alloy is also used for the sealing caps of sodium vapor lamps.

World consumption of niobium for the production of superconducting materials, such as Nb₃Sn and NbTi is estimated to be 60–70 t/a.

The addition of niobium to titanium–aluminum alloys imparts the ductility needed to fabricate this material for the aircraft and space industry [68].

Other newly developed alloys C 103 (NbHf10Ti1) and Nb 752 (NbW10Zr25) combined with a special coating technique enable niobium to be used in the manufacture of nozzles and combustion chambers for rocket propulsion [69].

28.8 Analysis

Extensive literature on the analytical determination of niobium is available in handbooks and monographs [70–73].

The determination of niobium in raw materials is carried out by X-ray fluorescence [72, 74, 75]. For this purpose, test pieces in tablet form are produced by reacting the niobium-containing material with borate to produce a melt, or by compressing it with binders such as wax or boric acid.

For ferroniobium, X-ray fluorescence analysis of HF solutions [76] or borate tablets is used. For umpire assay, it is usual to separate the niobium from the other material using ion-exchange resins with HF solutions, followed by gravimetric determination [77]. Small niobium contents in steels are determined photometrically [78].

Metallic impurities in niobium pentoxide or niobium metal are determined by atomic ab-

sorption spectrometry (AAS) or atomic emission spectrometry (ICP-OES, DCP-OES) in HF solution [79]. Emission spectrum analysis in a d.c. current plasma arc is also used. The nonmetals oxygen, nitrogen, hydrogen, carbon, and sulfur are determined by extraction at high temperature either with a carrier gas or under vacuum, or by combustion analysis in a stream of oxygen [80]. The hydride-forming elements arsenic, antimony, bismuth, selenium, and tellurium can be converted to their hydrides and detected with high sensitivity by the AAS method. The anions Cl[−] and F[−] are separated by distillation and determined photometrically, by ion-selective electrodes, or by ion chromatography.

In all the above-mentioned methods, the usual limits of detection are from the low µg/g region down to the ng/g region in routine quality testing. For the analysis of ng/g trace impurities it is necessary to separate and concentrate the material [81, 82]. The final determination is carried out using AAS with a graphite furnace, ICP-OES, DCP-OES, or voltammetry. Recently, ICP mass spectrometry has become a powerful additional method for many metallic impurities. Niobium metal is analyzed simply and quickly for metallic and nonmetallic impurities down to the lower ng/g region by glow discharge mass spectrometry (GDMS) [83]. The additional techniques of neutron activation analysis [84, 85] or proton activation analysis [86] are used for verification.

28.9 Economic Aspects

The world consumption of niobium has, since 1980, reached 16–20 × 10⁶ kg Nb₂O₅. The annual rate of increase is ca. 2%. More than 90% of total niobium production goes to the steel industry in the form of ferroniobium or niobium alloys, and therefore the demand for niobium is determined by the world market for iron and steel [87]. Figure 28.3 shows the clear relationship between steel production and niobium demand. Between 1984 and 1988, technical quality niobium pentoxide

was marketed in the price range \$14.3–15.2/kg. The price of standard grade ferroniobium is currently \$14.5/kg Nb. In mid 1987, the price of niobium concentrate ($> 65\%$ $\text{Nb}_2\text{O}_5 + \text{Ta}_2\text{O}_5$, 10:1) was \$5.5–6.4/kg Nb_2O_5 CIF Europe. Canadian pyrochlore concentrate was quoted at \$5.9/kg Nb_2O_5 FOB.

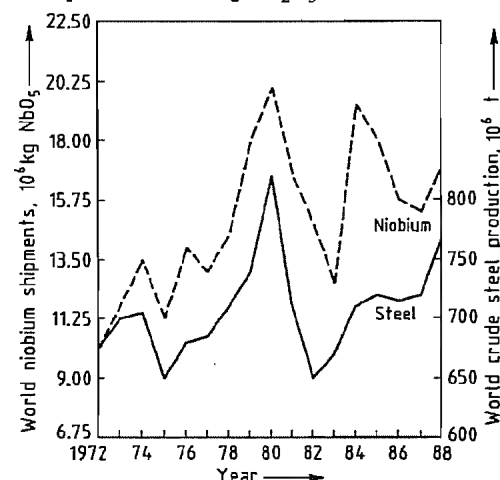


Figure 28.3: World niobium consumption compared to world crude steel production from 1972–1988 [87].

28.10 References

- R. Kieffer, H. Braun: *Vanadin-Niob-Tantal*, Springer Verlag, Berlin–Göttingen–Heidelberg 1963.
- I. Barin, O. Knacke: *Thermochemical Properties of Inorganic Substances*, Springer Verlag und Verlag Stahleisen GmbH, Düsseldorf 1973.
- C. English: "The Physical, Mechanical and Irradiation Behavior of Niobium and Niobium-Base Alloys" in H. Stuart (ed.): *Niobium-Proceedings of the International Symposium*, The Metallurgical Society of AIME, New York 1984, pp. 239–324.
- R.W. Balliett, M. Coscia, F. J. Hunkeler, *J. Met.* **38** (1986) no. 9, 25–27.
- (J. Perrault, E. A. Manker: "Geology and Mineralogy of Niobium Deposits" in H. Stuart (ed.): *Niobium-Proceedings of the International Symposium*, New York 1984, pp. 3–77.
- Tantalum–Niobium International Study Centre Brussels: *Int. J. Refract. Hard Met.* **7** (1988) no. 1, 3–7.
- Roskill: *The Economics of Niobium*, 5th ed., Roskill Information Services, London 1986, p. 1.
- Bureau of Mines, *Miner. Yearbook, Columbium and Tantalum*, 1987, p. 8.
- Roskill: *The Economics of Niobium*, 5th ed., Roskill Information Services, London 1986, p. 3.
- O. de Souza Paraiso, R. de Fuccio, *Min. Mag.* **146** (1982) no. 2, 134–147.
- G. Gabra: *CM Bull.* **78** (1985) no. 873, 80–85.
- Ullmann, 4th ed., 17, 305, 306.
- H. C. Starck, DE 2733193, 1977 (B. Krismer, H. Pungs).
- W. Rockenbauer: "Production of Niobium-Metal and Compounds from Tantalite, Columbite Natural Ores and Synthetic Tantalum–Niobium Concentrates" in H. Stuart (ed.): *Niobium-Proceedings of the International Symposium*, New York 1984, pp. 133–152.
- K. B. Higbie, J. R. Werning: Bureau of Mines, Report of Investigations 5239 (1956).
- Gesellschaft für Elektrometallurgie, H. C. Starck, DE-AS 1018036, 1957 (F. Brenthel, H. Rothmann, W. Keil).
- Fansteel Metallurgical Corp., US 3117833, 1958 (J. A. Pierret).
- T. H. Tunley, M. Fieberg: National Institute for Metallurgy South Africa, Report 1154 (1976).
- Gesellschaft für Elektrometallurgie, DE 3241832, 1984 (G. Bauer, J. Eckert).
- Hermann C. Starck Berlin GmbH & Co. KG, Product Information, *Tantalum and Niobium Compounds*, 1986.
- H. C. Starck, US 3407031, 1970 (H. Fürer, W. Rockenbauer).
- W. Rockenbauer: *Metall (Berlin)* **38** (1984) no. 2, 156–159.
- H. Schäfer, R. Gruehn, F. Schulte, *Angew. Chem.* **78** (1966) 28–41.
- H. J. Goldschmidt, *J. Inst. Met.* **87** (1958–59) 235–239.
- H. Schäfer, A. Dürkop, M. Jori, *Z. Anorg. Allg. Chem.* **275** (1954) 289–296.
- K. Tanabe, *Mater. Chem. Phys.* **17** (1987) 217–225.
- T. Ichimura: "Niobium Oxide in Optical Glass Manufacture" in H. Stuart (ed.): *Niobium-Proceedings of the International Symposium*, New York 1984, pp. 603–614.
- A. Räuber: *Current Topics in Materials Science*, vol. 1, F. Kaldis, North Holland Publishing Company, Amsterdam 1978, pp. 481–601.
- T. Wearden, *New Electronics*, 20th Mar. 1984, 29–31.
- D. Hennings, *Keram. Z. Beilage* **41** (1989) 1–6.
- S. L. Swartz, T. R. Shrout, *Mater. Res. Bull.* **17** (1982) 1245–1250.
- TDK Electronics Co., Ltd.; US 4265668, 1981 (S. Fujiwara et al.).
- N. Salo, M. Nassju, *High Temp. Mater. Processes* **8** (1988) no. 1, 39–46.
- Ullmann, 4th ed., 12, 523.
- E. K. Storms: "Phase Carbides and Nitrides" in L. E. J. Roberts (ed.): *MTP International Review of Science*, vol. 10, Solid State Chemistry, Butterworths, London 1972.
- B. Aronsson, L. J. Aschan: "Niobium in Cemented Carbide" in H. Stuart (ed.): *Niobium-Proceedings of the International Symposium*, New York 1984, 637–652.
- R. Kieffer, F. Benesovsky: *Harstoffe*, Springer Verlag, Wien 1963, pp. 127–135.
- R. Kieffer, F. Benesovsky: *Harstoffe*, Springer Verlag, Wien 1963, p. 405.
- N. P. Lyakishev, N. A. Tulin, Yu. L. Pliner: *Niobium in Steels and Alloys*, Companhia Brasileira de Metalurgia e Mineracao-CBMM, Sao Paulo 1984, pp. 38–40.
- M. Hansen, K. Anderko: *Constitution of Binary Alloys*, 2nd ed., McGraw-Hill, New York 1958.
- R. P. Elliott: *Constitution of Binary Alloys*, 1st Suppl., McGraw-Hill, New York 1965.
- G. Brauer, H. Müller, *J. Inorg. Nucl. Chem.* **17** (1961) 102–107.
- J. Krüger: "Use of Vacuum Techniques in Extractive Metallurgy and Refining of Metals" in O. Winkler, R. Bakish (eds.): *Vacuum Metallurgy*, Elsevier, Amsterdam–London–New York 1971, pp. 145–173.
- N. P. Lyakishev, N. A. Tulin, Yu. L. Pliner: *Niobium in Steel and Alloys*, Companhia Brasileira de Metalurgia e Mineracao-CBMM, Sao Paulo 1984, pp. 87–101.
- N. Krishnamurthy, R. Venkataramani, S. P. Garg, *Int. J. Refract. Hard Met.* **4** (1984) no. 1, 41–45.
- C. K. Gupta, D. K. Bose, N. Krishnamurthy, *J. Less Common Met.* **139** (1988) 189–202.
- N. P. Lyakishev, N. A. Tulin, Yu. L. Pliner: *Niobium in Steel and Alloys*, Companhia Brasileira de Metalurgia e Mineracao-CBMM, Sao Paulo 1984, pp. 101–114.
- H. A. Wilhelm, F. A. Schmidt, T. G. Ellis, *J. Met.* **18** (1966) 1303–1308.
- G. R. Kamat, C. K. Gupta, *Metall. Trans.* **2** (1971) 2817–2823.
- Rio Algam Mines, GB 1054163, 1967.
- Du Pont de Nemours and Comp., GB 863310, 1957.
- R. M. Haire, E. Hade, D. M. Hiller, H. W. Jacobsen in R. M. Kibby (ed.): *The Design of Metal Producing Processes*, AIME, New York 1969, pp. 300–308.
- T. T. Campell, F. E. Block, G. B. Robidart, J. L. Schaller, Bureau of Mines Report of Investigations 6080, 1962.
- T. Sugai, R. Watanabe: "Extraction of Niobium Metal by Chlorine Process", *Proceedings of International Symposium on Tantalum and Niobium*, Tantalum–Niobium International Study Center, Brussels, Belgium 1988, pp. 241–254.
- G. Jangg, R. Kieffer, P. Topic, *Monatsh. Chem.* **100** (1969) 379–384.
- W. Rockenbauer, *Chem. Ing.-Tech.* **41** (1969) no. 4, 159–162.
- K. K. Schulze, H. A. Jehn, G. Hörz, *J. Met.* **40** (1988) no. 10, 25–31.
- W. W. Albrecht, D. P. Ingals: *Raffinationsverfahren in der Metallurgie*, VCH Verlagsgesellschaft, Weinheim 1983, pp. 230–241.
- K. Schulze, O. Bach, D. Lupton, F. Schreiber: "Purification of Niobium" in H. Stuart (ed.): *Niobium-Proceedings of the International Symposium*, New York 1984, pp. 163–223.
- M. P. Schlienger, R. C. Eschenbach: "Recent Developments in Plasma Melting of Reactive and Refractory Metals" in R. Bakish (ed.): *Proceedings of the Conference Electron Beam Melting and Refining*, New York 1987, pp. 149–156.
- K. Mimura, M. Nanjo, *High Temp. Mater. Processes* **8** (1988) no. 1, 29–38.
- E. Drost, M. Hormann, *Metall (Berlin)* **41** (1987) no. 4, 382–385.
- M. Hörmann, *J. Less Common Met.* **139** (1988) 1–14.
- K. K. Schulze, *J. Met.* **33** (1981) no. 5, 33–41.
- D. Lupton, F. Aldinger, K. Schulze: "Niobium in Corrosive Environments" in H. Stuart (ed.): *Niobium-Proceedings of the International Symposium*, New York 1984, pp. 533–560.
- U. Gennari, E. Kny, T. Gartner: "Niobium–Titanium Oxide Alloy", *Proceedings of the International Plansee Seminar* **89**, vol. 3, 1989, pp. 587–614.
- Tantalum–Niobium International Study Center Brussels, Belgium: *TiC Bulletin* no. 46 (1986) 6–7.
- H. Inouye: "Niobium in High Temperature Applications" in H. Stuart (ed.): *Niobium-Proceedings of the International Symposium*, 1984, pp. 615–636.
- J. Lambert, "Aerospace brightens for Columbium, Tantalum + Columbium", Supplement to American Metal Market, New York 1988.
- R. Fresenius, G. Jander: *Handbuch der analytischen Chemie*, Part 3, "Quantitative Bestimmungs- und Trennungsmethoden", vol. 5b, "Elemente der 5. Gruppe. Vanadin, Niob, Tantal", Springer Verlag, Berlin 1957.
- O. G. Koch, C. A. Koch-Dedic: *Handbuch der Spurenanalyse*, Part 2, 2nd ed., Springer Verlag, 1974.
- R. W. Mosier: *Analytical Chemistry of Niobium and Tantalum*, Pergamon Press, New York 1964.
- I. M. Gibaldo: *Analytical Chemistry of Niobium and Tantalum*, Ann Arbor, 1970.
- A. Knight: *TiC Bulletin*, no. 45, Tantalum–Niobium International Study Center, Brussels, Belgium, 1964.
- A. M. E. Balaes, K. Dixon, G. J. Wall, *Appl. Spectrosc.* **41** (1987) no. 3, 509–512.
- Analyse der Metalle*, "First Supplementary Volume: I Schiedsanalyse, II Betriebsanalyse", Springer Verlag, Berlin 1980.
- Annual Book of ASTM Standards*, "Metal Test Methods and Analytical Procedures", vol. 03.05, "Chemical Analysis of Metals and Metal Bearing Ores", Faston 1987.
- Handbuch für das Eisenhüttenlaboratorium*, vol. 5, Verlag Stahleisen GmbH, Düsseldorf 1973.
- H. M. Ortner, P. Wilhertz in Tantalum–Niobium International Study Center, Brussels (ed.): *TiC Bulletin*, no. 49 (1987).
- D. Hirschfeld (ed.): "Gase in Metallen", *Vortrags-texte der Tagung Gase in Metallen*, Deutsche Gesellschaft für Metallkunde, Darmstadt 1984.
- R. Caletka, V. Krivan, *Fresenius Z. Anal. Chem.* **311** (1982) 177–182.
- H. N. Hecker, *Fresenius Z. Anal. Chem.* **293** (1978) 110–114.
- N. E. Sanderson et al., *Microchim. Acta (Wien)*, (1987) 275–290.
- R. Caletka, W. G. Faix, V. Krivan, *J. Radioanal. Chem.* **72** (1982) no. 1–2, 109–130.
- W. G. Faix, R. Caletka, V. Krivan, *Anal. Chem.* **53** (1981) 1594–1598.
- V. Krivan, *Anal. Chem.* **47** (1975) no. 3, 469–478.

87. H. Stuart, F. Heisterkamp: "The Niobium Market – A Perspective", *Proceedings of International Symposium on Tantalum and Niobium*, Tantalum-Nio-

bium International Study Center, Brussels, Belgium, 1988, pp. 71–89.

29 Tantalum

KLAUS ANDERSSON, KARLHEINZ REICHERT, RODIGER WOLF

29.1 Introduction	1417	29.6 Metallic Tantalum	1421
29.2 History	1417	29.6.1 Production	1421
29.3 Properties	1417	29.6.2 Semifinished Products	1421
29.4 Occurrence	1418	29.6.3 Tantalum Powder for Capacitors	1422
29.5 Extraction	1418	29.6.4 Other Uses	1422
29.5.1 Extraction and Processing of Ore Concentrates	1418	29.7 Compounds	1423
29.5.2 Obtaining Ta–Nb Concentrates from Tin Slags	1418	29.8 Analysis	1425
29.5.3 Processing Tantalum Scrap	1420	29.9 Economic Aspects	1426
		29.10 Toxicology	1426
		29.11 References	1427

29.1 Introduction

Tantalum has the electronic structure $1s^2 2s^2 p^6 3s^2 p^6 d^{10} 4s^2 p^6 d^{10} f^4 5s^2 p^6 d^3 6s^2$, which accounts for its principal oxidation states 2+ and 5+. There are two naturally occurring isotopes: ^{181}Ta and the weakly radioactive isotope ^{180}Ta (0.012%, half-life ca. 10^{13} years). A large number of artificial radioactive isotopes are also known.

29.2 History

Tantalum was discovered by EKEBERG in 1802 [1–2]. The discovery and history of tantalum and niobium are closely linked. The two elements usually occur together.

29.3 Properties

The physical properties of tantalum are as follows [1–7]:

Crystal structure	body-centered cubic
Lattice constant	$a = 0.33025 \text{ nm}$
Density	16.6 g/cm^3
Melting point	2996°C
Boiling point	5425°C
Heat of fusion	28.5 kJ/mol
Heat of vaporization at 3273 K	78.1 kJ/mol
Specific heat capacity at 20°C	$25.41 \text{ Jmol}^{-1}\text{K}^{-1}$
Linear coefficient of thermal expansion at 20°C	$6.5 \times 10^{-6} \text{ K}^{-1}$
Thermal conductivity at 20°C	$54.4 \text{ Wm}^{-1}\text{K}^{-1}$
Specific electrical conductivity	

at 20°C	$0.081 \Omega^{-1}\text{cm}^{-1}$
Superconductivity	4.3 K
Temperature coefficient ($0\text{--}100^\circ\text{C}$)	0.00383

The effect of temperature on electrical and thermal conductivity has been accurately determined [3].

The mechanical properties of the metal are strongly dependent on its purity, structure, and crystal defects, as is the case with almost all refractory metals. Even low concentrations of interstitial impurities increase the hardness and reduce the ductility. The yield strength is strongly temperature dependent, the value at 200°C being ca. 30% of that at 20°C [3]. The important mechanical properties are as follows [1, 3, 7, 8]:

<i>Tantalum, soft annealed</i>	
Tensile strength	240 MPa
Yield strength (0.2% offset)	210 MPa
Breaking elongation	40%
Vickers hardness	60–120 HV
Modulus of elasticity	177–186 MPa
Ductile–brittle transition temperature	4 K
Poisson's ratio	0.35
<i>Tantalum, cold formed</i>	
Tensile strength	400–1400 MPa
Yield strength (0.2% offset)	300–900 MPa
Breaking elongation	2–20%
Vickers hardness	105–200 HV
Recrystallization temperature	1200–1500 K

Like niobium, tantalum has principal oxidation states 2+ and 5+. Below 100°C , tantalum metal is extremely resistant to corrosion by most organic and inorganic acids, with the exception of hydrofluoric acid. This is due to a

dense adherent film of tantalum oxide, a characteristic which is utilized in the manufacture of electrolytic capacitors. Above ca. 300 °C, tantalum tends to form oxides, nitrides, hydrides, and carbides. All modern tantalum capacitor powders can be handled in air at temperatures up to ca. 100 °C. However, they are classified as flammable solids as they ignite at higher temperatures, forming Ta₂O₅.

Table 29.1: Tantalum deposits [11–15].

Location	Reserves, 10 ³ kg Ta ₂ O ₅	Production (1991, estimated), 10 ³ kg Ta ₂ O ₅	Annual production capacity (estimated), 10 ³ kg Ta ₂ O ₅
Australia	17 000	235	300
Brazil	18 000	100	245
Canada	3 000	80	130
Malaysia	2 000	80	130
Thailand	16 000	150	200
Africa	10 000	25	50
Russia	> 20 000	< 50	
China	17 000	100	200
Others	10 000	< 50	< 100

29.4 Occurrence

Tantalum is 54th in order of abundance of the elements in the Earth's crust (2.1 g/t). In many deposits, it occurs in association with the much more abundant niobium (24 g/t). The most important tantalum-containing minerals are tantalite, wodginite, microlite (the tantalum-rich end member of the pyrochlore series), and columbite [9]. The typical Ta₂O₅ concentration in processable pegmatitic deposits, which represent the principal raw material potential, particularly in Australia, is < ca. 0.1%. The uranium- and thorium-containing minerals yttriotantalite, strueverite, euxenite, and samarskite are sometimes highly radioactive, which limits their workability [10]. An important potential reserve lies in a belt stretching from China to Indonesia via Thailand and Malaysia, and consists of cassiterite (SnO₂) that contains some tantalum and niobium. During tin smelting, the tantalum and niobium become concentrated in the slag. The important deposits, with estimated current production capacities, are listed in Table 29.1, and the compositions of some tanta-

lum-containing minerals are given in Table 29.2.

29.5 Extraction

29.5.1 Extraction and Processing of Ore Concentrates

In the important Australian mines, the tantalum-containing minerals are present in finely divided form in hard pegmatitic rock. The rock is extracted by open-cast mining. Further processing, which is different from that used for the mainly niobium-containing deposits, is an initial size reduction to < 15 mm, followed by grinding in ball or rod mills to < 1 mm. Flotation is then carried out, and the soluble constituents are leached out from the concentrates. The latter are then dried, and the magnetic constituents are removed [18].

This ore concentrate, up to 40% Ta₂O₅, is dissolved in concentrated hydrofluoric acid, and is then separated from the niobium by extraction with methyl isobutyl ketone, so that the tantalum is obtained as H₂TaF₇. Potassium salts are added, and potassium heptafluorotantalate, K₂TaF₇, crystallizes out. This is reduced with sodium to metallic tantalum.

Major tantalum processing routes are summarized in Figure 29.1.

29.5.2 Obtaining Ta–Nb Concentrates from Tin Slags

Tantalum-containing tin slags represent an important source of tantalum; e.g., in 1980, ca. 50% of world demand was recovered from tin slags [19–21]. Owing to the low price of tin, its production is in continuous decline, so that the availability of tantalum-containing tin slags is decreasing. Moreover, the tantalum concentration in tin concentrates is also decreasing significantly. The fraction of the world demand for tantalum represented by Ta₂O₅ in tin slags is expected to fluctuate around 20%. The price of tin is not likely to reach a level at which more tantalum-rich tin

ores from Thailand and Malaysia can be processed economically.

The tantalum content of these slags fluctuates widely. Bolivian slags do not contain tantalum, but those from Thailand can have tantalum content 15–16% Ta₂O₅. The Ta:Nb ratio varies from 1:0.4 (Thailand) to 1:3 (Nigeria).

The most important grades of slag have the following tantalum and niobium content [19–21]:

	Ta ₂ O ₅ , %	Nb ₂ O ₅ , %
<i>High-grade</i>		
Thailand	13–16	9–10
Zaire	11	10
Australia	10	5–6
<i>Medium-grade</i>		
Thailand	4–6	4
Malaysia	3–4	3–4
Nigeria	4–5	12
South Africa	6–8	8–9
<i>Low-grade</i>		
Malaysia	0.8–2.5	0.8±2.5
Thailand	0.5–1	0.2–0.8
Brazil	1–2.5	1–2.5
Singapore	1–1.5	1–1.5

Table 29.2: Composition of important tantalum-containing minerals [9, 16, 17].

Mineral	Composition	Ta ₂ O ₅ content, %	Nb ₂ O ₅ content, %
Tantalite	(Fe, Mn)Ta ₂ O ₆	42–84	2–40
Microlite	(Na, Ca)(Ta, Nb) ₂ O ₆ F	60–70	5–10
Columbite	(Fe, Mn)(Nb, Ta) ₂ O ₆	1–40	40–75
Wodginite	(Ta, Nb, Sn, Mn, Fe) ₁₆ O ₃₂	45–56	3–15
Yttriotantalite	(Y, U, Ca)(Ta, Fe ³⁺) ₂ O ₆	14–27	41–56
Fergusonite	(RE ³⁺)(Ba, Ta)O ₄ ^a	4–43	14–46
Strueverite	(Ti, Ta, Nb, Fe) ₂ O ₃	7–13	9–14
Tapiolite	(Fe, Mn)(Nb, Ta) ₂ O ₆	40–85	8–15
Euxenite	(Y, Ca, Ce, U, Th)(Nb, Ta, Ti) ₂ O ₆	1–6	22–30
Samarskite	(Fe, Ca, U, Y, Ce) ₂ (Nb, Ta) ₂ O ₆	15–30	40–55

^aRE = rare earth element.

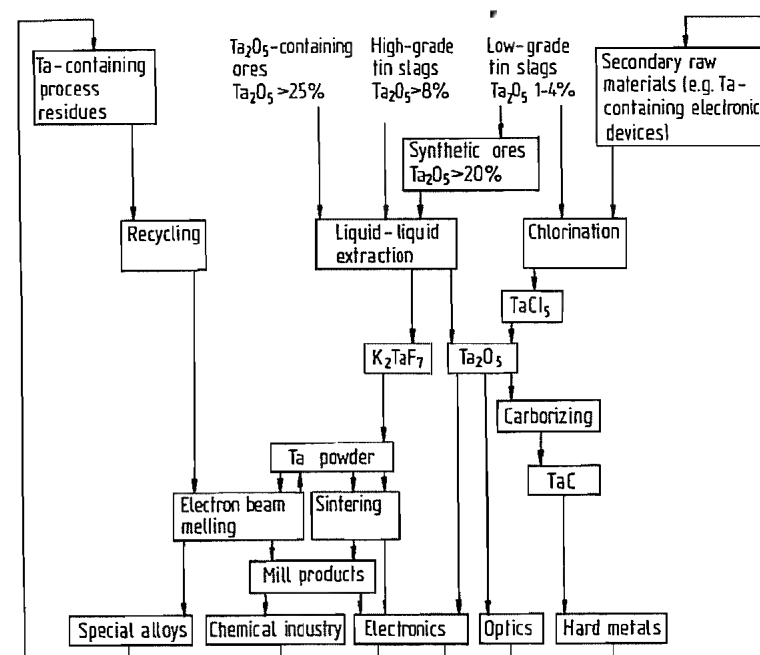


Figure 29.1: Major tantalum processing routes.

High-concentration slags are used directly in the wet chemical process (dissolution of the slag in hydrofluoric/sulfuric acid, followed by extraction and separation of tantalum and niobium).

From low-concentration slags, Ta/Nb concentrates containing 50–60% $\text{Ta}_2\text{O}_5/\text{Nb}_2\text{O}_5$ can be produced, e.g., pyrometallurgically. The Ta/Nb content of these synthetic concentrates is > 99% soluble in hydrofluoric acid, as is the case with natural ores.

In all the concentration processes so far developed, the slag is first melted in an electric furnace with addition of reducing agents, e.g., coke, and fluxing materials. This causes the Ta/Nb to collect in the carbide-containing ferroalloy produced, while some impurities remain in the slag. The solid ferroalloy is produced in relatively large blocks, which must be broken up and ground. The tantalum/niobium content is increased in further process steps, giving a concentrate containing 50–60% oxides of tantalum and niobium.

One method of enriching the tantalum and niobium consists of oxidizing the ferroalloy, which contains the Ta/Nb carbide, with Fe_2O_3 (e.g., as hematite). This causes undesired elements to be collected in the oxidic slag, while the Ta–Nb carbide is oxidized only as far as the metals and therefore remains in the metallic phase. In a final reaction stage, this is again oxidized with Fe_2O_3 to form a slag that contains tantalum and niobium oxides [22].

The partial oxidation can also be carried out in a single smelting stage using air, oxygen-enriched air, or pure oxygen. Under these conditions, the tantalum is converted to slag much more rapidly than the niobium, enabling the tantalum to be concentrated at the expense of niobium [23]. Ta/Nb carbide-containing ferroalloy can also be treated by wet leaching processes [24–26].

29.5.3 Processing Tantalum Scrap

When processing tantalum-containing waste materials, physical and chemical processes are used as much as possible, avoiding processes typically used in ore treatment, i.e.,

dissolution in hydrofluoric acid and solvent extraction. The tantalum scrap is divided into two categories which differ in difficulty of recycling:

- Scrap material of the first type can consist of pure unoxidized metallic tantalum, e.g., sintered tantalum powder pellets (anodes) from the manufacture of tantalum electrolytic capacitors, scrap foil, sheet, and wire, or of anodically oxidized sintered tantalum pellets containing 1.5–3% oxygen from capacitor manufacture and oxidized wire scrap arising from this process.

The following processing methods are commonly used for these scrap materials: ingot melting in an electron beam furnace, or conversion to brittle tantalum hydride, grinding, and dehydrogenation at > 600 °C in vacuo or under a protective gas to form metallic tantalum powder [1]. Alternatively, the ground tantalum hydride can be carburized with carbon black to form tantalum carbide [27].

The oxygen content of oxidized tantalum anodes can be reduced by deoxidation with magnesium or calcium to give high-grade scrap [28].

- Scrap of the second type consists of oxidized tantalum anodes coated with manganese dioxide or with conductive silver, or sometimes welded to nickel conductor wires. This category also includes faulty capacitors, in which the coated and welded tantalum anodes also have an encapsulation of synthetic resin or tinned brass.

Pure oxidized tantalum anodes can be recovered from coated anodes and brass-encapsulated capacitors by successive treatments with nitric and hydrochloric acid. Resin-encapsulated capacitors require complex treatment. These can be coarsely size-reduced in grinding mills, the tantalum being recovered by density separation. Foreign metals are removed by treatment with nitric and hydrochloric acid, leaving a residue of oxidized tantalum anodes in granular form [29].

Another method has been described for the

treatment of tantalum anode scrap containing manganese dioxide. This can be directly reduced in an argon/hydrogen plasma and melted to pure tantalum [30]. If the scrap capacitor materials are resin free, the tantalum can be recovered as its pentachloride by chlorination [31].

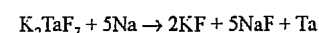
Some types of tantalum scrap which contain other impurities are roasted to form the oxide, and treated like ore concentrates. These include condensates formed during the melting of tantalum ingots, scrapped alloy materials; impure sawings and turnings, flue dust, and sediments from the wash liquors from the sodium reduction of potassium heptafluorotantalate.

Hard metals that contain tantalum carbide can be attacked by roasting and treating with caustic soda solution [32], anodic oxidation [33], or melting with sodium nitrate [34], converting the tantalum to its oxide for further recovery treatment.

29.6 Metallic Tantalum

29.6.1 Production

Metallic tantalum products (powder, semi-finished products, ingots) are produced almost exclusively by reduction of potassium heptafluorotantalate with sodium [35, 36]:



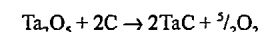
The strongly exothermic reaction is controlled by adding inert salts (KCl, NaCl, KF, NaF). The reduction can be carried out at constant temperature by controlled addition of one of the reactants, with controlled heat removal. Tantalum powder is recovered by leaching the salts out of the reaction product. Two processes are commonly used to obtain tantalum capacitor powder from this:

- The sodium-reduced metallic tantalum powder is purified and converted to a compactable and free-flowing product by further processing stages, e.g., high-temperature treatment in vacuo or under protective gas, deoxidation by magnesium [37], or a combination of these two processes [38]. Opti-

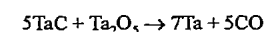
mum properties for capacitor production are obtained by the addition of dopants to control sintering of porous pellets [39–41].

- During ingot melting of compressed slugs of tantalum powder in electron beam or electric arc furnaces [42], volatile impurities are driven off, usually in two smelting operations. The ingot can be ground after hydrogenation. The powdered tantalum “hydride” is then dehydrogenated in vacuo [1] and agglomerated by high-temperature treatment.

In addition to the sodium reduction process, other processes have been described, i.e., the molten salt electrolysis of K_2TaF_7 with addition of Ta_2O_5 or TaCl_5 , and hydrogen reduction of TaCl_5 [1, 43], but these have not achieved economic importance. The carbo-thermic reduction of Ta_2O_5 in high vacuum [1, 4, 44] at ca. 1900 °C leads first to tantalum carbide:



This reacts above 2000 °C with residual Ta_2O_5 to metallic tantalum:



Because of the high quality standards for particle size and purity required by the producers of tantalum capacitors, this process is of minor importance.

29.6.2 Semifinished Products

Tantalum metal powder for producing semifinished products is also obtained by reducing K_2TaF_7 with sodium. Semifinished products such as sheet, wire, and shaped articles are produced by two different methods:

- Powders are compacted, and then sintered by passing an electric current at ca. 2500 °C (Coolidge process) or indirectly by resistance or induction heating in vacuo. Tantalum wire for tantalum electrolytic capacitor manufacture is produced by this process. It is advantageous to control the grain size, e.g., by adding dopants [45], to optimize the mechanical properties.
- Bars produced by powder compression are formed into ingots by electron beam or elec-

tric arc melting, and shaped by forging, rolling, extruding, and wire drawing. Intermediate heat treatment in vacuo is usually unnecessary as tantalum does not work harden. After 95% deformation, a tantalum product has typical hardness 180 HV, after an initial ingot hardness of 80–90 HV [46, 47].

As well as its use for electrolytic capacitors (wire, cans, foil), semifinished tantalum is also used in the chemical industry because of its excellent resistance to corrosion by hot, concentrated mineral acids, with the exception of hydrofluoric acid which strongly attacks tantalum. The passivation of the metal is a result of the dense, adherent oxide film, 1–4 nm thick, which forms spontaneously in air and in acidic media, and which is stable up to ca. 260 °C [48]. Welding of tantalum sheet is mainly carried out by the tungsten inert gas process, which allows complex heat exchangers and intricate heating equipment to be fabricated [49]. Impurity levels in commercial semifinished tantalum products are listed in Table 29.3.

Because of the high price of tantalum, large vessels and pipework are often merely clad with the metal. Plating of steel with tantalum can be carried out by the explosion method [50], or corrosion protection can be achieved by build-up welding of tantalum [51].

Table 29.3: Typical chemical composition of commercial tantalum semifinished products.

	Powder metal-lurgy grade	Electron beam melted grade
Ta	≥99.9%	≥99.98%
Impurity content, ppm		
O	250	100
C	75	30
N	75	30
H	15	10
Nb	10	20
W	10	20
Mo	5	10
Fe	75	10
Cr	15	3
Ni	20	2
Na	10	1
K	10	1

29.6.3 Tantalum Powder for Capacitors

Since the first report that tantalum could be used for electrolytic capacitors [52], the growth of this application has been such that it now accounts for the highest consumption of the metal [53]. The capacitor consists of an anode of tantalum metal powder compressed into a pellet, typically 20–200 mg. This anode is sintered to give electrical continuity and density of ca. 6–9 g/cm³. The electrical connection is provided by a tantalum wire, attached by sintering or welding. The whole of the pore surface of the sintered anode is coated with an amorphous dielectric layer of Ta₂O₅ by anodic oxidation, using an electrolyte of dilute H₃PO₄/H₂SO₄, sometimes with the addition of organic compounds [54, 55]. Ta₂O₅ has a resistivity of ca. 10¹⁵ Ωcm [56] and dielectric constant ε = 25. The anode is coated with a semiconducting layer of MnO₂ by impregnation with an aqueous solution of manganese nitrate, followed by pyrolysis. This solid electrolyte provides the cathodic contact. Research has been carried out into the effect of the pyrolysis temperature on the Ta₂O₅ layer [57] and its dielectric properties [58], and also into the effect of temperature on the capacity [59] and conductivity [60–62], and the effect of these on the leakage current of the capacitor [63]. Progressive improvements to powder quality [64] have doubled the specific capacitance of the tantalum metal powder (the product of capacitance and formation voltage per unit mass) [65]. Typical qualities and properties of capacitor grade tantalum powder are given in Table 29.4.

29.6.4 Other Uses

Tantalum is used in medicine because of its lack of toxicity and very good compatibility with tissue. Reports and discussions have been published on the suitability of inhaled tantalum powder as a contrast medium in X-ray diagnostics of the throat, trachea, larynx, bronchi, esophagus, and stomach [66–68], but the material has been rarely used, mainly for

cost reasons. Small tantalum spheres or tantalum wires are used in organs (e.g., the heart), in bone, or in implants as markers when controlling position and function by X rays [69–71].

Table 29.4: Typical properties of capacitor-grade tantalum powder.

Chemical impurities, ppm	Powder from electron beam melting		Powder from sodium reduction	
	QR 7 ^a	QR 3 ^a	VFI-18 KT ^b	STA-30 KD ^c
O	800	1500	1800	2200
C	10	10	35	40
N	20	40	50	70
H	15	15	50	50
Nb	<20	<20	<10	<10
W	<20	<20	<10	<10
Fe	<10	<10	25	25
Cr	<5	<5	10	10
Ni	<5	<5	20	20
Na	<1	<1	<2	<2
K	<1	<1	5	10
Specific charge, C/V/g (μF V/g)	3000	5000	15000	30000
Application working voltage, V	50–75	35–50	25–35	<25

^aH. C. Starck, Newton, United States.

^bH. C. Starck-V-tech, Tokyo.

^cH. C. Starck, Goslar, Germany.

Because of its stable oxide layer, tantalum in the body is completely bioinert. It has been shown in animal experiments that, if broken bones are held in position with tantalum rods, even in septic conditions with corrosive tissue reaction, healing is better than when chromium–nickel steel or niobium are used [72]. Tantalum implants in the jaw have shown good metal–bone contact over many years with no morbid reaction [73]. Tantalum has been largely replaced as a prosthetic implant material by titanium, as this has better strength properties and is sufficiently bioinert [74]. However, tantalum has an important use in clips for rapid occlusion of vessels in surgery, either temporary or permanent, [75–77]. In some cases, tantalum mesh and plate can be implanted in damaged areas of the skull [78–80].

The possible use of the very dense and ductile tantalum for the manufacture of heavy

missiles for armour penetration is under investigation [81].

29.7 Compounds

Oxides. Tantalum oxides in lower oxidation states are not industrially important. Tantalum(II) oxide, TaO, is the only lower oxide whose existence has been confirmed. It is produced from tantalum pentoxide by reduction with carbon at 1900 °C, or with hydrogen at 1100 °C. A possible use is for the production of heat-reflecting window glass [82].

No tantalum compound analogous to niobium(IV) oxide, NbO₂, is known. However, with tantalum pentoxide, the possibility exists of introducing interstitial tantalum atoms, so that TaO_x compounds can be obtained (x = 2–2.5). These oxides have metallic conductivity, but do not form discrete phases.

Tantalum pentoxide, Ta₂O₅ (*mp* 1880 °C, density 8.73 g/cm³), occurs in two thermodynamically stable modifications, α and β. The transition temperature from the orthorhombic β modification to the tetragonal α modification is ca. 1360 °C. The existence of an ε modification, produced hydrothermally from tantalum acid at 300–340 °C, is also known. This ε-Ta₂O₅ is isomorphous with β-Nb₂O₅, and is transformed to β-Ta₂O₅ by heating in air above 886 °C [83].

Two processes are used for the manufacture of tantalum pentoxide:

Wet Chemical Method. The raw materials (ores and/or tin slag concentrates) are dissolved in hydrofluoric acid at ca. 100 °C. Tantalum and niobium are extracted from this strongly acid aqueous solution, preferably with methyl isobutyl ketone. The impurities that are also extracted, SiF₆²⁻, FeF₆³⁻, AlF₆³⁻, SbF₆²⁻, etc., are washed out with sulfuric acid, and the tantalum and niobium are separated in a multistage operation. Ammonia gas or solution is added to the aqueous H₂TaF₇ solution, forming hydrated tantalum oxide, Ta₂O₅·nH₂O. This is washed, dried, and calcined above 800 °C to form the oxide [84].

Chloride Process. The ferroalloy produced by the pyrometallurgical method is chlorinated in an iron chloride-sodium chloride melt at 550–600 °C. The complex salt NaFeCl_4 present in the melt acts as a chlorine carrier. The iron loses a chlorine atom and is reduced from the trivalent to the divalent state, and the added chlorine gas causes the iron to be continuously reoxidized to Fe(III) . The $\text{TaCl}_5/\text{NbCl}_5$ mixture is separated by fractional distillation to obtain the chlorides of the two elements in a highly pure state. To obtain the oxide, the ground chlorides are hydrolyzed with steam in a fluidized bed, and then calcined.

In the optical industry, tantalum pentoxide is used in lanthanum borate glasses, characterized by their high refractive index and low optical scattering; since the 1980s, niobium pentoxide has been increasingly used for this application, as tantalum pentoxide is 3–5 times as expensive and has twice the density [85].

Tantalum pentoxide, and especially hydrated tantalum oxide $\text{Ta}_2\text{O}_5 \cdot n\text{H}_2\text{O}$, is used as an acid catalyst. In its amorphous form, its surface acidity can be as high as $H_0 \leq 8.2$ [86]. It therefore has good catalytic activity for alkylation, esterification, Beckmann rearrangement, aldol condensation, etc. [87–90].

Tantalates. Tantalates can be produced by calcination of oxide mixtures, or by dissolving tantalum pentoxide in molten alkali metal hydroxides or carbonates. Excess alkali metal hydroxides or carbonates leads to the formation of water-soluble tantalate isopolyanions $(\text{H}_x\text{Ta}_6\text{O}_{19})^{(8-x)-}$ where $x = 0, 1, \text{ or } 2$ [91].

The most industrially important tantalates are those of lithium and yttrium. Single crystals of lithium tantalate, LiTaO_3 , are pulled from the melt crucible by the Czochralski method [92]. The crystal growth rate for crystals 5–8 cm in diameter is ca. 2–3 mm/h. These ferroelectric single crystals in the unpoled state have domains that are statistically distributed in the crystal. They are poled on passing through the Curie temperature (665–618 °C) in an electric field and then have only

a single domain [93, 94]. Single-crystal wafers of LiTaO_3 are widely used as surface acoustic wave filters (SAW) for high-frequency applications in communication systems (intermediate-frequency filters in television and video equipment). Also, lithium tantalate is used in combination with lithium niobate in the manufacture of waveguides, frequency doublers (second harmonic generation), optical modulators, and optical switches.

Yttrium tantalate powder, YTaO_4 , produced in a solid state reaction, is applied as an emulsion to a film, and is used in diagnostic medicine as a phosphor for the amplification of X rays. It converts X rays to fluorescent light in very high yield, enabling the X-ray dose received by the patient to be significantly reduced [95].

Barium magnesium tantalate, $\text{Ba}_3\text{MgTa}_2\text{O}_9$, and barium zinc tantalate, $\text{Ba}_3\text{ZnTa}_2\text{O}_9$, are likely to play an increasingly important role in the future as the base material for microwave resonators for the stabilization of oscillators, or as frequency filters. These dielectric materials, which have the perovskite structure, have high dielectric constant and very low dielectric loss at high frequencies [96–99]. These high-quality resonators are especially necessary for the high carrier frequencies in satellite communication.

Halides. Tantalum pentafluoride, TaF_5 , (mp 96.8 °C, bp 229.5 °C) is produced by passing fluorine over metallic tantalum, or from tantalum chloride by adding anhydrous hydrogen fluoride [100–102]. Both tantalum pentafluoride and niobium pentafluoride are used in the petrochemical industry as isomerization and alkylation catalysts. The fluorides of both elements are also useful as fluorination catalysts for the manufacture of fluorochloro- and fluorinated hydrocarbons [103].

The oxyfluorides TaOF_3 and TaO_2F are also known, but have no industrial importance.

Potassium heptafluorotantalate (potassium tantalum fluoride), K_2TaF_7 , is an industrially important intermediate in the production of tantalum metal. It crystallizes in colorless, rhombic needles when K^+ ions (e.g., KCl or

KF) are added to solutions of tantalum in hydrofluoric acid (e.g., H_2TaF_7 solution) from the extraction process. If the acidity is not high enough, undesired oxyfluorides are formed in addition to K_2TaF_7 .

The solubility of potassium heptafluorotantalate in hydrofluoric acid solution decreases from 60 g/100 ml at the boiling point to < 0.5 g/100 ml at room temperature. As the corresponding stable niobium salt K_2NbOF_5 is significantly more soluble, tantalum can also be separated from niobium by fractional crystallization (Marignac process) [7].

Tantalum pentachloride, TaCl_5 , mp 216 °C, bp 242 °C, forms colorless, strongly hygroscopic, needle-shaped crystals. On an industrial scale, production of this chloride is exclusively by chlorination of metallic tantalum, ferrotantalum, or tantalum metal scrap. This process is mainly used in the production of high-purity oxides [104, 105].

Tantalum pentachloride is soluble in absolute alcohol, with formation of the corresponding alkoxide [106, 108]. Ultrafine tantalum oxide powder can be produced by hydrolysis of this alkoxide [108].

Tantalum pentachloride and tantalum alkoxides are suitable for use in the chemical vapor deposition of tantalum metal or tantalum oxide.

The other pentahalides, TaBr_5 and TaI_5 , are known, but are of no industrial importance.

Carbides. Tantalum carbide, TaC , is golden-brown, mp 3985 °C (one of the highest known). It is added as powder in the manufacture of hard metals. Tantalum carbide can be produced by the direct carburization of Ta metal by carbon, or preferably by reaction of Ta_2O_5 with carbon at ca. 1900 °C. In hard metal mixtures based on tungsten carbide, tantalum carbide is present at concentrations 0.5–10%. It improves the high-temperature fatigue strength and thermal shock resistance of the cutting tool.

Nitrides. Tantalum nitride, TaN , is a hard material, like tantalum carbide, with good wear resistance. It is produced by heating tantalum in a pure nitrogen atmosphere at ca. 1100 °C.

Tantalum nitride films are used as diffusion barriers in semiconductor technology [109, 110], and as protective coatings for moisture sensors [111]. Tantalum nitride is also sometimes found in small amounts (3–8%) in ceramics [base material Ti(C, N)].

Borides. The tantalum–boron phase diagram [112] shows the existence of Ta_2B , Ta_3B_2 , TaB , Ta_3B_4 and TaB_2 . These hard materials are of little industrial importance. The borides may be produced by heating tantalum and boron in vacuo at ca. 1800 °C, or by electrolyzing a melt of Ta_2O_5 , B_2O_3 , CaO , and CaF_2 .

Silicides. The silicides TaSi_2 and Ta_3Si_3 [113] are produced from the elements by heating in vacuo at 1000–1500 °C. Tantalum silicide targets were formerly used in the semiconductor industry for production of interconnections by sputtering [114], but tantalum silicides are no longer of any industrial importance.

29.8 Analysis

The analytical chemistry of tantalum is described in detail in several monographs [115–118]. Analysis for tantalum as a major or minor component or trace element in raw materials, ferroniobium–tantalum, scrap materials, and alloys must be distinguished from analysis for impurities in tantalum products. The classical method of analyzing for tantalum is by gravimetry after extraction as the fluoro complex on an ion-exchange resin [119]. Low concentrations, i.e., in the $\mu\text{g/g}$ region, are usually determined photometrically [118].

When tantalum is a major or minor component in ores, scrap, etc., it is usually determined by fusion with sodium or lithium borate, followed by X-ray fluorescence analysis ($\geq 0.01\%$ Ta) [120]. Analysis of solutions by emission spectrometry with plasma excitation (ICP-AES) is increasingly used. Tantalum in the ng/ml region can be determined by measurement at 296.5 nm.

Because of the high purity required for electronic components, optical glasses, and superalloys, sensitive multielement methods have been developed for the determination of

trace impurities in commercial products, e.g. potassium heptafluorotantalate, metallic tantalum, and tantalum oxide. The first methods were based on OES with vaporization in a carbon d.c. arc [121]. Additionally, many elements can be determined by plasma optical emission spectrometry (DCP-AES, ICP-AES) after dissolution by treatment with hydrofluoric or hydrofluoric/nitric acid under pressure [122]. Alkalis are determined by flame atomic absorption spectrometry, and arsenic, antimony, and other hydride formers by hydride techniques. Phosphorus, as a doping element in tantalum powders, can be very reliably determined photometrically [123]. Carbon and sulfur are determined by combustion analysis, and oxygen and nitrogen by hot extraction with a carrier gas.

As the optical spectrum of the tantalum matrix contains a very large number of lines, there are many possibilities for interference; trace element-matrix separation offers the possibility to overcome the problems [122, 124, 125]. For the final determination, ICP-AES, ICP-mass spectrometry, or neutron activation analysis are used. For trace determination in the sub-ppm region, glow discharge mass spectrometry is now the most sensitive routine method of determination [126].

29.9 Economic Aspects

Figure 29.2 shows how the price of tantalum has fluctuated over recent years. The most important tantalum processors have made long-term ore contracts with the large mining concerns [127]. World production of tantalum ores (Table 29.1) is well below capacity.

World demand for tantalum has changed little since 1970, remaining at ca. 1000 t/a. Forecasts based on increasing tantalum demand for electrolytic capacitors [128] have not been borne out, as developments in tantalum powders have meant that increasingly less tantalum powder is required for a given capacitor type [129]. However, the number of tantalum capacitors produced has grown continually, from ca. 2×10^9 in 1975 to ca. $9 \times$

10^9 in 1992 [53]. The most important area of use is for electrolytic capacitors, which account for > 50% of total world production of tantalum. The use of tantalum carbide as an additive in the hard metal industry, which was still important in 1980, has decreased in recent years [17] as TaC is being replaced by chromium and vanadium carbides for cost reasons. Figure 29.3 illustrates the shifting market shares of the various application areas over recent decades. Applications not included, e.g., Ta_2O_5 in optical applications and in X-ray phosphors, account for considerably less than 5% of the market.

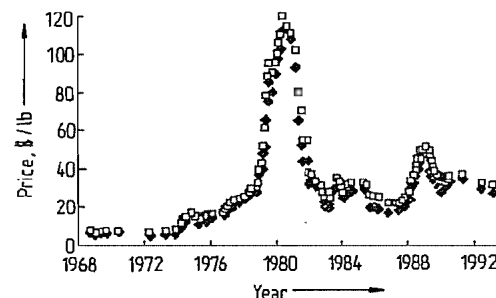


Figure 29.2: Tantalum ore prices. London Metal Bulletin 25/40% Ta_2O_5 , based on 30% Ta_2O_5 , cost, insurance, and freight.

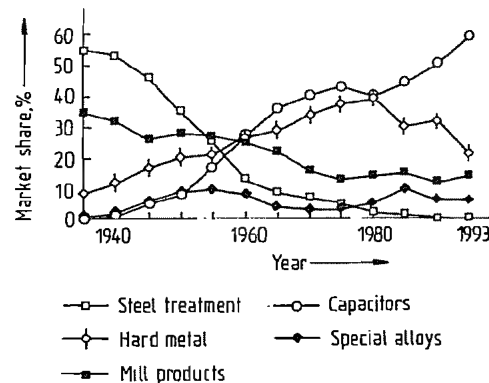


Figure 29.3: Market share of tantalum applications, 1935-1993.

29.10 Toxicology

Metallic tantalum is completely nontoxic and bioinert, and allergic reactions are unknown. This has enabled it to be used in X-ray

diagnostics and surgery (Section 29.6.4). Tantalum carbide is not known to have acute toxicity. Tantalum oxide is classified as nontoxic, although animal experiments indicate that the LD_{50} (rat, oral) is 8000 mg/kg (RTECS). For respirable dusts of metallic tantalum, the MAK value is 5 mg/m³. Tantalum chloride has a strongly corrosive and irritant effect, owing to the hydrolytic production of hydrogen chloride. The LD_{50} (rat, oral) is 1900 mg/kg (RTECS). MAK values have not yet been established for tantalum oxide, tantalum carbide, and tantalum chloride. Potassium heptafluorotantalate has toxic properties due to its fluoride content; LD_{50} (rat, oral) is 2500 mg/kg (RTECS), and MAK for dusts is 2.5 mg/m³ total dust (calculated as fluoride) [130].

29.11 References

1. R. Kieffer, H. Braun: *Vanadin-Niob-Tantal*, Springer Verlag, Berlin-Göttingen-Heidelberg 1963.
2. *Gmelin*, 50, part B1, pp. 1-4.
3. S. M. Cardonne, P. Kumar, C. A. Michaluk, H. D. Schwartz, *Adv. Mater. Processes* 1992, no. 9, 16-20.
4. R. Kieffer, G. Jangg, P. Ettmayer: *Sondermetalle*, Springer Verlag, Berlin-Heidelberg 1971.
5. O. Kubaschewski: *Atomic Energy Review, Tantalum: Physico-Chemical Properties of its Compounds and Alloys*, International Atomic Energy Agency, Vienna 1972.
6. W. Köck, P. Paschen, *J. Met.* (1989) no. 10, 33-39.
7. G. L. Miller: *Tantalum and Niobium*, Butterworths, London 1959, pp. 91-93.
8. E. Erben, R. Lesser, *Metall (Berlin)* 15 (1961) 679-686.
9. W. W. Albrecht: "Production, Properties and Application of Tantalum, Niobium and Their Compounds", in P. Möller, P. Cerný, F. Saupe (eds.): *Lanthanides, Tantalum and Niobium*, Springer Verlag, Berlin-Heidelberg 1989, pp. 345-358.
10. P. Borchers, G. J. Korinek: "Extractive Metallurgy of Tantalum", *AIIME Annu. Meet. 110th* 1981, 97-108.
11. TIC Tantalum-Niobium International Study Center Brussels, *Int. J. Refract. Hard Met.* 7 (1988) no. 1, 3-7.
12. L. D. Cunningham: *Mineral Industry Surveys, Columbium (Niobium) and Tantalum in 1993*, U.S. Bureau of Mines, Washington 1994.
13. R. Gaupp, G. Moteani, P. Möller, *Erzmetall* 36 (1983) 244-251.
14. H. C. Starck GmbH & Co. KG, Internal Raw Material Availability Survey, Goslar 1993.
15. TIC Tantalum-Niobium International Study Center Brussels, *TIC Bull.* 62-73 (1990-1993).
16. T. C. Pool (ed.): *Elements*, Concord Trading Corp., Denver 1992, pp. 12-17.
17. *The Economics of Tantalum*, 6th ed., Roskill Information Services, London 1986, p. 2.
18. C. Bird, *Met. Bull. Monthly* 1993, no. 5, 48-49.
19. W. Rockenbauer, *Metall (Berlin)* 35 (1981) 584-585.
20. W. Rockenbauer, *Metall (Berlin)* 38 (1984) 156-159.
21. J. Bonjer: "Proceedings of the Seminar on Production and Marketing of Associated Heaugh Minerals from South-East Asian Tin Deposit in Ipoh/Malaysia and Phuket/Thailand", in W. Gocht (ed): *Inter-technik* 26 (1985) 179-206.
22. Kawecki Berylko Ind., US 3721727, 1971 (R. A. Gustison).
23. Metallurgie Hoboken-Overpelt, DE 2844914, 1978 (M. C. F. van Hecke, J. Deweck).
24. Hoboken-lez-Anvers, US 2131350, 1937 (J. P. Lee-mans).
25. Kawecki Chemical Comp., US 3447894, 1966 (R. A. Gustison, W. Lawn, F. Gorcyca, J. A. Cenerazzo).
26. Kawecki Berylko Ind., US 3585024, 1968 (J. A. Cenerazzo, C. E. Mosheim, C. E. Marvasi).
27. R. Kieffer, F. Benesovsky: *Hartstoffe*, Springer Verlag, Wien 1963.
28. Western Electric Co., US 3697255, 1972 (W. M. Baldwin, E. O. Fuchs, D. J. Sharp, J. H. Swisher).
29. H. C. Starck, DE 2133104 C3, 1978 (H. Meyer).
30. K. Mimura, T. Takahashi, M. Nanjo, *J. Min. Mater. Proc. Inst. Jpn.* 106 (1990) no. 4, 187-192.
31. N. Sato, T. Takenaka, Y. Wei, M. Nanjo, *Tohoku Daigaku Senko Seiren Kenkyusho Iho* 46 (1990) no. 2, 96-104.
32. GTE Products Corp., US 4255397, 1981 (B. E. Martin, J. E. Ritsko, H. L. Acla).
33. G. P. Power, *Chem. Aust.* 46 (1979) no. 7, 303-307.
34. VEB Kombinat Metallaufbereitung, DD 207932, 1984 (G. Beyer, H. Bernhardt, H. Dam, H. K. Kiesling, W. Tomalik, A. Zimmermann).
35. NRC Inc., US 2950185, 1960 (E. D. Hellier, G. L. Martin).
36. NRC Inc., US 4141720, 1979 (H. Vartanian).
37. H. C. Starck, US 3635693, 1969 (H. J. Friedrichs, H. Meyer).
38. H. C. Starck, DE 3130392, 1983 (W. W. Albrecht, 33 U. Papp).
39. Fansteel, US 4356028, 1982 (V. T. Bates).
40. H. C. Starck, DE 3140248, 1983 (W. W. Albrecht, D. Behrens).
41. NRC Inc., US 4957541 (T. B. Tripp).
42. W. W. Albrecht, D. P. Ingalls: "Hochtemperaturreinigung von Tantal und Niob", in Gesellschaft Deutscher Metallhütten- und Bergleute (eds.): *Raffinationsverfahren in der Metallurgie*, Verlag Chemie, Weinheim 1983, pp. 229-242.
43. *Gmelin*, 50, part A2, pp. 490-491.
44. C. A. Hempel: *Rare Metals Handbook*, 2nd ed., Reinhold Publ. Corp., London 1961.
45. Fansteel, US 4859257, 1989 (V. T. Bates, C. Pokross).
46. E. Raub, E. Röschel, *Z. Metallkd.* 53 (1962) 93-103.
47. G. Jangg, R. Eck, *Metall (Berlin)* 31 (1977) 750.

48. G. D. Corey, *Proc. Int. Symp. Tantalum 1st* 1978, 61–82.
49. F. J. Hunkeler: "Properties of Tantalum for Applications in the Chemical Process Industry", in R. E. Smallwood (ed.): "Refractory Metals and Their Industrial Applications", *ASTM Spec. Tech. Publ.* 849 (1984) 28–49.
50. M. Hörmann, *Metall (Berlin)* 42 (1988) 400–406.
51. U. Draugelates, B. Bouaifi, H. Steinberg, *Werkst. Korros.* 44 (1993) 269–273.
52. R. L. Taylor, H. E. Haring, *J. Electrochem. Soc.* 103 (1956) 611–613.
53. Tantalum–Niobium International Study Center, *TIC Bull.* 73 (1993) 2–3.
54. M. Fernández, J. Baonza, J. M. Albella, J. M. Martínez-Duart, *Electrocomponent Sci. Technol.* 7 (1981) 205–210.
55. Sprague Electric Comp., US 4781802, 1988 (E. J. Fresia).
56. G. P. Klein, N. J. Jaeger, *J. Electrochem. Soc.* 117 (1970) 1483–1494.
57. T. Kudoh, M. Katoh, M. Watase, *Denki Kagaku oyohi Kogyo Butsuri Kagaku* 40 (1972) 701–705.
58. D. M. Smyth, G. A. Shirn, T. B. Tripp, *J. Electrochem. Soc.* 110 (1963) 1264–1270.
59. D. M. Smyth, T. B. Tripp, *J. Electrochem. Soc.* 110 (1963) 1271–1276.
60. D. M. Smyth, G. A. Shirn, T. B. Tripp, *J. Electrochem. Soc.* 111 (1964) 1331–1336.
61. D. A. Vermilyea, *J. Appl. Phys.* 36 (1965) 3663–3671.
62. D. A. Vermilyea, *J. Electrochem. Soc.* 112 (1965) 1232–1234.
63. M. Burnham, Hughs Aircraft Company Report, no. M 74-08, Culver City, CA, 1974.
64. K. Andersson, H. Naito, T. B. Tripp, *Proc. 6th Europ. Capacitor and Resistor Tech. Symp. CARTS-Europe*, Brugge 1992, pp. 1–6.
65. Tantalum–Niobium International Study Center Brussels, *TIC Bull.* 69 (1992) 6–8.
66. D. B. Plone, *J. Am. Osteopath Assoc.* 73 (1974) no. 4, 635–640.
67. P. J. Friedman, G. M. Tisi, *Radiology (Easton, PA)* 104 (1972) Sept., 523–535.
68. E. Kammler, W. Weller, W. T. Ulmer, E. Bruckmann, *Pneumologie* 146 (1972) 241–249.
69. G. T. Daughters et al., *J. Thorac. Cardiovasc. Surg.* 104 (1992) no. 4, 1084–1091.
70. T. Friden, L. Ryd, A. Lindstrand, *Acta Orthop. Scand.* 63 (1992) no. 1, 80–84.
71. B. Tjornstrand, G. Selvik, N. Eglund, A. Lindstrand, *Arch. Orthop. Trauma Surg.* 99 (1981) no. 2, 73–81.
72. L. Rabenseifner, W. Küßwetter, P. H. Wünsch, M. Schwab, *Z. Orthop.* 122 (1984) 349–355.
73. B. Heinrich et al., *Z. Stomatol.* 75 (1977) no. 6, 214–224.
74. P. Tetsch: *Erossale Implantationen in der Zahnheilkunde*, 2nd ed., Hanser Verlag, München 1991, pp. 46–47.
75. F. Kylberg, *Acta Chir. Scand.* 141 (1975) no. 3, 242–244.
76. F. Magistris, *Wien. Klin. Wochenschr.* 86 (1974) no. 8, 225–228.
77. F. Magistris, *Chirurg* 46 (1975) no. 11, 518–521.
78. H. Kobayashi et al., *Neurol. Res.* 8 (1986) no. 4, 221–224.
79. S. A. Wexler, B. R. Frueh, D. C. Musch, M. A. Pachtman, *Ophthalmology (Philadelphia)* 92 (1985) no. 5, 671–675.
80. H. J. Gerhardt, G. Muhler, D. Szdzuy, F. Biedermann, *Zentralbl. Neurochir.* 40 (1979) no. 1, 85–94.
81. J. Carleone, *TIC Bull.* 71 (1992) 5–10.
82. Central Glass Co., JP 04243935, 1992 (N. Takeuchi, T. Ito, M. Takayama, K. Furuyo, H. Nakajima, H. Iida).
83. F. Izumi, H. Kodama, *J. Less-Common Met.* 63 (1979) 305–307.
84. H. C. Starck, DE 4021207 A1, 1990 (W. Bludbus, J. Eckert).
85. T. Ichimura: "Niobiumoxide in Optical Glass Manufacture", in H. Stuart (ed.): *Niobium Proc. Int. Symp.* 1984, 603–614.
86. Mitsubishi Chem. Ind., JP 63051945, 1986 (H. Wada, T. Ushikubo).
87. Bayer, DE 4133675, 1991 (O. Immel, H. J. Buysch, G. Darsow).
88. Bayer, EP 433811, 1991 (O. Immel, H. Waldmann, R. Braden).
89. Mitsubishi Kasei Corp., JP 01050843, 1989 (H. Wada, T. Ushikubo).
90. Mitsubishi Kasei Corp., JP 63225329, 1988 (T. Maki, T. Yokoyama, Y. Sumino).
91. H. J. Lunk, S. Schönherr, *Z. Chem.* 27 (1987) 157–170.
92. B. C. Grabmaier, F. Otto, *J. Cryst. Growth* 79 (1986) 682–688.
93. S. Miyazawa, H. Iwasuki, *J. Cryst. Growth* 10 (1971) 276–278.
94. S. Miyazawa, H. Iwasuki, *Rev. Electr. Commun. Lab.* 21 (1973) 374–383.
95. AGFA-Gevaert, EP 0520094 A1, 1992 (D. Philip).
96. O. Renoult, J. B. Boilot, F. Chaput, *J. Am. Ceram. Soc.* 75 (1992) 3337–3340.
97. S. Kawashima, M. Nishida, I. Ueda, H. Ouchi, *J. Am. Ceram. Soc.* 66 (1983) 421–423.
98. D. A. Sagala, S. Nambu, *J. Am. Ceram. Soc.* 75 (1992) 2573–2575.
99. K. Tochi, *J. Am. Ceram. Soc. Jpn. Int. Ed.* 100 (1992) 1441–1442.
100. J. K. Gibson, *J. Fluorine Chem.* 55 (1991) no. 3, 299–311.
101. A. I. Papov, V. F. Sukhoverkov, N. A. Chumakovskii, *Zh. Neorg. Khim.* 35 (1990) 1111–1122.
102. E. I. Du Pont de Nemours, WO 92/03382, 1990 (M. Nappa).
103. Asahi Glass Co., WO 9008754 A2 090809, 1990 (S. Morikawa, S. Samejima, H. Okamoto, K. Ohnishi, S. Tatematsu, T. Tanuma, T. Ohmori).
104. Ciba, DE 1066194, 1957 (W. Scheller).
105. Ciba, DE 1056105, 1956 (F. Kern, W. Schornstein).
106. D. C. Bradley, B. N. Chakravarti, W. Wardlaw, *J. Chem. Soc.* 52 (1956) 2381–2384.
107. R. Gut, *Helv. Chim. Acta* 47 (1964) 2262–2278.
108. N. Sato, M. Nanjo, *High Temp. Mater. Proc.* 8 (1988) 39–46.
109. M. A. Nicolet, *Thin Solid Films* 52 (1978) 415–443.
110. J. R. Shappirio, *Solid State Technol.* 28 (1985) 161–166.
111. E. Jiang, C. Sun, J. Li, Y. Liu, *J. Appl. Phys.* 65 (1989) 1659–1663.
112. K. I. Portnoi, V. M. Romashov, *Sov. Powder Metall. Met. Ceram. (Engl. Transl.)* 11 (1972) 378–384.
113. S. P. Murarba, D. B. Fraser, W. S. Lindberger, A. K. Sinha, *J. Appl. Phys.* 51 (1980) 3241–3245.
114. K. Hieber, F. Neppel, *Thin Solid Films* 140 (1986) 131–135.
115. R. Fresenius, G. Jander: *Handbuch der analytischen Chemie*, Part 3, "Quantitative Bestimmungs- und Trennungsmethoden", vol. 5b, "Elemente der 5. Gruppe, Vanadin, Niob, Tantal", Springer Verlag, Berlin 1957.
116. R. W. Moshier: *Analytical Chemistry of Niobium and Tantalum*, Pergamon Press, New York 1964.
117. J. M. Gibalo: *Analytical Chemistry of Niobium and Tantalum*, Ann Arbor, London 1970.
118. O. G. Koch, G. A. Koch-Dedic: *Handbuch der Spurenanalyse*, Part 2, 2nd ed., Springer Verlag, Berlin–Heidelberg–New York 1974.
119. S. Kallmann, H. Obertin, R. Liu, *Anal. Chem.* 34 (1962) 609–613.
120. A. H. Knight, *TIC Bull.* 45 (1964) 7–8.
121. Autorenkollektiv: *Methoden zur Bestimmung von Spurenanalyse in Niob, Tantal und Wolfram*, VEB Deutscher Verlag für Grundstoffindustrie, Leipzig 1970.
122. J. Stummeyer, G. Wünsch, *Fresenius J. Anal. Chem.* 342 (1992) 203–206.
123. O. Hilmer, J. Peters, A. Breustedt, A. Hoppe: "Bestimmung des Phosphors in Refraktärmetallen und deren Verbindungen", in D. Hirschfeld (ed.): *Nichtmetalle in Metallen '90*, Deutsche Gesellschaft für Metallkunde (oGM), Oberursel 1990, pp. 85–92.
124. V. Krivan et al., *Fresenius J. Anal. Chem.* 341 (1991) 550–554.
125. R. Caletka, R. Hausbeck, V. Krivan, *J. Radioanal. Nucl. Chem.* 120 (1988) no. 2, 319–333.
126. N. Jakubowski, D. Stuewer, G. Tölg, *Int. J. Mass Spectrom. Ion Processes* 71 (1986) 183–197.
127. *Met. Week* 5 (1991) 21.
128. W. Gocht: *Handbuch der Metallmärkte*, 2nd ed., Springer Verlag, Berlin–Heidelberg–New York–Tokyo 1991, pp. 401–413.
129. I. Salisbury, *Proc. 5th Europ. Capacitor and Resistor Tech. Symp. CARTS-Europe*, Munich 1991, pp. 81–88.
130. H. C. Starck GmbH u. Co. KG, Sicherheitsdatenblätter für Tantal-Metall, Tantalcarbid, Tantaloxid, Tantalpentoxid, Tantalchlorid und Kaliumtantalfluorid, Goslar 1994 (in press).

30 Zirconium

RALPH H. NIELSEN

30.1 Introduction	1431	30.10.4 Bromides	1449
30.2 Properties	1432	30.10.5 Iodides	1449
30.3 Occurrence, Ores, and Mining	1434	30.10.6 Fluorides	1449
30.4 Production	1435	30.10.7 Sulfates	1450
30.4.1 Opening-up of Ore	1435	30.10.8 Carbonates	1450
30.4.2 Hafnium Separation	1437	30.10.9 Hydride	1450
30.4.3 Reduction to Metal	1439	30.10.10 Carbide	1451
30.4.4 Refining	1440	30.10.11 Nitrides	1451
30.5 Fabrication	1440	30.10.12 Borides and Borates	1452
30.6 Hazards in Handling Zirconium		30.10.13 Tungstate	1452
Metal	1442	30.10.14 Phosphate	1452
30.7 Grades and Specifications	1443	30.10.15 Nitrates	1453
30.8 Uses	1444	30.10.16 Carboxylates	1453
30.9 Economic Aspects	1444	30.10.17 Alkoxides	1453
30.10 Compounds	1445	30.11 Analysis	1453
30.10.1 Silicate	1445	30.12 Toxicology	1454
30.10.2 Oxides	1446	30.13 Storage and Transportation	1455
30.10.3 Chlorides and Hydroxide Chlorides	1447	30.14 References	1455

30.1 Introduction

On analyzing the gem mineral known as jargon from Sri Lanka. KLAPROTH in 1789 found it contained an oxide which he could not identify and which he later called "zirconerde". In 1824 BERZELIUS prepared the first zirconium metal, an impure black powder, by heating potassium hexafluorozirconate and potassium in a closed pot. LELY and HAMBURGER prepared the first relatively pure zirconium in 1904 by reduction of zirconium tetrachloride with sodium in a bomb, producing malleable, corrosion-resistant zirconium pellets. But it was a hundred years after BERZELIUS before VAN ARKEL, DE BOER, and FAST [1, 2] developed the iodide process which produced the first massive zirconium metal that could be cold worked and which exhibited good ductility at room temperature.

Early uses for zirconium metal were in pyrophoric devices such as fuses, ammunition primers, fireworks, photoflash powder, and flares. Zirconium powder was used exten-

sively as a gettering material in vacuum tubes. By 1946 the consumption of zirconium for these purposes was about 5 t/a. Less than 50 kg of ductile iodide metal was sold, at ca. \$700 per kilogram.

W. J. KROLL carried out the first inert-atmosphere magnesium reduction of zirconium tetrachloride in his Luxembourg laboratory in 1938 [3]. In 1944 the U.S. Bureau of Mines started a project to make ductile zirconium economically. KROLL was assigned to take over direction of the project in January, 1945. By 1947, a pilot plant was producing 30 kg of zirconium sponge per week. Concurrently, researchers at Massachusetts Institute of Technology and at Oak Ridge National Laboratory were evaluating the physical and atomic properties of metals as potential uranium fuel cladding materials for nuclear power stations. In 1948 hafnium-free zirconium was selected as most promising. By 1949 zirconium had been chosen as the structural material for the fuel core of the submarine thermal reactor, the land-based reactor prototype, and during

1949–1950 a satisfactory hafnium separation process was developed at Oak Ridge. By the end of 1950, 3000 kg of hafnium-free zirconium metal strip had been produced, and the zirconium metal producing industry was launched as an integral part of the beginning nuclear power industry.

30.2 Properties

Physical Properties. Zirconium is a lustrous, strong, ductile metal similar in appearance to stainless steel. Pure zirconium metal has three solid phases: ω -Zr, which is stable below 200 K at ambient pressure and up to 1000 K at 6 GPa [4]; α -Zr, which is stable from 200 K to 1125 K; and β -Zr, which is the stable form between 1125 K and the melting point. These transition temperatures change with the addition of α - or β -stabilizing alloying elements. The important physical properties are presented in the following:

Relative atomic mass	91.224
Atomic radius	15.90 nm (in metal lattice)
Ionic radius (Zr ⁴⁺)	7.5 nm
Electronegativity	1.22
Standard potential M/MO ₂	1.53 V
Melting point	1852 ± 2 °C
Boiling point	3850 °C
Crystal structure of ω -Zr	hexagonal open
α -Zr	hexagonal dense, $a = 32.3$ nm, $c = 51.5$ nm
β -Zr	body-centered cubic, $a = 36.1$ nm
Transformation temperatures	
$\omega \rightarrow \alpha$	-73 °C
$\alpha \rightarrow \beta$	862 ± 5 °C
Heat of fusion	2.30×10^4 J/mol
Heat of evaporation	5.96×10^5 J/mol
Electrical resistivity	3.89×10^{-5} Ω cm
Thermal conductivity at 25 °C	21.1 Wm ⁻¹ K ⁻¹
at 100 °C	20.4
at 300 °C	18.7
Specific heat at 25 °C	0.285 Jg ⁻¹ kg ⁻¹
at 865 °C	0.335
Thermal expansion coefficient	
α , bulk, at 25 °C	5.89×10^{-6} K ⁻¹
α -Zr, c axis	6.4×10^{-6}
α -Zr, \perp c axis	5.6×10^{-6}
β -Zr	9.7×10^{-6}
Density of α -Zr	6.50 g/cm ³
β -Zr	6.05
Effective cross section for thermal neutrons	1.9×10^{-29} m ² (0.19 barns)

Mechanical Properties. Although zirconium is a high-melting metal, its mechanical proper-

ties are similar to those of much lower melting metals: its elastic modulus is quite low, and its strength diminishes rapidly with increasing temperature. The mechanical properties of zirconium are strongly dependent on purity, especially the oxygen and nitrogen content, the amount of cold work, and the crystallographic texture. Forged or rolled zirconium shows marked anisotropy in mechanical properties in both the as-formed and annealed conditions. Pure zirconium is ductile at liquid-nitrogen temperatures but the metal is subject to hydrogen embrittlement whenever the hydrogen content sufficiently exceeds the hydrogen solubility at the operating temperature. Tables 30.1 and 30.2 gives typical values of the more important mechanical properties of zirconium and of Zircaloy 2 and Zircaloy 4 (see also Section 30.9).

Table 30.1: Mechanical properties of zirconium.

Property	20 °C	200 °C	300 °C
Tensile strength, MPa	300–450	200–250	150–180
Elastic limit 90.2%, MPa	200–300	110–130	75–85
Elongation, %	25–35	50–60	45–55
Modulus of elasticity, MPa	7.5×10^4	8.3×10^4	7.2×10^4
Brinell hardness	90–130		
Shear modulus	36 500		
Poisson's ratio	0.35		

Chemical Properties. Zirconium is a very reactive metal that, in air or aqueous solution, immediately develops a surface oxide film. This stable, adherent film is the basis for zirconium's corrosion resistance. In most media, zirconium is more resistant than titanium or stainless steel. Its acid resistance approaches that of tantalum, but unlike tantalum, zirconium is also resistant to caustic media.

Fluoride ions bond strongly to zirconium, and even a trace of fluoride in most media will drastically reduce its corrosion resistance.

The corrosion resistance in sulfuric acid is excellent at temperatures up to 150 °C and acid concentrations up to 70%, except that welds and adjacent heat-affected zones are susceptible to corrosive attack above 60% concentration. This can be alleviated by annealing.

Table 30.2: Mechanical properties of Zircaloy 2 and Zircaloy 4.

Property	Annealed			Recrystallized		
	20 °C	200 °C	400 °C	20 °C	200 °C	400 °C
Tensile strength, MPa	785	440	380	520	290	190
0.2% yield strength, MPa	600	360	300	370	150	130
Ultimate elongation (50 mm), %	17	20	20	34	45	55

Ferric, cupric, and nitrate ion impurities in sulfuric acid decrease the corrosion resistance at acid concentrations above 65%. Even at room temperature zirconium is rapidly attacked at concentrations above 75%.

The corrosion resistance in hydrochloric acid is excellent at temperatures up to 130 °C and concentrations up to 37%. However, even small amounts of ferric or cupric ions will lead to severe pitting and stress cracking.

The corrosion resistance in nitric acid is excellent at all concentrations up to 90% and temperatures up to 200 °C. In concentrations above 65%, stress corrosion cracking may occur if high tensile stresses are present [5].

The corrosion resistance in phosphoric acid is excellent in all concentrations up to 65 °C, and, at concentrations below 40%, up to 185 °C.

Zirconium is rapidly attacked by hydrofluoric acid, even at concentrations below 0.1%.

The corrosion resistance in sodium hydroxide and potassium hydroxide is excellent at all concentrations, up to the boiling temperature. Zirconium is resistant to molten sodium hydroxide up to 1000 °C.

Zirconium is very resistant to most organic compounds at all concentrations and temperatures. But, when air or moisture are not available to reform the surface oxide film, zirconium is attacked by anhydrous chlorinated organics at elevated temperatures and is etched by bromine or iodine dissolved in anhydrous organics. Stress corrosion cracking may also occur.

Zirconium reacts with most gases at relatively low temperatures.

Zirconium forms a visible interference color film in air starting above 200 °C. Above 400 °C the adherent oxide film is black.

Above 540 °C a loose gray-white oxide forms, the oxide layer becomes thicker as oxygen diffuses into the underlying metal, and the metal can become embrittled after prolonged exposure. The maximum continuous operating temperature of zirconium in air is ca. 450 °C. Short-term hot working such as forging, rolling, and extrusion are conducted at 550–1000 °C. Afterwards, the surface oxide and embrittled metal layer are mechanically and chemically removed. While solid zirconium metal is oxidized slowly in air, the oxidation is exothermic, and for high-surface-area forms, such as powder or sponge metal, the large heat release may cause ignition.

Oxygen-containing gases, such as carbon dioxide, carbon monoxide, sulfur dioxide, steam, and nitrogen oxides, oxidize zirconium somewhat slower than air. The maximum continuous operating temperature is about 400 °C.

Zirconium reacts more slowly with nitrogen than with oxygen because the reaction is less exothermic.

Zirconium readily absorbs hydrogen above 300 °C. The rate of absorption varies inversely with the thickness of the surface oxide film. Hydrogen solubility increases with temperature. On cooling, when the solubility is exceeded, zirconium hydride platelets precipitate, embrittling the metal. The reaction is reversible: hydrogen is removed on heating the metal above 600 °C in a high vacuum.

Zirconium's oxide film protects it from dry chlorine gas at room temperature, but any impact or abrasion that exposes a fresh metal surface may initiate an exothermic reaction producing zirconium tetrachloride vapor.

More information on the chemical behavior of zirconium metal can be found in [6].

30.3 Occurrence, Ores, and Mining

Zirconium is the ninth most abundant metal in the earth's crust, with an estimated concentration of 0.016–0.025% [7], about one twentieth that of titanium but more plentiful than nickel, copper, or zinc. Zirconium occurs only in fully oxidized form, never as free metal.

There are over 40 known zirconium minerals which can be grouped:

- Zirconium orthosilicates: Zircon and its metamict varieties
- Zirconium dioxide: baddeleyite and its altered varieties
- Zirconosilicates with sodium, calcium, iron, and other elements: eudialyte, eucolite, gittinsite and others
- Zirconium carbonates with sodium, calcium, and other elements: weloganite and others
- Others, including zirconolite ($\text{CaZrTi}_2\text{O}_7$)

Zircon is the predominant commercial zirconium mineral, but the minerals baddeleyite and eudialyte are also being used. All are obtained as by-products of other mineral recovery operations.

Zircon, ZrSiO_4 , occurs as an accessory mineral in silica-rich igneous rocks, particularly granite, nepheline syenite, and pegmatite, and also in metamorphic and sedimentary rocks. Zircon is rarely found in rocks in economically minable concentration. Weathering and erosion of these rocks frees the zircon grains, and the combined action of rivers, seas, and wind concentrate the heavier minerals by natural gravitation processes in placer deposits, deltas, and ocean beaches. As an ore, zircon is recovered from unconsolidated sands in beach deposits.

Large heavy mineral sands deposits are being extensively mined in Florida, West Australia, South Africa, India, Russia and Kazakhstan, with smaller operations in Sierra Leone, Sri Lanka, Madagascar, Malaysia, Brazil, Indonesia, Thailand, Ukraine and, Vietnam. In Canada, some zircon is obtained from

the processing of Athabasca tar sands. Undeveloped heavy mineral beach sand reserves containing zircon exist in New Jersey, the Carolinas, Georgia, Tennessee, Colorado, New Mexico, Oregon, Utah, Wyoming, Egypt, Malawi, Senegal, and Tanzania.

These heavy mineral sands deposits are mined to obtain the titanium minerals rutile, leucocoxene, and ilmenite to supply the titanium metal and titanium oxide pigment industries. Depending on the deposit's composition and current market pricing, zircon and other minerals are viable by-products. Australia and South Africa are major zircon exporters.

Mining of heavy mineral sands involves first removing a light sand overburden, followed by removal of the heavy sands layers using elevating scrapers and bulldozers, or by flooding the excavation and using dredges in the pond. The heavy minerals are concentrated by gravity separation, and the quartz, light minerals, fines, clay, and silt are returned to the back end of the excavation. Since the heavy mineral sands are only 4–7% of the deposit, the site can be rehabilitated close to the original elevation, topsoil replaced, and native vegetation replanted. The concentrate is hauled to a ore-dressing site where the grains may be scrubbed to remove surface coatings, dried, and separated into individual mineral components: rutile, leucocoxene, ilmenite, zircon, xenotime, monazite, staurolite, garnet, kyanite, and sillimanite. These separation steps utilize differences in the specific gravity, induced magnetism, and electrical conductivity of the individual minerals grains to gradually recover each mineral in good purity.

The various mining operations produce a range of zircon products from high grades with very low levels of impurities to lower grades where the impurities vary with the nature of the orebody and the type of separation process used. These various grades supply a range of applications: foundry sands, refractories, abrasives, opacifiers, zirconium chemicals, zirconium metal, and welding rod coatings. A typical analysis of zircon for the metal industry is 66.6% $(\text{Zr} + \text{Hf})\text{O}_2$, 0.2%

Al_2O_3 , 0.15% TiO_2 , 0.1% Fe_2O_3 , 0.1% P_2O_5 , 0.025% U, 0.020% Th.

Baddeleyite, ZrO_2 , has been found in Brazil, South Africa, Sri Lanka, and Russia. Brazilian baddeleyite often occurs mixed with zircon. The mixture is known as caldasite and usually contains 65–80% zirconium oxide. South African baddeleyite is a by-product of mining a volcanic orebody for copper and phosphate fertilizer. The baddeleyite concentrate contains 96% zirconium oxide. Russian baddeleyite from the Kola Peninsula is a by-product of open pit iron ore mining.

Eudialyte, $(\text{Ca}, \text{Na})_6(\text{Zr}, \text{Fe})(\text{Si}_3\text{O}_9)_2(\text{OH}, \text{Cl})_2$ has been found in Greenland, Norway, Brazil, Australia, Transvaal, and New Mexico. Some eudialytes contain 12–15% zirconium oxide, yttrium, and small amounts of niobium and rare earth metals.

Hafnium Content. All known zirconium minerals contain hafnium, usually in the range of 1.5–2.5% $\text{Hf/Zr} + \text{Hf}$, although higher hafnium contents have been found. There is a tendency for higher-hafnium ores to be also higher in uranium and thorium content. Hafnon, hafnium orthosilicate, with > 95% $\text{Hf/Zr} + \text{Hf}$ was found associated with a tantalum ore in Mozambique.

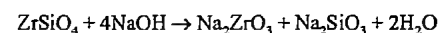
30.4 Production

Processing steps for the production of zirconium metal from zircon sand are shown in Figure 30.1.

30.4.1 Opening-up of Ore

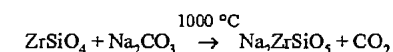
Zircon is a refractory mineral whose decomposition requires the use of high temperature and aggressive chemicals. Selection of a particular procedure depends on the subsequent product use or processing.

Caustic Fusion. Caustic fusion of zircon with a slight excess of sodium hydroxide at 650 °C (or sodium carbonate at 1000 °C) is the usual zircon decomposition process [8, 9]:



The cooled reaction mass is crushed and slurried in water. Water dissolves the sodium silicate and hydrolyzes the sodium zirconate to soluble sodium hydroxide and insoluble hydrous zirconia. The hydrous zirconia, recovered by filtration, can be fired to oxide, dissolved in mineral acid for further conversion to aqueous zirconium compounds, or dissolved in mineral acid for feeding to a hafnium extraction process.

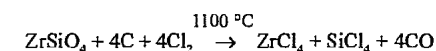
A variant of the caustic fusion process uses less caustic to produce an acid-soluble sodium zirconium silicate



The frit from this reaction is added to strong acid to yield a solution containing sodium and zirconium salts and silica gel:

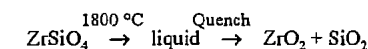


Chlorination. Fluidized-bed carbochlorination of milled zircon sand is the zircon decomposition process used by American and French zirconium metal producers. Chlorine is the fluidizing gas. The reaction is endothermic and supplemental energy is supplied, usually by induction heating of the interior graphite wall of the chlorinator.



The product gases are cooled to 200 °C in a primary condenser that collects zirconium (and hafnium) tetrachloride as a powder. The remaining gas mixture is cooled to –20 °C in a secondary condenser, collecting silicon tetrachloride as a liquid which is subsequently purified and used to make fumed silica, fused quartz, and fused-quartz optical fiber.

Thermal Dissociation. Thermal dissociation of zircon in an arc plasma forms zirconium oxide in droplets of liquid silica. Rapid quenching, to minimize recombination, produces intimately mixed crystals of zirconium oxide in a bead of amorphous silicon oxide [10].



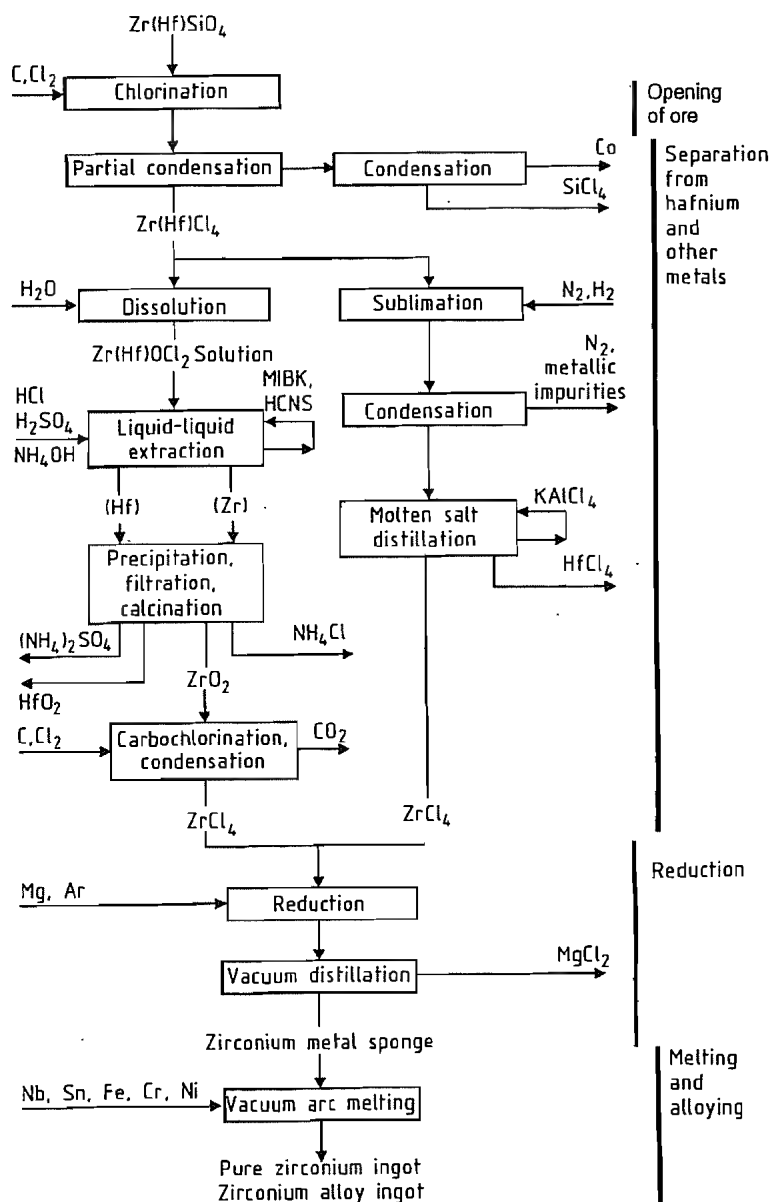
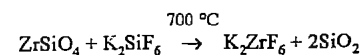


Figure 30.1: Flow diagram for production of zirconium.

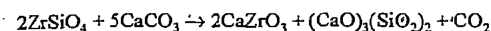
The mixture can be leached with sulfuric acid to yield a zirconium sulfate solution and insoluble silica, or leached with sodium hydroxide to yield a sodium silicate solution and insoluble zirconium oxide.

Fluorosilicate Fusion. The fusion of zircon and potassium hexafluorosilicate produces potassium hexafluorozirconate [11].



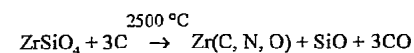
The fused mass is crushed, then the fluoride salt is dissolved with acidified hot water. The hot solution is filtered to remove silica and cooled to crystallize potassium hexafluorozirconate.

Lime Fusion. Fusion of zircon with limestone or dolomite produces calcium zirconate and calcium or magnesium silicate:



On cooling, the fused mass disintegrates into a very fine calcium silicate powder and coarse calcium zirconate crystals, which can be recovered by mechanical means. The acid-soluble calcium zirconate can be converted into zirconium salts or zirconium oxide.

Carbiding. An intimate mix of zircon sand and coke is continually fed into an open-top electric arc furnace. Insufficient carbon is used for complete conversion to carbide, so that silicon monoxide is vaporized at the arc temperature [12]:



A crude zirconium carbonitride ingot grows under the electrode, surrounded by unreacted mix, which acts as insulation for the steel furnace shell. When the furnace is full, it is moved to a cooling location. When cool, the ingot is separated from unreacted charge, which is recycled. The product is a dense block, having a silver to golden-yellow fracture surface, depending on nitrogen content. The block is broken and crushed to -75 mm chunks, which are subsequently chlorinated to zirconium tetrachloride. If the hot ingot is immediately removed from the furnace shell and unreacted charge, the ingot is oxidized to zirconium oxide containing ca. 5% silica.

High-Temperature Fusion. Direct electric arc smelting of baddeleyite or zircon is used to make fused zirconia or fused alumina-zirconia-silica (AZS). The silica is partially vaporized and recovered as fumed silica.

Baddeleyite is converted to zirconium sulfate by direct dissolution in concentrated sulfuric acid at ca. 200 °C. The recovery is low.

Better recoveries are obtained by first heating the baddeleyite with lime to yield calcium zirconate, which reacts with sulfuric acid to give zirconium sulfate and gypsum.

30.4.2 Hafnium Separation

Zirconium and hafnium are very similar chemically and metallurgically, and for most uses of zirconium their separation is unnecessary. Their separation is conducted only to produce hafnium-free zirconium metal for the nuclear power industry. Of the many methods developed since the discovery of hafnium, four are used industrially: fluoride salt crystallization, methyl isobutyl ketone extraction, tributyl phosphate extraction, and extractive distillation, in order of their development. In addition, ion exchange has been used for low-throughput, low-investment operations.

Fluoride Salt Crystallization. The first separation of zirconium and hafnium by repeated crystallization of potassium hexafluorozirconate from hot aqueous solution is credited to VON HEVESY [13]. The solution is acidified to minimize oxide-fluoride salt formation. At each step the salt crystals are depleted in hafnium. This multistep recrystallization procedure has been used for many years in Ukraine [14].

Methyl isobutyl ketone extraction developed at Oak Ridge National Laboratory and used by both American producers, is based on the preferred extraction of a hafnium dihydroxide thiocyanate complex from hydrochloric acid solution by methyl isobutyl ketone [15].

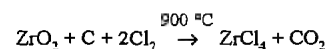
Zirconium-hafnium tetrachloride, produced by carbochlorination of zircon, is dissolved in water, with hydrolysis to form zirconium-hafnium dihydroxide chloride in a hydrochloric acid solution. This solution is contacted with methyl isobutyl ketone to extract iron as $HFeCl_4$ into the organic solvent. Then ammonium thiocyanate is added to the dihydroxide chloride solution, providing a mixed dihydroxide chloride/dihydroxide thiocyanate solution of zirconium and hafnium.

This solution is countercurrently contacted with a methyl isobutyl ketone/thiocyanic acid solution to preferentially extract hafnium dihydroxide thiocyanate into the organic phase. This is conducted in a series of mixer-settlers or a series of packed or internally agitated columns. Hafnium is recovered from the ketone solution by scrubbing with dilute sulfuric acid.

Zirconium is recovered from the hydrochloric acid solution by heating the solution above 90 °C, adding precisely two moles of sulfuric acid to each five moles of zirconium, and then carefully raising the pH to 1.2–1.5 with dilute ammonium hydroxide. This precipitates a granular zirconium basic sulfate, $Zr_5O_8(SO_4)_2 \cdot xH_2O$ which is easily filtered and washed to remove aluminum and uranium impurities. The sulfate filter cake is repulped with dilute ammonium hydroxide to convert it to zirconium hydrous oxide, which is fired to give pure zirconium oxide [16].

In this extraction process, methyl isobutyl ketone and thiocyanate are recovered and reused, but considerable quantities of hydrochloric acid, sulfuric acid, and ammonia are consumed. Zirconium produced typically contains 35–90 mg Hf/kg and the hafnium contains 200–2000 mg Zr/kg, but any degree of separation can be attained, without further chemical consumption, by providing fewer or more contacting stages during separation.

The zirconium oxide and hafnium oxide are each chlorinated in fluidized beds to give their tetrachlorides. Chlorination of the oxides is faster than that of the silicates, and can be efficiently conducted at a lower temperature.



The zirconium tetrachloride is then purified by sublimation at 350–400 °C in a nitrogen atmosphere containing 1–5% hydrogen. The hot gases pass through a filter to remove entrained particles before being cooled to condense the zirconium tetrachloride. This sublimation reduces the levels of oxide, iron, phosphorus, and aluminum.

Tributyl phosphate extraction, developed concurrently in Britain, France, and the United

States, was used commercially in the United States and is being used in India to obtain zirconium for the nuclear industry [17]. Hydrous zirconium–hafnium oxide from caustic fusion of zircon is dissolved in nitric acid. The nitric acid solution is countercurrently contacted with an organic solution of tributyl phosphate in kerosene. A zirconium tributyl phosphate complex is preferentially extracted into the kerosene, leaving hafnium and most metallic impurities in the aqueous phase. The zirconium is stripped from the kerosene solution with dilute sulfuric acid solution, precipitated, and fired to pure zirconium oxide.

Chloride Distillation. Hafnium tetrachloride is slightly more volatile than zirconium tetrachloride, and separation by fractional distillation would be feasible if the tetrachlorides could be handled as liquids. However, the tetrachlorides are either solid or gaseous, depending on temperature, unless kept under pressure while being heated to the triple point of zirconium tetrachloride (435 °C, 2.0 MPa). However a distillation process was developed in which the liquid phase was molten potassium chloroaluminate, in which zirconium and hafnium tetrachloride are soluble without forming compounds that could impede the separation or the recovery of separated chloride [18].

The zirconium–hafnium tetrachloride from chlorination of zircon is first purified by sublimation. The purified tetrachloride is revaporized and the vapor is introduced into the distillation column, above the midpoint. The potassium chloroaluminate liquid, equilibrated with hafnium-rich tetrachloride, is fed into the top tray of the distillation column, which is at 350 °C. As the liquid cascades down the column, it is gradually stripped of the more volatile hafnium tetrachloride while acquiring zirconium tetrachloride from the rising vapor. The zirconium tetrachloride in the liquid melt reaching the bottom of the column contains < 50 mg Hf/kg Zr.

In the boiler at the column bottom some of the zirconium tetrachloride is vaporized to provide the rising vapor in the column. From

the boiler the liquid melt goes to a short, hotter column where it is stripped with nitrogen to remove the product zirconium tetrachloride.

The stripped liquid melt is returned to an absorber–condenser above the distillation column where it is equilibrated with hafnium-rich tetrachloride vapor, then returned to the top of the distillation column. Unabsorbed hafnium-rich tetrachloride vapor ($HfCl_4$ content 30–50%) is led to a condenser. The hafnium-rich tetrachloride is accumulated until it can be reprocessed in the distillation column in a separate campaign to recover pure hafnium tetrachloride (< 1% $ZrCl_4$).

Control of the potassium to aluminum ratio in the melt is crucial. Excess potassium chloride preferentially bonds with hafnium tetrachloride, reducing its effective vapor pressure and thereby decreasing the separation efficiency. With a deficiency of potassium chloride, aluminum chloride is lost into the nitrogen stream in the stripper, contaminating the zirconium tetrachloride product.

This distillation process has a higher yield than the liquid–liquid extraction processes, does not consume large quantities of chemicals, and eliminates the rechlorination step. It is very capital intensive.

Other Processes. Although zirconium is not easily reduced except by very strong reducing agents, it can be reduced more easily than hafnium. This has led to several separation procedures. The most significant [19] involved both molten metal (zinc base) and molten halide salts for good contact between the phases and for the close approach to equilibrium needed for good separation factors.

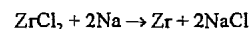
30.4.3 Reduction to Metal

Oxygen toughens zirconium metal, decreasing its ductility and therefore its formability as a metal. To produce ductile zirconium metal, the zirconium compound to be reduced and the reducing agent should be as free of oxygen (and nitrogen and carbon) as possible. Anhydrous zirconium tetrachloride or tetrafluoride are usually used.

Kroll Process. Ductile zirconium metal is produced by reduction of pure zirconium tetrachloride with molten magnesium under an inert gas (helium or argon). The reduction retort is a long, vertical cylinder composed of two sections. The lower third is a stainless-steel-lined crucible which holds the magnesium ingots. The upper two-thirds has a central annular pipe slightly shorter than the retort wall. The space between the wall and the central pipe is filled with zirconium tetrachloride powder, then the two sections are welded together and a lid is bolted to the top. The assembled retort is warmed to 200 °C, evacuated and filled with argon several times to remove the last traces of air. The retort is lowered into a furnace with heating zones for each retort section. The lower section is then heated to 850 °C to melt the magnesium, and argon is bled from the warming retort to maintain atmospheric pressure (the retort is not a pressure vessel). Zirconium tetrachloride vapor passes down through the central pipe, which communicates with the lower section, and is reduced by the molten magnesium. At the end of the reduction, the lower crucible contains a thick suspension, or mud, of tiny zirconium metal beads in liquid magnesium, under a layer of liquid magnesium chloride. The retort is cooled and unloaded. The stainless steel liner is separated from the reduction mass and the layer of magnesium chloride is mechanically removed from the zirconium–magnesium metallic regulus. Several reduction reguli are stacked and loaded into a distillation furnace for removal of magnesium and residual magnesium chloride. The distillation is conducted in a vacuum (< 1 Pa), with the charge located in the upper end of the retort. The bell furnace around the top of the retort is heated in programmed steps, reaching 980 °C in ca. 30 h. As the charge heats, the magnesium chloride melts and drains away, and the magnesium metal slowly evaporates, condensing on the water-cooled retort wall. As the magnesium evaporates, the zirconium beads come into closer contact and begin to sinter together. The final sintered porous mass is known as zirconium sponge. The heating schedule is critical:

If the magnesium receives heat faster than heat is removed by magnesium transpiration at the surface of the reguli, the reguli become soft and flow down out of the heated zone. After the retort is cooled and the sponge conditioned by slow, controlled exposure to air, the sponge regulus is removed from the retort. The regulus is broken into chunks by using a hydraulic chisel. The chunks are sorted into quality grades depending on color and relative location in the regulus. The chunks are crushed to less than 2 cm, and screened to remove -20 mesh fines, which are higher in impurities.

Other Reduction Processes. Ductile zirconium has been produced commercially in a two-step sodium reduction analogous to a titanium reduction process [20]. Zirconium tetrachloride vapor and liquid sodium are both slowly fed into an argon-filled stirred reactor containing granular sodium chloride to obtain a ZrCl_2 -NaCl mixture. This first step is very exothermic and the feed rate is controlled to allow excess heat to escape. The mixture is then transferred to a reactor by means of a screw conveyor. The reactor, already loaded with sodium, is sealed and heated to 800 °C:



The cooled mass was mechanically broken out of the reactor and leached with water to remove the sodium chloride from the zirconium. However, it was necessary to drip-melt the zirconium, forming splat-cooled chunklets, to remove the last traces of salt.

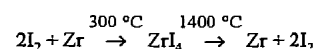
The Russian practice is to reduce potassium hexafluorozirconate with calcium metal in a sealed bomb. In Canada, zirconium tetrafluoride was reduced with calcium metal in a sealed bomb.

Zirconium oxide can be reduced by calcium or magnesium. Finely divided metal powder is recovered by leaching with cold hydrochloric acid. The powder has 0.3–0.5% oxygen, and would not be ductile or malleable if melted into ingot. The powder particles are 1–8 µm in diameter and are very pyrophoric.

Electrolysis. Electrowinning and electrorefining of zirconium have been conducted but are not in commercial use. A pilot electrolysis system tested for zirconium was used commercially for hafnium [21]. A summary of the difficulties in developing an electrolysis process is given in [22].

30.4.4 Refining

From 1925 to 1945 the van Arkel and de Boer iodide process was the only consistent method for obtaining pure ductile zirconium metal. Now Kroll zirconium is used for most applications and iodide zirconium is used only when the highest purity is needed. In the iodide process, iodine vapor is reacted with Kroll zirconium sponge or calcium-reduced zirconium metal powder to produce zirconium tetraiodide [23, 24]. The tetraiodide vapor diffuses to a heated filament, usually zirconium wire, where the iodide is thermally dissociated, depositing zirconium and releasing iodine to repeat the cycle:



The reaction is conducted in an Inconel vessel at an absolute pressure of 40 Pa. The wire filament diameter grows as zirconium is deposited on the wire. Bars up to 40–50 mm in diameter can be grown.

Electron beam melting is not usually used to purify zirconium because the metal's vapor pressure at its melting point is higher than that of most impurities. Iron and aluminum levels can be reduced by electron beam melting. The metal vapor pressure results in considerable evaporation loss in the high vacuum utilized in electron beam melting.

30.5 Fabrication

The procedures for melting zirconium sponge and for conversion of ingots to mill products are similar to those developed by the titanium industry, with the added requirement that high-neutron-cross-section materials such as boron be rigorously excluded.

Melting. Zirconium sponge is pressed into compacts, cylindrical or hexagonal discs, which then are stacked and surface-welded together in an electron beam furnace to form an electrode. The discs may be pure sponge, or may contain alloying ingredients added in the midst of each disc during pressing, or may be recycled clean turnings of the same intended composition. The welded electrode is then melted in a vacuum arc furnace. An electric arc is struck between the electrode and a starter pad of zirconium chips in the bottom of a water-cooled cylindrical copper crucible. The electrode is not cooled and it slowly melts off in the arc, producing a molten pool in the cooled copper crucible. The pool edge freezes on contact with the cool crucible wall so that the remaining pool is separated from the crucible wall. As melting continues, the electrode is consumed and the ingot grows in the crucible, cooling and solidifying from the bottom and sides as the pool moves upward. The outer skin contains impurities that vaporize during melting, primarily magnesium and magnesium chloride, and any possible copper pickup from sliding the ingot out of the crucible. The first-melt ingot is surface machined to remove the outer skin. Since the molten pool was, at any one instant, only a small portion of the ingot, distribution of alloying ingredients in the ingot is not homogenous after one melt. Two machined first-melt ingots are formed into a second electrode, first-melt bottom now at the top, which is again melted in a larger diameter copper crucible. A third melt assures complete homogeneity and dissolution of any inclusions. 750 mm diameter ingots of up to 9 t are produced.

Forming. Ingots are surface machined then heated to over 1000 °C and hot forged to 50–150 mm thick slabs, or to 200–400 mm diameter rounds. At the conclusion of hot working, the surface oxide scale is removed by sand-blasting and abrasive-wheel grinding. The underlying dark layer of oxygen-diffused metal is removed by pickling in dilute hydrofluoric-nitric acid solution [25].

Strip and sheet are formed by cold working the slabs in conventional rolling mills, including producing foil in a Sendzimir mill. The allowable cold deformation before annealing is 20–70%, depending on alloy toughness and the type of deformation process. Intermediate and final anneals are conducted in vacuum or inert-atmosphere furnaces.

For round products, the 200–400 mm rounds are cut to length, hot rotary forged to bar, cleaned, and swaged or drawn to rod or wire for welding use.

For hollow round products, short lengths of the rounds are drilled or trepanned to produce extrusion billets which are warm extruded to heavy wall tubeshells. Prior to extrusion the billets are coated with proprietary layers of glass, graphite, or copper. These coatings minimize oxidation of the surface and function as a lubricant during extrusion, but must be removed before subsequent cold working.

The extruded tubeshells are tube-reduced in pilger mills, with intermediate vacuum anneals, to produce thin-wall tube lengths. Zircaloy 2 or 4 (see Section 30.9) tubes are used as cladding for uranium oxide pellets for light-water nuclear fuel assemblies. This is the major use of zirconium metal.

Powder Metallurgy. Malleable zirconium and high-zirconium alloy powders are obtained by the hydride-dehydride process. Zirconium is hydrided by heating to 800 °C and cooling in a pure hydrogen atmosphere. The product is brittle and easily ground to powder in an argon-atmosphere chamber. The hydrogen is then removed by degassing in a vacuum above 650 °C. The metal powder is screened to obtain the desired particle-size distribution. The hydride powder can also be directly pressed and sintered, allowing for hydrogen outgassing.

Welding. Zirconium can be welded in argon or helium atmospheres. If welding is not conducted in an inert-gas chamber, the welding fixtures or jigs must be so arranged that argon or helium gas flooding is sufficient to keep air completely away from the welding zone. Care must be taken to avoid oxygen or hydrogen

pickup as these affect the ductility and corrosion behavior of the heat-affected zone. Electron beam welding is used for high-quality welds in repetitive situations such as nuclear fuel assembly.

While zirconium can be welded to titanium, hafnium, niobium or tantalum, joining of zirconium with other metals (i.e., copper, iron, nickel) by fusion welding is not practical because of the formation of brittle intermetallic phases. To join these metals, methods must be used that avoid formation of liquid phases but use mechanical interlocking: friction welding or explosive bonding, which is used for cladding of zirconium lining onto ferrous alloys. Welding of zirconium to titanium, niobium, or tantalum destroys the corrosion resistance.

30.6 Hazards in Handling Zirconium Metal

Solid zirconium is not hazardous, but any high-surface-area form of zirconium metal (powder, dust, chips, foil, sponge) is hazardous because of its easy ignition in air and its exothermic reaction with many other elements and compounds.

Zirconium chemical equipment, if used under conditions not recommended, such as sulfuric acid above 80% concentration or strong hydrochloric acid with ferric ion contamination, may suffer intergranular attack. This creates a highly pyrophoric surface layer, usually black, that is ignited easily when dry. The combination of γ -zirconium hydride and metallic particles has been suggested to be responsible for the pyrophoricity. Careful treatment in hot air or steam is recommended to stabilize this surface [26].

The ignition temperature of zirconium powder varies with particle size, method of production, and prior treatment. A < 40 mm powder prepared in inert atmosphere will immediately ignite upon exposure to air, unless it is first slowly exposed such as by gradually back-filling the airlock of a glove box, allowing the heat of surface oxidation to dissipate.

Zirconium powder produced wet, such as by acid leaching of a reduction mass, is usually safe if the water content is > 50%. This prevents localized temperature excursions. The powder should not be allowed to settle and compact for long periods of time, especially when freshly prepared. Hydrogen is still slowly generated, and accumulated gas bubbles in a compact powder mass can insulate some grains from the water, allowing localized heating to ignition.

Drying of wet powder is most hazardous. While wet powder is harder to ignite than dry powder, it burns much more vigorously because of the available oxygen from the water and is more explosive because of the generation of hydrogen and steam. The most hazardous water content is 5–10%. Powder is dried as a thin layer on warm-water-heated trays in a vacuum drier.

Machining of zirconium generates fine chips which can be ignited easily. Hot chips are the usual ignition source. The best metal removal procedures consistent with keeping chip temperatures down are: using slow cutting speeds with heavy feeds, and using an ample flood of water-soluble cutting oil as a coolant. Accumulation of chips should be avoided. Chips should be removed as generated and stored in water-filled drums kept outside in an isolated area. Coarse chips, if not contaminated, possibly may be chopped, cleaned, and recycled. Fine chips should be disposed of by burning in an incinerator or an open pit, feeding the fire in small increments of 1–2 kg.

Many unexpected flash fires have been caused by improper handling of machining chips resulting in more than one incident of fatal flash burns. Workers involved in handling, storing, cleaning, or disposal of machining chips or other zirconium fines should wear heat-reflectant clothing.

Zirconium fires can be controlled only by cutting off the supply of oxygen and other oxidants such as water, carbon dioxide, carbon tetrachloride, iron oxide, and limestone. Small fires can be smothered with dry silica sand or dry table salt, or with argon or helium if the

zirconium is enclosed in a container. Do not use water. Large fires are best left alone and allowed to burn out, keeping the surroundings from igniting.

Safe handling procedures for zirconium, including machining, grinding, welding, and descaling, are discussed in [27].

Solutions that corrode zirconium metal may react violently or explosively with zirconium powder. A solution of 83% concentrated H_2SO_4 and 17% $KHSO_4$ was added dropwise to 2 g of zirconium powder. Upon adding about 2 mL of the acid mixture, a violent explosion occurred.

30.7 Grades and Specifications

There are two parallel grading systems for zirconium: industrial (intended primarily for use as a construction material for equipment and piping in the chemical industry) and nuclear (intended for use as a construction material for fuel cladding and internal parts for nuclear power reactors). Some of these grades have little present usage.

The industrial grades are listed, showing first the ASTM designation, then any alternate designation:

- R 60701 (Zr 701) an unalloyed zirconium of low hardness and containing low levels of the impurities iron and chromium
 R 60702 (Zr 702) the usual unalloyed zirconium specified for general corrosion-resistant service

R 60703 (Zr 703) the least pure, available only as sponge metal, used primarily for alloying with other metals

R 60704 (Zr 704) an alloy containing tin and iron and used in chemical process applications where the higher strength of the alloy is needed and the corrosion resistance is sufficient

R 60705 (Zr 705) an alloy containing 2.5% niobium used where high strength is needed

R 60706 (Zr 706) a softer version of Zr 705 used specifically for severe forming applications

All of these grades may contain the usual 2% hafnium, or may be furnished hafnium-free. This does not affect the quality or usefulness in industrial applications.

Zirconium for use in nuclear service is supplied to meet individual company specifications (which usually use ASTM nuclear grades and specifications as a starting point). The nuclear grades are listed, showing first the ASTM designation, then any alternate designation:

- R 60001 unalloyed zirconium with a long list of controlled impurities to make it satisfactory for nuclear service. Primarily iodide zirconium for the first reactor core
 R 60802 (Zircaloy 2) an alloy containing 1.5 Sn, 0.15 Fe, 0.1 Cr, and 0.05 Ni used primarily in pressurized water reactors
 R 60804 (Zircaloy 4) an alloy containing 1.5 Sn, 0.2 Fe, 0.1 Cr used primarily in boiling water reactors
 R 60901 (Zr2.5Nb, 705) an alloy containing 2.5 Nb, used primarily for pressure tubes in the Canadian CANDU reactors

All of these grades are hafnium free, i.e., < 100 mg Hf/kg Zr.

U.S. and Canadian specifications for zirconium products are listed in Table 30.3.

Table 30.3: Specifications for zirconium and zirconium alloy products.

Zirconium product	Industrial		Nuclear		
	ASTM	ASME	ASTM	DOE	AECL
Sponge	B494		B349		
Ingot	B495		B350	M10-IT	MET 52
Forgings	B493			M2-9T	
Bar (rod) and wire	B550	SB550	B351	M7-9T	MET 62
Strip, sheet, and plate	B551	SB551	B352	M5-6T	MET 59
Tubes, seamless and welded	B523	SB523	B353	M3-8T	MET 92
Tubes, nuclear fuel cladding			B811		MET 56
Pipe, seamless and welded	B658	SB658			
Welding fittings	B653				
Bare welding rods		SFA2.54*			
Castings	B752				

* Also American Welding Society spec. A2.54.

30.8 Uses

Zirconium is produced almost exclusively as the hafnium-free metal. Most of this metal is used in zirconium alloys containing low levels of tin or niobium, for structural parts in the core of water-moderated nuclear reactors. For this use, zirconium has several desirable attributes: it is ductile, i.e., it can be formed. It has good strength up to 450 °C, i.e., it does not deform at reactor core temperature. Its alloys have hot-water and steam corrosion resistance, i.e., it lasts a long time in normal use. It has low thermal neutron cross section i.e., neutrons are not absorbed, shutting down the nuclear reaction. Its ore is readily available.

Zirconium is used for building chemical process equipment for those applications where its corrosion resistance is needed. In hot sulfuric acid up to 65% concentration, zirconium is used in facilities which produce hydrogen peroxide, acrylic films and fiber, methyl methacrylate, and butyl alcohol. Zirconium is used in the cooler condenser on a nitric acid absorption column. The operation conditions are 200 °C and 1035 MPa. One condenser constructed with zirconium tubes and zirconium/304L stainless steel explosion-bonded tubesheets contains over 18 km of zirconium tubing and has been in service for twelve years. Zirconium is used in contact with ammonium carbamate in urea production, in production of acetic and formic acid, and in many hydrochloric acid environments. In these applications zirconium's corrosion resistance is excellent and the long life of the equipment has justified the use of zirconium.

Zirconium foil, 0.002 mm, is used as the ignition-flash material in photographic flash bulbs, just as zirconium powder used to be one ingredient in the old open "flash pans" of earlier photographers, but this usage is fading because of built-in electronic flashes in newer cameras. Zirconium powder is still used in pyrophoric applications.

Zirconium and zirconium alloys with aluminum, iron, titanium, or vanadium are used for gettering in vacuum tubes [28], inert gases, and ultra-high-purity environments for the

semiconductor industry [29]. Heated zirconium absorbs, traces of oxygen, nitrogen, carbon monoxide, carbon dioxide, and water irreversibly. Hydrogen is reversibly adsorbed. The adsorbed materials diffuse into the bulk of the getter alloy, providing fresh surface for renewed adsorption. For ultra-pure inert gases, getters are used at the point of use to remove contaminants picked up from storage tanks or piping systems. Getters are used in gettering pumps for improving the quality of vacuum in ultra-high-vacuum systems.

Zirconium in the forms of clean, chopped machining chips, crushed sponge or magnesium-zirconium reguli turnings are often used in place of master alloys for zirconium additions to steel melts, super alloys, and nonferrous alloys.

30.9 Economic Aspects

Ores and Minerals. The four major producing countries for the world's current estimated annual production of 10^6 t of zirconium minerals are Australia 50%, South Africa 25%, United States 10%, and Ukraine 6%. Australia and South Africa are the major exporting countries. Europe, Japan, China and the United States are major importers.

There are no zircon mines. Zircon is recovered as a by-product of the extraction of the titanium-containing minerals rutile, ilmenite, and leucoxene. The producers of these minerals adjust their output to follow paint-market demand for titanium oxide pigment. Therefore, the supply and the demand for zircon are rarely in phase and zircon prices have wide swings. During 1975–1995, zircon prices ranged from \$75 per tonne to over \$1000 per tonne in late 1989. The price during 1990–1995 averaged \$250–300 per tonne, varying with quality.

Consumption of zirconium ores continues its gradual growth. In 1975, world production of zircon was 500 000 t and by 1995 it had essentially doubled. Currently, the growth in demand for zirconium materials is being led by

its use as a opacifier in glazed ceramic tile manufacture.

Metals. Less than 4% of the zirconium ores are used in the manufacture of zirconium metals. Since the incident at Three Mile Island, the meltdown at Chernobyl, and the ending of the cold war, the demand for commercial nuclear power and for military naval propulsion systems has diminished. It is estimated that in 1994 total world production was ca. 4000 t, compared to ca. 8000 t in 1982.

The United States has the largest production capacity with two producers: Teledyne Wah Chang in Albany, Oregon (nameplate capacity ca. 3000 t/a) and Western Zirconium in Ogden, Utah (nameplate capacity ca. 1500 t/a). In France, the Compagnie européenne du zirconium (CEZUS), owned jointly by Pechiney, Framatome and Cogema, has a capacity of ca. 2000 t/a. The capacity of the Pripirovsky plant in Ukraine is estimated to be 3000 t/a of calcium-reduced reguli, which is crystal-bar refined at Glasnov, Russia. The Indian plant in Hyderabad has a nameplate capacity of 300 t; production is consumed internally. Japan is not presently producing zirconium sponge.

Prices in 1994 were \$20–28 per kilogram of sponge and \$45–110 per kilogram for cold-rolled sheet, strip, or foil.

30.10 Compounds

In anhydrous halide-salt melts zirconium may exhibit valences of 4, 3, 2 or 1, but in aqueous solution its oxidation state is 4+. Zirconium compounds have coordination numbers of 6, 7, or 8. The colorless ion is hydrolyzed in aqueous solution. Because of the ion's high charge and small radius, zirconium has a great tendency to hydrolyze and to form polymers. It is believed that most zirconium in aqueous solution is present as a tetramer $[\text{Zr}_4(\text{OH})_4]^{8+}$ [30]. Therefore, $\text{ZrOCl}_2 \cdot 8\text{H}_2\text{O}$, by formula, is actually $[\text{Zr}_4(\text{OH})_4 \cdot 7\text{H}_2\text{O}]_4\text{Cl}_8$. Hydrolysis and further polymerization of these tetramer units occurs with time, by heating, or with decreasing acidity.

True equilibrium may take days or weeks. The following anions are listed with respect to their ability to form complexes with zirconium: $\text{I}^- \approx \text{Br}^- < \text{ClO}_4^- < \text{Cl}^- < \text{NO}_3^- < \text{SO}_4^{2-} < \text{F}^- \approx \text{C}_2\text{O}_4^{2-} \approx \text{PO}_4^{3-} < \text{CO}_3^{2-} < \text{OH}^-$.

30.10.1 Silicate

Zirconium silicate, ZrSiO_4 , occurs in nature as the mineral zircon. It can be made by heating an intimate mix of zirconia and silica to just above 1500 °C. The crystals are tetragonal with the zirconia and silica linked through shared oxygen atoms, forming edge-sharing alternating ZrO_8 triangular dodecahedra and SiO_4 tetrahedra [31]. Other, more complex silicates are also found in nature (see Section 30.5). Zirconium silicate is resistant to acids, aqua regia and cold alkali solutions. It is readily attacked by sodium oxide, by sodium hydroxide at 600 °C and by reaction with hot alkaline compounds. Above 800 °C zircon is reduced by carbon, the basis for the carbochlorination process.

Uses. Zircon's mechanical strength, chemical stability and high melting point make it a desirable refractory. Total world production of zircon was $(850\text{--}1060) \times 10^3$ t/a for 1990–1995. Of this ca. 35–40% is used in ceramic glazes and enamels, ca. 30–35% in refractories, 15–20% in foundry use, 8–12% in abrasives, and 8–12% in other uses including chemicals, metals and alloys, and glass constituents.

In the largest use, decorative ceramics, milled or micronized zircon is used as an opacifier for tile glazes and porcelain enamels. Zircon's high refractive index gives the glaze a white, opaque appearance.

Zircon is a popular refractory in the glass and steel industries. The glass industry uses fused zircon and AZS (alumina-zirconia-silica) refractories which have a high corrosion resistance to molten glass. The AZS refractories are made by electric furnace fusion of alumina and zircon. The steel industry uses zircon in ladles and continuous casting nozzles. Refractory applications were once the leading markets for zircon but they decreased

significantly following the zircon shortage in the late 1980s. Other less expensive refractories such as alumina spinels were substituted.

Zircon is used in foundries as a basic mold material and as a facing on other mold materials. The high thermal conductivity of zircon gives higher cooling rates than other mold materials. Zircon's high melting point, low coefficient of thermal expansion, and chemical stability make it the preferred mold facing, particularly in precision casting.

Alloyed AZ (alumina-zirconia) abrasives are made from 60–90% alumina-zirconia grains produced by fusing alumina with baddeleyite, or zirconia derived from zircon, in electric arc furnaces. The addition of zirconia toughens the alumina, reducing its brittleness. The abrasives have particular application in the grinding of steel and steel alloys because of high strength, hardness, and surface crystal sharpness, resulting in fast grinding and long wheel life.

Zircon is added to glass for television tubes because of its X-ray absorption properties and its ability to toughen the glass.

30.10.2 Oxides

Zirconium oxide occurs naturally as the mineral baddeleyite and is produced by calcining of other zirconium compounds. Three phases are stable at atmospheric pressure: cubic above 2370 °C, tetragonal above 1170 °C, and monoclinic below 1000 °C. Transformation of the monoclinic phase to the tetragonal phase begins at ca. 1050 °C and is complete at ca. 1170 °C. The transformation is accompanied by a volume shrinkage of 3–5%. The transformation has a thermal hysteresis: on gradual cooling the tetragonal phase is stable to ca. 1000 °C and only finishes conversion to monoclinic at ca. 800 °C. With rapid quenching the tetragonal phase is metastable to room temperature.

The high-temperature cubic phases can be stabilized down to room temperature by the addition of magnesia, calcia, yttria, or rare earth oxides, whose presence creates vacancies in the zirconium anion lattice. These sta-

bilized zirconium oxides contain from 3% yttria to 8% calcia. They have the same crystal structure from room temperature to melting, avoiding the catastrophic mechanical failure suffered by pure zirconia ceramic parts on transforming from the tetragonal to monoclinic phase while cooling.

Later, GARVIE [32] discovered that certain partially stabilized zirconias could be thermally cycled to precipitate metastable tetragonal zirconia within the grains of cubic zirconia. These materials had higher toughness than fully stabilized zirconias. The increased toughness of partially stabilized zirconia (PSZ) is the result of stress-induced martensitic transformation of the metastable tetragonal grains to the monoclinic form in the stress field of a propagating crack. This led to development of an entirely tetragonal zirconia, known as tetragonal zirconia polycrystal (TZP). The evolution of these materials and their growing application in structural ceramics can be followed in [33–38]. An introduction to zirconia ceramics is given in [39].

Zirconia also has a high-pressure (10 GPa) orthorhombic structure which can be stabilized to atmospheric pressure by addition of > 12 mol% of niobia or tantalum or a mixture thereof [40]. No transformation toughening was found [41].

Stable lower oxides of zirconium are not known, although oxygen dissolved in the zirconium metal lattice has led to the identification of some superstructures as $ZrO_{0.3}$ [42]. Zirconium monoxide, ZrO , has been observed in mass spectrographic measurements [43]. The black oxide surface on zirconium metal after exposure to water at 350 °C is a slightly substoichiometric $ZrO_{1.95}$.

Zirconia is very resistant to acids and alkalis, but slowly dissolves in concentrated hydrofluoric acid or hot concentrated sulfuric acid. Zirconia is resistant to many fluxes, molten glasses, or melts, silicate, phosphate, or borate, but is attacked by fluoride or alkaline melts. Zirconium oxide and alkaline oxides or caustics can be fired together to form solid-solution oxides, zirconate compounds, or a mixture of both.

Zirconium oxide is reduced by carbon, beginning at ca. 600 °C. With excess carbon, in a vacuum furnace, the reaction proceeds rapidly to zirconium carbide at 1500 °C. In the presence of chlorine the carbon reduction gives zirconium tetrachloride and carbon dioxide.

Uses. Zirconium oxide is used to coat the surface of titanium oxide pigment particles for some grades of exterior service paints. The coating minimizes ultraviolet excitation of the titania, which would interact with the organic paint binder, shortening the service life. Zirconia has been used in place of titania as the pigment of white camouflage paints for use in snow environments because zirconia more closely simulates snow in the infrared and microwave spectra. Over 300 t of single-crystal cubic zirconia are grown each year to provide low-cost gems for the jewelry trade [44]. Stabilized zirconia is being used in everyday applications such as fishing rod ferrules, knives, unbreakable shirt buttons, and golf putter heads.

While stabilized zirconias are insulators at room temperature, at elevated temperatures the vacancies in the anion lattice allow O^{2-} ions to diffuse and the zirconia becomes a solid electrolyte with applications in oxygen sensors and high-temperature fuel cells. Some stabilized zirconias can be used as resistors or susceptors. Inductively heated yttria-stabilized zirconia cylinders are used as heat sources to melt quartz boules for the drawing of quartz optical fibres.

Zirconia is a constituent of lead zirconate titanate (PZT) used in piezoelectric ceramics for applications as gas furnace and barbecue igniters, microphone and phonograph crystals, ultrasonic transducers for medical ultrasound imaging, for agitation in cleaning tanks, and for underwater sonar. With the further addition of lanthanum (PLZT), ferroelectric optically active transparent ceramics have become available [45].

Hydrous Oxide. Neutralization of an aqueous zirconium solution causes hydrolysis and condensation of the zirconium cations, forming a

white gel called zirconium hydroxide but generally considered to be a hydrous oxide. The freshly precipitated amorphous gel is generally considered to be a network of tetramer units $[Zr_4(OH)_8 \cdot 16H_2O]^{8+}$ linked through hydroxyl groups; it is easily dissolved by dilute or weak acids. As the gel ages some of the hydroxyl links are converted to oxo links, and the gel's reactivity decreases. Upon heating to 500 °C the gel yields monoclinic or metastable tetragonal oxide, or a mixture of these. The specific structure obtained has been attributed to the precursor zirconium salt [46], pH of the liquid in final contact with the condensed gel [47], electronegativity and pH [48], slow or rapid condensation from sol to gel, ageing, the presence during gelling of sulfate, sodium, potassium, or ammonium ions, and particle size [49].

Hydrous zirconium oxide in controlled particle size is prepared by hydrolysis of sodium zirconate [50].

Hydrous zirconium oxide sol is used in sol-gel processes to produce stabilized zirconias in spherical or fibrous form, and to form an oxidation-protective film on stainless steels.

30.10.3 Chlorides and Hydroxide Chlorides

The fully chlorinated form of zirconium is zirconium tetrachloride. The tetrachloride is normally produced by carbochlorination of zircon or zirconia [51] or by reacting zirconium metal with chlorine or hydrogen chloride. Chlorinated hydrocarbons, particularly carbon tetrachloride, chloroform, or hexachloroethane, are useful laboratory chlorinating agents. Zirconium tetrachloride can be formed by reacting ferrozirconium or silicozirconium with iron(II) chloride at elevated temperature [52].

Zirconium tetrachloride vapor is a tetrahedral monomer which crystallizes below 331 °C in a AB_4 type structure with $ZrCl_6$ octahedra coupled to each other by two edges to form a zigzag chain. Each zirconium has four bridging chlorine ligands and two terminal chlorines which are mutually *cis* [53]. Some

physical properties of zirconium tetrachloride are shown in Table 30.4.

Table 30.4: Physical properties of zirconium tetrahalides.

Property	ZrF ₄	ZrCl ₄	ZrBr ₄	ZrI ₄
Color	white	white	white	orange-yellow
Density, kg/m ³	4430	2800	3980	4850
Sublimation temperature (101.3 kPa)	903	331	357	431
Melting point, K	923	437	450	499
Critical temperature, K	932	503.5	532	686
Critical pressure, MPa		5.7	4.3	4.1
Crystal structure	mono-clinic	mono-clinic	cubic	cubic

Zirconium tetrachloride reacts rapidly with water, vapor or liquid, to exchange two chlorines for oxygen. Any handling of zirconium tetrachloride must be in moisture-free atmospheres to avoid degradation. Zirconium tetrachloride powder fed into water hydrolyzes to form a solution of zirconium hydroxide chloride and free hydrochloric acid. Zirconium tetrachloride vapor reacts with steam to yield zirconium oxide, and reacts with water to yield either an oxide slurry or hydroxide chloride solution.

Zirconium tetrachloride is used to form zirconium nitride coatings, to react electrochemically to form zirconia in high-temperature fuel cells, to react with alcohols to form alkoxides, and to produce zirconium organometallic compounds. Zirconium tetrachloride is reduced by molten alkali and alkaline earth metals, yielding zirconium metal.

Zirconium tetrachloride reacts reversibly with ammonium chloride, alkali metal chlorides, and alkaline earth chlorides to form hexachlorozirconates [54, 55]. Zirconium tetrachloride forms addition compounds with aluminum and iron trichlorides and phosphorus pentachloride, but FeZrCl_6 dissociates to FeCl_2 and ZrCl_4 above 350 °C.

Lower valent zirconium chlorides including zirconium trichloride, dichloride, monochloride, and zirconium chloride cluster phases $\text{Zr}_6\text{Cl}_{12}$ and $\text{Zr}_6\text{Cl}_{15}$ are produced by reduction of zirconium tetrachloride with zirconium metal or with zirconium monochloride in sealed tantalum containers. The reactions are slow, usually requiring weeks at 300 to

800 °C [56–58]. Zirconium monochloride reacts reversibly with hydrogen at 340 °C in a sealed tube to form ZrClH_x ($x \leq 1$) [59].

Hydroxide Chlorides. Zirconium hydroxide dichloride, empirically $\text{Zr}(\text{OH})_2\text{Cl}_2 \cdot 7\text{H}_2\text{O}$, has been known by several names: zirconyl chloride, zirconium oxychloride, zirconium oxide dichloride, all commonly identified as $\text{ZrOCl}_2 \cdot 8\text{H}_2\text{O}$. Structurally the hydroxide dichloride is really $[\text{Zr}_4(\text{OH})_8 \cdot 16\text{H}_2\text{O}]\text{Cl}_8 \cdot 12\text{H}_2\text{O}$ [60].

Zirconium hydroxide dichloride solution is formed by dissolving hydrous zirconium oxide or zirconium carbonate in hot hydrochloric acid, or by hydrolysis of zirconium tetrachloride in water. The solubility in hot water is quite high and the solubility is decreased by cooling and by adding hydrochloric acid. Excellent recoveries are obtained by crystallization ending with a 6 N hydrochloric acid mother liquor. This crystallization procedure also leaves most impurities dissolved in the mother liquor. Crystallization may be repeated to obtain very pure crystals.

Zirconium hydroxide dichloride crystals dissolve in their hydration water on gentle heating, and readily lose the hydrates outside the tetramer unit. With continued heating both water and hydrogen chloride are evolved until zirconium oxide remains [61, 62].

Zirconium hydroxide monochloride, $[\text{Zr}_4(\text{OH})_{12} \cdot 16\text{H}_2\text{O}]\text{Cl}_4$, is formed in solution by reacting equimolar portions of zirconium hydroxide dichloride and hydrous zirconium oxide or zirconium basic carbonate, or by the action of hydrogen peroxide upon zirconium hydroxide dichloride [63].

Anhydrous zirconium oxide chlorides have been prepared: the reaction of zirconium dioxide with zirconium monochloride at 980 °C produced ZrClO_x ($x < 0.42$) [64]. The reaction of zirconium tetrachloride powder in carbon tetrachloride with dichlorine oxide at –30 °C yielded ZrOCl_2 , which dissociated to ZrCl_4 and ZrO_2 above 200 °C [65].

30.10.4 Bromides

Zirconium tetrabromide, ZrBr_4 , can be prepared by heating zirconium metal or carbide above 400 °C in a stream of bromine, or similarly a fine mixture of zirconium oxide and carbon at 900 °C. Its behavior is similar to zirconium tetrachloride but, because of its higher cost, the tetrabromide is of little commercial interest. Some physical properties are shown in Table 30.4.

Zirconium tribromide, zirconium dibromide, zirconium monobromide, and zirconium monobromide hydride can be made by the same procedures used for their chloride analogues [66].

30.10.5 Iodides

Zirconium tetraiodide, ZrI_4 , is important because of its use in the van Arkel–de Boer refining process. The tetraiodide cannot be produced by heating fine zirconium oxide and carbon in iodine vapor, but is produced by heating zirconium metal to 300 °C in iodine. A temperature of ca. 1000 °C is required for a reasonably rapid reaction of iodine with zirconium carbide, carbonitride, or nitride. Zirconium tetraiodide is oxidized by dry air at about 200 °C. Some physical properties are shown in Table 30.4.

Lower-valence iodides have been made by reduction of zirconium tetraiodide with zirconium in sealed tantalum tubes or with zirconium or aluminum in aluminum iodide solvent [67]. Compounds formed include zirconium triiodide, zirconium diiodide ii (both α monoclinic and β orthorhombic forms), zirconium clusters Zr_6I_{12} , and zirconium monoiodide [68].

30.10.6 Fluorides

There are several methods for the production of zirconium tetrafluoride, ZrF_4 . Anhydrous zirconium tetrafluoride is produced in good purity by mixing hydrogen fluoride gas and zirconium tetrachloride vapor at 350 °C [69]. The hydrofluorination of zirconium oxide proceeds rapidly at 25 °C, followed by a

purifying sublimation in dry hydrogen fluoride at 825 °C [70]. Zirconium tetrafluoride monohydrate is precipitated by adding strong hydrofluoric acid to a concentrated zirconium nitrate/nitric acid solution. The filtered crystals are washed with nitric acid, dried, and dehydrated with hydrogen fluoride at 450 °C [71]. Zirconium metal or zirconium hydride can be fluorinated with hydrogen fluoride but unless the reaction is conducted above 800 °C, the tetrafluoride products coats the metal, impeding the reaction. Zirconium oxides mixed with ammonium hydrogen difluoride and heated to 200 °C yields ammonium heptafluorozirconate, $(\text{NH}_4)_3\text{ZrF}_7$, which, on heating to 500 °C, gives off ammonium fluoride. Some physical properties of zirconium tetrafluoride are shown in Table 30.4.

Zirconium tetrafluoride is hydrolyzed in water to a hydroxide fluoride $\text{Zr}_4(\text{OH})_6\text{F}_{10} \cdot 3\text{H}_2\text{O}$ with limited solubility. With increasing hydrofluoric concentration, $\text{ZrF}_4 \cdot 3\text{H}_2\text{O}$ crystallizes at 30–35% HF, $\text{HZrF}_5 \cdot 4\text{H}_2\text{O}$ at 30–35% HF, and $\text{H}_2\text{ZrF}_6 \cdot 2\text{H}_2\text{O}$ at 40–60% HF. In strong nitric or sulfuric acid containing excess hydrofluoric acid, the monohydrate crystallizes. Heating these hydrates produces ZrOF_2 at 300 °C.

Very high purity anhydrous zirconium tetrafluoride is a major constituent of some fluoride glasses, particularly ZBLAN, being developed because their transparency for near UV to mid IR (0.3–6 μm) was projected to be better than that of quartz optical fiber.

Potassium hexafluorozirconate production by fluorosilicate fusion is described in Section 30.6. This compound has been used to introduce zirconium into molten aluminum and magnesium as a grain refiner.

As mentioned in Section 30.7, zirconium metal is customarily pickled in dilute hydrofluoric acid/nitric acid solution. To minimize fluoride waste discharge the pickling solution is regenerated by adding sodium fluoride to precipitate sodium fluorozirconates. The particular salt precipitated varies with the sodium fluoride concentration: $\text{NaZrF}_5 \cdot \text{H}_2\text{O}$ is precipitated when the sodium fluoride concentration is less than 0.21%, and Na_2ZrF_6 is precipitated

if the sodium fluoride concentration is between 0.21 and 0.4%. At higher sodium fluoride concentration $\text{Na}_3\text{Zr}_2\text{F}_{13}$ and Na_3ZrF_7 precipitate.

Zirconium tetrafluoride forms many double fluoride compounds in different proportions with alkali fluorides, alkaline earth fluorides, and others as diverse as stannous hexafluorozirconate and zirconium hexafluorogermanate, both proposed for caries prophylaxis.

30.10.7 Sulfates

The sulfates of zirconium are classified as anionic, normal, or basic, depending on the sulfate to zirconium ratio. For anionic complexes this ratio is > 2 . Normal sulfates have a ratio of exactly two, and basic sulfates have less than two sulfates per zirconium. Basic sulfates made by hydrolysis of neutral sulfates usually have a ratio > 1 , while basic sulfates precipitated by adding sulfate ions to hot dilute solutions of zirconium hydroxide chloride have a ratio < 1 , usually 0.4–0.7.

Zirconium sulfate solutions can be generated by the action of strong sulfuric acid on hydrous zirconium oxide, zirconium oxide, zirconium carbonitride, zirconium metal, or basic zirconium sulfate. Normal zirconium sulfate, $\text{Zr}(\text{SO}_4)_2 \cdot 4\text{H}_2\text{O}$, also known as zirconium orthosulfate, can be crystallized from the above solution, or from a zirconium hydroxide chloride solution by adding sulfuric acid up to a concentration of 45% and allowing the solution to cool below 60 °C. A better purification is obtained during the crystallization if the solution contains some chloride ion.

Ammonium zirconium sulfates can be prepared by heating zirconium oxide with ammonium sulfate at 400 °C [72] or by precipitation from a zirconium sulfate solution [73]. A crude sodium zirconium sulfate can be prepared by adding sulfuric acid to sodium zirconate. Structure and composition of many sulfate variants are discussed in [30, 74, 75].

Basic zirconium sulfates containing less than one sulfate per zirconium are precipitated from hot acidic solutions of zirconium hydroxide chloride by adding 0.4–0.6 mol of sul-

fate per zirconium. The stoichiometric formula is $\text{Zr}_5\text{O}_{10-x}(\text{SO}_4)_x$ ($x = 1.8\text{--}3.5$). The most common basic sulfate is $\text{Zr}_5\text{O}_7(\text{SO}_4)_3 \cdot n\text{H}_2\text{O}$.

Normal zirconium sulfate is used for leather tanning, as a catalyst, to coat titanium oxide pigment powder, and for conversion to other zirconium chemicals. The basic sulfate is converted into other zirconium chemicals, many retaining the particle size developed during the controlled precipitation of the basic sulfate.

30.10.8 Carbonates

Basic zirconium carbonate is produced by adding basic zirconium sulfate to a sodium carbonate solution, and filtering the insoluble basic carbonate. The empirical formula is $\text{ZrO}_2 \cdot \text{CO}_2 \cdot x\text{H}_2\text{O}$ but the zirconium to carbonate ratio varies considerably.

The basic carbonate is reacted with organic acids to make soluble zirconium salts, such as the citrate, oxalate, and acetate, free of chloride and sulfate ions. The carbonate is used to make a zirconium–aluminum–glycine complex, an active ingredient of antiperspirant formulations.

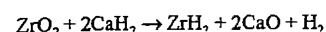
Zirconium basic carbonate is added to potassium carbonate or ammonium carbonate solutions to make water-soluble double carbonates. At room temperature, these solutions hydrolyze so slowly that they are considered to be stable for a month, but on heating carbon dioxide evolves and insoluble hydrous zirconium oxide forms. Ammonium zirconium carbonate, empirically $(\text{NH}_4)_3[\text{Zr}_2\text{O}(\text{OH})_3(\text{CO}_3)_3]$ is used extensively in bonding starch onto coated paper [76], and in controlling pitch deposition in pulp and papermaking systems [77].

30.10.9 Hydride

Zirconium hydride, ZrH_2 , is prepared by the reversible absorption of hydrogen into heated zirconium, usually sponge or ingot slices. The metal is heated above 600 °C in an inert atmosphere or vacuum to dissolve the

surface oxide film, then hydrogen is introduced. At 600 °C, hydrogen dissolves into the α -phase metal up to 6 atom%, when β -Zr appears. (Hydrogen is a β -phase stabilizer, lowering the transformation temperature from 863 to 550 °C). At 40 atom% the solubility in β -Zr is exceeded and δ -phase hydride appears. At 60–64 atom% only δ phase exists. Above 64 atom% the tetragonal ϵ -phase is stable [78]. To obtain fully hydrided ZrH_2 the charge is cooled to 300 °C in full hydrogen atmosphere.

The reduction of zirconium oxide with calcium hydride yields a fine (2–5 μm particles) hydride powder for use in pyrotechnics such as fuses or fireworks:



Extreme care must be used in dissolving the calcium oxide to recover the hydride powder.

Hydriding of zirconium sponge or ingot is the first step in producing coarse zirconium powder for powder metallurgy applications. Hydrided metal begins to lose its ductility above 40 atom% hydrogen, and above 60 atom% the hydrided metal is quite brittle and suitable for crushing, which is conducted in an inert atmosphere. During hydriding, the metal density decreases with increasing hydrogen content, going from 6.5 to 5.6 when fully hydrided.

Zirconium hydride loses hydrogen upon heating. For complete dehydriding the powder must be heated under vacuum (e.g., 700 °C until the vacuum falls to 10^{-3} Pa). Dehydriding is faster at higher temperatures but the powder begins to sinter.

Zirconium hydride contains about the same number of hydrogen atoms per volume as room-temperature water, and some alloys such as ZrNi and ZrCr_2 can hold even more [79]. Zirconium hydride has been used in the nuclear industry as a moderator for thermal neutrons in compact, high-temperature reactors. Zirconium hydride is of interest for hydrogen storage and nickel-base hydrogen battery applications.

Zirconium hydride is inert to air and water at room temperature. It ignites in air at 340 °C or lower, depending on powder size. Zirconium

hydride is resistant to corrosion by carbon dioxide up to 315 °C.

Zirconium hydride heated with carbon yields the hexagonal zirconium carbohydride, $\text{ZrC} \cdot \text{ZrH}_{1.46}$ [80]. Zirconium monochloride reversibly absorbs hydrogen up to ZrClH [81].

30.10.10 Carbide

Zirconium carbide, ZrC , is a hard, brittle metallic carbide. It is an electrical conductor and does not hydrolyze in water. It is an interstitial carbide with the carbon atoms occupying the octahedral interstices of the zirconium lattice, at 2000 °C, carbon is soluble in liquid zirconium up to 38.5 atom%. Zirconium carbide is a single phase within the concentration range of 38.5–49.4 atom% carbon with a congruent composition of 44 atom% carbon at the melting point of 3445 °C [82, 83].

Zirconium carbide can be produced from zircon by reduction with coke in electric arc furnaces [84]. An intimate mix of fine zirconium oxide and carbon black heated in vacuum or hydrogen in an induction-heated graphite crucible at 1600 °C yields a porous, light zirconium carbide. Milling and refining above 2200 °C gives a dense powder. Zirconium tetrachloride and methane in a hydrogen atmosphere are heated to 1200 °C to deposit zirconium carbide films on tool bits. Pure zirconium metal powder and fine graphite powder react exothermically, once ignited, to form zirconium carbide, usually to form a composite with an excess of one reagent.

30.10.11 Nitrides

Zirconium nitride, ZrN , is a golden-colored, hard, brittle metallic nitride. It is thermally and chemically stable, and has low resistivity. As with the carbide it is an interstitial compound with a NaCl cubic structure. At 2000 °C, nitrogen is soluble in liquid zirconium up to 39 atom% nitrogen. Zirconium nitride is a single phase within the concentration range of 39–50 atom% nitrogen [85, 86]. While 3253 K is the accepted melting point of zirconium nitride, the melting temperature of

3970 K as measured in a positive pressure of nitrogen [87] is compatible with a thermodynamic study of the Zr-N system.

Zirconium nitride has been made by heating zirconium or zirconium hydride powder in nitrogen at 1000 °C, and by heating a zirconium oxide/carbon mixture in a nitrogen atmosphere. The reaction of zirconium tetrachloride with ammonia or nitrogen and hydrogen has been used to produce nitride powder and to deposit coherent films on substrates at 1000–1200 °C. Very limited quantities of nitride have been made by the very exothermic reaction of lithium nitride and zirconium tetrachloride powders [88].

Metastable Zr_3N_4 has been made by dual ion beam deposition [89] and by reacting zirconium tetraiodide with ammonia at 500 °C and heating the product to Zr_3N_4 at 700 °C [90]. On further heating to 1000 °C ZrN is formed. Thin films of Zr_3N_4 have been grown by passing ammonia and tetrakis(diethyl-amido)zirconium over substrates at 200–400 °C [91].

Zirconium nitride has been used as a wear-resistant coating on steel drill bits and cemented-carbide tool bits, as decorative coating, as a protective coating on steel vessels handling molten metal, and as solar energy collector surface film.

30.10.12 Borides and Borates

While three zirconium borides, ZrB , ZrB_2 , and ZrB_{12} are found in the zirconium-boron system, only the diboride is chemically and thermally stable. Zirconium diboride is a gray refractory solid with a hexagonal crystal structure and a very high melting point of 3245 °C. Technical-quality zirconium diboride can be prepared by reacting zircon, boron oxide, and carbon in a submerged-electrode arc furnace [92]. Purer diboride can be produced by co-reduction of zirconium tetrachloride and boron trichloride with hydrogen or aluminum in a chloride bath. Zirconium diboride films can be produced by subliming zirconium tetrahydridoborate at 25 °C in a vacuum and passing the vapor over a substrate heated to 250 °C.

Zirconium diboride has high hardness, good oxidation resistance, and excellent thermal-shock resistance. It has been used as a diffusion barrier in semiconductors, as a container for molten metals, and as a burnable absorber in nuclear reactor cores.

Zirconium tetrahydridoborate, $Zr(BH_4)_4$, is prepared by reaction of zirconium tetrachloride with lithium tetrahydridoborate in diethyl ether, followed by double distillation at 20 °C [93]. It has a tetrahedral structure with three hydrogen atoms bridging the zirconium atom and each boron atom. Zirconium tetrahydridoborate is one of the most volatile zirconium compounds known: *mp* 29 °C; *bp* 118 °C; vapor pressure 2 kPa at 25 °C. Its decomposition near 250 °C forms the basis for a low-temperature method of depositing zirconium boride films. Zirconium tetrahydridoborate catalyzes the polymerization of unsaturated hydrocarbons. It reacts with aliphatic alcohols to form zirconium and boron alkoxides [94]. Zirconium tetrahydroborate inflames on contact with dry air.

30.10.13 Tungstate

Zirconium tungstate is precipitated as a white gel by simultaneous addition of dilute solutions of sodium tungstate and zirconium hydroxide dichloride to vigorously stirred water. After acidification the slurry is refluxed. The dried and fired product is ZrW_2O_8 [95]. Other studies indicate that ZrW_2O_8 is formed by the reaction of a mixture of ZrO_2 and WO_3 which is held between 1100 and 1400 °C for at least 24 h melts incongruently at 1257 °C and dissociates below 1105 °C [96]. ZrW_2O_8 is an unusual compound which contracts equally in each dimension when it is heated over the temperature range 1–1050 K [97].

30.10.14 Phosphate

Insoluble, amorphous zirconium phosphate is obtained when a zirconium salt is added to an excess of phosphoric acid. If the original salt was solid rather than in solution, the resulting phosphate will have a similar

physical size and shape: i.e., beads, granules, fibers. Refluxing the precipitate in strong phosphoric acid gives a crystalline product of constant composition, $Zr(HPO_4)_2 \cdot H_2O$. Zirconium bis(monohydrogenphosphate) with one water of hydration is known as α -zirconium phosphate. Below 80 °C a second water of hydration is added to form γ -zirconium phosphate. On heating α -zirconium phosphate, the water is lost between 300 and 650 °C, leaving β -zirconium phosphate. Conversion to zirconium pyrophosphate, ZrP_2O_7 , occurs between 800 and 920 °C [98].

Zirconium bis(monohydrogenphosphate) has ion exchange properties and, because of its structure and bonding between layers, can also act as an intercalation compound [99]. Zirconium phosphate shows excellent catalytic activity for the selective condensation of acetone to mesityl oxide, and when palladium is deposited on the phosphate surface the combination is an effective catalyst for the direct synthesis of methyl isobutyl ketone from acetone and hydrogen [100].

The addition of univalent ions Li, Na, K and compensating trivalent ions In, Y, Eu into ZrP_2O_7 produces a solid electrolyte [101]. Ultralow thermal expansion ceramics have been developed in the $Na_2O-ZrO_2-P_2O_5-SiO_2$ system [102], while the addition of vanadium to sodium zirconium pyrophosphate: $Na_2PrP_{2-x}V_xO_7$ yields a ceramic which shrinks when heated above 60 °C [103].

30.10.15 Nitrates

Zirconium hydroxide dinitrate, $Zr(OH)_2(NO_3)_2$, is formed by dissolving hydrous zirconium oxide in nitric acid or by dissolving zirconium hydroxide dichloride in nitric acid and distilling off the chlorine.

Zirconium tetranitrate, $Zr(NO_3)_4 \cdot 5H_2O$, can be precipitated from strong nitric acid at low temperature, less than 15 °C [104].

30.10.16 Carboxylates

Zirconium hydroxide carboxylates form upon adding carboxylate salts to a solution of

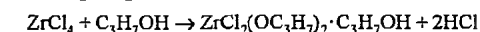
zirconium dihydroxide chloride, or carboxylic acids to zirconium basic carbonate. The general formula is $Zr(OH)_{4-n}(OOR)_n$, where n is 1–3 usually.

When zirconium basic carbonate paste is slowly stirred into a mineral spirit solution of octanoic acid, a solution of zirconium dihydroxide octanoate is produced which is of use in oil-based paints as a dryer catalyst.

Short-chain carboxylates may be soluble, i.e., zirconium dihydroxide diacetate. Longer aliphatic chain carboxylates (zirconium soaps) are water insoluble [105].

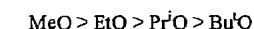
30.10.17 Alkoxides

Zirconium alkoxides are prepared by adding zirconium tetrachloride to anhydrous alcohols [106]:



If there is no steric hindrance, all four chlorines can be exchanged if ammonia is added to combine with the hydrogen chloride.

Alkoxides of different alcohols can be formed by alcohol exchange. This can be facilitated by removal of the more volatile alcohol, or a lower-boiling azeotrope with an inert solvent such as benzene. The conversion of zirconium tetramethoxide by refluxing with tertiary butanol proceeds only to zirconium methoxide tri-*tert*-butoxide because of steric factors. The following order was found in the interchange of alkoxy groups:



The reaction of *tert*-butanol with zirconium tetrahydridoborate yielded a double alkoxide complex of zirconium *tert*-butoxide with bis(*tert*-butoxy) borane [94].

Zirconium alkoxides hydrolyze quite easily. This provides a route to high-purity, high-surface-area zirconium oxide.

30.11 Analysis

Analysis for zirconium in ore, soil, vegetation in compounds, and as a minor alloying constituent involves bringing the zirconium into solution, then precipitating with mandelic

acid [107] and firing the precipitate to oxide. For the determination of zirconium in air samples, plasma emission spectroscopy is used.

Methods to determine the hafnium associated with the zirconium include atomic absorption spectroscopy, emission spectroscopy, mass spectroscopy, X-ray spectroscopy, and neutron activation.

Most impurities in zirconium and zirconium compounds are determined by emission spectroscopy, with arc-spark [108] or plasma excitation [109, 110]. Atomic absorption is also used to determine a variety of impurities [111].

Carbon and sulfur in zirconium are measured by combustion followed by chromatographic or IR determination of the oxides [112]. Hydrogen is determined by thermal conductivity after hot-vacuum extraction, or by fusion of zirconium with a transition metal in an inert atmosphere and subsequent separation by gas chromatography [113, 114].

Simultaneous determination of oxygen and nitrogen is accomplished by fusion of zirconium with a transition metal in the presence of carbon in an inert atmosphere and subsequent separation by gas chromatography [115, 116]. Nitrogen can be determined by the Kjeldahl technique [112].

Phosphorus may be determined by visible spectrophotometry using molybdenum blue [112] but can be determined more rapidly by phosphine, evolution and name emission spectroscopy.

Chloride at low level is determined indirectly by precipitation with silver nitrate and determination of the silver by X-ray or atomic absorption spectroscopy. Fluoride and higher levels of chloride can be measured by selective ion electrode techniques [117, 118].

30.12 Toxicology

Zirconium and its compounds are generally of low toxicity. However, the strongly acidic compounds such as zirconium tetrabromide, zirconium tetrachloride, zirconium tetrafluoride, zirconium tetraiodide, zirconium tetra-

trate and zirconium sulfate are strongly corrosive to eyes, lungs, skin, mouth, esophagus, and stomach. Exposure to these compounds should be avoided, not because they contain zirconium, but because of the acidic nature of their hydrolysis products generated upon contact with animal or plant tissue.

Inhalation of zirconium materials in the workplace has not resulted in significant toxicity in 40 years of considerable exposure if reasonable care was used. One case of pulmonary fibrosis is believed to have been induced by heavy and continued exposure to zirconium oxide dust while preparing slurries for lens polishing which developed after a 15-year latency period [119]. Severe respiratory tract irritation from inhaling zirconium acetoacetate disappeared after exposure ceased [120]. In 1978 the FDA banned the production of antiperspirant aerosols containing zirconium because of concern about possible lung granulomas.

Inhalation laboratory tests with insoluble zirconium oxide varied. Some showed no effect, some caused fibrosis. Russian tests with the insoluble compounds zirconium boride [121] and zirconium hydride [122] both showed fibrogenic action in the lungs of albino rats. Aerosols of soluble zirconium dihydroxide chloride and zirconium dihydroxide nitrate each caused intense irritation of upper breathing passages similar to the action of strong acid. The animals died with 30–40 min. Sodium zirconium lactate caused lung granulomatosis in rabbits [123], and it is indicated that a complex of zirconium chlorhydrate and aluminum chlorhydrate also induces granulomatous lung changes [124].

Antiperspirants and poison ivy remedies containing zirconium have caused skin granulomas as a delayed hypersensitivity reaction in a few users [125].

Toxicity tests on laboratory animals showed that the acute toxicity of inorganic zirconium salts is very low when administered orally. Administered intraperitoneally, both organic and inorganic compounds were 2–20 times more toxic.

An excellent summation of zirconium toxicology through 1975 is available [126]. Toxicity data for some zirconium compounds is shown in Table 30.5.

Table 30.5: Toxicity data (rat) for some zirconium compounds [127].

Compound	Oral LD ₅₀ , mg/kg	Inhalation LCLo, mg/m ³
Dihydroxide chloride	3500	500 for 30 min
Dihydroxide nitrate	2290	500 for 30 min
Sulfate	3500	
Tetrachloride	1688	3124 ppm HCl for 1 hour
Acetate	4100	

The OSHA exposure limit for zirconium and zirconium compounds as airborne particulate is 5 mg/m³ TWA and 10 mg/m³ STEL, as zirconium. In Germany, the MAK is 5 mg/m³ as zirconium. In Russia, MAK is 6 mg/m³ as zirconium.

30.13 Storage and Transportation

High-surface-area zirconium metal such as sponge or powder is a combustible solid which should be kept dry and stored away from sources of ignition and oxidizers.

The Department of Transportation has classified all dry zirconium powder as "spontaneously combustible", hazard class 4.2, with identification number UN 2008. The powders are subdivided into packing group I, II, or III, as evaluated by their burning rate in a standardized testing procedure. Group I is for very fine zirconium powder which is a pyrophoric material. Group I powder may not be shipped by air.

Some zirconium powder, usually fuse powder, is recovered wet and shipped wet. This powder is classified as a flammable solid, hazard class 4.1, UN 1358.

- Zirconium hydride is classified as a flammable solid, hazard class 4.1, UN 1437.
- Zirconium nitrate is classified as an oxidizer hazard class 5.1, UN 2728.
- Zirconium sulfate is classified as corrosive hazard class 8, NA 9163.

- Zirconium tetrachloride is classified as corrosive, hazard class 8, UN 2503.

30.14 References

1. A. E. van Arkel, J. H. de Boer, *Z. Anorg. Allg. Chem.* **148** (1925) 345–350.
2. J. H. De Boer, J. D. Fast, *Z. Anorg. Allg. Chem.* **153** (1926) 18.
3. W. J. Kroll, *J. Franklin Inst.* **260** (1955) 169–192.
4. O. Botstein, A. Rabinkin, M. Talianker, *Scr. Metall.* **15** (1981) 151–155.
5. T. L. Yau in C. S. Young, J. C. Durham (eds): *Industrial Applications of Titanium and Zirconium: Fourth Conference STP 917*, American Society for Testing and Materials, Philadelphia 1986, pp. 57–68.
6. T. L. Yau, R. T. Webster in: *Metals Handbook*, 9th ed., vol. 13, Corrosion, ASM International, Metals Park, OH, 1987, pp. 707–721.
7. B. Mason: *Principles of Geochemistry*, 3rd ed., Wiley & Sons, New York 1966, p. 45.
8. H. L. Gilbert, C. Q. Morrison, A. Jones, A. W. Henderson, *Bur. Mines Invest.* **5091** (1954).
9. H. S. Choi, *Can. Min. Metall. Bull. Trans.* **67** (1965) 65–70.
10. P. H. Wilks, *Chem. Eng. Prog.* **68** (1974).
11. Kawecki Chemical, US 2653855, 1953 (H. C. Kawecki).
12. A. J. Hudson, A. C. Haskell, Jr., *Electr. Furn. Conf. Proc.* **1958**, 211–220.
13. G. von Hevesy, *Chem. Rev.* **2** (1925) 1.
14. N. P. Sajin, E. A. Pepelyaeva, *Proc. Int. Conf. Peaceful Uses At. Energy*, 8th **1956**, 559–562.
15. J. M. Googin in F. R. Bruce, J. M. Fletcher, H. H. Hyman (eds.): *Progress in Nuclear Energy Series 3*, Process Chemistry, vol. 2, Pergamon Press, Oxford 1958, pp. 194–209.
16. R. H. Nielsen, R. L. Govro, *Bur. Mines Invest.* **5214** (1956).
17. N. P. H. Padmanabhan, T. Sreenivas, N. K. Rao, *High Temp. Mater. Process* **9** (1990) no. 2–4, 217–247.
18. L. Moulin, P. Thouvenin, P. Brun in D. G. Franklin, R. B. Adamson (eds.): "Zirconium in the Nuclear Industry: Sixth International Symposium", *ASTM Spec. Tech. Publ.* **824** (1984) 37–44.
19. J. A. Megy, H. Freun, *Metall. Trans. B* **10B** (1979) 413–421.
20. F. W. Starratt, *J. Met.* **II** (1959) 441–443.
21. A. P. Lamaze, D. Charquet in K. C. Liddell, D. R. Sadoway, R. G. Bautista (eds.): *Refractory Metals: Extraction, Processing and Applications*, The Minerals, Metals & Materials Society, Warrendale, PA, 1990 pp. 231–253.
22. S. N. Flengas, G. J. Kipouros, P. Tumidajski, *Met. Mater. Processes* **2** (1990) no. 3, 151–177.
23. Z. M. Shapiro in B. Lustman, F. Kerze, Jr. (eds.): *The Metallurgy of Zirconium*, McGraw-Hill, New York 1955, pp. 135–215.
24. R. F. Rolston: *Iodide Metals and Metal Iodides*, The Electrochemical Society, New York 1961.

25. ASTM Specification B614: Descaling and Cleaning Zirconium and Zirconium Alloy Surfaces.
26. T. L. Yau in R. T. Webster, C. S. Young (eds.): "Industrial Application of Titanium and Zirconium: Third Conference", *ASTM Spec. Tech. Publ.* 830 (1984) 124.
27. J. H. Schemel: "ASTM Manual on Zirconium and Hafnium", *ASTM Spec. Tech. Publ.* (1977).
28. R. I. Jaffee in Z. M. Shapiro in B. Lustman, F. Kerze, Jr. (eds.): *The Metallurgy of Zirconium*, McGraw-Hill, New York 1955, pp. 26-29.
29. D. A. Lorimer, E. J. Baker, M. Succi, D. K. Weber, *Solid State Technol.* 33 (1990) 77-79.
30. A. Clearfield, *Rev. Pure Appl. Chem.* 14 (1964) 91-108.
31. J. A. Speer in P. A. Ribbe (ed.): *Orthosilicates*, 2nd ed., Mineralogical Society of America, Washington DC, 1982.
32. R. C. Garvie, R. H. Hannink, R. T. Pascoe, *Nature (London)* 258 (1975) 703-704.
33. R. C. Garvie in A. E. Alper (ed.): *High Temperature Oxides*, part II, Academic Press, New York 1970, pp. 117-166.
34. A. H. Heuer, L. W. Hobbs (eds.): *Science and Technology of Zirconia*, American Ceramic Society, Columbus, OH, 1981.
35. N. Claussen, M. Rühle, A. H. Heuer (eds.): *Science and Technology of Zirconia II*, American Ceramic Society, Columbus, OH, 1984.
36. S. Somiya, N. Yamamoto, H. Yanagida (eds.): *Science and Technology of Zirconia III*, American Ceramic Society, Westerville, OH, 1988.
37. S. Meriani, C. Palmonari (eds.): *Zirconia '88 - Advances in Zirconia Science and Technology V*, Elsevier Appl. Sci., London 1989.
38. S. P. S. Badwal, M. J. Bannister, R. H. J. Hannink (eds.): *Science and Technology V*, Technomic Publishing Co., Lancaster, PA, 1993.
39. R. Stevens: *Zirconia and Zirconia Ceramics*, 2nd ed., Magnesium Elektron, Manchester, UK, 1986.
40. A. Pissenberger, G. Gritzner, *J. Mater. Sci. Lett.* 14 (1995) 1580-1582.
41. G. Gritzner, C. Puchner, J. Dusza, *J. Eur. Ceram. Soc.* 15 (1995) 45-49.
42. Y. Sugizaki et al., *J. Phys. Soc. Japan* 54 (1985) 2543-2551.
43. R. J. Ackerman, E. G. Rauh, C. A. Alexander, *High Temp. Sci.* 7 (1975) 304-316.
44. J. F. Menckus, *J. Crystl. Growth* 128 (1993) 13-14.
45. G. H. Haertling, C. E. Land, *Am. Ceram. Soc. Bull.* 49 (1970) 411.
46. R. Srinivasan, B. H. Davis, *Catal. Lett.* 14 (1992) 165-170.
47. G. T. Mamott et al., *J. Mater. Sci.* 26 (1991) 4054-4061.
48. M. Henry, J. P. Jolivet, J. Livage, *Struct. Bonding (Berlin)* 77 (1992) 153-206.
49. R. C. Garvie, *J. Phys. Chem.* 69 (1968) 1238-1243.
50. Société européenne des produits réfractaires, US 5149510, 1992 (J. Recasens, D. Urffer, P. Ferlanda).
51. W. W. Stephens, H. L. Gilbert, *J. Met.* 194 (1952) 733-737.
52. Electro Metallurgical Co., US 2433253, 1948 (W. J. Kroll, F. E. Bacon).
53. B. Krebs, *Angew. Chem. Int. Ed. Engl.* 8 (1969) 146-147.
54. M. Ohashi, S. Yamaoka, Y. Morimoto, M. Hattori, *Bull. Chem. Soc. Jpn.* 60 (1987) 2387-2390.
55. S. N. Flengas, P. Pint, *Can. Met.* 8 (1969) 151-166.
56. A. W. Strauss, J. D. Corbett, *Inorg. Chem.* 9 (1970) 1373-1376.
57. D. G. Adolphson, J. D. Corbett, *Inorg. Chem.* 15 (1976) 1820-1823.
58. J. D. Corbett, *Pure Appl. Chem.* 56 (1984) 1527-1543.
59. H. S. Marek, J. D. Corbett, R. L. Daake, *J. Less Common Metals* 89 (1983) 243-249.
60. A. Clearfield, P. A. Vaughan, *Acta Crystallogr.* 9 (1956) 555-558.
61. K. I. Arsenin, L. A. Malinko, I. A. Sheka, I. Ya Pishcai, *Russ. J. Inorg. Chem. (Engl. Transl.)* 35 (1990) 1327-1331.
62. M. D. Atherton, H. Sutcliffe, *J. Less Common Met.* 138 (1988) 63-70.
63. Teledyne, WO 94/12435, 1993 (J. A. Sommers).
64. L. M. Seaverson, J. D. Corbett, *Inorg. Chem.* 22 (1983) 3202-3210.
65. K. Dehnicke, J. Weidlein, *Angew. Chem. Int. Ed. Engl.* 5 (1966) 1041.
66. R. L. Daake, J. D. Corbett, *Inorg. Chem.* 16 (1977) 2029-2033.
67. E. M. Larsen, J. S. Wrazel, L. G. Hoard, *Inorg. Chem.* 21 (1982) 2619-2624.
68. D. H. Guthrie, J. D. Corbett, *Inorg. Chem.* 21 (1982) 3290-3295.
69. Teledyne, WO 89/1087, 1989 (J. A. Sommers).
70. M. Robinson, K. C. Fuller, *Mater. Res. Bull.* 22 (1987) 1725-1732.
71. W. J. S. Craigen, E. G. Joe, G. M. Ritchey, *Can. Met. Q.* 9 (1970) 485-492.
72. National Lead, US 5252474, 1950 (W. B. Blumenthal).
73. ICI Australia, WO 86/06362, 1986 (K. Ngian, A. J. Hartshoren, D. H. Jenkins).
74. I. J. Bear, W. G. Mumme, *Rev. Pure Appl. Chem.* 21 (1971) 189-211.
75. P. J. Squatrito, P. R. Rudolf, A. Clearfield, *Inorg. Chem.* 25 (1987) 4240-4244.
76. Hopton Technologies, US 5472485, 1995 (V. E. Pandian, C. V. Calcar, R. W. Wolff).
77. Nalco Chemical, US 5230774, 1993 (C. S. Greer, N. P. James).
78. T. B. Massalski (ed.): *Binary Alloy Phase Diagrams*, 2nd ed., ASM International, Materials Park, OH, 1990, pp. 2078-2080.
79. W. M. Mueller, J. P. Blackledge, G. G. Libowitz: *Metal Hydrides*, Academic Press, New York 1968, pp. 241-321.
80. J. Rexer, D. T. Peterson in: *Nuclear Metallurgy, International Symposium on Compounds of Interest in Nuclear Reactor Technology*, vol. X, AIME, New York 1964, p. 327.
81. A. W. Struss, J. P. Corbett, *Inorg. Chem.* 16 (1977) 360.
82. R. V. Sara, *J. Am. Ceram. Soc.* 48 (1965) 243-247.
83. E. Rudy: *Compendium of Phase Diagram Data*, Air Force Materials Laboratory, Wright-Patterson Air Force Base, OH, 1969.
84. Norton Co., US 3161470, 1958 (J. I. Scott).
85. T. Ogawa, *J. Alloys and Compounds* 203 (1994) 221-227.
86. W. E. Wang, D. R. Olander, *J. Alloys and Compounds* 224 (1995) 153-158.
87. M. A. Eronyan, R. G. Avarbe, *Inorg. Mater. (Engl. Transl.)* 10 (1974) 1850.
88. E. G. Gillan, R. B. Kaner, *Inorg. Chem.* 33 (1994) 5693-5700.
89. B. O. Johansson, H. T. G. Hentzell, J. M. E. Harper, J. J. Cuomo, *J. Mater. Res.* 1 (1986) 442-451.
90. R. Juza, A. Rabenau, I. Nitschke, *Z. Anorg. Allgem. Chem.* 332 (1964) 1-4.
91. R. Fix, R. G. Gordon, D. M. Hoffman, *Chem. Mater.* 3 (1991) 1138-1148.
92. J. C. McMullen, W. D. McKee, Jr., *Am. Ceram. Soc. Bull.* 44 (1965) 448-491.
93. B. D. James, B. E. Smith, *Synth. React. Inorg. Met. Org. Chem.* 4 (1974) 461-465.
94. L. A. Petrova, A. P. Borisov, V. D. Makhaev, *Sov. J. Coord. Chem. (Engl. Transl.)* 18 (1992) 425-428.
95. A. Clearfield, R. H. Blessing, *J. Inorg. Nucl. Chem.* 36 (1974) 1174-1176.
96. L. L. Y. Chang, M. G. Scroger, B. Phillips, *J. Am. Ceram. Soc.* 50 (1967) 211-215.
97. T. A. Mary et al., *Science* 272 (1996) 90-92.
98. A. Clearfield, J. A. Stynes, *J. Inorg. Nucl. Chem.* 26 (1964) 117-129.
99. U. Costantino in A. Clearfield (ed.): *Inorganic Ion Exchange Materials*, CRC Press, Boca Raton 1982.
100. Y. Watanabe, Y. Matsumura, Y. Izumi, Y. Mizutani, *Bull. Chem. Soc. Jpn.* 47 (1974) 2922-2925.
101. R. Sacks, Y. Avigal, E. Banks, *J. Electrochem. Soc.* 129 (1982) 726-729.
102. J. Alamo, R. Roy, *J. Am. Ceram. Soc.* 67 (1984) C78-82.
103. V. Korthuis et al., *Chem. Mater.* 7 (1995) 412-417.
104. W. B. Blumenthal: *The Chemical Behavior of Zirconium*, D. Van Nostrand, Princeton, 1958, p. 286.
105. W. B. Blumenthal in [104], p. 319.
106. D. C. Bradley, R. C. Mehrota, D. P. Gaur: *Metal Alkoxides*, Academic Press, London 1978, pp. 10-41.
107. R. B. Hahn, E. S. Baginski, *Anal. Chim. Acta* 14 (1965) 45-47.
108. R. Brayer, R. O'Connell, A. Powell, R. H. Gale, *Appl. Spectrosc.* 15 (1961) 10-13.
109. G. L. Beck, O. T. Farmer, *J. Anal. Spectrom.* 3 (1988) 771-773.
110. G. L. Beck, J. P. Fraley, Teledyne Wah Chang procedure ASP-OES-1 Rev. 0, 1988.
111. J. Schlewitz, M. Shields, *At. Absorpt. Newsl.* 10 (1971) 39-43.
112. R. VanSanten, J. Schlewitz, G. Beck, R. Walsh in F. D. Snell, L. S. Ettre (eds.): *Encyclopedia of Industrial Chemical Analysis*, vol. 14, Wiley-Interscience, New York 1971, pp. 103-148.
113. R. K. McGeary in: *Zirconium Alloys*, American Society for Metals, Cleveland 1953, pp. 168-175.
114. W. G. Guldner, *Talanta* 8 (1961) 191-202.
115. W. G. Smiley, *Anal. Chem.* 27 (1955) 1098-1102.
116. P. Ebling, G. W. Howard, *Anal. Chem.* 32 (1960) 1610-1613.
117. J. Surak, D. Fisher, C. Burros, L. Bate, *Anal. Chem.* 32 (1960) 117-119.
118. J. Lingane, *Anal. Chem.* 39 (1967) 881.
119. T. Bartter et al., *Arch. Intern. Med.* 151 (1991) 1197-1201.
120. M. Y. Longley et al.: *A Toxic Hazard Study of Selected Missile Propellants*, Technical Documentary Report no. ARML-TDR-64-28 Biomedical Lab., Aerospace Med. Res. Lab. Wright-Patterson Air Force Base, OH, 1964.
121. I. T. Brakhova: *Environmental Hazards of Metals. Toxicity of Powdered Metals and Compounds*, translated from the Russian (original publ. 1971) by S. L. Slep, Consultants Bureau, New York, NY, 1975.
122. I. T. Brakhova, G. A. Shkupko, *Gig. Sanit.* 37 (1972) 36-39.
123. J. T. Prior, G. A. Cronk, D. D. Ziegler, *Arch. Environ. Health* 1 (1960) 297-300.
124. "Aerosol Drug and Cosmetic Products Containing Zirconium. Proposed Determination", *Fed. Regist.* 40 (1975) 24327-24344.
125. W. B. Shelley, H. J. Jurley, Jr., in M. Sauter (ed.): *Immunological Diseases*, 2nd ed., Little, Brown & Co., Boston 1971, pp. 722-734.
126. I. C. Smith, B. L. Carson: *Trace Metals in the Environment*, vol. 3, Zirconium, Ann Arbor Science Publ., Ann Arbor 1978, pp. 173-371.
127. U.S. Registry of Toxic Effects of Chemical Substances.

31 Hafnium

RALPH H. NIELSEN

31.1 Introduction	1459	31.10 Uses.....	1466
31.2 Physical Properties.....	1459	31.11 Economic Aspects.....	1466
31.3 Chemical Properties.....	1459	31.12 Compounds.....	1466
31.4 Occurrence and Raw Materials.....	1460	31.12.1 Borides and Borates.....	1467
31.5 Production.....	1460	31.12.2 Carbide.....	1467
31.5.1 Opening-up of Ore.....	1460	31.12.3 Halides.....	1467
31.5.2 Separation of Zirconium.....	1462	31.12.4 Hydride.....	1468
31.5.3 Recovery of Metallic Hafnium.....	1463	31.12.5 Nitride.....	1468
31.5.4 Refining.....	1464	31.12.6 Dioxide.....	1468
31.6 Environmental Protection.....	1464	31.12.7 Other Derivatives.....	1468
31.7 Quality Specifications.....	1465	31.13 Toxicology and Occupational Health.....	1469
31.8 Analysis.....	1465	31.14 References.....	1469
31.9 Storage and Transportation	1465		

31.1 Introduction

The element hafnium, is always found in zirconium ore and is available as a by-product of the production of zirconium metal. The average concentration of hafnium in the earth's crust is estimated at 2.8–4.5 ppm. Six isotopes occur naturally: ^{174}Hf (0.16%), ^{176}Hf (5.2%), ^{177}Hf (18.6%), ^{178}Hf (27.1%), ^{179}Hf (13.7%), and ^{180}Hf (35.2%). Hafnium is used principally as a minor alloying element in nickel-based superalloys and as a thermal neutron absorber in nuclear power reactors. Annual world consumption is about 50 t.

31.2 Physical Properties

Hafnium is a heavy, hard, ductile metal similar in appearance to stainless steel. Although chemically very similar to zirconium, it has several physical differences: hafnium has twice the density of zirconium, a higher phase transition temperature, and a higher melting point. Hafnium also has a high thermal neutron absorption coefficient ($1.04 \times 10^{-26} \text{ m}^2$), whereas that for zirconium is very low ($1.8 \times 10^{-29} \text{ m}^2$). Some physical properties of hafnium are listed below:

<i>mp</i>	2227 °C
<i>bp</i>	4602 °C
Density	13.31 g/cm ³
Thermal conductivity (25 °C)	23.0 Wm ⁻¹ K ⁻¹
Coefficient of linear expansion (0–1000 °C)	$5.9 \times 10^{-6} \text{ K}^{-1}$
Specific heat (25 °C)	117 Jkg ⁻¹ K ⁻¹
Vapor pressure (1767 °C)	10 ⁻³ Pa
(2007 °C)	10 ⁻¹
Electrical resistivity (25 °C)	$3.51 \times 10^{-7} \text{ Wm}$
Thermal neutron absorption cross section	$1.04 \times 10^{-26} \text{ m}^2$
Crystal structure	
α-form	hexagonal close-packed (hcp)
β-form	body-centered cubic (bcc)
Temperature of α–β transformation	1760 °C

31.3 Chemical Properties

The ionic radii of hafnium and zirconium are almost identical because of the lanthanide contraction. Both elements exhibit a valence of four. Therefore, the chemistry of hafnium is similar to that of zirconium, and the elements are always found together in nature (see also Chapter 30).

Elemental hafnium reacts with hydrogen (> 250 °C), carbon (> 500 °C), and nitrogen (> 900 °C) to form brittle, nonstoichiometric interstitial compounds with metal-like conduc-

tivity. In molten salts, hafnium is normally quadrivalent, but in anhydrous molten halide salts, it can be reduced to hafnium(III) and hafnium(II).

In aqueous solution, hafnium is always quadrivalent, with a high coordination number (6, 7, or 8). In dilute acid, hafnium slowly hydrolyzes and polymerizes. Hafnium hydrous oxide precipitates from aqueous solution at ca. pH 2. The only inorganic compounds with significant solubility in neutral or slightly basic aqueous solution are the ammonium-hafnium carbonate and potassium-hafnium carbonate complexes. The tendency for hafnium to form inorganic complexes with anions decreases in the following order: $\text{OH}^- > \text{F}^- > \text{PO}_4^{3-} > \text{CO}_3^{2-} > \text{SO}_4^{2-} > \text{NO}_3^- \approx \text{Cl}^- > \text{ClO}_4^-$.

Reviews of zirconium chemistry [1, 2] are frequently useful for indications of the chemical behavior of hafnium, because of the similarity in chemical properties.

31.4 Occurrence and Raw Materials

Mineralogically, hafnium is always found with zirconium. Although about 40 known minerals contain these elements, the main commercial sources of zirconium and hafnium are *zircon* and *baddeleyite*, since they are available as by-products in the recovery of other minerals. Zircon sand is obtained during the processing of alluvial heavy mineral sands to recover the titanium minerals rutile and ilmenite. Commercially recoverable deposits of these heavy mineral sands are found in China, Malaysia, Thailand, India, Sri Lanka, Australia, South Africa, Madagascar, and the United States. Clean (high quality) zircon contains 64% zirconium oxide, 34% silicon dioxide, 1.2% hafnium dioxide, with the balance including aluminum, iron, phosphorus, rare earths, titanium, uranium, and thorium.

Worldwide, the hafnium content of zircon is usually ca. 2% of the zirconium content. A notable exception is a Nigerian zircon, available in commercial quantities during 1957–1965, that contained 6% hafnium (based on

zirconium). Two minerals, a Norwegian thortveitite and a Mozambican hafnon, have been reported to contain more hafnium than zirconium. Baddeleyite usually contains hafnium at < 2% of the zirconium content. At the Phalaborwa complex in South Africa, baddeleyite is recovered from process tailings in the extraction of copper and the extraction of apatite for phosphate fertilizers.

Although hafnium reserves are significant, demand is low and easily met as a by-product of the production of reactor-grade zirconium. Known hafnium reserves are listed in Table 31.1.

Table 31.1: Known hafnium reserves, $\times 10^3$ t.

Country	Annual zircon production	Zircon reserve ^a	Hf content of zircon reserve
Australia	480	32 000	390
United States	135	15 000	145
South Africa	135	15 000	145
Brazil	18	4000	38
India	15	9000	85
Sri Lanka	5	3000	29
Malaysia	3	3000	29

^aEstimated.

31.5 Production

Processing steps and alternative processes for the production of hafnium metal from zircon sand are shown in Figure 31.1.

31.5.1 Opening-up of Ore

Zircon is a refractory mineral, whose decomposition requires the use of aggressive chemicals and high temperature. Today, the commonly used techniques are caustic fusion, direct carbochlorination, or thermal dissociation; however, other procedures such as fusion with dolomite, fusion with potassium hexafluorosilicate, and a two-step process involving carbiding and exothermic chlorination of the crude carbide have all been used extensively to obtain zirconium and hafnium in more chemically active form.

The caustic fusion of zircon by using a slight excess of sodium hydroxide at 600 °C is the most common process for opening-up of zircon ore [3]:

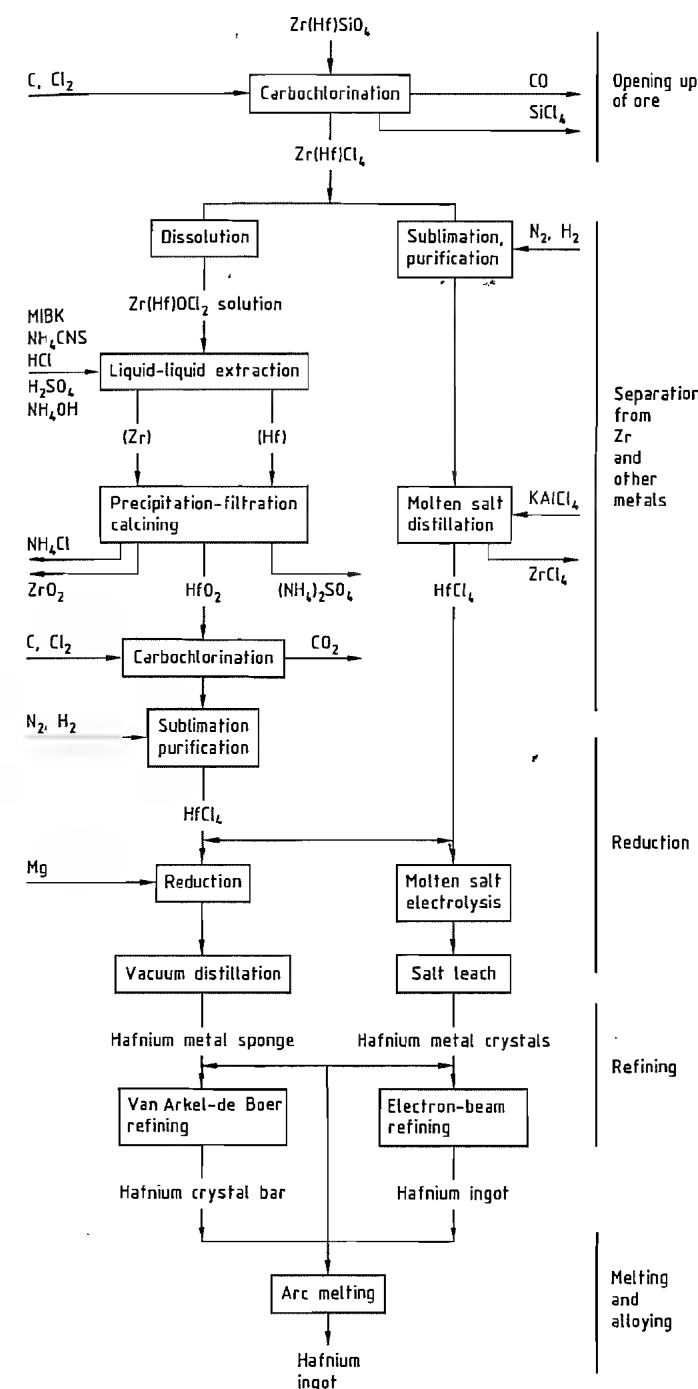
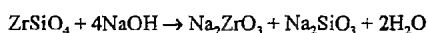


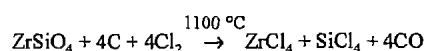
Figure 31.1: Flow diagram for production of hafnium.



The cooled reaction mass is broken up and slurried in water, which dissolves sodium silicate and hydrolyzes sodium zirconate to soluble sodium hydroxide and insoluble hydrous zirconia; the latter is recovered by filtering the slurry. Hydrous zirconia is soluble in strong mineral acid; hafnium can be recovered from the primary zirconium stream by ion exchange or liquid-liquid extraction.

Variations of this fusion process involve the use of sodium carbonate at 900 °C or the use of only half the quantity of sodium hydroxide to produce sodium zirconium silicate; the latter is subsequently treated with acid to form a soluble zirconium compound. These fusion processes are used worldwide to produce zirconium oxide, aqueous solutions of zirconium, and water-soluble zirconium compounds.

Fluidized-bed carbochlorination of zircon sand is the ore-decomposition process used by all three hafnium producers in the Western hemisphere: Teledyne Wah Chang Albany, CEZUS Division of Pechiney, and Western Zirconium Division of Westinghouse:



All the reaction products are gases when they leave the chlorinator. Zirconium and hafnium tetrachlorides are recovered as a powder by cooling the gas mixture to 200 °C in a large-volume space condenser. Silicon tetrachloride is then condensed by direct countercurrent contact of the remaining gas mixture with refrigerated (−40 °C) recycled liquid silicon tetrachloride.

Thermal dissociation of zircon in the high temperature of a plasma torch followed by rapid quenching is used to produce intimately mixed crystals of zirconium and silicon oxides. The oxides can be leached countercurrently with sodium hydroxide to yield zirconium oxide and a solution of sodium silicate, or leached with hot strong sulfuric acid to give a zirconium sulfate solution and silica. Both procedures are used by the Z-Tech Corporation Division of ICI.

31.5.2 Separation of Zirconium

Many well-known methods exist for separating hafnium from zirconium: ion exchange with a dilute sulfuric acid eluent [4]; *liquid-liquid extraction* of hafnium from hydrochloric acid solution by a methyl isobutyl ketone thiocyanic acid solution [5–8]; *distillation* of the mixed binary tetrachlorides at a pressure above the triple point [9]; and *extractive distillation* of hafnium tetrachloride from the mixed tetrachlorides dissolved in a molten halide solvent [10, 11].

Ion exchange is the easiest laboratory procedure. A dilute solution of $\text{Zr}(\text{Hf})\text{OCl}_2$ is introduced into a bed of strong cation-exchange resin and eluted with 0.25 M sulfuric acid. The eluate contains three components: (1) a small amount of unseparated metal, apparently polymerized, with minimum retention time; (2) a major fraction containing zirconium; and (3) a smaller fraction containing hafnium. A continuously fed rotating cylindrical bed system has been proposed for commercial separation of hafnium and zirconium [4].

Liquid-Liquid Extraction. The methyl isobutyl ketone (MIBK) liquid-liquid extraction is based on an analytical method for determining hafnium [12]. The process was developed at Oak Ridge National Laboratory to obtain hafnium-free zirconium to contain uranium fuel for nuclear-powered submarines. Recovery of hafnium as a by-product was initiated when uses were found for the hafnium.

The zirconium-hafnium dichloride oxide solution is introduced at the midpoint of a series of countercurrent contact stages in which the organic solvent is MIBK containing thiocyanic acid and the countercurrent aqueous solution is dilute hydrochloric acid. Hafnium is extracted preferentially into the organic solution as a hafnium oxide thiocyanate complex. The separation factor per stage is 4–5. After extraction, hafnium is recovered by treating the organic phase with dilute sulfuric acid, the water-soluble hafnium sulfate being more stable than the thiocyanate complex. The sulfuric acid is then neutralized to precipitate

hydrous hafnium oxide, which is calcined to hafnium oxide. This procedure is used by both U.S. producers of hafnium.

Fractional Distillation. Separation by fractional distillation would be feasible if the tetrachlorides could be handled as liquids; however, the tetrachlorides are solid or gaseous unless kept under pressure while heated to the triple point of zirconium tetrachloride (435 °C, 2.0 MPa). The operating range of a binary distillation system is limited because the critical temperature for zirconium tetrachloride is ca. 505 °C.

Extractive distillation of the mixed tetrachlorides from molten potassium chloroaluminate at atmospheric pressure was developed and used commercially by CEZUS [10, 11]. The crude tetrachloride product from carbochlorination is first purified by sublimation in an atmosphere of nitrogen with 1–5% hydrogen. The purified tetrachloride is then revaporized, and the vapor is introduced continuously above the midpoint of the distillation column. The potassium chloroaluminate solvent, equilibrated with hafnium-rich tetrachloride, is fed into the top of the distillation column, which is maintained at 350 °C. As the solvent cascades down the column it is gradually depleted of the more volatile hafnium tetrachloride, so that zirconium tetrachloride in the solvent reaching the bottom of the column contains < 50 ppm of the hafnium compound. The separation factor per stage is 1.4.

The solvent is fed to a boiler where much of the zirconium tetrachloride is vaporized and passed back up the column to become enriched in hafnium. Solvent from the boiler is fed into a stripper where it is treated with nitrogen to remove the remaining zirconium tetrachloride.

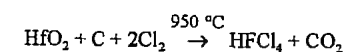
The stripped solvent is pumped to an absorber-condenser above the column where the solvent is equilibrated with the hafnium-rich tetrachloride and returned to the top of the distillation column. Unabsorbed hafnium-rich tetrachloride vapor (HfCl_4 content 30–50%) is collected in the hafnium condenser. This hafnium-enriched tetrachloride accumulates

until it can be reprocessed in the distillation column under different conditions to produce pure hafnium tetrachloride (< 1% ZrCl_4).

The degree of separation attained by these various processes is limited only by the number of stages provided in the separation equipment. Zirconium containing < 20 ppm hafnium and hafnium containing < 50 ppm zirconium have been produced.

31.5.3 Recovery of Metallic Hafnium

Hafnium dioxide from the separation process is converted first into hafnium tetrachloride by fluidized-bed carbochlorination:



The recovered hafnium tetrachloride is purified by sublimation in a nitrogen hydrogen atmosphere to reduce the levels of aluminum, iron, and uranium.

Kroll Process. Hafnium tetrachloride powder is placed in a vertical cylindrical steel retort welded onto a stainless steel-lined steel crucible containing cast ingots of magnesium. The two chambers are connected by a pipe rising through the center of the hafnium tetrachloride charge. The assembled retort is sealed, evacuated, and filled with argon several times to remove traces of air. The retort is lowered into a furnace; the lower section is then heated to 850 °C. Molten magnesium reduces the hafnium tetrachloride vapor as it sublimes out of the upper chamber. After the reaction is complete, the lower crucible contains hafnium metal, magnesium chloride, and excess magnesium. The retort is cooled and unloaded. The stainless steel liner is separated from the reduction mass, and the upper layer of magnesium chloride is physically removed from the hafnium magnesium metallic regulus. The latter is loaded into a vacuum distillation furnace for removal of magnesium and residual magnesium chloride. As the temperature gradually increases, magnesium sublimes, leaving a skeletal structure of hafnium sponge. Magnesium chloride melts and drains into the cool

lower portion of the retort. After the furnace is cooled and the sponge conditioned by slow, controlled exposure to air, the sponge is removed and placed in an argon atmosphere, where it is broken and chopped into pieces finer than 20 mm.

Electrowinning. Electrowinning of hafnium and zirconium has long been investigated as an alternative to metallurgical reduction. CEZUS recently began production of hafnium by electrolysis of hafnium tetrachloride dissolved in a molten equimolar bath of potassium and sodium chlorides [13]. Hafnium tetrachloride vapor is introduced periodically below the liquid level of the bath to replenish hafnium. The bath contains just enough sodium fluoride to convert dissolved hafnium into the hexafluorohafnate complex.

31.5.4 Refining

Applications of metallic hafnium require lower oxygen levels than commonly achieved by the Kroll process. Purification is accomplished by the *Van Arkel-de Boer* process, also known as the iodide-bar or crystal-bar process [14, 15]. Hafnium sponge is treated with iodine vapor to form volatile hafnium iodide, which diffuses to an electrically heated hafnium filament. Hafnium iodide dissociates at the filament temperature of 1400 °C, depositing hafnium on the filament and releasing iodine to repeat the diffusion cycle. The hafnium filament slowly grows from a 3-mm wire to a 40-mm crystal-faceted bar. Purification is effective in leaving behind interstitial impurities such as oxygen, carbon, and nitrogen. Metallic impurities generally transport poorly, depending on the behavior of individual iodides, so the hafnium filament is much purer than the sponge.

Electron beam melting can also be used to purify hafnium. Hafnium is slowly drip-melted into a superheated molten pool under extremely high vacuum. The more volatile metallic impurities and suboxides are boiled off at a much faster rate, relative to the vaporization of hafnium. Two slow melts are standard for hafnium.

Table 31.2: Typical impurity levels for hafnium metal, ppm.

	Kroll process sponge	Electrowon crystals	Electron-beam melting ingot	Van Arkel-de Boer crystal bar
Oxygen	875	670	320	< 50
Nitrogen	35	15	40	< 5
Carbon	< 30	40	< 30	< 30
Chlorine	100	50	< 5	< 5
Aluminum	200	10	< 25	< 25
Chromium	40	30	< 20	< 20
Iron	530	100	< 50	< 50
Magnesium	440	< 10	< 10	< 10
Manganese	15	10	< 10	< 10
Nickel	< 25	40	< 25	< 25
Silicon	25	< 25	< 25	< 25
Titanium	< 25	30	< 25	< 25

Typical impurity levels for Kroll-process hafnium sponge and electrowon hafnium crystals are shown in Table 31.2, together with the effectiveness of refining sponge by electron-beam melting or the Van Arkel-de Boer process.

31.6 Environmental Protection

Zircon contains traces of uranium and thorium in solid solution substitutionally and isomorphically in its structure. The retention of these elements and their radioactive decay daughter products are so complete that geological dating of rocks can be conducted by determining the radiological age of the zircon. Conversely, when the zircon structure is destroyed chemically, uranium, thorium, and their daughter products are released. If the attack on zircon is similar to carbochlorination, in which both zirconia and silica are converted to volatile species, the reaction residue may have sufficient concentrations of less volatile radioactive materials for special disposal procedures to be necessary.

Recovery of hafnia and zirconia from the acid solutions of liquid-liquid extraction results in process streams containing ammonium sulfate and ammonium chloride. Ammonia must be recovered for recycling or sale to avoid a heavy biological oxygen demand on effluent-receiving streams. Extreme

care must be taken to ensure that hypochlorite scrubbing solutions from chlorination do not come in contact with effluent streams containing traces of thiocyanate because the mixture produces cyanides.

31.7 Quality Specifications

For wrought hafnium the following U.S. specifications apply: ASTM B737-84 for Hot-Rolled or Cold-Finished Rod and Wire; ASTM B776-87 for Hafnium and Hafnium Alloy Strip, Sheet, and Plate; ASTM G2-88 and G2M-88 for Corrosion Testing of Products of Zirconium, Hafnium, and Their Alloys in Water at 680 °F (360 °C, 633 K) or in Steam at 750 °F (400 °C, 673 K); and ASTM C1076-87 for Nuclear-Grade Hafnium Oxide Pellets.

In Germany, VdTUV Material Sheet 463, Hafnium, 05.83, covers wrought hafnium sheet.

Hafnium for alloying purposes is sold in chunk or particulate form, at the particular chemical purity specified by the customer; the zirconium content is particularly important.

31.8 Analysis

Hafnium is chemically so similar to zirconium that most gravimetric, volumetric, or colorimetric methods of analysis result in a combined hafnium-zirconium determination. Methods that do not require prior separation of hafnium include atomic absorption spectroscopy, emission spectroscopy, plasma emission spectroscopy, mass spectroscopy, X-ray spectroscopy, and neutron activation [16]. Ores and compounds are frequently analyzed by precipitating hafnium and zirconium with mandelic acid [17], igniting the precipitate to give the combined oxides, and determining the relative proportion of each oxide by X-ray or emission spectroscopy.

Many analytical methods for determining impurities in zirconium can also be applied to hafnium [16, 18]. Carbon and sulfur in hafnium are measured by combustion, followed by chromatographic or IR determina-

tion of the oxides [16]. Hydrogen is determined by thermal conductivity after hot-vacuum extraction or by fusion of hafnium with a transition metal in an inert atmosphere and subsequent separation by gas chromatography [19, 20].

Simultaneous determination of nitrogen and oxygen is accomplished by a technique similar to that for hydrogen [21, 22]. Nitrogen can also be determined by the Kjeldahl technique [16]. Phosphorus may be determined by visible spectrophotometry using molybdenum blue [16] but can be determined more rapidly by phosphine evolution and flame emission spectroscopy.

Chloride at low level is determined indirectly by precipitation with silver nitrate and determination of silver by X-ray or atomic absorption spectroscopy. Fluoride and higher levels of chloride can be measured by selective ion electrode techniques [23, 24].

Other impurities are usually determined by emission spectroscopy either arc spark [25, 26] or plasma excitation [27, 28]. Many impurities can be determined rapidly and inexpensively. Atomic absorption is frequently used to determine a variety of impurities in hafnium metal and sponge [29].

31.9 Storage and Transportation

Hafnium metal powder is a flammable solid and should be kept dry, cool, and separate from potential oxidants. Dry hafnium powder, chemically produced, finer than 8.40×10^{-4} m (840 μ m, 20 mesh), or mechanically produced, finer than 5.3×10^{-5} m (53 μ m, 270 mesh), must have the following warning labels for shipping:

UN no. 2545

United States DOT: Flammable Solid

IAIA Dangerous Goods Regulations: Combustible Solid

IMDG Code: Combustible Solid

The same hafnium powder, wet, containing at least 25% water, must be labeled as a flammable solid for all shipping and hazard communication purposes (UN no. 1326).

Hafnium powder of the above descriptions, wet or dry, is forbidden on U.S. passenger aircraft by DOT. Dry hafnium metal powder, mechanically produced, finer than 3×10^{-6} m, or chemically produced, finer than 10×10^{-6} m, is forbidden from all air transportation by IATA.

Although not specifically required, hafnium hydride or hafnium carbide powder should be labeled, handled, and stored in similar fashion.

Hafnium tetrachloride must be shipped as a corrosive solid (UN no. 1759).

31.10 Uses

The major uses of hafnium involve the metal. The largest use is as an alloying additive (1–2%) in nickel-based superalloys. These alloys are used in turbine vanes in the combustion zone of jet aircraft engines. Addition of hafnium to some present-generation alloys has raised the allowable service temperature by 50 °C, improving engine efficiency. Hafnium forms stable precipitates at grain boundaries, improving high-temperature creep strength.

The second major use of hafnium is as control-rod material in nuclear reactors. In early reactors, bare hafnium metal in long cruciform shape was used because of the excellent hot-water corrosion resistance, good ductility, and machinability of hafnium, as well as its high thermal neutron absorption cross section. Hafnium clad in stainless steel is now replacing stainless steel-clad silver–indium–cadmium and stainless steel-clad boron carbide in some commercial nuclear power plants.

Hafnium is also used as an alloying element in niobium, tantalum, titanium, molybdenum, and tungsten alloys, as well as some new nickel aluminides.

Hafnium and hafnium–zirconium alloys have been suggested for use in spent nuclear fuel storage racks, and for tanks and piping in spent fuel reprocessing plants because of the neutron absorption capability of hafnium and its resistance to nitric acid. For a while, shred-

ded hafnium foil was used instead of zirconium foil as fuel in some photographic flashbulbs because hafnium provided a higher intrinsic color temperature and a greater light output. Pure hafnium has also been used as the active tip for plasma arc cutting tools.

Hafnium carbide–niobium carbide solid solutions have been used as a replacement for tantalum carbide in steel-cutting grades of cemented carbide tool bits.

Hafnium oxide has been used as a specialized refractory, including thermocouple insulation for short-term use above 2000 °C. Hafnium and hafnium oxide sputtering targets are used for coatings and specialized electronic applications.

Hafnium tetrachloride has been used to prepare hafnium metallocene Ziegler–Natta-type catalysts, which were the first catalysts to provide high yields of high molecular mass isotactic polypropylene [30]. Hafnium tetrafluoride is used in some heavy-metal fluoride glass cladding [31].

31.11 Economic Aspects

Production of hafnium oxide and hafnium tetrachloride has been steady since 1980, as a result of the leveling off of zirconium metal production for the nuclear energy program. The availability of hafnium still exceeds market demand. Annual Western hemisphere availability is estimated at 80 t, with consumption estimated at 50 t. Hafnium is produced commercially in the United States (Teledyne Wah Chang Albany and Western Zirconium Division of Westinghouse), France (CEZUS Division of Pechiney), and the former Soviet Union.

In 1988, hafnium oxide was available at \$100/kg; hafnium crystal bar, at \$200/kg; and hafnium wrought metal products (plate, sheet, wire, foil), from \$250 to \$500/kg.

31.12 Compounds

Compounds of hafnium have been studied mostly to develop methods of separating

hafnium from zirconium, producing the metal, and comparing properties with similar zirconium compounds. Although the properties of inorganic hafnium and zirconium compounds are generally comparable, differences in chemical behavior become more evident in organometallic compounds.

31.12.1 Borides and Borates

Hafnium boride, HfB_2 , is prepared by carbon reduction of hafnium oxide and boron carbide, by coreduction of hafnium and boron chlorides with magnesium or hydrogen, or from the elements. It is of interest because it is very refractory. Hafnium dodecaboride, HfB_{12} , has been synthesized by compressing the elements at 1660 °C and 6.5×10^3 MPa.

Hafnium tetrahydroborate, $\text{Hf}(\text{BH}_4)_4$, is prepared by reaction of hafnium tetrachloride with lithium borohydride in diethyl ether, followed by double sublimation under vacuum at 20 °C [32]. Hafnium tetrahydroborate is one of the most volatile hafnium compounds known: *mp* 29 °C, *bp* 118 °C, vapor pressure 2 kPa at 25 °C. Its decomposition at ca. 250 °C forms the basis for a low-temperature method of depositing amorphous hafnium diboride films [33].

31.12.2 Carbide

Hafnium carbide, HfC , is usually produced by carbothermic reduction of hafnium oxide in an induction-heated graphite-lined vacuum furnace. Hafnium carbide film can be deposited by reaction of hafnium tetrachloride and methane in a hydrogen atmosphere at 900–1400 °C. Hafnium carbide is a nonstoichiometric interstitial carbide with carbon atoms at octahedral interstices of the hafnium metal lattice. The hafnium–carbon phase diagram shows that hafnium carbide is single phase within the range 39.5–49.5 atom% carbon at 1400 °C [34]. Hafnium carbide is a hard refractory material with metallic conductivity.

31.12.3 Halides

Hafnium tetrafluoride, HfF_4 , can be made by addition of a stoichiometric amount of hydrofluoric acid to hafnium oxide chloride dissolved in 8 M nitric acid, to precipitate hafnium tetrafluoride monohydrate. The filtered crystals are dried in a stream of anhydrous hydrogen fluoride gas. Alternatively, anhydrous hydrogen fluoride can undergo an exchange reaction with hafnium tetrachloride powder or vapor, or ammonium fluorohafnate can be heated to drive off ammonium fluoride, leaving hafnium tetrafluoride as residue.

Potassium hexafluorohafnate K_2HfF_6 , can be crystallized from hafnium fluoride solution by adding a stoichiometric amount of potassium fluoride. The solution should be acidic to minimize hydrolysis. Other alkali metal hexafluorohafnates (Na_2HfF_6 , Rb_2HfF_6 , and Cs_2HfF_6) and the corresponding ammonium salts can be prepared similarly. With different proportions of alkali fluoride, other salts can be precipitated, including MHfF_5 , M_3HfF_7 , and $\text{M}_5\text{Hf}_2\text{F}_{13}$.

Hafnium tetrachloride, HfCl_4 , is prepared commercially by carbochlorination of hafnium oxide at 900 °C. Chlorination can be carried out with phosgene or carbon tetrachloride at 450 °C. Hafnium tetrachloride is used as starting material for the preparation of organic derivatives of hafnium, alkoxides, and alkali chlorohafnates. The partitioning of mixed tetrachloride vapor by alkali-metal salts, with preferential formation of alkali chlorohafnate and elimination of unreacted zirconium tetrachloride, has been proposed as a means of separating hafnium and zirconium [35, 36]. Hafnium tetrachloride vapor reacts with steam to form finely divided hafnium oxide. Solid hafnium tetrachloride reacts with water to form hafnium oxide chloride and hydrochloric acid.

Hafnium dichloride oxide, HfOCl_2 , is soluble in water and can be crystallized from hydrochloric acid solution as the octahydrate, $\text{HfOCl}_2 \cdot 8\text{H}_2\text{O}$. The solubility of hafnium dichloride oxide increases significantly with temperature and decreases with increasing

acidity up to 8.5 M hydrochloric acid. This crystallization procedure is the preferred method for obtaining pure hafnium dichloride oxide prior to the preparation of other hydrated hafnium compounds. Hafnium dichloride oxide is converted to the hydrous oxide $\text{HfO}_2 \cdot x\text{H}_2\text{O}$ on neutralization, at pH 2. On heating, hafnium dichloride oxide first loses water, then slowly releases water and hydrogen chloride, and is converted into granular hafnium oxide.

Hafnium tetrabromide, HfBr_4 , and hafnium tetraiodide, HfI_4 , are produced by reaction of the respective halogen with hafnium metal in the absence of air above 300 °C. Thermal dissociation of the tetraiodide is employed in the iodide-bar refining process.

Lower valence hafnium halides have been formed by reduction of tetrahalides with aluminum or hafnium in molten aluminum chloride or molten alkali halide baths. Zirconium is more easily reduced; this is the basis of several proposals for the separation of hafnium and zirconium [37, 38].

31.12.4 Hydride

Hafnium hydride, HfH_x , is formed as hafnium absorbs hydrogen. The proportion of hydrogen absorbed depends on temperature and hydrogen pressure. Above 500 °C, as hydrogen is absorbed, hafnium changes from hexagonal close-packed metal, to face-centered tetragonal hydride as the composition approaches the limiting solubility, with $x = 2$ [39]. At room temperature, hafnium hydride exists as the face-centered cubic form when $x = 1.7$ –1.8, and as the face-centered tetragonal form when $x \geq 1.87$.

Hafnium hydride is brittle and easily crushed. Crushing must be conducted in an argon atmosphere to avoid ignition of the fine powder. Hydrogen absorption is reversible; the process of hydriding, crushing, and dehydriding is therefore used to convert hafnium metal pieces into powder with little contamination. Hydrogen is removed by heating the hydride under vacuum.

31.12.5 Nitride

Hafnium nitride, HfN , is a nonstoichiometric interstitial nitride, which is single phase within the range 42–50 atom% nitrogen [40]. Hafnium nitride film can be deposited by reacting hafnium tetrachloride vapor with ammonia or nitrogen in a hydrogen atmosphere above 1000 °C. Above 1400 °C, nitride powder is produced. This film deposition process is used to coat cemented carbide tool bits. Hafnium nitride film is more effective than titanium nitride in reducing frictional forces and wear when machining steel [41].

31.12.6 Dioxide

Hafnium dioxide, hafnia, HfO_2 , is the only stable oxide of hafnium. It melts at 2900 °C and exists in three solid phases: a monoclinic phase stable up to 1475–1600 °C, above which hafnia changes into the tetragonal phase, the stable form up to ca. 2700 °C. Between 2700 and 2900 °C, hafnia has a cubic fluorite structure. Like zirconia, the tetragonal monoclinic transition is a martensitic transformation that exhibits considerable hysteresis. The cubic structure can be stabilized by addition of calcium oxide, yttrium oxide, or some of the rare-earth oxides, including those of cerium and europium. The use of stabilized hafnia for high-temperature engineered ceramics avoids the catastrophic 7% shrinkage that accompanies transformation from monoclinic to tetragonal form.

Hafnium dioxide is very stable and, except for strong hydrofluoric acid, is attacked only at elevated temperature. Hafnia reacts with carbon tetrachloride or phosgene above 400 °C, and with chlorine and carbon above 700 °C, to form hafnium tetrachloride. At high temperature, hafnia reacts with many metal oxides to form solid solution oxides or hafnate compounds such as CaHfO_3 .

31.12.7 Other Derivatives

Several excellent publications that cover the preparation and properties of hafnium

alkoxides, hydrides, and organic derivatives are available [42–44].

31.13 Toxicology and Occupational Health

Hafnium metal with a high surface area, such as thin machining chips, powder, sponge, or grinding dust, is extremely flammable, even pyrophoric. If the metal is slightly wet (5–15% H_2O) ignition can occur with explosive violence. Fires can be extinguished with a layer of dry salt or with a blanket of argon if the metal is in a container.

Water can be hazardous for fire fighting because it is a source of oxygen for the burning metal. The resulting hydrogen and steam may blow the burning chips throughout the area. Several reviews of methods for safe handling of hafnium and zirconium are available [45, 46].

Hafnium is essentially nontoxic. No health problems have been attributed to hafnium in more than 30 years of industrial experience with the metal and its compounds. Toxicological studies of ingestion indicate that the toxicities of hafnium and zirconium are similar. Hafnium was found to accumulate in the liver when hafnium compounds were injected intravenously or intraperitoneally into rats [47]. Chronic feeding of 1% hafnium tetrachloride to rats for 90 d caused liver damage [48]. The ACGIH TLV–TWA for hafnium is 0.5 mg/m^3 .

Hafnium tetrachloride and tetrabromide hydrolyze immediately on contact with water, releasing hydrochloric or hydrobromic acid fumes. These compounds should be handled with proper ventilation and personal protection.

31.14 References

1. A. Clearfield, *Rev. Pure Appl. Chem.* **14** (1964) 91.
2. R. Clark, D. Bradley, P. Thornton: *The Chemistry of Titanium, Zirconium, and Hafnium*, Pergamon Press, Oxford 1973.
3. H. S. Choi, *Can. Min. Metall. Bull.* **67** (1965) 65.
4. J. M. Begovich, W. G. Sisson, *Hydrometallurgy* **10** (1983) 11–20.

5. W. A. Stickney: "Zirconium–Hafnium Separation", USBM RI 5499, 1959.
6. J. M. Googin in F. R. Bruce, J. M. Fletcher, H. H. Hyman (eds.): *Progress in Nuclear Energy, Series III: Process Chemistry*, vol. 2. Pergamon Press, New York 1958.
7. J. H. McClain, S. M. Shelton in C. R. Tipton, Jr., (ed.): *Reactor Handbook*, vol. 1, Materials, 2nd ed., Interscience Publishers, New York 1960.
8. W. Fischer et al., *Angew. Chem. Int. Ed. Engl.* **5** (1966) 15–23.
9. E. I. DuPont de Nemours, US 2852446, 1956 (M. L. Bromberg).
10. Pechiney Ugine Kuhlman, US 4021531, 1976 (P. Besson, J. Guerin, P. Brun, M. Bakes).
11. L. Moulin, P. Thouvenin, P. Brun in D. G. Franklin (ed.): *Zirconium in the Nuclear Industry*, 6th Int. Symposium, ASTM STP 824, American Society for Testing and Materials, Philadelphia 1984, pp. 37–44.
12. W. Fischer, W. Chalybæus, *Z. Anorg. Allg. Chem.* **255** (1948) 277.
13. Pechiney, US 4657643, 1986 (M. Armand, J.-P. Garnier).
14. E. M. Sherwood, I. E. Campbell in D. E. Thomas, E. T. Hayes (eds.): *The Metallurgy of Hafnium*, US Government Printing Office, Washington, DC, 1960, 108–118.
15. R. F. Rolston: *Iodide Metals and Metal Iodides*, The Electrochemistry Society, New York 1961.
16. R. VanSanten, J. Schlewitz, G. Beck, R. Walsh in F. D. Snell, L. S. Ettre (eds.): *Encyclopedia of Industrial Chemical Analysis*, vol. 14, Wiley-Interscience, New York 1971, pp. 103–148.
17. R. B. Hahn, E. S. Baginski, *Anal. Chim. Acta* **14** (1956) 45–47.
18. R. B. Hahn in I. M. Kolthoff, P. J. Elving, E. B. Sandell (eds.): *Treatise on Analytical Chemistry*, Part II, vol. 5, Interscience, New York 1961, pp. 61–138.
19. R. K. McGeary in *A Symposium on Zirconium and Zirconium Alloys*, American Society for Metals, Cleveland 1953, pp. 168–175.
20. W. G. Guldner, *Talanta* **8** (1961) 191–202.
21. W. G. Smiley, *Anal. Chem.* **27** (1955) 1098–1102.
22. P. Elbling, G. W. Goward, *Anal. Chem.* **32** (1960) 1610–1613.
23. J. Surak, D. Fisher, C. Burros, L. Bate, *Anal. Chem.* **32** (1960) 117–119.
24. J. Lingane, *Anal. Chem.* **39** (1967) 881.
25. L. Carpenter, J. M. Nishi: "Analysis of High-Purity Columbium by Optical Emission Spectrography", USBM RI 6384, 1964.
26. R. Brayer, R. O'Connell, A. Powell, R. H. Gale, *Appl. Spectrosc.* **15** (1961) 10–13.
27. G. L. Beck, O. T. Farmer, *J. Anal. Atomic Spectrometry* **3** (1988) 771–773.
28. G. L. Beck, J. P. Fraley, *Teledyne Wah Chang procedure ASP-OES-I*, Rev. O, 1988.
29. J. Schlewitz, M. Shields, *At. Absorpt. Newsl.* **10** (1971) 39–43.
30. J. A. Ewen, L. Haspeslagh, J. L. Atwood, H. Zhang, *J. Am. Chem. Soc.* **109** (1987) 6544–6545.
31. D. C. Tran et al. in J. Lucas, C. T. Moynihan (eds.): *Halide Glasses I, Material Science Forum*, vol. 5, Trans Tech Pub., Switzerland 1985, 339–352.

32. B. D. James, B. E. Smith, *Synth. React. Inorg. Met. Org. Chem.* 4 (1974) 461-465.
33. J. A. Jansen, J. E. Gozum, D. M. Pollina, G. S. Girolami, *J. Am. Chem. Soc.* 110 (1988) 1643-1644.
34. E. Rudy: "Ternary Phase Equilibria in Transition Metal-Boron-Carbon-Silicon Systems", Part V, *Compendium of Phase Diagram Data*, AFML-TR-65-2, Air Force Materials Laboratory, Wright-Patterson AFB, Ohio, 1969, pp. 166-167.
35. S. Mazumdar, H. S. Ray, *J. Appl. Chem. Biotechnol.* 4 (1972) 565-576.
36. S. N. Flengas, J. F. Dutrizac, *Metal. Trans. B* 8B (1977) 377-385.
37. E. M. Larsen, J. W. Moyer, F. Gil-Armao, M. J. Camp, *Inorg. Chem.* 13 (1974) 574-581.
38. Teledyne Industries, US 4072506, 1975 (J. Megy).
39. W. M. Mueller, J. P. Blackledge, G. G. Libowitz: *Metal Hydrides*, Academic Press, New York 1968, pp. 321-330.
40. In [34], p. 671.
41. E. Rudy, B. F. Kieffer, E. Baroch, *Planseeber. Pulvermetall.* 26 (1978) 105-115.
42. D. C. Bradley, R. C. Mehrotra, D. P. Gaur: *Metal Alkoxides*, Academic Press, New York 1978.
43. D. J. Cardin, M. F. Lappert, C. L. Raston: *Chemistry of Organo-Zirconium and -Hafnium Compounds*, Ellis Horwood Ltd., Chichester 1986.
44. P. C. Wailes, R. S. P. Coutts, H. Weigold: *Organo-metallic Chemistry of Titanium, Zirconium, and Hafnium*, Academic Press, New York 1974.
45. J. Schemel: *ASTM Manual on Zirconium and Hafnium*, ASTM STP 639, Philadelphia 1977.
46. *National Fire Codes*, vol. 7, NFPA No. 482-1987, National Fire Protection Association, Boston 1988.
47. C. F. Kittle, E. R. King, C. T. Bahner, M. Bruler, *Proc. Soc. Exp. Biol. Med.* 76 (1951) 278-282.
48. T. J. Haley, R. Raymond, N. Komesu, H. C. Upham, *Toxicol. Appl. Pharmacol.* 4 (1962) 238-246.

32 Vanadium

GÜNTER BAUER (RETIRED), VOLKER GÜTHER, HANS HESS, ANDREAS OTTO, OSKAR ROIDL, HEINZ ROLLER, SIEGFRIED SATTELBERGER

32.1 History	1471	32.5.2 Production of Vanadium Metal and its Alloys	1480
32.2 Properties	1471	32.6 Uses	1482
32.3 Occurrence	1472	32.7 Compounds	1483
32.4 Processing of the Raw Materials	1475	32.8 Analysis	1485
32.4.1 Iron Ores and Titanomagnetites as Raw Materials	1476	32.9 Economic Aspects	1485
32.4.2 Processing of Other Raw Materials	1478	32.10 Environmental Protection and Toxicology	1486
32.5 Production of Vanadium	1480	32.11 References	1488
32.5.1 Reduction Behavior of Vanadium Oxides	1480		

32.1 History [1]

In 1801, MANUEL DEL RIO discovered vanadium in Mexican lead vanadate ore. In 1831, SEFTSTRÖM detected the element in converter slags from certain iron ores, and named it after the Norse goddess of beauty, Vanadis.

Vanadium metal was first produced in powder form by ROSCOE in 1867-1869 by reduction of vanadium dichloride with hydrogen. MARDEN and RICH obtained ductile vanadium by reducing vanadium pentoxide, V_2O_5 , with calcium metal.

The first major application of vanadium was in 1903 in England, where a vanadium-alloyed steel was produced on an 18 t scale [2]. In 1905 HENRY FORD recognized the advantages of vanadium steel and promoted its use in automobile construction. Today vanadium is of major importance as an alloying component in steel and titanium alloys and as a catalyst for chemical reactions.

32.2 Properties

Vanadium has two stable isotopes: ^{51}V (99.75%) and ^{50}V (0.25%). Unstable isotopes of relative atomic mass 48, 49, and 52 have half-lives ranging from 4 min to 600 d. The electronic configuration is $1s^2 2s^2 p^6 3s^2 p^6 d^3 4s^2$. Vanadium is steel gray with a bluish tinge.

It is ductile, and can be forged and rolled at ambient temperature.

Vanadium, together with niobium and tantalum, belongs to group 5 of the periodic table. It has a high melting point and good corrosion resistance at low temperature.

Physical Properties. The most important physical properties of vanadium are listed in the following [1, 3-6]:

Relative atomic mass	50.9415
Crystal structure	body-centered cubic
Lattice constant a	0.30238 nm
Density	6.11 g/cm ³
m_p	1929 \pm 6 °C
Heat of fusion	21 500 \pm 3000 J/mol
Specific heat at 298 K	24.35 \pm 0.10 Jmol ⁻¹ K ⁻¹
for 298-990 K	$C_p = 24.134 + 6.196 \times 10^{-2}T - 7.305 \times 10^{-7}T^2 - 1.3892 \times 10^{-12}T^3$
for 900-2200 K	$C_p = 25.9 - 1.25 \times 10^{-4}T + 4.08 \times 10^{-6}T^2$
for liquid V	47.43
Vapor pressure at 2190 K	3.73 Pa
at 2200 K	4.31
at 2300 K	12.53
at 2400 K	30.13
at 2500 K	87.86
at 2600 K	207.6
for liquid V, mbar	$\log p = -24.265 \times 10^3 T^{-1} + 9.65$
Heat of vaporization	465.9 kJ/mol
Linear coefficient of expansion	
at 20-200 °C	7.88×10^{-6}
at 20-500 °C	9.6×10^{-6}
at 20-900 °C	10.4×10^{-6}
at 20-1100 °C	10.9×10^{-6}
Specific electrical resistivity	
at 20 °C	$24.8 \times 10^{-6} \Omega\text{cm}$
Temperature coefficient	

for 0–100 °C	0.0034 μΩcm/K
Thermal conductivity at 100 °C	0.31 Jcm ⁻¹ K ⁻¹ s ⁻¹
at 500 °C	0.37
Superconductivity, transition temperature	5.13 K
Capture cross section for thermal neutrons	4.8 barn

Mechanical Properties. The mechanical properties of vanadium are strongly dependent on purity and hence on the production method used. In particular, the elements O, H, N, and C increase the hardness and tensile strength and decrease the ductility (elongation) [7]. The most important mechanical properties are listed in Table 32.1 [3, 4, 7].

Table 32.1: Mechanical properties of vanadium metal.

	Commercial purity	High purity
Tensile strength σ _B , N/mm	245–450	180
Extension, %	10–15	40
Vickers hardness HV 10, N/mm	80–150	60–70
Modulus of elasticity, N/mm	137 000–147 000	
Poisson's ratio	0.35	

Chemical Properties. Vanadium is stable in air below 250 °C. On prolonged storage the surface becomes bluish-gray to brownish-black, and significant oxidation takes place in air above 300 °C. Vanadium absorbs hydrogen in interstitial lattice sites at elevated temperatures (up to 500 °C). The metal becomes brittle and can easily be powdered. This hydrogen is liberated on heating to 600–700 °C in vacuum. At low temperature, a hydride phase ex-

Table 32.2: Principal vanadium minerals [12, 13].

Mineral and chemical formula	% V	% V ₂ O ₅	Occurrence
Roscoelite [KV ₂ (OH) ₂ /AlSi ₃ O ₁₀]	11.2–14.0	20–25	in uranium–vanadium ores; e.g., Colorado Plateau, USA
Montroseite (V, Fe)OOH	45.4	81.0	
Carnotite K ₂ [(UO ₂) ₂ /V ₂ O ₈]·3H ₂ O	10.3	18.3	
Tyuyamunite Ca[(UO ₂) ₂ /V ₂ O ₈]·5·8H ₂ O	11.1	19.8	
Francevillite (Ba, Pb)[(UO ₂) ₂ /V ₂ O ₈]·5H ₂ O	9.9	17.7	
Corvusite V ₂ ⁴⁺ ·V ₁₂ ⁵⁺ O ₃₄ ·nH ₂ O	40.8	72.8	
Vanadinite Pb ₂ [Cl/(VO ₃) ₃]	10.2	18.2	in Pb, Zn, Cu vanadate ores; e.g., Otavi Mountains, Namibia
Descloizite Pb(Zn, Cu)[OH/VO ₄]	12.7	22.7	
Mottramite Pb(Cu, Zn)[OH/VO ₄]	10.5	18.8	
Patronite VS ₄ or V ₂ O ₅	16.8	ca. 30	in asphaltites; e.g., Mina Ragra, Peru
Magnetite ^a Fe ₂ ²⁺ ·Fe ³⁺ O ₄	< 0.5–1.5	< 1.2–2.7	in titanomagnetite ores; e.g., Bushveld, South Africa

^a Several varieties exist in which there is partial replacement of Fe³⁺ by V, Ti, Al, and Cr, and of Fe²⁺ by Ti, Mg, Mn, and other elements. The vanadium- and titanium-containing magnetites are generally referred to as titanomagnetites.

ists in the V–H system [7]. Vanadium reacts with nitrogen at > 800 °C to form vanadium nitrides. It has a high affinity for carbon, forming carbides at 800–1000 °C. Data on the solubility of O, N, H, and C in vanadium and the reactions that occur with these elements can be found in [7, 8].

In its compounds, vanadium exhibits the oxidation state II, III, IV, or V. It is relatively stable towards dilute sulfuric, hydrochloric, and phosphoric acids, but is dissolved by nitric and hydrofluoric acids. Its corrosion resistance towards tap water is good, and towards seawater moderate to good, but pitting does not occur. Vanadium is resistant to 10% sodium hydroxide solution, but is attacked by a hot solution of potassium hydroxide [1, 3, 4, 9, 10]. Vanadium and some vanadium alloys have good corrosion resistance towards molten low-melting metals and alloys, especially alkali metals, which are used in nuclear reactors as coolants and heat-exchange media [11].

32.3 Occurrence

Vanadium is present in the earth's crust at a mean concentration of 150 g/t, and is therefore one of the more common metals. It is more abundant than copper and nickel, and of similar abundance to zinc. Vanadium forms several minerals, of which the most important are listed in Table 32.2 [12, 13].

In the early 1900s, vanadium was obtained almost exclusively from Peruvian patronite. As these deposits became exhausted, descloizite ores were mined in southern Africa, Namibia, and Zambia.

After World War II, the continental sedimentary uranium- and vanadium-containing carnotite deposits of the Colorado Plateau and the marine sedimentary vanadium-bearing phosphate deposits of Idaho became important. There are also uranium vanadium reserves in Yeellirie, Western Australia, and in the Ferghana Basin the Kirghiz, Tajik, and Uzbek Republics [13].

Vanadium production greatly increased from the mid-1950s with the mining and processing of titanomagnetites. This type of raw material can be used directly for vanadium extraction, or it can be employed to obtain vanadium-containing pig iron from which an oxidation slag highly enriched in vanadium is produced. This development began in Finland, followed by South Africa and smaller producers in Norway and Chile. Titanomagnetites have also been mined in the former Soviet Union and China in large quantities since the early 1960s and 1970s, respectively. The vanadium-bearing titanomagnetite deposits are of magmatogenic origin, and occur in many parts of the world. The most important reserves mined today include the Bushveld deposit in South Africa, Katschkanor in the Urals of Russia, Lanshan and Chienshan in the Sichwan province of China, and a deposit in New Zealand. The titanomagnetites of the Urals and in the Sichwan province are palaeozoic complexes.

The mines at Otanmäki and Mustavaara in Finland and RØdsand in Norway were shut down during the 1980s.

Production of lead zinc vanadates in Namibia had been discontinued by the end of the 1970s.

Since the 1980s, a new type of secondary raw materials has gained importance, i.e., residues of mineral oil processing. Most crude oils contain vanadium in amounts ranging from ca. 10 ppm (Middle East) to 1400 ppm (Central

America). In petrochemical refining, vanadium is retained in boiler residues and fly ashes from incineration, with vanadium contents between a few percent and 40%. The total amounts greatly exceed current world consumption.

Noteworthy is an aqueous emulsion of a highly viscous crude from the Orinoco basin in Venezuela (Orimulsion) whose combustion yields fly ashes containing 10% vanadium.^a

With environmental legislation becoming stricter, emission and deposition of these residues will be drastically reduced so that they will have increasingly to be processed.

Other, less important vanadium sources are: vanadium-containing waste salts from bauxite production, and spent catalysts from the chemical and petrochemical industries. The extraction of vanadium from currently available raw material sources (except direct processing of titanomagnetite) is always coupled with the production of other metals or energy. The most important sources are shown in Table 32.3.

Table 32.3: Vanadium production as a by-product.

Raw material	Coupled product	Vanadium by-product
Titanomagnetites	iron/steel	vanadium slag
Mineral oils	energy/petrochemicals	fly ashes boiler residues
Uranium–vanadium ores	uranium	petrochemical residue
Bauxite	alumina	vanadium salt
Phosphates	phosphorus	vanadium-containing Fe–P salamander
Lead vanadates	lead, zinc	vanadium slag

Table 32.4: Estimate of the world reserves and reserve base of vanadium in 10³ tonnes of vanadium content (% given in parentheses).

Geographic area	Reserves		Estimated reserves 1985
	1985	1990	
North America	185 (4.0)	135 (3.2)	2500 (13.7)
South America	25 (0.5)		130 (0.7)
Former USSR	2900 (60.4)	2631 (61.7)	4500 (24.6)
South Africa	950 (19.7)	862 (20.2)	8600 (47.0)
China	670 (14.0)	500 (14.2)	1800 (9.8)
Pacific	35 (3.1)	30 (0.7)	570 (3.1)
Total	4800 (100)	4267 (100)	18 300 (100)

Table 32.5: World production of vanadium-containing commodities by country, given in tonnes of vanadium content [14].

Countries	1985	1986	1987	1988	1989	1990	1991	1992	1993
China ^a	5 500	5 500	5 500	5 500	4 500	4 500	4 500	4 500	5 000
Finland	2 590								
South Africa ^b	17 000	18 600	17 300	19 900	16 500	17 000	15 500	14 300	16 000
Former USSR	11 500	11 500	11 600	11 600	9 600	9 600	8 000	6 000	7 900
United States (total)	4 000	3 600	3 800	3 500			5 600	5 300	5 500
from catalysts and ashes	2 970	2 560	2 760	2 480					
Japan ^c	925	1 020	1 020	1 020			600	800	
New Zealand							2 200	1 700	
Total	45 700	44 000	42 100	45 300	31 600	31 600	35 800	33 200	34 500

^a Estimated.^b South Africa: roughly 40% is pentoxide and vanadate products and 60% is vanadiferous slag products.^c Spent catalyst and petroleum ashes.

Resources and Production. Known and estimated mineral reserves are listed in Table 32.4.

In this table the vanadium containing carbonitic shells (very low concentration) and the petroleum ashes/residues are not included, although these oils contain tremendous amounts of vanadium.

Assessment of world reserves by studying the geology of deposits suggests that it will be possible to discover further workable deposits in the region of the widely distributed titanomagnetites in the old shields. The Indian shield in the Singhbhum (Bihar) and Magurbhanj (Orissa) regions, the Australian shield in Western Australia, the Canadian shield in Québec and Ontario, and the Finno-Scandinavian shield all show great promise. However, little is so far known about the Brazilian shield. The enormous vanadium reserves in the titanomagnetites cannot yet be even approximately quantified.

The world production of vanadium by country is listed in Table 32.5 [14].

Comparison of Tables 32.4 and 32.5 shows that the largest producers, South Africa and Russia, have also the largest mineral reserves. The next two producing countries China and the United States have comparatively small reserves of such origin.

Details of the Most Important Deposits. The Bushveld deposit in South Africa is an oval, bowl-shaped complex in a magmatic layer extending over an area of 65 000 km². The ores were deposited in the following order:

chromite, platinum ores, vanadium-containing titanomagnetites, and tin ores. In all, 21 magnetite layers have been found in the main and upper zones of this deposit. The titanomagnetites have the following chemical composition (%):

Fe	55.8–57.5	Cr ₂ O ₃	0.13–0.45
V ₂ O ₅	1.4–1.6	Al ₂ O ₃	2.5–3.5
TiO ₂	12.2–13.9	SiO ₂	0.9–1.5

The V₂O₅ content can be as high as 2.4% in exceptional cases.

Production by Highveld Steel & Vanadium is based on ore containing 1.6% V₂O₅ from the Mapochs mine, situated 90 km NNE of Middleburg. The reserves contain 200 × 10⁶ t ore. Mining is by the open pit method, and the maximum ore production capacity is 8000 t/d [13].

Other South African titanomagnetite deposits include the Kennedy's Vale mine, with a production capacity of 6000 t/d (though not currently producing) and two mines near Brits, each with a production capacity of 5000–6000 t/d.

There are a number of lead vanadate deposits in the Otavi Mountains in Namibia. Mount Aukas, near Grootfontein, has deposits of 2 × 10⁶ t ore containing 15% Zn, 4% Pb, and 0.5% V₂O₅. Deep mining has been discontinued since 1978. The mined ore, which was processed by flotation, yielded the following products: lead sulfide concentrate, zinc sulfide concentrate, willemite concentrate, cerussite concentrate, and a vanadium concentrate containing 17% V₂O₅, 43% Pb, and 17% Zn.

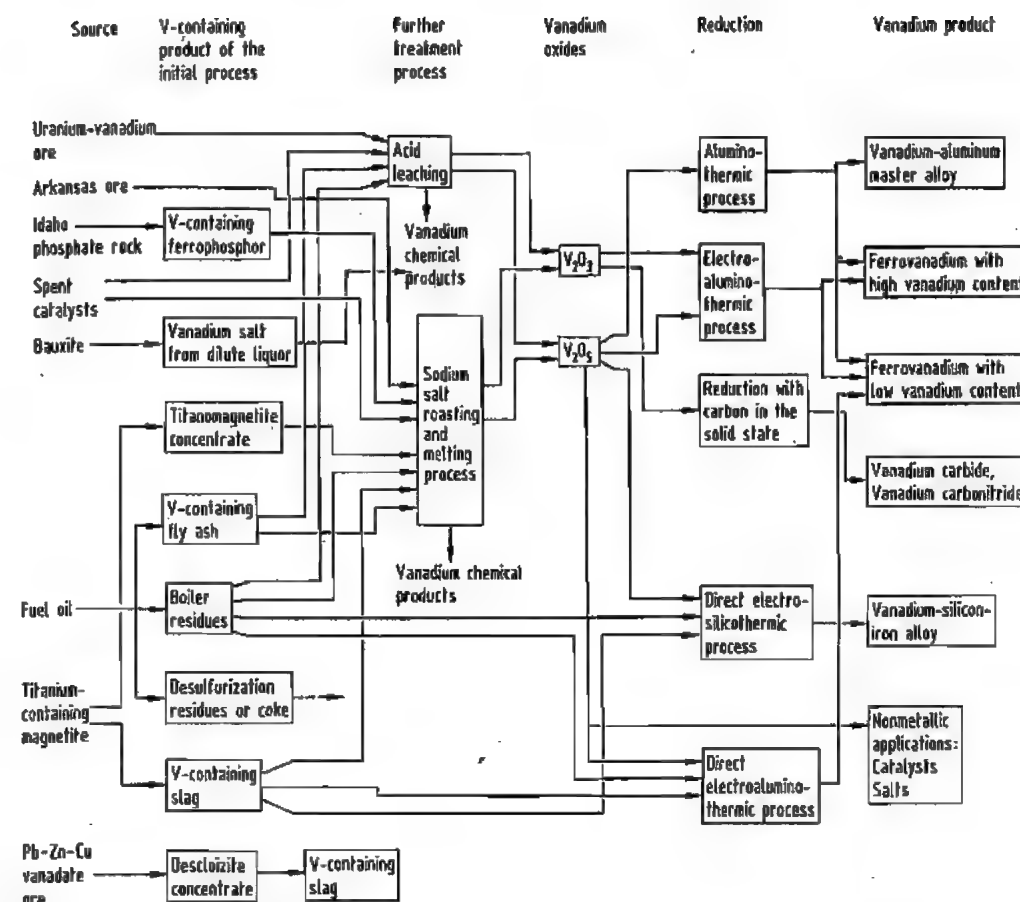


Figure 32.1: Treatment of vanadium raw materials [15].

The titanomagnetite deposits at Otanmäki and Mustavaara in Finland had reserves of 15 × 10⁶ t ore containing 35–40% Fe, 13% TiO₂, and 0.45 V₂O₅, and 40 × 10⁶ t ore containing 17% Fe, 3.1% TiO₂, and 0.36% V₂O₅ [14]. The production capacity of the Otanmäki deep mine was ca. 1 × 10⁶ t/a ore. Magnetite containing 69% Fe, 2.5% TiO₂, and 1.07% V₂O₅ together with ilmenite and pyrite were obtained by magnetic separation and flotation. Both mines were closed in the 1980s.

The Colorado Plateau in the United States contains the main mining area of the Uravan mineral belt, > 1100 km long, in SW Colorado and SE Utah. This belt contains irregular lenticular ore bodies, normally < 3000 t, with

0.2–0.3% U₃O₈ and 0.85–1.4% V₂O₅. The oxidation region contains the minerals carnotite, tyuyamunite, montroseite, and pascoite, and the unoxidized region contains the minerals coffinite, pitchblende, and corvusite. These ores are extracted in small deep mine workings which produce ca. 0.4 × 10⁶ t/a ore.

32.4 Processing of the Raw Materials

The raw materials used today include the titanomagnetite ores and their concentrates, which are sometimes processed directly, vanadium slags derived from the ores, oil combustion residues, residues from the

hydrodemetallization (HDM) process, and spent catalysts (secondary raw materials). A summary of the processing routes is given in Figure 32.1.

32.4.1 Iron Ores and Titanomagnetites as Raw Materials

Production of Vanadium Slags. The titanomagnetite ore in lump form, containing ca. 1.51–1.7% V_2O_5 (Mapoch mine in South Africa), is first prereduced by coal at ca. 1000 °C in directly heated rotary kilns. A further reduction is then performed in an electric arc furnace to obtain a pig iron which contains ca. 1.4% V_2O_5 . The slag that is also formed contains ca. 30% TiO_2 , and this is deposited on slag heaps. In a heat resistant shaking ladle the molten pig iron is oxidized with oxygen lances, causing the vanadium to be transferred to the slag. The vanadium slag contains vanadium in the form of a water-insoluble trivalent iron spinel, $FeO \cdot V_2O_3$, at a concentration corresponding to ca. 25% V_2O_5 . This slag is the world's principal raw material for vanadium production [16].

The largest slag and vanadium producer in the western world is South Africa (see Table 32.5), most of whose production is by the Highveld Steel and Vanadium Corp. [13]. Second largest producer is the Nizhny Tagil metallurgical plant in Russia; the slag contains ca. 12–18% V_2O_5 . Another producer of vanadium slag is the Pannang steelworks in Panzihua, China.

Vanadium slags were produced experimentally by W. L. GOODWIN and W. P. FIRTH in 1919, but the basic industrial process was developed by R. VON SETZ, and was first used by the Spigerverk plant in Oslo in the early 1930s. The process was then mainly used in conjunction with the Thomas process. The pig iron from the blast furnace was not directly converted to Thomas steel with addition of lime in the usual way. Instead, the vanadium was oxidized completely or partially before lime addition. As vanadium has a high affinity for oxygen, it was oxidized before the phosphorus and transferred to the slag. Slags con-

taining several percent of vanadium were obtained, depending on the vanadium content of the pig iron, whereas normal Thomas slags contain an average of only 0.5% V.

Oxidation of vanadium-containing pig iron to give vanadium-containing slag was carried out by the Röchling Iron and Steel Works in Völklingen from 1937 using a converter with a very acid lining or a continuously operating oxidizing drum. For details of these abandoned processes see [17].

Processing of Vanadium Slags. The main process used today to produce vanadium oxide from vanadium slags is alkaline roasting. The same process, with minor differences, is also used for processing titanomagnetite ores and vanadium-containing residues.

A vanadium slag has the following approximate composition: 14% V (= 25% V_2O_5), 1.5% Ca, 2.5% Mg, 2.0% Al, 0.01% P, 9% metallic Fe, 32% total Fe, 7% Si, 3.5% Mn, and 3.5% Ti. The presence of the elements Ca, Mg, and Al, which form water-insoluble vanadates during alkaline roasting, leads to a reduction in yield. Silicon can cause filtration difficulties during leaching of the calcine. Phosphorus, unless removed in a separate treatment, reports practically quantitatively to the vanadium oxide, and lowers the vanadium yield in the precipitation process.

The process is shown schematically in Figure 32.2. The vanadium slag is first ground to < 100 μm (1–11 in Figure 32.2), and the iron granules contained therein are removed. Alkali metal salts are then added, and the material is roasted with oxidation at 700–850 °C in multiple-hearth furnaces or rotary kilns (12–20) to form water-soluble sodium vanadate. During roasting, care must be taken to prevent agglomeration of the material by sintering and to ensure rapid cooling after the material leaves the furnace. The roasted product is leached with water (21 in Figure 32.2), and ammonium polyvanadate or sparingly soluble ammonium metavanadate is precipitated in crystalline form from the alkaline sodium vanadate solution by adding sulfuric or hydrochloric acid and ammonium salts at elevated

temperature (22–28). These compounds are converted to high-purity, alkali-free vanadium pentoxide by roasting. The usual commercial “flake” form of vanadium pentoxide is obtained by solidifying the melt on cooled rotating tables (29–31 in Figure 32.2).

The aluminothermic production of ferrovanadium described in Section 7.12 is also shown in Figure 32.2 (32–34), as well as wastewater purification (35–44), including the reduction of Cr(VI) to Cr(III) (35) and the crystallization of sodium sulfate (37).

In Russia, a combination of alkaline roasting and sulfuric acid leaching is used. A disadvantage of this process is the manganese content of up to 2% in the V_2O_5 , caused by acid leaching.

Direct Production of Vanadium Oxide from Titanomagnetite Ores and Clays. If the ores contain > 1% vanadium, they can be directly converted to vanadium pentoxide. The gangue material is first removed from the ore by flotation, and the ore is then mixed with sodium carbonate, pelletized, and roasted in shaft furnaces or rotary kilns at 1000 °C.

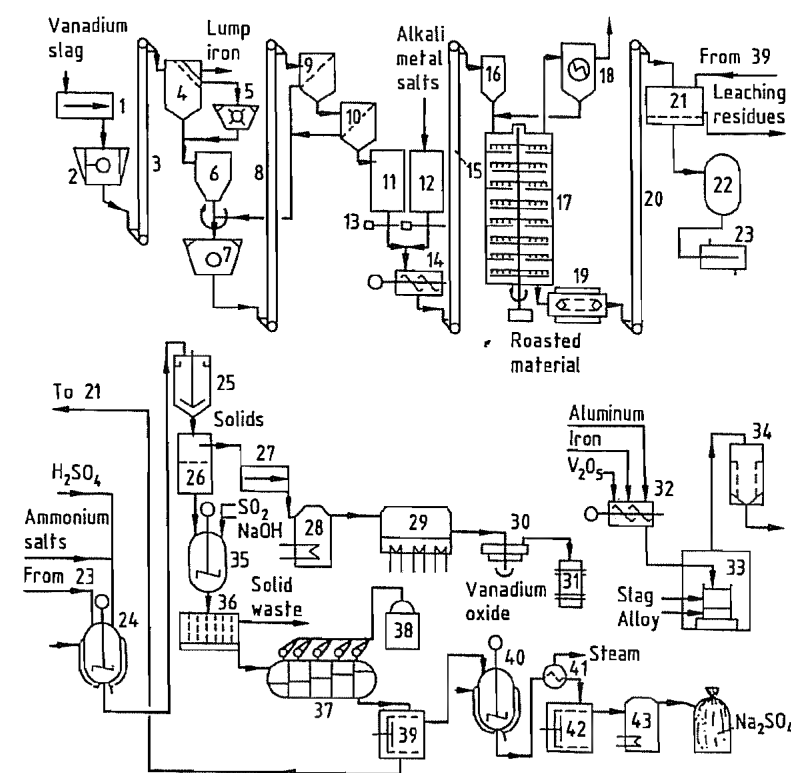


Figure 32.2: Production of vanadium from vanadium slags: process of the Gesellschaft für Elektrometallurgie. 1) Push feeder; 2) Jaw crusher; 3) Bucket conveyor; 4) Screen; 5) Impact mill; 6) Container with discharge device; 7) Mill; 8) Bucket conveyor; 9) Screen; 10) Air classifier; 11) Container for ground material; 12) Container for alkali metal salt; 13) Metering weighing machine; 14) Mixer; 15) Bucket conveyor; 16) Container with discharge device; 17) Multideck furnace; 18) Electrostatic precipitator; 19) Chain conveyor with cooling; 20) Bucket conveyor; 21) Leaching with filtration; 22) Storage container; 23) Double-tube heat exchanger; 24) Precipitation vessel; 25) Thickener; 26) Plate filter; 27) Continuous feeder; 28) Dryer; 29) Melting furnace; 30) Cooled rotary table; 31) Packing; 32) Mixer; 33) Aluminothermic reaction; 34) Bag filter; 35) Precipitation vessel; 36) Filter press; 37) Cooling with crystallization; 38) Steam generation; 39) Pusher centrifuge; 40) Melting vessel; 41) Heat exchanger; 42) Pusher centrifuge; 43) Dryer.

The sodium metavanadate formed is leached out with water, and vanadium pentoxide is obtained from this by the same method as that used in the roasting process for vanadium slags. The leach residue is used to produce pig iron if its ilmenite content is sufficiently low [15].

32.4.2 Processing of Other Raw Materials

Hydrometallurgical methods or a combination of pyrometallurgical and hydrometallurgical processes are used to produce vanadium oxides and salts from other raw materials. In the combined processes, thermal treatment is followed by alkaline or, more rarely, acid processing.

Acid Processes. Vanadium-containing oil residues and spent catalysts are digested with sulfuric acid, often under reducing conditions with addition of SO_2 . After removal of the impurities, the solution is oxidized, and polyvanadate and calcium or iron vanadate are precipitated by partial neutralization of the acid [13].

Acid digestion was formerly an important method of treating carnotite, a uranium–vanadium ore. After the uranium had been removed from the solution in sulfuric acid by solvent extraction, the vanadium was partially reduced with iron powder and solvent extracted. After re-extraction, the vanadium was in the form of an acid solution of vanadyl sulfate. This was oxidized with sodium chlorate at elevated temperature, and precipitated as red cake, a mixture of sodium and ammonium polyvanadate, by adding ammonia or ammonium salts. This precipitate was roasted to convert it into alkali-containing V_2O_5 [13, 18].

Historically, Pb–Zn–V concentrates from Namibia were subjected to acid treatment process. However, the mining of these ores became uneconomic and was discontinued in 1978.

The ore concentrate produced by flotation was ground and leached with dilute sulfuric

acid (10–15%). This led to the formation of insoluble lead sulfate. The solubility of the vanadium was considerably increased by simultaneously passing SO_2 through the liquor. Phosphorus was removed by adding sodium zirconate to precipitate sparingly soluble zirconium phosphate. The filtrate, which contained mainly ZnSO_4 and VOSO_4 , was treated with H_2S to precipitate As and Cu. The pH of the clear solution was increased to 1–2 by addition of sodium carbonate, and tetravalent vanadium was oxidized to the pentavalent state by heating with sodium chlorate. More sodium carbonate was added to the iron-containing solution to increase its pH to 4, precipitating a polyvanadate containing iron and sodium. This precipitate was filtered and treated with a solution of an ammonium salt to replace the sodium ions by ammonium ions. It was then dried and converted to V_2O_5 by fusion.

Zinc carbonate was precipitated from the filtrate after the polyvanadate precipitation.

Combination of Pyrometallurgical and Alkaline Hydrometallurgical Methods. This combined process, which is preferred in practice, is used to treat vanadium-containing residues and spent catalysts. (It was formerly also used for V-containing clays, phosphates, and Pb–Zn vanadates.) The vanadium, which is mainly trivalent, is oxidized at high temperature and converted to alkali metal vanadate, which can be leached with water.

The best known process is alkaline roasting, in one version of which the ore is pelletized with sodium carbonate or compacted. After leaching, the solutions are acidified and ammonium salts are added, precipitating the vanadium as polyvanadate, which is then converted to vanadium pentoxide by calcination.

In the treatment of Pb–Zn vanadates, the zinc and lead were first reduced with carbon in the presence of added sodium carbonate in short drum furnaces. The zinc was distilled off and the lead tapped off as molten metal. The vanadium was then present in the alkaline slag in water-soluble form.

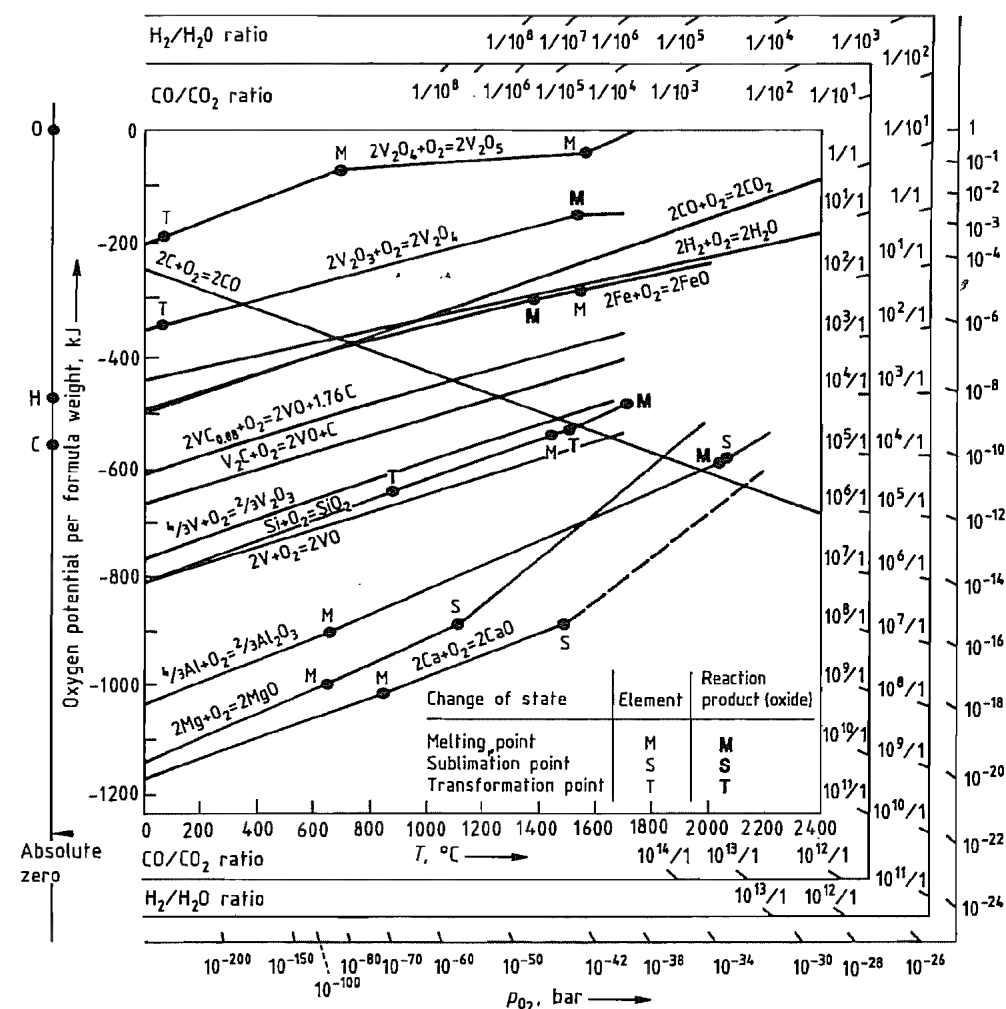


Figure 32.3: Oxygen potentials of oxides of vanadium and other elements as a function of temperature.

Production of Vanadium Pentoxide from Oil Residues and Boiler Ash. Appreciable amounts of vanadium are present in mineral oil, especially Venezuelan and Russian oils. The vanadium accumulates in the soot and ash of oil-fired boilers and in oil distillation residues and is sold in this form by power stations and refineries. These secondary raw materials, which sometimes contain > 50% V_2O_5 , can be blended in the pyrometallurgical/hydrometallurgical process [13] or treated separately.

The extraction of vanadium from mineral oil combustion residues is gaining in impor-

tance, since the asphalt-like oil deposits of the Orinoco basin in Venezuela can now be processed into a fuel resembling mineral oil by emulsification with water with addition of magnesium nitrate. The fuel is used for energy generation in power stations. The amount of vanadium in the resulting boiler ashes is expected to reach the same order of magnitude as is currently generated in vanadium slags.

Production of V_2O_5 during the Processing of Bauxites. Some deposits of bauxite contain high levels of vanadium, and during alumina production this ends up in the salt residue,

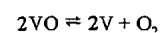
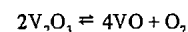
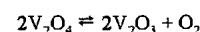
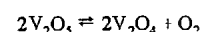
from which V_2O_5 can be obtained. This process is more expensive than vanadium production from slags and causes severe wastewater treatment problems due to the arsenic originating from the raw material [19]. Small amounts of vanadium are obtained by this method in India and Hungary [13].

32.5 Production of Vanadium

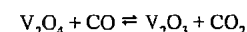
32.5.1 Reduction Behavior of Vanadium Oxides

The most important oxide obtained on treating raw materials is vanadium pentoxide, V_2O_5 (see Section 32.6).

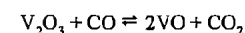
The oxygen partial pressure in equilibrium with the vanadium oxides in accordance with the equations



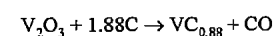
can be calculated from thermodynamic data [20]. The reactions are strongly endothermic, and have positive free enthalpies in the temperature range 298.15–2000 K (Figure 32.3). V_2O_5 is the only oxide which dissociates to a large extent, the oxygen pressure reaching 0.08 MPa at 2000 K. In the presence of reducing gases such as CO and H_2 , the higher oxides are reduced to V_2O_3 :



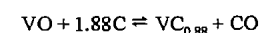
The reduction of V_2O_3 by CO or H_2 in accordance with the equation



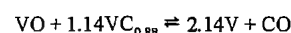
does not go to completion [20], but reduction by carbon is almost complete:



The reaction of VO with carbon initially gives vanadium carbide:



In the further reaction of oxide with carbide,



it can be calculated from thermodynamic data [20] that the CO pressure will reach ca. 600 Pa at 2000 K. However, VO and C are soluble in vanadium at high temperature. This does not favor carbothermic reduction to pure vanadium metal even under high vacuum, and it is difficult to obtain a metal with low C and O contents [1].

For the metallothermic reduction of vanadium oxide silicon, aluminum, calcium, and magnesium could be considered as possible reagents, of which calcium and magnesium have an especially strong reduction potential. However, reduction with aluminum is incomplete, the vanadium produced being either oxygen-containing and low in aluminum, or aluminum-containing and low in oxygen [21], which, in addition, leads to loss of vanadium in the slag. In the production of VAl, a low-oxygen, aluminum-containing alloy is refined in a second stage using a vacuum induction furnace and is adjusted to the derived final composition. The refinement of aluminum-free vanadium metal is performed in an electron-beam furnace. The even less complete reduction with silicon is only used in the production of ferrovanadium, as the reaction proceeds better in the presence of iron.

Reduction of the oxides with calcium and magnesium goes almost to completion. As these metals are volatile, it is advantageous to carry out the reaction in closed vessels.

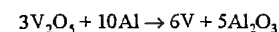
32.5.2 Production of Vanadium Metal and its Alloys

Reduction of Vanadium Oxide with Carbon. Carbothermic reduction of vanadium oxides is possible, but the vanadium produced is of high oxygen and carbon content; thus, this method is rarely used in practice. Also, the formation of a low-melting ternary eutectic (96.6% V, 2.8% C, 0.6% O; mp 1500 °C) prevents the reaction going to completion [22].

Avoidance of these problems by reducing vanadium oxide with vanadium carbide (carbidothermic production) has been proposed [23, 24]. High-purity vanadium ($\geq 99.8\%$ V) can be obtained by multiple sintering (two indirect sintering stages, one direct stage, and post-sintering).

Reduction of V_2O_5 with Calcium. A pressure vessel lined with pure magnesium oxide is used in this process. A mixture of high-purity V_2O_5 , double-distilled calcium chippings, and some high-purity sulfur as a booster is caused to react by heating [25]. This technique leads to a compact metal regulus (8–12 kg, 99.5–99.8% V) which is well separated from the slag. With a calcium excess of up to 70%, a vanadium yield of 85–90% is obtained. The Vickers hardness (HV 10) of this vanadium metal is 80–180, depending on the impurities present (mainly O, N, C, and Si) [1].

Reduction of V_2O_5 or V_2O_3 with Aluminum [26, 27]. The reduction



is self-sustaining, i.e., after initiation it proceeds without additional heating. The metal and slag are melted and separate well from each other. An excess of heat is produced during reduction. For process control, only a fraction of the material is ignited primarily and further material is then charged to the melt. To further decrease the exothermicity, a mixture of V_2O_5 and V_2O_3 is used. In the reduction of V_2O_3 with aluminum, boosters such as $KClO_3$ must be added to increase the reaction heat.

In the process developed by Teledyne Wah Chang Albany [28], a vanadium–aluminum alloy containing 13–15% Al is obtained by the aluminothermic reaction of high-purity V_2O_5 with aluminum powder in a closed vessel. The steel reaction vessel is lined with aluminum oxide at the bottom and in the reaction zone. After evacuation, it is purged several times with helium, and the charge is then electrically ignited with a heated resistance wire. The metal blocks obtained are refined in an electron-beam furnace by remelting several times. The high aluminum content leads to the re-

moval of most of the oxygen by volatilization of aluminum suboxides, but nitrogen and silicon cannot be removed by this method. A purity of 99.93% V can be achieved.

In a similar process [29], the metal produced in a closed reactor by the aluminothermic method is treated at 1700 °C and 10^{-4} Pa in a resistance-heated vacuum furnace, causing most of the aluminum to volatilize. Further purification by melting in an electron-beam furnace gives 99.93% pure metal.

Refining. Vanadium–aluminum alloys produced aluminothermically can be refined by molten salt electrolysis (electrorefining) [26]. A metal containing ca. 4.8% Al, 0.09% O, and 0.08% N can be refined by this method to give 99.6% pure vanadium.

The most effective purification of technically pure vanadium is achieved by the van Arkel process. Vanadium and iodine are heated together in a closed, evacuated tube, forming VI_2 and VI_3 . These are then sublimed and decomposed in a second reaction chamber on a tungsten or vanadium wire heated to 800 °C, yielding a 99.95% pure vanadium. The equipment required is complex and expensive, and the industrial potential is limited.

Production of Semifinished Products (Sheet, Rods, Tubes, Wire). The cast blocks of vanadium metal and alloys have a coarse structure which must first be converted into a fine-grained structure by extruding or forging at 900–1200 °C and then annealing. To prevent reaction of the vanadium with atmospheric oxygen and nitrogen, the blocks are encased in an iron or stainless steel cladding by vacuum welding. Owing to the good ductility of vanadium, subsequent metal working by rolling, forging, or drawing can be carried out at 100–500 °C. Pure vanadium can normally be formed at room temperature into thin sheets, wires, and tubes.

Vanadium and vanadium alloys can be welded using tungsten electrodes protected by an inert gas (TIG welding). Vanadium can be machined like niobium and tantalum. Excessive heating due to machining at high speeds must be avoided [30, 31].

32.6 Uses

Vanadium is mainly used as an alloying element in the steel industry, other major areas of use are [32, 33]

Steel	ca. 85%
Nonferrous alloys	ca. 9%
Chemical industry	ca. 4%
Others	ca. 2%

The second largest use area is in nonferrous alloys, mostly vanadium-containing titanium alloys and nickel-based superalloys for the aerospace industry. Additional uses are in vanadium-containing alloys for batteries and in grain refining of aluminum alloys. Vanadium compounds, principally the oxidation catalyst V_2O_5 , account for only ca. 3% of vanadium consumption [12].

Addition to Steel. Vanadium is added to steel mainly as ferrovanadium; technical vanadium carbide and vanadium carbonitride are also used. For the simultaneous addition of vanadium and nitrogen, nitrogen-containing Fe-V alloys are available.

Even small additions of vanadium increase the tensile strength and high-temperature strength of carbon steel [1, 46], and it has a grain refining and dispersion hardening effect in tempering steels.

Addition to Titanium. Alloying with vanadium improves the properties of titanium. The most important alloy is TiAl6V4, which has good strength properties at room temperature and good creep resistance. It is mainly used as a wrought alloy and casting alloy in airframe construction for load-bearing components and fixing devices, and in compressor disks and blades in jet engines. Other areas of increasing importance include power stations, shipbuilding, and reactor technology [13]. Other vanadium-containing titanium alloys with similar strength properties to TiAl6V4 include TiAl3V2.5, TiV15Cr3Sn3Al3, TiV10Fe2Al3, TiAl6V6Sn2, as well as TiV13Cr11Al3 [34, 35].

In light, corrosion-resistant titanium aluminides (intermetallic γ -TiAl phase) with high-temperature strength, small amounts of vanadium (as well as of chromium and man-

ganese) increase ductility at room temperature, which is an important criterion for usability and workability of this otherwise brittle material [36].

Other Uses. Alloys for Batteries. Intermetallic phases of the ZrV_2 type (Laves phases), in which vanadium is substituted partially by, e.g., Ni, Cr, Ti, or Mn, are used as electrode materials in metal hydride/nickel hydroxide batteries [37].

Coating materials containing vanadium and vanadium compounds are used in the electronics and glass industries as well as for wear protection.

Gettering materials based on Zr-V-Mn or Zr-V-Fe alloys are used for gas purification and for improving vacuums. The main component of these alloys, which contain up to 30% vanadium, is zirconium [38]. Gettering materials are specially adapted to individual applications; thus, with the exception of some products of the company SAES Getters, only a few standard alloys are marketed.

Vanadium Metal and Alloys. The use of vanadium as a principal component of alloys is in its infancy. As vanadium has higher thermal conductivity and strength and lower thermal expansion and density than stainless steel [39], it has been considered for cladding nuclear fuels for sodium-cooled fast breeder reactors, in the form of either pure metal or an alloy. In the United States, in the late 1960s, a large-scale development program on vanadium alloys was undertaken by the Atomic Energy Division at Westinghouse. Wide-ranging cooperative research projects in Germany in 1964–1971 are reported in [31, 40, 41]. A comprehensive review of these developments can be found in [7].

Of the vanadium alloys investigated, those in which titanium, niobium, chromium, and zirconium are the alloying elements seem the most promising.

The behavior of vanadium and its alloys in contact with lithium and sodium is described in [11, 41]. The effect of irradiation by neutrons on the strength properties of vanadium and its alloys is described in [42].

A further possible application of vanadium is in superconductivity. Vanadium-gallium alloys with composition V_3Ga are well known, but vanadium niobium alloys containing 30% Nb and vanadium-hafnium/zirconium alloys also have good superconducting properties.

32.7 Compounds

A large variety of vanadium compounds are used industrially: halides, oxides, nitrates, carbides, silicides, hydrides, vanadates, and organometallics.

Vanadium Oxides. *Vanadium pentoxide*, V_2O_5 , mp 690 °C, ρ 3.36 g/cm³, heat of formation $\Delta H^{298} = -1550.8$ kJ/mol, is orange yellow in color and is traded as fused flakes or powder. Reaction with alkali metal hydroxides or ammonium hydroxide gives vanadates. V_2O_5 is prepared by thermal decomposition of ammonium vanadates at 500–600 °C in an oxidizing atmosphere (air). It is by far the most important vanadium compound. V_2O_5 is used as an oxidation catalyst in heterogeneous and homogeneous catalytic processes for the production of sulfuric acid from SO_2 , phthalic anhydride from naphthalene or *o*-xylene, maleic anhydride from benzene or *n*-butane/butene, adipic acid from cyclohexanol/cyclohexanone, and acrylic acid from propane. Minor amounts are used in the production of oxalic acid from cellulose and of anthraquinone from anthracene.

V_2O_5 is used to lower the melting point of enamel frits for the coating of aluminum substrates. FeV and VAl master alloys are preferably produced from V_2O_5 fused flakes due to the low loss on ignition, low sulfur and dust contents, and high density of the molten oxide compared to powder.

Further uses of V_2O_5 are as a corrosion inhibitor in the CO_2 scrubbing solutions of the Benfield and related processes for the production of hydrogen from hydrocarbons, as cathode in primary and secondary (rechargeable) lithium batteries, as UV absorbent in glass, in YVO_4 : Eu³⁺ red phosphors for high-pressure mercury lamps and TV screens, for glazes

[43], for yellow (SnO_2/V_2O_5) and blue (ZrO_2/V_2O_5) pigments [13], as colloidal solution for antistatic layers on photographic material [44], and as a starting material for the production of carbides, nitrides, carbonitrides, silicides, halides, vanadates, and vanadium salts.

Vanadium trioxide, V_2O_3 , mp 1977 °C, ρ 4.99 g/cm³, heat of formation $\Delta H^{298} = -1218.8$ kJ/mol, black powder, is formed by thermal decomposition of ammonium vanadates at 600–900 °C in a reducing atmosphere (H_2 , CO, CH_4 , NH_3). The most important application is as an alternative to V_2O_5 in the production of FeV, VAl master alloys, high-purity vanadium metal, and vanadium carbides and carbonitrides [45].

Vanadium suboxides such as V_2O_4 , mp 1642 °C, heat of formation $\Delta H^{298} = -1427.37$ kJ/mol, dark blue in color, or V_6O_{13} , colored bluish black, are of minor industrial importance [46]. They are produced by heating stoichiometric mixtures of vanadium oxides or by reduction of ammonium vanadates or V_2O_5 in atmospheres of controlled reduction potential. Bronzes of V_6O_{13} or V_5O_{11} with Li_2O are used for lithium ion batteries.

Vanadates. The most important product is *ammonium metavanadate*, NH_4VO_3 , heat of formation $\Delta H^{298} = -1551.0$ kJ/mol, a white powder. Thermal decomposition starts at 70 °C. It is sparingly soluble in cold water (ca. 1%), but readily soluble in mono- and diethanolamine. It is precipitated from neutral alkali metal vanadate solutions by the addition of ammonium chloride or ammonium sulfate. Because of its ready conversion to V_2O_5 at elevated temperatures in oxidizing atmospheres, it is used as a substitute in the production of, e.g., DENOX catalysts and zirconium vanadium oxide yellow ceramic colorants.

Ammonium polyvanadate, $(NH_4)_2V_6O_{16}$, is an orange powder, produced by the addition of mineral acids and ammonium salts to alkali metal vanadates at pH 2–3 [47]. It is an intermediate product in the production of vanadium pentoxide.

Sodium ammonium vanadate, $2(\text{NH}_4)_2\text{O} \cdot \text{Na}_2\text{O} \cdot 5\text{V}_2\text{O}_5 \cdot 15\text{H}_2\text{O}$, an orange powder, is precipitated from sodium vanadate solutions by the addition of ammonium salts at pH 5–6. It is almost exclusively used as a soluble oxidation catalyst for the desulfurization of H_2S -containing gases by the Stretford process.

Sodium metavanadate, NaVO_3 , and **potassium metavanadate**, KVO_3 , both white powders, are water-soluble compounds. They are added as corrosion inhibitors to CO_2 washing solutions in the production of H_2 from hydrocarbons.

Vanadium Salts. **Vanadyl sulfate**, $\text{VOSO}_4 \cdot 5\text{H}_2\text{O}$, is produced by the reaction of V_2O_5 and SO_2 in aqueous media, and forms blue, water-soluble crystals. It is used in catalyst production as alternative to V_2O_5 . In multivitamin/multimineral pills it is the active component for fast energy supply to the muscles by enhancing glucose metabolism in the blood. It acts as an orally applied insulin mimic.

VOSO_4 , of blue color, and $\text{V}_2(\text{SO}_4)_3$, of green color, are the feed solutions for the vanadium redox battery. This battery contains vanadium(V) (yellow) and vanadium(II) (pink) in dilute sulfuric acid as electrodes when charged [48].

Vanadyl oxalate, VOC_2O_4 , forms blue, water-soluble crystals and is used in catalyst production as alternative to vanadates and vanadium oxides.

Vanadium Halides. Only **vanadium oxytrichloride** VOCl_3 , $mp -79.5^\circ\text{C}$, $bp 126.7^\circ\text{C}$, $\rho 1.82 \text{ g/cm}^3$, a bright yellow liquid, **vanadium tetrachloride**, VCl_4 , $bp 148^\circ\text{C}$, a red brown liquid, and **vanadium trichloride**, VCl_3 , boiling range $300\text{--}400^\circ\text{C}$ (disproportionates), a deep purple solid, are of commercial interest. Whereas VOCl_3 is stable, VCl_4 slowly decomposes into solid VCl_3 and Cl_2 . VOCl_3 is produced by the reaction of V_2O_5 and carbon with chlorine gas. For the production of VCl_4 , oxygen-free vanadium compounds such as vanadium carbide or vanadium carbonitride are reacted with chlorine gas. The chlorides are used as catalysts in the production of EPDM

(ethylene-propene-diene) rubber and polyethylene and are starting materials [49] for the preparation of organic vanadium compounds.

Organic Vanadium Compounds. Representatives of this class are vanadium(IV) and vanadium(III) acetylacetonates, naphthenates, octoates, and alkoxides (iso/*n*-butyl, iso/*n*-propyl), which are soluble in organic solvents. They are used in siccatives, antifouling paints, as catalysts for stereospecific organic synthesis, and in chemical vapor deposition.

Vanadium Carbides. The monocarbide, VC, has a theoretical carbon content of 19.08% and melts at 2830°C . It has a wide phase range. VC is isomorphous with VO and VN. Pure VC can be prepared by carburizing vanadium hydride powder with carbon in a vacuum [50]. Reaction at 800°C leads to vanadium carbide in which $\text{C}:\text{V} = 0.72\text{--}0.87$.

Industrial-grade VC is produced by heating V_2O_5 or V_2O_3 with carbon at 1100°C under a protective atmosphere of hydrogen [51], or by reacting V_2O_3 with carbon in a carbon-tube furnace. The crude carbide formed in the first stage is recarburized at $1700\text{--}2200^\circ\text{C}$ under vacuum. The final product contains 18.5–19% total-C and up to 0.5% free carbon. The VC is not completely free of oxygen because of its isomorphism with VO. VC is added to hard metals in amounts of 0.3–0.5%. It acts as a grain growth limiter [3]. Another carbide, V_2C , with a theoretical carbon content of 10.54%, also exists. This also has a large range of homogeneity, and decomposes at 1850°C . It is of no industrial importance as such, but is formed in all carbon-containing vanadium alloys.

Vanadium Nitrides. Three nitrides exist: VN, V_2N , and V_3N . The mononitride, $mp 2350^\circ\text{C}$, is a grayish-brown powder, isomorphous with VC and VO [52]. Its theoretical composition is 78.45% V, 21.55% N, but its range of homogeneity extends from $\text{VN}_{1.0}$ to $\text{VN}_{0.71}$. It can be obtained by the reaction of vanadium tetrachloride with mixtures of nitrogen and hydrogen gas, using the technique of growth on tungsten wires at $1400\text{--}1600^\circ\text{C}$. Although the

preparation of VN from vanadium oxides is difficult because of the isomorphism mentioned above, a product containing 78.3% V, 21.1% N, and 0.5% O can be obtained by reduction with carbon in an atmosphere of nitrogen [51].

As vanadium carbides and nitrides are mutually soluble, vanadium carbonitrides with a wide range of C:N ratios can be prepared at $1100\text{--}1400^\circ\text{C}$. This is true for both $\text{V}(\text{C}, \text{N})$ and $\text{V}_2(\text{C}, \text{N})$. Two broad three-phase regions extend continuously between the corresponding phases VC–VN and $\text{V}_2\text{C}\text{--}\text{V}_2\text{N}$.

Vanadium Silicides. VSi_2 , $mp 1650^\circ\text{C}$, can be prepared by sinter metallurgy. For example, the pure substance can be prepared by exothermic reaction sintering of vanadium and silicon powder [53]. In industry, it is obtained by the reaction of vanadium oxides with SiO_2 and carbon (or with SiC) at $1200\text{--}1800^\circ\text{C}$ under vacuum.

Vanadium Hydrides. In the H–V system [54] the following phases occur: β_1 , corresponding to ca. V_2H (low temperature), 33 atom% H; β_2 , corresponding to V_2H or VH , 33–50 atom% H; δ , corresponding to V_3H_2 , 40 atom% H; γ , corresponding to VH_2 , 66.7 atom% H.

32.8 Analysis

The most important analysis is the determination of vanadium in raw materials, especially vanadium-containing slags and the commercial products vanadium oxide and ferrovanadium [55].

To determine vanadium in raw materials, the sample is fused with sodium peroxide and sodium carbonate, the solidified product is leached with water, and the vanadium-containing solution so obtained is acidified with sulfuric acid. The vanadium is completely oxidized with potassium manganate(VII) to the pentavalent state, and the solution is back-titrated with iron(II) sulfate, with diphenylamine as indicator.

In the analysis of vanadium oxide, the sample is dissolved in sulfuric acid, completely re-

duced with iron(II) sulfate to the tetravalent state, and back-titrated potentiometrically with potassium manganate(VII) solution, using a calomel reference electrode.

Ferrovanadium is also analyzed potentiometrically. The sample is dissolved in sulfuric/nitric acid, and is then oxidized by potassium manganate(VII). The vanadium, now in pentavalent form, is reduced with iron(II) solution, and potentiometrically back-titrated with potassium manganate(VII) solution, using a calomel reference electrode.

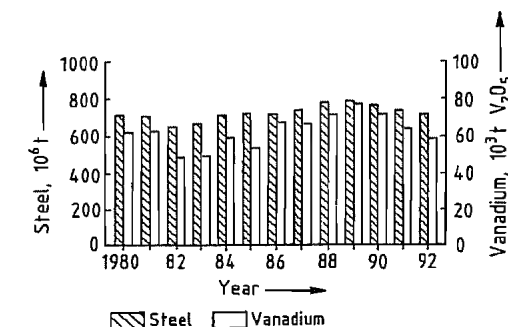


Figure 32.4: World production of steel and vanadium.

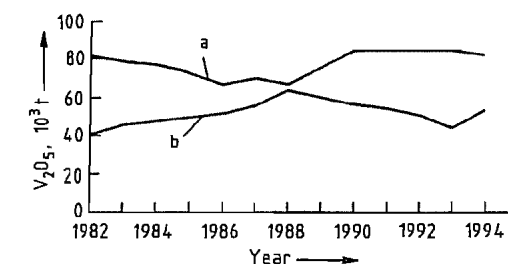


Figure 32.5: Worldwide vanadium capacity (a) and demand (b).

32.9 Economic Aspects

Consumption, Production Capacity, and Prices. The development of vanadium market prices is governed by consumer demand and existing production capacities. For main uses of vanadium and their shares see Section 32.6. The dependence of vanadium production on world steel production is shown in Figure 32.4 [56]. Total world demand is compared to available production capacities in Figure 32.5

[57]. This led to the price trend shown in Figure 32.6 [57].

For the vanadium demand of the western world, South Africa is the major exporter (Table 32.6). Vanadium in the form of slag and oxides was traded to converters in Europe, Japan, and the United States, for the production of ferrovanadium. Since 1994 most South African suppliers have installed their own ferrovanadium production capacity. This will eventually lead to the nonavailability of South African preproducts for the converters mentioned above. Their plants will have to use other raw materials, such as residues from mineral oil processing, or cease production.

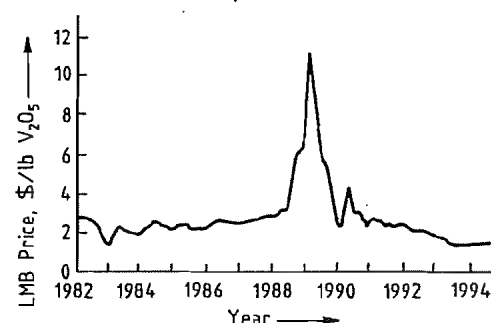


Figure 32.6: Vanadium price trends.

Table 32.6: World exports of vanadium, 1989–1992 [56] (in tonnes of V_2O_5).

Country	Exports				
	1989	1990	1991	1992	%
South Africa ^a	32 950	25 989	25 561	24 000	84.7
New Zealand ^b	2 000	4 000	4 500	3 000	10.6
CIS	1 500	1 350	1 200	1 200	4.2
Others ^c	200	150	150	150	0.5
Total	36 650	31 489	31 411	28 350	100

^a Including Republic of South Africa and Bophuthatswana.

^b Estimates.

^c China is considered to be a net importer of vanadium at present. Its re-exports are, therefore, not shown in this table.

Further suppliers of vanadium oxides are Russia, whose share for export strongly depends on its own economic development; and China, which is expected to turn from an exporter to an importer because of its high economic growth rate.

Ferrovanadium producers are listed in the following [51]:

Country	Company
Argentina	Pamet Stein Ferroaleaciones Sacifa
Austria	Treibacher Industrie AG
Belgium	SADACINV
Brazil	Termoligas metalurgicas SA Cia Paulista de ferro ligas
Canada	Masteralloy Products Inc.
China	Panzihua Iron and Steel Plant Emei Ferroalloy Plant Jinzhou Ferroalloy Plant
Czech Republic	Nikom Ferroalloy Plant
Germany	GfE Gesellschaft für Elektrometallurgie
Hungary	Ötvözetgyar, Hungaraloy
India	Birla
Japan	Awamura Metal Industry Co. Ltd. Taiyo Mining and Industrial Co. NKK Corp.
Mexico	Ferroaleaciones de México FERROMEX Ferralver SA
CIS	Chusovskoy Metallurgical Kombinat Tulachernet Kombinat
Spain	Ferroaleaciones especiales asturianas
South Africa	Highveld Steel and Vanadium Corp. Ltd. Vametco Vantech
United States	BEAR Metallurgical Corp. Shieldalloy Corp. Strategic Metal Corp., Stratcor

32.10 Environmental Protection and Toxicology

Soil. In sulfidic and oxidized form, vanadium is a ubiquitous element with an average abundance of 150 mg/kg in the earth's crust. The concentrations vary widely, between a few ppm and 1000 ppm. Depending on geological conditions, even higher values can be found, e.g., 1650 ppm vanadium in oil shales of permic copper schist [58]. The vanadium content of oil shale and mineral oil, in which it is present primarily as porphyrin complexes, is due to biological processes. Higher anthropogenic burdens can be found only in a few isolated geographic locations. In the upper layers of arable soils utilization of mineral fertilizers leads to accumulation of vanadium, which is retained and is only slightly mobile [59].

Air. Vanadium concentrations in uncontaminated air can reach 1 ng/m³, caused by whirled-up dust from weathered rock and by evaporation of water droplets driven off of surface waters by wind and waves. Increased

concentrations are recorded mainly in urban areas. They originate mainly from combustion of coal and especially heavy fuel oil. Concentrations of ca. 10–35 ng/m³ measured in the past (maximum values of up to 1000 ppm, recorded in London, 1962) are lower today, due to the use of efficient waste air purification systems. Industrial activities are of only minor, local importance in the pollution of the air with vanadium.

Water. Vanadium dissolved in water is present almost exclusively in the pentavalent form. In running waters, its concentration range is ca. 0.1–220 µg/L [60], the vanadium concentration in the water correlates to these in rocks near the river source in the river bed. The sediment of creeks also mirrors the abundance in the surrounding area. Seawater contains 0.3–29 µg/L vanadium [60]. Accumulation does not occur, since the vanadium input from running waters is transferred to the sediment by precipitation and biochemical processes.

Water contamination by vanadium takes place only to a minor extent. For removing vanadium from wastewater, single- or multiple-stage precipitation with iron or lime is employed.

Fauna and Flora. Vanadium is considered to be essential for a number of organisms [61–63]. In vertebrates the average concentration is 0.1 mg vanadium per kg dry matter. Considerably higher concentrations (≤ 0.1 g/kg) can be found in lower organisms. Especially in one order of invertebrates (ascidians), vanadium accumulates in unusually high amounts

[64]. In some species of these organisms, the vanadium is present in green blood cells (vanadocytes) and is complexed by pyrrole rings [65]. Data on vanadium concentrations in humans vary widely, between 100 µg [66] and 17–43 mg [67]. Fat tissue, bones, teeth, bone marrow, as well as serum are especially rich in vanadium.

In general, the vanadium concentration in plants is related to that in the soil. As with animals, plants vary widely in vanadium content. For example, in fly agaric (*Amanita muscaria*) concentrations 100 times as high as in other fungi are found, independent of location. The reasons for this are not yet known [64].

Toxicology. Toxicity data for some vanadium compounds are given in Table 32.7. The data show a correlation of toxicity with oxidation state and solubility. Toxicity decreases with decreasing oxidation state and decreasing solubility.

In investigations of neurobehavioral, neuropsychological, psychosomatic, and psychological parameters as a function of exposure to V_2O_5 in dust among workers in an industrial plant, no significant changes compared to uncontaminated persons were found, independent of the concentration of vanadium pentoxide [70].

Occupational Safety. For vanadium pentoxide, there is a total dust limit value (0.5 mg/m³) and a limit value for fine dust (0.05 mg/m³); in Germany, the definition of the latter is based on studies on volunteers [71].

Table 32.7: Toxicological data [68, 69].

	Oral LD ₅₀ (14 d), mg/kg body weight	Inhalative LC ₅₀ (14 d), mg/L	Dermal LD ₅₀ (14 d), mg/kg body weight
V_2O_5 , analytical grade	470 (male) 467 (female)	11.09 (male) 4.3 (female)	> 2500 (male) > 2500 (female)
V_2O_5 , technical grade	8713 (male) 5639 (female)	> 6.65 (male) > 6.65 (female)	> 2500 (male) > 2500 (female)
Ammonium metavanadate	218 (male) 141 (female)	2.61 (male) 2.43 (female)	> 2500 (male) > 2500 (female)
Potassium metavanadate	318 (male) 314 (female)	1.85 (male) 4.16 (female)	> 2500 (male) > 2500 (female)
BiVO ₄ –BiMoO ₄	> 5000	> 5.15	

32.11 References

1. R. Kieffer, G. Jangg, P. Ettmayer: *Sondermetalle*, Springer Verlag, Wien 1971.
2. A. M. Sage: "Discovery and History of Vanadium and its Contribution to Life in the Modern World", Metals Society, 1981.
3. R. Kieffer, H. Braun: *Vanadium, Niob, Tantal*, Springer Verlag, Berlin 1963.
4. W. Rostocker: *The Metallurgy of Vanadium*, Wiley, Chapman & Hall, New York 1958.
5. *Bull. Alloy Phase Diagrams* 2 (1981) no. 1, 40–41, 146; no. 2, 172.
6. I. Barin, O. Knacke: *Thermochemical Properties of Inorganic Substances*, Springer Verlag, Berlin, Verlag Stahleisen, Düsseldorf 1973.
7. D. L. Harrod, R. F. Gold, *Int. Met. Rev.* 25 (1980) 163–221.
8. E. Fromm, E. Gebhardt: *Gase und Kohlenstoff in Metallen*, Springer Verlag, Berlin 1976.
9. H. E. Dunn, D. L. Edlung: "Vanadium", in C. A. Hampel (ed.): *Rare Metals Handbook*, 2nd ed., Reinhold, Chapman & Hall, London 1961, pp. 640–642.
10. D. Schlain, C. B. Kenahan, W. L. Ackermann, *J. Less-Common Met.* 3 (1961) 458–467.
11. R. L. Ammon, *Int. et. Rev.* 25 (1980) 255–268.
12. M. Rühle, *Metall (Berlin)* 35 (1981) 1168–1172, 1282–1285.
13. Bundesanstalt für Geowissenschaften und Rohstoffe: *Untersuchungen über Angenot und Nachfrage mineralischer Rohstoffe, XIV, Vanadium*, Berlin-Hannover 1981.
14. P. Storm: "Vanadium Sources, Applications, and Markets", *Raw Materials Report*, vol. 10, no. 3, Royal Institute of Technology, Stockholm.
15. R. K. Evans: Vanitec, reprint from *Met. Mater.*, April 1978.
16. B. Rohrmann, A. G. Raper, *J. Iron Steel Inst. London* 1970, April, 336–341.
17. *Ullmann*, 3rd ed., 18, 56.
18. L. White, *Eng. Min. J.* 177 (1976) Jan., 87–91.
19. H.-J. Retelsdorf, *Metall (Berlin)* 35 (1981) 1166–1167.
20. A. D. Mah: "Thermodynamic Properties of Vanadium and its Compounds", *Bur. Mines Rep. Invest.* 6727 (1966).
21. W. Schmidt: "Untersuchungen an Vanadiummetall und seinen aluminothermisch hergestellten Legierungen mit Aluminium und Eisen", Ph. D. Thesis, RWTH Aachen 1969.
22. M. F. Joly: *2nd United Nations Int. Conf. on the Peaceful Use of Atomic Energy*, Geneva, May 1958, Paper No. A/Cnf. 15/P/1274.
23. R. Kieffer, H. Bach, H. Lutz, *Metall (Berlin)* 21 (1967) 19–22.
24. R. Kieffer, F. Lihl, E. Effenberger, *Z. Metallk.* 60 (1969) 94–100.
25. T. T. Campbell, F. E. Block, E. R. Anderson: "Reducing Vanadium Compounds in Bomb Reactors", *Bur. Mines Rep. Invest.* 6314 (1964).
26. P. V. S. Pillai, K. U. Nair, T. K. Mukherjee, C. K. Gupta, *Trans. Indian Inst. Met.* 26 (1973) no. 6, 24–30.
27. T. K. Mukherjee, C. K. Gupta, *J. Less-Common Met.* 27 (1972) 251ff.
28. C. T. Wang, E. F. Baroch, S. A. Worcester, Y. S. Shen, *Met. Trans.* 1 (1970) no. 6, 1683–1689.
29. O. N. Carlson, H. R. Burkholder, G. A. Martsching, F. A. Schmidt: *Extractive Metallurgy Refractory Metals Proc. Symp.* 1981, pp. 191–203.
30. R. W. Buckmann, Jr., *Int. Met. Rev.* 25 (1980) 158–162.
31. M. Rühle, *Metall (Berlin)* 33 (1979) 140–147.
32. R. Hahn: "Vanadin-Gewinnung und Verwendung", *Erzmetall* 40 (1987) no. 6, 298ff.
33. O. E. Kraus, *Stahl Eisen* 109 (1989) no. 11, 547–552.
34. H. B. Bomberger, F. H. Froes, P. H. Morton: "Titanium – A Historical Perspective, Titanium Technology: Present Status and Future Trends", *Tit. Dev. Ass.* 1985.
35. K. Rüdiger, *DVS-Ber.* 53 (1978) 39–47.
36. Y.-W. Kim, *J. Met.* 46 (1994) no. 7, 30.
37. A. Züttel, F. Meli, L. Schlapbach, *Z. Phys. Chem. (München)* 183 (1994) 355.
38. K. Ichimura, M. Matsuyama, K. Watanabe, *J. Vac. Sci. Technol. A* 5 (1985) no. 2, 3–4.
39. F. L. Yaggee, E. R. Gilbert, J. W. Styles, *J. Less-Common Met.* 19 (1969) 39–51.
40. M. Schirra, *Metall (Berlin)* 33 (1979) 455–465.
41. H. U. Borgstedt, *Metall (Berlin)* 33 (1979) 264–266.
42. R. E. Gold, D. L. Harrod, *Int. Met. Rev.* 25 (1980) 232–254.
43. *Nachr. Chem. Tech.* 16 (1968) no. 2, 23.
44. Eastman Kodak, FR 7522060, 1975.
45. R. Hahn: Dissertation, RWTH Aachen 1983.
46. Combustion Engineering, US 4486400, 1984.
47. U. M. Levanto, *Acta Polytech. Scand. Chem. Technol. Metall. Ser.* 82 (1969) 37.
48. M. Skylaskazacos et al.: "Characteristics and Performance of 1 kW UNSW Vanadium Redox Battery", *J. Power Sources* 35 (1991) 399–404.
49. Akzo Chemicals Inc.: "Polymerization Catalysts", Bulletin 92-03, 1992.
50. G. V. Samsonov, V. Ya. Vanmanko, L. N. Okhremchuk, B. M. Rud, *Izv. Akad. Nauk SSSR Neorg. Mater.* 10 (1974) no. 1, 52–56; *Chem. Abstr.* 80 (1974) 90458.
51. R. Kieffer, F. Benesovski: *Hartstoffe*, Springer Verlag, Wien 1963.
52. P. Ettmayer, R. Kieffer, F. Hattinger, *Metall (Berlin)* 28 (1974) 1151–1156.
53. F. Binder, *Radex Rundsch.* 1975, no. 4, 539–540.
54. J. F. Smith, D. T. Peterson, *Bull. Alloy Phase Diagrams* 3 (1982) no. 1, 55–60.
55. Chemiker-Ausschuß: *Analyse der Metalle*, vol. 1: Schiedsanalysen, vol. 2: Betriebsanalysen, Springer Verlag, Berlin 1961.
56. G. Grohmann: *World Vanadium Review*, Report R 14/93, Rep. of South Africa, Department of Mineral and Energy Affairs.
57. W. Beattie: "Overview of Vanadium and Tungsten Commodity Markets", *Metals Week Presentation*, reprint, 19th Sept. 1994.
58. H. Fauth, R. Hindel, U. Siewers, J. Zinner: *Geochemischer Atlas Bundesrepublik Deutschland*, Bundesanstalt für Geowissenschaften und Rohstoffe, Hannover 1985.
59. R. Schnabel, C. Koch, C. Bunke, G. Schmieder: "Zum Verhalten von Vanadin in der Umwelt", *Z. Gesamte Hyg. Ihre Grenzgeb.* 30 (1984).
60. Environmental Health Criteria 81: *Vanadium*, World Health Organization, Geneva 1988.
61. F. H. Nielsen, "Studies on the Essentiality of Some Elements Ascribed as Toxic – Arsenic, Boron, Lead, Tin and Vanadium", U.S. Department of Agriculture Agricultural Research Service, Grand Forks Human Nutrition Research Center, Grand Forks, ND.
62. E. J. Underwood: "Vanadium" in: *Trace Elements in Human and Animal Nutrition*, 4th ed., Academic Press, New York 1977, pp. 388–397.
63. R. Nechay: "Mechanism of Action of Vanadate", *Ann. Rev. Pharmacol. Toxicol.* 24 (1984) 501–524.
64. Natl. Res. Council, Committee on Biolog. Effects of Atmospheric Pollutants, "Vanadium", National Academy of Science, Washington, DC, 1977, p. 117104.
65. E. P. Levine, *Science (Washington, DC)* 133 (1961) 1352.
66. A. R. Byrne, L. Kosta: "Vanadium in Foods and in Human Body Fluids and Tissues", *Sci. Total Environ.* 10 (1978) 17–30.
67. H. A. Schroeder, J. J. Balassa, I. H. Tipton: "Abnormal Trace Metals in Man: Vanadium", *J. Chron. Dis.* 16 (1963) 1047–1071.
68. J. Leuschner, H. Haschke, G. Sturm: "New Investigations on Acute Toxicities of Vanadium Oxides", *Monatsh. Chem.* 125 (1994) 623–646.
69. H. Wienand, W. Ostertag: "Bismutvanadat/molybdat – ein neuartiges Farbpigment", *Farbe + Lacke* 9 (1986) 118ff.
70. Final Report Vanadium Pentoxide Investigation, Institute for Social Medicine, Innsbruck 1993/1994, unpublished.
71. C. Zenz, B. A. Berg, *Arch. Environ. Health* 14 (1967) 709.

33 Rhenium

HANS-GEORG NADLER

33.1 Introduction	1491	33.5 Rhenium as an Alloying Component	1495
33.2 Properties	1491	33.6 Uses	1496
33.3 Occurrence and Raw Materials	1492	33.7 Compounds	1496
33.3.1 Molybdenite	1492	33.7.1 Oxides and Chalcogenides	1496
33.3.2 Recovery from Spent Catalysts and Alloys	1492	33.7.2 Halides	1497
33.4 Production	1493	33.7.3 Carbonyls	1498
33.4.1 Recovery from Flue Gases in Molybdenite Roasting	1493	33.8 Uses of Rhenium Compounds	1498
33.4.2 Production of Pure Rhenium Compounds from Gas Scrubbing Solutions	1494	33.9 Analysis	1499
33.4.3 Production of Rhenium Metal Powder and Pellets	1495	33.10 Economic Aspects	1499
		33.11 Toxicology and Physiological Effects	1499
		33.12 References	1500

33.1 Introduction

Rhenium is present in the earth's crust at a very low concentration (ca. $7 \times 10^{-8}\%$, 0.7 ppm). The element was discovered in 1925, when TACKE, NODDACK, and BERG observed its X-ray spectrum in concentrates and compounds obtained from the beneficiation of columbite [5].

The discoverers isolated the first gram of rhenium from 660 kg of Norwegian molybdenite (MoS_2), which contained 2–4 ppm Re [6]. Rhenium is the most recently discovered refractory metal; it is a member of the group of high-melting metals that includes molybdenum, tungsten, niobium, and tantalum. It has the second highest melting point of all metals (3180 °C).

Industrial production of rhenium began in the 1930s at Kali Werke Aschersleben in the Harz region [7], and also at H. C. Starck, formerly Gebr. Borchers AG, in Goslar. The raw material consisted of furnace bottoms, by-products from the treatment of Mansfeld copper schists. The furnace bottoms were digested by fusion with sodium sulfate [8]. Then, after a complicated chemical separation process, rhenium was isolated as potassium

perrhenate, which was reduced with hydrogen to give the impure metal.

An important advance in rhenium technology was the production of the element from flue dusts from the roasting of molybdenite [9]. The amount recovered from the dusts was, however, only 10–15% of the total Re content of the MoS_2 concentrate. The introduction of accurate analytical methods [10] enabled material balances for rhenium extraction to be established. These showed that most of the rhenium was lost up the stack, and only a small amount remained in the flue dust or in the roasted product. The flue gas was therefore scrubbed intensively to ensure that the volatile oxides of rhenium were recovered when the molybdenite concentrate was roasted [11, 12].

33.2 Properties

Rhenium has the electronic configuration $[\text{Xe}] 4f^{14} 5d^5 6s^2$, and consists of the natural isotopes ^{185}Re (37.07%) and ^{187}Re (62.93%), β -emitter with a half-life of 10^{11} years). Fused or sintered rhenium has a silvery white luster, and the powdered metal is silver gray. It has a hexagonal close-packed structure (type A3), with $a_0 = 276$ pm and $c_0 = 446$ pm. Rhenium

retains this lattice up to its melting point and hence does not undergo a ductile-brittle transformation, in contrast to other refractory metals.

Other physical data are listed below:

Density (20 °C)	21.0 g/cm ³
Metallic radius	137 pm
Ionic radius (VII)	53 pm
Melting point	3180 °C
Boiling point	5870 °C
Heat of fusion	33 kJ/mol
Heat of sublimation ΔH_B (monoatomic gas)	+779 (± 8) kJ/mol
Enthalpy of formation of Re_2O_7	-1241 kJ/mol
Electrical conductivity	0.051 $\mu\Omega^{-1}\text{cm}^{-1}$
Specific resistivity (20 °C)	19.3 $\mu\Omega\text{cm}$
Superconductivity	1.699 K
Tensile strength (20 °C annealed)	12 MPa
Modulus of elasticity (20 °C)	459.9 GPa
Recrystallization temperature (depending on degree of working)	1300–1800 °C

Rhenium is a very heat-resistant metal, provided it does not come in contact with oxidizing agents. It is practically insoluble in hydrochloric and hydrofluoric acids. In oxidizing acids, it dissolves to form perrhenic acid (E^0 for Re/ReO_2 : 0.251 V).

Rhenium forms volatile oxides with oxygen at high temperature. In air at 350 °C, the heptoxide, Re_2O_7 , is formed. The rate of oxidation increases with increasing air flow rate. The stability of rhenium metal components is limited due to oxide formation even below 0.133 Pa [13]. When rhenium is heated with fluorine or chlorine, the fluorides or chlorides are formed. Rhenium reacts with silicon, boron, and phosphorus at elevated temperature to form silicides, borides, and phosphides.

33.3 Occurrence and Raw Materials

33.3.1 Molybdenite

Molybdenite, MoS_2 , especially from porphyry copper ore deposits, is the preferred host mineral for rhenium, which isomorphically replaces molybdenum in the MoS_2 lattice. The copper molybdenum porphyry ores contain 0.3–1.6% Cu and 0.01–0.05% Mo. The sulfides of copper and molybdenum are concentrated and separated by flotation, giving

a rhenium content in the MoS_2 concentrates of several hundred parts per million.

Rhenium contents (in ppm) of selected molybdenum concentrates of various origins are as follows:

Canada	
Island Copper	700–1300
HVC	200–400
Endako	< 100
United States	
Pinto Valley	1500–2000
Magma San Manuel	800
Bagdad	350
Sierrita	180
Bingham Canyon	250
Climax	30
Henderson	20
Mexico	
La Caridad	570
Peru	
Cuajone	580
Toquepala	600
Chile	
Chuquicamata	300
El Salvador	600
El Teniente	400
Iran	
Sar Cheshmeh	800

World rhenium reserves [14] (in t Re) are

Canada	32
Chile	1306
Peru	45
CIS	594
United States	386
Others	91
World total	2453

In copper concentrates, the rhenium content is 10–50 ppm, the molybdenum content 200–600 ppm. Copper concentrates are therefore a useful source of rhenium.

33.3.2 Recovery from Spent Catalysts and Alloys

Platinum-rhenium catalysts are used in the petroleum industry in the reforming process. When their activity is too low even after regeneration, the catalysts must be replaced. Valuable metals are recovered by dissolving the carrier (Al_2O_3) in sodium hydroxide solution or sulfuric acid. Platinum remains in the residue, from which it can be recovered. Rhenium, which goes into solution, can be recovered by solid or liquid ion exchangers [15].

In addition to this hydrometallurgical procedure, a pyrometallurgical process (fusion) allows rapid concentration of the valuable metals [16]. The resulting alloys are treated by dissolution and separation processes.

The high economic value of the WRe, MoRe, and rhenium-containing superalloys means that scrap alloys of these compositions must be processed. The following processes are suitable:

- Oxidation by atmospheric oxygen to form WO_3 and Re_2O_7 (*bp* 362 °C) which are separated by sublimation and distillation [17]
- Fusion with NaOH and oxidizing agents such as NaNO_3 and NaNO_2 [18].

These initial operations are followed by isolation of the elements and crystallization of their salts.

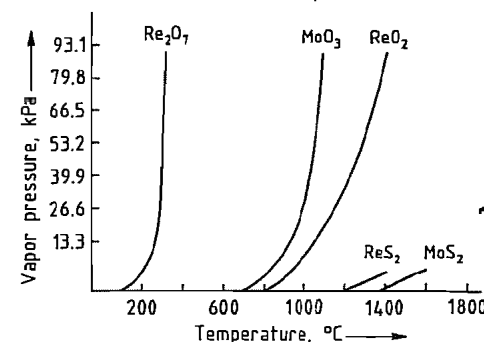


Figure 33.1: Vapor pressure of some oxides and sulfides of rhenium and molybdenum.

33.4 Production

33.4.1 Recovery from Flue Gases in Molybdenite Roasting

Porphyry copper ores containing 0.3–1.6% Cu and 0.01–0.05% Mo are ground and concentrated by flotation. Further treatment leads to almost quantitative recovery of molybdenite.

When molybdenite (90–95% MoS_2 , remainder: SiO_2 , Cu, Fe, etc.) is roasted at 500–700 °C to produce technical-grade molybdenum trioxide, MoO_3 , rhenium heptoxide, Re_2O_7 , sublimes due to its high vapor pres-

sure, and escapes with the flue gases. The vapor pressure curves of some oxides and sulfides of rhenium and molybdenum are given in Figure 33.1 [19].

The flue gases also contain sulfur dioxide, small amounts of sulfur trioxide, selenium dioxide, and large amounts of dust (MoO_3 , MoO_2 , and MoS_2). This dust can be recovered (> 99%) in high-temperature electrostatic filters and recycled to the roasting process. In the final gas scrubbing operation, the remaining dust fraction, rhenium heptoxide, selenium dioxide, sulfur trioxide, and some of the sulfur dioxide are removed from the flue gas. The scrubbing liquor is recirculated to increase the rhenium concentration, allowing the subsequent process stages to be operated economically.

The compound Re_2O_7 is readily soluble in water, forming HReO_4 , so that the recovery of rhenium from the flue gases is > 90%. Multi-stage pressure jet (venturi) scrubbers enable high rhenium recovery efficiencies to be achieved, effectively removing the finest dust fractions and causing rhenium oxides to be absorbed.

The venturi system operates with a pressure difference of 30 kPa in the first stage and 150 kPa in the second stage. The mist formed in the venturi washing process is trapped in a packed tower. This intensive gas purification produces waste gases that contain very pure SO_2 , which can be used for sulfuric acid production [11]. The recovery of rhenium from the flue gases in the roasting of molybdenite is shown schematically in Figure 33.2.

The roasted molybdenum concentrates are used mainly to produce MoO_3 for direct use in metallurgy (production of ferromolybdenum) and in molybdenum chemistry. For economic reasons, optimum conditions for rhenium recovery cannot always be maintained (temperature, air excess, etc.). The yield of rhenium is also limited by various impurities in the concentrates, especially alkali-metal and alkaline-earth elements, which form nonvolatile stable perrhenates under roasting conditions.

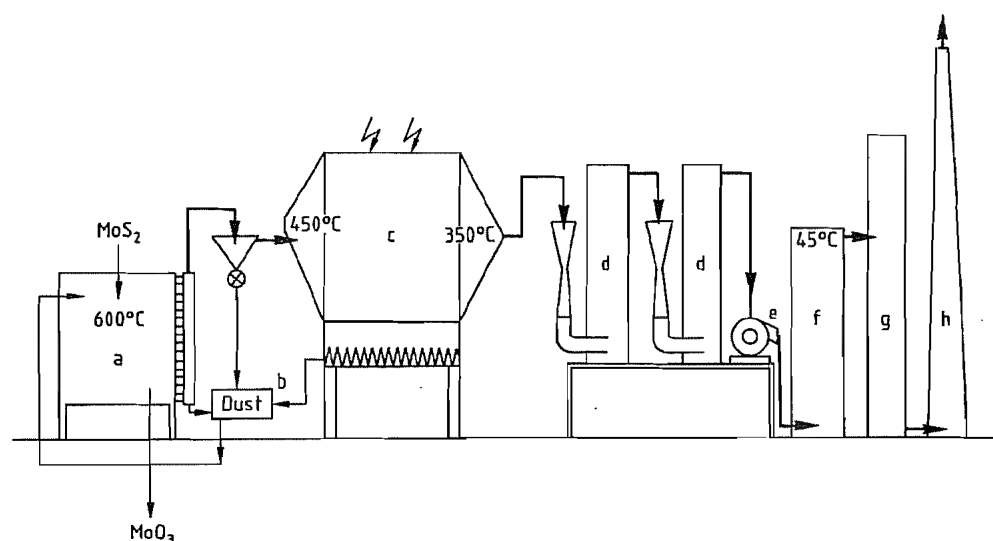


Figure 33.2: Flue gas purification with rhenium recovery by H. C. Starck: a) Roasting furnace; b) Dust chamber; c) Electrostatic filter; d) Venturi scrubbers; e) Ventilator; f) Secondary washer; g) SO_2 conversion; h) Stack.

Other possible processes for the treatment of molybdenum concentrates include electrooxidation [20] and treatment with O_2 or NH_3 at high temperature and pressure [21]. Yields of Mo and Re are ca. 98%. These processes have not been used thus far on an industrial scale.

33.4.2 Production of Pure Rhenium Compounds from Gas Scrubbing Solutions

Gas scrubbing solutions contain sulfuric acid and, typically, rhenium at 0.2–1.5 g/L. After removal of the solid constituents such as molybdenum oxides, sulfides, and selenium, rhenium can be precipitated as its sparingly soluble sulfide Re_2S_7 , or by cementation on iron or zinc. It can then be concentrated further.

However, the use of ion exchangers in solid or liquid form is preferable for recovering and concentrating rhenium. Primary, secondary, and tertiary long-chain amines, dissolved in organic solvents such as kerosene, can be used to extract rhenium and molybdenum at pH 1–2. At higher pH, quaternary amines are more effective [22]. Separation of molybdenum

from rhenium can be achieved by extraction at an optimum pH. Alternatively, both elements can be extracted from acidic solution and then separated by selective stripping with ammonia at different pH values [23].

Rhenium in neutral, alkaline, or sulfuric acid solution can be fixed by strongly basic solid ion exchangers. The molybdate ion is less strongly bound to the ion exchanger than the perrhenate ion, enabling the molybdenum to be removed by a displacement reaction. Rhenium can be eluted from the ion-exchange resin by strong mineral acids, especially perchloric acid, or ammonium thiocyanate [24].

Technical-grade ammonium perrhenate is produced by crystallization from the eluate solution. Further purification is carried out by recrystallization.

Solvent extraction, combined with the use of solid ion exchangers or crystallization, can be used to produce pure or highly pure ammonium perrhenate, which is the starting material for the production of many rhenium compounds as well as the metal [25]. A schematic of rhenium production is given in Figure 33.3.

Another method of rhenium production consists of solvent extraction combined with

electrowinning of the rhenium from perchlorate solutions [26].

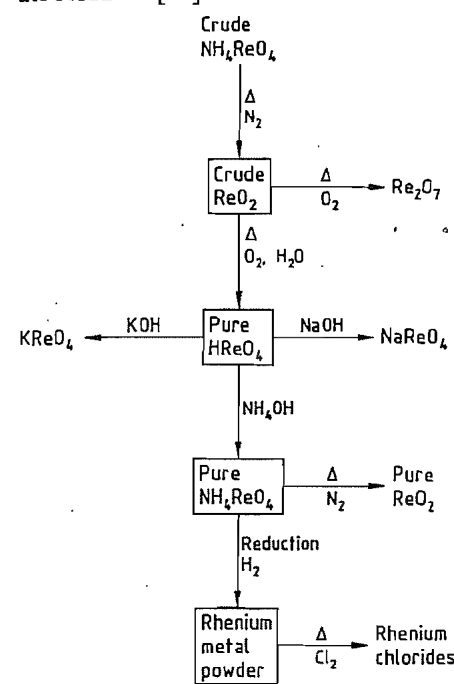


Figure 33.3: Rhenium production.

33.4.3 Production of Rhenium Metal Powder and Pellets

Rhenium powder can be produced by the reduction of pure ammonium perrhenate NH_4ReO_4 in a stream of hydrogen. This reduction is usually carried out in two stages:

- Reduction at 300–350 °C to form ReO_2
- Reduction of the ReO_2 to Re metal powder at 800 °C

The desired properties of the metal powder, such as grain size and surface area, can be achieved by adjustment of the reduction parameters.

In a further stage, the rhenium metal powder with added compaction agents is compressed into pellets and then sintered at ca. 1000–1500 °C under an atmosphere of hydrogen. To produce large workpieces, the powdered metal is charged into rubber containers, compressed isostatically at ca. 500 MPa, and

then sintered. Rhenium can be produced at almost its theoretical density by hot isostatic pressing (HIP) and by electron-beam or electric-arc melting.

Rhenium has very high strength at high temperature, as well as extremely good ductility and cold working properties. It is therefore a very useful high-temperature material. In some applications, the useful properties of rhenium can best be realized by chemical vapor deposition (CVD) [27]. Plasma coating with spheroidized rhenium metal powder is another possibility, producing dense rhenium coatings when combined with a sintering operation.

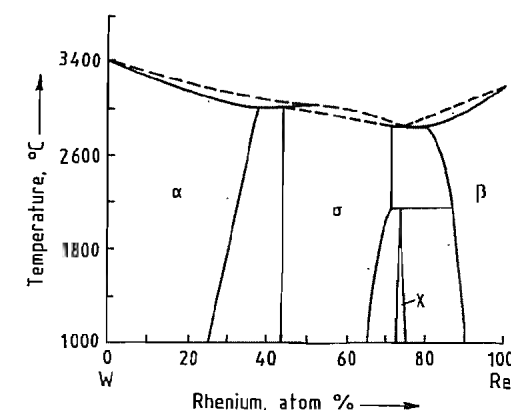


Figure 33.4: Tungsten-rhenium phase diagram [31].

33.5 Rhenium as an Alloying Component

When rhenium is used as an alloying component with the metals tungsten and molybdenum, which are difficult to work, ductility and strength are improved [28]. This is caused by alloy softening, which is defined as the reduction in the yield stress or hardness at low temperature. This effect is observed especially in body-centered cubic alloys. In addition to the improvement in ductility at low temperature, the strength at high temperature increases [29]. Tungsten rhenium alloys containing 25–30% Re have good cold ductility [30]. As indicated in Figure 33.4, rhenium is very soluble in tungsten, its solubility reaching 28% at

1600 °C and 37% at 3000 °C. Tungsten is also soluble in rhenium: 11% at 1600 °C and 20% at 2825 °C. Besides a tetragonal σ -phase, a cubic χ -phase exists in a very narrow range in the W-Re system [31].

The poor welding properties of common molybdenum alloys limit their use in high-temperature applications. The addition of rhenium enables these alloys to be welded and used as construction materials. Molybdenum rhenium alloys containing up to 50% Re show high tensile strength and good elongation over the temperature range 0–1800 °C [32].

Superalloys must have not only high strength, but also good corrosion resistance at elevated temperature. They may be divided into three groups: nickel-base alloys, cobalt-base alloys, and iron (nickel)-base alloys.

Other typical alloying elements include chromium, molybdenum, tungsten, niobium, tantalum, aluminum, titanium, boron, and zirconium. The addition 1–3% Re to a nickel-base alloy improves its toughness at high temperature and prevents fatigue fracture [33].

33.6 Uses

Rhenium in the form of the powdered metal or pellets is incorporated into alloys by various methods. The W-Re and Mo-Re alloys are used mainly in the manufacture of thermoelements. Other uses include semiconductors, heating elements, electrical and electronic applications, high-temperature welding rods, and metallic coatings [34].

Tungsten-rhenium alloys (W5Re, W10Re) are used in the manufacture of rotating X-ray anodes. For normal X-ray diagnosis, composite anodes, consisting of a very hard molybdenum base with an annular W-Re coating, are used. Computer tomography requires larger anodes, made by using a hybrid metal graphite construction combined with a W-Re coating [35]. An alternative technique is to deposit the metals or alloys by CVD or PVD processes [36].

Nickel-base alloys containing 1–3% Re are used mainly in the production of aircraft tur-

bine blades. They are monocrystalline and have high strength and resistance to oxidation. When these turbine blades are used in the hot zones of an engine, operating temperature can be increased, giving higher efficiency (lower fuel consumption). Similar effects are achieved by coating the gas turbine blades with rhenium-containing (1–20% Re) MCrAlY alloys [37].

33.7 Compounds

Rhenium closely resembles its neighbors in the sixth row (W, Os) and molybdenum (diagonal relationship) in its physical properties; many chemical parallels also exist. Eleven oxidation states of rhenium have been described [38]. In the most important rhenium compounds such as perrhenic acid, the perrhenates, and dirhenium heptoxide, rhenium has the oxidation state 7+. It exhibits its lowest oxidation states (as low as 3-) in carbonyl complexes.

33.7.1 Oxides and Chalcogenides

The yellow hygroscopic rhenium(VII) oxide, Re_2O_7 , is the most stable oxide of rhenium. It is formed from rhenium metal powder or other rhenium oxides in dry air or an oxygen atmosphere above 350 °C. The oxide Re_2O_7 is readily soluble in water, forming the colorless perrhenic acid, HReO_4 which is pale yellow at high concentration.

Perrhenic acid forms salts (MReO_4) with a tetrahedral ReO_4^- ion. Ammonium perrhenate, NH_4ReO_4 , is an important starting material, which can be reduced to Re metal and used for the production of many other rhenium compounds. The preparation of some rhenium compounds is shown in Figure 33.5. When Re_2O_7 is heated with rhenium powder, the oxides ReO_3 , Re_2O_5 , ReO_2 , and Re_2O_3 are formed.

In Re_2O_7 , ReO_4 tetrahedra and ReO_6 octahedra are linked alternately at their corners. ReO_3 disproportionates on heating to form Re_2O_7 and ReO_2 . The bluish black rhenium(IV) oxide, ReO_2 , which is insoluble in

water, has a distorted rutile structure and disproportionates at 900 °C into Re_2O_7 and metallic Re.

With sulfur, rhenium forms Re_2S_7 , ReS_3 and ReS_2 . The black rhenium(VII) sulfide is formed when hydrogen sulfide is passed into acidic solutions of perrhenates. Reduction of Re_2S_7 by hydrogen produces ReS_3 . The most stable sulfide ReS_2 is formed by the thermal decomposition of Re_2S_7 or by heating the elements together. The structure of ReS_2 (trigonal prismatic) is isomorphous with the rhombohedral modification of MoS_2 [38].

Table 33.1 lists the properties of some oxides and sulfides of rhenium.

Ammonium perrhenate reacts with aqueous ammonium polysulfide to form $(\text{NH}_4)_2(\text{Re}_2\text{S}_{16})$, a polynuclear sulfide having a metal-metal bond with marked double-bond character [39].

33.7.2 Halides

The most important rhenium halides can be prepared from the elements (Figure 33.5). Rhenium(VII) fluoride, ReF_7 , is the highest halide. It is formed at 400 °C under slight pressure.

Table 33.1: Properties of some rhenium oxides and sulfides [38].

Compound	mp/bp, °C	Structure	Oxidation state
Re_2O_7	300/360	alternating tetrahedra and octahedra	VII
ReO_3	> 300/750	cubic	VI
ReO_2	900 (decomp.) → $\text{Re}_2\text{O}_7 + \text{Re}$	rutile	IV
Re_2S_7	> 250 (decomp.) → $\text{ReS}_2 + \text{S}$		VII
ReS_2	1000 (decomp.) → $\text{Re} + \text{S}$	trigonal prismatic	IV

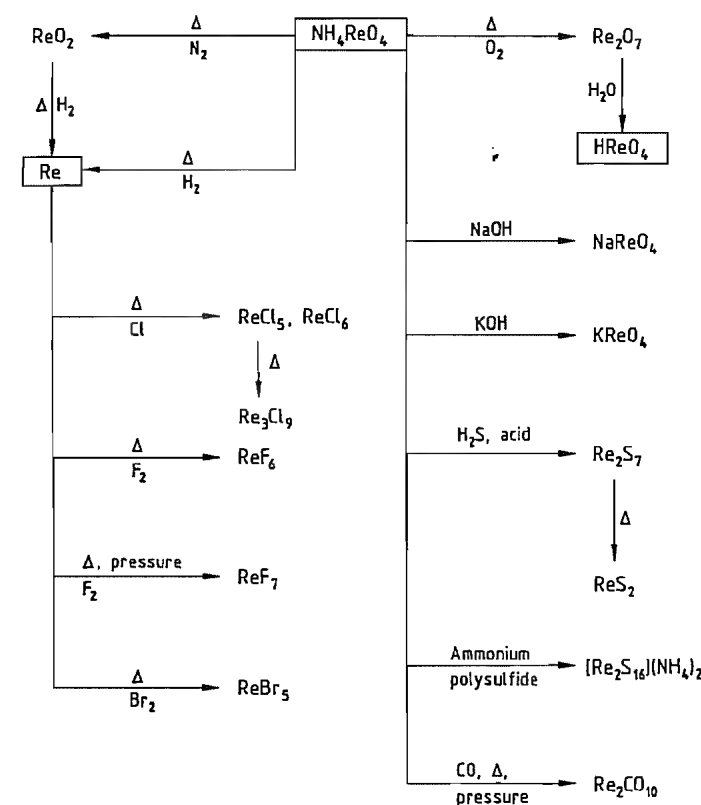


Figure 33.5: Synthesis of rhenium compounds.

Table 33.2: Rhenium halides.

Oxidation state	Fluorides	Chlorides	Bromides	Iodides
VII	ReF ₇ yellow mp 48.3 °C bp 73.7 °C			
VI	ReF ₆ yellow mp 18.5 °C bp 33.7 °C	ReCl ₆ brown-green mp 29 °C		
V	ReF ₅ yellow-green mp 48 °C bp 221 °C (extrapolated)	ReCl ₅ black-brown mp 220 °C	ReBr ₅ dark brown 110 °C (decomp.)	
IV	ReF ₄ blue mp 124.5 °C sublimes 300 °C	ReCl ₄ black-violet 300 °C (decomp.)	ReBr ₄	ReI ₄ (decomp. > room temperature)
III		(ReCl ₃) ₃ dark red sublimes 500 °C (decomp.)	(ReBr ₃) ₃ red-brown	(ReI ₃) ₃ black (decomp. on heating)

Rhenium(VI) fluoride, ReF₆, is formed from the elements at 125 °C. Rhenium(V) fluoride, ReF₅, and rhenium(IV) fluoride, ReF₄, can be prepared by reduction of ReF₆. Suitable reducing agents include H₂, metallic Re, SO₂, and Zn.

Rhenium pentachloride, Re₂Cl₁₀, is an important starting material for the synthesis of other rhenium compounds. It is formed from the elements at 500 °C. In the crystal, ReCl₆ octahedra form edge-sharing dimers. Rhenium(III) chloride, Re₃Cl₉, can be produced by thermal decomposition of the pentachloride. All rhenium(III) chlorides, bromides, and iodides contain the Re₃X₉ unit with Re₃ metal clusters.

ReBr₃ or ReCl₃ reacts with aqueous solutions of HBr to form ReBr₃·²/₃H₂O. Single crystals can be obtained by evaporation of the solution [40]. Rhenium(IV) bromide, ReBr₄, and ReI₄ are formed by the reaction of HReO₄ with HBr or HI.

Some properties of rhenium halides are given in Table 33.2 [38]. A large number of complex halides and oxyhalides of rhenium are known [41]. In the latter, rhenium is linked to oxygen by both single and double bonds. With nitrogen, triple, double, and single bonds are known [42].

33.7.3 Carbonyls

Rhenium carbonyl, Re₂(CO)₁₀, is formed by the reaction of CO with Re₂O₇ or Re₂S₇ at elevated pressure and temperature (20 MPa, 250 °C). It forms colorless crystals (mp 177 °C) and sublimes in vacuum. From the binary rhenium carbonyl, many cluster carbonyls, carbonyl hydrides, and complexes with a wide range of ligands in various oxidation states can be prepared [43].

33.8 Uses of Rhenium Compounds

Rhenium compounds are used in various areas of homogeneous and heterogeneous catalysis in petrochemistry, the pharmaceutical industry, and organic synthesis (e.g., alkylation, dehydroisomerization, dealkylation, isomerization, dehydrochlorination, hydrogenation, dehydrogenation, dehydrocyclization, oxidation, and reforming [44]).

Reforming is an important part of petroleum processing. It is used in the production of unleaded antiknock fuels for internal combustion engines and aromatic hydrocarbons for various syntheses [45]. Originally, molybdenum oxide was used for reforming, but it was soon found that platinum on aluminum oxide

(Al₂O₃) had better catalytic properties. An increase in catalytic activity, selectivity, and particularly stability was achieved with the development of platinum rhenium catalysts. The production of Pt-Re bimetallic catalysts by Chevron and UOP began in 1968 (Rheniform process). The rhenium components were solutions of NH₄ReO₄ or HReO₄. Today, multimetallic catalysts such as platinum rhenium indium have been developed from the earlier bimetallic catalysts [46]. The reforming process is still the most important catalytic application of rhenium compounds. In 1990, 45% of rhenium consumption in the United States was for this process [14].

New rhenium compounds such as methyltrioxorhenium, CH₃ReO₃, which can be produced fairly simply from Re₂O₇ and tetramethyltin, exhibit catalytic activity in the synthesis of alkenes (alkene metathesis), alkene oxidation, and alkenation of aldehydes [47].

Basic research in the field of rhenium compounds is expected to lead to the discovery of further catalytic properties of known rhenium compounds and of compounds as yet undiscovered.

33.9 Analysis

The analytical chemistry of rhenium includes the determination of rhenium in raw materials and intermediates, and the determination of trace impurities in high-purity rhenium products.

Rhenium can be determined by various analytical methods after separation by selective precipitation, distillation, extraction, and ion exchange. W. GEILMANN and H. BODE carried out important research into the analysis of rhenium in the 1940s and 1950s [48]. The most important practical application is the rapid and convenient determination of small amounts of rhenium in the presence of large amounts of molybdenum, which invariably accompanies it. After treatment of a sample with alkali, rhenium is determined in the Re(VII) state as the perrhenate ion. The accompanying elements

are separated and masked, and Re(VII) is then precipitated by addition of the tetraphenylarsonium cation and determined gravimetrically [49]. In acidic solution in the presence of SnCl₂, Re(VII) forms colored chelates with oximes and thiocyanates, which are extracted and determined by spectrophotometry [50]. Rhenium can be determined by atomic absorption spectrometry using the resonance line at 346.047 nm. Analysis of solutions by emission spectrometry uses the lines at 346.047 and 346.473 nm [51]. Polarographic methods are also available [52].

The determination of trace elements in high-purity rhenium products, such as NH₄ReO₄ or rhenium metal, is carried out by combustion analysis (C), hot extraction by carrier gas (N, O), and atomic absorption spectroscopy on solutions (metallic impurities) [53].

33.10 Economic Aspects

The largest world reserves of rhenium are located in Chile which is today the world's largest producer. Other producers include Germany, CIS, Sweden, the United States, and Japan. In Germany, rhenium is obtained from molybdenum concentrates, spent catalysts, and rhenium-containing scrap, and processed to produce high-purity NH₄ReO₄, HReO₄, and Re metal powder or pellets [54]. The largest consumer of rhenium is the United States, which imported ca. 15 t of Re in 1990. This could increase to 20 t/a in the next five years. Rhenium is used for aircraft turbine blades (60%), reforming catalysts (30%), and other applications (10%) [14].

33.11 Toxicology and Physiological Effects

No evidence exists that rhenium is an essential element for living organisms [55]. People who have worked over a long period of time in the extraction and production of rhenium metal and its most important compounds, perrhenic acid and ammonium

perrhenate, have not shown any toxic effects. Current toxicological investigations of rhenium and rhenium compounds are contradictory and do not enable any OECD guidelines to be issued [56].

Medical studies indicate that rhenium carboxylates have an antitumor effect [57]. ¹⁸⁸Rhenium and ¹⁸⁶rhenium are used in combination with monoclonal antibodies for the diagnosis and treatment of leukemia [58].

33.12 References

1. K. B. Lebedev: *The Chemistry of Rhenium*, Butterworths, London 1962.
2. R. D. Peacock: *The Chemistry of Technetium and Rhenium*, Elsevier, Amsterdam 1966.
3. B. W. Gonser (ed.): *Rhenium*, Elsevier, Amsterdam 1962.
4. A. Sutulov: *Molybdenum and Rhenium 1778-1977*, University of Concepción, Concepción, Chile 1976.
5. W. Noddack, I. Tacke, O. Berg, *Naturwissenschaften* **13** (1925) 567-574.
6. I. Noddack, W. Noddack, *Z. Anorg. Allg. Chem.* **183** (1929) 353-375.
7. W. Feit, *Angew. Chem.* **43** (1930) 459-462.
8. V. Tafel: *Lehrbuch der Metallhüttenkunde*, vol. 3, S. Hirzel, Leipzig 1954, pp. 224-230.
9. A. D. Melaven, J. A. Bacon, US 2414969, 1947.
10. S. Tribalat, *Anal. Chim. Acta* **3** (1949) 113-125; **4** (1950) 228-234.
11. H. G. Nadler, P. Borchers, *Erzmetall* **40** (1987) 293-298.
12. S. R. Zimmerley, E. E. Malouf, US 2809092, 1952.
13. H. Jehn, R. Völker, *Z. Metallkd.* **67** (1976) H. 11, 715-719.
14. J. W. Blossom: *Mineral Industry Surveys, Annual Review Rhenium in 1991*, U.S. Bureau of Mines, Washington, DC, 1992.
15. Universal Oil Products Comp., US 3672874, 1972 (C. L. Wiley, L. Blanchard).
16. Kennecott Corp., EP 0048823 A1, 1982 (P. Cichy).
17. M. J. Ferrante, F. E. Block, A. D. Fugate, F. A. Skirvin: *Recovery of Rhenium from Tungsten-Rhenium Alloy*, RI7254 U.S. Dept. of the Interior, Bureau of Mines, 1969.
18. GTE Products Corp., US 4557906, 1985 (A. D. Douglas, K. T. Reilly, J. E. Landmesser).
19. B. Jezowska-Trzebiatowska, S. Kopacz, T. Mikulski: *The Rare Elements*, Elsevier, Amsterdam 1990, p. 361.
20. B. J. Seheiner, R. E. Lindstrom, D. L. Pool: *Extraction and Recovery of Molybdenum and Rhenium from Molybdenite Concentrates by Electrooxidation: Process Demonstration*, RI8145, U.S. Bureau of Mines, 1976.
21. E. Gock, DE 3443806 A1, 1986.
22. E. Gock, J. Friedrich, J. Kähler, DE 3710725 A1, 1988.
23. American Metal Climax Inc., DE 2045308, 1971 (C. J. Hallada, H. F. Barry, R. W. McConnell).
24. G. M. Ritcey, A. W. Ashbrook: *Solvent Extraction*, Part II, Elsevier, Amsterdam 1979, pp. 421-425.
25. G. Huifa, Shell Jinglau, M. A. Hughes, *Hydrometallurgy* **25** (1990) 293-304.
26. J. Kähler, E. Gock, *Erzmetall* **41** (1988) no. 3, 132-137.
27. Kennecott Copper Corp., US 3558268, 1971 (J. D. Prater, R. N. Platzke).
28. H. G. Nadler, P. Borchers in GDMB Gesellschaft Deutscher Metallhütten- und Bergleute: *Die Anwendung von festen und flüssigen Ionenaustauschern bei der Gewinnung und Raffination von Metallen*, Heft 53, Clausthal-Zellerfeld 1989, pp. 162-174.
29. P. E. Churchward, J. B. Rosenbaum: *Sources and Recovery Methods for Rhenium*, RI6246, U.S. Bureau of Mines, 1963.
30. A. J. Sherman, R. H. Tuffias, R. B. Kaplan, *J. Met.* (1991) July, 20-23.
31. G. A. Geach, J. R. Hughes in F. Benesovsky (ed.): *The Alloys of Rhenium and Molybdenum or with Tungsten and Having good High-Temperature Properties*, *Plansee Proceedings*, Pergamon Press, London 1955, pp. 245-253.
32. E. Pink, R. J. Arsenault, *Prog. Mater. Sci.* **24** (1979) 1-52.
33. J. E. Peters, *J. of Met.* (1969) April, 27-30.
34. J. M. Dickinson, L. S. Richardson, *Trans. Am. Soc. Met.* **51** (1959) 758.
35. S. V. Nagender Naidu, P. Rama Rao, *J. Alloy Phase Diagrams* **6** (1990) no. 3, 129-136.
36. R. Eck, *Int. J. Refract. Hard Met.* **5** (1986) no. 1, 43-48.
37. General Electric Comp., EP 0403681 A1, 1990 (M. F. Henry).
38. H. Cross Comp.: *Rhenium and Rhenium Alloys*, Weekhawken, NJ.
39. H. Bildstein, BHM, *Berg Hüttenmänn. Monatsh.* **136** (1991) no. 9, 359-361.
40. Metallwerk Plansee, EP 0399621 A1, 1990 (P. Röthhammer).
41. Siemens AG, EP 0412397 A1, 1991 (N. Czech).
42. N. N. Greenwood, A. Earnshaw: *Chemistry of the Elements*, Pergamon Press, Oxford 1984.
43. A. Müller et al., *Angew. Chem.* **103** (1991) 1501-1503.
44. B. Jung, H. Ehrhardt, G. Meyer, *Z. Anorg. Allg. Chem.* **603** (1991) 49-56.
45. R. D. Peacock in J. C. Bailar, H. J. Emelius, Sir R. Nyholm, A. F. Trotman-Dickenson (eds.): *Comprehensive Inorganic Chemistry*, vol. 3, Pergamon Press, Oxford 1973, pp. 905-978.
46. K. Dehnicke, J. Strähle, *Angew. Chem.* **93** (1981) 451-463; **104** (1992) 978-1000.
47. F. A. Cotton, G. Wilkinson: *Anorganische Chemie*, VCH Verlagsgesellschaft, Weinheim 1985.
48. M. H. Corrigan, W. H. Davenport, J. W. Spelman: *A Bibliography on the Catalytic Applications of Rhenium*, Cleveland Refractory Metals, Weekhawken, NJ, 1968.
49. K. Weißermel, H. J. Arpe: *Industrielle Organische Chemie*, VCH Verlagsgesellschaft, Weinheim 1988, 334-337.
50. UOP Inc., US 4629551, 1986 (G. J. Antos, Li Wang).
51. Exxon Research and Engineering Company, EP 0106531 B1, 1984 (G. E. Markley, W. E. Winter).
52. W. A. Herrmann et al., *Angew. Chem.* **103** (1991) 183-185, 1704-1711.
53. M. E. Peterson, J. S. MacDuff, M. W. Hovey: *Isolation and Colorimetric Determination of Rhenium*, RI5889, U.S. Bureau of Mines, 1961.
54. *Gmelin*, System no. 70, Rhenium, Verlag Chemie, Berlin 1941, 69-72.
55. O. G. Koch, G. A. Koch-Dedic: *Handbuch der Spurenanalyse*, part 2, Springer Verlag, Berlin 1974, 976-986.
56. O. D. Bozhkov, N. Jordanov, L. V. Borissova, Yu. I. Fabelinskii, *Fresenius Z. Anal. Chem.* **321** (1985) 453-456.
57. H. Y. Chen, R. Neeb, *Fresenius Z. Anal. Chem.* **320** (1985) 247-251.
58. N. Jordanov, I. Hazevov, O. Bozhkov, *Fresenius Z. Anal. Chem.* **335** (1989) 910-913.
59. A. G. Khatchatrian, *J. Planar Chromatogr.* **2** (1989) April, 142-147.
60. Roskill: *The Economics of Rhenium*, 4th ed., Roskill Information Services Ltd., London 1988, pp. 7-8.
61. P. Jacquet in H. G. Seiler, H. Sigel, A. Sigel (eds.): *Handbook on Toxicity of Inorganic Compounds*, Marcel Dekker, New York 1988, pp. 557-560.
62. J. T. Haley, F. D. Cartwright, *J. Pharm. Sci.* **57** (1968) 321-323.
63. S. V. Suvorov, *Nov. Dannye Tskhikol. Redk. Met. Ikh Soedin.* **1967**, 45-51; *Chem. Abstr.* **71** (1969) 53274h.
64. G. W. Estland, G. Yang, T. Thompson, *Methods Find. Exp. Clin. Pharmacol.* **5** (1983) no. 7, 435-438.
65. Sloan Kettering Inst. Cancer, US 450918, 1989 (D. A. Scheinberg).

Part Eight

Scattered Metals

																H	He				
Li	Be															B	C	N	O	F	Ne
Na	Mg	Al												Si	P	S	Cl	Ar			
K	Ca	Sc	Ti	V	Cr	Mn	Fe	Co	Ni	Cu	Zn	Ga	Ge	As	Se	Br	Kr				
Rb	Sr	Y	Zr	Nb	Mo	Tc	Ru	Rh	Pd	Ag	Cd	In	Sn	Sb	Te	I	Xe				
Cs	Ba	La [†]	Hf	Ta	W	Re	Os	Ir	Pt	Au	Hg	Tl	Pb	Bi	Po	At	Rn				
Fr	Ra	Ac [†]																			

†	Ce	Pr	Nd	Pm	Sm	Eu	Gd	Tb	Dy	Ho	Er	Tm	Yb	Lu
---	----	----	----	----	----	----	----	----	----	----	----	----	----	----

‡	Th	Pa	U	Np	Pu	Am	Cm	Bk	Cf	Es	Fm	Md	No	Lr
---	----	----	---	----	----	----	----	----	----	----	----	----	----	----

For Hafnium and Rhenium, see *Refractory Metals*.

34 Germanium

JEAN SCOYER (§§ 34.1–34.11); FATHI HABASHI (§ 34.12); HANS UWE WOLF (§ 34.13)

34.1 Introduction	1505	34.7 Environmental Protection	1512
34.2 History	1505	34.8 Quality Specifications	1513
34.3 Physical Properties	1505	34.9 Chemical Analysis	1513
34.4 Chemical Properties	1506	34.10 Storage and Transportation	1514
34.5 Resources and Raw Materials	1507	34.11 Uses and Economic Aspects	1514
34.6 Production	1508	34.12 Compounds	1515
34.6.1 Production of Concentrates	1508	34.12.1 Germanium(IV) Compounds	1515
34.6.1.1 Bleiberg Bergwerks Union	1508	34.12.1.1 Germanium Hydrides	1515
34.6.1.2 Jersey Minière Zinc	1509	34.12.1.2 Polygermenes	1516
34.6.1.3 Musto Exploration	1509	34.12.1.3 Germanium(IV) Halides	1516
34.6.1.4 Peñarroya	1510	34.12.1.4 Germanium Dioxide, Germanic Acid, and Germanates	1517
34.6.1.5 Pertusola	1510	34.12.2 Germanium(II) Compounds	1518
34.6.1.6 Other Primary Producers	1510	34.13 Toxicology and Occupational Health	1518
34.6.2 Production of Germanium	1511	34.14 References	1519
34.6.3 Purification	1512		
34.6.4 Transformation Processes	1512		

34.1 Introduction

Germanium, a semiconducting element, has five natural isotopes: ^{70}Ge (20.53%), ^{72}Ge (27.43%), ^{73}Ge (7.76%), ^{74}Ge (36.54%), and ^{76}Ge (7.76%). Germanium also has some radioactive isotopes with greatly different half-lives, the isotope with the longest half-life being ^{68}Ge (287 days).

Germanium found its first industrial application in 1947 with the development of the transistor. Until the early 1970s, it was used extensively in the solid-state electronics industry, although it has been replaced almost entirely by the cheaper silicon.

The main use of metallic germanium currently is for infrared optics. Germanium tetrachloride is used in optical fiber production. Germanium dioxide is used mainly as a catalyst in the production of polyester and synthetic textile fiber.

The total consumption of germanium was estimated to be ca. 70 t of the element in 1986. The main producers of germanium end products are located in the United States, Belgium, France, Germany, and Japan.

Germanium is considered as a strategic material by the United States government. The erection of a stockpile with a capacity of 30 t of Ge was decided in 1984. The first delivery began in 1987 and the capacity may be increased to 140 t.

34.2 History

In 1871, MENDELEEV predicted the existence and the properties of an unknown element, ekasilicon, to be placed between silicon and tin in his periodic system of elements. In 1886, WINKLER isolated a new element from argyrodite, $4\text{Ag}_2\text{S} \cdot \text{GeS}_2$. This element, named germanium, showed properties remarkably close to those predicted by MENDELEEV.

34.3 Physical Properties

Although high-pressure polymorphs are known, germanium normally crystallizes in the diamond structure with comparatively weak covalent atomic bonding, yielding the typical hardness and brittleness, as well as the

semiconductor behavior of this gray amphoteric metal.

The specific structure of the forbidden energy gap (band gap E_g), the binding forces between the germanium atoms, and their mass determine the major electron-photon and photon-phonon interactions in the crystal lattice, which result in a broad optical transmission range for infrared radiation. The fact that this range covers a main atmospheric transmittance window between 7 and 14 μm , coinciding with the spectral emittance peak of a blackbody at room temperature, has promoted the use of germanium as an infrared optical material. Germanium's high refractive index results not only in high optical power and little spherical aberration, but also in the need for antireflection coatings. These materials often occur as exotic contaminants in recycling operations. Germanium's thermal properties sensitize this brittle material to thermal shock; crucible design and seeding techniques must also cope with a 6.6% volumetric expansion of germanium during solidification.

Due to the occurrence of a narrow band gap, most physical properties of germanium (e.g., resistivity) depend strongly on temperature as well as on minute concentrations of solutes. An updated and extensive compilation of the physical properties of germanium can be found in [1]; Typical room temperature values are summarized below.

<i>Mechanical</i>	
Lattice parameter	0.565790 nm
<i>mp</i>	1210.4 K
Density	5.3234 g/cm ³
Microhardness (Vickers-ASTM E384)	780 kg/mm ²
Tensile fracture strength	100 MPa
<i>Electrooptical</i>	
Band gap	0.67 eV
Intrinsic resistivity	47.6 Ωcm
Transmission wavelength range	2–16 μm
Absorption coefficient at $\lambda = 10.6 \mu\text{m}$	0.02 cm ⁻¹
Refractive index at $\lambda = 10.6 \mu\text{m}$	4.0027
<i>Thermal</i>	
Thermal conductivity	0.586 W cm ⁻¹ K ⁻¹
Specific heat	310 J kg ⁻¹ K ⁻¹
Linear thermal expansion	5.9×10^{-6} K ⁻¹

34.4 Chemical Properties

[2, 3]

Elemental Germanium. Metallic germanium is stable in air. At temperatures above 400 °C in oxygen, a passivating oxide layer is formed. This layer is destroyed by water vapor.

Germanium resists concentrated hydrochloric and hydrofluoric acids even at their boiling points, but reacts slowly with hot sulfuric acid. The dissolution of germanium in nitric acid proceeds faster than in sulfuric acid. In alkaline media in the presence of an oxidizing agent, e.g., hydrogen peroxide, germanium dissolves rapidly, even at room temperature. Germanium reacts readily with halogens to form tetrahalides.

Germanium and silicon are totally miscible and form a continuous range of alloys. The system with tin has a eutectic.

Germanium Compounds¹. Germanium can have valences of two or four. The divalent compounds are less stable and oxidize easily to the tetravalent compounds, which are similar to their silicon analogs.

Germanium dioxide, GeO_2 . Some properties of germanium dioxide are listed in Table 34.1. It exists in two crystalline forms and one amorphous form, all of which are white powders. The hexagonal form is obtained when germanium tetrachloride is hydrolyzed with water. This reaction leads to a voluminous gel that continuously releases its water during drying. The transformation to the tetragonal form occurs only on heating at 300–900 °C in the presence of a catalyst (e.g., an alkali metal halide).

The amorphous form is obtained by rapid solidification of molten GeO_2 or by reaction of GeCl_4 or GeO with oxygen in the gas phase. Moisture catalyzes the transformation from the amorphous to the hexagonal form.

Germanium monoxide, GeO , is obtained by the reaction of GeO_2 with reducing agents like germanium metal, iron, carbon, carbon mon-

¹ For more details, see Section 34.12.

oxide, or hydrogen above 600 °C. Germanium monoxide sublimes above 710 °C, and this property is used in some industrial processes to recover germanium from slags or residues (fuming of Ge). Germanium monoxide is insoluble in water.

Table 34.1: Properties of germanium dioxide.

Property	Structure		
	Hexagonal	Tetragonal ¹	Amorphous
Thermal stability, °C	1049–1116	<1049	
Density at 25 °C, g/cm ³	4.228	6.239	3.637
<i>mp</i> , °C	1116	1086	
Solubility in water at 25 °C, g/L	4.53	insoluble	5.18
water at 100 °C, g/L	13	insoluble	
HF, HCl, NaOH	soluble	insoluble	soluble

Germanium Halides. Of the germanium halides, only germanium tetrachloride has practical applications. The properties of the tetravalent halides are listed in Table 34.2. Germanium tetrachloride is obtained by reaction of chlorine gas with germanium metal and of hydrochloric acid with GeO_2 or germanates. Germanium tetrachloride is soluble in carbon tetrachloride. Industrial practice takes advantage of the insolubility of GeCl_4 in concentrated HCl (> 6 M) to purify GeCl_4 from trace impurities such as As, Cu, and B by solvent extraction with HCl.

Table 34.2: Properties of germanium tetrahalides.

Property	GeCl_4	GeF_4	GeBr_4	GeI_4
Form at 25 °C	liquid	gas	crystals	crystals
Color	colorless	colorless	gray white	red
Density at 25 °C	1.8755			
<i>mp</i> , °C	−49.5	−15	26.1	146
<i>bp</i> , °C	83.2	−36.5 (sublimes)	186.5	348

Germanium disulfide, GeS_2 , is obtained by the action of H_2S on acidic germanium solutions. Because GeS_2 is insoluble in acid media, this reaction is used industrially to obtain germanium concentrate.

Germanates are obtained in reactions at elevated temperature (800–1200 °C), in which glasses are produced from melts of GeO_2 and metal oxides or carbonates. The reactions also

occur at room temperature in aqueous solution; e.g., sodium germanate, $\text{Na}_3\text{HGe}_7\text{O}_{16}$, is formed by treatment of a NaOH solution of GeO_2 with sulfuric acid.

Germanides can be produced by melting other metals with germanium and freezing the melt, e.g., Mg_2Ge . Germanes (germanium hydrides) are evolved when germanides react with acids: monogermane, GeH_4 , digermane, Ge_2H_6 , and trigermane, Ge_3H_8 , can be separated by fractional distillation.

Organometallic Compounds. The organometallic compounds of germanium have few technical uses. Properties and methods of preparation have been extensively described [4].

34.5 Resources and Raw Materials [5, 6]

The concentration of germanium in the earth's crust averages 6.7 ppm, which is comparable to the concentration of zinc or lead. Thus, germanium is not scarce, but it is widely dispersed so that only a few minerals have been isolated. The most important are listed in Table 34.3.

Table 34.3: Germanium minerals.

Name and composition	Ge content, %	Mining location
Stottite, $\text{FeGe}(\text{OH})_6$	29	none
Schauerteite, $\text{Ca}_3\text{Ge}(\text{SO}_4)_2(\text{OH})_6 \cdot 3\text{H}_2\text{O}$	14	none
Briarite, $\text{Cu}_2(\text{Fe, Zn})\text{GeS}_4$	13–17	none
Germanite, $\text{Cu}_3(\text{Ge, Fe})\text{S}_4$	5–10	Tsumeb, Namibia
Renierite, $(\text{Cu, Fe, Ge, Zn, As})\text{S}$	6.3–7.7	Tsumeb, Namibia Kipushi, Zaire
Argyrodite, $4\text{Ag}_2\text{S} \cdot \text{GeS}_2$	1.8–6.9	Freiberg, Germany
Canfieldite, $4\text{Ag}_2\text{S} \cdot (\text{Sn, Ge})\text{S}_2$		

Germanium is present in the lattices of certain sulfides, such as sphalerite. The concentration of germanium in some germanium-rich deposits is given in Table 34.4.

Table 34.4: Germanium content of diverse deposits.

Type	Location	Estimated Ge content, ppm
Zinc	Gordonville, Tennessee, USA	400
	Nanisivik, Baffin, Canada	230
	Saint-Salvy, France	150
	Tsumeb, Namibia	250
	Lyon Lake, Ontario, Canada	200–250
	Salafosa, Italy	200
Copper	Apex, Utah, USA	640
	Northumberland, UK	300

In the past, germanite (Tsumeb) and renierite (Kipushi) were the principal sources of germanium. Currently, germanium is recovered mainly from by-products of the zinc industry.

The only mining operation specific for germanium (and Ga) is located at an old copper mine, the Apex, that has recently been reopened for this purpose.

At one time, germanium was recovered from the coal ash of electric power plants in England. This source of germanium vanished due to the decreased coal consumption for electric power production. The former Soviet Union, and probably China, still recover germanium from this source.

34.6 Production

The overall production processes can be divided into two steps: (1) production of germanium concentrate (primary production) and (2) production of germanium end products.

The first step varies depending on the raw materials processed and the chosen technology. Pyrometallurgical processes are based on the volatility of GeO and GeS. Hydrometallurgical processes are based on precipitation of germanium as its sulfide or hydroxide or with tannic acid.

More recently, solvent extraction has been reported using hydroxyoximes (e.g., LIX63), or oxime derivatives (e.g., Kelex 100, and LIX26) [7–18]. Fixation of germanium on resin impregnated with amines has also been patented [19]. However, published information on all of these is scarce and not always reliable.

The second step relies on the volatility of GeCl_4 as the separation–purification step. Because the processes used by the diverse producers are quite similar, this step can be described with one flow sheet (Figure 34.6).

34.6.1 Production of Concentrates

The flow sheets for the production of germanium concentrate from germanite and renierite as raw materials have been described [20].

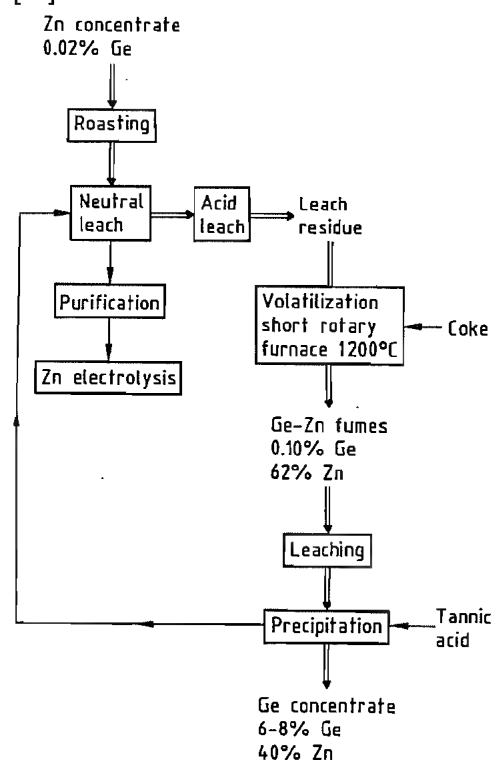


Figure 34.1: Production of a germanium concentrate: flow sheet of Bleiberg Bergwerks Union (BBU). Location: Arnoldstein, Austria; Bleiberg mine. Estimated Ge capacity: 6 t/a.

34.6.1.1 Bleiberg Bergwerks Union

Bleiberg Bergwerks Union (BBU) processes the leach residues of its own zinc plant by a thermic process in a modified Waelz oven (Figure 34.1). Germanium monoxide is sub-

limed at ca. 1200 °C. After the fumes are leached, germanium is precipitated with tannic acid. The germanium-free solution is recycled to the zinc plant and the germanium concentrate is sold as such.

The use of tannic acid leads to a relatively poor germanium concentrate. Care must be taken to avoid problems in the zinc electrolysis due to the recycling of unreacted tannic acid [21–23].

34.6.1.2 Jersey Minière Zinc

Jersey Minière Zinc produces zinc from its mines in Gordonville and Elmwood, Tennessee. Germanium is concentrated in the leach residue, which is dried and shipped to Metallurgie Hoboken-Overpelt (MHO), Belgium (Figure 34.2) [24].

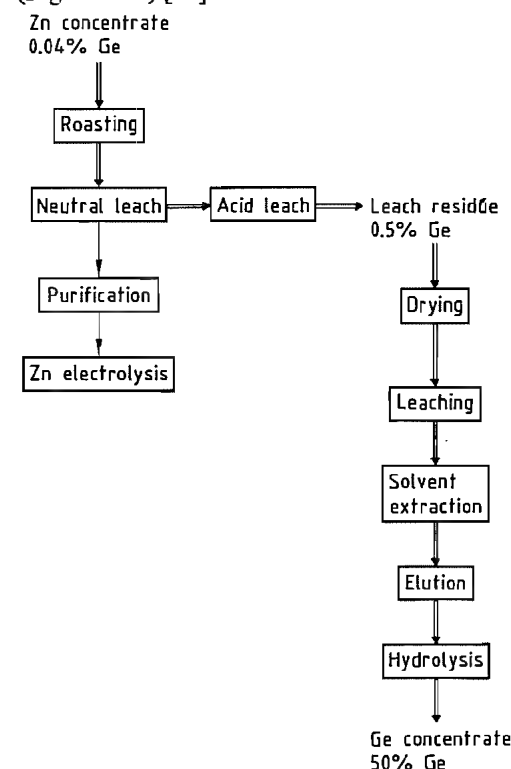


Figure 34.2: Production of a germanium concentrate: flow sheet of Jersey Minière Zinc (JMZ) and Metallurgie Hoboken-Overpelt (MHO). Location: JMZ at Clarksville, Tennessee, United States; Gordonville mine. MHO at Olen, Belgium. Estimated Ge capacity: 6 t/a.

At the Olen plant in Belgium, the germanium residue is leached, and germanium is separated by solvent extraction. After elution in an alkaline medium, a germanium concentrate is precipitated by hydrolysis [25]. The use of solvent extraction technology enables MHO to produce very rich germanium concentrates, regardless of the concentration in the feed [8–13].

34.6.1.3 Musto Exploration

The Ge–Ga concentrates from the company-owned Apex mine are leached in sulfuric acid with SO_2 to reduce trivalent iron (Figure 34.3). After cementation with iron to remove copper, H_2S is added to give a first sulfide concentrate. Gallium is then separated by solvent extraction. The germanium concentrate containing ca. 3% germanium is upgraded to GeO_2 of 98% purity before being sold to refiners. Exploitation started in 1985 [26].

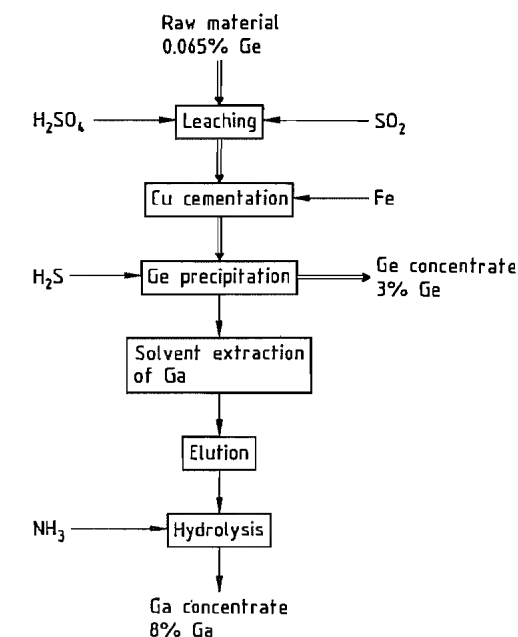


Figure 34.3: Production of a germanium concentrate: flow sheet of Musto Exploration. Location: St. George, Utah, USA; Apex mine. Capacity: 18 t/a of Ge and 10 t/a of Ga.

34.6.1.4 Peñarroya

Concentrates of Zn-Pb and germanium matte from Pertusola (Figure 34.5), a subsidiary of Peñarroya, are processed together by the Imperial Smelting Process. Germanium is collected in the zinc phase, which is further purified by distillation in New Jersey columns (Figure 34.4). Germanium is then concentrated in a residue by volatilization of zinc. However, due to ecological problems, thermal processes for zinc are losing importance compared with hydrometallurgical processes.

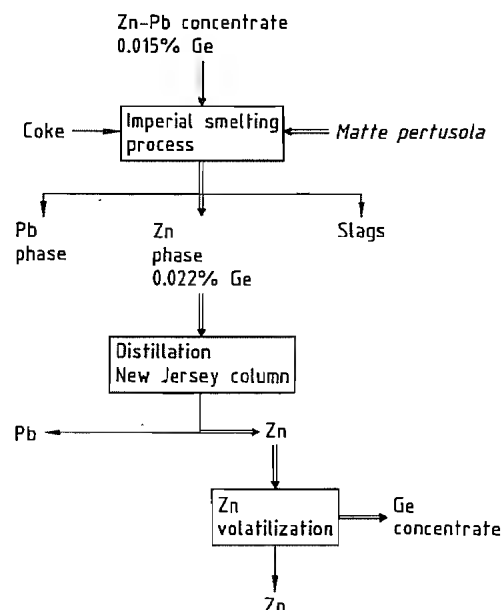


Figure 34.4: Production of a germanium concentrate: flow sheet of Peñarroya. Location: Noyelles-Godault, France; Saint-Salvy mine. Capacity: GeO_2 - GeCl_4 , 60 t/a; Ge metal, 30 t/a.

34.6.1.5 Pertusola

The zinc concentrates of Salafosa are treated at the refinery of Crotone (Figure 34.5). The leach and purification residues of the hydrometallurgical plant are thermally decomposed in a cubilot. Germanium is recovered in the Pb-Zn fumes, a small portion going into the matte phase, which is processed further by Peñarroya (Figure 34.4). After re-

leaching the fumes, a germanium concentrate containing 7–35% germanium is produced.

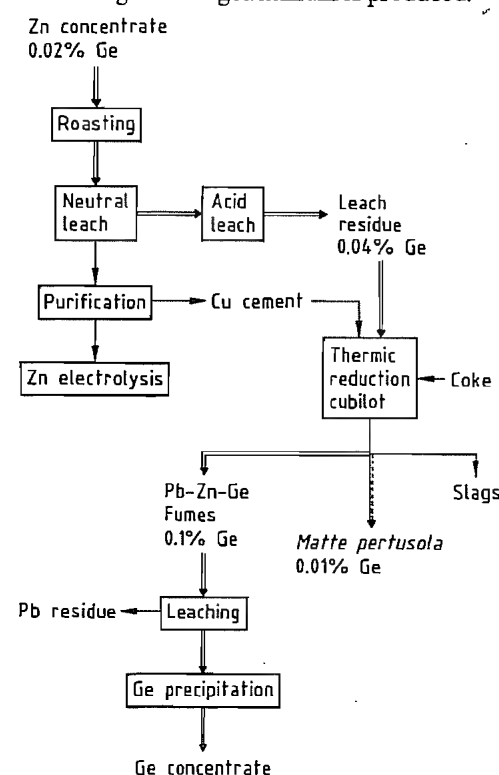


Figure 34.5: Production of a germanium concentrate: flow sheet of Pertusola. Location: Crotone, Italy; Salafosa mine.

34.6.1.6 Other Primary Producers

The Metallgesellschaft (Germany) recovers ca. 10 t/a of germanium from the hydrometallurgical plant of Datteln. China exports ca. 4 t/a of germanium. The production of the former Soviet Union is mainly used internally (estimated 40 t/a of germanium). Cominco (British Columbia, Canada) is developing a project for 10–20 t/a of germanium.

Eagle Picher (Quapaw, Oklahoma, USA) processed the residues of its zinc smelter by fuming in a Waelz oven at 1250 °C. Because this source is not economical at current prices, Eagle Picher now supplies its refining unit (25–40 t/a of germanium capacity) with purchased germanium concentrates [27]. Preus-

sag (15 t/a) and Otavi (5 t/a) (both Germany) processed germanite from Tsumeb before depletion, but they now buy concentrate [5].

34.6.2 Production of Germanium

The transformation of a germanium concentrate (mostly GeO_2) or germanium metal scrap to germanium (Figure 34.6) [28] begins with conversion to GeCl_4 :

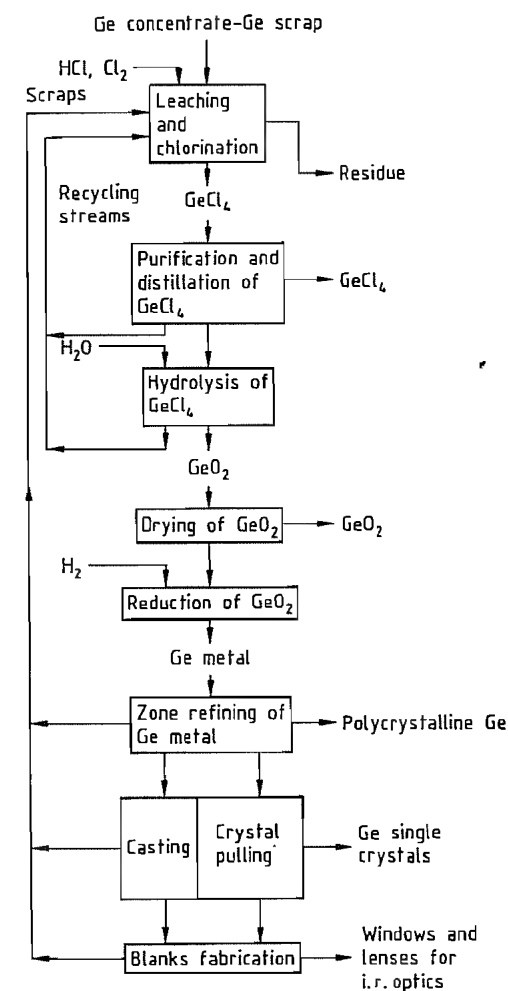
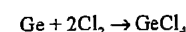
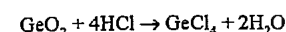
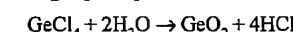


Figure 34.6: Flow sheet of the production of germanium metal from germanium concentrate.

The reactions are run at the boiling point of GeCl_4 (83.2 °C) in concentrated HCl (6 M) to avoid hydrolysis. Even when only GeO_2 is processed, a chlorine atmosphere is used to oxidize the volatile AsCl_3 to nonvolatile H_3AsO_4 .

The GeCl_4 , containing As^{3+} as the major impurity, is purified by fractional distillation. Traces of As, Sb, Cu, and B are extracted by HCl (> 6 M) saturated with chlorine. Other purification techniques have been reviewed [20].

The purified GeCl_4 is hydrolyzed with high-purity water,



After filtration and thorough washing, the GeO_2 is dried.

The usual method of producing elemental germanium is hydrogen reduction [29] of germanium dioxide in electrically heated tubular furnaces at ca. 650 °C, yielding a gray metallic germanium sponge. In industry, graphite and/or quartz boats and furnace linings are used. Quartz boats must be sandblasted and/or coated to avoid sticking and breakage.

Care must be taken to keep the temperature below 700 °C during reduction to avoid generation of volatile germanium monoxide. Adequate processing limits the germanium loss to less than 0.1 %.

As a result of the very stringent purity requirements, reduction processes [2] using carbon, flux electrolysis, or the direct reaction of germanium tetrachloride with zinc have lost industrial importance. The reaction of GeCl_4 with H_2 can be used to grow epitaxial germanium layers [30], but bulk germanium production is hampered by low metal yield and overall energy yield.

After complete reduction, the temperature is raised above the melting point (937 °C), and a polycrystalline germanium bar is solidified from one end to the other. Due to the different solubilities of the impurities in the liquid and solid phases, the impurities concentrate by segregation [31] in the first or the last melt fraction to solidify. Hydrogen is highly soluble in molten germanium; therefore, to avoid porosity and blow holes, the crystallization

speed must be limited to a few centimeters per hour.

34.6.3 Purification

To obtain semiconductor-grade germanium, the material must be further purified by zone refining [32, 33], under hydrogen, nitrogen, or another controlled atmosphere. Due to the low surface tension and high density of molten germanium, a crucible-free float zone-refining process never matured [34]. High-purity germanium is obtained by repeated passage of crude germanium through the zone-refining crucible. The number of efficient zone-refining passes which can be carried out in a single crucible is limited by the partition coefficient of the impurities between germanium and the crucible material. Eventually, an equilibrium between the concentration of impurities in the melt and in the crucible is reached. For this reason, a cyclic batch process, in which the zone refining is continued in a new crucible, is unavoidable if high-purity germanium is to be obtained. Between the successive refining steps, the less pure metal parts are mechanically cut away and recycled. A suitable etching technique [35] is required to clean and prepare the load as well as the crucible for the next refining step. Grain boundaries and other crystallographic imperfections (dislocations, vacancies, etc.) act as precipitation sites for impurities, impeding the ultrapurification.

Ultimate purity levels can therefore be obtained (and measured) only in single crystals grown in the most aseptic, dust-free environment. The physics and chemistry of ultrapurification of germanium have been discussed [36–38].

34.6.4 Transformation Processes

For most applications, the germanium must be processed further into a suitable size and crystallographic perfection and doped within a narrow range (e.g., 1–8 ppb) with a definite impurity (usually a group 13 or group 15 ele-

ment) to yield the specified electrooptical properties.

Two techniques are available for this transformation: (1) the *Bridgman process* [39] which entails horizontal or vertical, possibly seeded, directional solidification in a graphite crucible, often improperly called casting, and (2) the *Czochralski process* [40], by which a crystal seed is dipped into a germanium melt and allowed to grow by suitable control of pull speed and heat balance. The second process yields the most perfect material, e.g., dislocation-free single crystals. The fundamental physicochemical background of crystal-growth processes was reviewed recently [41–43]. Modern equipment handles up to 150-kg germanium loads and allows growth of single crystals up to 300 mm in diameter in a typical 48-h cycle.

Germanium crystals are ground, sliced, and milled with high precision microcomputer-controlled, diamond-tooled machines into the desired geometrical shape. This operation generates huge and costly amounts of scrap fines which have to be recycled. The brittleness of germanium and the need to preserve a near-perfect, strain-free crystal lattice do not allow germanium forging; segregation of the indispensable dopants hinders precision casting.

34.7 Environmental Protection

In the primary production of germanium, environmental problems are not specific to germanium, but are those of the zinc industry (e.g., SO_2 emission, cadmium pollution).

When solvent extraction units are used, special attention must be paid to fire protection and cleaning of the off-gas. The off-gas of GeCl_4 production must be scrubbed with alkaline solution to destroy HCl and chlorine. Monitoring the hydrogen content in the air avoids any risk of explosion in the reduction section.

34.8 Quality Specifications

Major impurities (< 10 ppm) in GeCl_4 are O, C, and H, all detectable by infrared spectrometry. The concentration of all metallic impurities can be depressed to or below their detection limits (typically < 5 ppb). Process-induced impurities in GeO_2 are H_2O (< 3000 ppm, ASTM F5-60) and Cl (< 300 ppm, turbidimetry). Often, C, F, and S are detected at ppm levels (conductimetry); all other elements are at or below their detection limit (< 10 ppb).

Density (ASTM B417-76, B 527-70) and grain size (ASTM B 330-76) obviously influence reduction kinetics, but the contamination risks inherent to all high-temperature processes suggest the use of all-quartz furnaces and synthetic quartz boats with palladium-diffused H_2 for the assessment of electronic grade GeO_2 by reduction (ASTM F 27-83).

The most commonly used characterization techniques for germanium metal are those that determine the electrical properties of semiconductors: e.g., transport properties (ASTM F 43-78, F 76-73, F 42-77) and crystallographic perfection (ASTM F 389-76). For evaluation of the optical quality of germanium, a number of routine spectroscopic and specialized interferometric techniques exist [44]. All of these methods are, however, sensitive to the surface preparation (polishing) of the sample. Since many of the optical and electronic properties of germanium are linked to one another [45, 46], the electronic properties, which can be more accurately and reliably measured, can be used to define the optical properties. Thus, for example, standard optical grade germanium is specified as n-type germanium with resistivity 5–40 Ωcm .

To determine the chemical nature and concentration of electrically active impurities, three sensitive (10^{-5} ppb) techniques are used: deep level transient spectroscopy (DLTS) [47], far infrared transmission (FIRT) [48] (Figure 34.7), and photothermal ionization spectroscopy (PTIS) [49].

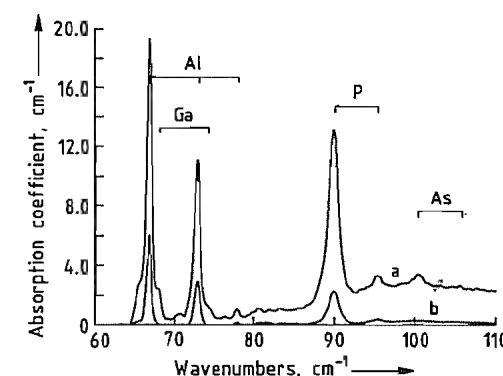


Figure 34.7: Purification by zone refining: a) 8K-FIRT spectra of germanium "as reduced" vs. b) after zone refining.

Impurity, ppb	"As reduced"	Refined
P	1.5	0.36
As	0.77	0.005
Al	1.1	0.27
Ga	0.031	0.005

The major residual impurities in high-purity germanium (H_2 < 100 ppb; C, Si, and O < 10 ppb) are process-induced and barely detectable by their lattice phonon absorption in the germanium matrix (ASTM F 120-75, F 122-74) or by autoradiospectrometry [50, 51]. The concentration of other impurities can be depressed below 10^{-3} ppb.

34.9 Chemical Analysis

The analytical determination of germanium has been reviewed recently [52].

Germanium can be determined by photometry at 510 nm after complexation with phenylfluorone. Atomic absorption spectroscopy at 261.1 nm is less sensitive than the previous method. X-ray fluorescence enables determination down to $5 \times 10^{-3}\%$. Polarographic methods such as differential pulse polarography and anodic stripping have been developed for the determination of germanium (and other impurities) in Zn electrolytes.

The determination of impurities in GeCl_4 , GeO_2 , and Ge can be achieved by graphite furnace atomic absorption spectroscopy [53] or spark source mass spectroscopy [54].

34.10 Storage and Transportation

Germanium tetrachloride is classified as a dangerous corrosive liquid subject to international regulations (ADR/RID-IMDG-IATA) under UN 1760 Class 8 Group II. The combination of these with the very stringent purity requirements of the optical fiber manufacturers demands the use of expensive packaging (e.g., glass/teflon, tantalum-coated steel).

The packaging should preserve the purity of the GeO_2 during transportation and storage. For relatively short storage, a hermetically sealed high-density polyethylene bottle is satisfactory. The quality degradation during longer storage is linked to diffusion of impurities through or deterioration of the polyethylene. In this case the use of fluorinated plastic foil or coating is advisable.

Germanium metal oxidizes slowly in air, therefore, its packaging should primarily take its brittleness into account.

34.11 Uses and Economic Aspects

Germanium is used in manufacturing a wide range of high-technology products. Table 34.5 summarizes these applications for the market economies with respect to market volume and trends, as well as the germanium compound used.

The use of germanium in *optical materials*, by far the most important today, represents ca. 50% of the world consumption. Germanium itself is the primary high-quality lens and window material for thermal imaging in the 8–12 μm wavelength range. The materials trade-off for this application was recently reviewed [55]. The replacement of silicon by germanium as a cation in optical glasses [56] extends their transmittance toward longer wavelengths and increases the refractive index. The second property is used to confine the signal within the core of telecommunication optical fibers. The chemistry of germanium in fiber manufacture is discussed in [57]. With As, Sb, and

Se, germanium forms nonoxide glasses [58], also used in IR optics (Figure 34.8), and whose photosensitivity yields high-resolution photoresists, a recent development reviewed in [59].

Table 34.5: Germanium market in 1986 (excluding East-bloc countries).

Application	Product	Consumption, t	Annual growth rate, %
Infrared optics	optical-grade Ge, shaped mono- and polycrystalline blanks	35	15
Optical fibers	high-purity GeCl_4	13	10
Catalysis	GeO_2 (hexagonal or amorphous), $\text{NaH}_2\text{Ge}_2\text{O}_6$	13	5
Electronics, optoelectronics	doped Ge single-crystal slices	2	5
High-energy radiation detectors	high-purity Ge single crystal	1	5
Luminescence	GeO_2	1	
Medical, alloys, and glasses	GeO_2 , Ge pellets, and powders	5	5
Total		70	11

Figure 34.8: Germanium for infrared optics: typical set of polished Ge blanks.

The second major use of germanium is as *catalyst* or *cocatalyst* [60] in the production of polyesters (e.g., poly(ethylene terephthalate)) and synthetic textile fibers. The more expensive germanium catalysts are used when the final product must be a colorless fiber or plastic, e.g., photographic films.

Some germanates crystallize as typical *phosphors*, which reemit absorbed energy as

visible radiation. Magnesium germanates and fluorogermanates, e.g., $\text{Mg}_{28}\text{Ge}_{10}\text{O}_{48}$ and $\text{Mg}_{56}\text{Ge}_{15}\text{O}_{66}\text{F}_{20}$, in which magnesium acts as activator, are used in lamps as a constituent of the fluorescent coating [61]. This is preferred to the cheaper arsenic-based phosphors, for which safety regulations are severe. Bismuth germanate, $\text{Bi}_4\text{Ge}_3\text{O}_{12}$, is an intrinsic phosphor that is used as a single crystal in high-energy gamma-ray scintillator detectors [62]. The stopping power is extremely high because of the high atomic number of bismuth.

The remaining interest for germanium in electronics is based on the advantageous mobility characteristics of charge carriers in this material. Typical applications are high-power devices with low energy loss and photodetectors [63]. The most demanding photodetector application involves *gamma-ray spectroscopy detectors* [64], for which germanium must be refined to an extremely low impurity level ($< 10^{-3}$ ppb) and grown in nearly perfect single crystals. Recent progress in producing stable insulating layers on germanium [65], as well as its crystal lattice match ($\Delta a/a < 5 \times 10^{-3}$) with GaAs (epitaxy) offers new hope for germanium as an electronic material in integrated circuits.

Another use of germanium, although limited virtually to Japan, is the industrial production of organogermanium compounds such as bis(carbamoyl)ethylgermanium sesquioxide, $(\text{GeCH}_2\text{CH}_2\text{CONH}_2)_2\text{O}_3$, for medical applications [66]. The use of germanium in alloys, e.g., high-precision resistors, is minor. The geographic production consumption pattern for 1986 is summarized in Table 34.6.

In consideration of the large internal scrap recycling coefficient of most production lines, care should be taken in evaluating the apparent refining overcapacity of many producers.

Table 34.6: Production-consumption pattern for Ge in 1986.

Country	Production, t	Consumption, t
North America	29	35
Western Europe	36	18
Asia	5	17

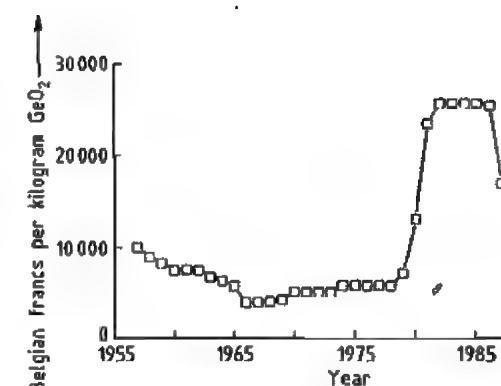


Figure 34.9: Belgian producer price for electronic-grade germanium dioxide (June 30 values from *Metal Bulletin*; the Belgian franc is the usual currency for the quotation of GeO_2).

Figure 34.9 illustrates the producer price evolution of electronic-grade GeO_2 , largely determined by the refining costs of low-grade ores. The price of germanium metal in its various commercialized forms reflects the stringent requirements for purity and crystallographic perfection and, therefore, depends strongly on the specifications.

34.12 Compounds [67, 68]

Halides, oxides and sulfides of both bivalent and quadrivalent germanium are known. The compounds of bivalent germanium are unstable. They have the tendency to be oxidized to germanium(IV) compounds.

34.12.1 Germanium(IV) Compounds

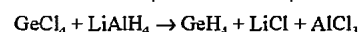
34.12.1.1 Germanium Hydrides

If zinc is allowed to react with sulfuric acid which contains germanium, the escaping hydrogen contains some germanium hydride, GeH_4 . If the gas mixture is passed through a strongly heated glass tube, the germanium is deposited on the wall as a bright metallic mirror, which appears red by transmitted light. Germanium hydride is obtained in good yield by the action of sulfuric acid on the alloy of composition Mg_2Ge , obtained when germa-

nium and magnesium are melted together. In addition to the ordinary gaseous germanium hydride (monogermane, *mp* -165°C , *bp* -90°C), formed as the main product, two germanium hydrides which are liquid at ordinary temperature are also formed:

- Digermane, Ge_2H_6 (*mp* -109°C , *bp* 29°C)
- Trigermane, Ge_3H_8 (*mp* -105.6°C , *bp* 110.5°C)

Monogermane is now prepared by the reduction of GeCl_4 with LiAlH_4 in ether:



34.12.1.2 Polygermenes

In addition to these volatile compounds, germanium forms highly unsaturated solid hydrides:

- $[\text{GeH}]$, a dark brown powder, which deflagrates upon admission of air when it is dry, is converted by oxidizing agents into germanium(IV) compounds, but does not react with dry hydrogen chloride.
- $[\text{GeH}_2]$, obtained by decomposing CaGe with dilute hydrochloric acid or with caustic soda. It is yellow in color, stable in the absence of air when dry, but at once ignites explosively in the air. With concentrated hydrochloric acid, it forms the series of volatile germanium hydrides — GeH_4 , Ge_2H_6 , and Ge_3H_8 — together with GeCl_2 and H_2 .

34.12.1.3 Germanium(IV) Halides

Table 34.7 indicates the most important physical properties of the germanium(IV) halides.

Table 34.7: Germanium halides.

	Color	<i>mp</i> , $^{\circ}\text{C}$	<i>bp</i> , $^{\circ}\text{C}$
GeF_4	colorless	-36.6 (subl.)	
GeCl_4	colorless	-49.5	83.1
GeBr_4	colorless	26	186
GeI_4	orange	144	> 300

Germanium Tetrafluoride. The action of concentrated hydrofluoric acid on germanium dioxide yields a clear solution, from which colorless, hygroscopic crystals of hydrated germanium tetrafluoride, $\text{GeF}_4 \cdot 3\text{H}_2\text{O}$, sepa-

rate. If the attempt is made to dehydrate the salt by heating, hydrolytic decomposition takes place. Part of the germanium simultaneously volatilizes as the anhydrous fluoride. The anhydrous fluoride is gaseous at ordinary temperature. When strongly cooled, it condenses to a white flocculent mass which sublimes without melting when it is warmed.

Potassium Fluorogermanate. $\text{K}_2[\text{GeF}_6]$ separates from a solution of germanium tetrafluoride to which potassium fluoride is added, in white hexagonal prisms or plates. It is not hygroscopic, sparingly soluble in cold water, insoluble in alcohol, and is decomposed when heated to a red heat.

Germanium Tetrachloride. GeCl_4 made by burning germanium in a stream of chlorine, or better by warming germanium dioxide with fuming hydrochloric acid in a pressure flask. It is a colorless liquid, density 1.88, *bp* 83°C , solidifying at -49.5°C . It is slowly hydrolyzed by water, with the formation of hydrated, finely divided germanium dioxide. In its concentrated hydrochloric acid solutions, germanium tetrachloride is present in the form of chlorogermanic acid, $\text{H}_2[\text{GeCl}_6]$, as is shown by the migration of the germanium towards the anode upon electrolysis. If germanium tetrachloride is heated with germanium, it undergoes partial reduction of the dichloride:



The compound $[\text{GeCl}]_x$ is prepared by heating GeCl_4 . The unstable Ge_2Cl_6 is formed at the same time, and also the dichloride GeCl_2 .

Germanium Oxychloride. GeOCl_2 is a colorless liquid solidifying at -56°C . It decomposes into Cl_2 and GeO when it is heated. The GeO is thereby obtained in a lemon yellow form, which passes into the ordinary black monoxide at 650°C .

Ge_2OCl_6 is obtained by the action of O_2 on GeCl_4 at 950°C . It is a colorless liquid, solidifying at -60°C , and decomposes with formation of GeO_2 when it is warmed.

Germanium Tetrabromide and Tetraiodide. Germanium tetrabromide, GeBr_4 (colorless regular octahedra, *d* 3.13, *mp* 26°C , *bp* 185.9°C), and germanium tetraiodide, GeI_4 (orange crystals, *d* 4.32, *mp* 144°C), can be prepared by methods similar to those for the chloride. They are vigorously decomposed by water and fume strongly in air. The iodide begins to decompose into GeI_2 and I_2 a little above its melting point.

34.12.1.4 Germanium Dioxide, Germanic Acid, and Germanates

Germanium dioxide. GeO_2 is formed by strongly heating germanium or germanium sulfide in a current of oxygen, or by oxidizing these substances with concentrated nitric acid. It is a white powder which melts at 1115°C after gradually softening, and solidifies from the melt as a glass. Germanium dioxide is volatile above 1250°C . It is sparingly soluble in water (solubility about 0.4 g in 100 g of water at 20°C , about 1 g in 100 g at 100°C).

The solubility of germanium dioxide is dependent on the quantity of solid phase present. This is because germanium dioxide is present in solution not only in molecular dispersion, but simultaneously in a colloidal state. The formation of a sol also explains the fact that although the solubility in the cold is considerably smaller than when hot, no turbidity results when a solution of germanium dioxide, saturated hot, is cooled. The solutions display an acid reaction, and have an appreciable electrical conductivity. From dialysis measurements at a pH of 8.4–8.8 it was shown that the ions present were $\text{Ge}_3\text{O}_{11}^{2-}$, and not GeO_3^{2-} as in strongly alkaline solutions.

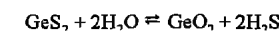
Germanium dioxide separates out in microscopic crystals when an aqueous solution is evaporated. It is dissolved with difficulty by acids, but readily by caustic alkalis. The compounds of germanium dioxide with strongly basic metallic oxides are called germanates; they can be obtained both from aqueous solution and by melting the components together, and display some relationships with the sili-

cates. The existence of germanates has been detected from melting point diagrams, e.g., Li_4GeO_4 (*mp* 1298°C), Li_2GeO_3 (*mp* 1239°C), Na_2GeO_3 (*mp* 1083°C), $\text{Na}_2\text{Ge}_2\text{O}_5$ (*mp* 799°C), $\text{Na}_2\text{Ge}_4\text{O}_9$ (*mp* 1052°C). Metagermanates — mostly as hydrates — usually crystallize from aqueous solutions.

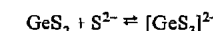
Germanium dioxide crystallizes not only in the water-soluble, hexagonal modification, having the low-quartz structure (*a* = 4.97 \AA , *c* = 5.65 \AA), but also in a tetragonal modification, insoluble in water, with the structure of rutile (*a* = 4.39 \AA , *c* = 2.86 \AA). This changes extremely slowly into the hexagonal modification above 1033°C .

If germanium dioxide is prepared by hydrolysis, e.g., of the tetrachloride, it separates out as a gel. The particles of oxide gradually undergo aggregation on standing under water. If it has aged sufficiently, the oxide loses its water on standing in air.

Germanium Disulfide and Thiogermanates. If hydrogen sulfide is passed into an aqueous solution of germanium dioxide, no precipitation is observed. Only when a sufficient quantity of a strong acid has been added is germanium disulfide, GeS_2 , formed as a white precipitate. The sulfide low solubility in water (0.455 g in 100 g of water); its aqueous solution gradually decomposes, hydrogen sulfide being evolved by hydrolysis:



The disulfide dissolves readily in ammonium sulfide, forming thiogermanate ions:

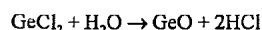


The thiogermanates are related to the naturally occurring double sulfides of germanium, the minerals germanite, $\text{Cu}_3(\text{Fe}, \text{Ge})\text{S}_4$ argyrodite, Ag_8GeS_6 , and canfieldite, $\text{Ag}_8(\text{Ge}, \text{Sn})\text{S}_6$.

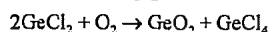
Germanium(IV) sulfate. $\text{Ge}(\text{SO}_4)_2$, obtained as a white powder of density 3.92 by the action of SO_3 on GeCl_4 . It is hydrolyzed by water, reacts vigorously and exothermically with caustic soda forming Na_2GeO_3 and Na_2SO_4 , and decomposes at 200°C .

34.12.2 Germanium(II) Compounds

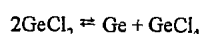
Germanium(II) chloride, GeCl_2 , is formed by passing GeCl_4 vapor over heated elemental germanium. It is a solid, reacts with water according to:



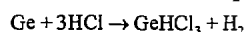
and with oxygen:



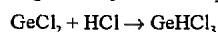
GeCl_2 is nearly colorless when cold, but turns orange when warmed. Decomposition occurs on stronger heating:



Trichlorogermane, GeHCl_3 , corresponds in composition to chloroform, and resembles it in many of its physical properties. The compound was first obtained by passing hydrogen chloride over heated powdered germanium:



A better process is to pass GeCl_4 over heated germanium, and to treat the product, consisting chiefly of GeCl_2 , with HCl :



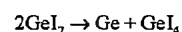
Trichlorogermane forms a colorless liquid, which turns milky on exposure to air, through the formation of oxychloride; *mp* -71°C , *bp* 75.2°C . Germanium must be present in this compound in the bivalent state, for it is decomposed by much water, depositing yellow germanium(II) oxide hydrate.

Germanium(II) bromide (colorless needles or leaflets, *mp* 122°C) can be obtained by the action of HBr on metallic germanium at 400°C ; GeHBr_3 is formed simultaneously, and may be reduced with zinc. The dibromide is hydrolyzed by water, with deposition of $\text{Ge}(\text{OH})_2$. GeBr_2 combines with HBr , to form tribromogermane, GeHBr_3 , a colorless liquid, solidifying at -24.5°C which decomposes again at high temperature.



Germanium(II) iodide, GeI_2 , (yellow hexagonal plates; crystal structure, sublimes at 240°C in vacuum) is prepared by the action of

concentrated hydriodic acid on $\text{Ge}(\text{OH})_2$. It is obtained only in poor yield by passing GeI_4 vapor over heated Ge , since it disproportionates according to



Germanium(II) Oxide. The decomposition of germanium(II) chloride with water or sodium hydroxide yields a yellow precipitate. If the precipitate is heated to 650°C in nitrogen, black crystalline germanium(II) oxide, GeO , is obtained.

Germanium(II) sulfide, GeS , can be obtained, by heating germanium(IV) sulfide, GeS_2 , in a stream of hydrogen. It forms leaflets, which are grey with metallic luster by reflected light, and bright red by transmitted light. It is thrown down as a red brown precipitate by the action of hydrogen sulfide on the hydrochloric acid solution of germanium(II) chloride. It is then soluble in caustic potash and, unlike the sulfide prepared by dry methods, also dissolves in hot concentrated hydrochloric acid and in ammonium polysulfide.

Germanium Selenides. GeSe (brown-black, tetragonal, density 5.30, *mp* 667°C and GeSe_2 (yellow, rhombic, density 4.56, *mp* 70°C) have been prepared like the sulfides, by precipitation from hydrochloric acid solutions, or by direct union of the components at 500°C .

34.13 Toxicology and Occupational Health

Germanium and most germanium compounds are comparatively low in toxicity because of pharmacological inertness, diffusibility, and rapid excretion. However, some exceptions exist, the most important being germanium hydride (germane). Surprisingly, soluble germanium compounds are more toxic by oral than by parenteral uptake. Intoxication is characterized by a lack of gross tissue changes in animals dying from oral uptake of germanium. Industrial exposure is due mainly to germanium fumes and dusts generated during production.

Absorption, Metabolism, Excretion, and General Effects. Gastrointestinal absorption of germanium oxides and cationic salts is poor; in contrast, the absorption of germanates from small oral doses is ca. 75% in 4 h and 96% in 8 h [69]. Inhaled germanates are quickly absorbed from the lungs into the blood [70]. Elemental germanium and germanium dioxide are excreted mainly via the urine in rats, rabbits, and dogs [71]. No reports of Ge accumulation in human or animal tissues exist. High exposure levels of germanium salts disturb water balance leading to dehydration, hemoconcentration, decrease in blood pressure, and hypothermia [72], without showing gross tissue damage.

Acute Toxicity. The symptoms of acute germanium toxicity in animals are listlessness, marked hypothermia, diarrhea, cyanosis, edema, hemorrhage of the lungs, petechial hemorrhage in the wall of the small intestine, peritoneal effusion, and edematous changes in heart muscle and in parenchymal cells of the liver and kidneys [73]. Germanium tetrafluoride and tetrachloride vapors irritate the eyes and mucous membranes of the respiratory tract [74]. Organic compounds, such as dimethylgermanium oxide, are only slightly toxic to rats [75], whereas triethylgermanium acetate shows considerable toxicity [76]. Germanium metal dust (particle size $1.7\text{ }\mu\text{m}$, concentration unknown) and GeO_2 (particle size $0.45\text{ }\mu\text{m}$, concentration unknown) had no adverse effects on rats after inhalation for 1 h [70]. In rats and mice, the acute oral toxicity of alkylgermanium compounds ranged between 300 and 2870 mg/kg [76, 77]. Triethylgermanium acetate has an LD_{50} value (rat, oral) of 250 mg/kg body weight. The LD_{100} for germane (mouse, inhalation) is 610 mg/m^3 [69].

Germanium hydride, GeH_4 , is a colorless, highly inflammable, toxic gas of low stability with a characteristic unpleasant odor. By inhalation, gaseous germanium hydride is the most toxic of germanium compounds. Inhalation of GeH_4 (70 mg/m^3 , minimally effective concentration) for 2–15 d caused nonspecific and nonpersistent changes in the nervous system,

kidneys, and blood composition. Like other metal hydrides such as AsH_3 , it shows hemolytic action in animals [78]. The lethal concentration in air is 150 ppm [79].

Chronic Toxicity. Symptoms of chronic germanium intoxication in experimental animals are mainly fatty degeneration of the liver and inhibition of growth: 1000 ppm neutralized GeO_2 (pH adjusted to 7) given in the diet of rats for 14 weeks depressed growth and caused 50% mortality; 5 ppm germanium administered as germanates in the drinking water of rats and mice resulted in decreased lifespan and mild fatty degeneration of the liver; 100 ppm GeO_2 in the drinking water for 4 weeks caused 50% mortality without hematological or gross pathological changes.

Exposure Limits. A TLV for germane of 0.2 ppm , equivalent to 0.64 mg/m^3 , was fixed by the TLV Committee of the American Conference of Governmental Industrial Hygienists in 1973 as an average limit of permissible exposure during an 8-h working day. No other TLVs for germanium or its compounds have been set in industrialized countries. Neither germanium nor its compounds are considered or suspected to exert a carcinogenic effect on humans or animals [80].

34.14 References

1. Landolt-Börnstein, GIII, 17a (1982) 87–126, 400–433.
2. Gmelin, System No. 45, Germanium Supplement Volume, 1958.
3. Kirk Othmer, 3rd ed. 11, pp. 791–802.
4. M. Lesbre, P. Mazerolles, J. Satge: *The Organic Compounds of Germanium*, J. Wiley & Sons, London 1971.
5. Roskill: *The Economics of Germanium*, 4th ed., Roskill Information Service Ltd., London 1984.
6. U.S.B.M., Minerals Yearbooks, U.S. Dept. of the Interior, Washington.
7. G. Cote, D. Bauer, *Hydrometallurgy* 5 (1980) 149–160.
8. A. De Schepper, *Hydrometallurgy* 1 (1976) 291–298.
9. MHO, US 3883634, 1975 (A. De Schepper, A. Van Peteghem).
10. MHO, US 4432951, 1984 (A. De Schepper, M. Coussemont, A. Van Peteghem).
11. MHO, US 4432952, 1984 (A. De Schepper, M. Coussemont, A. Van Peteghem).

12. MHO, EP 68540 B1, 1983 (A. De Schepper, M. Coussemont, A. Van Peteghem).
13. MHO, EP 68541 B1, 1983 (A. De Schepper, M. Coussemont, A. Van Peteghem).
14. Peñarroya, US 4389379, 1983 (D. Bauer, G. Cote, P. Fossi, B. Marchon).
15. Peñarroya, US 4568526, 1986 (G. Cote, P. Fossi, B. Marchon, D. Rouillard).
16. Peñarroya, EP-A 46437 A1, 1981 (D. Rouillard, G. Cote, P. Fossi, B. Marchon).
17. Peñarroya, EP-A 167414 A1, 1986 (D. Bauer, G. Cote, B. Marchon).
18. Preussag, DE-OS 3508041 A1, 1986 (K. Hanusch, W. Krajewski).
19. Cominco, US 4525332, 1985 (D. L. Ball, D. A. D. Boateng, G. M. Swinkels).
20. Ullmann, 4th ed., 12, 221-226.
21. P. Müllner, *Erzmetall* 30 (1977) no. 7/8, 326-329.
22. F. Hilbert, F. Stary, *Erzmetall* 35 (1982) no. 4, 184-189.
23. F. Stary, *Erzmetall* 35 (1982) no. 6, 311-313.
24. L. A. Painter, *Eng. Min. J.*, July 1980, 65-88.
25. I. de Ruijter, *Photonics Spectra* 21 (1987) no. 7, 55-59.
26. J. L. Hopkins, *Can. Metall. Bull.* 78 (1985) no. 879, 86-87.
27. P. B. Queneau, P. Avotins, L. Farais, *Can. Metall. Bull.* 79 (1986) no. 886, 92-97.
28. J. E. Hoffmann, *J. Met.* 6 (1987) 42-45.
29. R. Hasegawa, *Trans. Nat. Res. Inst. Metals (Jpn.)* 20 (1978) no. 2, 111-127.
30. V. J. Silvestri, *J. Electrochem. Soc.* 116 (1969) no. 1, 81-87.
31. V. N. Vigdorovich: *Purification of Metals and Semiconductors by Crystallisation*, Freund Publ. House, Tel Aviv 1971.
32. W. G. Pfann: *Zone Melting*, J. Wiley & Sons, New York 1958.
33. K. Hein, E. Buhrig: *Kristallisation aus Schmelzen*, VEB Deutscher Verlag für Grundstoffindustrie, Leipzig 1983.
34. A. F. Bogenschütz: *Ätzpraxis für Halbleiter*, Hause Verlag, München 1967.
35. P. J. Holmes: *The Electrochemistry of Semiconductors*, Academic Press, London 1962.
36. E. E. Haller, W. L. Hansen, F. S. Goulding, *Adv. Phys.* 30 (1981) no. 1, 93-138.
37. L. S. Darken, *J. Electrochem. Soc.* 126 (1979) no. 5, 827-833.
38. L. S. Darken, *IEEE Trans. Nucl. Sci.* NS 26 (1979) no. 1, 324-333.
39. P. W. Bridgman, *Proc. Am. Acad. Arts Sci.* 60 (1925) 305.
40. J. Czochralski, *Z. Phys. Chem.* 92 (1917) 219-221.
41. F. Rosenberger: *Fundamentals of Crystal Growth*, (Solid State Science no. 5) Springer Verlag, Berlin-Heidelberg-New York 1979.
42. J. C. Brice: *Crystal Growth Processes*, Blackie, Glasgow 1986.
43. A. A. Chernov, *Modern Crystallography III, Crystal Growth* (Solid State Science no. 36) Springer Verlag, Berlin 1984.
44. J. A. Savage, *Proc. SPIE Int. Soc. Opt. Eng.* 274 (1981) 175-179.
45. C. J. Hutchinson, C. Lewis, J. Savage, A. Pitt, *Appl. Opt.* 21 (1982) no. 8, 1490-1495.
46. L. Van Goethem, L. P. Van Maele, M. Van Sande, *Proc. SPIE Int. Soc. Opt. Eng.* 683 (1986) 160-165.
47. E. Simoen, P. Clauws, J. Vennik, *J. Phys. D:* 18 (1985) 2041-2058.
48. E. Rotsaert, P. Clauws, J. Vennik, L. Van Goethem, *Proc. Int. Conf. Shallow Impurity Centers, 2nd, Trieste* (1986).
49. G. Bambakidis, G. J. Brown, *Phys. Rev. B Condens. Matter* 33 (1986) no. 12, 8180.
50. E. Haller, W. Hansen, P. Luke, R. Murray, B. Jarrel, *IEEE Trans. Nucl. Sci.* NS 29 (1982) no. 1, 738-744.
51. W. Hansen, E. Haller, P. Luke, *IEEE Trans. Nucl. Sci.* NS 29 (1982) no. 1, 745-750.
52. G. Henze, *Fresenius Z. Anal. Chem.* 324 (1986) 105-110.
53. Y. A. Zololov, M. Grosserbauer, C. H. Morrison, Y. Karpov, *Pure Appl. Chem.* 57 (1985) no. 8, 1133-1152.
54. C. Verlinden, R. Gybels, F. Adams, *J. Anal. Atom. Spectr.* 1 (1986) 411-419.
55. J. A. Savage: *Infrared Optical Material and Their Antireflection Coatings*, Adam Hilger, Bristol 1985.
56. S. Musikant: *Optical Materials*, Dekker, New York 1985.
57. D. L. Wood, Kr. Walker, J. B. Macchesney, J. R. Simpson, R. Csencsits, *J. Lightwave Technol.* LT 5 (1987) no. 2, 277-285.
58. D. Hamed, G. Tilloc, *Proc. SPIE Int. Soc. Opt. Eng.* 400 (1983) 44-49.
59. P. Hugget, H. Lehmann, *J. Electron. Mater.* 14 (1985) no. 3, 205-230.
60. K. Wolf, B. Küsters, H. Helinger, C. Tchang, E. Schollmeyer, *Angew. Macromol. Chem.* 68 (1978) 23-27.
61. K. Butler: *Fluorescent Lamp Phosphors*, The Pennsylvania State Univ. Press, Pennsylvania 1980.
62. A. Horowitz, G. Kramer, *J. Cryst. Growth* 78 (1986) 121-128; 79 (1986) 296-301.
63. J. I. Pankove: *Optical Processes in Semiconductors*, Prentice Hall, Englewood Cliffs, NJ, 1971.
64. M. Van Sande, L. Van Goethem, H. Guislain, *Erzmetall* 38 (1985) no. 12, 588-593.
65. O. J. Gregory, E. C. Tisman, *Symposium on Integrated Circuit Fabrication and Technology* (Am. Chem. Soc.) 1984.
66. K. Asai: *Organic Germanium, A Medical Godsend*, Kogakusha, Tokyo 1977.
67. *Gmelin Handbook of Inorganic Chemistry*, System No. 45: Germanium, supplement volume, Springer Verlag, Berlin 1958.
68. H. Remy, *Lehrbuch der anorganischen Chemie*, volume 1, Akademische Verlagsgesellschaft, Leipzig 1965, pp. 637-643.
69. B. Venugopal, T. D. Luckey: "Metal Toxicity in Mammals", *Chemical Toxicity of Metals and Metalloids*, vol. 2, Plenum Press, New York-London 1978.
70. H. C. Dudley, *AMA Arch. Ind. Hyg. Occup. Med.* 8 (1953) 528.
71. H. C. Dudley, E. J. Wallace, *AMA Arch. Ind. Hyg. Occup. Med.* 6 (1952) 263.
72. G. Rosenfeld, E. J. Wallace, *AMA Arch. Ind. Hyg. Occup. Med.* 8 (1953) 466.
73. G. H. Bailey, B. P. Davidson, C. H. Bunting, *JAMA J. Am. Med. Assoc.* 84 (1925) 1722.
74. G. C. Harold, S. F. Meek, *Ind. Med.* 13 (1944) 326.
75. E. G. Rochow, B. M. Sindler, *J. Am. Chem. Soc.* 72 (1950) 1218.
76. J. E. Cremer, W. N. Aldridge, *Br. J. Ind. Med.* 21 (1964) 214.
77. NIOSH Registry of Toxic Effects of Chemical Substances, Washington, DC, 1976.
78. S. H. Webster, *J. Ind. Hyg. Toxicol.* 28 (1946) 167.
79. R. Kühn, K. Birett: *Merkmale Gefährliche Arbeitsstoffe*, vol. 5, Blatt Nr. C, 06, Verlag Moderne Industrie, München 1980.
80. Deutsche Forschungsgemeinschaft (ed.): *Maximale Arbeitsplatzkonzentration (MAK)*, Liste A1, A2, B, 1987, VCH Verlagsgesellschaft, Weinheim 1987.

35 Gallium

JÖRG FRIEDRICH GREBER (§§ 35.1–35.9); FATHI HABASHI (§ 35.10)

35.1 Introduction	1523	35.9 Toxicology and Industrial Medicine	1528
35.2 Physical Properties	1523	35.10 Compounds	1528
35.3 Chemical Properties	1523	35.10.1 Gallium(III) Compounds	1528
35.4 Occurrence and Raw Materials	1524	35.10.2 Gallium(II) and Gallium(I) Compounds	1529
35.5 Production	1524	35.10.3 Gallium Alkyls and Gallium Hydride	1530
35.6 Storage and Transportation	1527	35.11 References	1530
35.7 Uses	1527		
35.8 Economic Aspects	1527		

35.1 Introduction

Existence of gallium was predicted by MENDELEEV, and it was discovered by LECOQ DE BOISBAUDRAN in 1875. The metal was mainly of academic interest until 1970, when it was found that compounds of gallium with group 15 elements have semiconducting properties, and so began the extensive industrial use of the element. Gallium compounds are of particular value in optoelectronics, especially for light-emitting diodes.

35.2 Physical Properties

Gallium is a silvery-white metal, *mp* 29.78 °C, *bp* 2403 °C. The naturally occurring element contains two stable isotopes: ⁶⁹Ga (60.4%) and ⁷¹Ga (39.6%). The density of the liquid is 6.095 g/cm³ at 29.8 °C, and the density of the solid is 5.904 g/cm³ at 24.6 °C. There is a volume expansion of 3.2% on solidification.

Gallium forms orthorhombic crystals with the lattice constants *a* = 0.4523 nm, *b* = 0.45198 nm, and *c* = 0.76602 nm, and the physical properties are consequently strongly anisotropic. The thermal expansion coefficients are 1.65 × 10⁻⁵ K⁻¹ along the *a* axis, 1.13 × 10⁻⁵ K⁻¹ along *b*, and 3.1 × 10⁻⁵ K⁻¹ along *c*. The electrical properties are equally anisotropic, but it is not possible to quote reliable fig-

ures owing to the great influence of purity and temperature on the electrical conductivity.

35.3 Chemical Properties

[1–4]

Metallic gallium dissolves only slowly in dilute mineral acids, but rapidly in aqua regia and concentrated aqueous sodium hydroxide. It also dissolves slowly in solutions of hydrogen halides in ether.

In its compounds, the valency of gallium is usually 3. The monovalent state is unstable, although the monovalent gallium compounds Ga₂O and GaCl can be isolated. An oxidation state of 1+ has not yet been detected in aqueous solution, but some reactions of gallium indicate that it exists.

The oxygen compounds of gallium resemble those of aluminum in that there are high and low temperature forms of Ga₂O₃ and two hydroxides, Ga(OH)₃ and GaO·OH. Gallium halides have covalent character and therefore have good solubility in many nonpolar solvents in which they exist in dimeric form.

With elements of group 15, gallium forms binary compounds, of which GaP and GaAs are of great industrial importance. They may be prepared by direct combination of the elements at high temperature.

In aqueous solution, gallium forms octahedrally coordinated aquo ions [Ga(H₂O)₆]³⁺. There are many salts of oxoacids, such as the

sulfate, nitrate, and perchlorate, and also hydrated halides.

In aqueous solution, the hexaquo complex has an acid reaction owing to hydrolysis. Gallium salts of weak acids cannot exist in the presence of water for the same reason. Of the numerous anionic and cationic complexes, the most industrially important are the halide complexes, the $[\text{GaX}_4]^-$ ions, whose oxonium salts have good solubility in several organic solvents. This property is utilized in the extraction and purification of the metal. Other gallium complexes of industrial importance are the octahedrally coordinated chelates with p-diketones and 8-hydroxyquinolines, these also being soluble in organic solvents. Alcohols and organic derivatives may be prepared similarly to the analogous aluminum compounds.

Gallium forms a series of alloys with other metals, sometimes even at low temperatures. Some of these, containing up to 3% gallium, are useful in dentistry.

35.4 Occurrence and Raw Materials

With its natural abundance of 16 ppm, gallium is one of the rarer elements in the earth's crust. Gallium-containing minerals, the best known of which is a variety of germanite, do not have economic significance. Of the known locations, only the Apex mine in Utah has been commercially mined.

The greatest part of the world production of gallium is as a by-product of the production of aluminum oxide. The gallium concentration in bauxite ranges between 0.003 and 0.008%, depending on the location. The high contents occur in tropical bauxites such as Surinam bauxite, which contains 0.008% Ga, the highest average content known. The world supply of recoverable gallium in bauxite is estimated at 1.6×10^6 t based on bauxite reserves and their gallium contents [5].

The amount of gallium available from bauxite is determined by the amount of aluminum oxide that is produced. For the year 1986,

complete utilization of the gallium from aluminum oxide production would have corresponded to a theoretical production of ca. 2000 t of gallium. The gallium contained in zinc ore (sphalerite) has lost economic importance due to the changeover to hydrometallurgical methods of zinc extraction. The reserves of gallium in zinc ores worldwide has been estimated to be 6500 t [5].

The largest reserves of gallium are contained in phosphate ores and in coal of various kinds. When phosphorus is produced electrothermally from phosphate, the gallium is concentrated in the flue dust and may be recovered from it. Likewise, gallium may be obtained from the fly ash of coal, another material in which gallium is concentrated. Neither source is exploited at present because the gallium concentration is only 0.01–0.1%. It is not economic to treat these materials merely to extract the gallium. The total gallium reserves in phosphates and coals have been estimated at several million tonnes. They thus considerably exceed those in bauxite [5].

35.5 Production

The most important process for gallium production is the extraction of the metal from the circulating liquors in the Bayer process for aluminum oxide manufacture. These contain 70–150 mg/L of gallium, depending on the bauxite and on the concentration of the caustic liquor. The gallium content of the liquor is also determined by the dissolution process used. Bauxite which is high in boehmite ($\text{AlO} \cdot \text{OH}$) requires high temperatures for the dissolution process, leading to more complete release of the gallium and higher concentrations in the circulating liquors.

The gallium extraction plant is usually located within or very near to the aluminum oxide works. Part of the liquor stream is diverted for gallium extraction and then recycled. In some instances the liquor undergoes a preliminary purification process to remove certain heavy metals.

Three types of process are used to extract the gallium from the circulating liquor: (1) fractional precipitation, (2) electrolytic processes, and (3) extraction with chelating agents.

Fractional Precipitation. The basis of this process is that when the gallium-containing sodium aluminate solution is treated with carbon dioxide the first product precipitated is pure aluminum hydroxide. This increases the gallium content of the liquor. Further treatment then causes the gallium to separate along with more aluminum hydroxide. After this, fractional precipitation gives an aluminum hydroxide richer in gallium, and this is followed by one or more further fractional precipitations. The gallium-enriched aluminum hydroxide is dissolved in aqueous sodium aluminate and sodium gallate, from which gallium is obtained by electrolysis.

The precipitation process is used only to a small extent because of the expense of removing the by-product sodium carbonate unless thermal decomposition is used in the aluminum oxide works. Also, on account of the many precipitation stages involved, the process is labor intensive and can therefore be used only when energy and labor costs are low. China produces gallium at a rate of 5 t/a by this process.

Electrolytic Processes. The electrolytic process depends on the fact that mercury forms an amalgam with gallium from which the gallium may be extracted with a caustic soda solution. The gallium amalgam can be produced either directly (Alusuisse process) or indirectly (VAW/INGAL process).

In the Alusuisse process, the gallium is deposited directly onto the mercury cathode, using the appropriate conditions of temperature, agitation, and current density, and an amalgam is formed. In the VAW process, sodium amalgam is used to reduce the gallium present in the Bayer liquor. This gives an amalgam from which the gallium is removed by treatment with caustic alkali, and the mercury is then used again to produce sodium amalgam, i.e., the mercury circulates in a closed system.

Reduction processes have in recent years become less attractive because they require special conditions to be commercially viable. In particular, the aluminate solutions must contain over 150 g/L sodium and be very low in vanadium, tungsten, molybdenum, and iron so that the electrolytic current efficiency reaches economically acceptable values. However, such highly concentrated liquors are not produced in modern aluminum oxide plants, and therefore the electrolytic process can no longer be used in new installations. The environmental problems associated with mercury further discourage the use of electrolytic processes. These processes are, however, in operation in Hungary, former Czechoslovakia, and Germany. About 15–20 t/a of gallium is produced.

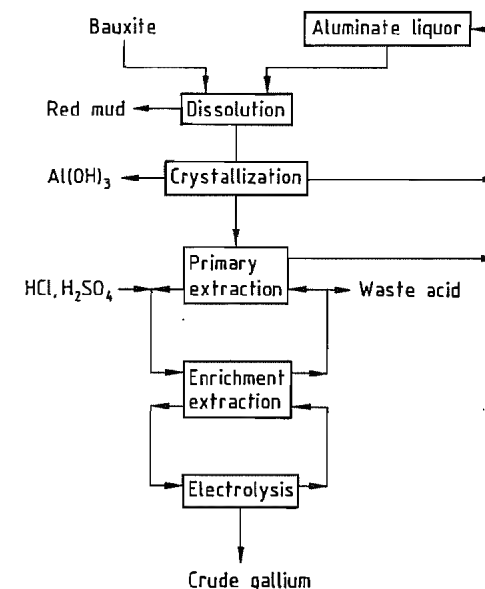


Figure 35.1: Flow diagram showing gallium extraction by the Rhône-Poulenc and Sumitomo processes.

Extraction with Chelating Agents. The discovery was made in 1974 that hydroxyquinolines could be used to extract gallium from sodium aluminate liquors (the Rhône-Poulenc process, Figure 35.1) [6], these substances having earlier been developed for the hydrometallurgical extraction of copper. The aluminate liquor is brought into contact with a

solution of Kelex 100 in kerosene. Gallium is thereby extracted from the liquor along with aluminum and sodium. Most of the elements extracted with the gallium may be stripped from the extraction medium by treatment with dilute acid. The gallium is then extracted with concentrated acid; either hydrochloric or sulfuric acid may be used. Gallium concentrations of 0.1–10 g/L may be reached in the acid extract, depending on the method used. The gallium to aluminum concentration ratio in the extract can reach values as high as 1, which corresponds to enrichment factors of up to 1000 in the primary extraction stage.

Further concentration of the gallium is achieved by anion- or cation-exchange treatment of the acid extract from the first stage. The metal can be isolated from this concentrate by direct electrolysis.

Although the process solutions are recirculated to a large extent, considerable quantities of waste acid are generated. This waste acid is contaminated with other extracted metals and residues from the extraction media. An important economic factor in the extraction process is therefore the possibility to dispose of these solutions cheaply or to make some use of them.

In the Sumitomo process (Figure 35.1) the first stage is extraction with the ion-exchange resin Duolite CS-346 (Diamond Shamrock) [7]. This resin contains amidoxime groups, which form chelate bonds to gallium. Unlike Kelex 100, this resin has the drawback that any vanadium extracted from the aluminate liquors blocks the ion exchange sites. Vanadium must therefore be removed from the circulating liquor of the aluminum oxide plant before gallium extraction. The rest of the Sumitomo process corresponds to the Rhône-Poulenc process.

Gallium is produced by extraction processes in France and Japan.

Purification. The gallium from extraction processes has a purity of 99–99.9%. For most applications, however, much higher purities are necessary, reaching 99.99999% (8N). Various procedures are used to remove the im-

purities. Volatile metals, such as mercury and zinc, are distilled off under vacuum. Further purification is effected by washing with aqueous acids and alkalis. The purest gallium is obtained by fractional crystallization, zone melting, or single crystal growth. Other methods of purification include the extraction of gallium chloride from acid solution and fractional distillation of liquid gallium compounds.

Environmental Protection. No harmful effects of gallium or its compounds have been reported. There are therefore no regulations concerning gallium concentrations in exhaust gases from gallium manufacturing plants. For the materials used in gallium manufacture, such as mercury or 8-hydroxyquinoline, the relevant legal requirements must be observed.

Quality. The commercially available materials include a crude grade and various pure grades of gallium. The crude metal contains 99–99.9% gallium. The material for semiconductor manufacture is used in purities from 99.9999% (6N) to 99.999999% (8N).

Analysis. Gallium is determined in raw materials and partially enriched intermediate products either by complexometric titration (high concentrations) or atomic absorption (low concentrations).

For the analysis of the purest grades of gallium it is necessary to have methods of determining impurities at parts per million to parts per billion levels. The most important technique is spark source or glow discharge mass spectrometry which enables heavy metals to be determined with sufficient accuracy. Lighter elements can be determined by activation analysis or by special mass spectrometric techniques.

A general assessment of gallium purity may be made from its residual resistance ratio. This is determined from the electrical conductivity of a gallium single crystal at room temperature and at liquid helium temperature. This ratio is very sensitive to the presence of impurities but is nonspecific. Typical values for high purity gallium are better than 55 000.

35.6 Storage and Transportation

The low melting point of gallium and the high purity requirements mean that care must be taken to prevent gallium from melting or being contaminated by the packing materials during storage and transportation. The metal is usually sold in lumps of 10 g–2 kg, individually packed and kept cold in plastic containers.

For short distances, gallium may be carried by truck or rail, provided that the temperature is not allowed to exceed 20 °C. For carriage over long distances, the method chosen is usually air transport, in which uninterrupted cooling is to be maintained. Regulations governing packaging for air transport have been laid down by IATA owing to the ability of gallium to form alloys with aluminum at normal temperatures, these alloys having very low mechanical strength. Gallium must be contained inside seven layers of packing material and in warm weather the container must be cooled. In this way, the danger of an accident in which the structural metal of the aircraft is attacked by liquid gallium can be reduced. In addition, there is a limit imposed on the amount of gallium which may be carried in an aircraft.

35.7 Uses

The main use of gallium is as a raw material in the manufacture of semiconductors which are formed by the combination of gallium with elements of group 15 (especially P and As). They have certain advantages over other semiconductor materials: (1) faster operation with lower power consumption, (2) better resistance to radiation and, most importantly, (3) they may be used to convert electrical into optical signals.

The largest proportion of the gallium produced worldwide goes to the manufacture of the arsenide or phosphide for the production of light-emitting diodes. The manufacture of integrated circuits using gallium arsenide is still at the development stage. A small proportion of the gallium produced is converted into

the oxide for manufacture of gallium–gadolinium garnets [8]. These are used to produce magnetic bubble memories.

35.8 Economic Aspects

In 1986, 50 t gallium was used worldwide (Figure 35.2), mainly in the manufacture of light-emitting diodes and other optoelectronic components.

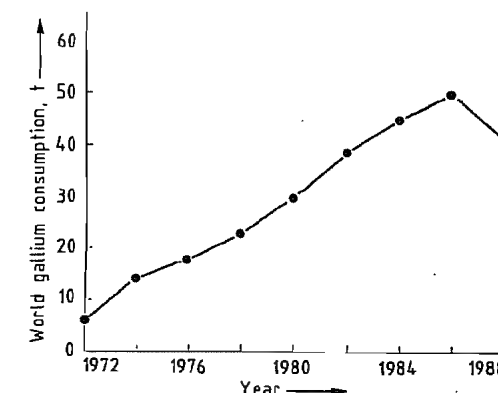


Figure 35.2: World gallium consumption.

About 65% of the market is in Japan, 20% in the United States, and 15% in Europe. The price has fallen continuously since 1970 and in 1986 reached \$450 or 77 000 yen per kg for 6N gallium. The total value of the gallium used worldwide in 1986 was therefore \$22 × 10⁶ (3.85 × 10⁹ yen). Gallium is extracted in Western Europe, Japan, and several countries of the Eastern Bloc. Production levels in the former Soviet Union, former East Germany, Hungary, and former Czechoslovakia are not known exactly as only a small part of the gallium produced there is exported.

The following companies produce gallium: INGAL (Germany), Rhône-Poulenc (France), Sumitomo (Japan), and Dowa Mining (Japan). Musto Mining (USA), Eagle Picher (USA), Alcan (Canada), and Cominco (Canada) have ceased production.

In addition to these producers of primary gallium, a number of companies recover pure gallium from gallium scrap. World gallium production increased from 17 800 kg in 1978

to 46 200 kg in 1984, but decreased to 40 000 kg in 1988 (Table 35.1).

Table 35.1: Gallium production in kilograms of gallium for 1978, 1984, and 1988.

Region and country	Year		
	1978	1984	1988
Europe			
Czechoslovakia		2 000	2 000
France	2 000	10 000	8 000
Germany	4 000	8 000	8 000
Hungary	1 000	3 000	2 000
Others	1 000	1 200	2 000
Asia			
Japan	200	13 000	12 000
China	600	5 000	5 000
United States	8 000	3 000	
Others	1 000	1 000	1 000
Total	17 800	46 200	40 000

35.9 Toxicology and Industrial Medicine

Gallium is only slightly toxic. No industrial injury caused by the metal or its compounds during gallium production and processing has been reported. An investigation in 1984 and 1985 by the Chemical Trade Association did not reveal any evidence of damage to health caused by gallium.

35.10 Compounds [9, 10]

Gallium is ordinarily trivalent in its compounds. The salts are colorless, and are more strongly hydrolyzed in solution than the salts of aluminum, which they closely resemble in properties. Like aluminum it is precipitated as the white oxide hydrate from solutions of its salts by any substance which disturbs the hydrolysis equilibrium by reducing the hydrogen ion concentration. Tartaric acid hinders the precipitation, by forming complexes with gallium, as it does with aluminum.

For bivalent gallium, the halides GaCl_2 and GaBr_2 , and the chalcogenides GaS , GaSe , and GaTe are known, but not gallium(II) oxide. Gallium(II) compounds readily undergo oxidation, or disproportionation to give gallium(III) compounds and gallium metal. Gallium(I) compounds are still less stable, and

in only a few cases has their existence been proved. The sulfide, Ga_2S_3 , and the selenide, Ga_2Se_3 , exist, but may be metastable at ordinary temperature. The existence of a volatile hydride of gallium is notable.

Table 35.2: Gallium halides.

	Density, g/cm ³	mp, °C	bp, °C	Heat of formation, kcal/mol
GaCl_3	2.47	77.9	201.3	
GaBr_3	3.69	121.5	279	92.4
GaI_3	4.15	212	346	51.0
GaF_3	4.47	800 (subl.)		

35.10.1 Gallium(III) Compounds

Table 35.2 summarizes gallium halides.

Gallium(III) chloride, GaCl_3 , forms long white crystals. It may be obtained by heating gallium in a stream of chlorine or of hydrogen chloride. Vapor density determinations have shown that in the neighborhood of the boiling point, the vapor consists of double molecules, Ga_2Cl_6 similar to Al_2Cl_6 . At 600 °C the vapor density corresponds to that required by the formula GaCl_3 . Fused gallium chloride is practically a non-conductor of electricity. The heat of formation of GaCl_3 is 125 kcal per mol. Gallium(III) chloride combines exothermically with water. It fumes in moist air, since it forms hydrogen chloride by hydrolysis. Its aqueous solution is acidic and readily deposits the hydroxide. Gallium(III) chloride can be extracted by means of ether from its 6-N HCl solutions and this property can be used to effect a separation of gallium from other elements.

Gallium Bromide and Gallium Iodide. Gallium bromide, GaBr_3 , and gallium iodide, GaI_3 , resemble the chloride in properties. Electron diffraction measurements show that both the chloride and bromide exist as dimeric molecules in the vapor state.

Gallium fluoride, GaF_3 , sublimes at 950 °C and is only slightly soluble in water or dilute hydrochloric acid. The hydrate, $\text{GaF}_3 \cdot 3\text{H}_2\text{O}$, obtained by dissolution of gallium(III) oxide hydrate in aqueous hydrofluoric acid, is soluble in dilute hydrochloric acid, and the gallium

must therefore be complexed. Addition of NH_4F to the solution yields octahedral crystals of $(\text{NH}_4)_3[\text{GaF}_6]$.

Gallium(III) oxide, Ga_2O_3 , is best obtained by heating the nitrate or sulfate. It is a white powder, which like aluminum oxide, loses its solubility in acids and caustic alkalis when it is strongly ignited. It is reduced to the metal when it is heated in hydrogen; Ga_2O may be formed as an intermediate stage. Gallium(III) oxide is polymorphic, like alumina. The modification stable below 600 °C (α - Ga_2O_3) has the corundum structure; the form stable at high temperatures (β - Ga_2O_3) is either rhombic or monoclinic. Ignition of gallium nitrate at low temperatures yields a modification (δ - Ga_2O_3). Ga_2O_3 also forms double oxides of spinel structure with MgO and ZnO .

Gallium Oxide Hydrate and Gallium Hydroxide. Substances which lower the hydrogen ion concentration throw down a white gelatinous precipitate from Ga(III) salt solutions. This precipitate is amorphous to x-rays and has a variable water content (gallium oxide hydrate, $\text{Ga}_2\text{O}_3 \cdot x\text{H}_2\text{O}$). It dissolves both in acids and in strong bases, and differs from aluminum oxide hydrate in being soluble in ammonia solutions. As the precipitate ages, its solubility in caustic alkalis diminishes.

A microcrystalline gallium(III) hydroxide of definite composition can be obtained by slow precipitation from both alkaline and acidic solutions. This is gallium oxide hydroxide, GaO(OH) , which has the α - AlO(OH) or diasporite structure. The same compound is formed by hydration of α - and δ - Ga_2O_3 with steam under certain conditions. Alkaline solutions of gallium hydroxide contain salts known as gallates.

Gallium(III) sulfide, Ga_2S_3 , is isolated by direct union of the elements. Reaction proceeds to completion only at high temperatures (1200 °C). Gallium(III) sulfide is yellow, with a mp of about 1225 °C and d 3.48. It is decomposed by water, with evolution of H_2S , and reduced by hydrogen at 800 °C to gallium(II) sulfide, GaS . This is a yellow solid, with a mp

of about 965 °C and d 3.75. It is stable towards water, but decomposes when it is heated in vacuum:



The gallium(I) sulfide so formed is a grey black sublimate (d 4.22), which decomposes into $\text{Ga}_2\text{S}_3 + \text{Ga}$ when it is heated again.

Gallium sulfate, $\text{Ga}_2(\text{SO}_4)_3$, crystallizes from aqueous solutions as an 18-hydrate similar to $\text{Al}_2(\text{SO}_4)_3 \cdot 18\text{H}_2\text{O}$, as white clusters. It can be dehydrated by heating, and decomposes above 520 °C with loss of SO_3 . With ammonium sulfate, it forms the double salt $(\text{NH}_4)_2\text{Ga}(\text{SO}_4)_2 \cdot 12\text{H}_2\text{O}$, ammonium gallium alum. Among the basic double sulfates, the compound $(\text{NH}_4)_2(\text{GaO})_2(\text{SO}_4)_2 \cdot 4\text{H}_2\text{O}$ is isotypic with the mineral alunite, $\text{K}(\text{AlO})_3(\text{SO}_4)_2 \cdot 3\text{H}_2\text{O}$.

Gallium nitrate crystallizes from nitric acid solutions as the octahydrate, $\text{Ga}(\text{NO}_3)_3 \cdot 8\text{H}_2\text{O}$, in colorless, highly refractive deliquescent prisms (mp ca. 65 °C). The hydrate is converted to the anhydrous salt, $\text{Ga}(\text{NO}_3)_3$, when it is warmed to about 40 °C in dry air.

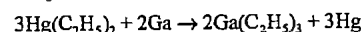
Gallium nitride, GaN , is obtained as a dark grey powder (d 6.10) by heating the metal in ammonia at 900–1000 °C. It is unattacked by most acids, but is slowly converted to Ga_2O_3 when it is heated in air.

35.10.2 Gallium(II) and Gallium(I) Compounds

Gallium(II) chloride, GaCl_2 , is formed by the incomplete combustion of gallium in chlorine, or by heating gallium(III) chloride with metallic gallium. It forms colorless transparent crystals (mp 170.5 °C, bp ca. 535 °C). At 1000 °C, the vapor density of gallium(II) chloride corresponds to the molecular formula GaCl_2 . At lower temperatures, polymeric molecules are also present and at higher temperatures some dissociation occurs. Gallium(II) chloride reacts vigorously with water with hydrogen evolution. Gallium(II) bromide resembles the chloride.

35.10.3 Gallium Alkyls and Gallium Hydride

Gallium triethyl. $\text{Ga}(\text{C}_2\text{H}_5)_3$, is obtained by the action of metallic gallium on mercury diethyl:



It is a colorless, unpleasant smelling liquid (d 1.058, mp -82.3°C , bp 142.8°C). It inflames in air, and is decomposed by water with explosive violence. Gallium trimethyl, $\text{Ga}(\text{CH}_3)_3$, (mp -15.8°C) can be obtained in the same way as the triethyl.

Gallium hydride. Gallium trimethyl reacts with hydrogen, under the influence of the electrical glow discharge, to form tetramethyl digallane, $\text{Ga}_2\text{H}_2(\text{CH}_3)_4$, a colorless, viscous liquid. When this is heated above 130°C , it decomposes into $\text{Ga}(\text{CH}_3)_3$, Ga, and H_2 . Acting on the hypothesis that this reaction involved a disproportionation into $\text{Ga}(\text{CH}_3)_3$ and Ga_2H_6 . The addition of trimethylamine, with which gallium trimethyl forms the stable compound $(\text{CH}_3)_3\text{Ga} \cdot \text{N}(\text{CH}_3)_3$, brought about reaction at ordinary temperature. Gallium

hydride could then be isolated without decomposition. It is a colorless, mobile liquid (mp -21.4°C , bp 139°C), which decomposes fairly rapidly above 130°C into Ga and H_2 . The molecular weight corresponds to the formula Ga_2H_6 (digallane), corresponding in complexity and structure (hydrogen bridged structure) to diborane.

35.11 References

1. F. A. Cotton, G. Wilkinson: *Advanced Inorganic Chemistry*, 4th ed., Wiley, New York 1980, pp. 326–351.
2. *Gmelin*, 8, System no. 36.
3. *Gmelin*, Organogallium Compounds, Part 1 (1987).
4. I. A. Sheka, I. S. Clans, T. T. Mityureva: *The Chemistry of Gallium*, Elsevier, Amsterdam 1966.
5. F. E. Katrak, J. C. Agarwal, *J. Met.* 33 (1981) no. 9, 33.
6. Rhône-Poulenc, FR 2307047, 1974 (J. Helgorsky, A. Leveque).
7. Sumitomo Chem. Comp., EP 0076404, 1983.
8. Vereinigte Aluminiumwerke AG, DE 2517292, 1975 (H. Pfundt, M. Fuchs, P. Voß).
9. *Gmelin Handbook of Inorganic Chemistry*, System No. 36: Gallium, Springer Verlag, Berlin 1936.
10. H. Remy, *Lehrbuch der anorganischen Chemie*, volume 1, Akademische Verlagsgesellschaft, Leipzig 1965, pp. 445–449.

36 Indium

NOËL FELIX

36.1 Introduction	1531	36.6 Quality Specifications	1537
36.2 History	1531	36.7 Analysis	1537
36.3 Properties	1531	36.8 Compounds	1537
36.4 Resources and Raw Materials	1532	36.9 Uses	1538
36.5 Production	1532	36.10 Economic Aspects	1539
36.5.1 Production from Zinc Circuits	1532	36.11 Toxicology and Occupational Health	1540
36.5.2 Production from Lead Circuits	1534	36.12 References	1540
36.5.3 Production from Tin Circuits	1536		
36.5.4 Recent Production Developments	1536		
36.5.5 Refining	1536		

36.1 Introduction

Indium, atomic number 49, is a metallic element of group 13 of the periodic table. Indium has two natural isotopes: ^{115}In (95.72%) and ^{113}In (4.28%). The abundance of indium in the earth crust is comparable to that of silver, i.e., 0.1 ppm [1].

36.2 History

Indium was discovered in 1863 by F. REICH and T. H. RICHTER during spectrometric analysis of sphalerite ores at the Freiberg School of Mines in Germany [2]. Indium is named after the indigo blue spectral lines that led to its identification.

36.3 Properties [3–8]

Indium is a crystalline, silvery white metal, which is very soft (softer than lead), ductile, and malleable. Indium retains its highly plastic properties at cryogenic temperatures. Indium can be deformed almost indefinitely under compression, is easily cold-welded, and, like tin, emits a high-pitched “cry” on bending.

Indium generally increases the strength, corrosion resistance, and hardness of an alloy system to which it is added. Even small con-

centrations of indium can have a considerable influence.

Molten indium wets clean glass. Indium has a low melting point (429.75 K) but a high boiling point (2353.15 K). Indium becomes superconducting at 3.37 K .

Some physical properties of indium are as follows [3, 5, 7]:

Electronic configuration	$[\text{Kr}] 4d^{10}5s^25p^1$
Thermal neutron cross section at 2200 m/s absorption	$(194 \pm 2) \times 10^{-28} \text{ m}^2/\text{atom}$
scattering	$(2.2 \pm 0.5) \times 10^{-28} \text{ m}^2/\text{atom}$
Crystal structure	tetragonal A6 $a_0 = 0.458 \text{ nm}$ $c_0 = 0.494 \text{ nm}$
Number of atoms per unit cell	4
Atomic radius (coordination number 12)	0.162 nm
Ionic radius (In^{3+} , coordination number 6)	0.081 nm
Atomic volume	$15.73 \times 10^{-6} \text{ m}^3/\text{mol}$
Density at 20°C	7.310 g/cm^3
mp	429.75 K
bp	2353.15 K
Enthalpy of fusion	3.26 kJ/mol
Enthalpy of vaporization	231.2 kJ/mol
Specific heat at 25°C	$26.70 \text{ kJ mol}^{-1} \text{ K}^{-1}$
Entropy at 25°C	$57.7 \text{ kJ mol}^{-1} \text{ K}^{-1}$
Entropy of fusion	$7.58 \text{ kJ mol}^{-1} \text{ K}^{-1}$
Entropy of vaporization	$98.56 \text{ kJ mol}^{-1} \text{ K}^{-1}$
Coefficient of linear expansion (0 – 100°C)	$3 \times 10^{-5} \text{ K}^{-1}$
Vapor pressure p , kPa, at temp. T , K, between mp and bp	$\log p = 9.835 - 12860/T - 0.7 \log T$
Thermal conductivity (0 – 100°C)	$71.1 \text{ W m}^{-1} \text{ K}^{-1}$
Surface tension at temperature T , N/m	$0.602 - 10^{-4}T$
Electrical resistivity at 3.38 K	superconducting

at 273.15 K	$8.4 \times 10^{-4} \Omega \text{m}$
temperature coeff. (0–100 °C)	$4.9 \times 10^{-3} \text{ K}^{-1}$
Standard electrode potentials	
$\text{In}^{3+} + 3\text{e}^- = \text{In}$	–0.338 V
$\text{In}^{3+} + 2\text{e}^- = \text{In}^+$	–0.40 V
$\text{In}^{2+} + \text{e}^- = \text{In}^+$	–0.40 V
$\text{In}^{3+} + \text{e}^- = \text{In}^{2+}$	–0.49 V
Brinell hardness	0.9
Tensile strength	2.645 MPa
Modulus of elasticity	10.8 GPa

Metallic indium is not oxidized by air or oxygen at room temperature. It reacts directly with arsenic, antimony, the halogens, oxygen, phosphorus, sulfur, selenium, and tellurium when heated. Indium dissolves only slowly in cold dilute mineral acids, but more readily in hot dilute or concentrated acids. Alkalis do not attack the massive metal. Indium forms alloys with most other metals. Extensive solid solutions are formed with lead, thallium, and mercury.

Table 36.1: Indium contents of some minerals [9]. (Reproduced from Roskill: *The Economics of Indium*, 4th ed., 1987, by permission of the publisher, Roskill Information Services Ltd.)

Mineral	Composition	Indium content, ppm
Sphalerite	ZnS	0.5–10 000
Galena	PbS	0.5–100
Chalcocite	Cu_2S	0–1500
Enargite	Cu_3AsS_4	0–100
Bornite	Cu_5FeS_4	1–1000
Tetrahedrite	$(\text{Cu, Fe})_{12}\text{Sb}_4\text{S}_{13}$	0.1–160
Covellite	CuS	0–500
Chalcocite	Cu_2S	0–100
Pyrite	FeS_2	0–50
Stannite	$\text{Cu}_3\text{FeSnS}_4$	0–1500
Cassiterite	SnO_2	0.5–13 500
Wolframite	$(\text{Fe, Mn})\text{WO}_4$	0–16
Arsenopyrite	FeAsS	0.3–20

36.4 Resources and Raw Materials [9]

Indium does not occur in the native state. It is widely spread in nature, generally in very low concentrations. The content of indium in the earth crust is estimated to be 0.1 ppm. Indium is found as a trace element in many minerals (Table 36.1).

Sphalerite is the most important indium-containing mineral followed by lead and copper sulfides. The amount of indium in sphalerite may vary widely even within a deposit. The

indium concentration is typically 10–20 ppm, but may be as high as 1% (10 000 ppm). A sphalerite deposit with a very high indium content (0.2–0.3%) is the Huari Huari zinc deposit in Bolivia. Tin deposits with high indium contents (up to 0.21%) are found in Cornwall (United Kingdom) and New Brunswick (Canada).

36.5 Production

During smelting processes for the recovery of base metals, indium concentrates in by-products such as residues, flue dusts, slags, and metallic intermediates. The processes for the recovery and production of indium are often complex and sophisticated; they are characterized by a low direct extraction efficiency. Therefore, the recycling of the indium contained in intermediate products is important.

36.5.1 Production from Zinc Circuits

A process for the recovery of indium from secondary zinc oxide is described in [10, 11]. The process is illustrated in Figure 36.1. In the first step, most of the zinc is removed by leaching with dilute sulfuric acid. The residue is leached with dilute hydrochloric acid to dissolve the indium. Tin is removed from the indium solution by neutralization to pH 1. Further neutralization then precipitates indium. The indium residue is leached with sodium hydroxide to give crude indium hydroxide as an intermediate product. Dissolution of this indium hydroxide in dilute hydrochloric acid gives an indium solution which is purified by cementation of copper and arsenic with iron, followed by cementation of tin and lead with indium. Indium is recovered from the purified solution by cementation with aluminum.

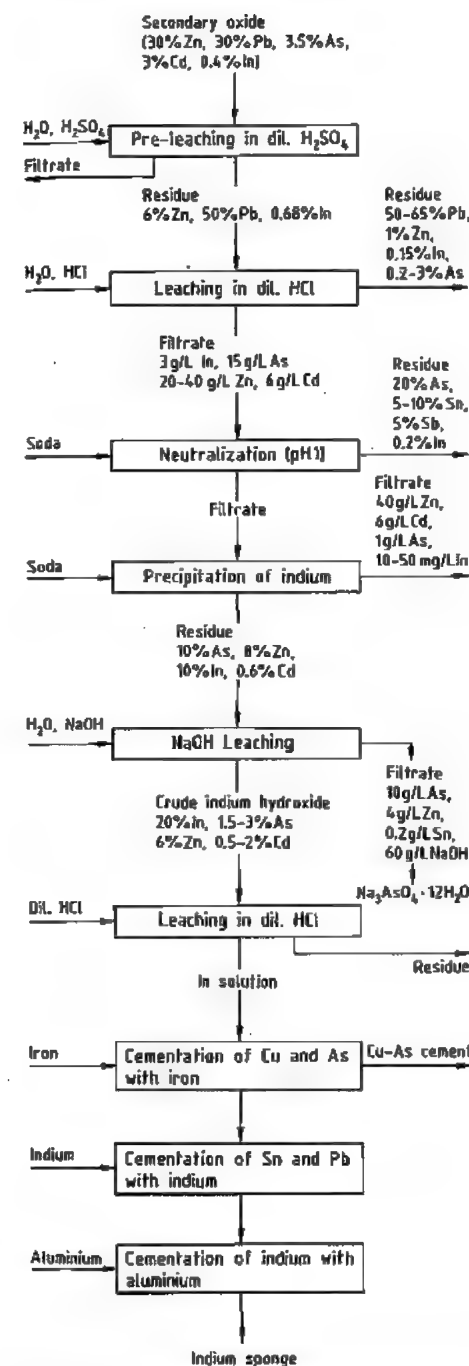


Figure 36.1: Recovery of indium from secondary zinc oxide [10, 11].

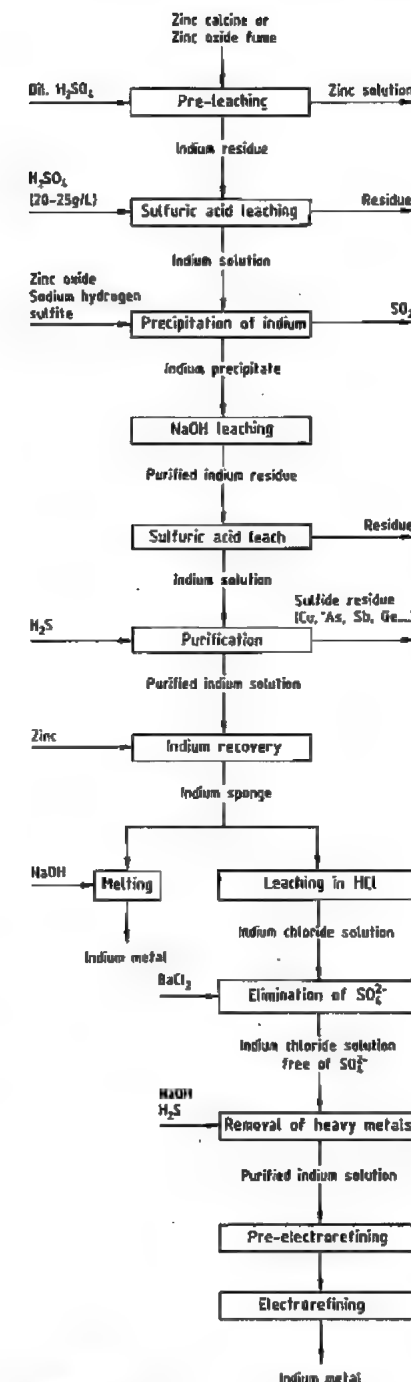


Figure 36.2: Indium recovery by Anaconda Copper Mining Company [12].

In the process developed by the Anaconda Copper Mining Company (Figure 36.2), indium is recovered from zinc calcine (roasted zinc blende) or zinc oxide fume [12]. Zinc calcine or zinc oxide fume is first leached in sulfuric acid at moderate pH, dissolving the bulk of the zinc and leaving indium in the residue.

In the second step, indium is dissolved from the residue by leaching with sulfuric acid (20–25 g/L H_2SO_4). Indium is precipitated from the resulting solution by adding zinc oxide and sodium hydrogen sulfite. The indium precipitate is purified by leaching with concentrated sodium hydroxide, washing with water and with dilute sulfuric acid to remove zinc. The purified residue is dissolved in sulfuric acid, heavy metals are precipitated with hydrogen sulfide, and indium is recovered as a sponge by adding zinc. The indium sponge may be melted with sodium hydroxide and cast into bars. Alternatively, the sponge may be purified by dissolving it in hydrochloric acid and adding barium chloride to remove sulfate, and hydrogen sulfide to remove heavy metals. After filtration, indium is recovered from the solution by electrolysis.

The extraction of indium from sphalerite of the Rammelsberg and Bad Grund deposits in Germany is described in [13]. On refining the retort zinc by distillation, indium remains with the lead. After oxidation of the lead residue, indium is recovered from the litharge, which contains 1–4% indium. The litharge is leached with sulfuric acid, which dissolves 88–97% of the indium. Indium is recovered by addition of zinc slabs to give a crude indium sponge containing ca. 95% indium. The crude indium is redissolved in sulfuric acid. The resulting solution is purified first by cementation with indium strips to remove tin and then with slabs of a zinc alloy, containing 1% indium and 0.3% cadmium, to remove thallium and cadmium. Indium with a purity of greater than 99.99% is recovered from the purified solution by precipitation with aluminum strips followed by melting under sodium hydroxide and sodium cyanide.

Chlorination of the lead retort residue under a molten salt cover for the extraction of in-

dium has been patented by Asarco [14]. The chloride slag is dissolved in water and indium is recovered by cementation on zinc or aluminum.

At the zinc refinery of Mitsubishi in Akita [15], indium is recovered from the leach residue (400 ppm In) of the zinc concentrate (120 ppm In). The residue is treated by a sulfation roasting process. Leaching of the sulfated product in sulfuric acid dissolves about 60% of the indium to give a leach solution containing 50–70 mg/L of indium. This solution is concentrated to an indium content of 2 g/L by double neutralization with calcium carbonate. The enriched solution is then subjected to solvent extraction followed by back extraction with hydrochloric acid. The aqueous solution is concentrated to 20–30 g/L indium. Indium is recovered by immersing aluminum plates in the solution. Indium sponge adhering to the aluminum plates is removed for melting and casting into anodes. Indium metal of 99.99% purity is then obtained by electrorefining.

36.5.2 Production from Lead Circuits

At Cominco's integrated lead–zinc smelter at Trail in Canada, tin and indium accumulate in the fumes of the continuous dressing furnace [16]. The flow sheet for the process is illustrated in Figure 36.3. A mixture of fumes, coke, and antimony-containing slag is melted in a direct-fired rotary furnace. Arsenic is removed by adding scrap iron to form iron speiss. The residual tin–indium–antimony–lead alloy is cast into anodes and electrolyzed in a fluorosilicate solution, giving a solder cathode (Sn–Pb alloy) and indium–antimony anode slimes. The slimes are roasted with sulfuric acid. Indium is dissolved from the sulfated product by leaching with water. Copper is removed from the indium solution by cementation on indium sheets. Indium is then recovered from the solution as a sponge by addition of aluminum or zinc. The indium sponge is melted and electrorefined to give indium of 99.99% purity.

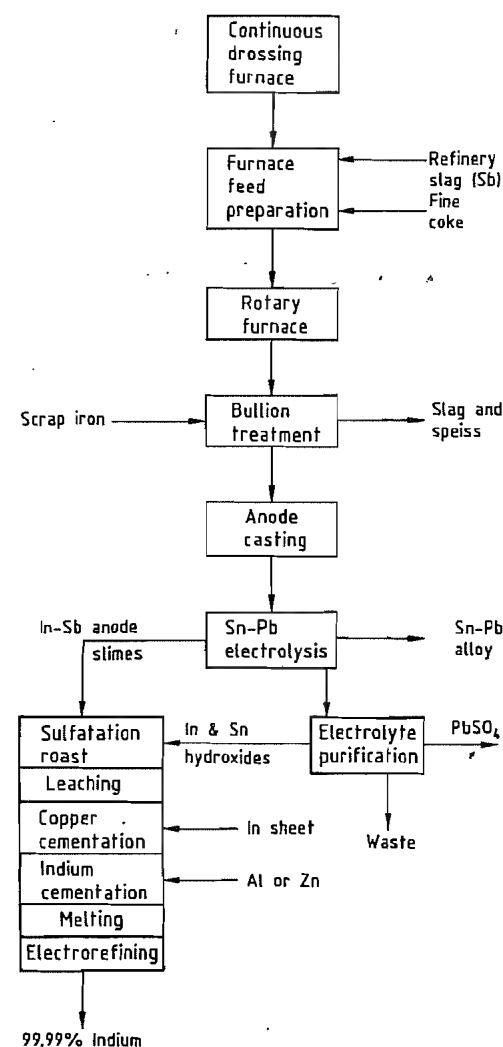


Figure 36.3: Indium recovery by Cominco [16]. (Previously published in the Proceedings of the Symposium on Quality Control in Non-Ferrous Pyrometallurgical Processes from the 24th Annual Conference of Metallurgists, August 1985. Reprinted with permission of the Canadian Institute of Mining and Metallurgy.)

Indium is recovered from lead bullion by Centromin of Peru at the La Oroya smelter, and by Metallurgie Hoboken-Overpelt (MHO) at the Hoboken smelter. At MHO, indium concentrates in a complex residue during refining of lead by the Harris process [17]. At the La

Oroya refinery, lead bullion is first drossed to remove copper, then tin and indium are removed at a higher temperature [18, 19]. The tin–indium dross is reduced to metal using coke, a mixture of lead and zinc chlorides is added, and indium is recovered as indium chloride in the slag.

The chloride slag of indium, lead, zinc, and tin is leached by wet grinding. The solution is purified by cementation of lead and tin on indium sheet. Indium is recovered as a sponge by adding zinc.

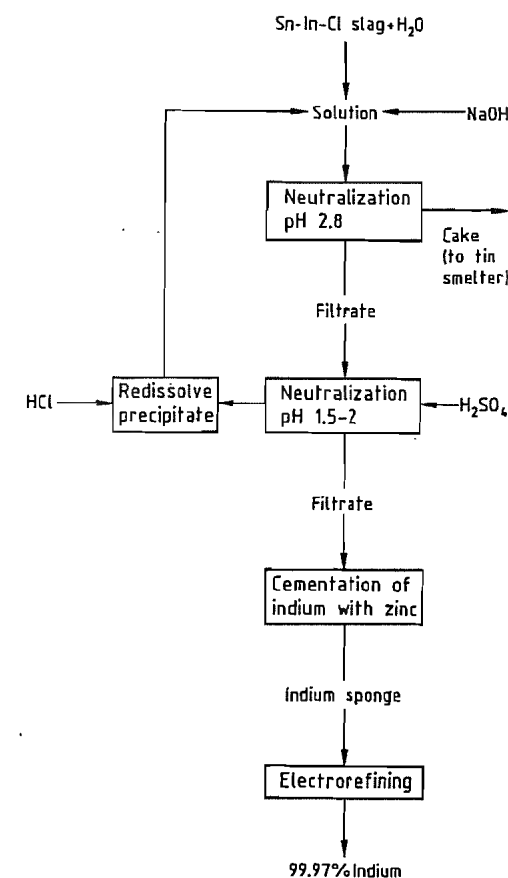


Figure 36.4: Indium recovery by Copper Pass [21]. (Reproduced by permission of the Institution of Mining and Metallurgy, from P. Halsall: Indium—Extraction from Lead, Zinc and Tin circuits (Figure 9). Trans. Instn. Min. Metall. (Sect. C: Mineral Process. Extr. Metall.) 97, 1977, C98.)

36.5.3 Production from Tin Circuits

At Capper Pass, chlorination of electrorefined tin gives a tin chloride slag which contains 2.7% indium [20]. This slag is treated as shown in Figure 36.4 [21]. Most of the tin is precipitated in the first neutralization stage. The precipitate from the second neutralization stage, which contains some indium, is recycled for indium recovery. Indium is recovered from the filtrate as a sponge by cementation with zinc. The indium sponge of 95% purity is electrorefined to give a 99.5% indium cathode, which is recast as the anode for the second electrorefining stage, in which indium of 99.97% purity is produced.

36.5.4 Recent Production Developments

Solvent extraction systems have been investigated to extract indium from various solutions.

The use of a mixture of hydroxyquinolines (Kelex 100 and LIX 26) to extract indium from acidic or alkaline aqueous solutions has been reported [22].

Di-(2-ethylhexyl) phosphoric acid (D2EHPA) in kerosene, and tributyl phosphate (TBP) in kerosene are used to extract indium from the solution obtained by leaching lead-containing residues with sulfuric acid [23]. The concentration of arsenic, cadmium, zinc, copper, antimony, and iron in the extract is greatly reduced. For good separation, iron should be present in the ferrous state.

Solutions of D2EHPA and TBP in kerosene are also reported to extract indium from sulfuric acid solutions that contain tin. The addition of soluble fluorides to the acid solution prior to solvent extraction inhibits the extraction of tin [24].

A process for the separation of indium from gallium and germanium in sulfuric acid solution using solvent extraction is described in [25].

Supported liquid membranes are used to extract indium from a copper-dross leach solu-

tion [26, 27]. The feed solution contains indium (0.5 g/L), copper (60 g/L), and sulfuric acid (30 g/L). The extractant is a 40% solution of D2EHPA in Escaid 100 (a mixture of 80% aliphatic and 20% aromatic long-chain hydrocarbons). A microporous polypropylenic support is used.

The recovery of indium and gallium from spent semiconductor material has also been reported [28].

Table 36.2: Standard potentials, in volts.

Cd^{2+}/Cd	-0.402
In^{3+}/In	-0.338
Ti^{4+}/Ti	-0.336
Sn^{2+}/Sn	-0.136
Pb^{2+}/Pb	-0.126

36.5.5 Refining

Sponge indium with a purity up to 99.5% requires upgrading for most uses. For the semiconductor industry, a purity of at least 99.9999% is required. Electrorefining is a commonly used technique.

In electrorefining, cotton-bagged indium anodes and pure indium cathodes are used. Metallic impurities collect as anode slime in the cotton bag, which thus prevents their entering the bulk electrolyte and contaminating the indium deposit. The electrolyte is generally a chloride solution, but the use of solutions of sulfate [29], cyanide [30], fluoroborate [31], and sulfamate [32] has also been reported.

A typical composition of the electrolyte is 20–75 g/L In, 80–100 g/L NaCl, 1 g/L glue, pH 2.2–2.5. The cathode current density is 1–2 A/dm². Apart from the dendritic nature of the indium deposit, the difficulty with electrorefining lies in the fact that impurities which generally accompany indium have standard potentials close to that of indium (Table 36.2).

For purities up to 99.9999%, multistage electrorefining is required [33], or electrorefining must be supplemented by vacuum distillation or zone refining or both of them.

The difference between the melting point and boiling point of indium is greater than for most other elements. This property allows the

elimination of impurities such as cadmium, sulfur, selenium, tellurium, zinc, lead, and thallium by vacuum distillation [34].

Elimination of cadmium, copper, zinc, gold, silver, and nickel by zone refining is described in [35]. Intensive cooling is necessary because of the low melting point of indium.

A method for refining indium to semiconductor grade, in which a chelating agent is used to absorb indium selectively from solution, has been reported [36].

36.6 Quality Specifications

Qualities ranging from 99.97% to 99.99999% indium are commercially available. Impurities may be metallic (Ag, Cu, Pb, Sb, Sn, Cd, Ti, Zn, Fe, Al, Ga) and nonmetallic (S, Cl, O, Se, N). Their concentrations depend on the origin of the indium-containing feed material and on the production and refining process.

Commercial grades are 99.97% (3N7), 99.99% (4N), 99.999% (5N), 99.9999% (6N), and 99.99999% (7N).

36.7 Analysis

Spectroscopic analysis enables the detection of indium down to 10 ppm due to its characteristic lines in the indigo blue region at wavelengths of 4511.36, 4101.76, 3256.09, and 3039.39 nm. The quantitative analysis of indium in ores, compounds, and alloys is described in [37]. Spark source mass spectrometry and graphite furnace atomic absorption spectrometry are used in the analysis of high purity indium ($\geq 99.9999\%$). About 40 elements can be determined with detection limits of 10–30 ppb by spark source mass spectrometry [38].

36.8 Compounds

The most common valence of indium is three. Monovalent and bivalent compounds of indium with oxygen, sulfur, and halogens are also known. The trivalent indium compounds

are the most stable. The lower valence compounds tend to disproportionate to give the corresponding trivalent compounds and indium metal.

The properties of some indium compounds are given in Table 36.3 [7, 39].

Indium(III) oxide, In_2O_3 , is formed by thermal decomposition of indium hydroxide, carbonate, nitrate, or sulfate in air, or by burning indium in air. It is a pale yellow, amorphous solid when formed at low temperature, but forms red-brown crystals when it is prepared at high temperature. The amorphous form is soluble in acids, but not in alkalis. Indium trioxide is reduced to indium by hydrogen, ammonia, sodium, aluminum, and carbon. *Indium(II) oxide*, InO , and *indium(I) oxide*, In_2O , are formed by reduction of indium(III) oxide under carefully controlled conditions.

Indium hydroxide, $\text{In}(\text{OH})_3$, is precipitated from solutions of indium salts by adjusting the pH in the range 4–10.

Indium trichloride, InCl_3 , is obtained by burning indium in excess chlorine. It is a white, crystalline substance which is easily sublimed, and is very soluble in water. *Indium dichloride*, InCl_2 , is obtained by the reaction of indium with hydrogen chloride at 200 °C. Indium monochloride, InCl , is formed by passing indium dichloride vapor over heated indium. The lower chlorides, InCl and InCl_2 , disproportionate in water to give indium trichloride and indium metal.

Indium orthoborate, InBO_3 , is prepared by melting a mixture of boric oxide and indium hydroxide.

Table 36.3: Properties of some indium compounds [7, 39].

Compound	Density, g/cm ³	mp, K	bp, K	Enthalpy of formation, kJ/mol
In_2O_3	7.180	2183		-925
InCl	4.190	498	881	-186
InCl_2	3.620	509	796	-362.4
InCl_3	3.450	856	771*	-535.0
InAs		1215		-57.7
InSb		798		-31.1
InP		1328		-75.2

*Sublimes.

Table 36.4: Estimated western-world consumption of indium in 1985 [9].

Use	Consumption, t
Low-melting alloys	12
Bearings	9
Dental alloys	7
Nuclear reactor control rods	3.3
Low-pressure sodium lamps	4-5
Electrical contacts	8
Alkaline dry batteries	6.8 ^a
Phosphors	6 ^b
Semiconductors	
Lasers, photodetectors, integrated circuits (Ga-As In-P, In-P)	5
CCDs in infrared video cameras (image orthicons, In-Sb)	3.5
Liquid crystal displays	7

^a 1987 data [40].^b 1986 data for Japan [41].

Indium forms alkyl and aryl compounds such as *trimethyl indium*, $\text{In}(\text{CH}_3)_3$; *triethyl indium*, $\text{In}(\text{C}_2\text{H}_5)_3$, and *triphenyl indium*, $\text{In}(\text{C}_6\text{H}_5)_3$. They are made by treating indium with the corresponding mercury alkyls or mercury aryls, or by reaction of indium trichloride with a Grignard reagent.

The semiconducting compounds *indium antimonide*, InSb , *indium arsenide*, InAs , and *indium phosphide*, InP , are prepared by direct combination of the high-purity elements at high temperature. Indium phosphide is also obtained by thermal decomposition of a mixture of a trialkyl indium compound and phosphine (PH_3).

36.9 Uses

Table 36.4 summarizes the western-world consumption of indium by end use [9, 40, 41].

Low-melting alloys represent a major use of indium. Indium is added to *solder alloys*, mostly composed of tin and lead, to increase thermal fatigue resistance, and to improve malleability at low temperature and corrosion resistance. Indium solders are used in *electronics* for fixing semiconductor chips to a base, for assembling semiconductor devices and hybrid integrated circuits, and to seal glass to metal in vacuum tubes. These solders are mainly used in the form of a paste, whose

main components are Pb, Ag, Cd, In, Sn, and an organic binder.

Fusible indium alloys are usually based on bismuth in combination with lead, cadmium, tin, and indium.

Fusible indium alloys are used to bend thin-walled tubes without wrinkling the wall or changing the original cross section. The alloy is cast in the tube, rendering it effectively solid. After bending, the alloy can be melted out using hot water.

These alloys are also used in fire-control systems. Restraining links that hold alarm, water valve, and door operating mechanisms in place are soldered with a low-melting alloy. A rise in temperature sufficient to melt the alloy results in the system coming into operation.

Fusible alloys are used for making disposable patterns and dies for the founding of ferrous and non-ferrous metals.

They are also used as temperature indicators in situations where other methods of temperature measurement are impracticable. Small rods of alloys of known melting point are inserted into equipment such as aircraft header tanks, test bearings, and experimental rigs. The melting of the alloy thus indicates the temperature attained in particular parts of the test system.

Addition of indium to lead-tin *bearings* for heavy-duty and high-speed applications provides particularly high resistance to fatigue and seizure. These bearings are used in piston-type aircraft engines, high-performance automobile engines (formula 1) and in turbo-diesel truck engines.

The addition of indium to gold *dental alloys* improves their mechanical characteristics and increases resistance to discoloring. Small amounts of indium are used to improve the machinability of gold alloys for *jewelry*.

Indium is used in *nuclear reactor control-rod* alloys (80% Ag, 15% In, and 5% Cd). The consumption of indium in this field is estimated at 3.3 t/a for the replacement of control rods in existing nuclear power plants [9].

In *low pressure sodium lamps* (SOX lamps), indium is applied as a thin layer of in-

dium-tin oxide on the inside of the outer glass envelope. The indium-tin oxide film increases the operating temperature and the efficiency of the lamp. Low pressure sodium lamps, characterized by their orange color, are mainly used in the United Kingdom, Belgium, and the Netherlands. The production of SOX lamps accounts for 4-5 t/a indium [9].

Indium is now used as a corrosion inhibitor in *alkaline dry batteries* as a substitute for mercury. This allows the mercury content of the amalgamated zinc powder used in their production to be reduced from 7% to 1-3% [42]. Currently, a target of very low mercury content, or even complete removal, is being pursued. The low-mercury zinc powders have corrosion and degassing characteristics which are similar to those of the 7% mercury powders.

Indium orthoborate is used as a *phosphor* in *cathode-ray tubes*, where it is applied as a thin layer. Indium phosphors emit light for a longer time than zinc sulfide phosphors but are more expensive. They are used particularly in computer monitors where image stability is of great importance. In Japan, consumption of indium for this application was 6 t in 1986 and 8 t in 1987.

Intermetallic compounds of indium find application as *semiconductors*. The development of the second generation of optical fiber communication systems in the early 1980s with substantially lower levels of attenuation at wavelengths near the infrared region of 1.3 μm and 1.55 μm has led to the development of new semiconductor lasers and photodetectors. *Laser diodes* based on indium-gallium arsenide phosphide emit in the 1.27-1.6 μm region. Indium-gallium arsenide *photodetectors* have high responsivity at 1.3 and 1.55 μm .

The development of integrated circuits and opto-electronic integrated circuits based on indium is still in the research phase.

High-purity indium is used for laser diodes, photodetectors, and integrated circuits.

Charge coupled devices operating in the infrared region are based on indium antimonide. Infrared detectors and infrared video cameras, such as orthicons, use indium antimonide.

Thin films of indium-tin oxide are able to transfer electricity to light emitting or light reflecting elements. They find application in *liquid crystal displays* and to a lesser extent in electroluminescent displays and touch panels.

Minor uses of indium include thin plastic films coated with indium-tin oxide that are being developed for use in touch panels (e.g., for computer screens), liquid crystal devices, and electroluminescent lamps. Indium oxide is used as a coating for *glass*. Window glass coated with an indium-tin oxide film to reflect infrared radiation is being investigated. Indium oxide films doped with tin oxide are used to prevent icing and fogging on aircraft windshields. Their application as windshield coatings in automobiles is in development, particularly in Japan. Indium antimonide is used in *Hall generators* to measure magnetic fields. *Solar cells* based on copper-indium diselenide are being developed [43]. Small amounts of indium compounds are used as additives for *lubricating oils*, and to produce *yellow glass*.

Table 36.5: Estimated indium production in 1986 [9].

Country	Company	Production, t
Belgium	Metallurgie Hoboken-Overpelt	15
France	Peñarroya	19
Italy	Pertusola	
United Kingdom	Capper Pass	3
	Johnson Matthey	2
Netherlands	Billiton	1
Germany	VEB	1
	Preussag	1
Japan	Nippon Mining	16
China		6
Former Soviet Union		6
Peru	Centromin-Peru	4
Canada	Cominco	6
Total		80

36.10 Economic Aspects

The world production of indium in 1986 has been estimated at 80 t. Table 36.5 lists the estimated indium production by country and company for 1986. The main producers are located in Belgium, Japan, France, and Italy. Important indium refiners are located in the United States (Indium Corporation of Amer-

ica, 25 t in 1986 [9]) and the United Kingdom (Mining and Chemical Products, 10 t in 1986 [9]).

Figure 36.5 shows the evolution of the producer price for standard grade indium (99.97%) from the Indium Corporation of America. For indium of 99.99% purity, a premium of \$2–5/kg is charged. Very pure indium (7N or 99.99999%) costs ca. \$1500/kg [9].

36.11 Toxicology and Occupational Health

There is no evidence of any health hazard from industrial use of indium. No systemic effects in humans exposed to indium have been reported [44]. The TLV for indium is 0.1 mg/m³.

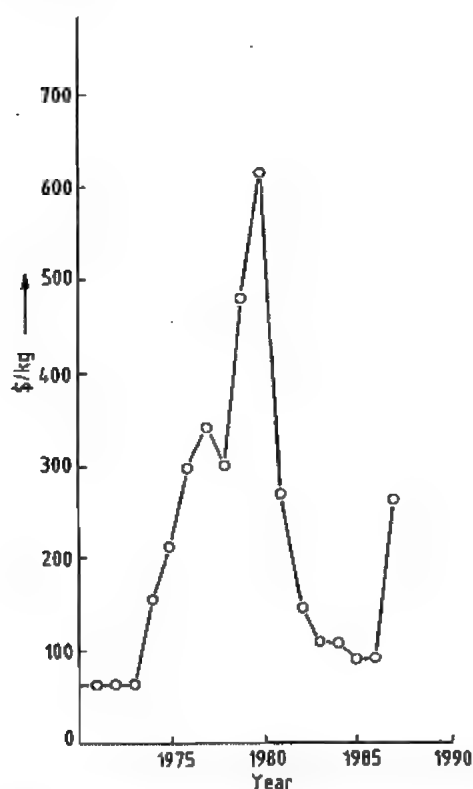


Figure 36.5: Evolution of the producer price for standard grade indium (99.97%) (Indium Corporation of America).

36.12 References

1. H. E. Suess, H. C. Urey, *Rev. Mod. Phys.* **28** (1956) 56.
2. F. Reich, T. H. Richter, *J. Prakt. Chem.* **89** (1863) 441.
3. *Kirk Othmer*, 3rd ed., **13**, p. 207.
4. J. R. Mills, R. A. King, C. E. T. White: *Rare Metals Handbook*, 2nd ed., Chap. 13, Reinhold Publishing Corporation, London 1961, p. 220.
5. *Ullmann*, 4th ed., **13**, 197.
6. *Handbook of Chemistry and Physics*, 62nd ed., The Chemical Rubber Co., Cleveland, OH, 1981/1982.
7. J. C. Bailar et al.: *Comprehensive Inorganic Chemistry*, 1st ed., Pergamon Press, Oxford 1973, pp. 983–1117.
8. J. W. Mellor, *A Comprehensive Treatise on Inorganic and Theoretical Chemistry*, vol. 5, Chap. XXXV, Longmans, Green and Co., London 1946.
9. Roskill: *The Economics of Indium 1987*, 4th ed., Roskill Information Services Ltd., London 1987.
10. E. Theurich, *Freiberg. Forschungsh.* **B90** (1963) 93.
11. L. Müller, *Freiberg. Forschungsh.* **B90** (1963) 105.
12. Anaconda Copper Mining Comp., US 2384610, 1940 (H. M. Doran et al.).
13. R. Kleinert, "Indium from the Rammelsberg Ores", *Min. Mag.* **83** (1950) 146.
14. Asarco, US 2433770, 1947 (Y. C. Lebedeff).
15. S. Takayanagi, K. Yajima, paper presented at the 22nd Annual Conference of Metallurgists of the Metallurgical Society of CIM, Edmonton, August 1983, paper no. 19.4.
16. E. F. Milner, W. A. Van Beek, "Rotary furnace reduction of lead drossing fume for recovery of tin and indium", paper presented at the 24th Annual Conference of Metallurgists of the Metallurgical Society of CIM, Vancouver, August 1985.
17. J. De Keyser, W. Jaspers, "The Harris Refinery of Metallurgie Hoboken-Overpelt", paper presented at the 110th AIME meeting, Chicago, Feb. 1981, AIME-TMS paper no. A-81-10.
18. J. Coyle, *Trans. Electrochem. Soc.* **85** (1944) 223.
19. T. Quarm, *Trans. Inst. Min. Metall.* **60** (1950) 77.
20. Copper Pass Limited, GB 2109008A, 1982 (P. Halsall).
21. P. Halsall, *Trans. Inst. Min. Metall. Sect. C* **97** (1988) 93.
22. Preussag Aktiengesellschaft Metall, US 4666686, 1987 (W. Krajewski, K. Hanusch).
23. Hazen Research, Inc. USA, CA 1188105, 1985 (E. Reynolds Jones, A. R. Williams).
24. Cominco Ltd., CA 1218237, 1987 (R. Perri et al.).
25. Tian Run-cang Zou Jia-yun, Zhou Ling-Zhi in M. J. Jones, P. Gill (eds.): *Mineral Processing and Extractive Metallurgy*, London IMM, 1984, pp. 615–624.
26. Samim Società Azionaria Mineraria Metallurgica S.p.A., BE 902890, 1986 (R. Guerziero et al.).
27. R. Guerziero, L. Meregalli, X. Zhang, *ISEC Int. Solvent Extr. Conf.*, Dechema, Frankfurt 1986, pp. 585–589.
28. Nippon Mining, JP-KK 88016338, 1988.
29. H. B. Linford, *Trans. Electrochem. Soc.* **79** (1941) 443.
30. Oneida Community Ltd., US 1965251, 1934 (M. S. Murray, D. Gray).
31. General Motors, US 2409983, 1946 (W. M. Martz).
32. Indium Corporation of America, US 2458839, 1949 (J. R. Dyer, T. J. Rowan).
33. G. S. Rao, G. H. Phatak, K. Gangadharan, *Indian J. Technol.* **12** (1974) 256.
34. A. Arkady et al., US 4287030, 1981.
35. U. Wiese, *Erzmetall* **34** (1981) no. 4, 190.
36. Sumitomo Chem. Ind., JP-KK 204830, 1986.
37. C. E. T. White, *Metal. Bull.* **47** (1977).
38. Y. D. Liu, J. Verlinden, F. A. Lams, E. Adriaenssens, *Bull. Soc. Chim. Belg.* **95** (1986) 309.
39. I. Barin, O. Knacke, O. Kubaschewski: *Thermochemical Properties of Inorganic Substances*, Springer Verlag, Berlin-Heidelberg-New York 1977.
40. D. B. Winter, *Metal. Bull.*, August 1988.
41. *Jpn. Ind. Rare Met. Ann. Rep.*, April 1988.
42. M. Meeus, Y. Strauven, L. Groothert, "Power Sources II", *Proc. Int. Power Sources Symp.*, 15th, (1987) 281–299.
43. C. E. T. White: *Advanced Materials & Processes Inc., Metal Progress*, December 1986, 69–72.
44. L. Friberg, G. F. Nordberg, V. Vouk: *Handbook on the Toxicology of Metals*, Elsevier/North-Holland Biomedical Press, Amsterdam 1979, pp. 429–436.

37 Thallium

HEINRICH MICKE (§§ 37.1–37.10); HANS UWE WOLF (§ 37.11)

37.1 Introduction	1543	37.7 Alloys	1547
37.2 History	1543	37.8 Compounds	1548
37.3 Properties	1543	37.9 Analysis	1552
37.4 Occurrence	1544	37.10 Economic Aspects	1553
37.5 Extraction	1544	37.11 Toxicology and Occupational Health	1553
37.6 Uses	1547	37.12 References	1555

37.1 Introduction

Thallium [1–18], atomic number 81, is in group 13 of the periodic table, and has electronic structure $1s^2 2s^2 p^6 3s^2 p^6 d^{10} 4s^2 p^6 d^{10} f^4 5s^2 p^6 d^{10} 6s^2 p^1$ [19]. It is a dense, fairly reactive metal, the fresh surface having a bluish-white luster. Thallium is softer than lead, but harder than indium, with a low *mp* 303 °C.

There are 20 known isotopes of thallium, of which two, atomic numbers 203 and 205, are relatively stable. The isotope ^{204}Tl is used for materials testing.

The only thallium-containing substances of commercial importance are the metal itself and thallium sulfate. As thallium compounds are prohibited for insect pest control in the United States and parts of Europe, methods of extraction have not been improved during the last 10 years. Several European producers have stopped production of thallium and its compounds.

37.2 History

Thallium was discovered in 1861 by the Englishman CROOKES and in 1862 by the Frenchman LAMY, probably independently. During spectrographic examination of a lead chamber slime, CROOKES found a green line that could not be ascribed to any known element. He was convinced that he had discovered a new element, and gave it the name thallium after the Greek word $\theta\alpha\lambda\lambda\omicron\varsigma$ a young

green branch. LAMY must have been the first person to isolate the element and establish its metallic character. A heated dispute over priority developed between the two investigators [20].

37.3 Properties

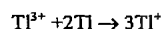
In many of its physical properties, thallium resembles its neighbor, lead. Its chemical behavior combines the properties of the alkali metals with those of silver, mercury, lead, and aluminum. Thallium is highly toxic.

Chemical Properties. Thallium is a very reactive metal. It oxidizes slowly in air, even at ca. 20 °C (more rapidly on heating), to thallium(I) oxide and thallium(III) oxide. Hydrogen peroxide and ozone oxidize the metal to thallium(III) oxide. In the presence of water, a hydroxide is formed. Thallium is therefore stored under petroleum spirit, glycerine, or de-aerated water. On prolonged storage under water with free access of air, metallic thallium becomes covered with large crystals of thallium(I) carbonate, and the water becomes saturated with this salt. To protect against oxidation, rods of thallium are coated with paraffin.

Thallium combines with fluorine, chlorine, and bromine at room temperature, and with iodine, sulfur, phosphorus, selenium, and tellurium on heating. Nitrogen, carbon, and molecular hydrogen do not react with the metal, which does not dissolve in liquid am-

monia. The metal is dissolved slowly by hydrochloric and dilute sulfuric acids, but more rapidly by nitric and concentrated sulfuric acids. Its slow reaction with hydrofluoric acid is noteworthy.

In the series of electrode potentials of cations, thallium has a similar normal potential to that of indium ($Tl/Tl^+ -0.335$ V, $In/In^{3+} -0.34$ V), lying between cadmium ($Cd/Cd^{2+} -0.402$ V) and tin ($Sn/Sn^{2+} -0.140$ V). Solutions of thallium(III) salts are not stable toward metallic thallium, reacting almost quantitatively:



The electrode potential of Tl^+/Tl^{3+} is +1.21 V.

Physical Properties. Thallium is a soft metal (Brinell hardness 29.4 N/mm², the value for lead being 39.2 N/mm²). Thallium exists in two allotropic crystal forms: α -thallium, hexagonal close-packed, stable at room temperature; and β -thallium, body-centered cubic, stable above 226 °C. A volume increase of 3.23% takes place on solidification. On bending, the metal emits a creaking sound similar to the "cry" of tin. It has good cold forming properties and low strength. It can be melted and worked like lead. Physical properties are as follows [21, 22]:

Atomic number	81
Isotope abundance	
²⁰³ Tl	29.52%
²⁰⁵ Tl	70.48%
Density at 20 °C	11.85 g/cm ³
Atomic volume	17.26 cm ³ /mol
Melting point	303.6 °C
Boiling point	1457 °C
Latent heat of fusion	30 J/g
Latent heat of vaporization at normal boiling point	800 J/g
Vapor pressure of melt, Torr	$\log p = -9300/T - 0.892 \log T + 11.1$
Thermal expansion of melt	3.1 4.3%/°C
Electrical resistivity at 2.38 K at 0 °C	superconducting $18 \times 10^{-6} \Omega \text{cm}$
Specific magnetic susceptibility	
Solid thallium	$-0.165 \times 10^{-6} \text{ cm}^3/\text{g}$
β -Thallium	-0.158×10^{-6}
Molten thallium	-0.22×10^{-6}
Surface tension	4.01 mN/cm
Tensile strength	9.8 kg/mm ²
Relative elongation	135%
Brinell hardness	3 kg/mm ²
Mohs hardness	1.2

Like mercury, lead, indium, etc., thallium can become superconducting, the average upper temperature limit being ca. 2.38 K [23]. Some compounds, e.g., Tl_3Bi , Tl_2Hg , and Tl_7Sb can also become superconducting [24]. It is especially valuable as a superconductor in ceramic materials at higher temperatures than are possible with other metals [25].

Vessels for containing liquid thallium can be made of Fe, W, Ta, Mo, Nb, and Co, in decreasing order of suitability.

37.4 Occurrence

Very variable figures are quoted for the concentration of thallium in the Earth's crust (1–3 ppm). It is said to be the 58th most abundant element [26]. In its occurrence, thallium shows a dual character. As a chalcophilic element, it occurs typically, though in low concentration, with the heavy metals that occur in sulfidic ores, usually associated with cadmium, mercury, indium, and germanium. Much more frequently, thallium accompanies the alkali metals potassium, cesium, and rubidium, where its concentration is also low, e.g., in carnallite, sylvine, leucite, lepidolite, feldspar, mica, etc. It is found in seawater, some mineral waters, and in native sulfur [1]. It also occurs in true thallium minerals, of which the following are the most common:

Lorandite	$TlAsS_2$
Pirotzite	$TlFe_2S_3$
Chalcothallite	Cu_3TlS_2
Vrbaite	$Hg_3Tl_4As_5Sb_2S_{20}$
Hutchinsonite	$(Pb, Tl)_2(Cu, Ag)As_5S_{10}$
Bukovite	$Cu_{3+x}Tl_xFeS_{4-x}$
Wallisite	$PbTlCuAs_2S_3$
Hatchite	$PbTlAgAs_2S_3$
Crookesite	$(Cu, Tl, Ag)_3Se$
Avicennite	$7Tl_2O_3 \cdot Fe_2O_3$

The thallium content of these minerals is 16–85%. For many years, only five true thallium minerals were known. Because of their extreme rarity, these are of no importance for the extraction of the metal [27, 28].

37.5 Extraction

Although the amounts of thallium in ores, including those of lead and zinc, are small

compared with the amounts in salts, rock, etc., only the former play a significant role in the winning of the metal. They can be economically worked only if the thallium becomes concentrated in the side products in the course of processing the ore to obtain the main metal, and if other metals are present in this side product to an extent that justifies their extraction. Only a small part of the thallium that occurs naturally is therefore available for extraction.

Thallium is present only as a trace element in nonferrous metal concentrates. Only in a few smelting works does the thallium become sufficiently concentrated in particular process steps for extraction to be practical.

The following companies are thallium producers: Vieille Montagne, Belgium; Cimkent, Russia; Toho Zinc, Japan; Cerro de Pasco, Peru; Preussag, Germany.

Thallium produced as a by-product of the extraction of nonferrous metals is of only minor importance, both quantitatively and economically.

If the raw materials are in solution, the thallium is precipitated by cementation, and is then processed like a solid raw material. The following concentration processes can be used for the treatment of solid raw materials.

Leaching and Precipitation. The simplest process is leaching with water without pretreatment. With airborne dusts from lead or zinc smelting works, or cementation slimes, a yield of 85–90% of the thallium can be obtained. The thallium-containing liquor, which usually also contains cadmium and zinc, is filtered, precipitated with zinc amalgam, and the relatively pure metal is obtained by an electrolytic process (Figure 37.1) [31].

There are many methods of pretreating the starting material before leaching. These include:

- Oxidative roasting at 500 °C
- Sulfatization at 175–250 °C
- Alkaline pretreatment

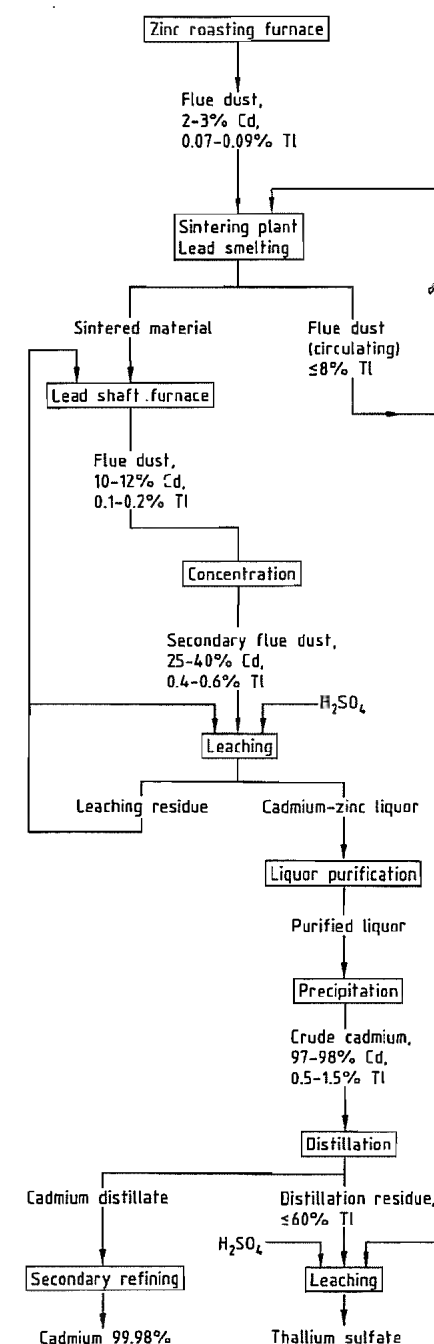


Figure 37.1: Simplified flow diagram of a plant for the combined recovery of cadmium and thallium sulfate from lead and zinc raw materials [29, 30].

Leaching of the raw material after pretreatment can extract 50–60% of the thallium. Flue dusts that contain bismuth, copper, zinc, iron, arsenic, cadmium, thallium, selenium, etc., are given an alkaline pretreatment (fusion with caustic soda and lead sulfide). The alkaline slag so formed is granulated with hot water. On cooling, sodium and thallium arsenates are precipitated, and processed to obtain the thallium [32].

The thallium is usually precipitated and recovered as a sparingly soluble salt (cementation thallium and thallium amalgam) from liquors produced in a variety of concentration methods, with and without pretreatment, and also from liquors that are themselves the raw materials.

Processing and refining of the precipitates obtained by cementation at the Duisburg copper refinery [33, 34] was discontinued in 1983.

Volatilization. In this process, crude arsenic containing 96% As_2O_3 and 0.2% Tl is treated by adding 5% H_2SO_4 and 5% lime and heating to 430 °C, causing 98% of the arsenic trioxide to be volatilized while 99% of the thallium remains in the residue. Sodium chloride is added, and the thallium is volatilized at 800 °C [33]. The volatilization process also gives good results with materials of complex composition from lead smelting. The secondary flue dust can be reprocessed. The most well-known process was that of the former company Zinkhütte Magdeburg [34].

Electrorefining. Electrorefining is operated in one or several stages, or as amalgam electrolysis. Depending on the purity of the starting metal and the operating conditions, thallium cathodes with variable thallium content (ca. 99.9–99.99% and above) are produced [35–37]. Metal of the highest purity can be obtained by multistage electrorefining, in which a perchlorate electrolyte containing 40–70 g/L TlClO_4 and 60–120 g/L NaClO_4 with small amounts of organic additives is used in the final stage. The current density is 0.3–0.6 A/dm². The sum of all the impurities in the

metal is < 1 g/t, i.e., the thallium produced has a purity of 99.9999% [38].

Wet metallurgical refining is normally combined with the concentration process. The high solubility of thallium sulfate in water is used when lead and other metals that form insoluble sulfates are precipitated. The insolubility of thallium sulfide in alkaline solvents is used to separate it from the group 1 metals, and its solubility in dilute acids is used to separate it from silver, mercury, bismuth, copper, arsenic, antimony, cadmium, etc. The solution is treated with hydrogen sulfide, or preferably with freshly precipitated thallium sulfide, so that an easily handled thallium sulfate precipitate is produced at the end of all operations [39]. Iron and arsenic can be removed after oxidation with air followed by neutralization, e.g., by adding zinc oxide. The high solubility of thallium carbonate in water is used to separate it from zinc, iron, cadmium, and other impurities, usually in combination with a concentration process. The low solubility of thallium chromate is then used for both concentration and refining.

Very pure metal can also be obtained by fractional dissolution of the impure metal or by fractional precipitation, mainly by fractional cementation of the impurities and the thallium from impure solutions. Impure thallium metal or thallium amalgam can be used as the starting material. When thallium amalgam is heated with 70–100% sulfuric acid to boiling, the thallium dissolves first. If dissolution is interrupted after almost all the thallium, but none of the impurities, has gone into solution, the solution contains pure thallium sulfate which can be the raw material for metal winning [40].

To obtain compounds of the highest purity for use as intermediates for producing very high-purity metal, several unusual reactions have been proposed. These include precipitation of the thallium as cyclopentadienyl thallium [41, 42], or extraction of thallium(III) chloride, TlCl_3 , from solution in hydrochloric acid (6–7 mol/L) with ether. First, however, the iron must be converted to the divalent form, and the heavy metals removed. Almost

complete removal of all impurities takes place by taking the impure starting substance into solution in hydrochloric, hydrobromic, or hydroiodic acid, and extracting the thallium complex with isopropyl ether at acid concentration 0.1–4 mol/L. The metal obtained by electrolysis of the purified compound has purity 99.9999–99.99999% [43].

During production of an ultrapure product from the already relatively pure metal by crystallization (especially zone melting and crystal pulling from the melt), the various impurities behave very differently. As well as the distribution coefficients, the operating conditions (mainly the migration rate of the zones and the crystallization rate) have a great influence on the refining. However, many other factors have an influence e.g., the rotation rate during zone melting, and the rotation rate of the seed crystal during crystal pulling from the melt. Secondary processes are also important, e.g., volatilization and oxidation of certain impurities. The behavior of some of the more common potential impurities for a given combination of operating conditions can make it difficult to obtain very pure end products.

Zone melting is generally carried out in graphite boats. The ingots used are 150–180 mm long, with a ca. 15 mm molten zone, the process being carried out in an atmosphere of purified nitrogen. With a zone migration rate of 0.5–1.0 mm/min and five passes, the copper content in most of the ingot can be reduced from 50 g/t in the starting metal to 2.7 g/t, and, under the same conditions, the silver content in approximately half the length of the ingot is reduced from 3 to < 0.3 g/t. By pulling crystals from the melt in vacuo (ca. 10^{-2} Pa, 10^{-4} mbar), crystals 100–220 mm long and 8–10 mm diameter can be obtained. With a crystallization rate of 0.4–0.5 mm/min, the manganese content is 0.2 g/t in the lower part and 0.1 g/t in the middle part of the crystal. After a second recrystallization, 0.05 g/t manganese is found in the middle and upper part.

Not all impurities can be removed by crystallization, e.g., lead and iron, and there is a group of impurities that can only be removed

by secondary processes. These include mercury, tin, and sulfur [44].

In Germany, thallium is produced solely by Preussag; annual production capacity is 4–5 t of 99.4–99.64% thallium [45]. Thallium is supplied as rods and granules in “4 nines” to “5 nines” quality (i.e., 99.99–99.999%). The catalogue also includes “pure” monovalent thallium compounds, including sulfate, bromide, chloride, and iodide. Other compounds can be produced on request.

37.6 Uses

No large application potential for thallium has so far been found. The unalloyed metal is unsuitable for direct use, owing to its unfavorable mechanical properties and marked tendency to oxidize. The radioactive isotope ^{204}Tl is a β -emitter with half-life ca. 3.5 years, and is used as a radiation source in materials testing, principally for thickness measurements on metals and nonmetals. It has been discovered that ^{205}Tl has the most constant atomic vibrations so far observed. This property has led to its use in atomic clocks.

These special applications require extremely pure grades. The very pure metal supplied by Unterharzer Berg- und Hüttenwerke contains > 99.999% Tl, i.e., the sum of all the impurities does not exceed 10 g/t [46]. American Smelting and Refining supply “high-purity thallium”, with the same purity. The following figures are quoted for the impurities [47]: Cu < 1 g/t; Pb 1 g/t; Fe < 1 g/t; Ag, Sn, Mg, and Si spectrographically undetectable, but < 1 g/t; other elements spectrographically undetectable.

37.7 Alloys

Thallium readily forms alloys with most other metals. There is complete mutual insolubility with iron, and limited solubility in the liquid state with copper, aluminum, zinc, arsenic, manganese, and nickel. The melting points of thallium lead alloys are higher than those of the pure metals, the maximum,

380 °C, being reached at 37.8% Pb. There is a resemblance to the two-component systems of lead, especially in alloys of thallium with copper, aluminum, zinc, and nickel. Gold, silver, cadmium, and tin form simple eutectics with thallium. Thallium also forms binary alloys with antimony, barium, calcium, cerium, cobalt, germanium, indium, lanthanum, lithium, magnesium, strontium, tellurium, and bismuth.

Alkali metals, alkaline earth metals, some metals of the rare earth group (e.g., lanthanum, cerium, praseodymium), and mercury form intermetallic compounds with thallium, some of which have unusually high melting points, e.g., CeTl (1240 °C) and PrTl (ca. 1150 °C). The compound with mercury, Hg₅Tl₂, has *mp* 14.5 °C and forms eutectics with thallium and mercury: Tl-Hg₅Tl₂ with 40.45% Tl melts at 0.6 °C and Hg-Hg₅Tl₂ with 8.5% Tl at -58.4 °C.

Of the systems with three or more components, the combinations with bismuth, lead, and cadmium have been much investigated. These have very low melting points over wide ranges, and in most cases form ternary or quaternary eutectics. For example, the melting point of the Bi-Pb-Tl eutectic with 11.5% Tl, 55.2% Bi, and 33.3% Pb is 90.8 °C, and the melting point of the quaternary B-Cd-Pb-Tl eutectic with 8.9% Tl, 44.3% Bi, 35.8% Pb, and 11.0% Cd is 81 °C [9].

The ternary alloys Tl-Pb-Bi, Tl-Al-Ag, In-Hg-Tl, Sn-Cd-Tl, Bi-Sn-Tl, and Bi-Cd-Tl are used as semiconductors or in ceramic compounds [48, 17].

The quaternary alloys Tl-Sn-Cd-Bi, Pb-Sn-Bi-Tl, and Pb-Cd-Bi-Tl are known [17].

Thallium, like tin, cadmium, lead, etc., has good wear resistance when used in bearings for steel shafts. As additions of thallium also increase the deformation resistance, breaking strength, yield, strength, and hardness of lead and its alloys, thallium-containing alloys are frequently recommended for bearings [49]. The alloy 72% Pb, 15% Sb, 5% Sn, and 8% Tl is superior to the best tin-based bearing metals with respect to yield strength and breaking strength. Bearing metals based on

Pb-Tl-Cd with high cadmium content can have compositions in the range 0.01–5% Tl, 5–40% Cd, the rest being Pb [47]. However, thallium has since been replaced by indium as an alloy constituent [45].

Addition of thallium to gold, silver, and copper contacts in the electronics industry (e.g., 0.05–20% Tl added to copper alloys) reduces the tendency to sticking [45].

In solid-state rectifiers, especially selenium rectifiers, addition of thallium increases the blocking resistance [50].

Addition of thallium can reduce the melting point of mercury from -39 °C to ca. -59 °C. One use for this low-melting Hg-Tl alloy is for low-temperature thermometers [51].

The increase in the melting point of lead by addition of thallium is used in special types of electrical fuses and in solder (thallium content ≤ 20%) where a higher melting point is required [5, 6].

37.8 Compounds

Thallium can be monovalent or trivalent, the stability of the 6s electron pair in the electronic structure making thallium preferentially monovalent in inorganic compounds. Thallium(I) compounds have a certain similarity to alkali metal compounds, e.g., high solubility of the sulfate, carbonate, and hydroxide in water. However, they also show similarities to compounds of silver, mercury, and lead, e.g., low aqueous solubility of the chloride, bromide, iodide, and sulfide.

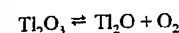
Thallium(I) oxide, Tl₂O, is formed by heating thallium in air at < 100 °C, or by dehydration of TlOH. It is reddish-black to black, volatile in air at higher temperatures, being converted to Tl₂O₃, and is very hygroscopic, forming a colorless, alkaline solution of TlOH with water. The enthalpy of formation is given by:



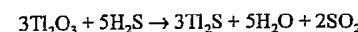
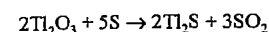
With B₂O₃, borates, or mixtures of borates and fluorides of alkali and alkaline earth metals, Tl₂O forms stable, clear, homogeneous

melts which can be used for the electrolytic production of metallic thallium.

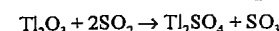
Thallium(III) oxide, Tl₂O₃, is more stable, and can be formed by heating Tl₂O to > 100 °C, treating thallium(III) salts with KOH or NH₃, or treating thallium(I) salts with oxidizing agents, e.g., TlCl with NaOCl. It is brown to black, forms cubic crystals with density (4–21 °C) 9.65 g/cm³, *mp* 717 ± 5 °C, and begins to sublime above 500 °C with partial decomposition:



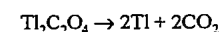
It can be reduced to Tl₂O, and even to the metal, by strongly heating with hydrogen, carbon, or carbon dioxide. It reacts very vigorously with sulfur and hydrogen sulfide, even at room temperature, doubtless in accordance with the equations:



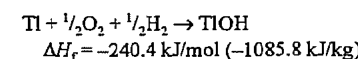
Treatment of an aqueous suspension with sulfur dioxide leads to Tl₂SO₄:



It is sparingly soluble in water, but does not form a hydroxide. It dissolves in hydrochloric, sulfuric, and nitric acids with formation of hygroscopic, unstable thallium(III) salts, from which it is precipitated unchanged by alkali. It is also dissolved by acetic and tartaric acids. With oxalic acid, the sparingly soluble oxalate is formed, which decomposes on heating:



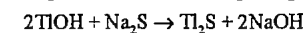
Thallium(I) hydroxide, TlOH (92.32% Tl), is formed on heating metallic thallium with water in the presence of air, or dissolving Tl₂O in water. It is white, becoming dark gray on exposure to light. Its enthalpy of formation is given by:



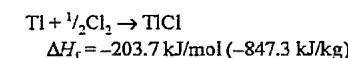
It dissociates to Tl₂O and H₂O on heating above 139 °C.

It is soluble in water, forming a colorless markedly alkaline solution which rapidly absorbs O₂ from the air, with formation of

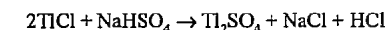
Tl₂CO₃, and rapidly oxidizes, forming Tl₂O₃. The aqueous solution is a stronger base than NaOH, attacking glass very strongly on heating. Sodium sulfide precipitates Tl₂S:



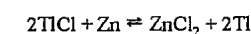
Thallium(I) chloride, TlCl, is formed when HCl or alkali metal chlorides are added to neutral thallium(I) salt solutions. The precipitated product is sparingly soluble in water, and is of some metallurgical importance. It is white, becoming gray-brown to blackish-brown on exposure to light. It forms cubic crystals, density 7.00–7.05 g/cm³, *mp* 427 °C, *bp* 806 °C, initial sublimation temperature ca. 360 °C, specific heat capacity *c_p* (2.8–45.3 °C) = 0.221 J g⁻¹K⁻¹. The enthalpy of formation is given by:



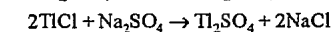
No thermal decomposition takes place at the melting point. On heating in a stream of chlorine, it is first converted to 3TlCl·TlCl₃, and then to TlCl₃. On melting with NaHSO₄, it is converted to Tl₂SO₄:



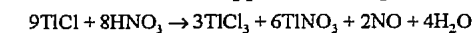
Metallic thallium is liberated on melting with alkali metal cyanides, or zinc:



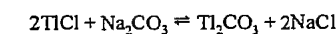
It is very sparingly soluble in water, 0.29 g dissolving in 100 g H₂O at 15.6 °C, and 2.41 g at 99.35 °C. It reacts with a dilute solution of Na₂SO₄ to form Tl₂SO₄:



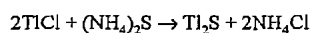
On heating with H₂SO₄, Tl₂SO₄ or TlHSO₄ are formed (see above). HNO₃ reacts in the cold to form 2TlCl·TlCl₃, and, on heating, the very soluble TlCl₃ (with some TlNO₃), in accordance with the approximate equation:



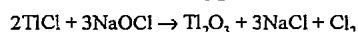
On treatment with a 20% solution of Na₂CO₃, Tl₂CO₃ is formed, which is converted to TlCl on addition of NaCl:



It reacts with ammonium sulfide to form Tl₂S:

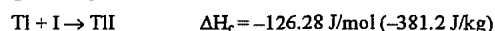


and with sodium hypochlorite to form Ti_2O_3 :

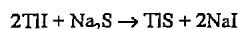


With CdCl_2 , TlCl forms a sparingly soluble double salt, $\text{TlCl} \cdot \text{CdCl}_2$, which decomposes again on boiling with water.

Thallium(I) iodide, TlI , is formed by direct combination of the elements or by precipitation from thallium(I) salt solutions by addition of alkali metal iodide. There are two modifications: a yellow rhombic form stable at room temperature, and a red cubic form stable above ca. 165 °C. The yellow form has density 7.1 g/cm³ and the red form 7.45 g/cm³, *mp* 440 °C, *bp* 824 °C. Sublimation starts at 355 °C. The specific heat capacity in Jg⁻¹K⁻¹ is given by $c_p = 0.152T + 3.43$. The enthalpy of formation is given by



Metallic thallium is liberated on melting with alkali metal cyanides. The following reaction takes place with sodium sulfide:

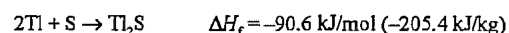


Its solubility in water is considerably less than that of TlCl , but is increased by addition of KOH . It is not attacked by sulfuric and hydrochloric acids, but nitric acid (dilute or concentrated) reacts with liberation of iodine.

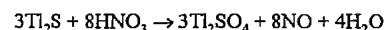
Thallium(I) fluoride, TlF , is very soluble in water, unlike the other thallium(I) halides, the solution is alkaline.

Thallium(I) sulfide, Ti_2S , is formed on melting together thallium and sulfur (along with Ti_2S_5 , depending on the mixing ratio). It is also precipitated from thallium(I) salt solutions on adding $(\text{NH}_4)_2\text{S}$, or an amorphous precipitate is formed when H_2S is added to very weakly acid solutions. This becomes crystalline on heating to 150–200 °C with a solution of $(\text{NH}_4)_2\text{S}$. From thallium(III) salt solutions, a mixture of Ti_2S and sulfur is precipitated. Ti_2S is also formed when a solution of Ti_2SO_4 is heated with $\text{Na}_2\text{S}_2\text{O}_3$. It is black, and the crystals have a blue metallic luster. Its density is 8.4 g/cm³, and its melting point 448 °C. It vaporizes on heating above 300 °C,

at first unchanged, but decomposing at higher temperatures (e.g., 900 °C). The enthalpy of formation is given by:



Precipitated Ti_2S is readily oxidized in air to Ti_2SO_4 . It is sparingly soluble in water and almost insoluble in alkaline solvents, but dissolves in boiling mineral acids (dilute H_2SO_4 and HNO_3). Reaction with fuming nitric acid leads to the sulfate:

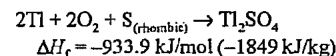


The other sulfides (Ti_2S_3 , Ti_2S_5) become increasingly insoluble as the sulfur content increases, and are converted to Ti_2S with liberation of sulfur on heating.

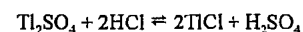
Thallium(I) sulfate, Ti_2SO_4 (80.97% Tl), is the most important starting material for thallium metal winning. Depending on its method of manufacture, it forms colorless, very lustrous rhombic crystals or a snow-white crystalline powder, density 6.765 g/cm³, *mp* 632 °C. It vaporizes unchanged at white heat. Above 900 °C, its vapor pressure increases rapidly. During the roasting of zinc concentrates (900 °C) and the sintering of lead concentrates (1000 °C), a considerable amount of thallium can volatilize as its sulfate. The effect of temperature on the vapor pressure can be approximately represented by:

$$\log p = -\frac{9300}{T} - 0.892 \log T + 11.1$$

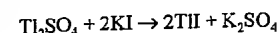
where p is in Torr (1 Torr = 133 Pa); T is in K. The enthalpy of formation is given by:



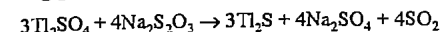
It is very soluble in water, e.g., 100 g boiling water dissolves 18.45 g Ti_2SO_4 . The solution is hardly hydrolyzed, and is therefore neutral. Addition of hydrochloric acid or alkali metal chlorides to the solution precipitates sparingly soluble TlCl , though never completely:



Potassium iodide addition can give complete precipitation:

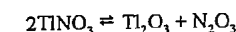


Addition of sodium thiosulfate at the boiling point produces Ti_2S :

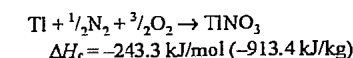


With excess sodium carbonate, partial hydrolysis of the Ti_2CO_3 formed, and oxidation of the TlOH , produces a black precipitate. Addition of $\text{Na}_2\text{Cr}_2\text{O}_7$ or Na_2CrO_4 produces sparingly soluble Ti_2CrO_4 , which can be redissolved to Ti_2SO_4 and CrSO_4 by treatment with dilute H_2SO_4 and NaHSO_4 . Treatment of Ti_2SO_4 with H_2SO_4 or treatment of TlCl with excess H_2SO_4 gives thallium(I) hydrogen sulfate, TiHSO_4 , or $\text{Ti}_2\text{SO}_4 \cdot \text{H}_2\text{SO}_4$, which melts at 115–120 °C and is converted to neutral Ti_2SO_4 with liberation of SO_3 by strong heating.

Thallium(I) nitrate, TlNO_3 , is formed when metallic thallium or Ti_2CO_3 is dissolved in HNO_3 . It is white, and forms rhombic crystals (a cubic modification is also known), density 5.55 g/cm³, *mp* 206 °C. It melts without decomposition, but decomposition begins at ca. 300 °C, and is complete at 450 °C:



The enthalpy of formation is given by:

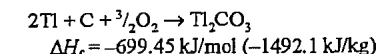


It is very soluble in water, the solubility increasing very rapidly with temperature, 100 g H_2O dissolving 7.93 g TlNO_3 at 15.4 °C and 593.93 g at the boiling point. Its solutions are neutral. H_2SO_4 reacts with TlNO_3 to form Ti_2SO_4 .

Thallium(I) carbonate is formed by the action of CO_2 on TlOH , or by reacting thallium(II) salt solutions with an alkali or alkaline earth hydroxide, e.g., $\text{Ba}(\text{OH})_2$, while passing CO_2 into the solution.

It is white, and forms monoclinic crystals, density 7.164 g/cm³, *mp* 272 °C, decomposing at elevated temperatures. The Ti_2O thus formed is soluble in molten Ti_2CO_3 , and is converted to Ti_2O_3 on prolonged heating.

The enthalpy of formation is given by:



It is fairly soluble in hot water (27.78 g Ti_2CO_3 dissolves in 100 g H_2O at 100 °C). On dilution, rapid hydrolysis takes place with formation of TlOH , so that the solution is alkaline. It is rapidly decomposed by acids.

Thallium metasilicate, Ti_2SiO_3 , is obtained by treatment of thallium(I) hydroxide with sodium metasilicate, Na_2SiO_3 , dissolved in a solution of NaNO_3 . The orthosilicate, Ti_4SiO_4 , is prepared by reacting thallium(I) hydroxide with sodium orthosilicate, Na_4SiO_4 . Both silicates are water soluble. Solid vitreous thallium silicate has a high refractive index.

The total quantity of thallium compounds in Germany does not exceed 500 kg (based on thallium metal), and is distributed in laboratories, universities, and research institutes.

Glasses and Single Crystals. Glasses composed of the three-component systems As–Tl–S and As–Tl–Se may be prepared by melting the elements together. They are very mobile liquids, even below 400 °C. Viscosity as low as 3 Pa·s has been observed at 250 °C for a composition of, e.g., 25% As, 45% Tl, and 30% S. The glasses are chemically very stable, and insoluble in dilute acids. They are very slightly attacked by alkalis. The electrical resistivity is ca. 10^6 – $10^{18} \Omega\text{cm}$. The glasses have good wetting properties toward many metals, and are extremely impervious. They are therefore suitable for hermetically sealing sensitive electrical equipment (capacitors, resistors, semiconductors, etc.) to protect them from moisture and atmospheric effects. The glasses can be vaporized in vacuo and directly condensed onto the article to be coated [52].

The properties of photochromic glass can be improved by the addition of 0.2–4% thallium (as TlCl added to AgCl).

Single crystals of three-component systems, e.g., Ti_3VS_4 , Ti_3NbS_4 , and Ti_3PSe_4 , are used in acoustical optical measuring equipment, e.g., laser modulators [53].

In the manufacture of quartz single crystals, Tl compounds can provide wavelength selection (optical windows) [54].

Uses. Since the 1970s, it has not been permitted to use thallium compounds for insect pest control in Europe and the United States, so that they are now sold only for special applications. Thallium compounds have also been proposed for impregnating wood and leather to kill fungal spores and bacteria, and for the protection of textiles from attack by moths. A solution of 0.2 g thallium(III) sulfate in 1 L water is suitable both for wood impregnation and seed treatment.

In the manufacture of ethylene oxide, catalysts containing 1 mmol Tl per kilogram catalyst have certain advantages [55]. When recycling polyurethanes at 120–200 °C, Ti_2O_3 0.01 mol/L and catalysts are added to the solutions [56].

Not only colloidal thallium metal, but also its compounds, especially the benzoate, oleate, and amyl alcoholate have been proposed as antiknock agents for internal combustion engines. These compounds are added to the fuel as insoluble suspensions or soluble compounds, or are introduced into the cylinders in other ways [57].

Binary mixed crystals of thallium halides, especially TlBr-TlI and TlCl-TlBr , are highly transparent in the infrared. They are used for the manufacture of plates, prisms, and lenses for infrared instruments [8].

Addition of thallium to the filling materials of high-pressure mercury vapor lamps improves light emission considerably. If thallium iodide is used in place of the metal, provided that certain operating conditions are observed, the spectrum can be modified, i.e., the shade can be corrected [58]. Thallium salts are also added to fluorescent materials as activators.

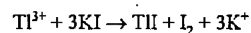
Thallium(I) sulfide is one of the most important photoconductors, and is used in the manufacture of photocells. These are mainly constructed as barrier layer photoconductive cells, i.e., the resistance of the cell is reduced by absorption of light. The cells are especially sensitive in the long wavelength visible and near infrared, and are superior to selenium cells at low radiation intensities [59].

Environmental Aspects. As the natural concentration of thallium in the Earth's crust is 1–3 ppm, it does not constitute a danger to groundwater or rivers (Rhine water, 2 ppb). The most important sources of air pollution are smelting and roasting plants for iron and nonferrous metals, and lignite power stations. Over 95% of the Tl is retained in cyclones and hot electrostatic filters [18]. The total thallium content of all the lignite used in Germany is 1.7 t/a. Of this, 95% is retained in the ash, and only 5% is released to the atmosphere (at an exhaust gas concentration $< 1 \mu\text{g}/\text{m}^3$).

37.9 Analysis

The quantitative determination of thallium is carried out with the aid of the grass-green coloration of the flame, and the spectral line at 535.1 nm, which is easily distinguished from the barium band at 534.7 nm by its sharpness and intensity. There are several wet chemical methods: precipitation of the monovalent ion by hydrochloric acid; the very sensitive reaction with potassium iodide to bright yellow thallium iodide (minimum detectable Tl concentration 1 in 3×10^5); precipitation from neutral solution as the yellow chromate, Ti_2CrO_4 ; or, the most sensitive detection method, precipitation with thionalide as a lemon-yellow complex (concentration limit 1 in 10^7).

Quantitative gravimetric determination is by precipitation as thallium(I) iodide or chromate. The reaction:



is used for volumetric determination, the liberated iodine being titrated against thiosulfate after addition of starch.

The Blumenthal permanganate precipitation is used to concentrate traces of thallium, ether being used to extract Ti^{3+} (Ti^+ cannot be extracted quantitatively with ether).

For the determination of thallium in the microgram and nanogram regions, atomic absorption spectrometry is used, by flame atomic absorption or flameless techniques. Optimal limits of detection are:

- Solid samples (ores, earth samples, dusts, etc.), 0.5 ppm
- Aqueous samples, 0.001 mg/L
- Biological materials, 0.004 ppm [60]

Field desorption mass spectrometry (FD-MS) enables detection and quantitative determination of metallic cations from biological samples and environmental samples in the picogram range, without a separate conversion to ash. With this new technique for the determination of trace and ultratrace quantities, the limits of detection for thallium are ca. 10^{-11} g. The extreme specificity of FD-MS makes elaborate sample preparation unnecessary, except for the tissue and cell components of samples, which must be homogenized and centrifuged; the time required per analysis is only ca. 20 min. The sample size need be only ca. 1 mg [61].

37.10 Economic Aspects

The limited demand can be fully met by suppliers, as the total world demand in 1988 was only ca. 6–8 t. No increase is expected for either the metal or its compounds. Annual production in 1975 was 15 t. The amount of thallium available annually from raw materials used in metal refineries is currently estimated as > 600 t/a.

The price of the metal has increased tenfold since 1975, and is currently ca. US\$170/kg. The price of the 99.999% metal is ca. US\$350/kg [62].

37.11 Toxicology and Occupational Health [64–66]

Thallium is a well-known, highly effective poison. Intoxications occurred in former times due to its use as a medicinal agent for many diseases such as venereal disease, dysentery, and tuberculosis. Another main source of accidental, suicidal, and homicidal exposures was its use as a rodenticide which, however, has been banned during the last decades in many countries. Thallium may be accumulated in mushrooms.

The toxicological significance of thallium is mainly restricted to some inorganic and organic salts of Ti^+ such as TlCl , Ti_2SO_4 (used as a rodenticide [67]), and thallium acetate. Intoxications by elemental thallium are comparatively rare. There is some evidence that, analogously to mercury, Ti^{3+} can be converted in the environment to methylated compounds by microbial action [68], and thus represents a potential cumulative hazard.

Toxicokinetics. Ti^+ ions are readily absorbed from the gastrointestinal tract and distributed into various tissues, resulting in high concentrations in kidneys, myocardium, testes, salivary glands, intestine, skeletal muscle, thyroid and adrenal glands. Uptake of thallium-containing dusts via the respiratory tract results in increased thallium toxicity. Transdermal absorption is also possible, especially after the use of thallium-containing ointments. Thallium ions are able to cross the placental barrier and can produce nail abnormalities and alopecia in fetuses exposed during the last trimester [69]. Thallium ions do not undergo metabolic reactions comparable to those of organic xenobiotics (e.g., hydroxylation and conjugation reactions).

Excretion of Ti^+ ions after strong acute intoxication mainly occurs via the feces. Due to pronounced enterohepatic circulation, the excretion half-life varies widely in the range 1.7–30 d. Only 3% of the entire body burden is excreted per day in the urine [64, 70].

The mechanism of toxicity is not completely understood. There is evidence for interaction of Ti^+ ions with thiol groups, resulting in reactions with a variety of proteins and in inhibition of enzymes such as succinic dehydrogenase. The exchange of the activating K^+ ion by the nonactivating Ti^+ ion leads to inhibition of Na^+ , K^+ -ATPase. Furthermore, Ti^+ is stored in axonal mitochondria, resulting in their destruction [71].

Acute and Chronic Toxicity. The most prominent and characteristic features of acute, subchronic, and chronic thallotoxicosis are seen in the nervous system, skin, and cardiovascular system. Concerning the clinical presenta-

tion, the time course for the development of symptoms can be divided into four stages [65, 72]:

- *During 3–4 h* onset of predominantly gastrointestinal symptoms such as nausea, vomiting, and diarrhea occurs. In severe cases, hematemesis may occur.
- *Within hours to days* various severe symptoms of the CNS (e.g., disorientation, coma, convulsions, psychosis, cerebral edema with central respiratory failure), PNS (combined motor and sensory neuropathy, including severe hyperesthesia of palms and soles), and ANS (tachycardia, hypertension, fever, salivation, and sweating) develop. Symptoms of the cardiorespiratory system, which may predominate in severe cases, include myocardial necrosis with dysrhythmia and pump failure, hypotension, and bradycardia. Skin symptoms include blue-gray lines on gums, dark pigmentation around the hair roots, and acne. The ophthalmologic symptoms are optic neuritis and ophthalmoplegias.
- *During 2–4 weeks* the skin becomes dry and scaly, and white stripes across the nails (Mees's lines), and scalp and facial hair loss appear as characteristic signs.
- *During several months* various CNS and PNS abnormalities such as ataxia, tremor, foot drop, and memory loss may persist.

Genotoxicity. Chromosome aberrations and an increased frequency of DNA breaks were found in embryonic cell cultures. After chronic thallium exposure, precancerous lesions in the female genital tract occurred in mice [64, 73].

Reproductive Toxicity. The reproductive system is highly susceptible to thallium toxicity; in humans some of the highest concentrations have been found in the testes after Tl poisoning [64]. Thallium has been shown to produce teratogenic effects in chick embryos, including achondroplasia, leg bone curvature, parrot beak deformity, microcephaly, and reduced fetal size; the results of teratological investigations in rats, mice, and cats are conflicting [73].

Toxicological Data and Analysis. The average lethal dose of thallium salts is ca. 1 g for adults (ca. 10–15 mg/kg body weight). Low blood thallium levels are only an indication for an exposure, but do not allow conclusions on the degree of an intoxication to be drawn. However, levels above 300 µg/L blood or 100 µg/L urine indicate severe intoxication (0.3 µg/L urine is the average level in unexposed persons). Moreover, the incorporation of thallium into scalp hair is of analytical significance, 7–15 ng/g hair being the normal range.

Treatment. Decontamination of the gastrointestinal tract such as by use of syrup of ipecac, lavage, serial doses of charcoal, and use of cathartics are useful during the first few hours after ingestion. Since thallium occurs as a monovalent cation, chelating agents used for the enhancement of excretion such as dithiocarb, CaNa_2EDTA , BAL (British anti-Lewisite, dimercaprol, 2,3-dimercaptopropanol), and penicillamine are not effective. The combination of hemodialysis (protecting the kidneys) and potassium diuresis has been recommended in the case of severe poisoning. However, hemoperfusion clearance seems to be superior to hemodialysis clearance.

Prussian blue, potassium ferricyanoferrate, in daily doses up to 24 g (combined with a mild cathartic) may be used to interrupt the marked enterohepatic circulation by exchanging Tl^+ for K^+ . The resulting compound cannot be absorbed and therefore causes only minor side effects [71]. Moreover, it does not liberate substantial amounts of cyanide.

Occupational Health. The MAK value is 0.1 mg/m³ soluble Tl compounds measured as total dust. In the United States and the United Kingdom the TLV-TWA is 0.1 mg/m³.

Occupational diseases caused by thallium are included in the list of the German Berufskrankheitenverordnung (Occupation Disease Regulations).

Since thallium tends to accumulate, persons exposed at the workplace should be monitored adequately even in cases of low chronic exposure.

37.12 References

1. Gmelin, Thallium, system no. 38. Ullmann, 3rd ed., 17, 299.
2. J. De Meit, H. C. Dake: *Rarer Metals*, Temple Press, London 1949.
3. N. Lowitzki: "Neueres Schrifttum über Thallium aus den Jahren 1938–1948", *Z. Erzbergbau Metallhüttenwes.* 3 (1950) 201.
4. H. E. Howe, A. A. Smith, Jr.: "Properties and uses of Thallium", *J. Electrochem. Soc.* 97 (1950) 167C.
5. L. Sunderson: "Thallium", *Can. Min. J.* 65 (1944) 624.
6. W. H. Waggaman, G. G. Heffner, E. A. Gee: "Thallium", US Dept. of the Interior, Bureau of Mines Information Circular 7553, 1950.
7. V. Tafel: *Lehrbuch der Metallhüttenkunde*, vol. 2, Hirzel, Leipzig 1953.
8. D. E. Eilertsen: "Thallium, Mineral Facts and Problems", US Dept. of the Interior, Bureau of Mines, Bulletin 585, 1960.
9. C. A. Hampel: *Rare Metals Handbook*, Reinhold Publ., New York 1961.
10. W. Schreiter: *Seltene Metalle*, vol. 3, VEB Deutscher Verlag für Grundstoffindustrie, Leipzig 1962.
11. R. Kleinert: "Thallium, ein seltenes Metall, ein Begleitmetall", *Erzmetall* 16 (1963) 67.
12. R. Kleinert: "Die Verwendung von Thallium", *Erzmetall* 18 (1965) 363.
13. A. G. Lee: *The Chemistry of Thallium*, International Idens. Inc., Philadelphia 1974.
14. H. R. Babitzke: "Thallium, Mineral Facts and Problems", US Dept. of the Interior, Bureau of Mines, Bulletin 667, 1975.
15. W. W. Stanzo, M. B. Tschernenko: *Die chemischen Elemente Antimon–Wismut, Bausteine der Erde*, vol. 3, Verlag MIR, Moskau, Urania Verlag, Leipzig 1976.
16. R. J. De Filippo: "Thallium, Commodity Data Summaries", US Dept. of the Interior, Bureau of Mines, 1977.
17. J. C. Smith, B. L. Carson: *Trace Metals in the Environment*, vol. 1, Ann Arbor Sci. Publ., Ann Arbor, MI, 1977.
18. Abfallwirtschaft: Forschungsbericht 10301327 des Bundesministers des Innern, Germany.
19. F. A. Cotton, G. Wilkinson: *Anorganische Chemie*, 2nd ed., Verlag Chemie, Weinheim 1970.
20. E. Pilgrim: *Entdeckung der Elemente*, Mondus, Stuttgart 1950.
21. W. Schreiter: *Seltene Metalle*, VEB Deutscher Verlag für Grundstoffindustrie, Leipzig 1960.
22. J. Fischer: "Die Dampfdruckkurve des Thalliums", *Festschrift der TH Breslau*, Verlag Korn, Breslau 1935.
23. W. Meißner, H. Franz, H. Westerhoff, *Ann. Phys. (Leipzig)* 13 (1932) 555.
24. C. J. Smithells: *Metals Reference Book*, Butterworth, London 1962.
25. *Am. Ceram. Soc. Bull.* 68 (1989) no. 5, 1070.
26. B. Mason: *Principles of Geochemistry*, Wiley, New York 1958.
27. P. Ramdohr: *Die Erzminerale und ihre Verwachsungen*, Akademie Verlag, Berlin 1960.
28. K. H. Wedepohl: *Handbuch der Geochemie*, Element 81, vol. 2, no. 3, Springer Verlag, Berlin 1972.
29. J. Feiser, *Erzmetall* 15 (1962) 578.
30. J. Feiser, personal communication, 1963.
31. M. T. Koslovskij et al., *Tr. Inst. Khim. Nauk Akad. Nauk Kaz. SSR* 3 (1958) 5.
32. Z. A. Serikov, S. M. Anisimov, *Izv. Vyss. Uchebn. Zaved. Chern. Metall.* 3 (1960) no. 6, 65.
33. I. D. Prater, D. Schlain, S. F. Ravitz, US Dept. of the Interior, Bureau of Mines, report of investigations no. 4900, 1952.
34. W. Langner, A. Göbel, *Erzmetall* 3 (1950) 370.
35. W. Kangro, F. Weingartner, *Erzmetall* 11 (1958) 70.
36. L. G. Plechanov, *Izv. Akad. Nauk Kaz. SSR Razdel. Metallurgii* 4 (1957) 38.
37. A. Gäumann, *Schweiz. Arch.* 21 (1955) 337.
38. A. A. Sokol, L. F. Kozin, *Ukr. Khim. Zh. Kiev* 25 (1959) no. 2, 249.
39. A. R. Powell, *The Institution of Mining and Metallurgy*, London 1950.
40. Duisburger Kupferhütte, DE 954236, 1954.
41. H. Meister, *Angew. Chem.* 69 (1957) 533.
42. Chem. Werke Huls, DE 942989, 1954.
43. Licentia Patentverwaltungs-GmbH, DE 1045999, 1957.
44. T. J. Darvojd, V. N. Vigdorovic, N. A. Jordanskaja, *Izv. Akad. Nauk SSSR Otd. Tekh. Nauk Metall. Topl.* 3 (1961) 55.
45. P. R. Mallory & Co., US 2180845, 1939.
46. F. Enßlin, *Erzmetall* 15 (1962) 419.
47. Unterharzer Berg- und Hüttenwerke, DE 740780, 1942.
48. *Chem. Abstr.* 68 (1968) 98239m.
49. A. E. Roach, C. L. Goodzeit, P. A. Totta, *Nature (London)* 172 (1953) 301.
50. A. Hoffman, F. Rose, *Z. Phys.* 136 (1953/54) 152.
51. H. Moser, *Phys. Z.* 37 (1936) 885.
52. S. S. Flaschen, *J. Am. Ceram. Soc.* 42 (1959) 450; 43 (1960) 168, 247.
53. Westinghouse Electric Corp., US 3929970, 1975; 3929976, 1975.
54. Schafer, *Proc. SPIE Int. Soc. Opt. Eng.* 285 (1981) 183.
55. US 4267073, 1981.
56. JP 8199244, 1981.
57. Ethyl Corp., US 3328440, 1967.
58. D. A. Larson et al., *Illum. Eng. (N.Y.)* Preprint no. 29 (1962).
59. W. Brugel: *Physik und Technik der Ultrarotstrahlung*, Vincentz, Hannover 1961.
60. H. R. Schulten, C. Achenbach, U. Bahr, F. Kochler, R. Ziskoven, *Angew. Chem.* 91 (1979) no. 11, 944. C. Achenbach et al., *J. Toxicol. Environ. Health* 6 (1980) 519–528.
61. M. Sager, G. Tolg: "Spurenanalytik des Thalliums", in: *Analytiker-Taschenbuch*, vol. 4, Springer Verlag, Berlin 1984, pp. 443–466.
62. *Am. Ceram. Soc. Bull.* 69 (1990) no. 5, 885.
63. L. Manzo, E. Sabbioni: "Thallium", in H. G. Seiler, H. Sigel, A. Sigel (eds.): *Handbook on Toxicity of Inorganic Compounds*, Marcel Dekker, New York 1988.
64. M. J. Ellenhorn, D. G. Barceloux: *Medical Toxicology, Diagnosis and Treatment of Human Poisoning*, Elsevier, New York 1988.

65. S. Moeschlin: *Klinik und Therapie der Vergiftungen*, 7. ed., Georg Thieme, Stuttgart 1986.
66. H. U. Wolf: "Thallium" in H. U. Wolf (ed.): *HAGERs Handbuch der Pharmazeutischen Praxis*, 5. ed., vol. 3: Gifte, Springer-Verlag, Heidelberg 1992.
67. W. P. Ridley, L. J. Dizikes, J. M. Wood, *Science* 197 (1977) 329.
68. S. Moeschlin, *Clin. Toxicol.* 17 (1980) 133-146.
69. W. Stevens et al., *Int. J. Clin. Pharmacol. Ther. Toxicol.* 10 (1974) 1-22.
70. P. S. Spencer et al., *J. Cell. Biol.* 58 (1973) 79-95.
71. F. H. Lovejoy, *Clin. Toxicol. Rev.* 4 (1982) 1-2.
72. E. Sabbioni, L. Manzo in L. Manzo (ed.): *Advances in Neurotoxicology*, Pergamon Press, Oxford 1980.
73. Berufskrankheitenverordnung, BK Nr. 1106: Erkrankungen durch Thallium oder seine Verbindungen.

38 Selenium

BERND E. LANGNER

38.1 Introduction	1557	38.6 Environmental Protection	1563
38.2 History	1557	38.7 Uses	1564
38.3 Properties	1558	38.8 Quality Specifications and Analysis	1566
38.4 Occurrence and Raw Materials	1559	38.9 Compounds	1566
38.5 Production	1560	38.10 Economic Aspects	1567
38.5.1 Primary Production	1560	38.11 Biological Activity and Toxicology	1568
38.5.2 Secondary Production	1562	38.12 References	1569
38.5.3 Refining	1563		

38.1 Introduction

Selenium, atomic number 34, is a member of group 16 of the periodic table and thus belongs to the chalcogens. Consonant with its position between the nonmetal sulfur and the metalloid tellurium, it has mainly nonmetallic properties.

Naturally occurring selenium consists of six stable isotopes: ^{74}Se (0.9%), ^{76}Se (9.0%), ^{77}Se (76%), ^{78}Se (23.5%), ^{80}Se (49.8%), and ^{82}Se (9.2%).

38.2 History

Selenium is 66th in order of natural abundance in the earth's crust, with an average concentration of 0.05 ppm. Selenium was discovered in 1817 by BERZELIUS in deposits in lead chambers used for the production of sulfuric acid from copper pyrites. The name selenium is derived from $\sigma\epsilon\lambda\eta\nu\eta$, the Greek word for moon, and reflects the close resemblance between selenium and tellurium (= earth), which was discovered about 20 years earlier.

Selenium is a by-product of the extraction of metals such as copper, zinc, and lead, and has many industrial applications based on its chemical and physical properties. Its semiconducting properties and the light-induced varia-

tion of its electrical conductivity are of particular importance.

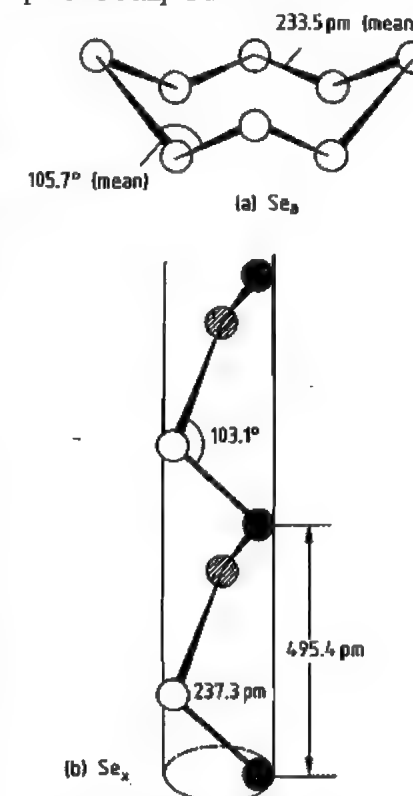


Figure 38.1: Structures of selenium: a) Se_8 molecule in red α -, β -, and γ -selenium; b) Helical chains in hexagonal gray selenium [4].

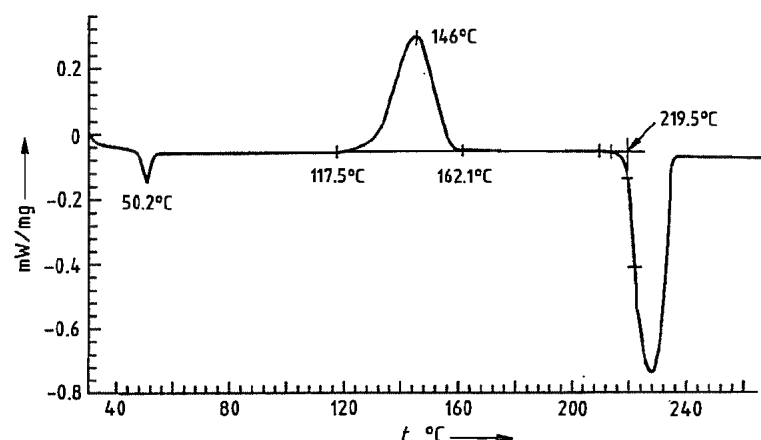


Figure 38.2: Differential thermal analysis of distilled high-purity selenium after 3 h at 450 °C to give a material of uniform structure [8].

38.3 Properties [1-4]

Like sulfur, selenium exists in several allotropic forms. The structures of these and the mechanism of transformation of one into another are not completely understood. Red selenium is a thermodynamically unstable, high-energy modification produced by precipitation at low temperature, crystallization of selenium from solution, or quenching of selenium vapor or molten selenium. The three modifications of monoclinic selenium (α -, β -, and γ -selenium) consist of Se_8 rings and differ only in the packing of these in the crystal (Figure 38.1). The red, amorphous form consists of chains in an irregular arrangement. It is soluble in carbon disulfide and to some extent in benzene, giving red solutions from which it can be crystallized. Red selenium is an electrical nonconductor. In the vapor phase, selenium exists mainly as Se_8 rings. At higher temperature these decompose into smaller units, eventually forming Se_2 molecules.

Thermodynamically unstable vitreous or amorphous forms are obtained by rapid cooling of molten selenium. The structure of these modifications is not yet fully understood. Presumably, high molecular mass selenium rings of various sizes are present, which explains the poorly defined melting point of industrial-grade vitreous selenium. This product softens

at ca. 50 °C to a rubberlike state and is transformed at > 100 °C into the gray, crystalline form, with release of the heat of crystallization. The black, nonconducting form is slightly soluble in carbon disulfide. Structures similar to those in vitreous selenium are present in molten selenium.

On heating to > 100 °C, both the red and the black forms are transformed into the stable, gray, hexagonal ("metallic") form in an exothermic reaction. This modification is also produced by reducing selenous acid with sulfur dioxide at high temperature. Unlike the ring structure of the unstable forms, it consists of helical chains in which the structure is repeated at every third atom (Figure 38.1). Gray selenium is a semiconductor whose electrical conductivity increases by a factor > 1000 under the influence of light (photoconductivity).

Impurities have a great influence on crystallizing properties, so results given in earlier research work, where impurity content is not quoted, are often erroneous. Also, the previous history of the material (e.g., high-temperature treatment) plays an important role in the transformations between various allotropic forms. The thermal properties of selenium can be conveniently investigated by differential thermal analysis [8]. Figure 38.2 shows the various transformations of distilled selenium on melting. The brittle vitreous form is trans-

formed at 50 °C into the ductile vitreous form (glass transition). Above ca. 120 °C, vitreous selenium changes into the stable hexagonal crystalline form, which melts at 220 °C.

Important physical properties of selenium are given below [1, 4]:

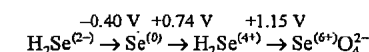
Electronic structure	[Ar] $3d^{10} 4s^2 p^4$
Oxidation states	2-, 0, 4+, 6+
Atomic radius	0.140 nm
Ionic radii	
Se^{2-}	0.191 nm ⁺
Se^{4+}	0.050
Se^{6+}	0.042
Ionization energy	940 kJ/mol
Ionization potential	
I	9.75 eV
II	21.5
Electronegativity (Pauling)	2.4
Density at 25 °C	
Hexagonal	4.189 g/cm ³
α -Monoclinic	4.389
Vitreous	4.285
Liquid (490 K)	3.975
Melting point	217 °C
Boiling point (101.3 kPa; 760 mm Hg)	684.7 ± 0.03 °C
Vapor pressure at 344.6 °C	0.133 kPa (1 mm Hg)
at 431.5 °C	1.333 (10)
at 547.4 °C	13.33 (100)
at 636.5 °C	53.32 (400)
Electrical resistivity ¹ at 25 °C	$10^{10} \Omega/\text{cm}$
at 400 °C	1.3×10^5
Glass transition temperature ² (vitreous modification)	30.2 °C

The electrical conductivity is strongly dependent on purity. Thus, the conductivity of selenium, including the poorly conducting amorphous form, can be increased considerably by traces (a few parts per million) of halide ions or by alloying elements such as tellurium or arsenic. Because the electrical properties are sensitive to the presence of crystal defects, the purity of selenium, which can be deliberately controlled by doping or alloying with other elements, plays an important role in its use in electrical and electronic applications.

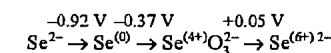
The chemical properties of selenium are intermediate between those of sulfur and those of the metalloid tellurium. In its compounds, it mainly exhibits the oxidation states 2-, 4+, and 6+. The oxidation state 6+ is considerably less stable than for sulfur, and in acid solutions

is attained only by the action of strong oxidizing agents such as chlorine or hydrogen peroxide. Selenate(VI) is more easily obtained by oxidation in alkaline solution. The redox potentials of selenium in acid and alkaline solution are as follows [4, 7]:

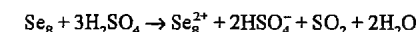
Acid:



Alkaline:



Selenium burns in air to form selenium dioxide, which has the smell of rotten radishes. Selenium is oxidized by nitric acid to selenous acid. No reaction occurs with nonoxidizing acids such as hydrochloric acid. Hot, concentrated sulfuric acid dissolves selenium, giving a green color and forming polymeric selenium cations, for example:



With chlorine, vigorous oxidation to selenium tetrachloride occurs. Selenium reacts with electropositive elements (e.g., many metals) to form selenides and is therefore strongly corrosive, especially at high temperature. With hydrogen, the toxic gas hydrogen selenide is formed. Selenium combines with sulfur to form nonstoichiometric alloys.

Selenium dissolves in solutions of strong alkali, disproportionating into selenide and selenite. It dissolves in alkali-metal sulfides, sulfites, and cyanides, with formation of addition compounds

38.4 Occurrence and Raw Materials

Pure selenium minerals are very rare. Thus, berzelianite (Cu_2Se), tiemannite (HgS), and naumannite (Ag_2Se) are never processed simply to obtain selenium. However, selenium occurs in various concentrations as an accompanying element in many sulfidic ores, although isomorphic substitution in copper pyrites, iron pyrites, or zinc blende cannot ex-

¹ Strongly dependent on purity and light intensity.

² Strongly dependent on purity.

ceed a theoretical maximum of 0.5% because of the larger ionic radius of selenium (Se^{2-} : 0.191 nm, S^{2-} : 0.174 nm). The selenium content of pyrites, zinc blende, galena, and molybdenite is too low for economic recovery. However, most copper concentrates from ore flotation contain ca. 100–400 g/t selenium and are hence the most important sources of selenium. Selenium production is therefore closely linked to copper production.

Selenium occurs in low concentrations (ca 15 g/t) in some types of coal and mineral oil.

In addition to extraction of selenium from copper ore, the recycling of photocopying drums and rectifiers is becoming an important source.

38.5 Production

38.5.1 Primary Production

Selenium is an accompanying element obtained during copper production. The sulfidic copper concentrate (e.g., chalcopyrite) is smelted in an oxidizing atmosphere to give a copper matte containing 40–70% Cu. This is then blown in a converter to yield crude copper. After reduction of excess copper oxide, the crude copper is cast into anodes. Along with other impurities, these copper anodes contain 25–70% of the selenium, depending on the smelting process. The rest of the selenium vaporizes during smelting, mainly as selenium dioxide. This is reduced to the element by the sulfur dioxide produced during smelting and collects in the slime formed in the gas purification equipment.

However, recovery is generally uneconomical due to the complex composition of the slime. Likewise, in the roasting of pyrites and zinc or lead ore, most of the selenium volatilizes and concentrates in the slime in the gas purification equipment. The selenium remaining in the copper anodes is mainly in the form of Cu_2Se , or sometimes CuAgSe and Ag_2Se , depending on the silver content. Because they are insoluble in the sulfuric acid electrolyte, these selenides remain in the anode slime dur-

ing electrolytic refining of the copper, as do the noble metals. As a result of the high stability of noble-metal selenides, the copper selenides initially present in the anodes can be converted to silver selenide or gold selenide under the influence of the electrolyte, depending on the noble-metal content. The selenium in the anode slime is therefore in the form of various compounds, depending on the silver content. The selenium content of the anode slime varies with the raw material and can reach > 20%.

Selenium contents (%) of anode slimes (from which residual copper has not been removed) from various copper tankhouses are as follows [9]:

CCR (Noranda), Canada	10.0
Chuquicamata, Chile	4.0
Copper Refineries Pty, Australia	0.7
IMI Refiners, United Kingdom	2.0
Inco, Canada	8.4
Kidd Creek, Canada	19.5
MHO, Belgium	5.1
Norddeutsche Affinerie, Germany	7.5
Palabora, South Africa	3.6
Phelps Dodge, United States	8.8
Southwire, United States	0.6

The precious metals can be recovered only by decomposing the very stable selenides with very strong acid or alkali, or by roasting. Selenium must be removed from the anode slime before the noble metals can be recovered. The important processes are [10]

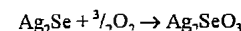
- Fusion with sodium carbonate
- Roasting with sodium carbonate
- Direct oxidation (roasting)
- Oxidative leaching with sodium hydroxide solution under pressure
- Roasting with concentrated sulfuric acid
- A hydrometallurgical process of chlorination in hydrochloric acid

In roasting with sodium carbonate, the anode slime is first treated with sulfuric acid solution to remove the copper and then mixed with sodium carbonate and water to give a stiff paste. The paste is extruded or pelletized, and dried. It is then roasted at 530–650 °C in a stream of oxygen air. Sodium carbonate prevents vaporization of the selenium as selenium dioxide by converting it completely into so-

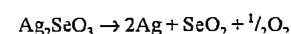
dium selenate. The roasted pellets are ground and leached with water to dissolve sodium selenate. The precious metals remain in the solid residue, which also contains tellurium in the form of sodium tellurate if higher roasting temperatures are used. The selenate is crystallized from solution and reduced with active carbon to sodium selenide, which is redissolved in water and oxidized with air to elemental selenium. However, this process leads to the formation of large amounts of wastewater.

Elemental selenium can also be precipitated from selenate solution by strongly acidifying with hydrochloric acid and reducing with iron(II) salts or sulfur dioxide. Alternatively, the sodium carbonate solution can be decomposed by adding acid to precipitate impurities such as tellurium. After filtration and further acidification, selenium is precipitated by reduction (Figure 38.3).

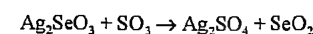
In the direct oxidation process, copper is removed first from the anode slime by sulfuric acid. The slime is then dried and mixed with inert materials that prevent sintering, and the selenium is volatilized as selenium dioxide vapor at 600–900 °C. Silver selenite is formed initially at < 400 °C



and decomposes at higher temperature



Selenium dioxide and some of the sulfur dioxide formed from the sulfate fraction of the anode slime are removed from the gas phase by scrubbing with water or sodium hydroxide solution. After acidifying the wash liquor, the selenium is reduced with sulfur dioxide (Figure 38.4). Very high volatilization rates are achieved at < 600 °C if the oxidative roasting is carried out in the presence of sulfur dioxide. The reaction is believed to occur via the intermediate formation of sulfur trioxide, which reacts with silver selenite:



This method is used by Outokumpu [11]. The selenium dioxide produced is absorbed in dilute sulfuric acid and immediately precipitated

as elemental selenium by the excess sulfur dioxide in the scrubbing equipment.

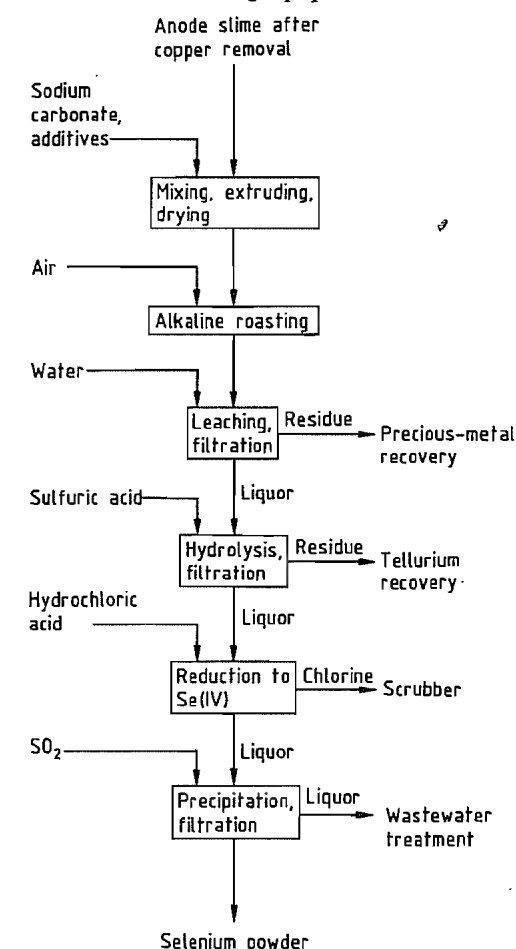


Figure 38.3: Recovery of selenium from copper anode slime by roasting with sodium carbonate.

Whereas roasting is carried out below the melting point of the anode slime, in the classical Doré process (Figure 38.5) the anode slime is melted after addition of fluxes. A matte consisting mainly of silver selenide and a high-lead slag containing precious metals are formed. The slag can be processed in a lead smelting works, or the noble metals can be recovered by flotation. The selenium-containing matte is oxidized in the molten state in a second stage, and selenium is vaporized as its dioxide and absorbed in a scrubbing stage. In a

process operated by the Canadian copper producer Noranda, these two stages are carried out in succession in a top blown rotary converter [12].

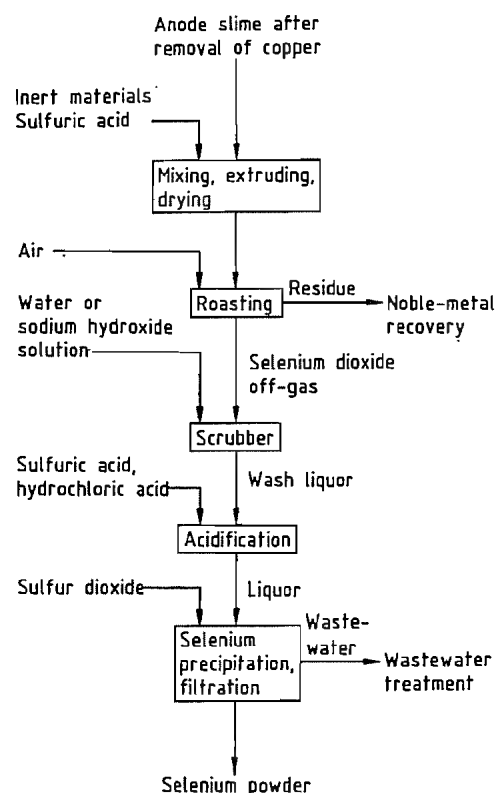


Figure 38.4: Recovery of selenium from copper anode slime by acidic roasting.

Alternatively, roasting with sulfation is carried out in the presence of concentrated sulfuric acid at 500–600 °C after removal of tellurium [9], although the large quantities of sulfur dioxide and sulfur trioxide aerosols formed can present environmental problems, and the severely corrosive properties of sulfuric acid at high temperature are difficult to deal with.

Apart from the widely used high-temperature processes, hydrometallurgical extraction of selenium from copper anode slimes is of some importance in small plants [13–15]. For example, in the copper refinery Austria-Metall [14], the anode slime is leached with hydro-

chloric acid and chlorine, whereby the gold, platinum metals, and selenium (as selenous acid) dissolve, and silver remains in the residue as silver chloride. Selenium is then precipitated from the hydrochloric acid solution by reduction with SO_2 .

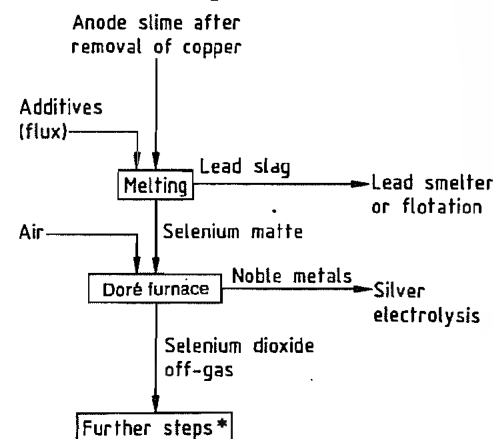
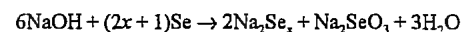


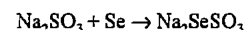
Figure 38.5: Recovery of selenium from copper anode slime by the Doré process. * See Figure 38.4.

38.5.2 Secondary Production

Although most selenium comes from primary production, recycling of the selenium in used rectifiers and photocopying drums is becoming increasingly important for environmental reasons. An older recovery process involves fusion with sodium hydroxide to dissolve the selenium, forming polyselenides:



Selenium is obtained by acidifying the solution, but toxic hydrogen selenide may be formed. This can be prevented if an alkaline solution of sodium sulfite is used in the treatment process. This dissolves selenium selectively, forming sodium selenosulfate:



Selenium can be recovered by acidification, which produces SO_2 .

In another process, selenium is treated with sodium hydroxide solution and hydrogen peroxide to give a mixture of sodium selenite and sodium selenate. The solution is acidified, and

selenium is precipitated by sulfur dioxide [16].

Selenium can also be removed mechanically from photocopying drums by using a water jet. The aluminum drum can be reused whether selenium is removed chemically or mechanically; the selenium on photocopying drums is thus 100% recyclable without any deterioration of its quality. Recycling of photocopying drums is currently performed on a large scale (e.g., by the company Retorte).

Selenium can be dissolved selectively from residues by leaching with ammonia or amines in an aprotic solvent in the presence of carbon monoxide, to form amine salts of selenocarbamic acid. It can then be precipitated in a pure state by heating, with recovery of carbon monoxide and the amine [17].

38.5.3 Refining [3]

The roasting processes, followed by precipitation with sulfur dioxide, gives selenium with a purity usually exceeding 99%, which is adequate for many chemical applications. However, for electronic applications or xerography, selenium must be purified further, because of the sensitivity of its physical properties to the presence of impurities.

The simplest method of purification is distillation at atmospheric pressure and ca. 650 °C, which gives a purity up to 99.99%. All the nonvolatile elements, such as copper, nickel, iron, and tellurium (if present as the dioxide), remain in the distillation vessel. However, sulfur and mercury (as HgSe) also distill over and are thus not removed. Therefore, the crude selenium should not contain mercury. A sufficiently pure product is obtained if some of the selenium is not distilled, ca. 50% being left behind in the distillation vessel to be returned later to the recovery process. The corrosive properties of selenium vapor cause problems during distillation, and purified selenium that is collected in cast iron vessels sometimes becomes contaminated with iron. Improved separation is obtained by vacuum distillation at 0.7–1.3 kPa and 360–400 °C, or at 0.1 Pa and 260 °C, which also reduces cor-

rosivity [18]. A further improvement in quality is obtained if the melt is selectively oxidized by atmospheric oxygen before distillation. This gives better separation of the more readily oxidized impurities.

An alternative to distillation for producing high-quality selenium is vaporization with oxidation, the selenium dioxide vapor formed being absorbed in pure water. Mercury can be removed from the solution by adsorption, and the other metallic ions by ion exchangers. Elemental selenium is then precipitated with high-purity sulfur dioxide. Purities > 99.99% can be achieved in this way [19]. After precipitation, the selenium powder is washed and can be remelted if desired (e.g., to produce granules or to homogenize the structure).

High-purity selenium is also obtained by the hydride process. Impure selenium is treated with hydrogen at ca. 550–685 °C to form hydrogen selenide, which is then decomposed at 1000 °C. Alternatively, it can be cooled to remove gaseous impurities before thermal decomposition is carried out [20].

38.6 Environmental Protection

Selenium is toxic at high concentration and must therefore be effectively removed from off-gases and wastewater. Since oxidizing processes are used, selenium is present in the off-gas as selenium dioxide. After cooling, it can be removed either by dust filters or, because of its high solubility, by absorption in water or sodium hydroxide solution in gas-scrubbing equipment. Because selenium dioxide is readily reduced by organic compounds or sulfur dioxide, the off-gas always contains a small amount of elemental selenium. The selenium-containing dust filtered out thus generally has a reddish color.

The wastewater treatment process and the minimum attainable selenium content both depend on the form in which selenium is present and on the other components in the wastewater. Although selenites in acid solution are reduced readily to insoluble selenium, complete

removal is often difficult, because the selenium sometimes precipitates as a colloid and the reduction is very slow, especially in dilute solution. Therefore, precipitation aids such as hydroxides of aluminum or iron must be added usually. Adsorptive precipitation then enables a final content of $< 10 \text{ mg/L}$ Se to be achieved in the wastewater.

Selenium-containing wastewater, as produced in the sour waters from petroleum refining, can be purified by ion exchange [21].

38.7 Uses [5, 6]

The uses of selenium and selenium compounds can be divided into the following categories [22]:

Electronic applications	ca. 25%
Pigments	ca. 10%
Glass	ca. 40%
Metallurgy	ca. 10%
Agricultural and biological applications	5%
Other uses (e.g., additives for rubber vulcanization, oxidation catalysts)	ca. 10%

Rectifiers. Selenium conducts electricity preferentially in one direction, and this property has been utilized since 1920 for converting alternating to direct current. A selenium rectifier consists of a steel or aluminum plate coated with nickel, with an additional coating of selenium, 50–60 μm thick. A sprayed cadmium alloy is used as a counterelectrode. Several of these rectifiers can be stacked in series. The efficiency of rectification is ca. 85%. Although selenium rectifiers have been increasingly replaced by germanium and silicon diode rectifiers, selenium is still used where the performance of the rectifier must be maintained even in the presence of high counter-voltage peaks.

Xerography [23]. The use of selenium in photocopying technology is based on its sensitivity to light. Selenium, which may be highly pure, doped, or alloyed, is deposited by a vaporization process to form a film, ca. 50 μm thick, on an aluminum drum. In the copying process, the selenium surface is first charged by a high-voltage corona discharge. The drum is then exposed to the projected light from the picture. Where the light falls on the drum, the

charge on the selenium flows away, and a latent picture is thereby formed. After the illumination stage, the thermoplastic toner powder is applied to the drum, attracted electrostatically to the charged parts (not illuminated), and then fixed by heat. A photograph of a used photocopier drum after 60 000 photocopying runs is shown in Figure 38.6. The pure, amorphous selenium originally used to coat the drums is very fragile and crystallizes at high temperature. Therefore, selenium stabilized with tellurium or arsenic is now often used (selenium tellurium alloys or arsenic triselenide), generally doped with small amounts of chlorine. The alloys containing high-purity tellurium enable copying rates to be increased and light of a wider spectral range to be used. A still-higher copying rate and wider spectral range are possible with arsenic triselenide, which has been used increasingly in recent years despite its toxicity and problems in manufacture. The drums also have a considerably longer life. The selenium-based system is now being replaced by organic photoconductors and amorphous silicon in low-cost applications. However, selenium is maintaining its position in industrial applications because of its long life and high photocopying capacity. Whereas a drum with organic photoconductors has a lifetime of ca. 10 000–30 000 copies, drums coated with selenium can withstand more than 100 000 copying operations.

A potential application of xerography with selenium as the photoconductor is in medicine. Here, X rays are used instead of visible light to form the latent image. The advantage of this process lies in the possibility for direct digitization without producing a copy or a film, so that the X-ray image is generated directly by a computer on a visual display unit, and can be stored and processed. Although several patents exist and comprehensive research has been carried out, the process is not yet in general use [24, 25].

Glass Manufacture. Selenium and selenium compounds are used in silicate glass both in decolorization and as a colorant for producing

intense yellow to red glass for special applications (selenium pink glass).

Figure 38.6: Selenium-coated photocopier drum after 60 000 copies.

The main application in glass manufacture is in the decolorization of glass, which is always colored green to yellow green by traces of iron(II) and iron(III). The addition of 30–150 g/t selenium compensates for this color by adding the pink of the selenium, with no apparent reduction in transparency [26]. Formerly, selenium was added mainly as the element. However, elemental selenium volatilizes below the melting temperature of glass, so the yields were usually $< 50\%$. Therefore, selenium compounds such as sodium selenite, sodium selenate, barium selenite, or zinc selenite are now increasingly used. Even so, some volatilization losses are unavoidable. If an excess of selenium is used, pink glasses are obtained that used to be important for artistic purposes.

The addition of cadmium sulfoselenide to glass gives intense colors such as those required for signal technology (e.g., traffic lights). The colors vary from yellow to red, depending on the CdSe content and melting conditions. Because of the volatility of selenium compounds, reproducible color control is difficult.

Pigments. Selenium is used as a pigment in the form of cadmium sulfoselenide. Replacement of part of the sulfur in cadmium sulfide by selenium changes the yellow color to an intense red. The pigment has good brightness and high stability. It is an important colorant for plastics, because the addition of up to 1.5% cadmium sulfoselenide does not significantly affect their physical properties; it is also stable at the temperatures used for injection molding and extrusion. However, the importance of these pigments has declined considerably because of the toxicity of cadmium compounds. In some areas, the use of cadmium sulfoselenide is prohibited.

Metallurgy. The addition of selenium to steel improves its machinability, resulting in higher cutting speeds, lower energy consumption, and a longer lifetime for the machine tool. Although this is often achieved by adding sulfur, selenium is always used where good hot and cold formability, corrosion resistance, and surface finish are also required. For stainless steel, the addition rate is ca. 0.1–0.3% Se. The machinability of copper can also be improved by addition of selenium, but tellurium is used more often. Addition of up to 0.1% selenium to magnetic silicon steels improves their magnetic properties for use in transformer cores. Selenium is also used in lead accumulators to improve the casting and mechanical properties of lead antimony alloys with low antimony content.

Ferroselenium, copper selenide, and nickel selenide are used in metallurgy.

Agriculture. Although the toxicity of soil with high selenium content has long been known, only much later was the need for selenium as an essential trace element in low concentrations discovered. A number of diseases formerly thought to be due to vitamin E deficiency are in fact the result of a deficiency of selenium. For example, the addition of 0.1–0.3 ppm selenium to the feed of chickens and pigs considerably increases their growth rate and prevents certain diseases, although the mechanism of this is not fully understood. Selenium may act as an antioxidant or free-radical trap.

The high rate of heart disease in Finland is thought to be due to a selenium deficiency, the soil being low in selenium, and the law now requires that 6–16 g/t selenium be added to fertilizers used there.

Selenium is added to fertilizers or animal feed in the form of sodium selenite or sodium selenate, which are absorbed more readily by plants.

Other Uses. Selenium and selenium compounds (e.g., Selenac, dialkylselenium carbamates) are added with sulfur in rubber manufacture. This improves the thermal stability of the product and controls the vulcanization rate.

Selenium compounds are used to a small extent as additives to oxidation catalysts for hydrocarbons. Selenium dioxide is also used as a selective oxidizing agent in organic chemistry.

Selenium acts as an absorbent for mercury, forming stable mercury selenide, in gas purification [27].

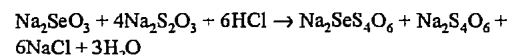
Addition of up to 5% selenium has been proposed in the preparation of dental amalgams [28].

38.8 Quality Specifications and Analysis

Standard-grade selenium containing 99.5% Se is adequate for chemical and metallurgical use, although many producers supply a 99.9% Se material. A special pigment grade containing 99.8% Se is also marketed. The standard grades are supplied as powders of various bulk densities, depending on precipitation conditions. The standard grade is used mainly as starting material for the production of high-purity selenium for photocopiers and electronic applications, which require a product containing > 99.999% Se. Here, the heavy-metal content must also be as low as possible, and the oxygen content should be much less than 5 ppm. Electronic-grade selenium is supplied in the form of granules, which can be produced by pouring molten selenium into deionized water. In addition to chemical anal-

ysis, the quality assessment of high-purity selenium includes measurement of electrical and especially the photoelectrical properties [29]. The crystallization temperature, determined by thermal analysis, can give a useful indication of the impurities in selenium (Figure 38.2), although interpretation of the results is not always unambiguous.

The methods of analysis for selenium depend on the matrix material. Direct spectroscopic determination in raw materials and intermediate products is usually impossible due to lack of standards. Hence, selenium-containing materials are first treated with nitric or sulfuric acid, for example, to dissolve the selenium as selenous acid. Most methods of determination involve reduction of selenous acid with various reducing agents, usually in solution in strong hydrochloric acid. Selenium can be determined gravimetrically after reduction with iron(II), for example, if the hydrochloric acid concentration is such that precipitation is complete and no loss of SeCl_4 vapor occurs [30]. The precipitated selenium is weighed, or redissolved and determined by atomic absorption spectroscopy, inductively coupled plasma, or direct coupled plasma spectroscopy [31]. In one of the oldest methods still in use, selenous acid is titrated with thiosulfate according to the equation:



Sodium monoselenopentathionate is formed, and the excess of thiosulfate is back-titrated iodometrically [32].

38.9 Compounds

Selenium forms a large number of chemical compounds, some of which are of major industrial importance.

Selenium Dioxide, Selenous Acid, Selenites. Volatile selenium dioxide (sublimes at 315 °C) is formed by the combustion of selenium-containing materials. Selenium dioxide dissolves readily in water (800 g/L at 85 °C) to form selenous acid. Unlike sulfur dioxide selenium dioxide and selenous acid are easily re-

duced to selenium by reducing agents such as sulfur dioxide. Even traces of organic material reduce part of the selenium dioxide to selenium, resulting in a slightly reddish color of the SeO_2 . The sensitivity to reduction is increased by the influence of light. Selenium dioxide is used to oxidize alkyl groups to carbonyl groups in organic chemistry, as a lubricant additive, and as an additive in the electrolysis of manganese. Selenous acid is more stable than sulfurous acid and can be isolated in the pure state in the form of colorless prisms. Selenous acid decomposes above 70 °C, forming selenium dioxide and water. Sodium selenite, zinc selenite, and barium selenite are important additives in glass manufacture. These salts are prepared by the reaction of selenous acid with the corresponding hydroxides or oxides, followed by crystallization.

Selenium Trioxide, Selenic Acid, Selenates. Selenous acid is oxidized to selenic acid by strong oxidizing agents such as chlorine, chloric acid, ozone, or anodic oxidation. Selenic acid is a hygroscopic solid that melts at 59.9 °C. It is a much stronger oxidizing agent than sulfuric acid; for example, a mixture of concentrated selenic acid with concentrated hydrochloric acid evolves chlorine. Selenic acid can be dehydrated with phosphorus pentoxide or by applying vacuum (200 Pa) at 160 °C to give the strongly oxidizing selenium trioxide (*mp* 118 °C). Above 185 °C, selenium trioxide decomposes into selenium dioxide and oxygen. Selenates are formed by the reaction of selenic acid with metal oxides or hydroxides, and resemble the isomorphous sulfates in both structure and solubility. Sodium selenate has recently become an important fertilizer additive.

Hydrogen Selenide, Selenides. Hydrogen selenide can be obtained either directly from the elements at ca. 400 °C or by decomposition of the selenides of iron, magnesium, or aluminum with hydrochloric acid. It is a colorless gas (*bp* -41.3 °C) smelling like rotten radishes, is even more toxic than hydrogen sulfide, and has a very irritating effect on the

mucous membranes, causing bronchial and nasal irritation. Hydrogen selenide is less stable than hydrogen sulfide and can be oxidized to selenium by air, especially in the presence of light. Heavy-metal selenides such as copper selenide form the basis of selenium extraction from ores. Cadmium selenide, produced from cadmium and selenium, is used in the pigment industry together with cadmium sulfide.

High-purity zinc selenide is an important infrared optical material. Single crystals can be produced by reacting zinc vapor with hydrogen selenide (chemical vapor deposition, CVD). Copper indium selenide could be the basis for solar cells of the future; light efficiencies of 14% at an energy flux density of > 100 W/m² can be achieved. However, the manufacturing process (CVD) is expensive [23, 33].

Selenium disulfide is formed by reaction of hydrogen sulfide with selenous acid or by direct combination of the elements. The red powder (*mp* ca. 100 °C) is used in concentrations of < 1% in shampoos and hair preparations for the treatment of dandruff.

Selenium Halides. The action of halogens or halides on elemental selenium yields various selenium halides, depending on the temperature and stoichiometric ratio. Selenium monochloride, Se_2Cl_2 (ρ 2.774 g/cm³), and selenium monobromide, Se_2Br_2 (ρ 3.604 g/cm³), are intensely colored, heavy liquids. SeCl_4 and SeBr_4 are crystalline substances that readily form complexes with alkali-metal halides. Selenium exhibits the oxidation state 6+ only in SeF_6 , the corresponding chloride and bromide being unstable. Of the oxyhalides, selenyl chloride, SeOCl_2 , is liquid at room temperature and is remarkable for its extreme reactivity, combining with almost all elements.

38.10 Economic Aspects

The total consumption of selenium in 1989/1991 was ca. 2100–2300 t/a (Table 38.1) [22, 34]. Average consumption in previous years was ca. 1700 t/a, although the published figures are unreliable due to the lack of informa-

tion from Eastern European countries. Of the total, about one-third is produced as high-purity selenium for electronic applications. Since selenium is a by-product of copper production, its price is subject to very wide variations due to over- or underproduction from time to time. In recent years, the price of selenium has decreased considerably (Table 38.1). However, most dealing takes place not on the open market, but directly between the producer and consumer, so the true prices differ from the published prices. The price for standard-grade selenium in 1990 was ca. \$10/kg, and for high-purity selenium ca. \$30–50/kg [22]. Manufacturers of elemental selenium in the Western world include the large copper producers Noranda Mines (Canada); Norddeutsche Affinerie AG (Germany), with its subsidiary Retorte producing selenium compounds and high-purity selenium; Metallurgie Hoboken-Overpelt (Belgium); Mitsubishi Metals, Nippon Mining, Sumitomo (Japan); Outokumpu (Finland); ASARCO, Kennecott, and Phelps Dodge (United States) [35]. Selenium compounds are also produced by Degussa (Germany).

Although the consumption of selenium compounds in the glass industry and as a fertilizer additive is increasing, the use of cadmium selenide in pigments is decreasing, and selenium is being replaced by organic photoconductors in some types of xerography. Therefore the total consumption of selenium is not expected to increase in the near future. However, the supply of selenium could decrease in the future if copper is produced partly by hydrometallurgical processes, which do not yield a selenium by-product.

38.11 Biological Activity and Toxicology

Although selenium is an important trace element in low concentrations, it is toxic at higher concentrations. It is an essential trace element in the selenoenzyme glutathione peroxidase. This enzyme, together with vitamin E, is important for the protection of cells from

oxidative attack. The activity of glutathione peroxidase in red blood corpuscles correlates well with the selenium concentration up to 100 µg/L [36, 37]. Low selenium levels in the blood cause heart disease. For instance, in China, Keshan disease, a cardiomyopathy, caused the deaths of a large number of people, especially children, until the daily consumption of selenium was found to be very low. The transition from essential trace quantities to toxic quantities of selenium in terms of intake in food is summarized below [37]:

Low-selenium area with Keshan disease	11 µg/d
Selenium adequate area	116 µg/d
National Academy of Sciences, Food and Nutrition Board "safe and adequate" range	50–200 µg/d
Lowest observed effect level (LOEL)	3200 µg/d
High-selenium area with chronic selenosis	4990 µg/d

Table 38.1: Estimated production (t), consumption (t), and price (\$/kg) of selenium [22, 35].

	1989	1990	1991
Production			
Belgium	275	360	260
Canada	270	340	240
Chile	40	40	40
Finland	10	25	25
Germany	110	110	100
Japan	534	550	631
South Korea	20	25	25
Mexico	25	25	25
Peru	20	20	20
Philippines	120	120	120
Sweden	60	30	30
United States	253	287	240
Yugoslavia	50	60	40
Zambia	50	60	40
Others	100	100	100
Total	1937	2052	1918
Consumption			
United States	560	530	500
Japan	283	289	263
Europe	830	800	770
China	200	300	350
Others	300	300	300
Total	2173	2119	2283
Average price	13.81	11.26	10.56

The concentration of selenium in the blood should be 60–100 µg/L. Although small amounts of selenium may reduce the risk of cancer, as indicated by some investigative studies, this has not been proved conclusively.

A chronic high selenium intake of > 5 mg/d gives rise to nonspecific symptoms such as

hair loss, changes to the fingernails, diarrhea, effects on the central nervous system, and nonspecific changes to the liver. Also, a loss of appetite and a tendency to walk in a circle can occur. High concentrations of selenium in the workplace can cause headaches and "selenium catarrh". Also, the breath can have a garliclike smell due to the formation of methyl selenide, although this effect is much less pronounced than with tellurium.

A few selenium compounds exhibit acute toxicity. Irritation of the mucous membranes of the digestive system, liver damage, and toxic edema of the lungs have been observed. The most toxic compound is hydrogen selenide, for which the MAK is 0.05 ppm, the MAK value for other selenium compounds being 0.1 ppm. In the United States, the TLV is 0.2 mg/m³. In a study carried out in Canada on people working in selenium production, if the TLV was exceeded slightly (up to 0.8 mg/m³) for limited periods, no symptoms resulted [38]. In Germany, the limit in drinking water is 0.008 mg/L [39], and in the United States, the EPA recommends a maximum contamination level (MCL) of 0.01 mg/L.

38.12 References

1. R. A. Zingaro, W. C. Cooper: *Selenium*, Van Nostrand Reinhold, New York 1975.
2. K. W. Bagnall: *The Chemistry of Selenium, Tellurium and Polonium*, Elsevier, Amsterdam 1966.
3. *Gmelin*, System no. 10, Teil A 1953, Teil B 1949, Ergänzungsbände 1979, 1980, 1981, 1984.
4. N. N. Greenwood, A. Earnshaw: *Chemie der Elemente*, VCH Verlagsgesellschaft, Weinheim 1988.
5. S. C. Caparella (ed.), *Proc. Int. Symp. Ind. Uses Selenium Tellurium 3rd* (1984).
6. S. C. Caparella (ed.), *Proc. Int. Symp. Uses Selenium Tellurium 4th* (1989).

7. A. J. Bard (ed.): *Encyclopedia of Electrochemistry of the Elements*, Dekker, New York 1975.
8. M. Nachtrab, Retorte Company, personal communication.
9. W. C. Cooper, *J. Met.* **42** (1990) Aug., 45.
10. J. E. Hoffmann, *J. Met.* **41** (1989) July, 33.
11. O. Hyvarinen, L. Lindroos, E. Yllö, *J. Met.* **41** (1989), July, 42.
12. Noranda Minerals, US 4581064, 1986 (B. H. Morrison, J. G. Lenz, J. Pageau, J. G. Bard).
13. H. Bußmann, K. F. Dobner, *Erzmetall* **43** (1990) 362.
14. Austria Metall, FP 0263910, 1986 (J. Bertha, J. Wallner, H. Wörz).
15. J. E. Hoffmann, *J. Met.* **42** (1990) Aug., 50.
16. L. A. Teixeira, R. E. Reber, L. Y. Tavares: "The Mineral, Metals & Materials Society", *EPD Congress 90*, Warrendale 1990, p. 209.
17. N. Sonoda, N. Hosoda, K. Hori, US 4663141, 1985.
18. F. Eckardt, H. Berg, *Naturwissenschaften* **45** (1958) 335–336.
19. Nippon Mining, JP 3108, 1956 (N. Imai, M. Endo); *Chem. Abstr.* (1957) 10858.
20. Bayer, DE-OS 1170912, 1962 (H. Giesekus, H. Schöning).
21. P. J. Marcantonio, US 4915928, 1990.
22. Gardener, *Met. Miner. Rev.* (1991) 91.
23. M. Caffaray, *Trans. Inst. Min. Metall. Sect. C* **97** (1988) C87.
24. Siemens, DE-OS 3236137, 1984 (K. Kempter).
25. U. Schiebel, T. Buchkremer, G. Frings, P. Quadflieg, *J. Non Cryst. Solids* **115** (1989) 216.
26. B. Simmingsköld in [5], p. 274.
27. K. Itagaki, A. Yazawa, *Erzmetall* **35** (1982) 358.
28. A. Sato, US 4528034, 1982.
29. M. Benson, H. J. Davis in [6], p. 241.
30. A. M. Seherfhauser, *Fresenius Z. Anal. Chem.* **164** (1958) 327.
31. M. Verlinden, H. Delestra, E. Adriaenssens, *Talanta* **28** (1981) 637.
32. J. F. Norris, H. Fay, *Am. Chem. J.* **20** (1898) 278.
33. K. Mitchell, C. Eberspacher, K. Pauls in [6], p. 572.
34. *Metall Bulletin* (1990) 15th March, p. 15.
35. D. Edelstein in [6], p. 7.
36. M. Piscator in [6], p. 88.
37. R. A. Goyer in [6], p. 97.
38. J. P. Robin in [6], p. 103.
39. Bundesgesetzblatt, "Trinkwasserverordnung", Part I, no. 16, 1975, p. 453.

39 Tellurium

GUY KNOCKAERT

39.1 Introduction	1571	39.7 Analysis	1576
39.2 History	1571	39.8 Compounds	1576
39.3 Properties	1571	39.9 Uses	1577
39.4 Resources and Raw Materials	1572	39.10 Economic Aspects	1579
39.5 Production	1573	39.11 Toxicology and Occupational Health	1579
39.6 Quality Specifications	1576	39.12 References	1580

39.1 Introduction

Tellurium, atomic number 52, is a metallic element of group 16 in the periodic table.

Tellurium has 8 natural stable isotopes, and is known to have a total of 21 artificial unstable isotopes. The natural abundance of the stable isotopes is: ^{120}Te (0.096%), ^{122}Te (2.60%), ^{123}Te (0.908%), ^{124}Te (4.816%), ^{125}Te (7.14%), ^{126}Te (18.95%), ^{128}Te (31.69%), and ^{130}Te (33.80%) [1]. The abundance of tellurium in the Earth's crust is comparable to that of platinum, 0.01 ppm.

39.2 History

Tellurium was discovered in 1782 by MÜLLER VON REICHENSTEIN and named by KLA-PROTH in 1798 (Latin, *tellus*, Earth) [2].

39.3 Properties [1, 3–12]

Tellurium is a crystalline, bright silver-white metal, which is rather brittle and easily crushed. Tellurium is relatively soft (2.3 Moh, nearly as hard as zinc).

The crystal structure is a three-point helical lattice with hexagonal symmetry, with the helical chains parallel to the hexagonal axis. Many physical and electrical properties, e.g., hardness, thermal expansion coefficient, Hall coefficient, resistivity, and diamagnetic susceptibility are anisotropic. The so-called

amorphous phase actually contains very small hexagonal crystals.

Tellurium, a *p*-type semiconductor, demonstrates the phenomenon of piezoelectricity and becomes superconductive at 3.3 K. Some tellurium compounds have excellent thermoelectric properties which are commercially interesting. Trace additives of tellurium to steel, lead, and copper and their alloys have a positive influence on the machinability of tools.

Tellurium has a relatively low melting (723 K) and boiling point (1327 K). On melting, the specific volume increases by ca. 5%. Tellurium vapor is yellow-gold and consists mainly of Te_2 molecules up to 2000 °C. Some physical properties of tellurium are:

Electronic configuration	[Kr] $4d^{10} 5s^2 p^4$
Thermal neutron cross section at 2200 m/s	
absorption	$(4.7 \pm 0.1) \times 10^{-28} \text{ m}^2/\text{atom}$
scattering	$(5 \pm 0.1) \times 10^{-28}$
Crystal structure	hexagonal lattice with trigonal symmetry (A3)
	$a_0 = 0.4457 \text{ nm}$
	$c_0 = 0.5929 \text{ nm}$
	bond angle $(103.2 \pm 0.1)^\circ$
Atomic radius	0.1285 nm
Ionic radius	
Te^{4+}	0.089 nm
Te^{2-}	0.221 nm
Atomic volume	$20.42 \times 10^{-6} \text{ m}^3/\text{mol}$
Density at 300 K	6.245 g/cm ³
<i>mp</i>	722.6 K
<i>bp</i>	1327 K
Enthalpy of fusion	17.489 kJ/mol
Enthalpy of vaporization (Te_2)	107.77 kJ/mol
Specific heat at 25 °C	25.707 Jmol ⁻¹ K ⁻¹
Entropy at 25 °C	49.497 Jmol ⁻¹ K ⁻¹
Entropy of fusion	24.201 Jmol ⁻¹ K ⁻¹

Entropy of vaporization	36.6 Jmol ⁻¹ K ⁻¹
Coefficient of linear expansion, mean value (anisotropic)	16.8 × 10 ⁻⁶ K ⁻¹
Vapour pressure <i>p</i> at 793 K	0.133 kPa
at 923 K	1.33
at 1111 K	13.3
Thermal conductivity at 293 K	0.060 Wm ⁻¹ K ⁻¹
Surface tension at temperature <i>T</i> , <i>T_{mp}</i> = melting point	0.178 – 2.4 × 10 ⁻⁵ (<i>T</i> – <i>T_{mp}</i>) N/m
Electrical resistivity at 3.3 K	superconducting
at 300 K	9.9 × 10 ⁻³ Ωm
Standard electrode potentials	
Te + 2e ⁻ → Te ²⁻	-0.92 V
Te ⁴⁺ + 4e ⁻ → Te	0.63
Tensile strength	11.0 ± 0.25 MPa
Modulus of elasticity	4140 MPa

Metallic tellurium has many properties similar to sulfur and selenium, but it is less reactive, more basic, more metallic, and strongly develops amphoteric properties. When metallic tellurium is heated in air, it burns with a blue-green flame; tellurium powder oxidizes at room temperature.

Tellurium reacts vigorously with halogens at room temperature, cannot be combined directly with sulfur, and reacts with hydrogen at high temperature (920 K). Tellurium does not react with carbon, boron, or nitrogen; it reacts with phosphorus only in a sealed tube heated above 595 K.

Tellurium is insoluble in water, dissolves in concentrated sulfuric and nitric acid, and only slightly in dilute hydrochloric acid. The solubility in caustic alkalis depends on the temperature; tellurium is, however, insoluble in ammonium hydroxide.

When heated in an evacuated ampule, stoichiometric amounts of tellurium and one or more other elements form binary or ternary tellurides. Molten tellurium corrodes iron, copper, and stainless steel.

39.4 Resources and Raw Materials [13]

Tellurium, a relatively rare element with a crustal abundance of 10 µg/kg, is found in close association with sulfur as well as with selenium. Unlike the latter, tellurium does not substitute in sulfide lattices, but forms discrete minerals or microsegregations in the host sulfide mineral [14].

Native tellurium has been observed, but the element is mainly found as a gold and/or silver telluride. The concentration of tellurium minerals in nature is insufficient to allow their economic recovery as principal mining products; its recovery therefore depends on its concentration during the processing of other nonferrous metals. In copper refining, tellurium accumulates together with precious metals and selenium in the anodic slimes generated by electrolysis. Other primary metals such as zinc, gold, and lead, concentrate tellurium during refining.

Reserves of tellurium are difficult to assess because of the limited knowledge of tellurium content in the copper or other ores from which it is recovered. Estimations of refinery production of tellurium are complicated by the trade in concentrates, blister, and anode copper, as well as other nonferrous residues.

As copper ores are the main sources for tellurium, public statistics are based on the copper industry. The United States Bureau of Mines estimates tellurium resources by applying fixed recovery factors (i.e., 0.065 kg Te per tonne of Cu) and quotes the figures in tonnes [15].

Continent, country	Tellurium reserves, t
North America	
United States	6 000
Canada	2 000
Others	3 000
South America	
Chile	6 000
Peru	2 000
Others	1 000
Europe	5 000
Africa	
Zaire	2 000
Zambia	2 000
Others	1 000
Asia	
Philippines	1 000
Others	1 000
Oceania	2 000
World	34 000

The results of these estimations do not include tellurium resources included in lead, zinc, or gold reserves.

39.5 Production [16–22]

Tellurium can be recovered as a by-product in the treatment of lead, copper, bismuth, precious metals, and nickel ores, and from sulfuric acid plants. The main source is copper anode slimes, which settle at the bottom of the refining tanks during the electrowinning of 99.9% pure copper. Copper anode slimes contain 0.5–10% tellurium (Table 39.1).

Table 39.1: Composition of copper anode slimes: selected examples [23–25].

Element	Typical concentration, %		
	Canadian Copper Refiners	Nippon Mining	Inco
Cu	20.3	4.73	17
Bi	0.36	1.6	0.1
Sb	0.95	0.95	0.05
Se	10.9	15.23	7
Te	3.19	3.64	2
Pb	8.5	6.54	1
Au		0.99	0.1
Ag	21.3	20.58	6
As	1.83	1.59	0.8
Ni	0.52	0.03	26

Tellurium is collected with the precious metals in the anode slimes, and has to be separated from these together with selenium, because they interfere with the separation and refining of the precious metals. Tellurium is mostly present in the form of intermetallic compounds of silver, copper, and sometimes gold [Ag₂Te, Cu₂Te, and (Ag, Au)Te₂]. Pretreatment of the slimes can dissolve the copper which is harmful in the further treatment of the slimes. It is normally followed by roasting or sulfatizing of the decopperized slimes, or a combination of these and alternative methods.

Pretreatment consists of dissolving residual copper and tellurium by dilute aerated sulfuric acid or by oxidative pressure leaching with dilute sulfuric acid (normally tankhouse liquid from the copper electrolysis). The first method dissolves 70–80%, the second > 90% of the tellurium. Pressure leaching takes place in an autoclave under an oxygen pressure of 250–350 kPa at 80–160 °C. Depending on the conditions, tellurium is converted to the tetravalent or hexavalent form. Tests have been performed at oxygen pressure up to 1000 kPa

whereby copper and tellurium are completely dissolved, together with part of the contained silver and selenium, which, after contact with a reducing agent (e.g., SO₂) at atmospheric pressure, reprecipitate [23]. The dissolved tellurium in the filtrate is consequently recovered as copper telluride (Cu₂Te) by cementation with copper above 80 °C. This can be performed in a rotating drum containing copper shot or in a fixed-bed reactor filled with copper chippings [26]. Other techniques use copper electrodes suspended in a bath containing the dissolved copper and tellurium sulfate, agitated by vibration or alternating current to the electrode to remove the deposited copper telluride [27, 28]. Figure 39.1 illustrates a possible pretreatment scheme.

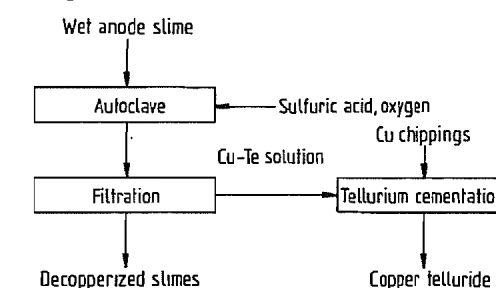
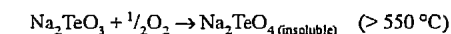
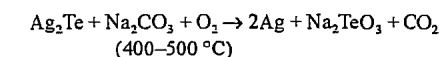
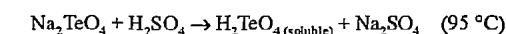


Figure 39.1: Anode slime pretreatment scheme.

Roasting. Pretreated decopperized slimes are roasted with soda ash, whereby tellurium is converted to insoluble sodium tellurite and tellurate:



Normally, complete conversion to hexavalent tellurium is preferred with roasting temperature 550–650 °C. Other processes operate below 400 °C or up to 750 °C, involving different process steps. After water leaching, selenium is recovered as soluble sodium selenate. The residue containing tellurium (as sodium tellurate), lead, and precious metals is either sent to a doré furnace, or treated with sulfuric acid:



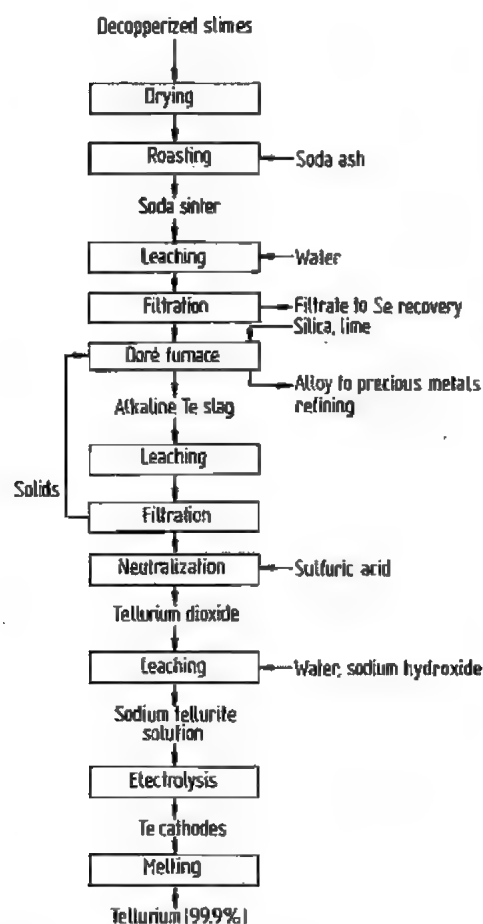
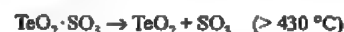
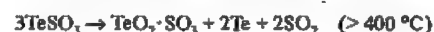
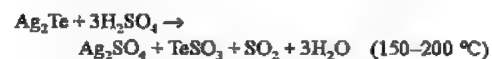


Figure 39.2: Soda ash roasting and doré furnace treatment.

In this processing step, the residue containing lead and precious metals is separated for further treatment. The telluric acid is reduced to tellurium by treatment with hydrochloric acid and sulfur dioxide, or reduced by sodium sulfite to tellurium dioxide, or precipitated as copper telluride by adding copper. If there is no preliminary sulfuric acid treatment, the residue still containing the sodium tellurate is smelted in a doré furnace, where the tellurium is collected in a soda slag leached with water to convert it to sodium tellurite. It is then neutralized with sulfuric acid to tellurium dioxide. Copper telluride and tellurium dioxide can be

leached with dilute sodium hydroxide (with aeration in the case of copper telluride) to form a sodium tellurite solution which is further prepared for electrolysis. Figure 39.2 shows a soda ash roasting process combined with a doré furnace.

Sulfation takes place in two stages: below 350 °C the sulfuric acid forms metal sulfates with the proper consistency to be roasted above 400 °C in the second stage. In this stage, selenium dioxide is eliminated. For tellurium, the following reactions take place:



The tellurium dioxide remains in the sulfated slimes, which are leached with water. Part of the tellurium is dissolved, and can be cemented with copper to yield copper telluride. The leach residue can be treated in the doré furnace. Alkaline leaching of the residues yields soluble sodium tellurite, but this process does not recover all the tellurium. Figure 39.3 shows a sulfatizing roasting process for the recovery of tellurium.

Other Techniques. The oxidation of slimes under pressure in alkaline solution can be used to give good separation of tetravalent selenium and hexavalent tellurium after oxidation. Sodium hydroxide concentration is 100–500 g/L, the temperature is ca. 200 °C, and the oxygen partial pressure is 170–1700 kPa. Pressure leaching with oxygen or hydrogen peroxide is also possible [29, 30]. Aqueous or dry high-temperature chlorination of slimes has been developed. Dry chlorination being difficult to control, wet chlorination is preferred. The slimes are sparged with chlorine gas or sodium chlorate at ca. 100 °C, and all selenium and tellurium is recovered in the soluble form.

The recovery of tellurium from secondary materials accounts for 10–20% of world tellurium production.

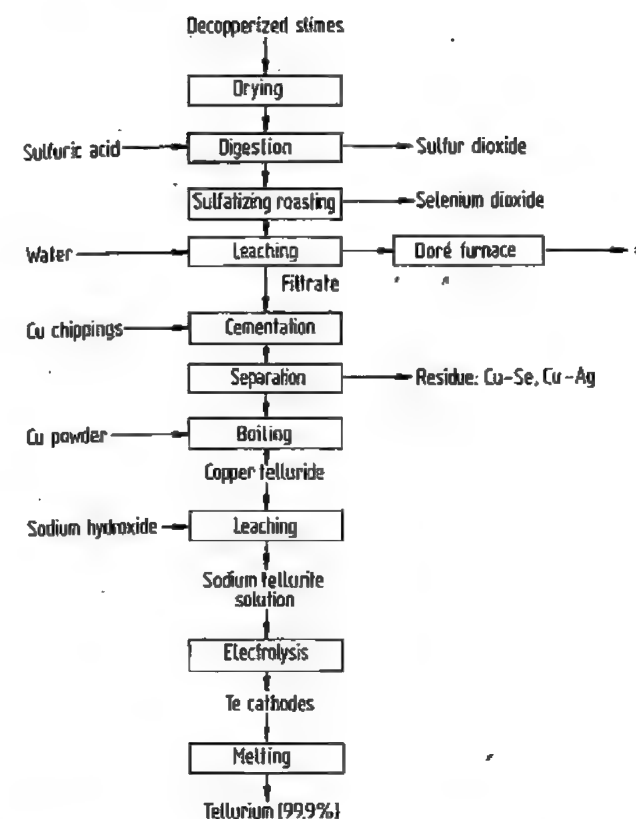


Figure 39.3: Sulfation roasting process. * As in Figure 39.2.

International Recoveries of the Philippines started producing tellurium dioxide and tellurium metal from copper telluride raw material in 1984, and other complex residues and waste products are now treated. Treatment of a tellurium tetrachloride residue was described in 1989 [31]. Small quantities of thermoelectric scrap are recycled by different tellurium producers.

Purification. The following reactions take place during the electrolysis of a tellurite solution:



Typical conditions in an electrolysis cell are: tellurium 100–200 g/L; free sodium hy-

dioxide 40 g/L; current density 160 A/m²; temperature 40–50 °C. After drying, melting, and casting in different shapes (or crushing to powder) the commercial tellurium grade is ready for sale. Direct precipitation with zinc is also possible instead of electrowinning.

Further refining consists of vacuum distillation and zone refining, and yields the higher-purity grades 99.99–99.9999%. As zone refining is unsatisfactory for some impurities, e.g., aluminum, bismuth, and iron, another process uses chlorination with HCl to tellurium tetrachloride; distillation and hydrolysis leads to the precipitation of tellurium dioxide of > 99.999% purity, which after reduction with hydrogen gas gives tellurium of the same purity [32].

39.6 Quality Specifications

Qualities ranging from 99.5% to 99.9999% tellurium are commercially available. Impurities may be metallic (As, Na, Ca, Pb, Cu, Ni, Sb, Sn, Se, Fe) and nonmetallic (S, Cl, O).

Commercial grades and forms are: 99.5–99.9% (2N5–3N) powder, sticks, or ingots; 99.99% (4N) ingots or lumps; 99.999% (5N) ingots; and 99.9999(9)% (6N–7N) ingots.

Tellurium dioxide powder is available with purity 99.5–99.9%.

39.7 Analysis (Table 39.2) [13, 33, 34]

Emission spectrometry (ES) is frequently used for the analysis of standard grade materials up to a purity of 99.99–99.999% (with pre-concentration if necessary). Atomic absorption spectrometry (AAS) is used for analysis down to sub-ppm levels; this method has, however, no multielement capability. AAS can be adapted with a graphite furnace (GFAAS) and coupled with a Zeeman background correction to allow detection limits at $\mu\text{g/kg}$ levels.

Techniques such as spark source mass spectrometry (SSMS) and glow discharge mass spectrometry (GDMS) offer panoramic elemental capability with low detection limits and maximum selectivity.

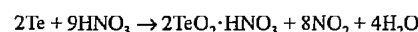
Table 39.2: Detection limits obtained by GFAAS, SSMS, and ES, $\mu\text{g/kg}$.

Element	GFAAS	SSMS	ES
Ag	10	1.0	100
Al	50	0.8	300
Bi	50	2.0	100
Cu	50	"	200
Fe	50	1.0	200
Mg	20	19	100
Ni	20	1.6	300
Pb	50	1.0	200
Sb	50	1.0	300
Sn	50	4.0	100

* Interference by doubly charged ions.

39.8 Compounds [5, 11, 35–37]

Tellurium dioxide, TeO_2 , is found in the minerals tellurite and paratellurite, which have a rhombic and a tetragonal lattice structure, respectively. It can be formed by burning tellurium in air, or by treating tellurium powder with nitric acid, followed by heating the nitrate:



The melting point of TeO_2 is 1005.8 K (732.6 °C), the clear, dark red liquid oxide vaporizes between 790 and 940 °. Tellurium dioxide is very soluble in water and is amphoteric, the minimum solubility is at pH 3.8–4.2, the isoelectric point. Tellurium dioxide is an important catalyst in oxidation, hydrogenation, and dehydrogenation processes; it is also used in chalcogenide glasses, and as a vulcanizing agent for rubber. Single crystals of TeO_2 are used in acousto-optic detectors and modulators. Other oxides of tellurium are tellurium monoxide, TeO , tellurium trioxide, TeO_3 , and tellurium pentoxide Te_2O_5 ; TeO_3 exists in a yellow α -form and a grey β -form.

Tellurium Halides. In tellurium halides, Te has valency 2, 4, or 6. Not all the halides are formed— TeI_2 and the Te_2X_2 halides do not exist. *Tellurium tetrachloride*, TeCl_4 forms white hygroscopic needle-like crystals which are soluble in benzene, nitrobenzene, toluene, ethylacetate, and methanol. It is used as a starting material for the synthesis of many organic tellurium compounds, and is also a catalyst for the chlorination of phenol and benzene, and the hydrogenation of acids and esters to alcohols. *Tellurium tetrafluoride*, TeF_4 , forms white hygroscopic needles. It reacts with water, glass, or silica to tellurium dioxide; metal tellurides are formed with copper, silver, gold, and nickel at 185 °C. Platinum is not attacked below 300 °C.

Hydrogen telluride, H_2Te , is a colorless, unstable gas which decomposes above 0 °C and is prepared by electrochemical reduction of tellurium, or by the addition of hydrochloric acid to Al_2Te_3 . It is used in the production of heavy metal tellurides.

Tellurous acid, H_2TeO_3 , is obtained by reaction of alkali tellurites with nitric acid, or by hydrolysis of a tellurium tetrabhalide. *Orthotelluric acid*, H_6TeO_6 , is made by oxidizing tellurium or tellurium dioxide. It is used in some chemical processes. *Sodium telluride*, Na_2TeO_3 , improves the corrosion resistance of electroplated nickel layers. Solutions of *sodium tellurate*, Na_2TeO_4 , containing Cu^{2+} ions are used for black or blue-black coatings on iron, steel, aluminum, and copper.

A large number of *metal tellurides* are known, and many are semiconductors (Table 39.3). The tellurides are used in infrared detectors ($\text{Cd}_x\text{Hg}_{1-x}\text{Te}$, PbTe , and $\text{Pb}_{1-x}\text{Sn}_x\text{Te}$) and laser diodes (PbTe and $\text{Pb}_{1-x}\text{Sn}_x\text{Te}$), thermoelectric elements (PbTe , Bi_2Te_3 , Sb_2Te_3 , GeTe), solar cells (CdTe), and γ -ray detectors (CdTe).

39.9 Uses

Consumption of tellurium (in t) according to end use in the western world in 1990 was estimated as follows [38]:

Steel additives	145
Nonferrous metals additives	55
Chemicals	45
Electronics	20
Others	5
Total	270

The machinability of steel can be improved by the addition of small quantities (up to 0.1%) of tellurium [39–42], added during the refining of leaded and/or resulfurized, or low-carbon steel in the form of powder, sticks, or cored wire. Manganese telluride alloys are most frequently used nowadays. Additions to cast iron help control the chill depth of rapidly

cooled surfaces and produce hard, wear-resistant top layers.

Tellurium steels and chilled castings are used in the automotive industry, in industrial machinery and tools, in mining, and in railroad equipment.

Many other positive effects of tellurium additions, e.g., deoxidation of liquid steel, refining of the grain size of castings, improvement of the magnetic anisotropy in electrical steels, and improvement of machinability of powder metallurgy steel have been reported.

The use of tellurium in steel could be affected because of decreased consumption of leaded steels owing to environmental constraints.

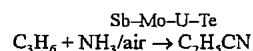
Traces of tellurium are added to many nonferrous metals [39, 41–43]. The tellurium content is mostly less than 1%. Tellurium–copper (which also contains some phosphorus) reduces cutting resistance, tool wear, heat of cutting, and chip size. It is used in forging, automotive radiators, vacuum applications, and as electrical, motor, and switch parts. Tellurium–copper can replace lead–copper in plumbing, as the latter is under environmental pressure in some countries.

Tellurium–lead is used in the sheathing of power and marine cables and in chemical equipment piping (mostly where sulfuric acid is used). In lead acid batteries, tellurium helps strengthen the battery grids. Other nonferrous alloys are tellurium bronze, tellurium–tin, tellurium–chromium, and tellurium–magnesium. Tellurium–cobalt–titanium is used in permanent magnets.

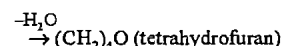
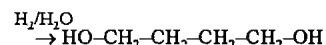
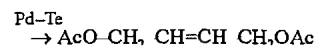
Table 39.3: Important tellurides and their properties.

Formula	Crystal type	Density, g/cm^3	Band gap at 300 K, eV	Carrier mobility at 300 K, $\text{cm}^2\text{V}^{-1}\text{s}^{-1}$		Melting point, °C
				μ_n	μ_p	
CdTe	cubic	5.86	1.5	1000	95	1092
HgTe	cubic	8.2	0.15	25 000	350	670
PbTe	cubic	8.16	0.29	1800	900	924
ZnTe	cubic	5.7	2.26	530	900	1238
Bi_2Te_3	hexagonal	7.86	0.15	1300	1200	588.5
Sb_2Te_3	hexagonal	6.52	0.24		360	621.5
GeTe	face-centered cubic	6.2	0.1		180	724

Tellurium is used in combination with other components in many catalysts. The chemical reactions involved are oxidation, ammoxidation, hydrogenation and dehydrogenation, halogenation and dehalogenation, and phenol condensation [44]. The two major industrial applications are the Nitto process: (acrylonitrile ammoxidation) and the Mitsubishi process (tetramethylene glycol synthesis) [45]:
Nitto: acrylonitrile ammoxidation catalyst:



Mitsubishi: tetramethylene glycol synthesis (Ac = acetate):



Tellurium is used as a secondary vulcanizing agent in natural, styrene-butadiene, and isobutylene-isoprene rubber [39, 41, 46]. The tellurium rubbers have improved aging and mechanical properties, and better resistance to heat and abrasion. They are used in portable cables, automobile tires, door and window seals, double glazing, and in conveyor belts for special applications. The use of tellurium in rubber has declined over the past few decades, and there is concern over the toxicity of tellurium handling in rubber production, which could further affect its usage.

Other uses of tellurium in chemistry are in heat- and vacuum-stable lubricants for electronics and aerospace applications, metal coatings for silverware, aluminum, and brass, in glass, pigments and fungicides, and in organic derivatives and radioactive isotopes for medicine and biology. Lately, the role of tellurium as a possible regulator in cholesterol synthesis has been studied [47].

In electronics, tellurium is a well-known additive in selenium(arsenic) photoreceptors [48, 49]. Tellurium has the property of increasing the sensitivity and broadening the

spectral response of the photoreceptor. Since organic photoconductors have been taking over the photocopier and laser printer market, starting with the slower machines (up to 20–30 pages per minute), the use of selenium-tellurium alloys is decreasing markedly, especially in the industrialized countries.

Polycrystalline cadmium telluride is used in photovoltaic solar cells [50]. CdTe has a direct band gap of 1.5 eV, which is optimal for solar energy conversion, and a high optical absorption coefficient. Research into higher efficiencies, lower cost, and better reliability has intensified in recent years, and the future of CdTe solar cells looks very promising. By the year 2000, the use of tellurium in solar cells could be more than 50 t/a [51].

Bismuth telluride and lead telluride are thermoelectric materials [52, 53]. Thermocouples of these materials convert electricity into heat (Peltier effect) and heat into electricity (Seebeck effect). In these thermocouples, dopants such as Sb and Se are needed to make *n*- and *p*-type materials.

Bi₂Te₃ is mostly used below 200 °C, PbTe at 200–500 °C. The efficiency of a thermoelectric material is expressed by its figure of merit *Z*, a function of the thermal and electrical conductivity and the Seebeck coefficient.

Thermoelectricity has found many applications in picnic boxes, water and food coolers, fiber optic circuits, blood analyzers, and other precision temperature control instruments, remote power generators, solar energy conversion, military equipment (e.g., refrigeration systems in submarines and infrared detectors), and aerospace. Especially the low-tech applications, such as picnic boxes and car drink coolers, have seen a steady rise in sales.

Now that systems based on chlorofluorocarbons are increasingly banned from refrigerators and air-conditioning devices, owing to their detrimental effect on the ozone layer, thermoelectricity could offer a viable alternative, but the present efficiency of the coolers is still too low and the cost too high to suggest a rapid growth in large cooling systems [54].

Optical disks are powerful tools for storing vast quantities of digitized information (up to

1 Gbyte). Different types of write-only and erasable disks exist, and some of their active layers use tellurium alloys which are sputtered onto the disk by vapor deposition techniques from targets containing, e.g., Te-Ge-Sb or Te-Se-Sb [55].

Cadmium-, cadmium zinc-, and cadmium selenium telluride single crystals are used in several electronic applications: γ -ray detectors for medical diagnostics and dosimetry, nonlinear optics, infrared electro-optic modulators, and photorefractive devices [34, 56]. These crystals are grown by vertical or horizontal Bridgman techniques, or the traveling heater method. They are also used as substrates for epitaxial cadmium mercury telluride (Cd_xHg_{1-x}Te) thin film detectors for infrared imagers [57], of which lead tin telluride (Pb_xSn_{1-x}Te) is an example. The detectors operate in the spectral ranges 3–5 μm and 8–14 μm . The thin films are grown by methods such as liquid phase epitaxy, organometallic vapor phase epitaxy, or molecular beam epitaxy [34]. The devices are normally cooled to 77 K with liquid nitrogen. The new generations of imagers use two-dimensional focal plane arrays to capture an entire image at once.

Research and development literature focuses on the different uses of tellurium in non-ferrous alloys (35%), optical storage (10%), cadmium- and cadmium mercury tellurides (20%), and 35% other applications.

39.10 Economic Aspects

World production of tellurium in 1990 has been estimated at 306 t. The estimated production (in t/a) by country and company for 1990 is listed below:

Japan	
Mitsubishi Metal	22
Mitsui Mining & Smelting	10
Nippon Mining & Smelting	12
Sumitomo Metal Mining	12
Belgium	
Union minière	90
Canada	
Noranda Mines	15
United States	
Asarco	40
Philippines	
Pacific Rare Metal	35

Former Soviet Union	50
Peru	10
China	10
Total	306

The main producers are in Belgium, the United States, the Commonwealth of Independent States, and the Philippines [41].

Figure 39.4 shows the evolution of the average annual price for standard-grade tellurium (99.5%) [41]. Tellurium 99.99% is normally 40–50% more expensive, 99.999% is more than double the standard-grade price, and $\geq 99.9999\%$ ranges from 400 to \$1200/kg.

The world economic recession of the early 1990s, particularly hitting the steel industry, and cheap material from the Commonwealth of Independent States, led to a price erosion of 50% between 1990 and 1993.

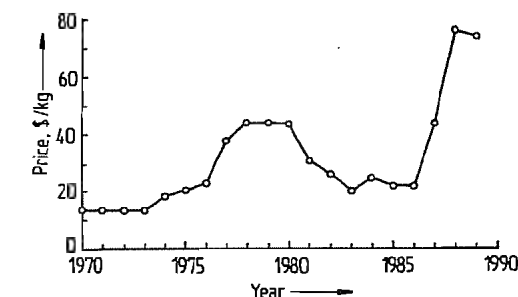


Figure 39.4: Average annual price for standard-grade tellurium (99.5%).

39.11 Toxicology and Occupational Health [58–62]

Elemental tellurium is considered to be less toxic than selenium. Organic compounds and reactive tellurides can be a health hazard. Hydrogen telluride (H₂Te) and tellurium hexafluoride (TeF₆) are both highly toxic, colorless gases. Some LD₅₀ values on ingestion of tellurium compounds are listed in Table 39.4. On the basis of new data for the LD₅₀ value for elemental tellurium, the Environmental Protection Agency of the United States has been asked to declassify tellurium as extremely hazardous [62].

Table 39.4: LD₅₀ values for different tellurium compounds.

Compound	Animal	Administration	LD ₅₀ , mg/kg
Te	rat, mouse	oral	> 5000
TeO ₂	unspecified	oral	> 3000
Na ₂ TeO ₃	white mouse	oral	20
Na ₂ TeO ₄	white mouse	oral	165

The acute inhalation toxicity value LC₅₀ (4 h) for rats is > 2.42 g/m³, the maximum attainable concentration [63].

Tellurium intoxication in the working environment can occur through inhalation and ingestion. No irritation of skin or eyes has been reported for elemental tellurium and tellurium dioxide. Exposure to tellurium fumes and dust cause a garlic odor of the breath and malaise, dryness of the mouth and metallic taste, anorexia, occasional nausea, and some other symptoms. Tellurium is accumulated in the liver, kidneys, bones, and neural cells. The elimination of tellurium in breath, sweat, urine, and feces is very slow. The typical garlic odor seems to result from the partial elimination of tellurium through the lungs as dimethyl telluride (CH₃)₂Te; it can be suppressed temporarily by administration of vitamin C (ascorbic acid), but the vitamin C may also enhance the toxic effects. Tellurium hexafluoride can cause a bluish-black pigmentation of the skin.

Tellurium intoxication symptoms do not appear when the tellurium concentration in the air is < 0.01 mg/m³ and in the urine < 1 µg/L. The TLV for tellurium and its compounds is 0.1 mg/m³ (calculated as tellurium). The TLV was established to prevent poisoning, but garlic breath may still occur. There is no specific antidote for tellurium poisoning.

There are no indications of carcinogenic, teratogenic, or mutagenic effects of tellurium or its compounds.

Unlike selenium, tellurium is not an essential trace element for humans or animals. Tellurium and its compounds cannot be used in cosmetics.

39.12 References

1. Gmelin, Suppl. A1, p. 205.

2. S. C. Carapella, Jr., in W. C. Cooper (ed.): *Tellurium*, Von Nostrand Reinhold Co., New York 1971, p. 1.
3. Ullmann, 4th ed., 22, 447.
4. *Handbook of Chemistry and Physics*, 66th ed., The Chemical Rubber Co., Cleveland, OH, 1985/1986.
5. J. C. Bailar et al.: *Comprehensive Inorganic Chemistry*, 1st ed., Pergamon Press, Oxford 1973, pp. 935–1009.
6. Kirk-Othmer, 22, 659–661.
7. S. C. Carapella, Jr.: *Metals Handbook*, 9th ed., vol. 2, American Society for Metals, Metals Park, OH, 1979, p. 806.
8. W. M. Becker, V. A. Johnson, A. Nussbaum in W. C. Cooper (ed.): *Tellurium*, Von Nostrand Reinhold Co., New York 1971, pp. 54–109.
9. D. M. Chizhikov, V. P. Shchastlivyi: *Tellurium and Tellurides*, Collet's Ltd., London 1970, pp. 1–30.
10. H. Lumbroso in P. Pascal (ed.): *Compléments au Nouveau Traité de chimie minérale*, vol. 8, Masson, Paris 1977, pp. 17–68.
11. W. A. Dutton in W. C. Cooper (ed.): *Tellurium*, Von Nostrand Reinhold Co., New York 1971, pp. 110–183.
12. I. Barin: *Thermochemical Data of Pure Substances*, part II, VCH Verlagsgesellschaft, Weinheim 1989.
13. M. Caffarey, *Proc. 8th Conf. on Thermoelectric Energy Conversion*, Nancy, France 1989, pp. 40–44.
14. W. C. Cooper (ed.): *Tellurium*, Von Nostrand Reinhold Co., New York 1971, pp. 1–13.
15. D. Edelstein in S. C. Carapella, Jr. (ed.): *Proc. 4th Int. Symp. on Uses of Selenium and Tellurium*, Banff, Canada 1989, pp. 4–13.
16. P. E. Skinner, *Trans. Inst. Min. Metall. Sect. C* 97 (1988) C83–C87.
17. P. H. Jennings in W. C. Cooper (ed.): *Tellurium*, Von Nostrand Reinhold Co., New York 1971, pp. 14–53.
18. Kirk-Othmer, 22, 662–663.
19. R. Bresee, D. Vleeschhouwer, J. Thiriar, *Proc. of the Symp. on Industrial Uses of Selenium and Tellurium*, Toronto, Canada 1980, pp. 31–49.
20. L. E. Hoffmann, *J. Met.* 41 (1989) no. 7, 32–38.
21. J. E. Hoffmann, *J. Met.* 42 (1990) no. 8, 50–54.
22. Ullmann, 4th ed., 22, 448–451.
23. Noranda Inc., CA 2049276, 1991 (P. L. Claessens, C. W. White).
24. Nippon Mining Co., JP 60208431, 1985 (T. Abe, Y. Takazawa).
25. J. E. Dutrizac, T. T. Chen in W. C. Cooper, G. E. Lagos, G. Ugarte (eds.): *Copper 87*, vol. 3, Universidad de Chile, Santiago, Chile 1988, p. 469.
26. T. Shibasaki, K. Abe, H. Takeuchi, *Hydrometallurgy* 29 (1992) 399–412.
27. Mitsubishi Metal Corp., Onahama Seiren Co., JP 01079008, 1989 (Y. Sugawara, J. Konishi, S. Hayashi, M. Hayashi).
28. Mitsubishi Materials Corp., US 5160588, 1992 (T. Shibasaki, K. Abe, H. Takenchi).
29. Nippon Shin Kinzuko K.K., JP 56084428, 1981.
30. Interlox Chemicals, EP 127357, 1984 (A. Broome).
31. R. J. Hisshion in S. C. Carapella, Jr. (ed.), *Proc. 4th Int. Symp. on Uses of Selenium and Tellurium*, Banff, Canada 1989, pp. 25–30.
32. Sumitomo Metal Mining Co., JP 63285106, 1988, JP 63286531, 1988 (M. Yukinobu, J. Oowa).
33. K. Swenters, J. Verlinden, R. Gijbels, *Fresenius Z. Anal. Chem.* 335 (1989) 900–904.
34. D. R. Nichols, B. E. Dean, C. J. Johnson in S. C. Carapella, Jr. (ed.): *Proc. 4th Int. Symp. on Uses of Selenium and Tellurium*, Banff, Canada 1989, pp. 282–299.
35. Ullmann, 4th ed., 22, 451–452.
36. D. M. Chizhikov, V. P. Shchastlivyi: *Tellurium and Tellurides*, Collet's Ltd., London 1970, pp. 145–259.
37. *The Economics of Tellurium 1991*, 4th ed., Roskill Information Services, London 1991, pp. 65–66.
38. E. Hoyne, *The Bulletin of Selenium-Tellurium Development Association Inc.*, Sept. 1989, pp. 1–4.
39. Kirk-Othmer, 22, 671–676.
40. E. S. Nachtmann in W. C. Cooper (ed.): *Tellurium*, Von Nostrand Reinhold Co., New York 1971, pp. 373–409.
41. *The Economics of Tellurium 1991*, 4th ed., Roskill Information Services, London 1991, pp. 51–98.
42. R. J. Raudebaugh, *Proc. of the Symp. on Industrial Uses of Selenium and Tellurium*, Toronto, Canada 1980, pp. 201–221.
43. P. W. Taubenblat, *Proc. of the Symp. on Industrial Uses of Selenium and Tellurium*, Toronto, Canada 1980, pp. 267–276.
44. W. C. Cooper (ed.): *Tellurium*, Von Nostrand Reinhold Co., New York 1971, pp. 410–430.
45. T. A. Koch in S. C. Carapella, Jr. (ed.): *Proc. 4th Int. Symp. on Uses of Selenium and Tellurium*, Banff, Canada 1989, pp. 661–672.
46. W. R. McWhinnie, J. E. Stuckey, K. G. Kamika Da Silva, *Proc. of the 3rd Int. Symp. on Industrial Uses of Selenium and Tellurium*, Stockholm, Sweden 1984, pp. 206–245.
47. A. D. Toews, S. Y. Lee, B. Popko, P. Morell, *J. Neurosci. Res.* 26 (1990) 501–507.
48. L. Cheung, G. M. Foley, P. Fournia, B. E. Springett, *Photogr. Sci. Eng.* 26 (1982) no. 5, 245–249.
49. R. C. Norton, *Proc. 7th Annual Photoreceptor & Components Conf.*, Santa Barbara, United States 1991.
50. K. Zweibel: "Toward Low Cost CdTe PV, NREL/TP413-4841", National Renewable Energy Laboratory, Golden, CO, April 1992.
51. M. C. King, Workshop Report. *Recycling of Cadmium and Selenium from Photovoltaic Modules and Manufacturing Wastes*, Golden, United States 1992, pp. 90–101.
52. C. H. Champness in W. C. Cooper (ed.): *Tellurium*, Von Nostrand Reinhold Co., New York 1971, pp. 322–372.
53. D. P. Burton, *Proc. 9th Int. Conf. on Thermoelectrics*, Pasadena, United States 1990, pp. 109–123.
54. P. M. Schicklin, *Proc. 9th Int. Conf. on Thermoelectrics*, Pasadena, United States 1990, pp. 381–395.
55. M. Hartmann, B. A. Jacobs, *Philips Tech. Rev.* 42 (1985) no. 2, 37–47.
56. M. Ohmori, Y. Iwase, R. Ohno, *Proc. Symposium on New Aspects of the Growth, Characterization and Applications of CdTe and Related Cd Rich Alloys of the 1992 E-MRS Spring Conf.*, Strasbourg, France 1992, pp. 283–290.
57. C. Lucas, *Sens. Actuators A* 25–27 (1991) 147–154.
58. J. R. Glover, V. Vouk in L. Friberg et al. (eds.): *Handbook on the Toxicity of Metals*, Elsevier/North Holland Biomedical Press, Amsterdam 1979, chap. 35, pp. 587–598.
59. W. C. Cooper in W. C. Cooper (ed.): *Tellurium*, Von Nostrand Reinhold, New York 1971, pp. 313–321.
60. Ullmann, 4th ed., 22, 453.
61. Kirk-Othmer, 3rd ed., 22, 666.
62. *Environmental Outlook*, vol. 3, no. 1, *Selenium-Tellurium Development Assoc.*, Grimbergen, Belgium 1992.
63. TNO Report V 92.008, TNO-Voeding, Zeist, Holland, Jan. 1992.

Part Nine

Radioactive Metals

																		H	He		
Li	Be															B	C	N	O	F	Ne
Na	Mg	Al													Si	P	S	Cl	Ar		
K	Ca	Sc	Ti	V	Cr	Mn	Fe	Co	Ni	Cu	Zn	Ga	Ge	As	Se	Br	Kr				
Rb	Sr	Y	Zr	Nb	Mo	Tc	Ru	Rh	Pd	Ag	Cd	In	Sn	Sb	Te	I	Xe				
Cs	Ba	La [†]	Hf	Ta	W	Re	Os	Ir	Pt	Au	Hg	Tl	Pb	Bi	Po	At	Rn				
Fr	Ra	Ac [‡]																			

†	Ce	Pr	Nd	Pm	Sm	Eu	Gd	Tb	Dy	Ho	Er	Tm	Yb	Lu
---	----	----	----	----	----	----	----	----	----	----	----	----	----	----

‡

40 General

HERBERT LUG (§ 40.1–40.3); CORNELIUS KELLER † (§ 40.4); JÖRGEN GRIEBEL, ALBRECHT M. KELLERER (§ 40.5)

40.1 History	1585	40.4.4 Francium	1592
40.2 The Law of Radioactive Decay	1587	40.4.5 Radium and Radon	1593
40.3 Activity	1587	40.4.6 Actinium	1593
40.4 Radioactive Elements	1588	40.4.7 Protactinium	1594
40.4.1 Promethium	1588	40.5 The Biological Effects of Radiation and Radionuclides	1595
40.4.2 Technetium	1589	40.6 References	1597
40.4.3 Polonium	1591		

40.1 History

1896: Discovery of Radioactivity. H. BECQUEREL discovered radioactivity one year after the discovery of X rays. Using photographic plates to study the fluorescence of uranium compounds, BECQUEREL found that uranium blackened plates even after a long period in the dark. Fluorescence, therefore, cannot be the cause of the blackening; the radiation comes spontaneously from the uranium, without prior excitation.

Radio-Thorium. MARIE CURIE made a systematic study of all elements to investigate which ones emit the newly discovered radiation. She discovered that thorium, two atomic numbers away from uranium, is also “radioactive”.

First Activity Unit, the Curie (Ci). In quantitative investigations with a galvanometer, M. CURIE found that the intensity of the radiation from uranium (the radioactivity) is proportional to the quantity of uranium.

1898: Polonium. From the pitchblende ore of a uranium deposit, M. CURIE isolated an element with atomic mass 210. She proposed the name “polonium” after her homeland.

1898: Radium. PIERRE and MARIE CURIE found element 88 in pitchblende from Joachimsthal and named it “radium”.

1899: Birth of Nuclear Physics. ELSTER and GEITEL stated the hypothesis that radioactivity originates from the transmutation of elements.

This hypothesis has ultimately become the basis for nuclear physics.

1899: Alpha and Beta Radiation. By measuring ranges, Rutherford determines that radioactive radiation consists of at least two distinct components which are designated α and β .

1903: Nobel Prize for Research on Radioactivity. H. BECQUEREL, M. SKŁODOWSKA-CURIE, and P. CURIE shared the Nobel Prize for Physics.

1903: Gamma Radiation. The third component of radioactivity, called γ radiation, was first reported in 1903 and later described in 1906 by P. VILLARD.

1905: Gamma Quanta. EINSTEIN postulated the existence of corpuscular light quanta (photons) and explained the photoelectric effect. Einstein’s postulate also explains the character of γ quanta.

First Decade of the 20th Century: Identification of Alpha and Beta Particles. The α particle was identified in 1903 by DES COUTURES, who determined the ratio of mass to charge of this particle, and in 1908 E. REGENER measured the charge. The α particle is found to have a mass identical to that of the helium nucleus. This result supplements the observation made by RAMSEY and SODDY (1903) that the noble gas helium is generated from “radium emanation”; this observation in turn supports ELSTER and GEITEL’s 1899 thesis of transmutation. In 1909, RUTHERFORD also

showed by spectroscopic measurements that α particles are helium nuclei.

For β particles, the deflection in electric and magnetic fields gives the ratio of charge to mass (KAUFMANN) and showed that the specific charge is the same as that of cathode rays, i.e., electrons.

1906: Equivalency of Mass and Energy. EINSTEIN stated that mass and energy are equivalent and can be transformed into each other. This equivalence is fundamental to all phenomena of radioactivity and nuclear physics.

1907: Three New Radioactive Elements. OTTO HAHN discovered the radioactive elements radiothorium, radioactinium, and "mesothorium" I and II.

1909: Isotropy. F. SODDY reported that lead atoms have different masses. The phenomenon of isotropy had not yet been explained until the discovery of the neutron in 1932.

1911: Second Nobel Prize for M. SKŁODOWSKA-CURIE. M. SKŁODOWSKA-CURIE received the Nobel Prize in Chemistry for the discovery of radium and polonium.

1911: The Atomic Nucleus. Rutherford's model of the atom has a small, heavy nucleus surrounded by a shell of electrons.

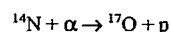
1913: Charge and Size of the Atomic Nucleus. H. GEIGER and E. MARSDEN obtained experimental confirmation of the Rutherford atomic model by measuring the charge and size of the nuclei.

1913: The Hydrogen Atom; Planck's Constant. NIELS BOHR described a planetary model of the atom. The spectral lines of the hydrogen atom were calculated with the help of Planck's constant.

1918: Protactinium. O. HAHN and L. MEITNER discovered the radioactive element protactinium.

1919: Discovery of the First Artificial Nuclear Reaction. While studying the range of α particles in nitrogen, RUTHERFORD observed components having a longer range but a lower

signal intensity on the scintillation screen. RUTHERFORD interpreted these unexpected components as protons:



1923: Compton Effect. A. H. COMPTON showed that X-ray quanta collide with electrons like discrete particles (1927 Nobel Prize).

1925: Pauli Exclusion Principle. The exclusion principle of W. PAULI, which holds for particles with spin $1/2$ and thus in particular for electrons in the atomic shell, explains the periodic system of the elements. It has also accounted for the nuclear systematics in the framework of the shell model. Protons and neutrons are also spin $1/2$ particles.

1926: Fermi Statistics. Fermi statistics apply to all spin $1/2$ particles ("fermions"), thus in particular to electrons and neutrons.

1927: Chemical Bonding. W. HEITLER and F. LONDON accounted for chemical bonding on a quantum-physical basis.

1927: Betatron Principle. R. WIDERÖE and F. STEENBECK described the betatron principle for accelerating electrons.

1928: Spin and Magnetic Moment of the Electron. P. A. M. DIRAC explained the angular momentum and magnetic moment of the electron by introducing the laws of relativity theory to extend quantum wave mechanics.

1928: Heisenberg's Uncertainty Principle. HEISENBERG stated that in the world of elementary particles, position and momentum cannot both be determined simultaneously.

1930: Prediction of the Positron. In the framework of his extended quantum theory, DIRAC predicted the existence of the positron, which was discovered experimentally in 1932.

1930: Cyclotron. E. LAWRENCE constructed the cyclotron.

1932: Discovery of the Positron. C. D. ANDERSON discovered the positron.

1932: Discovery of the Neutron. JAMES CHADWICK discovered the neutron. Nuclei consist of neutrons and protons.

1932: First Artificially Induced Nuclear Reaction. The first nuclear reaction initiated by artificially accelerated particles (150 keV protons) was accomplished by J. D. COCKROFT and E. T. S. WALTON. They received the Nobel Prize in 1951.

1932: Deuterium. H. C. UREY discovered deuterium (Nobel Prize 1934).

1932: Pair Production. I. CURIE and F. JOLIOT discovered pair production with the postulate that a γ quantum transforms into an electron-positron pair; mass and energy are equivalent (EINSTEIN, 1906).

1934: Annihilation Radiation. THIBAUD and JOLIOT discovered the emission of annihilation radiation when a positron and an electron interact and subsequently produce two γ quanta. As in the case of pair production, mass and energy are equivalent (EINSTEIN, 1906).

1934: Artificial Radioactivity. I. CURIE and F. JOLIOT discovered artificial radioactivity.

1934: Neutron-Induced Nuclear Reactions. E. FERMI initiated nuclear reactions with neutrons.

1934: Neutrino Theory. E. FERMI postulated the existence of the neutrino in order to account for β decay.

1935: Betatron. M. STEENBECK constructed the betatron, an electron accelerator.

1937: The μ Meson. The μ meson, predicted in 1935 by YUKAWA, was discovered in cosmic rays.

1937: Technetium. G. PERRIER and E. SGRÉ discovered element 43, technetium, as a nuclear reaction product. Because of its half-life of 4.2×10^6 a (^{98}Tc) or 210 000 a (^{99}Tc) is short on a cosmological scale, the element has never been found in nature. It is, however, certainly present in nature as a product of the very rare spontaneous fission of uranium.

1938: Neutron-Induced Nuclear Fission. HAHN and STRASSMANN discovered that the ura-

nium nucleus can be induced to fission by neutron bombardment.

1942: Chain Reaction. E. FERMI achieved the first nuclear chain fission reaction.

40.2 The Law of Radioactive Decay

In a tennis game, the ball occasionally lands among the spectators. This is neither the point of the game nor the intent of the players, it is a random event in the dynamics of play. When it will occur cannot be predicted; there is merely a certain probability that it will happen.

Comparable with the dynamics of a tennis game are the internal dynamics of an individual radioactive nuclide, which lives with the permanent risk of losing, e.g., four nucleons (an α particle in this situation) all at once. The nuclide suffers this loss at an unpredictable time and without external stimulation. Radioactive nuclides undergo such changes spontaneously, and radioactive decay must be regarded as a stochastic process.

The behavior of the stochastic occurrence in time is characterized by a decay constant λ . This constant is defined as a probability per unit time, specifically the (infinitesimal) probability $d\omega$ that a certain individual nucleus will decay in the infinitesimal time dt :

$$\lambda = d\omega/dt$$

or

$$d\omega = \lambda dt$$

The decay constant λ has the following properties:

- It is equal for all nuclides of a given species
- It is constant over time; Nuclides do not "age" and do not have any history

40.3 Activity

The physical quantity "activity" is defined as the number of decays per unit time. Since 1985, the unit of activity has been the number of decays per second:

$A = \text{decays} \cdot \text{s}^{-1}$

Its special name since 1985 has been the becquerel (Bq):

1 Bq = 1 decay $\cdot \text{s}^{-1}$

Up to 1950, the unit of activity was defined in terms of the activity of 1 g of uranium (special name: curie (Ci) after M. CURIE, who discovered the proportionality between the mass of radioactive uranium and the "intensity" of radiation). This definition was made numerically exact in 1950:

1 Ci = 1.700×10^{10} decays $\cdot \text{s}^{-1}$

By international convention, the unit curie may no longer be employed, but is, however, still frequently encountered. However, since radioactive decay is a stochastic process, sequential measurements of a radioactive source over time will not yield count rates $I(t)$ that correspond exactly to the exponential law $I(t) = I(0)e^{-\lambda t}$. The exponential law describes only the time dependence of the "expected" value $I(t)$. The individual measurements $\hat{I}(t_i)$ are Poisson distributed about the expected value $I(t_i)$. For "not too low" count rates \hat{I} ($\hat{I} > 20$), typical of all technical uses of radioactive sources, the skew-symmetric Poisson distribution can be replaced, to a good approximation, by the symmetric Gaussian normal distribution.

40.4 Radioactive Elements¹

40.4.1 Promethium

Promethium ($Z = 61$) was discovered after 1945 as a product of ^{235}U fission by neutrons (J. A. MARINSKY, L. E. GLENDENIN, C. D. CORYELL). The isotopes ^{130}Pm to ^{153}Pm are known, but only β^- -active ^{147}Pm ($t_{1/2} = 2.62$ a) has found some industrial importance. ^{145}Pm ($t_{1/2} = 17.7$ a) is the longest-lived promethium isotope but it can only be produced by nuclear

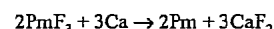
¹ Astatine, the heaviest halogen, a radioactive element ($Z = 85$), was discovered in 1940, and occurs in minute amounts as a short-lived intermediate product in the decay of ^{235}U and ^{238}U . Of no metallurgical interest.

reactions involving accelerators and is, therefore, only available in tracer quantities.

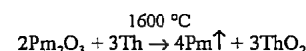
^{147}Pm is obtained from high active waste solutions of the PUREX process, together with other fission lanthanides. The waste solution is stored for at least several years and then extracted by a solution of di-(2-ethylhexyl)phosphoric acid in kerosene. Pure ^{147}Pm is subsequently separated by adsorption to a cation exchanger followed by elution with solutions of complexing agents such as nitrilotriacetic acid or ethylene diaminetetraacetic acid.

In its chemical and physical behavior, promethium (electronic configuration $[\text{Xe}] 4f^{14} 6s^2 p^1$) is a typical trivalent rare earth element.

Promethium crystallizes in the double-hexagonal close-packed (dhcp) structure ($a = 365$ pm, $c = 1165$ pm) and has a melting point of 1168°C . It is produced either by reduction of PmF_3 using calcium as a reductant



or in purer form by reduction of Pm_2O_3 with metallic thorium and subsequent sublimation and condensation.



Uses. All uses of ^{147}Pm are based on its inherent radioactivity. The heat released on ^{147}Pm decay (0.3 W/g ^{147}Pm) can be transformed into electric energy in isotope batteries via the thermoelectric effect. Backscattering of the electrons emitted by ^{147}Pm is applied for determination of the thickness of material that is composed of elements with low Z , for example a plastic cover on a metallic substrate.

Intimate mixtures of $^{147}\text{Pm}_2\text{O}_3$ and phosphors such as $\text{ZnS}(\text{Cu})$ are widely applied as luminescence materials for watches and space modules.

Handling. ^{147}Pm is a soft β emitter ($E_{\beta(\text{max})} = 225$ keV) so no special radiation shielding measures are necessary. However, when handling solid compounds in powder form tight glove boxes must be used to avoid contamination.

40.4.2 Technetium

Technetium (Tc, $Z = 43$), the lightest radioelement was discovered by G. PERRIER and E. SEGRÉ in 1937 after irradiation of molybdenum with deuterons at the Berkeley cyclotron (United States). SEGRÉ took the irradiated sample to Palermo (Italy) where he and PERRIER probably separated the isotope $^{97\text{m}}\text{Tc}$ ($t_{1/2} = 90$ d).

In 1992, all isotopes between mass numbers $M = 89$ [prepared by the reaction $^{60}\text{Ni}(^{32}\text{S}, p2n)$, with $t_{1/2} = 12.8$ s] and $M = 111$ (prepared by fission of ^{235}U after bombardment with 20 MeV protons, $t_{1/2} = 0.30$ s) were identified. ^{93}Tc ($t_{1/2} = 4.2 \times 10^6$ a) is the longest-lived isotope but it cannot be obtained in weighable amounts. The isotope ^{99}Tc ($t_{1/2} = 2.14 \times 10^5$ a) is used for chemical and physical studies of technetium and obtained by fission of ^{235}U with thermal neutrons in ca. 6% yield. This corresponds to formation of 2.8 g technetium per day and 100 MW_{th} power of a nuclear reactor (i.e., about 30 kg/a in a modern 1300 MW_e nuclear power reactor). ^{99}Tc can be recovered from high active waste solutions after reprocessing of spent fuel by the PUREX process.

The most important technetium isotope, however, is $^{99\text{m}}\text{Tc}$ ($t_{1/2} = 6.0$ h) which is currently the most frequently used radionuclide in nuclear medicine. Due to its short half-life, it must be separated from its mother nuclide ^{99}Mo ($t_{1/2} = 66$ h) by the use of a generator at the place of application.

Several types of $^{99}\text{Mo}/^{99\text{m}}\text{Tc}$ generators exist which can supply sterile $^{99\text{m}}\text{Tc}$ in high purity and good yield, e.g., by elution of technetium with NaCl solution from an alumina column loaded with ^{99}Mo (Figure 40.1).

^{99}Mo itself can be produced by two processes:

- Irradiation of ^{98}Mo -enriched molybdenum in a nuclear reactor via neutron capture $^{98}\text{Mo}(n, \gamma)^{99}\text{Mo}$

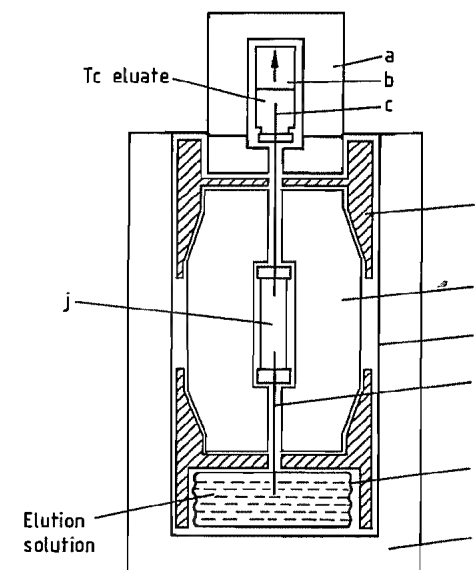


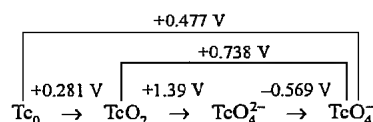
Figure 40.1: $^{99\text{m}}\text{Tc}$ generator "Tecegen" (Hoechst): a) Eluate shielding (lead glass); b) Evacuated eluate bottle, 13 mL, 5 mL calibration; c) Canula for eluate; d) Adapter for eluate; e) Transport shielding; f) Transport box; g) Canula for elution solution; h) Box containing elution solution in plastic container; i) Additional shielding; j) Generator column for fission Mo.

- Irradiation of highly ^{235}U -enriched ($\geq 20\%$) uranium in a nuclear reactor and separation of the fission product ^{99}Mo (fission yield $\approx 6\%$)

The second type of production is preferred because it yields ^{99}Mo with a high specific activity so that the eluted $^{99\text{m}}\text{Tc}$ is obtained in high concentration. In contrast, the product of ^{98}Mo irradiation only delivers ^{99}Mo with a much lower specific activity and, therefore, requires larger generators.

Nowadays, an adequate supply of $^{99\text{m}}\text{Tc}$ is provided by the so-called $^{99\text{m}}\text{Tc}$ generators. These generators are efficient and reliable and differ principally from common generators in the technique of separating technetium from molybdenum. Preferred separation methods are the adsorption of $^{99}\text{MoO}_4^{2-}$ onto a solid medium and elution of $^{99\text{m}}\text{TcO}_4^-$ with saline solution, selective extraction of $^{99\text{m}}\text{TcO}_4^-$ into organic solvents, and sublimation of ditechne-tium heptaoxide at high temperatures.

Technetium has the ground state electronic configuration of $[\text{Kr}] 4d^5 5s^1$. Its chemical properties are more similar to rhenium than to manganese. Valency states between 1- and 7+ are known, the most stable ones being Tc(IV) and Tc(VII). The most important redox potentials in acidic solution at 298.2 K are:



Metallic technetium can be easily prepared either by reduction of NH_4TcO_4 or TcO_2 with hydrogen at 700–900 °C or by electrodeposition from a 1 M solution of NH_4TcO_4 in sulfuric acid. Its most important *physical properties* are:

<i>mp</i>	2250 ± 50 °C
Density	11.47 g/cm ³
Crystal structure	hexagonal close-packed
Lattice dimensions (25 °C)	<i>a</i> = 274.07 pm <i>c</i> = 439.80 pm
Critical temperature (superconducting)	7.73 ± 0.02 K
Debye temperature	454 K
Standard entropy of formation	31 ± 0.8 Jmol ⁻¹ K ⁻¹
Magnetic susceptibility (25 °C)	270 × 10 ⁻⁶
Specific heat <i>C_p</i> (1000 K)	0.29 Jg ⁻¹ K ⁻¹

Chemical Properties. Solid technetium is-resistant to oxidation, but in sponge or powder form it is readily oxidized to the volatile hepta-oxide when heated in air. The metal dissolves in dilute or concentrated nitric acid, concentrated sulfuric acid, and bromine water, but not in hydrochloric acid. Technetium also dissolves in aqueous acid hydrogen peroxide solutions. It is oxidized by these solvents to pertechnetate, but in the case of bromine water $[\text{TcBr}_6]^{2-}$ is also formed.

TcO_2 reacts with fluorine to yield TcO_3F . Contrary to rhenium, no heptafluoride of technetium is known. Only TcF_5 and TcF_6 are obtained, for example, by fluorination of technetium metal at 400 °C. The corresponding reaction with chlorine or bromine at 550 °C produces the tetrahalides TcCl_4 and TcBr_4 . These halides can form hexahalide complexes with an octahedral TcCl_6^{2-} arrangement that are more stable than the corresponding tetrahalides, for example, K_2TcCl_6 .

TcOCl_4 and TcO_3Cl are formed if technetium reacts with chlorine that contains oxygen. Sulfur reacts with technetium at elevated temperature to give the disulfide, and carbon to give TcC . A technetium hydride of the composition $\text{TcH}_{0.73}$ is formed at 300 °C under a hydrogen pressure of ca. 0.2 GPa.

Only a few compounds have been prepared so far, with Tc in low oxidation states, including:

Tc(-1): $\text{HTc}(\text{CO})_5$
Tc(0): $\text{Tc}_2(\text{CO})_{10}$, $\text{CoTc}(\text{CO})_9$
Tc(+1): $\text{K}_2\text{Tc}(\text{CN})_6$, $(\text{C}_6\text{H}_5)_2\text{TcH}$, $\text{Tc}(\text{CO})_3\text{Cl}$
Tc(+2): $[(\text{C}_6\text{H}_5)_2\text{Tc}]_2$
Tc(+3): $[\text{Tc}(\text{o-phenylene-bis-dimethylarsine})_2\text{Cl}_2]\text{Cl}$
Tc(+4): TcO_2 , M_2TcX_6 (*X* = F, Cl, Br, I, SCN)

Oxidation of technetium metal by oxygen at 500 °C yields pale yellow Tc_2O_7 (*mp* 119.5 °C, *bp* 310.6 °C) which reacts with water vapor to form dark red HTcO_4 . Many pertechnetates such as LiTcO_4 or the sparingly soluble CsTcO_4 have been prepared and characterized.

Reduction of Tc(VII) solutions or thermal decomposition of NH_4TcO_4 at 450 °C in vacuum gives TcO_2 which has a distorted rutile structure. Brown-black Tc_2S_7 is precipitated from TcO_4^- solution by gaseous H_2S .

Uses. Technetium itself and some of its compounds and ions have properties that should make them suitable for broad industrial applications. However, their inherent radioactivity prevents their general use except in special applications, for example, $^{99\text{m}}\text{Tc}$ in nuclear medicine.

Metallic technetium supported on Al_2O_3 or SiO_2 is an excellent catalyst for hydrogenation, dehydrogenation, dehydrocyclization, and cracking reactions, particularly of C_6 and C_7 species. The reforming of naphtha to gasoline with higher aromatic content is catalyzed by technetium-promoted Cr_2O_3 catalysts, at a lower reaction temperature than other promoted catalysts. Technetium can, therefore, partly substitute for expensive platinum catalysts, especially as technetium catalysts are highly resistant to sulfur poisoning.

Metallic technetium is a weak-coupling type II superconductor with a high critical temperature ($T_c = 7.73$ K). Some technetium

alloys have still higher critical temperatures up to $T_c = 15.0$ K for a technetium molybdenum alloy with 60 atom% technetium.

TcO_4^- ions are excellent corrosion inhibitors even in the presence of corrosive media and at temperatures ≤ 250 °C. At pH ≈ 6 and 10 ppm Cl, a solution of 50 ppm technetium ($\approx 5 \times 10^{-4}$ M Tc) suppresses corrosion of a 0.1% carbon steel even after 20 years. The corrosion rate is at least four orders of magnitude less than in the absence of TcO_4^- ions. The surface concentration of technetium on the steel corresponds to about a tenth of a monolayer. Furthermore, technetium-coated stainless steel does not corrode in seawater.

^{99}Tc is used very often as a standard source of β radiation for radiometry and dosimetry. Such sources are safe and convenient to handle because of the lack of γ radiation.

In nuclear medicine, chemical compounds of $^{99\text{m}}\text{Tc}$ are widely used for radionuclidic imaging of the brain, liver, lung, and skeleton, and to a lesser extent in thyroid scintigraphy. $^{99\text{m}}\text{Tc}$ -labeled radiopharmaceuticals have been developed that are suitable for both static and dynamic evaluation of renal and cardiac pathology. Sales of $^{99\text{m}}\text{Tc}$ -labeled products account for about 75% of the total sale of radiopharmaceuticals in the United States; similar trends are observed in Europe.

Handling. ^{99}Tc is a soft β emitter so no special radiation protection measures are necessary. Tight glove boxes must be used to avoid contamination of work places and incorporation when handling powdered samples of ^{99}Tc compounds. Lead shielding is necessary for $^{99}\text{Mo}/\text{Tc}$ generators because ^{99}Mo also emits γ rays.

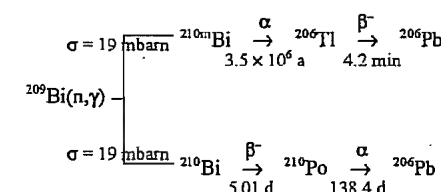
40.4.3 Polonium

Element 84 was discovered in 1894 by P. and M. CURIE. Its discovery was possible because of its inherent radioactivity.

Today, all isotopes between mass numbers $M = 193$ and $M = 218$ are known including many relatively long-lived isomers. The longest-lived isotope ^{209}Po ($t_{1/2} = 102$ a) is only available through charged-particle nuclear re-

actions and therefore not produced in weighable amounts. Nearly all the chemical and physical studies on polonium were performed with the pure α emitter ^{210}Po ($t_{1/2} = 138$ d).

Even though polonium was first discovered by the separation of ^{210}Po from uranium ores, due to the very small amount of ^{210}Po (equilibrium concentration 7.4×10^{-11} g $^{210}\text{Po}/\text{g}$ ^{238}U) in ores, nowadays most ^{210}Po is isolated in a different way. It is either separated from "old" radium samples or more recently by irradiation of very pure bismuth with neutrons in a nuclear reactor, even if the neutron capture cross section σ is low:



One year of irradiation of 1 kg bismuth at a neutron flux of 10^{14} ncm⁻²s⁻¹ gives 25 mg ^{210}Po (ca. 4×10^{12} Bq). The isolation of such quantities from natural sources is practically impossible. Following irradiation of bismuth, ^{210}Po is separated from molten bismuth by vacuum distillation. Final purification of polonium generally is accomplished by its spontaneous deposition on silver or copper powders. **Metallic polonium** is then easily prepared by sublimation of this deposit at about 700 °C. It is also obtained by reduction of polonium sulfide with hydrogen at 500 °C. Polonium sulfide itself is precipitated from an acid solution of polonium ion by gaseous H_2S .

Polonium with electronic configuration $[\text{Xe}] 4f^{14} 5d^{10} 6s^2 p^4$ is the heavy homologue to tellurium. The oxidation states 2-, 2+, 4+, and 6+ are known, but Po(IV) (ionic radius 102 pm) is the most stable one. Po(VI) (ionic radius 67 pm) is easily reduced to a lower oxidation state by its own radiation.

Important *physical properties* of polonium metal are:

<i>fp</i>	≈ 250 °C
<i>bp</i>	962 °C
Atomic radius	164 pm

Vapor pressure (438–745 °C), Pa	$\log p = (964.36 \pm 0.9064) - (716\,860 \pm 893)/T(^{\circ}\text{C})$
Structure α Po (< 18 °C) β Po (> 54 °C)	cubic, $a = 335.9$ pm rhombohedral, $a = 336.9$ pm, $\alpha = 98.23^{\circ}$
Density α Po β Po	9.142 g/cm ³ 9.352

Chemical Properties. Polonium is soluble in HCl and forms Po(II), in HNO₃ and aqua regia Po(IV) is produced.

Po(VI) solutions are obtained by the oxidation of Po(IV) with Cl₂, K₂Cr₂O₇, or Ce(IV)–HNO₃. SO₂ and N₂H₄ reduce Po(IV) to Po(II), by reduction with SnCl₂, Ti(III), and NaHSO₃, a precipitate of finely divided metallic polonium is formed.

Compounds. Polonides of several metals with the composition MPo (e.g., M = Mg, Mn, Y, rare earth element) are prepared by the interaction of polonium vapor with powdered metals. Most of these polonides dissociate at ca. 700 °C, only rare earth polonides are stable up to 1000 °C.

Polonium monoxide, PoO, is obtained by thermal decomposition of polonium selenide. The more stable PoO₂ is formed by thermal decomposition of, for example, PoO(OH)₂ or Po(IV) nitrate, or by reaction of metallic polonium and oxygen. It can be sublimed in an oxygen stream at 885 °C but decomposes in vacuum at 500 °C. PoO₂ vapor reacts with rare earth oxides to form compounds such as Pr₂O₃·PoO₂ and Dy₂O₃·PoO₂.

Halides such as PoCl₄ and PoBr₄ are formed when polonium metal reacts with chlorine or bromine at ca. 100 °C. At 200 °C these halides decompose to the corresponding polonium dihalides. Complex halides such as M₂PoX₆ (M = K, Rb, Cs; X = Cl, Br, I) of Po(IV) and MPoCl₃ and M₂PoCl₄ of Po(II) are also known.

Due to the high radioactivity of ²¹⁰Po, relatively unstable compounds such as PoH₂, PoF₆, PoO₃, and organometallic compounds could be identified only in tracer amounts but not in quantities that are needed for detailed investigations of their properties.

In aqueous solution, polonium ions are easily hydrolyzed even at pH ≈ 1, if not complexed by, for example, oxalic, citric, or tartaric acids. Po(IV) in particular, is readily extracted from aqueous solutions by, e.g., tri-*n*-butyl phosphate, dithizone–CHCl₃, and amines. Polonium is adsorbed as complex ions by anion exchangers in strong acid solution—elution must be performed rapidly due to the fast decomposition of the ion exchanger by α activity.

Uses. ²¹⁰Po is the only isotope that finds broad application. It is used as an energy source for radioisotope batteries. This isotope has the advantage that it does not emit γ rays therefore heavy weight shielding of the batteries can be avoided. The disadvantage is the short half-life of ²¹⁰Po. ²¹⁰Po (140 W_{th}/g) was especially used as an energy source in Soviet space missions, e.g., in Lunochod-1 and Lunochod-2. About 10¹⁵ Bq ²¹⁰Po are needed for a radioisotope battery that delivers 1 kW electric power. The polonium is mostly provided in the form of rare earth polonides.

²¹⁰Po is used also as an α emitter for (α , n) neutron sources. A BeO–²¹⁰Po source emits up to 93 neutrons per 10⁶ α particles.

Handling. Tracer amounts of ²¹⁰Po can be handled in well-working fume hoods but even microgram quantities of ²¹⁰Po require handling in tight glove boxes due to unavoidable α recoil and the consequent contamination of the working area.

40.4.4 Francium

Element 87 is the most unstable of all naturally occurring elements. It was discovered in 1939 by M. PEREY. ²²³Fr ($t_{1/2} = 21.8$ min) is the most stable of all 27 isotopes.

Relatively pure ²²³Fr solutions are obtained by its elution with NH₄Cl–CrO₃ from a cation exchanger loaded with ²²⁷Ac. The solution is further purified by passing it through a SiO₂ column loaded with BaSO₄.

Francium is only monovalent and shows a very similar behavior to the other heavy alkali

elements. Francium has the most negative standard potential of all elements.

No industrial applications or uses in nuclear medicine have yet been found.

40.4.5 Radium and Radon

Radium ($Z = 88$) was discovered in 1898 by P. and M. CURIE and G. BÉMONT. ²²⁶Ra ($t_{1/2} = 1600$ a) is the longest-lived of all the 25 radium isotopes known to date. Its concentration in uranium ores is 0.36 μg per gram uranium. ²²³Ra, ²²⁴Ra, and ²²⁸Ra also occur in nature.

According to its electronic configuration [Rn] 7s², radium shows the typical behavior of an alkaline earth element with a large ionic radius. It is obtained from uranium ores by a mixed precipitation–ion exchange procedure.

Radium metal is prepared by reduction of the oxide by aluminum at 1200 °C in vacuum. The pure metal has a cubic body-centered structure ($a = 515$ pm) such as barium and a mp of 700 °C. The known compounds, including the halides RaX₂ (X = F, Cl, Br, I), the oxide RaO, the carbonate RaCO₃, and the ternary oxides RaCeO₃ and RaMO₄ (M = Cr, Mo, W) are isostructural with corresponding barium compounds. Because of its large ionic radius, radium forms weak complexes and is not well extracted from aqueous solutions except at high pH values.

Uses. The use of ²²⁶Ra as a γ emitter in nuclear medicine for cancer therapy lost its importance when larger and cheaper ⁶⁰Co sources became available. Also most (α , n)-neutron sources based on ²²⁶Ra were replaced by ²⁴¹Am–Be sources even if the number of emitted neutrons in ²²⁶Ra sources are higher (for RaBeF₄: 1.84×10^6 neutrons per second and per gram ²²⁶Ra).

Today radium is mainly used to prepare ²²⁷Ac via neutron capture in a nuclear reactor.

Handling. ²²⁶Ra requires special precautions to work with because it is considered the most toxic radioelement. Handling of ²²⁶Ra is possible only in tight glove boxes where the circulating air stream must also be treated to avoid the escape of decay product ²²²Rn to the envi-

ronment. Special care must be taken when opening disused radium ampoules because of possible overpressure formed by the decomposition of water.

Radon, the heaviest noble gas, was discovered in 1900 as a decay product of radium by F. E. DORN.

Today, radon isotopes with atomic masses between 199 and 226 are known, of which ²²²Rn ($t_{1/2} = 3.82$ d), ²²⁰Rn ($t_{1/2} = 55.6$ s), and ²¹⁹Rn ($t_{1/2} = 3.96$ s) are members of natural decay series. On average, they contribute to about half of the natural radiation dose the population is exposed to.

Despite the fact that the chemical behavior of radon is only known from tracer experiments with the longest-lived ²²²Rn, there is no doubt that radon is the most reactive noble gas. Reaction of radon with fluorine or halogen fluorides, such as BrF₃, is likely to produce RnF₂ which can be reduced to radon by hydrogen only at temperatures > 500 °C. Radon fluoride can be sublimed at about 250 °C. It also seems to be possible to oxidize radon with O₃.

There are no known uses of radon, except application of ²²²Rn capsules for the treatment of cancer. The release of radon from solid substances (“emanation method” by O. HAHN) is often used to study structural changes of solids.

SbF₅ in the presence of ClF₃ and N₂F₂Sb₂F₁₁ might be suitable for the removal of radon from the air in uranium mines in order to reduce radiation dose to workers by the formation of RnF.

40.4.6 Actinium

The element with $Z = 89$ was discovered in 1899 by A. DEBIERNE, but F. O. GIESEL in 1902 was the first to have prepared pure actinium. Of all 25 known isotopes, only the longest-lived ²²⁷Ac ($t_{1/2} = 21.77$ a) has some importance. In uranium ores its amount is too low to be recovered (2×10^{-10} g per gram uranium), so currently nearly all ²²⁷Ac is obtained by irradiation of ²²⁶Ra. Three months irradiation at a neutron flux of 5×10^{14} ncm⁻²s⁻¹ transforms

2% of ^{226}Ra to ^{227}Ac . In the 1970s, about 18 g $^{227}\text{Ac}_2\text{O}_3$ were prepared by this method. The ^{227}Ac obtained was separated from ^{226}Ra and decay products by a precipitation ion exchange process.

Because of its electronic configuration $[\text{Rn}] 6d^1 7s^2$ and ionic radius ($r = 111$ pm for Ac^{3+}), actinium closely resembles lanthanum, but only few compounds [e.g., the oxide Ac_2O_3 , the sulfide Ac_2S_3 , the phosphate $\text{AcPO}_4 \cdot 0.5\text{H}_2\text{O}$, the halides AcX_3 , and oxide halides AcOX ($X = \text{F}, \text{Cl}, \text{Br}, \text{I}$)] have been synthesized up to now.

Actinium metal is obtained by reduction of Ac_2O_3 with thorium at 1750°C and 10^{-4} Pa. It crystallizes in the cubic β -lanthanum type structure with a lattice constant of $a = 531.5$ pm. In solution only Ac^{3+} occurs. The stability of Ac^{3+} complexes is low due to the large ionic radius. Because of this, actinium can only be extracted from aqueous solutions at relatively high pH values with low distribution coefficients. Most solution experiments were performed by using ^{228}Ac ($t_{1/2} = 6.13$ h), separated from ^{223}Ra ($t_{1/2} = 5.7$ a).

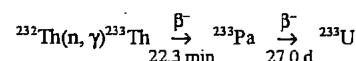
Uses. ^{227}Ac is a radionuclide with high specific power ($14.3 \text{ W}_{\text{th}}/\text{g}$) and besides ^{244}Cm , is the only radioisotope used for thermionic transformation of the heat of decay into electricity. For a thermionic battery that transforms 12% of heat into electricity, about 17 g $^{227}\text{Ac}_2\text{O}_3$ (equivalent to about 5×10^{13} Bq) are needed to obtain $250 \text{ W}_{\text{th}}$. Due to the instability of thermionic batteries compared to thermoelectric devices, the interest in ^{227}Ac is currently decreasing.

Handling. Handling of ^{227}Ac is possible only in tight glove boxes, gram-amounts require hot cells with γ shielding. Well-aerated fume hoods are sufficient for the handling of trace quantities of all actinium isotopes.

40.4.7 Protactinium

The element with $Z = 91$ was discovered in 1913. K. FAJANS and O. GÖHRING were probably the first to have separated pure protactinium.

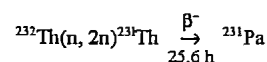
^{231}Pa ($t_{1/2} = 32\,480$ a) is the most important of all 24 known isotopes, even though ^{233}Pa is of special importance because it is formed as an intermediate in the production of fissile ^{233}U from nonfissile ^{232}Th by neutron capture



$\sigma = 7.4$ barn

This process is used in thorium high temperature reactors (THTR), which utilize the fivefold occurrence of thorium in nature compared to uranium.

The separation of ^{231}Pa from residues of uranium production is a difficult process. Nevertheless, around 1960 ca. 100 g pure $^{231}\text{Pa}_2\text{O}_5$ were isolated from residues of the uranium production at Springfield, United Kingdom, that contained 3.7 ppm ^{231}Pa . In future, larger quantities of ^{231}Pa might be recovered from nuclear waste originating from reprocessing of thorium fuels, because it is formed via



by the fast neutrons in a THTR nuclear reactor.

With its electronic configuration $[\text{Rn}] 5f^6 6d^1 7s^2$, protactinium is the first element to possess 5f electrons in the ground state. Both in the solid state and in solution protactinium can occur in the oxidation state Pa^{4+} ($r = 96$ pm) and Pa^{5+} ($r = 90$ pm). In its chemical and physical behavior protactinium is much more similar to tantalum than to typical 5f elements.

Protactinium metal is best prepared by the Van Arkel method using a $\text{PaCl}_3\text{-I}_2$ mixture. α Protactinium is tetragonal-body centered ($a = 393.1$ pm, $c = 323.6$ pm), β protactinium is cubic face-centered ($a = 501.9$ pm). The melting point of protactinium is $1572 \pm 20^\circ\text{C}$.

Compounds. The solid state chemistry of protactinium is quite well known. Binary compounds exist such as the tetrahalides PaX_4 and pentahalides PaX_5 and complex compounds including the sparingly soluble K_2PaF_7 . The very stable white Pa_2O_5 occurs in at least five modifications. The reduction of Pa_2O_5 with

pure hydrogen at 1550°C yields black PaO_2 . A protactinium peroxide of still unknown composition can be precipitated from diluted acids. This method is used to separate protactinium from tantalum and niobium which form soluble peroxide complexes.

Pa(V) is hydrolyzed in aqueous solution even in strong acids, if not complexed, for example, by F^- ions. No Pa^{5+} exists in solution. Only partly hydrolyzed species with two positive charges (in ca. 1 M HCl) or one positive charge (in 10^{-3} – 10^{-1} M H^+) could be identified. Pa(V) is readily adsorbed onto precipitates, surfaces (even metal surfaces), graphite, quartz, etc. The partly hydrolyzed protactinium species form very stable complexes with most organic ligands. Pa(V) can be extracted from aqueous solution by amines and most neutral and acid phosphoric and phosphonic extraction agents. The distribution coefficients are high.

Pa(IV) solution is obtained by reduction of Pa(V) solutions using chemical (e.g., zinc) or electrochemical methods. The behavior of Pa(IV) is very similar to all other actinides of oxidation state IV, however, its tendency to hydrolyse is much higher.

Due to the unavoidable hydrolysis and formation of radiocolloids, solutions of protactinium in various oxidation states must be freshly prepared before use. The large number of unexplainable results found in the literature are mostly due to using degraded protactinium solutions with partly hydrolyzed, nonspecified protactinium species that change composition by time, even in 6 M HCl.

Uses. Protactinium plays an important role in the THTR fuel cycle, especially because of the high neutron absorption cross section of ^{233}Pa ($t_{1/2} = 27.0$ d) that lowers the amount of fissile ^{233}U formed. Therefore, several processes, for example, for a "molten salt reactor", have been developed to separate protactinium continuously during reactor operation with the consequence that ^{233}Pa will decay outside the reactor core and, therefore, not absorb neutrons. However, many technological prob-

lems have to be solved before practical application.

Handling. ^{231}Pa must be handled in tight glove boxes, whereas tracer chemistry of protactinium (e.g., with ^{233}Pa) can be performed in well-aerated fume hoods.

40.5 The Biological Effects of Radiation and Radionuclides

The assessment of the health hazards arising from ionizing radiation has undergone a striking change in the course of this century. When RÖNTGEN announced in 1895 that he had discovered a new type of radiation, which he called X rays, the world reacted with an immense faith in progress. Although harmful side effects of X rays were soon encountered, no one thought about hazards or radiation protection. Inflammation similar to that caused by burns was observed on the hands of operators repeatedly testing X ray pictures and, later, the first cases of radiation-induced skin cancer became known. Only a decade after the discovery of X rays, an increased frequency of leukemia among radiologists was noticed [9]. This was not regarded as a warning sign but, at best, as an indication of the possible hazards arising from the long-term exposure to high doses of radiation.

The positive expectations that were aroused by this new agent are reflected in the application of X rays and natural radioactivity (which was discovered just a year later) in medicine within few weeks after the discovery by RÖNTGEN. X rays were being used extensively in the examination of the human body and first in simple medical diagnoses. Radioactivity was also quickly applied for all kinds of medical therapy and especially radium, with its penetrating γ radiation, was frequently and indiscriminately used at the start of this century in a large number of diseases and for the supposed stimulation of the organism. For instance, the application in the form of radium pillows was

common, even in the absence of disease and without medical supervision.

Early fundamental work in radiation biology, e.g., by the young FRIEDRICH DESSAUER [10], showed that higher doses of ionizing radiation destroy living cells. This finding quickly led to the introduction and subsequent improvement of radiation therapy for cancer patients. In spite of the accumulated results on the biological effects of ionizing radiation, the belief in the harmlessness of low doses of radiation persisted for decades.

The fate of hundreds of young women, especially in the United States, who painted the faces of clocks and instruments with luminous paint containing the long-lived, α -emitting ^{226}Ra was one of the first great tragedies resulting from unprotected exposure to radionuclides. Since they had not been warned of possible hazards, the workers sharpened their brushes soaked in luminous paint with their mouths, thus incorporating considerable amounts of activity. Many of them died of bone tumors [11, 12]. A young doctor published his suspicions, that the severe lesions in the jaws of the young women could be caused by radiation. In response, he was called a charlatan by a reader because, as was explained in the reader's letter, it was common knowledge that radiation was dangerous only in massive overdoses over long periods of time. The letter was written by the great scientist Marie Curie, who herself fell victim to radiation exposures later.

These and similar examples illustrate the consequences of the uncritical contact with ionizing radiation which took place in the first half of this century. A fundamental change in assessment of radiation hazards occurred, when the long-term effects of radiation exposure were discovered in the survivors of the atomic bombings of Hiroshima and Nagasaki. The possibility that leukemia might result from a single and relatively small dose of radiation was proposed by Lewis in the 1950s [13]. He inferred from the increased frequency of leukemia among the survivors of the atomic bombings—about a dozen cases per year—that leukemia could result from somatic muta-

tions, i.e., individual alteration in the DNA of single cells. This finding became the basis for the present philosophy of radiation protection, which holds the principle that unnecessary exposure to radiation should be prevented and unavoidable exposures should be reduced as far as possible.

The recognition that even the smallest doses of radiation can—with correspondingly low probability—cause hereditary defects or cancers and the fact that this possibility was recognized first for radiations, and only later for chemical carcinogens, may have led to the amazing change in the attitude to ionizing radiation. In the past, people had blind faith in the mysterious biopositive effects of radiation, but now the risks, which must indeed be taken seriously, are often overestimated in comparison with other risk factors.

Physical Radiation Effects. Several levels can be distinguished in the effects of ionizing radiation: physical, molecular, cellular, and tissue effects.

In spite of considerable differences in the energy transport and interactions with matter, all types of ionizing radiation act through the same physical primary processes and, as discussed later, they all act predominantly by damaging the DNA, i.e., the genetic material of the cell. *Indirectly ionizing radiation*, i.e., photons and neutrons, release fast particles in matter. The charged particles are, in turn, ionizing and produce secondary electrons which cause the major part of the ionizations and excitations. In the case of excitation, the excited molecule dissociates into radical or nonradical products or it gives up its energy to the environment without disintegrating. In comparison with ionizations, however, electron excitations are of secondary importance for radiation effects. In the case of *directly ionizing radiation*, such as electrons or α particles, charged particles are present from the start.

The photons of X rays or γ rays generated in nuclear decay and energy-rich neutrons have substantial penetrating power in tissue. The high-energy electrons produced in an accelerator can also penetrate deeply into tissue.

In contrast the electrons of β radiation, which are produced in radioactive decay, have a range of only a few millimeters in tissue. For this reason, β emitters are active primarily when they are incorporated. The same applies to α emitters. As a result of their short range, they are of importance only in the case of inhalation or ingestion of radionuclides.

Since the primary physical and chemical effects are identical for all types of ionizing radiation, the same quantity can be used to measure the extent of a radiation exposure. This quantity is called the *adsorbed dose*, D , or simply the dose. The unit used, to express the absorbed dose, is J/kg, or gray (Gy). In spite of the identity of the physical primary processes, the various types of radiation have, even at the same absorbed dose, different efficiency in the cell or tissue. The reason for the differences lies in the varying microscopic concentration of the energy transferred along the tracks of the various particles. *Sparsely ionizing radiations*, such as γ rays, X rays, or fast electrons, cause only a few dozen ionizations along their path through the cell. The resulting direct and indirect damage to DNA can be largely repaired. *Densely ionizing particles*, such as the relatively slow, heavy α particles or recoil nuclei triggered by neutrons, cause thousands of ionizations as they pass through the cell. The clustered DNA damage produced within a small site can often be only imperfectly repaired. The difference between the various types of radiation is quantified by the linear energy transfer (LET), i.e., the rate of energy loss per unit distance.

In the application of ionizing radiation in *tumor therapy*, the different efficiency of the various types of radiation must be carefully evaluated. Moreover, the effect ratio depends in a complicated manner on the dose and the dose distribution in time. Simplified evaluations of radiation quality are adequate for the purpose of *radiation protection*, where low doses are involved and, furthermore, only summary estimates are required of effects that are possible, but less likely to occur.

Radiation protection summarily takes into account the different efficiency of densely and

sparsely ionizing radiation through the *quality factor*, Q . This factor represents the relative biological effectiveness of the different types of radiation with regard to the production, through DNA damage, of stochastic, long-term effects, i.e., hereditary damage or carcinogenesis. The International Commission for Radiation Protection (ICRP) has defined the quality factor as a function of the LET [14] (Figure 40.2). The *dose equivalent*, H , is the product of the absorbed dose, D , times the quality factor, Q :

$$H = D \times Q$$

To differentiate between the absorbed dose and the dose equivalent, the latter is expressed in the unit sievert (Sv).

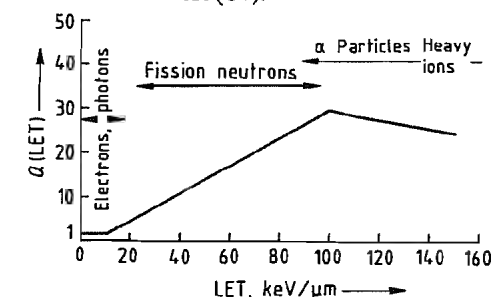


Figure 40.2: Quality factor as a function of the linear energy transfer, LET [14]. The corresponding ranges of LET are shown for some types of radiation.

40.6 References

1. Gmelin, 8th ed., Technetium, System no. 69, Suppl. vol. 1 and 2 (1982).
2. Gmelin, 8th ed., Polonium, System no. 12, Suppl. (1990).
3. Gmelin, 8th ed., Francium, System no. 25a, Suppl. (1983).
4. Gmelin, 8th ed., Radium, System no. 31, Suppl. vol. 1 and 2 (1977).
5. Gmelin, 8th ed., Actinium, System no. 40, Suppl. (1981).
6. Gmelin, 8th ed., Protactinium, System no. 51, Suppl. vol. 1 and 2 (1977).
7. E. J. Wheelwright: *Promethium Technology*, American Nuclear Society, Winsdale, IL, 1977.
8. F. Weigel, *Chem. Ztg.* **102** (1978) 287–299.
9. N. von Jagle, G. Schwarz, L. von Sienbenrock: "Blutbefunde bei Röntgenologen", *Berl. Klin. Wochenschr.* **48** (1911) 1220–1222.
10. F. Dessauer: "Über einige Wirkungen von Strahlen", *Z. Phys.* **12** (1922) 38.
11. H. S. Martland: "The Occurrence of Malignancy in Radioactive Persons: A General Review of Data

- Gathered in the Study of the Radium Dial Painters with Special Reference to the occurrence of osteogenic Sarcoma and the Interrelationship of Certain Blood Diseases", *Am. J. Cancer* **15** (1931) 2435-2516.
12. D. M. Taylor, C. W. Mays, G. B. Gerber, R. G. Thomas: "Risk from Radium and Thorotrast", *BIR Report* 21, EUR 12088, Brussels 1989.
13. E. B. Lewis: "Leukemia and Ionizing Radiation", *Science (Washington, DC)* **125** (1957) 965-972.
14. International Commission on Radiological Protection, ICRP Publication 60. 1990 Recommendations of the International Commission on Radiological Protection, Pergamon Press, Oxford 1991.

41 Uranium

MARTIN PEEHS, SABINE WALTER, THOMAS WALTER

41.1 Introduction	1599	41.7.4.8 Complete Plant for Production of UF_6 from Uranyl Nitrate	1626
41.2 History	1600	41.7.4.9 Enrichment of ^{235}U	1627
41.3 Physical Properties	1601	41.7.4.10 Production of UO_2 Pellets from UF_6	1631
41.3.1 Radioactivity	1601	41.7.4.11 Production of Uranium Metal	1635
41.3.2 Modifications	1601	41.8 Compounds	1637
41.3.3 Mechanical Properties	1604	41.8.1 Halides	1637
41.3.4 Thermal Properties	1604	41.8.1.1 Trivalent Halides	1637
41.3.5 Electrical and Electrochemical Properties	1605	41.8.1.2 Uranium Tetrahalides	1638
41.3.6 Magnetic Properties	1605	41.8.1.3 Uranium Pentafluoride	1638
41.4 Chemical Properties	1605	41.8.1.4 Uranium Hexafluoride	1638
41.5 Occurrence, Requirement, and Production Figures	1606	41.8.2 Carbides	1639
41.5.1 Occurrence	1606	41.8.3 Nitrides	1640
41.5.2 Resources, Requirement, and Production Figures	1607	41.8.4 Oxides	1640
41.6 Uses	1611	41.8.4.1 Uranium Dioxide	1640
41.7 Production	1612	41.8.4.2 Uranium Trioxide	1641
41.7.1 From Crude Ore to Yellow Cake ..	1612	41.8.4.3 Triuranium Octaoxide	1641
41.7.2 From Yellow Cake to UF_6	1612	41.8.4.4 Peroxides	1642
41.7.3 From UF_6 to the Nuclear Fuel UO_2 ..	1612	41.8.5 Nitrates	1642
41.7.4 Detailed Description of the Processes	1613	41.8.6 Sulfates	1643
41.7.4.1 Digestion and Leaching of Ores ..	1613	41.8.7 Tricarbonatodioxouranate	1643
41.7.4.2 Treatment of the Solution	1614	41.9 Safety	1643
41.7.4.3 Production of Uranium Concentrate	1617	41.9.1 Radiation Shielding	1643
41.7.4.4 Final Purification of Uranium Concentrate	1617	41.9.2 Safety Against Uncontrolled Criticality	1644
41.7.4.5 Production of UO_2 and UO_2 from Purified Uranyl Nitrate Solution ..	1619	41.9.3 Geometrically Safe Vessels	1644
41.7.4.6 Production of UF_6	1623	41.9.4 Apparatus with Heterogeneous Neutron Absorbers	1645
41.7.4.7 Production of UF_6 from UF_4	1625	41.9.5 Neutron Interactions in the UO_2 Fabrication Plant	1645
		41.9.6 Transportation	1645
		41.10 References	1646

The following abbreviations are used:

ADU	ammonium diuranate
AUC	ammonium uranyl carbonate
AVLIS	Atomic Vapor Laser Isotope Separation
BNFL	British Nuclear Fuels Limited
DC	Direct Conversion
GECO	General Electric Dry Conversion
DEHPA	2-ethylhexyl phosphate
IDR	Integrated Dry Route
LWR	light-water reactor
MLIS	Molecular Laser Isotope Separation
MTR	materials testing reactor
RIP	resin in pulp
TBP	tributyl phosphate
TOPO	triocetylphosphine oxide
USW	uranium separative work

UTK uranium tetrafluoride in kilns

41.1 Introduction

Uranium, atomic number 92, is a radioactive element that is transformed into the stable element lead via many intermediate stages involving the emission of α - and β -radiation. Uranium has the probable electronic configurations $4s^2p^6d^{10}f^4$, $5s^2p^6d^{10}$, $6s^2p^6d^4$, and $7s^2$, and is a member of the actinides in which the $6d$ shell is filled until uranium is reached, and the $5f$ shell is then filled from neptunium on-

ward to $5f^{14}$. Natural uranium consists of three isotopes whose concentrations in different resources are usually the same, even to the fourth decimal: ^{238}U , 99.2762 at%; ^{235}U , 0.7182 at%; ^{234}U , 0.0056 at%. However, uranium from one deposit in Gabon (the Oklo mine) is exceptional [8], the proportion of ^{235}U being lower (see below [9]):

Expected ^{235}U content	0.711 %
Measured ^{235}U content (July 7, 1972)	0.7078 %
Absolute discrepancy	0.0032 %
Relative discrepancy	0.45 %
Accuracy of measurement	± 0.0001 %

The somewhat lower percentage of ^{235}U in the Oklo deposit led to the discovery of natural reactors and the revelation that the first nuclear fission chain reaction was not brought about by humans in 1942 but by nature long before this. Since its discovery, the Oklo phenomenon has been investigated in great detail, and the results are documented in almost 100 papers. At least ten different reactor zones have been identified in Oklo. The individual reactors were active for 100 000 to 800 000 years. These periods of activity, which occurred 1.8×10^9 years ago, resulted in the release of 100×10^9 kWh thermal energy, equaling the output of a large-capacity power reactor over a three-year period. These natural reactors are the only ones discovered thus far in the world. During these periods of activity, natural uranium still had a ^{235}U content of ca. 3%; geochemical processes caused the U content to increase to 30% and higher. The thickness of the natural deposits reached 50 cm, and the presence of water as a moderator and coolant caused the configuration to become critical. The nuclear fission that then occurred was controlled by the properties of water. High power output led to evaporation of water, with consequent reduction of the moderating effect; lower power led to condensation and increased moderation. Decay products from earlier fission products and from the plutonium formed in the active zones of the natural Oklo reactor are still present without losses. This shows that these elements have not been dispersed but have been immobilized by simple geological barriers.

41.2 History

Uranium was discovered in 1789 by MARTIN HEINRICH KLAPROTH, who extracted it from pitchblende. He precipitated the yellow uranate and reduced this with charcoal, but obtained only a black oxide, probably UO_2 . In 1790, he named the putative metal uranium after the planet Uranus, which had been discovered in 1781 by HERSCHEL. In 1841, E. M. PÉLIGOT reported that he had obtained uranium metal by thermal reduction of anhydrous uranium tetrachloride with potassium in a platinum crucible. In 1856, he succeeded in producing the pure metal in compact form by reducing uranium tetrachloride with sodium with complete exclusion of air. A worth mentioning quantity of uranium metal was put on display at the Paris World Exhibition of 1867.

In the 1890s, H. MOISSAN developed new processes for producing metallic uranium. He obtained the purest metal (> 99% uranium) by electrolysis of sodium uranyl chloride. At the end of the 19th century, uranium found some almost unnoticed industrial applications, e.g., in glass and ceramics because of the beautiful colors of its different compounds.

The discovery of radioactivity by A. H. BECQUEREL on March 1, 1896, resulted from experiments with uranium. The fluorescence and phosphorescence of uranium compounds had been studied from about the mid-1800s. Following the discovery of X rays, the question arose of whether substances showing strong fluorescence or phosphorescence emitted penetrating rays of a similar kind. BECQUEREL exposed potassium uranyl sulfate to sunlight and observed that it emitted rays that darkened photographic plates. An interruption of these investigations due to cloud cover led to the discovery of intense darkening of the plates by uranium salts that had not been exposed to light. He concluded from this that uranium salts produced a special kind of radiation independent of light exposure.

The history of uranium is closely linked to the discovery of polonium and radium in pitchblende by P. and M. CURIE in 1898. The induced fission of the isotope ^{235}U was discov-

ered in 1938 by O. HAHN and F. STRASSMANN. This discovery was followed by intense research activity, that led to the first man-made nuclear chain reaction, which was brought about in Chicago by E. FERMI on December 2, 1942. World War II and U.S. decision to have a nuclear weapon led to intense activity in uranium research and nuclear development. Uranium enrichment plant based on the electromagnetic process was started in 1943 in Oak Ridge, Tennessee, followed a year later by another plant based on the gas diffusion principle.

After World War II, the search for uranium ores for the peaceful utilization of nuclear energy was intensified in most countries, and some large deposits were discovered. In the 1960s, military applications predominated; the peaceful use of nuclear energy gradually gained in importance in the late 1970s. Enriched uranium was required for the light-water reactors favored for energy production; thus, enrichment processes and techniques to manufacture fuel elements became important research and development topics. Enrichment by gas diffusion processes was used in the United States and France, whereas Germany, The Netherlands, and the United Kingdom developed a cooperative program based on three enrichment plants using the ultracentrifuge principle. The jet nozzle separation process, developed in Germany, is used in a demonstration plant in Brazil and South Africa.

Literature searches carried out for the present article have revealed that research and development of nuclear energy production and related technologies were largely complete in Western societies by the early 1980s. However, research continued into the technology of enrichment (laser and chemical processes), along with fundamental research into the band structure of uranium.

41.3 Physical Properties

41.3.1 Radioactivity

The natural uranium isotopes (^{238}U , ^{235}U , ^{234}U) are α -emitters. Tables 41.1 and 41.2 show the decay chains of the two most important isotopes. These chains terminate with the nonradioactive isotopes ^{206}Pb and ^{207}Pb .

Artificial uranium isotopes are formed in a nuclear reactor (e.g., by irradiation or decay of transuranics). Thus, after reprocessing of spent fuel elements, the following uranium isotopes are found in the purified uranium for a uranium burnup of 36 GW·d/t and an initial enrichment in the fuel elements of 3.5%:

^{232}U :	concentration 0.71 mg per tonne U; half-life 74 a; $\rightarrow ^{228}\text{Th}$
^{233}U :	concentration 7.4 mg per tonne U; half-life 1.6×10^5 a; $\rightarrow ^{229}\text{Th}$
^{234}U :	concentration 137 g per tonne U; half-life 2.5×10^5 a; $\rightarrow ^{230}\text{Th}$
^{236}U :	concentration 4490 g per tonne U; half-life 2.4×10^7 a; $\rightarrow ^{232}\text{Th}$

All four artificial isotopes are α -emitters with a certain amount of γ -emission and are transformed into the thorium isotopes indicated. Because of the comparatively short half-life of ^{232}U , associated γ -emission requires heavily shielded equipment for radiation protection. This hot-cell technology is also needed to handle the radioactive fission products in the reprocessing of spent fuel. Because it has an odd atomic number, ^{233}U is fissile by capture of a thermal neutron when it is reused in the reactor. However, ^{236}U in particular is purely a neutron absorber, so that on use of the reprocessed uranium, the fissile fraction (^{235}U) must be increased by ca. 0.15% to compensate for neutron capture by the $0.45\% ^{236}\text{U}$.

41.3.2 Modifications

The phase diagram of uranium is shown in Figure 41.1 [10, 11]. At atmospheric pressure, uranium occurs in three modifications with different crystal structures, depending on temperature [12]:

α -Uranium, $T < 942$ K, orthorhombic
Lattice constants: $a = 0.2858$ nm, $b = 0.5876$ nm, $c =$

0.4955 nm at 298.15 K.

β -Uranium, $T = 942\text{--}1049$ K, tetragonal
Lattice constants: $a = 1.0759$ nm, $c = 0.5656$ nm at 942 K (lower transformation point).

γ -Uranium, $T = 1049\text{--}1408$ K, body-centered cubic
Lattice constants: $a = 0.3524$ nm at 1049 K (lower transformation point).

The triple point of the three modifications is at 3.6 ± 0.2 GPa and 1078 ± 3 K [10]. Figures quoted for the mp at atmospheric pressure

cover the relatively narrow range between 1398 K (1125 °C) [13] and 1408 K (1135 °C) [14]. These small discrepancies are due to extremely low levels of impurities that cannot be avoided completely. The bp is said to be 4407 K. The theoretical density of α -uranium is 19.13 g/cm³, small variations in the experimental value again being due to impurities.

Table 41.1: Radioactive decay of ²³⁸U.

	Atomic number	Relative atomic mass	Penetration of α -particles in air at 15 °C and 0.1 MPa, cm	Half-life	Amount in radioactive equilibrium with ²³⁸ U contained in 1000 kg uranium, g
²³⁸ U	92	238.05	2.63	4.515×10^9 a	9.93×10^3
$\alpha \downarrow$ ²³⁴ Th	90	234		24.10 d	1.426×10^{-5}
$\beta \downarrow$ ²³⁴ Pa	91	234		1.16 min	4.76×10^{-10}
$\beta \downarrow$ ²³⁴ Pa	91	234		6.7 h	2.5×10^{-10}
$\beta \downarrow$ ²³⁴ U	92	234		2.32×10^5 a	50.1
$\alpha \downarrow$ ²³⁰ Th	90	230		8.3×10^4 a	17.6
$\alpha \downarrow$ ²²⁶ Ra	88	226.03	3.30	1590 a	3.32×10^{-1}
$\alpha \downarrow$ ²²² Rn	86	222	4.06	3.825 d	2.147×10^{-6}
$\alpha \downarrow$ ²¹⁸ Po	84	218	4.67	3.05 min	1.17×10^{-9}
$\beta \downarrow$ ²¹⁴ Pb	82	214		26.8 min	1.01×10^{-8}
$\beta \downarrow$ ²¹⁴ Bi	83	214		a few seconds	$ca. 1 \times 10^{-14}$
$\beta \downarrow$ ²¹⁴ Po	84	214		19.7 min	7.4×10^{-9}
$\beta \downarrow$ ²¹⁴ Rn	86	218		0.019 s	1×10^{-18}
$\beta \downarrow$ ²¹⁴ Po	84	214		1.45 $\times 10^{-4}$ s	9.1×10^{-16}
$\alpha \downarrow$ ²¹⁰ Tl	81	210		1.32 min	1.95×10^{-13}
$\beta \downarrow$ ²¹⁰ Pb	82	210		22.3 a	4.32×10^{-1}
$\beta \downarrow$ ²¹⁰ Bi	83	210		4.95 d	2.63×10^{-6}
$\beta \downarrow$ ²¹⁰ Po	84	210		138.8 d	7.37×10^{-5}
$\alpha \downarrow$ ²⁰⁶ Tl	81	206		4.23 min	7.6×10^{-16}
$\beta \downarrow$ ²⁰⁶ Pb	82	205.97		stable	∞

*99.96%.

Table 41.2: Radioactive decay of ²³⁵U.

	Atomic number	Relative atomic mass	Penetration of α -particles in air at 15 °C and 0.1 MPa, cm	Half-life	Amount
²³⁵ U	92	235.04	2.7	7.07×10^8 a	7.06×10^3
$\alpha \downarrow$ ²³¹ Th	90	231		24.6 h	2.75×10^{-8}
$\beta \downarrow$ ²³¹ Pa	91	231.04	3.62	3.2×10^4 a	3.14×10^{-1}
$\alpha \downarrow$ ²²⁷ Ac	89	227		21.7 a	2.09×10^{-4}
$\beta \downarrow$ ²²⁷ Tl	90	227	4.67	18.6 d	4.85×10^{-7}
$\alpha \downarrow$ ²²³ Ra	88	223		21 min	4.5×10^{-12}
$\alpha \downarrow$ ²¹⁹ Fr	87	223		11.3 d	2.93×10^{-7}
$\alpha \downarrow$ ²¹⁵ At	85	219		0.9 min	8×10^{-18}
$\beta \downarrow$ ²¹⁵ Pu	86	219		3.92 s	1.16×10^{-12}
$\beta \downarrow$ ²¹⁵ Bi	83	215		8 min	6×10^{-17}
$\beta \downarrow$ ²¹⁵ Po	84	215		0.00183 s	5.30×10^{-16}
$\alpha \downarrow$ ²¹¹ Pb	82	211		36.1 min	6.15×10^{-10}
$\beta \downarrow$ ²¹¹ At	85	215		$ca. 10^{-4}$ s	$ca. 1 \times 10^{-22}$
$\beta \downarrow$ ²¹¹ Bi	83	211		2.16 min	3.68×10^{-11}
$\beta \downarrow$ ²¹¹ Po	84	211		$ca. 0.005$ s	4.5×10^{-18}
$\alpha \downarrow$ ²⁰⁷ Tl	81	207		4.76 min	7.93×10^{-11}
$\beta \downarrow$ ²⁰⁷ Pb	82	206.98		stable	∞

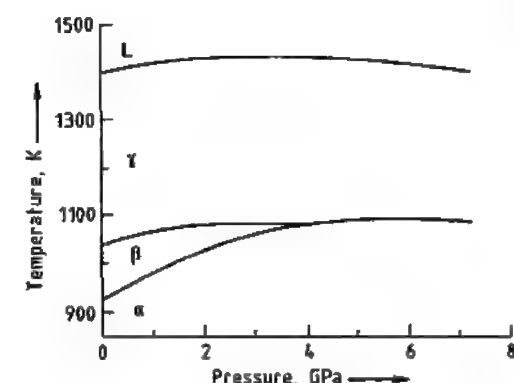


Figure 41.1: Phase diagram of uranium [10, 11]. Ranges of the α -, β -, and γ -modifications and of the liquid are shown.

Table 41.3: Mechanical strength of rolled uranium metal products annealed in the α - or β -region before measurement [15].

	Test temperature, °C	0.2% yield strength, MPa	Ultimate tensile strength, MPa	Elongation, %
Rolled at 570 °C				
α -annealed	20	298.6	766.0	6.8
β -annealed	20	169.3	439.9	8.5
Rolled at 1110 °C				
α -annealed	20	179.3	609.5	13.5
β -annealed	20	169.6	425.4	6.0
Rolled at 570 °C, α -annealed	299	120.7	242.7	49.0
Rolled at 570 °C, β -annealed	299	129.6	217.7	43.0
Rolled at 570 °C, α -annealed	499	35.2	76.7	61.0
Rolled at 1110 °C, α -annealed	499	37.6	72.0	57.0

Table 41.4: Hardness of annealed uranium metal.

Annealed for 1 h at	Rockwell hardness		Brinell hardness number
	150-kg weight	100-kg weight	
310 °C	36.6	109	341
490 °C	24.0	101	247
600 °C	22.0	99	240
720 °C	9.0	90	185
770 °C	0	92	152

41.3.3 Mechanical Properties

In the γ -phase (1049 K < T < 1408 K), the metal is soft, ductile, and easily worked. However, since this phase is readily oxidized in an oxidizing environment (e.g., air), uranium usually must be worked while in the α -phase at lower temperature (at 563 K).

Mechanical strength data for the α - and β -phases are given in Table 41.3 [15].

The hardness of the metal depends strongly on the annealing temperature (Table 41.4). The Rockwell hardness was measured at applied weights of 100 and 150 kg, and the Brinell hardness is given in Brinell numbers (applied weight of 300 kg divided by the penetration area of a 10-mm steel sphere).

The modulus of elasticity is also very dependent on the history of the material; it ranges between 155 GPa (α -phase, rolled; β -phase, annealed) and 207 GPa (γ -phase, extruded).

41.3.4 Thermal Properties

The specific and molar heat capacities of the three uranium modifications are given in Table 41.5 [12].

Table 41.5: Specific and molar heat capacities of uranium modifications.

	$c_p, \text{J kg}^{-1} \text{K}^{-1}$	$C_p, \text{J mol}^{-1} \text{K}^{-1}$
α -Uranium (298.15 K)	116	27.666
β -Uranium (942 K)	180	42.928
γ -Uranium (1049 K)	161	38.284

In the α - and β -phases, uranium is anisotropic; i.e., thermal expansion depends on direction. Thus, a crystal of α -uranium expands in only two directions and contracts in the third (Figure 41.2). The expansion coefficients for

α -uranium in the various crystal directions are given in Figure 41.3 [16, 17].

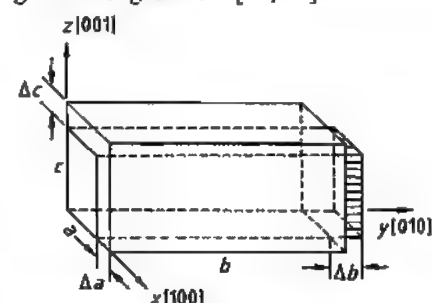


Figure 41.2: Dimensional change of α -uranium from 0 to 300 °C. Original dimensions: $a = 0.2852 \text{ nm}$; $b = 0.5985 \text{ nm}$; $c = 0.4945 \text{ nm}$; $\Delta a = +0.0015 \text{ nm}$; $\Delta b = -0.0006 \text{ nm}$; $\Delta c = +0.0339 \text{ nm}$.

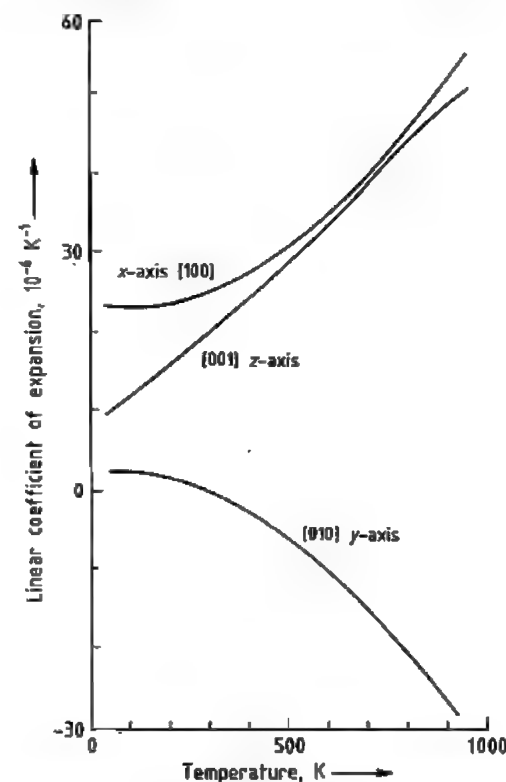


Figure 41.3: Linear expansion coefficient of α -uranium [16, 17].

For β -uranium in the range 959–998 K, the linear coefficients of expansion are

z-axis, $4.6 \times 10^{-6} \text{ K}^{-1}$
x-axis, $23.0 \times 10^{-6} \text{ K}^{-1}$

y-axis, $16.9 \times 10^{-6} \text{ K}^{-1}$

The linear coefficient of expansion of γ -uranium is the same for all three axes (i.e., ca. $18 \times 10^{-6} \text{ K}^{-1}$).

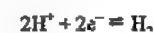
The thermal conductivity of uranium at 298 K is $27.60 \text{ W m}^{-1} \text{K}^{-1}$.

41.3.5 Electrical and Electrochemical Properties [18]

The specific electrical conductivity of uranium has been determined by several authors. The variations in the value obtained (3.0 – $3.38 \times 10^4 \Omega^{-1} \text{cm}^{-1}$) are due to variations in the purity and history of the metal. The values determined for specific electrical resistance naturally show similar variation, the mean value at room temperature being ca. $30 \mu\Omega \text{cm}$. The specific electrical resistance increases with increasing temperature to ca. $55 \mu\Omega \text{cm}$ at 873 K. At the transformation points of α - to β -uranium and of β - to γ -uranium, the curve shows a downward discontinuity but then rises again. The temperature coefficient of the specific electrical resistance in the range 273–373 K is 2.61 – 2.76×10^{-3} .

Uranium becomes superconducting at very low temperature, but the transition temperature T_c is very pressure dependent [10]. At atmospheric pressure, T_c has its lowest value (0.2 K), it reaches its highest value (2.25 K) at 1 GPa.

The standard electrode potential ε_0 for the reaction



at 25 °C with a 1 mol/L solution of metal ions and a hydrogen electrode is with water -0.414 V , with a 1 mol/L HClO_4 solution -0.631 V , and with a 1 mol/L HCl solution -0.640 V . The thermoelectric potential with copper is ca. 5 mV [19].

41.3.6 Magnetic Properties

Uranium is paramagnetic. The paramagnetic susceptibility varies with temperature and exhibits discontinuities at the phase trans-

formation points (Figure 41.4). The specific magnetic susceptibility at 298 K is $1.66 \times 10^{-6} \text{ cm}^3/\text{g}$.

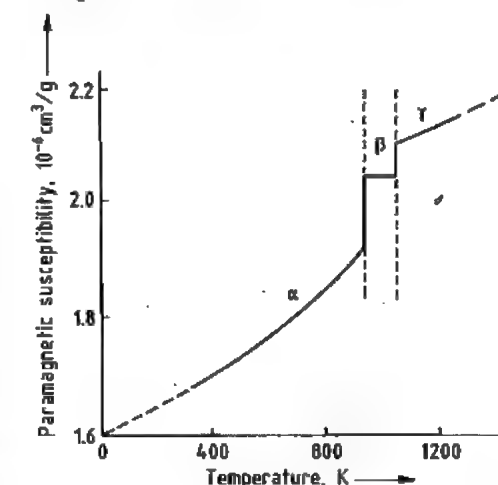


Figure 41.4: Paramagnetic susceptibility of uranium.

41.4 Chemical Properties

The freshly exposed surface of massive uranium metal has a silvery luster, but it is oxidized relatively rapidly in air. Within a few hours, the metal becomes covered with a thin oxide layer of iridescent colors and eventually turns black. The same mass of metal that is oxidized by steam at 593 K is oxidized by air only above 753 K. The enthalpy and the free energies of formation of oxides from the metal at 298 K are as follows [20]:



Uranium metal powder is pyrophoric and burns or smolders very readily in air, sometimes spontaneously if the powder has a large enough surface area. Mechanical machining of uranium metal by turning, lathing, and drilling must be carried out with adequate work fluids for lubrication of the cutting tools and for cooling the chippings formed. To store the chippings, they are wetted with a special oil or burned promptly in a controlled manner to form U_3O_8 . Uranium does not react with hydrogen at room temperature but combines

readily with it at 498 K to UH_3 , which decomposes again at 709 K. This behavior is utilized in the manufacture of the powdered metal from its compact form, in which UH_3 is produced as an intermediate. Also, to reduce the hazard involved in transporting tritium gas, it is currently absorbed by depleted uranium powder in flasks.

Uranium reacts very vigorously with *halogens* and *hydrogen halides*. It burns in fluorine gas to form UF_6 ("flame reactor"). The reaction with HF gas proceeds only to the UF_4 stage; reaction with aqueous HF leads to hydrated UF_4 ($\text{UF}_4 \cdot 0.75\text{H}_2\text{O}$, $\text{UF}_4 \cdot 2.5\text{H}_2\text{O}$). Uranium burns in a stream of chlorine to form UCl_6 and UCl_4 . With bromine and iodine, it reacts to only UBr_3 and UI_3 . With *sulfur*, grayish black US_2 is formed, which is stable up to 1273 K.

Powdered uranium reacts very vigorously with *water*; above 308 K the compact metal also reacts with water. Uranium is attacked vigorously by *dilute acids*, with the formation of salts. *Strong solutions of alkali* also attack the metal to form uranates.

41.5 Occurrence, Requirement, and Production Figures

41.5.1 Occurrence

The mean concentration of uranium in the earth's crust is $2 \times 10^{-4}\%$. For comparison, the abundances of cobalt, lead, and molybdenum are similar. Uranium is a typical lithophilic element, occurring mainly in the silicates of the earth's crust. Most of the uranium is distributed widely in small concentrations, both in acidic rocks such as granite, gneiss, and pegmatite, and in sedimentary rock such as schist and phosphatic ores. Basic rocks (basalt) have a lower uranium content than granite, for example. The wide distribution of uranium and the low degrees of enrichment in ores compared with other metals of similar abundance are the result of its ability to form a wide range of chemical complexes. Uranium occurs in more than 100 minerals; those of industrial importance are listed in Table 41.6.

Table 41.6: Uranium minerals of industrial importance (detailed information on uranium minerals is given in [21]).

Mineral	Chemical formula	Origin
<i>Oxides, hydrates, simple silicates (uranium, completely or primarily tetravalent)</i>		
Pitchblende	$x\text{UO}_3 \cdot y\text{UO}_2$	Canada, Congo, Western and Central Europe
Uraninite	UO_2 (with UO_3)	Canada, Colorado Plateau, Argentina
Coffinite	$x\text{USiO}_4 \cdot y\text{U}(\text{OH})_4$	Colorado Plateau
Uranothorite	$x\text{ThSiO}_4 \cdot y\text{USiO}_4$	Canada, Madagascar
<i>Complex deposits of uranium oxides with rare earths (titanates, etc.)</i>		
Brannerite	$(\text{U}, \text{Ca}, \text{Fe}, \text{Y}, \text{Th})_2\text{Ti}_2\text{O}_{16}$	Canada
Betafite (similar to am-pangabeite)	$(\text{U}, \text{Ca})(\text{Nb}, \text{Ta}, \text{Ti})_3\text{O}_9 \cdot x\text{H}_2\text{O}$	Madagascar
Davidite	$(\text{Fe}, \text{rare earths}, \text{U}, \text{Ca}, \text{Zr}, \text{Th})_x(\text{Ti}, \text{Fe}^{3+}, \text{V}, \text{Cr}, \text{Y})_y\text{O}_z$	
<i>Secondary minerals with hexavalent uranium</i>		
Gummite	$\text{UO}_3 \cdot x\text{H}_2\text{O}$ (also silicate, phosphate, of indefinite composition)	
Uranophane	$\text{CaO} \cdot 2\text{UO}_3 \cdot 3\text{SiO}_2 \cdot 6\text{H}_2\text{O}$	Colorado Plateau, Argentina
Schroëckerite	$\text{Na}_2\text{O} \cdot 3\text{CaO} \cdot \text{UO}_3 \cdot 3\text{CO}_2 \cdot \text{SO}_3 \cdot \text{F} \cdot 10\text{H}_2\text{O}$	Joachimsthal, Colorado Plateau, Argentina
Carnotite	$\text{K}_2\text{O} \cdot 2\text{UO}_3 \cdot \text{V}_2\text{O}_5 \cdot 3\text{H}_2\text{O}$	Colorado Plateau, Australia, Argentina
Tjujamunite	$\text{CaO} \cdot 2\text{UO}_3 \cdot \text{V}_2\text{O}_5 \cdot 8\text{H}_2\text{O}$	Turkestan, Colorado Plateau, Argentina
Autunite (torbernite)	$\text{CaO} \cdot 2\text{UO}_3 \cdot \text{P}_2\text{O}_5 \cdot 12\text{H}_2\text{O}$	

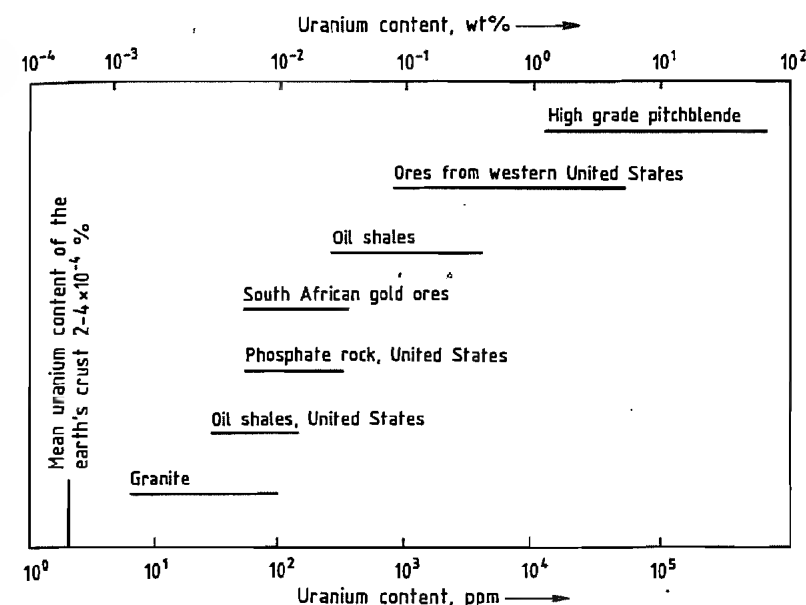


Figure 41.5: Uranium concentration in important uranium minerals.

Some materials not regarded as true uranium minerals are the poorly defined uranium-containing bituminous products known as kolm (Sweden), thucholite (Sweden, Canada, South Africa), and asphalt or asphaltite (Colorado Plateau, Argentina). An industrially important mineral, which contains uraninite or pitchblende as accompanying mineral, is monazite. Large deposits of monazite are found in India and Brazil.

Large reserves are also present in seawater because of its enormous volume. However, the uranium level (ca. 3 ppb = 3 $\mu\text{g/L}$) is very low. Nevertheless, attempts have been made since the 1950s to extract uranium from seawater. An enrichment factor of 10^5 has been achieved. However, the processes will be economical only if enrichment can be increased to ca. 10^6 ; the concentration would then correspond to that in a minable ore [22]. Uranium concentrations in the most important uranium-bearing ores in the earth's crust are shown in Figure 41.5 [23]. Approximately half of the annual uranium production comes from secondary minerals. One-third comes from conglomerates in which unweathered rock has been sedimented together with oxidized ura-

nium. The remaining uranium production is from veins or lodes and syngenetic-sedimentary ore deposits.

41.5.2 Resources, Requirement, and Production Figures

A 1991 report with data valid for January 1, 1991, issued jointly by the Nuclear Energy Agency of the OECD and the IAEA, gives data on deposits, production, and uranium requirements for 44 countries [24]. This report, for the first time, includes countries from the former Eastern Bloc.

Since then, the data from the former Eastern bloc have become more precisely known and have been more thoroughly evaluated. The development of uranium supply and demand has also changed considerably. Thus considerable quantities of uranium from military projects are now available for civil nuclear energy generation as a result of worldwide nuclear disarmament. Hence OECD/NEA [25] and The Uranium Institute [26] have revised and re-issued their existing reports. The market perspectives have been studied with respect to the question of how the

ever-increasing gap between uranium demand and uranium production can only be bridged by the release of military reserves [27–29].

The known world uranium resources, classified according to the IAEA system by the state of exploration and the anticipated costs per kilogram of uranium extracted, are listed in Table 41.7. The reserves of the following countries are not included in the IAEA classification:

Chile	0.23×10^3 t
China	55.1×10^3 t
India	66.15×10^3 t
Romania	26.0×10^3 t
Former Soviet Union	685.6×10^3 t
Bulgaria	45.0×10^3 t
Former Czechoslovakia	145.0×10^3 t
Poland	20.0×10^3 t
Total	1038.98×10^3 t

On the basis of reports on estimated and speculative reserves, it is assumed that worldwide reserves amount to $(8\text{--}13) \times 10^6$ t of uranium.

Table 41.7: World uranium reserves according to IAEA classification [24], in 10^3 t uranium.

Country	Reasonably assured resources		Estimated additional resources (category I)	
	up to \$80/kg U	\$80–130/kg U	up to \$80/kg U	\$80–130/kg U
North America (total)	247.90	323.90	149.00	80.70
Canada	146.00	68.00	149.00	80.00
Mexico	0.00	1.70	0.00	0.70
United States	101.90	254.20	0.00	0.00
Africa (total)	547.02	138.70	380.57	75.50
Algeria	26.00	0.00		
Central African Republic	8.00	8.00		
Gabon	11.00	4.65	1.30	8.30
Namibia	84.75	16.00	30.00	23.00
Niger	166.07	6.65	295.77	10.00
Somalia	0.00	6.60	0.00	3.40
South Africa	247.60	96.80	51.80	30.80
Zaire	1.80	0.00	1.70	0.00
Zimbabwe	1.80	0.00		
Europe (total)	58.27	74.25	23.05	51.35
Austria			0.70	1.00
Denmark	0.00	27.00	0.00	16.00
Finland	0.00	1.50		
France	23.80	15.70	4.20	3.90
Germany	0.60	4.00	1.60	5.70
Greece	0.30	0.00	6.00	0.00
Hungary	1.62	1.50	9.10	9.15
Italy	4.80	0.00	0.00	1.30
Portugal	7.30	1.40	14.45	0.00
Spain	17.85	21.15	0.00	9.00
Sweden	2.00	2.00	1.00	5.30
Australia	469.00	60.00	264.00	126.00
South America (total)	172.53	2.19	96.26	2.09
Argentina	8.74	2.19	0.54	1.95
Brazil	162.00	0.00	94.00	0.00
Peru	1.79	0.00	1.72	0.14
Asia (total)	4.32	27.53	0.00	3.20
Indonesia	4.32	0.00		
Japan	0.00	6.60		
Korea	0.00	11.80	0.00	3.00
Turkey	0.00	9.13		
Vietnam			0.00	0.20
Total	1449.04	626.57	912.88	338.84

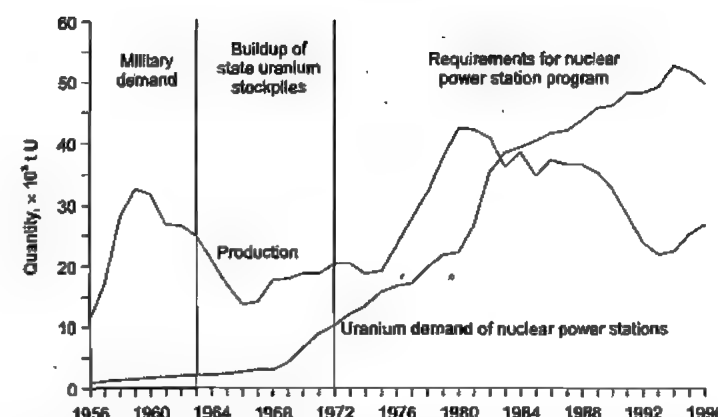


Figure 41.6: Uranium production and demand of the Western World (1956–1996).

Uranium Production of the Western Countries. Figure 41.6 shows the uranium production and uranium demand of the Western world in the period 1956 to 1995. In this part of the world, the uranium industry experienced its first boom in the early 1960s. At that time, almost the entire uranium production was consumed by the weapons programs of the western nuclear powers (United States, United Kingdom, France). The civil uranium demand for nuclear power stations began in the late 1960s and early 1970s. This was stimulated by the expansion programs that were established as a result of the oil crisis of 1973. However, the actual expansion in Europe and the United States failed to meet the planned level. Nevertheless, between 1975 and 1980, uranium production grew to meet the increased demand from civil nuclear energy generation. At this time, production of uranium as a by-product of phosphate-rock mining became important. The dramatic decrease in production since 1989 is due to increasing oversupply. Thus, in 1980 the uranium production of the western world was ca. 44 000 t U, but demand was only ca. 22 000 t U. While uranium production continued to decrease, the uranium demand of the civil nuclear energy program grew worldwide. The difference between supply and demand was covered by uranium from stockpiles.

The price development for uranium shows clearly that sufficient quantities of previously

produced uranium are reaching the market, since the uranium price has dropped (Figure 41.7) despite the fact that production has failed to meet demand. Up to 1973, the uranium price remained at a constant \$7/lb U but then increased greatly due to the oil crisis, reaching a peak of \$45/lb U in 1976. The overcapacity existing at this time led to a price drop and eventual stabilization at ca. \$23/lb in 1982. For the reasons discussed above, the uranium price fell slowly up to 1994 and has currently reached temporary stability at a low level.

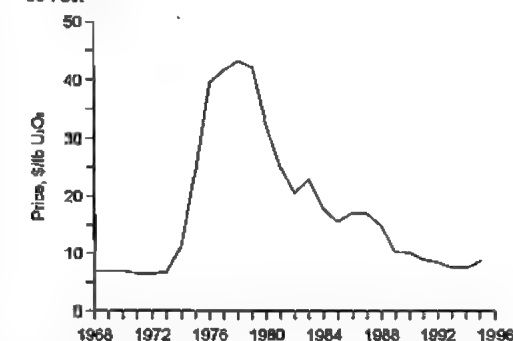


Figure 41.7: Uranium spot market price for European buyers (1968–1995).

Uranium Production of the Former Eastern Bloc. In the former Soviet Union, its satellite states, and China, ca. 630 000 t of uranium have been produced since the 1940s (Figure 41.8). Prior to the political and economic liberalization of Eastern Bloc in 1989/90, the majority of the uranium produced in the Soviet

sphere of influence was transported to the Soviet Union as a strategic material. Only Romania retained a few thousand tonnes for its CANDU reactor program. Of the uranium produced in the Soviet Union and imported from its satellites up to 1994, probably 450 000 t U was made available for military purposes, and 115 000 t U was used for the nuclear reactor program of the Soviet Union and Eastern Europe. Thus, today Russia should possess a stockpile of ca. 75 000 t U in the form of natural and enriched uranium. Figure 41.9 shows the uranium production of the CIS since 1991. Two of the largest producers, Kazakhstan and Uzbekistan, have essentially no nuclear energy program, so that their entire production should become available to the world market in the form of exports.

Uranium Production Today. World uranium production in 1995 was ca. 34 200 t U, 75% of which came from the Western countries and 25% from Eastern Europe, the CIS, and China (Figure 41.10). The 13 largest mines accounted for 70% of world uranium production. The three largest western uranium producers — Cogema, Cameco, and Uranerzbergbau — were responsible for ca. 44% of world uranium production. Figure 41.11 shows 1994 uranium production divided according to mine owners.

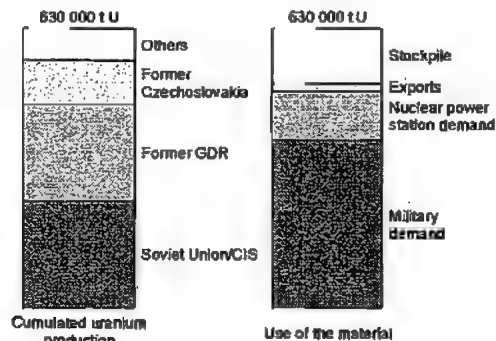


Figure 41.8: Cumulated uranium production in the former Eastern bloc and use of the material (1945–1994).

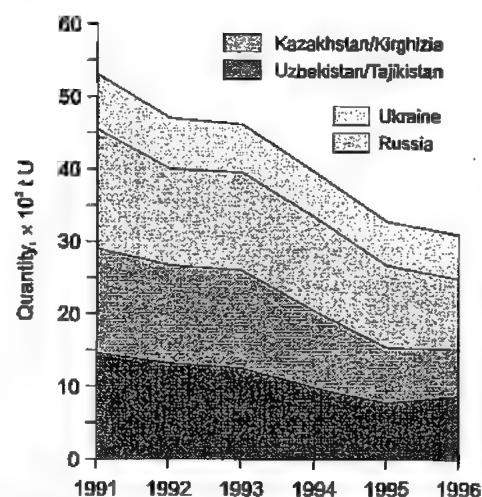


Figure 41.9: Uranium production in the CIS (1991–1996).

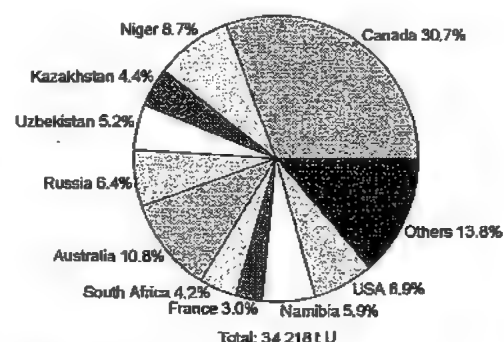


Figure 41.10: World uranium production in 1995 by countries.

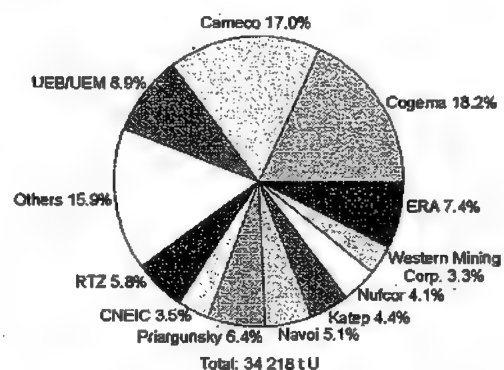


Figure 41.11: World uranium production in 1995, broken down by owners of mines.

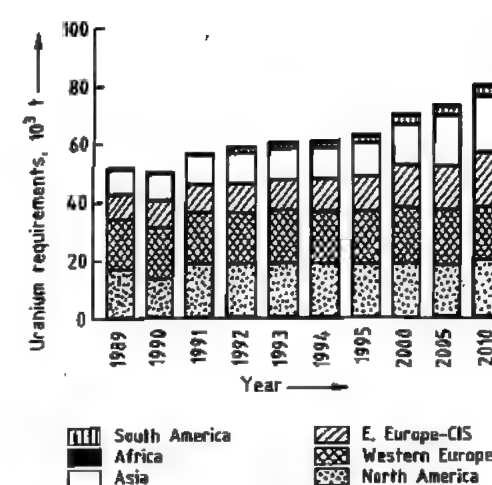


Figure 41.12: Projected uranium consumption for nuclear reactors [24].

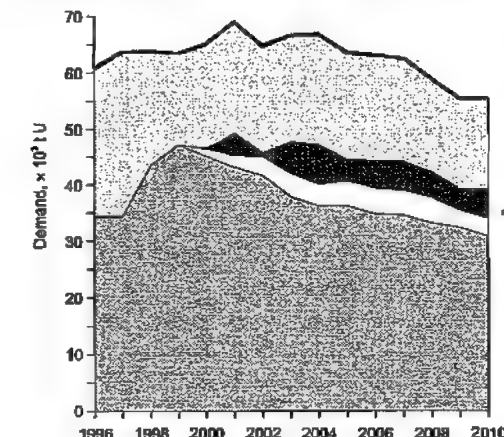


Figure 41.13: Contributions of the production of fresh uranium and uranium inventories to future uranium supply (1996–2010).

Future Supply/Demand Pattern. Figure 41.6 shows uranium demand and uranium production up to 1996. Figure 41.12 shows an OECD/IAEA estimate of future uranium demand dating from 1991. World uranium demand in 1991 was 49 300 t U, and this was distributed between the continents as shown in

Figure 41.12. On the basis of planned nuclear energy generating capacity, a uranium demand of ca. 77 700 t U is expected in the year 2010. New investigations of various reference scenarios of The Uranium Institute [26] give values between 70 000 and 80 000 t U. SCHREIBER [29] assumes a demand of less than 60 000 t U and predicts the uranium supply situation shown in Figure 41.13.

World uranium demand will increase slowly for about a decade, after which a downward trend can be expected if it is assumed that nuclear power stations are removed from the grid and not replaced when their licenses expire. This assumption is based on a projection of current energy policies.

Figure 41.13 compares world uranium demand with maximum achievable production capacity. Production capacity is divided into potential projects, mines held in reserve, and plants in operation or for which concrete plans exist. Figure 41.13 shows that world uranium production could double by 2002, but also that the operating, planned, and potential projects will not be sufficient to cover the uranium demand of the nuclear power stations. Hence, in future the existing civil uranium inventories and those that become available from military programs as a result of disarmament will have to be used to meet these demands.

41.6 Uses

The intermediate product “yellow cake” is produced from uranium ore. The industrially most important end product is UO_2 , which is the only nuclear fuel used in power station reactors, although uranium carbide (UC) is sometimes used in sodium-cooled fast breeder reactors because of its higher density and superior thermal conductivity compared with UO_2 .

Uranium metal is used as the fuel in materials testing reactors and Magnox reactors. Because of its extremely high density, it is also used in depleted form for trimming weights in large aircraft. A Boeing jumbo jet contains 360 kg of depleted uranium metal. The high

density of uranium metal also utilized in shielding materials for protection against radiation sources (e.g., in portable equipment for weld radiography and medical X-ray equipment).

U-Zr alloys are used as nuclear fuel in marine reactors and in research and materials testing reactors. *Hydrogenated U-Zr alloys* (UZrH_x) are used as combined fuel-moderator systems in spacecraft reactors. *Uranium silicides* could in principle be used as fuel in light-water reactors. However, uranium silicides are not utilized because undesired reactions with water, the cooling medium, can occur as a result of defects in the fuel elements. *Uranium-aluminum alloys* are used in materials testing and research reactors.

Uranium salts are now rarely added to ceramic products to produce luminous colors (e.g., in Merano glassware or tiles) because of the radiation problems involved.

41.7 Production

41.7.1 From Crude Ore to Yellow Cake

Mined crude ores are prepared for leaching by crushing and grinding. The chemical leaching process is selected according to the mineralogical nature of the ore. Acidic ores are treated with dilute H_2SO_4 , and alkaline ores with an aqueous solution containing sodium carbonate and sodium bicarbonate. Phosphatic ores are treated with acid.

Solid-liquid separation of leached ore is achieved by standard processes such as filtration, multistage decantation, and hydrocyclone separation; uranium is recovered from the solution by ion exchange or solvent extraction. Combining these two techniques, as in the Eluex process, is also advantageous. Yellow cake is then produced by precipitation from the acid liquor with ammonia or $\text{Mg}(\text{OH})_2$ or by precipitation from the alkaline liquor with NaOH.

Uranium is obtained as an accompanying element from phosphatic ores in which the

uranium content is very low (see Section 41.5.2). After acid treatment, uranium is purified and recovered by the stripping process. Uranium is precipitated as ammonium uranyl carbonate (AUC).

41.7.2 From Yellow Cake to UF_6

In the wet treatment process, yellow cake is dissolved in HNO_3 and purified by solvent extraction. The resulting solution of uranium in nitric acid can then be reacted chemically to form UO_2 or UO_3 by using either the ammonium diuranate (ADU) or the AUC process, or by denitrating evaporation.

UO_2 is converted into UF_6 in two stages: first UF_4 is produced by treatment with HF; UF_4 is then converted into UF_6 by treatment with fluorine gas. In principle, yellow cake can also be processed in the dry state. After size reduction and preliminary purification, yellow cake is calcined to form UO_2 , which is then converted into UF_6 as described above. However, the dry UF_6 so obtained must then be purified by fractional distillation.

41.7.3 From UF_6 to the Nuclear Fuel UO_2

If UF_6 is to be converted to the nuclear fuel UO_2 for light-water reactors, an enrichment process must be carried out for reasons of reactor physics until the ^{235}U isotope content is between 2 and 6%. Enrichment processes commonly used include the diffusion process, the nozzle process, and centrifugation.

Enriched UF_6 can be processed by either wet methods (e.g., AUC, ADU) or dry methods [e.g., Integrated Dry Route (IDR), Direct Conversion (DC), General Electric Dry Conversion (GECO)] to obtain UO_2 powder. After chemical conversion and before pelletization, the powder must be pretreated (except in the case of precipitation by the AUC process). Only after pretreatment do the various steps of pelletization (compression, sintering, and grinding) give an end product with the desired spectrum of properties.

41.7.4 Detailed Description of the Processes

41.7.4.1 Digestion and Leaching of Ores

Before ore digestion appropriate pretreatment is essential. This includes size reduction for which several stages are necessary. In the first stage, lumps of ore ca. 1 m in diameter are passed through gyratory or jaw crushers with a power consumption of 250–350 kW. These reduce the ore to lumps of ca. 200 mm diameter. Cone crushers with a power consumption of 30–40 kW are used in the second stage, giving pieces of ore ca. 65 mm in diameter. Particle sizes of < 10 mm are obtained in the third stage, in which fine cone crushers or roller crushers with power consumption of 15–20 kW are used [30, 31]. This degree of size reduction is adequate with most types of ore for which the much more usual sulfuric acid process is used. Finer grinding is necessary only for alkali treatment. Here screen mills and ball mills are used in succession to reduce the particle size of the ore to ca. 0.5 mm.

Consideration of the economics of the complete process of grinding and chemical treatment must include the question of whether preliminary removal of worthless material (gangue) might be beneficial. However, except for visual hand sorting of lump materials, no industrial process has thus far been used. Pilot-scale experiments in Elliot Lake, Canada, have been reported (Table 41.8) [32].

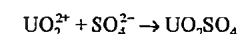
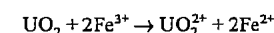
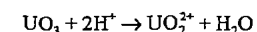
Table 41.8: Separation methods: amounts of worthless material removed and consequent uranium loss [32].

Method	Worthless material removed, %	U_3O_8 loss, %
Flotation after grinding to < 0.3 mm	62–80	8
Gravitational method	ca. 35	8
Radiometry method	ca. 20	8
Magnetic separation	ca. 85	14

Acidic Ores

Dilute sulfuric acid is always used for the acid treatment of ores. The rate of dissolution

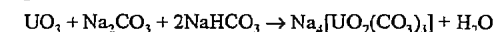
depends on acid concentration, temperature, and surface area of the ore particles. If the ore contains feldspar and clay, highly concentrated acid should not be used since it will dissolve aluminum silicates. If the particles are ground too finely, clarification of the cloudy solution can present some problems. If tetravalent uranium is present, an oxidizing agent (sodium chlorate or manganese dioxide) is added to the liquor, with dissolved iron acting as a catalyst. The following reactions occur during the dissolution process:



At higher acid concentration, complex anions such as $[\text{UO}_2(\text{SO}_4)_3]^{4-}$ are also formed, but these do not cause problems in later processing.

Alkaline Ores

Alkaline ores require treatment with alkaline solutions. Alkaline leaching is considerably slower than acid leaching, but is more effective for ores in which the gangue materials contain calcium compounds or other acid-consuming components. For alkaline treatment the ore must be more finely ground. Since carbonate solution does not attack this type of gangue, uranium is dissolved much more selectively than when acidic solutions are used, and the subsequent concentration stage is easier. The dissolution of uranium is due to the formation of a tricarbonato complex:



The above ratio of carbonate to hydrogen-carbonate should be maintained. If tetravalent uranium is present, oxygen is used as an oxidizing agent, and higher temperature and pressure are applied. This oxidation is catalyzed by copper sulfate and ammonia.

Digestion of Phosphate Rock

Uranium is present in phosphate rock at a mean concentration of 100–150 mg/kg. Flor-

ida phosphate rock, for example, contains 110 mg/kg uranium. Total uranium reserves in phosphate rock are currently estimated at ca. 7.1×10^6 t [24], which is nearly twice as much as the world reserves with beneficiation costs of <\$130 per kilogram uranium.

Most phosphate rock minerals are members of the apatite group, having the typical composition $\text{Ca}_{10}(\text{PO}_4)_6(\text{OH}, \text{F}, \text{Cl})_2$, in which calcium is replaced to a small extent by U^{4+} , which is of similar size (U^{4+} , 0.097 nm; Ca^{2+} , 0.099 nm). The presence of uranium is due to the formation of phosphate deposits from seawater, which contains 3 $\mu\text{g/L}$ uranium. In the presence of organic reducing agents or Fe(II) ions, U(VI) is reduced to U(IV) , which is incorporated into the apatite lattice.

When apatite is treated with dilute sulfuric acid at 80–135 °C to form crude phosphoric acid, uranium also goes into solution. However, if apatite is treated by the dry method or with concentrated sulfuric acid to form superphosphate, uranium is not dissolved but remains in the product. In Israel (only), uranium is first dissolved with hydrochloric acid when using the dry method. Two processes for extracting uranium from phosphoric acid solution have been put into practice, oxidation stripping and reduction stripping.

41.7.4.2 Treatment of the Solution

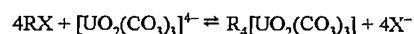
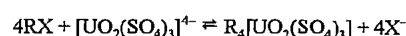
Uranium can be removed from the solution by ion exchange, solvent extraction, or a combination of the two processes known as the Eluex process. Undissolved solids, which would have a detrimental effect, are usually removed first from the liquor by sedimentation or decantation, or with hydrocyclones, filters, or centrifuges. The best process is vacuum filtration using plane, band, or drum filters, because the solution should be diluted as little as possible by washing of the filter cake.

Whereas slight cloudiness is tolerable for the ion-exchange process, the liquor must be clarified as much as possible before solvent extraction is carried out, because the expensive extraction agent can be lost by adsorption

by the solids, which can lead to environmental pollution.

Uranium Recovery by Ion Exchange

Anionic complexes of uranium are present in both acid and alkaline uranium solutions. Strongly basic ion exchangers are generally used to extract these complexes:



where R denotes the matrix and X the functional basic group of the ion exchanger.

The pH is adjusted to 1.5–2 in sulfuric acid solutions and to 9–10 in alkaline solutions for the ion-exchange process, which can be operated batchwise (fixed-bed process) or continuously.

Fixed-Bed Process. In the fixed-bed process, cylindrical columns of diameter 2–3 m, height 4–5 m, containing 10–30 m^3 resin are used. The ion-exchange resin is loaded at a flow rate of 5–20 m^3/h and eluted at 1–5 m^3/h . The resin pebble bed usually consists of spherical particles of diameter 0.3–0.8 mm, but 2-mm-diameter granules may be needed to prevent blockage of the columns if solutions are incompletely clarified. For such solutions, the resin in pulp (RIP) process was developed, in which large resin granules are held in sieve baskets that are moved to and from in a horizontal flow of unclarified liquor.

Elution can be carried out with 1 mol/L solutions of chlorides and nitrates. However, these anions interfere with subsequent loading of the resin, so elution with sulfates is often preferred. This proceeds more slowly but does not affect loading of the resin and is more cost-effective. The resin is first eluted with a 1 mol/L sulfate solution and subsequently treated with 10% sulfuric acid or, in the case of alkaline uranium solutions, with 1–2 mol/L sodium carbonate–sodium hydrogencarbonate solution.

Continuous Ion-Exchange Processes. Several types of columns have been developed for continuous ion exchange. The first is exempli-

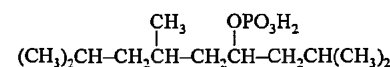
fied by the *Higgins column*, which has been operated successfully in Texas and Wyoming since 1955 [33]. Resin is loaded as it is pushed slowly upward through the column. It is washed at the overflow at the top and then passed to elution columns. Similar columns have been used successfully by the Bureau of Mines in South Dakota. In 1977, the *Himsley column* was installed in Ontario, Canada, and the *Cloete-streat column* in South Africa. In the *Porter column*, which was installed in Namibia in 1978, uranium solution flows upward and overflows from the top into a second ion-exchange column at a slightly lower level. The laden resin is drawn off from the bottom by means of compressed air and fed via an intermediate tank into elution columns.

Although ion-exchange resins have been improved considerably in recent years, the trend now is toward solvent extraction or a combination of ion exchange and solvent extraction (Eluex process) because these processes give better selectivity and, hence, improved product purity.

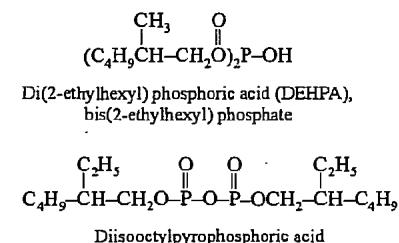
Uranium Recovery by Solvent Extraction

Two types of extraction solvents are used: the first includes alkylated phosphoric acids and pyrophosphoric acids; the second, higher aliphatic amines. Both types are dissolved in inert hydrocarbons, mostly high-purity kerosene. The mechanism of extraction is based on ion exchange in the liquid phase. Tributyl phosphate (TBP), which is used in the production of high-purity uranium, cannot be used for liquid–liquid extraction of sulfuric acid liquors because neutral extraction media are not suitable for uranyl sulfate solutions.

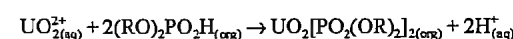
Solvent Extraction with Phosphoric Acids. The following three phosphoric acids have been found suitable for extraction of uranium:



Isododecyl phosphate



In the extraction process, acidic hydrogen atoms of phosphoric acids are replaced by the uranyl ion. The exchange therefore also depends on the pH of the solution. The complexes formed are soluble in the organic phase. In contrast to extraction with neutral organophosphorus compounds, the anion of the uranyl salt is not extracted at the same time:



Extraction can be much improved by adding tributyl phosphate to the phosphoric acid (synergistic effect). Concentrated mineral acids or sodium carbonate solutions are used to strip uranium from the organic solvent.

Solvent Extraction with Amines. Newer uranium processing plants use mainly amines as extraction solvents. These are usually commercially available mixtures of either highly branched dialkylamines or straight-chain trialkylamines. Solutions of these amines in hydrocarbons have a strong affinity for uranyl sulfate and form addition complexes of the type $(\text{R}_3\text{NH}^+)_2[\text{UO}_2(\text{SO}_4)_2]^{2-}$ that are soluble in organic solvents. Uranium can be stripped from these solutions by simple ion exchange with solutions of the nitrate or chloride of sodium or ammonium. Sodium carbonate solutions, which are sufficiently basic to convert the amine salt into free base, can also be used.

Technique of Solvent Extraction. Only a few column types are suitable for solvent extraction; these include the rotating disk column and the Scheibel column. However, the most suitable type is the mixer–settler in its various forms. A continuous mixer–settler consists of a mixing chamber and a settling chamber. The mixing chamber is provided with an agitator to mix the two phases (aqueous and organic).

The organic phase is fed by gravity from the preceding settling chamber into the inlet at the top of the mixing chamber, while the aqueous phase from the next settling chamber enters the mixing chamber from below. The mixed phases pass through an outlet at an intermediate height into the settling chamber in which the two phases separate. Thus, the phases flow countercurrently, and each mixer-settler constitutes one stage of the exchange process. Mixer-settlers are used for both the extraction and the stripping stages.

Four-stage mixer-settlers of various designs are used for industrial-scale solvent extraction. For example, in the Davy Power Gas mixer-settler, the mixed phases flow out centrally in upward direction. The Israel Mining mixer-settler contains lamellar internals to promote rapid phase separation [34]; these enable throughput rates to be improved by a factor of 20. The Lurgi MultiTray settler is aimed at a similar result [35]. Optimization of design and operation is described in [36].

Eluex Process

In the combined Eluex process, uranium is crudely separated by means of an ion-ex-

change resin, followed by solvent extraction [37]. The ion-exchange resin is designed so as to tolerate as much "cloudiness" as possible, and uranium is collected almost quantitatively. Breakthrough of foreign ions is acceptable since these are removed easily in the second (solvent extraction) stage. In this combined process, the first stage has the useful effect of increasing the concentration of uranium, with consequent reduction in the mass flow. This enables the second stage to be smaller by a factor of 20–30, and also improves the purification effect of this step as the uranium concentration in the feed is higher. An additional advantage is that the process can be used with relatively low uranium concentrations in the leach liquor (low-grade uranium ore). Thus, for example, the ion-exchange stage increases the concentration of a starting solution containing 0.02–0.5 g/L U_3O_8 to 9–12 g/L U_3O_8 and reduces the mass flow by the same factor. Four industrial plants processing 1000–1200 t/d ore are operating in the United States [38]. In South Africa, the technique was developed in 1963 under the name "BuMex Process", and full-scale operation followed.

Table 41.9: Specifications for uranium concentrate (yellow cake), contents in %.

	British Nuclear Fuel (UK)	Comurhex (France)	Eldorado (Canada)	Allied Chemical (USA)	Kerr McGee (USA)
U	40	60	50	75	60
Moisture	10	5	5.0	2.0	
Insolubles in HNO_3		0.1	0.1		0.1
Granulation, m	6.68	6	6.25	6.25	6.25
Th	not available	not available	2.0		2.0
Mo	< 0.6	0.45	0.15*	0.1	0.15*
V_2O_5	< 1.00	1.80	V = 0.1	0.1*	0.1*
Ca		1.15	1.0	0.05	1.0
P_2O_5	< 6	1.1	P = 0.35	$PO_4 = 0.1$	P = 0.35
Cl, Br, I	< 0.5	0.25	0.25*	0.05	0.25
F		0.15	0.15*	0.01	0.15
SO_4		10.50	S = 3.5	S = 3.00	S = 3.5
Fe				0.15	
As	< 2.00	1.0	1.0	0.05	1.00
CO_3	< 2.00	2.0	2.00	0.20	2.00
B	< 0.2	0.15	0.15	0.005	0.15
Na		not available		0.50*	
K		not available		0.1	
SiO_2	< 4.00				
Zr					2.00

*Maximum concentration without cost penalties.

41.7.4.3 Production of Uranium Concentrate

From Precipitation to Yellow Cake Production

Solutions obtained by the above processes contain uranium in the form of its sulfate or the carbonate complex $Na_4[UO_2(CO_3)_3]$. Uranium is precipitated from this as a uranate by addition of base, filtered, and dried. The uranium concentrate obtained, known as "yellow cake" because of its color and form, is the basic material for the production of nuclear fuels. Commercial uranium concentrates of various origins are listed in Table 41.9. Precipitation is carried out in large, agitated vessels. The precipitating agent for acidic, sulfate-containing solutions is ammonia or $Mg(OH)_2$, whereas carbonate complexes are precipitated by a 50% solution of NaOH.

Processing of Phosphate Liquor and Precipitation of AUC

Oxidation Stripping Process. In oxidation stripping, U(VI) is first converted into U(IV) by adding Fe(II) salts to the phosphoric acid; uranium is then extracted from the orthophosphoric acid by mono- and dioctylphenyl esters mixed with kerosene. Stripping is by oxidative treatment with phosphoric acid and sodium chlorate ($NaClO_3$). The U(VI) is again extracted from the stripping solution at 40–50 °C, this time by trioctylphosphine oxide (TOPO) and 2-ethylhexyl phosphate (DEHPA) dissolved in kerosene; it is then reductively stripped from this extract by addition of Fe(II). Multiple recycling of the stripping solution gives an enrichment factor of 40. The stripping solution is then reoxidized by $NaClO_3$ and extracted with DEHPA–TOPO–kerosene. Phosphoric acid is washed out of the extract, which is then stripped with $(NH_4)_2CO_3$ solution. An excess of ammonium carbonate is added in the cold to the complex salt solution obtained, precipitating ammonium uranyl carbonate, $(NH_4)_4UO_2(CO_3)_3$.

This is filtered off, washed, and calcined to give UO_{2+x} .

Reduction Stripping Process. Reduction stripping proceeds in an almost identical manner, except that only one extraction medium (DEHPA–TOPO–kerosene) is used. Uranium from the first stage is thus not reduced but extracted as U(VI). Both stripping stages are therefore reductive. Uranium does not require further purification in these cases and is usually purer than normal yellow cake.

41.7.4.4 Final Purification of Uranium Concentrate

Dissolution of Yellow Cake

Yellow cake produced by mining companies is not a single chemical substance, but a mixture of uranates. Its composition depends on the mined ores, as mentioned above, and on the chemistry of the treatment process suitable for those ores. The uranium content and the nature and concentration of impurities vary. However, the manufacture of nuclear fuel requires a product of high purity and constant composition, and the fine purification processes are intended to achieve this aim.

On an industrial scale, wet processes are used mainly to treat yellow cake, which must therefore first be brought into solution. This is achieved with hot nitric acid, which dissolves the uranium as uranyl nitrate. Impurities settle out to some extent or may also be dissolved as nitrates.

Extractive Purification

In the extractive stage of purification, uranium is separated from the accompanying impurities as far as possible. Removal of elements with a high cross section for thermal neutrons (e.g., boron, rare earths, cadmium, and lithium) is especially important.

Purification is carried out by dissolving the uranium concentrate in nitric acid and extracting uranium with selective solvents. Currently, TBP diluted with hydrocarbons is used in al-

most all known purification plants. A complex is formed according to



The complex is neutral, anhydrous, and undissociated, and has a higher solubility in the organic than in the aqueous phase. The uranyl nitrate solutions contain an excess of free nitric acid (sometimes nitrates of alkali metal, alkaline-earth metal, or aluminum are added), which has a salting-out effect and improves the distribution coefficient between the organic and inorganic phases. The tributyl phosphate solution is then treated with pure water, and uranyl nitrate is transferred back to the aqueous phase. The distribution coefficient is temperature dependent, and hot water (50–60 °C) is preferred for this stripping process.

Other heavy-metal nitrates can also form complexes with TBP. The more completely the amount of tributyl phosphate present in solution is bonded to $\text{UO}_2(\text{NO}_3)_2$, the smaller is the extent to which other heavy-metal nitrates are extracted. Therefore, a high degree of saturation of tributyl phosphate with uranyl nitrate is necessary. To reduce the density of tributyl phosphate (which is close to that of water) and to lower its relatively high viscosity, it is diluted with inert, saturated hydrocarbons. Kerosene and *n*-hexane are generally used, giving solutions that usually contain 25–35% TBP.

Harmful impurities in uranium solutions include gypsum and soluble silica, which can be deposited in the solvent extraction apparatus and reduce the efficiency of extraction. Also, some anions, especially sulfate and phosphate, cause problems by forming complexes with uranium. These complexes are not extracted and therefore lead to uranium losses. Fluorides and chlorides in the presence of nitric acid can cause severe corrosion of the vessel material.

Tributyl phosphate also contains impurities that interfere with extraction. Some of these are present in the commercial product as supplied; others are formed by chemical attack and by radiation. The main impurities are dibutyl- and monobutylphosphoric acids. Although dibutylphosphoric acid extracts ura-

nium more effectively, it is less selective than tributyl phosphate (i.e., impurities are extracted at the same time). These make the stripping of uranium more difficult. Acids can be removed by washing them out of the tributyl phosphate (e.g., with sodium hydroxide solution).

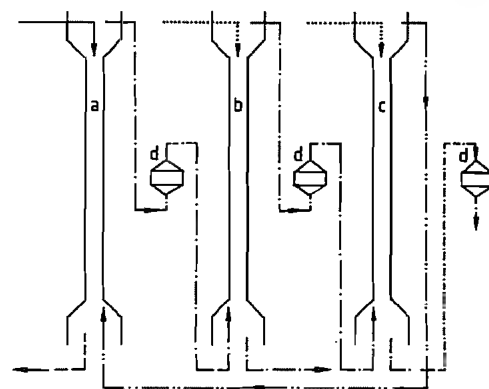


Figure 41.14: Schematic of a solvent extraction plant: a) Extraction column; b) Washing column; c) Stripping column; d) Diatomite filter. — Impure $\text{UO}_2(\text{NO}_3)_2$ solution containing 275 g/L U, 3 mol/L HNO_3 ; — Depleted solution (0.1 g/L U) passing out of extraction column; — Solution of uranyl nitrate in TBP; - - - Depleted solution (1–3 g/L U) of uranyl nitrate in TBP; ··· Water; — Aqueous solution of $\text{UO}_2(\text{NO}_3)_2$.

Technique of Solvent Extraction. The concentrate is dissolved in nitric acid, and the concentrations of uranium and nitric acid in the unfiltered solution are adjusted to the desired values, usually 250–350 g/L uranium and 1–3 mol/L free nitric acid. Before being fed to the solvent extraction plant, the solution is filtered in some plants. Various types of extractors (Figure 41.14) are used in solvent extraction plants. Pulsed sieve tray columns are the most popular, but mixer-settlers are also used in some cases. Pulsed columns and mixer-settlers are used both for solvent extraction and for washing and stripping. The columns contain perforated stainless steel plates ca. 50 mm apart. The holes are 3–5 mm in diameter, and the total area of all the holes is ca. 23–25% of the area of the plate. In the first column, uranyl nitrate is extracted by the solvent (25% TBP in kerosene). The volume ratio of the two phases is set such that maximum

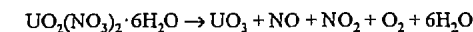
saturation of the organic phase with uranyl nitrate, together with almost quantitative extraction (> 99.9%) is achieved. In the second column (washing column), the organic phase is washed with a small amount of deionized water to remove impurities extracted at the same time. A volume ratio of organic phase: water = 10:1 is adequate. In this washing process, uranium is also partly transferred into the washing water. This solution is therefore recycled to the process. After the organic phase has been washed, it passes into the stripping column where uranyl nitrate is stripped out by hot (60 °C) deionized water. After treatment of the organic solvent with Na_2CO_3 to remove hydrolysis products of tributyl phosphate and the remaining uranium (a step not always included in the process), the organic solution is fed back to the first column.

41.7.4.5 Production of UO_3 and UO_2 from Purified Uranyl Nitrate Solution

Two different methods have been developed for the production of UO_3 and UO_2 from uranyl nitrate solution. In the first of these, the uranyl nitrate solution is evaporated until uranyl nitrate hexahydrate is completely crystallized; and this is then converted into uranium trioxide by thermal decomposition. Alternatively, uranium is precipitated in the form of an insoluble compound, and this precipitate (usually an ammonium salt) is converted into uranium trioxide. Common to both processes is reduction of the uranium trioxide UO_3 obtained to uranium dioxide UO_2 . The two processes are compared in Figure 41.15.

Evaporation of Uranyl Nitrate Solution and Denitration by Thermal Decomposition

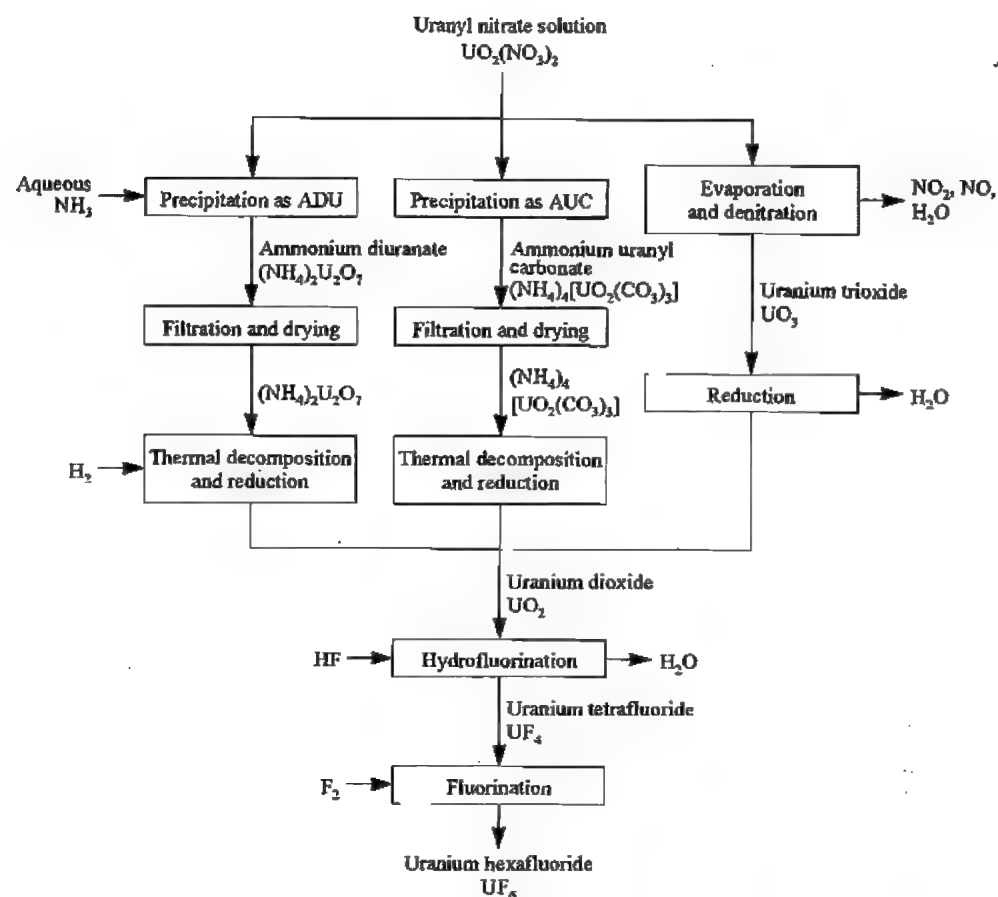
Solutions of uranyl nitrate are evaporated until uranyl nitrate hexahydrate, $\text{UO}_2(\text{NO}_3)_2 \cdot 6\text{H}_2\text{O}$, begins to crystallize. Further evaporation leads to the liberation of nitrogen oxides and water.



This decomposition and the phase diagram of the hydrated uranyl nitrate have been investigated thoroughly. The phase diagram (Figure 41.16) shows that the hexahydrate and the trihydrate have incongruent melting points at 60 and 113 °C, respectively. The uranyl nitrate–water system is stable up to 184 °C, the melting point of the dihydrate. Above this temperature, decomposition to uranium trioxide occurs with liberation of nitrogen oxides. This reaction becomes much more rapid above 300 °C. Since uranium trioxide loses oxygen above 430 °C [39], 400 °C is considered the optimum temperature for producing UO_3 . In order not to reduce the reactivity of UO_2 in later process steps (reduction, sintering, or hydrofluorination), avoiding higher temperatures, at which the U_3O_8 phase could be formed, is desirable.

Evaporation. The design of evaporation plants depends on the initial concentration of solutions to be evaporated. Since nitric acid at low concentration (up to 0.05 mol/L) is handled, the construction material is stainless steel. Vertical tube evaporators and evaporation tanks heated by internal steam pipes are commonly used. The final concentration of uranyl nitrate for the subsequent denitration stage is established by means of temperature control. Thus, a temperature of 120 °C corresponds to a uranium concentration of ca. 1000 g/L, and 143 °C to ca. 1285 g/L, the solution fed to the denitration stage being produced at a concentration between these two. The melting point of the less concentrated solution is 60 °C, and that of the more concentrated solution 116 °C. Because these melting points are relatively high, care must be taken to prevent the melt from solidifying in any part of the system (e.g., by heating the pipework). Concentrated uranyl nitrate solution is stored in heated tanks before being pumped to the denitration stage.

Denitration. *Batchwise denitration* was carried out in stainless steel pots containing fairly powerful agitators but the batch process is rarely used today.

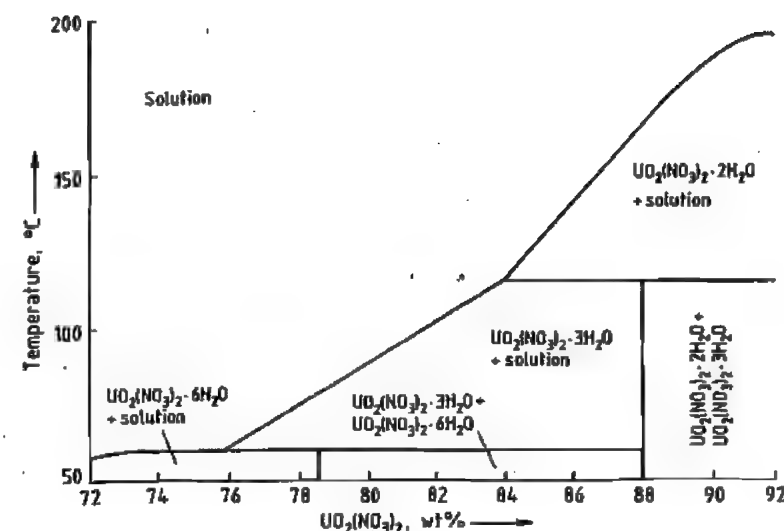
Figure 41.15: Methods for the production of UF_6 .

Continuous Denitration. The continuously operating furnace first used in 1956 in a plant in Hanford (Washington) consists of a horizontal trough with a central stirring device. Uranyl nitrate is fed via rotameters through the inlets to the decomposition trough, and the UO_3 formed flows out over a weir into a powder receiving vessel.

The temperature in the bed of powder largely determines the water and nitrate content of the powder. The nitrate content varies between 1.1% at 242 °C and 0.02% at 454 °C. At these temperatures, the water contents are 2.6 and 0.1%, respectively. Here, too, higher bed temperature leads to powder with lower reactivity.

The mean particle diameter of the powder is ca. 150 μm . In comparison to UO_3 powder produced by other processes, all powder produced by thermal decomposition of uranyl nitrate has a relatively high bulk density (ca. 3.5–4.3 g/cm^3) (i.e., the individual particles are very dense).

In the course of development work on equipment, Argonne National Laboratory started to develop a *fluidized-bed denitration furnace* as early as 1953. Fluidized-bed furnaces are now used widely not only in this stage but also in the reduction stage, for example.

Figure 41.16: Phase diagram of the system $\text{UO}_2(\text{NO}_3)_2\text{--H}_2\text{O}$.

Denitration is carried out by spraying uranyl nitrate solution onto a fluidized bed of hot particles of UO_3 . Carrier air is introduced from below through a porous metal filter and into the reaction tube where it fluidizes the bed of powder. Gaseous reaction products pass through sintered metal cartridges at the top of the reaction tube, and the nitrogen oxides are subsequently absorbed in water. The mean particle diameter is 150–200 μm . A fluidized-bed reactor of a type still often used today is illustrated in Figure 41.17.

Precipitation of Uranium by the ADU and AUC Processes

The sparingly soluble compounds ammonium diuranate (ADU), $(\text{NH}_4)_2\text{U}_2\text{O}_7$, tetraammonium dioxocarbonatouranate or ammonium uranyl carbonate (AUC), $(\text{NH}_4)_4[\text{UO}_2(\text{CO}_3)_3]$ and uranium peroxide, $\text{UO}_4 \cdot 2\text{H}_2\text{O}$, can all be used to precipitate uranium. All three compounds form uranium trioxide on thermal decomposition in air,

although precipitation of uranium peroxide is now rarely used industrially.

The ADU process was the first to be operated on an industrial scale and is still used widely today [40]. Precipitation of uranium from aqueous solution by ammonia gives a nonstoichiometric precipitate whose composition does not correspond to the chemical formula. Instead, the molar ratio $\text{NH}_3:\text{U}$ varies between 0.3 and 0.45. The properties of ammonium diuranate and of uranium dioxide produced from it can be influenced within limits by changing the operating conditions. Important parameters that determine particle size and particle-size distribution include temperature, precipitation time, initial concentration, and intensity of agitation. A relatively large size of agglomerated particles is obtained by using urea as the precipitating agent [41] or by passing a mixture of NH_3 and air into the solution [42]. Depending on the plant, precipitations can be carried out continuously or batchwise. The precipitate is separated from the mother liquor with the aid of continuous filters and centrifuges.

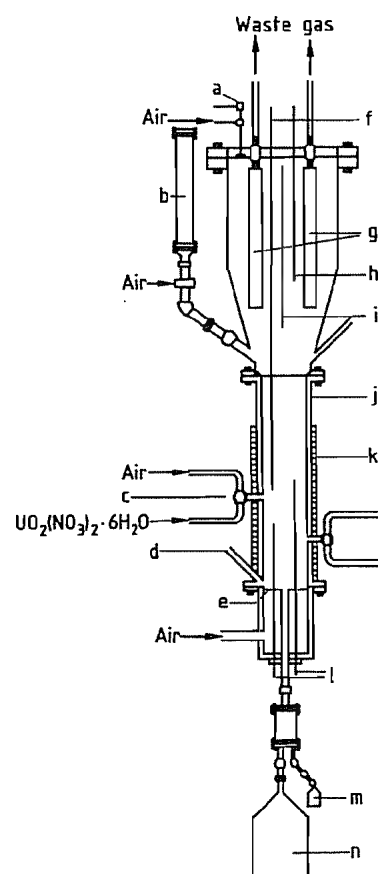
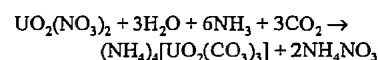
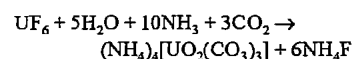


Figure 41.17: A 10-inch fluidized bed for denitration of $\text{UO}_2(\text{NO}_3)_2 \cdot 6\text{H}_2\text{O}$ (laboratory plant): a) Safety valve; b) UO_3 for charging; c) Spray nozzle; d) Pressure compensation; e) Porous filter plate (steel); f) Bed level detector; g) Porous filter; h) Separating plate; i) Thermocouple; j) Reaction tube; k) Heating element; l) Thermocouples; m) Sampling device; n) Receiver.

AUC Process [43, 44]. The AUC process was developed for precipitating uranium from fluorine-containing solutions (from the hydrolysis of UF_6) because the fluoride contained in precipitated AUC (produced by addition of NH_3 and CO_2) can be removed nearly completely by washing, in contrast to ammonium diuranate precipitated by NH_3 . Because of the high-quality UO_2 powder obtained from the precipitated product, this process was also used for uranyl nitrate solutions. The equations of these reactions are as follows:



Ammonia and carbon dioxide pass through a system of jets into a reaction tank filled with water, and uranyl nitrate solution is added at the same time at a controlled rate. The aqueous solution is pumped around a circulating system for the entire period during which reactants are added. The temperature of the water and the suspension increases because of liberation of heat of solution and reaction. When it reaches 60°C , the suspension is cooled to prevent excessive decomposition of the ammonium carbonate formed. After cooling to room temperature, the suspension is fed to a rotary disk filter, and after washing the precipitate with water, residual water is removed by suction until the moisture content is ca. 8%. If desired, the product can be dried further by washing with alcohol. The filter is discharged by rotating it while a knife fixed to a moving arm travels from the center to the edge of the filter over a period of up to 3–4 h, removing the filter cake in a thin layer. The powder is fed by a pneumatic suction device through the air lock of the fluidized-bed furnace.

Reduction of Precipitated Product to UO_2 Powder

Ammonium diuranate or ammonium uranyl carbonate can be reduced to uranium dioxide either immediately or after drying. The reduction temperature is $500\text{--}700^\circ\text{C}$. Hydrogen or cracked ammonia (i.e., an $\text{N}_2\text{--H}_2$ mixture) can be used as reducing agent. Most reducing furnaces used today are continuously or discontinuously operated fluidized-bed furnaces.

Batchwise Process. A discontinuously operated fluidized-bed furnace is used in the AUC process (Figure 41.18). The precipitated product in powder form is fed in small portions of ca. 0.5 kg through a cellular wheel sluice into the furnace, where it decomposes to uranium dioxide in the hot, reducing atmosphere of the

furnace. The gases liberated are passed through porous metal filter cartridges. Water vapor is used as the carrier gas for fluidization, and hydrogen is the reducing gas; these are fed through a fritted metal plate.

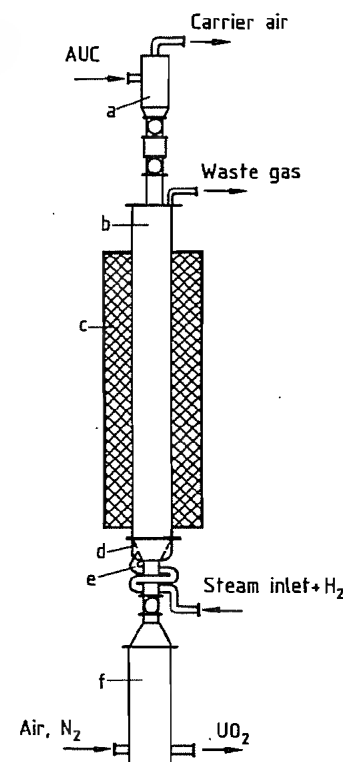


Figure 41.18: Fluidized-bed furnace for reduction of $(\text{NH}_4)_2\text{U}_2\text{O}_7$ (ADU) or $(\text{NH}_4)_4[\text{UO}_2(\text{CO}_3)_3]$ (AUC): a) Feed; b) Fluidized-bed furnace; c) Electrical heating; d) Sintered metal cone; e) Exterior heating coil for steam and H_2 ; f) Discharge vessel.

Continuous plants usually consist of several fluidized beds. The product is fed by a screw feeder into the first reactor where only partial reduction takes place; the powder then passes over an overflow into the second reactor where reduction is completed. *Moving-bed furnaces*, which are electrically heated cylindrical shafts through which a powder-granular material migrates continuously downward from above, produce a heterogeneous powder because of large temperature gradients in the furnace; these are now seldom used. However,

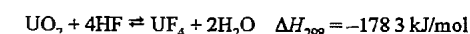
rotary kilns are sometimes employed and, like fluidized-bed furnaces, are in widespread use for other process stages in the thermal treatment of uranium compounds.

41.7.4.6 Production of UF_4

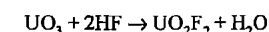
Uranium hexafluoride has always been produced on an industrial scale via the intermediate UF_4 , which is produced in a dry process by reaction of UO_2 with anhydrous hydrogen fluoride. If UO_3 is the starting material, it is first reduced to UO_2 . Uranium hexafluoride is then produced by reaction of UF_4 with elementary fluorine.

Hydrofluorination of UO_2

The reaction



is carried out at $300\text{--}600^\circ\text{C}$, depending on the reactivity of the UO_2 powder and the desired bulk density of the UF_4 product. Some difficulties are encountered due to the reversible nature of the hydrofluorination reaction and the possibility that eutectic $\text{UF}_4\text{--UO}_2$ mixtures may be formed that can lead to plastic flow and, hence, sintering at higher temperature. Uranium tetrafluoride always contains a small proportion of UO_2F_2 formed from the reaction of uranium trioxide with HF:



Fluidized-bed furnaces and rotary kilns are generally used to carry out the reaction. The LC reactor, which was developed in France, is of a special type (Figure 41.19), part of which resembles a moving-bed reactor (a) in which granulated uranium trioxide is reduced to uranium dioxide. The latter is then converted to UF_4 by passing anhydrous hydrogen fluoride over it in the next part of the equipment (d), which has vertical and horizontal sections. The powder flows by gravity through the moving bed and is then propelled forward in the horizontal section by a built-in screw feeder.

Hydration and Hydrofluorination of UO_3

In a process developed by British Nuclear Fuels Limited (the BNFL process) [44], uranyl nitrate solutions are concentrated continuously and denitrated to form UO_3 .

Reduction of UO_3 to UO_2 was formerly carried out in semicontinuous fluidized-bed reactors, and hydrofluorination of UO_2 to UF_4 in batch-operated fluidized-bed reactors. For economic and technical reasons, a change to continuous rotary kilns was made.

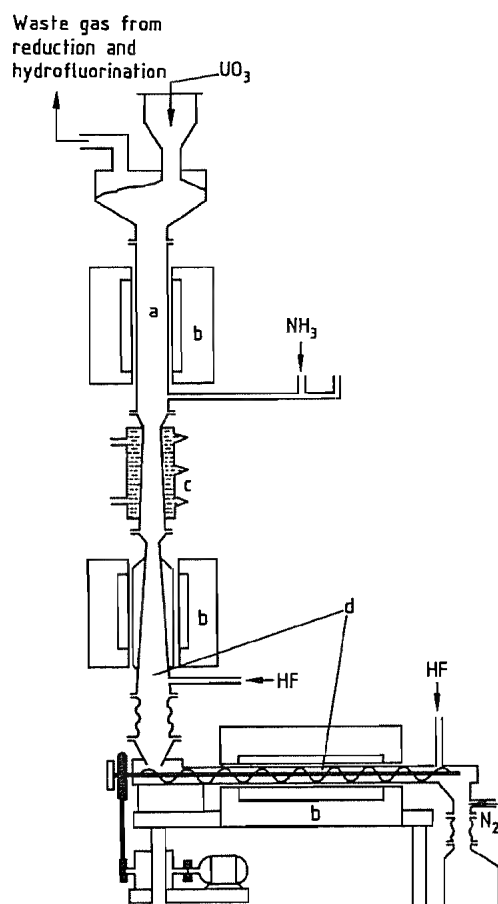


Figure 41.19: LC reactor for UF_4 production: a) Reduction section; b) Heating; c) Cooling; d) Hydrofluorination section.

The so-called UTK process (uranium tetrafluoride in kilns) has three principal stages (Figure 41.20):

- Exothermic hydration:
 $\text{UO}_3 + x\text{H}_2\text{O} \rightarrow \text{UO}_3 \cdot x\text{H}_2\text{O}$
- Endothermic dehydration and exothermic reduction:
 $\text{UO}_3 \cdot \text{H}_2\text{O} + \text{H}_2 \rightarrow \text{UO}_2 + 2\text{H}_2\text{O}$
- Exothermic hydrofluorination:
 $\text{UO}_2 + 4\text{HF} \rightarrow \text{UF}_4 + 2\text{H}_2\text{O}$

Uranium trioxide as produced by denitration in the fluidized bed consists of hard spherical particles with low surface area and inner porosity. To increase both of these parameters and thereby ensure rapid diffusion of the reacting gases, UO_3 is hydrated in jacketed vessels made of special steel. These contain screw feeders that operate intermittently, bringing the powder into contact with metered quantities of steam. Careful control of contact time and temperature ensures that the product is a dry, free-flowing powder.

Hydrated UO_3 powder is reduced in stainless steel rotary kilns (b) containing a system of pushers and retaining rings to give intimate contact with the countercurrent flow of hydrogen. The UO_2 formed is fed pneumatically under nitrogen into the feeder tank (c) of the hydrofluorination stage. The reaction temperature over the entire length of the kiln must be controlled carefully to ensure complete reduction of the product without any decrease in its chemical reactivity during the endothermic dehydration and exothermic reduction. Waste gases leaving the kiln contain nitrogen, steam, and excess hydrogen; they are passed first through filters that remove suspended particles of powder and then through water-cooled condensers and a flame. The gases are then discharged into the atmosphere.

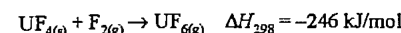
UO_2 is converted into UF_4 in a rotary kiln (h) containing similar powder feeding equipment, the material of construction being Inconel. Waste gases (nitrogen and small amounts of excess HF) are filtered and scrubbed with sodium hydroxide solution before being released to the atmosphere. The

NaF solutions produced are treated with hydrated lime.

41.7.4.7 Production of UF_6 from UF_4

Process Description

The only processes used on an industrial scale involve the use of elementary fluorine. Uranium tetrafluoride reacts with fluorine according to



The reaction proceeds fairly rapidly above 250°C . Reaction temperatures of 400°C are used for fluorination in fluidized-bed reactors, while name reactors operate at 1100°C .

If the conversion to UF_4 is incomplete, the product will contain UO_2 and UO_2F_2 , which also react with elementary fluorine. Large amounts of fluorine are consumed in these reactions, so the concentration of these compounds in UF_4 should be kept low. All metallic impurities react to give fluorides in which the metals are at their maximum oxidation states. Nonvolatile fluorides (e.g., AlF_3 , FeF_3 , and ThF_4) remain behind with unreacted UF_4 ; the volatile compound UF_6 contains volatile fluoride impurities (MoF_6 , VF_6 , SiF_4 , CF_4 , SF_6 , etc.). These impurities can be removed by dis-

tilling UF_6 and condensing it as a solid. For this, several condensers are used in series. Volatile fluorides of other elements contained as impurities (C, P, Si, B, and S) can be removed without problem during crystallization of UF_6 ; nonvolatile fluorides remain behind as solids at the bottom of the reactor. Most of the UF_6 can be recovered between $+5$ and -15°C in relatively large condensers; the remaining UF_6 is collected in much smaller condensers at ca. -50°C . Uranium hexafluoride is then melted out of the filled condensation vessels and collected in storage cylinders.

The heat-exchange surfaces of the condensers consist of nat ribbed plates that are fixed with baffles to the coolant pipes and steam pipes to give good contact. The tubes are U-shaped to reduce thermal stress to a minimum and to enable the condenser contents to be removed easily from the vessel.

Chemical Reactors

Fluidized beds can be used for all stages of the process, i.e., the production of UO_3 and its further reaction to UO_2 , UF_4 , and UF_6 . All of these are gas-solid reactions for which the fluidized-bed reactor is ideally suited, providing rapid mixing of the components and having only small temperature gradients within the bed volume.

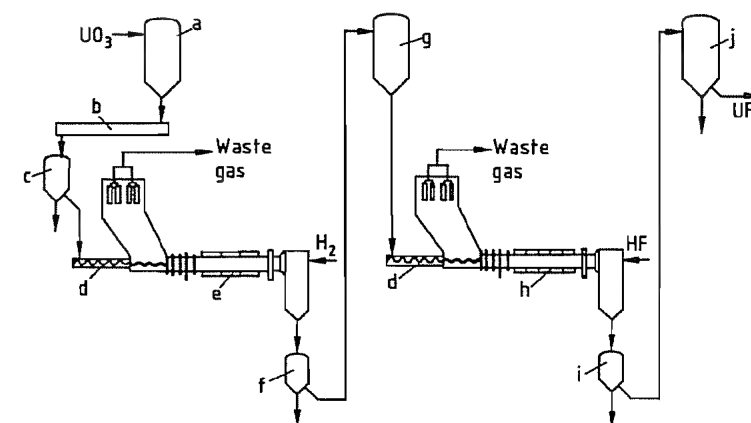


Figure 41.20: Flow diagram of UF_6 production plant in Springfield, United Kingdom: a) UO_3 storage vessel; b) UO_3 hydrator; c) $\text{UO}_3 \cdot \text{H}_2\text{O}$ storage vessel; d) Screw feeder; e) Rotary kiln for reduction; f) UO_2 intermediate storage vessel; g) UO_2 storage vessel; h) Rotary kiln for hydrofluorination; i) Intermediate storage vessel for UF_4 ; j) UF_4 receiver.

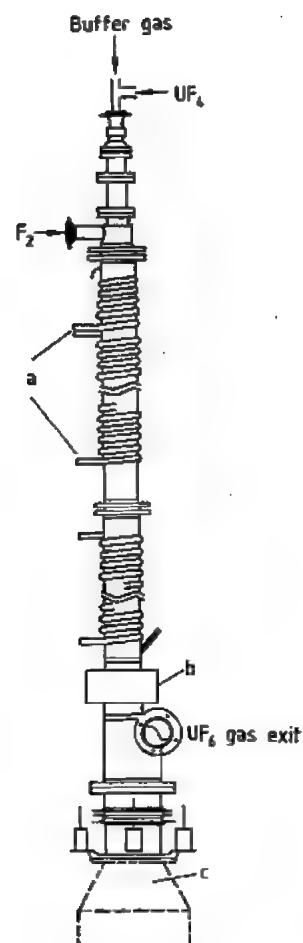


Figure 41.21: Flame reactor for fluorination of UF_4 : a) Cooling coils; b) Expansion compensator; c) Ash receiver.

Flame reactors, developed by Union Carbide Nuclear Corp., are also used. These reactors (Figure 41.21) consist of a vertical Monel tube surrounded by a cooling coil, with a device at the top to give good distribution of UF_4 , which is fed by a screw feeder. Fluorine, which is in excess, is fed through nozzles to the top of the reactor. Reaction of the two components produces a name at ca. 1100 °C inside the reactor. The upper part of the reactor, where most of the reaction occurs, must be cooled to give a wall temperature between 450 and 540 °C. This both minimizes corrosion of

the structural materials and prevents the formation of low-valence uranium fluorides.

Removal of Excess Fluorine from UF_6

To achieve complete fluorination of uranium, excess fluorine must be used; therefore, excess fluorine will still be present in the reaction gas after it has passed through the condenser. This fluorine comprises ca. 20–40% of the reaction gas and must be removed in an additional chemical reactor. This is similar to the fluorination reactor and operates with an excess of UF_4 . Not only is UF_6 formed, but also lower-valence intermediates such as UF_5 , U_2F_9 , and U_4F_{17} .

41.7.4.8 Complete Plant for Production of UF_6 from Uranyl Nitrate

French Process in Pierrelatte [45]

Uranyl nitrate solution (Figure 41.22) is pumped into a precipitation vessel (a) together with ammonia and water, which react to form ammonium diuranate. Temperature and pH are controlled during precipitation. The precipitate is filtered off by using a vacuum drum filter (b) and is transferred from this to a mixer (c), which converts it into a pumpable slurry by utilizing the thixotropic properties of the material. Ammonium diuranate is calcined to UO_3 in the first rotary kiln (d) and then reduced by a countercurrent flow of hydrogen further down this kiln. Uranium dioxide passes through a seal into a second rotary kiln where hydrofluorination occurs. A third kiln containing a screw feeder completes this reaction. The HF required for fluorination is fed from the exit end of the third rotary kiln in countercurrent flow to the solid. The UF_4 formed is conditioned in drums and then burned in a name reactor (a vertical Monel tube 4.40 m in length) to form UF_6 . The solid by-products UF_5 and U_2F_9 , which are formed in very small quantities, are removed by a screw and recycled to the top of the reactor.

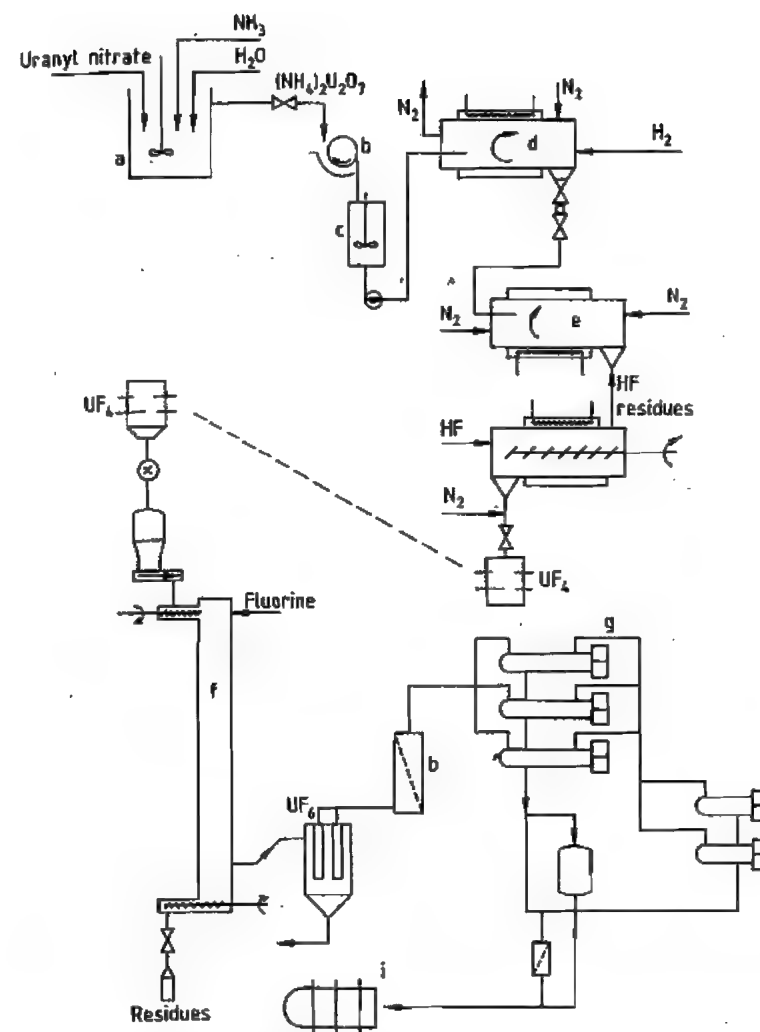


Figure 41.22: French process for UF_6 production: a) Precipitation; b) Filters; c) Mixer; d) Calcination and reduction; e) Hydrofluorination; f) Flame reactor; g) Primary crystallizers; h) Secondary crystallizers; i) UF_6 receiver.

Allied Chemical Process

Unlike the processes described above, the Allied Chemical process does not include final purification of uranyl nitrate by liquid-liquid extraction. Instead, UF_6 is purified by distillation [46] at a pressure and temperature above the triple point of UF_6 (64.05 °C at 151.1 kPa). Schematics of UF_6 production and distillation plants are shown in Figures 41.23 and 41.24, respectively.

41.7.4.9 Enrichment of ^{235}U

Three industrial processes are currently used for enrichment of uranium: the diffusion process, the ultracentrifuge process, and the less important jet nozzle process. Chemical enrichment, laser separation, and the plasma process are used on an experimental or laboratory scale. The three industrial processes employ gaseous UF_6 . Chemical enrichment requires the uranium to be in solution. Two la-

ser separation processes are in competition with each other. Metallic uranium is used in one of these, and gaseous UF_6 in the other. Metallic uranium is used in the plasma process as well.

Diffusion Process

Separation by diffusion occurs because isotopes diffuse through a semipermeable membrane at different rates owing to the \sqrt{m} effect. A schematic diagram of the process is given in Figure 41.25 [47]. The separation factor is small (i.e., 1.002–1.004 per stage). Many separation stages (1000–1500) are arranged in series in cascade to give an integral separation

effect. For improved maintenance and ease of replacement, 5, 8, 10, 16, or 20 separation cells are combined as a module. The heavier fraction (depleted in ^{235}U) that did not diffuse goes back to the previous stage. The heart of the separation cell is the diffusion membrane, which usually has a tubular shape. Diffusion is accelerated by a concentration difference between the outside and the inside induced by a pressure. The pressure difference is 1–10 kPa, depending on the membrane material, and the operating pressure in a cell is 10–30 kPa. Many materials have been tested as membrane materials, including Au, Ag, Ni, Al, Cu, Monel, Teflon, and Al_2O_3 .

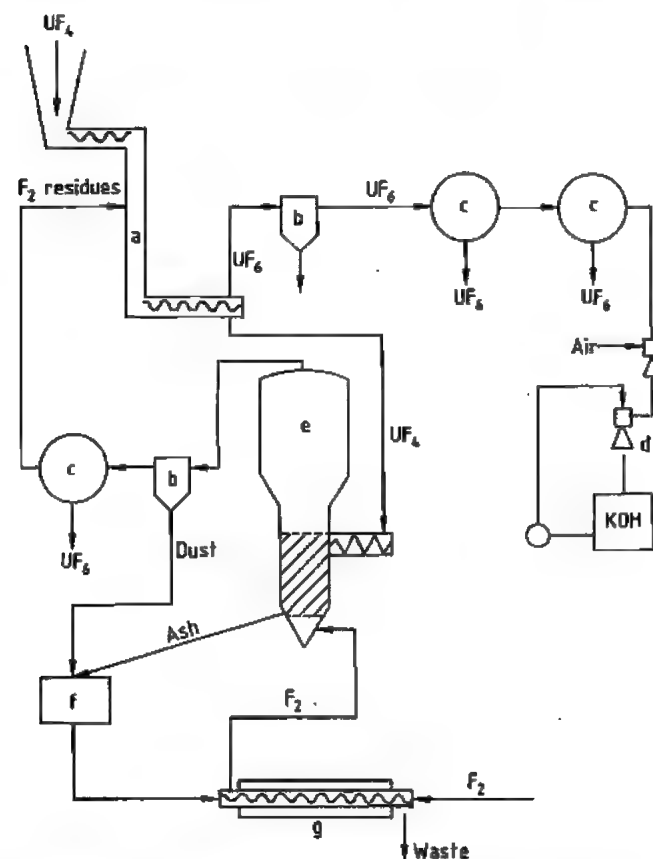


Figure 41.23: Flow diagram of an Allied Chemical UF_6 production plant: a) Tower reactor; b) Filter; c) Condenser; d) Scrubber; e) Fluorinator; f) Mill; g) Ash treatment.

Details of membranes are kept secret. They must be as thin as possible and have a pore size of 10 nm, but they must also have sufficient mechanical stability to withstand the pressure difference for years. One method of producing pores is to dissolve out a component of alloy foils (Ag–Zn, Au–Ag) selectively. Al_2O_3 membranes are produced from aluminum foil (13–30 μm thick) by anodically oxidizing it to completion in 5–10% sulfuric acid and then heat treating at 500–530 $^{\circ}\text{C}$. Water is evolved, and a porous membrane is formed with a permeability of ca. $0.1 \text{ cm}^3 \text{ cm}^{-2} \text{ s}^{-1}$. In the EURODIF plant in Tricastin, France, diffusers (diffusion cells) and compressors have been joined to form a single unit. The main disadvantage of the diffusion process is the high energy requirement for the work of compression. For example, the EURODIF plant, which provides 10 800 t USW/a (tonnes of uranium separative work per year), requires ca. 3000 MW electric power, for which four nuclear power stations, each of 925 MW capacity, have been constructed [48].

Ultracentrifuges

In 1942, P. HARTECK and W. GROTH first used centrifuge technology to separate uranium isotopes. The countercurrent centrifuge is illustrated in Figure 41.26 [47]. The separation factor of 1.2 formerly achieved has now been increased to 1.5 in modern equipment of this type. In Germany in 1970, a trilateral centrifuge project among the United Kingdom, The Netherlands, and West Germany was inaugurated (foundation of URENCO), and construction of three plants each with an enrichment capacity of 200 t USW/a was agreed upon. The German and Dutch plants are in Gronau, Lower Saxony, and Almelo, The Netherlands, respectively; the British plant is in Capenhurst, United Kingdom. Over the long period of operation, 99% plant availability has been achieved [49]. Ultracentrifuge plants of capacity > 100 t USW/a are competitive with diffusion plants and have two important advantages:

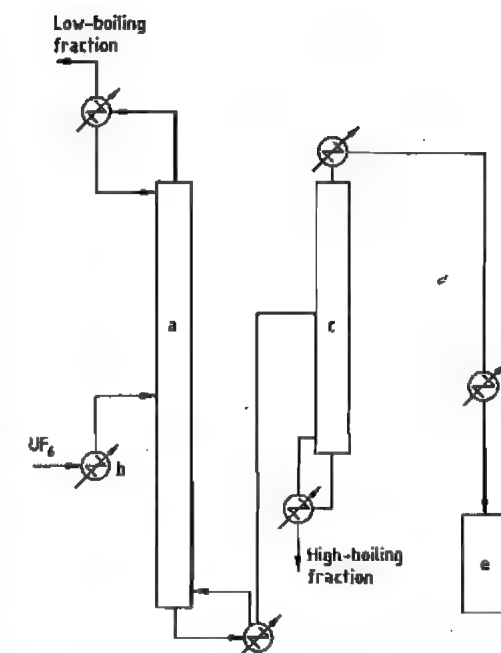


Figure 41.24: Flow diagram of the fine purification of UF_6 by the Allied Chemical process: a) Column I for low-boiling fraction; b) Evaporator; c) Column II for high-boiling fraction; d) UF_6 cooler; e) UF_6 receiver.

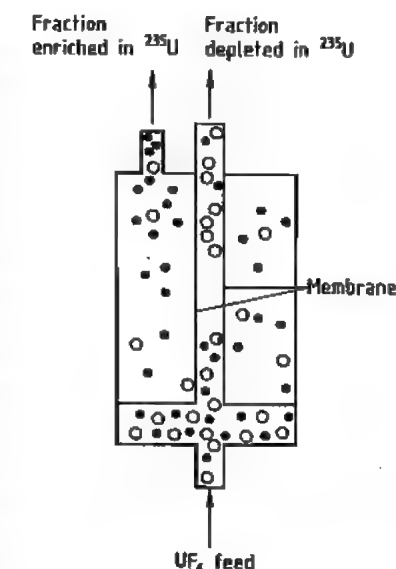


Figure 41.25: Schematic of a diffusion cell [47].

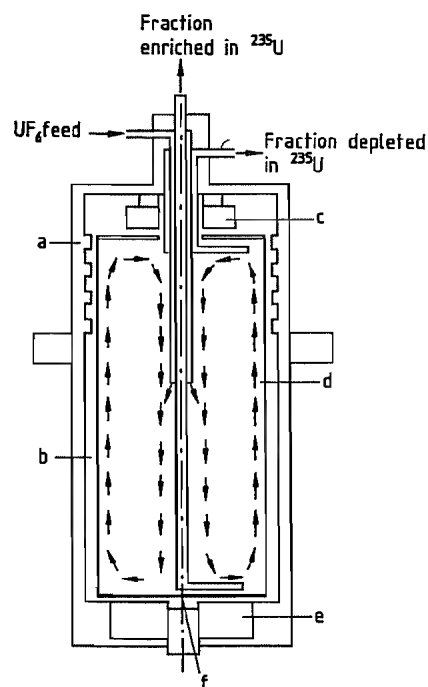


Figure 41.26: Cross section of a centrifuge [47]: a) Housing; b) Vacuum; c) Magnetic holding device; d) Rotor; e) Electrical drive; f) Needle bearing.

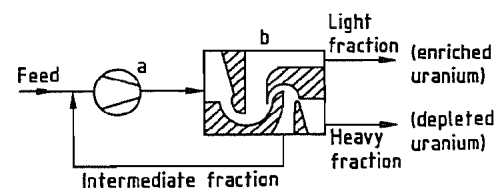


Figure 41.27: Schematic of the Brazilian nozzle separation system [47]: a) Compressor; b) Double deflecting system.

- The specific energy consumption using the centrifuge technique is 200 kWh/kg USW.
- The cascade for a low degree of enrichment (e.g., for light-water reactors) has only 15–20 separation stages, but diffusion equipment requires 1200 stages (EURODIF). A plant using the ultracentrifuge technique can be extended easily by the modular method using parallel connections.

Nozzle Process

This process, which was developed by E. W. BECKER in Karlsruhe, is the only one to which secrecy restrictions do not apply [50]. A modern nozzle with dimensional data is described [51]. The separation effect is improved by addition of a light gas. The nozzle principle is illustrated in Figure 41.27 [47].

A mixture of 4% gaseous UF_6 and 96% of a light carrier gas (e.g., H_2 or He) is expanded in the first jet. Due to the flow deflection in the carrier stream the heavier uranium isotopes become enriched in the outer flow region. Subsequently the outer flow region is separated by specially designed separation geometry from the inner flow region. The second jet works similar and is used to improve the efficiency of the stage.

The production of enriched uranium for light-water reactors requires several hundred stages in a cascade; i.e., the separation effect (0.015–1.026) is better than that obtained by the diffusion process and worse than that obtained by ultracentrifugation. The energy requirement is comparable to that of the diffusion process since high energies of compression are required. The process is operated on an industrial scale in Brazil and South Africa (the Helikon process).

Chemical Enrichment

The principle of chemical enrichment is based on the fact that in some chemical exchange processes (e.g., $\text{UX} + \text{Y} \rightleftharpoons \text{UY} + \text{X}$), different uranium isotopes have different tendencies to bond to substances X and Y. This mechanism is based on small differences in the preferred mean oxidation states of the particular isotopes in the given reaction environment. For industrial operation, the reaction must be rapid; the separation factor for the reaction must be acceptable; and the reverse reaction must occur readily. A pilot plant in operation in Japan [52] depends in principle on the equilibrium between U^{4+} and UO_2^{2+} in aqueous solution in the presence of an ion-exchange material. In this environment, the pre-

ferred valence of ^{238}U is 4 and that of ^{235}U is 6. The ion-exchange material has no preference for either isotope, but it preferably adsorbs hexavalent uranium isotopes. So the overall effect is a slight increase in ^{235}U concentration. Since the enrichment factor is very small (1.001 to 1.0014), many stages in the sequence are necessary. The integration of many stages into a continuously operating column was achieved in the pilot plant with the development of the self-generation reaction (Addox reaction) between the deactivated redox agents. A regeneration of ca. 70% is achieved in a semi-commercial plant. Figure 41.28 shows a schematic diagram of the plant.

In the column the zones are migrating continuously from top to bottom. In the adsorption zone the ion exchanger is loaded with ^{235}U . If the adsorption zone arrives at the valve, the adsorber is removed together with enriched uranium. The acceptor zone contains the depleted uranium. Uranium and regenerated ion exchanger material are introduced at the donor zone. The redox agents are regenerated in the addox boundary zone. Hydrogen and oxygen are fed in the area of the valve to complete regeneration of the redox agent.

In France, the equilibrium between U^{3+} and U^{4+} is utilized [53]. Separation occurs between an aqueous hydrochloric acid phase retaining trivalent ^{238}U and the phase of an organophosphorus compound, retaining $^{235}\text{UCl}_4$. The enrichment factor is ca. 1.025. This process also requires several thousand stages.

Laser Separation Process

Laser separation of isotopes is based on the fact that small differences exist between the absorption spectra of ^{235}U and ^{238}U . By using lasers of suitable wavelength, one isotope can be excited selectively. Two methods have been investigated, in one of which selective excitation is applied to uranium metal vapor, and in the other to gaseous UF_6 . The first of these is known as the Atomic Vapor Laser Isotope Separation (AVLIS) process. Here, the selectively excited uranium atom is ionized and then separated electrostatically from the

stream of metal vapor [54]. In the Molecular Laser Isotope Separation (MLIS) process, selectively excited UF_6 molecules dissociate into UF_5 and F. Fluorine must be bonded rapidly to suppress the reverse reaction. The UF_5 can then be separated from the stream of molecules [54]. Both processes require several stages despite the high separation factor. The AVLIS process is currently regarded as the most promising because the sequence of stages can be put together without problems. However, in the MLIS process, UF_5 must be converted back to UF_6 after each stage [54]. For this reason, research in the United States was formerly concentrated on the AVLIS process.

Two possible methods of incorporating the AVLIS process into the series of operations to convert uranium ore into nuclear fuel are illustrated in Figure 41.29.

Plasma Processes

Two effects suitable for isotope separation are under investigation.

The first utilizes the fact that uranium plasmas rotating in magnetic fields achieve considerably higher rotational speeds than those produced by a centrifuge. Thus, uranium isotopes can be separated by gravity. The second effect utilizes that in a homogeneous magnetic field the cyclotron frequency of the ions in the plasma depends only on magnetic field strength and ionic mass. Hence, the isotopes have different circulation paths in the cyclotron. Thus, isotopes are separated in a rotating plasma and collected separately by different collecting devices.

41.7.4.10 Production of UO_2 Pellets from UF_6

Conversion of UF_6 to UO_2

The industrially important processes for producing UO_2 pellets from UF_6 may be divided into wet and dry processes.

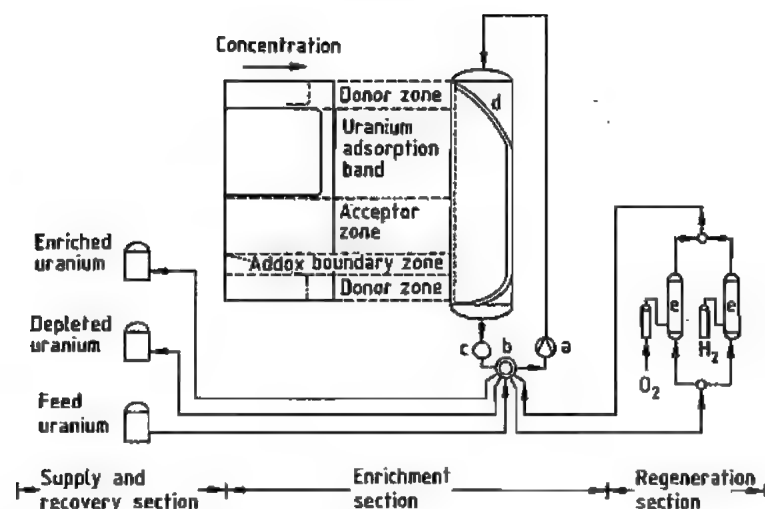


Figure 41.28: Schematic of the Japanese chemical enrichment plant: a) Pump; b) Valve; c) Detector; d) Enrichment column; e) Regeneration reactors.

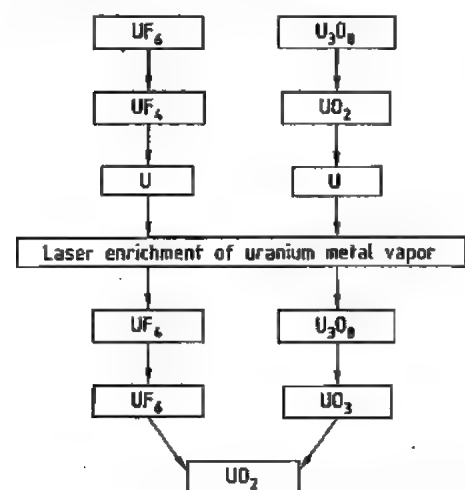
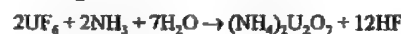


Figure 41.29: Example of incorporation of the AVLIS process into the chemical process chain of fuel element production.

Wet Processes. Wet processes include the precipitation of ADU and AUC, as described in Section 41.7.4.5 for obtaining UO_2 from high-purity uranyl nitrate. The apparatus for converting UF_6 to UO_2 is illustrated in Figures 41.30 and 41.31. The difference from the processes described in Section 41.7.4.5 is that the starting material is UF_6 . The following two reactions occur:

ADU process

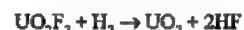


AUC process



Subsequent conversion of ammonium diuranate or ammonium uranyl carbonate to UO_2 powder is carried out by methods similar to those already described. However, since conditions in the calcination stage significantly affect the properties of the powder for later finishing operations, properties are optimized by controlling those conditions.

Dry Processes. Reaction equations for dry processes are given below in simplified form:



However, these dry processes vary considerably with respect to processing details and design of the chemical reactors. In the older processes, up to four separate reaction chambers were required, whereas modern processes use one or at most two reaction chambers. A schematic diagram of the Direct Conversion (DC) process is given in Figure 41.32. Construction materials must be chosen very carefully because of the corrosive properties of the

hot, gaseous hydrofluoric acid produced. However, satisfactory experience with this plant shows that reliable solutions to these problems have now been achieved by materials technology.

Possible Future Developments in the Conversion of UF_6 to UO_2 Powder

The wet ADU and AUC processes are used worldwide to convert UF_6 to UO_2 powder for the production of nuclear fuel pellets for light-water reactors. The combination of processes has been optimized within the limits of process parameters to enable the pellets to be pro-

duced economically and in accordance with quality specifications. The standards established are applicable to all later production developments, especially the dry conversion processes.

However, assessment of the wet processes shows that the following fundamental improvements are desirable:

- Avoidance of open-air handling of the powder in all process steps
- Reduction of radioactive secondary waste when treating process waste and purifying process materials from uranium

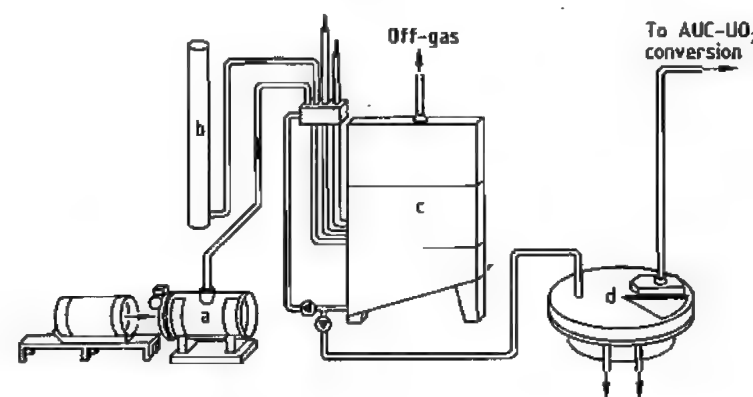


Figure 41.30: Conversion of UF_6 into AUC: a) UF_6 evaporation; b) NH_3 , CO_2 supply; c) Reaction tank; d) Rotating filter for AUC collection.

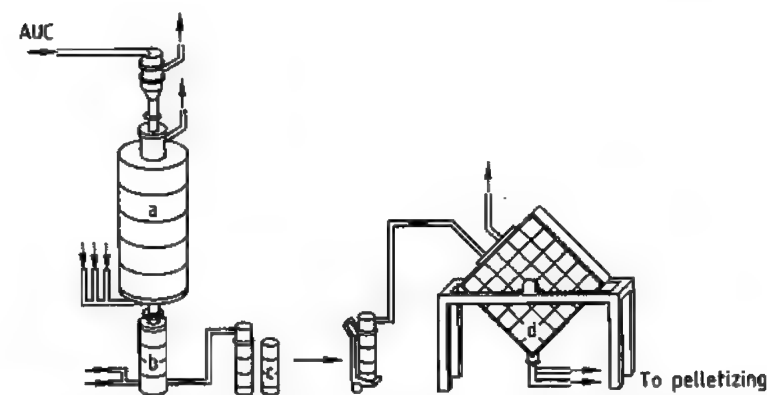


Figure 41.31: Conversion of AUC into UO_2 powder: a) Fluidized bed; b) Stabilization; c) Storage container; d) Homogenizer.

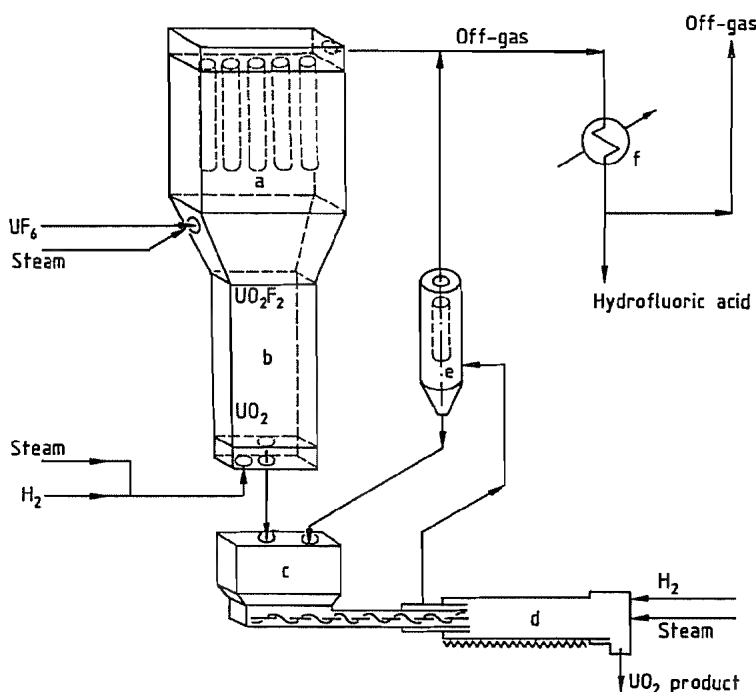


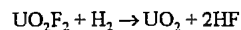
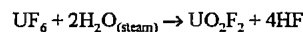
Figure 41.32: Schematic of Direct Conversion process: a) Reactor; b) Fluidized bed; c) Feed bin; d) Rotary kiln; e) Filter; f) Condenser.

Future Processes. In the production of UO_2 pellets, intermediate products in powder form can of course be avoided only by using *wet processes*. A possible approach is to use the sol-gel process [55–57] in which UF_6 is dissolved in aqueous uranyl nitrate solution and mixed with poly(vinyl alcohol). This solution is then sprayed into a second liquid with a very different surface tension, and ammonia is added. This causes hardening of the droplets to form particles, which are then washed in aqueous NH_3 solution to remove the undesired by-product NH_4NO_3 . A calcination process in air then decomposes the poly(vinyl alcohol) and the ammonium diuranate to UO_2 . The solid particles obtained can then be compressed directly into pellets. The process is carried out in such a way that the UO_2 pellets are of similar quality and have similar properties to those produced by conventional processes.

However, analysis of this process shows that the many washing and purification steps

and the considerable volume of materials used lead to a large volume of process and waste materials that must be cleaned and disposed of. Although very little dust is produced, the cost of cleaning and waste disposal is high. For this reason, the main interest in process development has now reverted to *dry processes* such as IDR, DC, and GECO, the industrial handling of dusts and aerosols having meanwhile been greatly improved.

All these processes convert UF_6 to UO_2 by the following reactions



These two reaction steps can be combined in one process as realized by the BNFL IDR process. Siemens prefers a two-step procedure. In a flame reactor UO_2 is formed together with minor amounts of UO_2F_2 . In a subsequent rotary kiln the UO_2 - UO_2F_2 mixture is converted to UO_2 which contains negligible impurities of fluorine. A common

feature of all processes is to provide a UO_2 powder with an acceptable sinterability and a low F content. Reducing the fluorine content requires a hydrogen treatment at higher temperature (500–800 °C), which results in an optimization of fluorine depletion and sinterability.

Table 41.10: Treatment of processing materials and residues in the AUC process (simplified).

Process step	Residual material ^a	Treatment	Disposal route
Precipitation	g: NH_3 g: CO_2	Waste-gas scrubbing	Stack
Filtration	l: NH_4F l: H_2O l: U (traces) l: Other activity	Peroxide precipitation Lime precipitation	Utilization
Washing	l: $(\text{NH}_4)_2\text{CO}_3$ l: H_2O l: U (traces)	ADU precipitation	Wastewater
AUC feed (AUC → UO_{2+x})	g: NH_3 g: CO_2 g: H_2O	Waste-gas scrubbing	Stack
Calcination	g: H_2 g: H_2O g: HF		

^ag = gaseous phase; l = liquid phase.

Chemicals and Residues in the AUC and DC Processes. Table 41.10 shows how the treatment (not presented in detail here) of processing chemicals and residues is integrated in such a way that it is compatible with the main process of $\text{UF}_6 \rightarrow \text{UO}_2$ conversion. Material flows are suitably interlinked to minimize consumption of raw materials and processing chemicals, and to recycle usable materials. At the same time, individual process steps must be optimized continuously to ensure compliance with steadily decreasing pollution limits.

In the *DC process*, the processing materials are steam, H_2 , and N_2 . In addition, HF is formed in amounts corresponding to the amounts of UF_6 treated. Gas streams passing from the reaction vessels are filtered several times to remove solids. After condensation of HF, the gas is recycled as far as possible for use as a processing material. Residual gas is passed over CaCO_3 to remove HF completely, the traces of HF reacting to form CaF_2 . The gas so obtained is flared off to remove H_2 , and

the waste-gas stream can be released from a stack since it contains only residual H_2 and H_2O . Fluorine introduced into the process in the form of UF_6 can be reused in the form of pure hydrofluoric acid. The small amounts of CaF_2 in CaCO_3 can be dumped without further treatment.

A comparison of the aqueous AUC process and the dry DC process shows that for the same product quality, the dry process has considerable advantages in the treatment of processing and waste materials. The DC process is consequently growing in importance, which shows how ongoing efforts to reduce pollution can also lead to process rationalization.

Pelletizing of UO_2 Powder

Some processes require preparation of the powder by compaction and granulation. When the AUC process is used, the UO_2 powder obtained can be compressed and sintered without any intermediate steps.

41.7.4.11 Production of Uranium Metal

The requirement for uranium metal is limited. Only Magnox reactors for power generation require uranium metal as fuel. Uranium metal is also needed for the production of U-Zr, U-Zr hydride, uranium silicide, and uranium-aluminum alloys. If laser enrichment processes such as the AVLIS process attain industrial importance, the requirement for elementary uranium will increase. Uranium metal is produced from UF_6 by a two-stage reduction; the intermediate product is UF_4 .

Reduction of UF_6 to UF_4

Two principal routes are used:

- Reduction of UF_6 by H_2 in the gas phase
- Reduction of UF_6 with chlorinated hydrocarbons (mainly unsaturated)

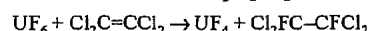
Reduction with Hydrogen. The throughput and degree of enrichment required are important considerations when selecting a process. Reduction of UF_6 by hydrogen in so-called

hot-wall and cold-wall reactors was reported at the Geneva Conference of 1958 [58]. The reaction is exothermic:



The heat of this reaction is not sufficient to give quantitative conversion. The *hot-wall reactor* is therefore provided with external heating to give a wall temperature of 630 °C. The *cold-wall reactor* obtains its energy from the highly exothermic reaction of fluorine (mixed directly with UF_6) with excess hydrogen.

Reduction with Tetrachloroethylene. Reaction of UF_6 with tetrachloroethylene (C_2Cl_4) in a fluidized-bed furnace was developed by United Nuclear Corp. [59]:

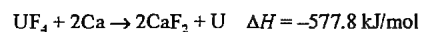


The reaction temperature is 260–295 °C. Nitrogen is added to tetrachloroethylene to act as a carrier gas.

Reduction of UF_4 to Uranium Metal

Calcium, magnesium, and sodium are thermodynamically suitable agents for the reduction of UF_4 to uranium metal, but only calcium and magnesium are of practical importance—calcium for small batches because of its higher heat of reaction, and magnesium for larger quantities because it is the cheaper metal.

Reduction with Calcium. The heat of reaction of reduction with calcium is very large:



With a calcium excess of 15% and adiabatic conditions during reduction, the temperature of the reaction mixture can rise to 1800 °C. This temperature is high enough to melt the slag formed (*mp* of CaF_2 1418 °C). Calcium granules (ca. 5 mm) are used, which must be very pure. High magnesium content may cause a violent reaction because the reaction temperature is higher than the boiling point of magnesium.

A mixture of UF_4 and calcium is charged into a steel reaction vessel whose inner walls are lined with high-purity CaF_2 (Figure 41.33). This interior lining prevents the container material from reacting with molten ura-

nium metal. Before reduction, the reaction apparatus is evacuated and filled with argon. The reaction mixture is then ignited electrically with an ignition pellet, and the reaction is complete after a few seconds. Molten uranium collects at the bottom of the reaction vessel and can be separated easily from the slag after the vessel is cooled. The yield of metal is ca. 98–99% of theory.

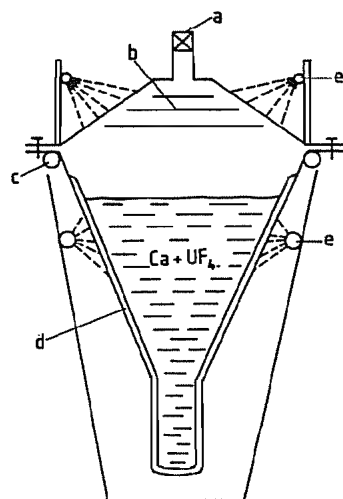
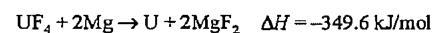


Figure 41.33: Reactor for reduction of UF_4 with calcium: a) Pressure control valve; b) Heat protection shields; c) Circular water pipe for flange cooling; d) CaF_2 lining; e) Circular pipe for water jets.

Reduction with Magnesium. Uranium reduction on a larger scale (several hundred kilograms of metal) is usually carried out with the much cheaper magnesium. Also, since its relative atomic mass is only about half that of calcium, the amount of magnesium required is smaller. However, the price advantage is counterbalanced partly by the lower heat of reaction:



which makes it necessary to heat the reaction mixture to ca. 600 °C. If the mixture is at room temperature when it is ignited, the melting point of uranium metal and of the MgF_2 slag (1263 °C) is not reached. By using an excess of 15% magnesium, the temperature reached is only ca. 900 °C under adiabatic conditions.

The interior walls of the reactor are often lined with dolomite. To obtain a good yield, the bulk density of UF_4 must be relatively high ($> 3 \text{ g/cm}^3$), giving good thermal conductivity. Briquetting the reaction mixture before loading it into the reactor vessel is therefore advantageous.

Production of Uranium Powder

Uranium powder can be obtained by reduction of UO_2 , electrolysis of fused salts, or decomposition of uranium hydride.

Reduction of UO_2 . Reduction of UO_2 with calcium or magnesium has not become widely established in industry because separation of the product from the slag is difficult. Also, the demand for uranium powder is limited.

Reduction with Calcium. The best reducing agent for UO_2 is calcium. A carefully prepared mixture of calcium granules and UO_2 is charged to a reactor whose walls are lined with CaO . The mixture is heated to 1200 °C under argon and kept at this temperature for at least 30 min. The temperature should reach the melting point of uranium (1132 °C) but should not cause CaO to melt. The uranium particles therefore become embedded in unmelted CaO . Excess calcium, which has low solubility in CaO , acts as a grain growth accelerator of the uranium.

After reaction, the mixture, which contains uranium and CaO together with excess calcium, is broken up and slurried with water. After careful addition of acetic acid (to buffer the solution at pH 5.5 by formation of calcium acetate), dilute nitric acid is added to leach out calcium. A temperature of 30 °C should not be exceeded in this leaching process because higher temperatures cause oxidation of the surface of the metal powder.

Reduction with Magnesium. The temperature during reduction with magnesium must be kept below 1270 °C; however, it should be above 1133 °C, which is higher than the *bp* of magnesium, so that large enough metal particles will be formed. The metal powder produced by reduction with magnesium is much finer than that obtained by reduction with cal-

cium. Magnesium chloride is often added to the reaction mixture to act as a flux.

Electrolysis of Fused Salts. The electrowinning of metal powder is carried out in fused fluoride or chloride salts. KUF_5 or UF_4 is dissolved in a molten salt mixture of 80% CaCl_2 and 20% NaCl , and electrolyzed at 900 °C in a graphite crucible, which forms the anode. When withdrawing the cathode from the molten salt, appropriate precautions must be taken to prevent burning of powdered metal that adheres to it. After cooling, soluble chlorides can be removed from the metal by washing with water.

Decomposition of Uranium Hydride. Hydrogen reacts very readily with uranium metal, forming uranium hydride (UH_3). The optimum hydrogenation temperature is 220 °C. Because of the large density difference between the hydride (10.8 g/cm^3) and the metal (19.06 g/cm^3), the brittle hydride breaks down during the reaction into a fine pyrophoric powder. This is decomposed thermally at 310 °C with application of a vacuum to draw off hydrogen. The metal powder so obtained is strongly pyrophoric and can be handled only under an inert gas atmosphere.

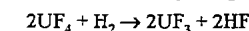
41.8 Compounds

41.8.1 Halides

The most important halides (Table 41.11) are the fluorides; polymers such as U_4F_{17} and U_5F_{22} are not included in this table because they have little technical importance.

41.8.1.1 Trivalent Halides

In general, trivalent halides may be prepared by reduction of the tetravalent compounds with hydrogen, e.g., [60]:



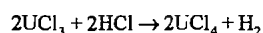
At 950 °C all of the UF_4 does not react; above 1080 °C, disproportionation of UF_3 into UF_4 and uranium occurs. Preparation of chlorides, bromides, and iodides involves similar problems.

Table 41.11: Halogen compounds of uranium (excluding polymeric compounds).

		Structure
Fluorides	UF ₃	hexagonal, LaF ₃ type
	UF ₄	triclinic (pseudomonoclinic), isomorphous with ThF ₄
	U ₂ F ₉	cubic
	α-UF ₅	tetragonal, chain structure
	β-UF ₅	tetragonal, three-dimensional lattice
Chlorides	UF ₆	rhombic, molecular lattice
	UCl ₃	hexagonal, La(OH) ₃ type
	UCl ₄	tetragonal
	UCl ₆	hexagonal, molecular lattice
Bromides and iodides	UBr ₃	hexagonal, La(OH) ₃ type
	UI ₃	rhombic, LaI ₃ type

Uranium trifluoride, UF₃, forms red-violet crystals. It is stable to moist air at room temperature, but is converted to oxide fluorides on heating and is oxidized to U₃O₈ above 900 °C. It is insoluble in cold water but is slowly oxidized to UF₄. In boiling water, further oxidation to uranyl fluoride occurs.

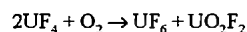
Uranium trichloride, UCl₃, forms dark red, very hygroscopic needles, *mp* 842 °C. In aqueous HCl solution, rapid transformation into a tetravalent green compound occurs, with liberation of hydrogen according to:



Uranium Tribromide and Triiodide. Uranium tribromide, UBr₃, *mp* 730 °C, and uranium triiodide, UI₃, *mp* 506 °C, are formed similarly to UF₃, and are also soluble in water.

41.8.1.2 Uranium Tetrahalides

Uranium tetrafluoride is a very important intermediate in the production of UF₆ for enrichment plants (see Section 41.7.2) and for production of the metal. It is a highly polymeric green solid that melts at 1034 [61] to 1036 °C [62]. Gaseous UF₄ is monomeric. The stability of solid UF₄ is explained by its complex crystal lattice (α-ZrF₄ structure). However, oxidation occurs in a stream of oxygen at 700–850 °C:



Uranium tetrafluoride is almost insoluble in water and is dissolved only by oxidizing acids and some concentrated acids.

Hydrated UF₄ can also be prepared by precipitation from U(IV) solutions with hydrofluoric acid. At room temperature, the very pale green UF₄·2.5H₂O [63] is formed, but at 80–100 °C the grass green compound UF₄·0.75H₂O is obtained. Both can be converted into anhydrous UF₄ by careful dehydration in a vacuum.

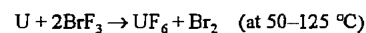
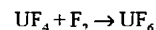
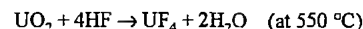
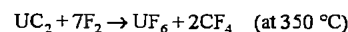
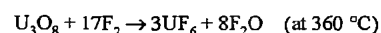
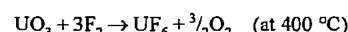
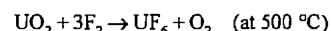
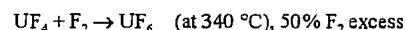
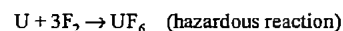
Other Halides. Uranium tetrachloride (*mp* 569 °C), UBr₄ (*mp* 518 °C), and UI₄ (*mp* 706 °C) can be produced by heating a mixture of uranium oxides and carbon in a stream of halogen. Uranium tetrachloride dissolves very readily in water, with evolution of heat; UBr₄ and UI₄ behave similarly.

41.8.1.3 Uranium Pentafluoride

The reaction of UF₄ with UF₆ produces UF₅, which is formed together with U₂F₉ and U₄F₁₇ as an intermediate in the production of UF₆ (see Section 41.7.4.7). UF₅ is now also important as an intermediate product formed during uranium enrichment using lasers (see Section 41.7.4.9). Other pentahalides are known but are of only theoretical interest.

41.8.1.4 Uranium Hexafluoride

Many possible methods can be used to produce UF₆, the more important are listed below:

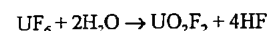


The only industrial route is from pure UF₄. The phase diagram of UF₆ is shown in Figure 41.34. At normal pressure, UF₆ sublimates at

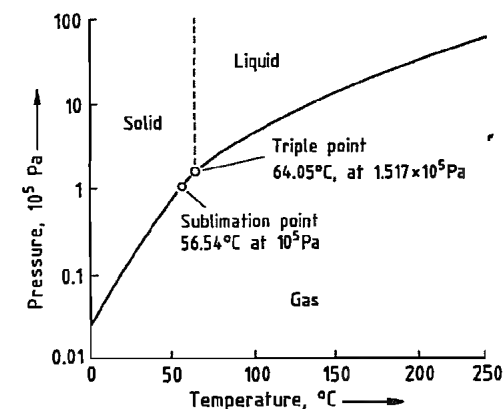
56.54 °C and melts only under a pressure of 1.517×10^5 Pa at 64.05 °C.

The critical constants for UF₆ are [64] ~ *T_c*, 230.5 ± 0.2 °C; *p_c*, (45.50 ± 0.50) × 10⁵ Pa; *p_c*, 1.375 g/m³; *V_c*, 0.256 L/mol.

Solid UF₆ has similarities to white phosphorus, having a colorless to yellowish appearance and being easily cut into pieces. However, in contrast to phosphorus, it reacts rapidly with moisture, hydrolyzing even in moist air to form the bluish compound UO₂F₂, which resembles cigarette smoke:



This fine bluish smoke enables the smallest UF₆ leak in pipework to be detected immediately. At increased temperatures, UF₆ gas reacts violently or explosively with organic substances, but metal and glass are not attacked in the absence of moisture. Comprehensive data on UF₆ can be found in [64].

**Figure 41.34:** Phase diagram of UF₆ [64].

41.8.2 Carbides

The three carbides UC, U₂C₃, and UC₂ appear in the U–C phase diagram [65]. Both UC and UC₂ are stable up to their melting points; U₂C₃ is an intermediate phase that disproportionates above 1800 °C into UC and UC₂ [66]. The carbide UC₂ is unstable below 1275–1500 °C, disproportionating to form U₂C₃ and carbon [67]. Above 1800 °C, UC₂ has the composition U/C = 1.86 ± 0.02 (atomic ratio) and a cubic structure, whereas a tetragonal

form exists between 1600 and 1800 °C with composition U/C = 1.96 ± 0.04. Various temperatures are quoted for the melting point. According to [68], the *mp* of UC is ca. 2350 °C, and that of UC₂ with the composition U/C = 1.9 is 2475 °C.

The carbides react very vigorously with water, and are therefore not used in water-cooled nuclear reactors because secondary damage could occur in the event of a defective fuel rod. However, they can be used as nuclear fuel if cooling is by gas or sodium, two generations of reactors that could be important in the future. Carbide fuels are therefore not yet available on the market except for testing purposes. In experimental fuel elements, UC is used mainly in the form of pellets, rods, or coated particles.

Uranium carbide is produced by three main methods:

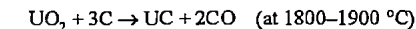
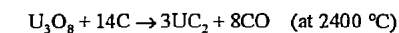
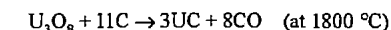
Reaction of Uranium Metal with Carbon. Stoichiometric UC is obtained when a mixture of uranium powder with carbon is compressed at 800–1000 °C [69]. The material so produced has a density of 98% of the theoretical value and a Vickers hardness of 700 kg/mm², a figure normally only obtainable with UC sintered at 2000 °C. A somewhat lower-density UC is formed by compressing uranium powder with carbon at 700–800 °C and then sintering the pellets at 1100 °C [70].

Very pure and dense UC is obtained by arc melting of uranium and carbon under vacuum or argon. This method gives densities of 98–99.5% of theory [71].

Reaction of Uranium Metal with Alkanes.

Very fine uranium powder (produced by decomposition of uranium hydride) is reacted with methane at 600–900 °C to give very pure and dense UC [72]. Reaction times are 0.5–2 h. Propane has also been used successfully.

Reaction of Uranium Oxides with Carbon. This is the only reaction of industrial importance. The following reactions can occur:



Nuclear fuels are produced by this method in a vacuum furnace or under a protective gas since UC is pyrophoric.

Production of UC Fuel Rods. Uranium carbide rods are produced by melting UC at ca. 2500 °C and casting in rod-shaped molds [73]. Of the possible melting processes (i.e., electron beam melting, induction melting, and arc melting), only the last has been developed to an industrial scale. Induction melting is particularly unsuitable because reaction with the walls of the graphite crucible occurs, converting UC to UC₂.

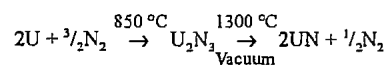
The process of melting UC in an electric arc furnace is known as skull melting; a solid shell of UC forms between the water-cooled copper crucible and the melt, preventing molten UC from reacting with the metal crucible. This ensures the required purity of the nuclear fuel. To be able to cast the melt, tilting furnaces or centrifugal casting furnaces are used.

41.8.3 Nitrides

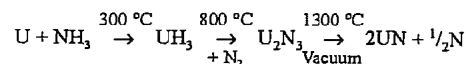
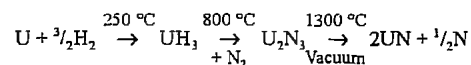
The nitrides UN, U₂N₃, and UN₂ are analogous to the carbides. The mononitride has a theoretical density of 14.32 g/cm³ [74]. Under N₂ at normal pressure (100 kPa), UN decomposes at 2800 °C in a uranium-rich melt with liberation of N₂. If the N₂ pressure is reduced to 10 Pa, the decomposition temperature decreases to 2080 °C. Above 2.5 × 10⁵ Pa, UN melts without decomposition [75]. At nitrogen pressures above atmospheric and 1300 °C, U₂N₃ disproportionates into UN + UN₂ with a 13% decrease in volume [76].

The *mononitride* is produced by three main methods [77]:

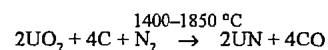
1. Reaction of uranium metal with nitrogen



2. Reaction of UH₃ with nitrogen



3. Reaction of uranium oxide with carbon and nitrogen



If method 3 is used, the nitride always contains some carbon and oxygen [77].

The nitrides have not yet become important nuclear fuels for power reactors, but the properties of uranium nitrides have recently been investigated again in detail with the aim of using them as nuclear fuels for special reactors (e.g., in space applications) [78–81].

41.8.4 Oxides

The following oxides of uranium are known:

- Uranium monoxide, UO, discovered by X rays, of no industrial importance
- Uranium dioxide, UO₂, an important reactor fuel
- UO_{2.3}, stable only above 500 °C, tetragonal crystal structure
- UO_{2.33}–U₃O₇, tetragonal crystal structure
- U₄O₉, formed as an intermediate from UO₂ at high temperature
- U₂O₅, monoclinic crystal lattice, red-brown
- U₃O₈, stable in all temperature regions (U₂O₅·UO₃), black
- UO₃, stable up to ca. 300 °C, orange
- Uranium peroxide, UO₄, light yellow

41.8.4.1 Uranium Dioxide

Production of the industrially important uranium dioxide is described in Section 41.7.4.5. Important physical properties are

Theoretical density	10.96 g/cm ³
mp	2860 ± 70.5 °C
Thermal conductivity at 500 °C	4.3 W m ⁻¹ K ⁻¹
at 1100 °C	2.6
at 1650 °C	2.15
at 2200 °C	4.3
Linear coefficient of expansion (4–2800 °C)	1.1 × 10 ⁻⁵ K ⁻¹
Specific heat capacity (32–315 °C)	237.4 J kg ⁻¹ K ⁻¹

The crystal lattice of UO₂ is face-centered cubic of the CaF₂ type. Stoichiometric UO₂ powder is pyrophoric and is oxidized in air to intermediate products (UO_{2.30} and UO_{2.33}) or to U₃O₈.

UO₂ powder with a large specific surface area is self-igniting. Therefore, handling of UO₂ powders with BET surfaces ≥ 2 mm²/g requires special precaution measures, e.g., surface oxidation in a controlled manner.

41.8.4.2 Uranium Trioxide

Normal decomposition at 300 °C of intermediate products obtained during uranium production always leads to orange-colored UO₃. At > 400 °C, this begins to change into black U₃O₈. Uranium trioxide occurs in five forms:

- α-UO₃ is formed by careful decomposition of UO₄ at 450–500 °C [82].
- β-UO₃ is formed by slow decomposition of ammonium diuranate at 450–500 °C [83].
- γ-UO₃ is formed by slow decomposition of uranyl nitrate hexahydrate (e.g., 4 h at 550 °C) [84].
- δ-UO₃ is red and is formed by dehydration of UO₃·H₂O in air at 375 °C [83].
- ε-UO₃ is brick red and is formed in a few minutes by oxidation of U₃O₈ with NO₂ at 350 °C [83].
- ζ-UO₃ is a brown powder produced by rapid decomposition of uranyl nitrate hexahydrate in the presence of 0.6% sulfamic acid [85]. The existence of this compound is not yet certain.

Uranium trioxide can be an intermediate in the production of nuclear fuel, but it is not itself used.

41.8.4.3 Triuranium Octaoxide

The polymorphism of U₃O₈ is extremely complex, and the data are to some extent conflicting. A summary is given below:

At normal pressure, four modifications exist denoted by α, α', α'', and β. Of these, α and β are base-centered rhombic, α' is body-cen-

tered rhombic, and α'' is hexagonal. The α-forms are stable at low temperature (room temperature) and the β-form at high temperature (> 730 °C). At 50 °C, the α-form changes to the α'-form [86]. The α-form changes to the β-form at high pressure or under shear forces at 1100–1500 °C in the presence of atmospheric oxygen [87]. However, β-U₃O₈ has a lower density and changes back to α-U₃O₈ at 50 °C. Therefore, the reported phase transitions depend on temperature, pressure, and redox reactions, which cause changes in density. The interrelationships between the different phases are thus very complex.

Another U₃O₈ (or UO_{2.67}) phase has been described, which is formed only at high pressure at ca. 627 °C and has a face-centered cubic structure. The combination of pressure and shear stress is said to be important for formation of this phase [86]. Thus, cubic U₃O₈ is obtained from α-U₃O₈ by prolonged milling in a ball mill, conversion being almost complete after one week. Considerable amounts of water are taken up during milling. Therefore, to obtain a pure product, α-U₃O₈ is first milled for 72 h; the mixture of α-U₃O₈ and cubic U₃O₈ obtained is heated to 750 °C; this is then milled again for 24 h in the absence of moisture. After milling for another 30 h in contact with atmospheric oxygen, an amorphous variety of α-UO₃ is formed.

Of four other possible modifications, the existence of two is fairly well established: γ-U₃O₈ is said to be formed at 940 °C from β-U₃O₈ with a heat of transformation of 4.63 ± 0.06 kJ/mol [88]. At 120 °C, this changes back irreversibly to α-U₃O₈, the heat of transformation being 4.40 ± 0.21 kJ/mol. The δ-U₃O₈ modification is formed above 1050 °C [89]. It crystallizes in a rhombic structure with unit cell dimensions *a* = 0.670 nm, *b* = 1.246 nm, and *c* = 0.851 nm. The density is said to be 7.86 g/cm³.

Oxygen is evolved when U₃O₈ melts, so the melting point cannot be determined; U₃O₈ vaporizes at 925–1525 °C with formation of mainly monomeric gaseous UO₃ [90].

The specific magnetic susceptibility of U₃O₈ does not obey the Curie law or the Cu-

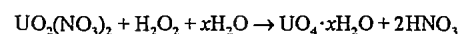
rie-Weiss law; this indicates that U_3O_8 should be written as $\text{U}_2\text{O}_5 \cdot \text{UO}_3$. The electrical conductivity of $\text{U}_3\text{O}_{8\pm x}$ depends strongly on temperature and the O:U ratio, so a generally valid value cannot be given. The oxide U_3O_8 is an *n*-type semiconductor. Conduction is thought to occur by electrons and also by holes. Because of its mixed oxide properties, electron transport from U(V) to U(VI) is assumed.

Chemical Properties. Triuranium octaoxide dissolves readily in oxidizing acids and is oxidized to the hexavalent state and hydrolyzed to uranyl salts [e.g., $\text{UO}_2(\text{NO}_3)_2$] in the aqueous phase. Uranyl chloride, UO_2Cl_2 , is formed by passing HCl gas over U_3O_8 at 700 °C. Triuranium octaoxide is insoluble in water and is oxidized rapidly to UO_4 (uranium peroxide) by hydrogen peroxide; it is reduced by hydrogen or ammonia to UO_2 at > 500 °C.

41.8.4.4 Peroxides

Of the uranium oxides containing a peroxide group, the existence of two is well established: UO_4 (crystallizing with two or four molecules of water) and U_2O_7 with or without water of crystallization.

The hydrate $\text{UO}_4 \cdot x\text{H}_2\text{O}$ can be precipitated easily from aqueous uranyl nitrate solutions at room temperature by addition of H_2O_2 :



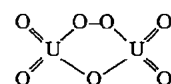
This precipitation easily can be performed continuously, and the precipitate can be dried to give a powder with good flow properties [91].

A UO_4 powder with good sintering properties is prepared from a solution of uranyl nitrate (90–120 g/L) in 0.5 mol/L HNO_3 to which ammonium nitrate (80 g/L) has been added. Precipitation at pH 1.5 and 40 °C occurs at a uranium:hydrogen peroxide ratio of 1:3. The UO_4 powder formed is a spheroidal to spherical agglomerate with a maximum particle size of 50 μm , although most particles are

ca. 20 μm . Calcination of this powder gives a product with good sintering properties.

The hydrate $\text{UO}_4 \cdot x\text{H}_2\text{O}$ is pale yellow; $\text{UO}_4 \cdot 4\text{H}_2\text{O}$ is the main product at a precipitation temperature of < 50 °C, $\text{UO}_4 \cdot 2\text{H}_2\text{O}$ at higher temperature. Careful dehydration in a vacuum at ca. 130 °C gives hydrated U_2O_7 , which decomposes with liberation of oxygen above 150 °C.

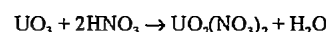
The structure of $\text{UO}_4 \cdot x\text{H}_2\text{O}$ has not yet been established, but U_2O_7 probably has the following structure [92]:



This is a brick-red to orange hygroscopic substance [93].

41.8.5 Nitrates

Uranium and its oxides dissolve in nitric acid to form uranyl nitrate:



The hexahydrate crystallizes from weakly acidic supersaturated solutions, but tri- and dihydrates can be obtained at higher concentration of HNO_3 (Figure 41.35). Upon evaporation of uranyl nitrate solutions to > 450 g/L uranium, $\text{UO}_2(\text{NO}_3)_2 \cdot 6\text{H}_2\text{O}$ (*mp* 60 °C) crystallizes on cooling [94]. The uranium content of a solution boiling at 120 °C is ca. 1000 g/L. The trihydrate melts at 113 °C, and the dihydrate at 184 °C. No decomposition occurs up to this temperature, but denitration begins above 300 °C. The UO_3 so produced has a relatively high bulk density (3.5–4.3 g/cm³) and, after reduction to UO_2 , is not very suitable for the production of compressed and sintered pellets. The nitrate of U(IV), $\text{U}(\text{NO}_3)_4$, can be obtained by treatment of uranyl nitrate with reducing agents such as hydrazine, iron(II) formate, or SO_2 , or by electrolytic reduction. Uranium(IV) nitrate is a green substance, in marked contrast to yellow $\text{UO}_2(\text{NO}_3)_2$. It oxidizes readily to U(VI) in air.

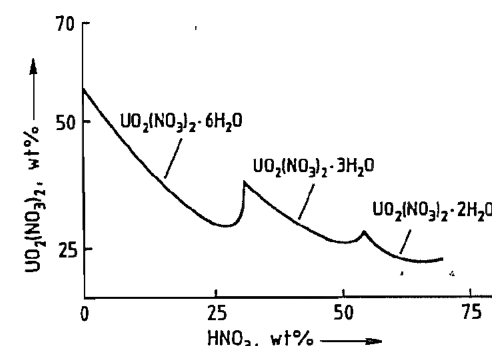


Figure 41.35: The $\text{UO}_2(\text{NO}_3)_2$ - HNO_3 - H_2O system.

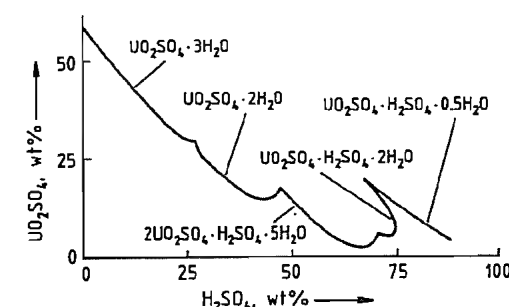


Figure 41.36: The UO_2SO_4 - H_2SO_4 - H_2O system.

41.8.6 Sulfates

The sulfates of uranium are important because uranium ores are usually digested with sulfuric acid (see Section 41.7.4.1), which generally leads to the formation of uranyl sulfate, UO_2SO_4 . The nature of the hydrates formed depends on the H_2SO_4 concentration (Figure 41.36). Sulfates of tetravalent uranium are more stable than nitrates. The following hydrates are known: $\text{U}(\text{SO}_4)_2 \cdot 8\text{H}_2\text{O}$, $\text{U}(\text{SO}_4)_2 \cdot 4\text{H}_2\text{O}$, $\text{U}(\text{SO}_4)_2 \cdot 9\text{H}_2\text{O}$, and $\text{U}(\text{SO}_4)_2 \cdot 2\text{H}_2\text{O}$.

41.8.7 Tricarbonatodioxouranate

Tricarbonatodioxouranate, $[\text{UO}_2(\text{CO}_3)_3]^{4-}$, is formed by alkaline digestion and in the AUC process. The ammonium salt of this anion (AUC) decomposes above 80 °C, liberating CO_2 and forming ammonium diuranate.

41.9 Safety

The normal safety precautions taken in the chemical industry when handling toxic, liquid, volatile, and gaseous substances must be observed also in the case of uranium, but in addition radiation protection and criticality safety must be included. These affect plant and equipment design and may necessitate the use of apparatus with dimensions not generally employed in chemical technology (see Section 41.9.3), but reflecting all considerations as regards chemical, nuclear, and radiological safety.

41.9.1 Radiation Shielding

Handling natural uranium that has not been irradiated does not present special problems. The danger of unacceptable emission of radiation is generally small, nevertheless, all processes are generally emboxed. Special attention must be given to cleaning UF_6 cylinders because buildup of ^{234}Th , which is in equilibrium with ^{238}U , can occur. After evaporation of UF_6 , the cylinder still contains residues in the form of uranium decay products. However, providing shielding against the intense β -radiation and bremsstrahlung emitted by these residues while they are being treated is not difficult.

In addition, the uranium content of atmosphere and contamination of the workplace are measured and controlled to protect personnel from uptake of or contamination by uranium. If legal limits are exceeded, respiratory protection must be provided. Workers must also be examined with a lung monitor at regular intervals, and the uranium content of urine must be determined. If uptake of uranium is suspected, whole-body measurements must be carried out.

Maximum permitted uranium concentrations in air at the workplace and in the form of surface contamination are given in Table 41.12.

Table 41.12: Maximum permitted uranium concentrations in the workplace (with figures for other toxic elements for comparison) [95].

	Outside atmosphere, mg/m ³	In the workplace	
		Inactive area, mg/cm ³	Active area ^a , mg/cm ³
Natural uranium	180	150	1500
Uranium with 5% ²³⁵ U	42	35	350
Uranium with 10% ²³⁵ U	24	20	200
HF	2000		
Pb	200		
Be	2.0		
²³⁹ Pu	0.000032	0.00017	0.0017

^a Workplace where radioactive materials are processed.

41.9.2 Safety Against Uncontrolled Criticality

Criticality safety includes all technical and organizational measures taken to prevent an uncontrolled chain reaction. Uranium with its natural isotopic composition becomes critical only under special reactor conditions. This means that a spontaneous chain reaction under the conditions of uranium processing is impossible. However, in contrast to uranium with a natural isotopic composition, enriched uranium can have a critical configuration under considerably simpler circumstances (e.g., during manufacture or storage of fuel elements). The critical mass depends mainly on the degree of enrichment of ²³⁵U, the composition of the material, and the moderating effect of the geometrical configuration.

In Germany, for example, plants for processing nuclear fuels can, therefore, be operated only if they are licensed under §7 of the Atomic Energy Law, which specifies essential criteria for the nuclear safety of personnel and of the environment. Similar regulations apply in other countries.

In older plants, the observance of limit values was ensured mainly by measures under the control of plant personnel, but in newer plants this has been superseded by automatic control

and is largely independent of human error. Exact and in licensing approved and validated computer codes enable a reduction of extra safety margins, so that larger vessels can be used with the knowledge that they are geometrically safe with respect to permitted criticality dimensions. In addition, more precise calculation of neutron interactions between individual vessels can be carried out with these methods; hence, a space-saving arrangement of components is possible.

41.9.3 Geometrically Safe Vessels

The nuclear safety of a critically safe ($k_{\text{eff}} < 0.95$) thickness of material is achieved by increasing the surface of a vessel, thereby increasing the loss of neutrons to the environment and preventing the neutron population necessary to reach a critical condition. The safe geometry is determined as follows:

A hypothetical optimum neutron reflector is assumed to be present at the vessel, whether or not this assumption corresponds to actual conditions. This assumed reflector reduces calculated neutron loss considerably, and, therefore, causes a calculated increase in activity exceeding that of the actual arrangement. The smallest dimensions of the vessel in which a self-sustaining chain reaction can occur are found, based on the combined effects of concentration of fissile material, degree of moderation, and neutron loss by leakage by using this conservative method of calculation. From these conservatively smallest critical dimensions for ideally reflected uranium-water systems, the largest safe subcritical dimensions for $k_{\text{eff}} = 0.95$ can be deduced, including safety factors (Table 41.13). Safe maximum amounts of uranium under all circumstances are listed in columns 2 and 3 of Table 41.13. The geometric dimensions in columns 4–6 apply to any amounts of uranium, provided $\rho_U < 3.5 \text{ g/cm}^3$.

Table 41.13: Safe masses and geometries for uranium salts and solutions as a function of degree of enrichment for a total density $< 3.5 \text{ g/m}^3$.

Degree of enrichment, % ²³⁵ U	Mass of ²³⁵ U max., kg	Total mass of U max., kg	Safe volume, L	Safe cylinder diameter, cm	Safe thickness of material, cm
100	0.350	0.35	4.4	12.70	3.81
75	0.360	0.46	5.0	13.21	4.06
50	0.390	0.76	6.0	14.48	4.83
40	0.410	1.025	6.7	15.24	5.08
30	0.440	1.467	7.7	16.00	5.59
20	0.480	2.4	9.5	17.53	6.86
15	0.520	3.467	11.0	18.80	7.87
12	0.583	4.858	12.5	19.81	8.64
10	0.600	6.0	14.0	20.83	9.14
8.0	0.6650	8.125	16.0	22.10	9.91
6.0	0.710	11.833	20.5	24.38	11.43
5.0	0.800	16.0	27.0	26.04	12.70
4.0	0.930	23.25	33.8	28.45	13.97
3.5	1.04	29.714	40.0	30.48	15.24
3.0	1.20	40.0	49.2	32.51	16.51
2.5	1.47	58.8	64.6	35.56	18.03
2.0	2.0	100.0	95.1	40.64	22.10
1.75	2.56	146.286	126	44.70	24.38

41.9.4 Apparatus with Heterogeneous Neutron Absorbers

The dimensions of safe vessels are often too small to allow desired throughputs to be achieved. In these cases, considerable benefit can be obtained by incorporating heterogeneous neutron absorbers (nuclear poisons), such as boron carbide or cadmium, into the equipment. Their effect is very dependent on the spatial arrangement of the no-absorption or intermediate vessel walls. For example, fluidized-bed furnaces are provided with a nuclear poison consisting of a central boron carbide rod with double cladding, and rotary UO_2 mixers with a surface covering or cladding consisting of securely attached cadmium sheets. This ensures nuclear safety even if water penetrates the fluidized bed or rotary mixer (accident safety).

41.9.5 Neutron Interactions in the UO_2 Fabrication Plant

A nuclear fuel production plant contains many individual processing stations. Therefore demonstrating that these will remain subcritical as individual units is not sufficient. Equally important is ensuring that no increase

in criticality is caused by interactions of the systems, plant, and equipment due to the way in which they are arranged. The entire layout of processing and storage operations must therefore be in the form of subcritical geometry.

41.9.6 Transportation

Plants for ore extraction, processing, and concentration are usually geographically remote from those for fuel assembly production; thus, uranium and its compounds must be transported between these plants. Since the materials being transported are often fissile and radioactive, special precautions must be taken and rules observed. For this reason, the IAEA has issued guidelines that are updated continuously according to the latest knowledge (Regulations for the Safe Transport of Radioactive Materials, IAEA, Vienna), in which national safety regulations are also considered. In its "Safety Series" of publications, the IAEA includes recommendations for methods of transporting radioactive materials, taking international and national regulations into account.

Since shipments often cross international boundaries, international harmonization of

rules and licensing procedures is necessary. This is controlled under the UNO umbrella [96]. The aim of the recommendations, guidelines, and regulations is to protect the general public, transport operatives, and private property from both the direct and the delayed effects of radiation during transportation [96].

This protection is secured by

- Restriction of the nature and activity of the radioactive material, which must be transported only in packaging of a specified type
- Specification of design criteria for each type of packaging
- Rules for handling and storage during transportation

The regulations are intended to prevent the release and uptake of radioactive materials into the human organism, to protect against radiation emitted by the materials being transported, and to ensure that unforeseen criticality events do not occur.

These aims are achieved in practice by

- Containment of the material being transported, the design and sturdiness of the packaging depending on the activity and nature of this material
- Limitation of the maximum dose level at the outer surface of the item being transported, by taking account of the contents of the package and storage techniques used in the transport system
- Protection of the transport container from external effects of an accident, again by taking into account the nature and activity of the material being transported
- Prevention of a criticality event by very restrictive assumptions with respect to the items being transported and the conditions that could arise from an accident

Experience with the transport of radioactive goods has justified the practices used internationally. In industrialized Western countries, no case of injury or death has resulted due to the release of radioactive materials in a transportation accident. This is supported by data from the following countries:

United States: A detailed study of 811 reported incidents between 1971 and 1981

United Kingdom: A study of 330 000 shipments of radioisotopes

Germany: A study of shipments up to 1984 [97]

The positions are underlined when assessing the Mont-Louis incident. In August 1984, the freighter Mont Louis, with a cargo of 350 t UF_6 , sank in 15 m water. Within 40 days, all of the containers were recovered undamaged from the wreck without any release of radioactivity.

41.10 References

- Gmelin, Uranium, Part A: The Element, Part B: The Alloys, Part C: The Compounds, Part D: The Chemistry in Solution, Part E: The Coordination Compounds.
- Uranium Ore Processing Panel Proceedings Series, printed by IAEA (Internat. Atomic Energy Agency) Vienna, Dec. 1976.
- S. Villani: Uranium Enrichment, *Topics in Applied Physics*, vol. 35, Springer Verlag, Berlin-Heidelberg-New York 1979.
- The Chemical Thermodynamics of Actinide Elements and Compounds, part I, 1976; part II, 1976; part III, 1978, IAEA, Vienna.
- Advances in Uranium Refining and Conversion, IAEA-TECDOC-420, Vienna 1987.
- J. H. Cavendish in W. W. Schulz, J. D. Navratil, T. Bess (eds): *Science and Technology of Tributyl Phosphate*, vol. 2: "Selected Technical and Industrial Uses", CRC Press, Boca Raton, FL, 1987.
- W. D. Müller: *Geschichte der Kerntechnik in der Bundesrepublik Deutschland*, Schäffer Verlag für Wirtschaft und Steuern, Stuttgart 1990.
- Int. Symposium on the Oklo-Phänomen, Libreville, Gabon, June 23-27, 1975; IAEA Proc. Series—STI/PUB/405.
- C. Keller: "Das Oklo Phänomen", *GIT Fachz. Lab.* 30 (1986) no. 5, 423-433; no. 6, 581-585.
- P. C. Sahu, M. Yousuf, K. Govinda Rajan, *Physica B + C* 183B (1993) 145-155.
- J. F. Cannon, *J. Phys. Chem. Ref. Data* 3 (1974) 801.
- ES Microwave, TAPP, Thermochemical and Physical Properties, Hamilton, OH, 1991.
- J. D. Grogan, *J. Inst. Met.* 77 (1950) 571.
- B. Blumenthal, *J. Nucl. Mater.* 2 (1960) 23.
- A. N. Holden, US-Report KAPL-480 (1950).
- R. W. Logan, *Metall. Trans. A* 14A (1983) 2337.
- L. T. Lloyd, C. S. Barrett, *J. Nucl. Mater.* 18 (1966) 55.
- M. A. Filyand, E. I. Seminova: *Handbook of the Rare Elements III*, Boston Technical Publ., Cambridge, MA, 1970 (translated by M. E. Alfieroff).
- A. F. Hollemann, E. Wiberg: *Lehrbuch der Anorganischen Chemie*, Walter de Gruyter Verlag, Berlin 1976.
- J. P. Coughlin, Bulletin 542 U.S. Bureau of Mines, "Contribution to the Data on Theoretical Metallurgy X, Heats and Free Energies of Formation of Inorganic Oxides", Washington, DC, 1954.
- E. Kohl: *Uran*, Enke Verlag, Stuttgart 1954.
- M. Rauboult: *Géologie de l'uranium*, Paris 1958.
- Gmelin, A1, 75-77.
- M. Benedict: *Nuclear Chemical Engineering*, McGraw-Hill, New York 1957.
- OECD and IAEA: *Uranium, Resources, Production and Demand*, 1991.
- OECD/NEA, *Uranium 1995 — Resources, Production and Demand*, Paris 1996.
- The Uranium Institute Market Report, Uranium Institute Report 1996.
- A. Max, T. Mason, *Vergangenheit und Zukunft der U-Produktion* 41 (1996) no. 2, February, p. 79.
- Uranversorgung der Welt 41 (1996) no. 7, Juli, p. 479.
- K. Schreiber, *Stand und Perspektiven der Uranversorgung, Vortrag Jahrestagung Kerntechnik*, 23.5.1996, Mannheim.
- H. Kirchberg: *Aufbereitung bergbaulicher Rohstoffe*, Gronau, Jena 1953.
- E. J. Pryor: *Mineral Processing*, 3rd ed., Elsevier, Amsterdam-London-New York 1965.
- M. E. Grimes, *Trans. Am. Inst. Min. Metall. Pet. Eng.* 254 (1973) 312-318.
- I. Higgins, *Environ. Sci. Technol.* 7 (1973) 1100-1140.
- P. Pfüller, F. J. Gogke, *Aufbereit. Tech.* 14 (1973) 555-560.
- G. Ritcey: "Extractive Metallurgy of Uranium", *Short Course Toronto Solvent Extraction 1978* 23-31.
- P. Niederer, *Verfahrenstechnik (Mainz)* 4 (1970) np. 12, 548-554.
- J. Wyllie, *World Min.* 32 (1979) 58.
- J. B. Rosenbaum: *Uranium Ore Processing*, IAEA Meeting, Nov. 24-26, 1975 Paper IAEA-AG/33-8, p. 6, Vienna 1976.
- J. K. Dawson, E. Wait, K. Alock, D. R. Chilton, *J. Chem. Soc.* 1956, 3531-3540.
- W. Biltz, H. Müller, *Z. Anorg. Allg. Chem.* 163 (1927) 257-296.
- General Electric Co., US 3579311, 1968.
- C. D. Harrington, A. E. Ruehle, *Chem. Eng. Prog.* 54 (1958) no. 3, 65-70.
- C. H. Chilton, *Chem. Eng. (N.Y.)* 65 (1958) no. 21, 138-141.
- P. S. Gentils, L. H. Talley, T. J. Coloppy, *J. Inorg. Nucl. Chem.* 10 (1959) 110-113.
- G. Wirths, L. Ziel, *Proc. U.N. Int. Conf. Peaceful Uses At. Energy 2nd*, 4 (1958) 16-21.
- Nukem, DE 1126363, 1960/62; DE 1592477, 1966; DE 1592478, 1967.
- F. Plöger, H. Vietzke, *Chem. Ing. Tech.* 37 (1965) 692-699.
- K. G. Hackstein, F. Plöger, *ATW Atomwirtsch. Atomtech.* 12 (1967) 524-526.
- T. J. Heal, J. E. Littlehild, H. Page, *Nucl. Eng. Int.* 25 (1980) 48-51.
- A. Ducouret, B. Kalthoff, *Ber. Jahrestag. Kerntechnik. Ges. Dtsch. Atomforum* 1980, 405-408.
- W. C. Ruch, D. A. Peterson, E. A. Gaskil, H. G. Tepp, *Chem. Eng. Prog. Symp. Ser.* 56 (1960) no. 28, 35-41.
- F. K. Pickert, H. J. Zech: *Brennstoffkreislauf*, Deutsches Atomforum, Bonn 1981.
- Urenco-Werkzeitschrift, Panorama, Gronau-Almelo-Capenhurst, Dec. 1980.
- H. Mohrhauer, E. Coester, *Atomkernenerg. Kerntechnik* 35 (1980) no. 3, 161-165.
- W. Becker, K. Bier, *Chem. Ing. Tech.* 39 (1967) no. 1, 1-7.
- P. Bley, W. Ehrfeld, U. Heiden, KFK report no. 2580, Kernforschungszentrum, Karlsruhe 1978.
- K. Takeda, H. Onitsuka, H. Obanawa in M. Abe, T. Kataoka (eds.): *New Developments in Ion Exchange*, Kodensha Ltd., Tokyo 1991, pp. 583-589.
- J. M. Lerat, C. Lorrain, *Conference on Solvent Extraction and Ion Exchange in the Nuclear Fuel Cycle*, Harwell, UK Sep. 3-6, 1985, pp. 53-61.
- I. D. Heriot: *Uranium Enrichment by Gas Centrifuge*, Commission of the European Communities 1988.
- H. Kühn, M. Peehs, K. Reichardt: "Thermische Bruterstudie", part 2, *Forschungsber. BMWF Inv. Reaktor* 37, April 1969.
- M. Peehs et al., *IAEA Tech. Committee on Utilization of Th-based Nuclear Fuel*, Vienna, Dec. 1985.
- M. Peehs, W. Dör, M. Hrovat, *IAEA Advisory Group Meeting on Advanced Fuel Technology and Performance*, EUR Würenlingen, Dec. 1984.
- S. H. Smiley, D. C. Brater, US-Report K-1379 1/18 (1958).
- J. A. Rode, US 594201, 1966.
- U. Berndt, B. Erdmann, *Radiochim. Acta* 19 (1973) 45-46.
- R. J. Sheil, US-Report ORNL-2061-Pt. 1-2-3 Del. 71 (1959).
- S. Langar, F. E. Blankenship, *J. Inorg. Nucl. Chem.* 14 (1960) 26-31.
- J. K. Dawson, R. W. M. D'Eye, E. A. Truswell, *J. Chem. Soc.* 1954, 3922-3929.
- R. DeWitt, US-Report GAT-280, p. 102 (1960).
- G. D. Oliver, H. T. Milton, J. W. Grisard, *J. Am. Chem. Soc.* 75 (1953) 2827-2829.
- M. W. Mallett, A. F. Gerds, H. R. Nelson, *J. Electrochem. Soc.* 99 (1952) 197-204.
- W. B. Wilson, *J. Am. Ceram. Soc.* 43 (1960) 77.
- J. M. Leitnacker, W. G. Wittemann, *J. Chem. Phys.* 36 (1962) 1445.
- S. Imoto et al., *Proc. of the Symposium at Harwell 1963*, vol. 1, McMillan, Basingstoke 1963, pp. 7-20.
- J. Dubuisson et al., *Proc. U.N. Int. Conf. Peaceful Uses At. Energy 2nd* 6 (1958) 551.
- E. Barnes, *Prog. Nucl. Energy Ser. 1* 1 (1956) 61.
- J. K. Dawson, R. G. Sowden: *Chemical Aspects of Nuclear Reactors*, vol. 1, Butterworths, London 1963.
- H. S. Kalish, US-Report TID-7614 (1961) 99-110.
- P. Himmelstein, H. Kühn, O. Pfahls, R. Lucas: "Verbesserung der Technologie bei der Fabrikation gegossener Urancarbidstäbe", *Euratom-Report EUR-4273d*.
- P. D. Shalek, *J. Am. Ceram. Soc.* 46 (1963) 155.
- R. M. Dell, M. Albutt, UKEA-Report AERE-R 4253 (1963).
- R. E. Rundle, N. C. Baenziger, A. S. Wilson, R. A. McDonald: "The Structure of Carbides, Nitrides and

- Oxides of Uranium", *J. Am. Chem. Soc.* **70** (1948) 99–105.
77. M. Smith, R. I. Honeycombe, *J. Inst. Met.* **83** (1954/1955) 421–426.
78. T. Matsui, R. W. Ohse, Commission of the European Communities, report EUR-10858, Order no. PB88-125356, 1986.
79. R. B. Matthews, *Space Nucl. Power Syst.* **8** (1989) 201–205.
80. S. L. Hayes, J. K. Thomas, K. L. Peddicord, *J. Nucl. Mater.* **171** (1990) nos. 2/3, 271–288.
81. G. Ledergerber, Z. Kopajtic, F. Ingold, R. W. Stratton, *J. Nucl. Mater.* **188** (1992) 28–35.
82. V. J. Wheeler, R. M. Dell, E. Wait, *J. Inorg. Nucl. Chem.* **26** (1964) 1829–1845.
83. H. R. Hoestra, S. Siegel, *J. Inorg. Nucl. Chem.* **18** (1961) 154–165.
84. V. G. Vlasov, Y. N. Semavin, *Zh. Prikl. Khim. (Leningrad)* **40** (1967) 1210–1215.
85. V. J. Wheeler, R. M. Dell, E. Wait, *J. Inorg. Nucl. Chem.* **26** (1964) 1829–1845.
86. A. N. Tsvigunov, L. M. Kuzvetsov, *Radiokhimiya* **16** (1974) 882–885.
87. H. R. Hoekstra, S. Siegel, L. H. Fuchs, J. I. Katz, *J. Phys. Chem.* **59** (1955) 136–138.
88. G. K. Khomyakov, V. I. Spitsyn, S. A. Zhvanko, *Issled. Obl. Khim. Urana* **1961**, 141–144.
89. A. F. Bessonov, *Kristallografiya* **15** (1970) 62–67.
90. H. Powers, E. Welch, J. B. Trice, NEPA-934-SCR-34 (1949 and 1961).
91. Nukem, DE 2623977, 1976 (P. Börner, H. Vietzke).
92. M. El-Chehabi, Dissertation University of Texas, 1957.
93. J. E. Boggs, M. El-Chehabi, *J. Am. Chem. Soc.* **79** (1957) 4258–4260.
94. W. L. Marshall, J. S. Gull, C. H. Secoy, *J. Am. Chem. Soc.* **73** (1951) 1867.
95. A. Pilgenröther, W. Thomas, *ATW Atomwirtsch. Atomtech.* **16** (1971) 74–77.
96. Bundesminister für Verkehr (eds.), bulletin "Die Beförderung radioaktiver Stoffe", Oct. 19, 1984.
97. Deutscher Bundestag, Drucksache no. 10/2160 Oct. 19, 1984.

42 Thorium

WOLFGANG STOLL

42.1 Introduction	1649	42.7 Metalworking	1673
42.2 Properties	1650	42.8 Intermetallic Compounds	1675
42.2.1 Physical Properties	1650	42.8.1 Thorium and Carbon	1675
42.2.2 Chemical Properties	1653	42.8.2 Thorium and Nitrogen	1675
42.3 Occurrence and Raw Materials	1654	42.9 Uses	1675
42.4 Production	1656	42.9.1 Nuclear Technology	1675
42.4.1 Concentration	1656	42.9.2 Conventional Applications	1678
42.4.1.1 Ore Preparation	1656	42.9.2.1 Illuminants	1678
42.4.1.2 Ore Digestion and Thorium		42.9.2.2 Electron Emitters	1678
Recovery	1656	42.9.2.3 Ceramics and Glass	1678
42.4.2 Fine Purification by Solvent		42.9.2.4 Catalysts	1679
Extraction	1661	42.9.2.5 Medicine	1679
42.5 Compounds	1663	42.9.2.6 The Demand for Thorium	1679
42.5.1 Oxides	1663	42.10 Product Quality and Analytical	
42.5.2 Halides	1665	Methods	1679
42.5.2.1 Tetrafluoride	1665	42.11 Toxicology	1681
42.5.2.2 Tetrachloride	1667	42.12 Industrial Safety	1681
42.5.2.3 Tetraoxide	1667	42.13 Environmental Protection	1682
42.5.3 Other Compounds	1668	42.14 Legal Aspects	1683
42.6 Production of Pure Thorium		42.15 References	1683
Metal	1669		

42.1 Introduction

Thorium was originally placed in group 4 of the periodic table under titanium, zirconium, and hafnium, following ^{89}Ac . However, the 5f electron shell is filled in the series of elements from ^{90}Th to ^{103}Lr . In analogy to the lanthanides, in which the 4f shell is filled, these elements are therefore referred to as the actinides, thorium being the first in the series [1, 2]. Its similarity to cerium and its mineralogical occurrence in association with the rare earths and uranium confirm this placing. The number of thorium isotopes known thus far, all radioactive, is 25 [3]. The most common of these has the relative atomic mass 232, and five others occur naturally in the decay chains of uranium and thorium. First isolated by BERZELIUS in 1828 from the silicate mineral thorite, thorium attained industrial importance in the late 1800s as a component of gas mantles. By World War II, total consumption world-

wide had amounted to ca. 8000 t, mainly for the production of gas mantles, reaching 250 t in some years. Thorium occurs in only a few regions of the earth's crust in minable amounts, although its average abundance is three to four times that of uranium [4]. After absorbing a neutron, thorium is transformed in several steps into fissile (i.e., fissionable by thermal neutron) ^{233}U . Thorium thus represents quantitatively by far the greatest energy reserve based on nuclear fission. Therefore, in the early years of nuclear technology, up to 900 t/a thorium was extracted and stockpiled as a strategically important raw material, and some hundreds of tonnes were irradiated in reactors although less than 3 t of ^{233}U was obtained from this.

However, for partly technical and partly economic reasons this route to energy production is now of little importance except in India. Therefore, since thorium is little utilized in the

nonnuclear field, consumption since 1990 has declined to a few tens of tonnes per year.

42.2 Properties

42.2.1 Physical Properties

Formation and Decay. The most abundant thorium isotope (exceeding the abundance of the other isotopes by a factor of several millions) is ^{232}Th . Its concentration in the earth's crust obeys Harkins' rule, which states that even-numbered isotopes are more abundant than odd-numbered ones [5]. However, its concentration overall is more than twice that expected from the decrease in abundance of nuclides with increasing atomic number. The half-life of ^{232}Th (a decay) is 1.4×10^{10} a, the longest of all actinides, and a calculation based on the half-lives of higher actinides shows that this concentration excess must be a result of the decay of primordial actinides such as plutonium and curium in the initial phases of the earth's history. Mineralogical evidence is provided by the fact that the very old thorium mineral bastnaesite, a thorium fluorocarbonate, is so far the only mineral in which traces of the longest-lived transuranic, the isotope ^{244}Pu with a half-life of 8.26×10^7 a, have been detected [6].

As early as 1922, the isotopic ratio ^{208}Pb : ^{206}Pb and the age-proportional Th:U ratio in old ores were thought to indicate that a parent nuclide to thorium must have existed, whose half-life was estimated to be $(5.9\text{--}6.3) \times 10^7$ a [7]. This closely matches that of ^{244}Pu .

Alpha decay of ^{232}Th leads to ^{228}Th , while in the uranium decay chain, ^{238}U gives the short-lived ^{234}Th and ^{230}Th , and decay of ^{235}U gives ^{231}Th and ^{227}Th . Because of the low concentration of ^{235}U (0.711%) in natural uranium and the short half-lives of the last two thorium isotopes, these are of little quantitative significance.

The thorium decay chain from ^{232}Th to ^{208}Pb is shown in Figure 42.1 [8].

The concentration ratio of ^{232}Th to ^{228}Th at equilibrium corresponds to the ratio of their

half-lives. In ^{232}Th irradiated in a reactor, an even higher proportion of ^{228}Th and of the follow-on daughter nuclides from ^{232}U decay chain is present, which is indicated, e.g., by the intensified 2.6-MeV γ -radiation from ^{208}Tl .

Neutron absorption leads to the formation of ^{233}Th from ^{232}Th . By two subsequent β decays ^{233}U is formed which decays to form the long-lived ^{233}Th (half-life 7340 a). The other thorium isotopes with mass numbers 212–225 are very short-lived α -emitters formed by decay of the corresponding uranium isotopes, and the isotopes ^{235}Th and ^{236}Th are short-lived β -emitters; all are produced by artificial transmutation and are of no industrial importance.

Like all other actinides, ^{232}Th also undergoes spontaneous fission with neutron emission, although, being the first member of the series, it has the longest half-life (i.e., $> 10^{21}$ a). The xenon isotopes expected as fission products can be found in old thorium ores, which also contain 1–10 cm³ of helium per gram from α -decay. The helium can be boiled out with water.

Where tetravalent uranium is present in primary ores, it is usually associated with thorium, whose principal valence is also 4. Therefore, the thorium isotopes present come from all three decay chains (^{235}U , ^{238}U , ^{232}Th). The isotope ^{230}Th (ionium), a decay product of ^{234}U , is important because of its relatively long half-life (75 400 a) and, at equilibrium, is present at a level of $1.76 \times 10^{-3}\%$ of the proportion of uranium in the thorium.

The activity of freshly separated ^{232}Th passes through two activity maxima due to the formation of decay products. The first of these, which gives approximately a threefold increase in activity, is due to the six short-lived decay products of ^{228}Th (half-life 1.9 a) and occurs after ca. 5 weeks. The second increase begins after ca. 4 a when ^{228}Th is formed from ^{228}Ra (half-life 5.75 a), and the original radiation level increases almost fivefold after 40 a (Figure 42.2).

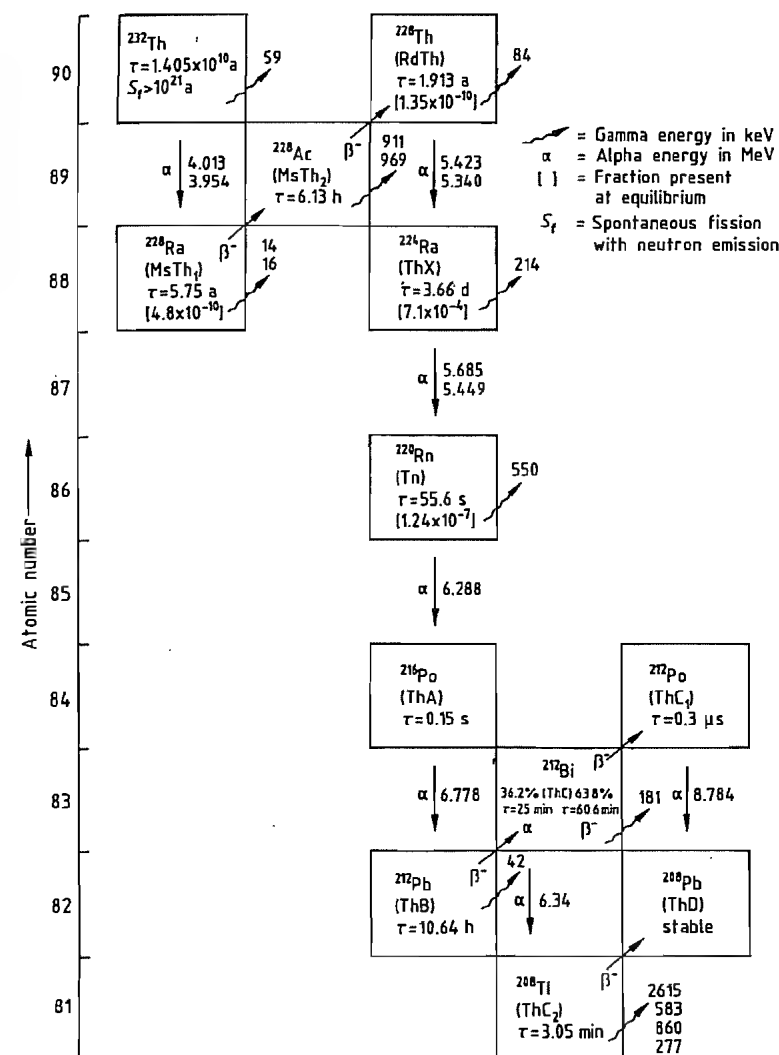


Figure 42.1: Thorium decay chain.

Pure thorium is a silvery-white, ductile metal, with low strength properties and chemical resistance [9]. It becomes gray on exposure to air. Finely divided thorium is pyrophoric. These disadvantages can be mitigated slightly by adding alloying elements. Solid thorium has the highest atomic density of all thorium compounds, which favors its use in nuclear reactors.

The physical properties and thermodynamic data of thorium are listed below. Tho-

rium exists in two solid phases, the α -phase (lattice constant 0.5068 nm) is stable at room temperature and is transformed to the β -phase (lattice constant 0.411 nm) at 1360 ± 10 °C (heat of transformation 3600 ± 125 J/mol). The phase transformation β -phase-liquid occurs at 1750 °C. Thorium has a b_p of 4702 °C. The molar heat capacities are as follows:

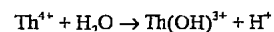
α -phase a : 25.5 J/mol
 $b \times 10^3$: 4.48 J/mol
 $c \times 10^{-5}$: -0.51 J/mol

trogen to form Th_2N_3 . Thorium reacts with hydrogen at 300–400 °C, with the evolution of heat, to form Th_4H_{15} , which itself decomposes above 1100 °C, probably forming ThH_2 , a gray-black powder that ignites spontaneously and is isomorphous with ZrH_2 . Thorium can therefore be melted only in an inert-gas atmosphere or in a vacuum.

Thorium reacts violently with the halogens and with sulfur on heating to 450 °C, producing a flame, and it reacts with fluorine even in the cold. The oxidation state of thorium is 4 in all the compounds formed. Thorium is hardly attacked at all by water, even when hot, but reacts at 800–900 °C with water vapor to form ThO_2 .

On heating with phosphorus, finely divided boron, or carbon, tetravalent compounds are formed immediately, as in the reaction with nitrogen. Alloys are formed with all actinides and lanthanides, iron- and platinum-group metals, alkali metals (except Li), Mo, W, Ta, Zn, Zr, Hf, Be, Al, and Si.

Thorium is stable toward dissolved or molten alkali and is attacked only slowly by dilute mineral acids. It is passivated in HNO_3 , but the effect disappears in the presence of small concentrations of HF or H_2SiF_6 (0.05 mol/L), and thorium is then dissolved rapidly. Thorium dissolves in aqua regia and concentrated HCl . Thorium salts generally contain tetravalent thorium. They have only a slight tendency to hydrolyze. A pH of 3.7 is required to remove the first hydrogen ion from the water molecule according to



The thorium ion forms anionic complexes with a large number of ions in acidic or neutral solution (e.g., CO_3^{2-} , $\text{C}_2\text{O}_4^{2-}$, SO_4^{2-} , HSO_4^- , PO_4^{3-} , citrate, and tartrate). Thorium forms positively charged complexes with F^- if the molar ratio of F^- to Th^{4+} is < 2 . Complexes are also formed with an excess of thiocyanide and nitrate. Thorium has a strong tendency to form double salts such as $\text{K}_2\text{ThF}_6 \cdot 4\text{H}_2\text{O}$, $\text{NaTh}_2(\text{PO}_4)_3$, $\text{MnTh}(\text{SO}_4)_3 \cdot 7\text{H}_2\text{O}$, and $\text{ThSO}_4\text{HPO}_4 \cdot 4\text{H}_2\text{O}$; it also forms basic salts such as $\text{ThOCO}_3 \cdot 2\text{H}_2\text{O}$. The strong adsorptive

forces of the Th^{4+} ion, which are exemplified by the formation of stable colloidal solutions in salt solutions with full gel-sol reversibility, especially in the system $\text{Th}^{4+}\text{-NO}_3\text{-OH}^-$, is used in industrial production of ThO_2 -particles of high density.

Some of the salts have very low solubility in acids (e.g., the iodates, peroxides, oxalates, fluorides, phosphates, complex sulfophosphates, ferrocyanides, and the double salt potassium thorium sulfate); these are used industrially to separate thorium. For more recent separation processes, the fact that thorium nitrate forms complexes with tributyl phosphate (TBP) and other organophosphates that are soluble in organic solvents is of great importance. These are useful for separating thorium from the rare earths (RE).

Although the readiness of the valence electrons to occupy the empty inner 5f shell is too small for any oxidation states other than 4 to be stable, it is deemed to be sufficient for covalent bonding. This gives thorium also a remarkable catalytic activity.

42.3 Occurrence and Raw Materials

Primary thorium deposits occur in acidic granitic magmas and pegmatites. They are locally concentrated, but of a small size. Secondary deposits are found in placer deposits at the mouths of rivers in granitic mountain regions (e.g., in India, Indonesia, and Brazil). In these deposits, thorium is enriched along with other heavy minerals.

Thorium, together with the related rare earths, is believed to have remained in the silicate layers during the phase separation of the earth because of their affinity for oxygen. Wherever these elements have not become bonded in the apatites formed in the initial crystallization, thorium became concentrated in the acidic residual magmas, especially in the nepheline syenite pegmatites, where it can be found at concentrations of ca. 80 mg/kg (Hungary) compared with the average level in granites (5–15 mg/kg Th). If these minerals

have been formed at high temperature, uranium is also present because of the isomorphism of UO_2 and ThO_2 , although at lower temperature in the presence of oxygen and water, uranium can migrate away as a hexavalent ion.

Since thorium minerals are attacked only slightly by reactive components of the atmosphere (e.g., oxygen, nitrogen) and by aqueous solutions, they have been deposited in a sedimentary sequence (monazite has a density of 4.3–5.6) along with other heavy minerals such as magnetite, rutile, cassiterite, garnet, ilmenite, and zircon in placer deposits, which sometimes also contain gold. If any thorium was present in the rivers in solution, it was precipitated together with dissolved iron as carbonate and fluoride on entering the sea.

Because of its low water solubility, thorium is scarcely present in water, soil, plants, or ani-

mals, even if the sand under a biotope contains thorium.

More than 100 different ores contain thorium minerals. The most important are listed in Table 42.3. No deposits exist that are worth extracting for thorium alone, so it is almost always extracted as a coupled product with the rare earths, which themselves can be a side product of the production of other heavy minerals when they are in the form of monazite from a gravity concentration process.

The most widely occurring and important mineral is monazite, a phosphate of rare earths and thorium, in which the content of individual metals varies with the origin of the mineral (Section 44.3). Typical compositions of monazite concentrates from five important deposits are given in Table 42.4 [12].

Table 42.3: Thorium minerals containing > 3% Th (mean value).

Name	Formula	Th content, %	Principal deposits
Oxides			
Thorianite	ThO_2	45.3–87.9	Sri Lanka
Uranothorianite	$(\text{U}, \text{Th})\text{O}_2$	15–48	Canada, Madagascar
Phosphates/silicates, carbonates			
Thorite	ThSiO_4	25.2–62.7	Langesundfjord (Norway)
Orangite	ThSiO_4		Madagascar, Idaho
Huttonite	ThSiO_4		New Zealand
Uranothorite	$(\text{U}, \text{Th})\text{SiO}_4$	20–42	Mid-Norway, Blind River (Canada)
Cheralite	$(\text{Ce}, \text{La}, \text{Pr}, \text{Nd}, \text{Th}, \text{Ca}, \text{U})(\text{PO}_4, \text{SiO}_4)$	25.9–27.7	Travancore (India)
Monazite	$(\text{Ca}, \text{La}, \text{Y}, \text{Th})\text{PO}_4$	3–26	India, Brazil, and most other deposits
Thorogummite	$\text{Th}(\text{SiO}_4)_{1-x}(\text{OH})_x$	18.2–50.8	Brazil, Jisaka (Japan)
Tscheffkinitite	silicates of RE, Fe, Mn, Mg, Ca, Al, Ti, Th, U	≤ 18.4	Madagascar
Pilbarite	$\text{PbO} \cdot \text{UO}_3 \cdot \text{ThO}_2 \cdot 2\text{SiO}_2 \cdot 4\text{H}_2\text{O}$	≤ 27.4	Western Australia
Allanite	$(\text{Ca}, \text{Ce}, \text{Th})_2(\text{Al}, \text{Fe}, \text{Mn}, \text{Mg})_3(\text{SiO}_4)_3\text{OH}$	≤ 3.2	Montana, Sri Lanka
Niobates/tantalates			
Pyrochlore	$(\text{Na}, \text{Ca}, \text{U}, \text{Th})(\text{Nb}, \text{Ta})_4\text{O}_{12}$	≤ 10	Colorado
Euxenite	$(\text{Y}, \text{Ca}, \text{Ce}, \text{U}, \text{Th})(\text{Nb}, \text{Ta}, \text{Ti})_2\text{O}_6$	≤ 4.5	Western Australia, Nigeria

Table 42.4: Composition of monazite concentrates (in %).

Constituent	India	Brazil	Florida beach sand ^a	South Africa Monazite Rock	Malagasy Republic
ThO_2	8.88	6.5	3.1	5.9	8.75
U_3O_8	0.35	0.17	0.47	0.12	0.41
$(\text{RE})_2\text{O}_3$ ^b	59.37	59.2	40.7	46.41	46.2
Ce_2O_3	(28.46)	(26.8)		(24.9)	(23.2)
P_2O_5	27.03	26.0	19.3	27.0	20.0
Fe_2O_3	0.32	0.51	4.47	4.5	
TiO_2	0.36	1.75		0.42	2.2
SiO_2	1.00	2.2	8.3	3.3	6.7

^a Florida beach sand contains about 70% monazite.

^b Rare earth oxides, including Ce_2O_3 .

The currently known and extracted deposits amounting to ca. 1.3×10^6 t are in India and Malaysia (30%); Egypt (20%); Canada and the United States (15%); and Brazil, Russia, and Australia (5%); the remainder is in Indonesia, Nigeria, Nyasaland, and South Africa. These deposits can meet the demand for the foreseeable future, so new deposits are not being sought.

The largest mining areas are in India in the province of Travancore, where the coastal sands over a distance of > 70 km contain monazite in the form of honey-yellow grains up to several millimeters in size.

The sands are usually subjected first to simple gravity concentration, which yields a concentrate containing 65–80% ilmenite (FeTiO_3), 3–6% rutile (TiO_2), zircon (ZrSiO_4), 1–5% sillimanite (Al_2SiO_5), and garnet [$(\text{Fe}, \text{Ca}, \text{Mg})_3\text{Al}_2\text{SiO}_4$], as well as some cassiterite (SnO_2) and a small amount of gold, together with 0.5–1% monazite.

42.4 Production [13]

The principal production stages are the concentration of thorium minerals, extraction of thorium from them, purification, and conversion to the metal or desired compounds, usually ThO_2 . Whereas up to 0.2% impurities, including rare earths, have no detrimental effects on conventional applications, nuclear technology demands a much lower level of impurities (by one or more orders of magnitude), especially of neutron-absorbing elements such as rare earths and boron, for which additional purification processes have been developed.

42.4.1 Concentration

42.4.1.1 Ore Preparation

The methods used for ore concentration are different for primary and secondary deposits. The process used by Molybdenum Corp. in the United States is described here as a typical example of beneficiation of a primary deposit. The pegmatites, which are usually obtained by

mining, are first coarsely and then finely ground. The ores are then subjected to a flotation process at 60 °C. This gives a 63% concentrate of rare earths and thorium. The alkaline-earth carbonates are dissolved out of this with HCl, further concentrating the ore to 73%. Thickening, filtration, and calcination yield a concentrate containing almost 90% Th and RE suitable for further processing.

For ore preparation from Indian coastal sands (*secondary deposit*), the sand is subjected to gravity separation on dredges just off the coast; i.e., the sand that is collected from the seabed is wet sorted in batteries of separators. Alternatively, after removal of the coarse fraction, the sand is sorted in a dry state on the coast. The second step is magnetic sorting using a series of magnets of increasing strength. Magnetite and ilmenite are first removed by the weakest magnets; garnet is removed by magnets of the next higher strength; and coarse and fine monazite is successively removed in the next two stages, the paramagnetism of monazite being due to its rare-earth content. The monazite concentrate obtained has a purity of up to 98%. Nonmagnetic residues are then usually treated by flotation to recover rutile, zircon, and gold, which are valuable by-products.

42.4.1.2 Ore Digestion and Thorium Recovery

Monazite is fairly inert chemically. The industrial chemical ore digestion process, which was started in the last century, was first based on the simplest possible methods (i.e., treatment with hot, concentrated sulfuric acid in cast iron vessels, followed by selective precipitation by dilution with water). Because of the low rate of solution and the simultaneous presence of rare earths, thorium, and the complexing ions phosphate and sulfate in the solution, only slight variation in operation was possible, and success depended on following the formulations precisely and also on the composition and grain size of the monazite. A number of other processes were therefore developed to avoid these problems. For eco-

nomie reasons, the only successful alternative method was to use alkaline digestion with hot sodium hydroxide solution. Although the process itself is a little more expensive than acid digestion, it removes phosphate and is therefore more suitable as a first stage before extractive separation to produce high-purity thorium. After some process development, it has been used mainly in the United States, India, and Brazil, where one of the target products is (or was) thorium of nuclear purity [14].

Acid Digestion

Digestion with sulfuric acid is usually carried out in two stages with 93% acid at 210–230 °C (see Figure 42.6). In the first stage, in which an acid excess of ca. 60% is used, the reaction mixture thickens as reaction products are formed—first to a slurry and then to a solid gray mass. Then, fuming sulfuric acid is added, and treatment is continued for additional 5 h at the same temperature. The acid concentration chosen is the result of a compromise between the reaction rate (which increases with concentration) and the viscosity (which also increases with concentration, thereby retarding the reaction). The completeness of the reaction depends on the grain size of the monazite sand, sand:acid ratio, temperature, and reaction time. Unfortunately, increasing the reaction temperature to 300 °C brings a risk of formation of insoluble thorium pyrophosphate and must therefore be avoided. Since the dissolution reaction is strongly exothermic, an upper limit exists to the rate of addition of monazite to the acid. In contrast, below 200 °C the reaction proceeds too slowly. If stoichiometric amounts of sand and acid could be used, the required amount of acid added would be only 60% of the sand mass. However, to keep the salts formed in solution and prevent blockage of the reactive surface of sand by the formation of precipitates, the mass of acid used must be twice the mass of sand (see Figure 42.7). To reduce acid consumption, reaction times of > 5 h are used to minimize the volume of solution after dilution. After the pasty mixture is cooled to 70 °C, it is diluted

with ten times its volume of cold water. The salts of rare earths and thorium remain in solution, while undissolved monazite rapidly settles out because of its high density. This can be recycled, and the finer and lower-density gangue materials are filtered off.

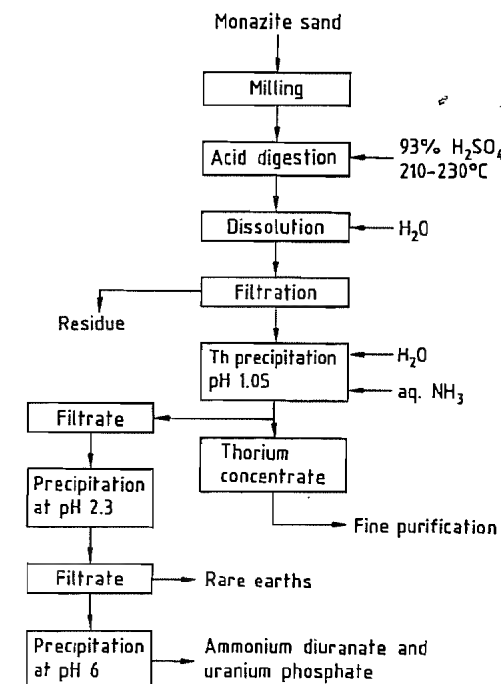


Figure 42.6: Digestion with sulfuric acid and thorium concentration.

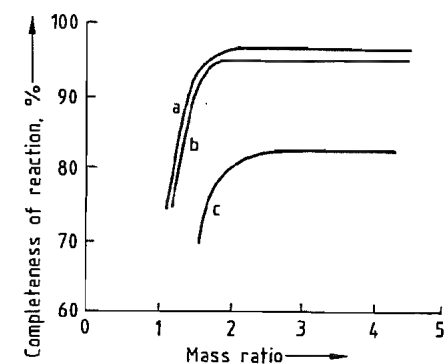


Figure 42.7: Effect of mass ratio of H_2SO_4 :monazite sand at 300 °C and 30-min digestion on completeness of reaction: a) Completeness of reaction of thorium fraction; b) Completeness of reaction of sand (overall); c) Completeness of reaction of uranium fraction.

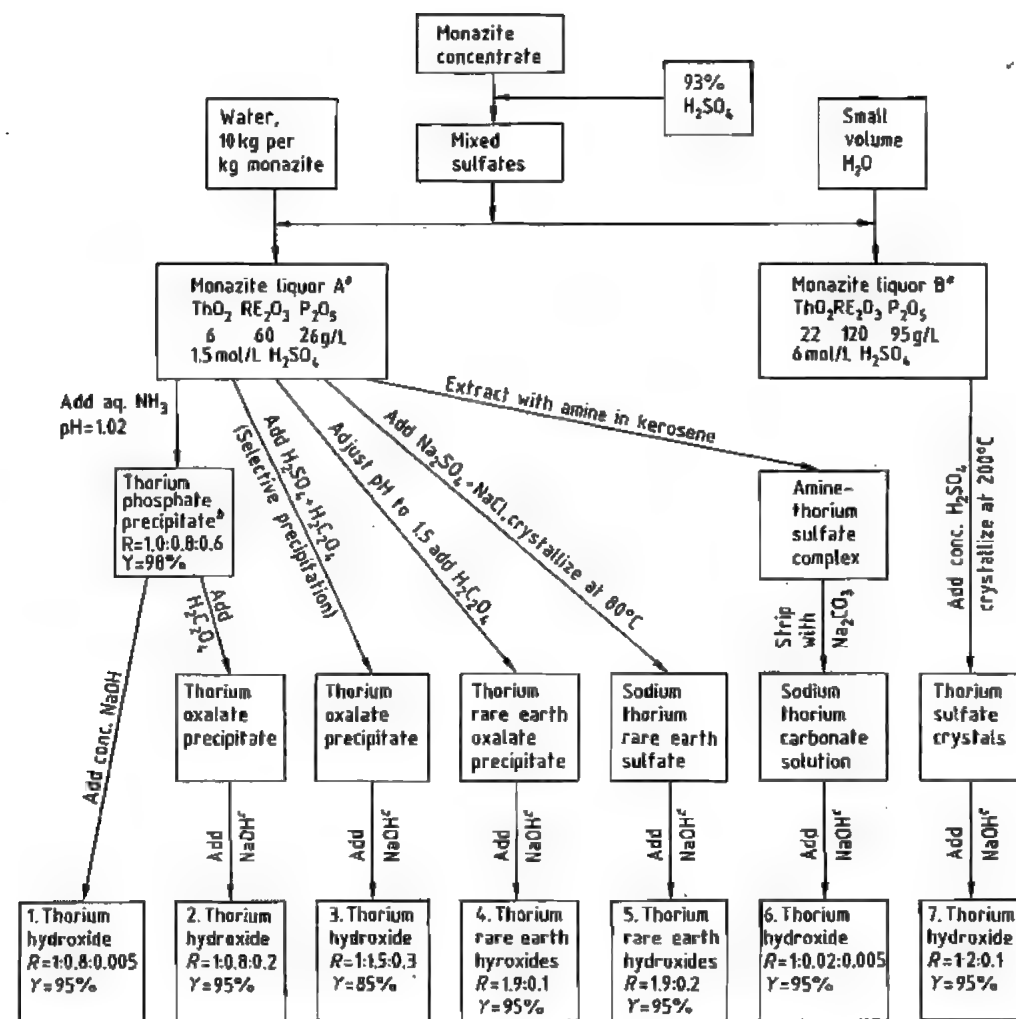


Figure 42.8: Principal processes for extracting thorium from monazite acid leach solution. R = Mass ratio $\text{ThO}_2:\text{RE}_2\text{O}_3:\text{P}_2\text{O}_5$; Y = Approximate overall ThO_2 yield in concentrate. ^a Filtered. ^b Washed. ^c 10% excess.

The subsequent separation of thorium and rare earths is based on the fact that thorium is almost completely precipitated as phosphate at pH values of ca. 1.3, while the main quantity of rare earths is precipitated later at a pH of ca. 2. Neutralizing agents such as sodium carbonate and ammonia must be added slowly and distributed homogeneously so that the pH limit is never exceeded, thus preventing local precipitation of rare earths, which do not redissolve. Furthermore, the slow rate of precip-

itation and the occlusive properties of the finely divided thorium precipitate must be kept in mind. The most uniform results would be obtained by diluting with pure water, but this is ruled out for practical reasons (i.e., excessive volume increase).

If the solution contains much uranium, simultaneous precipitation of thorium and rare earths by oxalic acid can be used—a selective, but expensive method of separation. Attempts have also been made to precipitate the rare

earths first as double sulfates by adding sodium sulfate; to selectively precipitate thorium along with uranium from the solution as peroxides; or to precipitate rare earths from the concentrated solution by phosphoric acid and then evaporate the solvent to achieve precipitation of thorium as a double salt (sulfate-phosphate) [15].

An overview of the principal proven process variations is given in Figure 42.8. None of the processes is sufficiently selective to be used without subsequent removal of the rare earths from thorium and vice versa. Also, sometimes one or more rare earths are the most marketable products and sometimes thorium is, the purity requirements being different in each case.

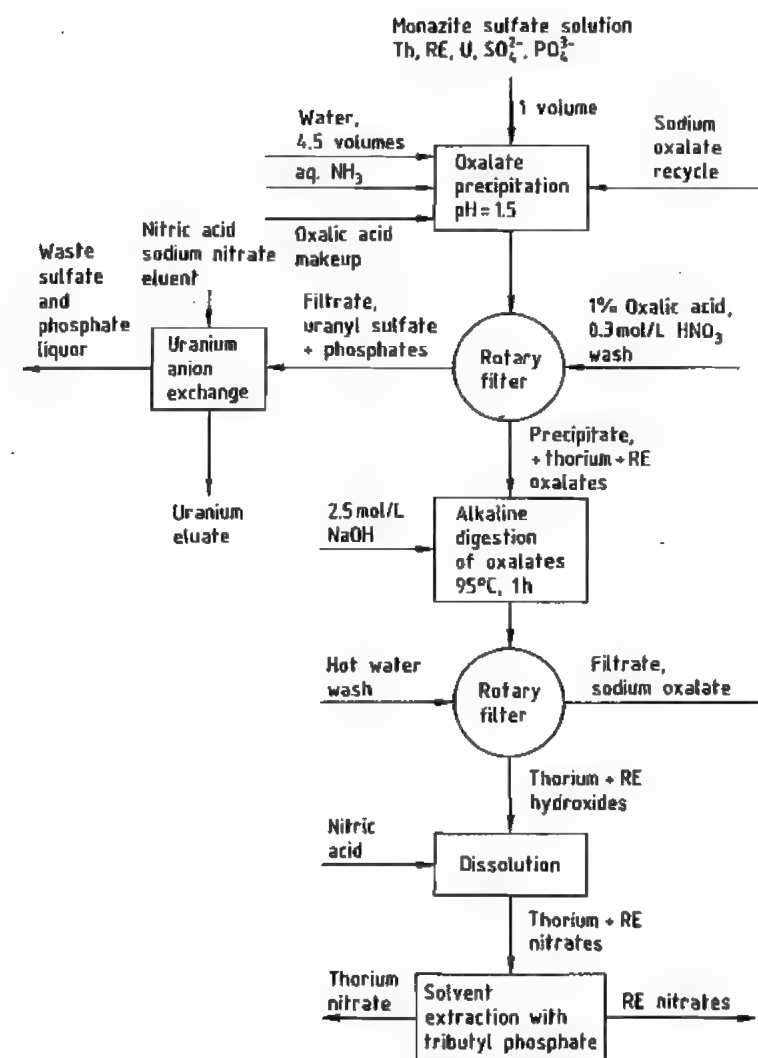


Figure 42.9: Iowa process for separating thorium, rare earths, and uranium from monazite sulfate.

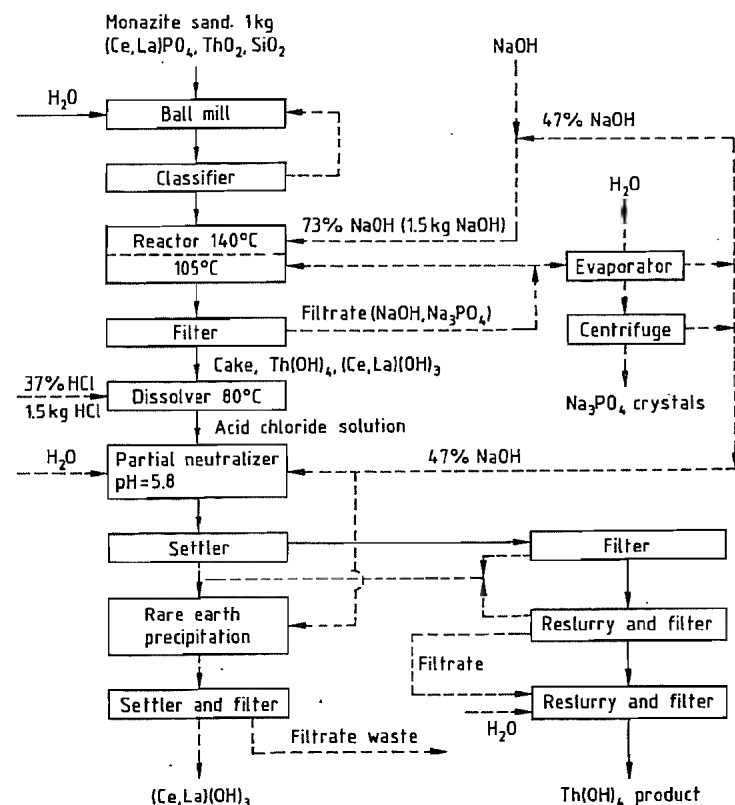


Figure 42.10: Caustic soda process for recovery of thorium from monazite.

In the early 1950s, interest in thorium of nuclear purity suddenly increased in the United States. This led to the development of the Iowa process in the Ames Laboratories of the USAEC [16] in which H_2SO_4 digestion was linked with purification by solvent extraction of the Th and RE nitrates with TBP. After acid digestion, phosphate and sulfate were removed by oxalate precipitation; the oxalates were digested with alkali to form hydroxide precipitates, which were subsequently dissolved in HNO_3 . The process was functionally reliable, but expensive, and produced a number of waste streams (variation 4 in Figure 42.8, with details in Figure 42.9).

Alkaline Digestion

As with acid digestion, treatment with sodium hydroxide solution (Figure 42.10) is lim-

ited by a number of factors. If the temperature is too high, a difficultly soluble thorium oxide is formed and too much uranium appears in the filtrate. If alkali concentrations are too low, the dissolution process takes too long. The optimum values appear to be 30–45% sodium hydroxide solution at ca. 140 °C and a reaction time of 3 h. However, these comparatively mild reaction conditions require finely ground monazite sand (particle size < 45 μm) to ensure adequate reaction. After filtration the filter cake contains rare earths and thorium as hydroxides and uranium as sodium diuranate; all of the phosphate is present in solution in the filtrate as trisodium phosphate. On cooling this below 60 °C, $\text{Na}_3\text{PO}_4 \cdot 10\text{H}_2\text{O}$ crystallizes. The uranium content of trisodium phosphate increases with the amount of dissolved SiO_2 , and it must be recrystallized before it becomes a saleable by-product.

Table 42.5: Distribution coefficients for uranium, thorium, and cerium between organic amines and aqueous sulfate solution.

Amine type	Examples of amines	Distribution coefficient ^a		
		U(VI)	Th(IV)	Ce(III)
Branched primary	primary JM ^b and 1-(3-ethylpentyl)-4-ethyloctylamine	5–30	> 20 000	10–20
Secondary with alkyl branching distant from the nitrogen	di(tridecyl)amine ^c	80	> 500	< 0.1
Secondary with alkyl branching on the first C	amberlite LA-1 ^d and bis(1-isobutyl-3,5-dimethylhexyl)amine	80–120	5–15	< 0.05
Tertiary with no branching or branching no closer than the third C	alamine 336 ^{e,f} and triisooctylamine ^{g,h}	140	< 0.03	< 0.01

^a 0.1 mol/L SO_4^{2-} ; pH = 1; = 1 g metal per liter; 0.1 mol/L amine in kerosene; 1:1 phase ratio.

^b Trialkylmethylamine, homologous mixture, 18–24 carbons.

^c Mixed C_{13} alkyls from tetrapropylene by oxo process.

^d Dodecyltrialkylmethylamine, homologous mixture, 24–27 carbons.

^e Trialkylamine with mixed *n*-octyl and *n*-decyl radicals.

^f Kerosene diluent modified with 3 vol % tridecanol.

^g Mixed C_8 alkyls from oxo process.

The hydroxides are dissolved in 37% HCl at 80 °C. After filtering off the undissolved material, 47% NaOH is added, and thorium along with uranium almost completely precipitates at pH 5.8. However, the alkaline filter cake must not be completely dried; otherwise, some Ce^{4+} is formed by contact with air, and this liberates chlorine from HCl. The rare earths are precipitated by further increasing the pH. Neutralization can be carried out with NaOH residues from the filtrate from alkaline digestion, provided concentrations of phosphate are low enough as not to precipitate insoluble RE phosphates.

If thorium and uranium are to be separated from rare earths by solvent extraction, the filter cake from alkaline digestion is preferably dissolved immediately in HNO_3 . However, complete dissolution of thorium cannot always be guaranteed, especially in the presence of titanium hydroxides, which bind large amounts of thorium. The good solubility of ThO_2 at 10 bar and 230 °C in HNO_3 was only discovered in 1986 [17], and has hitherto not yet been utilized on an industrial scale.

42.4.2 Fine Purification by Solvent Extraction

In recent decades, purification of chemically similar substances by techniques involving repeated transitions between solid and liquid phases has been replaced by technologi-

cally simpler liquid–liquid extractions. At the same time, purity requirements for thorium and its compounds have become more strict. Especially in nuclear technology, concentrations of elements with a high parasitic neutron capture cross section must be low. (For example, the maximum permitted concentrations equivalent to 4 mg/kg boron are only 8 mg/kg Sm, 2 mg/kg Er, or 1 mg/kg Gd.) Thus, the process of multiple solution and precipitation or recrystallization to separate rare earths from each other or from thorium and uranium has been replaced by multistage countercurrent solvent extraction methods. However, to give suitable distribution coefficients between the aqueous and organic systems, the chemical bonding of the ions that take part in the exchange must not be too different in the two systems. Thus, stable complexes of thorium and uranium that are soluble only in water, especially those with sulfate and phosphate ions, are unsuitable.

Hence, attempts to extract thorium and uranium directly from monazite sulfate solutions with TBP in organic solution were unsuccessful. Only the use of extraction media with strongly cationic character enabled successful extraction from these solutions to be carried out. Whereas the anionic character of UO_2^{2+} is strong enough for it to bond to quaternary nitrogen (in amines dissolved in organic solvents), the situation is less favorable in the

case of Th^{4+} . Some distribution coefficients are given in Table 42.5, which also shows the clear difference between thorium and uranium. This difference favors branched primary amines.

Amex Process. The use of a combination of different amines in three consecutive cycles (see Figure 42.11) is the basis of the prototype scale Amex process [18], which enables pure products (U, Th, RE) to be obtained directly from diluted solutions of monazite in sulfuric acid. However, in the absence of any large demand, this flow scheme has not yet been tested on a full scale.

Solvent Extraction with TBP. In the absence of phosphate ions (e.g., in the case of oxidic and carbonate-containing thorium ores) or if phosphate ions have been previously removed in the alkaline treatment method, the U, Th,

and RE nitrate complexes can be separated and purified by extraction with TBP in an organic solvent, preferably in kerosene. The overall process is simple and easily controlled. The effect of the molarity of nitric acid on the distribution coefficients of rare earths, uranium, and thorium is shown in Figure 42.12. With a mean acid concentration of 3 mol/L, the distribution coefficient (organic/aqueous) for rare earths is 0.02, for thorium 1, and for uranium 20, so that a multistage separation is possible [19]. Trivalent metallic ions such as Fe^{3+} can mask residues of phosphate. A suitable flow scheme is shown in Figure 42.13. Solvent extraction, which is optional in the purification of natural thorium compounds, is the only feasible method of separating thorium, ^{233}U , and fission products after irradiation in a reactor.

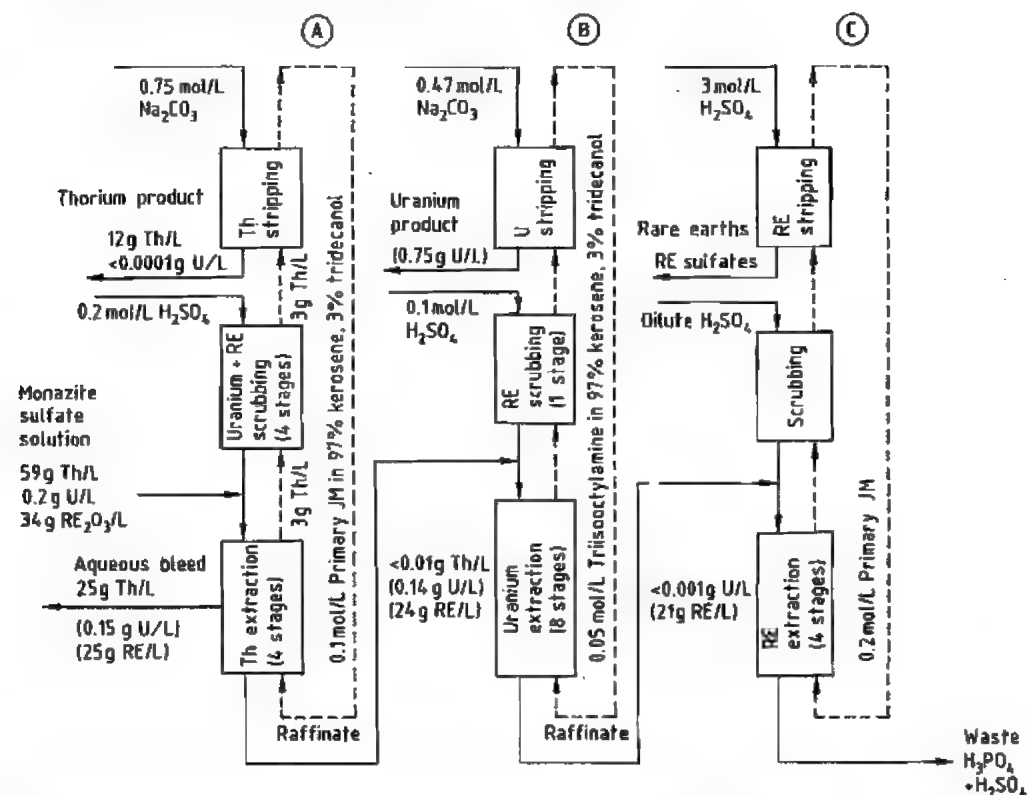


Figure 42.11: Separation of thorium, uranium, and rare earths from monazite by solvent extraction in Amex process. A) Thorium separation; B) Uranium separation; C) Rare earth separation.

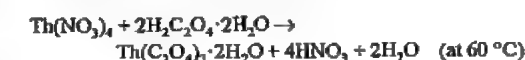
Canadian Blind River district), thorium is extracted with di(2-ethylhexyl)phosphoric acid.

42.5 Compounds

42.5.1 Oxides [20]

Two compounds, ThO and ThO_2 , exist in the oxygen-thorium system. The black compound ThO , which crystallizes with the sodium chloride lattice, is known only from coatings on the metal. It is probably an interstitial compound with an electron deficit structure. When ThO_2 is heated in an electric arc, ThO band structures appear in the spectrum.

The compound ThO_2 is the stable, well-known oxide, being formed if either a salt that contains a volatile anion or the oxidaquate is strongly heated. It is obtained as a very fine powder by precipitating and then strongly heating thorium oxalate, according to



and

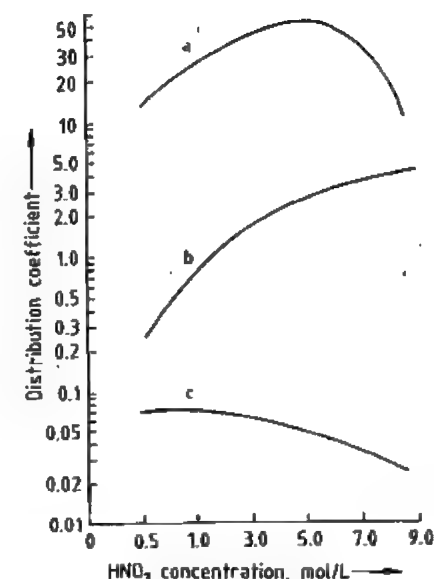
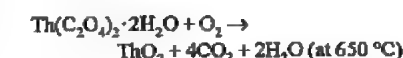


Figure 42.12: Effect of acid molarity on distribution coefficients (organic-aqueous phase) of nitrate complexes in TBP-kerosene extraction: a) Uranium; b) Thorium; c) Rare earths.

In an intermediate route that can be used in the presence of high concentrations of sulfate but in the absence of phosphate (e.g., in residual solutions from uranium extraction in the

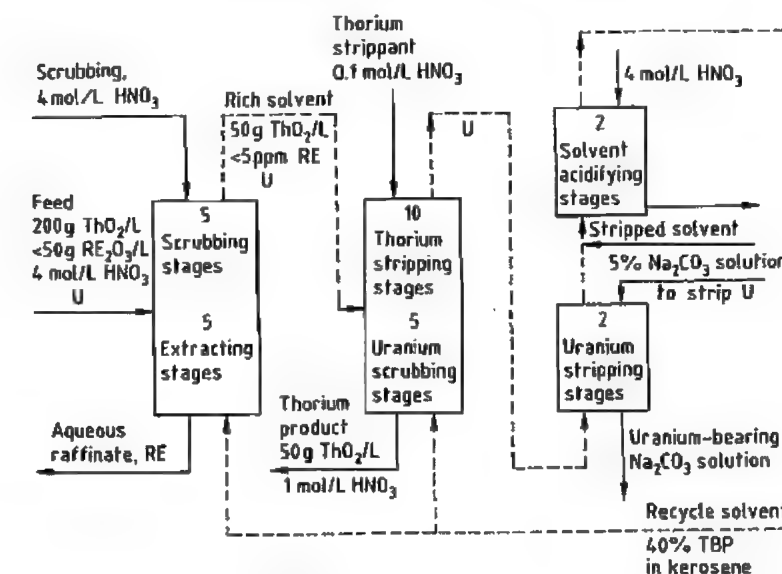


Figure 42.13: Thorium purification by solvent extraction with TBP — Aqueous phase; --- 40 vol% TBP in kerosene.

At pH 1 and with careful temperature control, the reaction with oxalic acid leads to a crystalline precipitate with good filtering properties. Precipitation can be carried out selectively also in the presence of trivalent metals, uranium, and titanium. Several other 1,2-dicarboxylic acids have been tested as alternatives, but only tetrachlorophthalic acid gave significantly improved selectivity against the rare earths [21].

The structure, decomposition temperature used, and calcination temperature can affect the rate of reaction of ThO_2 in other reactions. For example, ThO_2 freshly prepared by low-temperature thermal decomposition of thorium oxalate (meta- ThO_2) is catalytically active and fairly soluble in acids, whereas thorium oxide calcined at high temperature is very slowly attacked by acids. It can be dissolved only in hot, concentrated H_2SO_4 or in concentrated HNO_3 in the presence of F^- ions. Physical properties of ThO_2 are listed below [22]:

Color	white
Crystal system	face-centered cubic
Density (X ray, 25 °C)	10.00 g/cm ³
Linear expansion from 25 °C	9×10^{-3} at 1000 °C 20×10^{-3} at 2000 °C
Thermal conductivity (100 °C)	0.10 W cm ⁻¹ K ⁻¹
(600 °C)	0.04
Melting point	3370 ± 30 °C
Entropy (25 °C)	65.3 J K ⁻¹ mol ⁻¹
Heat of formation from elements (25 °C)	-1227.6 kJ/mol
Free energy of formation from elements (25 °C)	-1170.0 kJ/mol

The vapor pressure (atm) between 2180 and 2865 K can be calculated according to:

$$\log p = 8.00 - 3517/T$$

(ThO_2 dissociates partially into ThO and O_2 ; at low oxygen pressure the vapor pressure is somewhat higher.) The temperature dependence of the molar heat capacity (J/mol) between 298 and 3000 K is

$$C_p = 69.3 + 9.71 \times 10^{-3}T - 9.19 \times 10^{-5}T^2$$

Two crystal forms are known, i.e., a tetragonal modification similar to rutile that crystallizes from borate melts and a cubic form that crystallizes from phosphate melts. The lattice constants and densities are very similar

to those of the metal since the oxygen occupies interstitial locations. However, these densities are not reached by sintered oxides (maximum values: ca. 10.2 g/cm³). Thorium dioxide melts at 3370 °C and thus has the highest melting point of all ceramic materials. The tendency of meta- ThO_2 to form colloidal solutions (thorium oxidaquate) in the presence of nitrate ions is important, because these can be dried to form stable gels that can be sintered to give high-density ceramic bodies. Another important property of ThO_2 is the emission of long-wave red light on heating (a historical test of purity), and the shifting of the emitted wavelength further into the visible region by the addition of rare earths, especially cerium, which is an essential feature of gas mantle technology (see Section 42.9.2 for further details).

Coatings of ThO_2 on tungsten are used to promote the emission of electrons from incandescent cathodes. These coatings must be thin and uniform; they are produced by a simple process of dipping the cathodes into suspensions of thorium oxidaquate and various finely dispersed thorium oxide slurries or by electrophoretic deposition of the oxide from alcoholic suspensions. They must be "formed" by heating the cathodes to 2900–3000 °C.

Thorium oxide forms mixed crystals with a number of oxides of the actinides (e.g., U, Np, and Pu), with no miscibility gap. No phase transformation occurs up to the melting point.

When ThO_2 is used to form ceramics, for dimensional accuracy of the preformed bodies (crucibles, nuclear fuel pellets) the powders used must shrink by a small but definite amount during sintering/densification. Choice of the powder involves a compromise between less good sintering properties and minimized shrinkage. The meta- ThO_2 is preferably precalcined in an atmosphere of steam at 800–1000 °C before it is formed by pressing or slip casting. The effect of precipitation temperature and calcination temperature on the specific surface area of the powder is shown in Figure 42.14 [23].

Table 42.6: Physical properties of thorium tetrahalides.

Property	ThF_4	ThCl_4	ThBr_4	ThI_4
Color	white	white	white	yellow
Density at 25 °C, g/cm ³	6.12	4.62	5.72	6.00
Crystal system	monoclinic	tetragonal	orthorhombic	monoclinic
Low-temperature form		orthorhombic	tetragonal	orthorhombic
High-temperature form		(406)	≈ 420	?
Transition temperature, °C				
Melting temperature, °C	1110	770	679	570
Normal boiling point, °C	1782	942	905	853
Vapor pressure, atm				
$\log p = A - B/T$				
Solid, A	9.345	9.426	9.498	9.747
B, K	17 089	10 630	10 151	9894
Liquid, A	6.395	5.229	5.260	5.714
B, K	13 080	6346	6187	6425
Heat capacity, $C_p = A + 10^{-3}BT - 10^{-5}CT^2$				
Solid, A, J mol ⁻¹ K ⁻¹	112.0	120.4	127.7	129.8
B, J mol ⁻¹ K ⁻¹	24.51	23.84	15.1	13.0
C, J mol ⁻¹ K ⁻¹	7.56	6.15	6.15	6.15
Liquid, J mol ⁻¹ K ⁻¹	152.8	167.5	171.7	175.9
Heat of transition, J/mol		5.02	4.2	?
Heat of fusion, kJ/mol	44.0	61.5	(54.4)	48.1
Heat of vaporization at normal boiling point, kJ/mol	233.2	?	111.0	115.1
Heat of formation at 25 °C, kJ/mol	-2112.8	-1187.4	-966.3	-664.9
Free energy of formation $\Delta G = A + BT$				
Solid, A, kJ/mol	-2102.5	-1177.0	-1019.3	-783.1
Solid, B, J mol ⁻¹ K ⁻¹	293.6		283.5	290.8
Liquid, A, kJ/mol	-2031.0	-1093.3	-942.9	-716.0
B, J mol ⁻¹ K ⁻¹	240.3	201.4	211.7	210.4

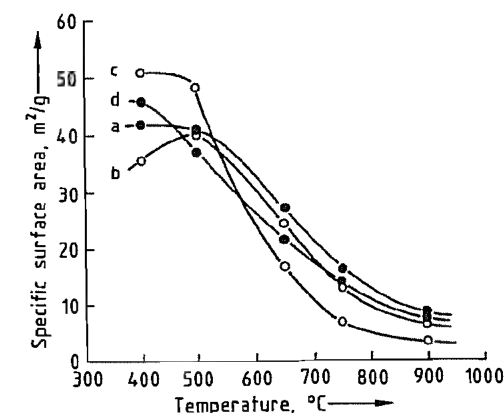


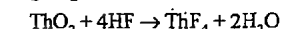
Figure 42.14: Effect of temperature on the specific surface of thorium oxide from thermal decomposition of thorium oxalate: a) 40% Precipitation; b) 10% Precipitation; c) 100% Precipitation; d) 70% Precipitation.

42.5.2 Halides

An overview of the properties of thorium halides is given in Table 42.6.

42.5.2.1 Tetrafluoride

Precipitation of thorium salt solutions with HF leads to the formation of gelatinous, white precipitates of ThF_4 hydrates with 8, 4, or 2 molecules of water of crystallization, but these hydrolyze to form mixtures of ThO_2 and ThOF_2 even on careful drying. Anhydrous ThF_4 can be obtained only by fuming ThF_4 hydrates many times with NH_4F or by dehydration in a stream of dry HF at 300–400 °C. Thorium tetrafluoride is therefore produced industrially by reaction of ThO_2 and HF in the gas phase:



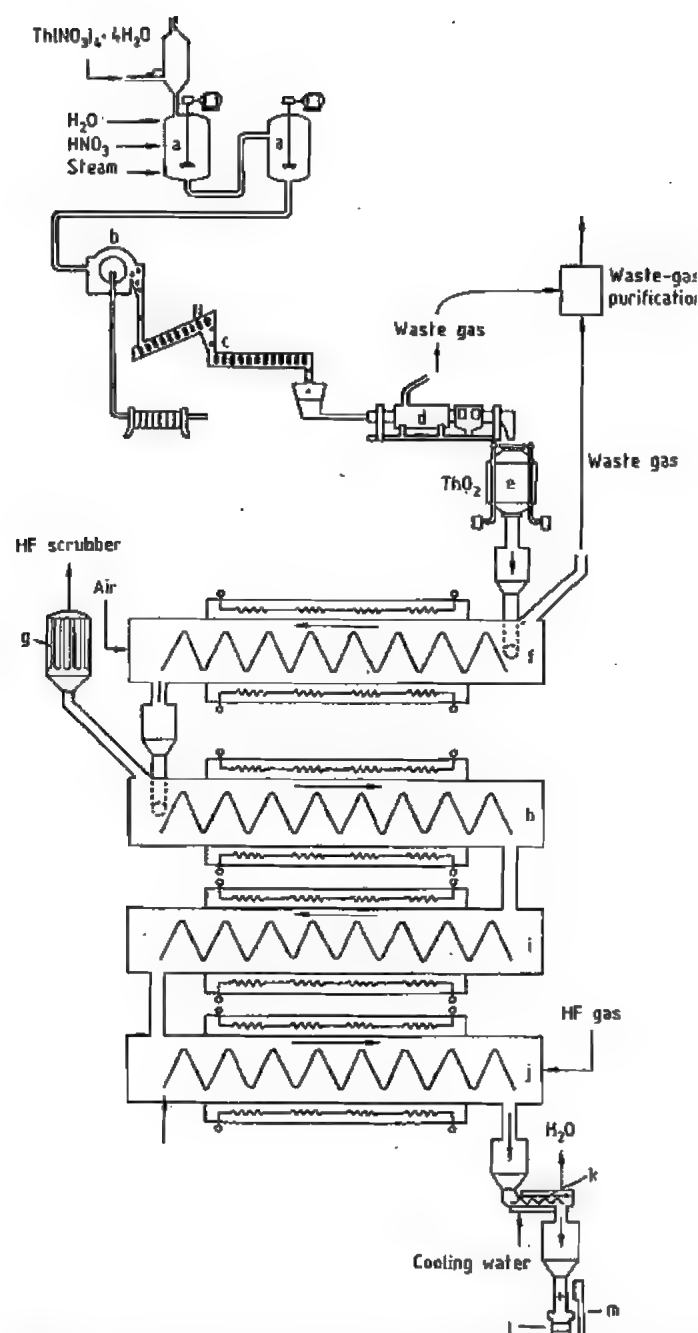


Figure 42.15: Production of ThF_4 by calcination and fluorination: a) Thorium oxalate precipitation; b) Drum filter to filter off $\text{Th}(\text{C}_2\text{O}_4)_2$; c) Band dryer; d) Calcination; e) Weighing; f) Calcination ($650\text{--}675^\circ\text{C}$); g) HF scrubber; h) Hydrofluorination (370°C); i) Hydrofluorination (370°C); j) Hydrofluorination (566°C); k) Cooling trough; l) ThF_4 collector; m) Weighing.

At 566°C the reaction is exothermic and at first proceeds rapidly, but thermodynamic equilibrium is attained very quickly, leaving an unreacted excess of HF. At lower temperature, the reaction goes to completion but proceeds much more slowly. A schematic of the production of thorium fluoride from the nitrate via the oxalate, as carried out by the National Lead Company (Fernald, Ohio), is shown in Figure 42.15 [11, p. 153]. The plant consists of four stainless steel tubular reactors arranged in series, each provided with exterior heating and interior screw conveyors made of Inconel. A countercurrent flow system with graded temperature increases utilizes HF to give complete conversion of ThO_2 . However, to obtain ThF_4 that does not contain oxide-fluoride, it was necessary to use excess anhydrous HF and produce and sell by-product aqueous HF (70%). New plants will probably be operated as fluidized-bed reactors following experience with uranium.

Thorium tetrafluoride is formed as a solid residue when enriched $^{235}\text{UF}_6$ is stored. The ^{234}U contained in uranium, which is also enriched, decays to form $^{230}\text{ThF}_4$. This remains behind after steaming out the UF_6 container and must be scrupulously removed because of its high α -toxicity.

In the electrolytic production of thorium from a fluoride melt, the double fluoride KThF_5 can be used as the starting material. The KThF_5 can be precipitated by adding KF to a solution of thorium nitrate according to

$$\text{Th}(\text{NO}_3)_4 \cdot 4\text{H}_2\text{O} + 5\text{KF} \cdot 2\text{H}_2\text{O} \rightarrow \text{KThF}_5 + 4\text{KNO}_3 + 6\text{H}_2\text{O}$$

and is dried at 120°C to give a product free of water of crystallization.

42.5.2.2 Tetrachloride

Depending on conditions, thorium tetrachloride crystallizes from aqueous solution with 11, 9, 8, 7, 4, or 2 molecules of water of crystallization, but oxide-chlorides are formed on drying. Anhydrous ThCl_4 , like anhydrous ThF_4 , can be produced only by reaction in the gas phase. All reactions that simultaneously reduce and chlorinate ThO_2

are suitable (see overview in Table 42.7), for example, chlorination of a mixture of ThO_2 and C above 600°C :



Table 42.7: Reaction of chlorine and ThO_2 with reducing agents.

ThO_2 type	Reducing agent	Temp., $^\circ\text{C}$	Time, h	Yield, %
$\text{Th}(\text{C}_2\text{O}_4)_2$	carbon	700	2	99
	CCl_4	800	4	10
$\downarrow > 675^\circ\text{C}$	sulfur	800	2	98
ThO_2	C_2Cl_6	400	5	25
	NH_4Cl	425	4	0
$\text{Th}(\text{C}_2\text{O}_4)_2$	carbon	600	2.5	99
	CCl_4	300	5.5	92
$\downarrow 445 \text{ to } 525^\circ\text{C}$	sulfur	500	3	99
ThO_2	C_2Cl_6	400	4	92
	NH_4Cl	500	1.5	99

Because the ThCl_4 formed contains carbon as an impurity, it must be distilled at 942°C . This step is complex due to the very hygroscopic and aggressive nature of the chloride. Distillation is not necessary if thorium oxalate is chlorinated with CCl_4 with a small addition of chlorine as a catalyst according to



The reaction is carried out at temperatures up to 525°C in several stages in a graphite reactor.

42.5.2.3 Tetraiodide

Thorium tetraiodide has an intense yellow color, an mp of 566°C , and a bp of 837°C , and can be produced by reaction of the elements. Thorium tetraiodide reacts with excess thorium to give subiodides of trivalent and divalent thorium, depending on the relative amounts of reactants and the temperatures and pressures used. Like the other halides, it can in principle be produced by reaction of intimate mixtures of carbon and ThO_2 with elementary iodine. In the production of pure metallic thorium, the main use of ThI_4 is not isolated as a separate product but is used only as an intermediate for gas-phase matter transfer between crude and pure thorium in the van Arkel-de Boer process [24].

42.5.3 Other Compounds

Thorium Nitrate. The compound from which almost all other thorium compounds are produced is thorium nitrate, $\text{Th}(\text{NO}_3)_4 \cdot 6\text{H}_2\text{O}$, which is highly soluble in water at room temperature (65%). Evaporation of the aqueous solution yields the tetrahydrate (one of seven hydrates) in the form of a finely crystalline white powder [25].

Thorium Hydrides. The hydrides ThH_2 and ThH_4 are known. On reduction of ThO_2 with excess magnesium in the presence of H_2 , a somewhat substoichiometric, highly flammable powder is formed, which is isomorphic with ZrH_2 and pseudoisomorphic with ZrC_2 and ThC_2 . The other compound, which is also substoichiometric, $\text{ThH}_{3.75}$, has a cubic crystal structure that does not resemble that of the metal. Both compounds can be used to produce finely divided thorium metal since they release all their hydrogen at 900 °C. Anhydrous thorium halides can be obtained by reaction of the hydrides with hydrogen halides.

Thorium hydroxide, $\text{Th}(\text{OH})_4$, is formed by precipitation from solutions of salts by adding alkali. This compound is not a true hydroxide, but an oxidaquate ($\text{ThO}_2 \cdot x\text{H}_2\text{O}$), a stable colloid that remains amorphous up to 340 °C.

Thorium peroxide, $\text{Th}_2\text{O}_7 \cdot 4\text{H}_2\text{O}$, is formed as a sparingly soluble precipitate when H_2O_2 is added to thorium salt solutions. Only the actinides react in this way. The reaction can be used to separate thorium from the rare earths.

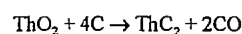
Thorium Nitrides. The compounds Th_2N_3 and ThN are known. The first, Th_2N_3 , is a hexagonal, dark red compound, which is formed from the elements, and decomposes in the presence of water to form NH_3 and ThO_2 .

ThN has the face-centered cubic structure like the nitrides of uranium, lanthanum, and cerium, in which nitrogen has a quasimetallic character similar to that of carbon.

Thorium Phosphide and Borides. The corresponding phosphide ThP_4 is stable toward all the usual solvents. The two borides ThB_4 and

ThB_6 are also very stable, hard materials, the latter forming dark red crystals.

Thorium Carbides. The mono- and dicarbide exist, although both compounds have a substoichiometric composition (i.e., 0.97 and 1.90). The monocarbide crystallizes with a face-centered cubic structure. The dicarbide is monoclinic up to 1410 °C and tetragonal above this temperature. The densities of ThC and ThC_2 are 9.6 and 8.76, respectively, and the melting points 2500 °C and 2640 °C. Depending on the availability of carbon, the carbides are formed readily from the elements or by reaction of an intimate mixture of graphite and thorium oxide at 1400 °C:



ThC has a metallic appearance and a thermal conductivity comparable to that of thorium metal. The dicarbide is readily oxidized to ThC at high temperature in the presence of oxidic substances. Partial mutual substitution of O_2 , N_2 , and carbon is possible, leading to relatively thermally stable compounds of the type $\text{Th}(\text{O}_{1-(x+y)}\text{C}_x\text{N}_y)$ when the sum of x and y is < 0.6 . The formation of solutions of carbon in thorium is described in Section 42.8.1.

Thorium sulfides are not readily formed from aqueous solution, but are formed by reaction of the elements. The compound ThS , which has a metallic appearance, is formed first and then converted in several stages to ThS_2 via the orthorhombic Th_4S_7 and other intermediates.

Thorium sulfate is important mainly because it is formed when monazite is digested with H_2SO_4 . Thorium sulfate forms five different hydrates, which contain up to nine molecules of water of crystallization. Also, sparingly soluble double salts are formed with alkali-metal sulfates.

Thorium Carbonate. When thorium salt solutions react with alkali-metal carbonate, a poorly defined basic carbonate of the type $\text{ThOCO}_3 \cdot 8\text{H}_2\text{O}$ precipitates. It dissolves in an excess of alkali-metal carbonate (similarly to the corresponding uranium) to form relatively stable complex double carbonates of the type

$\text{Na}_6\text{Th}(\text{CO}_3)_5$ or $(\text{NH}_4)_2\text{Th}(\text{CO}_3)_3 \cdot 6\text{H}_2\text{O}$. Thorium hydroxide does not precipitate from solutions of these substances.

42.6 Production of Pure Thorium Metal

Because of thorium's strongly negative standard electrode potential, its compounds cannot be reduced to the metal with carbon or hydrogen. The route to thorium metal is therefore reaction of the oxide or a halide with metals, electrolysis in molten salts, or thermal decomposition of a halide. The principal reactions that have led to production processes are summarized below:

- Electrolysis of fused salts:
 KThF_5 in NaCl
 ThF_4 in NaCl-KCl
 ThCl_4 in NaCl-KCl
- Reduction with reactive metals:
 ThO_2 with Ca
 ThCl_4 with Mg
 ThF_4 with Ca
- Thermal dissociation of ThI_4

The results of the processes are listed in Tables 42.8–42.11 [11, pp. 170–171].

The tolerable impurity level of intermediate products to be met when thorium metal is used in the nuclear industry are given in Table 42.12. In the production of thorium metal, problems arose because of its highly reactive nature and sensitivity to both air and moisture, as well as its high melting point (1750 °C). The following four production methods have been tested on a full scale.

Reduction of ThO_2 with calcium metal was first carried out in the United Kingdom at 1200 °C on a pilot plant scale in a reactor lined with CaO . In the United States, the reaction was carried out in molten CaCl_2 in an argon atmosphere to provide a more coarse-grained product, the heat of reaction being insufficient to melt the thorium. Both processes give thorium sponge, which requires many further

processing stages. These production processes were abandoned because of the high temperatures required and the cost of the apparatus.

Fused Salt Electrolysis. In fused salt electrolysis, KThF_5 is used as a 15–20% mixture with NaCl to give a eutectic. Thorium is produced in an argon atmosphere as a nonadherent finely crystalline powder deposited on molybdenum cathodes in graphite cells at 900 °C, using a current density of 20 A/dm². In fused salt electrolysis, only Cl_2 is formed at the anode, and the buildup of thorium powder in the electrolysis vessel causes short circuits. Thus, batchwise operation must be used. A continuous method of operation is possible if ThCl_4 is used in a mixture of NaCl and KCl as electrolyte at 800 °C with strict exclusion of moisture. A very pure, coarse-grained thorium metal is obtained. Plants of this type were operated briefly in the United Kingdom, the United States, and the Soviet Union.

Table 42.8: Production of thorium metal by reduction of halides or double halides.

Thorium halide	Reducing agent	Product
ThCl_4	Na or K	Th powder
KThCl_5	Na or K under H_2 atmosphere	Th powder
NH_4ThCl_5	Al	alloy
ThCl_4 (70%) in ThOCl_2 (30%)	Ca	powder
ThCl_4	Mg	powder
ThCl_4	$\text{Na}(\text{Hg})_x$	Th–Hg alloy
ThF_4	Ca with ZnCl_2 booster	Zn–Th alloy biscuit (sponge)

Table 42.9: Production of thorium metal by reduction of the oxide.

Thorium source	Reducing agent	Product
ThO_2	Mg	impure alloy
ThO_2	Al	Th beads
ThO_2	Ca	Th powder
ThO_2	Ca and CaCl_2	Th powder

Table 42.10: Production of thorium metal by thermal decomposition of halides.

Thorium source	Reducing agent	Product
ThI_4	hot-wire technique	crystal bar of thorium
	$\text{ThI}_4 \xrightarrow{\text{heat}} \text{Th} + 2\text{I}_2$	

Table 42.11: Production of thorium metal by electrolytic methods.

Thorium source	Electrolyte	Product
Aqueous solution		
Th(OH) ₄	HBF ₄	?
Thorium salts	HSO ₃ ·NH ₂	?
Organic solution		
Thorium salts	C ₂ H ₅ OH, CH ₃ OH, and other alcohols	thorium organic compounds
Complex Th salts	organic acids	?
Th(NO ₃) ₄	C ₂ H ₅ O with 15–20% Me ₂ CO ₃	ThO ₂
Fused salt solution		
ThCl ₄	KCl–NaCl	Th with ThO ₂ and C
KThF ₆	NaCl–KCl	Th powder
KThF ₆	NaCl	Th powder
ThCl ₄	NaCl and KCl–NaCl	Th powder
ThF ₄	NaCl–KCl	Th powder or Th in liquid Zn cathode

Table 42.12: Typical analyses of pure thorium products.

Element	Th(NO ₃) ₄	ThO ₂	ThF ₄
Th, % ^a	40.3	86	75.4
U, mg/kg ^a	8	2.5	16.3
Traces, mg/kg ^b			
Al	13	< 10	< 10
B	5.5	0.4	1.2
Ba	< 20	< 20	< 20
Be	< 1	< 1	< 1
Bi	< 2	< 2	< 2
Ca	< 200	< 200	< 200
Cd	< 0.2	< 0.2	< 0.2
Co	< 1	< 1	< 1
Cr	< 4	8.1	38
Cu	2	46	81
Fe	26	46	161
Mg	25	8	24
Mn	< 1	2	6
Mo	< 1	< 1	5
Ni	3	15.6	338
P	< 40	< 40	< 40
Pb	2	27	24
SiO ₂	109	207	33
Sn	< 1	6	< 1
V	< 10	< 10	< 10
Zn	< 10	< 10	29

^a Chemical analysis.^b Spectrochemical analysis.

Thermal decomposition of ThI₄ yields an extremely pure, ductile thorium metal. Thorium iodide is usually produced from impure metal pieces, which are first heated in a muffle furnace to > 500 °C for 24 h in a vacuum, and then reacted with iodine vapor, which is vaporized at 260 °C. Thorium iodide is formed between 450 and 480 °C, and purified by distillation. Thorium metal is deposited from the iodide on incandescent filaments of tungsten

or thorium at 900–1700 °C. The temperature range between 500 and 900 °C must be avoided because the tetraiodide decomposes to form thorium and nonvolatile ThI₃ at a little over 600 °C. The total reaction (formation of ThI₄ and decomposition) is carried out in long, stationary, heated tubes filled with iodine vapor. Concentric perforated sheet metal tubes retain unreacted pieces of crude thorium at the walls of the tube, and pure thorium is deposited on heated filaments at the center. The thickness of the thorium rod that forms in the center is limited only by the electric current used, which eventually reaches several hundred amperes. Both decomposition of the iodide and electrolysis give very pure metal, but these processes do not give high throughputs or yields in the present state of the technology.

Reduction of Halides. The larger quantities of thorium metal used in the nuclear industry are produced on an industrial scale mainly by the reduction of halides. The fluoride and chloride are not equivalent, as can be seen from the reaction enthalpies (Table 42.13). Thorium fluoride can be reduced only by calcium, whereas a choice of sodium, calcium, and magnesium exists for the reduction of the chloride. Two processes were developed in the United States almost simultaneously: the reduction of ThCl₄ with sodium amalgam (Metallex process, Oak Ridge, 1954 [26]) and reduction with magnesium in the Kroll process, which was favored because of the price of magnesium and its lower sensitivity to oxygen (1956).

Table 42.13: Free-energy change in reduction of thorium compounds to metallic thorium.

	Oxide	ThF ₄	ThCl ₄			
Reaction temperature T, K	1223	2023	1150			
Free energy of formation from elements at T, kJ/mol	ThO _{2(s)}	-998.4	ThF _{4(s)}	-1545.7	ThCl _{4(s)}	-831.8
	2Na ₂ O _(s)	-487.7	4NaF _(s)	-1303.0	4NaCl _(s)	-1219.7
	2MgO _(s)	-934.4	2MgF _{2(s)}	-1472.1	2MgCl _{2(s)}	-931.9
	2CaO _(s)	-1015.7	2CaF _{2(s)}	-1774.5	2CaCl _{2(s)}	-1241.2
Free-energy change in reaction, kJ/mol						
Th reduced with						
4 mol Na		+510.6	+243.4		-357.9	
2 mol Mg		+64.0	+73.6		-70.1	
2 mol Ca		-17.3	-255.5		-379.4	

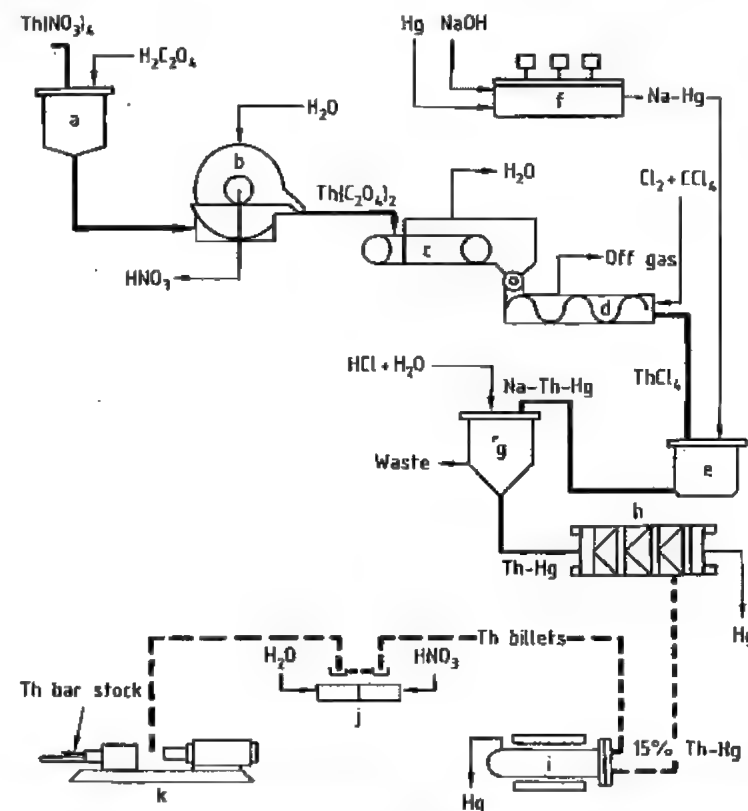


Figure 42.16: Schematic of Metallex process: a) Precipitator; b) Filter; c) Dryer; d) Chlorinator; e) Contractor; f) Electrolyzer; g) Scrubber; h) Hydraulic filter press; i) Retort; j) Pickler and washer; k) Extrusion.

Metallex Process. The flow diagram of the Metallex process, which requires relatively simple equipment, is shown in Figure 42.16. Originally, ThCl₄ was dissolved in propylene-diamine and reacted with liquid sodium amalgam. However, this step was then replaced for cost reasons by direct reaction of solid thorium chloride with the amalgam at 180–

300 °C in a kneader mixer, a conversion of 97% being obtained after 30 min. Excess sodium and sodium chloride were removed by washing with dilute HCl, and solid ThHg₃ was removed from excess Hg (in which thorium metal is soluble to < 0.1% at room temperature) by means of a filter press. Thorium amalgam was then decomposed in a steel retort at

1100 °C in vacuum, to remove mercury and produce a sintered solid. Since mercury as a high parasitic neutron capture cross section and can also attack the aluminum cladding on thorium rods in the reactor, it must be rigorously excluded. The process is consequently not without risk.

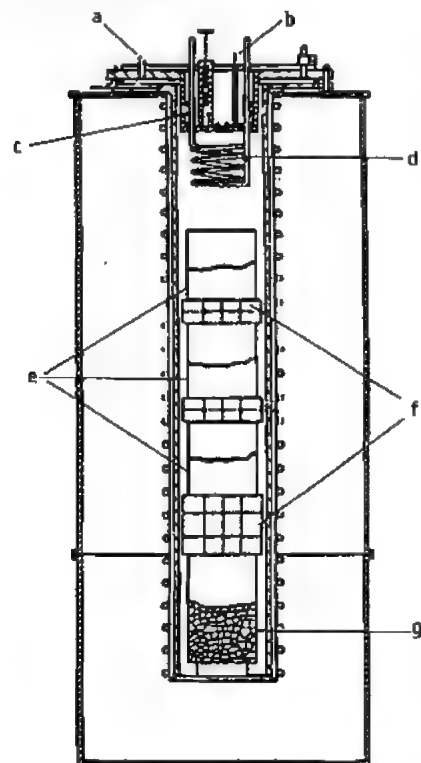


Figure 42.17: Furnace for ThCl_4 reduction (Kroll furnace): a) Vacuum connection; b) Thermocouple; c) Lift heater; d) Air-cooled condenser; e) ThCl_4 container; f) Distance disks; g) Melting crucible containing magnesium.

Kroll Process. The Kroll process, in which thorium chloride is reduced with magnesium [27], was developed at about the same time by the National Lead Company of Ohio. Although this process was originally expected to have a wide application for the treatment of all air-sensitive transition metals, it has in fact become widely used only for titanium, zirconium, hafnium, and thorium. In further development of the process by Ames Laboratories, thorium chloride is completely reacted

at 850–950 °C in a furnace provided with exterior heating, by using twice the stoichiometric quantity of magnesium to give a Th–Mg alloy (Figure 42.17). This alloy melts and forms a compact regulus. Magnesium chloride and excess magnesium are then distilled off at 950 °C in a high-vacuum furnace (Figure 42.18) and collected in collection vessels.

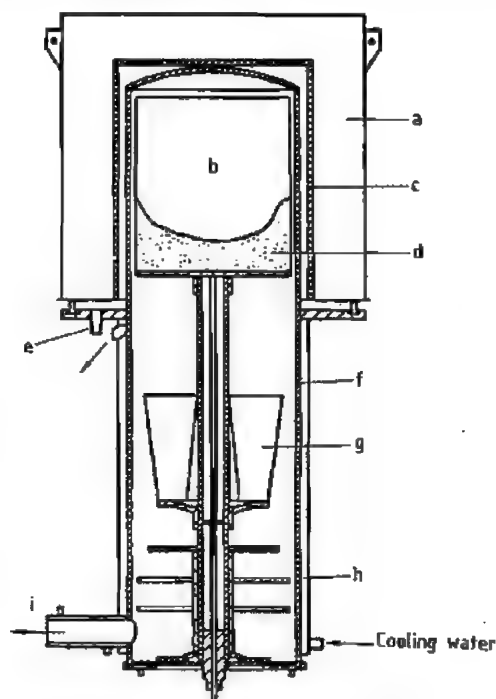


Figure 42.18: High-vacuum distillation furnace: a) Furnace; b) Distillation crucible; c) Heating element; d) Thorium sponge; e) Furnace vacuum connection; f) Inner wall of reactor; g) Collecting vessel; h) Cooling jacket; i) Reactor vacuum connection.

Reduction of ThF_4 with Calcium. Quantitatively, the most important method for producing thorium of nuclear purity in the United States was reduction of ThF_4 with calcium metal. The process developed by Ames Laboratories and Iowa State University [28] was analogous to the production of uranium metal. However, when calcium metal reacts with ThF_4 , the heat of reaction is insufficient to melt the thorium metal. Additional heat is therefore generated by reacting ZnCl_2 with calcium metal. This also produces a lower-

melting thorium–zinc alloy and a lower melting point eutectic of CaF_2 and CaCl_2 . The process requires careful preparation of the reactants since most of the metallic impurities in the reactants end up in thorium. Calcium metal must be sieved to remove fine-grained material after preliminary size reduction because this material contains most of the impurities. Zinc chloride must also be of high purity; it must be anhydrous and not too fine grained, otherwise the reaction with calcium can take place prematurely. The reduction furnace is illustrated in Figure 42.19. The furnace pot (e), which is made of nonscaling steel, is placed inside the muffle (g). This is heated by three heating elements (d, f, h), outside which is a lining of calcined dolomite. The reaction mixture consists of 75.3 kg of ThF_4 , 27.22 kg of granulated calcium metal, and 7.26 kg of anhydrous ZnCl_2 . A layer of dolomite powder is placed above and below the reactants to protect the walls. The furnace is heated to 660 °C, and when the contents reach 475 °C a strongly exothermic reaction begins, producing a Zn–Th alloy containing 18 mol% Zn. The furnace is operated behind safety walls because deflagrations occasionally occur. After cooling, the slag is removed, and 90% of the zinc can be distilled off in vacuum (<27 Pa). The thorium sponge is cooled in a protective gas and then inductively melted in a BeO crucible in vacuum. The remaining zinc evaporates, and the thorium is cast in graphite molds (yield 94–86%).

42.7 Metalworking [11, pp. 222ff; 29; 30]

Most production processes lead to thorium powder or sponge. This must therefore be compacted by sintering or melting before it can be worked in a metal-forming process. In the literature, densification by powder metallurgy is described in less detail than melting and casting.

Melting and Casting. To cast thorium metal, it is first melted at 1800 °C by inductive heat-

ing in vacuum to avoid the danger of picking up O_2 and N_2 . Also, zinc left behind from the production process (reduction of ThF_4 with Ca, see earlier) must be evaporated, and pickup of impurities from the crucible material must be as low as possible. For this, either zinc is removed first in graphite crucibles at a temperature at which thorium hardly picks up any carbon from graphite (1300 °C) and the actual melting is carried out later in BeO crucibles, or both processes are carried out together in a stabilized ZrO_2 crucible. Thorium metal has a very low heat of fusion and, when fused, attacks all known crucible materials, so that excessive heating must be avoided. Both the service life of the BeO crucible and the limitation of pickup of impurities by thorium are only moderately satisfactory.

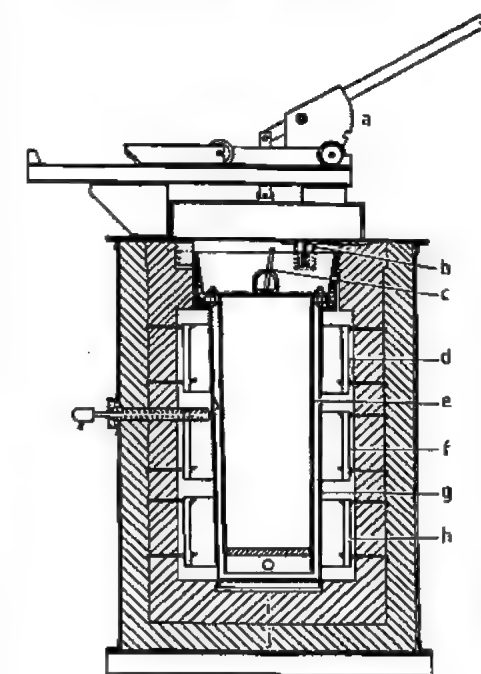


Figure 42.19: Section view of reduction furnace pot: a) Cover lifting mechanism; b) Muffle hanger; c) Pot alignment bar; d) Top element; e) Furnace pot (steel); f) Center element; g) Muffle; h) Bottom element; i) 2600 °C insulation brick; j) 1600 °C insulation brick.

Table 42.14: Average analyses of thorium ingots.

Type of analysis	Impurity	Induction melted; charge; 40% scrap, 60% virgin metal	Arc melted	
			Charge: virgin metal	Charge: virgin and scrap metal
Chemical	ThO ₂ , %	2.8	1.34	2.42
	ZrO ₂ , %	0.14		
	N, mg/kg	290	142	211
	C, mg/kg	465	211	193
Spectrochemical	Al, mg/kg	370	20	13
	B, mg/kg	3.9	0.4	0.5
	Fe, mg/kg	600	243	441
	Ni, mg/kg	520	324	486
	SiO ₂ , mg/kg	500	34	30
	Zn, mg/kg	10	128	43
	U, mg/kg	20	10	6
	Hardness, BHN ^a , 500-kg load	64	54	56
Density, g/mL		11.52	11.57	11.64

^aBHN = Brinell hardness number.

Table 42.15: Effect of carbon content on mechanical properties of iodide-source thorium (cold rolled to 85% reduction and annealed 30 min at 650 °C).

Carbon content, %	Yield strength (0.2% offset), MPa	Tensile strength, MPa	Elongation, %	Reduction of area, %	Hardness, VHN ^a
0.015	52.4	124.1	27.0	60	40
0.022	44.8	121.3	50.0	62	34
0.047	113.1	179.3		43	60
0.070	185.5	237.2	46.0	51	83
0.130	242.0	302.7	41.0	46	109
0.187	346.8	369.6	38.0	39	125
0.22	346.8	418.5	30.0	39	140

^aVHN = Vickers hardness number.

A two-stage electrode-consuming arc melting process is a better alternative for producing the cylindrical ingots generally used in nuclear technology. The molten thorium metal is subsequently solidified in water-cooled copper crucibles. The pieces of thorium sponge obtained from the first dezincification are sawed into strips in chambers filled with inert gas and then welded together to form electrodes. However, metal is lost in this laborious operation, and attempts have therefore been made to replace it by hot plastic forming of the sponge (casting or compaction). The properties of the ingots obtained by induction and arc melting are listed in Table 42.14.

In subsequent metalworking, thorium resembles soft iron in its ductile behavior. Even the presence of several percent oxygen does not cause problems, because oxygen is virtually insoluble in thorium and therefore only contained in inclusions of ThO₂. To prevent

surface oxidation—especially of the small pieces used during hot working by, e.g., rolling, hammering, or extruding—the pieces are encased in soft copper or iron cladding, which is later dissolved in acid. Welding of thorium is possible only in an inert-gas atmosphere. Thorium can be soft-annealed after cold working (e.g., rolling) by heating to 500–700 °C. No problems occur due to phase transition since these occur only above 1400 °C. Impurities picked up during the various production processes affect workability. Small amounts of oxygen and beryllium have little effect, but carbon causes hardening. As with steel, considerable precipitation hardening occurs on quenching from the soft-annealed state at 600–800 °C (see Table 42.15). Elements that form carbides (e.g., titanium, niobium, and tantalum) considerably counteract this effect.

The dimensionally accurate tubes—required for fuel elements used in breeder reac-

tors—were usually extruded at 600–700 °C, using a protective coating of copper or soft iron. Both of these metals form reaction zones with thorium that must subsequently be machined off. To prevent this, oxidic coatings on thorium were investigated. Alternatively thorium can also be preheated in a molten salt bath consisting of nitrites and cyanides of alkali metals. The adherent salt film acts as a protective and lubricating film. The method eventually favored was to coextrude thorium with an inner and outer cladding of aluminum. Zirconium of similar plasticity obtained by preheating zirconium ingots was used as cladding at a later stage. Process details are unknown for reasons of military secrecy.

42.8 Intermetallic Compounds

Thorium has limited solubility in carbon and nitrogen, and can form compounds of metallic character with both elements. These are described below and in Section 42.5.

42.8.1 Thorium and Carbon

Carbon is usually present as an impurity in thorium. Thorium produced by decomposition of thorium iodide contains 0.01–0.05% C, and from halide reduction 0.03–0.12% C. As mentioned in Section 42.7, carbon is one of the few elements that increases hardness and age hardening properties of thorium. Of all the elements that improve steel properties, only chromium can by itself (and even more in combination with carbon) produce comparable effects in thorium. Only indium seems to be more effective but is excluded from nuclear applications due to its neutron absorption. The other metals investigated (Ti, V, Mo) have a minor hardening effect, probably due to the formation of carbides with the carbon in thorium. However, the effect is partially negated by the hardness reduction caused by removal of carbon. The Th–C constitutional diagram (Figure 42.20) shows the two compounds ThC

and ThC₂ (see Section 42.5). The effect of temperature on the solubility of carbon in thorium is given below:

20 °C	0.35%
800 °C	0.43%
1018 °C	0.57%
1215 °C	0.91%

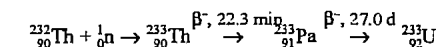
42.8.2 Thorium and Nitrogen

The compounds ThN and Th₂N₃ are described in Section 42.5. The solubility of nitrogen in thorium increases linearly with temperature, being 0.05% at 850 °C and 0.35% at 1500 °C. In thorium formed by halide reduction, nitrogen is usually present only at levels of 0.02%. The strength of thorium–nitrogen alloys increases moderately with increasing nitrogen content. Precipitation hardening (age hardening) of the alloy after annealing at 850 °C occurs only with quenching temperatures of < 300 °C.

42.9 Uses

42.9.1 Nuclear Technology [31]

Production of ²³³U. Use of thorium in the nuclear industry is based on its ability to behave as a breeder. It absorbs neutrons and forms ²³³U by successive release of two β-particles according to



The isotope ²³³U is notable for the fact that the ratio of neutrons liberated on fission to those absorbed is more favorable than the corresponding ratio of ²³⁵U and ²³⁹Pu. This has aroused interest in this nuclide—which is complicated to produce—in both the military and the civil areas. The ²³³U formed from thorium can either be separated from the breeder material by chemical methods or undergo fission in situ by absorption of further neutrons, thereby releasing energy. Both methods are subject to a number of limitations.

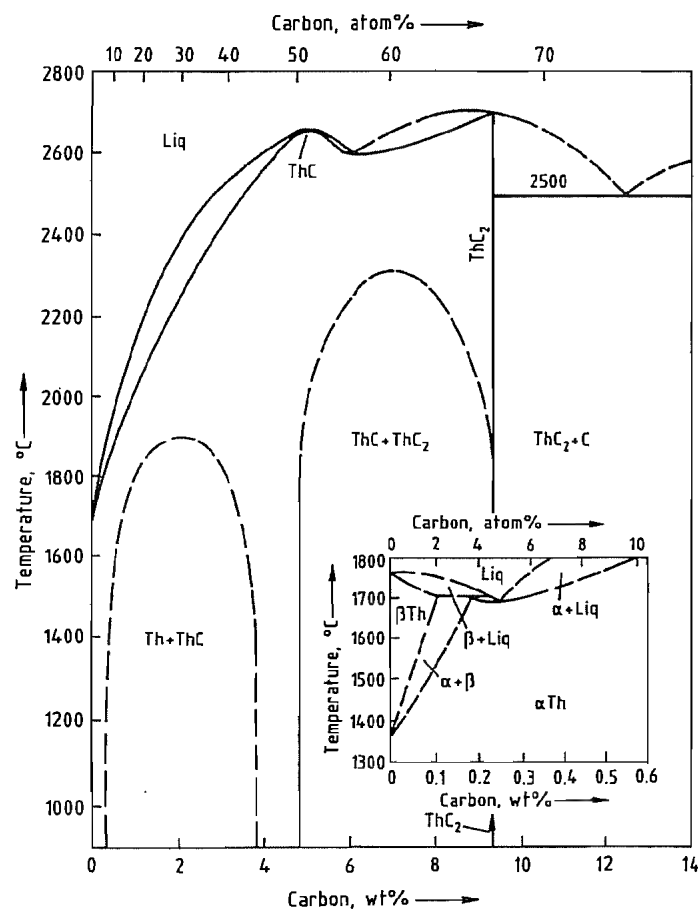


Figure 42.20: Phase diagram of the thorium-carbon system.

Chemical Separation of ^{233}U . In separating ^{233}U , it must be kept in mind that ^{232}U can be formed in an $n,2n$ reaction with neutrons with an energy of > 6.27 MeV from the ^{233}U already formed, and mainly from ^{232}Th via ^{231}Th and ^{231}Pa by further neutron capture. To avoid this reaction, thorium must be allowed to interact only with low-energy thermal neutrons. The same isotope ^{232}U is also formed with a cross section 14 times as large by low-energy neutron capture by ^{230}Th . Although ^{230}Th is present in thorium at a level of only a few parts per million, its concentration can be higher if thorium is a by-product of uranium production, in which case ^{230}Th is present as an α -decay daughter of ^{234}U .

Whereas ^{232}U is not itself harmful, a serious handling problem arises from the fact that it decays relatively rapidly to its daughter product ^{208}Tl , which emits penetrating γ -radiation with an energy of 2.62 MeV.

In practice, this means that thorium must not be used in a thermal neutron flux in molecular proximity to neutron sources (e.g., as a U-Th alloy, mixed oxide, or mixed carbide)—which would give optimum neutron capture—but should be kept separate from the neutron source ^{235}U (or ^{239}Pu) in breeder rods covered with a layer of moderator.

To give an idea of quantities, if 1 t of thorium is irradiated for some weeks in the carefully thermalized neutron flux and then cooled

for 150 d to enable the fission product iodine, which interferes with the separation process, to decay, this forms ca. 1 kg ^{233}U containing ca. 8 mg/kg ^{232}U . This then remains in a handleable state for some weeks without complicated gamma shielding. The overall complexity of this operation can be reduced by replacing the thorium metal rods with ceramic ThO_2 tablets, which are easier to produce but more difficult to dissolve later since $\text{HF} + \text{HNO}_3$ must be used. Even under these conditions, with a handling concentration limit of 10–20 mg/kg ^{232}U , an optimistic price estimate for ^{233}U is still twice that of highly enriched uranium [32]. According to published data, no more than 3 t ^{233}U has been produced worldwide, of which ≤ 800 kg in the United States. New fuel rods have been produced from this in only one full-scale experiment (Kilorod Facility, Oak Ridge, Tennessee [33]).

Attempts to irradiate thorium in the form of a fluid medium or of ThF_4 dissolved in fused salts [34] were finally not successful.

"In Situ" Fission. In an alternative method, ^{233}U is caused to undergo fission with generation of heat at the place where it is formed. Here, fewer possibilities exist for controlling the nuclear reaction, and thorium is by no means completely consumed, but the system is technically easier to realize. Also, a particular property of thorium can be utilized—i.e., its ability to form a series of solid solutions with other actinide oxides (UO_2 , PuO_2)—thereby stabilizing them at high temperature. This is mainly a property of ThO_2 , to a lesser extent of the carbide, and to a small extent of the metal. Also, since the formation of ^{232}U does not present a problem, the higher neutron flux (by at least an order of magnitude) of the fast breeder reactor is advantageous.

Thorium oxide forms a series of mixed crystals with a cubic fluorite structure with both UO_2 and PuO_2 , so that fuel elements can be produced in which thorium is the main component and which are stable when heated in air to $> 1200^\circ\text{C}$. This facilitates both production and safety analysis. The mixed crystals show no phase transformation up to their

melting point of $> 2600^\circ\text{C}$. However, used fuel elements of this type can be dissolved only in mixtures of HNO_3 and HF , which attack most available containment materials. Except in India where much thorium but comparatively little uranium is available, all fast breeder programs currently in operation are based on the uranium-plutonium cycle, and no thorium is used.

Thorium could be used in thermal reactors to extend the use of ^{239}Pu , which is produced as a fuel by transformation of ^{238}U . However, continuous hydrogenation of the cladding material (Zircaloy) limits the burnup in water reactors to ca. 50 000 MW·d/t, so that there is little advantage in using thorium, which is therefore limited to *graphite-moderated thorium high-temperature reactors* (THTRs), which allow ten times the burnup. Here, the fuel elements consist of small particles of uranium and thorium oxide or uranium and thorium carbide, embedded in a graphite matrix [35].

Owing to parasitic neutron capture in the thorium cycle, Th-U fuel required highly enriched uranium (93% ^{235}U), and the possible consequent proliferation of weapons-grade material led to concern on the part of source countries (United States). Therefore, new fuel variations are no longer based on thorium. Slightly enriched uranium (10% ^{235}U), which is not suitable for weapons, is used instead.

So far, high-temperature reactors have not reached the threshold of economic viability achieved by other methods of generating electricity. The safety advantage has not compensated for this disadvantage, and no power stations of this type are currently under construction or being operated.

Because of the wide variations in targeted burnups and the question of whether—and to what extent—thorium is recycled to the reactor, figures for thorium consumption fluctuate not only with reactor capacity but also according to the mode of operation. In using the minimum consumption figures that correspond to maximum recycling, the THTR reactor requires 7.3 t/a thorium for each 1000-MWe capacity, 340 kg ^{233}U can be recovered from the

used fuel elements, and 6.8 t Th (containing isotopes that interfere with a second burnup) must be disposed of as nuclear waste. The initial inventory of the reactor is ca. 60 t of thorium.

42.9.2 Conventional Applications

42.9.2.1 Illuminants

The most important application of thorium followed the discovery by AUER VON WELSBACH in 1892 that some rare earth oxides and thorium oxide, when introduced in the form of woven yarn into a gas flame, considerably increased the luminous efficacy of the flame. This emission of light is excited by cathode rays, heat, and UV radiation. Although pure cerium oxide converts the UV fraction of an oxidizing gas flame into visible light more efficiently than ThO_2 , it is not used in practice because so much light is emitted in the IR region that "cooling" of the gas flame occurs. Excitation of cerium oxide gives a gas flame temperature of only 1500 °C, whereas thorium oxide gives 1930 °C. Maximum luminous efficacy occurs with 1% cerium oxide in ThO_2 [36].

The requirements of maximum light-emitting surface area together with stability in a gas flame in which high flow rates occur at the zone of maximum temperature led to the development of the gas mantle, whose shape matches that of the combustion zone of the flame. Today, commercially available gas mantles are produced by soaking artificial silk (viscose or cellulose ester fibers) in a solution of thorium and cerium nitrates. The hydroxides are then formed by treatment with alkali and fixed to the fiber; the organic carrier material is burned off, and the remaining ash structure is fixed with collodion lacquer.

Modern gas mantles give a luminous efficacy of 3 lm/W with propane, which is even better than that produced by electric incandescent lamps. Gas mantles are expressly excluded from the restrictions on radioactive substances, although the inhalation of ash from used gas mantles, which can easily occur

on careless handling, can lead to harmful deposits in the lungs.

Thorium oxide also had limited application as a light converter (UV into visible light) in fluorescent lamps before modern oxide mixtures were developed.

42.9.2.2 Electron Emitters

In the production of incandescent filaments, the rate of recrystallization of tungsten is considerably reduced by adding 1% ThO_2 to the tungsten sintering powder before drawing the filaments.

A side effect of this addition was noticed: i.e., that a small addition of thorium oxide to the tungsten used in heated electrodes considerably reduces the work function of electrons (see Figure 42.4) [37]. This is probably due to the formation of a ThO dipole layer, which is constantly renewed from the interior of the electrode. Therefore, since 1922, thoriated tungsten wires have been used in electronic tubes and in the cathodes and anticathodes of X-ray tubes and rectifiers. Owing to the reactivity of thorium with O_2 and N_2 , it also acts as a getter for impurities in the evacuated tubes.

These applications decreased very much following the introduction of transistors in the 1950s, but reduction of the electron work function is still a useful phenomenon, having a beneficial effect on the process of welding in an inert gas (argon, helium), for which thoriated tungsten electrodes are used.

42.9.2.3 Ceramics and Glass

Thorium oxide crucibles represent the most refractory material known and can be used for melting pure, carbon-sensitive metals at 2300 °C. The crucibles are produced by sintering fused and ground thorium oxide—small additions of ZrO_2 , P_2O_5 , and cryolite being used as sintering aids. Although its application is very limited, ThO_2 is also used to increase the density of ZrO_2 crucibles.

Like ZrO_2 , ThO_2 increases the hardness of dispersion-hardened alloys, e.g., in an Ni-16Cr-(3–5)Al alloy for gas turbine blades.

The addition of ThO_2 to glass leads to extremely high refractive indices with low dispersions and densities lower than those of lead glass. However, this application is also limited because rare-earth oxides have a similar effect and are not α -emitters.

42.9.2.4 Catalysts [38]

The catalytic effect of ThO_2 seems to be due to an increase in the mobility of hydroxyl ions and hydrogen. Thus, a large number of hydroxylations, hydrogen additions, hydrogen eliminations, oxidations, and reductions have been documented in which thorium catalysts are used. The earliest use of thorium as a reactant and catalyst at the same time was the reaction of aliphatic dicarboxylic acids to give ring ketones (civetone, synthetic musk) by dry distillation of thorium salts [39].

Thorium oxide was used as a fixed-bed catalyst with nickel and cobalt on a kieselguhr carrier, first in ammonia synthesis and then in oil refining and the Fischer-Tropsch process. It was also employed in dehydrogenation, isomerization, and a number of other reactions.

An alloy of platinum with 10% thorium is a very good catalyst for the oxidation of ammonia to nitrogen oxides. However, a 5% rhodium alloy with platinum is now preferred because of its superior mechanical properties and longer lifetime in the form of a gauze.

In almost all cases, ThO_2 has been replaced by cheaper catalysts (e.g., based on rare earths) and is now hardly used.

42.9.2.5 Medicine

Thorium dioxide was used as a contrast medium (Thorotrast) when making X-ray photographs of hollow organs but has been replaced by nonirradiating substances.

^{225}Ra has been used experimentally for therapeutic irradiation, as this is the only isotope of radium that does not have a gaseous decay product. It is obtained either as a short-lived daughter nuclide of ^{229}Th , which is the most stable daughter nuclide (half-life 7340 a)

in the ^{233}U decay chain, or can be produced by neutron irradiation of ^{226}Ra .

42.9.2.6 The Demand for Thorium

In the first phase of utilization from 1893 to 1940, mostly for the production of gas mantles, worldwide consumption was ca. 8000 t ThO_2 , of which 3300 t came from India, 4000 t from Brazil, 370 t from the United States, 100 t from Indonesia, 60 t from Sri Lanka, and the rest from Norway, Australia, and a few other countries, together with a small amount of recycled material.

India, which produced 280 figures since development of the nuclear application. Nonnuclear use has in general decreased since 1950 [40].

In Germany in the 1990s, thorium consumption decreased to ca. 1.5 t/a, having been 3–5 t/a a few years before. Four companies produce thoriated tungsten electrodes, and one company produces electric discharge lamps. Gas mantles are mainly imported from France. Large quantities of thorium oxide, a coupled product from rare earth production, are stored in various parts of the former German Democratic Republic. This material will probably not be utilized but will be deposited as radioactive waste in a waste disposal site.

42.10 Product Quality and Analytical Methods

Product Quality. Thorium is commonly marketed in the form of solid thorium nitrate. Here, the thorium content and the level of certain impurities are important. Rare earths, magnesium, calcium, and heavy metals that can be precipitated by sulfide (mainly Fe) are determined.

Thorium nitrate used in the production of gas mantles is highly purified by multiple recrystallization or oxalate precipitation. Rare earths (except in concentrations < 1%) are undesirable because they stimulate the emission of IR radiation, thereby reducing the emission of visible light. Very small proportions

(> 0.02%) of SiO_2 lead to embrittlement of the gas mantle [41].

Sulfate in ThO_2 has a detrimental effect on crucible production and is removed by multiple dissolutions and precipitations of thorium as oxalate.

The rare earths are also undesirable in nuclear technology because some of them (e.g., erbium and gadolinium) are strong neutron absorbers. Therefore, these elements must be removed. If thorium is used in metallic form, the oxygen and carbon contents are important, the latter from the point of view of hardness properties. When processing irradiated thorium, uranium and thorium must be separated.

The determination of low concentrations of thorium is important in the quality control of alloys. Very low concentrations must be determined in geochemistry and environmental analysis, and when removing ^{230}Th from uranium compounds.

Analytical methods are based on the selective separation of thorium. The natural accompanying elements and compounds in thorium include La and lanthanides, Y, Sc, Ti, Zr, Hf, U, Fe, Al, Ca, SiO_2 , and P_2O_5 . Only a few reactions exist that are specific for thorium; moreover, it has a stable valence of four so redox separations are impossible. The most difficult precipitation separation is that of scandium, although large amounts of this element are seldom associated with thorium.

Precipitation processes usually start with solutions in relatively strong mineral acids. Precipitation of thorium as the oxalate, fluoride, peroxide, iodate, and hypophosphate gives the best selectivity, the last of these even against rare earths. Some organic dicarboxylic acids, especially tetrachlorophthalic acid, are more selective than oxalic acid. Dimethyl oxalate, which slowly hydrolyzes in warm solutions of mineral acids, can also be used to give slow formation of a precipitate that is free of inclusions.

Most of the compounds soluble in organic solvents that are used for *liquid-liquid extractions* in nuclear technology have been tested for the selective separation of thorium, mainly

from solutions in nitric acid, for analytical purposes. They include 1-(2-thenoyl-3,3,3-trifluoroacetone (TTA), mesityl oxide, dibutoxytetraethylene glycol ("penta ether"), long-chain amines (trilaurylamine), TBP [42], and a series of organic phosphonium compounds, especially bis(dialkylphosphinyl)methane [43]. The latter extractants, in particular, separate uranium and thorium selectively from the rare earths. Uranium is most effectively separated from thorium by means of the appropriate choice of ligands (branched or straight-chain) and of the concentrations of the acid and salt in aqueous stripping. Bis(dialkylphosphinyl)methanes are more selective extractants than trialkylphosphine oxides. The branched-chain, sterically hindered phosphine oxides extract U(VI) more effectively, whereas the straight-chain compounds extract thorium more effectively.

Good selectivity against the rare earths and selectivity against uranium can also be obtained by extracting thorium with TBP from nitric acid solution if the TBP concentration is 40% in the organic solution (instead of 10% as used with uranium). In contrast to uranium, stripping is best carried out by salting out with nitrates in the presence of moderately concentrated HNO_3 .

Few selective *analytical reagents* for thorium in solution are known. Their selectivity is generally considered to depend on the bond formed with inner electrons of thorium, as in the case of precipitation with dicarboxylic acids. The compounds formed are generally more sparingly soluble than the corresponding rare earth compounds.

Reagents include a series of weak organic acids with acid groups on adjacent carbon atoms, and other compounds that can form chelate-like complexes. The pink coloration produced by the reaction of ammoniacal solutions of pyrogallol with Th^{4+} has been known for some time, although this is only moderately stable and selective. The formation of star-shaped groups of red needles with Orange II (*p*-(2-hydroxy-1-naphthyl)azo]benzenesulfonic acid), is used for microchemical detection. The most selective reaction known is

the formation of a red coloration with thorin, 4-(2-arsonophenylazo)-3-hydroxy-2,7-naphthalenedisulfonic acid (in the absence of oxalate and fluoride). This coloration is measured at 54.5 nm in sulfuric acid solution, although a number of other compounds that react in a similar way (dibenzoylmethane, aurintricarboxylic acid, alizarin S) also give color reactions or form color lakes.

When impurities originating from production and processing of thorium metal and its compounds are to be analyzed most of the thorium must be separated first. The impurities can then be determined by the usual methods. This applies also to spectrographic analysis, for which most of the thorium should first be removed because of its complex line spectrum.

42.11 Toxicology

Thorium, its natural decay products, and its compounds are toxic both as heavy metals and as radioactive substances. However, their heavy-metal toxicity is low because of their low solubility in body fluids and organs, and has been compared with that of aluminum.

42.12 Industrial Safety

In addition to toxicological risks, the spontaneous flammability of thorium metal constitutes a handling hazard.

Thorium has been extracted and processed on an industrial scale since 1893, mostly as the oxide. However, the incidence of harmful effects associated with the handling of thorium is very low. In the absence of strong complex formers (e.g., citrates), water-soluble thorium compounds are immobilized close to the point of incorporation into the body in the form of insoluble hydroxides. Animal experiments first gave an LD_{50} of 1–2 g/kg. The low water solubility also prolongs the excretion process, mainly via the feces, and to a lesser extent the kidneys. Exposure to thorium occurs mainly by inhalation of dust into the tracheobronchial tract and the lungs. No toxic chemical effect

has thus far been observed in these areas, but radiation damage can occur in the lungs and from the small amounts of thorium transported to the bones.

Thorium is often compared with uranium, which has been well investigated radiologically. Thorium differs from uranium in the more rapid buildup of its daughter nuclides, which also have chemically different properties (Figure 42.1). Important daughter nuclides are ^{228}Ra , ^{228}Ac , ^{228}Th , ^{224}Ra , and ^{220}Rn . Other decay products are of little radiological importance. As shown in Figure 42.2, freshly separated thorium passes through two activity maxima, one after ca. 5 weeks and a second after ca. 60 a, with an intermediate activity decrease after 3 a. In addition to the relatively low β - and γ -radiation, α -radiation has a significant effect on the living organism due to the high ionization density that it produces. During chemical isolation of thorium from ores or residues that have been stored for a long time, ^{228}Ra and ^{224}Ra become concentrated in the filtrate (to > 70% in oxalate precipitation). These nuclides are precipitated with sulfate to concentrate them in sediment and prevent them from passing into receiving waters. Furthermore, phase transformations and chemical changes of thorium and its compounds cause the release of all the ^{220}Rn formed in the solid up to that point, which can lead to the buildup of significant α -activity in poorly ventilated areas. Table 42.16 gives the maximum permissible concentrations of thorium and its decay products according to the USAEC Regulations of 1955 (still in curies). The German legal requirements for thorium according to the Strahlenschutzverordnung are listed in Table 42.17. The recommended annual limits for incorporation (ALI) in the International Commission on Radiological Protection (ICRP) 30 Regulations are based on a metabolic inhalation model. This has been used to test the relationship between the uptake of thorium and biological detection in a large group of workers in a monazite processing plant [44]. It showed that the analysis of urine and feces correlated only moderately well with the short-term uptake of thorium.

After inhalation of insoluble thorium compounds urine analyses showed a maximum thorium uptake fraction of 1.4×10^{-3} , up to 12% were found in feces, both at the second day after incorporation. Almost all measurements yielded higher figures than the ICRP recommendation, although there was no detectable damage to health. Cytogenetic studies in parallel with this showed no correlation between the frequency of chromosomal aberrations and the duration of contact. Clearance from the lungs has a biological half-life of > 500 d, and from bones ca. 200 a.

The workplace should therefore be kept as dust free as possible.

42.13 Environmental Protection

Thorium occurs almost ubiquitously in nature in low concentrations. Because of its poor

solubility in water, it occurs in extremely low concentrations in the biological cycle, and because its use in industry is not increasing, special environmental protection measures are unnecessary. Only in a few locations where thorium was used or processed in the past are soil remediation operations occasionally required.

Table 42.16: Maximum permissible concentrations of thorium and the daughter products radium-228 and radium-224.

Element	Body limit, μC	Water MPC ^a , $\mu\text{C}/\text{cm}^3$	Air MPC ^a , $\mu\text{C}/\text{cm}^3$
²³² Th (soluble)	0.01	5×10^{-7}	3×10^{-13}
²³² Th (insoluble)	0.002 ^b		3×10^{-13}
²²⁸ Ra (soluble)	0.04	8×10^{-8}	1×10^{-11}
²²⁸ Ra (insoluble)	0.002 ^b		2×10^{-12}
²²⁴ Ra (soluble)	0.06	5×10^{-5}	8×10^{-9}
²²⁴ Ra (insoluble)	0.003 ^b		3×10^{-10}

^aMPC = maximum permissible concentration.

^bLung only.

Table 42.17: Exposure and annual limits for inhalation and digestion of radon, radium, actinium, and thorium.

Atomic no.	Element	Radionuclide	Exposure limit, Bq	Annual limit	
				Inhalation, Bq	Ingestion, Bq
86	radon	²²⁰ Rn	5×10^6	3×10^8	
		²²⁰ Rn ^a		5×10^5	
		²²² Rn	5×10^5	2×10^8	
		²²² Rn ^a		4×10^6	
88	radium	²²³ Ra	5×10^3	9×10^3	1×10^5
		²²⁴ Ra	5×10^4	2×10^4	2×10^5
		²²⁶ Ra	5×10^3	9×10^3	4×10^4
		²²⁸ Ra	5×10^3	2×10^4	5×10^4
89	actinium	²²⁷ Ac	5×10^3	9 ^b	4×10^3
				40 ^c	
				100 ^a	
		²²⁸ Ac	5×10^4	2×10^5 ^{a,b}	6×10^7
90	thorium	²²⁷ Th	5×10^3	4×10^3	2×10^6
				6×10^3	
		²²⁸ Th	5×10^3	200	1×10^5
		²³⁰ Th	5×10^3	100	9×10^4
				400	
		²³² Th	5×10^4	30	2×10^4
		²³⁴ Th	5×10^5	2×10^6	3×10^6
				3×10^6	
	Th-nat		5×10^4	50	3×10^4
				100	

^aIn equilibrium with decay products.

^bAll, except nitrates.

^cNitrates.

42.14 Legal Aspects

According to German atomic law (AtG), thorium that has not been irradiated is a "miscellaneous radioactive material" but is not a "nuclear fuel" so that according to § 3/§ 9 AtG it must be safely disposed of as a radioactive material. According to the nuclear nonproliferation treaty, thorium is classed as a controlled substance. Quantities of 20 t (source material) must be checked at least once per year, as also prescribed for Europe by Euratom Regulation no. 3227/76. Persons constructing and operating plants for the production, separation, utilization, and storage of thorium must report kilogram or higher quantities of thorium.

Exceptions to this duty to report include gas mantles, to which the limits imposed by the radiation protection regulations do not apply, although the amount of freshly purified thorium in a gas mantle represents the maximum permitted intake of activity for 100 person-years. Aged thorium contained in gas mantles could represent ten times this amount.

42.15 References

- G. T. Seaborg: *The Transuranium Elements*, Yale University Press, Washington 1958, p. 113.
- J. R. Naegele: "Surface Analysis of Actinide Materials," in U. Benedikt (ed.): *Transuranium Elements Today and Tomorrow*, North Holland Publ., Amsterdam 1989, p. 66.
- W. Seelmann-Eggebert, G. Pfennig, H. Münzel, H. Klewe-Nebenius: *Nuklidkarte*, Kernforschungszentrum, Karlsruhe 1981.
- S. Tilson: "The Earth's Crust", *Int. Sci. Technol. X* (1962) p. 24, Fig. 3.
- H. Remy: *Lehrbuch der Anorganischen Chemie II*, Akad. Verlagsgesellschaft, Leipzig 1942, p. 544.
- D. F. Peppard et al., *J. Am. Chem. Soc.* **73** (1951), 2529.
- G. Kirsch, *Ber. Wien. Akad.* **131**, IIa (1922) 551–568.
- G. T. Seaborg, *Chem. Eng. News* **26** (1948) 1902–1906.
- H. J. Vink, *Chem. Weekbl.* **44** (1948) 685–688.
- H. A. Wilhelm: *The Metal Thorium*, Am. Soc. for Metals, Cleveland, OH, 1956.
- J. R. Murray: "The Preparation, Properties and Alloying Behavior of Thorium," Report AERE-M/TN-12, 1952.
- R. K. Garg et al.: "Status of Thorium Technology," in: *Nuclear Power and its Fuel Cycle*, vol. 2, Inter-

- national Atomic Energy Agency, Vienna 1977, p. 457.
- F. L. Cuthbert: *Thorium Production Technology*, Addison-Wesley-Publ. Comp., Reading, MA, 1958, pp. 62ff.
- P. Krumholz, F. Gottdenker: "The Extraction of Thorium from Monazite," *Proc. Int. Conf. At. Energy* **8** (1956) 126–133.
- F. Soddy, GB 572411, 1949; *Chem. Abstr.* **42** (1948) 731.
- J. Barghusen, Jr., M. Smutz: "The Ames Process," *Ind. Eng. Chem.* **50** (1958) 1754.
- M. Steinhauser: "Löslichkeit von PuO₂ und ThO₂ in HNO₃", Ph.D. Thesis, Universität München 1987.
- D. J. Crause, K. B. Brown: "Recovery of Th, U, and SE from Monazite Sulfate Leach Liquors by the Amine Extraction (= Ames) Process", *Rep. Oak Ridge National Lab.*, no. 2720, July 16, 1959.
- R. A. Ewing et al.: "Purification of Thorium Nitrate by Solvent Extraction with TBP", *Fin. Rep. USAEC-BMI 946* (1952) pp. 3 ff.
- F. Sachs: "Preparation of ThO₂", *Nucl. Sci. Abstr.* **6** (1952) 647ff.
- L. Gordon, C. H. Vanselow: "Precipitation of Th from Homogeneous Solution," *Anal. Chem.* **21** (1949) 1323–1325.
- IAEA: "Thorium, Physicochemical Properties of its Compounds and Alloys," *At. Energy Rev. Spec. Iss.* Vienna (1975) Nov. 5.
- V. D. Allred, S. R. Buxton, J. P. McBride, *J. Phys. Chem.* **61** (1957) 117.
- N. D. Veigel et al.: "The Preparation of High Purity Thorium by the Iodide Process", *USAEC-Rep. AEC-3586*, BMI 1953.
- R. J. Meyer, A. Gumperts: "Reinheitskriterien von Thoriumnitrat", *Ber. Dtsch. Chem. Ges.* **38** (1905) 817–825.
- R. E. Blanco: "Status of the Metallex Process", *USAEC-Rep. CF-55-1-53*, ORNL 1955.
- T. C. Runion et al.: "Production of Thorium by Kroll Technique", *USAEC-Rep. NLCO-616*, National Lead Comp. of Ohio, 1956.
- F. H. Spedding: "Progress-Report in Metallurgy", *USAEC-Rep. ISC-6*, Iowa State College, 1947.
- H. A. Wilhelm: *The Metal Thorium*, Am. Soc. for Metals, Cleveland, OH, 1956.
- H. A. Wilhelm, B. A. Rogers: "The Physical Metallurgy of Thorium", *AIME-IMD Spec. Rep. Ser.* 1955, Oct. 17, 40.
- M. Benedict, T. Pigford, H. W. Levi: *Nuclear Chemical Engineering*, McGraw-Hill, New York 1981, pp. 283–317.
- E. D. Arnold: "Radiation Limitations on Recycle of Power Reactor Fuels", *Proc. 2nd Int. Thorium Fuel Cycle Symp.*, Gatlinburg, TN, May 3–6, 1966.
- R. E. Brooksbank, J. P. Nichols, A. L. Lotts: "The Impact of Kilorod Facility Operational Experience on the Design of Fabrication Plants for ²³³U-Th-Fuels," *Proc. 2nd Int. Thorium Fuel Cycle Symp.*, Gatlinburg, TN, Feb. 1968, pp. 321–339.
- W. R. Grimes, D. R. Cuneo: "Molten Salt Reactor Fuels," chap. 17, in C. R. Tipton Jr. (ed.): *Reactor Handbook*, 2nd ed., Interscience Publ., New York 1960.

35. E. R. Merz, G. Kaiser, E. Zimmer: "Progress in Th-²³³U-Recycle Technology," *Am. Nucl. Soc. Topical Meeting*, Gatlinburg, TN, May 1974.
36. F. Möglich, *Angew. Chem.* **53** (1940) 405-409.
37. I. Langmuir, *J. Am. Chem. Soc.* **38** (1916) 2221-2295.
38. R. Bastasz, C. Colmenares: *Catalytic Uses of Thorium and Uranium*, UCID 17499, Lawrence Livermore Laboratories, Livermore, June 1977.
39. L. Rusicka in P. Karrer (ed.): *Lehrbuch der Organischen Chemie*, Thieme Verlag, Stuttgart 1948, p. 789.
40. J. E. Crawford: "Thorium, Minerals, Facts and Problems," *Bull. U.S.-Bur. Mines* **556** (1956) pp. 1ff.
41. H. V. Hodgson, *J.-Soc. Chem. Ind Trans.* **41** (1922) 284.
42. K. Pan, Y. Mao Chen, S. Ti Lee: "A Study of Extraction of Thoriumnitrate with TBP", *J. Chin. Chem. Soc. Taiwan* **7** (1960) pp. 36ff.
43. J. R. Parker, C. V. Banks: "Some Bis(Dialkyl-Phosphinyl)Methanes as Solvent Extractants", Contract W-7405-eng-82, Ames-Lab., Iowa, June 1964, OTS.
44. J. L. Lipstein et al.: "Bioassay Monitoring Studies for Thorium," *Radiat. Prot. Dosim. Ser.* **26** (1989) nos. 1-4, 57-60.

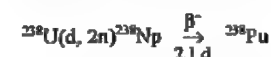
43 Plutonium

LOTHAR KOCH

43.1 Introduction	1685	43.3 Production	1688
43.2 Properties	1687	43.4 Compounds	1689
43.2.1 Physical Properties	1687	43.5 Toxicology	1691
43.2.2 Chemical Properties	1687	43.6 References	1692

43.1 Introduction

The first isotope of plutonium (Pu) to be discovered was ²³⁸Pu, which was generated by SEABORG, McMILLAN, KENNEDY, and WAHL in 1940 by bombarding uranium with deuterons:



The natural occurrence of plutonium was discovered later. In 1942, SEABORG, PEPPARD, GARNIER, and BONNIER isolated Pu from Canadian pitchblende and Colorado carnotite, in which traces of plutonium (U:Pu = 1:10⁻¹²) are formed continuously by neutron capture. Primordial ²⁴⁴Pu was isolated by HOFFMANN et al. from Precambrian bastnasite in 1971. In 1991, COWAN and ECONOMON discovered the double-beta decay of ²³⁸U to give ²³⁸Pu.

Larger quantities (ca. 10 t) of anthropogenic plutonium are distributed on earth as a

result of military activities (bomb tests, satellite accidents, bombers, rockets, etc.) and releases from nuclear facilities. Thus far, ca. 400 t of plutonium has been produced in nuclear power stations outside centrally planned economies (i.e., excluding the former Eastern-bloc countries). The ²³⁹Pu stockpiled in weapons is estimated to exceed 100 t.

Fifteen isotopes of plutonium have been synthesized; long-lived isotopes are listed in Table 43.1. They can be produced by multiple neutron capture by ²³⁸U and hence occur in spent nuclear fuel with varying abundances. Both ²³⁹Pu and ²⁴¹Pu are readily fissile with thermal neutrons, for which the absorption cross sections are higher by about two orders of magnitude. Consequently they have lower critical masses in aqueous solution since water moderates the velocity of neutrons. For ²³⁹Pu the critical mass given for metal spheres refers to H₂O reflectors only (Table 43.1).

Table 43.1: Nuclear properties of long-lived plutonium isotopes.

Mass number	Half-life, a	Decay ^a	Main α-radiation, MeV	Thermal cross section, barn		Critical mass, kg
				Capture	Fission	
238	87.7 4.80 × 10 ¹⁰	α s.f.	5.499 (70.9%) 5.457 (29.0%)	500	17	7.8 (metal sphere reflected by 10 cm iron)
239	2.41 × 10 ⁴ 5.50 × 10 ¹³	α s.f.	5.155 (73.3%) 5.143 (15.1%)	271	742	0.531 (in aqueous solution, fully H ₂ O reflected)
240	6.56 × 10 ³ 1.34 × 10 ¹¹	α s.f.	5.168 (72.8%) 5.123 (27.1%)	290	<0.08	
241	14.4	β > 99% α = 2.41 × 10 ⁻³ %	4.896 (83.2%) 4.853 (21.1%)	370	1011	0.260 (in aqueous solution, fully H ₂ O reflected)
242	3.76 × 10 ³ 6.80 × 10 ¹⁰	α s.f.	4.901 (74%) 4.857 (16%)	19	0.2	
244	8.26 × 10 ⁷ 6.60 × 10 ¹⁰	α s.f.	4.589 (81%) 4.546 (19%)	1.7		

^a α = α-decay; β = β-decay; s.f. = spontaneous fission.

Table 43.2: Structural data for plutonium (see also Figure 43.1).

Phase	Symmetry	Unit cell dimensions, pm	X-ray density, g/cm ³	Transformation temperature at STP, °C
α	simple monoclinic	at ca. 21 °C $a = 618.3 \pm 0.1$ $b = 482.2 \pm 0.1$ $c = 1096.3 \pm 0.1$ $\beta = 101.79 \pm 0.01^\circ$	19.86	
β	body-centered monoclinic	at ca. 190 °C $a = 928.4 \pm 0.3$ $b = 1046.3 \pm 0.4$ $c = 785.9 \pm 0.3$ $\beta = 93.13 \pm 0.03^\circ$	17.70	122 ± 4
γ	face-centered orthorhombic	at ca. 235 °C $a = 315.9 \pm 0.1$ $b = 576.8 \pm 0.1$ $c = 1016.2 \pm 0.2$	17.14	207 ± 5
δ	face-centered cubic	at ca. 320 °C $a = 463.71 \pm 0.04$	15.92	315 ± 3
δ'	body-centered tetragonal	at ca. 465 °C $a = 334 \pm 1$ $c = 444 \pm 4$	16.00	457 ± 2
ϵ	body-centered cubic	at ca. 490 °C $a = 363.61 \pm 0.04$	16.51	479 ± 4

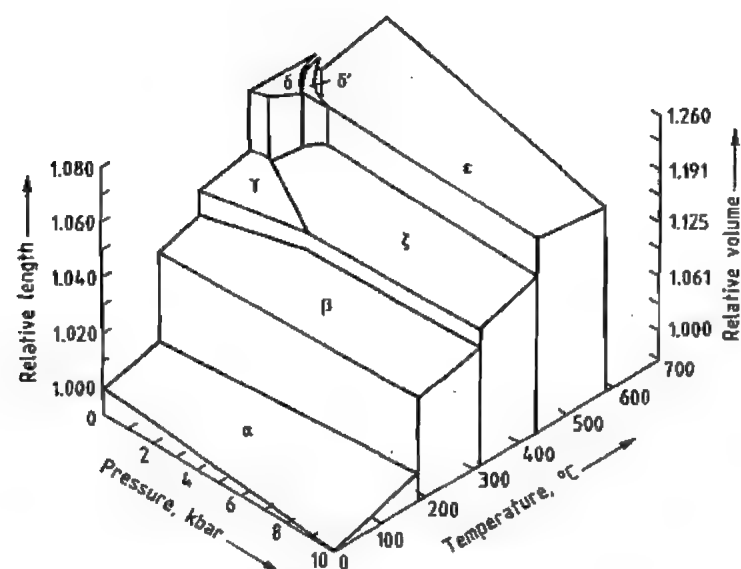


Figure 43.1: Pressure-temperature-volume diagram of plutonium.

43.2 Properties

43.2.1 Physical Properties

Plutonium is a silvery lustrous metal that exhibits five phase transitions (Table 43.2) between ambient temperature and its melting point ($640 \pm 2^\circ\text{C}$). Under pressure an additional phase occurs.

Because of the different densities of each phase, large changes in expansion are observed during phase transitions, which complicates the use of plutonium for military purposes and as a fuel in nuclear power stations (Figure 43.1). Table 43.3 lists expansion coefficients, Figure 43.2 shows the heat capacity, and Figure 43.3 the magnetic susceptibility of the different phases. For further properties, see [1].

Measurements of the thermal conductivity of the different plutonium phases are not in agreement. For α -Pu at ambient temperature it ranges from 0.084 to $0.041 \text{ W cm}^{-1}\text{K}^{-1}$.

Table 43.3: Linear thermal expansion of plutonium [1].

Phase	Principal coefficient	Temperature range, °C	Mean coefficient, $10^{-6} \text{ } ^\circ\text{C}^{-1}$
α	α_p	-186 to +101	42.3
	α_t	21-104	60
	$\alpha_s = \alpha_b$		75
	α_j		29
	α_p		54
β	$\alpha_s = \alpha_b$	93-190	94
	α_j		14
	α_p		19
	α_p		42
	α_p		42
γ	α_s	210-310	-19.7 ± 1.0
	α_p		39.5 ± 0.6
	α_p		34.3 ± 1.6
	α_p		34.6 ± 0.7
δ	α	320-440	-8.6 ± 0.3
	α_s	452-480	444.8 ± 12.1
δ'	α_s		-1063.5 ± 18.2
	α_p		-65.6 ± 10.1
	α_p		-65.6 ± 10.1
ϵ	α	490-550	36.5 ± 1.1
Liquid	α_s	664-788	93

43.2.2 Chemical Properties

Plutonium metal readily reacts with oxygen and moisture at ambient temperature, especially in bulk quantities due to self-heating.

The surface turns from grayish to dark blue and finally green oxide layers. In aqueous sodium chloride solution, it is converted to $\text{Pu}(\text{O})\text{H}$. Plutonium dissolves rapidly in hydrochloric or hydrobromic acid but is only slowly attacked by hydrofluoric acid. It undergoes passivation in nitric acid but dissolves in the presence of fluoride ions. Sulfuric acid converts plutonium slowly to its sulfate.

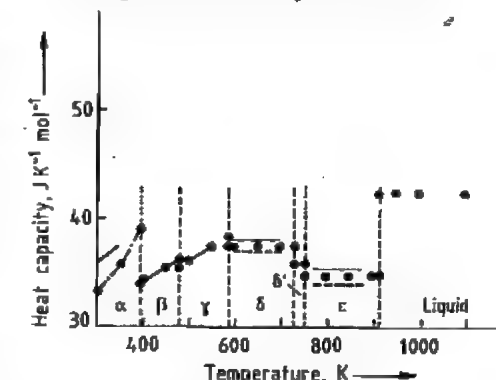


Figure 43.2: High-temperature heat capacity of plutonium metal. ● = Selected values.

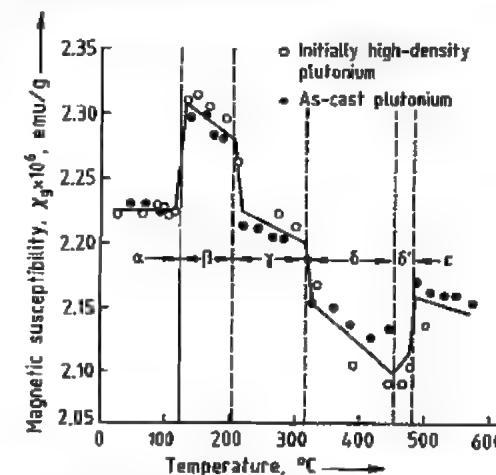


Figure 43.3: Magnetic susceptibility of plutonium as a function of temperature.

The behavior of plutonium in aqueous solution is unique. Five oxidation states exist: Pu^{3+} , Pu^{4+} , PuO_2^+ , PuO_2^{2+} , and PuO_3^{3-} (Table 43.4) of which up to four can be present simultaneously in significant quantities. The ions possess characteristic absorption bands that

are used in spectrophotometric analysis (Table 43.5). Standard potential schemes for plutonium in 1 mol/L HCl, neutral solution, and 1 mol/L OH⁻ at 25 °C are shown below:

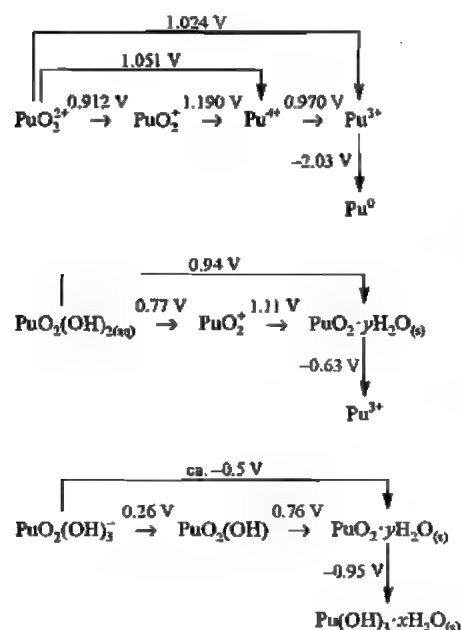


Table 43.4: Plutonium ions in aqueous solution.

Oxidation state	Form	Color
III	Pu ³⁺	blue
IV	Pu ⁴⁺	tan
IV	PuO ₂ ·nH ₂ O (polymer)	bright green, dark green
V	PuO ₂ ⁺	red-violet or pink
VI	PuO ₂ ²⁺	tan, orange (green)
VII	PuO ₃ ²⁻	blue

Table 43.5: Predominant absorption bands of plutonium ions.

Absorption bands, nm	Molar extinction coefficients			
	ε _{Pu(III)}	ε _{Pu(IV)}	ε _{Pu(V)}	ε _{Pu(VI)}
470	3.46	49.60	1.82	11.25
569	34.30	5.60	17.10	1.75
600	35.30	0.91	0.50	1.35
603	35.40	0.96	0.60	1.20
655	3.10	34.40	1.15	0.90
700	0.75	10.88	0.44	0.25
775	12.40	11.90	9.87	2.90
833	5.25	15.50	4.00	550
953	1.20	0.40	1.76	19.10

The plutonium cation Pu⁴⁺ is initially hydrolyzed to a monomer before a colloidal polymer forms, preferably in slightly acidic solution. Depolymerization is very slow and requires heating in strong acid or oxidation.

The PuO₂⁺ cation disproportionates readily at low acidity (Figure 43.4). The Pu⁴⁺ cation forms complexes with anions of inorganic acids. The nitrate complexes Pu(NO₃)_x^{(4-x)+} (with x = 1–4) are employed for the separation of plutonium by solvent extraction and anion exchange. With organic compounds, various complexes have been observed. Ethylenediaminetetraacetic acid forms complexes with plutonium cations of all valences and is often used to decontaminate surfaces or to wash out ingested plutonium.

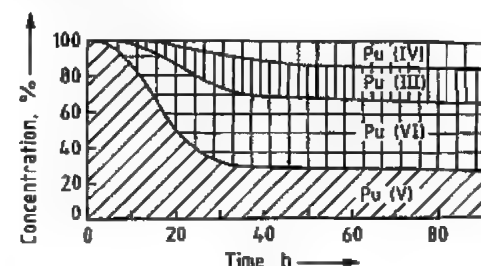


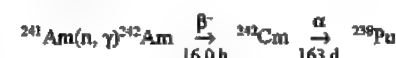
Figure 43.4: Change in composition of 0.1 mol/L HNO₃ Pu(V) solution by disproportionation.

43.3 Production

Bulk quantities of plutonium are produced through neutron capture by ²³⁸U in nuclear reactors. Thus plutonium is a by-product of nuclear energy generation. The ²³⁸Pu used as a heat source in nuclear batteries (for powering devices in space, pacemakers, etc.) is produced by the reaction



together with traces of ²³⁹Pu, or by the reaction



together with ²⁴²Pu (17%), formed by branching decay of ²⁴²Am.

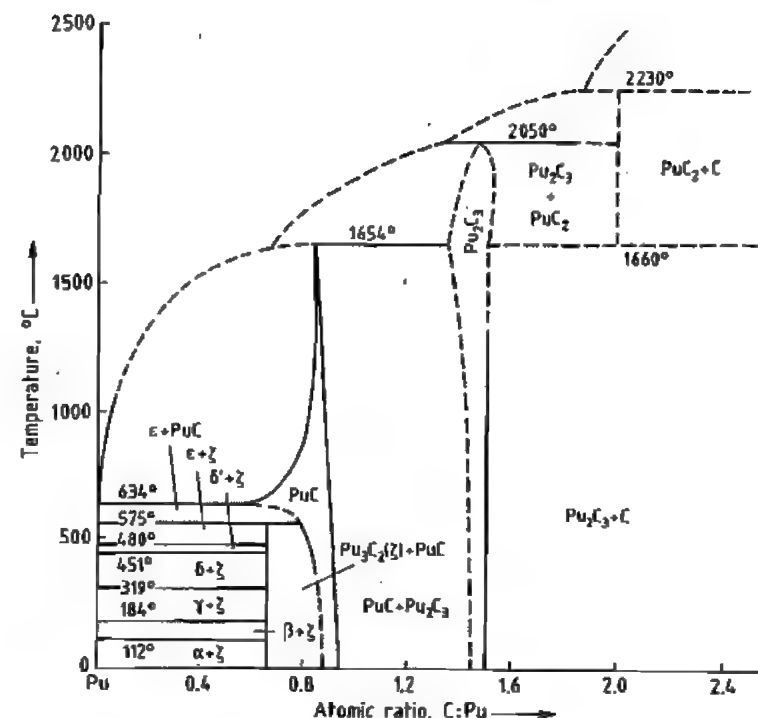


Figure 43.5: Phase diagram of plutonium-carbon system [4].

Plutonium from spent nuclear fuel is recovered by the PUREX process (liquid-liquid extraction of Pu with tri-*n*-butyl phosphate). Nonaqueous recovery by electrorefining from molten alkali-metal and alkaline earth metal chlorides is an alternative for metallic fuels. Plutonium metal is prepared from its oxide by reduction with calcium in molten CaCl₂ or CaCl₂-CaF₂.

43.4 Compounds [2, 3]

Like the other actinides, plutonium forms hard, black, metallic hydrides of the type PuH_{2+x} and PuH₃. They are inert to cold water but react slowly at 90 °C.

Four carbides of Pu exist: Pu₃C₂, PuC_{1-x}, Pu₂C₃, and PuC₂ (Figure 43.5). They decompose at high temperature with peritectic reactions, are oxidized when heated, and dissolve in oxidizing acids with the formation of CO₂ and carboxylic acids (e.g., malonic acid).

Several silicides have been observed: PuSi, Pu₃Si₂, PuSi₂, PuSi₃, and Pu₃Si₂. They have a metallic appearance and are hard, brittle, and pyrophoric. They are oxidized in air and are attacked by water.

Pnictides exist for the elements N, P, As, Sb, and Bi: PuN is black (*mp* 2570 ± 30 °C, under 100 kPa N₂), reacts slowly with cold but readily with hot water, and dissolves in mineral acids; PuP is a dark-gray compound that melts at 2600 °C under argon; PuAs has a gray metallic appearance; PuSb melts at 1980 ± 30 °C under 300 kPa Ar.

Chalcogenides exist for the elements O, S, Se, and Te: PuO₂ is a constituent of nuclear fuels. The plutonium oxygen phase diagram exhibits the existence of several oxides; their crystal data are listed in Table 43.6. The stoichiometric, metallically lustrous PuO, 5 melts at 2085 ± 25 °C and PuO₂ at 2390 ± 20 °C. Of technical relevance is the substoichiometric dioxide PuO_{2-x} (x = 1.61–1.98), which acts as an oxygen sink in nuclear fuels, absorbing ox-

ygen liberated during the fission process (and not bound by fission products). It is an olive-green compound like the stoichiometric PuO_2 , which ranges in color from dull yellow to green and finally to black depending on the starting material that is converted to the oxide. Depending on the Pu:O ratio, PuO_{2-x} has a melting point ranging from 2430 to 2510 °C.

Plutonium hydroxides and hydrated oxides are obtained by precipitation from aqueous solution. With excess alkali-metal hydroxides or NH_4OH , Pu^{3+} precipitates as blue or pale purple $\text{Pu}(\text{OH})_3 \cdot x\text{H}_2\text{O}$, Pu^{4+} as olive-green $\text{Pu}(\text{OH})_4 \cdot x\text{H}_2\text{O}$, and PuO_2^{2+} as $\text{PuO}_2(\text{OH})_2 \cdot \text{H}_2\text{O}$. Addition of H_2O_2 to solutions of Pu^{4+} in dilute acid leads to the formation of plutonium peroxide precipitates that contain about three peroxide groups per atom, together with varying amounts of anions (e.g., SO_4^{2-} , NO_3^-).

Table 43.6: Crystal structure data for plutonium oxides.

Compound	Space group	Unit cell dimensions, pm	X-ray density, g/cm ³	mp, °C
$\text{PuO}_{1.50}$	<i>P3m1</i>	$a = 384.1 \pm 0.6$ $c = 595.8 \pm 0.5$	11.47	2085 ± 25
$\text{PuO}_{1.51}$	<i>Ia3</i>	$a = 1104 \pm 2.0$	10.20	
$\text{PuO}_{1.51}$	<i>Ia3</i> or <i>Fm3m</i>	$a = 1095\text{--}1101$ or $a = 540.9$		
PuO_2	<i>Fm3m</i>	$a = 539.6 \pm 0.3$	11.46	2390 ± 20

Table 43.7: Annual limit of plutonium uptake.

Radionuclide	Form ^a	Exposure of operators		Exposure of public	
		Annual limits of incorporation by inhalation, 10^{-9} Ci	Derived concentration limits in air for an exposure of 2000 h/a, 10^{-12} Ci/m ³	Annual limits of incorporation by inhalation, 10^{-9} Ci	Annual limits of incorporation by ingestion, 10^{-6} Ci ^b
²³⁸ Pu	W	5.4	2.4	0.54	
	Y	16	8.1	1.6	(a) 0.81 (b) 8.1
²³⁹ Pu	W	5.4	2.2	0.54	
	Y	14	5.4	1.4	(a) 0.54 (b) 5.4
²⁴⁰ Pu	W	5.4	2.2	0.54	
	Y	14	5.4	1.4	(a) 0.54 (b) 5.4
²⁴¹ Pu	W	270	110	27	
	Y	540	270	54	(a) 27 (b) 270
²⁴² Pu	W	5.4	2.4	0.54	
	Y	16	8.1	1.6	(a) 0.81 (b) 8.1

^aW = week; Y = year.

^b(a) = all compounds, except oxides and hydroxides; (b) = oxides and hydroxides.

Several plutonium sulfides exist, including PuS , Pu_3S_4 , Pu_2S_3 , PuS_2 , and various nonstoichiometric sulfides. All are black powders except PuS , which is brown. The following oxysulfides are known: PuOS , $\text{Pu}_4\text{O}_4\text{S}_3$, $\text{Pu}_2\text{O}_2\text{S}$, and $\text{Pu}_2\text{O}_2\text{S}_3$. Three selenides have been identified: PuSe (mp 2075 ± 30 °C, 300 kPa Ar); Pu_2Se_3 (η and γ phase); and PuSe_{2-x} which decomposes above 600 °C.

In the Pu-Te system the following compounds have been observed: PuTe (mp 1870 \pm 30 °C, 300 kPa Ar); PuTe_2 , which decomposes when heated to give PuTe_{2-x} ; and two modifications of Pu_2Te_3 . The compound PuTe_3 is obtained by reacting plutonium hydride with excess tellurium.

The following halides and oxyhalides of plutonium are known:

PuF_3	violet-blue
PuF_4	pale brown
$\text{PuF}_4 \cdot n\text{H}_2\text{O}$	pink-white
$\text{PuF}_5 \cdot 2.5\text{H}_2\text{O}$	pink
PuF_6	reddish brown
PuCl_3	emerald green
$\text{PuCl}_3 \cdot 6\text{H}_2\text{O}$	blue
PuBr_3	green
$\text{PuBr}_3 \cdot 6\text{H}_2\text{O}$	blue
PuI_3	bright green
PuOF	metallic
PuOCl	blue-green
PuOBr	dark green
PuOI	green
PuO_2F_2	white
$\text{PuO}_2\text{Cl}_2 \cdot 6\text{H}_2\text{O}$	greenish yellow
PuO_2F_4	chocolate brown

The trifluoride and tetrafluoride hydrates are obtained by precipitation from aqueous solution. They undergo dehydration when heated in HF atmosphere to give PuF_3 and PuF_4 . Like its homologues, PuF_6 is volatile (mp 52 °C, bp 62.15 °C).

Figure 43.6: Glove box.

43.5 Toxicology

Because of its high radiotoxicity, plutonium is now handled exclusively in airtight glove boxes (Figure 43.6), which are under reduced pressure to prevent leakage of aerosols or volatile plutonium compounds in case of a containment rupture. Only very small quantities (in the range of microcuries) can be handled outside glove boxes with precautions, since the limits for ingestion and inhalation of plutonium are extremely low (Table 43.7). These limits [5] are based on the recommendations of the International Commission on Radiolog-

ical Protection. Compared to the radiological risks by incorporation, extracorporeal radiation by plutonium is relatively low. Here the same precautions are taken as for pure beta or gamma emitters.

Control of the Risk by Incorporation. In laboratories where plutonium is handled, personnel are protected against incorporation by

- Continuous monitoring of air
- Routine checks by body counters
- Routine urine analysis

For operations (e.g., bagging in and out of plutonium in glove boxes) where the risk of contamination exists, gas masks must be worn by the operator. Rooms housing glove boxes have reduced pressure and are vented through absolute filters. When leaving controlled laboratories, operators must check their clothing, hands, and feet for possible contamination.

Release of Plutonium to the Environment.

In addition to stratospheric injection from nuclear weapons testing, plutonium may be released into the troposphere during routine or accidental release from nuclear reactor operation or fuel reprocessing. Simulation tests under typical meteorological conditions have found that 99% of 0.3- μm particles are removed from the atmosphere in 3–60 d, whereas larger particles deposit more quickly. For plutonium deposited in the terrestrial ecosystem the transfer to humans via the food chain is reduced by a factor of at least 10^8 because of metabolic discrimination [6].

Characteristic discrimination factors (DF) for plutonium movement in the food chain are as follows:

Soil \rightarrow plant and root uptake	$\text{DF}_{\text{plant/soil}} 10^{-4}\text{--}10^{-6}$
Crop plant \rightarrow humans	$\text{DF}_{\text{human/plant}} 10^{-4}$
Forage plants \rightarrow grazing animals	$\text{DF}_{\text{animal/plant}} 10^{-4}$
Plant \rightarrow grazing animal \rightarrow human beings	$\text{DF} = 10^{-3} \times 10^{-4} = 10^{-8}$

where, for example, $\text{DF}_{\text{plant/soil}}$ is the ratio of the plutonium concentration in the plant to the plutonium concentration in the soil.

Discrimination against plutonium also occurs at each level of the food chain for the up-

44 General

IAN MCGILL

44.1 Introduction	1695	44.6.3 Separation by Ion Exchange	1711
44.2 History	1697	44.6.3.1 Ion Exchange with Chelating Agents	1711
44.3 Mineralogy, Abundance, Occurrence	1697	44.6.3.2 Separation Process	1712
44.4 Properties	1700	44.6.3.3 Industrial Processes	1713
44.4.1 Properties of the Nuclei	1700	44.6.3.4 Disadvantages of Ion Exchange	1713
44.4.2 Properties of the Atoms and Ions	1700	44.6.4 Separation by Liquid-Liquid Extraction	1714
44.4.2.1 Electronic Configuration, Position in the Periodic Table	1700	44.6.4.1 Theoretical Basis	1714
44.4.2.2 Oxidation States, Atomic and Ionic Radii	1701	44.6.4.2 Extractants	1715
44.4.2.3 Magnetic and Spectral Properties	1702	44.6.4.3 Industrial Liquid-Liquid Extraction	1719
44.4.2.4 Bonding, Coordination Numbers	1703	44.7 Production of the Metals	1722
44.4.3 Other Chemical and Physical Properties	1704	44.7.1 Fused-Salt Electrolysis	1725
44.4.4 Miscibility and Alloying Behavior	1704	44.7.2 Metallothermic Reduction	1726
44.4.5 Mechanical Workability	1704	44.7.3 Purification	1727
44.5 Digestion of Ores	1706	44.8 Analysis	1727
44.5.1 Wet Digestion; Fusion	1706	44.9 Compounds	1728
44.5.1.1 Monazite	1707	44.9.1 Hydrides	1728
44.5.1.2 Bastnaesite	1707	44.9.2 Oxides, Hydroxides, Peroxides, Salts of Inorganic Oxoacids, Double Salts	1728
44.5.1.3 Other Ores	1708	44.9.3 Halides	1730
44.5.2 Chlorination	1708	44.9.4 Chalcogenides	1731
44.6 Separation	1708	44.9.5 Nitrides	1731
44.6.1 Principles of Separation	1709	44.9.6 Carbides	1731
44.6.2 Separation by Classical Methods	1710	44.9.7 Complexes; Organic Compounds	1732
44.6.2.1 Fractional Crystallization	1710	44.10 Uses	1732
44.6.2.2 Fractional Precipitation	1710	44.11 Economic Aspects	1736
44.6.2.3 Separations Based on Oxidation State Changes	1710	44.12 Toxicology	1737
		44.13 References	1737

44.1 Introduction

The metallic elements known collectively as the rare earths (better: rare earth metals or rare earth elements, abbreviated to RE) are listed in Table 44.1. General reviews are given in [1–6]. Originally, the name was only used for the sesquioxides, RE_2O_3 , which are extraordinarily similar to one other in their chemical and physical properties and are therefore difficult to separate. Within the rare earth group, the elements scandium, yttrium, and lanthanum differ in their atomic structure (Table 44.2) from the elements cerium to lute-

tium (the lanthanides, Ln). The term lanthanoids has been proposed by IUPAC to include lanthanum and the lanthanides [7], but this usage is not yet universal. In the fields of mineralogy and geochemistry, the term cerium earths is used for the elements La and Ce to Eu, and yttrium earths for Y and Gd to Lu. Scandium occupies a special position with respect to this classification and its other properties, and therefore does not belong to either of these groups. The terms terbium earths for Eu, Gd, and Tb; erbium earths for Dy, Ho, Er, and Tm; and ytterbium earths for Yb and Lu are now hardly used. The rare earth elements al-

ways occur in nature in association with each other. The isolation of groups of rare earth elements or of individual elements requires costly separation and fractionation processes

owing to the great similarity of the chemical and physical properties of their compounds, which explains why the history of their discovery has extended over such a long period.

Table 44.1: Atomic numbers, relative atomic masses, and natural nuclides of the rare earth elements.

Element	Symbol	Atomic number	M_r	Mass numbers of the nuclides (abundance in %) ^a
Scandium	Sc	21	44.9559	45 (100)
Yttrium	Y	39	88.9059	89 (100)
Lanthanum	La	57	138.9055	138 (0.089; EC, 1.1×10^{11} a), 139 (99.91)
Cerium	Ce	58	140.12	139 (0.139), 138 (0.250), 140 (88.48), 142 (11.07; β^- , 5×10^{15} a)
Praseodymium	Pr	59	140.9077	141 (100)
Neodymium	Nd	60	144.24	142 (27.11), 143 (12.17), 144 (23.85; α , 1×10^{15} a), 145 (8.30), 146 (17.22), 148 (5.73), 150 (5.62)
Promethium	Pm	61	(145)	only radioactive isotopes
Samarium	Sm	62	150.4	144 (3.09), 147 (14.97; α , 1.06×10^{11} a), 148 (11.24; α , 1.2×10^{13} a), 149 (13.83; α , 4×10^{14} a), 150 (7.44), 152 (76.72), 154 (22.71)
Europium	Eu	63	151.96	151 (47.82), 153 (52.18)
Gadolinium	Gd	64	157.25	152 (0.20), 154 (2.15), 155 (14.73), 156 (20.47), 157 (15.68), 158 (24.87), 160 (21.90)
Terbium	Tb	65	158.9254	159 (100)
Dysprosium	Dy	66	162.50	156 (0.052), 158 (0.090), 160 (2.29), 161 (18.88), 162 (25.53), 163 (24.97), 164 (28.18)
Holmium	Ho	67	164.9304	165 (100)
Erbium	Er	68	167.26	162 (0.136), 164 (1.56), 166 (33.41), 167 (22.94), 168 (27.07), 170 (14.88)
Thulium	Tm	69	168.9342	169 (100)
Ytterbium	Yb	70	173.04	168 (0.135), 170 (3.03), 171 (14.31), 172 (21.82), 173 (16.13), 174 (31.84), 176 (12.73)
Lutetium	Lu	71	174.97	175 (97.41), 176 (2.59; β^- , 2.1×10^{10} a)

^a For the radioactive nuclides, the decay mode (EC = electron capture) and half-life is given in brackets as well as the abundance.

Table 44.2: Electronic configurations and spectroscopic terms of the gaseous rare earth elements in the ground state.

Symbol	RE ⁰	RE ²⁺	RE ³⁺
Sc	[Ar] 3d ¹ 4s ²	[Ar] 3d ¹ (2D _{3/2})	[Ar] (1S ₀)
Y	[Kr] 4d ¹ 5s ²	[Kr] 4d ¹ (2D _{3/2})	[Kr] (1S ₀)
La	[Xe] 5d ¹ 6s ²	[Xe] 5d ¹ (2D _{3/2})	[Xe] (1S ₀)
Ce	[Xe] 4f ¹ 5d ¹ 6s ²	[Xe] 4f ² (3H ₄)	[Xe] 4f ¹ (2F _{5/2})
Pr	[Xe] 4f ³ 6s ²	[Xe] 4f ³ (4I _{9/2})	[Xe] 4f ² (3H ₄)
Nd	[Xe] 4f ⁴ 6s ²	[Xe] 4f ⁴ (3I ₄)	[Xe] 4f ³ (4I _{9/2})
Pm	[Xe] 4f ⁵ 6s ²	[Xe] 4f ⁵ (6H _{5/2})	[Xe] 4f ⁴ (3I ₄)
Sm	[Xe] 4f ⁶ 6s ²	[Xe] 4f ⁶ (7F ₀)	[Xe] 4f ⁵ (6H _{5/2})
Eu	[Xe] 4f ⁷ 6s ²	[Xe] 4f ⁷ (8S _{7/2})	[Xe] 4f ⁶ (7F ₀)
Gd	[Xe] 4f ⁷ 5d ¹ 6s ²	[Xe] 4f ⁷ 5d ¹ (9D ₃)	[Xe] 4f ⁷ (8S _{7/2})
Tb ^a	[Xe] 4f ⁹ 6s ²	[Xe] 4f ⁹ (6H _{15/2})	[Xe] 4f ⁸ (7F ₆)
Dy	[Xe] 4f ¹⁰ 6s ²	[Xe] 4f ¹⁰ (3I ₆)	[Xe] 4f ⁹ (6H _{15/2})
Ho	[Xe] 4f ¹¹ 6s ²	[Xe] 4f ¹¹ (4I _{15/2})	[Xe] 4f ¹⁰ (3I ₆)
Er	[Xe] 4f ¹² 6s ²	[Xe] 4f ¹² (3H ₆)	[Xe] 4f ¹¹ (4I _{15/2})
Tm	[Xe] 4f ¹³ 6s ²	[Xe] 4f ¹³ (2F _{7/2})	[Xe] 4f ¹² (3H ₆)
Yb	[Xe] 4f ¹⁴ 6s ²	[Xe] 4f ¹⁴ (1S ₀)	[Xe] 4f ¹³ (2F _{7/2})
Lu	[Xe] 4f ¹⁴ 5d ¹ 6s ²	[Xe] 4f ¹⁴ 5d ¹ (2S _{1/2})	[Xe] 4f ¹⁴ (1S ₀)

^a For Tb⁰, possibly also 4f⁸ 5d¹ 6s².

Table 44.3: History of the discovery of the rare earth elements [6, 8].

Element	Year	Discoverer	Notes
Scandium	1879	NILSON	from ytterbium earths (DE MARIGNAC, 1878)
Yttrium	1843	MOSANDER	from yttrium earths (GADOLIN, 1794)
Lanthanum	1839–1841	MOSANDER	from cerium earths (KLAPROTH, BERZELIUS, HISINGER, 1803)
Cerium			
Praseodymium	1885	AUER V. WELSBACH	from didymium (MOSANDER, 1839–1841)
Neodymium			
Samarium	1901	DEMARCA	from the samarium fraction (LECOQ DE BOISBAUDRAN, 1879) of didymium (MOSANDER, 1839–1841)
Europium			
Gadolinium	1886	LECOQ DE BOISBAUDRAN	from didymium (MOSANDER, 1839–1841), independently of each other
	1880	DE MARIGNAC	
Terbium	1878	DE MARIGNAC	from terbium earth (DELAFontaine, 1878), originally named terbium earth (MOSANDER, 1843)
		DELAFontaine	
Dysprosium	1886	LECOQ DE BOISBAUDRAN	from the holmium fraction (CLEVE, 1879) of the erbium earth (DE MARIGNAC, 1878)
Holmium	1879	CLEVE	
Erbium	1879	CLEVE	from erbium earth (DE MARIGNAC, 1878)
Thulium	1879	CLEVE	from the holmium fraction (CLEVE, 1879) of erbium earth (DE MARIGNAC, 1878)
Ytterbium	1878	DE MARIGNAC	from ytterbium earth (DE MARIGNAC, 1878)
Lutetium	1907	URBAIN	from ytterbium earth, independently of each other (DE MARIGNAC, 1878)
		AUER V. WELSBACH	
		JAMES	

44.2 History

The discovery of the rare earths is summarized in Table 44.3, with the exception of the radioactive element promethium. Further details are given in [8]. The word “rare”, when used to describe this group of elements, originates from the fact it was thought that the rare earth elements could only be isolated from very rare minerals. Considering the abundance of the rare earth elements in the Earth's crust, the term rare is inappropriate.

44.3 Mineralogy, Abundance, Occurrence

The rare earth elements are lithophilic and are therefore concentrated in oxidic compounds such as carbonates, silicates, titanotantaloniobates, and phosphates, or form minerals of these types on their own [6, 9] (see also [1, parts A4, A5]). The formation of the minerals is influenced by variations in ionic radii, crystallochemical factors such as coordination number, basicity, potential for isomor-

phic replacement, tendency to form complexes, and differences in oxidation states [10], (see also [2, vol. 3, pp. 1–80]). These factors lead to the division of the rare earth elements into three groups, according to the mineralization process (REO denotes the rare earth sesquioxides):

- Minerals that contain lanthanum to neodymium, samarium, and europium, and in which cerium and, in some cases also lanthanum or neodymium, are present as the main components (cerium earths, Ce...). Typical examples of this group include bastnaesite (Ce...)FCO₃ (max. 75% REO content), monazite (Ce...)PO₄ (max. 65% REO content), and allanite (Ca, Ce...) (Fe, Al)₃ (SiO₄)₃(OH) (max. 28% REO content).
- Minerals with gadolinium to lutetium and yttrium as main components (yttrium earths, Y...). Typical examples of this group are xenotime (Y...)PO₄ (max. 62% REO content) and gadolinite (Y...)FeBe₂Si₂O₁₀ (max. 48% REO content). Typical compositions of bastnaesite, monazite, and xenotime from

various mineral resources are given in Table 44.4.

- Complex minerals in which both yttrium earths and cerium earths can be represented in the same mineral type, either of these groups of rare earths being the main one. Minerals of this type are oxidic ores containing titanium, niobium, tantalum, uranium, and thorium; for example:

Euxenite (Y..., Ce...)(Nb, Ta, Ti)₂O₆

Samarskite (Y..., Ce...)₄(Nb, Ta, Ti)₂O₆

Fergusonite (Y...)(Nb, Ti, Ta)O₄

Betafite (U, Ca, Y..., Ce...)₂(Nb, Ta, Ti)₂O₆(OH)

The minerals of the first two groups occur in pegmatites and metamorphic gneisses, as well as hydrothermal and pneumatolytic veins, and in skarns and carbonatites. The minerals of the third group are mainly found in pegmatites.

Useful concentrations (up to 5%) of rare earth elements occur in apatite Ca₅(F, Cl, OH)(PO₄)₃ (see typical composition in Table 44.4), and up to 10% in pyrochlore (Na, Ca, Ce...)₂(Nb, Ta, Ti)₂(O, OH, F)₇, and loparite (Na, Ca, Ce...)₂(Nb, Ta, Ti)₂O₆ in the Kola Peninsula (CIS), and also in most uranium minerals as trace substituents.

Scandium occurs in trace amounts in most rare earth minerals along with the true rare earth elements (e.g., as a substituent ion of the same valency). However, the amounts are very small. Thortveitite, Sc₂Si₂O₇; steretite, ScPO₄·2H₂O; and kolbeckite (Sc, Be, Ca) (SiO₄, PO₄)·2H₂O are genuine scandium minerals. Apart from scandium, thortveitite also contains yttrium, ytterbium, and lutetium.

In many minerals, scandium is present in a dispersed state. Wolframite and cassiterite can contain up to 1% scandium, so that scandium is a by-product of the production of tungsten and tin. Uranium minerals contain much smaller amounts of scandium, but, since uranium is produced in relatively large quantities, scandium is produced in appreciable quantities also.

The abundance of the rare earth elements taken together is quite considerable. Cerium, the most common rare earth, is more abundant than, e.g., Co. Yttrium is more abundant than, e.g., Pb, whereas genuinely rare REs such as Lu and Tm are as abundant as Sb, Hg, Bi, and Ag. Promethium in rare earth minerals is present only in amounts of < 10⁻¹⁹% as a result of nuclear reactions with cosmic rays or the spontaneous fission of ²³⁸U.

Table 44.4: Rare earth content (% of total REO) in typical minerals.

	Monazite		Bastnæsité		Xenotime	Apatite
	Australia	China	United States	China	Malaysia	CIS
Cerium earths	94.940	92.090	99.547	98.600	10.500	90.100
La ₂ O ₃	23.900	23.350	33.200	23.000	0.500	25.100
CeO ₂	46.030	45.690	49.100	50.000	5.000	45.000
Pr ₆ O ₁₁	5.050	4.160	4.340	6.200	0.700	3.900
Nd ₂ O ₃	17.380	15.740	12.000	18.500	2.200	14.000
Sm ₂ O ₃	2.530	3.050	0.789	0.800	1.900	1.600
Eu ₂ O ₃	0.050	0.100	0.118	0.200	0.200	0.500
Yttrium earths	5.060	7.910	0.315	1.400	89.500	7.250
Gd ₂ O ₃	1.490	2.030	0.166	0.700	4.000	1.500
Tb ₄ O ₇	0.040	0.100	0.016	0.100	1.000	0.100
Dy ₂ O ₃	0.690	1.020	0.031	0.100	8.700	1.000
Ho ₂ O ₃	0.050	0.100	0.005	trace	2.100	0.100
Er ₂ O ₃	0.210	0.510	0.004	trace	5.400	0.150
Tm ₂ O ₃	0.010	0.510	0.001	trace	0.900	0.020
Yb ₂ O ₃	0.120	0.510	0.001	trace	6.200	0.080
Lu ₂ O ₃	0.040	0.100	trace	trace	0.400	trace
Y ₂ O ₃	2.410	3.030	0.091	0.500	60.800	4.300
Total	100.000	100.000	99.862	100.000	100.000	97.350

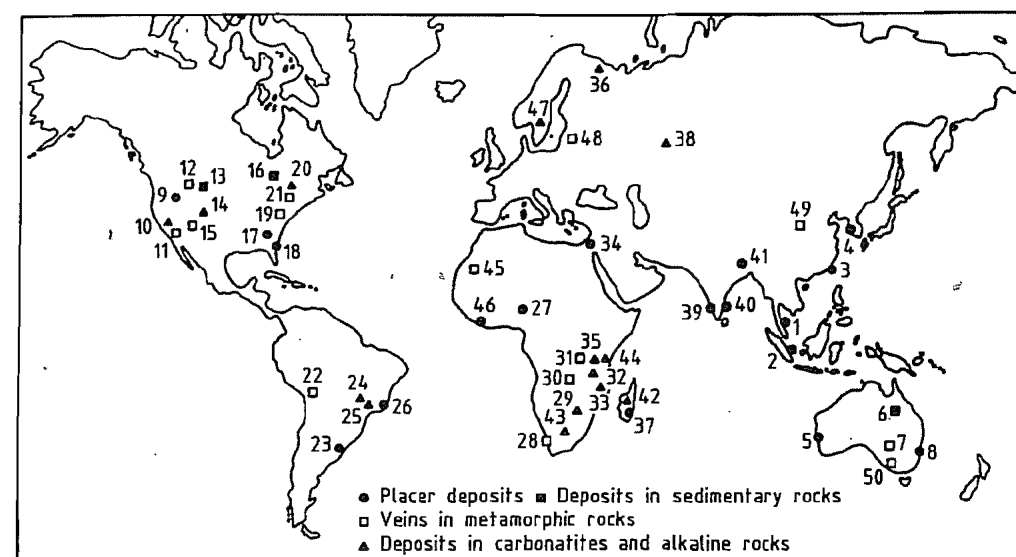


Figure 44.1: Important rare earth deposits [11]. 1) Malaysia; w) Singkep, Billit and Bangka, Indonesia; 3) Taiwan; 4) Korea; 5) Western Australia; 6) Mary Kathleen Mine, Australia; 7) Radium Hill, Australia; 8) New South Wales, Australia; 9) Bear Valley, Idaho/Montana; 10) Mountain Pass, California; 11) Music Valley, California; 12) Mineral Hill/Lenhi Pass, Idaho/Montana; 13) Bald Mountain, Wyoming; 14) Powderhorn and Wet Mountains, Colorado; 15) Gallinas Mountains, New Mexico; 16) Blind River/Elliott Lake, Ontario; 17) Piedmont, Georgia; 18) Atlantic Coast placer deposits; 19) Dover, New Jersey; 20) Oka, Québec; 21) Mineville, New York; 22) Llallagua, Bolivia; 23) Atlántida, Uruguay; 24) Araxa, Brazil; 25) Morro do Ferro, Brazil; 26) Espírito Santo, Brazil; 27) Jos Plateau, Nigeria; 28) Steenkampskraal, South Africa; 29) Glenover, South Africa; 30) Shinkolobwe, Zaire; 31) Karonge, Burundi; 32) Panda Hill, Tanzania; 33) Kangakunde Hill, Malawi; 34) Nile Delta, Egypt; 35) Mrima, Kenya; 36) Kola Peninsula, CIS; 37) Madagascar; 38) Vishnevye Mountains, CIS; 39) Kerala, India; 40) Sri Lanka; 41) Bihar and Bengal; 42) Iremo, Madagascar; 43) Pilanesberg, Bophuthatswana; 44) Wigu Hill, Tanzania; 45) Bon Nage Mauretania; 46) Monrovia, Liberia; 47) Fen, Norway; 48) Kangasala, Finland; 49) Bayan Obo, Inner Mongolia; 50) Roxby Downs, Australia.

The rare earth minerals of the three groups referred to above occur in distinct deposits (Figure 44.1) [11]. Perhaps the most important mined rare earth deposit is at the Mountain Pass Mine in California (carbonatite), where up to 40 000 t/a bastnæsité ore concentrate (70% REO) is produced by ore beneficiation. Other important bastnæsité deposits are in Burundi (carbonatite), Madagascar (alkali rock), and in Bayan Obo, near the town of Baotou in Inner Mongolia in China. The bastnæsité, with monazite, is associated with magnetite-hematite-fluorspar.

Monazite mainly occurs in secondary deposits in the heavy minerals of coastal sands. The extraction of monazite is closely linked with the extraction of rutile, ilmenite, and zircon in Australia, Brazil, India, and the United States, and with the extraction of cassiterite in

Indonesia, Malaysia, Thailand, Nigeria, and Zaire. However, this also means that the amount of monazite available depends on the demand for the main product. These monazites contain up to ca. 10% thorium. Xenotime is found in similar deposits, Malaysian monazite having particularly high xenotime contents.

Primary monazite deposits with high thorium contents are found in Brazil, and particularly in South Africa, though these are not extracted at present. Low-thorium monazites occur in primary carbonatitic deposits in Malawi and Burundi.

The minerals of the third group are extracted mainly for their Nb, Ta, and U contents.

In 1990, world reserves of rare earth minerals were estimated at ca. 84×10^6 t REO.

China has estimated reserves of 43×10^6 t REO (ca. 50% of the world reserves). The Baiyunebo deposit near Baotou in Inner Mongolia is the largest source of rare earth minerals in the world and accounts for over half of the Chinese production. The bastnæsité deposit at Mountain Pass, California, contains an estimated reserve of 4.3×10^6 t REO representing approximately 5% of world reserves. Total reserves within the United States currently amount to 12.6×10^6 t REO.

Reserves elsewhere have been estimated as follows: Australia: 5.1×10^6 t REO, India: 2.3×10^6 t REO, Canada: 0.95×10^6 t REO, CIS: 0.45×10^6 t REO, Brazil: 0.28×10^6 t REO, and others, excluding the United States and China, 19.63×10^6 t REO.

The production of bastnæsité concentrate at the Mountain Pass Mine, California reached a peak in 1984 of 25 312 t REO. In 1990, production totalled 22 829 t REO, representing approximately 27% of world production [12]. Estimated monazite production expressed as rare earth oxide (REO) in 1990 was as follows: Australia: 6500 t, Brazil: 1900 t, India: 2030 t, Malaysia: 1740 t, South Africa: 1000 t, United States: 2000 t, and the CIS: 1500 t.

Raw material prices in early 1990 for bastnæsité from the United States with 70% REO was \$1.3/lb, reflecting an increased use of cerium oxide in autocatalysts, glass additives, and polishing compounds. From 1988 to 1991, the price of Australian monazite with > 55% REO was stable between A\$800–900/t; Malaysian xenotime as 60% yttrium concentrate cost \$32–33/kg.

44.4 Properties

44.4.1 Properties of the Nuclei

Some naturally occurring nuclides of the rare earth elements are radioactive. Data on types of radioactive decay and half-lives are given in Table 44.1. Radioactive properties of artificial rare earth nuclides are given in [13]. Promethium, Pm, whose occurrence in nature was sought for a long time without success,

was first identified with certainty in 1945 by MARINSKY et al. as a radioactive fission product of uranium [14].

So far, 25 relatively short-lived isotopes of Pm are known (longest half life: 17.7 years for ^{145}Pm). ERÄMETSÄ [15] isolated traces of ^{145}Pm from the rare earth concentrate of an apatite in 1965, and deduced that the abundance of Pm in nature is $< 10^{-19}\%$. The question whether this is produced by natural uranium fission or by the action of cosmic rays on ^{146}Nd is the subject of debate.

The very high thermal neutron absorption cross section of several nuclides of Sm, Eu, and Gd is noteworthy.

44.4.2 Properties of the Atoms and Ions

44.4.2.1 Electronic Configuration, Position in the Periodic Table

The electronic configurations of neutral, isolated atoms of the rare earth elements in the ground state (Table 44.2) lead to the following position of the rare earth elements in the periodic table: the elements Sc, Y, and La are the first members of a series of transition elements (*d*-elements) with the valence electron configuration $ns^2(n-1)d^1$ ($n = 4, 5$, or 6). The 14 elements, Ce–Lu, constitute a series of inner transition elements ("*f*-elements") which must be inserted between La and Hf. These are the lanthanides, with valence electron configurations of the type $6s^2 5d^1 4f^{n-1}$ or $6s^2 4f^n$. Thus, all the rare earth elements belong formally to Group 3 of the Periodic System.

In the neutral atoms, the $5d$ and $4f$ electrons have similar energies. This fact explains the occurrence of the two typical electronic configurations referred to above within the lanthanide series (Table 44.2), whereby the configurations $4f^j$ (half-filled orbital) and $4f^{14}$ (completely filled orbital) are preferred owing to the high thermodynamic stability of such states. The irregularity of the configurations of the two elements immediately before the middle and the end of the lanthanide series, Eu and

Yb, are characteristic of the neutral atoms and the mono- and divalent ions. However, in the case of the trivalent ions, the $4f$ orbital is filled in a completely regular manner. The energy of the $4f$ orbital decreases with increasing atomic number and increasing ionic charge, so that when the valency is $3+$, which is characteristic of the rare earth elements, the $4f$ electrons represent well-defined "inner electrons" that take virtually no part in chemical bonding due to their proximity to the nucleus and shielding by the $5s^2 5p^6$ octet. Therefore, the regular filling of the $4f$ orbital from Ce^{3+} to Lu^{3+} determines the chemical properties, as the resulting electronic configurations resemble those of the rare gases, and lead to the great similarity of the Ln^{3+} compounds to each other, to the corresponding compounds of La^{3+} , Y^{3+} , and, to a limited extent, to those of Sc^{3+} .

Table 44.5: Atomic radii and effective ionic radii of the rare earth elements (in nm).

Symbol	Atom ^a	$\text{RE}^{2+ \text{ b}}$	$\text{RE}^{3+ \text{ c}}$	$\text{RE}^{4+ \text{ d}}$
Sc	0.1654		0.0730	
Y	0.1824		0.0892	
La	0.1884		0.1061	
Ce	0.1825		0.1034	0.096 ^e
Pr	0.1836		0.1013	0.095
Nd	0.1829		0.0995	
Pm	0.1825		0.0979	
Sm	0.1814	0.1232	0.0964	
Eu	0.1984	0.1220	0.0950	
Gd	0.1817		0.0938	
Tb	0.1803		0.0923	0.088
Dy	0.1796		0.0908	
Ho	0.1789		0.0894	
Er	0.1780		0.0881	
Tm	0.1769	0.1127 ^e	0.0869	
Yb	0.1932	0.1115	0.0858	
Lu	0.1760		0.0848	

^aHalf the interatomic distance for the modification stable at room temperature, calculated from lattice constants [17, 18].

^bFor coordination number 8 in difluorides with $r_{\text{F}^-} = 0.132$ nm [20].

^cFor coordination number 6 [19].

^dFor coordination number 8 in dioxides with $r_{\text{O}^{2-}} = 0.138$ nm.

^eEstimated.

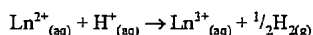
The regular filling of the $4f$ orbital is accompanied by a steady reduction in the Ln^{3+} ionic radii (Table 44.5, [17–20], and Figure 44.2)—the so-called lanthanide contraction. This steady shrinkage of the inner electron shell is mainly caused by the incomplete mu-

tual shielding of the $4f$ electrons against the increasing attraction of the nucleus.

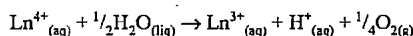
The peculiarities of the electronic structure of the rare earth elements described here lead to periodic changes in some physical and chemical properties of these elements and their compounds in the series La to Lu, while other properties show a steady or nonperiodic change. The typical similarity of the rare earth elements to each other, which is often emphasized, is in essence only exhibited for the nonperiodic properties. Thus, the regular change in the RE^{3+} radii leads to largely nonperiodic changes in properties that depend on ion size, such as solubility, basicity, normal potential, and enthalpy of hydration. Periodic variation in properties can have various causes and cannot be interpreted with certainty in all cases. Typically, maxima or minima occur at Eu and Yb, because they are situated immediately before the $4f$ shell is half filled ($4f^7$) or completely filled ($4f^{14}$) and attempt to achieve these stable configurations. Periodic variations are observed for atomic radii, molecular volumes, melting points, boiling points, and sublimation enthalpies of the elements. A similar periodicity is also observed in some dissociation enthalpies of gaseous molecules REX ($\text{X} = \text{chalcogenide}$) due to certain peculiarities in the electronic configurations [16]. Other types of pronounced periodicity occur, e.g., in magnetic moments and colors of the RE^{3+} ions.

44.4.2.2 Oxidation States, Atomic and Ionic Radii

The oxidation state $3+$ is characteristic for all rare earth elements, both for solid compounds and for solvated ions in various solvents. The oxidation state $2+$ can occur in pure solid compounds of Eu, and, to a slightly lesser extent, Yb, due to the higher stability of the configurations $4f^7$ and $4f^{14}$. It is also observed to a very limited extent with Sm and Tm. In aqueous solutions, Eu^{2+} ions are metastable. All the other Ln^{2+} ions react in acidic media as reducing agents:



The oxidation state 4+ can occur for Ce and Tb, which follow La and Gd respectively, and also to a very limited extent for Pr and Nd. Only the Ce^{4+} ion is metastable in aqueous solution; The other Ln^{4+} ions oxidize water as follows:



The general preference for the oxidation state 3+ in aqueous solution is probably a consequence of the similarity between the hydration enthalpy and ionization enthalpy of the ions. The standard electrode potentials listed in Table 44.6 [8] illustrate the behavior of the various RE^{n+} ions in aqueous solution, and show that the rare earths are a group of highly nonnoble elements. Figure 44.2 shows the atomic radii (in the metallic state) and ionic radii for the various typical valencies. The periodicity of the atomic radii described above (maxima for Eu and Yb) shows that in the metallic state these elements contribute only two electrons to the bond, so that their atomic volumes are similar to those of the alkaline earth metals. The radii of the Ln^{2+} ions, plus the radius of the Ba^{2+} ion, give a curve resembling the lanthanide contraction curve, and the term baride contraction has been suggested to describe this [21]. The radii of Eu^{2+} and Sr^{2+} are similar, as are the radii of Yb^{2+} and Ca^{2+} , which explains the commonly observed isomorphous replacement of alkaline earth ions by Ln^{2+} ions of similar size.

The similarity of the chemical properties of Ln^{3+} compounds to those of the corresponding compounds of La^{3+} and Y^{3+} can be explained by the similarities between the sizes of these ions. Therefore, as expected, in the case of those properties that are mainly determined by ion size, La should be placed near Ce, and Y between Ho and Er. However, for scandium, which has a comparatively small radius ($r_{\text{Sc}^{3+}} = 0.0730$ nm), there is a greater similarity to the chemistry of aluminum ($r_{\text{Al}^{3+}} = 0.0530$ nm) than to that of lutetium ($r_{\text{Lu}^{3+}} = 0.0848$ nm).

Table 44.6: Standard electrode potentials E°_{298} of the rare earth elements in volts [8] (much of the data is estimated).

Element	$\text{RE}_{(\text{s})}/\text{RE}^{3+}_{(\text{aq})}$	$\text{RE}^{2+}_{(\text{aq})}/\text{RE}^{3+}_{(\text{aq})}$	$\text{RE}^{3+}_{(\text{aq})}/\text{RE}^{4+}_{(\text{aq})}$
Sc	+2.077		
Y	+2.372		
La	+2.522		
Ce	+2.483		-1.74
Pr	+2.462		ca. -2.86
Nd	+2.431		
Pm	+2.423		
Sm	+2.414	+1.55	
Eu	+2.407	+0.43	
Gd	+2.397		
Tb	+2.391		-1.28
Dy	+2.353		
Ho	+2.319		
Er	+2.296		
Tm	+2.278		
Yb	+2.267	+1.15	
Lu	+2.255		

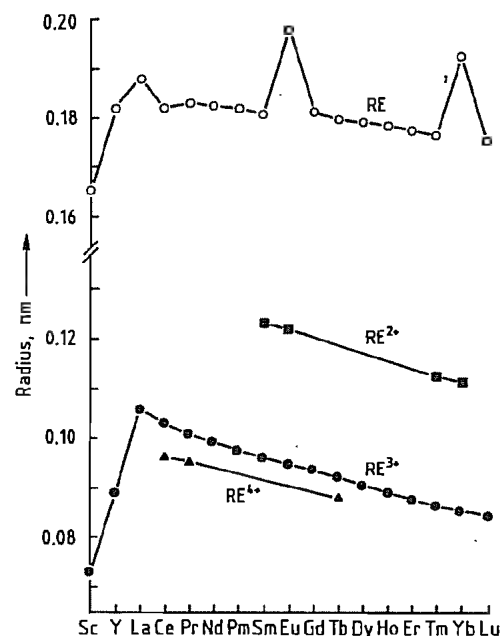


Figure 44.2: Atomic and ionic radii of the rare earth elements.

44.4.2.3 Magnetic and Spectral Properties

The electronic configurations and spectroscopic terms of the Ln^{3+} ions are largely unaffected by the type of compound in which they are situated, owing to the shielding of the 4f

electrons from the chemical environment by the $5s^2p^6$ octet. For these ions, with the exception of Sm^{3+} and Eu^{3+} , it is characteristic that the values of the total spins J applicable to the spectroscopic term of the ground state differ from each other fairly widely (difference at room temperature $> kT$) so that in the ground state practically only one J value is occupied. This peculiarity has interesting consequences for the magnetic properties of these ions. While Sc^{3+} , Y^{3+} , La^{3+} , and Lu^{3+} are diamagnetic due to their closed shells, the remaining Ln^{3+} ions are paramagnetic (Figure 44.3). The double maximum in the curve of permanent magnetic moments can be explained theoretically by the additive behaviour of the spin and orbital moments [3, vol. 1, pp. 310–350; 22]. These moments are in opposition for the elements before gadolinium, but additive for the elements that follow it. The magnetic moment of Gd^{3+} is due entirely to the electron spin. The magnetic moments of the Ln^{2+} and Ln^{4+} ions mainly correspond to those of the isoelectronic Ln^{3+} ions. Also, there is a noticeable difference between the magnetic properties of the lanthanides and those of the 3d transition elements, which are characterized by paramagnetism mainly due to spin.

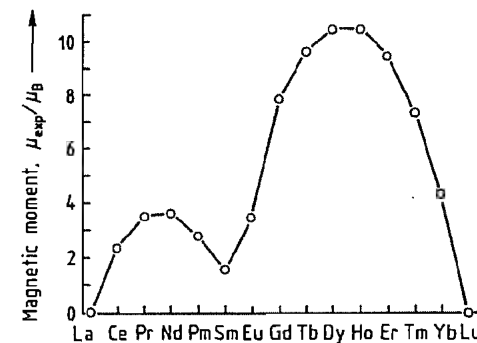


Figure 44.3: Magnetic moments of the RE^{3+} ions at 300 K.

The Ln^{3+} ions, with the exception of Ce^{3+} and Yb^{3+} , have very sharp absorption bands in the visible region and partly in the ultraviolet (Table 44.7). These bands are caused by $f \rightarrow f$ transitions. Their sharpness is due to the above-mentioned shielding of the 4f inner shell, which greatly hinders splitting of the

spectroscopic terms by external fields. The colors of the Ln^{3+} ions are given in Table 44.7 [8]. The sequence of colors in the series La to Gd is almost exactly repeated in the opposite direction in the series Gd to Lu. The ions Ce^{3+} and Yb^{3+} do not absorb in the visible region because an $f \rightarrow f$ transition is not possible for the configurations $4f^1$ and $4f^{13}$. The broad absorption bands of these ions in the ultraviolet region are due to configuration transitions of the type $4f^n \rightarrow 4f^{n-1} 5d^1$.

In aqueous solution, Eu^{2+} is pale yellow, Sm^{2+} is deep red, and Yb^{2+} is yellow.

Table 44.7: Colors and main absorption bands of RE^{3+} ions in the range 200–1000 nm [8].

Ion	Wavelength, nm	Color
La^{3+}		colorless
Ce^{3+}	210.5, 222.0, 238.0, 252.0	colorless
Pr^{3+}	444.5, 469.0, 482.2, 588.5	yellow-green
Nd^{3+}	354.0, 521.8, 574.5, 739.5, 742.0, 797.5, 803.0, 868.0	red-violet
Pm^{3+}	548.5, 568.0, 702.5, 735.5	pink
Sm^{3+}	362.5, 374.5, 402.0	yellow
Eu^{3+}	375.5, 394.1	colorless
Gd^{3+}	272.9, 273.3, 275.4, 275.6	colorless
Tb^{3+}	284.4, 350.3, 367.7, 487.2	very pale pink
Dy^{3+}	350.4, 365.0, 910.0	pale yellow-green
Ho^{3+}	287.0, 361.1, 416.1, 450.8, 537.0, 641.0	yellow
Er^{3+}	364.2, 379.2, 7487.0, 522.8, 652.5	pink
Tm^{3+}	360.0, 682.5, 780.0	pale green
Yb^{3+}	975.0	colorless
Lu^{3+}		colorless

44.4.2.4 Bonding, Coordination Numbers

The physical, chemical, and above all structural properties of the rare earth compounds indicate that these elements exhibit mainly ionic bonding.

In solution and in crystalline compounds, the RE^{3+} ions (except Sc^{3+}) generally have coordination numbers > 6 [8]. For scandium compounds, which can also be regarded as homologues of aluminum, coordination numbers > 6 do not occur. In general, the tendency of the lanthanides, including Y and La, to form complexes is smaller than for the d-transition elements, as the shielded 4f orbitals are not available for forming the hybrid orbitals that

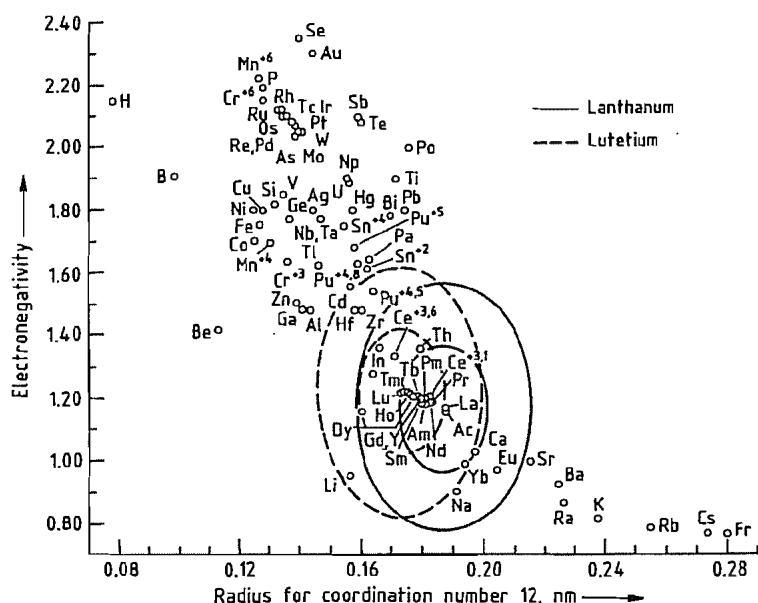


Figure 44.4: Darken-Gurry diagram for lanthanum and lutetium [27].

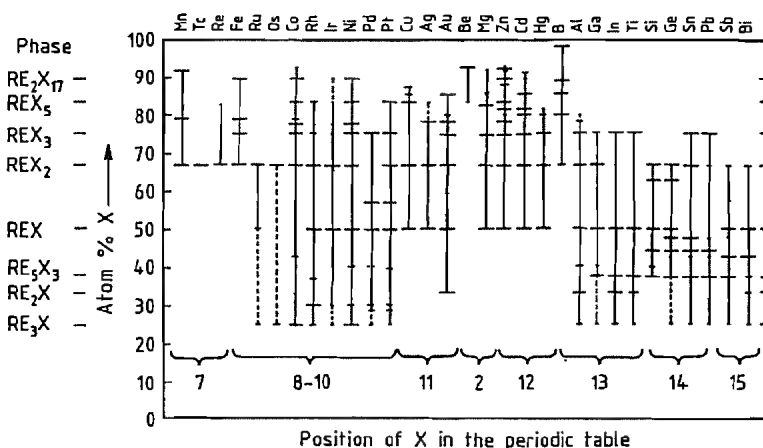


Figure 44.5: Compositions of binary rare earth alloys [2, vol. 2, chap. 13, pp. 1-54].

Rare earth metals can easily be extruded at temperatures just below the melting point. The presence of impurities, especially oxygen, has a detrimental effect on cold and hot rolling properties.

44.5 Digestion of Ores

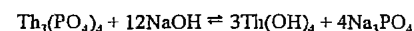
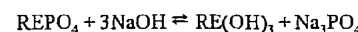
44.5.1 Wet Digestion; Fusion

The most important rare earth minerals monazite, bastnaesite, and xenotime are generally concentrated by physical processes such as heavy medium separation, flotation, and magnetic separation [1, part B1, pp. 60-67]. They are ground to 50 μm -1 mm and then di-

gested with acids or alkalis. Treatment with alkalis produces the hydroxides of the rare earth metals and thorium, which can then be dissolved in concentrated hydrochloric or nitric acid. Treatment of the ores with sulfuric or hydrochloric acid converts the rare earth metals into soluble sulfates or chlorides [1, part B1, pp. 67-104].

44.5.1.1 Monazite

Digestion by Alkalis. The reaction of rare earth phosphates with hot, concentrated alkali (50-75%) proceeds as follows:



This can be carried out at high temperatures in autoclaves (60% alkali, mass ratio 1:1) [32], or with more concentrated alkali at lower temperature (120 °C) and normal pressures [33].

The hydroxides produced are treated with hot water. The trisodium phosphate goes into solution, and the hydroxides are filtered off. The trisodium phosphate, a saleable by-product, crystallizes out. The washed hydroxides are then dissolved in hydrochloric or nitric acid. If the acid concentration is held at pH 4, a partial separation results, impure thorium hydroxide remaining behind while the rare earth hydroxides dissolve.

Sulfuric Acid Digestion. Monazite can be digested with 98% sulfuric acid at 200-230 °C. The rare earth sulfates formed are then dissolved out of the crystalline, hygroscopic reaction product with cold water. The thorium sulfate either remains undissolved or also goes into solution, depending on the reaction conditions [34].

The dissolved thorium, which was at one time the most important product, was formerly precipitated as sulfate. However, the sharpness of separation from the rare earth elements was poor. The method now used is to dissolve all the sulfates and separate the thorium by one of the following more effective methods:

- Precipitation of ThF_4 .

- Precipitation of thorium phosphate by increasing the pH or by dilution.
- Precipitation of the sodium/cerium earth double sulfates, while the corresponding much more readily soluble salts of thorium and the yttrium earths remain in solution. The thorium is then precipitated by adding oxalic acid, the solubility of thorium oxalate being much lower than that of the oxalates of the yttrium earths. The sparingly soluble double sulfates of the cerium earths are treated with boiling, concentrated alkali solution, forming the hydroxides, which are then dissolved in acid for subsequent fractionation.

44.5.1.2 Bastnaesite

Digestion with Acids. Many processes have been described for digesting bastnaesite with sulfuric acid. In one of these, the mineral is calcined to decompose the carbonates and then treated with 6 N sulfuric acid to dissolve the rare earth elements as sulfates [35].

In another process, the mineral is slurried with concentrated sulfuric acid and heated to 500 °C. The fluorine is driven off as hydrogen fluoride together with CO_2 and SO_2 , and the rare earth elements remain behind as their anhydrous sulfates [36]. These can then be treated like the products from the treatment of monazite with sulfuric acid.

In another process, the mineral is calcined at > 600 °C, and then treated with 16 N nitric acid, which is considerably more effective than 12 N hydrochloric acid or 18 N sulfuric acid [37].

In the Molycorp process, the mineral is concentrated to 60% by flotation and then calcined, converting the cerium to the tetravalent state. It is then treated with hydrochloric acid, which causes only the trivalent rare earth elements to go into solution, leaving behind 65-80% CeO_2 , which can be converted directly to a glass-polishing material by further calcination [38].

In another process, the carbonates are decomposed by hydrochloric acid. A fluoride residue is obtained, which is treated with al-

kali. The rare earth hydroxides obtained in this way are used to neutralize the excess acid from the chloride solution [39].

Digestion with Bases. Bastnaesite can be treated with concentrated alkali at ca. 200 °C to form rare earth hydroxides, which are then dissolved in acid [40].

44.5.1.3 Other Ores

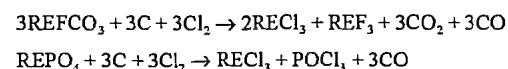
Xenotime is more difficult to digest than monazite. It is usually treated with concentrated alkali, like monazite, but under much more rigorous conditions. Rare earth silicate minerals are best digested with sulfuric acid at fairly high temperatures. Various methods have been described for the extraction of the rare earth elements from apatites during wet production of phosphoric acid [41, 42]. A process for the direct treatment of apatite with $\text{NOCl}/\text{NO}_2/\text{N}_2\text{O}_4$ at high temperatures is proposed in [43].

In the field of uranium production, only Denison Mines (Ontario) have so far produced an yttrium concentrate by solvent extraction of a sulfate solution.

44.5.2 Chlorination

The direct chlorination of rare earth ores in a shaft furnace at 1000–1200 °C produces two groups of chlorides, depending on the impurities present. These are firstly the chlorides volatile at this temperature such as AlCl_3 , FeCl_3 , POCl_3 , SiCl_4 , ThCl_4 , TiCl_4 , NbOCl_3 , NbCl_5 , and TaCl_5 , and secondly the nonvolatile chlorides of the alkali and alkaline earth metals as well as the rare earth chlorides, which collect at the bottom of the chlorinating furnace and are tapped off. The anhydrous rare earth chlorides can be treated, without further drying, by molten salt electrolysis to produce cerium mischmetal or they can be dissolved for further wet chemical processing.

The reaction of bastnaesite or monazite proceeds according to the following equations:



The rare earth ore, with a grain size of < 0.2 mm, is pelletized with charcoal powder and a binder. It is then dried and fed into the chlorination furnace (Figure 44.6). This consists essentially of a vessel lined with refractory bricks, inside which is a carbon cylinder that is the actual reaction space. A perforated graphite tube located inside this carbon cylinder contains a bed of coke through which the chlorine gas is passed to ensure even distribution before it passes through the solid feed material. The reaction is energetically self-sustaining, and only requires sufficient resistance heating to compensate for radiation losses. The rare earth chlorides collect in the melt space and are tapped off from time to time. A total of ca. 400 t rare earth chlorides can be produced during the working life of the carbon cylinder. The cylinder can be replaced without difficulty while hot. The output of a chlorination furnace of this type is ca. 100 t/month. The lining of the chlorination furnace has a lifetime corresponding to a total output of 1500 t rare earth chloride.

The chlorination furnace operates at a slight underpressure. The waste gases are passed into a combustion chamber, oxidized, and washed with alkali to remove residual chlorine. In principle, it is possible to recover the volatile chlorides of valuable elements from the off-gas stream (e.g., POCl_3 , NbCl_5 , TiCl_4 , TaCl_5 , ThCl_4 , UCl_4).

44.6 Separation

The separation of the rare earth elements poses one of the most difficult problems in inorganic chemistry. Due to the great similarity of the chemical properties, the methods are generally not very selective. In a few cases, much better separation can be achieved by conversion to another oxidation state of adequate stability ($\text{Ce}^{3+} \rightarrow \text{Ce}^{4+}$, $\text{Eu}^{3+} \rightarrow \text{Eu}^{2+}$).

A further difficulty is presented by the unfavorable distribution of concentrations of individual rare earth metals in the common minerals. The method of separation must therefore be selected to suit the existing ratios.

The first step is a preliminary separation into groups of elements that resemble each other very closely.

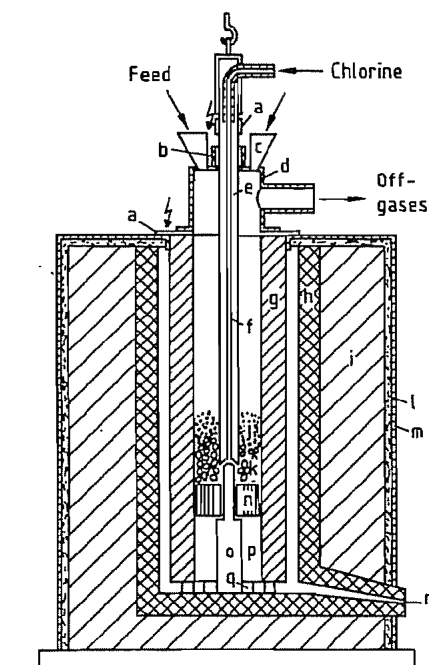


Figure 44.6: Diagram of a chlorination furnace [44, 45]: a) Electrical connection; b) Insulation and seal; c) Charging tunnel; d) Furnace hood; e) Central electrode; f) Central hole for chlorine feed; g) Insert; h) Inner refractory lining; i) Outer refractory lining; j) Charge materials; k) Layer of coke; l) Slag wool; m) Iron casing; n) Sieve plate; o) Sieve plate supports; p) Space for molten material; q) Exit holes in insert; r) Tapping hole.

44.6.1 Principles of Separation

Two principal types of process are used for the extraction of rare earth elements:

- Solid-liquid systems using fractional precipitation or crystallization, or ion exchange. Ion exchange processes are used in the production of small quantities of higher value heavy rare earth elements.
- Liquid-liquid systems using solvent extraction. This process is the most commonly used commercial process for the extraction of rare earth elements.

The distribution of two rare earth elements REA and REB between the two phases is given by the equilibrium constants k_A and k_B :

$$k_A = \frac{[\text{RE}_A]}{[\text{RE}_A]} \quad \text{and} \quad k_B = \frac{[\text{RE}_B]}{[\text{RE}_B]}$$

where $[\text{RE}]$ and $[\text{RE}]$ represent the concentrations in the aqueous and nonaqueous phase, respectively. The selectivity of this separation system is given by the separation factor $\alpha_{\text{RE}_B/\text{RE}_A}$, where

$$\alpha_{\text{RE}_B/\text{RE}_A} = k_B/k_A$$

More correctly, activities should be used instead of concentrations. In practice, apparent equilibrium constants based on concentrations are adequate. In the following discussion, these apparent constants are used throughout.

The processes of fractional crystallization or fractional precipitation are now mainly of historic interest only. The separation factor corresponds to the solubility ratio of the two rare earth elements in the aqueous phase.

In the case of ion exchange or liquid-liquid extraction, the ratio of the distribution coefficients is a measure of the different affinities of the rare earth metals for the two phases.

For the trivalent ions of neighboring rare earth elements, the separation factor is low for all methods. For precipitation or crystallization, $\alpha = 1.1$ to 5; for separation by ion exchange with addition of complexing agents, $\alpha = 1.1$ to 10; for liquid-liquid extraction, $\alpha = 1.1$ to 5.

For an effective separation, many repetitions of a single separation operation are necessary, which can be carried out batchwise or continuously.

With ion exchange separation, although the establishment of equilibrium is continually repeated, the overall process is discontinuous, since continuous feeding is not possible. However, it has the advantage that several rare earth elements can be separated at the same time.

A fully continuous liquid-liquid extraction process in countercurrent flow with partial recycle enables separation to be achieved into two groups or two individual rare earth ele-

ments of high purity. The production of three pure rare earth elements requires two batteries of separation equipment. This limitation is, however, compensated for by the advantage of continuous operation.

A further characteristic of a separation process is the size of the apparatus required. This depends on the concentration of the rare earth elements in the two phases. Cationic ion exchangers have a high capacity (ca. 150 g REO/L), but elution in the presence of complexing agents requires very dilute solutions (ca. 5–10 g REO/L). These separation plants are therefore very bulky.

In the liquid–liquid extraction process, the capacity of the solvent can be very high (170–190 g REO/L), and it is therefore often possible to work with aqueous solutions with concentrations of 100–140 g REO/L, i.e., approaching saturation. The equipment is therefore compact.

44.6.2 Separation by Classical

Methods [1, part B2; 3, vol. 1, pp. 30–61; 6]

44.6.2.1 Fractional Crystallization

Fractional crystallization was the first process for separating the rare earth elements, both in the laboratory and on the industrial scale. It is no longer of importance.

The purification effect decreases with increasing purity of the crystals. The achievable purity is therefore limited. Also, many intermediate fractions are produced that must be reprocessed.

In general, this process is more problematical for the yttrium earths than the cerium earths. The cerium earths were therefore separated by fractional crystallization and the yttrium earths by ion exchange. The cerium earths were converted to nitrates after oxidation of the cerium to the tetravalent state, and the double nitrates $\text{NH}_4\text{NO}_3 \cdot \text{RE}(\text{NO}_3)_3 \cdot 4\text{H}_2\text{O}$ were crystallized. Pechiney Saint Gobain produced 99.9% pure lanthanum in five crystallization stages, this salt being the most soluble. The yttrium was first precipitated as the dou-

ble chromate and then purified by ion exchange.

44.6.2.2 Fractional Precipitation

Fractional precipitation was only used for separating the rare earth elements into groups, due to filtration difficulties and the slow establishment of equilibrium.

The best known example is the precipitation of the hydroxides, which enables separation into three groups: (1) yttrium, (2) praseodymium, neodymium, and samarium, and (3) a fraction enriched in lanthanum and cerium.

Another process is the precipitation of double sulfates, $\text{Na}_2\text{SO}_4 \cdot \text{RE}_2(\text{SO}_4)_3$. The greater solubility of the yttrium earths enables a crude separation from the cerium earths to be carried out.

44.6.2.3 Separations Based on Oxidation State Changes

Cerium(IV) or europium(II) can be economically separated from the other rare earth metals by precipitation, ion exchange, or liquid–liquid extraction.

Cerium can be oxidized by oxidizing agents such as hypochlorite, H_2O_2 , atmospheric oxygen, or electrolytically at a suitable pH, precipitating it as cerium(IV) oxide hydrate. By adding chlorine and sodium hydroxide solution to a solution of cerium earth chlorides, cerium(IV) oxide hydrate is precipitated. This can be converted to a 90% pure cerium oxide that is suitable for use as a polishing material. The separation of tetravalent cerium from the trivalent rare earth elements by liquid–liquid extraction is described later.

Divalent europium has properties similar to those of the alkaline earths, especially strontium (insoluble sulfate, soluble hydroxide, etc.). The rare earth metals are usually reduced in hydrochloric acid solution by zinc amalgam or sodium amalgam. The subsequent precipitation of europium sulfate from the very dilute solution can be improved by coprecipitation of

strontium or barium sulfate. The europium can be further purified by precipitating trivalent elements as their hydroxides by using ammonia. Under these conditions, Eu^{2+} remains in solution [46]. The separation of divalent europium from the trivalent rare earth elements by liquid–liquid extraction is described later.

44.6.3 Separation by Ion Exchange

This process is based on work carried out on the separation of rare earth elements produced by uranium fission, and formed part of the Manhattan Project (1943–1947). The principles of separation by elution were developed by BOYD and coworkers in the Oak Ridge National Laboratory. The Ames Laboratory, Iowa State University, under the leadership of SPEDDING, investigated the production of rare earth metals on a large scale by displacement elution. SPEDDING and POWELL have provided review of the developments up to 1950 [5, pp. 55–73; 47]. Attempts to develop ion exchange column chromatography into a continuous process was realized with the development of the continuous annular chromatograph by researchers at Oak Ridge Laboratory in the mid 1970s. However, the process was designed for analytical requirements with low loading of the columns and was therefore not commercialized [48–50]. A more recent development, known as continuous displacement chromatography [51], shows greater promise for surpassing present industrial, batch, fixed-column displacement ion exchange processes.

44.6.3.1 Ion Exchange with Chelating Agents

Sulfonated polystyrene ion exchange resins, which possess high chemical stability, can combine with 0.5–0.8 mol of rare earth elements per 1 mol resin. However, differences in the affinities of the rare earth elements for the resin are very small, and the separation factor for two neighboring rare earth elements is only ca. 1.08 [52]. However, this can be con-

siderably improved by the addition of chelating agents.

The separation factor $F_{\text{RE}_B/\text{RE}_A}$ for two rare earth elements RE_A and RE_B between an aqueous solution and the cation exchanger (concentrations marked with a bar) is

$$F_{\text{RE}_B/\text{RE}_A} = \frac{[\overline{\text{RE}_B^{3+}}] \cdot [\overline{\text{RE}_A^{3+}}]}{[\overline{\text{RE}_A^{3+}}] \cdot [\overline{\text{RE}_B^{3+}}]}$$

On the addition of a chelating agent L , the equilibrium constants in solution are given by:

$$K_A = \frac{[\text{RE}_A\text{L}]}{[\text{RE}_A\text{L}^-] \cdot [\text{L}]} \quad K_B = \frac{[\text{RE}_B\text{L}]}{[\text{RE}_B\text{L}^-] \cdot [\text{L}]}$$

The constants depend on conditions in the medium, especially the pH of the aqueous phase. For large values of K_B and K_A and an excess of chelating agent (the concentration of the unchelated rare earth metals then being negligible), a new separation factor $F_{\text{RE}_B/\text{RE}_A}^*$ can be defined:

$$F_{\text{RE}_B/\text{RE}_A}^* = F \cdot \frac{K_B}{K_A}$$

Separation can therefore be much improved by using a chelating agent whose equilibrium constants K_A and K_B are very different from each other.

Certain carboxylic acids form 1:1 chelates over a large pH range with K values that differ considerably for neighboring rare earth elements and which are sufficiently soluble in water. Citric acid is only of historical interest; it was used in the Ames Laboratory to prepare rare earth oxides in kilogram quantities with a purity of 99.9% in 1947.

Later, polycarboxylic acids were replaced by aminocarboxylic acids, which form chelates with considerably improved stability, selectivity, and solubility.

Figure 44.7 shows the K values as a function of the atomic numbers of the rare earth elements. They vary between 10^{10} and 10^{20} . The selectivity F_L also varies widely, and can have values of between 1 and 10 for neighboring elements. For ethylenediaminetetraacetic acid (EDTA) and 1,2-diaminocyclohexanetetraacetic acid (DCTA), the selectivity for the cerium

earths is much higher than for the yttrium earths. The position of yttrium (dashed lines) varies with the chelating agent over a range from Pr to Dy.

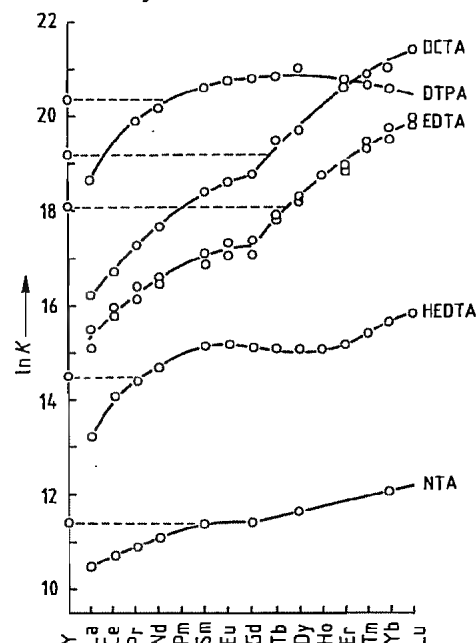


Figure 44.7: Stability constants K of selected rare earth chelates. — Position of yttrium.

The disadvantage of using chelates is their lower solubility. The most soluble chelates such as those of *N*-(hydroxyethyl)ethylenediaminetriacetic acid (HEDTA) or diethylenetriaminepentaacetic acid (DTPA) reach concentrations of ca. $(2-2.5) \times 10^{-2}$ mol/L at 25 °C.

44.6.3.2 Separation Process

The ion exchange resin is initially loaded with NH_4^+ . A solution of the salts of the rare earth elements to be separated is then passed through the column. The cations are absorbed by ion exchange onto the upper part of the column. The column is developed with a solution of the chelating agent, e.g., the triammonium salt of ethylenediaminetetraacetic acid.

In partition elution, the rare earth elements that form the most stable chelates are eluted first. The zones of the various rare earth ele-

ments are clearly separated from one other, but the eluted solutions are very dilute. This process is therefore used only for analytical purposes.

In displacement elution, a preliminary charge of a foreign ion (the so-called retarding ion) precedes the band of rare earth elements. This ion (denoted by R^{Y+}) has a lower affinity for the exchange resin than the rare earth elements. Displacement is now carried out using an ion that has a greater affinity for the resin than the rare earth elements. In some circumstances this ion can be NH_4^+ . The sequence of affinities for the resin is then given by $\text{NH}_4^+ > \text{RE}_B > \text{RE}_A > \text{R}^{Y+}$. NH_4^+ displaces the RE_B ions almost quantitatively, while the RE_A ions displace the R^{Y+} ions. A band of constant length containing the rare earth elements moves through the column, and the concentration of the rare earth elements in the band remains constant. Between the zone containing pure RE_A and the zone containing pure RE_B there is a narrow zone containing both RE_A and RE_B .

By this method, more highly concentrated solutions of separated rare earth elements can be obtained than with partition elution. The same amount of resin can therefore be used to produce considerably larger quantities of rare earth elements.

The theory of displacement elution is described in [53]. SPEDDING and coworkers [54] have shown that, if the separation factor F_L is large enough, the band requires only a minimum movement ϑ along the column to achieve a constant equilibrium state. This relationship can be described as follows:

$$\vartheta = \frac{1 + (F_L + 1)x_i}{F_L - 1}$$

where x_i denotes the mole fraction of the rare earth element in the original mixture that has the lowest affinity for the resin and, therefore, the greatest chelating ability. If $x_i = 0.5$ (equimolar mixture of two rare earth elements) and $F_L = 2$, the band must be moved along the column only 1.5 times its length to achieve equilibrium.

The cations in the equilibrium follow a logarithmic law. The molar fraction x_A of rare

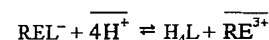
earth element A is a function of the number of theoretical plates n required to establish equilibrium:

$$x_A = \frac{F_L^{2n}}{1 + F_L^{2n}}$$

A refinement of the ion exchange model is given in [55, 56]. However, the equations given above are generally adequate for calculating the separation of the rare earth elements.

The main difficulty is the extrapolation from laboratory investigations to the industrial scale. The height equivalent to a theoretical plate (HETP) often becomes much greater.

Selection of Retarding Ions. The chelating ability of the weak aminopolycarboxylic acids increases with increasing pH. The H^+ ions can function as retarding ions:



where REL^- denotes the dissolved ionic chelate of the rare earth metal. Owing to their low solubility, the acids tend to crystallize in the column. Only DTPA and HEDTA are sufficiently soluble at normal temperatures to enable H^+ to be used as the retarding ion for the separation of rare earth elements. EDTA can be used at 95 °C [57].

Many cations, e.g., Fe^{3+} , Cu^{2+} , Ni^{2+} , Zn^{2+} , and Pb^{2+} have been investigated as possible retarding ions [58]. Of these, Cu^{2+} has been most widely used.

44.6.3.3 Industrial Processes

Ion exchange was first used for separating rare earth elements on an industrial scale in the late 1950s. However, it was largely replaced by liquid-liquid extraction during the 1960s, and only used if no suitable liquid-liquid extraction process was known. An example was the production of yttrium oxide [59–62], which, with europium oxide, is important as a red phosphor for TV tubes. However, yttrium oxide is now produced more economically by liquid-liquid extraction.

Since 1970, small amounts of rare earth elements have continued to be separated by ion

exchange [e.g., those required in high purity (> 99.9999%) for some electronic applications] or for the production of rare earth compounds with a very small market and which are only occasionally needed. A new phenol-based ion exchange resin was introduced by Unitika Ltd. of Osaka in 1989. The resin reportedly separates the elements to a purity approaching 99.999999% and at a faster rate than previous resins.

DTPA and HEDTA have proved to be the most suitable chelating agents for the production of high-purity rare earth compounds [63]. One process for producing small amounts of very pure rare earth compounds makes use of the temperature effect, which not only enables much more concentrated solutions of chelating agents to be used, but also enables the separation factor to be modified [64, 65].

44.6.3.4 Disadvantages of Ion Exchange

Chelating agents are expensive and must be recovered after use, but recovery is difficult and requires a large number of batch operations. Also, the low solubility leads to very dilute solutions of the rare earth elements (2–10 g REO/L), whereas with liquid-liquid extraction 10–50 times more concentrated solutions may be used. These high dilutions lead to bulky equipment and handling losses.

On the laboratory scale, theoretical plate heights of the order of millimeters are often possible. On conversion to the industrial scale, the HETP increases considerably, and can reach 10–20 cm in columns 230 cm high and 63 cm in diameter.

For reasons as yet unexplained, the purifying effect decreases with increasing purity. This effect is less significant if rare earth elements are required with impurity contents of ca. 50 ppm, but it makes it almost impossible to reduce the impurity content to, e.g., 5 ppm.

44.6.4 Separation by Liquid-Liquid Extraction

44.6.4.1 Theoretical Basis

The liquid-liquid extraction process for the separation of the rare earth elements was discovered by FISCHER et al. who showed that extraction of rare earth metal solutions in hydrochloric acid with an alcohol, ether, or ketone gives separation factors of up to 1.5 [66]. The principles of this separation technique are described in [1, part B2; 67; 68].

In the liquid-liquid extraction process used today, the organic phase usually consists of two or more substances. The active extractant has chelating properties and is mainly responsible for the transfer of the dissolved rare earth elements from the aqueous to the organic phase. In some cases, active extractants can be used neat, but they are usually highly viscous or even solid and must be dissolved in a solvent to ensure good contact between the two phases. Suitable solvents are kerosene and aromatics. Usually, a modifying agent is added to the organic phase to improve the hydrodynamics and sometimes also alter the separation factor.

Distribution Coefficient and Separation Factor. The distribution coefficient is the fundamental parameter in liquid-liquid extraction. It is strongly dependent on concentration and is given by:

$$k = \frac{[\text{RE}]_{\text{organic phase}}}{[\text{RE}]_{\text{aqueous phase}}} = \frac{[\overline{\text{RE}}]}{[\text{RE}]}$$

The separation factor for two rare earth elements RE_A and RE_B is thus

$$\alpha_{\text{RE}_B/\text{RE}_A} = \frac{k_B [\overline{\text{RE}}_B] [\text{RE}_A]}{k_A [\overline{\text{RE}}_A] [\text{RE}_B]}$$

Method of Operation. The flow diagram of a countercurrent extraction plant for the contin-

uous separation of two rare earth elements or two groups of rare earth elements is shown in Figure 44.8 [69]. The mixture of rare earths that is to be separated is fed into an intermediate stage of the liquid-liquid extraction plant operating in countercurrent flow. The extraction medium becomes preferentially charged with the rare earth metals (extract) that form the more stable chelates, while the less stable rare earth chelates remain preferentially in the aqueous phase (raffinate).

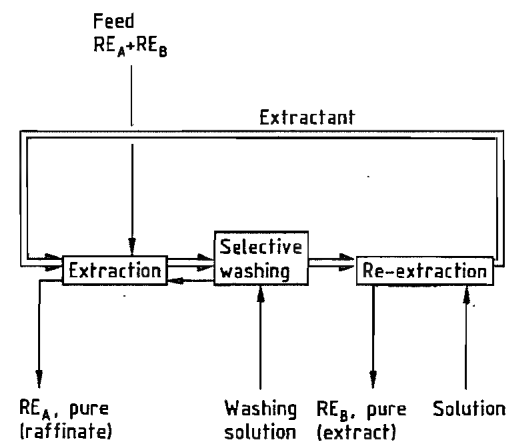


Figure 44.8: Principle of countercurrent liquid-liquid extraction.

This phase flows countercurrent to the extract, leading to further separation and preferential concentration of the more stable rare earth chelates in the extract (selective wash-out). The rare earth metals are re-extracted for further treatment and the extraction medium is treated for re-use. At both ends of the plant, partial recycle takes place. If the recycle was total, separation into individual rare earth elements would take place, but this method is not practical, as it can only be operated batchwise, and a very long time is necessary for the establishment of equilibrium. The separation effect can be calculated by the McCabe-Thiele method in simple cases (Figure 44.9).

Table 44.9: Separation factors with rare earth concentration, nitrate, media, with 50 vol% TBP in Shellsol A [70].

Aqueous phase REO concentration, g/L	Separation factors—yttrium/rare earths							
	Ce/Y	Nd/Y	Sm/Y	Gd/Y	Dy/Y	Ho/Y	Er/Y	Yb/Y
460		0.39	0.88	0.89	1.30	1.20	1.15	0.93
430		0.50		1.14	1.37	1.31	0.85	
310		0.69	1.41	1.51	1.76	1.65	1.35	
220	0.60	1.30	2.02	1.99	2.15	1.91	1.48	0.83
125	0.75	1.77	2.79	2.29	2.10	1.75	1.25	0.83
60		4.08	5.71	4.44	3.96	3.03	2.13	
	Separation factors—adjacent rare earth elements							
	Sm/Nd	Gd/Sm	Dy/Gd	Ho/Dy	Er/Ho	Yb/Er	α^2	
460	2.26	1.01	1.45	0.92	0.96	0.81		
430			1.20	0.96	0.65			
310	2.04	1.07	1.17	0.94	0.82			
220	1.55	0.99	1.08	0.89	0.78			
125	1.58	0.82	0.92	0.83	0.72			
60	1.40	0.18	0.89	0.77	0.70	0.63		

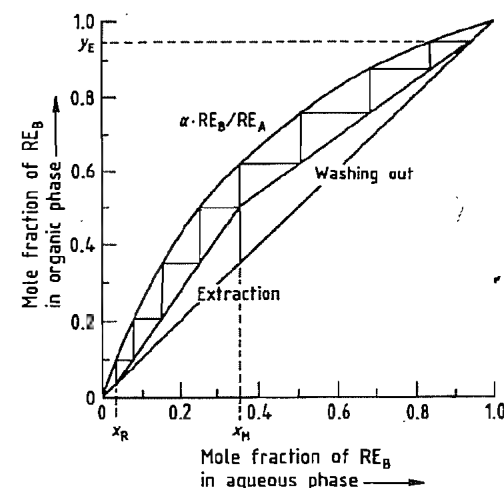
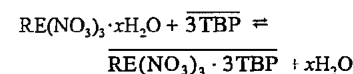


Figure 44.9: Mole fraction RE_B in the aqueous phase.

44.6.4.2 Extractants

Neutral Extractants

The most effective extractant tri-*n*-butyl phosphate (TBP), with which the nitrates of the rare earths are usually extracted by the following generalized process:



Separation factors between various rare earths and between the rare earths and yttrium are listed in Table 44.9 [70].

Concentrated nitric acid improves the selectivity. However, the strong acid solutions are difficult to handle, and the solubility of the rare earth nitrates in these is low. Furthermore, hydrolysis of the solvent takes place. A similar effect to that obtained with nitric acid can be achieved by adding nitrates that are not extracted by TBP, such as $\text{Al}(\text{NO}_3)_3$, alkali metal nitrates, or alkaline earth nitrates.

Pure TBP can be loaded with rare earth nitrates up to concentrations of 0.5 mol/L, corresponding to ca. 170–190 g REO/L. Temperature has a relatively small effect. The early development of mathematical models is described in [71]. A review of the many extraction processes with TBP is given in [72, 73]. Other salts of rare earth elements, e.g., perchlorates, chlorides, and thiocyanates have poor distribution coefficients or the selectivities are inadequate. The effect of low temperatures is described in [74].

Sulfoxides, $\text{RR}'\text{SO}$, behave analogously to TBP (Figure 44.10) [75]. Alcohols and ethers, which were used in the early days, are no longer of importance.

Acidic Extractants

Organophosphoric acids are the second most important extraction media after TBP.

44.7.2 Metallothermic Reduction

Metallothermic reduction of the rare earth oxides and anhydrous rare earth chlorides and fluorides can be used to produce high-purity rare earth metals, especially Gd to Lu, including Y. Metallothermic reduction is also used to produce rare earth mixtures with precisely controlled compositions that cannot be obtained by molten salt electrolysis. Alloys can also be produced by this process.

Alkali metals, alkaline earth metals, and aluminum are suitable reducing agents, as are alloys of these elements with each other. Lithium, which forms low-melting LiF, is of special importance, as is calcium. The use of Mg or Zn has the additional advantage of producing a low-melting alloy with the rare earth metal. The alloying elements can be removed by distillation, yielding the pure rare earth metal.

For the production of La, Ce, Pr, and Nd, the metallothermic reduction of the anhydrous rare earth chlorides is preferred. The reaction is carried out in crucibles lined with MgO at temperatures up to 1100 °C. At higher temperatures, reaction takes place between the rare earth metal and the MgO, and the rare earth chlorides vaporize. The process is not suitable for the production of Sm, Eu and Yb, which are merely reduced to the divalent state.

Gd to Lu and Sc, which have higher melting points, are obtained by reduction of the fluorides with Ca at 1500–1600 °C. The reduction is carried out in tantalum crucibles under a protective gas or in vacuum. The reaction temperature can be reduced by adding a “booster” such as iodine, which gives a slag with good flow properties that separates cleanly from the metal. Praseodymium is produced by reduction of the fluoride with lithium.

The Carlson–Schmidt apparatus is shown in Figure 44.18 [107]. This was used between 1957 and 1959 to produce high-purity yttrium metal in 50 kg batches.

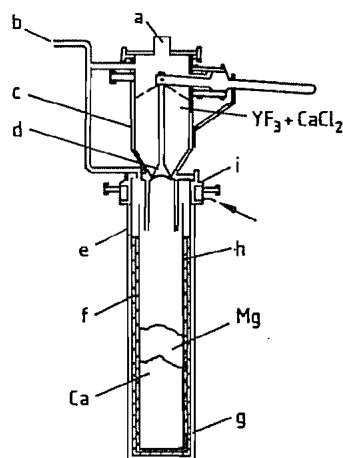


Figure 44.18: Reduction apparatus for the production of yttrium [107]: a) Sight glass; b) Vacuum connection and helium inlet; c) Charging tunnel; d) Charging shut-off mechanism; e) Steel reaction chamber; f) Titanium reaction crucible; g) Graphite insulation; h) Titanium or steel supporting crucible; i) Water cooling.

Sm, Eu, and Yb can be produced by reduction of the oxides with La or the cheaper cerium mischmetal at 1000–1300 °C. The rare earth oxides and the reducing metal are used in the form of pellets, prepared from chippings or thin disks. Sm, Eu, and Yb are volatile at the reaction temperature under vacuum ($< 10^{-4}$ bar), and can be distilled from the reaction space during the reaction and condensed on coolers. Thus, these metals can be separated from rare earth metals that are not volatile under these conditions and obtained in a pure state. Hence, the starting materials can consist of rare earth oxides in which Sm, Eu, and Yb have merely been concentrated. The principle of the reduction distillation apparatus is illustrated in Figure 44.19 [108]. Further purification can be carried out by a second distillation.

The calciothermic reduction of the rare earth oxides can be carried out such that a metal powder with a defined grain size distribution is produced. In this way, it is possible to produce alloys of rare earth metals with 3d metals that can be used to manufacture permanent magnets.

Methods of producing such alloys include, e.g., the coreduction process carried out under vacuum at 1000 °C for 3 h [109]:

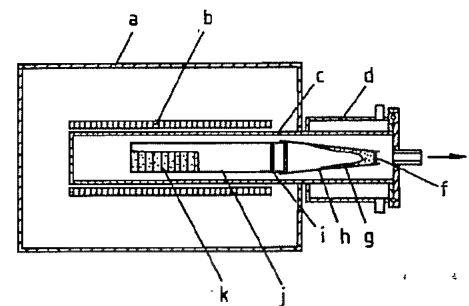
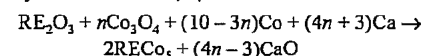
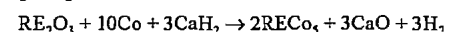


Figure 44.19: Reduction–distillation apparatus for the production of samarium, europium, and ytterbium [108]: a) Furnace; b) Heating element; c) Stainless steel container; d) Water cooling; e) Vacuum; f) Baffle; g) RE metal; h) Molybdenum condenser; i) Heat shield; j) Molybdenum crucible; k) Pelletized reactants.



where $n = 0-10/3$, or the reduction diffusion process carried out at 850–1150 °C for 5 h [110]:



The CaO formed can be removed without affecting the properties of the metal powder.

If C and Si are used as reducing agents, rare earth carbides or silicides are formed. Prealloys or inoculation alloys containing rare earth metals are produced by reducing rare earth oxide mixtures or rare earth ore concentrates with CaSi or FeSi in an electric arc furnace.

44.7.3 Purification

Production of the pure rare earth metals necessitates the removal of products of the reaction of the metals with the atmosphere, crucible materials, and coreactants. Suitable methods include melting under a protective gas or in a vacuum.

The high-boiling rare earth metals can also be purified by distillation. Tungsten powder is added to bind interstitial impurities (mainly C, N, O) as involatile compounds. Table 44.12 lists the temperatures at which the rare earth metals have vapor pressures of 1.3×10^{-3} to 1.3×10^{-5} bar [111].

Alloying elements and impurities such as Mg, Cd, Zn, and Ca are distilled off under vacuum. The remaining rare earth metal is then in

the form of a sponge, which can be consolidated by fusion in an electric arc furnace.

Zone melting, melt extraction, and melt filtration, e.g., through tungsten powder, degassing in a high vacuum, etc., are other recommended purification methods.

Table 44.12: Vapor pressure and distillation rate of the rare earth metals [111].

RE element	Temperature, °C		Distillation rate at 1.3×10^{-3} bar, $\text{gcm}^{-2}\text{h}^{-1}$
	1.3×10^{-5} bar	1.3×10^{-3} bar	
Sc	1397	1773	33
Y	1637	2082	43
La	1754	2217	53
Ce	1744	2174	53
Pr	1523	1968	56
Nd	1341	1759	60
Sm	722	964	83
Eu	613	837	90
Gd	1583	2022	59
Tb	1524	1939	60
Dy	1121	1439	71
Ho	1179	1526	69
Er	1271	1609	68
Tm	850	1095	83
Yb	471	651	108
Lu	1657	2098	61

44.8 Analysis

Analytical methods for the determination of the rare earth elements are reviewed in [5, pp. 570–593; 112]. Modern analytical methods are reported in [2, vol. 4; 113, 114].

Analysis may be divided into determination of individual rare earth elements, and group determination, in which the rare earth elements are coprecipitated as oxalates, hydroxides, or carbonates, and are then determined quantitatively after calcination to give the oxides. Complexometric titrations are also used for group analysis.

The ready conversion of cerium to the tetravalent state and of europium to the divalent state offer simple methods of titration for the single elements.

The determination of individual colored rare earth ions is normally carried out by spectrophotometry, emission spectroscopy, and spectroscopy in flames. Emission, absorption, or fluorescence methods are used. The tech-

nique and application of laser source mass spectrometry is discussed in [115].

X-ray fluorescence analysis can be used to determine concentrations in the range between 90% and ppm quantities with moderate sensitivity. It is useful to concentrate the rare earth elements (sometimes with the aid of a trace collector), and to determine the individual rare earth metals in the separated oxide, since a direct determination on the matrix can lead to erroneous results due to the presence of foreign elements or to the physical or chemical condition of the sample. For the determination of yttrium, the K lines are preferably used, although the L lines are preferred for the other rare earths due to the disturbance of the K lines by bremsstrahlung spectra. Inner standards such as strontium or zirconium with yttrium are used, or standard samples that should be as similar as possible to the sample being tested. The spectra can then be used for quantitative determinations. The samples are prepared by compressing the material for analysis with borax.

44.9 Compounds

44.9.1 Hydrides [2, vol. 3, chap. 26, pp. 299–336]

All the rare earth metals react with molecular hydrogen to form the dihydrides, REH_2 . Most rare earth metals will also react with hydrogen to produce the trihydrides, REH_3 . The rate of reaction depends on temperature, hydrogen pressure, and the surface condition of the metal. Both forms of the hydride are nonstoichiometric, showing wide ranges of homogeneity. The dihydrides of La, Ce, Pr, and Nd have ranges of homogeneity with a composition approaching REH_3 . The dihydrides of Sm, Gd to Tm, Lu, and Y have narrower ranges of existence and form a trihydride phase that is also nonstoichiometric. ScH_2 , EuH_2 , and YbH_2 are almost stoichiometric, but YbH_2 takes up additional hydrogen at very high pressures, up to the composition $\text{YbH}_{2.55}$. With the exception of EuH_2 and YbH_2 , which

form orthorhombic crystal structures similar to the alkaline earth hydrides, the dihydrides are cubic (fluorite structure). The trihydrides crystallize with a hexagonal structure.

Rare earth hydrides are brittle compounds, sometimes with a metallic luster. Similar to the transition metal hydrides, the rare earth dihydrides (except for YH_2 and EH_2) are metallic conductors. In particular, hydrogen-deficient dihydrides are better electronic conductors than their parent metals. In general, as the trihydride composition is approached the materials begin to show semiconducting properties.

Hydrides formed by the hydrogenation of binary rare earth solid solution alloys are usually considered to be solid solutions of the two parent rare earth hydrides, and as such their properties can be predicted with reasonable confidence from those of the constituent hydrides. In the case of binary alloys REM, where M is a non-rare-earth metal, the properties of the intermetallic hydride formed by hydrogenation of the alloy bear no relationship to those of the parent hydrides. They are therefore generally viewed as pseudobinary metal hydrides. Some of these materials can reversibly and efficiently absorb and desorb considerable amounts of hydrogen, and are therefore of commercial interest as a means of storing hydrogen. A review of hydrogen absorption in intermetallic compounds is provided in [116].

44.9.2 Oxides, Hydroxides, Peroxides, Salts of Inorganic Oxoacids, Double Salts

Aspects of the transformation and defect structures in rare earth sesquioxides is provided in detail in [117]. The sesquioxides, RE_2O_3 , of the rare earth elements, with the exception of Ce, Pr, and Tb, are obtained by oxidation of the metals with oxygen at elevated temperatures or by thermal or pyrohydrolytic decomposition of the hydroxides, halides, and certain oxosalts. In the case of Ce, Pr, and Tb, similar conditions yield the compounds CeO_2 , Pr_6O_{11} , and Tb_4O_7 , which can be reduced to

the sesquioxides by hydrogen at elevated temperature. The sesquioxides melt at very high temperatures (in the range of 2200–2400 °C) and have very high enthalpies of formation [–1907.9 kJ/mol (Sc_2O_3) to –1661 kJ/mol (Eu_2O_3)].

They crystallize in the hexagonal system (type A), monoclinic system (type B) or cubic system (type C), depending on the temperature and the radius of the cation. At temperatures near the melting point, high-temperature modifications, types H and X, are also formed. Most sesquioxides are polymorphic, not including the two high-temperature forms. La_2O_3 forms type A crystals; Ce_2O_3 to Nd_2O_3 form types A and C; Sm_2O_3 to Ho_2O_3 form types C and B; and Er_2O_3 to Lu_2O_3 , Y_2O_3 , and Sc_2O_3 form only type C crystals. Whether the observed modifications are thermodynamically stable or metastable has so far been established in only a few cases.

Cubic crystals (fluorite type) are formed both by the dioxides of Ce, Pr, and Tb and by their intermediate oxides, in which cations in the two oxidation states 3+ and 4+ are present together. With the exception of CeO_2 , which can be produced by air oxidation, the dioxides can only be obtained under strongly oxidizing conditions (e.g., oxygen at high pressure). The nonstoichiometric intermediate oxides have been extensively investigated in the system Pr–O [118]. Here, phases exist that are members of a series with the general composition $\text{Pr}_n\text{O}_{2n-2}$ ($n = 7, 9, 10, 11, 12$).

The compound EuO is fairly easy to obtain by reduction of Eu_2O_3 , e.g., with EuH_2 or $\text{Eu}_{(g)}$. With this exception, the condensed monoxides of the rare earth elements have only been observed as metastable compounds or as compounds stable under extreme conditions such as high pressure. For example, gaseous monoxides of all the rare earth elements have been observed at very high temperatures. EuO is a violet-black, cubic (NaCl type), ferromagnetic substance ($T_C = 70$ K). Eu also forms the oxide Eu_3O_4 , in which both Eu^{2+} and Eu^{3+} ions are present.

The hydroxides, $\text{RE}(\text{OH})_3$, are obtained as hydrates by the precipitation of RE^{3+} ions with

ammonia or other bases. The hydroxides and oxide hydroxides, REOOH , can be prepared in crystalline form by hydrothermal synthesis. The hydroxides are sparingly soluble in water. Their basicity and solubility decrease with increasing atomic number. This progressive change in properties is important both for the separation of the rare earth elements from one other (see Section 44.6) and for chemical analysis. The hydroxides react with carbon dioxide to form basic carbonates, the rate of reaction depending on their basicity.

So far, very little is known of the existence of peroxides of the rare earth elements. Cerium peroxide forms as a deep brown, hydrated compound when Ce^{3+} ions are precipitated with ammonia and hydrogen peroxide. This intense colour can be used for the detection of Ce in the presence of other rare earth elements.

Of the group of compounds of rare earths with inorganic oxoacids, the carbonates, sulfates, nitrates, and certain double salts are of importance for analytical and preparative chemistry. Precipitation of RE^{3+} ions by solutions of alkali metal carbonates yields the sparingly soluble hydrated or basic carbonates. These are readily decomposed by acids or on heating, liberating CO_2 . Apart from lanthanum sulfate, which forms a nonhydrate, the sulfates crystallize from aqueous solution as octahydrates. The hydrated sulfates can be thermally decomposed to the anhydrous form. They are fairly soluble, having a negative temperature coefficient of solubility, and are of industrial importance since sulfuric acid is used for digesting certain rare earth ores. Double sulfates, e.g., salts of the type $\text{RE}_2(\text{SO}_4)_3 \cdot \text{Na}_2\text{SO}_4 \cdot n\text{H}_2\text{O}$ are important in the separation of the cerium earths from the yttrium earths.

The rare earth nitrates crystallize from solution in dilute nitric acid in the form of hydrates, $\text{RE}(\text{NO}_3)_3 \cdot n\text{H}_2\text{O}$ ($n \leq 6$). These salts are very soluble in water and moderately soluble in various organic solvents (alcohols, ketones, esters), and are important in the separation of the rare earth elements from each other by liquid–liquid extraction. Certain double nitrates, e.g., of the type $2\text{RE}(\text{NO}_3)_3 \cdot$

$3\text{Mg}(\text{NO}_3)_2 \cdot 24\text{H}_2\text{O}$ were at one time important in the separation of the rare earth elements by fractional crystallization. A comprehensive review of inorganic complex compounds is provided in [119, 120].

44.9.3 Halides

The rare earth elements, except for europium, form trihalides, REX_3 , where $\text{X} = \text{F}, \text{Cl}, \text{Br}, \text{I}$. The trifluorides are sparingly soluble and are obtained from aqueous solution by precipitation with hydrogen fluoride. If these precipitates are dried at elevated temperatures, partial hydrolysis takes place, particularly of the more weakly basic elements. This can be effectively prevented by adding an excess of NH_4F or $\text{HF}_{(g)}$ during the dehydration process. With the exception of ScF_3 , the trifluorides crystallize in the hexagonal LaF_3 structure ("tysonite structure") or the orthorhombic YF_3 structure, depending on the radius of the cation and the temperature range. ScF_3 crystallizes in the cubic system (ReO_3 type). When dimorphism occurs, the YF_3 type is the low-temperature, and the LaF_3 type, the high-temperature modification. The trifluorides are high-melting compounds [1140 °C (HoF_3) to 1552 °C (ScF_3)]. EuF_3 and, to a very limited extent, YbF_3 , tend to liberate fluorine at high temperatures. A review of the rare earth fluorides is given in [117].

The trichlorides can be obtained as their hexa- or heptahydrates by careful evaporation of their solutions in hydrochloric acid. The dehydration of the hydrates must be carried out in a stream of HCl and/or in the presence of an excess of NH_4Cl to prevent hydrolysis. On an industrial scale, the anhydrous trichlorides are obtained by reacting oxidic ores with chlorine and carbon. They crystallize in the hexagonal UCl_3 type structure (LaCl_3 to GdCl_3) or the monoclinic YCl_3 type structure (DyCl_3 to LuCl_3 , YCl_3 , ScCl_3). They are very soluble in water and in certain organic solvents such as ethanol and pyridine. Their melting points are in the range 588 (TbCl_3) to 892 °C (LuCl_3). With the exceptions of EuCl_3 and YbCl_3 , which decompose on heating with liberation

of chlorine, all the other rare earth chlorides vaporize without decomposition or sublime (ScCl_3).

The tribromides and triiodides are obtained in the same way as the trichlorides. The tribromides, and more so the triiodides of Eu , Yb , and Sm , have a marked tendency to lose halogen on heating, since the 2+ oxidation state of the cation becomes more stable with increasing size of the anion. The melting points of the tribromides are in the range 664 (SmBr_3) to 960 °C (LuBr_3), and those of the triiodides in the range 738 (PrI_3) to 1045 °C (LuI_3). The trihalides react with the sesquioxides to form oxide halides of various compositions.

The existence of tetrahalides is limited to the tetrafluorides of Ce , Pr , and Tb . CeF_4 and TbF_4 are obtained by the reaction of the elements or the trifluorides with fluorine. PrF_4 can only be obtained by the extractive removal of NaF from the readily prepared Na_2PrF_6 by treating it with liquid hydrogen fluoride in a fluorine atmosphere. The tetrafluorides are white solids which crystallize in the monoclinic system (UF_4 or ThF_4 type). They are slightly soluble in water but decompose to the trifluorides and are thermally unstable. Cerium tetrafluoride is appreciably more stable than the tetrafluorides of praseodymium and terbium.

The dihalides may be divided into two groups: the mainly salt-like compounds, in which the cation has a valency of 2+, and those compounds whose properties (e.g., electrical conductivity) indicate that the bond has some metallic character, and can be represented, in a much simplified way, by the general formula $\text{Ln}^{3+}(\text{e}^-)\text{X}_2$. Important methods of preparation include reduction of the trihalides by hydrogen at elevated temperatures (dichlorides, dibromides, and diiodides of Eu , Yb , and Sm , as well as EuF_2), or by solid or gaseous rare earth metals.

Thermodynamically stable difluorides are known only for Eu , Sm , and Yb . However, the difluorides of almost all the other rare earth elements can be prepared as metastable compounds which crystallize in the cubic system (fluorite type). EuF_2 , YbF_2 , and SmF_2 can take

up considerable quantities of the corresponding trifluorides in solid solution. Other dihalides of many rare earth elements can be prepared, but it is difficult to give definite trends for the occurrence of salt-like or metallic properties. However, it can be stated that all the dihalides of Sm , Eu , and Yb are of a mainly salt-like nature.

44.9.4 Chalcogenides

The rare earth elements form chalcogenides with the general formula REZ , RE_3Z_4 , RE_2Z_3 (RE_5Z_7), and RE_2Z_4 (where $\text{Z} = \text{S}$ or Se) [3, vol. 3, pp. 149–248; 121]. With Te , compounds are known with the formulae RETe , RE_3Te_4 , RE_2Te_3 , RE_4Te_7 , RETe_2 , RE_2Te_5 , and RETe_3 , of which some must be regarded as intermetallic compounds. The rare earth chalcogenides exhibit a wide range of structural, electrical, and magnetic properties. Most of them are very sensitive to hydrolysis and can therefore only be prepared and handled if moisture is excluded.

The monochalcogenides are mainly prepared by direct synthesis from the elements, but may also be prepared in some cases (YbS , YbSe , SmS , SmSe [20, 122]) by the reduction of higher chalcogenides with the corresponding gaseous rare earth metal. EuS and EuSe are also obtained by the reaction of Eu_2O_3 with $\text{H}_2\text{S}/\text{H}_2$ or $\text{H}_2\text{Se}/\text{H}_2$ at ca 1100 °C. All the rare earth monochalcogenides crystallize in the cubic system (NaCl type) and have high melting and boiling points. Thus, for example, the compound CeS has been recommended as a sulfide ceramic material for coating vessels due to its inertness to many metals [123]. It begins to liquefy above 2100 °C, and melts at 2450 °C. Despite the 1:1 stoichiometry, only the monochalcogenides of Eu , Yb , and Sm can (within limits) be regarded as compounds of RE^{2+} . The other compounds have properties that show the simultaneous presence of ionic and metallic bonding.

The sesquichalcogenides, RE_2Z_3 ($\text{Z} = \text{S}$, Se , or Te), can also be prepared by direct synthesis from the elements (the only practical method for the tellurides), or by reaction of the sesqui-

oxides or trihalides with the hydrogen chalcogenides at high temperatures. When the oxides are used, very stable oxide chalcogenides such as $\text{RE}_2\text{O}_2\text{Z}$ can be produced as intermediate products. The sesquichalcogenides can exist in several modifications. The cubic modification is nonstoichiometric, with the approximate composition RE_3Z_4 (Th_3P_4 type).

Rare earth polychalcogenides include the polysulfides RE_2S_4 . With the exceptions of the polysulfides of Tm and Lu , they are obtained by heating the sesquisulfides with an excess of sulfur. They are interesting in that they are not RE^{4+} compounds, but contain two S^{2-} ions and one S_2 group per formula unit.

The crystal chemistry and phase equilibria of rare earth ternary systems with chalcogen elements is dealt with in [124].

44.9.5 Nitrides

The rare earth elements react with nitrogen to give nitrides of the type REN [125], and with the elements P , As , Sb , and Bi to give compounds with other stoichiometric compositions. The nitrides are formed in slow reactions of nitrogen with the metals or hydrides in very finely divided form at ca 1000 °C, or more readily by reaction with ammonia at ca. 700 °C. The nitrides are cubic (NaCl type) and have very high melting points and decomposition temperatures. They have a metallic appearance when in a compact form, and are ionic compounds with metallic conductivity or semiconductors. Apart from ScN , all the rare earth nitrides are very sensitive to hydrolysis, and can therefore only be handled when moisture is excluded.

44.9.6 Carbides

Of the rare earth compounds with elements of group 14, only the carbides are described here. Compounds with the formulae REC_2 , RE_2C_3 , RE_2C , and REC_{1-x} are known. Of these, the carbides REC_2 represent the largest group [3, vol. 3, pp. 284–342]. The carbides can be synthesized directly from the elements. The high-melting dicarbides are highly invol-

atile, crystallize in the tetragonal system (CaC_2 type), and are metallic conductors with approximately one conducting electron per C_2 group. Hydrolysis of the carbides under neutral or weakly acidic conditions leads to complex mixtures of unsaturated and saturated hydrocarbons, most of which are C_2 hydrocarbons due to the presence of C_2 groups in the crystal structure.

44.9.7 Complexes; Organic Compounds

From the point of view of complex-forming properties, the rare earth elements resemble the elements of group 2 more closely than those of the $3d$ transition elements, owing to the peculiarities described earlier. Only very strong ligands, with strong chelate-forming properties, are able to form thermodynamically stable, isolable rare earth complexes.

Many rare earth chelates are very difficult to isolate from aqueous solution, as water is an extremely strong ligand for rare earth ions. Also, ligand exchange reactions take place very rapidly in solution, which makes it impossible to isolate definite isomers. Of the rare earth chelate compounds so far prepared (e.g., [3, vol. 3, pp. 61–128; 126]), those useful for liquid–liquid extraction and separation of rare earth elements are of particular interest. The technically important chelating agents include certain ketones, but, above all, tri-*n*-butylphosphate (TBP) [3, vol. 1, pp. 89–109]. The chelates of the rare earth elements with 2,4-pentanedione (acetylacetone) and its derivatives are also important, these being characterized by great stability and sometimes considerable volatility [127].

When considering organic compounds [1, part D1–D3; 128], a distinction should be made between true organometallic compounds and salts of organic acids or coordination compounds with organic ligands. The relatively small number of true organic compounds (e.g., the tris(cyclopentadienyl) derivatives [129] and the triphenylene and anionic tetraphenyl complexes [130, 131]) are mostly very reactive, sensitive substances. Of the

large group of salts of organic acids, the oxalates deserve mention. These are formed as sparingly soluble precipitates from solutions in moderately concentrated hydrochloric acid and are important for the purification of the rare earth elements, and also for their quantitative determination. Organometallic compounds of the rare earth elements are discussed in [132].

44.10 Uses [3, vol. 1, pp. 416–500; vol. 2, pp. 190–297]

The rare earth metals and their compounds are used in numerous areas of industry for a wide range of purposes. The most important of these include metallurgy, catalysts in the chemical industry, coloring of glass and ceramics, the production of magnets, and phosphors.

Metallurgy. The importance of the rare earth metals in metallurgy is highlighted in [133, 134]. In 1990, ca. 22% by volume of rare earth consumption in the United States was devoted to metallurgical end use. The equivalent volume usage in Japan by contrast was ca. 10%. One of the most important areas of application, is based on their reactivity with water, hydrogen, nitrogen, sulfur, and the so-called tramp elements such as arsenic, antimony, and bismuth. Sulfur reacts to form rare earth sulfides or oxysulfides in spheroidal form which are not deformed under rolling conditions, and which form solid particles at the temperature of molten steel, thus improving the hot formability and flexibility of microalloyed steels, and reducing anisotropy in the notched toughness test. Rare earths are used in the form of mischmetal containing principally Ce, La, and Nd.

The addition of rare earth metals such as yttrium and cerium, or cerium mischmetal imparts improved oxidation resistance to heating element alloys, to substrate alloys for catalysts, and to superalloys. Rare earth metals improve the precipitation of spheroidal graphite in SG iron casting. Although for economic reasons cerium mischmetal is more often used

in these applications than the pure rare earth metals, the pure metals can give better results when used separately.

Addition of rare earths to copper and aluminum alloys, used as electrical conductors, improves the mechanical properties. In China, an yttrium magnesium aluminum alloy has been developed for transmission cabling. Yttrium improves tensile strength, heat resistance, vibration resistance and can raise electrical conductivity by 50%. Creep resistance and tensile strength at high temperatures are improved by addition of rare earth metal (mainly neodymium, praseodymium, and yttrium) to magnesium alloys for pressure casting and aircraft construction. Recent investigations have shown significant improvements to high strength Al–Mg and Al–Li alloys by the addition of scandium. Similar effects can be achieved with titanium and titanium alloys, and with alloys of niobium, tantalum, and vanadium.

The rare earth metals react readily with gaseous elements, and are therefore used as getters. Their pyrophoric properties are utilized in friction igniters (“flints”) and in military projectiles.

Alloys of the type LaNi_5 are capable of absorbing hydrogen, even from mixtures with other gases, forming rare earth hydrides. These are used to store hydrogen reversibly. In these alloys La can be partially replaced by Ce, Pr, and Nd, and Ni by Co, Cr, Cu, Fe, or Mn. They can also be used to separate D_2 from H_2 [135–138].

Rare earth alloys with $3d$ transition elements have magnetic properties [2, vols. 14, 16; 139, 140]. These alloys are of the type RE_2A_{17} , in which the rare earth metals can be cerium earths, especially Sm, and the $3d$ transition metals can be pure Co, or Co partially replaced by Fe, Mn, Cr, or Cu. These alloys give extremely stable magnets, having energy products, high remanence, and high coercive field strengths [141–143]. Some typical properties are given in Table 44.13. These high-power magnets are used in small motors, printers, quartz watches, headphones, loudspeakers, magnetic storage, traveling-wave tubes, etc., mainly in miniaturized equipment.

Rare earth alloys also exhibit very large magnetostriction at cryogenic temperatures. REFe_2 Laves phase compounds show very large magnetostriction but possess intrinsic magneto-crystalline anisotropy [2, vol. 2, chap 15, pp 231–258]. For many applications, high strain is required at low magnetic fields, and therefore anisotropy must be minimized. The most important material to emerge from research activity so far is the ternary alloy $\text{Tb}_{0.27}\text{Dy}_{0.73}\text{Fe}_2$, which shows promise for high power actuators, transducers, and sensors.

Catalysts [117, vol 5, chap 43, 217–320]. A further important use for rare earth elements (as their chlorides or nitrates) is in zeolite cracker catalysts for the improvement of gasoline yields and reductions in the formation of coke and light hydrocarbons. These catalyst compositions can correspond either to the natural composition of the cerium earths or can be based mainly on cerium [144].

Table 44.13: Characteristic properties of selected rare earth permanent magnetic materials.

Material	Energy product (BH) _{max} , kJ/m ³	Remanence B_r , mT	Coercivity before polarisation H_{cb} , kA/m	Coercivity after polarisation H_{cj} , kA/m
SmCo_5	160	920	2500	680
$(\text{Sm}_{0.4}\text{Pr}_{0.6})\text{Co}_5$	200	1050	1200	720
$(\text{Sm}_{0.2}\text{Mg}_{0.8})\text{Co}_5$	120	800	1000	580
$\text{Sm}(\text{Co}, \text{Cu}, \text{Fe})_5$	110	770	300	290
$\text{Sm}(\text{Co}, \text{Cu}, \text{Fe}, \text{Zr})_{6.9}$	240	1130	580	540
$\text{Sm}(\text{Co}, \text{Cu}, \text{Fe}, \text{Zr})_{7.5}$	210	1080	800	780
NdFeB	300	1300	1000	700
NdDyFeB	250	1100	2000	880

Rare earth elements are also used as catalysts for alkylation, isomerization, hydrogenation, dehydrogenation, dehydration, reforming of hydrocarbons, polymerization, oxidation of CO and hydrocarbons [145, 146], and reduction of the concentration of nitrogen oxides in automobile exhaust gases [147]. The formation of hydrides enables them to be used as methanation catalysts [148]. Cerium stabilizes $\gamma\text{-Al}_2\text{O}_3$ as a carrier for noble metal catalysts [149, 150]. Rare earth chelates with diketones can replace lead compounds as anti-knock agents [151].

Energy Production. Rare earth elements have a possible future use in energy production RENi_5 [152], La_2O_3 , Y_2O_3 , and CeO_2 , with Ni, Co, Cr, or Zn [153], can be used as electrodes in fuel cells, while the solid electrolyte can be ZrO_2 stabilized with Y_2O_3 , $\text{ZrO}_2\text{-Y}_2\text{O}_3\text{-Ta}_2\text{O}_5$, or $\text{ZrO}_2\text{-CeO}_2\text{-Y}_2\text{O}_3$ [154, 155].

Water, in the form of a photooxidizable compound with Eu^{2+} , is reduced in the first stage, and in the second stage the Eu^{3+} formed is reduced by a light-sensitive transition metal complex [156]. Water can be oxidized by Ce^{4+} in the presence of the redox catalyst PtO_2 or IrO_2 , and the Ce^{3+} produced reconverted photochemically to Ce^{4+} , with liberation of H_2 [157]. The low Curie point (20 °C) of Gd can be utilized to produce a heat pump [158].

In magnetohydrodynamic generators, LaCrO_3 [159] and LaCoO_3 [160] are used as electrodes, and LaB_6 [161] as an electron emitter.

Glass and Ceramics. Another important use of rare earth elements is in the glass and ceramic industries [162]. Rare earth oxides in their naturally-occurring composition or with an increased CeO_2 content (or pure CeO_2) are used as polishing agents in the glass industry. Other uses of Ce include the chemical decolorization of glass ($\text{Fe}^{2+} \rightarrow \text{Fe}^{3+}$) [163], reduction of UV transparency of glass containers for foodstuffs and medicines, and the prevention decolorization of television screens by X rays and γ rays.

Nd (blue to wine red), Pr (green), Er (pink), and Ho (blue) can be used both for coloring

glass and for color neutralization. Combinations of these with each other and with other elements such as Ti(+ Ce: yellow), Se(+ Nd: violet), and Ni(+ Nd: reddish) give further effects.

In optical glasses for lenses, La improves the refractive index and dispersion. La and Gd also improve chemical and mechanical properties, and enable these types of glass to be used under the demanding conditions of magneto-optical and electro-optical systems [120, chap. 58, pp. 1-90].

In very pure types of glass, Eu^{2+} and Ce^{4+} give a phototropic effect in sunlight.

In the ceramic industry, rare earth oxides are used as yellow pigments (Pr) [164], as opacifiers in glazes and enamels (Ce) [165], for radiation-shielding ceramics (Sm, Eu, Gd, Dy) [166], to improve the light fastness of lead chromate and titanium dioxide pigments, to impart "natural" fluorescence to artificial teeth (Eu, Sm, Ce) [167-169], and especially as stabilizers for cubic ZrO_2 [170]. An interesting application is in so-called lambda probes, in which Y_2O_3 -stabilized ZrO_2 is the solid electrolyte in a measurement/control system that optimizes oxidation and reduces the content of harmful gases in automobile exhausts [171]. In a similar application, it is used for determining the O_2 content of liquid steel [172].

CeS and Y_2O_3 can be used for the manufacture of crucibles and as temperature-resistant materials for gas turbines [173]. The mechanical properties of Si_3N_4 are improved by the addition of rare earths to promote sintering [174].

Electronics. Compounds of the type $\text{Pb}_{1-x}\text{La}_x(\text{Zr}_{1-y}\text{Ti}_y)\text{O}_3$ (PLZT) are used as electro-optical ceramics in displays [175], as electromechanical transducers [176], and for their piezoelectrical properties [177]. Lanthanum doped BaTiO_3 is used as a dielectric in capacitors [178], and in thermistors [179].

Compounds of the garnet type such as $\text{Y}_3\text{Al}_5\text{O}_{12}$ (YAG), $\text{Y}_3\text{Fe}_5\text{O}_{12}$ (YIG), and yttrium orthoaluminate YAlO_3 (YALO), doped with neodymium, are used as solid state lasers

[2, vol. 4, pp. 275-315]. Solid state Nd-YAG lasers, operating at 1064 nm wavelength, are most popular for cutting, welding and metal heat treatment. In Japan production is growing at ca. 10%/a. Recently, Ho-YAG and Er-YAG lasers, emitting at 2000 nm and 2900 nm, respectively, have been developed to partly replace CO_2 lasers for use in microsurgery. In 1986 Sumitomo Metal Mining Company produced single crystals of gadolinium-aluminum-scandium garnet (GASG). These laser materials doped with nickel and chromium are expected to capture some of the tunable and high-power laser markets. $\text{Y}_3\text{Fe}_5\text{O}_{12}$ (YIG) is also used in frequency control applications [180, 181]. $\text{Gd}_3\text{Ga}_5\text{O}_{12}$ (GGG) crystal contains 53.7% gadolinium oxide and is used for bubble type magnetic information storage [182] as well as in the doped form (ca. 3 atom% Nd) for high-power pulsed lasers. Rare earths used in laser technology are of very high purity (> 99.999%) and therefore have high added value.

Rare earth-transition metal alloys deposited onto glass or polycarbonate provide an excellent magneto-optical medium for high density data storage and retrieval. Films are generally deposited by sputtering, and the targets used in the process usually contain terbium, gadolinium, dysprosium, or neodymium together with cobalt and iron and other minor elements. Rare earth halides of Eu and Yb have semiconductor properties [183].

Phosphors [2, vol. 4, pp. 237-274]. Stimulation by UV, X rays, or electron beams causes certain rare earth elements to emit light of a definite wavelength. The energy is transferred from the host lattice to an activator. The following can act as host lattices: oxide sulfides and vanadates of Y, La, Gd, and Lu (favorable 4f electron configurations), and borates, aluminates, phosphates, silicates, tungstates, fluorides, compounds of the ruby type, etc. Phosphors containing rare earth oxides are

used in color cathode ray tubes, X-ray intensifying screens, and fluorescent lamps. The following are used as red emitting phosphors in cathode ray tubes for TV and VDU screens: $\text{YVO}_4\text{:Eu}^{3+}$ (4.5%), $\text{Y}_2\text{O}_3\text{:Eu}^{3+}$ (3.5%), and $\text{Y}_2\text{O}_2\text{S:Eu}^{3+}$ (3.65%). Examples of green-emitting phosphors are $\text{La}_2\text{O}_2\text{S:Tb}^{3+}$, CaS:Ce^{3+} , and $\text{SrGa}_2\text{S}_4\text{:Eu}^{2+}$. Blue phosphors include $\text{Sr}_5\text{Cl(PO}_4)_3\text{:Eu}^{2+}$ and ZnS:Tm^{3+} . Other rare earth activators are Ce^{3+} (UV, blue), Pr^{3+} (red, green, blue, UV), Nd^{3+} (IR, lasers), Sm^{3+} (orange), Eu^{2+} (blue, green), Tb^{3+} (green), Dy (yellow, white), Er (green, lasers), Ho (green, yellow, lasers), Tm (blue), and Yb (green). Other areas of use include high-sensitivity X-ray films, optical scanning devices, photocopying equipment, and scintillation crystals [184]. Rare earth fluorides and oxides are still added to the carbon of classical carbon arc lamps, e.g., for cinemas, to improve light emission [185]. In 1991, 73% by volume of the rare earths used in phosphors was associated with yttrium, 5% with europium, 4% with terbium, and 18% with other rare earth elements.

Reactor Technology. Sm, Eu, Gd, and Dy have high thermal neutron capture cross sections. Eu and Dy can take up five neutrons in succession. Therefore, they have a low rate of burn off when used in control rods or in ceramics for radiation protection [166]. Table 44.14 lists the thermal neutron capture cross sections of these elements.

Other Applications. Rare earth compounds are used in the paint industry as dryers [186]. They are also used in the textile industry [187] and as oxidizing agents for self-cleaning ovens [188, 189].

Europium complexes are used as shift reagents in NMR spectroscopy [190].

Rare earth elements can be used in the third stage of wastewater purification for the precipitation of phosphates [191].

Table 44.14: Thermal neutron capture cross sections of some rare earth elements in n, γ reactions.

Rare earth element	Number of absorbing isotopes	Relative atomic mass	Abundance in nature, %	Thermal neutron capture cross section, 10^{-28} m^2	
				For natural isotope mixture	For single isotopes
Sm	1	149	13.8	5 600	66 000
Eu	5	151	47.8	4 300	9 000
		152			5 000
		153	52.2		420
		154			1 500
Gd	2	155	14.9	46 000	13 000
		157	15.7		70 000
		157			180 000
Dy	5	160	2.3	950	130
		161	18.9		680
		162	25.5		240
		163	24.9		220
		164	28.2		2 780

44.11 Economic Aspects [192]

World production of rare earth minerals totalled ca. 96 500 t (57 000 t REO) in 1990, compared with an estimated output of ca. 107 500 t (64 000 t REO) in 1989. The decrease in mineral output over these two years has been associated with a decrease in Australian and Chinese production. In particular, up to 1988 production and pricing policy of raw materials and separated rare earth elements were essentially stable. Chinese production and export of these products increased dramatically between 1988 and 1990 without a parallel increase in market demand, thus causing some destabilization of world pricing policies. Prices of rare earth materials during this period dropped by between 20 and 70%, depending on the rare earth element China's export revenues also suffered a 40% decrease. Some stability has returned to the world market with China reducing output of rare earth minerals from 43 000 t (25 250 t REO) in 1989 to 27 500 t (16 500 t REO) in 1990. Exports of raw materials also dropped by 50% in 1990 and by 46% in 1991.

World rare earth consumption grew by less than 3% annually between 1980 and 1990 against a predicted growth of 6%. In 1980 the demand for rare earths expressed as oxide (REO) was ca. 27 000 t. Rare earth consumption in 1990 is estimated at 35 000 t with a

market value of ca. \$400 $\times 10^6$. Ores, concentrates and mixed rare earth compounds account for ca. 75% of the tonnage consumption but only 25% of the total market value.

Rare earths in the form of metals and separated high-purity oxide for use in applications such as phosphors, magnets and superconductors, demand much higher added value and account for nearly 75% of the market. This latter market sector is currently showing a reasonable growth rate of ca. 15%/a.

Current estimates of world rare earth consumption by end use for 1990 and predicted values for 1996 are shown in Table 44.15. However, as is shown in Table 44.16, the balance of consumption for end use applications varies significantly between the major user countries. This can reflect differences in technological status, future commercial strategies, and the availability of rare earth stock.

Table 44.15: World markets for rare earth consumption by end use [192].

Use	1990		Predicted for 1996	
	% vol	% by value	% vol	% by value
Phosphors	3	37	4	40
Magnets	7	20	15	23
Catalyst	40	16	35	11
Glass	18	12	17	10
Metallurgy	26	4	22	2
Ceramics	2	6	2	8
Other	4	5	5	6
Total	100	100	100	100

Table 44.16: Rare earth consumption by end use application [192].

Application	United States 1989		Japan 1990		China 1990	
	% vol	tonnes REO	% vol	tonnes REO	% vol	tonnes REO
Glass and ceramics	43	7 524	67	3639		
Catalysis	42	7 350			30	2200
Metallurgy	14	2 450	4	217	56.5	4100
Permanent magnets			18	978	3	216
Agriculture					6.5	480
Phosphors			5.5	299		
Other	1 ^a	175 ^a	5.5 ^b	299 ^b	4	260
Total	100	17 500	100	5432	100	7256

^a Includes permanent magnets, phosphors, and electronics.

^b Includes catalysis.

New developments based on the less common rare earth elements or requiring only a single rare earth element can affect the supply/demand situation. A favorable cost/price situation will only exist if there is a good market for all the principal rare earth elements that occur in nature, since rates of production of the elements by the rare earth industry are interdependent.

Prices of rare earths can vary significantly depending upon the abundance of the rare earth element in the ore, the source of the product, the purity of the element or compound required, and the quantity of material purchased.

Approximate prices of rare earth oxides are given in Table 44.17. Reviews of the rare earth industry are given in [14, 192–194].

Table 44.17: Approximate prices of rare earth oxides in 1990 [192].

Rare earth oxide	Rhône-Poulenc		Molycorp	
	Purity, %	\$/kg	Purity, %	\$/kg
Ce	99.50	25.75	99.0	19.25
Dy	95.00	132.00	96.00	132.00
Er	96.00	190.00	98.00	143.00
Eu	99.99	1960.00	99.99	1639.00
Gd	99.99	136.50	99.99	132.00
Ho	99.90	510.00		
La	99.99	23.00	99.99	19.25
Lu	99.99	7000.00		
Nd	95.00	20.00	99.90	88.00
Pr	96.00	38.85	96.00	37.00
Sm	96.00	175.00	96.00	143.00
Tb	99.90	880.00	99.90	825.00
Tm	99.90	3600.00		
Yb	99.00	230.00		
Y	99.99	115.50	99.99	115.50

44.12 Toxicology

The pure rare earth metals and their compounds are regarded as having low toxicities with respect to the Hodge Sterner classification system [195]. HALEY describes the rare earth elements as only slightly toxic [2, vol. 4, pp. 553–585; 196]; see also [1, part B2]. A further extensive review on this subject is provided by ARVELA [197].

Several authors investigations into the inhalation of rare earth oxides by humans (smoke from carbon arc lamps in cinemas) have been carried out [198–200]. Chest X rays show changes to the lungs caused by dust deposits, although these harmful effects are not caused by the rare earth elements, but by radioactive impurities, i.e., products of the radioactive decay of thorium and uranium. Modern methods of rare earth separation together with an increased use of bastnaesite have led to rare earth products that are virtually free from Th and U.

Experiments on animals showed that intravenous injection of rare earths caused impairment of liver function.

44.13 References

1. Gmelin, 8th ed. Seltene Erden, A2–A5, B1–B7, C1–C3, C4a, C5–C6, C8, D1–D3.
2. K. A. Gschneidner, Jr., L. Eyring, (eds.) *Handbook on the Physics and Chemistry of Rare Earths* vol. 1–4, North Holland Publ., Amsterdam 1979.
3. L. Eyring (ed.): *Progress in the Science and Technology of the Rare Earths*, vol. 1, 1964; vol. 2, 1966; vol. 3, 1968, Pergamon Press, Oxford.
4. J. A. Gibson, G. S. Harvey: "Properties of the Rare Earth Metals and Compounds", *Technical Report*

- AFML-TR-65-430, Wright Patterson Air Force Base, OH, 1966.
5. F. H. Spedding, A. H. Daane: *The Rare Earths*, J. Wiley, New York 1961.
 6. F. Trombe, J. Lories, P. Gaume-Mahn, Ch. H. La Blanchetais: "Scandium-Yttrium-Éléments des terres rares-Actinium" in P. Pascal (ed.): *Nouveau Traité de chimie minérale*, vol. 7, parts 1, 2, Masson, Paris 1959.
 7. International Union of Pure and Applied Chemistry (IUPAC): *Nomenclature of Inorganic Chemistry, Definition Rules 1970*, Butterworths, London 1971.
 8. Th. Moeller: "The Lanthanides" in I. C. Bailar, H. J. Emelius, R. Nyholm, A. F. Trotman-Dickenson (eds.): *Comprehensive Inorganic Chemistry*, vol. 4, Pergamon Press, Oxford 1971, p. 1.
 9. J. W. Adams, E. R. Iherall: "Bibliography of the Geology and Mineralogy of the Rare Earths and Scandium to 1971", *Geological Bulletin* 1366, Washington 1973.
 10. J. W. Adams: "Distribution of the Lanthanides in Minerals", *Proc. Rare Earth Res. Conf.* 7th (1968) 28-30.
 11. J. W. Adams: "Resources" in J. G. Parker, C. T. Baroch (eds.): *The Rare Earth Elements, Yttrium and Thorium. A Materials Survey*, chap. 3, USBM Information Circular 8476, Washington 1973, pp. 22-39.
 12. United States Bureau of Mines: Mineral Commodity Summaries, and Unocal Company Reports, Washington 1991.
 13. G. Friedlander, J. W. Kennedy: *Lehrbuch der Kern- und Radiochemie*, Thieme, München 1962.
 14. J. A. Marinsky, L. F. Glendenin, C. D. Coryell, J. Am. Chem. Soc. 69 (1947) 2781.
 15. O. Erämetsä, *Acta Polytech. Scand. Chem. Ind. Metall. Ser.* 37 (1965).
 16. D. A. Johnson, *J. Chem. Educ.* 57 (1980) 475.
 17. F. H. Spedding, B. J. Beaudry, *J. Less Common Met.* 25 (1971) 61.
 18. K. N. R. Taylor, M. I. Darby: *Physics of Rare Earth Solids*, Chapman and Hall, London 1972, pp. 1-324.
 19. R. D. Shannon, C. T. Prewitt, *Acta Crystallogr. Sect. B* B25 (1969) 925.
 20. T. Petzel, O. Greis, *Z. Anorg. Allg. Chem.* 396 (1973) 95.
 21. K. A. Gschneidner, Jr., *J. Less Common Met.* 17 (1969) 1.
 22. J. H. Van Vleck: *The Theory of Electric and Magnetic Susceptibilities*, Oxford University Press, Oxford 1932, pp. 1-395.
 23. K. N. R. Taylor, *Contemp. Phys.* 11 (1970) 423-454.
 24. H. R. Kirchmayr, *Z. Metallkd.* 60 (1969) 699-708.
 25. H. R. Kirchmayr, *Z. Metallkd.* 60 (1969) 778-784.
 26. W. E. Wallace: *Rare Earth Intermetallics*, Academic Press, New York 1973.
 27. K. A. Gschneidner, Jr.: *Rare Earth Alloys*, Van Nostrand, Princeton 1961.
 28. K. H. J. Buschow, *Rep. Prog. Phys.* 42 (1979) 1373-1477.
 29. M. Hansen, K. Anderko: *Constitution of Binary Alloys*, 2nd ed., McGraw-Hill, New York 1958, 1st Supplement R. P. Elliot, 1965, 2nd Supplement T. A. Shunk, 1969.
 30. W. G. Moffatt: *The Handbook of Binary Phase Diagrams*, General Electric, Schenectady 1978.
 31. K. A. Gschneidner, Jr., M. E. Verkade: *Selected Cerium Phase Diagrams, IS-RIC-7 Rare Earth Information Centre*, Iowa State University 1974.
 32. Soc. prod. chim. terres rares, FR 995112, 1949.
 33. A. E. Bearse, G. D. Calkins, J. W. Glegg, R. B. Filbert, *Chem. Eng. Prog. Monogr. Ser.* 50 (1954) 235-239.
 34. M. Smutz, G. L. Bridger, K. G. Shaw, M. E. Whatley, *Chem. Eng. Prog. Symp. Ser.* 50 (1954) 13, 167-170.
 35. American Potash and Chemical Corp., US 2900231, 1952.
 36. V. E. Shaw, *Rep. Inst. U.S. Bur. Mines RI* 5474 (1959) 1-12.
 37. Y. Hirashima, J. Shiokawa, *Nippon Kagaku Kaishi*, 1973 no. 3, 496-499; *Chem. Abstr.* 78 (1973) 152030.
 38. *Chem. Eng. (N.Y.)* 74 (1967) 2, 122-123.
 39. P. R. Kruesi, G. Duker, *J. Met.* 17 (1965) 847-849.
 40. D. J. Bauer, V. E. Shaw, *Rep. Invest. U.S. Bur. Mines RI* 6381 (1964) 1-15.
 41. B. I. Kogan, I. P. Skripka, *Redk. Elem.* 8 (1973) 3-57.
 42. H. Richter, A. Krause, *Chem. Tech. (Leipzig)* 17 (1965) 707-710.
 43. G. Trombe, DE-OS 2238665, 1973.
 44. W. Brugger, E. Greinacher, *J. Met.* 19 (1967) 32-35.
 45. Th. Goldschmidt AG, DT 956993, 1954.
 46. Soc. prod. chim. terres rares, FR 1209251, 1958.
 47. F. H. Spedding, J. E. Powell in F. C. Nachod, J. Schubert (eds.): *Ion Exchange Technology*, Academic Press, New York 1956, pp. 359-390.
 48. C. D. Scott, R. D. Spence, W. G. Sisson: "Pressurised Annular Chromatography for Continuous Separation", *J. Chromatogr.* 126 (1976) 381-400.
 49. J. M. Begovich, W. G. Sisson: "A Rotating Annular Chromatograph for Continuous Metals Separation and Recovery", *Resour. Conserv.* 9 (1982) 219-229.
 50. J. M. Begovich, C. H. Byers, W. G. Sisson: "A High Capacity Pressurised Continuous Chromatograph", *Sep. Sci. Technol.* 18 (1983) 1167-1191.
 51. V. T. Taniguchi, A. W. Doty, C. H. Byers: "Large Scale Chromatographic Separations using Continuous Displacement Chromatography (CDC)" in R. G. Bautista, M. M. Wong (eds.): *Rare Earths Extraction, Preparation and Applications*, The Minerals, Metals and Materials Soc., annual meeting, Las Vegas 1989, 147-161.
 52. J. P. Surls, Jr., G. R. Choppin, *J. Am. Chem. Soc.* 79 (1957) 855-859.
 53. S. W. Mayer, E. R. Tompkins, *J. Am. Chem. Soc.* 69 (1947) 2865-2874.
 54. J. E. Powell, F. H. Spedding, *Trans. Am. Inst. Min. Metall. Pet. Eng.* 215 (1959) 457-463.
 55. P. Conrad, M. Caude, R. Rosset, *Sep. Sci.* 7 (1972) no. 5, 457-463.
 56. P. Conrad, M. Caude, R. Rosset, *Sep. Sci.* 9 (1974) no. 4, 269-285.
 57. R. E. Linstrom, J. O. Wingert, *Rep. Invest. U.S. Bur. Mines RI* 6131 (1961) 1-21.
 58. D. B. James, J. E. Powell, F. H. Spedding, *J. Inorg. Nucl. Chem.* 19 (1961) 133-141.
 59. W. L. Silvermail, M. M. Woyski: "Commercial Ion Exchange Separation of the Rare Earths", *Proc. Rare Earth Res. Conf.* 6th, Gatlinburg, May 1967, 678-690.
 60. Santoku Metals Industry Co., JP 7028292, 1966.
 61. GTE Sylvania Inc., US 3482932, 1969.
 62. C. Persiani, J. F. Cosgrove, R. Walters, D. J. Bracco, *Sep. Sci.* 2 (1967) no. 6, 789-796.
 63. D. Asher et al., *Ind. Eng. Chem. Process Des. Dev.* 1 (1962) no. 1, 52-56.
 64. J. E. Powell, H. R. Burkholder, *J. Chromatogr.* 36 (1968) 99-104.
 65. J. E. Powell, H. R. Burkholder, *J. Chromatogr.* 29 (1967) 210-217.
 66. W. Fischer, W. Dietz, O. Jübermann, *Naturwissenschaften* 25 (1937) 348.
 67. W. Fischer, K. Biesenberger, J. Heppner, U. Neitzel, *Chem. Ing. Tech.* 36 (1964) 85-99.
 68. F. Horn, *Chem. Ing. Tech.* 36 (1964) 99-111.
 69. N. M. Rice, *Chem. Ind. (London)* 1977, Sept., 718-723.
 70. C. G. Brown, L. G. Sherrington: "Solvent Extraction used in Industrial Separation of Rare Earths", *J. Chem. Technol. Biotechnol.* 29 (1979) 193-209.
 71. R. F. Sebenik, B. M. Sharp, M. Smutz, *Sep. Sci.* 1 (1966) no. 4, 375-386.
 72. E. Hesford, E. E. Jackson, H. A. C. McKay, *J. Inorg. Nucl. Chem.* 9 (1959) 279-289.
 73. D. Scargill et al., *J. Inorg. Nucl. Chem.* 4 (1957) 304-314.
 74. Th. Goldschmidt AG, DT 1592120, 1967.
 75. Thorium LTD., GB 1180922, 1966.
 76. G. W. Mason, D. N. Metta, D. F. Peppard, *J. Inorg. Nucl. Chem.* 38 (1976) 2077.
 77. J. Alstad, J. H. Augustson, T. Danielssen, L. Farbu: "Comparative Study of the Rare Earth Elements in Extraction by HDEHP/Shell Sol T from Nitric and Sulphuric Acid Solutions" in G. V. Jeffreys (ed.): *Proc. Int. Solvent Extr. Conf.* 1974, 1083-1102.
 78. T. B. Pierce, P. F. Peck, *Analyst (London)* 88 (1963) 217-221.
 79. N. E. Thomas, S. Smutz, L. Burkhart, *Ind. Eng. Chem. Fundam.* 10 (1971) 453-458.
 80. D. S. Flett, G. W. Cutting, P. Carey, *Proc. Int. Miner. Process. Congr.* 10th (1973) Paper 23, (Pub. 1974) 1147-1167.
 81. D. E. Peppard, G. W. Mason S. W. Moline in R. G. Bautista, M. M. Wong (eds.): *Rare Earths: Extraction, Preparation and Applications*, The Minerals, Metals and Materials Soc., Warrendale 1989.
 82. D. E. Peppard, E. P. Horwitz, G. W. Mason in R. G. Bautista and M. M. Wong (eds.): *Rare Earths: Extraction, Preparation and Applications*, The Minerals, Metals and Materials Soc., Warrendale 1989.
 83. K. S. Han, K. Tozawa: "Thermodynamic Prediction of Coefficients for the Solvent Extraction of the Rare Earths" in R. G. Bautista, M. M. Wong (eds.): *Rare Earths: Extraction, Preparation and Applications*, The Minerals, Metals and Materials Soc., Warrendale 1989, pp. 115-128.
 84. C. F. Baes, Jr., *J. Inorg. Nucl. Chem.* 24 (1962) 707-720.
 85. Z. Kolarik, S. Drazanova, V. Chotivka, *J. Inorg. Nucl. Chem.* 33 (1971) 1125-1133.
 86. R. A. Alekperov, S. S. Geibatova, *Dokl. Chem. (Engl. Transl.)* 178 (1968) 29.
 87. R. D. Korpusov, G. L. Vaks, E. N. Petrusheva, *Russ. J. Inorg. Chem. (Engl. Transl.)* 14 (1969) 1004.
 88. F. J. Seelay, D. J. Crouse, *J. Chem. Eng. Data* 11 (1966) 42.
 89. F. J. Seelay, D. J. Crouse, *J. Chem. Eng. Data* 16 (1971) 393.
 90. US Atomic Energy Commission, US 3294494, 1966.
 91. J. S. Preston, A. C. DuPreez, *Rep. Mintek M378* (1988).
 92. P. Th. Gerontopoulis, L. Rigali, P. G. Barbanò, *Radiochim. Acta* 4 (1965) 75-78.
 93. Government of the United States, US 3323857, 1967.
 94. US Atomic Energy Commission, US 3409415, 1968.
 95. T. V. Healey, *J. Inorg. Nucl. Chem.* 19 (1961) 314-327.
 96. B. H. Lucas, G. M. Ritcey, *CIM Bull.* 68 (1975) no. 753, 124-130.
 97. B. Z. Zhang et al., *Hydrometallurgy* 9 (1982) 205-210.
 98. K. A. Gschneidner, Jr., *Rare Earths in the Electronics Industry* 88 (1991) 63-94; Royal Soc. Chem., Special Publication, Fine Chemicals for the Electronics Industry II.
 99. H. W. Harrah: Deco Trefoil, Denver Equipment Comp., Denver, CO, Nov.-Dec., 9, 1967.
 100. Forskningsgruppe for Sjeldne Jordarter, US 3751553, 1971.
 101. Molybdenum Corp., US 3640678, 1970.
 102. H. N. McCoy, *J. Am. Chem. Soc.* 63 (1941) 1622.
 103. E. Greinacher, K. Reinhardt: "Seltene Erden" in H. Harnisch, R. Steiner, K. Winnacker (eds.): *Chemische Technologie*, 4th ed., vol. 2, "Anorganische Technologie I", Hanser Verlag, München 1982, pp. 678-707.
 104. E. Morrice, M. M. Wong, *Miner. Sci. Eng.* 11 (1979) 125-136.
 105. Molybdenum Corp., US 3729397, 1970.
 106. T. A. Henrie, *J. Met.* 16 (1964) 978-981.
 107. O. N. Carlsson, J. A. Hæfling, F. A. Schmidt, F. H. Spedding, *J. Electrochem. Soc.* 107 (1960) 540-545.
 108. T. T. Campbell, F. E. Block, *J. Met.* 11 (1959) 744-746.
 109. Th. Goldschmidt AG, DT 2303697, 1973.
 110. R. E. Cech, *J. Met.* 26 (1974) 32.
 111. C. E. Habermann, A. H. Daane, P. E. Palmer, *Trans. AIME* 233 (1965) 1038-1042.
 112. A. Brusdeylins, *Chem. Ztg.* 97 (1973) 343-347.
 113. O. B. Michelsen (ed.): *Analysis and Application of Rare Earth Materials*, NATO Advanced Study Institute, Kjeller, Norway, 23-29 Aug., 1972, Universitetsforlaget, Oslo 1973.
 114. K. A. Gschneidner, Jr., L. Eyring (eds.): *Handbook on the Physics and Chemistry of Rare Earths*, vol. 13, North-Holland Publ., Amsterdam 1991.
 115. R. J. Conzemius, S.-K. Zhao, R. S. Houk, H. J. Svec, *Int. J. Mass Spectrom. Ion Processes* 61 (1984) 277.
 116. K. A. Gschneidner, Jr., L. Eyring (eds.): *Handbook on the Physics and Chemistry of Rare Earths*, vol.

- 6., chap. 47, North-Holland Publ., Amsterdam 1984, pp. 1-111.
117. K. A. Gschneidner, Jr., L. Eyring (eds.): *Handbook on the Physics and Chemistry of Rare Earths*, vol. 5, chap. 44, North-Holland Publ., Amsterdam 1982, pp. 321-386.
118. B. G. Hyde, D. J. M. Bevan, L. Eyring, *Phil. Trans. R. Soc. London Ser. A* 259 (1966) no. 1106, 583.
119. K. A. Gschneidner, Jr., L. Eyring (eds.): *Handbook on the Physics and Chemistry of Rare Earths*, vol. 8, chap. 56, part I, North-Holland Publ., Amsterdam 1986, 203-334.
120. K. A. Gschneidner, Jr., L. Eyring (eds.): *Handbook on the Physics and Chemistry of Rare Earths*, vol. 9., chap. 59, part II, North-Holland Publ., Amsterdam 1987, p. 320.
121. A. W. Sleight, C. T. Prewitt, *Inorg. Chem.* 7 (1968) 2282.
122. T. Petzel, *Inorg. Nucl. Chem. Lett.* 10 (1974) 119.
123. E. D. Eastmann et al., *J. Am. Chem. Soc.* 72 (1950) 2248.
124. K. A. Gschneidner, Jr., L. Eyring (eds.): *Handbook on the Physics and Chemistry of Rare Earths*, vol. 13., chap. 89, North-Holland Publ., Amsterdam 1990, pp. 191-281.
125. G. V. Samsonov: *High Temperature Compounds of Rare Earths with Nonmetals*, Consultants Bureau, New York 1965.
126. Th. Moeller et al., *Chem. Rev.* 65 (1965) 1.
127. R. E. Sievers, K. J. Eisentraut, C. S. Springer, Jr.: "Volatile Rare Metal Chelates of β -Diketones" in R. F. Gould (ed.): *Adv. Chem. Ser.* 71 (1967) 141-154.
128. H. Schumann, *Nachr. Chem. Tech. Lab.* 27 (1979) 393.
129. G. Wilkinson, J. M. Birmingham, *J. Am. Chem. Soc.* 76 (1954) 6210.
130. F. A. Hart, M. S. Saran, *Chem. Commun.* 1968, 1614.
131. F. A. Hart, A. G. Massey, M. S. Saran, *J. Organomet. Chem.* 21 (1970) 147.
132. K. A. Gschneidner, Jr., L. Eyring (eds.): *Handbook on the Physics and Chemistry of Rare Earths*, vol. 7., chap. 53, North-Holland Publ., Amsterdam 1985, p. 446.
133. A. Raman, *Z. Metallkd.* 68 (1977) 163-172.
134. A. Raman, *Z. Metallkd.* 67 (1976) 780-789.
135. H. Zulstra, *Chem. Tech. Technol.* 2 (1972) 280-284.
136. K. H. J. Buschow, A. R. Miedema: "Hydrogen Absorption in Rare Earth Intermetallic Compounds" in A. F. Andresen, A. J. Maeland (eds.): *Hydrides Energy Storage Proc. Int. Sym.*, 1977, (Pub. 1978) 235-249.
137. C. E. Lundin, R. W. Sullivan: "The Safety Characteristics of Lanthanum-Nickel (LaNi_5) Hydrides" in T. N. Veziroglu (ed.): *Hydrogen Energy Proc. Hydrogen Econ. Miami Energy Conf. 1974*, Plenum Publishing, New York 1975, pp. 645-658.
138. I. Lambert, A. Percheron-Guegan, J. Montel, *J. Chim. Phys. Phys. Chim. Biol.* 74 (1977) no. 3, 380-381.
139. K. A. Gschneidner, Jr., L. Eyring (eds.): *Handbook on the Physics and Chemistry of Rare Earths*, vol. 11, chap. 76, North-Holland Publ., Amsterdam 1988, pp. 293-321.
140. K. A. Gschneidner, Jr., L. Eyring (eds.): *Handbook on the Physics and Chemistry of Rare Earths*, vol. 12, chap. 83, North-Holland Publ., Amsterdam 1989, pp. 133-212.
141. *Goldschmidt Informiert*, 4 (35), 1-90 (1975).
142. *Goldschmidt Informiert*, 2 (48), 1-75 (1979).
143. *Proc. 7th Int. Workshop Rare Earth-Co Permanent Magnets and their Applications*, China Academic, Peking 1983.
144. Socony Mobil Oil Compl. Inc., US 3173854, 1961.
145. *Molycorp Application Report*, vol. 1, "A Bibliography. Six Years of Research in Catalysis with Rare Earth Elements", no. 7101, 1964-1970, vol. 2, "A Bibliography of the Research in Catalysis with the Rare Earth Elements", no. 7907, 1971-1976.
146. M. P. Rosynek, *Catal. Rev. Sci. Eng.* 16 (1977) 111-154.
147. S. C. Sorenson, J. A. Wrongkiewicz, L. B. Sis, G. P. Wirtz, *Am. Ceram. Soc. Bull.* 53 (1974) 446-449.
148. V. T. Coon, W. E. Wallace, R. S. Craig: "Methanation by Rare Earth Intermetallic Catalysts", in J. G. McCarthy, J. J. Rhyne (eds.): *Rare Earth Research Conf. 13th*, 1977, Plenum, New York 1978.
149. W. R. Grace, US 3903020, 1975.
150. Engelhard, US 4021185, 1977.
151. Government of the United States, US 3794473, 1972.
152. Allis-Chalmers Manufacturing Comp., US 3405008, 1965.
153. K. Shirili, S. Ihara, H. Sato, *Denshi Gijutsu Sogo Kenkyusho Iho* 38 (1974) 378-382; *Chem. Abstr.* 82 (1975) 173473c.
154. G. Robert, M. Forestier, C. Deportes, *Journ. Int. Etude Piles Combust. C. R. 3rd* (1969) 97-105.
155. Molycorp Inc.: "Overview of Application Possibilities", no. 48.
156. P. R. Ryason, US 4105517, 1977.
157. J. Kiwi, M. Gratzel, *Angew. Chem.* 91 (1979) 659-660.
158. B. Wyatt, *Ind. Res. Dev.* 21 (1979) June, 64-65.
159. General Refractories Co., US 3974108, 1974.
160. Tokai Rika Co., Ltd., JP 7652409, 1974.
161. P. H. Schmidt, D. C. Joy, *J. Vac. Sci. Technol.* 15 (1978) 1809-1810.
162. T. C. Shutt, M. Marlin, C. J. Lewis, J. Drobnick, *J. Can. Ceram. Soc.* 40 (1971) 29-37.
163. T. C. Shutt, G. Barlow, *Am. Ceram. Soc. Bull.* 51 (1972) 155-157.
164. Harshaw Chem. Co., US 2992123, 1959.
165. A. Nedeljkovic, R. L. Cook, *Vitreous Enameller* 26 (1975) 2-13.
166. W. Mialki, *Metall (Berlin)* 19 (1965) 16-21.
167. Dentists' Supply Comp., US 2895050, 1956.
168. National Research Development Corp., GB 1529984, 1976.
169. Zahnfabrik Bad Nauheim KG, DT 1813163, 1968.
170. L. Tcheichvili, M. N. P. DeMaeques, *Keram. Z.* 30 (1978) no. 3, 138-139; 30 (1978) no. 5, 252-254.
171. E. Hamann, H. Manger, L. Sleinke, *Automot. Appl. Sens. SAE Spec. Publ.* SP-418 (1977) 53-80.
172. D. Janke, W. A. Fischer, *Arch. Huttenw.* 48 (1977) 255-260.
173. Molycorp Inc.: "Overview of Application Possibilities", no. 40.

174. I. C. Huseby, G. Petzow, *Powder Metall. Int.* 6 (1974) 17-19.
175. J. R. Maldonado: *IEEE Int. Conv. Dig.* 1972, 190-191.
176. N. V. Philips' Gloeilampenfabrieken, DE-OS 2037197, 1969.
177. Matsushita Electric Industrial Co., Ltd., DE-OS 2055197, 1969.
178. J. B. Chesney, *J. Am. Ceram. Soc.* 46 (1963) 197-202.
179. Matsushita Electric Industrial Co., Ltd., US 3586642, 1968.
180. Molycorp Inc.: "Overview of Application Possibilities", no. 21.
181. Hitachi Ltd., JP 74129199, 1973.
182. Molycorp Inc.: "Overview of Application Possibilities", no. 54.
183. G. M. Schwab, F. Bohla, *Z. Naturforsch.* 32 (1968) no. 10, 1555-1558.
184. Molycorp Inc.: "Overview of Application Possibilities", no. 28.
185. R. E. Harrington, *Environ.* 13 (1967) March, 32-33; 13 (1967) June, 32-34; 13 (1967) Sept., 30-32.
186. Molycorp Inc.: "Overview of Application Possibilities", no. 38.
187. Molycorp Inc.: "Overview of Application Possibilities", no. 46.
188. A. B. Stiles, US 3266477, 1966.
189. Fedders Corp., US 3627560, 1970.
190. B. C. Milyo, *Chem. Soc. Rev.* 2 (1973) 49.
191. North American Rockwell Corp., DE-OS 1926969, 1968.
192. Roskill Information Services: *The Economics of Rare Earths and Yttrium*, 8th ed., London 1991.
193. B. Campna, *Bull. Ver. Schweiz. Pet. Geol. Ing.* 43 (1977) no. 104, 1-28.
194. *Inf. Chim.* 190 (1979) 67-70.
195. H. C. Hodge, H. S. Sterner, *Am. Ind. Hyg. Assoc. Q.* 10 (1943) 93.
196. Th. A. Haley, *J. Pharm. Sci.* 54 (1965) no. 5, 663-670.
197. P. Arvela in H. Grobecker et al. (eds.) *Progress in Pharmacology*, Publ. G. Fischer Verlag, Stuttgart 1979, 69-114.
198. R. Hoschek: "Die 'Cer-pneumokoniose' nach Einatmen von natürlichen Seltenen Erden", *Schriftenreihe Arbeitsmedizin-Sozialmedizin-Arbeits-hygiene*, vol. 18, Genter, Stuttgart 1968.
199. M. Menz, E. Kaufman, *Z. Unfallmed. Berufskr.* 65 (1972) no. 1, 62-73.
200. J. Sykora, F. Huzl, A. Kubat, M. Vykrocil, *Zentralbl. Arbeitsmed. Arbeitsschutz* 16 (1966) no. 1, 3-9.

45 Cerium

KLAUS REINHARDT, HERWIG WINKLER

45.1 Introduction	1743	45.3.1 Flint Alloy	1750
45.2 Cerium Mischmetal	1743	45.3.2 Permanent Magnets	1752
45.2.1 Preparation of the Raw Materials ..	1744	45.3.3 Hydrogen Storage	1752
45.2.1.1 Wet Chemical Attack	1744	45.4 Compounds	1753
45.2.1.2 Chlorination	1744	45.4.1 Production	1753
45.2.2 Fused-Salt Electrolysis	1745	45.4.2 Uses	1753
45.2.2.1 Iron and Graphite Cells	1745	45.5 Analysis	1754
45.2.2.2 Ceramic Cells	1747	45.6 Economic Aspects	1755
45.2.2.3 Oxide Process	1747	45.7 Toxicology and Occupational	
45.2.3 Properties	1748	Health	1755
45.2.4 Uses	1749	45.8 References	1756
45.3 Alloys	1750		

45.1 Introduction

Cerium is the most abundant rare-earth element and exceeds in abundance such well-known elements as tin, cobalt, and lead. The following article treats pure cerium and rare-earth mixtures in which cerium content either exceeds the naturally occurring composition or determines the overall properties or economics. The term cerium group, or light rare-earth elements, includes lanthanum through europium inclusively.

The presence of the rare-earth elements lanthanum to lutetium at the position of lanthanum (atomic number 57) in the periodic table is due to the fact that, starting with cerium ($[\text{Xe}] 4f^1 5d^1 6s^2$), 14 electrons are able to enter the inner $4f$ orbital. Lanthanum, which has an empty $4f$ level ($4f^0$), represents the stable electronic configuration. This configuration is also attained by tetravalent cerium, which explains why cerium has not only the normal rare-earth $3+$ oxidation state, but also a $4+$ state. This exceptional oxidation state simplifies separation of cerium from the other rare-earth elements.

Cerium was discovered in 1814 by BERZELIUS and named after the asteroid Ceres, which had been discovered in 1800–1801.

45.2 Cerium Mischmetal

Cerium mischmetal or more simply *mischmetal* is a mixture of rare-earth metals of the cerium group with cerium as the major constituent. Mischmetal is the lowest priced rare-earth metal because no expensive chemical separation is needed to produce it. It is produced predominantly by fused-salt electrolysis of rare-earth chlorides. Pure rare-earth metals of the cerium group are produced by fused-salt electrolysis of a mixture of chlorides and fluorides. The electrolytic reduction of rare-earth oxides of the cerium group dissolved in a fluoride electrolyte has been put into production recently. Metallothermic reduction of rare-earth chlorides or fluorides is also employed.

Mischmetal was first produced industrially in 1908 by AUER VON WELSBACH, who succeeded in finding an outlet for surplus rare earth in the production of lighter flints. At that time, monazite was used exclusively as the source of thorium needed for the manufacture of incandescent mantles.

45.2.1 Preparation of the Raw Materials

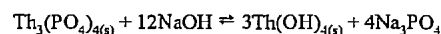
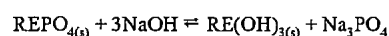
Rare-earth minerals in which cerium predominates over lanthanum, praseodymium, and neodymium (the other elements in the cerium group) are *monazite*, $(\text{RE}, \text{Th})\text{PO}_4$ from beach placers of India, Southeast Asia, Australia, South Africa, and Brazil, associated with cassiterite, rutile, ilmenite, and zircon and *bastnaesite*, REFCO_3 , from the carbonatitic deposit of the Mountain Pass mine in California and from the iron ore deposit of Bayan Obo in Inner Mongolia (China).

Monazite and bastnaesite are generally concentrated by physical methods such as gravity concentration, flotation, and magnetic separation [1, B1, pp. 60–67]. The rare-earth concentrates are converted into rare-earth chloride hydrates by wet chemical methods or into anhydrous rare-earth chlorides by high-temperature chlorination.

45.2.1.1 Wet Chemical Attack

After being ground (50 μm –1 mm), the concentrates are attacked by acids or caustic soda [1, B1, pp. 67–104].

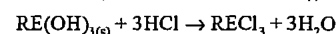
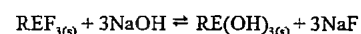
Monazite. At temperatures between 140 and 170 °C, concentrated sodium hydroxide solution (50–70%) reacts with the phosphates:



The attack is carried out in an autoclave [13]. More concentrated sodium hydroxide solutions (> 70%) react at lower temperature [14]. The rare-earth hydroxides are dissolved in hydrochloric acid. The thorium does not dissolve if the pH is kept close to 4. Trisodium phosphate is a saleable by-product after recrystallization.

Bastnaesite. The carbonates are attacked by hydrochloric acid. The residue of rare-earth fluorides is converted by alkaline treatment into rare-earth hydroxides, which can be used to neutralize the acid solution resulting from the hydrochloric acid attack [15]. Concen-

trated sodium hydroxide solution attacks bastnaesite to form rare-earth hydroxides, which are dissolved in hydrochloric acid [16].



The rare-earth chloride solution obtained by these various processes is evaporated to form the hexahydrates (*mp* 120–130 °C), which solidify on cooling. The rare-earth chloride hexahydrates must be dehydrated for fused-salt electrolysis. Dehydration is carried out under conditions that avoid excessive formation of rare-earth oxide chlorides by hydrolysis:



The dehydration is carried out either in vacuo or by adding salts like CaCl_2 , NaCl , or NH_4Cl that reduce hydrolysis.

Oxide chlorides increase the viscosity of the electrolyte and cause reoxidation of the rare-earth metals that are formed. However, rare-earth oxide chloride content near 5% is not detrimental, perhaps even desirable, for one special type of electrolytic cell, the ceramic cell. Dehydration can then be carried out in metal ovens or on heated rotating steel plates, at temperatures between 170 and 600 °C, depending on the process. In modern plants, spray drying and fluidized-bed drying are employed for the dehydration process. Special materials like titanium and Hastelloy can be used to avoid corrosion by the hydrochloric acid generated in the off-gas during drying.

45.2.1.2 Chlorination

The chlorination of rare-earth ores [17] in a shaft furnace at 900–1100 °C produces anhydrous rare-earth chlorides that can be used directly for fused-salt electrolysis. The reaction proceeds as follows:

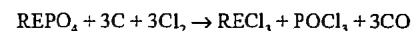
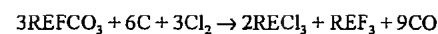


Table 45.1: Typical analyses of rare-earth chlorides from various sources.

Element, as oxide	RECl ₃ ·6H ₂ O from wet chemical treatment, % ^a						RECl ₃ from high-temperature chlorination, % ^a
	Brazil	China	France	India	Malaysia	United States	Germany
RE ₂ O ₃	458	45.8	47	46	46.1	46	65–67
REF ₃							6–10
CeO ₂ /TREO ^b	47.2	50.0	49	46	50.3	50	48–50
Na ₂ O				1	0.66		< 0.2
MgO				1		0.2	< 0.3
CaO	0.63		0.5	1	0.59	0.4	< 2
BaO						< 0.1	< 3
Fe ₂ O ₃	0.03			0.005		0.02	< 0.1
PbO	100 ppm	22 ppm	230 ppm	10 ppm	15 ppm		< 50 ppm
P ₂ O ₅	trace	trace	0.02	0.01			< 0.2
SO ₂	0.1	0.06	0.14	0.05			< 0.1
SiO ₂				0.05			< 0.1

^a Unless otherwise stated.

^b The cerium(IV) oxide content divided by the total rare-earth oxide content.

Bastnaesite yields a mixture of rare-earth chlorides and fluorides; monazite yields the chlorides. In the case of monazite, the radioactivity, caused mainly by radium, a disintegration product of thorium, remains with the rare-earth chlorides. In addition, ThCl₄ must be recovered from the off-gas to avoid environmental pollution. Therefore, thorium-free monazite should be used if available. The recovery of POCl₃ is an economic necessity.

Typical analyses of rare-earth chlorides from various sources are listed in Table 45.1.

45.2.2 Fused-Salt Electrolysis

For proprietary reasons, there are no modern detailed publications on the process technology for production of mischmetal by fused-salt electrolysis. The know-how of the producers covers optimization of electrolytic cell construction for continuous operations, special refractories resistant to the aggressive salt and metal melt, and maximization of current efficiency by the choice of the composition of the electrolyte, with a view to the viscosity, temperature, oxygen content, and solubility of deposited metal in the melt.

The kind of electrolytic-cell refractory characterizes the two main processes for the production of mischmetal: (1) iron/graphite and (2) ceramic [18, 19].

Independent of the type of cell, the amperage, voltage, electrode distance, and current

density are chosen to reach the reduction potentials of the rare-earth metals and to avoid an excessive electrolyte temperature, which may cause vaporization of the electrolyte, attack of the refractory lining by the electrolyte and metal, and formation of metal fogs.

Cerium deposits at a lower voltage than praseodymium, neodymium, and especially lanthanum. Samarium and europium are reduced at the cathode only to the 2+ oxidation state. Stirring by the chlorine liberated at the anode or diffusion allows both elements to migrate to the anode, where they are reoxidized [20]. Metal fogs reduce current efficiency similarly.

Added rare-earth fluorides and alkali and alkaline-earth chlorides and fluorides having decomposition voltages higher than those of the rare-earth chlorides lower viscosity, increase the conductivity, and improve the metal yield.

45.2.2.1 Iron and Graphite Cells

The iron or graphite crucible or pot serves directly as the cathode. Iron crucibles made of spheroidal cast iron are directly connected as the cathode, whereas graphite crucibles, which are protected by an iron housing against air oxidation, are connected via this iron housing.

Graphite-lined iron pots are connected directly. Crucibles up to an electrolyte volume

of 50 L are round; larger crucibles are rectangular. The schematic design of a rectangular graphite-lined iron cell is shown in Figure 45.1. The anodes consist of graphite or special carbon and can be moved vertically to adjust the amperage and current density.

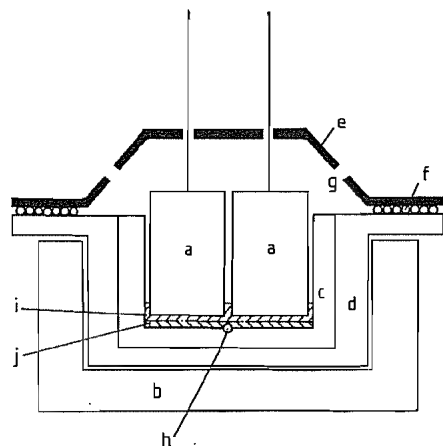


Figure 45.1: Schematic design of a rectangular graphite-lined iron cell (Th. Goldschmidt AG): a) Graphite anodes; b) Insulated housing; c) Graphite lining (cathode); d) Iron crucible; e) Hood; f) Seal; g) Feeding chute and chlorine suction; h) Bottom tap; i) Electrolyte melt; j) Mischmetal deposit.

The electrolysis is started via short-circuit heating by melting rare-earth chlorides and mischmetal down until a sufficient amount of melt is obtained for electrolysis. Already molten chloride, for example, from the chlorination process, also may be used. Fresh rare-earth chlorides are fed as solids.

As a result of the higher heat losses by the iron and graphite cathode, the so-called cooled cathode, the mischmetal is electrodeposited in the form of dendritic sponge or droplets, together with solidified electrolyte, at the bottom of the cell. The deposition of solid mischmetal diminishes the damage to the refractory lining.

Toward the end of the electrolysis, the metal is melted by increasing voltage and amperage or by external heating via gas or resistance heating. Before tapping, the temperature of the metal must be 850–950 °C. The temperature of the electrolyte at the surface may be 100 °C higher. Addition of iron scrap lowers

the melting point, making the melt easier to handle. The total content of the cell is cast into molds by tipping or bottom pouring; reoxidation of the molten metal is prevented by the residual electrolyte. The mischmetal settles to the bottom of the mold and is covered by the electrolyte, which can be removed after solidification with an air chisel. The separation of the residual electrolyte from the liquid metal can be accomplished via a mold that acts as part of a siphon: the metal collects at the bottom, while the electrolyte overflows. Mischmetal may be recast more cleanly.

Immediately after tapping, the electrolysis is restarted by feeding fresh rare-earth chlorides, which melt instantly in the hot cell.

The residual electrolyte, in which europium and samarium are enriched, especially when rare-earth fluorides are involved, may be recycled for further enrichment and later used for winning those two elements [21].

The cells are covered with a hood. The chlorine formed at the anode is removed from the exhaust gases by alkaline scrubbing: the resulting hypochlorite is either reduced to chloride or sold. Recovery of the chlorine itself is normally uneconomical because of dilution by air.

In modern plants, direct current is supplied by thyristor-controlled silicon rectifiers; in older plants, it is supplied by transformer-controlled selenium rectifiers. The rectifiers are connected in parallel, series, or individually to the cells. Cell voltage ranges between 6 and 15 V, depending on the radiative loss of heat. The amperage may be as high as 50 kA. The current density depends on the cell design: in large rectangular cells it is $\leq 2 \text{ A/cm}^2$, in smaller ones it is much higher. The current efficiency can reach 75%.

From 2 to 2.5 kg of rare-earth chlorides are consumed to produce 1 kg of mischmetal. The metal yield is between 85 and 95%, depending on the extent the residues are recycled. For a 50-kA cell, the daily production is nearly 1 t. The d.c. power consumption per kilogram of mischmetal produced is 10–15 kWh.

45.2.2.2 Ceramic Cells

Figure 45.2 shows the construction of a ceramic cell [19]. Electrolysis takes place in a ceramic crucible. The crucibles of small, simple cells have a diameter of ca. 30 cm and a height of ca. 50 cm. Further development resulted in the bigger ceramic cells now in operation.

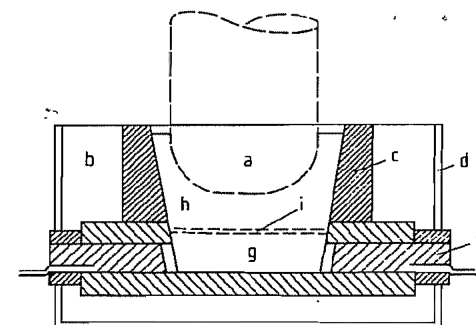


Figure 45.2: Ceramic cell [19]: a) Graphite anode; b) Insulation; c) Ceramic crucible; d) Iron housing; e) Current supply for cathode; f) Cathode; g) Mischmetal; h) Electrolyte melt; i) Rare-earth oxide chloride diaphragm.

A block of graphite or iron at the bottom of the crucible serves as the cathode. If iron cathodes are used, contamination of mischmetal with iron cannot be avoided. Mischmetal at the electrolysis temperature of ca. 900 °C attacks most of the construction materials in the electrolytic cell. The working life of the ceramic cells is limited to a maximum of 1 year.

The current density and voltage are controlled by raising or lowering an anode of amorphous carbon. Service life of the anode is between 30 and 50 d.

The electrolytic process in ceramic cells is started by short-circuit heating. The cells are filled with anhydrous rare-earth chlorides and short-circuited with an iron or carbon rod. If molten electrolyte from other cells is available, mischmetal lumps are placed in the melting pots and covered with melt. Electrolysis can be started immediately. The ceramic cells operate continuously. Anhydrous rare-earth chlorides are added as required.

Between metal at the bottom of the cell and the electrolyte is built up a diaphragm of rare-earth oxide chlorides, which operates as an

electrical resistance, generating the heat that keeps the deposited metal in liquid form.

One or two times a day, molten mischmetal is tapped, sucked, or ladled from the bottom of the crucible.

During the process the anode is consumed by oxidation. For this reason, the electrode must be adjusted from time to time. Oxidation results from contact with atmospheric oxygen or the chlorine produced or from reaction with oxide chlorides in the electrolyte. Therefore, a high oxide chloride content in the rare-earth chlorides causes considerable anode consumption.

The amount of molten electrolyte increases during operation. Enrichment of europium and samarium takes place. To maintain a constant level of electrolyte, a part, the so-called slag, is ladled out at regular intervals. This slag can be treated chemically to recover Eu_2O_3 and Sm_2O_3 . A typical composition of slag is presented in Table 45.2.

Table 45.2: Analyses of mischmetal slag, Treibacher Chemische Werke AG, Austria.

Element, as oxide	Relative content, % ^a
La_2O_3	26.6
CeO_2	31.9
Pr_2O_3	4.1
Nd_2O_3	19.8
Sm_2O_3	14.3
Eu_2O_3	0.4
Total	97.1
Total rare-earth oxide content is 41.9%.	

^a The element oxide content divided by total rare-earth oxide content.

45.2.2.3 Oxide Process

On the basis of a process developed by the U.S. Bureau of Mines [22, 23] and further improved by Santoku Metal Industries, Japan, Santoku now produces mischmetal from rare-earth oxides. The process is similar to aluminum electrolysis (Hall-Héroult process). It avoids emission of chlorine and the consequent expensive purification of off-gas.

Rare-earth oxides are dissolved in an electrolyte consisting of alkali fluorides (to improve conductivity), alkaline-earth fluorides (to reduce melting point), and rare-earth fluo-

rides (to improve the solubility of rare-earth oxides) and are reduced electrolytically to the rare-earth metals. The electrolysis cell (Figure 45.3) consists of a graphite crucible with graphite anode and molybdenum cathode, working under an inert-gas atmosphere to prevent oxidation of the construction materials. The electrolyte is initially melted by resistance heating. Electrolyte and electrodeposited rare-earth metals are kept liquid by the joule heat. A cell produces ca. 500 kg of metal per day. If bastnäsite is a raw material, it must be specially purified prior to electrolysis.

45.2.3 Properties

Table 45.3 shows typical analyses of mischmetal from various producers.

The physical and chemical properties of mischmetal are determined by the properties of its four main constituents—cerium, lanthanum, neodymium, and praseodymium [1, 24]. There can be no exact values for mischmetal because the composition depends on the type of raw material and treatment. However, the values correspond most closely to those of the main constituent, cerium. Table 45.4 lists several physical properties for the four main rare-earth metals.

Mischmetal is ductile. The freshly cut surface has a metallic gray appearance. In air, the

surface oxidizes to form yellow to greenish-gray rare-earth hydroxide carbonates or oxide hydrates. Some types of oil may protect the surface against corrosion, but only for a limited period of time. Alloying with 1–2% of magnesium increases corrosion resistance. Massive metal burns above 150 °C in pure oxygen; however, chips, turnings, and powder burn at this temperature even in air. Mischmetal dissolves in dilute mineral acids with evolution of hydrogen.

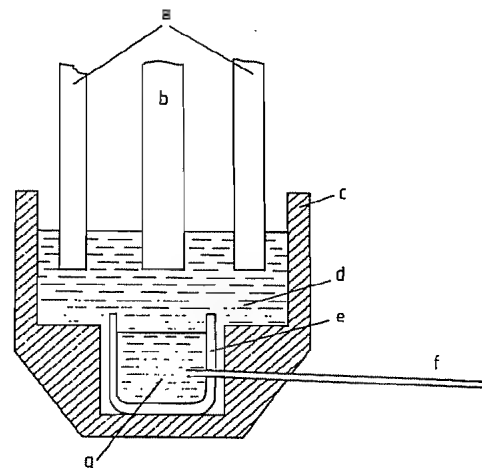


Figure 45.3: Electrolysis cell for the production of mischmetal from oxides [23]: a) Graphite anodes; b) Molybdenum cathode; c) Graphite crucible; d) Liquid electrolyte; e) Molybdenum crucible; f) Tapping pipe; g) Molten mischmetal.

Table 45.3: Typical analyses of mischmetal from various producers, weight percent unless otherwise specified.

Metal	Producer						
	Treibacher (Austria)	Ronson (United States)	Santoku (Japan)	Corona (Brazil)	Fluminense (Brazil)	Former USSR	Minmetals (China)
Total rare-earth metals	99.5	> 95	97.8	97.4	96.0	97	98.6
Relative content ^a		18–28					
La	23	50–55	22.9	17.5	17.9	25.1	19.6
Ce	49.8	4–6	51.9	54.2	55.3	53.2	54.9
Pr	5.6	12–18	5.4	5.6	7.3	5.2	6.1
Nd	18.6	< 0.1	16.2	16.0	17.4	14.0	17.1
Sm	0.2	< 2					0.4
Others	2.8		3.6	6.7	4.8	2.8	1.9
Al	0.05		0.14			0.05	0.1
Pb	50 ppm		343 ppm		90 ppm	227 ppm	4600 ppm
Fe	0.05	< 5	1	2.0	2.3	1.7	0.28
Si	0.20			0.1	0.54	0.1	0.05
Mg	0.03	< 0.5	0.20	0.20	0.2	0.033	0.35
Ca		< 0.1		0.02	0.1		0.013

^a The content of rare-earth metal divided by total rare-earth metals.

Table 45.4: Properties of lanthanum, cerium, praseodymium, and neodymium [1, 2, 4].

Property	Unit	La	Ce	Pr	Nd
Atomic number <i>z</i>		57	58	59	60
Atomic mass <i>A_r</i>		138.9055	140.115	140.90765	144.24
Crystal structure at 293 K		dhcp ^a	fcc	dhcp ^a	dhcp ^a
<i>a</i> ₀	nm	0.3774	0.51612	0.36725	0.36579
<i>c</i> ₀	nm	1.2159		1.18354	1.17992
Density <i>ρ</i>	g/cm ³	6.146	6.770	6.773	7.008
Melting point <i>m_p</i>	°C	918	798	931	1021
Heat of fusion <i>ΔH</i>	kJ/mol	6.2	5.5	6.9	7.1
Boiling point <i>b_p</i>	°C	3464	3433	3520	3074
Temperature at a vapor pressure of 133 Pa	°C	2208	2174	1968	1741
0.133 Pa		1581	1581	1360	1197
Specific heat at 25 °C	Jmol ⁻¹ K ⁻¹	26.2	27.0	27.0	27.5
Coefficient of linear thermal expansion at 25 °C	10 ⁻⁶ K ⁻¹	26.2	27.0	27.0	27.5
Thermal conductivity at 27 °C	J s ⁻¹ cm ⁻¹ K ⁻¹	0.135	0.114	0.125	0.165
Electrical resistivity at 0 °C	μΩ cm	61	77	71	64

^a Double hexagonal closest packed in the direction of the *c* axis.

The ingots may be easily machined. However, the pyrophoric character of mischmetal may cause autoignition of the turnings. Mischmetal may be easily extruded at temperatures just below its melting point. Rollability is adversely effected by oxygen content. Nearly all of the alloying elements cause brittleness.

45.2.4 Uses

The most important uses of mischmetal or cerium are metallurgical. The metallurgical importance of rare-earth metals is based on reactions to form solids with oxygen, hydrogen, nitrogen, sulfur, arsenic, bismuth, and antimony, reducing the effects of these elements on the properties of the metals [25]. To avoid the formation of harmful rare-earth oxide inclusions by secondary reactions of the mischmetal with refractories, slag, and atmospheric oxygen, the mischmetal is plunged into the molten metal or added under an inert-gas atmosphere. Metallurgical mischmetal can also be clad with aluminum or steel. Mischmetal is added as lumps, rods, doughnuts, or wire [26].

Iron and Steel [27]. Rare-earth sulfides and oxide sulfides are formed in liquid steel and precipitate as globular particles uniformly dispersed, which, unlike manganese sulfides, are not deformable during rolling and do not form stringers. This is called sulfide shape control and is used in microalloyed or HSLA (high-

strength low-alloy) steels to reduce anisotropy in toughness, notch toughness, and bend formability. This is especially important for pipeline steels used at subzero temperature in the Arctic.

Mischmetal may entrap hydrogen and diminish hydrogen-induced cracking.

Hot shortness in stainless steels can be reduced by removal of tramp elements (As, Bi, Sb) together with deoxidation and sulfide shape control. Heat and oxidation resistance can be increased by mischmetal, which forms protective surface layers of rare-earth oxides together with oxides of the steel components, for example, Cr₂O₃, that are resistant to scaling.

Mischmetal or cerium-containing master alloys are added to cast iron to improve ductility, toughness, and the microstructure. Cerium allows graphite to form nodules, causing nucleation in spheroidal and vermicular cast iron, and neutralizes the harmful effect of the tramp elements [28].

The addition rate depends on the application and preparation of the steel or iron melt. For sulfide shape control and nodularization of graphite, up to 1 kg of mischmetal is added per tonne. Other effects require even larger additions, up to 8 kg per tonne.

Nonferrous Metals [29]. Addition of mischmetal to copper alloys improves tensile

strength and deep-drawing properties. The heat resistance and ductility of aluminum conductor cables are improved without any significant decrease in electrical conductivity. Titanium alloys show a higher grade of grain refinement, better mechanical properties, and improved corrosion resistance as a result of mischmetal additions.

The need for improved galvanizing compositions (increased corrosion resistance, fluidity, wettability, and freedom from intergranular corrosion) without affecting formability, weldability, and paintability led to the development of Galfan, which is the classical zinc-aluminum eutectic alloy (95% Zn, 5% Al) with 0.05% mischmetal [30].

In nickel- and cobalt-based superalloys for turbine engines, cerium (yttrium is even better) increases oxidation and sulfidation resistance at high temperature. Similar effects are achieved in chromium-based alloys, and by removing gases cerium prevents embrittlement of niobium- and tantalum-based alloys.

Other Uses. Cerium and mischmetal are used as getters to absorb traces of gases in evacuated devices.

Mischmetal is said to increase the efficiency of fuel consumption and to decrease CO and NOX contents in the exhaust of internal combustion engines if steam is passed through mischmetal spirals before injection into the carburetor [31].

In some of these uses, mischmetal (= MM) can be replaced by CeSi, MMSi, or MMFeSi alloys produced directly from bastnaesite by reduction in an arc furnace.

The pyrophoric character of mischmetal alloyed with iron and magnesium is used for flints and pyrotechnics.

45.3 Alloys

The atomic radii of lanthanum, cerium, praseodymium, and neodymium differ only slightly so that miscibility is complete in the liquid state and close to the solidus curve. The liquidus curves correspond to those of ideal mixtures.

In the molten state the main constituents of mischmetal are completely miscible with nearly all non-rare-earth metals. Their large atomic radii and their low electronegativities are the reasons why there are only a few cases of their solid solubility in other metals. One such case, however, is the limited solid solubility of mischmetal in magnesium [32]. As solids they do not dissolve other metals; instead, they form intermetallic phases. With elements of the groups 4, 5, and 6 they do not form intermetallic phases [32, 33].

The intermetallic phases, with a degree of heteropolar bonding, may be brittle. Therefore, rare-earth metals and alloys are unsuitable as construction materials. Cerium phase diagrams are generally used in place of mischmetal phase diagrams [32, 34, 35].

Depending on the purity desired, alloying is done in crucibles made of tantalum, molybdenum, boron nitride, graphite, or clay graphite. An inert-gas atmosphere, vacuum, or inert slag cover are necessary.

45.3.1 Flint Alloy

Table 45.5: Analyses of lighter flints of different producers, %.

Metal	Producer			
	Treibacher (Austria)	Santoku (Japan)	Electro Centre (France)	Ronson (United States)
Total RE metals	76.2	78.3	76.7	77.0
Relative content ^a				
Ce	51	52.3	53.3	51.5
La	22.7	24.7	19.2	23.1
Nd	16.6	14.3	16.5	16.5
Pr	5.4	5.0	6.4	5.8
Sm	0.3	0.4	0.4	0.3
Fe	20.6	19.3	20.4	20.0
Mg	2.2	1.8	2.1	1.5
Al	0.09	0.28	0.04	0.05
Cu		0.02	0.03	
Si	0.22	0.29	0.22	0.2
Zn	0.54	0.03	0.34	0.5
C	0.02	0.08	0.06	0.01

^a The content of rare-earth metal divided by total rare-earth metals.

Pyrophoric Properties. None of the numerous developments of cerium-free pyrophoric alloys of the last decades has been able to re-

place the cerium-iron alloy invented and patented by AUER VON WELSBACH in 1903. Lighter flint alloy consists basically of mischmetal and iron. Some other metals are added in small amounts to modify the pyrophoric properties and to improve processing. Typical analyses of lighter flint alloys are shown in Table 45.5.

The frictional pyrophoric properties of cerium-iron are based on a combination of microstructure and mechanical and chemical properties of the alloy. The typical crystal structure of commercial alloy consists of tough, brittle primary crystals of $\text{Ce}_2\text{Fe}_{17}$ enclosed by a peritectic layer of CeFe_2 embedded in a soft matrix of CeFe_2 and Ce.

Mechanical friction generates primary cracks in the intermetallic compound, initially leading small particles with adherent matrix to break away. Residual frictional and deformation heat in the small particles heats them adiabatically to ignition temperature. On ignition, these particles burn totally. Heat is emitted predominantly by radiation, particle temperature reaching ca. 2000 °C. The size of these particles, which depends on the hardness of the lighter flint, influences the ignition behavior. Smaller particles ignite rapidly, resulting in quick adiabatic heating, whereas larger particles emit a higher local output of reaction heat.

Magnesium and cerium form an intermetallic compound that ensures a high heat of combustion. The temperature of the spark is also increased by alloying with aluminum, which in addition produces a spiky spark. Zinc and copper improve fluidity during extrusion.

Manufacture of Lighter Flints. Lighter flint alloy is produced by melting mischmetal, iron, and the other metals in clay graphite or other suitable crucibles heated in induction furnaces at 1000–1200 °C under a protective salt layer (CaCl_2 , BaCl_2). After removal of the salt layer, the alloy is cast into preheated molds.

For better shape control of the CeFe_2 crystallites, the melt is cooled slowly. The as-cast products are billets of 3–6 cm diameter. Average yield of alloy, based on raw material input,

is 95–98%. Losses arise from air oxidation and reaction with the crucible material.

After preheating at 400–500 °C, the flint billets are extruded to rods on horizontal or vertical extrusion presses at pressures between 20 and 50 MPa. Alloying with aluminum, magnesium, zirconium, titanium, and copper lowers the amount of pressure required. Extrusion pressure is also affected by impurities in the mischmetal, the rare-earth distribution, and the iron content of the alloy. During extrusion, the eutectic matrix liquefies. After extrusion, the rods are cooled rapidly in air or cooling oil. The diameter of the rods usually ranges between 2 and 6 mm.

These rods are cut on horizontal or vertical dies to the length of the lighter flint, usually between 4 and 12 mm. A subsequent heat treatment between 350 and 450 °C improves the pyrophoric properties considerably [36] by conversion of Ce-Fe mixed crystals, formed through rapid solidification during extrusion, into CeFe_2 and Ce.

The lighter flints are sized on sorting machines, generally with sorting sieves. These mechanically presorted flints are checked carefully by mechanical and optical sorting machines. Some producers make a final inspection by eye: flints are moved over a conveyor belt and imperfect flints are picked out by hand. Flints are checked for length, diameter, and straightness, as well as to see if the area of cut is circular as desired and if cavities or burrs are absent from the cut surface.

Durability of lighter flints is limited to 4–5 years normally. Humid air and a warm climate, such as prevails in the tropics, cause quick decomposition of the flint, visible as a dusting at the beginning of the decomposition process. For protection of the flint surface against corrosion, flints are normally coated and colored with lacquer.

Generally, there is a distinction between the normal lighter flints (most commonly 2.4 mm in diameter and 4 mm in length) and the lighter flints for disposable lighters. Flints for disposable lighters are manufactured in a length from 7 to 12 mm and a diameter from 2.3 to 2.5 mm, depending on the amount of

gas filling in the lighter. Such flints should ignite at least 1000 times before 50% of the flint is used up.

Accuracy of size is important for flints for disposable lighters because filling is carried out by machines and each faulty flint stops production. Maximum tolerances of ± 0.1 mm in length and in diameter are acceptable. One kilogram of lighter flints contains from 3000 to 10 000 flints.

45.3.2 Permanent Magnets

The classic RECo_5 permanent magnet alloys are based on samarium, which gives the best hard magnetic properties. Replacement of samarium, an expensive rare-earth metal, by cerium or even by inexpensive mischmetal reduces the hard magnetic properties, especially because of the lower crystal anisotropy field [37]. However, adding small amounts of samarium to the mischmetal and/or changing the composition of the mischmetal [38] or partial replacement of cobalt [39, 40] makes magnets with sufficient coercivity and energy product for less sophisticated uses and increases the range of uses because of the lower costs.

These alloys are manufactured by melting the metals or by calcinothemic reduction of oxide and metal-powder mixtures [41].

These magnets are used for electronic watches, microwave amplifier tubes, loudspeakers, headphones and microphones, magnetic coupling, bearings, sensors, clamp systems, switches, d.c. motors, servomotors, and step motors, mainly to achieve miniaturization.

Some magnetic properties are listed in Table 45.6.

45.3.3 Hydrogen Storage

LaNi_5 has a high storage capacity for hydrogen gas [42], up to the formula $\text{LaNi}_5\text{H}_{6.7}$. To decrease costs, lanthanum can be replaced by mischmetal [43]. However, to lower the higher hydrogen equilibrium pressure and form hydrides up to the formula $\text{MMNi}_5\text{H}_{6.3}$, the nickel must be partially replaced [44] by

aluminum [45], calcium [46], cobalt [47], chromium [48], copper [49], iron [50], or manganese [51]. Pressure composition isotherms are shown in Figure 45.4. Alloys of the type CeMg_{11}M ($\text{M} = \text{Ni}, \text{Cu}, \text{Zn}$) also absorb hydrogen [52].

These systems may be used for hydrogen transportation and storage; vehicular and stationary fuel supply, an ideal fuel from the ecological point of view; air conditioning; refrigeration; heat pumps; storing and regaining waste heat; and hydrogen-storage electrodes in alkaline batteries. These systems may also be used for purification [53] and isolation [54] of hydrogen and H_2/D_2 separation.

Table 45.6: Intrinsic magnetic properties of RECo_5 compounds at room temperature [40].

Property	SmCo_5	CeCo_5	MMCo_5^a
Saturation magnetization B_s , T	1.07	0.77	0.89
Anisotropy constant K , 10^6 Jm^{-3}	9.6	5.6	6.6
Anisotropy field H_A , MA/m	20	15.1	14.7
Curie temperature T_C , °C	724	347	520
Theoretical energy product $B_s^2/4$, kJm^{-3}	228	118	158

* The values for MMCo_5 are only approximate, for composition varies.

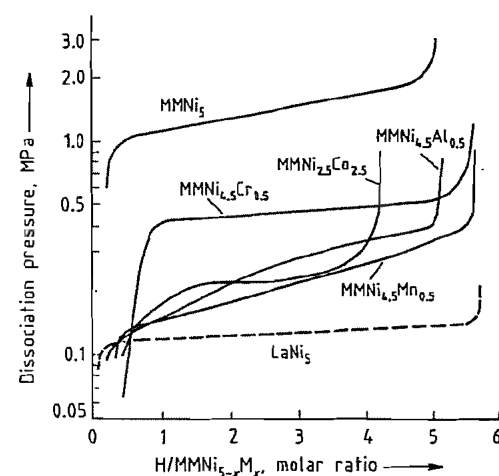


Figure 45.4: Pressure-composition isotherms for desorption in the $\text{LaNi}_5\text{-H}$, $\text{MMNi}_5\text{-H}$, and modified $\text{MMNi}_{5-x}\text{M}_x\text{-H}$ systems at 293 K [44]. MM represents mischmetal, and M represents a metal (here Al, Co, Cr, or Mn).

45.4 Compounds

Cerium is the most abundant rare-earth element. Nearly 50% of the available rare-earth raw material consists of cerium oxide. Cerium is also the only rare-earth element that can be easily separated from a mixture of rare-earth elements by simple chemical methods, for cerium has a tetravalent state.

45.4.1 Production

Cerium is separated from other rare-earth elements by oxidation of solutions resulting from attack of bastnaesite or monazite. The oxidizing agent can be H_2O_2 , hypochlorite, or atmospheric oxygen, or anodic oxidation can be used. Cerium precipitates as cerium(IV) oxide hydrate.

For example, cerium(III) rare-earth oxide hydrate is dried and oxidized by air to cerium(IV) rare-earth oxide hydrate. The oxidized hydrate is dissolved in nitric acid, and the solutions are neutralized slowly. Cerium(IV) oxide hydrate is collected by filtration. Initially, of the total rare-earth oxides 45–50% is CeO_2 . This is increased to 95% in the product.

In a process of Molycorp [55], ground bastnaesite ore concentrates are roasted, and cerium is oxidized with atmospheric oxygen. Roasted material is treated with hydrochloric acid to dissolve lanthanum, neodymium, praseodymium, etc. The pH is adjusted to 4, and a cerium-rich residue ($\approx 90\%$ CeO_2) is collected by filtration. This residue has high fluoride content and poor solubility. To get soluble cerium salts out of this material a subsequent digestion with sulfuric acid or caustic soda is necessary.

Cerium salts are produced today by liquid-liquid extraction from rare-earth cerium-containing solutions. Cerium can be extracted out of cerium nitrate-nitric acid solutions in a few steps in the form of a cerium(IV) nitrate complex in tributyl phosphate and therefore separated from the accompanying trivalent rare-earth elements, which form less stable nitrate

complexes. Purities of 99.99% and better can be achieved easily.

45.4.2 Uses

The principal uses for cerium compounds are as polishing agents and as a component in glass.

Cerium Oxide Polishing Compounds. Cerium(IV) oxide, CeO_2 , has now replaced other polishing oxides like iron oxide (red rouge), silica (white rouge), and zirconium dioxide almost completely. The special merits of cerium oxide are its 100% faster polishing speed and its cleanliness.

Cerium oxide is used for polishing glass mirrors, plate glass, television tubes, ophthalmic lenses, and precision optics. However, the advent of the Pilkington float process in the early 1970s significantly reduced the use of cerium oxide in the manufacture of plate glass.

Cerium oxide polishing powder is produced by calcining oxidic cerium mineral concentrates in rotary kilns or other furnaces at temperatures of ca. 1000 °C. Calcined concentrates are milled and cleaned by sieving or sifting afterwards. The impurities (CaO , SrO , non-rare-earth elements) must not exceed a certain level in the raw material; otherwise, cerium oxide will agglomerate during calcining and lose polishing capacity.

Polishing powders production can also start from cerium salt solutions. Cerium carbonates or hydroxides are precipitated and then calcined in rotary kilns or muffle furnaces to oxide at temperatures of ca. 1000 °C. The calcined oxides are milled and screened or sifted to get the desired grain size distribution and to remove scratching impurities.

Polishing powders made from mineral concentrates polish more slowly and less cleanly than precipitated products. The former are cheaper but are not used for high-performance polishing processes (precision optics).

Additives improve suspension properties of polishing powders in aqueous solutions and increase polishing rate, for instance, prevent-

ing foaming (antifoaming) and settling of cerium oxide (anticaking) in tanks and pipes.

Pure cerium oxide is yellowish white. Small amounts of Pr_6O_{11} in combination with other rare-earth oxides give a brown oxide. The color does not appear to affect the polishing properties for fixed CeO_2 content. Currently, standard concentrations are 50, 70, 90, and 100%. The polishing rate increases with CeO_2 content. The average grain size of polishing powders is normally 0.5–5 μm . A narrow grain size distribution is advantageous.

There are many theories about the mechanism of the polishing process [56]. According to these theories, both a chemical and a physical component, among others, are effective during polishing [57]. The glass surface is hydrolyzed by reaction with water (chemical theory) and the silica gel layer formed is removed mechanically by the polishing compound. Another theory states that glass is removed mechanically (wear theory) and to some extent by chemical reaction [58].

Cerium Oxide as a Glass Constituent. Cerium oxide can be used to decolorize soda lime glasses for bottles, jars, etc. [59]. The Ce^{4+} oxidizes Fe^{2+} impurities, which are always present in the raw materials and therefore in glasses, to Fe^{3+} . A change from the blue-green color of Fe^{2+} to the 10 times weaker yellow Fe^{3+} takes place. Arsenic, zinc selenite, or manganese are used for the same purpose. The combination of these materials with cerium reduces costs. Presently, cerium oxide has been replaced by less expensive decolorizers.

Cerium protects glass against solarization and browning, a discoloration caused by irradiation. It is therefore a constituent of glass for the faceplates of television screens, which are under constant bombardment by an electron beam [60]. Radiation-shielding windows for nuclear and radiochemical uses consist of lead glass stabilized by CeO_2 . Since maximum transmission is necessary for these thick windows, only 99.99% cerium oxide (15 ppm Fe max.) can be used.

For phototropic glasses, as in phototropic eye glasses, windshields, and window glasses

that darken in the sunlight and lighten in the shade, cerium is a sensitizer.

Other Uses. Cerium rare-earth fluorides improve the brightness of carbon arcs. Cerium fluoride oxide mixtures are mixed with carbon for electrodes. These electrodes are used on movie sets and as military searchlights to increase brightness as much as tenfold [61]. Cerium oxide (99.9%) is used as white pigment in enamels for tiles.

Basic oil-soluble cerium salts of organic acids, such as cerium alkyl sulfonates, alkyl sulfates, and alkyl phosphates, as well as cerium octoates, serve as driers in paints and varnishes. Cerium compounds that are soluble in organic liquids find use as combustion additives in fuels [62]. Particle emission in exhaust gases is reduced by 60%. Diesel oil savings in the range 2–3% are achieved. Cerium compounds added to silicones increase the thermal stability.

Cerium oxide is used in self-cleaning ovens as a catalyst [63].

In zeolitic cracking catalysts, cerium is a thermal and hydrothermal stabilizer to extend the life and increase the activity of the catalysts [64]. The following uses of cerium in noncracking catalysts are listed by PETERS and KIM [65]:

- Ammonia synthesis
- Hydrogenation
- Dehydrogenation
- Polymerization
- Isomerization
- Oxidation
- Automobile emissions control

45.5 Analysis

Mischmetal and cerium oxide can be analyzed for total rare-earth content and for individual rare-earth elements [6, 66].

The determination of the *total rare-earth content* is carried out by dissolving the rare-earth-containing material with acids or by alkaline fusion. The rare-earth elements are precipitated as hydroxides by adding NH_3 ,

dissolved in HCl or HNO_3 , and reprecipitated as oxalates, which are ignited to the oxides, RE_2O_3 , with the exception of cerium, which forms CeO_2 .

The individual rare-earth elements are determined by X-ray fluorescence (La), atomic absorption spectrometry (Y), and spectrophotometry (Nd, Pr, Sm). Analysis by means of optical plasma emission spectroscopy is a new, efficient method. Cerium can be determined by titration because it can be oxidized to the tetrapositive state.

45.6 Economic Aspects

Total rare-earth production in the Western world is 20 000–25 000 t of rare-earth oxides per year, of which 45–50% is cerium. Raw material prices have stabilized for bastnaesite at \$1 per pound total rare-earth oxide FAS Los Angeles, for monazite at A\$450 per tonne FOB Australia, and rare-earth chlorides ($\text{RECl}_3 \cdot 6\text{H}_2\text{O}$) at ca. \$0.70 per pound delivered.

The growing production of rare-earth raw material and products from China should only stabilize the market and not sensationally affect prices.

Rhône-Poulenc (France, compounds) and Molycorp-Union Oil (United States, bastnaesite and compounds) are the leading producers; other producers are Treibacher (Austria, metals, alloys, and compounds), Santoku (Japan, metals, alloys, and compounds), Ronson and Reactive Metals (United States, metals and alloys), Indian Rare Earths (India, compounds), and Corona and Fluminense (Brazil, metals and alloys). In Germany, Goldschmidt specializes in magnet alloys. Further magnet alloy producers are Hitachi and Research Chemicals (United States) and Sumitomo and Shin-Etsu (Japan).

Important producers of lighter flints in the Western world are Treibacher, Electro Centre (France), Santoku, and Ronson. Total world market for lighter flints is estimated at ca. 700 t/a. The share of flints for disposable lighters is more than 60%.

Modern steel technology has decreased demand for mischmetal substantially. The metallurgical uses of rare-earth metals consume less than 15% of the total rare-earth production. The production capacity for mischmetal is 4000–5000 t/a, but less than 50% is in operation. Mischmetal is sold at \$45 per pound, depending on quantity, shape, and size.

Total world demand for cerium-based polishing powders, the biggest consumer of cerium oxide at present, is estimated to be 3000–4000 t/a. The price for cerium polishing compounds depends on the cerium content and ranges between \$2 per pound for 50% CeO_2 and \$5 per pound for 99.9% CeO_2 .

The market for more sophisticated uses—electronics, magnets, etc.—is expected to grow.

The production of rare earths is profitable only if the market for all the rare-earth elements, which are produced in the relative amounts occurring in their minerals, is reasonably balanced.

45.7 Toxicology and Occupational Health

The rare-earth elements and compounds are considered to be only slightly toxic. No toxic effects during production or use have been reported in the rare-earth industry.

Progressive lung retention was observed after inhalation of dust containing rare-earth oxides and fluorides from carbon arc electrodes. The damage to the lung that was assessed by X ray did not seem to be attributable to the rare earths, but to thorium and its disintegration products. Continual progress in rare-earth processing has reduced the radioactive impurities in rare-earth products substantially, so they are practically free of radioactivity today. Intravenous injections of rare-earth salts damage the liver; oral administration has no pathological effect on animals [1, B2, pp. 282–283; 67].

45.8 References

1. Gmelin, system no. 39, Seltene Erden, A1 (1938); A2-A5, A7, A8, B1-B7, C1-C9, D1-D6 (1973 to date).
2. K. A. Gschneidner, Jr., L. Eyring (eds.): *Handbook on the Physics and Chemistry of Rare Earths*, vol. 1 (1978), vols. 2-4 (1979); vol. 5 (1982), vols. 6 and 7 (1984), vol. 8 (1986), North Holland Publ., Amsterdam.
3. L. Eyring (ed.): *Progress in the Science and Technology of the Rare Earths*, vol. 1 (1964), vol. 2 (1966), vol. 3 (1968), Pergamon Press, Oxford.
4. J. A. Gibson, G. S. Harvey: *Properties of the Rare Earth Metals and Compounds*, Technical Report AFML-TR-65-430, 1966.
5. F. H. Spedding, A. H. Daane: *The Rare Earths*, J. Wiley & Sons, New York 1961.
6. F. Trombe, J. Loriais, P. Gaume-Mahn, C. Henry La Blanchetais: "Scandium-Yttrium-Éléments des terres rares-Actinium", in P. Pascal (ed.): *Nouveau Traité de chimie minérale*, vol. VII, Fascicules 1 + 2, Masson, Paris 1959.
7. J. Helgorsky, A. Lévêque, T. Petzel, K. Reinhardt: "Seltene Erden", in *Ullmann*, 4th ed., 21, 235-271.
8. E. Greinacher, K. Reinhardt: "Seltene Erden", in *Winnacker-Küchler*, 4th ed., vol. 2, pp. 678-707.
9. K. A. Gschneidner, Jr. (ed.): *Industrial Application of Rare Earth Elements*, ACS Ser. no. 164, Washington, DC, 1981.
10. I. H. Jolly, R. P. Smith: "Availability of Rare Earths to Industry", in *Proc. Rare Earth Res. Conf.*, 12th, 1976.
11. C. R. Neary, D. E. Highley: "The Economic Importance of the Rare Earth Elements", *Dev. Geochem.* 2 (1984) 423-466.
12. J. Griffiths, *Ind. Min. (London)* 199 (1984) April, 19-37.
13. Soc. prod. chim. terres rares, FR 995112, 1949 (C. de Rhoden, M. Peltier).
14. A. E. Bearse, G. D. Calkins, J. W. Glegg, R. B. Filbert, *Chem. Eng. Prog.* 50 (1954) 235-239.
15. P. R. Kruesi, G. Duker, *J. Met.* 17 (1965) 847-849.
16. D. J. Bauer, V. E. Shaw, *Rep. Invest. U.S. Bur. Mines* no. 6381, Washington, DC, 1964.
17. W. Brugger, E. Greinacher, *J. Met.* 19 (1967) 32-35; Th. Goldschmidt AG, DE 956993, 1954 (W. Brugger).
18. I. S. Hirschhorn, *J. Met.* 20 (1968) 19-22. BIOS Final Rep. no. 22 (file no. XXXIII-31), 1947, p. 133.
19. BIOS Final Rep. no. 400 (item no. 21), 1945, p. 36.
20. D. Tang, R. Song, S. Du, M. Zao, Y. Minshou, W. Yu, *Proc. Int. Symp. Molten Salt Chem. Technol.*, 1st, 1983, 103-106.
21. Th. Goldschmidt AG, DE 2254245, 1974 (E. Greinacher).
22. T. A. Henrie, *J. Met.* 16 (1964) 978-981.
23. E. S. Shedd, J. D. Marchant, M. M. Wong, *Rep. Invest. U.S. Bur. Mines* no. 7398, Washington, DC, 1970.
24. B. J. Beaudry, K. A. Gschneidner, Jr. in [2], vol. 1, pp. 173-232.
D. C. Koskenmaki, K. A. Gschneidner, Jr. in [2], vol. 1, pp. 337-378.
25. K. A. Gschneidner, Jr., N. Kippenhan: *Thermochemistry of the Rare Earth Carbides, Nitrides, and Sulfides*, IS-RIC-5, Rare Earth Information Center, Iowa State University, Ames, IA, 1972.
K. A. Gschneidner, Jr., N. Kippenhan, O. D. McMaster: *Thermochemistry of the Rare Earths*, IS-RIC-6, Rare Earth Information Center, Iowa State University, Ames, IA, 1973.
26. K. Reinhardt: "Addition Techniques of Rare Earth Metals for the Treatment of Special Steels with Rare Earths", in *Proc. Rare Earth Res. Conf.*, 12th, 1976.
27. A. Raman, *Z. Metallkd.* 67 (1976) 780-789.
L. A. Luyckx: "The Rare Earth Metals in Steel", pp. 43-78 in [9].
28. B. Zao, E. W. Langer, *Scand. J. Metall.* 13 (1984) no. 1, 15-22, 23-31.
H. F. Linebarger, T. K. McLuhan: "The Role of the Rare Earth Elements in the Production of Nodular Iron", pp. 19-42 in [9].
29. A. Raman, *Z. Metallkd.* 68 (1977) 163-172.
30. S. F. Radtke, D. C. Herrschaft, *J. Less-Common Met.* 93 (1983) 253-259.
F. E. Goodwin, S. F. Radtke: *Galfan Galvanizing Alloy and Technology*, 2nd ed., Int. Lead and Zinc Res. Org., ILZRO, New York 1983.
31. Manassa, DE-OS 2551350, 1975.
32. K. A. Gschneidner, Jr.: *Rare Earth Alloys*, Van Nostrand, Princeton-London 1961.
33. H. R. Kirchmayr, *Z. Metallkd.* 60 (1969) 699-708, 778-784.
W. E. Wallace: *Rare Earth Intermetallics*, Academic Press, New York-London 1973.
34. K. H. J. Buschow, *Rep. Prog. Phys.* 42 (1979) 1373-1477.
M. Hansen, K. Anderko: *Constitution of Binary Alloys*, 2nd ed., McGraw-Hill, New York 1958.
R. P. Elliot: *Constitution of Binary Alloys*, First Supplement, 1965.
T. A. Shunk: *Constitution of Binary Alloys*, Second Supplement, 1969.
W. G. Moffatt: *The Handbook of Binary Phase Diagrams*, General Electric, Schenectady, NY, 1978.
K. A. Gschneidner, Jr., F. W. Calderwood: *Critical Evaluation of Binary Rare Earth Phase Diagrams*, ISRIC-PR 1-10 (to be continued), Rare Earth Information Center, Iowa State University, Ames, IA, 1981 on.
35. K. A. Gschneidner, Jr., M. E. Verkade: *Selected Cerium Phase Diagrams*, IS-RIC-7, Rare Earth Information Center, Iowa State University, Ames, IA, 1974.
36. Treibacher Chemische Werke AG, AT 342323, 1977 (H. Zeiringer).
37. H. R. Kirchmayr, C. A. Poldy in [2], vol. 2, pp. 55-230, especially pp. 197-230.
Proc. Int. Workshop Rare Earth-Cobalt Perm. Magnets Their Appl., 5th, 1981.
Proc. Int. Workshop Rare Earth-Cobalt Perm. Magnets Their Appl., 6th, 1982.
Proc. Int. Symp. Magn. Anisotropy Coercivity in Rare Earth-Transition Met. Alloys, 3rd, 1982.
Proc. Int. Workshop Rare Earth-Cobalt Perm. Magnets Their Appl., 7th, 1983.
38. K. Bachmann, *J. Magn. Magn. Mater.* 4 (1977) 8-12.
Ugimag Recoma AG, DE 2449361, 1976 (S. Gaiffi, A. Menth, H. Nagel).
39. G. Schäfer, H. H. Wiegand, *Metall (Berlin)* 29 (1975) no. 2, 113-121.
J. W. Walkiewicz, E. Morrice, M. M. Wong, *IEEE Trans. Magn. MAG-19* (1983) 2053-2055.
40. M. G. H. Wells, K. S. V. L. Narasimhan: "Developments in Mischmetal-Cobalt, and Low-Samarium Magnet Materials", *"Goldschmidt informiert..."* no. 48 (1979) pp. 15-22.
41. Th. Goldschmidt AG, DE 2303697, 1974 (H.-G. Domazer).
42. E. L. Huston, J. J. Sheridan III: "Applications for Rechargeable Metal Hydrides", pp. 223-250 in [9].
K. H. J. Buschow in [2], vol. 6, pp. 1-111.
43. J. Liu, E. L. Huston, *J. Less-Common Met.* 90 (1983) 11-20.
44. Y. Osumi, H. Suzuki, A. Kato, K. Oguro, M. Nakane, *J. Less-Common Met.* 74 (1980) 271-277.
45. G. D. Sandrock, US 4152145, 1979.
Y. Osumi, A. Kato, H. Suzuki, M. Nakane, Y. Miyake, *J. Less-Common Met.* 66 (1979) 67-75.
V. K. Sinha, W. E. Wallace, *J. Phys. Chem.* 88 (1984) 102-105.
46. G. D. Sandrock, *Proc. World Conf. Hydrogen Energy Systems*, 2nd, Zürich 1978, vol. 3, pp. 1625-1656.
International Nickel Co., US 4161402, 1979 (G. D. Sandrock).
47. R. A. Guidotti, G. B. Atkinson, M. M. Wong, *J. Less-Common Met.* 52 (1977) 13-28.
Agency of Industrial Science and Technology, US 4147536, 1979 (Y. Osumi, H. Suzuki, A. Kato, M. Nakane, Y. Miyake).
48. Agency of Industrial Science and Technology, US 4347082, 1982 (Y. Osumi, H. Suzuki, A. Kato, M. Nakane).
Y. Osumi, H. Suzuki, A. Kato, K. Oguro, M. Nakane, *J. Less-Common Met.* 79 (1981) 207-214.
49. F. Pourarian, W. E. Wallace, *J. Less-Common Met.* 87 (1982) 275-281.
50. International Nickel Co., US 4249940, 1981 (G. D. Sandrock, S. L. Keresztes).
51. C. E. Lundin, F. E. Lynch, *Altern. Energy Sources Proc. Miami Int. Conf. 1977*, 8 (1978) 3803-3820.
52. B. Darriet, A. Hbika, M. Pezat, *J. Less-Common Met.* 75 (1980) 43-50.
53. Shin-Etsu Chemical, DE-OS 2623213, 1976 (Z. Hagiwara, S. Matsui, S. Sakaguchi, Y. Yamanaka).
54. U.S. Atomic Energy Commission, US 3825418, 1973 (J. J. Reilly, R. H. Wiswall, Jr.).
55. H. W. Harrah: *Deco Trefoil*, Denver Equipment Co., Denver, CO, 1967, p. 9.
56. R. V. Horigan: "Rare Earth Polishing Compounds", pp. 95-100 in [9].
57. A. Kaller, *Silikattechnik* 31 (1980) 208-214.
58. T. Izumitani, S. Harada, *Wiss. Z. Friedrich-Schiller-Universität Jena, Math.-Naturwiss. Reihe* 28 (1979) no. 2-3, 389-413.
59. A. P. Herring, R. W. Dean, J. L. Drobnick: "Use of Cerium Concentrate for Decolorizing Soda-Lime Glasses", *Glass Ind.* 51 (1970) 316-322, 350-356, 394-399.
60. L. W. Riker: "The Use of Rare Earths in Glass Compositions", pp. 81-94 in [9].
61. MolyCorp-Union Oil: "Cerium", *Overview of Application Information and Possibilities*, no. 58.
62. Gulf Research & Development Co., US 4264335, 1981 (C. Bello, R. J. Hartle, G. M. Singerman).
63. E. I. Du Pont de Nemours & Co., US 3266477, 1966; US 3271322, 1966 (A. B. Stiles).
64. D. N. Wallace: "The Use of Rare Earth Elements in Zeolite Cracking Catalysts", pp. 101-116 in [9].
65. A. W. Peters, G. Kim: "Rare Earths in Noncracking Catalysts", pp. 117-131 in [9].
66. A. Brusdeylins, *Chem. Ztg.* 97 (1973) 343-347.
O. B. Michelsen (ed.): *Analysis and Application of Rare Earth Materials*, Universitetsforlaget, Oslo 1973.
Cheng Jai-Kai, *Inorg. Chim. Acta* 94 (1984) 249-258.
P. Melard: "Quality Control on an Industrial Scale at the LaRoche Rare Earth Plant", *Rare Earths Mod. Sci. Technol.* 2 (1980) 517-526.
67. T. J. Healey in [2], vol. 4, pp. 553-585.
P. Arvela: "Toxicity of Rare Earths", *Prog. Pharmacol.* 2 (1979) no. 3, 69-114.

Handbook of Extractive Metallurgy

Edited by Fathi Habashi

Volume IV: Ferroalloy Metals

Alkali Metals

Alkaline Earth Metals

Authors

Name Index

Subject Index

 **WILEY-VCH**

Weinheim • Chichester • New York • Toronto • Brisbane • Singapore

Professor Fathi Habashi
Université Laval
Département de Mines et de Métallurgie
Québec G1K 7P4
Canada

This book was carefully produced. Nevertheless, the editor, the authors and publisher do not warrant the information contained therein to be free of errors. Readers are advised to keep in mind that statements, data, illustrations, procedural details or other items may inadvertently be inaccurate.

Editorial Directors: Karin Sora, Ilse Bedrich
Production Manager: Peter J. Biel
Cover Illustration: Michel Meyer/mmada

Library of Congress Card No. applied for
A CIP catalogue record for this book is available from the British Library

Die Deutsche Bibliothek – CIP-Einheitsaufnahme
Handbook of extractive metallurgy / ed. by Fathi Habashi. –
Weinheim ; New York ; Chichester ; Brisbane ; Singapore ; Toronto :
WILEY-VCH ISBN 3-527-28792-2

Vol. 1. The metal industry, ferrous metals. – 1997

Vol. 2. Primary metals, secondary metals, light metals. – 1997

Vol. 3. Precious metals, refractory metals, scattered metals, radioactive metals, rare earth metals. – 1997

Vol. 4. Ferroalloy metals, alkali metals, alkaline earth metals; Name index; Subject index. – 1997

© VCH Verlagsgesellschaft mbH – A Wiley company,
D-69451 Weinheim, Federal Republic of Germany, 1997

Printed on acid-free and low-chlorine paper

All rights reserved (including those of translation into other languages). No part of this book may be reproduced in any form – by photoprinting, microfilm, or any other means – nor transmitted or translated into a machine language without written permission from the publishers. Registered names, trademarks, etc. used in this book, even when not specifically marked as such, are not to be considered unprotected by law.

Composition: Jean François Morin, Québec, Canada
Printing: Strauss Offsetdruck GmbH, D-69509 Mörlenbach
Bookbinding: Wilhelm Oswald & Co., D-67433 Neustadt/Weinstraße

Printed in the Federal Republic of Germany

Preface

Extractive metallurgy is that branch of metallurgy that deals with ores as raw material and metals as finished products. It is an ancient art that has been transformed into a modern science as a result of developments in chemistry and chemical engineering. The present volume is a collective work of a number of authors in which metals, their history, properties, extraction technology, and most important inorganic compounds and toxicology are systematically described.

Metals are neither arranged by alphabetical order as in an encyclopedia, nor according to the Periodic Table as in chemistry textbooks. The system used here is according to an economic classification which reflects mainly the uses, the occurrence, and the economic value of metals. First, the ferrous metals, i.e., the production of iron, steel, and ferroalloys are outlined. Then, nonferrous metals are subdivided into primary, secondary, light, precious, refractory, scattered, radioactive, rare earths, ferroalloy metals, the alkali, and the alkaline earth metals.

Although the general tendency today in teaching extractive metallurgy is based on the fundamental aspects rather than on a systematic description of metal extraction processes, it has been found by experience that the two approaches are complementary. The student must have a basic knowledge of metal extraction processes: hydro-, pyro-, and electrometallurgy, and at the same time he must have at his disposal a description of how a particular metal is extracted industrially from different raw materials and know what are its important compounds. It is for this reason, that this *Handbook* has been conceived.

The *Handbook* is the first of its type for extractive metallurgy. Chemical engineers have already had their Perry's *Chemical Engineers' Handbook* for over fifty years, and physical metallurgists have an impressive 18-volume *ASM Metals Handbook*. It is hoped that the

present four volumes will fill the gap for modern extractive metallurgy.

The *Handbook* is an updated collection of more than a hundred entries in *Ullmann's Encyclopedia of Industrial Chemistry* written by over 200 specialists. Some articles were written specifically for the *Handbook*. Some problems are certainly faced when preparing such a vast amount of material. The following may be mentioned:

- Although arsenic, antimony, bismuth, boron, germanium, silicon, selenium, and tellurium are metalloids because they have covalent and not metallic bonds, they are included here because most of them are produced in metallurgical plants, either in the elemental form or as ferroalloys.
- Each chapter contains the articles on the metal in question and its most important inorganic compounds. However, there are certain compounds that are conveniently described together and not under the metals in question for a variety of reasons. These are: the hydrides, carbides, nitrides, cyano compounds, peroxo compounds, nitrates, nitrites, silicates, fluorine compounds, bromides, iodides, sulfites, thiosulfates, dithionites, and phosphates. These are collected together in a special supplement entitled *Special Topics*, under preparation.
- Because of limitation of space, it was not possible to include the alloys of metals in the present work. Another supplement entitled *Alloys* is under preparation.
- Since the largest amount of coke is consumed in iron production as compared to other metals, the articles "Coal" and "Coal Pyrolysis" are included in the chapter dealing with iron.

I am grateful to the editors at VCH Verlagsgesellschaft for their excellent cooperation, in particular Mrs. Karin Sora who followed the project since its conception in 1994, and to

Jean-François Morin at Laval University for his expertise in word processing.

The present work should be useful as a reference work for the practising engineers and the students of metallurgy, chemistry, chemical engineering, geology, mining, and mineral beneficiation. Extractive metallurgy and the chemical industry are closely related; this *Handbook* will

therefore be useful to industrial chemists as well. It can also be useful to engineers and scientists from other disciplines, but it is an essential aid for the extractive metallurgist.

Fathi Habashi

Table of Contents

Volume I		Part Seven	Refractory Metals
Part One	The Metal Industry		26 Tungsten.....1329
	1 The Economic Classification of Metals.....1		27 Molybdenum.....1361
	2 Metal Production.....15		28 Niobium.....1403
	3 Recycling of Metals....21		29 Tantalum.....1417
	4 By-Product Metals.....23		30 Zirconium.....1431
Part Two	Ferrous Metals		31 Hafnium.....1459
	5 Iron.....29		32 Vanadium.....1471
	6 Steel.....269	Part Eight	Scattered Metals
	7 Ferroalloys.....403		34 Germanium.....1505
Volume II			35 Gallium.....1523
Part Three	Primary Metals		36 Indium.....1531
	8 Copper.....491		37 Thallium.....1543
	9 Lead.....581		38 Selenium.....1557
	10 Zinc.....641	Part Nine	Radioactive Metals
	11 Tin.....683		40 General.....1585
	12 Nickel.....715		41 Uranium.....1599
Part Four	Secondary Metals		42 Thorium.....1649
	13 Arsenic.....795		43 Plutonium.....1685
	14 Antimony.....823	Part Ten	Rare Earth Metals
	15 Bismuth.....845		44 General.....1695
	16 Cadmium.....869		45 Cerium.....1743
	17 Mercury.....891	Volume IV	
	18 Cobalt.....923	Part Eleven	Ferroalloy Metals
Part Five	Light Metals		46 Chromium.....1761
	19 Beryllium.....955		47 Manganese.....1813
	20 Magnesium.....981		48 Silicon.....1861
	21 Aluminum.....1039		49 Boron.....1985
	22 Titanium.....1129	Part Twelve	Alkali Metals
Volume III			50 Lithium.....2029
Part Six	Precious Metals		51 Sodium.....2053
	23 Gold.....1183		52 Potassium.....2141
	24 Silver.....1215		53 Rubidium.....2211
	25 Platinum Group Metals.....1269		54 Cesium.....2215

55	Alkali Sulfur Compounds.....	2221
<i>Part</i>	Alkaline Earth Metals	
<i>Thirteen</i>	56 Calcium.....	2249
	57 Strontium.....	2329
	58 Barium.....	2337
	Authors.....	2355
	Name Index.....	2375
	Subject Index.....	2379

Part Eleven

Ferroalloy Metals

																H	He
Li	Be											B	C	N	O	F	Ne
Na	Mg	Al											Si	P	S	Cl	Ar
K	Ca	Sc	Ti	V	Cr	Mn	Fe	Co	Ni	Cu	Zn	Ga	Ge	As	Se	Br	Kr
Rb	Sr	Y	Zr	Nb	Mo	Tc	Ru	Rh	Pd	Ag	Cd	In	Sn	Sb	Te	I	Xe
Cs	Ba	La†	Hf	Ta	W	Re	Os	Ir	Pt	Au	Hg	Tl	Pb	Bi	Po	At	Rn
Fr	Ra	Ac‡															
†			Ce	Pr	Nd	Pm	Sm	Eu	Gd	Tb	Dy	Ho	Er	Tm	Yb	Lu	
‡			Th	Pa	U	Np	Pu	Am	Cm	Bk	Cf	Es	Fm	Md	No	Lr	

46 Chromium

JAMES H. DOWNING (§§ 46.1–46.7); GERD ANGER † (§ 46.4); PAUL D. DEELEY (§ 46.8); HERBERT KNOPF, PETER SCHMIDT (§§ 46.9.1–46.9.5 EXCEPT 46.9.2.2; 46.9.10); JOST HALSTENBERG (§§ 46.9.1–46.9.6 EXCEPT 46.9.2.2; 46.9.10); MANFRED OHLINGER (§§ 46.9.2.2, 46.9.11, 46.10.3); KLAUS HOCHGESCHWENDER, GEORG UECKER (§§ 46.9.7–46.9.9); ULRICH KORALLUS (§ 46.9.11); MANFRED MANSMANN, DIETER RADE, GERHARD TRENCZEK, VOLKER WILHELM (§ 46.10.1); GERHARD ADRIAN, KARL BRANDT (§§ 46.10.2.1–46.10.2.4); GÜNTER ETZRODT (§§ 46.10.2.5, 46.10.4); HELMUT JAKUSCH, EKKEHARD SCHWAB, RONALD J. VEITCH (§ 46.10.3)

46.1 History	1761	46.9.4.3 Other Chromates	1790
46.2 Properties	1762	46.9.5 Other Chromium Compounds	1792
46.3 Resources and Raw Materials	1762	46.9.6 Analysis	1792
46.4 Ores	1763	46.9.7 Transportation, Storage, and Handling	1793
46.4.1 Ore Deposits	1764	46.9.8 Environmental Protection	1793
46.4.2 Ore Beneficiation	1767	46.9.9 Ecotoxicology	1794
46.5 Production	1767	46.9.10 Economic Aspects	1795
46.6 Uses	1770	46.9.11 Toxicology and Occupational Health	1795
46.7 Economic Aspects	1771	46.10 Pigments	1797
46.8 Alloys	1771	46.10.1 Chromium Oxide Pigments	1797
46.9 Compounds	1772	46.10.1.1 Properties	1798
46.9.1 Sodium Dichromate	1773	46.10.1.2 Production	1798
46.9.1.1 Alkaline Roasting	1774	46.10.1.3 Quality Specifications and Analysis	1800
46.9.1.2 Leaching of the Roast	1775	46.10.1.4 Storage and Transportation	1800
46.9.1.3 Acidification	1776	46.10.1.5 Uses	1800
46.9.1.4 Crystallization	1776	46.10.1.6 Economic Aspects	1801
46.9.2 Chromium Oxides	1777	46.10.1.7 Toxicology and Occupational Health	1801
46.9.2.1 Chromium(III) Oxide and Chromium Hydroxide	1777	46.10.2 Chromate Pigments	1801
46.9.2.2 Chromium(IV) Oxide (Chromium Dioxide)	1779	46.10.2.1 Chrome Yellow	1801
46.9.2.3 Chromium(VI) Oxide	1780	46.10.2.2 Chrome Orange	1803
46.9.3 Chromium(III) Salts	1782	46.10.2.3 Chrome Green and Fast Chrome Green	1803
46.9.3.1 General Properties	1782	46.10.2.4 Toxicology and Occupational Health	1804
46.9.3.2 Chromium(III) Sulfates and Chrome Tanning Agents	1783	46.10.2.5 Anticorrosive Chromate Pigments	1805
46.9.3.3 Other Chromium(III) Salts	1785	46.10.3 Chromium Dioxide	1806
46.9.4 Chromic Acids and Chromates(VI)	1787	46.10.4 Chromium Phosphate	1807
46.9.4.1 Chromic Acids	1787	46.11 References	1807
46.9.4.2 Alkali Chromates and Dichromates	1788		

46.1 History [1–5]

Chromium was discovered by VAUQUELIN, in the mineral crocoite, PbCrO_4 , in 1797. In 1798 he isolated chromium metal by reducing the oxide with carbon. Soon after the discovery of chromium, the commercial process for manufacturing chromates by roasting chromite with soda ash was developed.

During the 19th century, ferrochromium and chromium were produced by a variety of techniques. However, a commercial process was not developed until 1893, when MOISSAN produced ferrochromium in an electric furnace by the reaction of chromium oxide (Cr_2O_3) and carbon. In 1898, GOLDSCHMIDT produced chromium by the aluminothermic reduction of Cr_2O_3 . Other advances have included the application of silicothermics to the

production of low-carbon ferrochromium and chromium, production of chromium by aqueous electrolysis, and production of low-carbon ferrochromium and refining of electrolytic chromium by high-temperature vacuum processing.

Although chromium is found in many minerals, chromite is the only commercial source of chromium. Most of the mineral came from the Ural Mountains up to 1827, when deposits were discovered in the United States. These supplied a limited market up to about 1860, when large deposits were found in Turkey. Since that time chromite has been mined primarily in the eastern hemisphere.

Chromium was electrolyzed from a solution of chromium chloride by BUNSEN in 1854. However, large-scale commercial production of electrolytic chromium did not begin until 1954.

46.2 Properties [6-8]

At room temperature chromium is resistant to ordinary corrosive agents, which explains its use as an electroplated, protective coating. It dissolves in nonoxidizing mineral acids, such as hydrochloric and sulfuric acids, but not in cold aqua regia or nitric acid, which passivate the metal. At elevated temperature it reacts with halogens, silicon, boron, nitrogen, oxygen, and carbon.

Chromium and chromium-rich alloys are brittle at room temperature and this has limited their application [9]. Selected physical properties of chromium are as follows:

A_r	51.9961
Atomic number	24
m_p	1857 °C
b_p	2672 °C
Density ρ at 20 °C	7.19 g/cm ³
Crystal structure	cubic, body centered
Specific heat at 25 °C	23.25 Jmol ⁻¹ K ⁻¹
Molar entropy S_{298}^0	23.64 Jmol ⁻¹ K ⁻¹
Heat of fusion	16.93 kJ/mol
Latent heat of vaporization at b_p	344.3 kJ/mol
Linear coefficient of thermal expansion at 20 °C	6.2×10^{-6}
Resistivity at 20 °C	$12.9 \times 10^{-8} \Omega m$
Thermal conductivity at 20 °C	$67 W m^{-1} K^{-1}$

46.3 Resources and Raw Materials [4]

Chromite is a spinel $FeO \cdot Cr_2O_3$. In nature it is a mixture described by the formula $(Fe^{2+}, Mg)O \cdot (Cr, Al, Fe^{3+})_2O_3$. Chromite ore rarely contains more than 50% Cr_2O_3 ; other minerals such as SiO_2 can also be present.

Chromite is found in stratiform and podiform deposits. Stratiform deposits occur in layers up to a meter thick. The Bushveld Igneous Complex (Transvaal, Republic of South Africa), the Great Dyke (Zimbabwe) and the Stillwater Complex (Montana, United States) are examples. Podiform deposits range in size but a typical commercial deposit will be over 100 000 t. Deposits occur in the Ural Mountains, Albania, Zimbabwe, and the Philippines.

Table 46.1: Chromite production and reserves, 1983 [4].

	Production ^a , 10 ³ t	Reserves ^b , 10 ⁶ t	Reserve base ^{b,c} , 10 ⁶ t
North America			
Canada	0	—	4
South America			
Brazil	82	8	9
Cuba	8	3	3
Europe			
Albania	277	6	20
Finland	56	17	29
Greece	15	1	1
Former USSR	855	129	129
Africa			
Madagascar	13	7	7
Rep. South Africa	688	828	5715
Sudan	8	2	2
Zimbabwe	147	17	75
Asia			
India	112	14	60
Iran	16	1	1
Pakistan	—	1	1
Philippines	75	14	29
Turkey	103	5	73
Vietnam	5	1	1
Oceania			
New Caledonia	30	2	2
Australia	—	—	2

^a Estimated.

^b Shipping grade ore is deposit quantity and grade normalized to 45% Cr_2O_3 for high-Cr and high-Fe chromite, and 35% Cr_2O_3 for high-alumina chromite.

^c Reserve base includes deposits currently economic (reserves), marginally economic, and some currently subeconomic.

The 1983 production and reserves of chromite are shown in Table 1. Generally, richer lumpy Cr bearing ores have been preferred for smelting, whereas those with Cr_2O_3 content less than 40% have been used in refractories.

46.4 Ores [27-39]

The distribution of chromium in terrestrial rocks is closely linked to magmatic intrusions and their crystallization. The average content in the ten-mile crust of the earth is 100 ppm of chromium [33]. Table 46.2 contains a worldwide estimate of chromium ore resources.

The most important applications of chromium ores are in the manufacture of stainless steel, grey cast iron, iron-free high-temperature alloys, and chromium plating for surface protection. In the nonmetallic mineral industry, chromite is processed in conjunction with magnesite (sintered magnesia, calcined magnesia) and binders (clay, lime, gypsum, bauxite, corundum). The products are intended to have good resistance to pressure, fire, and temperature change, as well as good insulating properties between basic and acidic masonry. The chemical industry uses chromium ores in the production of chromium compounds. Table 46.3 shows quality requirements of chromium ores for different areas of application.

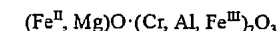
Table 46.2: Estimated reserves of chromium ore [93].

	Total	Reserves, 10 ⁶ t		
		Metallurgical ^a , > 45% Cr_2O_3	Chemical ^a , > 40% Cr_2O_3	Refractory ^a , > 20% Al_2O_3
South Africa	2000 ^b	100 (5%)	1900 (95%)	—
Zimbabwe	600	300 (50%)	300 (50%)	—
Turkey	10	9 (90%)	—	1 (10%)
Philippines	7.5	1.5 (20%)	—	6 (80%)
United States	8	0.4 (5%)	7.4 (92.5%)	0.2 (2.5%)
Canada	5	—	5 (100%)	—
Finland	7.5	—	7.5 (100%)	—
Others	11.35	8.175 (72%)	0.2 (2%)	2.975 (26%)
Total	2649.35	419.075 (16%)	2220.1 (84%)	10.175 (0.4%)
USSR and other Eastern bloc countries	51.5	26.5 (51%)	15 (29%)	10 (20%)
Total worldwide (rounded off)	2701	446 (17%)	2235 (83%)	20 (1%)

^a Graded according to Cr_2O_3 or Al_2O_3 contents.

^b Ores containing 30–50% Cr_2O_3 .

Minerals. Of the many minerals that contain chromium only the chromium spinels are of economic importance. The formula for the series of isomorphous mixtures of chromium spinels that form geological deposits is

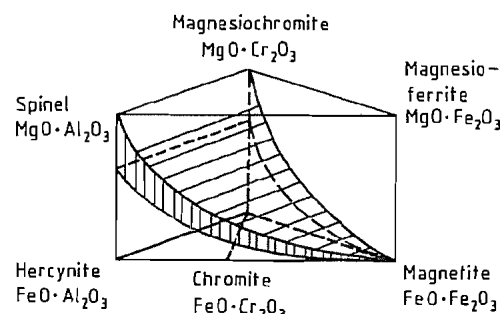


The proportion of Cr_2O_3 in the chromium spinels varies widely, causing the Cr:Fe ratio (also known as the Cr-Fe factor) to vary as well; this can have a profound effect on the evaluation of a deposit. In an ideal chromium spinel ($FeO \cdot Cr_2O_3$; 67.8% Cr_2O_3 , 32.2% FeO) the chromium:iron ratio is 2. As a result of the isomorphous inclusion of MgO , the Cr:Fe ratio may rise to between 2.5 and 5. Figure 46.1 shows the region of isomorphism with varying composition of the spinels. Natural chromium spinels usually contain 33–55% Cr_2O_3 , 0–30% Fe_2O_3 , 0–30% Al_2O_3 , 6–18% FeO , and 10–32% MgO . Table 46.4 lists some physical properties of chromium spinels.

Chromium also occurs in all groups of silicates where chromium replaces Al^{3+} , Fe^{3+} , and Mg^{2+} . Sulfidic chromium ores do not occur on earth. Chromates and chromium iodates are described, which originate from the weathering zone of sulfidic lead deposits (e.g., crocoite, $PbCrO_4$).

Table 46.3: Quality requirements (mass fractions in %) for chromium ores (according to U.S. Bureau of Mines).

	Metallurgical (high-Cr chromite)	Refractory (high-Al chromite)	Chemical (high-Fe chromite)
Cr:Fe ratio	3:1 or higher	—	—
Cr ₂ O ₃	> 48	> 31	> 44
Cr ₂ O ₃ + Al ₂ O ₃	—	> 58	—
Fe	—	< 12	—
SiO ₂	< 8	< 6	< 5
S	< 0.08	—	—
P	< 0.04	—	—
CaO	—	< 1	—

**Figure 46.1:** Ternary spinel system showing main isomorphous region.**Table 46.4:** Physical properties of chromium spinels.

Properties	Notes
Specific density: 3.8–4.8	increases as Fe and Cr contents increase
Mohs Hardness: 4.5–8	increases with increase in the ferrochromite component, very high for Al spinels
Melting point: 1545–1730 °C	inclusion of Mg raises melting point, inclusion of Fe ²⁺ reduces it
Color: dark brown to black	reddish with high Cr ₂ O ₃ content
Streak on porcelain plate; hammer striking mark: brown	important feature for differentiating from serpentine

46.4.1 Ore Deposits

Chromium ore deposits can be divided into two genetically different types:

- Seam-like deposits, also called stratiform or anorogenic deposits. Main representatives are Bushveld, Great Dyke, and Stillwater.
- Deposits which are shaped like sacks or tubes; they are called podiform or orogenic

deposits. Main representatives are Selukwe, Guleman, and Tiebaghi.

Various intermediate types such as adjacent "seam" pockets, striated chromite slabs, mottled ores, and vein-like deposits also occur. "Placer" deposits, i.e., enrichment due to chromite lumps and grains on or near primary deposits, are now achieving economic importance.

The seam-like deposits reveal layers or strata of chromite enrichment, with thicknesses ranging from centimeters to decimeters; the layers are regularly interlaminated with banded series of olivine-rich or pyroxene-rich rocks. The Main Seam of the Western Bushveld is, for example, 1.10–1.30 m thick and can be traced for over 65 km without any significant change in the mineral composition or thickness.

The demarcation between the chromite enrichment and the underlying bed is usually razor-sharp; in the direction of the overlying layer, disintegration into layers or mottled ores as a result of increased silicate content is observed.

The chromite bodies that are sack-like to tube-like in appearance are usually aligned with the direction of the magmatic stratification, i.e., the lowest sections are massive chromite ores; in the direction of the overlying layer, these merge into striated slabs or mottled ores.

The internal texture of the chromite ore bodies varies widely. The closest chromite crystal packing results in the formation of massive ores containing 75–85 vol% of chromite. Sphere or leopard ores, which consist of round chromite crystal aggregates 0.5–2 cm in diameter in a silicate matrix (olivine, pyroxene, serpentine), are also characteristic. Banded ores are closely related to the massive ores, but they are frequently richer in silicate and then form a link with the mottled ores (chromite single crystals in silicate matrix).

During transformation (serpentinization), the silicate content within the chromite ore bodies has resulted in the formation of friable and pulverizable masses (friable ore) which are encountered not only near the surface but

also at depths of several hundred meters below the present-day land surface.

Chromite transformation in the course of more recent tectonic superficial modification under pneumatolytic or hydrothermal conditions has resulted in the striking colors of recent uvarovite, smaragdite, and kammererite formations which act as pathfinders in prospecting and exploring for chromite deposits. Table 46.5 shows some analyses of selected chromium ores.

Former Soviet Union. The former Soviet Union is one of the most important producers of chromium ore in the world. All the deposits are distributed in ultrabasic massifs in the Central and Southern Urals.

The deposits that are most important at present were found in the late 1930s in the Akhtubinsk region (North Kazakhstan). The Donskoye deposit, which is associated with the mining settlement of Khrom Tau, contains high-grade chromium ores for ferrochromium production and low-grade ores for chemical purposes. Mining is carried on in numerous open-pit mines, which implies that the ore

bodies are small. A new open-cast mine was put into production near Donskoye, as is a processing plant with a throughput of 10⁶ t/a. Strong prospection effort for new occurrences is being made in the Northern Urals, but because of the rough climate no mine has been opened up to 1986.

Bushveld. In the Bushveld (South Africa) mining began in the 1920s in two districts: the Lydenburg district (Eastern Bushveld) and the Rustenburg district (Western Bushveld).

From a geological and petrological point of view this is a large intrusion of 500 × 250 km with a thickness of over 5 km. The chromite "seams" are located in the pyroxenite-norite zone of the basal section of the intrusion, always below the platinum-bearing Merensky Reef. In the case of Rustenburg there are up to 25 chromite seams on top of each other. The thickness of the individual seams varies from a few centimeters to 1.80 m. The seams are workable from 0.35 m upward, especially if they can be combined into mining units (Cr₂O₃ content in the crude ore 30–40%; Cr:Fe ratio = 1.6–2.3).

Table 46.5: Chemical analyses (mass fractions in %) of some chromium ores (crude ores, concentrates).

Country	Cr ₂ O ₃	FeO	SiO ₂	MgO	Al ₂ O ₃	CaO	V ₂ O ₅	Cr:Fe ratio
South Africa						n.d. ^b		
Rustenburg (c) ^a	44.5	26.4	3.5	10.6	14.1	0.4		1.7:1
Lydenburg (c)	44.3	24.6	2.3	11.2	16.1			1.8:1
Zimbabwe								
Great Dyke (m)	48.5	18.3	5.6	13.4	11.5	0.8		2.6:1
Great Dyke (r)	50.7	16.4	4.3	13.2	13.0	0.8		3.1:1
Selukwe (m)	47.0	12.0	5.7	15.5	12.6	1.8		3.9:1
Selukwe (r)	42.0	15.7	8.6	15.8	13.8	0.3		2.7:1
Turkey								
(m)	48.3	14.1	5.1	16.8	13.0	0.9		3.4:1
(r)	37.0	15.2	4.3	17.7	24.3	0.2		2.4:1
Philippines								
(Masinloc) (r)	33.3	13.2	4.6	19.6	28.2	0.4		2.5:1
Finland (Kemijoki)								
Crude ore	26.5	15.0	18.5	19.5	9.5	n.d.	0.04–0.1	1.8:1
Concentrate	45.7	33.8	0.4	2.9	13.6		0.1	1.4:1
Albania								
(m, r)	43.0	16.2	9.8	22.2	7.9	0.1		2.6:1
USSR								
(m)	53.9	12.6	5.8	13.3	9.6	1.1		4.3:1
(r)	39.1	14.0	9.4	16.1	17.4	0.7		2.8:1

^a (m) = metallurgical, (r) = refractory, (c) = chemical.
^b n.d. = not determined.

In the Lydenburg district, which is genetically very similar to the Rustenburg district, only two seams are being mined; the Cr_2O_3 content is 44% and the chromium:iron ratio 1.6–1.7. The iron content is frequently high, which may cause difficulties in the case of metallurgical ores; however, these ores are highly valued as chemical ores.

Great Dyke. The Great Dyke (Zimbabwe) is an intrusion which is 610 km long and 6–9 km thick — a remarkable length: thickness ratio which is unique in the world. The internal structure is similar to that of the Bushveld. From north to south, the individual complexes are Musengezi, Hartley, Selukwe, and Wedza. Selukwe consists of sack-like deposits containing 48% Cr_2O_3 and even more, with a chromium:iron ratio greater than 2.8 (a highly valued metallurgical ore). In the Hartley region, on the other hand, numerous bands and seams 2–75 cm thick are being mined; these are separated by serpentized peridotite layers, some of which are very thick and make mining very difficult. However, the Cr_2O_3 content varies between 48 and 57%, and the chromium:iron ratio is over 2.8 (Table 46.6).

According to conservative estimates, 1 km² of the Great Dyke contains around 1.4×10^6 t of crude ore, which corresponds to assured reserves of 600×10^6 t (geologically 4.6×10^9 t are possible).

Table 46.6: Analysis of chromium ores from Zimbabwe.

	Cr_2O_3 content, %	Cr:Fe ratio	Proportion, %
Metallurgical	over 48	over 2.8	80
Chemical	45–48	2.2–2.5	17
Refractory	42–46	1.8–2.0	3

Madagascar. On the island of Madagascar, chromium ores are being mined since 1967 with an annual production of around 60 000 t of metallurgical grade ore. Total output is calculated to be almost 2×10^6 t since the beginning of the operation (50–52% Cr_2O_3). The reserves are said to be around 5.5×10^6 t.

Turkey. Turkey still is the traditional country for chromite deposits of metallurgical quality, but because of falling prices on the world market and exhaustion of reserves, many mines

have been forced to close. The most important regions belong essentially to the alpidic era, e.g., Bursa, Mugla district, and Elazig, including the Guleman chrome ore field. Open-pit mining, and in some places underground mining at shallow depths, are employed.

Iran. Chromite deposits are described in two regions of Iran: northwest of Sabzawar near Mashad and 200 km northeast of the Gulf port of Bandar Abbas. These deposits are pocket-like, sometimes containing only 500 t of ore. Extraction is by open-pit mining and by primitive underground mining. Only hard lump ore for metallurgical applications is sometimes exported.

Philippines. On the Philippine island of Luzon the most important chromite deposits are to be found in the Coto region (near Masinloc, province of Zambales). These are chromite seams and pockets within layered dunites and harzburgites. They are classical metallurgical and refractory ores. More recently a new type of chrome ore has been put into production: chromite from lateritic soils. The concentrates are suited for the chemical industry.

Finland. In 1959 a fairly large deposit of chromite was discovered near Kemi, which has been developed into a productive mine. Chromium ore occurs in a serpentinite–anorthosite massif 12 km long and 1–2 km wide; the ore zone, however, is only 15 100 m thick and dips at an angle of 60° toward the north. The Cr_2O_3 content of the crude ore of the various ore bodies varies between 17.5 and 21.9% (locally even up to 30.5% Cr_2O_3); the chromium:iron ratio is low (0.81–1.87).

Yugoslavia. The deposits of chromite in Yugoslavia are restricted to the Raduša massif near Skopje, but the mining of metallurgical ores there has fallen considerably. Native ores are being processed in a new plant, whereas ores imported from Albania are being processed in the old one. The chromium ores are always associated with serpentized ultrabasic rocks. The striated slab type predominates, but massive chrome ores are encountered in some places.

Albania. Since 1960, Albania has become the third largest producer in the world. All actual data are based on estimates because the Albanian government withholds production and export figures. Albanian deposits belong to the podiform type and normal grades are reported to be 43% Cr_2O_3 with a Cr:Fe ratio of 3:1. The largest chrome ore mines are Bulquize and Matanesh with concentration plants of 300 000 t/a each.

46.4.2 Ore Beneficiation

The simplest method of concentrating chromite is by hand picking; this is still employed today at many pits, including those in Turkey, Brazil, Iran, and the Philippines. Because the mining of richer ores continues to decline, concentrating procedures, chiefly using the gravity method, have been developed to separate the serpentine from the chromite. For example, in South Africa or Brazil the chromite ores are enriched by crushing, milling, screening, and sophisticated gravity procedures. In South Africa, spirals and diamond pans are standard equipment. A combination of Reichert cones and Reichert spirals has also been employed. Although the costs are higher, the use of hydrocyclones for separating the fine chromite grains from waste is of great importance in the recycling of tailing dumps. Some chromium ores contain magnetite which can be removed by means of magnetic separation. However, if the magnetite is present as an individual phase within the chromite grains or as a fringe around the grains, this method is only suitable if Cr_2O_3 is further enriched. Flotation and electrostatic processes have so far enjoyed little success in the concentration of chromium ores. If the Cr_2O_3 content or the chromium:iron ratio is sufficient, fine-grained chromite concentrates can be briquetted or pelleted with the aid of binders.

The yield (65–85% of the chromite actually contained in the crude ore) depends on many factors including the nature of the chromite–serpentine intergrowth, grain size, and Cr_2O_3 content of the ore or individual grain.

At the chromite concentration plant at Kemi in Finland a fraction of the crude ore (70%) is crushed to below 10 mm in a primary crusher plant at the open-pit mine. After further grinding (rod and ball mill) and removal of sludge, the intermediate product is dried in a rotary kiln. The magnetic separation (a combination of weak and strong fields) produces two concentrates: concentrate 1 containing 45.9% Cr_2O_3 , which is sold or used as molding sand, and concentrate 2 containing 42.0% Cr_2O_3 for the production of ferrochromium.

46.5 Production¹

Extraction. Chromium is extracted from its ores by alkaline or acidic dissolution. In alkali dissolution, finely ground chrome ore is roasted with Na_2CO_3 under oxidizing conditions at ca. 1100 °C. The sodium chromate is leached from the calcine; most of the gangue is insoluble. The solution containing hexavalent chromium can be reduced with SO_2 and used for electrowinning, or $\text{Na}_2\text{Cr}_2\text{O}_7$ can be crystallized from it. The $\text{Na}_2\text{Cr}_2\text{O}_7$ can be converted to CrO_3 for use in electrolysis or to Cr_2O_3 for use in metallothermics.

Chrome ore can be dissolved in acid if an oxidizing agent is present. However, Fe, Al, and Mg also dissolve and must be removed. The preferred acidic dissolution technique is to reduce the ore with carbon, forming ferrochromium, which is ground and dissolved in sulfuric acid. The only significant impurity carried over is Fe, which is removed by crystallization as iron(II) ammonium sulfate. The chromium in the solution is in the +3 valence state and with additional purification is used to produce electrolytic chromium.

Production of Chromium Metal. Chromium metal is produced by the reduction of Cr_2O_3 or the electrolysis of Cr(III) solutions. The metal can also be obtained from Cr(VI) solutions by electrolysis, but the process is less efficient and is used primarily for plating.

¹ For Ferrochromium, see Section 7.5.

Aluminothermic Reduction. Aluminum is the most important reducing agent for producing chromium from Cr_2O_3 . Closely sized high-purity Al powder and Cr_2O_3 are blended and charged into a vessel lined with refractory, which is usually Al_2O_3 . The charge is ignited either with a KClO_4 -Al powder "wick" or electrically. The exothermic reaction results in a temperature greater than 2000°C , which leads to a clean separation of slag from metal. The purity of the chromium metal depends on the purity of the reactants, particularly the Cr_2O_3 . Originally this oxide was made by reduction of sodium chromate with sulfur, resulting in Cr_2O_3 of high sulfur content. Proprietary processes have been developed to produce Cr_2O_3 of higher purity. Analysis of aluminothermically reduced chromium is given in Table 46.7.

Chromium is also produced by *carbon reduction*. Chromium oxide and carbon are carefully weighed, mixed, briquetted, and heated in a furnace at 1400°C at a minimum pressure of 40 Pa. The heating cycle is 100 h. The C + O content is $\leq 1.5\%$ (Table 46.7).

Solutions suitable for *electrolytic production* of chromium can be derived from ore by oxidative roasting in alkali, or by direct solution of chromite in sulfuric acid; however, a commercial process was not achieved until the electrolyte was made by dissolving ferrochromium in H_2SO_4 and reduced anolyte. Figure 46.2 [10] shows the essential aspects of the process for electrolytic production of chromium metal.

Milled FeCr is leached with hot reduced recycled anolyte, chrome alum mother liquor, and makeup H_2SO_4 . The iron precipitates on cooling as iron(II) ammonium sulfate

$[\text{Fe}(\text{NH}_4)_2(\text{SO}_4)_2]$, which is recrystallized to recover the coprecipitated chromium.

The chromium is further purified by precipitation of chrome alum. Transformation of the Cr(III) to an insoluble salt requires aging at 30°C . After filtration the mother liquor is recirculated to the leach tank. The chrome alum crystals are redissolved to make the cathode feed. The overflow anolyte contains Cr(VI), which is reduced by SO_2 , thereby generating additional H_2SO_4 . The reduced anolyte is also cycled to the leach tank. The stripped catholyte is recycled. Dissolved chrome alum crystals are used to bring the chromium concentration in the catholyte feed up to the desired level.

The details of the cell reactions are shown in Figure 46.3 [11]. A diaphragm is necessary to prevent migration of Cr(VI) into the cathode compartment where its reduction by Cr(II) would lead to loss of current efficiency. Flow is maintained into the anode compartment from the cathode compartment by a higher level of solution in the latter. The pH of the catholyte must be controlled. At too low a value, H_2 evolution increases; at too high a value, precipitation of $\text{Cr}(\text{OH})_3$ occurs. This can be seen by an examination of the pH-potential diagram [12]. The pH is controlled by chromium concentration, current density, temperature, and differential height of solution between cathode and anode compartments. Water is fed to the anode to control the concentration of H_2SO_4 .

Chromium is plated onto stainless steel cathodes until it attains a thickness of ca. 3 mm. The plate is stripped from the cathode and degassed by heating at 420°C . The analysis of the flake is shown in Table 46.7.

Table 46.7: Analysis of various grades of chromium metal (in %).

	Cr	C	O	Si	S	P	N	Al
Aluminothermic ^a	99.4	0.05	0.10	0.10	0.010	0.010	0.02	0.10
Electrolytic ^b	99.1	0.02	0.5	0.01	0.03	0.01	0.05	0.01
Electrolytic ^{b,c}	99.5	0.05	0.02	0.05	0.04	0.01	0.002	0.0158
Carbon reduced ^b	98	1.5 ^d	—	—	0.1	0.02	0.001	0.1

^a Shieldalloy Corp.

^b Elkem Metals Co.

^c Vacuum treated.

^d C + O.

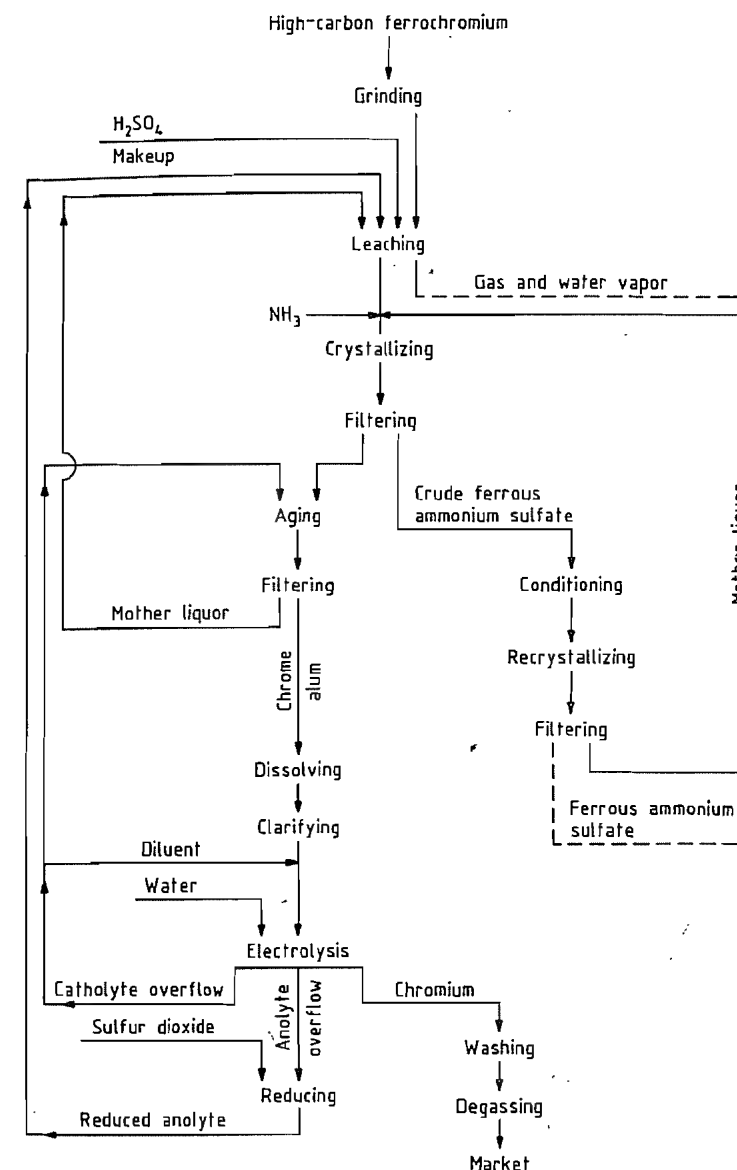


Figure 46.2: Flow sheet for producing electrolytic chromium from ferrochromium [10].

For many applications the oxygen content of the electrolytic chromium is too high. Deoxidation is carried out on a commercial scale by two techniques [13]. In the first either flake or briquettes of powdered flake are contacted with H_2 at elevated temperature. The procedure is less effective on chromium pro-

duced from chrome alum solutions than on chromium from hexavalent solutions [14]. The second technique involves heating briquettes of ground electrolytic flake and carefully controlled trace amounts of C in a vacuum furnace to form CO. The heating cycle is 90 h, the maximum temperature is

1400 °C, and the pressure is 13 Pa. The product is cooled in helium to prevent contamination. Analysis of the vacuum-treated product is shown in Table 46.7.

There are several other techniques for purifying chromium. These include iodide refining [9, 14], zone melting [9, 14], and treating chromium with a flux containing an alkaline earth metal [15]. Chromium prepared by these methods is purer but more expensive, and therefore is used only in, electronic applications.

46.6 Uses [4]

Chromium is used in ferrous and nonferrous alloys, in refractories, and in chemicals.

Chromium enhances an alloy's hardenability, creep and impact strength, and resistance to corrosion, oxidation, and wear. Ferrous alloys, mainly stainless steels, account for most of the consumption. These steels have a wide range of mechanical properties as well as being corrosion and oxidation resistant. Cast irons may contain from 0.5% to 30% Cr, which provides hardenability, toughness, hardness, and corrosion and wear resistance. Chromium is widely used in nonferrous alloys, including those based on nickel, iron-nickel, cobalt, aluminum, titanium, and copper. In Ni, FeNi, and Co, Cr is used for oxidation and corrosion resistance. In Al, Ti, and Cu it controls the microstructure.

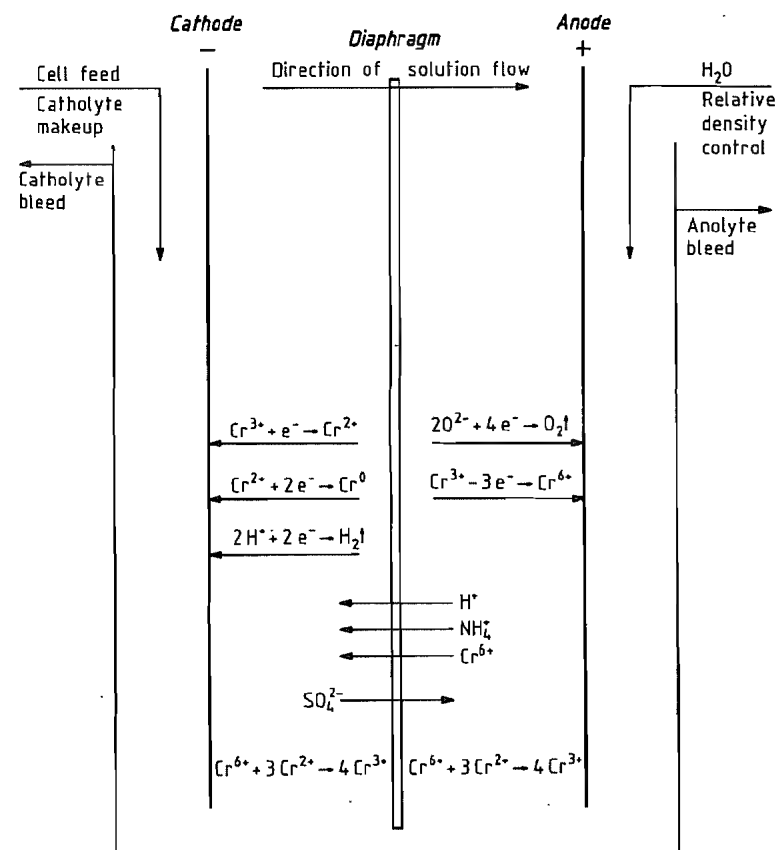


Figure 46.3: Idealized electrolytic cell reactions.

Chromium chemicals are used in a variety of applications. The largest amount is consumed to manufacture pigments for use in paints and inks. Other applications include leather tanning, metal corrosion inhibition, drilling muds, textile dyes, catalysts, and wood and water treatment.

Chromite is used in the refractory industry to make bricks, mortar, and ramming and gunning mixes. Chromite enhances thermal shock and slag resistance, volume stability, and strength.

46.7 Economic Aspects

The world production of chromium fluctuated between 1973 and 1983; however, growth is expected to the end of the century. Data for worldwide production are as follows [4]:

Year	Production, 10 ³ t	Year	Production, 10 ³ t
1973	1999	1979	2936
1974	2207	1980	2973
1975	2540	1981	2786
1976	2669	1982	2489
1977	2883	1983	2490
1978	2820	2000	5625 ^a

^aProbable projected demand.

46.8 Alloys

In the manufacture of steel, chromium is added usually in the form of ferrochrome. Pure chromium metal, produced by electrolytic or aluminothermic processes, is used for alloying nonferrous engineering materials. The most common materials are nickel-based and cobalt-based alloys, most of which are used at high temperature.

The only true chromium-based alloys that have been developed and used commercially are a few chromium-nickel alloys developed by the International Nickel Co. (INCO). These materials contain 50–60% chromium; the remaining percentage is nickel, with either niobium (columbium) or titanium specified as carbon and nitrogen scavengers. These alloys, as well as materials cited in [16, 17], often referred to as superalloys, are used in construct-

ing high-temperature exposed components in chemical and petrochemical industries.

Chromium-based alloys have found a unique application in power stations as supports for heat exchanger pipes. The balance of cobalt- and nickel-based high-chromium alloys are used mainly in components for gas turbine engines and for parts requiring resistance to elevated temperature, oxidation, and hot corrosion.

Chromium metal in powder form is used in the manufacture of *cermets* [18]. The cermets of commercial importance are as follows:

Cermet LT-1: 77% Cr, 23% Al₂O₃
 Cermet LT-1B: 59% Cr, 19% Al₂O₃, 20% Mo, 2% TiO₂
 Cermet LT-2: 25% Cr, 15% Al₂O₃, 6% W

These particular cermets have very good thermal stability and corrosion resistance.

Chromium metal from electrolytic or aluminothermic processes is used in a briquetted aluminum powder compact to provide the alloying addition to both cast and wrought aluminum products [19]. Two grades of smelted binary aluminothermic chromium-aluminum alloys (10% chromium and 20% chromium) are also used.

Other binary aluminothermic chromium alloys available for special alloying requirements are chromium-molybdenum (30% Mo) and niobium-chromium (30% Nb). Chromium-tungsten binary alloys were once used but are now redundant [20, 21].

Metallic chromium powders are used in both coated and cored welding electrodes. Small quantities of pure chromium are used for anodes in X-ray tubes and also for vacuum vaporization or sputtering.

Chromium powder, as well as ferrochromium powder, has been used in considerable quantities to produce *chromium coatings*.

The so-called pack chrome coating [21, 22] is applied to cast and wrought steel parts by immersing the article in a mixture of chromium powder, an inert material, e.g., kaolin, alumina, or magnesia; and mixtures of various salts, such as ammonium, iodide, or chloride. The packed part is then heated in an inert atmosphere at 900–1300 °C (heating time is dependent on part size).

Table 46.8: Uses of chromium compounds.

Branch of industry	Product	Use
Building industry	chromium(III) oxide	pigment for coloring building materials
Chemical industry	dichromates, chromium(VI) oxide	oxidation of organic compounds, bleaching of montan waxes, manufacture of chromium complex dyes
	chromium(III) oxide	catalysts
Printing industry	dichromates	photomechanical reproduction processes
	chromium(VI) oxide	chromium plating of printing cylinders
Petroleum industry	chromates(VI)	corrosion protection
Paints and lacquers	chromates, chromium(III) oxide	pigments
Refractory industry	chromium(III) oxide	additive for increasing slag resistance
Electroplating	chromium(VI) oxide	bright and hard chromium plating
Wood industry	chromates, chromium(VI) oxide	in mixtures of salts for protecting wood against fungi and insects
Leather industry	basic chromium(III) sulfates	tanning of smoothed skins
Metal industry	chromium boride, chromium carbide	flame sprays
	chromium(III) oxide	polishing agents
Metallurgy	chromium(III) oxide	aluminothermic extraction of pure chromium metal
Textile industry	dichromates	dyeing with chrome dyes
	basic chromium(III) acetates and chromium(III) fluorides	mordanting of textiles
Recording industry	chromium(VI) oxide	magnetic information storage
Pyrotechnics industry	dichromates	additive to igniting mixtures

Another procedure is the so-called gas chromium coating [22]. Steel parts and the chrome coating mixture are placed in a vessel at 1050–1250 °C. Volatile chrome compounds react with the steel components. The coating mixture consists mostly of chromium powder (both chromium metal and ferrochromium have been used [23]); inert materials (similar to those used in the pack chromium coating); and a relatively high concentration of a salt (fluoride, ammonia, or cryolite).

The gas chromium coating has been used to produce a so-called tin-free steel and to treat sheet steel on a continuous line.

Although chrome plating is used to produce a shiny as well as a hard satin finish, the source is from chromium salts rather than from aluminothermic or electrolytic chromium.

46.9 Compounds

Chrome iron ore (chromite) was discovered in 1798. A few decades later this ore was being subjected to oxidative roasting in the presence of soda and lime in manually operated furnaces to produce water-soluble sodium dichromate. This was processed further to yield yellow, red, and green chromium pig-

ments which were used among other things, for dyeing wallpaper; they replaced the toxic arsenic dyes that had been used until then. Chromium salts soon found their way into the textile industry as mordants for the dyeing of wool.

The importance of dichromates increased considerably in the period following 1870 when the rising coal tar dye industry needed large quantities for the oxidation of chemical intermediates. With the advent of the 20th century, chrome tanning was introduced in leather factories and in many areas replaced vegetable tanning.

The manufacture of chromium compounds received a further boost after 1930, when metallic chromium was successfully precipitated from chromic acid solutions by special additives. Since then this possibility has been used extensively in electroplating for bright and hard chromium plating.

Chromium compounds are used in numerous fields. In addition to the applications mentioned, chromates have long been used in printing as an aid in photomechanical reproduction. For some time, chromium dioxide has been a component of magnetic tapes for information storage. Table 46.8 lists important applications of chromium chemicals.

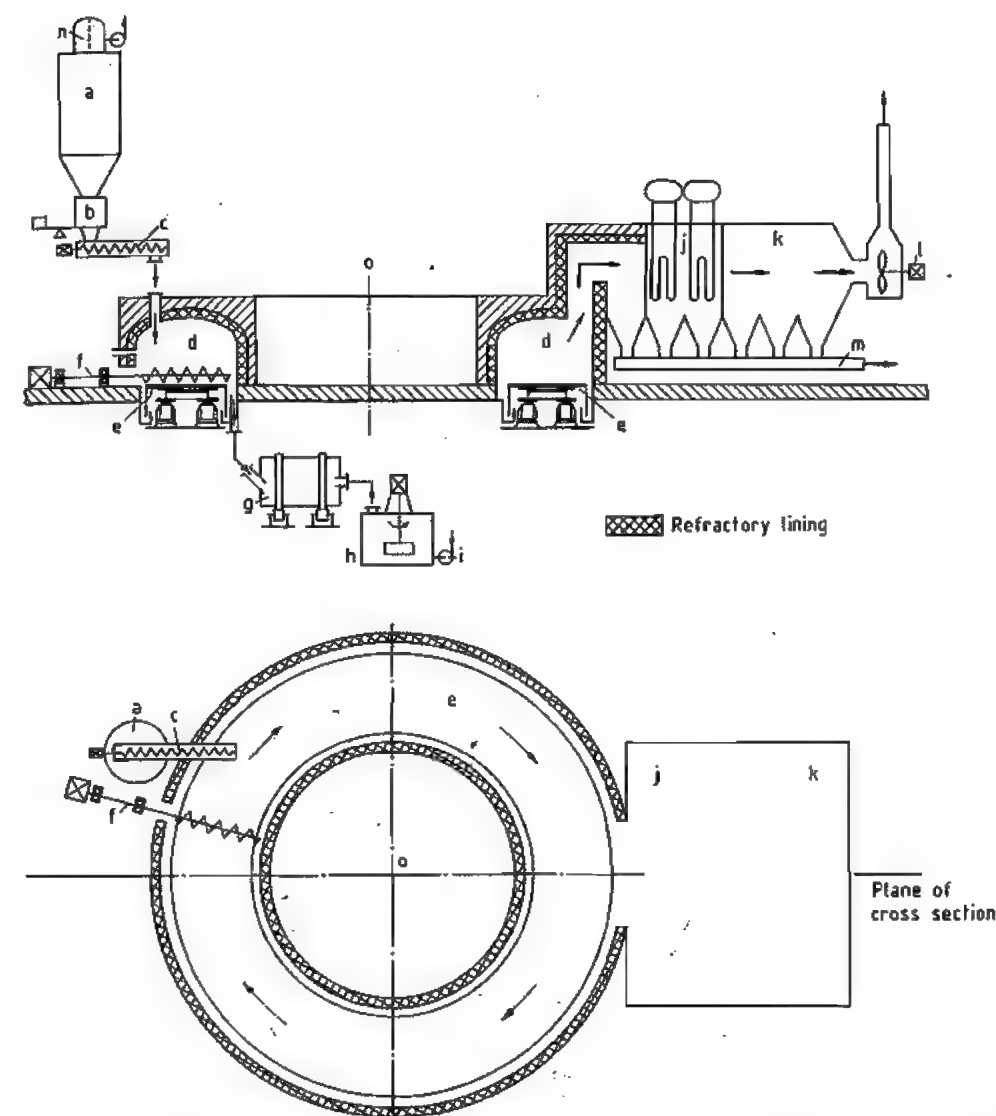
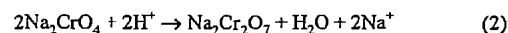
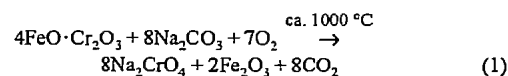


Figure 46.4: Annular hearth furnace: a) Mixture silo; b) Scales; c) Feed screw; d) Furnace; e) Annular hearth; f) Water-cooled ribbon screw; g) Wet tube mill; h) Stirred vessel; i) Pump for filtering system; j) Waste heat boiler; k) Electrostatic gas purification; l) Exhaust gas fan; m) Dust drag chain; n) Bin filter; o) Rotation axis.

46.9.1 Sodium Dichromate

Directly or via several intermediate stages, sodium dichromate, $\text{Na}_2\text{Cr}_2\text{O}_7 \cdot 2\text{H}_2\text{O}$, is the starting material for the production of all chromium compounds and pure chromium metal. Sodium dichromate is made in a three-step

process: (1) alkaline roast of chromite under oxidizing conditions (Equation 1), (2) leaching, and (3) conversion of sodium monochromate to sodium dichromate by means of an acid (Equation 2).



46.9.1.1 Alkaline Roasting

Soda ash (sodium carbonate) is generally used as the alkali component but sodium hydroxide may also be employed [40–42]. The degree of solubilization of chromites by the roasting process depends on their composition. For optimum results, the process is controlled by adding so-called carrier materials. These ensure sufficient porosity of the material so that oxygen can diffuse into the roast. Porosity is maintained by means of such materials as iron oxide, bauxite, or dried leach residue; CO_2 -emitting additives include lime and/or dolomite. The inert additives dilute the sodium carbonate and sodium chromate, which both melt at the reaction temperature. In the low-lime process the carbonates evolve CO_2 , decrease the reaction temperature to below 1000°C , and raise the melting point of the reaction products; the amount of lime added must be controlled so that the compound $5\text{Na}_2\text{CrO}_4 \cdot \text{CaCrO}_4$ [43] is produced in the roast. Temperatures above 1150°C must be avoided because they result in the subsidiary components of the ore being attacked. At still higher temperatures the degree of conversion is markedly decreased. The optimum temperature range is very narrow and depends strongly on the type of ore used and the composition of the mixture.

Process Description. A typical roast mixture contains 100 parts of ore, 60–75 parts of sodium carbonate, 0–100 parts of lime or dolomite, and 50–200 parts of inert materials. The components are first finely ground, then mixed, and fed into the furnace. Annular hearth furnaces or rotary kilns are commonly used in large plants today.

The *annular hearth furnace* (Figure 46.4) is made from steel with a refractory lining (inner diameter ca. 20 m; outer diameter ca. 30 m); it is driven by a gear wheel underneath and has rails running on rollers. The rotating hearth is

sealed from the stationary parts of the furnace by sheets of metal dipping into annular water troughs. The furnace is heated by several burners from the side or from the top with gas, coal dust, or oil. The exhaust gas can be utilized to preheat the burner air or to generate steam. The mixture is fed to the outer edge of the annular hearth by a feed screw. A water-cooled ribbon screw transports the mixture inward, each time the annular hearth revolves, and finally removes it in the middle.

In the annular hearth furnace, the mixture is uniformly heated to the reaction temperature and made to travel toward the center of the hearth with a well-defined layer thickness. The furnace process is fairly independent of the sintering of the roast; it allows the production of melts that contain 40% of water-soluble sodium chromate. The yield is 80–95%, based on the chromite feed. The roast takes 2–6 h, depending on the composition of the mix.

Most of the kiln tube of the *rotary kiln* (Figure 46.5) between the feed point and the reaction zone is used to heat the mixture. Shortly before the mix reaches the actual reaction zone, the soda melts and calcines. At this point the mixture bakes, and pellets or wreath-shaped cakes may be formed. If the furnace is operated inexpertly (temperature too high) or the composition of the mixture is wrong (too little carrier material) the kiln tube may get substantially clogged. In such cases, the constriction can be cleared by using an industrial gun.

The roast from the rotary kiln contains up to 30% of water-soluble sodium chromate. The yield is 75–90%, based on the chromite feed. The roast takes 3–8 h, depending on the composition of the mixture. The hot exhaust gas from the rotary kiln can be used to preheat the burner air.

Gas Purification. Exhaust gas purification systems able to achieve a high degree of separation are required for dust collection. They essentially consist of two components: (1) an exhaust gas cooling system, with optional energy recovery, for example, steam generation; and (2) the exhaust gas purification system, usually an electrostatic separator.

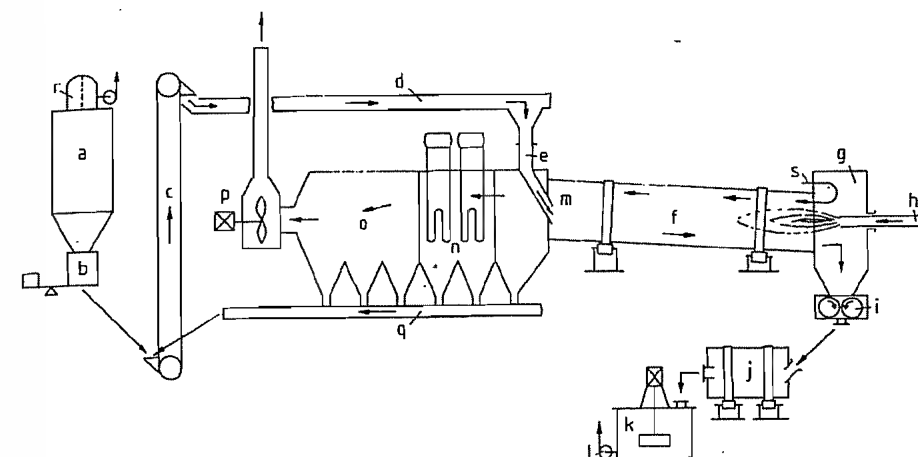


Figure 46.5: Rotary kiln for roasting chromium ores: a) Mixture silo; b) Scales; c) Elevator; d) Drag chain; e) Inlet tube; f) Rotary kiln; g) Combustion chamber; h) Burner; i) Crusher; j) Wet tube mill; k) Stirred vessel; l) Pump for filtering system; m) Kiln inlet; n) Waste heat boiler; o) Electrostatic gas purification; p) Exhaust gas fan; q) Dust drag chain; r) Bin filter; s) Air inlet.

The size and the design of the purification system depend on the type of furnace. In the rotary kiln, ca. 10% of the feed mixture is carried off by the exhaust gas, whereas in the annular hearth furnace, less than 1% is carried off. However, operation of the annular hearth furnace necessitates a considerable expenditure on gas cooling.

Other Processes. In the literature, other processes are proposed but so far these have not achieved any industrial significance. Thus, attempts have been made to roast chromium ore in a shaft furnace [44] or in a fluidized-bed reactor [45]. A fundamentally different process involves the reaction of the chromium ore and soda in a molten salt mixture with oxygen-containing gases being injected [46].

46.9.1.2 Leaching of the Roast

After the oxidative process, the roast is a mixture of soluble salts and insoluble components. It contains sodium chromate, sodium aluminate, magnesium oxide, sodium vanadate(V), iron(III) oxide, unused alkali, unchanged chromite, and small amounts of sodium chloride originating from the soda.

When the roast is extracted with hot water, a pH of 10.5–11.2 results. The pH is controlled

by adding acids or carbonates so that all chromate dissolves, whereas the alkali-soluble impurities hydrolyze and form a readily filterable precipitate along with the iron hydroxide and the unchanged ore components.

The roast is first cooled on a Fuller grate or in a cooling drum. Then it is either ground in a wet tube mill after addition of water or wash solution (see below) with carbonates or acids added, or it is dissolved in a stirred vessel. The insoluble residue is separated from the sodium chromate solution and thoroughly washed with a countercurrent of water. Nowadays continuous multistage Dorr plants or rotary filters are used; after separation, the insoluble residue is extracted two to three more times in counterflow. Dorr plants only exhibit satisfactory separation of residue and solution if the sodium chromate concentration is not too high. Rotary filter plants can be employed without difficulty for nearly saturated sodium chromate solutions; such filters are frequently preferred because the higher water consumption of the Dorr plant results in unnecessary steam costs in the subsequent evaporation process.

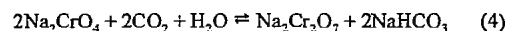
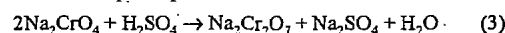
After removal of residual aluminum hydroxide and other undissolved components in a final purification process (e.g., thickener),

the concentrated sodium chromate solution is acidified (Section 46.9.1.3).

Some of the filter residue is dried and added to the roasting mix. The remainder is subjected to reducing treatment to convert the residual chromate content into an ecologically harmless form. To do this, the residue is suspended in water and treated with sulfuric acid and sodium hydrogen sulfite or iron(II) sulfate; chromate residues are converted into chromium(III) compounds in this way. Subsequent addition of alkali precipitates trivalent chromium (and iron(III), if present) as hydroxide. The suspension is then filtered and the cake (optionally after further removal of water) is dumped.

46.9.1.3 Acidification

The sodium chromate solution is converted into sodium dichromate solution by acidification with sulfuric acid (Equation 3) or carbon dioxide (Equation 4). The sequence of individual steps depends on the acid.



Sulfuric Acid Acidification. Sulfuric acid is added to the concentrated sodium monochromate solution in an agitated vessel until the pH is about 4. The sodium dichromate solution is then concentrated in a continuous evaporation plant. Each liter of sodium dichromate solution yields 400–500 g of anhydrous crystalline sodium sulfate. The sulfate is removed by centrifugation. The clear, dark-red sodium dichromate solution contains 900–1200 g of $\text{Na}_2\text{Cr}_2\text{O}_7 \cdot 2\text{H}_2\text{O}$ per liter and additional small amounts of sodium sulfate; it is dispatched in tanks, e.g., of steel. The solution is either used directly as an oxidizing agent or processed to yield dichromate crystals.

Carbon Dioxide Acidification. After filtration the sodium monochromate solution from the first filtration stage is concentrated to ca. 850 g of Na_2CrO_4 per liter. The saturated sodium chromate solution is then acidified with a countercurrent of carbon dioxide at 0.5–1.5 MPa (510 bar) to yield sodium dichromate and

sodium hydrogen carbonate. A series of stirred autoclaves is preferred for this reaction. They must be cooled to remove the heat of neutralization; the slurry leaves the last reactor at room temperature. The degree of conversion is about 80–90%.

The sodium hydrogen carbonate is removed by centrifugation or filtration, preferably under pressure to prevent reaction (4) from being reversed. After it has been washed, water can be removed in a pusher centrifuge. Still moist, the sodium hydrogen carbonate is then transferred to a calcining furnace. The carbon dioxide produced in the furnace may be fed back to the acidification autoclaves [25]; the sodium carbonate obtained is recycled for alkaline ore roasting [47].

To obtain commercial sodium dichromate solution, further evaporation to a concentration of 1000 g of sodium dichromate per liter is required. This is then followed by a second acidification with carbon dioxide or sulfuric acid.

Production of soda is the main advantage of carbon dioxide acidification. However, this is offset by a number of difficulties, particularly the formation of deposits on the evaporator during the concentration of the sodium monochromate solution. Other problems include mastering the pressure technology and cooling, separation of the sodium hydrogen carbonate, yield loss due to reverse reaction, and clogging of the calcination furnace.

46.9.1.4 Crystallization

For the purpose of crystallization the sodium dichromate solution (950–1200 g/L) is further concentrated and may, if necessary, be filtered while hot to remove additional sodium sulfate or sodium chromate. It is then slowly cooled to 30–35 °C with constant stirring to obtain orange-red crystals of $\text{Na}_2\text{Cr}_2\text{O}_7 \cdot 2\text{H}_2\text{O}$.

Today continuous vacuum crystallization is carried out to an increasing extent. The initial difficulties of this process, particularly in obtaining coarse, dust-free crystals, have largely been overcome. The crystalline slurry is continuously separated from the mother liquor

and dried. Precise control of the drying temperature is important because hydrated sodium dichromate is converted into anhydrous sodium dichromate above 84.6 °C and, therefore, cakes if overheated.

For reasons of occupational health, care should be taken to ensure that workplaces and production plants are dust free when sodium dichromate, especially the dried product, is being handled. In such locations, extensive ventilation and dust removal systems (wet scrubbers, electrostatic separators) are necessary.

46.9.2 Chromium Oxides

46.9.2.1 Chromium(III) Oxide and Chromium Hydroxide

Chromium(III) oxide, Cr_2O_3 , ρ 5.2 g/cm³, is green in finely dispersed form, whereas fairly large crystals have a blackish green hue and a metallic luster. The crystals have a hexagonal rhombohedral structure of the corundum type. The compound melts at 2435 °C, but begins to evaporate at 2000 °C to form clouds of green smoke; the boiling point is estimated to be 3000–4000 °C. The enthalpy of formation is –1141 kJ/mol. Macrocrystalline chromium(III) oxide has a hardness of 9 on the Mohs scale. An amorphous form of the oxide is also known; this crystallizes on heating.

Chromium(III) oxide does not dissolve in water, acid, alkali, or alcohols. It is converted by a molten bath of sodium peroxide into soluble sodium monochromate(VI). Chromium(III) oxide and chromates(III) are used in organic chemistry as catalysts, e.g., in the hydrogenation of esters or aldehydes to form alcohols and in the cyclization of hydrocarbons. They also catalyze the formation of ammonia from hydrogen and nitrogen.

Production. The industrial production of chromium(III) oxide involves the reduction of solid sodium dichromate, generally with sulfur. The finely divided components are thoroughly mixed, fed into a brick-lined furnace, and brought to dark-red heat. The reaction

proceeds exothermically. After the reaction mass has cooled, it is broken up and the sodium sulfate produced is leached out with water. The remaining solid is separated, rinsed, dried, and ground. To obtain 100 kg of chromium(III) oxide, 200 kg of sodium dichromate must react with at least 22 kg of sulfur, usually an excess of sulfur is used. Additives such as ammonium chloride or starch in the crude mixture affect the pigment properties. When sodium dichromate is replaced by the corresponding potassium salt, the hue of the pigment becomes more bluish.

The compound can also be prepared by a wet route involving reduction of sodium chromate by sulfur [48] with sodium thiosulfate being produced as a coproduct. The hydrate initially obtained is washed by decanting, filtered, and calcined to form the oxide.

Chromium(III) oxide destined for aluminothermic production of pure chromium metal must be heated additionally at 1000 °C to increase its grain size. If products particularly low in sulfur are to be produced for this purpose, charcoal can be used for the reduction instead of sulfur. High-purity oxides can also be obtained by thermal decomposition of chromium(VI) oxide or ammonium dichromate(VI), the latter yielding a material of very low density.

Chromium(III) oxide pigments contain 99.1–99.5% Cr_2O_3 . The aluminum oxide and silicon dioxide impurities each amount to ca. 0.1%; the annealing loss at 1000 °C is about 0.3%. The individual particles are spherical, with a diameter of 0.3 μm predominating. Chromium(III) oxide finds widespread application as a green pigment resistant to atmospheric conditions and heat. In addition, it is used as a colorant in glass products and printing inks, as a vitrifiable pigment in the ceramics industry, and as a polishing agent because of its considerable hardness.

Chromium(III) Aquoxides. Pure chromium(III) hydroxide, $\text{Cr}(\text{OH})_3$, can only be prepared with difficulty because the hydrates initially obtained by precipitation are subject to aging.

After drying in air, specimens prepared by precipitation with alkali in the cold from violet chromium(III) salt solutions have a composition corresponding to $\text{Cr}_2\text{O}_3 \cdot 9\text{H}_2\text{O}$, and are usually formulated as $\text{Cr}(\text{H}_2\text{O})_3(\text{OH})_3$. They are bright bluish green powders with limited life. All three hydroxyl groups react immediately with acids. Upon careful heating, dehydration occurs in steps and compounds containing 8, 5, 3, and 1 mol of water are formed. The density increases as the water content falls. Above 50 °C, conversion to a gelatinous green aging product occurs, and the solubility and chemical reactivity decrease; oxygen bridges are formed through the elimination of water, and polynuclear complexes are produced. The composition approaches that of chromium(III) oxide hydroxide, $\text{CrO}(\text{OH})$. Aging is accelerated by the presence of hydroxide ions.

In freshly precipitated hydroxides a crystalline phase isomorphous with bayerite $[\text{Al}(\text{OH})_3]$ is observed, whereas aged compounds are X-ray amorphous. The chromium(III) hydroxide hydrates are amphoteric compounds. With acids they form Cr^{3+} salts, whereas they dissolve in strong hydroxide solution to form chromates(III), e.g., the deep green sodium chromate(III), $\text{Na}_2\text{Cr}_2\text{O}_4$ (previously known as sodium chromite). When ammonium hydroxide is added, red solutions are formed. Oxidizing agents in the presence of alkali produce chromates(VI). With halogens this takes place immediately on gentle heating, but with oxygen several hours are required at a pressure of 4 MPa (40 bar) at 175 °C.

Chromium(III) hydroxide forms a stable colloid solution, whose isoelectric point is at pH 5. At higher pH the sol becomes negatively charged and adsorbs cations, whereas below pH 5 the charge is positive and anions are adsorbed. The adsorption capacity of chromium(III) hydroxide sols is higher than that of aluminum or iron(III) hydroxide sols. Sols containing 127 g of Cr_2O_3 per liter have been obtained from concentrated chromium(III) chloride solution by addition of ammonium carbonate and dialysis while the solution is hot [49].

Production. In industry chromium(III) hydroxide hydrates are usually produced from solutions of chromium(III) sulfate or chromium alum by precipitation with soda, sodium hydroxide solution, or ammonium hydroxide. Production by reduction of sodium chromate with sodium sulfide [50] has also been proposed.

For production from potassium chromium alum 54 kg of soda is dissolved in 300 L of water and a solution of 180 kg of alum in 900 L of water is added slowly. After the evolution of carbon dioxide has subsided, about 220 kg of moist chromium hydroxide containing 12% Cr_2O_3 is obtained by filtration. Chromium(III) hydroxide hydrates are used for the production of chromium(III) salts by reaction with the corresponding acids.

Hydrated chromium(III) oxide, $\text{Cr}_2\text{O}_3 \cdot x\text{H}_2\text{O}$, is a brilliant emerald-green pigment known as Guignet's green that consists of very finely divided chromium(III) oxide to which water is bonded by adsorption. It is produced by heating a ground mixture of one part by weight of potassium dichromate and three parts by weight of boric acid in a muffle furnace to a faint red heat, which results in the formation of chromium(III) and potassium tetraborates. The molten mass still contains 6–7% water and, after cooling, already has a deep green color. When this mass is boiled with water, it decomposes into chromium(III) oxide hydrate and boric acid. The product is coarse-grained and difficult to grind. Use of sodium dichromate as raw material results in a more yellowish color, whereas addition of thiourea or polysulfide to the reaction mixture produces a pigment with a bluish hue. The composition of the commercial products varies; typical values are: Cr_2O_3 79.3–82.5%, H_2O 16.0–18.0%, B_2O_3 1.5–2.7%.

Hydrated chromium oxide green is a pigment with properties similar to those of Guignet's green but with a somewhat less intensive coloration. This pigment is prepared by reducing sodium chromate or sodium dichromate in aqueous solution with sulfur or sodium formate in a stirred autoclave or pressure tube [51]. The temperature required is

250–270 °C. The solid is separated by filtration, washed, dried, and ground. The finished pigment consists of fine needles, with a particle size of $0.02 \times 0.1 \mu\text{m}$ predominating. The product contains 79–80% Cr_2O_3 , the annealing loss is about 19%, and the density 3.7 g/cm³. The coloration changes at elevated temperature. Because of its high reflecting power at infrared wavelengths the product had at times been of special importance in camouflage paints.

46.9.2.2 Chromium(IV) Oxide (Chromium Dioxide)

WÖHLER discovered ferromagnetic chromium dioxide in 1859 when he decomposed chromyl chloride [52]. About 100 years later, Du Pont produced it in pure form by decomposition of chromic acid under hydrothermal conditions [53, 54]. Industrial exploitation began after the morphological and magnetic properties had been modified by doping chromium dioxide with heavy metals [55, 56] in order to meet the requirements for a magnetic pigment [57]. The marketing of chromium dioxide at the beginning of the seventies initiated the development of cobalt-doped iron oxides which are nowadays used as an alternative to chromium dioxide for information storage.

Physical and Chemical Properties [58]. Chromium dioxide, CrO_2 , crystallizes in black tetragonal needles. The lattice is of the rutile type and belongs to the space group 4/mmm. The dimensions of the unit cell are $a = b = 44.21 \text{ nm}$ and $c = 29.16 \text{ nm}$. The X-ray density is 4.89 g/cm³, and the phase width is between $\text{CrO}_{1.89}$ and $\text{CrO}_{2.02}$ [59]. The enthalpy of formation is –590 kJ/mol [60]. The temperature coefficient for the c -axis is negative [61]. At 100 °C, agglomerated blocks have a linear coefficient of expansion of $-6 \times 10^{-6} \text{ K}^{-1}$ [62].

At room temperature chromium dioxide is ferromagnetic, the magnetic moment being 2 Bohr magnetons. The Curie temperature is 120 °C and increases to 155 °C as a result of doping with iron [63]. Finely crystalline nee-

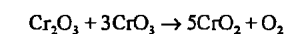
dle-shaped chromium dioxide has a specific magnetic saturation M_s/ρ of 77–92 Am²/kg, whereas in single crystals M_s/ρ rises to 100 Am²/kg [55]. The magnetocrystalline anisotropy constant is $22 \times 10^3 \text{ J/m}^3$ [64]. The coercivity H_c depends on the size of the crystals and on their shape and magnetocrystalline anisotropies. The coercivity is affected to differing extents by various heavy metals [65]. Iron, antimony, and tellurium increase H_c from 35 kA/m to 60 kA/m, whereas iridium increases it to 220 kA/m [66].

Chromium dioxide behaves as a metallic conductor [58, 67], with a specific electrical resistivity between 2.5×10^{-4} and $4 \times 10^{-2} \Omega\text{cm}$ [61, 68].

At room temperature and normal pressure chromium dioxide is metastable; when heated to temperatures above 350 °C, it decomposes into chromium(III) oxide and oxygen. Chromium dioxide has an oxidizing action on reactive organic compounds [69]; the reactivity is considerably decreased by enveloping it with iron(III) and chromium(III) oxides [70–72]. Chromium dioxide is insoluble in water. Reaction with water occurs at the crystal surface, with disproportionation to chromate and Cr^{3+} ions. The aqueous suspension has a pH of 3. However, chromium dioxide is soluble in concentrated sulfuric acid or concentrated alkali solution.

Production [73]. Chromium dioxide is made by decomposition of chromyl chloride, chromic acid anhydride [73], and chromium(III) chromate [74], or by oxidation of chromium(III) compounds with oxygen, hydrogen peroxide, chromic acid anhydride [75], or ammonium perchlorate [66].

Industrial production employs a process originally carried out under licence from Du Pont [65], which involves hydrothermal oxidation of chromium(III) oxide with excess chromic acid:



Iron(III) oxide and antimony(III) oxide are used as a dopant. Finely divided chromium(III) oxide is obtained either by thermal decomposition of ammonium dichromate or

by dehydration of chromium(III) hydroxide [75].

A highly viscous paste (50–100 Pa·s) is produced by intensively homogenizing the starting materials. This paste is heated at 300 °C and 35 MPa (350 bar) to form a hard agglomerate of fine chromium dioxide needles which must be drilled out of the reactor trays, broken, and carefully ground. If the residual moisture exceeds 5%, the product is reheated in a rotary kiln. The chromium dioxide is deagglomerated in an aqueous sodium sulfite suspension, and the crystal surface is simultaneously reduced; this forms a chromium(III) oxide hydroxide layer about 1 nm thick. To do this, the suspension is circulated through a mill which generates intense shear fields and the fine component is removed by using a hydrocyclone. After filtration and washing, drying is carried out in a spray tower. The chromium dioxide obtained has a bulk density of 0.8 g/cm³.

Production is carried out to a large extent in closed equipment. Less than 2 mg of dust is emitted per 1 m³ of exhaust air (STP). The chromium-containing wastewater from the production is worked up by reduction.

Use and Economic Importance. Chromium dioxide is used as a magnetic pigment. So far no other uses have achieved any significance [56].

In the audio field, chromium dioxide is used in mono- and multilayer tapes, the layers in the latter containing chromium dioxide of different coercivity. In video tapes, it is employed either on its own or mixed with cobalt-doped iron oxides. Because of its low Curie point, chromium dioxide allows high-speed thermomagnetic copying of prerecorded audio and video tapes [76]. Chromium dioxide has been used in digital data storage since 1985. Since the magnetostriction of chromium dioxide is low, repeated playing results in virtually no level losses [77]. Table 46.9 contains data on chromium dioxide powder intended for various applications.

In 1984 the demand for magnetic pigments was about 50 000 t, about 10% of this being chromium dioxide. The most important manufacturers are Du Pont (United States) and BASF (Germany). In addition, there is a chromium dioxide plant in the former Soviet Union.

46.9.2.3 Chromium(VI) Oxide

Chromium trioxide, chromic acid anhydride, chromic acid, CrO₃, ρ 2.7 g/cm³, forms dark red crystals which deliquesce in air. The enthalpy of formation is –594.5 kJ/mol. The oxide melts at 198 °C and starts to decompose, giving off oxygen and brownish red vapors with a pungent smell. The rate of decomposition reaches a maximum at 290 °C, chromium(III) oxide, Cr₂O₃, being produced as the final product via various intermediate stages. Chromium(VI) oxide dissolves in water to form chromic acids; the solubility depends only slightly on temperature. A saturated solution contains 166 g of CrO₃ at 20 °C and 199 g of CrO₃ at 90 °C per 100 mL of water. The compound also dissolves in sulfuric acid and nitric acid. Chromium(VI) oxide is a powerful oxidizing agent, particularly in the presence of acids. Reactions with alkali metals and numerous organic compounds, e.g., low-boiling hydrocarbons, acetone, or benzene and its derivatives, proceed explosively with considerable heat being produced. Esters of chromic acid are also known, e.g., with such cyclic tertiary alcohols as methylfenchol and methylborneol.

Chromium(VI) oxide is made by the reaction of sodium dichromate with sulfuric acid. The reaction can be carried out with solid sodium dichromate or with solutions or suspensions. Both methods are in use industrially.

The reaction proceeds rapidly and completely after the components have been mixed, with heat being evolved. Isolation of chromium(VI) oxide from the reaction mixture or purification of the crude product obtained from the aqueous solution is difficult.

Table 46.9: Powder data for typical chromium dioxide pigments.

Application	Particle geometry				Magnetic data ^a		
	SSA ^b , m ² /g	\bar{r} , μm	l/d^d	V^d , 10 ⁻⁴ μm^3	H_c , kA/m	M_r/ρ , Am ² /kg	M_s/ρ , Am ² /kg
Audio	28	0.29	9	2.5	41	35	77
Video	35	0.29	11	1.5	49	34	74
Data storage	24	0.32	8	3.5	39	35.5	79

^aMeasured with a vibration magnetometer, $H_m = 800$ kA/m.

^bSpecific surface area (SSA) determined by N₂ adsorption using the BET method (1-point measurement).

^cMean length l determined by electron microscope photography with a magnification of 20 000 times.

^dDiameter d and volume V calculated from SSA and l .

Quantitative separation of sodium hydrogen sulfate is possible only if the chromium(VI) oxide is melted, but at this temperature the product begins to decompose. The melting process must therefore be controlled very precisely.

Dry Process. Even today the old discontinuous process is in use to some extent. The reaction vessels are made from carbon steel or stainless steel. The conical containers are equipped with stirrer, exhaust facilities, and external heating. Sulfuric acid and sodium dichromate are added simultaneously with stirring. The paste heats up to 80 °C during mixing and is heated further to evaporate water. At 170 °C sodium hydrogen sulfate melts, followed by chromium(VI) oxide at 198 °C. As soon as the reaction products are liquid, the heating and the stirrer are turned off. After a few minutes the heavier chromium(VI) oxide (ρ 2.2 g/cm³) settles at the bottom, and is covered by a layer of the lighter sodium hydrogen sulfate (ρ 2.0 g/cm³). Liquid chromium(VI) oxide is drawn off the bottom and conveyed to a cooling drum where it solidifies to form scales. Sodium hydrogen sulfate is subsequently drained. The yield of chromium(VI) oxide is about 85%; 175 kg of sodium dichromate and 140 kg of 96% sulfuric acid are required to obtain 100 kg of chromium(VI) oxide. About 150 kg of sodium hydrogen sulfate is obtained as by-product.

Figure 46.6 shows a continuous dry process [78]. The raw materials are fed to a mixing screw for intimate mixing. A viscous paste of chromium(VI) oxide, sodium hydrogen sulfate, and water forms which is fed into a heated rotary kiln of stainless steel where it is melted. The heating must be controlled very

carefully. The melt flows into a separator, where the heavier chromium(VI) oxide collects at the bottom of the trough, is removed by means of a rising pipe, and is converted into scales on cooling drums. The upper sodium hydrogen sulfate layer leaves the separating cell via an overflow and is also cooled on drums. Exhaust air from the various pieces of equipment is purified in a wash tower. The yield of this process is over 90%.

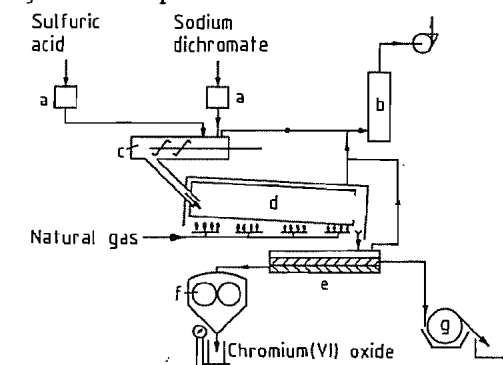


Figure 46.6: Continuous production of chromium(VI) oxide: a) Metering device; b) Wash tower; c) Mixer; d) Rotary kiln; e) Separation cell; f) Cooling drum for chromium(VI) oxide; g) Cooling drum for sodium hydrogen sulfate.

If a highly concentrated solution is used instead of dichromate crystals, the kiln can be heated directly [79].

Wet Process. A hot saturated solution of sodium dichromate, which may still contain dichromate crystals, reacts with sulfuric acid [80]. In the course of 30–60 min the chromium(VI) oxide precipitates from the hot solution. On filtration a crude product is obtained, with a yield of about 80%. Sodium hydrogen sulfate must be removed from the crude product by fusion. The filtrate can be re-

cycled for converting sodium monochromate into dichromate, it can also be used in a fresh reaction mixture [81] if sodium hydrogen sulfate is first crystallized and removed at 20–25 °C. The crude chromium(VI) oxide is purified by continuous successive fusion and decanting [82].

As an alternative to production by reaction with sulfuric acid, Diamond–Shamrock developed an electrochemical process [83–85] in which chromic acid is produced from sodium dichromate in a two- or three-compartment cell.

Chromium trioxide is usually sold in the form of flakes, but the coarsely or finely ground product is also marketed. Good commercial products contain 99.5–99.7% CrO₃ and a maximum of 0.1% of sulfate. In the form of flakes, the product has a bulk density of 1.1 kg/L whereas that of the ground product is 1.4 kg/L. Steel drums must be used as containers and they must be tightly sealed because the product absorbs moisture from the air.

Chromium trioxide is classified as a dangerous substance in the EEC list and must be marked as fire-promoting and corrosive. In the IMDG code chromic acid has been put in class 5.1., UN No. 1463. The MAK of CrO₃ is 0.1 mg/m³.

Electroplating is the most important field of application of chromium(VI) oxide. Numerous mixtures containing chromium trioxide are on the market; these “compounds” often contain hexafluorosilicates which improve the properties of the chromium coatings. Chromic acid solutions are also used for passivating zinc, aluminum, cadmium, and brass. Proprietary mixtures predominantly contain additions of fluoride, nitrate, and phosphate ions. Other uses for chromic acid are in the production of chromium dioxide and in wood preservation.

46.9.3 Chromium(III) Salts

46.9.3.1 General Properties

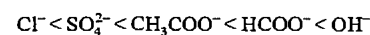
Water Content. In contrast to many other inorganic salts, chromium(III) salts occur in a variety of forms that depend on water content and on the particular conditions under which they are formed. Anhydrous compounds do not dissolve in pure water.

However, some of them, e.g., chromium(III) chloride or chromium(III) sulfate, dissolve in the presence of chromium(II) ions. In this process, one dissolved divalent ion transfers an electron via an anion bridge to a trivalent chromium ion in the solid crystal. Having become divalent, this ion detaches itself, acts in a similar manner on another chromium(III) ion in the crystal array, and reverts again to the trivalent state.

Complex Formation. Dissolved chromium(III) ions are always coordinated by various ligands. In the simplest case of the hexaaquochromium(III) ion, [Cr(H₂O)₆]³⁺, six water molecules surround the central chromium ion in an octahedral arrangement as ligands. In addition to the aquo complexes, numerous coordination compounds with other molecules are known, and research on them, particularly studies of the ammine complexes (NH₃ as ligand), has played an important part in the development of coordination compound chemistry [86].

When negatively charged ligands enter the chromium complex, the charge is decreased appropriately. If the sum of the negative charges is four or more, the complex becomes anionic, an example of this being the diaquodisulfatochromium(III) ion [Cr(SO₄)₂(H₂O)₂][−]. In this case, each sulfate radical with a double negative charge occupies the position of two ligands.

The tendency of negatively charged ligands to form complex compounds with chromium increases in the following order:



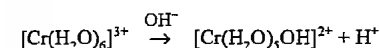
Nitrato complexes are unknown.

Hydrate Isomerism. Chromium(III) complexes exhibit hydrate isomerism due to the positioning of anions and water molecules. Thus chromium(III) chloride hexahydrate E_− is known in three different forms:

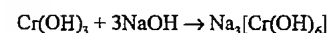
- Hexaaquochromium(III) chloride, [Cr(H₂O)₆]Cl₃, bluish grey
- Pentaquochlorochromium(III) chloride hydrate [Cr(H₂O)₅Cl]Cl₂·H₂O, bright green
- Tetraaquodichlorochromium(III) chloride dihydrate [Cr(H₂O)₄Cl₂]Cl·2H₂O, dark green

The anions that are directly bound to the central atom do not dissociate in water and consequently do not react with the common precipitating agents; therefore, in the two green chlorides, only one-half and one-third of the chloride ions, respectively, are precipitated by silver nitrate.

Basic Salts. Hydroxide ions form coordinate bonds, with central ion of the hexaaquochromium complex being hydrolyzed. In this process, the pentaquohydroxochromium(III) ion with a double positive charge is first formed:



When more alkali is added, chromium hydroxides are precipitated immediately. Finally, with a strong hydroxide solution, a soluble deep green hydroxo salt is produced:



Pentaquohydroxochromium(III) complexes are very weak bases. Their salts hydrolyze and the pH of aqueous solutions usually is 2. The basicity of these salts is defined as the ratio of hydroxyl groups (in percent) bound to chromium to the number of hydroxyl groups in chromium(III) hydroxide, that could theoretically be bound to chromium. Pentaquohydroxochromium(III) complexes therefore have a basicity of 33%. When a second hydroxyl group enters the complex the basicity increases to 67%. However, from a basicity of 60% onward, chromium(III) hydroxide precipitates and these compounds are not used in practice.

46.9.3.2 Chromium(III) Sulfates and Chrome Tanning Agents

Chromium(III) Sulfate. Anhydrous chromium sulfate, Cr₂(SO₄)₃, ρ 3.0 g/cm³, is a violet powder which is insoluble in water but dissolves to form complexes when reducing agents are added. For its preparation, chromium metal or chromite is heated over 250 °C with sulfuric acid.

The *octadecahydrate*, [Cr(H₂O)₆]₂(SO₄)₃·6H₂O, ρ 1.86 g/cm³, forms cubic crystals. The violet compound gives off water on heating and above 70 °C it is converted, with further loss of water, into a dark-green crystalline *pentadecahydrate*. As the water content diminishes, the solubility decreases.

Solutions of chromium(III) sulfates can be made by treating chromite with sulfuric acid in the presence of chromium(VI) compounds [87]. Since other components of the ore are solubilized at the same time, the solutions are strongly contaminated; separation of magnesium, aluminum, and iron presents such great difficulties that this process has not yet gone beyond the experimental scale. Chromium(III) sulfate solutions are also obtained by dissolving ferrochromium in sulfuric acid, a process in which iron(II) sulfate is obtained as a co-product. So far, the economical preparation of a pure product has been only partially successful.

Large quantities of chromium(III) sulfate solution are produced in the oxidation of organic substances with chromic acid or sodium dichromate in sulfuric acid solution. Examples of this are the preparation of anthraquinone from anthracene, the preparation of benzoquinone from aniline, or the bleaching of montan wax. These solutions are used to produce other chromium products; an electrolytic regeneration to dichromate is also possible.

Tanning Agents. Basic chromium(III) sulfates are used on a large scale as tanning agents for leather. Industrially, two processes are available for the reduction of sodium dichromate: (1) reaction with organic compounds (molasses, sugar) in the presence of

sulfuric acid and (2) reduction with sulfur dioxide.

Reduction with molasses is carried out in aqueous solution; about 30 kg of molasses or 15 kg of cane sugar is required for 100 kg of sodium dichromate dihydrate. The amount of sulfuric acid required depends on the desired basicity. To adjust the basicity to 33%, about 103 kg of 96% acid is needed. The reaction is strongly exothermic; water evaporates in abundance and must be continuously replenished. Lead-lined vats have proved successful as reaction vessels. The exhaust gases have an unpleasant smell, but this can be eliminated by scrubbing with water in a wash tower or by heating them after condensing the water vapor.

The properties of the final product are, to a certain extent, dependent on how the reaction is performed. If sulfuric acid is added first to the dichromate solution and the reducing agent is then added slowly, relatively few organic acids are produced as result of side reactions. The proportion of these acids becomes considerably larger if the dichromate solution is mixed first with the reducing agent and the sulfuric acid is added last. The organic acids form chromium complexes and mask the tanning agent. This masking delays the tanning process.

In the *reduction with sulfur dioxide* sulfuric acid is generated in such proportions that the tanning agent produced has a basicity of 33%. For the reduction of 100 kg of sodium dichromate dihydrate, 65 kg of SO_2 is theoretically required.

The reaction is carried out in lead-lined or brick-lined absorption towers containing ceramic packing material. Sulfur dioxide is produced by combustion of liquid sulfur which yields a gas containing 8–18% SO_2 ; SO_2 -containing gases from other manufacturing processes are also suitable for the reaction.

For the production of chrome tanning agents, chromium(III) sulfate solutions which are generated in the manufacture of organic intermediates may also be used. Impurities must be removed from such solutions, and the solutions are then converted to the correct basicity

by acidification or neutralization. They must also be concentrated by evaporation.

To manufacture *solid tanning agents*, the concentrated solutions are dried in spray driers made of stainless steel. With a basicity of 33%, the amorphous green powder obtained generally contains 24–26% Cr_2O_3 , 25–27% SO_3 , 22–25% Na_2SO_4 and 22–25% water. In air, the powder absorbs moisture and the particles stick together. Under the microscope, the individual particles, which are often hollow spheres or fragments of such spheres, have a glassy appearance.

The product obtained by spray drying is sold under numerous trade names, e.g., Chrometan (British Chrome and Chemicals, UK); Chromitan (BASF, Germany); Chromosal (Bayer, Germany); Salcromo (Stoppini, Italy); Tanolin (Hamblett & Hayes Co., Mass., USA).

Paper or jute sacks with watertight polyethylene liners or wrappings, or plastic sacks are used for packing.

Solutions of basic chromium(III) sulfate containing 12–18% Cr_2O_3 are also available commercially. Solutions of higher concentration must be kept warm because sodium sulfate precipitates at room temperature. The solutions are transported in rubber-lined rail or road tankers; lead-lined tankers are also suitable.

Besides the standard 33% basic type, a large number of products of higher basicity are available. To improve their stability toward alkali, these contain various quantities of organic acids. The market importance of chrome tanning agents containing 30% chromium oxide and having a basicity of 50% has increased.

In addition to the standard products, mixtures of chrome tanning agents have established themselves on the market. These contain basifying agents which react slowly and eliminate the need for the tedious basifying process. Mixed products containing special organic masking agents and having a high total basicity have recently been developed. These are used in combination with conven-

tional chrome tanning agents and afford a high degree of chromium exhaustion in the liquors.

Potassium chromium(III) sulfate, potassium chrome alum, $\text{KCr}(\text{SO}_4)_2 \cdot 12\text{H}_2\text{O}$, ρ 1.813 g/cm^3 , crystallizes in the cubic system forming violet regular octahedra which decay in air and melt at 89 °C, the color changing to green; the enthalpy of formation is -5788 kJ/mol . The solubility in water at 25 °C is 11.1%. The solution is violet when cold, but becomes green above 50 °C, this change being accompanied by a decrease in the molar conductance. For 0.125 M solution at 50 °C, the molar conductance is $221 \Omega^{-1}\text{cm}^2\text{mol}^{-1}$ for the violet form and $202 \Omega^{-1}\text{cm}^2\text{mol}^{-1}$ for the green form. This change is reversible and its rate is increased by acids. The green form always occurs as an amorphous solid and crystals are unknown.

In addition to the alum containing 12 molecules of water of crystallization, potassium chromium(III) sulfates containing one, two, and six molecules of water are known.

For the preparation of potassium chromium alum, a saturated potassium dichromate solution is reduced with sulfur dioxide in the presence of sulfuric acid.

During the reaction, the temperature must be kept below 40 °C by cooling to prevent the green modification being produced. Apart from sulfur dioxide, such organic compounds as formaldehyde, methanol, or starch are suitable as reducing agents. Crystallization starts after sulfuric acid has been added and the temperature is kept further below 40 °C. If the solution is allowed to settle in vats, large crystals are produced, whereas fine ones result if the solution is stirred. The industrial product contains 15% Cr_2O_3 and 0.01–0.03% Fe. The mother liquor may be reused in the production of the alum solution, but after several cycles it is so enriched in magnesium and sodium sulfate that crystallization of the alum is retarded. The trivalent chromium is then precipitated from the solution with alkali and may be recycled. Lead-lined equipment is used for the production.

The alum can also be prepared from ferrochromium. The reaction with sulfuric acid first results in a solution of chromium(III) and iron(II) sulfates. The majority of the iron(II) sulfate can be removed by crystallization. With potassium sulfate added, the filtrate yields the alum which is contaminated with 0.1–0.2% Fe.

Potassium chrome alum was formerly used on a large scale as a tanning agent in the leather industry, but its importance in this field has receded with the introduction of the basic chromium sulfates. Other fields of application are the textile industry and the film and photographic industry.

Ammonium chromium(III) sulfate, ammonium chrome alum, $\text{NH}_4\text{Cr}(\text{SO}_4)_2 \cdot 12\text{H}_2\text{O}$, ρ 1.72 g/cm^3 , crystallizes in the cubic system forming bluish violet octahedra which appear ruby red when held against the light and slowly decay in air. When heated to 70 °C they turn green, and at 94 °C the compound melts in its water of crystallization. Ammonium chrome alum is obtained from chromium(III) sulfate solutions by addition of a stoichiometric amount of ammonium sulfate. Ammonium chrome alum crystallizes much more easily than potassium chrome alum. The preparation of ammonium chrome alum from carbon-rich ferrochromium has assumed relatively great importance in the electrochemical production of pure chromium metal [88].

46.9.3.3 Other Chromium(III) Salts

Chromium(III) fluoride, CrF_3 , ρ 3.8 g/cm^3 . The anhydrous compound forms highly refractive rhombohedral crystals. It melts above 1000 °C and is distinctly volatile between 1100 and 1200 °C. Chromium(III) fluoride is insoluble in water if no divalent chromium is present. Double compounds are formed with other metal fluorides, e.g., green $\text{CrF}_3 \cdot 2\text{KF} \cdot \text{H}_2\text{O}$.

Hydrates are known which contain three to nine molecules of water. The violet hexaquo-chromium(III) fluoride, $[\text{Cr}(\text{H}_2\text{O})_6]\text{F}_3$, and its

trihydrate, $[\text{Cr}(\text{H}_2\text{O})_6]\text{F}_3 \cdot 3\text{H}_2\text{O}$, can be obtained from hexaaquochromium(III) salt solutions and alkali fluorides. Products containing less water are green. The composition of the industrial product corresponds approximately to $\text{CrF}_3 \cdot 3.5\text{H}_2\text{O}$ and the product contains about 30% chromium.

For the production of chromium(III) fluoride hydrate, chromium(III) oxide hydrate is dissolved in hot aqueous hydrofluoric acid and the green salt crystallizes. Chromium(III) fluoride is used in the textile industry for mordanting wool, for chromating dyestuffs, and in vigoureux printing. Recently, chromium(III) fluorides have also found application in rust-prevention paints as corrosion inhibitors.

Chromium(III) Chloride. *Anhydrous chromium(III) chloride*, CrCl_3 , forms hexagonal reddish violet flakes which sublime at 950°C yielding a vapor that dissociates above 1300°C . The enthalpy of formation is -554.8 kJ/mol . Chromium(III) chloride is insoluble in water if no reducing agent is present. On roasting in air, chromium(III) oxide is produced.

Anhydrous chromium(III) chloride is obtained along with iron(II) chloride by chlorinating roasting of chromite in the presence of carbon at $900\text{--}1050^\circ\text{C}$ [89]. Oxygen is added to the chlorine to prevent nonvolatile residues, in particular minor constituents of the ore, from sintering together. Fractionating condensation between 400 and 640°C has been suggested for separating the chloride vapors [90]. The compound can also be obtained by chlorinating chromium(III) oxide in the presence of reducing agents or by treating ferrochromium with chlorine [91].

Chromium(III) chloride can be prepared readily from chromyl chloride by reaction with carbon monoxide and chlorine. The reaction proceeds rapidly in the gas phase at $750\text{--}850^\circ\text{C}$ [92]. Since chromium(III) chloride evaporates only at a higher temperature, a considerable portion of the product, which varies as a function of the partial pressure, is produced in the form of fine crystals. As the smoke cools down, these act as crystallization nuclei for any gaseous chromium(III) chloride

still present. This procedure prevents the deposition of solid on the cooling surfaces.

Anhydrous chromium(III) chloride has been suggested for chromizing steel parts by surface diffusion; it can be used for the production of high-purity ductile chromium metal by reduction with magnesium and for the synthesis of organic chromium compounds.

Chromium(III) chloride hexahydrate is obtained in pure form by introducing hydrogen chloride and methanol into an aqueous solution of chromic acid. The reaction proceeds exothermally, and adequate cooling must be provided. Of the three isomeric hydrates the dihydrate of the tetraaquodichlorochromium(III) chloride crystallizes in the cold. This is used as an intermediate in the production of chromium complex dyes and other chromium salts, e.g., chromium stearates, which are of interest as impregnating agents for textiles or paper. The solution is also used as a mordant in the textile industry.

Chromium(III) Acetate. The bluish violet hexaaquo salt, $[\text{Cr}(\text{H}_2\text{O})_6](\text{CH}_3\text{COO})_3$, forms needle-shaped crystals. Basic chromium(III) acetates are green. For their preparation chromium(III) hydroxide hydrate is dissolved in dilute acetic acid, and the solid is obtained by drying on drums or in a spray drier. Basic chromium acetates are used as mordants in calico printing and worsted top printing, and also for fixing vigoureux dyes. Combinations of basic chromium(III) acetate and basic chromium(III) formate also find application in the textile industry as mordants. In addition, chromium(III) acetate is used as a starting compound in the production of organic chromium dyes.

Chromium(III) Nitrate. Normally, chromium(III) nitrate crystallizes with nine molecules of water, $[\text{Cr}(\text{H}_2\text{O})_6](\text{NO}_3)_3 \cdot 3\text{H}_2\text{O}$, $\rho 1.8 \text{ g/cm}^3$. The dark violet rhombic prisms become green above 36°C and melt at 66°C . The nitrate group is not bound to the trivalent chromium in a coordination compound. The salt is readily soluble in water, acid, alkali, and alcohol. To prepare chromium(III) nitrate, chromium(III) oxide hydrate is dissolved in

nitric acid and the nitrate is allowed to crystallize. The compound is also produced by reduction of chromic acid with methanol in the presence of nitric acid. During the exothermal reaction, the temperature is kept between 55 and 65°C by cooling. Chromium(III) nitrate is used to a limited extent as a mordant in cotton printing, usually together with basic chromium acetates. In addition, the salt is suitable for producing alkali-free catalysts.

Chromium(III) Phosphate. *Anhydrous chromium(III) phosphate*, CrPO_4 , $\rho 2.99 \text{ g/cm}^3$, is a black powder which belongs to the orthorhombic crystal system. It is insoluble in water, hydrochloric acid, and aqua regia but is attacked by boiling sulfuric acid. It is obtained by calcining its hydrates. The violet *hexahydrate*, $[\text{Cr}(\text{H}_2\text{O})_6]\text{PO}_4$, $\rho 2.12 \text{ g/cm}^3$, precipitates from chromium(III) salt solutions upon addition of phosphoric acid and disodium hydrogen phosphate. The crystals are triclinic and only sparingly soluble in water. Green chromium(III) phosphates precipitated hot contain two to three molecules of water after drying. A salt containing four molecules of water is also known. The green products are virtually insoluble in water. They are used to a small extent as pigments and have corrosion-inhibiting properties.

Chromium lignosulfonates are prepared by reaction of sulfite waste liquor from the pulp industry with sodium dichromate solution, the hexavalent chromium being reduced by the organic material to trivalent chromium. After filtration, the pH is adjusted by means of alkali and the product is dried in spray driers. It is a free-flowing, water-soluble powder and normally contains cations in the following quantities: ammonium $1.5\text{--}2.5\%$, chromium $2.5\text{--}4.2\%$, iron $0\text{--}5\%$, and sodium $1.5\text{--}2.5\%$. These saltlike compounds are used to a large extent in the petroleum industry as additives for lowering the viscosity of drilling muds and decreasing liquid loss [93].

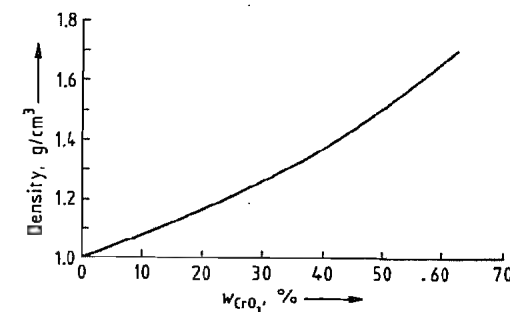


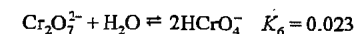
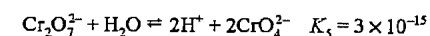
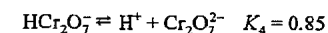
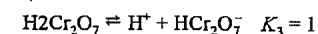
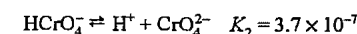
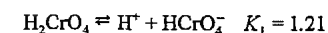
Figure 46.7: Density of aqueous chromic acid solutions at 15.6°C .

46.9.4 Chromic Acids and Chromates(VI)

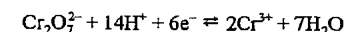
46.9.4.1 Chromic Acids

Chromic acids are not known in the free state. Depending on the method of preparation, mono-, di-, tri-, or tetrachromic acids are formed in aqueous solution. In alkaline or dilute solution, formation of the yellow monochromate ion is favored, but in acid solution or at high concentrations, the orange-red dichromate ion is formed preferentially. Aqueous solutions of chromic acids are, therefore, yellow or red depending on their concentrations. Figure 46.7 shows the density as a function of concentration.

Dissociation constants (at 25°C) are as follows:



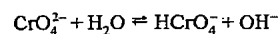
The standard redox potential for the reaction



is 1.36 V .

Chromic acid solutions are strong oxidizing agents with a strongly acidic character, they form salts with metals and bases. The mono-

chromates(VI), M_2CrO_4 , which are derived from chromic acid, hydrolyze in aqueous solution:



The easiest method of preparing chromic acid solutions is to dissolve chromium(VI) oxide in water. In industry, chromic acid is often produced from sodium dichromate(VI) and sulfuric acid.

Chromic acid solutions can also be prepared by anodic oxidation of chromium(III) sulfate solutions [94]; lead-lined cells with a diaphragm and lead electrodes are employed. To keep the concentration of sulfuric acid constant, the chromium(III) sulfate solution is introduced first into the cathode space, where it becomes depleted of sulfuric acid, and then into the anode space. Here, oxidation to chromic acid takes place and the concentration of sulfuric acid is restored to its original value.

In practice, several electrolytic cells are combined to form a unit. At a current density of 3 A/dm² the voltage is 3.5 V. Current efficiency is 80%. Lost chromium is periodically replenished by adding chromium(III) oxide. The electrolytic preparation of chromic acid can also start from chromium hydroxide hydrate with chromic acid as electrolyte [95].

Aqueous chromic acid solutions are used as pickling and chromium-plating baths in the metal processing and plastics processing industries.

46.9.4.2 Alkali Chromates and Dichromates

Sodium chromate, Na_2CrO_4 , *mp* 792 °C, ρ 2.723 g/cm³, ΔH_{298}^0 -1329 kJ/mol, crystallizes in the orthorhombic system in small yellow needles or columns; transformation to the hexagonal form takes place at 413 °C. The bulk density of the powder is 0.7 g/cm³; that of the crystals is 1.67 g/cm³. For solubility, see Table 46.10. The compound is hygroscopic and forms several hydrates: below 19.5 °C the decahydrate; between 19.5 and 25.9 °C, the

hexahydrate; and between 25.9 and 62.8 °C, the tetrahydrate which undergoes transformation into anhydrous sodium chromate above 62.8 °C.

To prepare the salt, sodium dichromate solution is usually mixed with a stoichiometric amount of sodium hydroxide, and the salt solution is then crystallized or spray dried. The 96.5–98.5% product (0.4% NaCl, 2% Na_2SO_4) is stored and dispatched in watertight steel drums.

Sodium chromate is used as a corrosion inhibitor in the petroleum industry and as a dyeing auxiliary in the textile industry.

Sodium Dichromate. The *dihydrate*, $Na_2Cr_2O_7 \cdot 2H_2O$, ρ 2.348 g/cm³, ΔH_{298}^0 -2194 kJ/mol, forms orange-red, monoclinic, translucent needles which are converted into the anhydrous salt above 84.6 °C. The bulk density is 1.2 g/cm³. For solubility, see Table 46.10. The heat of solution is -118 kJ/kg. The compound is very hygroscopic and deliquesces in air; in acid solution, it is a strong oxidizing agent.

Sodium dichromate is the most important of the industrial chromium chemicals and is used as the starting compound for almost all chromium compounds. Large quantities are used in numerous industrial fields. In the textile industry (wool, cotton, silk, and synthetics), sodium dichromate is used in mordanting and in after-treatment baths. The leather industry virtually no longer uses sodium dichromate. Sodium dichromate has a variety of uses in the surface treatment of metals, e.g., in the pickling of steel, aluminum, magnesium, and other metals and their alloys. The ability of the chromates to convert gelatin or protein into an insoluble form on exposure to light is exploited on a large scale in printing technology (lithography). A further field of application for the dichromates is in corrosion protection; they are added to crude oil in pipelines and to water in closed cooling systems as direct corrosion inhibitors. Sodium dichromate is also used for the manufacture of wood preservatives.

Table 46.10: Solubility (in %) of various chromates in water.

		Temperature, °C							
		20	25	40	50	60	75	80	100
Sodium chromate		44.3		48.8		53.5		55.8	56.1
Sodium dichromate dihydrate	70.6	73.18		77.09		82.04		88.39	91.43
Potassium chromate		39.96							45.0
Potassium dichromate	4.3	11.7		20.9		31.3		42.0	50.2
Ammonium chromate	19.78		27.02		34.4		41.2		
Ammonium dichromate	15.16	26.67		36.99		46.14		54.10	60.89
Silver chromate		0.0025			0.0053				0.0041

In the chemical industry, sodium dichromate is used as a strong oxidizing agent in numerous cases; the most important include oxidation of anthracene to anthraquinone (dyes), of aniline to quinone (hydroquinone for the photographic industry), of camphene to camphor, and of contaminants in oils, fats, tallow, and waxes (soap industry, wax bleaching).

To these classical applications, the wide field of catalysts and catalyst carriers containing chromium(III) oxide or chromates has been added over the past thirty years. These are important in a variety of oxidation and carbonizing processes.

Anhydrous sodium dichromate, $Na_2Cr_2O_7$, *mp* 356.7 °C, ρ 2.52 g/cm³, bulk density 1 g/cm³, heat of solution ca. -33.5 kJ/kg, forms light-brown to orange-red plates which are strongly hygroscopic. They decompose above 400 °C with the formation of sodium monochromate(VI), chromium(III) oxide, and oxygen.

Anhydrous sodium dichromate can be prepared by melting down sodium dichromate dihydrate, by crystallizing aqueous dichromate solutions above 86 °C, or by drying sodium dichromate solutions in spray driers.

Anhydrous sodium dichromate is required for cases in which the water content of the dihydrate has an interfering action. Thus, for example, the energy liberated in the oxidation with anhydrous sodium dichromate is greater than that liberated in the case of sodium dichromate dihydrate. Anhydrous sodium dichromate is, therefore, used in the preparation of chromium(III) oxide by the dry process, in pyrotechnics, and in anhydrous oxidation processes where it replaces the more

expensive potassium dichromate. Compared with sodium dichromate dihydrate, anhydrous sodium dichromate has the advantage that it can first absorb two molecules of water (13%) instead of deliquescing immediately when moisture is admitted.

Potassium chromate, K_2CrO_4 , *mp* 968.3 °C, ρ 2.73 g/cm³, ΔH_{298}^0 -1383 kJ/mol, occurs as the stable β -modification. The lemon-yellow, nonhygroscopic prisms are isostructural with K_2SO_4 . At 666 °C they are converted into hexagonal α -potassium chromate. For solubility, see Table 46.10. The heat of solution is -71.3 kJ/kg. The salt crystallizes from aqueous solution in anhydrous form and is thermally stable.

Potassium chromate is obtained by reacting potash with potassium dichromate. The potassium salt has been supplanted nearly completely by the cheaper sodium chromate and is used only for very specific purposes such as in the photographic industry.

Potassium dichromate, $K_2Cr_2O_7$, *mp* 397.5 °C, occurs in two modifications. α - $K_2Cr_2O_7$, tabular or prismatic, bright orange-red triclinic crystals, ρ 2.676 g/cm³, has a bulk density of about 1.3–1.6 g/cm³; at 241.6 °C α - $K_2Cr_2O_7$ transforms to β - $K_2Cr_2O_7$. For solubility, see Table 46.10. The heat of solution is -258.3 kJ/kg. The thermodynamic data are as follows: c_p 219.7 Jmol⁻¹K⁻¹, ΔH_{298}^0 -2033 kJ/mol, S_{298}^0 291.2 Jmol⁻¹K⁻¹, heat of fusion 36.7 kJ/mol. The substance is not hygroscopic and, above the melting point, decomposes into potassium chromate, chromium oxides, and oxygen.

Today potassium dichromate is obtained primarily by conversion of sodium dichromate with potassium chloride. Potassium dichro-

mate has largely been supplanted by the cheaper sodium dichromate but is still used whenever its advantage of being nonhygroscopic is important, for example, in the match, firework, film, and photographic industries. Potassium dichromate is of interest in the preparation of yellow and green zinc pigments.

Ammonium chromate, $(\text{NH}_4)_2\text{CrO}_4$, smells of ammonia and forms golden yellow needles, ρ 1.886 g/cm³, ΔH_{298}° -1152 kJ/mol, S_{298}° 656 Jmol⁻¹K⁻¹. For solubility, see Table 46.10. In air, it decomposes into ammonia, water, and ammonium dichromate. On heating it ignites and decomposes into chromium(III) oxide, ammonia, and nitrogen. Ammonium chromate is prepared from ammonium dichromate with the addition of ammonia.

Ammonium dichromate, $(\text{NH}_4)_2\text{Cr}_2\text{O}_7$, forms large, bright orange-red crystals, ρ 2.155 g/cm³, bulk density ca. 1.0–1.3 g/cm³. For solubility, see Table 46.10. The heat of solution is -230.9 kJ/mol. Ammonium dichromate crystallizes in anhydrous form from aqueous solution and is not hygroscopic. Decomposition, which is not preceded by melting, sets in on heating to 180 °C; this becomes self-maintaining at 225 °C and above. Decomposition proceeds with displays of fire and heat, and large amounts of gas are developed. The products of decomposition are chromium(III) oxide, nitrogen, and water vapor. Ammonium dichromate reacts very violently with organic solvents.

Ammonium dichromate is prepared by reaction of sodium dichromate with ammonium chloride or, less frequently, ammonium sulfate. Ammonium dichromate is used as the starting material for preparing very finely divided chromium(III) oxide and, in addition, finds application primarily in pyrotechnics, wood preservation, and photography (lithography) for the preparation of light-sensitive solutions of gelatin or proteins. Ammonium dichromate is also used to prepare catalysts for organic syntheses. A further field of application is the production of magnetic chromium(IV) oxide. Because of its self-ignition

properties and explosiveness, ammonium dichromate is subject to the German Explosives Law and the IMDG code, class 5.1, UN No. 1439. It is also distributed moist.

46.9.4.3 Other Chromates

Barium chromate, BaCrO_4 , mp 1400 °C (decomp.), ρ 4.498 g/cm³, ΔH_{298}° -1156 kJ/mol, crystallizes as light-yellow transparent rhombic crystals which are isomorphous with barium sulfate. Barium chromate is only sparingly soluble in water but dissolves readily in acids.

In the presence of excess alkali chromate or dichromate, barium chromate has a tendency to form double salts, among which special mention may be made of potassium barium chromate, $\text{K}_2\text{CrO}_4 \cdot \text{BaCrO}_4$, and ammonium barium chromate, $(\text{NH}_4)_2\text{CrO}_4 \cdot \text{BaCrO}_4$, both of which are light yellow.

These barium chromate double salts can be prepared by reaction of soluble barium salts or barium hydroxide with alkali chromate(VI) or dichromate(VI). In weakly acid solutions, as is the case, for example, if dichromates(VI) are used, the precipitation is incomplete. Quantitative precipitation is achieved by adding sodium acetate.

Yellow barium chromate and its double salts can be used for the production of chrome pigments for paints; the double salts, in particular, are excellent corrosion protection paints for all metals. They form sparingly soluble metal chromates, which prevent attack by moisture (condensation, seawater) even more readily than zinc chromate.

Calcium chromate, CaCrO_4 , mp 1020 °C (decomp.), ρ 3.12 g/cm³, is a yellow powder which is sparingly soluble in water (4.3% at 0 °C, 0.42% at 100 °C). The compound has acquired no industrial importance, but its preparation directly from chromium ores is described in several patents [96, 97].

Calcium dichromate, CaCr_2O_7 , ΔH_{298}° -1821 kJ/mol, is thought not to constitute a uniform crystalline phase but to be a mixture of phases consisting of calcium monochromate and

chromium(VI) oxide. The compound forms a series of readily soluble hydrates. Thus, below 10 °C, the hexahydrate $\text{CaCr}_2\text{O}_7 \cdot 6\text{H}_2\text{O}$ exists; between 20 and 40 °C, the pentahydrate; between 50 and 60 °C, the tetrahydrate; and above 70 °C, the monohydrate. A red deliquescent calcium dichromate trihydrate has also been prepared from the tetrahydrate.

Calcium dichromate can be made industrially by oxidative roasting of chromium-containing ores with calcium carbonate or calcium oxide and subsequent leaching of the cake with an acid e.g., chromic or sulfuric acid [97].

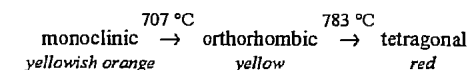
Copper Chromates. Neutral copper chromate, CuCrO_4 , is produced as a yellowish brown, water-containing compound by precipitation from a copper sulfate solution with sodium or potassium dichromate. The compound is used as the starting material for "chrome black" which is prepared by calcining the neutral salt under oxidizing conditions and subsequently leaching with hydrochloric acid.

The double salt *copper ammonium chromate* (cupric ammonium chromate) is required in dyeworks along with logwood and fustic extracts to obtain olive green wool or cotton dyes. Copper chromate is used as such or in reduced form as a catalyst in a number of petrochemical reactions.

Iron Chromates. No anhydrous iron(II) chromate is known. On the other hand, the water-soluble double salts, $\text{KFe}^\text{III}(\text{CrO}_4)_2 \cdot 2\text{H}_2\text{O}$ and $\text{NH}_4\text{Fe}^\text{III}(\text{CrO}_4)_2 \cdot 2\text{H}_2\text{O}$ do exist, and potassium iron(III) chromate is a corrosion inhibitor. A similar corrosion-inhibiting compound is also thought to be formed on steel surfaces that are treated with chromate solutions. Industrially, the compound is produced by the reaction of iron(III) chloride solution with potassium dichromate in an autoclave at 130–160 °C. The precipitate is filtered and dried.

Lead chromate, PbCrO_4 , mp 844 °C (with evolution of oxygen), ρ 6.123 g/cm³, ΔH_{298}°

-910 kJ/mol, is a yellowish orange powder which occurs in three modifications:



The solubility product in water is 1.5×10^{-14} at 18 °C. Lead chromate forms mixed crystals with lead(II) oxide, lead sulfate, and lead molybdate. All these salts are virtually insoluble in water; the molybdenum-containing compound is particularly well-known as molybdenum red. Lead chromate is prepared in a manner similar to that used for barium chromate. The composition, color, and quality of lead chromates depend on the conditions of precipitation; they are used widely as yellow to red pigments in the lacquer and paint industry.

Silver Chromate and Silver Dichromate. Ag_2CrO_4 , ρ 5.625 g/cm³, ΔH_{298}° -711.7 kJ/mol, S_{298}° 216 Jmol⁻¹K⁻¹, c_p 142.3 Jmol⁻¹K⁻¹, and $\text{Ag}_2\text{Cr}_2\text{O}_7$, ρ 4.770 g/cm³, ΔH_{298}° -1218 kJ/mol, form dark red crystals and are soluble in acids, ammonia, and potassium cyanide solutions but not in water. The salts can be precipitated from a silver salt solution with chromate or dichromate solution and are used in the photographic industry.

Zinc chromate, ZnCrO_4 , is sparingly soluble in water but dissolves readily in acids. A series of zinc chromate hydrates exists having the composition $n\text{ZnO} \cdot m\text{CrO}_3 \cdot x\text{H}_2\text{O}$. In industry zinc chromate is known as zinc yellow. Its color may be controlled by the mode of preparation. It is made by the reaction of either a suspension of finely ground zinc white (ZnO) in concentrated sulfuric acid or water-soluble zinc salts (ZnCl_2 , ZnSO_4) with potassium or ammonium dichromate. The zinc chromates prepared in this manner always incorporate potassium or ammonium ions into their lattice. Zinc chromate is used in lacquer primers as a corrosion inhibitor instead of minium (red lead) because of its ability to form insoluble iron(III) chromates with iron or to passivate metal surfaces by oxidation.

46.9.5 Other Chromium Compounds

Chromyl chloride, CrO_2Cl_2 , $mp -96.5^\circ\text{C}$, $bp 116.7^\circ\text{C}$, $p 1.912\text{ g/cm}^3$, is a blood red oily liquid with a pungent smell, $c_p 545\text{ J/kg}^\circ\text{K}^{-1}$, $\Delta H_{298}^\circ -567.8\text{ kJ/mol}$, $S_{298}^\circ 510\text{ J/kg}^\circ\text{K}^{-1}$, heat of fusion 268 kJ/kg . In the temperature range $178\text{--}390\text{ K}$ the vapor pressure obeys the equation

$$\log p = -3340T^{-1} - 9.08 \log T + 35.06$$

where p is in hPa (mbar) and T in K. The liquid is electrically conducting.

Chromyl chloride is easily hydrolyzed; it is an extremely powerful oxidizing and chlorinating agent and, therefore, reacts with organic solvents, often violently. It decomposes in daylight within a week via CrO_2 and Cl_2 to form a series of chromium oxides and chlorides with a low degree of oxidation.

Industrially chromyl chloride is produced from chromium(VI) oxide and hydrogen chloride gas, with concentrated sulfuric acid (>68%) being used primarily to bind the water of reaction. The higher density chromyl chloride is drained, distilled, and collected in cooled receptacles.

Chromyl chloride can also be prepared by using mixtures or molten baths of sodium chloride and alkali chromates or dichromates with fuming sulfuric acid. An elegant route involves the reaction of chromium(VI) oxide with liquid thionyl chloride; these reactants are converted quantitatively into chromyl chloride by elimination of SO_2 .

Hexacarbonylchromium, chromium hexacarbonyl, $\text{Cr}(\text{CO})_6$, $p 1.77\text{ g/cm}^3$, forms colorless, highly refractive crystals which belong to the orthorhombic system. The compound sublimes slowly even at room temperature; when heated in a sealed tube it melts at $149\text{--}150^\circ\text{C}$. The boiling point has been calculated to be 147°C . At 210°C , explosive decomposition occurs. The enthalpy of formation is -1077 kJ/mol . Hexacarbonylchromium is somewhat soluble in chloroform and carbon tetrachloride but insoluble in benzene, ether, alcohol, and acetic acid. It is resistant to water and dilute

acids at room temperature; there is no sign of attack even by concentrated hydrochloric acid or sulfuric acid in the cold, but concentrated nitric acid causes decomposition. No reaction with alkali occurs, but derivatives are produced with ammonia, pyridine, cyclopentadiene, and other organic ligands.

Attempts to synthesize hexacarbonylchromium directly from chromium and carbon monoxide have been unsuccessful. The action of carbon monoxide and a solution of phenylmagnesium bromide in ether on anhydrous chromium(III) chloride suspended in a mixture of benzene and ether produces intermediates that lead to hexacarbonylchromium upon addition of acid and distilling the ether in vacuo. Finely divided sodium can also be used for reduction instead of phenylmagnesium bromide. Yields of up to 80% are reported when very finely divided sodium reacts with anhydrous chromium(III) chloride below 0°C with carbon monoxide at a pressure of about 6 MPa (60 bar); the reaction proceeds in the presence of diethylene glycol dimethyl ether; the mixture is subsequently hydrolyzed while the carbon monoxide pressure is maintained [98].

Applications quoted for hexacarbonylchromium include the tempering and hardening of metal surfaces by chromizing, use as a fuel additive, an intermediate in the preparation of organic chromium compounds, and a catalyst for oxo-syntheses.

Chromium(II) Compounds. In general, compounds of divalent chromium are extremely unstable in air and, therefore, are of only minor importance in industry. Gaseous chromium(II) halides (for preparation, see [99]) are used to produce chromium diffusion layers on iron and nickel parts. Air stable sodium fluorochromate(II) is said to be suitable for the precipitation of metals in electroplating operations and for corrosion-protection coatings [100].

46.9.6 Analysis

Compounds that are insoluble in water and acids, for example, chromium ore, are solubi-

lized by roasting with sodium peroxide [101] in the presence of soda. Chrome-tanned leathers are incinerated before being treated with sodium peroxide. Under these conditions, chromium is completely converted into water-soluble chromate(VI). The roasted mass is leached with hot water and after cooling sulfuric acid is added. Compounds of lower oxidation state that are soluble in water or acids are oxidized with ammonium persulfate to chromate(VI) in dilute boiling sulfuric acid in the presence of silver ions as catalysts [102]. Chloride ions must be removed beforehand. Traces of chloride ions are precipitated by adding a few drops of silver nitrate solution. The chromate(VI) solutions obtained in this way or solutions of chromium(VI) compounds that are soluble in water or sulfuric acid, are then titrated with iron(II) sulfate solution after phosphoric acid is added [103]. The end point of this titration can be determined potentiometrically or by means of a redox indicator, e.g., sodium diphenylamine-4-sulfonate [103]. Iodometric titration of chromate(VI) is also possible [104]. For very low concentrations, e.g., in the analysis of water, atomic absorption spectrometry (AAS) and, in recent years, inductively coupled plasma atomic emission spectrometry (ICP-AES) have proved successful [106]. Trace amounts of chromium are also detected photometrically at 540 nm after oxidation to chromate(VI) and addition of diphenylcarbazide (formation of a reddish violet complex) [105].

46.9.7 Transportation, Storage, and Handling

The toxicity and the effects on the environment of chromium compounds are largely determined by the valency in which the chromium is present. Only tri- and hexavalent chromium compounds, and chromium(IV) oxide, CrO_2 , are of economic importance. Only chromium(VI) compounds are classified as dangerous in regulations relating to chemicals and transportation [107]. According to the IMDG code, the following classifications are applicable for transportation [108]:

$\text{Na}_2\text{Cr}_2\text{O}_7$, $\text{K}_2\text{Cr}_2\text{O}_7$: hazard class 6.1, UN No. 2811; $(\text{NH}_4)_2\text{Cr}_2\text{O}_7$: hazard class 5.1, UN No. 1439; CrO_3 (solid chromic acid): hazard class 5.1, UN No. 1463; chromic acid, solution: hazard class 8, UN No. 1755.

During handling and storage, chromates, dichromates, and chromic acid must not be brought into contact with readily oxidizable substances. The possible hazard to water supplies from chromium(VI) chemicals should also be borne in mind [109].

Throughout the world, the limit of $50\text{ }\mu\text{g/L}$ of chromium recommended by the WHO has been adopted in drinking water regulations. This figure was estimated by the U.S. Public Health Service from the toxicity data, the "No Observable Adverse Effect Level" (NOAEL), and the calculated "average daily intake" (ADI) for $\text{K}_2\text{Cr}_2\text{O}_7$ [110].

46.9.8 Environmental Protection

The following limits are specified in some regulations in Germany [111] and in Japan for the introduction of wastewater into sewage treatment plants: total chromium 2 mg/L max. , chromium(VI) 0.5 mg/L max.

In Germany, the emission of such carcinogenic chromates as calcium chromate, strontium chromate, chromium(III) chromate, and zinc chromate is limited to $1\text{ mg/m}^3\text{ max.}$ (specified as chromium) [112]; the emission of the other chromium compounds is limited to 5 mg/m^3 (specified as Cr).

Within the European Community, refuse that contains chromium(VI) compounds is considered hazardous [113]. In Germany, sewage sludge containing up to 1200 mg per kilogram of chromium may be applied to soil used for agricultural purposes provided the chromium content of the soil does not exceed 100 mg/kg before the application [114]. According to the U.S. Environmental Protection Agency, the chromium content of the soil should not be regarded as a limiting factor for the application of sewage sludge [115]. According to recent studies no harmful effect is to be expected from chromium ions when sewage sludge containing chromium hydroxide is applied to the

soil even if the level presently permitted is exceeded by a factor of 1000 [116].

46.9.9 Ecotoxicology

Insoluble inert chromium(III) oxide, Cr_2O_3 , is the stable mineral end product into which chromium compounds are converted in the environment as a result of natural processes.

Inland Waters. The mean concentration of chromium in surface waters is $< 1\text{--}10\ \mu\text{g/L}$ [117–119]. If trivalent chromium gets into an inland body of water it precipitates as chromium hydroxide in neutral regions. This ages

and becomes increasingly insoluble, with only a small proportion remaining in solution. If chromium(VI) compounds get into inland waters, they are reduced to chromium(III) compounds by the natural content of organic substances.

Table 46.11 summarizes toxicity data for chromium(III) and chromium(VI) compounds in relation to fish, bacteria, algae, daphnia, and plants.

The "water quality criteria documents" in the U.S. Federal Register [133], for example, specify limits for metals in freshwater (Table 46.12).

Table 46.11: Ecotoxicology of chromium compounds.

Species or medium	Chromium(III) compounds	Chromium(VI) compounds
Freshwater fish	CrCl_3 : LC ₅₀ (48 h) minnows, static, 400 mg/L LC ₅₀ (48 h) trout, static, $> 1000\ \text{mg/L}$ [120] LC ₅₀ (48 h) ides, static, 300 mg/L	$\text{K}_2\text{Cr}_2\text{O}_7$: 14 day no observable effect level (NOEL) for zebra fish (<i>Brachydanio rerio</i>) at 50 mg/L [127] or 80 mg/L [128]
Bacteria	$\text{KCr}(\text{SO}_4)_2 \cdot 12\text{H}_2\text{O}$: 100 mg/L proved not to be poisonous for bacteria of the genus <i>Escherichia</i> [121]	$\text{Na}_2\text{Cr}_2\text{O}_7 \cdot 2\text{H}_2\text{O}$: toxic limiting concentration for <i>Pseudomonas putida</i> 0.78 mg/L [129]
Algae	$\text{KCr}(\text{SO}_4)_2 \cdot 12\text{H}_2\text{O}$: incipient injurious effect at 4–6 mg/L (<i>Scenedesmus</i>) [121]	$\text{K}_2\text{Cr}_2\text{O}_7$ (<i>Scenedesmus subspicatus</i>): EC ₁₀ (96 h) 0.5 mg/L [127]; 0.3–1.3 mg/L [130]; 1.8 mg/L [128] EC ₅₀ (96 h) 1.4 mg/L [127]; 1.6–4.7 mg/L [130]
Daphnia	$\text{KCr}(\text{SO}_4)_2 \cdot 12\text{H}_2\text{O}$: marked injurious effect at 42 mg/L [121]	$\text{K}_2\text{Cr}_2\text{O}_7$ (21-day test): concentrations of $> 0.1\ \text{mg/L}$ markedly decreased the production of offspring [128]; swimming ability of <i>Daphnia magna</i> : EC ₀ = 0.3 mg/L; EC ₅₀ = 0.9 mg/L; EC ₁₀₀ = 2.2 mg/L [131]
Mammals (oral, rat)	$\text{Cr}(\text{NO}_3)_3$: LD ₅₀ 3250 mg/kg [122]	$\text{Na}_2\text{Cr}_2\text{O}_7 \cdot 2\text{H}_2\text{O}$: LD ₅₀ 150 mg/kg [132]
Soil mobility	low, only certain complex compounds are biologically available [123]	$\text{K}_2\text{Cr}_2\text{O}_7$: low since chromate is strongly adsorbed on the spodosol type of soil [128, 130] and is also reduced by organic soil constituents
Bioaccumulation	plants, particularly the parts above ground, do not absorb much chromium; accumulation of Cr is prevented at the very beginning of the food chain [124, 125]	$\text{K}_2\text{Cr}_2\text{O}_7$: carp (<i>Cyprinus carpio</i>): no bioaccumulation detected [128]
Higher plants EC ₅₀ * (14 d)	$\text{CrCl}_3 \cdot 6\text{H}_2\text{O}$: <i>Avena sativa</i> (oat) 560 mg of Cr/kg of soil [126] <i>Brassica rapa</i> (turnip) 230 mg of Cr/kg of soil [126]	$\text{K}_2\text{Cr}_2\text{O}_7$: oat: 27 mg/kg [127]; 32 mg/kg [128]; 96 mg/kg [130] turnip: 23 mg/kg [127]; 22 mg/kg [128]; 24 mg/kg [130]
Earthworm LC ₅₀ (28 d)	not known	$\text{K}_2\text{Cr}_2\text{O}_7$: $> 2000\ \text{mg/kg}$ of soil [127] no lethal effects at 1000 mg/kg [130]

*EC = effective concentration; at EC₅₀ growth is retarded by 50% compared with control.

Table 46.12: Limits for chromium and copper (for comparison) in freshwater, $\mu\text{g/L}$ [133].

Oxidation state	Water hardness, CaCO_3 , mg/L		
	50	100	200
Cr(III)	2200	4700	9900
Cr(VI)	21		
Cu(II)	12	22	43

Soil. The chromium content of soil varies very widely depending on the geological conditions. The range is from 5 to 1500 mg/kg, and the average level is about 50 mg/kg [134]. Chromium is found everywhere in the soil of Germany [135], and levels of over 1100 mg/kg may be reached. Such levels are caused solely by geological conditions.

Plants. Chromium occurs in soil in the form of chromium(III) compounds which are available to plants only to a small extent; consequently, chromium is not enriched in the food chain [124, 125, 136–138].

Animals. Grazing animals are not subjected unduly to chromium since only small amounts get into the parts of plants above the ground [131]. Less than 1% of the chromium contained in plants is available to animal and human organisms. To cover essential needs, the chromium must be in a special, biologically suitable form [139].

46.9.10 Economic Aspects [140–143]

The output of chromium ore is subject to considerable variations. Rich ores which are obtained easily by handpicking have declined. This shrinkage in output has to be counterbalanced by exploiting low-grade ores and upgrading them to saleable concentrates. The statistical documents are incomplete and contradictory.

Even the most pessimistic estimates of the worldwide reserves and the extraction possibilities in individual countries do not predict a chromium shortage before the end of this century. In addition, the huge lean-ore deposits in South Africa, Southeast Asia, and the United States, which are still completely untouched,

afford a replacement for the rich ores being mined at present.

In Table 46.13 the consumption of chromium ore is broken down according to products. The refractory brick share is declining because Siemens–Martin steel is being increasingly supplanted by oxygen-blown steel produced in converters with a basic lining.

Table 46.14 shows the share of individual applications in the consumption of chromium chemicals.

The starting material for virtually all chromium chemicals is sodium dichromate prepared from chromium ore.

Table 46.13: Estimated consumption of chromium ore in terms of products in 1984 [141, 144].

Product	World	United States
Ferrochromium, FeSi chromium, chromium metal, and foundry sands	72%	60%
Refractory bricks	12%	20%
Chemicals	17%	20%

Table 46.14: Estimated share (in %) of individual applications in the consumption of chromium chemicals, 1985 (excluding countries with state trading organizations).

	United States	Worldwide
Pigments	22	19
Metal processing	15	24
Tanning	12	32
Wood preservation	26	11
Corrosion protection	5	3
Petroleum industry	5	2
Textile dyes	2	1
Catalysts	2	1
Video tapes	2	2
Remainder	9	5

46.9.11 Toxicology and Occupational Health

Only the hexavalent chromium compounds are biologically active. Metallic chromium and the trivalent compounds, including those in chromium ores, are neither irritating, mutagenic, nor carcinogenic [145]. Sporadic incidences of skin sensitization supposedly caused by chromium(III) were probably caused by traces of chromium(VI) present.

Human Nutrition. Chromium is an essential trace element. The antidiabetogenic factor, a chromium-containing protein compound, is an example of a cofactor for the effect of insulin [146]. Some metabolic processes in animals and humans cannot proceed normally in the event of a chromium deficiency [147–149].

Most foodstuffs in the United States and Germany contain less than 0.1 mg of chromium per kilogram of fresh weight. Excessive levels of chromium in vegetable and animal food are unknown. On the contrary, the supply of chromium as an essential trace element tends to be too low rather than too high in Western industrial countries [150, 151]. The U.S. Food Nutrition Board recommends a daily intake of 50–500 µg for adults [152].

For chromium the gap between essential and toxic concentrations is particularly large. Mammals can tolerate 100 to 200 times the normal chromium content of their bodies without injury [153].

Chromium Dioxide. In a single administration, chromium dioxide is resorptively non-toxic; the lethal dose is greater than 17 000 mg/kg (rats, oral). In rabbits, chromium dioxide causes slight primary irritation of skin and mucous membranes.

Since any chromium dioxide in the normal atmosphere always contains traces of hexavalent chromium, care is taken during production and further processing to ensure that the concentration of chromium dioxide at the workplace does not exceed 0.08 mg/m³, which is approximately equivalent to the MAK of CrO₃ of 0.1 mg/m³. At higher concentrations breathing masks should be worn, for example, grade 2b (DIN 3180).

Employees of chromium dioxide plants are examined annually for chromium contamination. So far no indications have been found of any disease caused by chromium in chromium dioxide production plants.

Hexavalent Chromium Compounds. Particularly chromic acid and the alkali chromates corrode and irritate the skin and mucous membranes.

Acute Effects. Effects of longer exposure to hexavalent chromium compounds vary from irritation of the nasal mucous membrane to the formation of ulcers and perforations of the nasal septum [154].

Higher concentrations irritate the bronchial mucous membrane, thereby leading to bronchitis. Penetration of hexavalent chromium particles into small skin defects — not uninjured skin — causes ulcers which heal badly. Uptake by the digestive system (mostly in suicidal cases) causes serious intestinal inflammation, sometimes with loss of blood. Damage to the renal tubules occurs mainly after dermal absorption. This can lead to kidney failure if the spontaneous reduction capacity of plasma of about 2 ppm (20 minutes) is not sufficient to reduce chromium(VI) to the non-toxic chromium(III). The administration of high doses of ascorbic acid facilitates this reduction, and chromium(III) is then excreted in the urine without causing kidney damage [155].

Chronic Effects. Chronic irritation of the nasal mucous membrane can lead to its atrophy. Chronic bronchitis has been reported following long-term exposure to hexavalent chromium compounds, but this does not occur normally under today's manufacturing conditions [145]. Impairment of breathing has not been observed.

Hexavalent chromium compounds are capable of sensitizing the skin strongly, which may lead to chronic eczemas, particularly when the source is cement dust containing chromium(VI). In contrast, no sensitization of the respiratory tract occurs.

Mutagenicity. All hexavalent chromium compounds are mutagenic, but trivalent chromium compounds do not have any mutagenic potential. In some cases, the hexavalent compounds must first be solubilized to show a mutagenic effect. This effect is counteracted by the reduction of chromium(VI) to chromium(III), for example, by adding body fluids or organ homogenates [156, 157].

Carcinogenicity. Many animal experiments have been carried out to test the carcinogenicity of chromium compounds. These

include subcutaneous injection, inhalation, intratracheal instillation, and introduction of pellets into the bronchial tree [158–161].

According to these experiments the hexavalent compounds of chromium with calcium, strontium, zinc, and chromium(III) (chromic chromate) must be categorized as carcinogenic. Sodium dichromate showed a weak carcinogenic effect only upon intratracheal instillation of doses near to the toxic limits [162]. Lead chromate, chromic acid, and alkali chromates and dichromates are not carcinogenic. Generally, the easily water-soluble as well as the insoluble hexavalent chromium compounds are considered noncarcinogenic, whereas the slightly soluble compounds are carcinogenic [161].

Epidemiology. Trivalent chromium compounds have proved to be noncarcinogenic [163].

Earliest indications of increased incidences of lung cancer among workers in the chromate manufacturing industry were observed in the 1930s. More evidence in support of this observation came from a large number of epidemiological studies done after 1948 [164, 165]. Studies carried out between 1948 and 1956 showed a 25- to 29-fold increase in the incidence of lung cancer. In contrast, investigations carried out since 1979 reflect the effects of improved hygienic working conditions and production processes, for example, by avoiding the use of lime in the oxidative roast of chromium ores (low-lime process). These measures have led to a convergence between the observed and the expected incidences of lung cancer [154, 166–169].

An increased incidence of lung cancer was observed among persons employed in the chromate pigment industry only after exposure to zinc chromate. Lead chromate, on the other hand, showed no carcinogenic effect [170–172]. Results of epidemiological studies carried out during the handling of chromic acid, particularly during chromium plating, are blurred by confounding factors; a statistically significant increase in the rate of lung cancer was not observed [158, 173]. An in-

creased risk of lung cancer has also not been clearly established in the manufacture of ferrochromium [174, 175]. Occupational health care has been provided in the chromate-producing industry for several decades.

Classification. Germany: MAK list, appendix III, class A1: zinc chromate; class A2: calcium chromate, chromium(III) chromate, strontium chromate; class B: alkali chromates, chromium trioxide. The TRK value of calcium, chromium(III), strontium, and zinc chromate is 0.1 mg/m³ (as CrO₃ in total dust). For chromium trioxide, the MAK of 0.1 mg/m³ (as CrO₃) has been established.

United States: According to NIOSH [161], the following chromates are classified as noncarcinogenic: mono- and dichromates of hydrogen, lithium, potassium, sodium, rubidium, cesium, and ammonium, as well as chromic acid anhydride. All other hexavalent chromium compounds are classified as carcinogenic.

The threshold limit value (TLV) is as follows: chromium(VI) compounds 50 µg/m³ (TWA; as chromium); chromium (metal), chromium(II), and chromium(III) compounds 500 µg/m³ (TWA; as chromium).

Biological Monitoring. In addition to the classical assay for chromium in blood or urine, the degree of previous exposure to chromium can be estimated by determining the extent of bound chromium in erythrocytes [176].

46.10 Pigments

46.10.1 Chromium Oxide Pigments

Chromium oxide pigments, also called chromium oxide green pigments, consist of chromium(III) oxide, Cr₂O₃. Chromium oxide green is one of the few single-component pigments with green coloration. Chrome green is a blend of chrome yellow and iron blue pigments; phthalochrome green is a blend of chrome yellow and blue phthalocyanine pigments.

Natural, minable deposits of chromium oxide are not known. In addition to pigment grade, chromium oxide producers usually also offer a technical grade for applications based on properties other than coloration. These include:

- **Metallurgy:** aluminothermic production of chromium metal
- **Refractory industry:** production of thermally and chemically resistant bricks and lining materials
- **Ceramic industry:** coloring of porcelain enamels, ceramic frits, and glazes
- **Pigment industry:** raw material for the production of chromium-containing stains and pigments based on mixed metal oxide phases
- **Grinding and polishing agent:** chromium(III) oxide is used in brake linings and polishing agents due to its high hardness

Chromium oxide hydroxide and hydrated chromium oxide pigments (Grignets Green) have a very attractive blue-green color. They are of low opacity, but provide excellent light-fastness and good chemical resistance. Loss of water on heating limits the application temperature. These pigments are no longer of industrial importance [177].

46.10.1.1 Properties

Chromium(III) oxide crystallizes in the rhombohedral structure of the corundum type; space group $D_{3d}^6-R\bar{3}c$, ρ 5.2 g/cm³. Because of its high hardness (ca. 9 on the Mohs scale) the abrasive properties of the pigment must be taken into account in certain applications [178]. It melts at 2435 °C but starts to evaporate at 2000 °C. Depending on the manufacturing conditions, the particle sizes of chromium oxide pigments are in the range 0.1–3 μ m with mean values of 0.3–0.6 μ m. Most of the particles are isometric. Coarser chromium oxides are produced for special applications, e.g., for applications in the refractory area.

Chromium oxide has a refractive index of ca. 2.5. Chromium oxide green pigments have

an olive green tint. Lighter greens with yellowish hues are obtained with finely divided pigments, and darker, bluish tints with larger particle diameters; the darker pigments are weaker colorants. The maximum of the reflectance curve lies in the green region of the spectrum at ca. 535 nm (Figure 46.8, curve a). A weaker maximum in the violet region (ca. 410 nm) is caused by Cr–Cr interactions in the crystal lattice. Chromium oxide green pigments are used in IR-reflecting camouflage coatings because of their relatively high reflectance in the near infrared (Figure 46.8, curve b).

Since chromium(III) oxide is virtually inert, chromium oxide green pigments are remarkably stable. They are insoluble in water, acid, and alkali and are thus extremely stable to sulfur dioxide and in concrete. They are light-, weather-, and temperature-resistant. A change of the tint only occurs above 1000 °C due to particle growth.

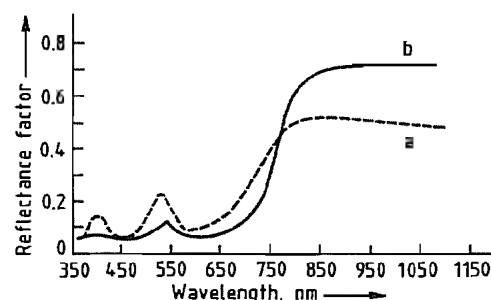


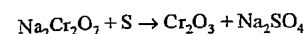
Figure 46.8: Dependence of the reflectance of chromium oxide on the wavelength: a) Regular pigment; b) Special product with larger particle size and high IR reflectance.

46.10.1.2 Production

Alkali dichromates are used as starting materials for the production of chromium(III) oxide pigments. They are available as bulk industrial products in the required purity. High impurity levels have an unfavorable effect on the hue.

Reduction of Alkali Dichromates. In industrial processes, solid alkali dichromates are reacted with reducing agents such as sulfur or carbon compounds. The reaction is strongly

exothermic, and with sulfur proceeds as follows:



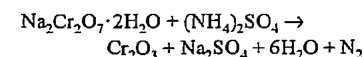
Sodium sulfate can then easily be separated by washing, because it is water soluble. The use of sulfur was first described in 1820 [179]. Roth described the use of $\text{K}_2\text{Cr}_2\text{O}_7$ in 1927 [180]. If charcoal is used in place of sulfur, Na_2CO_3 is formed as by-product [181].

Finely divided sodium dichromate (dihydrate or anhydrous) is mixed homogeneously with sulfur. This mixture is then reacted in a furnace lined with refractory bricks at 750–900 °C. An excess of sulfur is used to ensure completion of the reaction. The reaction mass is leached with water to remove water-soluble components such as sodium sulfate. The solid residue is then separated, dried, and ground.

If potassium dichromate is used instead of sodium dichromate, a green pigment with a more bluish hue is obtained.

If it is to be used as a pigment in paints and lacquers, chromium oxide green can be subjected to jet milling (micronization) to obtain the required properties (e.g., gloss).

Reduction of Ammonium Dichromate. Chromium(III) oxide can be obtained by thermal decomposition of ammonium dichromate. Above ca. 200 °C, a highly voluminous product is formed with elimination of nitrogen [182]. The pigment is obtained after addition of alkali salts (e.g., sodium sulfate) and subsequent calcination [183]. In the industrial process, a mixture of ammonium sulfate or chloride and sodium dichromate is calcined [184]:



The workup is then carried out as described above. A chromium oxide pigment obtained by this process typically contains (%):

Cr_2O_3	99.0–99.5
SiO_2	0.05 (max.)
Al_2O_3	0.1 (max.)
Fe_2O_3	0.05 (max.)
S	ca. 0.02
Water	ca. 0.3

Chromium oxides with a minimal sulfur content are preferred for metallurgical appli-

cations. These are obtained by reacting sodium dichromate with ammonium chloride or sulfate in a deficiency of 10 mol% [185]. Chromium(III) oxides with a low sulfur content can also be obtained by thermal aftertreatment [186]. Thermal decomposition of chromic acid anhydride (CrO_3) yields high-purity chromium(III) oxide [187].

The pigment properties of chromium oxides can be modified by precipitation of hydroxides (e.g., of titanium or aluminum), and subsequent calcining. This treatment changes the color to yellow-green, and decreases the flocculation tendency [188]. Aftertreatment with organic compounds (e.g., alkoxyated alkylsulfonamides) is also used [189].

Other Processes. Other production processes are suggested in the patent literature, but have not so far gained industrial importance. For instance, sodium dichromate can be mixed with heating oil and reacted at 300 °C. The soda formed must be washed out prior to calcining at 800 °C to avoid reoxidation in the alkaline melt [190].

In alkaline solution, sodium chromate can be reduced with sulfur at atmospheric pressure with formation of sodium thiosulfate. After neutralization, more sodium chromate is added to exhaust the reducing capacity of the thiosulfate. The mixture is calcined at 900–1070 °C [191].

Another process involves the shock heating of sodium dichromate in a flame at 900–1600 °C in the presence of excess hydrogen and chlorine to bind the alkali as sodium chloride [192]. This method is suitable for the preparation of pigment-grade chromium oxide of high purity, with an especially low sulfur content.

Environmental Protection. Since alkali dichromates or chromic acid anhydride are used as starting materials for the production of chromium(III) oxides, occupational health requirements for the handling of hexavalent chromium compounds must be observed [193]. The sulfur dioxide formed on reduction with excess sulfur must be removed from the

flue gases according to national regulations, e.g., by oxidation to H_2SO_4 .

Process wastewater may contain small amounts of unreacted chromates; recovery is uneconomical. Prior to release into drainage systems, the chromates in these wastewater streams must be reduced (e.g., with SO_2 or NaHSO_3) and precipitated as chromium hydroxide [194]. In Germany, for example, the minimum requirements for wastewater in the production of chromium oxide pigments are specified in [195].

46.10.1.3 Quality Specifications and Analysis

International, technical specifications for chromium oxide pigments are defined in ISO 4621 (1986), they must have a minimum Cr_2O_3 content of 96%.

Various grades are defined according to their particle fineness as measured by the residue on a 45- μm sieve: grade 1, 0.01% residue (max.); grade 2, 0.1% (max.); and grade 3, 0.5% (max.).

ISO 4621 (1986) also specifies analytical methods. Usually, analysis of chromium and the by-products is preceded by melting with soda and sodium peroxide. The content of water-soluble or acid-soluble chromium is becoming important from the toxicological and ecological point of view. It is determined according to DIN 53780 with water, or according to ISO 385615 with 0.1 mol/L hydrochloric acid.

46.10.1.4 Storage and Transportation

Chromium(III) oxide pigments are thermally stable and insoluble in water. They are not classified as hazardous materials and are not subject to international transport regulations. As long as they are kept dry their utility as a pigment is practically unlimited.

46.10.1.5 Uses

The use of chromium(III) oxide as a pigment for toys, cosmetics, and in plastics and paints that come in contact with food is permitted in national and international regulations [196–203]. Maximum limits for heavy metals or their soluble fractions are usually a prerequisite. Because pure starting materials are used, these limits are satisfied by most types of chromium oxide.

Chromium oxide is equally important as a colorant and in its other industrial applications. As a pigment, it is used predominantly in the paint and coatings industry for high quality green paints with special requirements, especially for steel constructions (coil coating), facade coatings (emulsion paints), and automotive coatings.

A series of RAL (Reichs Ausschuss für Lieferbedingungen) tints (e.g., Nos. 6003, 6006, 6011, 6014, and 6015) can be formulated based on chromium oxide. As mentioned previously, chromium oxide is also an important pigment for the formulation of green camouflage coatings (e.g., RAL 6031-F 9, Natogreen 285, Stanag 2338, and Forestgreen MIL-C-46168 C).

Except for the expensive cobalt green, chromium oxide is the only green pigment that meets the high color stability requirements for building materials based on lime and cement [204]. In plastics, however, chromium oxide green is only of minor importance because of its dull tint.

The industrial significance of chromium oxide is due to its chemical and physical properties. Its high purity makes it suitable as a starting material for the aluminothermic production of very pure chromium metal.

Since the late 1970s chromium oxide has gained significance as a raw material in the refractory industry. The addition of chromium oxide to bricks and refractory concrete based on alumina significantly improves their stability against slag in the production and processing of pig iron. Chromium oxide bricks containing ca. 95% Cr_2O_3 have become important in the production of E-glass fibers for

lining melting tanks. These linings have substantially improved furnace stability (i.e., prolonged furnace life).

The high hardness of chromium oxide resulting from its crystal structure is exploited in polishing agents for metals and in brake linings. Addition of a small amount of chromium oxide to magnetic materials of audio and video tapes imparts a self-cleaning effect to the sound heads.

46.10.1.6 Economic Aspects

Important producers are American Chrome and Chemicals (USA), Bayer (Germany), British Chrome and Chemicals (UK), and Nihon Denko (Japan).

Statistical data on the consumption of chromium oxide have not been published recently. However, it can be assumed that 37 000 t of chromium oxide, including 18 000 t as pigment, were consumed in 1990 worldwide excluding the former Eastern bloc and China. Chromium oxide is produced in the former Soviet Union and China, but reliable data on production and consumption are not available.

46.10.1.7 Toxicology and Occupational Health

Toxicological or carcinogenic effects have not been detected in rats receiving up to 5% chromium(III) oxide in their feed [205] nor in medical studies performed in chemical plants producing chromium(III) oxide and chromium(III) sulfate [206]. The oral LD_{50} for chromium(III) oxide in the rat is $> 10\,000\text{ mg/kg}$; it does not irritate the skin or mucous membranes.

Chromium(III) oxide is not included in the MAK list (Germany), the TLV list (USA), or in the list of hazardous occupational materials of the EC [207]. In practice, this means that chromium(III) oxide can be regarded as an inert fine dust with a MAK value of 6 mg/m^3 .

46.10.2 Chromate Pigments

The most important chromate pigments include the lead chromate (chrome yellow) and lead molybdate pigments (molybdate orange and molybdate red) whose colors range from light lemon yellow to reds with a blue hue. Chrome yellow, molybdate orange, and molybdate red are used in the production of paints, coatings, and plastics, and are characterized by brilliant hues, good tinting strength, and good hiding power. Special treatment of the pigments has allowed continual improvement of their resistance to light, weathering, chemicals, and temperature.

The chromate pigments are also combined with blue pigments (e.g., iron blue or phthalocyanine blue) to obtain high-quality chrome green and fast chrome green pigments. Molybdate orange and molybdate red pigments are often combined with red organic pigments, giving a considerable extension of the color range.

Lead chromates, lead molybdates, chrome greens, and fast chrome greens are supplied as pigment powders, low-dust or dust-free preparations, or as pastes.

46.10.2.1 Chrome Yellow

The chrome yellow pigments, C.I. Pigment Yellow 34:77600 and 77603, are pure lead chromate or mixed-phase pigments with the general formula $\text{Pb}(\text{Cr}, \text{S})\text{O}_4$ [208] (refractive index 2.3–2.65, density ca. 6 g/cm^3). Chrome yellow is insoluble in water. Solubility in acids and alkalis and discoloration by hydrogen sulfide and sulfur dioxide can be reduced to a minimum by precipitating inert metal oxides on the pigment particles.

Both lead chromate and lead sulfochromate (the latter is a mixed-phase pigment) can be orthorhombic or monoclinic; the monoclinic structure is the more stable [209]. The greenish yellow orthorhombic modification of lead chromate is metastable at room temperature, and is readily transformed to the monoclinic modification under certain conditions (e.g.,

concentration, pH, temperature). The latter modification occurs naturally as crocoite.

Partial replacement of chromate by sulfate in the mixed-phase crystals causes a gradual reduction of tinting strength and hiding power, but allows production of the important chrome yellows with a greenish yellow hue.

Production. In large-scale production, lead or lead oxide is reacted with nitric acid to give lead nitrate solutions, which are then mixed with sodium dichromate solution. If the precipitation solutions contain sulfate, lead sulfochromate is formed as a mixed-phase pigment. After stabilization the pigment is filtered off, washed until free of electrolyte, dried, and ground.

The color of the pigment depends on the ratio of the precipitating components and other factors during and after precipitation (e.g., concentration, pH, temperature, and time). According to WAGNER [210], the precipitated crystals are orthorhombic, but change very readily to the monoclinic form on standing; higher temperatures accelerate this conversion. Almost isometric particles that do not show any dichroism can be obtained by appropriate control of the process conditions. Needle-shaped monoclinic crystals should be avoided because they lead to disadvantages such as low bulk density, high oil absorption, and iridescence in the coating film.

Unstabilized chrome yellow pigments have poor lightfastness, and darken due to redox reactions. Recent developments have led to improvements in the fastness properties of chrome yellow pigments, especially toward sulfur dioxide and temperature. This has been achieved by coating the pigment particles with compounds of titanium, cerium, aluminum, antimony, and silicon [211–219].

Carefully controlled precipitation and stabilization provide chrome yellow pigments with exceptional fastness to light and weathering, and very high resistance to chemical attack and temperature, enabling them to be used in a wide field of applications. The following qualities are commercially available:

- Unstabilized chrome yellows (limited importance)
- Stabilized chrome yellows with high color brilliance, stable to light and weathering
- Highly stabilized chrome yellow pigments
 - very stable to light and weathering
 - very stable to light and weathering, and resistant to sulfur dioxide
 - very stable to high temperature, light, and weathering
 - very stable to high temperature, sulfur dioxide, light, and weathering

● Low-dust products (pastes or powders)

Lightfast chrome yellow pigments that are coated with metal oxides (e.g., of aluminum, titanium, manganese) are produced by Du Pont [212].

A chrome yellow that is coated with large amounts of silicate and alumina and which shows improved stability to temperature, light, and chemicals is also produced by Du Pont [213].

Bayer describes pigments containing lead chromate stabilized in aqueous slurry with silicate-containing solutions and antimony(III), tin(II), or zinc compounds [214].

ICI produces light- and weatherfast chrome yellow pigments stabilized with antimony compounds and silicates in the presence of polyhydric alcohols and hydroxyalkylamines [215].

Ten Horn describes a process for the production of lead sulfochromate containing at least 50% lead chromate [216]. This has a low acid-soluble lead content (< 5% expressed as PbO, by BS 3900, Part B3, 1965).

BASF produces temperature-stable lead chromate pigments with a silicate coating obtained by hydrolysis of magnesium silicofluoride [217].

Heubach has developed a process for the alternate precipitation of metal oxides and silicates [218, 219]. A homogenizer is used to disperse the pigment particles during stabilization. Products obtained have a very good temperature resistance and very low lead solu-

bility in acid (< 1% Pb by DIN 55770, 1986 or DIN/ISO 6713, 1985).

Continuous processes for the production of chromate pigments have been developed in the United States and Hungary [220, 221].

Uses. Chrome yellow pigments are mainly used for paints, coil coatings, and plastics. They have a low binder demand and good dispersibility, hiding power, tinting strength, gloss, and gloss stability. Chrome yellows are used in a wide range of applications not only for economic reasons, but also on account of their valuable pigment properties. They are important base pigments for yellow colors in the production of automotive and industrial paints.

Chrome yellow pigments stabilized with a large amount of silicate play a major role in the production of colored plastics (e.g., PVC, polyethylene, or polyesters) with high temperature resistance. Incorporation into plastics also improves their chemical resistance to alkali, acid sulfur dioxide, and hydrogen sulfide.

Chrome green and fast chrome green mixed pigments are produced by combining chrome yellow with iron blue or phthalocyanine blue.

World production of chrome yellow in 1996 was 37 000 t.

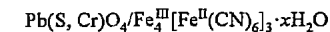
46.10.2.2 Chrome Orange

Chrome orange, C.I. Pigment Orange 21:77601, is a basic lead chromate with the composition $\text{PbCrO}_4 \cdot \text{PbO}$ but is no longer of technical or economic importance.

This product was obtained by precipitating lead salts with alkali chromates in the alkaline pH range. By controlling the pH and temperature, the particle size and thus the hue could be varied between orange and red.

46.10.2.3 Chrome Green and Fast Chrome Green

Chrome greens, C.I. Pigment Green 15:77510 and 77600, are combined or mixed pigments of chrome yellow and iron blue with the formula



Fast chrome greens, C.I. Pigment Green 48:77600, 74160, and 74260, are combinations of chrome yellow and phthalocyanine blue or phthalocyanine green. For high-grade fast chrome greens, stabilized and highly stabilized chrome yellows are usually used.

The density and refractive index of the chrome greens and fast chrome greens depend on the ratio of the components of the mixture. Their hues vary from light green to dark blue-green, again depending on the ratio of the components.

Production. Chrome green and fast chrome green pigments can be prepared by dry or wet mixing.

Dry Mixing. The yellow and blue or green pigments are mixed and ground in edge runner mills, high-performance mixers, or mills giving intimate contact of the pigment particles. Excessive increase of temperature must be avoided, because this can lead to spontaneous combustion [222]. Differences in the density and particle size of the components can lead to segregation and floating of the pigment components in the coating. Wetting agents are therefore added to avoid these effects [223].

Wet Mixing. Pigments with brilliant colors, high color stability, very good hiding power, and good resistance to floating and flocculation are obtained by precipitating one component onto the other. Solutions of sodium silicate and aluminum sulfate or magnesium sulfate are then added for further stabilization [224].

Alternatively, the components are wet milled or mixed in suspension and then filtered. The pigment slurry is dried, and the pigment is ground.

Uses. Chrome greens have very good dispersibility, resistance to flocculation, bleeding, and floating and very good fastness properties. This is especially true of the fast chrome greens that are based on high-grade phthalocyanine and highly stabilized chrome yellows. They are therefore used in the same applications as chrome yellow and molybdate red

pigments (i.e., for the pigmentation of coating media and plastics).

Pigments consisting of zinc potassium chromates combined with blue pigments are no longer of importance.

46.10.2.4 Toxicology and Occupational Health

Occupational Health. Precautions have to be taken and workplace concentration limits have to be observed when handling lead- and lead chromate-containing pigments. General regulations exist for all lead-containing materials [225]. Concentration limits are as follows:

MAK value (lead)	< 0.1 mg/m ³
BAT values	
Lead (blood)	< 70 µg/dL
Lead (blood – women < 45 years)	< 30 µg/dL
δ-Aminolevulinic acid	
(urine, Davies method)	< 15 mg/L
(women < 45 years)	< 6 mg/L
TLV-TWA value (lead)	< 0.15 mg/m ³

It is accepted that the BAT limit has been complied with if the blood lead level does not exceed 50 µg/dL (or for women of < 45 years, 30 µg/dL).

The EEC Directive EEC 82/605 specifies maximum lead concentrations in the air of < 150 µg/m³ and permitted blood lead levels of 70–80 µg/dL, with δ-aminolevulinic acid values of 20 mg/g creatinine [226].

MAK limits for lead chromates and lead chromate pigments are not given. They are classified as substances suspected of having carcinogenic potential (MAK: Group IIIB; TLV-TWA: 0.05 mg Cr/m³, A 2). However, extensive epidemiological investigations have given no indication that the practically insoluble lead chromate pigments have any carcinogenic properties [227, 228]. Such properties have been reported for the more soluble zinc chromate and strontium chromate pigments.

These chromate pigments can be safely handled if the various rules and regulations regarding concentration limits, safe working practices, hygiene and industrial medicine are adhered to.

Environmental Aspects. Dust emissions from approved manufacturing plants must not exceed 5 mg/m³ for lead and chromium with a total mass flow exceeding 25 g/h (TA-Luft) [229].

According to latest German wastewater legislation [230] for inorganic pigment manufacturing processes discharging directly into public stretches of water, mass limits for lead and chromium related to tonnes of average output (t_{prod}) are:

Lead	0.04 kg/ t_{prod}
Chromium (total)	0.03 kg/ t_{prod}

These requirements recently replaced earlier legislation dating from 1984 [231]. Lower limits might be set by local or regional authorities, even for “nondirect” discharges into municipal sewer systems.

Waste containing lead and lead chromate that cannot be recycled must be taken to a special waste disposal site under proper control.

Labeling. In the EC lead chromate and lead chromate pigments must be appropriately labeled. Such substances must be marked with a skull and crossbone (T) [232, 233]. Additionally, the following risk (R) and safety phrases (S) must be used:

R61	May cause harm to the unborn child
R62	Possible risk of impaired fertility
R33	Danger of cumulative effects
R40	Possible risks of irreversible effects
S53	Avoid exposure — obtain special instructions before use.
S45	In case of accident or if you fell unwell, seek medical advice immediately (show the label where possible).

In the 21st adaptation to EEC Council Directive 67/548, the lead chromate pigments C.I. Pigment Yellow 34 and C.I. Pigment Red 104 have been added individually [234]. These pigments are classified in the same manner as lead chromate and must be labeled with a skull and crossbone (T) and the above mentioned risk (R) and safety phrases (S).

According to the EEC Council Directive for the labeling of preparations [235] in conjunction with the 21st adaption to EEC Council Directive 67/548, Nota 1 [234], such materials containing more than 0.5% lead are labeled in the same way as the pure lead pig-

ment, with a skull and crossbone (T) and the corresponding R and S phrases.

With respect to improved protection of public health, special restrictions on carcinogenic and teratogenic substances and their corresponding preparations have been established by the 14th amendment of EEC Council Directive EEC 76/769 [236].

In accordance with the 14th amendment of EEC Council Directive EEC 76/769 [236] and revised ChemVerbV [237], lead chromate-based pigments and preparations are no longer permitted to be used by private consumers and have to be labeled with the phrase “Only for industrial purposes”.

Lead-containing coatings and paints with a total lead content exceeding 0.15% of the total weight of the preparation must carry the phrase “Contains lead. Should not be used on surface liable to be chewed or sucked by children” in accordance with EEC Council Directive 89/178 [238] and German GefStoffV [232].

Lead chromate pigments are not permitted for use as coloring materials for plastic for consumer goods [239] or for coatings for toys, according to European Standard EN 71 part 3 [240].

For transportation, the labeling to be used (GGVS/GGVE, ADR/RID) for the pigment as well as for its preparations is class 6.1, No. 62c, hazard symbol 6.1A, and a skull and crossbone, if the lead content soluble in hydrochloric acid [$c(\text{HCl}) = 0.07 \text{ mol/L}$] exceeds 5%.

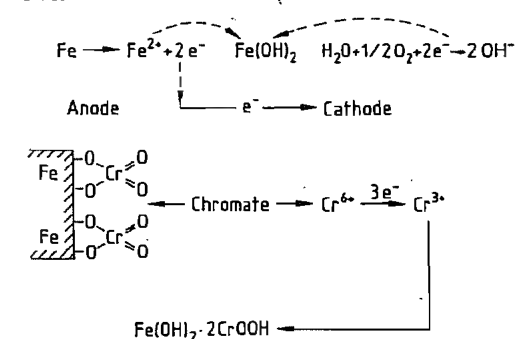


Figure 46.9: Passivation of iron by chromate pigments [248, 249].

46.10.2.5 Anticorrosive Chromate Pigments

Anticorrosive chromate pigments are summarized in Table 46.15.

The anticorrosive action of the chromate pigments is based both on chemical and electrochemical reactions [241–247]. Electrochemical passivation and chemical reaction are illustrated in Figure 46.9 [248, 249]. Passivation is based on electrochemical processes in the cathodic region. In addition, a protective film is also formed by reaction of chromate ions with metal ions at the surface of the substrate to form metal oxide hydrates.

The anticorrosive properties of this class of pigments depend on:

- The content of water-soluble chromate ions
- The ratio of water-soluble chromate ions to water-soluble corrosion-promoting ions (chloride and sulfate ions)
- The active pigment surface in the coating (i.e., particle size distribution and dispersibility)

Chromate-containing pigments are classified as toxic; their use is therefore very limited and they must be appropriately labeled [250, 251].

Zinc-Containing Chromate Pigments. Zinc chromate is produced by reacting an aqueous slurry of zinc oxide or hydroxide with dissolved chromate ions followed by neutralization, or by precipitation of dissolved zinc salts with dissolved chromate salts. Zinc tetraoxychromate is produced from zinc oxide and chromic acid in an aqueous medium. Basic zinc potassium chromate is obtained by reacting an aqueous slurry of zinc oxide with potassium dichromate and sulfuric acid. The pigments are washed, filtered, dried, and ground.

Table 46.15: Metallic anticorrosive chromate pigments.

Name	Formula	Synonym	Appearance	Solubility in water, g/L
Zinc chromate	ZnCrO ₄	chromic acid-zinc salt (1:1) zinc yellow C.I. Pigment Yellow 36	lemon yellow powder	insoluble
Zinc tetraoxycromate	ZnCrO ₄ ·4Zn(OH) ₂	basic zinc chromate ZTO chromate zinc tetrahydroxycromate C.I. Pigment Yellow 36	yellow powder	ca. 0.04
Basic zinc potassium chromate	4ZnO·K ₂ O·4CrO ₃ ·3H ₂ O	basic zinc chromate zinc chromate pigment lemon yellow C.I. Pigment Yellow 36	lemon yellow triclinic flakes	2.5-5
Zinc potassium chromate	KZn ₂ (CrO ₄) ₂ OH	chromic acid-potassium zinc salt (2:2:1) zinc yellow C.I. Pigment Yellow 36	yellow powder	sparingly soluble
Strontium chromate	SrCrO ₄	strontium chromate A strontium yellow C.I. Pigment Yellow 32	yellow powder	ca. 2

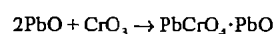
Trade names include Zinkchromat CZ20-CZ40 (SNCZ, France); Zinkchromat 1W (BASF, Germany); and Zinktetraoxichromat TC 20-TC 40, LOW DUST (SNCZ, France).

Strontium Chromate. Strontium chromate is precipitated from solutions of sodium dichromate and strontium chloride, followed by filtration, washing, drying, and grinding. A primer composition based on strontium and calcium chromates is described in [252, 253].

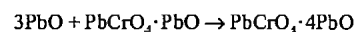
A *trade name* for strontium chromate pigments is Strontiumchromat L203 S-L203 E (SNCZ, France).

Lead Silicochromate [254]. Lead silicochromate, 4(PbCrO₄·PbO) + 3(SiO₂·4PbO), is an orange powder. This pigment is a core pigment, in which the active pigment substance (PbCrO₄) is precipitated onto an inert core (SiO₂).

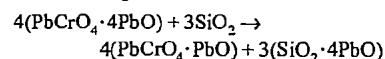
In the production process used by National Lead Industries, a solution of chromic acid is added to an aqueous slurry of lead oxide, finely ground silica, and a small amount of basic lead acetate:



The product is heated in a rotary kiln causing the excess lead oxide to react with the basic lead chromate, forming tetrabasic lead chromate:



On raising the temperature the following reaction takes place on the surface of the silica:



The pigment contains 47% PbO, 5.4% CrO₃, and 47.6% SiO₂. Properties are as follows: density 4.2 g/cm³, oil number 15 g/100 g, tamped volume 163 cm³/100 g, sieve residue (> 42 μm) 0.004%, moisture content 0.1%, and pH ca. 7.

A *trade name* for lead silicochromate is Onor (National Lead Chemicals, USA) [255].

46.10.3 Chromium Dioxide

In the course of the development of pigments for magnetic information storage, CrO₂ was the first pigment material that gave a higher recording density than γ-Fe₂O₃. In the field of audio recording this led to the IEC II standard or "chrome position".

Physical Properties. Chromium dioxide, chromium(IV) oxide, CrO₂, is a ferromagnetic material with a specific saturation magnetization M_s/p of 132 Am²/kg at 0 K corresponding to the spin of two unpaired electrons per Cr⁴⁺ ion. The M_s/p value of CrO₂ at room temperature is ca. 100 Am²/kg [256]; CrO₂ magnetic pigments reach values of 77-92 Am²/kg. The material crystallizes with a tetragonal rutile lattice in the form of small needles which have

the desired magnetic shape anisotropy. The morphology of the particles can be varied with several dopants, particularly antimony and tellurium [257]. The coercive field strength (in addition to shape) can be controlled by doping with transition metal ions which modify the magnetocrystalline anisotropy of the material; the Fe³⁺ ion being industrially important [258]. Depending on the iron content up to ca. 3 mol%, H_c values of CrO₂ may vary between 30 and 75 kA/m [259, 260]. Iron doping also increases the Curie temperature from 115 to ca. 170 °C. Because the Fe³⁺ ions are coupled antiferromagnetically with Cr⁴⁺ ions in the crystal lattice, the saturation magnetization (M_s/p) of CrO₂ decreases with increasing dopant levels [261].

Other important properties of CrO₂ when used as a magnetic pigment are its black color, electrical conductivity (2.5-400 Ω⁻¹cm⁻¹ [262]) and relatively high crystal hardness (Mohs hardness 8-9 [263]). Therefore, coating formulations based on CrO₂ require less or even no additives such as carbon black (good conductivity, black color) or refractory oxides such as alumina.

Chemical Properties. Pure CrO₂ slowly disproportionates in the presence of water. The CrO₂ crystal surface of commercial pigments is therefore topotactically converted to β-CrOOH which serves as a protection layer [264]. The conditions for this reaction have a great influence on the chemical properties of the pigment surface [265, 266]. Thus, the isoelectric point in water can vary between pH 3 and 7 [263], which affects dispersibility. In the absence of moisture, CrO₂ is stable up to ca. 400 °C; above this temperature it decomposes to form Cr₂O₃ and oxygen.

Uses and Economic Aspects. Chromium dioxide is used exclusively for magnetic recording media, e.g., tapes for audio, video, and computer applications. An application of particular interest depends on its relatively low Curie temperature. This allows thermomagnetic duplication at temperatures low enough for the base polymer of magnetic tapes, and is exploited in a commercial, high-speed copy-

ing process [267]. Chromium dioxide may also be used in combination with cobalt-modified iron oxides in the production of magnetic recording media. The world production of CrO₂ in 1990 amounted to 8000 t, ca. 12% of the total consumption of magnetic pigments. Producers are BASF and Du Pont.

Table 46.16: Composition and properties of chromium phosphate pigments.

Property (standard)	Chromium phosphate ZnPO ₄ ·3H ₂ O
Metal content, % (ISO 787, part 2)	ca. 27
Phosphate content, % (ISO 787, part 2)	ca. 47
Chloride content, % (ISO 787, part 13)	< 0.1
Sulfate content, % (ISO 787, part 13)	0.04
Water-soluble content, % (ISO 787, part 3)	0.4
Sieve residue, % (ISO 787, part 18)	max. 0.3
Density, g/cm ³ (ISO 787, part 10)	2.5
Specific surface area, m ² /g (DIN 66131/66132)	22
Loss on ignition, % (ISO 787, part 2)	26
Oil absorption value, g/100 g (ISO 787, part 5)	65
Conductivity, μS (ISO 787, part 14)	ca. 500
pH (ISO 787, part 9)	6.5
Color	green

46.10.4 Chromium Phosphate [268, 269]

Chromium phosphate, CrPO₄·3H₂O, is produced from chromium(III) salts and alkali phosphates. The physical and chemical properties are listed in Table 46.16 [268].

Chromium phosphate has a low solubility. It is therefore nearly always used in combination with other anticorrosive pigments. It is an extremely good long-term inhibitor, but is less effective during the initial phase of corrosion protection.

46.11 References

1. Gmelin, Chromium, Part A (1962) pp. 1-5.
2. J. W. Mellor: *Comprehensive Treatise on Inorganic and Theoretical Chemistry*, vol. 11, Longmans Green & Co., London 1931, p. 122.
3. M. J. Udy: *Chromium*, vol. 1, Reinhold Publ. Co., New York 1956, p. 1.

4. J. F. Papp: "Mineral Facts and Problems", U.S. Bureau of Mines Bulletin no. 675, 1985, Chapter on Chromium.
5. T. Matsumura, J. Hagiya, *Toya Soda Kenkyu Hokoku* 22 (1978) no. 2, 75-89.
6. C. L. Rollinson: *Comprehensive Inorganic Chemistry*, vol. 3, Pergamon Press, Oxford 1973, p. 624.
7. F. A. Cotton, G. Wilkinson: *Advanced Inorganic Chemistry*, Interscience, New York 1966, p. 818.
8. L. B. Pankratz: "Thermodynamic Properties of Elements and Oxides", U.S. Bureau of Mines Bulletin no. 672, 1982, p. 117.
9. A. H. Sully: *Chromium*, Academic Press, New York 1954, pp. 21-29.
10. M. C. Carosella, J. D. Mettler, *Met. Prog.* 69 (1956) no. 6, 51.
11. J. B. Rosenbaum, R. R. Lloyd, C. C. Merrill, U.S. Bureau of Mines, R.I. no. 5322, March, 1957.
12. M. Pourbaix: *Atlas of Electrochemical Equilibria*, Pergamon Press, Oxford 1966, p. 262.
13. H. F. Reichard, H. R. Spendelow, "Chromium", London Metal Bulletin Survey, London 1977.
14. A. N. Rakitskii, V. I. Trefilov, *Poroshk. Metall.* 160 (1976) no. 4, 20-30.
15. Shin Nippon Iron K.K., JP 54156013, 1979 (K. Katayama).
16. SAE, ASTM (eds.): *Metals & Alloys in the Unified Numbering System*, 4th ed., SAE, Warrendale, Pa., 1986, pp. 185-195, 209-211, 217, 359-361.
17. R. C. Gibbons: *Woldman's Engineering Alloys*, 6th ed., American Society for Metals, Metals Park, Ohio, 1979.
18. K. Wellinger, P. Gimmel, M. Bodenstein: *Werkstofftabellen der Metalle*, 7th ed., Kroner, Stuttgart 1972.
19. Union Carbide Corp., US 3592637, 1971.
20. P. D. Deeley, K. J. A. Kundig, H. R. Spendelow, Jr.: *Ferroalloys and Alloying Additives Handbook*, Shield-alloy Corp., Newfield, N.J., 1982, p. 29.
21. A. H. Sully, E. A. Brandes: *Metalurgy of the Rare-Earth Metals - Chromium*, 2nd ed., Butterworth, London 1967.
22. Alloy Surfaces Co., US 3222212, US 3375128, 1962.
23. G. M. Baughman, *Iron & Steel Eng.* 1972 (Sept.), 91-101.
24. Gmelin, System no. 52, Chrom.
25. M. J. Udy: *Chromium*, vol. 1, Reinhold, New York 1956.
26. A. H. Sully, E. A. Brandes: *Chromium*, 2nd ed., Butterworth, London 1967.
27. Minerals Yearbook U.S. Bureau of Mines, Washington, DC, 1983.
28. *Chromium minerals. World Survey of Production and Consumption*. ROSKILL Information Services Ltd., London 1972.
29. *Mining J. (London)*, Mining annual review 1985.
30. Mineral Facts and Problems, U.S. Bureau of Mines Bull. 650, 1970.
31. H. Borchert: "Principles of the genesis and enrichment of chromite ore deposits", in *Methods of prospecting for chromite*, OECD, Paris 1964, pp. 175-202.
32. S. Janković: *Wirtschaftsgeologie der Erze*, Springer, Wien 1967.
33. H. Kern: "Zur Geochemie und Lagerstättenkunde des Chroms und zur Mikroskopie und Genese der Chromerze", *Clausthaler Hefte zur Lagerstättenkunde und Geochemie der Mineralischen Rohstoffe*, no. 6, Bornträger, Berlin 1968.
34. T. Lukkariinen, L. Heikkilä: "Beneficiation of chromite ore, Kemi, Finland", *10th International Processing Congress 1973*, Inst. Min. Met., London 1973.
35. H. Schneiderhöhn: *Die Erzlagertätten der Erde*, vol. I, Gustav Fischer, Stuttgart 1958.
36. T. Shabad: *Basic industrial resources of USSR*, Columbia University Press, New York 1969.
37. H. Strunz: *Mineralogische Tabellen*, Akadem. Verlagsges., Leipzig 1966.
38. A. Sutulov: *Mineral resources and the economy of the USSR*, McGraw-Hill, New York 1973.
39. H. D. B. Wilson (ed.): *Magmatic ore deposits, a symposium*, monograph 4, Economic Geology Publ. Co., Lancaster, PA, 1969.
40. Bayer AG, DE-AS 1533076, 1966.
41. Bayer AG, FR 1531069, 1967.
42. Bayer AG, DE-OS 1926660, 1969.
43. S. K. Cirkov, *Zh. Prikl. Khim. (Leningrad)* 13 (1940) 521-527.
44. Associated Chemical Comp., DE-OS 1467298, 1963.
45. G. N. Bogachov et al., *Khim. Promst. (Moscow)* 1961, 655.
46. Produits chimiques Ugine Kuhlmann, DE-OS 2329925, 1972.
47. Bayer AG DE-AS 1533077, 1966.
48. C. K. Williams, US 2695215, 1950.
49. R. N. Mittra, N. R. Dhar, *J. Indian Chem. Soc.* 9 (1932) 315-327.
50. Pacific Bridge Co., US 2431075, 1945/47.
51. I. G. Farben, DE 492684, 1927.
52. F. Wöhler, *Justus Liebig's Ann. Chem.* 111 (1859) 117-121.
53. DuPont, US 2885365, 1959 (A. L. Oppegard).
54. DuPont, US 2956955, 1960 (P. Arthur).
55. T. J. Swoboda, P. Arthur, N. L. Cox, J. N. Ingraham, A. L. Oppegard et al., *J. Appl. Phys.* 32 (1961) 374-375.
56. F. Hund, *Farbe + Lack* 78 (1972) 11-16.
57. E. Köster, "Neue Werkstoffe für magn. Speicherschichten", in H. H. Mende (ed.): *Neuere magn. Werkstoffe und Anwendungen magn. Methoden*, Verlag Stahlisen, Düsseldorf 1983, pp. 149-170.
58. B. L. Chamberland, *CRC Crit. Rev. Solid State Mater. Sci.* 7 (1977) 1-31.
59. D. S. Chapin, J. A. Kafalas, J. M. Honig, *J. Phys. Chem.* 69 (1965) 1402-1409.
60. L. Brewer, *Chem. Rev.* 52 (1953) 9.
61. F. J. Darnell, W. H. Cloud, *Bull. Soc. Chim. Fr.* 1965, 1164-1166.
62. BASF, unpublished, 1983.
63. DuPont, US 3034988, 1962 (J. N. Ingraham, T. J. Swoboda).
64. F. J. Darnell, *J. Appl. Phys.* 32 (1961) 1269.
65. H. Y. Chen, D. M. Hiller, J. E. Hudson, C. J. A. Westenbroek, *IEEE Trans. Magn. MAG-20* (1984) 24-26.
66. CNRS, DE-OS 3209739, 1982 (G. Demazeau, P. Maestro, M. Pouchard, P. Hagenmuller et al.).

67. J. B. Goodenough, *Bull. Soc. Chim. Fr.* 1965, 1200-1207.
68. D. S. Rodbell, J. M. Lommel, R. C. DeVries, *J. Phys. Soc. Jpn.* 21 (1966) 2430.
69. J. Boháček, *J. Signalaufzeichnungsmater.* 8 (1980) 55-60.
70. DuPont, US 3512930, 1970 (W. G. Bottjer, H. G. Ingersoll).
71. BASF, DE-OS 2749757, 1977 (G. Vath, M. Ohlinger, H. J. Hartmann, M. Velic et al.).
72. Montedison, EP 29687, 1980 (G. Basile, G. Boero, E. Mello Ceresa, F. Montino).
73. W. Ostertag, W. Stumpf, R. Falk, M. Ohlinger, *Elektronik-Anzeiger* 11 (1972) 225-227.
74. Montedison, DE 2648305, 1976 (G. Basile, A. Mazza, M. Spinetta).
75. DuPont, US 3278263, 1966 (N. L. Cox).
76. G. R. Cole, L. C. Bancroft, M. P. Chouinard, J. W. McCloud, *IEEE Trans. Magn. MAG-20* (1984) 19-23.
77. P. J. Flanders, *IEEE Trans. Magn. MAG-12* (1976) 348-355.
78. Bayer AG, DE 1203748, 1961.
79. Aktjubinskij Sawod Chromowych Isdelij, DE-OS 2119450, 1971.
80. Bayer AG, DE 1065394, 1958.
81. Diamond Alkali Co., US 2993756, 1959.
82. Diamond Alkali Co., DE-OS 2018602, 1970.
83. Diamond-Shamrock Corp., DE-OS 3020260, 1980.
84. Diamond-Shamrock Corp., DE-OS 3020261, 1980.
85. Diamond-Shamrock Corp., DE-OS 3020280, 1980.
86. A. Werner, P. Pfeiffer: *Neue Anschauungen auf dem Gebiet der anorganischen Chemie*, 5th ed., Vieweg, Braunschweig 1923.
87. Griesheim Elektron, DE 369816, 1920.
88. R. B. Norden, *Chem. Eng.* 63 (1956) 308-311.
89. Degussa, FR 817502, 1936.
90. Pittsburgh Plate Glass Co., US 2185218, 1938.
91. I. G. Farben, DE 514571, 1925.
92. Bayer AG, DE 1467327, 1963.
93. W. F. Rogers: *Composition and Properties of Oil Well Drilling Fluids*, Gulf Publ. Co., Houston, TX, 1963, pp. 459-464.
94. Farbenfabriken Meister Lucius Bruning, DE 103860, 1898.
95. M. J. Udy, US 1739107, 1925.
96. M. J. Udy, GB 546681, 1940.
97. Ass. Chem. Comp., DE-AS 1467298, 1964.
98. Ethyl Corp., DE-AS 1159913, 1959.
99. G. Brauer: *Handbuch der präparativen anorganischen Chemie*, 2nd ed., vol. 2, Enke Verlag, Stuttgart 1962.
100. DuPont, DE-AS 1272909, 1960.
101. I. M. Kolthoff, P. J. Elving (eds.): *Treatise on Analytical Chemistry*, Part II, vol. 8, Interscience, New York-London 1963, pp. 301ff.
102. See [101], p. 326.
103. See [101], pp. 327-328.
104. See [101], p. 330.
105. See [101], pp. 338-339.
106. C. Veillon, K. Y. Patterson, N. A. Bryden, *Analytica Chim. Acta* 164 (1984) 67-76.
A. G. Cox, G. Cook, C. W. McLeod, *The Analyst* 110 (1985) 331-333.
107. EEC Directive of June 27, 1967 (67/548/EEC); EEC Directive of July 14, 1976, 1st amendmenf (69/907/EEC).
108. *International Maritime Dangerous Goods Code* (IMDG Code).
109. "Katalog wassergefährdender Stoffe" (List of water-hazard chemicals), Bundesministerium des Inneren, March 1, 1985 (GM Bl p. 175).
110. EPA: *Ambient Water Quality Criteria for Chromium*, Washington, DC, NTIS No. PB 81-117647, 1980.
111. State of Baden-Württemberg (FRG): *Wastewater Requirements*, June 28, 1978, no. 74-5040.
112. *Technische Anleitung zur Reinhaltung der Luft* (TA Luft), Febr. 28, 1986.
113. EEC Directive on poisonous and hazardous wastes, March 20, 1978 (78/319/EEC).
114. Klärschlammverordnung, June 25, 1982, BG Bl 1, p. 734.
115. EPA, Municipal Construction Div.: "Application of Sewage Sludge to Cropland. Appraisal of Potential Hazards of the Heavy Metals to Plants and Animals", NTIS PB-264015, EPA-430/9-76-013, Nov. 15, 1976.
116. G. Schmid, W. Pauckner, *Leder* 35 (1984) 165-171.
117. C. N. Durfor, E. Becker, *U.S. Geol. Survey Wafer Supply*, Paper No. 1812, 1964.
118. NAS-U.S. *Geochemistry and the Environment*, Washington, DC, U.S. Government Printing Office, 1974.
119. RIWA annual report 1983, Part A: *Der Rhein*, Aug. 1984, p. 60/61.
120. B. Hamburger, H. Häberling, H. R. Hirtz, *Arch. Fischereiwiss.* 28 (1977) 45-55.
121. G. Bringmann, R. Kühn, *Gesund. Ing.* 80 (1959) no. 4, 115-120.
122. NIOSH, Registry of Toxic Effects of Chemical Substances 1985.
123. R. A. Griffin et al., *J. Environ. Sci. Health Part A* A12 (1977) 431-449.
124. H. Rasp, *Leder* 32 (1981) 188-203.
125. D. Sauerbeck, *Zeitschrift des Verbandes Deutscher Landwirtschaftlicher Untersuchungs- und Forschungsanstalten (VDLUFA)*, Landwirtschaftliche Forschung, special issue no. 39, Kongressband 1982, pp. 108-129.
126. Unpublished results, Bayer AG, May 1985.
127. P. Friesel et al. (Bundesgesundheitsamt): *Überprüfung der Durchführbarkeit und der Aussagekraft der Stufe 1 und 2 des Chemikaliengesetzes*, Umweltbundesamt (UBA) Forschungsbericht 1984.
128. H. W. Marquart et al. (Bayer AG), in [127].
129. G. Bringmann, R. Kühn, *Haustech. Bauphys. Umwelttech. Gesund. Ing.* 100 (1979) 250.
130. W. Kördel et al. (Fraunhofer-Institut für Toxikologie und Aerosolforschung), in [127].
131. G. Bringmann, R. Kühn, *Z. Wasser Abwasser Forsch.* 15 (1982) 1-6.
132. Unpublished results, Bayer AG, 1978.
133. U.S. Federal Register 45, No. 231, of 28th Nov. 1980, p. 79331.
134. H. J. M. Bowens: *Environmental Chemistry of the Elements*, Academic Press, London 1979.

135. *Chrom, Bachsedimente* (creek sediments), Bundesanstalt für Geowissenschaften und Rohstoffe, Hannover 1984.
136. Umweltbundesamt, Jahresbericht 1982, Berlin 1983, pp. 33, 35.
137. D. J. Swaine, R. L. Mitchell, *J. Soil Sci.* **11** (1960) no. 2, 347–368.
138. S. Langard: *Biological and Environmental Aspects of Chromium*, Elsevier, Amsterdam 1982, p. 58.
139. S. Langard, in [138], p. 60, 62.
140. U.S. Geological Survey Circular 930-B, 1984.
141. U.S. Bureau of Mines: Mineral Commodity Summaries 1984.
142. U.S. Bureau of Mines: Mineral Commodity Summaries 1985.
143. T. Power: "Chromite – the non metallurgical markets", *Industrial Minerals* 1985, April, 17–51.
144. Minerals Bureau, International Report No. 86, Braamfontein.
145. D. Henschler: *Gesundheitsschäd. Arbeitsstoffe*, Verlag Chemie, Weinheim 1973.
146. W. Merz, K. Schwarz, *Am. J. Physiol.* **196** (1959) 614–618.
147. W. Mertz, *Proc. Nutr. Soc.* **33** (1974) 307–313.
148. R. A. Anderson, *Sci. Total Environ.* **17** (1981) 13–28.
149. J. A. Schouten, C. M. van Gent, *Diabetes Praxis* 1983, no. 1, 2–5.
150. Deutsche Forschungsgemeinschaft, Forschungsbericht Schadstoffe im Wasser, 1982, p. 411.
151. F. J. Diehl, in [125], p. 53.
152. S. Langard, in [138], p. 122.
153. T. D. Luckey et al.: *Heavy Metal Toxicity, Safety and Homology*, G. Thieme, Academic Press 1975, p. 49.
154. U. Korallus, H. Lange, A. Neiß, E. Wüstefeld, T. Zwingers, *Arb. Med., Soz. Med., Präy. Med.* **17** (1982) 159–167.
155. U. Korallus, C. Harzdorf, J. Lewalter, *Int. Arch. Occup. Environ. Health* **53** (1984) 247–250.
156. F. L. Petrilli, S. de Flora, *Appl. Environ. Microbiol.* **33** (1977) 805–809.
157. F. L. Petrilli, S. de Flora in: *Mutagens in our Environment*, A. R. Liss, New York 1982, pp. 453–464.
158. EPA Health Assessment Document for Chromium, August 1984 (EPA-600/8-83-D14F).
159. W. C. Hueper, W. W. Payne, *Arch. Environ. Health* **5** (1962) 445–462.
160. L. S. Levy, Fac. of Sc., University of London, 1975.
161. NIOSH (1975) Criteria for a recommended standard. Occ. exposure to chromium(VI), US DHEW, Washington, DC.
162. D. Steinhoff, C. Gad, G. T. Hatfield, U. Mohr, *Exp. Pathol.* (1986), in the press.
163. U. Korallus, H. Ehrlicher, E. Wüstefeld, *Arb. Med., Soz. Med., Präy. Med.* **3** (1974) 51–54; 76–79; 248–252.
164. W. Machle, F. Gregorius, *U.S. Publ. Hlth. Rep.* **63** (1948) no. 35, 1114–1127.
165. T. Mancuso, W. C. Hueper, *Ind. Med. Surg.* **20** (1951) 358–363.
166. M. R. Alderson, N. S. Rattan, L. Bidstrup, *Br. J. Ind. Med.* **38** (1981) 117–124.
167. R. B. Hayes, A. M. Lilienfeld, L. M. Snell, *Int. J. Epidemiol.* **8** (1979) 365–374.
168. W. J. Hill, W. S. Ferguson, *JOM J. Occup. Med.* **21** (1979) 103–106.
169. H. Satoh, Y. Fukuda, K. Teric, N. Chike Katsumo, *JOM J. Occup. Med.* **23** (1981) 835–838.
170. J. M. Davies, *Br. J. Ind. Med.* **41** (1984) 148–169.
171. R. Frentzel-Beyme, *J. Cancer Res. Clin. Oncol.* **105** (1983) 183–188.
172. S. Langard, T. Norseth, *Br. J. Ind. Med.* **32** (1975) 62–65.
173. H. Royle, *Environ. Res.* **10** (1975) 141–163.
174. G. Axelsson, R. Rylander, A. Schmidt, *Br. J. Ind. Med.* **37** (1980) 121–127.
175. S. Langard, A. Andersen, B. Gylseth, *Br. J. Ind. Med.* **37** (1980) 114–180.
176. J. Lewalter, U. Korallus, C. Harzdorf, H. Weidemann, *Internat. Arch. Occ. Environ. Health* **55** (1985) 305–318.
177. "Properties and Economics", *Pigment Handbook*, 2nd ed., vol. I, John Wiley & Sons, New York 1988, pp. 309–310.
178. S. Keifer, A. Wingen, *Farbe + Lack* **79** (1973) 866–873.
179. J.-L. Lassaigne, *Ann. Chim. Phys. Ser. 2* **14** (1820) 299–302.
180. H. C. Roth, US 1728510, 1927.
181. PPG Industries, US 4127643, 1977 (W. W. Carlin).
182. BASF, EP-A 0238713, 1986 (N. Müller et al.).
183. Pfizer Inc., EP 0068787, 1982 (V. P. Rao).
184. Bayer, US 4040860, 1976 (L. Mansmann, W. Rambold).
185. Bayer, DE 2635086, 1976 (W. Rambold, H. Heine, B. Raederscheidt, G. Tenczek).
186. British Chrome & Chemicals, US 4296076, 1981 (A. S. Dauvers, M. A. Marshall).
187. C. K. Williams & Co., US 2250789, 1940 (I. W. Ayers).
188. Bayer, DE 1257317, 1963 (F. Hund, D. Rade).
189. Bayer, DE-OS 2358016, 1973 (B. Knickel et al.).
190. Colores Hispania S. A., ES 438129, 1975.
191. C. K. Williams & Co., US 2560338, 1950 (C. G. Frayne); C. K. Williams & Co., US 2695215, 1950 (W. A. Pollock).
192. Bayer, US 3723611, 1971 (G. Broja, K. Brande, C. H. Elstermann).
193. Gefahrstoffverordnung – GefStoffV Dec. 16, 1987 (BGBl. I, 2721).
194. Bayer, DE 3123361, 1981 (J. Rademachers et al.).
195. 37. Abwasser VWV 05. Sept. 1984, GMBL Nr. 22, 344; Water Pollution Control Law, Law No. 138, Dec. 25, 1970 (Japan).
196. 178. Mitteilung BGesundhBl. 31 (1988) 363.
197. *Journal officiel de la République française* no. 1227 (1983) 75, 97, 109.
198. *Gazzetta Ufficiale della Repubblica Italiana*, Apr. 20, 1973, 3, 4.
199. *Belgisch Staatsblad – Moniteur belge* Sept. 24, 1976, 12030.
200. Verpakkingen – en Gebruiksartikelenbesluit (Warenwet) 01. Oct. 1980.
201. EG-Guidelines EEC 88/378, official gazette L 187 16. July 1988.
202. EEC Council Directive, EEC 76/768, on cosmetic products (18th Suppl.).
203. Japanese Pharmaceutical Affaires 1980.

204. E. Püttbach, *Betonwerk + Fertigteiltechnik* **2** (1987) 124–132.
205. S. Ivankovic, R. Preussmann, Ed. *Cosmet. Toxicol.* **13** (1975) 347–351.
206. U. Korallus, H. Ehrlicher, E. Wüstefeld, *ASP* **3** (1974) 51 ff.
207. EG-Guidelines 67/548/EEC 1967 and Suppl.
208. F. Hund, *Farbe + Lack* **73** (1967) 111–120.
209. L. J. H. Erkens et al., *J. Oil Colour Chem. Assoc.* **71** (1988) no. 3, 71–77.
210. H. Wagner et al., *Z. Anorg. Allg. Chem.* **208** (1931) 249; *Farben-Ztg.* **38** (1933) 932.
211. J. F. Clay & Cromford Color, GB 730176, 1951; H. Lesche, *Farbe + Lack* **65** (1959) 79, 80.
212. Du Pont, US 2808339, 1957 (J. J. Jackson).
213. Du Pont, DE-OS 1807891, 1969 (H. R. Linton).
214. Bayer, DE-OS 1952538, 1969 (C. H. Elstermann, F. Hund).
215. ICI, DE-OS 2049519, 1970 (Ch. H. Buckley, G. L. Collier, J. B. Mitchell).
216. Ten Horn Pigment, DE-OS 2600365, 1976 (J. J. Einerhand et al.).
217. BASF, DE 3323247 A1, 19X3 (E. Liedek et al.).
218. Heubach, DE 3806214 A1, 1988 (I. Ressler, W. Horn, G. Adrian).
219. Heubach, DE 3906670 A1, 1989 (I. Ressler, W. Horn, G. Adrian).
220. R. Williams, Jr.: "Continuous Chrome Yellow Process", *Chem. Eng. (N.Y.)* 1949, March.
221. Chemokomplex Vegyipari-Gep és Berendezes Export, Import Vallalat, DE-AS 1592848, 1971 (J. Scholtz et al.).
222. E. Renkwitz, *Farben-Ztg.* **28** (1923) 1066; H. Levecke, *Farbe + Lack* **42** (1936) 41–43; H. Berger, *Arbeitsschutz* **1941**, III/44.
223. *Paint Oil Chem. Rev.* **95** (1933) 86–92; A. E. Newkirk, S. C. Horning, *Ind. Eng. Chem. Ind. Ed.* **33** (1941) 1402–1407.
224. Sherwin-Williams, US 2237104, 1938 (N. F. Livingston).
225. *Internationale MAK-Werte-Liste* (1990) Ecomed Verlag; *TRGS 505 Blei* (1988), Carl Heymanns Verlag.
226. EEC Council Directive, EEC 82/605, July 28, 1982.
227. J. M. Davies, *Lancet* **2** (1978) 18; *Br. J. Ind. Med.* **41** (1984) 158–169.
228. W. C. Cooper, Dry Colour Manufacturers' Association, Arlington 1983.
229. TA-Luft (Technische Anleitung zur Reinhaltung der Luft) (1986), C. H. Beck'sche Verlagshandlung, München 1987.
230. 37. Anhang zur Rahmen-Abwasser-Verwaltungsvorschrift vom 27.08.1991; § 7 a Wasserhaushaltsgesetz.
231. 37. Abwasser VwV (05.09.1984) für Direkteinleiter (Herstellung Anorganischer Pigmente).
232. Gefahrstoffverordnung (GefStoffV) vom 26.10.1993, Stand 10.94, und Chemikalien-Verbotsverordnung (ChemVerbV) vom 26.10.1993, Stand 10.94, Deutscher Bundesverlag GmbH, Bonn.
233. EEC Council Directive EEC 67/548, June 27, 1967 together with EEC Council Directive EEC 93/21, April 27, 1993 (18th adaption to EEC 67/548) and EEC Council Directive EEC 93/72, Sept. 1st, 1993 (19th adaption to EEC 67/548).
234. EEC Council Directive EEC 94/46, Dec. 12, 1994 (21th adaption to EEC 67/548).
235. EEC Council Directive EEC 93/18, April 5, 1993 (3rd adaption to EEC 88/379).
236. Erste Verordnung zur Änderung chemikalienrechtlicher Verordnungen vom 12. Juni 1996, Deutscher Bundesverlag GmbH, Bonn.
237. EEC Council Directive EEC 94/60, Dec. 20, 1994 (14th amendment of EEC 76/769).
238. EEC Council Directive EEC 89/178, Feb. 22, 1989.
239. Lebensmittel- und Bedarfsgegenständegesetz vom 15.08.1974 (BGBl. S. 1945).
240. Sicherheit von Spielzeug (Safety of toys) EB 71 Part 3, Dec. 1994.
241. M. Cohen, F. J. Beck, *Z. Elektrochem.* **61** (1958) 696.
242. J. D'Ans, V. Groope, *Dtsch. Farben-Z.* **15** (1961) 51, 69.
243. U. R. Evans, *J. Chem. Soc.* 1927, 1020.
244. J. E. D. Mayne, *J. Chem. Soc.* 1948, 1932.
245. J. L. Rosenfeld, *Lakokras. Mater. Ik. Primen.* **1961** 50.
246. H. H. Uhlig, *Chem. Eng. News* **24** (1946) 3154.
247. G. H. Cartledge, *Corrosion (Houston)* **18** (1962) 316.
248. J. Ruf: *Korrosionsschutz durch Lacke und Pigmente*, A. W. Colomb, H. Heenemann GmbH, Stuttgart-Berlin 1972.
249. J. Ruf, *Farbe + Lack* **75** (1969) no. 10, 943.
250. GefStoffV, TRG A 602, part 2, 1987.
251. Verordnung über gefährliche Arbeitsstoffe (Arbeitsstoffverordnung – ArbStoffV) Feb. 11, 1982 (BGBl. I, 144).
252. Nippon Paint KK, JP 61276861, 1985.
253. Société nouvelle des couleurs zinciques, company information, Beauchamp 1990.
254. G. Lincke, O. Schroers, K. D. Nowak, *Farbe + Lack* **82** (1976) no. 11, 1003.
255. NL Chemicals: *Nalcin 2*, company information, Hightstown, NJ 1983.
256. M. Kryder et al., *IEEE Trans. Magn.* **MAG-23** (1987) 45.
257. Du Pont, US 2923683, 1957 (J. N. Ingraham et al.). Bayer, DE-AS 1467328, 1963 (F. Hund et al.).
258. Du Pont, US 3034988, 1958 (J. N. Ingraham et al.).
259. E. Köster in C. D. Mee, E. D. Daniel (eds.): *Magnetic Recording*, vol. I, McGraw-Hill, New York 1987.
260. H. Auweter et al., *IEEE Trans. Magn.* **MAG-26** (1990) 66.
261. M. W. Müller et al., *IEEE Trans. Magn.* **MAG-26** (1990) 1897.
262. Ullmann, A7, 77 ff.
263. BASF, unpublished.
264. M. Essig et al., *IEEE Trans. Magn.* **MAG-26** (1990) 69.
265. Du Pont, US 3512930, 1968 (W. G. Bottjer et al.).
266. BASF, EP-A 218234, 1985 (W. Steck et al.).
267. G. K. Cole et al., *IEEE Trans. Magn.* **MAG-20** (1984) 19.
268. Ten Horn Pigment bv., company information, Maas-tricht 1977.
269. H. Wienand, W. Ostertag, *Farbe + Lack* **88** (1982) no. 3, 183–188.

47 Manganese

PETER M. CRAVEN, JOHN W. WAUDBY, DAVID BRUCE WELLSBELOVED (§§ 47.1–47.9); ARNO H. REIDIES (§ 47.10)

47.1 History	1813	47.8.2 Legal Considerations and Nodule Recovery	1830
47.2 Properties	1814	47.8.3 Processing	1831
47.3 Occurrence	1815	47.8.3.1 Gaseous Reduction and Ammoniacal Leach Process	1831
47.4 Mining and Beneficiation	1816	47.8.3.2 Cuprion Ammoniacal Leach Process	1831
47.5 Reduction of Manganese Oxides ..	1818	47.8.3.3 Elevated Temperature and Pressure H_2SO_4 Leach Process	1832
47.5.1 Manganese–Oxygen System	1818	47.8.3.4 Reduction and HCl Leach Process ..	1832
47.5.2 Reduction of Manganese Oxides with Carbon Monoxide, Hydrogen, and Carbon	1819	47.8.3.5 Smelting and H_2SO_4 Leach Process	1834
47.5.3 Reduction of Mixed Oxides and Minerals Containing Manganese Oxides	1820	47.8.4 Economic Viability and Future Prospects	1835
47.5.4 Reduction of Manganese Oxides by Silicon	1821	47.9 Economic Aspects	1836
47.5.5 Reduction of Manganese Oxide by Aluminum	1821	47.10 Compounds	1837
47.6 Production of Manganese Metal ...	1821	47.10.1 Introduction	1837
47.6.1 Electrolysis of Aqueous Manganese Salts	1823	47.10.2 Oxides	1838
47.6.2 Electrothermal Process	1826	47.10.2.1 Manganese(IV) Oxide	1838
47.6.3 Aluminothermic Process	1826	47.10.2.2 Other Oxides	1844
47.6.4 Silicothermic Process	1827	47.10.3 Manganese(II) Salts	1846
47.6.5 Distillation of Ferromanganese ...	1827	47.10.4 Higher Oxidation-State Manganates	1848
47.6.6 Electrolysis of Fused Salts	1827	47.10.4.1 Potassium Manganates(V) and (VI)	1848
47.7 Manganese in the Iron and Steel Industry	1827	47.10.4.2 Potassium Permanganate	1848
47.8 Processing of Manganese Nodules and Encrustations	1828	47.10.4.3 Sodium Permanganate	1855
47.8.1 Occurrence, Origin, and Composition	1828	47.10.5 Miscellaneous Compounds	1856
		47.10.6 Occupational Health and Environmental Aspects	1856
		47.11 References	1857

47.1 History [1, 2]

There is some dispute over the origin of the name “manganese”. Deposits of manganese ore (probably pyrolusite) were apparently found near Magnesia in Asia Minor. This was referred to by PLINY around 50 B.C. as *magnesia negra* to distinguish it from *lapis magnes* (magnetite), which has a similar appearance and density. The name pyrolusite was derived only in 1826.

The useful properties of manganese were probably first identified in the mineral pyrolusite, which was used by the ancient Egyptians and Romans to control the color of glass.

Small additions of the ore removed the greenish yellow discoloration caused by iron impurities, while further additions imparted pink, purple, or black colorations.

During the 1400s the name braunstein was used for all the manganese oxide ores. SCHEEL recognized manganese as an element in 1774, and GAHN succeeded in isolating the metal for the first time during the same year. The name manganese was first used by BUTTMAN in 1808.

Manganese ore may have been used in ironmaking for centuries, but found formal usage in iron- and steelmaking only at the beginning

of the 19th century. Ferromanganese was first produced on an industrial scale in 1841 by POURCEL in France for use in crucible steels, and by 1850 spiegeleisen (an alloy of 20% manganese and iron) had been produced commercially in Prussia. The Bessemer process was made practical by MUSHET, who advised the addition of spiegeleisen in 1856/1857. The use of ferromanganese as an additive to steel to counteract the harmful effects of sulfur and phosphorus was patented by SIEMENS in 1866, and by 1875, POURCEL was making 65% ferromanganese in a blast furnace. HADFIELD developed a wear-resistant steel containing manganese as an alloying agent in 1888. Ferromanganese was first produced in an electric arc furnace during 1890.

A two-stage process for the production of refined ferromanganese with 1–2% carbon was proposed in 1908, and manganese metal was first produced industrially by an aluminothermic process in 1898. In 1866 LECLANCHE filed a patent for the $\text{MnO}_2\text{--NH}_4\text{Cl--Zn}$ dry-cell battery.

Table 47.1: Properties of manganese.

Property	$\alpha\text{-Mn}$	$\beta\text{-Mn}$	$\gamma\text{-Mn}$	$\delta\text{-Mn}$	Molten Mn
Atomic number	25				
Atomic mass	54.938				
Crystal structure	complex cubic	complex cubic	fcc	bcc	
Lattice parameter, nm	0.8894	0.6290	0.3774	0.3080	
Transition temperature, °C	$\alpha \leftrightarrow \beta$ 727	$\beta \leftrightarrow \gamma$ 1095	$\gamma \leftrightarrow \delta$ 1104	$\delta \leftrightarrow \text{liquid}$ 1244	liquid \leftrightarrow gas 2032
Standard electrode potential, V	1.134				
Magnetic susceptibility, m^3/kg	1.21×10^{-7}				
Density, g/cm^3	7.44	7.29	7.21		$7.55\text{--}1.2 \times 10^{-3}$ (1244–1500 °C)
Brinell hardness, MPa	3923–4119				
Hardness, J scale	5				
Volume increase on transition, %	$\alpha \leftrightarrow \beta$ 3.4	$\beta \leftrightarrow \gamma$ 0.8	$\gamma \leftrightarrow \delta$ 0.8	$\delta \leftrightarrow \text{liquid}$ 2.9	
Resistivity, Ωcm	$150\text{--}260 \times 10^{-6}$	90×10^{-6}	40×10^{-6}		
Compressibility, m^3/N	8.4×10^{-7}				
Coefficient of linear expansion, K^{-1}	22.3×10^{-6}	24.9×10^{-6}	14.8×10^{-6}	41.6×10^{-6}	
Latent heat of fusion, J/g	244				
Latent heat of vaporization, J/g	4020				
Heat of transition, J/mol	2240	2282	1800	14 655	219 901
Specific heat, $\text{Jg}^{-1}\text{K}^{-1}$	0.477	0.482	0.502		
Enthalpy, J/mol	4999		5112		
Entropy, $\text{Jmol}^{-1}\text{K}^{-1}$	32.0		32.3		173.8

47.2 Properties [1–5]

Manganese is a silver-grey metal, resembling iron. It is hard and very brittle, and its primary uses in a metallic form are as an alloying, desulfurizing, and deoxidizing agent for steel, cast iron, and nonferrous metals. Due to its high tendency to oxidize, annealing colors are often evident.

Manganese belongs to group 7 and period 4 of the periodic table with an atomic number of 25 and atomic mass of 54.94. Six isotopes have been produced, of which only ^{55}Mn is stable. The other isotopes, ^{51}Mn , ^{52}Mn , ^{54}Mn , ^{56}Mn , and ^{57}Mn , have half-lives ranging from 46 min to 310 d. Manganese exists in four allotropic forms: α , β , γ , and δ . Some important physical and thermodynamic properties are listed in Table 47.1. The vapor pressure of manganese in millibars is given by:

$$\log p = -13.625/T + 8.8237 \quad (770\text{--}885^\circ\text{C})$$

$$\log p = -13.994/T + 9.3360 \quad (957\text{--}1097^\circ\text{C})$$

$$\log p = -12.275/T + 8.3730 \quad (1250\text{--}1550^\circ\text{C})$$

and the molar heat capacity in $\text{Jmol}^{-1}\text{K}^{-1}$ as a function of temperature by:

$$\alpha\text{-Mn} (0.3\text{--}4.2\text{ K}):$$

$$C_p = [16T + 2.39T^2 + 0.0266T^3] \times 10^{-3}$$

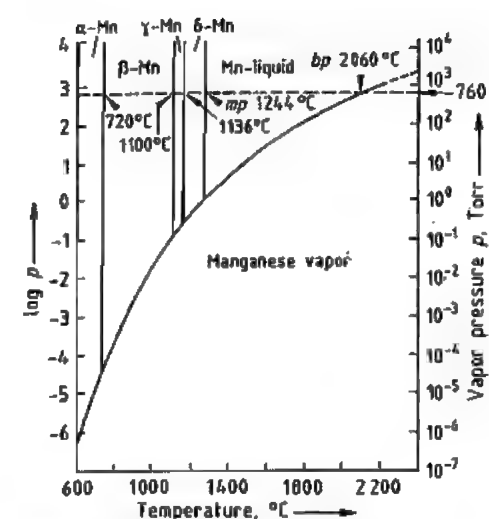


Figure 47.1: The vapor pressure of manganese [3].

$\alpha\text{-Mn}$ (298–1000 K):

$$C_p = 23.9 + 14.2 \times 10^{-3}T - 1.55 \times 10^{-5}T^2$$

$\beta\text{-Mn}$ (1000–1374 K): $C_p = 34.9 + 2.765 \times 10^{-3}T$

$\gamma\text{-Mn}$ (1374–1400 K): $C_p = 44.80$

$\delta\text{-Mn}$ (1410 K–mp): $C_p = 47.31$

Liquid Mn (mp–bp): $C_p = 46.06$

The vapor pressure diagram of manganese is shown in Figure 47.1.

Manganese exhibits certain similarities to its neighbors in the periodic table, iron and chromium. The electronic configuration is $1s^2 2s^2 2p^6 3s^2 3p^6 4s^2$.

Manganese occurs in all oxidation states between Mn(–III) and Mn(VII), with Mn(II) being the most stable. Trivalent manganese is less stable and readily disproportionates into Mn(II) and Mn(IV). The remaining oxidation states occur mainly in complexes.

The basicity of the oxides decreases with increasing valency of the manganese. Thus, manganese(II) oxide is the anhydride of a base $\text{Mn(OH)}_2 \rightarrow \text{MnO} + \text{H}_2\text{O}$

while manganese(VII) oxide Mn_2O_7 is an acid anhydride:



Manganese(IV) oxide (MnO_2) is amphoteric. The oxidation states Mn(II) and Mn(VII) are of industrial importance, forming a large

number of useful salts. In metallurgy, oxides of di-, tri-, and tetravalent manganese are important, especially Mn(II) oxide.

At normal temperatures, pure manganese is not attacked by oxygen, nitrogen, or hydrogen. At high temperatures it reacts violently with oxygen, sulfur, and phosphorus. It is therefore a powerful agent for deoxidizing and desulfurizing metals, whereby it is converted to a divalent oxide or sulfide. Reaction with chlorine forms manganese(II) chloride; with SO_2 the products are MnS and MnO .

Manganese dissolves in acids with liberation of hydrogen and formation of Mn(II) salts. Hot concentrated sulfuric acid dissolves manganese with evolution of SO_2 and nitric acid with evolution of hydrogen, nitrogen, and dinitrogen monoxide.

47.3 Occurrence [5–12]

Manganese is the twelfth most abundant element in the earth's crust, at 950 ppm [5].

Mineralogy. Manganese is contained in many minerals, of which approximately 250 can be regarded as true manganese minerals. The major ores, generally with manganese contents above 35%, are hydrated or anhydrous oxides. The silicates and carbonates occur to a lesser extent. The major manganese minerals are listed in Table 47.2.

Table 47.2: Manganese minerals of economic importance.

Mineral	Formula	Theoretical Mn content, %	Relative density
Pyrolusite	$\beta\text{-MnO}_2$	63.2	5
Braunite	$\text{Mn}^{2+}\text{Mn}_6^{3+}\text{SiO}_{12}$	66.6	4.7–4.9
Manganite	$\gamma\text{-MnOOH}$	62	4.3
Psilomelane	$(\text{Ba}, \text{Mn}^{2+})_3(\text{O}, \text{OH})_6 \text{Mn}_2\text{O}_{16}$	45–60	4.4–4.7
Cryptomelane	$\text{KMn}_8\text{O}_{16}$	62	4.3
Häusmannite	Mn_3MnO_4	73	4.7–5.0
Jacobsite	Fe_2MnO_4	23.8	4.8
Bixbyite	$(\text{Mn}, \text{Fe})_2\text{O}_3$	30–40	5
Rhodonite	$(\text{Mn}, \text{Fe}, \text{Ca})\text{SiO}_3$	42	3.4–3.6
Rhodochrosite	MnCO_3	47.6	3.3–3.6
Bentérite	$\text{Mn}_3\text{Si}_2\text{O}_7(\text{OH})_4$	43.2	3.5

Economically significant manganese deposits are all of sedimentary origin, having been dissolved from crystalline rocks and deposited as the oxide, hydroxide, or carbonate.

Wad is the term given to the soft, earthy, hydrous mixture of manganese and iron oxides of variable manganese content.

Ore Quality. Typically, only ores containing a minimum of 35% Mn are regarded as manganese ores. Ores containing 10–35% Mn are categorized as ferruginous manganese ores, and iron ores with 5–10% Mn are referred to as manganiferous ores. The three most important areas of application of manganese ores and the specific requirements, are as follows:

- Metallurgical grade ore for the iron and steel industry, which generally contains 38–55% Mn. The phosphorus content should preferably be below 0.1%, and the concentrations of Al_2O_3 , SiO_2 , CaO , MgO , and S are important. The manganese/iron ratio is critical; a 7.5:1 ratio, for example, is required for a standard ferromanganese alloy with 78% Mn.
- Battery-grade ore, containing 70–85% MnO_2 (44–54% Mn). The ore should generally contain less than 0.05% of metals more electronegative than zinc, such as copper, nickel, cobalt, and arsenic. The suitability of manganese dioxide for use in batteries depends on a number of factors, including the crystal structure, surface area, pore size distribution, particle shape and size, electrical conductivity, surface conditions, chemical composition, and structure defects [2].
- Chemical grade ore whose specifications vary considerably depending on the end use. Included in this category are feed stocks for electrolytic manganese and manganese dioxide, manganese chemicals, colorants and, in South Africa, an oxidant in uranium extraction.

Ore Deposits. The most important manganese ore deposits are located in South Africa, the former Soviet Union, Australia, Gabon in West Africa, and Brazil. The deposits in India and Mexico are of declining importance, and

the majority of the production is consumed domestically.

The largest known land-based manganese deposit is the Kalahari Field, located in the Northern Cape Province of South Africa, which contains ca. 78% ($13\,600 \times 10^6 \text{ t}$) of the world's potential resources. The surface area underlain by this deposit is approximately 320 km^2 . The deposit is sedimentary and interlayered with banded ironstone.

A breakdown of the world's total estimated manganese ore reserves is presented in Table 47.3.

Each of the major manganese producers offers a range of ore products, the detailed chemical and physical characteristics of which are given in [8]. Analyses of some typical commercial grades are presented in Tables 47.4 and 47.5.

Another potentially important source of manganese are the deep-sea nodules located over certain areas of the ocean floor.

47.4 Mining and Beneficiation

The methods employed for the mining and beneficiation of manganese ore vary widely depending on the size and nature of the deposit, ore type, end uses, and size of the operation.

Mining. The major producers of manganese ore utilize both underground and open-cast mining techniques. In South Africa, Samancor extracts ore from the open-cast Mamatwan Mine and the underground Wessels Mine. At Mamatwan the ore body attains a maximum thickness of 45.2 m and is overlain by, on average, 45 m of overburden. The open pit is approximately 1900 m by 300 m, and the ore is extracted from three benches by drilling, blasting, loading, and hauling to an in-pit crusher. At Wessels the ore body is located at a depth of ca. 300 m and a room and pillar mining system is employed. The average stope height is ca. 5 m, and the ore is drilled, blasted, loaded, and hauled to underground primary crushing facilities.

Table 47.3: Manganese reserves and production (1995).

	Ore reserves, 10^6 t	Ore production, 10^3 t	High-carbon ferromanganese production, 10^3 t^a	Silicomanganese production, 10^3 t
<i>Ore-producing countries</i>				
South Africa	13 600	3 040	433	266
Former Soviet Union	2 300	4 000	292	807
Gabon	400	1 930		
Australia	400	2 169	93	94
Brazil	160	2 500	142	230
China	100	3 700	550	524
India	60	1 700	191	100
Others	90	1 347		
<i>Non-ore-producing countries</i>				
Germany				
Japan			398	82
Mexico			78	65
Norway			233	210
United Kingdom				
France			437	89
Others			589	522
Total	17 110	20 386	3436	2989

^a Includes medium carbon ferromanganese production.

Table 47.4: Typical composition of some important metallurgical manganese ores (chemical content on % dry basis).

Producer	Product	Mn	Fe	P	SiO_2	Al_2O_3	CaO	MgO
Samancor, South Africa	Mamatwan Lumpy	37–38	4–6	0.04	4–6	0.5	14–16	4
	Mamatwan Ferruginous	32–34	4–6	0.04	4–6	0.5	14–16	5
	Wessels High Grade	50–51	9–11	0.05	5–7	0.5	4–6	1.5
	Wessels Low Grade	38–40	18–20	0.05	5–7	0.5	4–6	2
Groote Eylandt, Australia	Metallurgical Lump	49	2.5	0.06	6	4	0.05	0.1
	Siliceous Lump	44	2.5	0.06	15	4	0.05	0.1
Amapa, Brazil	Bitolado 48	48–49	5.5–6.9	0.08–0.11	2–3	3.7–5.5		
	Carbonate Grosso		2.5–4	0.04–0.10	10–14	2.0–3.8	3.3–5.2	2.2–4.5
CVRD, Brazil	Lumpy		3.7	0.08	3.6	9.8	0.25	0.3
Comilog, Gabon	Gabon Lumpy		3–5	0.11–0.14	2.5–4	6	0.11	0.07
Chiatura, Georgia	Chiatura Average	31	1.5	0.62	22.2	2.27	5.18	

Table 47.5: Typical composition of some important battery-grade manganese ores (chemical content on % dry basis).

Producer	MnO_2	Mn	Fe	Pb	Cu	Ni	As	Co
CVRD, Brazil	76.5	51.0	3.2	0.035	0.050	0.080	0.004	0.035
Comilog, Gabon	83.6		1.8		0.03	0.05		0.095

At Groote Eylandt, BHP operates Australia's only manganese mine by open-cut methods from various quarries, each limited to an area ca. 250 m long by 60 m wide and normally having a single bench [15].

The former Soviet Union's primary manganese source is the Nikopol field, where the thickness of the ore seam is 1.5–2.5 m on average occurring at a depth of 100–120 m. A combination of underground and open-cut mining methods are employed [16].

Beneficiation. Ore treatment varies from simple crushing, washing, and sizing plants to fairly sophisticated beneficiation techniques. Gravity separation techniques are frequently employed, such as the dense-medium separation plants at Groote Eylandt and Mamatwan. Extensive investigations on a pilot-plant scale have been undertaken by Samancor on ore sorting techniques, based on neutron activation or X-ray fluorescence; this has not as yet led to a commercial operation. Froth flotation

with fatty acids, amines, sulfates, sulfonates, and hydroxamates has been shown to be feasible on a laboratory scale [17], as have high-gradient magnetic separation techniques [18].

Beneficiation techniques are becoming progressively more complex as reserves of high-grade ores diminish and requirements for smelting and steelmaking become more stringent.

Intermediate treatment processes. Various intermediate treatment processes can be applied to manganese natural ores or concentrates prior to smelting to a ferroalloy or direct addition to a steelmaking process. These processes are employed for one or both of the following two reasons: 1) to convert a fine ore to a more suitable size, and 2) to calcine and/or reduce the ore to a more suitable final product.

Agglomeration processes include nodulizing, pelletizing, and briquetting. Reduction can be carried out in a rotary kiln or sinter plant.

Sintering has become the preferred process for intermediate treatment, and approximately ten manganese sinter plants currently exist, with sintering grate areas varying from 3 m² to 80 m² and production capacities of 2–300 t/h.

Sinter is produced on a moving grate from a mixture of fine ore, fine reductant/fuel, and recycled sinter fines. The fuel in the bed is ignited, and ignition is propagated by applying suction to the grate. A sufficiently high temperature is generated to fuse the ore particles together. During sintering, the ore is calcined and partially reduced. Some of the benefits derived from sintering ore are:

- Fine ore, which has a limited application and value in conventional smelting, is agglomerated and converted to a superior product.
- Reduced gas volumes, and hence fewer furnace eruptions, result when smelting sinter.
- Furnace availability and operating loads are increased.

47.5 Reduction of Manganese Oxides¹

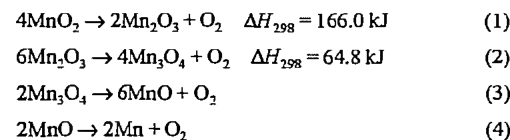
Manganese is only produced commercially from blends of ore in which manganese exists as an oxide. A knowledge of the thermodynamics of the reduction of these oxides [19] is therefore essential to the understanding of the production of alloys from manganese ores.

47.5.1 Manganese–Oxygen System

Of the known oxides of manganese (Mn₂O₇, MnO₂, Mn₅O₈, Mn₂O₃, Mn₃O₄, and MnO), the only oxides found naturally in manganese ores are MnO₂, Mn₂O₃, Mn₃O₄, and MnO.

Under normal conditions, manganese dioxide occurs as stable β-MnO₂; the other modifications, α, γ, δ, and ε, are not pure varieties of MnO₂. Dimanganese trioxide (Mn₂O₃) exists in the α-modification, which is cubic above 20 °C and rhombic below this temperature; the γ-modification is metastable. Trimanganese tetroxide (Mn₃O₄) exists at atmospheric pressure in the tetragonal α-modification and changes to the cubic β-form at 1170 °C. Manganese oxide (MnO) in normal conditions exists in only one modification. This oxide is, however, nonstoichiometric and is more accurately described as Mn_{1-x}O with x = 0–0.25 [20]. The complete phase diagram of the manganese–oxygen system above 1000 °C is given in Figure 47.2.

The equations for the thermal dissociation of the important manganese oxides are as follows:



The oxygen partial pressures exerted by these reactions are given as a function of temperature in Figure 47.3 [21]. According to the

¹ For Ferromanganese, see Section 7.4.

thermodynamic data in [22], the decomposition temperature at 101.3 kPa for reaction (1) is 500 °C and for reaction (2), 980 °C. For reaction (3) to occur at atmospheric pressure a reductant is necessary. Reaction (4) requires a high reducing potential. It is important, therefore, to consider the reduction of the oxides of manganese in the presence of carbon monoxide, hydrogen, and carbon. These are the reactions that usually take place in the blast furnaces and electric furnaces used to produce manganese alloys.

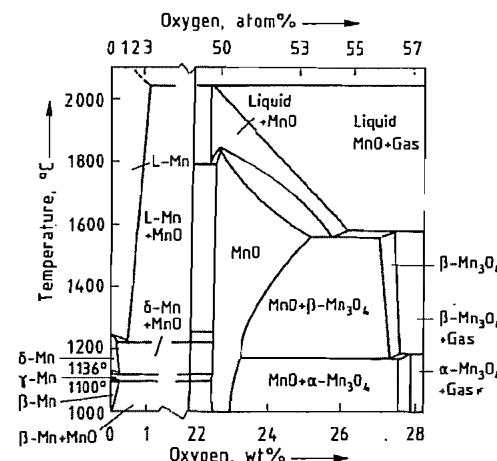


Figure 47.2: Mn–O phase diagram above 1000 °C.

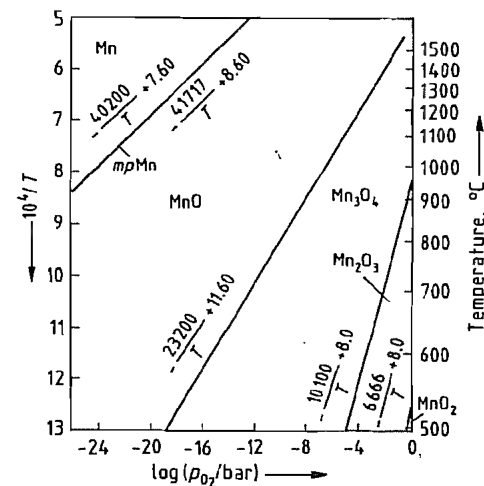
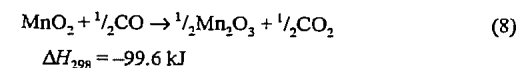
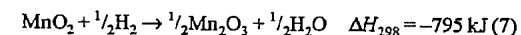
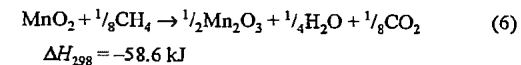
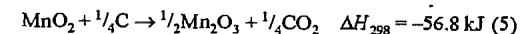


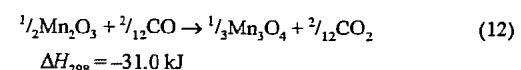
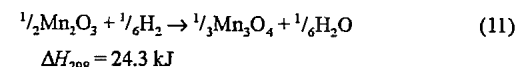
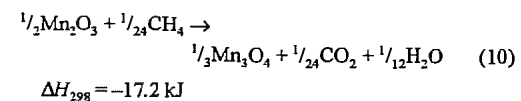
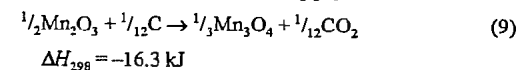
Figure 47.3: Variation of oxygen partial pressure in the Mn–O system with temperature.

47.5.2 Reduction of Manganese Oxides with Carbon Monoxide, Hydrogen, and Carbon

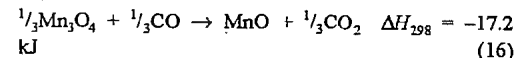
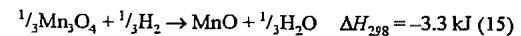
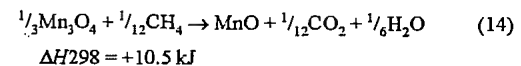
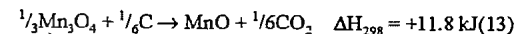
The reduction of MnO₂ to Mn occurs in four main steps (Equations 1–4). This reduction is strongly exothermic in the presence of carbon, methane, and carbon monoxide; the following equations apply:



The reduction of Mn₂O₃ in the presence of the same reducing agents is also exothermic. The following equations apply:



The third step is the reduction of Mn₃O₄, which is endothermic with carbon or methane and exothermic with hydrogen or carbon monoxide:

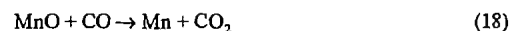


The last step, the reduction of MnO, is more difficult and requires a high reducing potential. The presence of carbon is therefore necessary and at a carbon monoxide partial pressure of 101.3 kPa a temperature of 1420 °C is necessary for the reaction to pro-

ceed. However, the formation of manganese carbides in the presence of carbon lowers the reaction temperature to 1300 °C. The following, highly endothermic overall reaction applies:



This reaction can be broken down into



and the reaction of CO_2 with C to produce CO



which ensures that a high reducing potential is maintained.

Due to the importance of both carbon monoxide and carbon as reducing agents in the commercial production of manganese-containing alloys, these are discussed in more detail. It is possible to predict the ratio CO/CO_2 that will reduce the individual manganese oxides by considering the relationship between the oxygen partial pressures and the equilibrium constants for the reactions (1–4)

$$K_{p(1-4)} = p_{\text{O}_2} \quad (20)$$

(assuming that the activities of the solid phases are unity) and the equilibrium constant of the reaction



which is

$$\frac{1}{K_p} = \frac{p_{\text{CO}}^2 \cdot p_{\text{O}_2}}{p_{\text{CO}_2}^2} \quad (22)$$

and the relationships

$$G^0 = -RT \ln K_p \quad (23)$$

and

$$G^0 = -RT \ln p_{\text{O}_2} \quad (24)$$

the oxygen potentials of the individual reactions at various temperatures can be calculated. This is shown graphically in the Richardson diagram [21] (Figure 47.5). The same applies to the use of hydrogen as a reductant. Although the reduction of MnO_2 , Mn_2O_3 , and Mn_3O_4 takes place at low partial pressures of CO, the presence of carbon is necessary for the reduction of MnO. In this case the following reaction is important:



for which

$$\log p_{\text{O}_2} = -11\,672/T - 9.16 \quad (26)$$

This reaction is pressure dependent due to the change in the number of moles of gas, and again the Richardson diagram can be used to predict under which conditions the reduction of MnO will occur (Equations 17, 18, and 19). However, manganese carbides are always formed during the reduction of MnO with carbon, and this lowers the temperature at which the reaction occurs.

The products produced in this process always contain carbon. The phase diagram for the manganese–carbon system is shown in Figure 47.4. The melting point increases with increasing carbon content [23]. Commercial ferromanganese (76% Mn, 16% Fe) contains ca. 7% carbon. The solubility of carbon decreases with increasing silicon content.

47.5.3 Reduction of Mixed Oxides and Minerals Containing Manganese Oxides

In the discussion of the reduction of manganese oxides it has been assumed that the activity of the solid phases is unity. However, this is usually not true in practice because in most manganese ores the manganese oxides are combined with iron oxides, silicates, aluminum oxides, calcium oxides, and phosphorus oxides.

The oxides FeO and P_2O_5 are reduced at lower temperature than MnO, and SiO_2 at only slightly higher temperature (Figure 47.5). Any iron oxides and oxides of phosphorus occurring in the ore, fluxes, and reductants used in commercial processes are reduced together with the manganese oxides and report to the product. A judicious choice of ores and raw materials is therefore necessary to limit the amount of these elements which report to the metal. The silica contained in the ores can also be reduced, and in the production of silicomanganese this is desirable. Quartz or quartz-

ite is therefore an important raw material for the production of silicomanganese.

The presence of other oxides in the ores reduces the activity of the manganese oxide. This must be compensated for by increasing the reducing potential by increasing the CO/CO_2 ratio of the gas mixture. Alternatively, the reduction temperature must be increased if the reaction is carried out with carbon.

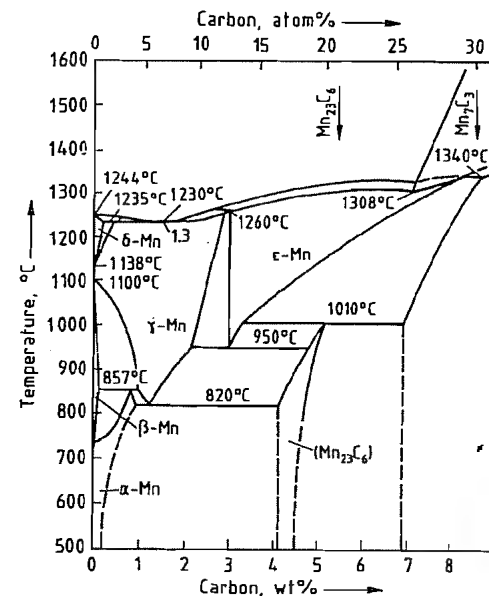
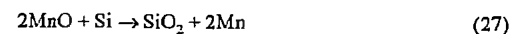


Figure 47.4: Phase diagram for the Mn–C system [23].

47.5.4 Reduction of Manganese Oxides by Silicon

Figure 47.5 shows that the reduction of manganese(II) oxide by silicon is also possible:



for which

$$K = \frac{a_{\text{SiO}_2} \cdot a_{\text{Mn}}^2}{a_{\text{MnO}}^2 \cdot a_{\text{Si}}} \quad (28)$$

This reaction is the basis of the Frisch process for the production of low-carbon ferromanganese and manganese metal from silicomanganese. The silicon content of the metal is

restricted by using a basic slag that reduces the activity of SiO_2 by reaction with CaO, displacing reaction (27) as far to the right as possible.

47.5.5 Reduction of Manganese Oxide by Aluminum

It is easier to reduce manganese(II) oxide with aluminum than with silicon because the differences in the oxygen potentials of the dissociation equilibria of MnO and Al_2O_3 are greater than for MnO and SiO_2 (Figure 47.5). As in the case of carbon and silicon, the higher oxides of manganese are also reduced if present in the ore. The aluminothermic process is used in the production of manganese metal (see Section 47.6.3).

47.6 Production of Manganese Metal [24, 25]

Pure manganese metal has only become an important commodity since ca. 1940. Today the world market is in excess of 140×10^3 t/a. Most of the high-purity manganese produced is consumed by the steel and aluminum industries, although the use of manganese for the production of manganese zinc soft ferrites has led to a demand by electronic component producers [26]. Whilst ferromanganese remains an economically sound additive for manganese steel producers, greater volumes of pure manganese metal are used in the formulation of specialty steels.

In aluminum production, manganese powder is added to the melt to make the product harder. Manganese powder has long been used in welding-rod fluxes, where it imparts superior flow properties to the melt forming the weld.

Producers of manganese chemicals enjoy the convenience of a pure, reactive starting material from which to manufacture manganese salts and compounds.

A number of methods for the production of relatively pure manganese metal are known:

- Electrolysis of aqueous manganese salts

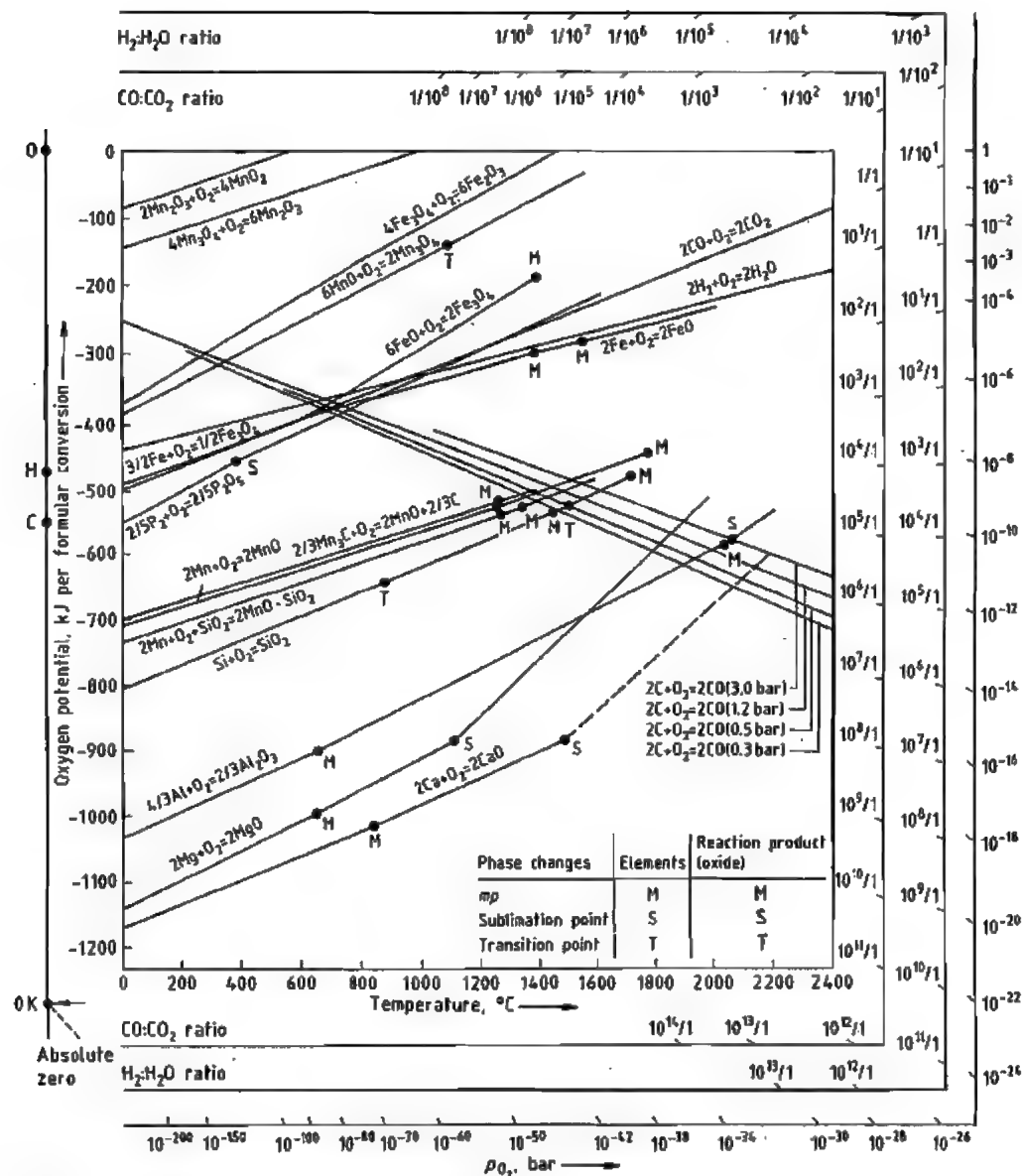


Figure 47.5: Temperature dependence and oxygen potentials of oxide systems [21].

- Electrothermal decomposition of manganese ores
 - Silicothermic reduction of manganese ores or slags
 - Aluminothermic reduction of manganese ores or slags
 - Distillation of ferromanganese
 - Electrolysis of fused salts
- The first two techniques are the most important.

47.6.1 Electrolysis of Aqueous Manganese Salts

The electrolytic route to manganese metal was first investigated in 1930 by DAVIS. However, the process did not become significant until 1939 when demand for manganese by the steel producers (for armaments manufacture) prompted the U.S. Bureau of Mines to build a 1 t/a pilot plant at Knoxville, Tennessee. The plant was redesigned in 1940, and by 1944 it was producing ca. 1500 t/a. Chuo Denki Kogyo of Japan commenced production in 1941. The U.S. Bureau of Mines built a second pilot plant at Boulder City in 1942 [27], and The Electrolytic Manganese Corporation of Krugersdorp, South Africa began production in 1955.

The Boulder City process forms the basis of modern electrolytic manganese plant operation and is encountered in many parts of the world. Production capacities according to country and company are listed in Table 47.6.

Table 47.6: Estimated production capacity for electrolytic manganese metal, 1988 [59].

Company	Country	Capacity, t
Fernvavi Industria e Comercio	Brazil	80
Chuo Denki Kogyo	Japan	3 600
Tosoh	Japan	6 000
Manganese Metal Company	RSA	43 300
Elkem Metals	United States	10 000
Kerr-McGee Chemicals	United States	11 250
State Organization	Former Soviet Union	3 000
Total		77 230

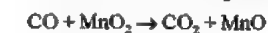
The Manganese Metal Company of South Africa is currently the largest supplier but high prices in the late 1980s have encouraged investment by other countries. The process may be conveniently divided into 3 stages:

- Milling and chemical reduction of a suitable ore
- Leaching of the soluble manganese and removal of deleterious solutes
- Electrowinning of manganese metal

Ore Milling and Reduction. To ensure reactivity in both the reduction and leaching steps,

the ore is milled to ca. 80–90% < 75 μm [28]. The surface area (BET) is 2–5 m^2/g . It is usual to dry mill the ore since the hydrometallurgical part of the process is closed and unnecessary dilution of the liquor must be avoided. Ball or vertical spindle mills are suitable for this purpose. Transport of the ore may be effected pneumatically at this stage.

Manganese ores usually occur in an insoluble form comprising minerals largely in the 4+ oxidation state. Carbonate ores, which are readily soluble, occur in some parts of the world. To render refractory ores soluble in acid, the manganese is usually converted to the 2+ oxidation state by calcining under a reducing atmosphere at 850–1000 $^{\circ}\text{C}$. Reductants are carbon sources and may include various combinations of anthracite, coal, charcoal, hydrocarbon oils, natural gas, coal gas, or liquefied petroleum gas. The reduction reactions can be simplified to:



Other species present are also reduced. Iron is reduced to the iron(II) state and in some cases to iron metal. The Fe(II) content of the calcined ore may be used as an indicator of the degree of reduction achieved; a calcine containing 1–3% Fe(II) can be assumed to have its manganese fully reduced to Mn(II).

The discharging calcined ore must be cooled to below 100 $^{\circ}\text{C}$ to exclude the possibility of reoxidation. The reactive nature of the calcine at this stage precludes pneumatic transport.

Reductive leaching has been investigated with bacteria [29] and with reducing chemicals such as sulfur dioxide, hydroquinone, and other organic compounds [30].

Leaching and Purification. The reduced ore is agitated with spent electrolyte which normally contains 2–5% sulfuric acid (generated at the diaphragm in the electrolysis stage). Other soluble species, notably iron(II), are also dissolved and must be removed prior to electrolysis. The pH of the leachate should be 5–6, and air oxidation of Fe^{2+} to Fe^{3+} ensures the precipitation of iron(III) hydroxide to re-

move soluble iron [31]. Other deleterious transition metals are removed by precipitation of their sulfides through pH manipulation and addition of a soluble sulfide [32]. Some manganese sulfide is necessarily coprecipitated during this process and the relative amount of this present in the sulfide precipitate is a measure of the efficiency of the reaction [33–36]. The manganese concentration at this point is ca. 10% expressed as the sulfate. If a substantial amount of soluble silica is present, it may be removed by coprecipitation with aluminum hydroxide. A solid-liquid separation is required to provide a perfectly clean solution for the electrolytic stage. Other current methods of purification include ion exchange and solvent extraction [37, 38].

Electrowinning of Manganese Metal. Although manganese has a strongly electronegative electrode potential (–1.13 V), its high hydrogen overvoltage allows electrowinning from aqueous solutions. Good current efficiencies are only obtained when other metallic solutes are absent from the catholyte.

The manganese is recovered in a diaphragm cell. The cathode may be made of titanium, stainless steel, or one of a number of proprietary alloys. The anode is usually a lead calcium or lead-silver alloy, but success has recently been achieved with anodes coated with platinum-group metals. Diaphragms are usually made of synthetic polymer canvas.

Prior to introduction to the cell, the solution is conditioned by addition of sulfur dioxide or, more recently, selenium dioxide [39]. These additives improve current efficiencies and ensure the deposition of the hard and brittle α allotrope of manganese. It has been reported that the current efficiencies have been increased to as much as 90% with selenium dioxide. However, the latter has the disadvantage that the metal obtained is often contaminated with selenium. This reduces the total manganese content of the metal and causes toxicological and environmental problems for the consumer. Addition of sulfur dioxide produces a metal with slightly higher sulfur content. Ammo-

nium sulfate is used in the cell solution as a supporting electrolyte.

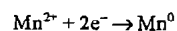
Typical cell operating conditions at the cathode are as follows:

MnSO ₄ concentration	4.0%
(NH ₄) ₂ SO ₄ concentration	13%
pH	7.0
Temperature	35–45 °C
Current densities:	
Anode	1000 A/m ²
Cathode	500
Potential	5–7 V

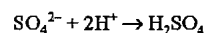
These values are approximate and vary considerably between installations. Current efficiencies are variable, depending on additives, the purity of the catholyte, and optimization of solute concentrations. Values between 42 and 62% are typical.

The following reactions occur [40]:

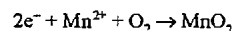
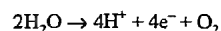
At the cathode



At the diaphragm



At the anode



The electrolysis of water is largely responsible for the inefficiency of the electrolytic procedure. Power consumption is typically 9000–12 000 kWh/t. Polymeric smoothing agents may be added to the electrolyte to prevent the formation of dendrites and nodules on the cathodes, which usually cause the metal to be of inferior quality. Deposition time is dependent on current densities and varies between 12 and 30 h. Current efficiencies tail off rapidly as the thickness of the metal increases, and a compromise must be made between high efficiencies and the production of the thick metal flake required by the market. A thickness of 1.5–2.0 mm is considered optimum.

Metal Treatment. The cathodes are removed from the electrolysis bath after the appropriate deposition period. Since the α -manganese deposited is hard and brittle, it is readily stripped from the cathode starter-sheet by mechanical shock. The metal is then washed and dried.

Absorbed hydrogen is removed by heating in air or under an inert atmosphere. The latter is necessary when manganese with a particularly low oxygen content is required. Metal destined to be milled must have hydrogen content < 0.0005% to minimize the explosion risk. A primary hydrogen explosion can initiate a secondary manganese dust explosion.

The metal is sold in flake, powder, or granular forms, depending on the end use. A generalization is that the steel industry requires thick flake, while the aluminum industry, welding-rod manufacturers, and manganese chemical producers require powders of various particle size distributions.

Other forms of manganese are also encountered; for example, powder and flake manganese which has had its surface passivated by mild oxidation. A market exists for briquettes of manganese and iron, or manganese and aluminum, which are conveniently added to melts of the appropriate metal to produce a particular alloy.

Quality Control and Analysis. Electrolytic manganese metal has a purity of > 99.5%; no reliable method exists to determine manganese content directly. The sum of the impurities is therefore deducted from 100% to obtain the assay of the metal.

A typical analysis (%) is:

Manganese	99.8
Oxygen	0.2
Nitrogen	0.005
Sulfur	0.02
Carbon	0.001
Iron	0.001
Copper	0.001
Cobalt	0.001
Nickel	0.001
Selenium	0.0005
Hydrogen	0.0006

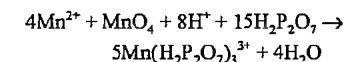
When selenium dioxide is used as a cell solution additive, typical values (%) are:

Manganese	99.4
Sulfur	0.01
Selenium	0.3

Analytical methods described in this section are applicable to all types of manganese metal.

In large amounts, manganese is best determined by titration and many methods exist.

The most reliable is the titration of the divalent ion with permanganate in a neutral pyrophosphate buffer that stabilizes the trivalent manganese species. A platinum redox indicator electrode is used with a suitable reference electrode. A microprocessor controlled automatic titrator facilitates precision and accuracy. The reaction can be summarized as:



The equivalence potential is ca. 0.47 V versus the saturated calomel electrode.

An alternative is to oxidize the manganese to permanganate with excess sodium bismuthate in the presence of nitric acid, add an excess of standard iron(II) solution and back-titrate with permanganate. This method has the advantage of not requiring sophisticated endpoint detection equipment but suffers from a number of interferences. Variations on this oxidation/titration method include silver-catalyzed oxidation by persulfate followed by an arsenate titration [41].

Metallic impurities in both metal and process liquors are usually determined by absorption or emission spectroscopy, though various voltammetric techniques have been used to determine traces in pure metals. The half wave potential of manganese is –1.57 V versus the saturated calomel electrode, making anodic stripping voltammetry ideally suitable for trace metal determination.

Nonmetallic impurities are universally determined by the use of commercially available equipment. The metal is usually heated above the melting point, in a gas stream, releasing the sought element in the form required. This is then determined in the gas phase by infrared absorption or thermal conductivity detectors. Nitrogen in greater than trace amounts has been determined by acid digestion, distillation, and colorimetric determination of ammonia (cf. Kjeldahl method for ammonia).

Summary. The electrolysis of aqueous solutions is the most important manufacturing route at present to high-purity manganese. Economic efficiencies are dependent on scrupulously clean solutions and strict control of

operating parameters. The metal produced may be > 99.7% pure and has many varied uses.

Manganese has also been produced by the electrolysis of aqueous solutions at a flowing mercury cathode. This process, which operates at high current efficiencies, can deliver the manganese in a variety of forms, and is less dependent on solution purities. High electrolysis temperatures, and the inconvenience of coping with toxic mercury are possible reasons why there are now no full-scale plants using this process.

47.6.2 Electrothermal Process

This practice is a refinement of the silicothermic reduction of manganese (see below). However, the purity of the product obtained from the electrothermal process is superior.

The production of bulk manganese by this method is a well protected secret and little information appears in the literature. It is essentially a multistage hot refining process based on the following principles. Manganese ore is smelted in an arc furnace with a limited amount of reductant. This preferentially reduces the iron to metal with a small amount of manganese to form a low-grade ferromanganese with a high phosphorus content. The slag is thus refined to a purified manganese starting material.

The slag is used to produce a high-silicon silicomanganese (> 30% Si) to ensure a low carbon content. Other ingredients such as quartz, limestone, and coke must be selected carefully to ensure a low contamination level. Coke, in particular, may have to be produced from special low-phosphorus coals.

The liquid silicomanganese is treated in two steps, with a liquid basic slag made from the purified manganese starting material. The operation is carried out in a ladle or a shaking ladle.

Typical analyses of electrothermal manganese are given in Table 47.7. From these analyses it can be seen that electrothermic manganese is a relatively pure product that competes in some areas with electrolytic man-

ganese. The sulfur content is particularly low. The aluminum industry is experimenting the use of these products as alternatives to electrolytic manganese.

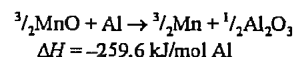
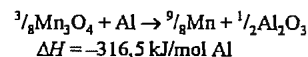
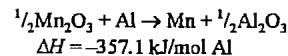
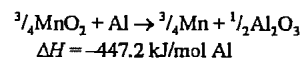
Table 47.7: Typical analyses of electrothermal manganese.

	Gimel* A	Gimel F	Gimel BF	Gimel LP
Mn (% min)	96	97	98	97
C (% max)	0.050	0.030	0.030	0.030
Si (% max)	0.50	0.30	0.30	0.30
P (% max)	0.050	0.030	0.030	0.020
S (% max)	0.008	0.008	0.008	0.008
Fe (% max)	3.0	2.0	1.5	2.0
H (ppm)	5	5	5	5
N (max)	0.035	0.035	0.035	0.035

*Gimel is a registered trade mark of Pechiney Électrometallurgie.

47.6.3 Aluminothermic Process

This production route is based on the well known thermite reaction in which a reactive metal liberates a less reactive metal from its oxide with the evolution of heat. The reactions possible for manganese oxides are:



A heat of reaction of between 272 and 314 kJ/mol aluminum is necessary to sustain the reaction and ensure that it is not explosive. Therefore, some ores may require modification of the relative proportions of the different manganese oxides prior to reaction. This is achieved by calcination at ca. 1000 °C. Certain circumstances require reduction of the ore by calcining in a reducing atmosphere.

Calcium oxide is added to the mix to improve the flow properties of the slag, ensuring good separation of slag and metal. Lime also decreases the amount of silica reporting to the metal phase.

The aluminothermic route to manganese production is attractive in that it requires simple technology which is well documented, and

low capital investment. Its disadvantages are that aluminum is expensive, and the exhaust gases from the process carry manganese and aluminum dust into the atmosphere. Efficiencies of up to 87% have been reported.

47.6.4 Silicothermic Process

The production of manganese by silicothermic reduction resembles that of low-carbon ferromanganese in electric arc furnaces of 1–3 MW power consumption [42, 43]. The raw material used is either low-iron manganese ore or a manganese slag concentrate. The silicon is in the form of a special silicomanganese with ca. 33% Si and < 3% Fe. It is made from a manganese slag concentrate or from pure ores. Reduction as complete as possible is ensured by the addition of lime, which forms a basic slag.

Many slag changes are carried out during the process, as in the silicothermic manufacture of low-carbon ferromanganese. The refined metal has the following typical percentage composition:

Manganese	93–97
Carbon	< 0.10
Silicon	1.5
Phosphorus	< 0.06

The system is moderately efficient and the manganese yield is 63–64%, with slag losses accounting for the remainder.

47.6.5 Distillation of Ferromanganese

Pechiney has filed patents dealing with the vacuum distillation of ferromanganese at 1200–1350 °C. The process has not been used on a large-scale since the manganese produced is inferior to electrolytic manganese and the production costs are prohibitive.

47.6.6 Electrolysis of Fused Salts

Manganese has been produced on a laboratory scale by the electrolysis of fused salts. A system in which an untreated manganese ore is dissolved in a fused mixture of calcium and manganese fluorides and electrolyzed at

1150–1200 °C has been described [44]. The cell potential was 5.5–6.5 V and current density was 9–11 A/cm² at the anode, and 2–2.5 A/cm² at the cathode. Manganese purity in the range 80–99.3% was obtained at current efficiencies of 53–65%.

47.7 Manganese in the Iron and Steel Industry [45]

More than 90% of the manganese mined is used in the steel industry (Figure 7.8). In the production of normal mild steel, high-carbon ferromanganese and silicomanganese are used; however, in special low-carbon steels, medium-carbon ferromanganese, low-carbon ferromanganese or electrolytic manganese is used. A steel producer has to weigh up the additional costs of the refined manganese alloys against the extra time in the argon oxygen decarburization process that would be necessitated by the use of carbon-containing alloys [46]. Manganese occupies a special place among all alloying elements as it is present in almost all types of steel and cast iron.

The addition of manganese to iron–carbon systems has the following effects:

- It retards the rate of transformation (i.e., it increases the hardenability).
- It lowers the martensitic start temperature. This effect is 40 °C at 1% addition of manganese and increases linearly to 200 °C with 5% addition.

Manganese has extensive solid solubility in austenitic iron; therefore, it has no solution hardening effect in austenite. The solubility of manganese in ferritic iron is limited to 3%. Hence, manganese exhibits a solution hardening effect in ferrite (30–40 MPa per % Mn).

Hadfield's austenitic manganese steels (which were developed from 1882) contain 1–1.4% carbon and 10–14% manganese. When they are quenched from 1000 °C the normal hardening transformation temperature is suppressed by the manganese and the steel remains austenitic at room temperature. These steels are exceptionally tough, have high tensile strength, and are wear resistant due to

work hardening. As a consequence, they are used extensively in the mining and earth moving industries.

Manganese is a milder deoxidant than silicon and aluminum. Manganese enhances the effectiveness of aluminum and silicon as deoxidizers of steel due to the formation of stable manganese silicates and aluminates.

The solubility of nitrogen in ferrite is increased by the presence of manganese. The solution hardening effect of manganese is considerably enhanced by nitrogen, which is valuable in high-temperature creep-resistant alloys. Both the yield and ultimate stress at elevated temperatures are increased by the presence of nitrogen in steel, and this effect is enhanced by the presence of manganese.

Nitrogen is a powerful austenizing agent in steels and can be used as a partial substitute for nickel in austenitic stainless steels. The solubility of nitrogen in stainless steels is increased by the addition of manganese, and this is the basis of the series 200 stainless steels.

Manganese has had a long association with the efforts of steel makers to remove sulfur and to minimize the harmful effects of residual sulfur in steel. In the absence of sufficient manganese, sulfur can concentrate in the interstitial liquid in the form of ferrous sulfide. This compound has a low melting point and can persist as a liquid down to low working temperatures. This can cause cracking (hot shortness) during steel rolling. Steel requires a manganese to sulfur ratio of 4 for adequate ductility in the hot working range (950–1150 °C). In practice, ratios of up to 20 are used.

One of the most significant properties of steel is its ability to harden with heat treatment. A number of alloying elements can influence the hardenability of steels but manganese has become virtually synonymous with hardenability due to its effectiveness, availability, and relatively low cost. Increasing the manganese content permits the use of lower heat treating temperatures for steel parts

where the use of higher temperatures would result in deformation.

Shortages, notably during the Korean War, originally prompted the use of manganese as a replacement for some of nickel in austenitic stainless steels.

47.8 Processing of Manganese Nodules and Encrustations

The primary economic interest in manganese deposits on the ocean floor has never been for the manganese content, but rather for the associated valuable metals, including nickel, copper, and cobalt. There are, however, some indications that the manganese content is becoming more attractive in its own right.

The deep ocean resources of manganese nodules were first discovered during the British HMS Challenger expedition of 1872–1876. The commercial potential of these resources was recognized in 1958 as a result of work undertaken at the University of California.

47.8.1 Occurrence, Origin, and Composition [47–50]

Occurrence. Manganese nodules occur over most of the deep ocean floor, but are currently considered to have economic potential in one primary and three subsidiary areas (Figure 47.6). The primary area is located in the northwestern equatorial Pacific (the Clarion Clipperton zone), and the subsidiary areas are in the South Pacific, western equatorial Pacific, and the central Indian Ocean. All of the main areas of potentially economically viable manganese nodules occur on the abyssal seafloor.

Limited quantities of ore-grade nodules have been identified within the Exclusive Economic Zones (EEZ) of some of the western Pacific islands.

Manganese encrustations occur on oceanic seamounts, primarily in the Pacific ocean.

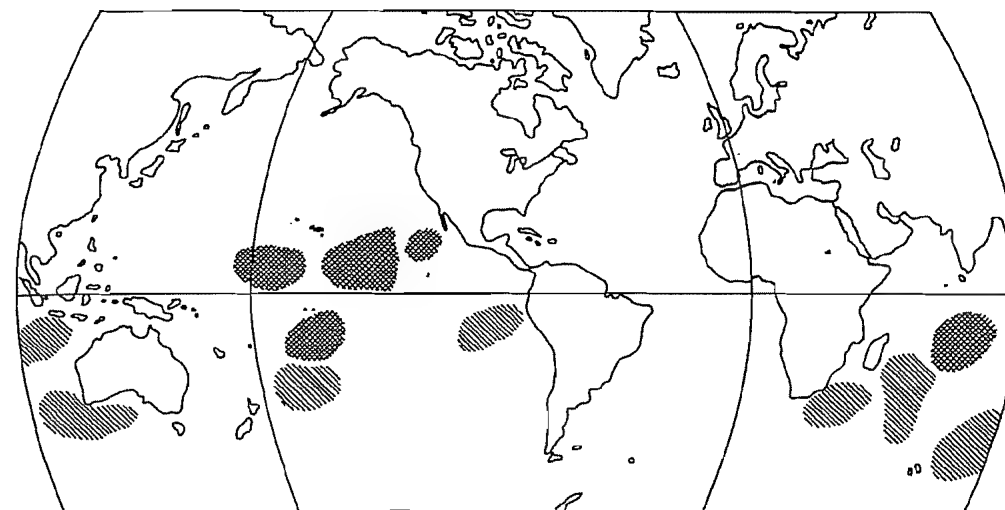


Figure 47.6: Manganese nodule occurrence. ■ Areas of high nodule concentration; ▨ Areas of potential economic viability.

Origin. Manganese on the ocean floor originates from two primary sources: runoff from the continents and submarine volcanic activity. It is believed that plankton extract the manganese and associated metals from seawater and carry them to the ocean floor after death.

The metals are liberated by organic decay processes into the pore water of the deep-sea muds, where, by a series of diagenetic reactions, they migrate to centers of nucleation within the uppermost sediments and precipitate to form manganese nodules. Encrustations are formed on exposed rocks.

Composition. The chemical composition of manganese nodules varies widely. Some 74 elements have been found to occur in manganese nodules and encrustations. The average chemical composition varies from ocean to ocean and with latitude, water depth, and mineralogy.

World averages of nodule composition are influenced by the disproportionately high number of stations located in the Pacific Clarion Clipperton zone, in which the nodules average 25.4% Mn, 6.66% Fe, 1.27% Ni, 1.02% Co. Excluding these values from the world averages decreases the average nickel, copper,

and manganese contents, increases the iron content, and has no effect on the cobalt content.

Principle metal contents, together with nodule concentration and depth, are listed in Table 47.8.

Table 47.8: Chemical composition of manganese nodules.

Element	Mean content, %	Range, %
Mn	18.60	0.04–50.3
Fe	12.47	0.30–50.0
Ni	0.66	0.01–1.95
Cu	0.45	0.101–1.90
Co	0.27	0.01–2.23

The top of a nodule is generally higher in Fe, Co, and Pb and lower in Cu, Ni, Mo, Zn, and Mn compared to the bottom. The nodule core is usually deficient in Fe, Co, and Pb.

Physical Characteristics. Manganese nodules generally exhibit five external shapes: spheroidal, ellipsoidal, discoidal, botryoidal, and flat faced. The surface textures, which may be smooth or granular, may vary on the opposite sides of the nodule. The size varies from 0.5–20 cm, with concretions larger than 20 cm generally assuming the form of slabs. The color is usually dark reddish brown to black. Some zonal pattern in nodule cross sec-

tion, produced by variation in mineral content of the growth layers, is generally present. The porosity is relatively high and relative density low (2.1–3.1).

Water comprises about 45–50% of nodules when removed from the ocean. Air drying removes about half of this water. Approximately 5–10% water is contained within the crystal structure.

Mineralogy. Nodules comprise a complex mixture of organic and colloidal matter, nucleus fragments, and crystallites of various minerals. The phases are fine grained, often metastable, poorly crystallized, and intimately intergrown.

Todorokite, birnessite, and vernadite are the predominant manganese oxide minerals, while various other MnO_2 modifications in the form of $\alpha\text{-MnO}_2$, $\beta\text{-MnO}_2$, and $\gamma\text{-MnO}_2$ have also been reported.

Iron is present as oxide, oxyhydroxide, and hydrated oxide phases, the most commonly observed being ferroxhyte, goethite, and lepidocrocite.

The accessory minerals can be divided into the following three categories: sheet silicates and zeolites, clastic silicates, volcanic minerals, and biogenic minerals.

Known minerals of nickel, copper, or cobalt have not been identified; Cu, Mo, Ni, and Zn are associated almost entirely with the manganese mineral phase. Ba, Cd, Ca, Mg, Sb, Sr, and V are usually associated with manganese but are also found in other phases. Pb and Ti are associated almost entirely with the Fe and Mn phases.

47.8.2 Legal Considerations and Nodule Recovery [47, 49, 51–54]

Legal Considerations. The Law of the Sea as pertaining to the exploitation of mineral resources is of major importance to the future viability and prospects of commercial venture.

During the early 1960s interest in deep-ocean mining increased and the Third UN Law of the Sea conference began in 1974. The

current Convention was eventually adopted by this conference in 1982.

The United States, Germany, and United Kingdom voted against the convention because of objections to certain provisions related to deep-sea mining.

The most important of the above regimes as pertaining to manganese nodule exploitation are the EEZ, extending to 200 nautical miles from the coastal state shoreline, and the so-called Area, extending beyond this limit. The coastal state has sovereignty over the EEZ, but the sea floor outside these zones falls under the jurisdiction of an International Seabed Authority which will be responsible for all mineral deposits and even mine these deposits through its own organization. The Authority would also license independent mining organizations to exploit these deposits, but in doing so would impose a number of conditions which some national governments and mining consortia find unacceptable.

The 200 mile EEZ would put under coastal state jurisdiction most of the minerals of the continental margins and, in some areas, those of the deep-ocean floor.

The convention also limits the amount of nickel that can be produced outside the EEZ over the first 20 years of commercial production in order to protect the markets of land-based producers.

The United States, Germany, France, the United Kingdom, the Soviet Union, and Italy have passed national deep-seabed mining legislation which, in many instances, is in contradiction of the UN Convention.

Nodule Recovery. Research into nodule recovery has been conducted since the 1960s and the technical feasibility, to a large extent, has been established.

Three main systems have been investigated: the continuous line bucket, the autonomous shuttle, and hydraulic pumping with a suspended conduit or dredge pipe.

Techniques based on continuous hydraulic pumping systems are the most technically and economically viable.

47.8.3 Processing

The following processes [48, 49, 55, 56] for recovering the metals of value (Mn, Co, Ni, Cu) from nodules have been identified as being potentially feasible:

- Gas reduction and ammoniacal leach
- Cuprion ammoniacal leach
- Elevated temperature and pressure H_2SO_4 leach
- Reduction and HCl leach
- Smelting and H_2SO_4 leach

The first three of the above options recover Co, Ni, and Cu, while Mn can be optionally recovered from the tailings. The last two are more suited to the recovery of all four metals.

Ammoniacal processes are similar to those used for the treatment of land-based nickeliferous laterites which, in some respects, are similar to manganese nodules. Cobalt, nickel, and copper are soluble in $\text{NH}_3\text{--NH}_4\text{CO}_3$ (the Caron process) and $\text{NH}_3\text{--(NH}_4)_2\text{SO}_4$ solutions.

These processes involve selective reduction of the metals and disruption of the nodule matrix to permit rapid, complete dissolution of the valuable metals. Acidic chloride solutions are also capable of dissolving the valuable metals including manganese. Acidic sulfate solutions can solubilize cobalt, nickel and copper. Nickel is recovered from laterites by sulfuric acid leaching at elevated temperature.

The diverse chemical, physical and mineralogical composition of the nodules exclude physical enrichment prior to the complex hydrometallurgical processing. Separation on the basis of density, magnetic properties, or flotation has not been successful.

The recovery of manganese from the tailings of the ammoniacal processes (routes 1 and 2 above) involves flotation of the MnCO_3 , which could then be converted to a manganese oxide product for further processing or sale. Manganese dioxide could be recovered from the H_2SO_4 process tailings (route 3 above) by dissolution and chemical treatment. Direct use of the tailings from all the processes above for ferromanganese production is probably pre-

cluded due to the unacceptably high levels of trace metals, sulfur, and phosphorus.

47.8.3.1 Gaseous Reduction and Ammoniacal Leach Process

This process (Figure 47.7) is an adaptation of the Caron process for nickeliferous laterites (see Chapter 12).

The MnO_2 is reduced to MnO at 625 °C by a producer gas rich in CO. The mineral structure is disrupted by this reduction and the contained metals can be dissolved by an aqueous solution of 10% ammonia and 5% CO_2 at 40 °C and atmospheric pressure. The pregnant solution is separated from the solids, and copper and nickel are isolated by solvent extraction and aqueous stripping. The products are recovered as cathode copper and nickel by electrowinning.

The aqueous $\text{NH}_3\text{--CO}_2$ solution is contacted with hydrogen sulfide, and insoluble cobalt sulfides and residual copper, nickel, zinc, and other metals are precipitated.

This precipitate is removed and contacted with air and H_2SO_4 to selectively redissolve the cobalt and the small amount of nickel still present. The cobalt and nickel are recovered from the liquid in powder form by selective reduction with hydrogen at 3.4 MPa and 185 °C.

The residual ammonia and carbon dioxide are removed from the nodule residue by steam at 120 °C and 0.2 MPa. The resulting mixture is condensed and, together with the mixture of ammonia carbon dioxide and steam arising from the cobalt extraction step, is recycled.

47.8.3.2 Cuprion Ammoniacal Leach Process

Manganese dioxide is reduced in an aqueous ammoniacal solution containing an excess of copper(I) ions at 50 °C. The cobalt, nickel, and copper are solubilized in an aqueous solution of ammonia and carbon dioxide at 50 °C and atmospheric pressure. The separation and purification of the metals is identical to the Caron gas reduction process (Figure 47.7).

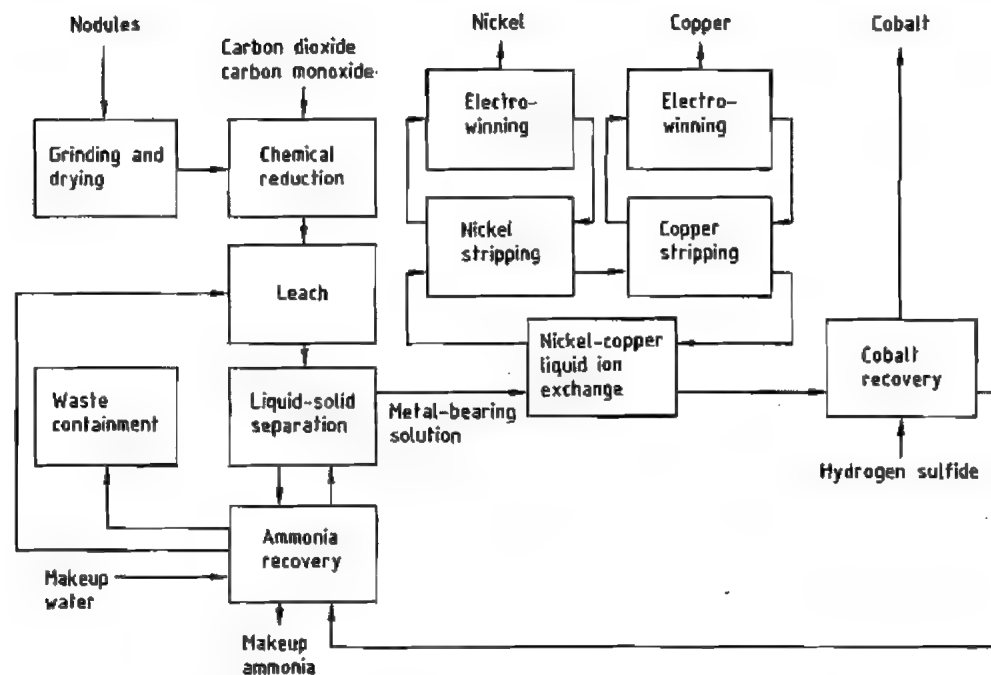


Figure 47.7: Gaseous reduction and ammoniacal leach process.

47.8.3.3 Elevated Temperature and Pressure H_2SO_4 Leach Process

In this process (Figure 47.8) the cobalt, nickel, and copper content of the milled nodules is dissolved in a 30% sulfuric acid solution at 245 °C and 3.54 MPa. Manganese and iron are not solubilized to any appreciable extent. The resultant slurry is cooled and the acid solution separated from the nodule residue. The pregnant solution is pH adjusted and the copper and nickel are selectively removed by extraction with an organic solvent. These metals are then stripped as copper and nickel sulfate in acidic aqueous solutions and subsequently recovered by electrowinning.

The cobalt is precipitated with hydrogen sulfide together with residual nickel, copper, and zinc. The precipitate is separated from the solution and contacted with air and H_2SO_4 at 100 °C to selectively redissolve the cobalt and

residual nickel, which are recovered as powders from the solution by reduction with hydrogen gas at 3.4 MPa and 185 °C.

The ammonia is recovered from the barren solution and recycled. The barren, ammonia-free solution is recycled for washing of the leached nodule material.

47.8.3.4 Reduction and HCl Leach Process

In this process (Figure 47.9) the manganese dioxide is reduced to soluble manganese chloride with hydrogen chloride at 500 °C and 0.1 MPa. A portion of the hydrogen chloride is oxidized to chlorine. The excess hydrogen chloride is separated from this chlorine and water vapor and recycled. Dissolution of the iron in the nodules is minimized by injection of steam, which results in the hydrolysis of iron chloride to insoluble ferric hydroxide.

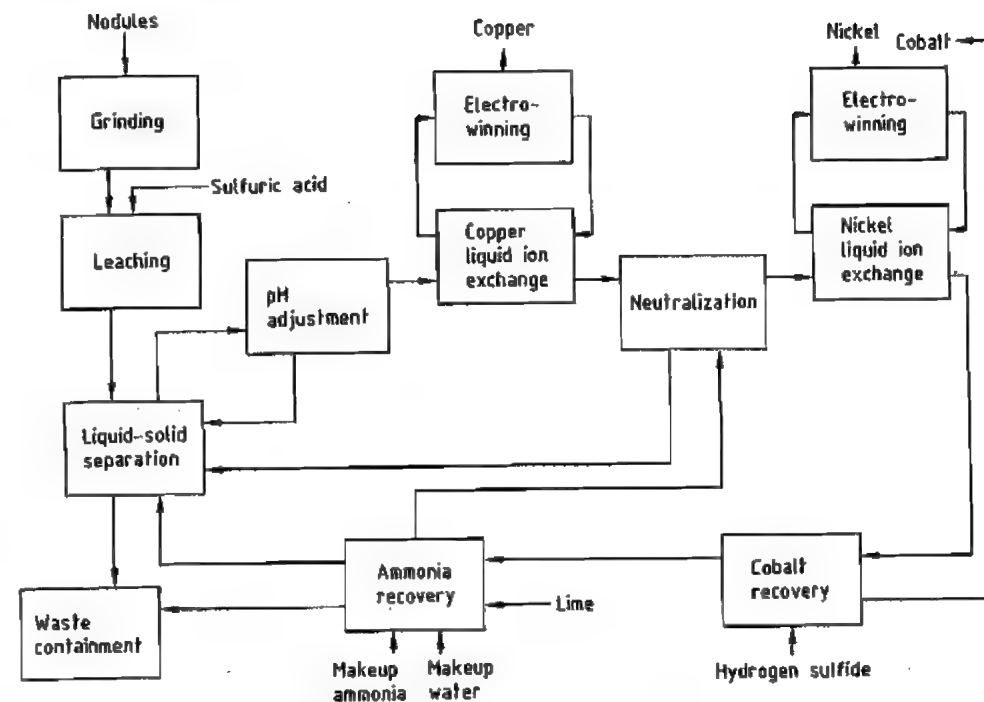


Figure 47.8: High-temperature, high-pressure sulfuric acid leach process.

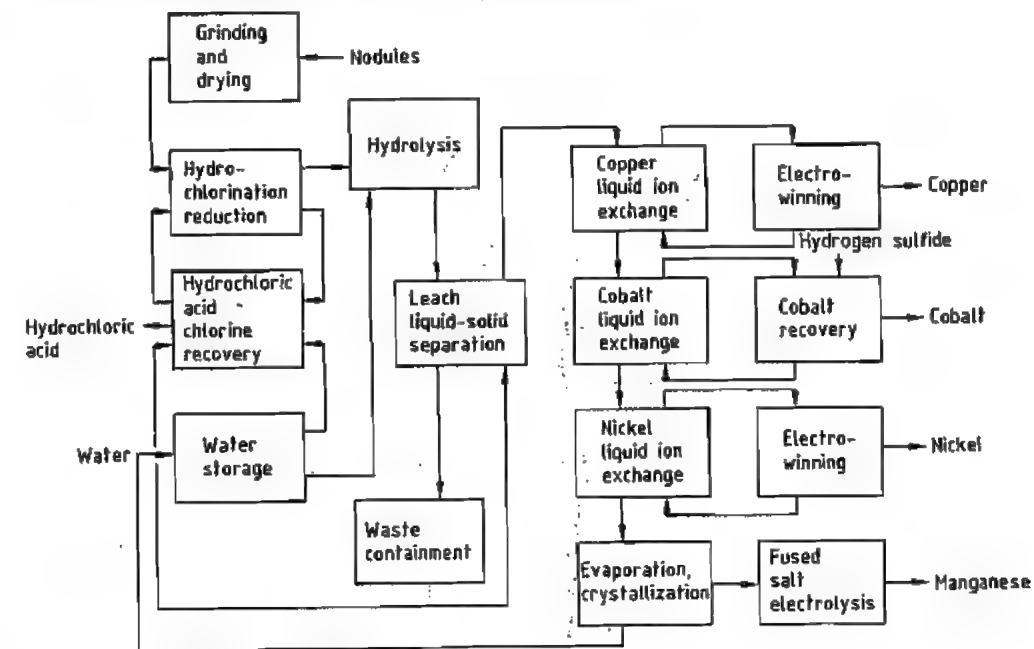


Figure 47.9: Reduction and hydrochloric acid leach process.

The soluble Co, Ni, Cu, and Mn chlorides are dissolved by leaching with HCl. Copper is selectively extracted by organic ion exchange and subsequently stripped into a strong H_2SO_4 solution. The copper is recovered by electro-winning.

The copper-free chloride solution is neutralized and cobalt is removed by a second selective solvent extraction stage. The cobalt is recovered as a powder by a sequence of stripping, precipitation as cobalt sulfide by hydrogen sulfide, selective leaching, and hydrogen reduction.

The copper- and cobalt-free solution is subjected to a third solvent extraction stage to remove nickel. The nickel is stripped into an acidic sulfate solution for subsequent electro-winning.

The final aqueous chloride solution can be dried to produce impure manganese chloride,

which can be charged to an electrolysis furnace where it dissolves in a molten alkali chloride bath. Molten manganese is tapped from the furnace and cast. Chlorine gas is also produced from the electrolysis furnace and, together with the chlorine resulting from the initial hydrochlorination stage, can be converted to hydrogen chloride for recycling.

47.8.3.5 Smelting and H_2SO_4 Leach Process

In the sulfuric acid leach process (Figure 47.10), the nodules are dried and the manganese dioxide and ferric oxide reduced to manganous and ferrous oxides at 625–1000 °C with coal and carbon-monoxide-rich producer gas. The reduced nodules, together with coke and silica, are hot-charged to an electric furnace.

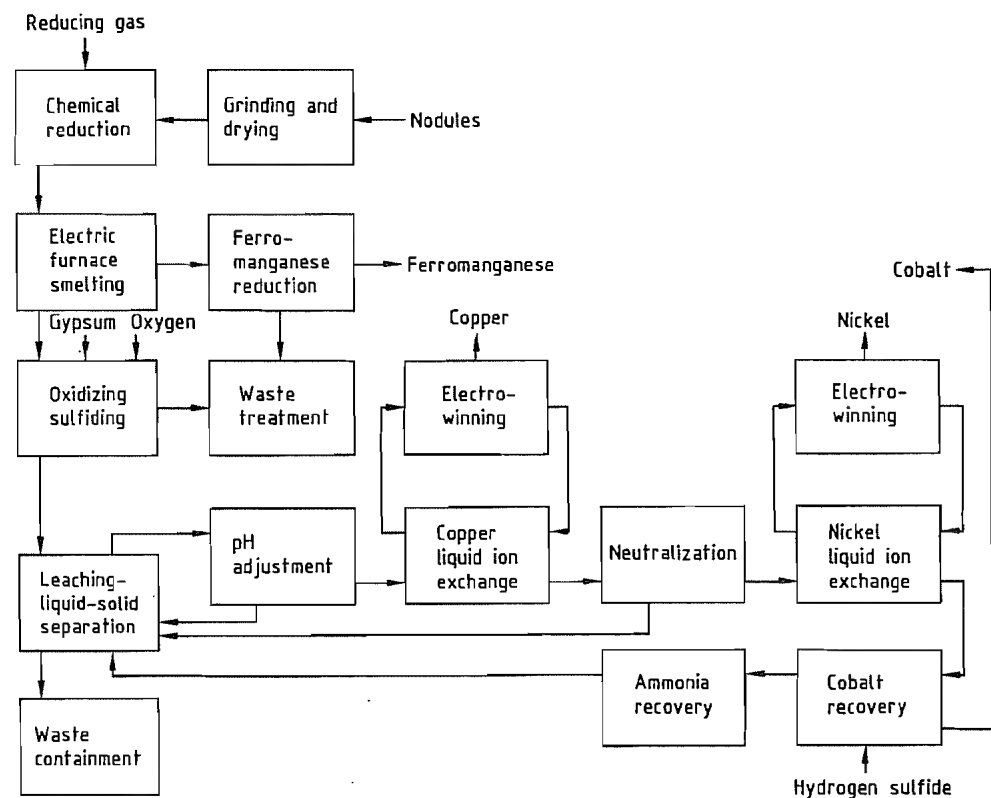


Figure 47.10: Smelting and sulfuric acid leach process.

In this step most of the Cu, Ni, Co, and Fe, and some of the Mn is reduced at 1425 °C to form a molten alloy phase, which separates by gravity from the unreduced management slag. The alloy is transferred to converters where, after the addition of further silica, the Mn and most of the Fe is reoxidized with air, separated as a slag, and recycled to the furnace. Gypsum, coke, and possibly sulfur are added to the alloy, producing a metal sulfide matte phase containing the Cu, Ni, and Co. These are separated in the converter and the slag is recycled to the electric furnace, while the matte is water quenched and granulated.

A ferromanganese alloy can be produced from the furnace slag by smelting, together with iron-rich slags and coke, in an electric furnace.

The metals are leached from the granulated matte with a 5% H_2SO_4 solution in the presence of oxygen at 1 MPa and 110 °C. Copper and nickel are recovered separately from this solution by selective solvent extraction. The pH of the solution is controlled by addition of ammonia. The metals are stripped into acidic aqueous solutions and the products recovered by electro-winning.

Cobalt and the residual other metals are recovered from the aqueous ammonium sulfate solution by precipitation with hydrogen sulfide. The separated precipitate is contacted with air and H_2SO_4 at 100 °C to selectively redissolve the cobalt and residual nickel, which are recovered in powder form by selective reduction with hydrogen at 3.4 MPa and 185 °C.

47.8.4 Economic Viability and Future Prospects [47, 49–51, 57, 58]

The constraints inhibiting the exploitation of the nodule reserves are complex a combination of economic, technological, sociological, and political. Any operation would have to satisfy several prerequisites: technical feasibility of mining and processing; economic or strategic viability; legal authorization and security of tenure; and environmental acceptability.

Although most of the results of the extensive research and development work undertaken by several nodule recovery consortia has not been published, sufficient successful announcements have been made to indicate that the recovery and processing of nodules is technically feasible.

Numerous environmental impact assessments indicate that nodule dredging totally destroys the area of operation. Adjacent undredged areas, however, appear to be unharmed and provide the basis for rehabilitation. Adverse environmental effects are therefore short-lived.

The estimated economic viability of mining and processing nodules has been well reported, covering a wide range of scenarios. Estimates of the internal rate of return range from 3 to 18%, with the more recent studies showing lower rates. The high degree of risk associated with nodule exploitation probably necessitates a rate of return of ca. 30% to warrant investment. The studies also exhibit very high sensitivity to variations in commodity prices, metal recoveries, and deposit grades. From an economic viewpoint only, it is most likely that nodules will not be mined and processed in the foreseeable future without significant financial incentives in the form of price supports, market protection, and tax breaks.

The considerable uncertainty currently existing as to the legal authorization for mining beyond the limits of national jurisdiction (that is, outside the EEZ) casts more doubt on the feasibility of commercial nodule mining for some years to come. The prospects of commercial exploitation of the extensive deposits of cobalt-rich manganese oxide crusts lying within the EEZ are better than those for the nodules. The technical feasibility of recovering these crusts has not yet, however, been developed and tested.

The supply and demand situation, coupled to strategic considerations, for the four metals of interest will probably be the ultimate determining factor for future exploitation. Most mining consortia have only considered the recovery of cobalt, nickel, and copper. Recent reappraisals of manganese and its perceived

value as a strategic metal (particularly in the United States) has led to an increasing interest in four-metal extraction. A modest increase in manganese usage is predicted in future, directly coupled to steel production. The perceptions of the instability of cobalt supply from African sources increase the strategic sensitivity of this metal.

Another important use for nodules is as a stack gas absorption mechanism. Elimination or reduction of sulfur and nitrogen oxides is possible by catalytic oxidation by compositions involving transition metals. Nodules possess the high specific surface area and transition metal oxide content required for an oxidation catalyst. This use of nodules also provides a primary stage for the recovery of the metals of value. The complex metal oxides in the nodules are readily reduced to sulfides as a contaminated gas stream is passed through the filter pack of ground nodules. Well defined processing techniques, as described before, can then be applied to recover the four metals of interest.

47.9 Economic Aspects [59]

Ninety percent of manganese produced is consumed in the steel industry, and the growth of the manganese industry is therefore directly related to that of the steel industry. Steel production in the Western world dropped sharply in the early 1980s and bottomed out in 1982–1983. Economic recovery in the Western industrialized countries in the late 1980s resulted in strong growth in the steel sector. Between 1986 and 1988 the world production of crude steel increased by 9% to 780×10^6 t and is likely to continue at this level into 1990, when a drop off is expected. Hereafter steel is expected to grow at ratio between 1% and 1.5% per annum however a migration of production capacity from developed to undeveloped countries will occur, China will become the world's largest producer of steel in the late nineties. As a consequence the demand for ferromanganese alloys has increased considerably. The increase in demand placed upward pressure on the price of ferromanganese and

silicomanganese in 1988 and 1989 and in terms of constant 1980 US\$ similar price levels are being achieved to those in the early 1980s (Figure 47.11). A sharp drop in the price of silicomanganese was experienced at the end of 1989 due to an excess of Chinese material in the market and the low ferrosilicon prices (Figure 47.12).

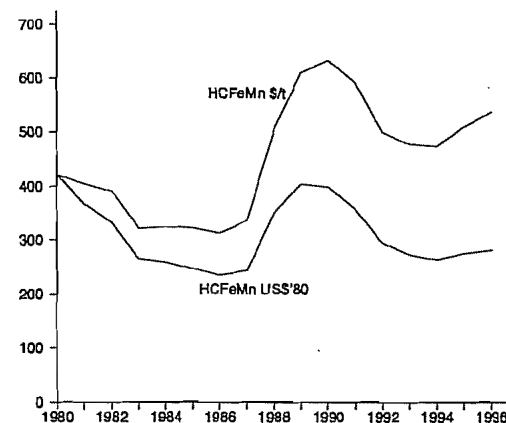


Figure 47.11: Price of ferromanganese.

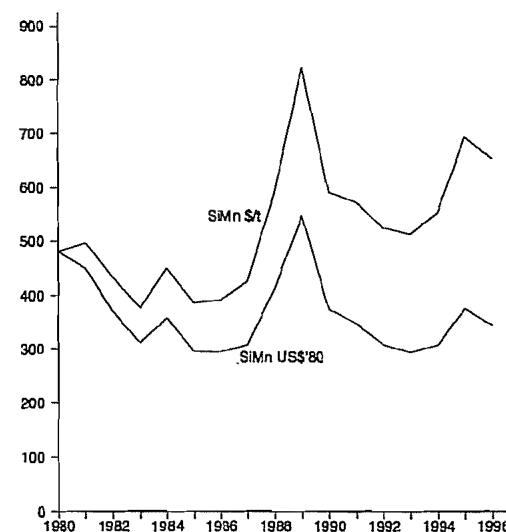


Figure 47.12: Price of silicomanganese.

Alloy prices remained low through the early nineties due to a stagnant world economy and a reorganization in the European steel industry. Recovery of prices began again in 1994 due to the rebuilding of the American

infrastructure and the collapse of the ex-Soviet steel industry.

In the future demand for alloys will shift to high- and medium-carbon ferromanganese from silicomanganese as mini mill steel producers increasingly introduce thin slab casting processes in their factories.

Prices of high and medium carbon ferromanganese should therefore remain reasonably firm, showing slight fluctuations as the steel goes through stocking and destocking cycles.

The increasing demand for high grade alloys has once again highlighted the shortage in the production capacity of high grade ores (as was the case in 1988–1989) (Figure 47.13). Traditional low grade ore producers, namely, the CIS, China and India are now becoming significant importers of high grade ore. China for instance imported 1.2 million tons in 1995. Ore prices are expected to flatten out at current levels and fluctuate in accordance with world electricity and coke prices.

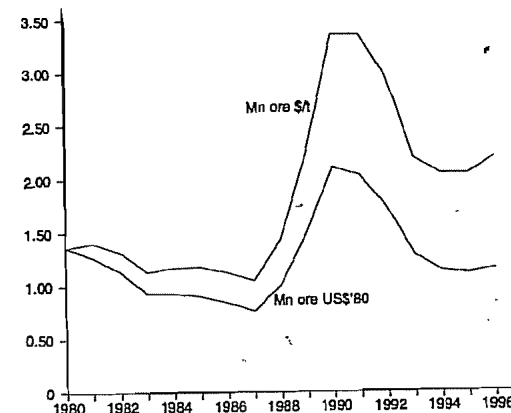


Figure 47.13: Manganese ore prices.

47.10 Compounds

47.10.1 Introduction [60]

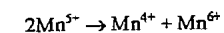
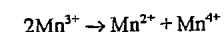
Manganese compounds occur in all oxidation states from 3– to 7+, with 2+, 4+, and 7+ being the most important. Most of the species in which Mn displays a negative valence state are anionic; for example, the ion $\text{Mn}(\text{CO})_5^{3-}$

[obtained by vigorous reduction of $\text{Mn}_2(\text{CO})_{10}$] contains Mn in the 3– state. The 2– oxidation state can be found in a complex of manganese with phthalocyanine, whereas manganese in the 1– state is represented by the manganese pentacarbonyl ion $\text{Mn}(\text{CO})_5^-$. Ions representing the various positive valences display characteristic colors, as indicated in Table 47.9. The color of a particular ion in solution is not always the same as that of the corresponding solid compound. Thus, solid MnO is light green, $\text{Mn}(\text{OH})_2$ is white, and Mn_3O_4 , Mn_2O_3 , and MnO_2 are black. Liquid Mn_2O_7 is green under reflected light but deep red under transmitted light.

Table 47.9: Ionic species of manganese.

Ion	Valence	Color
Mn^{2+}	2+	pink
Mn^{3+}	3+	red
Mn^{4+}	4+	brownish black
MnO_3^{3-}	5+	blue
MnO_4^{2-}	6+	green
MnO_4^-	7+	purple

Given the multitude of valence states for manganese compounds, redox reactions are of great importance. Under suitable pH conditions, compounds containing manganese with a valence of 3+ or more are effective oxidants. Furthermore, tri-, penta-, and hexavalent manganese compounds tend to undergo disproportionation reactions under the influence of H^+ and OH^- :



The divalent state is generally regarded as the most stable, at least in acid to neutral media. Tetravalent manganese is also quite stable as MnO_2 under moderately acid and moderately alkaline conditions, while the heptavalent state displays maximum stability around pH 7. Precipitated manganese(II) hydroxide is oxidized at room temperature by oxygen to tri- and tetravalent manganese oxides in the presence of traces of alkali, while conversion to manganates (i.e., the penta- and hexavalent states) requires much higher temperatures and high alkali concentrations ($\geq 180^\circ\text{C}$ for 60–

70% KOH). The basicity of the manganese oxides decreases (and the acidity increases) with increasing valency. Thus, MnO behaves as a basic anhydride, MnO₂ is amphoteric, and Mn₂O₇ is an acidic anhydride. Even though manganese in its highest valence state (7+) resembles chlorine (i.e., perchlorate), its general reactivity corresponds more closely to that of iron.

47.10.2 Oxides

47.10.2.1 Manganese(IV) Oxide

Properties

Manganese(IV) oxide, MnO₂, is deep black to dark brown and practically insoluble in water. It is more commonly referred to as manganese dioxide, occasionally as pyrolusite. Pyrolusite (German: Braunstein) is also the name of a specific MnO₂-containing mineral. The purest manganese dioxide—corresponding rather closely to the formula MnO₂—occurs in the form known as the β-modification. The compositions of other natural or synthetic manganese dioxides range from MnO_{1.7} to MnO_{2.0} with varying contents of lower-valent manganese, foreign cations (e.g., K⁺, Na⁺, Ba²⁺), hydroxyl ions, and water molecules. At least six distinct modifications of manganese dioxide have been characterized (α, β, γ, δ, ε, and ramsdellite) [61, 62], which differ according to their degree of crystallization and their content of foreign ions. The β-modification (as in the mineral pyrolusite) is not only the least reactive form of MnO₂ but also the most highly crystalline, and it comes the closest to having a stoichiometric composition. By contrast, γ-MnO₂ is nearly amorphous and much more reactive both chemically and electrochemically. When heated up to 500 °C, manganese dioxides frequently release water and/or undergo phase transitions; above 500 °C they liberate oxygen. Between 500 and 600 °C MnO₂ is converted into Mn₂O₃, and above 890 °C into Mn₃O₄. Manganese dioxide acts as an oxidant toward readily oxidizable

materials, its own valency changing from 4+ to 3+ or 2+. For example, under acidic conditions manganese dioxide oxidizes chloride ions to chlorine; hydrazine and hydroxylamine to nitrogen; iron(II) to iron(III); carbon monoxide to carbon dioxide; alkylbenzenes to aromatic carboxylic acids, ketones, and, in some cases, aldehydes; and oxalic acid to carbon dioxide.

In the presence of strong alkalis and at elevated temperature, however, manganese dioxide is itself readily oxidized by oxygen to manganese(V) and (VI) compounds. Other noteworthy properties of the various MnO₂ modifications include their sorptive and ion-exchange capabilities and their catalytic and electrochemical activities. The latter is of great importance to the dry-cell battery industry, which consumes large amounts of "battery-active" MnO₂ (especially the γ- and ε-modifications) for use as a depolarizer.

Natural Manganese Dioxide

Only about 5% of the world production of manganese ore (presently totalling about 27 × 10⁶ t/a) is consumed in nonmetallurgical applications. In 1976 (the latest year for which data have been published), the following approximate tonnages of manganese ore were associated with applications other than steel making [63, p. 331]:

For dry cell batteries (battery-active ore plus ore consumed in the production of battery-grade electrolytic manganese dioxide and chemical manganese dioxide)	500 000 t/a
In brick and ceramic coloring, including in glass manufacture	200 000 t/a
In welding rod manufacture	200 000 t/a
For the production of Mn chemicals and diverse chemical and metallurgical products	450 000 t/a
Total	1 350 000 t/a

Within limits, these consumption figures are probably still applicable, because world ore consumption in 1976 (24 × 10⁶ t/a) was only slightly less than that in 1986 (25 × 10⁶ t/a), and about 5% is still consigned to metallurgical uses. Organic MnO₂ oxidations are generally carried out in the presence of sulfuric acid, and they lead to manganese sulfate as a by-product. Oxidation of aniline by MnO₂ in

the presence of sulfuric acid was once the main industrial route to hydroquinone, but since the late 1960s this technique has been largely replaced by other methods, at least in the Western world. For more information on the synthetic applications of native manganese dioxide [64, pp. 36–37].

Several processes are known for the recovery of manganese from low-grade MnO₂-containing ores (Mn content < 20%) [65, pp. 727–731; 66], but they are currently of little practical significance since high-grade manganese ores (Mn > 40%) are widely available at moderate prices.

Synthetic Manganese Dioxides

Commercial Forms

Several types of synthetic manganese dioxide are produced commercially for specific end uses. In principle, synthetic manganese dioxide can be prepared either by a strictly chemical route (*chemical manganese dioxide*, CMD) or by electrochemical methods (*electrolytic manganese dioxide*, EMD).

Procedures leading to CMD include the oxidation of Mn(II) salts or lower manganese oxides, reduction of permanganates, thermal decomposition of manganese(II) nitrates, thermal decomposition/oxidation of manganese carbonate, and disproportionation of Mn(III) compounds.

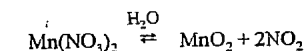
Manganese dioxides obtained by reduction of permanganate are commonly known as *manganites*. They correspond to the δ-modification of MnO₂ and should actually be regarded as salt-like combinations of hydrous manganese dioxide and cations of base-forming metals (e.g., K₂O · 4MnO₂). The metal portion is exchangeable against other cations. Such manganites [which are actually alkali manganates(IV)] are often obtained as by-products from technical permanganate oxidations, but they may also be synthesized intentionally by direct reduction of permanganate (e.g., with manganese(II) salts). Until the late 1960s, the manganites were important in the manufacture of dry cells because they are

highly active depolarizers. Manganites for this purpose were produced and sold in Europe under such trade names as Manganit and Permanox. However, in recent years they have been largely displaced by electrolytic manganese dioxide (EMD) and the other types of chemically prepared manganese dioxide (CMD) described later.

Also of interest is the *hydrated manganite*, better known as *active manganese dioxide*, used in organic syntheses under nonaqueous, neutral conditions. Manganese dioxide of this type is generally prepared from MnSO₄ and KMnO₄ under strictly controlled conditions. Numerous methods are available for the preparation of "active" manganese dioxide. Many involve oxidation of a Mn²⁺ salt with KMnO₄, but NaClO₃ or O₃ are also used as oxidants. In a typical procedure, a solution of manganese sulfate (151 g/2.87 L) is added with stirring to a solution of potassium permanganate (105 g/2 L), and the resulting suspension of hydrous MnO₂ is stirred at 60 °C for 1 h. After filtration and washing, the precipitate is dried to a constant weight at 60 °C [67, p. 122]. These conditions lead to precipitated MnO₂ in the poorly crystallized but very reactive γ-form. It is a specific oxidant whose uses include dehydrogenation (e.g., the preparation of unsaturated aldehydes and ketones from unsaturated alcohols) and coupling reactions.

Mention should also be made of the increasing use of manganese-dioxide-based *oxidation catalysts*, particularly for air pollution abatement (removal of volatile organics, destruction of Ozone) [68, 69].

Another commercial CMD is a *high-purity manganese dioxide* used in the manufacture of high-purity lower manganese oxides as well as ferrites (ceramic magnets) and thermistors for the electronics industry. This product (99.5% MnO₂) is obtained by thermal decomposition of manganese nitrate:



For a description of the original manganese nitrate process developed by IG Farbenindustrie (Bitterfeld) in the 1920s, see [70]. A later

modification of this process by Chemetals has been utilized at a plant in Baltimore since the early 1970s [71, 72] (Figure 47.14).

A concentrated solution of manganese nitrate (made from MnO_2 ore by reaction with NO_2) is first purified and then thermally decomposed at about 140°C in a well-agitated, externally heated reactor. The resulting β -manganese dioxide precipitates as a fine, free-flowing powder; the nitrogen dioxide coproduct is recycled to generate new manganese nitrate. Chemetals' production capacity for high-purity manganese dioxide is about 6000 t/a.

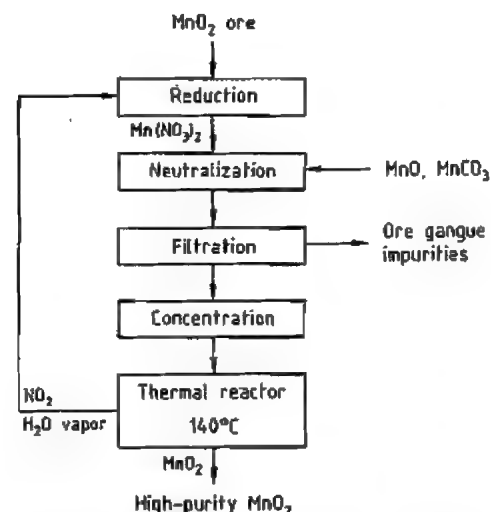


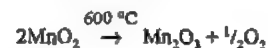
Figure 47.14: Manufacture of high-purity manganese dioxide MnO_2 (Chemetals process).

Synthetic Manganese Dioxides for Dry Cells

From a commercial standpoint the most important synthetic manganese dioxides are those that are electrochemically active and are therefore useful as depolarizers in dry-cell batteries. Electrochemical or battery activity of MnO_2 results from a favorable combination of such factors as crystal structure, surface area, porosity, and chemical purity. Battery activity is not readily predictable; the only reliable

way of establishing this property is by an actual performance test in a battery.

One important type is the so-called *activated manganese ore*, actually a semisynthetic product. It is made by roasting a high-grade oxidic manganese ore containing at least 80% MnO_2 but with low or no battery activity at 600°C . The product is then treated with hot sulfuric acid.



The second reaction is a disproportionation of trivalent manganese leading directly to battery-active γ - MnO_2 . The coproduct MnSO_4 must be separated by leaching with water. Activated manganese ore is somewhat less effective as a depolarizer than EMD or fully synthetic CMD (see below), but it is still produced in France at a rate of several thousand tonnes per year under the names Ergogene and Philodyne.

Chemical Manganese Dioxide (CMD). Much more important than activated ores are the CMD products manufactured by the Sedema Division of Sadacem S.A. in Belgium under the trade names Faradiser M (for Leclanché and magnesium cells) and Faradiser WSZ (for zinc chloride batteries). The chemical compositions of the two products are practically identical: ca. 90% MnO_2 (primarily the γ -modification), 2% water, plus minor amounts of lower manganese oxides. Critical trace impurities (Co, Ni, Cu, Mo) are kept below 0.001%. Types M and WSZ differ in such physical properties as surface area and density. Typical particle sizes are $80\% < 44 \mu\text{m}$ for type M and $85\% < 44 \mu\text{m}$ for type WSZ.

The first step in the production process [72, 73] (Figure 47.15) is the reduction of MnO_2 ore to MnO using heavy fuel oil and a temperature of ca. 900°C . The MnO is then treated with sulfuric acid to form manganese(II) sulfate. After careful neutralization with MnO to precipitate heavy metal impurities, solids are removed by thickening.

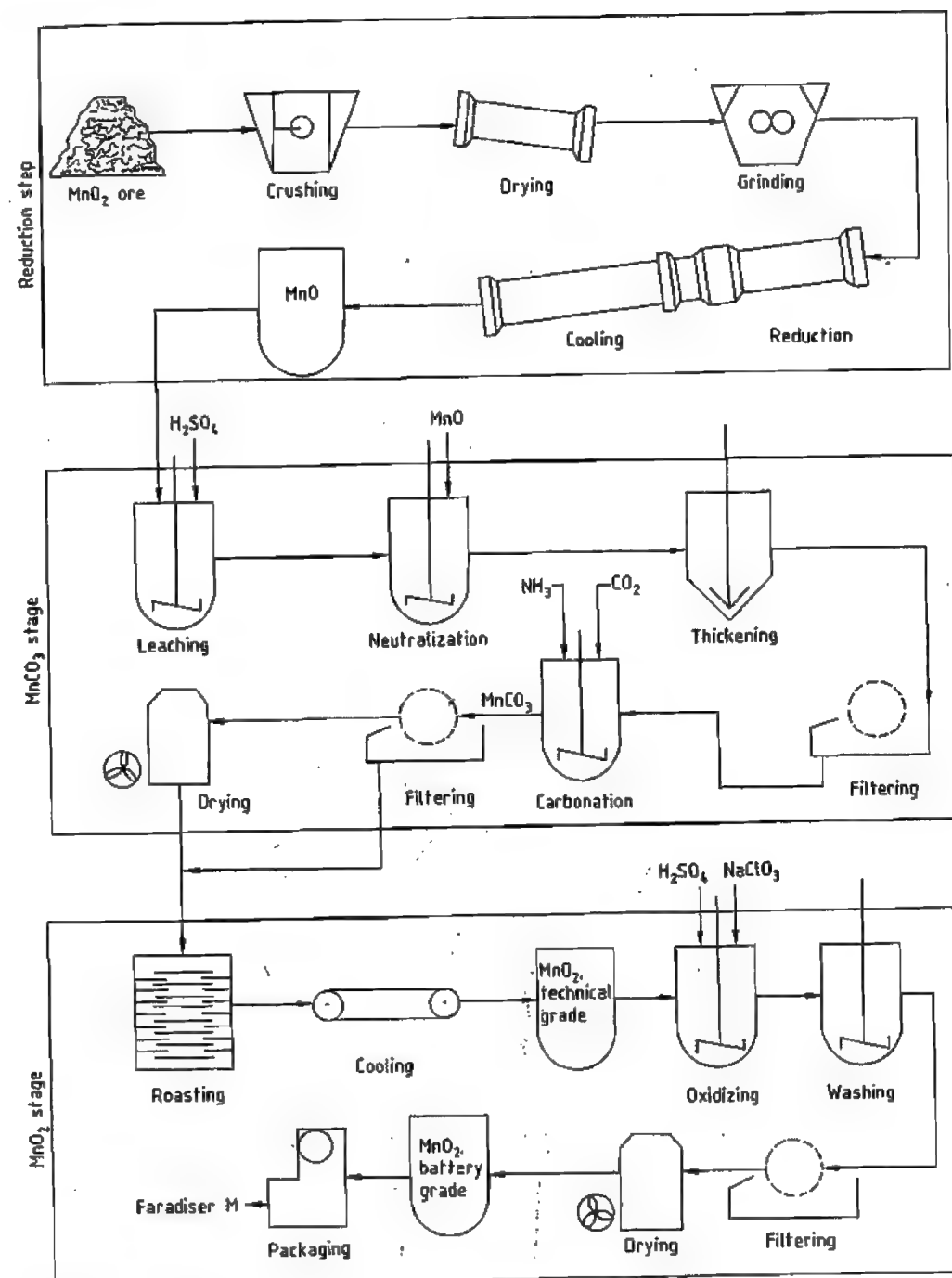


Figure 47.15: Production of chemical manganese dioxide (CMD) according to the Sedema process [72].

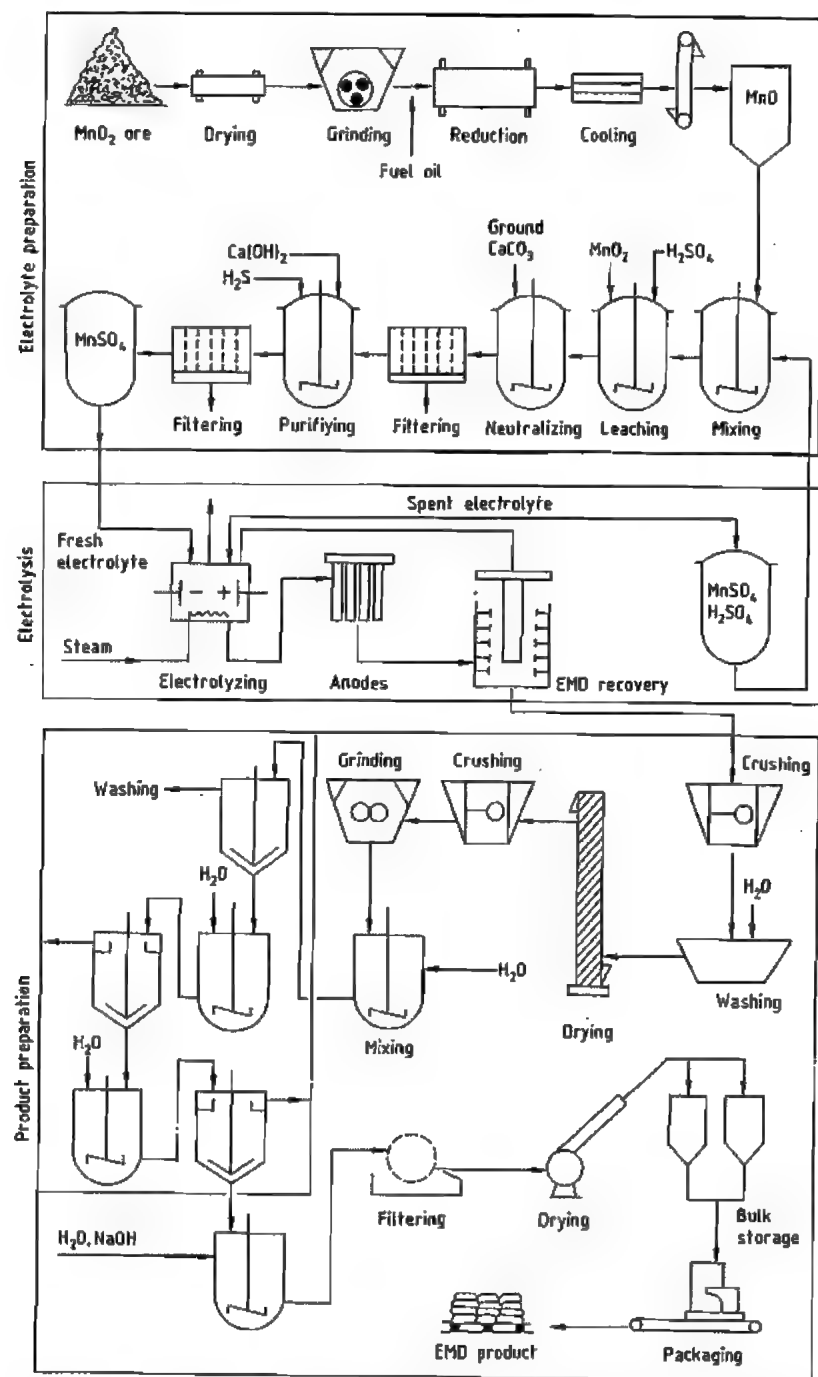
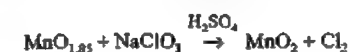
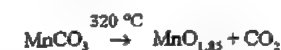


Figure 47.16: Production of electrolytic manganese dioxide (EMD) according to the process used by Tekkosha, Greece [72].

The solution of MnSO_4 is then treated with ammonium carbonate (by simultaneous addition of NH_3 and CO_2) to precipitate manganese(II) carbonate, ammonium sulfate being generated as a by-product. The MnCO_3 is separated and dry-roasted in the presence of air at about 320°C to form a higher manganese oxide with the approximate composition $\text{MnO}_{1.80-1.85}$. Complete oxidation to MnO_2 is achieved by treatment with NaClO_3 in the presence of sulfuric acid.

The key oxidation reactions may be represented as



Sedema has recently introduced a process improvement in the course of expanding their production in which the MnO_2 is transformed directly to $\text{Mn}(\text{NO}_3)_2$ by reaction with nitric oxides. The procedure is similar to the first step in the Chemetals synthesis of high-purity manganese dioxide. The $\text{Mn}(\text{NO}_3)_2$ solution thus obtained is treated with ammonium carbonate to give manganese carbonate (processed as before) and ammonium nitrate. The latter by-product is more readily marketed as a fertilizer than the previously obtained manganese sulfate [74].

Electrolytic manganese dioxide (EMD) is the most important of the synthetic manganese dioxides even though it is a relatively new commodity. Practically all the EMD produced is used in the manufacture of dry cells and electronic materials such as ferrites.

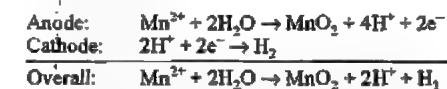
The electrolytic preparation of MnO_2 was discovered during the first half of the 19th century, but the outstanding suitability of the product as a depolarizer for dry cell batteries was not recognized until 1918 [75]. Commercial production started in Japan and the United States during the 1930s. By about 1952 the Japanese industry had perfected their technology to such an extent that the performance of dry cells made with EMD was about two to three times that of cells made with native bat-

tery ore [76]. Ever since, the Japanese EMD industry has maintained its world leadership in this field.

Electrolytic manganese dioxide is a black powder and typically contains 91% MnO_2 (mostly the hexagonal ϵ -modification [77]), 3–5% moisture, up to 1.3% sulfate, < 0.02% Fe, and very low residual concentrations (< 0.001%) of such metals as Pb, Cu, and Co. The balance consists largely of lower manganese oxides. The true density of EMD ranges from 4.0 to 4.3 g/cm^3 , and its tap density from 2.2 to 2.3 g/cm^3 . The BET surface area is 40–50 m^2/g [76] with a particle size of < 74 μm (< 200 mesh).

The outstanding performance of EMD as a battery depolarizer (especially in high-performance alkaline cells) is a result of its unique solid state properties (which permit free transport of protons through the lattice) and the virtual absence of elements that promote the corrosion of zinc metal [78].

Production of EMD usually starts from manganese dioxide ore [72; 79, p. 385; 80, p. 637; 81] (Figure 47.16), which is first reduced to MnO with either coal, heavy fuel oil, hydrogen, or natural gas. The MnO is then leached with sulfuric acid to form a manganese sulfate solution. Alternatively, if the rhodochrosite (manganese carbonate) is the starting material (as in Japan), only a leaching step with sulfuric acid is required. The acidic manganese sulfate solution is then purified by oxidation with MnO_2 and neutralized with lime to a pH of 4–6. This treatment precipitates any heavy-metal ions present (Fe, Pb, Ni, Co). Hydrogen sulfide may be added for even more complete purification. After filtration and adjustment of concentrations to 75–160 g/L MnSO_4 and 50–100 g/L H_2SO_4 , the manganese sulfate solution is subjected to electrolysis, which can be represented in simplified form by the following reactions:



The electrolytic cells generally consist of open steel troughs equipped with an acid-re-

sistant, electrically nonconductive lining (e.g., Hypalon, rubber, or ceramic). The anode is made from graphite, hard lead, or titanium. Anode current density is 70–120 A/m² at a cell voltage of 2.2–3.0 V. During the electrolysis, which is carried out at 90–98 °C (a paraffin layer is used to minimize evaporation), the concentration of MnSO₄ decreases and that of H₂SO₄ increases. Current yields range from 70% in older installations to > 90% in modern plants. In practically all commercial processes the EMD is deposited as a solid coating on the anode.

Electrolysis is terminated when the EMD deposit is 20–30-mm thick (requiring 14–20 d). The product is then mechanically removed from the anode, crushed, repeatedly washed with hot water, dried, and ground to the desired particle size (which depends upon the grade). The ground product is resuspended in water, adjusted to pH 6.5–7.0 with alkali, dried at 85 °C to a defined residual water content, and packaged.

Much of the recent progress toward economical production of high-quality EMD is related to technical advances in electrolytic cell (especially electrode) technology. Nevertheless, many EMD producers still use graphite and lead anodes (Table 47.10). The main disadvantage of graphite anodes lies in their relatively short life; lead anodes lead to undesirable product contamination. The modern trend is toward titanium anodes, which are mechanically and chemically stable and do not cause product contamination. One of the apparent limitations of titanium anodes is the formation of a passivated layer on the electrode surface at current densities > 80–90 A/m², but this problem has been overcome by the addition of a mixture of finely ground manganese oxides (MnO₂, Mn₂O₃, Mn₃O₄) to the electrolyte [83]. Cells are now operated at current densities ≥ 150 A/m², resulting in a substantial increase in productivity.

Economic Aspects. World capacity for CMD is estimated to be ca. 40 000 t/a. This includes the Sedema Division of Sadacem in Belgium, Chemetals Corporation in the United States,

and several plants in the former Soviet Union. Actual consumption is about 25 000 t/a [84]. Even though CMD has its own established niches in the battery industry, it also competes increasingly with EMD as a depolarizer in high-performance cells.

Electrochemical manganese dioxide is now the most important fastest growing synthetic manganese product due to the high growth rate of the dry-cell battery and electronic component markets. World production capacity for EMD is approximately 183 000 t/a (Table 47.10) and growing. The EMD capacities in Japan and the United States are 73 000 and 32 000 t/a, respectively. Additionally, two Japanese companies operate EMD plants in Ireland and Greece, with a combined capacity of ca. 25 000 t/a.

In view of the rapid growth of the EMD market in the 1980s (averaging about 10%/a), considerable interest has been stimulated in establishing new EMD production plants. Thus, announcements regarding the construction of new facilities were recently made by BHP in Australia (15 000 t/a), Metalman in Brazil (12 000 t/a), and CIA Minera Autlan in Mexico (13 200 t/a).

According to [85], the 1986 world demand for EMD was about 128 000 t/a, and current production is said to be 165 000 t/a [84]. Serious EMD oversupply and fierce competition among producers is already evident, and is expected to intensify in the future.

47.10.2.2 Other Oxides

Manganese(II) oxide, manganese monoxide, MnO, green, ρ 5.37 g/cm³, *mp* 1945 °C, is practically insoluble in water and occurs in nature as manganosite. It dissolves readily in most acids. Synthetic manganese monoxide is obtained by reduction of manganese dioxide or by thermal decomposition of Mn(II) carbonate under the exclusion of air. Depending on particle size (a function of the method of preparation), MnO reacts at varying rates with atmospheric oxygen even at room temperature, thereby forming Mn₃O₄.

Table 47.10: Major producers of electrolytic manganese dioxide (EMD).

Country	Producer	Location	Production capacity, 10 ³ t/a ^a	Anode material [82]
Japan	Toyo Soda	Hyuga	24	Ti
	Mitsui Mining and Smelting	Takehara	24	Ti
	Dai-ichi Carbon Company	Yokohama	6	C
	Japan Metals and Chemicals Company	Takaoka	18	Ti
Greece	Tekkosa Hellas	Thessaloniki	15	C
Ireland	Mitsui Denman	Cork	12	Ti
United States	Kerr McGee	Henderston, NV	11	C
	Eveready Battery Co.	Marietta, OH	7	C
	ESB Materials Company	Covington, TN	3	C
	Chemetals, Inc.	New Johnsonville, TN	10	Ti
Spain	Cegasa	Onate	5	Pb
Former Soviet Union	state	Rustavi	5	Pb
China	state		8	C
India	Union Carbide	Thaha	3	C
	T.K. Chemical	Trivandrum	1	C
Brazil	Union Carbide	Itapericera	4	C
South Africa	Delta	Nelspruit	6	Pb
Total world capacity			183	

Compiled by Hoechst AG, 1987.

Manganese monoxide has major significance as an intermediate in the manufacture of Mn(II) compounds (especially manganese sulfate and sequential products) from MnO₂ ores. Reducing agents for MnO₂ in the large-scale manufacture of manganese monoxide include finely powdered coal, hydrogen, carbon monoxide, natural gas, and heavy fuel oils. The reaction is carried out at 400–800 °C in a rotary kiln or shaft furnace. The freshly formed manganese oxide must be allowed to cool in a reducing atmosphere in order to ensure room-temperature stability with respect to atmospheric oxygen.

Manganese monoxide (in contrast to manganese dioxide) is readily assimilated by most plants. This fact accounts for its widespread use as a fertilizer for manganese-deficient soils.

The consumption of manganese monoxide in the United States for fertilizer applications (alone or in combination with MnSO₄) is about 20 000 t/a. A similar amount is used as an animal feed additive. Fertilizer/feed grade manganese monoxide (containing 77% MnO) is made by direct reduction of manganese ore.

High-purity manganese monoxide (obtained, for example, by reduction of 99.5% MnO₂) is used in the production of specialty

ceramics and glasses for electronic applications, in ferrites and thermistors, and for making welding rod fluxes and high-purity manganese chemicals.

Manganese(III) oxide, Mn₂O₃, decomp. > 900 °C, ρ 4.89 g/cm³, exists in α - (rhombohedral or cubic) and γ - (tetragonal) modifications. The hydrate Mn₂O₃·H₂O occurs as the mineral manganite and forms steel-gray, shiny, rhombic crystals. Manganese(III) oxide is made industrially from manganese dioxide by calcination at 600–800 °C, or by thermal decomposition and controlled air oxidation of manganese carbonate. Primary uses are the preparation of such electronic materials as ceramic magnets and semiconductors. It is a small-volume product, a few hundred tonnes are consumed annually.

Manganese(II, III) oxide, Mn₃O₄, *mp* 1562 °C, occurs naturally as hausmannite and crystallizes tetragonally (ρ 4.84 g/cm³). It may be obtained from the other manganese oxides by heating above 950 °C in the presence of air. According to a recently issued patent [86], high-purity Mn₃O₄ can also be made from an aqueous suspension of finely divided manganese metal by air oxidation at 30–100 °C in the presence of ammonium salts. The compound forms black crystals, but finely dis-

persed it appears as a red powder. Highly purified Mn_3O_4 is used in the manufacture of semiconductors and ceramic magnets. World production is estimated at ca. 2000 t/a.

Other Manganese Oxides. Oxides with penta-, hexa-, or heptavalent manganese have no industrial significance. Indeed, the hypothetical oxides Mn_2O_5 and MnO_3 have never been prepared. The anhydride of permanganic acid, Mn_2O_7 , forms readily from KMnO_4 and concentrated sulfuric acid. It is an unstable, highly explosive, green-black liquid.

47.10.3 Manganese(II) Salts

Manganese acetate, $\text{Mn}(\text{CH}_3\text{COO})_2 \cdot 4\text{H}_2\text{O}$, ρ 1.589 g/cm³, forms pink crystals that are soluble in water, methanol, and ethanol. The compound dehydrates between 80 °C and 130 °C, and decomposes at 350 °C to Mn_2O_3 . It is made industrially from acetic acid and either manganese carbonate, manganese(II) oxide, or electrolytic manganese metal. Its main use is as a catalyst (either alone or in combination with cobalt) in the liquid-phase air oxidation of hydrocarbons to carboxylic acids.

Manganese borate, $\text{MnB}_4\text{O}_7 \cdot 8\text{H}_2\text{O}$, is a white to pale reddish-white solid. It is insoluble in water and ethanol, but soluble in dilute acids. The compound is precipitated from aqueous solutions of manganese chloride and sodium borate, and is used as a siccative.

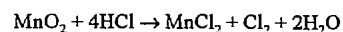
Manganese(II) carbonate, MnCO_3 , light pink, decomp. > 200 °C, ρ 3.125 g/cm³, occurs naturally as rhodochrosite. It is sparingly soluble in water (solubility product at 25 °C: 8.8×10^{-11}) but readily soluble in acids. It is produced commercially from manganese sulfate by precipitation with alkali-metal carbonates or hydrogen carbonates. If the presence of alkali-metal ions must be avoided in the product (as in the manufacture of ferrites), ammonium hydrogen carbonate may be used as the precipitating agent. According to a German patent [87], the use of ferromanganese as a starting material results in manganese carbonate of especially high purity. The precipitated MnCO_3 is filtered, washed, and dried at 110–

120 °C. Heating above 200 °C causes decomposition to MnO and CO_2 .

Manganese carbonate is used in the synthesis of other manganese(II) salts (by reaction with the corresponding acids) and also in the production of battery-active, chemical manganese dioxide (CMD). Manganese carbonate is also important in the preparation of high-quality manganese zinc ferrites for the television and computer industries [63, p. 180]. World production of MnCO_3 is estimated to be about 9000–10 000 t/a.

Manganese(II) chloride, MnCl_2 , ρ 2.977 g/cm³, *mp* 690 °C, *bp* 1190 °C, is readily soluble in water and exists in the anhydrous form and as di-, tetra-, and hexahydrates. Unless precautions are taken (see below), thermal dehydration of the hydrates to the anhydrous form may result in some hydrolytic decomposition, with formation of gaseous HCl and manganese oxychloride.

Industrial preparation of manganese chloride is based either on the reaction of aqueous hydrochloric acid with MnO_2 ore, MnO , MnCO_3 (rhodochrosite), or on direct chlorination of manganese metal or ferromanganese. The process currently employed in Bitterfeld (Germany) starts from manganese ore (MnO_2). Chlorine gas is generated



and is absorbed in a suspension of hydrated lime [65, p. 739]. An alternative process used by Chemetals avoids the formation of chlorine by prereluction of the MnO_2 to MnO .

The MnCl_2 solution thus obtained is purified by neutralization with MnCO_3 , causing iron and aluminum impurities to precipitate. After filtration and evaporation, the tetrahydrate crystallizes from the cooled solution in plate-like crystals. This material, which is itself a commercial product, requires very careful drying because it melts at 58 °C in its own water of crystallization. Dehydration requires a temperature above 200 °C. Fusion in the oven is avoided by addition of previously dehydrated product. The drying process may be carried out in the presence of excess dry HCl

gas if anhydrous manganese chloride free of oxychlorides is required.

Uses of manganese(II) chloride include dry cell manufacture, preparation of hard and corrosion-resistant magnesium alloys, synthesis of methylcyclopentadienylmanganese tricarbonyl brick coloring [63, p. 182].

Manganese(II) nitrate, $\text{Mn}(\text{NO}_3)_2$, decomp. > 140 °C, exists in the anhydrous form and as mono-, tri-, tetra-, and hexahydrates. The commercial product is the tetrahydrate, which is readily soluble in water. Manganese nitrate is prepared by nitric acid treatment of manganese carbonate or MnO , or by reaction of MnO_2 with nitric oxides. The compound is an important intermediate in the production of high-purity manganese oxides and is also used in the preparation of colorants for the ceramics industry.

Manganese(II) phosphates. The most important manganese phosphate is the water-soluble $\text{Mn}(\text{H}_2\text{PO}_4)_2 \cdot 2\text{H}_2\text{O}$, which is prepared by dissolving manganese carbonate, manganese(II) oxide, or manganese metal in phosphoric acid. This phosphate finds wide application in the phosphatizing of ferrous metals and is also used as a light stabilizer for polyamide fibers.

Manganese(II) sulfate, MnSO_4 , ρ 3.25 g/cm³, *mp* 700 °C, *bp* 850 °C (decomp.), is almost pure white in the anhydrous state; the corresponding mono-, tetra-, penta-, and heptahydrates are pink. Manganese(II) sulfate is readily soluble in water, but has a strongly negative solubility coefficient at temperatures > 24 °C. The solids content of a manganese sulfate solution saturated at 24 °C is 39.3%; at 100 °C the solids content drops to 26.2%.

The customary commercial product (technical grade) is the monohydrate, containing 99% $\text{MnSO}_4 \cdot \text{H}_2\text{O}$. Manganese sulfate is produced either directly by reaction of manganese(II) oxide (or manganese carbonate) with sulfuric acid or as a by-product from organic oxidations with manganese dioxide.

Until recently the manufacture of hydroquinone (by oxidation of aniline with MnO_2 and H_2SO_4) was a major source of fertilizer-

grade manganese sulfate, containing 78% MnSO_4 [88], but modern hydroquinone processes are based on either diisopropylbenzene/ O_2 or phenol and H_2O_2 .

Before 1977 Tennessee Eastman, a major U.S. hydroquinone producer, operated with a by-product manganese sulfate capacity of about 35 000 t/a. Eastman's manufacturing technology has since been changed, and manganese sulfate is no longer produced. Other organic oxidations are still carried out with MnO_2 as the oxidant (e.g., the manufacture of 4-*tert*-butylbenzaldehyde and *p*-anisaldehyde), but the output of manganese sulfate from these processes is no more than a few thousand tonnes per year, so the majority of U.S. manganese sulfate is now derived directly from MnO or MnCO_3 .

Manganese sulfate is commercially one of the most important manganese products. It is the starting material for electrolytic manganese metal, electrolytic manganese dioxide, fungicides such as Maneb, and other manganese compounds including manganese carbonate, manganese soaps (naphthenate, linolate, and resinate, all used as siccatives), and certain inorganic pigments. Manganese sulfate is also used in textile printing and glass making. Very significant in terms of volume is the use of manganese sulfate as a fertilizer for manganese-deficient soils, for example, in the vegetable- and citrus-growing areas of Florida. It is also valuable as a micronutrient additive for animal feeds [63, p. 187].

World production of commercial manganese sulfate is estimated to be about 120 000–130 000 t/a. Production in the United States is ca. 8000 t/a, with a demand of approximately 14 000–14 500 t/a. The deficit is covered by imports from Europe and China.

Major producers of manganese sulfate include: Eagle Picher (USA), production capacity 6000 t/a; Sulfamex (Mexico) 21 000 t/a (start-up delayed); and Sedema (Belgium) 22 000 t/a. For more economic information on manganese sulfate, see [89].

47.10.4 Higher Oxidation-State Manganates

47.10.4.1 Potassium Manganates(V) and (VI)

Potassium manganate(V), K_3MnO_4 , ρ 2.78 g/cm³, decomp. > 1000 °C, occurs as fine blue-green to turquoise crystals. In the presence of water it is readily hydrolyzed, disproportionating to K_2MnO_4 , $KMnO_4$, and MnO_2 . Solutions of K_3MnO_4 in 40% potassium hydroxide have limited stability even below -10 °C; however, in the presence of 75% KOH and under nitrogen, potassium manganate(V) is stable up to 240 °C. Pure potassium manganate(V) can be heated to over 900 °C without decomposition. It is an important intermediate in the production of potassium permanganate.

Potassium manganate(VI), K_2MnO_4 , ρ 2.703 g/cm³, decomp. 640–680 °C, exists in the pure state as brilliantly green, rhombic crystals. Upon aging, the color changes to black-green due to the formation of a surface film of $KMnO_4$. The compound is less prone to decomposition than K_3MnO_4 ; the deep green solutions in 15–20% potassium hydroxide (for solubilities in KOH see [90]) are quite stable even at 50–60 °C. In more dilute solutions, and especially in the presence of acid, K_2MnO_4 disproportionates to $KMnO_4$ and MnO_2 . Pure potassium manganate(VI) is stable up to ca. 600 °C; at higher temperatures it loses oxygen to form K_3MnO_4 and Mn_2O_3 . By far the largest part of the K_2MnO_4 produced industrially is converted to potassium permanganate; smaller quantities are used in the surface treatment of magnesium metal [91] and as a chemical oxidant [64, p. 175].

47.10.4.2 Potassium Permanganate

The best known of the manganates, potassium manganate(VII) (potassium permanganate) was introduced as a commercial product in 1862 [92]. It soon became a very important

chemical [93] not only industrially but also in the eyes of many generations of academic and industrial researchers. The former concerned themselves with the chemistry of $KMnO_4$ and its precursors, while the latter devised new and improved methods for its production. Unraveling the chemistry of the higher valence states of manganese (generally referred to as manganates) proved to be a major challenge. Since 1954 the roles of the various manganates [especially manganate(V)] in the industrial production of $KMnO_4$ have been fully clarified [94]. For more detailed historical information; see [95].

Properties

Potassium manganate(VII) $KMnO_4$, ρ 2.703 g/cm³, decomp. > 200 °C, gives dark purple to bronze-colored rhombic crystals. Its solutions are faint pink to deep violet, depending on concentration. The solids content of a saturated aqueous solution at 20 °C is ca. 6% $KMnO_4$ (11% at 40 °C and 20% at 65 °C). Permanganate solutions are most stable in the neutral or near-neutral pH region; acidic or alkaline solutions decompose with loss of oxygen. For solubilities in aqueous KOH see [90]. Potassium permanganate is also soluble in several organic solvents, including acetone, glacial acetic acid, methanol, and sulfolane (tetrahydrothiophene-1,1-dioxide). Such solutions usually have limited stability because the permanganate ion slowly attacks the solvent.

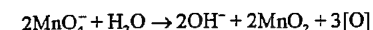
When dry potassium permanganate is heated to 200–300 °C, an exothermic, autocatalytic decomposition takes place with the evolution of oxygen. Contact with combustibles, especially water-soluble organic substances (such as polyhydroxy compounds), can lead to spontaneous ignition and potentially violent combustion.

The usefulness of permanganate as an oxidant is a result of several unique properties. One is the compound's ability to function as an oxidant at all pHs. Also interesting is the fact that permanganate oxidations can be carried out in both aqueous and several nonaque-

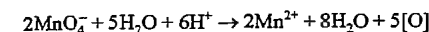
ous solvents. Phase-transfer catalysis greatly extends the range of usable solvents [96].

Permanganate oxidizes a wide variety of inorganic and organic compounds. It is often regarded as the oxidant of choice for olefins and aromatic side chains even though it can also interact with other functional groups [64, pp. 183–288; 97]. Permanganate oxidations can be used not only for specific modification of organic molecules but also to destroy such materials as in pollution abatement applications.

In moderately alkaline, neutral, or slightly acidic media, $KMnO_4$ donates active oxygen according to the following equation:



Only under substantially more acidic conditions, and with particular substrates, does permanganate oxidation follow an alternative course:



Production [6, pp. 741–762]

Most permanganate is made from MnO_2 -containing ore by fusion followed by electrolysis. However, all-electrolytic methods also exist. One such method, practiced in the Soviet Union since the late 1950s, involves direct single-step anodic oxidation of ferromanganese to permanganate [98]:



This process is not generally considered economical because of high energy consumption (about 15 kWh/kg), the high cost of preparing cast ferromanganese anodes, and the cost of cooling the electrolyte to the required operating temperature 20 °C).

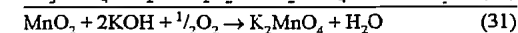
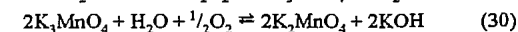
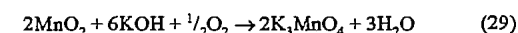
In another patented all-electrolytic process [99] a 10–25% suspension of precipitated manganese dioxide in aqueous KOH is electrolyzed at ≥ 60 °C:



It is not clear whether this process is, or has been, used commercially.

Fusion Processes [100]

The industrial preparation of potassium permanganate and its precursors (K_3MnO_4 and K_2MnO_4) begins with a finely ground MnO_2 ore which is subjected to alkaline oxidative fusion:



In a separate step, potassium manganate(VI) is subsequently converted to potassium permanganate, usually by anodic oxidation.

Several continuous or batch-type fusion processes are in current use, but they may be categorized in two groups:

- **Roasting processes** that employ a MnO_2 :KOH molar ratio of 1:2 to 1:3 (the reaction mixture is a solid).
- **Liquid-phase processes** with a MnO_2 :KOH molar ratio $\geq 1:5$.

Roasting processes usually involve two steps, with reactions (29) and (30) carried out sequentially. In the primary step, finely ground manganese dioxide is mixed with 50% KOH (frequently in a highly dispersed form) and treated with air or oxygen at 300–400 °C. The KOH/ MnO_2 reaction mixture is usually introduced as a fine spray into internally or externally heated rotary kilns (Figure 47.17). Stationary spray drier-like reactors are also in use. Most of the water quickly evaporates, and the highly concentrated KOH reacts within a few minutes with MnO_2 and oxygen to form K_3MnO_4 (Equation 29). The dry, blue-green reaction product is ground to increase its surface area and then subjected to secondary oxidation (Equation 30), in which it is exposed to a moisture-laden air or oxygen stream at 190–210 °C. Several hours are required to effect nearly complete conversion to the black-green K_2MnO_4 .

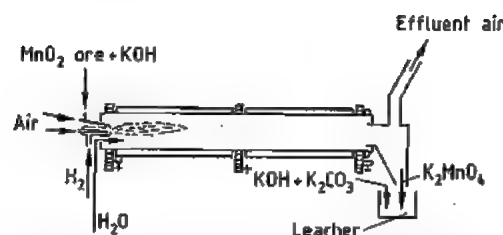


Figure 47.17: Rotary kiln with internal heating for the production of potassium manganate(VI).

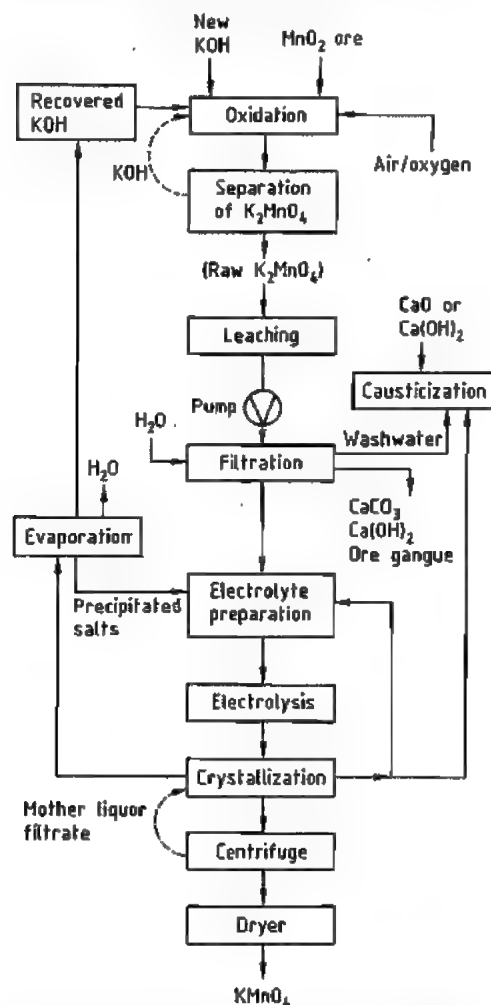


Figure 47.18: Production of potassium permanganate: liquid-phase oxidation process (overall flow schematic).

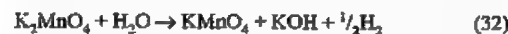
Rotary kilns are commonly employed for this step, but other types of solid gas contactor

(e.g., specially designed "plate" reactors) are also utilized. The removal of hard crusts that form on the inner walls of the reactor can cause substantial downtime.

Liquid-Phase Processes. In liquid-phase processes (Figure 47.18) finely ground MnO₂ ore is added to an excess of concentrated, molten potassium hydroxide (70–90%) at 200–350 °C. The reaction mixture is agitated vigorously and a stream of finely dispersed air or oxygen is passed through the molten mass. The MnO₂ is converted to K₂MnO₄ in a single step (Equation 31), although such an oxidation can also be effected in two stages [101–103]. Potassium manganate(VI) crystallizes from the melt, from which it must then be separated by suitable means (e.g., thickening, decantation, filtration, and centrifugation) [104, p. 870].

Anodic Oxidation of Manganate(VI)

Oxidation of the manganate(VI) to permanganate is always accomplished by electrolysis:



Crude manganate from the fusion process is first leached in dilute potassium hydroxide (90–250 g KOH per liter, depending upon the nature of the subsequent electrolysis). The resulting leach solution is usually filtered to separate insolubles, originating from the gangue portion of the ore (Figure 47.18).

Effective control of key parameters is decisive for the overall success of the electrolysis, including the concentrations of K₂MnO₄, KMnO₄, and KOH, as well as the temperature (usually ca. 60 °C).

Cell Design. Typical electrolysis cells employ voltages of 2.3–3.8 V and anodic current densities of 50–1500 A/m². Current yield depends on cell design and mode of operation, and ranges from 40–90%. Nickel or Monel Metal are the preferred materials for the anode, whereas iron is usually the metal of choice for the cathode.

Cells may be either monopolar or bipolar, rectangular or circular, and may be designed for either flow-through or batch operation.

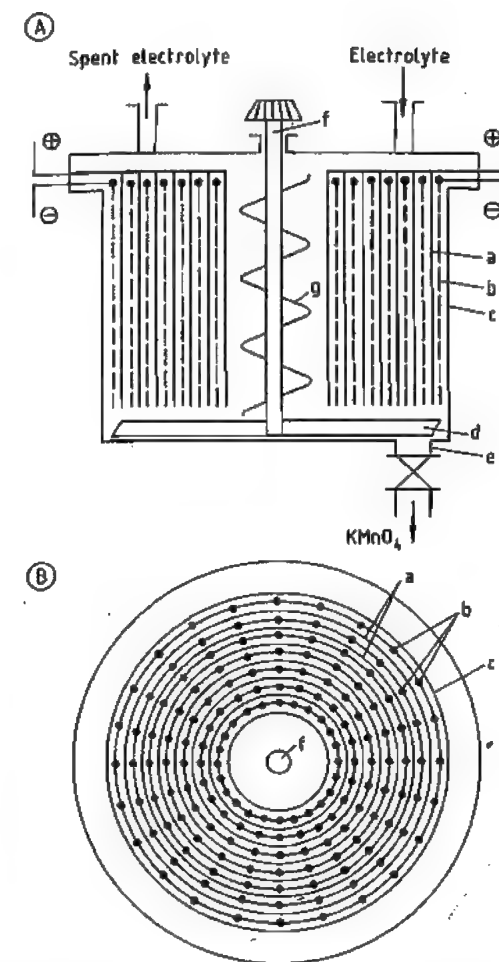


Figure 47.19: Electrolytic cell used in the Bitterfeld (Germany) process for the production of potassium permanganate. A) Vertical section; B) Cross section. a) Anode; b) Cathode; c) Rubber-lined cell trough; d) Agitator; e) Bottom discharge valve; f) Agitator shaft; g) Spiral agitator.

Cells used by the Chemiekombinat Bitterfeld in Germany [65, p. 749] (Figure 47.19), for example, have a volume of about 4 m³, are circular in shape, and are equipped with a built-in mechanical agitator. The electrode system is monopolar. These batch-operated cells use unfiltered electrolyte; the resulting KMnO₄ is allowed to crystallize within the cells and is drawn off periodically through a bottom valve. The crude product must be re-

crystallized to separate it from residual ore gangue.

In the cell developed by the Carus Chemical Company, numerous bipolar electrodes are combined in an arrangement resembling a filter press to form a closed, diaphragm-less, flow-through electrolyzer (Figure 47.20) [105–107]. The anodic side of each cell sheet consists of Monel Metal screens while the effective cathode area consists of a multitude of small steel protrusions. The rest of the cathode is covered with a corrosion-resistant insulating material. A lower surface area for the cathode than for the anode maximizes the anodic oxidation of MnO₄²⁻ and minimizes undesirable cathodic reduction of both manganate and permanganate. The resulting potassium permanganate is crystallized outside the carus cell in a continuous crystallizer system.

Crystallization. Crystallization of potassium permanganate is effected either directly in a specially designed electrolytic cell or in separate crystallizers. Modern installations use single- or multistage vacuum crystallizers, which produce a crystalline product directly from the mother liquor in such purity that only centrifugation and drying are required before the KMnO₄ is packaged and sold (Figure 47.21).

Removal of Impurities and Recycling. When the crude manganate is leached with dilute KOH a solid residue remains. This is composed of the insoluble portion of the ore gangue (e.g., iron oxide hydrates, precipitated aluminum silicate), unreacted MnO₂ ore, and some precipitated MnO₂ (from disproportionation of K₂MnO₄). These insoluble constituents are removed by the use of thickeners, vacuum filters, or filter presses. The Bitterfeld process operates with unfiltered electrolyte, but here the electrolyzers have been specially designed to cope with suspended matter.

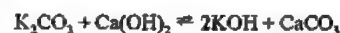
In order to recycle potassium hydroxide generated in the electrolysis step (Equation 32), the spent mother liquor is first concentrated by evaporation to a relative density of ca. 1.575–1.585. This "recovered" caustic potash is then recycled to the front end of the pro-

cess and added to either the roaster or the liquid-phase oxidizer. Alternatively, after removal of dissolved impurities, the recovered KOH can be treated with carbon dioxide to produce potassium carbonate. This method has the drawback that there is a limited market for the substantial quantities of potassium carbonate coproduct.

Dissolved impurities (in particular silicate and aluminate from the gangue portion of the ore) must be removed from the process liquors in order to avoid formation of rock-like deposits on pipeline and equipment walls. Equally undesirable is the buildup of carbonate in the process liquors due to reaction of atmospheric CO_2 with KOH. Excessive carbonate concentrations in the recycle system reduce the rate of conversion of ore into manganates and can

also cause low current efficiencies in the electrolytic cell.

All three major impurities (Si, Al, and carbonate) can be removed together with such minor impurities as Cu, Pb, Ni, and Co by treatment with calcium hydroxide [108]. Effective causticization of the potassium carbonate occurs according to



and requires that the potassium hydroxide concentration be kept < 80 g/L. The process used by Nippon Chemical Industrial Company [109] entails addition of $\text{Ca}(\text{OH})_2$ as early as the roasting step to prevent formation of soluble carbonate and the solubilization of other impurities.

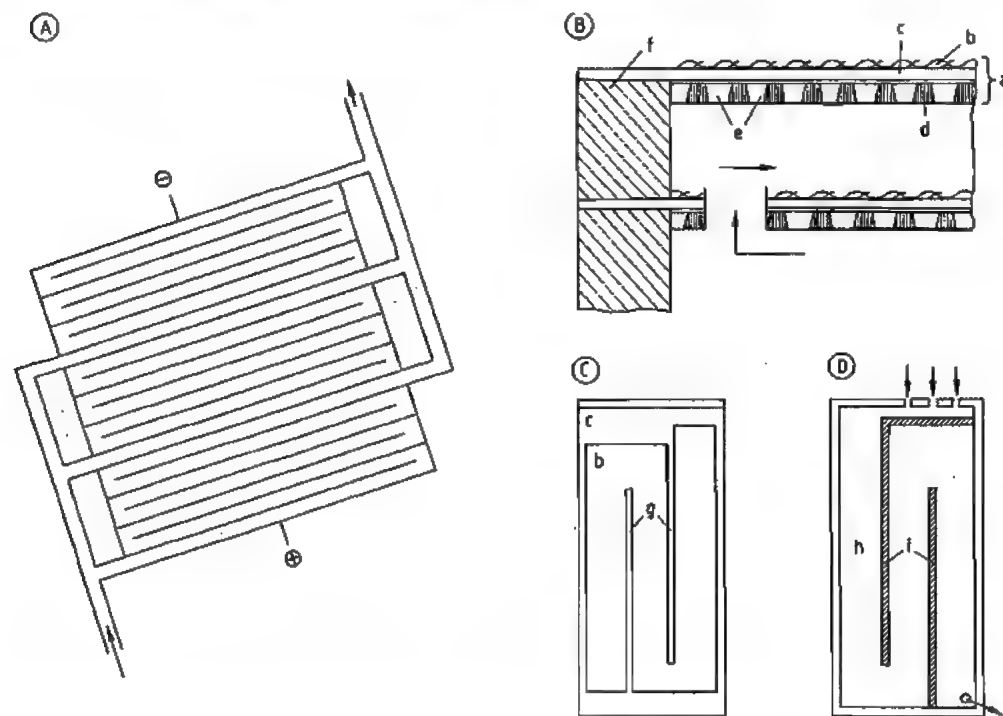


Figure 47.20: Carus Chemical electrolytic cell for the production of potassium permanganate from potassium manganate(VI) [106]. A) Schematic overview of the cell bank; b) Side elevation of an individual cell section; C) Cross section of the anode side of a bipolar electrode; D) Cross section of the cathode side of a bipolar electrode. a) Individual bipolar electrode; b) Anode (wire screen of Monel Metal); c) Base steel sheet; d) Steel cathode with perpendicular projections; e) Insulating plastic; f) Insulating spacer; g) Cutout for flow dividers; h) Cathode projections embedded in plastic; i) Flow dividers.

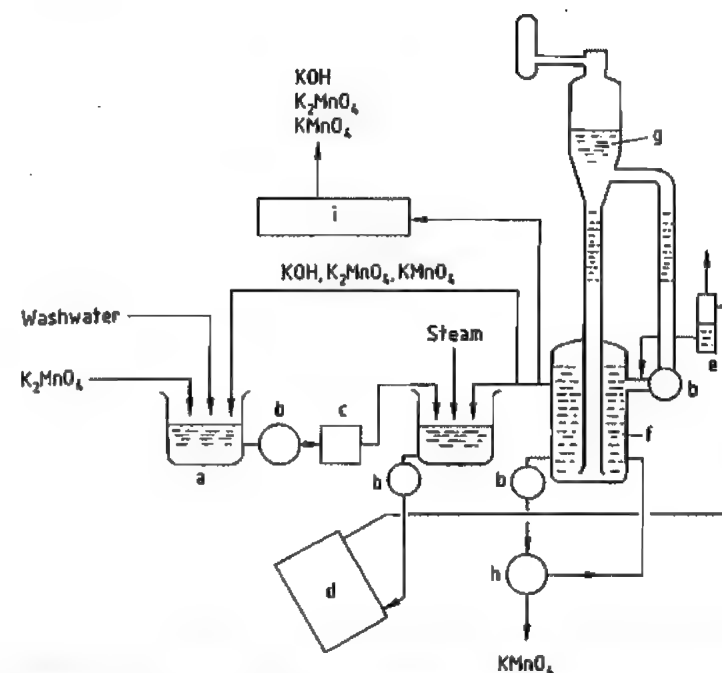


Figure 47.21: Production of potassium permanganate: continuous electrolyzing-crystallizing system: a) Leach tank; b) Pump; c) Filter; d) Electrolysis cell; e) Gas separator; f) Crystallizer; g) Vacuum evaporator; h) Centrifuge; i) Evaporator.

Waste Disposal. The treatment and disposal of solid wastes from permanganate production is an ecological as well as an economic problem. The waste product contains not only unreacted ore but also some-precipitated MnO_2 . The main constituents are derived from the insoluble portion of the ore gangue (Fe, Si, Al compounds) but these are accompanied by significant quantities of potassium and calcium salts. One permanganate producer has proposed recovering most of the adsorbed and chemically-bound potassium by treatment with calcium hydroxide. After washing, the treated waste could then be deposited in landfills [110]. The patent literature describes a number of potential uses for the waste from permanganate production, including extraction of residual manganese, or use of the waste as an absorbent for air pollutants [111], as a micronutrient additive for fertilizers [112], or in building materials [113].

Production Plants

This section gives a brief review of production plants for potassium permanganate in eight countries. Most of the reported production capacities are estimates.

Germany. The VEB Chemiekombinat Bitterfeld was built in 1920 and modernized recently (capacity 5000 t/a) [114]. Potassium manganate is produced by a two-stage roasting process. Electrolytic oxidation and crystallization of the resulting potassium permanganate occur in cylindrical, monopolar, batch-type cells.

India. Permanganate production began in India after World War II. Only one plant remains, that of Curti Chemicals (Goa) built in 1970 with a capacity of less than 1000 t/a. It uses a roasting step followed by electrolytic oxidation.

Spain. The Spanish permanganate plant in Trubia was established in 1940 and modernized in 1977. The plant is operated by As-

turquímica and capacity is 4000 t/a. A modified spray drier is used as the reactor in the first roasting step and a "plate" reactor for the second roasting step [115]. Electrolytic oxidation and vacuum crystallization occur continuously.

Japan. Nippon Chemical constructed a new, continuously operating plant in Aichi Prefecture in 1971 (capacity ca. 3000 t/a). An improved roasting process is employed for making the manganate intermediate, whereby the MnO_2 -KOH reaction mixture containing hydrated lime is dewatered in a separate step before it is introduced into the two-stage roaster system [109]. The electrolysis cells are arranged in cascade fashion and overflow from the final stage is passed to a vacuum crystallizer.

Former Soviet Union. The former Soviet Union operates three plants, built in the late 1950s and early 1960s. The plant in Rustavi has a capacity of 500 t/a and employs single-step anodic oxidation of ferromanganese [104, p. 875]. The second plant, in Saki, has a capacity of about 2500 t/a and uses technology similar to that of the Bitterfeld plant in Germany. The third plant is also in Saki and has a capacity of about 3000 t/a. It uses discontinuous liquid-phase oxidation in the manganate step [104, p. 870], followed by batch electrolysis and crystallization.

Former Czechoslovakia. The Czech plant (Spolek pro Chimickou a Hutní Vyrobu n.p., Usti n.L.) was built in the 19th century. It uses a two-stage roasting process with rotary hearth furnaces for the manganate step. Conversion of each batch of MnO_2 to K_2MnO_4 requires ca. 48 h. The monopolar, continuously operating electrolytic cells contain asbestos diaphragms and electrodes. Plant capacity in 1981 was stated to be 2000 t/a [116].

China. China, with ten state-owned plants, has become a major factor in the world permanganate market, especially as an exporter. Estimates of production capacity range from 7000–15 000 t/a. The largest most modern installation (with production of ca. 3000 t/a), es-

tablished in 1954 in Guangzhou, Canton, presumably uses a liquid-phase oxidation process in the manganate step. The other (smaller) plants are said to employ roasting methods.

United States. The Carus Chemical Company of La Salle, Illinois, has been a producer of potassium permanganate since 1915. New production technology was developed and installed during the late 1950s and early 1960s when patented processes included liquid-phase oxidation in the manganate step [101–103] and closed bipolar cells with continuous crystallization in the permanganate step [105–107]. Numerous improvements have since been introduced, and the current process is fully continuous, highly automated, and in full compliance with environmental regulations. Production capacity is ca. 15 000 t/a.

Commercial Grades, Packaging, and Transportation

Potassium permanganate is offered in several standard grades, including technical, technical free-flowing, U.S.P., and reagent. Guaranteed assays for the various products range from 97% KMnO_4 for the free-flowing grade (which contains an anticaking additive) to 98% for the technical grade and 99% for both U.S.P. and reagent grades (typical assays are usually approximately 0.5% above the guaranteed levels). In addition to assay requirements, reagent grade and U.S.P. grade potassium permanganate conform to specifications set forth in the U.S.P. [117] and the 7th Edition of Reagent Chemicals [118], respectively. Additional specialty grades are also available. Material intended for drinking water treatment must conform, for example, to NSF Standard 60 [119] in the United States and to DIN 19619 [120] in Germany. Packaging is in steel drums or, for large users, bulk containers, bulk cars, and trucks.

The following transportation regulations are applicable: IMDG code D 5187, class 5; RID/ADR class 5.1, number 9c; UN no. 1490; CFR 49:172.101 oxidizing material.

Uses

The United States is the leading consumer (followed by Western Europe and Japan) of permanganate intended for environmental applications, such as drinking water treatment (removal of tastes, odors, iron, and manganese [121]; control of trihalomethanes [122]); wastewater treatment (destruction of hydrogen sulfide [123] and other toxic and/or corrosive compounds, including phenols [124] and plating wastes [125]); and air purification (degradation of malodorous or toxic constituents in industrial off-gases) [126].

In other parts of the world (particularly Eastern Europe and India), the principal use of potassium permanganate is in chemical processing, especially the manufacture of synthetic organics (e.g., saccharine, chloroamphenicol, ascorbic acid, isonicotinic acid, pyrazinoic acid). Even in the Western world, chemical processing applications are significant. Thus, numerous intermediates for pharmaceuticals and pesticides are made via permanganate oxidation, as are many fine organics, including flavoring. Significant tonnage is also consumed for the oxidative destruction or precipitation of undesirable impurities, often ones that impart unwanted colors or odors. KMnO_4 is used in the purification of such chemicals as methanol, ethanol, acetic acid, caprolactam, adiponitrile, plasticizers, carbon dioxide for dry ice manufacture, zinc chloride, and hydrofluoric acid. In recent years, KMnO_4 has played a major role in the bleaching of indigo and other dyes for cotton twill fashion garments. This involves processes known as "frosting", "icing", or "acid washing". Permanganate is also used for bleaching beeswax, natural sponges, jute fibers, and certain clays.

Other important uses include surface treatment of carbon steels and stainless steels (descaling and desmutting, especially in wire manufacture), etching of rubber and plastics, and decontamination of nuclear reactors. Fish farmers utilize KMnO_4 to prevent oxygen depletion and to control fish parasites.

Economic Aspects

Even though potassium permanganate is not a large-volume chemical it is industrially very important. Especially in the manufacture of specific organic intermediates KMnO_4 is an indispensable oxidant.

World production capacity for potassium permanganate is estimated to be 43 000–51 000 t/a, although actual demand is less than 30 000 t/a. Most of the idle capacity is to be found in countries with free market economies: the United States, Western Europe, and Japan. Two of the three West European permanganate plants have been shut down since 1975: Rhône Poulenc's installation in France and the Boots Company plant in the United Kingdom.

Much of the permanganate output from countries with controlled economies enters Western markets at very low prices as a result of extremely low labor costs and virtually no environmental overhead. Government-imposed antidumping duties provide some relief, but not enough to ensure competition on a comparable-cost basis between the imported and domestic product.

47.10.4.3 Sodium Permanganate

Many permanganates other than KMnO_4 are known [103, pp. 859–860], but only sodium permanganate is currently of industrial significance. $\text{NaMnO}_4 \cdot \text{H}_2\text{O}$, ρ 1.972 g/cm³, mp 36.0 °C, can be made in several ways, including anodic oxidation of ferromanganese in Na_2CO_3 solution [65, p. 759], via aluminum permanganate [127], or from KMnO_4 by the hexafluorosilicate method [128]. The price of sodium permanganate is about 5 to 8 times that of KMnO_4 . This is mainly due to the fact that NaMnO_4 cannot be made in the same way as KMnO_4 because the oxidation of MnO_2 in a NaOH melt does not lead to the required Na_2MnO_4 (with hexavalent Mn) but only to Na_3MnO_4 with pentavalent Mn. The latter is very unstable in dilute NaOH solution (and therefore cannot be converted electrolytically to the desired NaMnO_4). Even if electrolytic

oxidation were possible, there would still be the difficult problem of isolating the extremely soluble NaMnO_4 from the alkaline mother liquor.

Sodium permanganate is readily soluble in water (900 g/L at ambient temperature) and is preferred for applications requiring high concentrations of the MnO_4^- ion. Thus, NaMnO_4 is used in the etching of plastic parts such as printed circuit boards [129], as well as in some special organic oxidation reactions, particularly if the presence of potassium ions is undesirable.

47.10.5 Miscellaneous Compounds

Manganese(III) fluoride, MnF_3 , ρ 3.54 g/cm³, is a red crystalline material, thermally stable to 600 °C, that is obtained by reacting Mn(II) halides with elemental fluorine at 200 °C. It decomposes in water and is used as a fluorinating agent for organic compounds.

Manganese hypophosphite, $\text{Mn(H}_2\text{PO}_2)_2 \cdot \text{H}_2\text{O}$, is soluble in water, forms pink, odorless crystals, and decomposes spontaneously upon heating to flammable phosphine. It is prepared from calcium hypophosphite and manganese sulfate. The compound is used as a stabilizer to improve the heat and light resistance of certain man-made fibers and as a food additive and dietary supplement.

Manganese(III) acetylacetonate, $\text{Mn(C}_5\text{H}_7\text{O}_2)_3$, mp 172 °C, is a brown to black crystalline solid that is insoluble in water but soluble in organic solvents. In the dry state it is relatively stable. It is synthesized by reacting manganese(III) sulfate, acetylacetone, and ammonia in an aqueous medium, and is used industrially as a catalyst for organic reactions (e.g., in the polymerization of 2-hydroxyethyl methacrylate to a soluble polymer [130]).

Manganese ethylenebis(dithiocarbamate), Maneb , $(\text{CH}_3\text{NHCS}_2)_2\text{Mn}$, is a yellow powder. It is prepared by the addition of an aqueous solution of ethylene diamine and ammonia to carbon disulfide, followed by neutralization with acetic acid and precipitation with MnSO_4

or MnCl_2 . The compound is an important fungicide.

Methylcyclopentadienylmanganese tricarbonyl (MMT), ρ 1.39 g/cm³, bp 233 °C, is a yellow liquid that is insoluble in water but soluble in organic solvents. Several synthetic routes exist for this compound. For example, manganese(II) chloride may be allowed to react with cyclopentadienylmagnesium bromide, $\text{C}_5\text{H}_4\text{MgBr}$, to form bis(cyclopentadienyl)manganese, an intermediate that reacts with carbon monoxide to give the tricarbonyl. This is then methylated in the presence of Friedel-Crafts catalysts. The product finds limited use as an antiknock additive in motor fuels and as a combustion aid in heating oils.

47.10.6 Occupational Health and Environmental Aspects

Manganese plays an important biochemical role in animal and plant life, and is regarded as an essential trace element [131]. It is added as a fertilizer (in the form of MnO or MnSO_4) to manganese-deficient soils and is also a constituent in dietary supplements for animals and humans.

The United States Food and Drug Administration has given GRAS (Generally recognized as safe) clearance to manganese chloride, manganese citrate, manganese gluconate, and manganese sulfate as direct human food ingredients [132]. Nevertheless, excessive intake and long-term exposure, especially to airborne manganese, can lead to toxic effects [133–136]. Acute poisoning with manganese compounds in humans is very rare, but a few cases involving potassium permanganate are mentioned in the literature, either in connection with its attempted use as an aborticide (abortifacient) or in cases of attempted suicide. The human LDLo for KMnO_4 is reported to be 143 mg/kg, with a TDLo for women of 2400 mg/kg⁻¹d⁻¹ [137].

Chronic manganese poisoning is of much greater concern [138]. Inhalation of manganese in the form of oxidic dust or as vaporized metal over extended periods of time (3 months to several years) increases susceptibility of the

respiratory organs to infection (manganese pneumonia). Manganese can also cause permanent damage to the central nervous system (manganism). The hazard of chronic manganese poisoning affects not only workers in manganese mines and manganese ore crushing/grinding facilities but also those employed in various manganese-consuming industries (e.g., the production and use of ferro- and silicomanganese in steelmaking, welding with manganese-containing welding rods, dry cell manufacture, and production of manganese chemicals) [139, 140]. The early symptoms of manganism are classed as psychological disturbances: fatigue, loss of appetite, incoordination, speech disorders, and psychotic behavior. Manganism at this stage is reversible provided exposure ceases. Continued exposure causes the disease to enter a second stage, in which permanent injury is inflicted on the central nervous system. Symptoms include severe rigidity of the limbs with jerky movements, gait problems, tremors, and excessive salivation and perspiration. There is some similarity between the symptoms of manganism and those of Parkinson's disease.

In the United States, Germany, Switzerland, and Japan a general ceiling value (MAK) has been set for manganese in air at 5 mg/m³. The ceiling value for Mn_3O_4 is 1 mg/m³ [141]. OSHA has recently proposed lowering the "Permissible Exposure Limit" to manganese at the workplace to 1 mg/m³ [142]. On the other hand, the United States Environmental Protection Agency decided not to designate manganese as a hazardous air pollutant under the Clean Air Act, mainly because public exposure to manganese is far below levels associated with serious noncarcinogenic health effects, and available data do not indicate that manganese is carcinogenic [143].

Detailed information about the location of major manganese air emission sources in the United States can be found in [144]. At current exposure levels, manganese does not constitute a general environmental risk [141]. The limit for manganese in drinking water in the United States and most West European countries is 0.05 ppm. This low value is based

largely on aesthetic rather than toxicological considerations [145].

47.11 References

1. J. S. Stanko: *Manganese for Steelmakers*, Council for Mineral Technology, Johannesburg, South Africa 1989.
2. S. A. Weiss: *Manganese—the Other Uses*, The Garden City Press Ltd., Letchworth 1977.
3. E. A. Brandes, R. F. Flint: *Manganese Phase Diagrams*, The Manganese Centre, Paris 1980.
4. O. Kubaschewski, E. L. Evans, C. B. Alcock: *Metallurgical Thermochemistry*, Pergamon Press, Oxford 1967.
5. L. Habraken: "Manganese—an Alloying Agent", *Proc. Semin. Non Ferrous Applications of Manganese*, The Manganese Centre, Paris 1977.
6. B. McMichael: "Manganese, EMD—the Power in the Market", *Ind. Miner.* (1989) May, 42–59.
7. J. F. Machamer: "A Working Classification of Manganese Deposits", *Min. Mag.* 157 (1987) no. 10, 348–351.
8. *Manganese Ores Analysis*, The Manganese Centre, Paris 1986.
9. A. S. E. Kleyenstuber: "The Correlation of the Mineralogy with the Sedimentary Cycles of the Proterozoic Manganese-Bearing Hotazel Formation in South Africa", *IAS Int. Symp. Sedimentology Related to Mineral Deposits*, 30th July–4 August 1988, Beijing.
10. C. J. Nel, N. J. Beukes, J. P. R. de Villiers: "The Mamatwan Manganese Mine of the Kalahari Manganese Field", in C. R. Anhaeusser, C. R. Maske (eds.): *Mineral Deposits of Southern Africa*, vol. 1, Geol. Soc. S. Afr., Johannesburg 1986, pp. 963–978.
11. S. Roy: *Manganese Deposits*, Academic Press, London 1981.
12. I. M. Varentson, G. Y. Graselty: *2nd International Symposium on the Geology and Geochemistry of Manganese*, Schweitzerbart'sche Verlagsbuchhandlung, Stuttgart 1980.
13. D. B. Wellbeloved: "Manganese in South Africa—an Overview", *Conference on Base Metals*, Johannesburg, May 17, 1988.
14. *Manganese Statistical Bulletin 1987*, The Manganese Centre, Paris 1988.
15. M. P. Sassos: "Manganese GFMCO Mines Huge Resources at Groote Eylandt", *Eng. Min. J.* 185 (1984) 57–58.
16. A. R. Chernenko, A. S. Sidorov: "Updating the Technology and Machinery for Underground Manganese Ore Mining", 12th World Mining Congress, New Delhi 1984.
17. M. C. Fuerstenau, K. N. Han, J. D. Miller: "Flotation Behaviour of Chromium and Manganese Minerals", in P. Somasundaran (ed.): *Advances in Mineral Processing*, Society of Mining Engineers, Littleton 1986, pp. 289–307.
18. J. Chen, D. Chen, T. Chen, S. Liu: "Technological Innovations and Theoretical Approach to Shear Washing for a Refractory Manganese Ore", *Zhongnan Kuangye Xueyuan Xuebao* 19 (1988) no. 4, 371–378.

19. O. Holta, S. E. Olsen: "Composite Briquettes of Manganese Ore and Coal", *Electr. Furn. Conf. Proc.* 43 (1986) 273-277.
20. K. P. Abraham, M. W. Davies, F. D. Richardson: "Determination of Manganese Oxide in Silicate Melts", *J. Iron Steel Inst. London* 196 (1960) 82-86.
21. F. D. Richardson: *Physical Chemistry of Melts in Metallurgy*, vol. 2, Academic Press, London 1974, p. 333.
22. I. Barin, O. Knacke: *Thermodynamic Properties of Inorganic Substances*, Springer Verlag, Berlin 1974.
23. J. H. Downing: "Fundamental Reactions in Submerged Arc Furnaces", *Electr. Furn. Conf. Proc.* 19 (1963) 288-296.
24. S. A. Weiss: *Manganese the Other Uses. A Study of the Non-Steelmaking Applications of Manganese*, Metal Bulletin Books Ltd. London 1977.
25. J. W. Mellor: *A Comprehensive Treatise on Inorganic and Theoretical Chemistry*, vol. XII, Longmans, London 1972.
26. E. C. Snelling: *Soft Ferrites, Properties and Applications*, 2nd ed., Butterworths, London 1988.
27. J. H. Jacobs et al.: "Operation of Electrolytic Manganese Pilot Plant, Boulder City, Nevada", *U.S. Dep. Inter. Bull.* 463 (1948).
28. G. L. Hubred, R. T. Lewis, US 4317730, 1982.
29. T. I. Mercz, J. C. Madgwick: "Enhancement of Bacterial Leaching by Microalgal Growth Products", *Proc. Australas. Inst. Min. Metall.* 283 (1982) 43-46.
30. F. N. Bender, C. Rampacek: "Percolation Leaching of Manganese Ores With Sulphur Dioxide", *U.S. Dep. Inter. Rep. of Investigation* 5233 (1957).
31. P. K. Sahoo, S. C. Das, S. K. Bose, S. C. Sircar: "Separation of Iron From Manganese Ore Roast-leach Liquor", *J. Chem. Tech. Biotechnol.* 29 (1979) 307-310.
32. S. Joris: "La cinétique de précipitation des sulfures de cobalt et de nickel par l'hydrogène sulfuré", *Bull. Soc. Chim. Belg.* 78 (1969) 607.
33. P. M. Ambrose, US 2316750, 1943.
34. J. Koster, US 2483287, 1949.
35. E. M. Wanamaker, W. D. Morgan, US 2325723, 1943.
36. P. M. Ambrose, US 2347451, 1944.
37. J. J. Harper, US 4311521, 1982.
38. J. E. Reynolds, N. J. Lombardo, US 4423012, 1984.
39. The Consolidated Mining and Smelting Company of Canada Ltd., GB 540228, 1939.
40. M. Harris, D. M. Meyer, K. Auerswald: "The Production of Electrolytic Manganese in South Africa", *J. S. Afr. Inst. Min. Metall.* 77 (1977) Feb. 137.
41. A. I. Vogel: *A Text Book of Quantitative Inorganic Analysis, Including Elementary Instrumental Analysis*, 3rd ed., Longmans, London, p. 953.
42. J. K. Tuset: "Silicothermic Reduction of Manganese", *Steelmaking Conf. Proc.* 69 (1986) 59-64.
43. M. M. Bourgeois: "Les alliages de manganèse à bas carbone: silicomanganèse et ferromanganèse", *Rev. Metall. (Paris)* (1979) June.
44. K. Venugopalan, M. Kamaludeen, N. G. Renganathan, V. Aravamudan: "Massive Manganese Metal By Fused Salt Electrolysis", *Trans. Indian Inst. Met.* 33 (1980) no. 1, 79-81.
45. J. S. Stanko: *Steel Makers Guide to Manganese*, Mintek, Randburg 1989.
46. T. Chisaki, K. Takervchi: "Electric Smelting of High Carbon Ferromanganese with Preheated Pre-reduced Materials at Kashima Works", Kashima 1971.
47. D. S. Cronan: "Marine Mineral Resources", *Geol. Today* 1 (1985) no. 1, 15-19.
48. B. W. Haynes et al.: "Pacific Manganese Nodules, Characterization and Processing", *U.S. Bur. Mines Bull.* 679 (1985) 2-32.
49. V. E. McKelvey: "Subsea Mineral Resources", *U.S. Geol. Surv. Bull.* 1689-A (1986) 72-95.
50. D. S. Cronan: "Manganese on the Ocean Floor", *Trans. Inst. Min. Metall. Sect. A* 94 (1985) July, 166-167.
51. W. D. Siapno: "Manganese Nodules: Overcoming the Constraints", *Mar. Min.* 5 (1986) no. 4, 457-465.
52. J. S. Chung: "Advances in Manganese Nodule Mining Technology", *Mar. Technol. Soc. J.* 19 (1985) no. 4, 39-44.
53. S. Wakabayashi, E. Kuboki, T. Saito, A. Takata, T. Linuma: "Research and Development Project of Manganese Nodule Mining System in Japan", *Proc. Fifth Int. Offshore Mechanics and Arctic Eng. Symp.*, Tokyo 1986.
54. D. C. Tolefson, J. P. Latimer, R. Kaufman: "Design Considerations for a Commercial Deep Ocean Mining System", *Proc. Fifth Int. Offshore Mechanics and Arctic Eng. Symp.*, Tokyo 1986.
55. S. B. Kanungo, R. P. Das: "Extraction of Metals from Manganese Nodules of the Indian Ocean by Leaching in Aqueous Solution of Sulphur Dioxide", *Hydrometallurgy* 20 (1988) no. 2, 135-146.
56. S. Anand, S. C. Das, R. P. Das, P. K. Jena: "Leaching of Manganese Nodules at Elevated Temperature and Pressure in the Presence of Oxygen", *Hydrometallurgy* 2 (1988) no. 2, 155-168.
57. C. T. Hillman, B. B. Gosling: "Mining Deep Ocean Manganese Nodules. Inf. Circ. No. 9013", *U.S. Dept. Inter. Bur. Mines*, Washington 1983, p. 1-15.
58. H. Bozon: "La future exploitation des nodules polymétalliques sous-marins", *JFE J. Four. Electr.* (1982) no. 9, 13-21.
59. Roskill Information Services: *The Economics of Manganese* 1989, 5th ed., 1989.
60. R. D. W. Kemmit: "Manganese" in J. C. Bailar, H. J. Emeleus, R. Nyholm, A. F. Trotman-Dickenson (eds.): *Comprehensive Inorganic Chemistry*, vol. 3, Pergamon Press Ltd., Oxford 1973, pp. 771-876. *Gmelin*, System-Number 56, Mangan.
61. O. Glemser, G. Gattow, H. Meisiek, *Z. Anorg. Allg. Chem.* 309 (1961) 1-19.
62. R. Giovanoli, E. Stähli, *Chimia (Aarau)* 24 (1970) 49-61.
63. S. A. Weiss: *Manganese - The Other Uses. A Study of the Non-Steelmaking Manganese Trade and Industry*, Metal Bulletin Books, London 1977.
64. D. Arndt: *Manganese Compounds as Oxidizing Agents in Organic Chemistry*, Open Court Publishing Company, La Salle, IL, 1980.
65. H. Marcy: "Anorganische Manganverbindungen", in F. Matthes, G. Wehner (eds.): *Anorganisch-Technische Verfahren*, VEB Deutscher Vlg. für Grundstoffindustrie, Leipzig 1964.

66. A. D. Little, Inc.: *Recovery of Manganese from Low-Grade Domestic Sources*, Bureau of Mines Open File Report 201-84 (1985), National Technical Information Service, U.S. Department of Commerce, Springfield, VA, under PB85-119378.
67. A. J. Fatiadi: "The Oxidation of Organic Compounds by Active Manganese Dioxide", in W. J. Mijs, C. R. H. L. de Jonge (eds.): *Organic Syntheses by Oxidation with Metal Compounds*, Plenum Press, New York-London 1986, pp. 119-260.
68. Lambeg Industrial Research Association, US 3900425, 1975 (E. Robinson).
69. Carus Corporation, US 4299375, 1981; US 4304760, 1981 (P. G. Mein, A. H. Reidies).
70. *Ullmann*, 4th ed., 16, 469.
71. Diamond-Shamrock Corp., US 3780158, 1973 (J. Y. Welsh).
72. E. Preisler, *Chem. Unserer Zeit* 14 (1980) no. 5, 137-148.
73. Manganese Chemicals Corp., US 2956860, 1960 (J. Y. Welsh).
74. E. Preisler, Hoechst AG, personal communication.
75. G. D. Van Arsdale, C. G. Meier, *Trans. Electrochem. Soc.* 33 (1918) 109.
76. A. Kozawa, I. Tanabe, *Proc. Electrochem. Soc.* 87 (1987) no. 14, (*Proc. Symp. Hist. Battery Technol.*, 1987), 39-46.
77. P. M. DeWolff, J. W. Visser, R. Giovanoli, R. Brüttsch, *Chimia* 32 (1978) 257-259.
78. E. Preisler, *Dechema Monographien* 102 (1986) 543-559; 109 (1987) 123-137.
79. K. v. Kordesch: *Batteries, Manganese Dioxide*, vol. 1, M. Dekker Inc., New York 1974.
80. E. Preisler, A. Reidies: "Manganverbindungen", in *Winnacker-Küchler*, vol. 2, 1982, 633-650.
81. G. Kano, *Mem. Fac. Eng., Fukui Univ.* 34 (1986) no. 2, 163-172.
82. A. Kozawa: "New Materials and New Processes", in *New Materials and New Processes*, vol. 3, JEC Press Inc., Cleveland, OH, 1985, p. 36.
83. Japan Metals and Chemicals, DE 3046913 C2, 1987 (M. Misawa et al.).
84. K. E. Anthony, Broken Hill Proprietary Co., Melbourne, Australia, personal communication.
85. H. Takahashi, *Jpn. Chem. Week* 27 (1986) 8.
86. Kerr-McGee Chemical Corp., US 4812302, (W. C. Laughlin, D. A. Schulke).
87. H. J. Koch, F. Henneberger, DD 45071, 1966.
88. *Ullmann*, 4th ed., 16, 472.
89. *Chem. Mark. Rep.*, Feb 15, 1988, 33; May 4, 1987, 50; Apr 23, 1984, 58.
90. R. Landsberg, P. Örgel, *Chem. Technol.* 13 (1961) 665-667.
91. H. A. Evangelides, US 2723952, 1952.
92. H. Cassebaum, *Pharmazie* 34 (1979) 740-744.
93. A. H. Reidies, *Water Conditioning and Purification*, 1987, 32-33.
94. R. Scholder, W. Klemm, *Angew. Chem.* 66 (1954) 463-465.
95. *Ullmann*, 4th ed., 16, 473; 3rd ed., 12, 229.
96. D. G. Lee: "Phase Transfer Assisted Permanganate Oxidations", in W. S. Trahanowski (ed.): *Oxidation in Organic Chemistry*, Academic Press Inc., New York 1980, Part D, pp. 147-206.
97. A. J. Fatiadi, *Synthesis* 1987, no. 2, 85-127.
98. G. R. Popov, *Khim. Ind. (Sofia)* 4 (1968) 166-169; *Chem. Abstr.* 69 (1968) 1023326.
99. Nippon Chemical Industrial Company Ltd., US 3986941, 1976 (T. Okabe, E. Narita, Y. Kobayashi, M. Mita).
100. W. Baronius, J. Marcy, *Chem. Techn.* 18 (1966) 723-727.
101. Carus Chemical Company, US 2940821, 1960 (M. B. Carus, A. H. Reidies).
102. Carus Chemical Company, US 2940822, 1960 (M. B. Carus, A. H. Reidies).
103. Carus Chemical Company, US 2940823, 1960 (A. H. Reidies, M. B. Carus).
104. A. H. Reidies in *Kirk-Othmer*, 14, 844-895.
105. Carus Chemical Company, US 2843537, 1958 (M. B. Carus).
106. Carus Chemical Company, US 2908620, 1959 (M. B. Carus).
107. Carus Chemical Company, US 3062734, 1962 (M. B. Carus).
108. Carus Chemical Company, US 3172830, 1965 (M. B. Carus).
109. Japan Chemical Industrial Company, JP 7230520, 1972 (S. Takasawa, Y. Kobayashi); *Chem. Abstr.* 78 (1973) 867066.
110. Carus Chemical Company, US 4085191, 1978 (P. G. Mein, H. Adolf).
111. Academy of Sciences, Kasakh SSR, SU 874135, 1981 (A. V. Kotova, N. S. Buyanova, S. T. Deikalo, Y. N. Kolesnikov); *Chem. Abstr.* 96 (1982) 37689q.
112. Nippon Chemical Industrial Co., JP Kokai 7411664 1974 (T. Takeda, K. Aihara); *Chem. Abstr.* 80 (1974) 144813s.
113. E. T. Berezhenko, B. M. Kuninets, E. V. Martynets, L. V. Pisarev, *Khim. Tekhnol. Kiev* 4 (1981) 29-30; *Chem. Abstr.* 95 (1981) 208465z.
114. *Chem. Tech. (Leipzig)* 33 (1981) no. 4, 209.
115. Industrial Química del Nalón S.A., BE 905130, 1986 (M. O. González García).
116. Spolek Pro Chemickov a Hutni Vyrobu n.p., Usti n. L., personal communication.
117. *The United States Pharmacopeia*, XIX revision (1975) p. 394; XX revision, 4th suppl. (1983) p. 711, United States Pharmacopeial Convention Inc., Rockville, MD.
118. *Reagent Chemicals*, 7th ed., American Chemical Society, Washington, DC, 1986, pp. 533-535.
119. NSF: *Standard 60 for Drinking Water Treatment Chemicals - Health Effects*, December 1987, revised June 1988, NSF, Ann Arbor, MI.
120. DIN 19619, *Kaliumpermanganat zur Wasseraufbereitung*, Technische Lieferbedingungen, Feb. 1975.
121. K. Ficek in R. L. Sinks (ed.): *Water Treatment Plant Design for the Practicing Engineer*, Ann Arbor Science Publications, Inc., Ann Arbor, MI, 1978, 461-479.
122. Ph. C. Singer, J. H. Borchardt, J. M. Colthurst, *J. Am. Water Works Assoc.* 72 (1980) 573-578.
123. K. S. Pisarczyk, L. A. Rossi, *Sludge Odor Control and Improved Dewatering with Potassium Permanganate*, paper presented at the 55th Annual Conference of the Water Pollution Control Federation in St. Louis, 5 Oct. 1982; J. H. Jackson, *Pulp & Pap.* 58 (1984) 147-149.

124. Hiyuga Scirenshe K.K., JP-Kokai 7830163, 1978 (K. Atsuchi, F. Hagiwara, K. Fujita).
125. C. Freudenberg K.-G., Langbein-Pfannhauser Werke AG, DE-OS 3335746, 1985 (L. Feikes, D. Schröder, P. Reyer); *Chem. Abstr.* 103 (1985) 26768b.
126. K. J. Ficek, *Paint Varn. Prod.* 63 (1973) no. 5, 45.
127. Carus Chemical Company, US 2504131, 1950 (T. Jaskowiak).
128. M. M. Kushnir, *Khim. Prom. Nauk. Tekhn. Zh.* 79 (1963); *Chem. Abstr.* 59 (1963) 4813.
129. Morton Thiokol Inc., US 4601783, 1986; US 4601784, 1986 (G. Krulik).
130. Leningrad Technological Institute, SU 1353780, 1987 (N. A. Lavrov, A. F. Nikolaev, N. A. Astafeva); *Chem. Abstr.* 108 (1988) 205263h.
131. Committee on Medical and Biologic Effects of Environmental Pollutants, National Research Council, Manganese, Washington, DC, 1973.
132. FDA: *Fed. Regist.* 50 (1985) 19164-19167.
133. EPA: *Health Assessment Document for Manganese, Final Report*, EPA-600/18-83-013F, NTIS PB 84-229954, Environmental Criteria Assessment Office, Cincinnati 1984.
134. EPA: *Health Effects Assessment for Manganese (and Compounds)*, EPA/540/11-861057, PB 86-134681, Office of Health and Environmental Assessment, Cincinnati 1984.
135. U.S. Department of Health and Human Services, Public Health Service, Centers for Disease Control, NIOSH: *Registry of Toxic Effects of Chemical Substances*, 13th ed., 1983-1984 cumulative supplement to the 1981-1982 ed.
136. WHO: *Task Group on Environmental Health Criteria for Manganese, Environmental Health Criteria 17: Manganese*, WHO, Geneva 1981.
137. Registry of Toxic Effects of Chemical Substances, ed. 1985/86, item 55171, U.S. Department of Health and Human Services DHHS (NIOSH), publication no. 87-114.
138. M. Tolonen: "Industrial Toxicology of Manganese", *Work, Environ. Health* 9 (1972) 53-60.
139. H. Roels et al., *Am. J. Ind. Med.* 11 (1987) 297-305.
140. H. Roels et al., *Am. J. Ind. Med.* 11 (1987) 307-327.
141. R. Schiele, *Met. Umwelt* 1984, 471-477.
142. NIOSH: *Fed. Regist.* 53 (1988) no. 109, 21000-21001.
143. EPA: *Fed. Regist.* 50 (1985) 36627-36628.
144. EPA: *Locating and Estimating Air Emission from Sources of Manganese*, EPA-450/14-83-007h, NTIS PB 86117587, Sep. 1985.
145. R. J. Bull, G. F. Craun: "Health Effects Associated with Manganese in Drinking Water", *J. Am. Water Works Assoc.* 69 (1977) 662-663.

48 Silicon

WERNER ZULEHNER (§§ 48.1-48.4); WALTER SIMMLER (§ 48.5); BERND NEUER, GERHARD RAU (§ 48.6); OTTO W. FLÖRKE, BRIGITTE MARTIN (§§ 48.7.1-48.7.2); LEOPOLD BENDA, SIEGFRIED PASCHEN (§ 48.7.3); HORACIO E. BERGNA, WILLIAM O. ROBERTS (§ 48.7.4); WILLIAM A. WELSH (§ 48.7.5); MANFRED EITTLINGER (§ 48.7.6); DIETER KERNER, PETER KLEINSCHMIT, JÜRGEN MEYER (§ 48.7.7); HERMANN GIES (§ 48.7.8); DIETMAR SCHIFFMANN (§ 48.7.9)

48.1 Introduction	1862	48.7.1.4 Silica Rocks	1911
48.2 History	1862	48.7.1.5 Crystalline Silica Products	1911
48.3 Properties	1862	48.7.2 Quartz Raw Materials	1917
48.4 Production	1863	48.7.2.1 Physical Forms and Occurrence	1917
48.4.1 Metallurgical Silicon	1863	48.7.2.2 Processing	1919
48.4.2 Semiconductor Silicon	1865	48.7.2.3 Uses	1921
48.4.2.1 Purification	1865	48.7.3 Kieselguhr	1925
48.4.2.2 Chemical Vapor Deposition	1866	48.7.3.1 Introduction	1925
48.4.2.3 Single-Crystal Growth	1868	48.7.3.2 Formation, Composition, and Quality Criteria	1925
48.4.2.4 Wafer Manufacture	1876	48.7.3.3 Occurrence and Mining	1927
48.4.2.5 Epitaxy	1877	48.7.3.4 Processing	1927
48.4.2.6 Characterization	1879	48.7.3.5 Analysis	1929
48.4.3 Solar Silicon	1879	48.7.3.6 Storage and Transport	1930
48.4.3.1 Crystalline Silicon	1880	48.7.3.7 Environmental and Health Protection	1930
48.4.3.2 Amorphous Silicon	1882	48.7.3.8 Uses	1931
48.5 Compounds	1883	48.7.3.9 Recycling	1932
48.5.1 Hydrides	1883	48.7.4 Colloidal Silica	1932
48.5.1.1 Monosilane	1884	48.7.4.1 Introduction	1932
48.5.1.2 Disilane	1885	48.7.4.2 Structure of Colloidal Silica Particles	1934
48.5.1.3 Purification	1885	48.7.4.3 Physical and Chemical Properties	1939
48.5.1.4 Uses	1885	48.7.4.4 Stability	1941
48.5.1.5 Safety Measures	1886	48.7.4.5 Production	1943
48.5.1.6 Photochemistry	1886	48.7.4.6 Analysis and Characterization	1945
48.5.2 Halides	1886	48.7.4.7 Uses	1945
48.5.2.1 Trichlorosilane	1886	48.7.4.8 Storage, Handling, and Transportation	1946
48.5.2.2 Tetrachlorosilane	1889	48.7.4.9 Economic Aspects	1947
48.5.2.3 Hexachlorodisilane	1892	48.7.5 Silica Gel	1948
48.5.2.4 Other Chlorides	1893	48.7.5.1 Introduction	1948
48.5.2.5 Fluorides	1893	48.7.5.2 Structure, Properties, and Characterization	1948
48.5.2.6 Bromides	1893	48.7.5.3 Production	1951
48.5.2.7 Iodides	1894	48.7.5.4 Uses	1952
48.5.3 Oxides	1895	48.7.5.5 Economic Aspects	1954
48.5.3.1 Monoxide	1895	48.7.5.6 Legal Aspects	1954
48.5.3.2 Sesquioxides	1896	48.7.6 Pyrogenic Silica	1954
48.5.3.3 Other Silicon-Oxygen Compounds	1897	48.7.6.1 Flame Hydrolysis	1954
48.5.4 Sulfides	1897	48.7.6.2 Electric-Arc Process	1962
48.5.5 Borides	1898	48.7.6.3 Plasma Process	1962
48.6 Silicides	1899	48.7.7 Precipitated Silicas	1962
48.6.1 General	1899	48.7.7.1 Introduction	1962
48.6.2 Calcium Silicon	1900	48.7.7.2 Production	1962
48.7 Silica	1902	48.7.7.3 Properties	1963
48.7.1 Silica Modifications and Products	1902	48.7.7.4 Uses	1965
48.7.1.1 Geochemistry and Crystal Structure	1902	48.7.8 Porosils	1967
48.7.1.2 Crystalline Silica Phases	1905		
48.7.1.3 Noncrystalline Silica Minerals	1911		

48.7.8.1 Introduction	1967	48.7.9.1 Experiences with Humans	1970
48.7.8.2 Physical and Chemical Properties	1967	48.7.9.2 Animal Experiments	1971
48.7.8.3 Manufacture of Porosils	1969		
48.7.9 Toxicology	1970	48.8 References	1973

48.1 Introduction¹

Silicon is a gray, metallically lustrous element with atomic number 14 and atomic mass 28.086. It is situated between carbon and germanium in the periodic table and has three natural isotopes: ²⁸Si (92.2%), ²⁹Si (4.7%), and ³⁰Si (3.1%). Corresponding to its position in the periodic table, silicon has four valence electrons, two of them in the 3s and two in the 3p levels. It crystallizes in the diamond structure like diamond, germanium, and α -tin. Silicon is a nonmetallic, semiconducting element with a resistivity of ca. 400 k Ω cm at room temperature in its purest state. Its electrical resistivity decreases with increasing temperature and increasing concentration of electrically active elements such as B, Al, Ga, In, Tl, P, As, and Sb. By doping silicon with boron, for example, its room-temperature resistivity can be reduced by nine orders of magnitude to ca. 0.4 m Ω cm. Except for very thin foil, silicon is impermeable to visible light, but it is highly permeable to infrared light. The IR permeability decreases with decreasing electrical resistivity.

After oxygen (50.5%), silicon is the second most abundant element (27.5%) in the lithosphere. It does not occur in elemental form, but only in oxides and silicates.

Modern electronics is almost exclusively (> 95%) based on silicon devices, both in low-power and in high-power electronics, a situation that will continue for at least the next few decades. Because of the eminent and ever increasing importance of electronics in technology and everyday life, silicon is one of the most important technical materials, although the quantity required for this application is relatively small (ca. 10 000 t of electronic-grade silicon in 1992). This small quantity results

from the very small dimensions of electronic devices (e.g., 0.5 \times 4 \times 4 mm).

Of secondary importance are the uses of silicon for metallurgy and chemistry (silicon compounds), although they consume the major portion of the silicon produced.

48.2 History

The name silicon derives from the Latin word *silex* (= flint). Even in ancient times, silicon compounds were used for the production of glass. The first attempts to obtain elemental silicon from silica were made in the 1700s, but only in 1810 did BERZELIUS succeed in isolating silicon from ferrosilicon by reduction with carbon and iron at the melting point of iron. In 1823, he obtained iron-free silicon by reducing SiF₄ with potassium metal.

In 1854, SAINTE-CLAIRE DEVILLE obtained coarse-grained silicon by fusion electrolysis of silicon-containing NaAlCl₄. Further important developments were achieved by WÖHLER (1855), WINKLER (1864), SCHEID (1899), and KÜHNE (1902). Commercial production of ferrosilicon (iron-rich silicon), which had proved to be an excellent deoxidant in steel production, began in the early 1900s as an offshoot of calcium carbide production. Ferrosilicon is produced in the same type of furnace as calcium carbide and is a by-product of calcium carbide production.

48.3 Properties

Some physical properties of silicon are as follows (values without references are taken from [1]):

Atomic number	14
A_r	28.086
Lattice constant (= edge length of the cubic unit cell)	0.3571 nm
Interatomic distance in (111) direction	0.2352 nm

¹ For Ferrosilicon, see Section 7.3.

Atomic density	5.00×10^{22} atoms/cm ³
Density at 300 K	2.329 g/cm ³
Density at melting point	2.30 g/cm ³
Solid	2.51
Liquid	
Volume increase at transition from liquid to solid	+ 9.1%
Specific heat (300 K)	0.713 J g ⁻¹ K ⁻¹
Thermal expansion (300 K)	2.6×10^{-6} K ⁻¹
Thermal conductivity (300 K)	1.5 W cm ⁻¹ K ⁻¹
mp	1687 K
bp	3504 K [2]
Critical temperature	5193 K
Critical pressure	145 MPa
Latent heat of fusion	50.66 kJ/mol
Heat of evaporation	385 kJ/mol
Combustion heat, H_c (Si/SiO ₂)	850 kJ/mol
Bulk modulus (300 K)	97.84 Pa
Vickers hardness	10.2 GPa
Mohs hardness	7
Surface tension at melting point	885 mJ/m ²
Band gap (300 K)	1.126 eV
Electron mobility	1440 cm ² V ⁻¹ s ⁻¹
Hole mobility	484 cm ² V ⁻¹ s ⁻¹

As an element of group 14 of the periodic table, silicon represents the transition from the base metals of groups 1, 2, and 13 to the metalloids and nonmetals of groups 15–17. With nonmetals of higher electronegativity, silicon forms predominantly nonpolar compounds such as Si₃N₄ or SiC, as well as more polar compounds such as SiO₂ and SiF₄ with oxidation state 4+. If Si–Si bonds are present, the mean oxidation state is lower (e.g., 3+ in Si₂I₆).

Silicon binds oxygen dissolved or present as compounds in metal melts to give SiO₂ or SiO, and it may partially evaporate in the form of the volatile SiO. With metals, silicon forms alloys, intermetallic compounds, or silicides.

Bulk silicon is very resistant to acid, including HF or HNO₃, but not to a mixture of HF and HNO₃. In this mixture, HF first etches away the SiO₂ layer from the silicon surface, then HNO₃ oxidizes silicon again, the new SiO₂ layer is removed by HF, and so on. Silicon reacts violently with even dilute alkaline solutions to generate hydrogen. Heating in an oxygen-containing atmosphere forms an SiO₂ layer that inhibits further oxidation. Above 520 K, silicon reacts with HCl to form SiHCl₃ and SiCl₄, and with CH₃Cl in the presence of copper to give alkylchlorosilanes. At ca. 620 K, silicon and HBr give SiBr₄ and SiHBr₃. At

room temperature, silicon and fluorine produce SiF₄.

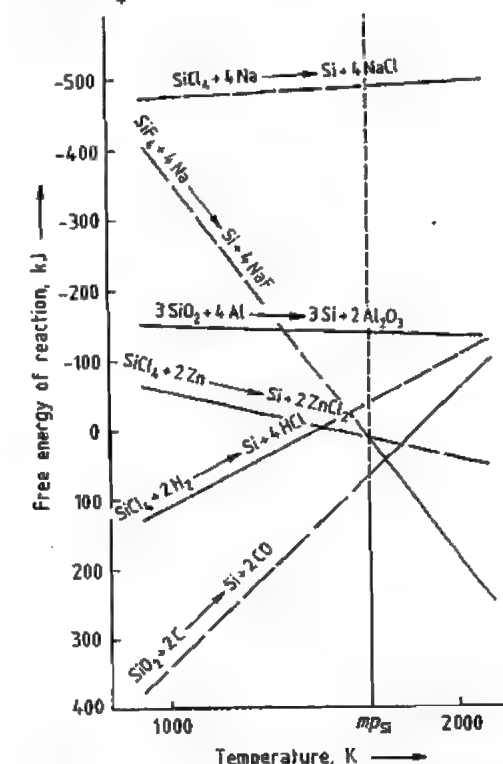
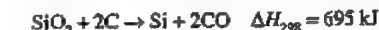


Figure 48.1: Free energy of selected reactions for production of silicon from SiO₂ and Silicon tetrahalides [5].

48.4 Production

48.4.1 Metallurgical Silicon

Since the turn of the century, silicon has been produced almost exclusively by carbothermal reduction of silicon dioxide:



Another way to produce silicon from SiO₂ is aluminothermic reduction:

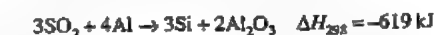


Figure 48.1 shows the free energy of reaction ΔG_0 of the two reactions for the range 900 to 2100 K. Whereas carbothermic reaction of SiO₂ is unattractive below 2000 K, reduction with aluminum is strongly exothermic over

the entire temperature range. In carbothermic reaction, the side reactions

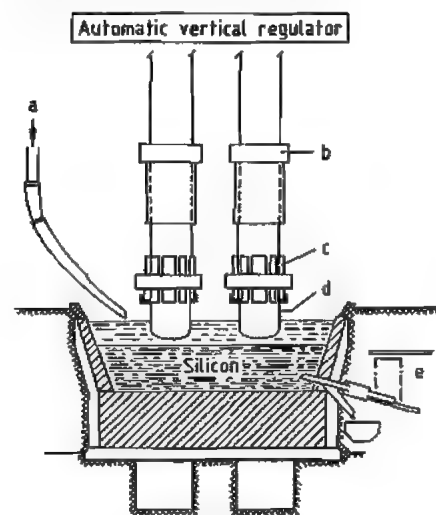


Figure 48.2: Arc furnace for silicon production [5]: a) Input of quartz and carbon; b) Electrode holder; c) Electric contact; d) Carbon electrode; e) Tapping electrode.



and



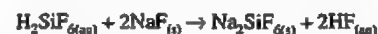
must be avoided.

For the carbothermal production of silicon and ferrosilicon, electric-arc furnaces (Figure 48.2) are used. For silicon production, graphite electrodes are used, whereas for the production of ferrosilicon, Söderberg electrodes (steel tubes filled with a mixture of coal powder, tar, and pitch) are employed. The carbothermal process yields silicon with a purity of ca. 98% (metallurgical-grade silicon, MG-Si), for which a typical analysis is 0.5% Fe; 0.4% Al; 100–400 ppm each of Ca, Cr, Mg, Mn, Ni, Ti, and V; and 20–40 ppm each of B, Cu, P, and Zr. The usual starting materials are chunks of quartzite, coke, as well as charcoal and wood chips for good ventilation of the charge. To produce 1 t of silicon, 2.9–3.1 t of quartz or quartzite, 1.2–1.4 t of coke (gas coke and petroleum coke), and 1.7–2.5 t of charcoal and wood are required. The consumption of electrode graphite is 120–140 kg/t Si, which must be added to the amount of reducing

agent, and of electrical energy is 12.5–14 MWh/t Si. The purity of the silicon produced depends primarily on the purity of these materials and secondarily on the purity of the graphite electrodes and the furnace lining.

The purity of silicon can be increased by using purer starting materials, by improving the furnace construction, and by optimizing the production process. Dow Corning [3, 4] has introduced an improved arc furnace, the so-called direct arc reactor (DAR), which yields purer silicon. With adequately pure starting and furnace materials and with optimized operation, the DAR process gives silicon with a purity of 99.99%. Residual impurities are Al, Fe (50–100 ppm each), and other metals, as well as B and P (< 10 ppm each).

Another method of producing silicon starts with silicon tetrafluoride, which is a by-product of the production of superphosphate fertilizer from phosphate rock. The ore contains CaF_2 , which is converted to HF when treated with H_2SO_4 ; HF then reacts with SiO_2 to form SiF_4 , with an estimated 75 000 t/a being recovered in the United States as fluosilicic acid, H_2SiF_6 . Sodium fluoride is added to the H_2SiF_6 to form sodium fluosilicate:



After filtration and drying, Na_2SiF_6 is decomposed at 920 K:



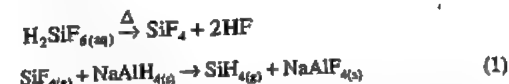
Then, SiF_4 is purified by passing it over iron at 1070 K to remove air and SO_2 , and by subsequent fractional distillation. Silicon tetrafluoride can be reduced readily to silicon by reaction with sodium:



The exothermic character of this reaction provides sufficient heat to maintain the process at 770 K. To separate silicon from NaF, the Si–NaF mixture is melted to form two immiscible phases for which liquid–liquid extraction (migration of impurities from silicon to NaF) provides additional purification. This reduction process is known as the SRI (Stan-

ford Research Institute International) process [6, 7]. Because the reduction reaction yields four times as much NaF as silicon, low-cost silicon is attainable only if the by-product can be sold.

An alternative way to transform $\text{H}_2\text{SiF}_6(\text{aq})$ into elemental silicon is used by Ethyl Corporation [8]:



Also, KAlH_4 or a mixture of NaAlH_4 and KAlH_4 can be used. NaAlF_4 is used in aluminum production, and SiH_4 is decomposed at ca. 1000 K to generate elemental silicon:



About 150 other reactions yield elemental silicon, but most of them are not used in industrial production.

Ferrosilicon production, ca. 2×10^6 t in 1992, constitutes the major part of industrial silicon production. Ferrosilicon is used in steelmaking, mainly as a deoxidizer, but also as an alloying element (e.g., for the production of transformer sheet metal).

World production of metallurgical-grade silicon in 1991 was ca. 650 000 t, with a market price of ca. \$1.5/kg. About 60% was used as an alloying element for nonferrous metals, particularly aluminum alloys; ca. 37% for the production of silicon compounds; and ca. 3% for electronic applications (electronic devices, solar cells, sensors, micromechanics). The main producer countries for MG silicon are Norway, the United States, France, Canada, the Republic of South Africa, the CIS, Italy, Spain, and Yugoslavia.

48.4.2 Semiconductor Silicon

48.4.2.1 Purification

For applications in electronics, photovoltaics, sensors, and micromechanics, metallurgical-grade silicon must be refined to a much higher purity. Purity requirements for the fabrication of high-efficiency solar cells, for ex-

ample, are nearly as high as those for advanced semiconductor devices.

At present, the main refining steps are the adsorption and distillation of a silicon compound. For this purpose, silicon is first converted into a compound such as SiHCl_3 , SiCl_4 , SiH_2Cl_2 , or SiH_4 . After purification, the silicon compound is transformed back into elemental, high-purity silicon by chemical vapor deposition (CVD). Alternative refining methods [5] have not been used in industrial production up to the present.

The starting material for the production of semiconductor-grade silicon (SG-Si) is about 90% carbothermal silicon and about 10% silicon produced by the Ethyl process [8].

Carbothermal silicon, milled to a sand or powder, is fed into a fluidized-bed reactor where it is fluidized by a stream of hydrogen chloride flowing through small orifices in the bottom of the reactor (Figure 48.3). The reactor is held at ca. 650 °C and the exothermic reaction yields predominantly trichlorosilane and hydrogen,



as well as silicon tetrachloride:



In addition to SiHCl_3 and SiCl_4 , other chlorosilanes and compounds of the impurities with chlorine or hydrogen are formed. After removal of silicon powder, impure trichlorosilane is condensed and stored in an intermediate tank, and subsequently purified by adsorption and distillation (Figure 48.3). Because of its favorable boiling point of 305 K, trichlorosilane can be purified effectively by fractional distillation. To improve the removal of boron and phosphorus, the two most important electrically active elements in silicon, boron(III) and phosphorus(III) chloride are transformed into less volatile compounds before distillation by use of complexing agents. In this way, the production of trichlorosilane with boron and phosphorus contents of < 1 ppba (parts per billion atomic) is possible.

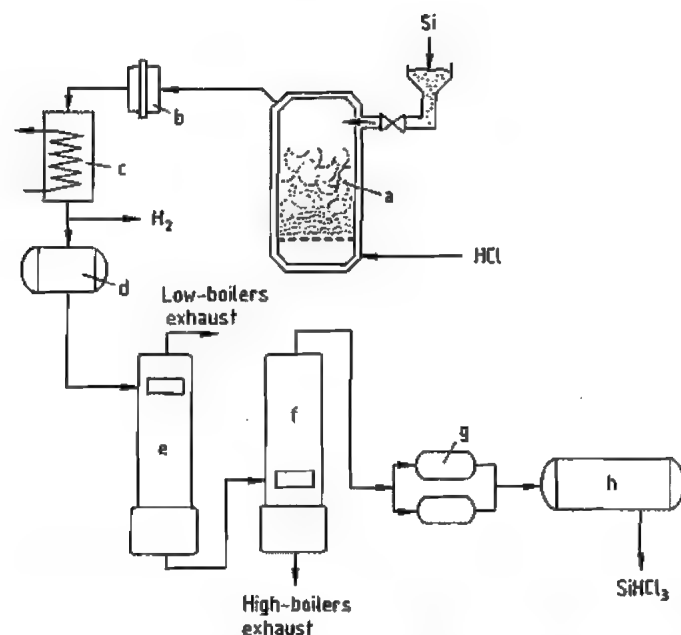


Figure 48.3: Flow chart of the preparation and refining of trichlorosilane: a) Fluidized-bed reactor; b) Dust filter; c) Condenser; d) Tanks; e) Distillation of low-boiling impurities; f) Distillation of high boilers; g) Tanks; h) Storage tanks.

From the point of view of chemical process engineering, trichlorosilane is easiest to handle and most economical. About 90% of the electronic-grade silicon is purified by distillation of trichlorosilane, and the rest by distillation of silane, SiH_4 . The distillation of SiH_4 is applied only after the Ethyl process (Equation 1). Silane is much more dangerous to handle than trichlorosilane.

48.4.2.2 Chemical Vapor Deposition

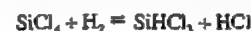
All semiconductor-grade silicon is produced by converting silicon compounds to elemental silicon by chemical vapor deposition (CVD). For ca. 75% of worldwide CVD production, trichlorosilane is used as the silicon compound (e.g., by Wacker, Hemlock, Tokuyama Soda, Kyundo, OTC, MEMC); for ca. 25%, silane (ASiMI, Ethyl), partly produced from trichlorosilane, is used.

The method of converting trichlorosilane into high-purity silicon was first developed by Siemens & Halske in 1952 and patented in

1956 [9]. It employs the reverse of Equation (3), which is strongly endothermic and therefore requires a high reaction temperature (ca. 1400 K). This reaction also yields much tetrachlorosilane as by-product:



The by-product SiCl_4 is partly converted back to trichlorosilane in the reactions



The remaining SiCl_4 is used for the production of highly dispersed SiO_2 (e.g., HDK from Wacker) and synthetic silica glass and glass fibers, and for silicon epitaxy in the production of electronic devices.

To avoid the deposition of silicon on unwanted and contaminating surfaces, the CVD arrangement shown schematically in Figure 48.4 is used. In a bell-jar reactor, three silicon slim-rods (ca. 8 mm in diameter, semiconductor grade, float zone pulled in a specially designed apparatus) are mounted in the form of an inverted U and are resistance heated electri-

cally to ca. 1400 K, while the bell jar is kept cold. In this way, the heat required for the reaction is available only on the surface of the silicon rods; silicon forms there exclusively and adheres to the rods. Elemental silicon not adhering to the rods is transformed back to a gaseous silicon compound at lower temperature (e.g., Equation 3) in the reactive atmosphere around the rods.

In the CVD process, the concentration of impurities is again reduced [10], in the case of boron and phosphorus by a factor of up to 1000. The trichlorosilane CVD process yields silicon with < 0.02 ppba boron and < 0.01 ppba phosphorus, so that further refining of the CVD silicon by zone melting for electronic applications is no longer necessary in most cases, in contrast to the situation at the beginning of semiconductor-grade silicon production.

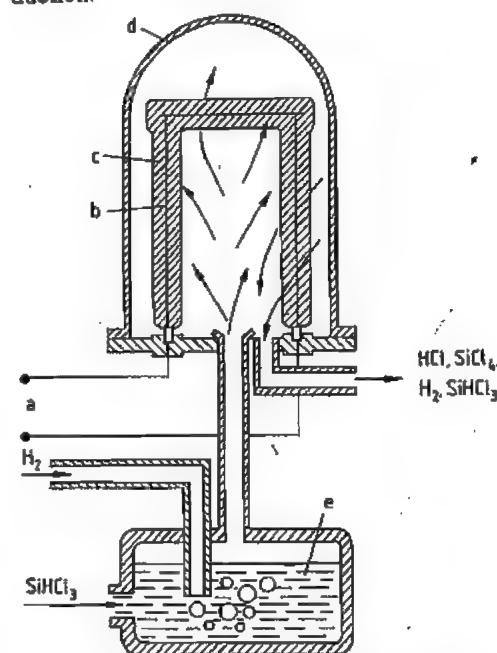


Figure 48.4: Chemical vapor deposition of silicon: a) Electrical current; b) Starting silicon slim-rod; c) CVD polycrystalline silicon rod (1400 K); d) Reactor (silica, metal); e) Saturator.

Silicon single crystals can also be grown by CVD if monocrystalline slim-rods are used. However, this process is very expensive be-

cause of the very low growth rate that must be used for single-crystal growth, and it yields low-quality single crystals. Therefore, the CVD silicon produced today is a fine-grained, polycrystalline material used as starting material for the melt growth of single crystals.

In the CVD process, much energy is lost by thermal radiation from the silicon rods. The radiant energy is absorbed largely by the cold reactor walls. Energy is therefore the primary cost factor in this process; thus endeavors are made to maximize the deposition rate. Theoretically, the highest growth rate is ca. 2 mm/h; however, growth rates used in industry are lower ca. 1 mm/h or less.

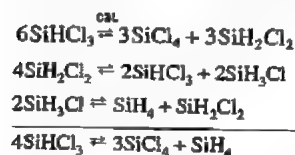
The upper limit for the deposition rate is determined by the required silicon quality, especially in the production of silicon rods for float-zone crystal growth, which requires long cylindrical silicon feed rods, free of cracks and voids, and with a smooth surface, as starting material. Too rapid a growth rate results in dendritic growth, which gives a rough surface, voids, and cracks in the material. Such a feed rod would either crack or emit silicon particles on melting during float-zone growth.

Whereas the diameter of the feed rods for float-zone growth is determined by the requirements of the crystal growth process (the diameter of the feed rods should be a little larger than that of the crystals to be grown), CVD silicon rods for the growth of crucible-pulled crystals may be of any diameter. Therefore, CVD rods for crucible pulling are always grown to the largest possible diameter for economic reasons: the CVD yield (kg/Wh) and the CVD output (kg/h) increase linearly with the radius of the rod at a constant deposition rate. However, the maximum diameter of CVD rods is ca. 25 cm, since at larger diameters, the center of the rod begins to melt and the rod system breaks down, causing damage to the reactor and contamination of the silicon. Therefore, the deposition process is stopped at a rod diameter known to exhibit no melting.

At present, CVD processes run automatically. Process parameters such as current, temperature, pressure, gas flow, and concentration

are measured continuously and are used by a computer to calculate new control parameters. Rod lengths > 2 m and rod numbers of 8–16 per reactor are usual today.

A different method of producing CVD silicon is used by ASiMI (formerly UCC), which transforms SiHCl_3 into SiH_4 and performs the CVD process with SiH_4 at ca. 1000 K. The CVD reactor and arrangement are similar to those used for deposition with SiHCl_3 (deposition on silicon rods, Figure 48.4). The transformation of trichlorosilane into silane occurs according to the following reactions:



The CVD reaction is the decomposition of silane:



A very different way of transforming silane into elemental silicon is used by Ethyl, United States [11], and KRICT, Korea [12], based on a Texas Instruments patent [13].

A mixture of ca. 20 mol% silane and 80 mol% hydrogen is fed through a gas-dispersing frit into the bottom of a reactor; a fine silicon powder is let in through an opening at the top of the reactor and fluidized by the upflowing gas. The silicon powder is heated to ca. 1000 K, and silane decomposes according to Equation (4) into silicon and hydrogen on the hot silicon particles. The silicon particles grow, and the larger ones fall to the bottom of the reactor where they are removed through an opening.

In the Ethyl process, the silicon particles are heated from outside the reactor by resistance heating (Figure 48.5). This leads to problems with unwanted deposition of silicon on the hot walls of the reactor.

This problem is overcome in the newer KRICT process. Silicon particles are heated with microwaves, and the reactor wall remains cold if it is made from an appropriate material (e.g., silica).

Granular CVD silicon has major advantages over rod-shaped CVD silicon for feeding, particularly for continuous feeding of the melt with silicon during crystal growth, because the round silicon granules flow much better than the sharp-cornered grains of broken CVD silicon rods. Moreover, breaking the rods contaminates the silicon severely.

In 1992, the world production of electronic-grade CVD silicon was ca. 10 000 t with a market value of ca. $\$500 \times 10^6$ (\$50/kg).

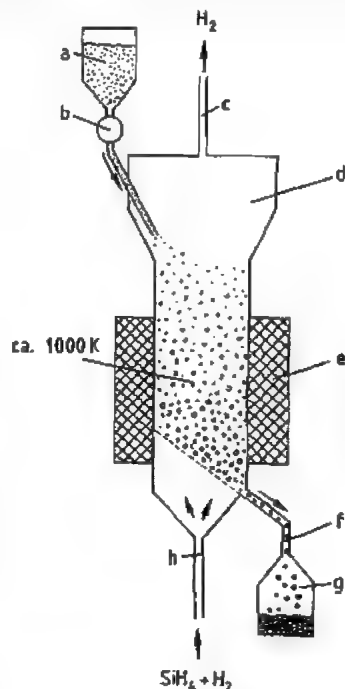


Figure 48.5: Chemical vapor deposition of granular silicon: a) Silicon powder; b) Powder-feeding device; c) Exhaust; d) Fluidized-bed reactor; e) Heating (resistance or microwave); f) Removal of coarse silicon granules; g) Container for silicon granules; h) Gas injection.

48.4.2.3 Single-Crystal Growth

More than 95% of all electronic devices are made from single-crystal silicon. In addition, single-crystal silicon is used at present for ca. 40% of all photovoltaic solar cells and for all micromechanical devices. Two crystal growth methods are used in industry for the production of silicon single crystals: the Czochralski

(CZ) method, which yields about 85% of all silicon crystals, and the float-zone (FZ) method, which yields 15% of the silicon crystals. The CZ crystals are used mainly for manufacturing highly integrated low-power devices, typically for microprocessors, RAMs, DRAMs, ASICs, etc., whereas the FZ crystals are used mainly for making discrete or low-integrated high-power devices such as diodes, transistors, and thyristors.

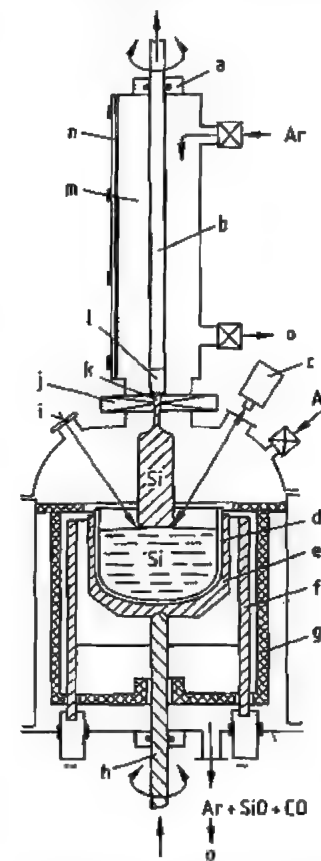


Figure 48.6: Czochralski silicon crystal puller: a) Seal; b) Seed shaft; c) Optical system; d) Silica crucible; e) Graphite crucible; f) Graphite heater; g) Thermal insulation; h) Crucible shaft; i) Viewing port; j) Separation valve; k) Seed crystal; l) Seed holder; m) Front opening chamber; n) Front opening door; o) Valve.

Czochralski Crystal Growth. The Czochralski method [14] uses a crucible for crystal pulling and is therefore also known as crucible pulling (see Figure 48.6; for more detailed in-

formation, see [15–17]). A silicon melt is held in a crucible and a single-crystal seed of the proper orientation is dipped into the melt and slowly withdrawn vertically. With suitable pulling speed and crystal and crucible rotation rate, a single crystal of the desired shape can be grown.

To eliminate dislocations, which always occur on immersing the seed crystal, a thin crystal neck (ca. 3–5 mm in diameter and several centimeters long) must be grown with a growth rate of several millimeters per minute. Because of the small diameter, the thermal strains in the neck are too low and the growth rate is too high for propagation of dislocations downward into the growing crystal, and the crystal neck becomes dislocation free after a few centimeters. The same procedure is used in float-zone pulling.

The dislocation-free state is stable, and large diameters can be grown despite the high cooling strains in large crystals. After neck growth, the diameter is increased to the nominal crystal diameter and then kept constant by adjusting the pulling rate and the heating power. Dislocation-free crystal growth can be completed by reducing the crystal diameter to nearly zero at the end of the crystal.

Usually, a small residual melt remains in the crucible, the amount of which depends on quality demands and economic factors. Owing to the segregation effect, the majority of the impurities remain in the melt since most of them have very low segregation coefficients (see Table 48.1).

The silicon melt reacts with all materials to some extent. Only silica can be used as crucible material, because the product of its reaction with the silicon melt, silicon monoxide (SiO), evaporates readily from the melt. Thus supersaturation of the melt with oxygen or SiO is prevented. Supersaturation of oxygen in the melt would cause supersaturation of oxygen in the crystal, oxygen precipitation, and the formation of dislocations in the crystal near the freezing interface. The growth of a dislocation-free crystal would be impossible. All other crucible materials either contaminate the silicon crystal with impurities (e.g., Al_2O_3 ,

or ZrO_2) or cause dislocated crystal growth by supersaturation (e.g., SiC and Si_3N_4).

Both to promote the evaporation and removal of SiO and to prevent the backflow of CO and other reaction and evaporation products, the furnace is purged with a strong argon stream and the pressure is kept low (generally 10–100 mbar). Table 48.2 gives an overview of the basic data for current industrial silicon crystal growth.

About 1.5 g of silica is dissolved per 1000 g of CZ-Si crystal during growth, but < 1% of the oxygen in the dissolved silica is found in the crystal. This indicates that the evaporation rate of SiO is very high and the oxygen content of the melt is exchanged every 10 min. Accordingly, oxygen transport from the crucible to the crystal and thus the oxygen content of the crystal can be manipulated over a wide range by influencing convective flows in the melt and the evaporation of SiO at the melt surface.

Table 48.2: Data for industrial silicon single-crystal growth.

Property	Maximum value ^a	Industrial standard production, 1992	
		CZ crystals	FZ crystals
Diameter, mm	≥ 300	≤ 200	≤ 150
Length, mm	≥ 2500	≤ 2000	≤ 1800
Weight, kg	≥ 100	≤ 100	≤ 50
Orientation	any	(100), (111), (110), (115)	(111), (100), (110), (115)
[B], cm^{-3}	≤ 3 × 10 ²⁰	1 × 10 ¹⁴ –1 × 10 ²⁰	5 × 10 ¹¹ –1 × 10 ¹⁷
[P], cm^{-3}	≤ 3 × 10 ²⁰	1 × 10 ¹⁴ –1 × 10 ¹⁸	1 × 10 ¹² –5 × 10 ¹⁸
[As], cm^{-3}	≤ 3 × 10 ²⁰	5 × 10 ¹⁸ –8 × 10 ¹⁹	
[Sb], cm^{-3}	≤ 3 × 10 ¹⁹	2 × 10 ¹⁷ –1 × 10 ¹⁹	
[Al], cm^{-3}	≤ 3 × 10 ¹⁷		
[Ga], cm^{-3}	≤ 3 × 10 ¹⁸		
[In], cm^{-3}	≤ 3 × 10 ¹⁷		
[C], cm^{-3}	≤ 3 × 10 ¹⁸	1 × 10 ¹⁵ –3 × 10 ¹⁶	1 × 10 ¹⁵ –3 × 10 ¹⁶
[N], cm^{-3}	≤ 3 × 10 ¹⁵	< 1 × 10 ¹⁴	< 1 × 10 ¹⁴ –1 × 10 ¹⁵
[O], cm^{-3}	≤ 3 × 10 ¹⁸	1 × 10 ¹⁷ –1 × 10 ¹⁸	1 × 10 ¹⁵ –2 × 10 ¹⁶
Crucible material		silica	no crucible
Crucible diameter, mm		≤ 600	
Rotation rate, rpm		≤ 50 crystal, ≤ 30 crucible	≤ 50 crystal, ≤ 2 feed rod
Growth rate, mm/min		≤ 2.5	≤ 4.5
Pressure, mbar		5–1000	5 × 10 ^{−4} –5000
Argon flow, L/h		400–5000	

^aThe maximum concentration for dislocation-free growth is generally lower than the maximum solubility in silicon (at ca. 1550 K) due to the effect of retrograde solubility for most of the elements (for most elements, solubility increases up to ca. 1550 K, then decreases continually up to the melting point of 1687 K). The maximum growth and rotation rates decrease with increasing crystal and crucible diameters.

^bConcentration in number of impurity atoms per cm^3 of silicon; 1 cm^3 Si contains 5.00×10^{23} atoms.

Table 48.1: Equilibrium distribution coefficients k_0 and typical concentrations of impurities in CVD-Si and CZ-Si.

Element	k_0	Impurity concentration, ppba	
		CVD-Si	CZ-Si
C	0.07	≤ 200	≤ 200
N	7×10^{-4}	≤ 4 ^a	< 4 ^a
O	ca. 1	≤ 100	ca. 15 000
A	0.8	≤ 0.02	ca. 0.2
Al	2.8×10^{-3}	≤ 0.01	≤ 0.4
Ga	8×10^{-3}	< 0.002 ^a	< 0.002 ^a
In	4×10^{-4}	< 0.002 ^a	< 0.002 ^a
P	0.35	≤ 0.01	ca. 0.1
As	0.30	ca. 0.01	≤ 0.01
Sb	0.023	ca. 0.0008	ca. 0.01
Li	0.01	< 0.3 ^a	≤ 0.1
Na	ca. 1×10^{-3}	< 0.3 ^a	≤ 0.1
K		< 0.2 ^a	< 0.1 ^a
Ti	2.0×10^{-6}	< 0.5 ^a	< 0.5 ^a
Cr	1.1×10^{-5}	< 0.02 ^a	< 0.004 ^a
Fe	6.4×10^{-6}	< 0.5 ^a	≤ 0.01
Ni	ca. 3×10^{-5}	ca. 0.4	≤ 0.01
Co	1.0×10^{-5}	ca. 0.002	< 0.001 ^a
Cu	8×10^{-4}	ca. 0.05	≤ 0.01
Ag	ca. 1×10^{-6}	0.01	< 0.0008 ^a
Au	2.5×10^{-3}	0.00001	< 0.00001 ^a
Zn	ca. 1×10^{-5}	ca. 0.1	< 0.05 ^a
Zr	< 1.5×10^{-7}	< 0.5 ^a	< 0.5 ^a

^aConcentration below the detection limit listed here.

crystal pullers allows completely automatic crystal growth. However, with monitoring and correction by an operator, the yield of the crystal grower can be improved. In 1992, the standard diameters of commercial CZ-Si crystals ranged from 50 to 200 mm, averaging 150 mm, and CZ-Si crystals 300 mm in diameter are being developed.

Float-Zone Crystal Growth. Figure 48.8 shows the basic arrangement for large diameter float-zone silicon crystal growth in a modern FZ puller. The FZ-Si method differs from the CZ-Si method mainly in the absence of a crucible and in the small melt volume. The absence of a crucible results in a very low oxygen content and in lower concentrations of impurities compared to CZ-Si crystals. The small melt volume leads to an axially constant boron or phosphorus concentration in contrast to CZ-Si (see Figure 48.9). Boron and phosphorus are the only dopants used in industrial FZ-Si production.

Figure 48.7: Removal of a large CZ silicon crystal (diameter 204 mm, weight 50 kg) that is still hanging from the seed crystal.

Impurities in the dissolved silica are absorbed by the silicon melt. However, only a small portion of impurities are incorporated into the crystal owing to the segregation effect, which is very strong for most elements (see Table 48.1). For example, from 100 000 iron atoms in the melt, only one atom is incorporated into the crystal. As a result of this strong segregation, the impurity content of the CZ-Si crystal is lower than that of the starting material for most elements.

Figure 48.6 shows the basic arrangement of a CZ-Si crystal puller, and Figure 48.7 shows a photograph of such a crystal puller during removal of a grown crystal. The best and most economical heating method is resistance heating with a graphite heating element. The soft silica crucible must be supported by a graphite crucible. The diameter of the crystal is monitored by an optical system (e.g., a CCD camera) and, in most cases, the melt and furnace temperatures are measured by pyrometers. The crystal and the crucible can be moved and rotated very precisely. A valve between the front-opening chamber and the furnace allows the removal of the crystal while the furnace is hot and refilling of the hot crucible (containing residual melt) with polycrystalline silicon and dopant. The growth control of modern

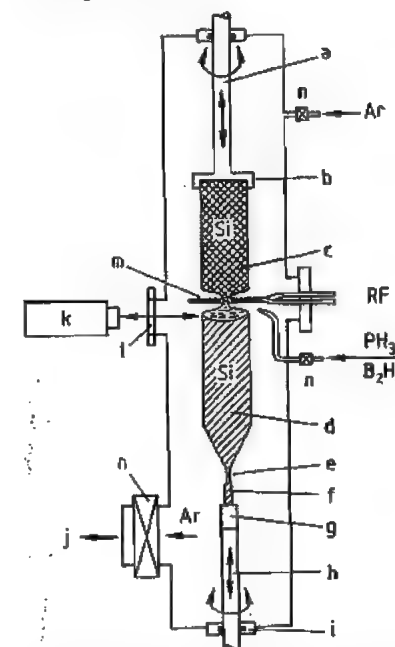


Figure 48.8: Float-zone silicon crystal puller: a) Feed rod shaft; b) Feed rod holder; c) Feed rod, polycrystalline; d) Single crystal; e) Neck; f) Seed; g) Seed holder; h) Seed shaft; i) Seal; j) To the vacuum pump; k) Camera; l) Viewing port; m) RF heating coil; n) Valve.

The starting material for the growth of an FZ-Si single crystal is a polycrystalline silicon feed rod clamped to a movable shaft. The feed rod can be unmelted CVD silicon or FZ-premelted silicon (CVD rods that have been float zone grown to give cylindrical, bubble- and crack-free polycrystalline rods). An induction coil melts the feed rod at the bottom, generating a large melt drop. A slim seed crystal is moved through the narrow opening in the center of the induction coil and brought into contact with the melt drop. Upon movement of the seed crystal downward the melt crystallizes on it and the seed crystal grows.

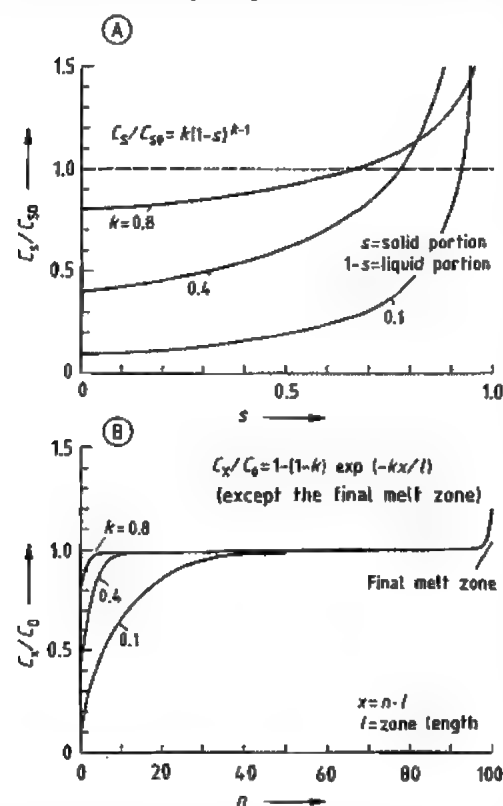


Figure 48.9: Relative axial concentration variation C/C_0 in silicon crystals produced from starting material (melt or feed rod) in which the impurities are distributed homogeneously. A) CZ crystals (normal freezing); B) FZ crystals (final melt zone freezes according to normal freezing); in this example, total length of feed rod is 100l, and a constant cylindrical shape and diameter is assumed for the system feed rod-FZ melt-FZ crystal. k = Distribution coefficient.

As in CZ-Si pulling, a dislocation-free state must be generated by growing a neck prior to growth of the large-diameter crystal. After the crystal diameter is increased, melt and crystal are heated from above by the induction coil, not laterally as in the case of small crystal diameters. The melt lies on top of the crystal and is held together mainly by its surface tension and partly by electromagnetic forces. It is connected to the feed rod by a slim melt neck through which the melt flows from the feed rod to the crystal. At the end of the crystal growth process, the FZ melt freezes on top of the crystal and generates dislocations. The dislocations multiply and propagate into the crystal over a distance of about one-half the crystal diameter.

The height of the melt at the edge of the crystal is only several millimeters and does not depend on crystal diameter. Therefore, the growth of large crystal diameters is not limited by heating problems, as was assumed earlier. The FZ-Si crystals can be grown to similar dimensions as CZ-Si crystals. The main problem in the growth of large-diameter FZ-Si crystals is the high thermal stress. The temperature gradients are larger in growing FZ-Si crystals than in growing CZ-Si crystals of the same diameter because FZ-Si rods cool faster. The CZ-Si crystals are reheated by thermal radiation from the melt, the crucible, and the heater. For the growth of large diameters, cooling of the FZ-Si crystals must be reduced.

Growing large-diameter crystals requires large amounts of energy and thus high RF voltages. To prevent sparkover at the induction coils, FZ-Si growth is carried out at higher gas pressures (> 1 bar). In contrast to CZ-Si growth, no argon flow takes place during FZ-Si growth; the FZ pulling chamber is first evacuated to high vacuum and then filled with argon to a certain pressure. The doping of silicon is currently realized during FZ crystal growth by the controlled addition of a doping gas (B_2H_6 or PH_3) to the argon during growth.

The monitoring and control of crystal diameter and the degree of automation of FZ-Si growth are similar to those of CZ-Si growth. Standard commercial production in 1992 (see

Table 48.2) had crystal diameters up to 150 mm (usually ca. 100 mm). Larger diameters could be developed if they were in industrial demand.

Float-zone crystals can be pulled with higher growth rates than CZ crystals, because the solidification energy of FZ crystals is removed more quickly. With FZ growth the entire environment of the cooling crystal is cold (ca. 300 K, see Figure 48.8), whereas the environment of the CZ crystal is very hot in places (melt, crucible, and furnace near 1700 K), and the growing CZ crystal receives much energy from thermal radiation.

The maximum growth rate depends strongly on the crystal diameter in both FZ and CZ growth. With increasing diameter the ratio between the heat-emitting surface (predominantly the parts of the surface hotter than 1200 K) and the heat-absorbing and generating growth interface becomes smaller, and additionally, the diffusion length of the heat increases owing to increasing distance between the crystal axis and the crystal surface. The maximum growth rate decreases from about 10 mm/min at 5-mm crystal diameter to about 1 mm/min at 150-mm crystal diameter for CZ-Si growth; the corresponding values for FZ-Si growth are 12 mm/min and 2 mm/min. In industrial production, the growth rates are lower than the maximum growth rates for reasons of yield and quality.

Segregation of Impurities. The axial variation of impurity concentration in CZ- and FZ-Si crystals due to segregation is shown in Figure 48.9. The segregation of impurities, in particular of dopants, has important qualitative and economical effects. Silicon device manufacturers demand silicon materials with tight resistivity tolerances, but CZ-Si crystal rods meet these tolerances only in small sections of their length.

In this respect, FZ-Si growth has major economic advantages. The resistivity of a boron- or phosphorus-doped FZ-Si crystal is nearly constant over its entire length. Strong variations occur only in the seed cone and in the finally freezing melt because of the small

FZ melt volume. The height and depth of the melt are only a few centimeters (near the crystal axis) and depend on the crystal diameter and the curvature of the concave solid-liquid interface. The melt volume in FZ growth is much smaller than in CZ growth and remains nearly constant during growth of the cylindrical crystal.

In CZ growth the silicon charge is melted completely at the beginning. The melt volume decreases and the dopant concentration increases continuously during crystal growth. This is valid for nonvolatile or moderately volatile dopants such as B, P, Al, and Ga. In the case of volatile dopants such as As, Sb, or In, the enrichment of the melt with dopant can be compensated or overcompensated by evaporation of the dopant. In FZ growth the enrichment of boron or phosphorus is continuously compensated by the supply of unenriched silicon.

Many attempts and developments have been made to eliminate the axial resistivity decrease during CZ-Si growth. A partial solution of this problem is to consume only a part (e.g., one-half) of the melt and then to refill the crucible by adding polycrystalline silicon chips or by immersion and melting of a polycrystalline silicon rod.

Conditions similar to those during FZ growth can be realized with small CZ melts that are fed quasi-continuously with silicon and dopant (Figure 48.10). The crucible is held in a fixed position and filled with melt to a certain level. A silica baffle is suspended from the cover of the furnace and dips several centimeters into the melt. The baffle has openings above the melt level to allow purging with argon. Additionally, a conical shield covers a large part of the melt surface to prevent the backflow and condensation of SiO on the feeding tube and baffle and to reduce heat losses by radiation. The silica feeding tube reaches to a short distance above the melt. Silicon granules and dopants are fed continuously through this tube at the same rate melt is removed by the growing crystal.

The problem with this technique is that fusion energy for the granules must be supplied

during crystal growth, resulting in higher temperature of the crucible walls and problems with corrosion of the silica, with oxygen content, and with dislocation-free growth. Additional problems result from silicon crystallites that "swim" underneath the baffle from outside to the growing crystal where they generate dislocations.

The fusion energy for the silicon need not be supplied to the melt from which the crystal is grown if the melt is fed with molten silicon.

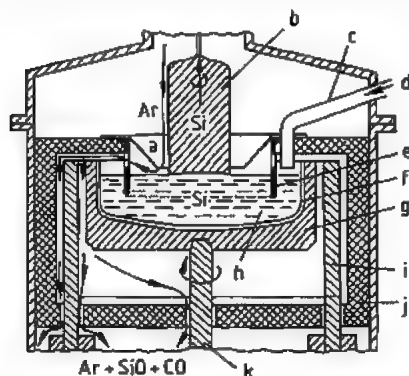


Figure 48.10: Quasi-continuous feeding of a CZ melt with silicon granules: a) Radiation shield, graphite; b) Crystal; c) Feeding tube, silica; d) Silicon granules; e) Baffle, silica; f) Crucible, silica; g) Susceptor, graphite; h) Melt; i) Heater, graphite; j) Thermal insulation, carbon; k) Crucible shaft, graphite.

Melt Flows. Constant-volume melts have the advantage that their convective flows are constant over time. On a macroscopic scale they give a constant oxygen content and a constant radial impurity distribution. Small melts have the advantage of more controllable convective flows because of their weaker thermal convection. The thermal convection in the CZ-Si melt depends on the Grashof number Gr :

$$Gr = \frac{g\alpha dTh^3}{\nu^2}$$

where g is the acceleration due to gravity, α is the volume thermal expansion coefficient, dT is the temperature difference in the melt, h is the height of the melt, and ν is the kinematic viscosity.

Owing to the dependence on h^3 and dT (the temperature differences in large melts are greater than in small melts), the convective

flows in large CZ-Si melts become very turbulent, unsteady, and nearly uncontrollable. The unsteady flows result in large temperature fluctuations at the solid-liquid interface and in large fluctuations in oxygen transport to the crystal.

Figure 48.11 shows schematically the various convective flows in a CZ-Si melt. In the classical "open" growth furnace, thermal convection is strongest. A thermocapillary convection—also called Marangoni convection—always occurs below the melt surface at the edge of the crystal and at the crucible wall. It is driven by the differences in surface tension due to differences in the melt temperature. The effects of thermocapillary convection are not well understood.

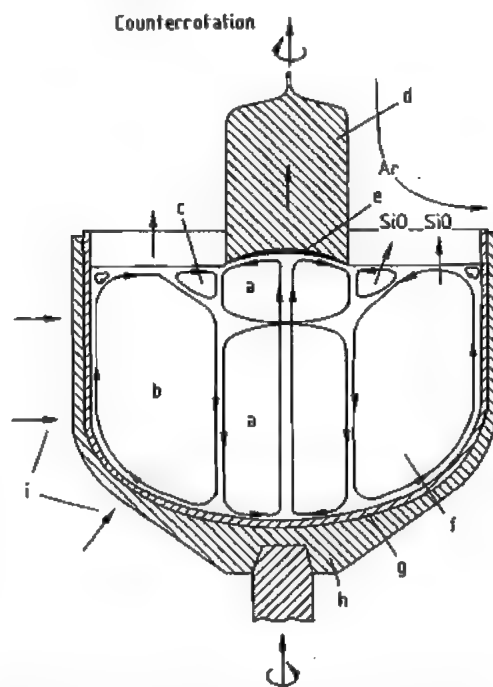


Figure 48.11: Schematic of the convective flows in a CZ silicon melt; flows are both temporally and locally inhomogeneous, creating temperature and concentration fluctuations. a) Mechanically forced convection; b) Thermal convection; c) Thermocapillary (Marangoni) convection; d) Crystal; e) Diffusion layer; f) Melt; g) Crucible; h) Susceptor; i) Heat flow direction.

Mechanically forced convection is generated by rotation of the crystal and crucible.

Crystal rotation must be used for two reasons. First, without rotation, the crystal would grow with a noncylindrical shape and dislocations would be generated; second, crystal rotation reduces the strong impurity enrichment toward the center of the crystal caused by thermocapillary convection and segregation.

The incorporation of impurities depends strongly on the thickness of the diffusion layer in the melt at the solid-liquid interface: the thicker the diffusion layer, the higher the incorporation of impurities into the crystal. The thickness of the diffusion layer is strongly influenced by melt flows.

Impurity Striations. Temperature fluctuations at the solid-liquid interface lead to unsteady growth and backmelting. These result in microscopic impurity variations in the crystal, also called impurity striations. Unsteady growth can be reduced by using a high crystal rotational velocity because, first, mechanically forced convection decreases the influence of unsteady thermal convection at the growth interface, and second, when the crystal is moved quickly over the temperature irregularities, temperature variations in the crystal are decreased owing to its thermal response time.

In general, the oxygen distribution does not correspond to the distribution of other elements; this is true on a microscopic scale as well. The effective distribution coefficient of oxygen is nearly unity and depends only slightly on the growth rate. However, the incorporation of oxygen into the growing crystal depends strongly on the pattern of convective flows in the melt. Therefore, unsteady melt flows result in an unsteady supply of oxygen and in oxygen striations in the crystal.

Modifying Melt Flows. Melt flows in a CZ-Si melt can be modified in several ways. In most cases, this is achieved by altering growth parameters such as crystal rotation rate, crucible rotation rate, melt dimensions, furnace dimensions, furnace construction, and so on.

A more expensive way to influence the flows in a silicon melt is by the application of magnetic fields, which interact with the free

electrons of the silicon melt and retard melt flows.

The easiest way to produce a magnetic field in a CZ-Si melt is to wind a magnetic coil around the furnace vessel and generate a vertical magnetic field in the melt. However, purely vertical fields were shown to result in poor radial impurity distributions. Better results were obtained with transverse magnetic fields, which damp the melt particularly in the vertical direction. This gives a more homogeneous radial impurity distribution of both oxygen and dopant and a low oxygen content. However, the isotherms in the melt are elliptically distorted, which causes backmelting at each revolution of the crystal and rotational striations of oxygen and dopants. Transverse magnetic fields up to 4000 G with diameters up to 100 cm are applied at present.

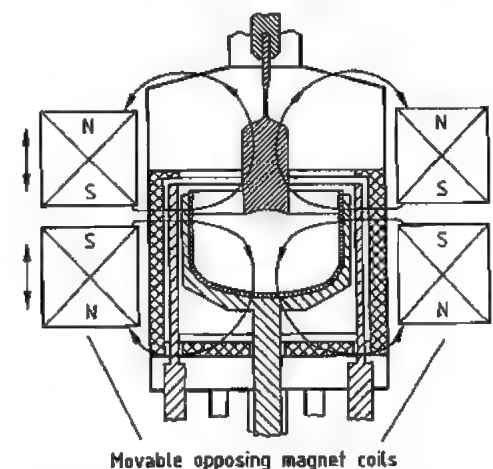
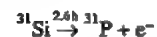


Figure 48.12: Growth of CZ silicon with two opposing vertical (also called cusp or configured) magnetic fields.

The third and newest method is the use of two opposing magnetic fields (see Figure 48.12); this is probably the best method of the three, but it is not yet fully developed. Two magnetic coils surround the furnace vessel and generate opposing vertical magnetic fields. The coils can be moved vertically to adjust the field to the requirements of the melt; this can also be done during crystal growth. The coils and the field strength are arranged in such a way that a strong field is present near the cru-

cible wall and a weak or zero field in the melt below the crystal. Thereby, melt flows are damped near the crucible wall and the transport of oxygen from the crucible to the crystal is reduced, but they are not damped below the crystal, where mechanically forced convection may result in a homogeneous radial impurity distribution. Good radial oxygen and dopant distributions and low oxygen contents are possible with this method.

Neutron Transmutation Doping. In the case of phosphorus doping, the problem of macro- and microscopical resistivity variation in silicon crystals can be overcome by neutron transmutation doping (NTD). The isotope ^{30}Si , which is present in natural silicon at 3.1 atom %, can be transformed to ^{31}P by absorption of a thermal neutron and emission of an electron:



In the nuclear reaction, the $^{31}\text{Si}/^{31}\text{P}$ atoms are displaced from their lattice sites and travel a short distance through the lattice, causing lattice defects. Annealing the crystal at ca. 1100 K restores the silicon lattice, and the ^{31}P atoms return to lattice sites.

The transformation takes place very homogeneously in silicon, because most of the neutrons pass through the silicon crystal without being captured, and each ^{30}Si atom in the crystal has nearly the same probability of capturing a neutron as of being transformed into phosphorus. Consequently, the ^{31}P atoms generated by transmutation are distributed very homogeneously in the crystal.

48.4.2.4 Wafer Manufacture

After they are grown, silicon crystals are not perfectly cylindrical and do not have the precise nominal diameter despite highly automated and sophisticated crystal pulling. There are always lines of small nodes (at $\langle 100 \rangle$ crystals) or facets (at $\langle 111 \rangle$ crystals) on the crystal surface parallel to the crystal axis and small variations in crystal diameter. Therefore, the

crystals are grown slightly larger in diameter and then ground precisely to cylinders of the stated diameter. To allow crystal-oriented positioning of the wafers in subsequent process steps, the wafers must have flats or notches at special crystallographic sites. For this purpose, planes or notches with defined crystal orientations (e.g., $\langle 100 \rangle$, $\langle 110 \rangle$, $\langle 112 \rangle$) are ground into the cylinders. After grinding, the ingots are polish-etched to remove grinding damage and to reduce wafer breakage on slicing.

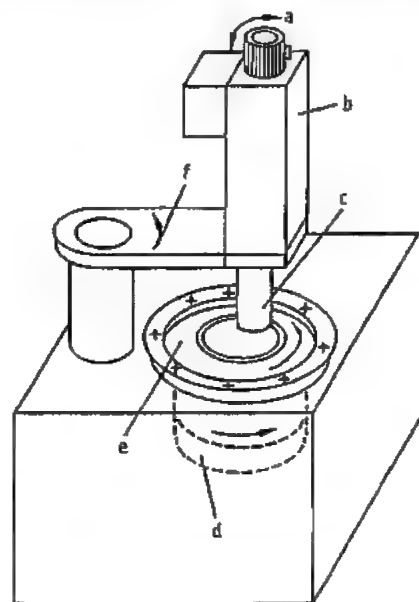


Figure 48.13: Inner-diameter (ID) sawing machine for slicing silicon: a) Crystal tilting; b) Crystal support and vertical feeding; c) Crystal; d) Saw-blade drive unit; e) ID saw blade; f) Horizontal crystal feeding.

Depending on the application of the wafers, the ingot is cut perpendicular to the crystal axis or with a well-defined misorientation of several degrees. These off-axis wafers, after polishing, are normally used as substrates for epitaxial processes. Slicing is performed with inner-diameter saws (see Figure 48.13), the saw blade of which is a 0.1-mm-thick high-grade steel foil clamped under high tension between two steel rings. The steel foil has a large circular opening in its center, the edge of which is covered with small diamonds at-

tached to the foil by a galvanic nickel layer. During sawing, the steel foil rotates at ca. 2000 rpm and consumes 0.3 mm of the ingot length (0.3-mm cutting loss). This method generates the flattest and most parallel cuts, and allows the cutting of silicon wafers down to ca. 150- μm thickness with little wafer breakage. For the manufacture of electronic devices, wafers with thicknesses between 150 and 1000 μm are cut.

After cutting, the wafers are edge-rounded in special machines, which enable the grinding of different round forms. Edge rounding substantially reduces chipping of the edges in subsequent process steps, imparts a higher mechanical strength to the wafers, and prevents the so-called epi-crown (irregular outgrowth of silicon at the wafer edge) in epitaxial deposition processes and the piling up of photoresist at the edges.

Especially for the mask printing techniques of modern VLSI (very large scale integrated) device manufacturing, the flatness and parallelism of the wafers must be improved by a lapping step. The silicon wafers are lapped between two large counterrotating steel disks, whereby the wafers are held and led by a lapping carrier. A suspension of an abrasive (a powder of silicon carbide, aluminum oxide, or a mixture of oxides with tightly specified grain size) is added to the process. After lapping, the wafers are etched to remove mechanical damage and then polished.

Figure 48.14 shows a schematic of a polishing machine for silicon wafers. Nowadays, polishing methods basically involve the combined action of chemical and mechanical forces. The polished wafer surface must be free of any residual damage, because such damage may cause stacking faults during subsequent oxidation treatments. Another very stringent demand on surface quality stems from modern photolithographic processing techniques. The polished surface must lie within the depth-of-focus range of the optical systems used to project a masking pattern on the photoresist covering the surface of the wafer.

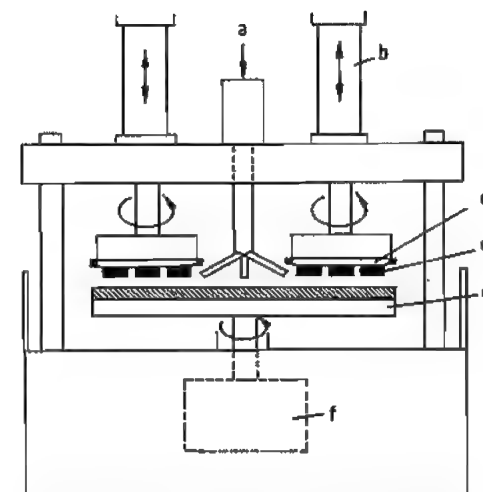


Figure 48.14: Polishing machine for silicon wafers: a) Polishing slurry feeding; b) Polishing pressure control; c) Wafer carrier; d) Wafers; e) Polishing plate; f) Drive unit.

With current technology, 200-mm-diameter wafers with both total flatness and total thickness variation of $< 1 \mu\text{m}$ are obtained. After polishing, a careful multistep cleaning process follows that yields a wafer free of particles ($> 0.2 \mu\text{m}$) and residues.

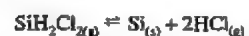
48.4.2.5 Epitaxy

In epitaxy a crystallographically oriented film is grown as an extension onto an oriented crystal substrate. The growth of an epitaxial film or layer may be realized either by chemical vapor deposition, by physical vapor deposition (e.g., molecular beam epitaxy, MBE), or by liquid-phase epitaxy (LPE). In industrial silicon epitaxy, chemical vapor deposition is employed [18, 19]. With this method, homoepitaxial silicon layers with thicknesses of 0.5–120 μm are deposited on perfectly polished single-crystal silicon wafers or substrates. The epitaxial or epi layers extend the crystal structure of the substrate exactly and differ only in resistivity and dopant. For device manufacturing, resistivities of ca. 0.03–50 Ωcm are generated in the layers by doping, mainly with boron, phosphorus, and arsenic.

Epitaxy is performed both on the whole wafer surface (after polishing and prior to device

manufacturing) and on small areas of structured wafers (during device manufacturing). In most cases, only one layer is deposited, but in some cases two or three additional layers of different thickness, resistivity, and dopant are deposited. The reasons for using epitaxial layers in device technology are numerous and various [18, 19]. The use of vapor-phase epitaxy in the semiconductor industry began in the early 1960s.

Epitaxial deposition of silicon is in principle the same process as the chemical vapor deposition used for the production of high-purity polycrystalline silicon. It is carried out at about the same temperature (usually ca. 1400 K) but with a lower growth rate and more precise control. Epitaxial deposition is possible down to ca. 1100 K. At lower temperature the silicon layer becomes polycrystalline or amorphous. The chlorosilanes SiCl_4 , SiHCl_3 , and SiH_2Cl_2 are used most frequently as silicon sources, with hydrogen as a reducing gas. The overall simplified reactions are



By using trichlorosilane, SiHCl_3 , and hydrogen at 1400 K, an epitaxial silicon layer grows at about 5 $\mu\text{m}/\text{min}$. Table 48.3 gives epitaxial growth rates for various silanes and temperatures [19].

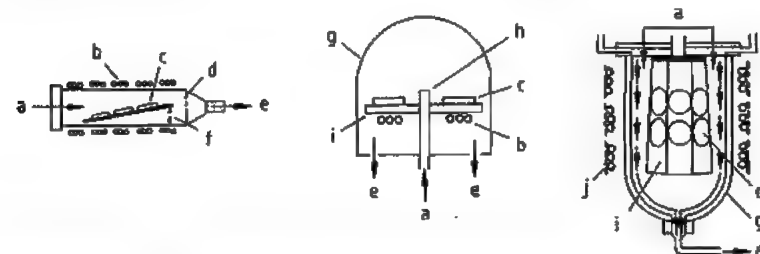


Figure 48.15: Three types of epitaxy reactors for silicon wafers: a) Gas inlet; b) Induction coil; c) Silicon wafers; d) Silica tube; e) Exhaust; f) Tilt angle; g) Silica belt; h) Inlet nozzle; i) Wafer susceptor; j) Radiant heaters.

Table 48.3: Chemical vapor epitaxial growth of silicon films.

Silane	Temperature range, K	Attainable growth rate, $\mu\text{m}/\text{min}$
SiCl_4	1420–1530	0.4–15.0
SiHCl_3	1370–1480	0.4–2.0
SiH_2Cl_2	1320–1430	0.4–3.0
SiH_4	1220–1330	0.2–0.3

Prior to deposition, the native oxide on the silicon wafer is removed by baking in hydrogen:



After that, a brief hydrogen chloride etch is generally applied to remove impurities from the wafer surface. During epitaxy, the wafer is held by a susceptor made of high-purity graphite coated with a layer of silicon carbide. The graphite susceptor is also hot during deposition and therefore is also covered with a silicon layer after epitaxy. This unwanted silicon layer is removed by etching with hydrogen chloride. In this way, deposition conditions are identical for each wafer.

To generate electrical doping in the epi layer, gases such as B_2H_6 , PH_3 , and AsH_3 are added to the chlorosilane hydrogen mixture. The doping gases decompose and the doping elements are absorbed or dissolved by the growing silicon layer. Because of their low diffusivity, the dopants diffuse only a short distance into the silicon substrate. Epitaxial layers with net charge carrier concentrations in the range of 10^{14} – 10^{20} cm^{-3} can be obtained readily. Figures 48.15 and 48.16 show schematically some epitaxial reactors.

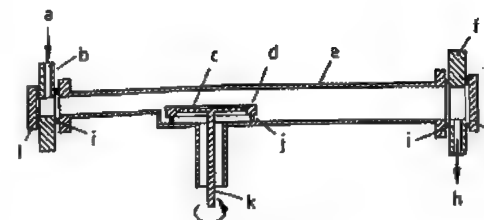


Figure 48.16: Single-wafer epitaxy reactor for large wafers (according to ASM): a) Gas injection; b) Gas injector flange; c) SiC-coated rotating wafer susceptor; d) SiC-coated saturn ring; e) Silica process tube; f) Back flange; g) Rear access port; h) Exhaust; i) O-ring; j) Silica saturn ring support; k) Rotating susceptor support; l) Gate valve.

48.4.2.6 Characterization

After crystal pulling, the properties of the silicon crystals, particularly the CZ-Si crystals for megabit devices, must be measured and tested in manifold respects. A great and constantly growing number of measuring and testing methods are employed on silicon. The extent of their application depends on the type and use of the respective material. The most common measuring and testing methods are described briefly below.

Bulk properties:

- Macroscopic axial and radial distribution of resistivity by two- and four-point probe measurements
- Microscopic resistivity distribution by spreading resistance measurements
- Oxygen and carbon concentrations by Fourier transform infrared absorption (FTIR) measurements
- Oxygen content in samples with high dopant concentration by gas fusion analysis
- Oxygen precipitation behavior in standardized annealings by FTIR measurements and microscopic visual or instrumental determination of the precipitate density and distribution
- Determination of the content of stacking fault nuclei by oxidation tests and microscopic analysis

- Testing of the gate oxide integrity by a gate oxidation and a subsequent electrical measurement
- Trap analysis by measuring the minority carrier diffusion length [e.g., with the surface photovoltage method]
- Concentrations of N, B, Al, Ga, P, As, Sb, C–O complexes, thermal donors, etc., by low-temperature (ca. 8 K) FTIR measurements
- Concentration of electrically active impurities (e.g., metals) and compounds (e.g., FeB) by deep-level transient spectroscopy
- Concentration of impurities by instrumental neutron activation analysis (INAA; detection limit = 0.00001–10 ppba depending on the element)

Geometrical and structural wafer properties:

- Thickness, parallelism, and flatness by diverse mechanical, optical, or electrical measurements ($\geq 0.1 \mu\text{m}$)
- Chipping off, scratches, spots
- Number and size of particles $> 0.15 \mu\text{m}$ on the wafer surface
- Roughness and haze on the surface by visual or instrumental optical inspection

Purity of the wafer surface:

- determination of diverse elements and compounds by
- Inductively coupled plasma mass spectrometry
- Total reflection X-ray Fourier analysis
- Inductively coupled plasma Auger electron spectroscopy
- Vapor-phase decomposition Auger electron spectroscopy
- Ion chromatography and other methods

48.4.3 Solar Silicon

Detailed information on solar silicon and its production is given in [5].

A distinction can be made between solar cells for terrestrial applications and solar cells for extraterrestrial applications. In the latter

case, the efficiency (output per square meter) is the most important factor; therefore, the best CZ silicon single-crystal qualities are used. Float-zone silicon is not used for extraterrestrial applications because it degrades too strongly on exposure to cosmic radiation, eventually reaching a lower efficiency than CZ silicon. The CZ silicon is more stable owing to its high oxygen content (ca. 15 ppma).

In the case of terrestrial photovoltaic solar cells, the prevailing opinion was initially that solar silicon should be as cheap as possible, and this led to the development of low-priced silicon of low efficiency for solar applications. However, the majority of the costs of a solar module come not from the silicon wafers but from costs that are proportional to the area of the module and are difficult to reduce. At present, about 30% of the module costs result from the silicon wafers, 30% from the manufacturing of the solar cell structures, and 40% from module costs (metals, glass, machining, etc.). Therefore, recent developments concentrate increasingly on the production of high-efficiency silicon of moderate or low price. High-efficiency silicon means that the purity and crystal quality of the material must be similar to those of silicon for electronic applications (i.e., monocrystalline and free of dislocations and microdefects). Consequently, solar-grade silicon and electronic-grade silicon will be produced by similar methods in the future.

This trend can already be seen in the development of the solar energy market. The market shares of amorphous silicon and nonsilicon solar materials such as CuInSe_2 and CdS are decreasing, while the market shares of multicrystalline silicon and, in particular, single-crystal silicon are increasing.

Table 48.4 shows the situation of the photovoltaic market in 1990 [20–22]. Photovoltaic (PV) modules for 48 MW_p (p = peak) were produced in total. The value of these PV modules (ca. $\$400 \times 10^6$) was about 0.5% of the value of the electronic devices made from silicon (ca. $\$90 \times 10^9$).

Table 48.4: Solar silicon market in 1990.

Type of material	Efficiency, %	Module price ^a , \$/W _p	Production MW _p	Share, %
Mono-Si	ca. 15	ca. 4.5	21	44
Multi-Si	ca. 13	ca. 4.5	12	25
α -Si:H	ca. 5	ca. 4.5	15	30
Others		in development		ca. 1

^a The selling prices are coupled to the output of the modules and not to the manufacturing cost.

48.4.3.1 Crystalline Silicon

At present, the industry uses the same starting material (high-purity CVD polycrystalline silicon) for the production of crystalline solar silicon as is used for the growth of single-crystal silicon for electronic devices. The production of CVD polycrystalline silicon is described in Sections 48.4.2.1 and 48.4.2.2. In 1990, ca. 8000 t of CVD polycrystalline silicon was produced, of which ca. 7000 t was consumed for the production of electronic devices, ca. 700 t for the production of solar cells, and the rest for other applications.

Monocrystalline Silicon. For terrestrial solar cells, CZ and FZ silicon single crystals of 0.5–5 Ωcm , mostly p-type and sometimes n-type, are used. Float-zone silicon has a market share of about 3% and is used only for manufacturing very high-efficiency solar cells for light concentrators.

For extraterrestrial applications, CZ crystals of higher resistivity (7–13 Ωcm) are used to reduce the degradation of the material by cosmic radiation. The resistivity chosen results from the optimization of the internal resistivity of the solar cell and the diffusion length of the minority charge carriers that are generated by photons and form the electrical current in the solar cell. Increasing the internal resistivity and decreasing the diffusion length reduce the efficiency of a solar cell. The diffusion length of the minority charge carriers is reduced by “traps” that capture the carriers and by too high a dopant concentration. Traps are formed by impurities (e.g., transition metals such as Fe, Mn, Cr, V, and Ti), by small impu-

rity precipitates, and by crystal defects having dangling bonds.

Single-crystal silicon for solar cells is produced in the same way as that for electronic applications. The cylindrical silicon crystals are cut to square ingots and then sawed into slices. Square slices give a more complete area covering than round slices.

At present, the efficiency of PV modules made from monocrystalline silicon reaches 18% in industrial production [23] and 24% in laboratory production [24].

Multicrystalline silicon is produced by ingot or sheet crystallization.

Ingot Crystallization. Several methods are used to produce multicrystalline silicon ingots:

1. Melting in a crucible and crystallization onto a cold plug, which is immersed in the melt and then withdrawn
2. Melting and solidification in the same crucible
3. Melting in a crucible, and casting and solidification in a mold (Figure 48.17)
4. Quasi-continuous melting in and pulling downward through a so-called cold crucible, which is open at the bottom (Figure 48.18)
5. Quasi-continuous casting through a cold crucible or graphite shaper analogous to (4)

Method (1) is not used for several reasons. Method (2) yields a good crystalline structure owing to its very slow crystallization but includes high crucible costs (crucible is not reusable). Method (3) is the most economical (reusable mold) and also yields good crystal quality. Methods (2) and (3) both yield square ingots, which is a major economic advantage (100% area coverage).

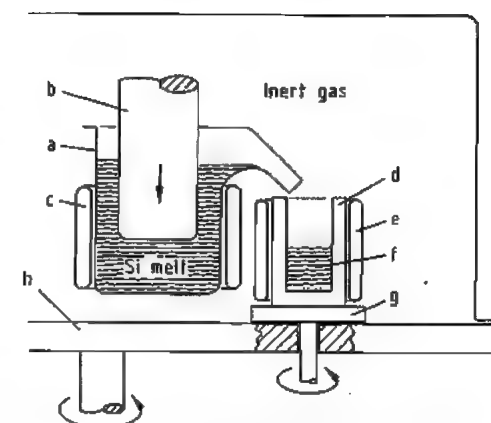


Figure 48.17: Equipment for semicontinuous production of multicrystalline silicon ingots by mold casting: a) Crucible; b) Piston; c) Heater; d) Mold; e) Heating; f) Cast ingot; g) Rotating cooling plate; h) Base plate.

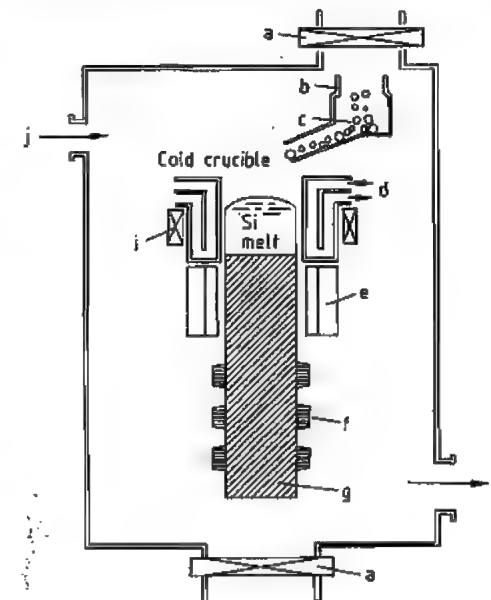


Figure 48.18: Cold crucible induction casting for multicrystalline silicon ingots: a) Valve; b) Granule feeder; c) Silicon granules; d) Cooling water; e) Auxiliary heater; f) Ingot puller; g) Ingot; h) Vacuum port; i) Induction coil; j) Inert gas inlet.

The ingots must be cut into thin slices (200–500 μm thick) for manufacturing solar cells. At present, inner-diameter saws (Figure 48.13) are generally used. However, multiple-wire sawing (Figure 48.19) is gaining in im-

portance. Multiple-wire sawing will be the slicing technique of the future for solar silicon because it results in lower material losses and can cut thinner slices.

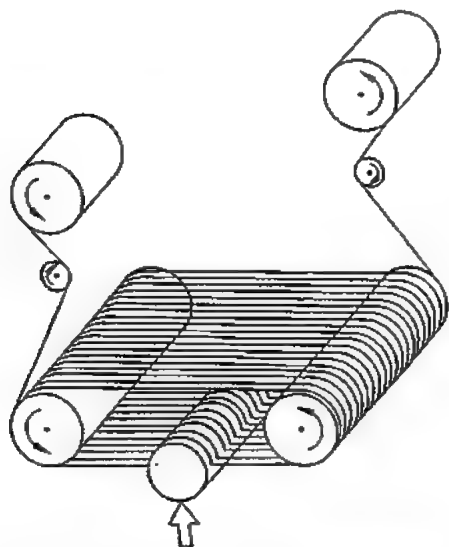


Figure 48.19: Multiple-wire slurry slicing technique. A single cutting wire is wound onto a delivery spool. The wire is arranged in multiple loops around grooved drive and idle rollers and fixed to the take-up spool.

The current efficiencies of multicrystalline solar cells reach 15%.

The advantage of sheet crystallization is that slicing, which causes high machining costs and material loss, is unnecessary. For economic reasons, sheet crystallization must be carried out at a very high growth rate. However, with such a growth rate, the segregation coefficients of the impurities become unity, and the impurities from the bulk and the surface of the starting polysilicon are incorporated completely into the silicon sheet. In contrast, at the low growth rates in single-crystal pulling or ingot crystallization the impurity concentration of the silicon is reduced drastically (e.g., by a factor of 105 for iron). Therefore, the starting silicon for sheet growth must be of a much higher purity than that for crystal or ingot growth.

A second disadvantage is that the very high growth rate leads to poor crystal quality (high density of dislocations and grain boundaries).

The higher content of both impurities and crystal defects results in lower solar cell efficiency. These two major drawbacks may not be overcome in the future.

Figures 48.20 and 48.21 give examples of multicrystalline silicon sheet growth. Many other methods exist for producing such materials [5, 25].

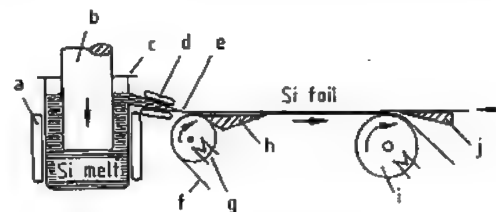


Figure 48.20: Continuous production of silicon ribbons: a) Heaters; b) Piston; c) Crucible; d) Heater; e) Die; f) Foil carrier; g) Heated cylinder; h) Ramp; i) Cooled cylinder; j) Separator.

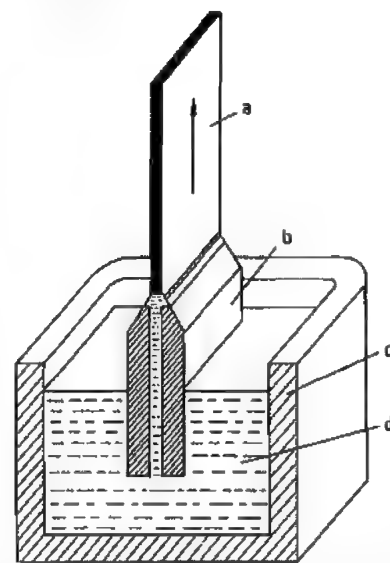


Figure 48.21: Edge-defined film-fed growth (EPG) or capillary action shaping technique (CAST) for the production of silicon ribbons: a) Silicon ribbon; b) Die; c) Crucible; d) Melt.

48.4.3.2 Amorphous Silicon

Amorphous silicon is often abbreviated to α -Si:H in contrast to c-Si for crystalline silicon. The H in α -Si:H stands for hydrogen, which is needed to neutralize the detrimental

dangling bonds. Most of the α -Si:H is used for photovoltaics and is prominent in consumer and low-power applications. In addition to photovoltaics, α -Si:H is employed for electrophotography, in photodetectors, and in accumulation-model field-effect transistors and other electronic devices. In particular, it can be used in integrated functions.

The α -Si:H solar cell is a typical thin-film device. The film is ca. 1 μm thick and is manufactured in large areas in integrated thin-film deposition lines (CVD at 470–530 K; see Section 48.4.2.2). The stabilized efficiency of modules in the field is ca. 5%. Multijunction devices incorporating α -Si:H/ α -Si:H tandems or α -Si:H/ α -Si:H/ α -Si,Ge:H triple junctions are under development for a stabilized efficiency of 8% [22].

48.5 Compounds

A number of inorganic compounds of silicon have gone through a remarkable development in the past years, prompted chiefly by the electronics industry and efforts of environmental protection. A tremendous growth of knowledge in physics and chemistry, as well as technical applications, has taken place around certain hydrides, halides, and oxides of silicon. Progress in solid state physics, the material sciences, and an increase in unwanted by-product formation in the course of production of large-scale silicon compounds have necessitated that one look anew at process engineering. Energy consideration is of direct bearing in this technology since most processes in technical silicon chemistry require high temperature.

Environmental protection and elimination of safety hazards during production and handling of the above silicon products has been the concern of all ever since these compounds became large-scale technical products. The moisture sensitivity of the halides, the oxygen sensitivity of the hydrides, and pyrophoric properties of some of the distillation residues from reaction steps involving elementary silicon or silicides have caused waste problems

and particular emphasis on process safety. Greater flexibility of chemical transformation within at least partly recycling procedures have both decreased waste and enhanced safety. Making use of by-products has been extended to comprise substances of the system C-Si-O-Hal, its phases and transformations. Alongside product making, by-product formation, its investigation, suppression, or transformation into useful silicon derivatives has been to some degree due to efforts of environment protection.

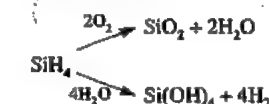
With respect to use, many new applications were found for special inorganic silicon compounds, optical fibers and solar cells being example for both surface as well as bulk properties.

Surface treatments, not necessarily confined to protective coatings but including migration beneath the surface, are carried out to increase hardness, thermal stability, to influence cohesion and adhesion, to resist oxidation, erosion, corrosion, and to enhance reflection, etc. Interfaces and multilayer ceramics and plastics need silicon in various bonding states as intermediates during production or permanently in a final product.

48.5.1 Hydrides

Silicon hydrides are sensitive to hydrolysis and oxidation; volatile higher silanes are spontaneously flammable [26–28]. The first five members of the homologous series $\text{Si}_n\text{H}_{2n+2}$ are known in the pure state (Table 48.5).

All silanes are decomposed in reactions of the type:



The thermal decomposition of monosilane takes place as follows:



Higher silanes decompose at lower temperature.

High-purity silicon can be produced in this way from pure silanes. Organosilicon compounds can be obtained by addition of silanes to unsaturated organic compounds.

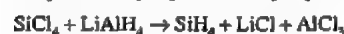
Table 48.5: Silanes $\text{Si}_n\text{H}_{2n+2}$

	mp, °C	bp, °C	d_4^{20}
SiH_4	-185	-112	0.68
Si_2H_6	-130	-14.5	0.69
Si_3H_8	-117	-53	0.72
Si_4H_{10}	-91	-108	0.79

48.5.1.1 Monosilane

Monosilane, SiH_4 , is formed by the hydrolysis of magnesium silicide (Mg_2Si) with 10% hydrochloric acid at 50 °C. It is, however, accompanied by higher homologues which must be removed by high-vacuum fractionation [29, 30]. However, if magnesium silicide is hydrolyzed with ammonium chloride in anhydrous ammonia under its own vapor pressure at room temperature, SiH_4 is obtained exclusively [31]. Ammonium bromide has also been used [32]. The ammonia is condensed out as far as possible, and any remaining traces are removed by washing the silane with dilute nitric acid.

Silane can readily be prepared from silicon halides and metal hydrides. The most convenient laboratory method is the reaction of SiCl_4 with lithium aluminum hydride in diethyl ether [33] or THF [34].



The hydrogenation can also be performed with alkali metal hydride/aluminum alkoxide or alkali metal hydride/boron triethyl in paraffin oil [35], or by alkali metal aluminum hydride/calcium aluminum hydride in other organic solvents [36, 37].

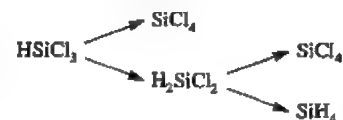
The alkali or alkaline-earth metal hydrides can be formed in situ by passing silicon tetrachloride and hydrogen into an electrolyzed melt of the metal halide [38].

In a two-step process, in which the rate of silane formation is adjusted by means of the temperature difference between the two stages, silicon halides other than the tetrafluoride are first reacted with excess alkali metal hydride or alkali metal aluminum hydride, fol-

lowed by degassing and then contacting the solid reaction product with excess silicon halide [39]. Monosilane is obtained in low yield but with sufficient purity to be used in the manufacture of semiconductors with toluene as a solvent instead of ethers [40].

Benzyltriethylammonium chloride or other quaternary ammonium salts are used as catalysts in concentrations up to 25 mol%. High yields of monosilane are obtained from the reaction of silicon halides with a mixture of aluminum products containing dialkyl aluminum hydrides, trialkylaluminum, ethylaluminum chloride, and aluminum powder in liquid paraffin at 40 °C.

Catalytic disproportionation of chlorosilane mixtures originating from various sources in the silicon industry provides a route to monosilane for the manufacture of polycrystalline solar silicon. For a mixture of trichloro- and dichlorosilane, copper [41], a mixture of silica and alumina at 300 °C [42], and quaternary ammonium groups bonded to carbon in an ion-exchange resin have been reported as catalysts for the main reaction



leading to monosilane [43].

The catalytic conversion of intermediate dichlorosilane can also be accomplished by alkyl or aryl nitriles on carbon carriers at 50 °C [44]. Boron catalysts, however, enhance the formation of dichlorosilane in chlorosilane mixtures obtained by high-pressure plasma hydrogenation of tetrachlorosilane [45]:



In-process purification is achieved by contacting part of the monosilane produced with the starting mixture of chlorosilanes, which contains the impurities as chlorides, chiefly those of arsenic, phosphorus, and boron. This procedure converts the contaminants into their more volatile hydrides, which are removed with the off-gas [43].

Properties and physical data of monosilane, particularly with regard to obtaining high-purity silicon by chemical vapor deposition, are compiled in [46].

48.5.1.2 Disilane

Increasing amounts of hexachlorodisilane are being produced as a by-product of the chlorosilane industry. Since it is of no immediate use, it is subjected to hydrogenation or disproportionation to convert it to useful derivatives, mainly tetra- or trichlorosilane. When the production of amorphous silicon from disilane became commercially viable, the hydrogenation of hexachlorosilane became a feasible alternative to disproportionation. The production of disilane resembles that of monosilane, the reducing agents being metal hydrides, mainly lithium aluminum hydride. The use of di-*n*-butyl ether as a solvent is reported to give a smooth reaction at 35 °C [47]. Addition of lithium hydride increases the yield molar ratios $\text{LiH}:\text{LiAlH}_4$ of 0.8, 2.0, 12.0, 20.0, and 40.0 resulted in yields of 83, 88, 90, 89, and 70 %, respectively. Lithium hydride can be used as the sole reducing agent if aluminum bromide or chloride is added to the ether solvent [48]. Lithium aluminum hydride in refluxing diethyl or diisopropyl ether gave disilane in 88 % yield [49].

48.5.1.3 Purification

Removal of boron compounds from silanes that are to be used for the production of high-purity silicon is very important. When SiH_4 is produced from alkali metal hydrides [37], it is recommended that water should be added to hydrolyze boron hydrides under the alkaline reaction conditions. Water vapor is added during distillation for the same reason [50]. Boron compounds can be removed from SiH_4 by adsorption from the gas phase onto activated carbon or silica carriers loaded with compounds that form complexes with boron compounds (AlCl_3 , FeCl_3 , $\text{C}_2\text{H}_5\text{CN}$, NH_2CN , PCl_3) [51].

If alkali metal hydrides MH are reacted in organic solvents, it is often unnecessary to in-

clude a special stage for removing boron compounds from the silicon compounds, as the former react to form boranate complexes under the following conditions:



A systematic study has been carried out on the liquid-vapor distribution coefficients of volatile trace impurities in the hydrides of boron, silicon, phosphorus, arsenic, sulfur, and selenium. Experimental and calculated data are reported for the temperature range between the boiling point and critical temperature. Linear regression coefficients for the temperature dependence of the impurity distribution coefficients are included [52].

48.5.1.4 Uses

Direct use of silicon hydrides involves their decomposition on surfaces, leading to deposition of elemental silicon or silicon compounds. Polycrystalline films of elemental silicon of controllable grain size are deposited on glass or silica-coated surfaces by heating them to 450–800 °C in an atmosphere consisting of monosilane and tetrabromo- or tetraiodosilane [53]. Chemical vapor deposition is generally followed by annealing and recrystallization with an energy beam. This is used to deposit silicon on insulator surfaces [54]. Amorphous silicon photoconducting layers on electrophotographic plates are made by using a plasma for silane decomposition and silicon deposition [55]. Liquid crystal displays, based on thin film transistors, for screens in monitoring devices, are made from amorphous silicon which is produced on alkali-free glass surfaces in situ by an electric discharge in an atmosphere of monosilane at reduced pressure. Residual bonds are saturated by hydrogen atoms to avoid diminishing the semiconductor effect [56]. On the surfaces of transition metals, cleaned by sputtering in an argon atmosphere, monosilane and the higher silicon hydrides can be thermally decomposed at ca. 300 °C to form metal silicides [57]. Exposure to air leads to the formation of silicon oxides.

48.5.1.5 Safety Measures

Silicon hydrides are combustible; the lower members are spontaneously flammable. Particular attention has been given to the system monosilane-oxygen and its explosibility [58]. Oxygen-rich mixtures (> 70% O₂) give water and silicon dioxide as combustion products. As the mixtures become richer in monosilane, hydrogen replaces water as a combustion product. For monosilane-rich mixtures (> 70% SiH₄) the products are hydrogen, silicon, and silicon oxides. The explosion of monosilane-rich mixtures is primarily a thermal explosion of monosilane itself.

Hazardous waste gases containing silicon hydrides and halides are passed through columns containing pelletized oxidants to remove the silicon compounds. The oxidants are made by treating a mixture of copper and zinc nitrate with sodium carbonate [59].

48.5.1.6 Photochemistry

Irradiation of silanes and silyl compounds leads to fragments, namely the silylene (:SiH₂) intermediate. Silane mixtures with boron trichloride [60] and hydrogen chloride [61] have been investigated with infrared laser techniques.

Monosilane and boron trichloride react along two pathways, one being hydrogenation of boron compounds, leading to boron dichloride, diborane, and trichlorosilane. In a side reaction, decomposition of silane takes place, forming hydrogen and amorphous silicon. Carrying out this procedure with methane instead of silane leads to a pyrolysis of methane, the released hydrogen partly converting the boron trichloride to hydrides.

In the presence of hydrogen chloride, the primary reaction seems to be the formation of intermediate silylene which in turn reacts with silane and hydrogen chloride. Simultaneous formation of chlorosilanes also occurs. The activation energy for the insertion of silylene into hydrogen chloride was determined to be < 1.3 kcal/mol. In general, silylene insertions are considered in the context of a triplet state,

and symmetry allows insertions to proceed without excitation energy when the antibonding orbital, relating to the bond into which the insertion occurs, is symmetrical with respect to the reaction coordinate [62].

Table 48.6: Melting and boiling points of halogenosilanes.

	mp, °C	bp, °C
SiH ₃ F		-98.6
SiH ₂ F ₂		-77.5
SiHF ₃	-131.5	-97.5
SiF ₄	-90.2 ^a	-98.6
SiH ₂ Cl ₂	-118	-30.5
SiH ₂ Cl ₂	-122	-8.5
SiHCl ₃	-134	36.5
SiCl ₄	-70	57.6
SiH ₂ Br ₂	-94	2.0
SiH ₂ Br ₂	-70	66
SiHBr ₃	-73.5	112
SiBr ₄	5	153
SiH ₂ I ₂	-56.5	46
SiH ₂ I ₂	-1	149.5
SiHI ₃	8	220
SiI ₄	121	290

^a At 1753 mbar triple point.

48.5.2 Halides

Silicon halides (Table 48.6) are mostly colorless liquids that fume in air, are readily hydrolyzed, and consequently have an irritating effect on the mucous membranes. Silicon hydridohalides with a high hydrogen content are spontaneously flammable. All 18 mixed silicon halides with the composition SiHal_n¹Hal_m² (n + m = 4) are known.

48.5.2.1 Trichlorosilane

Trichlorosilane, HSiCl₃, mp -134 °C, bp 36.5 °C (Table 48.6) is the most important silicon hydridohalide. The vapor is highly flammable; mixtures with oxygen or air explode violently on ignition or on contact with a hot surface. It is decomposed by water with the evolution of hydrogen.

Preparation from Elemental Silicon

Trichlorosilane was first prepared by F. WÖHLER, who used the same method as that

now used for laboratory and industrial scale production [63]:



A mixture of chlorinated silanes is produced when a mixture of hydrogen chloride and hydrogen at ca. 250–400 °C is passed over high-silicon (ca. 97% Si) ferrosilicon or silicon mixed with aluminum, nickel, or copper(I) chloride [64]. The process is sometimes carried out in a turbulent [65–67] or nonturbulent fluidized bed [68, 69].

Due to the growing demand for pure precursors for high-purity silicon, process improvements have been made continuously to raise the yield of trichlorosilane and to lower energy consumption as the chief cost cutting measures in production. The fluidized-bed reactor [70–79] has become the predominant process base for the manufacture of trichlorosilane from metallurgical-grade silicon or other silicon solids. Additional feed gases, both inert (e.g., nitrogen, argon, and helium) or reactive (e.g., chlorine) have been used [70, 71]; feeding hydrogen chloride in pulses is reported to give a higher yield [72]. Tetrachlorosilane added to the feed gas serves as a carrier and fluidizing agent when silicon residues are utilized as a source of silicon [73]. These residues can originate from the direct synthesis of organochlorosilanes. Higher-temperature in the fluidized bed followed by rapid quenching are reported to increase yield 1.8-fold. Quenching is effected by spraying the top of the bed with tetrachlorosilane at 20 °C such that the reaction gases leaving the reactor are cooled to 400 °C in less than one second [75].

Extremely fine particles of silicon (50–800 µm), obtained by atomizing molten elemental silicon in a nitrogen atmosphere, are claimed to give a high yield of trichlorosilane [76]. A screw conveyor has also been used for producing trichlorosilane from ferrosilicon [80]. Depending on the cooling rate the tetrachlorosilane to trichlorosilane ratio can be adjusted between 4:1 to 0.2:5.

In a two-step [81] process silicon is first reacted with tetrachlorosilane at 1100–1300 °C

and the resulting product is treated with hydrogen chloride. The conversion of tetrachlorosilane to trichlorosilane is 50–60%.

Adding tetrachlorosilane to the hydrogen chloride prior to contact with powdered silicon is claimed to enable complete conversion to trichlorosilane [82].

Silicon powder with 2% copper [83] or 6% copper [84], has been used at 350–600 °C. The yield of trichlorosilane was 7–27 mol% for 2% Cu, and 80–90 mol% for 6% Cu. Much lower temperatures (down to 260 °C) were possible when antimony pentachloride was used as a cocatalyst with copper; the trichlorosilane yield was 21% [85]. Silicon residues from direct synthesis of organochlorosilanes can also be reacted with hydrogen chloride to give trichlorosilane [86].

Preparation from Tetrachlorosilane

Tetrachlorosilane, up to now used as a starting material for silica fillers, quartz, and special glasses, has become an important precursor for trichlorosilane. The basic reaction is



Although use of a graphite heating element at 1100–1400 °C has been reported [87], most processes are operated between 800 and 1400 °C. The residence time is critical and is adjusted by quenching or by using a two-step process. The residence time of the feed should be < 2.5 s [88], and quenching carried out below 600 °C within < 1 s [89]. A feed stream of tetrachlorosilane hydrogen mixture with a molar ratio of 1:2 in the absence of silicon at 1100, 1200, and 1500 °C, gave trichlorosilane in 27, 31, and 35%, respectively.

In two-stage processes the reaction with silicon is carried out at lower temperature in the second-stage reactor.

Typical temperatures are 500–700 °C for the first stage, and 300–350 °C for the second [90]. The yield of trichlorosilane can be doubled by adding hydrogen chloride to the gas from the first reactor prior to entering the second [91]. A reaction mixture obtained by pass-

ing tetrachlorosilane and hydrogen through a reactor at 1050–1250 °C is then cooled to 250–350 °C and reacted with silicon in a second reactor [92], giving a product containing 38% trichlorosilane and 61% tetrachlorosilane. It is also possible to react the intermediate dichlorosilylene with hydrogen in a separate reaction chamber [93].

Single-step processes are mostly carried out in fluidized-bed reactors [94, 95] with quenching of the gaseous reaction products. For furnaces operating at ambient pressure, preheating the reactant gases [96], and removing surface oxide coatings from the silicon powder with aqueous acid or alkaline hydrogen fluoride solution raises the trichlorosilane yield to 70% [97]. Pretreatment of silicon can also be carried out with gaseous hydrogen chloride [98]. While particle size of the silicon and its distribution seems to have little influence on the reaction [99], it is strongly affected by catalysts. Copper, the main catalyst, is added as such to the silicon [100–106]. The reaction kinetics have been studied in the presence of copper chloride [107]. The hydrogenation of tetrachlorosilane has an activation energy of 20–25 kcal/mol which is lowered to 10–15 kcal/mol by the catalyst; conversion and throughput are improved.

Copper has also been used with cocatalysts such as metal oxides [108] and metal halides. Aluminum halides give trichlorosilane yields of 20–30 mol% [109–111]; iron and vanadium halides give comparable yields [112–114].

Using nickel salts as cocatalysts [115, 116] between 500 and 600 °C gave trichlorosilane yields of 36% whereas powdered nickel alone gave 27% [117]. Antimony chloride in a pressure reactor gave 21% [118].

Platinum compounds have also been used [119, 120]. Silicon with addition of 10^{-3} mol% platinum black [121] catalyzes tetrachlorosilane conversion at 550 °C to give an 80% yield of trichlorosilane. At the same temperature, platinum on carbon gives a mere 5% yield [122]. Carbon as the sole catalyst has also been reported in a two-step process [123], in a fluidized-bed reactor [124], and in a packed-bed reaction chamber [125], the latter

two giving trichlorosilane yields of 20 vol% and 11 mol%, respectively.

The conversion of tetrachlorosilane to trichlorosilane has also been effected electrolytically [126] with 1,2-dimethoxyethane as a solvent, hydroquinone as hydrogen donor, and tetrabutylammonium perchlorate as supporting electrolyte.

Purification

Extreme purification of trichlorosilane is necessary if it is to be used for production of high-purity silicon for semiconductors or photoconductors. This is mainly to remove impurities such as chlorides of calcium, aluminum, titanium, copper, magnesium, iron, boron, and phosphorus, which would remain in the silicon formed by hydrogen reduction. The trichlorosilane is treated with complexing agents such as thioglycolic acid, β -naphthylamine, and salts of ethylenediaminetetraacetic acid [127]. An extremely pure product is obtained by extraction with CH_3CN [128]. Other methods include adsorption of the impurities on columns of activated silica [129], activated carbon, ion exchangers [130, 131], titanium sponge [132], or by treatment with acetals [133] or salt hydrates, which cause partial hydrolysis of the impurities [134–136]. The purification of trichlorosilane [137, 138], the development of purity criteria, and industrial control of purity [139] are well developed subjects.

The ultimate aim in trichlorosilane purification is the elimination of trace amounts of boron and phosphorus. Both elements are retained in chemical processing in sufficient amounts to impede or even prohibit certain uses in electronics. Boron impurities are first converted from volatile halides or hydrides to nonvolatile acids or oxides, for example, by passing moist nitrogen into the boilers of a multistage distillation [140]. The addition of 0.1–1.0 g/t of trichlorosilane decreased the boron content from 1.6 ppm to 0.2 ppb. A similar procedure [141] gave 12 ppb residual boron in a one-step distillation. The addition of silica

with at least 0.25% of total hydroxyl groups is also claimed to effect partial hydrolysis [142].

Phosphorus, the other chief contaminant of silicon compounds, is present in chlorosilanes as phosphorous trichloride. During their distillation, it is trapped in the high-boiling residue by complex formation with molybdenum oxychloride and covalent nickel compounds. The phosphorus-metal complexes are thermally stable. Residual phosphorus contents of chlorosilanes distilled were below the analytical detection limit [143, 144]. Manganese dioxide is also reported as a purification agent. It forms phosphorus oxychloride which has a much higher boiling point than phosphorus trichloride and hence remains in the distillation residues [145]. Boron and phosphorus impurities in trichloro- or dichlorosilane can be oxidized with oxygen to give less volatile compounds [146]. Polycrystalline silicon prepared from purified chlorosilanes had residual impurities of 0.1 ppb boron and 0.18 ppb phosphorus.

Waste Disposal

The in-plant, partly on-line conversion of waste from chlorosilane manufacture and use has two chief sources: distillation residues and off-gases which are both hazardous materials. To provide safety, environment protection, and an economic conversion of material that can be used elsewhere or safely deposited, several procedures have been adopted. Distillation sludge is evaporated in the presence of metal chloride slurries giving chlorosilanes [147] and then hydrolyzed with steam in azeotropic hydrogen chloride which continuously gives additional hydrogen chloride [148].

Uses

The purity of trichlorosilane greatly influences its end use. High purity silicon is produced by the pyrolysis of trichlorosilane in the presence of hydrogen [149, 150], for which a large number of techniques have been used, e.g., pyrolysis in a fluidized bed [151], pyrolysis in or over molten silicon [152–154], and

epitaxial growth on silicon [155–157] or graphite [158]. Other processes reported include the production of polycrystalline silicon by the pyrolysis of trichlorosilane [159–162], the production of amorphous silicon coatings by CVD [163], and the production of solar silicon [164, 165]. A reactor made of silicon has been described for the pyrolytic process [166].

In fluidized-bed reactors caking of silicon on the inner wall is prevented by starting with a bed of polycrystalline silicon of grain size 700–3000 μm , fluidized by a mixture of trichlorosilane and hydrogen [167]. The polycrystalline silicon granules are continuously removed from the reactor.

Other important uses for trichlorosilane include the manufacture of very finely divided ("micronized") silica for use as a filler [168], the manufacture of silicon nitride ceramics, sometimes together with metal nitrides [169], the surface treatment of boron and borides [170], the production of free-flowing granulated fertilizers [171], and in screen printing [172].

48.5.2.2 Tetrachlorosilane

Silicon tetrachloride, SiCl_4 , m_p -69.4 °C, b_p 57.3 °C, T_c 234.0 , p_c 37.5 bar, V_c 326.3 $\text{cm}^3\text{mol}^{-1}$, is a clear, colorless liquid that fumes strongly in air and hydrolyzes rapidly in water, producing SiO_2 gel. When dry, it does not attack steel, and can therefore be transported in steel tanks. It is soluble in benzene, ether, chloroform, and petroleum ether. It reacts with alcohols to give esters of silicic acid. On partial hydrolysis (e.g., with ether–water mixtures), silicon oxychlorides, $\text{Si}_n\text{O}_{n-1}\text{Cl}_{2n+2}$, are formed as colorless, viscous liquids. These oxychlorides, together with the corresponding metallic chlorides, are formed when silicon tetrachloride reacts with metal oxides (e.g., of Mn, Cu, Ca, Zn, Mg, Ag, or Hg) in organic solvents [173].

Production

Silicon tetrachloride is prepared in the laboratory by the reaction of silicon or high-sili-

con ferrosilicon with dry chlorine at $> 400^\circ\text{C}$. At lower temperature, Si_2Cl_6 and other subchlorides are also formed [40].

In industry, SiCl_4 is mainly produced by reacting ferrosilicon, pure silicon, or silicon carbide with chlorine. Other possible processes include the reaction of SiO_2 or a SiO_2/SiC mixture with carbon and chlorine (or with COCl_2 or CO/Cl_2 mixture). This older process, which uses silica sand as the cheap raw material, has attracted renewed interest since the introduction of the fluidized-bed reactors.

From Ferrosilicon ($> 90\%$ Si) or Pure Silicon and Chlorine. The reaction between silicon and chlorine is exothermic. Therefore, after the reaction has been initiated, cooling must be provided. Ferrosilicon, with a high silicon content, is cheaper than pure silicon, and due to the greater reactivity of the iron, is more readily chlorinated. However, the temperature must be maintained at $> 400^\circ\text{C}$ so that the FeCl_3 formed is removed, and blockages in the pipework are prevented.

In the Dynamit Nobel process, large pieces of ferrosilicon containing $> 90\%$ silicon are continuously fed into a furnace at $> 500^\circ\text{C}$ fitted with a cooling jacket. Silicon tetrachloride is formed together with iron chloride and the chlorides of the other elements present in the ferrosilicon, mainly aluminum chloride, calcium chloride, and titanium tetrachloride. The nonvolatile chlorides (e.g., CaCl_2) remain in the furnace, and are removed from time to time together with unchlorinated components (e.g., SiO_2).

The volatile chlorides pass out of the furnace and are then partially condensed by cooling. The collecting vessel is maintained at such a temperature that the SiCl_4 distills over while the FeCl_3 and AlCl_3 remain behind. Most of the SiCl_4 is then condensed out, and the residual gases are cooled to -35°C , causing any remaining tetrachloride to separate.

The crude silicon tetrachloride still contains small quantities of iron and aluminum chlorides, and also some chlorine, titanium tetrachloride, and hexachlorodisiloxane formed by partial hydrolysis of SiCl_4 by the

traces of water that enter the furnace during charging. This is purified by simple evaporation and condensation, followed by fractional distillation. In the evaporation process, which is also applied to the residues from the fractional distillation, chlorides of iron and aluminum remain behind along with some of the medium boiling point compounds, i.e., hexachlorodisiloxane and titanium tetrachloride. The crude distillate obtained is fractionated in a double distillation column.

It has been proposed that a molten salt reaction medium should be used [174], and that inert materials such as carbon, aluminum oxide, and silica should be added in both the batch [175] and the continuous process [176].

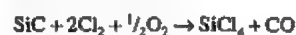
From Silicon Carbide and Chlorine.



The advantage of using the readily available industrial-grade silicon carbide as the starting material must be balanced against the disadvantages that the reaction with chlorine starts at a higher temperature, and the heat of reaction is not sufficient to maintain the material at the reaction temperature without heating. Also, the carbon formed remains behind as a residue.

Silicon is added to the silicon carbide to facilitate the reaction. The chlorination is carried out in a vertical shaft furnace made of steel or cast iron lined with carbon plates. The downstream condensation system includes a spray of liquid silicon tetrachloride to prevent blockage by the iron and aluminum chlorides formed from impurities in the raw material [177].

In a modified process, the chlorine is mixed with oxygen, which oxidizes some of the carbon formed in the reaction to carbon monoxide [178, 179]:



From Silica, Carbon, and Chlorine. Information on the temperature required for the reaction of various silica modifications with chlorine and carbon is given in [180].

Chlorides of alkali metals or alkaline earths can be mixed with the finely powdered coke

and kieselguhr or other silica-containing materials to lower the reaction temperature. The mixture is treated with chlorine at red heat [181]. In a variation of the process, the energy is provided by an electric arc, which is applied to the reaction mixture in a fixed [182] or fluidized bed [183].

As the reaction of SiO_2 with carbon and chlorine is endothermic, it is necessary to couple it with an energy-producing process, e.g., silicon and chlorine, ferrosilicon and chlorine, or silicon carbide and chlorine. In the Stauffer process [184], silicon carbide, silica sand, and coke are treated with chlorine gas in a fluidized-bed reactor. A separator removes any solid material from the gaseous reaction product, which is then cooled in heat exchangers. Silicon tetrachloride condenses out and is purified by the usual distillation process.

Other Processes. These include: treatment of silicon or a Si-Cu alloy with CCl_4 vapor at $260\text{--}300^\circ\text{C}$ [185], reaction of alkali metal silicofluorides (e.g., Na_2SiF_6) with AlCl_3 at 280°C [186] or with MgCl_2 at $500\text{--}1000^\circ\text{C}$ [187], and recovery of by-product silicon tetrachloride from the production of methylchlorosilanes.

The formation of incrustations in a fluidized-bed reactor can be prevented if a mixture of metallurgical silicon and silicon carbide with silicates of iron, titanium, vanadium, or chromium is used. Increases in yield of up to 12% have been observed [188].

Lower reaction temperatures, down to 200°C , and the use of silicides, preferably calcium silicide, yields substantial amounts of tetrachlorosilane together with an appreciable amount of hexachlorodisilane [189, 190]. The conversion of higher chlorosilanes into tetrachlorosilane is effected by tertiary amines in catalytic amounts below 160°C . Refluxing of hexachlorodisilane with 0.8 vol% of pyridine gave tetrachlorosilane [191].

Purification

The main aim of purification is to remove halides of boron and phosphorus by preferential hydrolysis, complexing agents, or the in-

corporation of adsorption stages in the distillation process. Examples include preferential hydrolysis of BCl_3 by adding water or ice [192, 193], adding substances to the distillation process that combine with BCl_3 such as CH_3CN and $(\text{C}_6\text{H}_5)_3\text{CF}$ [194, 195], substances that combine with PCl_3 such as AlCl_3 [196], and passing the silicon tetrachloride through adsorption columns charged with substances containing tertiary amine groups, quaternary ammonium groups [197], or water-containing oxides or silicates [198]. A countercurrent zone-melting process has also been developed for the purification of SiCl_4 [199].

Removing boron impurities is also accomplished by high-temperature hydrogenation, which converts boron trichloride, the chief impurity to volatile diborane [200]. The fact that considerable amounts of silicon hydrides, chiefly trichlorosilane and dichlorosilane, are formed as by-products, is of no apparent disadvantage since both can now be used in high-purity silicon manufacture.

Low-loss optical fibers require precursors with extremely low contents of hydroxyl-containing impurities. These are probably chloro hydroxy complexes of metals, mainly iron. They are removed by partial hydrolysis of the tetrachlorosilane with adsorption of the impurities on the in situ precipitated silica gel. The residual contaminant content is 12 ppm Fe, 2 ppm OH, and 18 ppm HCl [201].

Uses

High-purity silicon is produced by the thermal decomposition of SiCl_4 in the presence of hydrogen, and highly dispersed silica is produced by flame hydrolysis of SiCl_4 .

Corrosion-resistant silicon coatings are produced on metal surfaces, e.g., steel and iron [202, 203], molybdenum, tungsten, tantalum [204], molybdenum, or tungsten [205] by heating the metal component in an atmosphere of $\text{SiCl}_4\text{--H}_2$ or SiCl_4 at $1000\text{--}1400^\circ\text{C}$.

48.5.2.3 Hexachlorodisilane

For years, hexachlorodisilane was a typical by-product; its formation was suppressed as far as possible or a conversion to more versatile products carried out. It is now a compound of its own standing leading directly to the production of several special silicon products. The manufacturing processes, however, are still dominated by the basic reaction of silicon or silicides with chlorine giving a number of chlorosilanes, hexachlorodisilane being just one.

Production

To obtain hexachlorodisilane as a high share in a crude chlorosilane product mixture, conversion or degradation processes have been designed. Calcium silicide is the preferred raw material and a low reaction temperature of 200 °C is used [206]. Continuous production in a multicolumn reactor [207], and batch production [208] with a comproporation step have been described:



Reaction of ferrosilicon, with a silicon content of 50%, and chlorine at 160 °C in a vibrating reactor gave 55% hexachlorodisilane, and 44% tetrachlorosilane with a 70% ferrosilicon conversion [209, 210].

High-boiling residues, predominantly containing polychloropolysilanes, are cleaved by chlorine in a fluidized bed [211] at 250–450 °C.



At 500 °C on α -alumina beads [212] comproporation of tetrachlorosilane is readily achieved, with a conversion of 70%. The reverse reaction is carried out at a temperature of 700 °C aided by lithium-magnesium double oxides as catalysts and alumina as the carrier.



The reaction product consists of 50% unchanged tetrachlorosilane, 40% hexachlorodisilane, and 10% higher homologues [213].

Liquid-phase chlorination allows a lower reaction temperature to be used. Using ele-

mental silicon and a catalyst consisting of the chlorides of sodium, potassium, and zinc gives a product mixture that contains tetrachlorosilane, hexachlorodisilane, and tetrachlorodisilane in a weight ratio of 12:17:11 [214]. Suspension of silicides and antimony pentachloride can be chlorinated to hexachlorodisilane with 34% conversion [215]. In a solvent mixture in which some components exhibit catalytic properties [e.g., perfluoroalkanes, tris(perfluoroalkyl)amines, and cyclic perfluoroalkyl ethers] elemental silicon reacts with chlorine at 150 °C [216] to give hexachlorodisilane and octachlorotrisilane.

Uses

In most of its applications, hexachlorodisilane can be replaced by other special silicon compounds, but in some cases, the reactions take place at much lower temperature than with tetrachlorosilane or trichlorosilane. The deposition of elemental silicon by purely thermal decomposition has been carried out on silicon wire at 750 °C [217], on a quartz plate at 500 °C [218], or on quartz crucibles [219].

Hydrogen as a reducing agent has been used to make bulk polycrystalline silicon above 250 °C [220] or to produce atomic layers of silicon by homoepitaxy [221]. A viscous oil obtained by reacting hexachlorodisilane with tetrabutylphosphonium chloride at 200 °C can be pyrolyzed to give finely divided amorphous silicon [222]. The reaction of hexachlorodisilane with propane on graphite surfaces at 700 °C [223] gives β -silicon carbide. On a cobalt-containing substrate, silicon carbide whiskers are obtained [224]. Mixed carbides of silicon and titanium are made by hydrogenation of a mixture of hexachlorodisilane, titanium tetrachloride, and alkyl halide [225].

Optical fibers can be made by direct surface coating of preforms by flame hydrolysis of hexachlorodisilane [226, 227]. Ultrafine silica particles are formed by thermal decomposition of hexachlorodisilane in an oxygen atmosphere [228]. The method is suitable for

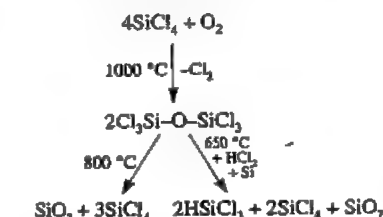
the manufacture of quartz glass as a substrate for wave guides [229].

48.5.2.4 Other Chlorides

Hexachlorodisiloxane, intermediate or by-product in oxidation or hydrolysis reaction, can be obtained as the chief product by reacting tetrachlorosilane with sulfur trioxide 500 °C.



By comparison, other monosilanes react differently. The bromide and hydride at room temperature give silicon dioxide, the fluoride, not at all even at 600 °C [230]. Formation and degradation of hexachlorodisiloxane can be shown by high-temperature reactions. It is formed from tetrachlorosilane and oxygen [231] together with other oligomeric siloxanes but with mono- and polycyclic siloxanes also. Thermodynamic studies indicate a certain metastability of halosiloxanes in general. No direct use has been made of hexachlorodisiloxane, conversion to chlorosilanes, i.e., recycling, is practised [232]:



An important intermediate is dichlorosilylene, the first reaction product of the attack of chlorine on silicon. Dichlorosilylene can be obtained directly in high-vacuum apparatus from the elements at 1250 °C [233, 234], and 1100 °C [235]; it is a transparent, amber-like solid.

48.5.2.5 Fluorides

Difluorosilylene. Silicon tetrafluoride and silicon react at 1200 °C in a high vacuum, yielding a condensate with the composition $(\text{SiF}_2)_x$. This turns yellow on cooling with liquid air and ignites on contact with atmospheric oxy-

gen. It loses its color on heating to –78 °C and becomes highly polymeric [236].

A plasma flame in an argon atmosphere [237, 238] can also be used as a reaction medium. A molar ratio of tetrafluorosilane to silicon of 0.8:1 gives a SiF_2 yield of 70%.

Difluorosilylene can be used to produce silicon difluoride filaments [239]. The production of amorphous silicon films from SiF_2 by chemical vapor deposition leads to material with residual Si–F groups [240], which is claimed to afford a higher doping efficiency [241] for boron and phosphorus.

Reacting SiF_2 with methane and hydrogen in a glow discharge [242] gives a photoconductive amorphous silicon carbide. Silicides can be prepared by reacting hexafluorides of tungsten or molybdenum with difluorosilylene in a hydrogen atmosphere at 300–600 °C [243]. Oxidation of SiF_2 with oxygen, nitrous oxide, or nitrogen dioxide [244] gives silicon dioxide with residual Si–F groups, suitable for the manufacture of optical fibers.

48.5.2.6 Bromides

Silicon tetrabromide, tetrabromosilane, SiBr_4 , is produced from silicon and bromine vapor at > 600 °C. It is a colorless liquid, with *mp* 5 °C and *bp* 153 °C.

With ferrosilicon powder a 70% yield of SiBr_4 is obtained. Crude tetrabromosilane is heated with zinc to remove residual bromine [245].

The main use for silicon tetrabromide is as a raw material for the production of silicon and its compounds. The reaction used is the reverse of the preparation method, i.e., it is pyrolytically decomposed [246, 247], usually together with silanes, using fluidized-bed processes [248], or crystal growth techniques [249]. These techniques are also used in the manufacture of optical fibers [250–253] and photoconductive silicon [254].

In a plasma, tetrabromosilane is readily cleaved to the elements, and the deposition of the silicon layer is much faster than with tetrachlorosilane [255]. Tribromosilane can be produced by reacting metallurgical-grade silicon

with tetrabromosilane at 600–800 °C in hydrogen atmosphere [256].

Other processes include the electrolytic deposition of silicon from solutions of silicon tetrabromide in aprotic organic solvents [257–259].

Silicon tetrabromide is also used to produce silicon nitride itself [260–263], as a coating, or to seal porous solids by exposing them to SiBr_4 vapor followed by reaction with ammonia [264]. Boron–silicon phases have been obtained by the coprolysis of halogenated silanes and boranes [265].

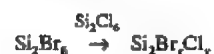
Silicon tetrabromide is used as an auxiliary in the production of SnO_2 whiskers [266], the etching of aluminum and its alloys [267], and the copolymerization of dienes and vinyl compounds [268].

The entire series of bromosilicon hydrides are obtained by disproportionation [269]. With Amberlite A 21 as catalyst at 135 °C the major product is dibromosilane. Fluorobromosilanes are made by reacting tetrabromosilane with antimony trifluoride [270].

Fluorobromosilicon hydrides are made by reaction with alkyltin hydrides [271] at room temperature under reduced pressure:



Comproportionation can be extended to the disilanes:



Separation of the products by distillation is difficult due to continuing halogen redistribution [272]. Since aryl groups on silicon can be cleaved by hydrogen halides in the presence of aluminum halide catalysts, this method can be used to prepare higher silicon bromides:



A well-defined, very reactive subhalide with the composition $(\text{SiBr}_2)_x$ is obtained by the reaction of SiBr_4 and silicon at 1150–1200 °C in a high vacuum. It is a transparent,

almost colorless, amber-like solid, soluble in benzene, xylene, and CCl_4 [40, 273, 274].

48.5.2.7 Iodides

Silicon iodide, SiI_4 , *mp* 121 °C, is a crystalline substance that is very sensitive to hydrolysis, decomposes into its elements on heating or on exposure to light, and reacts with oxygen at elevated temperature with liberation of iodine. SiI_4 is produced in 70% yield by passing a carrier gas saturated with iodine vapor over silicon containing 4% copper at 600–700 °C [40]. Silicon tetraiodide can be obtained on the kilogram scale in quantitative yield by passing nitrogen saturated with iodine vapor at ca. 200 °C over granulated silicon at 1150–1200 °C. Approximately 1.5 kg SiI_4 can be produced in 5 h by this method [275].

Other methods include the reaction of mixtures of iodine with bromine or chlorine with silicon at 600–800 °C [276], and heating alkali metal fluorosilicates with alkaline-earth iodides at 500–1000 °C [277] or with aluminum iodide at 300 °C [278].

Like the tetrachloride, tetraiodide can be used for the production of high-purity silicon by thermal decomposition (sometimes in the presence of hydrogen). The silicon tetraiodide can be purified beforehand by repeated sublimation and zone melting [279, 280].

Silicon tetraiodide has some value as an additional reactant in the pyrolysis of silicon hydrides for the production of high-purity silicon [160], in the reduction of other silicon halides in a fluidized bed [281], and for the purification of silicon by zone melting [247].

Silicon tetraiodide is used as a starting material for the preparation of high-purity silicon films for solar cells by electrolyzing a solution of SiI_4 in aprotic organic solvents [257, 258].

Special applications of silicon tetraiodide as a raw material include the manufacture of cermets [255], and of optical fibers with a germanium core and an outer coating of SiO_2 [282]. A subhalide having the composition of diiodosilylene has been reported [28].

48.5.3 Oxides

For silicon dioxide, see Section 48.7.

With the oxides, more so than with the halides, the growth of interest in use and production, i.e., formation, is brought about by the same driving forces as for the halides, i.e., electronics manufacture and environment protection.

Sources of silicon oxides are chiefly high-temperature processes in heavy industry like blast furnaces, carbide manufacture, coke making, and silicate processing. Main uses are found in high-tech precision preparation of chips, wafers, integrated circuits, layers, and coatings.

48.5.3.1 Monoxide

Silicon monoxide, SiO , is formed initially as a gas when SiO_2 and silicon, or SiO_2 and an amount of carbon insufficient for complete reduction, are heated to > 1250 °C. It therefore plays a part in the industrial production of silicon and silicon carbide from SiO_2 and carbon, and in the production of ferrosilicon [283, 284].

At lower temperature (ca. 600–1000 °C), SiO disproportionates into silicon and silicon dioxide:



There has, therefore, been prolonged controversy over the question whether SiO should be considered a true compound. Nevertheless, rapid chilling of the gas to room temperature enables the monoxide to be obtained in a solid metastable state. It has a wide range of uses as an additive in applied solid-state physics, and as a raw material in the production of other silicon compounds.

Production

A stoichiometric mixture of finely powdered SiO_2 and silicon in a reaction tube closed at one end is heated at its lowest point in a high vacuum for ca. 4 h at 1250 °C. A brown mixture of SiO_2 and Si, formed by disproportionation, collects in a short transition

zone in the part of the tube that just protrudes from the furnace, and the SiO collects as black, compact, shellac-like masses in the parts further away from the furnace.

If an intimate mixture of SiO_2 and silicon is heated for 9 h to 1300 °C and rapidly chilled, cubic crystals of SiO are formed [40]. On an industrial scale, the monoxide can be produced by heating SiO_2 with silica, carbon, or silicon carbide to 1500–1800 °C in a resistance furnace [285, 286].

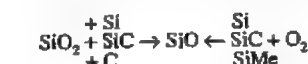
Heating the vapors of the reaction



to 1800 °C in an ammonia atmosphere gives amorphous silicon monoxide powders [287].

Silicon monoxide can be made directly in the form of fibers by reducing sand flour with methane at 2500 °C in a fluid-wall reactor [288].

The formation of silicon monoxide by side reactions or as a by-product of the main process takes place in the course of a number of industrial production streams. In terms of chemical categories these production steps are based on reductions as well as oxidations.



Properties

At room temperature, silicon monoxide is a light brown, finely divided powder, or, if it has been produced by slow condensation, it is a black or very dark brown, shellac-like, glassy mass. The lower limit of stability for gaseous SiO is not below 1025 °C, and is very probably > 1175 °C [289]. The best temperature range for its production from SiO_2 and Si is 1200–1400 °C [290–292].

At 600 °C, SiO decomposes in several hours, at 700–900 °C in ca. two hours, and at 1000–1200 °C almost instantaneously into SiO_2 and silicon [291, 293]. Oxygen causes surface oxidation to SiO_2 even at room temperature, and complete oxidation takes place at ca. 500 °C. Finely divided SiO is pyro-

phoric and burns with flame formation if there is rapid access of air.

With the increase in the number of possible uses for SiO, the silicon-oxygen system has been the subject of extensive investigations [294], particularly with regard to suppressing the formation of SiO during the production of high-purity silicon [295], and of Si-O-N mixed phases in atmospheres containing O₂ and N₂ [296].

Uses

Silicon monoxide is used in small quantities to produce protective films on semiconductors [297–299], vidicon targets [300], and in antireflective coatings on optical glass and plastics [301–304]. Silicon monoxide prevents the formation of anatase in rutile coatings on glass [305]. In entertainments electronics and data processing, silicon monoxide is used in recording tape, other types of data storage media, data transfer heads [306, 307], and in the alignment of liquid crystals for digital displays [308, 309]. Other applications include the coloring of glass surfaces by the simultaneous or sequential deposition of metals and silicon monoxide [310].

Another application of silicon monoxide electronics is the manufacture of heat-resistant films and devices in which corrosion resistance is required. It can be used as a heat-resistant protective layer in laser recording media [311], and in multilayer thermal heads for thermographic printers [312]. Multilayer devices consisting of aluminum, germanium, and silicon monoxide are selective solar absorbers for thermal conversion [313]. Ceramics consisting of silicon carbide whiskers in a graphite matrix can be reinforced by decreasing the porosity by filling the voids with silicon prepared in situ [314].

Silicon monoxide is used as a raw material, a construction material, and as an auxiliary. The best known application is the oxidation of gaseous silicon monoxide to amorphous finely divided silica [315]. Other uses include the production of silicon carbide [316, 317], silicon nitride [318–320], Si-O-N mixed phases

[321], and cermets [322, 323]. Silica can be removed from silica-containing materials (e.g., kaolin) by adding silicon and heating the mixture at 1450 °C in a vacuum [324–326]:



Silicon monoxide can be used to remove phosphorus from blast furnace slag, allowing it to be recycled [327].

Hard coatings of SiO₂ on metals, especially on metallic mirrors, can be produced by deposition of SiO from the vapor state. The SiO is then oxidized by atmospheric oxygen to form SiO₂.

In the production of silicon nitride ceramic powders, silicon monoxide is reacted with a reducing atmosphere consisting of a mixture of ammonia and hydrocarbons at 1000 °C. When methane is used as sole reductant, the product is cubic β-silicon carbide [328].

A convenient method to prepare members of the halosilane family is the reaction of silicon monoxide with hydrogen halides [329].

Low-silicon metals are produced by effecting silicon depletion of the melt by limited oxidation. In the production of high-purity vanadium, vanadium pentoxide is added to the melt and the silicon monoxide formed is evaporated [330]. Silicon in molten indium is oxidized with water in a hydrogen atmosphere at 800 °C; ca. 90 % of the initial silicon content is converted to SiO [331].

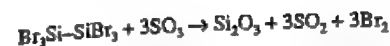
48.5.3.2 Sesquioxides

Depending on temperature and pressure, the following disproportionation steps can take place:



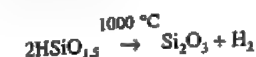
When the monoxide is evaporated at reduced pressure the vapor invariably condenses as the sesquioxide, Si₂O₃ [332].

The reaction of sulfur trioxide with hexabromodisilane at room temperature affords an almost quantitative yield of the sesquioxide; no cleavage of the Si-Si bond takes place [333]:



The sesquioxide can be prepared from hexachlorosilane by hydrolysis via a sol-gel route [334].

Polymeric silicon sesquioxide can be prepared by thermal dehydrogenation of silicon oxyhydride in high vacuum [335].



Silicon sesquioxide can be prepared in situ on surfaces. Plasma vapor deposition from a mixture of monosilane and nitrous oxide [336] gives a moisture-resistant film of silicon sesquioxide, used as a protective layer for *p*-Si substrates. On polycarbonate sheets, Si₂O₃ layers are prepared by electric discharge [337] or vacuum deposition [338]. On polyethylene [339] a Si₂O₃ layer has been applied by sputtering with an oxygen plasma, using silicon monoxide as the silicon source.

The suboxides, the sesquioxide being the predominant species, are present in semiinsulating films of polycrystalline silicon [340]. Annealing at 1100 °C converts the other suboxides to the sesquioxide only. The suboxides are also formed on etched surfaces of silicon [341] and in layers obtained by silicon implantation oxidation [342]. Thermal annealing leads to a composition corresponding to that of the sesquioxide when carried out at 600 °C.

Less for effects in high-tech physics than essentially in basic chemical processes, the sesquioxide has found quite different applications. Cleaning and purification spans from that of arsenic vapors [343] to the treatment of waste fluid from sweet potato processing [344]. Highly permeable membrane separation elements are made from a ceramic material based on alumina and silicon sesquioxide [345]. The material is stable in aqueous environment having a water penetration rate of 4.2 m³/m²h⁻¹. In ceramic material the sesquioxide has been used as an oxidizing agent during manufacture [346] and as bits for well-drilling [347]. Wear resistance is much lower though, than for tungsten carbide.

48.5.3.3 Other Silicon-Oxygen Compounds

Oxyhydrides of the composition (HSiO_{1.5})_x are obtained by the hydrolysis of trichlorosilane [348–350]. In organic solvents the product is formed as an amorphous powder or as transparent mica-like flakes [335], depending on the type of solvent. Well-defined, low molecular oligomers—the smallest [351, 352] being a cage of 8 silicon atoms arranged at the corners of a cube with 12 oxygen atoms forming the bridges along the edges—can be prepared by hydrolysis in a two-phase system [353–355]. Oligomers with *x* an even number ranging from 8 to 16 are obtained.

The Si₈-cube is also the smallest cage in zeolite structures; it is the 4-4 secondary building unit in zeolite A. Since the silver zeolite reacts with water evolving oxygen, ligand-to-metal charge transfers in the Si₈-cube are of interest in the context of processes involving photolysis of water by visible light [356]. By photochemical oxidation of tetrachlorosilane the trichlorosilanol is produced, a compound existing only in equilibria with others [357]. Utilizing structural possibilities new silicon-oxygen compounds were prepared, the oxygen taking part as the donor atom in penta-coordinate silicon alkoxide complexes. Alkoxysilanes react with metal hydrides to trialkoxy anions which then rearrange to the tetraalkoxy anion [358]



Likewise the reaction of silica with glycol is made possible through penta-coordinate complex formation around the silicon atom [359].

48.5.4 Sulfides

Silicon sulfide, SiS₂, *mp* 1090 °C, sublimation point 1130 °C, forms white, asbestos-like needles, which readily hydrolyze. It is formed from silicon and sulfur at 1100–1300 °C [360], but preferably at > 1400 °C [361, 362]. Silicides react with sulfur at > 700 °C, hydrogen sulfide at 1100–1200 °C, or sulfur chlo-

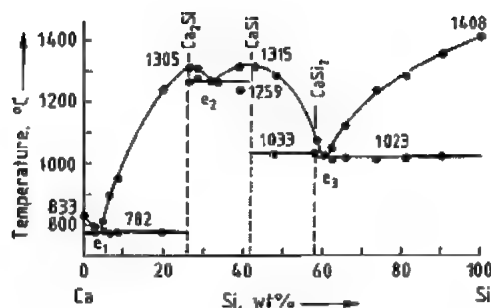


Figure 48.23: Calcium-silicon phase diagram [385].

48.6.2 Calcium Silicon

Like FeSi, calcium silicon [384] is produced carbothermally in submerged arc furnaces and is consumed in the iron and steel industry.

Physical Properties. The Ca-Si phase diagram (Figure 48.23) shows the existence of three compounds [385]: Ca_2Si (cubic, $a = 474$ pm), CaSi (orthorhombic, $a = 391$ pm, $b = 459$ pm, $c = 1080$ pm), and CaSi_2 (hexagonal rhombohedral, $a = 1040$ pm, $\alpha = 21.5^\circ$). Commercial CaSi contains ca. 30% calcium and 60% silicon; the remainder is iron and impurities. The alloy solidifies mainly as CaSi_2 with small amounts of primary and secondary eutectically precipitated silicon. The density of the commercial alloy is 2.2 g/cm^3 , and its melting range is $1050\text{--}1150^\circ\text{C}$.

Raw Materials and Production. The raw materials for the production of CaSi are quartz, lime, and coal. Whereas calcium carbide was formerly used as the source of calcium, it has now been replaced by lime with the following approximate specifications: CaO 94–97%, CO_2 1.5–3%, H_2O 0.5–1.5%.

The requirements for quartz and coal, as well as the particle size of the burden, correspond to those of ferrosilicon production.

The three-phase submerged arc furnaces generally used for the production of CaSi are similar to the furnaces used for the production of FeSi (see Figure 48.2). In practice, CaSi and FeSi are also produced alternately in the same furnace. Calcium silicon is produced only in open furnaces whose power consump-

tion is 8–30 MW, corresponding to a capacity of $(6\text{--}20) \times 10^3 \text{ t/a}$. The basic reaction of the commercial process is as follows:



In practice the processes are very complex. The process is sensitive to variations in the amount of reducing agent, which may also occur locally in the burden. An excess of carbon in the burden results in the formation of SiC and CaC_2 , which in the extreme case leads to the clogging of the furnace. The use of too little carbon results in the formation of lime-silicate slags that are difficult to reduce and are tapped with the metal, which lowers the capacity of the furnace.

Even with correct operation, up to 30% of slag is carried out with the CaSi. The slag, which is only slightly denser than CaSi, is separated after being tapped off into the pouring ladle. The slag sinks to the bottom, and the metal is then decanted by pouring into shallow molds. Some companies use a cascade of four to five tapping-off molds, which results in refinement because the slag preferably remains in the upper molds and the lower ones contain very pure metal. Careful separation from slag is the only feasible method for refining CaSi. The oxidative treatment used for FeSi is not possible because calcium has a high affinity for oxygen.

The slag, which also contains CaC_2 , is processed and recycled to the furnace. Typical values for the specific material and energy requirements of the CaSi process are as follows:

Quartz	1500–1800 kg/t
Lime	550–700 kg/t
Coal	680–800 kg/t
Recycled slag	250–300 kg/t
Söderberg paste	80–100 kg/t
Power consumption	9800–13 000 kWh/t

Environmental Protection. The large amount of dust generated in the CaSi process (up to 300 kg per tonne of CaSi) is a result of vapor losses of SiO_2 and calcium. Both components are oxidized in air and carried out of the furnace with the off-gas, from which they are separated in bag filters. The dust, which consists of ca. 60% SiO_2 and 30% CaO (remainder: MgO , carbon, Fe_2O_3), is dumped.

Table 48.7: Composition of CaSi (DIN 17580).

Name	Symbol	Material no.	Composition, %					
			Ca	Ca + Si (min.)	C (max.)	Al (max.)	P (max.)	S (max.)
Calcium-silicon	CaSi	0.3650	29–33	90	1.20	1.80	0.070	0.060
Calcium-silicon, low C	CaSiC 50	0.3655	29–33	90	0.50	1.80	0.070	0.050

Since all of the slag is reintroduced to the process, none remains to be disposed of.

Quality Specifications. The specifications for standard-grade commercial CaSi are summarized in Table 48.7. A number of multicomponent CaSi-based alloys contain up to 30% aluminum, manganese, barium, titanium, magnesium, mischmetal, or iron. These compositions are often specified by the customer and are not defined in standards.

DIN 17580 also defines procedures for analysis, testing, and arbitration [386, 387, 388].

Storage, Transport, and Toxicology. On contact with water, acid, or base, CaSi can produce hydrogen. The reaction proceeds extremely slowly with pure water and the alloy is therefore not classed as a hazardous substance in most countries (GGVS/GGVE) for transport by road.

For sea and air transport, CaSi is classed as a hazardous substance, Class 4.3 (IMDG-Code; UN no. 1405). Since fine CaSi dusts are explosive, inert gases (nitrogen or argon) must be used for pneumatic transport. The critical oxygen content for carrier or protective gases is 8%.

Calcium silicon should be stored in dry, ventilated rooms. On contact with moisture, slag impurities can release small amounts of phosphine, although with correct storage the concentrations are not critical.

Uses. Calcium silicon is used in steelmaking as a deoxidizer and desulfurizer, as well as for the modification of nonmetallic inclusions [389, 390]. Calcium is the active element in the alloy due to its high affinity for oxygen and sulfur; silicon serves as a carrier element and is alloyed in the steel melt, analogous to FeSi.

The efficiency of calcium is very low if the alloy is added in lumps because of the high va-

por pressure of calcium at the utilization temperature (p_{Ca} at 1600°C : 0.2 MPa) and the low solubility of calcium in molten iron (max. 0.03 %).

The efficiency has been improved by the development of injection techniques. Calcium silicon powder is blown deep into the steel melt through immersion lances, or CaSi-filled hollow wires are coiled rapidly into the pouring ladle. These techniques produce very good metallurgical results and are rapidly replacing conventional addition of the alloy as lumps.

The modification of inclusions by calcium improves the fluidity of steel in automated continuous casting plants. The calcium liquefies the suspended solid inclusions of aluminum oxide that are always present in aluminum-killed steels. Furthermore, the material properties of the steel are improved: the calcium aluminates formed are largely undeformable in the solidified steel and allow high isotropy of the material properties to be maintained after working of the steel.

Economic Aspects. The amount of CaSi required by the steel industry has decreased during the 1980s due to changes in process technology: the very efficient injection techniques, especially the cored wire process, greatly reduce the amount of CaSi required per tonne of steel.

In spite of the wide range of uses, world consumption fell from ca. $100 \times 10^3 \text{ t/a}$ in 1981 to ca. $80 \times 10^3 \text{ t/a}$ in 1991. In the Western steel-producing countries, ca. 50% is used in the form of filled wire, and this fraction will increase further.

Production capacity is estimated to be $120 \times 10^3 \text{ t/a}$, distributed evenly among the former Eastern-bloc countries, South America, and Western Europe.

48.7 Silica

48.7.1 Silica Modifications and Products

48.7.1.1 Geochemistry and Crystal Structure

Silica, silicon dioxide, SiO_2 , is the major constituent of rock-forming minerals in magmatic and metamorphic rocks; it accounts for ca. 75% of the Earth's crust [391]. It is also an important component of sediments and soils [392–394]. In rocks free silica predominantly occurs as quartz, which owes its important role to the action of water in rock-forming processes on Earth. Quartz makes up 12–14% of the Earth's crust. In silicate bodies that crystallized under dry conditions—moon rocks, and silicate slags, for example—quartz is rare; instead, cristobalite and tridymite crystallize. Micro- and noncrystalline silica minerals are described in [395]. The structural framework of crystalline SiO_2 phases can incorporate trace element impurities in two ways (Figure 48.24) [396]. The first is the substitution-addition mechanism (Figure 48.24): substitution of Si^{4+} by Al^{3+} or Fe^{3+} and addition of M^+ and M^{2+} at interstices ($\text{M}^+ = \text{Li}^+, \text{Na}^+; \text{M}^{2+} = \text{Mg}^{2+}, \text{Ca}^{2+}$).

The second is the formation of hydrolytic or alkaline nonbridging oxygens ("Trennstellen") in the framework. Incorporation of alkali metal and aluminum ions in stoichiometric proportions leads to stuffed derivatives [396], e.g.:

Structure type:	high quartz	high cristobalite	high tridymite
Stuffed derivative:	eucryptite $\text{Li}(\text{AlSiO}_4)$	carnegieite $\text{Na}(\text{AlSiO}_4)$	kalsilitite $\text{K}(\text{AlSiO}_4)$

Quartz has a very high geochemical purity, the dissolved trace elements rarely exceeding 100 ppm [395, 397, 398]. Water, however, can be incorporated in concentrations from hundreds to several thousands ppm (Figure 48.25). The transitions from structural incorporation to microstructural inclusion are fluent [399]. Sil-

ica has a strong affinity for water. At elevated temperatures and pressures water migrates rapidly through the structural framework, splitting Si-O-Si bonds and forming silanol groups. This mechanism of hydrolytic weakening activates reconstructive transformations, recrystallization, plastic deformation, and solid-state flow of quartz [400]. Traces of alkali metal oxides act as efficient transformation activators by forming alkaline Trennstellen (Figure 48.24) [401].

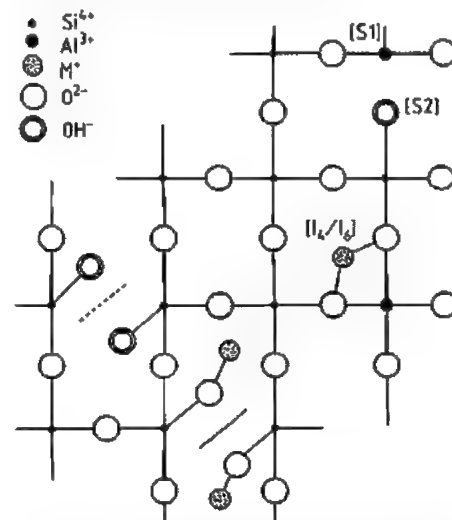


Figure 48.24: Two-dimensional scheme of chemical points defects in SiO_2 frameworks. — hydrolytic, — alkaline nonbridging oxygen (Trennstellen); [S] substitutional, [I] interstitial defects.

Apart from stishovite, which contains six coordinate silicon (Figure 48.26B), and silica W, with a tetrahedra-chain structure, the known crystalline silica phases are three-dimensionally linked, ordered frameworks of tetrahedra (Figure 48.26A) sharing all four corners, while the noncrystalline phases are random networks or clusters of all-corner sharing SiO_4 tetrahedra, whereby a few tetrahedra may possess some corners with nonbridging oxygen atoms. Four sp^3 hybrid orbitals on Si overlap with the $2p$ orbitals of oxygen, forming strong σ -bonds [402]. Additional minor bonding contributions arise from overlap of Si $3d$ orbitals with O $2p$ orbitals, which partly explains the shortening of Si-O

bond lengths with increasing Si-O-Si bond angle [403].

The approximately 1:1 ionic-to-covalent bond character favors compromise angles between 180° and 109° , averaging ca. 147° [404, 405]. Band theory treatment is given in [406]. In terms of ionic bonding, the radius of Si^{4+} in tetrahedral coordination with oxygen ($r_{\text{Si}^{4+}} = 0.127 \text{ nm}$) is 0.034 nm , and in octahedral coordination, 0.048 nm . The mean Si-O bond distance in tetrahedral polymorphs is 0.161 – 0.162 nm [407]. The mean O-O distance is 0.264 nm (Figure 48.26A). The short Si-O bond indicates high bond strength (452 kJ/mol in quartz), and in combination with the three-dimensional linking of tetrahedra, it results in high elasticity, melting point (cristobalite 2000 K), activation temperatures for reconstructive transformations (1300 K for quartz cristobalite at ambient pressure), the high transformation temperature of silica glass

(1300 K), and high hardness (quartz: Mohs hardness 7).

The variation in the Si-O-Si bond angles and the almost unrestricted rotation of adjacent tetrahedra around the bridging oxygen atom (Figure 48.26D) accounts for the topological and displacive variability of silica frameworks, the stacking polytypism of cristobalite-tridymite, complex growth and transformation twinning, and the tendency for glass formation. Generally, the favorable trans configuration of adjacent tetrahedra is adopted in the frameworks (Figure 48.26C). Rare exceptions with *cis* and *trans* configurations are the tridymites [401] and coesite [410]. In the *trans* configuration, the tetrahedra are nearly ideal, whereas the unfavorable *cis* configuration causes distortion of the tetrahedra in the tridymites [411] and is responsible for unusually high Debye-Waller temperature factors of the bridging oxygen atoms in coesite [412].

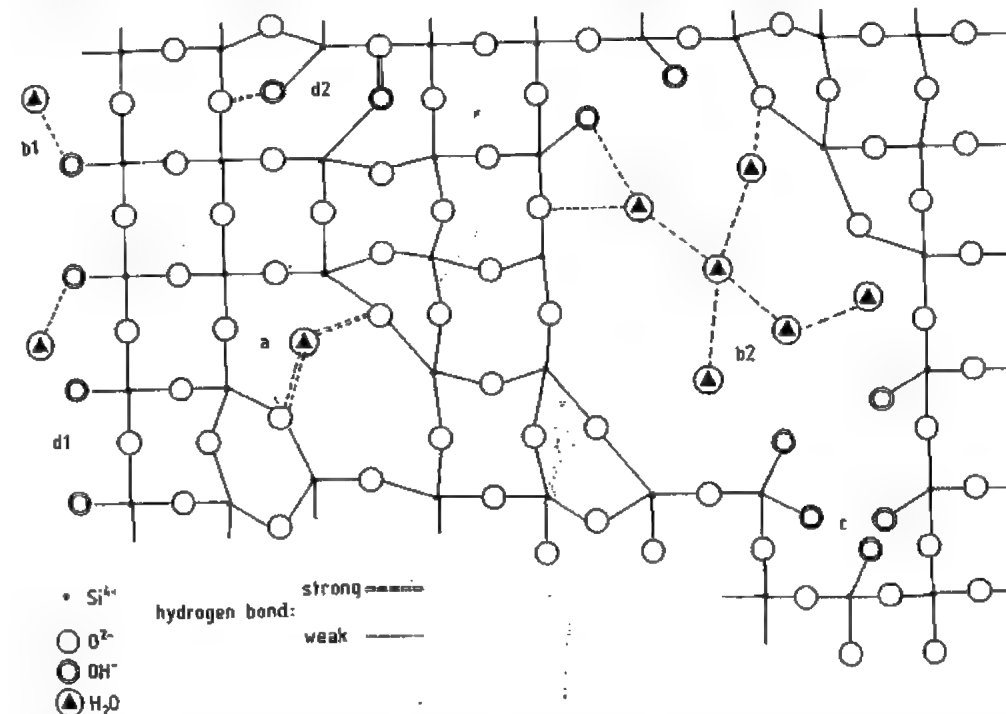


Figure 48.25: Two-dimensional scheme of water in and on the surface of quartz, as revealed by IR spectroscopy [408, 409]: a) H_2O strongly bonded in framework; b1) H_2O at outer surfaces; b2) H_2O clusters in framework ("freezeable water"); c) substitution of (SiO_4) by $(\text{OH})_4$; d1) surface silanol groups; d2) Trennstellen silanol groups.

Table 48.8: The crystalline silica minerals.

Mineral	Space group	Cell dimensions, nm			Crystal di- mensions ^a	Density, g/cm ³	Refractive indices ^b			Optical character	Displacive transforma- tion temperature ^c , K
		a	b	c			$\alpha, \beta, \gamma, ^\circ$	n_x	n_y		
Mineral phases											
Stishovite	P4 ₂ /mm	0.4177	0.2666		2	ca. 4.3	1.80		1.83 1.85	+	
Coesite	C2/c	0.7135	1.2396	0.7174	120.34	ca. 2.9 3.0	1.594	1.596	1.599	+	
Low quartz	P3 ₂ 1 R ^d P3 ₂ 1 L	0.4913	0.5405	1.20	1	2.65	1.5442		1.5533	+	846
High quartz (at 600 °C)	P6 ₃ 22 R ^d P6 ₃ 22 L	0.45	0.5	1.20							846
Moganite	I12/a1 ^e C12/c1	0.8758	0.4876	1.0715	90.1	ca. 2.5	1.52 1.53				
Low cristobalite ^f L-C ₀	P4 ₂ 2 ₁ 2 R ^d P4 ₂ 2 ₁ 2 L	0.4978	0.6948		1, 2 ^g	2.33	1.484		1.487	-	540 ^h
High cristobalite ^f H-C ₀	Rd3m ⁱ	0.7132			1, 2			1.485		-	540 ^h
Low cristobalite ^f L-C ₀		0.498	0.695		1, 2	ca. 2.33					
High cristobalite ^f H-C ₀		0.713			1, 2						
Low 1 tridymite ^j L1-T ₀	Cc	0.4991	2.5832	1.8495	117.75	2.27 2.28	1.47 1.48			+	380
Low 3 tridymite ^j L3-T ₀	C1	0.5008	0.8600	0.8217	91.51	2.26					340
High 5 tridymite ^j (at 95 °C) H5-T ₀	orthorhombic	0.9959	1.7440	8.179		2.24					ca. 340 380
High 4 tridymite ^j (at 155 °C) H4-T ₀	P2 ₁ 2 ₁ 2 ₁	0.4986	2.6171	0.8196		2.24					ca. 380 430
High 3 tridymite ^j (at 170 °C) H3-T ₀	monoclinic	0.5008	0.8748	0.8212	90.28	2.22					ca. 430 490
High 2 tridymite ^j (at 220 °C) H2-T ₀	C22 ₁	0.5024	0.8757	0.8213		2.21					ca. 490 690
High 1 tridymite ^j (at 420 °C) H1-T ₀	P6 ₃ /mmc	0.5047	0.8262			2.19					
Low 2-tridymite ^{k,m} L2-T ₀	F1	0.9933	1.7217	8.1865	1	ca. 2.28	1.48			+	
High 1 tridymite ^{k,m} H1-T ₀											
Melanophlogite ^a	Pm3n	1.3436			1, 2	ca. 2.0	1.47				

^a 1: macroscopic, 2: microscopic, 3: submicroscopic.^b Values in each column: optically biaxial; values in left and right column: uniaxial; values in middle column: mean value.^c Two values: intermediate high-modification.^d Handiness of enantiomorphic groups: R = right, L = left.^e 1: Settling for comparison with quartz structure.^f Stacking ordered cristobalite: C₀, tridymite, T₀.^g High-low transformation causes polysynthetic microtwinning.^h Transformation hysteresis low-high ca. 10 K, high-low ca. 20 K.ⁱ At 570 K.^j Average structure with six fold twinned domains.^k Stacking disordered cristobalite: C₀, tridymite: T₀.^m Tridymite S(trable)" or "metastable tridymite": redundant terms.ⁿ "Tridymite M(gasable)" or "terrestrial tridymite": redundant terms.^o With guest molecules.

48.7.1.2 Crystalline Silica Phases

The crystalline silica minerals are listed in Tables 48.8 and 48.9. Table 48.8 also lists the two known nonmineral crystalline phases.

Crystalline Silica Minerals

The *p*-*T* diagram of silica, with stishovite, coesite, quartz, and cristobalite, is shown in Figure 48.27 [413]. The existence field of tridymite is too small to be shown here.

Stishovite crystallizes in the rutile structure with [SiO₄] octahedra sharing two opposite edges and two corners [414, 415], resulting in very close packing of the oxygen atoms. At ambient pressure it transforms at ≥ 800 K rapidly into noncrystalline silica. Stishovite is almost insoluble in hydrofluoric acid; however, its solubility in water under ambient conditions is comparable to that of silica glass.

Coesite has its own structure type. Four-membered rings of tetrahedra are interlinked by Si₂O₇ groups, with the tetrahedra in the *cis* configuration and an apparent Si-O-Si angle of 180° at the bridging oxygen, which, however, appears to be the average structure of domains with more equilibrated tetrahedral configurations [410, 412]. Coesite is metastable, but at ambient pressure it persists up to ca. 1300 K. It is much less soluble in hydrofluoric acid than quartz, but the solubility in water under ambient conditions is similar to that of quartz. The occurrence of microcrystalline oxide precipitates with coesite-like structure in semiconductor silicon is still being discussed [416]. Stishovite and coesite are rare in nature and can be synthesized only in milligram quantities.

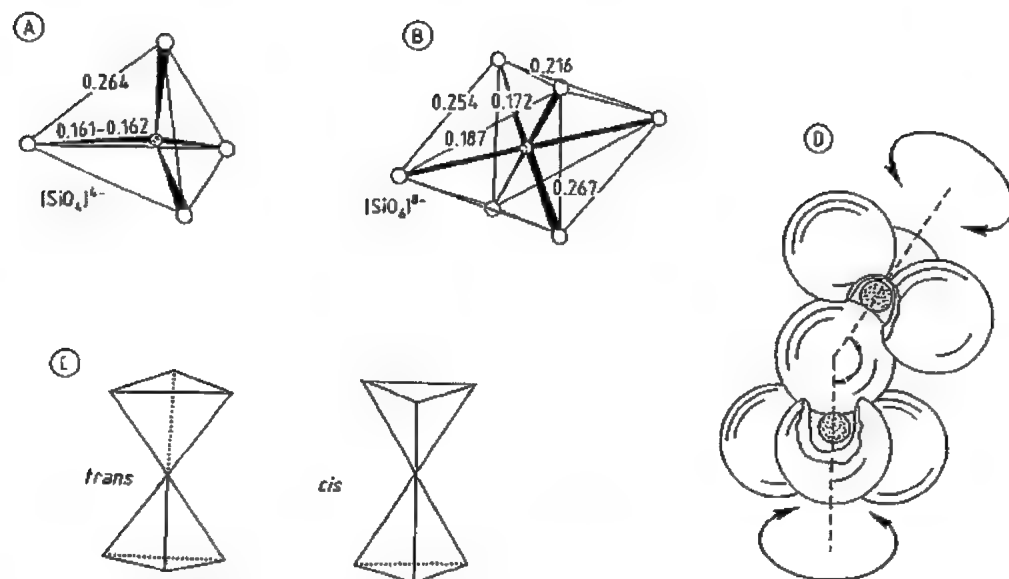


Figure 48.26: Details of silica crystal structures (see text for explanation).

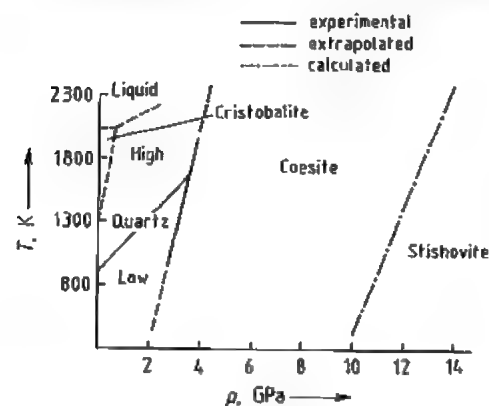


Figure 48.27: p - T diagram of SiO_2 system [413]. The borderline of tridymite to high quartz and high cristobalite runs along the ordinate from ca. 1200 to ca. 1800 K.

Quartz is the stable phase under ambient conditions. Due to the sluggish transformation the boundary to the coesite field at low pressures and temperatures can only be extrapolated. The same is true for the quartz-cristobalite boundary. The most important structural features are helices composed of tetrahedra along the c -axis. The helices have a repeat distance of 3 tetrahedra (T) (3T chain). The winding of the helices can be left- or right-handed, which results in the enantiomorphism of quartz crys-

tals [417, 418]. Six helices envelope structural channels with four-fold $[L_4]$ and six-fold $[L_6]$ oxygen-coordinated interstitial sites which alternate along the c -axis. Polarity along the a -axes accounts for the piezoelectricity of low quartz and its use in oscillator and voltage-pressure transducers. The low sensitivity, however, requires high-voltage amplification [419]. The low specific free surface energy of the rhombohedral faces $\{10\bar{1}1\}$ results in distinct cleavage [397]. The low thermal conductivity ($\lambda_{11} = 6.2 \text{ W m}^{-1} \text{ K}^{-1}$, $\lambda_{33} = 10.4 \text{ W m}^{-1} \text{ K}^{-1}$) and high thermal expansion ($\alpha_{11} = 13.3 \times 10^{-6} \text{ K}^{-1}$, $\alpha_{33} = 7.1 \times 10^{-6} \text{ K}^{-1}$) produce low thermal shock resistance, which can be exploited for crushing coarse quartz. Standard values of important properties are collected in [420], and relationships between structure and properties are given in [419].

The displacive transformation of low quartz to high quartz involves cooperative rotatory dislocation of the tetrahedra leaving the Si-O bonding topology unaffected. The transformation is rapid, reversible, and occurs without hysteresis. Starting with low quartz, the rotatory vibrational disorder increases continuously with temperature [418, 421].

Randomization reaches a maximum at the transformation temperature, which is illustrated by thermal expansion as a function of temperature (Figure 48.28). The difference in

specific volume between 300 and 850 K is 4%. The last jump between 825 and 850 K contributes about 1% [422]. The shape of the specific heat C_p curve is of the lambda type.

Table 48.9: The microcrystalline mineral species of quartz and of cristobalite-tridymite (opals).

Property ^a	Microcrystalline quartz species ^b			
	Microquartz MQ	Chalcedony CH_{LF}		Quartzine CH_{LS}
		CH-W _{LF}	CH-H _{LF}	
PLM				
Mean refractive index	ca. 1.54–1.55	ca. 1.533–1.543		ca. 1.542
Microstructure	granular, undulatory extinction	parabolic fiber bundles striations	radiating spherulites striations	parabolic fiber bundles (plait pattern) spherulites striations
Mean crystallite size (PLM, X-ray)	< ca. 20 μm	ca. 50–350 nm opal — CT matrix ca. 100–200 nm	ca. 100–200 nm
Texture (PLM, SEM)		parallel fibrous	parallel fibrous	plaited fibers
Texture (X-ray diffraction)		fiber axis: $\langle 11,0 \rangle$, $\langle 1\bar{1},0 \rangle$	fiber axis: $\langle 11,0 \rangle$, $\langle 1\bar{1},0 \rangle$	fiber axis: $\langle 00,1 \rangle$
TEM				
		polysynthetic twinning of R/L quartz lamellae		polysynthetic twinning of R/L quartz lamellae
		wrinkle-banding		
			Microcrystalline opals ^b	
		Opal-C O-C	Opal-CT O-CT	
		O-C _{LF}	O-C _M	O-CT _{LS} O-CT _M
PLM				
With crossed polarizers	birefringent	almost isotropic	birefringent fibrous-parabolic	almost isotropic
Mean refractive index	ca. 1.46	ca. 1.45	1.45–1.46	1.43–1.45
Microstructure				
SEM	parallel-platy after 111	tangled-platy	parabolic fiber bundles	lepidospheric tangled-platy
TEM		massy	fiber axis: $\langle 101 \rangle$ or $\langle 110 \rangle$	tangled-fibrous platelets intergrown at angles of ca. 70°

^a PLM: polarizing light microscope; SEM: scanning electron microscope; TEM: transmission electron microscope.

^b LF: optical character of fiber elongation negative; LS: optical character of fiber elongation positive; M: massy, tangled; W: wall-banded; H: horizontally banded.

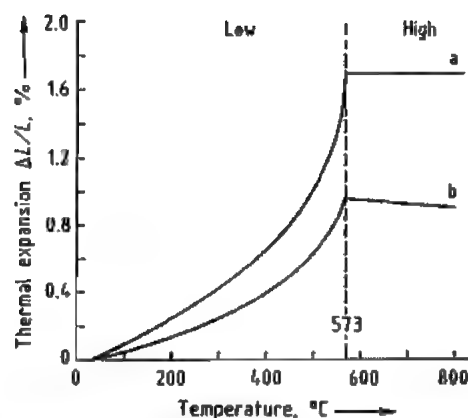


Figure 48.28: Thermal expansion of quartz: a) Parallel to a -axis; b) Parallel to c -axis.

Abnormal properties, such as optical biaxial character are due to inequivalent substitution of the three equivalent Si atoms of the structure by traces of Al or Fe during growth [423–425].

After passing through a region of retrograde solubility, under hydrothermal conditions the solubility of quartz in water increases strongly with pressure and temperature (Figures 48.29, 48.33) [426, 427]. Only above 400 K are equilibrium solubilities determinable at ambient pressure. At ambient temperature the solubility is ca. 6 ppm SiO_2 [428]. Quartz solubility plays an important role in the exploitation of geothermal energy (silica scaling in pipes and valves) [429]. Water in quartz (Figure 48.25) is highly mobile. The diffusion constant in the temperature range 625–1300 K is $D \approx 10^{-12} e^{-9510/T}$ [430]. Fluid inclusions found in nature are mainly H_2O , CO_2 , and CH_4 . Under ambient conditions NaCl may be partly precipitated from the saline fluid [431]. The diffusion coefficient of Na from 575 to 845 K parallel to the c -axis is $D_{\parallel c} = 0.68 e^{-8410/T}$, and perpendicular to the c -axis $D_{\perp c} = 400 e^{-11390/T}$ [432]. The diffusion depends strongly on the type and concentration of structural defects [433]. Perpendicular to the c -axis quartz is an insulator. However, alkali metal ions incorporated or deliberately introduced during growth in the c -direction result in electrolytic conduction [419].

Chalcedony and Quartzine. The microcrystalline quartz species chalcedony and quartzine (Table 48.9) [395] have dense microstructures of fibers composed of submicroscopic right-(R-) or left-(L-) handed quartz lamellae. Chalcedony occurs in agate nodules in masses of several kilograms. High hardness combined with high toughness and high purity (< 1% nonvolatiles, 0.5–2% H_2O) leads to high demand as an industrial mineral.

Quartz whiskers, in contrast to chalcedony and quartzine, are isolated single crystal fibers of ca. 1 μm diameter. They form by hydrothermal transport of silica with water [434].

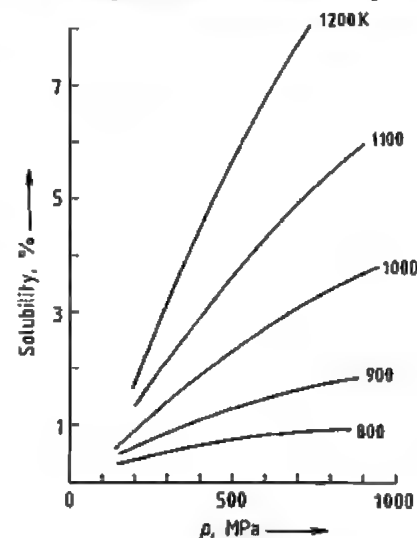


Figure 48.29: Hydrothermal solubility of quartz in water [426, 427] (isotherms in the high-pressure range).

Moganite. The crystal structure of moganite, a very rare microcrystalline silica mineral [435], consists of systematic twinning of one R- and one L-quartz {10T1} lattice slice per unit cell [436].

Cristobalite is the low-pressure, high-temperature modification of silica (Figure 48.27). The structure of high cristobalite is a derivative of the zinc blende type, with Si occupying the Zn and S positions. The framework consists of $\text{SiO}_4/2$ tetrahedra in *trans*-configuration, forming sheets of 6T rings with the tetrahedra in up-and-down positions (Figure

48.30). The sheets are in parallel orientation, stacked in a three-sheet sequence along the $\langle 111 \rangle$ directions. The structure has large interstitial cages. The apparently linear Si–O–Si bonds in high cristobalite are due to an average structure with six-fold domains; a true bond angle of 147° has been calculated [437]. The displacive high cristobalite–low cristobalite transformation is rapid, reversible, and cannot be frozen, though it shows a hysteresis of ca. 20 K. The sudden increase in specific volume on high low transformation is 4%, leading to characteristic “fish scale” microcracking. These scales are rectangular if the cristobalite is structurally ordered and become rounded with increasing stacking disorder [438]. Under nearly all conditions, the kinetics [439] prevent the growth of macrocrystals. Instead, repeated nucleation and dendrites are common growth features. The lack of suitable cristobalite macrocrystals limits the precise determination of properties and the extent of impurity incorporation. Coarse, refractory grade cristobalite crystals incorporate < 1% impurities [440]; natural cristobalite crystals, with a more complex microstructure, have higher contents of inclusions [441].

Tridymite is unstable to high pressures at elevated temperature. At ambient pressure it forms at 1200–1800 K; however, traces of foreign ions—preferably the alkali metals—are necessary. Formation is also favored by hydrothermal conditions [442]. Tridymite crystallization according to the nucleation-growth process [401] starts with cristobalite nuclei. The growth kinetics favor the formation of large tabular crystals [439]. The crystal structure is a derivative of the hexagonal wurtzite type with Si occupying the Zn and S positions. Sheets of 6T rings are stacked in antiparallel orientation to give a two-sheet sequence (Figure 48.30). With respect to bonding requirements the structure is much less balanced than that of cristobalite. As a consequence tridymite undergoes very complex high–low transformations. Trace ele-

ments are incorporated substitutionally and in open structural channels parallel to the c -axis [441]. In refractory grade crystals, trace element concentration is < 1% [443].

Cristobalite–Tridymite Stacking Polytypism. The close structural relationships enable stacking faults to occur during growth or reconstructive transformation. Intergrowth of tetrahedra sheets with cristobalitic or tridymitic stacking sequences and the transformation of cristobalite into tridymite and vice versa go off with mutual orientation [444]. Due to the nucleation-growth mechanism [401] and stacking polytypism several tridymite modifications and cristobalite may be intergrown in a single tridymite crystal [445]. Stacking disorder changes all properties, including temperature and heat of displacive transformation, as well as thermal expansion and X-ray diffraction, which are used for quantitative phase determination [446]. Unawareness of this fact led repeatedly to speculation about a “transition phase” occurring during quartz cristobalite–tridymite transformations [447, 448], which, however, does not exist. In any case it is necessary to discriminate between ordered and stacking disordered cristobalite (C_0 and C_D) and tridymite (T_0 and T_D). The terms tridymite S or meteoritic tridymite, and tridymite M or terrestrial tridymite are redundant synonyms for T_0 and T_D [411].

Melanophlogite, a very rare mineral with noteworthy occurrences known only in Agri-gento and Livorno, Italy [449, 450] is treated in Section 48.7.8.3.

Crystalline Nonmineral Silica Phases

Only two crystalline nonmineral silica phases are known, both of which do not occur in nature due to their instability (Table 48.8).

Keatite is synthesized as metastable microfibrillar parabolic bundles from noncrystalline silica under weakly alkaline hydrothermal conditions [451].

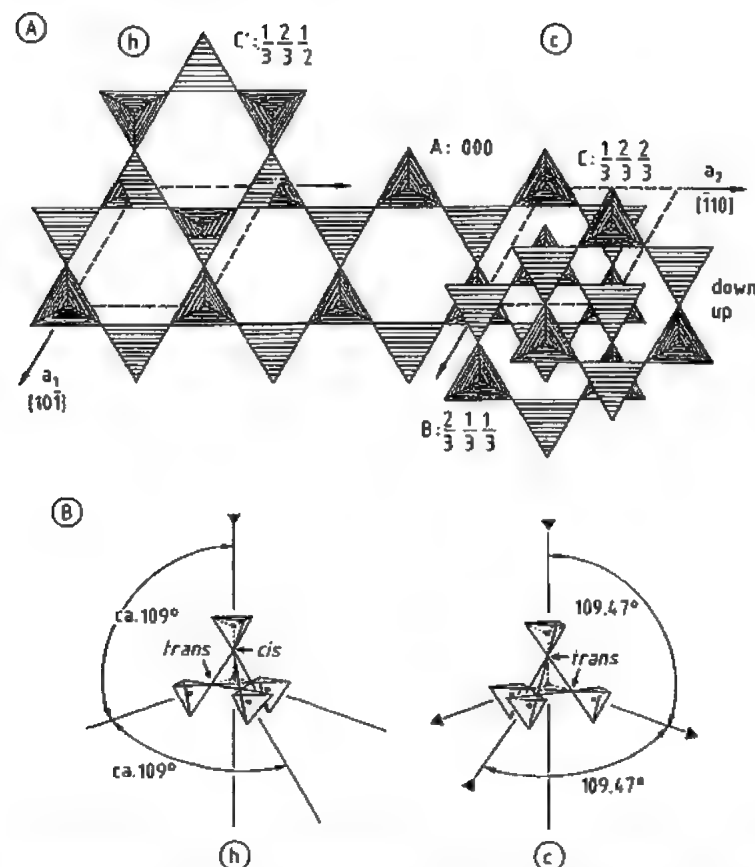


Figure 48.30: A) Stacking principles of idealized six-membered up and down ring tetrahedra sheets. c: Cristobalite, A, B, C sheets parallel; h: Tridymite, A and C' sheets in antiparallel position. B) Tetrahedra configurations in the framework. c: Cristobalite—all trans; h: Tridymite— $\frac{2}{3}$ trans, $\frac{1}{3}$ cis.

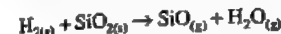
Table 48.10: The noncrystalline silica minerals.

Mineral or phase	Species	Microstructure (PLM/SEM)	Abbreviation ^a	Density, g/cm ³	Refractive index
Opal-A (noncrystalline silica with characteristic amounts of water)	opal-A _G		O-A _G	variable	ca. 1.45–1.46
	precious opal-A _G	close packing of homometric SiO ₂ ·nH ₂ O spheres	O-A _G -prec.		
	potch opal-A _G	irregular packing of heterometric SiO ₂ ·nH ₂ O spheres	O-A _G -potch		
	opal-A _N	botryoidal with striations	O-A _N	ca. 2.1–2.2	ca. 1.45–1.46
Lechätellierite (silica glass, almost free of water)	hyalite	bubbles from degassing			
	silica-fulgurite	relics of quartz grains cristobalite			
	meteoritic silica glass	pores schlieren meteoritic detritus and reaction products	LEC	ca. 2.2	ca. 1.458

^a A: noncrystalline; G: gel structure; N: network structure.

The tetrahedral framework of the keatite structure [452] contains 4T helices along the *c*-axis. 3T single chains [453] run parallel to the *a*-axes. The structure is not yet well refined; however, stuffed derivatives MAISI₂O₆ (M = H⁺, Li⁺, Na⁺, K⁺) have been structurally well characterized [454].

Silica W [455] forms above ca. 1500 K in the decomposition and vapor transport reaction



as metastable fibrous woolly aggregates. The crystal structure is isotypic with SiS₂. Infinite chains of edge-sharing tetrahedra run parallel to one another and are held together by weak interatomic forces. At ambient temperature, this very unstable configuration collapses immediately on coming into contact with traces of water. Tempering under the formation conditions produces cristobalite [455].

The substance known as SiO₂-X, is an alkali metal silicate hydrate with the approximate formula MSi₁₁O_{20.5}·3H₂O (M = K, Rb, Cs) [456].

48.7.1.3 Noncrystalline Silica Minerals

Noncrystalline silica minerals are listed in Table 48.10.

The lack of structural order and therefore of distinct stoichiometry makes the boundary between silica glass and silicate glasses fuzzy. For natural silica glass it can be arbitrarily drawn at ca. 3 mol % of nonsilica components.

Lechätellierites, which originate from silica melts formed by meteoritic impacts or lightning strikes on quartz sand or quartz rocks, are very rare [395, 397].

Opals-A_G are formed by flocculation of high-purity SiO₂·nH₂O spheres of ca. 100–500 nm diameter when colloidal silica percolates through water-permeable clays or metamorphosed volcanic rocks. The water is filtered and the spheres aggregate, with closest packing if they are homodisperse, or irregular packing if they are heterodisperse. Cubic close packing (ccp) is preferred because of its low

free surface energy. The ordered packings produce Bragg diffraction of visible light, while the disordered packings give rise only to Rayleigh scattering [457]. Biogenic opal-A_G is formed from skeletal silica remains of plankton. The water content of opals-A_G varies in the range ca. 58% with ca. 4–7% molecular water [395, 408].

Opal-A_N is a water-containing silica glass, formed by quenching of aqueous fluid silica solutions [395]. The opals-A are characterized by their microstructure and water content [408]. Opal-A_N with a continuous three-dimensional random tetrahedral network gives no small-angle X-ray scattering. Opal-A_G which consists of particle aggregates and water-filled microporosity [408] with discontinuous electron density, produces distinct small-angle X-ray scattering [458]. Opal-A_N contains ca. 3.5% water with 1.5% as silanol group water in the network and on the surfaces. The remainder is molecular water included in pores.

48.7.1.4 Silica Rocks

The classification of silica rocks is given in Table 48.11 [393, 459, 460]. Many special, trade, and trivial names exist, with varying meanings and often imprecise definitions. For example, "tripoli" is a friable porcellanite, and "ganister" a quartz sandstone cemented by chalcedony or opal-CT (cf. Table 48.11). Industrial silica rocks are treated in [461, 462]. Agates are siliceous fillings of vesicles and veins in volcanic rocks, consisting mainly of chalcedony with intergrown and interstratified granular microquartz, quartzine, opal-C, opal-CT, and coarse quartz [464, 465].

48.7.1.5 Crystalline Silica Products

Here, only silica products that are produced by crystallization from mobile mother phases or by transformation in the solid state are discussed.

Table 48.11: Silica rocks (> 90% SiO₂).

Classification	Name	Main constituent silica minerals; microstructure	Special, trade and trivial names (selection)
Metamorphic	quartzite	recrystallized quartz grains	crystalline quartzite, diamond quartzite, felsparquartz, tanusquartzit
Sedimentary detrital	quartz arenite	detrital quartz grains cemented by <ul style="list-style-type: none"> • direct contact • authigenic outgrowth • chalcedony, opal-CT 	quartz sandstone quartz sandstone orthoquartzite, ganister, silcrete, zementquartzit, findlingsquartzit
		<ul style="list-style-type: none"> • carbonates • argillaceous and ferric oxide minerals 	kitquartzit
Sedimentary non-detrital	diatomite	opal-A, detrital quartz; coherent diatom accumulations	kieselguhr [394]
	porcellanite	opal-CT; microporous (up to 50 vol %) dense and rather strong rock with conchoidal fracture; grades into chert	
	radiolarite	opal-A, opal-CT, chalcedony; coherent, friable	tripoli [463]
	chert	chalcedony, microquartz; nonporous tough rock with conchoidal fracture, containing scattered iron oxides, clay, and carbonate minerals	hornstein, jasper, novaculite [463]
	nodular chert	from chalk or limestone	flint*, silix, feuerstein
Volcanic	bedded chert	interbedding with mudstone or shale	phthanite, silica slate, radiolarite, lydit, kieselschiefer
	geyserite	opal-A _G , opal-CT; friable, porous	

* In the porcelain and earthenware industry in Europe, "flint" is used for ground flint, and in the United States, for ground quartz sand as well.

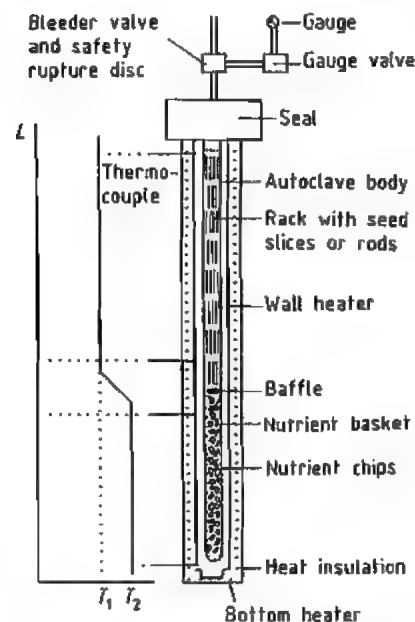


Figure 48.31: Autoclave for quartz single crystal bar growth.

In contrast to the many noncrystalline silica products, crystalline silica products are limited to hydrothermal cultured quartz crystals and thermochemically produced silica refractories.

Cultured quartz is of major economic importance and its use is growing rapidly. In contrast, the development of silica refractories has stagnated. They are used in certain high-temperature processes, and are generally produced batchwise when required, for example, when a new coke oven battery is installed, which can then be operated for up to 20 years with negligible silica consumption.

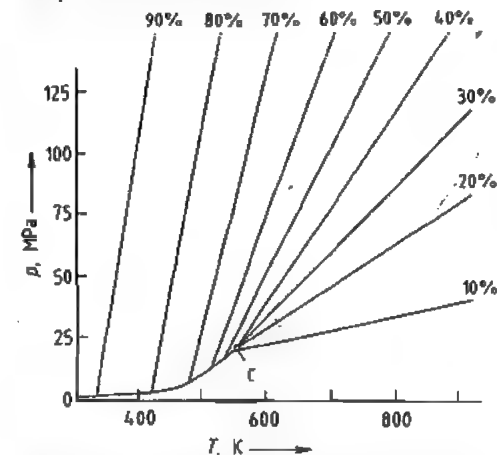
Cultured Quartz Single Crystals

The growth of quartz single crystals is carried out hydrothermally in sealed steel autoclaves with constant temperature difference and density-driven convection [466] (Figure 48.31). Hydrothermal syntheses are defined as growth or reaction at high pressure and tem-

perature in aqueous solution, both in the sub- and supercritical state [467].

Natural quartz [468] is fractionated into chips of controlled size distribution and surface area. They serve as nutrient and are filled into an iron wire basket which is placed in the lower part of the autoclave. The lower part is separated from the upper part by a baffle of defined opening. Seed slices or rods, cut with defined crystallographic orientation from natural or cultured quartz crystals that are untwinned and have a low content of structural defects, are hung in a rack and placed in the upper part of the autoclave. Preferred seeds are Z plates, cut parallel to {0001}, and Y rods, cut parallel to {1120} and {0001} and perpendicular to one of the *a*-axes.

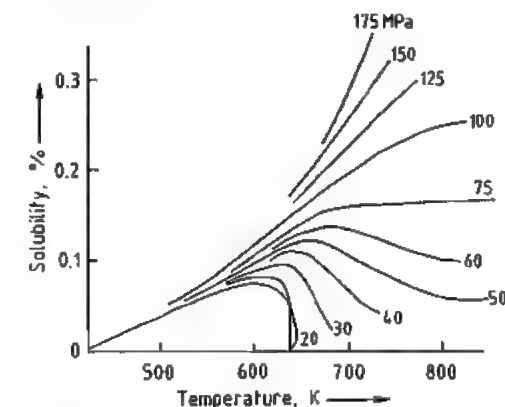
Aqueous growth solutions with different mineralizers (mainly 0.5–2.0 M NaOH or Na₂CO₃ and additives such as Li₂O) fill ca. 70–80% of the inner volume of the autoclave. Special syntheses such as growth of amethyst with incorporation of iron require K₂CO₃ or NH₄F solutions [469, 470].

Figure 48.32: *p*-*T* diagram of H₂O, isochores for various percentages of autoclave filling [471, 472]. C: critical point at 22.04 MPa, 547.4 K.

After sealing, the autoclave is electrically heated to a working temperature of ca. 675 K at the outer wall of the nutrient part (*T*₂) and ca. 20–40 K less at the seed part (*T*₁) (Figure 48.31). The actual temperature difference ΔT in the reactor is much smaller (5–10 K). With

increasing temperature, according to the percentage of filling, the pressure increases (Figure 48.32). Under working conditions it is ca. 100–150 MPa. A rupture disk in the pressure tubing at the autoclave seal prevents hazardous pressure increase.

During heating and cooling of the autoclave at pressures below ca. 80 MPa the system passes through a region of retrograde SiO₂ solubility. Above 80 MPa the solubility increases with temperature and pressure (Figure 48.33). The mineralizers increase the SiO₂ solubility, e.g., at 673 K and 100 MPa from ca. 0.15% for pure water to about 2–3%; the solubility is approximately proportional to the mineralizer concentration [473]. Concentrations of NaOH or Na₂CO₃ above 2 mol/L can lead to deposition of water glass at the bottom of the autoclave.

Figure 48.33: Solubility of SiO₂ in H₂O [473].

In the nutrient section SiO₂ goes into solution. Saturation, however, is not reached because the density of the solution is lower than that of the cooler solution in the seed section, and it therefore rises. Above the baffle it is cooled and becomes supersaturated with SiO₂, which deposits on the seed, which starts growing. The solution in the seed section has a higher density and sinks through the baffle into the nutrient section where it is heated and becomes subsaturated. It dissolves SiO₂ from the nutrient chips, ascends, and so on in a permanent density-difference driven circulation

until all nutrient is transported to the growing crystals.

The effective nonequilibrium distribution coefficient is defined as

$$k_{\text{eff}} = C_{\text{act}}/C_{\text{liq}}$$

where C_{act} is the actual trace element concentration in the solid, and C_{liq} the actual trace element concentration in the liquid. For $k_{\text{eff}} > 1$ the trace element impurities accumulate in the solution [474] and the cultured quartz bars are of higher purity than the nutrient. Doping with special components changes the trace element chemistry. For example, doping with LiF improves the electrical quality of quartz.

Increasing p , T , and ΔT increases the rate of SiO_2 transport and quartz growth. However, the high-temperature strength of the autoclave alloy limits p and T , and transition of convection from laminar to turbulent or even cellular flow restricts ΔT . Increasing face instability [474] and defect concentrations (channels, inclusions, dislocations) with increasing transport rates are further limiting factors.

The corrosion of the steel autoclave alloy is inhibited by formation of a dense coating of microcrystalline akmite, $\text{NaFe}^{3+}[\text{Si}_2\text{O}_6]$, and traces of emeulsite, $\text{LiNa}_2\text{Fe}^{3+}[\text{Si}_6\text{O}_{15}]$, on the inner wall. These minerals may also be found as inclusions in the crystal bars.

The duration of growth runs varies between 1 and 4 months, depending on the growth conditions. An autoclave with 250 mm inner diameter and an inner length-to-diameter ratio of 12 gives a yield of ca. 100 kg of quartz bars per month. The loss by removal of seeds from the bars is ca. 20%. Part of the cutting waste is used in the jewelry industry [475]. Growth parameters, which determine yield and quality of cultured quartz, are complexly coupled [476].

Maximum dimensions and yield capacities of autoclaves are summarized in Table 48.12.

Table 48.12: Dimensions and yield capacities of autoclaves for cultured quartz.

	Inner diameter, cm	Inner length, m	Inner volume, L	Yield per run, kg
Japan	65	13	4500	2000
USA	40	4.5	560	250

Worldwide quartz bar production in 1985 was ca. 1760 t (gross), i.e., 1410 t (net) after deduction of seed losses.

The largest production capacities exist in Japan and in the United States. Smaller capacities exist in Europe, Brazil, China, and South Africa. For 1992, growth capacities are estimated at 1400 t in Japan, 2300 t in the western world, 600 t in the CIS, and 300 t in China [475].

Small amounts of colored quartz [477, 478] for jewelry are cultured in the C.I.S. While blue (Co) and light green and yellow (Fe) quartz become colored in the growth process, the Al and Fe color centers for smoky quartz and amethyst must be activated by γ -irradiation after growth. The seeds for the first three color variations are Z-plates, whereas for smoky quartz and amethyst X-plates cut parallel to {0111} are used because of face-specific incorporation requirements of the dopants.

Filter and oscillator quartz must be free of twinning and of low defect concentration. Structurally incorporated impurities are determined by chemical trace analysis. Impurities that produce paramagnetic defects can be detected by electron spin resonance spectroscopy [479]. Dislocations produce diffraction contrast in X-ray topography [480, 481]. Water is determined by IR spectroscopy [482]. Inclusions are recognizable with X-ray diffraction, under the polarizing light microscope (PLM), and can be analyzed with an electron microprobe [483]. Brazil twinning can be seen with PLM, but Dauphine twinning can only be made visible by etching. Both types of twinning can be detected by X-ray topography [484, 485]. The quality of single-crystal quartz for vibrator uses is described by the electromechanical Q -value. Analogous to an electronic circuit resonating with the same frequency, this dimensionless quality-factor is defined as:

$$Q = \frac{2\pi fL}{R}$$

where f is resonance frequency, L inductance, and R resistance [486].

Q increases with decreasing energy loss due to relaxation and internal friction. The slower the decay of the vibration amplitude after cutting off the excitation, the higher is Q . A correlation exists between the IR absorptions of the structural OH groups at 3580 and 3410 cm^{-1} and the vibrational quality of quartz [487]. Therefore, an optical quality value a is defined that is derived from the absorption coefficients at 3580 and 3410 cm^{-1} and which is inversely proportional to Q .

Quartz with high Q is obtained by slow growth in the {0001}-sector (c- or Z-seed growth with Na_2CO_3 solutions).

In 1921 Cady described the first oscillator for generation of stable frequencies, cut from a natural quartz single crystal [488]. Today the uses of oscillator quartz are diverse and expanding (Figure 48.34), so that a comprehensive and detailed treatment cannot be given here. Electronic quartz component devices are principally used as filters, oscillators, timers, and sensors. Optical-grade quartz is used as a low-loss light transmitter. Cultured optical-grade quartz retains high transmissivity further into the UV and IR than natural quartz or silica glass. Whereas poly(vinylidene fluoride) layers are competing increasingly with quartz for piezoelectric devices, the importance of quartz as oscillator is unchallenged in applications such as high-sensitivity thermometers, thickness-measurement devices for vapor-deposited layers, in integrated circuits, microprocessors and synthesizers, and in color television, video and other communication systems.

Radiation, for example in space or from uranium or thorium impurities, affects the oscillator frequencies by action on alkali metal impurities. Therefore, quartz is cultured to extreme purity and the alkali metals are removed (swept) electrolytically after growth.

Electronic applications of cultured quartz are treated in [485, 488, 489]. Demand for quartz oscillator devices has increased from ca. 10^9 pieces in 1985 to 1.75×10^9 in 1989; for 1993, a demand of $(3-4) \times 10^9$ is estimated. Natural single-crystal quartz is now used only for a few special applications.

Despite the increasing demand, growth capacities are not markedly increasing because of improved cutting techniques, increasing miniaturization of oscillator devices, and the use of photolithographic etching. Quartz tuning forks for wrist watches are mass produced by this technique. Photolithography produces very high accuracies, allows any shape to be etched from large wafers, and lowers production costs.

Costs of cultured quartz in 1990 in \$/kg were [490]:

Y bar, as grown	60
Premium Q quartz	210
Optical-grade quartz	600
Swept, ultrapure quartz	1600

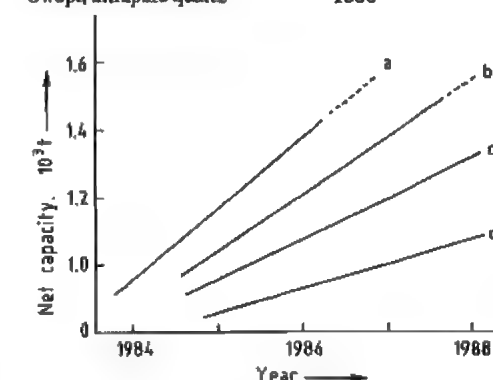


Figure 48.34: Net capacity (after seed removal) and usage of cultured quartz, Western world: a) Net capacity; b) Total usage; c) Oscillator usage; d) Optical usage.

Refractory Silica

By definition refractory silica must contain $\geq 93\% \text{SiO}_2$ [491].

Production. Silica bricks, containing 96–98% SiO_2 , are manufactured from mixtures of ground quartz arenite and quartzite in a mass ratio which keeps transformation during firing not too fast (arenite) and not too slow (quartzite). 1–3% CaO is added to the batch as milk of lime or as portlandite powder ($\text{Ca}(\text{OH})_2$), which, in combination with a soda-iron-silicate flux frit, acts as a transformation activator (mineralizer) and sintering aid. The batch is plastified, normally with 2% of thickened sulfite lye, to facilitate shaping by pressing, tamping, or hand molding and, in combination

with the lime, to give sufficient strength to the shaped and dried bodies in the green state. The batch must be very low in alumina ($< 1\%$); 9% of Al_2O_3 [492] lowers the melting temperature by ca. 140–180 K. Other impurities from the raw material are TiO_2 , Fe_2O_3 , Na_2O , and K_2O . Superduty silica bricks contain $< 0.5\%$ ($\text{Al}_2\text{O}_3 + \text{TiO}_2 + \text{Na}_2\text{O} + \text{K}_2\text{O}$) and ca. 3% CaO . Al_2O_3 here may be completely replaced by MgO and MnO . The bricks are fired in annular, chamber, or tunnel kilns at ca. 1725–1875 K. A firing cycle in a tunnel kiln takes 7–14 d. During firing an intergranular alkali calcium iron silicate partial melt forms (Figure 48.35), dissolving SiO_2 from the quartz grains and precipitating cristobalite and tridymite. Simultaneously, quartz is transformed into cristobalite in the solid state. At the beginning of firing the amount of cristobalite increases, but with time under the action of the mineralizers it is transformed into tridymite [494, 495]. The cold brick consists of nearly equal amounts of cristobalite and tridymite, residual quartz, and a glass phase (the frozen partial melt) from which wollastonite, CaSiO_3 , magnetite, Fe_3O_4 , calcium ferrite, CaFe_2O_4 , and dendritic cristobalite have crystallized.

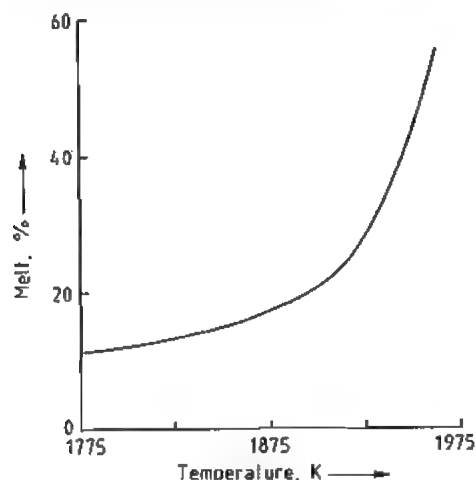


Figure 48.35: Fraction of Al-Ca silicate partial melt in the system Al_2O_3 - CaO - SiO_2 , with 1% Al_2O_3 and 2% CaO , as function of temperature [493].

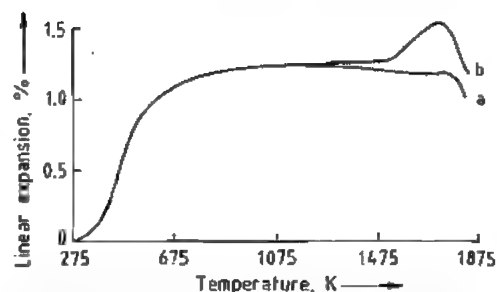


Figure 48.36: Thermal expansion of refractory silica bodies: structural volume change due to displacive (low temperature) and reconstructive (high temperature) transformations of silica polymorphs and microstructural volume change due to formation of microcracks [498]: a) $< 0.5\%$; b) ca. 5% residual quartz.

The crystalline phases in refractory silica are determined quantitatively by X-ray powder diffraction. This, however, is complicated by the extreme microcrystallinity of cristobalite formed in the solid state, the varying degree of stacking disorder of cristobalite and tridymite, and the diffuse background scattering from the glass phase, which can lead to wide error limits [496, 497]. An excess of residual quartz after firing must be avoided because of the volume increase (after-expansion) (Figure 48.36) that occurs when it is transformed into cristobalite tridymite during use. A small amount of quartz (1–5%) may be desirable for increasing the strength of a furnace vault, for example, by generation of compressive stress.

Properties. In comparison with fireclay products, refractory silica has outstanding high-temperature strength. This high load-bearing capacity enables its use under load up to 1920 K; super-duty bricks can be used up to 1980 K. Refractory silica does not shrink during use, and above 850 K it has excellent thermal shock resistance due to its very low thermal expansion. Thermal conductivity is low; it can be increased by admixture of SiC .

Silica bricks are highly resistant to attack by acidic iron silicate melts but they dissolve readily in glass melts. The open porosity varies between 15 and 25 vol%. Superduty bodies are less porous and less permeable to gases.

Table 48.13: Specifications for coke oven silica bricks.

Type	Open porosity, vol %	Component, %					Compression strength, MPa
		SiO_2	Al_2O_3	Fe_2O_3	CaO	$(\text{Na}_2\text{O} + \text{K}_2\text{O})$	
Low density	≤ 24.5	> 94.5	≤ 2.0	≤ 1.0	≤ 3.0	≤ 3.5	≥ 28
High density	≤ 22.0	≥ 94.5	≤ 1.5	≤ 1.0	≤ 3.0	≤ 3.5	$\geq 35-45$

Table 48.14: Physical forms of quartz raw materials.

Name	Formation and properties	Remarks, synonyms, and trivial names
Idiomorphic quartz	freely grown, euhedral faced, monocrystalline, possibly twinned, transparent colorless or smoky to dark brown or black	rock crystal, smoky quartz
Lump quartz	fragmented, anhedral, monocrystalline, may be twinned, transparent, colorless, smoky, milky, or white	chunk quartz, lascas, brazil pebbles, lump silica
Quartz pebbles	weathering product from quartz veins, worn by action of water, smoothly rounded, mono- or polycrystalline, transparent to white or yellowish white or gray	if transparent: rhinestone or rheinkiesel, grain size 2–60 mm
Granular quartz	xenomorphic product of natural (weathering) or industrial processing from granitic-pegmatitic rocks, monocrystalline, may be twinned, transparent to translucent, yellowish, gray, or smoky	grain size 0.5–1 mm [503]
Quartz sand	unconsolidated, wind- or water-eroded and transported weathering product of fragmental rocks, grumpled into mono- or polycrystalline grains, rounded or angular anhedral, the majority of grains are discernible with the naked eye, white to yellowish in bulk, in the individual grain transparent to translucent	silica sand, grain size 0.06–2.0 mm
Quartz powder	unconsolidated product of grinding or milling of coarser quartz, individual grains not discernible with the naked eye, white opaque in bulk	quartz flour, silica powder, silica flour, grain size 0.002–0.06 mm
Quartz rock	consolidated by intergrowth of grains or by cementation of grains by quartz	see text and Table 48.11

The principal disadvantage of silica bricks arises from displacive transformations of the SiO_2 polymorphs below 850 K (Table 48.8 and accompanying volume increase (Figure 48.36), which produces internal stress, cracking, and spalling unless extreme care is taken during heating and cooling in the range between ambient temperature and 850 K.

Uses of silica bricks include sprung arches of open-hearth furnaces, covers of electric furnaces, roofs of glass tank furnaces, blast preheaters, and coke and gas ovens [499, 500]. Specifications for coke oven silica bricks are listed in Table 48.13. Unshaped masses of refractory silica are used for monolithic constructions and repairs.

Cristobalite sand is produced from quartz sand in rotary furnaces at 1800 K, and cristobalite powder from flint in shaft furnaces with subsequent grinding. They are used as refractory mortars and ramming mixes in ceramic kilns and for blending with quartz or other mineral sands for various uses (e.g., in found-

ries). Heat-insulating lightweight (up to 60% porosity) silica refractories are produced by including a sufficient quantity of material that burns off during firing (e.g., sawdust, cork, fruit seeds, olive oil cake). Diatomaceous earth can also be used as raw material and already has a high porosity. Burned diatomite consists of about 80% crystalline silica—mainly cristobalite with some quartz and is an extremely lightweight heat-insulating material for use at temperatures up to 1200 K.

48.7.2 Quartz Raw Materials

48.7.2.1 Physical Forms and Occurrence

The range of quartz raw materials in nature is vast. Table 48.14 describes the physical forms of quartz raw materials [501–506].

Quartz gravel and sand are the most important raw materials on a volume basis; the construction industry consumes about 95% of

production (ca. 65% structural and ca. 30% civil engineering).

The main characteristics for quartz raw materials are chemistry, mineralogy, physical properties, and cost. Increasing demand for extremely pure quartz for silica glass production and in the quartz-oscillator industry, and the growing use of refined grades in many other industries makes consistency and long-term availability important [505].

Impurities and their accessibility to beneficiation processes are of major importance. In most cases, trace element analysis gives bulk composition and no information about the localization of impurities in the microstructure. Microstructural information, however, is es-

sential for choice of quartz processing methods. Figure 48.37 shows the principles of impurity distribution in a crystal.

Tripoli (see Table 48.11) contains ca. 98–99% SiO_2 . It occurs in sedimentary strata as a natural leaching product of calcareous cherts or siliceous limestones. White tripoli is low in iron impurities ($< 0.1\% \text{Fe}_2\text{O}_3$); "rose" or "cream" tripoli contains up to $1\% \text{Fe}_2\text{O}_3$. The quartz crystallites are submicroscopic; tripoli particles of $10\text{--}70 \mu\text{m}$ are crystallite aggregates. Southern Illinois (white) tripoli has the composition (%): SiO_2 99.5, Al_2O_3 0.009, Fe_2O_3 0.025, CaO 0.15, TiO_2 0.005.

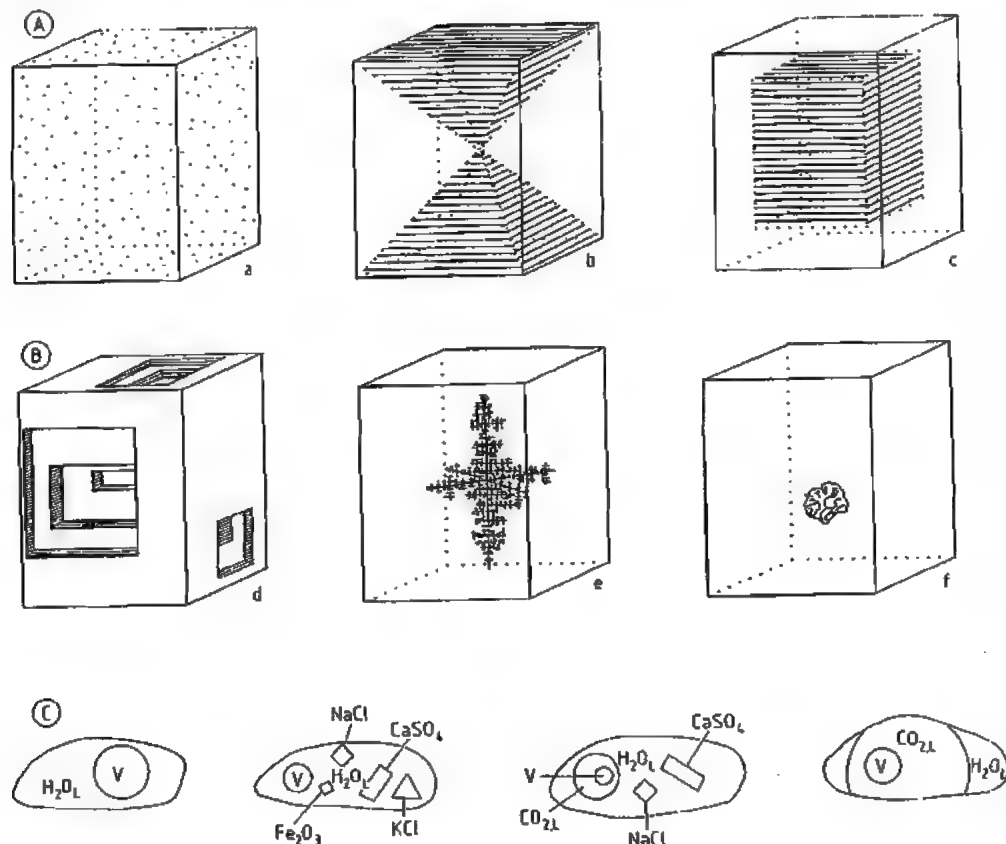


Figure 48.37: Principles of impurity distribution in a single crystal. A) Structural incorporation: a) Random; b) Growth sector specific; c) Zonal. B) Microstructural inclusion: d) Skeletal growth; e) Dendritic growth; f) Accumulated and accidental growth. C) Types of fluid inclusions in quartz [512]: V = vapor, L = liquid in the system $\text{H}_2\text{O}\text{--}\text{CO}_2$ (for other systems, e.g., $\text{H}_2\text{O}\text{--}\text{CO}_2\text{--}\text{CH}_4$, see [508]). Squares, rectangles, and triangles represent crystals.

Chalcedonies (Section 48.7.1.2) are classified according to their deposition as wall-banded CH-W or horizontally banded CH-H and according to the optical character of fiber elongation (chalcedony CH-W_{LF} or -H_{LF}; quartzine CH-W_{LS}). Chalcedony occurs in various geological environments, filling veins, vugs, and vesicles of magmatic volcanites and sediments [513].

In reflected light chalcedony CH-W is translucent bluish gray (or brownish if impregnated in nature with ferrous humic acid waters); CH-H is milky to white opaque, depending on the content of opal-CT [514].

The translucent CH-W possesses an open microporosity which makes it impregnable (e.g., with coloring solutions) and allows penetration of liquid impurities. However, the microstructure is monomineralic and of high toughness, which makes it a good material for milling devices and bearing stones.

CH-W_{LF} is slightly softer than CH-W_{LS}. Therefore, during use CH-W_{LS} layers which are always present, form a raised abrasion relief. However, since the resistance of CH-W_{LF} to etching with HF is higher than that of CH-W_{LS}, etch levelling is possible. CH-H has al-

most no open porosity, the space between the chalcedony spherulites (Table 48.9) being filled with opal-CT. The abrasion resistance of CH-H is low.

48.7.2.2 Processing

Impurities that are structurally incorporated in quartz are very difficult or impossible to remove. However, included impurities and those that form surface films can be removed by appropriate processing measures.

Purity grades of processed natural quartz raw materials are [503]:

Grade	Impurity content (ppm)
Low	> 500
Medium high	300–500
High	2–50
Ultrahigh	1–8

Processing of coarse monocrystalline quartz to lumps or lascas [503]:

- Removal of grown surfaces and visible adhering foreign minerals with a hammer (ca. 50% loss in mass)
- Size reduction to lumps or lascas (weight specification for lascas ca. 15–50 g)

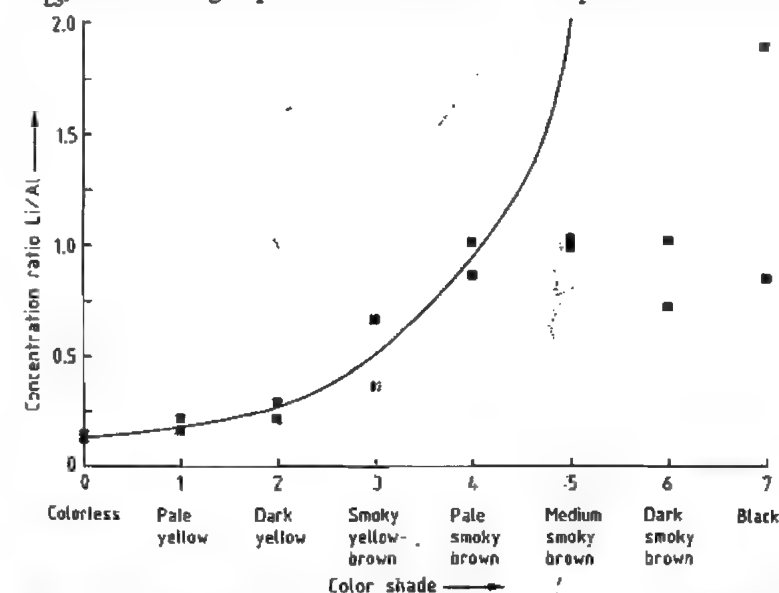


Figure 48.38: Irradiation (γ -radiation, dose 1 Mrad) color and Li/AI concentration relationship for initially colorless first-grade lascas (Minas Gerais, Brazil) [503].

- Sorting out of pieces with visible inclusions and for different transparency grades under visible light in water as immersion medium

- Sorting out of fluorescing pieces (inclusions of transparent and colorless foreign minerals and glass fragments)

Product: Various grades of lascar

The impurity content (ppm) of Arkansas-lascas of grade 1 (clear, free of crystal surfaces) and grade 4 (white opaque) is [505]:

	Al	Fe	Mg	Ca	Li	Na	K	Ti
Grade 1	15	2	1	1	1	2	2	25
Grade 4	20	5	1	1	1	25	10	64

Irradiation-aided processing of lascar [503]:

- γ -Irradiation (^{60}Co) with doses ≥ 1 Mrad [515]

- Color sorting of pieces with irradiation activated Al- and Fe-color centers. Irradiation color and depth is mainly a function of the Li/Al concentration ratio [503] (Figure 48.38)

- Thermoluminescence sorting

Product: medium high to high purity grade lascar

Processing of quartz lascar to granular quartz [503]:

- Cold washing in counterflow with aqueous 2% HF solution

- Heating to > 850 K (transformation into high quartz)

- Quenching in cold deionized water (fracturing by thermal expansion shock)

- Sorting out of red, iron-colored pieces and pieces with rutile-inclusions on a conveyor belt under visible light

- Grinding and sizing

- High-field magnetic and dielectric separation [516]

- Chlorination at ca. 1300 K to remove metal impurities and burn out organic impurities

Product: high purity grade granular quartz. Prices of processed quartz materials are listed in Table 48.15.

Table 48.15: Prices of processed quartz raw materials in January 1989 (in 1992, prices for lascar and granular quartz were about four times higher) [517].

Commodity	Grade	Price, DM/kg
Quartz sand	98.5% SiO_2	0.06*
Lump vein quartz	99.9% SiO_2	2.40
Lascar	99.9–99.997% SiO_2	
milky white	IV	1.50
dull milky	III	2.50
translucent	II	4.00
transparent	I	7.00
water clear	extra	10.00
Granular quartz (100–300 μm)	glass tank, optical	1.50
	lamp tubing	4.00
	semiconductor	7.00
	low alkali (LA)	10.00

* Prices increase by factors of 2–10 with decreasing impurity content.

Processing of quartz from feldspar-pegmatite [503]:

- Crushing and grinding

- Multistage flotation to separate mica, garnet and feldspar; reflation of the quartz tailings

- High-field magnetic separation

Product: medium high grade granular quartz (e.g., Quintus quartz from Spruce Pine pegmatite, North Carolina, United States, non-volatile impurity level < 400 ppm Si).

Worldwide capacity for production of granular quartz is ca. 17 000 t/a with more than 50% in the United States, with ca. 6000 t from Spruce Pine, North Carolina alone [517].

Processing of medium high purity quartz to high-purity quartz [503]:

- Sizing into 5 grain fractions and further processing of the individual fractions

- Acid (HF , HCl , H_2SO_4) leaching until HF is completely converted to fluorosilicic acid

- Elutriation by washing and decanting with deionized water until pH ≥ 6 is reached, and the suspended fine particles are removed

- Vacuum drying

- High-field magnetic separation

- Blending of the 5 fractions

- Treatment with HCl gas at ≥ 1400 K to remove metal impurities and water

Table 48.16: Analyses and prices of various IOTA quartz grades [503, 517].

Grade	Analysis, ppm								Price, \$/kg	
	Al	Fe	Ti	Mg	Ca	Li	Na	K	1989	1992
Lamp tubing (LT)	32.9	3.1		0.1	4.6		5.9	5.8	2.0	2.5
Standard (ST)	17.7	0.7	1.1	0.1	0.5	0.6	1.0	0.6	2.3	2.57
4	6.8	0.3	1.5	0.1	1.0	0.2	1.0	0.4	3.5	4.52
6	6.8	0.1	1.0	< 0.05	0.4	0.1	0.1	0.1	6.0	9.5

Product: high-purity granular quartz (e.g., IOTA quartz, impurity level < 30 ppm Si)

Trace element analysis (ppb) of high-purity granular quartz grades [517]:

Grade	Li	Na	K	Mg	Ca	Si
IOTA-6	100	100	100	< 50	400	< 50
Low-alkali	< 20	< 40	< 40	< 100	< 400	

Grade	Al	Ti	Ge	Zr	P	V
IOTA-6	6800	1000	600	100	< 50	< 50
Low-alkali	< 8800	< 1800	< 40	< 100	100	

Grade	Cr	Mn	Fe	Co	Ni	Cu	Zn
IOTA-6	< 50	< 50	100	< 50	< 50	< 50	< 50
Low-alkali	< 50	< 50	< 500	< 10	< 50	< 50	< 50

Analyses and prices of various IOTA grades are listed in Table 48.16.

Processing of quartz gravel:

- Separation of sand, blending with a given fraction of sand

- Washing to remove clay minerals

- Separation of residual sand

- Sizing and drying

Product: filter pebbles

Beach pebbles are already processed by nature (*product:* milling stones).

Processing of quartz sand [518, 519] varies depending on required grade. Important steps in the wet process are:

- Purification washing to remove loosely adhering impurities

- Friction washing (attrition), crushing and cleavage of agglomerated grains in acid (pH < 3 , H_2SO_4) or alkaline (pH 10, Na_2CO_3) water, rubbing off strongly adhering impurities (iron oxides, clay minerals)

- Screening Multistage flotation to remove a) micas; b) hematite, magnetite, rutile, andalusite, etc.; c) feldspars

- Chemical beneficiation with aqueous sulfuric and oxalic acid solution or dilute HF solution. Chlorination with HCl gas at ca. 600 K

- Physical beneficiation, magnetic and electrostatic separation of iron contaminants and feldspars

Products: quartz sand, various grades; sands for glass melting, foundry and chemical products.

Quartz powders are produced by dry grinding in encapsulated nodular-chert-lined mills with flint or corundum pebbles.

Processing of quartz rocks includes breaking, milling (with quartz rock lumps and steel balls), sieving, washing, and sizing [518, 519].

Biological removal of iron impurities with cultures of acid producing bacteria or fungi (e.g., *Aspergillus niger*) on a nutrient of molasses is discussed in [520].

48.7.2.3 Uses

Important uses of quartz raw materials or semifinished materials are listed below [505]:

Use	Raw or semifinished material
Abrasives and grinding media	sand, powder, tripoli, novaculite
Ceramics	quartzite, quartz-cemented sandstone, sand, powder
Chemicals	sand, powder
Construction of buildings and roads	gravel, sand, powder, quartzite, sandstone
Fillers, extenders	powder, tripoli
Filters	gravel, sand
Foundry	sand
Gems	monocrystalline quartz, chalcidony, agate chert
Glasses, enamels, glazes	sand, powder
Hydrothermal growth of quartz	lump quartz, granular quartz
Metallurgy	quartzite, sandstone, sand, powder
Milling	silex, chalcidony, flint, quartzite

Use	Raw or semifinished material
Optical and oscillator devices	monocrystalline cultured and natural quartz
Silicon metallurgical grade, silicon alloys	lump quartz, quartzite, quartz-cemented sandstone
Vitreous silica	lump quartz, granular quartz, sand
Well fracturing	sand

Abrasives and Grinding Quartz. Quartz sand and powder are used for grinding, scouring, and polishing. The conchoidal fracture, hardness, and brittleness provide and maintain during use particles with sharp cutting edges. The use of quartz in sandblasting is decreasing due to health hazards. Quartz sand is also of declining importance for sandpaper. Quartz powder is utilized in abrasive soaps and in scouring powders. Sandstones are used for grinding. Tripoli is friable, with a grain size of 0.1–5 μm , and its grains have no sharp edges. Tripoli grades with 98–99% SiO_2 are used for polishing [521]. Novaculite from Arkansas and Missouri, United States, has a microstructure of minute angular quartz grains with open porosity. It is used as oil-soaking whet- and honing stone. Whetstone grades range in porosity from 0.1 to 15% [521].

Ceramics. Batches for stoneware, porcelain, fireclays, and aluminum silicate refractories contain quartz as a nonplastic filler and glass former. White-burning, low-iron quartz powders produced from sand, flint, or quartz rocks (quartzite, novaculite) are used. Flint is calcined before grinding. In pottery and earthenware, quartz sand and powder act as nonplastic fillers [522].

Chemicals. A wide range of chemicals is produced from quartz. Here, only two important products that are representative of different reaction processes and reaction temperatures are mentioned.

Sodium or potassium silicate from the furnace route are melted from quartz sand and the alkali metal carbonate. Usually the sand is of container-glass grade with $\leq 0.1\%$ each of Al_2O_3 and CaO and a very low iron content ($\leq 0.02\%$ Fe_2O_3). Very high purity products require sand with $\leq 0.02\%$ Al_2O_3 and CaO each.

Melting is performed in tank furnaces at ca. 1700 K [523].

Water glass from the hydrothermal route is produced in autoclaves by reaction of quartz sand with aqueous NaOH solution at ca. 430–500 K.

Silicon carbide is produced from crushed lump quartz or sand with the specification in %: 99.5 SiO_2 , $< 0.1 \text{ Al}_2\text{O}_3$ and Fe_2O_3 each, $< 0.01 \text{ CaO}$, $< 5 \text{ H}_2\text{O}$ by reaction with coke and some ingredients at ca. 2300 K. Production of 1 t SiC requires ca. 1.5 t SiO_2 .

Construction of Buildings and Roads. Quartz sand is an integral part of mortar; quartz sand and gravel are additives for portland cement and asphalt. Tripoli is used as an inert filler and extender in asphalt.

Quartz sandstone, with various cementing materials and colors, and quartzite have long been used as building stones [524]. Bricks and tiles are fired from mixtures of quartz sand and clay. Since the early 1900s hydrothermally hardened lime-silica bricks (synonyms: calcium silicate bricks, sand-lime brick) have developed rapidly as building materials [525]. Quartz sand is reacted with hydrated lime and various additives in an autoclave at ca. 500 K and ca. 16 bar H_2O pressure. One of the essential process parameters is the grain-size distribution of the sand. Films of clay mineral or iron oxide on the quartz grains slow down the reaction of quartz with hydrated lime. The hardening reaction forms calcium silicate hydrate phases with very high water contents. This gives the material a high heat capacity, but the heat insulating capacity is low. It is increased by addition of slag granules or coal ash (power plant by-products).

Fillers and Extenders. Quartz powder and tripoli act as hard, inert fillers and extenders in paints and coatings, plastics, and rubbers. In paints quartz increases the resistance to acids and improves flowability, durability, and wear resistance. In plastics compressive and flexural strength and resistance to thermal shock and heat are improved. The insulator character of quartz and its surface leakage current resistivity make quartz fillers valuable for epoxy

resin encapsulation of electronic devices and for filling and fixing of coils. Quartz is used as a filler in rubbers instead of carbon black when colors other than black are required. In tire linings it gives improved heat aging, adhesion, and tear strength.

Filters. Quartz pebbles, preferably monocrystalline, and sand are the main filter materials for drinking water purification and softening.

Foundry Technology [504, 518, 519, 526]. Quartz sand is used in molds and cores. Refractoriness (i.e., the temperature at which sintering begins; ca. 1500–1700 K, depending on content of feldspar), thermal shock resistance, cohesiveness in the moist state, and high-temperature strength are the most important properties. For cast iron the mold must contain $\geq 85\%$ SiO_2 and for steel castings, $\geq 95\%$. Granulometric factors such as particle-size distribution, grain shape, state of grain surfaces, and surface area are also important. Coarse sand with low surface area requires less binding agent (usually montmorillonitic clay). Monocrystalline well-rounded grains ensure good permeability to gases evolved during casting. Mold surfaces made of fine sand give smooth molding surfaces that do not require machine finishing. The sands may naturally contain enough clay minerals for good mold strength, or require addition of binders, which increases costs.

Table 48.17: Quartz raw materials for glasses and enamel frits.^a

Glass type	Raw material	Composition, %							Grain size range ^b , mm
		SiO_2	Al_2O_3	Fe_2O_3	Cr_2O_3	Na_2O	K_2O	H_2O	
Optical and optical-thalamic ^c	sand, powder	99.7–99.9	0.02–0.05	0.004–0.0025	0.00005–0.0001	0.005–0.006	0.003–0.008	0.08–0.11	0.125–1 (mean 0.25)
Borosilicate	powder	99.88	0.04	0.013	0.0003	0.004	0.009	0.006	0.125–1 (mean 0.25)
Flat	sand	98–99	0.2–1.6	0.02–0.2				$\leq 5^d$	0.16–1 (mean 0.25)
Colored container green	sand	≥ 98.5	1–6	≤ 0.3			≤ 53		0.16–1 (mean 0.25)
brown	sand	≥ 98.5	1–6	≤ 1			≤ 53		0.16–1 (mean 0.25)
Enamel	powder	≥ 97.5	≤ 0.6	≤ 0.2					

^a Variation must be $\leq 0.03\%$ of the value; grains of difficultly dissolving accessory minerals (e.g., chromite, sillimanite, corundum) must be avoided or $\leq 0.2 \text{ mm}$.

^b MgO , CaO , TiO_2 : a few ppb.

^c Water aids melting.

Specifications for foundry sand grades of different refractoriness:

Beginning of sintering, K	> 1775	1575–1775	< 1575
Quartz, % (rest: feldspar and clay minerals)	> 99	95–99	< 95

Glasses, Enamels, and Glazes [505, 511, 523, 527–530]. Different types of glasses and enamels require various grades of quartz raw materials. The silica content of glazes is mainly supplied by the silicate ingredients (feldspar, clay). If additional SiO_2 is required, quartz or flint powder is added. Table 48.17 gives information on physical forms and grades of silica for glasses and enamel frits.

Hydrothermal Growth of Quartz [503]. Brazilian lascas were used worldwide as nutrient chips until the Brazilian quartz embargo 1974. Since then many other sources for high-purity low cost lump quartz and granular nutrient have been opened up. Iron plus aluminum impurities of $\leq 50 \text{ ppm}$ are allowed.

Metallurgical-Grade Silicon and Silicon Alloys. For chemical- or metallurgical-grade silicon, quartz lumps or pebbles (25–150 mm) are reduced with coke in electric-arc furnaces. The lumps and pebbles must not decrepitate during heating and therefore should preferably be monocrystalline and free of fluid inclusions. The grade of quartz raw material depends on the required grade of the products. Metallurgical-grade silicon with 99.0% Si requires (in %): $\geq 99.0 \text{ SiO}_2$, $\leq 0.2 \text{ Al}_2\text{O}_3$, $\leq 0.1 \text{ Fe}_2\text{O}_3$, $\leq 0.1 \text{ MgO}$ and CaO each, $\leq 0.02 \text{ TiO}_2$.

Low-grade silicon (98 % Si) for steel and aluminum production needs quartz with (in %): $98 \text{ SiO}_2, \leq 0.4 \text{ Al}_2\text{O}_3, 0.2 \text{ Fe}_2\text{O}_3, \leq 0.2 \text{ MgO}$ and CaO each, $\leq 0.1 \text{ P}_2\text{O}_5, \leq 0.002 \text{ TiO}_2$.

Production of 1 t metallurgical-grade silicon requires ca. 2.5 t of quartz. The worldwide silicon production is ca. 650 000 t/a.

Metallurgy. Quartz in the form of lumps or granules of vein quartz, quartzite, or sandstone is used as flux in smelting metal ores, for slagging iron oxides and basic oxides, and for balancing the silica/lime ratio of blast furnace burdens. In both cases the SiO_2 content must be > 90 % with lumps and granules in the size range of 0.8–2.5 cm.

For welding fluxes quartz powder is used with controlled grain-size distribution ≤ 0.25 mm with an average of 0.06 mm for coated standard electrodes. The size for quartz particles in agglomerated fluxes must be < 0.06 mm.

Milling. Nodular chert (silex) and very finely crystalline quartzite with > 96 % SiO_2 and homogenous microstructure serve as linings for mills. Rounded flint nodules are preferably used as grinding pebbles.

Belgian silex consists of chalcedonic silica with evenly distributed calcite as secondary mineral phase and represents a material with high overall toughness. Yugoslavian silex has a coarser microstructure and sometimes contains coarse quartzite, but is nevertheless of very good durability. Quartzite can only be used if it is free of accessory minerals. Translucent iron-free chalcedony from agates is used in ball mills and mortars for size reduction of high-purity quartz and silica glass.

Quartz for Optical and Oscillator Devices. Natural monocrystalline idiomorphic quartz is preferably used for optical devices as wafer

plates, Brewster windows and prisms, birefringent filters, and tuning elements for laser optics. Only small amounts of cultured quartz are used in these applications. Oscillator quartz devices, however, are almost exclusively made from cultured quartz, for reasons of quality (low damping) and cost advantages.

Vitreous Silica. Transparent silica glass is melted from lumps or granular quartz with an impurity content < 30 ppm, the latter being by far the most important feed. Translucent to white opaque fused silica is produced from quartz sand with an impurity content of ≤ 300 ppm Si. In both cases low aluminum- and iron-impurity levels are essential.

A titanium content indicates the presence of submicroscopic rutile crystallites, which cause bubble problems in transparent silica glass during tube drawing. Silica glass for semiconductor uses, if not produced from high-purity silicon compounds, must be very low in heavy metal impurities.

The impurity contents of quartz raw materials for various grades of vitreous silica are listed in Table 48.18.

Well Fracturing. For hydraulic fracturing of oil, gas, or geothermal wells a fluid with suspended quartz sand is pumped at high pressure into the well. Existing openings are enlarged and new voids created. When the fluid is withdrawn, the remaining sand holds the fractures open. Frac sand must have $\geq 98 \text{ % SiO}_2$ and well-rounded grains to make placement easier and to provide good permeability. It must consist of single crystalline grains which are clean and, in particular, free of adhering feldspar, clay, or carbonate minerals. The solubility in hydrochloric acid (a measure of the carbonate content) must be < 0.3 %. The content of soft particles must be < 1 %.

Table 48.18: Impurity contents of quartz raw materials for various grades of vitreous silica.

Glass grade ^a	Maximum impurity content, ppm														
	Al	Fe	Mg	Ca	Li	Na	K	B	P	Ti	Mn	Cr	Co	Ni	Cu
1	13	0.6	0.1	0.5	0.6	0.7	0.7	<0.1	0.2		0.1	0.08	0.01	<0.1	0.05
2	20–60	1–5	0.5–2	0.5–2	0.5–5	0.5–10	1–8			0.5–6				<1	
3	200	70	11	40	5	25	10			100				<1	

^a 1: Silica glass for semiconductor uses; 2: High-purity transparent silica glass; 3: White, opaque fused silica.

48.7.3 Kieselguhr

48.7.3.1 Introduction

The term kieselguhr (diatomite) refers to sedimentary rocks that are mainly composed of the skeletons of single-celled diatoms.

The low density, high porosity and thus high absorption capacity for liquids low thermal conductivity, and outstanding filtration properties make kieselguhr a versatile raw material [531–533].

Deposits with similar petrographic character or analogous physical properties, named according to their origin or area of application, include siliceous earth, "Bergmehl", "Saug-schiefer", "Polierschiefer", and tripolite, not all of which are true diatomites.

The designation "tripolite" is derived from the ancient name *terra tripolitana* (after the city of Tripolis). The name referred mainly to minerals used as grinding and polishing agents, but also as lightweight building blocks. Today, the term tripolite refers to extremely fine-grained quartz pelites of inorganic origin [534].

48.7.3.2 Formation, Composition, and Quality Criteria

Diatoms can be described as being almost "ubiquitous", occurring in marine, brackish and freshwater environments.

The plant organisms possess a silicified membrane and vary in size between several micrometers and ca. 2 mm (generally 10–150 μm).

The skeletons are composed of opal-like amorphous silica ($\text{SiO}_2 \cdot x\text{H}_2\text{O}$) and exhibit a wide range of porous fine structures and shapes. Including fossil forms, at least 15 000–20 000 different forms have been distinguished.

Rock-forming processes involving diatoms occurred worldwide from the Upper Cretaceous period onwards. Commercially exploitable deposits have been formed since the tertiary period.

The deposits are associated with sedimentation areas in which nutrients were abundant and the supply of silicates or dissolved silica was sufficient that a rich diatom flora developed and the frustules of the dead organisms accumulated to an appreciable thickness on the bed of the water body.

Such conditions are found worldwide, mainly in areas with volcanic activity, but also to a lesser extent in lakes with a largely decalcified environment and intensive chemical weathering of quartz sands or silicates (e.g., the German kieselguhr deposits) [534, 535].

Formation of diatomites of considerable thickness also occurred in marine coastal areas with continual subsidence, a periodical barrier to the open sea, and a regular supply of nutrients [536]. In addition, diatomites of brackish origin were formed in former saltwater lakes.

Important quality criteria for crude kieselguhr include the particle-size distribution, shape, and fine structure of the diatoms (Figure 48.39). However, these can be altered with regard to their structural framework (and porosity) by calcination (see Section 48.7.3.4) [537, 538], which is important for the various applications as filtration agents. Furthermore, the chemical and mineralogical composition plays an important role, since higher contents of certain components can limit economically viable processing and refinement of the crude product.

Apart from water and organic substances the most frequent additional components of diatomites are quartz, calcium carbonate, and clay minerals.

The content of water and organic substances is only of minor significance for quality assessment, since they can be removed by drying or calcination.

Quartz sands or other rock fragments of similar particle size can be removed by air classification. In this respect, the conventional specification of the SiO_2 content of a crude kieselguhr is not very informative. For the assessment of a diatomite it is not the total SiO_2 content which is decisive, but the content of opal (diatom skeletons).

Figure 48.39: Light micrographs of various kieselguhrs (diatom fraction). A, B) Lopoc, California, USA; C) Myvatn, Iceland; D, E) Munster-Breloh, Germany; F) Hetendorf/Hermannsburg, Germany; G) Neuohr/Unterlüß, Germany.

In contrast, the presence of fine-grained carbonates [CaCO_3 , $\text{CaMg}(\text{CO}_3)_2$] in amounts greater than 5–10 mol% is problematic because they form complexes during processing which adversely affect the filtration properties and lower the chemical inertness.

Clay minerals restrict the range of applications, but are advantageous for the production of insulating or refractory bricks or for use as powders.

Higher iron contents, particularly as pyrite or marcasite, require refinement by calcination (see Section 48.7.3.4). The color of the diatomites becomes reddish-gray or pink due to conversion into Fe_2O_3 . The filtration properties are hardly influenced, whereas the use as fillers can be affected considerably by this coloration. In the latter case, a Fe_2O_3 content of > 56% can already be a limiting factor.

48.7.3.3 Occurrence and Mining

Diatom deposits are distributed worldwide. Their economic exploitability and market potential depend on numerous factors such as mining conditions, and processing and transport costs. The size and quality of the deposit, exploitation costs, transport conditions as well as the question whether the kieselguhr is for a domestic market or whether it is to be exported play a significant role. In 1986, the world demand for kieselguhr was ca. 1.8×10^6 t/a [539].

The largest kieselguhr deposits in the world are found in the United States in the district of Lopoc, California. These are upper Tertiary (Miocene) marine deposits with an economically exploitable diatomite thickness of ca. 300 m. In addition, large quantities of marine and freshwater diatomites are mined in Georgia, Mississippi, Nevada, Oregon, and Washington. In 1986, the United States accounted for about one-third of world production (575 000 t), followed by Rumania, the CIS, and France, with outputs of $(246\text{--}272) \times 10^3$ t (1986). The production in Rumania and the CIS is almost entirely used in the building construction industry. Further, noteworthy deposits and production sites are located in Algeria, Argentina, Australia, Brazil, Germany, Iceland, Italy, Kenya, Korea, Mexico, Peru, and Spain, whereby in several of these countries the export of kieselguhr is of no significance [540]. Danish "Moler" is a clay-rich diatomite (diatomaceous earth), which is produced and exported in considerable quantities (63 500–72 600 t/a). It is used predominantly for the production of insulation materials (e.g., fire-resistant insulating bricks).

The only large, economically workable kieselguhr deposits in Germany are freshwater formations of Pleistocene age. They are situated on the edge of the Luneburger Heide in the area of Hetendorf/Hermannsburg, Neuohr/Unterlüß, and Munster-Breloh as well as in the Luhetal (Bispingen/Hützel/Schwindebeck). Here industrial usage began with the establishment of the first open-cast mine in 1863. Thus, German kieselguhr mining repre-

sents the earliest modern exploitation of this raw material. Up to World War I almost the total world requirement could be met, with an export quota of > 30%.

Kieselguhr is generally mined in open-cast mines, occasionally also by subsurface or underwater mining (Myvatn, Iceland). Mining by hand is now rare (Third World countries). Almost everywhere, modern, cost-effective mining methods are used, with excavators and wheel/ front loaders, and trucks or conveyor belts for transport.

48.7.3.4 Processing

Worldwide, the processing methods for crude kieselguhr differ only slightly from one another. The most important principle is minimization of mechanical damage to the structure of the diatom skeletons. Hollow forms should not be destroyed and pores not blocked (e.g., by sintering during calcination). The high porosity, the most important property of kieselguhr, must be retained. The processing steps are shown in Figure 48.40.

Preliminary size reduction of crude material is carried out with spiked rollers, charging boxes, or sieve kneaders to give a uniform grain size that ensures even heat transfer during further treatment. This is particularly important because of the low thermal conductivity of kieselguhr.

The following types of processed kieselguhr are produced.

Dried Kieselguhr. Depending on the climatic conditions at the production site, the crude kieselguhr from the deposits is either stored in the open for predrying or transported immediately to storage hoppers. Crude kieselguhr contains 30–65% water, which is removed in countercurrent driers. Simultaneous grinding and drying is also practiced, whereby preheated air is blown into the grinders. However, this is only possible for crude products with a low moisture content. Drying is followed by gentle grinding and screening. Granulation gives products that are used as absorbents (e.g., for oil) or as pet litter.

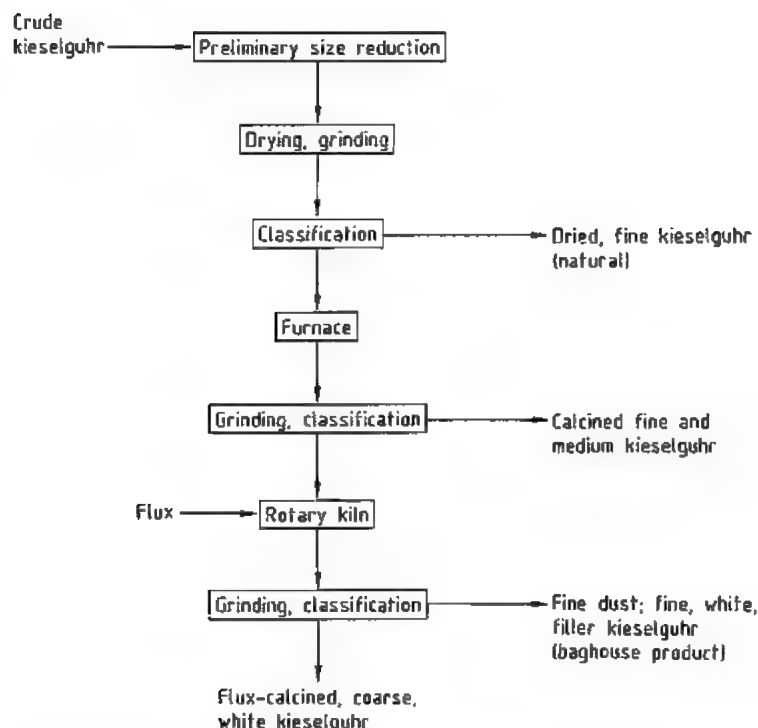


Figure 48.40: Kieselguhr processing.

Table 48.19: Chemical and physical properties of commercially available kieselguhrs.

Property ^a	1	2	3	4	5	6	7	8	9
Color	white-gray	yellow-brown	pink	yellow-brown	brown	white	white	white	yellow-brown
SiO ₂ , %	89.0	72.5	90.7	87.5	86.0	89.5	90.7	91.5	90.2
Al ₂ O ₃ , %	3.5	7.1	3.9	4.3	2.8	4.1	3.9	1.6	2.8
Fe ₂ O ₃ , %	0.9	5.0	1.4	2.9	4.7	1.6	2.1	0.7	2.5
CaO, %	1.1	1.2	0.5	1.9	0.6	0.5	1.0	4.4	0.7
Na ₂ O, K ₂ O, %	0.8	1.4	0.9	0.8	0.7	3.6	3.5	1.9	0.9
Ignition loss, %	2.0	4.7	0.5	0.7	0.3	0.2	0.1	0.1	0.4
Bulk density, %	107	290	120	140	125	229	200	195	209
pH value	7.0	5.2	7.3	6.9	7.0	10.0	9.7	9.5	6.7
Water uptake, %	255	200	250	205	201	156	160	200	196
Specific surface area, m ² /g	19.2	25.4	15.2	13.0	16.1	1.9	1.6	3.0	10.6
Average particle size, μm	14.2	19.3	15.9	14.1	13.9	22.5	30.1	6.5	14.7
Wet density, g/L	228	280	271	255	209	297	290	350	357
Permeability, Darcy	0.06	0.09	0.28	0.09	0.08	1.20	1.60		0.08
Crystalline content, %	2.0	2.2	7.6	9.2	9.8	58.1	59.7	62.7	10.3

^a 1) American filter kieselguhr, dried; 2) Danish filter kieselguhr, calcined; 3) American filter kieselguhr, calcined; 4) French filter kieselguhr, calcined; 5) German filter kieselguhr, calcined; 6) American filter kieselguhr, flux calcined; 7) French filter kieselguhr, flux calcined; 8) Spanish filter kieselguhr, flux calcined, very fine; 9) German regeneration filter kieselguhr, calcined.

If the starting material is of high purity and has a low content of organic substances, the dried kieselguhr can also be used as a filtration agent or catalyst support. These kieselguhrs

vary in color from white to yellowish or gray-brown, depending on their origin, and consist predominantly of amorphous silica with a low crystalline content (generally < 3 %).

Calcined Kieselguhr. To remove organic substances and alter the particle size, dried kieselguhr is calcined in gas- or oil-fired rotary kilns at 800–1000 °C. During calcination, the diatom frustules and their fragments are hardened and partially agglomerated by sintering. The degree of sintering can be controlled by altering the temperature and duration of the process. The kieselguhr is then ground and classified by cyclones and sorters into grades with different particle-size distributions (fine and medium calcined kieselguhrs). Iron impurities, present as Fe₂O₃ after calcination, color the products pink or yellowish to dark brown.

The old-fashioned furnaces with several decks, similar to pyrite-roasting kilns, are still used to a limited extent. They have the advantage of a slow calcination process at relatively low temperature which causes little damage to the structure. The kilns are loaded with moist crude kieselguhr, which is dried on the upper decks, calcined in the middle, and cooled on the lower decks.

Fluidized-bed drying and calcination processes were tested as early as the 1920s, but were unsuccessful due to technical problems. Nowadays modern fluidized-bed technology is also used for the processing of kieselguhr. Advantages include energy savings, short production times, mild treatment of the kieselguhr, and more compact design of the plants.

Flux-Calcined Kieselguhr. In this process, dried or calcined kieselguhr powder is calcined with the addition of alkaline fluxes. Sodium carbonate is generally used as flux in amounts of 1–6 %, either mixed with the kieselguhr before calcination or continuously added during calcination. The calcination temperature is 1000–1200 °C. The addition of sodium carbonate leads to the formation of a sodium silicate glass melt which binds the diatom frustules and their fragments into agglomerates. Since the iron contained in the kieselguhr is also bound, a white product is formed. The degree of agglomeration can be controlled by varying the temperature, the type and amount of flux, and the reaction time. This process is also known as activation. The

high calcination temperatures in the presence of alkali lead to a partial transformation (up to 65 %) of the amorphous silica into cristobalite, a crystalline silica modification. The porosity and the specific surface area are strongly decreased. The annealing and cooling processes are followed by grinding and classification, to give white filter kieselguhr (the main product) and a dust-like fine fraction which is used as white filler and auxiliary.

Commercially Available Forms, Products, and Producers. Powder kieselguhr is sold in paper sacks containing 15–25 kg as well as loose in big-bags and silo trucks. Granulated material is available in paper or plastic sacks containing 30 kg, sometimes also in big-bags or silo trucks.

Examples of commercial products are:

Celatom (Eagle-Picher Minerals Inc., Reno, USA)
 Celite (Celite Corp., Newark, USA)
 Clarcel (Ceca SA, Paris, France)
 Dicalite (Grefco Inc., Torrance, USA)
 Fina/Optima (Meyer-Breloh, Munster, Germany)
 Skamol (Skarrehage Molerværk a/S Nykøbing, Mors, Denmark)

Table 48.19 lists the chemical and physical properties of several commercially available kieselguhrs.

48.7.3.5 Analysis

Chemical and physical testing begins with the crude kieselguhr in the mine, continues during the individual production stages, and finishes with the test certificate of the end product. The results of the crude kieselguhr tests determine the working plan for the different regions of an open-cast mine.

The following analyses and tests are undertaken.

Chemical Analysis. The contents of silica, iron, aluminum, calcium, magnesium, manganese, titanium, sodium, potassium, and, depending on requirements, also other elements are determined after alkaline dissolution or acidic extraction. Filter kieselguhrs for breweries are also tested for beer-soluble iron, calcium, and sometimes other elements [541].

Physical Tests. Water content, loss on ignition (at 1050 °C), bulk density, tapped density, pH value (10% in water), water absorption capacity, and specific surface area are determined by conventional methods [541]. The particle-size distribution is determined by laser scattering or air-jet screening. For the fine fraction, the sedimentation method is used. The wet density is the density in g/L of a filter cake flushed with water. Since the majority of kieselguhr is used for filtration, the determination of the permeability is of major importance since it determines the performance and the retaining power of a filter kieselguhr. In general, the methods developed by the individual producers in which the rate of permeation of water is measured, are sufficient. The company CECA (France) possesses a patent for a permeameter which allows fully automatic measurement. The EBC filter is of simpler construction and allows Darcy values to be precisely measured [542]. Apart from the relative units used by the diverse producers, the Darcy has become generally accepted as the unit for the permeability of a filter agent. For filter materials with the permeability of 1 Darcy the flow rate of a liquid of viscosity of 1 mPa·s is 1 mL·s⁻¹·cm⁻² filter area for a filter-cake thickness of 1 cm and a pressure difference of 0.1 MPa. Since the permeability can be determined rapidly, this is a suitable method for differentiating between fine, medium, and coarse kieselguhrs [541, 543–545].

The amorphous silica content of a kieselguhr is determined by the alkali solubility. This property is of significance for catalyst kieselguhrs, or for kieselguhrs which serve as a silica source in cement, or as chemical reagents in other silica-containing products. The specific surface area is used to assess the porosity of a kieselguhr. It is generally determined by nitrogen adsorption (BET method). The degree of whiteness is measured with a leucometer.

48.7.3.6 Storage and Transport

Processed kieselguhr is stored in steel or stainless steel silos, mostly with a circular

cross section and equipped with various discharge aids, since kieselguhr tends to form bridges. Material packed in sacks is stored and transported on wooden palettes in amounts of 600–1000 kg enveloped by a shrink film, and also in big-bags made from plastic-coated webbing with a capacity of 600–1500 kg. Loose material is transported in silo road vehicles or rail containers with a capacity of 30–75 m³. The kieselguhr is conveyed pneumatically or with screw and vibrational conveyors.

48.7.3.7 Environmental and Health Protection

Kieselguhr rarely contains toxic compounds. Since, however, it can contain crystalline modifications of SiO₂ in addition to amorphous silica, dust safety measures are of special significance. This is especially true of white activated kieselguhrs, which can contain up to 65% crystalline cristobalite. The MAK value for uncalcined kieselguhr is 4 mg/m³ and for calcined kieselguhr, 0.3 mg/m³. The TLV for uncalcined kieselguhr is 10 mg/m³. The International Agency for Research on Cancer (IARC) published a monograph concerning crystalline silica in 1987 [546]. This summarizes the research results concerning the influence of crystalline silica on humans and concluded that apart from causing silicosis it may also cause cancer (see also Section 48.7.8). Hence, crystalline silica is classified in group 2A. As a result of this, the kieselguhr producers founded the International Diatomite Producers Association (IDPA), whose aims include informing personnel working in the kieselguhr industry and the consumer about these hazards, and to ensure adherence to the work protection regulations by increasing the information available [547, 548]. The regulations of individual countries concerning the handling of dusts containing crystalline silica differ widely:

United States: 29th Federal Statute book 1910.1000 from 19.01.89, which classifies crystalline silica as a hazardous substance and specifies tolerance levels.

EC: Directive 67/548/EEC from 18.09.79 concerning the classification, packaging, and labeling of hazardous substances.

United Kingdom: Control of substances which damage health No. 1857 from 1988.

Germany: UBG 119-4.86 Quartz: protection against dust dangerous to health; UBG 1004.85, rule G.1.1.: concerning the health precautions; GefStoffV 8.86: labeling regulations.

France: No. 50.1289 from 16. 10. 50 changed into No. 63576 from 11.06.63 concerning medical precautions against occupational silicosis. No. 11453 from 19.07.82 determines the dust concentration in the air of the work place. No. 87-200 from 25.03.87 regulates the content of safety data sheets for dangerous substances. L 231-6 from 10.10.83 lists dangerous substances and determines the packaging and labeling regulations.

Spain: from 27.11.85 classification and labeling of dangerous substances.

Italy: No. 256 from 29.05.74, No. 927 from 24.11.81, No. 141 from 20.02.88 concerning the classification, packaging, and information for hazardous materials.

48.7.3.8 Uses

The main uses of kieselguhr are the following: 60% of world production is used as a filtration agent; ca. 25% as filler kieselguhrs, including carrier materials; and ca. 15% for other uses.

Filtration Agents. Kieselguhr is used in both pressure and vacuum filters of various designs. Fine, medium, and coarse kieselguhrs, as well as mixtures thereof, are employed, depending on the desired clarity and flow rate [549]. Coarse kieselguhrs are used for precoat filtration in pressure filters in amounts of ca. 1 kg/m² of filter area. Fine and medium kieselguhrs are added to the slurry to be filtered, usually in amounts of 100–200 g/m² filter area. For use as filter aids kieselguhrs must fulfil the following requirements:

- Good preservation of the diatom structure
- Optimal particle-size distribution

- Low content of soluble components
- High volume and therefore high capacity for materials causing turbidity
- Formation of filter cakes with high permeability, low compressibility, and low tendency to form cracks

The most important uses of kieselguhr are for the filtration of beer, wine, fruit juice, sugar cane juice, swimming pool water, solvents for chemical cleaning, wastewater, varnishes, and paints etc. Large quantities of kieselguhr are used for the production of cellulose-based filter beds, filter candles, and special filter papers.

Fillers. Kieselguhr is used as filler and auxiliary, for example, to modify the rheological properties of polymers. It increases the thermal stability of bitumen, the Shore A hardness of silicone rubber, and is a reinforcing filler in plastics, rubber, and adhesives. Dust-like, white, activated kieselguhr is used as a delustering agent, for adjusting the viscosity of paints, and as an antiblocking agent for plastic films.

Insulators. Loose kieselguhr has long been used for insulating double-walled kilns made from fireclay bricks, as well as for producing insulating sheets and bricks. Danish Moler is especially well suited for producing insulating bricks, since its clay content functions as a ceramic binder. The most recent development in the insulation sector is the VSI process (vacuum super insulation), in which a special form of kieselguhr acts as a supporting and insulating layer in double-walled elements that contain a high vacuum. Thus, extremely high insulation values are achieved. The VSI process is being tested for long-distance heat transport.

Absorption Agents. Due to their high capacity for liquids, kieselguhrs are used to produce gas purification agents as well as absorption agents such as cat litter and drying agents. Kieselguhr is also used to ensure the flowability and to prevent clotting of foodstuffs, fire extinguisher powders, and seeds.

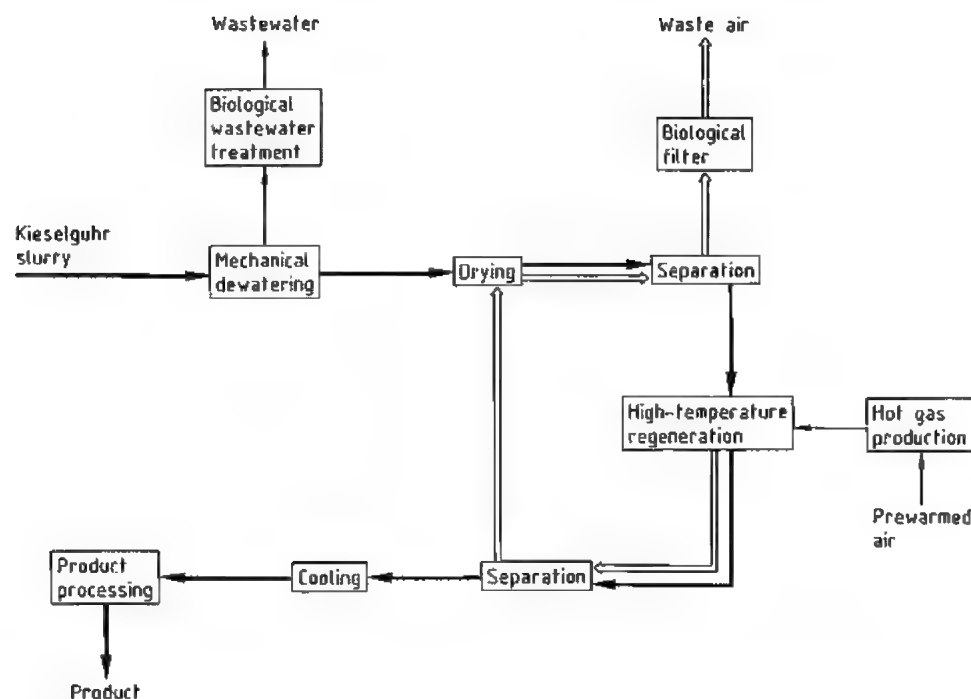


Figure 48.41: Flow sheet of thermal kieselguhr regeneration (Tremonis GmbH, Dortmund, Germany).

Other Uses. Kieselguhr serves as a fine scourer in polishes and cleaners such as car polishes, toothpastes, and silver polishes. Kieselguhr is employed as a catalyst support, for the production of pyrotechnics and matches, as a packing material for the transportation of hazardous liquids, and for the filling of acetylene bottles. In some countries it is used as the silica source for the production of cement and calcium silicate.

48.7.3.9 Recycling

Attempts to regenerate kieselguhr have been undertaken for many years [550]. This is only economically viable for kieselguhrs loaded with organic residues, which can be purified by leaching or calcination. In Germany, the company Tremonis operates a thermal process for recycling filter residues from breweries. The flow diagram of the plant is shown in Figure 48.41. The regenerated kie-

selguhr is classified as fine kieselguhr. It is added to the fresh kieselguhr for beer filtration in quantities of up to 50%.

48.7.4 Colloidal Silica

48.7.4.1 Introduction

Silica sols are stable disperse systems in which the dispersion medium (or continuous phase) is a liquid and the disperse or discontinuous phase is silicon dioxide in the colloidal state of subdivision. This state comprises particles with a size sufficiently small ($< 1 \mu\text{m}$) not to appear affected by gravitational forces but sufficiently large ($> 1 \text{nm}$) to show marked deviations from the properties of typical solutions.

The limits given for the colloidal size range are not rigid since they depend to some extent on the properties under consideration [551].

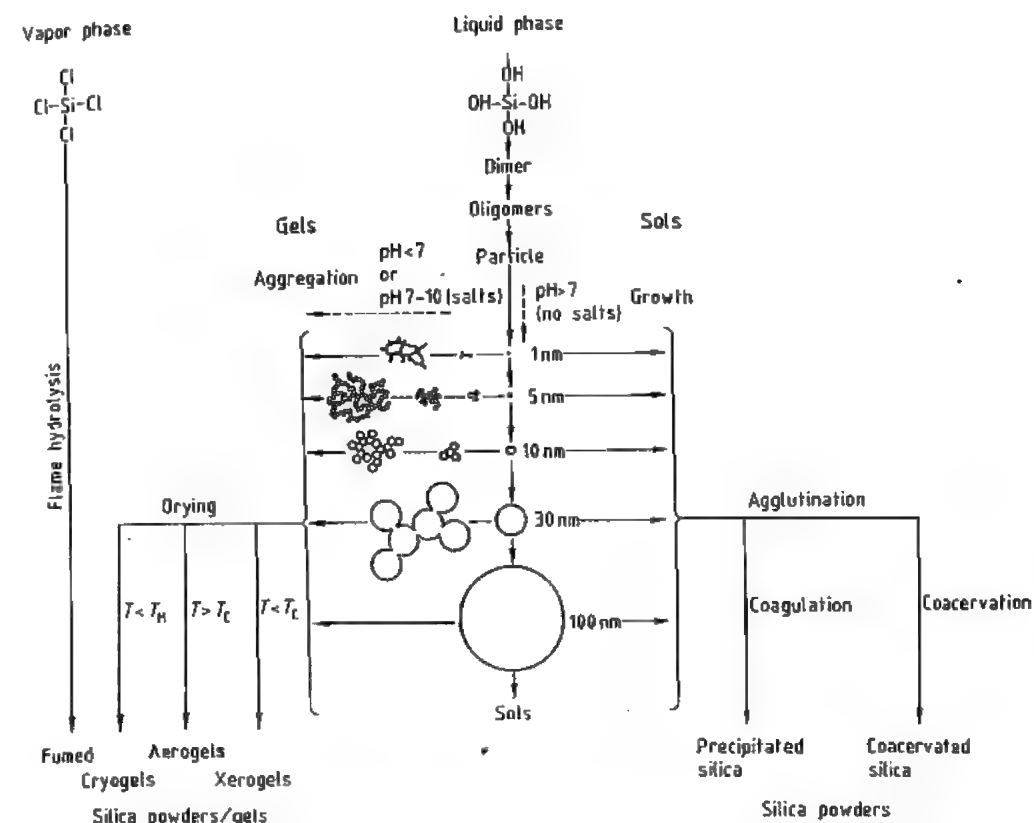


Figure 48.42: Formation of silica sols, gels, and powders by silica monomer condensation-polymerization followed by aggregation or agglutination and drying [552]. Growth of nascent colloidal particles with decrease in numbers occurs in basic solutions in the absence of salts. In acid solutions or in the presence of flocculating salts the colloidal silica particles form gels by aggregation into three-dimensional networks. Aerogels are made by drying wet gels under supercritical conditions, that is, above the critical temperature T_C and critical pressure of the liquid. Cryogels are made by drying wet gels below the melting temperature T_m of the liquid. Fumed or pyrogenic silicas are formed at high temperature by flame oxidation-hydrolysis of silicon halides.

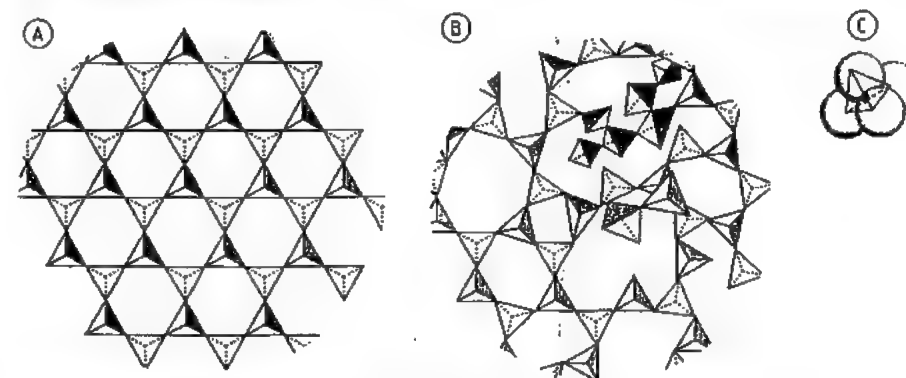


Figure 48.43: Tetrahedral configuration of crystalline (A) and amorphous (B) silica; (C) represents a silicon atom (filled circle) coordinated by four oxygen atoms (large atom spheres) [560].

Silica sols are commonly known as colloidal silica. Although the ultimate particles that constitute silica gels, xerogels, cryogels, aerosols, and pyrogenic (fumed), precipitated, and coacervated silica have lost their mobility by aggregation. They are also in the colloidal range of particle size and are therefore known as colloidal silicas. However, in this chapter the terms silica sol and colloidal silica are used as synonyms. Figure 48.42 illustrates the relationship between silica sols, gels, and powders [552].

In commercial silica sols the disperse silica is amorphous and the dispersion medium in most cases is water (aquesols or hydrosols). Dispersions in organic solvents are also commercially available (organosols). Silica sols are fluid and stable toward gelation and settling. Most commercial sols are close to monodisperse and consist of dense discrete spheres with a diameter range between ca. 4 or 5 nm and 100 nm. Also commercially available in the form of sols or powders are grades with particles between 0.1 and ca. 1.5 μm . Particle size, particle-size distribution, and concentration of solids determine the appearance of sols. Silica sols look milky if the particle size is large and the concentration is high, opalescent if the size is intermediate, or clear and almost colorless if the particles are of the smallest size range.

Although there are earlier references to what are now known as silica sols, it was GRAHAM [553] who coined the term *colloidal* in 1862 to refer to products such as the one he obtained by reacting acid with silicate and removing the electrolytes by dialysis. Stable and relatively concentrated silica sols were not available until the 1930s when I. G. Farbenindustrie first made 10% ammonia-stabilized silica sols [554]. However, the real breakthrough in colloidal silica technology came in 1941 when BIRD [555] patented a process for removing the alkali from a dilute solution of sodium silicate by ion exchange. The next landmark in the development of concentrated silica sols was the first process for making colloidal silica particles of uniform and con-

trolled size reported in 1951 by BECHTOLD and SNYDER [556].

By 1990 colloidal silica constituted a growing market valued at an estimated $\$50 \times 10^6$ in North America [557] and $\text{DM } 30 \times 10^6$ in Europe [558]. Applications of silica sols are based on characteristics such as particle size, high specific surface area that gives them good binding ability, stability towards gelation and settling, and surface properties. These characteristics enable colloidal silica to be used in a wide variety of applications. Major uses are in investment casting, silicon-wafer polishing, and fibrous ceramics.

48.7.4.2 Structure of Colloidal Silica Particles

The building block of silica is the SiO_4 tetrahedron, four oxygen atoms at the corners of a regular tetrahedron with a silicon ion at the central cavity or centroid [559]. The oxygen ion is so much larger than the Si^{4+} ion that the four oxygens of a SiO_4 unit are in mutual contact and the silicon ion is said to occupy a tetrahedral hole [559]. In amorphous silica the bulk structure is determined, as opposed to the crystalline silicas, by a random packing of $[\text{SiO}_4]^{4-}$ units, which results in a nonperiodic structure (Figure 48.43). As a result of this structural difference amorphous silica has a lower density than the crystalline silicas: 2.2 g/cm^3 versus 3.01, 2.65, 2.26, and 2.21 g/cm^3 for coesite, α -quartz, β -tridymite and β -cristobalite, respectively.

Figure 48.44 represents a two-dimensional random network of a dehydrated but fully hydroxylated amorphous silica particle.

Impurities such as Na, K, or Al, picked up during synthesis of silica aquesols in alkaline media, may be occluded inside the colloidal particles, replacing internal silanol protons (Na, K) or forming isomorphous tetrahedra (Al) with an additional negative charge on the surface or inside the particles (Figure 48.45). Sols obtained by hydrolysis of alkoxysilanes or by dispersion of pyrogenic silica in water or an organic solvent are pure and substantially free of alkali metals or aluminum.

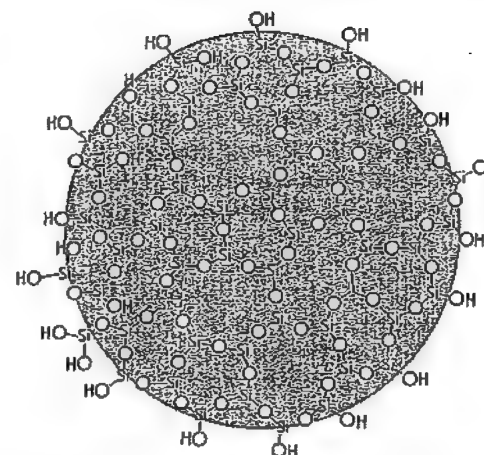


Figure 48.44: Two-dimensional random network of a dehydrated but hydroxylated colloidal silica particle. Four rules apply [561]: each oxygen ion is linked to no more than two silicon ions. The coordination number of oxygen ions about the central Si cation is 4 (the fourth oxygen not represented in the figure is directly above or below the Si cation). Oxygen tetrahedra share corners, not edges or faces. At least two corners of each tetrahedron are shared. Since the particle is fully hydroxylated each surface Si ion is bonded to one or two hydroxyl ions: the silanol number is 4.6 OH/nm^2 . Depending on the method of formation some internal Si ions may be linked to hydroxyl ions. Surface of occluded alkali-metal ion impurities may replace surface or internal protons. Aluminum ion impurities or added modifiers may replace internal or surface tetrahedral Si. The particle surface may be esterified, silanized (silylated), or ion exchanged. The concentration of OH groups on the surface decreases monotonically with increasing temperature when silica is calcined.

existence of silanol (Si-OH) groups on the silica surface. It is now generally accepted that surface silicon atoms tend to have a complete tetrahedral configuration and in an aqueous medium their free valence becomes saturated with hydroxyl groups forming silanol groups. Under appropriate conditions, silanol groups in turn may condense to form siloxane bridges: $\equiv\text{Si-O-Si}\equiv$.

In the meantime most of the following postulated groups have been identified on the surface or in the internal structure of amorphous silica (Figure 48.46).

- Single silanol groups, also called isolated or free silanol groups
- Silanediol groups, also called geminal silanols
- Silanetriols, postulated but existence not yet generally accepted [563]
- Hydrogen-bonded vicinal silanols (single or geminal), including terminal groups
- Internal silanol groups involving OH groups, sometimes classified as structurally bound water (Figure 48.46B)
- Strained and stable siloxane bridges
- Physically adsorbed H_2O , hydrogen-bonded to all types of surface silanol groups (Figure 48.46B)

Silanol groups are formed on the silica surface in the course of its synthesis during the condensation polymerization of $\text{Si}(\text{OH})_4$ or by rehydroxylation of thermally dehydroxylated silica with water or aqueous solutions.

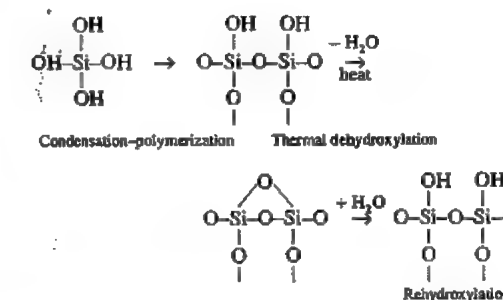


Figure 48.45: Internal structure of an amorphous silica particle showing an internal silanol group and occluded Na and Al ions.

Many of the adsorption, adhesion, chemical, and catalytic properties of colloidal silica depend on the chemistry and geometry of its surface. In 1934 HOFMAN [562] postulated the

The silanol groups on the silica surface may be classified according to their nature, multiplicity of sites, and type of association [564].

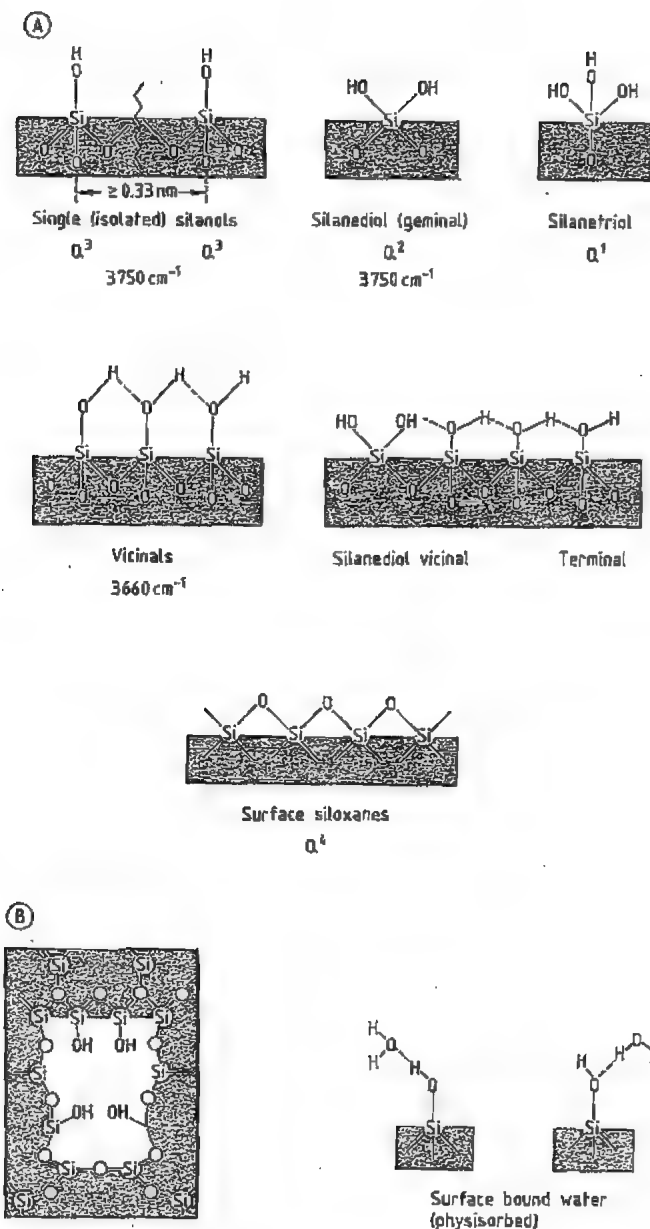


Figure 48.46: A) Possible types of silanol groups and siloxane bridges occurring on the surface of colloidal silica particles. Characteristic bands in the infrared spectrum and Q^n site designation is included (n is the number of bridging oxygens bonded to the central silicon atom); B) Surface bound water and internal silanols.

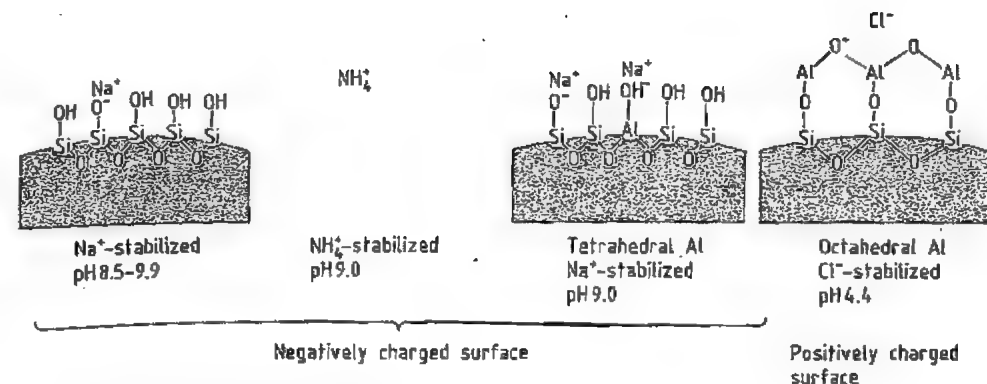


Figure 48.47: Modified colloidal silica surface.

An isolated silanol has an OH group sufficiently remote from neighboring hydroxyl groups that hydrogen bonding cannot occur ($\geq 0.33\text{ nm}$). A silicon site of this kind is designated as Q^3 in NMR Q^n terminology, where n is the number of bridging oxygens bonded to the central silicon. The isolated silanol shows a sharp band at around 3750 cm^{-1} in the IR spectrum [565, 566].

Geminal silanols are silanediol groups located on Q^2 silicon sites. Their existence was postulated by PERI [565-567] but only confirmed experimentally with the advent of solid-state ^{29}Si cross-polarization magic angle spinning nuclear magnetic resonance (CP MAS NMR) [568].

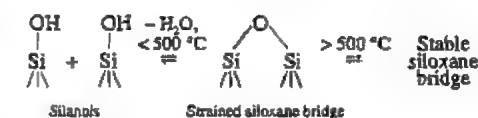
Vicinal or hydrogen-bonded or associated silanols are SiOH groups located on neighboring Si atoms such that the OH—O distance is sufficiently short for hydrogen bonding to occur. Hydrogen bonding causes a reduction in the O—H stretching frequency, the magnitude of which depends on the strength of the hydrogen bond and thus on the O—H—O distance [569]. The characteristic IR band of vicinal groups occurs at about 3660 cm^{-1} [570].

Geminal Q^2 silanol sites bonded to a neighboring Q^3 silicon through a single siloxane bridge also result in a hydrogen-bonded pair. The remaining OH group experiences very weak hydrogen bonding.

Silanol groups are also found within the structure of the colloidal particles. These groups are designated as internal silanols and

in some cases are erroneously referred to as structurally bound water. The concentration of internal silanol groups depends on the synthesis temperature and other variables.

Surface and internal silanol groups may condense to form siloxane bridges. Strained siloxane bridges are formed on the hydroxylated silica surface by thermally induced condensation of hydroxyl groups up to about 500°C . At higher temperature, the strained siloxane bridges are converted into stable siloxane bridges [569].



Strained siloxane groups undergo complete rehydroxylation on exposure to water in a matter of hours or a few days, depending on type of silica powder and conditions of exposure [570]. Stable siloxane groups are rehydroxylated at a slower rate. For example, a wide-pore sample of $340\text{ m}^2/\text{g}$ calcined in air at 900°C required five years of contact with water at room temperature for complete rehydroxylation [571].

Surface silanol groups are the main centers of adsorption of water molecules [571]. Water can associate by hydrogen bonding with all types of surface silanols, and in some cases with internal silanol groups.

Surface silanol groups of silica aquasols stabilized in an alkaline medium exchange

protons for ions such as Na^+ , K^+ , or NH_4^+ (Figure 48.47). The surface silanol groups can be esterified, as in the case of silica organosols, or silanized (silylated) (Figure 48.48). Derivatization, that is modification of the silica surface, is the basis for the use of silica in analytical and process chromatography.

The surface charge of pure silica aquasols is negative at a pH higher than ca. 3. The isoelectric point (IEP) is ca. 2. The IEP can be shifted by partial substitution of surface silicon groups by tetrahedral aluminum (Figure 48.47). In this way the pH range of stability of aquasols may be varied. The surface charge can be reversed by adsorption of octahedral aluminum ions such as those present in basic aluminum chloride [572] (Figure 48.47). Aquasols obtained in this manner are commercially available in various particle sizes and concentrations as *positive sols*.

The concentration of silanol groups on the silica surface α_{OH} expressed as the number of OH groups per square nanometer is the silanol number [571]. For a dehydrated but fully hydroxylated amorphous colloidal silica powder α_{OH} is 4.6 [571].

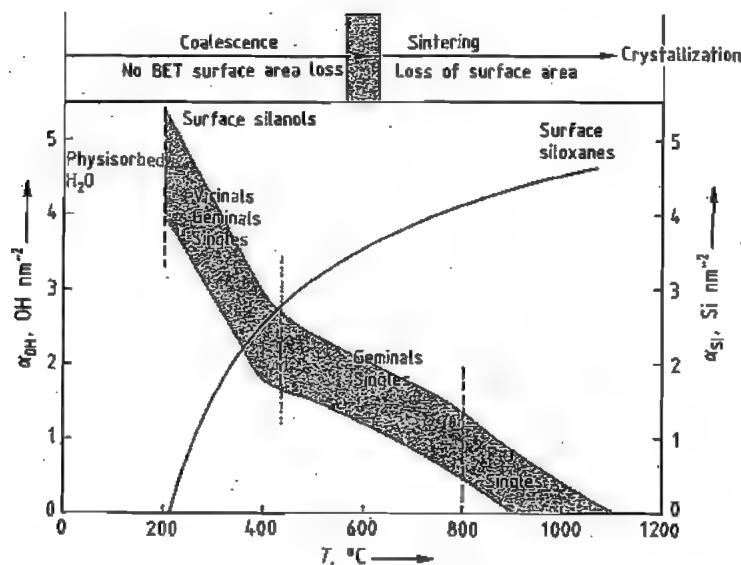


Figure 48.49: Effect of temperature on silanol groups on the surface of colloidal silica.

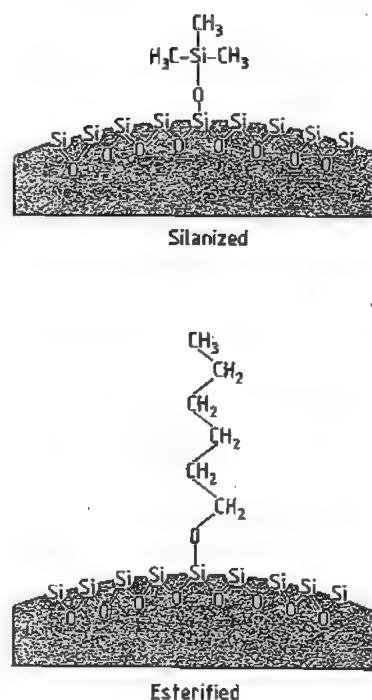


Figure 48.48: Silylated and esterified silica surface.

The threshold temperature corresponding to the completion of dehydration, that is removal of physisorbed water from the silica surface, and the beginning of dehydroxylation by condensation of surface OH groups, is estimated to be $190 \pm 10^\circ\text{C}$ [571].

The concentration of OH groups on the surface decreases monotonically with increasing temperature when silicas are heated under vacuum (Figure 48.49). Most of the physisorbed water is removed at about 150°C . At 200°C all the water from the surface is gone so that the surface consists of single, geminal, vicinal, and terminal silanol groups and siloxane bridges. At ca. 450 – 500°C all the vicinal groups condense yielding water vapor and only single, geminal, and terminal silanol groups and strained siloxane bridges remain. The estimated ratio of single to geminal silanol groups on the surface is 85/15 [571] and is believed not to change with temperature, at least up to ca. 800°C . Internal silanols begin to condense at ca. 600 – 800°C and in some cases at lower temperatures. Complete evolution of internal silanols occurs at higher temperatures. It appears that at temperatures from ca. 800°C to ca. 1000 – 1100°C , only isolated (single) silanol groups remain on the silica surface.

At a sufficient surface concentration, the OH groups make the silica surface hydrophilic, whereas a predominance of siloxane groups on the silica surface makes the surface hydrophobic.

48.7.4.3 Physical and Chemical Properties

Most commercial silica sols consist of dense, discrete, spheroidal particles typically 4–60 nm in diameter and amorphous to X-ray or electron diffraction. Because they are amorphous the silica particles are only slightly sol-

uble in water (100–150 ppm at 25°C and pH 2–8) and insoluble in alcohol or in inorganic acids except HF. They are soluble in organic bases such as tetramethylammonium hydroxide, forming water-soluble quaternary ammonium silicates, and, as opposed to crystalline silicas, are very soluble in hot sodium hydroxide solution. Specific surface areas vary with particle size, and for the common grades of silica sols are between 50 and $750\text{ m}^2/\text{g}$. Less typical grades have particle diameters between 60 nm and $1.5\text{ }\mu\text{m}$ with specific surface areas much lower than $50\text{ m}^2/\text{g}$, depending on their particle diameter. The specific surface area A in m^2/g of a system made of solid monodisperse amorphous silica spheres with a smooth surface and bulk density 2.2 g/cm^3 is:

$$A = 6000D/2.2$$

where D is the diameter of the spheres in nanometers.

Table 48.20 lists typical properties of representative commercial silica aquasols. The table also shows the dependence of relative density and viscosity on the silica content. Viscosity also depends on particle size and degree of cross-linking of the particles. In 30% silica aquasols it is generally $< 10\text{ mPa}\cdot\text{s}$.

Silica sols obtained by dispersion of pyrogenic silica powders generally differ from those synthesized in solution. The dispersion of pyrogenic silica to a sol of separate, discrete ultimate units is difficult, even using intense mechanical shearing forces, due to the extensive coalescence of the particles. Thus, the disperse product consists mainly of short chain-like aggregates made up of small silica particles. Typical properties of commercial sols made in this way are listed in Table 48.21.

Table 48.22 lists particle size, silica concentration, and viscosity of commercially available organosols.

Table 48.20: Typical properties of commercially available negative and positive silica aquasols (NA = not available) [573].

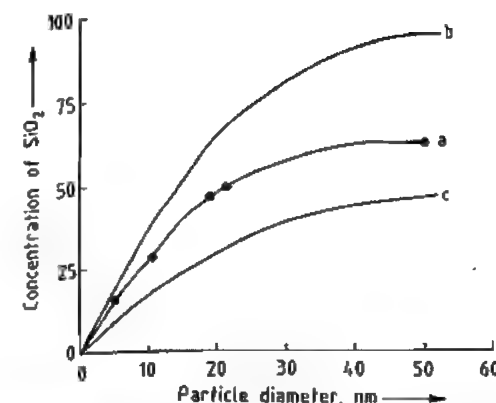
	Particle diameter, nm	Specific surface area, m ² /g	Silica, %	pH	Na ₂ O, %	Viscosity at 25 °C, mPa·s	Relative density at 25 °C
Negatively charged surface sodium stabilized	4	750	15	10.4	0.80	18	1.10
	7	360	30	9.9	0.56	6	1.22
	12	230	40	9.7	0.41	20	1.31
	21	130	50	9.0	0.21	35	1.40
	60	50	50	8.5	0.25	10	1.40
	50–80	NA	40	9–10	NA	NA	NA
	70–100	NA	40	9–10	NA	NA	NA
	100	NA	20	9–10	NA	NA	NA
	300	NA	20	9–10	NA	NA	NA
	500	NA	20	9–10	NA	NA	NA
alumina modified surface ammonium stabilized	12	230	30	8.9	0.24	11	1.21
	21	130	40	9.0	0.08	9	1.30
Positively charged surface chloride stabilized alumina surface	13–15	210	30	4.4	NA	NA	NA

Table 48.21: Typical properties of silica aquasols made of short chain-like aggregates of colloidal particles (NA = not available) [574].

Stabilizer	Ultimate particle size, nm	Solids, %	pH	Relative density	Viscosity, mPa·s
NH ₄ ⁺	7	12	7.5–7.8	1.07	< 100
	14	17	9.5–10.0	1.10	< 250
	14	12	5.0–5.5	1.07	< 100
	17	17	9.5–10.0	1.10	< 100
	30	20	5.0–5.5	1.12	< 100
K ⁺	17	18	8.6–9.0	1.11	< 150
	30	28	7.5–7.8	1.18	< 200
	30	30	10.0–10.3	1.19	< 150
Na ⁺	7	14	10.0–10.5	1.08	< 100
	8	15	9.5–10.0	1.09	< 100
	14	17	9.5–10.0	1.10	< 100
Acidic medium	11–14	20	2.0–4.0	NA	5–25

Table 48.22: Properties of commercially available silica organosols (NA = not available) [575].

Liquid phase	Particle diameter, μm	SiO ₂ , %	Viscosity at 25 °C, cP	Relative density
Methanol	0.01	30	1–5	NA
2-Propanol	0.01	30	3–20	NA
Water/2-propanol	0.02	30	10	NA
Ethylene glycol mono- <i>n</i> -polyether	0.01	20	5–20	NA
Dimethylacetamide	0.01	20	1–10	NA
Ethylene glycol	0.01	20	10–20	1.23
	0.18 ± 0.03	20		1.23
DMF	0.02	35	5	NA
Oil	0.02	50	80	NA
Ethylene glycol	0.28 ± 0.03	20		1.23
	0.43 ± 0.03	20		1.23
	0.50	20	10–20	1.23
	0.53 ± 0.03	20		1.23
	0.73 ± 0.03	20		1.23
	0.80 ± 0.04	20		1.23
	0.90 ± 0.05	20		1.23
	1.50 ± 0.10	20		1.23

Figure 48.50: Maximum concentration versus particle size in stable aqueous silica sols at about pH 9.5: a) Concentration in %; b) Concentration in grams SiO₂ per 100 mL; c) Volume fraction of SiO₂ (× 100) [576].

Silica sols are said to be stable because they do not settle or aggregate for long periods of time. Aggregation and rate of settling, as well as color, appearance, viscosity, density, growth, and solubility in water are functions of particle size. At optimum pH, electrolyte and SiO₂ concentration, aquasols of particle size 4 to ca. 40 nm are extremely stable to settling, whereas aquasols of particle size larger than ca. 60 nm tend to show some settling in a period of months. Particles larger than 100 nm settle on standing, leaving a clear upper layer after a few weeks or days. When the concentration of the silica aquasol is > 10–15% the particle size can be judged visually by the turbidity. If the particles are smaller than ca. 7 nm in diameter the sol is almost as clear as water; from 10–30 nm there is a characteristic opalescence or translucency when seen in bulk; above 40 or 50 nm the appearance is white and milky [554].

Commercial silica aquasols are stabilized near the optimum pH and are concentrated to the maximum concentration permitted by the particle size [576]: ca. 15% for 4–5 nm, ca. 30% for 8–9 nm, ca. 40% for 14 nm, ca. 50% for 22 nm (Figure 48.50).

When silica sols are gelled, dried, or frozen the original degree of dispersion cannot be restored without dissolution of the interparticle bonds that develop. Special dried grades are

made of particles with the surface esterified with primary or secondary C₂–C₁₈ alkoxy groups. These are organophilic and hydrophobic and can be dispersed in organic solvents or in organic products such as elastomers or plastics. Silica sols surface-modified with organic base cations such as (CH₃)₄N⁺ can be evaporated to a dry powder that disperses spontaneously in water [577].

48.7.4.4 Stability

Three types of stability may be distinguished in colloidal systems [578]:

- Phase stability, analogous to the phase stability of ordinary solutions.
- Stability to change in *dispersity* [578], that is particle size or particle-size distribution. For example, commercial concentrated silica sols, normally said to be 3 or 4 nm in particle size usually grow within hours or a few days to 5 nm or more on standing at room temperature. Concentrated sols normally labeled 7 nm, if not substantially homodisperse, may grow within months to 8–9 nm. This ripening effect also occurs for larger particle sizes, although at a much slower rate. A concentrated silica sol of 14 nm particle size was found to grow to 17 nm in twenty years at room temperature [579].
- *Aggregative stability* [578], the central issue in colloidal silicas, and for that matter in colloidal systems in general. In this case *colloidally stable* means that the colloidal particles do not aggregate at a significant rate [551]. The term aggregate is used to describe the structure formed by the cohesion of colloidal particles [551].

Two mechanisms of sol stabilization are generally believed to exist: electrostatic stabilization and steric stabilization. Electrostatic stabilization is based on an interplay of electrostatic repulsion between electrically charged colloidal particles and van der Waals forces of attraction between particles. The DLVO theory (Derjaguin, Landau, Verwey, and Overbeek) constitutes an attempt to describe quantitatively this interplay. Steric sta-

bilization is generally caused by long-chain molecules or macromolecules adhering on the colloidal particle surface (e.g., by grafting or by physical adsorption), thus preventing the particles from aggregating [580].

Colloidal silica particles aggregate by linking together and forming three-dimensional networks as is the case in gelation, coagulation or flocculation, or by coacervation [581]. In coacervation the silica particles are surrounded by an adsorbed layer of material which makes the particles less hydrophilic but does not form bridges between particles [582].

When a sol is gelled it first becomes viscous and then develops rigidity, filling the volume originally occupied by the sol. On the other hand when a sol is coagulated or flocculated, a precipitate is formed that settles out. A simple way to differentiate between a precipitate and a gel is that a precipitate encloses only part of the liquid in which it is formed [581].

Stability of silica aquasols against irreversible gelation decreases with increasing silica concentration, increasing electrolyte concentration of the aqueous medium, decreasing particle size, and increasing temperature. Water-miscible organic liquids have a similar destabilizing effect on silica aquasols as added electrolyte. The variation of stability as a function of pH and salt concentration is shown in Figure 48.51 [583].

According to ILER [584] the basic step in gel formation is the collision of two silica particles with sufficiently low charge on the surface that they come into contact so that siloxane bonds are formed, holding the particles irreversibly together. Formation of this linkage requires the catalytic action of hydroxyl ions (or, as interpreted by some, the dehydration of the surface of particles at higher pH). This is evidenced by the fact that the rate of gel formation in the pH range 3–5 increases with pH and is proportional to the hydroxyl concentration.

Above pH 6, scarcity of hydroxyl ions is no longer the limiting factor on the rate of gel-

ling. Instead, the rate of aggregation decreases because of fewer collisions between particles owing to the increasing charge on the particles and thus decreases with higher pH. Lines in Figure 48.51 schematically represent the increase in the catalytic effects of hydroxyl ions with increasing pH, and the decrease in the number of effective collisions between particles with increasing pH and particle charge. The net result of these two effects is a maximum in rate of gelling at around pH 5. In the pH range 8–10, sols are generally stable in the absence of salts.

There is also a region of temporary stability at about pH 1.5. Below pH 1.5, traces of HF catalyze aggregation and gelling [585]. In essentially all silicas, traces of fluoride ions, even less than 1 ppm, are present so that the concentration of HF increases with increasing acidity. The fluoride effect is influenced by the aluminum impurities present, since these inactivate some of the fluoride by forming complex ions such as AlF_6^{3-} and other species [586]. However, the gelling rate increases as the pH falls below 3 even when fluorine is absent.

Once the siloxane bonds have formed between particles, further deposition of silica occurs at the point of contact owing to the negative radius of curvature. This occurs rapidly above pH 5, and is slow at pH 1.5.

Since the curves shown in Figure 48.51 are constructed on the basis of irrefutable experimental evidence it is quite obvious that silica sols do not conform to the DLVO theory as originally formulated. For example, the DLVO theory predicts minimum stability at the point of zero charge (pH 2–3), whereas the experimental curve shows metastability. Also, the plot shows minimum stability in the pH range 4–7, whereas the DLVO theory predicts a continuous increase in stability in this pH range. Research is being conducted to study the possibility of modifying or amending the DLVO theory or developing a new theory of stability applicable to silica sols.

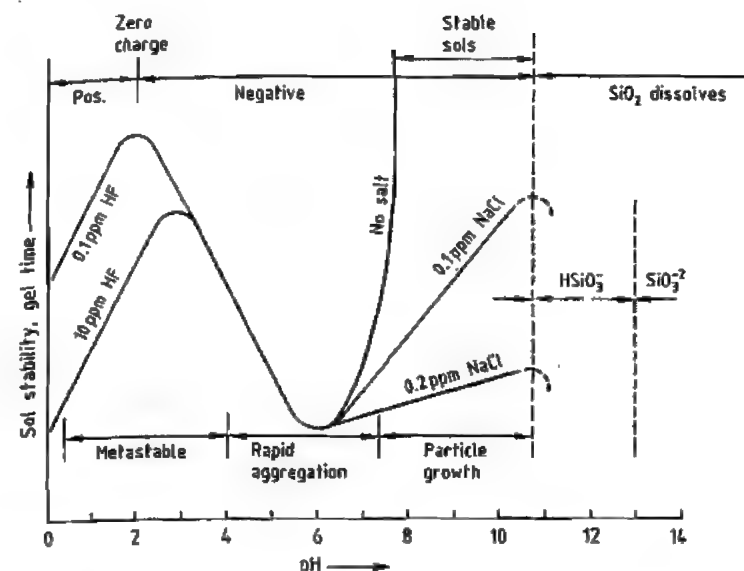


Figure 48.51: Effect of pH in the colloidal silica-water system [577].

In addition to common electrolytes such as NaCl, NH_4Cl , and KF, silica aquasols are destabilized and gelled by positively charged sols. When frozen at ca. 0 °C or lower, silica sols gel irreversibly. Long-chain nitrogen bases are effective flocculating agents for silica aquasols that form planar rather than spheroidal aggregates. Flocculation may also result from the addition of water-miscible organic solvents to alkali-stabilized silica sols.

Commercial silica aquasols are stabilized at pH 8.5–10.5 by alkalies, usually sodium hydroxide. Ammonia or potassium hydroxide is used when the presence of sodium ions is undesirable.

Surface-modified silica aquasols made by coating the silica particles with tetrahedral aluminum (e.g., sodium aluminate) are much more stable towards gelling in the pH range 4–6 where unmodified sols gel most rapidly. Silica sols modified in this manner are also less sensitive to salts [587].

Coating the negative silica surface with oxides of polyvalent metals such as Al, Cr, Ga, Ti, and Zr reverses the charge of the surface to produce positive aquasols stable at acid pH values [588]. An important characteristic of these sols is that they can be dried and reprecipitated.

Only polymeric hydrolyzed species such as $Al_2(OH)_5Cl$ and not the single Al^{3+} ion can cause charge reversal of silica sols [589, 590].

48.7.4.5 Production

The classic silica aquasols of particle size 5–100 nm are prepared by nucleation, polymerization, and growth in aqueous systems. The particle-size range can be extended to at least 300 nm by autoclaving. Silica organosols can be obtained by transferring aquasols to an organic solvent or by hydrolysis of a silane precursor in a mixture of alcohol/ammonia and sufficient water [591] followed by transfer to the solvent.

The most important processes to make silica sols are based on neutralization of soluble silicates with acids, ion exchange, hydrolysis of silicon compounds, dispersion of pyrogenic silica, electrodialysis, dissolution of elemental silicon and peptization of gels [592].

Currently, most commercial silica sols are prepared by ion exchange of dilute solutions of sodium silicate. Several methods have been proposed since the pioneering work of BIRD [555], BECHTOLD and SNYDER [556], ALEX-

ANDER [593], ATKINS [594], WOLTER and ILER [595], MINDICK and REVEN [596], and DIRNBERGER [597]. Sodium silicate can be deionized in a batch operation by adding simultaneously a dilute solution of sodium silicate and a cationic ion-exchange resin in the hydrogen form to a vigorously stirred weakly alkaline aqueous reaction medium in the pH range around 9, at 60–100 °C [595] (Figure 48.52). Under these conditions the system is stabilized against aggregation and the original silica nuclei grow while the sol concentration increases to about 10–15% silica. Rate of addition, pH, and temperature determine the particle size and quality of the sol.

After separation of the resin for regeneration, more sodium silicate is added to adjust the $\text{SiO}_2/\text{Na}_2\text{O}$ ratio as needed for further stabilization of the sol. The product is filtered and concentrated to the desired level. Sols of small particle size, such as 7 nm, may be used as "heels" to build up the particle size, for example, to 14 or 22 nm.

An alternative method of deionizing sodium silicate is to pass a relatively dilute solution through a bed of ion-exchange resin to produce a sol which is then stabilized with alkali and concentrated. The particles grow during evaporation. The addition of further deionized sol to the evaporating liquid allows

silica to build up on previously nucleated particles resulting in larger particle size.

Silica sols can also be made by dispersion of pyrogenic silica in water or in an organic solvent. Commercial pyrogenic silica, also known as fumed silica or aerosil, is made from silicon tetrachloride at high temperatures by a flame hydrolysis-oxidation process (see Section 48.7.6) [598]. The product is a highly aggregated silica powder. Pyrogenic silicas can be partially disaggregated and dispersed to obtain aquasols or organosols of relatively high silica concentration. The silica units in this case consist mainly of short chain-like aggregates composed of silica particles ca. 7–25 nm in diameter.

Monodisperse silica sols of exceptionally large particle size can be prepared by hydrolysis of tetraethoxysilane (TEOS) in a basic solution of water and alcohol [591]. It is claimed that the largest mean particle size that can be produced with TEOS is about 0.8 μm [599]. However, particles up to ca. 2 μm can be made by using tetrapentoxysilane [598], performing the reaction at low temperature [600], or growing the particles by adding more alkoxide after the particles have formed [600]. Wolf [601] has adapted the TEOS method to produce commercial quantities of silica sols.

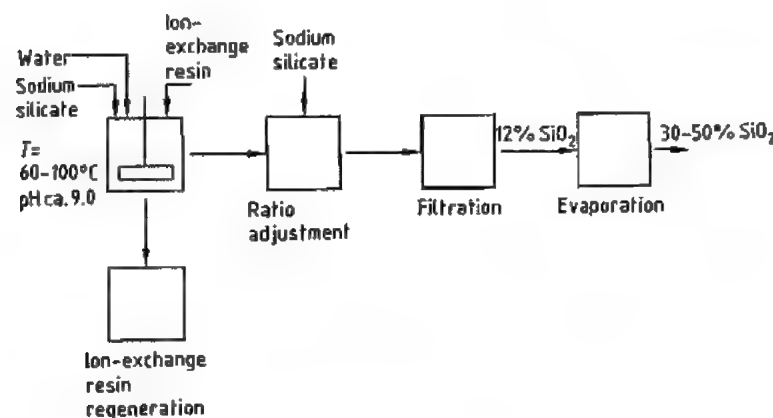


Figure 48.52: Ion-exchange process for silica aquasols.

Viable processes for making commercial silica sols are based on the electrodialysis of sodium silicate solutions to continuously remove sodium ions until a sol is obtained. In the ILER [602] and the BERGNA [603] processes there are three compartments separated by two parallel, closely spaced cation-exchange membranes between which the process or "heel" solutions of silica sol in dilute Na_2SO_4 as a conducting electrolyte are rapidly circulated at a specified temperature. Sulfuric acid is circulated in the anode compartment and an alkali in the cathode compartment where sodium hydroxide is generated. Dilute sodium silicate is fed to the third compartment to form SiO_2 by electrolysis. The silica or polysilicic acid that forms is deposited on the silica particles of the "heel" solution, and circulation of the solution is continued until the desired particle size is achieved. Sols of 25% silica, 15 nm particle-size can be prepared directly. Concentrated sols of ca. 8 nm particle size with very narrow particle-size distribution can be obtained by seeding in a first step at a lower temperature and raising the temperature in a second step to accelerate silica deposition [603].

Among the advantages of the electrodialysis process are that alkali, oxygen, and hydrogen can be recovered, and that there is much less salt-containing wastewater to be disposed of. The disadvantages of the process are higher electrical and maintenance costs.

48.7.4.6 Analysis and Characterization

Characterization of silica sols is aimed at identifying:

- Physical and chemical properties of the sol
- Compatibility and stability properties of the sol
- Purity of the sol
- Use-related characteristics

Selection of silica sols for commercial uses is commonly based on the nature of the liquid phase (water or organic solvent), particle size, particle-size distribution, degree of aggrega-

tion, pH, silica and counterion (stabilizing agent) concentration, viscosity, relative density, and specific surface area.

However, to fully understand and predict the behavior of silica sols and derived powders, it is necessary to determine other characteristics such as particle and particle surface structure; chemical composition including total carbon, organic carbon, soluble salts of alkali metals, total solids, nonsiliceous ash; and trace metals (especially Al and Fe); and physical properties such as turbidity, percent S (the percent by weight of silica in the dispersed phase of a silica sol [604]), refractive index, light scattering, sedimentation rate by ultracentrifugation, porosity, rate of dissolution of the particles, and coalescence factor of derived powders (the coalescence factor is the percent silica that must be dissolved to restore the light transmission under standard conditions of a silica powder redispersed in water [605]). In addition, most manufacturers of colloidal silicas use special tests for specific uses.

A new concept in the characterization of colloidal silica is the application of the fractal approach to sols and gels. The concept of fractal geometry, developed by MANDELBROT [606] in the early eighties, provides a way of quantitatively describing the average structure of certain random objects. For the application of the fractal concept to colloidal silica, see [560, 569].

48.7.4.7 Uses

This section gives a brief description of the major industrial uses of silica sols. The many minor uses are too numerous to be discussed here.

Colloidal silica is widely used as a binder in the modern version of the ancient lost wax process for casting metal [612]. In this process, known as *shell investment casting*, a wax original or a cluster of originals is dipped in a slurry of colloidal silica and refractory powder. Excess slurry is drained from the wax parts, and a dry refractory sand is applied to the wet surface. The coating is then allowed to dry. These coating steps are repeated until a

ceramic shell of sufficient thickness, usually about 5–10 mm, is built up around the wax.

The wax is then melted out, and the ceramic shell fired to increase its strength and to remove the last traces of wax. Molten metal is poured into the hollow left by the wax. When the metal has cooled, the shell is broken away and the metal, now an exact replica of the original wax shape, is recovered.

This process is widely used to produce jet engine components as well as a large number of other metal parts. The tolerances of the finished casting can be held very close to the final requirements, thus minimizing the need for additional finishing operations.

Refractory fibers can be bonded with colloidal silica to give *insulators* that have excellent high-temperature resistance. The process is similar to papermaking in that the fibers are suspended in water and the mixture passed through a screen which retains the fibers and allows the water to pass through and be recycled. The thickness of the fiber mat can vary from 0.1–10 cm depending on the insulating properties required. The screen is often contoured to give a shaped insulator. Usually, vacuum is used to assist the flow of water through the screen.

Colloidal silica is used two ways in this process. It is often used in small quantities together with starch in the original fiber suspension to help flocculate the fibers and the starch for better drainage and retention on the screen. The starch acts as the binder in the unfired or green state. Additional colloidal silica is often added to the final shape to stiffen and strengthen it and provide additional strength when the part is heated and the starch is burned out.

More recently, colloidal silica has been applied to the *papermaking* process itself. By adding small amounts of high surface area colloidal silica and a high molecular mass starch to the paper pulp, drainage rates and fiber and filler retention are improved. This allows for higher filler loadings, use of more recycled pulp, and in some cases, higher production rates [613–617].

Small amounts of colloidal silica increase the coefficient of friction of surfaces. One of the earliest uses of colloidal silica was to diminish the slipperiness of floor waxes while not affecting their gloss [618, 619]. It is widely used today to improve the frictional character of paper and boxboard, which facilitates handling and reduces breakage resulting from falling boxes [620].

Carpets and other surfaces coated with colloidal silica resist soiling because the colloidal silica occupies the sites which would most likely retain visible soil.

The strength and adhesion of latex-based adhesives and paints can be enhanced by the addition of colloidal silica.

Silicon wafers cut from silicon single crystals must be polished to an almost atomically smooth surface before being used as substrates for electronic chips [621, 622]. Colloidal silica is the main component of the final polishing compounds for these materials. They act both as a fine, uniform abrasive and as a scavenger for reaction products of polishing additives that chemically attack the silicon.

Colloidal silicas have been used to bond and improve the attrition resistance of catalyst powders used in streams of reacting gas or liquid. The silica provides sufficient strength and hardness to prevent the catalyst pellets from being broken down and swept away by the stream. Acrylonitrile is made from propylene and ammonia by such a fluidized bed reaction [623, 624]. Ammonia-stabilized colloidal silicas are generally used in these applications because of the poisoning effect of sodium.

Photographic films and papers often incorporate colloidal silicas as grain growth regulators or dye receptors.

Beverages, such as wine, beer, or fruit juices can be clarified using colloidal silica as an aid to the flocculation of the proteins which cause the materials to be hazy.

48.7.4.8 Storage, Handling, and Transportation

Colloidal silicas generally undergo irreversible precipitation of the silica if frozen.

Therefore, they are generally stored in heated buildings. If outdoor bulk storage is required, tanks should be heated and insulated in climates where freezing might occur. Heated trucks are typically used in cold climates for shipping colloidal silicas.

Colloidal silica is sometimes freeze-stabilized by addition of organic substances such as glycols. The amount added is insufficient to prevent freezing, but does prevent irreversible precipitation.

Storage in plastic, fiberglass-reinforced plastic, stainless steel or lined steel tanks is usually recommended.

Typically, the main hazard associated with colloidal silicas is their alkalinity. However, since the pH of most commercially available materials is < 10.5 they may irritate the skin or eyes, but do not cause irreversible burns. In applications where a respirable mist can be formed, operators should be protected by engineering design or suitable respirators. Since colloidal silica is amorphous, it is less toxic than crystalline silica.

48.7.4.9 Economic Aspects

Major manufacturers of colloidal silica and their trade names are as follows:

Bayer	Baykisol	(Germany)
Du Pont	Ludox	(United States)
Eka Nobel	Bindzil	(Sweden)
Hispano Quimica	Hispacil	(Spain)
Monsanto	Syton	(United Kingdom)
Nalco Chemical	Nalcoag	(United States)
Nippon Shokubai	Seabostar	(Japan)
Nissan	Snowtex	(Japan)
PQ Corporation	Nyacol	(United States)

Estimates of the colloidal silica market discussed in this section are based on [557, 558].

The U.S. market for colloidal silica is the largest in the world. The total market for North America is estimated at > 14000 t (100% silica basis) and valued at \$50 × 10⁶ [555]. These figures include ca. 1500 t consumed in Canada. Kline estimates that the total West European market for colloidal silica was 5500 t (100% silica basis) in 1992, valued at over DM 30 × 10⁶ [558]. In Japan colloidal silica production in 1988 was estimated at

4500 t (100% silica basis) and was expected to grow significantly [557].

The total annual capacity for the manufacture of colloidal silica in North America is estimated at 16 000–21 000 t (100% silica basis). The total capacity in Europe is estimated at 6000 t.

Nalco is the largest producer for the North American market followed by Du Pont and PQ Corporation. Eka Nobel of Sweden has a relatively small plant in the United States (ProComp Inc.). Alchem, a joint venture of C-I-L Inc. and Nalco in Ontario, is the sole Canadian producer.

In the United States, Monsanto imports colloidal silica from its plant in Wales and small amounts are also imported from Japan. Exports from the United States are believed to be relatively small at about 1800 t/a. Nalco and Du Pont are the main exporters, and Japan, Taiwan, and Canada are the principal destinations. Some colloidal silica is also exported to Europe.

The largest producers of colloidal silica in Western Europe are Bayer in Germany, Eka Nobel in Sweden, and Monsanto in the United Kingdom, followed by Akzo in the Netherlands and Hispano Química in Spain. There are a few smaller producers in Italy and France.

Western Europe imports some colloidal silica from the United States and exports relatively small amounts to the United States, Eastern Europe, the Far East, and the CIS.

In 1987–1988 the North American market for colloidal silica was expected to grow at an average rate of 5%/a, and the Western European market at 3.5%/a in volume. The author estimates that the actual growth for both markets has been lower due to the world economic situation.

Colloidal silica prices vary with grade, silica concentration, volume purchased, and country in which it is sold. In the United States the price is about \$1.80–1.95 per pound for electronic-grade material, and \$1.15–1.40 per pound for other grades (100% silica basis). In Western Europe the prices vary in the range 5.5–8.3 DM/kg (100% silica basis).

48.7.5 Silica Gel

48.7.5.1 Introduction

Silica gel has the nominal chemical formula $\text{SiO}_2 \cdot x\text{H}_2\text{O}$ and is a solid, amorphous form of hydrous silicon dioxide distinguished by its microporosity and hydroxylated surface. The structure of silica gel is an interconnected random array of ultimate polymerized silicate particles, called micelles, which are spheroidal and 2–10 nm in diameter (resulting in high surface areas of ca. 300–1000 m^2/g SiO_2). The properties of silica gel are a result of the silica micelles, their state of aggregation, and the chemistry of the micelle surface.

Control of the surface area, porosity, and surface chemistry of silica gel has led to numerous and diverse uses. Examples include adsorbents for water or other species, abrasives and thickeners in dentifrice, efficient matting agents in coatings, chromatographic media, and catalyst supports. The utility is reflected in an estimated world production of 90 000 t/a, excluding China, the CIS, and Eastern Europe [625].

The development of silica-gel science and technology began with the pioneering work of GRAHAM reported in 1861 [626], although observations of gelation had been reported earlier [627, 628]. Commercial production began at the Silica Gel Corporation (now part of W. R. Grace & Co.-Conn.) with the process invented by PATRICK in 1919 [629]. Commercial development and applications expanded worldwide [627], and the colloid chemistry of silica was explored further [630]. With the application of NMR spectroscopy, small-angle X-ray scattering, and fractal geometry [631], further fundamentals of silica gel chemistry are being elucidated.

48.7.5.2 Structure, Properties, and Characterization

Structure. Silica gel is prepared by the neutralization of aqueous alkali metal silicate with acid [627, 629, 630]; for example:



A complete synthesis of silica gel by this typical commercial route is outlined in Figure 48.53. Alternatively, stable silica sols may also be gelled [630]. Another method involves the hydrolysis of silicon alkoxides with water, catalyzed by acid or base [631].

The neutralization of sodium silicate initiates a polymerization of silicate tetrahedra in a random, amorphous manner to form small spheroids called micelles. The solution containing the micelles while still liquid is known as a hydrosol.

Gel formation occurs when the interaction of separate micelles through hydrogen bonding and eventual interparticle condensation becomes significant. The rate of gelation depends on many variables such as SiO_2 concentration, pH, temperature, and mixing; this is discussed in detail in [630, 631]. Polymerization and cross-linking continue after the hydrosol has solidified into a hydrogel. The random, amorphous structure is reflected in a lower skeletal density for silica gel of 2.1–2.2 g/cm^3 compared to quartz (2.65 g/cm^3) and the lack of X-ray crystallinity. The micelle, which is the ultimate particle, consists of SiO_2 in its interior and Si–OH on its surface. Solid-state ^{29}Si NMR indicates tetrahedral geometry about the silicon atoms and confirms the presence of bulk SiO_2 and surface Si–OH [632]. The micelle's size determines the specific surface area of the silica gel; a typical micelle size of ca. 2.5 nm in diameter corresponds to ca. 1000 m^2/g .

Once the gel network forms, several processing steps are performed to give the finished gel [633]. First, washing is normally performed to remove dissolved salts. Because silica gel has a very low ion-exchange capacity for cations or anions at moderate pH, salt removal is a diffusion-controlled dilution process. Next, if desired, the interaction between micelles and micelle growth can be accelerated by aging in aqueous media under conditions where silica is slightly soluble. A process in which silica dissolves from regions of positive curvature and redeposits at regions of

negative curvature reinforces the hydrogel network. Thus, a continuous gel structure is formed.

During the drying process, the surface tension of the solvent in the pores can act to shrink the hydrogel volume. In slow drying, as water is evaporated from a silica hydrogel, the structure collapses gradually due to the surface tension of water. Eventually a point is reached where even though water is still evaporating the gel structure no longer shrinks. At this point the gel is called a xerogel. Fast drying can minimize the shrinkage, and removal of water by solvent exchange followed by drying has the same effect. Materials that are dried with negligible loss of pore volume are known as aerogels.

Drying of silica gels can also be carried out under conditions where the solvent in the pores is above its critical point and is vented while maintaining temperature and pressure. KISTLER [634] dried gels supercritically after replacing the water of the hydrogel with alcohol. Alternatively the liquid in the pores can be exchanged for liquid CO_2 , which has more convenient critical-point properties [635, 636]. Considerable interest has been focused on such techniques recently due to the high porosity and mechanical properties achievable [631, 635, 637].

The resulting products from a scheme as in Figure 48.53 are high purity silica gels with controlled porosity. Transmission electron micrographs show the pore structure of silica gel. Typical properties are as follows:

Chemical analysis (dry basis) (%)

SiO_2	99.71
Al_2O_3	0.10
TiO_2	0.09
Fe_2O_3	0.03
Trace oxides	0.07

Physical analysis

Total volatiles	5–6.5%
Surface area	750–800 m^2/g
Pore volume	0.43 cm^3/g
Average pore diameter	2.2 nm
Apparent bulk density	0.72 g/cm^3
Skeletal density	2.19 g/cm^3
Specific heat	920 $\text{J}/\text{kg} \cdot ^\circ\text{K}^{-1}$
Thermal conductivity	522 $\text{J}/\text{m} \cdot \text{h} \cdot ^\circ\text{K}^{-1}$

Refractive index

1.45

Surface Chemistry and Stability. The physical microporosity of silica gel is an important property, as is the chemistry of its bulk and surface species (Figure 48.54). Pure silica gel has a hydroxylated surface covered with silanol groups. These hydroxyl groups are neither very acidic nor basic, with $\text{p}K_a \approx 6$ and an isoelectric point at ca. pH 2. The hydroxylated surface is hydrophilic and adsorbs moisture readily. This adsorbed moisture can be desorbed thermally at 100–200 $^\circ\text{C}$ leaving behind ≈ 5.5 OH/nm^2 (or ca. 5% silanol groups on a 300 m^2/g silica). These silanols are more difficult to remove but this can be done thermally by condensation to form siloxanes and water. Temperatures near 600–800 $^\circ\text{C}$ are required to dehydroxylate to ca. 1 OH/nm^2 . At this silanol concentration the surface is hydrophobic.

Characterization. Numerous methods have been developed to characterize the porosity, structure, and chemistry of silica gels [630] and new methods continue to be applied [631].

With regard to porosity, differently prepared silica gels can be described on the basis of pore diameter d as microporous ($d < 2$ nm), mesoporous ($d \approx 2$ –50 nm), or macroporous ($d > 50$ nm) [638]. The most generally useful methods for characterizing these structures with respect to surface area, pore volume, and pore-size distribution are nitrogen adsorption/desorption techniques. The primary method for surface area is the BET procedure [639] (ASTM D3663-84 or DIN 66131). Methods have been proposed to improve on the BET technique in small pores, such as the t -plot method [640], and the α_s method [641]. The related N_2 pore volume and pore-size distribution (pore volume as a function of pore diameter) methods are ASTM procedures D4222-83 and D4642-87, respectively. The porosity of a silica gel, determined by N_2 porosimetry, is shown in Figure 48.55. Alternative porosity measurement techniques include mercury porosimetry, water pore volume, and oil absorption.

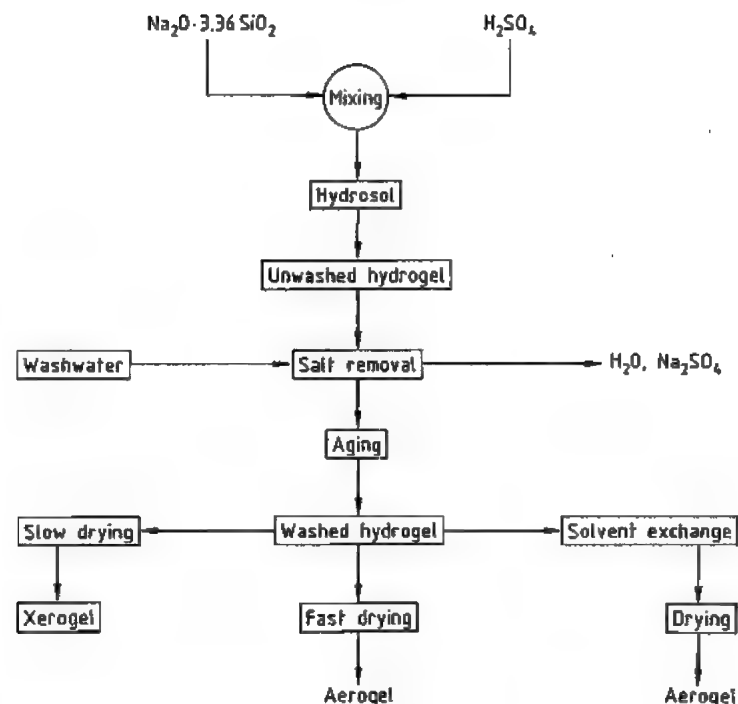


Figure 48.53: Schematic of silica gel manufacture.

Elemental analysis of silica gel focuses on trace elements in the range of $< 1\%$. Inductively coupled plasma atomic emission spectroscopy (TCP-ES) is becoming the preferred technique. pH measurement is performed on slurries and reflects the balance of residual trace elements (ASTM D1208, DIN ISO 787 1X, JIS K 5101/24).

The moisture content of silica gel is important to provide an anhydrous basis for chemical analysis and because the hydration of the surface and pores (Figure 48.54) is important to performance in applications. Most standards require two measurements: moisture loss on drying for 2 h at 105°C (ASTM D280, DIN ISO 787/11, or JIS K 5101/21) and loss on ignition after this drying by heating for 2 h at 1000°C (ASTM D 1208, DIN 55921, or JIS 5101/23). Another method often used in the United States prior to analysis to provide a solids basis is to measure total volatiles as a

weight per cent loss on heating for 1 h at 954°C .

The surface hydroxyl groups of silica gel can be characterized by thermogravimetric analysis [630], vibrational spectroscopy [631, 642], and nuclear magnetic resonance [631, 632, 643]. The information obtained concerns hydroxyl concentration, hydrogen bond interaction between hydroxyl groups, and distribution of $\equiv\text{Si}-\text{OH}$ and $=\text{Si}-(\text{OH})_2$ species on the surface. The adsorptive properties of variously hydroxylated silica materials are an indirect means of characterizing the surface.

Particle-size measurement is also important in silica-gel characterization (DIN 53206). The method for granular gel is standardized sieve screening (ASTM D4513). For particles less than ca. 0.1 mm in size, laser light scattering (ASTM D4464) and conductivity methods are preferred. For particles less than 100 nm, light scattering, electron microscopy, and small angle X-ray scattering are used.

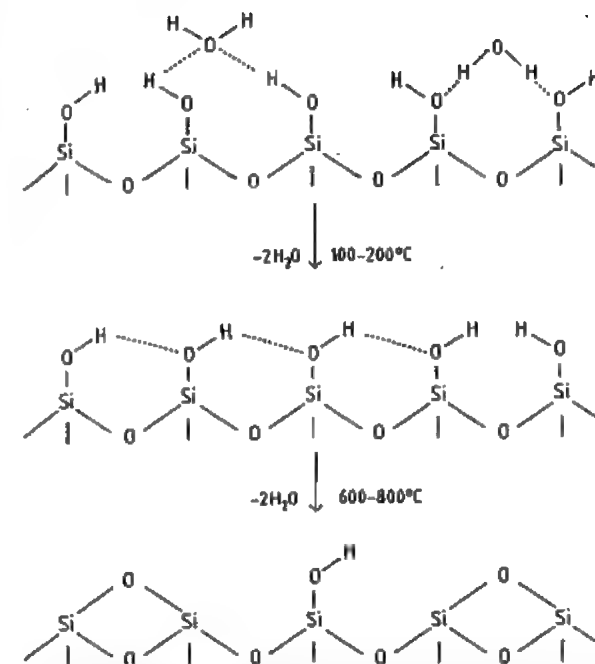
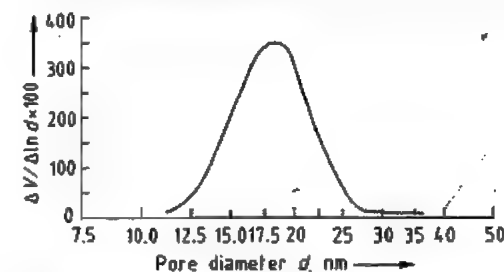


Figure 48.54: Schematic representation of the dehydration of a silica gel surface.

Figure 48.55: Nitrogen pore-size distribution of a silica gel similar to the fast dried sample of Table 48.23 (V = pore volume).

first at $75-120^\circ\text{C}$ then $300-400^\circ\text{C}$. A typical small pore gel made by this process is described in Table 48.23.

The Patrick gelation conditions, with relatively minor variation, have been the basis of most silica gel manufacture since. The next major change in silica gel products was the development of gels of higher pore volume and pore diameter by washing and aging hydrogels under basic conditions. Early references [644, 645] refer to this technology but large scale commercial introduction occurred around 1945. Base washing was a common industrial practice before 1950. In one example [646] a 17% SiO_2 hydrosol gelled in about one hour. The hydrogel was broken up and washed with an aqueous ammonia solution of pH 9 for ca. 45 h then tray dried. Similar conditions are described for intermediate-density gel [633]. One further variation involves fast drying [647] which increases the pore volume and diameter of such gels. Typical properties of acid-washed regular density, ammonia-washed intermediate density, and a flash-dried product are shown in Table 48.23.

48.7.5.3 Production

Processes. The original production process of PATRICK [629] as practiced by the Silica Gel Corporation starting in 1919 contains the main elements of modern processes using aqueous silicate raw materials. The initial step is the batch neutralization of sodium silicate ($1.185 \text{ g SiO}_2/\text{cm}^3$) at $35-80^\circ\text{C}$ with 10% HCl to form a hydrosol. A hydrogel then forms after 3-5 h at ambient temperature and is sized, washed with water to remove salts, and dried

Table 48.23: Typical properties of various silica gels.

Property	Regular density	Intermediate density	
	Slow dried	Slow dried	Fast dried
Total volatiles ^a	5	6	6
Na ₂ O dry basis, %	< 0.1	< 0.1	< 0.1
SiO ₂ dry basis, %	< 0.1	< 0.1	< 0.1
Al ₂ O ₃ dry basis, %	0.05	0.05	0.05
pH ^b	4.0	7.5	4.0
Specific surface area, m ² /g	750	325	390
Pore volume, cm ³ /g	0.40	1.1	1.8
Average pore diameter, nm	2.1	13.5	18.5
Water adsorption, %			
10% R.H.	7.5	2.0	
80% R.H.	35	17.0 ^c	

^a Weight loss after heating in air at 954 °C.^b pH of an aqueous slurry of the gel at 5% solids.^c > 90% water adsorption at 100% R.H.

Several methods of forming hydrogel, typically into spherical shapes, have been developed. Some methods employ a rapid gelation after mixing in a nozzle followed by spray setting [648–651], while others form beads in an oil phase immiscible with the hydrosol [652]. In some bead processes, recycled, dried, and powdered gel is mixed with the fresh sol to improve the physical integrity of the dried gels toward disintegration after contact with liquid water [653].

The supercritical preparation of aerogels has undergone a renaissance since earlier commercial production [654] because of renewed interest in the insulation and light-transmittance properties of these materials. The shift in applications toward large panels has created the need for what are described as aerogel monoliths [631]. One such process [635] forms a silica alcogel then exchanges the alcohol for liquid CO₂ before supercritical drying. The resulting monoliths show good light-transmittance properties. The monoliths, typically 500 × 500 × 2.5 cm, are used to fill the space in the middle of double-pane windows.

Environmental Protection. In the sodium silicate/H₂SO₄ processes the main environmental concerns are the fate of by-product process chemicals, normally aqueous Na₂SO₄ and small amounts of aqueous NH₃, and pH control of this stream.

Quality Specifications. Typical quality criteria for silica gel are chemical purity, moisture content, and porosity. These properties depend on manufacturing conditions such as concentrations, gelling and washing times, pH, and drying conditions. Typical properties of silica gels are reported in Table 48.23. Application-specific properties are often measured for certain end uses (see Section 48.7.5.4).

Silica gel has been described by numerous organizations for the purpose of defining the quality necessary for use in food, cosmetic, and pharmaceutical applications. In the United States, monographs for silica gel are included in the Food Chemicals Codex (1981) and The United States Pharmacopeia The National Formulary (1990). In Japan it is described in the Japanese Pharmacopeia, Standard for Cosmetic Materials, and JIS Z 0701. It is also on the "Positive" list for use in food-grade polyolefins. The EC is compiling permitted silica gel uses into a complete listing for member states. Until that listing is complete member states will maintain individual regulations.

48.7.5.4 Uses

Silica gel is used extensively in a wide variety of applications; here, some major uses are described.

Desiccants. The earliest well identified use for silica was as an adsorbent for water. The affinity of silica gel for water is affected by its

state of activation (or moisture loading) and the degree of saturation of the surrounding fluid by water vapor. A plot of the affinity of silica gel for water vapor as a function of equilibrium relative humidity at ambient temperature is shown in Figure 48.56. The properties of two silica desiccants have been described in Table 48.23.

Silica gel is widely used in the narrow pore form to keep enclosed spaces dry, such as in cable junctions, pharmaceutical containers, and consumer goods. Silica gel is also used for drying natural gas. The wider pore form of silica is used to prevent local condensation in high-moisture environments and to absorb condensed mists of moisture. Another application is to use silica gel to maintain a constant humidity environment around art objects [655].

Desiccants have been described in several countries by standards Mil-D-3716B (United States), DEF STAN 80-22 (United Kingdom), and JIS Z 0701-77. These descriptions include standard properties and methods of analysis.

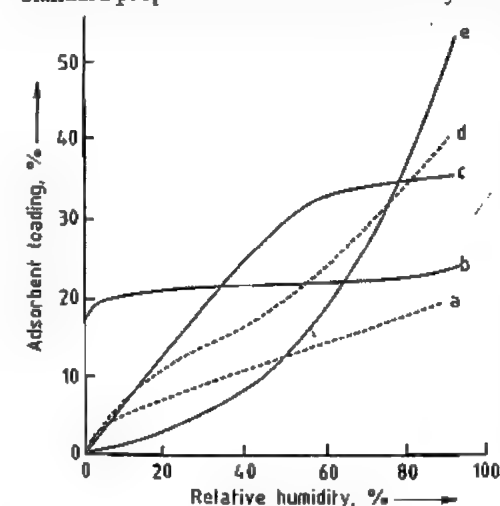


Figure 48.56: Water adsorption isotherms at room temperature as a function of relative humidity for several materials: a) Granular Al₂O₃; b) Zeolite A (Na⁺ form); c) Regular density silica gel; d) Spherical Al₂O₃; e) Intermediate density silica gel.

Adsorbents. Silica gel can adsorb many species other than water, particularly polar substances [656]. In addition to chemical

processing, silicas have many uses in food processing. Treatment of beer with hydrogels, hydrous gels, or xerogels to remove haze-forming proteins is one example [645, 657]. Another food use is the adsorptive purification of glyceride oils [658]. Silica gels also are used extensively in chromatography [659].

Dentifrice. Silica gels have long been components of dentifrice formulations [660] but more recently were employed more for their suitable abrasiveness for cleaning than simply as carriers or thickeners. Xerogels [661] and hydrous gels [662] are used, but must compete with precipitated silicas [663] in this application. The abrasiveness of a dentifrice can be measured [664] and generally correlates with how effectively it cleans the teeth.

Coatings. Fine sized silicas (2–15 μm) are used extensively to control the reflectance of coatings [646, 647, 654]. By interrupting the surface of the coating the gloss of the surface (as measured by ASTM D 523) is reduced but particles too large can harm the appearance of the surface. The fineness of grind (ASTM D1210-79) can be measured and specified. In clear coatings, the refractive index of the silica is important to maintain clarity. A typical matting agent has a particle size of ca. 10 μm, a pore volume of ca. 1.8 cm³/g, and a fineness of grind on the Hegman scale of > 4 (ASTM test).

Catalysts and Catalyst Carriers. The high surface area of silica gel makes it an attractive solid on which to effect catalysis. Silica itself does not catalyze many reactions of commercial significance. Silica aluminas have acidic catalytic properties best exemplified in catalytic cracking [627, 665]. Silica gel is also used as a support in olefin polymerization [666–668].

Suppliers. Silica gel suppliers (with trade names following in parentheses) are summarized: Akzo, Asahi, BASF (Silica-Perlen, Silica-Pulver), Crosfield Chemicals, Unilever Specialty Chemicals Group (Gasil, Lucilite), Eagle, Fuji Silysia (Sylopute, Art Sorb), Glidden (Silcron), W. R. Grace & Co.-Conn. (Sy-

loid, Sylobloc, TriSyl), Kali Chemie (KC-Trockenperlen), PQ (Britesorb), and Uetikon (Diamantgel).

48.7.5.5 Economic Aspects

Silica gel is but one form of synthetic amorphous silica. Published estimates of world production (excluding the Eastern bloc countries and China) of all amorphous silicas (t/a) include:

1974	475 000 [669]
1988	650 000 [670]
1990	1 000 000 [625]

Only the 1990 estimate specifically identified the silica gel tonnage at 90 000 t/a. Between 30–50% of silica gel is estimated to be used in desiccant applications.

48.7.5.6 Legal Aspects

Toxicology and Occupational Health. Silica gel is listed under TSCA in the United States, the Domestic Substances List (DSL) in Canada, the European Inventory of Existing Commercial Substances (EIECS), the Australian Inventory of Chemical Substances, and the Japanese Core Inventory (MITI).

Silica gel is generally classified as synthetic amorphous silica. Epidemiological studies have indicated low potential for adverse health effects in humans [671]. Silica gel is not listed on IARC, National Toxicology Program (NTP), or OSHA carcinogen lists.

Animal tests conducted in 1976–1978 (18-month exposure at 15 mg/m³) showed silica deposition in respiratory macrophages and lymph nodes, minimum lung function impairment, and no silicosis [671]. OSHA has established a PEL of 6 mg/m³ and ACGIH has established a TLV of 10 mg/m³.

Tests conducted for the U.S. DOT classification gave the following results for finely ground silica gel:

1-h LC ₅₀ (rat)	> 2 mg/L
48-h oral LD ₅₀ (rat)	> 31 600 mg/kg (estimated)
48-h dermal LD ₅₀ (rabbit)	> 2000 mg/kg (estimated)
Not considered an ocular irritant.	

Tests conducted for United States FDA approval for use in foods (see 21 CFR 160.105, 160.815, and 172.480) showed:

LD₅₀ (mouse) 8000 mg/kg (limit of test)
LD₅₀ (rat) 4500 mg/kg (limit of test)
6-month feeding tests (rat) at levels up to 10% of diet produced no effects.

A long-term bioassay of chronic toxicity on mice and rats concluded that "proper dietary administration of micronized silica has proven to be generally safe with no long-term toxic effects" [672].

Storage and Transportation. Silica gel should be stored in sealed containers to protect product quality, particularly to avoid moisture adsorption or desorption. Silica gel is not considered a hazardous material by the International Air Transportation Association (IATA Resolution 618, Attachment "A", 1992), the U.S. DOT (49 CFR), or in EEC Council Directive 67/548/EEC.

48.7.6 Pyrogenic Silica

The term pyrogenic silica refers to highly dispersed silicas formed from the gas phase at high temperature. Nowadays, the most important production process is flame hydrolysis. The electric-arc process is of little and the plasma process of no economic significance. The designation pyrogenic used in this chapter therefore always refers to silica produced by flame hydrolysis.

48.7.6.1 Flame Hydrolysis

The flame hydrolysis process was developed in the late 1930s and patented in 1942 [673]. The original aim was to develop a "white carbon" as a reinforcing filler for rubber. However, for technical and economic reasons precipitated silicas were adopted for this use.

In the meantime pyrogenic silica has found applications in numerous branches of industry.

Capacities for pyrogenic silicas amounted to ca. 100 000 t worldwide in 1991. Producers are Degussa (Aerosil), Cabot (Cab-o-sil), Wacker (HDK), and Tokuyama Soda (Reolasil).

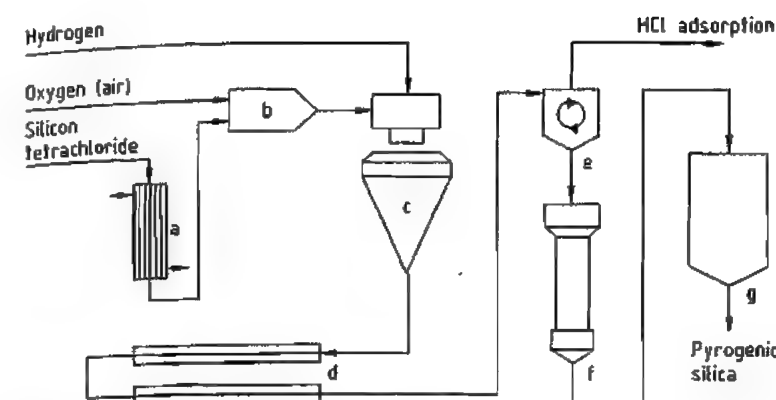
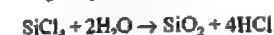


Figure 48.57: General process scheme of flame hydrolysis: a) Vaporizer; b) Mixing chamber; c) Burner; d) Cooling section; e) Separation; f) Deacidification; g) Hopper.

Production Process

Silicon tetrachloride is the usual raw material for flame hydrolysis. It is continually vaporized, mixed with dry air and then with hydrogen, fed to a burner, and hydrolyzed:



The gases leaving the reaction chamber contain all of the silica in the form of an aerosol.

The silica is separated almost quantitatively from the hydrochloric acid-containing off-gas by cyclones (centrifugal separators) or filters. Treatment with steam and air in a fluidized-bed reactor is then carried out to remove residual hydrochloric acid adsorbed on the large surface of the silica. The hydrogen chloride is washed from the off-gases in adsorption columns to give hydrochloric acid in commercial concentrations. The hydrochloric acid formed can be reused by reacting it with silicon to produce silicon tetrachloride and hydrogen.

The properties of pyrogenic silica can be controlled by varying reaction parameters such as flame composition and flame temperature. Thus, desired specific surface areas in the range 50 to 400 m²/g can be produced selectively.

The product, with a bulk density < 20 g/L, is pneumatically transported to packing machines, where the tapped density is increased

to 50–120 g/L by compacting rollers or vacuum packers.

A schematic of the flame hydrolysis process is shown in Figure 48.57.

It is also possible to use methyltrichlorosilane alone or mixed with silicon tetrachloride as raw material. In this case, however, simultaneous hydrolysis and oxidation is required, which requires modification of the production process.

Morphology

Flame hydrolysis produces extremely fine, mostly spherical particles with diameters of ca. 10 nm. The size of the average primary particles, which can be measured by transmission electron microscopy (TEM), ranges from 7 to 40 nm. The particle-size distribution becomes narrower with decreasing primary particle size (Figure 48.58).

The small particles give rise to high specific surface areas of ca. 50–400 m²/g. This consists almost entirely of outer surface, which is not formed by pores, and is readily accessible to diffusion processes. The specific surface areas determined by adsorption (e.g., by the BET method [674]) are in agreement with those determined by TEM within certain limits. Figure 48.59 shows the BET surface area as a function of the mean particle size measured by TEM.

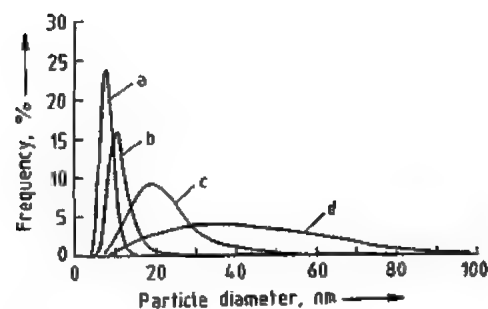


Figure 48.58: Primary particle-size distribution of pyrogenic silicas with various specific surface areas: a) 300; b) 200; c) 90; d) 50 m²/g.

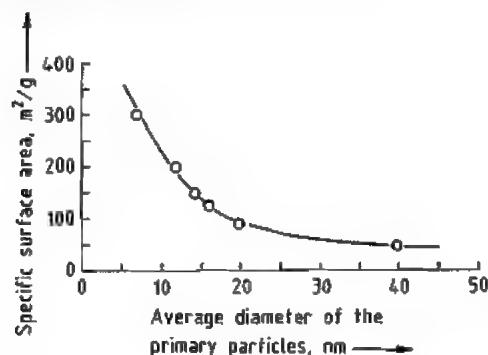


Figure 48.59: Correlation of the average primary particle size with the specific surface area of different pyrogenic silicas.

The primary particles do not occur in isolation, but form aggregates by intergrowth, and agglomerates through cohesion forces. In contrast to precipitated silicas, pyrogenic silicas cannot be produced in the form of defined aggregates or agglomerates. The primary particles can be identified by TEM, but it is not possible to distinguish aggregates from agglomerates [675].

The size of the agglomerates actually present in a liquid or powder mixture depends mainly on the dispersion and mixing intensity during preparation.

Figure 48.60 shows a TEM photograph of a pyrogenic silica with an average primary particle size of ca. 40 nm and a specific surface area of ca. 50 m²/g, while Figure 48.61 shows one with an average primary particle size of ca. 7 nm and a specific surface area of ca. 300 m²/g.

Solid-State Properties

Pyrogenic silicas are X-ray amorphous. For example, X-ray diffraction photographs with a detection limit of 0.2% for Aerosil 200, a hydrophilic pyrogenic silica with a specific surface area of ca. 200 m²/g, show no crystallinity [676]. This fact is of considerable significance for industrial hygiene, since current experiences indicate that the development of silicosis on inhalation of silica dust is associated with the crystallinity.

The refractive index of 1.45 is similar to that of silica glass. The particle size and the surface chemistry have a small but measurable influence on the refractive index. Transparent mixtures can be prepared from pyrogenic silicas and most organic polymers.

Pure pyrogenic silicas are thermally quite stable. Thus, heating for 7 d at 1000 °C results in no change of the morphology and no crystallization. The thermal stability is, however, significantly lower if other substances are present. Traces of alkali or alkaline-earth metal ions in particular act as mineralizers [677].

Since pyrogenic silicas are produced from readily vaporizable starting materials that can be easily purified by distillation, impurity concentrations resulting from the raw materials are very low. Generally, the silicon dioxide content is > 99.8% after ignition for 2 h at 1000 °C to remove chemically and physically adsorbed water. The content of hydrochloric acid by-product can be reduced to less than 250 ppm by suitable measures, which is adequate for most applications.

The purity of pyrogenic silicas is specified particularly for their use in pharmacy. The most important monographs concerning this are:

- European Pharmacopeia 2 (Silica Colloidal Anhydrica)
- DAB 10 (Hochdisperses Siliciumdioxid)
- U.S.P./National Formulary XVII (Colloidal Silicon Dioxide)

Figure 48.60: TEM photograph of a pyrogenic silica with an average primary particle size of ca. 40 nm and a specific surface area of ca. 50 m²/g.

Figure 48.61: TEM photograph of a pyrogenic silica with an average primary particle size of ca. 7 nm and a specific surface area of ca. 300 m²/g.

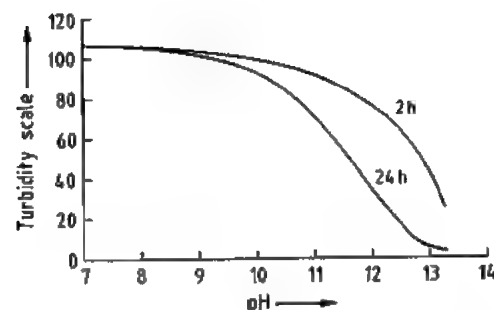


Figure 48.62: Time dependence of the solubility of a pyrogenic silica in caustic soda.

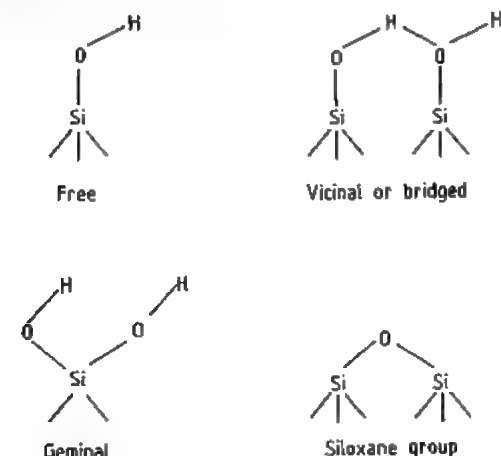


Figure 48.63: Siloxane and silanol groups on the silica surface.

Pyrogenic silicas are largely inert chemically. They dissolve in strong alkali solutions with silicate formation and in hydrofluoric acid with the formation of silicon tetrafluoride. The solubility in pure water is similar to that of quartz (ca. 150 mg/L). Figure 48.62 shows the solubility behavior of a pyrogenic silica with a specific surface area of 200 m²/g in the alkaline pH range.

Surface Chemistry

Siloxane and silanol groups occur on the surface of the silica particles. The former are hydrophobic while the latter are hydrophilic and make the pyrogenic silica wettable. The silanol groups can occur isolated, bridged, or geminal (Figure 48.63).

The silanol groups can be determined quantitatively by reaction with lithium aluminum hydride and measurement of the amount of hydrogen formed. The densities lie between 2.5 and 3.5 SiOH/nm² [678, 679]. The silanol groups are weakly acidic, which causes a zeta potential for the pyrogenic silicas of zero at a pH value of approximately two [680]. Pyrogenic silicas become preferably negatively charged by friction [681].

IR spectroscopy is important for the analysis of the surface chemistry of pyrogenic silicas [679, 682–685], although recent methods such as solid-state NMR spectroscopy promise further results. The following IR bands are of significance:

–O–D	2760 cm ⁻¹
–C–H	2900–3000 cm ⁻¹
–SiOH isolated	3750 cm ⁻¹
–SiOH bridged	3000–3800 cm ⁻¹
–SiOH combination band	4550 cm ⁻¹
H ₂ O adsorbed	5200 cm ⁻¹

Immediately after production pyrogenic silicas show mainly isolated silanol groups. In the course of time, adsorbed water reacts with strained siloxane groups and forms bridged silanol groups. This aging can easily be followed by IR spectroscopy (Figure 48.64) [679].

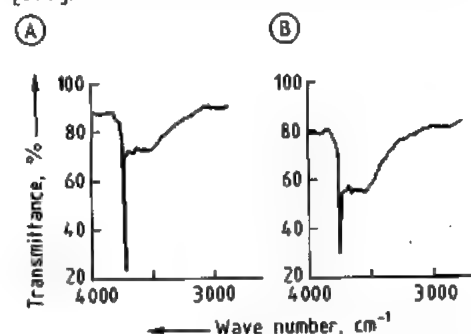


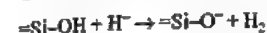
Figure 48.64: IR spectra of pyrogenic silica (200 m²/g specific surface area) shortly after production (A) and after storage for one year (B).

The desorption energies of both the chemically and physically bound water can be determined by gravimetric adsorption and temperature-programmed desorption [686]. Thus, the following energies were determined: 50 kJ/mol, for water hydrogen bonded to a silanol group, and 84 kJ/mol for water bonded to

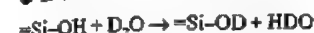
two neighboring silanol groups. The elimination of water from neighboring silanol groups and isolated silanol groups requires 122 kJ/mol and 130 kJ/mol, respectively.

The silanol groups undergo acid-specific reactions; examples include:

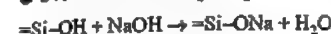
- With hydride ions (e.g., LiAlH₄) [678]



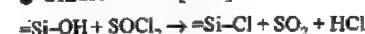
- Deuterium exchange [679]



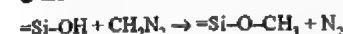
- Neutralization [687]



- Chlorination [688]



- Esterification with diazomethane [688]



Summaries of the surface chemistry of finely divided silicas are given in [689, 690].

Surface Modification with Silicon Compounds

Pyrogenic silicas are hydrophilic; however, a hydrophobic character is more favorable for some applications. This requirement can be met by reaction with dimethyldichlorosilane [691, 692]. The resulting silica thus is no longer wettable by water and was introduced on the market in 1962 under the name Aerosil R 972. Apart from chloroalkylsilanes, mainly hexamethyldisilazane, alkoxyalkylsilanes, and polydimethylsiloxanes are used.

Apart from methyl and longer chain alkyl groups, organofunctional groups can also be anchored on the surface of pyrogenic silicas by using silanes. This form of modification was first used on a large scale for applications in dental materials. A pyrogenic silica with a low specific surface area is treated with γ -methacryloxypropyltrimethoxysilane to give an active filler that can be chemically bonded to the polymethylmethacrylate matrix and provides the dental material with very good mechanical properties [693–695].

Another use of pyrogenic silicas modified with organofunctional silanes is in toners. Un-

til recently photocopiers generally fixed the latent electrostatic image on a positively charged selenium layer. An electrostatically negatively chargeable toner is required for development, which contains a hydrophobic pyrogenic silica to improve the flow behavior and chargeability. In more modern copier systems the latent image is formed on an organic semiconductor layer, which is negatively charged and requires a positively chargeable toner. However, pyrogenic silicas tend to become negatively charged due to the presence of silanol groups even in hydrophobized products. Hence, a surface modification is necessary to allow positive charging. This can be achieved by using aminofunctional silanes, which undergo hydrolysis-stable anchoring to the silica surface [696–698].

Characterization

Pyrogenic silicas can be characterized well on the basis of chemical and physicochemical data; however, these do not allow a definite assessment of their suitability for a particular use, which requires application testing. The following test methods have proved useful to test the suitability for many uses and also for the quality control of hydrophilic, pyrogenic silicas:

- BET surface area, m²/g (DIN 66131)
- Drying loss, % (2 h at 105 °C; DIN ISO 787/II)
- pH value (4% aqueous suspension; DIN ISO 787/IX)
- Silicon dioxide content, % (fuming with hydrofluoric acid, relative to the substance heated at 1000 °C for 2 h)

For hydrophobic or surface-modified pyrogenic silicas it is advisable to determine the carbon content instead of the silicon content, since the former provides information on the extent of surface loading.

Uses

Reinforcing Fillers. Pyrogenic silica is used in large quantities as an active filler in silicone

rubber. In RTV silicone sealants, both hydrophilic and hydrophobic pyrogenic silica are used (ca. 10%) to modify mechanical properties such as Shore hardness, tensile strength, and tear strength. High temperature vulcanizing (HTV) silicone rubber requires ca. 30% pyrogenic silica to improve the mechanical properties. Hydrophobic pyrogenic silicas with strongly reduced thickening action are used in liquid silicone rubbers. Theories of the reinforcing action of pyrogenic silica in silicone rubber are discussed in [699–701].

Pyrogenic silicas are also used as active fillers in natural and synthetic rubber, particularly if extremely high mechanical properties are required, as in cable sheathing, seals, or conveyor belts.

In fluoroelastomers, both hydrophilic and hydrophobic silicas improve the mechanical properties [702, 703], even under the action of aggressive gases.

Thickening and Thixotropization. An important application for pyrogenic silicas is the adjustment of the rheological properties of liquid systems such as paints, thermosetting resins, and printing inks. The increase in viscosity generally plays a minor role; thixotropization and the development of a yield value are decisive in practice. These effects are generally attributed to the formation of a three-dimensional network of silica agglomerates, which fixes the liquid in "cells" and thus increases the viscosity. The silica particles interact via silanol groups. The spatial network is destroyed by mechanical stress (e.g., stirring or shaking) to an extent which depends on the intensity and duration of energy input, whereby the viscosity decreases. The silica network regenerates when the stress is removed, and the original viscosity returns. This theory has proved suitable for simple, nonpolar liquids, but is not applicable to complex and/or polar systems, in which adsorption and solvation effects determine the rheological activity [704], especially in the case of hydrophobic pyrogenic silicas.

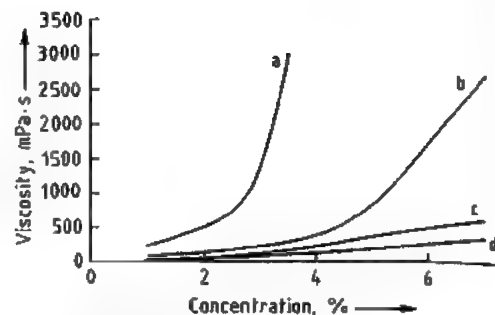


Figure 48.65: Thickening effect of a pyrogenic silica with 200 m²/g specific surface area (Aerosil 200) in various solvents: a) Xylene; b) Butylacetate; c) Diacetone alcohol; d) Butanol.

Hydrophilic pyrogenic silicas show the best thickening action in nonpolar liquids (Figure 48.65).

Antisettling Agents. Closely linked with the control of the rheological properties of liquid systems is the action of pyrogenic silicas as antisettling agents. The establishment of a flow limit hinders settling of suspended particles, depending on their density, size, and shape. If settling does occur, pyrogenic silica generally prevents caking of the sediment and ensures easy dispersibility.

This effect is mainly utilized in filler- or pigment-containing paints and plastics. Not only suspensions of lighter solids can be stabilized, such as silica-based matting agents, but also heavy anticorrosion pigments such as zinc dust or micaceous iron oxide. Both hydrophilic and hydrophobic pyrogenic silicas can be used as antisettling agents. The most suitable type must be determined for each individual case, whereby additional effects, such as the water repellency of hydrophobic products in corrosion protection systems, must also be taken into consideration [705, 706].

Dispersants. In solid-containing liquid systems, pyrogenic silicas reduce the reagglomeration of the solid particles during the dispersion process, whereby a more favorable state of distribution is achieved. This effect is particularly important in pigment-containing systems, where both the gloss and also the tinting strength, and in the case of carbon black pigments also the jetness, can be im-

proved by adding small quantities of pyrogenic silica [705].

Free Flow Agents. Some powders exhibit poor fluidity or they agglomerate on storage, particularly under the influence of pressure or moisture. The causes of agglomeration include solid bridges, which form by drying or pressure sintering processes, liquid bridges, electrostatic charging, and van der Waals forces [707, 708]. This can make use of the material difficult or even impossible. In many cases this can be remedied by the addition of hydrophilic or hydrophobic silicas. The reasons for this are complex. Thus, the small silica particles can envelop the powder particles and act as "ball bearings", hydrophilic pyrogenic silica can adsorb moisture and "render it harmless", or hydrophobic pyrogenic silica can slow down the absorption of moisture. The significantly smaller silica agglomerates can decrease the van der Waals forces between two powder particles by acting as spacers [708, 709]. Pyrogenic silica is used in fire-extinguisher powders, tablet mixtures, toners, powder coatings, and table salt.

Other uses of pyrogenic silica include:

- Adsorbents
- Antiblocking agents for plastic films
- Coatings
- Catalyst supports
- Matting agents

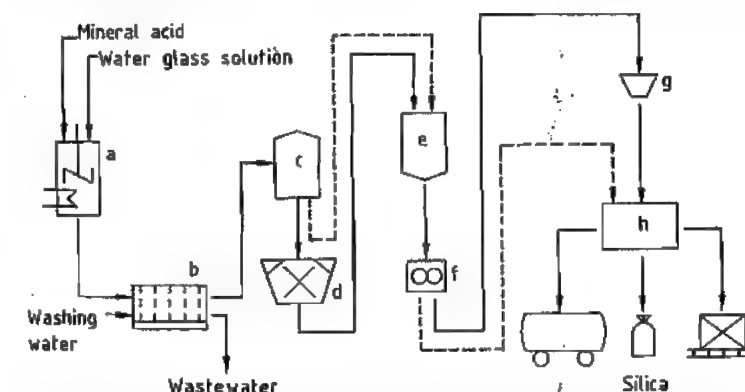


Figure 48.66: Process scheme for the production of precipitated silicas: a) Precipitation; b) Filtration; c) Drying; d) Milling; e) Storage; f) Compacting; g) Granulation; h) Packaging.

- Grinding agents
- Polishing agents
- Raw materials for silica glasses
- Thermal insulation
- Additive carriers

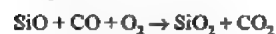
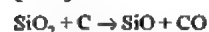
Industrial Hygiene and Safety

Pyrogenic silica does not cause silicosis on inhalation. So far no indication for this illness has been found for those employed in production who undergo regular medical tests [710]. However, since it can lead to irritation of the respiratory tract due to the fine particles, a MAK of 4 mg/m³ total dust in inhaled air was applicable in 1991. This MAK value is not exceeded if suitable precautions are taken, e.g., lowest possible dust development upon handling or extraction of air (ventilation). Otherwise dust masks should be used. According to the findings so far pyrogenic silica is basically harmless by oral intake [711, 712]. Pyrogenic silica can cause a feeling of dryness on the skin, which can be easily remedied by washing and creaming.

Pyrogenic silica is susceptible to electrostatic charging on handling. If it is likely to come into contact with combustible gases or vapors, it is necessary to take the corresponding safety measures, such as careful earthing and utilization of explosion-proof plants.

48.7.6.2 Electric-Arc Process

The reduction of quartz sand with coal in an electric-arc furnace gives gaseous silicon monoxide, which is oxidized to finely divided amorphous silica by atmospheric oxygen [713]:



In a variant of this process the thickening effect of the electric-arc silica is increased by adding steam during oxidation followed by thermal treatment [714].

The matting agent TK 900 used in paints is a silica produced by Degussa using this process.

48.7.6.3 Plasma Process

Finely divided amorphous silicas can be produced in plasma burners. In one case quartz sand is reduced to silicon monoxide with methanol at ca. 2000 °C. Subsequently, reduction with steam is carried out [715]. At present such silicas are not available commercially. A schematic of the plasma process can be found in [716].

48.7.7 Precipitated Silicas

48.7.7.1 Introduction

Precipitated silicas, like pyrogenic silicas and silica gels, are a synthetic, finely divided, white, amorphous form of silicon dioxide. Precipitated silicas have only been produced commercially since the 1940s. In the meantime, they have become the most important group of silica products on the basis of the amounts produced. Worldwide production capacity in 1990 was ca. 800 000 t, compared to ca. 400 000 t in 1970. Capacities in Europe, America, and Asia amount to 340 000, 260 000, and 200 000 t, respectively.

The largest producers worldwide are Degussa, Rhône-Poulenc, Akzo, and Crosfield in Europe, as well as PPG and Huber in the United States. The Asian market is additionally supplied by numerous local producers.

Among these, the companies with the largest capacities are Nippon Silica and Tokuyama Soda in Japan, and Sam Yung and Kofran in Korea.

48.7.7.2 Production

Raw materials for the production of precipitated silicas are aqueous alkali metal silicate solutions (e.g., water glass) and acids, generally sulfuric acid [717–732]. Precipitation with hydrochloric acid [733, 734], organohalosilanes [735, 736], carbon dioxide [737, 738], or a combination of the latter with mineral acids [739] are of minor economic importance.

In the reaction of alkali metal silicate solution with mineral acid, the silica precipitates according to the following equation:



In contrast to silica gels, which are produced under acidic conditions, in this case precipitation is carried out in neutral or alkaline media. The properties of the precipitated silicas can be influenced by the design of the plant equipment and by varying the process parameters.

The production process consists of the following steps; precipitation, filtration, drying, grinding, and, in some cases, compacting and granulation (Figure 48.66).

Numerous possibilities exist for carrying out the precipitation [717–739]. So far only batch precipitation processes have attained economic importance, although continuous precipitations have also been reported [732]. Generally, acids and alkali metal silicate solution are fed simultaneously into water in a stirred vessel with the formation of silica seeds. In the course of the precipitation, three-dimensional silica networks are formed, accompanied by an increase in viscosity. The networks are reinforced by further precipitation of oligomeric silica and grow further into discrete particles with a decrease in viscosity. The formation of a coherent system and thus a gel state is avoided by stirring and increasing the temperature.

The properties of the silica can be influenced by varying important precipitation parameters such as pH, temperature, duration, and solid concentration. Additionally, the rate of addition of the acid and the intensity of stirring, which can be supplemented by a shearing action, also influence the properties of the silica.

The separation of the silica from the reaction mixture and the washing out of the salts contained in the precipitate is carried out in filter aggregates such as rotary filters, belt filters, or filter presses (chamber, frame, and membrane filter presses).

The solids content of the washed filter cake is 15–25% depending on the type of silica and filter, therefore, drying requires the evaporation of large quantities of water. Depending on the desired properties of the end product, drying is carried out in turbine, plate, belt, or rotary driers. Special product properties can be achieved by spray drying the filter cake after redispersion in water or acid [722, 725, 740].

Figure 48.67 shows scanning electron micrographs of a spray-dried, unground silica and a conventionally dried, ground silica.

To control the desired fineness of the particles, various mills and, if required, separators [741] are used. Special degrees of fineness can be achieved by air-jet or steam-jet milling [722, 742]. The silica is separated from the air in cyclones or filters.

Processes for the compression and granulation of precipitated silica have been developed [743, 744] to reduce the volume for transport and for certain uses and also to decrease the formation of dust on handling and processing.

Bags, big bags, containers, or transport silos are used for packaging and shipping. Information about the different methods of packaging and shipping is given in [745]; dust-free handling of precipitated silicas is described in [746]. In Germany the general dust limit of 4 mg total dust/m³ air must be adhered to when handling precipitated silicas. Similar regulations apply in other countries.

A ↑

B ↓

Figure 48.67: REM photographs of precipitated silicas. A) Spray-dried unground silica; B) Conventionally dried, ground silica.

48.7.7.3 Properties

Physicochemical Properties

Precipitated silicas consist mainly of spherical primary particles, generally intergrown in three-dimensional aggregates. These aggregates can pack together to form larger agglomerates. The terms primary particle,

agglomerate, and aggregate are defined in DIN 53206.

Some important physicochemical properties of several precipitated silicas are listed in Table 48.24.

The specific surface area is generally determined by the BET method (DIN 66131), which measures both the outer surface and the surface of accessible pores. The specific surface area is of importance especially in reinforcement and adsorption applications. Precipitated silicas can be produced with specific surface areas of 25–800 m²/g.

The mean agglomerate size is important in the use of precipitated silicas as flatting or antiblocking agents for paint systems and plastic films. The agglomerate size can be determined by various methods either on the powder or after incorporation in a medium (e.g., water, paint, silicone rubber) [747].

The tapped density (DIN ISO 787/11) is a measure of the weight of the powder and thus gives indications of the spatial requirement for transportation and a general guide for han-

dling. The tapped densities of precipitated silicas lie in the range 50–500 kg/m³.

The loss on drying (DIN ISO 787/2) includes the majority of the water physically bound to the silica and for precipitated silicas generally lies between 2.5 and 7% (on leaving the supplier).

The loss on ignition (DIN 55921) includes the additionally chemically bound water (a siloxane group is formed from two neighboring silanol groups with the loss of a water molecule). Ignition losses for precipitated silicas generally lie between 3 and 7%.

Generally the pH value (DIN ISO 787/9) of precipitated silicas is ca. 7.

The dibutyl phthalate (DBP) absorption (DIN 53601) is a measurement of the adsorptive capacity and for precipitated silicas lies in the range of 175–320 g/100 g. The absorptive capacity is important for the conversion of liquids and pastes into powders.

The determination of the sieving residue (DIN ISO 787/18) provides an indication of the amount of difficultly dispersible fractions in a precipitated silica.

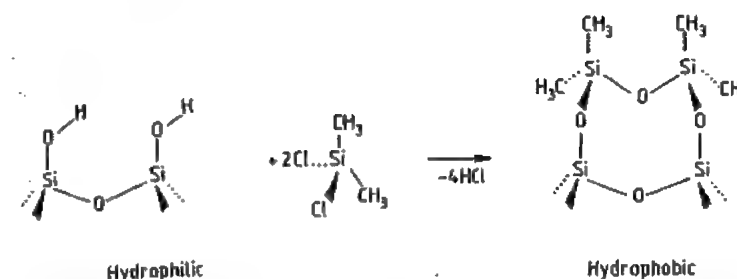


Figure 48.68: Schematic of the reaction of the surface silanol groups of a precipitated silica with dimethyldichlorosilane.

Surface Chemistry and Surface Modification

Precipitated silicas have two different functional groups on their surfaces: silanol (Si-OH) groups and siloxane (Si-O-Si) groups.

These two groups substantially influence the surface properties and hence the application properties of precipitated silicas. The surface has 5–6 silanol groups per nm², which results in the hydrophilic character of precipitated silicas. Whereas the siloxane groups are generally chemically inert, the reactivity of the silanol groups allows chemical surface modification [748] of precipitated silicas. Thus, the reaction with organosilanes [749–751] or silicone fluids [752, 753] leads to hydrophobic precipitated silicas.

Hydrophobization is carried out industrially both by wet processes (e.g., addition of organochlorosilane to the precipitate suspension; see Figure 48.68) and dry processes (e.g., the reaction of precipitated silicas with silicone fluids).

In coating processes, in contrast, no chemical reaction takes place; the coating agents are adsorbed on the silica surface. Wax coating with wax emulsions has become industrially important [722, 754, 755]. Surface modification is advantageous for certain applications (e.g., free flow agents, defoamers, and flatting agents; see Section 48.7.7.4).

Chemical Composition and Analysis

The chemical composition of precipitated silicas (Table 48.24) is generally less impor-

tant than the physicochemical data with regard to the application properties. Furthermore, commercially available precipitated silicas differ only slightly in their composition.

The SiO₂ content is determined gravimetrically by fuming with hydrofluoric acid (DIN 55921); the analysis of the metal-containing impurities is performed by atomic absorption spectrometry (AAS). The sulfate content is determined by complexometric titration (DIN 38405/5), colorimetric titration (DIN 2462/8), or potentiometric titration.

The carbon content of modified silicas is determined by converting the carbon-containing component into CO₂.

A survey of the chemical analysis of precipitated silicas is given in [756].

48.7.7.4 Uses

Precipitated silicas can be tailor-made to meet the requirements of various uses. Only the most important of the numerous applications (Figure 48.69) are mentioned here.

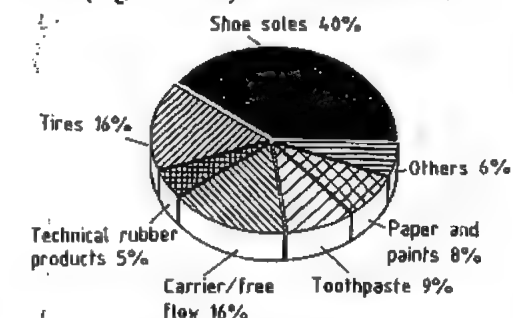


Figure 48.69: Worldwide consumption and use of precipitated silica in 1990.

Table 48.24: Physicochemical data and chemical composition of several precipitated silicas.

	Sident 12 DS	Utrasil VN 3	Sipemat 22	Sipemat 50 S	Intergarant Super 90	OK 412 ^a	Sipemat ^b D 17
Appearance	←		fluffy white powder				→
Behavior toward water	←		hydrophilic				hydrophobic
BET surface area, m ² /g	80	170	190	450	700		100
Mean agglomerate size, μm	6 ^c		100 ^d	3 ^e		3 ^e	10 ^f
Tapped density, g/L	200	260	270	100	180	120	150
Loss on drying ^g , %	6	6	6	6	6.5	ca. 5	3
Ignition loss ^h , %	4	5	5	5		ca. 11.5	7
pH value ⁱ	6.5	6.3	6.3	6.5	6.0	ca. 06	8 ^b
DBP absorption ^{k,l} , g/100 g			260	330			230
SiO ₂ ^l , %	98	98	98	98.5	99	ca. 99	99.5
Na ₂ O ^l , %	1		1	0.6			0.2
Fe ₂ O ₃ ^l , %	0.03	0.03	0.03	0.03			0.03
SO ₃ ^l , %	0.8		0.8	0.7			0.1
Sieve residue ^f , %			0.5	0.1			0.1

^a Flatting agent.

^b In water: methanol 1:1.

^c Coulter Counter, capillary 100-μm.

^d Alpine air-jet sieve.

^e Determined from SEM photos.

^f DIN ISO 787/18.

^g DIN ISO 787/2.

^h DIN 55921.

ⁱ Relative to substance dried for 2 h at 105 °C.

^j DIN ISO 878/9.

^k DIN 53601.

^l Relative to substance heated for 2 h at 1000 °C.

The oldest and most important use of precipitated silicas is the reinforcement of elastomer products such as shoe soles, technical rubber articles, cable, and tire compounds [757, 758].

The addition of 20–100 parts by weight of precipitated silica to 100 parts by weight of natural or synthetic rubber improves the tensile strength, hardness, tear strength, and abrasion resistance of the vulcanized material [759]. Furthermore, special precipitated silicas enable the production of transparent vulcanized materials.

The reinforcing effect of precipitated silica is superior to that of natural or mineral fillers and, in contrast to carbon blacks, they allow the production of white and colored rubber articles.

In cables, they are used mainly in sheathing compounds for cables that are not fixed and must be differentiated from the background by a colored exterior (e.g., mining or excavator-hauling cables). The high resistance of the cable sheath to friction and tearing protects the inside of the cable from abrasion and damage [760].

A further important use of precipitated silica is as reinforcing materials in tires. Furthermore, they are constituents of certain adhesive systems for the bonding of unvulcanized rubber to textiles (nylon, polyester) or steel tire cord.

In more recent developments, sulfur-containing bifunctional silanes are used to form covalent bonds between the silica filler and the unvulcanized rubber. The improved static and dynamic properties are being increasingly exploited in tire compounds for the running tread, side walls, and carcasses of highly stressed special tires [761–763].

Precipitated silicas are also used as reinforcing fillers in silicone rubber [764, 765], where they replace the more expensive pyrogenic silicas in certain formulations.

In thermoplastics, precipitated silicas are used to improve specific properties. They act as antiblocking agents and are used to prevent plate-out effects in films and film production.

They are also used to improve the mechanical properties of PVC flooring [766, 767].

A further major application is the use as carrier silicas for materials and as free flow agents for powder formulations, particularly of hygroscopic and adhesive substances. Of particular importance is high adsorptivity and good flowability of the silica, which can be achieved, for example, by spray drying.

Such precipitated silicas absorb liquids or solutions to give powder concentrates that contain up to 70% of the liquid [768]. In this way liquid materials are converted into a dry, free-flowing form, which can be mixed in any ratio with other dry substances. This is of particular importance in the animal-feed industry for the mixing of feed additives [769]. Materials converted into powder form include: choline chloride, ethoxyquin, molasses, and vitamin E acetate [770]. Fats can be converted into free-flowing powders for use as milk-substitute feeds [768, 770], mainly for the fattening of calves.

Precipitated silicas are used as carriers for crop protection agents and insecticides [771], in toothpastes as cleaning agents, since they clean effectively with a minimum of scratching [772, 773].

The surfaces of objects are matted for reasons of fashion but also to increase safety by avoiding dazzle. Special silica products have been developed for matting of paints and varnishes [722, 741, 755]. The matting effect is the result of roughening of the surface on the microscopic scale, whereby the light is diffused and no longer directionally reflected.

In the paper industry precipitated silicas are used in the production of special papers to ensure high depth of color and good contrast of the printed papers [774]. Here the silica fills the pores of the paper and gives a smooth surface.

Particularly, hydrophobic precipitated silicas are used increasingly in mineral-oil and silicone-oil antifoam agents to increase the antifoaming effect [775]. They are used as foam regulators in laundry detergents [776].

Further uses for precipitated silicas include additives in rolled asphalt and asphalt mastic

to increase the dimensional stability [777, 778], the purification and stabilization of beer [779], and the analysis of blood [780].

48.7.8 Porosils

48.7.8.1 Introduction

Porosils are crystalline porous silicas of the general composition $\text{SiO}_2 \cdot M$, where M is an organic or inorganic guest molecule residing within the pores of the silica host framework. R. M. BARRER coined the name porosils to differentiate between porous aluminosilicate zeolites and a new class of compounds of distinct composition [781]. Due to their porous crystal structure porosils have properties similar to the zeolites; however, differences in chemical composition are responsible for their specific properties in catalysis, sorption, and molecular sieving.

Work in the field was initiated in 1978 by FLANIGAN et al. [782] who reported on the synthesis and crystal structure of the siliceous analogue of the commercially most important zeolite ZSM-5.

The guest species M can be expelled by thermal treatment to give the pure silica form of the porosil. Therefore, porosils are considered to be the porous polymorphs of the structure family SiO_2 . Up to now, 24 porosil structure types have been made, either by template-directed synthesis or post-synthesis treatment of aluminosilicate zeolites [783]. In the synthesis of porosils the guest species M act as templates for the pores, defining their size and geometry [784]. During the post-synthesis treatment framework aluminum is substituted by silicon, and M is atmospheric gases or sorbate molecules [785].

Porosils are subdivided into zeosils and clathrasils according to the pore structure of the silica framework. Zeosils have channel-type pores with pore openings larger than 0.4 nm (Figure 48.70). The channels may intersect to give a two- or three-dimensional pore system. Clathrasils have cage-type voids with pore openings much smaller than the free di-

ameter of the cage and less than 0.45 nm (Figure 48.70).

With the exception of melanophlogite, a rare mineral formed by low-temperature, low-pressure metamorphism in, e.g., serpentine veins [786], all porosil structure types are synthetic materials. The ever increasing number of new porosil structure types reflects the efforts in the systematic investigation of the mechanism of formation of zeolites, for which porosils represent a simplified system. Besides porosils, water (clathrate hydrates), AlPO_4 (AlPO's), GaPO_4 , and other III–V oxides (e.g., arsenates) also form neutral inorganic porous framework structures when synthesized in the presence of structure-directing guest molecules [783].

48.7.8.2 Physical and Chemical Properties

The physical and chemical properties of porosils are closely related to their crystal structure and composition. Porosils are colorless materials of hardness close to that of quartz. Since they are framework silicas, they exhibit no pronounced cleavage. Refractive indices vary systematically with the density of the silica framework [787]. This confirms that the nature of the Si–O bond accounts for most of the physical properties and is closely related to the natural polymorphs of the SiO_2 structure family. The porosils are thermodynamically metastable and transform reconstructively to cristobalite at high temperature (e.g., melanophlogite: $T > 950^\circ\text{C}$ [788]).

Below 200°C structural phase transitions to lower symmetry space groups have been reported for melanophlogite [789], dodecasil 3 C [790], decadodecasil 3 R [791], silica-ZSM-5 [792], and silica-ZSM-11 [793].

For dodecasil 3 C, three consecutive phase transitions have been reported, with transformation from cubic to tetragonal, orthorhombic, and finally monoclinic symmetry [794]. This reflects the flexibility of the silica framework. Several phase transitions are ferroic (e.g., ferroelastic) indicating interesting physical properties for the material.

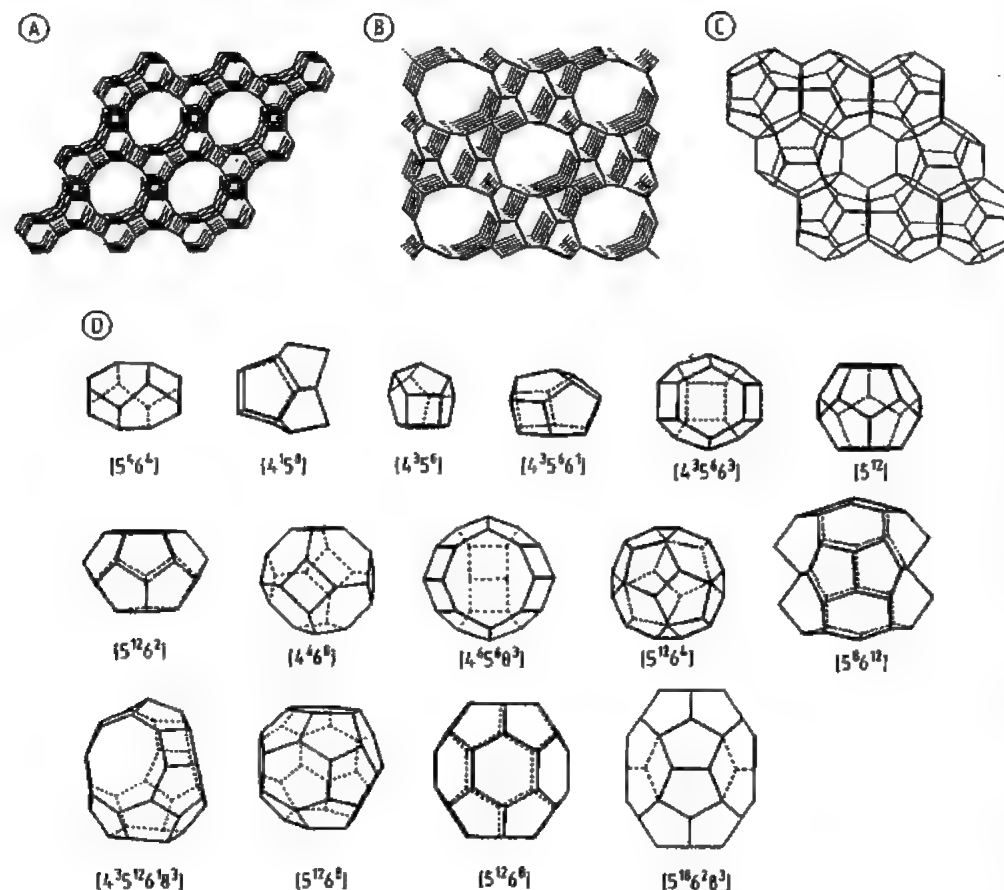


Figure 48.70: Skeletal projections of porosil framework structures. Si atoms are located in the nodes of the framework O atoms, which are close to the midpoint between 2 Si atoms, but are omitted for clarity. A) Projection of the AFI structure along the channel axis. The channel pore opening is confined by 12 Si atoms (12 MR); B) Projection of the FER, TON, MTT, MEL, and MFI structures along the straight channel axis. The channel pore opening is confined by 10 Si atoms (10 MR); C) Projection of the dodecasil layer. Pentagonal dodecahedra are arranged in layers which are the basic structural feature of DOH, MTN, DDR, and decadodecasil 3 H; D) Compilation of types of cage as found in clathrasil structure types ([5¹²] represents pentagonal dodecahedron, i.e., 12 five-membered rings).

Since the composition of the host framework is SiO_2 , porosils are electroneutral. The pores, therefore, contain only electroneutral guest species (i.e., ion pairs, molecules, and/or atoms). In contrast to aluminosilicate zeolites, porosils are hydrophobic [782, 795], preferentially sorbing aprotic organic molecules. The weak Lewis acidity of the electroneutral SiO_2 framework of the porosils reduces considerably their potential as materials for heterogeneous acid catalysis, for which the isostructural aluminosilicate zeolites are

widely used [796]. The pore geometry of the porosil structure types varies from zero-dimensional pores (i.e., cavities) to three-dimensional pore systems (i.e., intersecting channels). The pore openings are confined by $[\text{SiO}_4]$ units arranged in a ring (Figure 48.70) (e.g., ten-membered ring, 10 MR: 10 SiO_4 units per ring). In general the sorption properties of the materials are related to the largest pore opening of the structure, which provides for the release of guest molecules and the access of sorbates to the internal surface. In

clathrasils the maximum pore opening (6–8 MR) is too small for the exchange of the occluded species. The template-free material can be obtained only by calcination at $> 600^\circ\text{C}$. For 6 MR as maximum pore opening only very small atoms or molecules such as H_2 or He could be sorbed onto the silica framework. Zeosils with pore openings of 8–12 MR are calcined at lower temperatures and could be used for the selective sorption of, e.g., *n*-alkanes (8 MR materials) or *p*-substituted aromatic compounds (10 MR materials). Because of the uniform character of the pore opening and the possibility of tailoring the size of the pores, porosil-containing membranes, such as those already available for zeolites, could be useful for separation processes [797].

Zeosils

Physical and chemical properties specific to zeosils are related to their crystal structure. The channel-like pores allow access to the internal surface of the material for sorbates that meet the geometrical requirement of the pore window.

The free diameter of the individual materials, however, varies considerably due to the flexibility of the silica framework. Because of the hydrophobic properties of the silica framework and the geometry of the internal pore system, zeosils are of particular interest for various applications. In the presence of water zeosils sorb selectively hydrophobic organic molecules in the vapor and liquid phase [798]. Sorption of monomers into the silica framework followed by polymerization leads to one-, two-, or three-dimensional polymeric filaments inside the zeosil framework, as already demonstrated for zeolites [799]. The deposition of semiconducting materials [800] and metal atom clusters [801] inside, e.g., the zeosil cavity of silica-A or silica-faujasite creates new materials with interesting properties due to the limited size of crystallites built within the pores. The sorption of polar organic molecules such as *p*-nitroaniline also leads to changes in symmetry and polarization of the host-guest composites, leading, e.g., to non-

linear optical properties [802]. For a review on new applications of zeosils, see [803].

Clathrasils

The clathrasil structure types have cage-like pores. Species inside the cavities are too large to pass through the 4 MR, 5 MR, 6 MR, or 8 MR windows without their decomposition. In general, clathrasils in the as-synthesized form have no exchange capacity or sorption properties. After calcination at high temperature ($> 600^\circ\text{C}$) the decomposition of the guest species may lead to a guest-free porosil with very narrow pores that is suitable for sieving and sorption processes. The properties of clathrasils are, therefore, linked to properties introduced by the guest molecules clathrated in the formation process. Because of the high thermal and chemical stability of the silica host framework, clathrasils have been proposed as containers for radioactive gases (e.g., krypton) [804]. The synthesis of the clathrasil dodecasil 3 C with a number of nonglobular guest molecules leads to a distortion of the cubic symmetry of the silica framework. At room temperature the materials have acentric symmetry and, therefore, nonlinear optical properties [805]. The temperature of the phase transition to the acentric space group depends on the nature and the concentration of the guest molecule in the silica framework and is in the range between slightly below room temperature and ca. 200°C .

48.7.8.3 Manufacture of Porosils

With the exception of melanophlogite, all porosil structure types are synthetic materials made directly from an active form of SiO_2 or by dealumination of high-silica zeolites.

Synthesis of Porosils

Structure-directing templates play a key role in the synthesis of porous silicas [806]. Since the templates are occluded within the pores during synthesis, it is their size and shape which determine the size and shape of the pores of the silica framework. Organic

amines have proved to be the most efficient templates. Up to now ca. 100 different molecules have successfully been used for the synthesis of porosils [806–808]. Globular species such as xenon, quinuclidine, and 1-aminoadamantane preferentially stabilize the cage-like voids characteristic of clathrasils. Chain-like amines such as the α,ω -diamines of propane, butane, pentane, etc., stabilize channel-like voids. The size of the pore depends on the size of the template. Whereas pyrrolidine leads to preferential formation of dodecasil 3 C by occupying a 16-hedral cage, 1-aminoadamantane is occluded within a 20-hedral cage in dodecasil 1 H. Zeosil structure types with 10 MR channels are formed in the presence of aliphatic chain-like templates (α,ω -diamino-*n*-alkanes); 12 MR channels are formed with molecules containing sequences of *p*-substituted heterocycles (e.g., 4,4'-trimethylenedipiperidine).

Dealumination of Aluminosilicate Zeolites

Aluminum is selectively extracted from the silicate framework and replaced by silicon [809]. The dealumination procedure includes successive chemical and hydrothermal treatment of the material in order to extract and remove the framework aluminum atom. A typical procedure is the calcination of the synthesis product at 300–500 °C to expel the organic template, exchange of the cations with ammonium, and steaming at ca. 600 °C to remove the aluminum.

Formation of Melanophlogite

So far melanophlogite is the only known natural porosil. In synthesis experiments the conditions of formation have been simulated and are of low temperature (ca. 100–200 °C) and low (autogenic) pressure. The material has been described as a trace occurrence from five localities in very different geological settings. However, the nature of the porosil structure types and the wide range of structural features suggest that further natural variants

may exist, especially in hydrothermally active areas (e.g., geysers).

48.7.9 Toxicology

The effect of the dust that arises when working with silica is of primary importance from a toxicological point of view, especially in the case of long-term exposure of several hours per day. This applies to naturally occurring and synthetic as well as to crystalline and amorphous. As far as industrial medicine is concerned, local contact with the skin and mucous membranes is important. In the case of inhalation of the dust, the effect on the respiratory tract is significant.

The effect of silica-containing dust on the respiratory tract depends on:

- The physical and chemical properties (e.g., the particle or primary particle size and the specific surface area)
- The concentration administered
- The daily and total duration of exposure

48.7.9.1 Experiences with Humans

After long-term exposure at work, the effects of crystalline or amorphous SiO_2 dust on the respiratory tract of humans are well known and have been widely reported (for reviews, see [810–813]).

Crystalline Silica Dust. The classification into common, accelerated, and acute forms of silicosis [810] is based on the time interval between the beginning of exposure to silica and the first appearance of silicotic changes that are detectable in a X-ray picture. A rapid manifestation and an accelerated course of the disease are caused primarily by long-term inhalation of higher concentrations of SiO_2 dust.

The common form of silicosis (simple silicosis) occurs röntgenologically after about twenty or more years of exposure. The content of crystalline SiO_2 in the dust that causes silicosis in workers is often less than 30% [810].

The accelerated form of silicosis (5–15 years) develops after a shorter exposure to

higher concentrations of SiO_2 dust. Progressive massive fibrosis is often observed on the X-ray picture [810].

The acute form, also known as silicoproteinosis, develops in 1–3 years. The clinical symptoms include rapidly deteriorating function of the lungs, which is always fatal.

The progression of silicosis even after the termination of exposure is especially characteristic, and there is still no effective treatment.

For this reason, it is essential that the legal regulations for working with crystalline SiO_2 are obeyed [814–816].

Amorphous Silica Dust. *Amorphous Synthetic Silica.* From experimental long-term inhalation tests on rats, it is known that high concentrations of some synthetic amorphous silicas can cause nodular (fibrotic) changes in the lungs of the animals during the exposure phase [817]. However, the regression of the nodules (fibrosis) in the lungs after the termination of the exposure phase is characteristic of the biological action of these amorphous silica dusts. In a treatment-free, follow-up observation phase of several months, a clear time-dependent regression of the changes in the lungs of the experimental animals could be detected after three, eight, and up to twelve months (see below) [817, 818]. In the case of the neighboring lymph nodes, the regression of the morphological changes observed within the inhalation phase was established histologically [817, 818].

In-depth investigations carried out by company doctors over periods of up to 12 years [819] and from 1 to 32 years [820] have confirmed that until now long-term contact with amorphous synthetic silicas has not resulted in a single case of silicosis.

Established MAK [815] and TLV regulations [816] must be complied with when working with amorphous synthetic silicas. If these fixed limiting values are exceeded—especially for a longer period of time—an overtaxing of the respiratory passages and a corresponding biological defence reaction in

the bronchial tubes and, especially, in the lung tissue must be expected.

VITUMS et al. observed that fibrosis of the lungs was caused by exposure to flue dust containing silica with a wide particle-size distribution, such that as produced in the manufacture of ferrosilicon or quartz glass [821].

Amorphous Natural Silicas. A distinction is made between exposure to amorphous synthetic silica dust and exposure to natural amorphous silica dust (kieselguhr). The latter can contain small amounts of crystalline SiO_2 and, according to some studies, can cause silicosis in humans on long-term exposure [811].

Carcinogenicity of Silica Dusts in Humans.

In many cases, industrial workers exposed to silica dust exhibit a higher incidence of lung cancer. However, exposure to silica dust is often complicated by other hazards such as polycyclic aromatic hydrocarbons, asbestos, and smoking, which makes a causal analysis extremely difficult. According to GOLDSMITH et al. [822], at least two studies show a strong association between silicosis and lung cancer: the analysis of the Swedish pneumoconiosis register by WESTERHOLM [823] and a similar study by FINKELSTEIN [824] in Ontario, Canada. However, the same authors [822] also stated that a completely convincing causal relationship cannot be concluded. A possible association between silicosis and lung cancer is also discussed in [825], based on data from a clinical cancer monitoring register. A relationship between tumors of the upper intestinal tract and the ingestion of quartz particles in food in North China has been suggested [826]. A correlation was made between the incidence of cancer of the esophagus and the consumption of plant products that contain silica fragments and fibers for a region in North China, in northeast Iran, and in Transkei.

48.7.9.2 Animal Experiments

Long-Term Inhalation of Silica Dust. In specifically designed, practice-oriented long-term inhalation studies, various types of crystalline

and amorphous silica dust have been thoroughly tested on rodents. Rats [817, 818, 827, 828] were mainly used, but rabbits [818, 829, 830] and guinea pigs [818] were also employed.

The elimination rate in rats has been determined in an inhalation experiment with amorphous highly disperse silica. In the case of Aerosil 200, for example, after the termination of inhalation, 65–75% of the dust was eliminated in one month, 80–90% in two months, and 95% in three to five months. It is possible that the rate of solubilization of these hydrophilic silicas also plays a role [817].

It was found in retention studies on rats [817] that in the case of longer term inhalation (28 times four hours in 36 days) of highly disperse amorphous silica dust, the continuous elimination during the exposure phase is very high. This means that the formation of large SiO_2 deposits in the lungs is improbable [817]. In contrast, in long-term inhalation experiments with quartz dust the tendency towards formation of deposits was higher [817].

After the termination of a long-term inhalation study on rats with Aerosil 200 (12 months, 4 per day; concentration: 45 mg/m^3), some of the animals were subjected to treatment-free observation for another 3 to 8 months and then killed [817]. Subsequently, a histological investigation and chemical analysis of SiO_2 in the lungs and lymph nodes were performed. In the follow-up observation period, it was found that the nodules in the lungs were reduced to small residual foci. The lymph nodes, which were still enlarged after three months, had greatly regressed after eight months. Similar observations have also been made in previous inhalation experiments with Aerosil.

In a long-term inhalation experiment on rats with quartz [828] (12 months, 5 per day, 5 per week; concentration: 10 mg/m^3 , standard quartz No. 12, Dörentrup quartz), some of the animals were subjected to treatment-free observation for another 4 weeks to 6 months after the termination of exposure and then killed. In this follow-up observation period, it was possible to detect silicotic reactions in the

lungs and reticulohistiocytic cells typical of quartz in the lymph nodes. There was an increase in the silicotic nodules in the lungs after six months and fibrosis of the mediastinal lymph nodes had clearly increased.

Examination of lungs and accompanying lymph nodes of the individual groups of animals at various time intervals showed that in the case of quartz, a long residence time in the lungs must always be expected, but that deposits of finely divided amorphous silica are relatively quickly and extensively eliminated [817, 828]. This is true of amorphous silicas with a specific surface area of $> 100 \text{ m}^2/\text{g}$ [817].

Injection of Silica Dust. The tissue reaction typical of a particular silica dust can be determined in animal experiments by means of a single intratracheal or intraperitoneal injection.

The intratracheal injection of a high dose of quartz resulted in a massive local accumulation of dust [828]. The tissue reaction caused by an injection of this type is similar to the picture of acute silicosis. Fast reactions of this kind in the lung tissue—comparable with the exposure of workers to high concentrations of quartz [819]—can also be produced in animal experiments with very high inhalation concentrations (400 mg/m^3) [828].

The general effect of a particular dust (acute toxicity) and the local harmful (cytotoxic) effects are deduced from the tissue reaction observed in rats after intraperitoneal SiO_2 injections. Cytotoxicity can occur in the form of nodular fibrosis (dust nodules) or surface fibrosis that leads to extensive coalescence of the abdominal organs [817].

The reaction of lung tissue on longer term inhalation of SiO_2 dust cannot be directly inferred from the results of the intratracheal and intraperitoneal injections. Thus, the physiologically important reactions of the organism in the course of SiO_2 retention and SiO_2 elimination can be determined only in long-term inhalation tests with a sufficiently long, treatment-free, follow-up observation period.

The morphological changes in the lungs after long-term inhalation of natural crystalline SiO_2 progress after the termination of exposure, whereas with synthetic amorphous silica dust the morphological changes regress after the termination of exposure (reversibility).

Carcinogenicity of Silica Dusts in Animal Tests. Lymphomas have been found in rats after intrapleural, i.p., i.v., and direct application in the thymus gland of various silica modifications [831, 832]. The tumor incidence differed for various species of rat, and no tumors were observed in mice and hamsters. A synergistic effect has been reported for silica dust and benzo[a]pyrene [833], as has been found for other dusts (e.g., coal, TiO_2). This is presumably the result of chemico-physical surface effects, which may also be involved in tumor promotion. Tests have shown that Min-U-Sil causes tumors in rats in the intratracheal test [834]. Tissue scarring has been discussed as the cause. Min-U-Sil is strongly fibrogenic and extremely finely divided.

48.8 References

1. *Properties of Silicon*, EMIS Datareviews Series No. 4, INSPEC, London 1988.
2. *J. Phys. Chem. Reference Data* 14 (1985) 1.
3. L. P. Hunt, V. D. Dosaj, J. R. McCormick, *Quart. Rep. DOE/JPL-95 4559-76/2* 1977, Jan.
4. Dow Corning, DE-OS 3013319, 1979 (V. D. Dosaj, L. P. Hunt).
5. J. Dietl, D. Helmreich, E. Sirtl: *Crystals*, vol. 5, Springer-Verlag, Berlin 1981, p. 43.
6. A. Sanjurjo et al., *J. Electrochem. Soc.* 128 (1981) 179.
7. L. Nanis et al.: *Final Rep. DOE/JPL-95 4471* 1980, March.
8. Ethyl Corp., EP-A 0112151A1, 1984 (E. M. Marlett).
9. Siemens & Halske, DT 1102117, 1954 and DT 1140549, 1954. Siemens-Schuckertwerke, US 3042494, 1958 and 1962 (H. Gutsche).
10. E. Sirtl: *Festkörperprobleme VII*, Pergamon-Vieweg, Braunschweig 1967, p. 1.
11. Ethyl Corp., US 4784840, 1988 (M. F. Gautreaux, R. H. Allen); US 4820587 and 4883687, 1989 (M. F. Gautreaux, R. H. Allen).
12. KRIT, US 4900411, 1990 (Y. Poong, S. Yongmok).
13. Texas Instruments, US 3963838, 1976 (H. S. N. Seity, C. L. Yaws, B. R. Martin, D. J. Wangler).
14. J. Czochralski, *Z. Phys. Chem.* 92 (1917) 219.
15. W. Zulehner, D. Huber: *Crystals*, vol. 8, Springer-Verlag, Berlin 1982, p. 1.
16. W. Zulehner in *Materials Science Engineering*, vol. B4, Elsevier Sequoia, Lausanne 1989, p. 1.
17. W. Zulehner in K. Sumino (ed.): *Defect Control in Semiconductors*, Elsevier Science, North Holland 1990, p. 143.
18. S. B. Kulkarni in N. G. Einspruch, G. B. Larrabee (eds.): *VLSI Electronics: Microstructure Science*, vol. 6, Academic Press, New York 1983, p. 73.
19. T. L. Chu in N. G. Einspruch (ed.): *VLSI Handbook*, Academic Press, New York 1985, p. 285.
20. H. Herzer, *Proceedings of the 10th European Photovoltaic Solar Energy Conference*, Lisbon, Portugal, April 1991, p. 501.
21. New Energy Development Organization (NEDO, Japan), Report no. 1, 1990; *Photovoltaic Insider Report (PVIR)* 2 (1991).
22. S. Wagner, D. E. Carlson in [20], p. 1179.
23. N. B. Mason, D. Jordan in [20], p. 280.
24. M. A. Green in [20], p. 250.
25. A. Eyer, A. Räuber, A. Goetzberger, *Optoelectronics—Devices and Technologies* 5 (1990) no. 2, 239.
26. A. Stock: *Hydrides of Boron and Silicon*, Ithaca, New York 1933; *Z. Elektrochem.* 32 (1926) 341.
27. A. G. McDiarmid, *Quart. Rev.* 10 (1956) 208.
28. Gmelin, System no. 15, part B, 227ff.
29. A. Stock, C. Somieski, *Ber. Dtsch. Chem. Ges.* 49 (1916) 125, 155.
30. H. J. Emeleus, A. F. Maddock, *J. Am. Chem. Soc.* (1946) 1131.
31. H. Clasen, *Angew. Chem.* 70 (1958) 179.
32. W. C. Johnson, S. Isenberg, *J. Am. Chem. Soc.* 57 (1935) 1349.
33. A. E. Finholt, A. C. Brown, K. E. Wiltz, H. I. Schlesinger, *J. Am. Chem. Soc.* 69 (1947) 2692.
34. Internat. Standard Electric Corp., US 2888328, 1956.
35. Kali-Chemie, DT 1034159, 1956; DE-AS 1049835, 1956.
36. Allied Chem. Corp., DT 1080531, 1959.
37. Standard Telephone & Cables, GB 832333 and 832334, 1956.
38. W. Sundermeyer, O. Glemser, *Angew. Chem.* 70 (1958) 625.
39. Ethyl Corp., EP 300320, 1989 (J. A. Bossier, D. M. Richards, L. T. Crasto).
40. Ethyl Corp., US 4778668, 1988 (E. M. Marlett, R. N. DePriest).
41. Union Carbide, CA 1151305, 1983 (W. C. Brennan).
42. Tokuyama Soda, JP 59174516, 1984.
43. Union Carbide, CA 1184017, 1985 (W. C. Brennan, L. M. Coleman).
44. Tokuyama Soda, JP 60060917, 1985.
45. Solavolt International, US 4542004, 1985 (K. R. Sarma, C. S. Chanley).
46. J. Moriyama: "Production of High-Purity Silicon. A Review", *Suyokashi* 20 (1988) no. 10, 671–679.
47. Mitsui Toatsu Chemicals, JP 58156522, 1983.
48. Toa Gosei Chemical, JP 01234316, 1989 (S. Watanabe, T. Hattori).
49. Toa Gosei Chemical, JP 61191512, 1986 (O. Hirano et al.).
50. Bell Telephone, BE 566348, 1960.

51. Licentia Patentverwertung, DT 1073460, 1958.
52. V. V. Balabanov et al., *Vysokochist. Veshchestva* 6 (1990) 60-66.
53. Toshiba Corp., JP 58048417, 1983.
54. Seiko Instruments and Electronics, JP 63132420, 1988 (N. Shimizu, M. Shinho).
55. Canon, DE 3208494, 1982 (I. Shimizu, K. Ogawa, E. Inoue).
56. S. W. Depp, W. E. Howard, *Spektrum der Wissenschaft* 1993, 547.
57. Bell Laboratories, US 4579752, 1986 (L. H. Dubois, R. G. Nuzzo).
58. J. R. Hartmann, J. Famil-Ghiria, M. A. Ring, H. E. O'Neal, *Combust. Flame* 68 (1987) no. 1, 43-56.
59. Pioneer Electric Corp., JP 61090726, 1986 (K. Kitahara, T. Shimada).
60. A. Y. Adamova et al., *Kim. Vys. Energ.* 15 (1981) no. 4, 365-369.
61. C. B. Moore, J. Biedrzycki, F. W. Lampe, *J. Am. Chem. Soc.* 106 (1984) no. 25, 7761-7765.
62. T. N. Bell, K. A. Perkins, P. G. Perkins, *J. Chem. Soc. Chem. Commun.* 1980, no. 22, 1046-1047.
63. H. Buß, F. Wöhler, *Liebigs Ann. Chem.* 104 (1857) 94.
64. G. Braver: *Handbuch der präparativen anorganischen Chemie*, vol. 1, F. Enke, Stuttgart 1960.
65. Wacker, DT 1067010, 1951; BASF, DT 1105389, 1960.
66. Linde, US 2499009, 1947.
67. Union Carbide, US 2595620, 1948.
68. Dynamit Nobel, BE 856480, 1977.
69. Wacker, DT 623290, 1977.
70. Telecomunicações Brasileiras, BR 8006892, 1980 (J. W. C. Carvalho et al.).
71. A. C. F. de Arruda, L. C. Barbosa, *Congr. Ann. ABM, 35th*, vol. 3, Assoc. Brasileira Metais, Sao Paulo 1980, pp. 375-390.
72. V. F. Popenko et al., SU 833494, 1981.
73. General Electric, DE 3303903, 1983 (A. Ritzer, N. B. Shah, E. Daniel).
74. Toa Nenryo, JP 63170210, 1988 (H. Yamada, H. Ogawa, T. Hosokawa, M. Tachikawa).
75. Hüls, DE 3809784, 1989 (K. Ruff).
76. Elkem, DE 3938897, 1990 (K. Forwald, G. Schüller, O. Soerli).
77. High Pure Silicon Co., JP 02145413, 1990 (M. Takaguchi, N. Morioka).
78. T. C. Hwang, H. H. Hsieh, *Energy Res. Abstr.* 24 (1984) no. 24.
79. K. X. Li, S. H. Peng, T. C. Ho, *AIChE Symp. Ser.* 84 (1988) 114-125.
80. Nippon Aerosil Co., DE 3230590, 1983 (T. Ito, H. Hori).
81. Mitsubishi Kakoki Kaisha, JP 02172811, 1990 (K. Akaike).
82. C. Zhang, CN 87100535, 1987.
83. Shin-Etsu Chemical Ind., JP 58161915, 1983.
84. Osaka Titanium Co., JP 56073617, 1981.
85. Mitsui Toatsu Chemicals, JP 63100014, 1988 (K. Inoue et al.).
86. General Electric, US 4390510, 1983 (A. Ritzer, B. Shah, D. E. Silva).
87. Mitsubishi Metal Corp., JP 57003711, 1982.
88. Council of Sci. and Ind. Research, IN 166734, 1990 (V. G. Neurgaonkar et al.).
89. Denki Kagaku Kogyo, JP 60081010, 1985.
90. Motorola, EP 133209, 1985 (W. M. Ingle, S. M. Pefley, H. S. N. Setty).
91. High Pure Silicon Co., JP 51118017, 1982.
92. Wacker, DE 3024319, 1982 (A. Göppinger et al.).
93. Nippon Steel Corp., JP 63112410, 1988 (M. Onozawa).
94. Shin-Etsu Chemical Ind., JP 57140309, 1982.
95. Mitsubishi Kakoki Kaisha, JP 63008207, 1988 (K. Akaike).
96. Nippon Steel Corp., JP 62021707, 1987 (M. Onozawa).
97. Mitsubishi Metal Corp., JP 62288109, 1987 (E. Kimura, K. Ogi, T. Kurashige).
98. Wacker, DE 3341340, 1985 (A. Schnegg, R. Rüdiger).
99. J. Y. P. Mui, D. Seyferth, *Sci. Tech. Aerosp. Rep.* 19 (1981) no. 18.
100. J. Y. P. Mui, D. Seyferth, *Energy Res. Abstr.* 6 (1981) no. 6.
101. Rhône-Poulenc, EP 100266, 1984 (J. L. Lepage, G. Simon).
102. Osaka Titanium, JP 57140312, 1982.
103. Osaka Titanium, JP 57140311, 1982.
104. Osaka Titanium, JP 57129817, 1982.
105. Denki Kagaku Kogyo, JP 59035017, 1984.
106. Denki Kagaku Kogyo, JP 55045919, 1984.
107. W. M. Ingle, M. S. Peme, *J. Electrochem. Soc.* 132 (1985) no. 5, 1236-1240.
108. Mitsui Toatsu, JP 01313317, 1989 (K. Inoue et al.).
109. Mitsui Toatsu, JP 63 095107, 1988 (K. Inoue et al.).
110. Mitsui Toatsu, JP 63095108, 1988 (K. Inoue et al.).
111. Mitsui Toatsu, JP 63100015, 1988 (K. Inoue et al.).
112. Mitsui Toatsu, JP 63095109, 1988 (K. Inoue et al.).
113. Mitsui Toatsu, JP 63100016, 1988 (K. Inoue et al.).
114. Mitsui Toatsu, JP 63095110, 1988 (K. Inoue et al.).
115. Osaka Titanium, JP 57156319, 1982.
116. Osaka Titanium, JP 58011042, 1983.
117. Z. Shen, J. Wang, CN 85107465, 1987.
118. Mitsui Toatsu, JP 63095111, 1988 (K. Inoue et al.).
119. Nippon Kokan, EP 255 877, 1988 (N. Yoneda et al.).
120. Nippon Kokan, JP 01100011, 1989 (K. Ozaki et al.).
121. Mitsubishi Metal Corp., JP 62256713, 1987 (E. Kimura, K. Ogi, T. Kurashige).
122. Idemitsu Kosan, JP 62270413, 1987 (N. Tanaka).
123. High Pure Silicon Co., JP 57156318, 1982.
124. V. F. Kochubei, *Otkrytiya, Izobret., Prom. Obraztzy, Tovarnye Znaki* 1981, no. 45, 122.
125. Osaka Titanium, JP 62235205, 1987 (S. Morimoto).
126. Mitsui Toatsu, JP 63250484, 1988 (M. Murakami et al.).
127. Wacker, GB 906617, 1960.
128. Siemens & Halske, DT 955415, 1955.
129. Wacker, DT 1134973, 1958.
130. Union Carbide, DT 2507864, 1975.
131. Smiel, DT 2852598, 1979.
132. Bochkarev, SU 504699, 1976.
133. Dynamit Nobel, DT 1767667, 1976.
134. Wacker, DT 2546957, 1977.
135. Akademie der Wissenschaft, DL 135613, 1979.
136. Akademie der Wissenschaft, DL 136493, 1979.
137. A. A. Efremov, Y. D. Zel'venskii, *Tr. Mosk. Khim. Tekhnol. Inst. im. D. J. Mendeleeva* 96 (1977) 4-10.
138. Z. A. Elunika, V. J. Lobov, J. P. Polokhina, *Tr. Vuz. Met.* 1980, no. 3, 72-73.
139. Wacker, DT 2558183, 1977.
140. B. Köhler et al., DD 158322, 1983.
141. L. Y. Shvartsman et al., *Vysokochist. Veshchestva* 1989, no. 5, 136-140.
142. Dow Corning EP 107784, 1984 (R. S. Doornbos).
143. General Electric, DE 3423611, 1986 (W. D. Kray).
144. General Electric, JP 59097519, 1984.
145. General Electric, JP 59097518, 1984.
146. Motorola, US 440919, 1983 (R. D. Darnell, W. M. Ingle).
147. Union Carbide, DE 3709577, 1987 (W. C. Brennan, C. C. Yang, G. Henningsen).
148. Hüls Troisdorf, DE 3642285, 1988 (B. Falk, W. Grätz, K. Ruff).
149. Osaka Titanium, JA 73047500, 1973.
150. Mitsubishi Metal, JA 78097996, 1978.
151. Texas Instruments, US 3963838, 1976.
152. Permish, US 4176166, 1979.
153. Mitsubishi Paper Mill, JA 77144959, 1978.
154. Wacker, BE 857689, 1978.
155. Harris-Intertype, US 3935040, 1976.
156. Siemens, DT 2535813, 1976.
157. Hitachi, JA 77044166, 1977.
158. Dow Corning, US 3961003, 1976.
159. Kuratomi, JA 74076721, 1974.
160. Kuratomi, JA 74059729, 1974.
161. Union Carbide, US 3900660, 1975.
162. Motorola, NL 75008684, 1976.
163. Siemens, DT 2508802, 1976.
164. Hitachi, JA 76027077, 1976.
165. Nippon Electric, JA 76086080, 1976.
166. Siemens, BE 841241, 1976.
167. Osaka Titanium, JP 02279512, 1990 (M. Kuramoto, T. Nakai).
168. Cabot, BE 850891, 1977.
169. IBM, US 3974003, 1976.
170. Siemens, DT 2519572, 1976.
171. UKR Agric. Acad. ZAP, SU 660968, 1980.
172. Hiratsuka Resin, JA 76033149, 1976.
173. Dow Corning, US 2571884, 1950.
174. BASF, FR 1009837, 1948.
175. Monsanto, GB 815276, 1950.
176. Th. Goldschmidt, DT 685728, 1936.
177. Union Carbide Belge, BE 562868, 1956.
178. Stauffer Chem. Co., US 2739041, 1953.
179. Cabot, US 2843458, 1955.
180. E. Gruber, J. Elöd, *Z. Anorg. Allg. Chem.* 195 (1931) 269.
181. Konsort. für Elektrochem. Ind., GB 176811, 1922.
182. Degussa, DT 1079015, 1960.
183. Stauffer Chem. Co., GB 865939, 1959.
184. Stauffer Chem. Co., *Chem. Engng.* 69 (1962) 71.
185. L. V. Laine, SU 108316, 1957.
186. Kali-Chemie, DT 901412, 1954.
187. Horizons, GB 735617, 1953.
188. Union Carbide, EP 26860, 1979.
189. Mitsui Toatsu Chemicals, JP 59195519, 1984.
190. Mitsui Toatsu Chemicals, JP 59184720, 1984.
191. Wacker, DE 3503262, 1986 (R. Standigl, R. Griebhammer).
192. Int. Standard Electric, DAS 1074560, 1958.
193. Du Pont, US 2820698, 1954.
194. Bell Telephone Lab., US 2812235, 1955.
195. Westinghouse Electric, DT 1088473, 1957.
196. Western Electric, DT 1029811, 1956.
197. G. A. Wolff, US 2877097, 1958.
198. H. C. Theuerer, *J. Electrochem. Soc.* 107 (1960) 29.
199. G. G. Deryatykh, N. Kh. Agliulov, A. E. Wikolaev, E. M. Shcheplyagin, *Zh. Prikl. Khim. (Leningrad)* 53 (1980) no. 8, 1845-1848.
200. Denki Kagaku Kogyo, JP 02196014, 1990 (M. Fujimoto, M. Shinoyama, H. Matsumura).
201. Bell Telephone Lab., US 4282196, 1981 (T. Kometani, D. L. Wood).
202. General Electric, GB 309393, 1928.
203. Union chimique belge, GB 1042076, 1951.
204. Faustel Metallurgie, US 2665997, 2665998, 1950.
205. E. Fitzer, DE 178779, 1952.
206. Mitsui Toatsu Chemicals, JP 59162121, 1984.
207. Mitsui Toatsu Chemicals, JP 59232910, 1984.
208. Mitsui Toatsu Chemicals, JP 59207829, 1984.
209. Toa Gosei Chemical, DE 3623493, 1987 (M. Ito, T. Hattori, Y. Miwa).
210. Toa Gosei Chemical Industry, JP 63021211, 1988 (M. Ito, T. Hattori, Y. Miwa).
211. Mitsui Toatsu Chemicals, JP 61205614, 1986 (A. Hiai, K. Wakimura, T. Use).
212. Mitsui Toatsu Chemicals, JP 59207830, 1984.
213. Mitsubishi Metal Corp., JP 62070425, 1987 (H. Ikeda).
214. Mitsubishi Metal Corp., JP 63089414, 1988 (H. Ikeda, M. Tsunashima).
215. Mitsubishi Metal Corp., JP 62036014, 1987 (Y. Kuroda, K. Yamakawa).
216. Mitsubishi Metal Corp., JP 63091138, 1988 (H. Ikeda, M. Tsunashima, M. Sato).
217. Mitsubishi Metal Corp., EP 282037, 1988 (H. Ikeda, M. Tsunashima).
218. Mitsubishi Metal Corp., EP 264722, 1988 (H. Ikeda, M. Tsunashima, M. Sato).
219. Mitsubishi Metal Corp., JP 63210015, 1988 (H. Ikeda, M. Tsunashima, M. Sato).
220. Mitsubishi Metal Corp., JP 01192716, 1989 (K. Ogi, T. Kurashige, E. Kimura).
221. NEC Corp., JP 62296511, 1987 (A. Ishitani).
222. Dow Corning, FR 2486057, 1982 (J. H. Gaul, D. R. Weyenberg).
223. Toa Gosei Chemical, JP 61295372, 1986 (S. Motojima, T. Hattori, N. Ishikawa).
224. Toa Gosei Chemical, JP 63277599, 1988 (S. Motojima, T. Hattori, N. Ishikawa).
225. Mitsubishi Metal Corp., JP 01301507, 1989 (T. Hirai, H. Ikeda).
226. Mitsui Toatsu Chemicals, JP 62143839, 1987 (T. Iwao, K. Morii, Y. Tajima).
227. Mitsui Toatsu Chemicals, JP 62143840, 1987 (T. Iwao, K. Morii, Y. Tajima).
228. Mitsui Toatsu Chemicals, JP 61227914, 1986 (T. Iwao, K. Morii, Y. Tajima).
229. Wacker, DE 3518620, 1986 (R. Griebhammer, H. Herrmann, R. Standigl).
230. B. S. Suresh, D. K. Padma, *Polyhedron* 5 (1986) no. 10, 1579.

231. A. Kornick, M. Binnewies, *Z. Anorg. Anal. Chem.* 587 (1990) 157-166.
232. Dynamit Nobel, DE 3615509, 1987 (B. Falk, K. Ruff, K. Schrage).
233. P. Voss, Ph.D. thesis, Aachen 1961.
234. P. Voss, Dissertation, Aachen 1962.
235. H. Bloching, Dissertation, Freie Universität Berlin 1961.
236. Du Pont, US 2840588, 1956.
237. Kemira Oy, FI 82232, 1990 (V. P. Judin, A. Hayha, P. Koukkari).
238. Kemira Oy, US 5077027, 1991 (V. P. Judin, A. Hayha, P. Koukkari).
239. Semiconductor Energy Laboratory Co., JP 60054913, 1985.
240. M. Janai et al., *J. Appl. Phys.* 52 (1981) no. 5, 3622-3624.
241. H. Matsumura, H. Ihara, T. Uesugi, *J. Appl. Phys.* 57 (1985) no. 12, 5483-5485.
242. H. Matsumura, T. Uesugi, H. Ihara, *Mater. Res. Soc. Symp. Proc.*, 49 (1985) 175-180.
243. État français, FR 2620736, 1989 (Y. Pauleau, P. Lami, J. Pelletier).
244. Semiconductor Energy Laboratory Co., JP 60144940, 1985 (S. Yamazaki).
245. K. Zhang, Q. Yuan, *Huaxue Shiji* 23 (1982) no. 12, 353-354.
246. Schumacher, GB 2028289, 1980.
247. Ceres Corp., WP 8001489, 1980.
248. Schumacher, US 4084024, 1978.
249. Siemens, JA 77035605, 1977.
250. Western Electric, US 3932160, 1976.
251. Nippon Teleg. & Tel., JA 77088348, 1977.
252. Nippon Teleg. & Tel. and Furukawa Electric, JA 77104936, 1977.
253. Nippon Teleg. & Tel., JA 79127914, 1979.
254. Fuji Photo Film, JA 80167119, 1981.
255. Micron Technology Inc., US 5082524, 1992 (D. A. Cathey).
256. Schumacher, US 4318942, 1982 (L. M. Wörner, E. B. Moore).
257. Battelle Dev., US 3990953, 1976.
258. Exxon Res. & Eng., US 4192720, 1980.
259. Licentia Patentverwertung, DT 2929669, 1981.
260. Tokyo Shibaura Electric, JA 78140311, 1979.
261. UBE Industries GB 2020264, 1979.
262. Asahi Glass, JA 79134098, 1979.
263. Asahi Glass, JA 79160600, 1980.
264. Rosenthal, DT 2635167, 1977.
265. B. Armas, C. Combesure, G. Male, M. Morales, *Less-Common Met.* 67 (1979) no. 2, 449-453.
266. Toyota Cent. Res. & Dev., JA 75108183, 1977.
267. Hitachi, GB 19915, 1980.
268. Phillips Petroleum, BE 858462, 1978.
269. Asahi Glass, JP 62070219, 1987 (K. Sato et al.).
270. K. Zhang et al., *Huaxue Shiji* 5 (1983) no. 4, 251-253.
271. Dow Corning, EP 301678, 1989 (K. G. Sharp, J. J. D'Errico).
272. H. Schmäler E. Hengge, *J. Organomet. Chem.* 225 (1982) no. 1, 171-176.
273. M. Schmeißer, M. Schwarzmann, *Z. Naturforsch.* B116 (1956) 278.
274. Kali-Chemie, DT 955414, 1954.
275. K. Friedrich, Thesis, RWTH-Aachen 1964.
276. Licentia Patentverwertung, DT 1045381, 1957.
277. Morrizons, GB 735617, 1953.
278. Kali-Chemie, DT 901412, 1954.
279. B. Rubin, G. H. Moates, J. R. Wenier, *J. Electrochem. Soc.* 104 (1957) 656.
280. Japan Telegram & Telephone, JA 13669, 1988.
281. Texas Instruments, US 4154870, 1979.
282. Int. Telephone & Telegraph, US 3961926, 1976.
283. H. Schäfer, *Chem.-Ztg.* 75 (1951) 48.
284. E. Zintl et al., *Z. Anorg. Chem.* 245 (1940) 1.
285. Goodrich, DT 1079608, 1956.
286. O. K. Botoinkin, SU 139657, 1960.
287. Fumio Hori, JP 59008613, 1984.
288. J. M. Huber, EP 176770, 1986 (D. E. Schramm).
289. L. Brewer, *Chem. Rev.* 52 (1953) 39.
290. W. Blitz, P. Ehrlich, *Naturwissenschaften* 26 (1938) 188.
291. G. Grube, H. Speidel, *Z. Elektrochem.* 53 (1949) 339.
292. H. v. Wartenberg, *Z. Elektrochem.* 53 (1949) 343.
293. H. Schäfer, R. Hörnle, *Z. Anorg. Allg. Chem.* 263 (1959) 261.
294. J. Berak, D. Grzeskowiak, *Zesz. Nauk. Politech. Slask. Vhem.* 88 (1979) 154-155.
295. Kemanord, RD 199058, 1980.
296. A. Marcks, H. Hausner, *Therm. Anal. Proc. Int. Conf. 6th* 2 (1980) 223-228.
297. Hamatsu, NL 74006827, 1975.
298. Hitachi, DT 2365056, 1975.
299. Fujitsu, JA 79018689, 1979.
300. Stepanov, SU 423203, 1975.
301. Hoya Glass Works, DT 2443718, 1975.
302. Unitika, JA 74041469, 1975.
303. Richter, DL 120190, 1976.
304. Teijin Lens, JA 80110127, 1980.
305. BFG Glassgroup, BE 859428, 1978.
306. AS Phys. Metall. Inst., SU 609121, 1979.
307. Sony Corp., JA 79031721, 1979.
308. ITT Industries, FR 2362089, 1978.
309. Matsushita Elec. Ind., JA 79024866, 1979.
310. M. Schmitt, FR 2369103, 1978.
311. Matsushita Elec. Ind., JP 63276724, 1988 (K. Kimura et al.).
312. NHK Spring Co, JP 62071665, 1987 (T. Ebihara, T. Yokoo).
313. S. Yoshida, S. Misawa, *Denshi Gijutsu Sogo Kenkyusho Iho.*, 44 (1980) no. 1/2, 14-22.
314. United States Dept. of Energy, US 389802, 1983 (J. V. Milewski).
315. Lonza, DT 2531481, 1976.
316. Osaka Titanium, JA 74098807, 1975.
317. Suzuki, DT 2909104, 1979.
318. Toyota Chuv Kenkyusho, JA 76048799, 1976.
319. Lucas J. Industries, GB 1470171, 1977.
320. N. Azuma, T. Yamada, S. Kuwabara, *Yogyo Kyokai-shi* 86 (1978) no. 9, 418-424.
321. Ceraver, BE 858704, 1978.
322. Bludov, SU 438050, 1975.
323. Victor Co. of Japan, JA 75038200, 1976.
324. E. Zintl et al., *Z. Anorg. Allg. Chem.* 245 (1940) 1.
325. I.G. Farbenind., CH 215137, 1939.
326. Duisberg, US 2242497, 1939.
327. Kawasaki Steel, JA 78134794, 1979.

328. Toyota Motor Co., DE 3602647, 1986 (S. Abe, M. Ogawa).
329. Dow Corning, US 5051248, 1991 (G. N. Bokerman, J. P. Canady, C. S. Kuivida).
330. O. N. Carlson, F. A. Schmidt, *Proc. Vac. Metall. Conf. Spec. Met. Melting Process* 1985, 129-136.
331. L. M. Ericsson, SE 450391, 1987 (T. S. Ganey, M. Jansson).
332. K. L. Day, B. Donn, *Science* 4365 (1978) 307-308.
333. B. S. Suresh, D. Krishnamurthi Padma, *J. Chem. Soc. Dalton Trans.*, 1984, no. 8, 1779-1780.
334. V. Belot et al., *J. Non-Cryst. Solids* 127 (1991) no. 2, 207-214.
335. E. Wilberg, W. Simmler, *Z. Anorg. Allg. Chem.* 283 (1956) 401.
336. Hitachi, JP 59074637, 1984.
337. Asahi Glass, JP 55058230, 1980.
338. Asahi Glass, JP 55145739, 1980.
339. Toppan Printing Co., JP 02122924, 1990 (M. Sekiguchi et al.).
340. Y. Wang, C. Jiang, *Bandaoti Xuebao*, 7 (1986) no. 6, 596-601.
341. N. A. Takasaki, E. Ikawa, Y. Kurogi, *J. Vac. Sci. Technol. B* 4 (1986) no. 4, 806-811.
342. R. E. Stahlbush, W. E. Carlos, S. M. Prokes, *IEEE Trans. Nucl. Sci.*, NS-34 6 (1987) part 1, 1680-1685.
343. E. P. Bochkarev et al., *Vysokochist. Veshchestva* 1 (1989) 73-77.
344. Ei Shokusan K. K., JP 62183899, 1987 (F. Baba, K. Kozono, T. Hashiguchi, K. Maemura).
345. Kubota Ltd., JP 62250910, 1987 (Y. Okumura, Y. Okamoto, K. Yanai).
346. Unisearch Ltd., WO 8906222, 1989 (J. A. Bourdillon et al.).
347. I. N. Buyanovskii et al., *Trenie Iznas* 6 (1985) no. 1, 119-124.
348. A. Stock, F. Zeidler, *Ber. dtsch. chem. Ges.* 56 (1923) 986.
349. R. Müller, *Chem. Techn.* 2 (1950) 1.
350. G. H. Wagner, A. N. Pines, *Ind. Engng. Chem.* 44 (1952) 321.
351. R. Müller, R. Kohne, S. Sliwinski, *J. prakt. Chem.* 9 (1959) 71.
352. K. Larssow, *Ark. Kemi* 16 (1960) 215.
353. C. L. Frye, W. T. Collins, *J. Am. Chem. Soc.* 92 (1970) 5586.
354. H. Burgi, G. Calzaferri, *J. Chromatography* 507 (1990) 481.
355. P. A. Agaskar, *Inorg. Chem.* 30 (1991) 2707.
356. G. Calzaferri, *Nachr. Chem. Tech. Lab.* 40 (1992) 1106.
357. R. Gooden, J. W. Mitchell, *J. Electrochem. Soc.* 129 no. 7, 1619.
358. R. J. P. Corriu, *Organometallics* 10 (1991) 3574.
359. M. Laine, *Nature* 353 (1991) 642.
360. W. Humpel, V. Haary, *Z. Anorg. Allg. Chem.* 23 (1900) 32.
361. M. Schmeißer, H. Müller, W. Burgermeister, *Angew. Chem.* 69 (1957) 781.
362. L. E. Gorsh, G. N. Dolenko, *ZZV, Akad. Nauk. SSSR Neorg. Mater.* 15 (1979) no. 9, 1521-1523.
363. Kali-Chemie, DT 1008265, 1955, 1029810, 1957.
364. Mitsuishi Electric, JA 77070498, 1977.
365. Toyota Motor Corp., JP 63079716, 1988 (S. Abe, O. Kazuaki, M. Ogawa).
366. N. V. Tolstoguzov, *Izv. Vyssh. Uchebn. Zaved., Chern. Metall.* 1991, no. 4, 22-25.
367. Asahi Chemical Industry, JP 62252310, 1987 (Y. Yamada, N. Tamura, K. Makita).
368. Rockwell International Corp., US 4552740, 1985 (P. E. D. Morgan, E. A. Pugar).
369. Asahi Chemical Industry, JP 62252321, 1987 (Y. Yamada, N. Tamura, K. Makita).
370. R. Creus et al., *Mater. Sci. Eng. B* B3 (1989) no. 1/2, 109-112.
371. J. H. Kennedy, Z. Zhang, *J. Electrochem. Soc.* 136 (1989) no. 9, 2441-2443.
372. B. T. Ahn, R. A. Huggins, *Mater. Res. Bull.* 25 (1990) no. 3, 381-389.
373. S. Sahami, S. W. Shea, J. H. Kennedy, *J. Electrochem. Soc.* 132 (1985) no. 4, 985-986.
374. J. H. Kennedy et al., *Solid State Ionics* 18-19 (1986) no. 1, 368-371.
375. Matsushita Electric Industrial Co., JP 04133209, 1992 (K. Yamamura, K. Takada, S. Kondo).
376. J. H. Kennedy, Y. Yang, *J. Electrochem. Soc.* 133 (1986) no. 11, 2437-2438.
377. A. A. Godovikov, R. G. Kuryaeva, *Fiz. Khim. Stekla* 9 (1983) no. 4, 502-509.
378. H. Moissan, A. Stock, *Ber. Dtsch. Chem. Ges.* 33 (1900) 2125.
379. Allis-Chalmers, US 3427131, 1969.
380. Texaco Dev., US 4038292, 1977.
381. Aktiebolag Kautal, SW 201850, 1966.
382. R. Kiefer, F. Benesovsky: *Hartstoffe*, Springer Verlag, Wien 1963.
383. R. Kiefer: *Sondermetalle*, Springer Verlag, Wien 1971.
384. H. Walter in R. Durrer, G. Volkert (eds.): *Metallurgie der Ferrolegierungen*, Springer Verlag, Berlin 1972.
385. E. Schürmann, H. Litterscheid, P. Fünders, *Arch. Eisenhüttenwes.* 45 (1974) no. 6, 367-371.
386. *Handbuch für Eisenhüttenlaboratorium*, vol. 2, Verlag Stahleisen mbH, Düsseldorf.
387. "Probenahme", *Handbuch für das Eisenhüttenlaboratorium*, vol. 3, Verlag Stahleisen, Düsseldorf.
388. "Schiedsverfahren", *Handbuch für das Eisenhüttenlaboratorium*, vol. 4, Verlag Stahleisen, Düsseldorf.
389. B. Neuer, *Erzmetall* 42 (1989) no. 6, 239-243.
390. *Calcium Treatment Symposium Proceedings*, The Institute of Metals, London, 1988, Book 459.
391. K. C. Condie in K. H. Wedepohl (ed.): *Handbook of Geochemistry*, vol. II-2, Springer, Berlin 1970, Section 14.
392. R. Siever in [391].
393. H. Föchtbauer (ed.): *Sedimente und Sedimentgesteine*, 4th ed., Schweizerbart, Stuttgart 1988.
394. *Ind. Miner. (London)* 236 (1987) 22-39.
395. O. W. Flörke et al., *Neues Jahrb. Mineral. Abh.* 163 (1991) 19-42.
396. M. J. Buerger, *Am. Mineral.* 39 (1954) 600-614.
397. C. Frondel: "Silica Minerals", *The System of Mineralogy*, 7th ed., vol. III, Wiley, New York 1962.
398. M. J. Mombourquette, J. A. Weil, *Can. J. Phys.* 63 (1985) 1282-1293.
399. R. D. Aines, G. R. Rossman, *JGR J. Geophys. Res.* 89 (1984) 4059-4071.

400. A. Nicolas, J. P. Poirier: *Crystalline Plasticity and Solid State Flow in Metamorphic Rocks*. Wiley, London 1976, Chap. 5.9.
401. O. W. Flörke, A. Nukui, *Neues Jahrb. Mineral. Abh.* 158 (1988) 175–182.
402. L. Pauling, *Am. Mineral.* 65 (1980) 321–323.
403. R. J. Hill, G. V. Gibbs, *Acta Crystallogr. Sect. B* B35 (1979) 25–30.
404. M. O'Keefe, B. G. Hyde, *Acta Crystallogr. Sect. B* B34 (1978) 27–32.
405. W. H. Baur, *Acta Crystallogr. Sect. B* B36 (1980) 2198–2202.
406. W. A. Harrison: *Electronic Structure and the Properties of Solids*, Freeman, San Francisco 1980 pp. 257–288.
407. J. R. G. Da Silva, D. G. Pinatti, C. E. Anderson, M. L. Rudee, *Philos. Mag.* 31 (1975) 731–737.
408. K. Langer, O. W. Flörke, *Fortschr. Mineral.* 52 (1974) 17–51.
409. K. D. Aines, G. R. Rossman, *JGR J. Geophys. Res.* 89 (1984) 4059–4071.
410. L. Levien, C. T. Prewitt, *Am. Mineral.* 66 (1981) 324–333.
411. H. Grätsch, O. W. Flörke, *Z. Kristallogr.* 195 (1991) 31–48.
412. G. V. Gibbs, C. T. Prewitt, K. J. Baldwin, *Z. Kristallogr.* 145 (1977) 108–123.
413. E. M. Lewien, C. R. Robbins, H. F. McMurdie in M. K. Reser (ed.): *Phase Diagrams for Ceramists*, suppl., Amer. Ceram. Soc., Columbus 1969.
414. C. B. Sclar, A. P. Young, L. C. Carrison, C. M. Schwartz, *JGR J. Geophys. Res.* 67 (1962) 4049–4054.
415. M. A. Spackmann, R. J. Hill, G. V. Gibbs, *Phys. Chem. Miner.* 14 (1987) 139–150.
416. R. Wörner, O. F. Schirmer, *Phys. Rev.* B34 (1986) 1381–1383.
417. J. D. H. Donnay, Y. Le Page, *Acta Crystallogr. Sect. A* A34 (1978) 548–594.
418. K. Kihara, *Eur. J. Mineral.* 2 (1990) 63–77.
419. R. F. Newnham: *Structure-Property Relations*, Springer, Berlin 1975.
420. S. Haussühl: *Kristallphysik*, Verlag Chemie, Weinheim 1983, Chap. 11.4.
421. H. Grimm, B. Dörner, *J. Phys. Chem. Solids* 36 (1975) 407–413.
422. H. Salmang, H. Scholze: *Keramik*, 6th ed., vol. 1, Springer, Berlin 1982.
423. T. Barry, P. McNamara, W. Moore, *J. Chem. Phys.* 42 (1965) 2599–2606.
424. V. Rumyantsev, A. Novozhilov, *Sov. Phys. Crystallogr. (Engl. Transl.)* 25 (1980) 75–78.
425. R. Paulkath, *Phys. Chem. Miner.* 17 (1991) 681–689.
426. G. C. Kennedy, *Econ. Geol.* 45 (1950) 629–653.
427. G. M. Anderson, C. H. Burnham, *Am. J. Sci.* 263 (1965) 495–511.
428. G. M. Morey, R. O. Fournier, J. J. Rowe, *Geochim. Cosmochim. Acta* 26 (1962) 1029–1043.
429. S. H. Chan, *Geothermics* 18 (1989) 49–56.
430. P. Cordier, B. Boulogne, J.-C. Doukhan, *Bull. Mineral.* 111 (1988) 113–137.
431. J. Mullis in M. Frey (ed.): *Low Temperature Metamorphism*, Blackie, Glasgow 1987, Chap. 5.
432. H. Frischat, *Ber. Dtsch. Keram. Ges.* 47 (1970) 238–243, 313–316.
433. N. G. Stenina, L. S. Bazarov, M. Y. Sherbakova, R. J. Mashkorts, *Phys. Chem. Miner.* 10 (1984) 180–186.
434. O. W. Flörke, *Krist. Tech.* 7 (1972) 159–166.
435. O. W. Flörke, U. Flörke, U. Giese, *Neues Jahrb. Mineral. Abh.* 149 (1984) 325–336.
436. G. Miehe, H. Grätsch, *Eur. J. Mineral.* 4 (1992) 693–706; 182 (1988) 183–184.
437. A. F. Wright, A. J. Leadbetter, *Philos. Mag.* 31 (1975) 1391–1401.
438. O. W. Flörke, H. Schneider, *cfi/Ber. Dtsch. Keram. Ges.* 63 (1986) 368–372.
439. O. W. Flörke, *Glastechn. Ber.* 32 (1959) 1–9.
440. U. Seifert-Krauß, H. Schneider, *Ceramics Intern.* 10 (1984) 135–142.
441. H. Schneider, *Neues Jahrb. Mineral. Monatsh.* 1986, 433–444.
442. O. W. Flörke, K. Langer, *Contrib. Mineral. Petrol.* 36 (1972) 221–230.
443. H. Schneider, O. W. Flörke, *Neues Jahrb. Mineral. Abh.* 145 (1982) 280–290.
444. H. Schneider, O. W. Flörke, *Z. Kristallogr.* 175 (1986) 165–176.
445. A. Nukui, O. W. Flörke, *Am. Mineral.* 72 (1987) 167–176.
446. O. W. Flörke, *Ber. Dtsch. Keram. Ges.* 34 (1957) 343–353.
447. A. C. D. Chaklader, *J. Amer. Ceram. Soc.* 46 (1963) 66–71, 192–193.
448. U. Steinicke et al., *Cryst. Res. Technol.* 22 (1987) 1255–1261.
449. M. Grassellini Troysi, P. Orlandi, *Atti. Soc. Tosc. Sci. Nat., Mem.* A79 (1972) 245–250.
450. H. Gies, H. Gerke, F. Liebau, *Neues Jahrb. Mineral. Monatsh.* 3 (1982) 119–124.
451. B. Martin, K. Röllner, *Neues Jahrb. Mineral. Monatsh.* 1990, 462–466.
452. J. Shropshire, P. P. Keat, P. A. Vaughan, *Z. Kristallogr.* 112 (1959) 400–413.
453. F. Liebau, *Am. Mineral.* 63 (1978) 918–923.
454. B. Baumgartner, G. Müller, *Eur. J. Mineral.* 2 (1990) 155–162.
455. Al. Weiß, Ar. Weiß, *Z. Anorg. Allg. Chem.* 276 (1954) 95–112.
456. O. W. Flörke, J. B. Jones, U. Köster, E. Robarick, *Acta Crystallogr. A* 46 (1990) Suppl. C-247.
457. P. J. Darragh, A.-J. Gaskin, J. V. Sanders, *Sci. Am.* 234 (1976) 84–95.
458. H. Grätsch, A. Mosset, H. Gies, *J. Noncryst. Solids* 119 (1990) 173–180.
459. F. J. Pettijohn: *Sedimentary Rocks*, 3rd ed., Harper & Row, New York 1975, pp. 195ff., 300ff., 392ff.
460. H. Williams, F. J. Turner, C. M. Gilbert: *Petrography*, 2nd ed., Freeman, San Francisco 1982.
461. A. Peschel: *Natursteine*, 2nd ed., Dtsch. Verlag Grundstoffind., Leipzig 1983, pp. 77–80, 243–251, 274–275.
462. S. J. Lefond (ed.): *Industrial Minerals and Rocks (Nonmetallics other than Fuels)*, 4th ed., Amer. Inst. Mining Metallurg. Petrol. Eng. AIME, New York 1975.
463. P. Harben, *Ind. Miner. (London)* 184 (1983) 28–29, 32.

464. O. Brätsch, *Heidelb. Beitr. Mineral. Petrogr.* 5 (1957) 331–372.
465. O. W. Flörke, B. Köhler-Herbertz, K. Langer, I. Tönges, *Contrib. Mineral. Petrol.* 80 (1982) 324–333.
466. M. Smith, *Ind. Min. (London)* 203 (1984) 19–25.
467. K.-T. Wilke: *Kristallzüchtung*, H. Deutsch, Thun 1988, p. 1027–1058.
468. E. D. Kolb et al., *J. Crystal Growth* 36 (1976) 93–100.
469. V. S. Balitsky, *J. Crystal Growth* 41 (1977) 100–102.
470. C. G. Kennedy, W. L. Knight, W. T. Holser, *Am. J. Sci.* 256 (1958) 590–595.
471. W. T. Holser, C. G. Kennedy, *Am. J. Sci.* 257 (1959) 71–77.
472. C. G. Kennedy, *Econ. Geol.* 45 (1950) 629–653.
473. R. A. Laudise, E. D. Kolb, *Endeavour* 28 (1969) 114–117.
474. N. B. Hannay (ed.): "Change of State", *Treatise on Solid State Chemistry*, vol. 5, Plenum Press, New York 1975.
475. J. Hoffmann, Frank & Schulte GmbH, Essen, personal communication.
476. V. A. Kuznetsov, A. N. Lobachev, *Sov. Phys. Crystallogr.* 17 (1973) 775–803.
477. G. Lehmann, H. U. Bambauer, *Angew. Chemie* 85 (1973) 281–289.
478. K. Nassau, B. Prescott, *Mineral. Mag.* 41 (1977) 301–312.
479. J. A. Weil, *Phys. Chem. Mineral.* 10 (1984) 149–165.
480. A. C. McLaren, C. F. Osborne, L. A. Saunders, *Phys. Stat. Solidi* 4 (1971) 235–247.
481. A. C. McLaren, R. F. Cook, S. T. Hyde, R. C. Tobin, *Phys. Chem. Miner.* 9 (1983) 79–94.
482. M. S. Paterson, *Bull. Mineral.* 105 (1982) 20–29.
483. J. Flicstein, M. Schieber, *J. Cryst. Growth* 24/25 (1974) 603–609.
484. P. P. Phakey, *Phys. Stat. Solidi* 34 (1969) 105–119.
485. A. C. McLaren, P. P. Phakey, *Phys. Stat. Solidi* 31 (1969) 723–737.
486. D. R. Hale in S. J. Lefond (ed.) in [462].
487. D. M. Dodd, D. B. Frazer, *J. Phys. Chem. Solids* 26 (1965) 673–686.
488. W. G. Cady: *Piezoelectricity*, Dover Publ., New York 1964.
489. P. Profos (ed.): *Handbuch der industriellen Meßtechnik*, 4th ed., Vulkan-Verlag, Essen 1987.
490. G. Lindemann, personal communication.
491. H. Salmang, H. Scholze: *Keramik*, 6th ed., vol. 2, Springer, Berlin 1983.
492. M. K. Reser (ed.): *Phase Diagrams for Ceramists*, 2nd ed., Amer. Ceram. Soc., Columbus, OH, 1964, No. 313, 314 and 1975 Suppl., No. 4373.
493. J. Mackenzie, *Trans. Br. Ceram. Soc.* 51 (1952) 136–171.
494. H. Schneider, K. Wohleben, A. Majdic, *Mineral. Mag.* 43 (1980) 879–883.
495. H. Schneider, A. Majdic, *Neues Jahrb. Mineral. Monatsh.* (1984) 559–568.
496. O. W. Flörke, *Ber. Dtsch. Keram. Ges.* 34 (1957) 343–353.
497. I. Patzak, *Tonind. Ztg.* 96 (1972) 291–297.
498. A. Majdic, *Keram. Ztg.* 34 (1982) 89–92.
499. H. J. Koschlig in L. J. Trostel Jr. (ed.): *UNITECR Proc.*, vol. 1, Amer. Ceram. Soc., Columbus, OH, 1989, pp. 244–283.
500. P. Das, N. R. Sircar, R. Choudhury, *InterCeram.* 38 (1989) 23–24.
501. F. Press, R. Siever: *Earth*, 4th ed., Freeman, San Francisco 1986.
502. B. J. Skinner, S. C. Parker: *Physical Geology*, Wiley-Interscience, New York 1987.
503. L. Jung: *High Purity Natural Quartz*, part I: "High Purity Natural Quartz for Industrial Uses"; Part II: "High Purity Natural Quartz Markets for Suppliers and Users", Quartz Technology Inc., Liberty Corner, NJ, 1992.
504. R. Weiß: *Formgrundstoffe*, Gießerei-Verlag, Düsseldorf 1984.
505. J. Griffith, *Ind. Miner. (London)* 235 (1987) 25–43.
506. H. Fuchtbauer (ed.): *Sedimente und Sedimentgesteine*, 4th ed., Schweizerbart, Stuttgart 1988.
507. E. Roedder in H. L. Barnes (ed.): *Geochemistry of Hydrothermal Ore Deposits*, 2nd ed., J. Wiley & Sons, New York 1979.
508. J. Mullis in M. Frey (ed.): *Low Temperature Metamorphism*, Blackie, Glasgow 1987, pp. 162–199.
509. C. Müller (ed.): *Databook für Keramik-Glas-Baustoff-Produktion*, 2nd ed., Sprechsaal-Verlag, Coburg 1975.
510. R. Weiß, *Ber. Dtsch. Keram. Ges.* 55 (1978) 82–91.
511. *Ind. Miner. (London)* 197 (1984) 19–37, 39–45.
512. J. T. Nash, T. Theodore, *Econ. Geol.* 66 (1971) 385–399.
513. C. Frondel: "Silica Minerals", *The System of Mineralogy*, 7th ed., vol. 3, J. Wiley & Sons, New York 1962.
514. H. Grätsch, O. W. Flörke, G. Miehe, *Phys. Chem. Miner.* 14 (1987) 249–257.
515. B. Sawyer, US 3837826, 1974.
516. L. Jung, US 4882043, 1989.
517. G. Lindenmann, private communication.
518. Ullmann, 4th ed., 21, 444–450.
519. R. Weiß, *Erzmetall* 27 (1974) 169–177; 31 (1978) 450–457.
520. S. N. Groudev, V. J. Groudeva, *Ind. Miner. (London)* 222 (1986) 81–84.
521. P. Harben, *Ind. Miner. (London)* 184 (1983) 28–29, 32.
522. H. Scholze (ed.): "Keramische Werkstoffe", *Keramik*, part 2, 6th ed., Springer Verlag, Berlin 1983.
523. B. M. Coope, *Ind. Miner. (London)* 298 (1989) 43–55.
524. A. Peschel: *Natursteine*, 2nd ed., Dtsch. Verlag Grundstoffindustrie, Leipzig 1983.
525. H. Gundlach: *Dampfgehärtete Baustoffe*, Bauverlag, Wiesbaden 1973.
526. H. Insley, V. D. Fréchet: *Microscopy of Ceramics and Cements*, Academic Press, New York 1955.
527. R. Weiß, *Glastechn. Ber.* 49 (1976) 12–25.
528. J. Lange: *Rohstoffe der Glasindustrie*, Dtsch. Verlag Grundstoffind., Leipzig 1980.
529. A. G. Pincus, D. H. Davies (eds.): "Major Ingredients", *Raw Materials in the Glass Industry*, part 1, Ashlee Publ., New York 1983.
530. H. Petzold, H. Pöschmann: *Email und Emailtechnik*, Springer, Berlin 1987.

531. N. Severinghaus, Jr. in S. J. Lerond (ed.): *Ind. Miner. Rocks* 1975, 235-249.
532. Roskill Inform. Serv. Ltd.: *The Economics of Diatomite*, 2nd ed., London 1981, p. 73.
533. L. Petitfer, *Ind. Miner. (London)* 175 (1982) 47-69.
534. L. Benda, H. Brandes, *Geol. Jahrb. Reihe A* 21 (1974) 3-85.
535. L. Benda, *Schriften: GDMB* 38 (1981) 134-140.
536. W. B. Clark, *Calif. Geol.* 31 (1978) 3-9.
537. L. Benda, B. Mattiat, *Geol. Jahrb. Reihe D* 22 (1977) 3-107.
538. F. L. Kadey, Jr. in S. J. Lerond (ed.): *Ind. Miner. Rocks* 1975, 605-635.
539. *Ind. Miner. (London)* 1987, May, 22-39.
540. Ullmann, 4th ed., 21, 452-456.
541. Mitteleuropäische Brautechnische Analysenkommission (MEBAK): *Methodensammlung*, Freising 1982, III, pp. 651-659.
542. Supplier: VEL Geldenaakbeaan 464, B-3030 Leuven (Heverlee), Belgium.
543. S. Ward: "Liquid Filtration Theory", in M. J. Matteson, C. Orr (eds.): *Filtration, Principles and Practices*, New York-Basel 1987.
544. J. Kierer: "Kieselgurfiltration", *Bräunwelt* 40 (1990) 1730-1749.
545. E. Krüger, N. Wagner, B. Lindemann: "Einflußgrößen bei der Bierfiltration", *Bräunwelt* 50 (1989) 2434-2444.
546. International Agency for Research on Cancer (IARC): "Silica and Some Silicates", *Carcinogenic Risk of Chemicals to Humans*, no. 42, Lyon 1987.
547. International Diatomite Producers Association (IDPA): *Silica Facts Questions and Answers; Health and Safety Aspects of Diatomaceous Earth. The Nature and Safe Handling of Diatomaceous Earth*, San Francisco 1989.
548. *Br. J. Ind. Med.* 46 (1989) 289-291.
549. O. Walton: "Filter Media", *The Brewer* 64 (1978) 261-265.
550. F. Kainer, *Kieselgur*, 2nd ed., Enke, Stuttgart 1951, pp. 39-43.
551. D. H. Everett: "Definition Terminology and Symbols in Colloid and Surface Chemistry", *Symbols and Terminology for Physicochemical Quantities and Units*, Appendix II, part 1, International Union of Pure and Applied Chemistry, Butterworths, London 1971.
552. R. K. Iler: *The Chemistry of Silica*, J. Wiley & Sons, New York 1979, p. 174.
553. T. Graham, *Justus Liebigs Ann. Chem.* 121 (1862) 36.
554. R. Griessbach, *Chem. Ztg.* 57 (1933) 253.
555. P. G. Bird, US 2244325, 1945.
556. M. F. Bechtold, O. E. Snyder, US 2574902, 1951.
557. "Silicates and Silicas Report", *Chemical Economics Handbook*, SRI International, Menlo Park 1990.
558. *Opportunities in Specialty Silicas*, Kline & Co., Fairfield, NJ, 1992.
559. E. S. Gould: *Inorganic Reactions & Structures*, Henry Holt & Company, New York 1957.
560. G. J. Fine, *J. Chem. Ed.* 68 (1991) 765.
561. W. D. Kingery, H. K. Bowen, D. R. Uhlmann: *Introduction to Ceramics*, 2nd ed., J. Wiley & Sons, New York 1976.
562. V. Hofman, K. Endell, D. Wilm, *Angew. Chem.* 30 (1934) 539-558.
563. V. Khavryutchenko et al.: "Abstracts of Papers", in R. K. Iler (ed.): *Memorial Symposium on the Colloid Chemistry of Silica*, Washington, DC, 1990, Paper no. 100.
564. A. P. Legrand et al., *Adv. Colloid Interface Sci.* 33 (1990) 91-330.
565. R. S. McDonald, *J. Phys. Chem.* 62 (1958) 1168.
566. M. L. Hair: *Infrared Spectroscopy in Surface Chemistry*, Marcel Dekker, New York 1967, p. 82.
567. J. B. Peri, A. L. Hensley, Jr., *J. Phys. Chem.* 72 (1968) no. 8, 2926-2933.
568. G. E. Maciel, D. W. Sindorf, *J. Am. Chem. Soc.* 102 (1980) 7606-7607.
569. K. D. Unger: "Porous Silica", *J. Chromatogr. Libr.* 16 (1979).
570. M. L. Hair in A. T. Bell, M. L. Hair (eds.): "Vibrational Spectroscopies for Adsorbed Species", *ACS Symp. Ser.* 137 (1980).
571. L. T. Zhuravlev: "Abstracts of Papers", in R. K. Iler (ed.): *Memorial Symposium on the Colloid Chemistry of Silica*, Washington, DC, 1990, Paper no. 93.
572. R. K. Iler in [552], p. 410.
573. Du Pont Company, Nalco Inc., and Nissan Chemicals, based on product information sheets (not specifications).
574. Cabot Corp., and Nissan Inc. and Nissan Chemicals, based on product information sheets (not specifications).
575. Nalco Inc., Nissan Chemicals, and Nippon Seahostar, based on product information sheets (not specifications).
576. R. K. Iler in [552], p. 325.
577. R. K. Iler in [552].
578. B. V. Derjaguin: *Theory of Stability of Colloids and Thin Films*, Consultants Bureau, New York 1989.
579. G. W. Sears, R. K. Iler, private communication.
580. D. H. Napper: *Polymer Stabilization of Colloidal Dispersions*, Academic Press, London 1983.
581. R. K. Iler in [552], p. 364.
582. R. K. Iler in [552], p. 396.
583. R. K. Iler in [552], p. 367.
584. R. K. Iler in [552], p. 366.
585. R. K. Iler, *J. Phys. Chem.* 56 (1952) 680.
586. E. Matijevic et al., *J. Phys. Chem.* 73 (1969) 564.
587. R. K. Iler in [552], p. 409.
588. G. B. Alexander, A. H. Bolt, US 3007878, 1961.
589. J. T. Overbeek, private communication, 1955, unpublished.
590. E. Matijevic, *J. Colloid Sci.* 19 (1964) 333.
591. W. Stober, A. Fink, *J. Colloid Interface Sci.* 26 (1968) 62.
592. R. K. Iler in [552], p. 331.
593. A. B. Alexander, A. H. Bolt, US 3007878.
594. R. C. Atkins, US 3012973, 1961.
595. R. K. Iler, F. J. Wolter, US 2631136, 1953.
596. M. Mindick, L. E. Reven, US 3468813, 1969.
597. L. A. Dirnberger, US 2703314, 1955.
598. J. Klöpfer, DT 762723, 830786, 1942.
599. C. J. Brinker, G. W. Scherer: *Sol-Gel Science*, Academic Press, San Diego 1990.
600. C. G. Tan et al., *J. Colloid Interface Sci.* 118 (1987) 290-293.
601. J. Wolf, private communication.
602. R. K. Iler, US 3668088, 1972.
603. H. E. Bergna, US 4410405, 1983.
604. G. B. Alexander, US 2750345, 1956.
605. H. E. Bergna, F. A. Simko, Jr., US 3301635, 1967.
606. H. H. Mandelbrot in D. Avnir (ed.): *A Fractional Approach to Heterogeneous Chemistry*, J. Wiley & Sons, New York 1989.
607. S. Brumauer, P. H. Emmett, E. Teller, *J. Am. Chem. Soc.* 60 (1938) 309.
608. G. W. Sears, *Anal. Chem.* 28 (1956) 1981.
609. R. K. Iler in [552], p. 354.
610. T. Allen, R. Davies in R. K. Iler (ed.): "Abstracts of Papers", *Memorial Symposium on the Colloid Chemistry of Silica*, Washington, DC, 1990, Paper no. 37.
611. J. Kirkland in H. E. Bergna (ed.): "Colloid Chemistry of Silica", *Adv. Chem. Ser.* 234, in press.
612. P. F. Collins, US 2380945, 1945.
613. P. G. Batelson, CA 1154564, 1983.
614. K. Anderson et al., *Nord. Pulp Pap. Res. J.* (1986).
615. K. A. Johnson, US 4643801, 1987.
616. S. C. Sofia et al., US 4795531, 1989.
617. J. D. Rushmore, US 4798653, 1989.
618. R. K. Iler, US 2597871, 1947.
619. R. K. Iler, US 2726961, 1955.
620. I. V. Wilson, US 2643048, 1953.
621. R. J. Walsh, A. H. Herzog, US 3170273, 1965.
622. G. W. Sears, US 3922393, 1975.
623. J. L. Callahan, US 2974110, 1961.
624. J. L. Callahan et al., US 3322847, 1967.
625. H. Ferch in H. Bergna (ed.): "The Colloid Chemistry of Silica", *Adv. Chem. Ser.* 234, in press.
626. T. Graham, *Philos. Trans. R. Soc. London* 252 (1861) 204.
627. J. G. Vail: "Soluble Silicates", *ACS Monograph Series*, vol. 2, Reinhold, New York 1952, p. 549.
628. Ullmann, 4th ed., 21, pp. 458-462.
629. W. A. Patrick, US 1297724, 1918.
630. R. K. Iler: *The Chemistry of Silica*, J. Wiley & Sons, New York 1979.
631. C. J. Brinker, G. W. Scherer: *Sol-Gel Science*, Academic Press, San Diego 1990.
632. Wijnen et al., *J. Colloid Interface Sci.* 145 (1991) 17.
633. M. E. Winyall in B. E. Leach (ed.): *Applied Industrial Catalysis*, vol. 3, Academic Press, Orlando 1984, p. 43.
634. S. S. Kistler, *J. Phys. Chem.* 36 (1932) 52.
635. P. H. Tervari, A. J. Hunt, US 4610863, 1986.
636. BASF, US 4667417, 1987 (F. Graser, A. Stange).
637. L. C. Klein (ed.): *Sol-Gel Technology for Thin Films, Fibers, Preforms, Electronics, and Specialty Shapes*, Naves, Park Ridge, New Jersey, 1988.
638. M. B. Kenny, K. S. W. Sing in H. Bergna (ed.): "The Colloid Chemistry of Silica", *Adv. Chem. Ser.* 234, in press.
639. S. Brumauer, P. H. Emmett, E. Teller, *J. Am. Chem. Soc.* 60 (1938) 309.
640. R. W. Cranston, F. A. Inkley, *Adv. Catal.* 9 (1957) 143.
641. K. Sing in G. Parfitt, K. Sing (eds.): *Characterization of Powder Surfaces*, Academic Press, New York 1976, p. 34.
642. R. L. White, A. Nair, *Appl. Spectrosc.* 44 (1990) 69.
643. P. Wijnen, T. Beelen, R. van Santen in H. Bergna (ed.): "The Colloid Chemistry of Silica", *Adv. Chem. Ser.* 234, in press.
644. V. K. Markov, N. A. Nagornaya, *J. Applied Chem. (USSR)* 10 (1937) 853.
645. E. Heimann, US 2316241, 1938.
646. Davison Chemical, US 2625492, 1949 (L. O. Young).
647. W. R. Grace & Co., US 2856268, 1954 (L. O. Young).
648. Houdry, US 2232727 (A. G. Peterkin, H. A. Shabaker).
649. Mizusawa Ind. Chem., DE 1442778, 1963 (T. Kuwata, Y. Sugahara, T. Nakazawa).
650. Asahi Chem. Ind., JP 48013834, 1966 (K. Takizawa, Y. Ohba).
651. BASF, DE 2103243, 1979 (G. Merz, H. Gehrig, W. Chorbacher).
652. Socony-Vacuum Oil Comp., US 2385217, 1945 (M. M. Marisic).
653. Kali-Chemie, DE 1567617, 1970 (J. Dultz).
654. J. F. White, I. V. Wilson, *Ind. Eng. Chem.* 33 (1941) 1169.
655. Fuji-Davison, Art-Sorb®-Technical Information (in English), 4.11.27 Meieki, Nagoya-shi, Japan 450.
656. R. S. McDonald, *J. Am. Chem. Soc.* 79 (1975) 850.
657. Crosfield, US 3617301, 1968 (D. Barby, J. P. Quinn).
658. W. R. Grace & Co., US 4629588, 1984 (W. A. Welsh, Y. O. Parent).
659. A. Bertod, *J. Chromatogr.* 549 (1991) 1.
660. J. Freng, GB 203248, 1922.
661. Lever Bros., US 3538230, 1966 (M. Pader, W. Wiesner).
662. W. R. Grace & Co., US 4303641, 1978 (R. B. DeWolf, R. Glemza).
663. J. M. Huber, US 4340583, 1977 (S. K. Wason).
664. M. Pader: *Oral Hygiene Products and Practice*, Marcel Dekker, New York 1988.
665. J. S. Magee, J. J. Blazek in J. A. Rabo (ed.): "Zeolite Chemistry and Catalysis", *ACS Monogr.* 1976, no. 171, 615.
666. Phillips Petroleum, US 3378540, 1964 (D. R. Witt).
667. F. Karol et al., *J. Polym. Sci., Polym. Chem. Ed.* 10 (1972) 2621.
668. Exxon Chemical, US 4701432, 1986 (H. C. Welborn).
669. H. Ferch, *Chem. Ing. Tech.* 48 (1976) 922.
670. B. M. Coops, *Ind. Miner. (London)* 1989, no. 3, 43.
671. D. D. Dunnorn (ed.): *Health Effects of Synthetic Silica Particulates*, ASTM Special Technical Publication, no. 732, Philadelphia 1981.
672. Y. Takizawa et al., *Acta Med. Biol. (Nagata)* 36 (1988) 27.
673. Degussa, DE 762723, 1942 (H. Klöpfer).
674. S. Brumauer, P. H. Emmett, E. Teller, *J. Am. Chem. Soc.* 60 (1938) 309.
675. H. Ferch, K. Seibold, *Farbe Lack* 90 (1984) 88.
676. Degussa, *Schriftenreihe Pigmente*, Paper no. 11, Frankfurt 1992.
677. M. Schmücker, "Untersuchungen an nichtkristallinen technischen Kieselensäuren unter besonderer Berücksichtigung des thermischen Transforma-

- tions-verhaltens", Diplomarbeit, Ruhr-Universität, Bochum 1988.
678. H. Wistuba, "Die Silanolgruppen der Siliciumdioxidoberfläche und ihre chemischen Reaktionen", Dissertation, Universität Heidelberg 1967.
679. J. Mathias, G. Wannemacher, *J. Colloid Interface Sci.* **125** (1988) 61.
680. D. Kerner, W. Leiner, *Colloid Polym. Sci.* **253** (1975) 960.
681. H. Ferch, *Seifen Öle Fette Wachse* **101** (1975) 17, 51.
682. B. A. Morrow, A. J. McFarlan, *J. Non Cryst. Solids* **120** (1990) 61.
683. B. A. Morrow, A. J. McFarlan, *Langmuir* **7** (1991) 1695.
684. K. Yoshinaga et al., *Chem. Lett.* **1991**, 1129.
685. C. P. Tripp, M. L. Hair, *Langmuir* **7** (1991) 923.
686. G. Hellwig, *Farbe Lack* **81** (1975) no. 8, 705.
687. A. Meffert, A. Langenfeld, *Fresenius Z. Anal. Chem.* **249** (1979) 231.
688. H.-P. Böhm, M. Schneider, *Z. Anorg. Allg. Chem.* **301** (1959) 326.
689. H.-P. Böhm, *Kolloid Z. Z. Polym.* **227** (1968) 17.
690. H.-P. Böhm, *Angew. Chem.* **78** (1966) no. 12, 617.
691. Degussa, DE 1163784, 1962 (H. Brünner, J. Diether, D. Schütte).
692. Degussa, DE 3211431, 1982 (H. Klebe et al.).
693. Ivoclar, DE 3632215, 1986 (V. M. Rheinberger, T. Büchl).
694. Blendax, WO 8503220, 1985 (W. Kuhlmann).
695. Kulzer, DE 2405578, 1974 (A. Groß, R. Schäfer).
696. Canon, EP 369443, 1989 (Y. Sato, T. Kukimoto).
697. Nippon Aerosil Corp., JP 58185405, 1983 (N. Furuya, T. Morii).
698. Canon, EP 216295, 1986 (K. Tanaka et al.).
699. V. M. Litvinov et al., *Acta Polym.* **39** (1988) no. 5, 244.
700. G. Berrod, A. Vidal, E. Papirer, J. B. Donnet, *J. Appl. Polym. Sci.* **23** (1979) 2679; **26** (1981) 833 1015.
701. P. Vondracek, M. Schätz, *J. Appl. Polym. Sci.* **21** (1977) 3211.
702. L. A. Peters, J. C. Vicic, D. E. Cain, *GAK Gummi Asbest Kunstst.* **44** (1991) no. 2, 69.
703. H. Ferch, A. Reiser, R. Bode, *Kautsch. Gummi Kunstst.* **39** (1986) 1084.
704. Degussa, *Schriftenreihe Pigmente*, Paper no. 23, Frankfurt 1986.
705. Degussa, *Schriftenreihe Pigmente*, Paper no. 68, Frankfurt 1985.
706. Degussa, *Schriftenreihe Pigmente*, Paper no. 18, Frankfurt 1989.
707. K. Borio et al., *Chem. Ing. Tech.* **63** (1991) no. 8, 792.
708. H. Rumpf, *Chem. Ing. Tech.* **46** (1974) no. 1, 1.
709. R. Tawashi, *Pharm. Ind.* **25** (1963) 64.
710. H. Ferch, H. Gerofke, H. Itzel, H. Klebe, *Arbeitsmedizin Sozialmedizin Präventivmedizin* **22** (1987) 6, 23.
711. F. Leuschner, unpublished results.
712. J. J. Sarre, unpublished results.
713. Degussa, DE 1180723, 1963 (H. Biegler, W. Neugebauer, H. Kempers).
714. Degussa, DE 1933291, 1969 (A. Illigen, W. Neugebauer).
715. Lonza, DE 2337495, 1972 (C. Schnell, M. Wüller, K. Hengartner).
716. E. R. Schnell, S. M. L. Hamblin, K. Hengartner, M. Wüller, *Powder Technol.* **20** (1978) 15.
717. Degussa, DE-AS 1467019, 1963 (A. Becker, P. Nauroth).
718. Degussa, DE-AS 1168874, 1962 (G. Roderburg, P. Nauroth).
719. Degussa, DE-AS 1299617, 1965 (H. Reinhardt, K. Achenbach, P. Nauroth).
720. Degussa, EP 0078909, 1982 (P. Nauroth, H. Esch, G. Türk).
721. Degussa, DE 1767332, 1968 (G. Türk, J. Welsch).
722. Degussa, EP-A 0341383, 1989 (D. Kerner, A. Wagner, F. Schmidt, D. Bauer).
723. Degussa, DE-OS 3114493, 1981 (P. Nauroth, R. Kuhlmann, G. Türk, A. Becker).
724. Akzo, DE-AS 2020887, 1970 (G. Steenken, E. Seeburger).
725. Rhône-Poulenc, EP 0018866, 1980 (J.-L. Ray, M. Condurier).
726. Rhône-Poulenc, EP 0170578, 1985 (Y. Chevallier).
727. Rhône-Poulenc, EP-A 0396450, 1990 (Y. Chevallier).
728. Degussa, DE-OS 3639845, 1986 (H. Reinhardt, A. Becker, R. Kuhlmann, P. Nauroth).
729. Tokuyama Soda, JP-Kokai 59141416, 1983.
730. Crosfield, US 4127641, 1977 (D. Aldcroft, D. Barby, A. L. Lovell, J. P. Quinn).
731. Huber, US 4260454, 1978 (S. K. Wason, R. K. Mays).
732. Sifrance, DE-AS 2224061, 1972 (J.-B. Donnet, B. Baudru, M. Condurier, G. Vrisakis).
733. Degussa, DE 966985, 1950 (K. Andrich).
734. Nippon Silica, JP 0375215, 1989 (Y. Mikamoto, K. Sakata).
735. Degussa, DE 1229504, 1962 (G. Kallrath).
736. Bayer, DE-OS 3525802, 1985 (L. Puppe, O. Schlak, J. Ackermann, T. Naumann).
737. Degussa, DE-AS 1192162, 1962 (L. Hüter, G. Steenken).
738. PPG, DE-AS 1131196, 1955 (F. S. Thornhill, E. M. Allen).
739. PPG, DE 1283207, 1961 (C. B. Lagerstrom).
740. Degussa, DE-AS 2505191, 1975 (B. Brandt, P. Nauroth, A. Peters, H. Reinhardt).
741. Degussa, DE-OS 1467437, 1965 (G. Bretschneider, K. Pfeiffer, R. Schwarz, K. Laun).
742. Degussa, DE-AS 1293138, 1965 (H. Reinhardt, P. Nauroth).
743. Degussa, US 4179431, 1979 (E. Kilian, A. Kreher, P. Nauroth, G. Türk).
744. Degussa, DE-AS 1567440, 1965 (H. Biegler, K. Trebinger).
745. Degussa, *Schriftenreihe Pigmente*, Paper no. 70, 2nd ed., Frankfurt/Main 1984.
746. Degussa, *Schriftenreihe Pigmente*, Paper no. 28, 5th ed., Frankfurt/Main 1991.
747. Degussa, *Schriftenreihe Pigmente*, Paper no. 32, 4th ed., Frankfurt/Main 1989.
748. H. Ferch, *Chem. Ing. Tech.* **48** (1976) no. 11, 922.
749. Degussa, DE 1172245, 1963 (G. Kallrath).
750. Degussa, DE 2513608, 1975 (H. Reinhardt, K. Trebinger, G. Kallrath).
751. Degussa, DE 2729244, 1977 (P. Nauroth et al.).
752. Degussa, DE 1074559, 1959.
753. Degussa, DE 2628975, 1976 (P. Nauroth et al.).
754. Degussa, DE 1667465, 1967 (P. Nauroth, R. Kuhlmann).
755. Degussa, DE 1592865, 1967 (O. Kühnert, G. Türk, E. Eisenmenger).
756. Degussa, *Schriftenreihe Pigmente*, Paper no. 16 4th ed., Frankfurt/Main 1990.
757. H. J. Bachmann, J. W. Sellers, M. P. Wagner, R. F. Wolf, *Rubber Chem. Technol.* **32** (1959) 1286.
758. G. Kraus, *Reinforcement of Elastomers*, Interscience, New York 1965.
759. S. Wolff, *Kautsch. Gummi Kunstst.* **41** (1988) no. 7, 674.
760. Degussa, *Schriftenreihe Pigmente*, Paper no. 5, Frankfurt/Main 1982.
761. S. Wolff, *Kautsch. Gummi Kunstst.* **34** (1981) no. 4, 280.
762. S. Wolff, *Kautsch. Gummi Kunstst.* **36** (1983) no. 11, 969.
763. Degussa, DE-OS 3305373, 1983 (S. Wolff, P. Golombeck).
764. R. Bode, A. Reiser, *Kautsch. Gummi Kunstst.* **32** (1979) no. 2, 89.
765. P. Vondracek, M. Schätz, *Kautsch. Gummi Kunstst.* **33** (1980) no. 9, 699.
766. Degussa, *Schriftenreihe Pigmente*, Paper no. 13, 4th ed., Frankfurt/Main 1986.
767. Degussa, *Schriftenreihe Pigmente*, Paper no. 43, 1984.
768. K. H. Müller, *Mühle Mischfüttertech.* **114** (1977) 28.
769. K. H. Müller, *Kraftfutter* **53** (1970) 436.
770. Degussa, *Schriftenreihe Pigmente*, Paper no. 30, 3rd ed., Frankfurt/Main 1990.
771. Degussa, *Schriftenreihe Pigmente*, Paper no. 1, 5th ed., Frankfurt/Main 1989.
772. O. Pfeingel, *Fette Seifen Anstrichm.* **63** (1961) no. 5, 445.
773. Degussa, *Schriftenreihe Pigmente*, Paper no. 9, 3rd ed., Frankfurt/Main 1988.
774. Degussa, *Schriftenreihe Pigmente*, Paper no. 2, Frankfurt/Main 1983.
775. Degussa, *Schriftenreihe Pigmente*, Paper no. 42, 3rd ed., Frankfurt/Main 1986.
776. W. Leonhardt, *Speciality Chemicals* **1989**, 441.
777. K. H. Müller, W. Barthel, *Die Asphaltstraße* **1990**, no. 6, 22.
778. Degussa, EP-A 0434944, 1990 (K. H. Müller, W. Barthel).
779. Degussa, DE 1517900, 1965 (H. Reinhardt, P. Nauroth, K. Achenbach).
780. General Electric, US 4018564, 1975 (J. H. Wright).
781. R. M. Barrer, "Porous Crystals: A Perspective" in Y. Murakami, A. Jijima, J. W. Ward (eds.): *New Developments in Zeolites Science and Technology*, Kodansha, Tokyo, and Elsevier, Amsterdam, Tokyo 1986, pp. 3-11.
782. E. M. Flannigan et al., *Nature* **271** (1978) 512-516.
783. W. M. Meier, D. H. Olson: *Atlas of Zeolite Structure Types*, Butterworth, London 1987.
784. H. Gies, B. Marler, *Zeolites* **12** (1992) 42-49.
785. R. Szostak: "Modified Zeolites" in H. van Bekkum, E. M. Flannigan, J. C. Jansen (eds.): *Introduction to Zeolite Science and Practice*, Elsevier, Amsterdam 1991, pp. 153-199.
786. H. Gies et al., *Neues Jahrb. Mineral. Monatsh.* **3** (1982) 119-124.
787. B. Marler, *Phys. Chem. Miner.* **16** (1988) 286-290.
788. J. F. Cooper, Jr., G. E. Dunning, *Am. Mineral.* **57** (1972) 1494-1499.
789. C. A. Fyfe, H. Gies, *J. Inclusion Phenom.* **8** (1990) 235-239.
790. H. Gies, *Z. Kristallogr.* **167** (1984) 13-82.
791. C. A. Fyfe et al., *Zeolites* **10** (1990) 278-282.
792. C. A. Fyfe et al., *J. Am. Chem. Soc.* **110** (1988) 3373-3380.
793. C. A. Fyfe et al., *J. Am. Chem. Soc.* **111** (1989) 2470-2474.
794. J. A. Ripmeester et al., *J. Chem. Soc., Chem. Commun.* **1988**, 608-611.
795. N. Y. Chen, *J. Phys. Chem.* **80** (1976) 60-64.
796. D. H. Olson et al., *J. Catal.* **61** (1980) 390-396.
797. R. M. Lago et al.: "The Nature of the Catalytic Sites in HZSM-5-Activity Enhancement" in Y. Murakami, A. Jijima, J. W. Ward (eds.): *New Developments in Zeolite Science and Technology*, Elsevier, Amsterdam 1986, pp. 677-684.
798. T. Bein et al.: "Molecular Sieve Films from Zeolite-Silica Microcomposites" in P. A. Jacobs, R. A. van Santen (eds.): *Zeolites: Facts, Figures, Future*, Elsevier, Amsterdam 1989, pp. 887-896.
799. Y. S. Lin, Y. H. Ma: "A Comparative Study of Adsorption and Diffusion of Vapor Alcohols and Alcohols from Aqueous Solutions in Silicalite" in P. A. Jacobs, R. A. van Santen (eds.): *Zeolites: Facts, Figures, Future*, Elsevier, Amsterdam 1989, pp. 877-886.
800. P. Enzel, T. Bein, *J. Phys. Chem.* **93** (1989) 6270-6272.
801. S. D. Cox, G. D. Stucky, *J. Phys. Chem.* **95** (1991) 710-720.
802. N. Herron, Y. Wang, *J. Phys. Chem.* **91** (1987) 2757.
803. S. Miyazaki, H. Yoneuyama, *Denki Kagaku* **58** (1990) 37-40.
804. S. T. Homeyer, W. M. H. Sachtler: "Design of Metal Clusters in NaY Zeolite" in P. A. Jacobs, R. A. van Santen (eds.): *Zeolites: Facts, Figures, Future*, Elsevier, Amsterdam 1989, pp. 975-984.
805. K. Möller et al., *J. Phys. Chem.* **93** (1989) 6116-6120.
806. S. D. Cox et al., *Chem. Mater.* **2** (1990) 609-619.
807. G. Ozin et al., *Angew. Chem.* **101** (1989) 373-390.
808. H. Gies et al., *Angew. Chem.* **94** (1982) 214-215.
809. H. K. Chae et al.: "Clathrasils: New Materials for Nonlinear Optics" in G. Stucky (ed.): "New Materials for Nonlinear Optics", *Am. Chem. Soc. Symp. Ser.* **1991**.
810. H. Gies: "Clathrasils and Zeosils: Inclusion Compounds with Silica Host Framework" in J. L. Atwood, J. E. D. Davies, D. D. McNicol (eds.): *Inclusion Compounds*, vol. 5, Inorganic and Physical Aspects of Inclusion, Oxford University Press, Oxford 1991, pp. 1-36.
811. K. R. Franklin, B. M. Lowe, *Zeolites* **8** (1988) 491-516.
812. E. W. Valyocsik, L. D. Rollman, *Zeolites* **5** (1985) 123-125.
813. G. T. Kerr, *J. Phys. Chem.* **71** (1967) 4165.
814. C. A. Fyfe et al., *J. Chem. Soc., Chem. Commun.* **1984**, 1093-1094.

810. "Silica Flour: Silicosis", *NIOSH, Current Intelligence Bulletin* no. 36, 1981. *DHHS (NIOSH) Publication* no. 81-137, 1981.
811. Information Profiles on Potential Occupational Hazards, vol. II, Chemical Classes: Amorphous Silicas, NTIS, no. PB81-147886, 1979.
812. *Patty*: 3rd ed., 2B, p. 3012.
813. D. D. Dunnom (ed.): "Health Effects of Synthetic Silica Particulates", *ASTM Spec. Tech. Publ.* 732 (1981) no. 04-732000-17.
814. E. Quellmalz: "Silikogener Staub", *Das neue Chemikaliengesetz: Arbeitsstoffverordnung Anhang II, 12/2.8*, WEKA-Verlag, Kissing 1982.
815. Deutsche Forschungsgemeinschaft (ed.): *MAK- und BAT-Wert-Liste*, VCH, Weinheim 1992, pp. 96-102.
816. *Documentation of the Threshold Limit Values*, 4th ed. 1980, Suppl. Docum. 1981, Silica (amorphous), p. 362, Silica (fused), p. 363, Silica (quartz), p. 364. *Am. Cong. Gov. Ind. Hyg.*, Cincinnati, OH, 1981.
817. V. Klosterkötter, *Arch. Hyg. Bakteriologie* 149 (1965) 577-598.
818. W. H. Schepers et al.: *AMA Arch. Ind. Health* 16 (1957) 125-146.
819. H. Volk, *Arch. Environ. Health* 1 (1960) 125-128.
820. H. Geroftke: *Beobachtungen an Beschäftigten des Aerosil-Betriebes*, Rheinfelden 1981, unpublished.
821. V. C. Vitums et al.: *Arch. Environ. Health* 32 (1977) no. 2, 62-68.
822. F. D. Goldsmith, T. L. Guidotti, D. R. Johnston: *Am. J. Ind. Med.* 3 (1982) 423.
823. P. Westerholm: *Scand. J. Work Environm. Health (Suppl.)* 2/6 (1980) 1.
824. M. Finkelstein, R. Kusiak, G. Suranyi: *J. Occup. Med.* 24 (1982) 663.
825. H. Gulbergsson, K. Kurppa, H. Koskinen, M. Vasama: "Association between Silicosis and Lung Cancer: A Register Approach", *VI. International Pneumoconiosis Conference*, Bochum, Sept. 20-23, 1983.
826. C. G. O'Neill et al.: *Lancet* 202 (1982) 1202.
827. W. Klosterkötter, H. J. Einbrodt: *Arch. Hyg. Bakteriologie* 149 (1965) 367-384.
828. W. Klosterkötter: *Retention, Penetration und Elimination von Quarz bei einem Langzeit-Inhalationsversuch (Konzentration 10 mg/m³)* vol. 9, Verlag Glückauf, Essen 1973, p. 177.
829. H. Gärtner: *Arch. Hyg. Bak.* 136 (1952) 451-461.
830. K. W. Jötten: *Gutachtliche Untersuchung und Beurteilung der Wirkung von Aerosilstaub auf das Lungengewebe von Versuchstieren*, Deutsche Gold- und Silber-Scheideanstalt, Frankfurt am Main 1952.
831. M. M. E. Wagner: *J. Natl. Cancer Inst.* 57 (1976) 509.
832. M. M. E. Wagner, J. C. Wagner, R. Davies, D. M. Griffiths: *Br. J. Cancer* 41 (1980) 908.
833. F. Stenback, J. Rowland: *Oncology* 36 (1979) 63.
834. L. M. Holland, M. Gonzales, J. S. Wilson, M. I. Tillery: "Pulmonary Effects of Shale Dusts in Experimental Animals", *Environmental Health Conference*, Park City, April 6-9, 1982.

49 Boron

ULRICH BAUDIS (§ 49.1 EXCEPT 49.1.1); ROBERT A. SMITH (§§ 49.1.1, 49.7-49.13); ROBERT J. BROTHERTON, C. JOSEPH WEBER (§§ 49.2-49.3); CLARENCE GUBERT, JOHN L. LITTLE (§§ 49.4-49.5); JOSEPH A. CORELLA (§§ 49.4-49.5); ALFRED LIPP, KARL A. SCHWETZ (§§ 49.6); GÜNTER ETZRODT (§ 49.14)

49.1 The Element	1985	49.4.1.3 Uses	2000
49.1.1 Occurrence	1986	49.4.2 Borohydrides	2001
49.1.2 Structure and Polymorphism	1987	49.5 Toxicology and Occupational Health	2001
49.1.3 Physical Properties	1988	49.6 Metal Borides	2002
49.1.4 Chemical Properties	1988	49.6.1 Properties	2002
49.1.5 Production	1989	49.6.2 Production	2005
49.1.6 Chemical Analysis, Storage, Safety	1990	49.6.3 Uses	2005
49.1.7 Uses, Economic Aspects	1991	49.7 Boric Oxide	2006
49.2 Boron Halides	1991	49.7.1 Physical Properties	2006
49.2.1 Physical Properties	1991	49.7.2 Chemical Properties	2006
49.2.2 Chemical Properties	1992	49.7.3 Production	2007
49.2.2.1 Exchange Reactions	1992	49.8 Boric Acid	2007
49.2.2.2 Halide Displacement Reactions	1992	49.8.1 Physical Properties	2007
49.2.2.3 Boron Trihalides as Lewis Acids	1993	49.8.2 Chemical Properties	2010
49.2.2.4 Reduction Reactions	1993	49.8.3 Production	2010
49.2.3 Production	1993	49.9 Aqueous Borate Solutions	2011
49.2.4 Quality Specifications, Chemical Analysis	1994	49.10 Sodium Borates	2012
49.2.5 Sources, Handling, and Transportation	1994	49.11 Other Metal Borates	2016
49.2.6 Uses of Boron Trihalides	1994	49.11.1 Calcium and Calcium Sodium Borates	2016
49.2.7 Pollution Control, Toxicology, and Occupational Health	1995	49.11.2 Lithium, Potassium, and Ammonium Borates	2016
49.2.8 Fluoroboric Acid and Fluoroborates	1995	49.11.2.1 Lithium Borates	2016
49.2.8.1 Physical and Chemical Properties	1995	49.11.2.2 Potassium Borates	2017
49.2.8.2 Production	1996	49.11.2.3 Ammonium Borates	2017
49.2.8.3 Quality Specifications, Chemical Analysis	1996	49.11.3 Zinc Borates	2018
49.2.8.4 Sources, Handling, and Transportation	1996	49.12 Borate Glasses	2018
49.2.8.5 Uses	1997	49.13 Miscellaneous Data	2019
49.2.8.6 Pollution Control, Toxicology	1997	49.13.1 Quality Specifications	2019
49.2.9 Boron Subhalides	1997	49.13.2 Uses	2019
49.3 Boron Sulfide	1998	49.13.3 Economic Aspects	2020
49.3.1 Physical and Chemical Properties	1998	49.13.4 Toxicology and Occupational Health	2021
49.3.2 Production	1998	49.14 Pigments	2021
49.3.3 Uses	1998	49.14.1 Borosilicate Pigments	2021
49.4 Boranes	1998	49.14.2 Borate Pigments	2021
49.4.1 Diborane and Higher Boranes	1998	49.15 References	2021
49.4.1.1 Physical and Chemical Properties	1999		
49.4.1.2 Production	2000		

49.1 The Element

The nonmetallic element boron is situated in the top position of the third main group in

the periodic table. Boron is not found free in nature but is always bound to oxygen. It occurs as orthoboric acid and as alkali-metal and alkaline earth metal borates. The most impor-

tant sources of boron are the minerals rasorite and kernite, which are found in extensive deposits in California in the Mojave desert. There are also large ore deposits in Turkey and the former USSR. Although widespread in nature, boron constitutes only about 3 ppm of the earth's crust [9].

Boron was discovered concurrently by the French chemist GAY-LUSSAC and the English chemist SIR HUMPHRY DAVY in 1808. HENRI MOISSAN [10] first obtained considerable quantities of boron (of 86% purity) by reduction of boric oxide with magnesium in 1895. The Moissan process is still the basis for commercial production of amorphous low-purity boron.

In 1909 WEINTRAUB [11] succeeded in preparing 99% pure boron by decomposition of BCl_3 in an electric arc. Since then numerous methods have been developed, but still research continues to find methods for producing commercial quantities of pure boron.

49.1.1 Occurrence

In nature boron always occurs in the oxygenated state, mainly as borates. The structure of these covalently bonded boron-oxygen compounds consists of either planar BO_3 units with 120° between bonds or tetrahedral BO_4 units. In addition, boron is the only light element having two abundant isotopes, ^{10}B (18.8%) and ^{11}B (81.2%).

Boron is found in the earth's crust at an average concentration of about 10 ppm. Large deposits of commercially valuable boron minerals are only found in a few localities, usually sites of earlier intense volcanic activity. There are about 150 known boron-containing minerals [12], and of these only tincal, colemanite, ulexite, kernite, probertite, and szaibelyite are of significant commercial importance (Table 49.1).

The Arabic word for borax, baurach, is found in old manuscripts from ancient Persia and Arabia dating 2000 years ago. Tincal, the mineral name for borax decahydrate, derives

from tincana, the Sanskrit word for borax. Borates were known before Babylonian times to be useful as a flux for welding gold and have been found in enamels from China as early as 300 B.C. At the end of the 13th century Marco Polo brought borax from Mongolia to Europe. This became the primary European source for use as a soldering and enameling agent. In Turkey borates have been known since the 13th century but have been little used until recently. In 1772 boric acid or sassolite was discovered in hot springs located in Tuscany, Italy. About 1836, borates were discovered in Chile and Argentina, and these deposits quickly became the major source of world borates until the end of the century. By 1864 borates had been discovered in California and Nevada (USA).

The large sodium borates deposit of United States Borax & Chemical Corp. was discovered in California in 1913. Production began in 1927, and this has become the principal world source of refined sodium borates and boric acid. Reserves include tincal, kernite, and ulexite. American Borate Corp. near Death Valley in California produces colemanite and ulexite. Kerr McGee Chemical Corp. extracts borates from brines located at Searles Lake in California.

Reserves and production of borates in Turkey are operated by Etibank, a government controlled corporation [13]. A large sodium borates deposit found at Kirka has reserves of tincal and kernite, estimated at 500×10^6 t, which are very similar to the deposit in California. The Kirka reserve is by far the largest known borate deposit. A new refinery designed to produce sodium borates is near completion at Kirka. Much smaller deposits of colemanite are found at Bigadic, Keatelek, and Hisarcik. Ulexite is also found at Bigadic. Colemanite and ulexite are the principal minerals mined and sold today. However, major expansion for production of refined products is reported to be under construction.

Table 49.1: Important borate minerals.

Mineral	Formula	Formula	%		Location
			B_2O_3	H_2O	
Tincal, borax	$\text{Na}_2\text{O} \cdot 2\text{B}_2\text{O}_3 \cdot 10\text{H}_2\text{O}$	$\text{Na}_2\text{B}_4\text{O}_7 \cdot 10\text{H}_2\text{O}$	36.5	47.2	Boron, California, USA; Turkey; Argentina
Tincalconite	$\text{Na}_2\text{O} \cdot 2\text{B}_2\text{O}_3 \cdot 5\text{H}_2\text{O}$	$\text{Na}_2\text{B}_4\text{O}_7 \cdot 5\text{H}_2\text{O}$	47.8	30.9	California, USA; Turkey; Argentina
Kernite	$\text{Na}_2\text{O} \cdot 2\text{B}_2\text{O}_3 \cdot 4\text{H}_2\text{O}$	$\text{Na}_2\text{B}_4\text{O}_7 \cdot 4\text{H}_2\text{O}$	50.9	26.4	Boron, California, USA; Argentina
Ulexite	$\text{Na}_2\text{O} \cdot 2\text{CaO} \cdot 5\text{B}_2\text{O}_3 \cdot 16\text{H}_2\text{O}$	$\text{NaCaB}_3\text{O}_6 \cdot 8\text{H}_2\text{O}$	43.0	35.6	California, USA; Nevada, USA; Argentina; Chile; Peru; Tibet; Turkey
Colemanite	$2\text{CaO} \cdot 3\text{B}_2\text{O}_3 \cdot 5\text{H}_2\text{O}$	$\text{Ca}_2\text{B}_6\text{O}_{11} \cdot 5\text{H}_2\text{O}$	50.8	21.9	Turkey, California, USA; Nevada, USA; Mexico
Pandermite, priceite	$4\text{CaO} \cdot 5\text{B}_2\text{O}_3 \cdot 7\text{H}_2\text{O}$	$\text{Ca}_4\text{B}_{10}\text{O}_{19} \cdot 7\text{H}_2\text{O}$	49.8	18.1	Turkey
Hydroboracite	$\text{CaO} \cdot \text{MgO} \cdot 3\text{B}_2\text{O}_3 \cdot 6\text{H}_2\text{O}$	$\text{CaMgB}_6\text{O}_{11} \cdot 6\text{H}_2\text{O}$	50.5	26.2	Caucasus, Russia; Argentina
Inyoite	$2\text{CaO} \cdot 3\text{B}_2\text{O}_3 \cdot 13\text{H}_2\text{O}$	$\text{Ca}_2\text{B}_6\text{O}_{11} \cdot 13\text{H}_2\text{O}$	37.6	42.2	Kazakhstan; Argentina
Ascharite, szaibelyite	$2\text{MgO} \cdot \text{B}_2\text{O}_3 \cdot \text{H}_2\text{O}$	$\text{Mg}_2\text{B}_2\text{O}_5 \cdot \text{H}_2\text{O}$	41.4	10.7	Former USSR; China
Datolite	$2\text{CaO} \cdot \text{B}_2\text{O}_3 \cdot 2\text{SiO}_2 \cdot \text{H}_2\text{O}$	$\text{Ca}_2\text{B}_2\text{Si}_2\text{O}_9 \cdot \text{H}_2\text{O}$	21.8	5.6	Kazakhstan
Meyerhofferite	$2\text{CaO} \cdot 3\text{B}_2\text{O}_3 \cdot 7\text{H}_2\text{O}$	$\text{Ca}_2\text{B}_6\text{O}_{11} \cdot 7\text{H}_2\text{O}$	46.7	28.2	Turkey
Inderite	$2\text{MgO} \cdot 3\text{B}_2\text{O}_3 \cdot 15\text{H}_2\text{O}$	$\text{Mg}_2\text{B}_6\text{O}_{11} \cdot 15\text{H}_2\text{O}$	37.3	48.3	Argentina
Howlite	$4\text{CaO} \cdot 5\text{B}_2\text{O}_3 \cdot 2\text{SiO}_2 \cdot 5\text{H}_2\text{O}$	$\text{Ca}_4\text{B}_{10}\text{Si}_2\text{O}_{31} \cdot 5\text{H}_2\text{O}$	44.4	11.5	Mexico; Turkey
Probertite	$\text{Na}_2\text{O} \cdot 2\text{CaO} \cdot 5\text{B}_2\text{O}_3 \cdot 10\text{H}_2\text{O}$	$\text{NaCaB}_3\text{O}_6 \cdot 5\text{H}_2\text{O}$	49.6	25.6	California, USA
Sassolite	$\text{B}_2\text{O}_3 \cdot 3\text{H}_2\text{O}$	H_3BO_3	56.3	43.7	Tuscany, Italy
Boracite	$5\text{MgO} \cdot \text{MgCl}_2 \cdot 7\text{B}_2\text{O}_3$	$\text{Mg}_3\text{B}_2\text{O}_5\text{Cl}$	62.2	—	Turkey

Both tincal and ulexite are found in Argentina and ulexite is found in Peru. Borate reserves in Kazakhstan are found in the Inder district, and consist principally of szaibelyite and hydroboracite. Although production in the former USSR is relatively small, reserves are believed to be extensive. Ascharite, a magnesium borate, is the source of most borates produced in China.

49.1.2 Structure and Polymorphism

There are several allotropic forms of boron. Well established are amorphous boron, α -rhombohedral boron, and β -rhombohedral boron. In addition, four tetragonal forms have been described. However, these are probably stabilized by small amounts of nitrogen or carbon [4].

The β -rhombohedral form is the thermodynamically stable modification at all temperatures. Amorphous boron slowly converts to

the β -rhombohedral form at $\approx 1200^\circ\text{C}$ and to α -rhombohedral boron above 1500°C . Any type of boron recrystallizes in β -rhombohedral structure when heated above the melting point and cooled.

The unit cell of β -rhombohedral boron contains 105 boron atoms grouped $84\text{B} + 2 \times 10\text{B} + 1\text{B}$ in a complex arrangement. The structure of α -rhombohedral boron can be described as a slightly deformed cubic close packing of B12 icosahedra. The unit cell contains 12B atoms at the vertices of the icosahedron.

Amorphous boron exhibits broad reflections in the x-ray diffraction pattern. It is believed to be a frozen-in intermediate between the α - and β -modifications or a microcrystalline deposit of β -rhombohedral boron [4]. Amorphization can be achieved by intensive milling of β -rhombohedral samples [14]. Structures of the other polymorphs are too complex to be described in a few words; however all boron structures have been discussed thoroughly elsewhere [4].

49.1.3 Physical Properties

Determination of precise physical properties of boron is made more complicated by the structural polymorphism and purification problems. Some recent values, rather arbitrarily collected from the literature, are listed below.

Atomic number	5
Relative atomic mass	10.811
Melting point (°C)	2050 ± 50
Sublimation point (°C)	2550
Density (20 °C)	2.3
(g/cm ³)	2.35
	2.46
	2.99
	2.13
Crystal structure	amorphous, α-rhombohedral, β-rhombohedral, four tetragonal
Hardness (Knoop)	2390
(kg/mm ²)	2690
Electrical resistivity	7.5 × 10 ²
(300 K) (Ωcm)	7 × 10 ³
	10 ⁶ –10 ⁷
Heat capacity C _p	12.054
(JK ⁻¹ mol ⁻¹)	11.166
	33.955
	39.063
Entropy S (298 K)	6.548
(JK ⁻¹ mol ⁻¹)	5.875
Enthalpy of fusion	50.2
ΔH _f (kJ/mol)	
Enthalpy of sublimation	572.7
ΔH _s (kJ/mol)	

Boron is the second hardest element, the diamond allotrope of carbon being the hardest. α-Rhombohedral boron is red to brown; β-rhombohedral boron lustrous gray black; and amorphous material is brown to gray. The electrical resistivity changes drastically with temperature, varying from 10¹¹ Ωcm at -160 °C to 10⁶ Ωcm at 20 °C and to 0.1 Ωcm at 700 °C [4] for polycrystalline β-rhombohedral boron, behavior characteristic of a semiconductor. Detailed information about optical, magnetic, electrical, thermodynamic, and other properties of the various boron polymorphs are given in the literature [4, 5].

Boron is composed of two stable isotopes, ¹⁰B and ¹¹B. Their nuclear properties are summarized in Table 1. The nuclear spin permits NMR spectroscopy. The high value of thermal neutron cross section of the isotope ¹⁰B makes

boron useful as a neutron absorber in nuclear power plants.

49.1.4 Chemical Properties

The chemical properties of boron are determined to a large extent by its small atomic radius (0.25 nm) and high ionization potentials.

Ionization energy (kJ/mol)	
B → B ⁺	798 (8.27 eV)
B ⁺ → B ²⁺	2426 (25.15 eV)
B ²⁺ → B ³⁺	3658 (37.92 eV)
Standard electrode potential	
B + 3H ₂ = OH ₃ BO ₃ + 3H ₂ + 3e ⁻	-0.73 V
Electron affinity (kJ/mol)	
	32 (0.332 eV)
Electronegativity	
	2.04 (Pauling)
	2.01 (Mulliken)
Ionic radius (nm)	
	0.25
Atomic radius (nm)	
	0.80–0.95 (depending on type of bonding)
Standard enthalpy of formation (kJ/mol)	
BF ₃	-1136
BCl ₃	-402
BBBr ₃	-239
B ₂ O ₃	-1269
BN	-256

The electronic configuration 2s²2p¹ dictates predominant trivalency. However, simple B³⁺ ions do not exist.

Because boron has more orbitals available for bonding than electrons (4 orbitals, 3 electrons), it is an electron-pair acceptor, a Lewis acid, and it has a tendency to form multi-center bonds. Other dominant characteristics are the high affinity for oxygen and the tendency to combine with most metals to give refractory alloylike metal borides.

Table 49.2: Nuclear properties of boron.

Property	Nuclide	
	¹⁰ B	¹¹ B
Relative atomic mass	10.0129	11.0093
Natural abundance, %	19.8	80.2
Nuclear spin	+3	-3/2
Magnetic moment, nuclear magnetons ^a	+1.80063	+2.68857
Quadrupole moment, barn ^b	+0.074	0.036
Cross section for (n,α), barn ^b	3837	0.005

^a 1 nuclear magneton = 5.0508 × 10⁻²⁷ Am².

^b 1 barn = 10⁻²⁸ m².

The chemical behavior of elemental boron depends upon the morphology and particle size. Generally speaking, crystalline boron is rather unreactive, whereas amorphous boron does react more readily. At room temperature all modifications of boron are relatively resistant to chemical attack.

No direct reaction occurs with hydrogen, but indirect synthesis leads to a variety of boron hydrides.

The halogens react to form the trihalides:



Fluorine reacts spontaneously at room temperature; chlorine, at 500 °C; and bromine, at 600 °C [15].

Reaction with oxygen starts at ≈ 600 °C but is restrained by the formation of a glassy liquid B₂O₃ film on the boron particles [16]. Boron reacts with sulfur to form glassy B₂S₃ and with Se to form B₂Se₃, both at ≈ 600 °C. There is no reaction with Te. With nitrogen, boron nitride, BN, is formed at 1100 °C. Phosphorus reacts completely at 1000 °C to give BP. Arsenic forms BAs at 800 °C under pressure.

Boron and carbon react to give B₁₂C₃ above 2000 °C; with silicon, B₄Si and B₆Si are formed. Heterocyclic compounds containing C, N, S, O, and boron have interesting structures and properties. There is also a large variety of organoboron compounds [17].

When it does react, elemental boron is an effective reducing agent. Water vapor is reduced at 800 °C to give H₂ and B₂O₃. Carbon monoxide is reduced at 1200 °C; boron burns in carbon dioxide at red heat. Nitrogen oxides are reduced to give BN and B₂O₃. Sulfur dioxide is also reduced. When transition metal oxides like Fe₂O₃, TiO₂, and Cr₂O₃ are reacted with elemental boron, B₂O₃ and metal borides form. Up to 1400 °C alkaline-earth oxides and aluminum oxide do not react with boron.

Boron is not attacked by aqueous NaOH but reacts completely with molten Na₂CO₃ or molten mixtures of sodium carbonate and sodium nitrate.

Boiling nonoxidizing acids, such as HF, HCl, HBr, or dilute sulfuric or phosphoric acid, do not attack boron. However, vigorous

reaction occurs with concentrated HNO₃ or with HNO₃-H₂O₂ mixtures.

The chemical properties of boron are summarized in [19].

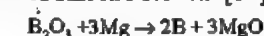
49.1.5 Production

A variety of preparative methods have been described. The following are the most important methods [6]:

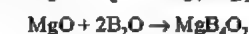
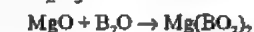
- Reduction of boric oxide with magnesium
- Reduction of boron halides or fluoroborates with sodium or another metal
- Reduction of boron halides with hydrogen
- Thermal decomposition of boron compounds, especially boron halides and hydrides
- Electrolysis of molten borates or fluoroborates

The modification of boron formed depends primarily on temperature and reaction time, only secondarily on the method [20]. As a rule of thumb, temperature below 900 °C and short reaction time produce amorphous boron; temperature above 1400 °C and long reaction time produce β-rhombohedral or the tetragonal modifications. The optimum conditions for formation of α-rhombohedral boron are in between.

The usual method for commercial production of large quantities of amorphous boron is the reduction of boron trioxide with magnesium in a thermite-like reaction [21–23]. The principles of this method date back to the work of HENRI MOISSAN [10].

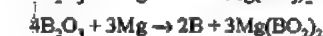
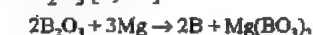


Simultaneously MgO reacts with excess B₂O₃:



The reduction is very quick and highly exothermic; finely divided material may react explosively [7].

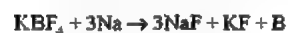
Reaction is smoother if there is an excess of B₂O₃ [7, 24]:



The optimum ratio $B_2O_3:Mg$ is about 1.8:3 [7]. Reaction is carried out in vertical steel re-ports shielded from oxygen by a flow of argon. It is initiated by electric spark and igniter mixture or by external heating.

After cooling, the reaction mass is crushed to 1-mm particles and leached twice with hydrochloric acid. Crude amorphous boron of 86–88% purity is obtained [23]. This material can be upgraded by treatment with B_2O_3 [24] or KHF_2 and KBF_4 [25, 26], subsequent leaching with acid, and final heating in a vacuum to remove boron suboxide and metals [27]. The boron content is then 90–92 or 95–97%, adequate for use in pyrotechnics and fluxes.

Reduction of KBF_4 by sodium



was used for the commercial production of boron in Germany until the end of the 1950s [28].

A common problem of metallothermic reduction is incomplete reaction and formation of nonremovable metal borides.

Samples of very pure boron, > 99% B, can be obtained by reduction of boron halides with hydrogen, especially BBr_3 [29, 30] and BCl_3 [31–34]. This is also the method of choice for laboratory synthesis [29, 31]. The halides can be purified by distillation prior to reduction [4, 29]. However, the efficiency of the hydrogen reduction process is rather low [21], yields of 5–25% being the usual. Unreacted boron halide must be recycled [32], washed out, or removed by other methods [35]. This complicates the process and makes it expensive.

Very pure boron is also obtained by thermal decomposition of BI_3 [36, 37], BBr_3 [38], or boron hydrides [39, 40] on tungsten wires or another type of incandescent filament. Boron of 99.9999% (six nines) purity was obtained by decomposition of diborane and subsequent zone melting [41].

Electrolysis of molten borates or KBF_4 [42] is not an important method for commercial or laboratory preparation although it has been mentioned in numerous articles.

Boron can be refined either by zone melting [6, 37, 41, 43, 44] or volatilization of impurities in high vacuum or hydrogen at 2000 °C [27, 37].

49.1.6 Chemical Analysis, Storage, Safety

Analysis. Boron content in elemental boron is generally determined quantitatively by decomposition to borate with fused carbonate in a platinum crucible subsequent acid leaching neutralization addition of mannitol and titration of boric acid. The mixture $HNO_3-H_2O_2$ also decomposes boron samples. Metal impurities in boron, such as Mg Na and Fe are determined by atomic absorption or emission spectrometry after decomposition of the sample [45]. Chlorine and fluorine are determined by titration [46]. The elements O, N, H, P, Si, and C are difficult to determine. However vacuum hot extraction and combustion methods [44, 45] or spark source mass spectrography [37, 47] can be used.

A sensitive qualitative test for boron is the green flame test. The sample is usually decomposed to methyl borate by heating a mixture of the sample sulfuric acid and methanol to ignition.

Storage. Dry boron is not very sensitive to oxidation. It is packaged in airtight metal drums, cardboard or plywood containers, or glass bottles [48]. Boron powder, like other combustible material, presents a dust explosion hazard. The lower explosive limit was determined to be 125 g/m³ in air [49].

Boron ignites in air at 600–800 °C but does not burn violently because of the formation of a glassy boric oxide film that prevents the material from oxidizing rapidly [16]. Burning boron should be covered with sand, aluminum oxide, sodium chloride, or the like. Water must not be used, because of the formation of inflammable hydrogen. Boron is an explosion hazard when mixed with strong oxidizing agents, such as nitrites, chlorates, lead dioxide, and silver fluoride. Such mixtures can react violently and even explode [15, 16, 18].

Safety. Elemental boron is considered to be nontoxic because of its chemical inertness and insolubility. In contrast, most boron compounds, especially the hydrides, are extremely toxic [50]. During the production process leading to boron the possible formation of any toxic boron hydrides must be either avoided or controlled.

49.1.7 Uses, Economic Aspects

Relatively large quantities of amorphous boron (90 and 95% B) are used as additives in pyrotechnic mixtures, especially in flares, igniters, and delay compositions; solid rocket propellant fuels [51]; and explosives [52]. Some boron is needed for the preparation of refractory metal boride additives for cemented carbides. Boron is also a useful reducing additive in fluxes for soldering stainless steel.

Use of boron in electronics is limited to high-purity boron (> 99.99%). It is used as a ppm additive for germanium and silicon to make *p*-type semiconductors [53]. Crystalline high-purity boron is used in thermistors [54, 55] and delay lines [56]. Boron filaments have been developed as reinforcing material for light-weight, stiff composites for use in commercial and military aircraft [57]. Epoxy resins [58], polyamides, aluminum, magnesium, and other materials are the matrix [59, 60]. However, today graphite filaments have replaced boron filaments in many applications.

In nuclear technology thin films of boron are used in neutron counters [54]. Boron powder dispersed in polyethylene castings is used for shielding against thermal neutrons [61]. In addition, composites of boron with Al or Fe, especially when enriched in ^{10}B , are used as neutron shields and absorbers in nuclear reactors [61].

Boron is an effective deoxidizing agent, e.g., for production of pure copper [62]. It also is important in the preparation of amorphous magnetic metals and alloys [63]. Boron, as ferroboration, is used in microalloyed steel (0.001% B). This steel exhibits excellent resistance to stress cracks as well as improved tensile strength and hardness.

Amorphous boron of 90–92% purity costs about DM 250–300 (= \$100) per kg (1984). Material of higher purity is much higher in price: very pure boron (> 99.99%, four nines) may cost up to DM 10 000 (= \$3500) per kg and more. Boron enriched in ^{10}B costs \$9–10 per gram [61].

The leading producers are H. C. Stark, Goslar, Germany, and Kerr McGee Chemical Corp., Oklahoma, United States. There are further production facilities at Degussa AG, Frankfurt am Main; Elektroschmelzwerk Kempton, München; Union Carbide Chemical Corp., New York; NL Industrial Corp., Wilmington, Delaware, United States; Murex Ltd., Rainham, United Kingdom; and Kawecki-Billiton Corp., Arnhem, the Netherlands [64]. Boron is also produced in the former Soviet Union.

Total production is estimated to be 30–50 t/a.

Table 49.3: Physical properties of boron halides [69, 70].

	BF_3	BCl_3	BBr_3	BI_3
mp, °C	–127.1	–107	–46	49.9
bp, °C	–99.9	12.5	91.3	210
Density, g/mL	1.57*	1.359	2.618	—
H^0 fusion, kJ/mol (at 25 °C)	–1136 [71]	–403 [72]	–240 [72]	–47 [72]
ΔS^0 , J mol ^{–1} K ^{–1} (at 25 °C)	254 [71]	290	324	—
$c_{p(B)}$, J mol ^{–1} K ^{–1} (at 25 °C)	50.5	62.6	68.0	—
Electron affinity, $\times 10^{-19}$ J	<0 [73]	0.53 [73]	1.31 [73]	1.81 [73]
B–X Bond energy, kJ/mol	154.3	106.1	88.0	63.7
B–X Bond length, μm	0.129	0.175	0.187	0.210

* At –100 °C.

49.2 Boron Halides

49.2.1 Physical Properties

Boron forms trihalides, sometimes called trihaloboranes, with fluorine, chlorine, bromine, and iodine. The trifluoride, BF_3 , and trichloride, BCl_3 , are gases at room temperature. The tribromide, BBr_3 , is a liquid, and the

triiodide, BI_3 , is a solid. All four trihalides are colorless, but the tribromide and triiodide discolor on exposure to light. A summary of some physical properties of these compounds is given in Table 49.3.

All four compounds have trigonal symmetry with X-B-X angles of 120°C . A crystal structure has been reported for a metastable phase of BF_3 at 142 K in which boron atoms are trigonal prismatic with B-X_{eq} bond lengths of 0.126–0.131 nm and B-X_{ax} bond lengths of 0.268–0.271 nm [74].

49.2.2 Chemical Properties

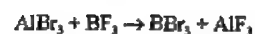
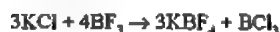
Trivalent boron halides are coordinatively unsaturated and their chemistry is dominated by the unfilled boron p_z orbital. The compounds are Lewis acids and readily form adducts with a variety of electron donors. Overlap of the unfilled boron p_z orbital with nonbonding filled orbitals on the halides decreases the electron acceptor ability of the molecule but increases the strength of the B-X bonds. The B-F bond in BF_3 is the strongest single bond known. The boron-halide p_z overlap decreases with increasing size of the halide. Thus, the acceptor strength increases as $\text{BF}_3 < \text{BCl}_3 < \text{BBr}_3 < \text{BI}_3$. However, the strength of the B-X bond decreases from BF_3 to BI_3 . Boron trifluoride chemistry is dominated by Lewis acid base reactions, whereas BBr_3 and BI_3 adducts are relatively unstable and halide displacement reactions predominate.

49.2.2.1 Exchange Reactions

All of the boron halides undergo halide exchange reactions, but of the mixed halide species only BBr_2I and BBri_2 have been isolated. Exchange reactions are also known with trialkyl, triaryl, trialkoxy, and triaryloxy boranes:



Exchange reactions between BF_3 and metal halides may be used to prepare other boron trihalides:



49.2.2.2 Halide Displacement Reactions

Boron halides, with the exception of boron trifluoride, react readily with compounds that have active hydrogen atoms, including water, alcohols, thiols, amines, phosphines, and arsines. Because of the strength of the boron-fluorine bond, halide displacement reactions occur to a lesser extent with BF_3 than with other boron halides. Boron trifluoride reacts with water to give a number of partially hydrolyzed fluoroborate species including BF_3OH^- , $\text{BF}_2(\text{OH})_2^-$, and $\text{BF}(\text{OH})_3^-$, in addition to boric acid and the fluoroborate anion, BF_4^- . Two hydrated species, $\text{BF}_3 \cdot \text{H}_2\text{O}$ and $\text{BF}_3 \cdot (\text{H}_2\text{O})_2$, can be isolated at low temperature. The dihydrate is formulated as $\text{BF}_3\text{OH}_2 \cdot \text{H}_2\text{O}$ based on recent structure analysis [75].

In contrast to the slow substitution reactions of BF_3 , other boron trihalides react vigorously with water:

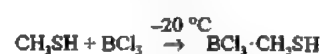
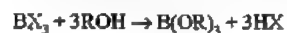


The reaction of BBr_3 or BI_3 with water may be explosive.

Most halide displacement reactions with BF_3 require either elevated temperature or an active nucleophile, such as a Grignard reagent:



Halide displacement reactions between other boron halides and compounds with active hydrogen atoms are quite facile. The first step is often the formation of an adduct, which may be isolated at low temperature, followed by the elimination of the hydrogen halide:



In general the reactivity of boron trihalides toward compounds with active hydrogen atoms increases with decreasing B-X bond energy,

in the order $\text{BF}_3 < \text{BCl}_3 < \text{BBr}_3$. Side reactions leading to alkyl halides and boric acid rather than simple halide displacement are more common with the triiodide and sterically hindered alcohols.

49.2.2.3 Boron Trihalides as Lewis Acids

Boron trifluoride forms adducts with a large number of electron donors including ethers, alcohols, ketones, amines, phosphines, arsines, thiols, and selenides. Those complexes with large electron donor atoms or sterically hindered bases tend to be less stable. Boron trichloride also forms many stable complexes with electron donors, but these are more prone to halide displacement reactions than are the BF_3 adducts. Few stable adducts are known with BBr_3 or BI_3 .

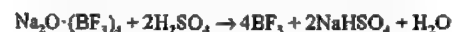
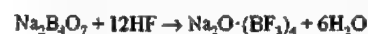
49.2.2.4 Reduction Reactions

Reaction of boron halides with hydrogen, hydrides, or alkali metals often yields boron subhalides or elemental boron. If hydrogen or a hydride is used, boranes may result, e.g., in the following convenient preparation of diborane:



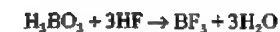
49.2.3 Production

Boron Trifluoride. Boron trifluoride was first prepared by the reaction of boric acid and fluorspar (CaF_2) at red heat [76]. Commercially, BF_3 has been produced by the stepwise addition of hydrofluoric acid and sulfuric acid to anhydrous borax (sodium tetraborate):



Another method involves addition of sulfuric acid and fluorspar and a source of boron, such as anhydrous borax or boric oxide (B_2O_3).

Recently, Polish workers have developed a process in which BF_3 is obtained by the reaction of HF and boric acid, using oleum as a dehydrating agent [77].



Boron trifluoride is now made commercially in the United States by a proprietary process from boric acid and hydrofluoric acid.

A variety of synthetic routes are available for the production of small quantities of BF_3 , including thermal decomposition of diazonium fluoroborate.

The diethyl etherate adduct, $\text{BF}_3 \cdot \text{O}(\text{C}_2\text{H}_5)_2$, produced by bubbling BF_3 into diethyl ether, provides a convenient source of BF_3 for many synthetic applications.

Boron Trichloride. This compound can be prepared by the reaction of boric oxide, a reducing agent, and chlorine in a melt at high temperatures, for example:



The product BCl_3 is recovered by fractional condensation. Sodium tetraborate $\text{Na}_2\text{B}_4\text{O}_7$ can be used in place of B_2O_3 . Molten sodium chloride, formed as a by-product, settles to the bottom of the reactor [78]. A molten combination of aluminum chloride and an alkali-metal chloride has also been used as a medium for reductive chlorination of borates [79].

Free-radical chlorination of borate esters also yields BCl_3 :



A modification of this process, in which a free-radical initiator is used, has recently been reported [80, 81]. A low reaction temperature, 40–90 $^\circ\text{C}$, and the use of an initiator decrease the consumption of Cl_2 and prevent the formation of phosgene, COCl_2 .

Commercially, boron trichloride is prepared by the reaction of boron carbide with chlorine in a borate melt. This reaction can also be done with dry B_4C in a fluidized-bed reactor using a transition metal halide as a catalyst [82].

Contamination of BCl_3 with COCl_2 from the chlorination of carbon oxides is a serious problem in BCl_3 manufacturing. Because of similar vapor pressure-temperature curves, BCl_3 and COCl_2 cannot be separated by fractional distillation. Thermal or photochemical

conversion of COCl_2 to CO and Cl_2 followed by fractional distillation has been used to purify BCl_3 .

Boron trichloride can be prepared in the laboratory by the reaction of boron trifluoride and aluminum chloride.

Boron Tribromide. This compound can be prepared by the reaction of boric oxide, carbon, and bromine, or from boron carbide and bromine analogous to the chlorine reactions.

Small quantities of BBr_3 can be made by the reaction of boron trifluoride and aluminum tribromide. A five-fold excess of AlBr_3 increases the yield of BBr_3 .

Boron Triiodide. Boron triiodide can be prepared by the reaction of a borohydride and iodine:



where M is lithium, sodium, or potassium.

The reaction between sodium borohydride and iodine in dimethylformamide (DMF) results in $\text{BI}_3 \cdot 4\text{DMF}$ [83]. Boron triiodide can also be made by exchange reactions between AlI_3 and BF_3 , or between LiI and LiBH_4 . Contrary to an earlier report, boron triiodide can be prepared from the elements by the reaction of amorphous boron with iodine at 870°C [84].

49.2.4 Quality Specifications, Chemical Analysis

Boron trifluoride is available in quantity as a 99% pure gas. Boron trichloride is typically sold as a 99.9% pure liquid. Boron tribromide is offered in grades up to 99.9999% for electronic applications.

Common impurities in BF_3 include air, silicon tetrafluoride, and sulfur dioxide. The major impurities in boron trichloride are phosgene and chlorine. Boron tribromide typically contains traces of bromine.

The boron halides may be analyzed by hydrolysis followed by analysis of B_2O_3 and the halide, or by base titration. The concentration of phosgene (COCl_2) in BCl_3 may be determined by infrared spectroscopy. The trifluo-

ride, trichloride, and tribromide may be purified by fractional distillation.

49.2.5 Sources, Handling, and Transportation

Allied Corp. is the major producer of boron trifluoride. Boron trifluoride complexes with monoethylamine, phenol, and diethyl ether are also available in large quantities from Allied. Complexes of BF_3 with water, dimethylamine, monoethylamine, phosphoric acid, and piperidine are available from Harshaw/Filtrol. Kerr-McGee Corp. is the major producer of BCl_3 and BBr_3 . Boron trifluoride and trichloride are available in steel cylinders. Boron tribromide is available in glass bottles. Boron tribromide for use in electronics is supplied by J. C. Schumacher Co. in specially sealed glass vessels equipped with teflon valves. Boron triiodide is available in small quantities from the Ventron Division of Morton-Thiokol Inc.

Boron trifluoride and boron trichloride sold for \$6.83/kg (\$3.10/lb) and \$8.38/kg (\$3.80/lb) in bulk in 1984. The 1982 price for BBr_3 was \$57/kg (\$26/lb) in large quantities from Kerr-McGee.

Boron trifluoride is the largest volume boron halide. The total annual production of BF_3 and its adducts is about 2300–4500 t/a. The annual production of BCl_3 is about 225–450 t/a. The annual production rate of BBr_3 is significantly less than that of BCl_3 .

The boron trihalides are nonflammable. But because they hydrolyze easily, care should be taken to avoid exposure to moisture. The DOT classification for BCl_3 and BBr_3 is corrosive liquid; BF_3 is classified as a nonflammable gas. Equipment for conveying the compounds should be flushed with dry air prior to use. Stainless steel lines and valves are suitable for use with all dry boron halides.

49.2.6 Uses of Boron Trihalides

Boron Trifluoride. Boron trifluoride is the most widely used boron halide. Most applications take advantage of its strong Lewis acidity. The most important uses are in organic

syntheses. Boron trifluoride is commonly used as a catalyst for Friedel-Crafts alkylation reactions. It also is used to catalyze the cleavage of ethers to alcohols, to catalyze esterification reactions, and in the nitration and sulfonation of aromatic compounds. Many olefin polymerization reactions use BF_3 as an initiator, in conjunction with a proton donor, such as water. Also BF_3 is used to catalyze the isomerization of alkenes and alkanes and in petroleum cracking and desulfurization. Amine complexes of BF_3 are used as epoxy curing agents.

Boron Trichloride. One of the most important uses of BCl_3 is in the preparation of boron fibers. Typically an electrically heated tungsten filament is passed through a chamber containing BCl_3 and hydrogen. The BCl_3 is reduced, and boron is deposited on the filament, producing a stiff, strong boron fiber.

Boron trichloride, like the trifluoride, has been used as a Lewis acid catalyst in organic synthesis in the polymerization of olefins and phosphazenes, as well as in catalysis of other organic reactions. Boron trichloride is also used in plasma etching of aluminum and silicon, in semiconductor manufacturing, and as a source of boron for chemical vapor deposition. Steel is boronized by contacting it with a reactive mixture of hydrogen, hydrocarbons, and BCl_3 at high temperatures.

Boron Tribromide. The primary use of boron tribromide is as an initiator for the polymerization of olefins and as a catalyst in other organic reactions. It is also used in the electronics industry as a source of bromine for ion implantation in semiconductors, and for plasma etching in semiconductor device manufacturing.

Boron Triiodide. There are no important commercial uses for boron triiodide.

49.2.7 Pollution Control, Toxicology, and Occupational Health

Boron halides are not major pollution sources. Fluoride, from the hydrolysis of BF_3 , can be precipitated from waste water as CaF_2 by the addition of a calcium salt [85–87].

Aqueous boron (boric acid or borates) can be precipitated by the addition of calcium salts at high pH.

Boron halides are quite toxic and contact with skin or eyes should be avoided. A TLV ceiling limit of 1.0 ppm, 3 mg/m³ (TWA), has been set for BF_3 by the ACGIH. The MAK values are the same. For BBr_3 , the adopted TLVs are 1 ppm, 10 mg/m³ (TWA); 3 ppm, 30 mg/m³ (STEL). The LCs in air for BF_3 and BCl_3 in male rats (1 h exposure) are 387 and 2.54 ppm, respectively [88]. These compounds are not known to be carcinogenic.

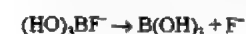
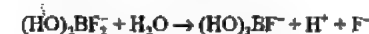
49.2.8 Fluoroboric Acid and Fluoroborates

49.2.8.1 Physical and Chemical Properties

In the older literature and in some commercial usage, HBF_4 and its salts are referred to as fluoboric acid and fluoborates. Nomenclature based on fluoroboric and fluoroborates has now become generally accepted in the literature and is used throughout this chapter [93].

The fluoroborate anion, BF_4^- , is essentially the adduct of BF_3 and F^- . The ion is tetrahedral, with B–F bond lengths of about 0.140–0.145 nm compared to a B–F bond length of 0.129 nm in BF_3 .

The fluoroborate anion hydrolyzes in water in a stepwise manner to give first hydroxyfluoroborates, then boric acid:



Concentrated solutions of alkali-metal fluoroborates are stable toward hydrolysis; the anion is more easily hydrolyzed in solutions of transition-metal fluoroborates. Concentrated aqueous solutions of fluoroboric acid, tetrafluoroboric acid, HBF_4 , can be made, but HBF_4 has not been isolated. Solvated species have been crystallized, including $\text{H}_3\text{O}^+ \cdot \text{BF}_4^-$.

$\text{H}_2\text{O}_2 \cdot \text{BF}_4$ and $[\text{H}(\text{CH}_2\text{OH})_2] \cdot \text{BF}_4$ [94]. The term fluoroboric acid, as used commercially, always refers to an aqueous solution of HBF_4 .

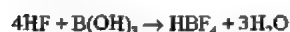
Many transition-metal fluoroborates are quite soluble in water. Alkali-metal salts are less soluble. Ammonium, sodium, and potassium fluoroborate crystallize as anhydrous salts. Transition-metal salts all crystallize with various degrees of hydration. Many metal fluoroborates are also soluble in methanol and ethanol. Silver and copper(II) fluoroborate are soluble in diethyl ether and aromatic solvents.

Solid fluoroborate salts decompose upon heating, evolving BF_3 . The heat of dissociation increases with cation size for the alkali-metal fluoroborates [95]. The reaction has been used as a convenient source of BF_3 for laboratory applications:



49.2.8.2 Production

Fluoroboric acid is usually made by the reaction of hydrofluoric acid and boric acid in water:



The reaction is exothermic.

Most of the commonly used fluoroborate salts can be prepared by reacting metal oxides, hydroxides, or carbonates with fluoroboric acid.

Ammonium fluoroborate can be made from ammonia and fluoroboric acid. Fluoroborate salts can also be prepared by the reaction of BF_3 with a metal fluoride in a nonaqueous, inert solvent, such as HF , BrF_3 , or SO_2 .

49.2.8.3 Quality Specifications, Chemical Analysis

Fluoroboric acid is available from Harshaw/Filtrol in two grades, Electropure and Fluopure, a lower purity material. Specifications for Electropure fluoroboric acid are given in Table 49.4.

Table 49.4: Specifications for Harshaw/Filtrol Electropure fluoroboric acid.

Component	Specification	Typical average
HBF_4	48–50%	48.5%
H_2BO_3	0.5–1.5%	0.75%
Fe	10 ppm max.	4 ppm
Cu	1 ppm max.	< 1 ppm
Pb	1 ppm max.	< 1 ppm
Zn	1 ppm max.	< 1 ppm
Cl	3 ppm max.	< 3 ppm
SO_4	50 ppm max.	< 50 ppm
Ni	2 ppm max.	< 1 ppm

Solid alkali-metal fluoroborates may contain some hydroxyfluoroborates and boric acid as contaminants. Metal fluoroborate solutions may contain free boric acid or fluoroboric acid as well as trace amounts of metallic impurities.

Fluoroboric acid can be analyzed by hydrolysis, followed by precipitation of fluoride with calcium and titration for the borate. Metal fluoroborates have been analyzed by electrolytic reduction followed by mannitol titration for boric acid [96]. A BF_4^- ion selective electrode is available from Orion. The tetrafluoroborate ion can also be analyzed by ion chromatography [97, 98].

49.2.8.4 Sources, Handling, and Transportation

Fluoroboric acid is available from Allied Corp., Harshaw/Filtrol, C.P. Chemicals, Fidelity Chemicals, Harstan, and Ozark-Mahoning. A variety of fluoroborate salts is produced by C.P. Chemicals, Harstan, Allied, Harshaw/Filtrol, and Fidelity Chemicals. Transition-metal fluoroborates are commonly sold as aqueous solutions. They may contain a slight excess of boric acid, added as a stabilizer. Information on commercial fluoroborates is given in Table 49.5.

Fluoroboric acid and solutions of fluoroborates are corrosive and are shipped in plastic drums or polyethylene pails. Glass vessels should not be used for containing these solutions.

Table 49.5: Commercial fluoroborates.

Compound	Formula	Commercial form
Fluoroboric acid	HBF_4	49% solution
Alkali-metal salts		
Ammonium	NH_4BF_4	crystalline solid
Potassium	KBF_4	crystalline solid
Sodium	NaBF_4	solid
Transition-metal salts		
Antimony(III)	$\text{Sb}(\text{BF}_4)_3$	solution
Cadmium(II)	$\text{Cd}(\text{BF}_4)_2$	50% solution
Cobalt(II)	$\text{Co}(\text{BF}_4)_2$	solid
Copper(II)	$\text{Cu}(\text{BF}_4)_2$	45% solution
Indium(III)	$\text{In}(\text{BF}_4)_3$	solution
Iron(II)	$\text{Fe}(\text{BF}_4)_2$	41% solution
Lead(II)	$\text{Pb}(\text{BF}_4)_2$	51% solution
Nickel(II)	$\text{Ni}(\text{BF}_4)_2$	45% solution
Silver(I)	AgBF_4	powder
Tin(II)	$\text{Sn}(\text{BF}_4)_2$	50% solution
Zinc(II)	$\text{Zn}(\text{BF}_4)_2$	40% solution

Solutions of fluoroboric acid and fluoroborates are classified as corrosive materials for shipping.

49.2.8.5 Uses

The primary use of fluoroboric acid is in the preparation of other fluoroborate salts. Fluoroboric acid is also used in electroplating and in dipping solutions for surface treating of aluminum. It has been recommended as a pickling agent for hot rolled steel [99], and has been patented for use as an etchant for silicon and glass in the electronics industry [100, 101].

Molten alkali-metal and ammonium fluoroborates are good solvents for metal oxides and are commonly used in fluxes for soldering and brazing.

A mixture of LiF and NaBF_4 has been studied as a nuclear reactor coolant [102] and as a solvent for fissionable materials. Mixtures of NH_4BF_4 with nitro compounds are useful as explosives [103].

Alkali metal fluoroborates and fluoroboric acid have also been used as catalysts in organic synthesis and in polymerization reactions.

Lithium fluoroborate is used as an electrolyte in lithium-sulfur batteries.

The fluoroborate anion is similar to perchlorate, ClO_4^- , in its size, shape, and lack of

ability to form coordinate bonds with transition metals. Fluoroborates are often used in transition metal chemistry where a noncoordinating anion is required.

The primary use of transition metal fluoroborates is in electroplating. The fluoroborate ion is electrochemically inert and solutions of fluoroborates are highly conductive. Metals plated from fluoroborate solutions include cadmium, copper, indium, iron, lead, nickel, silver, tin, and zinc.

49.2.8.6 Pollution Control, Toxicology

Aqueous solutions of fluoroborates can be hydrolyzed and treated with calcium compounds to precipitate calcium fluoride for pollution control [104–106]. Reverse osmosis has also been used to purify waste streams containing potassium fluoroborate [107].

Protective equipment used with hydrofluoric acid should also be used when handling solutions of fluoroboric acid or fluoroborates.

Little information is available in the literature on the toxicity of fluoroborates. Fluoroborate given intravenously to rats depressed levels of L-thyroxine [108], and ammonium fluoroborate was shown to be nontoxic to fresh water minnows at concentrations less than 600 mg/L [109].

49.2.9 Boron Subhalides

All of the compounds, B_2X_4 , where X is F, Cl, Br, or I, are known. The tetrafluoride is the most stable, but all four compounds decompose at room temperature to BX_3 and other boron halides. The compounds are Lewis diacids and form 1:2 complexes with amines and other Lewis bases. Boron tetrachloride, which is the most commonly used of these tetrahalides, can be prepared by reduction of BCl_3 in an electrical discharge apparatus. The most important use of B_2X_4 compounds is in diboration reactions, i.e., the addition of B_2X_4 to unsaturated organic molecules. These reactions are analogous to hydroboration reactions with diborane. Some of the decomposition

products of B_2Cl_4 have been characterized. They include B_4Cl_4 , B_8Cl_8 , and B_9Cl_9 .

49.3 Boron Sulfide

49.3.1 Physical and Chemical Properties

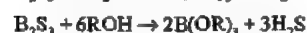
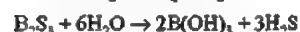
Boron sulfide, B_2S_3 , is a colorless compound normally obtained as an amorphous glass. It is extremely difficult to purify and often contains traces of silicon (from glass vessels), oxygen, or sulfur, which may impart a yellow color to the material [110]. The amorphous form does not have a well-defined melting point but begins to sublime at about 300 °C. Some of the physical properties are given in Table 49.6.

Table 49.6: Physical properties of B_2S_3 .

mp (crystalline form), °C	563 [111]
Flow point (amorphous form), °C	310 [110]
bp, °C	≈ 300, sublimes [110]
Density ρ , g/cm ³	1.92 [112]
B-S bond energy, kJ/mol	360 [113]
Heat of fusion, kJ/mol	150 [110]
Heat of vaporization, kJ/mol	252 [114]
Average B-S bond length, nm	0.1808 [112]

An X-ray analysis of crystalline B_2S_3 indicates it is composed of $(BS)_3$ and $(BS)_2$ rings linked through bridging sulfur atoms in a two-dimensional lattice [112].

Boron sulfide reacts with a variety of protonic reagents [115]:



The reaction with water is quite violent.

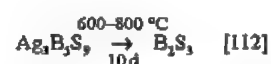
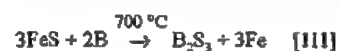
Boron sulfide inflames in chlorine, and is oxidized at high temperature by carbon dioxide or by oxygen [115]. At high temperature it also readily attacks quartz and silicate glass [110]. Boron sulfide reacts with sulfur to give B_8S_{16} , a planar molecule [116]. A variety of other higher molecular mass boron sulfides is also known [117].

Boron sulfide can also act as a sulfidizing agent [118] and can be used to replace a terminal oxygen atom with a terminal sulfur atom in

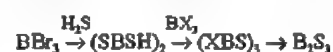
both organic and inorganic systems [119, 120].

49.3.2 Production

Boron sulfide is difficult to prepare in a pure form. The reaction of boron hydrides or metal borides with sulfur or sulfur compounds yields impure B_2S_3 [110]. Higher purity product is obtained by the reaction of amorphous boron with H_2S or sulfur. Other preparative reactions that have been reported are:



The recommended route for the synthesis of pure B_2S_3 is the decomposition of $(XBS)_3$, where X is Cl, Br, or I [110, 115]:



49.3.3 Uses

Boron sulfide has been used in organic synthesis to reduce sulfoxides to thiols [121], and to convert ketones to thioketones [119, 122]. Recently it was found that the sulfide glasses, $M_2S-B_2S_3$, where M is Li or Na, have electrical conductivities 10^3 times greater than the corresponding oxide glasses [123]. Electrically conducting boron sulfide glasses have also been made incorporating LiI [124] and other glass-forming sulfides [125, 126]. These glasses have potential as electrolytes in batteries or fuel cells.

Boron sulfide is available in research quantities from the Alfa-Ventron Division of Morton-Thiokol (USA).

49.4 Boranes

49.4.1 Diborane and Higher Boranes

Introduction. ALFRED STOCK and co-workers began working on the hydrides of boron in 1912 [127]. From then until 1936, he discov-

ered a series of boron hydrides of the composition B_nH_{n+4} and B_nH_{n+6} , which he named boranes.

Research on boron hydrides was started in the United States by H. I. SCHLESINGER, who with A. BURG published a new preparation of diborane in 1931 [128]. Impetus was added by government sponsorship of various military programs to develop high-energy fuels for rockets and aircraft during World War II. Boron fuels (alkyl penta- and decaboranes) created great interest because they possessed much higher heats of combustion than conventional hydrocarbon fuels. Large quantities of boron fuels were manufactured under projects HEF (Olin Matheson Chemical Corp.) and ZIP (Callery Chemical Co.).

Attention has been expanded to other chemical properties of the boranes since 1956, when H. C. BROWN discovered hydroboration procedures [129] (1979 Nobel Prize). His work has opened new avenues of research, one of which was to obtain chiral and optically specific compounds required in biological activity.

Progress in borane research was thwarted by inconclusive theories of structure and reactivity until the second half of the century, when W. LIPSCOMB and co-workers defined the structural and theoretical aspects of the boron hydrides through X-ray diffraction studies [130] (1976 Nobel Prize). This breakthrough in borane chemistry gave new impetus to boron research and to the discovery of the most thermodynamically and kinetically stable class of boranes, the polyhedral anions, carboranes, and metaboranes.

Collectively, boranes are compounds of very complex structure with $B-H^A-B$ and (open or closed structured) $B-B^A-B$ tricentered bonds, with H^A equal to linking hydrogen atoms. Explanation of structures and unusual bonding of these compounds has furthered the theory of chemical bonding [131]. Nomenclature of these compounds has been confusing, however, and recommendations to clarify their structures have been made by IUPAC and ACS [132].

Table 49.7: Physical properties of boranes.

Formula	mp, °C	bp, °C (101.3 kPa)	ΔH° fusion, kJ/mol
B_2H_6	-164.9	-92.6	35.5
B_4H_{10}	-120	18	66.1
B_5H_9	-46.6	48	73.2
$B_{10}H_{14}$	99.7	213	31.5

49.4.1.1 Physical and Chemical Properties

The lower boranes are very reactive to oxygen and moisture. Diborane(6), B_2H_6 , and air mixtures containing 75–98% diborane detonate in air when sparked, and concentrations over 0.5 vol% can lead to explosions in air or oxygen even without an ignition source. For recent investigations of oxidation see [133–135]. Pentaborane(9), B_5H_9 , a volatile liquid, reacts readily with air and moisture. Solid decaborane(14), $B_{10}H_{14}$, should be handled in an inert atmosphere; exposure should be avoided because of the compound's toxicity (see Table 49.8). Solutions of $B_{10}H_{14}$ and carbon tetrachloride are explosive and more shock sensitive than nitroglycerine [136]. Some physical properties of the most commercially available boranes are given in Table 49.7.

As a Lewis acid, the borane(3), BH_3 , group complexes with Lewis bases, analogous to coordinate compounds of the Werner type; the ligands NH_3 , NH_3R , and NR_3 are common to the two cases [137]. The Lewis acid BH_3 combines with another borane (Lewis acid) to give the relatively stable borane(6); hence borane groups may be considered as operational "electron-deficient" bases as well as Lewis acids: How the nature of the base or nucleophile affects the cleavage of diborane is controversial and has been discussed [138]. With neutral bases the two modes of cleavage, symmetric or unsymmetric, may occur to give molecular or ionic fragments as shown in Figure 49.1. Generally with large bases or weaker donor atoms symmetric cleavage occurs. Base displacement reactions readily occur and the relative stability of the complexes is:

Group V: $P > N$

Group VI: $S > O$

Group V > Group VI

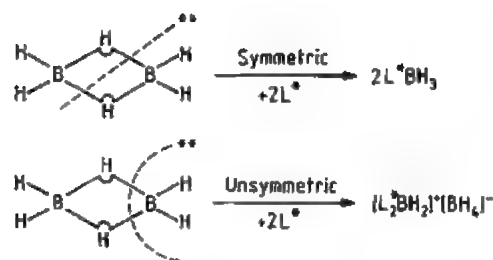


Figure 49.1: Cleavage of diborane. * L is any ligand. ** Modes of cleavage.

Lewis bases react with decaborane, without deprotonation, evolving hydrogen with the ligands coordinating at the 6,9 position. This species, B₁₀H₁₂L₂, is a key intermediate in the synthesis of the very stable and useful *closoboranes*, [B₁₀H₁₀]²⁻ and carbaboranes (where carbon is inserted in the 1,2 position of the polyhedron, i.e., 1,2-C₂B₁₀H₁₂).

Bridge hydrogens of the boranes are acidic as demonstrated by titration of B₁₀H₁₄ and by deuterium exchange [139, 140]. Abstraction of a proton forms hypopolyborate anions, such as B₅H₈⁻. They are useful intermediates in the formation of higher boranes, heteroboranes, and metalloboranes. These anions, containing a B-B edge bond, can be reacted with diborane to expand the polyhedron [141].

49.4.1.2 Production

Diborane(6) is available from Callery Chemical Co., Callery, Pennsylvania (USA). The method preferred for the commercial preparation is the addition of boron trifluoride to a stirred solution of sodium borohydride in diethylene glycol dimethyl ether (diglyme):



Currently, diborane is shipped either as a compressed gas (ambient) or as a liquid (cylinder over packaged with dry ice). It is packaged as a hazardous material regulated by the DOT [142].

Tetraborane(10), B₄H₁₀, can be obtained by the action of acid on borides [143-145]. It has been prepared from the decomposition of diborane at 120-180 °C [146] and under pressure

[147]. Tetraborane can also be prepared from the reaction of acid on commercially available B³H₈⁻ salts, e.g., NaB₃H₈.

Pentaborane is obtained by passing diborane through a hot tube. Careful control of temperature, pressure, and flow are required to obtain good yields and avoid further pyrolysis to higher hydrides.

Decaborane can be produced by several procedures, none of which give high yields; all require extensive preparatory time or equipment. It is best produced by the pyrolysis of diborane between 120-240 °C. The solids thus produced are removed from the reactor by dissolution and further purified by sublimation.

49.4.1.3 Uses

Most of the boranes are highly reactive. This property makes them useful and important chemicals, but also necessitates special care in their application.

Diborane serves as a strong but selective reducing agent in organic chemistry. It is an electrophilic reagent and reacts markedly different from the nucleophilic alkali-metal boron and aluminum hydrides. The rates of reduction with diborane were found to decrease in the order: carboxylic acids > olefins > ketones > nitriles > epoxides > esters > acid chlorides [148]. Reductions of several other organic substrates have been studied, for example, oximes [149], perfluorinated olefins [150], diene polymers [151], and organic acid amides [152].

Hydroboration, the addition of diborane or borane to olefins, has found great significance in preparative chemistry [129]. Hydroboration is applicable to multiple bonds between C-C, C-O, C-N, N-N, N-O. Diborane catalyzed by the presence of an ether adds, in an anti-Markownikoff mode, virtually quantitatively to the carbon-carbon double bond of olefins, forming an alkyl borane.

Other important derivatives of diborane are Lewis base adducts, carbonyl adducts, and oxygen-containing products. Further areas of application for diborane are the doping of

semiconductor silicon and germanium. Diborane is readily decomposed at high temperature (600-700 °C) [153] to give fine-powder, high-purity elemental boron. Copolyrolysis of diborane with hydrocarbons yields boron carbide, and with NH₃ yields boron nitride. These materials, deposited on metal substrates as thin, hard layers, are used in ceramics, tools, and wear-resistant parts. Boron fibers are formed from the decomposition of diborane on substrates and used for light-weight structural components.

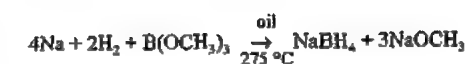
The large cross-sectional area of the ¹⁰B isotope for neutron capture makes these compounds especially useful in nuclear applications. Borane is also supplied as stable liquid adducts (CH₃)₂S·BH₃ (Callery Chemical Co., Aldrich Chemical Co.), and as a 1 M solution in tetrahydrofuran (THF) (Aldrich Chemical Co., Ventron Div. of Morton-Thiokol Inc.).

49.4.2 Borohydrides

Of the borohydrides or hydroboron ions, the most common and most completely studied is the tetrahydromonoborate(1-). The oxidation state of the central atom in the higher hydroboron ions is fractional in ions containing several boron atoms and the charge is listed as a suffix in parentheses [154]. Generally, the borohydrides are highly polarizable [155] and the bonding may vary from essentially ionic to essentially covalent.

All of the alkali-metal tetrahydroborates have been prepared and are white crystalline solids with markedly different solubilities. Sodium tetrahydroborate(1-), NaBH₄, is stable in dry air, reacting slowly with moisture. Hydrolysis is catalyzed by acid, but can be terminated with sufficient sodium hydroxide [156]. Salts of the ions B³H₈⁻, B₁₁H₁₄²⁻, B₁₀H₁₀²⁻ and B₁₂H₁₂²⁻ are all white crystalline solids. The latter two salts are extremely stable thermally, especially their halo derivatives B₁₀X₁₀²⁻, B₁₂X₁₂²⁻.

Production. Sodium tetrahydroborate is made by the addition of methyl borate to hydrogenated sodium in mineral oil [157, 158]:



Separation of the sodium methoxide from NaBH₄ was accomplished by such methods as extraction with amines [159], and extraction with water followed by a counterextraction with a solvent, such as 2-aminopropane [160]. Sodium borohydride is produced commercially by Ventron Div., Morton-Thiokol (USA) [161].

A simple preparation for B₃H₈⁻, adaptable to large scale, involves the addition of B₂H₆ to NaBH₄ in diglyme at 100 °C [162]. Further addition of B₂H₆ to the B₃H₈⁻ at higher temperature yields B₁₂H₁₂²⁻ [163].

Uses. A concentrated aqueous solution of NaBH₄ stabilized by NaOH is used to reduce hydrogen sulfite to dithionite in the bleaching of ground wood pulp [164]. Also, NaBH₄ has extensive and important use as a reducing agent in organic synthesis. Other hydroborates can be obtained by reaction with NaBH₄ to give different reductive capabilities (e.g., NaBH₃CN) [165].

Additional applications are extensive, e.g., electroless plating [166], blowing agent for cellular plastics [167], removal of heavy metals from waste streams [168], polymerization catalyst [169], and hydrogen source for fuel cells [170]. The B₃H₈⁻, B₁₀H₁₀²⁻, and B₁₂H₁₂²⁻ may also find use in the latter application. The quaternary ammonium salt of B₃H₈⁻ is used as a fogging agent in photographic film [171]. Chloro derivatives of B₁₀H₁₀²⁻ and B₁₂H₁₂²⁻ lithium salts have been used as battery electrolytes [172]; B₁₂H₁₁SH²⁻ was useful in a study of neutron-capture therapy in brain tumors [173].

49.5 Toxicology and Occupational Health

The toxicology of boron compounds has been reviewed recently [174]. Experimental animal toxicity data, cases of human exposures, industrial hygiene, and medical treatments are discussed. There are also other

readily accessible sources of information [175, 176].

Diborane(6) is primarily a pulmonary irritant [177]; TLVs and MAKs are given in Table 49.8 [178]. Overexposure causes respiratory tract injury, and secondary infections may follow [180]. Prolonged exposure to low concentrations causes headaches and other central nervous system (CNS) effects [181]. Diborane is a flammable gas and must be handled in a closed system.

Pentaborane(9) and decaborane(14) affect the CNS and can have effects that may be delayed for up to 48 h [181]. TLVs have been set (Table 49.8) [178]. Pentaborane(9) is a liquid which should be treated as pyrophoric and must be handled in a closed system. Decaborane(14) is a solid but has sufficient vapor pressure at room temperature to make it a hazard by inhalation, as well as by the dermal and oral routes [182].

Animal toxicity testing of amine boranes has shown that they also affect the CNS [183]; however, no TLVs or MAKs have been set for them. Toxicity is affected by the number and kind of substituents and varies from compounds that are highly toxic to those with low toxicity [183, 184].

The few toxicity studies on borohydrides show that they are corrosive to the skin and eyes [185]. When ingested, sodium borohydride produced death from gas embolism in animals.

The lower trialkylboranes have some toxicity to small rodents at nonpyrophoric concentrations in air [174, 186].

Table 49.8: Maximum concentrations in the work environment [178, 179].

	TWA		STEL		MAK	
	ppm	mg/m ³	ppm	mg/m ³	ppm	mg/m ³
Diborane(6)	0.1	0.1	—	—	0.1	0.1
Pentaborane(9)	0.005	0.01	0.015	0.03	0.005	0.01
Decaborane(14)	0.05	0.3	0.15	0.9	0.05	0.3

Toxicity of carbaboranes depends mainly on the nature of the substituents [174, 187].

49.6 Metal Borides

Boron combines with a large number of metals and semimetals to form binary or higher solid compounds, the so-called borides. Most binary borides, especially those formed from transition metals having high melting points, are metallic high-temperature materials that can be grouped with the carbides, nitrides, and silicides as refractory hard metals [188]. Although a great number of metal borides were prepared by MOISSAN around the turn of the century [194], they have not established themselves in modern technology to the same extent as the refractory metal carbides. Thus it has not been possible to develop metal boride materials that combine the extreme hardness of refractory borides with toughness in analogy with cemented tungsten carbide.

Nevertheless, metal borides have some unique properties and are used in some specialized fields of modern industry, especially when the requirements cannot be met by other materials. More information about metal borides is available in [190, 191, 195–203].

49.6.1 Properties

Metal borides are unique in the number of stoichiometries; compositions corresponding to at least 24 M:B ratios between 5:1 and 1:66 are known. However, the most common are the monoborides, MB; diborides, MB₂; tetraborides, MB₄; hexaborides, MB₆; dodecaborides, MB₁₂; and hectoborides, MB₆₆. The binary compounds of boron are given in the form of a periodic table in Table 49.9. As can be seen, many metal–boron systems contain three or more intermediate phases.

A classification of borides was first given by KIESLING [204] on the basis of boron structural elements typical for various M:B ratios.

Table 49.9: Binary compounds of boron.

Main group elements									
H ₂ B ^a	Be ₂ B		(B ₁₂ C)	BN	BO		BF ₃		
Li ₂ B ₄	Be ₂ B		(B ₁₂ C ₂)		B ₂ O ₂				
LiB ₆	BeB ₂		B ₁₂ C ₃		B ₂ O ₃				
LiB ₁₀	BeB ₄				BO ₂				
	(BeB ₁₂) ^b				BO ₃				
					B ₁₂ O ₂				
NaB ₆	MgB ₂	AlB ₂	(B ₁₂ Si)	B ₁₂ P ₂	B ₁₂ S ₂		B ₂ Cl ₄		
NaB ₁₃	MgB ₄	AlB ₁₂	B ₁₂ Si ₂	B ₁₂ P ₂	BS		BCl ₃		
	(MgB ₆)		B ₁₂ Si ₃	BP	B ₂ S ₃				
	MgB ₇				B ₂ S ₄				
	(MgB ₁₂)				BS ₂				
					B ₂ S ₃				
KB ₆	CaB ₄			B ₁₂ As ₂	BSe		BBr ₃		
	CaB ₆			B ₁₂ As ₂	B ₂ Se ₃				
				BAs	BSe ₂				
(RbB ₆)	SrB ₆						BI ₃		
(CsB ₆)	BaB ₆								
Transition metals									
ScB ₂	TiB	V ₂ B ₂	Cr ₂ B	Mn ₂ B	Fe ₂ B	Co ₂ B	Ni ₂ B		
ScB ₁₂	TiB ₂	VB	Cr ₂ B ₃	MnB	FeB	Co ₂ B	Ni ₂ B		
		V ₂ B ₆	CrB	Mn ₂ B ₄		CoB	Ni ₂ B ₃		
		V ₂ B ₄	Cr ₂ B ₄	MnB ₂			NiB		
		V ₂ B ₃	CrB ₂	MnB ₄					
		VB ₂	CrB ₄						
YB ₂	ZrB ₂	Nb ₂ B ₂	Mo ₂ B	Ta ₂ B	Ru ₂ B ₃	Rh ₂ B ₃	Pd ₂ B	(AgB ₂)	
YB ₄	ZrB ₁₂	NbB	MoB	Ta ₂ B ₃	Ru ₂ B ₆	Rh ₂ B ₄	Pd ₂ B		
YB ₆		Nb ₂ B ₄	MoB ₂	TaB ₂	RuB	RhB	Pd ₂ B ₃		
YB ₁₂		NbB ₂	MoB ₂		Ru ₂ B ₃		Pd ₂ B		
YB ₆₆			Mo ₂ B ₃		RuB ₂				
			Mo _{1-x} B ₃						
*	HfB	Ta ₂ B	W ₂ B	Re ₂ B	OsB	IrB _{0.9}	Pt ₄ B	(AuB ₂)	
	HfB ₂	Ta ₂ B ₂	WB	Re ₂ B ₃	Os ₂ B ₃	IrB _{1.1}	Pt ₂ B		
		TaB	WB ₂	ReB ₂	OsB ₂	IrB _{1.3}	PtB _{0.7}		
		Ta ₂ B ₄	W ₂ B ₃						
		TaB ₂	W _{1-x} B ₃						
Lanthanides and actinides									
* LaB ₂	CeB ₄	Pr ₂ B ₃	Nd ₂ B ₃	PmB ₄	Sm ₂ B ₃	EuB ₆	Gd ₂ B ₃	TbB ₂	DyB ₂
	CeB ₆	PrB ₄	Nd ₂ B ₃	PmB ₆	SmB ₄		Gd ₂ B ₂	TbB ₄	DyB ₄
		PrB ₆	Nd ₂ B ₆		SmB ₆		Gd ₂ B ₄	TbB ₆	DyB ₆
			Nd ₂ B ₆₆		SmB ₆₆		Gd ₂ B ₆	TbB ₁₂	DyB ₁₂
							Gd ₂ B ₆₆	TbB ₆₆	DyB ₆₆
**	ThB ₄	UB ₂	NpB ₂	PuB ₂	AmB ₄	CmB ₄			
	ThB ₆	UB ₄	NpB ₃	PuB ₃	AmB ₆	CmB ₆			
	ThB ₆₆	UB ₁₂	NpB ₆	PuB ₆	(AmB ₁₂)	(CmB ₁₂)			
			NpB ₁₂	PuB ₁₂	AmB ₆₆	CmB ₆₆			
			BpN ₆₆	PuB ₆₆					

^a And higher boranes.

^b Parentheses around a compound indicate that the existence of the compound has not been confirmed.

Table 49.10: Physical properties of some refractory borides [191].

Boride	Density ρ , 10 ³ kg/m ³	Melting point m_p , K	Electrical resistivity, 10 ⁻⁸ Ω m	Knoop hardness, load 0.1 kp
TiB ₂	4.52	3470	9-15	2600
ZrB ₂	6.09	3520	7-10	1830
ZrB ₁₂	3.61	2520	60-80	2580
HfB ₂	11.2	3650	10-12	2160
VB ₂	5.10	2670	16-38	2110
NbB ₂	7.21	3270	12-65	2130
TaB ₂	12.60	3370	14-68	2500
CrB ₂	5.20	2170	21-56	1100
Mo ₂ B ₃	7.48	2370	18-45	2180
W ₂ B ₅	13.1	2470	21-56	2500
Fe ₂ B	7.32	1663	—	1800
FeB	7.15	1820	30	1900
CoB	7.32	1535	26	2350
NiB	7.39	1325	23	—
LaB ₆	5.76	2985	7-15	2010
EuB ₆	4.91	2890	80-170	1870
UB ₄	9.38	2768	30	1850
UB ₁₂	5.65	2500	22	2630
CaB ₄	2.46	2540	160	1650
SiB ₆	2.43	2140	2 × 10 ⁵	2140
B ₄ C	2.52	2720	10 ⁵ -10 ⁷	3000
β -B	2.35	2420	10 ¹²	2600

With increasing M:B ratio the tendency to form boron-boron bonds increases, and pairs (M₂B₂), zigzag chains (MB), branched chains (M₁₁B₉), double chains (M₃B₄), plane nets (MB₂), and finally three-dimensional arrays of boron atoms, including cross-linked nets (MB₄), interconnected B₆ octahedra (MB₆), B₁₂-cubo-octahedra (MB₁₂), and interconnected B₁₂-icosahedra (MB₆₆) all are found.

The most characteristic properties of the metal borides are their high melting points, extreme hardness, and in many cases high electrical and thermal conductivities, fair corrosion resistance, good wear resistance, and thermal shock resistances superior to those of oxide ceramics. Some physical properties of the most common and typical metal borides are given in Table 49.10. The most stable binary borides at high temperatures are the diborides of titanium, zirconium, and hafnium, each melting above 3000 °C. The melting points of the boron-rich borides MB_n, $n \geq 2$, are generally higher than those of the parent transition metals. On the other hand, melting points of metal-rich borides are often

as low as those of their parent metals. Most of these borides are paramagnetic. Knoop hardness numbers HK-0.1 usually fall in the range of 1100-2600 for diborides, 1650-2100 for hexaborides, and 2300-2600 for dodeca- and hectoborides [205]; therefore, many borides are harder than WC or α -Al₂O₃, two cutting and grinding materials widely used. Hardness and high melting points reflect the properties of the rigid, three-dimensional boron frameworks.

The electrical characteristics, however, cover the entire spectrum: semiconductors, the MB₆₆, MB₆, and MB₁₂ phases of Be, Mg, Ca, Eu, Al, and Si; metallic conductors, TiB₂, ZrB₂, and the majority of transition-metal borides; superconductors, NbB, YB₆, and ZrB₁₂.

In addition, LaB₆ and other lanthanoid and actinoid borides (YB₆, ThB₆, GdB₆, etc.) belong to the best-known high-temperature electron emitters. Most of these borides are intensively colored: for example, ZrB₁₂ is pink, GdB₆ is blue, LaB₆ is purple, and ThB₆ is scarlet [191, 205].

The metal borides display resistance to oxidation in air at elevated temperatures, most of them up to 1000 °C, and to attack by molten metals, basic slags, and molten salts. Except for alkali-metal and alkaline earth metal borides, which are saltlike and ionic, they are not readily attacked by nonoxidizing acids and aqueous alkalis. Resistance to oxidation is greatest for the transition metal diborides and is lower for greater boron contents. The controlling factor is the surface layer of parent boron and transition-metal oxides, which prevents further oxidation up to temperatures at which boric oxide has appreciable volatility. Most metal borides are inert in hydrogen, nitrogen, and carbon, even at high temperatures. Chlorine and fluorine react vigorously with all borides, fluorine even at 400 °C. All types of borides are readily attacked by oxidizing molten salts such as nitrates and carbonates and hydroxides in the presence of air, and this is a usual method of decomposition for chemical analysis [206].

49.6.2 Production

Metal borides can be prepared by the following high-temperature reactions [191]:

1. Synthesis from the elements by melting, sintering, or hot-pressing
2. Borothermic reduction of metal oxides
3. Aluminothermic, silicothermic, or magnesiothermic reduction of metal oxide boric oxide mixture
4. Carbothermic reduction of metal oxide-boric oxide mixtures, e.g.,

$$\text{TiO}_2 + \text{B}_2\text{O}_3 + 5\text{C} \rightarrow \text{TiB}_2 + 5\text{CO}$$
5. Reduction of metal oxide with carbon and/or boron carbide, i.e., the boron carbide method e.g.,

$$2\text{ZrO}_2 + \text{B}_4\text{C} + 3\text{C} \rightarrow 2\text{ZrB}_2 + 4\text{CO}$$

$$\text{Eu}_2\text{O}_3 + 3\text{B}_4\text{C} \rightarrow 2\text{EuB}_6 + 3\text{CO}$$
6. Electrolysis of fused salts containing metal oxide and boric oxide
7. Auxiliary-metal bath method, M + B being dissolved in molten Al, Cu, Sn, or Pb
8. Deposition from the vapor phase involving coreduction of a metal halide-boron halide mixture by hydrogen, optionally as a plasma [207]

Reactions 1, 2, 6, 7, and 8 give pure products but are almost always restricted to the laboratory. For large-scale production, borides are prepared by reactions 4 and 5 followed by purification. These reactions are usually carried out in electric furnaces much like those for production of boron carbide. Molten metal borides often contain up to 3% carbon and boron carbide, although these impurities can be scavenged with additional metal oxide or boric oxide on reheating the powdered mixture above 1400 °C under a partial vacuum. After cooling, the metal boride is crushed and milled to its final grain size. Monolithic boride shapes usually are fabricated from commercial boride powders by powder metallurgy techniques:

- Cold forming — isopressing, slip casting, etc. — followed by pressureless sintering of the powder compact [207-210]

- Axial hot-pressing [211-214] and hot isostatic pressing [210, 215]

49.6.3 Uses

The principal use for metal diborides is as a crucible material for nonferrous metals, especially for aluminum, copper, magnesium, zinc, tin, and lead. Monolithic shapes of dense TiB₂ [216] are used for the electrolytic production of aluminum with the Hall-Héroult cell [217]. Their inertness to molten aluminum and cryolite and excellent electrical conductivity suggest titanium diboride and zirconium diboride as cathode leads, electrodes, and thermocouple sheaths in aluminum metallurgy [218]. Related uses are TiB₂-BN-AlN hot-pressed composite crucibles, so-called evaporation boats, for the continuous evaporation of aluminum metal for vacuum metallizing [219]. The world production of TiB₂ is \approx 100 t/a, much of this for the manufacture of these resistance-heated boats. The price of TiB₂ powder is \$15-35 per kg.

Calcium hexaboride, CaB₆, is used as a deoxidizer for high-conductivity copper [220-222]. A major established use of NiB, CrB, and CrB₂ is the production of welding and hard facing alloys based on nickel-chromium-boron-silicon, called colmonoy [223].

The hardness and wear properties of borides are utilized economically as thin coatings on metal surfaces, prepared by the so-called boronizing process. Lanthanum hexaboride is useful as a high-current-density electrode for electron microscopes, electron-beam furnaces, and other devices of highest electronic emissivity. The lifetime of LaB₆ electrodes is reported to exceed that of tungsten cathodes by two orders of magnitude [224-225].

The refractory hexaboride of europium was suggested as a neutron absorber to control the power of fast breeder reactors. As a neutron absorber EuB₆ is equivalent to 35 mol% ¹⁰B-enriched boron carbide, and its nuclear worth is \approx 15% higher than europium sesquioxide [189, 192, 193].

49.7 Boric Oxide

Boric oxide (B_2O_3) exists as vitreous glass and as two crystalline forms. The *vitreous form* is a colorless, hard, tough, glasslike solid, commonly prepared by dehydration of boric acid. The most common crystalline B_2O_3 has a *hexagonal* or α -form and is crystallized at 200–250 °C at ambient pressure. A less common *monoclinic* β -form can be crystallized at 4000 MPa and 600 °C [226].

49.7.1 Physical Properties

Vitreous B_2O_3 is difficult to obtain in a completely anhydrous state even when heated at > 1000 °C [227]. Many physical properties of B_2O_3 are sensitive to small amounts of residual water. Very dry B_2O_3 can be prepared by heating at 200–400 °C in high vacuum [228]. Vitreous B_2O_3 softens between 325 and 450 °C and the melt is still quite viscous at > 1000 °C. The dynamic viscosity of the melt is:

$t, ^\circ\text{C}$	$\eta, \text{Pa}\cdot\text{s}$	$t, ^\circ\text{C}$	$\eta, \text{Pa}\cdot\text{s}$
300	4.4×10^8	800	26
400	1.6×10^8	900	12
500	3900	1000	7.4
600	480	1100	4.3
700	85		

The density (ρ) of the vitreous form is dependent on both its thermal history and moisture content. Commercial boric oxide has a density of 1.84 g/cm³, whereas very dry B_2O_3 has a density of 1.82 g/cm³ at 20 °C. The density at high temperature has been investigated [229]. Annealed B_2O_3 has a greater density compared to rapidly cooled melt (1.53 g/cm³ when quenched from 1000 °C), implying a higher degree of molecular order in the annealed material [230]. The heat of formation of amorphous B_2O_3 glass is 1260 kJ/mol [231].

Crystalline hexagonal or α -form, *mp* 450 °C, ρ 2.42–2.46 g/cm³; monoclinic or β -form, *mp* ca. 510 °C [232], ρ 2.95 g/cm³; the β -form is much more resistant to attack by water and dilute HF than the α -form.

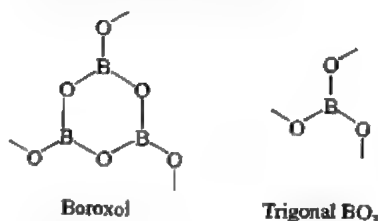
The heat of formation for crystalline B_2O_3 is 1274 kJ/mol. Its heat capacity increases

with temperature from 1.05 Jg⁻¹K⁻¹ at 100 °C to 1.82 Jg⁻¹K⁻¹ at 275 °C [233]. The heat of vaporization is calculated as 391.6 kJ/mol at 1800 °C [234], and the heat of sublimation is 431.4 kJ/mol at 25 °C [235]. The electrolytic conductivity (κ) is only 5×10^{-4} S/cm at 300 °C [236]. The refractive index (n_D) varies between 1.4502 and 1.4633, depending on the thermal history [228]. The vapor pressure of B_2O_3 melt is [232, 237]:

$t, ^\circ\text{C}$	1163	1270	1673	1810	2000	2146
$p_{B_2O_3}, \text{kPa}$	0.0005	0.005	1.5	5.7	24	80

The vapor composition (by mass spectrometry) is predominantly $B_2O_3^+$ with about 7% each of $B_2O_2^+$ and BO^+ and 2% B^+ . Boric oxide has been observed to be more volatile in steam than in a dry atmosphere. The green color of B_2O_3 in a flame has been attributed to BO_2 as the emitting species.

Historically there has been considerable controversy over the molecular structure in liquid and vitreous B_2O_3 . The structure is believed to consist of a random network of trigonal BO_3 units and boroxol rings with short-range localized order. There is disagreement over the relative amounts of these two structural units. A summary of the structural data has been reported [238].



Apparently the structure interpretation can be influenced by the presence of residual moisture.

49.7.2 Chemical Properties

Molten B_2O_3 is corrosive to most metals and alloys at temperatures exceeding 1000 °C. This is because of the fluxing character of B_2O_3 , which keeps the metal surface clean and vulnerable to attack by oxygen in the air. Molybdenum and nickel alloys are resistant to

corrosion below 1000 °C, whereas silicon carbide is resistant above 1200 °C.

Reduction of B_2O_3 at high temperatures by aluminum, magnesium, or alkali metals produces $B_{12}O_3$ and other boron suboxides. Above 900 °C carbon reacts with B_2O_3 in a nitrogen atmosphere to form boron nitride, which can also be made by reacting B_2O_3 with ammonia at 600–900 °C.

Vitreous B_2O_3 reacts exothermically with 3 mol of water to form crystalline boric acid, with a heat of hydration of –76.5 kJ/mol [239]; heat of hydration of crystalline B_2O_3 is –8.2 kJ/mol. Above 135–140 °C boric oxide reacts with water to form metaboric acid.

Sodium hydride reacts with B_2O_3 at 330–350 °C to give sodium borohydride in about 60% yield [240]. Reaction of either B_2O_3 or boric acid with anhydrous H_2SO_4 or oleum forms the acid $HB(HSO_4)_4$ [241].

49.7.3 Production

High-purity B_2O_3 (99%) is made by fusing refined boric acid. A 96% grade of B_2O_3 is made commercially by fusing a mixture of sodium tetraborate plus sulfuric acid at 800 °C. Two molten layers are formed, an upper layer of boric oxide and a lower layer of sodium sulfate. The molten B_2O_3 layer is separated and cooled on chill rollers. The resulting glass is ground, sized, and packaged in moisture-proof containers. The product B_2O_3 contains 3–4% sodium sulfate.

Boric oxide can also be prepared by thermal decomposition of ammonium pentaborate, $NH_4B_5O_{16} \cdot 4H_2O$, at 500–900 °C and through direct reaction of boron with oxygen [242].

49.8 Boric Acid

Boric acid can be viewed as a hydrate of boric oxide and exists both as a trihydrate, orthoboric acid ($B_2O_3 \cdot 3H_2O$ or H_3BO_3), and as a monohydrate, metaboric acid ($B_2O_3 \cdot H_2O$ or HBO_2). Only the more stable orthoboric acid form is of commercial importance and is usually referred to simply as boric acid. The terms “pyroboric acid” and “tetraboric acid”

are sometimes encountered in the literature, but these acids do not actually exist as solid-phase compounds.

49.8.1 Physical Properties

Boric acid crystallizes from an aqueous solution as odorless, white, waxy platelets. Crystalline orthoboric acid (*mp* 170.9 °C, heated in a closed space) is monoclinic, having a sheet lattice structure. Sheets consist of coplanar $B(OH)_3$ molecules linked by hydrogen bonds. These sheetlike layers are held together only by van der Waals forces. This allows easy cleavage into flakes which feel slippery.

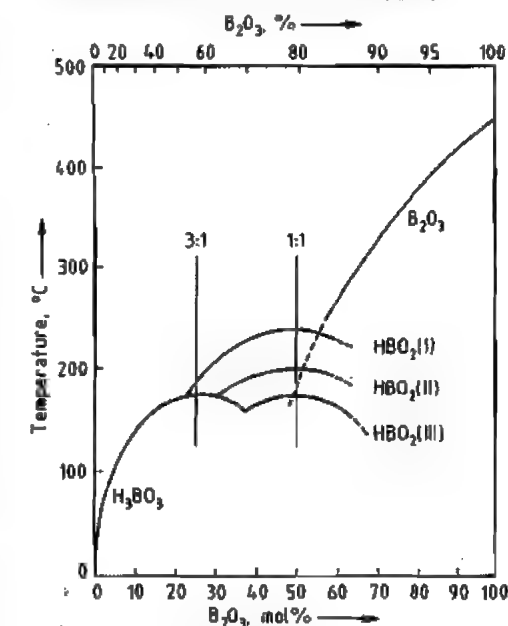


Figure 49.2: Solubility diagram for the system B_2O_3 - H_2O .

The three known crystalline modifications of metaboric acid are shown in the B_2O_3 - H_2O solubility phase diagram (Figure 49.2) [243]. Orthoboric acid slowly dehydrates at 100–130 °C to form flaky crystals of orthorhombic $HBO_2(III)$ (α -form, d 1.784, *mp* 176 °C). After disappearance of the residual H_3BO_3 at temperatures up to 160 °C, a coarsely crystalline monoclinic $HBO_2(II)$ (β -form, d 2.044, *mp* 201 °C) is formed. At yet higher tempera-

tures (200–250 °C) a highly viscous liquid is formed from which cubic $\text{HBO}_2(\text{I})$ (γ -form, d 2.486, mp 236 °C) slowly crystallizes. With about 1% moisture remaining, $\text{HBO}_2(\text{I})$ acts as seed for crystallization of hexagonal (α) boric oxide. The structures of these metaborate forms range from all trigonal borons in

$\text{HBO}_2(\text{III})$, to one-third tetrahedral borons in $\text{HBO}_2(\text{II})$, to all tetrahedral borons in $\text{HBO}_2(\text{I})$.

The solubility of boric acid in water is increased by addition of salts, such as KCl , KNO_3 , RbCl , K_2SO_4 , and Na_2SO_4 , whereas addition of LiCl , NaCl , and CaCl_2 tends to lower the solubility.

Table 49.11: pH values of aqueous boric acid and borate solutions as a function of concentration.

Compound	$t, ^\circ\text{C}$	pH at % of compound						
		0.1	0.5	1.0	2.0	4.0	10.0	15.0
$\text{B}(\text{OH})_3^a$	20	6.1	5.6	5.1	4.5	3.9		
$\text{Na}_2\text{B}_4\text{O}_7 \cdot 10\text{H}_2\text{O}$	20	9.3	9.2	9.2	9.2	9.3		
$\text{Ba}_2\text{B}_4\text{O}_{11} \cdot 5\text{H}_2\text{O}^b$	23			8.5	8.4	8.1	7.6	7.3
$\text{Na}_2\text{B}_4\text{O}_{11} \cdot 4\text{H}_2\text{O}$	20			8.5	8.5	8.1	7.6	7.3
$\text{K}_2\text{B}_4\text{O}_{11} \cdot 4\text{H}_2\text{O}$	25	9.2	9.1	9.1	9.2	9.3		
$\text{KB}_3\text{O}_8 \cdot 4\text{H}_2\text{O}^c$	25	8.4	8.4	8.4	8.1	7.9		
$(\text{NH}_4)_2\text{B}_4\text{O}_7 \cdot 4\text{H}_2\text{O}$	25	8.8	8.9	8.8	8.8	8.8	8.9	
$\text{NH}_4\text{B}_3\text{O}_8 \cdot 4\text{H}_2\text{O}$	25	8.5	8.4	8.3	8.2	7.9	7.3	
$\text{NaBO}_2 \cdot 4\text{H}_2\text{O}$	20	10.5	10.8	11.0	11.2	11.4	11.7	11.9

^a Saturated solution at 20 °C, pH 3.7 at 4.7%.

^b At 40 °C, pH 6.9 at 20%, pH 6.5 at 30%.

^c pH 7.6 at 5.0%.

Table 49.12: Solubility of boric acid and borates in water.

Compound	Solubility, % (anhydrous salt), at temp., °C										
	0	10	20	30	40	50	60	70	80	90	100
$\text{LiBO}_2 \cdot 8\text{H}_2\text{O}^a$	0.9	1.4	2.5	4.6	9.4						
$\text{LiBO}_2 \cdot 2\text{H}_2\text{O}$					7.4	7.8	8.4	9.5	10.6	11.9	13.4
$\text{Li}_2\text{B}_4\text{O}_7 \cdot 3\text{H}_2\text{O}$	2.5		2.8	3.0	3.2	3.5	3.8	4.1	4.4	4.9	5.4
$\text{LiB}_3\text{O}_8 \cdot 5\text{H}_2\text{O}^b$				17.9	18.7	20.9	24.3	28.0	32.0	36.6	41.42
$\text{NaBO}_2 \cdot 4\text{H}_2\text{O}^c$	14.5	17.0	20.0	23.6	27.9	34.1					
$\text{NaBO}_2 \cdot 2\text{H}_2\text{O}$							38.3	40.9	43.7	47.4	52.4
$\text{Na}_2\text{B}_4\text{O}_7 \cdot 10\text{H}_2\text{O}^d$	1.0	1.6	2.5	3.8	5.9	9.5	16.0				
$\text{Na}_2\text{B}_4\text{O}_7 \cdot 5\text{H}_2\text{O}$							16.4	19.5	23.4	28.1	34.6
$\text{Na}_2\text{B}_4\text{O}_7 \cdot 4\text{H}_2\text{O}^e$						14.2	14.7	17.0	19.7	23.0	27.2
$\text{NaB}_3\text{O}_8 \cdot 5\text{H}_2\text{O}$	5.8	7.5	10.6	13.7	17.5	21.7	26.9	35.0	38.1	44.3	51.0
$\text{B}(\text{OH})_3$	2.4	3.5	4.7	6.2	8.8	10.3	13.0	15.8	19.1	23.3	27.5
$\text{KBO}_2 \cdot 4\text{H}_2\text{O}^f$	34.2	38.2	43.8								
$\text{KBO}_2 \cdot 1.3\text{H}_2\text{O}^g$	35.5			44.4	45.5	46.4	47.5	48.5	49.6	50.6	51.6
$\text{K}_2\text{B}_4\text{O}_7 \cdot 4\text{H}_2\text{O}$	6.3	9.0	12.1	15.6	19.4	24.0	28.5	33.3	38.2	43.3	48.4
$\text{K}_4\text{B}_{10}\text{O}_{17} \cdot 5\text{H}_2\text{O}$					23.2	24.9	26.9	28.6	31.0	32.5	33.8
$\text{KB}_3\text{O}_8 \cdot 4\text{H}_2\text{O}^h$	1.6	2.1	2.8	3.8	5.1	6.9	9.0	11.7	14.7	18.3	23.3
$\text{KB}_3\text{O}_8 \cdot 2\text{H}_2\text{O}^i$	2.0	2.6	3.2	3.8	5.0	6.4	7.8	9.2	10.6	13.9	15.3
$\text{Na}_2\text{B}_4\text{O}_{11} \cdot 4\text{H}_2\text{O}$	1.9	3.7	7.8	18.1	22.9	26.4	28.9	39.3		37.4	
								(75 °C)		(94 °C)	
$(\text{NH}_4)_2\text{B}_4\text{O}_7 \cdot 4\text{H}_2\text{O}$	3.8	5.3	7.6	10.8	15.8	21.2	27.2	34.4	43.1	52.7	
$\text{NH}_4\text{B}_3\text{O}_8 \cdot 4\text{H}_2\text{O}$	4.0	5.4	7.1	9.1	11.4	14.4	18.2	22.4	26.4	30.3	

^a Transition of the 8-hydrate to the 2-hydrate at 36.9 with 7.2% LiBO_2 .

^b Incongruent solubility below 37.5 or 40.5 °C.

^c Transition to the 4-hydrate to the 2-hydrate at 53.6 °C with 36.9% NaBO_2 .

^d Transition of the 10-hydrate to the 5-hydrate at 60.7 °C with 16.6% $\text{Na}_2\text{B}_4\text{O}_7$.

^e Transition of the 10-hydrate to the 4-hydrate at 58.2 °C with 14.6% $\text{Na}_2\text{B}_4\text{O}_7$.

^f Transition of the 4-hydrate to the 1.3-hydrate at 24 °C with 43.8% KBO_2 .

^g Metastable below 24 °C.

^h More stable below 46 °C.

ⁱ More stable above 46 °C.

Table 49.13: Solubility of boric acid and sodium tetraborate hydrates in organic solvents.

Solvent	$t, ^\circ\text{C}$	Solubility, %			
		$\text{B}(\text{OH})_3$	$\text{Na}_2\text{B}_4\text{O}_7 \cdot 10\text{H}_2\text{O}$	$\text{Na}_2\text{B}_4\text{O}_7 \cdot 5\text{H}_2\text{O}$	$\text{Na}_2\text{B}_4\text{O}_7$
Methanol	20	20.68			
	25		19.9	16.9	16.7 ^c
Ethanol	25	94.4 ^b			
Aqueous ethanol (46.5%)	15.5		2.48		
<i>n</i> -Butanol	25	42.8 ^b			
<i>n</i> -Propanol	25	59.4 ^b			
2-Methylbutanol	25	35.3 ^b			
Isoamyl alcohol	25	2.39			
Ethylene glycol	25	18.5	41.6	31.2	15.5 ^c
Propylene glycol	25	15.06		21.9	
Diethylene glycol	25	13.6		10.0	
Glycerol (86.5%)	20	21.1	47.2		
Glycerol (98.5%)	20	19.9	52.6		
Glycerol	25	17.55			
Mannitol (10%)	25	6.62			
Acetone	25	0.6			
Methyl ethyl ketone	20	0.7			
Methyl butyl ketone	20	0.23			
Ethyl acetate	25	1.5	0.14		
Acetic acid (glacial)	30	6.3			
Diethyl ether	20	0.008			
Dioxane	25	$\approx 15^b$			
Aniline	20	0.15			
Pyridine	25	$\approx 70^b$			
Ammonia (liquid)	25	1.88			
Formamide	25				40.6 ^b
Fuel oil	25	2.46			
Water	25	5.46			
	20	4.72			

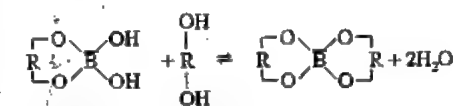
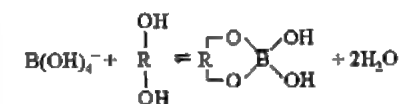
^a Finely divided solid.

^b Solubility, g/L.

^c Viscous solution.

Boric acid behaves as a weak acid in aqueous solutions, pK_a of 9.23 at 25 °C [244]. As shown in Table 49.11, pH decreases as concentration increases. This is because of formation of trimeric and tetrameric species. The pH also increases with temperature. The solubility of boric acid in water is shown in Table 49.12.

The solubility of boric acid in many organic solvents is shown in Table 49.13. Boric acid is particularly soluble in polyhydric alcohols capable of forming complexes. Normally, boric acid is too weak an acid to titrate directly. Use of a polyhydric complexing agent, such as mannitol, enhances the acidity of boric acid sufficiently to allow accurate titration using phenolphthalein as the indicator.



where $\text{R} = -(\text{CHOH})_4-$ (mannitol).

The vapor pressure of boric acid is primarily due to water from dehydration equilibria. Vapor below 160 °C is composed of water and boric acid molecules. At higher temperatures, HBO_2 is also found in the vapor phase, and above 940 °C (HBO_2)₃ becomes significant [245].

Boric acid is volatile with steam. Distillate from a boiling saturated solution contains

about 0.18% of boric acid [246]. Boric acid is particularly volatile from concentrated solutions made acidic by strong acids. The volatile loss from low molecular mass alcohol solutions can be attributed to ester formation.

49.8.2 Chemical Properties

Boric acid reacts with strong bases to form metaborate ion, $B(OH)_4^-$, and with alcohols to form borate esters. Boric acid reacts with fluoride ion to form tetrafluoroboric acid and with hydrofluoric acid to form trifluoroboric acid $H(F_3BOH)$, which can be distilled at reduced pressures (58.5–60.0 °C at 0.16 kPa) [247].

49.8.3 Production

Boric acid is manufactured industrially from borate minerals and brines [248]. Alkali and alkaline-earth metal borates, such as borax, kernite, colemanite, ascharite, ulexite, or hydroboracite, react with strong mineral acids to form boric acid. In the United States boric acid is made primarily from sodium borate minerals, whereas in Europe it is made from colemanite imported from Turkey. In Kazakhstan magnesium borates from the Inder region are used to make boric acid. Borates found in saline lake brine in California at Searles Lake are extracted and recovered as boric acid.

The world's largest and most modern boric acid plant was constructed by U.S. Borax in 1981 at Boron, California. Crushed kernite ($Na_2O \cdot 2B_2O_3 \cdot 4H_2O$) ore is reacted with sulfuric acid in recycled weak liquor (contains low concentration of borates) at 100 °C. Coarse gangue is separated by rake classifiers and fine particles are settled in a thickener. The boric acid strong liquor (high borate concentration) is nearly saturated with sodium sulfate. Complete solubility of sodium sulfate is maintained throughout the process by careful control of pH and temperature. The strong liquor is filtered at 98 °C and boric acid crystallized in two stages using continuous evaporative crystallizers. The temperature is dropped to 70 °C in the first stage and to 35 °C in the second. Crystals are filtered and washed

with progressively weaker liquor in a counter-current fashion. The final product is dried in rotary driers and screened for packaging. Weak liquor at 35 °C, nearly saturated in sodium sulfate, is heated to 100 °C and returned to the reactor. Sodium sulfate is removed from the process as solid in gangue and in effluent from a second-stage thickener, and is pumped to sealed solar ponds. The plant has a capacity of 113 000 t/a (expressed as B_2O_3).

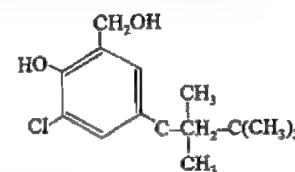
In Europe boric acid is produced from crushed colemanite ($2CaO \cdot 3B_2O_3 \cdot 5H_2O$) ore by reaction with sulfuric acid at 90 °C. By-product gypsum ($CaSO_4$) and gangue are filtered and the hot mother liquor cooled to crystallize boric acid. The weak liquor is recycled to the reactor.

Magnesium borate ores, primarily of ascharite (szaibelyite, $2MgO \cdot B_2O_3 \cdot H_2O$), and hydroboracite ($CaO \cdot MgO \cdot 3B_2O_3 \cdot 6H_2O$), are finely ground and decomposed to boric acid with sulfuric acid at 95 °C. Insoluble gypsum and gangue are filtered and the mother liquor is cooled to 15 °C to crystallize boric acid. The weak liquor is nearly saturated in magnesium sulfate ($MgSO_4 \cdot 7H_2O$), which is crystallized by concentration of the liquor at elevated temperature; the concentrated liquor is then recycled to the reactor.

Datolite ($2CaO \cdot B_2O_3 \cdot 2SiO_2 \cdot H_2O$) is the most common silicoborate mineral. Ore containing 5% B_2O_3 is finely ground and digested with sulfuric acid. Silica in the mother liquor is coagulated upon heating to 95 °C. The resulting boric acid solution is nearly free of silicic acid.

At Searles Lake, California, borax is found in brine at a concentration of about 1.5% (expressed as anhydrous borax); a number of other salts are also present. A process using liquid-liquid extraction is used to separate borax selectively from brine. Borax is extracted into a water-insoluble solvent, such as kerosene, by use of an aromatic polyol that efficiently complexes the borate ion, e.g., 3-chloro-2-hydroxy-5-isooctylbenzenemethanol. The organic phase is isolated and acidified with sulfuric acid, giving an aqueous solution of boric acid and sodium sulfate. Af-

ter concentrating by evaporation, the liquor is cooled to crystallize boric acid.



3-Chloro-2-hydroxy-5-isooctylbenzenemethanol

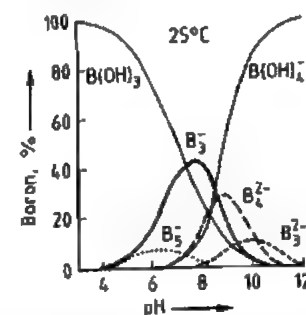
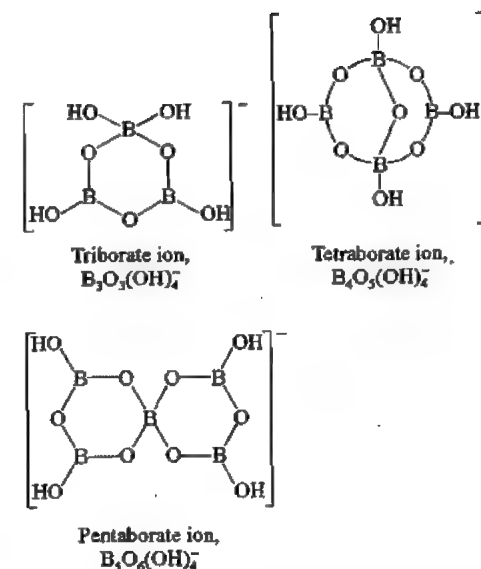


Figure 49.3: Distribution of borate polyanion species in aqueous solution: $B_1^- = B_3O_3(OH)_1^-$; $B_2^- = B_3O_3(OH)_2^-$; $B_3^- = B_3O_3(OH)_3^-$; $B_4^- = B_4O_5(OH)_4^-$; $B_5^- = B_5O_6(OH)_6^-$ [243].

49.9 Aqueous Borate Solutions

Dilute borate solutions contain only monomeric species. Solutions of boric acid below 0.1 M contain monomeric boric acid molecules, $B(OH)_3$, and solutions of metaborate salts contain monomeric metaborate ions, $B(OH)_4^-$. Solutions made from mixtures of boric acid and metaborate salts contain a mixture of $B(OH)_3$ molecules and $B(OH)_4^-$ ions.

Polymeric borate anions form in more concentrated borate solutions. In addition to monomeric $B(OH)_3$ and $B(OH)_4^-$, concentrated borate solutions contain the polyions $B_3O_3(OH)_4^-$, $B_3O_3(OH)_5^{2-}$, $B_3O_3(OH)_6^{3-}$, $B_4O_5(OH)_4^{2-}$ (Figure 49.3). These polyion species are all in rapid dynamic equilibrium and their distribution is dependent on the $Na_2O-B_2O_3$ molar ratio, temperature, and borate salt concentration, but is essentially independent of the cation [249].



The pH of borate salt solutions varies with both concentration (see Table 49.11) and temperature as a consequence of these polyions. At the isohydric point the pH value is independent of borate concentration. This occurs at a pH of 8.9 and a $Na_2O-B_2O_3$ molar ratio of 0.41 for a sodium borate solution. Borate solutions with a $Na_2O-B_2O_3$ molar ratio less than 0.4 become more acidic at higher concentrations, whereas solutions with a $Na_2O-B_2O_3$ molar ratio greater than 0.4 become more alkaline with increasing concentration (Figure 49.4). Borax, with a $Na_2O-B_2O_3$ molar ratio of 0.5 makes an excellent buffer solution.

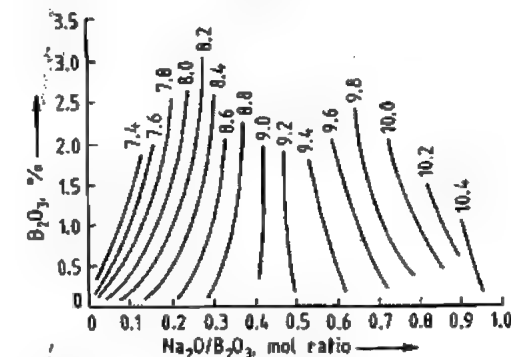


Figure 49.4: pH values in the system $Na_2O-B_2O_3-H_2O$ at 25 °C [250].

49.10 Sodium Borates

The lack of a uniform system of nomenclature for naming metal borate salts has led to ambiguities in the past. Today metal borates are most commonly described by an empirical formula with the number of cations and boron atoms in the simplest stoichiometric units. The descriptive name is derived from this formula. In addition, an oxide formula is also in common use with the derived portions of metal oxide, boric oxide, and water in the simplest molar ratio. Many metal borates are also described using the mineral name, e.g., tincal for borax, $\text{Na}_2\text{B}_4\text{O}_7 \cdot 10\text{H}_2\text{O}$. Although useful for cataloging metal borates these formulas give no indication of the molecular structure of the borate anion found in the solid crystals. The solubilities of the borates described in this chapter are summarized in Table 49.12. Of the sodium borates discussed, only borax decahydrate and borax pentahydrate are sold in large commercial volume.

Sodium tetraborate decahydrate, borax, tincal, $\text{Na}_2\text{O} \cdot 2\text{B}_2\text{O}_3 \cdot 10\text{H}_2\text{O}$ or $\text{Na}_2\text{B}_4\text{O}_7 \cdot 10\text{H}_2\text{O}$, crystals are odorless, white, monoclinic prisms with a relative density of 1.715. Based on the crystal structure, borax is best represented by the formula $\text{Na}_2[\text{B}_4\text{O}_5(\text{OH})_4] \cdot 8\text{H}_2\text{O}$, with 2 mol of water existing as hydroxyl groups and 8 mol as water of crystallization [251]. The water in borax can be maintained at exactly 10 mol by storage in a closed container with a relative humidity produced by a solution saturated in both sucrose and salt [252].

Borax decahydrate slowly dehydrates at ambient conditions, depending on the relative humidity, to a water content of about 7 mol. The dehydration path is dependent on the thermal history of the sample [252]. Freshly crystallized borax previously heated to about 50 °C has a vapor pressure of 1.33 kPa at 19.8 °C and follows a stable dehydration path. That is, it dehydrates reversibly to borax pentahydrate at ambient temperature with a heat of dehydration of 54.17 kJ/mol. Further dehydration under vacuum produces an amorphous

product containing 2 mol of water. Freshly crystallized borax decahydrate maintained below 50 °C has a vapor pressure of only 0.22 kPa at 20 °C and follows an unstable dehydration path. At ambient pressure and temperature over H_2SO_4 it undergoes irreversible dehydration leading directly to the amorphous hydrate (2 mol H_2O), bypassing borax pentahydrate. This hydrate can rehydrate first to borax pentahydrate and then to borax decahydrate.

Borax heated in a closed container melts in its own water of hydration at about 60 °C. Borax loses 5 mol of water by heating from 50 to 100 °C and loses an additional 3 mol up to 160 °C (determined by thermal gravimetric analysis). The remaining 2 mol of water are slowly lost during heating to about 400 °C. Anhydrous borax fuses at 742 °C forming a clear glass.

Rapid heating of borax decahydrate causes puffing [253]. Puffed borax consists of small glassy hollow spheres with a void volume as high as 90% and a bulk density of about 0.07 g/cm³.

Borax has a heat of formation of -6264.3 kJ/mol [254], and a specific heat of 1.611 kJ kg⁻¹K⁻¹ at 25–50 °C [255].

Borax decahydrate crystallizes from aqueous solution below 60.8 °C, the decahydrate-pentahydrate transition temperature (Figure 49.5). This transition temperature is lowered by addition of either boric acid or sodium hydroxide [256]. In a solution saturated with sodium sulfate this transition temperature drops to 49.3 °C; with sodium chloride it drops to 39.6 °C; and when saturated with sodium chloride and potassium sulfate it drops to 35.5 °C. The solubility of borax in organic solvents is shown in Table 49.13.

The pH value of a borax solution increases slightly with increasing concentration (Table 49.11), and drops slightly with increasing temperature [257].

Sodium tetraborate pentahydrate, tincalconite, $\text{Na}_2\text{O} \cdot 2\text{B}_2\text{O}_3 \cdot 5\text{H}_2\text{O}$ or $\text{Na}_2\text{B}_4\text{O}_7 \cdot 5\text{H}_2\text{O}$, crystals have rhombohedral symmetry and resemble octahedra; their relative density is

1.880. This pentahydrate has the same polyanion structure as borax decahydrate and is best represented by the formula $\text{Na}_2[\text{B}_4\text{O}_5(\text{OH})_4] \cdot 3\text{H}_2\text{O}$, with 3 mol of water of crystallization and 2 mol of water existing as hydroxyl groups. Pure borax pentahydrate actually contains 4.75 mol rather than 5.0 mol of water because of apparent vacancies in the crystal structure [258].

Borax pentahydrate rapidly crystallizes from aqueous solution above 60.8 °C (Figure 49.5). Solid pentahydrate in equilibrium with its saturated solution is metastable to kernite at all temperatures above 58.2 °C. When a solution saturated with borax pentahydrate is heated for one day or more, kernite crystals slowly form [259]. The solubility of tincalconite in organic solvents is shown in Table 49.13.

From thermogravimetric analysis 3 mol of water are lost on heating borax pentahydrate at 160 °C. The last 2 mol are slowly lost up to about 400 °C. Pentahydrate dehydrates reversibly to an amorphous dihydrate on heating at 80 °C and 0.3 kPa pressure or at 140 °C in air.

Like borax decahydrate, borax pentahydrate puffs when rapidly heated [253].

The heat of formation for borax pentahydrate is -4784 kJ/mol [254] and the specific heat is 1.318 kJ kg⁻¹K⁻¹ [255].

Production. Refined borates are almost exclusively produced as a sodium salt, with a minor amount of potassium salt and even smaller amounts of lithium and ammonium salts.

The largest source of refined sodium borate products in the world is currently located at the U.S. Borax mine and refinery in Boron, California.

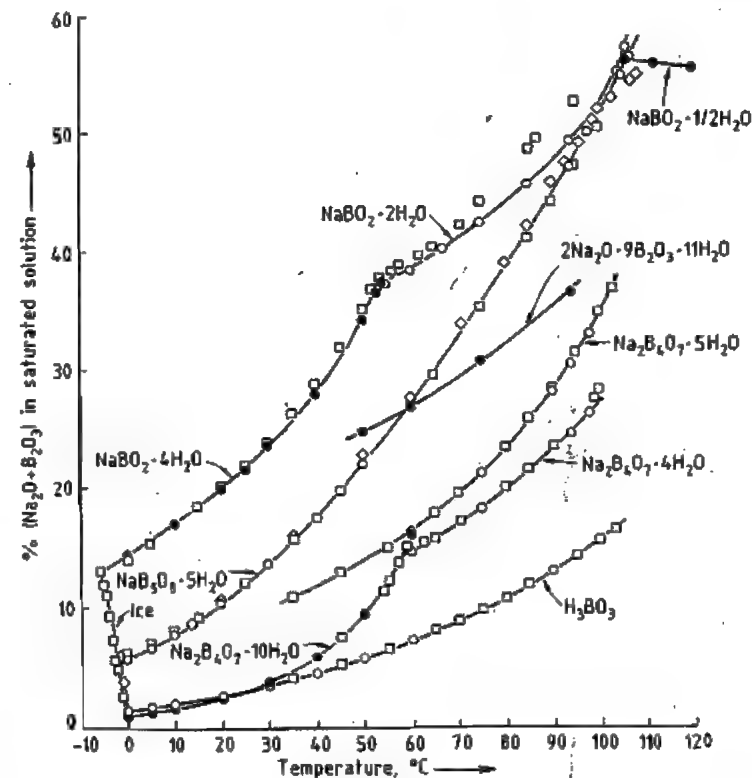


Figure 49.5: Solubility versus temperature curves for borate hydrates [256].

Sodium borate ore consisting primarily of tincal and clay is crushed, mixed with Trona, and dissolved in weak liquor at 100 °C. The coarse gangue is separated on a screen and strong liquor and fine insolubles are transferred to a primary thickener. Clarified strong liquor is used to produce borax pentahydrate in continuous vacuum crystallizers at a temperature above the borax penta-decahydrate transition temperature of 60.8 °C. Borax decahydrate product crystallizes below this transition temperature. Crystals are filtered using a continuous centrifuge and dried in rotary driers. Borax crystals are washed with a weak boric acid solution leaving a very thin surface coat of pentaborate, which inhibits caking. Thickened underflow from the primary thickener is washed in a countercurrent fashion through four thickener stages with progressively weaker liquor in each stage. Fresh water is added to the last stage thickener. Liquid effluent is pumped to sealed solar ponds. The plant B_2O_3 capacity is 2030 t/d.

Calcium and sodium calcium borate ores were once a major source for borax production, but since the discovery of the high-grade borax deposit in California they are of less importance. Ulexite ($Na_2O \cdot 2CaO \cdot 5B_2O_3 \cdot 6H_2O$) is preferred over calcium borates and borosilicates because less alkali is required and less insoluble calcium salts are produced. Ulexite (ca. 38% B_2O_3), which is finely ground and preferably calcined at 390 °C, is heated with aqueous sodium carbonate and sodium hydrogen carbonate to a near boil for several hours. The insoluble calcium carbonate is filtered and borax crystallized from the mother liquor in about 91–96% yield.

Borax is recovered from upper lake brines by Kerr McGee at Searles Lake in California by heating and evaporating water to precipitate $NaCl$, Na_2CO_3 , and Na_2SO_4 . The hot liquor, which is nearly saturated in KCl , is then rapidly cooled in a vacuum crystallizer to precipitate KCl . The cool mother liquor, which is supersaturated with borax, is treated with $NaHCO_3$ to crystallize crude borax pentahydrate. This crude material is washed with brine and recrystallized as either borax deca- or pen-

tahydrate. In a carbonation process borax is recovered from the lower brines by treatment with purified flue gas, causing $NaHCO_3$ to precipitate. The filtrate is neutralized with raw brine and cooled to crystallize crude borax.

A very pure grade of borax can be produced by reacting refined boric acid with hot $NaOH$ solution and crystallizing the resulting borax.

Anhydrous sodium tetraborate, anhydrous borax, $Na_2O \cdot 2B_2O_3$ or $Na_2B_4O_7$. Fused borax forms an amorphous glass when rapidly cooled (density 2.36 g/cm³). When slowly cooled orthorhombic crystals (α -form) are obtained. A β - and γ -form also exist [260]. The α -form is the most stable form with a congruent melting point at 742.5 °C. Its heat of formation has been calculated as -3290 kJ/mol [261], and its vapor pressure is 0.73 kPa at 1200 °C, 1.73 kPa at 1250 °C, and 3.39 kPa at 1300 °C. Anhydrous borax dissolves more slowly in water than hydrated forms, giving off a large amount of heat; heat of hydration is 161 kJ/mol. The integral heat of solution in water to give a 2.5% solution is -192.6 J/g at 51.5 °C and 190.5 J/g at 60 °C. The solubility in several organic solvents is shown in Table 49.13.

The melt attacks most refractories at 800 °C. Many metal oxides are soluble in borax glass giving characteristic colors. Anhydrous borax reacts with carbon at 1200 °C in the absence of oxygen to form B_4C_3 and Na_2C_2 , and reacts with metallic sodium to form elemental boron.

Production. Anhydrous borax is produced commercially by dehydration of hydrated sodium tetraborates in large fusion furnaces to form a borate glass. Anhydrous borax melts at 742 °C and this melt readily supercools to an amorphous glass. A crystalline form can be obtained by prolonged annealing or by seeding. The melt is very corrosive to furnace refractories and methods have been devised to keep borax away from the furnace walls [262].

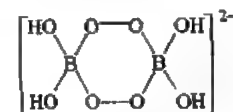
Sodium metaborate tetrahydrate, $Na_2O \cdot B_2O_3 \cdot 4H_2O$ or $NaBO_2 \cdot 4H_2O$, crystals are triclinic with a density of 1.743 g/cm³. From X-ray studies the structure is best represented by

the formula $NaB(OH)_4 \cdot 2H_2O$, containing $B(OH)_4^-$ ions [263]. Crystals begin to melt in their own water of hydration at 53.5 °C. At low humidity water is lost forming the dihydrate. By differential thermal analysis (DTA) 1 mol of water is lost at 130 °C, a second at 140 °C, and a third at 280 °C; the remaining water is slowly lost up to 800 °C. Heat of hydration is 52.51 kJ/mol.

Sodium metaborate tetrahydrate is the stable solid phase in contact with its saturated solution between 11.5 and 53.6 °C. Solutions are easily supersaturated. Both crystals and solutions absorb carbon dioxide from air forming borax and sodium carbonate. The pH of aqueous solutions increases with concentration (Table 49.11).

Production. Sodium metaborate tetrahydrate is made commercially by crystallization (< 30 °C) from a solution containing borax and a slight excess of sodium hydroxide.

A solution of sodium metaborate, prepared from borax pentahydrate and sodium hydroxide, is reacted with hydrogen peroxide on a large commercial scale to produce sodium perborate tetrahydrate, $NaBO_3 \cdot 4H_2O$ or $Na_2O \cdot B_2O_3 \cdot 2H_2O_2 \cdot 6H_2O$, containing about 10% available oxygen. Sodium perborate crystallizes in transparent monoclinic crystals, which are comparatively stable in air [264]. Its aqueous solution slowly decomposes; decomposition is accelerated by catalysts or elevated temperature.



Perborate anion

Sodium metaborate dihydrate, $Na_2O \cdot B_2O_3 \cdot 4H_2O$ or $NaBO_2 \cdot 2H_2O$, crystals are triclinic with a relative density of 1.909. The dihydrate is crystallized from aqueous solutions at 53.6–105 °C. When solutions are cooled rapidly very small needles, which are difficult to filter, form. Large platelike crystals form over several days during slow crystallization at 54–80 °C [265].

Sodium metaborate dihydrate slowly loses water at ambient temperatures and becomes sticky when heated. The heat of dehydration is 58.2 kJ/mol [266]. A monohydrate can be produced by dehydrating the dihydrate or by crystallization from highly basic solutions above 40 °C. Anhydrous sodium metaborate, $NaBO_2$, formed by heating to 350 °C, is very hygroscopic. At 966 °C it melts forming a clear glass.

Sodium pentaborate pentahydrate, sborgite, $Na_2O \cdot 5B_2O_3 \cdot 10H_2O$ or $NaB_5O_{13} \cdot 5H_2O$, crystals are triclinic with a density of 1.713 g/cm³. The heat capacity, heat content, and entropy and other thermal functions have been reported from 0 to 345 K [267].

Sodium pentaborate is stable in contact with its saturated solution between 2 and 59.5 °C. Below 2 °C borax forms, and above 59.5 °C, $2Na_2O \cdot 9B_2O_3 \cdot 11H_2O$, Taylor's borate (*d* 1.903), slowly crystallizes if seeds are present. Supersaturated aqueous solutions of Taylor's borate easily form up to the boiling point. Still lower hydrates of 4, 2, 1, and 0 mol of water crystallize at temperatures above 100 °C under pressure [268].

Production. Sodium pentaborate can be made by gradually heating borax and boric acid (1:6 molar ratio) in a rotary drier from 30 to 66 °C [269]. It is also made by spray drying a borate solution of the appropriate composition.

Disodium octaborate tetrahydrate, $Na_2O \cdot 4B_2O_3 \cdot 4H_2O$ or $Na_2B_8O_{13} \cdot 4H_2O$, is a spray-dry product. It is an amorphous solid, and is sold under the trade name Polybor, boron content is high (67.1% B_2O_3), as is solubility in water. It is easily dissolved in cool water to give supersaturated solutions of considerable concentration. Above 60 °C, concentrated solutions become quite viscous. In aqueous solution the pH decreases with concentration (Table 49.11).

Disodium tetraborate tetrahydrate, kernite, $Na_2O \cdot 2B_2O_3 \cdot 4H_2O$ or $Na_2B_4O_7 \cdot 4H_2O$, forms monoclinic crystals (*d* 1.908) consisting of infinite linear chains of the polyanion

$[\text{B}_4\text{O}_6(\text{OH})_2]_n^{2-}$ made up of fused six-membered rings [270]. The heat of formation at 24 °C is -4489.0 kJ/mol [254]. Crystal cleavage forms long fibrous needles.

Borax pentahydrate is metastable to kernite when in contact with its saturated aqueous solution above 58.2 °C (Figure 49.5). However, the rate of crystallization and of dissolution of kernite is very slow compared to borax pentahydrate. Calcined kernite dissolves at a considerably faster rate compared to the tetrahydrate.

Kernite hydrates irreversibly to borax decahydrate under ambient conditions. It dehydrates reversibly to the dihydrate, metakernite, over P_2O_5 in a vacuum or by heating at 100–120 °C. Further dehydration by heating to 190 °C causes irreversible dehydration forming an amorphous monohydrate. Rehydration of this monohydrate forms borax penta- and decahydrate.

Heating kernite to 180 °C results in the loss of 3 mol of water (DTA). The last mole of water is slowly lost up to 400 °C.

49.11 Other Metal Borates

49.11.1 Calcium and Calcium Sodium Borates

Calcium and calcium sodium borates are next to sodium borates in commercial importance. This includes the minerals colemanite, ulexite, and probertite.

Colemanite, $2\text{CaO} \cdot 3\text{B}_2\text{O}_3 \cdot 5\text{H}_2\text{O}$ or $\text{Ca}_2\text{B}_6\text{O}_{11} \cdot 5\text{H}_2\text{O}$, is the most widely occurring calcium borate mineral. Crystals of pure colemanite are monoclinic with a relative density of 2.42 and heat of formation of -3469 kJ/mol. Its crystal structure is represented by the formula $\text{Ca}_2\text{B}_6\text{O}_{11}(\text{OH})_6 \cdot 2\text{H}_2\text{O}$ and is made up of polymeric chains of $[\text{B}_3\text{O}_4(\text{OH})_3]^{2-}$ anions [271]. The solubility in water at 25 °C is about 0.18% as B_2O_3 and 0.38% at 100 °C. At about 350 °C, colemanite decrepitates violently losing all its water of hydration.

Ulexite, $\text{Na}_2\text{O} \cdot 2\text{CaO} \cdot 5\text{B}_2\text{O}_3 \cdot 16\text{H}_2\text{O}$ or $\text{NaCaB}_5\text{O}_8 \cdot 8\text{H}_2\text{O}$, forms triclinic needles with a density of 1.955 g/cm³. The crystal structure consists of discrete pentaborate rings and is represented by the formula $\text{NaCaB}_5\text{O}_8(\text{OH})_6 \cdot 5\text{H}_2\text{O}$ [272]. By DTA ulexite dehydrates losing 4 mol of water at 70–90 °C, and another 8 mol between 100 and 120 °C; the remaining water is gradually lost up to about 400 °C.

The solubility of ulexite in water is about 0.49% as NaCaB_5O_8 at 25 °C. Calcination at 200–500 °C increases the solubility to 9–13 g/L [273].

Ulexite can be prepared by reacting borax, calcium metaborate, and water at 20 °C for 119 d or at 40 °C for 60 d [259]. Also moistened probertite heated at 80–100 °C forms ulexite in about four weeks [274].

Probertite, $\text{Na}_2\text{O} \cdot 2\text{CaO} \cdot 5\text{B}_2\text{O}_3 \cdot 10\text{H}_2\text{O}$ or $\text{NaCaB}_5\text{O}_8 \cdot 5\text{H}_2\text{O}$, exists as monoclinic crystals with a density of 2.14 g/cm³. It has a crystal structure of $\text{NaCaB}_5\text{O}_8(\text{OH})_4 \cdot 3\text{H}_2\text{O}$ and is made up of pentaborate rings linked in polymeric chains [272]. Probertite is a commonly found scale in borax refineries. By DTA 2 mol of water are lost at about 100 °C, 4 mol more between 100 and 180 °C, and the last 4 mol are slowly lost up to 400 °C. Probertite can be prepared by heating borax and calcium metaborate for 8 d at 105 °C [229].

49.11.2 Lithium, Potassium, and Ammonium Borates

Borates of lithium, potassium, and ammonium are of much smaller commercial volume than those described in Section 49.11.1.

49.11.2.1 Lithium Borates

Lithium metaborate octahydrate, $\text{Li}_2\text{O} \cdot \text{B}_2\text{O}_3 \cdot 16\text{H}_2\text{O}$ or $\text{LiBO}_2 \cdot 8\text{H}_2\text{O}$, with a trigonal crystal structure, is the stable solid in contact with saturated aqueous solutions below 36.9 °C [275]. Heating the crystals causes rapid loss of 6 mol of water below 70 °C, forming orthorhombic crystals of a dihydrate, $\text{Li}_2\text{O} \cdot \text{B}_2\text{O}_3 \cdot 4\text{H}_2\text{O}$ or $\text{LiBO}_2 \cdot 2\text{H}_2\text{O}$, with a

density of 1.825 g/cm³. This dihydrate is the stable solid in contact with its saturated solution above 36.9 °C.

Lithium pentaborate pentahydrate, $\text{Li}_2\text{O} \cdot 5\text{B}_2\text{O}_3 \cdot 10\text{H}_2\text{O}$ or $\text{LiB}_5\text{O}_{10} \cdot 5\text{H}_2\text{O}$, has an incongruent solubility reported as both < 37.5 °C and 40.5 °C. By DTA the solid loses 3.7 mol of water when dehydrated between 110 and 200 °C and an additional 0.8 mol are lost up to 300 °C; it becomes anhydrous at 450 °C.

Dilithium tetraborate trihydrate, $\text{Li}_2\text{O} \cdot 2\text{B}_2\text{O}_3 \cdot 3\text{H}_2\text{O}$ or $\text{Li}_2\text{B}_4\text{O}_7 \cdot 3\text{H}_2\text{O}$, has a density of 1.88 g/cm³. When crystallized from an aqueous solution, a variety of hydrates form; when boiled the trihydrate forms [275]. Dehydration occurs at 260 °C and fusion at about 890 °C.

49.11.2.2 Potassium Borates

Potassium tetraborate tetrahydrate, $\text{K}_2\text{O} \cdot 2\text{B}_2\text{O}_3 \cdot 4\text{H}_2\text{O}$ or $\text{K}_2\text{B}_4\text{O}_7 \cdot 4\text{H}_2\text{O}$, is the most common of this class. Crystals are orthorhombic, having a relative density of 1.92 and a borate anion structure similar to borax [276]. The solid loses 2 mol of water between 112 and 180 °C, with a heat of dehydration of 86.6 kJ/mol; the last 2 mol are gradually lost between 180 and 420 °C. Potassium tetraborate is more soluble than the corresponding sodium tetraborate. In contact with its saturated solution above 56 °C, it is metastable to tetrapotassium decaborate pentahydrate, $2\text{K}_2\text{O} \cdot 5\text{B}_2\text{O}_3 \cdot 5\text{H}_2\text{O}$ or Auger's potassium borate. This Auger's form is very slow to crystallize in the absence of seed. The pH value of aqueous potassium tetraborate solutions increases slightly with concentration (Table 49.11).

Potassium tetraborate can be crystallized from aqueous solutions of potassium hydroxide and boric acid with a B_2O_3 - K_2O molar ratio of 2.0. It can also be crystallized from borax solutions by addition of potassium chloride.

Potassium pentaborate, $\text{K}_2\text{O} \cdot 5\text{B}_2\text{O}_3 \cdot 8\text{H}_2\text{O}$ or $\text{KB}_5\text{O}_{10} \cdot 4\text{H}_2\text{O}$, crystals are orthorhombic with a relative density of 1.74, mp 780 °C, and heat capacity of 330.5 Jmol⁻¹K⁻¹ at 298 K

[267]. The heat of dehydration is 110.8 kJ/mol between 106 and 134 °C. Potassium pentaborate is less soluble than the sodium analog. The pH value of its aqueous solution decreases with concentration (Table 49.11). Potassium pentaborate can be crystallized from a solution of potassium hydroxide and boric acid with a B_2O_3 - K_2O molar ratio of about 5.0.

49.11.2.3 Ammonium Borates

Ammonium pentaborate octahydrate, $(\text{NH}_4)_2\text{O} \cdot 5\text{B}_2\text{O}_3 \cdot 8\text{H}_2\text{O}$ or $\text{NH}_4\text{B}_5\text{O}_{10} \cdot 4\text{H}_2\text{O}$, exists in two crystalline forms: an orthorhombic α -form with a relative density of 1.567 and heat capacity of 359.4 Jmol⁻¹K⁻¹ at 301.2 K, and a monoclinic β -form. The crystal structure of ammonium pentaborate has the same borate ion $[\text{B}_5\text{O}_{10}(\text{OH})_4]^-$ found in sodium and potassium pentaborates. Unlike diammonium tetraborate the pentaborate is very stable to ammonia loss. At 150 °C all but 2 mol of water are lost, with less than 1% ammonia loss [250]. At 200 °C and 0.1 kPa one more molecule of water is lost with only 2% ammonia loss.

Ammonium pentaborate tetrahydrate can be crystallized from an aqueous solution of ammonia and boric acid with a B_2O_3 - $(\text{NH}_4)_2\text{O}$ molar ratio of 5.0 [277]. To determine its solubility in water, long equilibration times are required. For this reason solubility data published prior to 1966 are suspect [278]. The pH value decreases with solution concentration (Table 49.11).

Diammonium tetraborate tetrahydrate, $(\text{NH}_4)_2\text{O} \cdot 2\text{B}_2\text{O}_3 \cdot 4\text{H}_2\text{O}$ or $(\text{NH}_4)_2\text{B}_4\text{O}_7 \cdot 4\text{H}_2\text{O}$, has a crystal density of 1.58 g/cm³. The solid is somewhat unstable, with an appreciable vapor pressure of ammonia at ambient pressure and temperature. It is crystallized from a solution of ammonium hydroxide and boric acid with a B_2O_3 - $(\text{NH}_4)_2\text{O}$ molar ratio of about 2.0. Aqueous solutions up to 10% concentration have an invariant pH of 8.8. The crystal structure can be described by the formula $(\text{NH}_4)_2\text{B}_4\text{O}_7 \cdot (\text{OH})_4 \cdot 2\text{H}_2\text{O}$ [279].

Other metal borates are of comparatively smaller commercial volume. They are generally prepared by reacting an aqueous solution of boric acid or alkali metal borate with a metal oxide or soluble metal salt.

49.11.3 Zinc Borates

Several hydrates of zinc borate are known. These include $2\text{ZnO} \cdot 3\text{B}_2\text{O}_3 \cdot 3.5\text{H}_2\text{O}$ or ZB 2335, which has a crystal density of 2.69 g/cm^3 and thermal stability to dehydration up to $290\text{--}300^\circ\text{C}$ [280]. It is made commercially from an aqueous boric acid solution with zinc oxide above 70°C in the presence of product zinc borate seed. An induction period of 1–2 h is followed by a highly exothermic reaction.

A zinc borate of composition $2\text{ZnO} \cdot 3\text{B}_2\text{O}_3 \cdot 7$ to $7.5\text{H}_2\text{O}$ or ZB 237, has a crystal density of 2.44 g/cm^3 , and, from its X-ray structure, has the formula $\text{Zn}[\text{B}_3\text{O}_3(\text{OH})_2] \cdot \text{H}_2\text{O}$ [281]. Six mol of water are lost when ZB 237 is heated from 120 to 170°C .

The nine hydrate, $2\text{ZnO} \cdot 3\text{B}_2\text{O}_3 \cdot 9\text{H}_2\text{O}$ or ZB 239 is made using the same conditions as for ZB 2335 below 70°C .

The zinc borate, $\text{ZnO} \cdot \text{B}_2\text{O}_3 \cdot 2\text{H}_2\text{O}$ or ZB 112, is thermally stable to dehydration up to 190°C . Several hydrated zinc borates are of commercial importance as fire retardant and smoke suppressant agents for polymers and coatings, most notably in PVC, halogenated polyesters, and nylon. For example, ZB 2335 is sold under the trade name Firebrake ZB or ZB 2335 (U.S. Borax & Chemical Corp., USA); it has a mean particle size of $5\text{--}10 \mu\text{m}$. Its high-thermal stability is an important physical property because of the high temperatures required in some plastic processing. The zinc borate ZB 112 is sold by Humphrey Chemical Co. (USA) and Storey Brothers (U.K.). In addition Humphrey sells zinc borates described as ZB 235 and ZB 237, which are prepared by dry mixing boric acid with zinc oxide. The resulting product is actually a mixture of zinc

borate $2\text{ZnO} \cdot 3\text{B}_2\text{O}_3 \cdot 9\text{H}_2\text{O}$ or ZB 239 and unreacted starting materials.

49.12 Borate Glasses

Various alkali-metal oxides, when fused with boric oxide, form a viscous melt, which on supercooling readily forms glasses. Mixtures of alkali-metal borates, boric acid, and alkali-metal carbonates or hydroxides can be used. Many physical properties of these glasses have maxima and minima with increasing alkali-metal oxide to borate ratio. This has been termed the *boron anomaly*, and has been observed in such properties, as viscosity, density, thermal expansion, and heat content [264]. This anomaly has been shown to be a result of structural changes in the glass, and of the variation in proportion of tetrahedral coordination of the boron in BO_4 groups and trigonal coordination in BO_3 groups.

The viscosity of $\text{Na}_2\text{O}\text{--}\text{B}_2\text{O}_3$ and $\text{K}_2\text{O}\text{--}\text{B}_2\text{O}_3$ glass has a maximum value at $20\text{--}25 \text{ mol\%}$ metal oxide below 900°C [282], and the density increases from 1.85 g/cm^3 in pure B_2O_3 to a maximum of 2.36 in mixtures containing $27\text{--}33 \text{ mol\%}$ metal oxide at 900°C [283]. Maximum hardness is achieved with a composition of $25\% \text{ Na}_2\text{O}$ [284]. Thermal expansion reaches a minimum up to about 13 vol\% Na_2O . The index of refraction (n_D) is 1.48 at 6 vol\% Na_2O , and 1.51 at 24 vol\% Na_2O .

Silica is quite soluble in molten sodium borate, giving a viscous liquid. The use of boric oxide in silica glass imparts many desirable properties. Borosilicate glass approaches the desirable properties of quartz glass, except the melting range and workability of the glass melt is significantly improved. Addition of boric oxide to alkali-metal silicate glass imparts increased hardness and decreased expansivity, lowers the melting range, and increases furnace production and durability of the glass. In ceramic glass, B_2O_3 improves resistance to weathering and chemicals.

49.13 Miscellaneous Data for Sections 49.7–49.12

49.13.1 Quality Specifications

Product specifications for boric oxide, boric acid, and borax are listed in Tables 49.14 and 49.15.

49.13.2 Uses

The glass and ceramic industry in the United States consumes about one-half of the total domestic B_2O_3 . This includes borosilicate glasses, insulation fiberglass, textile fiberglass, porcelain enamels, and ceramic glazes. The largest market is for insulation fiberglass, with typically $5\text{--}7\%$ of contained B_2O_3 from borax pentahydrate, ulexite, or probertite; whereas textile fiberglass typically has $8\text{--}9\%$ of contained B_2O_3 from boric acid or colemanite. Borosilicate glass has $12\text{--}15\%$ of contained B_2O_3 largely from borax pentahydrate. Borates are used as a flux in the manufacture of porcelain enamels and ceramic glazes. Of the total United States domestic B_2O_3 consumption, about 15% is used in the form of boric acid and metal borates as fire retardants in cellulosic insulation and plastics; 4% as soluble borates in agriculture as a fertilizer to amend boron-deficient soils and as a herbicide at high dosages; 10% from borax decahydrate and sodium perborate for cleaning and bleaching of laundry products;

and 2% as corrosion inhibitors in aqueous systems, especially automotive antifreeze.

In Western Europe about one-half of the B_2O_3 is used in the manufacture of glass-related products. Sodium perborate accounts for about one-third of the total boron consumption as a bleach in high-temperature laundry products.

In Japan 70% of B_2O_3 consumption is used in glass-related products.

Other minor uses of boric acid and metal borates are listed below.

• Boric acid

- Flux in welding and brazing
- Bacteriostat and fungicide
- NF grade as a mild, nonirritating antiseptic
- Cockroach control
- Protection of wood products against insect damage
- Use in nuclear reactor cooling water
- Manufacture of refractories and abrasives
- Catalysts for air oxidation of hydrocarbons

Table 49.14: Specification for commercial B_2O_3 .

	% Maximum	% Typical
Na	0.1	0.015
SiO_2	0.21	0.15
Al_2O_3	0.14	0.08
Fe_2O_3	0.02	0.009
CaO	0.03	0.013
MgO	0.15	0.05
SO_4	0.41	< 0.20

Table 49.15: Maximum specifications for grades of boric acid, borax, and borax pentahydrate.

	Boric acid		Borax		Borax pentahydrate
	technical	special quality	technical	special quality	technical
$\text{H}_3\text{BO}_3\text{--Na}_2\text{B}_4\text{O}_7 \cdot 10\text{H}_2\text{O}$	>99.5	>99.9	>99.5	>99.9	0.08
SO_4	0.10	0.00015	0.06	0.0001	—
PO_4	—	0.001	0.001	0.001	—
Cl	0.01	0.00004	0.07	0.00004	0.05
Fe_2O_3	0.0007	0.0002	0.003	0.00028	0.004
Heavy metals as Pb	—	0.0002	—	0.001	—
Mn	—	0.0001	—	—	—
As	—	0.0005	—	0.0002	—
Ca	—	0.005	—	0.005	—
Na	—	0.001	—	—	—
Water insolubles	—	0.001	0.02	0.001	—

- **Sodium borates, Calcium borates**
 - Manufacture of refractories and abrasives
 - Metallurgical flux (smelting)
 - Neutron absorber in nuclear reactors
- **Sodium metaborate**
 - Photographic chemical
 - Herbicides
 - Detergents and cleansers
 - Textile-finishing compounds
 - Adhesives
- **Potassium borates**
 - Nonsodium alkaline borate source
 - Lubricant component
 - Solvent for casein
 - Welding and brazing flux for stainless steels and various nonferrous metals
- **Ammonium tetraborate**
 - Nonalkaline metal borate source
- **Ammonium pentaborate**
 - Component in electrolytes for electrolytic capacitors
 - Flameproofing formulations
 - Paper coating
- **Lithium meta- and tetraborates**
 - Glass-making
- **Barium borates**
 - Fire retardants
 - Mildew inhibitor in latex, paints, plastics, textile, and paper products
 - Preservative in protein-based glues
- **Copper metaborate**
 - Rot and mildew inhibitor
 - Fungicide in lumber and other cellulosic materials
 - Oil pigment
- **Manganese borate**
 - Printing ink drier

49.13.3 Economic Aspects

The estimated world reserves of borate minerals and world production of boron products for 1980 through 1982 are listed in Table

49.16. Of the total world borates the United States produces 62%, Turkey 29%, and all other sources 9%, based on B_2O_3 . World borate consumption in the United States is 30%, Western Europe 37%, Japan 5%, and all other countries 28%. The European and Japanese borate requirements are served through imports largely from the United States and Turkey. Almost all B_2O_3 production in Turkey and about one-half the production in the United States is exported.

Nearly 99% of the sales volume of borate products consists of borax pentahydrate, borax decahydrate, boric acid, boric oxide, anhydrous borax, colemanite, and ulexite. Borax pentahydrate is the highest volume commercial borate.

Until mid-1984, U.S. Borax exported a crude borax pentahydrate, trade name Rasorite-46, containing less than 1% clay. This product is now exported without clay as borax pentahydrate. Prices of the primary borate products are shown in Table 49.17.

Table 49.16: Estimated world borate reserves and mine production (as B_2O_3).

Country	Reserves, kt	Production, kt		
		1980	1981	1982
United States	70 000	710	670	550
Turkey	70 000	339	320	320
South America	35 000	—	—	—
Argentina	—	—	30	27
Chile	—	—	1	4
Peru	—	—	3	3
Soviet Union	65 000	—	40	40
China	30 000	—	5	5
World total	270 000	1049	1069	949

Table 49.17: Borate prices (285).

Product	\$/t
Borax, decahydrate, technical, granular, 99.5%, bulk cartons	193 ^a
Borax, pentahydrate, technical, granular, 99.5%, bulk cartons	222 ^a
Borax, anhydrous, technical, 99%, bulk cartons	622 ^a
Boric acid, technical, granular, 99.9%, bulk cartons	609 ^a
Tincal	148–185 ^b
Ulexite	120–170 ^b
Colemanite, glass quality	255–325 ^b
Colemanite, refining grade	160–190 ^b

^a FOB (free on board) rail cars in California, United States.

^b FOB ship Bandirma, Turkey.

There has been a significant decline in production of anhydrous products because of the rapid increase in fuel costs. In addition there is a trend to use colemanite for the manufacture of textile fiberglass.

49.13.4 Toxicology and Occupational Health

Boron is present in animal tissue at about 1 ppm, but has no known essential biochemical function [286]. Humans absorb about 10–20 mg of boron in a normal daily diet, mainly from fruits and vegetables. Inhalation of boric acid and borate dust causes only irritation without permanent injury. It is not absorbed when contacted with healthy skin, but can be toxic when used on large areas of burned or abraded skin. The handling of boric acid and sodium borates is not generally considered hazardous [289].

Boric acid has an acute oral LD_{50} (rats) of 4 g/kg; for borax the oral LD_{50} (rats) is 6 g/kg. The TLV and MAK data are given in Table 49.18 [287, 288].

Boron is an essential trace element in higher plant nutrition [290]. At high levels boron becomes toxic, with damage manifested in deformation of leaves, which curl at the edge, often accompanied by necrosis. Fertilizers with calcium tend to reduce this damage [254].

Table 49.18: Maximum concentrations in the work environment.

Substance	TWA, mg/m ³	STEL, mg/m ³	MAK, mg/m ³
Sodium tetraborates			
Anhydrous	1	—	—
Decahydrate	5	—	—
Pentahydrate	1	—	—
Boron oxide	10	20	15

49.14 Pigments

49.14.1 Borosilicate Pigments

Borosilicate pigments usually contain calcium or zinc ions in a matrix of silicon dioxide and boron trioxide, $x(Ca, Zn) \cdot ySiO_2 \cdot zB_2O_3$.

Aqueous slurries of this white pigment are alkaline (pH > 9). Borosilicate pigments are recommended as nontoxic alternatives to basic lead silicate. Their main field of application is in waterborne binders and electrodeposition coatings [291–293].

A trade name for calcium borosilicate is Halox CW291, -2230 (Halox Pigments, USA).

49.14.2 Borate Pigments

Barium metaborate, $BaO \cdot B_2O_3 \cdot H_2O$ [294], and zinc borophosphate, $ZnO \cdot xB_2O_3 \cdot yP_2O_5 \cdot 2H_2O$, are colorless pigments. Their properties are listed in Table 49.19. They both have a relatively high water solubility. Barium metaborate is coated with silica to reduce this.

Table 49.19: Properties of metal borate pigments.

Property	Barium metaborate	Zinc borophosphate
Density, g/cm ³	ca. 3.3	2.8
pH	9–10	8
Water-soluble content, %	0.4	1–1.5
Use	primer, topcoat	primer

The anticorrosive effects of these pigments depend mainly on their ability to maintain high pH values in the coating. They are most effective in the initial phase of corrosion protection. The borate ion neutralizes acidic foreign ions and binder decomposition products, but is also thought to act as an anodic passivator, forming a protective film. The effectiveness of metal borate pigments in aqueous air-dried anticorrosive coatings is described in [295].

The metal borate pigments are classified as having a relatively low toxicity [296, 297].

Examples of trade names are Butrol (Buckmann Laboratories, USA) for barium metaborate and Sicor BZN (BASF, Germany) for zinc borophosphate.

49.15 References

1. V. I. Matkovich (ed.): *Boron and Refractory Borides*, Springer Verlag, Berlin 1977.

2. R. M. Adams: *Boron, Metallo-Boron Compounds and Boranes*, J. Wiley & Sons, New York 1964.
3. R. F. Gould (ed.): "Borax to Boranes", *Adv. Chem. Ser.* 1961, no. 32, pp. 27-52.
4. Gmelin, Boron (system no. 13), main vol. (1926), supplement vol. (1954), supplement vol. 2 (1981).
5. N. N. Greenwood: "Boron", in J. C. Bailar (ed.): *Comprehensive Inorganic Chemistry*, vol. 1, Pergamon Press, Oxford-New York 1973, pp. 680-689.
6. R. Naslain in P. Hagenmuller (ed.): *Preparative Methods in Solid State Chemistry*, Academic Press, New York 1972, pp. 439-485.
7. A. F. Zhigach, D. C. Stasinevich: "Methods of Preparation of Amorphous Boron", in V. I. Matkovich (ed.): *Boron and Refractory Borides*, Springer Verlag, Berlin 1977, pp. 214-240.
8. H. S. Cooper: "Boron", in C. A. Hampel (ed.): *Rare Metals Handbook*, 2nd ed., Reinhold Publ. Co., London 1961, p. 77.
9. B. Mason: *Principles of Geochemistry*, John Wiley & Sons, New York 1952, p. 41.
10. H. Moissan, *Ann. Chim. Phys.* 6 (1895) 296.
11. E. Weintraub, *Trans. Am. Electrochem. Soc.* 16 (1909) 165.
12. R. C. Erd: *Supplement to Mellor's Comprehensive Treatise on Inorganic and Theoretical Chemistry*, vol. 5, Longman, New York 1980, Part A, Section A1, p. 7.
13. T. Dickson, *Ind. Miner. (London)* 12 (1983) 63.
14. K. P. Tsomaya et al., *J. Less Common Met.* 47 (1976) 249.
15. J. Cueilieron, *Ann. Chim.* 19 (1944) 459.
16. Y. Hara et al., *Kenkyu Hokoku Asahi Garasu Kogyo Gijutsu Shoreikai* 26 (1975) 255; *Chem. Abstr.* 87 (1977) 44 716 p.
17. G. Wilkinson (ed.): *Comprehensive Organometallic Chemistry*, vol. 1 pp. 253-554, vol. 7, pp. 111-364, Pergamon Press, Oxford 1982.
18. L. Bretherick (ed.): *Hazards in the Chemical Laboratory*, 3rd ed., Royal Society of Chemistry, London 1981, p. 203.
19. J. Cueilieron, F. Thevenot: "Chemical Properties of Boron", in V. I. Matkovich (ed.): *Boron and Refractory Borides*, Springer Verlag, Berlin 1977, pp. 203-211.
20. L. Vandenbulcke, G. Vuillard, *J. Less Common Met.* 67 (1979) 65.
21. D. Z. Hobbs, T. T. Campbell, F. E. Block, *Rep. Invest. U.S. Bur. Mines* 6456 (1964) 1-14.
22. B. I. Silbergleit et al., *SU* 1004262, 1981.
23. J. C. Schuhmacher, US 3 001855, 1961.
24. H. Mazza et al., US 2866688, 1958.
25. W. J. Kroll, N. P. Nies, E. W. Fajans, US 2893842, 1959.
26. J. Yannacakis, N. P. Nies, *Boron Synth. Struct. Prop. Proc. Conf.* 1959 1960, 38-41.
27. L. Markovskii, *Electron Technol.* 3 (1970) 95.
28. H. C. Starck, GB 747287, 1956 (H. Haag).
F. Müller, H. Haag, DE 936745, 1955.
H. Haag, DE 957299, 1957; US 2794708, 1957.
29. R. Naslain, *Inorg. Synth.* 12 (1970) 145.
30. T. Sugaya et al., *J. Less Common Met.* 47 (1976) 49.
31. H. J. Becker: "Boron", in G. Brauer (ed.): *Handbuch der Präp. Anorg. Chemie*, 3rd ed., vol. 2, Enke Verlag, Stuttgart 1978, pp. 787-788.
32. G. H. Fetterly, US 2542916, 1951.
33. D. Stern, L. Lynds, *J. Electrochem. Soc.* 105 (1958) 676.
34. A. J. Laubengayer et al., *J. Am. Chem. Soc.* 65 (1943) 1924.
35. Elektroschmelzwerk Kempton, DE 2115810, 1982 (G. Wiebke et al.).
36. J. Cueilieron, J. C. Viala, *J. Less Common Met.* 65 (1979) 167.
37. J. Cueilieron, J. Viala, *J. Less Common Met.* 67 (1979) 333.
38. A. van Arkel, US 1774410, 1930; *Metallwiss. Metalltech.* 13 (1934) 405.
39. H. Schlesinger, G. W. Schaeffer, US 2528514, 1950.
40. J. Lagrenaudie, *J. Chem. Phys.* 50 (1953) 629.
41. W. H. Dietz, H. A. Herrmann, *Electron Technol.* 3 (1970) 195.
42. N. P. Nies, *J. Electrochem. Soc.* 107 (1960) 817.
43. W. Borchert et al., *Z. Angew. Phys.* 29 (1970) 277.
44. G. V. Tsagareishvili et al., *J. Less Common Met.* 67 (1979) 419.
45. F. Thevenot, J. Cueilieron, *Analisis* 5 (1977) 105; *Met. Abstr.* 1977, 23-0637.
46. F. Ehrenberger, *Fresenius Z. Anal. Chem.* 305 (1981) 181.
47. F. Thevenot, J. C. Viala, *Analisis* 3 (1975) 76.
48. Military Specification MIL-B-51092/ORD (1962).
49. Degussa, Research Dept. Phys. Chem., internal measurements (1983).
50. S. Moeschlin: *Klinik und Therapie der Vergiftungen*, Thieme Verlag, Stuttgart 1980, pp. 206-208.
51. R. J. Markle, S. G. Stephenson, *Int. J. Powder Metall. Powder Technol.* 18 (1982) 243.
52. W. C. Goss, US 2415946, 1947.
53. Winnacker-Küchler, 4th ed., vol. 3, pp. 408-440.
54. G. K. Gaulé et al., *Boron Prep. Prop. Appl. Pap. Int. Symp.* 1964 2 (1965) 317-338.
55. G. F. Girri et al., 3rd Int. Conf. Thin Films, Budapest 1975, p. 215; *Met. Abstr.* 1976, 63-0163.
56. J. T. Milek, S. J. Wellers, *Boron, Electronic Prop. Inf. Center, Hughes Aircraft Co., Culver City, Calif.*, Data Sheet DS 151 (1967).
57. J. L. Christian et al., *Met. Prog.* 97 (1970) 113.
58. G. Lubin, S. Dastin, *Mod. Plast.* 48 (1971) 62.
59. D. Kuehl, *Nat. SAMPE Symp. Exhib. Proc.* 20 (1975) 67; *Met. Abstr.* 1975, 61 0384.
60. M. Miller, A. Robertson, *Hybrid Sel. Met. Matrix Compos.* 1977, 99-157; *Met. Abstr.* 1979, 62-0211.
61. Kirk-Othmer, 3rd ed., vol. 16, p. 163.
62. *Met. Abstr.* 1981, 46-0040.
63. Kirk-Othmer, 3rd ed., vol. 2, pp. 537-569.
64. H. P. Munster, G. Kirchner: *Taschenbuch des Metallhandels*, Metall Verlag, Berlin 1982, pp. 151-153.
65. Gmelin, vol. 34, sect. 1 & 9, 332 pp.
66. Gmelin, vol. 53, sect. 2 & 19, 341 pp.
67. Gmelin, vol. 2(1), pp. 255-316.
68. Gmelin, vol. 2(2), pp. 1-154.
69. N. N. Greenwood, B. S. Thomas in J. C. Bailar (eds.): *Comprehensive Inorganic Chemistry*, vol. 1, Pergamon Press, Oxford 1973, p. 956.
70. G. Urry in E. Muettteries (ed.): *The Chemistry of Boron and Its Compounds*, J. Wiley & Sons, Inc., New York 1967, pp. 325-375.
71. J. D. Cox, *J. Chem. Thermodyn.* 10 (1978) 903-906.
72. A. Finch, P. J. Gardiner in R. J. Brotherlon, H. Steinberg (eds.): *Progress in Boron Chemistry*, vol. 3, Pergamon Press, New York 1970, p. 200.
73. E. W. Rothe, B. P. Mathur, G. P. Reck, *Inorg. Chem.* 19 (1980) 829-831.
74. D. Mootz, M. Steffen, *Angew. Chem.* 92 (1980) 481; *Angew. Chem. Int. Ed. Engl.* 19 (1980) 483-484.
75. D. Mootz, M. Steffen, *Acta Crystallogr. Sect. B*, B37 (1981) 1110.
76. J. L. Gay-Lussac, L. J. Thenard, *Ann. Chim. (Paris)* 69 (1809) no. 1, 204-220.
77. B. Zawadzki, A. Bulinska, E. Wilk, *Mater. Ogolnopol. Symp. Zwiastki Fluorowe* 1980 (Publ. 1981) 113-117.
Chem. Abstr. 95 (1981) 189416.
78. Kerr-McGee Chemical Corp., US 4125590, 1978 (L. F. Schmoeyer).
79. Alcoa, US 4024221, 1977 (A. J. Becker, D. R. Careatti).
80. PPG Industries, Inc., US 4210631, 1980 (N. R. De-lue, J. C. Crano).
81. PPG Industries, Inc., US 4213948, 1980 (J. C. Crano).
82. H. Kral, DE 2826747, 1980.
Chem. Abstr. 92 (1980) 113123.
83. V. S. Khain, V. P. Val'kova, E. S. Kotelevets, *Zh. Neorg. Khim.* 22 (1977) 338.
84. J. Cueilieron, S. C. Viala, *J. Less Common Met.* 58 (1978) 123.
Chem. Abstr. 89 (1978) 15952.
85. Showa Koji K. K., JP-Kokai 7768754, 1977 (H. Yasutomi, N. Takeshima, T. Matsuno, H. Momo).
Chem. Abstr. 87 (1977) 206078.
86. Morita Kagaku Kogyo Co. Ltd., JP-Kokai 7896260, 1978 (T. Tatsuno, K. Momota).
Chem. Abstr. 90 (1979) 11870.
87. Asahi Glass Co. Ltd., JP-Kokai 8047119, 1980 (M. Noshiro, T. Yaita, S. Kobayashi).
Chem. Abstr. 94 (1981) 7204.
88. E. H. Vernot, J. D. MacEwen, C. C. Haun, E. R. Kinkead, *Toxicol. Appl. Pharmacol.* 42 (1977) 417-423.
Chem. Abstr. 88 (1978) 84173.
89. H. S. Booth, D. R. Martin: *Boron Trifluoride and Its Derivatives*, J. Wiley & Sons, New York, p. 87.
90. D. W. A. Sharp in M. Stacey, J. C. Tatlow, A. G. Sharpe (eds.): *Advances in Fluorine Chemistry*, vol. 1, Butterworths Scientific Publications, London 1960, p. 68.
91. Gmelin, vol. 2(1), p. 276.
92. Gmelin, vol. 2(2), p. 31.
93. R. M. Adams, *Pure Appl. Chem.* 30 (1972) 683.
94. D. Mootz, M. Steffen, *Z. Anorg. Allg. Chem.* 482 (1981) 193.
95. N. V. Krivtsov, K. V. Titova, V. Ya. Rosolovskii, *Zh. Neorg. Khim.* 22 (1977) 679.
96. R. Wilmutte, J. Benezech, *Galvano-Organico* 45 (1976) 313.
97. C. J. Hill, R. P. Lash, *Anal. Chem.* 52 (1980) 24.
98. J. P. Wilshire, W. A. Brown, *Anal. Chem.* 54 (1980) 1647.
99. United States Steel Corp., US 3933605, 1976 (T. J. Butler, R. M. Hudson, C. J. Warning).
100. RCA Corp., US 3979238, 1976 (H. W. Justice).
101. Rockwell International Corp., US 4004957, 1977 (L. J. Quintana).
102. Y. Nakao, H. Nakeshima, M. Ohta, K. Furukawa, *J. Nucl. Sci. Technol.* 15 (1978) 76.
Chem. Abstr. 88 (1978) 96218.
103. United States of America, US 4207124, 1980 (K. O. Christe).
104. Morita Chemical Industry Co., Ltd., JP-Kokai 76116060, 1976 (Y. Mochida, T. Tatsuno).
Chem. Abstr. 87 (1977) 90347.
105. Dart Industries, Inc., US 4008162, 1977 (T. F. Korenowski, J. L. Penland, C. J. Ritzert).
106. Showa Koji K. K., JP-Kokai 7692561, 1976 (H. Yasutomi, N. Takeshima, T. Matsuno, H. Momo).
Chem. Abstr. 85 (1976) 166268.
107. Nitto Electric Industrial Co., Ltd., JP-Kokai 82162692, 1982.
Chem. Abstr. 98 (1983) 59412.
108. P. Langer, H. Kokesova, K. Gschwendtova, *Acta Endocrin. Copenhagen* 81 (1976) 516.
Chem. Abstr. 85 (1976) 40748.
109. M. W. Curtis, C. H. Ward, *J. Hydrol. (Amsterdam)* 51 (1981) 359.
Chem. Abstr. 95 (1981) 55868.
110. E. L. Muettteries: *The Chemistry of Boron and Its Compounds*, J. Wiley & Sons, New York 1967, pp. 647-667.
111. H.-Y. Chen, B. R. Conard, P. W. Gilles, *Inorg. Chem.* 9 (1970) 1776-1777.
112. H. Diercks, B. Krebs, *Angew. Chem.* 89 (1977) no. 5, 327; *Angew. Chem., Int. Ed. Engl.* 16 (1977) no. 5, 313.
113. E. G. Zhukhov, S. A. Dembovskii, *Izv. Akad. Nauk SSSR Neorg. Mater.* 16 (1980) 37-41.
Chem. Abstr. 92 (1980) 117432.
114. M. P. Morozova, G. A. Rybakova, *Vestn. Leningr. Univ., Fiz., Khim.* 23 (1968) no. 22, 161-163.
Chem. Abstr. 71 (1969) 7162.
115. N. N. Greenwood, B. S. Thomas in J. C. Bailar (ed.): *Comprehensive Inorganic Chemistry*, vol. 1, Pergamon Press, New York 1973, pp. 909-916.
116. B. Krebs, H. U. Huerter, *Angew. Chem.* 92 (1980) 479; *Angew. Chem., Int. Ed. Engl.* 19 (1980) 481-482.
117. H.-Y. Chen, P. W. Gilles, *J. Am. Chem. Soc.* 92 (1970) 2309-2312.
118. J. H. Holloway, D. C. Puddick, G. M. Staunton, D. Brown, *Inorg. Chim. Acta* 64 (1982) L209-L210.
119. R. R. Schumaker, E. M. Engler, *J. Am. Chem. Soc.* 99 (1977) 5521-5522.
120. K. P. Callahan, P. J. Durand, *Inorg. Chem.* 19 (1980) 3211-3217.
121. R. D. Baechler, S. K. Daley, *Tetrahedron Lett.* 1978, no. 2, 101-104.
122. E. R. Squibb & Sons, Inc., US 4018761, 1977 (C. M. Cimarusti, P. Wojtkowski, J. E. Dolfini).
123. A. Levasseur, R. Olazcuaga, M. Kbal, M. Zahir et al., *C.R. Séances Acad. Sci. Sér. 2* 293 (1981) 563-565.
Chem. Abstr. 96 (1982) 186016.
124. H. Wada, M. Menetrier, A. Levasseur, P. Hagenmuller, *Mater. Res. Bull.* 18 (1983) no. 2, 189-193.
125. S. Susman, L. Boehm, K. J. Volin, C. J. Delbecq, US Appl. 3755257 1983.
Chem. Abstr. 100 (1984) 124156.

126. S. Susman, L. Boehm, K. J. Volin, C. J. Delbecq, *Solid State Ionics* 5 (1981) 667-669.
127. A. Stock: *Hydrides of Boron and Silicon*, Cornell University Press, Ithaca, New York 1933.
128. H. I. Schlesinger, A. B. Burg, *J. Am. Chem. Soc.* 53 (1931) 4321.
129. H. C. Brown: *Hydroboration*, W. A. Benjamin Inc., New York 1962.
130. W. N. Lipscomb, *Science* 196 (1977) 1047.
131. W. N. Lipscomb, *Adv. Inorg. Chem. Radiochem.* 1 (1959) 156.
132. *Pure Appl. Chem.* 30 (1972) 683.
R. M. Adams, *Inorg. Chem.* 7 (1968) 1945.
J. B. Casey, W. J. Evans, W. H. Powell, *Inorg. Chem.* 22 (1983) 2245.
133. T. P. Fehlner, R. L. Strong, *J. Phys. Chem.* 64 (1960) 1526.
134. R. F. Porter, F. A. Grimm, *Adv. Chem. Ser.* 72 (1969) 100.
Chem. Abstr. 68 (1968) 110276.
135. M. D. Carabine, R. G. W. Norrish, *Proc. R. Soc. (London), Ser. A* 296 (1967) 1.
136. A. E. Newkirk, H. R. Broadly, A. L. Marshall, General Electric Co. Report No. 55 248, March 20, 1950.
137. R. W. Parry, L. J. Edwards, *J. Am. Chem. Soc.* 81 (1959) 3560.
138. E. Muetterties (ed.): *Boron Hydride Chemistry*, Academic Press Inc., New York 1975, Chapter 3.
139. G. A. Guter, G. W. Schaeffer, *J. Am. Chem. Soc.* 78 (1956) 3546.
140. M. F. Hawthorne et al., *J. Am. Chem. Soc.* 82 (1960) 1825.
141. H. D. Johnson, II, S. G. Shore, *J. Am. Chem. Soc.* 93 (1971) 3798.
142. Callery Chemical Co., *Diborane Handling Bulletin*, 1982.
143. A. Stock, C. Massenz, *Ber. Dtsch. Chem. Ges.* 45 (1912) 3539.
144. E. Wiberg, K. Schuster, *Ber. Dtsch. Chem. Ges.* 67B (1934) 1807.
145. V. I. Mikheeva, V. Y. Markina, *Zh. Neorg. Khim.* 1 (1956) 619.
146. M. J. Klein, B. C. Harrison, I. Solomon, *Abstr. 131st ACS Meeting*, Miami, FL, April, 1957.
147. C. R. Dillard, Ph.D. Thesis, University of Chicago, 1949.
148. H. C. Brown, W. Korytnik, *J. Am. Chem. Soc.* 82 (1960) 3869.
149. S. Ikegami, S. Yamada, *Chem. Pharm. Bull. (Tokyo)* 14 (1966) no. 12, 1399.
Chem. Abstr. 66 (1967) 65377.
150. R. L. Johnson, D. J. Burton, *Tetrahedron Lett.* 1965, no. 46, 4039-4084.
151. H. Ikeda, A. Kogure, K. Shuna, Y. Minoura, *Kogyo Kagaku Zasshi* 68 (1965) 1107.
Chem. Abstr. 66 (1965) 56346.
152. E. M. Fedneva, V. N. Konoplev, V. D. Krosnaperova, *Zh. Neorg. Khim.* 11 (1966) 2051.
Chem. Abstr. 66 (1967) 28367.
153. R. M. Adams: *Boron Metallo-Boron Compounds and Boranes*, Interscience, New York 1964, p. 249.
154. R. Ewens, H. Bassett, *Chem. Ind. (London)* 68 (Feb., 1949) 131.
155. A. P. Altschuler, *J. Am. Chem. Soc.* 77 (1955) 5455.
156. Metal Hydrides, US 2970114, 1961 (R. W. Bragdon).
157. Mine Safety Appliances, US 2744810, 1956 (C. B. Jackson).
158. Callery Chemical Co., GB 774728, 1957 (W. H. Schacter).
159. A. E. Finhold, A. C. Bond, Jr., H. I. Schlesinger, *J. Am. Chem. Soc.* 69 (1947) 1199.
160. Ventron Div., Morton-Thiokol Inc., DE 1218413, 1959; DE 2429521, 1974 (E. R. Winiarczyk).
161. M. M. Cook, E. A. Sullivan, R. C. Wade: *13th Northeast Regional ACS Meeting*, Hartford, CT, June, 1983.
162. D. F. Gaines, R. Schaeffer, F. Tebbe, *Inorg. Chem.* 2 (1963) 526.
163. H. C. Miller, N. E. Miller, E. L. Muetterties, *J. Am. Chem. Soc.* 85 (1963) 3885.
Inorg. Chem. 3 (1964) 1456.
164. G. S. Pauson, L. E. Weill, *J. Inorg. Nucl. Chem.* 15 (1960) 184.
165. R. O. Hutchins, N. R. Natale, *Org. Prep. Proced. Int.* 11 (1979) 246.
166. Ventron Div., Morton-Thiokol Inc., US 2942990, 1960 (E. A. Sullivan).
167. Ventron Div., Morton-Thiokol Inc., US 2930771, 1960 (R. C. Wade).
168. E. A. Sullivan: *Third International Meeting on Boron Chemistry*, Munich and Ettal (FRG), July 5-9, 1976, Pergamon Press, Oxford 1977, p. 132.
169. GAF Corp., US 3306886, 1967 (F. Grosser, E. V. Hart, A. Schwartz).
170. Union Carbide, US 3374121, 1968 (J. N. Hgsett).
171. Eastman Kodak, FR 1548122, 1968 (C. C. Bard, H. W. Vogt).
172. W. Boden, *J. Electrochem. Soc.* 129 (1982) 1252.
173. H. Hatanka, *J. Neurol.* 209 (1975) 81.
174. W. Kliegel: *Bor In Biologie, Medizin und Pharmazie*, Springer Verlag, Berlin 1980, pp. 636-803.
175. G. D. Clayton, F. E. Clayton (ed.): *Patty's Industrial Hygiene and Toxicology*, J. Wiley & Sons, New York 1981, pp. 2978-3005.
176. R. L. Tatken, R. J. Lewis, Sr.: *Registry of Toxic Effects of Chemical Substances*, vols. 1, 2, 3, U.S. Dept. of Health and Human Services, NIOSH Publ. No. 83-107, 1981-1982.
177. C. C. Comstock, L. Feinsilver, L. H. Lawson, F. W. Oberst, Army Chemical Corps Medical Laboratories, Research Report No. 258, 1954.
178. ACGIH (ed.): *Threshold Limit Values (TLV)*, ACGIH, Cincinnati, OH, 1985.
179. DFG (ed): *Maximale Arbeitsplatzkonzentrationen*, Verlag Chemie, Weinheim 1984.
180. E. M. Cordasco, R. W. Cooper, J. V. Murphy, C. Anderson, *Chest* 41 (1962) 68.
181. H. J. Lowe, G. Freeman, *AMA Arch. Ind. Health* 16 (1957) 523.
182. E. H. Krackow, *AMA Arch. of Ind. Hyg. Occup. Med.* 8 (1953) 335.
183. R. M. Adams: *Boron, Metallo-Boron Compounds and Boranes*, Interscience, p. 731, New York 1964.
184. L. H. Hall, C. O. Starnes et al., *J. Pharm. Sci.* 69 (1980) 1025.
185. C. T. Blaisdell, Army Chemical Corps Medical Laboratories, Research Report no. 351, 1955.

186. W. E. Reinhart, *Am. Ind. Hyg. Assoc. J.* 21 (1960) 389.
187. R. A. Spryskhova, L. I. Karaseva, V. A. Bratsev, N. G. Serebryakov, *Med. Radiol. (Mosk.)* 26 (1981) 62.
Chem. Abstr. 95 (1981) 108411.
188. R. Kieffer, F. Benesovsky: *Hartstoffe*, Springer Verlag, Wien-New York 1963.
189. R. A. Murgatroyd, B. T. Kelly, *At. Energy Rev.* 15 (1977) 3-74.
190. V. I. Matkovich: *Boron and Refractory Borides*, Springer Verlag, Berlin-Heidelberg-New York 1977.
191. K. A. Schwetz, K. Reinmuth, A. Lipp, *Radex Rundsch.* 1981, no. 3, 568-585.
192. K. Reinmuth, A. Lipp, H. Knoch, K. A. Schwetz, "Borhaltige, keramische Neutronenabsorberwerkstoffe", *J. Nucl. Mater.* 124 (1984) 175-184.
193. K. A. Schwetz, A. Lipp, *ATW Atomwirtsch. Atomtech.* 18 (1973) 531.
194. H. Moissan: *Der elektrische Ofen*, Verlag M. Kroyer, Berlin 1900.
195. J. L. Hoard, R. E. Hughes in E. L. Muetterties (ed.): *The Chemistry of Boron and Its Compounds*, J. Wiley & Sons, New York 1967, pp. 22-154.
196. T. Lundström, *Ark. Kemi* 31 (1969) 227-266.
197. H. Nowotny in L. E. J. Roberts (ed.): *Solid State Chemistry*, vol. 10, Butterworths, London 1972, pp. 151-183.
198. E. Rudy, *Tech. Rep. AFML-TR 652*, Part V. Compendium of Phase Diagram Data (1969).
199. K. E. Spear: *Phase Diagrams*, vol. IV, Materials Science and Technology, Academic Press, New York 1976, pp. 91-159.
200. G. V. Samsonov, T. I. Serebryakova, V. A. Neronov, *Boridy (Borides)*, Atomizdat Publ., Moscow 1975.
201. R. Thompson in J. Brotherton, H. Steinberg (eds.): *Progress in Boron Chemistry*, vol. 2, Pergamon Press, Oxford 1971, pp. 173-230.
202. F. Binder, *Radex Rundsch.* 1975, no. 4, 531-557; 1977, no. 1, 52-71.
203. H. Pastor, F. Thevenot, *Inf. Chim.* 178 (1978) 151-173.
204. R. Kiesel, *Acta Chem. Scand.* 4 (1950) 209.
205. K. A. Schwetz, Thesis, Technical University, Vienna 1971.
206. F. Thevenot, J. Cueileroq, *Analisis* 5 (1977) 105-121.
207. PPG, DE-OS 2523423, 1975.
208. PPG, DE-OS 2818418, 1978 (R. R. May, Jr.).
209. H. Pastor in [190], pp. 457-493.
210. ESK GmbH, DE-OS 3301841, 1984.
211. E. Fitzer, *Arch. Eisenhüttenwes.* 44 (1973) no. 9, 703-709.
212. R. D. Holliday, R. Mogstad, J. L. Henry, *Electrochem. Technol.* 1 (1963) 183-190.
213. S. K. Dutta, G. E. Gazza, *Bull. Am. Ceram. Soc.* 52 (1973) 552-554.
214. F. Rigby: "Development of Hot Pressing Techniques at Springfield Nuclear Laboratories", *Spec. Ceram.* 7 (1981) 249-258.
215. K. Hunold, *CFI Ceram. Forum Int.* 60 (1983) 182-189.
216. W. Grellner, K. A. Schwetz, A. Lipp, *Radex Rundsch.* 1983, no. 1/2, 146-151.
217. Aluminum Corporation of America, US 4071420, 1978.
218. C. E. Ransley, *J. Met.* 14 (1963) 129.
219. ESK GmbH, DE 2240655, 1972.
220. K. S. S. Murthy, *Br. Foundryman* 67 (1974) 335.
221. ESK GmbH, US 4118256, 1976.
222. K. G. Schmitt-Thomas, H. Meisel, S. Mirdamadi-Therani, *Metall (Berlin)* 32 (1978) 1103.
223. O. Knotek, E. Lugscheider, H. Eschnauer: *Hartlegierungen zum Verschleißschutz*, Verlag Stahleisen, Düsseldorf 1975.
224. G. V. Samsonov, Yu. B. Paderno, V. S. Fomenko, *Sov. Powder Metall. Met. Ceram. (Engl. Transl.)* 6 (1963) 24.
225. M. Futamoto, M. Nakazawa, U. Kawabe, *Surf. Sci.* 100 (1980) 470-480.
226. F. Dachille, R. Roy, *J. Am. Ceram. Soc.* 42 (1959) 78.
J. D. Mackenzie, W. F. Claussen, *J. Am. Ceram. Soc.* 44 (1961) 79.
227. D. White, D. E. Mann, P. N. Walsh, A. Sommer, *J. Chem. Phys.* 32 (1960) 481, 488.
H. J. Emeleus, A. G. Sharpe: *Advances in Inorganic Chemistry and Radiochemistry*, vol. 5, Academic Press, New York 1963.
228. P. Wulff, S. K. Majumdar, *Z. Phys. Chem.* B31 (1936) 319.
229. H. Menzel, H. Schultz, *Z. Anorg. Chem.* 245 (1940) 157.
230. A. Cousen, W. E. S. Turner, *J. Chem. Soc.* 1928, 2654.
231. E. J. Prosen, W. H. Johnson, F. Y. Pergiel, *J. Res. Nat. Bur. Stand.* 62 (1959) 43.
Chem. Abstr. 53 (1959) 15746.
232. W. F. Claussen, J. D. Mackenzie, *J. Am. Chem. Soc.* 81 (1959) 1007.
233. S. T. Benson, G. S. Parks, *J. Phys. Chem.* 35 (1931) 2091.
234. A. Buechler, J. B. Berkovitz-Mattuk, *J. Chem. Phys.* 39 (1963) 286.
235. D. L. Hildebrand, W. F. Hall, N. D. Potter, *J. Chem. Phys.* 39 (1963) 296.
236. K. Yu. Kazema, A. K. Lindpere, L. A. Luts, *Tr. Inst. Fiz. Astron., Akad. Nauk Est. SSR* 7 (1958) 34.
Chem. Abstr. 54 (1960) 19188.
237. F. T. Greene, J. L. Margrane, *J. Phys. Chem.* 70 (1966) 2112.
238. J. Dulat in [12], Section A4, p. 186.
239. J. C. Southard, *J. Am. Chem. Soc.* 63 (1941) 3147.
240. H. T. Schlesinger, H. C. Brown, A. E. Finhold, *J. Am. Chem. Soc.* 75 (1953) 205.
241. R. Flowers, R. J. Gillespie, J. V. Oubridge, *J. Chem. Soc.* 1956, 1925.
242. Olin Mathieson Chemical Corp., US 2867502, 1959 (H. Stange, S. L. Clark).
243. F. C. Kracek, G. W. Morey, H. E. Merwin, *Am. J. Sci.* 35A (1938) 143.
244. G. G. Manov, N. J. DeLollis, S. F. Acrea, *J. Res. Nat. Bur. Stand.* 33 (1944) 287.
Chem. Abstr. 39 (1945) 1348.
245. D. White, D. E. Mann, P. N. Walsh, A. Sommer, *J. Chem. Phys.* 32 (1960) 488.
D. J. Meschi, W. A. Chupka, J. Berkowitz, *J. Chem. Phys.* 33 (1960) 530.

50 Lithium

RICHARD BAUER, ULRICH WIETELMANN

50.1 Introduction	2029	50.5.2 Ore Digestion and Production of Lithium Compounds	2036
50.2 History	2029	50.5.2.1 Acid Digestion	2037
50.3 Properties	2030	50.5.2.2 Alkali Digestion	2038
50.3.1 Physical Properties	2030	50.5.2.3 Ion-Exchange Processes	2039
50.3.2 Chemical Properties	2031	50.5.3 Production of Lithium Carbonate from Brines	2040
50.4 Occurrence	2032	50.6 Lithium Metal and Lithium Alloys	2041
50.4.1 Minerals	2032	50.6.1 Production of Metal	2041
50.4.1.1 Lithium Aluminum Silicates	2032	50.6.2 Uses	2042
50.4.1.2 Micaceous	2033	50.6.3 Alloys	2043
50.4.1.3 Lithium Phosphates	2033	50.7 Compounds	2044
50.4.1.4 Other Minerals	2034	50.8 Quality Specifications and Analysis	2048
50.4.2 Reserves	2034	50.9 Toxicology and Occupational Health	2049
50.4.3 Lithium in Natural Brines	2035	50.10 Economic Aspects	2049
50.5 Production of Primary Lithium Compounds	2036	50.11 References	2049
50.5.1 Mining of Ore and Production of Concentrate	2036		

50.1 Introduction

Lithium (from the Greek word for stone, λίθος), A_r 6.941, is the lightest element that is solid at normal temperature. Its natural isotopes ^6Li , A_r 6.015, natural abundance 7.42% and ^7Li , A_r 7.016, natural abundance 92.58%, are not radioactive. The artificial isotopes ^5Li , ^8Li , and ^9Li have half-lives of 10^{-21} , 0.855, and 0.17 s, respectively. The electronic configuration of the free atom is $1s^2 2s^1$. The atomic radius is 0.155 nm (in the metal), and the ionic radius is 0.086 nm [1].

Lithium is a member of group 1 of the periodic table and thus has a valence of 1+. In many respects (e.g., the strong alkalinity of lithium hydroxide solutions and the reactivity of the metal) it has the character of an alkali metal, but it also exemplifies the diagonal relationship in the periodic table in its resemblance to magnesium: the metal forms only the oxide on combustion (not the peroxide), and with nitrogen it forms the nitride directly. Lithium carbonate, fluoride, and phosphate are very slightly water soluble. In contrast to

sodium chloride, lithium chloride is soluble in polar organic solvents such as methanol.

50.2 History

The lithium minerals petalite and spodumene were discovered between 1790 and 1800 by JOSÉ DE ANDRADA in an iron ore deposit on the Swedish island of Utö. In 1817 AUGUST ARFVEDSON discovered the element lithium in this petalite deposit after finding discrepancies in his analytical values. BERZELIUS named the element lithion to indicate its occurrence in a stone. In 1818 DAVY and BRANDÉ first prepared lithium metal in extremely small amounts by electrolysis of lithium oxide with a voltaic pile. At about the same time, GMELIN discovered the red flame coloration produced by lithium salts. In 1825 BERZELIUS determined the lithium content of various mineral sources. The first preparation of the metal in gram quantities was achieved in 1854 by BUNSEN and MATTHIESSEN by electrolysis of molten lithium chloride.

For a long time, lithium and its compounds were of only minor interest (e.g., in pharmaceutical applications and as additives to glazes). Only after World War I did an appreciable demand for lithium develop, owing to its use in lithium-containing (0.04%) lead-based alloys (Bahnmittel) for bearings. This was the reason for the first industrial production of lithium carbonate and lithium metal in 1923 based on the mineral zinnwaldite by the Hans-Heinrich works of the Metallgesellschaft in Langelsheim, Germany. The availability of lithium carbonate in tonnage quantities made its industrial use possible, at first mainly in the ceramic industry. In 1929, the Maywood Chemical Works in the United States began production of lithium metal and lithium compounds based on German know-how. Lithium production in the United States increased substantially during World War II due to the use of lithium hydride as a convenient source of hydrogen, especially for small balloons carrying transmitter aeriels for emergency use by ships and aircraft in distress and by lifeboats. This has been followed in the last 50 years by increasing use of lithium-based soaps in multipurpose lubricating greases for automotive and industrial use. A further upsurge in demand came from the nuclear industry: the isotope ^6Li yields tritium when subjected to a neutron flux.

The world market for lithium and lithium compounds is now supplied mainly from production facilities in the United States, from the Salar de Atacama in Chile (Cyprus Foote Mineral, formerly Foote Mineral, Lithium Corporation of America), and from production by Chemetall GmbH (a subsidiary of Metallgesellschaft), Frankfurt/Main in Europe. In addition, China and the former Soviet Union export some lithium carbonate and hydroxide and, to a lesser extent, lithium chloride and lithium metal. The small production facilities in Japan are for domestic use only. Between 1960 and 1964, lithium carbonate was produced by Québec Lithium in Canada. Other minor producers of lithium carbonate and hydroxide, e.g., Maywood Chemical Works, Montecatini in Italy, Rhône-Poulenc in

France, and Associated Lead Manufacturers in the United Kingdom, have all since ceased production for economic or technical reasons.

50.3 Properties

50.3.1 Physical Properties

Lithium, a silvery white metal, is the least dense of all known solids at room temperature, m_p 180.54 °C, heat of fusion 431.4 J/g, b_p 1342 °C. It has a very low Mohs hardness of 0.6 and is therefore very easy to form.

The density at 20 °C is 0.534 g/cm³, and the density of the liquid between 200 and 1600 °C is given very accurately by the equation [2]

$$\rho = 0.515 - 1.01 \times 10^{-4} (t - 200)$$

The vapor pressure at the melting point is calculated to be 1.88×10^{-6} Pa. Between 800 and 1400 °C, it is given by the relationship [2]

$$\log p = 10.4038 - 8283.1/T - 0.7081 \log T$$

The heat of vaporization is 22 705 J/g. The dynamic viscosity at 180.5 °C is 0.599×10^{-3} Pa·s; between this temperature and 1000 °C, it follows the equation [2]

$$\log \eta = -1.5064 - 0.7368 \log T + 109.95/T$$

The surface tension σ at the melting point is 398 mN/m and, between 500 and 1600 °C, is given by [2]

$$\sigma = 0.16(3550 - T) - 95$$

The mean linear coefficient of thermal expansion α_m between 273 and 368 K is 56×10^{-6} K⁻¹, and the mean coefficient of cubical expansion β_m between 291 and 453 K is 180×10^{-6} K⁻¹. Lithium melts with a volume change of +1.5%. The volume of the molten metal between 185 and 235 °C is given by [3]

$$V_T = V_{298} [1 + 174.106 \times 10^{-6} (T - 453)]$$

The specific heat c_p of lithium metal between 20 and 180 °C is 3.3–4.2 J/g. For the molten metal at 450 °C, a value of 4.2 Jg⁻¹K⁻¹ is quoted. Between the melting point and 421.8 °C, the following equation is valid:

$$c_p = 1.083 - 2.00 \times 10^{-4} t$$

and from 421.8 to 895.3 °C:

$$c_p = 1.006 - 1.73 \times 10^{-4} t$$

The critical data are as follows: $T_c = 3223 \pm 600$ K; $p_c = 68.9$ MPa; $V_c = 66 \pm 19$ mL/mol; and $\rho_c = 0.120 \pm 0.033$ g/cm³.

The thermal conductivity, in Js⁻¹m⁻¹K⁻¹, between 250 and 950 °C is given by

$$\lambda = 42.3 + 12.3 \times 10^{-4} t$$

The enthalpy, in J/g, between 500 and 1300 °C is given by [2]

$$\Delta H = -21.248 + 4.1902 \times 10^{-4} t - 21.658/t$$

The ionization energy is 5.37 eV, and the electrode potential of the half cell ($\text{Li} \rightleftharpoons \text{Li}^+ + e^-$) is 3.024 V.

Values in the range 0.23–0.31 nm have been quoted for the radius of the hydrated ion [4].

Metallic lithium has good electrical conductivity. The resistivity at 0 °C is 8.55 $\mu\Omega\text{cm}$, and between 200 and 1000 °C it is given by

$$R = 18.33 + 3.339 \times 10^{-2} t - 6.795 \times 10^{-4} t^2$$

The electrical resistance increases with increasing density under pressure [3].

Between -180 °C and the melting point, lithium crystallizes in a body-centered cubic system ($a = 0.35$ nm at 20 °C). At ca. -190 °C, an allotropic transformation of α -lithium into a hexagonal modification with densest close packing occurs.

Very thin lithium films are reddish brown by transmitted light, a color similar to that observed with colloidal dispersions of lithium in inert liquids. Pure lithium vapor emits a red light. The arc spectrum of lithium between 607.82 and 230.22 nm exhibits more than 42 lines, the strongest of which is the red line at 670.8 nm; the orange line at 610.3 nm is also excited in a Bunsen flame. The red spectral line at 670.8 nm can be used to detect lithium chloride in amounts as low as 1.26×10^{-6} mg.

50.3.2 Chemical Properties

Lithium metal is very reactive, though considerably less so than other alkali metals. The presence of sodium as an impurity, even in amounts of 0.5–1%, increases its reactivity,

e.g., for the formation of lithium alkyls from lithium metal and organic halides.

A freshly cut surface of lithium metal has a silvery luster. At room temperature in dry air with a relative humidity of less than 1%, the surface remains shiny for several days, although a very thin passive surface layer is formed that is hardly visible to the naked eye and consists mainly of lithium carbonate and oxygen-containing compounds [5]. Lithium metal can therefore be processed in dry air. However, in moist air a dull gray coating, consisting mainly of lithium nitride, lithium oxide, and lithium hydroxide, forms within a few seconds. If lithium ingots are allowed to remain in contact with air for some weeks, the reaction with atmospheric nitrogen extends into the interior of the metal with the formation of reddish brown lithium nitride and can lead to ignition. Even at room temperature dry nitrogen reacts slowly with lithium metal.

Protective gases for lithium metal include the noble gases, dry carbon dioxide, or pure sulfur hexafluoride up to 225 °C. Mineral oil is also suitable as a protective medium.

Lithium burns with a very luminous white flame, forming a dense white smoke consisting mainly of lithium oxide; the flame temperature is almost 1100 °C.

Burning lithium metal reacts with silicates (e.g., sand and concrete) and carbon dioxide. These substances are therefore unsuitable as fire-fighting agents, as is sodium hydrogen carbonate. Powdered limestone (calcium carbonate) and fire-extinguishing powders based on sodium chloride are suitable for fighting lithium fires. Another suitable material is Graphex (from the company CECA), a graphite-sulfate complex whose volume increases many times at high temperature, thereby effectively smothering the burning lithium.

Lithium reacts with water with formation of hydrogen, which ignites under normal conditions only if the metal is finely divided. Molten lithium reacts explosively with water. Lithium reacts with hydrogen to form lithium hydride. This reaction is carried out on an industrial scale at 600–1000 °C. Lithium reacts with gaseous ammonia at elevated tempera-

ture to form lithium amide. The vigorous reaction with halogens produces incandescence. Organic compounds containing active hydrogen or halogen usually react with lithium to form the corresponding organolithium derivative.

Lithium also reacts with boron, silicon, phosphorus, arsenic, antimony, and sulfur upon heating.

A suitable container material for molten lithium metal is low-carbon steel, which has good resistance up to ca. 700 °C. Because lithium reacts with carbides, carbon-steel vessels in contact with liquid lithium are destroyed by decarburization. Up to 1000 °C, niobium, tantalum, or molybdenum can be used; nickel is satisfactory up to 225 °C. Aluminum, calcium, magnesium, silver, platinum, and gold are attacked by molten lithium.

Lithium metal dissolves readily in liquid ammonia, the concentration of the saturated solution at -33.2 °C being 9.8%. A saturated solution of lithium in ammonia has a density of 0.477 g/cm³ at 19 °C, and is thus the lightest known liquid at this temperature. The concentrated solution has a bronze color, whereas dilute solutions show the blue color typical of alkali metals. Solutions of lithium in ammonia are used to produce lithium acetylide and for Birch reductions in organic chemistry.

50.4 Occurrence

Lithium is present in the earth's crust to the extent of ca. 0.006%; it is the 27th most abundant element. Approximately 150 lithium minerals are known. Lithium enrichment in minerals took place in geological time by the fractional crystallization of molten magma. Lithium migrated to the low-viscosity molten phase which eventually solidified as pegmatite. Sometimes lithium ore deposits are also formed in the pneumatolytic phase, as shown by the frequent association of lithium minerals with pneumatolytically formed cassiterite. Typical examples of this are provided by the spodumene deposit at Manono in Zaire and at Kamativi in Zimbabwe. The lithium found in

mineral water sources in magmatic zones was probably formed in a similar manner.

The four most important lithium minerals are amblygonite, spodumene, petalite, and lepidolite. Of these, spodumene and petalite are used directly in the form of ores or concentrates, especially in the glass industry, whereas spodumene concentrate is used in the production of lithium carbonate.

Natural brines with a high lithium chloride content, which are the end result of a natural leaching and evaporation process, are also important in the industrial production of lithium. Given the technology currently available, seawater, which has a lithium content of only ca. 0.17 ppm, cannot be regarded as a viable raw material for economic lithium production.

50.4.1 Minerals

Analytical data for the commercially important lithium minerals are given in Table 50.1.

Table 50.1: Typical analyses of lithium minerals, %.

	Amblygonite	Spodumene concentrate	Spodumene glass-grade	Petalite	Lepidolite
Li ₂ O	min. 7	min. 7	min. 4.8	min. 4	min. 3.5
K ₂ O	ca. 0.2	ca. 0.7	0.12	ca. 0.2	8-12
Na ₂ O	0.4-1.1	0.5-0.8	0.09	0.4-1.4	0.3-1.1
Al ₂ O ₃	34-37	26-29	17-18	16-18	20-28
SiO ₂	ca. 2.5	60-65	74-80	74-78	49-55
F	ca. 3.5	ca. 0.2	max. 0.1	ca. 0.1	4-6
Fe ₂ O ₃	ca. 0.2	0.5-2	0.1-0.2	0.03-0.2	0.1-2
P ₂ O ₅	44.5-50	ca. 0.5	max. 0.1	ca. 0.3	ca. 0.5
CaO	ca. 1	0.1qP0.5	ca. 0.06	ca. 0.4	ca. 0.4
MgO	ca. 0.1	0.1-1	ca. 0.05	0.2-0.4	ca. 0.2

50.4.1.1 Lithium Aluminum Silicates

Spodumene (triphanes), LiAlSi₂O₆, has a theoretical Li₂O content of 8.03%, but usually contains 6-7.5% because of partial replacement of Li⁺ by Na⁺ and K⁺. Spodumene has a monoclinic pyroxene structure consisting of -SiO₃- chains linked together by aluminum ions, with the balance of the positive charge provided by lithium ions. Spodumene sometimes occurs in the form of large single crystals.

tals. Its color varies from white to gray-green to reddish. Very pure and transparent single crystals are regarded as semiprecious stones (kunzite). The high hardness value of spodumene (6.5-7 on the Mohs scale) leads to considerable abrasive effects when the material is worked. At ca. 1000 °C, naturally occurring α-spodumene undergoes an irreversible phase change to β-spodumene, whereby the volume increases greatly and the density decreases from 3.2 to ca. 2.4 g/cm³. Spodumene ores consist of pure spodumene combined with quartz or feldspar; the Li₂O content ranges from less than 1% to more than 5%.

Petalite, LiAlSi₄O₁₀, has a theoretical Li₂O content of 4.9% but usually contains only 3.5-4.5%. It crystallizes in the form of monoclinic prisms and is white, gray, or reddish in color. It has a density of 2.4 g/cm³ and a Mohs hardness of 6.5. Petalite decomposes at 1100 °C into β-spodumene and SiO₂. This transformation (and that of α-spodumene) is important in digestion of the ore.

Eucryptite, LiAlSiO₄, is a relatively rare lithium mineral that occurs mainly in combination with petalite, e.g., in Bikita, Zimbabwe. It has the highest Li₂O content (11.1%) of the lithium aluminum silicates.

The three minerals are distinguished by their SiO₂ content:

Eucryptite: Li₂O·Al₂O₃·2SiO₂

Spodumene: Li₂O·Al₂O₃·4SiO₂

Petalite: Li₂O·Al₂O₃·8SiO₂

Thus, thermal transformation of petalite into β-spodumene and quartz can be regarded as a decomposition reaction.

50.4.1.2 Micas

The mica minerals form a subgroup of the aluminosilicates. They are sometimes formed by direct crystallization from molten magma but often owe their origin to pneumatolytic decomposition.

Lepidolite, K[Li, Al]₃[Al, Si]₄O₁₀[F, OH]₂, lithium mica, is the most important representative of this group. Depending on its origin

and the weathering it has undergone, lepidolite can contain between 3.3 and 7.74% Li₂O. Economic deposits contain 3-4% Li₂O. The mineral is often pink to grayish violet and frequently contains 3-5% rubidium and cesium oxides.

Zinnwaldite, which has the general formula K[Li, Al, Fe]₃[Al, Si]₄O₁₀[F, OH]₂, can be regarded as a variety of lepidolite with a high iron content. The Li₂O content varies with the actual composition of the mineral. The deposit in Zinnwald (Erzgebirge) contains 2-3% Li₂O. Zinnwaldite is silvery to grayish brown, sometimes also tinged with red. The emerald green variety known as cryophyllite, found in Massachusetts, contains up to 5% Li₂O.

50.4.1.3 Lithium Phosphates

Commercial amblygonite is a complex phosphate with the general formula (Li, Na) Al(F, OH)PO₄. Its principal constituents are pure amblygonite, LiAlFPO₄, with a theoretical Li₂O content of 10.1%, and its hydroxyl substitution product, montebrasite, LiAl(OH)PO₄, with 10.3% Li₂O. Amblygonite is milky white to gray in color, sometimes also with a brown or green tinge; it may have a sheen resembling a solidified stream of molten glass or a pearly luster. Deposits suitable for mining have an Li₂O content of 7-9%, the highest of the commercially exploited lithium ores. However, amblygonite is never found in large accumulations but is widely distributed in small, usually lenticular deposits, often associated with other lithium minerals. Although amblygonite once was an important source of lithium, it is no longer regarded as a suitable source of raw material for today's large-scale lithium carbonate production plants.

Triphylite, LiFePO₄, and lithiophilite, LiMnPO₄, have a theoretical Li₂O content of 9.5%. The known deposits yield a raw material with 8-9% Li₂O; however, they have not been commercially exploited because of their small size.

50.4.1.4 Other Minerals

Lithiophorite, $[\text{Li, Al}]\text{MnO}_2(\text{OH})_2$, is often found in veins of manganese ore.

Hectorite, which has the approximate composition $\text{LiNaMg}_2(\text{Si}_4\text{O}_{10})_3[\text{F, OH}]_6$ and contains ca. 1.2% Li_2O , is the only lithium mineral that occurs in sedimentary rock and clay; it is classified in the montmorillonite group.

The unusual mineral zhabuyelite [6] was discovered recently in salt deposits in the Zha Buye lake in Tibet. It consists of colorless, transparent, monoclinic crystals of almost pure lithium carbonate.

50.4.2 Reserves [7, 8]

The only mineral used as a raw material for the production of lithium compounds at present is spodumene, the largest known deposits of which are at Manono in Zaire. Reserves have been estimated to be over 2×10^6 t of lithium [9, 10]. New investigations by Lithium Australia into their own pegmatite deposits in Greenbushes (Western Australia) [11] have revealed reserves with 7×10^5 t of lithium, of which ca. 10% is in the form of spodumene with more than 4% Li_2O , ca. 50% with more than 2.5% Li_2O , and ca. 40% with ca. 1.5% Li_2O .

The U.S. producers Cyprus Foote Mineral and Lithium Corporation of America base their operations on deposits in the "tin-spodumene belt" of North Carolina, which may contain as much as 2.8×10^6 t of lithium [9, 10].

The Canadian deposits at La Corne, which provided raw material for Québec Lithium, are estimated to contain 10^5 t of recoverable lithium, with potential reserves of about twice this amount. Deposits belonging to Tantalum Mining Co. at Bernic Lake amount to ca. 60×10^3 t. The total known reserves in Canada are quoted as 6×10^5 t of lithium [12].

The deposits at Bikita in Zimbabwe consist mainly of petalite and lepidolite with some spodumene and eukryptite. They contain between 7.5×10^4 and 10^5 t of lithium. Russia has deposits of spodumene and lepidolite at Krivoj Rog and in Chita in Transbaikalia. Other lithium minerals occur in the Altai mountains and on the Kola peninsula. No details are available concerning the extent of these reserves.

In northwest China, considerable reserves of spodumene containing ca. 1.5% Li_2O have been reported in the southern slopes of the Altai mountains in the Koktohay-Aletai region. This provides raw material for lithium carbonate and hydroxide production in Urumchi. No details are available.

In addition to the principal reserves described above, a number of smaller ones exist in the United States, Canada, Australia, Zimbabwe, and China. Lithium minerals have also been found in Afghanistan, Argentina, Brazil, India, Madagascar, Mali, Mozambique, Namibia, and South Africa [13, 14].

The reserves in Europe are all of minor importance and so far have not proved worth mining. This is also true for the spodumene deposit that has recently been investigated in the Koralpe of Austria [15]. This contains 5×10^6 t of ore with an average of 1.7% Li_2O . Spodumene has also been found in Lalin and near Cáceres in Spain, Dublin in Ireland, and Tammela in Finland. Lepidolite deposits exist in France (Massif Central), Portugal, the island of Elba, Sweden, and central Finland. Petalite also occurs on Elba and at Utö in Sweden.

The confirmed lithium reserves based on pegmatite in the Western world are estimated at 3×10^6 t of lithium if recent figures from Greenbushes are included [16]; potential reserves amount to an additional 4×10^6 t [9].

Lithium ores are used directly or as flotation concentrate (sometimes mixed with other materials), e.g., in the glass industry or as slag formers in the foundry industry.

Table 50.2: Typical analyses of brines, %.

	Li^+	Na^+	K^+	Mg^{2+}	Ca^{2+}	SO_4^{2-}	Cl^-	Br^-
Clayton Valley (Nevada)	0.02	7.5	1.0	0.03	0.05	0.75	11.7	
Salar de Atacama (Chile)	0.15	7.6	1.8	0.96	0.03	1.78	16.00	trace
Salar de Uyuni (Bolivia)	0.024	9.42	0.51	0.44	0.05	0.72	15.91	trace
Salar del Hombre Muerto (Argentina)	0.06	9.8	0.6	0.09	0.05	0.82	15.9	trace
Salar del Rincón (Argentina)	0.05	10.8	0.7	0.4	0.12	0.7	16.7	trace
Zha Buye Lake (Tibet)	0.12	14.17	3.96	0.001	trace	4.35	15.63	0.6
Dachaidan, Qinghai (China)	0.02	10.6	0.4	1.3	0.04	2.25	18.7	7.0
Dead Sea (Israel/Jordan)	0.002	3.0	0.6	4.0	0.3	0.05	16.0	0.4
Great Salt Lake (Utah)	0.004	7.0	0.4	0.8	0.03	1.5	14.0	
Bonneville (Utah)	0.007	9.4	0.6	0.4	0.12	0.5	16.0	
Seawater	0.000017	1.8	0.038	0.013	0.04	0.027	1.94	0.0004

50.4.3 Lithium in Natural Brines

Recently, lithium-containing brines have become important raw materials. Their industrial exploitation began at Searle's Lake, California, in 1938 by Kerr-McGee Chemical, and in Clayton Valley, Nevada in 1966 by Foote Mineral (now Cyprus Foote Mineral).

In 1984, production of lithium carbonate from the brines of the Salar de Atacama in Chile was started by the Sociedad chilena de litio Ltda (SCL), now a 100% affiliate of Cyprus Foote Mineral [17]. At the same Salar also, Minsal S.A., a subsidiary of the Chilean mining company Sociedad química y minera de Chile S.A. (SQM Soquimich) started its commercial lithium carbonate production based on brines.

In Argentina, at the Salar de hombre muerto, FMC Corp. is in the process of building a brine-based lithium extraction plant. This project is set for a start-up in 1997.

Because of the extremely high solubility of lithium chloride in water, the basic concentration process for lithium-containing brines is natural evaporation such as occurs only in dry regions of the earth in particular geological formations [18]. The evaporation process leads first to increased lithium content in salt lakes, such as the Dead Sea or the Great Salt Lake. Further enrichment of lithium then takes place if the surface of the lake is completely dried out as in Searle's Lake and Clayton Valley. This enrichment also occurs in the last brines to be formed, which are enclosed in cavities. The surrounding salts can be practi-

cally lithium free or can contain up to 1500 ppm of lithium.

Important reserves of lithium-containing brines are found in western North and South America and in western China (Tibet and Qinghai Province) [6, 19, 20]. Their lithium contents vary greatly (Table 50.2).

The reserves of lithium in these brines are sometimes considerable. It is estimated that the Salar de Atacama in Chile contains more than 1.1×10^6 t of lithium, Clayton Valley 7×10^5 t of lithium, and the Great Salt Lake 4.5×10^5 t of lithium. The quantities of lithium that can be recovered economically from these reserves are, however, much smaller. For the Clayton Valley they are estimated to be 4×10^4 t of lithium and for the Great Salt Lake, with coproduction of other salts, 2.6×10^5 t [9]. On the other hand, the amount of recoverable lithium from the Salar de Atacama, because of the higher concentration, is considerably larger (up to 8×10^5 t). A study by Amax Exploration of the recovery of 15×10^3 t/a of lithium carbonate as a coproduct with potassium chloride, potassium sulfate, and boric acid has been completed [21].

Not only is the lithium yield from brines reduced due to dilution caused by replacement of the withdrawn brine by fresh water, lithium is also lost through inclusion in salt crystals that form upon evaporation and in the sludge produced when magnesium is precipitated with lime.

The verified reserves of lithium from salt lakes are estimated to be 1.8×10^6 t, and the potential reserves 18×10^6 t.

The recovery of lithium from material of low lithium content is also interesting, because of the importance of lithium to nuclear technology. An example is the proposed extraction from the Dead Sea by precipitation as lithium aluminate, $\text{LiH}(\text{AlO}_2)_2 \cdot 5\text{H}_2\text{O}$ [22]. Also under investigation is the recovery of lithium from seawater [23] which, although it contains only 0.17 ppm of lithium (Table 50.4), represents a total lithium reserve of 2.5×10^{11} t.

Another potential source of lithium is provided by subsurface brines associated with mineral oil. The brine lies beneath the oil layer and is often recovered at the same time as the oil. In Texas, the brines contain up to 692 mg of lithium per liter, but only rarely does the lithium content exceed 100 mg/L [24]. However, the high magnesium content presents a serious technical problem. For example, in the Smack-over brines in Arkansas the magnesium concentration is 20 times that of lithium. Given the other lithium resources available, industrial exploitation of the lithium in these brines does not appear to be considered anywhere at present.

50.5 Production of Primary Lithium Compounds

50.5.1 Mining of Ore and Production of Concentrate

Lithium ores are recovered by quarrying or open-cut mining according to their location. Because the veins of ore are often only a few meters thick, the mining operation has to follow the veins, or open-pit mining must be used, which involves the removal of relatively large volumes of overburden. The ratio of overburden to ore is usually 3:1–5:1. An important exception is the Greenbushes deposit in Australia, which has veins of ore up to 250 m thick.

If the lithium minerals are largely separated from the accompanying rock, preliminary sorting can be carried out by hand on a conveyor belt. In this way, it is possible to pro-

duce spodumene containing 4–5.5% Li_2O from raw material containing 1–1.5% Li_2O . A mechanical separation process, based on the difference in reflective properties between ore and gangue material, can also be used. This can give good results if the material is first suitably reduced in size.

The concentration of lithium ores by heavy-medium separation always entails large losses of lithium and has therefore not been used commercially.

A flotation process is employed on an industrial scale especially for spodumene [25]. The material is first ground to a grain size of less than 0.3 mm by using rod mills. Material finer than 0.075 mm is then removed (e.g., by hydrocyclone) because it would result in lower recoveries in the flotation process. Flotation agents such as anionic fatty acids in alkaline medium and sulfonated oils in acid medium are recommended. The use of cationic surfactants in hydrofluoric acid solution has also been proposed. The flotation process is carried out in a series of stages. Quartz, feldspar, and mica are concentrated in the foam and spodumene is floated off. The spodumene concentrate contains 5.5–7.5% Li_2O . It can be sieved into fractions with different lithium contents; the coarser fractions have the higher lithium contents. The yield of lithium from the raw mineral after concentration by flotation is 60–80% depending on the milling conditions used.

50.5.2 Ore Digestion and Production of Lithium Compounds

The digestion of lithium ore can be carried out with acid or alkali, or by an ion-exchange process using salts. Various processes are reviewed in [26]. Depending on the process and the digestion agent, the product obtained is lithium carbonate, lithium hydroxide, or lithium chloride.

Although amblygonite, triphylite, and lepidolite can be treated directly with the appropriate digestion agent, spodumene and petalite require pretreatment (decrepitation) to convert α -spodumene to β -spodumene, and petalite to

β -spodumene and quartz. Decreptionation is carried out in rotary kilns at 1000–1100 °C. It results in a 30% increase in the mineral's volume and a considerable improvement in its grindability.

50.5.2.1 Acid Digestion

The sulfuric acid digestion process can be used for all lithium ores. It is usually carried out at 250–400 °C, although 850–900 °C is recommended for amblygonite because this leads to the formation of insoluble aluminum phosphate which facilitates removal of the insoluble residue.

Sulfuric acid digestion gives a product that contains an insoluble residue, together with lithium sulfate which is leached from the crushed product with hot water. To remove alkaline-earth metals, aluminum, and iron, the solution is neutralized with lime and soda and then filtered. Lithium carbonate is precipitated by adding concentrated sodium carbonate solution. This is carried out near the boiling point, to take advantage of the decreasing solubility of lithium carbonate at higher temperature.

The sulfuric acid process gives good yields of lithium (ca. 90%) and has a relatively favorable energy balance compared with other processes for the production of lithium compounds from ores. Digestion by hydrochloric acid or hydrogen chloride gas at 935 °C has been suggested for the production (by sublimation) of lithium chloride from lepidolite. This process has, however, little significance compared to the sulfuric acid process.

The production of lithium carbonate from spodumene (petalite) by using sulfuric acid is described in detail in [25]. The flow sheet for the process is shown in Figure 50.1. The ore is first crushed to a particle size of 20–80 mm. Alternatively, flotation concentrate, which is already finely divided, is used. The crushed ore is fed into an oil-, coal-, or gas-fired rotary decrepitation kiln, which attains the required temperature (1050–1100 °C) over at least 10 m of its length. The spodumene takes ca. 4 h to pass through the rotary kiln, the dwell time in

the decrepitation zone being 15–30 min, which results in practically complete transformation into β -spodumene.

The heat efficiency is improved by using a countercurrent flow of material and hot gas. The exhaust gases are used to preheat the ore, to heat the roasting furnace, and to concentrate the liquors by evaporation. The spodumene is quite hot as it leaves the rotary kiln, and sometimes a rotary cooler, which can also be used to preheat the combustion air, is necessary.

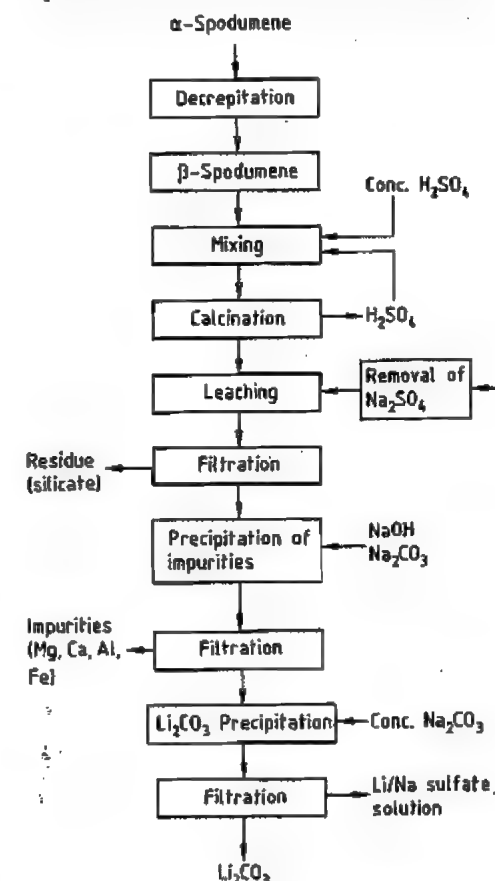


Figure 50.1: Flow sheet for lithium carbonate production from spodumene.

If the starting material is in lump form, the β -spodumene produced by decrepitation is crushed to a grain size of less than 0.1 mm. Sulfuric acid (93%, in 35% excess) is then added either by a mixer conveyor or by spray-

ing onto a band conveyor fitted with a deflector plate. The digestion process, in which lithium in the ore is converted into soluble lithium sulfate, is carried out at ca. 250 °C in a lined rotary furnace or on a conveyor heated by exhaust gases, which carries the spodumene through a tunnel directly to the leaching stage. Digestion is usually complete in less than 1 h.

The lithium sulfate formed is leached out of the reaction product with hot water in Pachuca tanks agitated by compressed air or in stirred vessels. A continuous leaching process, in which the material and the water move countercurrently through several stirred vessels in series, has proved advantageous. After leaching, aluminum silicate residues are removed by a rotary vacuum filter, and the filtrate is treated with lime and soda to precipitate alkaline-earth metals and iron. After repeated filtration, the solution is neutralized with sulfuric acid. During neutralization and in the subsequent evaporation, which concentrates the solution to 200–250 g/L of lithium sulfate, aluminum hydroxide precipitates and is removed together with any purifying additives (e.g., activated charcoal).

The precipitation of lithium carbonate by concentrated sodium carbonate solution is carried out near the boiling point. Lithium carbonate is removed by filtration or centrifugation and washed with hot water to remove the adhering mother liquor (mainly sodium sulfate). It is then dried with a vacuum plate dryer, a band dryer, or a vacuum screw conveyor dryer.

The particle size of lithium carbonate depends strongly on the concentration during precipitation, the temperature, and the rate of addition of sodium carbonate.

Mother liquor from lithium carbonate precipitation always contains ca. 1 g of lithium per liter and is therefore recycled. Before the liquor is returned to the leaching stage, sodium sulfate is removed by crystallization at low temperature. This is a valuable by-product and improves the economic viability of the process.

The use of fluidized-bed furnaces has recently been proposed for the decrepitation process, enabling it to be carried out under mild conditions (Figure 50.2). Recycling of excess sulfuric acid from the dissolution process has also been proposed [27].

50.5.2.2 Alkali Digestion

Spodumene and lepidolite can also be digested by reaction with quicklime. Decrepitation of spodumene, calcination of limestone, and digestion are carried out in a single operation. Three parts of limestone are wet milled with one part of lepidolite, or 3.5–4 parts of limestone with one part of spodumene. The mixture is dried in a rotary furnace and then heated to the clinker point to give calcium orthosilicate and lithium aluminate together with excess lime.

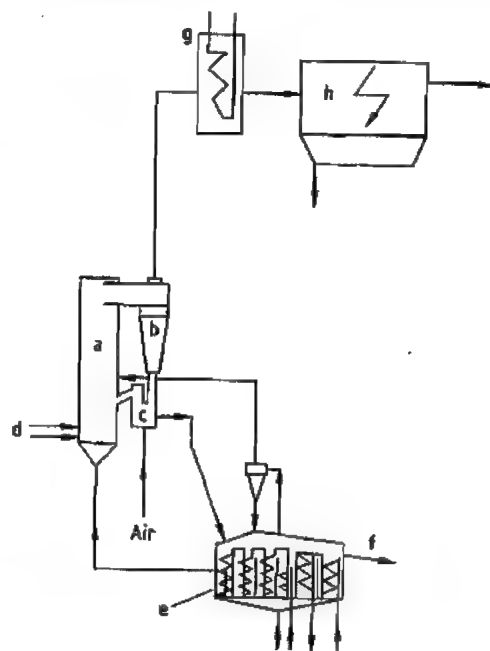


Figure 50.2: Schematic of a fluidized-bed reactor for spodumene decrepitation: a) Fluidized-bed reactor; b) Cyclone; c) Oversize return; d) Raw material feed and fuel supply; e) Countercurrent cyclone cooler; f) Product offtake; g) Heat exchanger (waste-heat boiler); h) Electrostatic precipitator.

The process is critically dependent on the temperature; lepidolite requires ca. 900 °C, and spodumene ca. 1040 °C. If the temperature is too high, a glassy clinker is formed, which severely hinders subsequent leaching of lithium hydroxide; too low a temperature leads to incomplete reaction. Control of the kiln is complicated because of caking and building up of the reaction mixture. In the case of lepidolite, the clinker obtained must be quenched immediately so that no reverse reaction occurs. Spodumene clinker may be cooled slowly, but quenching produces a clinker with better grindability.

After the clinker has been ground in ball mills, lithium hydroxide is leached out with water in several stages. The residues are then separated, and the solution is concentrated in multistage vacuum evaporators to crystallize lithium hydroxide monohydrate. The process has a relatively high energy requirement and gives a lithium yield appreciably below that of the sulfuric acid process. The lower yield is due to the problem of precisely controlling the kiln. For this reason, only the sulfuric acid process is used in the Western world. It is sometimes followed by the conversion of the lithium carbonate into lithium hydroxide. The production of lithium chloride by sublimation from spodumene mixed with calcium chloride and calcium oxide in a one-stage process with decrepitation at 1100 °C also has not become established.

50.5.2.3 Ion-Exchange Processes

Ion-exchange processes involve heating a lithium ore with a sodium or potassium salt. This leads to replacement of Li^+ ions in the ore by Na^+ or K^+ and formation of the soluble lithium salt of the anion used.

The digestion of lepidolite by potassium sulfate at 825–875 °C has attracted much interest. Lithium is leached out as lithium sulfate and then separated from excess potassium sulfate. After evaporation, potassium sulfate is crystallized, and lithium carbonate is precipitated by addition of sodium carbonate to the solution. The potassium sulfate is then reused

in the dissolution stage [28]. However, the loss of potassium in the form of potassium aluminum silicate in the insoluble residues is far from negligible, and for this reason the process is no longer used. If lithium production from lepidolite were to be resumed, the sulfuric acid process would probably be favored over ion exchange, because it also produces aluminum sulfate as a by-product and is therefore more economical.

The digestion of β -spodumene with sodium or potassium acetate is carried out at ca. 400 °C [29]. It produces lithium acetate from which lithium carbonate is precipitated by addition of sodium carbonate; the resulting sodium acetate is recycled. In theory, the process consumes an amount of sodium carbonate equivalent to the lithium carbonate produced, the sodium acetate acting only as a carrier and remaining in the system. However, so far, the process has apparently been operated only on a pilot-plant scale.

The Québec process of the Québec Lithium Corporation is a modification of the acetate process in which β -spodumene is treated with aqueous sodium carbonate solution (30% excess) at ca. 200 °C and 5 MPa for at least 10 min. A slurry of sodium aluminum silicate and lithium carbonate is formed, and subsequent treatment with carbon dioxide at low temperature dissolves the lithium, forming the soluble bicarbonate. The insoluble residue is a sodium zeolite that can be marketed. Lithium carbonate is precipitated from the solution by heating to the boiling point. The carbon dioxide generated is used again for the dissolution of lithium carbonate [30].

This process was used on an industrial scale until 1966. It requires considerably more energy than the sulfuric acid process because of the repeated heating of large quantities of water. Furthermore, sodium carbonate is lost through formation of sodium hydrogen carbonate during dissolution of the lithium carbonate with carbon dioxide.

In a further development of the Québec process, pressure digestion of β -spodumene is carried out at 250 °C with aqueous sodium chloride solution made alkaline by the addi-

tion of 0.1–0.2% calcium hydroxide. Lithium carbonate can be precipitated from the resulting liquor by addition of sodium carbonate. Alternatively, lithium chloride can be isolated by solvent extraction (e.g., with *n*-butanol) [31].

50.5.3 Production of Lithium Carbonate from Brines

The lithium in brines is at present extracted commercially only at Clayton Valley and the Salar de Atacama. In Clayton Valley, the brines are pumped from wells up to 100 m deep into a series of solar ponds, in which the lithium concentration increases continuously while the accompanying salts precipitate due to oversaturation. The production process requires the lithium concentration to be at least 5000 ppm. If the initial concentration is 200 ppm, the enrichment factor must be at least 30 to obtain solutions suitable for the production process, because lithium losses take place by inclusion in precipitated salts and by seepage of the solution through the solar ponds. This means that at least 95% of the water in the original brine must be evaporated. Such a process can only be operated economically where

solar energy is sufficient to provide high rates of evaporation, i.e., in hot, dry regions of the earth. Brines containing 100 ppm of lithium can be concentrated economically if the magnesium content is low. The concentrated brine is purified and then sodium carbonate solution is added at high temperature to precipitate lithium carbonate, which is separated and dried.

Brines containing less than 100 ppm of lithium (e.g., from Searle's Lake) require a different process to recover the lithium, e.g., by precipitating it first as lithium sodium phosphate, Li_2NaPO_4 . This lithium concentrate, known as licon, which contains 20–21% Li_2O is then treated with concentrated sulfuric acid, converting it to phosphoric acid and a solid mixture of lithium and sodium sulfates. This is dissolved, and lithium carbonate is precipitated from the solution by addition of sodium carbonate. The yield of lithium in this process is ca. 88%, which is very good in view of the low starting concentration. The economic viability of the process depends on the recovery of associated by-products such as potassium chloride, sodium sulfate, sodium carbonate, borax, phosphoric acid, and bromine [32]. Lithium production at Searle's Lake was abandoned in the 1970s.

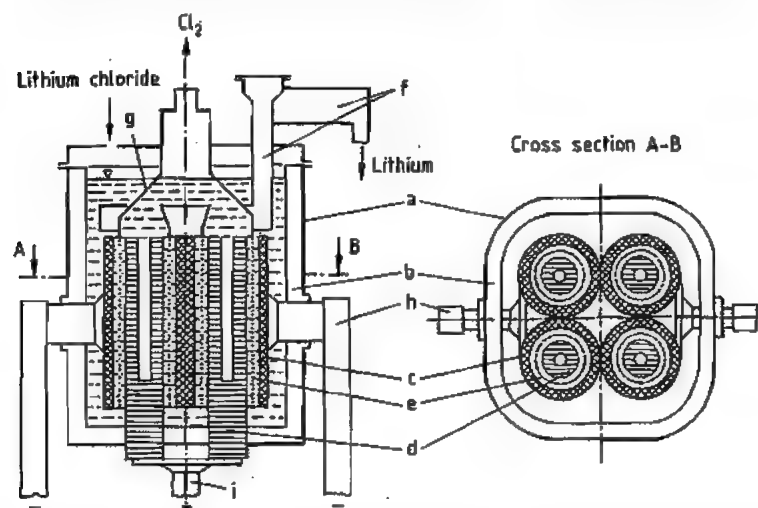


Figure 50.3: Schematic of an electrolytic cell for the production of lithium: a) Steel casing; b) Ceramic lining; c) Cathode with supporting arm; d) Anode; e) Diaphragm; f) Annular collection zone with riser pipe and overflow for lithium; g) Dome for chlorine collection and removal; h) Cathode conductor rail; i) Anode conductor rail.

50.6 Lithium Metal and Lithium Alloys

50.6.1 Production of Metal

Lithium metal is currently produced only by the electrolysis of molten lithium chloride, whose melting point of 614 °C is lowered by addition of potassium chloride. The lithium chloride potassium chloride eutectic, with 44.3% lithium chloride, melts at 352 °C. The salt mixtures used in industry contain 45–55% lithium chloride, which allows electrolysis to be carried out at 400–460 °C.

The electrolytic cells most commonly employed (Figure 50.3) resemble the Downs cell used for the production of sodium [33].

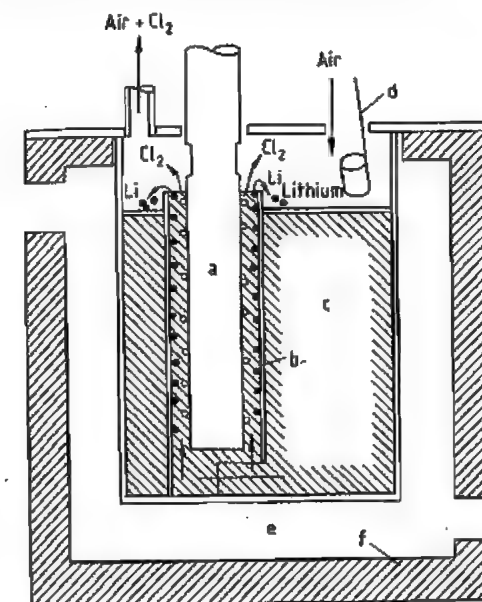


Figure 50.4: Schematic of an American lithium electrolysis cell: a) Graphite anode; b) Steel cathode; c) Melt; d) Ladle; e) Heating chamber; f) Insulation.

The cell and the cathode are constructed from steel, whereas the anode is made of graphite. Four cathode tubes are combined to form a unit, with each tube enclosing an anode cylinder. The anodes enter the electrolysis space from below, and the cathodes are supported by arms attached to the cell sides. The

anode and cathode are separated by a wire-mesh steel diaphragm. The cell is equipped with an insulating inner lining, because both electrodes are introduced below the surface of the melt. Lithium metal is formed at the cathode, rises to the top, and is collected under an argon atmosphere.

In the United States, lithium cells are sometimes operated without a diaphragm or ceramic insulating lining (Figure 50.4) [34]. This greatly prolongs the lifetime of the cells but results in greater power consumption.

Another recently developed lithium electrolysis cell (Figure 50.5) has neither ceramic insulation nor a diaphragm [35]. In this cell, a molten salt mixture containing the lithium metal formed rises continuously in the electrode space and is collected in an annular trough at the top of the cathode near the surface of the melt. It is then transferred through a siphon-like tube to a separation vessel connected to the cell, but isolated from the chlorine gas.

Here, the lithium metal is separated from the electrolyte under an inert-gas atmosphere; the electrolyte is recycled, and the lithium metal is recovered.

The output of an individual cell is usually 200–300 kg of lithium metal per day. The decomposition voltage of lithium chloride is ca. 3.68 V, but in practice 6.0–6.8 V is usually required. The theoretical power consumption is 14.2 kWh/kg of lithium, but the actual figure is 28–32 kWh/kg of lithium. The current efficiency is ca. 90%.

Lithium metal is shipped in steel drums or cans under an argon atmosphere or under a coating of oil. Lithium metal can be stored indefinitely in the absence of air.

Molten lithium can be cast in low-carbon steel molds without special precautions. Its low hardness enables it to be easily extruded or rolled. However, to maintain the silvery luster of lithium, the operation must be carried out in air of very low moisture content or under an inert-gas atmosphere.

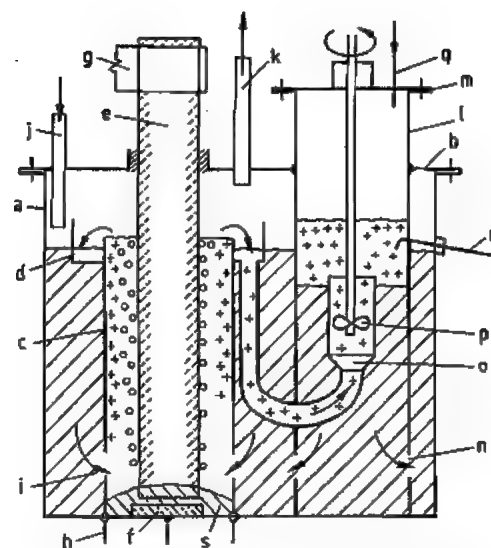


Figure 50.5: Schematic of a special electrolytic cell for production of lithium: a) Electrolysis cell; b) Cover plate; c) Cathode; d) Collecting trough; e) Graphite anode; f) Insulating material; g) Anode connection; h) Cathode connection; i) Openings in cathode wall; j) Charging pipe for lithium chloride; k) Chlorine outlet; l) Separating cylinder; m) Cover plate; n) Openings in wall of separating cylinder; o) Pipe connecting trough to separating cylinder; p) Agitator; q) Inlet for inert gas; r) Outlet pipe for lithium; s) Solidified melt.

50.6.2 Uses

The largest application of lithium metal is the production of organolithium compounds, principally butyllithium, and lithium hydride.

Lithium is used as a reducing agent in organic chemistry, as a solution in liquid ammonia for Birch reductions, and in the synthesis of vitamins [36].

A rapidly growing application of lithium metal is in sacrificial anodes in batteries. Lithium has a high electrochemical equivalent (3.86 A·h/g) and a low electrochemical potential (−3.045 V). The main advantages of lithium batteries are high power output, extremely good storage properties (low rate of self-discharge), and relatively small power loss at low temperature. Commercially produced primary cells have counterelectrodes made of manganese dioxide, chromium oxide (CrO₂), or graphite loaded with sulfur dioxide

or thionyl chloride, and electrolytes consisting of lithium salts dissolved in organic solvents such as propylene carbonate or dimethoxyethane. They have cell voltages up to 3 V and energy densities up to 300 Wh/kg [37]. Secondary lithium cells, some based on aluminum lithium alloys, are currently being investigated extensively [38, 39].

Lithium metal is becoming increasingly important as an alloying component; it is also used as a deoxidizing and desulfurizing agent, especially for copper, nickel, and alloy steels.

Lithium and its compounds play a number of important roles in the nuclear industry, e.g., in the production of tritium, as a heat-exchange cooling medium, as a shielding material, and in the form of a molten salt mixture, as a solvent for other nuclear fuels.

These applications depend on the extremely large difference in neutron capture cross section and absorption distance between the two stable lithium isotopes (Table 50.3) [40].

Table 50.3: Thermal neutron absorption cross section σ and absorption distance λ for lithium.

Absorbent	$\sigma, \times 10^{-24} \text{ cm}^2$	$\lambda, \text{ mm}^2$
Natural isotopic mixture	71	3
⁶ Li	945	0.2
⁷ Li	0.0033	8000

*Distance at which radiation energy has decayed to 1/e of the original intensity.

Table 50.4: Thermonuclear reaction energies.

Reaction	Energy, MeV
⁶ Li(n, T) ⁴ He	4.8
⁷ Li(n, nT) ⁴ He	2.5
⁷ Li(p, γ) ⁴ He	19.7
T(D, n) ⁴ He	17.6
T(T, 2n) ⁴ He	11.3

Production of Tritium. The extremely large amount of energy released in thermonuclear reactions (Table 50.4) is illustrated by the hydrogen bomb, in which tritium or its parent substance lithium in the form of ⁶Li²D reacts with deuterium nuclei. Several fusion reactions have been proposed for power generation. Of these the reaction between deuterium and tritium



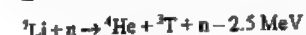
has the best prospect of success because it requires the lowest plasma temperature [41]. The tritium required for the reaction is produced from ⁶Li by irradiation with thermal neutrons:



The overall equation for the fusion reaction is [42]:



This reaction takes place with loss of neutrons; therefore, neutron multiplication reactions (n, 2n) are used to breed tritium, e.g., based on beryllium or using ⁷Li as the starting material according to the equation



Calculations based on this reaction show that 1 kg of natural lithium could produce 5×10^{13} J of energy.

Coolants. In addition to helium at ca. 5 MPa, the following coolants have been proposed for the cooling jacket of a fusion reactor: molten lithium metal, molten LiF–BeF₂, and molten lead containing 17 atom% lithium. In the latter materials the tritium breeding reaction can take place [41, 43]. An important parameter is the product of density and specific heat which shows that, compared with sodium as a coolant, a lower circulation rate of lithium metal (by a factor of 1.9) can be used. For LiF–BeF₂, this factor is 4.5 [44].

Solvents for Nuclear Fuels. Owing to the low neutron capture cross section of ⁷Li, a mixture of ⁷LiF (72 mol%), beryllium fluoride (16 mol%), thorium fluoride (12 mol%), and uranium tetrafluoride (< 1 mol%) has been proposed as a molten salt fuel for breeder reactors. In these reactors, which are envisaged as small power plants (e.g., in aircraft), the LiF–BeF₂ molten salt mixture acts as a solvent for the nuclear fuel [45].

Isotope Separation. The nuclear powers from time to time offer on the world market relatively large quantities of lithium hydroxide in which the natural ⁶Li content is reduced by ca. 50%. Separation of the lithium isotopes is carried out either by an isotope-exchange reac-

tion between lithium amalgam and a lithium compound in solution [46] or by continuous ion-exchange chromatography of lithium salt solutions on special ion-exchange resins [47]. The isotopes ⁶Li and ⁷Li can be purchased with purities of 95–96% and up to 99.9% respectively.

Lithium isotopes are supplied by the Isotopes Sales Department of the Oak Ridge National Laboratory and the US Energy Research and Development Administration.

50.6.3 Alloys

Lithium readily forms alloys with other metals such as lead, copper, silver, magnesium, boron, and aluminum [48]. Lithium often completely changes the properties of metals to which it is added, e.g., the hardness of aluminum and lead, or the ductility of magnesium.

The lead alloy Bahmetall, which was developed in Germany in 1918 and contained 0.04% lithium, is no longer important, it was used as a bearing metal for railroad cars until ca. 1955. A eutectic mixture of lead with 17% lithium is used in nuclear fusion technology as a breeder and cooling medium.

The first aluminum–lithium alloy, containing 0.1% lithium, was developed in 1924 in Germany under the name Skleron. In the United States in 1957, the alloy X-2020 (4.5% Cu, 1.3% Li, remainder Al) was used in the wings and horizontal tail surfaces of naval aircraft. During the 1980s, aluminum lithium alloys have been developed continuously, especially by Alcoa, Alcan, and Pechiney. The low density of these materials, compared with the usual aluminum alloys, is of great interest to the aircraft industry. They will probably be used in the foreseeable future for military and large passenger aircraft, despite competition from carbon fiber-reinforced plastics.

Lithium is the only element, apart from beryllium, that simultaneously reduces the density of aluminum and increases its modulus of elasticity; furthermore, formation of the Al₃Li phase gives improved strength. Modern aluminum lithium alloys are now based almost

without exception on the system Al-Li-Cu-Mg-Zr [49]. The alloy 8090, for example, has the composition 2.3% lithium, 1.3% copper, 0.8% magnesium, 0.12% zirconium, and the remainder aluminum. Such alloys have a density about 10% lower, and a modulus of elasticity ca. 10% higher, than aluminum.

Aluminum-lithium alloys with the composition 50 mol% aluminum and 50 mol% lithium are used in primary thermal batteries in which the electrolyte (a mixture of salts) is melted before the battery is used.

50.7 Compounds [50]

Lithium amide, LiNH_2 , ρ 1.18 g/cm³, mp 373 °C, is a colorless compound that forms cubic crystals. It is converted to lithium imide, Li_2NH , above 400 °C, with loss of ammonia.

Production. Lithium amide is produced industrially by heating lithium metal or lithium hydride in a stream of ammonia. It also forms slowly when lithium metal dissolves in liquid ammonia.

Uses. Lithium amide is now used in many reactions in preference to sodium amide for safety reasons, and because it often shows greater selectivity. It is used as a catalyst for Claisen and aldol condensations; as an alkylation catalyst for amines, nitriles, ketones, and monosubstituted alkynes; and as a polymerization catalyst for acrylonitrile and methyl methacrylate.

Lithium acetate, CH_3COOLi , is available commercially in the anhydrous form or as the dihydrate. Both are colorless powders that dissolve readily in water to give slightly alkaline solutions.

Production. Lithium acetate is produced by reacting lithium carbonate or lithium hydroxide with acetic acid.

Uses. Lithium acetate is used to a limited extent in pharmaceuticals. The technical grade is used as a component of catalysts for the production of polyesters [poly(ethylene terephthalate)] or as an additive to improve their physical properties. It is also added to organ-

opolysiloxanes and acrylic polymers to prevent adhesion of ice.

Lithium benzoate, $\text{C}_6\text{H}_5\text{LiO}_2$, is used in the production of some synthetic polymers (e.g., to harden polyepoxides) [51].

Lithium citrate, $\text{C}_6\text{H}_7\text{Li}_3\text{O}_7$, is commercially available mainly as a di- or tetrahydrate and is used in the treatment of certain types of manic-depressive illness.

Lithium bromide, LiBr , mp 547 °C, ρ 3.463 g/cm³, is a colorless, highly hygroscopic salt. The saturated aqueous solution at 20 °C contains 59.8% lithium bromide and, at 100 °C, 69.9%. The vapor pressure of water above aqueous 52% lithium bromide is 0.53 kPa at 25 °C, 4.98 kPa at 65.6 °C, and 48.1 kPa at 121 °C [52, 53].

Production. Lithium bromide is produced by treating an aqueous suspension of lithium carbonate with hydrobromic acid or by reacting lithium hydroxide with bromine. The latter reaction also produces lithium hypobromite, which is reduced to lithium bromide with formic acid or ammonia.

Uses. A 50–60% aqueous solution of lithium bromide is used in air conditioners operating by the absorption principle. Solid lithium bromide is a component of oxidation and hydroformylation catalysts. It is also used for deprotonation and dehydration of organic compounds having acidic protons. Mixtures of lithium bromide and lithium carbonate in dimethylformamide are used to carry out mild dehydrohalogenation reactions [36, 54]. Lithium bromide is also used for the purification of steroids and prostaglandins, with which it reversibly forms complexes [55].

Lithium carbonate, Li_2CO_3 , ρ 2.11 g/cm³, crystallizes as colorless monoclinic prisms that melt with slight decomposition at 732 °C. The technical product is a fine white powder with a bulk density of ca. 0.8 kg/L. Carbon dioxide dissociation pressures over lithium carbonate are as follows:

Temperature, °C	610	620	740	840	1000	1200
Pressure, kPa	0.1	0.3	1.9	3.8	9.2	30.4

Lithium carbonate is only slightly soluble in water; its solubility decreases with increasing temperature.

Temperature, °C	0	20	40	60	80	100
Solubility, g/100 g water	1.54	1.33	1.17	1.01	0.85	0.72

Lithium carbonate dissolves in aqueous carbon dioxide to form lithium hydrogen carbonate. Concentrations of 70 g/L of lithium carbonate at 20 °C and 0.1 MPa carbon dioxide pressure can be reached. Lithium hydrogen carbonate cannot be isolated. Aqueous solutions decompose on heating to form lithium carbonate and carbon dioxide. This reaction is used in the Québec process and for the purification of technical-grade lithium carbonate. Lithium carbonate reacts with acids stronger than carbonic acid to form the corresponding salts. Reaction with calcium hydroxide yields lithium hydroxide.

Production. Lithium carbonate is produced entirely from minerals or naturally occurring brines. The solution of lithium salts initially obtained (lithium sulfate, lithium chloride) is reacted with sodium carbonate solution and lithium carbonate is precipitated, or lithium hydrogen carbonate is formed first and then decomposed thermally.

Uses. Lithium carbonate is the starting material for the industrial production of all other lithium compounds and is itself used in industry in large quantities. It is an additive in glass, enamels, and ceramics [56, 57] (as are many lithium ores, e.g., spodumene and petalite). The lithium oxide generated by lithium carbonate is a very active flux for silica. It is increasingly replacing fluorspar (CaF_2) for environmental reasons. Its function is generally based on reduction of melting point (particularly important for enamels), reduction of viscosity of molten glass (leading to higher throughput and smaller wall thickness), increased surface tension (giving improved reflexivity to enamels and glazes), and improved chemical resistance. Lithium aluminum silicates with compositions in the range LiAlSiO_4 – $\text{LiAlSi}_4\text{O}_{10}$ are produced that have extremely low or negative thermal expansion coefficients. These compounds and high-lith-

ium glasses are used in heat-resistant ovenware.

The addition of lithium carbonate to cement or concrete leads to quicker setting. Amounts of 1–5% are used to control setting times [58]. In quick-setting tile adhesives, faster adhesion of the tiles is achieved.

Lithium carbonate is also used as an additive to molten salt baths for the electrolytic production of aluminum. It reacts with aluminum trifluoride in the melt to form lithium fluoride. The concentration used is 2–5%, preferably 3.5%, of lithium fluoride. The following effects are produced: reduction of melting point (by 10–25 °C), density, and viscosity of the melt and an increase in electrical conductivity of ca. 10%. This results in a reduced operating temperature, reduction in fluorine emission (up to 50%), and savings in energy (2–3%) and anode carbon (ca. 2%). It is possible to operate existing electrolytic cells at higher loading (ca. 10%), thus increasing capacity without additional capital investment [59–62].

Specially prepared high-purity lithium carbonate (conforming to the national pharmacopoeias, e.g., U.S.P., DAB, E.P., B.P., J.P.) is used increasingly for the treatment of manic-depressive conditions [63–65]; daily doses of ca. 150–500 mg of lithium carbonate are used. The successful treatment of herpes, alcoholism, and cancer by lithium carbonate assisted chemotherapy has also been reported [65]. Mixtures of lithium and potassium carbonate are used as electrolytes in molten carbonate fuel cells (MCFCs). The MCFC, operating at high temperatures (600–650 °C), is especially suited for 21st-century coal-fired baseload electric utility plants or in natural gas units. The high-quality waste heat can be used for industrial cogeneration or internal reforming [82].

Lithium chloride, LiCl , mp 614 °C, bp 1382 °C, ρ 2.07 g/cm³, crystallizes in a cubic system. Its solubility in water is as follows:

Temperature, °C	20	40	60	80	100
Solubility, g/100 g water	83.2	89.8	98.4	111.9	128.3

Its solubility in ethanol at 25 °C is 2.5 g/100 g, and in methanol, 17 g/100 g.

Production. The known methods of producing lithium chloride from lithium ores have not been adopted commercially. At present, it is produced exclusively by reaction of lithium carbonate and hydrochloric acid, with special steel or nickel equipment because of the extreme corrosivity of lithium chloride. Concentration of the solution (e.g., in a vacuum evaporator) causes lithium chloride to crystallize. It is then separated from the mother liquor, dried, and packed in moisture-proof containers.

Uses. Lithium chloride is extremely hygroscopic; thus, like lithium bromide, it is used for drying gases and in air conditioners of the absorber type. Because molten lithium chloride readily dissolves metallic oxides, it is used as a component of fluxes and dipping baths for welding and brazing aluminum and light metal alloys. Most of the lithium chloride produced is used as starting material for the production of lithium metal by molten salt electrolysis.

Lithium cobalt(III), LiCoO_2 , ρ 5.16 g/cm³, can be used as cathodic material in secondary lithium ion batteries [83]. The active dark material with a theoretical specific capacity of 137 Ah/g is prepared by sintering Li_2CO_3 with CoCO_3 at 900 °C. The first cells with a cylindrical design have been commercialized by Sony Corp. [84].

Lithium hypochlorite, LiOCl , is produced by reacting either chlorine with lithium hydroxide solution, or calcium hypochlorite (bleaching powder) with lithium sulfate. Unlike sodium hypochlorite, it may be obtained in solid form (e.g., by spray drying), although overheating must be avoided because oxygen is liberated above 100 °C.

Lithium hypochlorite is increasingly used as a disinfectant and bleaching agent for swimming pools and in food preparation areas (e.g., dairies and butcher shops). Its action in swimming pools is analogous to that of the cheaper calcium hypochlorite, but it does not increase the hardness of water and is completely soluble.

Lithium perchlorate, LiClO_4 , ρ 2.428 g/cm³, crystallizes from aqueous solution as the trihydrate (mp 95.1 °C), which is converted into the anhydrous compound at 130–150 °C via the dihydrate stage. Anhydrous lithium perchlorate melts at 236 °C and is stable up to 400 °C. Like lithium chloride, it is readily soluble in water (56.3 g/100 g water at 20 °C; 196.9 g/100 g water at 95.1 °C).

Lithium perchlorate is produced by reaction of lithium hydroxide or lithium carbonate with perchloric acid. It is used as a conducting salt in electrolytes for lithium batteries.

Further on, solutions of LiClO_4 in polar aprotic solvents (e.g., diethyl ether) produce a dramatic acceleration of Diels–Alder reactions due to the Lewis acid character of the lithium ion [85].

Lithium tetrafluoroborate, LiBF_4 , ρ 2.04 g/cm³, and lithium hexafluoroarsenate, LiAsF_6 , are of potential interest as conducting salts for the electrolytes in lithium batteries.

Lithium hexafluorophosphate, LiPF_6 , dec. 130 °C, is highly soluble in aprotic solvents like ethers, carbonates, etc., and decomposes slowly in water under formation of HF . Due to its high solubility and electrochemical stability, it is the most preferred conducting salt for secondary lithium batteries [86].

Lithium chromate, Li_2CrO_4 , is used as a corrosion inhibitor in air conditioners that contain lithium chloride or bromide solutions. It is made from lithium hydroxide and chromic acid.

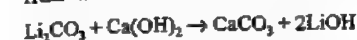
Lithium fluoride, LiF , ρ 2.6 g/cm³, mp 870 °C, is used as a flux for enamel and glass, and for brazing and welding light metals.

Lithium hydride, LiH , ρ 0.82 g/cm³, is used increasingly as a selective reducing agent for polar groups (e.g., esters, amides, nitriles) in organic compounds, although the complex hydrides are of much greater importance: e.g., lithium tetrahydridoaluminate, lithium aluminum hydride, LiAlH_4 , and lithium tetrahydridoborate, lithium borohydride, LiBH_4 . It can be used for the hydrogenolysis of Si–Cl bonds, e.g., in the production of monosilane (SiH_4)

by the Sundermeyer process [66] or SiH-containing polymers [87].

Lithium hydroxide monohydrate, $\text{LiOH} \cdot \text{H}_2\text{O}$, ρ 1.83 g/cm³, loses water on heating to form anhydrous lithium hydroxide, LiOH , ρ 1.46 g/cm³, mp 462 °C.

Production. The production of lithium hydroxide monohydrate by digestion of spodumene with lime has been replaced for economic reasons by the reaction between lithium carbonate and calcium hydroxide:



This yields solutions containing up to 3.5% lithium hydroxide. Attempts to work at higher concentration lead to loss of lithium carbonate in the calcium carbonate residue, because the solubility of lithium carbonate is reduced by the presence of lithium hydroxide. The reaction between these sparingly soluble starting materials requires intensive agitation and gives yields just over 95% after many hours. The insoluble residue (mainly calcium carbonate) is removed, and lithium hydroxide monohydrate is crystallized from the mother liquor by evaporation, under vacuum if required. It is then separated and dried at 130–140 °C. Further heating to 150–180 °C produces calcined lithium hydroxide (LiOH). The removal of water can be accelerated by use of vacuum.

Other production processes that have been proposed include the reaction of lithium sulfate solution with barium hydroxide and the reaction of lithium carbonate with silicic acid in the molten state followed by hydrolysis of the lithium silicate formed. These processes are, however, of little more than academic interest.

The solubility of lithium hydroxide monohydrate in water is as follows:

Temperature °C	20	40	60	80	100
Solubility, g/100 g water	21.6	22.0	23.1	25.6	29.6

Uses. Lithium hydroxide is used mainly for the production of lubricating greases. Over 50% of the greases used today in motor vehicles, aircraft, and heavy machinery contain lithium stearates, mainly lithium 12-hydroxystearate. These greases have good viscosity

properties up to 200 °C and are practically insoluble in water.

Lithium hydroxide is also used in the production of dyes [67]. It has attained some importance as an additive to nickel–iron accumulators and, in its calcined form (98% LiOH), as an absorbent for carbon dioxide in breathing apparatus, especially for crews of submarines and space vehicles. One gram of anhydrous lithium hydroxide absorbs 450 mL of carbon dioxide, so that ca. 750 g of lithium hydroxide is sufficient to absorb the carbon dioxide generated by one person in one day. Lithium hydroxide is also used in the building industry. As additive to the mix water, it helps to prevent the so-called “alkali–silica reactivity”, that is a source of distress (cracking).

Lithium iodide, LiI , ρ 4.0 g/cm³, is a yellowish crystalline powder that is prepared by reaction of lithium hydride with iodine in diethyl ether. It is used in organic syntheses to accelerate the aldol condensation of ketones with enolizable or nonenolizable aldehydes [68] and to cleave methyl esters and oxides [69]. Lithium iodide is also of interest for the manufacture of rapid solid ionic conductors [70]. **Lithium iodide trihydrate,** $\text{LiI} \cdot 3\text{H}_2\text{O}$, ρ 2.5 g/cm³, is prepared by reaction of lithium hydroxide with hydriodic acid.

Lithium manganese oxide, LiMn_2O_4 , ρ 4.28 g/cm³, is a ternary spinel-type double oxide commonly prepared by sintering a manganese oxide (MnO_2 or Mn_2O_3) with Li_2CO_3 at high temperatures. This salt is a possible low-price candidate for cathodes in high-power secondary lithium ion batteries. Practical specific capacities are between 90–120 mAh/g [83, 89].

Lithium nitrate, LiNO_3 , ρ 2.37 g/cm³, is used, with other salts, to produce eutectic molten salt baths for vulcanization [71]. A salt mixture consisting of lithium and potassium nitrate is available under the trade name “Sabalith®” [88]. Unless conventional nitrite (e.g., NaNO_2)-containing salt mixtures, Sabalith® is not classified as a toxic substance and helps to reduce emissions of nitrous gases and carcinogenic nitrosoamines.

Lithium nitride, Li_3N , ρ 1.38 g/cm³, could attain industrial importance as a solid ionic conductor. It is also used together with magnesium boride and hexagonal boron nitride to prepare cubic boron nitride [72].

Lithium oxide, Li_2O , ρ 2.01 g/cm³, is formed when lithium hydroxide is heated to 800 °C in vacuum. It is also obtained by the reaction of lithium metal with oxygen, which proceeds without formation of lithium peroxide.

Lithium peroxide, Li_2O_2 , ρ 2.297 g/cm³, is formed by reaction of lithium hydroxide solution with hydrogen peroxide; it can be isolated by careful evaporation in vacuum. It has some importance as a hardener for the formation of special polymers and for air purification in sealed spaces (submarines, breathing apparatus, space travel). One gram of Li_2O_2 produces 0.348 g of oxygen and absorbs 0.96 g of carbon dioxide.

Lithium double oxides are also known as lithium ceramics, and are used to a small extent in the ceramic and enamel industries. They include lithium aluminate, LiAlO_2 ; lithium borate, LiBO_2 ; lithium cobaltite, LiCoO_2 ; lithium manganite, Li_2MnO_3 ; lithium molybdate, Li_2MoO_4 ; lithium silicate, Li_2SiO_3 ; lithium titanate, Li_2TiO_3 ; and lithium zirconate, Li_2ZrO_3 .

Lithium aluminate is of some importance as a construction material in fusion reactors [73] and fuel cells [74].

Lithium tetraborate, $\text{Li}_2\text{B}_4\text{O}_7$, either pure or doped with beryllium or strontium as an internal standard, is used as a flux in X-ray spectroscopy and optical emission spectral analysis. It also has limited application in the manufacture of special lithium-containing, high-performance lubricating greases.

Lithium phosphate, Li_3PO_4 , ρ 2.537 g/cm³, is sparingly soluble in water (ca. 0.04%). It is prepared by precipitation from solutions of lithium salts by addition of phosphates or phosphoric acid. It has some importance as a component of protective optical heat filters, in the corrosion protection of vessels for poly-

mer production, and in the catalytic production of allyl alcohol.

Lithium sulfate, Li_2SO_4 , ρ 2.221 g/cm³, m_p 860 °C, is a colorless salt produced from lithium carbonate and sulfuric acid. It is used in the anhydrous or hydrated form for the treatment of manic-depressive conditions [40]. It has also been considered for the production of quick-setting cements.

Other Lithium Salts. Lithium azide, borate, cyanide, molybdate, and salicylate, are prepared by reaction of lithium carbonate or lithium hydroxide with the corresponding acids. Lithium niobate and lithium tantalate single crystals are used as ferroelectric materials and also have acousto-optical properties that can be utilized in optical data transmission systems.

50.8 Quality Specifications and Analysis

Lithium metal of standard grade has a purity in excess of 99%, and contains ca. 0.5% sodium. Battery grade lithium contains less than 200 ppm of sodium. Standard quality lithium is usually produced in the form of bricks or cylinders 0.1–1 kg in weight, rods with a diameter of 10–20 mm, or granules with a diameter of ca. 2.5 mm. Battery grade lithium is supplied as foil with a thickness down to 0.05 mm.

Lithium is detected qualitatively by its characteristic red flame coloration; this is also used for quantitative determination by flame emission spectroscopy, in which the emission line at 670.8 nm is measured. Analysis is carried out by using diffraction or refraction spectrometers. In the presence of interfering ions, especially other alkali metals, a calibration curve should be used to obtain adequate accuracy ($\pm 1\%$) [75].

Lithium can also be determined by gravimetric, titrimetric, and colorimetric methods, after precipitation as the periodate, phosphate, zinc uranyl acetate, aluminate, or fluoride [76]. Lithium sulfate can be used as a primary

standard. Lithium hydroxide and organolithium compounds can be determined easily by acidimetric methods. Indirect methods for the determination of lithium salts are also used, e.g., separation of the lithium by ion exchange followed by titration of the acid produced and, for lithium salts of organic acids, by titration with perchloric acid in nonaqueous media [77].

Analysis of lithium hydrides can be carried out by measuring the volume of gas evolved on hydrolysis. For low concentrations of lithium, ion-exchange chromatography is most suitable [78].

50.9 Toxicology and Occupational Health

The lithium ion is considerably more toxic than the sodium ion; for example, 5 g of lithium chloride can cause fatal poisoning. On the other hand, lithium salts have received widespread clinical use for over 30 years in the treatment of manic-depressive illness. Thus therapeutic doses of 170–280 mg/d Li in the form of mainly lithium carbonate are administered over long periods.

Lithium is an environmental trace element, the background exposure is estimated to be about 2 mg/d Li and to have beneficial effects [90].

In Europe and in the United States, there are no special regulations concerning lithium in waste waters. Lithium is included as a part of the allowed salt emissions.

No industrial disease caused by ingestion of lithium compounds has been reported thus far. Lithium hydroxide has caustic properties similar to those of other alkali-metal hydroxides; the caustic action of lithium hydride and lithium aluminum hydride is due to the lithium hydroxide formed by hydrolysis. Details of the toxicity and therapeutic possibilities of lithium are given in [63, 65].

50.10 Economic Aspects

The information available concerning world production of lithium ores is incomplete [79]. Including those amounts used for lithium carbonate production, it can be estimated at 6×10^5 t/a.

In 1992, estimated consumption of lithium minerals in the Western World for direct use (e.g., in the glass, ceramics, and metallurgical industries) was 8.55×10^4 t/a (corresponding to about 1.2×10^4 t lithium carbonate equivalents). An additional 1.5 – 2.0×10^5 t were used in the production of lithium chemicals.

The bulk prices (FOT Amsterdam) in May 1995, in U.S. dollars per ton, were

Petalite (4.2% Li_2O)	147
Spodumene concentrate (> 7.5% Li_2O)	385
Glass-grade spodumene (5% Li_2O)	175

The consumption of lithium compounds (calculated as lithium carbonate) in the Western world was ca. 3.2×10^4 t in 1989, with an annual rate of increase of ca. 3–4%. Approximately 40% of the lithium production was consumed by the United States, where, together with Chile, the main ore and brine deposits are to be found. The capacity available at present together with the projected expansion will ensure that the market remains satisfied. About 25% of the lithium produced is used in the lubrication industry, 25% in the aluminum industry, 25% in the enamel, glass, and ceramic industries, and the rest for miscellaneous uses such as chemicals, pharmaceuticals, catalysts for the rubber industry, additives for welding materials, and absorbers in air conditioners.

Bulk prices in the United States in November 1996, in U.S. dollars per kg, were:

Lithium carbonate	4.25
Lithium hydroxide monohydrate	5.73
Metallic lithium	89.51
Lithium chloride	8.91
n-Butyllithium	47.18

50.11 References

1. M. F. C. Ladd, *Theor. Chim. Acta* **12** (1968) 333–336.

2. E. J. Cairns, F. A. Cafasso, V. A. Maroni: *Chemistry of Fusion Technology*, Plenum Publishing Corp., New York 1972, pp. 91-160.
3. Landolt-Börnstein, 6th ed., IV, Part 2, pp. 326-330.
4. Gmelin, System no. 20, Lithium, p. 150.
5. H. Roy, E. Geiss, *Microbeam Analysis 1981*, San Francisco Press, San Francisco 1981, pp. 303-308.
6. Xiang Jun: "Study of Zha Buyesaline/Lake Tibet", *Scientific papers on geology for the 27th Internat. Geol. Congr.* 4 (1985) 173-184, Geol. Publ. House, Beijing.
7. I. A. Kunasz, "Lithium Raw Materials", in S. J. Le-fond (ed.): *Industrial Minerals and Rocks*, 5th ed., American Institute of Mining, Metallurgical and Petroleum Engineers, New York 1983, vol. 2, pp. 869-880.
8. D. London, D. M. Burt: "Lithium Minerals in Peg-matites", *Short Course Handb. Mineral. Assoc. Can.* 8 (1982) 99-133.
9. R. K. Evans: "Lithium Reserves and Resources", *Energy* 3 (1978) 379-385.
10. I. A. Kunasz: "Lithium how much?" *Foote prints* 44 (1980) no. 1, 23-27.
11. K. R. Suttill, *Eng. Min. J.* 188 (1987) 40-43.
12. Minister Energy, Mines, Resources Canada, "Lithium, an Imported Mineral Commodity", *Mineral Bulletin MR 212*, Canadian Government Publishing Centre, Ottawa 1986, p. 24.
13. G. Aubert: "Le Lithium", *Éditions Bureau recherches géologiques et minières, Paris XV* (1963) no. 2, 23-93.
14. M. L. Deshpande: "Lithium Resources in India", *Indian Miner.* 32 (1978) no. 4, 41-47.
15. "Minerex explores for Lithium", *Ind. Miner.* 1984, no. 8, 9.
16. D. I. Bleiwas, J. S. Coffman: "Lithium Availability Market Economy Countries", Bureau of Mines, U.S. Dept. of Interior, Inf. Circular 9102, Washington, DC, 1986.
17. M. Coad: "Lithium Production in Chile's Salar de Atacama", *Ind. Miner.*, Oct. 1984, 27-33.
18. J. R. Davis, J. D. Vine: "Stratigraphic and Tectonic Setting of the Lithium Brine Field, Clayton Valley, Nev.", *Basin and Range Symp.*, Oct. 7-11, 1979, Rocky Mountain Assoc. Geol. 1979, pp. 421-430.
19. "China Finds Lithium", *Min. Mag.* 155 (1986) no. 4, 303.
20. Qian Ziqiang, Xuan Zhiqiang: "Borate Minerals in Salt Lake Deposits at Chaidam Basin, China", *Sixth Intern. Sympos. on Salt*, Salt Institute, vol. I, 1983, 185-194.
21. "Chile Aims at Top Producer Slot", *Metal Bull. Monthly*, Jan. 1983, p. 61.
22. D. Kaplan, *Isr. J. Chem.* 1 (1963) 115-120.
23. M. Steinberg, Vi-Duong Dang: "Preliminary Design and Analysis of a Process for the Extraction of Lithium from Seawater", *Lithium Resources and Requirements by the Year 2000, Geological Survey Professional Paper*, no. 1005, US Government Print Office, Washington 1976, pp. 79-88.
24. A. G. Collins: "Lithium Abundances in Oilfield Waters", in [23], pp. 116-123.
25. A. E. Schreck, *U.S. Bur. Mines. Inf. Civ.* 1961, no. 8053, 36-41.
26. G. G. Gabra, A. Torma: "La métallurgie extractive du lithium", *L'Ingénieur* (Montréal, École polytechnique), March, April 1977, 10-15.
27. Metallgesellschaft AG, *Verfahren zur Gewinnung von Lithiumcarbonat*, DE-OS 3622105 A1, 1988 (P. Brödemann, G. Krüger, H. Heng).
28. G. von Girssewald: "Lithium", *Mitt. d. Metallgesellschaft* 2 (1929) 13-20.
29. J. Tixhon, *Ind. Chim. Belge Suppl.* 1 (1959) 752.
30. M. Archambault, US 3112171, 1963.
31. G. G. Gabra, A. E. Torma, C. A. Olivier, *Can. Metall. Q.* 14 (1975) no. 4, 353-358.
32. L. E. Rykken: "Lithium Production from Searles Valley" in [23], pp. 33-34.
33. W. Hinrichs, L. Lange in Winnacker, Küchler (eds.): *Chemische Technologie*, 4, Carl Hanser Verlag, München-Wien 1986, p. 334.
34. R. Bauer, *Chem. Ing. Tech.* 44 (1972) 147-151.
35. H. Lauck: "Galvanische Zellen mit organischen Elektrolyten", *BMFT-Forschungsbericht T 74-02*, 1974.
36. F. J. Kruger, H. Lauck, E. Voss, *Chem. Ing. Tech.* 50 (1978) 284.
37. J. O. Besenhard, G. Eichinger, *J. Electroanal. Chem.* 68 (1976) 1-18.
38. Metallgesellschaft AG, EP 0217438 A1 (J. Möller, R. Bauer, B. Sermond, E. Dolling).
39. L. F. Fieser, M. Fieser: *Reagents for Organic Synthesis*, J. Wiley & Sons, New York 1967, pp. 54-56.
40. J. P. Gaban: *Lithium Batteries*, Academic Press, New York 1983.
41. K. M. Abraham in R. O. Bach (ed.): *Lithium—Current Applications in Science, Medicine and Technology*, J. Wiley & Sons, New York 1985, pp. 155-175.
42. D. Vissers, Z. Tomczuk, L. Redey, J. Battles in R. O. Bach (ed.): *Lithium—Current Applications in Science, Medicine and Technology*, John Wiley & Sons, New York 1985, pp. 121-153.
43. A. Klemm, *Angew. Chem.* 70 (1958) 21-24.
44. R. Klingelhöfer, *Chem. Ztg.* 111 (1987) 85.
45. C. M. Braams, *9th World Energy Conference*, Paper 4.1-11, London 1974, pp. 181-190.
46. H. U. Borgstedt, V. Coen, S. Malang: "Flüssige Bruststoffe", *Jahrestagung Kerntechnik 1987*, Deutsches Atomforum e.V., Bonn 1987.
47. W. Danner, *Reaktortagung*, Hamburg 1972, Deutsches Atomforum e.V., Bonn 1972, pp. 747-750.
48. C. F. Baes, Jr., *J. Nucl. Mater.* 51 (1974) no. 1, 149-162.
49. Commissariat à l'énergie atomique, DAS 1244750, 1960 (E. Saito, G. sur Yvette, G. Dirian, S.-O. Pal-laiseau).
50. CEER, *Chem. Econ. Eng. Rev.* 15 (1983) 32.
51. P. D. Frost, *Batelle Tech. Rev.* 8 (1959) 3-8.
52. M. Peters, K. Welpman, *Metall* 39 (1985) 1141-1144.
53. W. A. Hart, O. F. Beumel, Jr.: *Comprehensive Inorganic Chemistry*, vol. 12, Pergamon Press, Oxford-New York 1972, pp. 331-367.
54. Shell B.V., DE 1914004, 1969 (G. Rossa).
55. W. Pennington, *Refrig. Eng.* 63 (1955) 57-61.
56. D. S. Davis, *Chem. Eng.* 64 (1957) 292-294.
57. Sterling Drug Inc., US 885776, 1978 (M. R. Bell, J. L. Hermann, V. Akullian).
58. Searle, DE 3207470, 1981 (J. B. Hill, R. A. Erickson).
59. J. H. Fishwick: *Application of Lithium in Ceramics*, Cahners Publ. Comp., Boston, MA, 1974.
60. B. R. Franklin, L. C. Klein: "Lithia in Container Glass", *Am. Ceram. Soc. Bull.* 62 (1983) 209.
61. H. R. Carroll, J. I. Angelo: "Adding Lithium Can Improve Melting-Forming Performance", *Glass Ind.*, Nov. 1983, 14-18.
62. Woellner Werke, DE-OS 2725524, 1978 (W. R. Semle).
63. Armstrong World Industries, DE-OS 3541614, 1986 (J. O. Presley).
64. Tokuyama Soda Co., IP 77121632, 1977 (T. Fukunaga, H. Iwakura, T. Uchiyama, H. Kono).
65. K. Grjotheim et al.: *Aluminium Electrolysis, the Chemistry of the Hall-Héroult Process*, Aluminium-Verlag, Düsseldorf 1977.
66. R. Pawlek: Übersicht über das Verhalten lithiumhaltiger Salze in der Tonerdeschmelzflußelektrolyse, Schweizerische Aluminium AG, Zürich 1981.
67. H. Kvande: "The Optimum Bath Composition in Aluminium Electrolysis, does it exist?" *Erzmetall* 35 (1982) 597-604.
68. K. Grjotheim, H. Kvande, K. Matiasovsky: "Addition of LiF and MgF₂ to the Bath of the Hall-Héroult Process", *Light Metals*, March 1983, 397.
69. S. Gershon, B. Shopsin: *Lithium—its Role in Psychiatric Research and Treatment*, Plenum Press, New York-London 1973.
70. F. N. Johnson (ed.): *Lithium Research and Therapy*, Academic Press, London-New York 1974.
71. R. O. Bach (ed.): *Lithium—Current Applications in Science, Medicine and Technology*, John Wiley & Sons, New York 1985, pp. 337-407.
72. W. Sundermeyer, O. Glemser, *Angew. Chem.* 70 (1958) 625.
73. Hoechst AG, DE 3443305, 1986 (F. Meininger, L. Schläfer).
74. Mitsubishi Chemical Industries Co. Ltd., EP 216296, 1987 (Y. Narita, H. Takimoto, H. Sano).
75. R. G. Kelleher, M. A. McKevey, P. Vibuljan, *J. Chem. Soc. Chem. Commun.* 1980, 486.
76. J. E. McMurtry, *Org. React.* 24 (1976) 187.
77. W. Weppner, W. Welzel, R. Kniep, A. Rabenau, *Angew. Chem.* 98 (1986) 1105-1106.
78. Furukawa Electric Co. Ltd., JP 8259742, 1982.
79. Showa Denko, JP 5957905, 1984; JP 5973411, 1984.
80. J. Raeder: "Der Entwicklungsstand der Kernfusion", *Kernforsch.* 6 (1977) 253.
81. S. B. van der Molen, E. J. Siewers, H. den Uil, M. J. A. A. Goris: "Porous MCFC Component Development at ECN", *International Seminar Fuel Cell Technology and Applications*, Den Haag 1987.
82. J. A. Dean: *Flame Photometry*, McGraw-Hill, New York 1960, pp. 153-160.
83. S. Kallmann: *The Alkali Metals, Treatise on Analytical Chemistry*, vol. I, part II, J. Wiley & Sons, New York 1961.
84. I. Gyenes: *Titration in nichtwässrigen Medien*, Ferdinand Enke Verlag, Stuttgart 1970.
85. J. Weiß: *Handbuch der Ionenchromatographie*, VCH Verlagsgesellschaft, Weinheim 1985.
86. Roskill Info. Services, London: *The Economics of Lithium*, 5th ed., 1987.
87. J. A. Ober: "Lithium", *U.S. Dep. Inter. Bur. Mines Miner. Yearb.* 1986, 1-7.
88. D. J. Kingsnorth: "Lithium Minerals in Glass", *Ind. Miner.*, Jan. 1988, 49-52.
89. K. Kordes, G. Simader, *Fuel Cells and their Applications*, VCH, Weinheim 1996.
90. K. Brandt, *Solid State Ionics* 69 (1994) 173-183.
91. K. Ozawa, *Solid State Ionics* 69 (1994) 212-221.
92. A. Loupy, B. Tchoubar, *Salt Effects in Organic and Organometallic Chemistry*, VCH, Weinheim 1992.
93. J. M. Tarascon, D. Guyomard, *Solid State Ionics* 69 (1994) 293-305.
94. Goldschmidt AG, EP 266633, 1986 (K. Koerner, C. Weitemeyer, D. Wewers).
95. Sabalith®, *Nitrite-Free Heat Transfer Salt*, brochure published by Chemetall GmbH, June 1994.
96. J. M. Tarascon, E. Wang, F.K. Shokoohi, W. R. Kimmon, S. Colson, *J. Electrochem. Soc.* 138 (1991) 2859-2864.
97. G. N. Schrauzer, K.-F. Klippel, *Lithium in Biology and Medicine*, VCH, Weinheim 1991.

51 Sodium

GABRIELE HARTMANN, ALFRED KLEMM, LUDWIG LANGE, WOLFGANG TRIEBEL (§§ 51.1–51.12); GISEBERT WESTPHAL (§ 51.13, INTRODUCTION); T. BAUER, GERHARD KRISTEN (§ 51.13.1); WOLFGANG HERDE (§ 51.13.2); WILHELM WEGENER † (§ 51.13.3.1); PETER AMBATELLO (§ 51.13.3.2); BERNARD CLERCX, HELMUT GEYER (§ 51.13.3.3); CHRISTIAN BODART, BERNARD EPRON (§ 51.13.3.4); KARL SEEBODE (§ 51.13.4); ULRICH KOWALSKI (§ 51.13.5); FRANZ-RUDOLF MINZ (§ 51.14); CHRISTIAN THIEME (§ 51.15); HELMOLD VON PLESSSEN (§ 51.16); TAKAO MAKI (§ 51.17)

51.1 Introduction	2054	51.13.5.2 Packaging, Transport, and Storage	2094
51.2 History	2054	51.14 Sodium Hydroxide	2094
51.3 Properties	2055	51.14.1 Properties	2094
51.4 Occurrence	2059	51.14.1.1 Properties of Sodium Hydroxide	2094
51.5 Production	2059	51.14.1.2 Properties of Sodium Hydroxide Solution	2095
51.5.1 Chemical Processes	2059	51.14.2 Production	2096
51.5.2 Electrolytic Processes	2059	51.14.2.1 Production of Sodium Hydroxide Solution	2096
51.5.2.1 Development of Molten Salt Electrolysis of NaOH and NaCl	2059	51.14.2.2 Production of Solid Sodium Hydroxide	2099
51.5.2.2 Description and Operation of NaCl Molten Salt Electrolytic Cell	2061	51.14.2.3 Forming	2100
51.5.2.3 Properties of the Electrolyte	2065	51.14.2.4 Specifications	2100
51.5.2.4 Other Electrolytic Processes	2066	51.14.2.5 Storage, Packaging, and Transportation	2101
51.6 Safety	2066	51.14.3 Uses	2101
51.7 Uses	2067	51.14.4 Safety Precautions	2102
51.8 Alloys	2069	51.14.5 Economic Aspects	2102
51.9 Packaging and Transport	2070	51.15 Sodium Carbonates	2104
51.9.1 Sodium Metal	2070	51.15.1 Sodium Carbonate	2104
51.9.2 Transport Regulations	2070	51.15.1.1 Properties	2104
51.9.3 Break-Bulk Packaging	2071	51.15.1.2 Sodium Carbonate Minerals	2105
51.9.4 Portable Tanks	2072	51.15.1.3 Production	2106
51.10 Quality Specifications and Analysis	2072	51.15.1.4 Quality Specifications	2117
51.11 Health and Safety	2073	51.15.1.5 Producers	2118
51.12 Economic Aspects	2073	51.15.1.6 Storage and Transport	2119
51.13 Sodium Chloride	2073	51.15.1.7 Uses	2119
51.13.1 Properties	2074	51.15.1.8 Toxicology	2120
51.13.2 Formation and Occurrence of Salt Deposits	2076	51.15.2 Sodium Hydrogencarbonate	2120
51.13.3 Production	2077	51.15.2.1 Properties	2120
51.13.3.1 Mining of Rock Salt	2077	51.15.2.2 Production	2121
51.13.3.2 Production of Crude Brine by Mining Methods	2080	51.15.2.3 Uses and Quality Specifications	2121
51.13.3.3 Controlled Solution Mining	2083	51.16 Sodium Sulfates	2121
51.13.3.4 Production of Sea Salt	2086	51.16.1 Sodium Sulfate	2121
51.13.4 Production of Pure Salt by Evaporation of Brine	2089	51.16.1.1 History and Natural Occurrence	2121
51.13.4.1 Purification of Crude Brine	2090	51.16.1.2 Properties	2122
51.13.4.2 Evaporation of Brine	2090	51.16.1.3 Extraction and Production	2123
51.13.4.3 Recrystallization	2091	51.16.1.4 By-product Sodium Sulfate	2129
51.13.4.4 Other Process Steps	2092	51.16.1.5 Uses	2132
51.13.4.5 Salt Quality	2092	51.16.1.6 Occupational Health and Environmental Protection	2132
51.13.5 Economic Aspects	2092	51.16.1.7 Economic Aspects	2132
51.13.5.1 Commercial Grades	2092	51.16.2 Sodium Hydrogensulfate	2132
		51.17 Sodium Benzoate	2133
		51.18 References	2133

51.1 Introduction

Sodium is the best-known alkali metal. The amount of sodium metal produced industrially exceeds that of all other alkali metals. It is a member of group 1 of the periodic table, with the relative atomic mass 22.9898 and the atomic number 11.

Sodium has only one naturally occurring isotope, ^{23}Na . Several artificial isotopes are also known [1]. The isotope ^{24}Na is used as a tracer in industrial and medicinal applications.

Few basic chemicals are used in as many areas as sodium metal. Elemental sodium can be considered both a fine chemical whose properties make it indispensable for industrial applications ranging from pharmaceuticals to heavy inorganic chemicals, and a readily liquefied metal with a wide range of metallurgical and physical uses. A large number of products derived from sodium metal are used in the chemical industry.

51.2 History

The German name *Natrium* is derived from the Egyptian *neter*, meaning sodium carbonate [2-4], while the English name sodium is derived from soda [3]. Sodium was discovered in 1807 by DAVY, who electrolyzed molten sodium hydroxide in a platinum dish, by contacting it with a platinum wire using a voltaic pile as the source of electricity [3].

However, this electrolytic process could not be used for industrial production at that time, because no economic source of direct current was available. Powerful d. c. generators first became available after the discovery of the dynamo principle by W. SIEMENS in 1867.

The history of the industrial production of sodium, which extends over more than 100 years, can be divided into four periods, in which four different processes were used [5].

Thermochemical reduction processes were used between 1854 and 1890. A mixture of sodium carbonate, wood charcoal or coal, and quicklime was heated to $> 1100^\circ\text{C}$, and the

sodium vapor formed was condensed (SAINT-CLAIRE DEVILLE, Paris, 1854). An annual production of 5-6 t of sodium was achieved by this process. In a later development, sodium carbonate was replaced by sodium hydroxide, and the wood charcoal or coal by a mixture of iron and coal (CASTNER, 1886). Using this process, the Aluminium Company Limited in Oldbury produced ca. 150 t/a sodium between 1888 and 1890 [4].

Between 1891 and 1920, sodium was produced by electrolysis of molten sodium hydroxide, to which sodium chloride and sodium carbonate were added to lower the melting point (Castner process). The Castner process [6] was the only important industrial process for producing sodium during this period.

In the 1900s, attempts were made in Switzerland (Ciba), Germany (Degussa), and the United States (Rössler & Hasslacher Chemical Co.) to use the cheaper starting material sodium chloride in a molten salt electrolysis process. In 1921, DOWNS succeeded in constructing a cell for electrolyzing sodium chloride [7], the basic principle of which is still used today. The electrolyte used from ca. 1925 onward for industrial production was a mixture of sodium chloride and calcium chloride. Since ca. 1950, a modified Downs cell has been used, with an electrolyte consisting of a ternary mixture of NaCl , BaCl_2 , and CaCl_2 . This process has since become established worldwide.

The industrial use of sodium has also undergone a change. The only demand for large-scale production of sodium in the mid-1800s came from the aluminum industry, where it was used for reducing aluminum trichloride. However, around 1890, aluminum producers began to switch to a molten salt electrolysis process. Sodium was also used in the production of sodium cyanide (for extracting gold from its ores) and sodium peroxide. It was later used in the production of lead-containing antiknock agents for gasoline and special metals such as titanium.

51.3 Properties

Physical Properties. The properties of sodium are directly related to its structure [8]. The electronic configuration of sodium is $1s^2 2s^2 2p^6 3s^1$. The atomic volume is therefore large, and the cohesive forces in the sodium lattice are relatively low. Thus, like all alkali metals, sodium has a lower density than the alkaline-earth metals, as well as lower hardness; lower melting and boiling points; and lower energies of sublimation, vaporization, and dissociation [5, 9].

Sodium crystallizes from the melt with a body-centered cubic crystal lattice. It has typical metallic properties, including high thermal and electrical conductivity, the electrical conductivity of sodium at 20°C being about one-third that of copper. It is liquid over a wide temperature range from 97.8 to 881.4°C and has a fairly low vapor pressure, which is an important requirement for production in an electrolytic cell [10].

Alkali metals give characteristic flame coloration. Their outer electrons can easily be raised to an excited state, which is the basis for their analytical determination by flame photometry and atomic absorption spectroscopy. Sodium and sodium salts color the flame of a Bunsen burner yellow. The sodium D doublet at 589 and 589.6 nm is due to the $3s^1-3p^1$ transition in sodium atoms formed by the reduction of Na^+ in the flame [9].

Sodium is monoatomic in the vapor state, although dimers and tetramers have also been reported [10].

Some physical properties of sodium are listed below [8, 10]:

Atomic number	11
Relative atomic mass	22.98977
Melting point	97.83°C
Heat of fusion	113 J/g
Volume expansion on melting	2.7%
Boiling point	881.4°C
Heat of vaporization	3750 J/g
Atomic radius in metallic lattice	189.6 pm
Ionic radius	$95-98\text{ pm}$
Ionization potential	5.139 V
Standard electrode potential	2.714 V

Electrical resistivity at 20°C	$4.77 \times 10^{-8}\ \Omega\text{m}$
Critical temperature	$2508.7 \pm 12.5\text{ K}$
Critical pressure	$25.64 \pm 0.02\text{ MPa}$
Critical density	206 kg/m^3
Specific heat capacity at 20°C	$1.22\text{ Jg}^{-1}\text{K}^{-1}$
Thermal conductivity at 20°C	$132.3\text{ Wm}^{-1}\text{K}^{-1}$
Density	
at 20°C	0.968 g/cm^3
at 120°C	0.927 g/cm^3

The density (kilograms per cubic meter) of solid sodium in the range $273-370.98\text{ K}$ is given by the following equation [8]:

$$\rho_s = 972.5 - 20.11 \times 10^{-2}(T - 273.15) \times 10^{-4}(T - 273.15)^2$$

For liquid sodium in the range $370.98-1644.24\text{ K}$, the following equation applies [8]:

$$\rho_l = 1011.8 - 0.22054T - 1.9226 \times 10^{-5}T^2 + 5.637 \times 10^{-9}T^3$$

The specific heat capacity ($\text{Jg}^{-1}\text{K}^{-1}$) as a function of temperature at $273.15-370.98\text{ K}$ is given by [8]

$$c_p = 1.1987 + 6.4894 \times 10^{-4}(T - 273.15) + 1.053 \times 10^{-5}(T - 273.15)^2$$

In the range $370.98-1173.15\text{ K}$, the following equation applies [8]

$$c_p = 1.4361 - 5.8024 \times 10^{-4}(T - 273.15) + 4.621 \times 10^{-7}(T - 273.15)^2$$

The thermal conductivity ($\text{Wm}^{-1}\text{K}^{-1}$) from 370.98 to 1173.15 K is given by [8]

$$\lambda = 91.8 - 4.9 \times 10^{-3}(T - 273.15)$$

The vapor pressure (kilopascals) at $300-2500\text{ K}$ is [8]

$$\log p = 10.182516 - 5693.8776/T - 1.0948 \log T + 8.5874946 \times 10^{-5}T$$

The viscosity ($\text{mPa}\cdot\text{s}$) at $< 773\text{ K}$ is given by [8]

$$\eta = (0.1235 \pm 0.0018) \times (p/1000)^{1/3} \times e^{(597 \pm 9)/(1000T)}$$

Above 773 K , the equation is [8]

$$\eta = (0.0815 \pm 0.0013) \times (p/1000)^{1/3} \times e^{(1040 \pm 19)/(1000T)}$$

The surface tension (newtons per meter) in the range $370.98-1300\text{ K}$ is given by [8]

$$\sigma = 206.7 \times 10^{-3} - 1.0 \times 10^{-4}(T - 273.15)$$

Figure 51.1 shows some properties of sodium as a function of temperature.

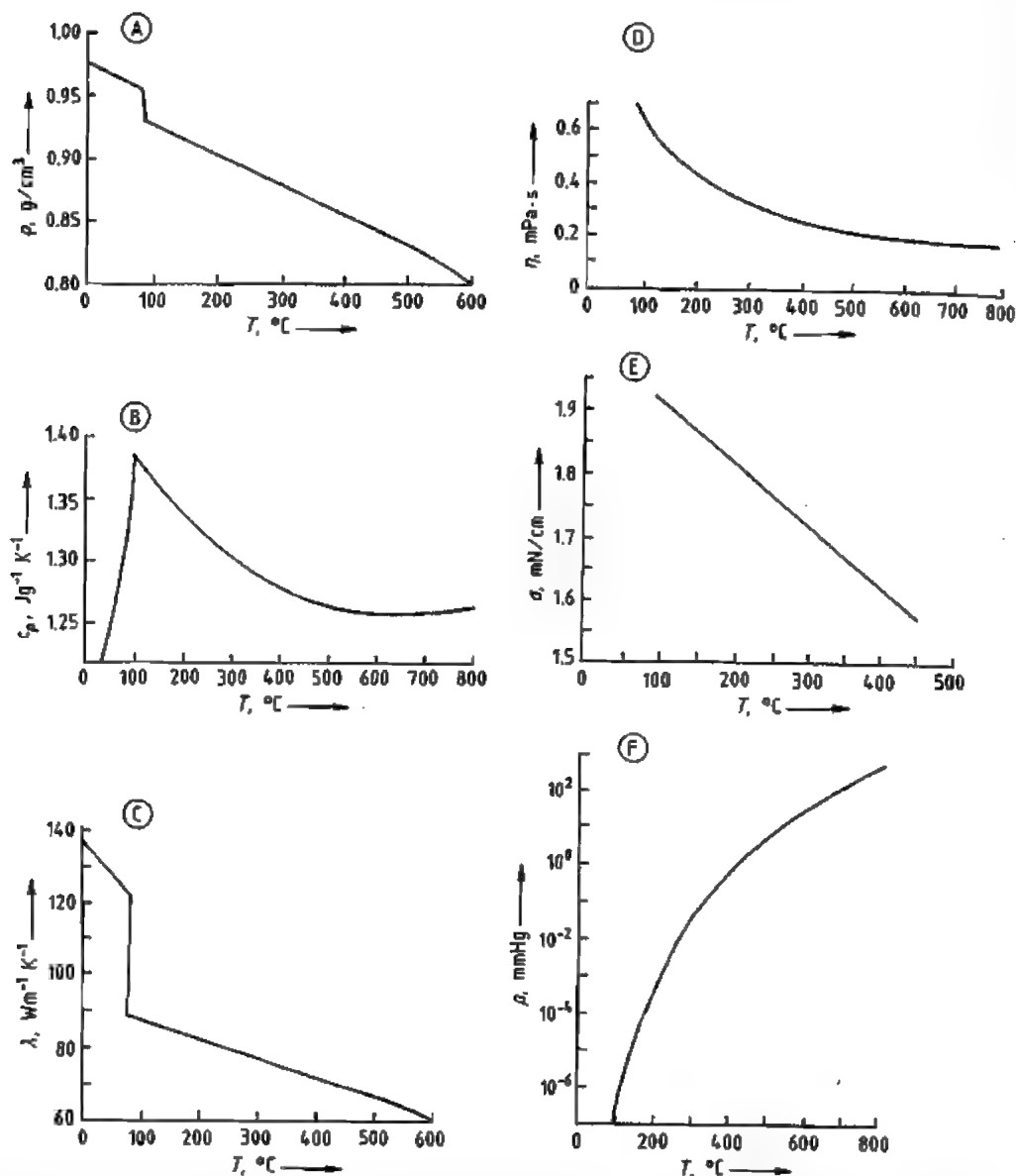
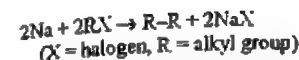
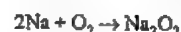
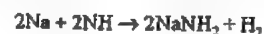
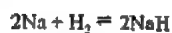


Figure 51.1: Some properties of sodium as a function of temperature [11]. A) Density; B) Specific heat capacity; C) Thermal conductivity; D) Viscosity; E) Surface tension; F) Vapor pressure.

Chemical Properties. The reactivity of sodium can be illustrated by the following equations [12, 13]:



The high reactivity of sodium is a result of its electronic configuration [14]. Sodium, like the other alkali metals, has only one s electron in its outer shell, which is very weakly bound due to shielding from the atomic nucleus provided by the completely filled rare gas shells.

• Sodium reacts with hydrogen at ca. 200–300 °C to form sodium hydride. In NaH, hydrogen is present as hydride ion. In organic syntheses, sodium hydride has little reducing action [15], its most important chemical property being high basicity. Sodium hydride reacts as a strong base not only with all acids, but also with all organic and inorganic compounds that contain an active hydrogen atom. Sodium hydride is more strongly basic than sodium amide [16]. However, in molten NaOH or eutectic salt baths, NaH behaves as a strong reducing agent toward metallic salts and oxides [17]. The system Na–H₂–NaOH–Na₂O has been investigated extensively [18, 19].

• Titanium was first produced in large quantities in 1910 by HUNTER, who reacted titanium tetrachloride with sodium in an evacuated steel bomb. In 1956, ca. 1500 t of titanium sponge, representing ca. 10% of the total world output, was produced by ICI by reducing titanium tetrachloride with sodium [20]. Also, Reactive Metals, Inc., of Ashtabula, Ohio, until recently, used sodium as the reducing agent in the production of titanium. However, by far the largest amount of titanium has been produced by the magnesium-based Kroll process. More recently, the electrolysis of TiCl₄ has become important.

The Hunter process is representative of many reactions in which the halides of most of the metals in periods 4–6 of the periodic table can be reduced with sodium to the metal, with formation of the corresponding sodium salt. Examples include the production of aluminum by using sodium as the reducing agent (Deville and Bunsen process, 1854) [4] and of thorium from thorium tetrachloride [4, 21–23] or

K₂ThCl₆ [24]. The elements potassium, beryllium, magnesium, boron, and aluminum can also be produced by this method. The reduction of KCl by sodium appears to go against the normal order of reactivity (K > Na). At 850–880 °C, the following reaction takes place:



Since potassium is more volatile, it is more readily distilled, so the equilibrium is shifted to the right and the reaction proceeds [9].

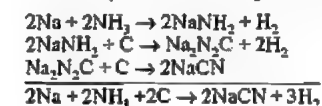
• Sodium amide is produced industrially by the reaction of molten sodium with ammonia at 300–400 °C.

Sodium dissolves in liquid ammonia to give a blue color that changes to a coppery red with increasing concentration. Solutions of alkali metals in liquid ammonia are powerful and selective reducing agents. Aromatic systems are reduced smoothly to cyclic mono- or dialkenes, and alkynes are stereospecifically reduced to *trans*-alkenes [9].

Sodium does not react with molecular nitrogen under normal conditions. Hence, nitrogen is a suitable protective gas, even at high temperature, for the production, storage, and transport of sodium [10].

Sodium azide, NaN₃, can be prepared by the reaction of dinitrogen oxide with sodium amide at 200 °C. The existence of Na₃N is very doubtful. The heavier alkali metals do not appear to form compounds of this type, possibly for steric reasons [9].

Prior to the 1960s (i.e., before modern catalytic methods for producing hydrogen cyanide became available [12]), sodium cyanide was produced via sodium amide and sodium cyanamide by the Castner process [12]:



Metallic silver and gold form complexes with NaCN in a smooth reaction under mildly oxidizing conditions. This is used in the extraction of these metals from ores or gold-bearing sand [12].

With carbon, sodium forms compounds of the acetylide type, M_2C_2 , and with graphite it forms a layered compound [8]. Sodium acetylide can be produced by the reaction of sodium with acetylene or by the thermal decomposition of $NaHC_2$ in a vacuum. Sodium acetylide can be used in the preparation of alkynes.

The reaction between graphite and sodium gives an intercalation compound with the approximate formula $C_{64}Na$ [8].

Sodium formate or oxalate can be produced in the reaction between carbon dioxide and sodium. Burning sodium reacts explosively with solid carbon dioxide; thus CO_2 extinguishers are unsuitable for sodium fires [10]. Alkali metals in liquid ammonia react with carbon monoxide to form colorless crystals of $Na_2C_2O_2$, which contain linear groups, $NaOC \equiv CONa$, linked together to form chains [9].

- Sodium reacts with oxygen to form the following oxides: monoxide (Na_2O), peroxide (Na_2O_2), and hyperoxide (NaO_2). The ozonide NaO_3 is also known [25].

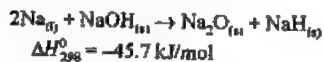
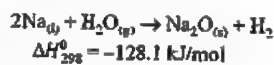
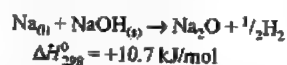
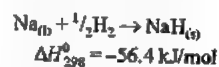
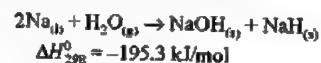
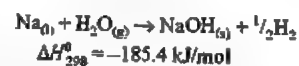
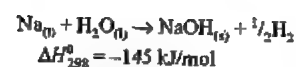
The reactions to form the monoxide and the peroxide are exothermic. The peroxide is manufactured in a rotating drum reactor. In the first stage, sodium reacts with air to form sodium monoxide, which reacts with oxygen or oxygen-enriched air in the second stage to form sodium peroxide [25].

The structure and chemical properties of the oxygen compounds of alkali metals have been investigated thoroughly [26].

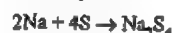
In normal atmospheric air, molten sodium can ignite at $> 115^\circ C$, but higher temperature is necessary in dry air. Combustion is exothermic, with the evolution of much smoke, and an intense white-yellow light is emitted with the formation of Na_2O and Na_2O_2 [10].

Sodium reacts with water to form sodium hydroxide and hydrogen. If the hydrogen evolved mixes with air, the gas mixture formed can explode with great violence [10]. The reaction of excess sodium with high-pressure steam in the absence of air gives sodium hydroxide and sodium hydride [8].

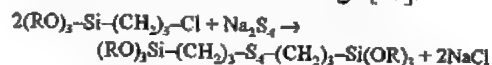
The heats of reaction of the individual reaction steps are given below [8]:



- Molten sodium reacts with stoichiometric amounts of molten sulfur under an inert atmosphere to form disodium tetrasulfide.



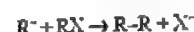
Disodium tetrasulfide is used industrially for the production of organofunctionalized silanes [27] by reaction with 3-chloropropyltrialkoxysilanes. In a nucleophilic reaction, the tetrasulfide anion displaces the chlorine atoms and links two propyltrialkoxysilane molecules with formation of a sulfur bridge [27].



- Halogens react with sodium with varying degrees of vigor. With fluorine, ignition takes place at room temperature, but no reaction occurs in liquid chlorine. With gaseous, dry chlorine, negligible reaction takes place at room temperature, but molten sodium burns in a stream of chlorine to form sodium chloride. This reaction takes place to a small extent in the Downs cell. Sodium is fairly stable toward bromine. Sodium and iodine can be melted together without reaction [10].
- Lower and primary alcohols react readily with sodium to form alkoxides. Higher and branched alcohols generally react very slowly due to the decreasing acidity of the hydroxyl group. The reaction velocity can be increased by raising the temperature and

by using finely divided sodium. Alkoxides are condensation agents of high basicity, used in the alkylation of carbon, nitrogen, and oxygen atoms (e.g., the mono- and dialkylation of malonic esters, acetoacetic esters, cyanoacetic esters, benzyl nitrile) and for base-catalyzed ring closure reactions to form nitrogen-containing heterocyclic compounds. Alkoxides are used as synthetic building blocks in the Williamson ether synthesis [11].

- The reactions of alkali metals with alkyl halides (Wurtz reaction) are heterogeneous and probably very complex [28]. Alkanes are formed when the alkylsodium compound initially formed displaces the halogen atom from an alkyl halide molecule:



Organometallic compounds of group IV A metals can be prepared by a variation of this synthetic method. For example, tetraethyllead can be prepared by reacting chloroethane with a lead-sodium alloy [29]:



51.4 Occurrence

Sodium is strongly electropositive, very reactive, and does not occur in nature in the elemental state, but always in cationic form in salts. Sodium is the seventh element in order of abundance in the Earth's crust (2.27%). It occurs in several minerals in association with other alkali metals. Extensive deposits of relatively pure sodium salts were formed by the evaporation of prehistoric lakes, a process that can still be observed [e.g., in the Great Salt Lake (Utah) and the Dead Sea].

Industrially important naturally occurring sodium compounds include rock salt (sodium chloride), trona (sodium carbonate), Chile saltpeter (sodium nitrate), mirabilite (sodium sulfate), and borax or kernite (sodium borate). Sodium chloride ($NaCl$) is the most used raw material in the inorganic chemical industry [9].

51.5 Production

51.5.1 Chemical Processes

Sodium can be obtained from many of its compounds by high-temperature reduction [4]. In the older thermochemical methods, sodium carbonate or sodium hydroxide was reacted with charcoal or coal, sulfur, or iron. Other compounds of sodium, such as the chloride, sulfide, sulfate, and cyanide were also used. A serious disadvantage of thermochemical methods was that reverse and secondary reactions occurred. Despite these problems, patents were applied for, covering many variations of the thermochemical methods of production [10]. In a Du Pont patent, sodium carbonate or sodium hydroxide was reduced with coal. The gases formed in the reaction were passed through molten tin, which absorbed the sodium vapor. Sodium was then recovered from the tin in an additional process step. According to a patent of Pechiney S. A., $NaCl$ vapor is passed over calcium carbide at $800-1000^\circ C$, and the sodium formed is collected in oil. In a Dow Chemical Co. process, sodium carbonate is reduced with coal at $> 1200^\circ C$. The sodium vapor formed is condensed in liquid sodium [10].

51.5.2 Electrolytic Processes

51.5.2.1 Development of Molten Salt Electrolysis of $NaOH$ and $NaCl$

Using the same principle by which DAVY discovered sodium, CASTNER developed a process for producing the metal on a large scale from molten sodium hydroxide in an electrolytic cell (Figure 51.2). This process was operated at Niagara Falls (United States) and Rheinfelden (Germany), and was the only practical method for sodium production from 1881 to the mid-1920s. Cheap hydroelectric power was available at both locations.

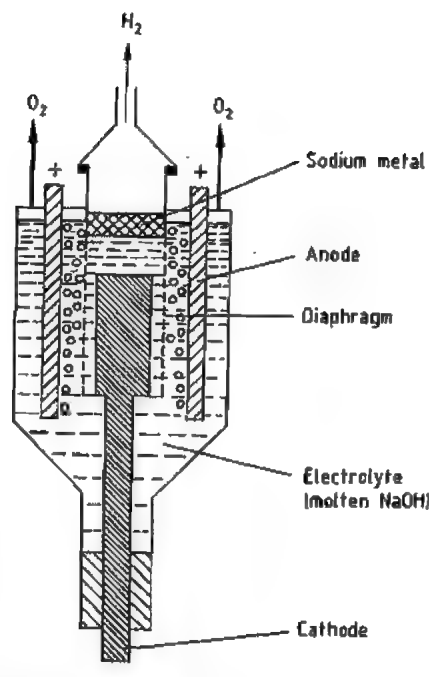
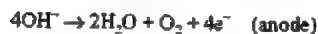
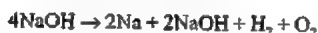


Figure 51.2: Production of sodium by the Castner process (1891).

The Castner process yields sodium, hydrogen, and oxygen:



The overall reaction is:



Thus the current efficiency cannot exceed 50%. In practice, current efficiencies of < 45%, were achieved.

Before sodium can be produced by this method, sodium hydroxide must first be obtained (e.g., by electrolysis of aqueous sodium chloride). Much research was therefore aimed at producing sodium by direct electrolysis of sodium chloride, which has the following advantages over sodium hydroxide as a starting material:

- Higher current efficiency during sodium production
- Cheaper raw material

- Easier handling
 - Production of chlorine as by-product
- Its disadvantages are:

- The need to install a plant for chlorine purification and sometimes also for chlorine liquefaction
- Increased technical problems associated with chlorine
- Higher melting point

Many cells were developed at this time, but only the Downs cell solved the problems encountered with other cells. With the Downs cell, the foundations were laid for large-scale sodium production. Along with the Hall aluminum cell and the Dow magnesium cell, this is one of the most successful molten salt electrolysis cells ever developed [30].

In the Castner cell (Figure 51.2) a cylindrical nickel anode surrounds the copper cathode concentrically. If NaOH is replaced by a molten salt containing NaCl, the collection and containment of the chlorine evolved cause problems, which are solved only when the positions of the anode and cathode are reversed, as in the Downs cell in which the anode is surrounded concentrically by the cathode.

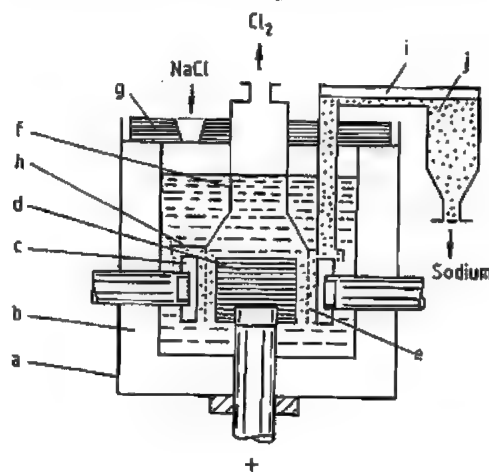


Figure 51.3: The Downs cell (original form): a) Steel vessel; b) Ceramic lining; c) Iron cathode; d) Graphite anode; e) Wire gauze diaphragm; f) Dome for collecting chlorine gas; g) Insulating lid; h) Channel with riser pipe for collecting sodium; i) Sodium overflow; j) Sodium holding vessel.

Figure 51.3 is a schematic of the Downs cell in its original form [13, 31]. It consists of a lined steel vessel in which the graphite anodes pass through the floor, and the two electrical conductors connected to the cathodes pass through the walls. The anode is surrounded by the cylindrical iron cathode.

The Downs process used a mixture of 60% CaCl_2 and 40% NaCl at an operating temperature of 560–585 °C. This composition represents a compromise between the melting point of the salt mixture and the sodium content. The eutectic mixture, which contains 66.8% CaCl_2 and 33.2% NaCl , melts at ca. 505 °C. Although increasing the CaCl_2 content reduces the melting point of the binary mixture, it also decreases the concentration of sodium in the cathode space due to the equilibrium



The operating temperature of ca. 580 °C is well below the temperature of maximum solubility of sodium in the molten salt. The density of the salt is 1.89–1.94 g/cm³. Along with sodium metal, calcium (ca. 3.5–4%) is deposited at the cathode. Because of the high melting point of calcium (804 °C) and its low solubility in sodium, the alloy phase Na–Ca can accumulate in the sodium and cause blockages in the equipment for continuous removal of sodium from the cell. These solid deposits must be scraped off the walls of this equipment. Most of the calcium can react with NaCl in the melt (by the above reversible reaction), again forming calcium chloride. A further quantity of calcium is removed from the sodium by filtration at 110 °C. The sodium purified in this way contains < 400 ppm calcium. Some of the early cell types used for sodium production (e.g., the Castner, Ciba, McNitt, and Downs cells) are described in detail in [4, 13].

51.5.2.2 Description and Operation of NaCl Molten Salt Electrolytic Cell

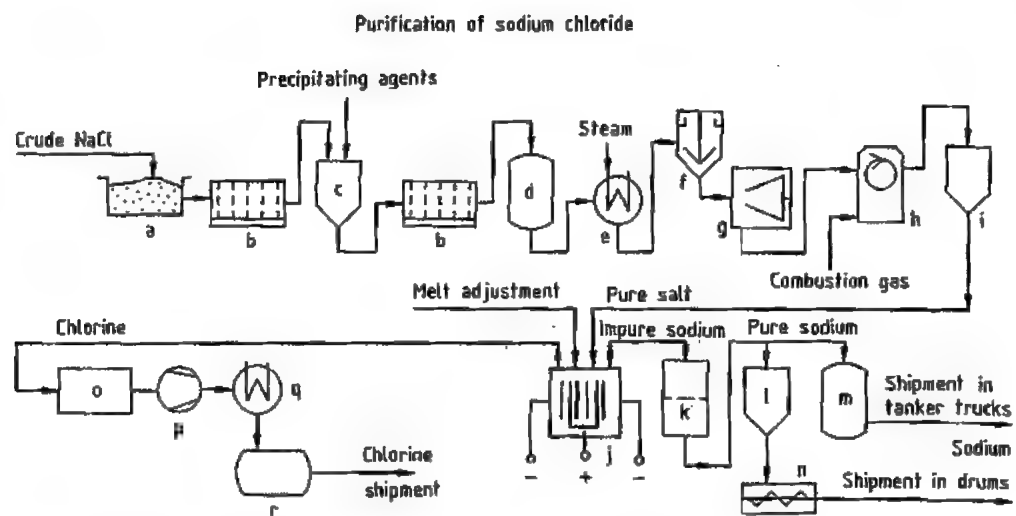
Large sodium production plants have 40–50 d.c. electrolytic cells connected in series to

achieve optimum efficiency. The voltage of each cell depends on the operating conditions (current, temperature, melt composition, sodium production rate) and changes with time.

Today, electrolytic cells are usually operated at up to 45 kA, with outputs of up to 800 kg/d sodium. For problem-free operation, the individual electrolytic cells, with their associated equipment, must be electrically insulated from neighboring cells and from the ground. The graphite used to make the anodes in the electrolytic cell is resistant to nascent chlorine in the chloride melt even at high temperature, and its electrical conductivity is adequate at the operating temperature. However, all oxygen-containing compounds must be removed from the salts used to prevent corrosion of the graphite. Salts of heavy metals and salts of aluminum and magnesium also cause problems in molten salt electrolysis.

Because of the requirement for high-purity raw materials, extensive facilities are required to purify the salt used in the electrolytic process [5]. Sodium chloride is first dissolved in water to give a saturated brine. Barium chloride and sodium carbonate are added, mainly to remove CaSO_4 . The precipitate of BaSO_4 and CaCO_3 forms a sediment together with clay minerals present in the crude salt. The filtered solution is then evaporated to crystallize the salt, which is recovered by centrifugation and dried to a water content of < 600 ppm, which is important for optimum operation of the electrolytic cells [5]. A process for the purification of sodium chloride by recrystallization alone, without the use of precipitating agents, has been reported recently [32]. A schematic of a sodium production process is given in Figure 51.4.

At the melting point of sodium chloride (808 °C), chlorine would severely corrode all the cell components that come in contact with it. Also, the vapor pressure of sodium is high at this temperature (50 kPa), and its solubility in molten salt is also high (4.2%). Therefore lower melt temperatures must be used. A ternary salt mixture is normally employed (NaCl – BaCl_2 – CaCl_2). The temperature of the molten salt in the cell is ca. 600 °C.



Purification and liquefaction of chlorine

Electrolytic production and purification of sodium

Figure 51.4: Flow sheet of sodium production: a) Dissolution vessel; b) Filter; c) Precipitation vessel; d) Vessel for pure brine; e) Evaporator; f) Thickener; g) Centrifuge; h) Rotary dryer; i) Pure salt bunker; j) Electrolysis cell; k) Sodium filter; l) Sodium storage; m) Sodium tank; n) Casting; o) Chlorine purification; p) Chlorine compressor; q) Liquefier; r) Chlorine storage vessel.

From this molten salt mixture, ca. 1% calcium is deposited on the cathode with the sodium. The crude sodium removed from the cell also contains 0.3% calcium oxide, 0.3% sodium oxide, and small quantities of entrained molten salt. A product of marketable quality [10] is made by cooling the sodium to ca. 120 °C and removing the impurities that separate with the aid of a candle filter equipped with gauze. The filter cake obtained consists of calcium, sodium, chlorides, and oxides. Various methods of recovering calcium or calcium alloys from the filter cake have been proposed, but none has had commercial success [1, 33, 34].

In modern cells (Figure 51.5) the cathode and anode are subdivided into four pairs of electrodes. Four steel tubes, welded together, surround the four cylindrical graphite anodes concentrically. The cell design has been developed over the course of time [13, 35–40].

The anodes usually take the form of a hollow cylinder with slits in the wall [41, 42]. Al-

ternatively, anode blocks can be made with conical central holes, which increases the proportion of graphite and decreases the resistance along the length of the anode [43].

The four steel cathodes are connected to the electrical supply by two conducting rods that pass through the side walls of the cell. The annular gap between the anode and the cathode is < 50 mm wide. A cylindrical iron mesh is placed in this gap, forming a diaphragm to separate the products, sodium and chlorine. The cylindrical diaphragm is attached to a device that collects sodium and chlorine from the four electrode pairs. Above the cathode space (between the cathode and the diaphragm) is a channel with a closed roof to collect the liquid sodium that rises through the melt in the form of droplets. Four shafts lead gaseous chlorine from the four anode spaces upward into a dome. Chlorine collects in the dome above the surface of the melt and is removed via an outlet at the top.

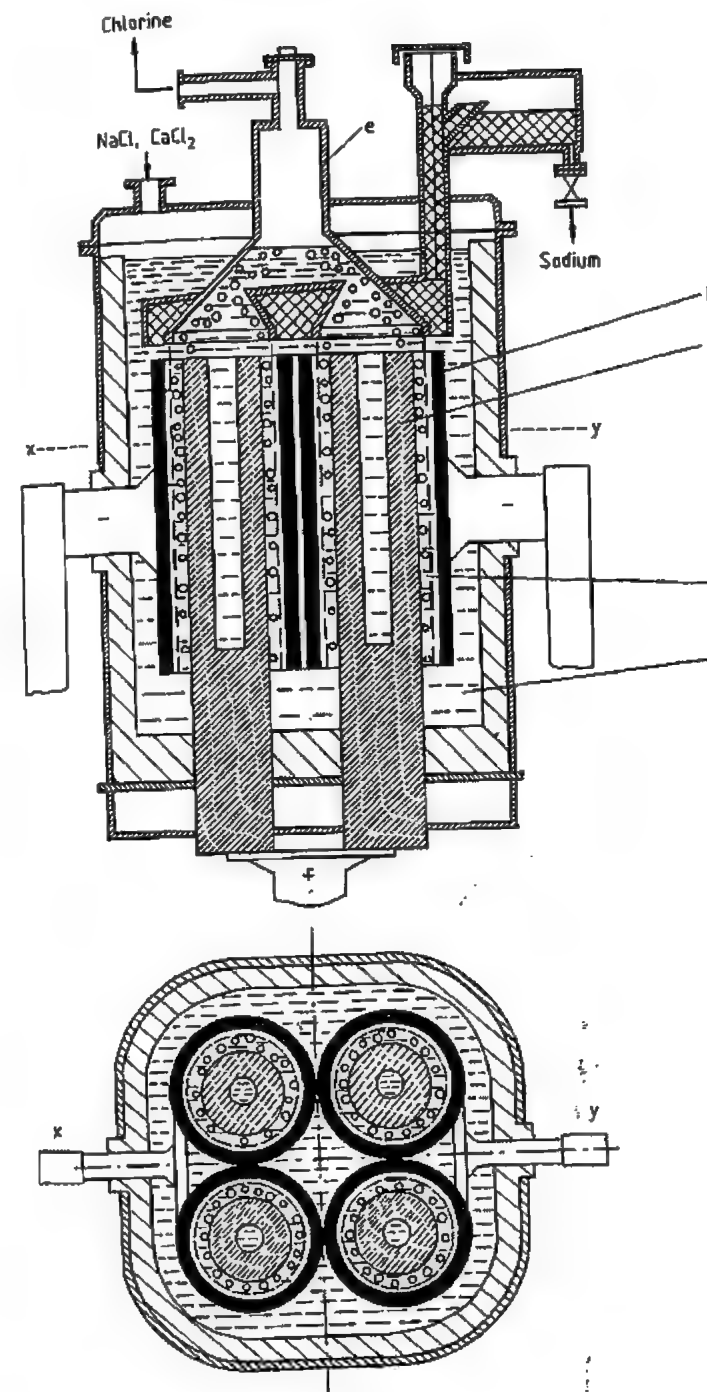


Figure 51.5: Modified Downs cell: a) Anode; b) Cathode; c) Molten salt; d) Diaphragm; e) Chlorine dome.

The chlorine pipe leading from the top of the dome is fitted with an access cover that is used to monitor the extraction of chlorine from the cell into the collection device. This cover can be provided with a tongue-and-groove seal to prevent intake of air into the chlorine [44].

The roof of the sodium-collecting device usually slopes upward, so that sodium flows smoothly into the vertical riser pipe. The device for collecting the sodium and chlorine may also include a tube for promoting circulation of the melt. The chlorine bubbles that form and rise at the graphite anodes improve the circulation of the melt in the anode space. The rising gas bubbles cause the surface of the melt to rise in the chlorine collection hood, so that the salt level is higher inside the hood than outside. Circulation of the molten catholyte is improved by the upward flow of the sodium. Downward flow of the catholyte takes place by natural convection at the inactive outer walls of the cathodes. By including a circulation tube, the flow of the catholyte can be improved, enabling the electrolyte from the chlorine-collecting hood to flow downward into the central cathode space [45].

Sodium flows from the riser pipe of the collecting device into a closed collection vessel [6]. The calcium dissolved or suspended in the sodium separates as a solid on the inner walls of the riser pipe. Blockage is prevented by means of an agitator inside the riser pipe that scrapes calcium from the walls. Since the density of calcium is higher, it sinks down through the sodium to the salt level, where partial reaction with NaCl of the ternary salt mixture occurs to form calcium chloride and sodium. Various designs of this agitator mechanism in the riser pipe have been described [46, 47]. Calcium, oxides (e.g., Na_2O_2 and CaO), and entrained melt settle at the bottom of the collection vessel, which is therefore equipped with a stirrer [48]. A design has also been described in which this stirrer is combined with the agitator in the riser pipe [49].

A characteristic of another possible design [49] is, that the open overflow is replaced by

an overflow pipe between riser pipe and collecting vessel (Figure 51.5).

If the overflow pipe is at the correct height, the hydrogen liberated occasionally at the cathode and the chlorine diffusing into the cathode space do not enter the collector. The gases that collect above the sodium in the gas space of the riser pipe are removed by a stream of inert gas (e.g., nitrogen) [50].

An overview of the procedures for starting up a Downs cell is given in [51].

The salt used for the initial melting operation can be a solid salt mixture or a powdered, solidified melt. Melting is achieved by short-circuiting the electrodes with so-called starter blocks. A number of these starter blocks are wedged between the anode and cathode, and the cell is then filled with salt mixture. In order to melt the mixture, a low electric current is passed through the cell. When sufficient salt has melted, the starter blocks are removed, the current is increased to the normal operating level, and the diaphragm is inserted.

In an improved technique, the cell is filled with solid powdered electrolyte or salt mixture until the level is just below the top of the electrodes [52]. The part of the cathode that is not covered is then heated to a temperature well above the melting point of the salt mixture. If a small amount of liquid melt is introduced from another cell, a low electric current can be passed between the electrodes. While solid salt mixture is being added, the electric current is slowly increased until the cell is filled with molten salt mixture to the correct height. The diaphragm is then introduced. A further improvement in the procedure for starting up a cell has now been developed, in which the cell is preheated, and sufficient liquid melt from neighboring cells is added to enable the diaphragm to be introduced and the electric current to be applied immediately to the cell [51]. Sodium production can then begin without the need for the complicated procedures described above.

Cells normally used today have a capacity of ca. 8.4 t molten salt with a density of ca. 2.7 g/cm³. Cells have a working life of about three years. They are normally taken out of commis-

sion when the cell voltage and hence the energy consumption become too high due to wear of the anodes. Operating data for a Downs molten salt cell are [5]:

Operating temperature	590–610 °C
Lifetime of cell	1100–1200 d
Cell voltage	6.5–7 V
Cell current	≤ 45 kA
Current efficiency	80–90%
Consumption of electrical energy	9.8–10.5 kWh/kg Na

The voltage required for the electrolysis of sodium chloride is ca. 3.4 V, which is ca. 50% of the cell voltage.

In the course of a working life, various changes in the operating conditions of the Downs cell take place that lead to increased energy consumption. These changes are mainly a result of loss of graphite from the anodes due to corrosion and erosion, and buildup of impurities in the melt, leading to the accumulation of precipitated material on the cell floor [53]. A cell that consumes ca. 280 kW per day to produce 700 kg sodium uses ca. 116 kW for decomposing the NaCl to sodium and chlorine, which corresponds to a power efficiency of ca. 41%. Heating the charge of NaCl from room temperature to the operating temperature requires 9.9 kW, and an additional 11.1 kW is required for melting, amounting to ca. 8% of the total power consumption. To maintain a constant melt temperature, a cooling power of 143 kW is required (i.e., ca. 51% of the total power consumption). The difficulty in operating a cell consists in maintaining an optimum balance of the continually changing rate of heat production due to the internal resistance of the cell, recombination of sodium and chlorine to form sodium chloride, and the rate of removal of excess heat. Here, care must be taken that the flow pattern and hence the cell resistance are not disturbed by the adjustments made to control the cooling [53].

Electricity consumption figures for large installations for the production of sodium by molten salt electrolysis are given in [54]. The consumption of electrical energy for the electrolysis is 9.8–10.5 kWh/kg pure sodium, depending on the length of time that the cell has been in operation. If the associated equipment

(ventilation, heating of vessels, and equipment) is included, this increases to 11.5–12.0 kWh/kg pure sodium. If a plant for purifying the raw salt and a plant for the purification and liquefaction of the chlorine produced is taken into account, the total energy consumption is 12.0–13.0 kWh/kg pure sodium.

51.5.2.3 Properties of the Electrolyte

The electrolyte consists of a mixture of NaCl, CaCl_2 , and BaCl_2 . Some properties of these salts are listed in Table 51.1.

Table 51.1: Physical properties of salts used in the Downs cell.

Property	NaCl	CaCl_2	BaCl_2
Melting point, °C	58.45	110.99	208.27
Density of molten salt at mp, g/cm ³	1.6	2.1	3.2
Electrical conductivity of the molten salt at mp, $\Omega^{-1}\text{cm}^{-1}$	3.6	2.0	2.0

The melting point of the ternary eutectic of these salts is 450 °C. However, the eutectic mixture is not suitable as a working electrolyte since the CaCl_2 content of ca. 50% would result in an unacceptably high proportion of calcium in the sodium product. A mixture of 28% NaCl, 25% CaCl_2 , and 47% BaCl_2 (51 mol% NaCl, 24 mol% CaCl_2 , 25 mol% BaCl_2) is suitable. This mixture melts at 570 °C, and the calcium content of the sodium produced is ca. 1%.

If the rate of sodium chloride addition varies during electrolysis, the NaCl content of the mixture and its melting point fluctuate, but the BaCl_2 – CaCl_2 weight ratio remains practically constant at 1.88. For example, melting points of the mixture are 550 °C for 26% NaCl and 600 °C for 32% NaCl.

The current efficiency would be 100% if pure sodium were deposited at the cathode, and no back reaction of sodium with chlorine occurred to form sodium chloride. The diaphragm prevents sodium droplets formed at the cathodes from reacting with the chlorine bubbles formed at the anodes.

However, another possible mechanism for the back reaction, associated with the slight

solubility of sodium in the melt, causes the melt to become a partial electronic conductor [55]. The dissolved sodium dissociates into sodium ions and electrons [56]. The electrons and surrounding cations form color centers, called F-centers, that impart a bluish appearance to the melt.

If dissolved sodium is present in the cathode compartment, electrons migrate in the electric field from the cathode across the diaphragm where they react with sodium ions to form sodium. This sodium recombines with the gaseous chlorine present in the anode compartment, which decreases the current efficiency.

To remove dissolved metal (mainly sodium) from the electrolyte, two methods of regeneration have been proposed. In both of these, regeneration of the melt takes place outside the cell. The melt can be melted repeatedly and allowed to solidify, so that the dissolved metals coagulate and separate from the salt melt [57], or the dissolved metals can be oxidized by passing air through the salt melt [58].

Under some circumstances (e.g., during a plant shutdown), the sodium production rate of a cell may have to be reduced for a period of time without interrupting the ohmic resistance heating of the cell. To achieve this, 0.1–0.5% aluminum oxide can be added to the melt [59]. Solid bridges of aluminum form between the cathode and the diaphragm, and the latter starts functioning as the cathode. Recombination of sodium with chlorine is no longer prevented and the current efficiency is drastically decreased. Since the melting point of aluminum (660 °C) is above the operating temperature of the cell the aluminum bridges do not melt. To restore the current efficiency to its normal value, the bridges are broken by shaking the diaphragm or replacing it.

51.5.2.4 Other Electrolytic Processes

Sodium can be deposited electrolytically on a molten lead or mercury cathode to form an alloy [31]. Using this principle, ASHCROFT has

designed a double cell, in whose primary cell an amalgam is formed by electrolysis of aqueous NaCl with a mercury cathode. Alternatively, molten sodium chloride is electrolyzed with a molten lead cathode. The alkali-metal alloy is then transferred to the secondary cell where the molten salt electrolyte (*mp* ca. 200 °C) is NaNH_2 , NaCN, or an NaOH–KOH mixture. In the secondary cell, the alloy is anodically decomposed into its constituents, whereby the alkali metal is deposited on the cathode and the alloying metal is returned to the primary cell. However, the Ashcroft process could not compete with other electrolytic processes.

In the Szechtman process, a sodium–lead alloy is produced by electrolysis of molten sodium chloride with a molten lead cathode. The sodium is then recovered from the alloy formed by distillation [31].

Sodium can be recovered by electrolysis of the amalgam produced in the chlor-alkali electrolysis process. Several electrolytic methods have been developed for recovering sodium from the amalgam, but they have not been used commercially (e.g., the Tekkosha process [10, vol. 17, p. 151]).

Reference [60] describes the use of a solid ceramic that conducts sodium ions (as used in the sodium-sulfur battery) as a divider for a two-compartment cell. This method allows low-melting sodium salts or salt mixtures to be used to produce sodium [1, vol. 21, p. 193; 60–64]. This type of cell should give current efficiencies approaching 100% with 30% lower energy consumption, as well as producing high-purity sodium. The process has, however, not been operated on a large scale [1].

51.6 Safety

If appropriate regulations and special safety precautions are observed, sodium can be handled safely in inert systems or even in the open air, provided its temperature is < 115 °C [11]. The possibility of leakage from pipework and vessels containing molten sodium must be guarded against, because spontaneous ignition

can occur at > 115 °C [65]. Effectively fighting sodium fires requires a detailed knowledge of the combustion properties of sodium [66]:

- In sodium fires in vessels in the open air, the temperature in the reaction zone is 900–1000 °C. Even in unfavorable conditions, the temperature of the sodium remains below its boiling point. Hence, high rates of combustion, such as those observed with boiling liquids, do not occur with sodium.
- For any equipment carrying molten sodium, a special system of containment must be provided that safely retains sodium escaping from a leak and effectively prevents contact with air so that a fire cannot develop.
- The preferred material for insulating sodium-carrying pipework and vessels is rock wool or slag wool with a low content of free silica. For higher temperature, ceramic fibers are suitable. Fibrous insulation made from molten materials is less hygroscopic than powdered or foamed porous material and is therefore preferable. The action of burning sodium on concrete has been studied in detail [67, 68].

The question of an optimum extinguishing agent has been discussed in the literature. The provision of inert-gas atmospheres such as nitrogen or argon in areas at risk from fire is generally too expensive. For pure sodium fires, which take place at the surface, a special expanded graphite is a very suitable fire-fighting material [69]. This powder floats on liquid sodium and thus prevents access of oxygen. Other powders, however, sink in the sodium and hence fail to provide a covering layer. The amount of such powder used on a vessel of molten sodium must therefore always be sufficient to absorb all the sodium and shield it against air [66]. To extinguish small spillages of sodium that have caught fire, powders specially developed and permitted for metal fires (Class D fires), as well as dry salt, dry sand, and anhydrous sodium carbonate, are suitable [11]. Water, foam, halons, CO_2 , and fire-extinguishing powders of Classes A, B, and C must not be used under any circumstances [11].

Sodium burns to form sodium oxide (Na_2O) and sodium peroxide (Na_2O_2). With surface fires, 10–30% of the sodium forms an atmospheric aerosol with a typical particle size of 0.001–0.002 mm. They combine with atmospheric moisture within a few seconds to form sodium hydroxide. This is followed by reaction with carbon dioxide to form sodium carbonate or hydrogencarbonate, which takes about 3–5 min [70–72].

To clean equipment contaminated with sodium, the sodium-containing residues are first removed mechanically and then disposed of (e.g., by controlled combustion). The remaining sodium can then be converted into hydroxide by steam. The excess steam renders the reaction zone inert [11]. The removal of sodium by melting and cleaning out with steam and an alcohol water mixture (isopropanol with 5% water) is described in [73]. Small amounts of sodium in the laboratory can be converted to alkoxides, first with isopropanol, then with ethanol, and finally with methanol. Only when hydrogen evolution has ceased should the solution be treated with water. Very small amounts of sodium can be disposed of by storage under paraffin oil in an open beaker, which results in gradual conversion to the hydroxide.

51.7 Uses

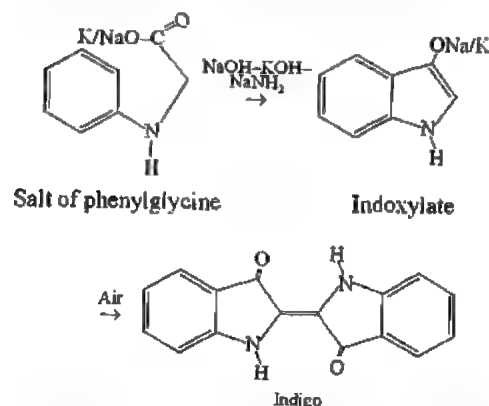
Sodium Compounds. Some sodium compounds are important because of their nucleophilic properties.

Sodium hydride [74] is produced from sodium and hydrogen at 200–350 °C. Large quantities are reacted with trimethyl borate to form sodium borohydride



which is a very good hydrogenation and reducing agent. Its reducing power can be controlled by selection of the solvent and by adding ionic compounds. Sodium hydride reacts with the following compounds to give their sodium salts [103]: alcohols, phenols, thiols, amines, ketones, alkynes, and carboxylic acids.

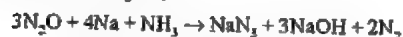
Sodium amide [74], which is produced from sodium and ammonia, is used mainly to synthesize indigo by the Heumann-Pfleger reaction and to produce sodium azide for the explosives industry. In the Heumann-Pfleger indigo synthesis, sodium amide is used to cyclize phenylglycine, forming indoxyl in very high yield [12, 74]. The reaction is carried out in molten sodium amide at 180–200 °C.



Sodium azide is synthesized by reacting molten sodium amide with dinitrogen oxide:



On an industrial scale, liquid ammonia is used as a solvent. In a variation of the method, sodium and ammonia are used without isolating NaNH_2 [9]



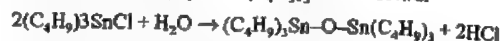
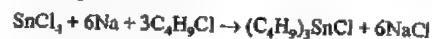
Sodium alkoxides [74] are used for C-, N-, and O-alkylation reactions (e.g., of malonic esters, acetoacetic esters, cyanoacetic esters, and benzyl nitrile) and in ring-closure reactions to form nitrogen-containing heterocycles. Alkoxides are used as synthetic building blocks in the Williamson ether synthesis.

Organometallic Compounds. The production of organometallic compounds is an important use of sodium. Organometallic compounds of group IV B metals can be prepared by a modified Wurtz synthesis [74].

Organotin compounds can be produced by the reaction

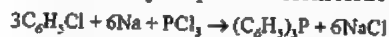


which, however, is used less often than other methods. Tributyltin oxide is an effective wood preservative:

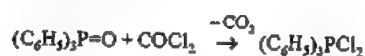


Tetrachyllead, PbEt_4 , is produced by reacting a sodium-lead alloy with chloroethane. Use of the antiknock agents [75] PbEt_4 and PbMe_4 is being increasingly restricted as a result of environmental legislation.

Synthesis of Vitamin A. The preferred method for the production of vitamin A involves the Wittig reaction, i.e., the reaction of methylenetriphenylphosphorane with benzophenone to give triphenylphosphine oxide and 1,1-diphenylethylene [76]. Triphenylphosphine is produced from chlorobenzene, sodium, and phosphorus trichloride [76].



Since the expensive triphenylphosphine is irreversibly converted to triphenylphosphine oxide in the Wittig reaction, ways have been sought to reuse the latter. An economic process has been developed in which the phosphine oxide is reacted with phosgene to give the dichloride, which is coproportionated with phosphorus [76].



Metallurgy. Metals such as titanium, zirconium, tantalum, hafnium, and niobium can be produced in high purity by reacting their chlorides with sodium. Pure titanium was first prepared in 1887 by two Swedish chemists, using the reaction



This method of preparation became known as the Hunter process. The reaction of sodium with titanium tetrachloride is usually carried out by placing the two reactants in an evacuated steel bomb and initiating the reaction by passing an electric current through a wire. Other methods of production are now available (e.g., a process involving direct electrolysis of titanium tetrachloride).

Small amounts of sodium are used in lead refining, for optimizing aluminum silicon melts and improving the properties of bronzes [11]. Sodium treatment [77] of Al-Si melts prevents anomalous crystallization, characterized by the precipitation of needle-like or lamellar silicon [78–80]. Sodium leads to supercooling processes [81, 82] that result in rounded eutectic silicon, normal fine eutectic solidification, and improved material properties, especially tensile properties [83].

Sodium-Sulfur Batteries. Rechargeable batteries with liquid sodium as the anode, sulfur-sodium polysulfide as the cathode, and sodium-doped aluminum oxide as the solid electrolyte are available for testing in the automobile industry [5, 84].

The two active materials, sodium and sodium polysulfide, are separated by a solid electrolyte of β -aluminum oxide, which conducts sodium ions. The operating temperature of the battery is 300–350 °C [85]. The most important component of a sodium-sulfur cell is the tube of solid electrolyte that separates the two molten electrodes. This material must be highly permeable to sodium ions and have a long lifetime to give a sodium-sulfur battery with a high power density and long working life [86].

Sodium as a Heat-Transfer Medium. The alkali metals, particularly sodium, were first used on a large scale as heat-transfer media by the nuclear energy industry. Today, liquid sodium is used worldwide as a coolant in fast breeder reactors. Power stations may contain several thousand tonnes of the metal. Both its nuclear properties and its very favorable thermal properties have led to the choice of sodium to cool fast breeder reactor cores, where the heat flux is high. Alkali metals are also used to a limited extent as heat-transfer media outside the nuclear industry [87]. In a solar energy plant in the Mojave Desert, California, sodium is used to store energy and transfer it from the collector to the steam generator [88].

51.8 Alloys

Sodium-potassium alloys [89] are used mainly in heat exchange systems, because of their good thermal conductivity and the wide temperature range over which they are liquid. The physical properties of two typical Na-K alloys are listed in Table 51.2. A review of physical properties and chemical reactions is given in [13]. Large-scale production is described in [5]. The ternary alloy, 12% Na, 47% K, and 41% Cs, has the lowest known melting point (–78 °C) of all metallic systems [9].

Table 51.2: Physical properties of Na-K alloys [8].

Property	Composition, % K	
	44	78
Melting point, °C	19	–12.67
Boiling point, °C	825	784
Density, kg/m ³ (100 °C)	886	847
Viscosity, mPa·s (250 °C)	0.316	0.279
Heat capacity, kJ/kg·K ^{–1} (200 °C)	1.096	1.045
Thermal conductivity, Wm ^{–1} K ^{–1} (200 °C)	26.36	25.10

Sodium Amalgams. Sodium and mercury form the following intermetallic compounds: NaHg_4 , NaHg_2 , Na_2Hg_8 , NaHg , Na_3Hg_2 , Na_5Hg_2 , and Na_3Hg [90, 91]. A liquid amalgam containing ca. 1% sodium is an intermediate product in chlor-alkali electrolysis and is used to produce sodium hydroxide solution. Amalgams with higher sodium content (1.25%) are viscous liquids. Still higher sodium contents result in silvery-white crystalline solids [10]. The physical properties, chemical reactions, and production of sodium amalgam are described in [13].

Many attempts have been made to utilize the reducing properties of sodium amalgam in chemical syntheses [92]. Sodium dithionite is produced on a large scale by the reduction of SO_2 with sodium amalgam. Other uses of sodium amalgam include the production of sodium sulfide, reduction of salicylic acid to salicylaldehyde, and reduction of nitrobenzene to azobenzene. These reactions are no longer of industrial importance. The reaction of sodium amalgam with alcohols in a vessel

filled with graphite spheres to form alkoxides is used to a limited extent [92].

Sodium amalgam formation can be used to recover mercury from mercury-containing button cells. After treatment with molten sodium, the nonextractable solids are removed, and the amalgam is decomposed electrolytically into its constituents with a solid electrolyte made of sodium-ion-conducting $\beta\text{-Al}_2\text{O}_3$ [93].

51.9 Packaging and Transport

51.9.1 Sodium Metal

Alkali metals are often marketed in shaped pieces of various sizes and weights. However, sodium is supplied to the customer mainly in the form of cast blocks produced by pouring the molten metal into containers and allowing it to cool and solidify. The shaped pieces are produced primarily by melting and casting the liquid metal. Alkali metals, especially sodium, are also pressed into variously shaped billets while in the solid state. The most serious disadvantage of these processes is the formation of impurities by reaction of the metal with air and atmospheric moisture. Also, the high pressure required for pressing the solid metal leads to wear. Pressing solid alkali metals is always a batch operation. The output of the machine is therefore limited, and the labor costs are high compared to a continuous process.

The production of alkali metal billets by continuous casting under pressure has also been described. In the presence of a lubricant the molten metal is forced by a pump through a die cooled to below the melting point of sodium [94].

In the extrusion molding process described in [95], molten metal is charged batchwise into the so-called feeder and, after cooling, until it is in a hot plastic state, is formed into an ingot, which is then extruded to form a billet by means of a plunger.

In the technique described in [96], two separate sets of machinery are used for extrusion

of the alkali metal. The molten metal is fed into a gear pump, which delivers liquid metal. In a cooler, which is separate from the pump, the liquid alkali metal is cooled below its melting point and pressed into a solid shape under pressure from the gear pump (ca. 15 MPa).

In a state-of-the-art process [97], liquid alkali metal is fed into a twin-screw extruder, which is cooled such that the temperature falls to slightly below the melting point of the metal just before the extrusion die. The alkali metal is thus solid but sufficiently ductile for extrusion. The extrusion pressure at the outlet is 3–5 MPa.

The alkali-metal billet produced can be cut by an automatic cutting device, sometimes under a protective gas, to produce lengths suitable for packing. Figure 51.6 shows a schematic of an extrusion plant for the production of alkali-metal billets [97].

After manufacture, sodium is in the molten state and can be filled immediately into freight containers. The following types are available:

- Rail tank cars with a capacity of up to 45 t sodium
- Road tank vehicles with a capacity of up to 20 t sodium
- Iso-containers with a capacity of up to 20 t sodium
- Special containers with a net capacity of up to 5 t sodium, and smaller packaging units in the form of drums of various types

Sodium is usually transported in the solid state for safety reasons and therefore must be remelted before it is emptied from the containers. This method of shipment allows the metal to be delivered in a very pure form. However, special handling equipment at the unloading site is required.

51.9.2 Transport Regulations

Sodium metal is a Class 4.3 hazardous material for all kinds of transport [98]. Detailed transport classifications read:

- Road and Rail (Europe), ADR/RID: Class 4.3, No. 11a

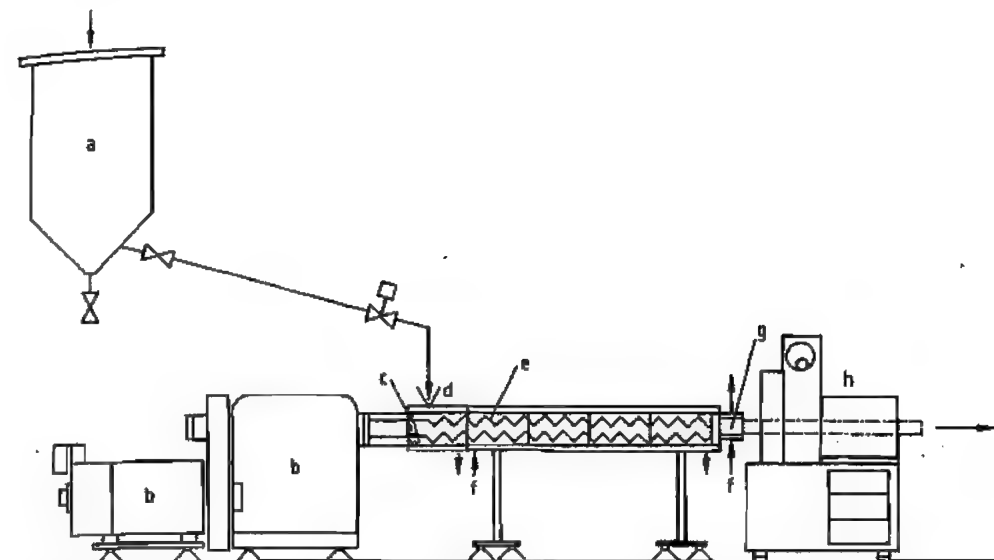


Figure 51.6: Schematic of an extrusion plant for the production of alkali-metal billets [97]: a) Sodium storage tank, heated; b) Drive; c) Sealing layer of sodium; d) Feeding nozzle; e) Twin-screw extruder; f) Heating and cooling jacket; g) Extrusion die; h) Cutting machine.

- Inland Waterways (Europe), ADNR and ADN: Class 4.3, No. 11a
- Sea Cargo (Worldwide), IMDG Code: Class 4.3, UN No. 1428, PG. I
- Air Cargo (Worldwide), ICAO-TI and IAT-ADGR: Class 4.3, UN No. 1428, PG. I

The European transport regulations were harmonized with the UN-recommendation-based regulations for sea and air transport of January 1, 1993. Thus sodium metal may be transported worldwide by using a unified packing system. However, different weight limits and packaging requirements are specified for various methods of transport.

51.9.3 Break-Bulk Packaging

For all kinds of transport UN-approved PG. I packaging has to be used. PG. I means the highest test standard for performance-oriented packaging. The packaging must have no venting device.

Road and Rail Transport in Europe. Sodium metal must be hermetically sealed, so that neither moisture nor any other substance can penetrate the packaging and come in con-

tact with the contents. The provision to cover the sodium with an inert gas or protective liquid is no longer required.

The following types of packaging are permitted: single packaging such as drums and canisters with removable head (made of steel or plastic) with a maximum capacity of 450 L or a net weight of 400 kg, as well as combination packaging (such as glass containers of 5-kg capacity, plastic containers of 30-kg capacity, or metal containers of 40-kg capacity) inside outer packages such as wooden, cardboard, or metal boxes with a maximum permissible net weight of 400 kg.

European Inland Waterways. Packaging regulations for European inland waters are identical with those for road and rail transport.

Sea Transport. In contrast to land transport, a distinction is made between lumps and solid fused goods (i.e., those poured into the container in a molten state) in sea transport.

Lumps have to be packed in hermetically-sealed (vapor-tight closure) packaging and must be completely covered by a protective liquid (flash point > 50 °C) or covered with nitrogen. The following types of packaging are

permitted: Steel drums with removable head with a maximum net weight of 250 kg, or combination packaging such as glass bottles (max. 1 kg gross) packed in wooden boxes (max. 5 kg gross), metal boxes or cans (max. 15 kg net) packed in wooden boxes (max. 115 kg gross), or cardboard boxes (max. 40 kg gross).

Solid fused sodium must be packed in effectively closed (liquid-tight closure) drums with removable head with a maximum net weight of 250 kg.

Air Transport. Sodium metal may be transported only by cargo aircraft; transport by passenger aircraft is not permitted. The net weight per package must not exceed 50 kg. Special conditions and permitted types of packing are described in packing instruction No. 418 of the air transport regulations ICAO-TI/IATA-DGR¹².

51.9.4 Portable Tanks

Portable tanks include rail tank cars, road tank vehicles, and demountable tanks. Rail tank cars have a capacity up to ca. 45 t; tank containers and road tanker trucks, up to ca. 25 t.

Tanks for transporting sodium metal must be tested to a minimum pressure of 0.4 MPa. The temperature on the tank shell must not exceed 70 °C during transportation. Insulating material must be nonflammable. The atmosphere inside the tank must be inerted by an inert gas.

Road and Rail Transport in Europe. Although the transport of molten sodium metal is allowed, many producers allow the fused sodium to solidify the outer layer, so that escape of liquid sodium is prevented in case of leakage. Openings below the surface level of the material are permitted.

Portable tanks for sodium metal must undergo testing at eight-year intervals after the first certification, including testing of the condition of the inside and outside of the vessel and pressure testing with a liquid. In addition, a leakproofness test of the tank with its equip-

ment and a check of the satisfactory operation of the equipment must be carried out at least at four-year intervals.

Transport by European Inland Waterways. Regulations for inland waterways are identical with those for the road and rail transport of movable large containers.

Sea Transport. IMO tank type 1 containers with a minimum wall thickness of 6 mm and a minimum test pressure of 0.4 MPa must be used. IMO tank type 1 tanks have a capacity of > 450 L, with a maximum permitted operating pressure of 175 kPa or above. Road tank vehicles and rail tank cars used to transport sodium on seagoing vessels have to comply with the IMO tank type 1 provisions too. In contrast to the land transport regulations, the sea transport regulations do not permit openings below the surface level to the material, i.e., the tank must be equipped with top openings. For sea transport, the sodium metal must be in the solid state.

51.10 Quality Specifications and Analysis

Sodium is marketed with a purity of > 99%. Depending on the production method, standard-quality sodium can contain between 400 and 600 ppm of calcium [11]. Purification of sodium is described in [8].

Methods based on filtration and cooling depend on the low solubility of many elements in liquid sodium just above its melting point. Impurities remain in the filtration residue or settle out in solid form in cool traps.

The affinity of some of the impurities in sodium for oxygen is also utilized in purification processes since the oxides formed are easily removed from the sodium. For example, calcium is reacted with Na₂O or Na₂O₂ at 300–400 °C, and the calcium oxide formed is filtered off [5, 99].

The trace elements in sodium are listed in Table 51.3, with typical analysis figures and analytical methods [11]. Sodium can also be obtained in special grades [100].

Table 51.3: Trace impurities in sodium: Typical analysis figures and methods of determination [11].

Element	Concentration, ppm	Methods of determination
Aluminum	0.5	AAS, Zeeman
Arsenic	< 1	AAS, Zeeman
Barium	< 5	AAS, Zeeman
Boron	< 1	Photometric
Calcium ^a	450	Titrimetric
	5	AAS
Carbon	2	Dissolve, filter, GC
	7	Vacuum distill, GC
Chlorine	4	Nephelometry
Chromium	< 0.5	AAS, Zeeman
Cobalt	< 0.5	AAS, Zeeman
Copper	< 0.5	AAS, Zeeman
Iron	4	AAS, Zeeman
Lead	< 0.5	AAS, Zeeman
Lithium	< 1	AAS
Magnesium	< 1	AAS, Zeeman
Nickel	< 0.5	AAS, Zeeman
Oxygen ^b	7	Amalgam process, AAS
Phosphorus	< 0.5	Photometric
Potassium	70	AAS
Silicon	< 1	AAS, Zeeman
Silver	< 1	AAS, Zeeman
Strontium	5	AAS, Zeeman
Sulfur	< 4	AAS
Tin	< 1	AAS, Zeeman
Zinc	0.3	AAS, Zeeman

^a Specification: normal grade < 600 ppm, nuclear grade < 10 ppb.

^b Owing to the high affinity of sodium for atmospheric oxygen, moisture, and carbon dioxide (formation of oxides, hydroxide, and carbonate), the figures given apply only to sodium that has come in contact with dry inert gas atmospheres (O₂ < 1 ppm, H₂O < 1 ppm) during filling, storage, and handling.

51.11 Health and Safety

Sodium can be handled safely without endangering the health of personnel concerned, provided appropriate precautions are taken to deal with possible hazards [101]:

- Spontaneous ignition of sodium in moist air at > 115 °C
- Severe caustic effects of the combustion products of sodium
- Fire explosion associated with uncontrolled chemical reaction between sodium and acid, water, aqueous solutions, alcohol

Sodium must always be stored, transported, and handled under dry and inert conditions. Direct contact with the skin must be prevented by wearing gloves and clothing made of

flame-resistant material. The eyes are protected by spectacles, goggles, or shields in all circumstances.

Information and advice about necessary technical, organizational, and personal protective measures can be obtained from company publications [11, 102] and leaflets available from chemical industrial trade associations [101]. Methods for safe working with sodium in the laboratory are described in detail in [8, 11].

51.12 Economic Aspects

Until recently, sodium was used mainly for the production of lead-containing antiknock agents for gasoline and for the production of titanium. However, the increasing use of lead-free gasoline and the manufacture of titanium by other processes have led to a drastic reduction in sodium capacity worldwide [103, 104]. In 1979, world sodium capacity, excluding the former Eastern-bloc states, was estimated at 250 000 t/a [10]. By 1986, this had decreased to 200 000 t/a [5]. In 1993 it is expected to be ca. 80 000 t/a. The most important sodium producers in the Western world, with their 1993 capacities are listed below:

Du Pont, Niagara Falls, United States	51 000 t/a
Associated Octel, Ellesmere Port, United Kingdom	20 000 t/a
Métaux spéciaux, Pomblière, France	12 000 t/a

51.13 Sodium Chloride

The history of mankind is also a history of salt [105–110]. Although it is not clear how man learnt of its effects and its savory properties, salt has been mentioned in literature for thousands of years.

In the Odyssey, HOMER wrote: "travel ... until you meet mortals who do not know the sea and who never eat food seasoned with salt." Elsewhere he refers to salt as "holy". CASSIODORUS said: "Gold can be dispensed with, but not salt." Other notable historical sources that refer to salt include PLUTARCH, PLINY, HERODOTUS, the Old and New Testaments, and ancient Chinese writings.

Before the industrial revolution in the 1800s, salt was used almost entirely as a food-stuff and as a preservative. Its importance led people of all cultures to strive to find ways of obtaining this important, life-sustaining substance. The coastal regions of the Earth were the favored areas for salt production. Possibly the oldest mine in the world was worked in ca. 1000 B.C. at Hallstatt, Austria which gave its name to the "Hallstatt Culture". In Germany, salt was probably first won in Schwäbisch Hall in ca. 500 B.C. The well-known salt deposit in Wieliczka, Poland was first mentioned in the 1100s. Wherever natural brine was available or early methods of brine production were practiced, a large number of salt works came into being between the 1100s and 1700s.

Salt was used universally, but was not everywhere available from natural sources, so that trading rapidly became important. The extent to which salt was used as an article of commerce is shown by the appearance of the famous salt roads in China, Africa, and Europe, and by the foundation of towns such as Salzburg, Salzach, Hall, Hallein, and Heilbronn (Celtic: *hal* = salt). Also, salt was used as currency (hence the word "salary") and as source of tax revenue. Ancient Rome had a salt tax, and salt monopolies were established in many countries and continue to exist in Austria and Switzerland. Starting in 1765, Prussia demanded an annual salt payment from its citizens, and in Germany a tax of DM 120/t was levied on all salt used in food. The total revenue from this in 1990 was DM 47×10^6 . This tax was discontinued at the beginning of 1993, following the establishment of the European single market.

With the advent of the industrial revolution, the use of salt as a chemical raw material increased rapidly. Industrial salt production, whether by evaporation in salt works or from mined rock salt, continually increased in importance.

Another important process of recent decades is controlled solution mining.

Although salt is no longer the cause of war-like confrontations, it has certainly lost none of its fascination, whether as a life-giving con-

diment or as an indispensable, versatile raw material.

Many museums, e.g., the German Museum in Munich and the German Salt Museum, Lüneburg, have comprehensive exhibitions on the history of salt.

51.13.1 Properties [111]

Sodium chloride, NaCl, is a colorless salt with good solubility in water. Chemically pure NaCl crystallizes from aqueous solutions in well-formed cubes, which under the influence of surface tension often grow together into funnel-shaped, hollow, square-based pyramids. In the presence of impurities, octahedra or dodecahedra are sometimes formed. Crystallization from hydrochloric acid solution gives long, fibrous, needle-shaped crystals.

During crystallization, small amounts of water can be trapped in holes in the crystals. When this vaporizes on heating, it causes the crystals to explode with audible decrepitation. In salt from natural deposits, inclusions of gases such as methane, carbon dioxide, and hydrogen sulfide can occur.

In the crystal, the Na and Cl ions alternate. The ions of each type form a face-centered cubic lattice, in which each ion is surrounded octahedrally by six ions of the other type at a distance of $a/2$ (lattice constant $a = 0.56273$ nm). The modulus of elasticity perpendicular to the surface of the cube is 41 074 MPa. Under high pressure, slow flow takes place. Sodium chloride is highly transparent to light of wavelength between 200 nm (ultraviolet) and 15 μ m (infrared). Ionizing radiation causes lattice defects (color centers) which give the salt a blue color. On heating to ca. 250 °C, this color disappears.

Some important physical properties are listed below and in Tables 51.4–51.6.

Melting point	801 °C
Boiling point	1465 °C
Density at 25 °C	2.1615 g/cm ³
Mohs hardness	2–2.5
Brinell hardness	14 HB
Dielectric constant	5.9
Refractive index n_D^{20}	1.5443
Electrical resistivity at 20 °C	$4.6 \times 10^{16} \Omega \text{cm}$
at 100 °C	1.38×10^{15}

Sodium

Thermal conductivity at 17 °C	0.072 W cm ⁻¹ K ⁻¹
Linear coefficient of expansion	40.5 μ m/mK
Specific heat capacity at 25 °C	850 J kg ⁻¹ K ⁻¹
Enthalpy of formation at 25 °C	-410.9 kJ/mol
Entropy at 25 °C	72.36 J mol ⁻¹ K ⁻¹
Latent heat of fusion	0.52 kJ/g
Latent heat of evaporation	2.91 kJ/g
Viscosity of saturated aqueous solution	1.93 mPa·s
Density of molten NaCl at 801 °C	1.549 g/cm ³
Viscosity of molten NaCl at 850 °C	1.29 mPa·s
Surface tension of molten NaCl at 850 °C	110 mN/m
Electrical conductivity of molten NaCl at 850 °C	3.7 S/cm

Thermodynamic properties of aqueous solutions are given in [112].

In the system NaCl–H₂O (Figure 51.7), only one hydrate, NaCl·2H₂O, exists. It crystallizes as monoclinic, thin, bevelled platelets that decompose to solid sodium chloride and saturated brine at 0.15 °C. Below this temperature it is the stable solid phase. However, it crystallizes so slowly that, on rapid cooling, the phase diagram follows the broken curve in Figure 51.7. The metastable eutectic point reached is ca. 1.3 K below the true cryohydric point at -21.12 °C. Its property of depressing the freezing point of water enables sodium chloride to be used in freezing mixtures and as a deicing salt. The saturated aqueous solution boils at 108.7 °C.

Table 51.4: Solubility of NaCl in water.

Temperature, °C	g NaCl/100 g H ₂ O	NaCl, %	Density of solution, g/cm ³	NaCl content of solution, g/L
0	35.76	26.34	1.2093	318.5
20	35.92	26.43	1.1999	317.1
40	36.46	26.71	1.1914	318.2
60	37.16	27.09	1.1830	320.5
80	37.99	27.53	1.1745	323.3
100	39.12	28.12	1.1660	327.9
180	44.9	30.99		

Table 51.5: Density of aqueous solutions of NaCl.

NaCl, %	Density, g/cm ³				
	0 °C	20 °C	40 °C	60 °C	80 °C
4	1.03038	1.02680	1.01977	1.0103	0.9988
8	1.06121	1.05589	1.04798	1.0381	1.0264
12	1.09244	1.08566	1.07699	1.0667	1.0549
16	1.12419	1.11621	1.10688	1.0962	1.0842
20	1.15663	1.14779	1.13774	1.1268	1.1146
24	1.18999	1.18040	1.16971	1.1584	1.1463

Table 51.6: Vapor pressure of aqueous solutions of NaCl (in kPa).

Temperature, °C	NaCl content				
	5%	10%	15%	20%	25%
0	0.59	0.57	0.55	0.51	0.47
20	2.26	2.18	2.09	1.97	1.81
40	7.13	6.88	6.58	6.20	5.72
60	19.26	18.58	17.78	16.76	15.53
80	45.75	44.16	42.49	39.97	37.09
100	97.89	94.43	90.44	85.52	79.67

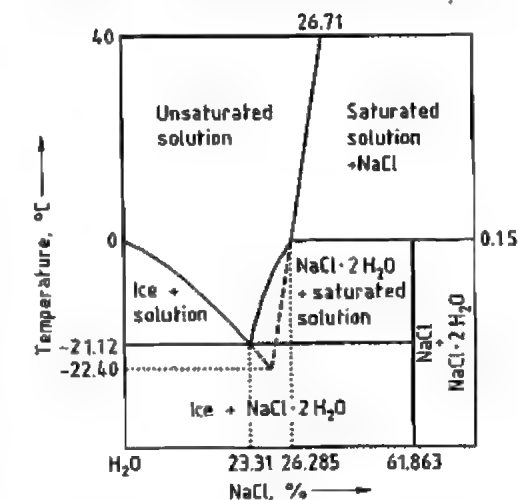


Figure 51.7: Phase diagram of H₂O–NaCl system (schematic, not to scale).

Table 51.7: Solubility of sodium chloride in aqueous ammonia at 20 °C [113].

[NH ₃], g/L	15.38	30.06	62.56	92.97
[NaCl], g/L	303.46	294.05	273.01	257.60
ρ , g/cm ³	1.186	1.175	1.147	1.124

Sodium chloride has good solubility in aqueous ammonia (Table 51.7). At low temperatures, fine white needles of composition NaCl·5NH₃ separate out. Addition compounds with urea, glucose, and sucrose also exist. Solubilities in pure methanol and pure ethanol at 25 °C are 1.31 and 0.065 g NaCl/100 g solvent, respectively. Sodium chloride is also soluble in glycerine, and dissolves in high pressure steam, the solubility being 0.1% at 17 MPa, and 0.6% at 19.5 MPa. Chemically pure sodium chloride is not hygroscopic, but if magnesium salts are present as an impurity it becomes so. Sodium chloride solutions are corrosive to base metals, and

therefore dilute solutions of NaCl are used in corrosion tests (e.g., DIN 50907). Solutions of pure NaCl are more corrosive than those that also contain salts of Mg or Ca [114]. Iron and steel are attacked only fairly slowly by pure NaCl solutions, but much more quickly when the solutions contain oxygen. Corrosion by NaCl solutions is accelerated by the presence of local electrolytic cells [115]. Mixtures of organic acids with sodium chloride, (e.g., in perspiration) are highly corrosive [116].

51.13.2 Formation and Occurrence of Salt Deposits [117]

When rocks are chemically weathered, salts are dissolved, carried into natural running waters, and collect in the oceans and inland lakes and seas. Where evaporation is predominant, the salts become concentrated until the solutions become supersaturated and crystallization occurs.

The proportion of sodium chloride in the salts of seawater is ca. 78%. Although the oceans contain the largest quantity of dissolved salts, the majority of salt is bound in the form of solid deposits. In Germany alone, the quantity is estimated to be ca. 100 000 km³.

The chemical-sedimentary genesis of salt deposits has been accepted ever since OCHSENIUS (1877) proposed his bar theory. Inspired by the contemporary example of the Kara-Bugaz bay (Caspian Sea), he suggested that bodies of seawater became almost completely isolated from the open sea by bars. Then, due to the evaporation that took place in arid climatic regions, the seawater became concentrated. The sparingly soluble carbonates and sulfates were the first to crystallize, followed by the more soluble chlorides.

In the case of the most important European salt deposit, the Zechstein Formation, communication with the North Sea has been proved by fossil finds, thus demonstrating the marine origin of the Zechstein salts, which extend over ca. 500 000 km² from England to Central Poland, and from Denmark to Thuringia/Hessen (Germany). The bar theory can satisfactorily

account for even the 800–1000 m thickness of the Zechstein salt deposit, and is valid even today, in modified form, for marine salt deposits. A depth of 100 m seawater produces a salt layer only 1.5 m thick on complete evaporation.

It is now believed that, for the European Zechstein salt deposit, the salt lakes were connected to the ocean by an extended saturation shelf lake where considerable amounts of CaSO₄ were deposited. The minor and major salt lakes were filled with salts during four largely identical deposition cycles, each having the sequence clay, calcium–magnesium carbonates and calcium sulfate, sodium and potassium chlorides, and ending with a recessive transition [sodium chloride, calcium sulfate (anhydrite), and clay] to the next cycle. The concentrations of the various soluble salts reached saturation successively as the seawater became gradually more concentrated, so forming the geographical sequence of salts. This explains why the composition does not correspond to that of normal seawater at any point in the salt profile, why all the types of salt are not deposited everywhere, why salts of differing solubilities are precipitated simultaneously at different saturation regions, and why the chlorides of potassium and magnesium are deposited only at the centers of the lakes.

The intermediate layers of clay sediments in each cycle are the result of influxes of fresh seawater. Eolian (airborne) transportation of clay minerals into the salt basin can also occur.

The depths of the brine in the deposition basins have been calculated from the bromine contents for each phase of deposition. The results obtained were: first cycle (Werra region) 330 m, second cycle in the Staßfurt region 860 m, and third cycle in the Leine region 95 m. In some cases the salt basin dried out during the third cycle. Sediments of younger formations covered and protected the Zechstein salts from dissolution.

In the North West German depression zone, a layer of overlying rock up to 5 km thick was formed. The pressure due to this denser rock, together with the interior heat of the Earth,

caused metamorphosis of the salt, which became plastic and migrated. It accumulated in zones of deformation and ascended, forming salt domes (diapirs) which sometimes extended as far as the earth's surface. These were slowly dissolved by groundwater, leading to the formation of very flat secondary intermediate layers next to the overlying rock.

The upward movement of the salt during the formation of salt domes deformed the salt layers into folds, with predominantly steeply inclined strata. Under the thinner overlying rocks at the edge regions, the flat deposits remained undisturbed. Marine rock salt deposits occur in most geological formations.

51.13.3 Production

51.13.3.1 Mining of Rock Salt

Rock salt has been mined in Europe for 3000 years. A salt deposit near ground level in the Eastern Alps was developed by tunnelling and worked by excavation around 1000 B.C.

Salt-bearing regions are revealed by the presence of surface springs of saline water, and these were the areas where the possibility of mining was always investigated by sinking shafts. The main precondition for success is the presence of dry overlying rock, and it was this circumstance that enabled the first German salt mine to be opened in 1825 near Schwäbisch Hall. In other parts of Europe, salt was mined long before this, e.g., in Poland before 1000 A. D., and in England since the 1600s.

Total world production of solid salt by conventional mining and brine by solution mining is ca. 190×10^6 t. Annual production of salt in West Germany in 1989 was ca. 13×10^6 t.

The purity of the salt mined from rock salt deposits is between 90 and 99% NaCl, and sometimes higher. The other minerals present in the rock salt are mainly clay and anhydrite, often intimately intergrown.

Rock salt and potassium chloride have the same marine origin, often occurring together in a single deposit, and have essentially the same mechanical strength properties. Hence,

the development and mining of rock salt deposits is similar to that of potash mineral deposits.

Mine Shafts. Access from the surface to the salt deposit is usually by vertical shafts 5 m in diameter. There must be at least two shafts, so that in case of damage to one of them, the underground workforce has an emergency route to the surface.

To sink the shaft, the rock is broken up by drilling and explosives. The rock debris is loaded into skips by grabs, and taken to the surface. In most cases, the upper layers of the overlying rock are water-bearing, and sometimes consist of unstable loose rock and moving sand capable of exerting pressure. Therefore, before sinking the shaft, these strata must be solidified and stabilized. This can be achieved by freezing via holes drilled around the area where the shaft is to be sunk. The freezing equipment must be kept in place for the duration of the sinking of the shaft.

Another method of preventing the movement of water in the overlying strata and immobilizing loose rocks is the injection of cement, synthetic resins, or other hardening materials via boreholes. This technique is also suitable for sealing the mine shaft against the ingress of water and for stabilizing the rock at the bottom of the shaft.

As rock salt is a water-soluble mineral, it is especially important to ensure that the lining of the shaft is watertight when it is sunk through water-bearing strata. In older shafts, the sealing system consists of ring-shaped sections of cast iron or steel bolted together. Newer shafts have a watertight lining consisting of a welded sheet-steel cylinder, an inner hollow cylinder of reinforced concrete, and an outer asphalt-filled ring.

Material is hoisted up the shaft in 20 t skips at rates of up to 1000 t/h. These travel between wooden or steel guide rails, or in a few cases between tensioned guide cables.

If the salt deposit appears as an outcrop, or is at low depth (< 100 m), the salt can be extracted by drift mining (tunnelling) or by means of an inclined shaft. In these cases, the

salt can be transported to the surface with conveyor belts.

Mining Methods. As with any mining operation, the method of extracting salt depends on the thickness and spatial formation of the deposit.

A characteristic feature of salt mining is that the haulage and ventilation tunnels servicing the excavation chambers are driven through rock salt, whereas in other types of mine they are often coated in the adjacent rock. In salt mining this is generally not necessary, as the deposits are usually thicker. Furthermore, drilling and tunnelling into the adjacent rock should be avoided as far as possible to prevent ingress of water or gas from these strata into the mine.

Mining in Level Deposits. In most salt mines, a systematic extraction procedure is possible due to the uniformity of the deposit over large areas.

In salt deposits with horizontal or gently inclined seams, the standard method is room and pillar mining. In this method, the extraction process produces large chambers with rectangular cross sections of ca. 50–400 m² and lengths of up to 500 m. The parallel extraction chambers are separated from each other by rock salt pillars left behind during mining. These pillars must be of such dimensions that they can carry the weight of the overlying rock. Generally, additional support is not required, and the ground above is protected against subsidence.

The pressure exerted by the overlying rock increases with depth, so that the salt pillars must be wider. For example, in a salt mine at a depth of 200 m, the pillars are 15 m wide and the chambers 15 m; at a depth of 500 m, the pillars are 30 m wide and the chambers 20 m; and at a depth of ca. 700 m, the pillars are 50 m wide, and chambers 22 m. The salt pillars result in a ca. 40–70% loss of product, depending on their dimensions.

The salt extraction process starts with the construction of a central haulage tunnel. At right angles to this, tunnels leading to the working faces are driven. The tunnels are de-

veloped upward or downward to form chambers if the deposit is so thick that it extends above or below them. The salt pillars produced by this mining technique are usually not cut through.

If the deposits have a workable thickness of < 10 m, the pillar and chamber method with long pillars is often changed to one with short, square pillars (room and pillar system). Here, the transverse tunnels usually have the same height and width as the long ones.

Fresh air is provided by an inlet ventilation road above the haulage tunnel. The used air is removed through return air galleries and by the main ventilating fan, which is usually underground, and blown through the exhaust shaft to the surface.

The mining of the salt during the construction of the tunnels and in the extraction chambers is by drilling and the use of explosives. Other possible methods, such as cutting the salt by part-face heading or full-section cutting machines, are used where there are special restrictions, e.g., where the winning process must be vibration free.

Various drilling and blasting processes are used. In the undercutting method, the working face is undercut to a distance of 4–5 m. The cut, 15–20 cm wide, is produced by a machine resembling a chain saw. An electro-hydraulic mobile drilling machine drills 35–38 mm diameter holes for the explosive. In another process, a wide hole up to 7 m in length and 0.45 m in diameter is drilled into the middle of the working face to provide an initial extension space for the salt at the moment of explosion, a function that is performed in the undercutting process by the undercut.

The extraction chambers are created by widening the access tunnels. If these are driven through the lower part of the deposit, this is performed by the use of explosives in long inclined boreholes directed upwards. If the tunnel runs through the upper part of the deposit, the salt is extracted from the floor, i.e., by drilling long holes downwards into the salt.

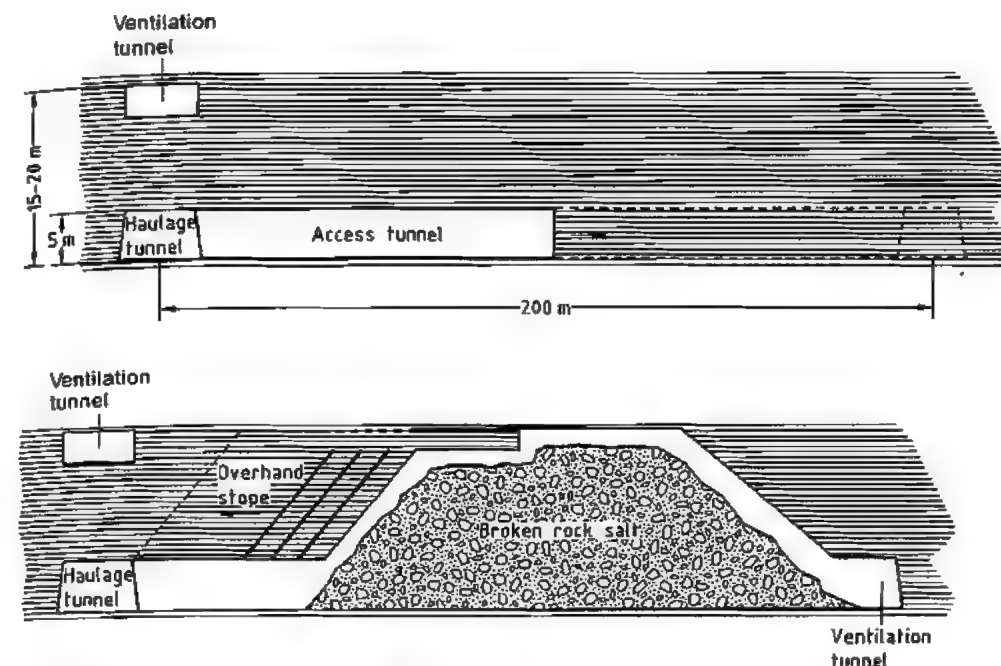


Figure 51.8: Vertical section through a South German salt mine.

Figure 51.8 shows a vertical section through a South German mine where the rock salt deposit is 20 m thick and 200 m deep. The haulage and working roads are located in the lower part of the deposit, and the main ventilation road in the upper part. In the main extraction phase, the salt that has been broken up by explosives is left lying in the space created, and the final position of the roof of the chamber is created by blasting, working from the top of the heap of loose salt. After scaling the roof can then be collected without the danger of roof falls.

The most commonly used explosive is ANFO (ammonium nitrate fuel oil mixture) in the form of loose prills. It is charged pneumatically into the boreholes.

Due to the strength of the salt rock, it is possible in most mines to keep the mined space open without supports. At great depths, where the pressure is high, or where breakup of the deposit leads to danger to the miners from roof falls of salt, rock bolts are used.

Mining Steeply Inclined Deposits. Steep to vertical rock salt deposits are generally mined by the stepped face method, as used, for example, in North German mines at depths of 400–850 m, with working levels at vertical intervals of 100–250 m and intermediate sublevels at intervals of 15–20 m. Between the sublevels, there are working faces which are drilled and blasted, beginning with the lowest, using long boreholes. In one mine, the openings produced are 20 m wide, 42 m high, and 100 m long, and, in another, 20 m wide, 100 m high, and 60 m long.

To maintain stability of the rock, salt masses must also be left behind using the grid wall system, the vertical pillars being 10–30 m thick, and the horizontal pillars between the sublevels, 8 m thick.

Loading and Haulage. To load the mined material after blasting and to transport it to the first crusher, diesel-powered front loaders with bucket capacities of up to 18 t are used (LHD: Load, Haul, Dump System). For economic reasons, there should be a straight road

between loading and discharging points not longer than ca. 300 m. For longer distances, the interrupted system is more economic, with special loading equipment and dumper trucks of up to 50 t capacity.

After crushing the salt to < 300 mm using equipment near to the working face, it is transported by band conveyors to the hoisting shaft.

In mines where the salt has a purity of > 99% NaCl, the salt can be marketed directly after grain-size classification.

Where the natural purity is lower (e.g., 94% NaCl in South German mines), impact mills are used in the first processing stage. As rock salt is more brittle than the clay and anhydrite inclusions, it is more readily size reduced. A screening operation follows, separating the two size fractions, which increases the NaCl content by 2–3% compared to the crude salt. Further purification of the salt to > 99% NaCl for industrial use is carried out in heavy media hydrocyclones.

Utilization of the Chambers. Salt mining is mainly carried out without back-filling, i.e., the chambers produced during mining need not be backfilled with other material to support the roof of the mine and increase the load-bearing capacity of the salt pillars.

Where processing of the rock salts produces residues that must be disposed of, these are usually dumped in the empty chambers.

Hence salt mines do not produce heaps of tailings at ground level.

In some cases, empty chambers are utilized for disposing of waste materials, e.g., wastes from combustion processes and the chemical industry.

51.13.3.2 Production of Crude Brine by Mining Methods

The principle of all mining methods for the production of crude brine (NaCl solution) is the use of "solution mining".

The rock salt, which may be present in a pure state (e.g., geologically undisturbed crystalline salt deposits) or in a mixed mineral in finely divided form (e.g., in alpine salt deposits), is dissolved by the action of fresh water on the rock formation and converted to a concentrated salt solution (brine with an NaCl content of 312 g/L or 27%).

In all processes, the brine is produced in underground excavations made by conventional mining or solution mining [118–124]. The extraction processes result in formation of chambers [125]. Between the chambers in which the brine is produced and extracted, pillars of considerable size are left behind to maintain stability of the rock [126, 127]. Figure 51.9 gives a survey of brine mining methods.

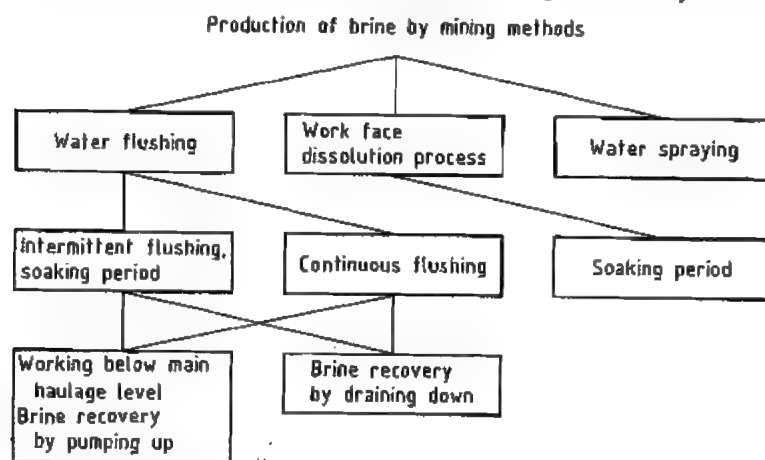


Figure 51.9: Classification of brine mining methods.

Mining of brine is no longer widely used. It is employed in alpine salt deposits and in a few rock salt mines. The most widely used and most economic process today is solution mining [118, 119]. In a few cases, subsurface solution mining is also carried out at depths of 100–140 m [128, 129].

Water flushing (intermittent or continuous dissolution in chambers) is the extraction process usually used in the alpine salt deposits in West Germany and Austria [118, 119, 122–124]. Tunnels, shafts, and chambers are usually first produced by mining techniques. A single worked stratum is divided into separate districts of a given size in which several extraction chambers are set up. A block of definite dimensions (length, breadth, and height) is allocated to each chamber based on a predetermined degree of extraction. The block encompasses a space of irregular configuration produced by the extraction process and the pillars left between the extracted spaces, which are also of irregular shape. An initial space is first created, which is a funnel-shaped (Germany), or circular chamber (Austria). A shaft or tunnel is first driven from the main tunnel or a transverse tunnel to the center of the intended block at the bottom of the worked strata. A shaft is then sunk by mining techniques from which the initial chamber of a specific size is created at the lowest point by drilling and explosive methods (Austria). In Berchtesgaden, Germany, the initial space (Figure 51.10) required for excavation is created by drilling and water-injection processes. An important feature of this process [124, 126] is that the initial space is funnel shaped, and is generated by controlled dissolution, starting from a wide borehole, so that the insoluble components of the deposit can be raised by airlifting equipment and removed by a hydraulic pump as a solid-brine mixture. The production of the initial space is usually divided into the following stages (Figure 51.10): sinking a borehole for examination of the deposit in the region to be excavated, vertical development by sinking a wide borehole, further widening of the borehole by controlled dissolution, forming a funnel-shaped space at a

depth extending from 100 to 125 m. During this phase, the space normally attains a volume of 3000–5000 m³, depending on the quality of the deposit, with a height of 4–6 m and a diameter of 30–32 m. The creation of the initial space completes the preparation for the extraction process. The space is next extended further, conditions now having been established for continuous, high yield, cost effective brine production. The initial space (chamber) is slowly filled with fresh water, which dissolves salt from the side walls and roof. The insoluble components, such as clay, anhydrite, and polyhalite sink to the floor of the chamber. Fresh water is continuously added, raising the liquid level, so that water remains continuously in contact with the roof of the chamber until the water in the chamber is completely saturated. The dwell time depends on the salt content of the rock, the size of the chamber, the ease of dissolution of the salt, and the surface area of the chamber roof, and is usually between 10 and 30 days. After complete saturation has been attained (312 g/L), the brine is removed either by pumping out of the excavated space (if working below the tunnel level), or by draining off to the level below. The space is then refilled with fresh water. This procedure (filling, saturation, emptying), is known as intermittent water flushing, and is repeated until the chamber roof area has reached ca. 3000–3200 m². The chamber is then ready for continuous brine production by the continuous water flushing process. The water flows at a rate appropriate for the parameters of the deposit, with simultaneous removal of concentrated brine by draining or pumping. The brine production is now almost invariably carried out below the main haulage level (Germany and Austria), i.e., working upwards from the bottom. Each day, 1–1.5 cm rock salt is dissolved from the surface of the roof of the chamber. The chambers take on a funnel-shaped to cylindrical configuration (Figure 51.10). Chamber heights in Austria [123, 128, 129] are 20–30 m (normal working) or 50–80 m (deep working), depending on the diameter. In Berchtesgaden, Germany, the exploitable height of the chamber is

100 m. The initial space is created in the region between 100 m and 125 m below the level of the tunnel.

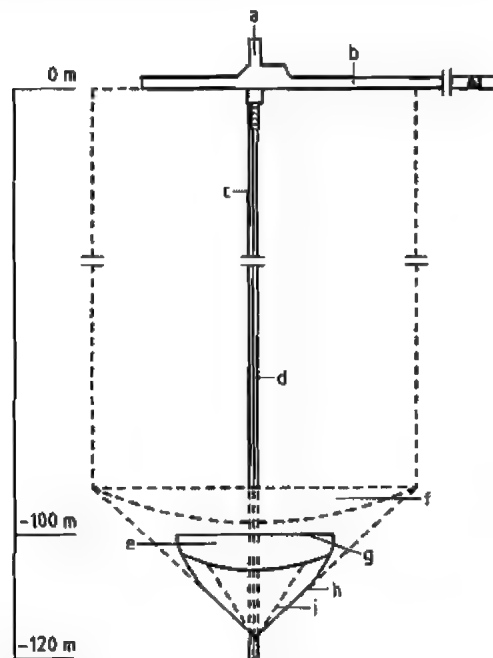


Figure 51.10: Production of the initial extraction chamber by drilling and water flushing, and brine production operating below the main tunnel (Salzbergwerk Berchtesgaden, Germany): a) Drilling chamber; b) Main tunnel; c) Borehole (76 mm); d) Wide borehole (670 mm); e) Initial extraction space; f) Developed extraction space; g) Chamber roof; h) Angle of boundary; i) Angle of repose of solid residues.

To calculate the efficiency of extraction of the deposit, the salt content of the rock and the size of the rock mass assigned to the particular operation point (cavern), including the horizontal safety pillars, must be taken into account. In Berchtesgaden, Germany, when the size of the horizontal and vertical pillars, the average salt content of alpine deposits (50%), and the usable height of the chamber (100 m) are taken into account, the total quantity of brine available per chamber is $1.1 \times 10^6 \text{ m}^3$. This corresponds to an extraction efficiency of ca. 12% [124, 126]. In Austrian salt extraction operations, the following total available quantities of brine have been quoted, depending on the type of extraction chamber [128] and

[129]: 200 000–400 000 m^3 for normal operations, and 700 000–1 000 000 m^3 for deep operations.

The *work face dissolution process*, in which dissolution is carried out in chamber-like tunnel sections, is similar in principle to the intermittent water flushing process, and is also not widely used. In some mining operations in Germany and Poland [119, 121] it is still operated alongside other brine production processes (e.g., solution mining using boreholes drilled from the surface).

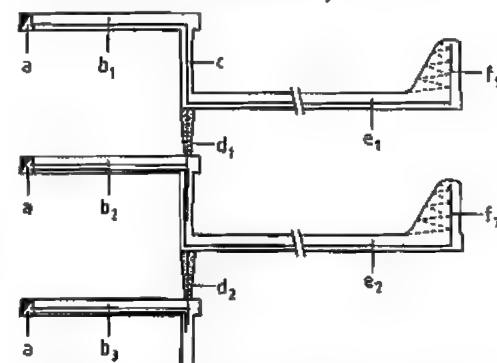


Figure 51.11: Production of brine work-face dissolution: a) Access tunnels; b₁–b₃) Transverse tunnels for work faces 1–3; c) Borehole widened to make a shaft; d) Brine removal; e) Transverse tunnels; f₁, f₂) Spraying equipment.

To obtain the brine, transverse tunnels are driven one above the other on both sides of the main tunnel (Figure 51.11). The transverse tunnels are linked together at their ends by a borehole. Passing from one tunnel to the next, the borehole is widened to a shaft of 1 m diameter and provided with an outlet to the lower tunnels. About 10 m below each tunnel, a tunnel for brine production is driven from the widened borehole, a work face is produced by cutting upwards at the end, and spraying equipment is installed at that point. This creates a cut which moves backwards at a fixed height until it meets the widened borehole. After the initial work has been finished, the working is filled with water or unsaturated brine. The water or brine remains in the working until saturation is reached. The concentrated brine is then removed via the lower work face. In contrast to the water flushing

process described above, the salt is only removed from the work faces until the planned chamber width is produced.

The production of brine by means of water jets is only used to a small extent, being employed in a few cases to solve special problems, e.g., to speed up excavation during intermittent water injection at the development stage, or to regulate the configuration of the chamber during the water flushing process in large chambers.

51.13.3.3 Controlled Solution Mining

Controlled solution mining is the modern economical method of extracting rock salt from underground deposits, and contrasts with conventional mining (see Section 51.13.3.1). However, for this method certain preconditions must be fulfilled, especially with regard to the geology of the deposit (type, formation, and depth of the salt). Economic operation of the solution mining process requires that the deposit—whether a diapir (salt dome) or a flat stratum of salt—should fulfill the following geological conditions:

- Adequate thickness and extent of the salt deposit
- High purity of the rock salt without inclusions of potassium chloride
- Largely undisturbed stratification at medium depth

In addition, an adequate supply of water must be available.

Drilling and Construction of the Borehole

The drilling and completion of the trial boring and the design and installation of the brine wells (also known as the cavern wells) closely resemble those of petroleum and natural gas wells. The method of operation and the geological conditions determine the size, type, and position of the casing that protects the walls of the borehole against the effects of permeable strata, and prevents solid material

from the rock from falling into the borehole. A standard pattern for the casing diameters in a cavern well (see Figure 51.12) is as follows:

1. 0–15 m: 24.5 inch pipe
2. 0–300 m: 16 inch pipe
3. 0–20 m (max.) beyond the projected roof of the cavern in the deposit: 11.75 inch pipe

The casings described in (2) and (3) above are cemented up to ground level.

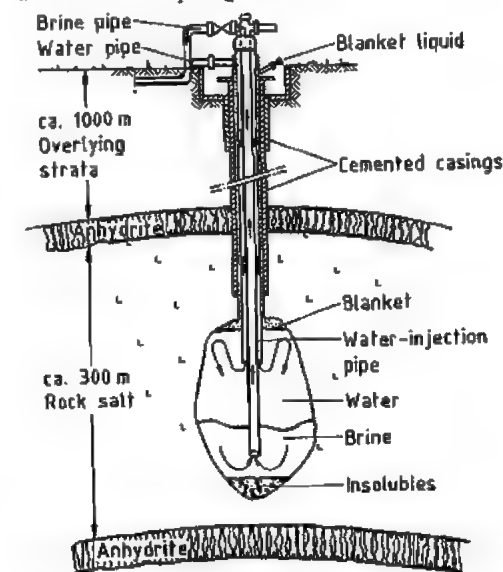


Figure 51.12: Method of brine production.

Geophysical borehole measurements and tests on the cores obtained during sinking of the borehole not only give information about mineralogical composition, but also yield physical data about the overlying rock and the salt deposit. The most important characteristics of the overlying rock are its thickness and strength. Also, to enable the dimensions of the cavern and the proposed extraction process to be decided upon, the strength and thickness of the salt deposit and the solubilities of its component parts must be known.

The outer casing must be installed and cemented with special care, and each individual joint as well as the whole casing must be tested for tightness. After this, the well is completed by inserting two concentric pipes (of di-

iameter between 8.625 and 5.5 inches), the final preparative work being the assembly of the well head and making all the pipe connections (Figure 51.12).

The Process of Solution Mining

As shown in Figure 51.12, fresh water is pumped into the borehole through the annular space between the two inner pipes. The water dissolves salt from the walls of the cavern. The solution sinks as its salt content increases, and the saturated brine formed then rises to the surface in the central pipe due to the applied pressure.

Dissolution of salt from the roof is prevented by injecting a protective liquid or gas blanket through the annular space between the outer casing and the pipe carrying the fresh water. This blanket forms a layer above the water due to its lower density, so protecting the roof. Insoluble materials collect at the bottom of the cavern.

The desired cavern shape is produced by stepwise adjustments to the depth of the water-injection pipe and the level of the blanket [130-133].

The extraction process is controlled by continuously measuring the salt content of the brine, the blanket pressure, and the quantity of brine extracted. The cavern space produced is calculated from these data by computer, and the spatial extent of the cavern is continuously determined by echometric surveying. The actual cavern produced can then be continuously compared with the planned cavern.

Planning of the Extraction Process

The safety of caverns can be ensured if pillars of adequate width are left between neighboring caverns and if there is a thick enough mass of solid salt at the top of each cavern. The width of the pillar and the thickness of the roof depend on the planned cavern dimensions, the cavern shape, and, in particular, on the mechanical properties of the salt deposit. The latter have been investigated in detail [133-139].

Furthermore, correlations and formulas have been derived that enable the forces produced in the rock to be calculated from the size and shape of the cavern, the interior pressure produced by the solution mining process or subsequent use for storage purposes, the depth and thickness of the overlying rock, and the mechanical properties of the surrounding rock formations. The decrease in the volume of large caverns (convergence) caused by elastoplastic properties of the rock salt are determined from formulas, confirmed by data from practical experience [134-143].

Irrespective of the widths of the pillars calculated with these equations, the wells in a brine field should be arranged in a hexagonal pattern (Figure 51.13), which gives optimum utilization of the available area.

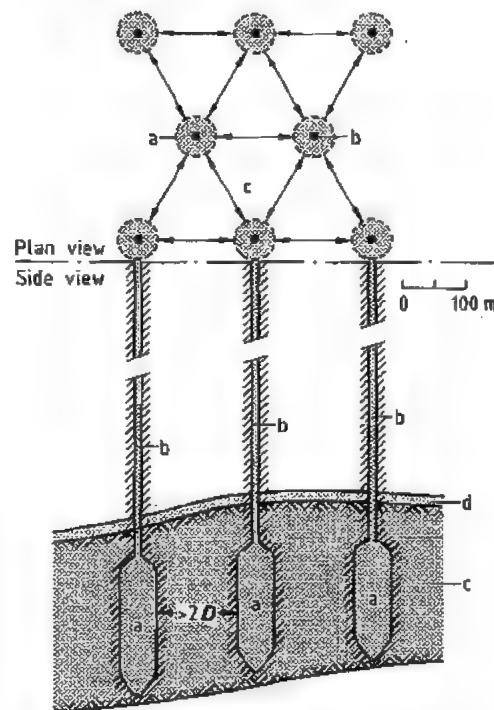


Figure 51.13: Hexagonal arrangement of caverns in a brine field with a level salt deposit: a) Cavern (diameter $D = 60-100$ m); b) Borehole; c) Pillar of stable rock salt (thickness of pillar: $2D$); d) Upper layer of anhydrite.

The distance between the brine wells is the sum of pillar width, the maximum cavern diameter, and a safety factor to allow for devia-

tion of the borehole from the vertical. If a borehole must be relocated due to the situation at ground level, the hexagonal arrangement below ground can be maintained by adjusting the drilling direction (Figure 51.14).

Other Systems

Individual boreholes for extracting brine can generally only be operated economically in thick salt deposits or salt domes. However, thin salt deposits can also be exploited economically in some cases. Here, two or three boreholes are linked together by injecting water to dissolve the salt and to fracture it by hydraulic action [132, 144, 145]. Fresh water enters via the first borehole, and the brine is collected from the second or last borehole. Here also, dissolution of the roof is prevented by a blanketing medium. The floor is dissolved first, then the roof. With thin seams of salt, the strength and impermeability of the overlying strata are very important.

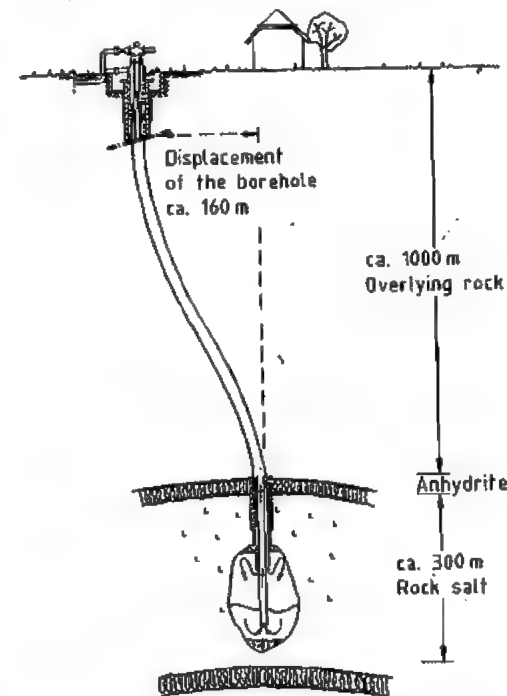


Figure 51.14: Directional drilling in the production of a cavern.

Control of this method of solution mining is more difficult than with individual brine wells. The stability of the cavern spaces cannot be guaranteed, as there is a risk of uncontrolled dissolution processes. Thus, this method of solution mining is only used in countries with few salt deposits where there are sparsely populated areas above thin salt strata.

Equipment

The equipment requirements normally consist of

- Equipment for supplying water, sometimes including a pipeline
- A pumping station with a distribution system delivering water to the individual solution mining operations
- A pipeline for transporting the brine to the consumers
- A central system for supervising and controlling the entire processing equipment

The water is injected by high-pressure centrifugal pumps at a pressure determined by the difference in the densities of the two media (water and brine) and the friction losses in the pipes. The salt at the working face dissolves and passes through the central pipe as saturated brine to the well head and into the piping system. The low residual brine pressure at this point is sufficient to deliver it to the pumping station, where delivery pumps force the brine into the pipeline that takes it to the consumer industries.

Storage Caverns

The caverns remaining after extraction of the sodium chloride can be used for storage of mineral oil, mineral oil products, and gases such as natural gas and ethylene.

Emergency reserves of mineral oil or mineral oil products can be injected through a pipeline into the brine-filled caverns by a high-pressure pump. In place of the two concentric pipes used in solution mining, a brine removal pipe is suspended in the cavern with its open end just above the sump region. The mineral oil is forced into the annular space be-

tween the outer pipe and the brine removal pipe and displaces the brine, which rises through the brine removal pipe to the surface and is fed into the brine network, and thence to the production plant. To discharge the oil, the process is reversed.

Caverns in rock salt are also suitable for gas storage. For example, natural gas is stored to compensate for seasonal and daily variations in demand. The conversion of a cavern to a gas-storage system is more complex than conversion to liquid storage. To protect the outer piping against pressure and temperature variations during operation, a protective pipe is fitted. The annular space between this pipe and the outer pipe is pressurized so that the welded pipes are under a constant load. For the first filling operation with gas, a brine extraction pipe is lowered to the bottom of the cavern. The gas in the annular space between the protective pipe and the vertical central pipe is compressed to a high pressure, and displaces the brine from the cavern until the latter is completely empty. The gas storage system operates by the principle of compression-decompression. The gas in the cavern required to maintain the minimum residual pressure required for stability of the cavern is called the cushion gas, but when it is filled up to its maximum operating pressure, it is known as the working gas.

Descriptions of cavern storage systems can be found in [146-149]. A worldwide information exchange service is provided by the Solution Mining Research Institute (SMRI), Woodstock, Illinois.

51.13.3.4 Production of Sea Salt

Introduction. In his *Historia Naturalis*, PLINY THE ELDER already referred to the technique of producing salt by the natural evaporation of sea water. Even today, this method of exploiting the oceans, seas, salt lakes, and chotts is still widespread. It is practiced in nearly all regions of the world where climate and topography allow.

While some methods have changed very little, such as those of the "Paludiers" working

the salt marshes along the Atlantic coast of Portugal and France, other modern methods are now applied, combining productivity with strict environmental protection. This applies to the vast majority of salt fields in the Mediterranean basin, on the west coast of Australia, and Guerrero Negro, the world's largest salt field in Mexico at the southernmost tip of Baja California.

The Raw Material: Sea Water

The water of the seas and oceans contains all the known elements, most of them present in small amounts [150]. Sodium chloride is the most important compound in terms of concentration, averaging 28 g/L.

Sea water also contains significant amounts of magnesium, sulfur, and calcium, the other important sea-water-based process being the production of magnesium compounds.

The salinity (grams of salt per kilogram of sea water) of ocean and sea water varies with location and depth [151]. This dispersion, due either to dilution by precipitation or drainage pattern, or to local overconcentration caused by strong evaporation, is more evident in inland seas.

The average salinity is 3.5%, corresponding to a relative density of 1.026. It reaches 4.1% in the Red Sea and is only 3% in the Baltic Sea.

The salt mixture in sea water has the following typical composition (in %) [47]:

NaCl	77
MgCl ₂	10
MgSO ₄	6
CaSO ₄	3.9
KCl	2

The Main Factors Governing Production of Sea Salt

To produce sea salt economically, the amount of water evaporating must exceed the amount of precipitation (rain or dew) for a long and continuous period of at least three months during the year.

Table 51.8 lists the main types of climate compatible with the production of sea salt. In

Taiwan, a borderline case, sea salt production calls for a maximum of ingenuity. In Western Australia, by contrast, the climate is ideal, notwithstanding the risk of cyclones, and sea salt can be produced all year round.

In practice, evaporation at a given production site is measured over fresh water with an evaporimeter. Since the total concentration of dissolved salts is known, the evaporation is determined approximately from an empirical curve, an example of which is shown in Figure 51.15 [152].

Table 51.8: Typical climatology of solar saltfields [151].

	South of France	Australia	Indonesia	Taiwan
Annual evaporation ^a , mm	1700	3600	1850	1660
Annual rainfall, mm	550	300	1300	1400

^a Fresh water.

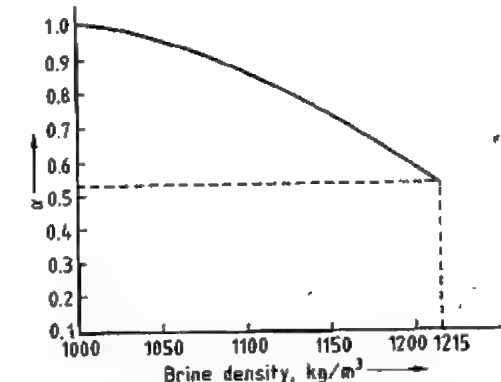


Figure 51.15: Evaporation coefficient α as a function of density.

1 cm of evaporation over fresh water corresponds to a cm for the body of water in question; a normally ranges from 0.95 for sea water to 0.55 for saturated brines depositing their salt.

In addition to a favorable climate, a particular topography is required, and the ground must be as impermeable as possible to minimize brine seepage.

The pond areas containing the brines or saline solutions must also be as level as possible, ideally below sea level, and stepped in elevation. This reduces the number of intermediate

pumping stations required and helps to optimize the design of the ponds, dikes, channels, and culverts making up the salt field.

These conditions are often satisfied in the deltas of large rivers. The Rhône delta in France's Camargue is one example, and is the location of two large salt fields: Aigues-Mortes and Salin de Giraud.

Concentration of Sea Brines. After being pumped from the sea, the sea water passes through the salt field from pond to pond. As it passes through the ponds, the NaCl concentration in the sea water rises from 28 g/L to roughly 260 g/L, corresponding to an increase in relative density from 1.026 to 1.215. At this point, the brine begins to deposit its salt. Most of the calcium carbonate (CaCO_3) and calcium sulfate ($\text{CaSO}_4 \cdot 2\text{H}_2\text{O}$) has already crystallized before this point, as shown in Figure 51.16, while the magnesium salts continue to become concentrated without crystallizing.

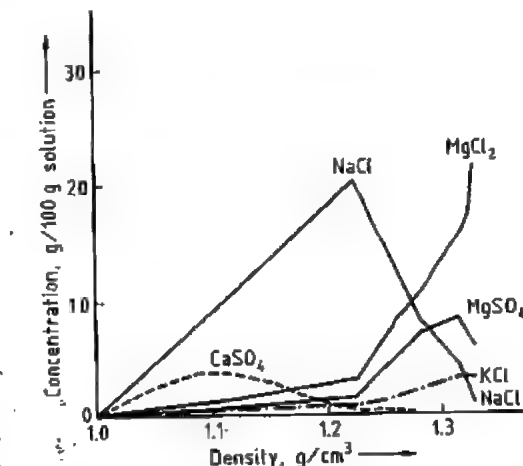


Figure 51.16: Brine composition as a function of density [153]. Values for CaSO_4 concentration are multiplied by a factor of ten.

Crystallization of Sodium Chloride. When the brines approach the NaCl saturation point, they are fed through feed channels into the crystallizers, which represent the production units. The floors of the crystallizers must first be carefully prepared by compacting and levelling to ensure easy separation of the salt from the ground and a uniform layer of brine.

The surface area of these crystallizers generally represents ca. 10% of the total area of the salt field.

From this point on, the salt worker's job is to monitor the brine strengths and purge the bitterns from the ponds when the concentration of secondary salts, particularly magnesium salts, is liable to lower the quality of the salt. The ponds are then filled with fresh or pure brine with a low magnesium salt content.

The salt is produced in the form of a layer of tangled crystals whose density and grain size depend on the characteristics of the bittern and, especially, on the turbidity or cloudiness. If the brine is turbid, the suspended fine particles act as seed crystals. If, however, the brine is clear and well settled, the number of seed crystals is greatly reduced, and crystal growth occurs in preference to germination.

The thickness of the salt layer varies from one site to another, and also, at a given site, from one year to another, depending on weather conditions. In the South of France where the production period runs from May to September, the thickness at the end of the season averages 10 cm. At other latitudes, layers may be over 20 cm thick.

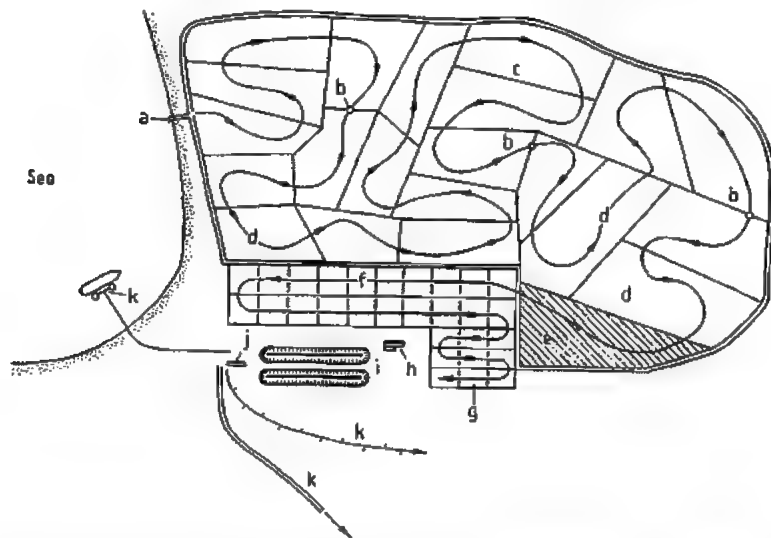


Figure 51.17: Modern salt field [151]: a) Sea water intake; b) Pumping station; c) Dikes; d) Condensers; e) Brine storage tanks; f) Crystallizers; g) Bitterns areas; h) Washing plant; i) Salt storage areas; j) Packaging plant; k) Dispatch.

Production Stages in a Modern Salt Field

Figure 51.17 shows the main components of the infrastructure of a modern salt field, from sea water intake to the production facilities for processing and packaging the salt.

The production process features the following stages:

- **Seawater pumping:** the salt field is supplied with sea water by a pumping station. In some parts of the world, such as Australia, the salt fields are gravity fed with sea water in accordance with the tides. Several million cubic meters of sea water are required annually to produce several hundred thousand tonnes of sodium chloride (the Aigues-Mortes salt field in France pumps $50 \times 10^6 \text{ m}^3$ of sea water for an average annual output of 400 000 t).
- **Concentration of sea water in the ponds:** in this stage, the water flows through shallow ponds and is allowed to concentrate until approximately 90% of the initial water content has evaporated. The brines are moved pond to pond by gravity or by pumping as dictated by the local topography.

Table 51.9: Percentage compositions of rock salt from various sources.

	Borth, Germany	Malagash, Canada	Northwick, England	Staßfurt, Germany	Retsof, USA
NaCl	98.5	99.095	93.43	97.53	98.1
MgCl ₂	0.13	0.026	0.14		0.00
MgSO ₄				0.23	
CaCl ₂		0.118	0.01		
CaSO ₄	0.75	0.401	1.16	1.49	1.60
Na ₂ SO ₄	0.44		0.04	0.43	
NaHCO ₃			0.01		
Insolubles	0.1	0.360	5.25		0.27
Water					0.03

- **Deposition of NaCl in the crystallizers:** for a salt field with a single production season during the year, the crystallizers are first filled with brine kept from the previous year, which has been protected from rain dilution in deep storage ponds. A few weeks later, the old brine is replaced by the new concentrated brine leaving the ponds. By the time the relative density of the brine reaches 1.215, when NaCl crystals start to form, the brine has already precipitated 80% of the calcium sulfate in the form of gypsum. The bitterns are then removed before the specific density reaches 1.260 to avoid codeposition of magnesium salts. Where bitterns are present in sufficiently large quantities, and if the climate allows, the bitterns can be concentrated on a bittern salt field to extract the magnesium bromide, magnesium sulfate, and even magnesium chloride.
- **Salt harvesting:** in batch-operated salt fields, salt harvesting begins at the end of the salt production period. For continuous salt fields, harvesting is performed at regular intervals to ensure that the level of the salt does not exceed the operating height of the harvesting machines. The harvester is generally carried by a tractor of the type often used for civil engineering projects. The salt is first scooped off the floor of the crystallizer by a large blade up to 3.6 m wide pushed along by the tractor. It is then lifted by slotted or bucket conveyors. The salt is then evacuated and poured into trailers by a conveyor belt.
- **Transport, washing, and storage:** the harvested salt is loaded onto trucks or tractor-

drawn trailers for transport to a washing plant where most of the impurities are removed.

Washing removes all solid impurities from the salt (substances insoluble in water) along with the accompanying bitterns (solutions of magnesium or potassium compounds). The salt is kept in suspension in saturated brine. The salt-brine mixture is then dewatered and centrifuged. The salt travels up an inclined gantry conveyor and is poured on top of one of the huge salt stockpiles that are a familiar feature of salt production sites.

- **Processing and packaging:** The salt reclaimed from the salt stockpile may be washed a second time, which increases the sodium chloride content to 99%. The salt is then generally dried, crushed, and screened, and anticaking agents are added. Other substances added at this stage include iodide or fluoride in salt for human consumption. The salt is then packaged in various containers (e.g., boxes, polyethylene bags), as required by the consumer.

51.13.4 Production of Pure Salt by Evaporation of Brine

Salt can be produced by evaporation of saturated brine. The brine is generally obtained by dissolving crude salt that contains many impurities. The production of high-purity salt requires chemical purification of the brine. The high purity is the major difference to rock salt (Table 51.9). Purification is also necessary to avoid scale formation in the evaporation equipment. Also, when pure salt is used in in-

dustrial processes, much less waste is produced than when rock salt is used, and this aspect is of ever-increasing importance.

51.13.4.1 Purification of Crude Brine

The most common and most problematic impurities in crude salt are the sulfates and carbonates of calcium and magnesium, and polyhalite ($K_2SO_4 \cdot 2CaSO_4 \cdot MgSO_4 \cdot 2H_2O$). The principal impurities of crude brine are therefore calcium, magnesium, and sulfate ions. The following chemical methods are used to purify crude brine [154].

Purification with Lime or Caustic Soda and Soda Ash. Magnesium ions are precipitated from the crude brine as magnesium hydroxide by adding calcium or sodium hydroxide. Calcium ions are precipitated as calcium carbonate by adding sodium carbonate or by purging the alkaline brine with carbon dioxide, usually in the form of combustion gas. Salt is obtained from the purified brine by evaporation, which is stopped prior to the onset of sodium sulfate crystallization. The mother liquor has a high sodium sulfate content and can be used for sodium sulfate production.

Purification in a Circulating System. Here, the brine is usually treated in two stages. In the first stage, crude brine, mother liquor, and calcium hydroxide suspension or sodium hydroxide solution are brought together and thoroughly mixed. This causes magnesium hydroxide and calcium sulfate to precipitate. Other metal ions are precipitated in addition to the alkaline earths. After removal of these solids, sodium hydroxide solution and/or sodium carbonate solution are sometimes added to the clear brine, which is saturated with calcium hydroxide, in the second stage. Also, carbon dioxide (usually as combustion gas) is passed through, whereby calcium carbonate crystallizes and is removed. The clarified brine is fed to the evaporator, and evaporated until sodium sulfate just fails to crystallize. The salt is recovered, and the mother liquor, which has a

high sodium sulfate content, is recycled to the first stage of the brine purification process.

Design of Brine Purification Plants. The brine purification processes described above were formerly carried out as batch operations, but today continuous processes are more common. In both methods, the impurities are allowed to settle and then removed. Sedimentation is accelerated by adding flocculating agents, usually polyacrylamides sometimes in combination with iron hydroxide. In the continuous process, the solid impurities are removed in thickeners. Modern brine purification plants are often fully automated, and are controlled by means of automatic analyzers.

51.13.4.2 Evaporation of Brine

As the solubility of sodium chloride increases only slightly with temperature (Table 51.4), the salt is normally crystallized out in an evaporative crystallizer at 50–150 °C. Both pure brine and crude brine are evaporated.

When evaporating crude brine, the gypsum slurry process is used, in which a certain quantity of crystalline calcium sulfate is maintained in the suspension of salt crystals. The calcium sulfate that precipitates deposits on these gypsum crystals and hence does not form a scale on the heating surfaces or the walls of the vessel.

Salt was formerly produced by evaporation in open pans. Due to the high heat consumption and relatively poor performance, this method is now hardly used [154, 155]. To achieve the best possible utilization of heat, multistage evaporation and vapor recompression were developed.

In the multistage evaporation process, improved heat utilization is achieved by compressing the vapors from the first evaporator and using these for heating the second. The vapors from the second evaporator are then used to heat the third, and so on. The plant generally has four, five, or six stages. The brine is preheated in preheaters which are heated with vapor and condensate from the evaporators.

The heat of the vapor can be used in the same evaporator if the vapor is compressed to a higher pressure [156]. This system is widely used where cheap electrical energy is available. In this case, only one evaporator is required. Reductions in power costs and hence operating costs can be achieved by switching off the electrically powered turbine compressor during periods of peak electricity consumption.

Hybrid systems are also used, which can be operated as multistage or vapor-compression evaporators [157]. Combined methods are also used in which high-pressure steam is passed through back pressure turbines, and the exhaust steam heats a multistage evaporation plant. The mechanical power is available for compressing the vapors.

In general, three types of crystallizers are used [158, 159]:

Type 1: Evaporators with forced circulation and external heating.

Type 2: Evaporators with internal heaters and a circulating pump in the central pipe producing forced circulation.

Type 3: Oslo crystallizers (Figure 51.18)

In Oslo crystallizers, recirculating brine and fresh brine are heated in the heat exchanger and evaporated in the evaporator. The supersaturated crystal-free brine passes down the central pipe into the crystallizer, and from there passes upwards through the bed of crystals.

The choice of crystallizer depends on the desired crystal size. If crystal size is not important, Type 1 crystallizers are generally used. These produce cubic crystals with 50% > 400 μm (by sieve analysis). If somewhat coarser salt is desired, Type 2 crystallizers are used, giving cubic crystals with rounded corners, with 50% > 650 μm (sieve analysis). Type 3 crystallizers produce a granular product, with lenticular or spherical particles, ca. 1–2 mm in size.

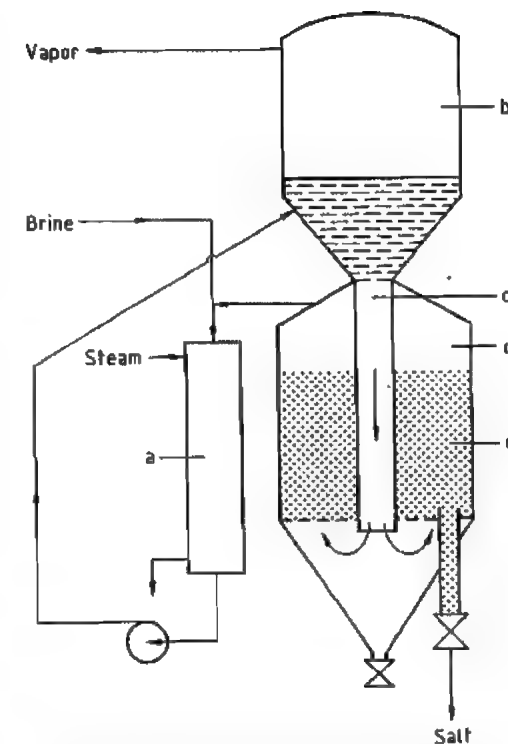


Figure 51.18: Oslo evaporator: a) Heat exchanger; b) Vacuum evaporator; c) Down pipe; d) Crystallizer; e) Bed of crystals.

51.13.4.3 Recrystallization

The recrystallization process utilizes the fact that the solubility of calcium sulfate in brine decreases with increasing temperature, while that of sodium chloride increases slightly. The process is suitable for producing a fairly pure salt from fine or waste salt [154, 160].

The process consists of three stages:

- **Dissolution:** Fine salt is heated with mother liquor from the evaporator to ca. 105 °C in a dissolving vessel by passing steam into it. The sodium chloride dissolves, but not the calcium sulfate, because the brine from the mother liquor is already saturated with calcium sulfate.
- **Filtration:** Removal of solid calcium sulfate and other solid impurities from the brine.

● **Crystallization:** The clear brine is pumped to the crystallizer, which is an expansion evaporator with forced circulation but without heaters. On expansion, evaporation and cooling take place. The salt suspension is removed from the evaporator and the mother liquor is returned to the dissolution vessels.

Heat exchangers are not generally used in this process, which can be carried out in one or several stages.

51.13.4.4 Other Process Steps

Manufacture of Special Salt Crystals. Salt crystals with special shapes can be produced by adding substances that affect crystal growth to the brine in the evaporation equipment. The addition of soluble iron(II) cyanide complexes in amounts of ca. 10 mg/kg (expressed as the amount of additive in the product) produces dendritic crystals. This salt has a very low bulk density of ca. 0.8 g/cm³. Other suitable additives include nitrilotriacetic acid, nitrilotriacetamide, sodium hexametaphosphate, and cadmium chloride [161, 162].

Coarse salt is also produced by compressing fine salt to form tablets or briquettes, or into compacted sheets that are then broken up to form coarsely granular salt [154].

Construction Materials. To avoid corrosion [154, 163], the material of the evaporator is usually made of steel plated with a monel alloy. Less critical parts of the equipment can be made of steel. Rubber-coated equipment is also used. The tube sheets are of steel or monel metal and the heat-exchanger tubes are generally made of copper nickel alloy or titanium.

Removal of the Crystals. The crystal suspension is removed from the evaporators, which are often conical at the bottom. Fresh brine is often fed in through a discharge branch, which washes the salt crystals and causes thickening of the suspension.

Salt Drying. The mother liquor is removed from the crystal suspension in centrifuges. Sometimes the salt crystals are washed in a pusher centrifuge. If washing is not required, a screw centrifuge can be used. After centrifug-

ing, the salt still contains ca. 2–3% moisture. Further drying can be carried out in rotary driers, but fluidized bed driers are now more common. At the end of the fluidized-bed dryer there is usually a cooling zone into which cold air is blown, or a separate cooler can be used. The dried salt is often passed through a classification process.

51.13.4.5 Salt Quality

Typical analyses of salt produced by the evaporation of crude or purified brine are given in Table 51.10. Anticaking agents such as sodium, potassium, or calcium ferrocyanide are added at a concentration of 5–15 mg/kg. Purity requirements for salt are continually increasing, especially for industrial applications such as chlor-alkali electrolysis. As salt purity improves, the amount of waste decreases, and the environmental pollution caused by the wastewater is substantially reduced.

Table 51.10: Typical analyses of salt from evaporation processes.

	From crude brine [154]	From purified brine
NaCl, %	99.7	99.95
SO ₄ , mg/kg	1900	300
Ca, mg/kg	900	7
Mg, mg/kg	20	0.5

51.13.5 Economic Aspects

51.13.5.1 Commercial Grades

Salt for Food. Salt intended for human consumption is known as cooking salt or table salt. Apart from its function as a seasoning in foods, it is of vital importance for the human organism. The average daily salt requirement for humans is 7 g [164]. In Germany, the fraction of total salt consumption used for food is only 3%. In 1990, the consumption of table salt was ca. 398 000 t. The largest use in the food industry is for food preservation. Only ca. 100 000 t is sold in small packages for household use [165]. Caking of table salt is prevented by adding anticaking agents such as calcium or magnesium carbonate, or sodium or potassium ferrocyanide [166].

Table salt is used as a carrier for various active substances. Iodized table salt is important worldwide in the prevention of diseases of the thyroid gland. Fluoridized table salt is used to prevent tooth decay.

In Europe, ca. 90% of all meat products are preserved with nitrite pickling salt, which consists of sodium chloride and various amounts of sodium nitrite [165].

Treated Salt. Salt that is used neither as a foodstuff nor for the chemical industry is denatured in many countries for tax reasons. The consumption of this type of salt in Germany in 1990 was ca. 800 000 t.

Salt that is not suitable for human consumption or food production is produced on demand by the addition of denaturants such as eosin, patent blue, or soda ash.

Treated salt is used for water softening, textile treatment, in the leather industry, in animal food production, and in many other fields.

Of the above, the regeneration of water softeners is a very important application [167]. Water softening is essential owing to the widespread occurrence of hard water, and so far there is no alternative to the long-established

and well proven method based on ion exchangers and salt.

Industrial salt is salt that is used as raw material for producing other compounds [168, 169]. The main applications of industrial salt in the chemical industry are in chlor-alkali electrolysis and sodium carbonate production.

The products obtained form the basic raw materials for innumerable other products, including glass, dyes, washing and cleansing agents, medicines, plastics, aluminum, and paper (Figure 51.19).

In Germany in 1990, ca. 4.5×10^6 t crystalline salt was used, and ca. 5.9×10^6 t in the form of brine.

As with all forms of salt, industrial salt is subject to tax laws, but it may be used without being denatured if a salt license has been issued. For technical reasons, no anticaking agents are added to industrial salt.

Deicing Salt. Rock salt and sea salt can be used for deicing road surfaces to give safe driving conditions for traffic in winter. The chemical processes (hydration) that take place when deicing salt comes into contact with snow and ice on the roads in winter effectively eliminate slippery conditions [171].

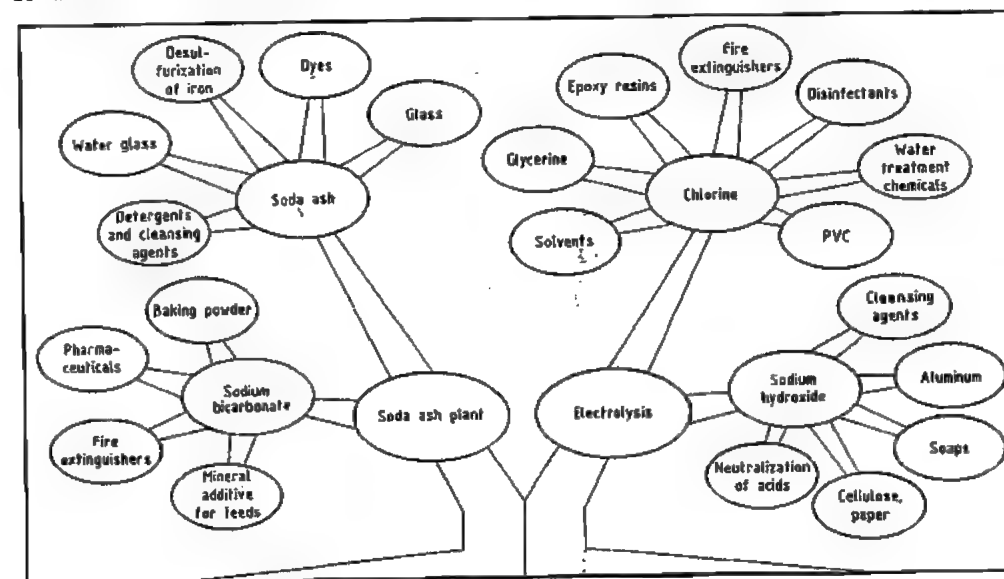


Figure 51.19: Family tree of salt chemistry [170].

The effect of deicing salt on the environment has been the subject of controversy. However, in the wake of mounting evidence from scientifically based investigations, there is now little opposition to the sparing application of deicing salt to ensure the safety of traffic, and the frequency of accidents caused by snow and ice can be drastically reduced.

The development and use of suitable technology have contributed greatly to decreasing the amount of deicing salt used and hence to reduction of environmental pollution. This technology makes use of modern electronic equipment for automatically adjusting the salt spreading process to the width of the road and the speed of the gritting vehicles, and the spreading of moist salt.

For the spreading of moist salt, the dry salt is wetted with a 5–30% solution of sodium chloride, calcium chloride, or magnesium chloride. Moistening prevents windblown losses and gives a more rapid deicing effect [171].

In the 1960s, at least 40 g/m² deicing salt was required, but subsequent technical developments have enabled an optimum deicing effect to be achieved with only 10 g/m². In 1990, ca. 630 000 t of deicing salt was used in Germany.

51.13.5.2 Packaging, Transport, and Storage

Salt is supplied both loose and in packaged form. Salt for human consumption is available in big bags, in plastic and paper sacks, and in small packets. Denatured salt and deicing salt are supplied loose or in packages, but salt intended for large-scale industrial use is only supplied in loose form.

Salt is transported by canal and river boats, or by road in tipping trucks, flat trucks, or silo trucks.

51.14 Sodium Hydroxide

Pure sodium hydroxide, NaOH, is a colorless solid. It does not occur in nature, but is manufactured on a large scale from fairly

readily obtainable raw materials and is used in numerous chemical processes. Because of its corrosive action on many substances, it is known as caustic soda.

Sodium hydroxide solution is one of the oldest man-made chemicals. The reaction of sodium carbonate with calcined limestone (causticization of soda) was already known in early Afro-Oriental cultures. Alabaster vessels containing 3% sodium hydroxide solution have been found in Egyptian tombs dating from 3rd century B.C. near the Pyramid of Cheops. The first written records of caustic soda production during the early years A.D. came from Egypt and India.

51.14.1 Properties

Because pure sodium hydroxide has a high affinity for water, the physical and chemical properties of the pure substance are difficult to determine. Many of the data are obtainable only by extrapolating values for impure sodium hydroxide. The same is true for the concentration-dependent physical properties of aqueous solutions of sodium hydroxide, since these solutions have a strong tendency toward supersaturation.

51.14.1.1 Properties of Sodium Hydroxide

Some physical properties of solid sodium hydroxide are as follows:

Appearance	white, crystalline
Density (liquid, 350 °C)	1.77 g/cm ³
mp (soda and water free)	322 ± 2 °C
Heat of fusion	6.77 kJ/mol
Boiling point at 0.1 MPa	1388 °C (calculated)
Specific heat capacity at 20 °C	3.24 J kg ⁻¹ K ⁻¹

Pure sodium hydroxide is strongly hygroscopic. It dissolves in water with liberation of heat and forms six defined hydrates (Figures 51.20, 51.21, and Table 51.11). When transporting and storing sodium hydroxide solution, the containers must be heated or insulated because the melting points of some of the hydrates are much greater than 0 °C. In the presence of moisture, NaOH reacts readily with atmospheric carbon dioxide to form so-

dium carbonate. Sodium hydroxide reacts with carbon monoxide under pressure and in the presence of moisture to yield sodium formate.

The high affinity of sodium hydroxide for water causes a reduction in water vapor pressure (e.g., to 0.36 kPa for 50.3%, NaOH at 30 °C). Sodium hydroxide is therefore a very effective drying agent. It is fairly readily soluble in methanol and ethanol.

Anhydrous sodium hydroxide reacts very slowly with most substances. For example, it attacks many metals only slightly at room temperature (e.g., Fe, Mg, Ca, and Cd). However, corrosion rates increase rapidly with increasing temperature. More noble metals such as nickel, silver, gold, and platinum are attacked only slightly even when heated, especially if oxidizing atmospheres are excluded. Anhydrous sodium hydroxide does not react with dry carbon dioxide.

51.14.1.2 Properties of Sodium Hydroxide Solution

Physical Properties. The concentrations of the aqueous solutions in equilibrium with solid NaOH at various temperatures are given below:

<i>t</i> , °C	10	18	30	40	53	64
% NaOH	49.8	51.0	53.3	55.4	59.7	69.0

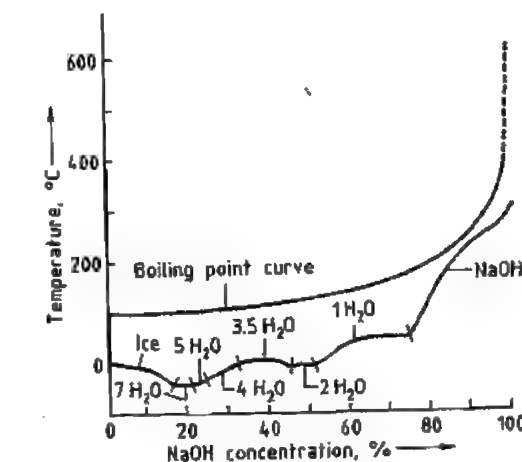


Figure 51.20: The NaOH-H₂O system.

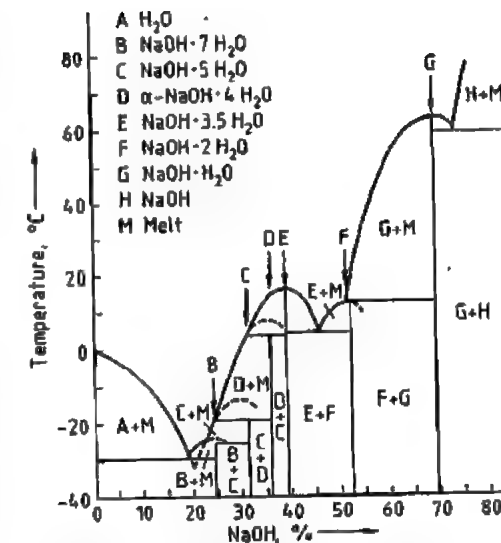


Figure 51.21: The NaOH-H₂O system [172].

Table 51.11: Stability of the hydrates of sodium hydroxide.

Formula	Stability range, °C
NaOH·7H ₂ O	-23.5 to -28.3 ^a
NaOH·5H ₂ O	-12.2 to -31.9 ^a
α-NaOH·4H ₂ O	+7.6 to -21.4 ^a
β-NaOH·4H ₂ O (unstable)	-1.7 to -14.5 ^a
NaOH·3.5H ₂ O	+15.6 to -8.8 ^b
9NaOH·28H ₂ O (unstable)	+2.7 to -2.5 ^a
NaOH·2H ₂ O	0 to +12.5 ^c
NaOH·H ₂ O	+4.5 to +64.3 ^b

^a Unstable melting point.

^b Clearly defined melting point.

^c Melting point can be determined only by extrapolation.

The heat of solution is ca. 44 kJ/mol at 18 °C. The surface tension at 20 °C increases from 7.46×10^{-2} N/m for a 5% solution to 0.1 N/m for a 35% solution [173]. A 1 mol% solution has a surface tension of 7.43×10^{-2} N/m at 20 °C, which decreases to 6.23×10^{-2} N/m at 90 °C. The density of aqueous sodium hydroxide solution in the concentration range 0–20% can be calculated from the formula:

$$d_1 = d_2 + (1.16027 \times 10^{-3} - 2.511 \times 10^{-5} t + 1.0222 \times 10^{-7} t^2 p - (1.0817 \times 10^{-5} - 3.6748 \times 10^{-7} t + 2.034 \times 10^{-10} t^2) p^2)$$

where d_1 (g/cm³) = density of solution at t °C, t (°C) = temperature, p (%) = g NaOH/100 g solution, d_2 (g/cm³) = density of water at t °C.

The densities of more concentrated aqueous sodium hydroxide solutions at 20 °C are as follows:

[NaOH], %	Density, g/cm ³
20	1.219
30	1.328
40	1.430
50	1.525

The boiling point curve is shown in Figure 51.20. In the concentration range 0–60%, NaOH, the boiling point increases approximately linearly with temperature.

NaOH concentration, %	5.9	23.1	33.8	48.3	54.6
Boiling point, °C	105	110	120	140	150

A 5-g/L solution of sodium hydroxide in water is almost completely dissociated. Activity coefficients are in the range $\alpha = 0.784$ (0.1 M at 10 °C) and $\alpha = 3.922$ (15 M at 70 °C).

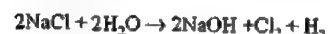
Chemical Properties. Amphoteric metals such as zinc, aluminum, tin, and lead are attacked by dilute sodium hydroxide solution at room temperature. Iron, stainless steel, and nickel are fairly resistant.

51.14.2 Production

Sodium hydroxide is produced commercially in two forms: a 50% solution (the most common form) and in the solid state (caustic soda) as prills, flakes, or cast shapes.

51.14.2.1 Production of Sodium Hydroxide Solution

Electrolysis of Sodium Chloride. Sodium hydroxide solution is produced industrially mainly by the electrolysis of sodium chloride. This yields sodium hydroxide solution, chlorine, and hydrogen in the mass ratio 1:0.88:0.025 in accordance with the following overall equation:



In the early 1980s, the membrane process was introduced, the other processes in operation at that time being the amalgam and diaphragm processes. Chlor-alkali production in 1990 was divided between these three processes as shown in Table 51.12.

Table 51.12: Distribution of chlor-alkali production among the three most widely used processes (percentage of installed capacity in 1994) [174, 175].

Process	North America	Western Europe	Japan
Amalgam	14	65	0
Diaphragm	78	25	15
Membrane	6	6	85
Others	2	4	0

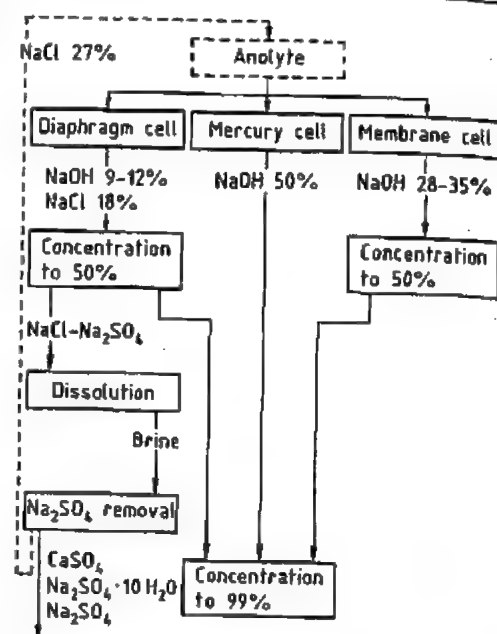


Figure 51.22: Treatment of the sodium hydroxide solution from electrolysis cells [176].

In Japan, by 1988 all plants based on the amalgam process had been either shut down or converted to the membrane process. Some Japanese diaphragm plants were also replaced by membrane plants for reasons of both cost and quality.

Treatment of the liquor from the electrolytic cell is shown schematically in Figure 51.22. In the amalgam process, sodium hydroxide solution is produced from sodium amalgam and water over a graphite catalyst at 80–120 °C. The 50% solution produced is very pure. It is cooled, mercury is removed by centrifugation or filtration through cartridge or pressure plate filters, and it is then sold without further treatment.

In the diaphragm cell, the depleted sodium chloride solution from the anode compartment is transferred quantitatively to the cathode compartment, so that the cell liquor produced there contains ca. 18% sodium chloride and 9–12% sodium hydroxide. During evaporation to give a 50% NaOH solution, all the impurities carried over with the depleted sodium chloride solution are removed to their limiting solubility by fractional crystallization; thus the sodium chloride content can only be reduced to ca. 1–1.5%. In the DH process of the PPG Company, further purification is carried out by extraction with anhydrous liquid ammonia. This gives a product comparable to that from the amalgam process (rayon quality), but the process is seldom used because of cost. This is also true of a Japanese process in which a relatively pure sodium hydroxide solution is obtained by cooling the 50% diaphragm liquor and recovering the crystals of pure NaOH·3.5H₂O formed. Methods of optimizing the various evaporation systems used for treating liquor from the diaphragm cell are described in [177].

In the membrane process, a hydraulically impermeable membrane prevents mixing of the electrolytes. This process produces a high-purity, virtually chloride-free sodium hydroxide solution comparable to that of the amalgam process. However, the chloride content increases by a factor of ca. 10 if operation of the cell is interrupted, due to diffusion of Cl⁻ ions through the membrane. The sulfate and chlorate present in the anolyte also affect the concentration of these impurities in the caustic liquor from the membrane cell, since the cation-selective membrane has an appreciable residual permeability for anions. Most membrane cells give optimum economic performance at an NaOH concentration of 30–35%. An ion-exchange membrane has now been developed that enables a 50% sodium hydroxide solution to be produced in the cell [178], although a considerable increase in

voltage is required. Such membranes are viable only if steam costs are high and electricity costs low [179]. The 30–35% sodium hydroxide solution is usually concentrated in a two- or three-stage falling-film evaporator (depending on steam costs and plant size) to give a commercial 50% solution (see Figure 51.23). For a three-stage evaporator, the steam consumption is 0.55 t/t NaOH (100%), and for a two-stage evaporator, 0.71 t/t NaOH (100%), with sodium hydroxide solution and steam in countercurrent flow.

The evaporation of membrane cell liquor (unlike that of diaphragm cell liquor) does not produce any solid material that can foul the heat exchanger or erode the pipework. The pickup of metals during evaporation is < 1 ppm if appropriate construction materials are used (nickel, stainless steel). The various evaporation techniques are described in [176], with special reference to the concentration of membrane cell liquor.

As shown in Table 51.13, the three electrolytic processes have different energy requirements. The membrane process consumes the least electrical energy (2300–2500 kWh/t NaOH) but requires an additional 180 kWh/t NaOH in the form of steam to produce a 50% solution. The diaphragm process consumes less electrical energy than the amalgam process but requires 900 kWh/t NaOH as steam for the evaporation stage and therefore has the highest total energy requirement.

Table 51.13: Energy requirements for the production of 1 t of sodium hydroxide (as 50% solution) by the three electrolytic processes.

Energy, kWh/t NaOH*	Process		
	Amalgam	Diaphragm	Membrane
Electricity	2800–3200	2500–2600	2200–2500
Steam (equivalent)	0	799–900	90–180
Total	2800–3200	3200–3500	2290–2680
Relative energy costs, %	90	100	70

* The energy requirement given is based on the production of NaOH, Cl₂, and H₂.

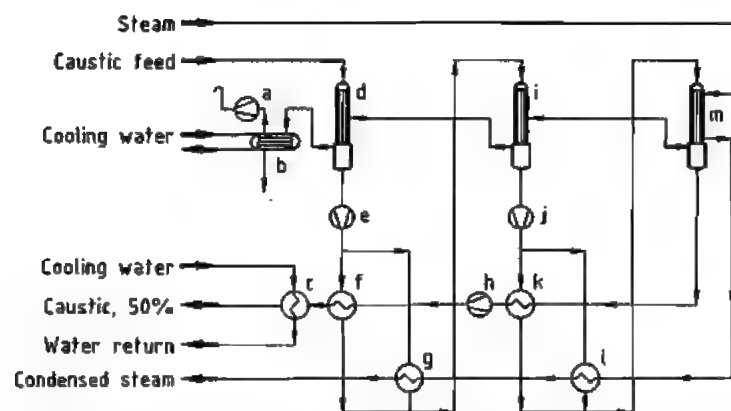


Figure 51.23: Membrane cell caustic evaporation (Bertrams process): a) Vacuum pump; b) Condenser; c) Caustic cooler; d) First evaporator; e) Caustic pump; f) First caustic heat exchanger; g) Second heat exchanger; h) Caustic pump; i) Second evaporator; j) Caustic pump; k) Second caustic heat exchanger; l) First heat exchanger; m) Third evaporator.

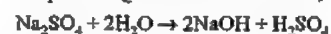
Because of the high consumption of electrical energy, much research has been aimed at reducing the cell voltage. A ca. 1 V reduction can be achieved by using an oxygen-consuming cathode (as in a fuel cell) in the membrane cell process, although in this case no by-product hydrogen is produced. These cells have not been used on a production scale because of major technical difficulties.

The electrolysis of fused NaCl at 350 °C with a β - Al_2O_3 diaphragm is also of interest. In laboratory-scale cells, a power consumption of 2350 kWh/t NaOH can be attained [180]. This technique, too, has yet to be used on a commercial scale.

Other Processes. Processes not linked to chlorine production are currently coming back into favor, as future world demand for sodium hydroxide solution is expected to exceed that for chlorine [181, 182]. The causticization of sodium carbonate solution is the oldest method of producing sodium hydroxide and was the only method available until the introduction of electrolysis. Although it had almost disappeared from use, it is now of special interest for companies with access to synthetic sodium carbonate from the Solvay process or to natural sodium carbonate (e.g., trona, $\text{Na}_2\text{H}(\text{CO}_3)_2 \cdot 2\text{H}_2\text{O}$). In this process, a hot, ca. 12% solution of sodium carbonate is mixed

with quicklime. The calcium carbonate that precipitates according to the equation $\text{Na}_2\text{CO}_3 + \text{CaO} + \text{H}_2\text{O} \rightarrow 2\text{NaOH} + \text{CaCO}_3$ is removed, and the ca. 12% solution of sodium hydroxide is evaporated in several stages. The impurities that precipitate, mainly NaCl and Na_2SO_4 , are filtered off. In a process operated by Tenneco, the calcium carbonate produced is converted back to calcium oxide and recycled. In 1991, this company started a new plant producing 75 000 t/a of 50% sodium hydroxide from trona in Green River, Wyoming. Further details on the causticization of sodium carbonate are given in [183].

In a combination of electrolytic and dialysis cells, sodium salts can be split into the corresponding acids and alkalis, e.g.,



This reaction can be carried out in a two-chamber cell with a cation- or anion-exchange membrane; in a three-chamber cell with a cation-exchange and an anion-exchange membrane; or in a multichamber cell with a combination of cation, anion, and bipolar membranes [184–187]. However, in all industrially operated cells, the product is a dilute sodium hydroxide solution (15–30%), which also contains some of the salt used as starting material. For this reason, this type of process is most suitable for treating sodium-salt containing wastewater from processes in which

the dilute sodium hydroxide solution obtained can be recycled for neutralization purposes.

An alternative method of producing sodium hydroxide solution for small paper pulp plants, the ferrite recovery process, is described in [188]. Here, waste liquor containing sodium salts and organic substances is evaporated, and the residue is mixed with Fe_2O_3 and calcined. The sodium ferrite formed is decomposed by water to give NaOH and Fe_2O_3 .

51.14.2.2 Production of Solid Sodium Hydroxide

Solid sodium hydroxide (caustic soda) is obtained by evaporating sodium hydroxide solution until the water content is < 0.5–1.5%. The most efficient utilization of energy is achieved with multistage equipment. A flow diagram of a plant constructed by Bertrams, Basel (Switzerland), is shown in Figure 51.24.

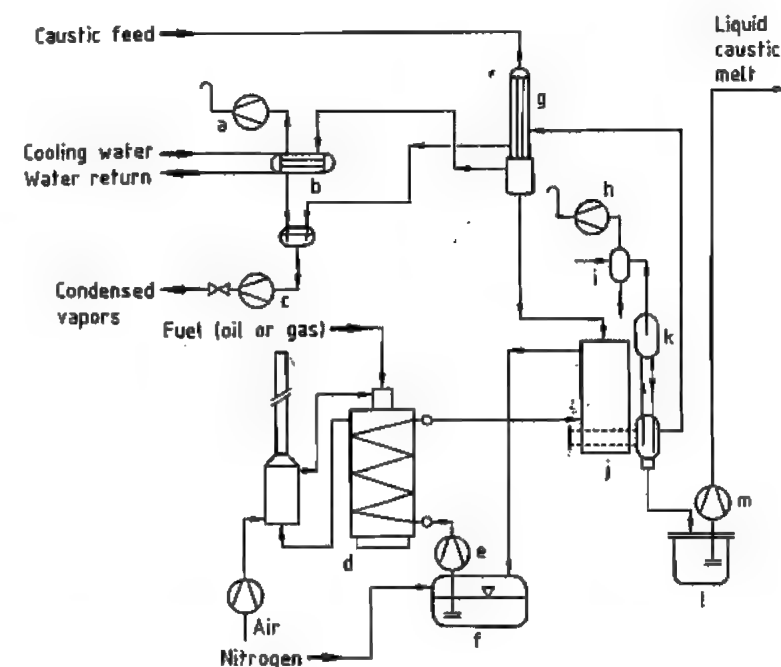


Figure 51.24: High-concentration unit for caustic soda (Bertrams process): a) Vacuum pump; b) Condenser; c) Condensate pump; d) Furnace unit; e) Salt melt pump; f) Heated salt melt tank; g) Pre-concentration unit; h) Vacuum pump; i) Condenser; j) Falling-film concentrator; k) Flash evaporator; l) Heated caustic melt tank; m) Caustic melt pump.

A 50% solution is vacuum evaporated in a pre-concentration unit, by using the heat of the vapor from the main concentrator, until the concentration reaches ca. 60%. In the second stage, a concentration of ca. 99% is attained by heating with a molten salt heat-transfer medium (NaNO_2 – NaNO_3 – KNO_3) at > 400 °C in a falling-film evaporator. The product is fed to a flash evaporator that operates as a gaslift pump. Molten NaOH is raised by vacuum into a heated riser pipe, causing the remaining water to evaporate. The rising steam bubbles lift the melt to the highest point of the system, where the steam is pumped off. The almost anhydrous melt passes through a downcomer pipe into the holding vessel, from which it is pumped to the conditioning plant. The holding vessel, pumps, and pipes must be heated to prevent premature crystallization.

51.14.2.3 Forming

When the NaOH melt is cooled and formed, both the solidification point of NaOH (322 °C) and that of the monohydrate, NaOH·H₂O (62 °C), must be passed through quickly to prevent caking due to unsolidified monohydrate.

Solid sodium hydroxide is supplied in the form of flakes, prills, cast blocks, and less commonly as tablets, briquettes, or granules. Flakes have a bulk density of ca. 0.9 kg/dm³, a thickness of ca. 1.5 mm, and a diameter of 5–20 mm, and are easily broken so that some dust is always formed on handling. Prills have a bulk density of > 1 kg/dm³ and consist of spheres with a diameter of 0.1–0.8 mm (microprills) or 0.5–2.5 mm.

Flakes. To produce flakes, molten NaOH is fed into a trough in which an internally cooled drum rotates. The molten material solidifies on the surface of the partially immersed drum and is scraped off by a knife, which breaks up the sheet of NaOH into flakes. These are taken to a small intermediate storage silo and packed as soon as possible in sacks or steel drums. The material tends to bridge due to its particle shape, so that it cannot be stored in large silos or be transported by compressed air.

Prills are produced by spraying the molten material at ca. 360 °C to form droplets. The spray equipment used can be nozzles (outdated), or a spinning disk or basket. The finely divided melt forms spheres of fairly uniform diameter due to surface tension. These are cooled to ca. 250 °C as they fall down a shaft in which air flows upward. The prills are collected in a funnel from which they run into a cooling drum where they are cooled to ca. 50 °C. The finished product is stored in silos (Figure 51.25).

Unlike flakes, prills are free flowing. Also, they do not cake as readily and thus can be stored in silos, transported in containers or other large vessels, or moved by compressed air, because they are almost dust free.

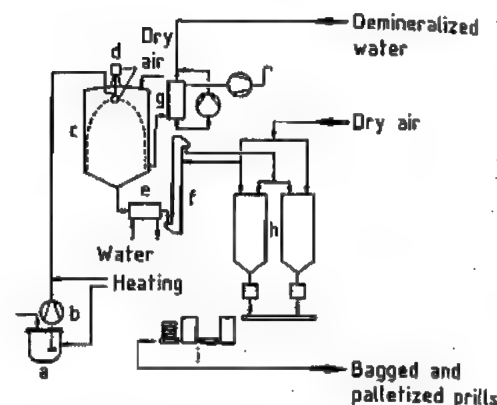


Figure 51.25: Production of sodium hydroxide prills (Bertrams process): a) Caustic melt tank; b) Caustic melt pump; c) Spray tower; d) Rotating spray system; e) Product cooler; f) Elevator; g) Exhaust air treatment; h) Silo; i) Bagging and pelletizing.

Cast Blocks. Molten NaOH is directly cast into iron drums or similar containers. The drums are externally cooled intensively by spraying with water, so that a solid film of sodium hydroxide forms immediately on the walls of the container, preventing further contamination by the iron.

Special Shapes. Tablets, pills, or pellets are produced by the droplet process. Molten NaOH drops from a special device made of silver onto a slowly rotating cooled table or conveyor belt (pill machine). The product has a very low content of metallic impurities, so that this process is especially suitable for producing small quantities (e.g., for analytical purposes).

51.14.2.4 Specifications

Diaphragm liquor cannot be used in all applications (e.g., for artificial silk manufacture or various organic processes) because of the amounts of chloride, chlorate, and heavy metals present.

When corrosion-resistant materials are used for sodium hydroxide production (nickel and stainless steel), the pickup of metal (Ni, Fe) is < 1 ppm. Solid caustic soda should have a pure white appearance. The most important

impurities in solid sodium hydroxide are listed in Table 51.14.

Table 51.14: Product quality: typical percentage analyses of sodium hydroxide from chlor-alkali electrolytic processes.

	Amalgam process	Diaphragm process
NaOH	99–99.5	98–99
NaCl	0.03–0.05	1–2
Na ₂ CO ₃	0.2–0.4	0.65
Na ₂ SO ₄	0.03	0.035
Ca	0.002	0.001
Mg	0.0005	0.0004
Fe	0.001	0.0006–0.0015
Al	0.001	0.0005
Ni	0.0002–0.0004	0.0002–0.0004
Hg	0.000001–0.00001	
mp, °C	322	322

51.14.2.5 Storage, Packaging, and Transportation

Iron, stainless steel, and nickel are suitable materials for containers used for transport and storage, as well as for pipelines. However, corrosion resistance is not the sole criterion for the choice of material. Stress corrosion cracking, changes in the crystal structure, and pitting can cause sudden material failure, so that a more expensive material is often chosen for safety reasons.

Vessels for holding aqueous solutions of sodium hydroxide are usually constructed of alkali-resistant steel. However, at > 50 °C or in the presence of oxygen, iron is slowly attacked by sodium hydroxide solution. For a high-quality product (e.g., with iron content < 1 mg/kg), cladding (rubber or plastic coating) is required. At < 50 °C the solution can be transported by pipes of alkali-resistant steel or plastic (e.g., PVC). Iron pipes are always kept full to prevent corrosion due to ingress of air and consequent black coloration of the solution. At higher temperature, coated materials such as rubber-lined steel, austenitic Cr–Ni steel (e.g., DIN 1.4541), nickel, Hypalon, epoxy resin, polypropylene, or glass fiber-reinforced composites are suitable. In the latter case, an inner lining must be used to prevent contact between the glass fiber and the solution. Heat exchangers are usually constructed

of nickel, nickel alloys, or stainless steel because of the high temperature. For equipment handling highly concentrated solutions, nickel is the most commonly used material because of its outstanding corrosion resistance. Metals that have been in contact with solutions are difficult to weld, so that repairs to pipework and equipment which have carried sodium hydroxide solutions are difficult. A comprehensive review of materials that can be used with sodium hydroxide is given in [189].

Pipelines carrying 50% sodium hydroxide solution in cold regions are provided with thermostatic heating. Solutions are transported by road, rail tanker, or ship.

Caustic soda prills are stored in steel or stainless steel hoppers with a capacity of 30–50 m³. The hoppers have conical bases with an angle of 25° to the vertical and are provided with external hammering equipment. Even when the product is stored under dry air, a storage time of 3–6 d should not be exceeded to ensure that the prills do not cake under their own weight. Solid sodium hydroxide is usually packed in 25–50-kg hermetically sealed polyethylene sacks. For transport, the sacks are stacked on wooden pallets and shrink wrapped in polyethylene. Caustic soda prills are also carried in 50- or 200-kg steel drums, loose in 1000-kg-capacity steel or flexible containers, or in transportable hoppers. In the closed system delivery (CSD) method of the PPG Company, containers coated with epoxy resin are transported by road and rail. Pneumatic transport is carried out with dry air and causes very little damage to the product [190].

51.14.3 Uses

Most users of sodium hydroxide require dilute aqueous solutions.

The sodium hydroxide produced in Europe (8.67 × 10⁶ t/a NaOH) in 1990 was divided among various areas of use as shown in Figure 51.26. More than 48% of production is used in the chemical industry:

- In inorganic chemistry, sodium hydroxide is used in the manufacture of sodium salts,

for alkaline ore digestion, and for pH regulation.

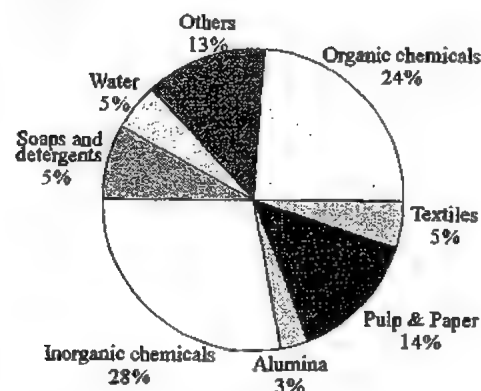


Figure 51.26: Consumption of sodium hydroxide in Europe (total: 40.96×10^6 t/a in 1995).

- The organic chemical industry uses sodium hydroxide for saponification reactions, production of nucleophilic anionic intermediates, etherification and esterification, basic catalysis, and the production of free organic bases. Sodium hydroxide solution is used for scrubbing waste gases and neutralizing wastewater.
- In the paper industry, sodium hydroxide solution is used for cooking wood (removal of lignin).
- The textile industry uses sodium hydroxide solution to manufacture viscose and viscose staple fibers. The sodium hydroxide solution used must contain only traces of chloride ions (rayon quality). The surface of cotton can be improved by treatment with sodium hydroxide solution (mercerization).
- Considerable quantities of sodium hydroxide are used for sodium phosphate production in the detergent industry. Soaps are manufactured by the saponification of fats and oils with sodium hydroxide solution, and detergents are produced from organic sulfonic acids and sodium hydroxide.
- In the aluminum industry, sodium hydroxide is used mainly for the treatment of bauxite.
- Waterworks use dilute sodium hydroxide solution to regenerate ion exchangers for

water purification and wastewater treatment.

- Other users of sodium hydroxide include electroplating technology, the natural gas and petroleum industries, the glass and steel industries, and gold extraction (cyanide leaching). In the food industry, sodium hydroxide is used for degreasing, cleaning, and for peeling potatoes.

51.14.4 Safety Precautions

Because of its strongly caustic action, all contact with sodium hydroxide during handling must be prevented by the use of suitable protective equipment (protective goggles, safety gloves, and, if needed, dust masks). Any clothing or shoes that come in contact with sodium hydroxide must be removed immediately and can be reused only after thorough cleaning. First aid to affected parts of the body consists of washing with copious amounts of water. The skin can be neutralized with a dilute solution of a buffered weak acid (e.g., acetic acid-sodium acetate). For irrigation of the eyes, a special hygienic eyewash solution is used. The product poses no direct environmental risk and has therefore been removed from the list of chemicals (e.g., in the United States) whose emission must be reported to local and national environmental authorities.

51.14.5 Economic Aspects

Methods of manufacture of sodium hydroxide have changed often throughout the years (see also [191]). Decisive factors have included the availability of raw materials (sodium carbonate, sodium chloride, or sodium sulfate), process economics, and product quality. The coproduction of chlorine in the electrolytic process and of sulfuric acid in the electrodialysis process together with their environmental implications may also have an effect on future production of sodium hydroxide solution.

Total world production in 1995 was 40.96×10^6 t/a NaOH, the largest amount being pro-

duced in the United States (Figure 51.27). Production of chlorine and alkali since 1920 in the United States is shown in Figure 51.28. Growth was almost exponential until 1965, after which it flattened out considerably during the next 20 years. As shown in Figure 51.29, world production increased by 40% from 1976 to 1995, while the corresponding increase during the same period in the United States was only ca. 26%, and in Germany only 13%. An annual growth of 2–2.2% as can be seen starting from 1992–1993 is forecast up to 2000, with the greatest increase in Asia-Pacific region [192, 193], especially in China and in countries with low energy price. By that time, world consumption will probably be ca. 43×10^6 t/a NaOH and world capacity ca. 50×10^6 t/a [190]. Because the growth rate of the coproduct chlorine is estimated to be in the same range, or even higher, a world shortfall of electrolytic sodium hydroxide solution is not expected until the year 2000 [175].

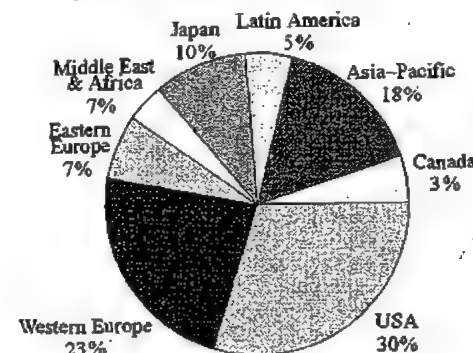


Figure 51.27: World production of sodium hydroxide by region (total: 38.43×10^6 t/a in 1990).

The conversion of sodium carbonate to sodium hydroxide by causticization has been revived since 1990, but the possibilities for producing sodium hydroxide solution from natural sodium carbonate are limited by the rather high transport costs, because natural deposits of sodium carbonate are much rarer than those of sodium chloride. At present, the process is used only in the United States. Synthetic sodium carbonate produced by the Solvay process has the disadvantage that the wastewater contains chloride.

Supply-demand restructuring and a technical breakthrough for alternative techniques such as salt splitting forced by increasing prices have not taken place so far and cannot be seen coming.

Increasing prices could lead to supply-demand restructuring and to a technical breakthrough for alternative techniques such as salt splitting.

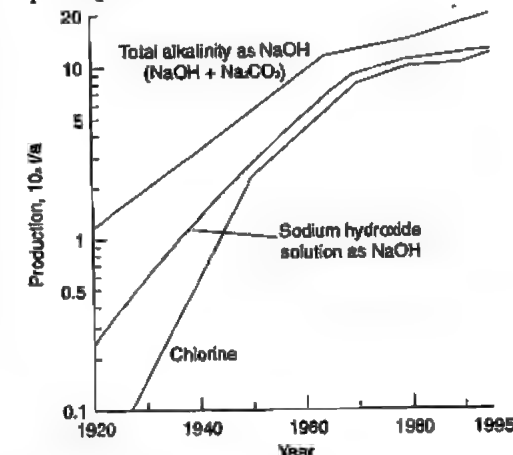


Figure 51.28: U.S. production of chlorine, sodium hydroxide solution, and total alkali.

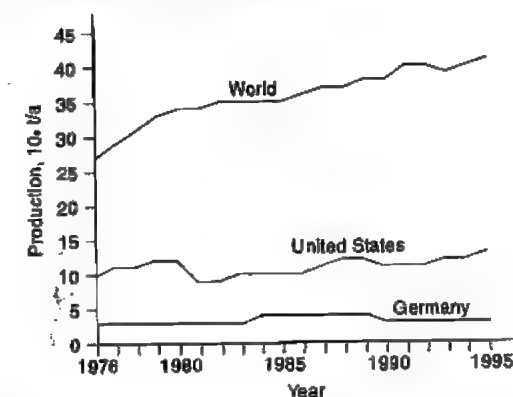


Figure 51.29: Growth of sodium hydroxide production in West Germany, the United States, and the world from 1976 to 1995.

51.15 Sodium Carbonates

51.15.1 Sodium Carbonate

Sodium carbonate (soda ash) is the neutral sodium salt of carbonic acid. It is one of the most important raw materials used in the chemical industry, and has been known by humans since ancient times. Sodium carbonate had many uses even then (cleaning and glass manufacture) for which it is still indispensable. Sodium carbonate from the deposits in Wadi Natrun (4% Na_2CO_3 , 25% NaHCO_3) was traded in ancient Egypt.

Production of the alkaline materials sodium carbonate and potassium carbonate (which were recognized rather late as chemically distinct) was carried out from ancient times until the 1800s by the combustion of marine and land vegetation, followed by calcination at red heat and leaching of the ash. The term soda ash originates from this process.

The soda ash obtained in this way was a low-percentage material; e.g., Spanish barilla contained 25–30% Na_2CO_3 , varec from Normandy 3–8%, and Scottish kelp 10–15%. The soda ash produced from plants was very expensive, and the processes used were too primitive for mass production and consumed vast quantities of vegetation.

Large-scale production was possible only after the development of a new process, named after its inventor **LEBLANC** (1742–1806). In 1790, the first plant was built in Saint-Denis, France. Initially, production was 300 kg/d. In the following years, the soda industry developed rapidly in England due to the increasing demand for soda ash to clean cotton from the colonies. In 1878, production in England was 8 t per week, and in the rest of the world, 4 t a week.

However, in the second half of the 1800s, the Leblanc soda ash process experienced serious competition from the Solvay process. In

the first half of the 1800s, investigations were already being carried out into the industrial use of the double decomposition reaction of NaCl with NH_4HCO_3 , but without success. However, the Belgian **ERNEST SOLVAY** (1838–1932) brought the development of the process to a successful conclusion during 1861–1865. The first plant was started up in 1865 in Couillet, Belgium, with an initial production of 1.5 t/d. The first Solvay plant in Germany was built in 1880 in Wyhlen on the upper Rhine.

The technically and economically superior Solvay process displaced the Leblanc to such an extent that by the early 1900s only a few Leblanc works ceased operation around 1923. Since then, the Solvay process has remained predominant. Since World War II, soda ash has been increasingly obtained from trona, especially in the United States.

51.15.1.1 Properties

Physical Properties. In addition to anhydrous sodium carbonate, Na_2CO_3 , the following hydrates exist: sodium carbonate monohydrate, $\text{Na}_2\text{CO}_3 \cdot \text{H}_2\text{O}$; sodium carbonate heptahydrate, $\text{Na}_2\text{CO}_3 \cdot 7\text{H}_2\text{O}$; and sodium carbonate decahydrate, $\text{Na}_2\text{CO}_3 \cdot 10\text{H}_2\text{O}$. The physical properties of these compounds are listed in Table 51.15. Solubilities of the hydrates of sodium carbonate are shown in Figure 51.30. The relationship between the concentration of an aqueous solution of Na_2CO_3 and its pH at 25 °C is shown in Figure 51.31.

Chemical Properties. Thermal Behavior: The thermal decomposition of sodium carbonate to sodium oxide and carbon dioxide in a vacuum in the absence of chemically activating substances such as water vapor begins at ca. 1000 °C. The dissociation pressure is ca. 200 Pa and increases to 10.3 kPa at 1450 °C [196].

Table 51.15: Physical properties of sodium carbonate and its hydrates.

	Anhydrous	Monohydrate	Heptahydrate	Decahydrate
Formula	Na_2CO_3	$\text{Na}_2\text{CO}_3 \cdot \text{H}_2\text{O}$	$\text{Na}_2\text{CO}_3 \cdot 7\text{H}_2\text{O}$	$\text{Na}_2\text{CO}_3 \cdot 10\text{H}_2\text{O}$
Density at 20 °C, g/cm ³	2.533	2.25	1.51	1.469
Melting point, °C	851	105 ^a	35.37 ^b	32.0
Heat of fusion, J/g	316			
Specific heat capacity at 25 °C, J g ⁻¹ K ⁻¹	1.043	1.265	1.864	1.877
Heat of formation, J/g	10.676			
Heat of hydration, J/g		133.14	646.02	858.3
Crystal structure	monoclinic	rhombic	rhombic-bipyramidal	monoclinic-pseudo-hexagonal
Refractive indices n_x , n_y , n_z	1.410, 1.537, 1.544	1.420, 1.506, 1.524	197	1.405, 1.425, 1.440
Heat of solution ^c , J/g	-222	-79.6		243

^a In its own water of crystallization.

^b Incongruent.

^c Integrated enthalpy of solution at infinite dilution.

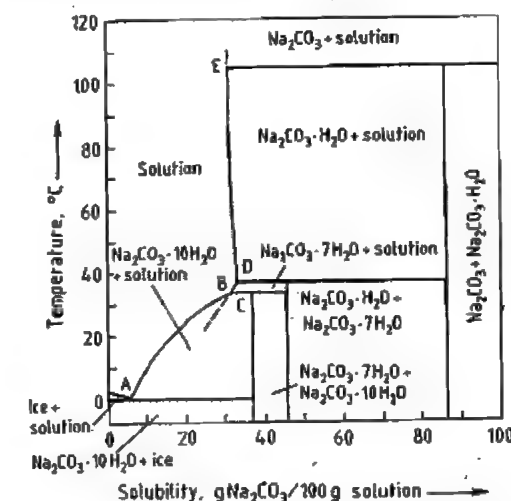


Figure 51.30: Solubilities in the system $\text{Na}_2\text{CO}_3\text{--H}_2\text{O}$ [194]. Temperatures and concentrations of the two-salt points and the cryohydric point.

Two-salt point	T , °C	Solubility, g Na_2CO_3 /100 g solution	Solid phases
A	-2.1	3.93	ice + $\text{Na}_2\text{CO}_3 \cdot 10\text{H}_2\text{O}$
B	32.0	31.26	$\text{Na}_2\text{CO}_3 \cdot 10\text{H}_2\text{O}$ + $\text{Na}_2\text{CO}_3 \cdot 7\text{H}_2\text{O}$
C	32.96	33.35	$\text{Na}_2\text{CO}_3 \cdot 10\text{H}_2\text{O}$ + $\text{Na}_2\text{CO}_3 \cdot \text{H}_2\text{O}$ (metastable)
D	35.37	33.21	$\text{Na}_2\text{CO}_3 \cdot 7\text{H}_2\text{O}$ + $\text{Na}_2\text{CO}_3 \cdot \text{H}_2\text{O}$
E	105 ± 5	31.15	$\text{Na}_2\text{CO}_3 \cdot \text{H}_2\text{O}$ + Na_2CO_3

Reaction with Water and Carbon Dioxide. Sodium carbonate is hygroscopic. In air at 96% R.H. its weight can increase by 1.5%

within 30 min [197]. If sodium carbonate is stored under moist conditions, its alkalinity decreases due to absorption of moisture and carbon dioxide from the atmosphere



Water vapor reacts with sodium carbonate above ca. 400 °C to form sodium hydroxide and carbon dioxide [198].

Reaction with Elements. Sodium carbonate reacts exothermically with chlorine above ca. 150 °C to form NaCl , CO_2 , O_2 and NaClO_4 [199].

The elements platinum, gold, vanadium, titanium, zirconium, aluminum, molybdenum, tungsten, and iron (1200 °C) are attacked by fused Na_2CO_3 , with liberation of CO_2 and formation of complex metal oxide sodium oxide compounds. At higher temperature, the Na_2O formed reacts with excess metal to form sodium metal vapor [200]. Sodium carbonate reacts very slowly with copper and nickel at high temperature (> 1500 °C).

51.15.1.2 Sodium Carbonate Minerals

Whereas the production of sodium carbonate from the ashes of plants that grow in salty soil near the sea is only of historical interest, extraction from soda-containing minerals, especially trona, is of increasing importance.

The most important deposits are located in Wyoming (Green River District), California (Owens Lake and Searles Lake), East Africa

(Magadi Lake), and Lower Egypt (Wadi Natrun).

The proportion of Na_2CO_3 in the salt mixture in such deposits seldom exceeds 40%. The accompanying compounds include sodium hydrogencarbonate, borax, sodium sulfate, sodium chloride, and potassium chloride.

For example, the concentrations of dissolved salts in the water of Owens Lake are [201]

9% Na_2CO_3 , 1% $\text{Na}_2\text{B}_4\text{O}_7$, 16% NaCl
1.2% NaHCO_3 , 3% Na_2SO_4 , 1.5% KCl

Deposits of Na_2CO_3 -containing minerals occur worldwide:

Trona $\text{Na}_2\text{CO}_3 \cdot \text{NaHCO}_3 \cdot 2\text{H}_2\text{O}$
Natron $\text{Na}_2\text{CO}_3 \cdot 10\text{H}_2\text{O}$
Thermonatrite $\text{Na}_2\text{CO}_3 \cdot \text{H}_2\text{O}$
Hanksite $2\text{Na}_2\text{CO}_3 \cdot 9\text{Na}_2\text{SO}_4 \cdot \text{KCl}$
Pirssonite $\text{Na}_2\text{CO}_3 \cdot \text{CaCO}_3 \cdot 2\text{H}_2\text{O}$
Gaylussite $\text{Na}_2\text{CO}_3 \cdot \text{CaCO}_3 \cdot 5\text{H}_2\text{O}$

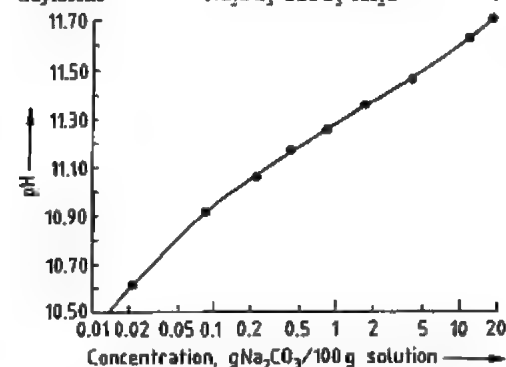


Figure 51.31: pH values of aqueous solutions of Na_2CO_3 at 25 °C [195].

Concentration, g Na_2CO_3 /100 g solution	pH at 25 °C
0.055	10.274
0.0217	10.612
0.0884	10.919
0.2246	11.063
0.4376	11.171
0.8609	11.254
1.806	11.357
4.241	11.453
12.034	11.617
18.555	11.699

Only trona is of commercial importance. These Na_2CO_3 -containing minerals were formed from the original rock by the erosive action of air, water, heat, and pressure, followed by chemical changes caused by the ac-

tion of atmospheric carbon dioxide. The carbonate-containing salts formed were leached by water and then concentrated and crystallized by evaporation.

51.15.1.3 Production

Ammonia-Soda Process

General and Theoretical Principles

The ammonia-soda process is based on the formation of sparingly soluble sodium hydrogencarbonate (known in the soda industry as bicarbonate) by reacting sodium chloride with ammonium hydrogencarbonate in aqueous solution:



The process includes the following stages:

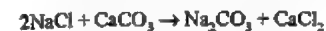
1. Production of a saturated salt solution
 $\text{NaCl} + \text{H}_2\text{O}$
2. Burning of limestone or chalk (the CO_2 liberated is used in stage 4)
 $\text{CaCO}_3 \rightarrow \text{CaO} + \text{CO}_2$
3. Saturation of the salt solution with ammonia
 $\text{NaCl} + \text{H}_2\text{O} + \text{NH}_3$
4. Precipitation of bicarbonate by the introduction of carbon dioxide (from stages 2 and 6)
 $\text{NaCl} + \text{H}_2\text{O} + \text{NH}_3 + \text{CO}_2 \rightarrow \text{NH}_4\text{Cl} + \text{NaHCO}_3$
5. Filtering and washing of precipitated bicarbonate
 $2\text{NaHCO}_3 \rightarrow \text{Na}_2\text{CO}_3 + \text{H}_2\text{O} + \text{CO}_2$
6. Thermal decomposition of bicarbonate to sodium carbonate (the CO_2 evolved is recycled to stage 4)
7. Production of milk of lime
 $\text{CaO} + \text{H}_2\text{O} \rightarrow \text{Ca(OH)}_2$
8. Recovery of ammonia by distillation of the mother liquor from stage 4 (bicarbonate precipitation) with milk of lime (the ammonia liberated is recycled to stage 3)
 $2\text{NH}_4\text{Cl} + \text{Ca(OH)}_2 \rightarrow 2\text{NH}_3 + \text{CaCl}_2 + 2\text{H}_2\text{O}$

Table 51.16: Reciprocal pair $\text{NaCl} + \text{NH}_4\text{HCO}_3 \rightleftharpoons \text{NaHCO}_3 + \text{NH}_4\text{Cl}$ 15 °C isotherm, monovariant points (mol/1000 g H_2O).

Point	NaCl	NaHCO_3	NH_4Cl	NH_4HCO_3	Solid phase
a	6.12				NaCl
b			6.64		NH_4Cl
c				2.36	NH_4HCO_3
d		1.05			NaHCO_3
I	6.06	0.12			$\text{NaCl} + \text{NaHCO}_3$
II	4.55		3.72		$\text{NaCl} + \text{NH}_4\text{Cl}$
III			6.40	0.81	$\text{NH}_4\text{Cl} + \text{NH}_4\text{HCO}_3$
IV		0.71		2.16	$\text{NaHCO}_3 + \text{NH}_4\text{HCO}_3$
P ₁	0.51	0.93	6.28		$\text{NH}_4\text{Cl} + \text{NH}_4\text{HCO}_3 + \text{NaHCO}_3$
P ₂	4.44	0.18	3.73		$\text{NH}_4\text{Cl} + \text{NaCl} + \text{NaHCO}_3$

The liquid remaining after distillation is usually discarded in its entirety, because only a small fraction can be used for calcium chloride production, depending on demand.

The process can be represented by the following simplified equation:



In aqueous solution, the reaction proceeds from right to left due to the low solubility of calcium carbonate. The role of ammonia is to promote the formation of sodium bicarbonate via the intermediate ammonium bicarbonate.

The reaction that takes place in aqueous solution



is determined by the solubilities of the individual salts in the presence of other components of the reciprocal salt pairs. These solubility relationships have been investigated by FEDOTIEFF [202].

The basic principles can be explained by using the 15 °C isotherm (Figure 51.32), based on the values given in Table 51.16. The figure is the orthogonal projection of a three-dimensional diagram (i.e., a four-sided pyramid whose edges represent the coordinates of NaCl , NH_4Cl , NH_4HCO_3 , and NaHCO_3). This diagram shows the ranges of existence of the individual solid phases that are in equilibrium with their saturated solutions at 15 °C:

Area a-I-P ₂ -II:	NaCl
Area II-P ₂ -P ₁ -III-b:	NH_4Cl
Area P ₁ -III-c-IV:	NH_4HCO_3
Area I-P ₂ -P ₁ -IV-d:	NaHCO_3

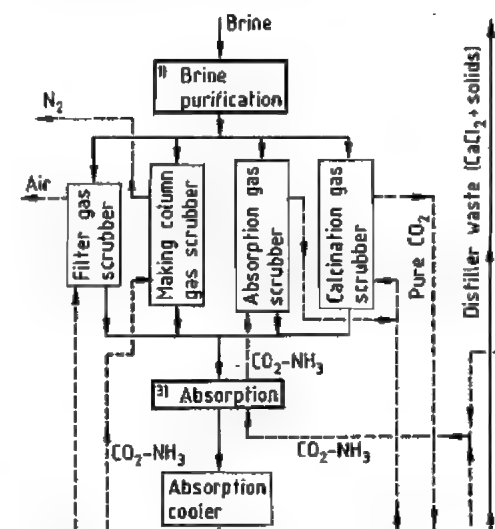


Figure 51.32: The 15 °C isotherm for the reciprocal salt pair $\text{NaCl} + \text{NH}_4\text{HCO}_3$ (concentration in mol/1000 g H_2O are shown on the ordinate and abscissa).

Along the lines I-P₂, II-P₂, P₂-P₁, P₁-III, and P₁-IV, two solid phases coexist, and at the points P₁ and P₂, three solid phases coexist. These two points are thus monovariant because in the presence of three solid phases, a change in concentration is possible only by changing the temperature.

The point P₁, at which the three salts NH_4Cl , NH_4HCO_3 , and NaHCO_3 coexist, is of special importance for the ammonia-soda process, because this point has the highest NH_4Cl concentration in the entire range. If point P₁ is reached by the precipitation of bicarbonate, it represents the maximum attainable sodium yield. Nevertheless, working so that neither the point P₁ nor the lines P₁-P₂ and P₁-IV are

actually reached is advisable, to avoid coprecipitation of NaHCO_3 , NH_4Cl , or NH_4HCO_3 . The coprecipitation of NH_4Cl has a particularly detrimental effect on the quality of the soda, because it is converted to NaCl on calcination:



or



An end point that is as close as possible to P_1 but lies within the hatched area in Figure 51.32 is best.

The course of bicarbonate precipitation can be followed clearly in the square diagram of JANECKE [203]. Figure 51.33 shows the 30 °C isotherm of the system in such a diagram. This diagram does not represent absolute solubilities, but percentages of salts in the total salt content of the solution. Thus, the corners represent pure salts or solutions of a single salt, and the lines joining two corners represent mixtures of two salts. Points within the square represent mixtures or solutions of three salts. The solubilities can be found from the diagram if the appropriate water value is given for each point of equilibrium (the salt value being 1 kmol in all cases). This can be shown by means of lines of equal water content (isohydric lines).

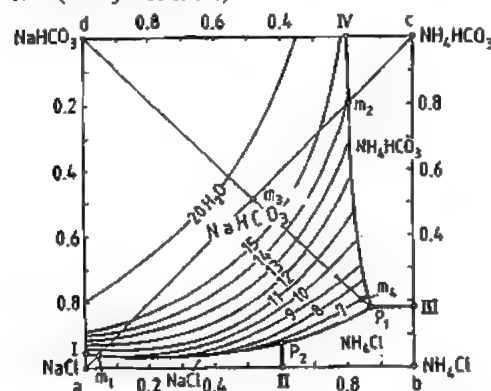


Figure 51.33: The 30 °C isotherm for the reciprocal salt pair $\text{NaCl} + \text{NH}_4\text{HCO}_3$. On the ordinate and abscissa of the square diagram, the amount of each salt is shown as a molar fraction of the total salt content of the solution.

The points, lines, and areas in Figure 51.33 have the same significance in principle as

those in the 15 °C isotherm diagram of Figure 51.32. The corner point (a) corresponds to a solution of pure sodium chloride. If NH_4HCO_3 is added (by passing carbon dioxide and ammonia into the solution), the mixture moves from point (a) toward point (c) (NH_4HCO_3). In the case of saturation, systems represented by points on line m_1 – m_2 are in equilibrium with NaHCO_3 as solid phase.

In the ammonia-soda process, point (a) represents a solution that is not completely saturated (9.7 instead of 9.01 kmol H_2O /kmol NaCl). Point (m_3) on line a–c is reached by the introduction of CO_2 and NH_3 in an equimolar ratio. At this point, the water content necessary to give a saturated solution is ca. 17.5 kmol/kmol dissolved salt (see isohydric lines in Figure 51.33). However, the proportion of water introduced with the brine, which is further reduced by the reaction of NH_3 with CO_2 to form NH_4HCO_3 , is only ca. 7 kmol/kmol dissolved salt. This leads to the precipitation of sodium bicarbonate.

The precipitation process consists of separation of the supersaturated system (m_3) into the solid pure component NaHCO_3 (point d) and the saturated mother liquor (m_4).

In the Solvay process the degrees of utilization of Na^+ and NH_4^+ are both important. These can be calculated from the composition of the mother liquor (determined by chemical analysis) by using the equations:

$$U_{\text{Na}^+} = \frac{100(\text{Cl}^- - \text{Na}^+)}{\text{Cl}^-}$$

$$U_{\text{NH}_4^+} = \frac{100(\text{NH}_4^+ - \text{HCO}_3^-)}{\text{NH}_4^+}$$

In these equations, Cl^- , Na^+ , NH_4^+ , and HCO_3^- denote the concentrations in moles per kilogram of H_2O , and U_{Na^+} and $U_{\text{NH}_4^+}$ denote the percentage utilization of Na^+ and NH_4^+ . The values for U_{Na^+} and $U_{\text{NH}_4^+}$ depend on the starting concentrations, and maximum Na^+ utilization does not correspond to maximum NH_4^+ utilization. These relationships are illustrated by the values given in Table 51.17.

Table 51.17: Percentage utilization of Na^+ and NH_4^+ in the reaction of NaCl with NH_4HCO_3 at 15 °C and various initial concentrations.

Initial concentration of solution, mol/1000 g H_2O		Point	Solution produced, gmol/1000 g H_2O				Utilization, %	
NaCl	NH_4HCO_3		HCO_3^-	Cl^-	Na^+	NH_4^+	Na^+	NH_4^+
8.188	3.730	P_2	0.18	8.188	4.62	3.730	43.58	95.17
7.658	4.552	\downarrow	0.31	7.658	3.39	4.552	55.73	93.19
7.128	5.450		0.51	7.128	2.19	5.450	69.28	90.64
6.786	6.272	P_1	0.92	6.786	1.44	6.272	78.78	85.33
6.000	5.640		0.99	6.000	1.34	5.640	77.67	82.45
5.403	5.210	\downarrow	1.07	5.403	1.27	5.210	76.49	79.46
5.025	4.919		1.12	5.025	1.23	4.919	75.52	77.23
4.000	4.135	IV	1.30	4.000	1.16	4.135	71.00	68.56

For economic operation of the process, the utilization of Na^+ should be high, rather than that of NH_4^+ , since unconsumed NH_4^+ is recycled. Therefore, in practice, Na^+ utilization is between 72 and 76%, and NH_4^+ between 69 and 71%. However, note that consideration of phase rule theory gives no information about kinetic effects such as rates of reaction, nucleation, and crystallization.

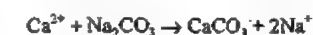
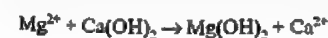
A comprehensive treatment of the phase rule theory is given in [204, pp. 125–160].

Technology

The Solvay ammonia-soda process is shown schematically in Figure 51.34. The main operational stages are shown in the numbered bold rectangle:

Stage 1: Brine Purification. The sodium chloride used as a raw material in the Solvay process can be obtained by conventional or solution mining [205].

The brine always contains inorganic impurities that lead to production problems and impair the quality of the final product. For example, calcium and magnesium ions can cause scaling in the equipment and pipework due to the formation of basic carbonates during ammonia absorption, which can seriously interfere with the process. Purification of the brine, which should be as near saturation as possible to achieve optimum Na^+ utilization, is best carried out by the lime-soda process. Magnesium ions are precipitated as hydroxide, and calcium ions as carbonate:



The reagents used in this precipitation are prepared by dissolving soda ash or milk of lime in brine (Na_2CO_3 concentration: 65–80 kg/ m^3 ; $\text{Ca}(\text{OH})_2$ concentration: 170–185 kg/ m^3). Reaction times, crystallization rates, and settling rates are improved if the brine with the added reagent solutions is mixed with a recycled seed slurry. Under these conditions, precipitates of calcium carbonate and magnesium hydroxide can be produced with settling rates up to 1 m/h, and in some cases even 3 m/h.

Stage 2: Limestone Calcination and Lime Slaking. The limestone must be of very high purity (SiO_2 : < 3%; Fe_2O_3 – Al_2O_3 : < 1.5%). From it, both carbon dioxide for the carbonation stage and calcium oxide for the distillative recovery of ammonia are produced by calcination with coke (see Section 56.5).

The quantity of limestone used per tonne of soda ash produced is determined solely by the amount of calcium oxide required for ammonia recovery. Hence, the excess carbon dioxide is either released to the atmosphere or supplied to other consumers.

The consumption of 95% pure limestone varies between ca. 1100 and 1200 kg/1000 kg sodium carbonate, and is therefore approximately 10–20% higher than the theoretical value.

In the system $\text{CaCO}_3 \rightleftharpoons \text{CaO} + \text{CO}_2$, the equilibrium pressure of CO_2 , p_{CO_2} , varies logarithmically with absolute temperature T

$$\log p_{\text{CO}_2}(\text{bar}) = -\frac{8580}{T(\text{K})} + 7.26$$

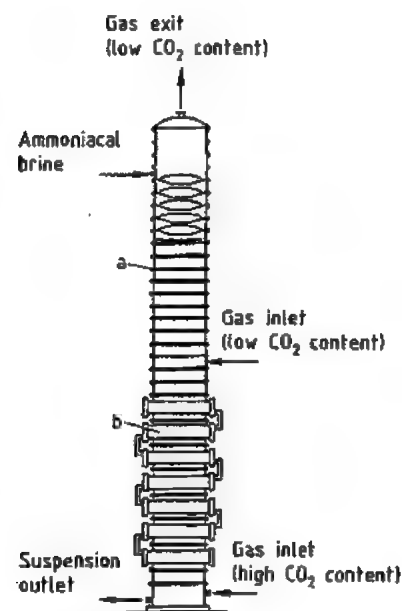


Figure 51.36: Making column: a) Double tray; b) Cooling tube bundle.

A few soda ash plants still use the Honigmann process, in which carbonation is carried out in three to five vessels. CO_2 -containing gas is bubbled through a central dip tube into the ammoniacal brine. Gas with the highest CO_2 content (calcination gas) is supplied to the vessel with the most strongly carbonated ammoniacal brine, and weak gas is fed to the vessel that contains fresh solution.

The temperature profile in both column and vessel processes exhibits a maximum of $50\text{--}60^\circ\text{C}$. The suspension of bicarbonate in mother liquor leaves the carbonation stage at 30°C .

Stage 5: Filtration of Bicarbonate. Bicarbonate is generally separated from the mother liquor in continuous rotary vacuum filters or band filters, and sometimes in centrifuges. Mother liquor adhering to the bicarbonate crystals is washed off with condensate produced during the production process or with softened water. The quantity of washing water required depends on the particle size of the precipitated product and varies between 0.3 and $1\text{ m}^3/\text{t}$ of bicarbonate.

Crude bicarbonate has the following approximate composition: NaHCO_3 , 75.6%; Na_2CO_3 , 6.9%; NH_4HCO_3 , 3.4%; NaCl + NH_4Cl , 0.4%; H_2O , 13.7%.

Centrifuged products contain only 7–9% water. Calcination of 1 t of crude bicarbonate yields ca. 520–560 kg of soda ash.

Stage 6: Calcination of Bicarbonate. Thermal decomposition of crude bicarbonate to carbonate liberates carbon dioxide, ammonia, and water vapor. The product is technical-grade soda ash, which contains sodium chloride. The main reaction is



and side reactions are



The heat requirement for the calcination of crude bicarbonate is 0.92 GJ/t soda, not including that required for drying the moist, filtered product. The total heat requirement for calcination in rotary calciners is 3.7 GJ/t soda. This heat is supplied at ca. 180°C ; the decomposition temperature of NaHCO_3 is 87.7°C at a total CO_2 - H_2O pressure of 0.1 MPa .

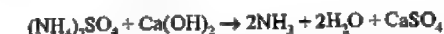
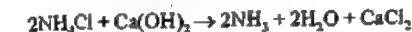
Today, calcination is almost always carried out in rotary calciners. These are heated either externally with oil, gas, or coal, or internally with steam, which passes through heating tubes in the calciner countercurrent to the flow of solid material. Condensing steam gives much better heat transfer than combustion gas, so that the output from steam-heated rotary calciners is considerably higher than that of calciners heated by combustion processes. The advantages of steam-heated calciners compared with those heated by combustion include the absence of thermal damage to the calciner, smaller space requirements and hence lower equipment costs, and ca. 15% less fuel consumption.

Gases extracted from the calciners contain CO_2 , NH_3 , H_2O , and some leakage air, together with large amounts of dust (sodium carbonate and bicarbonate), which is removed in cyclones or electrostatic filters. Before this gas is used in the carbonation stage, it is

cooled and washed with brine and water until it is free of ammonia. The condensate produced at this point is fed to the ammonia recovery stage.

If the soda ash is required in the form of solution or hydrated crystals, wet calcination can be used. This is carried out in a tower with steam in countercurrent flow. In this thermal decomposition, a sodium carbonate sodium bicarbonate equilibrium is established, which limits the yield to 85–88%.

Stage 7: Recovery of Ammonia. Ammonia, present in the filtrate as ammonium carbonate, hydrogencarbonate, sulfate, and chloride, is recovered by distillation followed by absorption. Both $(\text{NH}_4)_2\text{CO}_3$ and NH_4HCO_3 are completely decomposed at $85\text{--}90^\circ\text{C}$, liberating all of the carbon dioxide and a small part of the ammonia from solution. Liberation of ammonia from NH_4Cl and $(\text{NH}_4)_2\text{SO}_4$ requires reaction with milk of lime:



This reaction must be preceded by thermal decomposition of $(\text{NH}_4)_2\text{CO}_3$ and NH_4HCO_3 to avoid precipitation of calcium carbonate and consequent consumption of additional milk of lime. Free ammonia is displaced from solution with low-pressure steam.

A distillation plant is shown schematically in Figure 51.37. Distillation gas, which contains NH_3 and CO_2 , is cooled to ca. $55\text{--}60^\circ\text{C}$ in the still condenser and still preheater. At this temperature, no danger exists of blocking the pipework with crystallized salts formed by ammonia and carbon dioxide. The stripping still removes CO_2 and NH_3 by thermal decomposition of $(\text{NH}_4)_2\text{CO}_3$ and NH_4HCO_3 , and in the preliher, NH_4Cl and $(\text{NH}_4)_2\text{SO}_4$ are reacted with milk of lime. In the distillation column the ammonia content of the liquor is lowered to ca. 0.5 kg/t sodium carbonate by steam treatment. The CO_2 - NH_3 -containing condensate from the gas cooler and heat exchanger is recycled to the stripping still or distilled in a special condensate tower.

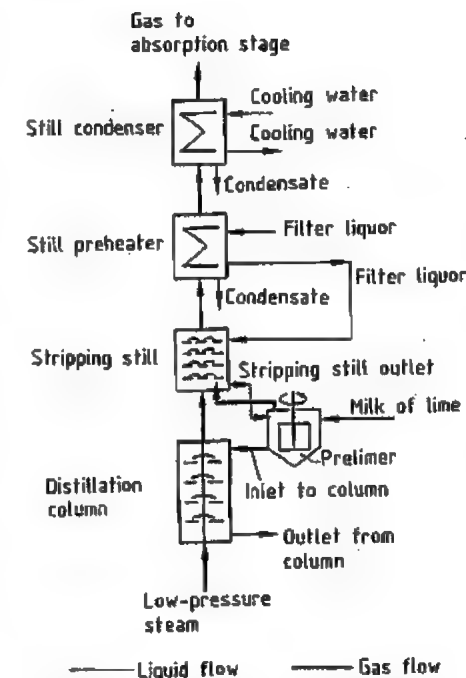


Figure 51.37: Flow diagram of stripping equipment.

Modified Ammonia-Soda Process

Many variants of the ammonia-soda process exist [213]. Here, only the dual process, developed and operated in Japan, is described. This process combines soda ash production with ammonium chloride production. The importance of the process in Japan is due to the high cost of imported rock salt and use of the ammonium chloride as a fertilizer.

In the dual process [206] (Figure 51.38), ammonia is absorbed by the bicarbonate mother liquor, and solid sodium chloride is added. On cooling, ammonium chloride separates, is recovered in centrifuges, and is then dried in rotary dryers with air at 150°C . The mother liquor is recycled to the carbonation towers where sodium bicarbonate is precipitated.

Important differences exist between equipment used for the conventional Solvay process and that used for the ammonium chloride-soda process. In the dual process, ammonia is not recovered; hence no distillation equipment

is required. Also, lime kilns are not required if other sources of CO_2 are available. Because of the extremely corrosive properties of NH_4Cl -containing solutions, they are produced in equipment made of special cast iron or plastics. As the mother liquor is recycled, special attention must be paid to the water balance of the system. The amount of water introduced into the system (e.g., for washing sodium bicarbonate and ammonium chloride) must be controlled continuously to maintain the correct quantity and composition. The quantity of sodium carbonate produced in 1970 by the dual process amounted to ca. 4.7% of world production [207].

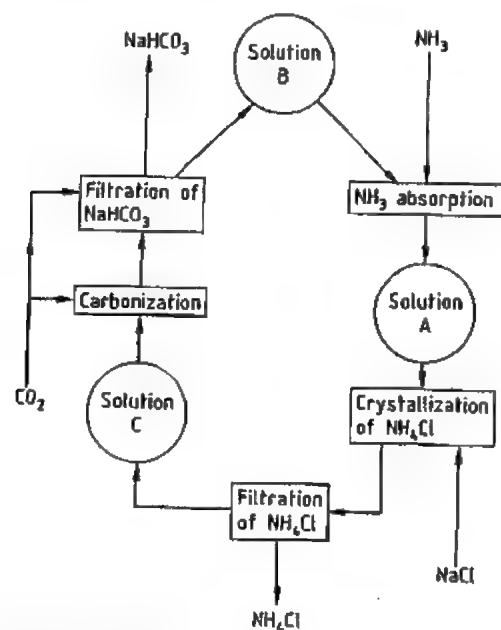


Figure 51.38: Flow diagram of the dual process. Solution A: 4.1 mol/L NH_4Cl + 1.05 mol/L NaCl ; $\rho = 1.108 \text{ g/cm}^3$; $t = 20^\circ\text{C}$. Solution B: 3.45 mol/L NH_4Cl + 1.1 mol/L NaCl ; $\rho = 1.110 \text{ g/cm}^3$; $t = 5^\circ\text{C}$. Solution C: 1.86 mol/L NH_4Cl + 3.73 mol/L NaCl ; $\rho = 1.187 \text{ g/cm}^3$; $t = 10^\circ\text{C}$.

Production from Trona and Other Sodium Carbonate-Containing Minerals

The production of soda ash from trona in the United States has become significant since

World War II. The raw material is either a naturally occurring brine containing sodium carbonate (e.g., from Searles Lake in California) or a trona deposit (e.g., from the Green River region of Wyoming).

Sodium carbonate brines are pumped from the lake and treated with CO_2 gas to precipitate sodium bicarbonate, which is filtered, washed, and calcined to form sodium carbonate.

In another process, the liquor is evaporated in solar ponds until trona ($\text{Na}_2\text{CO}_3 \cdot \text{NaHCO}_3 \cdot 2\text{H}_2\text{O}$) crystals separate. The trona contains ca. 45% Na_2CO_3 , 35% NaHCO_3 , 2% NaCl , 1.5% Na_2SO_4 , 0.1% SiO_2 , 0.2% insolubles, and 16% H_2O . Calcination yields a product containing 95–96% sodium carbonate.

In 1937, a large deposit of trona was discovered in the Green River region of Wyoming, but its significance was not recognized at first. Drilling work, which continued from 1944 to 1947, gave the first indication of the size of the deposit, which was subsequently extracted by the companies FMC, Stauffer Chemical, Allied Chemical, Texas Gulf (after 1976), and Tenneco Oil (after 1982) [208]. At first, mined trona (ca. 40 000 t/a) was simply calcined to produce crude sodium carbonate, but by 1952 an FMC plant was producing 300 000 t/a of purified sodium carbonate. Drilling work during the last 30 years has revealed reserves of $> 50\,000 \times 10^6 \text{ t}$, mainly at depths of 250–450 m.

Natural trona from these deposits is a colorless or white mineral with a density of 2.13 g/cm^3 and a Mohs hardness of 2.5–4. The deposits generally contain $> 90\%$ trona, with halite (NaCl), shortite ($\text{Na}_2\text{CO}_3 \cdot 2\text{CaCO}_3$), pyrite (FeS_2), shale, and other rock minerals. The United States now obtains its sodium carbonate entirely from trona; production capacity in 1991 was $9.88 \times 10^6 \text{ t}$ [208].

Processing is carried out mainly by the monohydrate process (Figure 51.39). Trona is crushed to $< 6 \text{ mm}$ and calcined at 300°C in a rotary furnace to remove water of crystallization and convert the bicarbonate to carbonate.

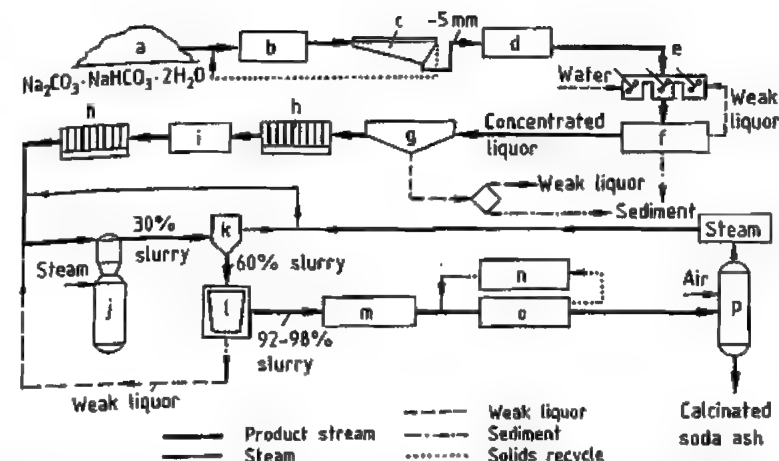


Figure 51.39: Conversion of trona to calcined soda ash (simplified flow diagram): a) Trona storage; b) Crusher; c) Screen; d) Rotary furnace; e) Agitated dissolver; f) Classifier; g) Thickener; h) Filter press; i) Activated carbon filter; j) Vacuum crystallizer; k) Cyclone; l) Centrifuge; m) Dryer; n) Grinding mill; o) Classifier; p) Product storage.

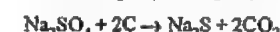
The calcined material is agitated with water to dissolve the crude soda ash. Insoluble components such as silica, sodium silicate, and gangue are removed by classifiers. The insoluble residues are then extracted with water. The concentrated liquor containing dissolved sodium carbonate is transferred to a thickener where the remaining finely divided insoluble residues are precipitated with flocculating agents. The clarified concentrated liquor is further purified by filter presses, and residual organic impurities are removed with activated carbon. The almost saturated solution is then evaporated in multiple-effect evaporators to give a 30% slurry of $\text{Na}_2\text{CO}_3 \cdot \text{H}_2\text{O}$. This is followed by concentration to a 60% solids content in hydrocyclones and centrifugation. The centrifuged monohydrate crystals, which still contain 2–8% water, are calcined in rotary furnaces, while the filtrate is recycled to the process. The calcined product is ground to the required particle size and then sent to the storage silo.

In the sodium sesquicarbonate process, trona is first subjected to a multistage solution process to remove impurities. After vacuum crystallization, the sesquicarbonate crystals produced are separated from the mother liquor by centrifugation and calcined in rotary furnaces.

The largest trona deposit outside the United States is located at Magadi Lake in Kenya. This has an area of 65 km^2 and a thickness of 30 m, and is extracted by open-cast mining. Since 1990, the production capacity of the Magadi-Soda Co. (a subsidiary of Penrice Soda Products of Australia) has been 275 000 t/a [208–211].

Other Processes

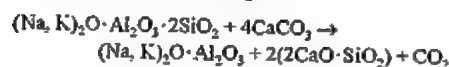
Le Blanc Process. The Le Blanc process, which is now of only historical interest, is based on the following reactions:



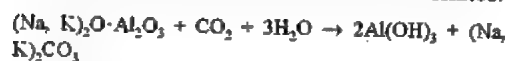
The first plant using this process began operating in 1790 with a production of 300 t/d. By 1870, England had 40 factories and Germany 20. From 1885, Leblanc soda ash production declined because of competition from the more economical Solvay process, which also resulted in a higher-quality product. In England, the United Alkali Co. ceased production by the Leblanc process in 1916, and in Germany, Chemische Fabrik Rhenania in Stolberg, the last company using the process, operated until 1923.

A major disadvantage of the Leblanc process compared to the Solvay process is that it involves mainly solid-phase reactions and consumes large amounts of energy (at red heat or just below). The waste products calcium sulfide and hydrochloric acid are another disadvantage. Calcium sulfide caused both atmospheric and water pollution.

Production from Nepheline. In the former Soviet Union, pottery clay is produced from nepheline; the process also yields some sodium carbonate [212]. Finely ground nepheline is intimately mixed with very pure limestone, and the mixture is sintered. The following reaction takes place:



The clinker produced is ground with water to dissolve the sodium and potassium aluminates. The aluminate solution is then treated with CO_2 -containing gas (e.g., combustion gas), to precipitate aluminum oxide hydrate and give a solution of alkali-metal carbonates:



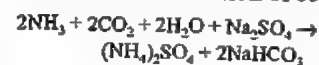
The solution is evaporated and separated into fractions containing various proportions of sodium and potassium carbonate, which differ in solubility. The bicarbonates present in these solutions are converted to carbonates by treatment with alkali-metal hydroxide solution before evaporation.

In the process for converting nepheline to aluminum oxide, 4 t of nepheline gives ca. 1 t of sodium carbonate.

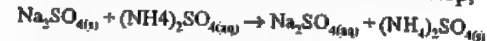
Other Proposed Modifications of the Ammonia-Soda Process. Attempts to produce sodium carbonate by other methods have been unsuccessful [213, 214]. A few proposals are mentioned here, although these have not been adopted industrially.

- According to [215], recovery of ammonia by distillation can be avoided by using an intermediate salt; hydrochloric acid is produced in addition to sodium carbonate. The process consists of two stages. In the first,

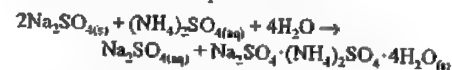
sodium bicarbonate is precipitated from an ammoniacal solution of sodium sulfate:



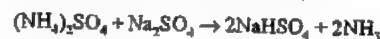
In the second stage, sodium sulfate is regenerated from the mother liquor produced in the above reaction. Here, either pure ammonium sulfate is precipitated in the first step,



or a double salt is produced:

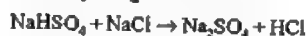


The solid ammonium sulfate obtained is heated with sodium sulfate:

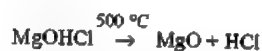
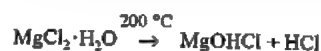


Ammonia is thereby recovered and recycled to the process.

Then, NaHSO_4 is fused with NaCl , to produce hydrogen chloride:



- The following variation of the Solvay process is proposed in [216]: Ammonia from the bicarbonate mother liquor is recovered by reaction with magnesium hydroxide, not calcium oxide. Magnesium chloride and sodium chloride are present in the distillation liquor after removal of ammonia. Magnesium chloride is recovered as the monohydrate by evaporation and then decomposed:



The hydrogen chloride liberated is sold as such or after oxidation to chloride, and magnesium oxide is recycled to the process. Apart from the fact that the hydrogen chloride produced is difficult to market, doubts exist that the decomposition of MgCl_2 is feasible in practice because of corrosion problems.

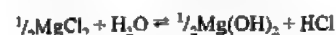
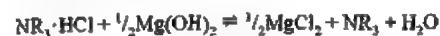
- The following proposal was made by BLUMBERG et al. [217, 218]. In the equation



the reaction proceeds to the right if hydrogen chloride is removed. This is achieved by reac-

tion with a $\text{C}_8\text{--C}_{12}$ tertiary amine dissolved in *n*-pentanol. The amine is regenerated by reaction with magnesium hydroxide. The 26% solution of MgCl_2 produced is thermally decomposed to hydrochloric acid and magnesium oxide, which is recycled to the regeneration stage.

The starting material is brine containing 24–26% NaCl and CO_2 dissolved at a partial pressure of ca. 0.3 MPa. Sodium bicarbonate is precipitated as a solid salt and recovered from the bottom of the vessel. The liquid separates into two phases: a solution of NaCl , which is recycled, and organic solvent saturated with hydrogen chloride. The equations are as follows:



The process is problematic because it results in pollution of the environment with amines and organic solvents. Another problem is the hydrogen chloride by-product.

- The combined production of sodium carbonate, chlorine, and a mixture of ammonium and sodium nitrates has been proposed in [219]. Sodium chloride is oxidized by excess nitric acid, to produce sodium nitrate and chlorine:



The sodium nitrate solution is neutralized with ammonia and then reacted with carbon dioxide to form sodium bicarbonate.

After the bicarbonate is filtered off, a mixture of ammonium and sodium nitrates that can be used as a fertilizer is recovered from the filtrate.

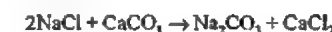
Wastewater Problems in Sodium Carbonate Production [220]

In the recovery of ammonia by distillation with milk of lime, an end liquor (ca. 7–10 m³/t sodium carbonate) is produced at its boiling point. This liquor has the following approximate composition: 120–180 g/L CaCl_2 , 1.0–

1.7 g/L $\text{Ca}(\text{OH})_2$, 50–75 g/L NaCl , 1.0–1.5 g/L CaSO_4 , and 20–30 g/L suspended solids. These solids originate mainly from impurities in the limestone and coke, and include uncalcined or dead-burnt limestone. Also, some solid material results from the reaction of milk of lime with residual carbon dioxide not removed in the stripping still.

The solid material consists of ca. 67% CaCO_3 , 10% $\text{Mg}(\text{OH})_2 + \text{Ca}(\text{OH})_2$, 10% $\text{CaSO}_4 \cdot 2\text{H}_2\text{O}$, 10% SiO_2 , and 3% $\text{Fe}_2\text{O}_3 + \text{Al}_2\text{O}_3$. It is very finely divided and therefore difficult to remove. The liquor is often clarified in large settling basins or ponds. However, mud with a high chloride content is produced, which presents disposal problems. Therefore, the end liquor is frequently diluted with used cooling water and discharged directly into the receiving water body. This method of disposal is generally recognized as safe because calcium carbonate, which is the main solid component in the wastewater, reacts with carbon dioxide in the water to form calcium bicarbonate solution.

The amount of CaCl_2 in the end liquor is given by the overall equation for the Solvay process:



This shows that the reaction produces 1 mol CaCl_2 in the end liquor for each mole of Na_2CO_3 produced. The end liquor also contains some NaCl resulting from incomplete reaction. Removal of chloride from the end liquor should be considered only if at least some of it can be used to produce calcium chloride. However, this is carried out in only a few sodium carbonate plants, because the demand for this chemical is relatively low.

51.15.1.4 Quality Specifications

The product obtained by the ammonia-soda (Solvay) process is, after calcination, an anhydrous, technical-grade sodium carbonate. The two main commercial forms are light soda ash and dense soda ash, which differ in particle size and bulk density. Light soda ash

has a bulk density of 0.5–0.6 kg/L; dense soda ash 1.05–1.15 kg/L.

The quality of the product is normally assessed by the following tests:

1. Loss on heating at 250 °C
Method: Drying of sample at 250 °C for 2 h in a crucible furnace
2. Water-insoluble material
Method: Determination of residues insoluble in water at 50 °C
3. Total alkalinity expressed as Na₂CO₃
Method: Titration with 1 M hydrochloric acid, with methyl orange as indicator
4. Sodium bicarbonate (NaHCO₃)
Method: Winkler titration—conversion of NaHCO₃ to Na₂CO₃ by addition of a known amount of NaOH; precipitation of total CO₂ as BaCO₃; back titration of excess NaOH with HCl (indicator: phenolphthalein)
5. Sodium carbonate (Na₂CO₃)
Calculation: Total alkalinity (method 3) minus alkalinity due to NaHCO₃ (method 4)
6. Sodium chloride (NaCl)
Methods: a) Mohr's titration against 0.1 M AgNO₃ with K₂CrO₄ as indicator
b) Argentometrically with potentiometric determination of the end point
7. Sodium sulfate (Na₂SO₄)
Method: Gravimetrically by precipitation of the sulfate as BaSO₄
8. Iron oxide (Fe₂O₃)
Method: Colorimetric (photometric) determination of the concentration of Fe(II) dipyriddy complex
9. Water (H₂O)
Calculation: Weight loss at 250 °C (method 1) minus weight loss due to CO₂ + H₂O determined from decomposition of NaHCO₃ (NaHCO₃ by method 4)

A typical analysis is given below:

Na ₂ CO ₃	99.6%	Fe ₂ O ₃	0.002%
NaCl	0.15%	CaO	0.01%
Na ₂ SO ₄	0.02%	MgO	0.02%

In addition to its chemical analysis, the product is also characterized by particle size and bulk density.

For soda ash produced from trona, the following are typical analysis figures:

Na ₂ CO ₃	99.6%	Fe ₂ O ₃	0.001%
NaCl	0.035%	CaO	0.01%
Na ₂ SO ₄	0.1%	MgO	0.003%

The difference in particle-size distribution between light and dense soda ash is shown by the following value:

	Light ash (%)	Dense ash (%)
> 2mm	0.1	0.2
2–1 mm	0.5	5
1–0.5 mm	1	26
0.5–0.25 mm	10	50
0.25–0.125 mm	30	14
0.125–0.063 mm	38	4
< 0.063 mm	20.4	0.8

Soda ash of the quality described above is suitable for most applications and is usually adequate for the food industry.

Other special grades include dense granulated soda and briquetted soda. So-called washing soda crystals, the decahydrate Na₂CO₃ · 10H₂O, is now of minor importance. This is produced from calcined sodium carbonate by dissolving it in boiling water until the density is 30–40 °Bé. Hard crystals are obtained only if the solution contains some sulfate, and a small percentage of this substance is therefore added to the solution. The solution is clarified by allowing solid impurities to sediment. The solution is then cooled to 38 °C in crystallizing troughs to obtain soda crystals. A typical analysis of the commercial product is 36.6% Na₂CO₃, 0.03% NaCl, 0.15% Na₂SO₄, 63.22% H₂O.

51.15.1.5 Producers

Western Europe producers of soda ash are listed in Table 51.18.

In Eastern Europe plants in the following countries are producing soda ash by the Solvay process: Bulgaria, Poland, Romania, the former Yugoslavia, and the CIS.

The United States has the following production plants:

FMC Corporation	Green River, WY
General Chemical Corp.	Green River, WY
North American Chemical	Argus, CA

Rhône-Poulenc
Solvay Minerals (formerly Temleco)
in partnership with Asahi Glass
Texasgulf Chemical Co.

Green River, WY

Green River, WY

Green River, WY

The most important producers outside Europe and the United States are China, India, and Japan.

Table 51.18: Western Europe producers of soda ash.

Country	Company	Location
Germany	Solvay Deutschland GmbH	Rheinberg, Heilbronn, Bernburg
	Chemische Fabrik Kalk GmbH*	Köln-Kalk
	Matthes & Weber GmbH	Duisburg
	Sodawerk Staßfurt GmbH	Staßfurt
Belgium	Solvay S.A.	Couillet
France	Solvay S.A.	Dombasle
	Rhône-Poulenc	La Madeleine
Italy	Solvay S.A.	Rosignano
Netherlands	AKZO	Delfzijl
Portugal	Soda Pova S.A.R.L. (Solvay subsidiary)	Pova de Santa Iria
Spain	Solvay S.A.	Torrelavega
United Kingdom	Penrice Soda Products Ltd.	Winnington

* Closure planned for end of 1993.

51.15.1.6 Storage and Transport

Calcined soda ash is hygroscopic, gradually taking up moisture and carbon dioxide during transportation and storage. This converts the surface of sodium carbonate to the bicarbonate and leads to a weight increase of up to 17%. Soda ash is therefore best stored in closed, dry areas.

Soda ash is supplied either bulk in silo wagons that can be discharged pneumatically or in paper sacks.

Soda crystals (washing soda) can effloresce or dissolve in the water of crystallization, depending on the temperature and relative humidity. They melt at 32–33 °C. At lower temperature, they are stable, provided the relative humidity is within the limits listed below:

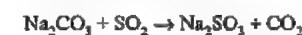
T, °C	0	10	15	25
R.H., %	59–98	64–96	68–94	76–87

At lower humidity, soda crystals effloresce, and at higher humidity the surface becomes wet.

51.15.1.7 Uses

Soda ash is an important raw material for the chemical industry. Its sodium content results in fluxing properties that make it important in the glass and silicate industries. It is used to neutralize inorganic and organic acids or acidic salts, and to maintain a constant pH in processes where acids are liberated. It is also utilized in the production of sodium salts (e.g., phosphates, nitrates, chromates, citrates, tartrates, salts of fatty acids).

Soda ash can be used in aqueous solution to remove sulfur dioxide from process gas or off-gases, forming sodium sulfite and sodium bicarbonate:



These reactions are also important in the production of paper pulp by the sulfite process.

Other uses of sodium carbonate are as follows:

Chemical industry: production of bleaching agents, borax, chromates and dichromates, fertilizers, dyes, fillers, tanning agents, industrial cleaning agents, catalysts, cryolite, adhesives, metal carbonates, sodium nitrate, perborates, phosphates, silicates, ultramarine pigments, soluble silicates, etc.

Detergent and soap industry: manufacture of detergents and saponification of fats.

Petrochemicals: neutralization.

Pulp and paper industry: cooking wood; neutralization, cleaning, bleaching, and treatment of recycled paper.

Artificial silk industry: deacidification of artificial silk.

Textile industry: dyeing, bleaching, and finishing of wool and cotton.

Coke ovens, gasworks, and hydrogenation plants: gas purification (desulfurization).

Iron and steel industry: removal of sulfur and phosphorus from pig iron, cast iron, and steel; ore beneficiation, flotation agents, and fluxing agents.

Heavy-metal industry: digestion and beneficiation of ores (e.g., of antimony, lead, chrome, cobalt, nickel, bismuth, and tin).

Glass industry: raw material for the glass melt and for reacting with sand.

Aluminum industry: reaction with bauxite.

Ceramics industry: production of refractory materials and glazes.

Enamel industry: as a flux.

Food industry: hydrolysis of proteins, production of margarine and starch, and softening of sugar beet juice.

Various branches of industry: water treatment, metal degreasing.

Environmental protection:

- Purification of flue gases by injecting sodium carbonate or sodium hydrogencarbonate (dry process).
- Regeneration of acidic lakes by the introduction of briquettes of sodium carbonate, so that organic sediments exhibit an alkaline reaction over a long period.

51.15.1.8 Toxicology

The lowest known lethal dose of sodium carbonate is 4000 mg/kg (rat, oral). Toxic effects do not occur under normal working conditions. For humans, oral ingestion of > 15 g is potentially lethal. In case of ingestion, vomiting should not be induced, but copious amounts of water and dilute lemon juice or vinegar (two tablespoons per glass of water) should be drunk. The stomach can be carefully irrigated for 15 min at most, with the usual precautions, but use of this treatment for longer periods is strongly contraindicated (danger of perforation). Medical help should be sought.

Because of its alkaline reaction, sodium carbonate has a irritating effect on the skin and mucous membranes. If skin is attacked, the affected part should be thoroughly washed with copious quantities of water, and a nonirritant dressing applied if necessary. If eyes are splashed with sodium carbonate, the eyelids should be held open while the eye is treated for several minutes with running water or sa-

line solution. Medical help should be sought from a specialist.

51.15.2 Sodium Hydrogencarbonate

51.15.2.1 Properties

Some physical properties of sodium hydrogencarbonate are given below:

Density	2.22 g/cm ³
Specific heat capacity (25 °C)	87.7 kJmol ⁻¹ K ⁻¹
Enthalpy of solution	-18 kJ/mol
Enthalpy of formation	950 kJ/mol
Refractive indices	1.380, 1.500, 1.586
Dielectric constant (25 °C)	4.39

Solubility properties are listed in Table 51.19. Solubility is lower in the presence of sodium carbonate.

Table 51.19: Solubility of sodium hydrogencarbonate in water.

T, °C	Solubility	
	g/100 g solution	g/100 g H ₂ O
-2.35	6.26	6.68
0	6.4	6.9
10	7.6	8.2
20	8.7	9.6
30	10.0	11.1
40	11.3	12.7
50	12.7	14.5
60	14.2	16.5
80	16.5	19.7
100	19.1	23.6

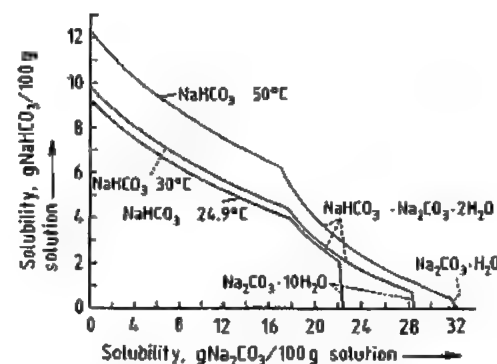


Figure 51.40: Solubilities in the system H₂O-NaHCO₃-Na₂CO₃ at 24.9 °C, 30 °C, and 50 °C [222].

In the system H₂O-NaHCO₃-Na₂CO₃, the double salt trona NaHCO₃·Na₂CO₃·2H₂O occurs at > 21.3 °C. The isotherms at 24.9 °C,

30 °C, and 50 °C are shown in Figure 51.40, which indicates the ranges of existence of the solid phases at these temperatures [222, 223].

On heating, sodium hydrogencarbonate decomposes into sodium carbonate, carbon dioxide, and water:



Dissociation pressures of carbon dioxide at equilibrium are as follows:

T, °C	30	50	70	90	100	110
p _{CO₂} , kPa	0.825	3.99	16.013	55.102	97.236	166.596

At room temperature, sodium hydrogencarbonate is fairly stable because of its low rate of decomposition. The aqueous solution has an only slightly alkaline reaction due to the small extent of hydrolysis.

51.15.2.2 Production

Sodium hydrogencarbonate is an intermediate in the ammonia-soda process. However, because of the content of ammonium salts, a product that satisfies the quality requirements of consumers (mainly in the food industry) cannot be obtained by drying crude bicarbonate. Moreover, a sufficiently pure product cannot be obtained by recrystallization. Therefore, it is necessary to start with an aqueous solution of sodium carbonate which is obtained either by dissolving calcined soda ash or by decomposing crude bicarbonate with steam. This is then filtered and carbonated with pure concentrated carbon dioxide, with cooling to remove the heat of reaction:



As carbonation proceeds, sodium hydrogencarbonate precipitates. It is recovered by centrifuging and then dried with hot air (e.g., in tray dryers).

51.15.2.3 Uses and Quality Specifications

Sodium hydrogencarbonate is used in the manufacture of baking powder, as a medication for neutralizing stomach acid, as a component of effervescent powders, in animal feed, and as a dry-powder fire extinguisher.

The following analysis is typical for the food-grade product: NaHCO₃, 99.7%; Na₂CO₃, 0.2%; NaCl, 0.004%; H₂O, 0.05%; insolubles, 0.003%.

Sodium hydrogencarbonate tends to form lumps in the presence of moisture or under pressure. On heating to > 60 °C, appreciable decomposition to sodium carbonate occurs. The bicarbonate readily picks up odors from its surroundings and should therefore be stored under dry, airtight conditions.

51.16 Sodium Sulfates

51.16.1 Sodium Sulfate

51.16.1.1 History and Natural Occurrence

Sodium sulfate has been known since the 1500s. Its use in the form of spa water or as a salt goes back even further. It was first described in 1658 by J. R. GLAUBER. It was known as sal mirabile Glauberi [224], was prepared from common salt and sulfuric acid, and was used medicinally as a laxative. Many kinds of spa water and the salts obtained from them contain sodium sulfate (e.g., Karlsbad salt, which contains 44% sodium sulfate) [225].

Processes for the manufacture of soda and hydrochloric acid that developed in the 1800s involved the production of sodium sulfate (salt cake) [226]. This method has now declined in importance compared to extraction from natural deposits and production as a by-product of chemical processes. By-product sodium sulfate must be removed from wastewater for reasons of environmental protection, which allows largely closed recirculating systems to be established (e.g., for spinning baths in the viscose-fiber industry [227, 228]).

Sodium sulfate not only occurs in salt deposits in ancient geological formations but can also be produced on an industrial scale from continuously formed reserves in salt lakes in Canada, the United States, South America, the

Commonwealth of Independent States, and other countries.

Anhydrous sodium sulfate occurs naturally as thenardite, sometimes in high purity, and Glauber's salt occurs as mirabilite, $\text{Na}_2\text{SO}_4 \cdot 10\text{H}_2\text{O}$. In marine salt deposits and in the crystalline deposits that are being produced in salt lakes at the present time, many double salts containing sodium sulfate occur such as astrakhanite, $\text{Na}_2\text{SO}_4 \cdot \text{MgSO}_4 \cdot 4\text{H}_2\text{O}$; glaserite, $\text{Na}_2\text{SO}_4 \cdot 3\text{K}_2\text{SO}_4$; glauberite, $\text{Na}_2\text{SO}_4 \cdot \text{CaSO}_4$; loewite, $6\text{Na}_2\text{SO}_4 \cdot 7\text{MgSO}_4 \cdot 15\text{H}_2\text{O}$; d'Ansite, $\text{MgSO}_4 \cdot 9\text{Na}_2\text{SO}_4 \cdot 3\text{NaCl}$; vanthoffite, $\text{MgSO}_4 \cdot 3\text{Na}_2\text{SO}_4$; burkeite $\text{Na}_2\text{CO}_3 \cdot 2\text{Na}_2\text{SO}_4$; and hanksite, $\text{KCl} \cdot 2\text{Na}_2\text{CO}_3 \cdot 9\text{Na}_2\text{SO}_4$. Hence, the industrial production of sodium sulfate can be combined with the production of common salt, soda, or potash salts [229–233].

51.16.1.2 Properties

Physical Properties. Table 51.20 compares the properties of thenardite (anhydrous sodium sulfate) and Glauber's salt (the decahydrate). The heptahydrate, $\text{Na}_2\text{SO}_4 \cdot 7\text{H}_2\text{O}$, is unstable (Figure 51.41) and can be detected on cooling saturated solutions to $< 12^\circ\text{C}$ [234–236].

Table 51.21 lists the solubility of sodium sulfate in water [234, 235, 237–239]. Sodium sulfate is polymorphic; above 240°C , four other modifications are formed from thenard-

ite (Table 51.21) [237]. In the sodium sulfate–water system, a transformation occurs at a temperature that has been determined with great accuracy (32.384°C) and is suitable as a fixed point. Above this temperature, anhydrous thenardite crystallizes from saturated solutions, and below it, Glauber's salt (Figure 51.41).

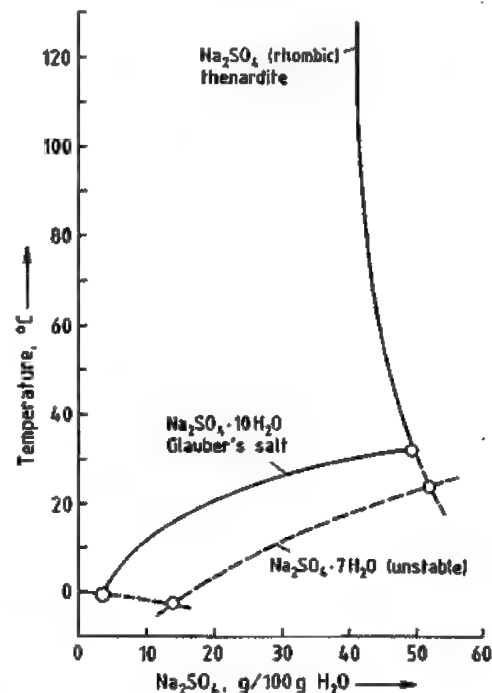


Figure 51.41: Solubility of sodium sulfate.

Table 51.20: Properties of thenardite and Glauber's salt.

Property	Thenardite, Na_2SO_4	Glauber's salt, $\text{Na}_2\text{SO}_4 \cdot 10\text{H}_2\text{O}$
Water of crystallization, %	0	55.914
mp, $^\circ\text{C}$	884.0 (decomp. $> 884^\circ\text{C}$)	"melts" at 32.384°C in its own water of crystallization (decomp. $> 32.384^\circ\text{C}$)
Crystal habit	rhombic	monoclinic
Unit cell dimensions	0.586, 1.23, 0.982	1.143, 1.034, 1.290 (angle = $107^\circ 40'$)
No. of molecules in unit cell	8	4
Refractive indices n_D	1.464, 1.474, 1.485	1.394, 1.396, 1.398
Density, g/cm^3	2.697	1.468
Specific heat capacity c_p at 300 K, $\text{J}/\text{kg}^\circ\text{K}^{-1}$	899.2	1825.7
Heat of fusion, kJ/kg	147.98	214.52
Heat of sublimation at 18°C , kJ/kg	16.2	–243.8
Enthalpy of formation, kJ/mol	–138.5	–4327
Entropy S° , $\text{J}/\text{mol}^\circ\text{K}^{-1}$	149.60	588.2
Dielectric constant (at 10^3 Hz)	7.80	7.90
Mohs hardness	2.7	1.5–2

Table 51.21: Solubility of sodium sulfate in water.

Temperature, $^\circ\text{C}$	g Na_2SO_4 in	
	100 g H_2O^a	100 g solution
–1.2	3.9a	3.8
0	4.5b	4.3
5	6.2b	5.8
10	9.0b	8.3
15	13.2b	11.7
18	16.4b	14.1
20	19.0b	16.0
22	22.1b	18.1
24	25.8b	20.5
25	27.8b	21.8
30	41.2b	29.2
32.4	49.7b,c	33.2
35	49.1c	32.9
40	48.1c	32.5
50	46.4c	31.7
60	45.3c	31.2
70	44.2c	30.7
80	43.2c	30.2
90	42.6c	29.9
100	42.2c	29.7
110	42.0c	29.6
150	42.2c	29.7
200	44.1c	30.6
240	44.9c,d	31.0
250	44.0d	30.5
260	41.8d	29.5
270	38.8d	28.0
280	35.2d	26.0
290	30.8d	23.5
300	24.8d	19.9
310	18.5d	15.6
320	13.1d	11.6
330	7.3d	6.8
340	4.2d	4.0
350	2.4d	2.3
360	0.9d	0.9
382	0.38d	0.38

^a Solid phases: a = $\text{Na}_2\text{SO}_4 \cdot 10\text{H}_2\text{O} + \text{ice}$; b = $\text{Na}_2\text{SO}_4 \cdot 10\text{H}_2\text{O}$; c = Na_2SO_4 , rhombic (thenardite); d = $\gamma\text{-Na}_2\text{SO}_4$, hexagonal (transforms into rhombic $\beta\text{-Na}_2\text{SO}_4$ on cooling below 240°C and into monoclinic $\alpha\text{-Na}_2\text{SO}_4$ on cooling below 180°C ; this is unstable in aqueous solution and transforms into thenardite).

The decrease in solubility of sodium sulfate resulting from the presence of sodium chloride can be utilized in the industrial production of sodium sulfate from aqueous solutions. This effect is shown by the three-component system sodium sulfate–sodium chloride–water (Table 51.22) [225, 240, 241].

The system sodium sulfate–sulfuric acid–water shows first an increase and then a decrease in the solubility of sodium sulfate with

increasing sulfuric acid concentration [225, 238, 241]. The reaction to form sodium hydrogensulfate is of industrial importance.

The low solubility of sodium sulfate in organic solvents or mixtures of these with water can be used in the precipitation crystallization of thenardite [228, 238, 242].

Table 51.22: Solubility (%) of sodium sulfate in water and sodium chloride solutions.

Temperature, $^\circ\text{C}$	NaCl content of solution, %				
	0	10	14	17	20
10	8.25a ^a	3.9a	3.3a	3.2a	3.3a
15	11.7a	6.4a	5.5a	5.2a	5.5a
17.5	13.7a	8.1a	7.4a	6.8a	7.1c
25	21.8a	15.7a	14.9a,b ^b	11.8b	9.2c
30	29.9a	19.2a,b ^b	14.2b	10.8b	8.5c
33	33.2a,b ^b	18.9b	14.2b	11.2b	8.9c
50	31.7b	18.3b	13.7b	10.3b	6.7c
75	30.4b	17.3b	13.0b	9.9b	8.1c
100	29.7b	16.7b	12.8b	10.0b	7.8c

^a Solid phases: a = $\text{Na}_2\text{SO}_4 \cdot 10\text{H}_2\text{O}$; b = Na_2SO_4 (thenardite); c = mixtures with NaCl.

^b The transformation temperature of 32.384°C is depressed to 17.9°C by NaCl.

Chemical Properties. In moist air, anhydrous sodium sulfate takes up water of crystallization with a considerable increase in volume, which reaches a factor of 4.17 on complete conversion to the decahydrate (Glauber's salt) and can lead to damage if the change occurs in cracks in buildings. Buildings constructed with cement, especially those made of concrete, can be destroyed by solutions containing sodium sulfate. Glauber's salt is not hygroscopic. It effloresces and is converted to an almost anhydrous sulfate after a few days in a cold current of air.

On heating below its melting point (884°C), thenardite decomposes slowly. Above 1200°C , the weight loss of the molten material can be several percent. If sodium sulfate is added to molten glass, sodium silicates are formed, and sulfur dioxide and oxygen are released (see Table 51.25).

51.16.1.3 Extraction and Production

Of the world production of sodium sulfate (ca. 4.6×10^6 t in 1988), approximately 50% is

a by-product of the chemical industry, the remainder being extracted from natural deposits. World reserves of sodium sulfate are estimated at 3400×10^6 t [243, 244].

The extraction of sodium sulfate from wastewater from the chemical industry has a beneficial effect on the environment and has the further advantage that it is independent of weather conditions, in contrast to production from natural sources [228, 243]. Furthermore, the production plant is usually close to the consumer of the sodium sulfate, whereas production from natural deposits often takes place in remote regions.

Glauber's salt is not a commercial product, owing to its high content of water of crystallization (56%) and consequently high transportation costs, its low melting point (32.4 °C), and its tendency to effloresce. However, it is an important intermediate product in many processes.

Crystallization and Calcination

The principle of the crystallization process is to cool the solution to < 20 °C, causing Glauber's salt, $\text{Na}_2\text{SO}_4 \cdot 10\text{H}_2\text{O}$, to crystallize [225, 245]. Multistage vacuum-cooled crystallizers are used, usually of the horizontal type. Glauber's salt is recovered and calcined to form anhydrous sodium sulfate (thenardite) in the next stage. Glauber's salt "melts" in its own water of crystallization at 32.38 °C, forming a saturated solution of sodium sulfate that contains anhydrous sodium sulfate as a solid phase (37% of the sodium sulfate from the Glauber's salt). In older processes, the saturated sodium sulfate solution, after removal of the precipitated sodium sulfate, was once again vacuum cooled, and the Glauber's salt that crystallized was again recovered and melted. If Glauber's salt was again crystallized from the residual mother liquor, up to 85% of the total Glauber's salt could be recovered as anhydrous sulfate.

This energy-intensive process was superseded by evaporative crystallization of the saturated sodium sulfate solution obtained on melting Glauber's salt [246–251]. The energy

consumption was reduced further by using multistage evaporation, in which the vapor was employed as heating steam for the following stage, which was operated at lower pressure. Further savings resulted from the use of mechanical or thermal compression of the vapor [252–254].

The formation of encrustations in the heat exchangers presented a problem, especially in the heat exchangers of the Glauber's salt melting vessels because of the decreasing solubility of sodium sulfate above 32 °C [225, 255]. For this reason, unheated melting vessels were often used, in which Glauber's salt was melted by mixing with approximately 15 times the amount of hot, saturated sodium sulfate solution from the evaporation stages [249].

The formation of encrustations can also be prevented if the heating medium for the melting vessel has such a low temperature (e.g., vapor from the last evaporation stage) that the temperature increase of the circulating melt solution in the heat exchanger is limited to 1–3 °C per pass [256].

In another process, part of the sodium sulfate solution is evaporated at 108–114 °C and pressures of up to 0.15 MPa absolute [257]. In this temperature range, the solubility curve of sodium sulfate exhibits a minimum, so that crust formation in the heat exchanger of the evaporator is greatly reduced. The vapor from this first stage is used as the heating medium for the evaporator of the second stage, which operates with vapor compression.

The purity of the sodium sulfate produced can be controlled by varying the amount of mother liquor removed at the calcination stage. Here, the saturation concentrations of the dissolved impurities must not be exceeded [258]. These processes can then yield a very pure sodium sulfate ($> 99.9\%$). The mother liquor can be fed to a biological wastewater treatment plant or worked up to yield Glauber's salt [259].

Figure 51.42 shows a flow diagram of a plant for the production of sodium sulfate from wastewater [228].

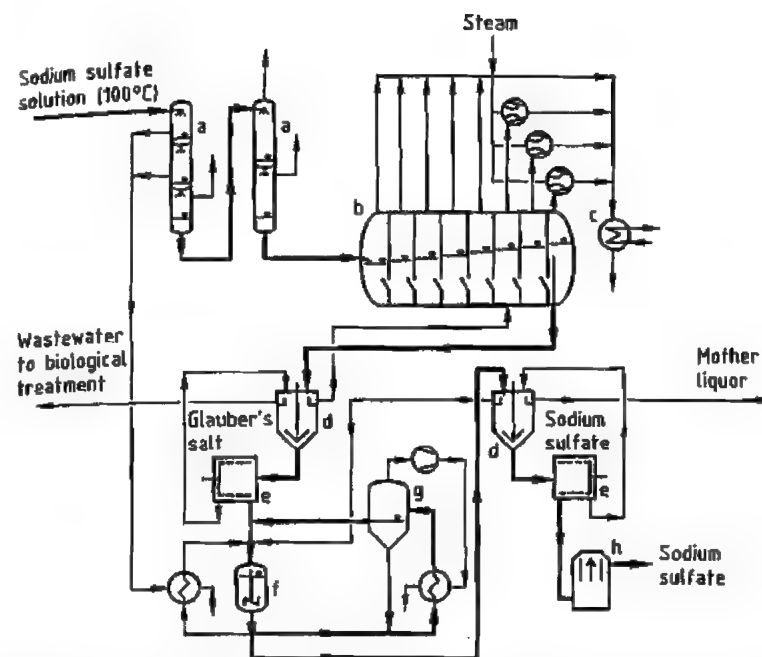


Figure 51.42: Production of sodium sulfate by crystallization and calcination: a) Evaporative cooler; b) Vacuum cooling crystallizer; c) Cooler; d) Thickener; e) Centrifuge; f) Melting vessel; g) Evaporator; h) Dryer.

The formation of encrustations during the thermal dehydration of Glauber's salt can be largely prevented by the use of air, spray, or fluidized-bed dryers, which have no solid heat-exchange surfaces. For example, in the Holland evaporator, predried Glauber's salt is heated by combustion gases at 870–980 °C in a rotary dryer to produce thenardite. If the Glauber's salt is melted and thenardite is separated, the mother liquor can be spray-dried with hot combustion gases. The specific energy consumption can be reduced if molten Glauber's salt in the form of a crystal slurry is sprayed into a rotary dryer heated to 150–400 °C. In fluidized-bed drying, thenardite is produced with hot air at 450 °C, giving a waste gas temperature of 80–100 °C. The fines are recirculated, producing a dust-free sodium sulfate with a grain size that can be controlled up to 4.8 mm.

In these processes, the entire water of crystallization is evaporated, so that the impurities in Glauber's salt remain in the sodium sulfate [225, 260–262]. Sodium sulfate can be precipi-

tated as thenardite from aqueous solutions by adding water-soluble organic solvents such as methanol [225, 263–266]. This process is used in the treatment of solutions containing Na_2SO_4 and sulfuric acid from the cellulose industry [267, 268].

Sodium sulfate can also be obtained from Glauber's salt by using submerged combustion heaters. However, the burner must be cleaned or changed frequently due to corrosion and encrustation [225, 243].

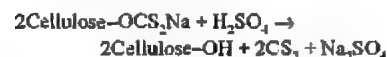
Sodium sulfate can be separated from mixtures of solid salts by flotation. This process is being investigated for the treatment of salt mixtures from natural deposits [269].

Production as a By-product of the Chemical Industry

Solutions of sodium sulfate are produced in numerous reactions of sodium compounds with sulfuric acid or with sulfur dioxide and oxygen. These solutions must be treated to prevent water pollution. Sodium sulfate is ob-

tained from them by crystallization and calcination. The quantities of sodium sulfate produced as a by-product from various sources depend very much on the state of the market for the main products and the state of the technology. In spite of this, total production of by-product sodium sulfate has hardly changed since 1980 [243].

From Viscose-Fiber Spinning Baths. Fibers are produced by spinning viscose in a sulfuric acid precipitation bath in which the following reaction takes place:



The precipitation bath contains ca. 10% H_2SO_4 , 20% Na_2SO_4 , and 1% ZnSO_4 . The spinning process produces ca. 1 kg of sodium sulfate for each kilogram of viscose fiber. Sulfuric acid must therefore be added continuously to the bath, and sodium sulfate removed [225, 227].

The treatment process for the bath consists of multistage evaporation, followed by cooling of the concentrated solution from 50 °C to 0.5 °C in a crystallizer. Glauber's salt is removed by centrifuges, and the mother liquor is recycled to the spinning bath. The zinc sulfate

dissolved in the spinning bath does not crystallize. Thenardite containing 99.6–99.9% sodium sulfate is produced by calcination of Glauber's salt in evaporating crystallizers with partial recycle of the mother liquor [246, 270–273]. In Western Europe in 1988, 305 000 t of sodium sulfate was produced from viscose-fiber manufacture, and in the United States in 1989, 89 000 t [243].

From Sodium Dichromate Production. Sodium sulfate is produced by the acidification of sodium chromate solution with sulfuric acid according to the equation:



If the reaction is carried out above 32.4 °C, thenardite (> 99% Na_2SO_4) precipitates. This still contains 0.2% dichromate, which can be removed by dissolving, reducing with SO_2 , and filtering off chromium(III) oxide. If the sodium sulfate is used in the sulfate cellulose (Kraft) process, the dichromate is reduced and therefore does not cause problems [244, 274, 275].

Quantities of sodium sulfate obtained from sodium dichromate production in 1988–1989 were 70 000 t/a in western Europe and 110 000 t/a in the United States [243].

Table 51.23: Sodium sulfate as a by-product of chemical processes.

Process	Reaction	References
Production of boric acid	$\text{Na}_2\text{B}_4\text{O}_7 + \text{H}_2\text{SO}_4 + 5\text{H}_2\text{O} \rightarrow 4\text{H}_3\text{BO}_3 + \text{Na}_2\text{SO}_4$	
Production of chlorine dioxide	$2\text{NaClO}_3 + \text{SO}_2 \rightarrow 2\text{ClO}_2 + \text{Na}_2\text{SO}_4$	[267, 277–279]
Production of hydroxylamine	$2\text{HON}(\text{SO}_3)_2(\text{Na}, \text{NH}_4) + 4\text{H}_2\text{O} \rightarrow (\text{HONH}_2)_2 \cdot \text{H}_2\text{SO}_4 + \text{Na}_2\text{SO}_4 + 2\text{NH}_4\text{HSO}_4$	[280, 281]
Production of lithium carbonate	$\text{Li}_2\text{SO}_4 + \text{Na}_2\text{CO}_3 \rightarrow \text{Li}_2\text{CO}_3 + \text{Na}_2\text{SO}_4$	[243]
Production of resorcinol or naphthol	$\text{C}_6\text{H}_4(\text{ONa})_2 + 2\text{NaHSO}_3 + 2\text{H}_2\text{SO}_4 \rightarrow \text{C}_6\text{H}_4(\text{OH})_2 + 2\text{Na}_2\text{SO}_4 + 2\text{SO}_2 + 2\text{H}_2\text{O}$	[243, 282, 283]
Production of methionine	$2\text{CH}_3\text{S}-\text{CH}_2\text{CH}_2\text{CH}(\text{NH}_2)-\text{COONa} + \text{H}_2\text{SO}_4 \rightarrow 2\text{CH}_3\text{S}-\text{CH}_2\text{CH}_2\text{CH}(\text{NH}_2)-\text{COOH} + \text{Na}_2\text{SO}_4$	[243]
Production of formic acid	$2\text{HCOONa} + \text{H}_2\text{SO}_4 \rightarrow 2\text{HCOOH} + \text{Na}_2\text{SO}_4$	[243, 284]
Neutralization of waste sulfuric acid	$2\text{NaOH} + \text{H}_2\text{SO}_4 \rightarrow \text{Na}_2\text{SO}_4 + 2\text{H}_2\text{O}$	[285–288]
Roasting and chlorination of pyrite cinder	$2\text{Cu}_2\text{S} + 4\text{FeSO}_4 + 8\text{NaCl} + 5\text{O}_2 \rightarrow 4\text{Na}_2\text{SO}_4 + 4\text{CuCl}_2 + 2\text{Fe}_2\text{O}_3 + 2\text{SO}_2$	[225, 243, 246, 289]
Desulfurization of flue gases	$2\text{Na}_2\text{SO}_3 + \text{O}_2 \rightarrow 2\text{Na}_2\text{SO}_4$; $2\text{Na}_2\text{SO}_3 + \text{SO}_3 \rightarrow \text{Na}_2\text{SO}_4 + \text{Na}_2\text{S}_2\text{O}_3$; $2\text{Na}_2\text{SO}_3 + \text{Na}_2\text{S}_2\text{O}_3 \rightarrow 2\text{Na}_2\text{SO}_4 + \text{Na}_2\text{S}_2\text{O}_3$	[290–294]

* See Section 49.8.

From Ascorbic Acid Production. In the synthesis of ascorbic acid by the Reichstein-Grössner process, sulfuric acid is used in the production of the diacetone-L-sorbose intermediate. The sulfuric acid is neutralized with sodium hydroxide solution in a later stage of the process [276]. On removal of the solvent, a saturated solution of Na_2SO_4 is produced, from which thenardite (> 99.9% Na_2SO_4) is obtained by evaporative crystallization. For each tonne of ascorbic acid, 1.5 t of sodium sulfate is produced. In 1988–1989, 45 000 t/a Na_2SO_4 was produced in this way in western Europe, and 17 000 t/a in the United States [243].

From Other Processes. Sodium sulfate is also produced in various quantities from a large number of other chemical processes (Table 51.23).

Production from Natural Sources

The most important production plants for sodium sulfate from natural sources are located in Canada, Spain, Mexico, Turkey, the United States, and the CIS. The output from these countries in 1987–1989 was ca. 2×10^6 t/a [243].

Owing to the varying compositions of the salt mixtures in the deposits, many types of processes for the production of sodium sulfate and other compounds have been developed [225, 269, 295, 296]. A review of some important production methods is given here.

Production in Canada. The Canadian deposits are located in Alberta and Saskatchewan, and are in the form of shallow lakes with only a few inlets. These contain sodium sulfate in the form of brines or deposits of mirabilite ($\text{Na}_2\text{SO}_4 \cdot 10\text{H}_2\text{O}$). Mirabilite dissolves from the deposits to an extent that depends on annual temperature variations, amount of water entering the lake, and evaporation. Various processes are used to recover the product.

Brine is pumped into shallow basins, from which some of the water evaporates during the summer. In winter, mirabilite crystallizes (ca. 600 kg/m³ brine) and collects at the bottom of

the basin. Excess brine is pumped back into the lake. Mirabilite is then collected by means of drag lines or other equipment and taken for further treatment.

Other operations use floating dredges to mine permanent deposits of mirabilite from the lake beds. The slurry of mirabilite and brine is sent by pipeline for further treatment.

In a third method, brine is produced by dissolving the salt in situ with hot water, which is injected via a large number of boreholes into the body of salt lying under the brine. The solution produced is taken to the next stage of treatment, which consists of precipitating crude salt in cooling towers [225, 243, 295, 297, 298].

In some cases, dry deposits of mirabilite are mined conventionally, and the crude salt can then be transported to the processing plant.

The crude salt is charged into evaporators, where it "melts" in its own water of crystallization. The crystal suspension is then evaporated with hot combustion gases and transported to rotary dryers by belt conveyors.

In operations that send a brine for processing, Glauber's salt is crystallized by cascading the brine in contact with cold air [243, 298]. Entrained clay slime can be removed in centrifuges. The Glauber's salt melt is then evaporated by the submerged combustion of natural gas. Sodium sulfate (97–99.8% Na_2SO_4) with a controlled grain size is produced by grinding and screening. Total production in Canada in 1987–1988 was 312 000 t/a sodium sulfate [243].

Production in Spain. Glauberite deposits are mined in the provinces of Burgos, Toledo, and Madrid. The Castellar mine at Toledo produces a crude salt containing 67% Na_2SO_4 , 19% CaSO_4 , and 12% clay and shale, from which sodium sulfate can be produced in various ways [225, 230, 299, 300]. For example, sodium sulfate can be leached from the crude salt at 35–40 °C (stage 1). The residue contains slime (clay) and glauberite ($\text{Na}_2\text{SO}_4 \cdot \text{CaSO}_4$), which is stable above 29 °C. Below 29 °C, this solid material yields additional sodium sulfate solution, which is

recycled to the first stage. Thenardite is produced from the leachate by vacuum evaporation. The three deposits yielded 510 000 t of sodium sulfate in 1988 [243].

Production in the United States, Mexico, Turkey, and the Commonwealth of Independent States. Sodium sulfate is obtained from natural deposits in California, Texas, and Utah.

Brine containing sodium carbonate is obtained by sinking wells into the deeper layers below the salt crust of Searles Lake in California. The brine is treated with carbon dioxide to precipitate sodium hydrogencarbonate, from which sodium carbonate is obtained. The filtrate is then cooled to 15 °C to precipitate borax, which is filtered off. Further cooling to 5–6 °C causes Glauber's salt to crystallize. The decahydrate still contains some finely divided borax, which can be removed by hydraulic screening. Only Glauber's salt with a grain size of > 0.8 mm is dehydrated to form thenardite. The fine crystals are used as crystallization seeds [225, 243, 295, 301]. In 1989, 218 000 t of sodium sulfate was produced.

In Texas, brine from deposits close to the surface is treated. In Seagraves, Glauber's salt is separated from brine saturated with sodium chloride at –7 to –10 °C. The product obtained is melted and evaporated by submerged gas burners to produce thenardite. The thenardite suspension is centrifuged and dried to yield a product containing 99.7% Na₂SO₄ [225, 243, 295, 302]. In 1989, ca. 140 000 t of sodium sulfate was produced by this method [20].

A sodium sulfate production plant in Utah uses brine from the Great Salt Lake. The brine is pumped into solar evaporation ponds with a surface area of ca. 80 km². Each year, stepwise crystallization of sodium chloride, potassium salts, and Glauber's salt takes place. These are removed by scrapers and transported by road vehicles for treatment. The crude salt is dissolved, the saturated solution is filtered, and sodium chloride is added to precipitate thenardite, which, after filtration and drying, contains > 94% Na₂SO₄. Recrystallization gives thenardite containing > 99.7% Na₂SO₄ [225,

229, 243, 303]. In 1989, 25 000 t of Na₂SO₄ was produced [243].

Sodium sulfate production figures for Mexico, Turkey, and the Soviet Union are listed in Table 51.24.

Table 51.24: Production of sodium sulfate in Mexico, Turkey, and the Soviet Union in 1987–1988.

Country	Starting material	Sodium sulfate production, t/a	References
Mexico	Brine from salt lakes	420 000	[243]
Turkey	Crude salts from salt lakes	157 000	[243]
Soviet Union	Water from the Caspian Sea, etc.	375 000	[243, 295]

Production

In addition to production methods based on by-product material or natural deposits of sodium sulfate, processes are also operated in which sodium sulfate is manufactured from compounds that contain sodium and sulfate.

From Sodium Chloride and Sulfuric Acid (Mannheim Process). The thermal reaction



which takes place via the intermediate formation of sodium hydrogensulfate, was developed as part of the Leblanc sodium carbonate process [226]. The reaction produces sodium sulfate and hydrogen chloride, which are of comparable economic importance [243].

This process is often carried out in Mannheim furnaces [225, 244, 286, 304, 305], which have a diameter of 6 m and produce 25 t/d sodium sulfate and 37.5 t/d hydrochloric acid (31%) by addition of 93–96% sulfuric acid to sodium chloride. One tonne of sulfate requires 3.6×10^6 kJ (88 kg of fuel oil), 65 kWh, 1.4 m³ of process water, and 26 m³ of cooling water. The product contains 97–99.7% Na₂SO₄. The small amounts of free sulfuric acid in the product are neutralized during cooling in a rotary cooler by the addition of sodium carbonate. The commercial product is obtained by grinding and screening.

The Climax Chemical Co., United States, operates a plant in which sodium chloride and sulfuric acid are reacted by the Cannon fluid-

ized-bed process. Production costs are lower than with the furnace process [225, 243, 306].

In 1988–1989, ca. 390 000 t/a sodium sulfate was produced from sodium chloride and sulfuric acid [243].

Sodium sulfate can be produced from dilute sulfuric acid and sodium chloride in a spray evaporator [285, 307].

The Hargreaves Process. Up to 1983, the Morton Chemical Co. in Louisiana, United States, operated the Hargreaves process, which is based on the reaction



This process is of interest owing to its low energy consumption compared to other production processes. Mannheim furnaces were used for the reaction, but rotary kilns or fluidized-bed reactors have been proposed [225, 243, 305, 308–310].

Metathesis. Several processes have been developed for the conversion of sodium chloride to sodium sulfate, for example,



Of these processes, the reaction of sodium chloride with kieserite (MgSO₄·H₂O) is the most important, because of all the crude salts from German potash production, kieserite is the cheapest source of sulfate.

To obtain a good yield of Glauber's salt, it is important to have the optimum NaCl/MgSO₄ ratio in the starting liquor. In the five-component system Mg–Na₂–SO₄–Cl₂–H₂O, an optimum point exists for the composition of the starting liquor. During dehydration of Glauber's salt, sodium chloride is added to the mother liquor, causing thenardite to precipitate. The mother liquor can then be used to produce the starting liquor. The process produces thenardite containing 98.7–99.5% Na₂SO₄ [225, 229, 263, 311–313]. In 1988, ca. 118 000 t of Na₂SO₄ was produced [243].

51.16.1.4 By-product Sodium Sulfate

Sodium sulfate is produced in a number of chemical processes and must be utilized or

disposed of. Hence, processes for converting sodium sulfate into its constituents (sodium hydroxide and sulfuric acid) or into other useful chemicals are of interest [228, 243].

Electrochemical Decomposition of Sodium Sulfate

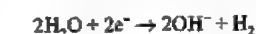
The electrochemical decomposition of sodium sulfate takes place according to the overall reaction:



The anodic decomposition of water produces H⁺ ions and oxygen



and the corresponding cathodic reaction produces OH[–] ions and hydrogen



If sodium hydroxide solution and sulfuric acid are required, reverse reaction between H⁺ and OH[–] must be prevented. This can be achieved by using a mercury cathode or a diaphragm cell [228].

The use of cation- and anion-selective ion-exchange membranes has led to new developments in recent years. Figure 51.43 shows the principle of Na₂SO₄ decomposition by electrodialysis in a cell divided into three zones by a cation-exchange membrane (CM) and an anion-exchange membrane (AM). The sulfate solution flows through the central zone. Sodium hydroxide and hydrogen are formed in the cathode space, and sulfuric acid and oxygen in the anode space. Sulfuric acid (5–15%) and sodium hydroxide (15–20%) are obtained with an energy consumption of 3500–4000 kWh/t NaOH and a current efficiency of 60–80%. The consumption of electrical energy can be reduced by using the reaction gases H₂ and O₂ in a fuel cell, or by the use of electrodialysis cells with gas-diffusion electrodes [314, 315].

Further improvements in electrodialysis are achieved by using anion-exchange membranes composed of styrenedivinylbenzene copolymer with strongly basic quaternary ammonium groups and a hydronium ion blocker.

This gives improved current efficiencies and more concentrated sodium hydroxide and sulfuric acid [316].

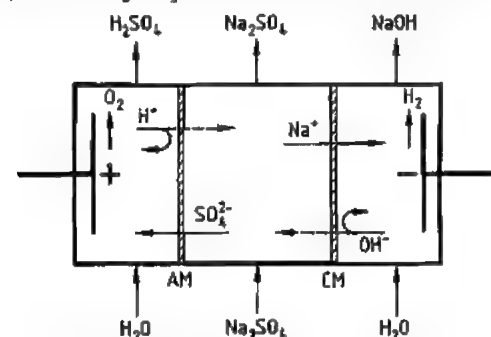


Figure 51.43: Decomposition of sodium sulfate by electrodialysis.

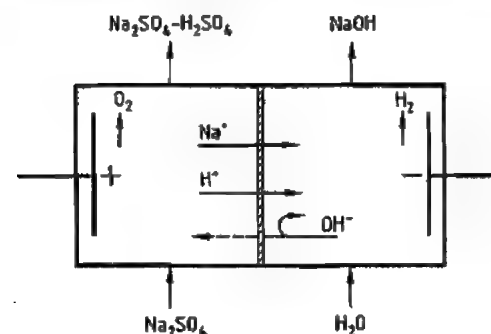


Figure 51.44: Electrolysis of sodium sulfate solution.

Figure 51.44 shows a two-compartment cell divided by a cation-exchange membrane. The sulfate solution is charged into the anode space where it becomes enriched in sulfuric acid; only salt-containing acid can be produced. The sodium hydroxide in the cathode space is almost free of sulfate [317]. As the acid concentration increases and the salt concentration decreases, more H^+ ions contribute to the transport of current. Therefore, the current efficiency depends not only on the selectivity of the membrane and the sodium hydroxide concentration in the catholyte, but also on the H^+/Na^+ ratio in the anolyte. High current efficiencies are obtained only with an excess of Na^+ ions. For example, if the molar H^+/Na^+ ratio in the anolyte is 1:1, 5–10% sulfuric acid and 15–25% sodium hydroxide are obtained with current efficiencies of 65–70%.

Electrolysis of highly concentrated sodium sulfate solutions (up to 39% Na_2SO_4) gives sulfuric acid concentrations of 10–20% and sodium hydroxide contents of 15–20% with current efficiencies of 65–80% [318].

In the Sulfomat process, sodium sulfate is electrolyzed to give sodium sulfate-containing sulfuric acid and caustic soda solution. The latter is used for absorption of SO_2 in flue gas desulfurization, giving a solution of sodium sulfite. Acidification with the Na_2SO_4 -containing sulfuric acid gives SO_2 and reforms sodium sulfate, which is electrolyzed [319]. Also, spinning bath solutions from the viscose-fiber industry can be regenerated electrochemically [320, 321].

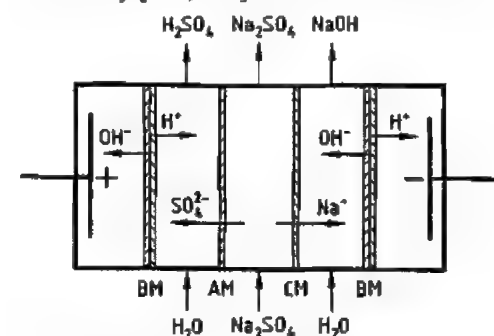


Figure 51.45: Electrodialysis of sodium sulfate with bipolar membranes.

A development by Allied Signal of electrodialysis with bipolar membranes is of interest due to the low energy consumption [322–325]. In these bipolar membranes (BM), a cation-exchange membrane is bonded to an anion-exchange membrane [326]. Water molecules diffuse to the phase boundary CM-AM, where they dissociate in the electric field. The H^+ and OH^- ions diffuse in opposite directions. If the bipolar membranes are combined with CM and AM, as shown in Figure 51.45, the sulfate can be decomposed without the formation of hydrogen and oxygen. A large number of individual BM-AM-CM elements can be fitted between the two end electrodes. Decomposition of H_2O at the electrodes is then negligible. The only energy required is the dissociation energy of the water (0.022 kWh/mol). Laboratory investigations showed

an energy consumption of 1450–1700 kWh/t $NaOH$ when 12–16% sodium hydroxide and 5–10% sulfuric acid are produced. Allied Signal supplies cells for pilot- and full-scale operation.

Conversion Processes

Metathesis with Hydrogen Chloride. Owing to the high cost of electricity in the sodium sulfate electrolysis process, early attempts were made to bring about metathesis with hydrogen chloride:



If the reaction is carried out in 40–60% sulfuric acid, sodium chloride precipitates and can be obtained in 99.2% yield (with 40% H_2SO_4 at 30 °C) [228, 275, 327–329]. The concentrations must be such that enough HCl is taken up by the reaction mixture. A stoichiometric amount of HCl is sufficient for the reaction to proceed. Of this, approximately one-third distills off during the process, and must be recycled to the reactor.

The sodium chloride obtained can be used for the chlor-alkali electrolytic process [328]. The 40–60% sulfuric acid produced in the industrial process contains 1–2% residual Na_2SO_4 [328] and is preferably recycled to the process in which the sodium sulfate is formed or used for reactions with sodium compounds, such as the production of chlorine dioxide from sodium chlorate, whereby Na_2SO_4 is reacted continuously with HCl in a decantation-washing column [330].

Table 51.25: Use of sodium sulfate for reduction processes.

Process	Reaction	References
Le Blanc process	$Na_2SO_4 + 2C + CaCO_3 \rightarrow Na_2CO_3 + CaS + 2CO_2$	[228, 234, 339]
Production of sodium sulfide	$Na_2SO_4 + 2C \rightarrow Na_2S + 2CO_2$ $Na_2SO_4 + CH_4 \rightarrow Na_2S + CO_2 + 2H_2O$	[228, 243, 340–343]
Production of aluminum oxide (Peniakoff process)	$2Al_2O_3 \text{ (bauxite)} + 2Na_2SO_4 + C \rightarrow 4NaAlO_2 + 2SO_2 + CO_2$ $2NaAlO_2 + CO_2 + 3H_2O \rightarrow 2Al(OH)_3 + Na_2CO_3$	[344–348]
Digestion of phosphate rock for fertilizer production	$Ca_3(PO_4)_2 + 2Na_2SO_4 + 8C \rightarrow CaNa_4(PO_3)_2 + 2CaO + 8CO$	[349, 350]
Production of sodium silicate (water glass)	$2Na_2SO_4 + 2SiO_2 + C \rightarrow 2Na_2SiO_3 + 2SO_2 + CO_2$	[228]

The metathesis of Na_2SO_4 with HCl in dilute sulfuric acid was carried out in 1951 in a pilot plant [328].

Carrying out the metathesis at 800–900 °C in a melt allows pure sulfuric acid and pure sodium chloride to be obtained [331].

Conversion to Potassium Sulfate. The reaction



has been thoroughly investigated [228, 300, 332, 333]. It occurs in two stages: In the first stage, glaserite ($Na_2SO_4 \cdot 3K_2SO_4$) is formed, which is decomposed by more potassium chloride to form K_2SO_4 and $NaCl$ in the second stage:



The reactions can be carried out at 20–40 °C. If Glauber's salt is used, temperatures of > 32 °C are preferred. In a modern plant, K_2SO_4 yields of 98–99% are obtained [334, 335]. The reaction crystallization process is carried out in a loop-type bubble column [336].

The process has been operated since 1984 in a Russian plant that consumes 40 000 t/a Na_2SO_4 . The Potash Corporation of Saskatchewan (PCS) has operated an experimental plant since 1985 in Cory, Canada, with a consumption of 25 000 t/a Na_2SO_4 [243, 335].

Single-stage processes for carrying out this reaction have been proposed [337, 338].

Reduction Processes

Sodium sulfate can also be used in reductive processes (Table 51.25).

Table 51.26: Consumption of sodium sulfate in 1987 (in 10^3 t/a).

Use	Consumption		References
	Western world ^a	United States	
Cellulose industry	714	271	[243, 351, 352]
Glass production and others	456	128	[243, 353]
Detergents	1736	354	[243, 354]

^aIncluding United States.

51.16.1.5 Uses

World consumption of sodium sulfate in 1987 was ca. 4.6×10^6 t [243].

The most important consumers were the cellulose-fiber industry and manufacturers of glass and detergents (Table 51.26).

Other users are from a wide range of industries [225, 243], including dyeing technology [355], electrochemical metal treatment [356], animal feeds [225], heat accumulators [243], and sponge manufacture [243].

51.16.1.6 Occupational Health and Environmental Protection

Sodium sulfate is a permitted food additive [357] and is a common component of spa waters [225].

Inhalation of sodium sulfate dust causes irritation of the mucous membranes, and prolonged skin contact has a drying effect. The laxative effect of oral ingestion is well known and is used medicinally.

Sodium sulfate in wastewater can be recovered as thenardite. However, if the solutions are very dilute ($< 5\%$ Na_2SO_4), the crystallization process is energy intensive. In such cases, treatment of the wastewater by a membrane process [358], a precipitation process [359], or by biochemical methods [259] can be considered.

51.16.1.7 Economic Aspects

Demand for sodium sulfate in the Western industrialized nations has decreased during the last decade, but further reduction is ex-

pected to be balanced by increasing consumption in other parts of the world. The cellulose and glass industries and detergent manufacture account for ca. 80% of the sodium sulfate consumed. Environmental regulations have a great influence on the market for sodium sulfate, affecting both its production and its consumption. Owing to the large natural reserves of sulfate and the large quantities produced as a by-product of the chemical industry, prices are not expected to increase greatly. The most important producing countries in 1988 were the United States 16%; the Soviet Union 14%; Spain 13%; Mexico 10%; Canada 7%; Japan 6%; and Belgium 6%. The remaining 28% came from a number of sources [243].

51.16.2 Sodium Hydrogensulfate

Sodium hydrogensulfate [360] occurs as the monohydrate, $\text{NaHSO}_4 \cdot \text{H}_2\text{O}$, in the system sodium sulfate-sulfuric acid-water [238, 241] or exists as the solid phase NaHSO_4 at a sulfuric acid concentration of 62%. The monohydrate is converted to the anhydrous salt at 58.45 ± 0.05 °C.

The thermal decomposition represented by the equation



takes place near the melting point, which can be determined only approximately (ca. 183 °C) with a water vapor pressure of 2500 Pa (25 mbar). Conversion to sodium disulfate is complete after heating for ca. 4 h at 240–260 °C. Sodium disulfate decomposes above 400 °C to form sodium sulfate with liberation of sulfur trioxide.

Production. Sodium hydrogensulfate is formed as an intermediate in the production of hydrochloric acid by the Mannheim process (Section 1.3.4) and is a by-product of the manufacture of chromium(VI) oxide [274, 279, 286, 361]. The reaction between sulfuric acid and sodium chloride may be carried out by the old process using cast iron retorts heated with gas or oil, or by the use of submerged combustion equipment in brick-lined vessels [305, 362]. The addition of a stoichiometric amount

of sulfuric acid to sodium sulfate or Glauber's salt at 200–280 °C produces molten sodium hydrogensulfate [363]. The same reaction can be utilized to produce sodium hydrogensulfate in aqueous solution at 80 °C directly [363].

Uses. Sodium hydrogensulfate is used in the manufacture of household cleaners, in the textile industry, for the regeneration of rubber, for metal surface treatment, and as a flux for low-melting metals and their alloys [225].

51.17 Sodium Benzoate

$\text{C}_6\text{H}_5\text{O}_2\text{Na}$, white granules or powder of sweetish taste. Between 0 and 50 °C the solubility in water is nearly constant, but at higher temperatures it increases sharply. At –13.5 °C, the eutectic mixture with water consists of 44.9 g of the salt and 100 g of water. The densities of the aqueous solutions at various concentrations are given in Table 51.27. The aqueous solution is slightly alkaline (pH ca. 8). Sodium benzoate is soluble to the extent of 0.8 g in 100 mL of ethanol, 8.2 g in 100 mL of methanol, and over 20 g in 100 mL of ethylene glycol.

Table 51.27: Densities of aqueous sodium benzoate solutions at 20 °C.

Concentration, %	Density, g/cm ³
22.0	1.09
24.53	1.1
26.84	1.11
29.0	1.12
31.06	1.13
33.14	1.14
35.3	1.15
36.7 (saturated)	1.154

Dry sodium benzoate is electrically charged by friction and forms an explosive mixture when its dust is dispersed in air. It absorbs moisture from the air to some extent.

Upon heating in an inert atmosphere sodium benzoate carbonizes and forms sodium carbonate. In the presence of air, it burns to give carbon dioxide and sodium carbonate. Chlorination of sodium benzoate gives rise to a complex mixture of the salts of chlorobenzoic acids. Sodium benzoate reacts with benzoyl chloride to form benzoic anhydride.

Other salts of benzoic acid can be prepared by metathesis reactions with the salts of particular cations. The aqueous and alcoholic solutions of sodium benzoate possess a remarkable ability to passivate the surfaces of metals and alloys.

Sodium benzoate is produced by the neutralization of benzoic acid with sodium hydroxide. Direct oxidation of toluene in sodium hydroxide solution is not currently in use. The other production methods include the hydrolysis of benzoic esters or benzonitrile. Purification is essential to the production of high-purity product.

Table 51.28 shows the specifications required in Japan by JP 10 for sodium benzoate used as a food additive. The FAO and WHO limit some additional items which are not mentioned in Table 51.28. These include readily oxidizable substances, readily carbonizable substances, polycyclic acids, organic chlorine compounds, and lead.

The principal use of sodium benzoate is as an anticorrosive. The expansion of the motor industry has increased the demand for it. It is added mainly to antifreeze coolants. Sodium benzoate is also used in food preservatives. In the pharmaceutical field, it is used as a diagnostic reagent for liver functions. It is also used in combination with caffeine as a nerve stimulant.

Table 51.28: Specifications for high-purity sodium benzoate (Japanese document JP 10).

Assay	min. 99%
Appearance	white granules or powder, odorless
Solubility	pass test
Free alkaline	max. 0.04% as NaOH
Chlorine compounds	max. 0.085% ^a
Sulfate	max. 0.12% as SO_4
Phthalate	pass test
Arsenic	max. 4 mg/kg as As_2O_3 ^b
Heavy metals	max. 20 mg/kg
Weight loss at 110 °C	max. 1% ^c

^aFood Chemicals Codex (USA) max. 0.07.^bFAO/WHO max. 3 mg/kg.^cFAO/WHO max. 1.5%.

51.18 References

1. Kirk-Othmer, 3rd ed., 21, p. 181.

2. Hofmann, Rüdorff: *Anorganische Chemie*, 21st ed., Vieweg & Sohn, Braunschweig 1973, p. 420.
3. C. Berger, H. Fickenscherichs, R. Peper, W. Jansen: *Prax. Naturwiss. Chem.* 40 (1991) no. 6, 2.
4. M. Sittig: *Sodium, its Manufacture, Properties and Uses*, Reinhold Publ. Co., New York 1956, pp. 1-9.
5. *Winnacker-Küchler*, 4th ed., 4, p. 326.
6. H. Y. Castner, US 452030, 1891.
7. Röbber & Haßlacher Chem. Co., US 1501756, 1921 (J. C. Downs).
8. H. U. Borgstedt, C. K. Mathews: *Applied Chemistry of the Alkali Metals*, Plenum Press, New York 1987.
9. N. N. Greenwood, A. Earnshaw: *Chemie der Elemente*, 1st ed., Verlag Chemie, Weinheim 1988, pp. 97.
10. *Ullmann*, 4th ed., 17, p. 143.
11. Degussa, Geschäftsbereich Chemie: Natrium, Eigenschaften, Handhabung, Anwendung, Company brochure, Ch 621-0-2-1089H, Hanau.
12. G. Dittich, H. Offermanns, H. Schlosser, Jr., *ChET Chem. Exp. Technol.* 3 (1977) 151-162.
13. "The Alkali Metals", *Mellor's Comprehensive Treatise on Inorganic and Theoretical Chemistry*, vol. 2, suppl. 2, part 1, Longmans, London 1961.
14. Linus Pauling: *Chemie, Eine Einführung*, 7th ed., Verlag Chemie, Weinheim 1967.
15. P. Caubère, *Angew. Chem.* 95 (1983) 597-611.
16. Degussa, Geschäftsbereich Chemie: Natriumhydrid, Eigenschaften, Reaktionen, Anwendung, Company brochure, C 25-0-1-772 Vol, Hanau.
17. O.-A. Neumüller: *Römpps Chemie-Lexikon*, 8th ed., Franck'sche Verlagsbuchhandlung, Stuttgart 1985.
18. A. Klemenc, E. Svetlik, *Z. Anorg. Allg. Chem.* 269 (1952) 153.
19. K. M. Myles, F. A. Cafasso, *J. Nucl. Mater.* 67 (1977) 249-253.
20. *Ullmann*, 3rd ed., 17, p. 415.
21. J. J. Chydenius *Ann. Phys. (Leipzig)* 2 (1863) no. 119, 43-56.
22. W. v. Bolton, *Z. Elektrochem. Angew. Phys. Chem.* 14 (1908) 768-770.
23. D. Lely, Jr., L. Hamburger, *Z. Anorg. Chem.* 87 (1914) 209-228.
24. L. F. Nilson, *Ber. Dtsch. Chem. Ges.* 15 (1882) 2537-2547.
25. *Ullmann*, 4th ed., 17, p. 711.
26. N. Korber, W. Assenmacher, M. Jansen, *Prax. Naturwiss. Chem.* 40 (1991) no. 6, 18.
27. U. Deschler, P. Kleinschmitt, P. Panster, *Angew. Chem.* 98 (1986) 237-253.
28. A. Streitwieser, C. H. Heathcock, *Organische Chemie*, Verlag Chemie, Weinheim 1980, pp. 192-194.
29. F. A. Cotton, G. Wilkinson: *Advanced Inorganic Chemistry*, 4th ed., John Wiley & Sons, New York 1980.
30. National Distillers and Chem. Corp.: *Sodium Monography*, Company brochure, New York.
31. *Winnacker-Küchler*, 3rd ed., 6, 81.
32. Nippon Soda, JP 59050021, 1982.
33. The Dow Chemical Comp., US 3265492, 1963 (P. R. Juckniess).
34. Ethyl Corp., US 2660517, 1952 (F. L. Padgitt).
35. R. E. Hulse, US 2130801, 1938.
36. Ethyl Corp., US 2944950, 1957 (G. O. Hayes).
37. Du Pont, US 3037927, 1962 (C. T. Gallinger).
38. J. S. Honea, US 2770364, 1956.
39. Ethyl Corp., US 2770592, 1956 (A. L. Feutress).
40. Olin Mathieson Chem. Corp., US 3085967, 1960 (G. T. Motock).
41. Ethyl Corp., US 2755244, 1952 (C. C. Harvey).
42. Du Pont, US 2921894, 1957 (T. O. Callaghan).
43. Du Pont, US 3544444, 1967 (V. J. Reilly).
44. Du Pont, US 4376028, 1981 (R. D. Marczewski, F. J. Ross).
45. Du Pont, US 3118827, 1961 (S. E. Eckert, F. J. Ross).
46. ICI, US 2861938, 1955 (R. D. Glascodeine).
47. Ethyl Corp., US 3463721, 1967 (L. L. Harris).
48. Du Pont, US 4305671, 1980 (F. J. Ross).
49. Du Pont, FR 1567424, 1967 (C. T. Gallinger).
50. Du Pont, US 4092228, 1977 (F. J. Ross).
51. S. Crowther, US 3776823, 1967.
52. National Distillers and Chem. Corp., US 2913381, 1967 (W. F. McFadyen, C. E. Buterbaugh).
53. K. A. Ruppert, Degussa AG, Company information, Frankfurt/Main 1992.
54. K. H. Meier, Degussa, Company report, Frankfurt/Main 1992.
55. M. A. Bredig in M. Blander (ed.): *Molten Salt Chemistry*, Interscience, New York 1964, pp. 367-425.
56. N. H. Nachtrieb in J. Prigogine, S. A. Rice (eds.): *Advances in Chemical Physics*, vol. 31, John Wiley, New York 1975, pp. 465-480.
57. Du Pont, US 3558451, 1971 (R. E. Svadlenak).
58. Du Pont, US 3560353, 1971.
59. Du Pont, US 4139428, 1979 (A. J. Dean, F. J. Ross).
60. Ford Motor Co., US 3488271, 1966 (J. T. Kummer, N. Weber).
61. Du Pont, US 4203819, 1978 (S. A. Cope).
62. Du Pont, US 4133728, 1978 (S. A. Cope).
63. Du Pont, US 4089770, 1977 (C. H. Lemke).
64. ICI, US 3607684, 1967 (A. T. Kuhn).
65. F. Huber, P. Menzenhauer, W. Peppler, W. Tell: "Untersuchung des Brandverhaltens von flüssigem Natrium", *KFK Nachr.* 4 (1972) no. 3, 9-13.
66. F. Huber, P. Menzenhauer, W. Peppler, W. Till, Verhalten von Natrium-Bränden und Erprobung von Schutzsystemen, KFK-1970, Kernforschungszentrum Karlsruhe, April 1974.
67. W. Cherdron: *Jahrestagung Kerntechnik 1989*, Düsseldorf, p. 231.
68. W. Cherdron, W. Schütz: *Jahrestagung Kerntechnik 1993*, Köln.
69. P. Menzenhauer, G. Ochs, W. Peppler, Erprobung eines Löschpulvers auf der Basis von Graphit für Flüssigmetallbrände, KFK-2525, Kernforschungszentrum Karlsruhe, Nov. 1977.
70. F. Huber, P. Menzenhauer, W. Till, *KFK-1970*, Kernforschungszentrum Karlsruhe, April 1974.
71. W. Cherdron, S. Jordan, W. Lindner, *KFK-1338*, Kernforschungszentrum Karlsruhe, Nov. 1990.
72. S. Jordan et al., *Nuclear Technol.* 81 (1988) no. 2, 183.
73. P. Menzenhauer et al., "Experience with Cleaning of Sodium-Wetted Components and Decontamination at Nuclear Research Centre Karlsruhe", *IAEA Meeting on Sodium Removal and Decontamination*, Richland, WA, Aug. 1978, pp. 30-37.

74. E. Bilger, L. Lange, *Prax. Naturwiss. Chem.* 40 (1991) no. 6, 12.
75. J. F. Cordes, *Chem. Unserer Zeit* 3 (1977) no. 11, 65.
76. H. Pommer, *Angew. Chem.* 89 (1977) 437-443.
77. K. W. Stoffregen, Fa. Dr. Riedelbauch & Stoffregen GmbH, Company report, Meisenheim/Glau.
78. A. Pacz, DT 117773, 1925.
79. E. Dunkel, *Gießerei* 58 (1971) no. 24, 782.
80. Metallgesellschaft, "Silumin, die Al-Gußlegierung", Company brochure, Frankfurt/Main.
81. G. Gürtler, *Z. Metallk.* 44 (1953) 503.
82. S. Justi, K. Körber, K. Löhberg, *Gießereiforschung* 24 (1972) no. 1, 37-44.
83. R. Irmann: *Aluminium in Sand und Kokille*, Aluminium Verlag, Düsseldorf 1953, p. 104.
84. Asea Brown Boveri AG, "Hochenergiebatterie und Elektroauto", Company brochure no. DHB 1310881 (1987), DHB 1253871 (1988), Heidelberg.
85. F. Beck, *Chem. Ing. Tech.* 54 (1982) no. 9, 809-817.
86. W. Fischer, F. J. Rohr, *Chem. Ing. Tech.* 50 (1978) no. 4, 303-305.
87. H. U. Borgstedt, G. Frees, *Werkst. Korros.* 38 (1987) 725-737.
88. K. Förster, G. Ruloff: "Flüssigmetalle als Wärmeübertragungsmittel", CAV, Konradin Verlag, Leinfelden-Echterdingen 1988, p. 182.
89. H. U. Borgstedt, C. Guminski, *Metals in Liquid Alkali Metals*, IUPAC Solubility Data Series, in press.
90. O. J. Foust: *Sodium Na-K, Engineering Handbook*, Gordon & Breach, New York 1972.
91. C. Hirayama, Z. Galus, C. Guminsky, "Metals in Mercury", in A. S. Kertes (ed.): *Solubility Data Series*, vol. 25, International Union of Pure and Applied Chemistry, in press.
92. H. Hund, F. R. Minz in H. Harnisch, R. Steiner, K. Winnacker (eds.): *Chemische Technologie*, 4th ed., vol. 2, Carl Hanser Verlag, München 1982, p. 400.
93. Kernforschungszentrum Karlsruhe, DE 4034137 C1, 1990 (H. U. Borgstedt).
94. E. Hermann: *Handbuch des Stranggießens*, Aluminium Verlag, Düsseldorf 1958, pp. 764-765.
95. Metall Invent S.A., DT 2457423, 1974.
96. Unilever, GB 1236233, 1968 (W. H. De Groot, M. H. Hilder).
97. Degussa AG, DE 3016173, 1980 (W. Hinrichs et al.).
98. R. Neureiter, Degussa AG, Company report, Frankfurt/Main 1992.
99. Métaux spéciaux S.A. Paris, DT 2454051, 1974 (B. Batoux, A. Laurent-Atthalin, M. Salmon).
100. Métaux spéciaux S.A., "Sodium", Company brochure, 92087 Paris la Défense, Frankreich.
101. O. Pfeffer: Berufsgenossenschaft der chemischen Industrie, Merkblatt Natrium, M 019,5/84, Jedermann-Verlag, Heidelberg 1984.
102. Du Pont, Sodium Data Sheet, Chemical Safety Data Sheet, Wilmington, Delaware 1989 SD-47, Sodium Manufacturing Chemists Association, Washington, DC, 1978.
103. A. Huber: "Sodium (Metal)-United States", (E. H. Data Summary, Chemical Information Services, Stanford Research Institute, CA, 1990).
104. G. Busch: "Sodium Makers Adjust to Changing Market Place", *Chem. Mark. Rep.* 240 (1991) 27.
105. W. Botsch: *Salz des Lebens*, Kosmos Gesellschaft der Naturfreunde, Franck'sche Verlagshandlung, Stuttgart 1976.
106. H. Seidel, R. Woller: *Das Geschenk der Erde*, ECON Verlag, Düsseldorf 1980.
107. M. J. Schleiden: *Das Salz, seine Geschichte, seine Symbolik und seine Bedeutung im Menschenleben*, Verlag Wilhelm Engelmann, Leipzig 1875.
108. S. Falkenberg: *Salz ist Leben, seine Bedeutung für Ihre Gesundheit*, Ariston Verlag, Genf 1987.
109. P. Meier: *Die Würze des Lebens, Salz*, Schweizer Verlagshaus, Zürich 1983.
110. J. F. Bergier: *Die Geschichte vom Salz*, Campus Verlag, Frankfurt-New York 1989.
111. W. Kaufmann: *Sodium Chloride*, Reinhold Publ. Co., New York 1960, pp. 587ff.
112. *J. Phys. Chem. Ref. Data* 11 (1982) 15-81; 13 (1984) 1-102. *Gmelin* 8th ed., System No. 21, pp. 309ff. *Landolt-Börnstein*, 6th ed., 2, part 8, 46ff.
113. Te-Pang Hou: *Manufacture of Soda*, Reinhold Publ. Co., New York 1942, p. 118.
114. S. K. Coburn, *Corrosion* 10 (1954) no. 5, 1.
115. W. W. Bradley, *Corrosion (Houston)* 11 (1955) 383.
116. DECHEMA-Werkstoffabelle, Blatt Nr. DWT 1043ff, 3. Bearbeitung, DECHEMA, Frankfurt/Main 1962.
117. S. T. Lefond: *Handbook of World Salt Resources*, Plenum Press, New York 1969.
118. G. Spackeler: *Lehrbuch des Kali- und Steinsalzbergbaues*, VEB Wilhelm Knapp Verlag, Halle (Saale) 1957, pp. 243-254.
119. H. Jendersie: *Kali- und Steinsalzbergbau*, vol. 2, VEB Deutscher Verlag für Grundstoffindustrie, Leipzig 1969, pp. 150-154.
120. G. Brückner, *Freiburg. Forschungsh.* A418 (1967) 11-46.
121. G. Brückner, *Bergakademie* 10 (1961) 625-629.
122. P. Ambatiello, *5th Symp. on Salt*, vol. 2, The North, Ohio Geol. Soc. Corp., Cleveland, OH, 1978, pp. 213-218.
123. K. Thomanek, *5th Symp. on Salt*, vol. 2, The North, Ohio Geol. Soc. Corp., Cleveland, OH, 1978, pp. 171-182.
124. P. Ambatiello, *Glückauf* 118 (1982) 1183-1188.
125. G. Dorstewitz, C. H. Fritzsche, H. Prause, *Glückauf* 95 (1959) 1245-1250.
126. P. Ambatiello, *Felsbau* 8 (1990) 180-184.
127. G. Feder, M. Hoscher, *Felsbau* 5 (1987) 114-149.
128. K. Thomanek, *BHM Berg Hüttenmänn. Monatsh.* 127 (1982) 381-389.
129. M. Hoscher, *BHM Berg Hüttenmänn. Monatsh.* 126 (1981) 234-238.
130. K. Schmidt, *Tech. Mitt.* 68 (1975) 363-368.
131. H. Gorm, J. Hieblinger, G. Kühn, *Erdöl Erdgas Z.* 93 (1977) 83-90.
132. H. K. Röhr, *Erdöl Kohle Erdgas Petrochem.* 22 (1969) 670-679, 734-741.
133. S. Meister, G. Kuhr, *Erdöl Erdgas Z.* 88 (1972) 248-257.
134. H. Borchert, W. Dreyer: Gutachten über die Standfestigkeit und Konvergenz von Kavernen im Salzstock, Mineralog.-petrograph. Inst. d. TU Clausthal, 10 Dec. 1967.
135. W. Dreyer, *Kali Steinsalz* 5 (1971) 473-478.

136. S. Serata: "Continuum Theory and Model of Rock Salt Structures", 2nd Symp. on Salt, Northern Ohio Geol. Soc., Cleveland 1965.
137. R. W. Durie, F. W. Jessen, *Soc. Pet. Eng. J.* 1964 183-190.
138. W. Dreyer: *Gebirgsmechanik im Salz*, Enke Verlag, Stuttgart 1974.
139. K.-H. Lux: *Gebirgsmechanischer Entwurf und Felderfahrungen im Salzkavernenbau*, Enke Verlag, Stuttgart 1984.
140. F. Schöber, A. Sroka: "Die Berechnung von Bodenbewegungen über Kavernen unter Berücksichtigung des zeitlichen Konvergenz- und Gebirgsverhaltens", *Kali Steinsalz* 8 (1983) March, no. 10.
141. A. Sroka, F. Schöber: "Die Berechnung der maximalen Bodenbewegungen über kavernenartigen Hohlräumen unter Berücksichtigung der Hohlraumgeometrie", *Kali Steinsalz* 8 (1972) Aug., no. 8.
142. A. Sroka: "Abschätzung einiger zeitlicher Prozesse im Gebirge", Schriftenreihe Lagerstättenforschung und -darstellung, Bodenbewegungen und Bergschäden Ingenieurvermessung Kolloquium, Leoben, 15-16 Nov. 1984.
143. A. Sroka, A. Hartmann: "Die Überwachung von Speicherkavernen mittels geodätischer und physikalischer Beobachtungen", Proceedings 5th. International Congress, International Society of Mine Surveying Harrogate, 9-13 Sept. 1985.
144. H. von Schonfeldt, L. Remoline in A. H. Coogan (ed.): "Mechanism of Solution and Cavity Control in a Two-Well-System with Emphasis on Jetting", 4th Symp. on Salt, Northern Ohio Geol. Soc. Inc., Cleveland 1974, pp. 189-202.
145. K. Henderson: "Methods of Joining Two or More Wells for Brine Production", in [144], pp. 211-218.
146. H. Rischmüller, *Erdöl Erdgas Z.* 88 (1972) 240-248.
147. H. G. Haddenhorst et al., *Erdöl Erdgas Z.* 90 (1974) 154-161, 197-204.
148. H. Bresson, *Rev. fr. énerg.* 26 (1969) 527-543.
149. M. Klafki, H.-J. Kretschmar, W. Menzel, W. Schreiner: "Auslösung von Gasspeicher-Kavernen in mächtigen Salzlagerstätten", *Neue Bergbautech.* 20 (1991) March, no. 3.
150. E. F. Armstrong, L. M. Miall: *Raw Materials from the Sea*, Chemical Publishing Co., Brooklyn 1946.
151. Compagnie des Salins du Midi et des Salines de l'Est (C.S.M.E.): *Le Sel*, Presses universitaires de France, Paris.
152. Laboratoire C.S.M.E., Aigues-Mortes, France, personal communication.
153. Central Research Institute, Japan Monopoly Corporation, Figures for Salt Production, Tokyo 1954.
154. D. W. Kaufmann: *Sodium Chloride*, Reinhold Publ. Co., New York 1960.
155. *Ullmann*, 3rd ed., 12, 674.
156. J. v. Rozičky: in [144], vol. 2, p. 425.
157. Escher-Wyss-Mitteilung 1961/2-3; 1975/2.
158. C. M. van Land, K. J. A. de Waal: *Industrial Crystallisation*, J. W. Mullin, New York 1976, pp. 449ff.
159. C. M. van Land, B. G. Wienk: *Industrial Crystallisation*, J. W. Mullin, New York 1976, pp. 51ff.
160. L. J. Theilgard, 1st Symposium on Salt, Northern Ohio Geol. Soc. Inc., Cleveland, OH, 1963, pp. 417ff.
161. M. A. van Damme et al.: *Influence of Additives on the Growth and Dissolution of Sodium Chloride Crystals*, Drukkerij Smit, Hengelo 1965.
162. E. G. Cooke in [136], vol. 1, p. 259.
163. Salt Institute, Recent successes and Failures in Combating Corrosion in Salt Plants, Seminar Chicago, Ill. June 1977.
164. Verein Deutsche Salzindustrie e.V. (VDS): *Salz III - Ein Nahrungsmittel*, Hanser Verlag, München 1985, pp. 17ff.
165. G. Reimer, Ch. Thieme, *Natriumchlorid*, Hanser Verlag, München 1982, pp. 492-494.
166. VDS: *Salz I - Geschichte und Bedeutung*, Hanser Verlag, München 1983, p. 64.
167. VDS: *Salz V - In der Wasserenthärtung*, Hanser Verlag, München 1989, pp. 37ff.
168. W. Botsch: *Salz des Lebens*, Franckh'sche Verlagshandlung, Stuttgart 1976, pp. 69ff.
169. VDS: *Salz II - Rohstoff in der Chemie*, Hanser Verlag, München 1984, pp. 36-38.
170. Deutsche Solvay Werke GmbH: *Das Salz der Chemie*, Solingen 1983, pp. 28-29.
171. VDS: *Salz IV - Im Winterdienst*, Hanser Verlag, München 1985, pp. 10-15.
172. S. U. Pickering, *J. Chem. Soc.* 63 (1893) 890.
173. *Gmelin*, 8th ed., System no. 21.
174. H. S. Burney, J. B. Talbot, *J. Electrochem. Soc.* 138 (1991) 3140-3169.
175. Hariman report (1996) 03/1995, Tecnon Ltd., London.
176. R. Winkler, *Chem. Ind.* 36 (1984) 152-155.
177. S. A. McCluney, J. W. Van Zee, *J. Electrochem. Soc.* 136 (1989) 2556-2564.
178. C. B. Kelly, I. L. Walker, Staff of the Chlorine Institute, Inc. (eds.): *The Second Chlor-Alkali Symposium, World Chlor-Alkali. An Industry in Transition*, Proceedings, Washington, DC, 1990.
179. D. C. Brandt, paper presented at the Chlorine Institute Meeting, Washington, DC, April 1989.
180. M. Kamaludeen et al., *Transactions of the SAEST* 21 (1986) no. 1, 53-56.
181. B. A. Friedfeld in T. C. Wellington (ed.): *Modern Chlor Alkali Technology*, vol. 5, Elsevier, London 1992, pp. 1-12.
182. J. Young, *Chem. Week* 150 (1991) Oct. 2, 14.
183. *Ullmann*, 3rd ed., 12, pp. 659-660.
184. S. Sridhar, *Chem. Ing. Tech.* 61 (1989) 428-429.
185. H. v. Plessen et al., *Chem. Ing. Tech.* 61 (1989) 933-940.
186. G. Kreysa, *Chem. Ing. Tech.* 62 (1990) 357-365.
187. J. Jörissen, K. H. Simmrock, *J. Appl. Electrochem.* 21 (1991) 869-876.
188. G. Venkoba Rao, *IPPTA* 24 (1987) no. 3, 20-29.
189. I. K. Nelson in B. J. Moniz, W. I. Pollock (eds.): *Process Industries Corrosion*, NACE, Houston, TX, 1986.
190. CSD, PPG Industries, Company Brochure, Pittsburgh, PA.
191. *Ullmann*, 4th ed., 17, p. 206.
192. Tecnon Market Analysis, Caustic Soda into the 1990s, London 1990.
193. *Chem. Bus.* 1989, Dec., 24-25.
194. *International Critical Tables*, vol. III, p. 372, vol. IV, pp. 237, 259, McGraw-Hill, New York 1928.

195. L. Lortie, P. Demers, *Canadian J. Res.* 18 (B) (1940) 164.
196. A. F. Newkirk, J. Aliferis, *Anal. Chem.* 30 (1958) 982-984.
197. W. L. W. Ludekens, T. Thirunamachandran, *Chem. Ind. (London)* 1954, 1263-1266.
198. C. Kröger, E. Fingas, *Z. Anorg. Allgem. Chem.* 212 (1933) 257-268, 264.
199. F. Ishikawa, F. Murooka, H. Hagisawa, *Abstr. Rikawagaku-Kenhyo-jo Iho* 5 (1932) 23-24; *Sci. Rep. Tohoku Imp. Univ.* 22 (1933) 1179-1196.
200. E. G. Bunzel, E. J. Kohlmeier, *Z. Anorg. Allgem. Chem.* 254 (1947) 1-30.
201. Te-Pang Hou: *Manufacture of Soda*, 2nd ed., Reinhold Publishing Corp., New York 1942, p. 17.
202. P. P. Fedodoff, *Z. Anorg. Chem.* 17 (1904) 1644-1659.
203. E. Jänecke, *Z. Angew. Chem.* 20 (1907) 1559-1564.
204. Z. Rant: *Die Erzeugung von Soda nach dem Solvay Verfahren*, F. Enke Verlag, Stuttgart 1968, pp. 76-83, 125-160.
205. H. Börger, *Bergbau Rundschau* 4 (1952) 84-88.
206. M. Imamura, *Ind. Eng. Chem.* 54 (1962) no. 2, 35-39.
207. United Nations Economic and Social Council, *ECE/CHEM* 14 (1976) Sept. 20, p. 5.
208. *The Economics of Soda Ash*, 6th ed., Roskill Information Services, London 1991.
209. B. M. Coope, P. W. Harben: "Soda Ash", in P. W. Harben (ed.): *Raw Materials for the Glass Industry*, Industrial Minerals Consumer Survey, 1977.
210. *Ind. Chem.* 31 (1955) no. 370, 547.
211. *Ind. Min.* 1975, no. 96, Sept., 23-27.
212. N. L. Talmud, *Khim. Promst. Moscow* 1961, 226-232.
213. *Ullmann*, 3rd ed., 12, p. 656.
214. *Winnacker-Küchler*, 2nd ed., 1, pp. 210-213.
215. E. Stiers, DE-OS 1592039, 1967.
216. S. Lynn et al., US 3792153, 1972.
217. R. Blumberg, J. E. Gai, K. Hajdu, *Proceedings International Solvent Extraction Conference 1947*, vol. 3, pp. 2789-2802, Soc. Chem. Ind., London 1974.
218. Israel Mining Industries Institute for Research and Development, Israel, IL 33552, 1969.
219. E. Pischinger, St. Bursa, H. Koneczny, J. Straszko, *Przem. Chem.* 54 (1975) 593-594.
220. F. Meinck, H. Stoeff, H. Kohlschütter: *Industrie-Abwasser*, G. Fischer-Verlag, Stuttgart 1968, pp. 245-248.
221. Industrial Minerals Glass Survey 1977, pp. 39-49.
222. *Gmelin*, 8th ed. System no. 21, pp. 764-766, 1358-1363.
223. A. E. Hill, L. R. Bacon, *J. Am. Chem. Soc.* 49 (1927) 2487.
224. J. F. Henkels: *Pyritologia oder Kieselhistorie*, Großische Handlung, Leipzig 1754, p. 705.
225. *Ullmann*, 4th ed., 17, 211-229.
226. G. Lunge: *Handbuch der Soda-Industrie*, 3rd ed., vol. 2, Vieweg, Braunschweig 1909.
227. H. Furkert in F. Ebel (ed.): *Chemische Berichte*, Reichsamt für Wirtschaftsausbau, Berlin, January 1943, pp. 28-33.
228. H. v. Plessen et al., *Chem. Ing. Tech.* 61 (1989) 933-940.
229. Great Salt Lake Minerals and Chemicals Corp., US 3575688, 1969.
230. Mannesmann, DE-OS 3721667, 1987.
231. Intermountain Res. Dev. Corp., US 4519806, 1982.
232. Techemet, ZA 87/09599, 1987.
233. *Ullmann*, 4th ed., 13, 450.
234. *Gmelin*, 8th ed., Natrium (1928).
235. *Gmelin*, 8th ed., Aun., Natrium, Erg.bd. (1964-1970).
236. In [235], part 3, 1117.
237. In [235], part 3, 1092-1095.
238. A. Seidell, W. F. Linke: *Solubilities of Inorganic and Metal-Organic Compounds*, 4th ed., vol. 2, American Chemical Society, Washington, DC, 1965, pp. 1121-1123.
239. H. Stephen, T. Stephen: *Solubilities of Inorganic and Organic Compounds*, vol. 1/1, Pergamon, London 1963, pp. 126-127.
240. A. Seidell: *Solubilities of Inorganic and Metal Organic Compounds*, 3rd ed., vol. 1, Van Nostrand, New York 1940, pp. 1234-1235.
241. H. L. Silcock (ed.): *Solubilities of Inorganic and Organic Compounds*, vol. 3/2, Pergamon, Oxford 1979 pp. 827-848, 971-972.
242. R. E. Vener, A. R. Thompson, *Ind. Eng. Chem.* 41 (1949) 2242-2247; 42 (1950) 171-174.
243. *The Economics of Sodium Sulphate 1990*, 6th ed., Roskill Information Services, London 1990.
244. SRI International: *Chemical Economics Handbook*, May 1982, p. 771, 1000 G-T.
245. R. C. Kerr et al., *Nature (London)* 340 (1989) no. 6232, 357-362.
246. In [235], part 1, 231-234.
247. *Winnacker-Küchler*, 4th ed., 1-7, 1981-1986.
248. In [247], 2, 76-78.
249. Metallgesellschaft AG DE 1150368, 1960.
250. Standard-Messo, DE 1467244, 1963.
251. Standard-Messo, DE 1519911, 1965.
252. W. Linstadt, G. Hofmann, *Chem. Ind. (Düsseldorf)* 31 (1979) 329-333.
253. R. J. King, *Chem. Eng. Prog.* 80 (1984) no. 7, 63-69.
254. D. J. Neville, *Cryst. Precip. Proc. Int. Symp.*, 1987, pp. 109-116.
255. T. Messing, W. Wöhlk, *Chem. Ing. Tech.* 45 (1973), 106-109.
256. Metallgesellschaft AG, DE-OS 2904345, 1979.
257. Ebner & Co, DE-OS 2246568, 1972.
258. Standard-Messo, DE-OS 1519910, 1965.
259. R. Hürzeler, G. Stücki, *GWG Gas Wasserfach: Wasser Abwasser* 131 (1990) 231-244.
260. P. G. Rueffell: *Proc. 3rd Symp. Salt 1969* (Publ. 1970) p. 429-451.
261. Ebara Inflico, DE-AS 1567941, 1967.
262. Escher-Wyss, DE-OS 2543721, 1975.
263. Wintershall AG, DE-AS 2029984, 1970.
264. Multifibre Process, AT 355517, 1978.
265. W. Fleischmann, A. Mersmann, *Process Technol. Proc.* 1984, no. 2 (Ind. Cryst.), pp. 165-170.
266. W. Fleischmann, A. Mersmann, *Chem. Ing. Tech.* 57 (1985) 178-179.
267. D. Lobley, K. L. Pinder, *Waste Treat. Util. Proc. Int. Symp.* 2nd 1980 (Publ. 1982) pp. 63-70.

268. G. Mina-Mankarios, K. L. Pinder, *Can. J. Chem. Eng.* 69 (1991) 308-324.
269. M. R. Bhatt et al., *Res. Ind.* 37 (1992), no. 1, 34-35.
270. T. Kobayashi, *CEER Chem. Econ. Eng. Rev.* 8 (1976) no. 6, 42-48.
271. M. Driesen, *Br. Chem. Eng.* 15 (1970) 1154-1158.
272. Politechnika Szczecińska DD 265390, 1986.
273. *Chem. Abstr.* 107 (1987) 24670x.
274. Allied Chem. Corp., DE-OS 2151323, 1970.
275. Occidental Chem. Corp., US 5393503, 1991.
276. *Ullmann*, 4th ed., 23, 688.
277. Kema Nord AB, US 4678653, 1985.
278. Tenneco Canada, US 4780304, 1987.
279. Lundberg, US 4483740, 1983.
280. G. Gurato et al., *Chim. Ind. (Milan)* 69 (1987) no. 12, 140-147.
281. G. Gurato et al., *J. Cryst. Growth* 66 (1984) 621-631.
282. In [247], 6, 182-183.
283. E. M. Arnoldov et al., *Sov. Chem. Ind. (Engl. Transl.)* 11 (1979) 549-550.
284. Poliofi, EP-OS 245719, 1986.
285. FIAT, Microfilm AA-216, Frames 8-15, 65-156 (PB, 73556).
286. J. B. Hunter, EP-OS 65412, 1981.
287. B. Asano, M. Olper, *Proc. 43rd Int. Waste Conf.* 1988 (Publ. 1989) 45-50.
288. R. M. Reynolds et al., *Proc. World Symp. Metall. Environ. Control 1990*, 119th TMS Annu. Meet., pp. 1001-1056.
289. *Ullmann*, 3rd ed., 11, 185-187.
290. Balcke-Dürr AG, EP-OS 301452, 1987.
291. Chemieanlagenbaukombinat Leipzig-Grimma, DD 293098, 1987.
292. Metallgesellschaft AG, DE-OS 3616508, 1986.
293. D. J. Wahl, *Umwelt* 20 (1990) no. 3, L4-L10.
294. S. Weiß, H. Wanko, *Chem. Tech. (Leipzig)* 43 (1991) 177-188.
295. In [235], part 1, 214-224.
296. G. Lesino et al., *Sol. Energy* 45 (1990) no. 4, 215-219.
297. W. A. MacWilliams, R. G. Reynolds, *CIM Can. Inst. Mining Met. Bull.* 66 (1973) no. 734, 115-119. Alberta Sulphate, CA 1007563, 1975.
298. P. L. Broughton, *Ind. Miner. (London)* 1977 no. 121, 51-59.
299. MINERSA, ES 504459, 1981.
300. O. K. Yanateva et al., *J. Appl. Chem. USSR (Engl. Transl.)* 52 (1979) 388-389.
301. Kerr-McGee Chem. Corp., US 4291002, 1977; US 4478599, 1982.
302. W. I. Weisman, *Chem. Eng. Prog.* 60 (1964) no. 11, 47-49.
303. P. Behrens, *Bull. Utah Geol. Min. Surv.* 1980, no. 116, 233-238.
304. *Chem. Ing. Tech.* 37 (1965) 666.
305. *Ullmann*, 3rd ed., 15, 71-73.
306. C. W. Cannon, US 2706145, 1955.
307. IG Farbenindustrie AG, DE 694409, 1936.
308. FIAT, Microfilm AA-216, Frames 174-188 (PB, 73556).
309. In [235], part 1, 228-229.
310. Morton Int., DE-AS 1293139, 1961.
311. Winnacker-Küchler, 3rd ed., 1, 150-151.
312. In [235], part 1, 227.
313. H. Picht, *Hung. J. Ind. Chem.* 17 (1989) no. 2, 179-183.
314. J. Jörissen et al., *DECHEMA-Monogr.* 124 (1991), 21-35.
315. J. Jörissen et al., *J. Appl. Electrochem.* 21 (1991) 869-876.
316. BASF, EP-OS 449071, 1990.
317. B. Pieper, *Fortschr. Ber. VDI Reihe 3* 132 (1987).
318. Imperial Chem. Ind., EP-OS 532188, 1991.
319. K. Tomiie, Y. Hayashi, *New Mater. New Processes Electrochem. Technol.* 1 (1981) 284-288.
320. H. Kau, *DECHEMA-Monogr.* 98 (1985) 291-298.
321. Lenzing AG, EP-OS 399993, 1989.
322. K. Nagasubramanian et al., *J. Membr. Sci.* 2 (1977) 109-124; 3 (1978) 71-83.
323. Allied Corp., US 4116889, 1978.
324. Allied Corp., US 4140815, 1979.
325. K. N. Mani et al., *Desalination* 68 (1988) 149-166.
326. H. Strathmann et al., *DECHEMA-Monogr.* 125 (1992) 83-100.
327. BASF, DE 868742, 1941.
328. C. F. Linström, *Chem. Tech. (Leipzig)* 4 (1952) 375-380.
329. K. Altenbach, Hoechst AG, personal communication, Frankfurt/Main 29.11.1991.
330. Erco Industries, DE-OS 2856504, 1978.
331. C. F. Hoppe, Dissertation Dortmund 1995, Aachen: Shaker Verlag, 1996.
332. *Gmelin*, 8th ed., Kalium, Erg.bd. (1970), 26-37.
333. H. Scherzberg et al., *Chem. Tech. (Heidelberg)* 20 (1991) no. 6, 41-48.
334. Forschungsinstitut Leningrad, DE 2820445, 1978.
335. U. Neitzel, *Kali Steinsalz* 9 (1986) 257-261.
336. G. Z. Zelmanov, V. G. Terio, *Sov. Chem. Ind.* 18 (1986) no. 5, 46-48.
337. Graessor Contactors, GB 2270308, 1992.
338. Mannesmann, DE 4340839, 1993.
339. FIAT, Microfilm H-45, Frames 7834-7842 (PB, 70041).
340. BIOS Final Report no. 855.
341. Waagner-Biro, Chemiefaser Lenzing, AT 349494, 1976.
342. Rockwell International, EP-OS 91948, 1981.
343. J. H. Cameron et al., *Ind. Eng. Chem. Fundam.* 24 (1985) 443-449.
344. BIOS Final Report no. 288.
345. H. L. Murray: Office Publication Board, Report No. 223 (*Bibl. Sci. Ind. Rep.* 1 (1946) 7).
346. Metallgesellschaft AG, EP-OS 540072, 1991.
347. H. Röter in F. Ebel (ed.): *Chemische Berichte*, Reichsamt für Wirtschaftsausbau, Berlin Dec. 1941, p. 201-208.
348. FIAT Final Report no. 989.
349. Metallgesellschaft AG, GB 473520, 1936; 513744, 1937.
350. BIOS Final Report no. 107.
351. *Ullmann*, 4th ed., 17, 555-556.
352. *Kirk-Othmer*, 3rd ed., 19, 395-406.
353. In [247], 3, 117.
354. Henkel, EP-OS 302403, 1988.
355. *Ullmann*, 4th ed., 22, 643, 660.
356. Allegheny Ludlum, US 4824536, 1988.

357. Zusatzstoff-Verkehrsordnung vom 10.07.1984, BGBl. I, no. 30 (1984), 897-901, and Anlage 2, p. 64.
358. S. N. Gaeta, *Chem. Sep. Dev. Sel. Pap. Int. Conf. Sep. Sci. Technol. 1st* 1986, no. 2, 95-106.
359. Walhalla-Kalk, EP 250626, 1986.
360. In [235], part 1, 226, 246-247; part 3, 1149-1159.
361. *Ullmann*, 4th ed., 9, 612-613.
362. Hoechst, DE-OS 2810693, 1978.
363. Mannesmann, DE-OS 3723292, 1987.

52 Potassium

JÖRG BRÖNING, ELIZABETH R. BURKHARDT (§§ 52.1–52.2, 52.5–52.10); HEINZ SCHULTZ (RETIRED) (§§ 52.3, 52.4 INTRODUCTION, 52.4.2.3, 52.4.3–52.4.5, 52.11 EXCEPT 52.11.3 AND 52.11.7, 52.12, 52.17, 52.18); GÜNTER BAUER (RETIRED), ERICH SCHACHL (RETIRED) (§§ 52.4.1–52.4.2.2); FRITZ HAGEDORN (§§ 52.11.3, 52.11.7); PETER SCHMITTINGER (§§ 52.13–52.15); TAKAO MAKI (§ 52.16)

52.1 Introduction	2142	52.11.3.6 Processes	2178
52.2 Properties	2142	52.11.4 Electrostatic Separation	2180
52.3 History	2143	52.11.4.1 Theoretical Basis	2180
52.4 Occurrence	2144	52.11.4.2 Equipment and Processes	2181
52.4.1 Potash Salt Deposits	2145	52.11.5 Heavy-Media Separation	2182
52.4.1.1 Minerals	2145	52.11.6 Debrining and Drying	2183
52.4.1.2 Geology of Potash Deposits	2146	52.11.7 Process Measurement and Control	2184
52.4.2 Mining of Potash Salts	2147	52.11.8 Waste Disposal and Environmental Aspects	2185
52.4.2.1 Shaft Mining	2147	52.11.9 Granulation	2187
52.4.2.2 Extraction, Conveying, and Haulage	2147	52.11.10 Quality Specifications	2188
52.4.2.3 Solution Mining	2148	52.11.11 Toxicology and Occupational Health	2189
52.4.3 Treatment of Potash Ores	2149	52.11.12 Economic Aspects and Uses	2189
52.4.3.1 Intergrowth and Degree of Liberation	2149	52.12 Potassium Sulfate	2190
52.4.3.2 Grinding	2151	52.12.1 Properties	2190
52.4.4 Potash–Magnesia	2152	52.12.2 Raw Materials	2191
52.4.5 Production of Potassium Salts from Other Raw Materials	2153	52.12.3 Production	2191
52.4.5.1 The Dead Sea	2153	52.12.3.1 From KCl and H ₂ SO ₄ (Mannheim Process)	2191
52.4.5.2 The Great Salt Lake	2153	52.12.3.2 From KCl and MgSO ₄	2193
52.4.5.3 Searles Lake	2154	52.12.3.3 From KCl and Langbeinite	2194
52.4.5.4 Other Sources	2154	52.12.3.4 From KCl and Kainite	2195
52.5 Production of the Metal	2155	52.12.3.5 From KCl and Na ₂ SO ₄	2195
52.6 Analytical and Test Methods	2155	52.12.3.6 From KCl and CaSO ₄	2196
52.7 Economic Aspects	2156	52.12.3.7 From Alunite	2196
52.8 Health and Safety Factors	2156	52.12.3.8 From Natural Brines and Bitterns	2196
52.9 Potassium–Sodium Alloys	2157	52.12.4 Granulation	2196
52.10 Uses	2158	52.12.5 Quality Specifications	2197
52.10.1 Potassium Bases	2158	52.12.6 Toxicology and Occupational Health	2197
52.10.2 Potassium Graphite (C ₆ K)	2158	52.12.7 Economic Aspects and Uses	2197
52.10.3 Potassium Hydride	2159	52.13 Potassium Hydroxide	2198
52.10.4 Potassium Superoxide	2159	52.13.1 Properties	2198
52.11 Potassium Chloride	2159	52.13.2 Production	2198
52.11.1 Properties	2160	52.13.3 Quality Specifications	2199
52.11.2 Production by Crystallization from Solution	2160	52.13.4 Economic Aspects and Uses	2199
52.11.2.1 Phase Theory	2160	52.14 Potassium Carbonate	2199
52.11.2.2 Hot Leaching Process	2162	52.14.1 Properties	2199
52.11.2.3 Processing of Carnallite	2166	52.14.2 Production	2200
52.11.2.4 Equipment	2170	52.14.3 Quality Specifications and Analysis	2202
52.11.3 Flotation	2174	52.14.4 Storage and Transportation	2203
52.11.3.1 Potash Ores Suitable for Flotation	2174	52.14.5 Economic Aspects and Uses	2203
52.11.3.2 Carrier Solutions	2175	52.15 Potassium Hydrogencarbonate	2204
52.11.3.3 Flotation Agents	2175	52.15.1 Properties and Production	2204
52.11.3.4 Theory	2175	52.15.2 Uses	2204
52.11.3.5 Flotation Equipment	2177	52.16 Potassium Benzoate	2204
		52.17 Storage and Transportation	2204

52.1 Introduction

Potassium is the third element in the alkali-metal series. The name is derived from the word *potash*. The German name *Kalium*, is derived from the Arabic word *qalia* and is the source for the element symbol K. The ashes of these plants (*al qalia*) were the historical source of potash for preparing fertilizers or gun powder.

Potassium ions are essential to plants and animals. They play a key role in carbohydrate metabolism in plants. In animals, potassium ions promote glycolysis, lipolysis, the breathing of tissue, the synthesis of proteins and acetylcholine. Potassium ions are also believed to function in regulating blood pressure.

Potassium and sodium share the position of the seventh most abundant element. Common minerals such as alums, feldspars and micas are rich in potassium. The largest potassium chloride deposit is in Saskatchewan, Canada while the largest deposit of the double salt, $\text{KCl} \cdot \text{MgCl}_2 \cdot 6\text{H}_2\text{O}$ is in Solikamsk, Russia. Potassium metal, a powerful reducing agent, does not occur in nature.

52.2 Properties

Physical Properties. Potassium, a soft, low density, silver-colored metal, has high thermal and electrical conductivities, and a very low ionization energy. One very useful physical property of potassium is that it forms liquid alloys with other alkali metals such as Na, Rb, and Cs. These alloys have very low vapor pressures and melting points.

Potassium has three naturally occurring isotopes: ^{39}K (93.22%), ^{40}K (0.01%) and ^{41}K (6.77%). The radioactive decay of ^{40}K to Argon (^{40}Ar), half-life of 1.25×10^9 years, makes it a useful tool for geological dating.

Some physical properties of potassium are summarized below [1-3]:

Atomic weight	39.102
Atomic radius	0.235 nm

Ionic radius	0.133 nm
Pauling electronegativity	0.8
Crystal lattice	body-centered cubic
Analytical spectral line	766.4 nm
Melting point	63.7 °C
Boiling point	760 °C
Density at 20 °C	0.76 g·cm ⁻³
Specific heat	0.741 J g ⁻¹ K ⁻¹
Heat of fusion	59.591 J/g
Heat of vaporization	2.075 kJ/g
Electrical conductance at 20 °C	0.23 μs
Surface tension at 100 °C	86 mN/m (dyn/cm)
Thermal conductivity at 200 °C	44.77 W m ⁻¹ K ⁻¹

Chemical Properties. Potassium has an electron-configuration of $1s^2 2s^2 2p^6 3s^2 3p^6 4s^1$. All alkali-metals (Li, Na, K, Rb, Cs) are good reducing agents. They have a strong tendency to attain inert-gas electron configuration by giving away the single, unpaired valence electron. Reducing power increases from lithium to cesium. The alkali metals share many common features, yet they differ in size, atomic number, ionization potential, and solvation energy. As a result, each maintains its own individual chemical characteristics.

Cesium and rubidium are too reactive for safe handling and are not commercially available in large quantities. Potassium is the most electropositive reducing agent used in industry. Among K, Na and Li compounds, potassium compounds are more ionic and more nucleophilic. Potassium ions form loose or solvent-separated ion-pairs with their counteranions in polar solvents. Large potassium cations tend to stabilize delocalized (soft) anions in transition-states. In contrast, lithium compounds are more covalent, more soluble in non-polar solvents, and usually existing as aggregates (tetramers and hexamers) in the form of tight ion pairs. Small lithium cations stabilize localized (hard) counteranions. Sodium chemistry is intermediate between that of potassium and lithium.

The superb reducing power of potassium metal is clearly demonstrated by its facile displacement of protons in the weakly acidic hydrocarbons, amines, and alcohols (Table 52.1) and reactions with inorganics and gaseous ele-

ments (Table 52.2). In addition, oxides, hydroxides and salts of numerous metals are reduced by potassium to the metallic state.

Table 52.1: Potassium products from hydrocarbons, amines and alcohols.

Starting material	pK _a [*]	Product
1,3-Diaminopropane	35	$\text{KNH}(\text{CH}_2)_3\text{NH}_2$
Ammonia	35	KNH_2
Hexamethyldisilazane	28	$\text{KN}[\text{Si}(\text{CH}_3)_3]_2$
Aniline	27	KNHC_6H_5
Acetylene	25	$\text{KC}\equiv\text{CH}$
tert-Butanol	18	$\text{KOC}(\text{CH}_3)_3$
Methanol	16	KOCH_3
Phenol	10	KOC_6H_5

*pK_a refers to the pK_a of the conjugate acid of the potassium base.

Table 52.2: Typical chemical reactions of potassium.

Reactant	Reaction	Product
H ₂	begins slowly at 200 °C, rapid above 300 °C	KH
O ₂	begins slowly with solid, fairly rapid with liquid	K ₂ O, K ₂ O ₂ , KO ₂
H ₂ O	extremely vigorous and frequently results in hydrogen-air explosions	KOH, H ₂
C (graphite)	150-400 °C	KC ₂ , KC ₈ , KC ₃₆
CO	forms unstable carbonyls	(KCO)
NH ₃	dissolves as K; iron, nickel, and other nmetals catalyze in gas and liquid phase	KNH ₂
S	molten state in liquid ammonia	K ₂ S, K ₂ S ₂ , K ₂ S ₄
F ₂ , Cl ₂ , Br ₂	violent to explosive	KF, KCl, KBr
I ₂	ignition	KI
CO ₂	readily, but sometimes explosive	CO, C, K ₂ CO ₃

52.3 History

Before the discovery and exploitation of potassium salt deposits, the production of potassium compounds consisted almost entirely of potash (K_2CO_3) obtained from natural sources such as wood ash, residues from distilleries, Bengal saltpeter, wool grease, and mother liquors from sea salt production. Quantities were small and were used only for the production of soap, glass, and explosives.

In 1840, J. von LEBIG laid the foundations of the theory of mineral fertilizers in his paper "The Application of Organic Chemistry to

Agriculture and Physiology". This spread the knowledge that potassium was one of the most important plant nutrition elements. In 1851, some deep mine workings in Stassfurt struck minerals containing potassium and magnesium, although these could not be used as fertilizers. In 1861, ADOLPH FRANK started the first plant using the process that he developed for producing from carnallite a potassium salt that could be employed as a fertilizer. This soon led to the development of other processes and to the establishment of many potash mines and works. Many attempts were made up to the end of World War I to hinder the building of new factories in Germany, which had a world monopoly in the production of potash fertilizers, and attempts were made to ration production and supply, and to regulate prices. In spite of this, 69 factories were in existence in 1910, and 198 in 1918. When World War I ended, Alsace was returned to France, and the potash works that were built there shortly after 1900 became French property, so that Germany lost her monopoly in potash.

The German national assembly of 1919 enacted the potash regulations and the so-called closure order, which reduced the number of operating factories to 29 by the year 1938. This also caused production to be concentrated in a few large potash companies [95, 96].

After the end of World War II, ca. 60% of German production capacity went to the area that was later to become the German Democratic Republic, and became the VEB Kombinat Kali. After German unification in 1990, the newly formed Mitteldeutsche Kali AG took over these operations. In West Germany, several groups of works were formed, leading in 1970 to the formation of the company Kali und Salz AG following a series of amalgamations. This company owns seven potash works, all located in the former Federal Republic of Germany [97, 98].

Most of the French potash works in Alsace were nationalized after World War I. During World War II, production was greatly increased. Several of the deposits have now become exhausted, and many of the works have

been closed. Production has been concentrated in two large works, although these are likely to be closed down soon after the end of this century [99].

Potash production in Spain began in 1926 with the start up of a factory in Catalonia. Other factories were established later both there and in Navarra.

The kainite deposits in Sicily have been worked since 1959–1960; the salts are used for potassium sulfate production [100].

The Soviet Union began potash production in 1931 at a plant in the Northern Urals. In 1939, plants that had been operating in Eastern Poland since 1920 were taken over by the Soviet Union. In 1963, the first plant was started to exploit a very extensive deposit in White Russia. The CIS today has several large operations in the Urals and White Russia, giving it the largest capacity of all potash-producing countries.

In the United States, potash production began during World War I because the United States economy could no longer buy German potash fertilizers. Potassium salts were obtained from Searles Lake in California and in northern Nebraska. Most of these operations ceased production in the 1920s. After the discovery of potash deposits in the area of Carlsbad, New Mexico, a large number of potash works were founded since 1931 [101]. Since the foundation of the Canadian potash industry, which has the United States as its main outlet, the number of works in the Carlsbad region and their production rate have continually declined. New potash works were started in southern Utah at Moab in 1964 and at the Great Salt Lake in 1970 [102].

The most important potash deposit in North America was discovered during World War II in Saskatchewan, Canada. After initial problems due to its great depth and the presence of water-bearing overlying rock, which was difficult to deal with, several potash works were founded in the early 1960s, and today Canada is second only to the CIS as a potash producer. Two more potash plants were established in the 1980s in New Brunswick on the east coast of Canada.

In 1986, a potash plant began production at Sergipe in Brazil.

In 1974, a potash mine was opened in Yorkshire, United Kingdom.

Potash production in Palestine began on the north bank of the Dead Sea in 1931. Potash plants have now been producing since 1952 at the southern end on the Israeli side and since 1982 on the Jordanian side.

Potash ores are treated today by three basic processes: leaching–crystallization, flotation, and electrostatic treatment. Gravity separation is of minor importance because of the small density differences between salt minerals.

The oldest process is leaching–crystallization. In this process, salt solutions were originally cooled in open vessels. Vacuum cooling of the solutions in crystallizers was introduced in 1918 in the United States, so that much less energy was required and cooling times were reduced from days or weeks to minutes. Flotation was introduced in 1935 in the United States. This proved so efficient, especially for the treatment of sylvinitic ores, that it is now the main potash treatment process worldwide. The electrostatic process was first used on a large scale in the German potash industry in 1974. It is now widely used in Germany for treating complex hard salts.

52.4 Occurrence

Potassium occurs in nature only in the form of its compounds. It is one of the ten most common elements in the earth's crust. Several widely distributed silicate minerals contain potassium, in particular, the feldspars and micas. The weathering of these minerals produces soluble potassium compounds, which are present in seawater and occur in extensive salt deposits. Potassium is important in the metabolism of plants and animals, and is therefore found in ash from plant materials and in the bodies of animals. Potassium compounds are obtained almost entirely by the mining of salt deposits.

52.4.1 Potash Salt Deposits

52.4.1.1 Minerals

Potash salt deposits were formed by the evaporation of seawater [103]. Their composition is often affected by secondary changes in the primary mineral deposits. More than 40 salt minerals are now known, which contain some or all of the small number of cations Na^+ , K^+ , Mg^{2+} , and Ca^{2+} ; the anions Cl^- and SO_4^{2-} ; and occasionally Fe^{2+} and BO_3^{3-} , as well. Most of these are listed in Table 52.3 [104].

The more important salt minerals are halite, anhydrite, sylvite, carnallite, kieserite, polyhalite, langbeinite, and kainite. Gypsum occurs at the edges of salt deposits and in the overlying strata. Bischofite, tachhydrite,

glauconite, thenardite, glaserite, and leonite occur additionally in some deposits [82, 105, 106].

Other minerals, not described in detail here, are useful in elucidating difficult geological questions with regard to the origin of salt deposits. In special geochemical investigations, small amounts (ppm) of Rb^+ and Cs^+ in place of K^+ ; Sr^{2+} replacing Ca^{2+} ; Mn^{2+} replacing Fe^{2+} ; Br^- replacing Cl^- ; etc., are important [107, 108]. The individual minerals can be identified microscopically (grains or thin sections) and by X-ray analysis.

Potassium salt deposits always consist of a combination of several minerals (Table 52.4). The German term *Harzsalz* (hard salt) refers to the greater hardness of sulfate-containing potash minerals in potash deposits.

Table 52.3: Principal salt minerals.

Mineral	Formula	Crystal system/ crystal class	Refractive indices $n_a:n_b:n_c$, or n_{opt} , optical activity	Density, g/cm ³	Hardness (Mohs)
Anhydrite	CaSO_4	rhombic, D_{2h} -mmm	1.570:1.575:1.614, opt. +	2.96	3.8
Ascharite	$\text{Mg}_3[\text{B}_2\text{O}_3] \cdot \text{H}_2\text{O}$	monoclinic, C_{2h} -2/m	1.575:1.646:1.650, opt. –	2.70	3
Astrakhanite	$\text{Na}_2\text{Mg}(\text{SO}_4)_2 \cdot 4\text{H}_2\text{O}$	monoclinic, C_{2h} -2/m	1.483:1.486:1.487, opt. –	2.23	3
Bischofite	$\text{MgCl}_2 \cdot 6\text{H}_2\text{O}$	monoclinic, C_{2h} -2/m	1.495:1.507:1.528, opt. +	1.60	1.5
Boracite (stassfurtite; lumpy form of boracite)	$\text{Mg}_3[\text{Cl}/\text{B}, \text{O}_{13}]$	rhombic, C_{2v} -mm 2	1.662:1.667:1.673, opt. +	2.95	7
Carnallite	$\text{KMgCl}_3 \cdot 6\text{H}_2\text{O}$	rhombic, D_{2h} -mmm	1.467:1.475:1.495, opt. +	1.60	2.7
D'Ansire	$\text{Na}_2\text{Mg}[\text{Cl}_3(\text{SO}_4)_{10}]$	cubic, T_d -43 m	1.489	2.65	
Epsomite	$\text{MgSO}_4 \cdot 7\text{H}_2\text{O}$	rhombic, D_2 -222	1.432:1.455:1.461, opt. –	1.68	2.5
Glaserite	$\text{K}_2\text{Na}(\text{SO}_4)_2$	trigonal, D_{3d} -3 m	1.491:1.498, opt. +		
Glauconite	$\text{CaNa}_2(\text{SO}_4)_2$	monoclinic, C_{2h} -2/m	1.515:1.532:1.536, opt. –	2.85	3
Gypsum	$\text{CaSO}_4 \cdot 2\text{H}_2\text{O}$	monoclinic, C_{2h} -2/m	1.521:1.523:1.530, opt. +	2.32	2
Halite (rock salt)	NaCl	cubic, O_h -m3m	1.5443	2.168	2.5
Kainite	$(\text{KMg}(\text{ClSO}_4))_4 \cdot 11\text{H}_2\text{O}$	monoclinic, C_{2h} -2/m	1.494:1.506:1.516, opt. –	2.13	3
Kieserite	$\text{MgSO}_4 \cdot \text{H}_2\text{O}$	monoclinic, C_{2h} -2/m	1.518:1.531:1.583, opt. +	2.57	3.7
Koenerite	$[\text{Mg}_2\text{Al}_4(\text{OH})_{23}][\text{Na}_4(\text{CaMg})_2\text{Cl}_{12}]$	trigonal, D_{3d} -3 m	1.55:1.58, opt. +	2.15	1
Langbeinite	$\text{K}_2\text{Mg}_2(\text{SO}_4)_3$	cubic, T -23	1.534	2.83	4.2
Leonite	$\text{K}_2\text{Mg}(\text{SO}_4)_2 \cdot 4\text{H}_2\text{O}$	monoclinic, C_{2h} -2/m	1.479:1.483:1.488, opt. +	2.20	2.7
Löweite	$\text{Na}_{12}\text{Mg}_7(\text{SO}_4)_{13} \cdot 15\text{H}_2\text{O}$	trigonal, C_{3i} -3	1.495:1.478, opt. –	2.34	2.5–3
Mirabilite (Glauber's salt)	$\text{Na}_2\text{SO}_4 \cdot 10\text{H}_2\text{O}$	monoclinic, C_{2h} -2/m	1.394:1.396:1.398, opt. –	1.49	1.7
Polyhalite	$\text{K}_2\text{MgCa}_2(\text{SO}_4)_4 \cdot 2\text{H}_2\text{O}$	triclinic, C_1 -1	1.548:1.562:1.567, opt. –	2.78	3–3.6
Rinneite	$\text{K}_2\text{Na}(\text{FeCl}_4)$	trigonal, D_{3d} -3 m	1.588:1.589, opt. +	2.35	3
Schönite	$\text{K}_2\text{Mg}(\text{SO}_4)_2 \cdot 6\text{H}_2\text{O}$	monoclinic, C_{2h} -2/m	1.461:1.463:1.476, opt. +	2.03	2.6
Sylvite	KCl	cubic, O_h -m3m	1.4903	1.99	2
Syngenite	$\text{K}_2\text{Ca}(\text{SO}_4)_2 \cdot \text{H}_2\text{O}$	monoclinic, C_{2h} -2/m	1.501:1.517:1.518, opt. –	2.58	2.5
Tachhydrite	$\text{CaMgCl}_6 \cdot 12\text{H}_2\text{O}$	trigonal, D_{3d} -3 m	1.520:1.512, opt. –	1.67	2
Thenardite	Na_2SO_4	rhombic, D_{2h} -mmm	1.471:1.477:1.484, opt. +	2.67	2.7
Vanthoffite	$\text{Na}_2\text{Mg}(\text{SO}_4)_2$	monoclinic, C_{2h} -2/m	1.485:1.4876:1.489, opt. –	2.69	3.6

Table 52.4: Marine salt rocks: mineral constituents (A = anhydrite; Bi = bischofite; C = carnallite; Dol = dolomite; Kai = kainite; Ki = kieserite; La = langbeinite; Mag = magnesite; Na = halite; Po = polyhalite; Sy = sylvite; Ta = tachhydrite).

Salt rock	Main components	Secondary components
Rock salt	Na	A, Po, Ki, La, clay minerals, etc.
Anhydrite	A	Na, Dol, Mag, gypsum, Sy, C, clay minerals, borates
Carnallite	C, Na	Ki, Sy, A
Sylvinite	Sy, Na	C, Ki, A
Hard salt		
Kieserite	Na, Ki, Sy	C, A, La, Po, borates
Langbeinite	Na, La	Ki, A, Sy, C
Anhydritic	Na, Sy, A	Ki, C
Kainite	Na, Kai	Ki, Sy, C
Bischofite	Bi, C and/or Ta	Na, Ki, Po, A, borates
Tachhydrite	Ta, Bi	C, Na
Claystone	Clay minerals, quartz, mica, A, Dol, Mag	Na, Sy, C, Bi, Ta, La, coccaenite, rinneite

52.4.1.2 Geology of Potash Deposits

Potash deposits occur worldwide in almost all geological systems. The most important deposits were formed in the Devonian, Carboniferous, Permian, Cretaceous, and Tertiary periods [82, 103, 105, 109–115]. All major potash deposits are of marine origin. Bodies of seawater became isolated from the open ocean when bars formed under the water surface, and under arid climatic conditions, the seawater became concentrated, finally depositing the dissolved salts. The important feature is that exchange between normal seawater and concentrated salt solution generally does not occur. During sedimentation, the less soluble salts were deposited first, and the most soluble salts last. In most salt-forming sea basins, this process was repeated many times, resulting in cyclical salt formation [114, 116].

A complete salt deposition cycle begins with basic carbonates (limestone, dolomite, and sometimes magnesite), followed by sulfates (gypsum and anhydrite), rock salt, and finally potassium and magnesium salts (Table 52.3). Intermediate layers of clay sediments are the result of repeated influxes of fresh water, which can lead to partial redissolution of

the salt deposits. Also, eolian (airborne) transportation into the basin can occur. A recent example of a salt deposition basin is provided by the Kara-Bugas, a lagoon on the eastern side of the Caspian Sea.

In the course of the earth's history, the deposited salts underwent many changes, often leading to the formation of a modified mineral constitution. The original formations were affected by relatively low-temperature thermal and hydraulic metamorphoses, and sometimes by volcanic action, producing the mineral compositions that exist today (Table 52.4) [117, 118].

Rock movements have changed the original horizontal stratification in many salt deposits. Salt migration, folding, and upward movement to form diapirs have led to tilting of the potash layer, sometimes to an acute angle; to thinning; or to local accumulation. As a result of movements, salt deposits often came into contact with groundwater and were partially or completely redissolved.

Table 52.5 shows the distribution of potash deposits, with estimates of the reserves [82, 115, 119].

The concept of a reserve presupposes the possibility of economical extraction, which depends on the presence of a useful potash content together with usable quantities of other materials. Other important factors are the type of deposit, a uniform and usable seam thickness at a depth that is neither too great nor too low (water problems), economic workability, the possibility of solution extraction, and above all, proximity to consumers and profitability. Losses incurred during the extraction process (10–20%) must be deducted from the total size of the reserve.

The two largest known potash deposits in the world, which are in Saskatchewan (Canada) and White Russia, are of Devonian origin. The Permian deposits (Germany, United States, and CIS) were for a long period the classical salt deposits and were the most important potash reserves, but these lost their economic importance after World War II.

Table 52.5: Mineable potash reserves in units of 10^6 t K_2O .

Canada, Saskatchewan (conventional mining only)	4500–6000
New Brunswick	60–80
United States	100–150
Brazil	10–40
Chile and Peru	30–50
Congo	ca. 20
Germany	400–800
United Kingdom	30–50
Italy	10–20
France	ca. 20
Spain	20–30
Commonwealth of Independent States	2000–3000
Dead Sea (Israel and Jordan)	100–200
China	10–100
Thailand	up to 160
Laos	up to 20
World ^a	7500–10 000

^aIf reserves only extractable by solution mining are included (particularly those in Saskatchewan, but also including those in the CIS), the figure for the total mineable reserves increases by a factor of 4 or 5. Other deposits of potash salts are either unimportant or of minor local importance compared with the above figures. These exist in Australia, Ethiopia, Iran, Libya, Morocco, Poland, and Tunisia.

However, the known potential of extractable potash deposits is so large that the world supply is guaranteed for many hundreds of years.

Salt Lakes and Subterranean Brines. *Israel and Jordan.* Potassium chloride, magnesium chloride, rock salt, soda, chlorine, and bromine are obtained from the Dead Sea [82, 115].

United States. Potassium and sodium sulfate are extracted from the Great Salt Lake [82, 115]. Potassium and magnesium chloride are obtained from subterranean brines from the Great Salt Lake Desert [82]. Potassium chloride and sulfate, sodium borate, and boric acid are obtained from subterranean brines in Searles Lake [82, 115].

Australia. Langbeinite is obtained from subterranean brines at Lake McLeod.

China. Tsaerhan Lake, a dry lake, ca. 1100 km northeast of Lhasa, the largest salt lake in the Chaidamu basin, appears to be the most important potential reserve of potassium chloride in China [82, 115].

52.4.2 Mining of Potash Salts

52.4.2.1 Shaft Mining

Mineral salts are very soluble, and therefore any flow of water into the mine from the overlying strata, which are normally water bearing, must be prevented. This causes difficulties when sinking a shaft, and severe accidents have been caused by influxes of water. The freezing technique, especially deep freezing, is comparatively safe and is currently used to sink most mineshafts. The shaft itself is protected from water-bearing rocks by the use of tubings, which are segments bolted together to form rings and are usually made from cast iron or steel-reinforced concrete. The shafts generally have a diameter of 5–7 m, and the depth can exceed 1000 m.

52.4.2.2 Extraction, Conveying, and Haulage

In most potash mines, the salt is mined from subhorizontal deposits. Generally, rooms are created by removing the salt, and pillars are left between these to prevent the cover rocks from collapsing. This enables an extraction rate of 25–60% to be achieved. For cost reasons the mined-out rooms are not backfilled. In some mines, the total ore is extracted, which causes substantial subsidence of the overlying strata (Alsace).

In steeply dipping deposits (e.g., in the salt domes of northern Germany), roof mining was originally carried out. This was later replaced by floor mining and then by funnel mining, which is now being used increasingly in numerous variations [121]. Entry drifts are driven one above the other at intervals of 15–20 m, and the remaining potash salt is mined by sublevel stopping. Material loosened by explosives falls via the lowest funnel-shaped region into the main haulage level underneath. The mined-out room, 100–250 m in height, is usually backfilled with salt waste after mining. Funnel mining is much safer and cheaper than roof mining, because both ore stopping and backfilling take place under gravity, and

the mined room need not be reentered. During drilling of the blast holes, the miners are protected by horizontal pillars between the sub-levels.

Drilling and blasting operations are carried out with the help of trackless vehicles. Large holes with a diameter of ca. 40 cm and a length of 7 m are drilled by mobile drilling equipment, and another mobile drilling rig is used to drill blast holes around the larger hole in a predetermined pattern. The explosive (generally ammonium nitrate with addition of oil) is brought to the workplace in tanks carried by diesel vehicles and is blown into the shot holes by compressed air.

In predominantly horizontal sylvinitic deposits, the most frequent method of extraction is by cutting with heavy machinery (180 t per unit) at high cutting rates. These machines produce material suitable for transport by conveyor belt, enabling continuous extraction in 30–60-m sections.

Extraction by borers with two to four rotors is mainly used to produce long pillars in a room and pillar system (Canada), the length of the chambers being as much as 1000 m. In longwall mining, however, which is usually carried out as a caving operation, two or three drum shearers are used (e.g., in Alsace and the CIS). These machines enable daily outputs between 1500 and 4000 t to be achieved.

The recovered material is transported by trackless diesel or cable-fed electric front-end loaders with a capacity of 15 t. Transport along underground roads is increasingly by conveyor belts but also by electric or diesel trains with 30-t-capacity wagons or by dumper trucks with a hopper capacity of 40 t. For transportation by conveyor belt, the material must first be broken into suitably sized pieces.

The network of roadways for conveying, traveling, and ventilation usually extends > 100 km in large potash works. A radio communication system is generally used.

Since the introduction of very heavy machinery and diesel-powered vehicles, extra attention must be given to ventilation. Powerful fans supply fresh air at up to 30 000 m³/min.

In hoisting shafts, the skips have a capacity of up to 25 t. These operate automatically and supply large intermediate storage bins in the filling station, so that the continuously operating manufacturing plants can be supplied with ore at a steady rate. Average daily throughput can be ca. 30 000 t of ore.

Improvements in mining methods and the introduction of new techniques have enabled the output per worker underground to be increased considerably. In Germany during 1965–1974 the output of potash ore increased by 20%, despite a > 50% reduction in the number of employees.

52.4.2.3 Solution Mining

Solution mining is an alternative to conventional mining for the extraction of potash ore. The advantages of this method are that the high expense of sinking a shaft is eliminated and reserves can be exploited where conventional mining is impossible (e.g., at great depth). Also, this method can be used where existing mine workings are available but conventional mining methods are no longer feasible, even though extensive reserves may still exist.

Since 1964, Kalium Chemicals in Saskatchewan has operated a plant in which brine extracted from a potash deposit at a depth of ca. 1500 m is used to produce very pure potassium chloride. The process is based on a series of patents [122], but details have not yet been published. Water or an unsaturated solution of potassium chloride is passed through a system of boreholes into the potash seam, which is 20–25 m thick; potassium chloride and sodium chloride are dissolved. The almost saturated solution is pumped to the surface and fed to the production plant. Rock salt above the potash seam is protected from dissolution by an oil or air cushion (see Figure 52.1). The brine produced passes through multiple-effect evaporators in which sodium chloride crystallizes. Potassium chloride is then crystallized in a series of vacuum coolers [123].

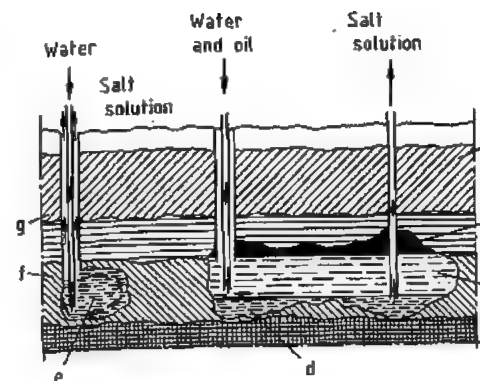


Figure 52.1: Solution mining: a) Overlying rock; b) Oil cushion; c) Partly unsaturated salt solution; d) Saturated salt solution; e) Cavity produced by dissolution; f) Potash deposit; g) Sodium chloride layer.

In Utah (United States), where it was necessary to terminate a conventional mining operation due to severe geological and technological problems, operation was resumed in 1972 by using solution mining. Shafts and underground cavities were flooded, providing a route for the brine formed when water was fed in to dissolve the salt. The brine was passed into surface ponds where solar evaporation caused a mixture of potassium chloride and sodium chloride to crystallize, which was treated in a flotation plant to produce 60% K₂O potassium chloride [124].

In Canada a conventional mining operation was also converted to the solution mining method after penetration of water led to complete flooding of the mine and forced operations to cease. Water is passed via boreholes into the flooded mine and is converted into a concentrated brine, which is withdrawn and cooled in a pond during the very cold Canadian winter. The potassium chloride that crystallizes is recovered and processed to give a salable product [125].

In the former German Democratic Republic, extensive research into the solution mining of carnallite or potassium chloride from carnallitic deposits has been carried out. An experimental plant with a KCl capacity of ca. 50 000 t/a was operated for a long period [126].

52.4.3 Treatment of Potash Ores

52.4.3.1 Intergrowth and Degree of Liberation [127, 128]

The salt minerals in potash ores are intergrown to varying extents. Before the minerals can be separated and the useful components recovered, the ore must be sufficiently reduced in size so that individual components are accessible to the processing method to be used. In the hot leaching process, sylvite is extracted, and therefore it must first be liberated (i.e., it must not be occluded inside other minerals). To achieve this, it is sufficient to break down the ore to a particle size of 4–5 mm or less.

For the mechanical treatment processes (i.e., flotation, electrostatic treatment, and gravity separation), liberation of the minerals must be complete (i.e., individual grains must consist as much as possible of pure minerals). The extent to which the minerals in the potash ore are intergrown can vary greatly from deposit to deposit (see Figure 52.2), which means that the crude salt must be size-reduced to varying degrees before further processing.

The degree of intergrowth of individual minerals can be determined by examination of a thin section. A photomicrograph shows the sizes and shapes of individual minerals in relation to each other [129]. The disadvantage of this method is that a thin section gives only a two-dimensional view of a relatively small region of the salt mineral, and a very small sample of the substance is examined. The three-dimensional arrangement of minerals present and their distribution are not observed. For these reasons, and also because of the high cost of preparing thin sections, this method is now of only minor importance for the industrial processing of potash ores.

More usually, the degree of liberation in size-reduced samples is determined. The degree of liberation of a mineral means the percentage ratio of fully liberated mineral particles to the total content of the mineral in the sample.

liberated, nonintergrown fraction of useful mineral in each grain size range must be determined. Two methods for doing this are possible:

- Visual estimation (by counting under the microscope) of the proportion of intergrown particles
- Heavy-medium separation of the free or almost free grains

The first method is easy to apply to salt minerals because the intergrowth effects are readily recognized owing to the transparency of the grains. For coarse-grained materials such as those usually found in ground products from coarsely intergrown potash ores, this process cannot be used.

The separation of free or nearly free mineral grains from a size fraction is carried out by using heavy liquids of appropriate density, such as tetrabromoethane-toluene mixtures. A float-sink separation is carried out to determine the fraction of free mineral grains. This method cannot be used for salt particles with a grain size < 0.5 mm because of the agglomeration of fine grains. In this case, the method of counting under the microscope must be used, or the degrees of liberation of the coarser size ranges must be extrapolated.

The results are expressed in liberation curves, which give the degree of liberation as a function of grain size (Figure 52.3).

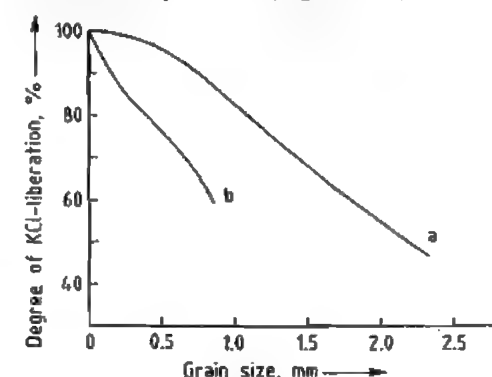


Figure 52.3: Liberation curves of sylvinite ores: a) Coarsely intergrown sylvinite ore (from New Brunswick, Canada); b) Finely intergrown sylvinite ore (from a north German salt deposit).

Figure 52.2: Thin sections of sylvinite ores. A) Coarsely intergrown (potash works in Lanigan, Canada); B) Finely intergrown (Kaliwerk Sigmundshall, Germany).

Degree of liberation:

$$\frac{\% \text{ Free mineral}}{\% \text{ Free} + \% \text{ Intergrown mineral}} \times 100\%$$

The degree of liberation L depends not only on the grain size achieved by the grinding operation but also on the type of grinding. It can be given for particular ranges of grain size so that the way in which it depends on grain size can be determined, or it can be expressed as an average for the total sample (the integral degree of liberation \bar{L}). The arithmetic mean of the degree of liberation of each range of grain sizes is obtained from the following formula:

$$\bar{L} = \frac{\sum_{i=1}^n L_i p_i a_i}{100a}$$

where p_i is the mass fraction of the i th size range in percent; a_i the percentage of useful mineral in the i th size range; and a the percentage of useful mineral in the total sample. Apart from the fraction of useful mineral a , which is determined by chemical analysis, the

52.4.3.2 Grinding [130, 131]

Potash salts are easily size-reduced. Therefore, fines may be formed, which can cause problems in later stages of processing. Great care must be taken in selection of the equipment for various stages of grinding.

The maximum grain size to which the potash ore is ground depends on the processing method used and the degree of intergrowth of the ore. For the hot leaching process, an upper grain size limit of 4–5 mm is adequate. For mechanical processing, the ore must be ground to a degree of liberation > 75%. For German sylvinite ores and hard salts, this is achieved by grinding to a maximum grain size of 0.8–1.0 mm. For the much coarser sylvinite ores of New Mexico, a maximum grain size limit of 2.4 mm is sufficient. The sylvinite ores of Saskatchewan are even more coarsely intergrown, so that size reduction to < 9 mm would give adequate liberation. However, such large crystals cannot be treated by conventional flotation, and the material is therefore normally ground to < 2.3 mm. One large Canadian manufacturer produces a coarse crystalline product by grinding the potash ore to < 9 mm, removing grains < 1.7 mm, and treating this fine material by conventional flotation. The remaining fraction (1.7–9 mm) is treated in a heavy-medium separation plant (see Section 52.11.5), giving a product with 60% K_2O (95% KCl) and a size distribution of the granular commercial grade.

The preliminary size reduction of potash ore is carried out by underground mobile crushers, usually in the vicinity of a mining operation. When the ore is mined by continuous mining this gives sufficient size reduction for it to go directly to the haulage line. Further size reduction to the grain size required for processing is carried out in two stages on the surface. An initial size reduction with impact or hammer mills is always carried out to produce 4–12-mm particles, depending on the raw material and processing method to be used. A coarse grinding plant usually includes two grinding and screening stages (Figure 52.4).

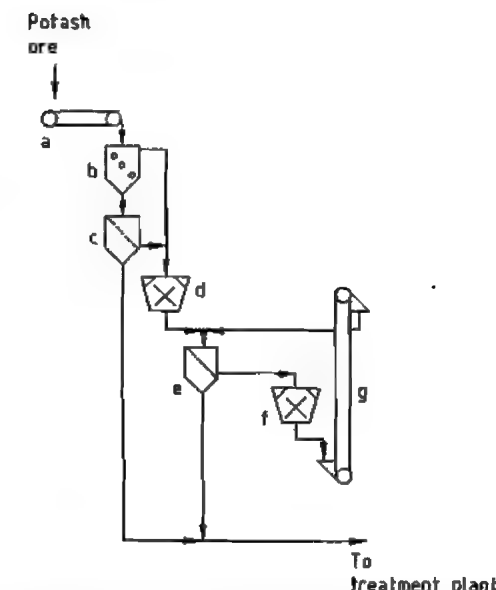


Figure 52.4: Two-stage grinding system: a) Conveyor belt; b) Grid; c) First screening stage; d) First grinding stage; e) Second screening stage; f) Second grinding stage; g) Bucket elevator.

The final fine grinding stage is carried out either by wet grinding in rod mills or by dry grinding with rollers or impact crushers (Figures 52.5 and 52.6). Wet grinding with rod mills in a recirculating system with classification is standard for most flotation plants. Classification is by spiral classifiers, vibrating screens, curved screens, or cyclones. Wet screening produces only a small amount of fines and has the further advantage of providing a scrubbing effect that facilitates the removal of clay from clay-bearing ores, a necessary step before the flotation process.

The production of a fine product by dry grinding is rarely used in flotation plants. It is indispensable as a preparation for electrostatic processing, which is not compatible either with the changes to the mineral surfaces caused by aqueous solutions or with excess moisture. The grinding operation must be carried out carefully to give a product low in fines. Roller mills and impact mills can be used. Roller mills have the disadvantage that throughputs are relatively low and maintenance costs are high. Although this was the

preferred method in the early days of electrostatic processing owing to its gentle grinding action, it has now been largely replaced by impact grinding, which is also used for size reduction of the middle product from electrostatic separation [132].

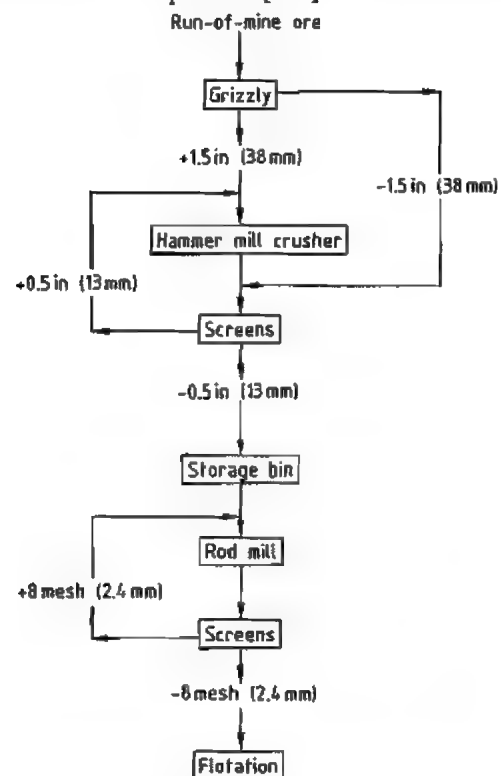


Figure 52.5: Wet grinding and screening of coarsely intergrown potash ore for flotation [83]. Reprinted with permission of the Society for Mining, Metallurgy, and Exploration, Inc.

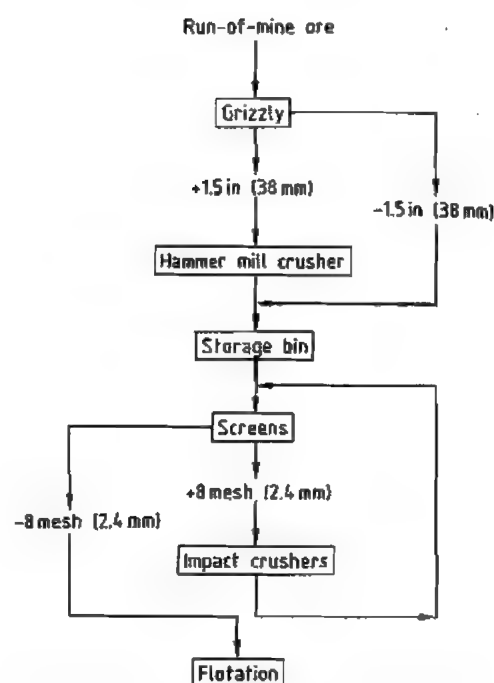


Figure 52.6: Dry grinding and screening of coarsely intergrown potash ore for flotation [83]. Reprinted with permission of the Society for Mining, Metallurgy, and Exploration, Inc.

52.4.4 Potash-Magnesia

Crops sensitive to chloride can be fertilized with potassium sulfate alone or by fertilizers containing the sulfates of potassium and magnesium. These consist either of a mixture of the two sulfates or of the double sulfates schönite, leonite, or langbeinite in dehydrated form.

Formerly, large quantities of a mixture of fine-grained potassium sulfate and kieserite were marketed under the name potash-magnesia (K_2O : 27–30%, MgO : 9–12%). This has since been almost completely replaced by a granulated potash magnesia fertilizer, which is produced by first mixing potassium sulfate and kieserite at 95 °C with hot synthetic langbeinite. The hot mixture is granulated in a drum granulator, and the product is quickly cooled to < 60 °C. It contains 29–30% K_2O and 10% MgO .

Langbeinite from the potash deposits in Carlsbad, New Mexico (United States), can be used in the pure state directly as a potash magnesia fertilizer. Crude langbeinite also contains halite and varying amounts of sylvite, and the method of purification utilizes the low rate of dissolution of langbeinite in water. If the sylvite content is low, the potash ore is first ground to < 6 mm and then simply washed with water to dissolve the halite. The langbeinite that remains is dried and screened to obtain the commercial size gradings. For higher sylvite content, an additional stage is required to separate the components by a combination of gravity separation and flotation. The langbeinite produced has a K_2O content of 20–22% and an MgO content of 18–19%, and is marketed as Sulpomag or K-Mag.

52.4.5 Production of Potassium Salts from Other Raw Materials

Potassium salts occur not only in salt deposits, but also in solution in many types of inland lakes and in seawater. Where the concentration of the salt solution is high enough and the climatic and topographical conditions are suitable, potassium chloride or potassium sulfate can be produced by solar evaporation. Typical analyses of some of the more important sources are listed in Table 52.6.

Table 52.6: Composition of some natural brines compared with seawater (in %).

	Dead Sea	Wendover brine	Great Salt Lake	Seawater
K^+	0.6	0.6	0.7	0.04
Na^+	2.9	9.4	7.6	1.08
Mg^{2+}	3.4	0.4	1.1	0.13
Ca^{2+}	1.3		0.016	0.04
Cl^-	17.0	16.0	14.1	1.94
SO_4^{2-}	0.04	0.2	2.0	0.27
Br^-	0.5		0.01	0.006
H_2O	74.3	73.3	74.5	96.5

52.4.5.1 The Dead Sea

Potash production by solar evaporation began at the northern end of the Dead Sea in 1931. Later, production switched to the south-

ern end but was interrupted by the war of 1947–1948. In 1952, potash production was resumed in Sodom by the Israeli State *Dead Sea Works*. The capacity was built up in several stages and now amounts to $> 2 \times 10^6$ t of potassium chloride in all the usual commercial grades [260, 261].

Brine from the lake is concentrated in evaporation ponds with a total area of ca. 90 km², from which the crystallized salts are recovered. Most of the dissolved sodium chloride separates out first in the primary evaporation ponds. A mixture of carnallite and sodium chloride then crystallizes in the main production ponds. This is removed as a suspension by suction dredgers and pumped to the works where the crystals are filtered off and treated by the carnallite cold decomposition process. Most of the resulting NaCl–KCl mixture is then treated in a hot leaching plant, where potassium chloride with > 60% K_2O is produced in crystallizers. Part of the crop of crystals from the main production ponds is treated by a cold crystallization process developed by the Dead Sea Works. This decomposition process directly yields a product containing > 60% K_2O .

A potash works was started by the *Arab Potash Co.* in 1982 on the southeast bank of the Dead Sea near Safi, Jordan. Evaporation and carnallite production are carried out in a pond system with a total area of 100 km². The process resembles that of the Dead Sea Works. Magnesium chloride is removed from carnallite in a cold decomposition process, and the salt mixture formed is then treated in a hot leaching plant to give potassium chloride [260, 262].

52.4.5.2 The Great Salt Lake [263]

The Great Salt Lake is the result of the shrinkage by evaporation of the former Lake Bonneville and lies in the eastern part of the basin. It has a high salt content and is the reason for the existence of several plants that produce sodium chloride and, since 1968, potassium salts.

At the western end of the Great Salt Lake, in the Great Salt Lake Desert near Wendover, are the Bonneville Salt Flats. Here, under a salt crust, are porous sediments containing brines, which are regenerated by water from atmospheric precipitation. Potassium chloride has been produced from these brines since 1937. They are collected by a system of ditches and evaporated in ponds. A mixture of potassium and sodium chloride crystallizes, from which potassium chloride is obtained by flotation [264].

Unlike the Wendover brines, the Great Salt Lake brines contain considerable amounts of sulfate (see Table 52.6). The process used in Wendover cannot therefore be used here. The opportunity exists of obtaining substantial quantities of valuable potassium sulfate rather than potassium chloride, which has been carried out since 1970 in the Great Salt Lake Minerals & Chemicals Corporation (GSLM & CC) plant at Ogden on the east bank. Sodium chloride is first crystallized in the 56-km² pond system until the solution is saturated in potassium salts. Further solar evaporation then takes place in the main production ponds, producing a mixture containing varying proportions of kainite, carnallite, and schönite, with small amounts of sodium chloride [265]. This mixture is converted into schönite in the plant by treatment with recycled process brine. The sodium chloride that is not dissolved by this reaction must be removed before further treatment. This is carried out by flotation of a side stream [180]. Schönite is then decomposed by water, which produces very pure potassium sulfate. The brine from this decomposition stage has a high potassium content and is recycled to the first stage of the process. The brine produced by the reaction at this stage is recycled to the evaporation pond. The sulfate content of the main crop of crystals is higher than the potassium content, so that further potassium sulfate can be produced by addition of potassium chloride from an external source [266].

The level of the Great Salt Lake increased so much during the 1970s and 1980s that the pond system of the Great Salt Lake Minerals

& Chemicals Corporation (GSLM & CC) overflowed during 1984, and production had to stop [267]. The lake level then fell, the pond system was reinstated, and production started again in 1989.

52.4.5.3 Searles Lake [268]

In Trona, on the northwest bank of the almost dry Searles Lake, brines are obtained that contain not only sodium and potassium chlorides, but also considerable quantities of sulfate, carbonate, and borate ions. Recycled process brines are first added, and evaporation produces sodium chloride and the double salt burkeite, Na₂CO₃·3Na₂SO₄. Potassium chloride is obtained by vacuum cooling of the potassium- and borate-containing mother liquor. Part of the chloride is reacted with part of the burkeite to form glaserite, Na₂SO₄·3K₂SO₄, an intermediate stage in potassium sulfate production. Another reaction used for potassium sulfate production is that of potassium borate in the end brines with sulfuric acid, to form potassium sulfate and boric acid:



52.4.5.4 Other Sources

In addition to the sources mentioned under potassium sulfate, other salt lakes exist whose potassium content would appear to offer the possibility of extracting potassium salts. In 1969 at Lake McLeod in Western Australia, a works produced langbeinite, K₂SO₄·2MgSO₄, for a short period of time but ceased operations for unknown reasons. In China, in the Qinghai Province, potassium chloride production has been carried out for several years at Tsarhan Lake by using solar evaporation. Large increases in production are planned [269].

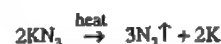
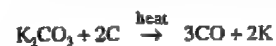
Seawater has a low potassium content (Table 52.6) so that economical extraction of potassium salts is not possible. The production of sea salt by solar evaporation in salt gardens yields residual brines with increased potassium content. In some places (e.g., India), small quantities of low-percentage potassium

salts are produced from these bitters. However, economical production of potash fertilizers of marketable quality is not possible from the amounts of mother liquor available from even the largest sea salt producers.

52.5 Production of the Metal

Potassium was first obtained by H. DAVY in 1807 by electrolysis of potassium hydroxide. Historically, Degussa operated an electrolytic process developed in the 1920s with an electrolyte of 66% KOH, 19% K₂CO₃, and 15% KCl. Later, use was made of a salt mixture (melting point approximately 600 °C) of potassium chloride and potassium fluoride with a few percent of potassium carbonate [4]. Application of the Down's electrolytic sodium process to produce potassium has not been successful.

On the laboratory scale, potassium can be prepared using the following reactions:



However, these reactions are not easily adaptable to a commercial scale.

Currently in industry, chemical reduction is preferred over electrolytic processes for potassium production. Mine Safety Appliances Company (MSA, USA) developed a reduction process using sodium and KCl to produce potassium metal in the 1950s at Callery, Pennsylvania [5].



The technology is based on the rapid equilibrium established between sodium, potassium, potassium chloride and sodium chloride at high temperatures. The equilibrium shifts to the product side when potassium is removed continuously by distillation through a packed column. This process can produce high purity potassium metal. Appropriate adjustments of

conditions give a wide range of potassium-sodium alloys of specified compositions.

The commercial production equipment consists of a furnace, heat-exchanger tubes, a fractionating column packed with Raschig rings, a KCl feed, a waste-removal system, and a vapor-condensing system (see Figure 52.7).

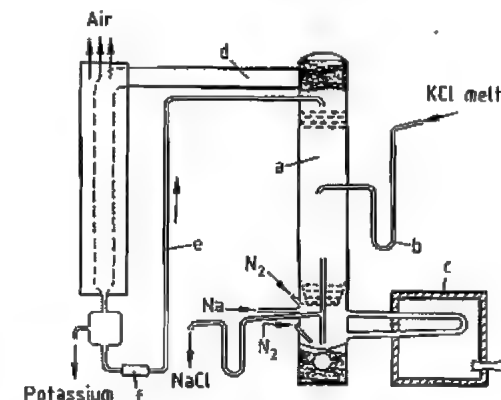


Figure 52.7: Commercial production of potassium: a) Packed column; b) Trap; c) Furnace; d) Condenser; e) Reflux; f) Electromagnetic pump.

During operation, KCl is melted and introduced through a trap to the column. Molten sodium is fed to the bottom of the column. The lower portion of the column serves as a reactor whereas the upper portion is a fractionator. Potassium vapor is fractionated and condensed in an air-cooled condenser with the reflux pumped back to the top of the column. Waste sodium chloride is continuously removed from the bottom of the column through a trap.

52.6 Analytical and Test Methods

The only major impurity in potassium metal is sodium. Potassium's purity can be accurately determined by a melting point test (Figure 52.8) or atomic absorption after quenching with alcohol and water. Traces of nonmetallic impurities such as oxygen, carbon, and hydrogen can be determined by chemical and physical methods [7].

52.7 Economic Aspects

Total U.S. production of potassium is less than 500 metric tons per year. There are few commercial producers worldwide, although some companies produce potassium for their own needs. The more prominent producers are Callery Chemical Company (a division of Mine Safety Appliances Company), USA, and China. Potassium may be manufactured in Russia as well. Strem Chemicals (USA) supplies small quantities in ampoules.

Prices (1996) are as follows:

Bulk potassium	\$40–60/kg
As NaK (78% K)	\$15–30/kg

Potassium up to 99.99% purity can be produced by zone refining or further distillation of commercial potassium. Technical grade potassium (minimum 99% purity) is packaged under nitrogen.

52.8 Health and Safety Factors

Reactions of potassium with water and oxygen are violent to explosive, therefore safe handling is a concern. Potassium oxidizes slowly in air at room temperature, but it usually ignites if molten potassium sprays into the air. The peroxide and superoxide products may explode in contact with free potassium metal or organic materials including hydrocarbons. Thus, packaging under oils is less desirable than packaging with inert cover gas or vacuum because potassium can react with entrapped air in oils to form superoxide. The incrustation of potassium with superoxide (as a yellow crust) developed during storage has been known to detonate by friction from cutting. Potassium incrustated with peroxide and superoxide should be destroyed immediately by careful, controlled disposal [8].

Potassium forms corrosive potassium hydroxide and liberates explosive hydrogen gas upon reaction with water and moist air. Airborne potassium dusts or potassium combustion products attack mucous membranes and skin causing burns and skin cauterization. In-

halation and skin contact must be avoided. Safety goggles, full face-shields, respirators, leather gloves, and fire-resistant clothing and a leather apron are considered minimum safety equipment.

Steam treatment of equipment under nitrogen or argon may be used to destroy potassium residues. It is imperative that equipment be designed to permit substantially complete drainage of potassium metal prior to steam cleaning. Precautions must also be taken to avoid hydrogen–air explosions by using an inert cover gas. Small quantities of the metal can be safely destroyed under nitrogen by adding *tert*-butanol or high boiling alcohols, followed by methanol and then water. The caustic aqueous potassium waste should be disposed of in compliance with local regulations.

Fire Fighting. Potassium metal reacts violently with water releasing flammable, explosive hydrogen gas. Dry soda ash, dry sodium chloride, or Ansul's Met-L-X should be used to extinguish potassium or potassium alloy fires. Water, foam, carbon dioxide or dry chemical fire extinguishers should never be employed. A NIOSH/MSHA approved self-contained breathing apparatus with full facepiece operated in a positive pressure mode and full protective clothing should be worn when removing spills and fighting fire.

Packaging and Shipping. Potassium of 98–99.5% purity is supplied in carbon steel or stainless steel drums and cylinders under nitrogen cover. Sodium–potassium alloy is shipped in carbon or stainless steel containers (3, 10, 25, 200, 750 lbs) with dip-tubes and valves. Commercially, the eutectic composition of 78% K, 22% Na (melting point of -12°C) is most commonly handled, but other ratios of sodium and potassium are available.

Transport regulations are as follows [6]:

Metal/alloy	Identification number
Potassium	UN 2257
Potassium–sodium alloys	UN 1422

Potassium and the alloys are classified as "water-reactive" (Hazard Class 4.3) by U.S. Department of Transportation regulations. A

blue background label with a "Flame" pictogram, the words "dangerous when wet", and the number 4 are required for ground transportation. The words "dangerous when wet" are omitted for air and ocean shipment labels. Quantities less than 1 kilogram may be shipped via United Parcel Service (UPS), packaged in mandatory exemption packaging specified in UPS's *Guide for Shipping Ground and Air Hazardous Materials* (1995). Larger quantities are shipped in DOT Specification 4BW240 cylinders via common carrier, regulated under 49 CFR. Air shipments are restricted to cargo air craft only, 15 kg (max.) and packaged under packing instruction 412 of IATA "Dangerous Goods Regulations" (37th ed., 1996) or ICAO "Technical Instructions for the Safe Transport of Dangerous Goods by Air" (1995–1996).

52.9 Potassium–Sodium Alloys

Potassium–sodium alloys represent a commercial use for direct reaction of potassium metal. The alloys (called NaK alloy or "nack" in the USA) are liquid at ambient temperature over the weight percent range of 40–90% potassium (Figure 52.8). The physical properties such as excellent thermal and electrical conductivities combined with the wide range of compositions in a liquid state, render the alloys ideal for use as heat-exchange fluids [17–19], cooling liquids in hollow valve stems [20], contact liquids for high temperature thermostats and homopolar generators, and hydraulic fluids [21]. Potassium or potassium–sodium alloys had been used as working fluids on a power plant topping cycle during the 1940s and 1950s.

Potassium alloyed with other metals generates compounds of lower reactivity than potassium metal. Most intermetallic compounds are less ductile than the pure metal. Another low melting alloy of interest is a ternary eutectic (3% Na, 24% K, 73% Cs) which melts at -76°C .

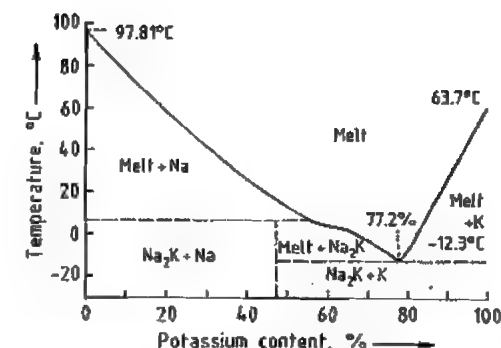


Figure 52.8: Sodium–potassium thermal equilibrium diagram [22].

The eutectic at 77.8% potassium has a freezing point of -12.56°C . The physical properties of NaK are listed below [2]:

Composition	78% K, 22% Na
Melting point	-12.6°C
Boiling point	$\approx 785^{\circ}\text{C}$
Density at 20°C	0.867 g/cm^3
100 $^{\circ}\text{C}$	0.855
550 $^{\circ}\text{C}$	0.749
Electrical resistance at -12.6°C	$33.5\text{ }\mu\Omega\text{cm}$
20 $^{\circ}\text{C}$	38.0
Thermal conductivity at 20°C	$2.18 \times 10^{-3}\text{ Wm}^{-1}\text{K}^{-1}$
550 $^{\circ}\text{C}$	2.62×10^{-3}
Specific heat at -12.6°C	$0.975\text{ Jg}^{-1}\text{K}^{-1}$
100 $^{\circ}\text{C}$	0.937

The liquid NaK alloy, usually used as a dispersion and on an inert support, provides a more reactive surface area than either potassium or sodium metal alone, thus enhancing its reactivity and permitting reaction to proceed at low temperatures (e.g., -12°C). NaK alloys are suitable for chemical reactions involving unstable intermediates such as carbanions and free radicals.

NaK alloys have been used successfully in the following applications: side-chain alkylation of toluenes and xylenes [23], isomerization of α -olefins to internal olefins [24, 25], free-radical [26] and condensation [27–30] polymerization, reduction of metal halides to highly reactive metal powder [31], reduction of organic functional groups such as arenes, ketones, aldehydes and alkyl halides [32, 33], cleavage of functional groups containing C–X, C–O, O–S bonds [34–38], interesterification of tallow with cotton seed oil to improve the pour and clarification temperatures [39,

40], and impurity scavenging of acetylenic and allenic contaminants [41].

52.10 Uses

The understanding of potassium chemistry has been greatly expanded over the last 30–40 years [9–16] and has led to numerous important industrial applications. Potassium, potassium–sodium alloys, and potassium derivatives (alkoxides, amides, and hydride) are extensively used both industrially and academically, to synthesize organic and inorganic materials. Some key applications are highlighted in the following sections.

52.10.1 Potassium Bases

Potassium bases are prepared synthetically by reaction of the metal with alcohols and amines.

Potassium Alkoxides. The most widely used potassium bases are potassium *tert*-butoxide (KTB) and potassium *tert*-amylate (KTA). These strong alkoxide bases offer such advantages as base strength (pK_a 18), solubility (Table 52.7), regio- and stereo-selectivity (due to the bulky *tert*-alkyl groups), and stability (because of the lack of α -protons). Solid KTB and KTA have long shelf lives under an inert atmosphere.

Table 52.7: Solubilities of KTA and KTB at 25 °C (%)

Solvent	KTA	KTB
Tetrahydrofuran	> 50	44
2-Methoxyethyl ether	47	42
<i>tert</i> -Butyl methyl ether	~ 30	2.0
Toluene	36	2.3
Cyclohexane	27	0.4
Hexane	30	0.3

KTB and KTA are superior to alkali metal hydrides for deprotonation reactions because they have good solubilities, produce no hydrogen, and leave no oil residue. Furthermore, reactions of KTA and KTB can be performed in hydrocarbon solvents as sometimes is required for mild and nonpolar reaction conditions. Potassium alkoxides [42] are used in large quantities for condensation, esterification, transesterification, isomerization and

alkoxylation reactions. In combination with butyl lithium, KTB or KTA acts as a "super-base" forming potassium carbanions [13, 43].

Potassium Amides. The strong, extremely soluble, stable and non-nucleophilic potassium amide base, potassium hexamethyldisilazane (KHMDS), $\text{KN}[\text{Si}(\text{CH}_3)_3]_2$ (pK_a 28), was recently commercialized [44]. Available in both THF and toluene solutions, KHMDS is ideal for regio- and stereo-specific deprotonation and enolization reactions. It has demonstrated benefits for reactions involving kinetic enolates [45], alkylation and acylation [46], Wittig reaction [47], epoxidation [48], Ireland-Claisen rearrangement [49], isomerization [50], Darzen reaction [51], Dieckmann condensation [52], cyclization [53], chain [54]/ring expansion [55], and elimination [56].

Potassium 3-aminopropylamide, (KAPA), $\text{KNHCH}_2\text{CH}_2\text{CH}_2\text{NH}_2$ (pK_a 35), can be prepared by the reaction of 1,3-diaminopropane with potassium metal or potassium hydride [57–59]. KAPA powder has been known to explode during storage under nitrogen in a drybox, and is therefore made *in situ*. KAPA is extremely effective in converting an internal acetylene or allene group to a terminal acetylene [60].

52.10.2 Potassium Graphite (C_8K)

Potassium, rubidium, and cesium react with graphite and activated charcoal to form intercalation compounds: C_8M , C_{24}M , C_{36}M , C_{48}M and C_{60}M [61, 62]. Gold colored flakes of potassium graphite, C_8K , are prepared by mixing molten potassium with graphite at 120–150 °C under an inert atmosphere.

Potassium graphite is a powerful solid reducing agent because of the free electrons from the ionized potassium trapped inside the graphite lattice. In packed columns or beds, it can effectively eliminate undesired organic contaminants such as halogenated hydrocarbon impurities from gas streams and liquid solutions. The scope of its reducing reactions include [61]: Birch-type reactions of α - and β -unsaturated ketones, carboxylic acids, and

Schiff's bases; reductive cleavage of vinylic and allylic sulfones; selective alkylation of aliphatic esters, imines, and nitriles; and reductive decyanation of nitriles. Potassium graphite has been used to prepare active metals supported on graphite [62]: Zn–Gr for Reformatsky reactions, Sn–Gr for allylic organometallics, Ti–Gr for coupling carbonyl compounds, Fe–Gr for debromination, Pd–Gr for vinylic and allylic substitution, and Pd–Gr, Ni–Gr for hydrogenation, etc. Potassium graphite has also been applied in polymerization reactions [63].

52.10.3 Potassium Hydride

Potassium hydride, KH is made from reaction of molten potassium metal with hydrogen at about 200 °C or at lower temperatures with a catalyst [64]. Pressure Chemical Company (USA) is a major supplier of KH in an oil dispersion. KH is much more effective than NaH or LiH for enolization reactions [65]. KH used as a base and nucleophile is reviewed elsewhere [66].

A noteworthy development is the use of KH for complexing alkylboranes and alkoxyboranes to form mild reducing agents used in the pharmaceutical industry. Potassium tri-*sec*-butylborohydride, $\text{KB}[\text{CH}(\text{CH}_3)\text{C}_2\text{H}_5]_3\text{H}$ and potassium tri-*sec*-amylborohydride $\text{KB}[\text{CH}(\text{CH}_3)\text{CH}(\text{CH}_3)_2]_3\text{H}$ are made by complexing KH with tri-*sec*-butylborane and tri-*sec*-amylborane respectively. Potassium tri-*iso*-propoxyborohydride can be made by the reaction of KH with isopropyl borate [67].

The potassium trialkylborohydrides find a variety of uses as selective reducing agents [68]. Because of their bulky nature, they exhibit high stereoselectivity in the reduction of hindered cyclohexenones [69]. Regioselective reduction of unsymmetrical cyclic anhydrides by trialkylborohydrides delivers lactones [70]. Potassium tri-*sec*-butylborohydride cleanly reduces α - and β -unsaturated enones in a 1,4-addition to give ketones [71]. In addition, potassium trialkylborohydrides and potassium triisopropoxyborohydride

have been used in organometallic synthesis [72].

52.10.4 Potassium Superoxide

Potassium, rubidium and cesium form superoxide (MO_2) upon oxidation by oxygen or air. However, sodium gives the peroxide, Na_2O_2 , while lithium yields the oxide, Li_2O , when oxidized under comparable conditions. Mine Safety Appliances Company first developed potassium superoxide (KO_2) for use as an oxygen source in self-contained breathing equipment since it liberates oxygen in contact with moisture and carbon dioxide [73].

The unique chemical behavior of KO_2 is a result of its dual character as a radical anion and a strong oxidizing agent [74]. The reactivity and solubility of KO_2 is greatly enhanced by a crown ether [75]. Its usefulness in furnishing oxygen anions is demonstrated by its applications in SN_2 -type reactions to displace methanesulfonate and bromine groups [76], the oxidation of benzylic methylene compounds to ketones [77], and the syntheses of α -hydroxyketones from ketones [78].

52.11 Potassium Chloride

Potassium chloride, KCl, mineral name sylvite, forms colorless nonhygroscopic crystals. It occurs in many salt deposits (see Section 52.4.1.2) mixed with halite and other salt minerals. Natural sylvite is usually opalescent or milky white, as are crystals obtained from an aqueous solution. Sylvite is often colored red by hematite. With magnesium chloride it forms the double salt carnallite, $\text{KCl} \cdot \text{MgCl}_2 \cdot 6\text{H}_2\text{O}$, which is also commonly found in salt deposits. Potassium chloride is produced in large quantities from mined potash ores and from salt-containing surface waters. More than 90% of the potassium chloride produced is used in single- or multi-nutrient fertilizers, either directly or after conversion to potassium sulfate. The remainder has various industrial uses and is the raw material for the manufacture of potassium and its compounds.

52.11.1 Properties

Potassium chloride crystallizes in the cubic system, usually as actual cubes. Some physical properties described are as follows:

Melting point	771 °C
Crystal system and type	cubic, O_h^5
Refractive index n_D^{20}	1.4903
Density	1.987 g/cm ³
Specific heat c_p	693.7 J/kg ⁻¹ K ⁻¹
Heat of fusion	337.7 kJ/kg
Enthalpy of formation DH0	-436.7 kJ/mol
Entropy S0	82.55 J/mol ⁻¹ K ⁻¹
Dielectric constant (at 106 Hz)	4.68
Thermal coefficient of expansion (15–25 °C)	33.7×10^{-6} K ⁻¹

Solubilities in water at various temperatures appear in Table 52.8, and the phase diagram of the system KCl–H₂O is shown in Figure 52.9.

Table 52.8: Solubility of potassium chloride in water (G/100 g) [94].

Temperature, °C	Solubility	Temperature, °C	Solubility
0	28.1	60	45.9
10	31.2	70	48.6
20	34.2	80	51.3
30	37.2	90	53.8
40	40.2	100	56.2
50	43.1		

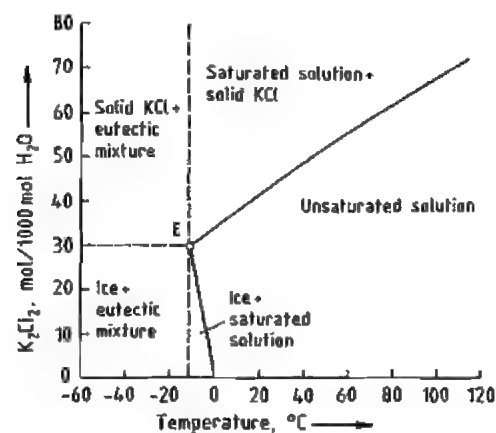


Figure 52.9: Solubility curves for potassium chloride in water. E = cryohydric point: ice–potassium chloride solution.

In the system KCl–H₂O, the only solid phases formed are KCl and ice. The cryohydric point (ice + KCl) is -10.7 °C (29.7 mol K₂Cl₂/1000 mol H₂O). The boiling point of the saturated solution at 1.013 bar is 108.6 °C (71.6 mol K₂Cl₂/1000 mol H₂O).

52.11.2 Production by Crystallization from Solution

52.11.2.1 Phase Theory

The salt deposits were formed by the evaporation of seawater, which contains the principal ions Na⁺, K⁺, Mg²⁺, Ca²⁺, Cl⁻, and SO₄²⁻. With water, these ions constitute a six-component system. The concentration of Ca²⁺ in the most interesting region of the system is negligibly small, so that the system reduces to quinary. It is nevertheless very complicated with, 23 different salts being formed between 0 and 100 °C, depending on the temperature and the ratio of concentrations of the components.

Understanding how the salt deposits were formed and how they behave in dissolution processes requires knowledge of the solution equilibria.

The theoretical foundations for this were laid by VAN'T HOFF et al., who between 1896 and 1906 investigated the formation of oceanic salt deposits [133]. Many investigators have continued this work up to the present.

J. D'ANS critically evaluated all published data up to 1933, expressing his results in graphical form [134]. In the same book, he described experimental methods for determining solution equilibria and gave recommendations for the graphical representation of experimental results [135].

Much of the equilibrium data published up to 1967 are given in [136, 137].

In the years following World War II, in the Kalifornische-Institut (Potash Research Institute) of Hannover, AUTENRIETH carried out comprehensive and detailed research into the stable and metastable equilibria of most relevance to potash production (especially from hard salt), giving the results in a form suitable for practical application [138–144].

The intensive investigations carried out into the quinary system make it the most thoroughly investigated system with more than four components. However, only parts of the system that are of most relevance to potash production have been thoroughly investigated.

An obstacle in the application of equilibrium data to practical problems is that such a complex system is very difficult to represent in a two-dimensional diagram. However, by fixing parameters, working with projections on a plane, and using diagrams showing lines of constant parameters, even nonexperts can work with them.

The best-known region is that in which the solutions are saturated with sodium chloride. This is also the most important region for potassium chloride manufacture, both by the hot leaching process and by flotation, because in both cases a solution saturated with sodium chloride is used. The most important part of the so-called NaCl saturation space at 25 °C is shown in Figure 52.10 as a three-dimensional view.

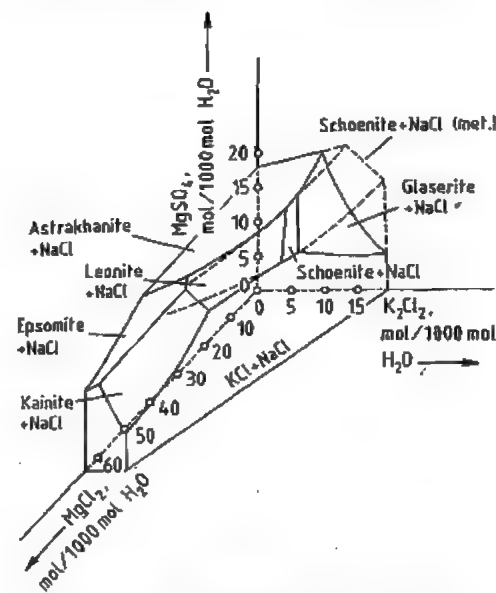


Figure 52.10: Three-dimensional view of the quinary system (saturated with NaCl) at 25 °C with 0–65 mol MgCl₂/1000 mol H₂O showing stable and metastable regions.

Each point in the interior of this space corresponds to a solution saturated with NaCl, in which the concentrations of MgCl₂, K₂Cl₂, and MgSO₄ are given by the distance of the point from the axes. For practical reasons, the concentration figures are given in moles per 1000 mol of H₂O, and the concentrations of

KCl and NaCl are given in double moles. If one or more of the salt concentrations increase, and if the saturation concentration of another salt is exceeded, this salt separates out. Its identity depends on the concentration ratio in the solution. Such two-salt solutions (saturated with two salts) lie on two-salt surfaces, which form the boundaries of the saturation space. Of the twelve other salts whose saturation spaces form the boundary of the NaCl saturation space, seven can be seen on the figure because their two-salt surfaces lie in the concentration range of Figure 52.10.

The KCl–NaCl two-salt surface on the front side of Figure 52.10 is of special significance for the potash industry, because it allows solutions to be made up that are saturated with both salts at 25 °C. Such solutions are important in the treatment of sylvinitic potash ores.

In many instances, a salt does not crystallize spontaneously when its concentration exceeds that indicated on a two-salt surface. Instead, highly supersaturated solutions are formed, which can remain stable for hours or days, depending on temperature and composition. These supersaturated solutions are termed metastable. They become stable saturated solutions by crystallization of a salt. In Figure 52.10, continuations of the stable schönite–NaCl two-salt surface to the right and left into the unstable region are shown as broken lines. In potash manufacture, stable solution equilibria are seldom attained. This is particularly true for hard salt processing in which NaCl-saturated solutions with high MgSO₄ content often lead to the undesired crystallization of double sulfates such as schönite, leonite, langbeinite, and glaserite. Here, the rates of dissolution, nucleation, and crystallization of these salts as a function of temperature and composition of the solutions are especially important [142–144].

For practical application of equilibrium data, the boundary surface of the NaCl saturation space is projected, for example, in the direction of the K₂Cl₂ axis in the MgSO₄–MgCl₂ plane. In Figure 52.11, the two-salt surface NaCl–KCl for the stable and metastable 25 °C

isotherm is shown. The indicated K_2Cl_2 and Na_2Cl_2 lines of constant concentration enable the complete composition to be read off for each of the solutions shown here. By using this diagram, the dissolution and crystallization processes possible in this part of the quinary system can be described quantitatively. To control the crystallization of potassium chloride from 90 °C solutions in an industrial plant, for example, the most important boundary surfaces of the 90 °C isotherm of the system (Figure 52.12) are additionally required.

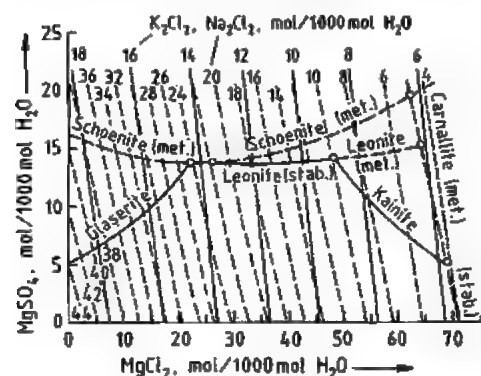


Figure 52.11: 25 °C isotherms of the quinary system saturated with NaCl. Stable (—) and metastable (---) surfaces saturated with KCl and NaCl. Concentrations of K_2Cl_2 (—) and Na_2Cl_2 (---) are indicated by lines of equal concentration.

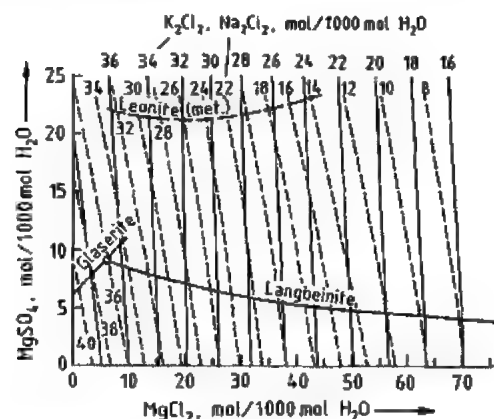


Figure 52.12: 90 °C isotherms of the quinary system saturated with NaCl. Stable (—) and metastable (---) surfaces saturated with KCl and NaCl. Concentrations of K_2Cl_2 (—) and Na_2Cl_2 (---) are indicated by lines of equal concentration.

If any of the components of the quinary system are present in such small quantities that they have a negligible effect on the process, the mathematical treatment can be simplified by dealing only with the remaining subsystem. The following subsystems are of importance:

- Na^+ , K^+ , Mg^{2+} , Cl^- , and H_2O with NaCl saturation (see Figure 52.19) for the conversion of carnallite into potassium chloride and bischofite
- K^+ , Mg^{2+} , Cl^- , and H_2O (see Figure 52.18) for the decomposition of carnallite
- Na^+ , K^+ , Cl^- , and H_2O [135] for the selective dissolution of NaCl (e.g., from crystalline product obtained from hard salt in the hot leaching process)
- K^+ , Mg^{2+} , Cl^- , SO_4^{2-} , and H_2O [139] for the production of potassium sulfate and potash-magnesia
- Na^+ , Mg^{2+} , Cl^- , SO_4^{2-} , and H_2O [135] for the production of thenardite or Glauber's salt

52.11.2.2 Hot Leaching Process

The hot leaching process is the oldest industrial process used to produce potassium chloride from potash ore. It was first used in 1860 in Stassfurt and since then has been developed further in Germany, where it is still the dominant process. It is especially suitable for treating very finely intergrown ores or ores that contain other salt minerals or insoluble minerals in addition to the sylvite and halite. It enables a high-purity product with a uniform grain size to be produced. In many plants, especially in Canada, where flotation is the main production process, small hot leaching plants are also operated, in which the product fines (< 0.2 mm) are recrystallized, or potassium chloride is extracted and crystallized from the flotation residues or thickened clay slurries. These procedures give a considerable improvement in total yield and result in a very pure, completely water-soluble product.

Two different processes are used, depending on the composition of the ore. In the *sylvinitic* hot leaching process, the other salts

present in addition to KCl and NaCl play only a minor role in the process solutions. In *hard salt* leaching, process solutions contain appreciable amounts of $MgCl_2$ and $MgSO_4$. In the case of carnallite-containing hard salts, preliminary carnallite decomposition must be carried out if the amount of carnallite present exceeds a critical level.

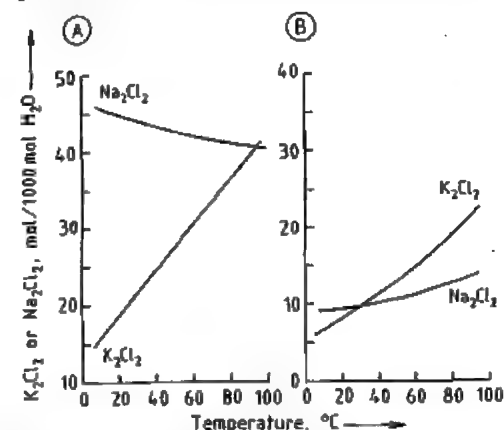


Figure 52.13: Solubility curves for KCl and NaCl (schematic). A) Sylvinitic leaching (with nonevaporative cooling); B) Hard salt leaching.

The different solubility properties of sodium chloride and potassium chloride are shown in Figure 52.13. The solubility of potassium chloride is lower in hard salt solutions than in sylvinitic solutions. The difference between the potassium chloride contents of saturated solutions at low and high temperatures is less for solutions of hard salt than for solutions of sylvinitic, so that the amount of potassium chloride that can be crystallized from a given amount of solution is smaller, which has a marked effect on the energy requirement. Furthermore, an important difference between the two solution types is that the solubility of sodium chloride in sylvinitic solutions decreases with increasing temperature, whereas it increases in hard salt solutions. This is apparent in Figure 52.13B, which shows the behavior of process solutions in a carnallitic hard salt plant with a magnesium chloride content of ca. 240 g/L. This dependence of the solubility of sodium chloride on temperature and magnesium salt content explains why the sodium

chloride contents of crystallized products differ, depending on whether they came from the treatment of sylvinitic or hard salt.

The Process (Figure 52.14). The potash ore, ground to a fineness of < 4–5 mm, is stirred in a continuous dissolver with leaching brine heated to just below its boiling point. The leaching brine is the mother liquor from the crystallization stage of a previous cycle of the process. The quantity of leaching brine required is determined by the amount of potassium chloride in the ore. The potassium chloride should be extracted from the ore as completely as possible, and the resulting product solution should be as nearly saturated as possible. The residue consists of two fractions of different particle size. The coarse fraction is removed from the dissolver and debrined. The fine fraction (fine residue or slime) is removed from the dissolver along with the crude solution, which is clarified with the aid of clarifying agents. The slime that separates is filtered off, and the filtrate from the coarse and fine residues is recycled to the recirculating brine. The residues are washed with water or plant brines low in potassium chloride to remove the adhering crude solution, which has a high potassium chloride content. The residues are then disposed of by dumping.

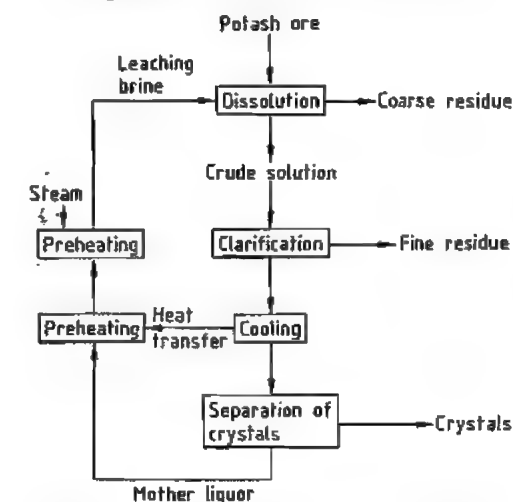


Figure 52.14: Overall schematic of a hot leaching process.

The hot, clarified, crude solution is cooled by evaporation in vacuum equipment. Potassium chloride and sodium chloride crystallize as the water is removed. The sodium chloride content of the crystals formed can be controlled by complete or partial replacement of the evaporated water during crystallization. The crystals formed are separated from the mother liquor and processed further. The mother liquor is heated and recycled to the dissolver as leaching brine.

The leaching process is usually carried out in two stages in a main dissolver and a secondary dissolver. The ground ore is first added to the main dissolver where it is mixed with the already partially saturated solution from the secondary dissolver. This causes the solution to be almost completely saturated, and it is then removed from the leaching equipment. The partly extracted ore is next fed to the secondary dissolver where it comes in contact with fresh leaching brine, and the potassium chloride that was not extracted in the main dissolver is taken up by the solution, which is then fed to the main dissolver. The leaching process in the main dissolver can be cocurrent or countercurrent (Figure 52.15).

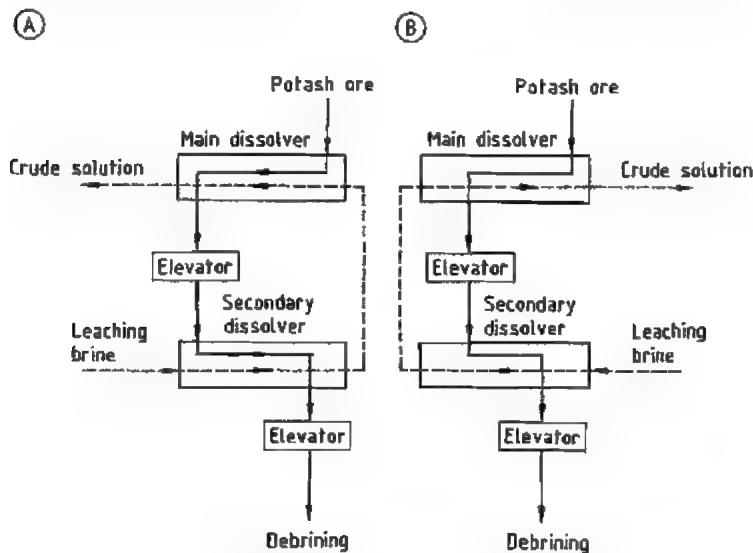


Figure 52.15: Schematic arrangements of a hot leaching apparatus. A) Cocurrent flow; B) Countercurrent flow.

The residence time in the leaching equipment is insufficient to give complete KCl-NaCl equilibrium. The crude solution always contains less potassium chloride and more sodium chloride than corresponds to equilibrium. Another reason for the potassium chloride concentration to be maintained below saturation is that complete recovery of potassium chloride from the ore is possible only if the hot solution at the end of the leaching process still has a small capacity for dissolving potassium chloride. Also, the crude solution cools by 1–2 °C as it travels from the main dissolver to the overflow from the following hot clarification stage. If the solution leaving the main dissolver were completely saturated in potassium chloride, the potassium chloride would begin to crystallize at this point, leading to losses in the slime.

For the crystallization process the potassium chloride content should be maintained as near to saturation as possible in the leaching equipment, so that the concentration difference between the mother liquor and the hot crude solution is as great as possible. The greater this difference, the smaller is the amount of solution used, and the lower is the energy consumption.

Also, a high concentration of potassium chloride in the solution leads to a high potassium chloride content in the crystalline product obtained on cooling. If the solution is unsaturated with respect to potassium chloride, a corresponding amount of sodium chloride in excess of its saturation concentration is taken up by the solution to compensate for the missing potassium chloride. This means that, on cooling, a quantity of sodium chloride crystallizes, causing a decrease in the potassium chloride content of the product even in sylvinic solutions in which the solubility of sodium chloride increases with decreasing temperature.

Cooling the crude solution by evaporation increases the concentration of salts present below saturation, and the salts with which the solution is saturated crystallize. Unwanted crystallization of sodium chloride can be prevented by adding water to the vacuum cooling equipment, especially in the case of solutions from sylvinite ore leaching. If the required potassium chloride content in the crystalline product cannot be obtained by adding water to the solution, which is often the case when hard salt is being processed, the same result can be obtained by treating the product with cold water. A product containing 60% K₂O (95% KCl) is usually required. By this cold-water treatment technique, it is even possible to obtain a product with 62% K₂O (98% KCl). The spent solution is recycled to the process.

For KCl of analytical or pharmaceutical quality, potassium chloride produced by the hot leaching process must be purified by single or multiple recrystallization.

Processing of Hard Salt. Unlike the sylvinic potash ores, whose principal constituents are sodium and potassium chloride, hard salts contain not only the alkali chlorides but also large amounts of kieserite, usually with varying amounts of carnallite, langbeinite, and anhydrite. Therefore, process brines produced by the leaching of hard salt are characterized by high contents of magnesium chloride and magnesium sulfate, which make potassium chloride production more difficult.

Magnesium sulfate comes mainly from kieserite, which is very soluble (Figure 52.16) but has a slow rate of dissolution that becomes even slower if large amounts of dissolved MgCl₂ are present. The amount of magnesium sulfate that dissolves depends on the grain size of the ore fed to the dissolving equipment, the kieserite content of the ore, the time for which the crude salt solution mixture is stirred, the temperature, and the magnesium chloride content of the brine.

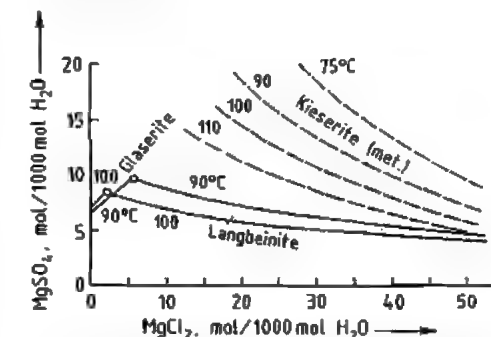


Figure 52.16: Metastable solubility of kieserite in the quinary system saturated with KCl and NaCl between 75 and 110 °C, and solubilities of langbeinite and glaserite at 90 and 100 °C.

Magnesium chloride results from reaction of dissolved magnesium sulfate with potassium chloride to give sulfate-containing double salts, and also from any carnallite (KCl·MgCl₂·6H₂O) present in the hard salt. In general, the MgCl₂ and MgSO₄ contents are kept constant in the circulating brines, so that the rate at which magnesium is taken up from the ore is balanced by the rate at which it leaves the system in the residues and products. If the ore contains large amounts of carnallite, part of the circulating brine must be removed continuously from the system to prevent the MgCl₂ level becoming too high.

Because of the large amounts of magnesium salts in process brines, the hard salt leaching process has three important disadvantages compared with the sylvinite process:

- In solutions of hard salt, the range of solubilities is considerably less than in solutions of sylvinite (Figure 52.13). To extract a given amount of potassium chloride, much

more liquor, and hence more energy, is required compared with sylvinite.

- With solutions of hard salt, crystallization of double sulfates such as schönite, leonite, and langbeinite often occurs. These salts can appear in the residue or the product, which leads either to potassium losses in the residue or to a lower K_2O content of the product. Also, double salts can crystallize in pipelines, vessels, and pumps, interfering with the process and in extreme cases bringing it to a standstill. The particular double salt that crystallizes depends on the $MgCl_2$ content of the solutions, the temperature, and other operating conditions (Figures 52.11 and 52.12). The extent of supersaturation with double sulfates must therefore be controlled to prevent uncontrolled crystallization of double salts and consequent introduction of impurities into the product or disturbance of the process. To achieve this, the circulating brine, or part of it, is fed to a reactor in which it is agitated intensively in the presence of nuclei (20–40%) of the double salt to be removed until the brine is no longer supersaturated with respect to it [145].

- Another disadvantage of the hard salt leaching process is that, with higher magnesium salt contents, the temperature dependence of the solubility of NaCl becomes unfavorable (Figure 52.13), that is, when the potassium chloride is crystallized by cooling, considerable amounts of sodium chloride can also crystallize (Figure 52.17). In practice, equilibrium is not completely reached when the KCl–NaCl is dissolved, and cooling of the solution often occurs by water removal, so that the K_2O content of the crystals formed is usually only a little more than 40%. Since the usual potassium chloride for fertilizers (excluding special products) has a minimum potash content of 60% K_2O , this primary product was formerly crystallized in a second leaching plant. Alternatively, a product can be made with 60% K_2O directly, if the crystallization of sodium chloride during vacuum cooling is prevented by addition of

sufficient water before or during crystallization of the solution to ensure that only potassium chloride crystallizes [145]. The K_2O content in the product of a primary crystallization can be increased to the required level by treating the product with water or a plant solution unsaturated with respect to sodium chloride. Both the excess water added during vacuum cooling and the water used for treating the product must be removed from the recirculating system of the plant. Both cause a loss of yield whose extent depends on operating conditions. To avoid this, excess water must be evaporated from process liquors.

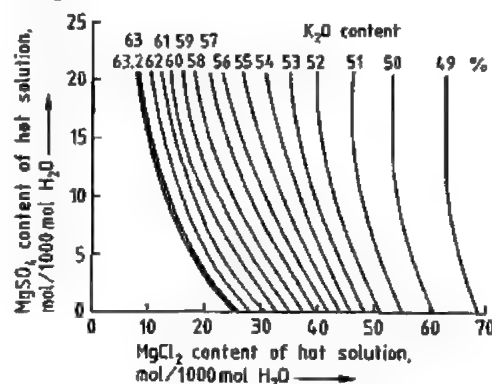


Figure 52.17: K_2O content of the crystalline product obtained by cooling an equilibrium solution saturated with NaCl and KCl from 90 to 25 °C without evaporation while maintaining saturation.

52.11.2.3 Processing of Carnallite

Carnallite, $KCl \cdot MgCl_2 \cdot 6H_2O$, is the most abundant potassium mineral in salt deposits and occurs widely in mixtures with halite or with halite and kieserite in the form of carnallite ore. In the early days of the potash industry in Germany, it was the preferred starting material for the production of potassium chloride. Today, sylvinitic ores and hard salts are used almost exclusively, because the extraction and processing of carnallite ore are considerably more difficult and expensive for the following reasons:

- Carnallite ore has unfavorable mechanical properties that make mining more difficult.

- The K_2O content of pure carnallite is ca. 17%, compared with ca. 63% for pure sylvite.
- Whereas the separation and purification of sylvite from sylvinitic ore can usually be carried out by flotation, which does not involve a phase change, the extraction of potassium chloride from carnallite ore necessitates dissolution or decomposition of the carnallite, and a high energy consumption for decomposition or purification of the decomposition product, depending on the process.
- The treatment of carnallite generates large quantities of concentrated magnesium chloride solution, which must be disposed of.

For these reasons, mined carnallite ore is today seldom used as a raw material. However, carnallite is often a major component in mixed salts of the hard salt type, and hence influences the choice of processing method.

Large quantities of a carnallite halite mixture obtained by solar evaporation of water from the Dead Sea are used for the production of potassium chloride in Israel and Jordan.

Theoretical Basis. The theory of the production of potassium chloride from carnallite and carnallite-containing mixed salts is based on the KCl– $MgCl_2$ – H_2O system shown in Figure 52.18, which is valid between –3 and 117 °C. In van't Hoff coordinates (moles of salt per 1000 mol H_2O) the points representing the composition of water (P_{H_2O}), bischofite ($P_{\text{bischofite}}$), and carnallite ($P_{\text{carnallite}}$) are indicated. All possible mixtures of water and carnallite are shown on the straight line between P_{H_2O} and $P_{\text{carnallite}}$, the molar ratio $K_2Cl_2:MgCl_2$ here being always 1:2, as in carnallite. The curve from L_1 via R and E to point L_0 represents an arbitrary isotherm, and indicates compositions in which solutions are in equilibrium with the corresponding solid phase. Point L_0 gives the solubility of KCl in water, and the solutions L_1 are in equilibrium with KCl as the solid phase. Solution E is in equilibrium with the solid phases KCl and carnallite, and the solutions L_2 are in equilibrium with carnallite only. Solution R is in equilibrium with bischofite and

carnallite. The solutions L_3 are in equilibrium with bischofite, and point L_4 indicates the solubility of bischofite in water.

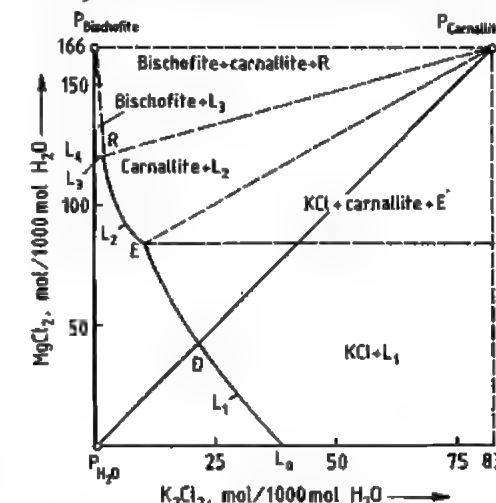


Figure 52.18: The system KCl– $MgCl_2$ – H_2O (not to scale) represented by using van't Hoff coordinates.

If carnallite is dissolved in water, the composition of the solution follows the straight line P_{H_2O} – $P_{\text{carnallite}}$, which intersects curve L_1 at point D. Here, the solution is saturated with KCl, and further addition of carnallite results in dissolution of $MgCl_2$ and crystallization of KCl until point E is reached. This incongruent solubility is the basis for the simple method of processing carnallite (i.e., cold decomposition by mother liquor).

Carnallitic potash ores or crystallized products from solar evaporation always contain so much halite that solutions produced during processing are saturated with sodium chloride. Figure 52.19 is a section from the quaternary system KCl–NaCl– $MgCl_2$ – H_2O saturated with NaCl, showing the 25 °C and 105 °C isotherms. The kieserite content in the ore in the region of the solutions E has in practice a negligible effect on the composition of the solutions. Some analyses of equilibrium solutions of the quaternary system are given in Table 6.

Processing Methods. Many processes for the treatment of carnallite have been described in the literature and used [88], but only a few are important today. By far the most important is

cold decomposition by mother liquor. The complete dissolution process is still used occasionally.

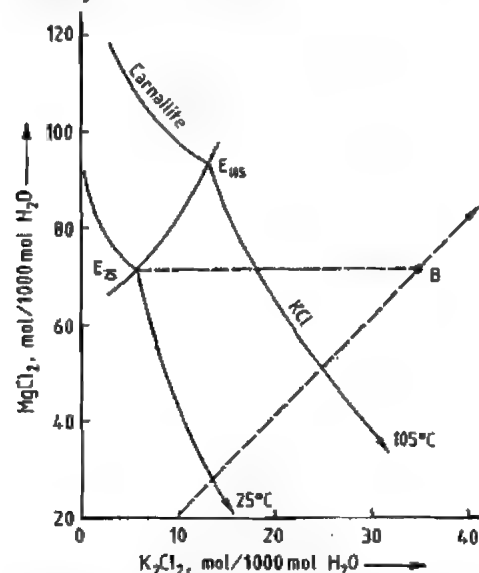


Figure 52.19: Quaternary system (K_2Cl_2 - $MgCl_2$ - Na_2Cl_2 - H_2O) saturated with NaCl. See text for explanation.

Table 52.9: Composition of stable saturated solutions in Figure 52.19.

Point*	Temperature, °C	Density, g/cm ³	Concentration, mol/1000 mol H ₂ O			
			K ₂ Cl ₂	MgCl ₂	MgSO ₄	Na ₂ Cl ₂
E ₂₅	25	1.275	5.8	70.8		4.4
Q ₂₅	25	1.291	5.8	68.0	5.2	4.2
E ₁₀₅	105	1.328	13.2	93.7		4.4
Q ₁₀₅	105	1.325	13.7	92.9	1.0	4.3

* Solutions Q₂₅ and Q₁₀₅ are saturated with MgSO₄ and NaCl, and correspond to solutions E₂₅ and E₁₀₅, which are saturated with NaCl.

Cold decomposition is carried out at ambient temperature (e.g., 25 °C). Carnallite ore is mixed and agitated with water or with a solution of low MgCl₂ content such that the composition of the mixture corresponds to point B in Figure 52.19. This causes the crystallization of an amount of potassium chloride corresponding to the line B-E₂₅, with formation of a solution of composition E₂₅. The very fine potassium chloride produced still contains fine, salted-out sodium chloride, undissolved halite, and sometimes kieserite and clay, depending on the composition of the car-

nallite ore used. Approximately 85% of the potassium chloride contained in carnallite can be obtained as a crystalline product by this process. The yield can be increased by evaporative concentration of the decomposition mother liquor E₂₅ or Q₂₅ (analyses are given in Table 52.10). During evaporation, sodium chloride and sometimes magnesium sulfate crystallize and must be removed. The synthetic carnallite that crystallizes when the concentrated solution is cooled is fed to the cold decomposition process.

Table 52.10: Typical grain-size distribution in potash fertilizers (cumulative percentage retained).

Mesh width, mm	Tyler mesh	Cumulative subsieve fraction		
		Granular	Coarse	Standard
+3.36	+ 6	2-12		
+2.38	+ 8	30-45	2-20	
+1.68	+ 10	75-90	25-50	
+1.19	+ 14	95-98	70-90	5-15
+0.84	+ 20	99	90-98	20-45
+0.60	+ 28		99	50-75
+0.42	+ 35			70-90
+0.30	+ 48			85-95
+0.21	+ 65			96-98
+0.15	+100			97-99

Potassium chloride from the decomposition, which consists of very finely divided particles and is rather impure, must be purified. Purification by flotation is difficult owing to the fineness of the decomposition product. For this reason, purification is nearly always carried out by the hot leaching process, which yields a very pure, completely water-soluble, coarse-grained product.

The mother liquor E₂₅ or Q₂₅ from the decomposition process can take up a certain amount of sodium chloride (see Table 52.10). If the carnallite used in the cold decomposition contains only small amounts of halite and if water is used for the decomposition, potassium chloride can be produced that requires no further purification, because sodium chloride has dissolved in the decomposition liquor. In Israel, a large proportion of the carnallite-halite mixture recovered from the Dead Sea by solar evaporation is so completely freed from halite by fractional crystallization and hydraulic classification that a grade of potassium

chloride with > 60% K₂O can be produced directly by cold decomposition. This so-called cold crystallization process is carried out so that the crystals produced have the same grain size as those from the crystallization plant of

the hot leaching process and no further increase in grain size is required. A schematic diagram showing various processes used in the treatment of carnallite from the Dead Sea is given in Figure 52.20.

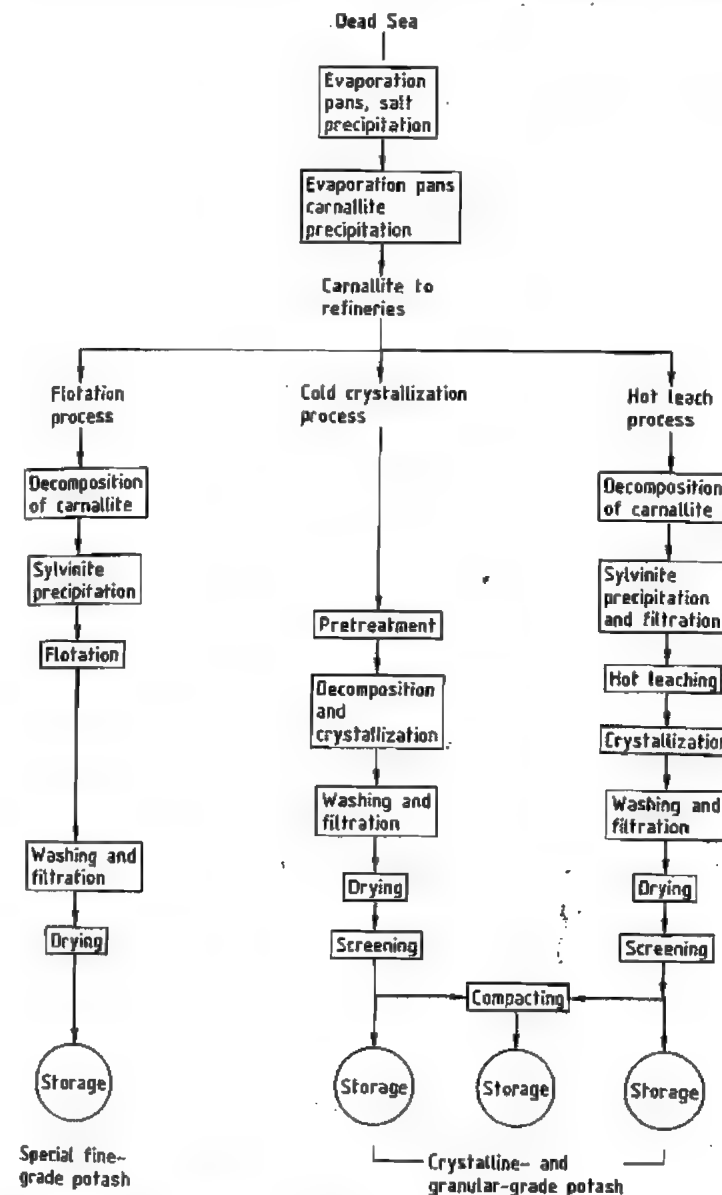


Figure 52.20: Flow diagram for potassium chloride production by the Dead Sea Works Ltd. (Israel) [82]. Reproduced from [82] with permission.

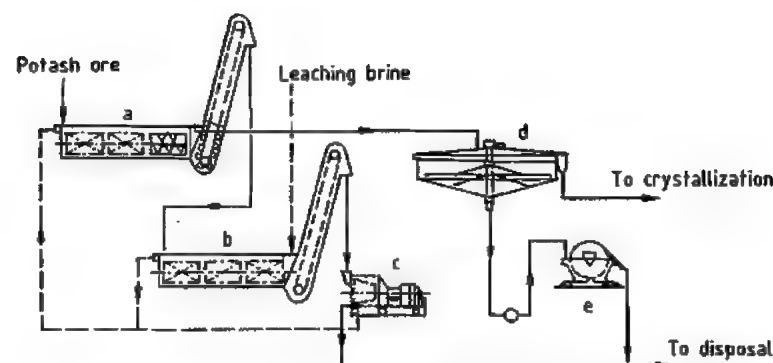


Figure 52.21: Leaching system with residue debrining: a, b) Screw leachers with draining elevators; c) Vibratory screen centrifuge; d) Hot clarifier; e) Rotary filter.

In the electrostatic treatment of carnallitic hard salts, concentrates can be produced that contain various amounts of halite together with sylvite and carnallite. These concentrates are reacted with suitable process brines or with water to bring about cold decomposition of the carnallite. The K_2O content of the product, and hence its potential use, depend on the halite content of the concentrate.

The complete dissolution process is used in an experimental plant in central Germany in which carnallite is extracted from a salt deposit by solution mining [126].

The crude salt is dissolved by a solution in which the magnesium chloride content is adjusted so that at the chosen temperature of ca. 80 °C, no decomposition of carnallite takes place, and hence no crystallization of potassium chloride, and the carnallite is completely dissolved. The solution, which is almost saturated with carnallite, is pumped out, evaporated, and cooled, causing crystallization of the carnallite, which is then treated by the cold decomposition process to produce potassium chloride.

For mixed salts containing less than ca. 15% carnallite, carnallite decomposition is generally dispersed with, and the ore is treated directly by the hot leaching process. The magnesium chloride that enters the process in the carnallite must be removed from the brine circuit in appropriate process brines. If the carnallite content of the ore is high, a carnallite

decomposition stage is carried out before the hot leaching process.

52.11.2.4 Equipment

Leaching. The choice of leaching equipment depends on the properties of the material to be leached and the throughput required. The techniques used in plants in which the potash is completely leached (e.g., in many German and French plants) differ fundamentally from those in plants (e.g., in Canada) where only the fine materials from a screening operation, cyclone fines, and slimes are recrystallized or extracted.

Potash ores are leached at rates of up to 1000 t/h salt, producing up to 2000 m³/h solution. Screw dissolvers, up to 14 m long and 3 m in diameter, are widely used (Figure 52.21). High material transfer is achieved by fitting partitions in the upper part of the dissolver at intervals of 2–3 m. These are immersed in the suspension of crystals and force the solution to flow perpendicular to the main flow direction. At the outlet of the dissolver, the solids are scooped from the solid-liquid mixture by an elevator system with perforated buckets from which liquid drains during conveying; the residual water content is ca. 15–20%. Alternatively, bucket wheels can be used.

Elevators or bucket wheels remove only the coarse residue (ca. 75% of the total residue) from the screw dissolver. The amount of po-

tassium chloride-containing solution adhering to the coarse residue is usually lowered to 2–4% by centrifugation.

The fine residue (ca. 25% of the total residue), which consists of very fine salt and insoluble components of the ore (mostly anhydrite and clay), flows with the raw solution from the screw dissolver into the hot clarifier, where flocculation agents are added and sedimentation occurs. Sealed, insulated circular clarifiers are used. The fine residue is removed from the hot clarifier as a suspension with a solids content of ca. 50% and debrined on rotary filters to a residual water content of 10–16%. To avoid losses of potassium chloride, the solution adhering to the residue must be removed. For small quantities of residue, this is done by washing on the filter with water or a process brine having a low potassium chloride content. For large amounts of residue, two- or three-stage water washing is used; the filter cake is slurried with the water, and the resulting suspension is filtered. This treatment is repeated once or twice.

In North America, where the flotation process predominates and only small quantities of

ore are treated by the hot leaching process, a series of agitated vessels is used. The leaching process takes place in either cocurrent or countercurrent flow. Between the stages of countercurrent leaching, solid-liquid separation is carried out with hydrocyclones or hydroclassifiers [146]. The layout of a leaching plant including crystallization is shown in Figure 52.22.

Crystallization [147, 148]. The hot solution from the clarifier of the leaching plant is almost saturated with potassium chloride and is cooled by expansion evaporation in vacuum equipment to cause crystallization. The vapors are condensed in surface or barometric condensers, with process brines used for higher temperatures and cooling water for lower temperatures. The amount of heat that can be recovered depends on the number of stages in the cooling system. In the past, vacuum cooling plants were constructed with up to 24 stages, to give maximum possible heat recovery. However, the number of stages in a modern plant is usually between four and eight.

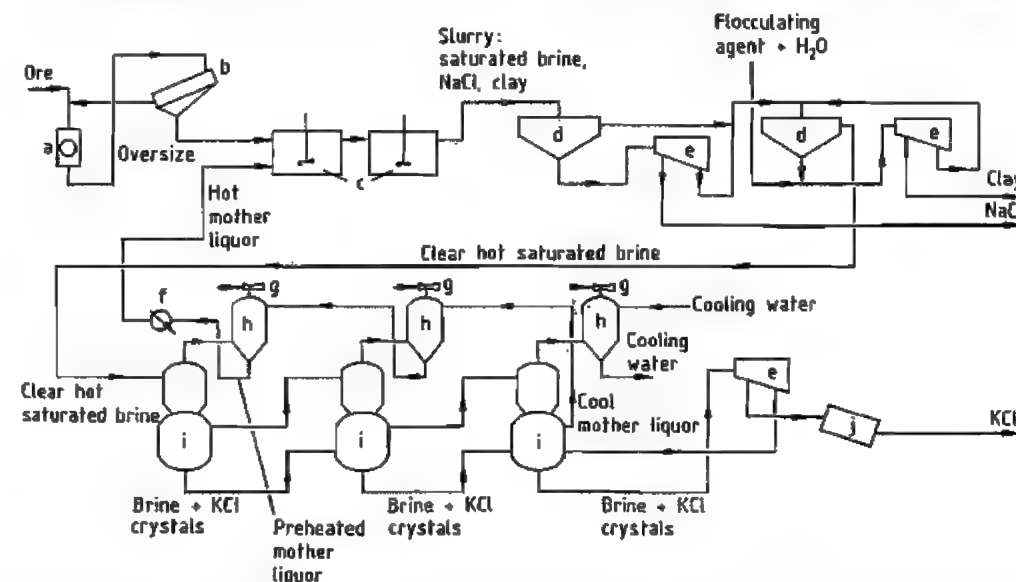


Figure 52.22: Leaching-crystallization process for production of potassium chloride from potash ore [86]. Reproduced from [86] with permission. a) Crusher; b) Screen; c) Leach tanks; d) Thickener; e) Centrifuge; f) Heater; g) Steam ejector; h) Barometric condenser; i) Vacuum cooler-crystallizer; j) Dryer.

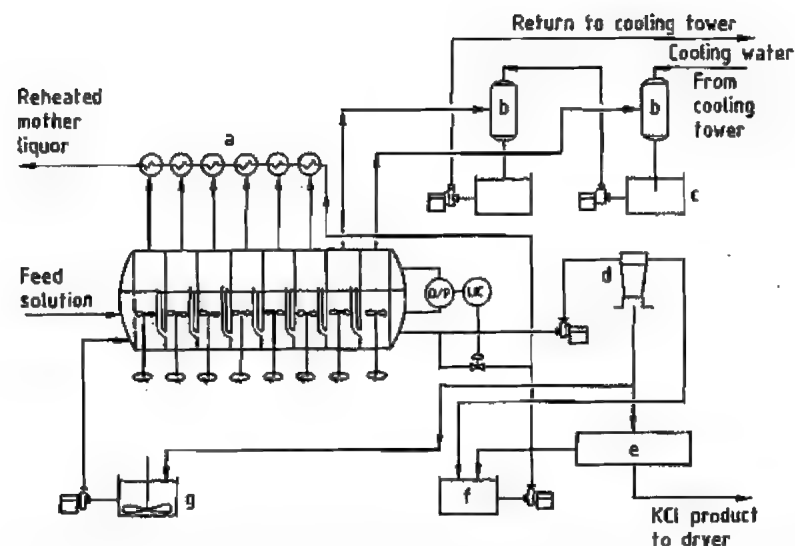


Figure 52.23: Eight-stage horizontal crystallizer: a) Surface condensers; b) Barometric condenser; c) Hot well; d) Cyclone; e) Centrifuge; f) Filtrate tank; g) Slurry holding tank. Reprinted with permission from E. M. McKercher et al., *Proc. 1st Int. Potash Technol. Conf.*, Oct. 3-5, 1983, Pergamon Press.

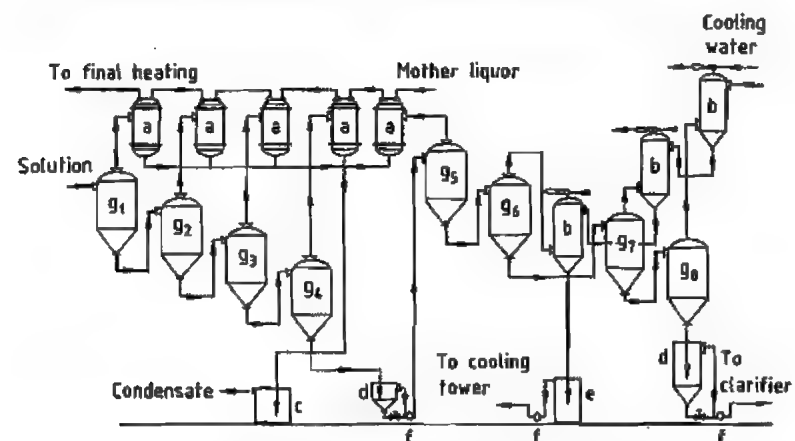


Figure 52.24: Conical-based evaporator-crystallizer plant with eight evaporation stages: a) Surface condensers; b) Barometric condensers; c) Barometric collection vessel for condensate; d) Barometric collection vessel for salts and brines; e) Barometric collection vessel for cooling water; f) Pumps; g₁-g₈) Evaporators.

The high cooling rate of a vacuum plant results in a high degree of supersaturation that produces very fine crystals, unless the design of the plant and the crystallizing conditions are optimized to give a coarse product. Several suitable crystallizers are now available.

If it is not important to have coarse crystals (e.g., if they are to be reprocessed), stirred crystallizers or conical-based evaporators are

used. The former consist of horizontal cylindrical vessels divided into chambers by vertical walls. The solution or suspension flows from chamber to chamber through openings in the walls as it is cooled. These crystallizers are provided with mechanical stirrers or air agitation (Figure 52.23).

The conical-based evaporator consists of a vertical cylinder with a lower conical section.

The solution is sprayed into the top, and much of the water evaporates. A certain liquid level is maintained in the evaporator, into which liquid from the nozzle falls as a supersaturated solution. Several evaporators are arranged in series one above the other so that the suspension flows through each stage in the direction of decreasing pressure without the need for intermediate pumps (Figure 52.24). The advantage of this arrangement lies in its very simple and economical construction, with no moving parts. However, the product is very finely divided.

The aim of the crystallization process is usually a dust-free product with optimum grain size. Two main requirements must be met to achieve this: the solution must have only a slight degree of supersaturation, and this should be removed by crystallization on seed crystals that are already present. The slight degree of supersaturation is achieved by providing internal circulation within each crystallization stage, in which the cooled solution is mixed with the added hot solution in an exactly controlled ratio. The continuous presence of seed crystals is ensured by keeping the solids content in each crystallizer at ca. 30%.

These conditions are fulfilled by two types of crystallizer: the fluidized-bed (Oslo) type and the draft-tube agitated type.

In the Oslo crystallizer (Figure 52.25), the solution is supersaturated in a separate evaporator and flows into a crystal slurry vessel below, where the supersaturation is removed by crystallization on KCl crystals already present. To reduce the degree of supersaturation in the evaporator, a large amount of clarified solution is pumped from the crystal slurry vessel into the evaporator, together with the incoming hot feed solution. Clarified solution for the next stage is removed from the vessel at another takeoff point. A crystal suspension is also removed from the vessel at a rate corresponding to the rate of crystallization, and is fed either to the next stage as seed crystals or to the debrining stage. Crystallizers of this type are constructed by companies such as Lurgi, Swenson, and Struther-Wells.

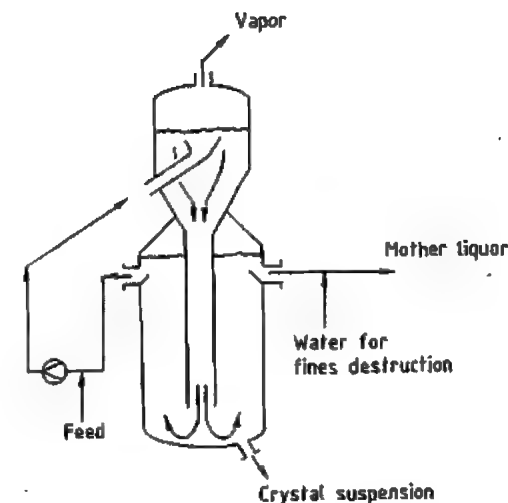


Figure 52.25: Oslo crystallizer.

In draft-tube agitated crystallizers, a state of supersaturation is created and removed in the same crystallizer. This type is manufactured by Swenson (DTB = draft tube baffle), Standard-Messo, and Kali und Salz. In the Swenson and Standard-Messo crystallizers, the entire suspension is brought into continuous contact with the evaporator surface by a propeller stirrer that provides internal circulation; immediately after supersaturation is achieved, a large quantity of salt is made available to remove the state of supersaturation. The coarser crystals collect preferentially in the lower part of the crystallizer, where they are removed as a suspension and fed to the next stage or to the debrining stage. The hot solution is passed through a clarifying zone and is fed to the next stage.

All the processes described so far are operated cocurrently (i.e., the crystallizing salt is transported with the cooling solution from one stage to the next). In contrast, the Kali und Salz process (Figure 52.26) operates countercurrently [149]. The salt produced in each crystallizer is passed through a classifier at the bottom of the crystallizer as soon as a predetermined minimum crystal size has been reached; then, unlike the other systems, it is passed to the next hottest stage. The classifier is fitted with equipment that enables the up-

ward flow rate, and hence crystal concentration and product crystal size, to be controlled independently of the throughput rate of the solution. Mixing of the cooler solution with the hotter solution in a crystallizer is prevented by transferring the salt with the help of the solution from the stage into which it is pumped.

52.11.3 Flotation

Since the early 1900s, ores of many different kinds have been processed by froth flotation.

Investigations into the flotation of potash ores began in the early 1930s in the United States and the Soviet Union [150, 151]. The first full-scale plant began production in 1935 in Carlsbad (New Mexico, United States) [152].

The first reports of investigations into the flotation of potassium salts in Germany appeared in 1939 [153]; the first full-scale plant began operating in 1953 [154, 155].

At present, most of the worldwide production of potash fertilizers is by flotation. This is the most widely used process in Canada, the United States, the CIS, and France. Small hot

leaching plants are often attached to the flotation plants for treating slimes and intermediate products. The flotation process is not widely used in Germany, where a combination of electrostatic treatment with the hot leaching process predominates.

52.11.3.1 Potash Ores Suitable for Flotation

Various types of crude potash salts can be treated by flotation:

Sylvinite ores are mixtures of sylvite (KCl) and halite (NaCl) in varying ratios. They represent the majority of potash ores treated. The sylvinites of Canada, the United States, and the CIS also contain up to 8% clay components [156].

Hard salts contain kieserite ($\text{MgSO}_4 \cdot \text{H}_2\text{O}$), as well as sylvite and halite, and sometimes also anhydrite (CaSO_4).

Mixed salts consist of a mixture of sylvinite ore or hard salt with carnallite ($\text{KCl} \cdot \text{MgCl}_2 \cdot 6\text{H}_2\text{O}$)

Polymineal salts contain not only sylvite, halite, and kieserite, but also langbeinite ($\text{K}_2\text{SO}_4 \cdot 2\text{MgSO}_4$), kainite ($4\text{KCl} \cdot 4\text{MgSO}_4 \cdot 11\text{H}_2\text{O}$), polyhalite ($\text{K}_2\text{SO}_4 \cdot \text{MgSO}_4 \cdot 2\text{CaSO}_4 \cdot 2\text{H}_2\text{O}$), and clay.

52.11.3.2 Carrier Solutions

In the flotation of water-soluble salts the carrier liquids are salt solutions that are saturated with the components of the raw material.

Thus, sylvinite ore flotation is carried out in a KCl - NaCl solution. For the flotation of hard salt, the brine also contains various amounts of magnesium sulfate and magnesium chloride.

52.11.3.3 Flotation Agents

The *collectors* are the true flotation agents, which selectively coat the surface of the component to be floated. For the flotation of sylvite, straight-chain primary aliphatic amines are used in the form of their hydrochlorides or acetates [157]. Mixtures of amines of various chain lengths, which largely eliminate the effects of pulp temperature variation, are extremely useful. A typical flotation amine has, for example, the following composition: 5% $\text{C}_{14}\text{-NH}_3\text{Cl}$, 30% $\text{C}_{16}\text{-NH}_3\text{Cl}$, 65% $\text{C}_{18}\text{-NH}_3\text{Cl}$, iodine number: 4.

Foamers contribute to the dispersion of long-chain amines and to the stabilization and homogeneous distribution of amine micelles [158]. The following substances are preferred: aliphatic alcohols with chain lengths $> \text{C}_4$, terpene alcohols, alkylpolyglycol ethers, and methyl isobutyl carbinol, which is used mainly in Canada and the United States.

Extenders for sylvite flotation are nonpolar materials, especially oils of various types. They are probably incorporated in the micelles and increase their hydrophobic properties. Extenders are especially effective in the flotation of coarse particles [159].

Clay depressants are used in salt flotation to block clay components, which would otherwise bind large amounts of flotation agent. Clay contents of 1.5–2% can be controlled by treatment with these depressants. If larger

amounts are present, additional steps must be taken (clay flotation or classification). Clay depressants include guar and starch products, carboxymethyl cellulose, and polyacrylamide [156].

52.11.3.4 Theory

The combinations of reagents used for sylvite flotation have been found by empirical investigation.

Theoretical studies of the separation of potassium and sodium chloride by flotation have led to various interpretations.

The theories developed up to 1961 are thoroughly discussed in [160], which also describes experimental results that have contributed greatly to the understanding of salt flotation.

The most important theories are reviewed below:

According to the *exchange theory* [161–163], hydrophobic properties can be imparted to a mineral if the polar group of a collector can be incorporated into the crystal lattice in place of an ion. In the flotation of sylvinite ore, for example, exchange between the K^+ ion (radius: 0.135 nm) and the NH_3^+ group of the amine (radius: 0.143 nm) is assumed to occur, whereas the Na^+ ion (radius: 0.095 nm) is too small (Figure 52.27). This does not account for the fact that kieserite ($\text{MgSO}_4 \cdot \text{H}_2\text{O}$), for example, is readily floated by amines in water although the Mg^{2+} ion has a radius of only 0.065 nm.

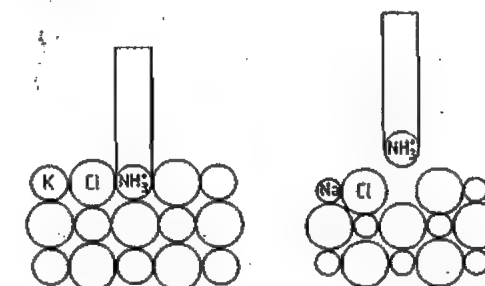


Figure 52.27: Incorporation of a polar group of the collector into the crystal lattice [161]. Reprinted with permission of the Society for Mining, Metallurgy, and Exploration, Inc.

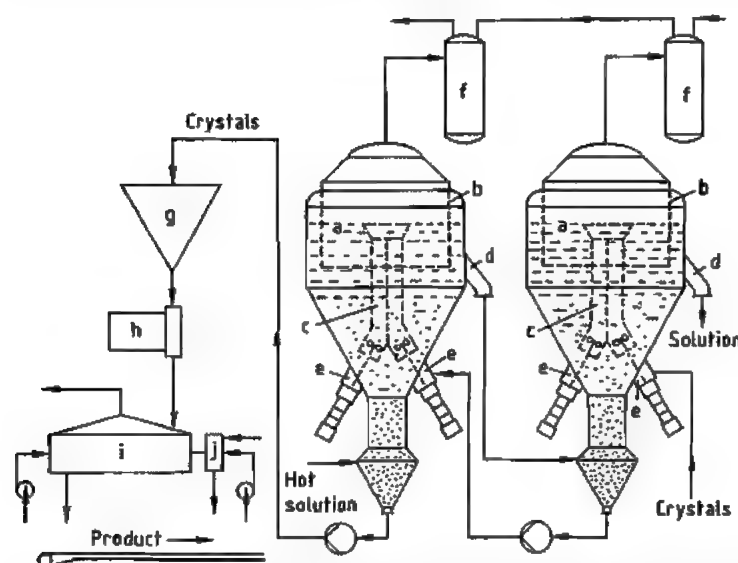


Figure 52.26: Kali und Salz countercurrent crystallization process: a) Crystallizers; b) Bells; c) Draft tubes; d) Liquor overflow; e) Stirrers; f) Condenser; g) Thickener; h) Centrifuge; i) Dryer; j) Combustion chamber.

The *structure theory* [164] postulates that the interanion distance in the crystal lattice of the salt matches the intermolecular distance in the lattice of the amine hydrochloride within $\pm 20\%$. In sylvite, this condition for oriented growth of the collector on the crystal is fulfilled, whereas the interionic distance of 0.398 nm in the halite lattice is too small. However, langbeinite has good flotation properties, although these steric requirements are not met [164].

According to the *hydration theory* [165], flotation of a mineral is impossible if it has a positive heat of solution, whereas salts with negative heats of solution can be floated. If heat is evolved when a salt dissolves, more energy is produced by hydration of the ions than is required for breakdown of the lattice. This suggests that such salts are strongly bonded to water molecules, preventing adhesion of the collector. A comment on this theory is given in [166].

Another hydration theory is based on new information on the hydration of ions in dilute solutions [167]. This differentiates between positive local hydration (in which the ion reduces the mobility of the neighboring water molecules) and negative local hydration (water molecules close to the ions are more mobile than in pure water).

According to [168], in the case of positive local hydration (e.g., with Na^+ ions), the Cl^- ions are shielded by water molecules, so that the bond between a cationic amine and sodium chloride can only be weak. In the case of negative local hydration (e.g., with K^+ ions), formation of a bond with the collector is unhindered. Application of these theories, developed for dilute electrolyte solutions, to the hydration state of salt surfaces is difficult, but should be qualitatively valid [168].

The G zone theory ($G = \text{Grenzflächen} = \text{interfaces}$) [169] applies both to the flotation of sylvinites with amines and to the flotation of kieserite with an anionic surfactant (the sodium salt of a highly sulfated fatty acid). In both cases, adsorption of the collector proceeds by the same mechanism.

Amines and the anionic surfactant, in a saturated solution of salts that can be floated with these reagents, are present either as micelles or in true solution. In the usual carrier brines, flocculation (amines) or formation of very small droplets occurs (anionic surfactant).

Based on experimental results, zones are assumed to be formed on the surfaces of crystals suspended in a mixed-salt solution (carrier liquid) in which ions from the lattice are present in the form of a saturated solution.

When collectors are introduced into the suspension, they migrate to the zones where their solubility is greatest due to their thermodynamic tendency to dissolve (i.e., to the boundary zones of those particles that they cause to float). The bonding of the collectors in these zones is reinforced if their solubility in the surrounding carrier brine is low. The success of flotation depends on the strength of this bond (Figure 52.28).

Froth cannot be produced in the usual carrier liquids either by collectors or by foaming agents. The collision of an air bubble with a crystal coated with the collector material causes the latter to spread over the surface of the bubble, stabilizing it and causing the crystal to float.

Large-scale operations of sylvite and kieserite flotation has thus been placed on a good unified theoretical foundation.

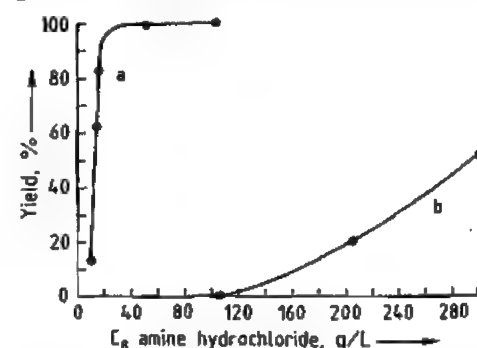


Figure 52.28: Flotation of potassium chloride with octylamine in saturated solutions of KCl and KCl + NaCl (Feed material: 20% KCl, 80% NaCl; 0.1–0.315 mm): a) Carrier liquid saturated in KCl and NaCl (low solubility of octylamine); b) Carrier liquid saturated only in KCl (high solubility of octylamine).

52.11.3.5 Flotation Equipment

The flotation equipment used in the potash industry resembles that used for flotation of other ores.

Mechanical flotation cells operate with a rotor stator system that causes both thorough mixing of the pulp and thorough distribution of the air, which can be drawn in by suction or injected from a compressed air network.

In recent decades, high-capacity flotation has been introduced almost everywhere. In this process, several stirrers operate in a single trough [170].

Agitair high-capacity flotation equipment is used in Germany, and the preconcentrate is purified in individual cells of the Denver type. Wemco high-capacity machines are used by the French potash industry, and Mechanobr high-capacity cells by the former Eastern-bloc countries.

Modified Mechanobr M 7 fluidized-bed units (Figure 52.29), manufactured by Meserjakov, are standard equipment in the CIS [171, 172]. Typical features include the presence of a grid and circulation of the suspension via a box on the front wall of the cell, connected to the agitator by a circulation pipe.

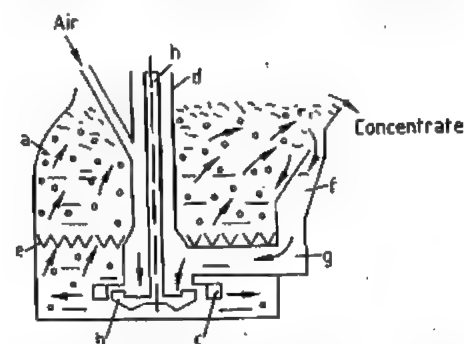


Figure 52.29: Mechanical flotation cell with fluidized bed: a) Flotation cell; b) Stirrer; c) Stator; d) Tube of the stirrer system; e) Grid; f) Circulation box; g) Circulation pipe; h) Shaft.

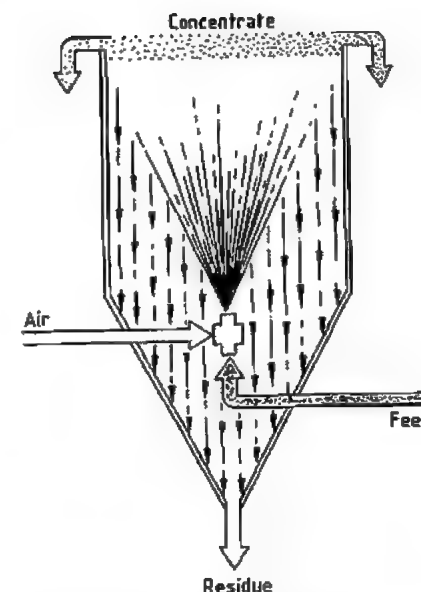


Figure 52.30: Principle of pneumatic free-jet flotation. Reproduced from [173] with permission.

Pneumatic flotation equipment operates without stirrers. In the free-jet flotation process developed in Germany [173], the conditioned pulp is pumped through an aerator fitted with a porous gas distributor or annular nozzle, either outside or inside the separation vessel, and flows as a free jet into the separation vessel. Air bubbles with the adhering minerals rise to the top and form a froth that flows over the edge of the vessel into a channel (Figure 52.30). The pneumatic flotation process has been tested successfully for a special case of sylvite flotation. It is used industrially for the recovery of kieserite from leaching residues.

In the CIS, a pneumatic flotation cell has been developed for the treatment of coarse sylvinites ores with a maximum grain size of 3–5 mm [174, 175] (Figure 52.31). The conditioned pulp is fed from above onto a layer of froth immediately above the perforated-tube aeration system. The hydrophobic sylvine crystals are retained in the froth, so that mechanical damage of the bubble-crystal combination is kept to a minimum. The flotation rate is very high.

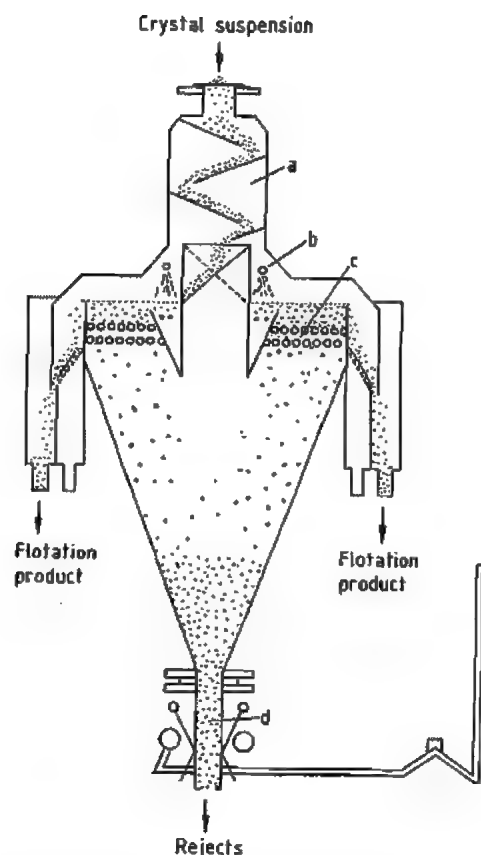


Figure 52.31: Pneumatic coarse-grain flotation cell (Gogorchimproect type) [174]. Reproduced from [174] with permission. a) Feeding device; b) Spray nozzle; c) Aeration system (perforated rubber tubes); d) Device for removing reject material.

52.11.3.6 Processes

Sylvinite Ore Flotation. Pure sylvinite of German origin can be floated without serious problems. The components of the ore are relatively strongly intergrown [128] and must be broken down by grinding until each grain consists as far as possible of only one component.

The ore is first ground to a particle size of < 4 mm, screened to remove fines, and then slurried with carrier brine and ground to a grain size of < 0.8–1.0 mm in a circulating system that includes rod mills, spiral classifiers, or wet screens (Figure 52.32).

The solids content of the flotation pulp is adjusted to 30–40%, and it is then mixed with flotation agents (ca. 40 g of oil, 20 g of foaming agent, and 40–80 g of collector per tonne of crude salt). As much of the desired product as possible is then extracted by the three-stage high-capacity rougher flotation. The rougher tails are classified in hydrocyclones, debrined (the coarse fraction in centrifuges, and the fine fraction in rotary filters), and dumped. Since the filtrate still contains finely divided salt, it is clarified in a thickener and recycled for slurrying the ore.

The material floated in the rougher flotation is then concentrated in a cleaner flotation process, usually in three stages. This does not produce a marketable product (with > 60% K_2O). The concentrate is therefore separated from the brine and washed with water in salt washing equipment.

This washing process dissolves more halite than sylvite, producing a potash salt that meets quality requirements. The washing liquor is removed by centrifuges, and the product is dried and conveyed to silos.

The cleaner flotation process also produces some intermediate-quality product with a fairly high K_2O content, whose coarse particles contain most of the residual intergrown material from the ore. They are therefore recovered by hydrocyclones and fed to the screening-grinding stage for size reduction. The energy consumption for the entire process is ca. 10 kWh/t ore.

The treatment of sylvinite ores from Canada, the United States, and the CIS is more difficult owing to the clay content of up to 8%. The clay components disintegrate in the brine, forming very fine slimes that absorb large quantities of flotation agent. The flotation process is therefore sometimes preceded by a desliming stage (Figure 52.33). The clay is first detached from the surface of the salt by vigorous agitation in scrubbers, so that it can be floated in a separate operation. The clay is usually removed by multistage classification [176]. The fine material is then thickened and washed with water to reduce losses of K_2O .

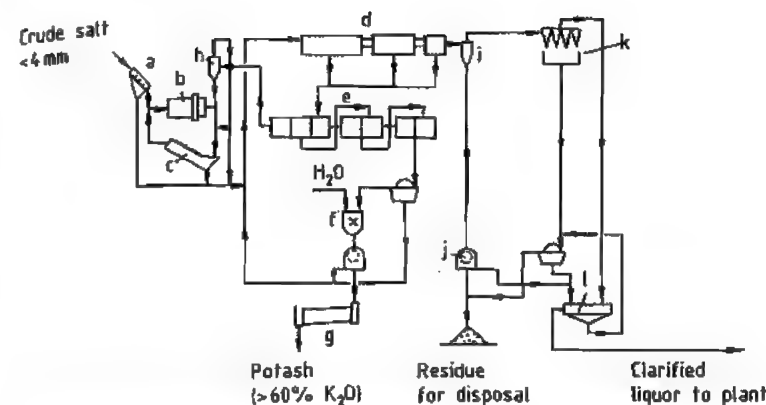


Figure 52.32: Flow diagram of the flotation of potash ores: a) Fine screen; b) Wet grinding; c) Classification; d) Rougher flotation (high volume); e) Cleaner flotation (three stage); f) Water washing for concentrate and debrining; g) Drying; h) Classification of intermediate-quality product; i) Residue (tails) collection; j) Residue debrining; k) Cyclone; l) Clarification of brine for recirculation.

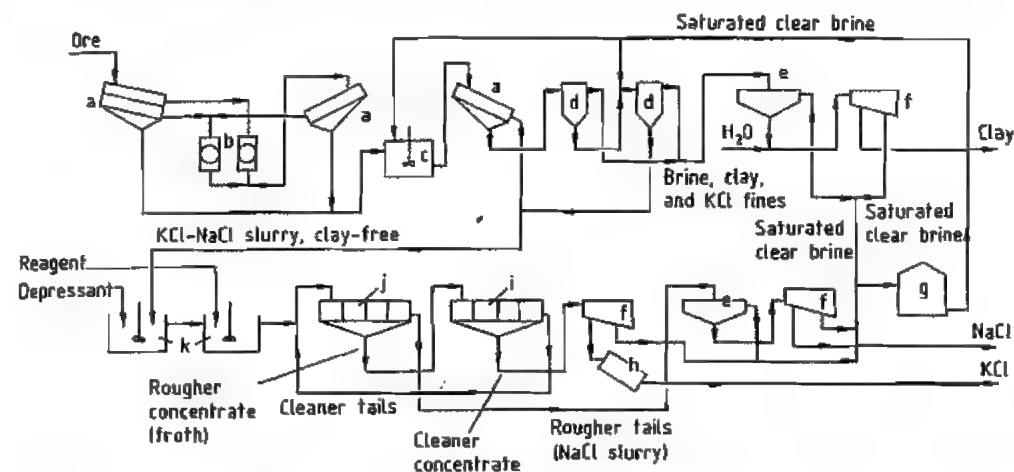


Figure 52.33: Schematic of flotation of potash ores: a) Screen; b) Crushers; c) Scrubber; d) Classifier; e) Thickener; f) Centrifuge; g) Brine tank; h) Dryer; i) Cleaner flotation cells; j) Rougher flotation cells; k) Conditioners. Reproduced from [176] with permission.

Up to 1.5–2% of residual clay in the crude salt can be handled by adding clay depressants.

An advantage of clay-bearing sylvinite ores is that they are usually sufficiently liberated at grain sizes of < 3–5 mm. Sometimes, coarse crystals are floated separately from fine crystals.

Hard-salt flotation is similar to the sylvinite flotation process (Figure 52.32). However, the flotation product also contains kieserite,

which cannot be removed by washing because it dissolves only slowly in water.

Sylvite, which is intergrown with kieserite, must therefore be liberated as fully as possible, which leads to increased grinding costs. Because of the increased production of fines, more flotation agent is needed. Also, in warm summer months, potassium-containing double salts (leonite, schönite) can separate from the circulating brine. Since these salts end up in the residue, the yield is reduced.

Mixed-Salt Flotation. Carnallite ($\text{KCl} \cdot \text{MgCl}_2 \cdot 6\text{H}_2\text{O}$) in the mixed salt is usually decomposed by a brine with low MgCl_2 content. The potassium chloride produced has a grain size of < 0.04 mm and is accompanied by sylvinite ore or hard salt components.

In the 1980s, this complex salt mixture was successfully treated by flotation alone for the first time [177, 178].

Potassium chloride produced by the decomposition is first floated with a fairly small amount of amine in pneumatic or stirred flotation cells; then the sylvite component of the sylvinite ore or hard salt is floated with a further measured amount of amine, and a discardable residue is obtained. The flotation froth is then treated by flotation in cleaner cells to give a concentrate with $> 55\%$ K_2O . A final washing process gives a potash fertilizer salt containing $> 60\%$ K_2O .

Polyminerals are rarely treated by flotation. Potash ore from Stebnik (CIS) contains not only sylvite, halite, and clay materials, but also large amounts of kainite, langbeinite, and polyhalite [179]. Clay depressants are added first, followed by flotation of halite with a mixture of C_7 – C_9 fatty acids. Sodium hydroxide solution is used to adjust pH [179].

Schönite can be floated from a salt mixture by using coconut oil acids as the collector [180]. The flotation of anhydrite to produce a salt mixture of kieserite, langbeinite, and polyhalite is recommended in [181].

A combination of cold leaching and flotation for the treatment of salt mixtures containing langbeinite and polyhalite is described in [182].

52.11.4 Electrostatic Separation

Electrostatic separation depends on the directional movement of electrically charged bodies or particles in an electric field. The processes used differ according to the various methods of producing or separating the charges and according to the separation equipment used. The separation of mixtures of salt minerals (e.g., in the treatment of crude potash ores) invariably involves the selective ex-

change of electric charges that takes place on contact between the various mineral particles, followed by separation in free-fall separators. Although roll separators are widely used for treating other minerals, they have not been used for salts, mainly because of their low throughput.

The first investigations into the industrial-scale separation of potassium chloride and sodium chloride were carried out after World War II by the International Minerals & Chemical Corp. in Carlsbad, New Mexico [183]. The ore, which contains alkali-metal chlorides and various amounts of clay and sulfate minerals, was ground, heated to ca. 500°C , cooled to ca. 110°C , and separated in a free-fall separator with a field strength of 2–6 kV/cm. Results were not encouraging and the method was abandoned.

Research in the Kaliforschungs-Institut in Hannover in 1956 led to an industrial breakthrough. The addition of organic and inorganic reagents much improved the electrical charge exchange between the mineral components, and the separating temperature could be reduced to $< 100^\circ\text{C}$ [184, 185]. The potash works of Neuhof-Ellers, a subsidiary of Kali und Salz, was the first industrial plant to use this process to produce kieserite in 1974. In the following years, plants for the electrostatic production of kieserite and potash concentrates, and for the dry removal of residues, were installed in three other factories, with capacities up to ca. 1000 t/h [186]. Investigations aimed at the introduction of this process for processing sylvinite ores from the potash deposits in Saskatchewan, Canada, have been carried out by PCS Mining, Saskatoon [187].

52.11.4.1 Theoretical Basis

The basis of the process is the mutual selective exchange of electrical charge between the salt components, which occurs on contact. The direction, selectivity, and intensity of the charge exchange can be influenced by a large number of reagents (conditioning agents) [188]. In addition to this chemical conditioning, treatment with air of specific relative hu-

midity is necessary. This is usually controlled by means of the air temperature and should be between 5 and 25% [188, 189]. By the appropriate choice of conditioning agent and relative humidity, the charging properties of the individual mineral components in a potash ore can be controlled so that the desired components are recovered. In this way, an ore of complex composition can be completely separated into its components [190].

The mechanism of charging by contact depends on the transfer of electrons between the touching mineral surfaces, which must have suitable surface properties (i.e., surface energies appropriate for the exchange of charge). These energies are influenced (or created) by chemical conditioning agents and partial water vapor pressure [191–193].

52.11.4.2 Equipment and Processes

Before the separation process, the potash ore must be size-reduced to give complete liberation of its components. Fine particles (< 0.1 mm) behave nonselectively in an electrostatic field, so the grinding process must be carried out as carefully as possible (e.g., by impact grinding). The conditioning agents (20–100 g/t ore) are added to the ore in a mixer or introduced in the vapor state into the fluidized-bed dryer that heats the salt to the separation temperature (25 – 80°C), whereby the relative humidity is adjusted to a suitable value for selective charging of the salt particles [194–196]. Alternatively, a rotary dryer can be used. Depending on the conditioning agent used and the relative humidity and temperature, sylvite generally becomes positively charged, whereas halite and kieserite can be positive or negative. Accompanying minerals such as langbeinite, carnallite, or kainite can be separated individually or together with other mineral components [197–200].

Separation of the mixture of charged minerals is carried out in free-fall separators with an electrical field strength of 4–5 kV/cm. For a distance between the electrodes of 25 cm, the applied voltage is 100–125 kV. Formerly, ver-

tical belt separators were common, but they are now used only for special applications. The electrodes consist of rotating rubber belts with conducting coatings. Brushes on the side opposite the electric field remove salt fines, which otherwise settle on the electrode surface, forming a coating that weakens the electric field and hinders separation. The separator used exclusively today is the tube free-fall separator (Figure 52.34), which was developed by the potash industry [201]. It consists of two opposed rows of steel tubes, ca. 2 m long. The tubes rotate on their axes, and salt fines are removed by brushes on the side remote from the falling salt. The maximum working length of separators of this type is ca. 10 m. The charged salt mixture leaving the fluidized bed is fed to the top of the separator and falls through the electric field between the electrodes. This causes the particles to move sideways, the direction depending on the sign of the charge. At the bottom of the separator, adjustable flaps enable a cathodic fraction, an anodic fraction, and a middle fraction to be recovered. These fractions are then treated further or removed from the process as product and waste (or middlings).

With currently available separator designs and achievable electric fields, the particle sizes for complete liberation should not exceed 1.5–2 mm for sylvite and halite, or 1.2 mm for kieserite, because the movement of particles in the electric field of the separator is determined by both the horizontal electrical force and the vertical effect of gravity. Since the electrical force depends on the charge on the particle, which in turn is a function of the surface area, the surface volume ratio is a very important factor in determining the extent of sideways movement in the electric field. For fine materials, the effect of the electrical force is the greater; the converse is true for coarse particles.

Modern tube free-fall separators have a throughput of 20–30 $\text{th}^{-1}\text{m}^{-1}$. Their energy consumption is very low because for this throughput the current is only ca. 2 mA.

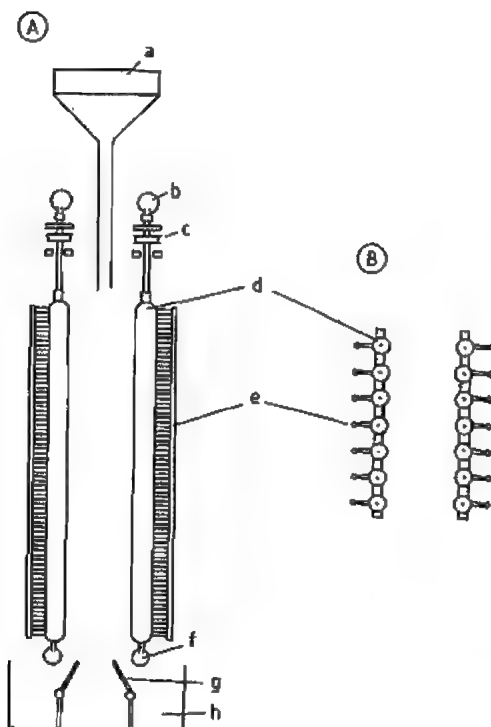


Figure 52.34: Tubular free-fall separator. A) Cross section; B) Plan view. a) Salt feed; b) Upper bearing; c) Motor; d) Tubes; e) Brushes; f) Lower bearing; g) Flaps; h) Receiver for products.

Generally, even for a single-stage separation step two free-fall separators are arranged one above the other so that the concentrate and waste material from the upper separator bypass the lower one, while the middlings flow directly to the lower separator where further separation occurs. In most cases, multistage separation or treatment is necessary, in which the concentrate produced in the first stage is purified or concentrated in another single stage or in multistage separation.

Electrostatic separation has thus far been used industrially on a large scale only for the treatment of hard salts with the principal components sylvite, halite, kieserite, and various percentages of carnallite. Three basic methods of separation into the individual components are

1. Separation of sylvite in the first stage [183, 189, 202], and separation of kieserite and halite in the second stage
2. Separation of kieserite in the first stage [203, 204], and separation of sylvite and halite in the second stage
3. Separation of halite in the first stage [205–207], and separation of kieserite and sylvite in the second stage

In all cases, carnallite appears in the sylvite fraction.

The first stage of method 2 is used to produce kieserite on a large scale, and method 3 is used in several variations for the production of a dry halite residue and of kieserite and potash concentrates [186]. So far, these plants have been operated almost entirely in association with leaching and flotation plants because electrostatic treatment alone gives unsatisfactory yields.

52.11.5 Heavy-Media Separation

Heavy-media separation is not used widely in the potash industry because of the generally unfavorable extent of intergrowth and the small density difference between the main components sylvite ($\rho = 1.99$) and halite ($\rho = 2.17$). However, the process can be used for very coarsely intergrown high-quality sylvinite ores as mined in Saskatchewan. International Minerals & Chemical Corporation (IMCC) operates a plant of this type in Esterhazy, Saskatchewan [208]. The heavy medium is a suspension of magnetite in a saturated salt solution whose density is adjusted to 2.10. Small salt crystals (< 1.7 mm) are very difficult to separate from magnetite; therefore, only materials with a particle size of 1.7–8 mm are treated by this process. Separation is carried out in hydrocyclones in two stages. A process scheme is given in Figure 52.35.

IMCC also operates a heavy-media separation plant in Carlsbad, New Mexico, where langbeinite ($\rho = 2.83$) is recovered from a potash ore in which sylvite and halite are the other main components.

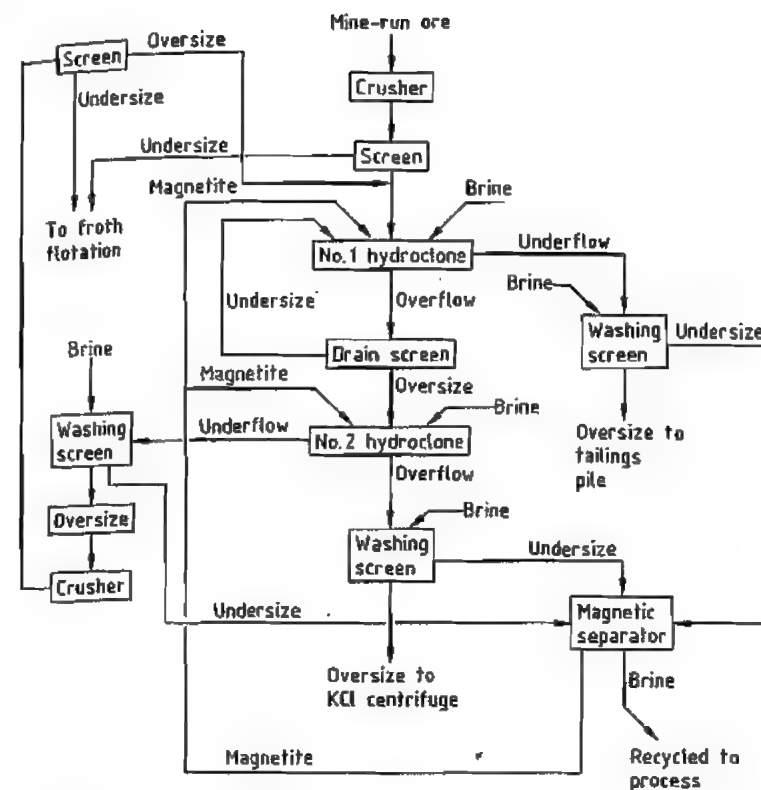


Figure 52.35: Heavy-media separation of potash ore [208]. Reprinted from [208] with permission of John Wiley & Sons, Inc.

52.11.6 Debrining and Drying

The products and waste from all the treatment processes except for the dry electrostatic process are obtained as suspensions with various solids contents and must be debrined. The two main aims of debrining potassium chloride product are (1) to achieve as low a moisture content as possible to minimize drying costs and (2) to remove as much of the adhering brine as possible to maximize product purity. As the brine adhering to the residues contains potassium chloride, its recovery minimizes yield losses. Suspensions must often be thickened in circular thickeners or hydrocyclones before debrining.

The choice of equipment is determined mainly by the particle size of the material to be treated. The extent to which adhering brine

can be removed by washing with water is also important.

Pan filters are used where debrining of a fine-grained product is combined with water washing to increase the K_2O content and when the product is to be stored intermediately. Residual moisture content in this case is 12–14%.

Drum filters are generally used for debrining fine residues or when washing of the filter cake is necessary; they give a residual moisture content of 9–11%. Alternatively, belt filters are used because they have a high capacity and allow the filter cake to be washed with recovery of the washing liquids.

The most commonly used debrining apparatus consists of centrifuges of various designs [209]. In potash works in Canada, the United States, Jordan, and the CIS, screen-bowl and

solid-bowl centrifuges of 1400-mm diameter are in general use. Screen-bowl centrifuges have throughputs of 60–110 t/h and achieve a residual moisture content of 3–8%. They are used to treat both products and residues. Solid-bowl centrifuges mostly are used for fine residues, and achieve throughputs of 70–120 t/h and a residual moisture content of 6–8%. In European and some Canadian factories, large-diameter (> 900 mm) pusher centrifuges are used, with throughputs of 40–50 t/h and a residual moisture content of 3–6%. For coarse products and residues, vibratory screen and screw screen centrifuges are generally used. These have a diameter of 900–1200 mm and a throughput of 35–70 t/h, and give a residual moisture content of 2–4%.

The products are usually dried in drum dryers with diameters up to 3 m and lengths of 20 m [210]. They are heated with oil or gas in cocurrent flow at throughputs up to 120 t/h. The dryers are fitted with internals to promote heat exchange and prevent caking of the salt. Exhaust gases are dedusted, first by cyclones and then by electrostatic filters, wet scrubbers, or fabric filters. The main reasons for the widespread use of drum dryers are their ruggedness, safe operation, lack of sensitivity to throughput variations, and adaptability to differing grain sizes and moisture content.

Since the early 1960s, fluidized-bed dryers have been used to an increasing extent. At first, they were used mainly for coarse products (> 0.5 mm) with low initial moisture content. Later, improvements in fluidized-bed technology enabled products with grain size down to 0.1 mm and initial moisture content up to 8% to be dried. Their most important advantages compared with drum dryers are improved heat and mass transfer, more efficient use of energy, and much smaller floor space requirement. Cyclones and bag or electrostatic filters are used for dedusting the exhaust gases from a fluidized-bed dryer.

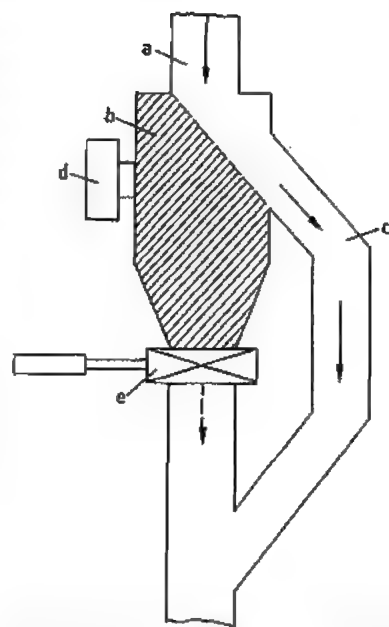


Figure 52.36: Equipment for radiometric determination of potassium in solid materials: a) Inlet for material to be analyzed; b) Container for material to be analyzed; c) Bypass; d) Detector; e) Time-controlled valve.

52.11.7 Process Measurement and Control

The methods normally used in the chemical industry for measuring and controlling process parameters are also used in potash plants. Special methods include the analytical determination of potassium by means of its natural radioactivity [211], the use of flame photometry for so-called ratio analysis, and mineral analysis by infrared spectrometry.

The natural mixture of potassium isotopes includes ca. 0.012% of the radioactive isotope ^{40}K , which is both a β and a γ emitter. Both types of radiation are measured to determine potassium content. The β emissions are usually measured in the laboratory, whereas on-line measurement of γ emissions is widely used for process control. Owing to the great penetrating power of γ rays, the reliability of measurement is strongly dependent on the geometry of the measuring equipment. Equipment for the radiometric determination of

potassium in bulk products is shown in Figure 52.36 [212].

The on-line method of ratio analysis [213, 214] of KCl–NaCl mixtures is based on measuring the potassium and sodium contents of a sample with a double-beam flame photometer, and calculating the ratio from the measured data. Since this ratio is independent of the weight and dilution of the sample wet materials with varying water content can be analyzed without weighing the sample. Ratio analysis is used for determining residual NaCl content in flotation concentrates that have been water washed. The NaCl content is used to determine the amount of washing water required, and enables losses of K_2O due to excessive use of washing water to be avoided. The method has also been used for controlling the K_2O content in products from leaching–crystallization plants.

Infrared spectroscopy is suitable for continuous determination of carnallite or kieserite in crude potash salts. Reflection photometry can be used to measure water of crystallization, and hence the content of these minerals. In some circumstances, the carnallite content can be determined even when kieserite is present [214].

52.11.8 Waste Disposal and Environmental Aspects [215, 216]

The main environmental problem of the potash industry is disposal of process waste. The total world production of potash ore is ca. 250×10^6 t/a, whose processing necessitates the disposal of ca. 200×10^6 t of waste without damage to the environment [215]. In the Canadian province of Saskatchewan alone, 300×10^6 t of solid waste has been generated during the last 30 years, covering an area of ca. 35 km^2 with solid and liquid materials [217].

The composition of the waste depends on the type of ore treated. Waste from the treatment of sylvinites consists mainly of halite. Waste materials from hard salt treatment are halite and kieserite, and from carnallite ore processing, halite and magnesium chloride, which is always produced in the form of an

aqueous solution. Salt solutions that must be disposed of are also generated during the production of potassium sulfate from potassium chloride and magnesium sulfate, and during the recovery of kieserite from residues from the treatment of hard salt by dissolving the halite.

Four methods for disposing of waste are dumping, backfilling, pumping into the ground, and discharge into natural water systems.

The disposal of waste by dumping is by far the most important method. Salt solutions that run off the dumped materials must be demonstrated not to harm the environment when they are absorbed into the ground. Salt solutions can originate from the brine adhering to wet residues or from the carrier liquid for transporting solid waste to the dump, or they can form when atmospheric precipitation dissolves the salt from waste material. If the ground underneath the dump is not impermeable, it must be sealed by layers of clay or plastic sheeting, or a combination of the two. The salt-containing runoff water is collected in ditches at the edges of the dump, and as much as possible is returned to the recirculating brine system in the plant. Excess brine is disposed of along with other liquid waste. In Germany, solid waste is formed into steep conical heaps after drying or debrining as fully as possible. This reduces the amount of salt-containing runoff water formed by atmospheric precipitation and also minimizes the ground area required. In most Canadian installations, filtration residues (tails) are slurried with brines and pumped as a suspension into a large lagoon surrounded by dykes. Flat deposits are formed over a very large area. The brine that runs off is pumped back to the plant and reused for slurring solid waste (Figure 52.37) [218, 219]. If the salt solution enters groundwater-bearing layers despite sealing, boreholes are sunk, and salt-bearing groundwater is pumped back into the lagoon. Attempts to cover dumped waste material to prevent the formation of salt-containing water by the leaching effect of rainfall have in the long run proved unsuccessful [217].

Under certain geological conditions, and if mining methods are suitable, solid residues can be transported underground for backfilling. Since the bulk density of the residue is much lower than that of the potash ore, often only a part of the residue can be accommodated by the space left after extraction of the ore. Backfilling is the main method of waste disposal in North German salt works where the salt beds are steeply inclined, as well as the potash works of New Brunswick in Canada. In most potash works, where the potash is mined from level deposits, backfilling is not possible for technical and economic reasons.

Pumping salt solutions back into the ground is possible if certain geological requirements are met. The formation used for this purpose must possess sufficient porosity and permeability, and must have no contact with formations that could provide a water supply or contain salt deposits. Salt solutions are generally pumped under pressure through lined boreholes into the porous formation.

Since 1926, in the Werra potash region of Germany, large quantities of brine have been pumped into a porous dolomite layer 20–25 m thick. Injection wells have an absorption ca-

capacity up to 1000 m³/h at head pressures up to 11 bar [220]. Since most of this waste brine comes from kieserite production, the amount produced has decreased drastically with the introduction of electrostatic ore treatment [221]. In Saskatchewan, excess brine is pumped into deep formations of dolomite or sandstone. The capacity of these wells is up to ca. 200 m³/h at head pressures up to 60 bar. Kalium Chemicals, Saskatchewan, has been disposing of waste brine since 1979 in caverns produced by solution mining.

The possibility of disposing waste brine in rivers and lakes depends very much on the location. Sea disposal, as practiced in the United Kingdom and by one of the potash works in New Brunswick, presents few major problems if the outfall is sufficiently remote from the coast. The potash works on the Dead Sea can dispose of waste brine in the Dead Sea itself without harmful consequences. The Potash Company of America in Saskatchewan discharges its solid and dissolved wastes into the southern end of the salt-containing Lake Patience, which is isolated from the rest of the lake by a dam.

For most potash works, waste brine cannot be disposed in natural salt water. If underground disposal is impossible, disposal into flowing natural water is the only alternative. In all countries, this is subject to ever-stricter regulation. One particular problem, for which a solution in the foreseeable future is being sought, is the high salt content in the Werra River due to brine from the potash works in the eastern part of the Werra region [221].

The only significant atmospheric pollution caused by potash works is salt dust emitted by the drying plant and from the handling of the ore and products during production and supply. Dust removal from waste gases from dryers is discussed in Section 52.11.6. The dusts produced during production and conveying are usually removed by air extraction, and trapped in fabric filters or wet scrubbers. During the drying of products containing magnesium chloride brines, hydrolysis of the magnesium chloride can lead to the emission of hydrogen chloride, which can be removed from the gas by wet scrubbing or absorption in calcium hydroxide in combination with a woven filter [222]. This procedure can also greatly reduce the level of sulfur dioxide if it is present in the exhaust gas.

52.11.9 Granulation [223–227]

Potassium chloride can be produced in a wide range of crystal sizes, depending on the composition of the potash ore, its degree of intergrowth, and the process used. Different particle-size distributions are needed for various applications. To meet these requirements, the potash industry offers products with standardized size distributions (see Section 52.11.10) obtained by screening to give the various fractions. The resultant distribution of the product among the various standardized grades does not always correspond to market requirements. Demand for products with a particle size of ca. 1–5 mm (coarse and granular grades) exceeds their normal production rate in a potash works. Most potash works must therefore increase the proportion of coarse

product by granulating part of the primary product.

The main reason for the high demand for granulated potassium chloride is the technique of applying fertilizers that was developed mainly in North America and Western Europe in the postwar years. This technique, which is now the most widely used, requires coarse particles with a rather narrow size range. This is needed both for single nutrient fertilizers and for bulk-blended materials, which are widely used in North America. Also, granulated potassium chloride has a lower tendency to cake or form dust than the fine product.

Two methods of granulation are commonly used in the fertilizer industry: agglomeration of molten or wet material in rotating drums or dishes, or compaction of dry material in roll presses. The latter is the method most often used for potash fertilizers.

The starting material for compaction usually consists of a mixture of fine material from the production process with recycled material from the grinding and screening system of the compaction plant. Although dusts from the plant can also be compacted, a high proportion of fines (< 0.1 mm) must be avoided because they cause problems in the compaction equipment. Amines from the flotation process on the surfaces of the particles can also interfere with compaction and must be destroyed or rendered inactive by heat or chemical treatment.

Roll presses used in the potash industry usually have 60–125-cm-long rolls with diameters of 60–100 cm. The feed material, which is usually at 100–120 °C, is generally predensified by force feeders that feed it into the nip between rolls, where it is deaerated and compressed, with plastic deformation of each particle, to produce a dense sheet of material. The compression force is 40–50 kN/cm of roller length. The sheet of material is fed to a pre-breaker that size-reduces it for ease of transportation. It then goes to a grinding sieving plant, which produces either a granular product or granular and coarse products. Undersize material is recycled to the compaction press.

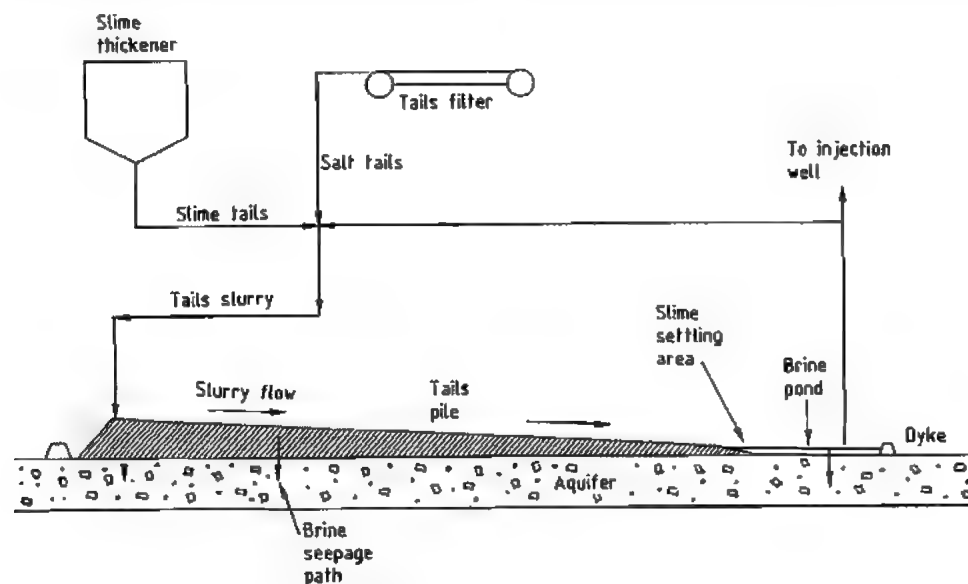


Figure 52.37: Conventional potash waste handling in Saskatchewan [217]. Reproduced with permission.

The compaction product consists of irregularly shaped angular particles. Handling causes abrasion of the edges and corners to form unwanted dust. The granular material is therefore usually treated with water after screening and then dried in a fluidized-bed dryer at 180–200 °C. This smooths the corners and edges, and gives a dense surface to the granules. Another method of dust reduction is to treat the granules with liquids that bind the dust formed by abrasion.

52.11.10 Quality Specifications

The main application of potassium chloride is in potash fertilizers, either as a single-nutrient fertilizer or as the potash component in mixed or complex fertilizers. In English-speaking areas and on the international market it is often called muriate of potash (MOP).

Single-nutrient fertilizers, which were formerly the most common type, have been replaced largely by complex or mixed fertilizers. Also, the finely divided fertilizers formerly used have increasingly been replaced by granulated products. Single potash fertilizers often contain the additional nutrient magnesium sulfate.

Potassium chloride must have differing grain structure and nutrient content depending on its intended use, e.g., for the production of granulated NPK or PK fertilizers, for application as suspension or liquid fertilizers, for bulk blending with other components, or as a single-nutrient fertilizer. The potash industry has developed internationally accepted quality standards.

The three main grades differ in grain size:

Standard	0.2–0.8 mm
Coarse	0.8–2.0 mm
Granular	1.2–3.5 mm

Other products, such as those designated soluble, special standard, or special fine, can contain a high proportion of grains < 0.2 mm. Grain-size distributions of the principal grades are listed in Table 52.10. Products from various manufacturers can diverge considerably from these specifications.

The granular and coarse products are used for bulk blending with other granulated fertilizers

or as single-nutrient fertilizers. The standard and other fine materials are used in the manufacture of granulated multinutrient fertilizers, and for suspension and liquid fertilizers.

The potassium chloride content, which for fertilizers is usually given as % K_2O (100% $KCl = 63\% K_2O$), is generally at least 60% K_2O (95% KCl) for this application. The main impurities include sodium chloride, or magnesium sulfate, and sometimes anhydrite or clay minerals, depending on the raw materials and production method. Fertilizer-quality potassium chloride produced by flotation is often colored red to red-brown by hematite inclusions or salt clay.

For single-nutrient fertilization, especially in European agriculture, potash fertilizers with a low K_2O content are often used. These generally contain a guaranteed level of water-soluble magnesium salts. In Germany, for example, two granulated potash fertilizers with a guaranteed MgO content are widely used: 40er Kornkali with MgO (40% K_2O , 6% MgO) and Magnesia-Kainit coarse (11% K_2O , 5% MgO , 24% Na_2O).

About 5% of the potassium chloride produced worldwide is used as an industrial chemical, mainly for the production of potassium hydroxide (see Section 52.13) and chlorine by chlor-alkali electrolysis. Material of this quality is produced by recrystallizing low-purity potassium chloride. A distinction is made between industrial-grade and chemical-grade material, depending on the impurity content and area of use. Typical analyses of these products are

Industrial grade:	KCl :	99.0–99.5%
	$NaCl$:	0.8–0.3%
Chemical grade:	KCl :	99.8–99.9%
	$NaCl$:	0.05–0.03%

The remaining impurities consist mainly of bromide and alkaline-earth sulfates, depending on the raw material and production process.

Dust content and free-flowing properties are important quality criteria, and depend on chemical composition and grain size. With granulated materials, dust formation by abrasion occurs due to handling during manufacture and transport even if the materials are

specially treated during production. To bind the dust, the granulated material is treated with conditioning agents such as polyglycols, mineral oil products, vegetable oils and waxes, or mixtures of these. The addition rates are usually 0.3–5.0 kg/t [228, 229]. Various methods have been developed to assess or measure the abrasion resistance and dust content of the granulated product. Abrasion resistance is tested by subjecting samples of the granules to a process of screening or rolling in a rotating drum with steel spheres or rods, and weighing the fine material formed after a given time [230]. Dust content is determined by air blowing a sample under precisely defined conditions and weighing the dust collected [228].

Fine potassium chloride (standard quality or finer) tends to cake on storage or transport over long distances. Anticaking agents are therefore generally added, usually mixtures of aliphatic amines, or sometimes higher fatty acids. Salt products that do not contain alkaline-earth sulfates are treated with potassium hexacyanoferrate(II). Addition rates for organic anticaking agents are 50–300 g/t, but potassium hexacyanoferrate(II) is effective even at 15–25 g/t [228, 229]. Anticaking agents can affect the wettability of potassium chloride, which in turn can affect its granulation properties when complex fertilizers are being produced. The anticaking treatment must therefore suit the user's requirements exactly [231].

52.11.11 Toxicology and Occupational Health

No toxic hazards are associated with the normal handling of potassium chloride. According to USP XVII of 1970, the usual therapeutic dose (e.g., for treating potassium deficiency) taken orally would be 1–10 g/d. The LD_{50} (oral, guinea pig) is 2500 mg/kg.

Protective measures for storage and handling and personal protection such as breathing apparatus or gloves are unnecessary.

52.11.12 Economic Aspects and Uses [82, 232, 233]

Germany was the sole producer up to World War I, and was later joined by France and the United States, and then Spain, the Soviet Union, and Poland. After World War II, the leading producers were the central and western European countries and the United States. In the 1960s, the Soviet potash industry grew strongly, and the Soviet Union became the leading producer. Also in the 1960s, the first potash works in Saskatchewan was started up. In a few years, several large potash works were in operation there, and Canada became the second largest producer after the Soviet Union. The capital investment in the Soviet Union and Canada and the rapidly increasing use of fertilizers in agriculture in the 1960s and 1970s led to a steep increase in world potash production. Since 1980, the average annual increase in world potash production has been only 0.7%.

Almost two-thirds of world potash production is exported. All the potash-producing countries are exporters except for Brazil and China. Canada is by far the largest exporter.

The economic situation, particularly in developed countries, greatly influences the extent and regional distribution of exports. Both the quantity exported and its distribution among consumers are greatly affected by the state of their agriculture, especially in developed regions, and by the demand for or availability of convertible currency in the exporting or importing country. Transport costs for potash fertilizers have a considerable bearing on total cost to the consumer, and logistical considerations also influence the direction and size of exports or imports. Finally, fluctuations in the rate of exchange of currencies between the countries concerned are very important.

Because of the conditions described above, certain special regional relationships developed. The agricultural requirements of the former COMECON countries were satisfied by the Soviet and East German potash industries only. In western Europe, the market was supplied almost entirely by western European

producers. In North America, Canadian and United States producers were in a dominating position. Canada had a good export market in Asia, as did Europe and Jordan. The Latin American market was supplied mainly by Canadian producers, together with East Germany and the Soviet Union. In recent years, the political and economic changes in the former Eastern Bloc, the unification of Germany, and the collapse of the dollar have all led to changes in the supply demand relationships described above, although the distance between the producer and the consumer is still of overriding importance. The future development of potash exports will be influenced greatly by imports into China and Brazil. Both countries have only minimal production and are compelled to import fertilizers on a large scale. Problems associated with their internal economies and with foreign exchange have thus far limited imports [234, 235].

The capacities of the potash producers in various countries for 1990–1991 (in 10^3 t K_2O) were [233]:

Middle and Western Europe	8 700
Germany	5 700
France	1 500
Spain	750
Italy	250
United Kingdom	500
North America	13 028
United States	1 838
Canada	11 190
Soviet Union	12 880
Western Asia	2 220
Israel	1 380
Jordan	840
Brazil	150
China	50
Others	200
Total	37 218

Estimated world demand for potash fertilizers in the business year 1990–1991 by regions (in 1000 t K_2O) was as follows:

Europe	7 520
Eastern Europe	2 120
Western Europe	5 400
Soviet Union	5 600
America	7 320
North America	5 100
Central America	350
South America	3 190
Asia	4 705
Western Asia	155
Southern Asia	1 360
Eastern Asia	3 190

Africa	522
Oceania	260
World	25 927

In using these figures, it should be borne in mind that the capacities quoted by individual producers are generally too high and that only ca. 95 % of the total potash production is used in the form of fertilizers. Hence, the total consumption of products of the potash industry is ca. 1.5×10^6 t of K_2O higher than the figure given above. Nevertheless, considerable overcapacity exists worldwide, as can be seen by comparing the two tables.

Industrial-grade and chemical-grade potassium chloride are used mainly for the electrolytic production of potassium hydroxide. Other important uses include the production of drilling fluids for the oil industry, aluminum smelting, metal plating, production of various potassium compounds, and applications in the food and pharmaceutical industries [236].

52.12 Potassium Sulfate [237]

Potassium sulfate, K_2SO_4 , mineral name arcanite, forms colorless, nonhygroscopic crystals. It occasionally occurs in nature in the pure state in salt deposits (e.g., in Germany, the United States, and the CIS) but is more widely found in the form of mineral double salts in combination with sulfates of calcium, magnesium, and sodium (Table 52.3). Potassium sulfate is, after potassium chloride, the most important potassium-containing fertilizer, being used mainly for special crops. Potassium sulfate constitutes ca. 5 % of the world demand for potash fertilizers.

52.12.1 Properties

Potassium sulfate forms orthorhombic crystals, which transform to the trigonal modification at 583 °C. Some properties of potassium sulfate are listed below:

f_p	1069 °C
Crystal system and type	orthorhombic, D_{2h}^{16}
Phase change at	583 °C
Crystal system and type at > 583 °C	trigonal, D_{3d}^{13}
Refractive indices n_D^{20}	1.4933; 1.4946; 1.4973
Density	2.662 g/cm ³

Specific heat capacity c_p	752.9 J kg ⁻¹ K ⁻¹
Heat of fusion	197.4 kJ/kg
Heat of transformation (orthorhombic/trigonal)	48.5 kJ/kg
Enthalpy of formation ΔH°	-1438 kJ/mol
Entropy S°	175.6 J mol ⁻¹ K ⁻¹
Dielectric constant (at 4×10^4 Hz)	6.3
Thermal coefficient of expansion (cubic)	130×10^{-4} K ⁻¹

Apart from the naturally occurring double-salt minerals mentioned above, potassium sulfate also forms double salts and mixed crystals with ammonium sulfate and the sulfates of beryllium, magnesium, calcium, strontium, barium, and lead. It is reduced to potassium sulfide or potassium polysulfides by reducing agents such as hydrogen and carbon monoxide at high temperature.

The solubility of potassium sulfate in water is listed in Table 52.11. The cryohydric point is -1.51 °C (7.1 g K_2SO_4 /100 g H_2O), and the boiling point of the saturated solution is 101.4 °C (24.3 g K_2SO_4 /100 g H_2O). The solid phases formed in the system K_2SO_4 - H_2O are K_2SO_4 , $K_2SO_4 \cdot H_2O$, and ice. In aqueous ammoniacal solution, the solubility decreases rapidly with increasing ammonia concentration [238]. Potassium sulfate is virtually insoluble in industrial organic solvents.

Table 52.11: Solubility of potassium sulfate in water (g/100 g) [93].

Temperature, °C	Solubility	Temperature, °C	Solubility
0	7.35	60	18.4
10	9.24	70	20.0
20	11.1	80	21.5
30	12.9	90	22.8
40	14.8	100	24.0
50	16.6		

52.12.2 Raw Materials

Potassium sulfate is produced from single or mixed minerals or brines, or by the reaction of potassium chloride with sulfuric acid or sulfates [239]. The economically important minerals include the deposits of hard salt in Germany, langbeinite in New Mexico (United States), and kainite in Sicily. In the United States, sulfate-containing crystalline products from the evaporation of water from the Great Salt Lake (Utah) and Searles Lake (California)

are also used for the production of potassium sulfate.

Potassium chloride is usually converted to potassium sulfate by reaction with sulfuric acid, but SO_2 -air mixtures can also be used. Reactions with sodium sulfate and gypsum have recently become of interest. Small amounts of potassium sulfate are obtained during the production of alumina from alunite.

52.12.3 Production

The choice of production method and the location of a potassium sulfate plant depend on having a plentiful economic supply of the starting materials and being able to utilize or dispose of the by-products or waste. Most production plants are located on salt deposits from which at least some of the raw materials can be obtained. Plants in which potassium chloride is reacted with sulfuric acid with liberation of hydrogen chloride are usually located in regions with a demand for hydrochloric acid, (e.g., for an acidification of petroleum boreholes), or they operate in conjunction with a chemical works having a process that uses hydrogen chloride. In such cases, the exploitability of hydrogen chloride determines the capacity of the potassium sulfate plant.

52.12.3.1 From KCl and H_2SO_4 (Mannheim Process)

The reaction of sulfuric acid with potassium chloride takes place in two stages:



The first reaction step is exothermic and proceeds at relatively low temperature. The second is endothermic and must be carried out at higher temperature. The relationship between total reaction time and temperature is shown in Figure 52.38. In practice, the process is operated at 600–700 °C. To minimize the chloride content of the product, a small excess of sulfuric acid is used, which is later neutralized with calcium carbonate or potassium carbon-

ate, depending on the purity requirements for the product.

The reaction is usually carried out in so-called Mannheim furnaces (Figure 52.39) [240].

The furnace has a closed dish-shaped chamber, with diameter up to 6 m, heated externally by an oil or gas burner. Potassium chloride and sulfuric acid are fed into the chamber in the required ratio at an overhead central point. The mixture reacts with evolution of heat and is mixed by a slowly moving stirrer fitted with stirring arms with scrapers (rabblers), which propels the mixture from the center of the chamber to the periphery. Potassium sulfate leaves the reaction chamber at this point and is neutralized and cooled. It normally contains 50–52% K_2O and 1.5–2% chloride. Hydrogen chloride gas formed is absorbed in water to form hydrochloric acid or used in gaseous form.

The Mannheim process is the most widely used method of producing potassium sulfate due to its simplicity, high yield, and the many ways in which the by-product can be utilized. Hydrogen chloride is used to produce dicalcium phosphate, vinyl chloride, or calcium chloride if it cannot be sold as hydrochloric acid.

Disadvantages of the process include high energy consumption, severe corrosion, and high capital cost. In the United States, reductions in corrosion and energy consumption are

achieved by using the Cannon process, in which the reaction is carried out in a directly fired fluidized bed.

Another variation is the Hargreaves process, which is also used in the United States. Briquetted potassium chloride is heated in reaction chambers in a stream of sulfur dioxide from the combustion of sulfur, excess air, and water vapor. The yield and the degree of conversion are both ca. 95 %.

The Mannheim and Hargreaves processes are also used to produce sodium sulfate from sodium chloride and sulfuric acid. Mannheim furnaces can be used to produce potassium and sodium sulfates alternately. Recent research into the reaction of potassium chloride with sulfuric acid in a liquid-liquid extraction process did not result in the construction of a production plant [241, 242].

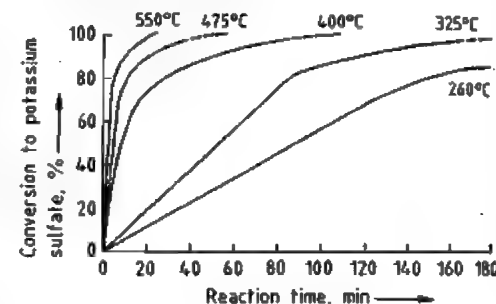


Figure 52.38: Temperature dependence of the reaction between chloride and sulfuric acid. Reproduced from [240] with permission.

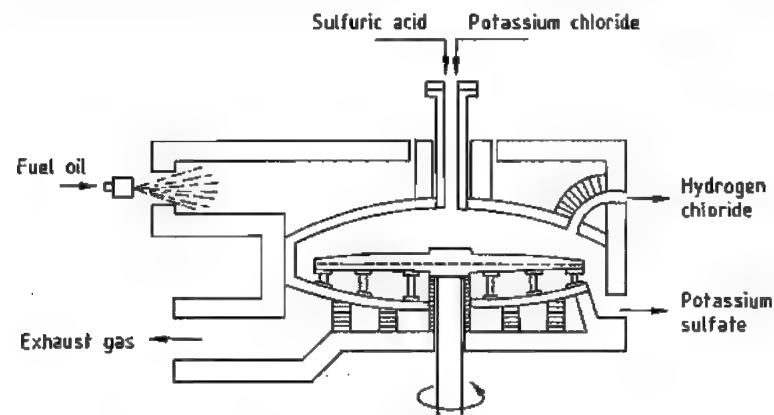


Figure 52.39: Schematic diagram of a Mannheim furnace. Reproduced from [240] with permission.

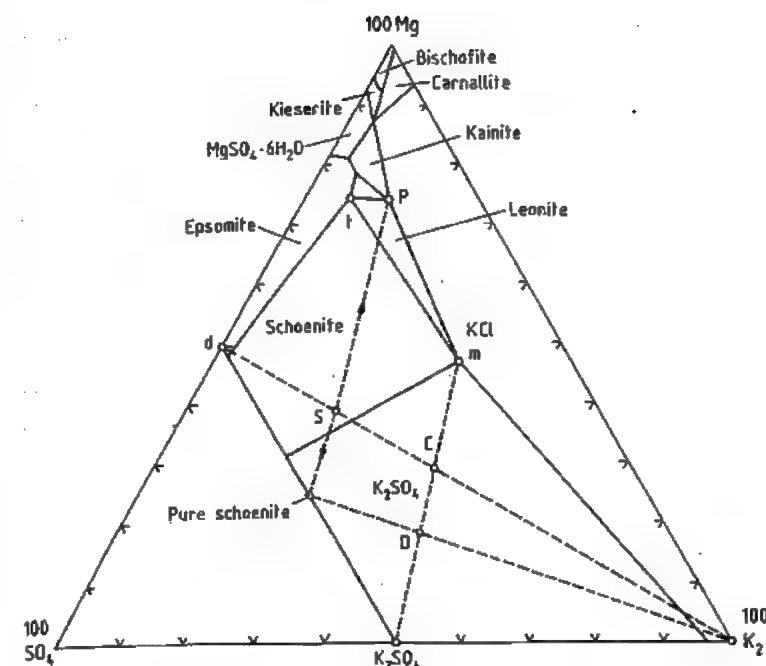


Figure 52.40: Isothermals of the system $K_2-Mg-Cl_2-SO_4-H_2O$ at 25 °C according to JÄNECKE.

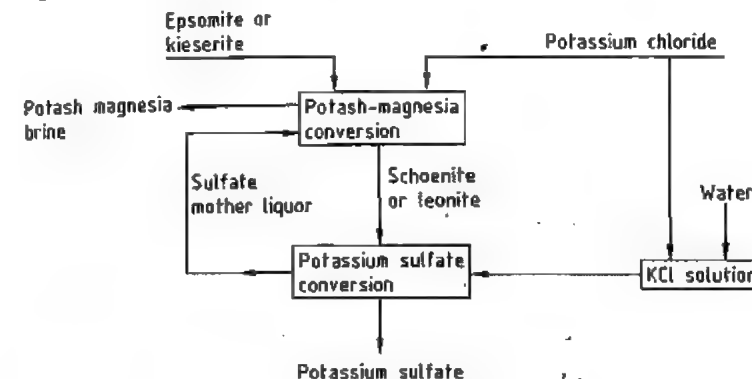


Figure 52.41: Flow diagram of the two-stage production of potassium sulfate from potassium chloride and magnesium sulfate.

52.12.3.2 From KCl and $MgSO_4$ [243, 244]

In a process used mainly in Germany, the sulfate required is provided by kieserite, $MgSO_4 \cdot H_2O$, a component of German hard salt deposits. The reaction can be represented by the following overall equation:



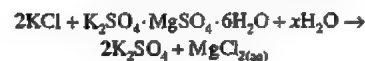
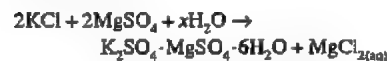
Kieserite reacts very slowly and must be ground finely before reaction. Alternatively, it can first be recrystallized to give epsomite, $MgSO_4 \cdot 7H_2O$.

The basis of the process is explained in Figure 52.40. The fundamental relationships for the single-stage process of KUBERSCHKY and the two-stage process of KOELICHEN and PRZI-

BYLLA are shown as broken lines on the isotherm diagram.

For the single-stage process, the most favorable mixing ratio of the starting materials is given by point C. In the presence of sufficient water, this mixture reacts to form potassium sulfate and a sulfate mother liquor (point m). This solution has the highest magnesium chloride content attainable by direct reaction, which determines the yield. The magnesium content of solution m reaches a maximum at 25 °C, and the process is therefore carried out at this temperature. The single-stage process achieves a theoretical potassium yield of only 46.1% and sulfate yield of 67.5%.

For this reason, the two-stage process is now used exclusively. In this process, the starting materials are first mixed in the presence of a definite quantity of water corresponding to point S to form schönite, $K_2SO_4 \cdot MgSO_4 \cdot 6H_2O$. So-called potash-magnesia liquor, which has a high magnesium chloride content (point P), is also formed. The schönite is reacted with additional potassium chloride (point D) to form potassium sulfate and sulfate mother liquor:



This process gives a theoretical potassium yield of 68% and sulfate yield of 83.7%.

The flow diagram of the process is shown schematically in Figure 52.41.

In the first stage, called the potash-magnesia stage, schönite or leonite, $K_2SO_4 \cdot MgSO_4 \cdot 4H_2O$, is produced by stirring solid epsomite or finely ground kieserite with potassium chloride in sulfate mother liquor recycled from the second stage. The suspension produced is filtered on rotary filters; the potash-magnesia brine, which contains 180–200 g/L magnesium chloride, is removed; and the solid crystalline product, also known as potash-magnesia, is fed to the next stage, sometimes after being washed with sulfate mother liquor, where it is stirred with potassium chloride solution at ca. 70 °C. The temperature of the

mixture is 35–40 °C, and solid potassium sulfate is formed. This is thickened, debrined by centrifuges, and dried in drum or fluidized-bed dryers.

If the sulfate reaction is carried out in a classifying crystallizer at a high solids content [245], a very pure, coarsely crystalline product is obtained with K_2O content of 53% and chloride content of < 0.5%.

In the industrial process, sodium chloride is always present. If the molar ratio of $Na_2:K_2$ in the sulfate mother liquor exceeds 2:5, glaserite, $3K_2SO_4 \cdot Na_2SO_4$, is formed instead of potassium sulfate. To prevent this, the potassium chloride used must be of adequate purity.

The yield is determined by losses to the waste brine. The higher the magnesium chloride content of the potash-magnesia brine is, the lower is the potassium content, and therefore the potassium loss. Excess potassium-rich sulfate mother liquor must be recovered.

52.12.3.3 From KCl and Langbeinite [246]

Large deposits of langbeinite, $K_2SO_4 \cdot 2MgSO_4$, can be found in New Mexico (United States). Langbeinite can be converted to potassium sulfate according to the following overall equation:



The potash ore also contains halite and varying amounts of sylvite, from which langbeinite is separated by gravity separation, flotation, and dissolution of halite, giving various crystal sizes. The coarser langbeinite fraction is sold as potash-magnesia fertilizer, and the finer fraction is reacted with potassium chloride to produce potassium sulfate. A flow diagram for the process is given in Figure 52.42.

Potassium

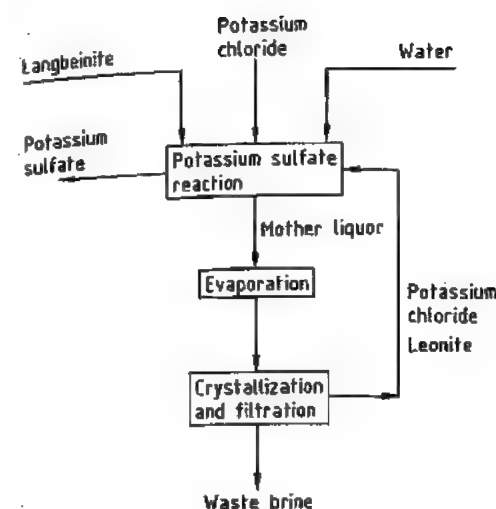


Figure 52.42: Flow diagram of the production of potassium sulfate from langbeinite.

The potassium sulfate formed is granulated and marketed in three different grain sizes: granular (0.8–3.4 mm), standard (0.2–1.6 mm), and special standard. The latter has a high content of grains < 0.2 mm.

52.12.3.4 From KCl and Kainite [239]

In Sicily, kainite, $KCl \cdot MgSO_4 \cdot 2.75H_2O$, is obtained from a potash ore by flotation. It is then converted into schönite at ca. 25 °C by stirring with mother liquor containing the sul-

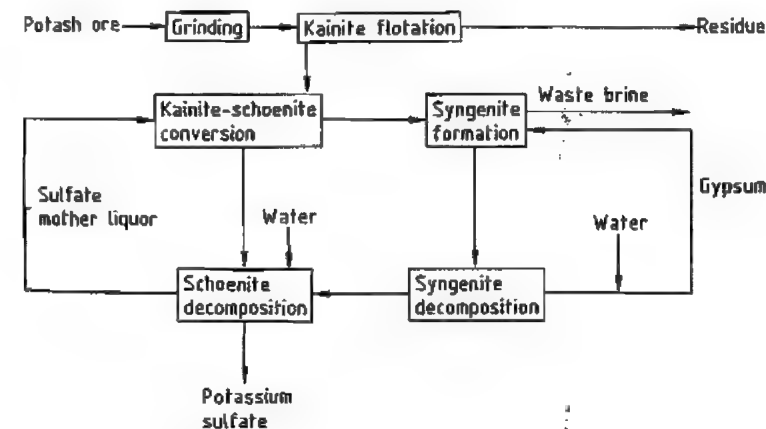


Figure 52.43: Flow diagram of the production of potassium sulfate from kainite.

fates of potassium and magnesium from the later stages of the process. Schönite is filtered off and decomposed with water at ca. 48 °C. This causes magnesium sulfate and part of the potassium sulfate to dissolve and most of the potassium sulfate to crystallize. The crystals are filtered and dried. The sulfate mother liquor is recycled to the kainite-schönite conversion stage. The mother liquor produced there, which still contains ca. 30% of the potassium used, is treated with gypsum, $CaSO_4 \cdot 2H_2O$, causing sparingly soluble syngenite, $K_2SO_4 \cdot CaSO_4 \cdot H_2O$, to precipitate. Syngenite is decomposed with water at ca. 50 °C, which dissolves potassium sulfate and reprecipitates gypsum. The potassium sulfate solution is recycled to the schönite decomposition stage, and gypsum is reused to precipitate syngenite. A simplified flow diagram of the process is given in Figure 52.43.

52.12.3.5 From KCl and Na_2SO_4 [242]

The production of potassium sulfate from potassium chloride and sodium sulfate takes place in two stages, with glaserite, $Na_2SO_4 \cdot 3K_2SO_4$, as an intermediate, according to the following equations:



Potassium chloride and sodium sulfate are reacted at 20–50 °C in water and recycled process brines to form glaserite, which is filtered and then reacted with more potassium chloride and water to form potassium sulfate. Because the mother liquor from the glaserite stage has a high potassium and sulfate content, the maximum potassium yield is 73%, and the maximum sulfate yield is 78%. The yield can be increased considerably by cooling the mother liquor to produce more crystals and by including a final evaporation stage.

A production plant in the CIS uses the glaserite process [244], and an experimental plant is operating in Canada [247].

Alternatively, sodium sulfate solution can be used to charge an anion exchanger with sulfate, which reacts with potassium chloride solution to give a high yield of potassium sulfate [248, 249]. This process is used at Quill Lake, Saskatchewan, Canada, which has a high sodium sulfate content.

52.12.3.6 From KCl and CaSO₄

Processes based on gypsum, CaSO₄·2H₂O, have often been proposed, because it is so readily available. Two processes have been tested in experimental plants:

- Reaction with potassium chloride in strongly ammoniacal solution
 - Reaction with anion exchangers
- Potassium chloride reacts with gypsum in water to give syngenite. If the reaction is carried out in a concentrated solution of ammonia at low temperature, potassium sulfate with a very low syngenite content is obtained [241, 250, 251].



By carrying out the reaction in two or more stages, high concentrations of calcium chloride in the waste brine can be produced, and hence very high yields. The ammonia required for the reaction medium must be recovered by distillation. This process has recently attracted some interest [252].

The anion-exchange process is carried out in two stages [253]. First, the ion-exchange

resin (R) is treated with a suspension of gypsum, charging it with sulfate. The charged resin is then treated with a concentrated solution of potassium chloride, to replace the dissolved chloride by sulfate. Potassium sulfate crystallizes from the solution, sometimes after the addition of solid potassium chloride. The process takes place according to the following equations:



52.12.3.7 From Alunite [254]

Alunite, K₂SO₄·Al₂(SO₄)₃·4Al(OH)₃, occurs in several extensive deposits. On being heated to 800–1000 °C, it decomposes with liberation of sulfur trioxide to form a mixture of alumina and potassium sulfate. The latter can be extracted from the mixture. A plant in the CIS uses this process.

52.12.3.8 From Natural Brines and Bitterns

In the United States, large quantities of potassium sulfate are produced from the brines of the Great Salt Lake and smaller amounts from the brines of Searles Lake. Extensive investigations and project studies have been carried out in various countries into the extraction of potassium sulfate from the mother liquors (bitterns) produced when salt is extracted from seawater, and from concentrated brines in Tunisia and the Atacama desert of Chile [242].

52.12.4 Granulation

The demand for granulated potassium sulfate has increased greatly in recent years for the same reasons that the demand for potassium chloride has increased. The method of production with compaction rolls is widely used (see Section 52.11.9), although potassium sulfate does not behave under pressure like potassium chloride, which undergoes plastic deformation with merging of the grain boundaries. However, the granulated product is much more dense and solid if the potassium

sulfate is wetted before compaction by adding up to 2% water, or if steam is introduced through force feeders located above the compaction rolls. Also, the pressure used must be considerably higher than that for potassium chloride [255, 256]. A compaction plant for potassium sulfate is otherwise similar to that for potassium chloride, although the throughput is much lower.

52.12.5 Quality Specifications

The important quality specifications for agricultural-grade potassium sulfate, known in the English-speaking world and on the international market as sulfate of potash (abbreviated to SOP), are the K₂O and chloride content. All producers guarantee a minimum K₂O content of 50% (92.5% K₂SO₄), typical values being 50.5–51.0%. A completely water-soluble potassium sulfate with K₂O content of > 52% is supplied for the production of liquid fertilizers.

The maximum permissible chloride content is 3%, according to EC Guidelines, but the usual commercial upper limit is 2.5%. The chloride content depends very much on the production method, and some producers offer potassium sulfate with chloride content < 0.5%.

The most common impurities, apart from alkali chlorides, are the sulfates of calcium and magnesium.

The demand for granulated potassium sulfate as a single-nutrient fertilizer and for bulk blending has greatly increased. The crystal size and size distribution of the products granular, coarse, and standard are the same as those for potassium chloride.

Potassium sulfate does not cake as readily as potassium chloride and is therefore not treated with anticaking agents. Dust-reducing agents are added at the rate of 5 kg/t to the fine and granulated products; the same additives are used as for potassium chloride.

Industrial-grade potassium sulfate with a K₂SO₄ content of 99.6–99.9%, purified by recrystallization, is supplied as a raw material for the production of other potassium com-

pounds and as an auxiliary material or reagent for various branches of industry. Specifications with respect to chemical purity and crystal size distribution are suited to the individual user's requirements and can sometimes be very detailed.

52.12.6 Toxicology and Occupational Health

No health hazard is associated with potassium sulfate if it is handled in accordance with regulations. According to Swiss law relating to toxic substances, it is a Class 4 material (LD₅₀: 500–5000 mg/kg). Otherwise, the information given in Section 52.11.11 for potassium chloride applies.

52.12.7 Economic Aspects and Uses

Potassium sulfate accounts for ca. 5% of world production by the potash industry, expressed in K₂O units. It is produced in 11 countries. Of the total, ca. two-thirds comes from Belgium and Germany. Other European producers are Italy, Spain, Finland, and Sweden. Potassium sulfate is also produced by the CTS. Other production plants are in the United States, Japan, South Korea, Taiwan, the Philippines, and recently, China. Present world production and consumption both exceed 1.5 × 10⁶ t K₂O [257, 258].

Potassium sulfate is up to twice as expensive as potassium chloride based on K₂O content due to the costs of the raw material (potassium chloride) and processing. It is therefore only used as a potash fertilizer for applications where it performs much better than potassium chloride.

The sulfur content of potassium sulfate is an advantage where there is a deficiency of sulfur in the soil. Also, it has only a slight oversalting effect on soil in arid or semiarid areas. It is useful for fertilizing crops that are sensitive to chloride or whose quality is improved by chloride-free fertilization. This applies particularly to tobacco, vegetables,

potatoes, vines, and citrus or various other fruit [257, 259].

Potassium sulfate is used in industry for the production of other potassium compounds, accelerators for rapid-setting cements, synthetic rubbers, desensitizers for explosives, lubricants, powdered fire extinguishers, dyes, explosives, and pharmaceuticals.

52.13 Potassium Hydroxide

[273–276]

52.13.1 Properties

Pure, solid potassium hydroxide, KOH, caustic potash, ρ 2.044 g/cm³, *mp* 410 °C, *bp* 1327 °C, heat of fusion 7.5 kJ/mol, is a hard, white substance. It is deliquescent and absorbs water vapor and carbon dioxide from the air. Potassium hydroxide dissolves readily in alcohols and water (heat of solution 53.51 kJ/mol). The solubility of KOH (g KOH/100 g H₂O) in water is shown below:

Temperature, °C	0	10	20	30	50	100
Solubility	97	103	112	126	140	178

The mono-, di-, and tetrahydrates are formed with water. Aqueous potassium hydroxide is a colorless, strongly basic, soapy, caustic liquid, whose density depends on the concentration:

Concentration, %	10	20	30	40	50
Density, g/cm ³	1.092	1.188	1.291	1.395	1.514

Technical caustic potash (90–92% KOH) melts at ca. 250 °C; the heat of fusion is ca. 6.7 kJ/mol.

52.13.2 Production

Today, potassium hydroxide is manufactured almost exclusively by potassium chloride electrolysis. The diaphragm, mercury, and membrane processes are all suitable for the production of potassium hydroxide, but the mercury process is preferred because it yields a chemically pure 50% potassium hydroxide solution.

In the *diaphragm process*, a KCl-containing, 8–10% potassium hydroxide solution is initially formed, whose salt content can be reduced to ca. 1.0–1.5% KCl by evaporation to a

50% liquor. Further purification is complicated, and the quality of liquor from mercury cells cannot be achieved.

In the *mercury process* a very pure KCl brine must be utilized, because even traces (ppb range) of heavy metals such as chromium, tungsten, molybdenum, and vanadium, as well as small amounts (ppm range) of calcium or magnesium, lead to strong evolution of hydrogen at the amalgam cathode. The very pure potassium hydroxide solution running off the decomposers is cooled, freed from small amounts of mercury in precoated filters, and in some cases sent immediately to the consumer as a 45–50% liquor in drums, tank cars, or barges.

Since about 1985, new cell rooms for the manufacture of potassium hydroxide solution have used the *membrane process*. At present, the cell liquor has a low chloride content (10–50 ppm); the KOH concentration is 32%. Before dispatch, it is concentrated to 45–50% by evaporation.

Nonelectrochemical processes have been proposed for the manufacture of chlorine and potassium hydroxide from KCl by thermal decomposition of potassium nitrite in the presence of Fe₂O₃ [277].

This method involves reacting KCl with NO₂ to obtain Cl₂ and potassium nitrite, reacting the KNO₂ with iron(III) oxide and oxygen to give potassium ferrate (K₂Fe₂O₄), and reacting the ferrate with water to produce KOH. Another method consists of reacting an aqueous solution of KCl with NO₂ and O₂ to give Cl₂ and KNO₃, which is reacted with water in the presence of Fe₂O₃ to produce KOH.

Largely water-free, ca. 90–95% potassium hydroxide (caustic potash) is obtained by evaporating potassium hydroxide solution. The residual content of 5–10% H₂O is bound as a monohydrate.

Suitable evaporation processes are single- or multistage falling-film evaporators [278], Badger single-tube evaporators, or boilers connected in cascade. Heating is carried out with steam or by means of heat-transfer agents (salt melts, Dowtherm). Flash evaporators are

used as the final stage in large-capacity plants [279].

To counter the strong corrosiveness of the potassium hydroxide solution and retain the purity of the caustic potash, the equipment is made largely from high-purity nickel (LC 99.2) or is silverplated. The equipment is often protected by polarization.

For dispatch, caustic potash comes on the market poured directly into drums or packed in polyethylene bags after cooling; in blocks, molded pieces, flakes, prills, and as a powder. Potassium hydroxide is classified as a corrosive material:

UN no.	1814 (for aqueous solution)
UN no.	1813 (for dry material)
GGVS/GGVE	Class 8
RID/ADR	Class 8
Handling is described in [280].	

52.13.3 Quality Specifications

Potassium hydroxide solution is supplied in pure quality [total alkalinity 49.7–50.3%, KOH 48.8% (min.), NaOH 0.5% (max.), CO₃²⁻ 0.1% (max.)] or in technical quality [total alkalinity 49.7–50.3%, NaOH 1.0% (max.), CO₃²⁻ 0.3% (max.)]. The contents of Cl⁻, SO₄²⁻, Fe²⁺, and Ca²⁺ are < 30 ppm. Solid caustic potash produced from amalgam liquor has a total alkalinity (calculated as KOH) of 89–92%, NaOH 1.5% (max.), CO₃²⁻ 0.5% (max.), Cl⁻ 0.01% (max.). The values for SO₄²⁻, Fe²⁺, and Ni²⁺ are < 50 ppm. Caustic potash from diaphragm electrolysis has a Cl⁻ content of 2.5–3.0% and higher content of heavy metals.

52.13.4 Economic Aspects and Uses

Pure-quality potassium hydroxide is used as a raw material for the chemical and pharmaceutical industry, in dye synthesis, for photography as a developer alkali, and as an electrolyte in batteries and in the electrolysis of water. Technical-quality KOH is used as a raw material in the detergent and soap industry; as a starting material for inorganic and organic potassium compounds and salts (e.g.,

potassium carbonate, phosphates, silicate, permanganate, cyanide); for the manufacture of cosmetics, glass, and textiles; for desulfurizing crude oil; as a drying agent; and as an absorbent for carbon dioxide and nitrogen oxides from gases.

World production is estimated at ca. 700–800 × 10³ t/a. Main producers are the United States [281], Germany, Japan, and France. Other important producer countries are Belgium, the United Kingdom, Italy, Spain, South Korea, India, Israel, Yugoslavia, former Czechoslovakia, Sweden, and Romania.

52.14 Potassium Carbonate

[273–276]

Potassium carbonate was produced in antiquity and used for many purposes. In the Old Testament, potash is mentioned in Jeremiah (written in the 7th century B.C.). ARISTOTLE describes the extraction of wood ash with water; the Romans manufactured soap from fat and potash. LAVOISIER identified potash as potassium carbonate.

The production of potash from wood ash for the manufacture of glass and soap was a flourishing industry in the Middle Ages in areas having a plentiful supply of wood such as Russia and also in Scotland. Since 1860, potash salts have replaced wood as a raw material for the manufacture of potassium carbonate.

In Anglo-American usage, the term potash today includes potassium carbonate as well as all potassium salts, such as KCl, K₂SO₄, and K₂SO₄·MgSO₄·xH₂O, that are used as fertilizers; the potassium content is given as K₂O.

Potassium carbonate occurs in small amounts in a few African lakes (e.g., Lake Chad and in the vicinity of Lake Victoria), as well as in the Dead Sea.

52.14.1 Properties

Anhydrous potassium carbonate, K₂CO₃, ρ 2.428 g/cm³, *mp* 891 °C, is a white, hygroscopic, powdery material that deliquesces in moist air. It is readily soluble in water with the formation of an alkaline solution. The solubil-

ity of K_2CO_3 (g K_2CO_3 /100 g H_2O) in water is given below:

Temperature, °C	Solubility	Temperature, °C	Solubility
0	105.5	60	126.8
10	108.0	70	133.1
20	110.5	80	139.8
30	113.7	90	147.5
40	116.9	100	155.7
50	121.2		

On addition of acid, potassium carbonate reacts with the evolution of carbon dioxide:



K_2CO_3 forms several hydrates, of which $K_2CO_3 \cdot 1.5H_2O$ is the stable phase in contact with the saturated solution from 0 °C to ca. 110 °C. This hydrate (ρ 2.155 g/cm³) crystallizes in glassy, virtually dust-free crystals. It is also hygroscopic and deliquesces in moist air. It is completely dehydrated at 130–160 °C.

52.14.2 Production

From Caustic Potash and Carbon Dioxide. The most important process for the manufacture of potassium carbonate begins with electrolytically produced potassium hydroxide solution. The almost chemically pure solution obtained by the mercury process is reacted with carbon dioxide or CO_2 -containing off-gases (flue gas, lime kiln gas).



Solid potassium carbonate is then obtained by crystallization (under vacuum and with cooling) from liquors or in the fluidized-bed process.

In the continuous crystallization process (Figure 52.44), the filtered, fresh carbonate solution is mixed with mother liquor and concentrated in several preliminary evaporators connected in series until the hydrate $K_2CO_3 \cdot 1.5H_2O$ finally precipitates in the crystallizer after cooling under vacuum [282]. The mother liquor is separated from the crystal suspension in hydrocyclones and centrifuges, filtered, and fed back to the process. The crystals are dried at ca. 110–120 °C in rotary kilns or fluidized-bed dryers and packed for sale as

potash hydrate, or they are calcined at 200–350 °C to give 98–100% K_2CO_3 . Impurities such as soda, sulfate, silicic acid, and iron that concentrate in the mother liquors can be partially removed [283] by removing a partial stream of the mother liquor, which is either used for brine purification in the electrolysis process or sold as a low-grade potassium carbonate solution, or by crystallizing the double-salt $NaKCO_3$ at elevated temperature in a separate crystallization and drying process.

The resulting potassium carbonate is very pure and meets the requirements of USP, BP, DAB, and JP if the process is operated in appropriate manner.

Starting from potassium carbonate solution, prills can be produced in a combined reactor, in which spray drying and fluidized-bed granulation take place simultaneously [284].

In the fluidized-bed process, aqueous potassium hydroxide solution is sprayed into a fluidized-bed reactor from above and exposed to a countercurrent of CO_2 -containing hot gas (Figure 52.45) [285, 286]. Carbonization and calcination take place in the same reactor. Hard, spherical potassium carbonate prills are formed having a high packing density. The prills are discharged and sieved. The coarse grains are ground and returned to the reactor together with the very fine grains, where they act as crystallization seeds. The salable, dust-free, medium grains are cooled and packed. Because no mother liquor is formed, the quality of the potassium carbonate depends on that of the raw materials. Compared to the crystallization process the chloride, soda, and sulfate contents are usually higher, but the investment and production costs are lower.

Amine Process. In the Mines de potasse d'Alsace process, potassium chloride is reacted under pressure in autoclaves with carbon dioxide in precarbonated isopropylamine solution. Potassium hydrogencarbonate precipitates and is filtered off, carefully purified of amine by intensive washing, and dried. It can be converted to potassium carbonate by calcination. Free amine, containing carbon dioxide, is recovered from the mother liquor by distillation

and recycled. The chloride, predominantly present in the mother liquor as amine chlorohydrate, is reacted with hydrated lime to give

free amine and an aqueous solution of calcium chloride [287].

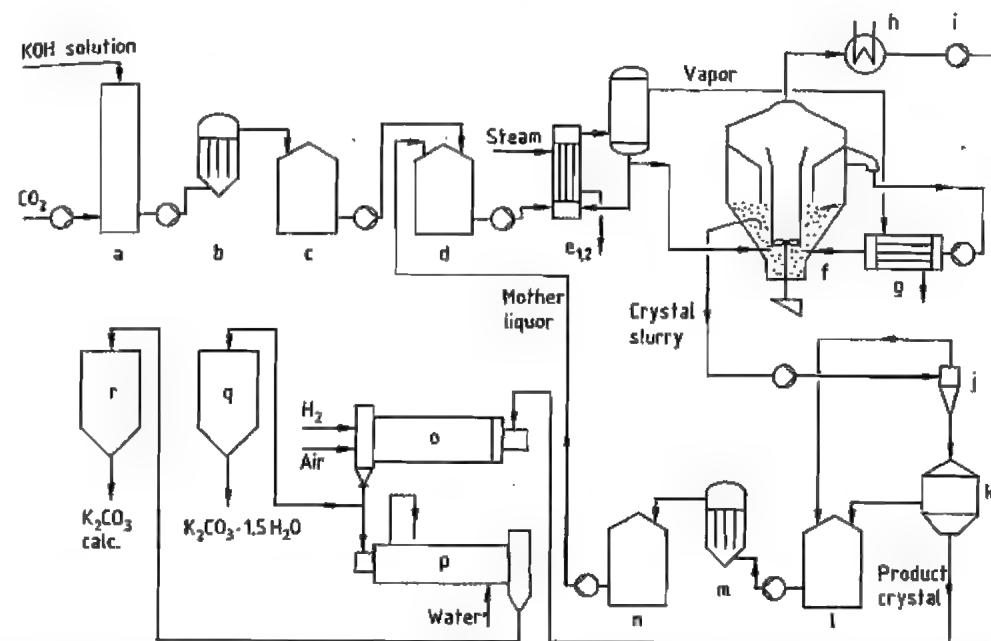


Figure 52.44: Preparation of potassium carbonate with continuous crystallization: a) Carbonization; b) Crude liquor filter; c) Fresh liquor tank; d) Mixed liquor tank; e₁, e₂) Preliminary evaporation; f) Vacuum/cooling crystallization (Chemietechnik Messo system); g) Preheater; h) Vapor condenser; i) Vacuum pump; j) Hydrocyclone; k) Centrifuge; l) Centrifuge liquor tank; m) Filter for mother liquor; n) Mother liquor tank; o) Drying or calcining rotary kiln; p) Cooling device for calcined K_2CO_3 ; q) Storage for hydrated potash; r) Storage for calcined potash.

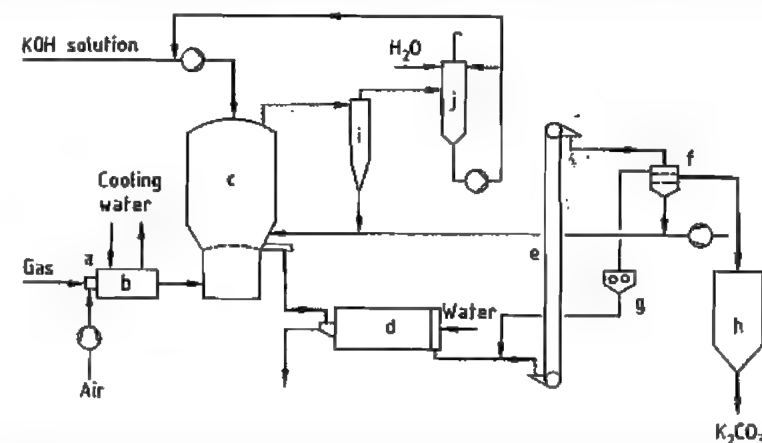
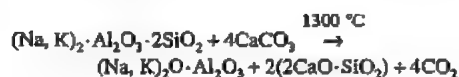


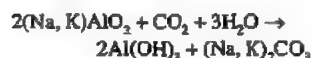
Figure 52.45: Production of potassium carbonate by the fluidized-bed process: a) Burner; b) Gas cooler; c) Fluidized-bed reactor; d) Cooler; e) Elevator; f) Screen; g) Mill; h) Silo; i) Cyclone; j) Exhaust gas scrubber.

The use of triethylamine [288], hexamethylenimine [289], or piperidine [290] is also patented. All the processes have the disadvantage that calcium chloride liquor is obtained, which can be utilized today only to a small extent and therefore represents an environmental pollutant.

Nepheline Decomposition Process [291]. In the CIS, considerable amounts of potassium carbonate are formed as a by-product in the nepheline decomposition process for aluminum hydroxide production. The mineral nepheline is decomposed with limestone by sintering at 1300 °C:



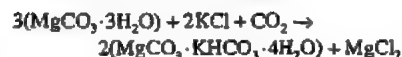
Alumina, portland cement, soda, and potash are obtained from the product in a complex process. The sinter product is leached with an Na_2CO_3 - NaOH solution. After filtration, a filter cake is obtained that is processed to give portland cement and an aluminate solution containing silicic acid. After precipitation of the silicic acid as alkaline aluminum silicate the purified aluminate solution is reacted with carbon dioxide:



The aluminum oxide hydrate is filtered off, and the carbonate solution is concentrated by fractional crystallization in a three-stage process and separated into sodium carbonate and $\text{K}_2\text{CO}_3 \cdot 1.5\text{H}_2\text{O}$.

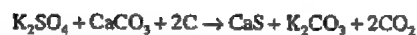
Feldspar (KAlSi_3O_8) and leucite (KAlSi_2O_6) can also be decomposed analogously and used for alumina, cement, and potassium carbonate manufacture [292].

The magnesia process (Engel-Precht process) is of limited interest:



In hot water the double salt ($\text{MgCO}_3 \cdot \text{KHCO}_3 \cdot 4\text{H}_2\text{O}$) decomposes under pressure into magnesium carbonate and dissolved potassium carbonate.

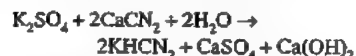
Other processes. Le Blanc process:



Formate process:



"Piesteritz" process:



These processes are uneconomical today because of high energy consumption and poor product quality, and are no longer used.

In the decomposition of chromium ores with potassium hydroxide solution, a chromate-containing potassium carbonate is obtained as by-product. The production of potassium permanganate yields considerable amounts of potassium carbonate solution [293].

Organic raw materials, such as sunflower stalks, molasses, and suint, are used to a small extent for potash manufacture. They are ashed, leached with water, and processed to potash by fractional crystallization and calcination [294].

Ion-Exchange Process [295, 296]. An acidic ion exchanger loaded with ammonium ions is charged with KCl solution, K^+ being absorbed and an ammonium chloride solution running off. The ion exchanger is then eluted with an excess of ammonium carbonate solution (regeneration of the exchanger). The eluate, a K_2CO_3 - $(\text{NH}_4)_2\text{CO}_3$ solution, is separated by thermal cleavage to give ammonia and carbon dioxide. The ammonium chloride is reacted with magnesium hydroxide to give magnesium chloride and ammonia, which is recycled.

52.14.3 Quality Specifications and Analysis

Depending on the intended use, potassium carbonate is offered in varying commercial forms and degrees of purity: as granules, as powder, and as potassium carbonate hydrate ($\text{K}_2\text{CO}_3 \cdot 1.5\text{H}_2\text{O}$). The material manufactured from mercury-process potassium hydroxide

solution is of high purity, particularly with respect to chloride content. In the amine process, the chloride content is higher and the sodium carbonate content lower, while nepheline decomposition gives high sodium carbonate contents and relatively high sulfate contents (Table 52.12).

Analysis. The *total alkalinity* includes $\text{K}_2\text{CO}_3 + \text{KOH} + \text{Na}_2\text{CO}_3$; it is determined with 0.5 NH_4SO_4 by potentiometric titration or with a methyl orange indicator (change to brown-red). Sodium is determined by flame photometry. The *chloride content* is determined by turbidity measurement after addition of AgNO_3 . The *sulfate content* is determined by ion chromatography or gravimetrically after precipitation as barium sulfate. The *metal content* is determined by atomic absorption spectroscopy or photometrically by complex formation (Fe^{2+} as sulfosalicylate, Si^{4+} as the molybdate complex, Cu^{2+} as pyrrolidinothiocarbamate, and Ni^{2+} as the diacetylgyloxime complex). Test methods for *photographic-grade* potassium carbonate, anhydrous are described in ISO 3623-1976 (E).

52.14.4 Storage and Transportation

Potassium carbonate is stored in bunkers; the ventilation air must be dry because of the hygroscopicity of the product.

Silo vehicles and bulk containers are used for dispatch to bulk customers. Smaller amounts are packed in polyethylene valve sacks of 25–50 kg. The material is not hazardous; for pharmaceutical use it is classified as GRAS (generally recognized as safe) by FDA [297].

Table 52.12: Analyses of calcined potassium carbonate of varying origin (data in %, remainder H_2O).

	From potassium hydroxide solution				
	Mercury process		Diaphragm process	Amine process	Nepheline decomposition
	Crystallization	Fluidized bed			
K_2CO_3	98.0–99.8	98.5–99.5	97–99	99	97.5–98.5
Na_2CO_3	0.1–0.5	0.1–0.5	0.5–1.0	0.01	0.1–1.0
Cl	0.001–0.002	0.004–0.013	0.2–1.0	0.19	0.01–0.03
SO_4	0.003–0.005	0.005–0.013	0.005–0.010		0.25–0.60
Si + Ca	0.005	0.006	0.010	0.009	
Fe	0.0003–0.0005	0.0002–0.0006	< 0.0005	< 0.0024	0.0007–0.0021

52.14.5 Economic Aspects and Uses

The glass industry is the most important consumer of K_2CO_3 . Large amounts are also required for potassium silicate manufacture.

Potassium carbonate is used for many organic syntheses. Numerous inorganic and organic potassium salts are manufactured from potassium carbonate (potassium phosphate, bromide, iodide, dichromate, cyanide, and ferrocyanide); in addition it is a starting material for drying, neutralization, and condensation agents. As a regenerable absorbent for carbon dioxide, hydrogen sulfide, and sulfur oxides, it is attaining importance in environmental protection. Potassium carbonate is used as a fertilizer for acidic soil.

Other users are the electrical industry, the dye industry, the printing trade, the textile industry, the leather goods industry, and the ceramic industry. Soft soap manufacture has lost its earlier importance as a customer. Potash solutions are used as fire retardants and as cooling brines (freezing point -36 °C at 576 g/L = 40.5% K_2CO_3).

The food industry uses potassium carbonate as a leavening agent in baked goods, as a debitterizing agent for cocoa beans, and as an additive for drying raisins. Potash in DAB quality is frequently used in the pharmaceutical industry as a raw material and auxiliary.

The most important producer countries for potassium carbonate are the CIS, France, Germany, the United States, and Japan. Other producers are Israel, Spain, India, South Korea, Belgium, Italy, former Yugoslavia, and China.

52.15 Potassium Hydrogencarbonate [273-275]

52.15.1 Properties and Production

Potassium hydrogencarbonate KHCO_3 , ρ 2.17 g/cm³, is a white, crystalline powder that is sparingly soluble in water and insoluble in alcohol. When heated above 120 °C, it decomposes into potassium carbonate, water, and carbon dioxide.

It is manufactured industrially by passing carbon dioxide into concentrated potassium carbonate solutions or exposing these to a countercurrent of purified, cold flue gas in trickle towers (overcarbonization). Because of its low water solubility (22.4 g of KHCO_3 in 100 mL of H_2O at 20 °C) it precipitates in crystalline form, is separated by centrifugation, and dried at ca. 110 °C. In some potassium carbonate production processes, potassium hydrogencarbonate is obtained as a precursor.

The total alkalinity of the industrial material, calculated as KHCO_3 , is at least 98–100% [KHCO_3 98% (min.), Na^+ 0.1% (max.), Cl^- 0.01% (max.), SO_4^{2-} 0.02% (max.); for analysis see potassium carbonate, Section 52.14.2].

52.15.2 Uses

Potassium hydrogencarbonate is used in the manufacture of fire extinguisher powders, in the food industry as a leavening agent, and in the chemical and pharmaceutical industry for the manufacture of high-purity potassium carbonate and other pure potassium salts. Producing countries are the United States, Germany, and France.

52.16 Potassium Benzoate

At 17.5 °C, a saturated aqueous solution of $\text{C}_6\text{H}_5\text{O}_2\text{K}$ contains 41.1% of the salt. Potassium benzoate is a key compound in the production of terephthalic acid from benzoic acid.

52.17 Storage and Transportation

The demand for potash fertilizers fluctuates greatly throughout the year, but because potash plants need to produce at as steady a rate as possible, large storage capacities are needed to accommodate periods of low demand. Therefore, potash plants usually have high-capacity product storage facilities. Also, in seaports, where fertilizers are loaded onto ships, the largest potash companies or their subsidiaries have large storage capacities. In both cases, long storage sheds are used, usually with walls sloping to match the angle of repose of the potash salt. The sheds are usually filled by means of conveyor belts located under the shed roof. They are emptied either by bucket loaders or scrapers that move the salt into a channel under the floor of the silo or onto a conveyor belt at the side, which carries it via sloping bands or elevators to the loading plant. More recently, especially where there is a shortage of land, round silos have been used, often arranged in rows. These too are filled from above by conveyor belts and are emptied through openings at ground level. The majority of potash fertilizer is transported in bulk in self-discharging wagons with a capacity up to 100 t, by rail, truck, or inland waterway. Transport from potash plants remote from a seaport or the main consuming area is usually by special trains that run on a fixed timetable between the potash plant and the seaport or intermediate storage facility. For example, the transport of potash fertilizers from Saskatchewan to a cargo-handling plant in Vancouver uses continuous-loop train tracks that enable 10 000 t to be delivered in 102 wagons with a capacity of 98 t each [270].

A small proportion of potash salts is supplied in sacks, usually containing 50 kg. The sacks are filled either by the supplier or at the loading plant at the seaport by automatic sack-filling machines. The sacks are usually palletized.

52.18 Analysis of Potassium Compounds

Potassium is usually determined gravimetrically. In the United States, it is precipitated as the hexachloroplatinate [271]. Precipitation as the tetraphenylborate is another widely used method, being the standard ISO method for fertilizers, and can be either a gravimetric or a volumetric procedure (ISO 5318 and 5310) [272]. Precipitation as the perchlorate or tartrate is seldom used. Flame photometry is used for both laboratory and process control analysis. Recently, X-ray fluorescence has also been used for the analysis of solids or brines.

52.19 References

1. J. W. Mellor, *Supplement III to Mellor's Comprehensive Treatise on Inorganic and Theoretical Chemistry*, Vol. II, John Wiley & Sons, Inc., New York 1963.
2. O. J. Foust (ed.): *Sodium and Sodium-Potassium Engineering Handbook*, Vol. I, Gordon and Breach, New York 1972, Chap. 2.
3. *Landolt-Börnstein* (1965) 4, 2C, 351.
4. *Winnacker-Küchler*, 4th ed., 6 (1973) p. 102. R. Thilenius, *Z. Elektrochem.* 37 (1931) p. 740.
5. Mine Safety Appliances Company, US 2480655, 1949 (C. B. Jackson, R. C. Werner).
6. *Fed. Reg.* 55 (1990) Dec. 21, 52402–52729; 56 (1991) Dec. 20, 66124–66287; 59 (1994) Dec. 29, 67390–67556.
7. R. E. Lee and S. L. Walter, *Techniques of Sampling and Analyzing Hot Flowing Sodium-Potassium Alloy TR-4*, MSA Research Corp., Evans City, PA, 1950.
8. J. W. Mausteller, F. Tepper, and S. J. Rodgers, *Alkali Metal Handling and Systems Operating Techniques*, Gordon and Breach Scientific Publishers, Inc., New York 1967.
9. M. A. Armour, L. M. Browne and G. L. Weir, *Hazardous Chemical Information and Disposal Guide*, 2nd Edition, Univ. of Alberta, Edmonton, Alberta, 1984, p. 202.
10. A. A. Morton, *Solid Organoalkali Metal Reagents*, Gordon & Breach, New York 1964.
11. H. Pines, W. M. Stalick, H. B. Injovanovich (eds.), *Base-Catalyzed Reactions of Hydrocarbons and Related Compounds*, Academic Press, New York 1977.
12. M. Szwarc, *Carbanions, Living Polymers, and Electron Transfer Processes*, Interscience, New York 1968.
13. E. Grovenstein, Jr., K. W. Chiu, B. B. Patil, *J. Am. Chem. Soc.* 102 (1980) p. 5848.
14. E. Grovenstein, *Adv. Organomet. Chem.* 16 (1977) p. 167.
15. L. Lochmann, J. Pospisil, D. Lim, *Tetrahedron Lett.* 7 (1966) pp. 257–262.
16. L. Lochmann, J. Petranek, *Tetrahedron Lett.* 32 (1991) p. 1483.
17. L. Lochmann, J. Trekoval, *J. Organomet. Chem.* 326 (1987) pp. 1–7.
18. M. Schlosser, S. Strank, *Tetrahedron Lett.* 25 (1984) pp. 741–744.
19. *Chem. Eng. News* 33 (1955) p. 648.
20. M. A. Turchin et al., *Appl. Therm. Sci.* 1 (1988) no. 1, pp. 39–43.
21. W. G. Anderson et al., *Proc. 25th Intersoc. Energy Convers. Eng. Conf.* 25 (1990) no. 5, pp. 268–273.
22. R. N. Lyon (ed.), *Liquid-Metals Handbook*, 2nd ed., U.S. Government Printing Office, Washington, DC, 1952, p. 5.
23. D. A. Wallace et al., *Proc. Intersoc. Energy Convers. Eng. Conf.* 26th (1991) no. 5, pp. 349–354.
24. W. Mialki, *Metall. (Berlin)* 3 (1959) p. 174.
25. US 4929783, 1990 (R. S. Smith).
26. US 4720601, 1989 (G. S. Osaka, M. F. Shiga).
27. EP-A 211448, 1987 (G. Suzukamo, M. Fukao, M. Minobe, A. Sakamoto).
28. GB 820263, 1959 (Z. Karl).
29. C. W. Carlson, R. West, *Organometallics*, 2 (1983) no. 12, pp. 1972–1977.
30. P. A. Bianconi, T. W. Weidman, *J. Am. Chem. Soc.* 110 (1988) no. 7, pp. 2342–2344.
31. H. Y. Qui, Z. D. Du, *Gaodeng Xue Xue Huaxue Xuebao* 10 (1989) no. 4, pp. 423–425.
32. US 4800221, 1989 (O. W. Marko).
33. R. D. Rieke, *Acc. Chem. Res.* 10 (1988) p. 301.
34. R. M. Schramm, C. E. Langlois, *Prepr. Div. Petr. Chem. Am. Chem. Soc.* 4 (1959) no. 4, p. B-53.
35. PCT Int. Appl., WO 8607097, 1986 (W. R. B. Martin).
36. T. Ohsawa, T. Takagaki, A. Haneda, T. Oishi, *Tetrahedron Lett.* 22 (1981) no. 27, pp. 2583–2586.
37. T. Ohsawa et al., *Chem. Phar. Bull.* 30 (1982) no. 9, pp. 3178–3186.
38. C. A. Ogle, T. E. Wilson, J. A. Stowe, *Synthesis* 1989, no. 6, pp. 495–496.
39. T. A. Thornton et al., *J. Am. Chem. Soc.* 111 (1989) no. 7, pp. 2434–2440.
40. Jpn. Kokai Tokyo Koho, JP 63218705, 1988 (M. Ohata et al.).
41. Thomas Hedley & Co., Ltd., GB 785147, 1957.
42. D. Kazimierz, *Tluszcz i Srodki Piorace* 5 (1961) pp. 143–149.
43. DD 235184, 1986 (G. Houbelein, D. Stadermann, H. Hartung, W. Muller).
44. For a review of KTB chemistry: D. E. Pearson, C. A. Buehler, *Chem. Rev.* 72 (1974) pp. 45–86.
45. L. Lochmann, H. Jakubov, L. Brandsma, *Collect. Czech. Chem. Commun.* 58 (1993) pp. 1445–1451.
46. US 5025096, 1991 (K. W. Chiu, L. C. Yu, J. R. Strickler).
47. J. Tsuji, I. Minami, I. Shimizu, *Tetrahedron Lett.* 24 (1983), p. 1973.
48. G. M. Coppola, *Synth. Commun.* 15 (1985) p. 135. P. J. Dunn, R. Haner, H. Rapoport, *J. Org. Chem.* 55 (1990) pp. 5017–5025.
49. E. J. Corey, M. M. Mehrotra, *Tetrahedron Lett.* 27 (1986) p. 5173.

48. W. C. Still, V. J. Novack, *J. Am. Chem. Soc.* 103 (1982) p. 1282.
49. A. B. Smith, et al., *J. Am. Chem. Soc.* 104 (1982) p. 4105.
J. Kallmerter, T. J. Gould, *J. Org. Chem.* 51 (1986) p. 1155.
50. Y. Ikeda, H. Yamamoto, *Tetrahedron Lett.* 25, 1984, p. 5581.
Y. Ikeda, J. Ukai, N. Ikeda, H. Yamamoto, *Tetrahedron Lett.* 25, 1984, p. 5177.
51. Pfizer, EP 0076643, 1982 (P. Weeks).
52. D. Heissler, J. Riehl, *Tetrahedron Lett.* 21 (1980) p. 4707.
53. K. Takeda et al., *J. Org. Chem.* 51 (1986) p. 4735.
54. D. Home, J. Gaudino, W. J. Thompson, *Tetrahedron Lett.* 25 (1984) p. 3529.
55. T. Tekahashi, S. Hashiguchi, K. Kasuga, J. Tsuji, *J. Am. Chem. Soc.* 100 (1978) p. 7424.
56. S. Hanessian, A. Ugolini, P. J. Hodges, D. Dube, *Tetrahedron Lett.* 27 (1986) p. 2699.
57. C. Heathcock, J. A. Stafford, *J. Org. Chem.* 57 (1992), p. 2566.
58. C. Almonsa, A. Moyano, M. A. Pericas, F. Serratos, *Synthesis* 1988, p. 707.
59. J. H. Wouiz, P. M. Barelski, D. F. Koster, *J. Org. Chem.* 38 (1973) p. 489.
60. C. A. Brown, A. Yamashita, *J. Am. Chem. Soc.* 97 (1975) p. 891.
US 5062998, Nov. 5, 1991 (F. L. Herman, A. C. L. Savoca, M. L. Listermann).
61. R. Csuk, B. I. Glanzer, A. Fursiner, *Adv. Organomet. Chem.* 28 (1988) p. 85.
62. H. Kamimura, *Synth. Met.* 23 (1988) pp. 171-174.
W. Rudorff in H. J. Emeleus, A. G. Sharpe (eds.), *Graphite Intercalation Compounds, Advances in Inorganic Chemistry and Radiochemistry*, Vol. 1, Academic Press, New York 1959, pp. 224-264.
G. R. Henning in F. A. Cotton (ed.), *Interstitial Compounds of Graphite, Progress in Inorganic Chemistry*, Vol. 1, Interscience, New York 1959, pp. 125-205.
63. W. Uhlig, *Z. Naturforsch. B: Chem. Sci.* 50 (1995) p. 1674-1678.
B. Lacave-Goffin, L. Hevesi, J. Devaux, *J. Chem. Soc. Chem. Commun.* 7 (1995) pp. 769-770.
64. Y. Zhang, S. Liao, Y. Xu, *J. Mol. Cat.* 84 (1993) pp. 211-221.
65. C. A. Brown, *J. Org. Chem.* 39 (1974) p. 3913.
66. C. A. Brown, *Synthesis* 1975, p. 326.
67. H. W. Pinnick, *Org. Prep. Proced. Int.* 15 (1983) p. 199.
68. H. C. Brown et al., *J. Org. Chem.* 49 (1984) p. 885-892.
H. C. Brown et al., *Inorg. Chem.* 23 (1984) p. 2929-2931.
69. S. Krishnamurthy, *Aldrichimica Acta* 7 (1974) p. 55.
C. A. Brown, *J. Am. Chem. Soc.* 95 (1973) p. 4100.
US 5428159, June 27, 1995 (W. C. Shieh, J. A. Carlson).
70. S. Krishnamurthy, W. B. Vreeland, *Heterocycles* 18 (1982) pp. 265-270.
71. J. M. Fortunato, B. Ganem, *J. Org. Chem.* 41 (1976) pp. 2194-2200.
B. Ganem, *J. Org. Chem.* 40 (1975) p. 146.
72. J. A. Gladysz, *Aldrichimica Acta* 12 (1979) pp. 13-17.
73. J. W. Mausteller in M. L. Nuckols, K. A. Smith (eds.), *Charact. Carbon Dioxide Absorbing Agents Life Support Equip., Winter Annu. Meet. Am. Soc. Mech. Eng.* 1982, pp. 23-31.
CA 98:68148.
74. D. T. Sawyer, J. S. Valentine, *Acc. Chem. Res.* 14 (1981) no. 12, p. 393.
E. Lee-Ruff, *Chem. Soc. Rev.* 6 (1977) p. 195.
L. Sotirion, W. Lee, R. W. Giese, *J. Org. Chem.* 55 (1990) pp. 2159-2164.
75. T. Itoh, K. Nagata, M. Okada, A. Ohsawa, *Tetrahedron Lett.* 31 (1990) p. 7193.
76. R. A. Johnson, E. G. Nidy, L. Baczyński, R. R. Gorman, *J. Am. Chem. Soc.* 99 (1977) p. 7738.
N. A. Porter, J. D. Byers, R. C. Mebane, D. W. Gilmore, J. R. Nixon, *J. Org. Chem.* 43 (1978) p. 2088.
77. Y. H. Kim, K. S. Kim, H. K. Lee, *Tetrahedron Lett.* 30 (1989) no. 46, pp. 6357-6360.
78. C. Betancor, C. G. Francisco, R. Freire, E. Suarez, *J. Chem. Soc., Chem. Commun.* 1988, p. 947.
79. Fertilizer Manual, International Fertilizer Development Center, Muscle Shoals, AL, 1979, pp. 225-247.
80. Kirk-Othmer, 3rd ed., 18, 920-950.
81. Winnacker-Küchler, 4th ed., 2, 268-333.
82. The British Sulphur Corporation, *World Survey of Potash Resources*, London 1985.
83. V. A. Zandon in N. L. Weiss (ed.), *SME Mineral Processing Handbook*, Society of Mining Engineers, New York 1985, section 22.
84. R. M. McKerchel (ed.), "Potash Technology", *1st International Potash Technology Conference*, Saskatchewan, Canada, Oct. 3-5, 1983, Pergamon Press, Toronto 1983.
85. W. H. Eatock: "Potash Refining in Saskatchewan", *Min. Eng. (Lincoln, CO)* 34, (1982) no. 9, 1350-1353.
86. M. P. Kurtanek: "Mining and Beneficiating Potash, Recent Developments and Trends outside North America", *Phosphorus Potassium* 128 (1983) Nov./Dec., 26-31.
87. Gmelin, System no. 22.
88. F. Serowy: *Verarbeitungsmethoden der Kalisalz*, W. Knapp, Halle/Saale 1952.
89. H. Schubert: *Aufbereitung fester mineralischer Rohstoffe*, VEB Deutscher Verlag für Grundstoffindustrie, Leipzig, vol. I, 1968; vol. II, 1986; vol. III, 1984.
90. D. Fulda et al.: *Kali, das bunte, bittere Salz*, VEB Deutscher Verlag für Grundstoffindustrie, Leipzig 1990.
91. A. Heinz, R. v. d. Osten (eds.): *ABC Kali und Steinsalz*, VEB Deutscher Verlag für Grundstoffindustrie, Leipzig 1982.
92. I. Barin: *Thermochemical Data of Pure Substances*, VCH, Weinheim 1989.
93. M. Broul, J. Nývlt, O. Söhnel: *Solubility in Inorganic Two-component Systems*, Elsevier, Amsterdam 1981.
94. Ullmann, 4th ed., 13, 447-496.
95. R. Slotta: "Die Kali- und Steinsalzindustrie", *Technische Denkmäler in der Bundesrepublik Deutschland*, vol. 3, Deutsches Bergbaumuseum, Bochum 1980.
96. D. Hoffmann: *Elf Jahrzehnte Deutscher Kalisalzbergbau*, Verlag Glückauf, Essen 1972.
97. Kaliverein e.V.: *Die Kaliindustrie in der Bundesrepublik Deutschland*, 6th ed., 1988.
98. *Phosphorus Potassium* 166 (1990) March/April, 17-19.
99. R. Weissenberger: *Chronique des mines de potasse d'Alsace*, Ziegler, Bergholtz 1985.
100. *Phosphorus Potassium* 168 (1990) July/Aug., 12-13.
101. J. W. Turrentine: *Potash in North America*, Reinhold Publ., New York 1943.
102. *Phosphorus Potassium* 68 (1973) Nov./Dec., 39-43.
103. O. Braitsch: *Entstehung und Stoffbestand der Salzlagerstätten*, Springer Verlag, Berlin 1962.
104. In [94], p. 450.
105. M. A. Zharkov: *Paleozoic Salt Bearing Formations of the World*, Springer Verlag, Berlin 1984.
106. E. A. Vysotsky, V. Z. Kislik: "Epochs of Bishofite Deposition in Geological History", *Int. Geol. Rev.* 29 (1987) no. 2, 134-139.
107. R. Kühn, *Kali Steinsalz* 1 (1955) no. 9, 3-16.
108. R. Kühn, *Geol. Jahrb.* 90 (1972) 127-220.
109. H. Borchert: *Ozeane Salzlagerstätten*, Bornträger, Berlin 1959.
110. F. Lotze: "Steinsalz und Kalisalz", *Die wichtigsten Lagerstätten der "Nicht-Erde"*, vol. III, part 1, Bornträger, Berlin 1938.
111. F. Lotze: *Steinsalz und Kalisalz*, 2nd ed., part 1, Bornträger, Berlin 1957.
112. F. Lotze: *Die Salzlagerstätten in Zeit und Raum*, Arbeitsgem. Forsch. Landes Nordrhein-Westfalen, no. 195, Westdeutscher Verlag, Köln-Opladen 1969.
113. G. Richter-Bernburg: "Salzlagerstätten", in Bentz-Martini (ed.), *Lehrbuch der Angewandten Geologie*, vol. 2, part 1, Enke Verlag, Stuttgart 1968, pp. 916-1061.
114. G. Richter-Bernburg, *Z. Dtsch. Geol. Ges.* 105 (1953) 593-645.
115. M. Brongersma, *Mar. Geol.* 11 (1972) 123-144.
116. C. Kippenberger et al.: *Untersuchungen über Angebot und Nachfrage mineralischer Rohstoffe, XX Kali*, BGR Hannover-DIW Berlin, Schweizerbart, Stuttgart 1986.
117. J. D'Ans, *Naturwissenschaften* 34 (1947) 295-301.
118. J. D'Ans, R. Kühn, *Kali Steinsalz* 3 (1960) 69-84.
119. H. Mayrhofer: "World Reserves of Mineable Potash Salts Based on Structural Analysis", *Proceedings of the 6th International Symposium on Salt*, vol. 1, The Salt Institute, Alexandria, USA, 1983.
120. P. A. Ziegler, *Geological Atlas of Western and Central Europe*, Elsevier, Amsterdam 1982.
121. E. Messer, *Kali Steinsalz* 5 (1970) 244-251.
122. Pittsburgh Plate Glass Co., US 3058729, 1962 (J. B. Dahms, B. P. Edmonds); CA 627308, 1963 (J. B. Dahms); US 4007964, 1977 (E. L. Goldsmith); US 3262741, 1966 (B. P. Edmonds, J. B. Dahms); US 3433530, 1969 (J. B. Dahms, B. P. Edmonds); US 4329287, 1980 (F. L. Goldsmith).
123. *Phosphorus Potassium* 138 (1985) July/Aug., 32-33.
124. D. Jackson, *Eng. Min. J.* 174 (1973) no. 7, 59-68.
125. *Phosphorus Potassium* 168 (1990) July/Aug., 23-28.
126. G. Duchrow, I. Fitz, N. Grischow, *Phosphorus Potassium* 167 (1990) May/June, 26-32.
127. H. Schubert in [90], vol. 1, 72-84.
128. R. Kühn, *Kali Steinsalz* 5 (1970) 307-317.
129. R. Kühn, *Erzmetall* 8 (1955) Suppl. B93-B107, B115.
130. H. Autenrieth, O. Braun, W. Otto in [81], 281-283.
131. V. A. Zandon in [83], 22-4-22-5.
132. J. Gotte, *Kali Steinsalz* 10 (1990) 261-264.
133. J. H. van't Hoff: *Untersuchungen über die Bildungsverhältnisse der ozeanischen Salzlagerungen*, Akad. Verlagsges., Leipzig 1912.
134. H. D'Ans: *Die Lösungsgleichgewichte der Systeme der Salze ozeanischer Salzlagerungen*, Verlagsges. für Ackerbau, Berlin 1933.
135. J. F'Ans, *Z. Elektrochem.* 56 (1952) 497-505.
136. Gmelin, System no. 22.
137. A. B. Sdanowsky, E. I. Lyakhowskaya, R. E. Schleyemowitch: *Handbuch der Löslichkeit der Salze*, Gaskhimisdat, Leningrad, vol. I, 1953; vol. II, 1954; vol. III, 1961; vol. IV, 1963 (Russ.).
138. H. Autenrieth, *Kali Steinsalz* 1 (1953) no. 2, 3-17.
139. H. Autenrieth, *Kali Steinsalz* 1 (1954) no. 7, 3-22.
140. H. Autenrieth, *Kali Steinsalz* 1 (1955) no. 11, 18-32.
141. H. Autenrieth, *Kali Steinsalz* 2 (1958) no. 6, 181-200.
142. H. Autenrieth, *Kali Steinsalz* 5 (1969) no. 5, 158-165.
143. H. Autenrieth, *Rev. chim. minér.* 7 (1970) 217-229.
144. H. Autenrieth, *Kali Steinsalz* 5 (1970) no. 9, 289-306.
145. G. Peuschel, *Kali Steinsalz* 9 (1986) no. 9, 296-303.
146. W. P. Wilson, A. G. McKee: *Proceedings of the 4th Symposium on Salt*, vol. 1, The Northern Ohio Geological Society, Cleveland, OH, 1974, 517-525.
147. W. P. Wilson: *Proceedings of the 3rd Symposium on Salt*, vol. II, The Northern Ohio Geological Society, Cleveland, OH, 1969, 20-29.
148. J. H. Wolf in [84], 711-716.
149. H. Domning, *Kali Steinsalz* 7 (1977) no. 4, 155-160.
150. W. H. Coghill, J. R. De Vancy, J. B. Clemmer, S. R. B. Cooke, Report of Investigations of the U.S. Bureau of Mines, Report no. 3271, 1935.
151. A. S. Kusin, *Kalit* 6 (1937) 17-27.
152. R. A. Pierce, L. D. Anderson, *Eng. Min. J.* 143 (1942) 38-41.
153. Kreller, *Kali, Verw. Salz Erdöl* 33 (1939) 35-37, 46-47, 53-57.
154. E. Rusberg, *Chem.-Ing.-Tech.* 27 (1955) 1-4.
155. O. Karsten, in W. Gründer: *Erzaufbereitungsanlagen in Westdeutschland*, Springer Verlag, Berlin 1955, 343-345.
156. V. A. Arscntiev, J. Leja, *CIM Bull.* 3 (1977) 154-158.
157. Du Pont, US 2088325, 1937 (J. F. Kirby).
158. C. M. Aleksandrovic, *Freiberg. Forschungsh.* A544 (1975) 73-81.
159. H. Schubert, *Aufbereit. Tech.* 7 (1967) 365-368.
160. A. Singewald, *Chem.-Ing.-Tech.* 33 (1961) 376-393, 558-572, 676-688.

161. D. W. u. M. C. Fuerstenau, *Min. Eng. (Littleton, CO)* 8 (1956) 302-307.
162. A. F. Taggart, *Elements of Ore Dressing*, John Wiley & Sons, New York 1951.
163. A. M. Goudin, Testimony in Transcript of Evidence, Civil Action no. 1829, District of New Mexico, p. 1255.
164. R. Bachmann, *Erzmetall* 8 (1955) Suppl. B109-B116.
165. J. Rogers, J. H. Schulman: *Second International Congress of Surface Activity*, vol. II, Reprints, Butterworths, London 1957, 330-338.
166. A. Singewald, *Erzmetall* 12 (1959) 121-135.
167. O. J. Somojlov: *Struktur von wässrigen-Elektrolytlösungen*, B. G. Teubner, Leipzig 1961.
168. H. Schubert, *Aufbereit. Tech.* 6 (1966) 305-313.
169. F. Hagedorn, *Kali Steinsalz* 10 (1991) 315-328.
170. D. Uhlig, *Neue Bergbautech.* 5 (1975) 145-155.
171. H. Köhler et al., *Neue Bergbautech.* 16 (1986) 45-50.
172. N. F. Mescerjakov, Y. W. Rjabov, V. N. Kuznetsov, *Freiberg. Forschungsh.* A594 (1978) 33-54.
173. A. Bahr, K. Legner, H. Lüdke, F. W. Mehrhoff, *Aufbereit.-Tech.* 1 (1957) 1-9.
174. N. F. Mescerjakov: *Flotacionnye mashiny*, Isdatel'stvo Nedra, Moskau 1972.
175. H. Schubert, *Neue Bergbautech.* 4 (1974) 223-228.
176. *Phosphorus Potassium* 145 (1986) 29-33.
177. Kali & Salz, DE 3435124, 1987 (F. Hagedorn, G. Peuschel, A. Singewald).
178. F. Hagedorn, *Kali Steinsalz* 9 (1986) 232-238.
179. H. Köhler, W. Kramer, *Neue Bergbautech.* 11 (1981) 362-366.
180. R. B. Tippin, *Chem. Eng. (N.Y.)* 184 (1977) no. 15, part 1, 73-75.
181. VEB Kali, DD 220237, (L. Herrmann et al.).
182. S. Mildner, R. Ecke, DD 35637, 1965.
183. I. M. Le Baron, W. C. Knopf, *Min. Eng. (Littleton, CO)* 10 (1958) 1081-1083.
184. H. Autenrieth, *Kali Steinsalz* 5 (1969) 171-177.
185. Kali-Forschungsanstalt, DE 1056551, 1957 (H. Autenrieth).
186. G. Fricke, *Kali Steinsalz* 9 (1986) 287-295.
187. D. Larmour in [84], 597-602.
188. R. Bock, *Chem.-Ing.-Tech.* 53 (1981) 916-924.
189. Kali & Salz, DE 1249783, 1966 (A. Singewald, G. Fricke).
190. A. Singewald, U. Neitzel in [84], 589-595.
191. L. Ernst, *Kali Steinsalz* 9 (1986) 275-286.
192. L. Ernst, *Ber. Bunsenges. Phys. Chem.* 93 (1989) 857-863.
193. L. Ernst, *Ber. Bunsenges. Phys. Chem.* 94 (1990) 1435-1439.
194. Kali & Salz, DE 3603166, 1986 (G. Fricke, L. Giesler, R. Diekmann).
195. Kali & Salz, DE 3603165, 1986 (H. Balzer, H. Burghardt, F. Maikranz).
196. Kali & Salz, DE 3603167, 1986 (U. Neitzel, G. Fricke).
197. Kali & Salz, DE 1077611, 1959 (H. Autenrieth, G. Peuschel).
198. Kali & Salz, DE 1142802, 1961 (H. Autenrieth, G. Peuschel, G. Weichart).
199. Kali & Salz, DE 2007677, 1970 (A. Singewald, G. Fricke, D. Jung).
200. Kali & Salz, DE 2052993, 1970 (A. Singewald, G. Fricke, D. Jung).
201. Kali & Salz, DE 1154052, 1960 (H. Autenrieth, H. Dust).
202. Kali & Salz, DE 1076593, 1957 (H. Autenrieth).
203. Kali & Salz, DE 1261453, 1967 (A. Singewald, G. Fricke).
204. Kali & Salz, DE 1667814, 1968 (G. Fricke, A. Singewald).
205. Kali & Salz, DE 1283772, 1967 (H. Autenrieth, H. Wirries).
206. Kali & Salz, DE 1792120, 1968 (A. Singewald, G. Fricke).
207. Kali & Salz, DE 1953534, 1969 (A. Singewald, G. Fricke).
208. W. B. Dancy in [80], 931-933.
209. T. E. Burus, B. J. Clarke, W. B. Coome, A. H. Newcombe in [84], 541-546.
210. R. Diekmann: Lecture held at *Int. Potash Technol. Conf.*, 2nd, Hamburg, May 26-29, 1991.
211. E. Weps, *Kali Steinsalz* 8 (1981) 177-183.
212. Kali & Salz, DE 3434190, 1984 (O. Pföh, C. Radick, H. Thenert).
213. F. Hagedorn, *Kali Steinsalz* 7 (1977) 161-164.
214. T. Fleischer, *Kali Steinsalz* 9 (1986) 304-313.
215. H. J. Scharf: "Environmental Aspects of K-Fertilizers in Production, Handling and Application", *Development of K-Fertilizer Recommendations*, International Potash Institute, Worblaufen-Bern 1990, 395-402.
216. *Phosphorus Potassium* 148 (1987) March/April, 30-35.
217. M. D. Haug, K. W. Reid: Lecture held at *Int. Potash Technol. Conf.*, 2nd, Hamburg, May 26-29, 1991.
218. J. F. Tallin, D. E. Pufahl in [84], 755-760.
219. K. W. Reid, G. A. Maki: Lecture held at [217].
220. H. E. Schroth, *Phosphorus Potassium* 67 (1973) Sept./Oct., 38.
221. A. Singewald, *Die Weser* 57 (1983) no. 516, 1-8.
222. N. Knöpfel in [217].
223. H. Stahl, *Aufbereit. Tech.* 20 (1980) 525-533.
224. W. B. Pietsch in [84], 661-669.
225. L. Medemblik in [84], 653-659.
226. A. S. Middleton, D. A. Cormode, J. E. Scotten in [84], 647-651.
227. *Phosphorus Potassium* 173 (1991) May/June 28-36.
228. K. Kahle, G. Leib: Lecture held at [217].
229. L. I. Skvirski, A. A. Chityakov, Z. L. Kozel: Lecture held at [217].
230. H. Rieschel, K. Zech, *Phosphorus Potassium* 115 (1981) Sept./Oct., 33-39.
231. H. Rug, K. Kahle, *Phosphorus Potassium* 170 (1990) Nov./Dec., 23-27.
232. International Fertilizer Industry Association (IFA): *Potash Statistics 1989*, Paris.
233. Prognose-Arbeitsgruppe Weltbank/FAO/Unido, 1991, unpublished.
234. C. Childers, *Phosphorus Potassium* 169 (1990) Sept./Oct., 16-20.
235. O. Walterspiel, *Kali Steinsalz* 10 (1989) 168-174.
236. *Phosphorus Potassium* 165 (1990) Jan./Febr., 1819.

237. *Gmelin*, System no. 22, Suppl. vol., pp. 1280-1338.
238. J. Nather, H. H. Emons, *Bergakademie* 21 (1969) 310-313.
239. *Phosphorus Potassium* 156 (1988) July/Aug., 27-34.
240. *Phosphorus Potassium* 122 (1982) Nov./Dec., 36-39.
241. N. P. Finkelstein, S. H. Garnett, L. Kogan in [84], 571-576.
242. U. Neitzel, *Kali Steinsalz* 9 (1986) 257-261.
243. H. Autenrieth, O. Braun, W. Otto in [81], 320-322.
244. H. Scherzberg, G. Döring: Lecture held at [217].
245. Kali & Salz, DE 3418147, 1984 (E. Meuche, H. G. Diehl, H. Eberle).
246. W. B. Dancy in [80], 945.
247. D. K. Storer in [84], 577-582.
248. R. Phinney, EP 0199104, 1986.
249. Kali & Salz, DE 3607641, 1986 (S. Vajna, G. Peuschel).
250. Société d'études chimiques pour l'industrie et l'agriculture (SECIPIA), DE 956304, 1954 (J. Lafont).
251. J. A. Fernandez Lozano, A. Wint, *Chem. Eng. J. (Lausanne)* 23 (1982) 53-61.
252. *Phosphorus Potassium* 167 (1990) May/June, 11.
253. Superfos A/S, Vedbæk, DK, DE 3331416, 1983 (K. C. B. Knudsen); US 4504458, 1983 (K. C. B. Knudsen).
254. *Chem. Eng. (N.Y.)* 81 (1974) 98-99.
255. Kali & Salz, DE 2810640, 1978 (N. Knöpfel, F. Wartenpfehl, A. Hollstein).
256. A. Hollstein, *Kali Steinsalz* 7 (1979) 498-500.
257. *Phosphorus Potassium* 141 (1986) Jan./Feb., 17-21.
258. *Phosphorus Potassium* 151 (1987) Sept./Oct., 16-21.
259. G. Kemmler, *Kali Steinsalz* 9 (1985) 167-169.
260. In [82], pp. 62-64.
261. *Phosphorus Potassium* 24 (1966) 40-44.
262. A. M. Amarin, K. Manastrah, *Proc. IFA-NFC Joint Middle East-South Asia Fertilizer Conference*, Lahore, Pakistan, Dec. 3-6, 1988.
263. *Kirk-Othmer*, 2nd ed., Suppl. vol., 438-467.
264. In [82], pp. 38-39.
265. U. Neitzel, *Kali Steinsalz* 5 (1971) 327-334.
266. P. Behrens, *Industrial Processing of Great Salt Lake Brines*, *Utah Geological and Mineral Survey Bulletin* 116, 1980, 223-228.
267. *Phosphorus Potassium* 132 (1984) July/Aug., 6.
268. In [82], pp. 42-43.
269. In [82], p. 70.
270. *Phosphorus Potassium* 173 (1991) May/June, 26-27.
271. W. Horwitz (ed.): *Official Methods of Analysis of the AOAC*, 11th ed., Association of Official Analytical Chemists (AOAC), Washington, DC, 1970.
272. Verband Deutscher Landwirtschaftlicher Untersuchungs- und Forschungsanstalten (LUFA): "Die Untersuchung von Düngemitteln", *Methodenbuch*, vol. II, Verlag J. Neumann-Neudamm, Melsungen 1972, method 4.1.
273. *Kirk-Othmer*, 3rd ed., 18, 936-939.
274. J. Ford: "Caustic potash", *Encycl. Chem. Process. Des.* 7 (1978) 22-34.
275. *Ullmann*, 4th ed., 13, 489-496.
276. Hüls, *Handbook KOH-, K₂CO₃-, KHCO₃-Products*, Marl 1992.
277. N. Takeuchi, *Soda to Enso* 39 (1988) no. 461, 277-290.
278. Bertrams, *Concentration Plants for NaOH-, KOH-, Na₂S- and CaCl₂-liquors*, Muttenz, Switzerland, 1979.
279. Sulzer-Escher-Wyss, US 4927494, 1990 (R. Winkler et al.).
280. Oxy-Occidental Chem. Corp., *Caustic Potash Handbook*, Irving 1987.
281. *Oil Paints Drugs, Chemical Marketing Reporter*, 28th May, 1990.
282. Messo Chemietechnik Brochure, Mass Crystallization, Duisburg, Germany, 1990.
283. Mannesmann, DE 3816061, 1989 (R. Schmitz).
284. VEB Kombinat Kali, DD 255328A, 1986 (K. Will, G. Elberling).
285. Bertrams, *Fluid Bed Processes*, Muttenz, Switzerland, 1979.
286. Diamond Shamrock Corp., *Company brochure*, Cleveland, OH, 1969.
287. *Inf. Chim.* 99 (1971) Aug./Sept., 125.
288. Kali-Chemie, DT 1220401, 1962 (P. Schmid).
289. J. N. Shokin et al., *Khim. Promst. (Moscow)* 9 (1978) 685.
290. FMC Corp., BE 616193, 1962 (A. B. Gency, M. J. McCarthy).
291. D. M. Ginzburg, A. A. Tripolskii, *Tr. Gos. Nauchno-Issled. Proekt. Inst. Osnov. Khim.* 30 (1973) 26.
292. IMC Corp., US 3073443, 1960 (R. E. Snow).
293. A. Schmidt, *Angewandte Elektrochemie*, Verlag Chemie, Weinheim 1976, p. 183.
294. Lemar Developments, AU 563487, 1987 (B. W. Levy).
295. *Chem. Age Int.*, 29th Sept., 1972.
296. Dynamit Nobel, DT 1812769, 1968 (D. Labriola et al.).
297. FDA, *Fed. Regist.* 48 (1983) no. 224, 52440-3.

53 Rubidium

WOLFRIED LENK, HORST PRINZ

53.1 Introduction	2211	53.6 Storage and Transportation.....	2213
53.2 Properties	2211	53.7 Uses and Economic Aspects.....	2213
53.3 Raw Materials and Production	2211	53.8 Toxicology and Occupational Health.....	2213
53.4 Inorganic Compounds.....	2212	53.9 References.....	2214
53.5 Quality Specifications and Analysis.....	2212		

53.1 Introduction

Rubidium was discovered in 1861 by BUNSEN, who found hitherto unknown spectral lines during experiments on cesium salts obtained from spa water from Bad Dürkheim, Germany. Soon after this, he succeeded in preparing rubidium metal from its tartrate.

53.2 Properties

Rubidium, the penultimate alkali metal element that is used in industry, is named after two characteristically colored spectral lines (Latin: *rubidus* = dark red). It is a very reactive soft metal with a silvery luster and has the typical chemical properties of an alkali metal. It ignites spontaneously in air and burns with a violet flame. It reacts explosively with water to form colorless rubidium hydroxide, the second strongest base after cesium hydroxide. Rubidium forms four oxides, all of which are colored [1]. Rubidium is monovalent in all its compounds. The isotopic composition of natural rubidium is 72.15% ^{85}Rb , a stable isotope, and 27.85% ^{87}Rb , a β^- emitter. Eighteen artificial isotopes are known. Between mass numbers 79 and 84, these are mainly β^+ emitters, and between mass numbers 85 and 95 they are exclusively β^- emitters. Some important physical properties of natural elementary rubidium are:

Atomic number	37
Relative atomic mass	85.468
Melting point	39 °C
Boiling point	696 °C

Ionization potential	4.16 eV
Work function	2.19 eV
Normal electrode potential	-2.99 V
Electrical conductivity (at 0 °C)	$8.86 \times 10^{-4} \Omega^{-1}\text{cm}^{-1}$
Thermal conductivity (liquid)	$29.30 \text{ W m}^{-1}\text{K}^{-1}$
Specific heat capacity	
Solid	0.332 J g $^{-1}$ K $^{-1}$
Liquid (from mp to 1093 °C)	0.368
Gas	0.242
Heat of fusion	25.71 J/g
Heat of sublimation (at 25 °C)	1004.3 J/g
Heat of vaporization	887.6 J/g
Vapor pressure (427–1093 °C)	$\log(p/\text{mbar}) = 7.0493 - 3891.8 \text{ K}/T$
Mohs hardness	0.3
Atomic radius	0.243 nm
Covalent radius	0.211 nm
Ionic radius	0.149 nm
Density at 18 °C	1.522 g/cm 3
at mp, liquid	1.472
Crystal structure	body-centered cubic

53.3 Raw Materials and Production [2–6]

Rubidium is very widely distributed and always occurs in combined form owing to its high chemical reactivity. Unlike its homologues lithium and cesium, it is not a major component of any mineral. Nevertheless, it is more abundant in the Earth's crust than lithium and cesium (ca. 120 g/t). Its ionic radius [3] is similar to that of potassium, and it is found in association mainly with this element, but also with the other alkali metals. The lithium-containing mica lepidolite has a high rubidium content (ca. 3% Rb_2O). Also, pollucite, a cesium aluminum silicate from Bernic Lake in Canada, can contain ca. 1% Rb_2O .

Due to the similarity in their ionic radii, rubidium is always found in potash salt deposits, e.g., carnallite, sylvite, and langbeinite, which contain 10–300 g/t rubidium oxide, Rb_2O .

Rubidium is also widely distributed in very small concentrations in spring water, rivers, lakes, and seas.

Although rubidium is more abundant than lithium and cesium, it is much more difficult to extract than the other alkali metals. Owing to its very widespread distribution and consequent low concentration in ores, rubidium production is nearly always linked to the production of lithium, potassium, and cesium [7]. The process based on the fractional crystallization of carnallite is now only of historical interest. The more selective methods of recovering rubidium from potash salts (in which the quantities of rubidium are large but the concentrations are very low) are based on extraction processes using substituted benzenes as extractants [8–10]. Other techniques include the use of liquid crystals in a d.c. electric field [11], selective cation exchangers based on nitrated and sulfonated polystyrene [12–14], and inorganic cation exchangers consisting of complex salts based on hexacyanoferrates [15, 16]. Acidic MnO_2 can be used in an adsorption-elution cycle to concentrate rubidium [17]. The liquid waste from the production of cesium from pollucite can also be treated to give rubidium.

Rubidium is obtained from the mixed alkali metal carbonates that are a by-product of the abandoned production of lithium from lepidolite in the United States. After precipitating the less soluble dicesium hexachlorostannate, the rubidium is precipitated as dirubidium hexachlorostannate. It is converted to rubidium chloride by pyrolysis. Rubidium carbonate is obtained by precipitating dirubidium zinc hexacyanoferrate(II) followed by thermal oxidation. In all processes, the main difficulty is separating the rubidium from the potassium and cesium.

In more recently published research work, the following processes are described: the extraction from weathered rocks by sodium chloride solution in a high-frequency electri-

cal field or with dipicrylamine and ultrasound [18], and the thermal decomposition of rubidium alum (rubidium aluminum sulfate) in the presence of calcium oxide followed by dissolution to form rubidium sulfate [19]. Another proposal is the recovery of rubidium from intermediates that arise in the production of aluminum oxide from bauxites and nephelines by means of solvent extraction with long-chain *p*-alkylphenols [20].

53.4 Inorganic Compounds

Rubidium hydroxide, RbOH , mp: 301 °C, solubility in water: 180 g/100 mL at 15 °C

Rubidium carbonate, Rb_2CO_3 , mp: 837 °C, solubility in water: 450 g/100 mL at 20 °C

Rubidium hydrogencarbonate, RbHCO_3 , mp: 175 °C (decomp.), solubility in water: 54 g/100 mL at 20 °C

Rubidium fluoride, RbF , mp: 775 °C, bp: 1410 °C, solubility in water: 130.6 g/100 mL at 20 °C

Rubidium chloride, RbCl , mp: 715 °C, bp: 1390 °C, solubility in water: 77 g/100 mL at 0 °C

Rubidium bromide, RbBr , mp: 682 °C, bp: 1340 °C, solubility in water: 98 g/100 mL at 5 °C

Rubidium iodide, RbI , mp: 642 °C, bp: 1300 °C, solubility in water: 152 g/100 mL at 17 °C

Rubidium nitrate, RbNO_3 , mp: 310 °C, bp: ca. 1700 °C, solubility in water: 44 g/100 mL at 16 °C, solubility in water: 42 g/100 mL at 10 °C

These inorganic compounds are colorless or white, and have the properties typical of salts of alkali metals. They are mostly prepared by wet chemical reactions.

53.5 Quality Specifications and Analysis

Rubidium salts are marketed with purities up to > 99.5%. Rubidium metal is obtainable with purities of 99.5% and 99.8% [2].

Metallic impurities are usually determined by atomic absorption spectroscopy, and more recently with ICP (inductively coupled plasma) excitation. The elements are then detected by conventional optical detectors or by mass spectroscopy (ICP-MS). The homologous elements sodium, potassium, and cesium can be analyzed by emission spectroscopy. The analysis of rubidium metal must be preceded by reaction to give an aqueous salt solution. Anions can be determined photometrically (e.g., sulfate, phosphate) or argentometrically (chloride).

53.6 Storage and Transportation

Because rubidium metal is very reactive toward water, steam, ice, air, and many other gases and substances, special precautions are necessary. The metal is shipped in sealed evacuated glass ampoules, or is hermetically sealed in metal containers packed in vermiculite and enclosed in a second outer metal container. Due to its low melting point (mp 39 °C), melting cannot be prevented during transportation to or through hot climatic zones. Rubidium salts are hygroscopic and must be protected from moisture during storage and transport. Radioactive rubidium preparations are subject to special storage and transport regulations.

53.7 Uses and Economic Aspects

Uses. Rubidium compounds are used in psychiatry and medicine [21], in magneto-optic modulators [22], solid-state lasers [23], phosphors (rubidium aluminate) [24], Rb–C molecular sieves for hydrogen absorption [25], paper pigments [26], glass hardening by ion exchange [27], components of electrolytes for fuel cells [28], in Na–Rb zeolites for separating mixtures of hydrocarbons [29], and for density gradient centrifugation. In the early investigations of the Fischer–Tropsch synthe-

sis, RbOH was used to activate the iron catalyst [30]. Owing to its high ionic conductivity silver rubidium iodide, RbAg_4I_5 , is of interest as a solid electrolyte for primary and secondary cells [31] and as an electrographic picture recording material [32].

The use of rubidium compounds to activate catalysts of various types may increase in terms of quantity. However, potassium and cesium often compete with rubidium in this application. Three types of catalyst may be distinguished. The most important group includes rubidium-activated transition metal oxide catalysts for the production of organic chemicals, e.g., the oxidation of acrolein to acrylic acid [33] or of C_4 hydrocarbons to maleic anhydride [34], the ammoxidation of isobutene to methacrylonitrile [35], or the oxidation of *o*-xylene or naphthalene to phthalic anhydride [36]. The second category includes the activation of metallic catalysts, e.g., silver contact catalysts for ethylene oxide manufacture [37]. The third category comprises rubidium compounds that themselves have catalytic properties, e.g., Rb_2O used in polyester production by polycondensation [38] and in NH_3 synthesis [39], and RbOH for the dehydrocyclization of 1-hexene to form benzene [40].

Economic Aspects. Rubidium manufacturers do not publish production or sales figures. World consumption in 1979 was estimated to be ca. 2 tonnes [2], and has increased slightly since then. The demand for the metal is small compared to the demand for its compounds. In 1996, the price of 99.5% pure metal was \$0.70–1.00/g, and for 99.8% pure metal, \$0.80–6.00/g. Current prices for rubidium compounds (99.5%) are in the range ca. \$250–550/kg, and for > 99.5% pure compounds, \$550–750/kg.

53.8 Toxicology and Occupational Health

It is not possible to give a precise assessment from the small amount of available data on the toxicity of rubidium. In plasma and blood, the properties of rubidium are not dis-

similar to those of potassium, as far as can be determined from physiological investigations. The hazard potential is therefore regarded as low [41].

Rubidium metal is designated as a "flammable solid" and "dangerous when wet", and should be handled with great care under a protective gas or inert solvent.

In its compounds, the precautions and protective measures to be taken are determined by the anion. Thus, RbOH is very caustic, RbF shows the toxicity typical of the alkali metal fluorides, and RbClO₄ and RbNO₃ are oxidizing agents.

53.9 References

1. Kirk-Othmer, 3rd ed., 17, pp. 492-499.
2. Gmelin, 8th ed., System-no. Rubidium, 24.
3. Ullmann, 4th ed., 20, pp. 295-297.
4. C. E. Berthold: "Rubidium and Cesium - Where are they going?" *J. Met.* **34** (1962) 355-358.
5. E. G. Kuznetsova, L. A. Kulikova, A. K. Ru, *Sovrem. Khim.-Metallurg. Metody Pererab. Kompleks. Rud. Syrta, M.* 1985, 102-106; *Chem. Abstr.* **107**, 25536.
6. E. Schroll, *BHM Berg Hüttenmänn. Monatsh.* **131** (1986) 110-115.
7. Li, Minqian, CN 85101989, 1986; *Chem. Abstr.* **107**, 179516.
8. E. M. Kuznetsova, N. A. Kresova, G. M. Panchenkova, *Zh. Fiz. Khim.* **41** (1967) 1041-1046; *Chem. Abstr.* **67**, 57665.
9. V. E. Plyushchev et al., SU 323459, 1970; *Chem. Abstr.* **79**, 22004.
10. L. I. Pokrovskaja et al., *Zh. Prikl. Khim.* **50** (1977) 546-549; *Chem. Abstr.* **87**, 9148.
11. V. N. Golubev, A. G. Petrov, V. N. Verkhovtsov, SU 1279650, 1986; *Chem. Abstr.* **106**, 140437.
12. R. Ratner, L. Kogag, D. Kohn, *J. Chromatogr.* **148** (1978) 539-544.

13. E. Kh. Ismailov, R. G. Osichkina, *Vzh. Khim. Zh.* (1988), no. 5, 56-58; *Chem. Abstr.* **110**, 138080.
14. R. Ratner, J. Mittelman, D. H. Kohn, *J. Chem. Technol. Biotechnol. Chem. Technol.* **35A** (1985) no. 5, 209-216; *Chem. Abstr.* **104**, 112171.
15. S. A. Kolesova, V. V. Volkhin, V. V. Alikin, SU 552105, 1975; *Chem. Abstr.* **87**, 137936.
16. R. M. Shklovskaya, S. M. Arkhipov, SU 1245555, 1986; *Chem. Abstr.* **105**, 136478.
17. V. V. Volkhin, G. V. Leonteva, SU 295399, 1968; *Chem. Abstr.* **81**, 51787.
18. Jiucheng Li, Xiaohong Li, Xian-Gan Li, CN 1037127, 1989; *Chem. Abstr.* **113**, 194434.
19. S. M. Arkhipov, N. I. Kashina, SU 1546425, 1990; *Chem. Abstr.* **112**, 237478.
20. A. M. Reznik, V. I. Vukin, L. G. Romanov, A. O. Baikovrova, *Trav. Chem. Int. Etude Bauxites Alumine Alum.* **17** (1982) 63-66; *Chem. Abstr.* **99**, 91593.
21. H. L. Meltzer, R. R. Fieve, *Curr. Dev. Psychopharmacol.* **1** (1975) 203-242.
22. IBM, US 3527577, 1968.
23. Optical Materials Inc., US 3506584, 1966.
24. Toshiba, JA 7490689, 1973.
25. Ichiro Kato, JA 7401487, 1972.
26. Bayer, DE-OS 2148599, 1971.
27. Daini Seikosha Co., JA 7223885, 1970.
28. Leesona Corp., US 34883035, 1965.
29. Esso Research and Engineering Co., US 3674425, 1966.
30. F. Fischer, H. Tropsch, *Brennst. Chem.* **5** (1924) 201-216.
31. B. Scrosati, *J. Appl. Chem. Biotechnol.* **21** (1971) 223-228.
32. Nippon Electric, JA 7416440, 1972.
33. Standard Oil of Ohio, DE-OS 2634791, 1976.
34. Standard Oil of Ohio, US 4087444, 1976.
35. Montedison, DE-OS 2403716, 1973.
36. BASF, DE-AS 2546268, 1975.
37. Hoechst AG, DE-AS 2740480, 1977.
38. Mitsubishi Rayon, JA 7413635, 1968.
39. Chevron Research Co., US 3653831, 1968.
40. Phillips Petroleum, DE-OS 2832654, 1978.
41. U.S. Department of Health, Education and Welfare, NIOSH, Health Hazard Evaluation, Report 71-72, July 1973.

54 Cesium

MANFRED BICK, HORST PRINZ

54.1 Introduction	2215	54.7 Storage and Transportation	2217
54.2 Resources	2215	54.8 Uses	2217
54.3 Production	2216	54.9 Economic Aspects	2218
54.4 Compounds	2216	54.10 Toxicology and Occupational Health	2218
54.5 Quality Specifications	2217	54.11 References	2218
54.6 Analysis	2217		

54.1 Introduction

Cesium (from the Latin word *caesius*, gray blue, which characterizes the pale blue color of the emission of thermally excited cesium atoms) is a soft, gold-colored metal, which melts slightly above room temperature. Physical properties of elemental cesium are summarized below [4, 5]:

Atomic number	55
Relative atomic mass <i>A_r</i>	132.90543
Melting point <i>m_p</i>	28.7 °C
Boiling point <i>b_p</i>	685 °C
Atomic radius (12-coordinate metal)	0.274 nm
Ionic radius (6-coordinate salt, empirical)	0.165 nm
Density <i>p</i> at 20 °C	1.873 g/cm ³
Specific heat, liquid	0.236 Jg ⁻¹ K ⁻¹
Heat of fusion	2.13 kJ/mol
Heat of vaporization at 0.1 MPa	65.9 J/mol
Ionization potential	3.87 eV
Standard electrode potential	-2.923 V
Work function	1.91 eV
Electrical conductivity solid, 25 °C	4.9 × 10 ⁴ Ω ⁻¹ cm ⁻¹
vapor, 1250 °C	2.0 × 10 ²
Vapor pressure <i>P</i> , kPa	log <i>P</i> = -0.2185 <i>A/T</i> + <i>B</i>

T, K	A	B
200-350	17543.0	6.0739
279-690	17070.7	5.8889

Cesium belongs to the alkali-metal group. The metal reacts with most elements, to form alloys when reacted with metals or to form typical salts when reacted with halogens. In the salts, cesium is strictly monovalent, and its chemistry is typical of an alkali metal. Because of its extremely low ionization potential, cesium is usually far more reactive than

lithium, sodium, or potassium and still pronouncedly more reactive than rubidium. When cesium is exposed to air, an explosion-like oxidation to form cesium superoxide, CsO₂, occurs; contact with water results in a vigorous reaction to form cesium hydroxide and hydrogen gas, which may ignite spontaneously.

Naturally occurring cesium consists only of the stable isotope ¹³³Cs. Radioactive cesium isotopes, such as ¹³⁷Cs (half-life of 30.1 a), are generated in fuel rods during operation of nuclear power plants.

54.2 Resources

Cesium is the 40th most abundant among the elements, occurring about as frequently as germanium. Resources can be categorized into two groups. One, of no commercial importance, consists of the diffuse occurrence of the few grams of cesium per ton contained in potassium salt deposits, sedimentary rocks, and seawater [3].

The only sources of cesium of commercial importance originated during the solidification of residual melts of silicate magmas. After the initial formation of huge granite masses, the remaining melt rich in rare elements like lithium, rubidium, cesium, tantalum, niobium, beryllium, and tin then crystallized to form a type of ore body well-known under the name *pegmatite*. Under favorable conditions, which seem to have existed only in relatively few cases, these pegmatites differentiated into separate bodies.

Sodium, potassium, and rubidium formed feldspar-type minerals of considerable mutual solubility, while lithium and cesium, because of the considerable difference in ionic radii from the other alkali metals, formed separate minerals. In the case of cesium, this seems to have occurred in far fewer cases than for lithium, yielding the only commercial cesium mineral, *pollucite* [6, 7].

Pollucite is a cesium aluminum silicate, which typically contains 18–26% cesium oxide. The theoretical content is 42%, but usually pollucite contains considerable quantities of quartz. Its appearance is also very similar to that of quartz. For this reason and because the demand for cesium has not been great enough to result in any systematic exploration for cesium minerals, possibly further deposits may be discovered. Well known are the large deposits at Bernic Lake in Canada, at Bikita in Zimbabwe, and in South-West Africa. In the CIS, a new mineral, *cestitantite*, a mixed cesium–antimony–tantalum oxide, was reported [8], and pollucite findings have been reported in some deposits of lithium, niobium, and tantalum minerals [9, 10]. Apparently, pollucite also occurs in Afghanistan [11]. Small concentrations of cesium, less than one percent, are found in lepidolite, a lithium mineral.

54.3 Production

For any of the production methods described, pollucite must be powdered first. Production processes can be categorized as (1) decomposition with bases and (2) acid digestion. The second category includes the group of processes used industrially.

Alkaline decomposition can be carried out either by mixing ore with lime and calcium chloride and heating to 800–900 °C followed by leaching of the residue [12] or by heating pollucite with sodium chloride and soda ash to 600–800 °C followed by leaching [13]. In both cases, solutions of impure cesium chloride result. Recently, hydrothermal alkaline leaching with $\text{Ca}(\text{OH})_2$ [14] has been developed as an industrial process to yield a low-

purity cesium hydroxide directly from pollucite [15, 16]; operating conditions are 200–280 °C and high pressure.

Acid digestion can be carried out with hydrochloric acid, sulfuric acid, or hydrobromic acid. Treatment of pollucite with hydrochloric acid at elevated temperature produces a solution of chlorides of cesium, aluminum, and alkali metals, which is separated from the silica residue. The cesium is precipitated as mixed chloride with lead, antimony, or tin. Hydrolysis precipitates the auxiliary metal [17]. Alternatives are precipitation with hydrogen sulfide or recovery of cesium by solvent extraction from the leach liquor [18] or ion exchange from cesium chloride solution.

Treatment of pollucite with sulfuric acid [12, p. 5] yields sparingly soluble cesium alum, cesium aluminum sulfate, which is roasted with carbon to convert the aluminum to alumina and the sulfate sulfur to SO_2 . The residue is leached to obtain a cesium sulfate solution, which can be converted to the desired salts by ion exchange, treatment with ammonia or lime (to precipitate aluminum), or solvent extraction [19]. Hydrobromic acid converts pollucite into a solution of bromides of cesium, aluminum, and impurity metals, from which cesium can be precipitated by addition of alcohol. Leaching the precipitate with bromine selectively extracts cesium as CsBr_3 [20].

Cesium metal can be produced as an amalgam by electrolyzing concentrated cesium salt solutions on a mercury cathode [21], but reduction of solid cesium salts, especially the halides, with calcium or barium at elevated temperature and removal of cesium by vacuum distillation is the usual method [22].

54.4 Compounds

Cesium carbonate, Cs_2CO_3 , 81.58% Cs, is a colorless, hygroscopic powder, decomp. at 610 °C, ρ 4.07 g/cm³, solubility of 261.5 g in 100 g of water, basic solution.

Cesium hydrogencarbonate, CsHCO_3 , 68.54% Cs, colorless crystalline powder, de-

comp. at 175 °C, solubility of 209 g in 100 g of water, basic solution.

Cesium chloride, CsCl , 78.9% Cs, colorless, crystalline, hygroscopic powder, mp 642 °C, ρ 3.983 g/cm³, solubility of 186 g in 100 g of water.

Cesium hydroxide, CsOH , 88.66% Cs, anhydrous, colorless, lumpy solid, mp 272 °C, ρ 3.68 g/cm³, solubility of ca. 400 g in 100 g of water. The solution is a strong base and very caustic.

Cesium hydroxide monohydrate, $\text{CsOH} \cdot \text{H}_2\text{O}$, 79.14% Cs, colorless, crystalline, hygroscopic powder, mp 205–208 °C, ρ 3.5 g/cm³, solubility of ca. 860 g in 100 g of water. The solution is a strong base and very caustic.

Cesium iodide, CsI , 51.2% Cs, colorless, slightly hygroscopic powder, mp 621 °C, ρ 4.51 g/cm³, solubility of 74 g in 100 g of water.

Cesium nitrate, CsNO_3 , 68.19% Cs, colorless crystalline powder, mp 414 °C, ρ 3.69 g/cm³, oxidant.

Cesium sulfate, Cs_2SO_4 , 73.46% Cs, colorless hygroscopic powder, mp 1010 °C, ρ 4.243 g/cm³.

54.5 Quality Specifications

Cesium metal and cesium salts are marketed in purities from 99% for technical grades to 99.999% for high-purity compounds. For some applications, a crude form with approx. 85% purity can also be produced.

54.6 Analysis

Assays and purities of commercial products are derived by subtracting the sum of analyzed impurity levels from unity. Alkali-metal impurities are analyzed by emission spectroscopy, whereas alkaline-earth metals are determined by atomic absorption. Other metals and anions, such as phosphate and sulfate, can be determined by photometric methods; chloride is established argentometrically.

54.7 Storage and Transportation

Special precautions are necessary for cesium metal, which is shipped in evacuated glass ampules or steel containers with an appropriate outer packing to ensure that the metal is kept from air and moisture under any conditions.

Many cesium salts, especially halides, are hygroscopic and must be stored dry. Transportation regulations, where they exist, are governed by the anion, i.e., the hydroxide being caustic, the nitrate being an oxidant, because nothing inherent in the cesium cation calls for special precautions.

54.8 Uses

Cesium metal is used in frequency standards, especially the time standards known as atomic clocks, which lock in on one frequency of excited gas-phase cesium. The metal is also used in the production of various types of vacuum tubes, where it acts as a scavenger to reduce residual gaseous impurities after the tubes have been sealed. The cesium is normally generated in situ by firing the tube to convert a pellet of cesium chromate mixed with a metal powder to elemental cesium vapor.

In ion thrusters, cesium metal is the propellant. It is ionized in a vacuum chamber, and cesium ions are then accelerated through a field and ejected through a nozzle, producing a high specific impulse because of their high atomic mass. Devices of this type are used in satellites for orientation control.

Recognition that the reserves of fossil fuels are limited has focused considerable research on conversion of solar energy into electricity. One approach to achieve this uses thermionic converters, which require cesium. Direct conversion of heat from nuclear reactors into electricity by generating a voltage difference across a cesium vapor-filled vacuum tube between hot and cold electrodes has been proposed [23]. Another potential use of cesium

metal for energy generation is its use as a plasma seeding agent in closed-cycle magnetohydrodynamic generators that use high-temperature nuclear reactors as their heat source.

Of the compounds, the halides (especially the chloride), the trifluoroacetate, and the sulfate are used in ultracentrifuges, where aqueous solutions of high-purity grades are a medium for separation and purification of nucleic acids (DNA and RNA) for biochemical research. At high rates of rotation, these solutions form a density gradient that separates nucleic acids according to their densities [24].

Various catalysts can be doped with cesium salts as activators, much like the corresponding potassium salts. High-purity cesium halides are transparent to infrared radiation; therefore, they are used for cuvettes, prisms, and windows for spectroscopic equipment. Cesium iodide can be doped to make it a scintillator [25]; single crystals are used in scintillation counting equipment. Cesium fluoride is used for fluorination in organic chemistry.

Open-cycle magnetohydrodynamic generators could offer a considerable potential for cesium compounds as a plasma seeding agent. These devices are under development, especially in North America and the former Soviet Union, with the hope that they can boost the overall efficiency of power plants that depend on fossil fuels from ca. 35 to ca. 45%. Hot combustion gas is seeded with potassium or cesium carbonate to make a highly conductive plasma, which is passed through a magnetic field. At right angles to both the field and the direction of plasma flow, there is a voltage difference [26]. Nevertheless, the higher seeding efficiency of cesium compounds must compete with the lower price of potassium compounds.

Recently, the very low toxicity of the cesium cation and the pronounced physical and chemical properties of cesium formate to form clear solutions of high density (up to 2.3 tonnes/m³) have attracted considerations to use these solutions as brines in oil and gas well drilling [27], alone or in mixtures with sodium or potassium formate.

54.9 Economic Aspects

The producers do not publish production or consumption figures. The U.S. Bureau of Mines estimated world consumption in 1978 at about 20 t of cesium, as metal and in compounds. At that time prices for cesium salts were \$64–81 per kg for technical grades and \$147–170 per kg for high-purity products. The price levels in 1996 are \$35–85 per kg for technical and pure grades, and \$85–150 per kg for high-purity salts.

54.10 Toxicology and Occupational Health

The cesium ion itself is only very slightly toxic, more toxic than the sodium ion, but less toxic than the potassium ion. Typical LD₅₀ values of cesium salts are 1400 mg/kg (rat, intraperitoneal) and 1000 mg/kg (rat, oral) [28]. Exceptions are caused by the toxicity of the particular anion. Cesium hydroxide is strongly caustic, cesium nitrate is an oxidant, and cesium fluoride exhibits the typical toxicity of fluoride. Special precautions are necessary when handling the metal because exposure to this substance results in severe caustic burns.

54.11 References

1. Gmelin, system no. 25, Cesium (1938).
2. Kirk-Othmer, 3rd ed., vol. 5, pp. 327–338.
3. C. A. Hampel: *Rare Metals Handbook*, 2nd ed., Reinhold Publ. Co., New York 1969.
4. W. Peek, *Chem.-Zig.* 87 (1963) 315–318.
5. *Handbook of Chemistry and Physics*, 53rd ed., CRC Press, Cleveland 1972–1973.
6. V. M. Goldschmidt: *Geochemistry*, Clarendon Press, Oxford 1954.
7. V. V. Gordiyenko, *Int. Geol. Rev.* 13 (1970) no. 2, 134.
8. P. Černý: *Mineralogy of Rubidium and Cesium, Short Course Handb. Mineral. Assoc. Can.* 8, 1982, 149–161.
9. V. F. Durnev, G. B. Melentyev, V. A. Sokolov, Y. N. Pokrovskiy, G. A. Cherepivskaya, *Doklady Akademii Nauk SSSR* 213 (1973) no. 1, pp. 180–183.
10. L. G. Kuznetsova, B. M. Shmakin, *Zap. Vses. Mineral. O-va* 110 (1981) 1, 59–70.
11. L. N. Rossovskii, *Doklady Akademii Nauk SSSR* 236 (1977) no. 1, pp. 216–219.
12. K. C. Dean, P. H. Johnson, I. L. Nichols, *Rep. Invest. U.S. Bur. Mines* 6387 (1964).

13. W. D. Arnold, D. J. Crouse, K. B. Brown, *Ind. Eng. Chem.* 4 (1965) 249.
14. Y. G. Goroshchenko, E. B. Panasenko, V. A. Roi, V. P. Izotov, *Tsvetnye Metally* 2 (1961) no. 5, pp. 57–59.
15. Metallgesellschaft AG, DE 4237954 C1 (M. Wegner, K. Köbele, H. Hoffmann, H. Prinz).
16. Metallgesellschaft AG, DE 4339062.5–41 (K. Schade, K. Köbele, H. Hoffmann, H. Prinz).
17. J. C. Bailor, Jr.: *Inorganic Syntheses*, vol. 4, McGraw-Hill, New York 1965.
18. *Chem. Eng. News* 41 (1963) no. 51 (Dec. 23), 35.
19. H. W. Parsons, J. A. Vezina, R. Simard, H. W. Smith, *Can. Dept. Mines, Mineral Branch, Tech. Bull.* 50 (1963), reprint of *Can. Metall. Q.* 2 (1963) 1–13; *Chem. Abstr.* 58 (1963) 12199c.
20. V. A. Stenger, US 2481455, 1949.
21. R. E. Davis: "Electrowinning of Rubidium and Cesium", *Encyclopedia of Electrochemistry*, Reinhold Publ. Co., New York 1964.
22. L. Hackspill, *Helv. Chim. Acta* 11 (1928) 1003.
23. J. Raloff, *Sci. News (Washington, DC)* 113 (1978) no. 13, 202.
24. J. Vinograd, J. E. Hearst: *Equilibrium Sedimentation of Macromolecules and Viruses in a Density Gradient*, Springer-Verlag, Wien 1962.
25. P. Brinckmann, US 3446745, 1966.
26. J. Melcher, *Min. Eng. (Littleton, CO)* 29 (1977) no. 12, 34.
27. Shell Internationale Research Maatschappij B.V., Europe Patent Application 0259939 A3 (A. J. Clarke-Sturman, P. L. Sturla).
28. K. W. Cochran et al., *Arch. Ind. Hyg. Occup. Med.* 1 (1950) 637.

55 Alkali Sulfur Compounds

LUDWIG LANGE, WOLFGANG TRIEREL (§§ 55.1–55.8); JOSÉ JIMÉNEZ (§ 55.9); ADOLF METZGER (§ 55.10); MANFRED R. WOLF (§ 55.11)

55.1 Introduction	2221	55.9.5 Sodium Hydrogensulfite	2235
55.2 Compounds of the System $\text{Na}_2\text{S-S}$	2221	55.9.6 Sodium Sulfite	2235
55.2.1 Physical Properties	2221	55.9.7 Analysis of Alkali-Metal Sulfites	2236
55.2.2 Chemical Properties	2224	55.9.8 Toxicology	2236
55.3 Production of Compounds of the System $\text{Na}_2\text{S-S}$	2226	55.10 Thiosulfates	2236
55.3.1 Sodium Tetrasulfide	2226	55.10.1 General Properties	2236
55.3.2 Sodium Disulfide	2227	55.10.2 Sodium Thiosulfate	2236
55.3.3 Sodium Monosulfide	2227	55.10.3 Ammonium Thiosulfate	2238
55.4 Sodium Hydrogensulfide	2228	55.10.4 Toxicology	2239
55.4.1 Properties	2229	55.11 Sodium Dithionite	2239
55.4.2 Production	2229	55.11.1 Introduction	2239
55.5 Uses of Sulfides	2229	55.11.2 Properties	2240
55.6 Safety and Environmental Aspects	2232	55.11.3 Production	2241
55.7 Economic Aspects	2233	55.11.4 Quality Specifications and Analysis	2241
55.8 Transportation	2233	55.11.5 Trade Names and Uses	2242
55.9 Sulfites and Disulfites	2234	55.11.6 Safety and Environmental Aspects; Storage and Transport	2242
55.9.1 General Properties	2234	55.11.7 Economic Aspects	2243
55.9.2 Ammonium Sulfite	2234	55.11.8 Toxicology	2243
55.9.3 Potassium Disulfite	2234	55.12 References	2243
55.9.4 Sodium Disulfite	2234		

55.1 Introduction

Sulfur-sulfur bonds occur in numerous inorganic, organic, and biologically interesting compounds. One reason for this is the high bond energy of the S-S single bond (265 kJ/mol). This is the third strongest single bond, after H_2 (435 kJ/mol) and the C-C single bond (330 kJ/mol) [1].

Of the compounds of sulfur with metals, only the alkali and alkaline earth sulfides, which contain the S^{2-} ion [2], and the corresponding hydrogensulfide, are soluble in water. The sulfides of the alkali and alkaline earth metals undergo addition of sulfur with conversion to polysulfides, which can also be regarded as salts of the sulfanes [3].

55.2 Compounds of the System $\text{Na}_2\text{S-S}$

55.2.1 Physical Properties

The $\text{Na}_2\text{S-S}$ phase diagram has been widely investigated [4–8], with essentially consistent results being obtained [9]. Above 285 °C the phase diagram (Figure 55.1) contains two liquid regions: a sodium-rich, single-phase region in which the composition moves continuously towards Na_2S_5 as the sulfur content increases, and a two-phase region where two immiscible liquids— Na_2S_5 saturated with sulfur, and sulfur saturated with Na_2S_5 —coexist [5, 10]. In the sodium-rich part of the diagram, the liquidus curve between Na_2S_2 and Na_2S_4 shows an eutectic, which lies at 235 °C according [5], and at 240 ± 2 °C according to [11]. According to [5], the eutectic corre-

sponds to the composition Na_2S_3 ; earlier investigations indicated the composition $\text{Na}_2\text{S}_{3.24}$. X-Ray diffraction experiments have shown that Na_2S_3 does not exist as a defined polysulfide in the solid state [12]. The solid product with the stoichiometric composition Na_2S_3 contains only Na_2S_2 and Na_2S_4 [13].

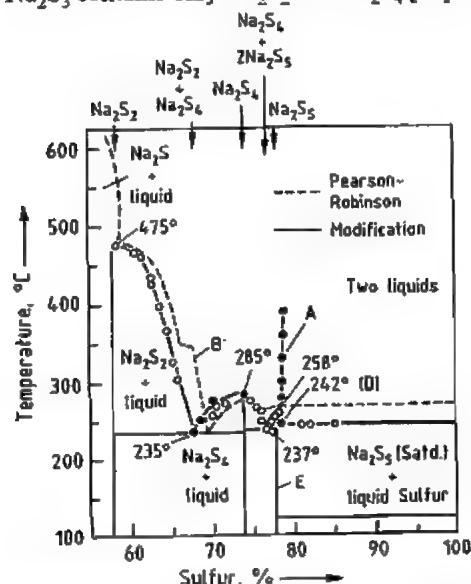
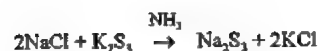


Figure 55.1: Phase diagram of the Na-S system between the compositions Na_2S_2 and 100% S [7].

Although the above results show that solid sodium trisulfide is unstable, the situation is different for the molten state [14]. A melt with the composition Na_2S_3 consists of a mixture of Na_2S_2 , Na_2S_4 , and Na_2S_6 [14]. In spite of the undoubted presence of the S_3^{2-} ion in K_2S_3 , BaS_3 , etc., Raman spectroscopy shows that in molten Na_2S_3 the ion disproportionates into S_2^{2-} and S_4^{2-} ions [15]. Thus, the compositions of the known alkali polysulfides are as listed below [8]:

Li_2S	Li_2S_2	Na_2S_4	Na_2S_5
Na_2S	α , β - Na_2S_2	K_2S_4	K_2S_5
K_2S	K_2S_2	Rb_2S_4	Rb_2S_5
Rb_2S	Rb_2S_2	Cs_2S_4	Cs_2S_5
Cs_2S	Cs_2S_2	Na_2S_6	Na_2S_7

The following route to Na_2S_3 has been proposed on the basis of the differing solubilities of NaCl and KCl in liquid ammonia (NaCl : 3.02 g/100 g solution; KCl : 0.04 g/100 g solution) [8, 11].



The question of whether Na_2S_3 can be synthesized was partially elucidated when it was shown that the compound can exist as an ammoniate [11]. X-Ray and thermogravimetric measurements at various temperatures on powdered samples showed that ammonia can be removed at 370 K without fundamentally changing the structure [11]. The eutectoid decomposition reaction is hindered, at least kinetically, at low temperature [11].

Experiments on the melting and crystallization processes in the sodium sulfur cell show remarkable behavior by some sodium polysulfide compounds [16]. The melting temperatures of, e.g., polycrystalline Na_2S_4 and Na_2S_5 are reproducible for the first melting process, but in subsequent melting and crystallization cycles, the two compounds behave like the products of eutectic composition. With the exception of the disulfide, the polysulfides can form supercooled melts, and vitreous states have been observed. Some data on the melting behavior of polysulfides are given in Table 55.1 [16].

Table 55.1: Melting behavior of polysulfides.

Polysulfide composition	1st melting		Remelting	
	mp, °C	ΔH_{fus} , kJ/mol	Remelt cycles	mp, °C
Na_2S_2	474	7.48	3	474
$\text{Na}_2\text{S}_{3.0}$	234	15.62	3	234
$\text{Na}_2\text{S}_{3.1}$			2	241
$\text{Na}_2\text{S}_{4.0}$	283	28.85	3	240
$\text{Na}_2\text{S}_{4.2}$			3	207–234
$\text{Na}_2\text{S}_{4.6}$			2	240–260
$\text{Na}_2\text{S}_{4.8}$			3	213–231
$\text{Na}_2\text{S}_{5.0}$	258	32.55	2	220–241
$\text{Na}_2\text{S}_{5.2}$	255	30.41	10	219–247
$\text{Na}_2\text{S}_{5.3}$			11	236–246
$\text{Na}_2\text{S}_{6.1}$	254	27.89	4	205–247
$\text{Na}_2\text{S}_{6.8}$	254	29.36	3	205–265

Sodium monosulfide, Na_2S , like Li_2S , K_2S , Rb_2S , Li_2O , Na_2O , and K_2O , crystallizes with the antifluorite structure, in which each S atom is surrounded by a cube of 8 Na atoms, and each Na atom by a tetrahedron of 4 S atoms [15]. The mp is $1170 \pm 10^\circ\text{C}$ [17], the heat of fusion $\Delta H_{\text{fus}} = 30.1 \text{ kJ/mol}$ [20], the standard

entropy $S_{298}^\circ = 90.3 \text{ JK}^{-1}\text{mol}^{-1}$ [17], and the heat of formation $\Delta H_{298}^\circ = -386.6 \text{ kJ/mol}$, based on [19, 20].

Sodium disulfide crystallizes in two modifications [12]. The transformation from the α - to the β -modification takes place in the temperature range $150\text{--}250^\circ\text{C}$ [12]. The change in structure is irreversible. Products that solidify from the melt or are tempered at high temperature have the β -structure, which is isotypical with that of Li_2O_2 [21]. Sodium disulfide isolated from alcoholic solution exists in the α -modification, isotypical with the structure of Na_2O_2 [21]. The sodium disulfide was prepared in alcoholic solution by the method proposed in [22] in which an alcoholic solution of sodium tetrasulfide is reduced with sodium metal [12].

The specific heat capacity c_p of α - Na_2S_2 was found to be constant at $1071 \text{ Jkg}^{-1}\text{K}^{-1}$ over the temperature range $97\text{--}167^\circ\text{C}$ [16].

For β - Na_2S_2 in the range $191\text{--}267^\circ\text{C}$, c_p is $1113 \text{ Jkg}^{-1}\text{K}^{-1}$ [16]. The relative density d_{20} of α - Na_2S_2 is 2.01, and that of β - Na_2S_2 , 2.05. The color of Na_2S_2 is yellow to orange.

Sodium Tetrasulfide. The crystal structure of Na_2S_4 is described in [23]. The structure of the S_4^{2-} ions in sodium tetrasulfide is shown in Figure 55.2 [24].

The interatomic distance d of the sulfur atoms is 207 pm, the valency angle α is 109.8° , and the torsion angle τ is 98° [24].

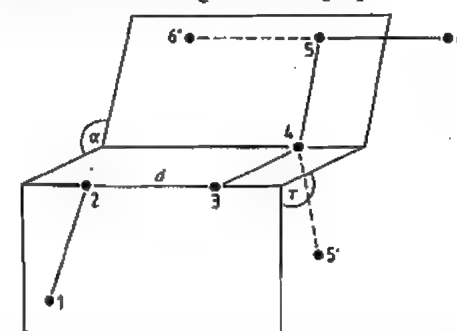


Figure 55.2: Structural principle of the ions S_4^{2-} , S_5^{2-} , and S_6^{2-} [24]. In S_4^{2-} , atoms 5 and 6 or 5' and 6' are absent, and in S_5^{2-} , atom 6 or 6' is missing. In $\text{gg}'\text{-S}_5^{2-}$, the fifth atom is in position 5. Likewise, the last atom of $\text{ggg}'\text{-S}_6^{2-}$ would be in position 6'.

According to [24], reliable IR and Raman spectra of sodium tetrasulfide were first published in [25], the Na_2S_4 spectra available until then having been falsified by the presence of lines due to the pentasulfide. The relative density of sodium tetrasulfide is $d_{20} = 2.08$ [12].

Sodium Pentasulfide. Like Na_2S_2 and Na_2S_4 , Na_2S_5 in the solid state forms a structure that appears uniform by X-ray diffraction, and is therefore a true chemical compound with a definite chain length [12, 26]. The structure, shown in Figure 55.2 as $\text{gg}'\text{-S}_5^{2-}$, is based on the Raman spectrum of Na_2S_5 [24]. The relative density of Na_2S_5 is $d_{20} = 2.08$ [12].

Some physical properties of anhydrous alkali metal sulfides are listed in Table 55.2 [27].

Table 55.2: Physical properties of the anhydrous alkali metal sulfides.

Compound	ΔH_f , kJ/mol	mp, °C	Density, g/cm ³	H_{ion} , 0 °C, kJ/mol
NaHS	-238.4	350	1.79	16.0
KHS	-263.9	455	1.68–1.70	0.4
RbHS	-262.1			0.0
CsHS	-264.2			-1.7
Na_2S	-376.6	1180	1.856	65.1
K_2S	-420.0	840	1.805	94.5
Rb_2S	-349.4	530	2.912	103.4
Cs_2S	-340.6	510		114.4
Na_2S_2	-443.6	445		
K_2S_2		470	1.973	
Rb_2S_2		450	2.79	
Cs_2S_2		460	3.83	
Na_2S_3	-450.7	275		
K_2S_3		252	2.102	
Rb_2S_3		210	2.68	
Cs_2S_3		217	3.47	
Na_2S_4	-413.3	285	2.08	41.2
K_2S_4	-474.6	145		5.0
Cs_2S_4		160		
Na_2S_5		253	2.08	
K_2S_5		206		
Rb_2S_5		230	2.67	
Cs_2S_5		211		
K_2S_6		196	2.02	
Rb_2S_6		201		
Cs_2S_6		186		

Molten Sodium Polysulfide. Conductivity data for some molten sodium polysulfides are plotted in Figure 55.3 [28]. The values are in the range expected for ionic liquids. At 340°C , the conductivity κ of Na_2S_4 is 0.45

$\Omega^{-1}\text{cm}^{-1}$, which compares with $1.11\ \Omega^{-1}\text{cm}^{-1}$ for NaNO_3 and $0.87\ \Omega^{-1}\text{cm}^{-1}$ for NaSCN at the same temperature.

The conductivity increases with decreasing sulfur content approximately twofold from Na_2S_5 to Na_2S_3 . This is partly a result of the increasing ionic concentration as the proportion of sulfur decreases.

The conductivity of pure molten sulfur and of molten sulfur saturated with Na_2S_3 is shown in Figure 55.4. The two "types of sulfur" show only small differences in their conductivities, in contrast to the conductivity of molten Na_2S_3 . This shows that the solubility of Na_2S_3 in sulfur is extremely low [28].

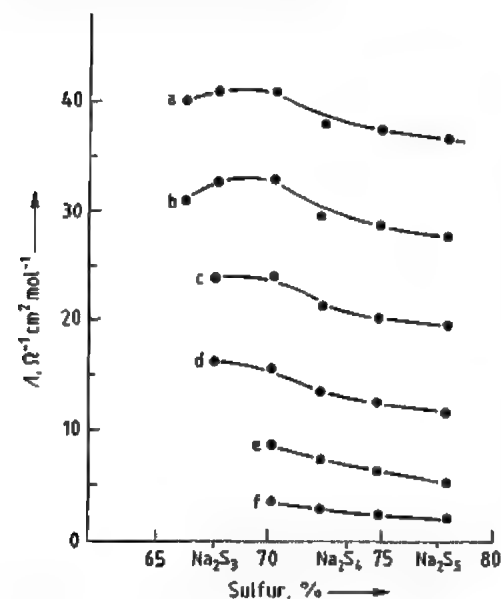


Figure 55.3: Equivalent conductivity plotted against % sulfur for fused sodium polysulfides [28]: a) 420 °C; b) 380 °C; c) 340 °C; d) 300 °C; e) 260 °C; f) 220 °C.

Table 55.3: Values of parameters in the equation $\rho = D + E(T - 600)$, describing the density of fused sodium polysulfides [29].

Melt	S, %	Temperature range, K	$D, \text{g/cm}^3$	$10^4 E, \text{g cm}^{-3} \text{K}^{-1}$
Na_2S_3	67.6	590–683	1.887	-5.65
$\text{Na}_2\text{S}_{3.5}$	69.7	576–689	1.901	-7.96
$\text{Na}_2\text{S}_{3.7}$	72.0	563–669	1.926	-5.47
$\text{Na}_2\text{S}_{4.1}$	75.4	571–680	1.869	-6.66
$\text{Na}_2\text{S}_{4.8}$	77.0	573–683	1.876	-7.16

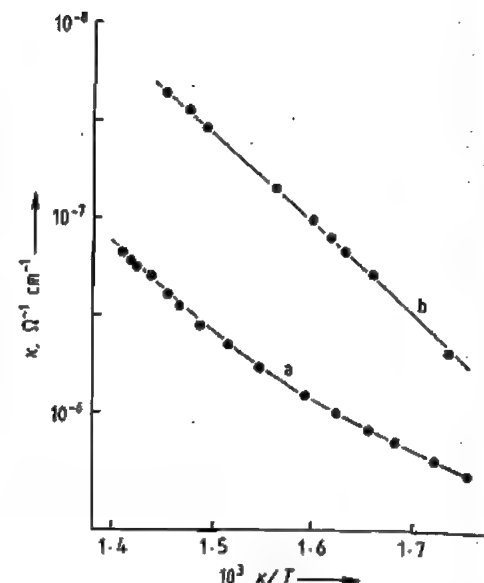


Figure 55.4: Temperature dependence of conductivity for liquid sulfur (a) and sulfur saturated with Na_2S_3 (b) [28].

Density values for some sodium polysulfide melts are listed in Table 55.3 [29]. Comparing the densities of solid and liquid Na_2S_4 and Na_2S_5 shows that the transformation from solid to liquid is accompanied by a volume increase of ca. 8–10% [29].

55.2.2 Chemical Properties

Sodium Monosulfide. The chemical properties of sodium sulfide are described in detail in [30–32]. Anhydrous Na_2S is a white solid that readily reacts with moist air to form sodium sulfite and carbonate. Pure NaHS can be obtained by the action of H_2S on anhydrous Na_2S .

Sodium sulfide is very soluble in water. The concentration of a saturated solution of Na_2S at various temperatures is given below [33]:

$\text{g Na}_2\text{S}/100\text{ cm}^3$	12.2	16.0	21.3	28.0	33.0	40
$T, ^\circ\text{C}$	0	20	40	60	80	90

The relationship between % Na_2S y and density x at various temperatures is given by [32]:

$$y = -98.24 + 98.28x \text{ at } 20^\circ\text{C}$$

$$y = -98.73 + 99.01x \text{ at } 30^\circ\text{C}$$

$$y = -98.40 + 99.01x \text{ at } 40^\circ\text{C}$$

Aqueous solutions [33] of sodium sulfide react alkaline due to hydrolysis:



Iron compounds dissolve in hydrolyzed sodium sulfide solutions, forming thio complexes with an intense brown-red color. Iron metal is also attacked by concentrated Na_2S solutions.

Na_2S solutions can dissolve sulfur up to a composition corresponding to Na_2S_3 .

Sodium sulfide solutions are oxidized by NaOCl solutions; depending on the concentration of the reactants, the temperature, and the pH, various amounts of sulfur and sulfate are formed [32]. For dilute solutions of approximately constant concentration, the ratio of sulfur to sulfate formed is constant. With a large excess of sulfide, the formation of sulfur increases, and for a large excess of NaOCl , the formation of sulfate increases. Sulfate formation is favored by increased temperature. Maximum sulfate formation is observed at pH 10 [32].

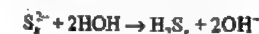
Sodium sulfide is oxidized by the Karl Fischer reagent, presumably by the reaction [32]



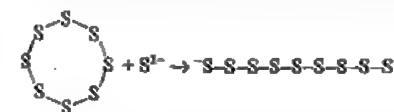
Sodium sulfide is appreciably soluble in the lower alcohols (methanol, ethanol) [33].

Sodium Polysulfides. The chemical properties of the sodium polysulfides are described in detail in [30, 31, 34, 35].

Sulfur dissolves readily in alkali metal sulfide solutions with formation of alkali metal polysulfides [35]. These solutions are strongly alkaline owing to the reaction



The S_8 ring is broken by the thiophilic S^{2-} and SH^- ions in accordance with the equation

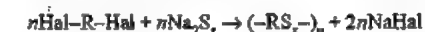


leading to the formation of nonasulfide ions which can break down to form shorter chains.

At the same time, longer chains are formed from S^{2-} ions (e.g., S_2^{2-} , S_3^{2-} , etc.) which can also undergo degradation. In solutions of alkali polysulfides produced from alkali sulfide and sulfur, these reactions take place in single steps and, therefore, constitute a complex dynamic equilibrium between sulfide ions of various chain lengths. This explains why aqueous solutions of polysulfide ions of definite chain length cannot be obtained by reaction of stoichiometric amounts of sulfur with sulfide. Addition of such solutions to cold hydrochloric acid always gives a mixture of sulfanes [35]. Furthermore, of the alkali metal polysulfides M_2S_n , only the pentasulfide dissolves without decomposition, dissociating to form S_5^{2-} ions [26]. Higher polysulfides with $n > 5$ also form pentasulfide ions with precipitation of the excess sulfur, while the lower polysulfides ($n < 5$) disproportionate into monosulfide, tetrasulfide, and pentasulfide ions, which are in pH-dependent equilibrium with each other [26, 36]:



Free polysulfide ions consist of sulfur chains [36]. The sulfur atoms of an S_3^{2-} chain are necessarily coplanar, but for longer chains there are possibilities for isomerism, as shown in Figure 55.5. Thus, for the structure of the S_4^{2-} ion there are two possibilities (Figure 55.5A and B), for the S_5^{2-} ion there are the possible structures (C) and (D), and for the S_6^{2-} ion, the structure (E) [36]. The equilibrium between the polysulfide ions in aqueous solution also appears to influence the production of polymeric polysulfides, represented by the general equation



This is essentially a nucleophilic exchange between the halogen and the polysulfide anion. The exact nature of the polysulfide ions that react with the dihalides is not yet clear. The polymer initially formed on addition of dihalide to aqueous sodium polysulfide contains less sulfur than expected.

The degree of sulfur substitution (sulfur grade) is the average number of sulfur atoms

in each repeating unit of the polymer. However, if a polymer with, for example, a sulfur grade of 4, is treated with 1 mol Na_2S_4 , the sulfur grade in the polymer decreases to 3.1, while that of the polysulfide solution increases by a corresponding amount [37].

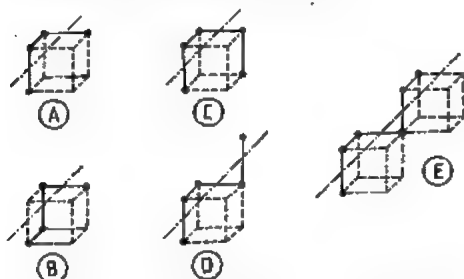


Figure 55.5: Idealized stereochemistry (dihedral angle equal to 90°) for polysulfide ions [36]. A, B) *d*- and *l*- S_3^{2-} ; C, D) *cis*- and *trans*- S_3^{2-} ; E) *trans,trans*- S_4^{2-} .

For reactions that must be carried out under anhydrous conditions, anhydrous polysulfide reagents can be prepared according to the following reaction scheme [38]:



where Cp = cyclopentadienyl and M = Ti, Zr, Hf, V. The so-called Super-Hydride method has been found to be very versatile for the preparation of polysulfide complexes of transition metals [38].

55.3 Production of Compounds of the System Na_2S -S

Sodium tetrasulfide is nowadays produced from the elements in the absence of water and solvents on an industrial scale; sodium disulfide and sodium monosulfide can be prepared similarly on the laboratory scale [39-43].

A summary of the processes is given in Figure 55.6. The production of Na_2S_4 , Na_2S_3 , and Na_2S is briefly described below.

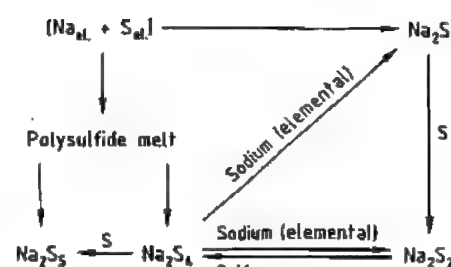


Figure 55.6: Some production routes to anhydrous, solvent-free sodium monosulfide and polysulfides.

55.3.1 Sodium Tetrasulfide

Sodium tetrasulfide is now produced on an industrial scale in high purity from the elements in the absence of water and solvents.

Molten polysulfide is charged into a cylindrical reactor, with no added water or solvent [39]. Molten sodium and sulfur are added alternately and are mixed with the melt by vigorous agitation. The heat of reaction is removed by a heat-transfer oil in contact with the outer wall of the reactor.

For optimum process operation, the temperature of the polysulfide melt should be in the range 340 – 360°C .

As the molten polysulfide is extremely corrosive, the choice of construction materials is very important. The alloy AlMg appears to be sufficiently resistant. The atmosphere in the reactor is inerted with argon [39].

The preparation of the sodium polysulfides Na_2S_3 , Na_2S_4 , and Na_2S_5 on the laboratory scale by synthesis from the elements is described in [13]. An equimolar amount of sulfur is added to molten sodium in small amounts with agitation. The reaction product, consisting mainly of Na_2S_2 , is cooled, size reduced, and then mixed at room temperature with the required amount of sulfur. The mixture is then melted. Unreacted sodium recovered from the size-reduced reaction product is then added to this polysulfide melt [13].

In another laboratory method, based on early work [5, 22], Na_2S_4 was prepared in alcoholic solution from sodium, hydrogen sulfide, and sulfur [12]. In a widely cited preparation of sodium tetrasulfide or polysul-

fides from Na_2S and sulfur, alkali metal sulfide, prepared by the reduction of Na_2SO_4 , is added to molten sulfur [44].

55.3.2 Sodium Disulfide

Sodium disulfide, Na_2S_2 , is produced by adding a higher sodium polysulfide and sodium, either simultaneously or alternately, to a polysulfide melt [40]. As the melting point of Na_2S_2 (474°C) is higher than the boiling point of sulfur, it is preferable to use sodium tetrasulfide. Thus, sodium disulfide free of water or solvent can be produced in an easily controlled process. The process has three variations [40]. The whole of the polysulfide can be premelted, and the sodium added to the melt until the desired stoichiometric composition is obtained, or sodium and, for example, Na_2S_4 can be added to the melt either alternately or simultaneously [40].

There are many literature references to other methods of producing sodium disulfide. For example, sodium tetrasulfide can be dissolved in alcohol and then reduced with sodium metal to give sparingly soluble Na_2S_2 [22]. It has not been possible to prove conclusively that the product so obtained, which contains 4-6% alcohol, represents a defined alcoholate [12]. High-purity Na_2S_2 can be produced from the elements in liquid ammonia [12].

Small amounts of sodium polysulfide for the investigation of thermodynamic properties have been prepared by melting together Na_2S and sulfur in a small sealed capsule [16].

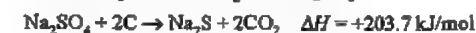
Sodium disulfide is produced on an industrial scale from sodium hydroxide solution and sulfur [45], and is used for the production of polysulfide polymers [37] (see Section 55.5).

55.3.3 Sodium Monosulfide

The most important processes for the production of Na_2S are described in detail in [30-32, 46]. Of these, the reduction of sodium sulfate with carbon is described in detail here.

Sodium sulfide is produced in large quantities by the reaction of anhydrous sodium sul-

fate with carbon in a process that has been used for decades. The reaction, which is carried out at 700 – 900°C , is represented by the following overall equation [33]:



At ca. 730°C , the evolution of CO_2 begins, and the reaction mass becomes very fluid. On further heating, it becomes pasty, and finally solid. This behavior can be explained by means of the sodium sulfate-sodium sulfide phase diagram (Figure 55.7) [33].

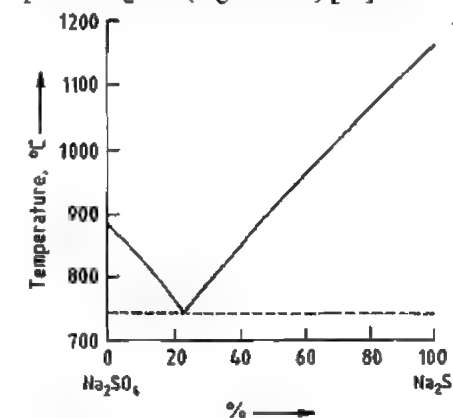


Figure 55.7: Phase diagram of the system Na_2SO_4 - Na_2S [31].

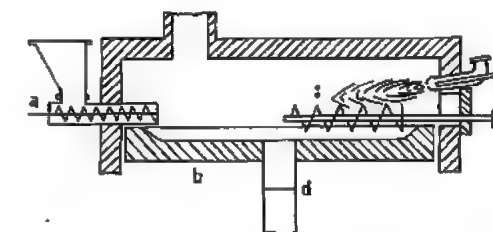


Figure 55.8: Rotating-hearth furnace [33]: a) Screw feeder; b) Rotating hearth; c) Transporting screw feeder; d) Discharge shaft; e) Burner.

The process details and the operation of the reactors or furnaces are described in patents [30]. The rotating-hearth furnace (Figure 55.8) operates fully continuous. The sulfate-carbon mixture is delivered by a water-cooled screw feeder (a), onto the outer part of the rotating hearth (b) [33]. As the hearth rotates, a second screw feeder (c) moves the mixture nearer to the center of the plate where the melt passes through the discharge shaft (d).

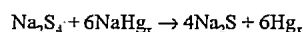
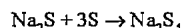
To ensure sufficient heat transfer to the reaction mixture, the temperature in the gas space of the furnace must be ca. 1100 °C. The furnace lining is strongly attacked by Na₂S.

The sodium monosulfide so produced contains excess carbon, ash components, Na₂CO₃, Na₂S₂O₃, and Na₂SO₃. The product is leached with water, and the undissolved components are removed by filtration. The solution is concentrated by evaporation to 60–62% Na₂S. The concentrated solution, which solidifies at ca. 90 °C, is converted to the solid form by cooling on rolls or in pans [33]. Depending on process conditions, the purity of the sodium monosulfide obtained can vary between 50 and 98% [30]. The product can be purified in various ways, e.g., by removal of the strongly colored iron compounds from the sodium sulfide solution [47].

High-purity sodium monosulfide can be obtained by treating the reaction product with methanol to dissolve the sulfide, instead of water [48]. Unlike its hydrates, anhydrous sodium sulfide is very soluble in alcohols. The solubility of Na₂S in methanol is 160 g/L at 20 °C, whereas that of Na₂S·9H₂O in methanol is only 30 g/L [48]. Other aliphatic, aromatic, and polyhydroxy alcohols can also be used as extractants: the solubility of Na₂S in ethanol is 90 g/L, and in ethylene glycol > 200 g/L. The sodium sulfide obtained by evaporating the extractant is free of water, iron, sulfite, sulfate, and thiosulfate [48].

Sodium sulfide can also be obtained by reducing Na₂SO₄ with hydrogen (Sulfigran process) [33], methane, or other hydrocarbons [30, 33, 46].

The reduction of sodium polysulfides with sodium amalgam to give high-purity monosulfide proceeds according to the following equation [33]:



Anhydrous sodium monosulfide is obtained from moist, anhydrous sodium sulfide in a two-stage process [49].

Pure Na₂S can be prepared on a laboratory scale from the elements using liquid ammonia

as solvent [12] or without the use of solvents [41–43]. Na₂S has been prepared in the laboratory in two steps:

In the first step, one of three processes was carried out in a preheated kneading machine:

1. Solid Na₂S₄ was charged into the machine and ground. Liquid sodium was then slowly added, maintaining the temperature of the reaction mixture at 120–250 °C by means of a heat-transfer oil [41]; or
2. Liquid sodium was charged into the machine, and solid sulfur was slowly added, maintaining the temperature of the reaction mixture at 120–250 °C by means of a heat-transfer oil [42]; or
3. Sulfur and sodium were added alternately to powdered sodium monosulfide, prepared by method 1 or 2, maintaining the temperature of the reaction mixture at 120–250 °C by means of a heat-transfer oil [43].

All of these first stages gave a blue-black powder as intermediate product.

In the second stage, the intermediate product was placed in a small reactor. The unreacted residues of sodium and sulfur in the black intermediate product were then allowed to react at 250–480 °C. A white sodium monosulfide was produced from all three products of the first stage. The purity of the Na₂S so obtained was consistently > 95% [41–43].

55.4 Sodium Hydrogensulfide [33]

Sodium hydrogensulfide, NaHS, *mp* 350 °C, *d* 1.79, is a colorless to yellow solid. The anhydrous salt (95–98% NaHS) is of minor importance. In industry, the following low-iron hydrated products are used [46]:

- Sodium hydrogensulfide solution (30% NaHS)
- Sodium hydrogensulfide flakes (70% NaHS)
- Sodium hydrogensulfide powder (95% NaHS)

55.4.1 Properties [33]

Sodium hydrogensulfide is very soluble in water [32]. The variation of solubility with temperature is shown below:

g NaHS/100 cm ³	41	50	55	60	65	72
T, °C	5	22	35	39	43	65

Sodium hydrogensulfide forms two hydrates, NaHS·2H₂O and NaHS·3H₂O. The aqueous solution has an alkaline reaction.

The solid products are strongly hygroscopic, and are oxidized by atmospheric oxygen.

55.4.2 Production [33]

Sodium hydrogensulfide is usually obtained by the action of hydrogen sulfide on sodium sulfide or sodium hydroxide solution. If hydrogen sulfide is passed over anhydrous high-percentage sodium sulfide at ca. 300 °C, high-percentage sodium hydrogensulfide is obtained [50]. According to a patent, anhydrous sodium hydrogensulfide is obtained by the reaction of sodium metal with hydrogen sulfide in inert organic solvents [51], and high-percentage solid products can be obtained by the evaporation of aqueous solutions [52].

Hydrated products are obtained by reacting hydrogensulfide with solutions of sodium sulfide or sodium hydroxide (e.g., in spray towers). If sodium hydroxide solution is used, it should be noted that the sodium sulfide formed as an intermediate is less soluble than the end product. Problems arising from this can be avoided by a patented method [53]. Another patent [54] describes how the difference between the solubilities of sodium sulfide and sodium hydrogensulfide can be exploited by allowing hydrogen sulfide to react with sodium sulfide (60% Na₂S) in lump form in a tower, controlling the temperature so that the sodium hydrogensulfide runs off, leaving behind the sodium sulfide as a solid.

The hot solutions obtained using pure hydrogen sulfide can be converted to solid products by cooling without intermediate treatment. If the hydrogen sulfide contains carbon dioxide, Na₂CO₃ is formed in the solu-

tions in addition to NaHS. A process for obtaining pure products from such solutions is described in a patent [55]. Another patent describes how NaHS solutions can be produced from H₂S-containing gaseous by-products of petroleum refining [56].

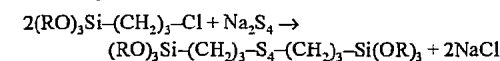
55.5 Uses of Sulfides

Much of the new knowledge of the system Na₂S–S mentioned above has come from research into sodium sulfur cells. However, the Na₂S_{*n*} compounds that are formed and decomposed in these cells are initially produced from the elements sodium and sulfur, so that the batteries that contain these cells have no economic implications for the production and use of anhydrous, solvent-free sodium polysulfide compounds [10, 57].

An established application is in the production of *sulfur dyes* [58], which are produced by the two methods:

- The polysulfide bake method, where sulfur or sulfur–sodium sulfide is heated in the dry state with aromatic amino or nitro compounds or with nitrogen-free organic substances such as cresol, anthracene, or decacyclene
 - The polysulfide melt method, in which organic compounds are refluxed with polysulfide in an aqueous or alcoholic medium
- The water-insoluble sulfur dyes are dissolved by reduction to the leuco form, generally with sodium sulfide. The leuco dyes become attached to the fibers, and the sulfur dye is then fixed on the fiber by oxidation with peroxides or perborates [58].

Anhydrous, solvent-free sodium tetrasulfide is extensively used in the production of *organosilanes*, which are used in the rubber industry:



The ethyl derivative of bis(trialkoxysilylpropyl) tetrasulfide (Si 69) is one of the most important organofunctionalized silanes [59]. Organosilanes are used in the rubber industry in combination with various fillers to produce

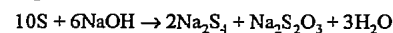
elastomers with improved static and dynamic vulcanizate properties [60]. These silanes have two different reactive groups that react with the silanol groups of fillers during compounding in rollers or kneaders, and form chemical bonds to the polymer and cross-linking agents during vulcanization. Si 69 can also be used as a sulfur donor that gives reversion-free vulcanization (equilibrium cure system) [60].

Another example of the use of an anhydrous sulfide is in a process for producing poly(phenylene sulfide) [34, 61, 62]. In the production of poly(phenylene sulfide), 1,4-dichlorobenzene and sodium sulfide are reacted at ca. 280 °C under pressure in a polar aprotic solvent, usually *N*-methyl-2-pyrrolidone [63]. While aliphatic polysulfides can easily be prepared by nucleophilic exchange reactions of chloride with sulfide, the reaction with aromatic compounds is much more difficult because of the considerably lower reactivity of the aromatically bonded chlorine [34]. It has been suggested that formation of poly(phenylene sulfide) does not proceed like a normal polycondensation [64]. The reaction is a one-electron transfer process in which radical cations act as reactive intermediates [64]. Poly(phenylene sulfide) can be used with very high contents (up to 70%) of fillers such as glass fiber, carbon fiber, or minerals. Its good chemical resistance (PPS is practically insoluble in all the usual solvents) and inherent flame-retardant properties enable it to be used under severe thermal and chemical conditions. Reinforced PPS can replace metals in many applications, e.g., in the construction of machinery and equipment, pump housings, and gear wheels [63].

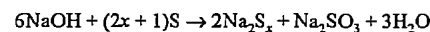
Sodium sulfide, sodium hydrogensulfide, and sodium polysulfide are sometimes used in the same fields of application [32]. This is also true to some extent of the sulfanes, although their instability prevents their large-scale use [33]. Examples are the manufacture of polysulfide polymers and the sulfide reduction of polynitroaromatics, both described below.

Aliphatic polysulfides of the thiokol type have the general formula $(C_xH_{2x}S_y)_n$. These

find wide application [61] as sealants and, in combination with epoxy resins, as adhesives and mastics. These products have a marked ability to expand and contract, are elastic over a wide temperature range, and are resistant to seawater, solvents, and many chemicals. The best known commercial products are the Thiokols, which are polyalkyl- and polyalkoxy polysulfides. They are produced by the condensation of Na_2S_n with dichloroalkyls and bischloroalkylformals [66, 67]. Trichloroalkanes [68], epichlorohydrin [69], condensation products of α -monochlorohydrin formaldehyde [70], and monochloro alcohols [67] are also used as modifiers in the condensation reaction. The basic properties of these polysulfides mainly depend on the sulfur content [37]. The Na_2S_n compounds can be obtained by the reaction of NaOH with sulfur [45]. At temperatures of < 110 °C and with NaOH concentrations of < 30%, polysulfide and thiosulfate are formed according to the equation

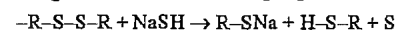


whereas at higher NaOH concentrations (up to 35%) and higher temperatures (100–320 °C) sulfite is also formed [45]:

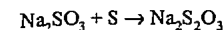


The autoxidation of aqueous polysulfide solutions in the temperature range 23–40 °C, the kinetics of polysulfide–thiosulfate disproportionation [71, 72], and equilibria of polysulfide ions in solution [73] should be mentioned in this connection [74]. The reaction usually proceeds very rapidly from sulfite to thiosulfate, so that only small amounts of sulfite remain. However, as sulfite crystallizes from concentrated NaOH solution, small amounts of thiosulfate remain in the solution [75].

The polymers produced by the reaction of alkyl chlorides with sodium polysulfide are obtained as high molecular mass, rubber-like products with a very limited range of uses. The polymers can be selectively cleaved by the action of sodium hydrogen sulfide on the disulfide groups, allowing the average chain length to be controlled [76].

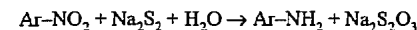
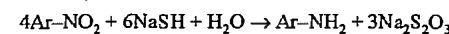
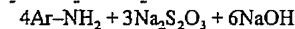
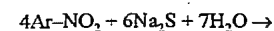


The sulfur liberated in this reaction reacts with added sodium sulfite to form sodium thiosulfate [76]:



The bis(vinylarylalkyl) polysulfides [77], obtained by reacting 4-vinylbenzyl chloride with Na_2S-S , are used as coatings and sealants in the form of copolymers with halogenated alkanes.

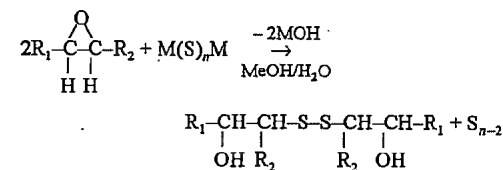
Aromatic amino compounds can be prepared by the reduction of polynitroaromatics with sulfide [78]. Sulfide reductions are carried out in industry with Na_2S , NaHS, Na_2S_2 , or ammonium sulfide solutions. The reactions are not exactly stoichiometric, proceeding approximately in accordance with the following equations:



Some other important products obtained by using the sulfide reaction are 1,2-diamino-4-nitrobenzene from 2,4-dinitroaniline and NaSH; 2-amino-4-nitrophenol from 2,4-dinitrophenol and NaSH; and 4,6-dinitro-2-aminophenol (picraminic acid) from picric acid and NaSH [78].

To reduce friction and increase load-bearing capacity, EP (extreme-pressure) and AW (antiwear) oil additives are added to engine oils, transmission oils, turbine oils, and machining oils and their emulsions [79, 80]. It is known that sulfur-containing compounds in which the sulfur is in "available" form perform especially well in this application. Especially suitable are those compounds with polysulfide bridges in which the sulfur atoms are in a labile, active form, are liberated at elevated temperature, and can form metal sulfide coatings on the metal surface. These coatings usually have a lower coefficient of friction than the metal itself and thus improve frictional behavior [79, 80].

These sulfur-containing compounds can be prepared by reacting epoxides with an alkali metal disulfide or tetrasulfide [79]:



In accordance with the above reaction scheme, elemental sulfur is liberated when Na_2S_4 is used [79].

Oil additives can also be produced by the reaction of Na_2S or Na_2S_n , often in combination with elemental sulfur, with chlorinated organic compounds. These compounds can be formed by the addition of an S–Cl compound (e.g., S_2Cl_2) to a double bond (e.g., isobutene), and then condensed with Na_2S-S [81–86]. Other products may be obtained from the reaction of aromatic hydroxy compounds (e.g., 2,6-di-*tert*-butylphenol or 2,4,6-tri-*tert*-butylphenol) with aldehydes or ketones and Na_2S [87].

The reaction of 4-chlorotetrahydropyran with Na_2S in a methanol/ethanol mixture, followed by hydrogen peroxide oxidation of the resulting thiol group leads to bis(tetrahydropyranyl)disulfide, which is used as a lubricant additive [88].

Dialkylbenzyl disulfides, which are used as oil additives, are produced from a catalytically cracked naphtha fraction (boiling range 164–250 °C), which is chloromethylated with formaldehyde–HCl, and then reacted with Na_2S_2 [89].

In a similar process, benzyl chloride and Na_2S_2 are reacted at 80–90 °C for 20 h to produce dibenzyl disulfide, which is used as a component of an oil additive [90].

The production of additives for high-pressure lubricants is described in [91]. A mixture of xylol isomers is chloromethylated and then reacted with Na_2S_3 (a mixture of Na_2S_2 and Na_2S_4) to form a polysulfide.

A group of microcrystalline Al–Na silicates with various sulfur contents have been referred to as ultramarines [92]. Analysis gives an approximate empirical formula of $(Na_8Al_6Si_6O_{24}S_4)_n$, suggesting the name sodium aluminum silicate polysulfide.

The production of an *ultramarine* and a green pigment from zeolites and Na_2S_3 by heating to $> 300^\circ\text{C}$ has been reported [93]. The color of the ultramarines may be due to singly charged polysulfide(-1) radical ions [94, 95].

Sodium monosulfide solutions mixed with FeSO_4 , $\text{Ca}(\text{OH})_2$, and a polymeric flocculating agent are used to remove copper from aqueous solutions, process liquors, and wastewater [96]. Lead can be removed by using a mixture of caustic soda solution, sodium monosulfide solution, and aluminum chloride [97].

55.6 Safety and Environmental Aspects [98]

Sodium sulfide and Na_2S_n are classified as irritants in GefStoffV [99], as indicated by the hazard symbol C.

The following R and S phrases are applicable:

R31: "Toxic gases produced on contact with acids"

R34: "Causes irritation"

S26: "On contact with eyes, rinse immediately with plenty of water, and seek medical help"

S45: "In case of accident or illness, seek medical help immediately. Show this label if possible."

In accordance with GefStoffV vessels containing Na_2S or Na_2S_n should carry the name of the substance in permanent printed letters, the hazard symbol "irritant", the hazard information R 31-34, and the safety advice S 26-45 [100, 101].

Aqueous solutions of Na_2S , NaHS , and sodium polysulfides must always be maintained at a pH of > 10 to prevent liberation of toxic hydrogen sulfide [3]. The hazardous properties of hydrogen sulfide and its effects on humans are described in [33].

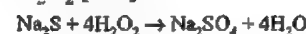
Solid sodium sulfide, sodium hydrogensulfide, and sodium polysulfide form strongly alkaline solutions when dissolved in water, and these can cause severe irritation of the eyes and skin. Goggles must therefore be worn. When working with larger quantities, impermeable protective clothing consisting of rubber boots (not leather-soled shoes) and long rubber gauntlets must also be worn.

If dust is formed, respirators with combination B/P2 type filters (color code: gray with white ring) must be worn [100].

In case of fire, respiratory equipment with an independent air supply must be used, completely sealed chemically-resistant clothing must be worn while fighting the fire, and the auxiliary equipment used must be resistant to caustic solutions [100]. Note that sulfide solutions can emit hydrogen sulfide on heating, which can represent a potential hazard during storage or in production [32].

Industrial safety data for sodium sulfide, sodium polysulfide, and sodium hydrogensulfide are given in [98, 102].

Sulfide is classified as a hazardous substance according to § 7a of the German Water Management Act [103]. In accordance with the current state of the art of the process in which by-product sulfide is formed, the sulfide content of wastewater has to be reduced. This can be carried out in various ways, e.g., by oxidation of the alkaline solution with H_2O_2 [104]:



The limit values for the sulfide content of wastewater are taken from the Framework Wastewater Directive or a recommendation of the German wastewater technical association (ATV) for indirect dischargers. Some values (in mg/L) are listed below [105]:

Appendices to Framework Wastewater Directive (1992)	
Appendix 25 (leather manufacture, fleece treatment, leather fiber production): wastewater from soaking, liming, and deliming, including washing	2
Appendix 37 (manufacture of inorganic pigments):	
Source type 1.1.3 (lithopone, zinc sulfide pigment, and precipitated barium sulfate)	1
Appendix 39 (manufacture of nonferrous metals)	1
Appendix 40 (metal working and treatment)	
Source type 1.1.1 (electrolytic)	1
Source type 1.1.2 (pickling)	1
Source type 1.1.4 (burnishing)	1
Source type 1.1.7 (printed circuit manufacture)	1
Source type 1.1.8 (battery manufacture)	1
Source type 1.1.9 (enamelling)	1
Appendix 47 (scrubbing of furnace combustion gases)	0.2
34th Framework Wastewater Directive (manufacture of barium compounds)	1
38th Framework Wastewater Directive (textile manufacture)	0.1
43rd Framework Wastewater Directive (synthetic fibers): Source type 2.1.3 (manufacture of viscose spun fiber)	15

Wastewater technical association (ATV)
Information sheet A 115 (yellow printing)

2

55.7 Economic Aspects [106]

Sodium monosulfide is supplied commercially in the form of flakes containing 60-62% Na_2S .

Major producers of the monosulfide include Tessenderlo Chemie (Belgium) and Foret (Spain). There are also producers in Germany, Italy, and France.

The output of sodium monosulfide in Western Europe is estimated to be 50 000 t/a. Excluding the considerable quantities exported to the African copper mines, this consumption is distributed among the following areas of use:

Dehairing agents for the leather industry	40%
Precipitation of heavy metal ions (chemical industry)	30%
Production of sulfur dyes	20%
Other uses	10%

Sodium hydrogensulfide is supplied in the following forms:

- In powder form with a purity of 95%
- In flake form with a purity of 70-74%
- As a 30% solution

Sodium hydrogensulfide is manufactured by the sodium monosulfide producers mentioned above, and also by Goldschmidt, Rhodanid Chemie, and Leuna. The main producers in the United States are Jupiter Chemical, PPG Industries, and Ethyl Corp.

As sodium hydrogensulfide is used in the same areas as Na_2S , no reliable information is available concerning the production and consumption of NaHS in Western Europe. In the United States, about two-thirds of annual production (i.e., ca. 180 000 t/a) is of lower quality (low grade, 20-30% NaHS) and is used in the cotton industry.

For many years, sodium polysulfide has been available only in solution. Sodium polysulfide solution is supplied by Goldschmidt (Germany), Witton (United Kingdom), PPG (United States), and Sankyo Kasei (Japan).

Approximately 25 000 t/a polysulfide solution, produced mainly by Morton International

(United States), Toray Thiokol (Japan), and Akros (Greiz-Dolau, Germany), is used in the production of polysulfide elastomers.

Sodium polysulfides are also available in anhydrous and solvent-free form, but the price of this material is considerably higher than that of the aqueous solution.

55.8 Transportation [107]

Sodium sulfide with at least 30% water of crystallization is classified as follows:

RID/ADR	Class 8, no. 45 b
IMDG Code	Class 8, UN no. 1849, PG II
ICAO-TI/IATA-DGR	Class 8, UN no. 1849, PG II

Approved packaging for sodium sulfide has been harmonized for all means of transport. Intermediate bulk containers are permitted for land and sea transport. Portable tanks (rail tank cars, road tank cars, tank containers) are permitted for land and sea transport.

Sodium sulfide with less than 30% water of crystallization is classified as follows:

RID/ADR	Class 4.2, no. 13b
IMDG Code	Class 4.2, UN no. 1385, PG II
ICAO-TI/IATA-DGR	Class 4.2, UN no. 1385, PG II

Approved packaging has been harmonized for all means of transport, and must be hermetically sealed. Bags are not permitted for sea transport. Bags may be used for land transport provided they are loaded on pallets and forwarded as full load. Intermediate bulk containers are only permitted for land and sea transport. Portable tanks (rail tank cars, road tank cars, tank containers) are permitted only for land transport.

Sodium hydrogensulfide with at least 25% water of crystallization is classified as follows:

RID/ADR	Class 8, no. 45 b
IMDG Code	Class 8, UN no. 2949, PG II
ICAO-TI/IATA-DGR	Class 8, UN no. 2949, PG II

Packaging has been harmonized for all means of transport. Intermediate bulk containers and portable tanks are permitted for land and sea transport.

Sodium hydrogensulfide with less than 25% water of crystallization is classified as follows:

RID/ADR	Class 4.2, no. 13 b
IMDG Code	Class 4.2, UN no. 2318, PG II

ICAO-TI/IATA-DGR Class 4.2, UN no. 2318, PG II

Packaging has been harmonized for all means of transport, and must be hermetically sealed. Bags are not permitted for sea transport, but can be used for land transport provided they are loaded on pallets and forwarded as full load. Intermediate bulk containers are permitted for land and sea, and portable tanks only for land transport.

Sodium polysulfides are not specifically named in the transport regulations, but should be classified as follows:

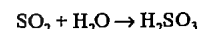
RID/ADR	Class 8, no. 45 b
IMDG Code	Class 8, UN no. 1759, PG II (solid)
	Class 8, UN no. 1760, PG II (solid)
ICAO-TI/IATA-DGR	Class 8, UN no. 1759 PG II (solid)
	Class 8, UN no. 1760 PG II (liquid)

Packaging has been harmonized for all means of transport. Intermediate bulk containers and portable tanks are permitted for land and sea transport, with restrictions for solid polysulfide in portable tanks.

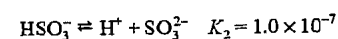
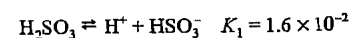
55.9 Sulfites and Disulfites

55.9.1 General Properties

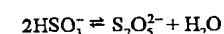
Sulfurous acid is formed on passing sulfur dioxide into water:



Since the equilibrium lies almost completely on the left-hand side and gas hydrates are formed on cooling the solution, isolation of the anhydrous acid is not possible. The acid dissociates in two steps:



The dissociation constants K refer to 25 °C [108]. At higher concentrations the disulfite ion is formed:



The neutral alkali-metal sulfites M_2SO_3 and hydrogensulfites MHSO_3 are readily soluble in water. The latter cannot be isolated, since

they are converted to disulfites on concentrating the solution.

Sulfurous acid and its salts are used as reducing agents. Aqueous solutions of halogens are reduced to hydrogen halides, iodates to iodides, and dichromates to chromium(III). However, sulfurous acid behaves as an oxidizing agent in the presence of stronger reducing agents; for example, with sulfur, thiosulfates are formed.

55.9.2 Ammonium Sulfite [109]

Solutions of ammonium sulfite, $(\text{NH}_4)_2\text{SO}_3$, are produced by treating sulfur dioxide with aqueous ammonia. They are mainly used for the production of ammonium thiosulfate.

55.9.3 Potassium Disulfite [110]

The industrial production of potassium disulfite, $\text{K}_2\text{S}_2\text{O}_5$, is similar to that of sodium disulfite. It is used for combatting fungi on vines and in wine production.

55.9.4 Sodium Disulfite [111]

Sodium disulfite, $\text{Na}_2\text{S}_2\text{O}_5$, dissolves readily in water with the formation of sodium hydrogensulfite NaHSO_3 (see Figure 55.9) [112].

The fine crystalline salt can be stored without any problem if kept cool, dry, and with the exclusion of air. When moist it is oxidized by atmospheric oxygen to the sulfate.

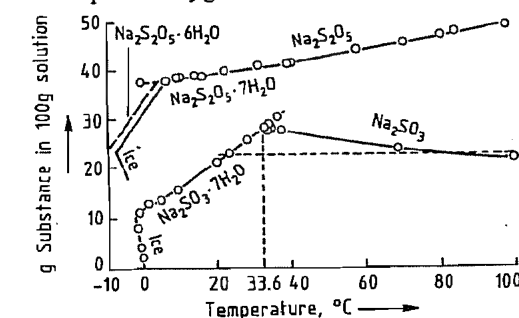


Figure 55.9: Solubility of $\text{Na}_2\text{S}_2\text{O}_3$ and $\text{Na}_2\text{S}_2\text{O}_5$ in water as a function of temperature.

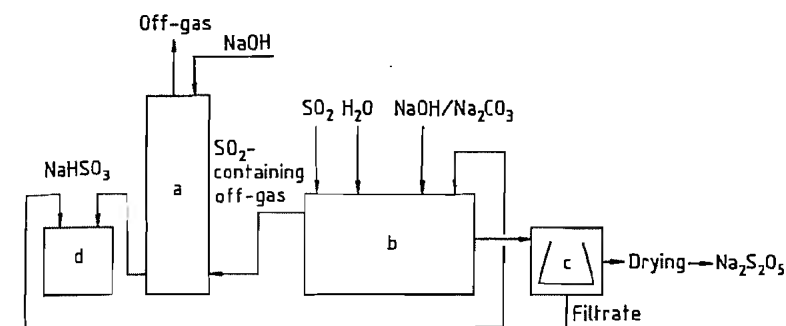


Figure 55.10: Production of sodium disulfite and sodium hydrogensulfite solution: a) Scrubber; b) Production plant; c) Centrifuge; d) Storage vessel for sodium hydrogensulfite solution.

Sodium disulfite is produced by treating 50–70% sodium hydroxide or a suspension of sodium carbonate with sulfur-dioxide-containing gases in saturated sodium hydrogensulfite solution (Figure 55.10) [113–116]. The sodium disulfite is removed by centrifugation and then dried. The saturated mother liquor from the centrifuge is mixed with the liquor from the waste-gas scrubber and adjusted to the usual commercial concentration.

Sodium disulfite production is coupled with the formation of sodium hydrogensulfite solution, for which, therefore, a demand must also exist. Production processes that use an anhydrous route, involving treatment of sodium sulfite or sodium carbonate with sulfur dioxide, have not achieved industrial importance.

Equipment and storage containers are predominantly made from 1.4571 grade stainless steel. Fiberglass-reinforced plastic containers are also suitable for storage. Paper or plastic sacks, steel barrels, or big bags made of synthetic fibers are used for transportation.

The commercial product has a content of ca. 97% $\text{Na}_2\text{S}_2\text{O}_5$, 1–2% Na_2SO_3 , and ca. 1% Na_2SO_4 .

Sodium disulfite is used in the photography and fiber industries, for preserving foodstuffs, for wastewater treatment, and in the paper, textile, and leather industries.

55.9.5 Sodium Hydrogensulfite [111]

Sodium hydrogensulfite, NaHSO_3 , is not known in the solid state. On concentrating an aqueous solution, solid sodium disulfite crystallizes. Sodium hydrogensulfite is oxidized in air. Solutions of high purity can be produced by dissolving sodium disulfite in water. Commercial solutions are produced as the mother liquor in the production of sodium disulfite or by treating a suspension of sodium hydroxide, or sodium sulfite or sodium carbonate with sulfur dioxide until a pH of 3.5–4 is reached. The equipment is mainly made of 1.4571 grade stainless steel. For storing the solution, fiberglass-reinforced plastic containers are also suitable.

55.9.6 Sodium Sulfite

Sodium sulfite, Na_2SO_3 , is predominantly marketed as the anhydrous salt. It is produced by treating a suspension of sodium hydroxide or sodium carbonate with sulfur dioxide. The temperature is maintained at 60–80 °C for optimal crystal separation. The sodium sulfite suspension formed is centrifuged and the salt dried. Today part of the sodium sulfite is obtained from scrubbing of SO_2 -containing off-gases. Production processes using an anhydrous route have not yet achieved industrial importance.

Sodium sulfite is sold in various purity grades containing 90–98% Na_2SO_3 . The salt can be stored for long periods if kept dry, with

the exclusion of air. It is transported in plastic and paper sacks. Sodium sulfite is used as a reducing agent, for the production of sodium thiosulfate, in the photography, paper, and textile industries, for treating boiler water, and as a food preservative.

55.9.7 Analysis of Alkali-Metal Sulfites

The total sulfur dioxide content is titrated iodometrically. Sulfate is determined, after acidification of the solution with HCl and driving off the SO₂ with CO₂, either titrimetrically or as barium sulfate. To determine sulfite in sodium hydrogensulfite or sodium disulfite, the sample solution is treated with formalin and the NaOH liberated is titrated in the presence of phenolphthalein.

55.9.8 Toxicology

Oral administration of a few grams of sodium sulfite causes dizziness, vomiting, and diarrhoea [117]. Small doses of sodium hydrogensulfite are oxidized to sulfate in vivo, whereas larger doses cause considerable irritation of the gastrointestinal tract.

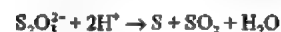
55.10 Thiosulfates

55.10.1 General Properties

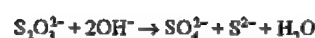
Thiosulfates are the salts of thiosulfuric acid, H₂S₂O₃. Whereas thiosulfuric acid is highly unstable, thiosulfates are quite stable, even in aqueous solution.

Most thiosulfates are readily soluble in water, with the exception of the moderately soluble barium salt and the sparingly soluble silver and lead salts. The soluble salts are readily crystallized. Acid salts do not exist.

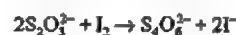
The following properties are characteristic of thiosulfates: decomposition to sulfur and sulfur dioxide in acid solution:



decomposition in alkaline solution according to the equation:



oxidation by weak oxidizing agents (I₂, Fe³⁺, and Cu²⁺) to give tetrathionate:



and oxidation by strong oxidizing agents (Cl₂, Br₂, MnO₄⁻, and Cr₂O₇²⁻) to give sulfate:



The use of thiosulfates as antichlorines for removal of chlorine (e.g., from bleached materials) is based on the last-mentioned reaction. With heavy metals (e.g., silver) the thiosulfate ion forms soluble complexes [Ag(S₂O₃)₂]³⁻. This property is used in photography for fixing.

Sodium and ammonium thiosulfates are important industrial chemicals.

55.10.2 Sodium Thiosulfate

Sodium thiosulfate is produced and sold as the anhydrous salt, and as the pentahydrate Na₂S₂O₃·5H₂O. The hydrated product was formerly known as antichlorine, because of the earlier wide use for removal of residual chlorine.

Properties. Sodium thiosulfate crystallizes from aqueous solution as short, colorless prisms or elongated crystals. It effloresces in dry air, particularly at temperatures above ca. 33 °C. At 48 °C the crystals dissolve in their own water of crystallization. The solution tends to become supersaturated and can be kept in this state for weeks at room temperature. Spontaneous crystallization only occurs on supercooling to -30 °C or below. On heating, preferably with stirring and under reduced pressure, the anhydrous salt is obtained as a heavy, white, crystalline powder. Anhydrous Na₂S₂O₃ is also produced by dehydration of Na₂S₂O₃·5H₂O in a stream of dry air at temperatures of up to 60 °C. At 223 °C sodium thiosulfate decomposes, predominantly giving sodium sulfate and pentasulfide:



The pentahydrate, which exists in two modifications, is stable below 48 °C. Four modifi-

cations of anhydrous Na₂S₂O₃ are known [118].

Aqueous solutions of sodium thiosulfate are of neutral pH. They can be kept for months in the dark with the exclusion of air, but decompose on prolonged boiling in air. On addition of acid sulfur precipitates and sulfur dioxide is liberated. The densities of aqueous Na₂S₂O₃ solutions at 20 °C are listed below:

[Na ₂ S ₂ O ₃], %	ρ, g/cm ³
1	1.0065
2	1.0148
4	1.0315
8	1.0654
10	1.0827
12	1.1003
16	1.1365
20	1.1740
24	1.2128
28	1.2532
30	1.2739
35	1.3273
40	1.3827

Table 55.4 lists the solubility in water; other properties are given in Table 55.5 and [119].

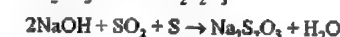
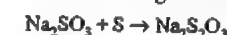
Table 55.4: Solubility of sodium thiosulfate in water.

Solid phase	T, °C	%
Ice	-3.9	15.0
	-11	30.0
Na ₂ S ₂ O ₃ ·5H ₂ O	0	34.4
	20	41.2
	40	50.6
Na ₂ S ₂ O ₃ ·2H ₂ O	48	62.0
	50	62.9
	60	67.4
Na ₂ S ₂ O ₃ ·0.5H ₂ O	65	69.5
	70	70.0
	75	70.8
Na ₂ S ₂ O ₃	80	71.0
	100	72.7

Table 55.5: Properties of sodium thiosulfate.

	Na ₂ S ₂ O ₃ ·5H ₂ O	Na ₂ S ₂ O ₃
Crystal system	monoclinic	monoclinic
ρ at 25 °C, g/cm ³	1.749	2.267
Specific heat capacity at 0 °C, J/kg·K ⁻¹	1453	924
Heat of fusion, kJ/kg	148.1	
Heat of solution at 25 °C, kJ/kg	190.6	
Heat of hydration at 18 °C, kJ/mol	55.7	
Enthalpy of formation, kJ/mol	2601	

Production of sodium thiosulfate is based on the following reactions:



The raw materials are usually used in a technically pure form and consist of sulfur (solid or liquid), sodium sulfite, sodium hydrogensulfite, sodium hydroxide, and sulfur dioxide. The latter is used either as a pure gas or as a sulfur combustion gas containing ca. 18% SO₂.

The addition of sulfur to sodium sulfite is carried out in stirred vessels. The reaction rate depends on the temperature, the excess of sulfur, and the intensity of stirring. The reaction lasts for several hours.

Polysulfide solutions are also produced to some extent as intermediates and react with disulfite to give thiosulfate [120]. Processes have also been described involving the production of sodium thiosulfate by oxidation of aqueous sodium sulfide solutions in the presence of catalysts [121–123].

The sodium thiosulfate solutions are filtered hot, sometimes with the addition of decolorizing charcoal. The excess sulfur is recycled. The Na₂S₂O₃·5H₂O is crystallized by cooling the filtrate. The mother liquor still contains ca. 5% Na₂S₂O₃ at 20 °C. Further sodium thiosulfate can be obtained from this mother liquor by evaporation. The crystalline salt is separated by centrifugation. The pentahydrate must be dried below ca. 40 °C because at higher temperatures water of crystallization is lost. Pneumatic-conveyor or fluidized-bed driers are used.

Anhydrous sodium thiosulfate is produced by dehydration of the pentahydrate at 60–105 °C at atmospheric or reduced pressure. Another possibility is crystallization from sodium thiosulfate solution above 70 °C.

The standard commercial particle sizes are obtained by using continuous or batch crystallization equipment.

Quality Specifications and Analysis. For photographic purposes the degree of purity laid down in the ASA and DIN/ISO standards is, usually adequate (99% for Na₂S₂O₃·5H₂O).

and 97% for anhydrous $\text{Na}_2\text{S}_2\text{O}_3$). The content of sodium thiosulfate is determined potentiometrically by titration of the diluted solution with iodine solution [124–126].

Both types of sodium thiosulfate are produced in Germany at Chemiewerk Bad Köstritz and anhydrous $\text{Na}_2\text{S}_2\text{O}_3$ is produced by Th. Goldschmidt AG, Werk Mannheim; Brotherton, England; and Foret, Spain, for example.

Uses. Anhydrous sodium thiosulfate is now only added in small quantities to ammonium thiosulfate. The hydrated salt is used as an antichlorine in bleaching, in wastewater purification, for reduction of dichromate in chromed leather production, and as a solvent for silver chloride in the chloride roasting of silver-containing minerals.

Table 55.6: Solubility of ammonium thiosulfate.

T, °C	Solubility	
	in water	in NH_3 -saturated water
0	60.0	
10	61.6	
20	63.1	25.8
30	64.7	38.1
40	66.3	46.5
50	67.9	58.2
60	69.4	65.9
70	71.0	70.7
80	72.6	72.4
90	74.2	

55.10.3 Ammonium Thiosulfate

Properties. Ammonium thiosulfate, $(\text{NH}_4)_2\text{S}_2\text{O}_3$, crystallizes in an anhydrous form as shiny plates or sword-shaped crystals. No hydrates are known. On heating to 150 °C it sublimes with partial decomposition into $(\text{NH}_4)_2\text{SO}_3$, S, NH_3 , and H_2S . Ammonium thiosulfate is hygroscopic; the stability limit is at 64% relative humidity. It is readily soluble in water, sparingly soluble in acetone, and insoluble in alcohol. The solubility in water is lowered by the presence of NH_3 . The solubilities are listed in Table 55.6. The densities of aqueous solutions at 20 °C are listed below:

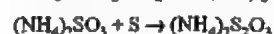
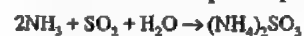
$(\text{NH}_4)_2\text{S}_2\text{O}_3$, %	ρ , g/cm ³
56	1.303
57	1.310
58	1.314

59	1.319
60	1.324
61	1.329
62	1.334

The data are for technical grades, which contain ca. 0.2% NH_3 and small quantities of sulfate and sulfite. Aqueous ammonium thiosulfate solutions decompose slowly on heating above 40 °C with formation of sulfur and sulfate. A small quantity of sulfite stabilizes the solutions considerably. Some other properties are as follows:

100% $(\text{NH}_4)_2\text{S}_2\text{O}_3$	
Crystal system	monoclinic
ρ at 25 °C, g/cm ³	1.71
Heat of solution, water, 25 °C, kJ/kg	105
58–60% $(\text{NH}_4)_2\text{S}_2\text{O}_3$ (aq)	
Thermal conductivity, $\text{kJ m}^{-1}\text{h}^{-1}\text{K}^{-1}$	1.84
Specific heat capacity, $\text{kJ kg}^{-1}\text{K}^{-1}$	2.45
Vapor pressure, kPa at 20 °C	1.7
at 40 °C	5.4
at 60 °C	14.2

Production of ammonium thiosulfate is based on the reaction of sulfur, or occasionally ammonium sulfide and polysulfides [127], with ammonium sulfite in an aqueous ammoniacal medium. The ammonium sulfite is produced from ammonia or ammonia water and SO_2 in the same or in a separate process step:



The sulfur dioxide is used neat (gaseous or liquid) or as sulfur combustion gas, and sulfur is used in liquid or solid form.

The rate of reaction of sulfur with ammonium sulfite depends on the temperature, the intensity of stirring, and the excess of sulfur. At 110 °C the reaction is complete after 1–2 h. Increased pressure with higher reaction temperatures and shorter reaction times can also be used [128]. A one-step process is also possible. Solutions containing ca. 60% ammonium thiosulfate are produced to be sold as such, and 70–72% solutions for production of the solid salt. The latter are filtered hot, sometimes with the addition of charcoal. The 60% solutions can be filtered hot or after cooling.

To obtain the salt the filtered solution is cooled to ca. 20–30 °C. The crystallized salt is separated by using sieve-screw centrifuges. Drying must be carried out carefully; a prod-

uct temperature of 50 °C must not be exceeded. The ca. 60% mother liquor is recycled.

Crystalline ammonium thiosulfate tends to cake. It can be rendered free-flowing by the addition of 5–10% anhydrous sodium thiosulfate (ammonium thiosulfate 90/10). The stability to storage is increased by the addition of ca. 1–2% Na_2SO_3 . The stability to storage of ammonium thiosulfate solutions can be increased by adding $(\text{NH}_4)_2\text{SO}_3$ or Na_2SO_3 .

Ammonium thiosulfate can also be produced by the reaction of ammonium polysulfide solutions with gaseous SO_2 [129, 130]. In a process developed by the company Foret $(\text{NH}_4)_2\text{S}_2\text{O}_3$ is obtained from H_2S , NH_3 , and water at ≤ 45 °C in the first step and subsequent reaction with SO_2 [130, 131].

Quality Specifications and Analysis. Commercially the degrees of purity and analysis methods laid down in the ASA, DIN, and ISO standards are valid [124–126] (Table 55.7). In some cases particle size and particle-size distribution are also specified.

Table 55.7: Specifications for photo-quality ammonium thiosulfate.

Analysis	Solid (ASA)	Aqueous solution (DIN 19080 T82, ISO 3619)
$(\text{NH}_4)_2\text{S}_2\text{O}_3$, %	≥ 97	57–61
Sulfite (as SO_3), %	≤ 14	≤ 0.7
Sulfate (as $(\text{NH}_4)_2\text{SO}_4$), %		max. 1
H_2O , %	≤ 0.5	—
$(\text{NH}_4)_2\text{S}$, ppm	≤ 10	≤ 5
Insolubles, %	≤ 4	≤ 0.2
Combustion residue, %	≤ 2	≤ 0.2
Heavy metals (as Pb), ppm	≤ 20	≤ 10
Iron, ppm	≤ 50	≤ 10

Titration with iodine solution gives the combined thiosulfate and sulfite content; titration in the presence of formaldehyde gives the thiosulfate content.

Uses. Ammonium thiosulfate is used almost exclusively as a photographic fixing salt. Its advantage compared with sodium thiosulfate lies in the shorter fixing times, the increase in the efficiency of the fixing baths by ca. 50%, and shorter washing periods. The recovery of the silver from spent fixing baths is easier. In

Western Europe almost only ammonium thiosulfate is now used for fixing. By far the greatest proportion of the demand is covered by solutions.

The following are commercially available as solids:

Ammonium thiosulfate	98/100
Ammonium thiosulfate	90/10
Rapid fixing salt U3	70% $(\text{NH}_4)_2\text{S}_2\text{O}_3$, 20% $\text{Na}_2\text{S}_2\text{O}_3$, 10% Na_2SO_3

Some producers of ammonium thiosulfate in Europe are: Th. Goldschmidt, Chemiewerk Bad Köstritz, Germany; Foret, Spain; W. Blythe & Co., United Kingdom.

55.10.4 Toxicology

For sodium thiosulfate, the LDLo for subcutaneous application in rabbits is 4000 mg/kg, and in frogs 6000 mg/kg [132].

For $\text{Na}_2\text{S}_2\text{O}_3 \cdot 5\text{H}_2\text{O}$, the oral TDLo in humans is 300 mg/kg (oral intake during 7 days). For dogs, the intravenous LDLo is 3000 mg/kg [132].

According to [133], $\text{Na}_2\text{S}_2\text{O}_3 \cdot 5\text{H}_2\text{O}$ has low oral toxicity. Larger doses (up to 12 g daily) have a severe laxative effect.

The following values have been determined for ammonium thiosulfate [132]: LD₅₀ (oral, rat) 2890 mg/kg, LD₅₀ (oral, guinea pig) 1098 mg/kg.

55.11 Sodium Dithionite [134]

55.11.1 Introduction

Sodium dithionite, $\text{Na}_2\text{S}_2\text{O}_4$, is the only industrially important salt of dithionous acid ($\text{H}_2\text{S}_2\text{O}_4$), which has not been isolated. The importance of sodium dithionite lies in its powerful reducing capacity, which allows, for example, vat dyes to be reduced at room temperature. It is also used as a bleaching agent, mainly in the textile and paper industries.

STAHL first prepared dithionite unwittingly in 1718 when he treated iron with aqueous sulfur dioxide and obtained a yellow solution. In 1789 BERTHELOT showed that no hydrogen was produced in this reaction. In 1852 SCHÖNBEIN

used this solution for the reduction of indigo. SCHÜTZENBERGER isolated dithionite as the dihydrate and gave it the name hydrosulfite. In 1881 BERNTHSEN established that hydrosulfite did not contain any hydrogen, but corresponded to the formula $\text{Na}_2\text{S}_2\text{O}_4$. In 1905 BAZLEN introduced the zinc-dust process for the production of anhydrous sodium dithionite. He also suggested using sodium amalgam as reducing agent.

55.11.2 Properties

Sodium dithionite is known as the dihydrate $\text{Na}_2\text{S}_2\text{O}_4 \cdot 2\text{H}_2\text{O}$ and as the anhydrous salt. The dihydrate crystallizes in thin, yellowish shiny, soft prisms of density 1.58 g/cm^3 . The anhydrous salt forms monoclinic white crystals of density 2.38 g/cm^3 . The solubility in water of both forms is shown in Figure 55.11. Solutions with anhydrous undissolved solute are labile below 72°C . The solubility and the position of the transformation point are strongly influenced by foreign salts, particularly sodium salts, and water-miscible organic solvents.

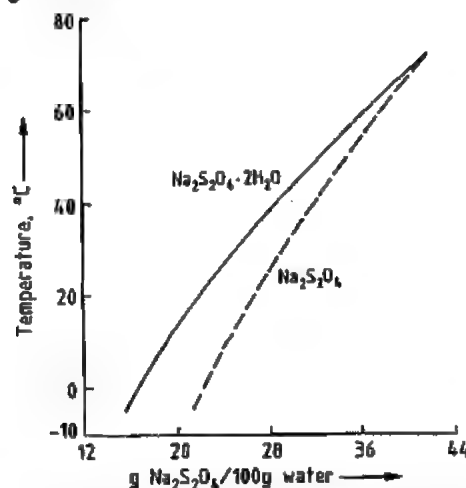
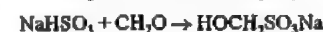
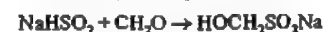
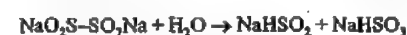


Figure 55.11: Solubility of sodium dithionite in water.

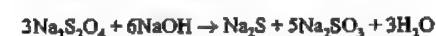
Sodium dithionite dihydrate is very sensitive toward atmospheric oxygen in the finely crystalline state. The heat of oxidation can lead to ignition. The anhydrous salt decomposes exothermically in air on prolonged heat-

ing above 90°C . The main decomposition products are sodium sulfate and sulfur dioxide. Above ca. 150°C , with exclusion of air, sodium dithionite decomposes in a vigorous reaction, giving mainly sodium sulfite, sodium thiosulfate, sulfur dioxide, and a small amount of sulfur. In the absence of air, moisture only causes a small degree of decomposition. Sodium dithionite in powder form can decompose in air on contact with a small amount of water with such intense heat formation that it burns with a flame.

Aqueous dithionite solutions decompose slowly in the cold and rapidly in the warm, whereby hydrolysis to hydrogensulfoxylate and hydrogensulfite occurs first. The hydrolysis products can be trapped as sodium 1-hydroxyalkanesulfinates and 1-hydroxyalkanesulfonates by addition of aldehydes or ketones:



In weakly acidic solution dithionite decomposes rapidly, especially under warm conditions, to give the thiosulfate and disulfite or hydrogensulfite, and in alkaline solution to give the sulfide and sulfite:



The decomposition in alkaline solution is accelerated by thiosulfates and polysulfides. On addition of strong acids the dithionite solution first becomes yellow-red, and after a short time complete decomposition occurs with precipitation of sulfur. The dithionite can be recovered if the solution is rapidly neutralized before the sulfur precipitates. Weak alkalis (pH 8–13) stabilize dithionite solutions, which can then be kept for weeks below 10°C with the exclusion of air. In the presence of air the dissolved dithionite is converted rapidly into sulfate and sulfite at room temperature, with or without stabilizer.

The industrial applications of sodium dithionite are determined by its strong reduc-

ing properties, due to the S–S bond and the oxidation state of the sulfur in the compound.

With relatively strong oxidizing agents, such as potassium permanganate and iodine, sulfate is formed; with weaker ones, such as vat dyes, sulfite is formed. With MnO_2 , dithionate can be formed.

55.11.3 Production

All processes for the production of dithionite start with the reduction of sulfurous acid, which can either be present in the free form or as hydrogensulfite. The production processes with zinc dust, sodium amalgam, sodium formate, sodium borohydride, and electric current as the reducing agent are important industrially.

Zinc-Dust Process. Some important producers still use the zinc-dust process, which was developed by BASF. The basic reactions are:



An aqueous slurry of zinc dust is treated in a stirred reactor with cooling at ca. 40°C with liquid or gaseous sulfur dioxide to give zinc dithionite. After completion of the reaction the solution is passed through a filter press to remove unreacted zinc dust and impurities from the zinc.

The zinc is then precipitated from the zinc dithionite by adding sodium carbonate or sodium hydroxide in stirred vessels. The zinc carbonate or hydroxide is removed in filter presses. Anhydrous sodium dithionite is precipitated from the clarified sodium dithionite solution by concentration under vacuum and addition of sodium chloride at $> 60^\circ\text{C}$. It is filtered, washed with methanol, and dried at 90 – 100°C .

Besides the evaporation process the salting out process, which was more widely used previously, is still known. In this process the dithionite is obtained from the solution by the addition of sodium chloride and methanol.

The zinc carbonate or hydroxide formed as side products can be further processed to give zinc salts or zinc oxide.

Amalgam Process. In the amalgam process, sodium hydrogensulfite is reduced to sodium dithionite in aqueous solution in a cooled, stirred vessel using the sodium amalgam of a chlor-alkali electrolysis cell. The sodium-free mercury is returned to the electrolysis cell where it is recharged with sodium. During reaction of the amalgam with the hydrogensulfite solution a pH of 5–6 must be maintained. The product is obtained by precipitation with salts or methanol or both.

Formate Process [135]. Sodium formate, dissolved in 80% aqueous methanol, is charged to a stirred vessel. At a pressure of 2–3 bar sulfur dioxide and sodium hydroxide are introduced into this solution such that a pH of 4–5 is maintained. The reaction can be described by the following equation:



Under the above conditions anhydrous sodium dithionite precipitates as fine crystals. It is filtered, washed with methanol, and dried.

Sodium Borohydride Process. Sodium borohydride is stable in strong aqueous alkali and can be used in this form for the production of sodium dithionite by adding SO_2 and sodium hydroxide:



Electrolytic Process [136]. The electrolytic process, developed by BASF and by Olin, is used in only one small plant.

In a bipolar electrolysis cell, with the cathode and anode spaces separated by a semipermeable membrane, disulfite ions are reduced to dithionite at the cathode at pH 5–6. At the anode chloride ions, for example, are oxidized to chlorine. For charge equalization sodium ions pass through the membrane from the anode space to the cathode space. This process gives a dithionite solution which can be further processed as in the amalgam process.

55.11.4 Quality Specifications and Analysis [137]

Commercial sodium dithionite generally has a purity of ca. 88%. It contains ca. 3% of

each of the following: sodium disulfite, sodium sulfite, sodium sulfate, and sodium carbonate. The latter stabilizes the $\text{Na}_2\text{S}_2\text{O}_4$. The total heavy metal content is generally < 20 ppm. The product from the zinc-dust process has a zinc content of up to 300 ppm.

The sodium dithionite content can most readily be determined iodometrically. It is dissolved in a neutral formaldehyde solution in a standard flask. The dithionite, which is sensitive to oxidation, reacts immediately on dissolving to give the more stable sodium hydroxymethanesulfonate, which can be titrated.



However, this method of analysis does not differentiate between dithionite and any thiosulfate which may be present. Since no acid is formed in the iodometric oxidation of thiosulfate, but is formed in the dithionite titration, the proportion of dithionite can be determined by subsequent titration of the solution with alkali.

55.11.5 Trade Names and Uses

Sodium dithionite is sold as the 88% product, for example, under the names Hydrosulfit (BASF, Brüggemann, Germany; Prayon, Belgium; Hoechst-Celanese, USA; Hoechst-UK, UK, etc.), Blankit (BASF), Albite A (Idrosol, Italy), and Konite (Akzo, Holland). Hydrosulfit mixtures are sold, for example, under the names Blankit (with index, BASF), Blancolen (Brüggemann, Germany), Albite LA (Idrosol, Italy), Konite TP (Akzo, Holland), Zepar (Du Pont), Burmol (BASF), Arostit (Sandoz).

All uses of sodium dithionite are based on its reducing properties. It is used predominantly in the textile industry as a dyeing and printing auxiliary and as a bleaching agent in the textile and paper industries.

In dyeing and printing, sodium dithionite is used to convert insoluble vat dyes to the soluble leuco form. High-purity sodium dithionite (e.g., Blankit) is used to bleach wool, cotton,

silk, bristle, straw, horsehair, coconut fiber, raffia, soaps, glues, clay, sand, bauxite, and in some countries for bleaching sugar, syrup, fruit, edible oils, edible fats, and gelatin.

For special applications in the paper or textile industries complexing agents such as trilon or phosphates, or also optical brighteners are added to dithionite-containing products.

The reducing action of sodium dithionite is also used in preparative and analytical chemistry. It can reduce azo, diazo, nitro, nitroso, and carbonyl groups.

55.11.6 Safety and Environmental Aspects; Storage and Transport

Above a certain dithionite concentration, mixtures in powder form decompose if subjected to prolonged exposure to high temperatures or come into contact with water. In the case of very finely divided products this decomposition can already occur at 80 °C. Product that is decomposing must be covered immediately with dry sand or powder extinguisher, or dissolved by shovelling into large quantities of water. If sodium dithionite packed in iron drums ignites, the SO_2 gas produced must be allowed to escape by opening the container or drilling holes in the wall. The contents of the container are destroyed by throwing them into large quantities of water. The aqueous solution thus formed must be treated as it contains reducing agent and must be slowly introduced into an appropriate wastewater-treatment plant. Gloves and respiratory protection must be worn while extinguishing fires.

Dithionite is classified in the German water hazard class 1 as posing a slight hazard to water.

The wastewater from all production processes contains approximately equal quantities of reducing agent, which must be removed in a wastewater-treatment plant. The CO_2 formed in the formate process (Section 55.11.3) must be freed from SO_2 , methanol, and thiols before being released into the atmosphere.

Commercial sodium dithionite (e.g., Hydrosulfit and various product mixtures, which contain Hydrosulfit) are spontaneously combustible hazardous goods (Class 4.2, UN no. 1384), and are therefore subject to the corresponding transport regulations [138–142].

Because of the danger of spontaneous ignition sodium dithionite and its mixtures must be stored dry and in a cool place. Storage or transport together with sodium nitrite, sodium nitrate, and ammonium nitrate is forbidden. Transport containers must always be kept closed. Product should only be removed in a dry area using dry equipment.

55.11.7 Economic Aspects

World consumption of sodium dithionite is ca. 300 000 t/a, corresponding to ca. 60% of production capacity. The zinc dust process accounts for ca. 35% of the capacity, the formate process 40%, the amalgam process 15%, and the sodium borohydride process 10%.

55.11.8 Toxicology [143]

The LD_{50} (rat, oral) is ca. 2500 mg/kg. In the rabbit the product has no irritant effect on the skin, but has an irritant effect on the mucous membrane (rabbit's eye). Therefore, in an emergency or as first aid measures it is sufficient to wash the skin thoroughly with water and to rinse the eyes for 10 min. with running water. An eye specialist should then be consulted.

The 48-h LC_{50} in golden orfe is 10–100 mg/L.

55.12 References

1. R. Steudel, *Angew. Chem.* 87 (1975) no. 19, 683.
2. F. A. Cotton, G. Wilkinson, P. L. Gaus: *Grundlagen der Anorganischen Chemie*, VCH Verlagsgesellschaft, Weinheim 1990, p. 160.
3. *Römpp* 9th ed., 5, 4377.
4. T. G. Pearson, P. C. Robinson, *J. Chem. Soc.* 1930, 1473.
5. N. K. Gupta, R. P. Tischer, *J. Electrochem. Soc.* 119 (1972) 1033.
6. E. Rosen, R. Tegman, *Chem. Scr.* 2 (1972) 221.
7. D.-G. Oei, *Inorg. Chem.* 12 (1973) 435.
8. D.-G. Oei, *Inorg. Chem.* 12 (1973) 438.

9. B. Cleaver, S. M. Upton, *Electrochim. Acta* 36 (1991) no. 3/4, 673–677.
10. W. Fischer: "Die Natrium-Schwefel-Batterie", *Elektrochem. Energietechn. Entwicklungsstand Aussichten* 1981, 185–205.
11. P. Bottcher, *Z. Anorg. Allg. Chem.* 467 (1980) 149–157.
12. F. Fehér, H. J. Berthold, *Z. Anorg. Allg. Chem.* 273 (1953) 144.
13. A. P. Brown, J. E. Battles, *Synth. React. Inorg. Met. Org. Chem.* 14 (1984) no. 7, 945–951.
14. B. Cleaver, S. J. Sime, *Electrochim. Acta* 28 (1983) no. 5, 703–708.
15. N. N. Greenwood, A. Earnshaw: *Chemie der Elemente*, 1st ed., VCH Verlagsgesellschaft, Weinheim 1988, p. 893.
16. G. J. Janz, D. J. Rogers, *J. Appl. Electrochem.* 13 (1983) 121–131.
17. B. Wamqvist, *Thermochim. Acta* 37 (1980) 343–345.
18. R. Tegman, *Chem. Scr.* 9 (1976) 158–166.
19. E. Rosén, *K. Tek. Hoegsk. Handl.* (1960) 159.
20. E. Rosén, *Sven. Kem. Tidskr.* 76 (1964) 195.
21. H. Föppel, E. Busmann, F.-K. Frorath, *Z. Anorg. Allg. Chem.* 314 (1962) 12.
22. J. S. Thomas, A. Rule, *J. Chem. Soc.* 105 (1914) 177.
23. R. Tegman, *Acta Crystallogr. Sect. B: Struct. Sci.* B29 (1973) 1463.
24. R. Steudel, F. Schuster, *Z. Naturforsch. A: Phys. Phys. Chem. Kosmophys.* 32A (1977) 1313–1319.
25. H. H. Eysel, G. Wiegardt, H. Kleinschmager, G. Weddigen, *Z. Naturforsch. B: Anorg. Chem. Org. Chem.* 31B (1976) 415.
26. H. Köpf, B. Block, *Chem. Ber.* 102 (1969) 1504–1508.
27. T. P. Whaley in A. F. Trotman-Dickenson (ed.): *Comprehensive Inorganic Chemistry*, vol. 2, Pergamon Press, Oxford 1973, p. 369.
28. B. Cleaver, A. J. Davies, M. D. Harnes, *Electrochim. Acta* 18 (1973) 719–726.
29. B. Cleaver, A. J. Davies, *Electrochim. Acta* 18 (1973) 727–731.
30. B. Cleaver: "Properties of Polysulfide Melts", in R. P. Tischer (ed.): *The Sulfur Electrode Fused Salts and Solid Electrolytes*, vol. II, Academic Press, New York 1983, pp. 36–78.
31. *Mellor's Comprehensive Treatise on Inorganic and Theoretical Chemistry*, vol. II, suppl. II, part I, Longman Group Ltd., London 1961, p. 991.
32. *Gmelin*, 21, 1049.
33. *Kirk-Othmer*, 3rd ed., 21, 256.
34. Ullmann, 4th ed., 17, 167.
35. M. Schmidt, *Inorg. Macromol. Rev.* 1 (1970) 101–113.
36. M. Schmidt, W. Siebert: "Sulfane", in *Comprehensive Inorganic Chemistry*, vol. 2, sect. 2.1, Pergamon Press, Oxford 1973, pp. 826–842.
37. A. Müller, E. Diemann, *Adv. Inorg. Chem. Radiochem.* 31 (1987) 89.
38. L. Hockenberger, *Chem. Ing. Tech.* 36 (1964) no. 10, 1046.
39. T. B. Rauchfuss, M. Draganjac, *Angew. Chem.* 97 (1985) 745–760.
40. Degussa, US 4640832, 1985.

40. Degussa, US 5080881, 1989.
41. Degussa, US 5075098, 1990.
42. Degussa, US 5039506, 1990.
43. Degussa, US 5039505, 1990.
44. I. G. Farbenind., DE 590278, 1933 (E. Reißmann, H. Wolff).
45. Thiokol Chem. Corp., US 2796325, 1951 (E. R. Bertozzi).
46. Winnacker-Küchler: *Chemische Technologie*, 4th ed., 2, 83.
47. Kali-Chemie, DE 842789, 1950.
TH. Goldschmidt, DE 920010, 1949.
R. Bolton, US 1736741, 1927.
I. G. Farbenind., DE 499417, 1925.
48. Bayer, DE 1016242, 1958 (H. Beyer).
49. Sankyo Kasei, EP 0361998 A1, 1990 (Maeda, Kanosuke).
50. Verein. Chem. Fabr. Mannheim, DE, 194882, 1907.
51. Degussa, DE-AS 1084701, 1959.
52. BASF, DE-AS 1122045, 1960.
53. BASF, DE-AS 1102114, 1959.
54. Bayer, DE 814140, 1949.
55. Solvay Process, US 2376433, 1944; US 2376434, 1944; US 2376435, 1944.
56. Deutsche Erdöl-AG, DE-AS 1144241, 1961.
57. J. L. Sudworth, A. R. Tilley: "The Sodium-Sulfur Battery with β -Alumina Electrolyte", in R. P. Tischer (ed.): *The Sulfur Electrode Fused Salts and Solid Electrolytes* vol. VII, Academic Press, New York 1983, pp. 235-325.
58. Winnacker-Küchler, *Chemische Technologie*, 4th ed., 7, 41.
Kirk-Othmer, 3rd ed., 22, 168.
59. U. Deschler, P. Kleinschmit, P. Panster, *Angew. Chem.* 98 (1986) 237-253.
60. Degussa AG, Geschäftsbereich AC; Company brochures:
„Organosilane für die Gummiindustrie“ Jan. 1994/Nr. 6000.0.
Schriftenreihe Pigmente, Nr. 75, „Degussa-Silane“ Fig. 75-2-3-1087 DD, Okt. 1987.
„Si 69X 50-SX50“ Verstärkungsadditiv Information für die Gummiindustrie PT68-2-3-691 Ha.
61. *Kirk-Othmer*, 3rd ed., 18, 793.
62. *Ullmann*, 5th ed., 21, 429.
63. H. Cherdron, F. Herold, A. Schneller, *Chem. Unserer Zeit* 23 (1989) no. 6, 181.
64. W. Koch, W. Heitz, *Makromol. Chem.* 184 (1983) 779-792.
65. *Kirk-Othmer*, 3rd ed., 18, 793.
66. Société nationale des pétroles d'Aquitaine, DE 2157575, 1972 (J. B. Signouret, Y. Labat, C. Esclamadon).
67. Société nationale Elf Aquitaine S.A., DE 2757148, 1978.
68. J. Kausch, DD 156709, 1982.
69. K. Negoro, T. Watanabe, *Nippon Gomu Kyokaishi* 43 (9), 743-752; *Chem. Abstr.* 73 (1970) 121333b.
70. Toray Industries, JP 46014671, 1971 (S. Tanemoto, M. Takahashi).
71. W. Schulz, Universität Frankfurt/Main 1979, Ph. D. Thesis: "Untersuchungen an Verbindungen mit verschiedenartigen Sulfidbrücken".
72. W. F. Giggenbach, *Inorg. Chem.* 13 (1974) 1730.
73. W. F. Giggenbach, *Inorg. Chem.* 13 (1974) 1724.
74. R. Steudel, G. Holdt, R. Nagorka, *Z. Naturforsch. B: Anorg. Chem. Org. Chem.* 41B (1986) 1519-1522.
75. M. B. Berenbaum: *Encyclopedia of Polymer Science and Technology*, vol. 11, Wiley-Interscience, pp. 425-447.
76. G. Wilhelm, *Adhäsion* 5 (1976) 156.
77. Dow Chemical, US 4438259, 1984 (V. E. Meyer, T. E. Dergazarian).
78. Winnacker-Küchler, *Chemische Technologie*, 4th ed., 6, 2.14.
79. Henkel, DE 3604793 A1, 1986 (G. Borggreffe).
80. *Ullmann*, 4th ed., 20, 552.
81. E. Cooper, EP 32281, 1981 (A. G. Papay, J. P. O'Brien).
82. Mobil Oil, EP 7735, 1980 (A. G. Horodysky, S. Landis).
83. Lubrizol, US 4119549, 1978 (K. E. Davis).
84. E. Cooper, US 4563302 A, 1986 (P. G. Griffia, W. Y. Lam).
85. Mobil Oil, US 4123372, 1978 (R. F. Bridger, P. S. Landis).
86. Institut français du pétrole, FR 2588881 A1, 1987 (M. Born, L. Briquet, G. Parc).
87. Lubrizol, US 86838234, 1986 (C. P. Bryant, S. Q. A. Rizvi, K. B. Grover, J. N. Vinci).
88. Phillips Petroleum, US 3759956, 1973 (P. R. Strapp).
89. A. M. Kuliev, F. I. Gasanov, F. N. Mamedov, *Prisadki Smaz. Maslam* 2 (1969) 27-9; *Chem. Abstr.* 72 (8) 33982m.
90. A. M. Kuliev, K. I. Sadykhov, R. K. Mamedova, N. S. Kerimov, S. M. Abutalybova, *Azerb. Neft. Khoz.* 53 (1973) 40; *Chem. Abstr.* 80 (10) 50087f.
91. Magyar Asvanyolaj Ész Foldgaz Kiserleti Intezet, GB 2193957 A1, 1988 (R. Csikos, S. Borzsonyi, P. L. Farkas).
92. R. Bötcher, S. Wartewig, W. Windisch, A. Zschunke, *Z. Naturforsch. A: Astrophys. Phys. Phys. Chem.* 23A (1968) 1766-1770.
93. Toyo Soda Mfg., JP 55071761, 1980; *Chem. Abstr.* 93 (16) 151794h.
94. F. Seel, H. J. Güttler, *Angew. Chem.* 85 (1973) 416.
95. F. A. Cotton, J. B. Harmon, R. M. Hedges, *J. Am. Chem. Soc.* 98 (1976) 1417.
96. Nitto Chemical Industry Co., JP 50060050, 1975 (I. Watanabe); *Chem. Abstr.* 83 (12) 102984w.
97. Yuasa Battery, JP 56058 582, 1981; *Chem. Abstr.* 95 (16) 138034g.
98. F. Holdinghausen, D. Männig, R. Wenzl, company report, Degussa AG, Frankfurt/Main 1994.
99. Gefahrstoffverordnung, 4th ed., 12/1993, Deutscher Bundes-Verlag, Bonn 1993.
100. Köln-Birret-Merkblätter, 13. Erg.-Lfg. 11/80-N 19-2, Ecomed Verlagsgesellschaft, Landsberg.
101. Roth-Weller: *Sicherheitsfibel Chemie*, 5th ed., Ecomed-Verlag, Landsberg/Lech 1991.
102. Daten Chemischer Stoffe, 28. Erg.-Lfg. 12/92, Ecomed-Verlag, Landsberg/Lech 1992.
103. Wasserhaushaltsgesetz (WHG) in der Fassung der Bekanntmachung vom 23. Sept. 1986, Bundesgesetzblatt I, p. 1529.
104. Degussa AG: brochure "Umwelt und Degussa" no. CH 460 4-05-290 and leaflet no. CH 337-3-05491, Degussa AG, Hanau 1991.
105. Allgemeine Rahmen-Verwaltungsvorschrift über Mindestanforderungen an das Einleiten von Abwasser (Rahmen-Abwasser-VwV) in Gewässer, Gemeinsames Ministerialblatt Nr. 25 vom 22. Sept. 1989.
106. H. W. Sonntag, company report, Degussa AG, Frankfurt/Main 1994.
107. R. Neureiter, Degussa AG, company information, Frankfurt/Main 1994.
108. G. Nickless: *Inorganic Sulfur Chemistry*, Elsevier, Amsterdam 1968, pp. 509-533.
109. *Gmelin*, system no. 23, Ammonium, 1936, 256-259.
110. *Gmelin*, system no. 22, Kalium, 1938, 702-708.
111. *Gmelin*, system no. 21, Natrium, 1928, 515-535; suppl. 1964-1970, 205-213, 1079-1090, 1876.
112. F. Foerster et al., *Z. Phys. Chem. (Leipzig)* 110 (1924) 435-496.
113. Hoechst, DE-OS 2221298, 1973 (W. Schreiber, A. Metzger, J. Scholderer).
114. BASF, DE-OS 1186450, 1965 (W. Spormann, J. Heinke).
115. BASF, DE-OS 1809507, 1970 (W. Spormann).
116. Allied Chem., DE-OS 2611190, 1976 (S. L. Bean).
117. M. W. Wirth: *Toxikologiefibel*, Thieme Verlag, Stuttgart 1962.
118. H. V. Benda, *Z. Naturforsch. B Anorg. Chem. Org.* 34B (1979) 957-968.
119. *Gmelin*, system no. 21, 3rd ed., 1162-1176.
120. *Chem. Abstr.* 99 no. 20, 160805p.
121. *Chem. Abstr.* 104 no. 10, 71120r.
122. *Chem. Abstr.* 110 no. 10, 78385b; *Chem. Abstr.* 111 no. 12, 99852z.
123. *Chem. Abstr.* 82 no. 12, 77551f; *Chem. Abstr.* 82, no. 4, 19032b.
124. American Standards Association INC., Specifications PH 4, New York 1960, pp. 250-251.
125. ISO Norm 3619, 1976.
126. DIN 19080, Part 82, August 1978.
127. Th. Goldschmidt, DT 1184330, 1963; DT 1265146, 1966.
128. Allied Chem., CA 82159, 1967.
129. *Chem. Abstr.* 70 no. 20, 89265f.
130. *Chem. Abstr.* 80 no. 14, 72539g.
131. *Chem. Abstr.* 107 no. 20, 179463f.
132. NIOSH: *Registry of Toxic Effects of Chemical Substances*, Cincinnati 1983.
133. W. Braun, *Vergiftungsfibel*, Thieme Verlag, Stuttgart 1980.
134. M. Schmidt, W. Siebert: *Comprehensive Inorganic Chemistry*, vol. 2, Pergamon Press, Oxford 1973, p. 881.
G. Nickless: *Inorganic Sulfur Chemistry*, Elsevier, Amsterdam 1968, p. 519.
135. Mitsubishi Edogawa, DE 1592013, 1978 (Y. Yoshikawa, H. Okazaki, T. Yamaguchi).
BASF, DE-AS 2442418, 1974 (E. Voelkl et al.).
136. BASF, DE 2646825, 1976 (B. Lautner et al.).
Olin Corporation, US 4836903, 1989 (D. W. Cawfield).
137. G. Nickless: *Inorganic Sulfur Chemistry*, Elsevier, Amsterdam 1968, pp. 220, 227.
138. Bundesgesetz Blatt 11, p. 838 (1990).
139. Bundesgesetz Blatt 1, p. 1001 (1990).
140. Bundesgesetz Blatt 1, p. 860 (1992).
141. Bundesgesetz Blatt 1, p. 1714 (1991).
142. Bundesgesetz Blatt 1, p. 1221 (1990).
143. BASF: safety data sheets, 1983.

Part Thirteen

Alkaline Earth Metals

																H	He		
Li	Bc												B	C	N	O	F	Ne	
Na	Mg	Al													Si	P	S	Cl	Ar
K	Ca	Sc	Ti	V	Cr	Mn	Fe	Co	Ni	Cu	Zn	Ga	Ge	As	Se	Br	Kr		
Rb	Sr	Y	Zr	Nb	Mo	Tc	Ru	Rh	Pd	Ag	Cd	In	Sn	Sb	Te	I	Xe		
Cs	Ba	La [†]	Hf	Ta	W	Re	Os	Ir	Pt	Au	Hg	Tl	Pb	Bi	Po	At	Rn		
Fr	Ra	Ac [†]																	

†	Ce	Pr	Nd	Pm	Sm	Eu	Gd	Tb	Dy	Ho	Er	Tm	Yb	Lu
‡	Th	Pa	U	Np	Pu	Am	Cm	Bk	Cf	Es	Fm	Md	No	Lr

For Beryllium and Magnesium, see *Light Metals*.
For Radium, see *Radioactive Metals*.

56 Calcium

STEPHEN HLUCHAN (§§ 56.1–56.4); JOSEPH A. H. OATES (§ 56.5); FRANZ WIRSCHING (§ 56.6); SUZANNE E. KEEGAN, ROBERT KEMP (§ 56.7); PETER FORGIONE (§ 56.8)

56.1	Introduction	2250	56.6.3	Production	2291
56.2	Properties	2250	56.6.3.1	Natural Gypsum to Calcined Products	2291
56.3	Production	2250	56.6.3.2	FGD Gypsum to Calcined Products	2297
56.4	Uses	2251	56.6.3.3	Phosphogypsum to Calcined Products	2299
56.5	Lime and Limestone	2252	56.6.3.4	Anhydrite Plaster	2301
56.5.1	Introduction	2252	56.6.4	Use and Properties of Gypsum Plasters and Products and Anhydrite Plasters	2301
56.5.2	Limestone	2253	56.6.4.1	Hydration, Setting, Hardening	2301
56.5.2.1	Physical and Chemical Properties	2255	56.6.4.2	Prefabricated Gypsum Building Components	2304
56.5.2.2	Formation and Occurrence	2256	56.6.4.3	Gypsum Plaster	2305
56.5.2.3	Production	2256	56.6.4.4	Other Uses	2306
56.5.2.4	Uses and Specifications	2257	56.6.4.5	Properties of Gypsum Building Products Installed <i>in Situ</i>	2308
56.5.3	Quicklime	2258	56.6.5	Material Testing and Chemical Analysis	2309
56.5.3.1	Physical and Chemical Properties	2258	56.6.5.1	Standards	2309
56.5.3.2	Raw Materials	2260	56.6.5.2	Testing	2309
56.5.3.3	Production	2262	56.6.5.3	Chemical Analysis	2310
56.5.3.4	Uses and Specifications	2269	56.6.5.4	Phase Analysis	2310
56.5.4	Hydrated and Slaked Lime	2271	56.6.6	Economic Aspects	2311
56.5.4.1	Physical and Chemical Properties	2271	56.7	Calcium Chloride	2311
56.5.4.2	Raw Materials	2272	56.7.1	Physical Properties	2311
56.5.4.3	Production	2273	56.7.2	Chemical Properties	2313
56.5.4.4	Uses and Specifications	2274	56.7.3	Production	2314
56.5.5	Environmental Protection	2276	56.7.4	Environmental Protection	2314
56.5.6	Physical Testing and Chemical Analysis	2277	56.7.5	Quality Specifications	2315
56.5.6.1	Sampling and Sample Preparation	2277	56.7.6	Chemical Analysis	2315
56.5.6.2	Physical Testing	2278	56.7.7	Storage and Transportation	2315
56.5.6.3	Chemical Analysis	2278	56.7.8	Uses	2316
56.5.7	Storage and Transportation	2278	56.7.9	Economic Aspects	2317
56.5.8	Economic Aspects	2279	56.7.10	Toxicology and Occupational Health	2317
56.5.9	Toxicology and Occupational Health	2280	56.8	Calcium Cyanamide	2317
56.5.9.1	Toxicology	2280	56.8.1	Physical Properties	2317
56.5.9.2	Occupational Health	2281	56.8.2	Chemical Properties	2318
56.6	Calcium Sulfate	2281	56.8.3	Production	2318
56.6.1	The $\text{CaSO}_4\text{--H}_2\text{O}$ System	2282	56.8.3.1	Overall Process	2318
56.6.1.1	Phases	2282	56.8.3.2	Manufacture	2319
56.6.1.2	Laboratory Synthesis	2284	56.8.3.3	Processing of Technical Calcium Cyanamide	2322
56.6.1.3	Industrial Dehydration of Gypsum	2285	56.8.4	Quality Specifications	2323
56.6.1.4	Energy Aspects	2285	56.8.5	Storage and Transportation	2323
56.6.1.5	Structure, Mixed Compounds, Solubility	2286	56.8.6	Uses	2323
56.6.2	Occurrence, Raw Materials	2287	56.9	References	2324
56.6.2.1	Gypsum and Anhydrite Rock	2287			
56.6.2.2	Flue-Gas Desulfurization (FGD) Gypsum	2288			
56.6.2.3	Phosphogypsum	2290			
56.6.2.4	Fluoroanhydrite	2290			
56.6.2.5	Other By-product Gypsums	2291			

56.1 Introduction

Calcium metal was discovered in 1808 independently by SIR HUMPHRY DAVY and by J. J. BERZELIUS and POUTIN. Its name derives from the Latin "calx", for lime. It is the fifth most abundant element in the earth's crust. Some important, naturally occurring compounds are the carbonate (limestone), the sulfate, and complex silicates.

56.2 Properties

Calcium, stable isotopes 40, 42, 43, 44, 46, 48, electronic configuration 2-8-8-2, is a silvery white metal. Its major properties are:

Density (20 °C)	1.55
Melting point	838 °C
Boiling point	1440 °C
Specific heat (0-100 °C)	0.624 Jg ⁻¹ K ⁻¹
Heat of fusion	217.7 J/g
Heat of vaporization	4187 J/g
Thermal expansion (0-400 °C)	22.3 × 10 ⁻⁶ K ⁻¹
Electrical resistivity (0 °C)	3.91 × 10 ⁻⁶ Ωcm
Thermal conductivity (20 °C)	1.26 W cm ⁻¹ K ⁻¹
Lattice constant (Fcc)	0.5582 nm

Calcium is relatively unstable in moist air, rapidly forming a hydration coating. It can be stored in dry air (less than 30% R.H.) at room temperature. Calcium reacts spontaneously with water to form Ca(OH)₂ and hydrogen gas; when finely divided, it will ignite in air.

One of the alkaline earth group of metals, group IIA, calcium exists in the face centered cubic form at room temperature, transforming to a body centered cubic structure at 448 °C, and melting at 838 °C.

The predominate stable isotope of calcium is ⁴⁰Ca. Calcium exhibits only one valence state, 2+, in all of its reactions. It is slightly less active than barium and strontium in the same series. Calcium is a very ductile metal and can be formed by casting, extrusion, rolling, etc. Table 56.1 presents mechanical properties of calcium.

Calcium is noted for its high reactivity, especially the high heat of formation of some of its compounds. Examples are given in Table 56.2. The low density and relatively low-electrical resistivity make calcium one of the most efficient electrical conductors on a mass basis.

Table 56.1: Mechanical properties of calcium metal.

Mechanical properties	Annealed	Cold worked
Tensile strength, N/mm ²	4800	11 500
Yield strength, N/mm ²	1370	8500
Elongation, %	51	7
Modulus of elasticity, MN/mm ²	2.2-2.6	
Hardness, Rockwell B	16-18	

Table 56.2: Heats of formation ΔH_f of calcium compounds.

Compound	ΔH_f , kJ/mol	Compound	ΔH_f , kJ/mol
CaBr ₂	-675.3	Ca ₃ N ₂	-432.1
CaCl ₂	-795.5	CaO	-636.0
CaF ₂	-1215.4	CaO ₂	-659.4
CaH ₂	-188.8	Ca ₃ P ₂	-504.5
Ca ₂	-535.1	CaS	-482.7

56.3 Production

Calcium is produced in the United States by Minteq Int'l Inc. at Canaan, Connecticut; in Canada by Timminco Ltd; and in France by Pechiney. Prior to World War II, the major production method was electrolysis of fused calcium chloride, but this method has been discontinued. The world capacity is 8000 t/a. The United States accounts for over 50% of the world's consumption of calcium. Total world capacity utilization is under 65%; pricing has been stable.

The process used today is thermal reduction of lime with aluminum. The reactants, lime and aluminum powder, are briquetted and charged into a high-temperature alloy retort. The reaction vessel is evacuated to 0.1 Pa or less; it is then heated to 1200 °C. The aluminum reduces the lime producing calcium metal vapor. The calcium then is removed from the reaction by condensation, thus allowing the reaction to continue in the desired direction.

High-purity grade calcium metal requires highly purified lime and aluminum. A further vacuum distillation step is also required because the calcium produced in the reduction reaction is contaminated with aluminum. In addition this second operation reduces the level of other contaminants, such as manganese. Table 56.3 shows the purity after both the first and the second purification steps.

Table 56.3: Chemical analysis of typical commercial and redistilled calcium.

Element	Commercial grade, %	Redistilled grade, %
Mg	0.50	0.50
N	0.08	0.02
Al	0.30	0.001
Fe	0.008	0.001
Mn	0.01	0.002
Co	—	0.0002
Li	—	0.0001
Be	—	0.0001
Cr	—	0.0002
B	—	0.0001
Ca and Mg	99.5	99.9

56.4 Uses

Calcium is used in the production of energy-efficient materials: high-strength steels, maintenance free automotive batteries, and advanced magnetic materials.

The major use of calcium is to improve the quality of steel. For decades, calcium containing ferroalloys have been used as tap stream additions to the molten metal, or calcium compounds were injected through a refractory lance using argon, a carrier gas. Although the benefits of using pure calcium metal were known, they were difficult to obtain; calcium is highly volatile, boiling well below steel-making temperatures.

In the early 1970s, wire feeding technology was introduced. A steel clad calcium wire is fed through a delivery system which propels the wire well below the surface of the molten steel. The steel cladding protects the calcium until it reaches a depth where the ferrostatic pressure suppresses the vaporization. Systems have been developed for ladle, tundish, and degasser application. For large tonnage use, a wire-lance system combines the advantages of wire feeding, gas control of fluid dynamics, and treatment with pure calcium. This has resulted in the efficient production of improved quality ultraclean steels.

Calcium is important in steel chemistry because it is a strong oxide and sulfide former; furthermore, it has the uncommon ability to alter the oxides and sulfides. Treatment with calcium modifies the melting point of inclu-

sions which rapidly float out of the steel, and also alters the morphology of any remaining inclusions, rendering them spherical in shape, very small, and finely dispersed. The result is a fundamental quality improvement, especially in the mechanical properties: formability, drawing, impact, tensile, machinability, resistance to cracking and tearing, and improved surface and internal cleanliness. Calcium also improves resistance to hydrogen induced cracking in line pipe associated with high-sulfur oil and gas pipelines.

In the maintenance free automotive battery, calcium improves electrical performance and battery life. The antimony-lead used in the conventional lead-acid battery is replaced with a 0.1% Ca-Pb grid alloy. The calcium improves the conductivity and current capability of the cell; it significantly reduces gassing, permitting the cell to be closed (preventing water loss and extending life).

High-energy density magnetic materials are produced using calcium. Samarium cobalt magnets with energy products of between 8 and 16 × 10⁴ T·A/m have found applications in miniature transducers and other devices requiring high energy or volume restrictions. The reaction is:



The development of neodymium ferro boron magnets involve the use of calcium metal as a reductant. This is an important development because these magnets have energy products approaching 40 × 10⁴ T·A/m, over twice the value as for samarium cobalt. In addition, the availability of the raw materials is significantly greater than for samarium cobalt; both the quantity and stability of raw material supply limited the growth of samarium cobalt magnets. Therefore, neodymium ferro boron magnet materials are less expensive to produce.

The energy density is sufficient to permit the replacement of armature windings in motors, transducers, and generators with permanent magnets. The mass of an automotive starting motor was reduced from 3.6 kg to 1.8 kg; the size and cost of the motor were com-

mensurately reduced as well. This technology is finding extensive applications in automotive, computer peripheral, medical, home appliance, and military markets.

There are two methods of producing the neodymium ferro boron raw material, a neodymium iron alloy. One is the calcium thermal reduction method:



The second method is by electrolysis:



The calcium thermal reduction process is preferred. It has the greatest flexibility in producing the basic neodymium iron and alloy variations. The by-products are not toxic as they are in the electrolytic process. The calcium process is less capital intensive and readily scaled in volume to meet market demands.

In the *debismuthizing of lead* by the Kroll-Betterton process, calcium metal is combined with bismuth which then floats out in a dross:



Lead ores are thus refined to commercial soft lead with 0.02% or less Bi.

Calcium metal is readily reacted with zirconium fluoride to refine *zirconium*; the high heat of reaction melts the zirconium. The zirconium ingot produced by this method is remelted under vacuum for purification. To produce *thorium* and *uranium*, the oxides are mixed with a stoichiometric excess of calcium and reduced under an atmosphere of argon. The resulting metals are leached with acetic acid to remove the lime produced as a by-product of the reaction.

Calcium metal is readily hydrided for use as a portable source of *hydrogen gas*. It also is used in the production of the B-complex vitamin calcium pantothenate.

Calcium ferroalloys are used in the production of nodular iron castings. In magnesium ferrosilicon, calcium reduces the reactivity, enhances nucleation, and improves morphology. The ratio of calcium to magnesium varies

from 0.15 to 0.50. Pieces of the ferroalloy are placed in a protected pocket cut in the refractory lining of the ladle prior to tap. The molten iron is then poured into the ladle where it reacts with the alloy. The treated, nodularized iron is then cast into molds.

In the recent in-mold process, granularized ferroalloy is placed in a special reaction chamber formed in the channels of the mold. This permits the reaction to occur when the iron is cast; it enhances the effectivity of the ferroalloy and results in improved castings. The process can be automated for high productivity.

Alloys of calcium also are used to deoxidize magnesium, to strengthen lead electrodes, and to produce special aluminum alloys.

Calcium is used to improve the mechanical properties of lead. A proprietary process for improving the integrity and formability of the lead used in yacht keels was developed in Australia and contributed to the nation's success in winning the America's Cup in 1984.

56.5 Lime and Limestone

56.5.1 Introduction

Limestone is a naturally occurring mineral that consists principally of calcium carbonate but may also contain magnesium carbonate as a secondary component. It is found in many forms and is classified in terms of its origin, chemical composition, structure, and geological formation. Limestone occurs widely throughout the world and is an essential raw material for many industries.

Quicklime is produced by the thermal decomposition of limestone. It consists mainly of calcium oxide. Its quality depends on many factors, including physical properties, degree of sintering, and chemical composition. As the most readily available and cost effective alkali, quicklime plays an essential part in a wide variety of industrial processes.

Hydrated lime and slaked lime are produced by reacting quicklime with water; they consist mainly of calcium hydroxide. In gen-

eral, hydrated lime refers to a dry calcium hydroxide powder, while slaked lime refers to an aqueous suspension of calcium hydroxide particles in water. Hydrated and slaked lime are widely used in aqueous systems as low-cost alkalis.

The term lime refers to quicklime and, less frequently, to hydrated or slaked lime. It is, however, sometimes used incorrectly to describe limestone, which is a frequent cause of confusion.

History. Limestone was probably used in the Stone Age. The first records relate to the Egyptian Second Dynasty (ca. 2800 B.C.), when it was employed in the construction of the Giza Pyramids. Marble, a highly crystalline form of limestone, was used by the Greeks shortly after this period for statues and the decoration of buildings. Limestone was widely used by the Romans for building roads.

There is evidence of the widespread use of quicklime and hydrated lime for building by many civilizations by about 1000 B.C., including the Greeks, Egyptians, Romans, Incas, Mayas, Chinese, and Mogul Indians. The Romans employed hydraulic lime in many construction projects, including the Appian Way.

Lime was also well known to the Romans as a chemical reagent. In 350 B.C. XENOPHON referred to the use of lime for bleaching linen. The medical use of limewater was recorded by DIOSCORIDES in 75 A.D.

The burning of limestone in kilns was mentioned by CATO in 184 B.C. PLINY THE ELDER (ca. 70 A.D.), in his "Chapters on Chemical Subjects" described the production, slaking, and uses of lime, and stressed the importance of chemical purity.

The use of limestone and lime in building spread throughout Europe in the 1400s.

In the 1700s, JOSEPH BLACK gave the first sound technical explanation of the calcination of limestone, including the evolution of gaseous carbon dioxide. LAVOISIER confirmed and developed BLACK's explanation. In 1766, DE RAMECOURT, published a detailed account of "The Art of the Lime Burner" which covered

the design, operation, and economic aspects of limestone quarrying and lime burning.

Terminology. Because the quarrying of limestone and the production of quicklime and hydrated lime are long-established industries, they have generated many traditional expressions which frequently cause confusion. The following definitions cover the most common terms. A more comprehensive list has been published [6].

Air-slaked lime is produced by excessive exposure of quicklime to the atmosphere. It contains varying proportions of the oxides, hydroxides, and carbonates of calcium and magnesium.

Agricultural lime is a term which includes any limestone, quicklime, or hydrated lime product used to neutralize soil acidity.

Aragonite is one of the less abundant crystalline forms of calcium carbonate.

Available lime is an analytical term for the calcium oxide content of quicklime or hydrated lime that is able to react with sucrose under specified conditions.

Bituminous limestone — see carboniferous limestone.

Carbonaceous limestone contains organic matter as an impurity. It is often dark gray and has a musty odor.

Carboniferous limestone was deposited in the carboniferous period of the Palaeozoic era.

Calcitic limestone refers to a high-calcium limestone.

Calcite is the most abundant crystalline form of calcium carbonate.

Cement is produced by calcining limestone with materials containing silica, alumina, and iron oxide to produce a controlled blend of calcium silicates, aluminates, and ferrates in the form of a clinker. The clinker is then ground with gypsum and other materials to form cement.

Chalk is a naturally occurring form of limestone, which has been only partially compacted and, therefore, has a high porosity.

Chemical quality limestone is a high-calcium or dolomitic limestone with low levels of

impurities, which meets the requirements of the chemical industry.

Dead-burned dolomite is a highly sintered form of dolomitic quicklime which is used primarily as a basic refractory.

Dolime refers to calcined dolomite.

Dolomite is strictly speaking the double carbonate containing 54–58% of CaCO_3 and 40–44% of MgCO_3 . This term is, however, frequently used to describe dolomitic limestone.

Dolomitic limestone is generally understood to contain 20–44% of MgCO_3 .

Fine quicklime generally refers to screened products with a top size below 0.6 cm.

Free lime is an analytical term for the calcium oxide component of quicklime or hydrated lime. It excludes calcium oxide in CaCO_3 , Ca(OH)_2 , and calcium silicates.

Granular quicklime usually refers to screened products with a top size of 0.5–2.5 cm.

Ground quicklime refers to powdered products produced by milling.

Hard-burned quicklime is a sintered form of quicklime with low reactivity to water.

High-calcium limestone is a general term for limestone consisting mainly of CaCO_3 and having a low content of MgCO_3 (max. 5%). Similarly, high-calcium quicklime contains mainly CaO and not more than 5% MgO .

Hydrated lime is a dry powder produced by reacting quicklime with controlled amounts of water.

Hydraulic limestone is an impure carbonate containing considerable amounts of silica and alumina. Calcination of hydraulic limestone produces hydraulic lime, which, after mixing with water, has cementing (or hydraulic) properties and is capable of setting under water.

Iceland spar is a rare and very pure form of crystalline limestone. It is transparent and has been used in optical instruments.

Light-burned quicklime is quicklime that is lightly sintered and has a high reactivity to water.

Lime putty is a viscous dispersion of calcium hydroxide in water.

Lump quicklime usually refers to products with a top size above 2 cm.

Magnesian limestone is generally understood to be mainly CaCO_3 with 5–20% of MgCO_3 .

Marble is a highly crystalline carbonate rock which may be high-calcium or dolomitic limestone. It occurs in many colors with veined and mottled effects.

Marl is an impure, soft, earthy rock which contains clay and sand. If it contains more than 50% CaCO_3 , it is classified as a limestone.

Milk of lime is a fluid suspension of hydrated lime in water.

Neutralizing value is an analytical term for that proportion of limestone, quicklime, or hydrated lime (expressed as CaO) that is capable of reacting with hydrochloric acid under specified conditions. It includes the contribution of CaCO_3 , CaO , Ca(OH)_2 , and the acid soluble fraction of the calcium silicates, aluminates, and ferrates.

Pebble quicklime usually refers to screened products with a top size of 1.5–6 cm.

Precipitated calcium carbonate (PCC) is produced by blowing carbon dioxide into milk of lime, thereby precipitating finely divided calcium carbonate with a mean particle size in the range 0.02 to 0.2 μm .

Reactivity of quicklime is a measure of the rate at which it reacts with water. There are many reactivity tests (see Section 56.5.3.1).

Slaked lime generally describes an aqueous suspension of mainly calcium hydroxide. It includes milk of lime and lime putties. The term slaked lime is sometimes used to describe hydrated lime.

Soft-burned quicklime — see light-burned quicklime.

Solid-burned quicklime — see hard-burned quicklime.

Total lime is an analytical term for the total CaO plus MgO content of a limestone or lime, expressed in terms of CaO equivalent. It includes the carbonates, oxides, hydroxides, silicates, aluminates, and ferrates.

Type N or normal hydrated lime is defined in ASTM specification C-207 [7]. It is gener-

ally produced by hydrating high-calcium quicklime at ca. 100 °C.

Type S hydrated lime is also defined in ASTM specification C-207 [7]. It is produced by heating high-calcium or magnesian lime in an autoclave at ca. 180 °C. It may contain up to 8% of unhydrated oxide.

Whiting is a finely powdered product produced by milling and classifying limestone (generally chalk). The nominal top size varies from 75 to 10 μm .

56.5.2 Limestone

56.5.2.1 Physical and Chemical Properties

The physical and chemical properties of limestones vary widely as a result of the origin of the deposit, its microstructure, and impurities. The information given below is typical of most commercially exploited deposits.

Color. Pure calcite is white. Chalk and marble are also generally white, although impurities in the latter can produce a variety of colors and patterns. Many limestones, however, contain carbonaceous material, which produces various shades of gray. Iron compounds can introduce a red color. Some impurities produce a surface coloration on weathering.

Odor. Any odor possessed by limestone generally arises from its content of carbonaceous material. The smell is musty or earthy.

Structure. All limestones are crystalline. The grain size increases with the amount of recrystallization that has occurred during formation of the deposit. Thus, shell limestones have a grain size of ca. 1 μm , marls and chalks from 2 to 5 μm , dense limestones from 5 to 250 μm , and marbles and calcite spar from 250 to 1000 μm . Calcite and dolomite have rhombohedral crystal structures, and aragonite is orthorhombic.

Porosity. The porosity of limestone decreases with increasing levels of compaction. Thus, marls have up to 50% porosity, chalks 20–

40%, dense limestones 1–10%, and calcite spar < 1%.

Density. For pure calcite, the density is 2.71 g/cm^3 at 20 °C; for aragonite and dolomite, it is 2.93 g/cm^3 and ca. 3.0 g/cm^3 , respectively. The porosity of limestone results in apparent densities of 2.1–2.5 g/cm^3 for chalk, 2.5–2.7 g/cm^3 for high-calcium limestone, and 2.75–2.9 g/cm^3 for dolomitic limestones.

Bulk Density. The bulk density depends primarily on the apparent density of the limestone and its particle size distribution. Crushed, screened limestone with a 2:1 size ratio generally has a bulk density of 1300–1450 kg/m^3 . Crushed limestone, including the fines, has a bulk density of 1600–1750 kg/m^3 .

Impurities. Magnesium carbonate is not generally regarded as an impurity. Impurities may be dispersed homogeneously as a result of their being present during the recrystallization process. Alternatively they may be present heterogeneously in features such as faults, bedding planes, or nodules. Silica and alumina, in the form of clay, silt, and sand, are commonly found as homogeneous impurities, but also occur as heterogeneous impurities. Similarly, iron can exist homogeneously as iron carbonate and heterogeneously as pyrite and limonite. Sulfur from sulfates and organic remains generally exists as a homogeneous impurity. Other trace impurities such as lead are often found in the vicinity of faults where mineralization has occurred. Typical levels of trace elements are given in Table 56.4.

Hardness. Pure calcite has a hardness of 3 Mohs. Naturally occurring limestones lie in the range 2–4 Mohs.

Strength. The compressive strength of limestone varies from 10 MPa for some marls and chalks to 200 MPa for some marbles.

Specific Heat. The specific heats of high-calcium limestone and dolomite at 20 °C are 817 and 880 $\text{J kg}^{-1} \text{K}^{-1}$, respectively. They increase with temperature [8].

Solubility. The solubility of calcite in distilled water free of carbon dioxide has been reported

as ca. 15 mg/L at 20 °C [6]. The solubility in distilled water in equilibrium with atmospheric carbon dioxide is approximately double the above value. Dolomite has been reported as being somewhat more soluble than calcite [6].

Reaction with Acids. Calcium carbonate reacts with acids with evolution of carbon dioxide and heat (reported to be about 19 kJ/mol in hydrochloric acid [9]).

pH. Both limestone and dolomite are essentially neutral products, giving pHs of 8.5–9.0.

Thermal Dissociation. The heat of dissociation of calcium carbonate is 3180 kJ/kg of CaO relative to 25 °C, and 3010 kJ/kg relative to 900 °C (760 kcal/kg and 720 kcal/kg, respectively). The corresponding values for magnesium carbonate are 3010 kJ/kg MgO relative to 25 °C, and 2850 kJ/kg relative to 700 °C.

Table 56.4: Typical trace element concentrations in limestone.

Element	Concentration	Element	Concentration
Al	0.05–0.6%	Ni	1–5 mg/kg
Ba	0.02–0.2%	P	0.02–0.2%
B	1–50 mg/kg	K	0.01–0.5%
C	0.05–1%	Ag	0.2–0.5 mg/kg
Cd	0.1–2 mg/kg	Na	0.01–0.2%
Cr	10–500 mg/kg	Si	0.2–5%
Cu	0.5–10 mg/kg	Sr	20–2000 mg/kg
Co	0.5–5 mg/kg	S	0.01–0.2%
Fe	0.01–0.1%	Sn	ca. 20 mg/kg
Pb	1–100 mg/kg	Ti	0.01–1%
Mn	20–300 mg/kg	V	5–50 mg/kg
Hg	< 1 mg/kg	Zn	1–200 mg/kg
Mo	ca. 20 mg/kg		

56.5.2.2 Formation and Occurrence

Limestone is widely distributed throughout the world in deposits of varying sizes and degrees of purity. Information regarding the deposits in a given country is generally best obtained by contacting the appropriate national geological society.

The process of limestone formation is believed to have started with the extraction of calcium salts from the earliest forms of igneous rocks by the combined effects of erosion

by the weather and corrosion by dissolved acids, e.g., sulfurous acid and carbon dioxide.

Under certain conditions of concentration and temperature, calcium carbonate precipitated from the solutions of calcium salts. Deposits with such chemical origins are generally thin, of limited extent, and therefore of little commercial importance.

When the solutions of calcium salts drained into the sea, marine life extracted the dissolved calcium hydrogen carbonate component to build shells and skeletons of calcium carbonate. These gradually accumulated on the bed of shallow tropical seas to produce deposits, many of which were massive. The calcium carbonate became contaminated by waterborne clays and silts, and by airborne volcanic ash. The extent of contamination depended on the distance from estuaries and volcanoes. In general the purest deposits originated from mid-ocean banks remote from land.

The limestone deposits became covered with other materials and were subjected to solvent action under high pressure and temperature. This consolidated the deposits and caused recrystallization to varying degrees. The sequence marl, chalk, limestone, and marble shows progressive consolidation and change of structure. Soft marls are porous and contain well-defined fossils. Marble is particularly dense, highly crystalline, and contains no discernible fossils. The grain size ranges from less than 5 µm for marls and chalks to over 250 µm for some marbles and calcite. Such rocks in which the original marine deposits have recrystallized are termed sedimentary clastic rocks, while the process of structural change is known as metamorphism.

56.5.2.3 Production

Most limestone is produced by open-cast quarrying. A small proportion (less than 5%) is extracted by underground mining and a still smaller proportion (less than 1%) as cut dimension-stone.

The first operation in open-cast quarrying is to remove the overburden (i.e., the soil, clay,

and loose rock overlying the deposit). Various techniques and types of earth moving equipment are used for this.

The next stage is generally to drill the bedrock. Rotary and percussive drills are widely used to drill the holes. The spacing between holes and the burden (distance between the holes and the quarry face) is carefully controlled. The diameter of the holes varies from 5–25 cm, depending on the design of the blast.

The drill holes are then filled with controlled amounts of explosive. A mixture of ammonium nitrate and fuel oil (ANFO) is widely used; it is initiated with a high explosive. In a typical blast, 5000–50 000 t of stone is fragmented with about 140 g of explosive per 1 t limestone.

It is important to control the blast. Too little fragmentation produces oversize boulders which have to be broken using secondary blasting or a drop ball. Too much fragmentation produces an excessive amount of fine particles and increases the risk of throwing rock away from the quarry face. Optimum fragmentation is obtained by selection of the correct diameter and spacing of holes, time delay between holes, thickness of burden, and quantity of explosive.

Some soft rocks, e.g., chalk and marl, are broken by using heavy rippers. Other soft deposits, as found in lakes or in the sea, are extracted with dredgers. Underground mining is used when the overburden is thick, or when the limestone deposit is overlain by other rocks. Most operations use the room and pillar technique.

After blasting, the rock is loaded into dump trucks, generally by front-end shovels or hydraulic excavators and transported to the crushing and screening plant. In the crushing and screening plant, the larger lumps of rock are broken in a primary crusher to a size which suits the needs of the business and the characteristics of subsequent equipment. The rock is then screened into oversize (e.g., +15 cm), large (e.g., –15 +5 cm), medium (e.g., –5 +0.6 cm), and fine (e.g., –0.6 cm) fractions. The oversize stone is frequently recrushed and rescreened. The fine fraction is rich in impurities

such as clay, and is often tipped. In some plants clay and the fine fractions are removed more efficiently by washing and screening.

Compression machines such as jaw, gyratory, and roll crushers are generally selected when the amount of fine fraction must be minimized and when slabby lumps can be tolerated. Impact crushers such as hammer mills and impact breakers are selected when cubical lumps are required and increased fines production can be tolerated. Impact crushers have the advantage of being able to achieve a greater size reduction at lower capital cost. Although the major demand for limestone is in the –2.5 +0.1 cm size range, specialized requirements exist for very finely divided products, which are produced in a variety of mills, generally by dry grinding.

Dimension-stone production (for facing buildings and ornamental use) is a specialized process in which blocks are cut from the rock face with channelling machines or wire saws. The blocks are then cut, shaped, and, if required, polished to make the finished product.

56.5.2.4 Uses and Specifications

Construction. Limestone is the most widely used crushed rock, although it is generally out-sold by sand and gravel.

The quality specifications for construction stone relate mainly to its physical properties. Thus the stone must be clean, strong, dense, durable, free from cracks, and have the required particle size distribution. Some specifications limit the amounts of organic matter, clay, or water-soluble components (e.g., alkali-metal salts and gypsum). Specifications for the stone in the top dressing of roads (particularly in the vicinity of junctions) sometimes require a high resistance to polishing; this excludes the use of limestone. Standards for the testing and size distribution of road-stone and construction stone are given later.

Cement. The production of cement is the main use for chalk, and a major use for dense, high-calcium limestone. Approximately 1.1 t of limestone is required for 1 t cement. For the

estimated worldwide production of cement in 1987 of 1050×10^6 t [10], the consumption of limestone was ca. 1150×10^6 t.

Because cement is a mixture of calcium silicates, aluminate, and ferrate, the presence of SiO_2 , Al_2O_3 , and Fe_2O_3 in the feedstone is acceptable, provided the level is uniform. When the composition of the limestone is variable, elaborate arrangements are made to produce a consistent chemical analysis by blending. The magnesium carbonate content, however, must be below 5%.

Quicklime. Approximately 1.8 t of limestone is required per 1.0 t of quicklime. Further details are given later.

Agriculture. Many crops grow best under neutral to slightly acid conditions (i.e., pH 6–7). Thus soils which are more acidic than pH 6 generally benefit from the application of limestone. The limestone also helps to replace the calcium and magnesium removed by crops. Other benefits include an increase in the supply of other chemical nutrients, an increase in the organic matter of the soil, an increase in beneficial soil microorganisms, improved soil tilth, an improved supply of trace elements, and an increase in the efficiency with which fertilizers are used by the crop [6].

It is important that the limestone used for agriculture is in the correct physical state; a top size of ca. 0.1 cm is generally required. The delivered cost per tonne of carbonate is an important factor. In some cases, the magnesium content of dolomite gives it an advantage over high calcium limestone.

Limestone is also used in animal feeds and poultry grit. In animal feeds, trace elements may be restricted (e.g., lead levels below 10 mg/kg).

Metal Refining. When limestone is used in metal refining it is initially converted to quicklime, which reacts with acidic oxides (e.g., SiO_2 , Al_2O_3 , and Fe_2O_3) to produce molten slags. Most is used in blast furnaces for the production of iron, where the slag typically contains 40–50% CaO . Smaller amounts are used in the production of copper, lead, zinc,

and antimony. The quality requirements are as for chemical-quality stone. Some magnesium carbonate is acceptable but not essential.

Flue Gas Desulfurization. A growing use of limestone is in the treatment of flue gas to remove sulfur dioxide. The limestone is finely ground to 90% less than 45 μm and reacted with flue gases in a scrubber. The resulting calcium sulfate may be converted to salable gypsum, in which case the MgCO_3 content should not exceed 1%.

Other Uses. There are many other uses of limestone, e.g., production of alumina, glass, wood pulp, paper, ceramics, mineral wool, fillers, whiting, and coal-mine dusts, neutralization of acids and construction of filter beds; they are described in [6].

56.5.3 Quicklime

56.5.3.1 Physical and Chemical Properties.

Color. Most quicklimes are white. Impurities can result in gray, brown, or yellow tints. When quicklime is produced by solid fuel firing, a gray surface contamination is produced.

Odor. Quicklime has a slight earthy odor.

Porosity. The porosity of commercially produced quicklime can be as high as 55%, if a highly porous limestone is lightly burned. Exposure to elevated temperature results in sintering (Figure 56.1) which can reduce the porosity to below 25%. Dead-burned dolomite has a porosity of ca. 10%.

Density. The true density of calcium oxide is ca. 3.3 g/cm^3 . The apparent density of lumps can be as low as 1.4 g/cm^3 for highly porous quicklime. This can rise to over 2.3 g/cm^3 after sintering (Figure 56.2).

Calcined dolomite is generally denser than high-calcium quicklime, if given the same heat treatment. Dead-burned dolomite has an apparent density of ca. 3.2 g/cm^3 .

A

B

C

Figure 56.1: Scanning electron micrographs of quicklimes. A) Apparent density 1.5 g/cm^3 ; B) Apparent density 1.9 g/cm^3 ; C) Apparent density 2.3 g/cm^3 .

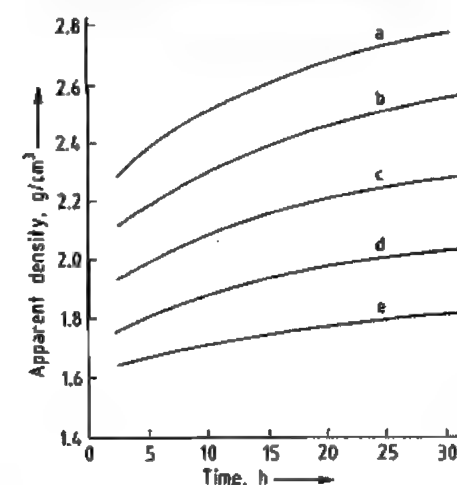


Figure 56.2: Variation of apparent density with temperature and time for a dense, high-calcium quicklime: a) At 1400°C ; b) 1300°C ; c) 1200°C ; d) 1100°C ; e) 1000°C .

Bulk Density. The bulk density depends on the mean apparent density of the particles and on the voidage between them. The latter is related to the particle size distribution and the particle shape. Most screened commercial quicklime products have compacted bulk densities of $900\text{--}1200 \text{ kg/m}^3$. Inclusion of fines can increase the bulk density by 30%.

Hardness. Most commercial quicklime products have a hardness of 2–3 Mohs. The value for dead-burned dolomite is in the range 3 to 5 Mohs.

Melting Point. The melting points for calcium oxide and magnesium oxide are 2570°C and 2800°C , respectively, with calcined dolomite being intermediate [11].

Specific Heat. The mean specific heats for high-calcium and dolomitic quicklime at 20°C are 760 and $830 \text{ J kg}^{-1}\text{K}^{-1}$, respectively. They increase with temperature [8].

Angle of Repose. The angle of repose for cubical, well-graded pebble quicklime is about 35° . This increases, however, as the fines content increases. For bunker design, valley angles of not less than 60° are recommended.

Heat of Hydration. The heat liberated by the reaction of quicklime with water is 1140 kJ/kg of CaO . The value for dolime is 880 kJ/kg of $\text{CaO}\cdot\text{MgO}$.

Reactivity to water may be measured by the rate of release of the heat of hydration [12, 13, 14] or by the rate at which an aqueous suspension reacts with hydrochloric acid [15]. The relationships between some reactivity tests are shown in Figure 56.3. Reactivity is related to the mean apparent density of quicklime produced from a given source stone (Figure 56.4).

It should be noted that the reactivity of quicklime can be markedly affected by impurities in the water. For this reason, distilled water should be used as a reference standard.

The low reactivity of calcined dolomite probably arises mainly from the low solubility of $\text{Mg}(\text{OH})_2$ in water. Sintering of MgO , which forms at lower temperatures than CaO may also be a factor.

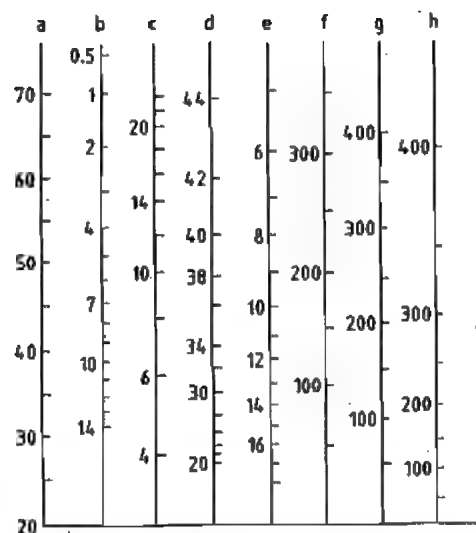


Figure 56.3: Comparisons between reactivity tests for a high-calcium quicklime: a) BS 6463, temperature after 2 min, °C [12]; b) DIN 1060, time (min) to 60 °C [13]; c) ASTM 110, temperature rise after 30 s, °C [14]; d) ASTM C 110, maximum temperature rise, °C [14]; e) ASTM C 110, time (min) to maximum temperature [14]; f) Acid titration, mL at 3 min [15]; g) Acid titration, mL at 5 min [15]; h) Acid titration, mL at 10 min [15].

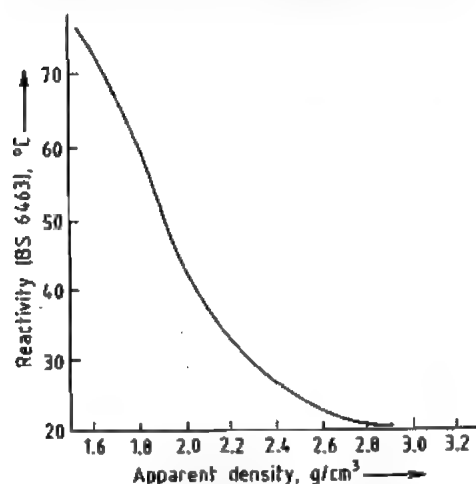


Figure 56.4: Relationship between reactivity and apparent density for a high-calcium quicklime.

Affinity for Water. Quicklime has a high affinity for water and is a more efficient desiccant than silica gel. Because of its high affinity for water vapor and (after partial hydration) for carbon dioxide, care should be taken to

minimize exposure of quicklime to the atmosphere. Relatively small amounts of air slaking (less than 1.5%, of combined water) can reduce the reactivity significantly.

The reaction of quicklime with water is associated with an increase in volume. This can cause the expansion of products that contain some lime which is not fully hydrated.

Reaction with Carbon Dioxide. In the absence of calcium hydroxide, quicklime only reacts with dry carbon dioxide above ca. 300 °C and below ca. 800 °C, depending on the carbon dioxide pressure. Partial recarbonation in the absence of calcium hydroxide can occur in lime kilns under certain abnormal conditions. It can produce an unexpectedly low reactivity and markedly affects the normal relationship between reactivity and mean apparent specific gravity.

Acid Neutralization. Quicklime is used extensively to neutralize acidic oxides, such as SiO_2 , Al_2O_3 , and Fe_2O_3 , in high-temperature nonaqueous systems (e.g., in steel making). Temperatures are generally selected so that the resulting calcium and magnesium salts produce molten slags.

Reaction with Carbon. Above 1700 °C, carbon reduces calcium oxide to produce calcium carbide and carbon monoxide.

56.5.3.2 Raw Materials

Limestone

Size. The ratio of the top to bottom sizes in the stone fed to lime kilns should preferably be 2:1 and certainly no more than 3:1. This gives an open, porous bed which offers a low resistance to gas flow and heat transfer. The narrow size range also helps to limit sintering of the smaller sizes while the larger are still dissociating. Selection of the size is influenced by the cost and availability of the stone and by the limitations imposed by the design of the lime kiln.

Shape. While a cubical shape is generally preferred for lime kilns, the slabby shapes pro-

duced by jaw and roll crushers are acceptable, providing they do not lead to a packed bed with low porosity.

Strength and Abrasion Resistance. Both the stone and the quicklime should be sufficiently strong to resist the physical forces to which they are exposed in the kiln and the handling and storage system. Excessive breakage in the kiln increases the resistance to gas flow and heat transfer. Breakage reduces the yield of granular products, which are usually at a premium, and increases the yield of fines, which are usually in surplus. Various empirical tests have been developed by kiln manufacturers to quantify the above factors.

Thermal Degradation. Some limestones, and particularly highly crystalline ones, are prone to break-down as a result of the heating, calcining, or thermal cycling processes within the kiln. Various empirical tests have been developed to quantify these effects.

Water. Some chalks are highly porous and may contain 10% water, which reduces the temperature of the kiln exhaust gas and may cause condensation problems in dust collectors.

Impurities. When limestone is burned in a kiln, most of the impurities persist in the quicklime. Permissible levels of SiO_2 , MgO , Al_2O_3 , Fe_2O_3 , S, Pb, and F depend on the quality specifications for the quicklime. Heterogeneous impurities (e.g., those arising from contamination with clay) tend to concentrate in the smaller sizes of quicklime. Removal of the fines (e.g., -6 mm) by screening generally improves product quality. Much of the sodium and potassium compounds and some of the sulfur compounds are removed during calcination. Sulfur oxides, most of which may arise from the fuel, are reabsorbed onto the surface of the quicklime at the start of the calcining zone and concentrate in the fine fraction.

Fuel

In lime burning, the fuel is more than a source of heat. It interacts with the process,

and the combustion products react with the quicklime. Many different fuels are used in lime kilns. The most common is coal. Coke, fuel oil, and natural gas are also widely used.

Selection of the correct fuel is important to the lime producer. Its cost per tonne of quicklime frequently represents 50% of the total production cost. Some fuels cannot be used in certain kilns. Other fuels may markedly affect the heat usage, output, and product quality. Some require different refractory linings to be used.

The selection of a new fuel, e.g., a different coal, is often a matter of trial and error. The selection for a new kiln should be made with great care. Most kilns can be operated on more than one fuel, and enable the operator to select the ones which give the optimum economic performance for his situation.

The major factors relating to the performance and acceptability of fuel are discussed briefly below. Further details are available in [6].

Calorific Value. The calorific value coupled with the unit cost of the fuel and the kiln heat usage enables the cost of the fuel per unit of quicklime to be calculated. Some confusion arises between the gross (or upper) and the net (or lower) calorific values. The former includes the latent heat of condensation of the water produced by combustion; it is used in North America and the United Kingdom. The net value more logically excludes the latent heat; it is widely used in, for example, continental Europe and Japan.

Sulfur. Some of the most important markets for quicklime, notably steelmaking, require low sulfur levels. Sulfur from the fuel is absorbed by quicklime in the cooler part of the calcining zone of lime kilns as calcium sulfate. In the more efficient kilns, e.g., shaft kilns, most of this sulfur is retained in the quicklime. In the less efficient units, e.g., some rotary kilns, much of the sulfur from the fuel may be eliminated from the kiln in the kiln gases by operating the calcining zone with low levels of excess air and high temperatures, and by limit-

ing contact between the kiln gases and the quicklime in the cooler part of that zone.

Combustion Characteristics. The combustion characteristics of fuels vary markedly. Pulverized coal tends to burn with a short, hot, and highly (infrared) emissive flame. Natural gas and wood burn with longer, cooler flames which have lower emissivities. These differences can affect many aspects of quality, and particularly the relationship between the residual CaCO_3 content and the reactivity to water.

Particle Size. Solid fuels should be of the correct particle size. In some cases they need to have adequate strength. Their coking properties may be critical, as may be the amount of volatile matter. The ash generally contaminates the lime to some degree with silica, iron oxide, and alumina. It may cause bridging between particles, and can also combine with lime dust and with volatile alkalis (sodium and potassium) to form troublesome deposits.

Ash Fusion. The properties of the fuel ash can have a marked effect on the acceptability of the fuel. Key properties include the ash content of the fuel, the ash fusion temperature (which is affected by lime dust and by the concentration of oxygen and carbon monoxide in the atmosphere), and the level of alkalis.

56.5.3.3 Production

Calcination

The chemical reaction for the decomposition of calcium carbonate by heat is:

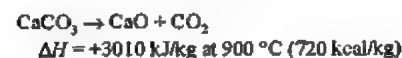


Figure 56.5 shows the variation of the partial pressure of carbon dioxide above calcium carbonate with temperature. The pressure is 101 kPa at ca. 900°C . Thus, although surface calcination can proceed at lower temperatures, complete calcination only occurs above 900°C .

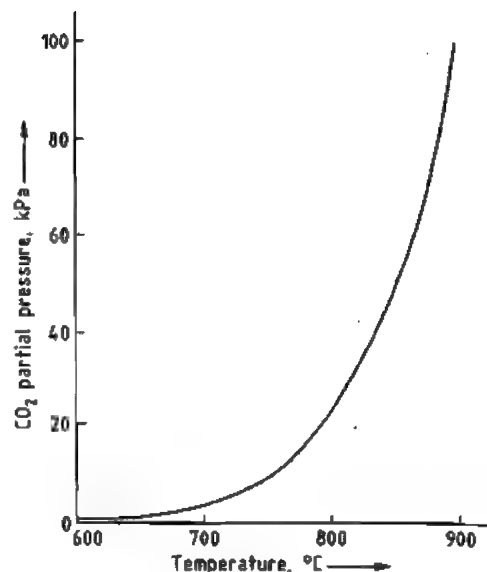


Figure 56.5: Variation of the CO_2 partial pressure above CaCO_3 with temperature.

The calcination mechanism is complex and involves several stages: heat transfer to the surface of the particle and through the outer layer of lime. The heat is absorbed by the chemical reaction at the lime-limestone interface. The carbon dioxide so generated migrates to the surface of the particle counter to the heat flow and then diffuses from the surface into the kiln gases.

The rate-determining stage in the above process depends on the particle size, temperature, amount of calcination that has already taken place, and the composition of the kiln gases. Although attempts have been made to produce a mathematical model to account for observed effects in practical lime burning, none has proved applicable over wide ranges of the above variables.

Figures 56.6 and 56.7 summarize smoothed results for calcining spheres of U.K. carboniferous limestone. Although the results do not apply accurately to the random shapes encountered in practice or to other limestones, they serve as a useful guide to the relative effect of changing residence time or temperature.

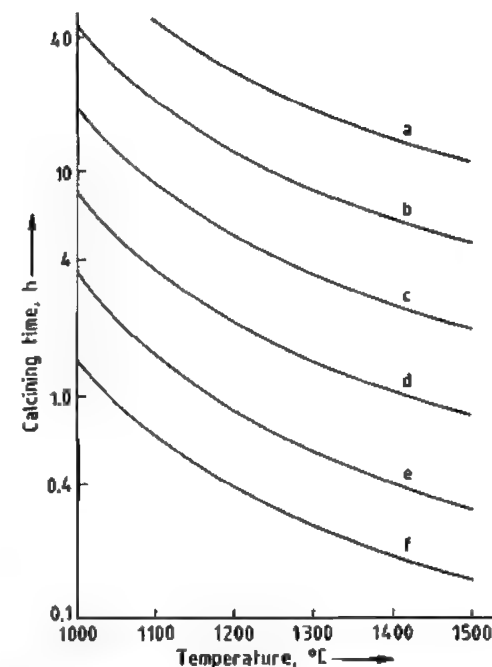


Figure 56.6: Calcining times for spheres of a dense, high-calcium limestone: a) 15 cm; b) 12.5 cm; c) 10 cm; d) 7.5 cm; e) 5 cm; f) 2.5 cm diameter.

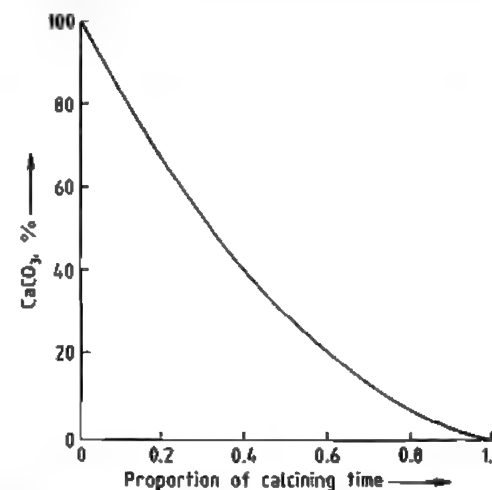


Figure 56.7: Progression of calcination of limestone spheres.

Figure 56.6 shows the marked variation in the time for complete calcination caused by changes in particle size. This is one of the reasons why the size range of stone fed to lime

kilns is generally in the ratio of 2:1. The other reasons are the effects on sintering and on the porosity of the stone bed, which must be sufficiently high to allow rapid gas flow and efficient heat transfer.

When a high-calcium limestone particle is decomposed at low temperature (950°C or below), its external dimensions do not change significantly. Calcination of limestone with 2% porosity theoretically produces quicklime with a porosity of 54%, corresponding to an apparent density of 1.5 g/cm^3 .

Prolonged heating of quicklime above 900°C causes sintering, a reduction in porosity, and an increase in apparent density (see Figure 56.2). This sintering process markedly reduces the reactivity of the quicklime to water (see Figure 56.4).

In lime kilns, variations in heat distribution, temperature, and solids residence time further complicate the calcination process. As a result the quicklime particles discharged from the kiln can be grouped into three categories:

- Particles that are not fully calcined (i.e., with a central CaCO_3 core), the lime layer of which has a low apparent density and a high reactivity to water
- Particles that are just fully calcined and have a low apparent density and a high reactivity to water
- Particles that have sintered to varying degrees and which have an increased apparent density and a reduced reactivity to water

The relative quantities of product in the above categories are influenced by the kiln design. In most kilns, the quicklime is exposed to gas temperatures of $1200\text{--}1300^\circ\text{C}$ just before it enters the cooling zone. Generally, such kilns only produce highly reactive quicklime from high-calcium limestone if the residual CaCO_3 content is relatively high. Some designs complete the calcination at a lower temperature (ca. 1100°C), and produce a highly reactive quicklime with low levels of CaCO_3 . In some kilns, changing the air fuel ratio can affect the characteristics of the quicklime. A low ratio lengthens the flame, and hence the calcining zone, and reduces maximum gas

temperatures. This leads to a higher reactivity for a given CaCO_3 content. It may, however, increase unit heat usage.

If the quicklime is exposed to kiln gases containing carbon dioxide at 600–800 °C, recarbonation occurs. This increases the CaCO_3 level and reduces the active CaO content slightly. The most marked effect, however, is the reduction in the reactivity of the quicklime.

A small amount of recarbonation always occurs in the cooling zone of the kiln as a result of air slaking. The quantities involved are, however, small and the effect on the quality of the quicklime is negligible.

Any magnesium carbonate in the limestone decomposes at ca. 700 °C. Its heat of calcination is lower than that of calcium carbonate. The resulting magnesium oxide does not contribute significantly to the reactivity towards water.

Lime Kilns

Early lime kilns were constructed of stone and were generally built into the side of a hill [16]. An amount of fuel, originally wood, was placed on a hearth at the base of the kiln. Large stones were placed above the fuel, followed by layers of increasingly smaller stone. The fuel was then lit and allowed to burn for a few days. After the fire had burned out and the lime had cooled, the kiln was drawn-down by hand from the hearth. The product often contained substantial amounts of both over- and under-burned lumps, and the thermal efficiencies were very low.

It was then recognized that a continuously operating lime kiln would be more productive and more thermally efficient. For the purpose of heat transfer, a kiln should be regarded as consisting of three zones (Figure 56.8).

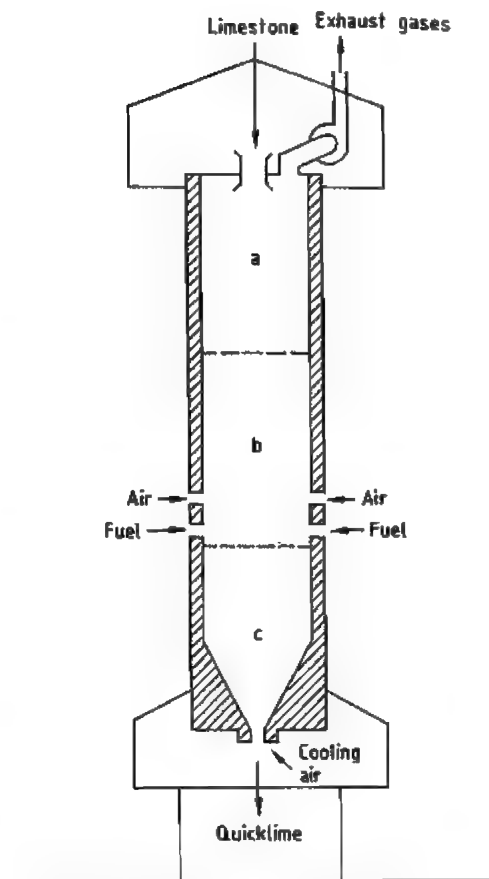


Figure 56.8: Schematic of a vertical shaft kiln: a) Preheating zone; b) Calcining zone; c) Cooling zone.

In the pre-heating zone, limestone is heated from ambient temperature to over 800 °C by the heat of the gases emerging from the calcining zone. In the calcining zone, the calcium carbonate is decomposed into calcium oxide, thereby absorbing some of the heat of combustion produced by burning the fuel and preheated air. In the cooling zone, quicklime is cooled by part or all of the combustion air, which in turn is preheated.

Subsequently, vertical shaft, mixed-feed kilns were developed in which layers of stone were alternated with layers of fuel (initially wood or coal). Calcined quicklime was drawn from the base of the kiln and further layers of fuel and stone were charged into the top of the

kiln. The thermal efficiencies of these designs were better than those of the earlier kilns, but were still poor, owing to the incomplete combustion of the volatile matter. Use of coke overcame this problem and high thermal efficiencies were obtained. A large number of shaft kilns were developed [16]. Kiln outputs were often increased by the use of fans to increase the gas and air flows.

Most of the kilns in current use are based on either the vertical shaft or on the rotary design. There are a few other kilns based on different principles. All of these designs incorporate the concept of the three zones. In some kilns, they are incorporated into one unit, in others they exist as separate units (Figure 56.13).

Vertical Shaft Designs. Figure 56.8 shows a schematic of a vertical shaft kiln. The major problem with shaft kilns is obtaining uniform heat release across the shaft. Fuel injected at a wall usually does not penetrate more than 1 m into a packed bed. This limits the kiln width (or diameter) to 2 m. Increased fuel penetration can be achieved in larger shafts by:

- use of the mixed feed technique,
- use of central burners or lances,
- injecting the fuel via tuyères which penetrate ca. 1 m into the kiln,
- injection of the fuel underneath arches, or
- injection of air or recycled kiln gas above the fuel.

In general, vertical shaft kilns have relatively low heat usages because of efficient heat transfer between the gases and the packed bed. However, they retain most of the sulfur in the fuel so that low-sulfur quicklime can only be produced if a low-sulfur (and generally expensive) fuel is used to calcine a low-sulfur stone. Older designs tend to produce quicklime with a low to moderate reactivity and a relatively high CaCO_3 content. Modern designs incorporate features which enable highly reactive lime to be produced with low CaCO_3 levels. The four designs which are used extensively throughout the world are described below.

Mixed-Feed Shaft Kiln. Modern mixed-feed kilns use limestone with a top size in the range 5 to 15 cm and a size ratio of ca. 2:1. The most widely used fuel is a dense grade of coke with low reactivity and low ash content. The coke size is only slightly smaller than that of the stone so that it moves with it rather than trickling through the interstices. The stone and coke are mixed together and are charged into the kiln in such a way as to minimize segregation.

The net heat usage can be very low at ca. 3560 kJ/kg (850 kcal/kg). This advantage is offset by the high cost of coke compared to competitive fuels. Another advantage of the mixed-feed shaft kiln is that it produces kiln gas with a very high CO_2 content. For processes which can use both the quicklime and the CO_2 (e.g., the precipitated calcium carbonate process, the Solvay process, and the sugar beet process), this is an important factor in the overall economics.

The quality of the quicklime tends to be moderate, with the reactivity being considerably lower than that obtained by rotary kilns at the same CaCO_3 level. This, however, can be an advantage for certain uses. The retention of sulfur from the fuel is high.

Double-Inclined Shaft Kiln. In the double-inclined kilns (Figure 56.9), the stone moves downwards under gravity past an upper and then a lower hearth, both of which are inclined at about 60°. Opposite each hearth are burners mounted underneath arches. The products of combustion and calcination travel upwards through the stone and are removed by an exhaust fan. Most of the combustion air is drawn through the cooling zone.

These kilns accept stone with a top size as low as 2 cm and as large as 10 cm. They produce a reactive, low-carbonate quicklime at a net heat usage of about 4600 kJ/kg (1100 kcal/kg). Although various fuels can be used, they should be selected to avoid excessive build-ups caused by fuel ash and calcium sulfate deposits.

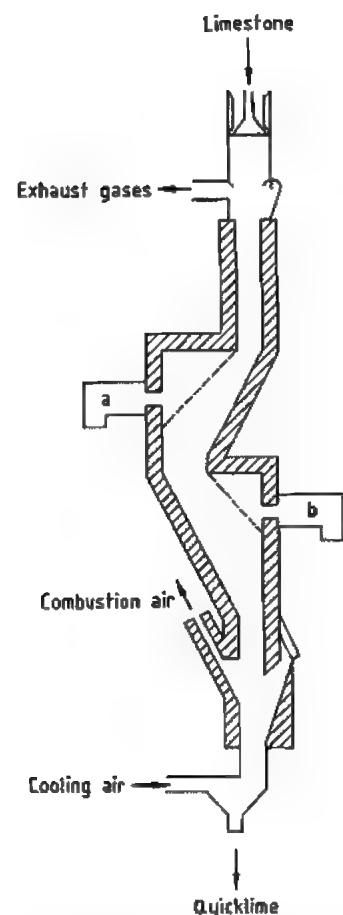


Figure 56.9: Schematic of a double-inclined shaft kiln: a) Upper burners; b) Lower burners.

Annular Shaft Kiln. The major feature of the annular shaft kiln (Figure 56.10) is a central cylinder which restricts the width of the annulus, and ensures good heat distribution. The central column also enables part of the combustion gases from the lower burners to be drawn down the shaft and to be injected back into the lower burner chamber. This recycle moderates the temperature at the lower burners and ensures that the final stages of calcination occur at low temperature. Both effects help to manufacture a product with a low CaCO_3 level and high reactivity.

The annular shaft kiln accepts stone with a top size of 5–11 cm. Use of a heat recuperator,

in which 30% of the kiln gases are used to pre-heat part of the combustion air, reduces the net heat usage to about 4180 kJ/kg (1000 kcal/kg). The kiln can be fired by gas, oil, or solid fuel.

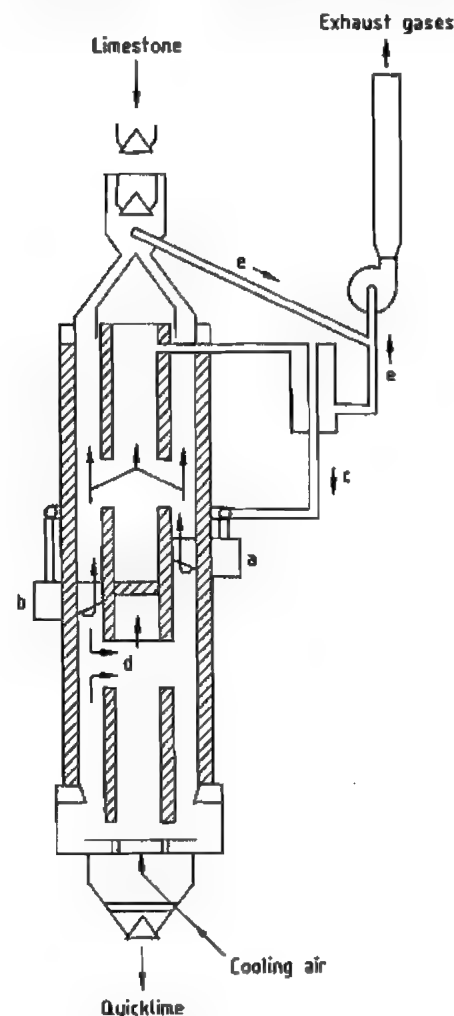


Figure 56.10: Schematic of an annular shaft kiln: a) Upper burners; b) Lower burners; c) Combustion air to upper burners; d) Combustion air to lower burners; e) Kiln gases.

Parallel-Flow Regenerative Kiln. The parallel-flow regenerative (or Maerz) kiln (Figures 56.11 and 56.12) consists of two or three interconnected vertical shafts. The following description relates to the two-shafted design.

The operation consists of two equal stages, which last about 12 min.

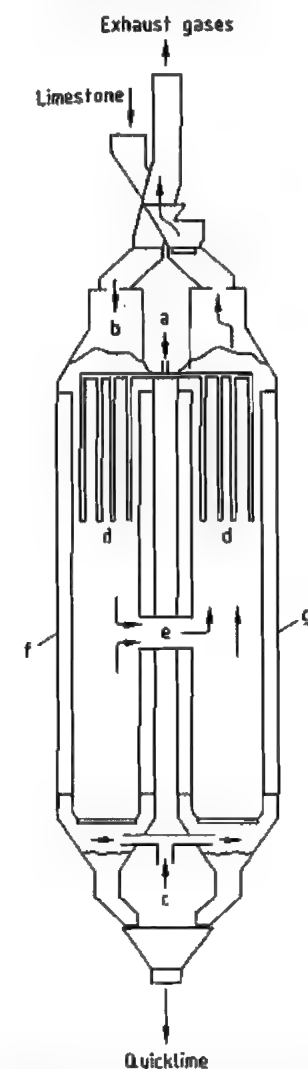


Figure 56.11: Schematic of a parallel-flow regenerative kiln: a) Fuel; b) Combustion air; c) Cooling air; d) Lances; e) Cross-duct; f) Shaft 1; g) Shaft 2.

In the first stage, fuel is injected through lances into shaft 1 and burns with combustion air blown down the shaft. The heat released is partly absorbed by calcining the limestone in shaft 1. Air is blown into the base of each shaft to cool the lime. The air in shaft 1 mixes with the combustion gases, including the carbon di-

oxide from calcination. The mixture passes through the cross-duct into shaft 2, at about 1050 °C. In shaft 2, the gases from shaft 1 mix with the cooling air blown into shaft 2 and pass upwards. In so doing, they heat the stone in the pre-heating zone of that shaft.

Figure 56.12: Two 300 t/d parallel-flow regenerative kilns.

During the second stage of the operation, the converse applies. The same amounts of fuel and combustion air are added to shaft 2. The combustion gases plus cooling air pass upwards in shaft 1, heating the stone in the pre-heating zone of that shaft.

The two key principles of the above operation are:

- The stone-packed preheating zone in each shaft acts as a regenerative heat exchanger in addition to pre-heating the stone to calcining temperature. The surplus heat in the gases is transferred to the stone in shaft 2 during the first stage. It is then transferred from the stone to the combustion air in the second stage. As a result, the combustion air is preheated to about 800 °C. The net heat

usage of the kiln is very low at below 3770 kJ/kg (900 kcal/kg) of quicklime.

- The calcination of the quicklime is completed at the level of the cross-duct at a moderate temperature of about 1100 °C. This favors the production of a highly reactive quicklime, which may, if required, be produced with a low CaCO_3 content. The kiln accepts stone with a top size of 5–12 cm, and it can be fired with gas, oil, or solid fuel.

Rotary Kilns. There are many designs and variants of the rotary kiln (Figure 56.13). Most use a feedstone with a top size in the range 1 to 6 cm. They operate well on gaseous, liquid, or solid fuels.

Heat usages for rotary kilns are generally much higher than those of shaft kilns and their capital costs tend to be higher. These adverse factors are often offset by their ability to produce a high-quality quicklime with lower CaCO_3 and sulfur levels and high reactivity, when fired by less expensive fuels.

In the earliest rotary kilns, stone was charged into the elevated end of the rotating section (generally inclined at about 4°). It was preheated by the gases drawn from the calcining zone at the other end of the kiln, and then calcined as it moved towards and under the

flame. The hot lime was then discharged into a pit to cool.

In later designs, the thermal efficiency of the rotary kiln is improved by:

- fitting lime coolers which preheat the combustion air,
- fitting raised sections of refractory (i.e., dams or mixers) in the calcining zone to improve heat transfer,
- installing refractory trefoils, metal lifters, or similar devices in the pre-heating zone of the rotating section, or
- using a stone pre-heater, followed by a shorter rotary section.

Net heat usages of rotary kilns range from over 8370 kJ/kg (2000 kcal/kg) for the simplest gas-fired units, to about 5020 kJ/kg (1200 kcal/kg) for the more complex coal-fired installations.

One complication often associated with rotary kilns is the build-up of "rings" on the refractory material in the rotary section. They are produced by the combination of lime dust with clay, ash (if present), and sodium and potassium salts. They can be particularly troublesome in kilns fitted with preheaters and in coal-fired kilns. In the latter case, fine grinding of a well selected coal generally minimizes ring formation.

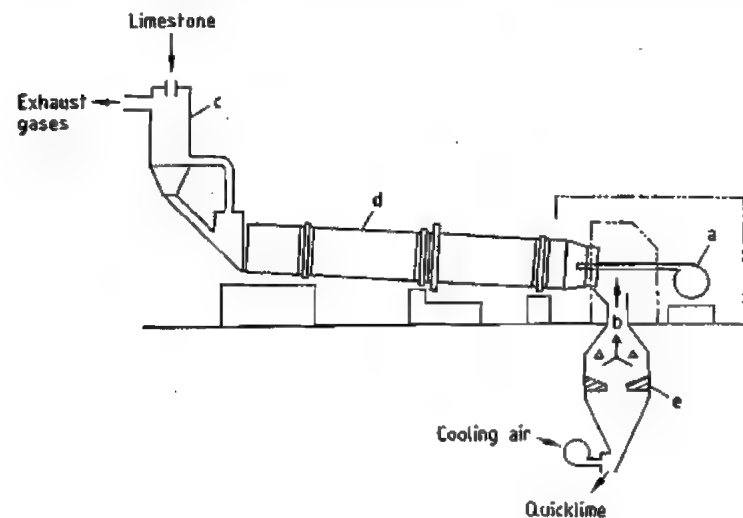


Figure 56.13: Schematic of a rotary kiln: a) Burner; b) Combustion air; c) Preheater; d) Kiln; e) Cooler.

A particular advantage of rotary kilns without preheaters is that it is possible to eliminate most of the sulfur introduced with the fuel. This enables low-sulfur lime to be made with cheaper, high-sulfur fuels. Use of a preheater increases the contact between the combustion gases and the partially calcined stone, increases the absorption of sulfur dioxide, and reduces the ability to eliminate sulfur. Calcium sulfate build-ups in the kiln or in the preheater can be troublesome.

Many lime producers have found that rotary kilns complement shaft kilns, because they use a smaller feedstone and produce quicklimes with different characteristics, which meet the requirements of certain customers.

Other Kilns. Various designs of lime kilns have been developed, based on the technology used in modern cement kilns. These accept small sizes of stone, e.g., below 0.6 cm, and carry out the calcination in fluidized beds or in a high-temperature gas stream by means of refractory-lined cyclones. They have not, as yet, proved to be viable.

The rotary hearth, or Calcimatic, kiln challenged the rotary kilns in the late 1960s and early 1970s, but generally failed to match them as they became more sophisticated and more economical.

Dolomite Kilns. Dolomite is calcined in both shaft and rotary kilns. The principles of making lightly burned dolomite are similar to those of making quicklime. Heat usages are lower owing to the lower heat of calcination and the lower calcination temperature of MgCO_3 .

Dead-burned dolomite for brick making is generally produced in mixed-feed, coke-fired shaft kilns and in coal-fired rotary kilns, at temperatures of about 1800 °C, to give a density of 3.2 g/cm³. It should be low in iron content.

When dolomite is used for fettling purposes to protect the refractory lining of steelmaking vessels, 5–10% of iron oxide may be added and the product is sintered at 1400–1600 °C [6, 17].

Quicklime Processing

The major demand is for the screened grades of quicklime in the range 4 to 0.6 cm. To obtain the maximum yield of those sizes, particularly from shaft kilns, it is generally necessary to crush the lime. Roll crushers are often used because they minimize formation of fines. Surplus grades (generally <0.6 cm) are often used as feed for the production of hydrated lime or ground quicklime.

The production of finely ground quicklime has expanded markedly in recent years. As various grades are required, ranging from 30 to over 99% passing 75 µm, they are generally produced in mills fitted with a variable speed classifier which returns coarse particles to the mill and controls the fineness of the finished product.

56.5.3.4 Uses and Specifications

Iron and Steel. A small amount of lime is used in the production of iron ore agglomerates from fines. The main advantage of adding 1 to 6% of quicklime to the ore is a marked increase in the production capacity of the sinter strand. Ground quicklime is also used for the desulfurization of iron in the ladle before charging into the steelmaking furnace.

The major use of quicklime, however, is in the Basic Oxygen Steelmaking Process. Its usage varies from about 35 to 70 kg/t of steel. The quicklime neutralizes the acidic oxides, SiO_2 , Al_2O_3 , and Fe_2O_3 , to produce a basic molten slag. Correct formation of the slag is essential for the refining process.

A typical U.K. specification for steelmaking-quality quicklime is given in Table 56.5. The CaCO_3 content is limited to avoid excessive cooling of the melt through its decomposition to quicklime. The specifications for SiO_2 content and neutralizing value ensure that the quicklime has a high effective CaO content (1% of SiO_2 neutralizes about 2.8% of CaO). The grading and reactivity requirements ensure that the quicklime has an adequate surface area and reacts rapidly to

produce the slag without excessive loss of fines from the vessel.

Table 56.5: Quicklime specification for BOS steelmaking.

Specification	Criterion	Value
Sulfur	max. average	0.03%
	maximum	0.05%
Neutralizing value (CaO)	min. average	95.0%
	at least 95% greater than	93.0%
Silica (SiO ₂)	max. average	1.0%
	maximum	1.5%
Loss on ignition due to CO ₂	max. average	2.0%
	at least 95% less than maximum	2.5%
Reactivity (BS 6463)	minimum	46 °C
Grading	nominal top size	38 mm
	nominal bottom size	5 mm
	max. amount passing 3 mm	10%

Further information on the role of quicklime and the slag in removing phosphorus and sulfur from steel is given in the literature [18].

Calcined dolomite is also added to the BOS vessel to give about 6% MgO in the slag, thereby reducing slag viscosity and attack of the basic refractory lining.

The electric arc steelmaking process uses quicklime to react with acidic oxides and produce a molten slag. The specification is similar to that for the BOS process.

Quicklime is also used in the argon oxygen decarburization process, for which a -1.5 +0.6 cm product is required with less than 0.15% C and 0.04% S.

Calcium carbide is produced by reacting quicklime [19] with coke in furnaces which are heated electrically to 2000 °C. It is used to produce acetylene by reaction with water. The by-product is an impure form of hydrated lime.

Aerated Concrete. Ground quicklime is used in the production of aerated concrete blocks, with densities of ca. 0.7 g/cm³. The quicklime is mixed with an active form of silicon (either ground silica sand or pulverized fuel ash), sand, water, aluminum powder and, depending on the quicklime quality, cement. The reaction of quicklime with aluminum powder generates hydrogen bubbles which cause the "cake"

to rise. At the same time the quicklime reacts with the water, generating heat and causing the cake to set. Close control of the process results in a green set, which enables the cake to be removed from the mold and cut into blocks before autoclaving at elevated temperature and pressure.

The key aspect of the quicklime specification for this use is consistent reactivity (which includes a measure of the total free lime content). The product should have at least 90% less than 75 µm and its MgO content should be less than 2%.

Soil Stabilization. Quicklime and hydrated lime can considerably increase the load carrying capacity of clay-containing soils. They do this by reacting with finely divided silica and alumina to produce calcium silicates and aluminates, which possess cementing properties.

Quicklime has the advantage over hydrated lime of drying out the soil. It does this by absorbing 30% of its own weight of moisture and also by generating heat which accelerates evaporation.

Soil stabilization is used in road and rail construction to strengthen subgrades, thereby reducing construction depths. It may also be used to produce a sub-base in place of aggregate. It is used on clay-rich construction sites for placement and compaction of on-site material. In some countries lime piling is used to pin unstable soils and to provide support for building slabs.

The U.K. specification for quicklime used in soil stabilization is given in a Department of Transport publication [20].

Other Uses. Small quantities of quicklime are used in other processes [6], e.g., the production of glass, calcium aluminate cement, and organic chemicals. About 50% of the total production, however, is converted to calcium hydroxide before use.

Specifications. Because of the dominance of steelmaking customers, most of the quicklime is produced to meet their chemical requirements. High reactivity is an advantage in soil stabilization. Consistent reactivity is essential

in the aerated concrete process. The particle size requirements often depend on the customers' handling, conveying, and blending systems.

56.5.4 Hydrated and Slaked Lime

56.5.4.1 Physical and Chemical Properties

Color. Most hydrated limes are white. High levels of impurity can result in a gray or buff color.

Density. High-calcium hydrated lime has a density of about 2.3 g/cm³. The values for partially and fully hydrated dolomitic lime are about 2.7 and 2.5 g/cm³, respectively.

Bulk Density. The compacted bulk density is in the range 550 to 650 kg/m³. In the as-poured state, it can be as low as 350 kg/m³, owing to air entrainment.

Specific surface area may be measured by air permeability [12], or by surface absorption of nitrogen (BET surface area). The former method generally gives areas of 1000–2000 m²/kg; the latter gives results which are some 20 to 30 times greater.

Angle of Repose. In the fluidized state, the angle of repose is 0°. In the compacted state, and particularly with 1% or more of excess water, the angle of repose can be over 80°. With bunker aeration, valley angles of 70° have proved to be satisfactory.

Hardness. This is between 2 and 3 Mohs.

Specific Heat. The specific heat of calcium hydroxide rises from 1130 J/kg⁻¹K⁻¹ at 0 °C to 1550 J/kg⁻¹K⁻¹ at 400 °C [21]. That of dolomitic hydrate is believed to be about 5% higher [6].

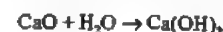
Solubility. This decreases from about 1.85 g Ca(OH)₂/L water at 0 °C to 0.71 g/L at 100 °C for commercial calcium hydroxide, depending on impurity levels [22].

Some inorganic compounds affect the solubility [23]. Calcium sulfate is of particular interest; a 2 g/L solution reduces the solubility to

0.06 g Ca(OH)₂/L. Organic compounds can increase the "solubility" of calcium hydroxide. Sugar has the greatest effect, as a result of the formation of calcium saccharate [23].

Magnesium hydroxide is only sparingly soluble in water (ca. 0.01 g/L) [24].

Carbon Dioxide. Calcium hydroxide reacts readily with carbon dioxide in the absence of water at temperatures below its dissociation point (ca. 540 °C). The reaction of quicklime with carbon dioxide below 300 °C only proceeds in the presence of some water vapor via formation of calcium hydroxide.



Acid Neutralization. Hydrated lime, whether Ca(OH)₂, Ca(OH)₂·MgO, or Ca(OH)₂·Mg(OH)₂, reacts readily with acids and acidic gases. The rate of reaction depends in part on the particle size of the hydrated lime.

Silica and Alumina. Hydrated lime reacts with pozzolans (materials containing reactive silica and alumina) in the presence of water to produce hydrated calcium silicates and aluminates. The reactions may take months to proceed to completion at ambient temperatures (e.g., in mortars and soil stabilization), but proceed within hours at elevated temperature and water vapor pressures (e.g., at 180 °C and a steam pressure of 1 MPa). This pozzolanic reaction is the basis of the strength generated by hydraulic quicklime.

pH. Because calcium hydroxide is a strong base, a concentration of 0.1 g Ca(OH)₂/L gives a pH of about 11.3 at 25 °C. A saturated solution at 25 °C, containing 1.8 g/L, gives a pH of 12.45. Magnesium hydroxide gives a pH of about 10.5, owing to its lower solubility. The pH of dolomitic hydrate is dominated by its Ca(OH)₂ content and is similar to that of calcium hydroxide.

Thermal Dissociation. Calcium hydroxide decomposes at about 540 °C to quicklime and water. The quicklime so produced has an exceptionally high reactivity to water.

Causticization. Hydrated lime reacts with soluble metal carbonates to produce insoluble calcium carbonate and the metal hydroxide. This reaction is used to produce caustic soda (see Section 56.5.4.4).

56.5.4.2 Raw Materials

Raw Materials For Dry Hydrated Lime

Dry hydrated lime can be produced from any quicklime. In commercial practice, however, the quicklime quality should be within well-defined limits to enable the processing plant to be selected to produce salable products economically.

Reactivity. The reactivity of the quicklime should be compatible with the characteristics of the plant.

Thus highly reactive quicklime (over 55 °C, BS 6463) tends to produce a water-burned gritty hydrate with a particle size up to 3 mm. The grit is believed to be formed by very rapid hydration on the surface of a quicklime particle, leading to the production of a putty which bakes into a hard layer and holds the particle together. If the plant includes a mill which has the capacity to grind the product to substantially less than 75 µm, such grit does not present any quality problems.

Quicklime of intermediate reactivity (30–55 °C, BS 6463) generally hydrates well, providing it is given adequate residence time in the hydrator.

Quicklime of low reactivity (below 30 °C, BS 6463) also tends to produce a gritty hydrate, unless given a long residence time. This grit consists largely of particles of unreacted solid-burned lime with a coating of hydrate. This must be ground to substantially less than 75 µm and returned to the hydrator if a fully hydrated product is required. Any free lime eventually hydrates and expands. This can cause expansion in, for example, sand-lime bricks, and may result in cracking, surface defects, and unsoundness in, for instance, plaster.

Calcium Carbonate. The permissible CaCO_3 content of the feed quicklime depends on the ability of the plant to reject a fraction rich in CaCO_3 and on the CaCO_3 specification for the finished hydrated lime. In some cases, with a hydrated lime specification of 2% CaCO_3 , feed quicklime CaCO_3 levels of up to 10% can be accepted; in others the level must be below 2.6%. The CaCO_3 is removed by screening or air classification.

Particle Size. The particle size of the quicklime fed to hydrators is generally below 5 cm and sometimes as low as 0.6 cm, depending on the design of the plant.

Magnesium Oxide. As MgO does not hydrate readily, the normal hydration process does not convert it to the hydrate. Providing the MgO content is below about 2%, the consequent unsoundness and expansion potential do not present problems. Higher MgO contents limit the markets into which the hydrated lime can be sold. Quicklimes with high MgO contents are often hydrated in the autoclave process, which produces a fully hydrated product with a high plasticity.

Other Impurities. Some customers place limits on the permissible levels of impurities in hydrated lime, which in turn place constraints on the impurities in the feed lime. These include lead, iron, silicon, and fluorine (see Section 56.5.4.4).

Raw Materials For Slaked Lime

In the slaking process, quicklime is reacted with a controlled excess of water to produce a milk or putty. The quicklime should be of a quality which gives the required quality of milk or putty, and which is compatible with the slaker used.

Reactivity. It is generally necessary to specify the reactivity to match the characteristics of the slaker and to obtain the required physical properties of the milk or putty.

Calcium Carbonate. Although many slakers remove grit rich in CaCO_3 by settling or filtration, their capacity to do so is limited. There-

fore, the CaCO_3 content should also be limited. In other slakers, most or all of the CaCO_3 in the quicklime is included in the slaked lime; its content should be limited according to the acceptable level in the slaked lime.

Particle Size. This is generally determined by the handling and processing equipment. In some cases a –2 cm quicklime is required. In others a ground quicklime is specified.

Magnesium Oxide. In applications where unsoundness or expansion potentials must be low, the MgO content in the quicklime should be below 2%.

Water. The presence of impurities in water can have a marked effect on the reaction of quicklime with water in the reactivity test (see Section 56.5.6). However, water quality does not generally affect the industrial production of slaked lime.

Restrictions on other impurities in the quicklime are as for the production of dry hydrated lime.

56.5.4.3 Production

Normal Hydration Process

The normal hydration process, leading to the production of Type N hydrate, as defined in ASTM specification C-207 [7], is carried out at atmospheric pressure and ca. 100 °C. There are many designs of equipment, the choice of which depends on the reactivity and chemical purity of the quicklime, its particle size, and on the requirements for the finished product.

In a typical plant, the quicklime is mixed rapidly with about twice the stoichiometric amount of water in a premixer and is then passed into the main hydrating vessel, which is agitated and fitted with a weir at the discharge end to give an average solids residence time of 10–15 min.

As the hydration reaction proceeds, part of the water boils off vigorously, producing a partially fluidized bed. Coarse particles of

gritty hydrate or unreacted lime are retained behind the weir, while fine particles of hydrate flow over it. A purge paddle close to the weir prevents excessive build up of coarse particles by lifting them over the weir.

The raw hydrate is then conveyed along one or more tubes, which serve to complete the hydration and evaporate excess water. The hydrate is discharged at about 90 °C and contains less than 1% excess water.

The raw hydrate is fed to an air classifier, in which a recycling air stream removes fine particles into an outer settling chamber and allows coarse particles to fall to the base of the inner feed chamber. The fine particles make up the finished product. The coarse particles may then be rejected as a stream rich in CaCO_3 . Alternatively, they may be milled, with the product being recycled to the hydrator, added to the fines from the air classifier, or reclassified.

The steam generated in the hydrator, together with any air drawn into the process, may be de-dusted in a wet scrubber before discharge to the atmosphere, in which case the milk of lime from the scrubber is fed to the premixer.

Some plants use aging silos to retain damp hydrate at elevated temperature for about 24 h to increase the extent of hydration. They are generally used when the feed quicklime has a low reactivity; with dolomitic hydrate; or when a product with a particularly low expansion potential is required.

Pressure Hydration Process

Type S hydrate, as defined in ASTM specification C-207 [7], is produced by reacting quicklime (generally dolomitic) and water under a steam pressure of ca. 1 MPa and at a temperature of ca. 180 °C. After hydration the product is dried, milled, and air classified.

Slaking

There are many ways of slaking quicklime, ranging from the batch process to sophisticated continuous slakers.

In the batch process, water and quicklime are added as required to maintain the milk at about 90 °C. With reactive quicklime, care should be taken to avoid local overheating which can lead to water-burning and a gritty hydrate. With cold water, this technique produces a viscous suspension with 35–40% solids. Grit arising from uncalcined limestone and from unreacted and water-burned lime settles on the floor of the vessel.

There are various designs of continuous slakers, which produce either milk of lime or lime putty. Some feature automatic grit removal.

Slaking at ca. 90 °C produces the finely divided particles of calcium hydroxide required by most users. If the slaking temperature drops, e.g., to 70 °C, the resulting increase in particle size reduces both the viscosity and reaction rate.

Aging the slaked lime for 30 min generally ensures complete hydration. Aging for a day generally improves the physical properties, e.g., higher viscosity and greater workability.

Some operators achieve the same benefits by subjecting the slaked lime to high shear (e.g., by use of a colloid mill). Milk of lime produced in this way, with dispersing agents, may be stored in unstirred tanks.

56.5.4.4 Uses and Specifications

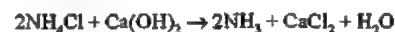
Uses

In this Section, the term hydrated lime is used to describe both dry hydrate and slaked lime, unless otherwise specified.

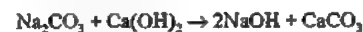
There is little reliable information about the proportion of quicklime which is hydrated before use. The author's estimate for European countries is that it is roughly 50%, of which about one-third is initially converted into dry hydrated lime and two-thirds are initially slaked to give milk of lime or lime putty.

Hydrated lime is used in a large number of processes. The more important ones are described briefly below. More detailed information is available in the literature [6].

The Solvay Process. A key step in the Solvay (or ammonia-soda) process for the production of soda ash and sodium hydrogen carbonate is the recovery of ammonia from an ammonium chloride solution by reaction with milk of lime.



Causticization. Caustic soda is produced by reacting sodium carbonate with milk of lime. Before the development of the electrolytic cell, this was the normal method of production of caustic soda.

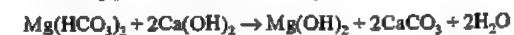


In addition to its use in the Bayer alumina process (see below) this reaction is used for the regeneration of caustic soda in wood pulp plants for the production of kraft or sulfate paper.

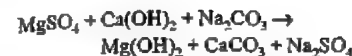
Nonferrous Metallurgy. Hydrated lime is used in the production of alumina by the Bayer process to regenerate sodium hydroxide from sodium carbonate solutions (see above). It is used in flotation processes to beneficiate copper ore and to extract gold and silver. It is an essential chemical for the extraction of uranium from gold slimes and for the recovery of nickel and tungsten after smelting.

Hydrated lime is used in the production of magnesia and magnesium metal. In the seawater processes, a high-calcium hydrate is used to precipitate magnesium hydroxide, while in the Dow natural brine process, dolomitic hydrated lime is used.

Water Treatment. Hydrated lime is used to remove temporary and permanent hardness. Calcium and magnesium hydrogen carbonates react with calcium hydroxide to produce insoluble calcium carbonate and magnesium hydroxide.



Permanent hardness caused by calcium and magnesium chlorides and sulfates can be removed by hydrated lime plus sodium carbonate.



Water can be purified by raising the pH to above 11 for 1–2 d, followed by recarbonation to pH 8–9. In addition to killing bacteria, this treatment removes temporary hardness. Acid water may be neutralized by the addition of lime. Specifications have been published for limes used in the United States for water treatment [19, 25]. A European standard is in preparation.

Sewage Treatment. Treatment of sewage sludge with hydrated lime in conjunction with ferrous sulfate is an effective way of removing solids and phosphorus compounds, and for destroying pathogens. It produces a sludge which dewateres well and can be used as a fertilizer.

Industrial Wastes. Hydrated lime is used widely to neutralize acid wastes and precipitate heavy metals in effluents from a wide range of industries. In some cases it is also used to assist with the clarification process.

Flue Gas Desulfurization. Of the many flue gas desulfurization processes, three use hydrated lime.

In the wet scrubbing process, milk of lime is sprayed through the gases. The product is a suspension of calcium sulfite, which may be oxidized to produce salable gypsum. Up to 95% removal of sulfur dioxide has been reported, with over 90% utilization of the hydrated lime [26].

In the dry scrubbing process, milk of lime is fed into a spray drier in which the product is a dry powder consisting of calcium sulfite and hydrated lime. Up to 85% removal of sulfur dioxide and 40–60% utilization of the hydrated lime have been obtained [26]. Sulfur dioxide may also be removed by injection of dry hydrate either into the boiler, or downstream from the boiler. The reaction products are collected with the fly ash for disposal. Only 50–60% of the sulfur dioxide is removed, and the utilization of normal hydrated lime is less than 40% [26]. Hydrated lime products, with

higher specific surface areas than those of normal hydrate, have been developed for this use.

Sugar Refining. In the refining of sugar beet, the crude solution of sugar is treated with milk of lime to precipitate calcium salts of organic and phosphonic acids. After filtering, the solution is neutralized with carbon dioxide, calcium carbonate is removed by filtration, and a purified sugar solution is produced.

As the process requires a large quantity of both lime (about 250 kg/t of sugar) and carbon dioxide, producers of sugar from beet generally operate their own lime kilns as part of their process.

Because cane sugar is purer, its refinement requires much less hydrated lime (typically 5 kg/t).

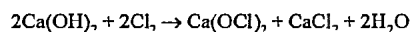
Sand-Lime Bricks. There is a substantial market in Europe for sand lime bricks. These are made by mixing hydrated lime with sand, followed by autoclaving for several hours under a steam pressure of ca. 1 MPa (180 °C). In some processes, it is essential that the hydrated lime is not expansive, because the expansion can occur in the autoclave and result in the production of oversize bricks.

Mortars. Hydrated lime is used in lime cement sand mortars in various proportions. The required compressive strength of the mortar is obtained by adjusting its composition [54]. The lime confers several benefits. It increases the plasticity and water retentivity of the wet mortar and increases the bond strength of the mortar to the masonry. The mortar is more flexible and less prone to cracking.

Soil Stabilization. Both dry hydrated lime and milk of lime are used in soil stabilization. Dry hydrate disperses readily when making a soil tilth. Milk of lime has advantages when the soil is dry; it can also be injected under pressure.

Agriculture. The advantages of adjusting soil pH with limestone are described in Section 56.5.2.4. Hydrated lime has the additional advantage of being quick acting.

Bleaching. Chlorine is reacted with hydrated lime to produce a powdered mixture of calcium hypochlorite and calcium chloride, commonly known as bleaching powder.



Calcium hypochlorite solution is used in bleaching wood pulp.

Precipitated calcium carbonate (PCC) is produced by blowing gases containing carbon dioxide through milk of lime. By controlling the conditions, a very finely divided calcium carbonate with a high reflexivity and a median particle size of 0.02–0.2 μm is produced. Some PCCs are coated with compounds which facilitate their blending with organic substances (e.g., plastics and rubber).

Inorganic Salts and Bases. Hydrated lime is used in the production of mono-, di-, and tri-calcium phosphates as well as other calcium salts. It is used in the Solvay process to produce calcium chloride as a by-product. Lithium and barium hydroxides are made by causticization.

The brine purification process uses sodium carbonate and milk of lime to remove dissolved calcium and magnesium.

Other Uses. There are a wide range of other uses such as the production of calcium silicate insulation products, plasters, lubricants, pigments, soda lime, organic compounds and calcium salts. Hydrated lime is also used in the petroleum industry, glass manufacture, solid waste disposal, and leather tanning [6].

Specifications

In many countries, the most widely recognized specifications for dry hydrated lime relate to its use in building [7, 13, 27, 48]. These set minimum values for fineness, neutralizing value, and other properties. In practice, most dry hydrated limes meet these requirements with ease. A typical quality specification is given in Table 56.6.

Table 56.6: Typical specification for high-calcium hydrated lime.

Specification	Criterion	Value
Carbon dioxide	maximum	6% ^a
Acid insoluble matter	maximum	1% ^a
CaO + MgO	minimum	65% ^a
MgO	maximum	4% ^a
Residue on 200 μm	maximum	2% ^a
90 μm	maximum	7% ^a
Soundness expansion	maximum	20 mm ^a
pat test	pops or pits	nil
Excess moisture	maximum	1%

^a As required by BS 890 (1995).

Some end uses require especially low levels of impurities such as silica, iron oxide, magnesium oxide, and fluoride. Others require uniform surface areas.

Dry hydrated lime for use in the production of sand lime bricks should have an expansion below 1.0 cm [27] and less than 4% MgO (unless it is Type S).

56.5.5 Environmental Protection

Standards. The emission of dust from stone processing, lime kilns, and solids handling is often the major environmental problem associated with the production of lime and limestone products.

In many countries, emissions of dust to the atmosphere are limited to below 50 mg of solids per cubic meter (at 0 °C and 101 MPa) of exhaust gas or air.

In the United Kingdom, the Pollution Inspectorate gives practical advice on control methods for all aspects of limestone processing and the production of quicklime and hydrated lime [28, 29].

Equipment. A variety of techniques are used to control dust emissions from stone processing operations. Dust suppression, which uses water with a wetting agent to cause dust to adhere to larger particles, can be an effective and inexpensive method. It may, however, cause undesirable surface contamination of screened products with fines and increase downstream dust problems.

As the effluent gases from stone processing and local exhaust ventilation systems are generally at relatively low temperatures, bag filters or high-energy wet scrubbers are widely used. The dust collected by bag filters can often be sold as a filler for concrete production.

The temperature of the effluent gases from lime kilns is commonly 200–400 °C. In the past, high efficiency multi-cyclones were widely used to collect the dust. They had the advantage of being relatively inexpensive to install and operate. However, their efficiency is generally no longer adequate in the context of current emission requirements.

Electrostatic precipitators can handle gases at the above temperatures. Although their capital cost is high, their operating costs are moderate.

Gravel bed filters can be operated at high temperatures. They are efficient but have higher capital and operating costs than electrostatic precipitators. Consequently, they are not widely used.

Bag filters are widely used when the gas temperatures are below 200 °C. They are lower in capital cost than precipitators, have a high collection efficiency, but have high operating costs. The reverse-jet method of cleaning the bags has generally been found to be the most effective.

The dust collected from lime kilns is generally high in CaCO_3 but is contaminated with quicklime and possibly fuel ash. It is usually tipped.

Wet collectors are not widely used with quicklime. They are, however, generally the preferred method of controlling dust from hydrating plants. The collected milk of lime is fed back to the process.

Dust collection from the handling, storage and loading of quicklime and hydrated lime generally involves bag filters. The collected dust usually has a high lime content and is sold.

56.5.6 Physical Testing and Chemical Analysis

56.5.6.1 Sampling and Sample Preparation

The most common cause of disagreement between laboratories arises from the failure to obtain representative samples. Sampling solids, and particularly granular solids made from naturally occurring minerals, is especially difficult. The problem is compounded when, as in the case of quicklime, the quality of the sample is affected by exposure to the atmosphere. In general, if quicklime contains 1% or more of combined water, it has not been correctly handled, and its reactivity to water will have been reduced.

Guidance on the sampling of limestone, quicklime, and hydrated lime is given in BS 6463, Part 1 [12]. Similar advice is given in ASTM D 75 for limestone and in ASTM C 110 and C 50 for lime products [14, 30, 31]. The sampling of aggregate and the reproducibility and repeatability of test results is described in BS 812, Parts 1, 101, and 102 [32].

Samples should be taken from a falling stream whenever possible. Precautions should be taken to ensure that segregation within the stream does not lead to bias. Samples may also be taken from conveyor belts; precautions are required to obtain a representative sample. It is very difficult to obtain a representative sample from the body of a truck or from a stockpile. Careful checks should therefore be made to establish whether the sampling method is valid.

Each sample should consist of not less than 10 increments. Each increment should be of an adequate volume (e.g., 10 L for lumps with a maximum size of 10 cm, decreasing to 2 L for a maximum size of 1 cm, and to 1 L for powders). There are many mechanical aids to sampling ranging from augers to automatic samplers [33].

Some physical tests are performed on the sample as taken. For other physical tests and for chemical analysis, it is necessary to crush,

subdivide and pulverize the product to less than 300 μm . This should be done on a separate sample from that used for the physical tests, and in such a way as to avoid bias and, in the case of quicklime and hydrated lime, to avoid excessive exposure to the atmosphere.

All quicklime and hydrated lime samples should be stored in well sealed containers or bags. It is good practice to double-wrap samples which are to be stored for prolonged periods. Quicklime should not be stored in a desiccator because it removes water from some commonly used desiccants.

56.5.6.2 Physical Testing

Limestone. In the United Kingdom, limestone is generally processed to meet either BS 882 (Aggregates from Natural Sources for Concrete) [34] or to BS 63, Part 1 (Road Aggregates) [35]. The latter is generally referred to in specifications for drainage material and for feed for tarmac coating plants. Most of the physical tests are described in BS 812, Parts 1–4 [32].

The susceptibility of crushed stone to frost damage may be tested using a Road Research Laboratory method [36]. With regard to resistance to the alkali silica reaction, the cause of so-called concrete cancer, limestone is generally regarded as being inert. Requirements for coated macadam are given in BS 4987 [37], which includes their composition, manufacture, testing, and transport. Corresponding U.S. methods are available [6].

Quicklime and Hydrated Lime. Physical test methods for quicklime and hydrated lime are given in BS 6463 [12]. The corresponding U.S. standard is ASTM C 110 [14]. Test methods for building limes are given in European standard DD ENV 459-1 [48].

56.5.6.3 Chemical Analysis

The methods for chemical analysis of limestone, quicklime, and hydrated lime are closely related and are described in BS 6463, Part 2. The corresponding U.S. standard is

ASTM C 25 [38]; DIN 1060, Part 2 [13] relates to building limes.

Increasingly, test methods using atomic spectrometry are being used for the analysis of minor components and trace elements, e.g., [49, 50].

56.5.7 Storage and Transportation

Limestone. Screened sizes of limestone are stored in bunkers and in outside stockpiles. Fine grades are generally stored in sealed bunkers.

As most screened limestone is distributed to a large number of sites, generally within 40–80 km of the quarry, it is mainly transported in sheeted tipper road vehicles. Use of rail or water transport becomes more economic as the volume of business to a given site increases and as the distance becomes greater. It has been estimated that over 75% of limestone is transported by road [6]. Fine grades of limestone are transported by air pressure discharge vehicles, generally by road, but suitable railroad cars are also available.

Quicklime. Quicklime is stored in enclosed bunkers with well-sealed discharge mechanisms to minimise the reaction with atmospheric water and carbon dioxide and to control dust emission. Storage capacities equivalent to 2 to 5 days' production are usually necessary.

Screened grades of quicklime (generally 0.5 cm and above) may be transported in tipper trucks. Effective sheeting is essential to minimize atmospheric attack on the quicklime and to control dust emission. Air pressure discharge vehicles are used to transport fine grades of quicklime (below 0.5 cm) and, increasingly, screened grades up to 2 cm. Where appropriate, use of rail or water transport can extend the economic delivery distance.

A small amount of quicklime is packaged. Plastic containers and sacks are used for amounts up to 50 kg. Intermediate bulk containers, both rigid and flexible, are being used increasingly for quantities up to 1 t. There is a

small international market for packaged quicklime.

Where totally enclosed bunkers cannot be provided, quicklime should be stored on a concrete base, preferably in a separate bay within a building. It should be used as soon as possible after delivery. It can be kept longer by covering the pile with a close-fitting impermeable sheet. Open reception hoppers should be protected from the elements.

Contact of quicklime with flammable materials should be avoided, especially when there is a risk of water penetration. The heat of hydration has been known to cause fires.

Further details on the delivery, storage and handling of quicklime are often available from the supplier, for example [39].

Hydrated Lime. Hydrated lime is stored in enclosed silos to minimize reaction with atmospheric carbon dioxide and to control dust emissions.

Most hydrated lime is transported in air pressure discharge vehicles, both by road and rail. A substantial amount, however, is sold in paper sacks (generally 25 kg in the United Kingdom). Use of intermediate bulk containers holding up to 1 t is increasing. There is a significant international market for packaged hydrate.

The flow characteristics of hydrated lime are very variable. The angle of repose varies from 0–80° according to the amounts of entrained air and excess water, and other factors. Silos may need to be fitted with devices to cope with bridging of the powder above discharge points and to encourage flow (e.g., bin activators and air pads).

Hydrated lime in paper sacks is generally placed on pallets and stored under cover. By fitting impermeable slip sheets under the bags and shrink wrapping a cover over the loaded pallet, it may be stored out of doors for several months.

Further details on the delivery, storage and handling of hydrated lime are often available from the supplier, for example [40].

56.5.8 Economic Aspects

Statistics on the production of limestone are not widely available and are often complicated by the inclusion of other crushed rock. The United States is probably the largest producer with over 700×10^6 t/a. Russia is believed to produce ca. 500×10^6 t/a, and Japan 200×10^6 t/a. Production in the United Kingdom is about 120×10^6 t/a.

The major uses of limestone (including chalk) in the United Kingdom and United States are compared in Table 56.7 [41, 51].

The quantities of dense, high-calcium limestone, dolomite, and chalk consumed in the United Kingdom by the main user industries are given in Table 56.8 [42].

The ex-works price for construction stone in the United Kingdom is in the range £1–5/t (1996). Chemical quality limestone for lime burning and glass manufacture commands higher ex-works prices.

Ground limestone products, often known as whiting, can command prices of £20–200/t, depending on grading and quality. Precipitated calcium carbonate is a specialist chemical which sells for £200–1000/t (1996).

Table 56.7: Main uses of limestone.

Use	Market share, %	
	UK (1993)	USA (1987)
Construction (mainly concrete and roadstone)	79	75
Cement	8	10
Lime (including dead-burned dolomite)	4	4
Agriculture	2	5
Flux stone (mainly for iron production)	2	3
Other	5	3

Table 56.8: Consumption of limestone, in the United Kingdom (1986).

1	Dense, high-calcium limestone, 10^6 t/a	Dolomite, 10^6 t/a	Chalk, 10^6 t/a	Total, 10^6 t/a
Construction	65.9	12.7	0.9	79.5
Cement	9.1	0	9.6	18.7
Agriculture	1.3	1.2	0.6	3.1
Iron, steel, chemical and other uses	4.9	1.7	1.0	7.6
Total	81.2	15.6	12.1	108.9

Table 56.9: Estimated world quicklime production, 1994.

Country	Production, 10 ⁶ t/a
Former Soviet Union	20.0
China	19.5
United States	17.1
Japan	10.5
Germany	6.6
Brazil	5.7
Italy	4.4
Mexico	4.0
Romania	3.0
France	2.2
Belgium	2.1
United Kingdom	1.3
Others	23.2
Total	122.2

Table 56.10: Main uses of quicklime.

Use	Percentage of total market				
	United States	Japan	Germany	France	United Kingdom
Steel and iron	41	49	36	55	36
Chemical and industrial	36	27	23	23	34
Construction and roads	7	7	26	9	11
Agricultural	< 1	3	6	9	19
Refractories	5	14	9	4	
Other	11				

The estimated production of quicklime (including hydrated lime) in various countries is given in Table 56.9 [51, 52]. The total is just over 100×10^6 t/a. The major producers are the former Soviet Union, China, United States, and Japan.

Comparison of statistics on uses of quicklime for different countries is complicated by the use of different classifications. Table 56.10 lists information from various sources [17, 41, 42] for five countries. In all five, the iron and steel industry dominates the market. There are a large number of uses in the chemical and construction industries (including building), as well as in general industry.

The ex-works price of lime products in the United Kingdom is generally in the range £30–60/t (1996). Specialist products, which are tailored to the needs of individual markets, generally command higher prices. The prices of ground quicklime and hydrated lime are

typically some 25% higher than screened quicklime and reflect the capital and operating costs of the additional processing stage.

56.5.9 Toxicology and Occupational Health

56.5.9.1 Toxicology

Limestone. Limestone is a practically non-harmful material. It is regarded as a nuisance dust and has a recommended occupational exposure limit of 10 mg/m³ for total, and 5 mg/m³ for respirable dust [43]. These limits are not affected by the presence of crystalline silica at levels below 1%. Lower limits may apply at higher silica levels. The subject is under review.

The dust may irritate the eyes and cause discomfort. It is nonirritant to the skin. Exposure to high levels of dust can cause discomfort as a result of its drying effect on the mouth and upper respiratory tract.

Calcium carbonate is a recognized ingredient of human and animal foodstuffs. It is used as an antacid. The therapeutic dose is 1–5 g. Chronic effects are unlikely to be encountered in industry. There are no occupational diseases known to be connected with the handling of limestone.

Quicklime and Hydrated Lime. The recommended occupational exposure limits for quicklime and hydrated lime (8-h TWA) are 2 mg/m³ and 5 mg/m³, respectively, for total dust [43]. The dusts are irritant to the upper respiratory tract. Gross inhalation may result in inflammation of the respiratory passages, ulceration and perforation of the nasal septum, and possible pneumonitis. With minor exposures, only transitory effects may occur.

Quicklime and hydrated lime in the eye can be very painful and may cause chemical burns which could lead to impairment or total loss of vision if immediate attention is not received. Speed of treatment is essential.

Both products are irritant to the skin and cause chemical burns in the presence of moisture, including perspiration. Prolonged and re-

peated contact may cause the skin to become dry and cracked if proper care is neglected. They may cause dermatitis. Ingestion causes corrosion of, and damage to, the gastrointestinal tract.

56.5.9.2 Occupational Health

Limestone. The quarrying industry in general has a poor safety record. In the United Kingdom, the risk of a fatal accident in quarrying is ca. 17 times greater than that in manufacturing industry [44].

While the use of explosives is generally perceived to be the greatest hazard in quarrying, it causes less than 5% of the deaths and major injuries [45] and is generally well covered by legislation. Dump trucks, mechanical shovels, and other mobile equipment, however, are the cause of over half of the deaths and major injuries. This category includes falls associated with mobile equipment.

In limestone mines, rock falls account for about one-third of deaths and serious injuries, with haulage and transport being the next most significant category [46]. Special electrical precautions (e.g., high integrity earthing and use of low voltage portable tools) are essential as water percolates into most mines.

Stone processing involves a number of mechanical operations. The largest category of injuries caused by these processes generally arises from inadequate guarding of moving machinery and from failure to electrically isolate equipment when carrying out maintenance.

Stone processing generates high noise levels. Measures are required to reduce or contain the noise at source, or to exclude it from work areas. Use of television cameras and monitors can reduce the exposure of operators to high sound levels. Effective personal hearing protection is also required. In dusty areas, suitable respiratory and eye protection equipment should be used.

Quicklime and Hydrated Lime. The lime industry has a lower accident rate than quarry-

ing. Tripping and falling constitute the largest category of accidents [47].

Both quicklime and hydrated lime are dusty, alkaline products. A common injury associated with them is grit or dust in the eye. The use of adequate eye protection in all lime production and handling areas is essential. Eye wash facilities should be provided in all work areas so that the eye can be irrigated immediately.

Skin contact removes the natural oils and causes the skin to become dry. Sweating can result in chemical burns. Porous gloves protect the skin and reduce the risk of sweating. Use of skin cream after exposure helps to moisturize the skin.

Milk of lime, if splashed, presents a serious hazard to the eyes and skin. Use of suitable goggles, gloves and protective clothing is recommended.

Lime processing involves a number of mechanical operations. Adequate guarding of moving machinery and effective electrical isolation when carrying out maintenance are essential.

56.6 Calcium Sulfate

Both gypsum, CaSO₄·2H₂O, and anhydrite, CaSO₄, are widely distributed in the earth's crust. Only in volcanic regions are gypsum and anhydrite rock completely absent. In addition, large quantities of gypsum and anhydrite are obtained from industrial processes when flue gases are desulfurized or calcium salts are reacted with sulfuric acid. In these cases calcium sulfate is usually obtained as a moist, fine powder.

Gypsum is useful as an industrial material because (1) it readily loses its water of hydration when heated, producing a partially or totally dehydrated calcined gypsum, it reverts to the original dihydrate — the set and hardened gypsum product. These two phenomena, dehydration and rehydration, are the basis of gypsum technology:

Dehydration



Rehydration



The apparent density of the rehydrated calcium sulfate is much lower, 0.5–1.5 t/m³, than the density of the calcium sulfate rock, 2.3 t/m³.

Gypsum and anhydrite are nontoxic.

Both gypsum plaster and lime were used as mortar in antiquity. Gypsum was called gatch in Persian, γυψος in Greek, and gypsum in Latin. Iranians, Egyptians, Babylonians, Greeks, and Romans were familiar with the art of working with gypsum plaster, examples being the walls of Jericho, the pyramid of Cheops, the palace of Knossos, and the decorated interior walls of Pompeii. In Germany gypsum plaster was used as mortar in walls and buildings during the early Middle Ages, e.g., the monastery at Walkenried in the Harz Mountains. It gained popularity tremendously, reaching its peak during the Baroque and Rococo periods. Examples are the Wessobrunn school for stucco workers [71] and the stucco decorations in Charlottenburg palace, Berlin. The expansion of the cement industry in the second half of the nineteenth century also considerably increased the use of gypsum.

Over the centuries the gypsum industry has developed empirically out of the old craft of gypsum plastering. The distinctions between gypsum plaster and lime, however, remained obscure up to the eighteenth century. Research into the principles of gypsum technology was begun in 1765 by LAVOISIER, and has continued to this day. However, a craft so firmly steeped in tradition was slow to accept scientific conclusions, and only in the last few decades has gypsum manufacture developed into a modern industry [55].

56.6.1 The CaSO₄–H₂O System

56.6.1.1 Phases

The CaSO₄–H₂O system is characterized by five solid phases. Four exist at room temperature: calcium sulfate dihydrate, calcium sulfate hemihydrate, anhydrite III, and anhydrite II. The fifth phase, anhydrite I, only exists above 1180 °C [72], and it has not proved possible to produce a stable form of anhydrite I below that temperature. Table 56.11 characterizes the phases in the CaSO₄–H₂O system. The first four phases are of interest to industry.

Calcium sulfate dihydrate, CaSO₄·2H₂O, is both the starting material before dehydration and the final product after rehydration. Calcium sulfate hemihydrate, CaSO₄·½H₂O, occurs in two different forms, α and β, representing two limiting states [74]. They differ from each other in their application characteristics, their heats of hydration, and their methods of preparation (see Table 56.18) [75]. The α-hemihydrate (Figure 56.14) consists of compact, well-formed, transparent, large primary particles. The β-hemihydrate (Figure 56.15) forms flaky, rugged secondary particles made up of extremely small crystals.

LEHMANN et al. [76] postulated three limiting stages for anhydrite III, also known as soluble anhydrite: β-anhydrite III, β-anhydrite III', and α-anhydrite III. The three stages of anhydrite III were characterized by X-ray analysis, differential thermal analysis, scanning electron microscopy, mercury porosimetry, and measurement of the specific surface area. Anhydrite II is the naturally occurring form and also that produced from calcining the dihydrate, hemihydrate, and anhydrite III at elevated temperature.

The most important physical properties of the calcium sulfate phases are shown in Table 56.12.

Table 56.11: Phases in the CaSO₄–H₂O system.

Characteristic	Calcium sulfate dihydrate	Calcium sulfate hemihydrate	Anhydrite III	Anhydrite II	Anhydrite I
Formula	CaSO ₄ ·2H ₂ O	CaSO ₄ ·½H ₂ O	CaSO ₄	CaSO ₄	CaSO ₄
Thermodynamic stability, °C	< 40	metastable ^a	metastable ^b	40–1180	> 1180
Forms or stages		two forms: α, β	three stages: β-anhydrite III, β-anhydrite III', α-anhydrite III	three stages: AII-s, slowly soluble anhydrite, AII-u, insoluble anhydrite, AII-E, <i>Estrichgips</i>	
Other names, often based on the application	raw gypsum FGD gypsum synthetic gypsum chemical gypsum by-product gypsum set gypsum hardened gypsum	α-form: α-hemihydrate autoclave plaster α-plaster β-form: β-hemihydrate stucco plaster β-plaster plaster of Paris	soluble anhydrite	raw anhydrite natural anhydrite synthetic anhydrite chemical anhydrite by-product anhydrite calcined anhydrite	high-temperature anhydrite
Synthesis conditions: temperature, °C, and atmosphere	< 40	α-form: > 45, from aqueous solution β-form: 45–200, in dry air	α- and β-AIII: 50 and vacuum or 100 in air β-AIII': 100 in dry air	200–1180	> 1180
Production temperature, °C	< 40	α-form: 80–180 β-form: 120–180	β-AIII and β-AIII': 290 α-AIII: 110	300–900, specifically AII-s: < 500 AII-u: 500–700 AII-E: > 700	not produced commercially

^aMetastable in air saturated with water vapor.

^bMetastable in dry air.

Figure 56.14: α-Hemihydrate (scanning electron micrograph), 200 ×.

Figure 56.15: β-Hemihydrate (scanning electron micrograph), 200 ×.

Table 56.12: Physical properties of the $\text{CaSO}_4 \cdot x\text{H}_2\text{O}$.

Property	Calcium sulfate dihydrate	Calcium sulfate hemihydrate		Anhydrite III	Anhydrite II	Anhydrite I
		α -form	β -form			
Water of crystallization, %	20.92	6.21	0.00	0.00	0.00	0.00
Density, g/cm^3	2.31	2.757	2.619–2.637	2.580	2.93–2.97	undetermined
Mohs hardness	1.5	—	—	—	3–4	—
Solubility in water at 20 °C, g per 100 g of solution	0.21	0.67	0.88	hydrates to the hemihydrate	(0.27)	—
Refractive indices n_a	1.521	1.559 ^a	1.501	1.570	undetermined	undetermined
n_b	1.523	1.5595 ^a	1.501	1.576	undetermined	undetermined
n_c	1.530	1.584	1.546	1.614	undetermined	undetermined
Optical character	+	—	+	+	undetermined	undetermined
Optical orientation	$n_b \parallel b$ $n_{xc} = 52^\circ$	$c \parallel n_y$	$c \parallel n_y$	$n_a \parallel c$ $n_b \parallel c$	undetermined	undetermined
Axial angle $2V$	58–60°	14°	= 0°	42–44°	undetermined	undetermined
Lattice symmetry	monoclinic	monoclinic	orthorhombic	orthorhombic	cubic	undetermined
Space group	I 2/a	I 121	C 222	Amma	undetermined	undetermined
Lattice spacing, nm, a	0.5679	1.20317	1.20777	0.7006	undetermined	undetermined
b	1.5202	0.69269	0.69723	0.6998	undetermined	undetermined
c	0.6522	1.26712	0.63040	0.6245	undetermined	undetermined
β	118.43°	90.27°				

^a Average.

56.6.1.2 Laboratory Synthesis

The thermodynamic stability ranges for the calcium sulfate phases are shown in Table 56.11. Below 40 °C, i.e., under normal atmospheric conditions, only calcium sulfate dihydrate is stable. The other phases are obtained at higher temperatures by progressive dehydration of the calcium dihydrate in the following order:

dihydrate \rightarrow hemihydrate \rightarrow anhydrite III \rightarrow anhydrite II

Under normal atmospheric conditions hemihydrate and anhydrite III are metastable, and below 40 °C in the presence of water or water vapor they undergo conversion to the dihydrate, as anhydrite II does. However, between 40 °C and 1180 °C anhydrite II is stable.

To synthesize pure phases in the laboratory, β -hemihydrate is made from the dihydrate by heating at a low water-vapor partial pressure, i.e., in dry air or vacuum, between 45 °C and 200 °C. Further careful heating at 50 °C in a vacuum or up to \approx 200 °C at atmospheric pressure produces β -anhydrite III.

At very low water-vapor partial pressure, if water vapor is released rapidly and particle size is small β -anhydrite III' forms directly from the dihydrate, without formation of an intermediate hemihydrate. The specific surface area of such β -anhydrite III' can be up to ten times that of β -anhydrite III.

α -Hemihydrate is obtained from the dihydrate at high water-vapor partial pressure, e.g., above 45 °C in acid or salt solutions, or above 97.2 °C in water under pressure (e.g., 134 °C, 3 bar). Further careful release of water at 50 °C in a vacuum or at 100 °C under atmospheric pressure yields α -anhydrite III.

Anhydrite III is difficult to prepare pure because anhydrite II begins to form above 100 °C, and anhydrite III reacts readily with water vapor to form hemihydrate.

The β -hemihydrates from β -anhydrite III and β -anhydrite III' differ in their physical properties [77]. Therefore hemihydrates from β -anhydrite III' should be designated as β -hemihydrate'. α -Anhydrite III absorbs water vapor to form α -hemihydrate. Likewise, the hemihydrates, in humid air, reversibly adsorb

up to 2% of their weight in water without converting to dihydrate. This nonstoichiometric water in the hemihydrate can be completely removed by drying at 40 °C.

Gypsum dehydration kinetics have been investigated by several authors.

Neutron and x-ray powder diffraction studies have shown that the dehydration (and hydration) mechanism is strongly topotactic in the temperature range of 20–350 °C [78, 79].

In neutron thermodiffraction experiments it was found that gypsum decomposes to $\text{CaSO}_4(\text{H}_2\text{O})_{0.5}$, then to anhydrite III, and finally to anhydrite II. With high local steam pressure, a subhydrate with 0.74 H_2O was found [79].

According to another paper three phases of the α -hemihydrate type can be prepared as pure samples: $\text{CaSO}_4(\text{H}_2\text{O})_{0.6}$, $\text{CaSO}_4(\text{H}_2\text{O})_{0.5}$, and anhydrite III. The crystal structures of these phases were determined; data for $\text{CaSO}_4(\text{H}_2\text{O})_{0.5}$ and for anhydrite III are listed in Table 56.12. The structure of the subhydrate $\text{CaSO}_4(\text{H}_2\text{O})_{0.6}$ was found to be monoclinic, space group I 121, with $a = 1.19845$, $b = 0.69292$, $c = 1.27505$ nm and $\beta = 90^\circ$. The density is 2.74 g/cm^3 [80].

In general the hemihydrate $\text{CaSO}_4(\text{H}_2\text{O})_{0.5}$ is considered to be the kinetically most stable subhydrate. Table 56.12 also lists the well-established crystallographic data of gypsum [81] and of anhydrite II [82, 83].

Anhydrite II is formed at temperatures between 200 °C and 1180 °C. Above 1180 °C, anhydrite I forms; below 1180 °C it reverts to anhydrite II.

Another mechanism for conversion of gypsum directly to anhydrite II has been found in the catalytic action of small quantities of sulfuric acid on moist, finely divided gypsum at 100–200 °C. In this case anhydrite II with orthorhombic crystal structure is produced by neoformation [84].

56.6.1.3 Industrial Dehydration of Gypsum

Industrially it is most important that dehydration is achieved in the shortest time with the lowest energy consumption, i.e., that the costs be held to a minimum. Because of kinetic inhibitions calcination is carried out at much higher temperatures than those used in the laboratory (Table 56.11). Rarely are pure phases produced during manufacture; rather, mixtures of phases of the $\text{CaSO}_4\text{--H}_2\text{O}$ system are produced. Three types of calcined anhydrite II (anhydrous gypsum plaster or overburnt plaster) are manufactured, depending on burn temperature and time:

- Anhydrite II-s (slowly soluble anhydrite), produced between 300 and 500 °C
- Anhydrite II-u (insoluble anhydrite), produced between 500 and 700 °C
- Anhydrite II-E (partially dissociated anhydrite; floor plaster, *Estrichgips*), produced above \approx 700 °C

In use the difference among these products lies in the rates of rehydration with water, which for anhydrite II-s is fast, for anhydrite II-u slow, and for anhydrite II-E in between, a little faster than anhydrite II-u (Figure 56.23). Transitions between these different stages of reaction are possible.

Anhydrite II-E consists of a solid mixture of anhydrite II and calcium oxide formed by the partial dissociation of anhydrite into sulfur trioxide and calcium oxide when raw gypsum is heated above 700 °C. The presence of impurities lowers the normal dissociation temperature of anhydrite II, \approx 1450 °C.

56.6.1.4 Energy Aspects

KELLY et al. made a thorough study of the thermodynamic properties of the $\text{CaSO}_4\text{--H}_2\text{O}$ system [85, 86]. Tables 56.13 and 56.14 list the heats of hydration and dehydration of the various phase changes that are of industrial significance.

Table 56.13: Heats of hydration.

Phase change	Heats of hydration per mole (gram) of dihydrate at 25 °C, J
$\beta\text{-CaSO}_4 \cdot \frac{1}{2}\text{H}_2\text{O} + \frac{1}{2}\text{H}_2\text{O}_{(l)} \rightarrow \text{CaSO}_4 \cdot 2\text{H}_2\text{O}$	19 300 \pm 85 (111.9 \pm 0.50)
$\alpha\text{-CaSO}_4 \cdot \frac{1}{2}\text{H}_2\text{O} + \frac{1}{2}\text{H}_2\text{O}_{(m)} \rightarrow \text{CaSO}_4 \cdot 2\text{H}_2\text{O}$	17 200 \pm 85 (100.00 \pm 0.50)
$\beta\text{-CaSO}_{4(m)} + 2\text{H}_2\text{O}_{(l)} \rightarrow \text{CaSO}_4 \cdot 2\text{H}_2\text{O}$	30 200 \pm 85 (175.3 \pm 0.50)
$\alpha\text{-CaSO}_{4(m)} + 2\text{H}_2\text{O}_{(l)} \rightarrow \text{CaSO}_4 \cdot 2\text{H}_2\text{O}$	25 700 \pm 85 (149.6 \pm 0.50)
$\text{CaSO}_{4(m)} + 2\text{H}_2\text{O}_{(l)} \rightarrow \text{CaSO}_4 \cdot 2\text{H}_2\text{O}$	16 900 \pm 85 (98.0 \pm 0.50)

Table 56.14: Heats of dehydration.

Phase change	Heat of dehydration per mole or tonne of dehydration products at 25 °C	
	J/mol	kJ/t
$\text{CaSO}_4 \cdot 2\text{H}_2\text{O} \rightarrow \beta\text{-CaSO}_4 \cdot \frac{1}{2}\text{H}_2\text{O} + \frac{1}{2}\text{H}_2\text{O}_{(l)}$	86 700	597 200
$\text{CaSO}_4 \cdot 2\text{H}_2\text{O} \rightarrow \alpha\text{-CaSO}_4 \cdot \frac{1}{2}\text{H}_2\text{O} + \frac{1}{2}\text{H}_2\text{O}_{(l)}$	84 600	582 700
$\text{CaSO}_4 \cdot 2\text{H}_2\text{O} \rightarrow \beta\text{-CaSO}_{4(m)} + 2\text{H}_2\text{O}_{(l)}$	121 800	895 700
$\text{CaSO}_4 \cdot 2\text{H}_2\text{O} \rightarrow \alpha\text{-CaSO}_{4(m)} + 2\text{H}_2\text{O}_{(l)}$	117 400	863 100
$\text{CaSO}_4 \cdot 2\text{H}_2\text{O} \rightarrow \text{CaSO}_{4(m)} + 2\text{H}_2\text{O}_{(l)}$	108 600	798 000

56.6.1.5 Structure, Mixed Compounds, Solubility

Crystal Structure. All structures in the $\text{CaSO}_4\text{-H}_2\text{O}$ system consist of chains of alternate Ca^{2+} and SO_4^{2-} ions. These CaSO_4 chains remain intact during phase changes.

Calcium sulfate dihydrate has a layered structure, and the water of crystallization is embedded in between the layers.

When calcium sulfate dihydrate is dehydrated to hemihydrate, a tunnel structure is formed with wide channels parallel to the CaSO_4 chains. In the subhydrates the tunnels are filled with water molecules; in anhydrite III they are empty.

The relative ease of escape of these water molecules explains the facile conversion from subhydrate to anhydrite III.

Anhydrite II exhibits closest packing of ions, which makes it the densest and strongest of the calcium sulfates. However, lacking empty channels, it reacts only very slowly with water.

The α - and β -forms of calcium sulfate hemihydrate exhibit no crystallographic differences. The β -forms of calcium sulfate hemihydrate are active states of the α -form [87].

Isomorphism. Isomorphic incorporation of chemical compounds into the lattice of $\text{CaSO}_4\text{-H}_2\text{O}$ phases is of interest in connec-

tion with gypsums from flue-gas desulfurization and wet phosphoric acid processes. Isomorphic incorporation of calcium hydrogenphosphate dihydrate occurs because the $\text{CaHPO}_4 \cdot 2\text{H}_2\text{O}$ has lattice spacings almost identical with those of $\text{CaSO}_4 \cdot 2\text{H}_2\text{O}$ [88]. Monosodium phosphate, NaH_2PO_4 , can also be incorporated into the gypsum lattice [89]. KITCHEN et al. [90] consider isomorphism between the ions AlF_6^{3-} and SO_4^{2-} a possibility. EPELTAUER [74, 91] reports on further isomorphism, incorporation of the anion FPO_3^{2-} as well as the incorporation of Na^+ , $\leq 0.2\%$ in the hemihydrate lattice, but only 0.02% in the dihydrate lattice. Chlorides are not incorporated.

Double and Triple Salts. Gypsum forms double salts with alkali-metal or ammonium sulfate, some of which occur in nature, such as syngenite, $\text{CaSO}_4 \cdot \text{K}_2\text{SO}_4 \cdot \text{H}_2\text{O}$.

There are triple sulfates of calcium with the divalent ions of the iron and zinc subgroups and of manganese, copper, and magnesium along with the univalent alkali metals, also including ammonium. A good example is the well known polyhalite, $2\text{CaSO}_4 \cdot \text{MgSO}_4 \cdot \text{K}_2\text{SO}_4 \cdot 2\text{H}_2\text{O}$, which also occurs in natural salt deposits.

Ettringite, $3\text{CaO} \cdot \text{Al}_2\text{O}_3 \cdot 3\text{CaSO}_4 \cdot 32\text{H}_2\text{O}$, is important in cement chemistry [92], as are syngenite [93] and thaumasite [94].

Adducts. Gypsum forms sulfuric acid adducts in concentrated sulfuric acid: $\text{CaSO}_4 \cdot 3\text{H}_2\text{SO}_4$ and $\text{CaSO}_4 \cdot \text{H}_2\text{SO}_4$ [95].

Calcium sulfate dihydrate can combine with four molecules of urea to form an addition compound.

Solubility and Supersaturation. Gypsum is slightly soluble in water (Table 56.12). The solubilities of the various forms of calcium sulfate are strongly affected by the presence of other solutes. The references [58, 61] can be consulted for particulars on the solubility of gypsum in acids, especially sulfuric acid, phosphoric acid, and nitric acid. Gypsum is readily soluble in glycerol and sugar solutions and in aqueous solutions of chelating agents, such as EDTA. All calcium sulfates have a tendency to supersaturation [58].

56.6.2 Occurrence, Raw Materials

56.6.2.1 Gypsum and Anhydrite Rock

Gypsum and anhydrite deposits are found in many countries. They originated from supersaturated aqueous solutions in shallow seas, which evaporated and deposited first carbonates, then sulfates, and finally chlorides, i.e., in order of increasing solubility [59, 60].

Gypsum and anhydrite are almost always found in the Permian, Triassic, and Tertiary formations. The Permian includes the Upper Permian (Zechstein deposits, Germany). The Triassic consists of Lower (*Buntsandstein*), Middle (*Muschelkalk*), and Upper Triassic (*Keuper*). The Tertiary deposits include the Eocene (Spain, Persia, Near East), the Oligocene (Paris), and the Miocene deposits (Mediterranean area, North Africa). The Jurassic and Cretaceous formations, which lie between the Triassic and Tertiary, are almost devoid of useful gypsum deposits, as are the older pre-Permian formations — at least in the Old World — as, for example, the Carboniferous formation.

The currently accepted view is that gypsum, $\text{CaSO}_4 \cdot 2\text{H}_2\text{O}$, was formed upon initial crystallization. The best known deposits of primary gypsum are those of the Paris Basin and the areas around the Mediterranean. Under increased pressure and thus temperature, anhydrite could have developed locally from the original gypsum [96, 97]. However, uptake of surface water can convert the anhydrite back into gypsum. This gypsum is therefore a secondary rock, especially in formations older than the Middle Tertiary [98].

The various gypsum and anhydrite deposits differ in purity, structure, and color. The major impurities are calcium carbonate (limestone), dolomite, marl, clay; less frequently, silica, bitumen, glauberite, syngenite, and polyhalite. If these are present in the gypsum and anhydrite from its formation, they are called *primary impurities*. A distinction is drawn between carbonate-sulfate deposits, mainly found in the Upper Permian (Zechstein), and the clay-sulfate deposits, which predominate in the Triassic [99]. *Secondary impurities* are formed during exposure to materials flushed into cracks and leached cavities, but may also be introduced into the rock as waste material during mining. Gypsum is readily soluble in water, even if it is only slightly soluble, and therefore gypsum rock is leached by surface water. The chemical composition of some calcium sulfates is shown in Table 56.15.

Workable gypsum and anhydrite rock are structurally quite distinct from one another. The most important types of native gypsum are sparry gypsum, also called gypsum spar or flaky gypsum (selenite), fibrous gypsum, alabaster (grainy gypsum), gypsum rock (common gypsum, also massive gypsum), porphyritic gypsum, earthy gypsum (gypsite in the United States), and gypsum sand (contaminated with Glauber's salt $\text{Na}_2\text{SO}_4 \cdot 10\text{H}_2\text{O}$). Anhydrite, always crystalline, can either be sparry (anhydrite spar), coarse to close grained, or even rod shaped.

Table 56.15: Chemical composition of some calcium sulfates.

	Natural gypsums		Natural anhydrites		Phosphogypsums			Fluoroanhydrite
	Zechstein	Keuper	Zechstein	Keuper	a	b	c	d
Mineralogical analysis								
CaSO ₄ ·2H ₂ O	91.6	96.4	6.0	3.8	93.0	97.6	96.5	0.0
CaSO ₄ II	6.4	0.9	88.8	83.7	0.0	0.0	0.0	94.7
MgCO ₃	0.1	0.6	2.0	3.6	0.0	0.0	0.0	0.0
CaCO ₃	1.9	1.3	3.1	5.3	0.0	0.0	0.0	0.0
Chemical analysis								
Combined water	19.1	20.1	1.3	0.8	19.5	19.2	19.2	0.0
SO ₃	46.4	45.4	55.1	51.0	43.2	45.4	46.9	56.4
CaO	33.6	32.5	40.3	38.7	32.2	32.5	32.1	40.8
MgO	0.05	0.28	0.95	1.71	0.01	0.01	0.01	0.13
SrO	0.07	0.16	0.07	0.14	0.06	2.05	0.05	0.0
Fe ₂ O ₃ + Al ₂ O ₃	0.01	0.08	0.01	0.39	0.27	0.70	0.93	0.27
HCl-insoluble residue	0.10	0.47	0.10	2.49	1.51	1.00	0.68	0.69
Na ₂ O	0.02	0.01	0.04	0.11	0.47	0.14	0.02	0.03
Total P ₂ O ₅	0.0	0.0	0.0	0.0	1.01	0.11	0.30	0.0
F	0.0	0.0	0.0	0.0	1.76	0.14	0.29	0.92
Others								0.11 ZnO 0.69 K ₂ O
Organics	0.0	0.0	0.0	0.0	0.08	0.03	0.04	0.0
Ignition loss	0.54	0.71	2.08	4.45	1.38	0.34	0.43	0.14
pH	6-7	6-7	6-7	6-7	3	9	4	10-12

^aFrom Moroccan raw phosphate, dihydrate process.

^bFrom Kola raw phosphate, dihydrate/hemihydrate process, after rehydration to dihydrate.

^cFrom Moroccan raw phosphate, hemihydrate/dihydrate process.

^dFrom hydrofluoric acid production, Zechstein is an Upper Permian deposit; Keuper, an Upper Triassic.

Gypsum can be pure white. If it contains iron oxide, it is reddish to yellowish. If clay and/or bitumen is present, it is gray to black. Very pure anhydrite is bluish white, but usually it is gray with a bluish tinge. The white veins sometimes found on the boundary between gypsum and anhydrite consist largely of glauberite (CaSO₄·Na₂SO₄) or Glauber's salt (Na₂SO₄·10H₂O).

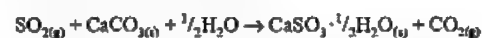
56.6.2.2 Flue-Gas Desulfurization (FGD) Gypsum

FGD gypsum is produced from the desulfurization of combustion gases of fossil fuels (coal, lignite, oil) in power stations as a product with a specification and quality standards. The internationally accepted definition of FGD gypsum is: "Gypsum from flue gas desulfurization plants (FGD gypsum, desulfogypsum) is moist, finely divided, crystalline, high-purity calcium sulfate dihydrate, CaSO₄·2H₂O. It is specifically produced in a flue gas desulfurization process incorporating after lime(stone) scrubbing, a refining process in-

volving oxidation followed by gypsum separation, washing, and dewatering." [100]

FGD gypsum is produced in four stages:

- **Desulfurization:** In a first circuit the dedusted flue gas is sprayed with a limestone suspension in counterflow. The reaction, which takes place at pH 7-8, produces insoluble calcium sulfite:



- **Forced oxidation:** In a second circuit the calcium sulfite reacts spontaneously with atmospheric oxygen at pH 5, initially forming soluble calcium bisulfite, which is then oxidized to calcium sulfate dihydrate:



During this procedure the gypsum crystals grow by continuous circulation to the required average size of 30-70 μm.

- **Gypsum separation:** In a hydrocyclone, the calcium sulfate dihydrate crystals produced in the quencher slurry are separated and solid impurities are removed.

- **Gypsum washing and dewatering:** The calcium sulfate crystals are separated from the process water in filters or centrifuges and washed with clean wash water to remove unwanted water-soluble chlorides and sodium and magnesium salts. The resulting

FGD gypsum contains < 10% free moisture by weight. About 5.4 t of gypsum is produced per tonne of sulfur in the fuel.

Figure 56.16 shows a typical flow diagram of a flue gas desulfurization plant for producing FGD gypsum.

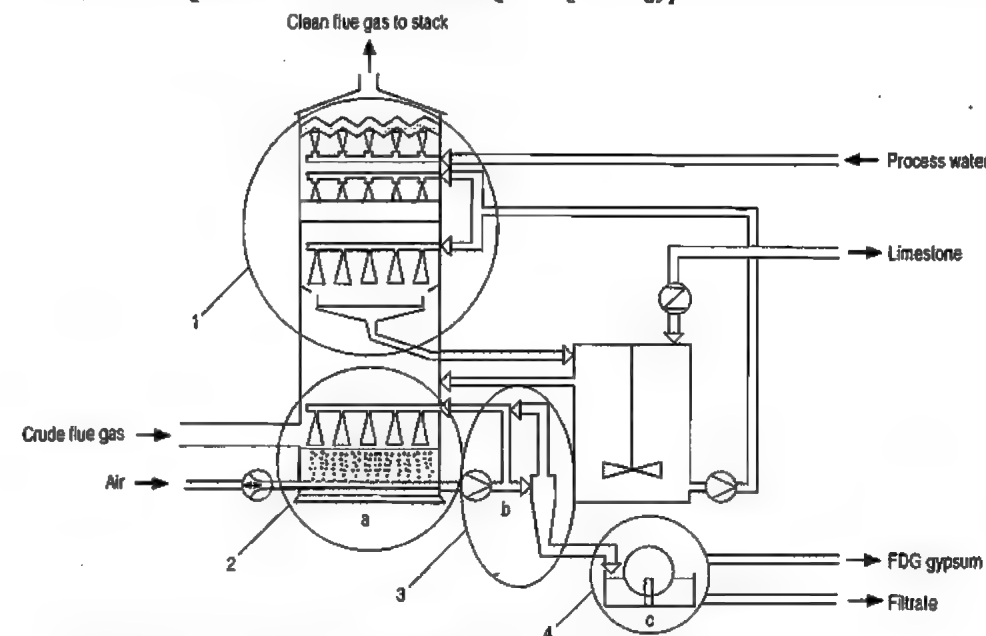


Figure 56.16: Flowsheet of a flue gas desulfurization plant for producing FGD gypsum with the four operation stages 1 to 4 (see text for explanation): a) Quencher; b) Hydrocyclone; c) Filter.

Sometimes FGD gypsum from lignite-fired power stations is darker than that from coal-fired power stations. Therefore a special "overflow cleaning" operation was developed to improve the color of lignite FGD gypsum. Such lignite FGD gypsum meets international quality specifications and can be used for all applications. This could be important, for example in Germany, where lignite FGD gypsum will predominate in the future [101].

A large-scale investigation has been carried out to compare FGD gypsum to natural gypsum in the production, processing, utilization, and disposal of building materials. The conclusion was that the differences in chemical composition and in trace element content between FGD gypsum and natural gypsum are insignificant. FGD gypsum can be used for the production of all building materials [102].

Table 56.16 lists quality standards for FGD gypsum.

Table 56.16: Quality standards for FGD gypsum.

Quality parameters	Quality standards
Free moisture	< 10.0%
Calcium sulfate dihydrate	> 95.0% ^a
Magnesium oxide, water soluble	< 0.10%
Sodium oxide, water soluble	< 0.06%
Chloride	< 0.01%
Sulfur dioxide	< 0.25%
pH	5-9
Color	white ^b
Odor	neutral
Toxicity	nontoxic

^aThe reduction of the calcium sulfate dihydrate content by inert elements is not detrimental to the different areas of application.

^bDifferent color values may apply depending on the use of the FGD gypsum and the final products.

FGD gypsum is not regarded as a waste and is therefore not included in the European Waste Catalogue (EWC).

FGD gypsum is used directly in the gypsum industry (and small quantities in the cement industry) without any further treatment, and is equivalent to natural gypsum.

The predicted quantities of FGD gypsum from coal-fired and lignite-fired power stations in Europe, the United States and Canada, and Japan and Taiwan in 1996 are listed in Table 56.17 [101].

Table 56.17: Predicted quantities of FGD gypsum in 1996.

Country	Quantity of FGD gypsum, 10 ³ t
Germany	4920
Denmark	340
Finland	190
Great Britain	1200
Italy	40
Netherlands	360
Austria	100
Poland	770
Russia	60
Czech Republic	40
Ukraine	85
Total for Europe	8225
USA and Canada	3000
Japan and Taiwan	2300

In Germany the quantities of FGD gypsum will rise from 4.9×10^6 t in 1996 to 6.3×10^6 t in the year 2000 due to lignite FGD gypsum from new power stations in the former Democratic Republic.

In Spain, France, Italy and Turkey, fairly large quantities are to be expected after 1996.

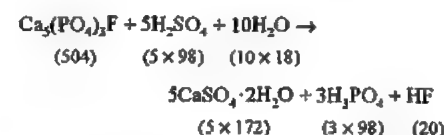
The quantities of FGD gypsum produced in Japan and Taiwan of ca. 2.3×10^6 t are expected to remain stable after 1996 [137].

The quantities of FGD gypsum predicted for the United States and Canada will probably be attained later than predicted above, i.e., only after 1996.

56.6.2.3 Phosphogypsum

By far the largest amount of by-product gypsum is obtained from the production of wet phosphoric acid from phosphate rock

(usually fluorapatite) and sulfuric acid ($n \times M_r$):



Worldwide, about 100 Mt/a of phosphogypsum are currently obtained. Phosphogypsum is a waste and therefore listed in the EWC as follows [105]:

06 00 00: Wastes from inorganic chemical processes

06 09 01: Phosphogypsum

In the OECD lists on the Control of Transfrontier Movements of Wastes, phosphogypsum is listed as follows [106]:

Amber list AB 140: Gypsum arising from chemical industry processes

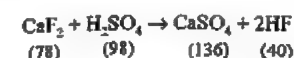
This phosphogypsum is a moist, fine powder with a free water content of ≈ 20 –30% and considerable amounts of impurities, the exact impurities and their amounts depending on the rock and the specific process. The radioactive substances present in small amounts in phosphate rock are partly transferred to the phosphogypsum as ^{226}Ra , leading to slightly increased radioactivity of such gypsums [68]. About 1.7 t of gypsum are produced per tonne of raw phosphate, corresponding to 5 t of gypsum per tonne of phosphorus pentoxide produced.

Currently < 4% of the phosphogypsum obtained is utilized. The principal difference in using phosphogypsum compared to FGD gypsum is the need to refine phosphogypsum by washing, flotation, and recrystallization to remove harmful impurities and to modify its unsuitable particle shape. However, today it is simply cheaper to use natural gypsum or FGD gypsum than to purify and process phosphogypsum. The quantity of phosphogypsum obtained annually is nearly equal to world demand for natural gypsum and anhydrite of ca. 100×10^6 t/a.

56.6.2.4 Fluoroanhydrite

Anhydrite is a by-product in the production of hydrofluoric acid from fluorspar and sulfuric acid, to the extent of 2–3 Mt per year ($n \times M_r$):

ric acid, to the extent of 2–3 Mt per year ($n \times M_r$):



One tonne of fluorspar produces 1.75 t of anhydrite. Fluoroanhydrite is used as a raw material for the gypsum industry only in Germany and some of its neighbors.

56.6.2.5 Other By-product Gypsums

Calcium sulfate dihydrate is obtained as a waste in small quantities in the production or treatment of organic acids (e.g., tartaric acid, citric acid, and oxalic acid) or inorganic acids (e.g., boric acid). All these acids are produced by reaction of their calcium salt with sulfuric acid.

The amounts of industrial by-product gypsums are expected to increase from treating sulfate-containing waste waters and neutralizing dilute sulfuric acids that are produced in the processing of minerals (e.g., zinc ore) and the manufacture of pigments (e.g., titanium dioxide). Especially titanogypsum is obtained in large quantities and can be used in the gypsum industry if it is produced in the titanium dioxide industry with specification and quality standards similar to FGD gypsum. Several 100 000 tonnes are already used in the gypsum industries of Japan, the United States and Europe [137].

Gypsum scrap from the ceramic industry and metal foundries has likewise not been used so far as a raw material for the gypsum industry, although efforts continue to be made in that direction [107]. The quantities are small and recovery operations are very costly because of the impurities originating from slip casting.

56.6.3 Production

Although a dozen industrial processes for the preparation of cementitious calcium sulfates are well known, only a few are used extensively in the industrial countries. The

processes characterized by low capital and operating costs, simple design and operation, robust and long-lasting equipment, and uniform high-grade calcined gypsum product subsequently used to manufacture gypsum building components and gypsum plaster are discussed in the following chapter.

Since the two major raw materials — natural gypsum and FGD gypsum — are processed differently, they are discussed separately, as is the processing of phosphogypsum.

56.6.3.1 Natural Gypsum to Calcined Products

Natural gypsum is mined by the open-pit method [108] and by underground mining [109]. In open-pit mining the gypsum is recovered by drilling and blasting, mostly on one or more levels. In deep mining, chamber blasting is used [110]. The blasted rock consists of large lumps, containing 0–3% free moisture (quarry water). The amounts of explosives needed are about 250 g/t for open-cast mining and 400 g/t for underground mining.

The coarse rock is conveyed to the crushing plants, normally at the gypsum works, by means of trackless loading and haulage gear. Impact crushers, jaw crushers, and single-roll crushers with screen and oversize return are all suitable for coarse size reduction. Impact pulverizers or roller mills are used for intermediate size reduction; and hammer mills, ball mills, or ring-roll mills are used for fine grinding. The degree of size reduction is determined by the calcining unit or the intended use of the gypsum:

Rotary kiln	0–25 mm
Kettle	0–2 mm
Kettle with combined drying and grinding unit	0–0.2 mm
Conveyor kiln	4–60 mm
Gypsum and anhydrite for cement	5–50 mm

If transport by ship or truck to distant gypsum or cement plants is necessary, the material is reduced to required size for further treatment prior to transport.

Cleaning or beneficiating the blasted rock is no longer common practice, except for gypsum with much Glauber's salt, which is

readily removed by leaching with water. This is still done in Britain [108].

Often the mined and crushed rock is homogenized before being calcined. This is done in homogenizing plants with capacities of about one week's production.

The final stage in gypsum open-pit mining is the restoration of the quarry site and its re-inclusion in the environment of the area.

β -Hemihydrate Plasters. Stucco and plaster of Paris are prepared by dry calcination between 120 °C and 180 °C, either in directly fired rotary kilns or else in indirectly heated kettles, to produce the β -hemihydrate. The kettles may be upright or horizontal.

The *rotary kiln* (capacities up to 600 t/d) is particularly suitable for calcining granular (0–25 mm) gypsum rock. This, without predrying, is fed continuously to the kiln in cocurrent flow with the hot gases with a weigh-belt feeder and cellular wheel sluice (Figure 56.17). The hot gases are produced in a brick-lined combustion chamber ahead of the gypsum feed. The shell of the rotary kiln is not brick-lined but consists of thick steel plates with steel inserts to ensure an even distribution of gypsum particles across the furnace cross section.

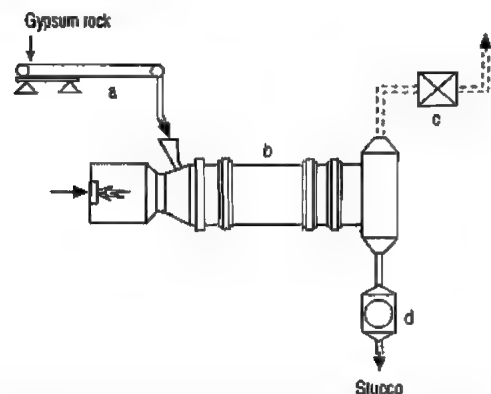


Figure 56.17: Production of stucco (plaster of Paris, β -hemihydrate plaster) by the rotary kiln process: a) Weigh-belt feeder; b) Rotary kiln with combustion chamber; c) Cyclone; d) Pulverizer.

High thermal efficiency is achieved by the direct transfer of heat from the hot gases to the gypsum. The residence time of the gypsum rock in the kiln is self-regulating. It increases with the size of the grains, but complete calcination can be achieved regardless of particle size, to produce β -hemihydrate of uniform quality and invariant properties after fine grinding and air classifying. Any gypsum not dehydrated to hemihydrate at start-up or shut-down is collected in a bin and added in small quantities to the calcined gypsum. Rotary kiln plants are fully automatic and usually can be controlled by one worker.

The externally heated *kettle*, of capacity up to 760 t/d, is the first of a series of similar calcining units heated indirectly. The gypsum is predried and ground to < 2 mm. In modern plants fine grinding, which used to follow the calcining process, is combined with the predrying and carried out in drying-grinding units to produce particles < 0.2 mm (Raymond mill, Claudius Peters mill, Attritor). The properties of the product hemihydrate are shown in Table 56.18. The phase composition of plaster of Paris is shown in Table 56.19.

In the 1960s [112, 113] the kettle process was improved and made continuous, especially in England (British Plaster Board Ltd.) and North America. Predried and finely ground gypsum is fed continuously from above. As it dehydrates, the gypsum sinks to the bottom, the water vapor set free keeping the gypsum bed fluidized. The calcined gypsum settles at the bottom of the kettle, where it is continuously discharged through a pipe connected to the side of the kettle.

Figure 56.18 shows a flow diagram for such a plant. The thermal balance is not quite as good as for directly fired rotary kilns, but the waste gases are less dust laden. Up to 760 t of hemihydrate plaster per day can be produced in this type of plant.

Table 56.18: Properties of calcined gypsum [111].

Manufacturing process	Type of plaster	g plaster/100 g H ₂ O	Water-to-plaster ratio	Setting time, min		Strength of hardened plaster ^a , N/mm ²			Density of hardened specimen, kg/m ³
				Start	End	Flexural	Compressive	Hardness	
Rotary kiln	β -hemihydrate	137	0.73	13	28	4.8	11.2	19.1	1069
Conveyor kiln	multiphase	167	0.60	6	35	5.1	15.5	25.9	1225
Kettle	β -hemihydrate	156	0.64	9	22	5.2	14.0	26.8	1133
Autoclave	α -hemihydrate	263	0.38	10	22	12.8	40.4	92.0	1602

^a 40 × 40 × 160 mm specimen.

Table 56.19: Phase compositions, in %, of overburnt plaster, plaster of Paris, and multiphase plaster (impurities not considered).

	Plaster of Paris (rotary kiln)	Overburnt plaster (conveyor kiln)	Multiphase plaster, a mixture of plaster of Paris and overburnt plaster
Dihydrate, CaSO ₄ · 2H ₂ O	0	0	0
β -Hemihydrate, β -CaSO ₄ · 1/2 H ₂ O	75	6	27
β -Anhydrite III, β -CaSO ₄ III	20	19	15
Anhydrite II, CaSO ₄ II ^a	5	75	58

^a Consisting of reaction stages, AII-s (slowly soluble A), AII-u (insoluble A), and AII-E (Estrichgips).

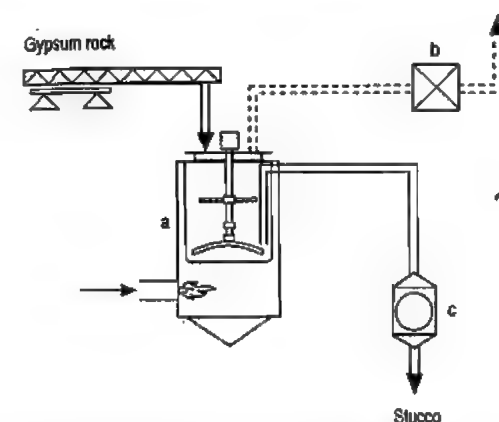


Figure 56.18: Production of stucco (plaster of Paris, β -hemihydrate plaster) by the continuous kettle process: a) Kettle with combustion chamber and ascending pipe; b) Cyclone; c) Pulverizer.

Recently the *submerged combustion* method — more specifically indirect heat transmission of the externally heated boiler casing combined with direct heat transmission — has been introduced. The advantages are high thermal efficiency and low energy consumption. Kettles heated only by submerged combustion are being tested at present. Existing kettles can also be fitted with submerged combustion burners, which reduces energy consumption and increases the flow rates. Figure 56.19 shows a kettle with such a burner

that is designed for continuous operation [113].

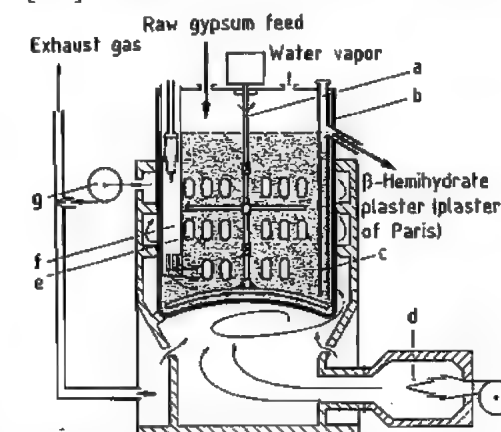


Figure 56.19: Kettle with submerged combustion burner for continuous production of β -hemihydrate (plaster of Paris): a) Agitator; b) Outer casing of kettle; c) Ascending pipe for stucco plaster discharge; d) Combustion chamber; e) Cross pipes for hot gases; f) Submerged pipe with submerged combustion burner; g) Ventilating fan for exhaust and circulating gas.

Batch horizontal kettles, with capacities of 5–10 t/h, are popular in France under the name of Beau.

Almost the total world production of β -hemihydrate is carried out in plants of the types just described. Today in North America indirectly heated kettles and directly heated

rotary kilns are in use in a proportion of about 5:1, whereas earlier only the kettle had been used. In Britain and France, the indirectly heated kettle is widely used, and in Germany, the rotary kiln and the kettle.

Most of the β -hemihydrate or stucco produced is used in gypsum building components; to a lesser extent β -hemihydrate is used in special building plaster.

Other calcining processes for the manufacture of β -hemihydrate have also been used industrially. In a grinding-calcining process [114], the raw gypsum is continuously crushed and calcined to β -hemihydrate in one single unit (Claudius Peters) (Figure 56.20). A few plants produce β -hemihydrate and to some extent also multiphase plaster in a fluidized bed [115–117] — the dried and finely ground gypsum rock is calcined in the stream of hot gases (Thyssen-Rheinstahl). Another development is the indirectly heated, continuously operated horizontal kettle. Externally it resembles a rotary kiln. In this unit the hot gases first pass through a central tube in cocurrent flow and then through further heating tubes in countercurrent flow. Similar is the continuously operated Holoflute calcining unit, using hot oil or superheated steam as the heat exchange medium. In this case the gypsum is moved along on a screw conveyor that has hot oil passing through it [118].

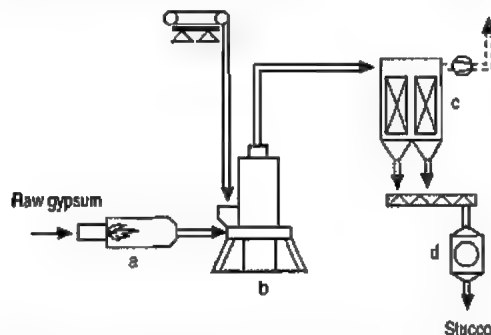


Figure 56.20: Production of stucco (plaster of Paris, β -hemihydrate plaster) by the grinding-calcining process: a) Combustion chamber; b) Grinding-calcining unit; c) Separating cyclone; d) Pulverizer.

Calcined Anhydrous Plasters and Multiphase Plasters. Overburnt plasters are pro-

duced in dry calcining processes at temperatures between 300 and 900 °C. For the most part they are calcined anhydrite. There are three reaction stages:

- AII-s, slowly soluble anhydrite, < 500 °C
- AII-u, insoluble anhydrite, 500–700 °C
- AII-E, *Estrichgips*, > 700 °C

The properties and final phase compositions of overburnt plaster are shown in Tables 56.18 and 56.19.

In overburnt plaster, and also in multiphase plaster, these three stages of reaction have to have a definite ratio, which is determined jointly by the raw material and the calcining process. In some of these processes [55] the gypsum is calcined in such a way that the anhydrite phase is obtained along with the hemihydrate. In other processes the overburnt plaster is produced separately and mixed with β -hemihydrate afterwards. These plasters are designated as multiphase plasters, *Putzgips* in Germany (Tables 56.18 and 56.19).

A modern calcining unit for overburnt plaster and multiphase plaster is the conveyor kiln developed by KNAUF [119] (Figure 56.21). Today, capacities up to 1200 t/d are usual, making it the most efficient kiln used for gypsum. Before being fed to the conveyor kiln, the gypsum rock is crushed to size 4–60 mm and split into three or four sieve fractions (e.g., 7–25 mm, 25–40 mm, and 40–60 mm or 4–11 mm, 11–25 mm, 25–40 mm, and 40–60 mm). The fractions are piled on the continuous conveyor grate, the smallest on the bottom. The grate, which moves continuously at a speed of 20–35 m/h, passes through a calcining hood. There the hot gases are drawn through the gypsum bed by exhaust fans. The top layer can reach a temperature up to 700 °C; the bottom layer, up to 300 °C. The temperature of the heat-resistant plates of the conveyor grate does not exceed 270 °C. The gypsum is not mixed during calcination, and therefore little dust is formed. About half the hot gases are discharged into the atmosphere as waste gas, issuing from the chimney at about 100 °C; the remainder (at \approx 270 °C) is recirculated to the combustion

chamber together with air (\approx 230 °C) drawn through the calcined gypsum bed to cool it. The thermal efficiency of such a conveyor kiln is high, greater than 70%. In Germany and elsewhere conveyor kilns with a total capacity of more than 2 Mt/a are currently in operation.

Figure 56.22 shows a flow diagram of a process producing construction plaster. In addition to a conveyor kiln it also uses a rotary kiln in which raw gypsum of small particle size (0–4 mm or 0–7 mm) is calcined to β -hemihydrate and subsequently mixed with anhydrous plaster that has been ground to the required fineness. In this way, multiphase plasters are produced. They differ from each other in their setting properties and also from β -hemihydrate plaster in that they are coarser (see Table 56.19 for composition, Table 56.18 for properties, Figure 56.23 for representation as three-component diagram) [55].

Multiphase plasters are used to finish interior walls and ceilings. Since 1965 machine-applied plaster has been produced in large quantities by incorporating chemical additives to one such multiphase plaster. Even pure construction plasters (Saarland construction plaster, southern German *Doppelbrandgips*),

which have been used in Germany for years, but which recently have declined in importance, can be prepared in these types of plants. This is also true for the construction plasters used in Latin countries, North Africa, and the Near East [120].

Other calcining plants producing anhydrous plasters operate on the principle of a countercurrent rotary kiln (Vernon). For example, in France an overburnt plaster, *surcuit*, is produced and mixed with β -hemihydrate to produce *Paris construction plaster* [121]. In such a countercurrent rotary kiln, the gypsum enters at the end opposite to the combustion chamber and travels into hot gases. The dehydrating gypsum reaches its maximum temperature, \approx 500 °C, just before exiting the kiln. These kilns, with capacities of 15–30 t/h, are sometimes linked together and used to produce anhydrous plaster and β -hemihydrate simultaneously [122]. This improves the efficiency and offers the opportunity of cooling the anhydrous plaster obtained at very high temperatures advantageously. The problem of cooling has also been solved by making use of the planetary cooling system of the cement industry.

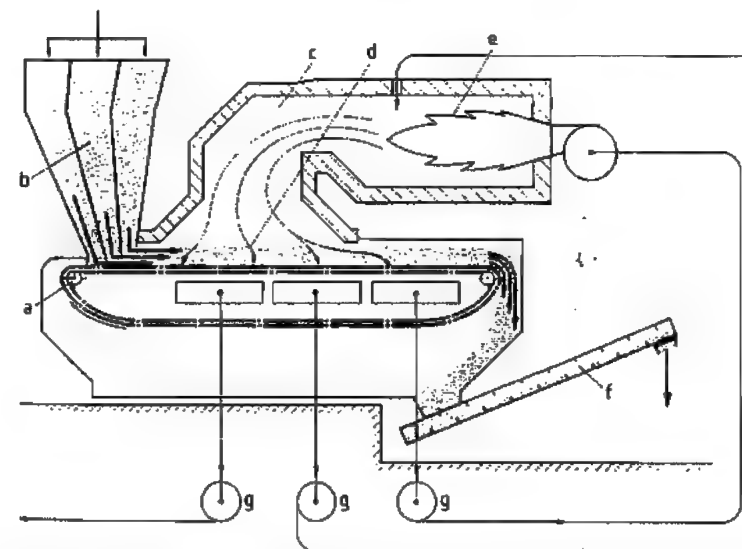


Figure 56.21: Conveyor kiln for the production of anhydrous plaster: a) Conveyor grate; b) Feed hoppers; c) Calcining hood; d) Layers of gypsum; e) Combustion chamber; f) Discharger; g) Circulating and cooling air fans for exhaust gas.

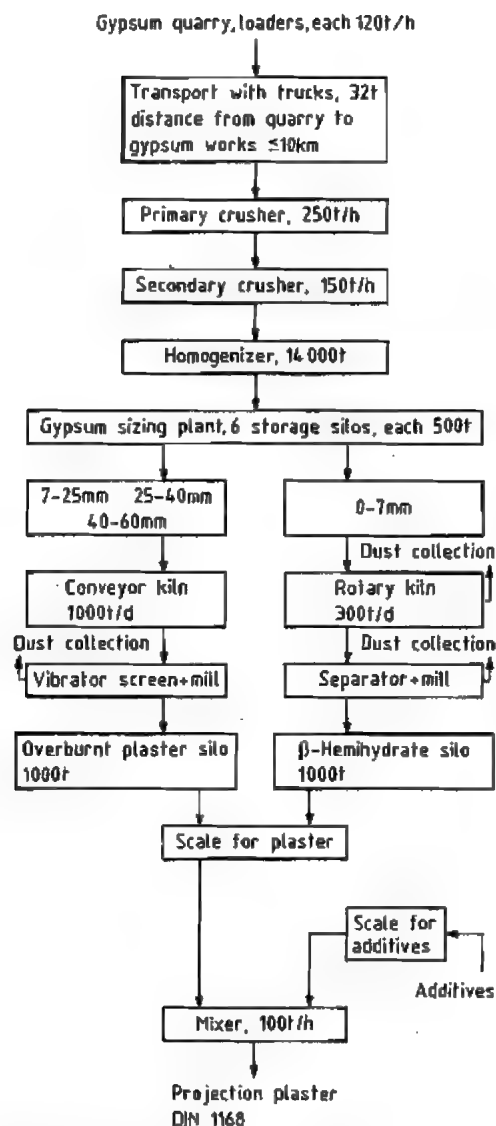


Figure 56.22: Flow diagram for production of projection plaster with a conveyor kiln.

α-Hemihydrate can be produced by wet calcining processes, either under elevated pressure in autoclaves or at atmospheric pressure in acids or aqueous salt solutions between ≈ 80 and 150°C . However, only the autoclave pro-

cesses have so far achieved industrial importance for the small amounts produced.

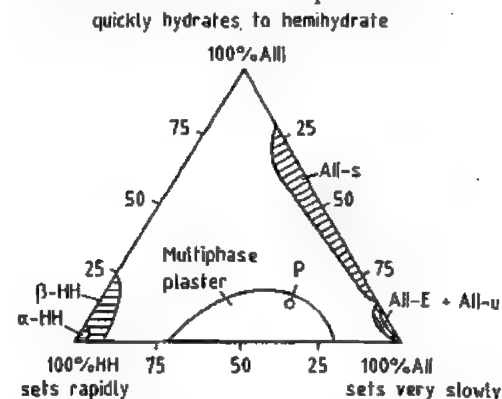


Figure 56.23: Three-phase composition diagram of calcined gypsums [55]. Point P indicates the composition of a multiphase plaster consisting of 26% β-hemihydrate, 14% anhydrite III, and 58% anhydrite II, the composition given in Table 56.19 for multiphase plaster.

α-Hemihydrate from natural gypsum is nearly always batch-processed. For instance, gypsum rock (particle size $150\text{--}300\text{ mm}$, $> 95\%$ $\text{CaSO}_4 \cdot 2\text{H}_2\text{O}$, rocklike) is put in wire baskets, and either stacked in upright autoclaves or wheeled into horizontal autoclaves with capacities of $0.5\text{--}10\text{ m}^3$. The autoclaves are heated directly or indirectly with steam at $130\text{--}135^\circ\text{C}$. The heating is carried out so that after about four hours a pressure of 4–5 bar has built up. The autoclave is then emptied; the α-hemihydrate formed is immediately transferred in the baskets to a chamber to be dried at 105°C under atmospheric pressure. It is subsequently ground to the desired particle size and size distribution. Variation in pressure and temperature during dehydration and drying can be used to affect the properties of the products (Table 56.18).

α-Hemihydrate is often mixed with β-hemihydrate. For that reason processes have been developed that produce a mixture of α- and β-hemihydrates in a single operation [123]. In one such process the α-hemihydrate is dried in a rotary kiln, which at the same time serves to both calcine the β-hemihydrate and blend the two types of material.

Table 56.20: Examples of characteristic energy data in manufacturing calcined gypsum.

Parameter	Rotary kiln (β-hemihydrate)	Kettle (β-hemihydrate)	Conveyor kiln (Putzgips)	Autoclave (α-hemihydrate)
Calcined gypsum capacity, t/d	600	760	1200	150
Theoretical energy requirement, kJ/t	598 600	584 000	770 400	560 000
Practical energy requirement, kJ/t	892 000	800 000	1 100 000	1 590 000
Thermal efficiency, %	67	73	70	35
Moisture content of gypsum rock, %	1.5	1.5	1.6	0.0
Crude gypsum purity, %	90.0	90.0	94.0	95.0
Water of crystallization, raw gypsum, %	18.8	18.8	19.7	19.9
Water of crystallization, calcined gypsum, %	3.0	5.5	1.0	5.8

Process Control. Dry gypsum calcining processes are usually equipped with dry dust collection systems. The amount of dust formed depends on the type of calcining unit. For the most part electrostatic filters are used for dust collection, but recently mechanical filters have also been used (see the B Series). Sieves and grinders, as well as conveying equipment, for calcined gypsum are fitted with flat screen-type filters for internal dust collection. The dust collected is added to the calcined gypsum.

The water liberated in the process is discharged as vapor through outlet stacks into the atmosphere. There are no wastes or by-products. No environmental problems are encountered, provided the processing of the gypsum plaster proceeds normally.

The energy consumption of a gypsum plant is the sum of the fuel used in the calcination of the gypsum and the electric power needed to operate the machinery. Table 56.20 shows the energy consumption of various types of processes based on experience. Mainly oil and gas have been used as the fuel. However, coal is being used increasingly, chiefly in grate firing, pulverized coal firing, and fluidized firing systems [124]. To improve the energy consumption of these units, the design is optimized and the waste heat is utilized. At the same time large modern gypsum plants are increasingly using automatic process control.

56.6.3.2 FGD Gypsum to Calcined Products

FGD gypsum is used directly as a major raw material by the gypsum and the cement industries.

β-Hemihydrate and Multiphase Plasters

FGD gypsum is a finely divided powder with less than 10% surface moisture. It therefore differs considerably in its state of aggregation from natural gypsum and requires treatment not needed for natural gypsum.

To produce β-hemihydrate for the manufacture of gypsum plasterboards and other gypsum building components, FGD gypsum must be dried before calcination. This can be carried out in cocurrent drying units in which the hot gases come into direct contact with the moist gypsum (e.g., flash dryers), or in tube dryers heated indirectly with steam. After drying the gypsum is calcined to β-hemihydrate in kettles [125, 126].

FGD gypsum used for the production of multiphase plaster and gypsum building plaster must be treated further. Its particle structure, which ranges from cubic (bulk density 1200 kg/m^3 narrow particle size distribution $40\text{--}60\text{ }\mu\text{m}$) are unsuitable for the production of multiphase plaster [127]. It is this particle structure that is the cause of its thixotropy if it is used as multiphase plaster. As plaster it also lacks smoothness, and its volume yield is too variable.

Agglomeration processes have been developed to modify the particle structure of flue-gas gypsum and convert it into a lump product. Of all the agglomeration processes—briquetting with a compacting press, granulating with extrusion presses, pelletizing—briquetting has proved the most effective and is the most widely accepted. In this process the flue-gas gypsum is compacted in the dry state without addition of bonding agents or additives to

produce briquettes 2 cm thick and 6 cm long, in their mechanical properties comparable to natural gypsum [128].

Their point strength exceeds 500 N, and their apparent density is $\approx 2.15 \text{ g/cm}^3$. These briquettes are exceptionally abrasion resistant. They can be stored in the open and are unaffected even by frost or rain. In this form all types of flue-gas gypsum have bulk density of $\approx 1.1 \text{ t/m}^3$ and can be used alone or mixed with natural gypsum.

Figure 56.24 shows a flow diagram for a plant processing FGD gypsum by drying and briquetting. Several of these plants operate in Germany.

The flue-gas gypsum briquettes can be processed to multiphase gypsum plaster in the calcining units used for natural gypsum.

The extra energy input per tonne of dry $\text{CaSO}_4 \cdot 2\text{H}_2\text{O}$ consists of (a) 550 000 kJ of thermal energy and 12 kWh of electrical energy for drying to 10% moisture and (b) 10 kWh of electrical energy for agglomeration into briquettes.

The value of FGD gypsum can be established from a cost comparison between pro-

cessing FGD gypsum and natural gypsum. A second major factor is the transport of the FGD gypsum from power station to gypsum plant. In comparison with the transport of natural gypsum from the quarry to the gypsum plant, the transport of FGD gypsum is associated with additional costs, e.g., for intermediate storage due to seasonal differences in production of the power station and consumption of the gypsum plant.

For a gypsum plant the long-term security of supply of FGD gypsum is vital. In times of FGD gypsum shortages it must therefore be possible to fall back on natural gypsum. The surplus quantities of FGD gypsum that will be available in the future in parts of Europe should be placed in intermediate storage locally in artificial deposits as a future raw material reserve. An environmental compatibility study is at present being prepared. With such a gypsum reserve it would be possible to fulfill the requirement of the gypsum industry for an assured long-term supply of raw material over the life-time of the power station [101, 129].

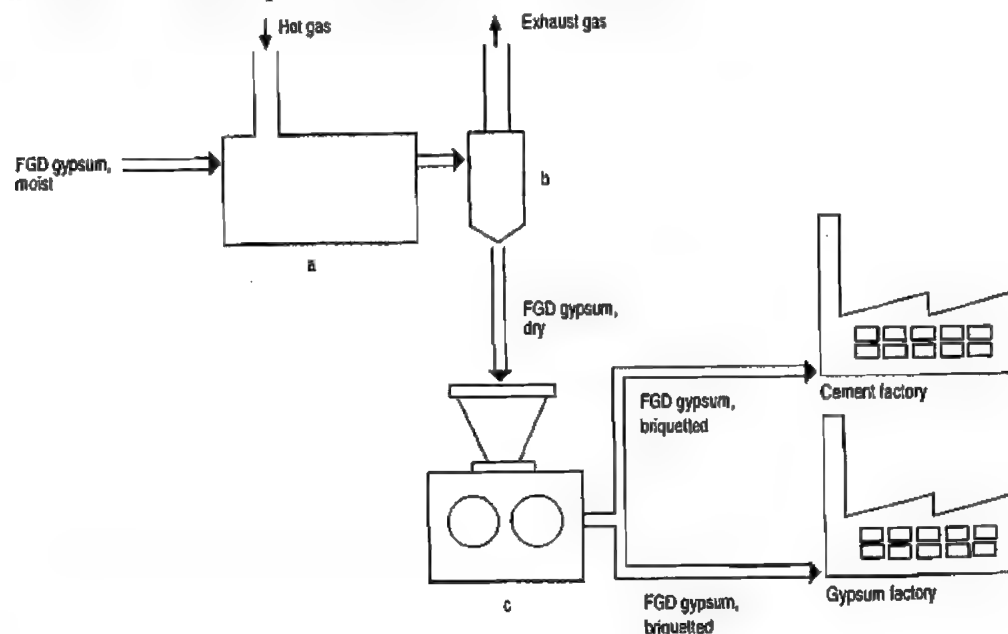


Figure 56.24: Flowsheet of a FGD gypsum drying and briquetting plant: a) Dryer; b) Cyclone; c) Press.

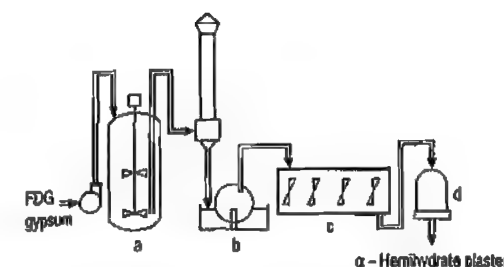


Figure 56.25: Production of α -hemihydrate plaster by the continuous autoclave process (Nitto Gypsum-Knauf): a) Autoclave; b) Expander; c) Vacuum filter; d) Dryer; e) Pulverizer.

α -Hemihydrate Plaster from FGD Gypsum

FGD gypsum is an ideal raw material for manufacturing α -hemihydrate plaster by the continuous autoclave process (Nitto Gypsum-Knauf). The gypsum is used in its original moist, finely divided state without predrying. In the continuous autoclave process, shown schematically in Figure 56.25, FGD gypsum having a free water content of 10% is slurried with water (one part gypsum, two parts water) and pumped continuously into the autoclave where it is dehydrated to α -hemihydrate under controlled conditions (135°C , 2 h). Additives in the suspension change the crystal habit of the α -plaster and yield a product of defined, consistent properties. The α -hemihydrate produced is withdrawn as an aqueous suspension and dewatered in a vacuum filter. The product that has a free water content of ≈ 10 –15% is immediately dried at $\approx 150^\circ\text{C}$ in an indirectly heated dryer and ground. This dry α -hemihydrate can then be used for all types of α -hemihydrate plasters and products.

Today the continuous autoclave process is also used industrially for the processing of finely divided natural gypsum and synthetic gypsum.

Another α -hemihydrate plaster process was recently developed especially for utilizing lignite FGD gypsum (ProMineral-SICOWA). The moist, finely divided FGD gypsum is mixed with auxiliaries, pressed into stable stackable blocks and converted into α -hemi-

hydrate plaster in large hot pressure autoclaves. The resulting blocks of α -gypsum are dried and ground. Important applications for this type of α -gypsum are the manufacture of self-levelling floor plaster, floor slabs and mining mortar.

Other continuous autoclave processes have ceased operations within a few years (Giulini), never got beyond the pilot stage (ICI), or remained dormant in patents.

Processes in which α -hemihydrate is produced without pressure in sulfuric acid, nitric acid, or salt solutions are found in the literature, but they never came into operation.

All efforts to produce an α -hemihydrate plaster similar in its properties to β -hemihydrate plaster have so far been unsuccessful.

56.6.3.3 Phosphogypsum to Calcined Products

Moist, finely divided phosphogypsum is a waste from the production of wet phosphoric acid [67]. It is available as filter cake with free water content of 20–30%. The content of impurities is high and the impurities must be removed or rendered harmless by operations such as washing, flotation, and recrystallization before phosphogypsum can be used by the gypsum industry.

All phosphogypsums contain inorganic impurities such as phosphates, nitricfluorides, and sodium salts. They affect the properties of the gypsum.

Organic impurities and small amounts of radiation (^{226}Ra) are present in sedimentary phosphate rocks (Morocco), part of which appears in the gypsum. Magmatic phosphate rocks (Kola) contain no organic impurities and no radioactive matter.

The unsuitable crystal shape of all phosphogypsums must be modified by fine grinding or by recrystallization.

The one- and two-stage phosphoric acid processes that have been developed for the manufacture of wet phosphoric acid produce different qualities of phosphogypsum. In the

one-stage processes, phosphogypsum is obtained as dihydrate (dihydrate process, e.g., that of Prayon, altogether representing 84% of all phosphogypsum produced) or hemihydrate (hemihydrate process, e.g., that of VEBA [130] or Fisons [131], but representing less than 1%).

In the two-stage phosphoric acid processes, either gypsum or hemihydrate is produced in the first stage. In the second stage it is converted to another state of hydration before being removed by filtration. These processes include the hemihydrate-dihydrate process (e.g., Nissan [132]; 15% of all phosphogypsum produced) and the dihydrate-hemihydrate process (e.g., Central Prayon [133], less than 1%). Generally, gypsum obtained from the two-stage processes is of better quality in regard to inorganic impurities such as phosphate, fluorine, and sodium.

The gypsum industry is faced with the need for recovery operations if it attempts to use phosphogypsum [134, 135]. Removal of organic impurities, which discolor the gypsum, and of water-soluble inorganic contaminants, which cause efflorescence, involves first remashing the phosphogypsum with water, then subjecting it to flotation, classification (hydrocyclone), thorough washing, and filtering. Up to 5 t of water per tonne of phosphogypsum is consumed. Gypsum purified in this way is obtained as filter cake with a free water content of 20–30%.

For production of β -hemihydrate intended for gypsum building components the filter cake is dried (e.g., rapid dryer from Hazemag, or the contact dryer from Serapic) and then calcined to β -hemihydrate in the same way as finely ground natural gypsum. Today this method is still the principal one used by the gypsum industry in Japan, where this method was developed in 1940 by Yoshino.

For use in gypsum building plaster and multiphase plaster, phosphogypsum is made unsuitable by its particle shape, fineness, and isomorphous acid phosphate impurities. Its particle shape and fineness seriously impair the workability of the multiphase plaster, i.e., the plaster is thixotropic. The cocrystallized

acid phosphates cause calcined products to develop lime sensitivity, which interferes with setting and development of the strength [136].

In order to overcome these deficiencies the phosphogypsum is dried, calcined, and after addition of aqueous calcium hydroxide suspension simultaneously agglomerated and recrystallized in a pelletizer. Such alkaline-recrystallized pellets are used as starting material for gypsum building plaster and multiphase plaster.

In one process *phosphohemihydrate* gypsum is the starting material. If the process is carried out with adequate care, the phosphohemihydrate is sufficiently pure that the gypsum recovery phase can be dispensed with. The fine phosphohemihydrate, having a residual water content of ≈ 20 –25%, is mixed immediately with a calcium hydroxide suspension or calcium hydroxide powder so that the calcium sulfate crystallizes into coarse-grained dihydrate. Part of the moisture and all of the acid phosphate are bound chemically, and the particle size and structure are satisfactory.

The phosphogypsum pellets or lumps thus produced can then be calcined and further processed in rotary kilns or, after grinding, in kettles to produce a β -hemihydrate plaster similar in composition to plaster of Paris. They can be converted on a conveyor grate into overburnt plaster, which consists of coarse particles and is comparable to multiphase plaster. These plasters can be processed into all kinds of machine-applied and premixed plasters.

Such processing methods were developed and put into operation by Knauf in 1962 and 1970. Most other processes designed to use phosphogypsum (e.g., those of Rhône-Progil, Charbonnages de France, Chimie-Air Industrie, Imperial Chemical Industry, Buell) have not resulted in viable commercial operation.

The recovery operations required by phosphogypsum involve additional capital expenditure and operating costs, jeopardizing its competitiveness with natural gypsum and generally rendering phosphogypsum uneconomical for commercial use. The repercussions felt after the first energy crisis, in 1973, because

the extra treatment is energy intensive, were an additional set-back.

Phosphoric acid producers do not pay for the extra treatment required by the gypsum manufacturer. In summary, the conclusion must be drawn that the chance of phosphogypsum ever being utilized on a large scale worldwide is extremely remote, even though disposal of phosphogypsum is becoming more of a problem [104].

Only Japan has so far managed to continuously use phosphogypsum, an accomplishment favored by its total lack of natural gypsum resources. South Korea also uses phosphogypsum as a source of gypsum.

56.6.3.4 Anhydrite Plaster

Anhydrite plaster is produced by grinding anhydrite rock in tube mills or impact pulverizers to a particle size below 0.2 mm. Activators to promote setting are added together with the gauging water. However, the very fine grinding is expensive.

The activators are mixtures of alkali-metal or heavy-metal salts and calcium hydroxide, up to $\approx 2\%$ of the anhydrite. Acid activators, e.g., potassium hydrogensulfate or iron(II) sulfate, can also be used [138].

Fluoroanhydrite, a dry fine powder, is neutralized with calcium hydroxide and ground very finely for use as an anhydrite plaster. Sulfates, e.g., potassium sulfate and zinc sulfate, and calcium hydroxide or Portland cement are activators [139], which are usually added and mixed with the anhydrite powder in the factory.

Natural anhydrite and fluoroanhydrite differ from each other in crystal structures. Fluoroanhydrite consists of very small primary crystals that have been agglomerated to secondary particles with a high specific surface area and high reactivity, whereas natural anhydrite consists of large primary particles, which are rendered reactive by fine grinding.

Recently, a process has been developed for the manufacture of thermal anhydrite from FGD gypsum using the suspension gas calcining process (POLCAL® process). The appara-

tus consists of one or more preheating cyclones, a reactor with integrated separating cyclone, and a cyclone coder. The conversion temperature is above 700 °C, and the residence time of the small gypsum particles in the reactor is a few seconds.

Thermal anhydrite from FGD gypsum is used as a binder component in self-levelling floor plasters [101].

56.6.4 Use and Properties of Gypsum Plasters and Products and Anhydrite Plasters

56.6.4.1 Hydration, Setting, Hardening

Calcium sulfate hemihydrate, anhydrite III, and anhydrite II undergo hydration under ambient conditions, converting into calcium sulfate dihydrate. If hydration is carried out with just enough water to produce a homogeneous, fluid, stable, nonsedimenting slurry, then this mixture sets and hardens because the calcium sulfate dihydrate forms needles that intergrow and interlock.

Much research has gone into the mechanism of hydration. Around 1900, LE CHÂTELIER [140, 141] established the theory of crystallization, which gained universal acceptance [142, 143]. According to this theory the calcium sulfate hemihydrate in water first forms a saturated solution, about 8 g/L at 20 °C. However, this solution is actually supersaturated, because at 20 °C calcium sulfate dihydrate has a solubility of only 2 g/L, and $\text{CaSO}_4 \cdot 2\text{H}_2\text{O}$ precipitates.

CAVAZZI [145], and later BAYKOFF [146], put forward a colloid theory, which states that the hydration proceeds via a colloidal intermediate involving formation of a type of gel or an adsorption complex between the calcium sulfate hemihydrate and water. However, this gel has not yet been demonstrated experimentally.

In recent years the Le Chatelier theory of crystallization has been supplemented by the detection of topochemical reactions taking place during hydration [147]. The two mecha-

nisms are not mutually exclusive, because transformation into dihydrate in both cases takes place via the solution phase. The topochemical hydration is an internal hydration of the hemihydrate particles taking place over very short distances.

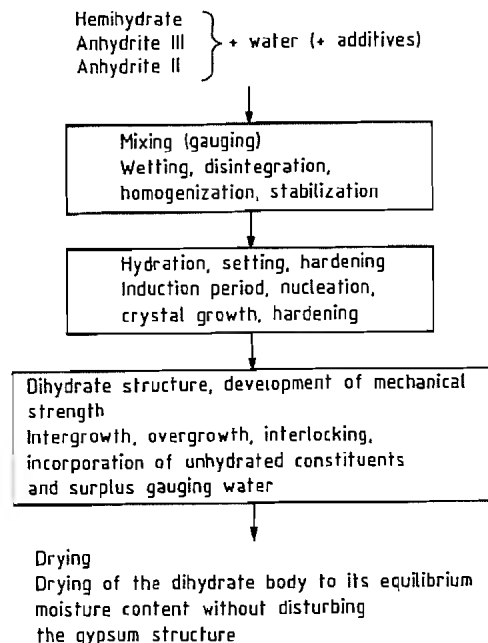


Figure 56.26: Stages of hydration, setting, and hardening of calcium sulfates.

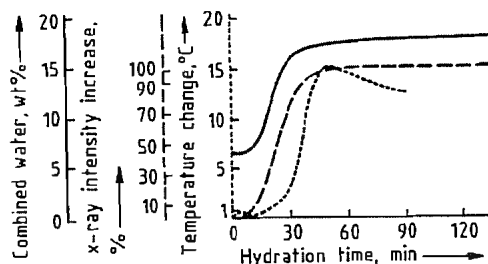


Figure 56.27: Rate of hydration of β -hemihydrate demonstrated by combined water content (—), intensity of x-ray diffraction (---), and temperature increase from heat of hydration (···) [150].

Formation of dihydrate crystals conforms to the laws of nuclei formation and crystal growth (Figure 56.26). Mixing and wetting of the hemihydrate powder, which causes disintegration of the hemihydrate particles, is fol-

lowed by a short induction period, after which nuclei begin to form from the supersaturated solution. The accumulation of very small dihydrate crystals with much excess water has been described by KRÖNERT et al. as clustering [148]. Subsequently, after this nucleation, crystal growth begins, which at least initially is accompanied by continuous recrystallization [144]. The rate of nuclei formation is proportional to the relative supersaturation (von Weimarn's theory), and the rate of crystal growth is proportional to the absolute supersaturation (Nernst-Noyes equation). Hemihydrate is converted directly into dihydrate; there are no intermediate stages. Anhydrite III is converted via the hemihydrate, and anhydrite II is converted directly into dihydrate, without anhydrite III or hemihydrate intermediates. If the proportion of water is correct for setting and hardening, the slurry hardens by forming a dihydrate structure, a final crystallization, which according to LUDWIG et al. [149] consists of intergrown, overgrown, and interlocking dihydrate crystals and inclusions of unhydrated components. Excess water can be removed by drying.

The rate of hydration of β -hemihydrate as shown in Figure 56.27 is demonstrated by combined water content, intensity of the X-ray diffraction, and rise in temperature due to the heat of hydration [148].

There are many ways in which these processes of hydration, setting, and hardening can be applied in practice. Parameters for characterizing these processes are the water-to-plaster ratio on mixing, the consistency of the mixture, the initial and final set, the rate of strength development, and the strength and density of the final dry gypsum product.

The method of manufacture of the plaster influences the gypsum technology to a very large extent. For instance, β -hemihydrate from a rotary kiln requires more water to produce a fluid slurry of uniform consistency than does plaster from a kettle. The latter, in turn, requires more water than multiphase plaster, which, in turn, requires more than autoclave plaster. This water-to-plaster ratio (water capacity of the gypsum plaster), an inverse of the

quantity of gypsum plaster in grams per 100 g of water, is related to the strength and density of the set and hardened gypsum product.

α -Plasters, which are workable with little water, can be simply turned into gypsum products of high strength and high density. However, these products are avoided in the building industry on account of their brittleness.

β -Plaster and multiphase plaster require more water than α -plaster to obtain a fluid consistency. They produce products of average strength, higher elasticity, and lower densities, and are used universally in the construction industry.

The particle shape, particle-size distribution, and specific surface area also determine the quantity of water required to give a specific consistency. Generally, very fine plaster requires more water than coarse-grained plaster. Rod-shaped particles also increase the amount of water needed. β -Hemihydrate particles may disintegrate on first contact with water, breaking up into a multitude of very fine loose particles, thus changing their particle size distribution [151]. The particle size distribution of multiphase plasters determines their workability to a great extent.

When stored, calcined gypsums are subject to changes in their properties, called *aging*. This aging is caused to some extent by the uptake of water vapor from the air. The degree of aging affects the water needed for given consistency; more water is needed for fresh calcined gypsum than for aged. If a considerable amount of water vapor is adsorbed, dihydrate nuclei may form, accelerating the hydration process. However, the reactions taking place on aging have not yet been entirely elucidated [150, 152]. Natural aging of calcined gypsum produces gradual changes in the properties of the plaster over a period of months. To avoid this, methods have been developed to bring about aging artificially, so that the plaster undergoes no significant changes during storage. One process is called aridization: calcium chloride or similar salts are added in quantities up to about 0.2% to the raw gypsum before calcination [153]. Aging of calcined gypsum

is also achieved by injecting small quantities of water containing a wetting agent to prevent the formation of a dihydrate [154, 155].

The mixing and gauging of calcined gypsum with water to form a slurry of specific consistency can be affected by various wetting agents. Most of these, called *plasticizers* or water-reducing agents, lower the water demand. They include alkylarylsulfonates, lignosulfonates, or melamine resins [156]. It is also possible to increase the water requirement by adding flocculating agents, e.g., polyethylene oxide [157]. Chemicals that thicken, e.g., cellulose and starch ethers, can be added to stabilize the water plaster slurry or prevent sedimentation and segregation; however, these have little effect on water demand [158].

Setting and hardening can be accelerated or retarded by numerous additives [159, 160]. Many inorganic acids and their salts are useful as *accelerators*, especially sulfuric acid and its salts. Calcium sulfate dihydrate is regarded as a special additive in this respect. Finely divided, it acts as a strong accelerator and therefore must be completely removed when raw gypsum is calcined. The accelerating effect of these substances is due to an increase in solubility and the rate of dissolution of the calcined gypsum and to an increase in the rate of nuclei formation.

Retarders are usually organic acids [161] and their salts and organic colloids that are the decomposition and hydrolysis product of biopolymers such as proteins as well as salts of phosphoric acid or boric acid. The mechanism of retardation varies: high molecular mass colloids prolong the induction period because they are nuclei poisons. Other retarders slow down the rate of dissolution of the hemihydrate or the growth of the dihydrate crystals. The hydration of anhydrite II usually does not have to be retarded since it is slow enough and almost always requires acceleration.

In every case, temperature affects the rate of hydration of plaster, the rate increasing up to $\approx 30^\circ\text{C}$, after which it decreases [162].

The *strength* of set dried gypsum is directly proportional to its density, therefore dependent only on its porosity or, less directly, on

the water-to-plaster ratio and the size and structure of the pores [163, 164]. The strength is affected by moisture or additives without a change in density. The strength of gypsum products with a moisture content exceeding 5% is only about one half that of air-dried gypsum products. When a gypsum product dries, the strength begins to increase below 5% moisture content, becomes evident around 1% moisture content, and reaches its final value in the region of its equilibrium moisture content [65].

Persistently moist conditions reduce strength, because crystalline and textural changes, especially recrystallization, take place as a result of the solubility of gypsum in water [165]. The deformation or creep of moist gypsum products under mechanical stress is likewise the result of structural change. Additives induce a change in structure by changing the crystal habit of the dihydrate so that without a change in density strength is changed even in the dry state.

An extreme example of reducing strength is the effect of citric acid, commonly used as a retarder. Used sparingly, less than 0.1%, it does have a retarding effect and lessens the strength only slightly. More, say, above 0.2%, changes the crystal habit of the dihydrate to such an extent that hardening of the gypsum is no longer possible because the crystals no longer interlock and intergrow [166].

MURAT [167] has studied the morphology of natural and synthetic calcium sulfate dihydrates with up-to-date techniques and the effects of additives upon the crystal habit of the dihydrate.

56.6.4.2 Prefabricated Gypsum Building Components

Prefabricated gypsum building components are manufactured in large quantities: plasterboards, partition panels, ceiling tiles, and fiber-reinforced boards. These are light, porous, dry, and nonbrittle products possessing excellent workability. β -Hemihydrate is the starting material for all these because it sets quickly and easily meets the building industry's de-

mand for certain properties for the finished product.

The plants for the manufacture of gypsum building components are usually built adjacent to gypsum works.

Gypsum *plasterboards* are large thin gypsum panels covered with cardboard; they have a density of 750–950 kg/m³. They are manufactured by feeding β -hemihydrate plaster into a continuous mixer from controlled feeding devices, mixing it continuously with water and additives, e.g., adhesives, to form a homogeneous and rapidly setting slurry. This slurry is spread on a continuous sheet of cardboard about 0.5 mm thick (200–300 g/m²). The slurry is then covered with a second sheet of cardboard and passed over a molding platform to be shaped into a completely encased strip, 1.20–1.25 m wide and 9.25, 12.5, 15.0, 18.0, or 25.0 mm thick. This strip of gypsum plasterboard, initially soft, hardens within minutes and is cut into separate panels. These panels, with approximately one third of their weight being free water, are dried immediately in a continuous tunnel dryer heated either indirectly with steam or directly with gas or oil. The finished gypsum plasterboard, consisting of a gypsum core tightly encased and bonded to cardboard, is considered to be a laminated building material.

Many different types of gypsum plasterboards are manufactured, depending on their intended use. Distinctive features are size, edge configuration, weight, water resistance, structural behavior, and strength. Gypsum plasterboards with specific fire-resistant properties incorporate fiberglass. The noncombustible gypsum lightweight board is a recent development, making use of a laminate of glass fiber mat with a lined-on glass silk scrim to replace the cardboard [168]. Modern plants for the manufacture of plasterboards have a capacity of about $(20\text{--}40) \times 10^6$ m² per year and an annual consumption of 150 000–300 000 t of hemihydrate plaster.

Plasterboard is used in interior finishing, e.g., for wall and ceiling panelling. It is screwed to wooden or metal frames or pasted on masonry or concrete with special building

plaster (adhesive plaster, the German *Ansetzgips*). The joints are covered and finished with special paper and joint filler to form a smooth surface. Plasterboard can also be used for the construction of dismantable partitions and lightweight dividing walls having various characteristics (weight, sound proofing, fire resistance) in concrete or steel-framed buildings as well as in prefabricated dwellings. Plasterboard undergoes further processing in factories into special-sized panels, coffers, or lightweight laminated panels with intermediate layers of polystyrene or polyurethane, the last called insulating board. Multilayered plasterboards are used for dry floorings and for the construction of lift shafts. Factory-made tiles with decorative surface finishes such as plastic sheet or special coats of paint or else an aluminum foil to prevent water vapor transmission are available.

Gypsum *partition panels* consist of set gypsum plaster. To produce them β -hemihydrate plaster is mixed with water (water-to-plaster ratio 0.9–1.0) and the slurry, which sets quickly, is poured into molds. After 5–8 min the panels are taken out of the molds and dried [169].

The standard size of gypsum partition panels is 500 × 666 mm, with a thickness of 60, 70, 80, or 100 mm and a density of 700–900 kg/m³. They are used in interiors as lightweight dividing walls, the tongue and groove joints being bonded with joint plaster. The partition walls can be single or multilayered. Characteristic features are low weight, average to good sound insulation, and excellent fire resistance.

Gypsum *ceiling tiles* are produced by mixing β -hemihydrate, water, and small amounts of glass fiber and pouring the slurry into rubber molds. The molds allow for designs of individual choice.

Ceiling tiles are used as decorative tiles, ventilation tiles, heating tiles, or sound-proofing tiles with mineral wool bonded on the back. They are screwed to a base frame and fitted into the framework. They are normally 625 × 625 mm in size and weigh between 10 and 20 kg/m².

Gypsum *fiber board* and fiber-reinforced gypsum elements are another group of gypsum building components manufactured from hemihydrate plaster and paper fibers, glass fibers, or another type of fiber material [170–174]. Glass fiber, as mat or web, can be incorporated [175]. The proportion of fiber in these components, evenly distributed in the plaster, ranges up to 15%. These fiber boards have an apparent density between 800 and 1200 kg/m³.

Factories for the manufacture of gypsum partition panels and ceiling tiles have capacities up to 1 000 000 m²/a, consuming about 50 000 t/a of hemihydrate plaster, or else gypsum fiber boards up to 10×10^6 m²/a, consuming the same amount of hemihydrate.

56.6.4.3 Gypsum Plaster

Calcined gypsum is used for plastering. Best is multiphase plaster (Table 56.19) because its phase composition results in quick initial setting and gradual final setting; smoothness, plasticity, and high coverage; single-coat application without additives or aggregates; rapid drying of the finished plasterwork; and suitable density and high strength.

β -Hemihydrate plaster without additives is not suitable for plastering because the initial setting occurs too late and the final setting too early. Also its particle size distribution is not suitable for plaster. However, additives permit β -hemihydrate to be made into certain types of plastering material, known as retarded hemihydrate gypsum plaster and premixed lightweight gypsum plaster. Because of inadequate setting properties, lack of smoothness, and insufficient coverage, α -plasters are not used in construction [65, 176].

Over the past twenty years considerable progress has been made in Germany towards development of a factory-made machine-applied gypsum plaster. Ordinary multiphase plaster is used as the starting material. Mixed with additives it is processed into a material that can be used for continuous machine application in single coats. The rate of setting and

the hardening process have been adjusted to suit the longer working cycle for material applied over a large surface area. Too rapid water uptake is controlled by adding water-retaining hydrophilic colloids, e.g., methyl cellulose. In this way the soft plaster slurry remains plastic until the work has been completed, resulting in better bonding to the base. The uniformity of the properties and the homogeneity of these plasters are particularly good when they are manufactured in large plants.

Such plants are equipped with high-capacity mixing and handling devices (Figure 56.22) and can produce up to 400 000 t/a. At the construction site the dry plaster is fed continuously into the plastering machine (e.g., Gipsomat) where it is mixed with water at a metered rate to form a slurry applied in a single coat to the base by means of a screw pump and hose. A smooth and even surface is obtained with an electrically powered felting tool (e.g., Power Float, Gipsoglätt).

Table 56.21: Application properties of projection plaster, bonding plaster, and premixed plaster [64]. Tests conform to German (DIN) standard 1168 [111].

Property	Projection plaster	Bonding plaster	Lightweight plaster
Water:plaster ratio	0.45–0.65	0.60–0.80	0.55–0.75
Initial setting, min	60–120	40–90	40–90
Final setting, min	120–240	60–120	60–120
Strength of set and hardened gypsum, N/mm ²			
Flexural strength	1–2	1–2	1–2
Compressive strength	2.5–5	2.5–4	2.5–4
Apparent density of dry gypsum, kg/m ³	1000–1200	850–1000	900–1100
Coverage, m ² per 100 kg of plaster	> 60	> 120	> 110

In some countries, especially in Great Britain, the two- or three-coat method of plastering is still employed. The undercoat is browning plaster, a factory-processed hemihydrate plaster containing a retarder, which is mixed with sand or expanded perlite either in the factory or on the building site. It takes several hours to set, i.e., far longer than premixed plaster. The next day a smooth finishing coat of plaster of Paris and hydrated white lime is applied.

In France, Spain, some countries in North Africa and the Near East, and to some extent in southwest Germany, especially in the Saarland, pure multiphase plaster containing no additives (Paris construction plaster, southern

Plastering machines operated inside buildings are supplied with plaster directly from bins or containers installed just outside the building by pneumatic conveyor pumps through flexible hoses. Such a plastering machine can be operated by one person.

Premixed gypsum plasters (bonding plaster, lightweight plaster), factory-processed from β -hemihydrate plaster (or multiphase plaster) containing additives and aggregates, e.g., expanded perlite or vermiculite, are worked batchwise on site. The plasters are mixed with water and applied in one coat on all types of concrete and masonry. Premixed plasters already contain the necessary additives to ensure good workability. Only water need be added by the plasterer, who can then apply the plaster, independent of the weather, without fear of making a mistake. The application properties of these plasters are listed in Table 56.21.

German *Doppelbrandgips*, Saarland multiphase plaster) is used for single-coat and multicoat plasterwork. In countries with a dry climate, e.g., Iran, multiphase plaster is also used as mortar for brickwork and for external claddings.

56.6.4.4 Other Uses

Anhydrite capable of setting and α -hemihydrate plaster are extensively used as a binder for mining mortar and as a flooring plaster, uses where its brittleness is not a handicap [177].

Substantial amounts of natural anhydrite are consumed by the mining industry for the construction of roof supports for galleries and

ventilating air structures in coal mines. Dry mining anhydrite having a specified particle size distribution, e.g., 0–6 mm, and containing an accelerator is used in underground coal mines worked by the long-wall method. With the aid of large blowers the anhydrite is conveyed pneumatically through hoses and wetted at the site of use before being sprayed in layers to form a barrier. The anhydrite barriers rapidly develop a high initial compressive strength of about 15 N/mm², their strength exceeding 40 N/mm² after 28 d. They serve to support the gallery and roofs in the roadways [178]. α -Hemihydrate plaster is also used as a binder for mining mortars [179].

Finely ground natural anhydrite, processed fluoroanhydrite and α -hemihydrate plaster, all capable of setting, are used as binders for self-levelling floor plasters. When used for laying floor screeds, the cementitious material is first mixed with sand in the proportions of 2:5 and then batch-mixed with water in a pan mixer until it attains a stiff consistency. Piston pumps and hoses pump the mix to the different floors and rooms, where it is spread on the floors. More recently α -hemihydrate plaster, with or without additives, mixed with water to form a fluid slurry, has been used as machine-applied floor plaster (self-levelling floor plaster). Since calcium sulfate floor screeds do not shrink, they can be laid free of joints and, when properly done, free of cracks over a large surface area.

Substantial quantities of natural gypsum, FGD gypsum, and anhydrite rock are used as a retarder for Portland and blast-furnace cements. In compliance with German (DIN) standards, the maximum permissible calcium sulfate content of cement is 3% SO₃ for Portland cement and 4% SO₃ for blast-furnace cement [180]. Gypsum rock or FGD gypsum (briquettes) or anhydrite rock, or a mixture with a particle size range 5–50 mm, is directly added to the cement clinker before grinding. It is then present in the cement in a finely divided reactive form [181]. More than 50% of the entire gypsum and anhydrite rock production is consumed by the cement industry.

In Russia a *gypsum cement* mortar is manufactured by calcination of raw gypsum in combination with certain types of cement and active silica. Because of its water-resistant properties, this mortar is used for the production of prefabricated washrooms, occasionally also for exterior wall elements of prefabricated cottages. However, pure gypsum building components have not found widespread use externally because of the solubility of gypsum in water [66, 182, 183].

α -Hemihydrate is used as a high-strength molding material for roofing tile, cast metal, and dental materials [69]. Mixed with β -hemihydrate, α -hemihydrate is the favored molding plaster — especially for ceramics — because its expansion on setting and the strength and absorbency of the final mold can be varied by varying the α : β hemihydrate ratio [184]. Addition of high molecular mass compounds perhaps improves the stability of gypsum molds without adversely affecting the plaster. Molding plaster is used to make surgical casts and orthopedic bandages.

Calcium sulfate dihydrate is used as a soil stabilizer and to displace sodium in soils too high in sodium salts, e.g., those soils flooded by seawater. It also serves as a fertilizer in soils deficient in sulfur, especially in North America [185].

The classical Müller-Kühne process (gypsum-sulfuric acid-cement process) has once again become of interest for treating secondary materials such as unrefined calcium sulfite and calcium sulfate from FGD or SAP spray absorption residues (OECD Amber List AB 150) [106], gypsum wallboard or plasterboard from demolished buildings (OECD Green List GG 20) [106], or fly ash. Today in Wolfen, Germany, 100 000 t/a of cement is produced by the Müller-Kühne process [186].

Unrefined calcium sulfite and calcium sulfate from FGD or SAP spray absorption residues, together with fly ash and activating additives, can be converted to a stabilized back-filling material for landfills and mining caverns [187].

The Merseburg process for the manufacture of ammonium sulfate from natural gypsum or

phosphogypsum has never been important because the demand for ammonium sulfate has always been met from the large quantities arising as by-product in the chemical industry [188].

Anhydrite III is an effective drying agent (Drierite) in laboratories and in industry.

Fillers made from FGD gypsum have been investigated thoroughly and their application in adhesives, paints and plastics gave good results. In principle, it is possible to produce calcium sulfate fillers from FGD gypsum, but the economic situation compared to competitive fillers is unsatisfactory [189].

Also coating pigments produced from FGD gypsum for the paper industry have been developed, showing new fields of application of FGD gypsum outside the construction industry [190].

Natural gypsum and anhydrite are insufficiently pure and therefore not suitable for producing fillers and coating pigments.

In the beverage industry, especially breweries, pure natural gypsum is used to obtain and standardize the desired water hardness.

Processes for the manufacture of calcium sulfate whiskers, developed in the United States and Japan, have not yet become established [191].

Pure finely ground anhydrite has found a ready market in the glass industry as a substitute for sodium sulfate because of its low price.

56.6.4.5 Properties of Gypsum Building Products Installed in Situ

Gypsum building materials are suitable for the construction of non-load-bearing interior finishes in dry locations. Gypsum building components and prefabricated units are dried at the factory. Gypsum plasters dry after application, with ventilation within a few days. These plasters adhere to the base well [192, 193]. Once gypsum building materials are sufficiently dry, i.e., moisture content < 2%, they can be decorated immediately with interior coatings, wallpaper, ceramic tiles, and other facings. The surfaces of gypsum building materials are inert [194].

Table 56.22: Gypsum building materials and their properties.

	Plasterboard, 9.5 mm thick	Finished gypsum projection plaster
<i>Apparent density and porosity</i>		
Density, kg/m ³	900	800–1200
Pore volume, %	60*	50–65
Pore radius, μm	≈ 99% > 0.05	≈ 99% > 0.05
<i>Climatic properties</i>		
Heat conductivity λ, W m ⁻¹ K ⁻¹ (DIN 4108)	0.21	0.35
Heat penetration coefficient b (equivalent) 1/2 h test, Js ^{-1/2} m ⁻² K ⁻¹	412	1200
2-h test	489	1400
Resistance to transmission of water vapor μ (DIN 4108)	8	10
Water vapor absorption coefficient a, m/h		
untreated surface	2.29	
rough fiber coated	2.98	2.5
wallpapered	2.66	
<i>Heat expansion and equilibrium moisture content</i>		
Linear coefficient of thermal expansion α, K ⁻¹	(13–20) × 10 ⁻⁶	20 × 10 ⁻⁶
Equilibrium moisture content at 20 °C and 65% relative humidity, %	0.6–1.0	0.3
Modulus of elasticity, N/mm ²	2000–2500	2800

*Core.

to fire because of the fibers in the material [63, 196].

56.6.5 Material Testing and Chemical Analysis

56.6.5.1 Standards

Today there are international standards for gypsum products (ISO — International Standards Organisation), European standards (CEN — Comité européen de coordination des normes), and national standards (e.g., DIN, Germany; AFNOR, France; B.S., United Kingdom; ASTM, United States; GOST, Russia; J.I.S., Japan).

Eurogypsum, the Association of European Gypsum Industries, through its scientific and technical committee, constantly exchanges information with the International Standards Organisation [197] and RILEM, the International Union of Testing and Research Laboratories for Materials and Structures. The German standards for gypsum comprise material standards [111, 198–201] and application standards [202–215].

European standards (EN) for gypsum building materials are in preparation. Quality assurance systems and standards, in accordance with ISO 9000, are being introduced into the gypsum industry.

56.6.5.2 Testing

The German (DIN) standard methods of testing for gypsum building plasters comprise tests on particle size by sieving, initial set with a water: plaster ratio defined by the water capacity of the plaster or the spread in a flow table test, flexural strength, compressive strength, and hardness. A test for bond strength, e.g., for bonding plaster to concrete, is also recommended. Gypsum partition panels and gypsum ceiling tiles are characterized by apparent density, dimensions, weight, and breaking load. Plasterboards are characterized by dimensions, weight, breaking load, and permanent deflection after specified loading and unloading.

Figure 56.28: Structure of set and hardened gypsum (scanning electron micrograph). The structure shown in the photograph of set hemihydrate plaster is typical of rehydrated gypsum: the characteristic features are determined by needle-like particles that interlock and intergrow and by the high degree of porosity (2000×).

Table 56.22 summarizes some of the most important properties of gypsum building products installed in situ [64, 195]. Set and hardened gypsum has low density and high pore volume and thus has a low thermal conductivity. The large pore size allows rapid absorption and desorption of water vapor, resulting in high breathing capacity. Gypsum walls and ceilings in living and working rooms feel warm to the touch; they do not sweat. Figure 56.28 shows a scanning electron micrograph of the structure of set and hardened gypsum.

Gypsum building materials have volume stability, only slight changes in size resulting from changes in temperature or moisture content. Their equilibrium moisture content is below 1%; however, permanent wetting and continuous exposure to temperatures above 60 °C change the crystal structure, and should be avoided.

Gypsum building materials promote fire protection because of the combined water of the dihydrate, which, in case of fire, evaporates, not allowing the other surface of the gypsum to reach much above 100 °C. Plasterboard and fiber-reinforced gypsum boards retain their structural integrity during exposure

A method for determining the Blaine specific surface area is used for comparative testing [216]. A simple and inexpensive device for the determination of impact strength can be used for comparative and routine testing, especially for building components [217, 218].

The ceramic industry, which itself has not yet established any guidelines for the testing of molding plaster, determines additional properties, such as setting and final expansion and water absorption coefficient. A standardized vacuum mixer is used to gauge the gypsum slurry and to remove air bubbles from the mixture [219].

Classification of gypsum building materials with regard to their behavior during fires is set out in DIN 4102. Gypsum building materials come within Class A, rated as noncombustible building materials. Materials with no combustible components (such as plaster, partition panels, and ceiling tiles) are classified as Class A1. Gypsum plasterboard is classed as Class A2. For materials classified under Class A2 there are limits for smoke density and toxicity.

Gypsum building materials and components that comply with DIN 4102 are ideal for structures ranging from fire-retardant to highly fire-resistant walls, partitions, ceilings, steel columns, and supporting beams. Test certificates issued for built-in components are based on compliance with Classes F30, F60, F90, F120, and F180 — fire retardant to highly fire resistant. The figures 30–180 denote the fire resistance rating (period of time in minutes) of the components for a given temperature–time curve.

56.6.5.3 Chemical Analysis

Conventional chemical analysis [57] is used in arbitrational analysis. Free water content in raw gypsum, calcined gypsum, and set and hardened gypsum is determined by drying at 45 °C. Combined water content is determined by drying at 360 °C.

Calcium sulfate in solution is qualitatively determined by precipitation of syngenite, $\text{CaSO}_4 \cdot \text{K}_2\text{SO}_4 \cdot \text{H}_2\text{O}$.

Today the following methods of analysis are used for routine quantitative testing in the laboratories of the gypsum industry: complexometric titration of calcium and magnesium; flame photometry for sodium and potassium; and atomic absorption for sodium, potassium, magnesium, calcium, strontium, iron, aluminum, and sulfate, the last indirectly, via barium [220]. The phosphates contained in phosphogypsums are determined spectrophotometrically or gravimetrically with ammonium molybdate. Water-soluble, citrate-soluble, and total phosphates are distinguished. Fluorine can be determined titrimetrically. Organic substances can be determined by oxidation with potassium permanganate. Acidity is determined by titration with alkali using methyl orange or bromophenol blue. Calcium sulfite is determined via SO_3 ; chlorine, by the Volhard method or with a chloride electrode.

56.6.5.4 Phase Analysis

Phase analysis differentiates between dihydrate, hemihydrate, anhydrite III, and anhydrite II, including its three reaction stages AII-s, AII-u, and AII-E. This differentiation of calcined gypsum according to phases is not possible by chemical analysis.

Phase analysis can be carried out by x-ray diffraction, infrared spectroscopy, microscopy, and calorimetry. However, it takes considerable experience to reach $\pm 5\%$ accuracy [221]. The conventional method in any industrial laboratory is the gravimetric determination utilizing the differing rates of hydration [55, 57, 222, 223].

The determination of dihydrate is not especially accurate, particularly when small quantities ($\leq 5\%$) are involved. In such cases, however, an exact determination is possible by differential thermal analysis [224, 225].

The determination of anhydrite II by exposure to moisture is a matter of definition. Thus the anhydrite hydrating within three days is designated as AII-s, anhydrite hydrated in seven days as AII-u, and anhydrite that after seven days remains nonhydrated is assigned to

the nonhydrated constituents and can be determined by an additional measurement. (By the addition of a 1% aqueous potassium sulfate solution in place of distilled water the seven-day period can be reduced to a few hours [55].) The stages AII-s and AII-E can be distinguished from each other by measurements of the pH value, which for AII-E is above 9, but is otherwise 6–7.

Distinction between α - and β -hemihydrates is not possible by hydration methods. Today α -hemihydrate and β -hemihydrate are usually determined by microscopy, the quantitative proportions are simply estimated.

56.6.6 Economic Aspects

The estimated world consumption of natural gypsum and natural anhydrite in the gypsum and cement industries was ca. 95×10^6 t/a in 1995.

The cement industry, as the largest consumer of raw gypsum and raw anhydrite, used ca. 55×10^6 t/a for a world cement production of 1400×10^6 t in 1995.

The gypsum industry uses ca. 40×10^6 t/a natural gypsum and anhydrite and ca. 5×10^6 t/a FGD gypsum. Less than 2×10^6 t/a of phosphogypsum is used, mainly in Japan, Korea, and Europe. Titanogypsum and fluoroanhydrite consumption is less than 1 Mio t/a worldwide.

The most important gypsum building materials are gypsum plasterboards with a per capita consumption of 8 m²/a in the United States; 6 m²/a in Japan; and 2 m²/a in the EU, with the highest consumption in France and Great Britain (ca. 3 m²/a), and the lowest in Spain and Portugal (0.35 m²/a). Machine-applied plaster is important in Central Europe, and multiphase plaster in Spain, Italy, North Africa, and the Near East.

Since 1985 the demand for calcium sulfate has increased at an average annual rate of 5% in Asia, 3% in Western Europe, and 1% in North America [226].

The gypsum and cement industries will remain the prime consumers. In only a few

countries, perhaps China and the countries in Eastern Europe, the states around the Persian Gulf, and some rapidly developing areas in the Far East, is gypsum consumption expected to rise in response to increased building activities.

56.7 Calcium Chloride

Calcium chloride is found in small quantities, along with other salts, in seawater and in many mineral springs. It is found in higher concentrations in natural brines in California and Michigan (USA), in the mineral antarcticite, $\text{CaCl}_2 \cdot 6\text{H}_2\text{O}$; in the yellow colored mineral tachhydrite (from the Greek word meaning easily soluble), $2\text{MgCl}_2 \cdot \text{CaCl}_2 \cdot 12\text{H}_2\text{O}$; and in the mineral chlorocalcite, KCaCl_3 . Calcium chloride is reportedly also contained in small amounts in the mineral carnallite, KMgCl_3 [227–230].

Calcium chloride appears to have been discovered as early as the 15th century but apparently received little attention or study until the latter part of the 18th century. All of the work was done with laboratory prepared samples because it was not commercially produced until after the development of the Solvay ammonia–soda process in the mid-1800s. This process was originally designed to produce soda ash (crude sodium carbonate). Calcium chloride was considered a waste product until uses for it were developed some years later. Its importance has grown continuously to the extent that it is now invaluable for various uses, including ice and dust control, oil well drilling, refrigeration, coal thawing, and food processing. Natural brines now account for as much as 70–75% of United States calcium chloride production [231, 232].

56.7.1 Physical Properties

Calcium chloride, CaCl_2 , is a white, odorless, extremely water soluble salt that forms hydrates with properties as indicated in Table 56.23.

Table 56.23: Properties of pure calcium chloride, anhydrous and hydrates (Courtesy Allied Corp.).

Property	CaCl ₂	CaCl ₂ ·H ₂ O	CaCl ₂ ·2H ₂ O	CaCl ₂ ·4H ₂ O	CaCl ₂ ·6H ₂ O
CaCl ₂ , %	100.00	86.03	75.49	60.63	50.66
mp, °C	772	260	176	45	30
bp, °C	1670	—	—	—	—
ρ (25 °C), g/cm ³	2.22	2.24	1.85	1.83	1.72
Heat of formation (18 °C), kJ/kg	-7190	-8160	-9490	-10 980	-11 911
Heat of fusion, kJ/kg	256 (772 °C)	—	—	—	170 (30 °C)
Heat of hydration (anhydrous salt), kJ/kg	—	-240	-295	-600	-840
Heat of solution ^a (hydrate, 291 °C), kJ/kg	-680	-380	-290	-50	+80
Specific heat (hydrate), JK ⁻¹ kg ⁻¹	670	840	1170	1340	1420

^aOne mol solute in 400 mol of water, except monohydrate, which is in 300 mol.

Table 56.24: Data for Figure 56.29 (Courtesy Allied Corp.).

Area	Saturation curve for	% CaCl ₂		Temperature, °C		Liquid phase contains % CaCl ₂		Solid phases	Solid phase transition at	
		from	to	at and below	from	from	to		% CaCl ₂	°C
A	ice	0	29.8	0	-55	0	29.8	ice		
B		0	50.7	-55				ice	29.8	-55
C	CaCl ₂ ·6H ₂ O	29.8	50.7	-55	+29.8	29.8	50.3	CaCl ₂ ·6H ₂ O		
D		50.7	60.6	+29.8				CaCl ₂ ·6H ₂ O		
E	CaCl ₂ ·4H ₂ O	50.3	60.6	+29.8	45.3	50.3	56.6	CaCl ₂ ·4H ₂ O		
F		60.6	75.5	45.3				CaCl ₂ ·4H ₂ O	56.6	45.3
G	CaCl ₂ ·2H ₂ O	56.6	75.5	45.3	175.5	56.6	74.9	CaCl ₂ ·2H ₂ O		
H		75.5	86.0	175.5				CaCl ₂ ·2H ₂ O	74.9	175.5
I	CaCl ₂ ·H ₂ O	74.9	86.0	175.5	260.0	74.9	86.0	CaCl ₂ ·H ₂ O		
J	Area above saturation curve							unsaturated solutions		

Calcium chloride is highly soluble in water over a wide temperature range, with maximum solubility of approximately 75% at temperatures above 175 °C. Although calcium chloride dissolves readily in water to form highly concentrated solutions, due account must be taken of the temperature at which solid hydrates precipitate from these solutions. A detailed diagram of the solid and liquid phases, showing temperatures and concentrations of calcium chloride and water, is given in Figure 56.29. The solubility data in this diagram were obtained with pure calcium chloride. The saturation curve and the freezing points of solutions of commercial calcium chloride up to a concentration of 29.8% CaCl₂ are practically the same as for pure solutions; above 29.8% CaCl₂, the curve follows the

same general pattern (and direction) but falls slightly to the left of the curve for pure calcium chloride. The difference in the curves is small between 29.8% and 50% CaCl₂ but increases somewhat at higher concentrations.

The effect of a small percentage of sodium chloride and other minor impurities is to raise the saturation temperature slightly for any given concentration of calcium chloride. Thus, a 40% CaCl₂ solution becomes saturated when cooled to ca. 13 °C, whereas a pure 40% CaCl₂ solution is saturated at ca. 12 °C.

Calcium chloride forms solutions with high densities. This property is commonly used to determine the strength of calcium chloride brines. Density data for commercial calcium chloride solutions are presented in Table 56.25.

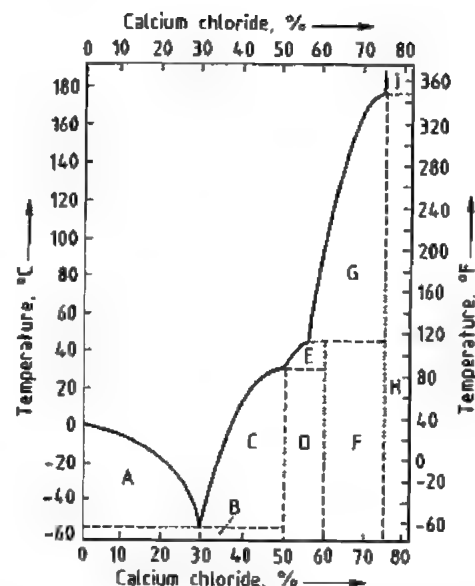


Figure 56.29: Solubility of pure calcium chloride in water-freezing point diagram (Courtesy Allied Corp.). Data for areas A-J given in Table 56.24.

Table 56.25: Densities and crystallizing temperatures of commercial calcium chloride solutions (Courtesy Allied Corp.).

c _{CaCl₂} , %	ρ (15.5 °C), g/cm ³	Crystallizing temperature, °C
0	0.999	0
2	1.017	-0.9
4	1.033	-1.9
6	1.051	-2.9
8	1.068	-4.1
10	1.086	-5.4
12	1.104	-7.1
14	1.124	-9.2
16	1.144	-11.6
18	1.164	-14.5
20	1.185	-18.0
25	1.238	-29.4
30	1.294	-46.0
35	1.349	-9.8
40	1.409	+13.3

Calcium chloride is extremely hygroscopic and deliquescent when the vapor pressure of the air equals or exceeds that of the saturated solution at the prevailing temperature. Data on calcium chloride solutions in equilibrium with air at various temperatures and relative humidities are presented in Figure 56.30.

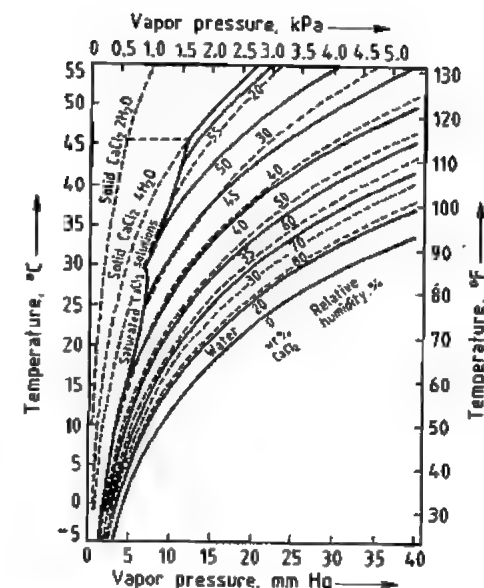


Figure 56.30: Vapor pressure of calcium chloride solutions (Courtesy Allied Corp.).

Freshly prepared solutions of commercial calcium chloride are somewhat alkaline due to the presence of a small amount of lime (CaO). Although these solutions may exhibit a relatively high pH (pH ≤ 10.3), they have little acid-neutralizing value because of the small percentage of lime present.

Calcium chloride solutions exposed to air gradually absorb carbon dioxide to form calcium carbonate from the lime, thus reducing the pH of freshly prepared solutions [231, 233].

56.7.2 Chemical Properties

Calcium chloride is a source of soluble inorganic calcium and reacts with carbonates, fluorides, and sulfates to form insoluble or moderately soluble salts. Calcium chloride forms water soluble compounds with ammonia, e.g., CaCl₂·8NH₃, and with alcohol, e.g., CaCl₂·C₂H₅OH. Calcium chloride reacts with sodium tungstate, Na₂WO₄, to form calcium tungstate, CaWO₄, also known as synthetic scheelite [233-237].

Table 56.26: Calcium chloride standards.

	ASTM ^a D 98-80			AASHTO ^b M 144-78		Food Chemicals Codex ^c	
	77%	90%	94%	77%	94%	77%	94%
Calcium chloride, % min.	77	90	94	77	94	74.7 to 80.8	93
Total alkali chlorides, % max. as NaCl	6.8	8	8	2	5	—	—
Magnesium, % max. as MgCl ₂	0.43	0.5	0.5	0.5	0.5	—	—
Magnesium and alkali salts, % max.	—	—	—	—	—	4	5
Other impurities excluding water, % max.	0.85	1	1	1	1	—	—
Arsenic, ppm max. as As	—	—	—	—	—	3	3
Fluoride, % max. as F	—	—	—	—	—	0.004	0.004
Heavy metals, % max. as Pb	—	—	—	—	—	0.02	0.02
Lead, ppm max. as Pb	—	—	—	—	—	10	10

^a American Society of Testing Materials specification is based on 90.5% calcium chloride; for comparison, the values shown have been adjusted and are on an "as received" basis.

^b American Association of State Highway & Transportation Officials.

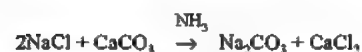
^c Food Chemicals Codex actually specifies a range of 99–107% for calcium chloride dihydrate assay; for comparison, this range has been converted to actual calcium chloride content.

56.7.3 Production

Calcium chloride is produced in commercial quantities by several processes: (1) refining of natural brines, (2) the reaction of calcium hydroxide with ammonium chloride in Solvay (synthetic) soda ash production, and (3) the reaction of hydrochloric acid with calcium carbonate. The refining of natural brines and calcium chloride recovered from synthetic soda ash production together account for over 90% of calcium chloride production [232].

Natural brines in California and Michigan contain a mixture of chloride salts of calcium, magnesium, and sodium. Magnesium is removed by precipitating magnesium hydroxide, Mg(OH)₂, with lime. The solution remaining after filtration is concentrated. Sodium chloride precipitates because it is only slightly soluble in calcium chloride solutions.

In the *ammonia-soda* (Solvay) process, ammonia serves as a catalyst for the reaction of sodium chloride with calcium carbonate. Although this process is actually quite complicated, it can be summarized as follows:



The calcium chloride solutions produced by the purification of natural brines and by the Solvay process are relatively dilute. Part of the solution is concentrated by evaporation to 30–45% calcium chloride and marketed as such.

An additional part is concentrated to ca. 75% solids, corresponding to calcium chloride dihydrate, CaCl₂·2H₂O. This material is flaked and dried to the commercial calcium chloride dihydrate (77–82% CaCl₂) and anhydrous (94–97% CaCl₂) products [238–240]. Anhydrous pellets can be produced by substituting an agglomeration procedure in place of the flaker [241, 242].

56.7.4 Environmental Protection

Calcium chloride is not generally considered harmful to the environment. However, as with any chemical, calcium chloride spills should be promptly contained and disposed of in accordance with local ordinances.

The taste threshold of calcium chloride in potable water is reported as 150–350 ppm. However, depending on the calcium hardness of the water, even concentrations as low as 50 ppm can be objectionable [243].

In high concentrations (> 1000 ppm), calcium chloride retards plant growth and can damage foliage. Because calcium is a nutrient for plants, these effects are most likely caused by accumulation of the chloride ion in the plant tissue. High chloride concentrations are seldom found in U.S. water supplies, even in areas of high salt usage for dust and ice control [243–245].

Calcium chloride concentrations of 10 000 to 20 000 ppm in water have been shown to be

hazardous to animals and fish because of differences in osmotic pressure. The effects vary from reduced growth rate and impaired reproduction to death. Such high concentrations are readily detected by the presence of an unpleasant saline taste. In general, the environmental effects of calcium chloride are quite similar to those of rock salt (sodium chloride) [243, 246].

56.7.5 Quality Specifications

The major uses of calcium chloride (ice and dust control) do not require high chemical purity. However, the calcium chloride must be free of materials that are harmful to the environment. Commercial calcium chloride from the three main processes contains low levels of heavy metals and organic compounds and is relatively innocuous.

The current standards established by various organizations are perhaps the best indication of calcium chloride quality (Table 56.26) [247–249].

Total alkali chlorides are generally the impurities of concern to calcium chloride producers. These impurities, essentially sodium chloride with smaller amounts of potassium chloride, are known to be harmful when included in cement. Because calcium chloride is utilized in cement, its total alkali chlorides content must be kept at a reasonable level.

In general, commercial calcium chloride meets the requirements of the Food Chemicals Codex. However, food-grade calcium chloride is not currently available from the major producers and is marketed regionally by companies that generally refine the commercial material. Because of the high quality of commercial calcium chloride, the FDA has granted variances covering some commercial grades of calcium chloride for use in vegetable brining and apple dipping. However, direct addition of commercial grades of calcium chloride to foods, such as cheese, continues to require food-grade material.

56.7.6 Chemical Analysis

Routine analytical tests performed on calcium chloride include: assay, total alkali chlorides, percent sodium chloride, percent potassium chloride, and various granulation tests [250–253].

The concentration of calcium chloride is most easily determined by an ethylenediaminetetraacetic acid (EDTA) titration. This procedure determines total calcium, which is expressed as calcium chloride. In the determination of total alkali chlorides, sodium chloride, and potassium chloride, atomic absorption spectroscopy is most widely used. Sodium and potassium are determined individually, and these results are combined and expressed as total alkali chlorides.

56.7.7 Storage and Transportation

Calcium chloride is not classified as a hazardous material by the DOT and is, therefore, not subject to specific handling regulations [254]. The various modes of transportation include: bulk rail cars (30–90 t), bulk trucks (up to 20 t), box rail cars, and van and flat-bed trailers. Depending on whether the shipments are in liquid or dry form, there are several variations to the above general classifications.

Dry bulk calcium chloride can be stored in bins fabricated from most construction-grade steel materials. Care should be taken to minimize moisture. Venting should be limited to times of filling and discharging calcium chloride from the storage bin. Liquid calcium chloride can be stored in either horizontal or vertical cylindrical tanks constructed of steel. Fiberglass and plastic may also be used within limits of strength and temperature.

Because calcium chloride is hygroscopic, the common safety precautions involved in the handling of chemicals should be observed: wearing gloves, boots, long-sleeve shirts, and safety glasses, and if dry products are being handled, dust protection must be insured.

56.7.8 Uses

Calcium chloride's versatility is related to its unique combination of physical properties: moisture attraction and retention, high solubility, high heat of solution, and freezing point depression of solutions. Calcium chloride is most widely known for its deicing and dust-controlling abilities.

The largest market for calcium chloride (30% of total production) is for *deicing* of roads, sidewalks, and parking lots (Table 56.27). Calcium chloride melts ice at temperatures as low as -51°C (-60°F). Because it liberates heat when exposed to moisture, ice is melted quickly, usually within 15–30 min of application. Calcium chloride is also used in conjunction with rock salt (sodium chloride) to enhance and sustain the effectiveness of the rock salt.

Table 56.27: Calcium chloride end uses in the United States.

	%
Deicing	30
Dust control, road stabilization	25
Industrial (refrigerant, coal thawing, etc.)	15
Oil and gas drilling fluids	10
Concrete	5
Tire ballast	4
Miscellaneous	11

Dust control accounts for ca. 25% of calcium chloride production. Its hygroscopic and deliquescent properties make it ideal for this use. Calcium chloride absorbs moisture from the air and forms a solution that acts to coat dust particles and bind them together, greatly reducing dusting. Calcium chloride solutions are slow to evaporate because of their low vapor pressure and are, therefore, useful in the compaction of road surfaces.

Calcium chloride is used in the *cement* and *concrete* industries. Addition of 1–2% calcium chloride accelerates the setting time of concrete, resulting in earlier strength development. Calcium chloride should not be considered as an antifreeze in concreting; however, the addition of calcium chloride to concrete mixes poured at temperatures below 21°C

(70°F) largely offsets the retarding effects of the lower temperatures [255].

Calcium chloride solutions, because of their low freezing points, are used extensively as heat-transfer media in *food processing*. Calcium chloride brine greatly increases the heat-transfer rate compared to chilled air or to a sodium chloride brine. Contact time between the brine and the various food molds is decreased, resulting in higher production rates [256].

Calcium chloride is also used in the food industry to increase the firmness of fruits and vegetables and to prevent spoilage during processing.

In the *petroleum* and *petrochemical industries* calcium chloride is used as a desiccant for hydrocarbons. It is also used in drilling fluids, packer fluids, completion fluids, and workover fluids in oil well drilling.

Other uses for calcium chloride include:

Adhesives	humectant lowers gel temperature
Animal feed supplement	source of calcium
Tractor tire weight	lowers freezing temperature of water improves traction by increasing tire weight
Highway shoulder and base stabilization	retains moisture which improves compaction of soils
Freezeproofing of coal	lowers freezing point of residual water
Paper manufacture	increases web strength of corrugated media
Rubber manufacture	coagulates latex emulsions
Steel and pig iron manufacture	eliminates alkalis that attack furnace refractory
Wastewater treatment	precipitates fluorides breaks oil emulsions densifies floc

Table 56.28: World calcium chloride production from the Solvay process (1979).

Continent	Production (100% basis), 10^3 t
Europe*	15 480
Asia	3 390
North America	1 460
Australia	290
South America	210
Africa	10
Total	20 840

* Includes the USSR.

Table 56.29: United States calcium chloride producers (1983).

Producer	Capacity (100% basis), 10^3 t
Allied	263
Dow	900
Hill Brothers	4
Leslie Salt	27
National Chloride	13
Occidental	6
Reichhold	6
Texas United	32
Wilkinson Salt	15
Total	1266

56.7.9 Economic Aspects

The majority of the world's calcium chloride is a by-product from synthetic (Solvay) soda ash production. About 1 t of calcium chloride (anhydrous basis) is produced with each ton of synthetic soda ash. Synthetic soda ash production worldwide was ca. $20.8 \times 10^6\text{ t}$ (1979), and a similar quantity of calcium chloride was also produced. However, most of this material is produced as a 5–10% waste solution and is simply discarded. World production of calcium chloride (waste and refined) from the Solvay process is shown by continent in Table 56.28 [257].

In the United States, synthetic soda ash has been largely replaced by natural material from Sweetwater County, Wyoming. As a result, natural brines now account for ca. 70% of the U.S. calcium chloride production. The major calcium chloride producers and their capacities are shown in Table 56.29.

Because of the widespread use of calcium chloride in deicing and dust control, demand for this chemical is erratic (demand, 100% basis, 1000 t):

Year	1975	1979	1980	1981	1982
Demand	550	690	550	670	590

Demand is expected to grow at a rate of 3% per year through 1986 [232, 258].

56.7.10 Toxicology and Occupational Health

Calcium chloride is not generally considered toxic; however, prolonged exposure may

be detrimental to health. Contact with skin may cause irritation. Calcium chloride can irritate or burn eyes. Inhalation of product dust may irritate nose, throat, or lungs. Ingestion could irritate the mouth, esophagus, or stomach. In rats calcium chloride has an acute oral LD_{50} of 1 g/kg. No TLV or MAK has been established for calcium chloride in air [259].

56.8 Calcium Cyanamide

Calcium cyanamide was probably first obtained in the laboratory in 1877 by heating calcium carbamate to red heat [268]. In 1889 it was prepared in larger quantities by heating thoroughly mixed, finely pulverized urea and calcium oxide [269]. A commercial process for the nitrogenation of calcium carbide, the Frank-Caro process, was patented in Germany in 1895 [270]. A calcium cyanamide plant using a batch oven furnace was erected at Piano d'Orta, Italy, in 1905. At about the same time, the Polzeniusz-Krauss channel furnace was put into service. By 1910, plants were established in Germany (Bayerische Kalkstickstoffwerke; AG für Stickstoffdünger), France, Japan, Sweden, Switzerland, and the United States (Amer. Cyanamid).

Calcium cyanamide, $\text{CaNC}\equiv\text{N}$, is the neutral salt of cyanamide, NH_2CN ; it is also known as lime nitrogen, nitrolime, and kalkstickstoff.

Industrial-grade calcium cyanamide contains, in addition to CaCN_2 , ca. 20% CaO and 10–12% free carbon, which gives the product its gray-black color. It also contains a small amount of nitrides formed from silica and alumina. The total nitrogen content varies from 22 to 25%, depending on the raw materials used. Of the total nitrogen, 92–95% is present as cyanamide and 0.1–0.4% as dicyandiamide; the remainder is present as nitrides.

56.8.1 Physical Properties [270]

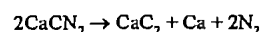
Pure calcium cyanamide is a colorless hygroscopic salt, which forms rhombohedral crystals. In a nitrogen atmosphere, it melts

with decomposition at 1300 °C. Other physical properties are given below.

Density at 25 °C	2.36 g/cm ³
Heat of fusion	54 kJ/kg
Specific heat, 20–100 °C	909 J/kg
Enthalpy of formation ΔH_{298}	-348 kJ/mol
Free energy of formation ΔF_{298}	-303 kJ/mol
Normal entropy S	87.1 Jmol ⁻¹ K ⁻¹

56.8.2 Chemical Properties [271]

Calcium cyanamide decomposes above 1000 °C in a way that depends on the temperature, the partial pressure of nitrogen, and impurities present. The principal decomposition products formed by heating under vacuum or in an inert gas are calcium carbide, calcium metal, and nitrogen:



Decomposition at higher nitrogen pressure gives primarily cyanide products. Calcium nitride and carbon are always formed.

Calcium cyanamide reacts with oxygen and carbon dioxide, starting at ca. 475 °C, with formation of nitrogen and calcium carbonate, calcium oxide forms above 850–900 °C. Carbon present as an impurity cannot be removed by oxidation, which attacks calcium cyanamide preferentially.

Carbon monoxide and calcium cyanamide react above 1000 °C to form CaO and calcium carbide.

The reactions of calcium cyanamide in aqueous solution are determined primarily by temperature and pH [272]. At room temperature, monocalcium cyanamide, $\text{Ca}(\text{HCN}_2)_2$ forms; when heated at pH 9–10, this is converted to calcium hydroxide and dicyandiamide, $(\text{NH}_2)_2\text{CNCN}$. Below 40 °C, cyanamide is obtained at pH 6–8; lime is precipitated with carbon dioxide.

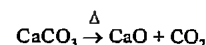
Urea forms in the presence of acid and catalysts, thiourea in the presence of sulfides.

At 200 °C under pressure, calcium cyanamide is hydrolyzed to ammonia and calcium carbonate in an alkaline medium. The reaction was employed to produce ammonia early in this century.

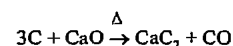
56.8.3 Production

56.8.3.1 Overall Process

Calcium cyanamide is manufactured in three steps. First, lime is made by heating high-grade limestone:

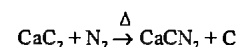


Second, calcium carbide is synthesized from lime and coke or coal in an electric furnace:



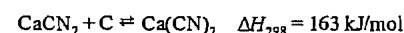
A smothered electric arc is used to melt the lime and effect the reaction with the coke.

Third, calcium cyanamide is synthesized from calcium carbide and nitrogen. This reaction is exothermic but requires heating of a portion of the reaction mixture to the initiation temperature of 900–1000 °C:



The heat source is then removed [272]. The reaction continues by controlled addition of nitrogen; it produces 286.6 kJ/mol at 1100 °C and 295 kJ/mol at 0 °C.

Mechanism. It is believed that calcium cyanamide is formed through a number of intermediates, such as $\text{Ca}(\text{CN})_2$, CaC_2N_2 , CaC , and Ca_2N_2 [273–275]. However, in the nitrogenation of calcium carbide, the main products are calcium cyanamide and carbon. Above 1000 °C, cyanide also forms and is in equilibrium with cyanamide and carbon:



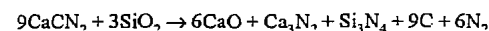
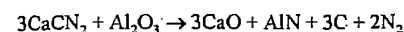
This reaction is endothermic, whereas the nitrogenation is exothermic.

Above 1160 °C, the system $\text{CaCN}_2/\text{C}/\text{Ca}(\text{CN})_2$ melts, with over 60% cyanamide present at equilibrium.

Small amounts of cyanide present at the usual reaction temperatures of 1000–1100 °C are rapidly converted to calcium cyanamide by slow cooling; the cooled product is practically free of cyanide.

When the cyanide-containing melt is cooled in the presence of alkali-metal compounds, complete conversion to cyanamide does not take place. This is the basis of the fusion cyanide process, which is still used at the present time. Commercially, cyanide (ca. 50% NaCN equivalent) is prepared by melting and cooling a mixture of calcium cyanamide and sodium chloride [276]; the product is used mainly for precious metal extraction.

Nitrogenation By-products. Technical-grade calcium carbide contains impurities that, during nitrogenation, lower the yield of desired product. This is due to the fact that silica and alumina, which are only partially reduced in the carbide furnace, are present in the carbide raw materials. In the nitrogenation, Al_2O_3 and SiO_2 react with CaCN_2 to form nitrides.



Industrial-grade calcium carbide also contains calcium hydroxide, $\text{Ca}(\text{OH})_2$, and calcium carbonate, CaCO_3 . On heating, water and carbon dioxide are liberated; reaction with carbide gives acetylene. As a result, hydrogen, formed by decomposition of acetylene, is always found in the exhaust gas of the nitrogenation furnaces.

These side reactions and the inadvertent introduction of some oxygen during the nitrogenation reduce the overall yield by ca. 10%. The purest possible raw materials give the most favorable results economically.

Catalysts. Various catalysts that act as fluxes are used to accelerate the reaction or lower the required temperature. The most commonly used are calcium chloride and calcium fluoride. Their function is not completely clear, but they may provide a liquid phase in which the reaction can occur. The product is in the form of a well-sintered pig, indicating the presence of a liquid phase at some stage of the reaction.

Rate studies have shown that calcium fluoride reduces the temperature of optimum reac-

tivity and increases the reaction rate 4.5 times at 1000 °C [277].

Reaction Kinetics. The conversion rate depends on temperature, partial nitrogen pressure, carbide purity, and additives present. The crystallite size also plays a part. High-grade carbide with a coarse crystal structure reacts more slowly than fine material of a lower grade. As indicated above, metal halides accelerate the reaction.

In the nitrogenation of calcium carbide, the reaction proceeds inward from the grain surface. The rate of nitrogen transport through the porous layer is a determining factor at lower temperature, whereas the chemical reaction at the boundary layer governs at higher temperature and in the presence of additives. The dependence of the rate constants on temperature, additives, and nitrogen pressure has been reported [278]. Figure 56.31 shows the effect of nitrogen pressure.

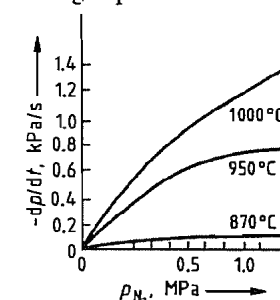


Figure 56.31: Rate of calcium carbide nitrogenation as a function of nitrogen pressure [278]. Powdered CaC_2 (67%) containing 1.2% CaF_2 used.

56.8.3.2 Manufacture

Both batch and continuous processes have been used to prepare calcium cyanamide [287]. The more important processes include the Frank-Caro batch furnace process, the Polzeniusz-Krauss channel furnace process, the Trostberg rotary furnace process, and the Fujiyama shaft furnace process. Other processes have been explored, but have not achieved comparable importance.

In these processes, the exothermal reaction between carbide and nitrogen takes place between 1000 and 1150 °C. In the continuous ro-

tary furnace process, the reactants, except at the beginning, are heated exclusively by the heat of reaction, whereas the batch furnace process requires ignition for each batch.

All processes use finely ground high-grade calcium carbide and control of the reaction temperature by the addition of lime nitrogen (crude calcium cyanamide). This dilution of the carbide prevents a temperature rise that would decompose the cyanamide and promotes homogeneity and nitrogen diffusion. This type of temperature control is of particular importance in the Trostberg rotary furnace process to prevent caking on the furnace wall.

Frank-Caro Batch Oven Process [277]. The batch oven process is widely used in North America. It employs a batch reactor filled with ground calcium carbide. After an initial ignition, the reaction proceeds spontaneously. Large stationary furnaces with and without basket inserts have been used in several variations. A basket insert with a capacity up to 10 t is filled with ground carbide and inserted into a steel furnace equipped with nitrogen inlets and a current supply. Graphite heating rods (up to 3.5 m long) are inserted into the carbide, and contact is established with the cover and grounded furnace shell. Before application of the electrical charge, nitrogen is introduced through inlets in the lower part of the furnace shell. When the walls of the channels glow after being heated for 3–4 h, the current is turned off and the reaction is allowed to go to completion. After being initiated, the exothermic reaction is self-sustaining.

During the reaction, the contents sinter to a block or pig. In an 8–10-t furnace, the reaction is completed and the mixture partially cooled in ca. 70 h. Although calcium cyanamide is white, the pig is black because of graphite formed during the reaction. It contains ca. 70% calcium cyanamide, 10% free lime, 12% graphite, and 0.5% unreacted carbide. The pig is broken into pieces and milled.

Furnaces and Electrodes. The batch oven furnaces used in North America by Amer. Cyanamid are cylindrical, firebrick-lined steel shells (Figure 56.32). The firebrick floor of

the furnace (20 cm is adequate) is covered with carbon blocks cemented with pitch. This refractory material withstands the high temperature and alkalinity of the molten lime. The sides of the furnaces are not subjected to vigorous conditions because they are insulated by a mass of charge and product. The external dimensions of a typical large furnace are 12.5 × 13.8 m at the top, 8.8 × 3.3 m at the bottom, and a height of 5.5 m [277].

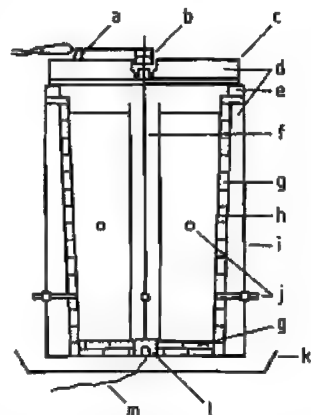


Figure 56.32: Self-heating nitrogenation oven: a) Insulator; b) Graphite contact; c) Steel cover; d) Diatomaceous earth; e) Sand seal; f) Graphite rod; g) Firebrick; h) Paper lining; i) Steel shell; j) Nitrogen inlets and outlets; k) Sand tray; l) Graphite ground contact; m) Ground lead.

A number of electrode systems have been used in batch furnaces. In one system the electrodes are equipped with one to three composite rectangular rods made of electrolytic-grade carbon held in a line to give a composite cross-section of 510 × 280 cm when all are used. Another system uses sliding contacts, permitting the addition of electrode components without removing the assembly from the furnace. Component electrodes have also been replaced with continuous electrodes of the Söderberg type, where a paste of carbonized anthracite, coke fines, and tar is packed into the top of a 12.2-m thin steel tube. The tube serves as an electrode and is fed into the furnace as it burns away from the bottom. As the paste moves closer to the surface of the charge, it is slowly baked, conferring great mechanical strength when it reaches the 2-m

section below the sliding electrical contacts [277].

Polzeniusz-Krauss Channel Furnace Process. In the channel furnace process, the carbide mixture is diluted with lime nitrogen (ca. 67% carbide solids) and 2–3% calcium chloride or fluorspar. This mixture is loaded into iron boxes of ca. 1800 kg capacity and rolled into the channel furnace by a rail assembly. The furnace is 50–80 m long and can be closed by gastight doors made of brickwork in the reaction zone and of sheet metal mufflers in the cooling zone (Figure 56.33). A significant advantage of the channel furnace is its flexibility of operation, which can be modified, depending on the quality of the carbide, the duration of the reaction, and the temperature of the cooling zone. To accelerate ignition at 750 °C, a small amount of calcium nitrate is added.

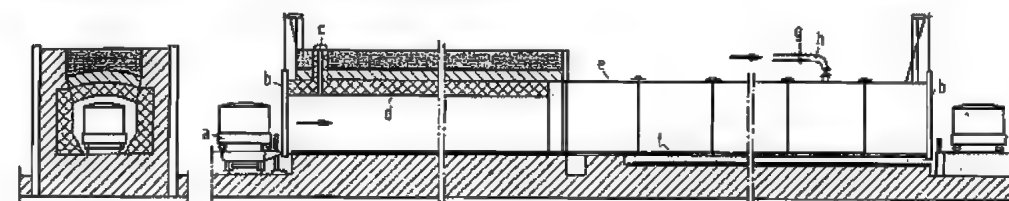


Figure 56.33: Channel furnace: a) Cast steel carriage; b) Doors; c) Temperature measuring connection; d) Refractory walls; e) Sheet metal muffler; f) Rails; g) Orifice gauge; h) Nitrogen inlet tube.

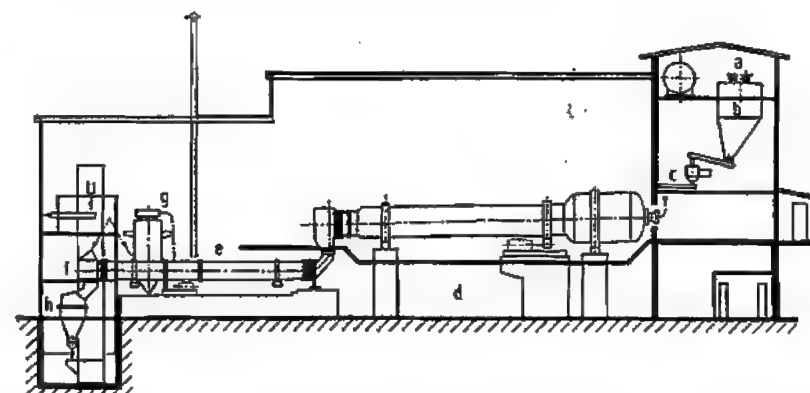


Figure 56.34: Trostberg rotary furnace: a) Feed; b) Silo for ground material; c) Metering; d) Reaction section; e) Cooling unit; f) Discharge; g) Filter; h) Hammer mill.

After conversion, the carriages are pulled from the furnace and cooled. The product is easily crushed because the blocks have a coke-like structure and readily fall apart. Up to 30 t/d of calcium cyanamide can be produced in a single furnace.

Trostberg Rotary Furnace Process. In this continuous nitrogenation process, ground lime nitrogen is metered onto a material bed in a broadened part of the rotary furnace in such a way as to keep the carbide concentration in the bed as low as possible. The process is controlled by varying the carbide content.

The rotary furnace developed by Süddeutsche Kalkstickstoff-Werke is ca. 20 m long and includes the broadened furnace head, where the main reaction takes place [279]. The furnace is lined with fireclay (Figure 56.34).

Ground carbide with a CaC_2 content of 55–60% is continuously mixed with calcium fluoride and ground lime nitrogen and is blown into the furnace with nitrogen. The average residence time of the solid is between 5 and 6 h. The resultant reaction product is a granular or powdered lime nitrogen, which is transferred from the rotary furnace to a cooling drum. The heat released by the reaction is sufficient to bring the starting materials to the desired temperature of 1000–1100 °C. After the furnace has been started, it remains in operation without external heating for many months. The capacity of a unit is about 25 t/d of fixed nitrogen. For the manufacture of calcium cyanamide, crude calcium carbide (ca. 3.36×1.68 mm or 6×12 mesh) can be used; for cyanamide and dicyandiamide a 74- μm (200-mesh) anhydrous carbide is used.

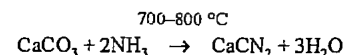
Knapsack Rotary Furnace Process [280]. The Knapsack rotary kiln process was developed 20 years before the Trostberg process, but has not been in operation at Knapsack since 1971. It is the only industrial process that does not use finely ground calcium carbide and that operates without dilution with lime nitrogen. Granular carbide, up to 2 mm in diameter, is nitrogenated in the presence of 1–2% of calcium chloride in a cylindrical rotary drum, giving a product of the same grain size as the starting carbide. A typical kiln can produce 12–13 t/d of fixed nitrogen; the product can be sold without further processing.

Fujiyama Process. This Japanese process employs a shaft furnace equipped with a continuous charging unit for ground carbide and a scraping device at the lower end of the furnace where the calcium cyanamide is formed.

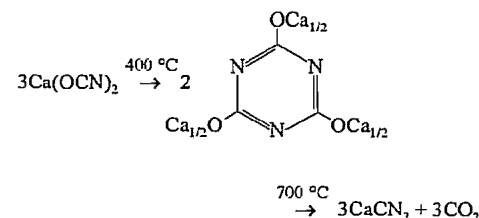
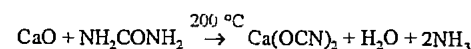
Carlson Process. This fluidized-bed process, operated in a furnace with stirrers, was used for a few years in Sweden. It failed because of the tendency of the reaction material to agglomerate [281]. A combination of this approach with a rotary furnace was explored, but was not adapted commercially [282].

Other Processes. Because large amounts of energy are consumed, particularly in the prep-

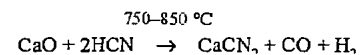
aration of calcium carbide, less energy intensive methods for manufacturing calcium cyanamide have been examined. Between 600 and ca. 1000 °C many reactions of lime with nitrogen compounds containing hydrogen or carbon lead to calcium cyanamide. Compounds such as hydrocyanic acid, dicyanogen, urea, and dicyandiamide form calcium cyanamide with lime. Another example is the reaction of limestone with ammonia [283]:



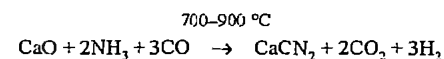
Lime and urea form calcium cyanate [284, 285], which on heating is converted to calcium cyanurate and finally to calcium cyanamide:



Lime reacts with hydrogen cyanide [286]:



An ammonia–carbon monoxide mixture produces 99% calcium cyanamide:



The above processes give white calcium cyanamide, whereas the product obtained from limestone and coal always contains carbonaceous impurities. None of these processes have yet been commercialized because of cost or poor yield [287].

56.8.3.3 Processing of Technical Calcium Cyanamide

Crude calcium cyanamide is reduced in size and ground in tube mills to allow passage through a 0.2-mm screen. If calcium cyana-

mid is sold in granular form, grinding is omitted and the desired grain size is separated by screening.

When the carbide content is above 0.1%, as in the Frank–Caro process, calcium cyanamide is degassed by treatment with water to convert the carbide to acetylene and calcium hydroxide. For safety reasons, the acetylene is dispersed with an inert gas [277].

Granulation. Because of the dust problems associated with finely ground calcium cyanamide in fertilizer applications, the product is oiled. Attempts have also been made to convert it to a more compact form by granulation or compression. A stable, abrasion-resistant granular material is produced by a two-stage process, in which ground calcium cyanamide is initially treated with a small amount of water or an aqueous solution to hydrate any free calcium oxide. In the second stage, the material is moistened, granulated, and dried or pressed [288].

Beads. Granulation with calcium nitrate solutions gives a fine, finished calcium cyanamide bead. This form affords a nitrate nitrogen system that can be used directly in the plant as starter nitrogen. In addition, it affords a slowly acting cyanamide nitrogen source [289]. This product has an almost unlimited storage life, because the free calcium oxide is completely hydrated and no expansion can occur. In Europe, the Trostberg plant of Süddeutsche Kalkstickstoff-Werke is the main producer of beaded calcium cyanamide.

Encapsulation of Granular Calcium Cyanamide. Various coating methods have been used to protect crushed granular calcium cyanamide against decomposition. Waxes and resins have been investigated, but only sulfur is used in practice [289]. It functions by limiting the diffusion of water into the material, and it permits fertilizing action in use.

56.8.4 Quality Specifications

Commercial-grade calcium cyanamide has approximately the following composition:

Total nitrogen	19–20%
----------------	--------

Cyanamide nitrogen	ca. 15%
Nitrate nitrogen	ca. 2%
Dicyandiamide nitrogen	0.4–0.7%
Other nitrogen	2.0–2.5%
Total calcium oxide	53–55%
Water (chemically bound)	7–8%

Total nitrogen is determined by the Kjeldahl or Dumas method.

56.8.5 Storage and Transportation

Calcium cyanamide is stored in warehouses or silos, but storage life with free calcium oxide is limited because the latter is expanded by moisture.

Production-grade ground calcium cyanamide, with a nitrogen content of 22–24%, is adjusted to the usual commercial nitrogen content of 19–20% by adding a diluent such as ground limestone. Oiling may be used to prevent dusting.

Valve bags are used almost exclusively for packaging. Bags used for ground and granular calcium cyanamide must be moisture-tight to prevent grain breakdown and expansion. Polyethylene valve bags in combination with multilayer paper bags are excellent for granular calcium cyanamide. Paper and plastic bags are used for the less sensitive, beaded product. Loose beaded calcium cyanamide may be transported in special containers in Germany. For agricultural applications, 50-kg bags are used; smaller packages of finely beaded product are sold for horticultural applications.

56.8.6 Uses

In Europe, cyanamide and calcium cyanamide are used as fertilizers, weed killers, and defoliants. In North America these applications have been practically discontinued. In fertilizer applications, calcium cyanamide is broken down by soil moisture into highly reactive lime and free cyanamide; the latter is converted by soil microbes to urea and then ultimately to ammonia. Nitrifying bacteria convert ammonia to nitrate [290]. Calcium cyanamide is particularly valuable for acid soils in need of lime. It can also be used in mixed fertilizers, although if it is used in excess, the resultant high alkalinity reduces solu-

ble phosphate. Calcium cyanamide is used on asparagus and onions as a weed killer. Heavy applications approximately 1 month before planting control soil-borne plant disease and weed seed.

Calcium cyanamide has been used to control animal pests. On grasslands it is used to kill the dwarf water snail, the intermediate host of the liver fluke. It also kills gastric and intestinal parasites in domestic animals and destroys salmonellae in liquid sewage.

Nitrogen oxides are removed from waste gases with over 99% efficiency by scrubbing with calcium cyanamide [291]. In portland cement, cyanamide and calcium cyanamide improve set characteristics, increase compression strength, and reduce freeze-thaw damage [292].

Pharmaceutical-grade calcium cyanamide is used to treat alcoholism. A small pill, taken once a day, subjects the alcohol user to an unpleasant cyanamide flush (see Section 56.8.5), which discourages drinking [293]. Calcium cyanamide is used for steel nitridation [294] and, to some extent, for desulfurization [295]. It has various uses in the production of cyanamide, dicyandiamide, melamine and other substituted triazines, thiourea, and guanidines.

56.9 References

1. *Metals Handbook*, 9th ed., vol. 1. American Society for Metals, Metals Park, OH, 1978.
2. J. W. Robison: "Ladle and Mold Treatments with Steel-Clad Metallic Calcium Wire", *Scaninject III*, MEFOS, Luleå, Sweden, 1983, pp. 35.1–35.23.
3. D. C. Brown: "High Quality Strand Cast Steel", *33 Metal Producing* 1982 (Sept.) 62–66.
4. R. D. Prengaman: *Advanced Lead Alloys for Maintenance-Free Batteries*, Lead Development Assoc., London, England, 1980.
5. S. E. Hluchan: *Calcium Alloys for Battery Grid Production*, Lead Development Assoc., London, England, 1983.
6. R. S. Boynton: *Chemistry and Technology of Lime and Limestone*, John Wiley, New York 1980.
7. ASTM C-207 Specification for Hydrated Lime for Masonry Purposes, American Society for Sampling and Testing.
8. J. Murray: "Specific Heat Data for Evaluation of Lime Kiln Performance", *Rock Prod.*, Aug. 1947, 148.
9. H. Bäckström, *J. Am. Chem. Soc.* **47** (1925) 2432, 2443.
10. Cem. Bureau, World Statistical View, 1988.
11. Schumacker, *J. Am. Chem. Soc.* **48** (1926) 396.
12. BS 6463: Quicklime, Hydrated Lime and Natural Calcium Carbonate.
13. DIN 1060: Building Limes, 1982.
14. ASTM C 110: Methods of Physical Testing of Quicklime, Hydrated Lime and Limestone.
15. N. E. Rogers, *Cem. Lime Gravel*, June 1970, 149–153.
16. A. B. Searle: *Limestone and Its Products*, E. Benn, London 1935.
17. M. O'Driscoll, *Ind. Miner.*, May 1988, 23–51.
18. A. Jackson: *Oxygen Steelmaking for Steelmakers*, Butterworths, London 1969.
19. ASTM C911: Specification for Quicklime, Hydrated Lime and Limestone for Chemical Uses.
20. Specification for Highway Works, Part 2, Aug. 1986, HMSO.
21. International Critical Tables, 5, McGraw Hill, New York 1929, pp. 98–99.
22. R. Haslam et al., *J. Am. Chem. Soc.* **46** (1924) 308.
23. A. Seidell: *Solubilities of Inorganic and Metal Organic Compounds*, Van Nostrand, Princeton 1965, pp. 309–310.
24. N. Knibbs, *Lime and Magnesia*, E. Benn, London 1924, p. 71.
25. AWWA Standard B 202–83 American National Standards Institute.
26. D. H. Stowe, Lime for F. G. D., 6th International Lime Congress, 1986, International Lime Association.
27. BS 890 (1972): Specification for Building Limes.
28. Notes on Best Practicable Means Requirements for Mineral Works, BPM 13, Health and Safety Executive, Department of Environment, London.
29. Notes of Best Practicable Means Requirements for Lime Works, BPM 2/78, Health and Safety Executive, Department of Environment, London.
30. ASTM D 75: Methods for Sampling Aggregates.
31. ASTM C 50: Sampling, Inspection, Packing and Marketing of Lime and Limestone Products.
32. BS 812 (1975): Testing Aggregate. Parts 1, 2 & 3.
33. BS 1017 (1977): Methods for Sampling of Coal and Coke, Part 1.
34. BS 822 (1983): Specification for Aggregates from Natural Sources for Concrete.
35. BS 63 (1987): Road Aggregates.
36. P. G. Roe, D. C. Webster, Road Research Laboratory, Scientific Report, 829, HMSO, London 1984.
37. BS 4987 (1988): Coated Macadam for Roads and Other Paved Areas.
38. ASTM C-25: Method for Chemical Analysis of Limestone, Quicklime and Hydrated Lime.
39. *Quicklime—Delivery, Storage and Handling*, TS/E/37/3, ICI Chemicals and Polymers Ltd., Buxton 1986.
40. *Hydrated Lime—Delivery, Storage and Handling*, TS/E/34/3, ICI Chemicals and Polymers Ltd., Buxton 1987.
41. *Minerals Yearbook*, 1987, U.S. Bureau of Mines, Washington.
42. U. K. Business Monitor, PA 1007, 1986, HMSO.
43. Occupational Exposure Limits, Health and Safety Executive, Guidance Note EH 40/96, HSE Books.
44. Health and Safety Commission and Health and Safety Executive Reports from 1985/6 and 1986/7 and HSE, "Quarries" Report for 1984/5, HMSO.
45. "Safety in Quarries" (Part 1), J. M. Hobbs, 1988, Private Publication.
46. Health and Safety Executive Report "Mines" 1985/6, HMSO.
47. N. G. Grice, personal communication, Jan. 1990.
48. DD ENV 459-1, 1995, *Building Lime*.
49. EN ... TC 164 (in preparation), *Test Methods for Calcium Carbonate, High-Calcium Lime, and Half-burnt Dolomite used for Treatment of Water for Human Consumption*.
50. BS 6463, Part 102 (in preparation), *Methods for Chemical Analysis of Quicklime, Hydrated Lime, and Natural Calcium Carbonate*.
51. *Statistical Year Book*, 1995, British Aggregate Construction Mineral Industries.
52. *International Lime Association—Statistics*, 1994.
53. *European Minerals Yearbook*, 1994.
54. EN 998, *Specification for Mortars for Masonry*.
55. H. E. Schwiete, A. N. Knauf: *Gips—Alte und neue Erkenntnisse in der Herstellung und Anwendung der Gipse*, Merziger Druckerei u. Verlags-GmbH, Merzig 1969.
56. *Winnacker-Küchler*, 4th ed., vol. 3, pp. 262–277.
57. A. Voellmy, W. Albrecht: "Die Prüfung der Gipse und Gipsmörtel", in O. Graf (ed.): *Handbuch der Werkstoffprüfung*, 2nd ed., vol. 3, Springer Verlag, Berlin 1957, pp. 520–576.
58. *Gmelin*, system no. 28, Calcium, Main B3 (1961), pp. 675–785.
59. A. W. Groves: *Gypsum and Anhydrite, Overseas Geological Surveys*, Her Majesty's Stationery Office, London 1958.
60. F. Lotze: *Steinsalz und Kalisalz, Geologie. Die wichtigsten Lagerstätten der „Nichterze“*, 2nd ed., 1st part, Verlag Gebr. Bornträger, Berlin 1957.
61. A. V. Slack: *Phosphoric Acid*, Marcel Dekker, New York 1968, parts I, II.
62. M. Sekiya: *Gypsum*, K. K. Gihodo, Tokyo 1964.
63. K. Volkart: *Bauen mit Gips*, Bundesverband der Gips- u. Gipsbauplatten-Industrie, Darmstadt 1981.
64. *Gips-Datenbuch*, Bundesverband der Gips- und Gipsbauplattenindustrie, 1995.
65. W. Albrecht: *Stuckgips und Putzgips, Fortschritte und Forschungen im Bauwesen*, no. 15, Franckh'sche Verlagshandlung, Stuttgart 1953.
66. A. V. Volzenskij, A. V. Ferronskaja: *Gips, Bindemittel und Erzeugnisse (Technologie, Eigenschaften, Anwendung)*, Strojizdat, Moscow 1974.
67. S. D. Ewjentschik, A. A. Novikov, *Phosphogips und seine Anwendung*, Moskow "Chimija" 1990.
68. *Die Strahlenexposition von außen in der Bundesrepublik Deutschland durch natürliche radioaktive Stoffe im Freien und in Wohnungen unter Berücksichtigung des Einflusses von Baustoffen*, Der Bundesminister des Innern, Bonn 1978.
69. G. Franz: *Dentalgipse*, Hanser Verlag, München-Wien 1981.
70. H. Hanusch: *Gipskartonplatten Trockenbau Montagebau-Ausbau*, Verlagsgesellschaft Rudolf Müller, Köln-Braunsfeld 1978.
71. G. Beard: *Stuck—Die Entwicklung plastischer Dekoration*, Schuler Verlagsgesellschaft, Herrsching 1983.
72. M. Murat, M. Foucault: "Sulfates de calcium et matériaux dérivés," *Colloques internationaux de la RILEM*, Paris 1977.
73. R. M. Gruver, *J. Am. Ceram. Soc.* **34** (1951) 353–357.
74. E. Eipeltaufer, *Zem. Kalk Gips* **11** (1958) 264–272, 304–316.
75. W. C. Riddell, *Rock Prod.* **53** (1950) 68–71, 102.
76. H. Lehmann, K. Rieke, *Tonind. Ztg. Keram. Rundsch.* **97** (1973) 157–159.
77. S. M. Mehta: *Dissertation*, Techn. Universität, Clausthal 1974.
78. K. Reisdorf, W. Abriel, *Neues Jahrbuch Miner. Abh.* **157** (1987) 35–46.
79. W. Abriel, K. Reisdorf, J. Parmetier, *J. Solid State Chem.* **85** (1990) 23–30.
80. C. Bezou, A. Nonat, J.-C. Mutin, A. Norlund Christensen, M. S. Lehmann, *J. Solid State Chem.* **117** (1995) 165–176.
81. B. F. Pedersen, D. Semmingsen, *Acta Crystallogr.* **B38** (1982) 1074–1077.
82. A. Kirfel, G. Will, *Acta Crystallogr.* **B36**, (1980) 2881–2890.
83. G. C. H. Cheng, J. Zussman, *Acta Crystallogr.* **16** (1963) 767–769.
84. F. Wirsching, R. Hüller, B. Kimmer, *Zem. Kalk Gips* **47** (1994) 278–286.
85. K. K. Kelley, J. C. Southard, C. T. Anderson: *U. S. Bur. Mines Tech. Paper* **625** (1941).
86. A. Krus, H. Späth, *Tonind. Ztg. Keram. Rundsch.* **75** (1951) 341–351, 395–399.
87. H. J. Kuzel, M. Hauner, *Zem. Kalk Gips* **40** (1987) 628–632.
88. Nippon Kokan Kabushiki, GB 1016007, 1962 (K. Araki).
89. H. J. Förster, *Chem. Ing. Tech.* **44** (1972) 969–972.
90. D. Kitchen, W. J. Skinner, *J. Appl. Chem. Biotechnol.* **21** (1971) 53–55, 56–60, 65–67.
91. E. Eipeltaufer, *Tonind. Ztg. Keram. Rundsch.* **97** (1973) 4–8.
92. U. Ludwig, *Zem. Kalk Gips* **21** (1968) 81–90, 109–119, 175–180.
93. S. Sprung, *Zem. Kalk Gips* **27** (1974) 259–267.
94. G. Leifeld, W. Münchberg, W. Stegmaier, *Zem. Kalk Gips* **23** (1970) 174–177.
95. D. Hass, E. Kemnitz, B. Grunze, R. Sebowksi, H. Worzala, *Z. anorg. allg. Chem.* **525** (1985) 173–178.
96. H. Borchert, E. Baier, *Neues Jahrb. Mineral. Abh.* **86** (1953) 103–154.
97. E. Posnjak, *Am. J. Sci.* **238** (1940) 559–568.
98. A. Herrmann, *Silik. J.* **3** (1964) 443–466.
99. D. Ostwald, *Tonind. Ztg. Keram. Rundsch.* **78** (1954) 137–142, 173–177.
100. F. Wirsching, R. Hüller, D. Olejnik, *Zem. Kalk Gips* **47** (1994) 65–69, 683–688.
101. H. Hamm, *Zem. Kalk Gips* **47** (1994) 443–451.
102. J. Beckert, H. J. Einbrodt, M. Fischer, Bericht und gutachterliche Stellungnahme zu FGD gypsum und natural gypsum, VGB-Forschungsförderung Essen, Bundesverband der Gips- und Gipsbauplattenindustrie Darmstadt (1990).

103. Proceedings from the 4th International Conference on FGD and Synthetic Gypsum, Ortech Corporation, Mississauga, Ontario, Canada.
104. W. Kumpf, K. Maas, H. Straub: *Handbuch Müll- und Abfallbeseitigung: Rückstände aus der Phosphorsäureproduktion*, vol. 5, E. Schmidt Verlag, Berlin 1964, no. 8581 (1982).
105. Official Journal of the European Communities L5/22, Vol. 37, 7 January 1994.
106. Official Journal of the European Communities L288/36-46, Vol. 37, 9 November 1994.
107. E. Eipeltauer, S. Stojadinovic, *Ber. Dtsch. Keram. Ges.* 37 (1960) 442-447.
108. J. R. Gunn, *Gypsum J.* 49 (1968) 14-18.
109. W. Kreuter, *Zem. Kalk Gips* 27 (1974) 222-225.
110. P. Joest, *Ind. Steine Erden* 71 (1961) 23-29; *Glückauf* 92 (1956) 504-506.
111. DIN 1168, Gypsum building plasters (1975).
112. BPB Ind., DE 1258321, 1962 (R. C. Blair).
113. A. J. T. Ward, *Zem. Kalk Gips Ed. B* 33 (1980) 594-600.
114. W. Lahl, H. E. Schwiete, *Zem. Kalk Gips* 12 (1959) 345-351, 582.
115. J. Steinkuhl, O. Wiechmann, K. Moldan, *Zem. Kalk Gips* 25 (1972) 383-386.
116. E. Eipeltauer, Ch. Stein, *Zem. Kalk Gips* 52 (1963) 45-53.
117. P. Sörgel, J. Bergmann, G. Fietsch, *Silikattechnik* 22 (1971) 225-230.
118. National Gypsum Co., US 2788960, 1954 (S. D. Skinner).
119. Gebrüder Knauf, DE 1143430, 1961 (A. N. Knauf).
120. H. Hamm, F. Wirsching, *Zem. Kalk Gips* 27 (1974) 226-229.
121. P. Landrieu, J. Gibaru, C. Collomb, *Zem. Kalk Gips* 17 (1964) 455-460.
122. D. Roddewig: "Erfahrungen beim Brennen von Gips im Kompaktdehnen", *15th Eurogypsum Congress*, Venice, Sept. 1982.
123. Roddewig & Co., CH 445359, 1964 (H. Roddewig, sen.).
124. D. Böcker, H. Kreusing, *Zem. Kalk Gips Ed. B* 34 (1981) 221-226.
125. H. Remmen, M. Grünwald, G. Hilsdar, *Zem. Kalk Gips* 42 (1989) 217-222.
126. H. Jurkowitsch, R. Hüller, *Zem. Kalk Gips* 43 (1990) 583-588.
127. H. Scholze, M. Hurbancic, Conradt, *Zem. Kalk Gips* 42 (1989) 248-251.
128. F. Wirsching, *Umwelt* 13, 435-438.
129. H. Hamm, *Zem. Kalk Gips* 44 (1991) 593-604.
130. A. Kurandt, *ISMA Tech. Conf.* 1974.
131. Fisons, GB 1135951, 1966 (N. Robinson).
132. Nissan Kakasu KKK, US 3653826, 1968 (T. Ishihara).
133. Société de Prayon, DE 1567821, 1966 (E. Pavonet).
134. "Getting Rid of Phosphogypsum I-IV", *Phosphorus Potassium* 87 (1977) 37; 89 (1977) 36; 94 (1978) 24; 96 (1978) 30.
135. *International Symposium on Phosphogypsum*, 5-7 Nov. 1980, Florida Institute of Phosphate Research (47 Papers).
136. J. Beretka, T. Brown, *J. Chem. Technol. Biotechnol.* 32 (1982) 607-613, 33A (1983) 299-308.
137. "Supply-Demand Trend of Gypsum, Lime and Cement in 1994", *Inorganic Materials* 2 (1995) no. 258, 426-438.
138. D. Israel, *ZKG International* 49 (1996) 228-234.
139. K. Schaupp, K. Metz, *Zentralbl. Industriebau* 4 (1965) 180-184.
140. M. H. Le Chatelier, *C. R. Hebd. Séances Acad. Sci.* 96 (1883) 1668-1671.
141. J. H. Van't Hoff, E. F. Armstrong, W. Hinrichsen, F. Weigert, G. Just, *Z. Phys. Chem. Stoechiom. Verwandtschaftsl.* 45 (1903) 257-306.
142. J. R. Clifton, *Report NBS-TN 755* (1973) 1-28.
143. M. J. Ridge, J. Beretka, *Rev. Pure Appl. Chem.* 19 (1969) 17-44.
144. W. Krönert, P. Haubert, *Zem. Kalk Gips* 25 (1972) 553-558.
145. A. Cavazzi, *Z. Chem. Ind. Kolloide* 12 (1913) 196-201.
146. M. Baykoff, *C. R. Hebd. Séances Acad. Sci.* 182 (1926) 128-129.
147. K. W. Fischer, *Wiss. Z. Hochsch. Archit. Bauwes. Weimar* 10 (1963) 351-371.
148. W. Krönert, P. Haubert, unpublished results, RWTH Aachen.
149. U. Ludwig, J. Kuhlmann, *Tonind. Ztg. Keram. Rundsch.* 98 (1974) 1-4.
150. H. Lehmann, H. Mathiak, P. Kurpiers, *Ber. Deutsch. Keram. Ges.* 50 (1973) 201-204.
151. M. K. Lane, *Rock Prod.* 71 (1968) no. 3, 60-63, 108; no. 4, 73-75, 116, 117.
152. R. A. Kuntze, *Mater. Res. Stand.* 7 (1967) 350-353.
153. Certain-Teed Products Corp., US 2067762, 1934 (G. A. Hoggatt).
154. B. Lelong, *Zem. Kalk Gips Ed. B* 37 (1984) 205-218.
155. Gebrüder Knauf, DE-AS 2023853, 1970 (A. N. Knauf).
156. A. Aignesberger, H. Krieger, *Zem.* 21 (1968) 415-419.
157. Imperial Chem. Ind., GB 1049184, 1963 (K. G. Cunningham).
158. Imperial Chem. Ind., DE 1126792, 1959 (K. G. Cunningham).
159. G. Benz, *Stuckgewerbe* 1969, no. 12, 533-544.
160. A. N. Knauf, W. Krönert, P. Haubert, *Zem. Kalk Gips* 25 (1972) 546-552.
161. T. Koslowski, U. Ludwig: *Zitronensäure*, Institut für Gesteinshüttenkunde der RWTH, Aachen (1983).
162. K. Aichinger, B. Wandser, *Zem. Kalk Gips* 1 (1948) 33-37, 50-51.
163. H. Engelke, *Zem. Kalk Gips* 32 (1979) 560-568.
164. M. Rößler, *Dissertation*, Techn. Universität, Claus-thal 1983.
165. B. Wandser, *Zem. Kalk Gips* 15 (1962) 437-438.
166. M. J. Ridge, H. Surkevicius, *J. Appl. Chem.* 11 (1961) 420-434.
167. M. Murat, *Tonind. Ztg. Keram. Rundsch.* 97 (1973) 160-164; 98 (1974) 33-37, 73-78.
168. G. Neuhauser, *Bundesbaublatt* 31 (1982) 566-569.
169. E. Aepli, *Eurogypsum*, Stockholm 1972.
170. N. W. Knauf, DE 1104419, 1957 (A. N. Knauf).
171. FERMA Gesellschaft für Rationelle Fertigbaumethoden und Maschinenanlagen mbH & Co., CH 505674, 1969 (K. Schäfer).

172. M. A. Ali, F. J. Grimer, *J. Mater. Sci.* 4 (1969) 389-395.
173. J. Kazimir, *Tonind. Ztg. Keram. Rundsch.* 91 (1967) 22-25.
174. G. Kossatz, K. Lempfer, *Holz Roh. Werkst.* 40 (1982) 333-337.
175. G. Kossatz, *Baustoffindustrie* 9 (1966) 1-5.
176. A. N. Knauf, *Stuckgewerbe* 1961, no. 3, 1-4.
177. Forschungsgemeinschaft Bauen und Wohnen: *Estriche im Hochbau*, no. 80, Verlagsgesellschaft R. Müller, Köln-Braunsfeld 1966.
178. F. Henrich, *Glückauf* 107 (1971) 1-13; *Neue Bergbautech.* 9 (1979) 409.
179. P. Thien, *Glückauf* 128 (1992) 750-757.
180. DIN 1164, Portland-, Eisenportland-, Hochofen und Traßzement (1978).
181. H. E. Schwiete, U. Ludwig, P. Jäger, *Zem. Kalk Gips* 17 (1964) 229-236.
182. T. Matyszewski, G. Ambrozewicz, *Baustoffindustrie, Ausg. A* 16 (1973) no. 5, 18-20.
183. Stroitelnykh i Njerudnykh Materialow, DE 1241330, 1963 (P. W. Lapschin).
184. W. Reingen, *Zem. Kalk Gips* 27 (1974) 252-258.
185. J. C. Rinehart, G. R. Blake, J. C. F. Tedrow, F. E. Bear, *Bull. N.J. Agric. Exp. Stn.* 772 (1953).
186. "The WSZ Schwefelsäure und Zement GmbH — Unique or a Model for the Future?" *ZKG International* 49 (1996) A33-A34.
187. F. Wirsching, E. Weißflag, *VGB Kraftwerkstechnik* 68 (1988) 1131-1141; 1269-1278.
188. E. Sacher, *ISMA Tech. Conf.* 1968.
189. F. Wirsching, R. Hüller, H. Hamm, H. Hoffmann, A. Pürzer, *ZKG International* 48 (1995) 241-256.
190. H. Hamm, K. Kraft, J. Trummer, F. Wirsching, *Wochenblatt für Papierfabrikation* 123 (1995) 88-94.
191. Franklin Key, Inc., US 3822340, 1974 (J. J. Eberl).
192. H. Scholze, M. Hurbancic, H. Engelke, *Zem. Kalk Gips Ed. B* 34 (1981) 318-338.
193. H. Scholze, *Tonind. Fachber.* 108 (1984) 170-172.
194. H. Haagen, *Farbe Lack* 87 (1981) 543-550.
195. F. Wirsching, *ZKG International* 44 (1991) 248-252.
196. D. Schumann, *Bauwirtschaft* 26 (1972) 88-97.
197. Ch. Collomb, *Zem. Kalk Gips* 17 (1964) 451-454.
198. DIN 4208, Anhydrite binder (1984).
199. DIN 18163, Gypsum partition panels (1978).
200. DIN 18169, Gypsum ceiling panels (Draft 1979).
201. DIN 18180, Gypsum plasterboards (1978).
202. DIN 4102, Behaviour of building materials and components in fire (Parts 1 + 4, 1981; Parts 2 + 3, 1977; Parts 5-7, 1977; Part 8, Draft 1977).
203. DIN 4103, Non-loadbearing partitions (Part 1, Draft 1982; Part 2, Draft 1983).
204. DIN 4108, Thermal insulation in buildings (1981).
205. DIN 4109, Noise-control in buildings (1962).
206. DIN 18168, Light ceiling linings and underceilings (Part 1, 1981; Part 2, Draft 1982).
207. DIN 18181, Gypsum plasterboards for building construction (1969).
208. DIN 18182, Accessories for the use of gypsum plasterboards (Part 1, Draft 1983; Parts 2-4 in preparation).
209. DIN 18183, Lightweight partitions of gypsum plasterboards (Draft 1975).
210. DIN 18184, Gypsum plaster sandwich boards (1981).
211. DIN 18350, Plaster and stucco works (1979).
212. DIN 18550, Plaster and rendering (Parts 1 + 2, Draft 1979).
213. DIN 18555, Testing of mortars with mineral binders (Parts 1-3, 1982; Part 4, Draft 1983; Part 5 in preparation).
214. DIN 18560, Floor screeds in building construction (Parts 1-5, Draft 1983).
215. DIN 13911, Dental materials; gypsum; requirements, testing (1976).
216. L. Chassevent, *Zem. Kalk Gips* 15 (1962) 509-512.
217. F. Wiwhing, W. Poch, *Zem. Kalk Gips* 27 (1974) 240-244.
218. Wissenschaftlich-Technische Kommission von Eurogypsum, *Tonind. Ztg. Keram. Rundsch.* 97 (1973) 145-157.
219. K. Litzow: *Handbuch der Keramik, Gruppe VA*, 7, Verlag Schmid, Freiburg i. Brg. 1969.
220. G. Neuhauser, *Zem. Kalk Gips* 27 (1974) 240-244.
221. H. Lehmann, *Tonind. Ztg. Keram. Rundsch.* 91 (1967) 8-14.
222. *Ullmann*, 4th ed., vol. 12, p. 312.
223. Phasenanalyse von Gips, Forschungsvereinigung der Gipsindustrie e.V., Darmstadt (1988).
224. R. A. Kuntze, *Mater. Res. Stand.* 2 (1962) 640-642.
225. V. Schlichenmaier, *Tonind. Ztg. Keram. Rundsch.* 98 (1974) 223.
226. A. Miels, *Intern. Cem. Review* Nov 1992, 20-29; Nov. 1995, 31-32.
227. J. C. Bailar, H. J. Emeleus, R. Nyholm, A. F. Trotman-Dickenson (ed.): *Comprehensive Inorganic Chemistry*, 1st ed., vol. 1, Pergamon Press, Oxford 1973, pp. 630-633.
228. C. Palache, H. Berman, C. Frondel: *The System of Mineralogy*, 7th ed., vol. 2, J. Wiley & Sons, New York 1951, pp. 91-96.
229. G. E. Dunning, J. F. Cooper, Jr., *Am. Mineral.* 54 (1969) 1018-1025.
230. J. F. Thorpe, M. A. Whiteley: *Thorpe's Dictionary of Applied Chemistry*, 4th ed., vol. 2, Longmans, Green & Co., New York 1938, pp. 212-214.
231. "Calcium Chloride", *Technical and Engineering Service Bulletin* No. 16, Allied Corp., Morristown, NJ, 1978.
232. "Calcium Chloride", *Chemical Products Synopsis*, Mansville Chemical Products, Mansville, NY, June, 1983.
233. National Research Council: *International Critical Tables*, McGraw-Hill, New York 1928.
234. G. F. Hüttig, *Z. Anorg. Allg. Chem.* 123 (1922) 31-42; *Chem. Abstr.* 16 (1922) 4153.
235. W. H. Nebergall, F. C. Schmidt, H. F. Holtzclaw, Jr.: *College Chemistry with Qualitative Analysis*, 2nd ed., D. C. Heath & Co., Boston 1963, pp. 654-655.
236. H. Stephen, T. Stephen (ed.): *Solubilities of Inorganic and Organic Compounds*, vol. 1, Macmillan Publ. Co., New York 1963, Part 1, pp. 243-261.
237. D. J. Treskon: "Tungsten", *Chemical Economics Handbook*, Stanford Research Institute, Menlo Park, CA, 1977, Section 789.1000-789.1001 M.
238. T. P. Hou: *Manufacture of Soda With Special Reference to the Ammonia Process*, 2nd ed., Reinhold Publ. Co., New York 1942, pp. 252-253.

239. Solvay Process Co., CA 314878, 1927 (C. Sundstrom).
240. Dow Chemical Co., US 1660053, 1928 (A. K. Smith).
241. Dow Chemical Co., US 2646343, 1953 (W. R. Bennett, L. N. Carmouche).
242. Dow Chemical Co., US 4076776, 1978 (W. G. Moore).
243. J. E. McKee, H. W. Wolf (eds.): *Water Quality Criteria*, 2nd ed., The Resources Agency of California State Water Quality Control Board, Publication No. 3-A, pp. 152-153.
244. F. W. Holmes, J. H. Baker: "'Salt Injury to Trees', II. Sodium and Chloride in Roadside Sugar Maples in Massachusetts", *Phytopathology* 56 (June, 1966) no. 6, 633-636 (reprint).
245. F. E. Hutchinson: *The Influence of Salts Applied to Highways on the Levels of Sodium and Chloride Ions Present in Water and Soil Samples*, U.S. Department of the Interior, Project No. A-007-ME, U.S. Gov't. Printing Office, Washington, DC, June, 1969.
246. "Primary Skin Irritation Test-Rabbits", Hazelton Laboratories, Inc., March 1963, unpublished paper.
247. R. P. Lukens, J. L. Cornillot, R. A. Prieman, D. J. Felty et al.: *Annual Book of ASTM Standards*, ASTM, Philadelphia 1981, Part 14, pp. 183-186.
248. American Association of State Highway and Transportation Officials, *Standard Specification for Calcium Chloride: M144-78*, AASHTO, Washington, DC, 1978.
249. National Research Council: *Food Chemicals Codex*, 3rd ed., National Academy Press, Washington, DC, 1981, pp. 47-49.
250. Allied Corp., Assay of Calcium Chloride, CA 4-12A, revised June, 1983.
251. Allied Corp., Determination of Sodium and Potassium in Calcium Chloride, CA 4-56, June, 1983.
252. Reference [247], Part 30, pp. 1041-1046.
253. Reference [247], Part 35, pp. 644-647.
254. General Services Administration: "Transportation", Title 49 Code of Federal Regulations, U.S. Gov't. Printing Office, Washington, DC, 1982, Part 172.
255. National Ready Mixed Concrete Association: *Cold Weather Ready Mixed Concrete*, Silver Spring, MD, 1968, pp. 11-12.
256. ASHRAE Handbook 1981 Fundamentals, American Society of Heating, Refrigerating, and Air Conditioning Engineers, Inc., Atlanta, GA, 1981, pp. 18.2-18.5.
257. *The Economics of Soda Ash*, 1st ed., Roskill Information Services Ltd., London 1981, pp. 20-26.
258. "Calcium Chloride", *Chemical Profiles*, Schnell Publishing Co., New York, April, 1982.
259. N. I. Sax: *Dangerous Properties of Industrial Materials*, 5th ed., Van Nostrand Reinhold Co., New York 1979, pp. 460-461.
260. M. Wildhagen: *Handbook of Industrial Electrochemistry*, vol. 5, Akademie-Verlag, Leipzig 1953, Part 1.
261. A. Brauer, J. D'Ans: *Progress in Industrial Chemistry*, Springer, Berlin 1937.
262. "SKW-Cyanamide Products", Südd. Kalkstickstoff-Werke, Trostberg, Germany, 1973, 82 pp.
263. "Cyanamide", Amer. Cyanamid, Wayne, NJ, 1966, 49 pp.
264. *Beil.* 3, 91; 3(2), 42; 3(2), 75; 3(3), 167.
265. "Dicyandiamide", Südd. Kalkstickstoff-Werke, Germany, 1973.
266. "Aero Dicyandiamide", Amer. Cyanamid, Wayne NJ, 1970, 20 pp.
267. E. Drechsel, *J. Prakt. Chem.* 16 (1877) 180-200.
268. F. Emich, *Monatsh. Chem.* 10 (1889) 321-352.
269. N. Caro, A. Frank, DE 88363, 1895.
270. *Gmelin*, system no. 28, Calcium, Parts B1-2 (1956) pp. 179-195.
271. *Gmelin*, system no. 14, Carbon, Part D1 (1971) pp. 258-297.
272. *Gmelin*, system no. 28, Calcium, Part B3 (1961) pp. 962-971.
273. T. Aono, *Bull. Chem. Soc. Jpn.* 16 (1941) 92-98.
274. V. Ehrlich, *Z. Elektrochem.* 32 (1926) 187-188.
275. F. E. Polzeniusz, *Chem. Ztg.* 31 (1907) 958.
276. H. H. Frank, H. Heimann, *Z. Elektrochem.* 33 (1927) 469-475.
277. M. L. Kastens, W. G. McBurney, *Ind. Eng. Chem.* 43 (1951) 1020-1033.
278. H. Rock, *Chem. Ztg. Chem. Appar.* 88 (1964) 191-271.
279. Südd. Kalkstickstoff-Werke, DE 917543, 1952 (F. Kaess et al.).
280. Südd. Kalkstickstoff-Werke, US 2838379, 1958 (F. Kaess et al.).
281. BASF, DE 965992, 1950 (G. Hamprecht, H. Gettert).
282. Südd. Kalkstickstoff-Werke, DE 972048, 1953 (T. Fischer et al.).
283. A. A. Pimenova et al., *Tr. Tashk. Politekh. Inst.* 107 (1973) 49.
284. Amer. Cyanamid, unpublished results.
285. V. G. Golov et al., *Tr. N.-I i Proekt. In-Ta Azot. Prom.-St i Produktov Organ. Sintez* 28 (1974) 49-52; *Chem. Abstr.* 84 (1975) 159006n.
286. "Cyanamide by Cyanamid", Amer. Cyanamid, Wayne, NJ, 1961.
287. O. I. Polyanshikov et al., *Vopr. Khim. Tekhnol.* 39 (1975) 136.
288. *Gmelin*, system no. 28, Calcium, Part B1-2 1956-1957, pp. 179-196.
289. Ferto Chemical Sales Co., DE 623600, 1932.
290. Südd. Kalkstickstoff-Werke, DE 1097457, 1961 (T. Fischer et al.).
291. K. Rathack, *Landwirtsch. Forsch.* 6 (Special ed.) (1954) 116-132.
292. Nukem, DE 2926107, 1981 (H. Qui Umann).
293. Amer. Cyanamid, US 3503766, 1970 (F. De Maria). R. E. Dwyer, US 4049465, 1977.
294. K. Arikawa, K. Inanaga, *Folia Psychiat. Neurol. Jpn.* 27 (1973) no. 1, 9.
295. Goerig Co., DE 1771827, 1973 (P. Birk, K. Wohlge-muth).
296. K. Deutzmann, DE 2136450, 1973 (W. Blank O. Vorbach).
297. Südd. Kalkstickstoff Werke, DE 2252795, DE 2252796, 1974 (W. Meichsner).

57 Strontium

PAUL MACMILLAN (§§ 57.1, 57.2, 57.7); ROLF GERSTENBERG, KARL KOHLER, JAI WON PARK, HEINZ WAGNER, PETER WALL-BRECHT (§§ 57.3-57.6, 57.8)

57.1 Introduction	2329	57.6.2 Strontium Nitrate	2332
57.2 Properties	2329	57.6.3 Strontium Chloride	2333
57.3 Occurrence	2330	57.6.4 Strontium Chromate	2333
57.4 Mining and Processing	2330	57.7 Strontium Metal	2333
57.5 Digestion of Ores	2331	57.8 Toxicology	2335
57.6 Inorganic Compounds	2331	57.9 References	2335
57.6.1 Strontium Carbonate	2331		

57.1 Introduction

Strontium belongs to group 2 of the periodic table and is one of the alkaline earth metals. Strontium, with atomic number 38, lies between calcium and barium in this group. Strontium was first discovered by A. CRAWFORD in 1790. The discovery of strontium carbonate, which was originally thought to be barium carbonate, is associated with a lead mine located in Strontian, Scotland, hence the name strontium. In 1791 T. C. HOPE confirmed CRAWFORD's discovery, distinguishing strontium carbonate from calcium and barium carbonates.

In 1808 H. DAVY [8] produced strontium metal from strontium carbonate originating from the Strontian deposit. DAVY produced an oxide from the carbonate, and electrolyzed a mixture thereof with mercuric oxide to produce a strontium amalgam.

57.2 Properties

Strontium metal is silvery white and lustrous, but it readily forms a white surface coating when exposed to air and water. Strontium is allotropic and displays three crystal structures; at temperatures below 215 °C it is face-centered cubic. The crystal system properties are summarized in Table 57.1. Some other properties are listed below:

Atomic number 38

Atomic mass	87.62
Stable isotopes	
⁸⁴ Sr	0.56%
⁸⁶ Sr	9.96%
⁸⁷ Sr	7.02%
⁸⁸ Sr	82.56%
Density, g/cm ³	2.63
Melting point, °C	768
Boiling point, °C	1381
Heat of fusion, kJ/kg	104.7
Electrical resistivity, μΩ/cm	22.76

Table 57.1: Strontium crystal structures.

Temperature, °C	Structure	Atomic radius, pm	Lattice constants, pm	
			a	c
< 215	fcc	213	607	
215-605	hcp	202	431	705
> 605	bcc	195	484	

Strontium is generally more reactive than magnesium and calcium and less reactive than barium. Strontium reacts with H₂O, O₂, N₂, F₂, and S producing compounds which correspond to its valence of two.

Common practice for the analysis of strontium is based on the use of spectral emissions. Strontium and strontium compounds impart a bright crimson color to a flame. Some of the lines useful in the quantitative analysis of strontium are listed below (wavelength in nm):

Arc spectra	460.7, 421.6
Spark spectra	407.8, 421.6
Flame photometry	460.7, 407.8
Atomic absorption	460.7, 407.8

Strontium, while less reactive than the alkali metals, is a strong reducing agent and requires appropriate handling. Strontium reacts

vigorously with water to form SrOH, liberating H₂ in the process.

57.3 Occurrence

Strontium is present in the earth's crust at an average concentration of 0.04%, and is therefore 15th in abundance. In seawater it is the 10th most abundant element, having a concentration of 0.0008% [9].

Of the naturally occurring strontium compounds, only the minerals strontianite (strontium carbonate, SrCO₃) and celestite (strontium sulfate, SrSO₄) are of economic importance.

Celestite can be formed as a direct precipitate in a series of marine salt deposits. Hydrothermal formation is also possible [10]. In addition, it seems possible that strontium sulfate could be formed by modification of primary strontium-bearing minerals (aragonite, calcite, anhydrite), whereby part of the strontium included in the crystal lattice is liberated and then precipitated as celestite by sulfate-containing solutions [11]. Strontianite can be formed both as a primary mineral from the hydrothermal phase and as a secondary mineral from, e.g., celestite [12].

Celestite occurs principally as nodules, lenses, beds and materials filling crevices in sedimentary rocks such as carbonates, gypsums, clays, and evaporites. The economic importance of celestite is considerably greater than that of strontianite.

Very large, exploited deposits occur in Spain, Mexico, Turkey, China, and Iran. There are much less important deposits in Algeria, Cyprus, Argentina, and Morocco. Mining in the United Kingdom, the traditional producer, ended in 1992. Little is yet known of the deposits and their extraction in the former eastern bloc [13, 14].

57.4 Mining and Processing

Celestite ores are obtained by both open-cast and underground mining. In most cases, only coarsely intergrown rich ores are worked,

which can be further enriched by hand picking to give a material containing > 90% SrSO₄. Demands for increasing purity in chemically produced strontium salts together with the growth of mechanized mining techniques necessitate a continually increasing amount of processing.

Finely divided impurities are removed by desliming. By means of density separation, celestite ($\rho = 3.8\text{--}3.9\text{ g/cm}^3$) is separated from limestone, quartz, gypsum, and dolomite, which have densities of < 3 g/cm³, giving end products containing > 95% SrSO₄. In Spain, a flotation plant for separating finely intergrown celestite ores has been in operation since 1990. The introduction of this technology has markedly increased the number of deposits worldwide that can be profitably worked.

Many important deposits cannot be mined because of unacceptably high levels of barium and deposit-specific trace elements that cannot be removed by available processing technologies.

Economic Aspects. Whereas strontianite was the principal starting material used in the production of strontium compounds between 1870 and 1920, it has now been almost completely replaced by celestite for this purpose.

Practically the only use for celestite is the production of other strontium compounds. It is used only to a small extent as a white filler in competition with ground barite (barium sulfate).

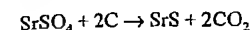
World production of celestite in the early 1990s was estimated at ca. 250 000–300 000 t/a. The most important producing countries, with their production figures, are listed in Table 57.2.

Table 57.2: Estimated production of celestite (10³ t).

Country	1988	1991
Spain	45	70
Turkey	55	65
United Kingdom	20	2
China	20	25
Mexico	40	90
Iran	10	20
Morocco	2	4

57.5 Digestion of Ores

Reduction with Carbon. Celestite, floated or ground to 0.1–1 mm, is chemically reduced according to the equation



The reduction is carried out at 1100–1200 °C with coal in a rotary kiln, heated by fuel oil, natural gas, or coal dust in countercurrent flow. The conditions used depend in particular on the type of celestite and its impurities.

The light gray to grayish-black crude strontium sulfide (75–80% SrS) produced is extracted with hot water. The insoluble solids are removed in a series of thickeners. The solution obtained is generally used to produce strontium carbonate.

Reaction with Sodium Carbonate. Ground celestite (SrSO₄) is converted to strontium carbonate by adding it to hot sodium carbonate solution. Numerous variations of this process have been proposed. Typically, an excess of Na₂CO₃ solution is used. The crude product so obtained is not usually acceptable without further treatment. A product sufficiently pure for most applications is obtained by dissolving the crude material in hydrochloric acid, neutralizing with sodium carbonate solution to precipitate iron and aluminum, filtering, and reprecipitating with caustic soda. This process also produces impure sodium sulfate solution as a by-product which must be further treated or disposed of. The high consumption of sodium carbonate is a further drawback.

Other Processes. Celestite can be reacted with ammonium carbonate in a continuous countercurrent reactor to form strontium carbonate and ammonium sulfate [15]. The ammonium sulfate is treated with calcium oxide or calcium carbonate to form calcium sulfate, ammonia, and carbon dioxide, which are re-used for producing ammonium carbonate.

In the Odda process for producing orthophosphoric acid, phosphate rock is reacted with nitric acid. The strontium present in many types of phosphate rock is converted to strontium nitrate, which remains in the insoluble

residues if the concentrations of HNO₃ and Ca(NO₃)₂ are kept within certain limits. It can then be recovered by extraction with water.

57.6 Inorganic Compounds

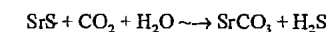
Like the compounds of the other alkaline reagents, the compounds of strontium are white or colorless. The sulfate and the carbonate are of low solubility, being intermediate between the corresponding compounds of calcium and barium in this respect.

Strontium compounds give a striking carmine red color to a flame. This property is used both for the rapid detection of strontium compounds and in pyrotechnics. Quantitative analysis of the industrial strontium compounds is usually carried out by means of titrimetry, X-ray fluorescence spectroscopy, and atomic absorption spectroscopy.

57.6.1 Strontium Carbonate

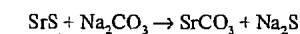
Strontium carbonate, SrCO₃, ρ 3.70 g/cm³, *mp* 1497 °C (6.99 MPa) forms rhombic crystals (aragonite type) below 924 °C, and hexagonal crystals (calcite type) above this temperature. Its solubility at 25 °C is 10^{−3} g/100 mL. Strontium carbonate is produced from strontium sulfide, SrS.

Precipitation by Carbon Dioxide. Strontium carbonate is precipitated from the clarified solution of strontium sulfide with carbon dioxide. Strontium carbonate and hydrogen sulfide are formed.



The carbon dioxide is obtained from natural wells or from industrial processes. The reaction is carried out in gas-tight reactors, and is so controlled that the hydrogen sulfide produced has a low CO₂ content. The hydrogen sulfide is converted to sulfur in a Claus plant.

Precipitation with Sodium Carbonate. Sodium carbonate can be used instead of carbon dioxide in the above reaction.



In addition to strontium carbonate, a dilute solution of sodium sulfide is formed, which is

concentrated to give a 60% solution; the solidified product is marketable.

The choice of production method depends on the comparative availabilities of carbon dioxide and sodium carbonate, and the opportunities for exploiting the by-products sulfur and sodium sulfide.

The two processes lead to products with different properties. The impurities in the strontium carbonate depend partly on the raw materials used. Also, the concentrations, temperatures, and reaction times lead to different values of bulk density, particle size distribution, and concentrations of sulfur and heavy metals.

The strontium carbonate powder is often converted into granules in a further process.

Quality Specifications. Typical specifications for strontium carbonate from the two precipitation processes are as follows:

SrCO ₃	98.0–98.5%
BaCO ₃	1.0–2.5%
Sulfur (as SO ₃)	0.3–0.5%
HCl insolubles	0.1–0.6%
Fe ₂ O ₃	0.005–0.01%

For powder:

Bulk density	0.4–1.2 g/cm ³
Fraction of particles < 3 μm	95–100%

For granules:

Bulk density	1.2–1.8 g/cm ³
Grain size > 850 μm	0–5%
< 150 μm	5–15%

Transport. Strontium carbonate is stored in silos, and transported in 25 or 50 kg multi-ply paper sacks, 1 t big bags, or silo wagons. Strontium carbonate is not listed as a dangerous material in current regulations.

Uses. Strontium carbonate is by far the most important industrial compound of strontium. Its main use is in the manufacture of X-ray-absorbing glass for cathode ray tubes. Strontium carbonate is also used in the manufacture of ceramic permanent magnets (strontium ferrite), for removing lead from solutions of zinc sulfate in the electrolytic zinc process, and for the production of strontium metal, electrocer-

amics, and oxide superconductors [14, 16]. Strontium carbonate is also the starting material for the production of other strontium compounds. For example, heating strontium carbonate with carbon in an electric furnace gives strontium oxide, which is used for production of strontium metal.

Between 1980 and 1990, world consumption of strontium carbonate increased from ca. 80 000 t/a to > 150 000 t/a. Percentage consumption of strontium carbonate in 1990 was [14]:

Glass for cathode ray tubes	74
Electroceramics	12
Pyrotechnics	5
Electrolytic zinc extraction	2
Other uses	7

57.6.2 Strontium Nitrate

Strontium nitrate, Sr(NO₃)₂, ρ 2.986 g/cm³, mp 570 °C, forms face-centered cubic crystals. Below 29.3 °C, the solid phase in equilibrium with an aqueous solution on strontium nitrate is strontium nitrate tetrahydrate, Sr(NO₃)₂ · 4H₂O. The solubility of strontium nitrate (in grams per 100 g solution) at various temperatures is as follows:

Temperature, °C	20	29.3	60	105
Solubility	40.7	47.0	48.3	51.2

Production. Strontium nitrate is obtained by dissolving strontium carbonate in 60% nitric acid.

If the solution is maintained above ca. 30 °C during the evaporation, colorless crystals of the anhydrous compound are formed. After the carbonate, the nitrate is the strontium compound produced commercially in the largest quantities.

Uses. Strontium nitrate has long been used in pyrotechnics and as a component of signalling devices. Related devices are used in the United States and Japan as alternatives to portable electric lamps in motor trucks [14].

Packaging and Storage. Strontium nitrate is packed in 50 kg polyethylene bags. The following transport regulations apply:

RID/ADR:	Class 5.1, 22 C
IMDG Code:	Class 5.1, UN no. 1507

57.6.3 Strontium Chloride

Strontium chloride, SrCl₂, ρ 3.052 g/cm³, mp 875 °C, forms cubic crystals. Its solubility at 20 °C is 34.5%.

Production. Strontium chloride is obtained by dissolving strontium carbonate in concentrated hydrochloric acid. The hexahydrate, SrCl₂ · 6H₂O, is formed on crystallizing below 61 °C. On dehydration, the hexahydrate dissolves in its water of crystallization at 61 °C. After passing through the di- and monohydrate stages, strontium chloride becomes fully dehydrated at 320 °C.

Uses. Strontium chloride is mainly used as an intermediate in the production of other strontium compounds. Compared with the sulfide, it has the advantage of not reacting with oxygen and carbon dioxide, which facilitates industrial handling.

Strontium chloride hexahydrate is used in toothpastes for sensitive teeth [17].

Strontium chloride is not classified as a dangerous material in transport regulations.

57.6.4 Strontium Chromate

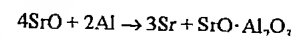
Strontium chromate, SrCrO₄, ρ 3.895 g/cm³, forms monoclinic crystals. Strontium chromate is included in dangerous materials regulations [18] (symbol: T).

Production. Strontium chromate is produced by precipitating a solution of chromate ions with a strontium salt, or by reacting strontium hydroxide solution with chromic acid.

Uses. Strontium chromate (strontium yellow) is used as an anti-corrosion primer for aluminum and its alloys in aircraft and ship construction [19].

57.7 Strontium Metal

Production. Commercial strontium production relies on a variant of the Pidgeon process, exploiting the reaction proposed by GUNTZ [20]:



Produced under vacuum, the strontium evolves as a gas and is transported through the production retort to a cooler end where precipitation occurs. The strontium precipitates as a solid and when the production cycle is complete the vacuum is broken and the product removed. Strontium is produced by Timminco Limited in Canada, Pechiney Électrometallurgie in France, and Cal-Stron Corporation in the United States. In addition, production may well occur in the CIS and China but the extent of production, if any, is unknown.

Strontium metal is commercially available as pure metal, and as an alloy with aluminum or aluminum and magnesium.

A typical percentage chemical analysis of commercial strontium is as follows:

Sr	99.0 min.
Mg	0.20
Ca	0.10
Ba	0.50
Na	0.07
N	0.03
Al	0.01
Fe	0.015

Transportation, Storage, and Safety. Due to its reactive nature strontium must be handled with care. The pure metal and the commercial eutectic alloy, 90% Sr–10% Al, are classified as alkaline earth metals n.o.s. (not otherwise specified), UN no. 1393, for the purposes of transportation [21]. This classification is indicative of materials requiring special approved packaging for transport. These two forms of commercial strontium are packed under an inert atmosphere to prevent formation of an oxide coating. Strontium is a strong reducing agent and forms explosive hydrogen gas when in contact with water. Strontium is therefore classified as a flammable solid. Hence strontium is a Class 4.3 material, i.e., one that emits a flammable gas on contact with water. Strontium should therefore be stored in a well ventilated dry place, avoiding all contact with water. It is recommended that protective gloves and glasses should be worn when handling pure strontium. However, commercial alloys of strontium, such as the Sr–Mg–Al master alloy or the family of aluminum-strontium master alloys which contain up to 10 per-

cent strontium do not require these special precautions.

Uses. Metallic strontium and master alloys containing strontium have experienced significant expansion in application in modern foundry practice. In aluminum foundries strontium is used as an additive to Al-Si alloys to enhance their mechanical properties and improve the machining performance. Strontium improves the mechanical properties of Al-Si castings by changing the morphology of the eutectic silicon phase. In an unmodified Al-Si alloy this eutectic silicon phase precipitates as coarse acicular plates, which causes the casting to exhibit poor mechanical properties. Modification causes the silicon to assume a fine, interconnected fibrous morphology, resulting in higher tensile strength and greatly improved ductility. Impact resistance and machining characteristics are also enhanced through modification.

The optimum strontium level to achieve the best possible mechanical properties in hypoeutectic Al-Si alloys is 0.005–0.015 percent strontium [22]. The impact of strontium is also influenced by the solidification rate, with faster rates producing better properties.

Early foundry practice utilized sodium as a modification agent. In 1920, Pacz outlined a process by which the solidification structure of Al-Si alloys was modified by the addition of sodium to the melt. The sodium addition produced a fibrous eutectic structure which showed improved mechanical properties, especially elongation.

The principal drawback with sodium is that the effect of the sodium rapidly dissipates as sodium is lost by evaporation and/or oxidation during the holding of the molten alloy.

Strontium has the advantage of imparting a semi-permanent modifying effect, as it is less prone to the fading observed with sodium. This allows the production of so called pre-modified aluminum ingots which can be sold to end users. Nevertheless, many foundries for economic and logistical reasons chose to modify in house.

Recent developments in aluminum metallurgy now suggest that strontium also acts to improve the properties and processing of wrought aluminum alloys.

Strontium appears to act on both the mechanical and forming properties of 6xxx series wrought alloys. These improvements are reported to occur when, in the presence of strontium, the complex intermetallic compounds found in these alloys are precipitated in more favorable crystal structures [23]. Under normal or nonstrontium treated conditions the formation of β -AlFeSi intermetallic is favored. The presence of this compound can contribute to surface defects upon extrusion of 6xxx series alloys. The controlled addition of strontium promotes the less detrimental α -AlFeSi leading to better surface quality in the extrusion and faster extrusion speeds.

In the 7xxx series of wrought alloys it has been reported that strontium, at levels of at least 0.005 percent, refines the intermetallic phases, including Mg_2Si , Al-Cu-Mg, and Al-Cu-Fe. When these phases are refined the alloy has enhanced toughness, finer grain size, and can be processed more quickly due to shortened homogenizing times compared to strontium-free alloys [24].

In an aluminum alloy sheet which requires high formability the presence of strontium is reported to reduce the number of intermetallic precipitates. This improves the alloy's formability and reduces the incidence of edge cracking [25].

In ferrous metallurgy strontium finds application as a component in certain foundry grades of ferrosilicon, used as inoculants in gray iron casting. The addition of 0.65–1.05% strontium controls the carbon structure in an iron casting and inhibits the chill. The chill, which is in some cases a desired phenomena, is a rapidly solidified zone in a casting where the formation of mottled iron (cementite and graphite) is favored over a pearlite structure with graphite. By controlling the chill the foundry may be able to decrease the minimum section size in a casting keeping it free from the brittle carbides which would most likely form without inoculation. In addition stron-

tium-bearing inoculants are particularly effective in helping to control internal shrinkage in these castings and thereby enhancing the pressure tightness of the casting [26].

57.8 Toxicology

Strontium carbonate is not considered to have any dangerous properties. There are no known occupational diseases associated with handling strontium carbonate, the most important industrial strontium compound.

The strontium ion is slightly toxic. The toxic action of strontium compounds is thus closely associated with the anion of the compound concerned. Strontium behaves similarly to calcium both chemically and biologically. The biological effects of strontium and its compounds have been described in detail [27].

Strontium is deposited preferentially in the bones and teeth of the human body. Strontium salts are not readily absorbed via the intestinal tract.

Symptoms of acute toxicity are excessive salivation, vomiting, colic and diarrhea, and possibly respiratory failure.

The LD₅₀ values (oral) of various strontium salts (nitrate, hydroxide, chloride, fluoride) are > 2000 mg/kg body weight [28].

Strontium nitrate was administered orally in the food of rats at a concentration of 50 mg/kg (1030 ppm daily for 8 weeks) without harmful effects. Strontium lactate at a level of 16 000 ppm, after more than one year, caused temporary cessation of growth and reduction of bone mineralization [14].

The inhalation of ca. 50 mg/m³ strontium nitrate (4 h daily for one month, particle size mainly < 5 μ m) was less well tolerated by male rats. As well as local effects on the respiratory tract, functional and histological systemic changes took place, especially in the liver and kidneys [29].

Strontium oxide and strontium hydroxide have a strongly irritant effect on the skin and mucous membranes, especially the eyes.

No special hygienic measures are taken in the industrialized countries, except in the case of strontium chromate. The TLV/MAK value for strontium nitrate is 1 mg/m³, and for strontium sulfate and strontium carbonate, 6 mg/m³ [30]. However, these values are still the subject of debate.

Strontium chromate is included in the list of MAK values for carcinogenic industrial materials in Group I11, A2 [31]. The TRK of strontium chromate (SrCrO₄) is 0.1 mg/m², calculated as CrO₃.

57.9 References

1. Kirk-Othmer, 2nd ed., 19, 48–49.
2. *Metals Handbook*, 9th ed., vol. 2, American Society of Metals, Metals Park, OH, 1979.
3. C. L. Mantell: "Strontium" in C. A. Hampel (ed.): *Rare Metals Handbook*, 2nd ed., Reinhold Publ. Co., London 1961, pp. 27–31.
4. J. E. Gruzleski, B. M. Closset: *The Treatment of Liquid Aluminum-Silicon Alloys*, American Foundrymen's Society, Des Plaines, IL, 1990, pp. 25–105.
5. *CRC Handbook of Chemistry and Physics*, 67th ed., CRC Press, Boca Raton, FL, 1986.
6. R. D. Goodenough, V. A. Stenger: "Magnesium, Calcium, Strontium, Barium and Radium" in J. C. Bailar (ed.): *Comprehensive Inorganic Chemistry*, vol. 1, Pergamon Press, Oxford 1973, pp. 591–664.
7. *The Economics of Strontium 1992*, 6th ed., Roskill Information Services, London 1992.
8. H. Davy: "Elements of Chemical Philosophy" in J. Davy (ed.): *The Collected Works of Sir Humphrey Davy*, vol. 4, Smith Elder and Company, Cornhill 1840, p. 253.
9. B. Mason, C. B. Moore: *Grundzüge der Geochemie*, Enke Verlag, Stuttgart 1985.
10. H. Gundlach, *Geol. Jahrb.* 76 (1959) 637–712.
11. E. Usdowski, *Contrib. Mineral. Petrol.* 38 (1973) 177–195.
12. H. Harder, *Beitr. Mineral. Petrogr.* 10 (1964) 198–215.
13. J. Griffiths, *Ind. Miner. (London)* 293 (1992) 21–33.
14. Roskill: *The Economics of Strontium 1992*, 6th ed., Roskill Information Service Ltd., London 1992.
15. Proinsur, WO 9201630 A1, 1992 (A. Piedrafita Palacios).
16. H. Maeda, Y. Tanaka, M. Fikutomu, T. Asano, *Jpn. J. Appl. Phys.* 27 (1988) 209.
17. M. L. Schole et al., US 3699221, 1972.
18. EC Guideline 91/325, March 1, 1991, EC Number: 024-009-00-4.
19. US Department of the Interior, Bureau of Mines: *Strontium – Uses, Supply, and Technology*, IC 9213, Washington 1989.
20. A. Guntz, F. Benoit, *Bull. Soc. Chim. Fr.* 35 (1924) no. 4, p. 712.

21. International Maritime Organization (IMO): *International Maritime Dangerous Goods Code*, vol. 3, London 1990, p. 4325.
22. B. Closset, J. Gruzleski, *Metall. Trans. A* 13A (1982) 945-951.
23. Alcan Research and Development, US 3926690, 1975 (L. R. Morris, F. B. Miners).
24. Aluminum Company of America, US 4711762, 1987 (W. D. Vernam, B. W. Lifka).
25. Kobe Steel Inc, JP 62-207 849, 1987 (N. Shinano).
26. *Metals Handbook*, 9th ed., vol. 1, American Society of Metals, Metals Park, OH, 1979, p. 21.
27. G. Thiedemann, *Wiss. Umwelt* 1 (1979) 48-51.
28. US Department of Health and Human Services: Registry of Toxic Effects Chemicals Substances, NIOSH-RTECS-File, Washington 1992.
29. *Patty*, 3rd ed., 2A, 1894.
30. N. Ju. Tarasenko, Ju. V. Zjuzjukin, *Gig. Sanit.* 5 (1976) 28.
31. Deutsche Forschungsgemeinschaft (ed.): MAK- und BAT-Werte-Liste, Mitteilung 28, VCH Verlagsgesellschaft, Weinheim 1992.

58 Barium

ULRICH BAUDIS (§ 58.1); PAUL JÄGER, H. HERMANN RIECHERS, HARTMUT SMOLEIT †, HEINZ WAGNER, LUDWIG WALTER (§ 58.2); HANS UWE WOLF (§ 58.3)

58.1 Introduction	2337	58.2.1.3 Blanc Fixe	2344
58.1.1 Physical Properties	2337	58.2.2 Barium Sulfide and Polysulfides	2345
58.1.2 Chemical Properties	2337	58.2.3 Barium Carbonate	2346
58.1.3 Production	2338	58.2.4 Barium Chlorate	2348
58.1.4 Analysis	2339	58.2.5 Barium Chloride	2348
58.1.5 Transportation, Storage, Safety	2339	58.2.6 Barium Ferrite	2349
58.1.6 Uses	2339	58.2.7 Barium Oxide	2349
58.1.7 Economic Aspects	2340	58.2.8 Barium Hydroxide	2350
58.2 Inorganic Compounds	2340	58.2.9 Barium Nitrate	2351
58.2.1 Barium Sulfate	2342	58.2.10 Barium Titanate	2352
58.2.1.1 Properties	2342	58.3 Toxicology	2352
58.2.1.2 Barite	2342	58.4 References	2352

58.1 Introduction

Barium is 19th in atomic abundance. Its average content in the earth's crust is estimated to be 250 g/t [10].

The metal is very reactive and does not occur free in nature. However, its compounds are widely distributed. Its major minerals are barium sulfate (barite, heavy spar) and barium carbonate (witherite). Barium sulfate occurs in large deposits throughout the world, and it is the most important raw material for all other barium chemicals.

DAVY first prepared barium metal by electrolyzing mixtures of barium oxide and mercuric oxide and subsequently evaporating the mercury [11]. He proposed the name barium (βαρύς, heavy). The principles of the reduction of the oxides of alkaline-earth metals with aluminum were described by MALLET [12] as early as 1878, but GUNTZ [13] is considered to be the first who obtained a considerable amount of barium of good purity by aluminothermic reduction of the oxide.

58.1.1 Physical Properties

Barium has a body-centered cubic crystal structure at standard temperature and pressure. It is a soft silvery-white metal of medium spe-

cific weight and good electrical conductivity (see Table 58.1). Ultrahigh-purity barium is described as slightly golden yellow [14]. The color changes into silvery white as soon as the surface is contaminated. It is not easy to obtain samples of ultrahigh purity, and therefore accurate measurements of some physical properties of barium metal are difficult to carry out. In fact, the values for some physical properties are still the subject of controversy.

58.1.2 Chemical Properties

Barium is clearly metallic and is strongly electropositive. In all of its compounds it has an oxidation state of 2+. Barium is very reactive, and its compounds have high energies of formation. Barium forms stable salts with nearly all oxoacids. Table 58.2 summarizes the physicochemical properties that are associated with the chemical properties of the element.

Generally speaking, barium is more reactive than magnesium, calcium, or strontium. On heating, it readily combines with the halogens in strongly exothermic reactions. It also reacts with the chalcogens to form BaO, BaS, BaSe, and BaTe [15]. These compounds are also formed by reduction of the carbonate, sulfate, selenate, or tellurate [16]. Barium com-

biners with oxygen even at room temperature. Therefore, the metal must be protected from oxidation by storage under paraffin oil or an inert gas. A series of phosphides can be isolated [17]. Reaction of barium with nitrogen starts at about 250 °C. The compound Ba_3N_2 is formed [16, 18].

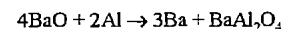
Silicon reacts with barium at 1150 °C to form the silicides BaSi , BaSi_2 , and Ba_3Si_4 [19]. Barium combines with carbon to form the carbide BaC_2 [20]. At moderately elevated temperatures barium reacts with hydrogen to form the hydride BaH_2 [16]. Barium reacts vigorously with water, liberating hydrogen, to form the strong base barium hydroxide. The metal reacts similarly with alcohols to form the alkoxides and hydrogen. Barium dissolves readily in liquid ammonia. The blue or black solutions contain ammine complexes such as $\text{Ba}(\text{NH}_3)_6$. Evaporation of the solvent leaves residues of barium amide, $\text{Ba}(\text{NH}_2)_2$, imide, $\text{Ba}(\text{NH})$, and nitride, Ba_3N_2 [21, 22].

Little is known about organobarium compounds. Alkyl- and arylbarium halogenides, R_2BaX , as well as dialkyl- and diarylbarium, R_2Ba , have been synthesized [23, 24].

Barium forms many alloys, and many binary phases have been described [25]. Nevertheless, only the system barium–aluminum has commercial importance.

58.1.3 Production

On an industrial scale barium metal is produced in a vacuum by reduction of its oxide with aluminum:



The two-stage process is similar to that for calcium. The raw material is barium oxide.

The barium oxide is mixed with aluminum granules, and the mixture briquetted and charged into long tubular retorts of heat-resistant steel. These are evacuated and heated to ≈ 1100 °C at the end containing the charge, while the other end is kept cool. Molten aluminum and aluminum vapor react with the solid barium oxide, releasing barium vapor, which condenses in the cooler part of the apparatus

[26], where it is collected and cast into chill molds under argon.

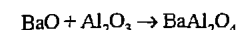
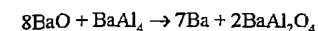
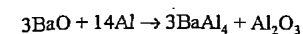
Table 58.1: Physical properties of barium.

Property	Value
Atomic number Z	56
Relative atomic mass A_r	137.34
Mass number (natural abundance, %) of stable isotopes	130 (0.101), 132 (0.097), 134 (2.42), 135 (6.59), 136 (7.81), 137 (11.3), 138 (71.7)
Density ρ at 20 °C	3.74 g/cm ³
Melting point m_p	726.2 °C
Boiling point b_p at 101.3 kPa	1637 °C
Hardness (Mohs scale)	1.25
Crystal structure	body-centered cubic
Lattice constant a_0 at 20 °C	0.5025 nm
Coefficient of thermal expansion α_l (mean, 0–100 °C)	$1.8 \times 10^{-5} \text{ K}^{-1}$
Modulus of elasticity E	$1.265 \times 10^{10} \text{ N/m}^2$
Heat of fusion ΔH_m	7.98 kJ/mol
Heat of vaporization ΔH_v	140.3 kJ/mol
Specific heat capacity c at 20 °C	192 J kg ⁻¹ K ⁻¹
at 900 °C	230
Vapor pressure P at 630 °C	1.33 Pa
730	1.33×10^1
860	1.33×10^2
1050	1.33×10^3
1300	1.33×10^4
1520	5.33×10^4
1637	1.013×10^5
Electrical resistivity ρ	
Commercial purity	$40 \times 10^{-6} \Omega \text{ cm}$
Extra high purity	30×10^{-6}
Liquid barium at m_p	314×10^{-6}
Thermal coefficient of electrical resistivity $d\rho/dT$ (mean, 0–100 °C)	$6.5 \times 10^{-3} \text{ K}^{-1}$

Table 58.2: Physicochemical properties of barium.

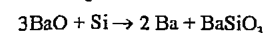
Property	Value
Work function Φ	$3.38 \times 10^{-19} \text{ J}$ or 2.11 eV
Ionization potential	
First	$8.33 \times 10^{-19} \text{ J}$ or 5.212 eV
Second	$1.60 \times 10^{-18} \text{ J}$ or 10.00 eV
Standard electrode potential $\text{Ba}^{2+} + 2e^- \rightarrow \text{Ba}$	-2.91 V
Electronegativity (Pauling)	1.02
Ionic radius (Ba^{2+} , Pauling)	0.135 nm
Atomic radius	0.217 nm
Enthalpy of hydration (Ba^{2+})	1290 kJ/mol
Standard heats of formation (25 °C)	
BaO	-558 kJ/mol
BaCl ₂	-858
BaH ₂	-191
Ba ₃ N ₂	-377

BaAl_4 is an intermediate [27], and the net reaction is actually the sum of three reactions:



In the laboratory the aluminothermic reduction of barium oxide is also the most useful method of preparation [7, 21, 28–31]. It is also the method of choice for preparing of high-purity samples [32].

Silicon powder can be used to reduce barium oxide, but somewhat higher temperatures are required, 1200 °C in a vacuum [33]:



Either no reduction or only partial reduction combined with alloying occurs when barium oxide is treated with magnesium, calcium, sodium, or potassium. Barium can be isolated by reaction of barium iodide with sodium, whereas the chloride does not react. Electrolytic methods are not useful for industrial production and are only rarely useful for laboratory synthesis because of the solubility of barium in its molten halides [34]. It is unlikely that barium has ever been isolated in sufficient purity by electrolysis, even though this method has been mentioned numerous times [2].

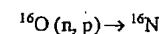
58.1.4 Analysis

Volatile barium compounds impart a pale green color to flames, and this is an effective, simple qualitative test for barium (455.4, 493.4, 553.6, and 611.1 nm).

Barium is separated from magnesium, strontium, and calcium by precipitation from a dilute solution in nitric or hydrochloric acid with a solution of potassium dichromate in aqueous acetic acid. Barium is determined gravimetrically by precipitation of the sulfate [35]; small quantities are determined spectrometrically [36].

The metallic impurities in commercial barium (Table 58.3) are determined by atomic absorption and flame emission spectroscopy. Trace impurities are best determined by inductively coupled emission spectroscopy (ICP) [38]. The carbon content in barium is determined by combustion; nitrogen, by the

Kjeldahl method; and hydrogen, by vacuum hot extraction. Vacuum hot extraction is not useful for analysis of oxygen. Neutron activation analysis based on the reaction



is the recommended method for determination of oxygen in alkaline-earth metals [39].

Table 58.3: Chemical analysis of commercial barium [37].

Element	Percentage
Ba	99.3 ± 0.3
Sr	0.8
Ca	0.25
Al	0.05
Mg	0.02
N	0.02
Fe	0.01
Cl	0.01
C	0.01
Li, Na, K	0.01

58.1.5 Transportation, Storage, Safety

Barium metal is commercially available in bars of 5–20 kg or in rods 22 mm in diameter and 400 mm in length. The rods can be cut into small pieces or extruded into wires.

Barium is packaged in air-tight steel drums containing up to 100 kg of the metal under argon or paraffin oil. Smaller amounts (1–10 kg) are packaged in tin cans, and even smaller samples are packaged in hermetically sealed glass bottles [40, 41].

Barium is a flammable solid and cannot be mailed. If it comes into contact with water, there is always the danger of explosion on account of the liberated hydrogen. Therefore barium should always be stored in a dry, well ventilated place and every contact with moisture and air avoided. Protective glasses and safety gloves should be worn while handling barium. Burning barium can be extinguished with sand, aluminum oxide, etc.

58.1.6 Uses

The main use of barium and barium–aluminum alloys is as *getter* to remove the last traces of unwanted gases from television pic-

ture tubes, transmitter valves, and other vacuum tubes [42–48]. Barium and its aluminum alloys also are used in incandescent lamps [49, 50]. Barium is particularly well suited as a getter because it has a low vapor pressure at the working temperatures of the tubes and is very reactive toward undesired gases, such as oxygen, nitrogen, hydrogen, carbon dioxide, water vapor, even removing residues of inert gases by inclusion.

Many other uses of barium have been described in the literature, but they are minor. For example, barium has been used in bearing alloys [51]; in lead–tin soldering alloys, where it increases creep resistance [52]; in nickel alloys for spark plugs [53]; in alloys with calcium, silicon, aluminum, and manganese that are used as deoxidizers for high-grade steel [19, 54]; and as an inoculant for steel and cast iron [55, 56]. Barium has also been used as a modifying agent for silumin, instead of strontium or sodium, because barium also refines the structure of the eutectic aluminum–silicon alloy [57]. Barium is also a good reducing agent; however, it is not normally used for this purpose because of its high atomic mass and its relatively high price, one kilogram of the metal costing about DM 100 (\$260) in 1983.

58.1.7 Economic Aspects

The leading producer is Degussa AG, Germany. Production is about 30 t/a of pure metal and 10 t/a of barium–aluminum alloy [58], essentially covering the demand in the West. Some barium metal, perhaps about 6 t/a, is produced by Union Carbide Corp. in the United States. There may also be production facilities at Pfizer Inc. (United States) and Chromasco Corp. (Canada), but no metal is produced there at present [59]. Nothing is known about production in the former USSR, although facilities doubtlessly exist.

It is difficult to predict the future demand for barium. However, the replacement of television picture tubes by liquid crystal displays, or similar systems, is likely to decrease demand and production over the long term.

58.2 Inorganic Compounds

History. The first mention of barium compounds dates from the year 1602 when V. CASCIOROLUS, in Bologna, realized that barite heated in the presence of organic substances, phosphoresces in the dark. Much later, after 1774, C. W. SCHEELER discovered barium oxide and described its properties. He noted that a precipitate formed when sulfuric acid was added to barium oxide dissolved in water.

J. G. GAHN recognized that this was a reaction of the oxide to form barite, i.e., that the oxides were a new class of compounds. At that time the oxide was given the name baryta ($\beta\alpha\rho\upsilon\varsigma$ = heavy), which in some countries is still the name for technical grades: caustic baryta for the oxide, hydrate of baryta for the hydroxide. Today, however, the mineral heavy spar, BaSO_4 , is meant by baryta or barite. Barium carbonate also occurs in nature. Native barium carbonate was named witherite, for W. WITHERING discovered the mineral in Cumberland, Great Britain, in 1783.

Raw Materials and Processing. The most important barium mineral is barite (barytes, heavy spar, barium sulfate, BaSO_4), today almost exclusively used as the raw material for the production of barium compounds. Barite occurs all over the earth in hydrothermal vein and sedimentary deposits. The main deposits of the mineral witherite (BaCO_3) are situated in England, Romania, and the former USSR, but witherite is no longer of economic importance. No other mineral containing barium is used as a raw material for barium or its compounds at present.

The maximum world output of barite was $\approx 8.3 \times 10^6$ t (1981); however, only 7–8% of this was used for the production of other barium compounds. Figure 58.1 shows how dressed barite is converted into other barium compounds. The barite is first reduced with carbon to give water-soluble barium sulfide, which is used mainly as an intermediate for the production of all other barium compounds and lithopone [60–64].

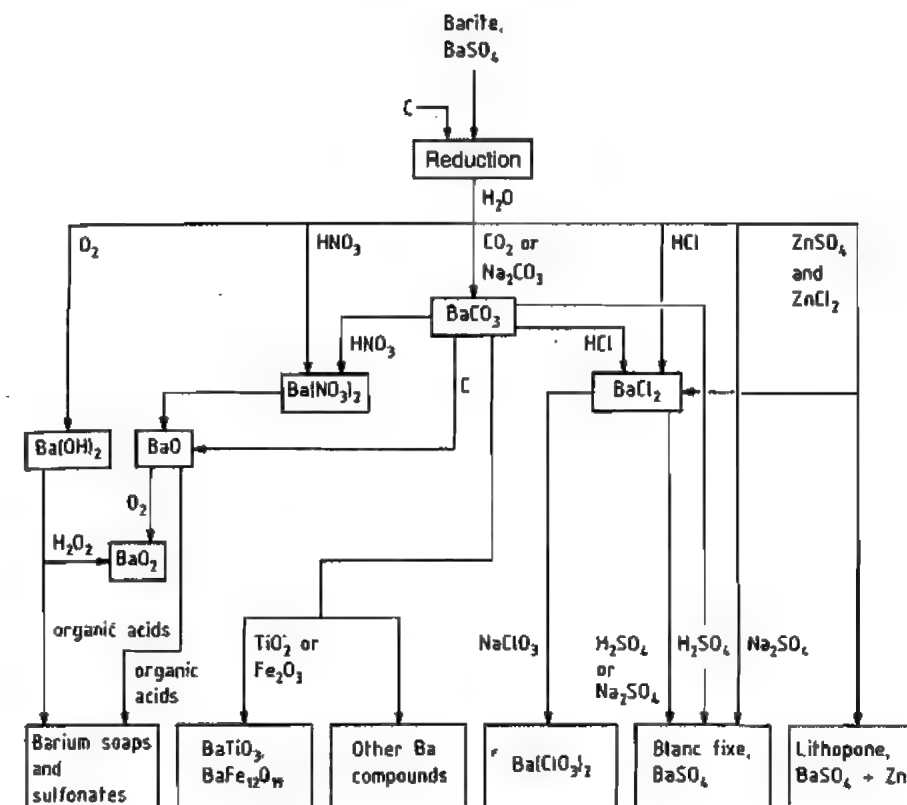


Figure 58.1: Production pathways to various barium compounds starting from barite.

Chemical Analysis. All barium compounds may be identified by the green color imparted to flames. For quantitative analysis, atomic absorption spectroscopy, flame emission spectroscopy, X-ray spectroscopy, complexometry, and gravimetry are suitable.

Economic Aspects. Production data is available only for barium sulfate, the most important barium compound and the starting material for the production of most other barium compounds. The reason for this is the small number of producers of barium compounds worldwide, and these release only a limited amount of production information. The worldwide production of barite (BaSO_4) has increased from 3900 kt in 1970 to 8300 kt in 1981. This dramatic increase in production was the result of increased exploration and drilling for oil and gas, itself a result of the oil

crisis of the early 1970s. Coupled with a reduction in exploration and drilling in 1982, the production of BaSO_4 fell in 1982 to about 7300 kt, a trend that has continued. At this rate of production the known and probable reserves, estimated at 400 Mt worldwide, will last at least 60 years. The production by country is shown in Table 58.4.

Table 58.4: Estimated production of barium sulfate, $\times 10^3$ t.

Country	1980	1981	1982
United States	2030	2590	1800
Canada	86	82	77
Mexico	270	318	254
South America	845	820	800
Western Europe	1200	1100	1030
Comecon	800	810	820
Africa	480	600	580
Middle and Far East	1810	1960	1890
World production	7520	8280	7250

Around 88–90% of the world production of barite is used to increase the density of drilling muds. About 7–8% is used to produce barium compounds. Over one half of this amount is used to produce barium carbonate. Other important compounds are the chloride, the hydroxide, and blanc fixe. Only about 3–5% of the world production is used as a filler — both bleached and unbleached — in paints, rubbers, etc.

58.2.1 Barium Sulfate

Barium sulfate is the most important barium compound, and the mineral barite, BaSO_4 , also called heavy spar or baryte, is by far the most important barium mineral.

58.2.1.1 Properties

Barium sulfate, BaSO_4 . The industrially precipitated product is called blanc fixe. Pure BaSO_4 forms colorless rhombic crystals of refractive index ≈ 1.64 , hardness 3–3.5 (Mohs scale), and density ρ 4.48 g/cm³. Heating BaSO_4 decomposes it, the rate increasing with temperature over the range 1100–1500 °C. The main products are BaO , SO_2 , and O_2 . For this reason melting points given in the older literature 1345 °C or 1580 °C differ. Barium sulfate is almost insoluble in water, the solubility being $2.5 \times 10^{-4}\%$ at 20 °C and $3.9 \times 10^{-4}\%$ at 100 °C. Barium sulfate is more soluble in hot concentrated sulfuric acid and in melts of alkali-metal salts. The most important reaction of barite is its reduction with carbon to produce barium sulfide.

58.2.1.2 Barite

In nature barite rarely occurs as a pure white mineral; generally, its color is yellowish, pink, reddish brown, dark gray, or black. The main impurities are quartz, calcium carbonate, iron and manganese oxides, fluorite, strontium sulfate, pyrite, lead glance, zinc blende, and sometimes bituminous substances, the impurities and their amounts depending on the particular deposit. To remove these impurities before the barium sulfate is

used industrially, in most cases barite is given a preliminary treatment to increase the BaSO_4 content to 90–97%.

Deposits. Barite deposits are found in all regions of the world. The most important in Europe are found in Ireland, France, Italy, Germany, and Greece, but barite is also mined in Spain, Turkey, and Yugoslavia. Another important producer of barite is the former USSR.

The most significant deposits in the Americas are found in the United States, but other large deposits are mined in Canada, Mexico, Peru, and Argentina.

Morocco is the most important producing country in Africa. Smaller quantities are mined in Algeria, Tunisia, and Egypt. Large deposits are situated in China, India, Thailand, and Iran.

Mining and Dressing of the Ore. Barite is usually mined in open cuts, only sometimes in open pits or underground galleries. The ore is washed in trommels to remove adherent argillaceous impurities, then crushed in breakers, and classified. The various grain sizes are liberated from the mostly quartz gangue in jigs, thus enriching the barium sulfate. This wet mechanical dressing is adequate for many uses. If there is a high degree of intergrowth of quartz and barite and if the ore contains much iron, lead, or zinc, flotation is required. This produces 98% BaSO_4 [65]. Sometimes barite is a by-product of the flotation of pyritiferous ores. The flotation agents and the pH depend, among other things, on the impurities present in the crude ore [66]. Generally the barite is wet ground to a grain size of 0.1 mm before flotation. Sodium oleate, tall oil, oleic acid, and most recently alkyl sulfonates and sulfates have been used as collectors. Water glass is the preferred depressant, especially for quartz and iron oxides. Flotation processes to depress the BaSO_4 and float the impurities are confined to a few special cases, e.g., ore rich in fluorite [67].

Another method applicable only to special barite types is based on the tendency of these barites to decrepitate. The broken ore is heated to 700 °C in rotary kilns, the barite crystals

bursting while the gangue is unaffected. The decrepitated fines rich in barite are screened off from the gangue. The yield depends above all else on the suitability of the barite for this treatment.

Barite grades with special properties are produced for the various industrial uses.

Drilling Muds. About 88–90% of the world output of barite is ground and used to increase the density of drilling muds, especially for drilling oil and gas wells. The muds consist of an aqueous clay suspension and additives. The large amount of barite that can be added to this suspension allows adjustment of the density to a high value without the viscosity being affected significantly. The increased density allows faster discharge of cuttings and prevents blowouts. The standards for drilling-mud-grade barite vary from country to country; for instance, they are described in the OCMA or API standards [68]. However, in every case the barite must be free from water-soluble salts because these cause clay suspension to flocculate [69].

For the production of barite for drilling muds, generally it is sufficient to jig the ore to increase the density by removing the quartz. In most cases the other impurities do not cause trouble. On the other hand, barite that has been floated must be heated or treated in some other way to destroy its hydrophobic character.

Raw Material for Barium Chemicals. The 7–8% of the total barite production to be used as a raw material for other barium compounds is always reduced to barium sulfide as the first stage. The BaSO_4 content must be > 95%, and the BaSO_4 should contain as little silica and iron as possible, as these impurities reduce the yield of water-soluble barium sulfide. Fluor-spar (fluorite) and lead glance interfere with the reduction. Such barite is generally shipped in bulk as coarsely broken material, either granular (jigged) or ground (floated).

White Ground Barite Filler. Ground barite is used as a filler owing to its resistance to chemicals and weathering, its wettability and dis-

persibility, and its low adsorption of binders. The properties of barite flour vary, depending on the commercial grade:

Grain size	0.1–40 μm
Brightness (reference, $\text{MgO} = 100$)	85–95
Refractive index n_D	≈ 1.64
Oil requirement	10–12 g of oil/100 g
Bulk density, tamped	1.4–2.2 g/cm ³
Density	4.0–4.25 g/cm ³

Some white barite grades may be ground directly without further treatment. More usual, however, is to subject the spar to coarse crushing and gravity dressing. Then the granular material is treated in bleaching vats with hot dilute acid, preferably sulfuric or hydrochloric acid, to remove the colored iron or manganese oxides, washed, and dried. The bleached spar is dry-milled in edge or ball mills to obtain the desired grain size, then air classified.

There is a more economical procedure: the coarsely crushed, gravity dressed barite is ground to the desired grain size by continuous wet milling in lined ceramic tubes. The screened suspension of ground material is bleached in agitator vessels, with dilute sulfuric or hydrochloric acid along with reducing agents (e.g., sodium sulfite) or oxidizing agents (e.g., nitric acid), depending on the kind of impurities, then washed, decanted, and dried. If floated barite is used in this process, then the barite must be floated again after bleaching to remove the decomposed organic material [70].

A third bleaching procedure lacks economic importance: here the barite is heated in a rotary kiln by adding alkali-metal salts, e.g., sodium chloride or sodium hydrogensulfate. This procedure is confined to special cases due to its high cost.

The specifications for ground barite are given in DIN 55911 for Germany and ISO 3262 internationally. The requirements of the buyers differ in regard to grain size and whiteness. Some products, such as EWO-Albaryt grades of the Deutsche Baryt-Industrie, Bad Lauterberg/Harz, are equivalent to synthetic blanc fixe in many respects. White ground barite is generally shipped in 50-kg paper bags.

Barite flours are mainly used as fillers and extenders in paints, varnishes, plastics, rubber, linoleum, sealing compounds, stoppers, plasters, and adhesives (3–4% of the total barite production). High-quality grades can be used as an X-ray-opaque medium in medicine, insofar as the grades meet the requirements of the individual countries as given in USP, EP, JP, DAB, etc.

58.2.1.3 Blanc Fixe

Precipitated barium sulfate is usually called blanc fixe. It is mainly used as a filler and extender, in some fields also as a white pigment. The most important properties for the consumer are its insolubility in water and organic binders, its high degree of whiteness, and its homogeneous granulation:

Grain size	0.1–20 μm
Average grain size	0.2–2 μm
Brightness (reference, $\text{MgO} = 100$)	95–99
Refractive index n_D	≈ 1.65
Oil requirement	12–22 g of oil/100 g
Bulk density, tamped	0.9–2.2 g/cm^3
Density	4.0–4.4 g/cm^3

Production. Blanc fixe is usually precipitated in stirred tanks from solutions of barium chloride or barium sulfide by adding dilute sulfuric acid or sodium sulfate solutions. The sulfuric acid or the sodium sulfate solution must be free from heavy metals that can impart color to the product.

The method of manufacture and the reaction conditions depend on the ultimate use of the blanc fixe, especially the desired grain size. For example, fine-grained blanc fixe is produced by rapid precipitation from highly concentrated solutions at high pH and low temperatures. Coarse blanc fixe is produced from dilute solutions at high temperatures, say 80–100 °C. The use of seed crystals and prolonged residence time, e.g., by stirring for an extended period at low pH, produces a larger average grain size in the finished product. The precipitated blanc fixe is filtered or centrifuged and washed. It is drawn off and packed as paste, slurry, or powder, the last involving an additional process step of drying and perhaps one of regrinding.

A special problem in preparing blanc fixe from barium sulfide and sodium sulfate solutions is washing out the sodium sulfide. However, this problem can be overcome by enlarging the particle size of the extremely fine material by sintering (at 300–1000 °C) with fluxes like sodium sulfate and extracting the clinker [71].

Another procedure for the manufacture of blanc fixe is based on the conversion of an aqueous suspension of barium carbonate with dilute sulfuric acid, sometimes in the presence of small amounts of hydrochloric acid. The resulting product is characterized by its whiteness [72].

Formerly blanc fixe was obtained as a by-product of hydrogen peroxide production by reaction of barium peroxide and sulfuric acid—but today hydrogen peroxide is prepared by other procedures.

Quality Specifications. In Germany, the standards for blanc fixe, the methods of analysis, and tests are defined in DIN 55911. The various grades differ mainly in grain size. The smaller the grain diameter the higher the luster. In fact, grades are still sometimes characterized as mat, semimat, or lustrous.

The standards for blanc fixe to be used as X-ray-opaque medium in medicine are described and defined for the various countries in USP, EP, JP, DAB, etc. The standards deviate slightly from one to another.

Shipping and Packing. Blanc fixe is shipped as powder (25- or 50-kg paper bags, 1000-kg bags, or in silo trucks); slurry (30–40% water in 460-kg plastic barrels or in tank trucks); and agglomerate-free paste (25–35% water in 50-kg polyethylene-lined iron barrels). Because blanc fixe is nontoxic, it is not classified as a dangerous good.

Uses. About 70% of the blanc fixe consumed in Western Europe is used in paint and varnish as well as in printing ink as a filler. It is used as a coating pigment to upgrade the surface of paper and is sometimes used as a pulp filler. Photographic paper requires grades free from sulfur and heavy metals, but recently this mar-

ket has lost significance. Blanc fixe is also used as a filler in plastics, rubber, and adhesives and as an additive in the negative plates of lead storage batteries. Special grades are used as a medium opaque to X rays for medical purposes (stomach X rays).

58.2.2 Barium Sulfide and Polysulfides

The principal intermediate between barium sulfate and other barium compounds is barium sulfide.

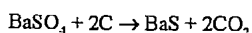
Properties. Pure barium sulfide, BaS, ρ 4.3 g/cm^3 , forms colorless cubic crystals. It melts above 1200 °C. Its heat capacity c_p is 287 $\text{J kg}^{-1} \text{K}^{-1}$. At room temperature barium sulfide is unaffected by dry air, but over the range 500–1000 °C it is oxidized to barium sulfate, at an ever-increasing rate. In humid air containing carbon dioxide, some barium carbonate forms, and the odor of hydrogen sulfide is noticeable. The solubility of barium sulfide in water depends strongly on the temperature, the maximum being near 90 °C:

°C	0	20	40	60	80	90	100
% BaS	2.8	7.3	13.0	21.7	33.3	40.2	37.6

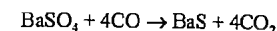
Owing to complete hydrolysis a solution of sulfide is actually an equimolar solution of barium hydroxide, $\text{Ba}(\text{OH})_2$, and barium hydrosulfide, $\text{Ba}(\text{SH})_2$. Accordingly, barium sulfide does not precipitate when the solution is cooled; instead, a double salt of composition $\text{Ba}(\text{OH})_2 \cdot \text{Ba}(\text{SH})_2 \cdot 10\text{H}_2\text{O}$ precipitates. Excess hydrogen sulfide converts the barium hydroxide in solution quantitatively to barium hydrosulfide, which can be precipitated as $\text{Ba}(\text{SH})_2 \cdot 4\text{H}_2\text{O}$ by addition of ethyl alcohol.

Aqueous barium sulfide reacts with carbon dioxide to form barium carbonate, BaCO_3 , and the solution is also susceptible to atmospheric oxygen, which easily oxidizes the hydrosulfide to polysulfide, thiosulfate, and sulfite.

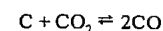
Production. Barium sulfide is produced by reducing barite (BaSO_4) with carbon. The net reaction is



However, the thermodynamic data suggests that the actual reducing agent is carbon monoxide [73]:



Barium sulfite, BaSO_3 , is an intermediate [74]. The CO forms in the reaction between carbon and CO_2 , the Boudouard equilibrium:



The barite should have a BaSO_4 content $\geq 95\%$. Large amounts of impurities, especially silica and iron oxide, reduce the yield of water-soluble barium sulfide by forming the insoluble barium silicates and ferrates. The spar is ground to 0.1–2 mm and mixed with low-ash reducing carbon or coke, one part of carbon to 4–6 parts of barite.

Today the reduction is usually carried out in a continuous process centered around rotary kilns up to 50 m long. A burner at the outlet of the kiln fired with fuel oil, natural gas, or coal dust provides countercurrent heating. Reduction takes place at 1000–1200 °C; average residence time is 90–120 min. The operating conditions must be carefully controlled to prevent secondary reactions with the gangue and to impede caking. The barium sulfide melt should be obtained in a fine-grained condition. The sulfide melt leaves the kiln continuously through a cooling drum. Generally further grinding is not necessary.

The older batch method, using rotary kilns, is still in use, especially in smaller companies. Essentially the operating conditions correspond to those of the continuous process. However, batch operation is characterized by lower output and higher unit operating cost.

Recently, various processes using a fluidized-bed kiln have been reported. Here, the pulverized spar, e.g., from flotation, is granulated together with carbon and reacted in a fluidized bed, a part of the carbon being used for heat generation and a part for reduction [74, 75]. Other processes use a reducing gas, e.g., carbon monoxide or methane, instead of carbon. The gas serves three functions: it provides heat upon combustion, it supports the fluidization, and it is the reducing agent. The

advantages are a reduction temperature below 1000 °C, a residence time less than 1 h, and a more favorable energy balance [76, 77]. However, large-scale plants of this kind have not been reported.

Crude barium sulfide (black ash) is leached countercurrently with 50–70 °C water to dissolve the barium sulfide. This leaching is carried out batchwise in batteries of Shank leaching vats or continuously in closed agitated vessels followed by several thickeners. The suspended matter is filtered off, and the lye, containing 13–18% BaS, is immediately treated further to prevent oxidation or crystallization. At this point the barium sulfide solution is very pure.

The residue still contains 50% barium, in the form of compounds insoluble in water, such as silicates and ferrates of barium and unreacted barite. The silicates and ferrates can be dissolved with hydrochloric acid to form barium chloride; however, this process is often uneconomical because of the cost of purifying the barium chloride solution. To avoid these problems a recent method proposed that the leaching residue be resuspended in water and, by adding hydrogen sulfide, the portion of barium compounds that are insoluble in water be converted into readily soluble barium hydrosulfide that can be led back into the sulfide lye [78].

Quality Specifications. Barium sulfide is available only as a technical-grade, granular, dark gray crude product called black ash. It contains 75–85% water-soluble BaS, barium compounds soluble in hydrochloric acid (8–10% as BaO), 2–4% SiO₂, 2–3% Fe₂O₃ and Al₂O₃, 2–4% BaSO₄, and 1–2% carbon. The economic value depends directly on the content of water-soluble BaS, which is determined analytically by acidimetry and iodometry.

Packing and Shipping. Barium sulfide is packed in multilayered paper bags with an inner polyethylene bag or in 50-kg polyethylene bags. Shipment is governed by TMDG Class 6.1, UN 1564, and RID/ADR Class 6.1, 71.

Uses. Barium sulfide is mainly used for the production of other barium compounds, especially lithopone. Some BaS is used for the production of hydrogen sulfide; in this case, barium chloride is the by-product. Other uses (depilatories, purification of mineral acids) are far less important.

Barium Polysulfides. The polysulfides have the general composition BaS_x (x = 2–5). They include barium disulfide, BaS₂; barium trisulfide, BaS₃; barium tetrasulfide, BaS₄; barium tetrasulfide monohydrate, BaS₄·H₂O; barium tetrasulfide dihydrate, BaS₄·2H₂O; and barium pentasulfide, BaS₅. Polysulfides form when barium sulfide solutions are oxidized by air, when sulfur is dissolved in barium sulfide solutions, when barium sulfide is fused with sulfur in a vacuum, etc.

The isolation of individual polysulfides from solution is difficult because of their tendency to decompose. Technical barium polysulfide is produced by grinding barium sulfide with sulfur (Ba:S = 1:4–5). It is marketed as a grayish-yellow powder. The formation of polysulfide does not take place until the powder is dissolved.

A new process, however, produces a mixture of true barium polysulfides, BaS_{4–5}, by sudden evaporation of a solution in a spray dryer [79]. The resulting light yellow powder is stable and dissolves in water without leaving a residue.

As a 1–3% solution barium polysulfide is a fungicidal and acaricidal agent used in fruit and grape growing.

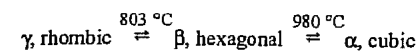
Shipment of barium polysulfides is governed by the IMDG Class 6.1, UN 1564, or RID/ADR Class 6.1, 71.

58.2.3 Barium Carbonate

Barium carbonate is the most important manufactured barium compound. It occurs in nature as witherite, which has little economic significance due to rareness, inevitable impurities, and almost fully depleted deposits.

Properties. Barium carbonate, BaCO₃, mp 1360 °C accompanied by loss of CO₂. Pure

barium carbonate is a white fine crystalline powder having several modifications:



The rhombic modification is isomorphous with the carbonates of calcium (aragonite), strontium (strontianite), and lead (cerussite).

Barium carbonate has a density of 4.29 g/cm³. Its solubility in water at 20 °C is only 2 × 10⁻³%, although it is a little more soluble in water containing CO₂. Its refractive index is ≈ 1.6. Its heat capacity *c_p* at room temperature is 433 J/kg·K⁻¹.

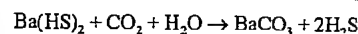
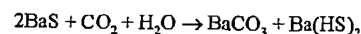
When barium carbonate is heated, it loses carbon dioxide and forms barium oxide. The dissociation is promoted by traces of water. Barium carbonate and its decomposition product barium oxide are partially soluble in each other at elevated temperatures, at 1000 °C ≈ 10 mol% oxide in the carbonate and 5 mol% of carbonate in the oxide — this partial solubility was not adequately appreciated in the older literature. Moreover, there is a eutectic at 1060 °C with 34 mol% barium oxide. The equilibrium CO₂ pressure above barium carbonate saturated with oxide increases rapidly above 1000 °C [80, 81]:

°C	900	1000	1100	1200	1250	1300	1360
kPa	0	0.21	1.6	10.1	21.6	46.4	101.3
Torr	0	1.6	12	76	162	348	760

Production. Barium carbonate is produced almost exclusively by precipitation from barium sulfide solutions. There are two processes:

- precipitation with carbon dioxide
- precipitation with soda

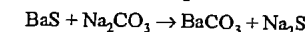
The first is based on the reactions



The carbon dioxide is usually available from combustion gases or native carbonic acid. The precipitation is carried out batchwise in gastight vessels, several of which may be arranged in series to absorb the carbon dioxide that breaks through with the hydrogen sulfide in fresh lye; a utilizable hydrogen sulfide poor in carbon dioxide is produced in this

way. Also there are continuous processes, e.g., using precipitation columns [82, 83].

The second process is based on the reaction



The barium sulfide lye containing 15–18% BaS is run into 30% soda solution in agitator vessels.

The decision to favor one or the other of the two processes does not depend only on the availability and relative cost of carbon dioxide or soda. Above all else the value or sales prospects of the by-products, H₂S or Na₂S, is decisive. The hydrogen sulfide must be worked up to sulfur, sulfuric acid, sodium hydrosulfide, or sodium sulfide. The dilute sodium sulfide solution produced in the soda process in most cases is upgraded to crystalline sodium sulfide hydrate (60% Na₂S).

The main impurity in BaCO₃, sulfur as sulfide, elementary sulfur, or sulfate, is the major problem. Patents offer a number of solutions: adding aluminum powder to the barium sulfide lye to reduce the polysulfide sulfur [84], continuously maintaining a residual barium sulfide content in the solution of 0.5% during the precipitation with carbon dioxide to keep the sulfur dissolved [85]; or a careful step-by-step precipitation, perhaps first to BaCO₃ and Ba(HS)₂ and then to BaCO₃ and H₂S [82, 83].

Quality Specifications. Purity, bulk density, and grain-size distribution depend on the particular use. Usually, low sulfur and heavy-metal content is demanded. The manufacturers of electroceramics require low strontium content. The numbers below refer to products of various origin, quality, and process and should only be regarded as reference values:

Barium carbonate	≥ 98.5%
Sulfur	0.08 (0.02)%
Strontium	0.5–1.4 (0.3)%
Iron	6–20 × 10 ⁻⁴ %
Insoluble in HCl _(reln)	0.1–0.6%
Density	4.29 g/cm ³
Bulk density, tamped	0.4–1.8 (202) g/cm ³
Grain size, < 5 μm	80–95%

An important standard for barium carbonate as a sulfate-binding agent is its reactivity. This is determined by conversion of barium carbonate with known quantities of sulfate, as gypsum water or sodium sulfate solution.

Packing and Shipping. Barium carbonate is stored in silos and shipped in 50-kg multilayer paper bags, \approx 1000-kg bags, or silo wagons. Shipment is governed by the IMDG Class 6.1, UN 1564, or RID/ADR Class 6.1, 71.

Uses. Barium carbonate is used to remove the detrimental sulfate ion from the input solutions of the alkali-metal chloride electrolysis, e.g., the mercury process, as well as from industrial waters of various kinds. In brick production barium carbonate is a binder for the soluble sulfates in the raw mixture. The formation of insoluble barium sulfate prevents discoloration (efflorescence) during production. Moreover, barium carbonate reduces the tendency of baked bodies to effloresce on exposure to moisture. Barium carbonate is used to incorporate barium oxide into special fine glassware, apparatus glass, and many optical glasses. The barium oxide increases the workability of the glass melt, improves the mechanical and chemical resistance, and increases the refractive index of the glass. Barium in television screens prevents the leakage of X rays.

Barium carbonate is also used in enamels, the electroceramic barium titanate and the magnetoceramic barium ferrites. These last two uses require high-purity BaCO_3 .

58.2.4 Barium Chlorate

Barium chlorate monohydrate, $\text{Ba}(\text{ClO}_3)_2 \cdot \text{H}_2\text{O}$, forms monoclinic short prismatic crystals of density 3.18 g/cm^3 . Its solubility in water is 21.2% at 10°C and 51.3% at 100°C . Near 120°C barium chlorate begins to lose its water of crystallization, and above 250°C oxygen is lost. The anhydrous salt melts at 415°C ; however, explosions can occur on fusion or if a mixture with sulfur or organic substances is heated even at 110°C . Barium chlorate is a good oxidant.

Barium chlorate is produced on an industrial scale by mixing concentrated barium chloride solution into hot concentrated sodium chlorate solution. On cooling, barium chlorate monohydrate crystallizes. Although it crystallizes in a rather pure form, barium chlorate can be purified even further by recrystallization.

This double conversion is more economical than electrolysis of a barium chloride solution, a process that is no longer used.

Barium chlorate is almost exclusively used in pyrotechnics, where it produces a green color. In addition, it has been used as an oxidizing agent, e.g., in textile printing. Shipment is governed by IMDG Class 5.1, UN 1445, or RID/ADR, Class 5.1, 4a.

58.2.5 Barium Chloride

Anhydrous barium chloride BaCl_2 , *mp* 962°C , ρ_{20} 3.91 g/cm^3 , crystallizes in two modifications: α - BaCl_2 (rhombic, mostly lamelliform) and β - BaCl_2 (cubic). The conversion temperature is 925°C . Barium chloride is soluble in water:

$^\circ\text{C}$	0	20	40	60	80	100
% BaCl_2	23.6	26.3	29.0	31.6	35.0	36.6

The enthalpy of fusion is 193 kJ/kg , and the entropy of fusion is $87.7 \text{ Jkg}^{-1}\text{K}^{-1}$. The heat capacity c_p is $361.8 \text{ Jkg}^{-1}\text{K}^{-1}$ near room temperature.

Barium chloride crystallizes from aqueous solutions as the dihydrate in monoclinic colorless plates, ρ 3.097 g/cm^3 . Water of crystallization is not lost much before 110°C , this process being finished around 160°C .

Production. Today the production of barium chloride on an industrial scale is carried out by the reaction of 15–18% barium sulfide solution with 31–32% hydrochloric acid. In addition, the reaction of barium sulfide solution with chlorine is of commercial interest.

In both methods reaction is continued until the solution becomes acid to assure complete conversion of the barium sulfide and to remove from solution the hydrogen sulfide formed. The reaction with hydrochloric acid is often followed by oxidation with air or chlorine to convert any dissolved sulfur compounds into barium sulfate, which removes the sulfur from the solution. In both methods the solution is neutralized afterwards with barium carbonate or sodium hydroxide to precipitate heavy metals.

The solubility of BaCl_2 in water does not depend strongly on temperature. If the barium chloride is to be crystallized, this is carried out by evaporative crystallization. In most cases vacuum evaporation is used, the salt crystallizing as the dihydrate. Normally it is only dried but it can be dehydrated further if necessary. The mother lye, which still contains barium chloride, can be processed to produce insoluble blanc fixe (BaSO_4) or barium carbonate. The by-product hydrogen sulfide from the hydrochloric acid process is usually converted into sodium sulfide or sodium bisulfide.

In the chlorine process the by-product is sulfur, usually containing barium carbonate and heavy metals.

By-product barium chloride is obtained in the production of lithopone grades containing more than 30% zinc sulfide, for in these cases barium sulfide is reacted with zinc sulfate and zinc chloride. Another source of barium chloride is the black ash leaching residues. These are reacted with hydrochloric acid by some manufacturers. However, the resulting barium chloride solutions contain such a concentration of impurities that they must be purified extensively before further use.

The literature reports various procedures to convert barite directly into barium chloride. These procedures, e.g., the reaction of barite with carbon and calcium chloride or the chloridizing reduction of barite, no longer have significance in Western Europe or America, for they are now uneconomical. Direct conversion still seems to be of interest in Eastern Europe, where numerous scientific papers and patents on direct conversion are issued, e.g., [86]. The industrial production of barium chloride from barium sulfate, carbon, and calcium chloride is reported only from China.

Quality Specifications, Packing, Shipping. Both the dihydrate and anhydrous barium chloride are marketed as technical grades of 99–99.5%, the dihydrate also being available as a high-purity grade (\approx 100%). They are packed in 50-kg multilayer paper bags with polyethylene covers or liners to make the bags

moistureproof. Shipment is governed by IMDG Class 6.1, UN 1564 (harmful, keep separate from foodstuffs), or RID/ADR Class 6.1, 71.

Uses. Along with other chlorides barium chloride is used as a component of melt quenching baths for steel. It is used as a starting material for the production of blanc fixe and, instead of barium carbonate, to remove sulfate from solutions. Finally, it has a limited importance as a stabilizer for plastics.

58.2.6 Barium Ferrite

Barium hexaferrite, $\text{BaFe}_{12}\text{O}_{19}$, forms hexagonal needle-shaped ferrimagnetic crystals. It is usually manufactured in a two-stage solid-state reaction, first stage at 650 – 750°C , second stage $> 850^\circ\text{C}$. An intermediate is barium monoferrite, BaFe_2O_4 .

58.2.7 Barium Oxide

Barium oxide, caustic baryta (an older term), BaO , *mp* $\approx 1920^\circ\text{C}$, sublimes $\approx 2000^\circ\text{C}$. Pure commercial barium oxide is a white fine crystalline powder, whereas technical grades are often gray due to carbon impurities. Barium oxide forms face-centered cubic crystals. The densities reported in the literature vary considerably, perhaps depending on preparation. The most likely value is $\approx 5.7 \text{ g/cm}^3$.

Usually barium oxide is very reactive. However, its reactivity depends on the preparative conditions, the reaction temperature, and the coreactant. In the absence of water BaO often reacts very slowly with carbon dioxide. In the presence of small amounts of water, however, it is converted by carbon dioxide into barium carbonate in a very exothermic reaction. The conversion of barium oxide by water into barium hydroxide is also very exothermic. Self-ignition may occur on contact with wet organic substances. Barium oxide is soluble in methanol: 20% dissolves at 15°C , and therefore barium oxide can be purified by recrystallization before it is used as a starting material for organic barium com-

pounds or for incorporation, as a methyrate, into organic systems.

Production. Barium oxide is mainly produced by decomposition of barium carbonate in the presence of carbonaceous material at high temperature. The use of carbon significantly lowers the temperature at which the barium carbonate decomposes, which to a large extent avoids unwanted corrosion of the reactor when barium carbonate is decomposed by heat alone at 1400 °C. Also important is the decomposition of barium carbonate mixed with channel black (6.21% C) in retorts of silicon carbide–corundum externally heated to \approx 1250 °C.

The modern procedures tend to use continuous fluidized beds. Barium carbonate-soot pellets are used [87, 88], or the carbon is added to the fluidized bed as methane [89]. The advantages are, among others, that the low reaction temperatures give less-sintered products, i.e., more reactive BaO.

There are also procedures using electrical arcs in a core zone [90]. In such processes a steep temperature drop is maintained between the hot core zone and the reactor shell, to provide a protective layer for the shell material. Addition of carbon is not absolutely necessary.

The crude barium oxide can be reacted [88, 89] in a second stage with carbon for more complete conversion.

The latest literature reports preparation of barium oxide by direct decomposition of barium sulfate or barium carbonate on a plasma torch, although production using this method has not been reported.

Quality Specifications. Barium oxide is marketed in grades of a purity of 97–99%. The main impurities are 1–3% barium carbonate, \leq 1% barium peroxide, and a few tenths of a percent of nonconverted carbon.

Storage and Shipping. Barium oxide is shipped mainly in iron drums or, for smaller quantities, in tin cans. Shipment is governed by the regulations on the transport of harmful

goods of the IMDG Class 6.1, UN 1884, or RID/ADR Class 6.1, 71.

Uses. Barium oxide, like barium hydroxide, is mainly used for the preparation of additives for oils and greases; however, this is losing significance. In addition, barium oxide is used as a starting material for organic barium salts used in plastics. Barium oxide is frequently incorporated into fluorescent material, recently also into polyphenylene sulfide sealing pastes.

58.2.8 Barium Hydroxide

The anhydrous hydroxide has only a secondary industrial importance; the monohydrate and octahydrate are used in industry on a far larger scale.

Properties. Barium hydroxide octahydrate, hydrate of baryta, caustic baryta, $\text{Ba}(\text{OH})_2 \cdot 8\text{H}_2\text{O}$, forms monoclinic pseudotetragonal crystals, often plates when rapidly crystallized. It melts at 78 °C in its own water of crystallization, releasing the water when heated above 108 °C to yield the monohydrate. The density is \approx 2.18 g/cm³. The specific heat capacity c_p of the solid is 1250 J kg⁻¹ K⁻¹, of the melt 1675 J kg⁻¹ K⁻¹ at 80 °C.

The solubility in water depends on the temperature dramatically:

°C	0	20	40	60	78
% $\text{Ba}(\text{OH})_2 \cdot 8\text{H}_2\text{O}$	3.0	6.9	14.1	32.6	100.0
g BaO/100 g H ₂ O	1.5	3.48	7.35	18.8	94.7

The solutions are strongly alkaline and tend to supersaturate.

Like all soluble hydroxides, barium hydroxide, especially in aqueous solution, reacts readily with acidic gases. The most important example in practice is carbon dioxide, to form barium carbonate.

Barium hydroxide monohydrate, $\text{Ba}(\text{OH})_2 \cdot \text{H}_2\text{O}$, crystallizes as often radially intergrown needles. Its density ρ_{20} is \approx 3.74 g/cm³. The monohydrate does not react with dry carbon dioxide.

Anhydrous barium hydroxide, $\text{Ba}(\text{OH})_2$, $mp \approx$ 407 °C. The course of the dehydration, i.e., the temperatures and times, from mono-

hydrate to anhydrous $\text{Ba}(\text{OH})_2$ depends on the reactivity of the monohydrate. Molten anhydrous hydroxide is so corrosive, attacking steel and most ceramics, that the conversion of barium hydroxide into barium oxide, which takes place at 800 to 850 °C, is not carried out on an industrial scale.

Production. Barium hydroxide octahydrate is produced by hydration of barium oxide. The barium oxide is suspended in recycled mother lye and heated for several hours to destroy peroxides. The insolubles, e.g., BaCO_3 , are separated, and the hydroxide is precipitated by crystallization at low temperatures in stainless steel vessels. The crystals are removed from the mother lye by centrifugation.

Another industrial method is based on the oxidation of a barium sulfide solution [91–93]. Air is passed into the stirred solution containing barium hydroxide and barium hydrosulfide, the hydrolysis products of barium sulfide, until the hydrosulfide is oxidized to form polysulfide. Then the barium hydroxide octahydrate is crystallized at low temperatures and separated with a centrifuge. The polysulfidic mother lye is partly recycled, the rest usually processed for other barium compounds.

The monohydrate is generally produced on a commercial scale by dehydration of the octahydrate in heated vacuum driers. A monohydrate of especially high reactivity is obtained with drum driers [94]. This highly reactive monohydrate is particularly suitable for the production of oil additives.

Storage, Packing, Shipping. Both the monohydrate and the octahydrate are packed and stored in 50-kg polyethylene-lined multilayer paper bags. Shipping is governed by IMDG Class 6.1, UN 1564, or RID/ADR Class 6.1, 71.

Uses. Barium hydroxide, especially the monohydrate, is used to produce organic barium compounds such as additives for oil and stabilizers for plastics. In addition, barium hydroxide is used for dehydration and deacidification, especially for removing sulfu-

ric acid from fats, oils, waxes, and glycerol. In some applications, e.g., removal of sulfate from water and as starting material for other barium compounds, barium hydroxide to some extent replaces barium carbonate. The earlier use of the hydroxide in some countries for extracting the residual sucrose from molasses is no longer of much significance. The recent patent literature describes a procedure in which barium hydroxide is reacted with hydrogen peroxide to produce barium peroxide monohydrate [95].

58.2.9 Barium Nitrate

Barium nitrate, $\text{Ba}(\text{NO}_3)_2$, mp 593 °C, colorless cubic crystals, often octahedra, ρ_{20} 3.24 g/cm³. The solubility of barium nitrate in water increases with temperature:

°C	0	10	20	50	100
% $\text{Ba}(\text{NO}_3)_2$	4.8	6.5	8.4	14.6	25.4

On heating, barium nitrate decomposes into barium oxide, barium peroxide, nitric oxide, nitrogen, and oxygen. The gaseous products formed and their proportions depend largely on the temperature and rate of heating [96]. The presence of sulfur or organic substances may cause an explosion.

For the production of barium nitrate various procedures are possible, starting from BaCO_3 , $\text{Ba}(\text{OH})_2 \cdot 8\text{H}_2\text{O}$, BaS, or BaCl_2 . However, for industrial production there are two main procedures. In the first, barium carbonate is suspended in recycled mother lye and reacted with nitric acid. If necessary, heavy metals are precipitated, and the solution is filtered hot. The nitrate is then crystallized, if necessary with vacuum evaporation. The second procedure consists of reacting a barium sulfide solution, directly or after the removal of barium hydroxide, with nitric acid. After carefully removing any sulfur formed and the heavy metals, the barium nitrate is crystallized at low temperatures.

The preparation of $\text{Ba}(\text{NO}_3)_2$ by double conversion of barium chloride and sodium nitrate or calcium nitrate is described in the Eastern European patent literature.

Barium nitrate is packed and stored in 50-kg polyethylene-lined multilayer paper bags. Shipping is governed by IMDG Class 5.1, UN 1446, or RID/ADR Class 5.1, 7c.

One of the main uses, a component in pyrotechnics to produce a green color, requires very pure barium nitrate, 99.5–99.8%. The content of other flame colorants — sodium, strontium, calcium — must be extremely low. Barium nitrate is used as a plaining agent in the manufacture of special glasses and optical glasses in place of the combination alkali-metal nitrate-arsenic. In addition it is used to incorporate barium oxide into catalysts, in luminescent cathode-ray screens, and as a component of metallurgical hardening agents.

58.2.10 Barium Titanate

Barium titanate, BaTiO_3 , m_p 1625 °C, ϵ_{20} 6.02 g/cm³, has phase transitions and both ferroelectric and piezoelectric properties.

58.3 Toxicology

Water-soluble barium compounds are toxic, as is shown in Table 58.5. Most barium poisonings are caused by mistaking soluble barium compounds, such as barium carbonate, for the insoluble — and therefore nontoxic — barium sulfate, which is used as a contrast agent in X-ray diagnosis.

Table 58.5: Acute lethal doses of soluble barium compounds.

Compound	Toxicity	Ref.
Barium carbonate	TDL ₀ 29 mg/kg (human, oral)	[97]
Barium nitrate	LD ₅₀ 8.5 mg/kg (mouse, i.v.) LD ₅₀ 355 mg/kg (rat, oral)	[98] [99]
Barium chloride	LDLo 11.4 mg/kg (human, oral)	[100]
Barium oxide	LD ₅₀ 50 mg/kg (mouse, subcutaneous)	[101]
Barium fluoride	LD ₅₀ 250 mg/kg (rat, oral)	[102]

The symptoms of poisoning are convulsions of both striated and smooth muscles, including the heart, followed by paralysis of the peripheral nerve system. These effects on the nerve system are accompanied by severe inflammation of the gastrointestinal tract.

Barium carbonate is often used in the ceramics industry. Detailed examination of workers exposed to BaCO_3 dust for 7–27 years did not reveal any specific chronic poisoning [103]. Damage to the lungs is often caused by contaminants in the barium compounds, such as quartz [104] or zinc sulfide [105]. However, it is possible that BaSO_4 causes benign pneumoconiosis (barytosis) because, unlike BaCO_3 , BaSO_4 is not absorbed by the organism [106, 107].

For soluble barium compounds an exposure limit of 0.5 mg/m³ (as Ba) has been established by both TLV and MAK commissions (1983). According to the MAK, short-term exposure limits may be as high as 10 mg/m³ (average over 30 min, four times within 8 h).

58.4 References

- Ullmann, 4th ed., vol. 8, p. 301.
- Gmelin, Barium (system no. 30), main volume, 1932; supplement volume, 1960.
- R. Fromageau, *Monogr. Mét. Haute Pureté* 1977, no. 2, 153–183.
- Kirk-Othmer, 3rd ed., vol. 3, pp. 457–463.
- R. D. Goodenough, V. A. Stenger: "Magnesium, Calcium, Strontium, Barium and Radium", in J. C. Bailar (ed.): *Comprehensive Inorganic Chemistry*, vol. 1, Pergamon Press, Oxford 1973, pp. 591–664.
- J. Alexander, M. Steffel: "Calcium, Strontium and Barium", in F. Korte (ed.): *Methodicum Chimicum*, vol. 7, Georg Thieme Verlag, Stuttgart 1976, pp. 97–106.
- Winnacker-Küchler, vol. 6: Metallurgie, pp. 81–107.
- C. L. Mantell: "Barium", in C. A. Hampel (ed.): *Rare Metals Handbook*, 2nd ed., Reinhold Publ. Co., London 1961, pp. 25–31.
- Römpfs Chemie-Lexikon, 8th ed., vol. 1, Franckh'sche Verlagshandlung, Stuttgart 1979, p. 365.
- B. Mason: *Principles of Geochemistry*, J. Wiley & Sons, New York 1952, p. 41.
- H. Davy, *Nicholson's J.* 21 (Suppl. 1808) 366; 22 (1809) 54.
- J. W. Mallet, *Justus Liebigs Ann. Chem.* 190 (1878) 62.
- A. Guntz, *C.R. Hebd. Séances Acad. Sci.* 143 (1906) 339; *Ann. Chim. Phys.* 10 (1907) 441.
- J. Evers, A. Weiss, *J. Less Common Met.* 30 (1973) 83.
- E. Miller et al., *Trans. Metall. Soc. ADME* 218 (1960) 978.
- P. Ehrlich, H. J. Seifert in G. Brauer (ed.): *Handbuch der Präparativen Anorg. Chemie*, vol. 2, Enke Verlag, Stuttgart 1978, pp. 917–934.
- K. E. Maas, *Z. Anorg. Allg. Chem.* 374 (1970) 1.

- R. Schmid: "Nitride der Hauptgruppenmetalle", in F. Korte (ed.): *Methodicum Chimicum*, vol. 7, Georg Thieme Verlag, Stuttgart 1976, pp. 59–62.
- I. Obinata et al., *Metall (Berlin)* 19 (1965) 21; also see [6] and the literature cited there.
- J. J. Alexander: "Carbide der Elemente der 1.–4. Hauptgruppe", in F. Korte (ed.): *Methodicum Chimicum*, vol. 7, Georg Thieme Verlag, Stuttgart 1976, p. 67.
- W. Biltz, G. Hüttig, *Z. Anorg. Allg. Chem.* 114 (1920) 241.
- R. Juza, H. Schuhmacher, *Z. Anorg. Allg. Chem.* 324 (1963) 278.
- Houben-Weyl, 13 (2a), 542–543.
- W. Lindsell in G. Wilkinson (ed.): *Comprehensive Organometallic Chemistry*, vol. 1, Pergamon Press, Oxford 1982, pp. 223–252.
- M. Hansen: *Constitution of Binary Alloys*, McGraw-Hill, New York 1958; 1st Supplement, R. P. Elliott (ed.), New York 1965; 2nd Supplement, F. A. Shunk (ed.), New York 1969.
- H. Seliger, *Freiberg. Forschungsh. B* 34 (1959) 80.
- J. Krüger in O. Winkler, R. Bakish (eds.): *Vacuum Metallurgy*, Elsevier, Amsterdam 1971, pp. 207–212.
- I. S. Bystrova et al., *Proizvod. Ferrosplavov* 1977, no. 5, 31–37; *Chem. Abstr.* 87 (1977) 120951.
- O. Orman, E. Zembala, *Pr. Inst. Hutn.* 4 (1952) 437.
- E. Fujita, H. Yokomizo, *Tokyo Kogyo Shikensho Hokoku* 47 (1952) 291.
- P. S. Danner, *J. Am. Chem. Soc.* 46 (1924) 2382.
- J. Evers, G. Oehlinger, A. Weiss, *J. Less Common Met.* 81 (1981) 15.
- C. Matignon, *C.R. Hebd. Séances Acad. Sci.* 156 (1913) 1378.
- W. Sundermeyer, *Angew. Chem.* 77 (1965) 245.
- Ges. Deutscher Metallhütten- und Bergleute: *Analyse der Metalle*, 2nd ed., vol. IV/1, Springer Verlag, Berlin 1961, pp. 139–145.
- L. Edelbeck, P. W. West, *Anal. Chim. Acta* 52 (1970) 447.
- Degussa, Geschäftsbereich Technische Metallzeugnisse, Lieferprogramm Sondermetalle, Hanau, Germany.
- G. Tölg, *Fresenius Z. Anal. Chem.* 294 (1979) 1; also see [27], pp. 22–23.
- L. Melnick, L. Lewis, B. Holt (eds.): "Determination of Gaseous Elements in Metals", *Monographs on Analytical Chemistry*, vol. 40, J. Wiley & Sons, New York 1974.
- IMDG, Class 4.3, p. 4147; UN 1400; 4.3/1A RID, ADR, GGVS, GGVE.
- I. Sax (ed.): *Dangerous Properties of Industrial Materials*, 4th ed., Van Nostrand Reinhold Co., New York 1975, p. 430.
- S. Wagoner, *Z. Angew. Phys.* 6 (1954) 433.
- J. Maley, J. Moscony, *J. Vac. Sci. Technol.* 6 (1969) 51.
- K. Marquard, *Residual Gases Electron Tubes Proc. Int. Conf. 4th* 1971, 315–334; *Chem. Abstr.* 77 (1972) 106–735.
- M. Malev, *Vacuum* 23 (1973) 359.
- J. Turnbull, *J. Vac. Sci. Technol.* 14 (1977) 636.
- U.S.-Philips Corp., US 4077899, 1978; *Chem. Abstr.* 88 (1978) 181336.
- A. Misumi et al., *Shinku* 23 (1980) 183; *Chem. Abstr.* 93 (1980) 178254.
- Phillips Electronic, GB 1182883, 1970; *Chem. Abstr.* 72 (1970) 115999.
- P. Ward, *J. Illum. Eng. Soc.* 9 (1980) 194; *Chem. Abstr.* 93 (1980) 190370.
- W. Cowan et al., *Trans. Am. Electrochem. Soc.* 40 (1921) 27.
- P. Paschen et al., *Metall (Berlin)* 23 (1969) 786.
- D. Randolph, *Trans. Electrochem. Soc.* 66 (1934) 85.
- Union Carbide Corp., US 3734714, 1973.
- V. Nikolaev, V. Vasilev, *Liteinoe Proizvod.* 1980, no. 4, 6; *Chem. Abstr.* 93 (1980) 135988.
- V. D. Povolotskii et al., *Izv. Vyssh. Uchebn. Zaved. Chern. Metall.* 10 (1982) 69; *Met. Abstr.* 16 (1983) 45-0527.
- Z. Zhou et al., *Gießerei Prax.* 1983, no. 4, 49–52.
- K. Adam, *Metall (Berlin)* 37 (1983) 733.
- P. Münster, G. Kirchner: *Taschenbuch des Metallhandels*, 7th ed., Metall-Verlag GmbH, Berlin 1982, pp. 148–149.
- E. Sibbing: "Schwerspat: Rohstoffbasis für Fullstoffe und Bariumchemikalien", part 1, *Kunstst. J.* 8 (1974) no. 10, 30–36.
- E. Sibbing: "Schwerspat: Rohstoffbasis für Fullstoffe und Bariumchemikalien", part 2, *Kunstst. J.* 8 (1974) no. 11, 26–31.
- Barytes — Its Uses Outside Drilling Muds, *Ind. Miner. (London)* 1978, no. 133, 33–43.
- J. Massonne: "Technology and Uses of Barium and Strontium Compounds", *Ind. Miner. (London)* 1982, no. 177, 65–69.
- D. Rohe: "Nicht nur Masse, sondern auch Qualität durch mineralische Fullstoffe, part III: Sulfate", *Chem. Ind. (Düsseldorf)* 35 (1983) 369–373.
- Gmelin, Barium (system no. 30), main volume, 1932; supplement volume, 1960.
- M. Clement, H. Surmatz, H. Hüttenhain, *Z. Erzbergbau Metallhüttenwes.* 20 (1967) 512–522.
- Klöckner Humboldt-Deutz, DE-OS 1783014, 1968.
- Oil Companies Material Association (OCMA): Specification No. DFCP 3, Cecil Chambers, London 1973.
- American Petroleum Institute (API): *API RP 13B*, 6th ed., Washington, DC, 1976.
- K.-H. Grodde: *Bohrspülungen und Zementschlämme in der Tiefbohrtechnik*, Verlag O. Vieth, Hamburg 1963.
- Sachtleben, DE-OS 1955881, 1969.
- Sachtleben, DE 567348, 1930.
- Titan Co., GB 427220, 1933.
- R. Maivald, Dissertation 1977, Bergakademie Freiberg.
- A. A. Rawdel, N. A. Nowikowa, *Zh. Prikl. Khim. (Leningrad)* 36 (1963) 1433–1442.
- Forschungsinstitut für NE-Metalle, DE-OS 1567512, 1965.
- G. Salvi, A. Fiumara, *Riv. Combust.* 12 (1958) 525–561.
- N. S. Safiullin, S. F. Gawrilowa, *Khim. Promst. (Kiev)* 1965, no. 3, 32–35.
- Kali-Chemie, DE-OS 2034065, 1970.
- Kali-Chemie, DE 1800866, 1968.
- E. H. Baker, *J. Chem. Soc.* 1964, 699–704.

81. M. M. Evstigneeva, A. A. Bundel, B. V. Kondakov, *Tr. Mosk. Khim. Tekhnol. Inst. im. D. I. Mendeleeva* 62 (1969) 291-294; *Zh. Fiz. Khim.* 43 (1969) 2613-2614; 44 (1970) 2607-2609.
82. A. Schulze, DD 58501, 1966.
83. Kali-Chemie, DE 1907440, 1969.
84. A. Schulze, DD 45070, 1964.
85. PPG Industries, US 3467494, 1966.
86. A. F. Lozhkin, SU 245047, 1967.
87. Columbia Southern Chem., US 2772948, 1952.
88. Columbia Southern Chem., US 2772949, 1952.
89. Columbia Southern Chem., US 2915366, 1956.
90. FMC, US 3031266, 1959.
91. IG Farbenind., DE 519891, 1929.
92. IG Farbenind., DE 526796, 1930.
93. Kali-Chemie, DE 1792505, 1968.
94. FMC, DE 1186841, 1962.
95. Peroxid-Chemie, DE-OS 203063, 1983.
96. F. Lazarini, B. S. Brčić, *Monatsh. Chem.* 97 (1966) 1318.
97. *Israel J. Med. Sci.* 3 (1967) 565.
98. *Toxicol. Appl. Pharmacol.* 22 (1982) 150.
99. J. V. Marhold: *Sbornik Výsledků Toxicologického Výšetření Láték a Přípravků*, Institut Pro Vychovu Veducion Pracovníků Chemického Průmyslu, Praha 1972, p. 10.
100. T. Sollmann (ed.): *Manual of Pharmacology and its Applications to Therapeutics and Toxicology*, 7th ed., Saunders, Philadelphia 1942, p. 478.
101. *Zh. Vses. Khim. Ova.* 19 (1974) 186.
102. *Vestn. Akad. Med. Nauk SSSR* 32 (1977) 28.
103. H.-G. Essing, G. Böhlmeier, G. Kemmerer, R. Procharka, *Arbeitsmed. Sozialmed. Präventivmed.* 11 (1976) no. 12, 299-302.
104. E. Browning: *Toxicity of Industrial Metals*, 2nd ed., Butterworths, London 1965.
105. E. Wende, *Arch. Gewerbepathol. Gewerbehyg.* 15 (1956) 171.
106. Z. Marešić, *Med. Klin. (München)* 52 (1957) 1950-1953.
107. E. P. Pendergrass, R. R. Gruning, *Arch. Ind. Hyg. Occup. Med.* 7 (1959) 44-48.

Authors

Jörg Adel

● §§ 15.12.1-15.12.4
BASF Aktiengesellschaft
EPM/EE, H 201
67056 Ludwigshafen
Germany

Gerhard Adrian (retired)

● § 27.7.4.1
● §§ 46.10.2.1-46.10.2.4
Dr. Hans Heubach GmbH & Co. KG
Postfach 1160
38679 Langelsheim
Germany

Fritz Aldinger

● Chapter 19
Leybold-Heraeus GmbH
Wilhelm-Rohn-Straße 25
63450 Hanau
Germany

Peter Ambatiello

● § 51.13.3.2
Südsalz GmbH
Salzbergwerk Berchtesgaden
Bergwerkstraße 83
83471 Berchtesgaden
Germany

Klaus Andersson

● Chapter 29
H.C. Starck GmbH & Co. KG
Werk Goslar
Postfach 2540
38615 Goslar
Germany

Knut Andreassen

● §§ 20.1-20.10
Norsk Hydro a.s.
P.O. Box 2594, Solli
N-0203 Oslo 2
Norway

Gerd Anger †

● § 46.4
Bayer AG

GB-SP-Chrom, Geb. T18
51368 Leverkusen
Germany

Terje Kr. Aune

● §§ 20.1-20.10
Norsk Hydro a.s.
P.O. Box 2594, Solli
N-0203 Oslo 2
Norway

Ulrich Baudis

● § 49.1 except 49.1.1
● § 58.1
Durferrit GmbH
Degussa ZN Wolfgang
Rodenbacher Chaussee 4
63457 Hanau
Germany

Günter Bauer (retired)

● § 7.12
● Chapter 32
● §§ 52.4.1-52.4.2.2
Kali und Salz AG
Friedrich-Ebert-Str. 160
34119 Kassel
Germany

Richard Bauer

● Chapter 50
Anemonenstraße 10
83346 Bergen
Germany

T. Bauer

● § 51.13.1
Solvay Alkali GmbH
Postfach 10 13 61
47493 Rheinberg
Germany

Leopold Benda

● § 48.7.3
Niedersächs. Landesamt f. Bodenf.
Postfach 51 01 53
30631 Hannover
Germany

Gerhard Berger

● § 16.12
BASF Lacke + Farben AG
Pigmente und Hilfsmittel
Postfach 1163
74354 Besigheim
Germany

Horacio E. Bergna

● § 48.7.4
The Du Pont Company
Du Pont Experimental Station
P.O. Box 80262
Wilmington, DE 19880-0262
USA

Udo Bertmann

● § 5.22.7
DMT-Gesellschaft für Forschung und Prüfung mbH
Franz-Fischer-Weg 61
45307 Essen
Germany

Robert Besold

● § 8.12
● § 10.9.8
● § 21.11.3
Carl Schlenk AG
Postfach 4548
90024 Nürnberg
Germany

Manfred Bick

● Chapter 54
Chemetall GmbH
Reuterweg 14
60323 Frankfurt
Germany

Christian Boidart

● § 51.13.3.4
CIE Salins du Midi et Salines de l'Est
68, Cours Gambetta
F-34063 Montpellier Cedex 4
France

Bernhard Bonn

● § 5.22.7
DMT-Gesellschaft für Forschung und Prüfung mbH
Franz-Fischer-Weg 61
45307 Essen
Germany

Thomas B. Bonney

● § 21.8
Aluminum Company of America
Alcoa Technical Center
Alcoa Center, PA 15069
USA

Karl Brandt

● § 27.7.4.1
● §§ 46.10.2.1–46.10.2.4
Dr. Hans Heubach GmbH & Co. KG
Postfach 1160
38679 Langelsheim
Germany

Robert J. Brotherton

● §§ 49.2–49.3
U.S. Borax Research Corp.
Chemical Research
412 Crescent Way
Anaheim, CA 92801
USA

Volker Brückmann

● § 6.8
Wirtschaftsvereinigung Stahl
Postfach 10 54 64
40045 Düsseldorf
Germany

Jörg Brüning

● § 52.1–52.2, 52.5–52.10
Callery Chemical Company
P.O. Box 429
Pittsburgh, PA 15230
USA

Heinz-Lotbar Bünningel

● § 5.13
● § 6.8
Wirtschaftsvereinigung Stahl
Postfach 10 54 64
40045 Düsseldorf
Germany

Andreas Buhr

● § 5.7
Krupp Hoesch Stahl AG
Abt. 20 GWT-STP Feuerfeste Stoffe
44120 Dortmund
Germany

Elizabeth R. Burkhardt

● §§ 52.1–52.2, 52.5–52.10
Callery Chemical Company
P.O. Box 429
Pittsburgh, PA 15230
USA

Alfred Richard Burkin

● §§ 27.2–27.3, 27.8
Dept. of Mineral Resources Eng.
Imperial College
Prince Consort Rd.
London, SW7 2AZ
England

Gunter Buxbaum

● § 5.21.1
Bayer AG
Werk Uerdingen, R & G
Postfach 166
47812 Krefeld
Germany

Dodd S. Carr

● § 9.13
Int. Lead Zinc Res. Organization
P.O. Box 12036
Research Triangle Park, NC 27709-2036
USA

Douglas A. Church

● § 27.9
Climax Metals Co.
Amax Center
Greenwich, CT 06836-1700
USA

Bernard Clercx

● § 51.13.3.3
Salzgewinnungsgesellschaft Westfalen mbH
Graeser Brook 9
48683 Ahaus
Germany

Joseph A. Corella

● §§ 49.4–49.5
Callery Chemical Co.
P.O. Box 429
Pittsburgh, PA 15230
USA

William Brian Cork

● § 21.11.1

155 Newland Park
Hull
North Humberside HU5 2DX
England

Peter M. Craven

● § 7.4
● §§ 47.1–47.9
Samancor House
88 Marshall St.
Johannesburg 2001
Republic of South Africa

John C. Crelling

● §§ 5.22.1–5.22.4, 5.22.9–5.22.11
Department of Geology
Southern Illinois University
Carbondale, IL 62901
USA

Winfried Dahl

● § 6.6.3
RWTH Aachen
Institut für Eisenhüttenkunde
Intzestraße 1
52072 Aachen
Germany

Max Danner

● §§ 21.10.5.2–21.10.5.3, 21.10.6
Hoechst Aktiengesellschaft
Werk Gersthofen
-Chemikalien-
86368 Gersthofen
Germany

Max Daunderer

● § 17.14
Kreuzeckstraße 9
82049 Pullach
Germany

Robert K. Dawless

● § 21.5
Aluminum Company of America
Alcoa Technical Center
Alcoa Center, PA 15069
USA

Paul D. Deeley

● § 46.8
Paul Deeley & Associates
27 Lonesome Pine Trail

Yalaha, FL 34797-3060
USA

Herbert Diskowski

● § 7.7
Fasanenaue 4
50374 Erfstadt
Germany

John Dallas Donaldson

● §§ 18.1-18.11
Brunel University
Dept. of Chemistry
Uxbridge, Middx UB8 3PH
England

Robert R. Dorfler

● §§ 27.4.1-27.4.4
Cyprus Minerals Company
Green Valley, AZ 85622
USA

James H. Downing

● §§ 46.1-46.7
Elkem Metals Company
P.O. Box 1344
Niagara Falls, NY 14302
USA

Franz Ludwig Ebenhöch (retired)

● § 5.17.6
Philipp-Stempel-Straße 9
67069 Ludwigshafen
Germany

Joachim Eckert

● § 7.10
● Chapter 28
H. C. Starck GmbH & Co. KG
Postfach 2540
38615 Goslar
Germany

Ralf Emmert

● § 5.21.5
● § 9.14.5
● § 15.12.5
● § 22.7.11
Rona
Bayonne, NJ 07002
USA

Hartmut Endriß

● § 16.12
BASF Aktiengesellschaft
-EPM/TP, J 550-
67056 Ludwigshafen
Germany

Bernard Epron

● § 51.13.3.4
Compagnie des Salins du Midi et des Salines de l'Est
Dép. Coopération technique
53, Rue des Mathurins
F-75008 Paris
France

Semih Eser

● § 5.22.13
404 Academic Activities Bldg.
The Pennsylvania State Univ.
University Park, PA 16802
USA

Manfred Ettlinger

● § 48.7.6
Degussa AG
-AC-KS-AT/AE-
Postfach 1345
63403 Hanau
Germany

Günter Etzrodt

● § 5.21.4
● §§ 9.14.1-9.14.4
● §§ 10.9.2.8, 10.9.3-10.9.7
● § 21.11.2
● § 27.7.4.2
● §§ 46.10.2.5, 46.10.4
● § 49.14
BASF Aktiengesellschaft
-EPM/KK - J 550-
67056 Ludwigshafen
Germany

Harald Fabian †

● §§ 8.1-8.10
Buchholzer Weg 1a
21079 Hamburg
Germany

Noël Felix

● Chapter 36
Metallurgie Hoboken-Overpelt
R + D Department

A. Greinerstraat 14
B-2710 Hoboken
Belgium

Horst Ferch

● § 5.21.2
Justus-Liebig-Straße 13
63486 Bruchköbel
Germany

Rudolf Fichte

● §§ 7.1, 7.5, 7.9
Karl-Giermann-Straße 14
90473 Nürnberg
Germany

Wilhelm Flick

● § 20.11.3.5
An der Wierlmaar 16
51143 Köln
Germany

Jürgen Flückenschild

● § 5.11
Deutsche Voest-Alpine
Industrieanlagen GmbH
Postfach 26 01 52
40094 Düsseldorf
Germany

Otto W. Flörke

● §§ 48.7.1-48.7.2
Wagenfeldstraße 11
58456 Witten
Germany

Peter Forgione

● § 56.8
120 Little Hill Dr.
Stamford, CT 06905
USA

Lothar Formanek

● § 5.10 except 5.10.1
Lurgi Metallurgie GmbH
Lurgiallee 5
60295 Frankfurt/Main
Germany

William B. Frank

● §§ 21.1-21.9
Aluminum Company of America

Alcoa Technical Center
Alcoa Center, PA 15069
USA

Klaus-Dieter Franz

● § 5.21.5
● § 9.14.5
● § 15.12.5
● § 22.7.11
E. Merck KGaA
Abt. PK FO PE
Frankfurter Straße 250
64271 Darmstadt
Germany

Gabriele Friedrich

● § 5.17.6
BASF Aktiengesellschaft
ZAA-A, M300
67056 Ludwigshafen
Germany

Harald Gaedcke

● §§ 5.21.6-5.21.7
● § 10.9.2.9
● § 18.12
● § 22.7.12
BASF Aktiengesellschaft
Lacke und Farben AG
Gustav-Siegle Straße 19
74354 Besigheim
Germany

Wolfgang Gatzka

● § 5.22.12
Bredeneyer Straße 141
45133 Essen
Germany

Rolf Gerstenberg

● §§ 57.3-57.6, 57.8
Solvay Barium Strontium GmbH
Postfach 220
30002 Hannover
Germany

Helmut Geyer

● § 51.13.3.3
Schelverweg 13
48599 Gronau-Epe
Germany

Hermann Gies

● § 48.7.8
Ruhr-Universität Bochum
Institut für Mineralogie
Postfach 10 21 48
44780 Bochum
Germany

James C. Gilliland (retired)

● §§ 27.10-27.11
Amax Mineral Resources Co.
1626 Cole Boulevard
Golden, CO 80401-3293
USA

Hans-Jürgen Grabke

● § 6.6.2
Max-Planck-Institut für Eisenforschung GmbH
Abt. Physikalische Chemie
Postfach 14 04 44
40074 Düsseldorf
Germany

Günter G. Graf

● §§ 10.1-10.6
● Chapter 11
Schulweg 17b
09599 Freiberg/Sachsen
Germany

Douglas A. Granger

● § 21.6
Aluminum Company of America
Alcoa Technical Center
Alcoa Center, PA 15069
USA

Jörg Friedrich Greber

● §§ 35.1-35.9
Am Weingarten 16
38154 Königslutter
Germany

Jürgen Griebel

● § 40.5
Forschungsz. f. Umwelt u. Gesund.
(GSF) Inst. f. Strahlenbiologie
Ingolstädter Landstraße 1
91465 Ergersheim
Germany

Wolf-Dieter Griebler

● § 10.9.1

Sachtleben Chemie GmbH
Dr.-Rudolf-Sachtleben-Straße 4
47198 Duisberg
Germany

Horst Großman

● §§ 13.1-13.9
Rosa-Luxemburg-Straße 14
44534 Lünen
Germany

Clarence Guibert

● §§ 49.4-49.5
Callery Chemical Co.
P.O. Box 429
Pittsburgh, PA 15230
USA

Volker Güther

● §§ 7.11-7.12
● Chapter 32
Gesellschaft für Elektrometallurgie
Postfach 2844
90013 Nürnberg
Germany

Fathi Habashi

● Chapters 1-4
● §§ 5.1, 5.2, 5.4-5.6 except 5.5.6-5.5.11, 5.8-5.9, 5.14-5.16, 5.17.1, 5.18-5.19
● § 7.2 (introductory paragraph)
● § 8.11.3.4
● § 22.13
● § 34.12
● § 35.10
Laval University
Department of Mining and Metallurgy
Sainte-Foy, Québec
G1K 7P4
Canada

Fritz Hagedorn

● §§ 52.11.3, 52.11.7
Kali und Salz AG
Friedrich-Ebert-Str. 160
34119 Kassel
Germany

Fred W. Hall

● § 7.2 (except introductory paragraph)
537 Fulwood Road
Sheffield S10 3QG
South Yorkshire

England**Jost Halstenberg**

● §§ 46.9.1-46.9.6 except 46.9.2.2; 46.9.10
Bayer AG
-GB-SP-Chrom, Geb. T18-
51368 Leverkusen
Germany

Rudolf Hammer †

● §§ 6.3.5.1-6.3.5.3
Im Kirchbruch 23
46535 Dinslaken
Germany

Kunibert Hanusch

● §§ 13.1-13.9
● §§ 14.1-14.10, 14.12-14.13
Hüttenwerke Kayser AG
Kupferstraße 23
44532 Lünen
Germany

Gabriele Hartmann

● §§ 51.1-51.12
Degussa AG
Werk Wesseling
Postfach 1164
50375 Wesseling
Germany

Hartmut Härter

● § 5.21.5
● § 9.14.5
● § 15.12.5
● § 22.7.11
E. Merck
-Pigment-Sparte-
Frankfurter Straße 250
64271 Darmstadt
Germany

Turid Haugerød

● §§ 20.1-20.10
Norsk Hydro a.s.
P.O. Box 2594, Solli
N-0203 Oslo 2
Norway

Rolf Hauk

● § 5.11
Deutsche Voest-Alpine
Industrieanlagen GmbH

Postfach 26 01 52
40094 Düsseldorf
Germany

Warren E. Haupin

● §§ 21.1-21.9
Aluminum Company of America
Alcoa Technical Center
Alcoa Center, PA 15069
USA

Otto Helmboldt

● §§ 21.10.2-21.10.3
Giulini Chemie GmbH & Co. OHG
Postfach 15 04 80
67029 Ludwigshafen
Germany

Robert Hentrich

● § 6.3.5.4
Thymianweg 10
57078 Siegen
Germany

Karl-Albert Herbst

● §§ 13.1-13.9
● §§ 14.1-14.10, 14.12-14.13
Rosa-Luxemburg-Straße 14
44534 Lünen
Germany

Wolfgang Herde

● § 51.13.2
Husarenweg 11
38272 Burgdorf
Germany

Hans Hess

● § 7.12
● Chapter 32
Gesellschaft für Elektrometallurgie mbH
Postfach 2844
90013 Nürnberg
Germany

Stephen Hluchan

● §§ 56.1-56.4
Speciality Minerals Inc.
The Chrysler Building
405 Lexington Avenue
New York, NY 10174-1901
USA

Klaus Hochgeschwender

● §§ 46.9.7-46.9.9
Bayer AG
AI-S/8K + Si, Geb. 01
51368 Leverkusen
Germany

Hans-Georg Hoff

● § 5.13
Wirtschaftsvereinigung Stahl
Postfach 10 54 64
40045 Düsseldorf
Germany

Hans Hougardy

● § 6.6.1
Max-Planck-Institut für Eisenforschung GmbH
Postfach 14 04 44
40074 Düsseldorf
Germany

Nils Ove Høy-Petersen †

● §§ 20.1-20.10
Norsk Hydro a.s.
P.O. Box 2594, Solli
N-0203 Oslo 2
Norway

L. Keith Hudson (retired)

● §§ 21.10.1, 21.10.3.1
Aluminum Company of America
Corporate Research & Development
Alcoa Technical Center
Alcoa Center, PA 15069
USA

Hatto Jacobi

● §§ 6.3.5.1-6.3.5.3
Mannesmannröhrenwerke AG
Mannesmann Forschungsinstitut
Postfach 25 11 67
47251 Duisburg
Germany

Paul Jäger

● § 58.2
Kali-Chemie AG
Hauptverwaltung, C-AF
Postfach 220
30002 Hannover
Germany

Helmut Jakusch

● § 5.21.3.4
● § 46.10.3
BASF Aktiengesellschaft
-EPR/P, J653-
67056 Ludwigshafen
Germany

Robert James

● § 21.9
Aluminum Company of America
Alcoa Technical Center
Alcoa Center, PA 15069
USA

Dieter Janke

● § 6.3.2
TU Bergakademie Freiberg
Institut für Eisen- und Stahltechnologie
09596 Freiberg
Germany

José Jiménez

● § 55.9
Geisenheimer Straße 90
60529 Frankfurt
Germany

Heinrich J. Johnen †

● § 10.7
Bruchweg 38
41564 Kaarst
Germany

Mark W. Johns

● § 23.4.3
MINTEK
Privat Box X3015
Randburg 2125 TVL
Republic of South Africa

Peter Jönk (retired)

● § 17.11
Rosenstraße 4
63480 Roßdorf
Germany

Sigurd Jönsson

● Chapter 19
Leybold-Heraeus GmbH
Wilhelm-Rohn-Straße 25
63450 Hanau
Germany

Hendrik Kathrein

● §§ 5.21.3.1-5.21.3.3
Bayer Corp.
Industrial Chemicals Division
100 Bayer Road
Pittsburgh, PA 15205-9741
USA

Suzanne E. Keegan

● § 56.7
Allied Corporation
P.O. Box 6
Solvay, NY 13209
USA

Cornelius Keller †

● § 40.4
Kernforschungszentrum Karlsruhe
Schule für Kerntechnik
Postfach 3640
76021 Karlsruhe
Germany

Albrecht M. Kellerer

● § 40.5
Forschungsz. f. Umwelt u. Gesund
(GSF) Inst. f. Strahlenbiologie
Ingolstädter Landstraße 1
85758 Oberschleißheim
Germany

Robert Kemp

● § 56.7
Allied Corporation
P.O. Box 6
Solvay, NY 13209
USA

Robert C. Kerby

● §§ 9.6.2, 9.11
General Manager R + D
Cominco Ltd.
Trail
British Columbia V1R 4L8
Canada

Derek G. E. Kerfoot

● § 7.6
● §§ 12.1-12.15
Sherritt International Corporation
P.O. Box 3388
Fort Saskatchewan, Alberta T8L 2P2
Canada

Dieter Kerner

● § 48.7.7
Degussa Corp.
65 Challenger Road
Ridgefield Park, NJ 07660
USA

M. Rashid Khan

● § 5.22.13
U.S. Dept. of Energy
Morgantown Energy Tech. Center
Morgantown, WV 26505
USA

Peter Kleinschmit

● § 48.7.7
Degussa AG
Kieselsäuren und Chemiekatal.
Forschung u. Anwendungstechnik
Postfach 1345
63403 Hanau
Germany

Alfred Klemm

● §§ 51.1-51.12
Max Planck Institut für Chemie
Otto Hahn Institut
Beuthener Straße 25
55131 Mainz
Germany

Guy Knockaert

● Chapter 39
UM-Ge & Special Metals
A. Greinerstraat 14
B-2660 Hoboken
Belgium

Herbert Knopf

● §§ 46.9.1-46.9.5 except 46.9.2.2; 46.9.10
Bertha-von-Suttner-Straße
51373 Leverkusen
Germany

Lothar Koch

● Chapter 43
Institute for Transuranium Elements
Nuclear Chemistry
P.O. Box 2340
76125 Karlsruhe
Germany

Karl Köhler

● §§ 57.3–57.6, 57.8
Solvay Barium Strontium GmbH
Postfach 220
30002 Hannover
Germany

Manfred Koltermann

● § 5.7
Krupp Hoesch Stahl AG
Abt. 20 GWT-STP Feuerfeste Stoffe
44120 Dortmund
Germany

Morgan Kommer

● § 21.7
Aluminum Company of America
Alcoa Technical Center
Alcoa Center, PA 15069
USA

Ulrich Korallus (retired)

● § 46.9.11
Walter-Flex-Straße 25
51373 Leverkusen
Germany

Ulrich Kowalski

● § 51.13.5
Südsalz-Vertriebs GmbH
Postfach 1254
74174 Bad Friedrichshall
Germany

Gerhard Kristen

● § 51.13.1
Solvay Alkali GmbH
Postfach 10 13 61
47493 Rheinberg
Germany

Joachim Krüger

● §§ 15.1–15.10
RWTH Aachen
Institut für Metallhüttenwesen und Elektrometallurgie
52056 Aachen
Germany

Lothar Kucharzik

● § 6.3.5.5
Am Kothen 7
40822 Mettmann
Germany

Brigitte Kühborth

● § 5.17.6 (Toxicology and Occupational Health)
BASF Aktiengesellschaft
Toxikologie ZST, Geb. 470
67056 Ludwigshafen
Germany

John M. Laferty (retired)

● §§ 27.4.1–27.4.4
Clinmax Molybdenum Company
Wheatridge, CO 80033
USA

Ludwig Lange

● §§ 51.1–51.12
● §§ 55.1–55.8
Degussa AG
Abt. USAN
Postfach 11 05 33
60287 Frankfurt
Germany

Bernd E. Langner

● Chapter 38
Norddeutsche Affinerie AG
Forschung und Entwicklung
Hoferstraße 50
20539 Hamburg
Germany

Keith Lascelles

● §§ 12.17 except 12.17.2 and 12.17.5
INCO Europe Ltd.
Clydach, Swansea SA6 5QR
Wales
Great Britain

Erik Lassner

● §§ 26.1, 26.2.2, 26.3–26.11
Grazerstraße 34 C
A-8045 Graz
Austria

Gerhard Leichtfried

● §§ 27.4.5–27.4.8, 27.5
Plansee AG
A-6600 Reutte
Austria

Dieter Leininger †

● § 5.22.6
Bergbauforschung GmbH
Franz-Fischer-Weg 61

45307 Essen
Germany

Lutz Leitner

● §§ 5.21.3.1–5.21.3.3
Bayer AG
-GB A1-
51368 Leverkusen
Germany

Winfried Lenk

● Chapter 53
Chemetall GmbH
Reuterweg 14
60323 Frankfurt
Germany

Marcel de Liedekerke

● §§ 10.9.2.1–10.9.2.7
Graaf de Gelooslaan 8
NL-6245 AS Eysden
Netherlands

Alfred Lipp

● §§ 49.6
Bürgermeister-Singer-Str. 15
86825 Bad Wörishofen
Germany

John L. Little

● §§ 49.4–49.5
Callery Chemical Co.
Research & Development
Boron Labs.
Callery, PA 16024
USA

Manfred Lück

● §§ 15.1–15.10
RWTH Aachen
Institut für Metallhüttenwesen und Elektrometallurgie
52056 Aachen
Germany

Eberhard Lüderitz

● § 7.8
● §§ 15.1–15.10
World Resources Company (WRC) GmbH
Büro Wurzen
Lüptitzer Straße 24c
04808 Wurzen
Germany

Heribert Luig

● § 40.1–40.3
Universität Göttingen
Institut für Nuklearmedizin
Robert-Koch-Straße 40
37075 Göttingen
Germany

J. Paul Lyle

● § 21.10
Aluminum Company of America
Alcoa Laboratories
Alcoa Center, PA 15069
USA

Paul MacMillan

● §§ 57.1, 57.2, 57.7
493 Fortington St.
Renfrew, Ontario K7V 1E3
Canada

Takao Maki

● § 21.10.7
● § 51.17
● § 52.16
Mitsubishi Chemical Industries Ltd.
Research Center
1000 Kamoshida-cho
Midori-ku, Yokohama
Kanagawa 227
Japan

Manfred Mansmann

● § 22.7.10
● § 46.10.1
Bayer AG
Geschäftsbereich PK, Geb. R20
51368 Leverkusen
Germany

Brigitte Martin

● §§ 48.7.1–48.7.2
Ruhr-Universität Bochum
Fak. f. Geowiss., Inst. f. Mineralog.
Postfach 10 21 48
44780 Bochum
Germany

Wilfried Mayer

● § 5.21.2
Degussa AG
Abt. US-IT
Postfach 1345

63403 Hanau
Germany

Gernot Mayer-Schwinning

● § 5.12
Lurgi Umwelt GmbH
Forschung und Entwicklung
Gwinnerstraße 27-33
60388 Frankfurt
Germany

Ian McGill

● Chapter 44
4 Sheepwalk
Surley Row
Caversham
Reading RG4 8NE
England

Albert Melin

● §§ 9.1-9.6
Cockerillstraße 69-73
52222 Stolberg
Germany

Heinrich Meiler

● § 5.3
Bomstraße 65
65719 Hofheim
Germany

Adolf Metzger

● § 55.10
Matterhornstraße 3
65199 Wiesbaden
Germany

Jürgen Meyer

● § 48.7.7
Degussa AG
GB Anorg. Chemieprodukte F + E
Postfach 1345
63403 Hanau
Germany

Hartmut Meyer-Grünow

● § 7.13
SKW Metals + Alloys Inc.
3801 Highland Avenue
Niagara Falls, NY 14305
USA

Heinrich Micke

● §§ 37.1-37.10
Am Domacker 77
47447 Moers
Germany

Edward F. Milner

● §§ 9.1-9.9
Cominco Ltd.
Research and Development
Trail, British Columbia
Canada V1R 4L8

Franz-Rudolf Minz

● § 51.14
Hans-Sachs-Straße 14
41542 Dormagen
Germany

Chanakya Misra

● §§ 21.10.1, 21.10.3.1
Aluminum Company of America
Corporate Research & Development
Alcoa Technical Center
Alcoa Center, PA 15069
USA

Philip C. H. Mitchell

● § 27.6
The University
Dept. of Chemistry
Whiteknights 5
Reading RG6 2AD
England

Lindsay G. Morgan

● § 12.17.5
Glynteg
Park Road
Ynystawe, Swansea SA6 5AP
Great Britain

Hans-Georg Nadler

● Chapter 33
H. C. Starck GmbH & Co. KG
Werk Goslar
Postfach 2540
38615 Goslar
Germany

Bernd Neuer

● § 7.3
● § 48.6

SKW Trostberg AG
Postfach 1140
83302 Trostberg
Germany

David Nicholls

● § 12.17.2
University of Liverpool
Department of Chemistry
Liverpool L69 3BX
England

Ralph H. Nielsen

● Chapter 30
● Chapter 31
3424 SW Takena St. SW
Albany, OR 97321-3603
USA

Katsuhisa Nitta

● § 5.21.5
● § 9.14.5
● § 15.12.5
● § 22.7.11
Merck Japan
970/04 Onahama
Japan

Tony Oates

● § 56.5
Limetec Quality Services
19 Macclesfield Road
Buxton, Derbyshire SK17 9AH
England

Manfred Ohlinger

● § 5.21.3.4
● §§ 46.9.2.2, 46.9.11, 46.10.3
BASF Aktiengesellschaft
EPR/P, J 653
67056 Ludwigshafen
Germany

Andreas Otto

● § 7.12
● Chapter 32
Gesellschaft für Elektrometallurgie mbH
Postfach 2844
90013 Nürnberg
Germany

Walter Otto (retired)

● §§ 20.11.2, 20.11.4

Pappelweg 2
34292 Ahnatal-Weimar
Germany

Dag Øymo

● §§ 20.1-20.10
Norsk Hydro a.s.
P.O. Box 2594, Solli
N-0203 Oslo 2
Norway

Roger Pankert

● §§ 6.4-6.5
Nöretherstraat 144
B-4700 Eupen
Belgium

Jai Won Park

● §§ 57.3-57.6, 57.8
Solvay Barium Strontium GmbH
Postfach 220
30002 Hannover
Germany

Siegfried Paschen (retired)

● § 48.7.3
Innsbrucker Str. 63
28215 Bremen
Germany

Martin Peehs

● Chapter 41
Siemens AG
Power Generation (KWU) — BP
P. O. Box 3220
91050 Erlangen
Germany

Günter Petzow

● Chapter 19
Max-Planck-Inst. f. Metallforschung
Seestraße 92
70174 Stuttgart
Germany

Gerhard Pfaff

● § 5.21.5
● § 9.14.5
● § 15.12.5
● § 22.7.11
E. Merck KGaA
Abt. FK FOPE
Frankfurter Straße 250

64271 Darmstadt
Germany

Magnus Piscator

● § 16.11
The Karolinska Institute
Dept. of Environmental Hygiene
P.O. Box 60400
S-104 01 Stockholm
Sweden

Helmold von Plessen

● § 51.16
Hoechst Aktiengesellschaft
Verfahrenstechnik
Postfach 800302
65926 Frankfurt
Germany

David Prengaman

● § 9.12
RSR Corporation, Res. & Develop.
Tenth Floor
1111 West Mockingbird Lane
Dallas, TX 75247
USA

Otto P. Preuss

● § 19.16
Brush Wellman Inc.
1200 Hanna Building
Cleveland, OH 44115
USA

Helmut Printzen

● § 5.21.1
Bayer AG
Werk Uerdingen, R 36
Postfach 166
47812 Krefeld
Germany

Horst Prinz

● Chapter 53
● Chapter 54
Chemetall GmbH
Reuterweg 14
D-60271 Frankfurt am Main
Germany

Dieter Råde

● § 22.7.10
● § 46.10.1

Bayer AG
GB Pigmente + Keramik
Rheinuferstraße 7-9
47812 Krefeld
Germany

Ljubisa R. Radovic

● § 5.22.13
The Pennsylvania State Univ.
404 Academic Activities Bldg.
University Park, PA 16802
USA

Gerhard Rau

● § 7.3
● § 48.6
SKW Trostberg AG
Forschung und Entwicklung
Postfach 1140
83302 Trostberg
Germany

Karlheinz Reichert

● Chapter 29
H.C. Starck GmbH & Co. KG
Werk Goslar
Postfach 2540
38615 Goslar
Germany

Arno H. Reidies

● § 47.10
Carus Chemical Company
Research Library
P.O. Box 1500
La Salle, IL 61301-3500
USA

Rainer Reimert

● § 5.22.8
Universität Karlsruhe
Engler-Bunte-Institut
Postfach 6980
76128 Karlsruhe
Germany

Klaus Reinhardt

● Chapter 45
Th. Goldschmidt AG
Bosselberg 14
45134 Essen
Germany

Hermann Renner

● Chapter 23 except § 23.4.3
● Chapter 24
● Chapter 25
Zoznegger Str. 5
78333 Stockach
Germany

Hugh Wayne Richardson

● § 8.11 except 8.11.3.4
Phibro-Tech. Inc.
P.O. Box 1979
Sumter, SC 29150
USA

H. Hermann Riechers

● § 58.2
Solvay Barium Strontium GmbH
Am Güterbahnhof
53557 Bad Honningen
Germany

Gary G. van Riper

● § 27.10
Amax Mineral Resources Co.
1626 Cole Boulevard
Golden, CO 80401-3293
USA

Rafael Rituper

● § 5.20
Keramchemie GmbH
Postfach 1163
56425 Siershahn
Germany

William O. Roberts

● § 48.7.4
Du Pont Chemicals
Du Pont Experim. Station 262/328
P.O. Box 80262
Wilmington, DE 19980-0262
USA

Dieter M. M. Rohe

● §§ 10.8.1-10.8.5
Grillo-Werke AG
Weseler Str. 1
47169 Duisburg
Germany

Oskar Roldl

● §§ 7.11-7.12

● Chapter 32
Gesellschaft für Elektrometallurgie
Postfach 2844
90013 Nürnberg
Germany

Heinz Roller

● § 7.12
● Chapter 32
Gesellschaft für Elektrometallurgie
Postfach 2844
90013 Nürnberg
Germany

Fritz Rose

● § 5.10 except 5.10.1
Lurgi Metallurgie GmbH
Lurgiallee 5
60295 Frankfurt/Main
Germany

Gerhard Rose

● §§ 13.1-13.9
● §§ 14.1-14.10, 14.12-14.13
Rosa-Luxemburg-Straße 14
44534 Lünen
Germany

Siegfried Sattelberger

● § 7.12
● Chapter 32
Gesellschaft für Elektrometallurgie mbH
Postfach 2844
90013 Nürnberg

Dieter Sauter

● §§ 5.22.5, 5.22.8
Am Jungfernborn 25
61130 Nidderau
Germany

Alan Scaroni

● § 5.22.13
C211 Coal Utilization Lab.
The Pennsylvania State Univ.
University Park, PA 16802
USA

Erich Schachl (retired)

● §§ 52.4.1-52.4.2.2
Kali und Salz AG
Friedrich-Ebert-Str. 160
34149 Kassel

Germany

Klaus Schäfer

● §§ 6.3.3–6.3.4
Am Pavillon 6
49124 Georgsmarienhütte
Germany

Dieter Schauwinhold

● §§ 6.1, 6.7.1
Scheibenstraße 21
40479 Düsseldorf
Germany

Dietmar Schiffmann

● § 48.7.9
Universität Rostock
Fachbereich Biologie
Institut für Zoologie, Tierphysiologie und Genetik
Universitätsplatz 2
18051 Rostock
Germany

Peter Schmidt

● §§ 46.9.1–46.9.5 except 46.9.2.2; 46.9.10
Bayer AG
GB-SP-Chrom, Geb. T18
51368 Leverkusen
Germany

Peter Schmittinger

● §§ 52.13–52.15
Germanenstraße 42
53859 Niederkassel
Germany

Klaus Schneider

● § 5.21.2
Degussa AG
Abt. AC-GKP
60287 Frankfurt
Germany

Wolf-Dieter Schubert

● §§ 26.1, 26.2.2, 26.3–26.11
Grazer Straße 34C
A-8045 Graz
Austria

Karl-Heinz Schulte-Schrepping

● §§ 16.1–16.10
Eichenbachstraße 8

53639 Königswinter
Germany

Heinz Schultz (retired)

● §§ 52.3, 52.4 (introduction), 52.4.2.3, 52.4.3–52.4.5,
52.11 except 52.11.3 and 52.11.7, 52.12, 52.17, 52.18
Gehrenweg 11
34292 Ahnatal
Germany

Ekkehard Schwab

● § 5.21.3.4
● § 46.10.3
BASF Aktiengesellschaft
AG-EPR/P, J 653
67056 Ludwigshafen
Germany

Stefanie Schwarz

● § 16.12
BASF Aktiengesellschaft
EPM/TP, J 550
67056 Ludwigshafen
Germany

Karl A. Schwetz

● §§ 49.6
Elektroschmelzwerk Kempten GmbH
Postfach 1526
87405 Kempten
Germany

Jean Scoyer

● §§ 34.1–34.11
Union Minière Research
Kasteelstraat 7
B-2250 Olen
Belgium

Roger F. Sebenik

● §§ 27.1, 27.4.1–27.4.4
P.O. Box 3299
Englewood, CO 80155
USA

Karl Seebode

● § 51.13.4
Akzo Nobel Salz GmbH
Postfach 1729
21657 Stade
Germany

Margarete Seeger

● §§ 20.11 (introduction), 20.11.1, 20.11.3.1–20.11.3.4
Vesouler-Straße 35
70839 Gerlingen
Germany

Heinz Sibum

● §§ 22.1–22.6, 22.8–22.12
Deutsche Titan GmbH
Altendorfer Straße 103
45143 Essen
Germany

Jack Silver

● § 5.17.7
School of Chemical and Life Sciences
University of Greenwich
Woolwich Campus, Wellington Street
London SE18 6PF
England

Walter Simmler

● § 48.5
Schlinghofenerstraße 10
51519 Odenthal-Glöbusch
Germany

Hartmut Simoleit †

● § 58.2
Kali-Chemie AG
Postfach 220
30002 Hannover
Germany

Matthias Simon

● §§ 17.1–17.10, 17.13–17.14
Rheinzink GmbH
Bahnhofstraße 90
45711 Datteln
Germany

Ole Skåne

● §§ 20.1–20.10
Norsk Hydro a.s
P.O. Box 2594, Solli
N-0203 Oslo 2
Norway

Reiner Skroch

● § 5.12
Lurgi GmbH
Lurgiallee 5
60295 Frankfurt

Germany

Robert A. Smith

● §§ 49.1.1, 49.7–49.13
U.S. Borax Research Corp.
412 Crescent Way
Anaheim, CA 92801
USA

Hans Stark

● §§ 5.17.4–5.17.5
● §§ 21.10.5.1, 21.10.6
BASF Aktiengesellschaft
RCA/N-B516
67056 Ludwigshafen
Germany

Rolf Steffen

● § 6.3.1
VDEh
Sohnstraße 65
40237 Düsseldorf
Germany

Wolfgang Stoll

● Chapter 42
Ameliastraße 25
63452 Hanau
Germany

F. Werner Strassburg

● § 12.16
Comeniusstraße 5
47906 Kempen
Germany

Charles A. Sutherland

● §§ 9.1–9.9
Cominco Ltd.
Research and Development
Trail, British Columbia VIR 4L8
Canada

Herbert Teindl

● § 9.10
Cominco Ltd.
Research and Development
Trail, British Columbia VIR 4L8
Canada

Stanley A. Thielke

● § 27.11

Climax Metals Co.
Amax Center
Greenwich, CT 06836-1700
USA

Christian Thieme

● § 51.15
Schwanenstraße 124
42697 Solingen
Germany

Manfred Toncourt

● § 6.2
VDEh
Informationszentrum Stahl und Bücherei
Sohnstraße 65
40237 Düsseldorf
Germany

Gerhard Trenczek

● § 46.10.1
Bayer AG
Rheinuferstraße 7-9
47812 Krefeld
Germany

Wolfgang Triebel

● §§ 51.1-51.12
● §§ 55.1-55.8
Degussa AG
Werk Wesseling
Postfach 1164
50375 Wesseling
Germany

Georg Uecker (retired)

● §§ 46.9.7-46.9.9
Emil-Nolde-Str. 78
51375 Leverkusen
Germany

Ronald J. Veitch

● § 5.21.3.4
● § 46.10.3
BASF Akriegengesellschaft
EPR/PM
67056 Ludwigshafen
Germany

Tore Vrålstad

● §§ 20.1-20.10
Norsk Hydro a.s.
P.O. Box 2594, Solli

N-0203 Oslo 2
Norway

Mark S. Vukasovich (retired)

● § 27.7 except §§ 27.7.4.1-27.7.4.2
1457 Woodland Drive
Ann Arbor, MI 48103
USA

Heinz Wagner

● §§ 57.3-57.6, 57.8
● § 58.2
Solvay Barium Strontium GmbH
Postfach 220
30002 Hannover
Germany

Peter Wallbrecht

● §§ 57.3-57.6, 57.8
Solvay Bario e Derivati S.p.A.
Via Oliveti, 84
54100 Massa
Italy

Ludwig Walter

● § 58.2
Kali-Chemie AG
Hauptverwaltung, C-AF
Postfach 220
30002 Hannover
Germany

Sabine Walter

● Chapter 41
Universität Hannover
Institut für Werkstoffkunde
30167 Hannover
Germany

Thomas Walter

● Chapter 41
PreußenElektra Aktiengesellschaft
Tresckowstr. 5
30457 Hannover
Germany

John W. Waudby

● § 7.4
● §§ 47.1-47.9
Samancor House
88 Marshall St.
Johannesburg 2001
Republic of South Africa

C. Joseph Weber

● §§ 49.2-49.3
U.S. Borax Research Corp.
Chemical Research
412 Crescent Way
Anaheim, CA 92801
USA

Karl Wefers

● §§ 21.10.1, 21.10.3.1
Aluminum Company of America
Corporate Research & Development
Alcoa Technical Center
Alcoa Center, PA 15069
USA

Wilhelm Wegener †

● § 51.13.3.1
Hegelmaierstraße 26
74076 Heilbronn
Germany

Maurice W. Wei

● § 21.7
Aluminum Company of America
Corporate Research & Development
Alcoa Technical Center
Alcoa Center, PA 15069
USA

David Bruce Wellbeloved

● § 7.4
● §§ 47.1-47.9
Samancor Ltd.
P.O. Box 8186
Johannesburg 2000
Republic of South Africa

William A. Welsh

● § 48.7.5
W. R. Grace & Co. — Conn
7500 Grace Drive
Columbia, MD 21044-4098
USA

Klaus Wessiepe

● § 5.10.1
Schliepersberg 33A
45257 Essen
Germany

Axel Westerhaus

● §§ 22.7.1-22.7.9

Bayer AG
Rheinuferstraße 7-9
Postfach 166
47812 Krefeld
Germany

Gisbert Westphal

● § 51.13 (introduction)
Damaschkestraße 7
42655 Solingen
Germany

Henning Wienand

● §§ 15.12.1-15.12.4
BASF Aktiengesellschaft
-EPM/DA, J 550-
67056 Ludwigshafen
Germany

Ulrich Wietelmann

● Chapter 50
Chemetall GmbH
Reuterweg 14
60271 Frankfurt
Germany

Egon Wildermuth

● §§ 5.17.2-5.17.3
Rückertstraße 1
51373 Leverkusen
Germany

Volker Wilhelm

● § 22.7.10
● § 46.10.1
Bayer AG
PK-P-BZ, Geb. R 32
51368 Leverkusen
Germany

Heinrich Winkeler

● § 5.21.2
Degussa AG
Postfach 13 45
63403 Hanau
Germany

Reinhard Winkelgrund

● § 6.7.2
Stahl-Informations-Zentrum
Breite Straße 69
40213 Düsseldorf
Germany

Herwig Winkler

● Chapter 45
Neckheimgasse 42
A-9020 Klagenfurt
Austria

Peter Winkler

● §§ 15.1–15.10
RWTH Aachen
Institut für Metallhüttenwesen und Elektrometallurgie
52056 Aachen
Germany

Franz Wirsching

● § 56.6
Gebrüder Knauf Westdeutsche Gipswerke
Postfach 10
97343 Iphofen
Germany

Peter Woditsch

● §§ 22.7.1–22.7.9
Bayer AG
AI-Geschäftsfeldleitung IP, Geb. 54
47829 Krefeld
Germany

Hans Uwe Wolf

● § 10.8.6
● § 13.10
● § 14.14
● § 15.11
● § 22.14
● § 26.12
● § 34.13
● § 37.11
● § 58.3
Universität Ulm
Pharmakologie und Toxikologie
Oberer Eselsberg N26
89069 Ulm
Germany

Manfred R. Wolf

● § 55.11
BASF Aktiengesellschaft
Abt. RCA/S, D 404
67056 Ludwigshafen
Germany

Rüdiger Wolf

● Chapter 29
H.C. Starck GmbH & Co. KG
Werk Goslar
Postfach 2540
38615 Goslar
Germany

Gabriele Wühl-Couturier

● § 17.12
Thor-Chemie GmbH
Landwehrstrasse 1
67346 Speyer
Germany

Jun-Ichiro Yagi

● §§ 5.5.6–5.5.11
Inst. for Advanced Materials Processing
Tohoku University
1-1, Katahira, 2-chome Aobaku
Sendai 980-77
Japan

Werner Zulehner

● §§ 48.1–48.4
Wacker-Siltron AG
Abteilung FE
Postfach 1140
84479 Burghausen
Germany

Authorless Sections

● § 14.11 (Antimony, § 10)
● § 26.2.1 (Tungsten, § 2.1) (provient de Ullmann 4, Hugo M. Ortner)

Name Index

A

Achard, F. C. 1270
Africanus, Constantinus 824
Agricola, Georgius 492, 642, 824, 845, 891
Anderson, C. D. 1586
Arfvedson, August 2029
Aristotle 795, 2199
Ashcroft 2066

B

Barrer, R. M. 1967
Bayer, Karl Josef 1044, 1072
Bazlen 2240
Becker, E. W. 1630
Beckett, F. M. 439
Becquerel, Henri 1585, 1600
Bedson, George 278, 282
Bémont, G. 1593
Berg 1491
Bergman, Torbern Olof 716, 924, 1330
Berthelot, M. 154, 1269, 2239
Berthier, P. 1044, 1068
Berzelius 1040, 1431, 1557, 1649, 1697, 1743, 2029
Bessemer, Henry 278, 280
Black, Joseph 2253
Böhm 1062
Bohr, Niels 1586
Bonnier 1685
Boyd 1711
Brandé 2029
Brandt, G. 924
Brown, H. C. 1999
Bunsen 1040, 2029, 2211
Burg, A. 1999
Bussy 955, 981
Buttman 1813

C

Casciorolus, V. 2340
Castner 2054, 2059
Cato 2253
Chadwick, James 1587
Champion 642
Chaptal 1106
Chirkov, N. A. 468
Claus, C. 1270
Cleve 1697
Cockroft, J. D. 1587

Compton, A. H. 1586
Coolidge, W. D. 1330
Cort, Henry 277, 279
Coryell, C. D. 1588
Courtois 673
Cowan 1685
Cramer 673
Crawford, A. 2329
Creusot 278
Cronstedt, Axel F. 716, 1330
Crookes 1543
Curie, Irène 1587
Curie, Marie 1585, 1593, 1600
Curie, Pierre 1585, 1593, 1600

D

D'Ans, J. 2160
Daelen, Rainer 278, 282
Dalton 1040
Darby, Abraham 31, 277, 278
Davy, Humphry 981, 1040, 1986, 2029, 2054, 2059, 2155, 2329, 2337
de Andrada, José 2029
de Boer 1164, 1431
de Elhuyar, F. 1330
de Elhuyar, J. J. 1330
de Marignac 1697
de Ramecourt 2253
de Ulloa, A. 1270
Debiérne, A. 1593
Delafontaine 1697
Demarcay 1697
Des Coudres 1585
Dewey 1062
Dickinson, J. 966
Dießhach 179
Dioscorides, Pedanios 795, 823, 2253
Dirac, P. A. M. 1586
Doebereiner, J. W. 1270
Dony 643
Downs 2054
du Faur, Faber 278
du Monceau, H. I. 1330
Dwight 586

E

Economon 1685
Einstein, Albert 1587
Ekeberg 1417

Elkington, J. B. 493, 531
 Elster 1585
 Elyutin 483
 Ercker, Lazarus 824, 1329

F

Fajans, K. 1594
 Faraday 981
 Fast 1431
 Fermi, Enrico 1587
 Firth, W. P. 1476
 Fischer 1714
 Fleur 277
 Ford, Henry 1471
 Forest 1190
 Frank, Adolph 2143
 Frank, K. D. 467
 Fremy, E. 438
 Fricke 1062
 Fritz, John 282

G

Gadolín 1697
 Gahn, J. G. 1813, 2340
 Garnier, Pierre 716, 1685
 Gay-Lussac 1261, 1262, 1986
 Geiger, H. 1586
 Geiss 643
 Geitel 1585
 Giesel, F. O. 1593
 Gilchrist, Percy C. 278, 280
 Glauber, J. R. 2121
 Glendenin, L. E. 1588
 Gmelin, Christian 1116
 Göhring, O. 1594
 Goldschmidt, H. 406, 465, 966, 1761
 Goodwin, W. L. 1476
 Gregor 1129
 Greville 1062
 Groth, W. 1629
 Guimet, J. B. 1116
 Guntz 2337
 Gusarov, V. N. 463

H

Hahn, Otto 1586, 1601
 Hall 1040
 Hall, Charles Martin 1044
 Hamburger 1431
 Hanamann 1330
 Hanbury, John 277
 Hannibal, Paulus 278
 Harteck, P. 1629

Hatchett 1403
 Haüy 1062
 Haynes, E. 924
 Heberlein 586
 Heisenberg 1586
 Heitler, W. 1586
 Herodotus 1062, 1183
 Hérault, Paul L. T. 278, 281, 1040, 1044
 Herschel 1600
 Hisinger 1697
 Hoffmann 1685
 Hofman, W. 1935
 Hope, T. C. 2329
 Humboldt, Alexander von 1270
 Hunter 1130
 Huntington 586
 Huntsman, Benjamin 277, 279

I

Ilgner 282

J

James 1697
 Jean, G. 439
 Joliot, F. 1587
 Just 1330

K

Kennedy 1685
 Khodorovsky, Y. 465
 Kisselbach, Clemens 282
 Klapproth, Martin Heinrich 1130, 1431, 1600, 1697
 Kreutzer, H. W. 285
 Kroll 1162
 Kroll, W. J. 1130, 1431
 Kühne 1862
 Kunkel 642

L

Lamy 1543
 Langer, Carl 746
 Lavoisier 1040, 2199, 2253, 2282
 Lawrence, E. 1586
 Le Châtelier 1072, 2301
 Lebeau 955
 Leblanc 2104
 Leclaire 673
 Lecoq de Boisbaudran 1523, 1697
 Lely 1431
 Lemery, N. 824
 Leonardo da Vinci 924
 Lewis, W. 1270
 Libavius, Andreas 642, 824

Lipscomb, W. 1999
 Lloyd 586
 Löhneyss 642
 London, F. 1586

M

Magnus, Albertus 796, 845
 Mallet 2337
 Manhès 493, 519
 Mannesmann, Max 278, 282
 Mannesmann, Reinhard 278, 282
 Manuel del Rio 1471
 Marden 1471
 Marggraf 642, 1062
 Marinsky, J. A. 1588, 1700
 Marsden, E. 1586
 Martin, Pierre-Émile 278, 281
 Matthiessen 2029
 Matuschka, A. 466
 McArthur 1190
 McMillan 1685
 Meitner, L. 1586
 Mendeleev 1505, 1523
 Merensky, Hans 1276
 Miller 1185
 Milori 179
 Moissan, Henri 439, 465, 1330, 1600, 1986, 1989
 Mond, Ludwig 154, 746
 Morgan, Charles 278, 282
 Mosander 1697
 Müller von Reichenstein 1571
 Mushet 1814

N

Nasmyth, James 278
 Neilson, Jean Beaumont 278
 Niclassen 1062
 Nilson 1697
 Noddack 1491

O

Olympiodorus 795
 Ørsted, Hans Christian 1040, 1111
 Østerheld 955
 Ostwald 1309
 Oxland, R. 1330

P

Paracelsus 796, 824, 845, 1105
 Pattinson 1226
 Pauli, W. 1586
 Paynet, John 277
 Péligot, E. M. 1600

Peppard 1685
 Perey, M. 1592
 Perrier, G. 1587, 1589
 Pidgeon, L. M. 981
 Plattner 1185
 Pliny the Elder 823, 1062, 1813, 2086, 2253
 Polhems, Christoph 277
 Pott 845
 Pourcel 1814
 Powell 1711

Q

Quincke, L. 154

R

Ramazzini 623
 Ramsey 1585
 Rchiladze, V. G. 805
 Regener, E. 1585
 Reich, F. 1531
 Rich 1471
 Richter, Jeremias 716
 Richter, T. H. 1531
 Riss, M. 465
 Roscoe 1471
 Rose 1403
 Ruberg 642
 Rutherford 1586

S

Sack, H. 282
 Sainte-Claire Deville, H. 1040, 1862, 2054
 Scaliger, J. C. 1270
 Scheele, C. W. 796, 1330, 1361, 1813, 2340
 Scheid 1862
 Schinkel 643
 Schlesinger, H. I. 1999
 von Schlippenbach 586
 Schönbein 2239
 Schröder 796
 Schützenberger 2240
 Seaborg 1685
 Seaman, I. J. 282
 Searles Lake 2154
 Segré, E. 1587, 1589
 Shemtschushny 480
 Siemens, Friedrich 278, 281
 Siemens, Wilhelm 278, 281, 2054
 Soddy 1585
 Solvay, Ernest 2104
 Spackman 192
 Spedding 1711, 1712
 Stahl 642, 2239

Steenbeck, F. 1586
 Stock, A. 966
 Stopes 192
 Strassmann, F. 1587, 1601
 Strohmeyer 869

T

Tacke 1491
 Tennant, S. 1270
 Theophrast 795
 Thomas, Sidney G. 278, 280
 Torney 1062

U

Urbain 1697
 Urey, H. C. 1587

V

Valentinus, Basilius 824, 845
 van Arkel 1130, 1164, 1431
 van Nordstrand 1062, 1064
 van't Hoff 2160
 Vauquelin 955, 1062, 1106, 1761
 Villard, P. 1585
 Vivian, A. C. 966
 von Hevesy 1437
 von Leonhard, K. C. 1330
 von Liebig, Justus 2143
 von Nägeli 1264

von Setz, R. 1476
 von Welsbach, Auer 1678, 1697, 1743, 1751

W

Wahl 1685
 Walton, E. T. S. 1587
 Wartman 1130
 Watson, W. 1270
 Weidenhammer, P. 924
 Weintraub 1986
 Westwood, John 277
 Wetherill, S. 673
 Widerøe, R. 1586
 Wilkinson, J. 281, 1310
 Winkler 214, 1505, 1862
 Withering, W. 2340
 Wöhler, Friedrich 1040, 1862
 Wohlwill, E. 493, 531, 1185
 Wollaston, W. H. 1270
 Wood, C. 1270

X

Xenophon 2253

Y

Yukawa 1587

Z

Zadra 1193

Subject Index

A

Abrasion-resistant alloy 471
 Abrasive hydroxide 1096
 Abrasives 1012, 1921
 Absorption agents 1931
 Accumulators 874
 Acetaldehyde from ethanol 1258
 Acetylene 215
 Achrematite 1363
 Acicular goethite 153
 Acid digestion 1657
 Acid pressure leaching 741
 Acrylate-acrylamide copolymers 1079
 Actinides 1650
 Actinium 11, 1593
 Actinon 10
 Activated aluminas 1096
 Activated carbon 210, 215, 905, 1191, 1199, 1259, 2158
 Activating agent 665
 Active manganese dioxide 1839
 Acute effects of lead 625
 Additive to fodder 149
 Additives for gasoline 633
 Adducts 2287
 Adsorbents 1096, 1953
 Adsorption
 of gold by carbon 1191
 of hydrogen fluoride 1094
 of water on activated alumina 1098
 Aerated concrete 2270
 Affination 1185, 1194, 1197
 Age-hardenable copper alloys 955
 Agglomeration 41, 43, 215, 737, 1081
 Agitation leaching 526
 Air for blast furnace 54
 Air pollution control 132, 133
 Aircraft turbine blades 1499
 Akmite 1914
 Albite 1092
 Alcan cell 991
 Alcohol dehydration 1099
 Alcohulates 1110
 Aldoxime 1296
 Algicidal action 672
 Alginite 194
 Aliphatic carboxylic acids 873
 Aliphatic polysulfides 2230
 Aliphatic sulfides 205
 Aliquat 1370

Alkali aluminate 1121
 Alkali amalgam 909
 Alkali dichromates 1798
 Alkali metal billets 2070
 Alkali metal cyanides 1187
 Alkali metal peroxides 1187
 Alkali metal polysulfide 1187
 Alkali metal silicofluorides 1891
 Alkali metals 3, 12
 Alkali polysulfides 2222
 Alkali sulfur compounds 2221
 Alkali-metal niobates 1408
 Alkaline cyanide solutions 1198
 Alkaline digestion 1660
 Alkaline-earth metals 3, 13
 Alkaline-earth soaps 678
 Alkaline-earth titanates 1172
 Alkanes 2059
 Alkoxides 2058, 2067
 Alkoxyalkyl mercury 919
 Alkoxysilanes 1897, 1934
 Alkyl tin halides 712
 Alkyl tin hydrides 1894
 Alkyl xanthates 1366
 Alkylation 2157
 Alkylmercury compounds 919
p-Alkylphenols 2212
 Allanite 1655, 1697
 Allenite 1030
 Allotropic forms of boron 1987
 Allotropic forms of cobalt 925
 Alloy steels 9, 385
 Alloyed cast iron 342
 Alloying elements 283, 404
 Alloys with ceramic veneers 1315
 Alluvial gold 1185
 Alluvial placers 687
 ALNICO 40
 Alum 962
 Alum-containing ores 1104
Alumen 1062, 1105
 Alumina 1062, 1110
 chemicals 1095
 desiccant 1098
 gels 1097
 in catalytic processes 1099
 production 1091
 -supported catalysts 1100
 Alumina-zirconia abrasives 1446
 β -Aluminas 1068

Aluminates 1068, 1109
 Aluminosilicate lattice 1116
 Aluminosilico reactions 409, 414
 Aluminothermic Mn 406
 Aluminothermic processes 406, 468, 1768
 Aluminothermic production of ferroboreon 467
 Aluminothermic reduction of niobium oxide ores 472
 Aluminum 7, 18, 1039
 alloys 1000
 casting 1055
 cell emissions 1056
 chlorination 1112
 coating 355
 electrodes 1115
 in drinking water 1000
 industry 2120
 master alloys 469
 oxidation 1042
 pigments 1116
 powder 414
 Aluminum alkoxides 1110
 Aluminum Association 19
 Aluminum borohydride 1113
 Aluminum carbide 1053
 Aluminum chloride 1111
 Aluminum chloride hydroxides 1114
 Aluminum fluoride 1046, 1054, 1096
 Aluminum hydrogen phosphate 1121
 Aluminum hydroxides 1062, 1095
 Aluminum hydroxychlorides 1114
 Aluminum *iso*-propoxide 1111
 Aluminum-lithium alloy 2043
 Aluminum-magnesium alloys 1000
 Aluminum-niobium 472
 Aluminum oxide 1042, 1045, 1062
 Aluminum oxide chlorination 1112
 Aluminum oxide hydroxide 1063, 1065, 1097
 Aluminum oxychloride 1111
 Aluminum phosphate 1122
 Aluminum phosphates 1085
 Aluminum-refining cell 1054
 Aluminum *sec*-butoxide 1111
 Aluminum-silicon alloy 1054
 Aluminum suboxide vapor 1053
 Aluminum sulfate 1102, 1116
 Aluminum sulfate neutralization 1097
 Aluminum zinc phosphate 1121
 Alums 150, 938, 1105
 Alumite 1093, 2196
 Amalgam electrolysis 653
 Amalgamation 6, 1189, 1217, 1224, 1232
 Amalgams 709, 908, 1188, 1281, 2101
 Aman process 1018
 Amax process 769
 Amblygonite 2033, 2036
 Amex process 1662
 Amidosulfuric acid 613
 Amine boranes 2002
 Amine process 2200
 Amine tungstates 1351
 Amines 1615, 1718
 Aminocarboxylic acids 1711
o-Aminomethylphenols 873
 Ammonia
 absorption 2111
 oxidation 1309
 recovery 2113
 synthesis 1100
 Ammonia-soda process 2106, 2110, 2121
 Ammoniacal leaching 738, 931
 Ammonium alum 1108
 Ammonium alum neutralization 1097
 Ammonium aluminum sulfate 1108
 Ammonium amalgam 909
 Ammonium borates 2017
 Ammonium carnallite 1010
 Ammonium chloride 1120
 Ammonium chromate 1790
 Ammonium chromium(III) sulfate 1785
 Ammonium dichromate 1790, 1799
 Ammonium dimolybdate 1369
 Ammonium diuranate 1620, 1622
 Ammonium ferric sulfate for tanning 150
 Ammonium fluoroborate 1996
 Ammonium-hafnium carbonate 1460
 Ammonium heptamolybdate 1376, 1382
 Ammonium hexachloroiridate(IV) 1298, 1300
 Ammonium hexachloropalladate(IV) 1297, 1303
 Ammonium hexachloroplatinate 1270
 Ammonium hexachlororhodate(III) 1294, 1298, 1300
 Ammonium hexachlororuthenate(III-IV) 1300
 Ammonium hydrogen sulfide 766
 Ammonium magnesium arsenate(V) 812
 Ammonium metavanadate 1483, 1487
 Ammonium paratungstate 1338, 1340
 Ammonium pentaborate 2017, 2020
 Ammonium perthenate 1494, 1496, 1499
 Ammonium persulfate 164
 Ammonium polyvanadate 1483
 Ammonium sulfamate 739
 Ammonium sulfate 739, 742
 Ammonium tetraborate 2020
 Ammonium tetrafluoroberyllate 964
 Ammonium tetrathiomolybdate 1379, 1381
 Ammonium thiocyanate 1494
 Ammonium thiosulfate 2234, 2238
 Ammonium uranyl carbonate 1620, 1621, 1622
 Ammonium vanadate 864
 Ammonium zirconium carbonate 1450

Ammonium zirconium sulfates 1450
 Amorphous alloys 467
 Amorphous boron 1987, 1991
 Amorphous silicon 1882
 Amphoteric metal 1122
 Analysis of metallic tin 707
 Analysis of platinum group metals 1305
 Anatase 1069, 1134-1137, 1143
 Andorite 1221
 Andrussov process 1309
 Anglesite 584
 Anhydrite 2145, 2174, 2281
 Anhydrite plaster 2301
 Anhydrous aluminum chloride 1116
 Anhydrous copper sulfate 562
 Anhydrous iron(III) chloride structure 150
 Anhydrous magnesium chloride 1004, 1009
 Anhydrous magnesium nitrate 1003
 Anhydrous magnesium sulfate 1032
 Anion-exchange membranes 2129
 Anion-exchange resins 1199
 Anionic complexes 1718
 Anisometric forms of Fe_3O_4 186
 Anisotropic structures in coke 237
 Annealing 347
 Anode baking furnaces 1057
 Anode effect 1050, 1165
 Anode slimes 533, 615, 704, 832, 1047, 1218, 1228, 1284, 1560, 1573
 of electrolytic lead refinery 852
 Anodic dissolution of silver scrap 1236
 Anodic oxidation of potassium manganate(VI) 1850
 Anodized aluminum 944
 Anorthite 1092
 Anorthosite 1092
 Antarcticite 2311
 Anthoinite 1333
 Anthracite 199, 203, 205, 1045
 Anthraquinone production 1113
 Anticaking agents 2092, 2189
 Anticor 679
 Anticorrosive pigments 189, 676, 678
 Anticorrosive zinc oxide 677
 Antidandruff agent 666
 Antidotum Thalii 184
 Antiknock agent 634
 Antimonates 839
 Antimonial copper ores 833
 Antimonial lead 833, 840
 Antimonic acid 839
 Antimonite 825, 894
 Antimony 6, 823, 846
 black amorphous 823
 explosive 823
 native 825
 red 825
 scrap 833
 spots 842
 yellow 823
 Antimony bloom 838
 Antimony(III) chloride oxide 837
 Antimony hydride 843
 Antimony-lead alloys 832
 Antimony oxide 838, 840
 Antimony(III) oxide 826, 838, 842, 843
 Antimony(IV) oxide 826, 839
 Antimony pentachloride 838, 843
 Antimony pentafluoride 838, 843
 Antimony pentasulfide 839, 843
 Antimony pentoxide 839, 843
 Antimony sulfate 840
 Antimony sulfides 839, 841
 Antimony tribromide 838
 Antimony trichloride 836, 837, 843
 Antimony trifluoride 838, 843
 Antimony triiodide 838
 Antimony trisulfide 839, 842, 843
 Antiperspirants 1116
 Antlerite 498
 Apatite 34, 39, 1085, 1698
 Aqua regia 1043, 1197, 1285, 1306
 Aquamarine 961
 Aqueous chemistry of molybdenum 1377
 Aqueous electrolysis 1313
 Aqueous oxidation of iron sulfides 164
 Aqueous oxidation prior to cyanidation 34
 Aqueous thiosulfate 1232
 Aragonite 2253
 Arbiter process 529
 Arenite 1915
 Argentiferous copper ores 1222
 Argentiferous lead ores 1222
 Argentiferous tetrahedrite 830
 Argentite 1221
 Argentometry 1262
 Argentopyrite 1221
 Argyrodite 1221, 1505, 1507
 Argyropyrite 1221
 Armaments 1346
 Armco process 112
 Arsenates 799
 Arsenates(III) 796, 810
 Arsenates(V) 812
 Arsenic 6, 653, 795, 820
 black 795
 brown 795
 crystalline 805
 high-purity 806

native 797
white 795
Arsenic acid 165, 811, 812
Arsenic acid hemihydrate 820
Arsenic(III) bromide 814
Arsenic(III) chloride 814–820
Arsenic(V) chloride 814
Arsenic(III) fluoride 814, 820
Arsenic(V) fluoride 814
Arsenic halides 814
Arsenic hydride 796, 814
Arsenic(III) iodide 814
Arsenic oxides 797, 925
Arsenic(V) oxychloride 814
Arsenic pentoxide 796, 811, 820
Arsenic poisoning therapy 818
Arsenic precipitation 808
Arsenic(III) sulfide 817
Arsenic sulfides 797, 813
Arsenic trioxide 796, 797, 809, 817, 820
refined 803
Arsenical materials roasting 799
Arsenical war gases 818
Arsenic-containing by-products 807
Arsenic-containing copper concentrate 801
Arsenic-containing gold ores 1185
Arsenic-containing pyrite concentrates 801
Arsenides 796, 815
Arsenites 796
Arsenolite 809
Arsenopyrite 33, 164, 165, 797–801, 805, 928
Arsenous acid 796, 810
Arsine 814, 815, 819, 820
Artists' colors 1120
Arylmercury compounds 919
ASARCO shaft furnace 535
Asbestos 32, 1003, 1032
Asbolite 928
Ascharite 1987, 2145
Ascorbic acid production 2127
Asphaltites 1472
Assay methods 1306
Astatine 1588
Astrakhanite 1030, 2122, 2145, 2161
Astringent 666
Atacamite 498, 528
Atmospheric corrosion 365
Atomic hydrogen arc welding 1255
Atomic volume of iron 373
Atomizing molten aluminum 1122
Attrition mill 967
Audio cassettes 186
Augustin process 1232
Auranofin 1202

Aureolin yellow 944
Austenite 143, 144
Autoclaves 656, 671, 739, 757, 767–768, 931, 964
Autoclaves for cultured quartz 1914
Autogenous smelting 513
Automobile catalytic converters 1279, 1284, 1310, 1320
Autooxidation 164
of disulfide ion 164
Autunite 1606
Avicennite 1544
Awaruaite 32
Azurite 498

B

Bacillus subtilis 843
Bacterial leaching 526
Bactericidal effect of silver 1264
Bactericide 6
Bacteriostatic compound 1253
Bad Dürkheim 2211
Baddeleyite 405, 1434, 1435, 1460
fusion 1437
Bahnametall 2030, 2043
Bainite 645
Bai-Yin copper smelting process 512
Balbach–Thum electrolysis 1242
Balling 216
Barite 670, 2342
Barium 13, 2337
Barium aluminates 1110
Barium borates 2020
Barium carbonate 188, 2346
Barium chlorate 2348
Barium chloride 1054, 2348
Barium chromate 1790
Barium ferrite 2349
Barium ferrite pigments 188–189
Barium fluoride 1054
Barium hexaferrite 188
Barium hydroxide 2350
Barium magnesium tantalate 1424
Barium nitrate 2351
Barium oxide 409, 2349
Barium peroxide 411
Barium polysulfides 2346
Barium sulfate 673, 2342
in lithopone 669
Barium sulfide 2345
Barium titanate 2352
Barium zinc tantalate 1424
Barringtonite 1003
Baryta 2340
Basalt 32, 1070
BASF-Grünkupper 572

Basic aluminum chloride 1114, 1116
Basic aluminum sulfate 1107
Basic beryllium acetate 973
Basic beryllium carbonate 964, 973
Basic copper(II) acetate 564
Basic copper(II) sulfates 562, 572
Basic iron(III) acetate 160
Basic lead acetate 629
Basic lead carbonate 629, 636
Basic nickel carbonate 764, 766, 776
Basic oxygen furnaces 1022
Basic potassium aluminum sulfate 1107
Basic zinc phosphate 678
Basic zinc potassium chromate 1806
Bastnæs site 1685, 1697, 1707, 1708, 1723, 1744
Batac jig 206
Batteries 4–6
Battery types 616
Battery-grade manganese ores 1817
Bauxite 10, 25, 1068, 1090, 1104, 1106, 1473, 1524, 2212
Bauxite residue, see *Red mud* <Default ¶ Font>
Bayer process 1069, 1072, 1109, 1524
Bayerite 1062, 1063, 1098
Baykisol 1947
Bearing alloys 6
Bearings 5
Béchamp reaction 176
Bedded chert 1912
Beehive ovens 251
Behavior of impurities in blast furnace 55
Belonesite 1363
Bementite 1815
Beneficiated feed to blast furnace 61
Beneficiation
of iron ore 39
of nickel sulfide ores 722
of ores 2120
Benz[*a*]anthracene 1057
Benzo[*a*]pyrene 1057
Benzofluoranthene 1057
Berlin blue 179, 1104
Berlin white 179
Bernic Lake, Canada 2211
Bertrams process 2099, 2100
Bertrandite 961, 963
Beryl 960
Beryl Picker 961
Beryllides 971, 973
Berylliosis 976
Beryllium 6, 13, 955, 1000
disease 976, 977
pebbles 966
powder 967

single crystals 968
Beryllium ammonium phosphate 973
Beryllium bromide 973
Beryllium carbide 972
Beryllium chloride 965, 973
Beryllium chloride electrolysis 966
Beryllium chloride reduction 965
Beryllium–copper 976
Beryllium fluoride 964, 973
Beryllium fluoride reduction 965
Beryllium hydride 972
Beryllium hydroxide 963, 973
Beryllium magnesium fluoride slag 965
Beryllium nitrate 973
Beryllium nitride 960, 972
Beryllium orthophosphate 973
Beryllium oxide 956, 972
Beryllium oxide chlorination 965
Beryllium perchlorate 973
Beryllium-rich alloys 971
Beryllium sulfate 973
Berzelianite 1559
Berzelius' reduction of K_2TaF_7 by Na 406
Bessemer converter 493, 519
Bessemer process 17, 31
Betafite 1606, 1698
Betatron 1587
Betts process 614
Beverage cans 21
Bimetallic powders 1313
Binary compounds of boron 2003
Bindzil 1947
Biochemical coalification 195
Biocidal paints 6
Bioleaching 1190
Bipolar membrane process 171
Bimessite 1830
Bischofite 983, 1007–1011, 1018, 2145, 2162, 2167
Bismite 846
Bismuth 6, 845
alloys 857
compounds 859
dross 613, 851
from copper and tin concentrates 854
from lead concentrates 849
in medicine 859
pigments 863
separation from tin concentrates 855
Bismuth chloride oxide 859, 863
Bismuth glance 846
Bismuth molybdate catalysts 1384
Bismuth nitrate 864
Bismuth nitrate oxide 863
Bismuth ochre 847

Bismuth oxides 860
 Bismuth oxychloride 863, 865
 Bismuth pentafluoride 859, 860
 Bismuth pentoxide 861
 Bismuth phosphate 861
 Bismuth telluride 1578
 Bismuth titanate 863
 Bismuth tribromide 859, 860
 Bismuth trichloride 859, 860
 Bismuth trifluoride 859, 860
 Bismuth triiodide 859, 860
 Bismuth trinitrate 860
 Bismuth trinitrate pentahydrate 859
 Bismuth trioxide 859, 860
 Bismuth trisulfide 859, 861
 Bismuth vanadate 863, 864
 Bismuth vanadate molybdate 864
 Bismuth vanadate pigments 865
 Bismuth-containing drosses 851
 Bismuth-containing molybdenum ores 848
 Bismuthine 860
 Bismuthinite 1364
 Bismuthyl carbonate 859, 860
 Bismutite 847
 Bismutospherite 847
Bismutum 845
 Bittersalz 1030
 Bitumen 216
 Bituminite 194
 Bituminous coal 199, 203, 205
 Bixbyite 1815
 Black amorphous antimony 823
 Black-and-white photography 1258
 Black arsenic 795
 Black copper 529
 Black Fe_3O_4 pigments 174
 Blanc fixe 671, 2344
 Blancolen 2242
 Blankit 2242
 Blast furnace 133, 276
 as a countercurrent heat exchanger 58
 flue dust 53
 gas 55
 plant 97
 slag 55, 137
 sludge 137
 Blast humidity control 62
 Blister copper 529
 Blister steel 279
 Bloedite 1030
 Bloomery furnace 31, 275
 Blooms 31
 Blue Shield 572
 Blue ultramarine 1116

Blumenfeld method 1142
 Boehmite 1062–1065, 1068, 1072–1075, 1097
 Bog iron ore 33
 Boiler ash 1479
 Boliden electric furnace 597
 Boliden Kaldo 597, 599
 Bolzano process 993, 994
 Bonding of elements in coal 204
 Boracite 466, 468, 1987, 2145
 Boranes 1998
 Borates 1986
 glasses 2018
 in seawater 1017
 ores 468
 pigments 2021
 Borax 1987, 2059
 Bordeaux mixture 571
 Boric acid 468, 748, 2007, 2019, 2021, 2126
 Boric oxide 466, 468, 2006
 Boride-forming metals 467
 Borides 467, 1988, 2002
 Bornite 33, 498
 Borohydrides 2001
 Boron 12, 1011
 allotropic forms 1987
 binary compounds 2003
 minerals 466
 pigments 2021
 Boron carbide 12
 Boron halides 1991, 1995
 Boron nitride 12
 Boron subhalides 1997
 Boron sulfide 1998
 Boron tribromide 1994, 1995
 Boron trichloride 1886, 1993, 1995
 Boron trifluoride 1993, 1994
 Boron triiodide 1994, 1995
 Boron trioxide reduction 1989
 Borosilicate pigments 2021
 Boroxol 2006
 Boulangerite 584
 Bourmonite 498
 Brannerite 1606
 Brass 4, 641
 Braunite 1815
Braunstein 1838
 Brazing 1168, 1343, 1374
 Breeder reactor 11
 Breithauptite 719
 Breunnerite 1014
 Briarite 1507
 Bright coal 199
 Brilliant primrose yellow 863
 Brine purification 2109

Briquetting 210
 Brixlegg process 513
 Brochantite 498
 Bromargyrite 1221
 Bromide in seawater 1017
 Bromine 987
 Bromosilicon hydrides 1894
 Bromyrite 1221
 Bronze 4
 Bronze blue 179
 Brookite 1134, 1136
 Brown arsenic 795
 Brown coal 200, 201, 220
 Brown pigments 174
 Brucite 983
 Bukovite 1544
 Bullion 591
 Bunsen process 2057
 Burkeite 1085, 2122, 2154
 Busbars 18
 Bustamente furnace 896
 Bustle pipe 58
 Butyl rubber production 1113
 Butyllithium 2042, 2049
 By-product cobalt 770
 By-products of copper smelting 673

C

Cable sheathing 4, 619
Cadmia 642, 673, 869
 Cadmium 5, 24, 594, 806, 846, 869, 877
 alloys 875
 cementation 871
 coatings 874
 distillation 873
 electrolytic deposition 872
 emission 878
 in blood 883
 in cigarettes 883
 in soil 879
 in tobacco 880
 pigments 873, 884
 poisoning 881
 recycling 873
 Cadmium antimonide 837
 Cadmium carbonate 870, 876
 Cadmium chloride 876
 Cadmium cinnabar 886
 Cadmium consumption 880
 Cadmium-containing alloys 871
 Cadmium-containing waste 873
 Cadmium cyanide 876
 Cadmium hydroxide 876
 Cadmium mercury sulfide 886
 Cadmium mercury telluride 1579

Cadmium nitrate 877
 Cadmium oxide catalyst 876
 Cadmium oxides 876, 880
 Cadmium red 885, 887
 Cadmium selenide 875, 1565, 1567
 Cadmium–selenium–indium alloy 875
 Cadmium sulfate 877
 Cadmium sulfate in electroplating 877
 Cadmium sulfide 870, 880, 884, 885, 888
 Cadmium sulfite 876
 Cadmium sulfoselenide 880, 885, 1565
 Cadmium telluride 1578
 Cadmium–tin alloys 873
 Cadmium yellow 885, 887
Calam 642
 Calamine 645
 Calcination of $\alpha\text{-FeOOH}$ 174
 Calcination of $\text{Al}(\text{OH})_3$ 1086
 Calcined alumina 1101
 Calcined dolomite 1003
 Calciothermic production of titanium alloys 1167
 Calcite 34, 1014, 2253
 Calcium 2249
 content of Al_2O_3 1085
 ferroalloys 2252
 Calcium aluminate 1092
 Calcium arsenate 608, 612, 809, 812, 820
 Calcium borates 2016, 2020
 Calcium carbide 215, 2059, 2270
 Calcium carbonate 2087
 Calcium chloride 699, 1144, 2311
 Calcium chromate 1790
 Calcium chromite 409
 Calcium cyanamide 2317
 Calcium cyanate 2322
 Calcium cyanide 1190
 Calcium cyanurate 2322
 Calcium dichromate 1790
 Calcium ferrite 44, 50, 678, 1916
 Calcium fluoride 1047, 1057
 Calcium hexacyanoferrate(II) 180, 1104
 Calcium hydroxide 1016
 Calcium–manganese–silicon 404
 Calcium molybdate 1333, 1370
 Calcium oxide 509
 Calcium plumbate 635
 Calcium silicate slags 293
 Calcium silicon 404, 1900
 Calcium–silicon–aluminum 404
 Calcium–silicon–barium 404
 Calcium–silicon–magnesium 404
 Calcium–silicon–titanium alloys 475
 Calcium–silicon–zirconium 404
 Calcium sodium borates 2016

Calcium stannate 608, 612
 Calcium sulfate 2087, 2090, 2281
 Calcium sulfide 2116
 Calcium thiosulfate 1218
 Calcium titanate 1172
 Calomel 911
 Calorific value 202, 220
 Canfeldite 1507
 Canga 37
 Cannon process 2192
 Capacitors 9
 Carat 8
 Carbides 996
 Carbiding of zircon 1437
 Carbido-carbonyls 939
 Carbochlorination of zircon 1435, 1462
 Carbon black 215
 Carbon bricks 101
 Carbon regeneration 1194
 Carbonaceous material 198
 Carbon-in-leach 1194
 Carbon-in-pulp 1191, 1192
 Carbonitrides 1173
 Carbonization 211
 Carbonization assay 202
 Carbonization of coal 211
 Carbonyl complexes of cobalt 940
 Carbonyl iron 143, 157, 159
 Carbonyl iron oxide 158
 Carbonyl process 752, 933, 1283
 Carbothermal silicon 1865
 Carbothermic ferroboration 467
 Carbothermic production of ferrotitanium 475
 Carbothermic production of ferrotungsten 464
 Carbothermic reduction 441, 983
 Carbothermic reduction of MoO_3 478
 Carboxylic acids 1718
 Carburization 370
 Carcinogenicity 625, 883
 Carnallite 983, 987, 1004, 1007–1009, 2143, 2145, 2153, 2154, 2159, 2162, 2166, 2174, 2180, 2212, 2311
 decomposition 2169
 dehydration 988
 Carnegieite 1902
 Carnotite 1472, 1606
 Caron process 758, 764, 767, 776, 1831
 Carrollite 928, 930
 Case hardening of steels 370
 Case-hardened steels 471
 Cassiterite 686, 689, 1418, 1656
 Cassiterite-sulfide deposits 687
 Cast house dedusting 135
 Cast iron 1, 146, 341
 ductile 2
 grey 2
 malleable 2
 white 1
 with vermicular graphite 342
 Cast steel 338
 Casting 318, 1374
 Casting of anodes 531
 Casting thin slabs 334
 Castner process 2057, 2060
 Catalan forge 31, 275
 Catalyst in organic syntheses 676
 Catalyst poisoning 1310
 Catalyst support 1105
 Catalyst-forming methods 1099
 Catalysts 4, 6, 9, 10, 21, 152, 665, 1308, 2213
 Catalytic aluminas 1096, 1099
 Catalytic dehydrogenation of methanol 1258
 Catalytic hydrolysis of benzotrichloride 665
 Cathode lining 1057
 Cathode-ray tubes 1539
 Cathodic protection 661
 Cathodic sputtering 1255, 1314
 Cation complexation 873
 Cattierite 928
 Caustic magnesia 1020, 1021
 in agriculture 1024
 in building industry 1024
 Causticization 1075, 2274
 Celestite 2330
 Cell design 1094
 Cell gas dry scrubbing 1094
 Cell heat loss 1051
 Cement 2253, 2257
 Cement copper 529
 Cementation 527, 656
 of cadmium 871
 with zinc 657
 Cementation furnaces 278
 Cemented carbides 936
 Cemented tungsten carbide 1357
 Cementite 145, 146
 Centre d'information cuivre, laitons et alliages 545
 Centrifuge 208
 Ceramic capacitors 1409
 Ceramic coatings 944
 Ceramic industries 1374
 Ceramic method 188
 Ceramic silicon carbide 1373
 Ceramic uses of alumina 1101
 Ceramic-bonded bricks 1023
 Ceramic-grade niobium pentoxide 1409
 Ceramics 943, 1921
 Cerargyrite 1221

Cerium 12, 1743, 1749
 Cerium earths 1695, 1698
 Cerium(IV) oxide 1753
 Cermets 1771
 Cerro Matoso ferronickel 457
 Cerulean blue 944
 Cerussite 584
 Cervantite 825
 Cesium 2215
 Cestibantite 2216
 Chain reaction 11
 Chalcantite 498
 Chalcidionies 1919
 Chalcedony 1907, 1908
 Chalcocite 498, 930, 1363, 1367
 Chalcopyrite 24, 33, 34, 152, 498, 719, 1277, 1363, 1367
 chlorination 509
 leaching 152
 reduction 509
 Chalcothallite 1544
 Chalk 2255
 Challenger expedition 1828
 Chamotte 696, 1023
 Champion WP 572
 Changing technology 17
 Char 242, 243, 244
 Characterization of coals 202
 Char-forming reactions 244
 Chemical detinning 706
 Chemical manganese dioxide 1840
 Chemical structure of coal 200
 Chemical vapor deposition 159, 1865, 1866, 1868
 Chemically bonded bricks 1023
 Chemically resistant steels 270
 Chemico process 931
 Cheralite 1655
 Chert 1912
 Chevrel phases, see *Ternary molybdenum chalcogenides*
 Chiles anodes 527
 Chillagite 1363
 Chinese blue 179
 Chloanthite 797, 815
 Chlor-alkali electrolysis 2096, 2188
 Chlorhydrol 1116
 Chloride distillation 1438
 Chloride leach processes 743
 Chloride process 1141, 1143, 1150
 Chloridization 504, 694, 834
 Chloridizing roasting of copper ores 1218
 Chlorinated organic compounds 999
 Chlorinating agents 1161
 Chlorination 151, 963, 1406, 1744
 of aluminum 1112

 of aluminum oxide 1112
 of beryllium oxide 965
 of chalcopyrite 509
 of ferroalloys 1406
 of magnesia 984
 of magnesite 984
 of pyrite cinder 2126
 of titanium dioxide 1160
 Chlorine 2062
 Chlorine dioxide 2126
 Chloroantimonic acid 836
 Chlorobenzenes 999
 Chlorocalcite 2311
 Chlorodibenzofurans 999
 Chlorodibenzo-*p*-dioxins 999
 Chloromethanes 999
 Chloropentamminerhodium(III) chloride 1294
 Chlorosilanes 1878
 Chloro-*tris*-(triphenylphosphine)rhodium(I) 1304, 1310
 Chromate pigments 1801, 1805
 Chrome green 1803
 Chrome orange 1803
 Chrome yellow 1801
 Chrome-magnesia 101
 Chromia-impregnated alumina catalyst 1100
 Chromic acid 453
 Chromic acids 1787
 Chromite 33, 1762
 Chromite ores 439, 441
 Chromium 12, 405, 1761
 master alloys 448
 ores 1022, 1763
 spinel 1764
 Chromium(III) acetate 1786
 Chromium alum 1106
 Chromium(III) aquoxides 1777
 Chromium(III) chloride 1786
 Chromium-coated steel 359
 Chromium(II) compounds 1792
 Chromium dioxide 1779, 1796, 1806
 Chromium(III) fluoride 1785
 Chromium hydroxide 1777
 Chromium lignosulfonates 1787
 Chromium-molybdenum master alloys 449
 Chromium-niobium 472
 Chromium-niobium master alloys 449
 Chromium(III) nitrate 1786
 Chromium nitrides 448
 Chromium oxide pigments 1797
 Chromium(III) oxide pigments 1777
 Chromium oxides 413, 1777, 1797, 1800
 Chromium phosphate 1807
 Chromium(III) phosphate 1787
 Chromium rutile yellow 1156
 Chromium(III) salts 1782

- Chromium(III) sulfate 1783
 Chromium trioxide 1780
 Chromyl chloride 1779, 1792
 Chrysene 1057
 Chrysoberyl 961
 Chrysocolla 498
 Cinnabar 893, 895, 911
 Circofer process 118
 Circored process 117
 Cladding 362
 Classification of coal 199
 Classification of TiO_2 pigments 1150
 Clathrasils 1969
 Claus process 1099
 Clay activation 1119
 Clay depressants 2175
 CLEAR process 529
 Clinobisvanite 863
 Coagulant 150
 Coal 191
 carbonization 211
 classification 199
 coking 210
 combustion 215
 conversion 210
 dewatering 207
 for smelting-reduction processes 123
 gasification 210, 213
 hydrogenation 212
 liquefaction 210, 212
 mineral matter content 219
 organic components 200
 petrology 191
 pyrolysis 191, 211, 224
 thermoplastic properties 224
 Coal tar 215
 Coal tar pitch 253
 Coalification 193–196
 Coarse quartz 1911
 Coating of silver sulfide 1220
 Coating systems 361
 Cobalt 5, 923, 1370
 as a catalyst 945
 corrosion 937
 electroplating 947
 electrowinning 743
 extraction 743
 from arsenide ores 933
 from laterite ores 933
 from nickel ores 770
 in igneous rocks 928
 in ZnS lattice 670
 powders 936
 separation from other metal ions 933
 Cobalt acetate 944
 Cobalt(II) acetate 942
 Cobalt alum 1106
 Cobalt arsenide minerals 930
 Cobalt blue 944, 950
 Cobalt boron 469
 Cobalt(II) carbonate 942
 Cobalt carbonyl complexes 940
 Cobalt carbonyls 934, 939
 Cobalt carboxylates 935
 Cobalt(II) carboxylates 943
 Cobalt(II) chloride 942
 Cobalt(II) complexes 938
 Cobalt(II) compounds 938
 Cobalt(III) compounds 938
 Cobalt Development Institute 19
 Cobalt(II) dicobalt(III) tetroxide 940
 Cobalt fluoride 946
 Cobalt hydroxide 938
 Cobalt(II) hydroxide 941
 Cobalt(III) hydroxide 741, 748
 Cobalt ion reduction 935
 Cobalt molybdenum–alumina catalysts 1100
 Cobalt(II) nitrate 942
 Cobalt(II) oxalate 943
 Cobalt(II) oxide 935, 938, 940, 948
 Cobalt(III) oxide 938, 940
 Cobalt oxides 940
 Cobalt(III) pentammine complex 931
 Cobalt(II) phosphate 942
 Cobalt sulfamate 947
 Cobalt(II) sulfate 942
 Cobalt sulfide 937, 945
 Cobalt tripotassium hexanitrite 943
 Cobalt violet 944
 Cobaltamines 938
 Cobalt-base superalloys 1375
 Cobalt–chromium–molybdenum 449
 Cobalt-containing iron oxide pigments 187
 Cobalt-containing pigments 944
 Cobalt-containing plating baths 947
 Cobaltite 797, 928, 930
 Cobalt–niobium 472
 Cobalt–tungsten alloys 947
 Cobre Nordox 572
 Cobre Sandoz 572
 Cochranite 1173
 COED pyrolysis process 255
 Coesite 1903, 1904, 1905
 Coffinite 1606
 COGAS process 254
 Coil coating 360
 Coin process 132
 Coinage 1251, 1307
 Coinage alloys 1205, 1223
 Coke 31, 53

- consumption 53
 microstructure 233
 Coke oven gas 211
 Coke oven silica bricks 1917
 Coke ovens 251
 Coke properties 252
 Coking 211
 Coking of coal 210
 Colcord process 604
 Cold press welding 1255
 Colemanite 466, 468, 1987, 2010, 2016
 Collectors 2175
 Colloidal gold 1188
 Colloidal hydrous ferric oxide 148
 Colloidal silica 1932, 1945, 1946, 1947
 Colloidal silica surface 1937
 Colloidal silica–water system 1943
 Colloidal silver 1250, 1259
 Colloidal silver sols 1253
 Colmonoy 471
 Color photography 1258
 Colored gold alloys 1205
 Colored quartz 1914
 Coloring of silver 1252
 Columbite 33, 472, 686, 1404, 1418, 1419
 Combismelt process 126
 Commercial forms of nickel 771
 Compact cassettes 186
 Complex antimony sulfide ores 833
 Complex compounds of iron 148
 Complex iron(II) cyanides 179
 Complex oxides 33
 Complex silicides 1374
 Complex tin concentrates 689
 Complexation of cations 873
 Composite metals 1256
 Composite MgO-C anodes 983
 Composites 1255, 1256
 Composition
 of brines 983
 of dolomites 983
 of ferrophosphorus 460
 of ferrotungsten 461
 of seawater 1017
 Compressibility of iron 374
 Computer control of electric furnaces 438
 Computer tapes 186
 Concrete reinforcing steel 473
 Condensation 2157
 Condensation of mercury 898
 Conical cathodes 993
 Conseil intergouvernemental des pays exportateurs de cuivre 545
 Conseil international pour le développement du cuivre 545
 Constructional steel 1
 Consumable electrode remelting processes 336
 Consumable electrodes 1167
 Consumption of cadmium 880
 Contact breakers 1256
 Conterfey 642
 Continemelt process 531
 Continuous casting 327
 Continuous casting of copper 536
 Continuous converting 521
 Continuous production of potassium 2155
 Continuous rod casting 537
 Contop process 524
 Control grids 1374
 Control rods 10, 875
 Controlled cooling 747
 Controlled oxidation of Fe_3O_4 174
 Conversion of iron(II) sulfate to gypsum 149
 Converter gas cleaning 380
 Converter slags 518, 732
 Converting 518
 Cooperite 1276
 Copper 4, 18
 alloys, age-hardenable 955
 anionic complexes 567
 and the environment 569
 anode slimes 855, 1228, 1229, 1283
 anodes 534
 cathodes 532
 converter 519
 dross 611
 electrical conductivity 495
 electrowinning 741, 742
 from secondary materials 524
 grades 539
 hydrometallurgy 525
 ions 547
 matte 833
 mechanical properties 494
 minerals 497
 ore deposits 499
 pigments 571
 porphyry ores 1365
 powder 538
 refining 529
 thermal properties 495
 Copper(I) acetate 563
 Copper(II) acetate monohydrate 563
 Copper(II) acetoarsenite 564
 Copper(II) arsenate 564
 Copper(II) arsenite 564
 Copper(II) *bis*-(1,8-dihydroxyquinoline) 568
 Copper boron 469
 Copper(I) bromide 564
 Copper(II) bromide 564
 Copper(II) carbonate hydroxide 552

Copper chloride 871
Copper chloride complexes 567
Copper(I) chloride 528, 553
Copper(II) chloride 555
Copper(II) chromate(III) 565
Copper(II) chromate(VI) 564
Copper chromates 1791
Copper(I) cyanide 565
Copper(I) cyanide complexes 568
Copper Development Association 545
Copper(II) diphosphate hydrate 566
Copper(II) formate 565
Copper(II) hydroxide 550
Copper indium selenide 1567
Copper(I) iodide 565
Copper metaborate 2020
Copper(II) nitrate trihydrate 565
Copper(II) oxalate 566
Copper(I) oxide 548
Copper(II) oxide 549
Copper(II) oxychloride 556
Copper(II) phosphate trihydrate 566
Copper(II) selenide 566
Copper(II) soaps 566
Copper(I) sulfate 557
Copper(II) sulfate monohydrate 562
Copper(II) sulfate pentahydrate 557
Copper sulfide 10
Copper(I) sulfide 566
Copper(II) sulfide 567
Copper telluride 1573
Copper(II) tetrafluoroborate 567
Copper(I) thiocyanate 567
Copperas 149
Copperas process 173
Copperas reds 173
Copper-chromium master alloys 449
Copper-plate amalgamation process 1224
Copper-silicon alloy 527
Copper-precipitation 1100
Cordierite 1028
Core of the earth 31
Corex process 127, 142
Corrosion 364
 of cobalt 937
 of stainless steels 366
 of titanium 1133
Corrosion protection 661
Corsican forges 275
Corundum 1063, 1066
Corundum concrete 103
Corvusite 1472
Cosmetic industry 866
Countercurrent decantation 1079

Covellite 498, 1365, 1367
Cresol 704
Cresolsulfonic acid 704
Crevice corrosion 366
Cristobalite 1902, 1904, 1908, 1916
Cristobalite sand 1917
Crocoite 584, 1763
Crookesite 1544
Crucible steel 279
Crucibles 1346
Crust breaker 1047
Cryogels 1933
Cryogenic steels 270
Cryolite 1045
Cryptocrystalline magnesite 1014, 1022
Cryptomelane 1815
Crystal growth 50, 1869
Crystal silver 1250
Crystal structure of iron blue 179
Crystalline arsenic 805
Crystalline boron 1989
Crystalline nonmineral silica phases 1909
Crystalline quartzite 1912
Crystalline silica phases 1905
Crystalline silica products 1911
Crystalline silicon 1880
Crystallization 739, 742
 of K_2NbF_7 1406
 of sodium chloride 2087
Cubanite 719
Cupellation 1203, 1226, 1227, 1230
Cupola furnace 343
Cuprasol 572
Cupravit-Forte 572
Cupravit-Spezial 572
Cuprion ammoniacal leach process 1831
Cuprite 498
Cupronickel coin 716
Cuprotungstite 1333
Curie 1588
Curie temperature 372, 374
 of α -iron 376
Current efficiency 1050
Cutinite 194
Cyanidation process 1185, 1190, 1218, 1225
Cyanide 1058
Cyanide-containing melts 1313
Cyanide-insoluble silver compounds 1225
Cyano complexes 179
Cyanogen 55
Cyanogen bromide 1187, 1225
Cyclone crystallization 167
Cyclone smelting 517, 828
Cyclones 97

Cylindrite 686
Cymet process 529
Czocharski silicon crystal 1869

D
D'Ansire 2122, 2145
D2EHPA 748, 964, 1536, 1716
Datolite 1987, 2010
Davidite 1606
Dawsonite 1093
De re metallica 492, 642, 824
Deactivation of alumina catalyst 1100
Dead Sea 2153
Debismuthizing 610
Debismuthizing of lead 2252
Decaborane 2000, 2002
Decarburization 294, 316, 372
Decarburization of high-carbon ferrochromium 445
Decolorizing agents 1096
Decomposition of carnallite 2169
Decomposition of diborane 1990
Decomposition points of coal 232
Decoppering 604
Degussa process 1162, 1309
Dehydrated carnallite 984
Dehydration 1385
 of alcohols 1100
 of aluminum hydroxide 1097
 of aqueous magnesium chloride 986
 of *n*-butane 1100
 of carnallite 988
 of gypsum 2285
 of magnesium chloride 984
 of silica gel 1951
Dehydrogenation 316, 1385
Dehydrogenation of isopropanol 1258
Deicing salt 2093
Delft china 944
Demag electrolysis 1236
Demonetization of silver 1218
Denitrating 372
DENOX catalysts 1353
Dense-media separation 40, 206
Densification cycle 757
Densities of ferrotitanium alloys 474
Density of mercury 892
Dental amalgams 1224
Dental materials 1208, 1314
Dentifrice 1953
Deoxidation 297, 313
Deoxidation diagram for Al-Si-O 298
Deoxidation of killed steel 474
Deoxidized copper 540
Dephosphorization 102, 295, 314

Deposition of silver alloys 1254
Descloizite 1472
Desiccants 1952
Desilication reaction 1091
Desilicization 102
Desilvering 608
Desilvering of silver-plated material 1239
Desulfurization 102, 296, 313, 1000, 2258
 of coal gas 149
 of flue gases 2126
 of petroleum 1384
Detergents 1120
Determination of boron in ferroboration 470
Determination of Sn 706
Detinning 21
Detinning tin slags 701
Deuterium exchange 1959
Deutsches Kupfer-Institut 545
Dewatering 207
Dewatering of coal 207
Deyerite 863
Dezincing 609
Di-(2-ethylhexyl) phosphonic acid 934
Di-(2-ethylhexyl) phosphoric acid, see *D2EHPA*
Diagenesis 195
Dialkylphosphoric acid 1010
Dialkylselenium carbamates 1566
Diammine silver complexes 1247
trans-Diamminedichloropalladium(II) 1297, 1303
Diammonium tetraborate 2017
Diamond quartzite 1912
Diaphragm cells 830, 2097, 2101
Diarsenide ion 34, 164
Diarylmercury 915
Diaspore 171, 1063, 1065, 1074, 1075
Diatomite 1912, 1925, 1927
Diborane 1998, 1999, 2000
Diborane decomposition 1990
Dibutyl carbitol 1196
Dibutyltin dichloride 712
Dicalcium ferrite 1015
Dicalcium phosphate 2192
Dicalcium silicate 1015
Dicalcium silicate slag 995
Dichlorodiamminepalladium(II) 1298, 1300
Dickite 34
Dicyandiamide 2318
Dicyanoaurate complex 1188
Die casting 4, 662
Diehl process 1187
Dielectric layer of Ta_2O_5 1422
Dielectric materials 1424
Diethyldithiocarbamate 707
Dietzel electrolysis 1236

Diffusion deoxidation 297
 Diffusion process 1628
 Difluorosilylene 1893
 Digenite 498
 Digermane 1516
 Digestion of ores 2120
 Digital audio 186
 Dilithium tetraborate 2017
 Dimethylglyoxime 657, 1305
 Dimethylmercury 915
 Dinitro-diammineplatinum(II) 1302
 Diodes 6, 1346
 Dioptase 498
 Dioxane 1005, 1009
 Diphenylamine 704
 Direct reduction 21, 104, 136, 287
 Direct rolling 334
 Dirhenium heptoxide 1496
 Disadvantage of metallothermic reduction 406
 Disilane 1885
 Disilver fluoride 1246
 Disodium arsenate 820
 Disodium ethylenediaminetetraacetate 1115
 Disodium octaborate 2015
 Disodium tetrasulfide 2058
 Dispersants 1960
 Dispersion-hardened platinum 1307
 Disproportionation 1385
 Dissolution of silver 1220
 Distillation
 of ferromanganese 1827
 of mercury 906
 of osmium(VIII) oxide 1295
 of ruthenium(VIII) oxide 1295
 under reduced pressure 872
 Distribution coefficient 1714
 Disulfide ion 34, 164
 Disulfide ion autooxidation 164
 Disulfides 33
 Disulfites 2234
 Dithiocarbamates 1383
 Dititanium trioxide 1171
 Divalent mercury 910
 DK process 103
 Dodecacarbonyltetracobalt 939
 Dolime 2254
 Dolomite 13, 983, 1004, 2254
 Dolomite-magnesia 101
 Domeykite 815
 Doré bullion 534
 Doré furnace 1230
 Doré metal 1283
 Double bell system 58
 Double sulfides 33

Doubling period 17
 Dow cell 992
 Dow Chemical process 986, 988, 1005
 Down's process 2155
 Downdraft sintering 586
 Downs cell 2041, 2060, 2063
 Driers 941, 944
 Drilling muds 547, 2343
 Drinking water from seawater 1258
 Dross 1232, 1233, 1279, 1283
 Dressing 604
 Dry coke quenching 136, 211
 Dry scrubbers for controlling cell emission 1057
 Dry stacking 1089
 Drying agents 1096
 Ductile cast iron 2
 Dump leaching 526
 Dust catchers 96
 Dust emission 378
 Dust-recovery system 96
 Dyes 215
 Dyna Whirlpool 40
 Dysprosium 12

E

EDTA 1254, 1711, 2287
 Effect of temperature on precipitation 1082
 Effect of temperature on silanol groups 1938
 Effects of chlorine in oxidation 370
 Efficient operation of blast furnace 61
 El Teniente converter 519, 520
 Elastic properties of iron 374
 Electric arc furnace 308, 425, 475, 1022
 Electric arc melting 1342
 Electric batteries 1257
 Electric furnace smelting 512, 728
 Electric furnaces 425
 Electric induction furnace 309
 Electric slag furnaces 514
 Electric steel dusts 645
 Electric steel process 306
 Electrical conductivity of copper 495
 Electrical industry 1223
 Electrical insulator 1026
 Electrical lamps 9
 Electrical properties of iron 375
 Electrical resistivity of aluminum 1043
 Electrical technology 1255, 1312
 Electrically conducting TiO_2 pigments 1154
 Electroceramics 1155
 Electrochemical apparatus 1308
 Electrochemical decomposition of sodium sulfate 2129
 Electrochemical deposition 657

Electrocrystallization 535
 Electrodes 215
 Electrodes made of SnO_2 711
 Electrodeposition 1945
 Electroforming 1208, 1314
 Electrogravimetry 1307
 Electrolysis
 of aqueous solutions of iron(II) salts 143
 of beryllium chloride 966
 of magnesium chloride 983
 of magnesium oxide 983
 of molten borates 1990
 of molten lithium chloride 2041
 of pickle solution 168
 of sodium chloride 2096
 Electrolysis cell 1748
 Electrolytic capacitors 1418
 Electrolytic coating 356
 Electrolytic copper powder 539
 Electrolytic deposition of cadmium 872
 Electrolytic detinning 705
 Electrolytic galvanizing 662
 Electrolytic manganese 406
 Electrolytic manganese dioxide 1843
 Electrolytic oxidation of nickel(II) hydroxide 741
 Electrolytic production of zinc 658
 Electrolytic production of zinc dust 653
 Electrolytic reduction of silver nitrate solutions 1250
 Electrolytic refining 1218
 Electrolytic refining of lead 613
 Electrolytic route to manganese 1823
 Electron beam melting 1372, 1412, 1440, 1464
 Electron beam refining 1461
 Electron beam remelting 338
 Electron beam welding 1168
 Electron beam zone melting 1342
 Electron emitters 1678
 Electronic applications of cultured quartz 1915
 Electronic tubes 1346
 Electronics industry 1223, 1254, 1312
 Electroplating 4, 12, 356, 1208, 1772
 Electroplating industry 1279
 Electroplating of cobalt 947
 Electrorefining 24
 of silver 1227
 of tin 704
 of zirconium 1440
 Electro-slag remelting 338
 Electrostatic concentration 40
 Electrostatic precipitators 98
 Electrostatic separation 2180
 Electrostatic separation of kieserite 1031
 Electrothermal process for manganese 1826
 Electrowinning 527
 of hafnium 1464

 of manganese 1824
 of nickel 750
 of titanium 1165
 of zinc 653
 of zirconium 1440
Electrum magicum 1185
 Elemental silicon 1886
 Elemental silver 1224
 Elemental sulfur 655, 703
 Elemental sulfur from pyrrhotite 165
 Elred process 126
 Eluex process 1615, 1616
 Elution with organic solvents 1194
 Embalming 1105
 Embolite 1221
 Emeleusite 1914
 Emerald 961
 Emergency batteries 1257
 Emission control 545
 Emulsion breaker 665
 Enamel industry 1110
 Enameling of steel 944
 Enamels 663, 941, 1923
 Enargite 498, 797
 Energy saving 21, 437
 English cupellation furnace 1228
 Engraving 149
 Enrichment of ^{235}U 1627
 Enstatite 1028
 Environmental aspects of nickel smelting 732
 Environmental aspects of steel production 377
 Environmental protection 132
 Environmental protection in ferrochromium production 453
 Eosite 1363
 Epitaxy 1877
 Epsom salt 1019, 1023, 1030, 1031
 from langbeinite 1032
 from magnesite 1032
 from seawater 1032
 Epsomite 1007, 1030, 2145, 2161, 2193
 Equilibrium data for iron pentacarbonyl 155
 Erbium 12
 Erbium earths 1695
 Erythrite 928
 Eschka's gravimetric method 906
 Esterified silica surface 1938
 Etchant for aluminum 149
 Etching 152
 Etching solutions 568
 Etherification 1385
 Ethyl process 1865
 Ethylene 241
 Ethylene glycol 1009

Ethylenediaminetetraacetic acid, see *EDTA*
 Ettringite 2286
 Euclase 961
 Euclite 1434
 Eucryptite 1902, 2033
 Eudialyte 1434, 1435
 Eugenite 1221
 Eukryptite 2033
 Europium 12
 Europium oxide separation 1722
 Euxenite 1405, 1419, 1655, 1698
 Evaporation
 of brine 2089
 of magnesium chloride solutions 1010
 of seawater 1007, 2086
 Evaporative cooler 2125
 Exhaust-gas catalysts 1311
 Exinite 193
 Expansion coefficient of iron 373
 Explosion hazards and alloy formation 1320
 Explosion hazards of silver compounds 1264
 Explosive antimony 823
 Explosive cladding 1169, 1255
 Explosive silver compounds 1247
 Extenders 1921, 1922
 Extenders for sylvite flotation 2175
 External scrap 21
 Extraction 18
 of silver from gold ores 1223, 1232
 of silver from tin ores 1232
 Extrusion dies 1374
 Exudatinitite 194

F

Faber du Faur furnace 613
 Factors influencing recycling 385
 Falcondo ferronickel process 458
 Faraday's law 989, 1050
 Fatty alcohol sulfates 1031
 Fatty amines 1008
 Fehling's solution 568
 Feldspar 2202
 Felsparazit 1912
 Ferberite 462, 1334
 Fergusonites 1405, 1419, 1698
 Ferric alums 148
 Ferric arsenate precipitates 165
 Ferric chloride 148, 150
 Ferric compounds 147
 Ferric ion hydrolysis 166
 Ferric molybdate 1384
 Ferric oxide 50
 Ferricyanide complex 148
 Ferrimagnetic γ -Fe₂O₃ 173

Ferrimagnetic iron oxide 185
 Ferrimolybdate 1363
 Ferrite-based permanent magnets 40
 Ferrites 177
 Ferritungstite 1333
 Ferroalloy metals 3, 12
 Ferroalloys 404
 Ferroboron 404, 414, 465
 Ferrocromium 404, 438, 449, 450, 1769
 by Perrin process 447
 by Simplex process 447
 consumption 453
 dust emissions 454
 Ferrocolumbium, see *Ferroniobium*
 Ferrocyanides 148
 Ferroelectric materials 2048
 Ferroelectric perovskites 1409
 Ferroelectric single crystals 1424
 Ferromanganese 404, 420, 1814, 1835
 distillation 1827
 electric arc furnaces 430
 Ferromolybdenum 404, 412, 414, 477, 1493
 Ferronickel 32, 404, 454, 758, 760, 762
 refining 459
 smelting 770
 Ferroniobium 404, 414, 472, 1405, 1413
 Ferroniobiumtantalum 404
 Ferrophos 189
 Ferrophosphorus 404, 460
 Ferroselenium 404
 Ferrosilicochromium 404, 439, 449, 451
 Ferrosilicomanganese 404
 Ferrosilicon 404, 415, 993, 995, 1890
 Ferrosilicon-aluminum alloy 481
 Ferrosilicon-titanium alloys 474
 Ferrosilicozirconium 404
 Ferrotitanium 404, 414, 473
 Ferrotitanium-silicon 475
 Ferrotungsten 404, 412, 414, 460
 carbothermic production 464
 composition 461
 from scheelite 465
 Ferrous carbonate 164
 Ferrous chloride 153
 Ferrous compounds 147
 Ferrous halides 147
 Ferrous hydroxide 147
 Ferrous ion oxidation 165
 Ferrous metals 1
 Ferrous oxalate 162
 Ferrous oxide 162
 Ferrous sulfate 147
 Ferrous sulfide 33, 147
 Ferrovanadium 404, 414, 476, 1477, 1486
 Ferroxyhite 1830

Ferrozirconium 404
Ferrum 31
 Fertilizers 12, 13, 149, 1024
 for acidic soil 2203
 for vines 184
 Feuerstein 1912
 Fick's law 300
 Fillers 1096, 1921, 1922, 1931
 Film coatings 361
 Findlingsquarzit 1912
 Fior process 116
 Fire assay 1203
 Fire extinguisher powders 2204
 Fire refining 529
 Fire retardants 6, 2203
 Fireclay 1916
 Fire-resistant ceramic products 1116
 Fisan silver powder 1252
 Fischer-Tropsch synthesis 946
 Fission 11
 Fixed carbon 218
 Flake zinc pigments 679
 Flame hydrolysis 1954
 Flame retardants 840, 1025, 1033
 Flash calciner 1086
 Flash converting 521
 Flash evaporation 1088
 Flash smelting 730
 Flash smelting furnaces 505
 Flat set 530
 Flints 1733, 1912
 Float-zone crystal growth 1871
 Flocculant 1079
 Flocculating agents 152, 153
 Flotation 24, 40, 207, 1190, 2154, 2174
 equipment 2177
 of kieserite 1031
 of potash ores 2179
 of potassium chloride 2176
 of primary tin ores 688
 Flue dust 55
 Flue gas desulfurization 2126, 2275
 Fluid dynamics in Al cell 1052
 Fluid-bed dry scrubbing 1094
 Fluidized-bed
 electrolysis 905
 processes 115, 646
 reactors 505, 725
 regeneration of pickling solution 168
 Fluoboric acid 613
 Fluorapatite 13
 Fluorescent macerals 194
 Fluorescent materials 871
 Fluorescent tubes 1346
 Fluoride in drinking water 1099

Fluoride-crystallization 170
 Fluorinating agents 941
 Fluorination catalysts 1424
 Fluorinite 194
 Fluoroanhydrite 2290
 Fluoroborates 1997
 Fluoroboric acid 1995, 1996, 1997
 Fluorobromosilicon hydrides 1894
 Fluorocarbon compounds 1050
 Fluorosilicate fusion of zircon 1436
 Fluorotitanates 1172
 Fluorspar 687
 Fluosilicic acid 613
 Flux for welding 663
 Fluxes 409
 Fly ashes 1473
 Foamers 2175
 Foil 18
 Forging dies 1374
 Formation
 of intermetallic compounds 410
 of magnetite 518
 of silicon carbide 418
 of whiskers 50
 Formic acid 2126
 Forsterite 983, 1015, 1027
 Foundry iron 140
 Foundry technology 1923
 Fountain pen nibs 1278
 Fractional crystallization 1055, 1710
 Francevillite 1472
 Francium 12, 1592
 Franckeite 686
 Frank-Caro process 2317
 Franklinite 645
 Free energy change
 in oxide formation 407
 in reduction of oxides by aluminum 408
 in reduction of oxides by silicon 408
 Free flow agents 1961
 Freibergite 1221
 Freieslebenite 1221
 Frequency doublers 1409, 1424
 Frequency filters 1424
 Friction igniters 1733
 Friedel-Crafts catalyst 1113
 Friedel-Crafts syntheses 152, 1111
 Fuel element cans 1413
 Fuel injection in blast furnace 62
 Fulminating gold 1200, 1201
 Fulminating silver 1248
 Fungicides 6, 184, 546, 666
 Fungurai 572
 Fused alumina 1101

Fused barium sulfide 670
 Fused magnesia 1026
 Fused magnesium oxide 1026
 Fused zircon sand 1028
 Fused-salt electrolysis 1725, 1745
 Fusible alloys 845, 858
 Fusible indium alloys 1538
 Fusinite 195
 Fusion of baddeleyite 1437

G

Gabbro 1070
 Gadolinite 1697
 Gadolinium 12
 Galena 584
 Galfan 355
 Gallium 10, 25, 846, 1069, 1523
 content of Al_2O_3 1084
 Gallium alkyls 1530
 Gallium alum 1106
 Gallium arsenide 815, 837
 Gallium bromide 1528
 Gallium(II) chloride 1529
 Gallium(III) chloride 1528
 Gallium fluoride 1528
 Gallium hydride 1530
 Gallium hydroxide 1529
 Gallium iodide 1528
 Gallium nitrate 1529
 Gallium nitride 1529
 Gallium oxide hydrate 1529
 Gallium(III) oxide 1529
 Gallium sulfate 1529
 Gallium(II) sulfide 1529
 Gallium triethyl 1530
 Galvalume 355
 Galvanizing 643, 661, 668
 Galvanizing baths 666
 Galvannealed 355
 Gamma-ray spectroscopy detectors 1515
 Ganister 1911, 1912
 Garnet 1656
 Garnierite 719, 758
 Gas cleaning 437
 Gas discharge lamps 1346
 Gas sensors 1312
 Gas turbine 5
 Gas turbine components 473
 Gaseous products in coal pyrolysis 240
 Gaseous SiO 418
 Gasification of coal 210
 Gasoline additives 4, 620
 Gaylussite 2106

Gécamines process 932
 Gelatinous aluminum hydroxide 1097
 Gemstones 961, 1921
 Genesis of bauxites 1070
 Geology of potash deposits 2146
 German cupe 1228
 German Salt Museum 2074
 German silver 4, 5, 1253
 Germanates 1507, 1517
 Germane 1518
 Germanic acid 1517
 Germanides 1507
 Germanite 1507, 1524
 Germanium 10, 654, 846, 1505
 Germanium(II) bromide 1518
 Germanium(II) chloride 1518
 Germanium dioxide 1506, 1517
 Germanium disulfide 1507, 1517
 Germanium halides 1507
 Germanium(IV) halides 1516
 Germanium hydrides 1515, 1518, 1519
 Germanium(II) iodide 1518
 Germanium monoxide 1506
 Germanium organometallic compounds 1507
 Germanium(II) oxide 1518
 Germanium oxychloride 1516
 Germanium selenides 1518
 Germanium(IV) sulfate 1517
 Germanium(II) sulfide 1518
 Germanium tetrabromide 1517
 Germanium tetrachloride 1516
 Germanium tetrafluoride 1516
 Germanium tetraiodide 1517
 Gersdorffite 719, 797, 928
 Geyserite 1912
 Gibbsite 1062, 1063, 1068, 1072, 1074, 1109
 Gibbsite bauxite 1075
 Gilding 1188, 1208
 Gittinsite 1434
 Glaserite 2122, 2145, 2154, 2161, 2195
 Glass crystallization method 189
 Glass industry 815, 1033, 1308, 2203
 Glasses 943, 1551, 1923
 Glass-melting furnaces 1375
 Glauber's salt 2122, 2145, 2162
 Glauberite 2122, 2127, 2145
 Glauconite 928
 Glazes 663, 1923
 Glue 704
 Goethite 171, 172, 190, 719, 767, 1069, 1084, 1830
 Goethite process 655
 Gold 8, 18, 1183, 1280
 alloys 1202, 1204
 amalgam 909

bronze pigments 572
 coins 1204
 compounds 1199
 deposits 1188
 foil 906
 in electronics 1207
 in medicine 1186
 leaf 1209
 plating 1207
 recovery from surface-coated materials 1198
 recovery from sweeps 1197
 refining 1194
 separation from silver 1185
 solders 1205
 Gold(I) acetylide 1202
 Gold aurates 1187
 Gold(I) chloride 1202
 Gold(III) chloride 1202
 Gold(I) complexes of diphosphines 1202
 Gold(I) cyanide 1202
 Gold(III) hydroxide 1200-1202
 Gold malate 1202
 Gold mercaptides 1202
 Gold(III) oxide 1202
 Gold ruby glass 1201
 Gold(III) selenate 1202
 Gold sulfides 1202
 Gold sulforesinates 1202
 Gold thiosulfate 1202
 Gold-copper alloys 1197, 1207
 Gold-copper-nickel alloys 1207
 Gold-germanium alloys 1207
 Gold-manganese alloys 1207
 Gold-nickel alloys 1207
 Gold-palladium alloys 1207
 Gold-palladium gauze 1209
 Gold-platinum alloys 1208
 Gold-rich alloys 1197
 Gold-silicon alloys 1207
 Gold-silver alloys 1197, 1284
 Gold-silver-copper alloys 1202, 1207
 Gold-silver-palladium alloy 1208
 Gold-tin alloys 1207
 Gossan 36
 Grades of titanium 1131
 Granular quartz 1917, 1920
 Granulated kieserite 1031
 Granulated potassium chloride 2187
 Graphex 2031
 Graphite 101
 Graphite retorts 675
 Gravity concentration 1189
 Gravity separators 40
 Gray iron 341
 Gray tin 684

Great Salt Lake 2153
 Green vitriol 149
 Greenockite 870
 Grey cast iron 2, 146
 Grignard reagents 915, 1003, 1009
 Grignard syntheses 998, 1000
 Grinding aluminum powder 1122
 Grindstones 1012
 Growth rate 16
 Guignet's green 1778
 Gummite 1606
 Gutzeit arsenic test 814
 Gypsum 13, 656, 2145, 2281
 Gypsum dehydration 2285
 Gypsum plaster 2305

H

Hafnium 10, 1000, 1459
 electrowinning 1464
 metal powder 1465
 production 1461
 Hafnium boride 1467
 Hafnium carbide 1466, 1467
 Hafnium dichloride oxide 1467
 Hafnium hydride 1468
 Hafnium hydrous oxide 1460
 Hafnium iodide 1464
 Hafnium nitride 1468
 Hafnium oxide 1466, 1468
 Hafnium tetrabromide 1468, 1469
 Hafnium tetrachloride 1466, 1467, 1469
 Hafnium tetrafluoride 1467
 Hafnium tetrahydroborate 1467
 Hafnium-free zirconium 1431, 1462
 Hafnium-zirconium alloys 1466
 Halite 2145, 2174
 Halkyn process 603
 Hall generators 1539
 Hall-Héroult cell 1046, 1072
 Haloantimonates 837
 Halogen lamps 1346
 Halogenosilanes 1886
 Halostannates(IV) 710
 Halox Zinc Phosphate 678
 Hanksite 2106, 2122
 Hard coal 220
 Hard metal alloys 936
 Hard metals 1345, 1355
 Hargreaves process 2129, 2192
 Harlake process 559
 Harris process 604, 607, 832
 Hastelloys 1301
 Hatchite 1544
 Hausmannite 1815

Hazlett casting system 531
 Hazelwoodite 32, 719
 Heap leaching 526
 Heat balance in Al cell 1051
 Heat economy system 100
 Heat treatment of beryl 961
 Heating elements 1346
 Heats of formation
 of compound oxides 410
 of intermetallic compounds 410
 of oxides 407
 Heat-storage medium 1023
 Heat-transfer medium 2069
 Heavy-media separation 2182
 Hectrite 2034
 Hematite 33, 166, 171, 172, 1084
 Hematite enrichments 37
 Hematite iron 140
 Hematite process 656
 Hematite-quartzite ores 38
 Hematological effects of lead 625
 Hemimorphite 644
 Henry's law 497
 Heraklith 1024
 Herbicides 6, 815
 Hercynite 1764
 Herzenbergite 686
 Hessite 1221
 Heterocyclic sulfur compounds 205
 Heterogenite 928
 Heteropolymolybdates 1382, 1383
 Heteropolytungstates 1351
 Heucophos 678, 1121
 Hexacarbonylchromium 1792
 Hexachlorodisilane 1892
 Hexachlorodisiloxane 1893
 Hexachloroiridic(IV) acid 1304
 Hexachloroplatinates 1299, 1302
 Hexachloroplatinic(IV) acid 1301, 1314
 Hexachlororhodic(III) acid 1303
 Hexachlororuthenate(III) 1295
 Hexachlororuthenic(III) acid 1314
 Hexachlorosilane 1885
 Hexachlorozirconates 1448
 Hexacyanocobaltates(III) 939
 Hexagonal ferrites 188
 Hexahydroxyantimonates 839
 Hexamethylenetetramine 1005
 Hexamethylenimine 2202
 Hexanitritocobaltates(III) 939
 Hexavalent chromium compounds 1796
 Heyrowski reaction 364
 Hieber reaction 154
 Higgins column 1615

Higgins furnace 1027
 High-carbon ferrochromium 438, 442
 High-carbon ferromanganese 423
 High-intensity dry magnetic separators 40
 High-purity aluminum 1054
 High-purity arsenic 806
 High-purity magnesium 999
 High-purity quartz 1920
 High-purity tungsten 1348
 High-speed steels 461, 1345
 High-temperature alloys 4, 936
 High-temperature electrolysis 1313
 High-temperature steels 369, 1345
 High-tungsten tin concentrates 695
 High-vacuum distillation furnace 1672
 Himsley column 1615
 Hismelt process 131
 Hispacil 1947
 Hispafos 678
 Hoboken converter 519, 520
 Hofmann-Sand reaction 915
 Höganas process 114
 Holmium 12
 Horizontal crystallizer 2172
 Horizontal retorts 649
 Horizontal strand casting 333
 Hornstein 1912
 Hot blast stoves 102
 Hot metal 52, 283
 Hot pressing 968
 Hot-dip coating 351
 Hot-metal mixer 52
 Howlite 1987
 HSLA steels 471, 473
 Hübnerite 462, 1334
 Hulsite 686
 Humboldt continuous copper refining 531
 Humic acids 1085
 Humphreys' spiral 40
 Hunter process 1162, 2057, 2068
 Huntite 1004, 1014
 Hutchinsonite 1544
 Huttonite 1655
 Hybinette process 746
 Hydrargillite 1062, 1063, 1110
 Hydrate isomerism 1783
 Hydrated chromium(III) oxide 1778
 Hydrated iron oxides 33
 Hydrated manganite 1839
 Hydrated tantalum oxide 1424
 Hydrazine 1283
 Hydroboracite 1987
 Hydroboration 2000
 Hydrobromic acid 1287

Hydrocassiterite 686
 Hydrochloric acid by-product 1019
 Hydrochloric acid pickling solutions 168
 Hydrochloric acid-bromine mixtures 1286
 Hydrochloric acid-chlorine mixtures 1286
 Hydrochlorination of ethanol 665
 Hydrocyclones 41
 Hydrofluoric acid 1423
 Hydrofluoric acid pickling solutions 169
 Hydrofluorination 1623
 Hydrogen 241
 in coal 205
 overvoltage 659
 storage 1752
 Hydrogen attack 372
 Hydrogen chloride dehydration 987
 Hydrogen chloride process 1093
 Hydrogen cyanide 55
 Hydrogen embrittlement 367
 Hydrogen fluoride 1057
 Hydrogen fluoride adsorption 1094
 Hydrogen peroxide production 1099
 Hydrogen reduction 757
 Hydrogen selenide 885, 1563, 1567
 Hydrogen sulfide 739, 765
 Hydrogen telluride 1576, 1579
 Hydrogenation 1385
 Hydrogen-induced cracking 364
 Hydrogenolysis 1385
 Hydrolysis
 of ferric ion 166
 of titanium sulfate 1142
 of trichlorosilane 1897
 Hydromagnesite 1014
 Hydrometallurgy
 of copper 525
 of nickel concentrates and mattes 737
 of nickel oxide ores 763
 of zinc 652
 Hydrophobic agent 1116
 Hydropyrolysis 247, 254
 Hydrosulfit 2242
 Hydrothermal barium ferrite 189
 Hydrothermal crystallization 177
 Hydrothermal growth of quartz 1923
 Hydrothermal reactions 1189
 Hydrothermal reactor 186
 Hydrothermal solubility of quartz in water 1908
 Hydrous ferric oxide 148
 Hydrous zirconium oxide 1447, 1462
 Hydrox 572
 Hydroxylamine 2126
 Hydroxylated colloidal silica 1935
 Hydroxyquinolines 1536
 Hydrozincite 645

HyL process 114

I

Iceland spar 2254
 Idiomorphic quartz 1917
 IG Farben cell 990
 IG Farben process 984
 Ilmenite 33, 34, 103, 149, 474, 1134, 1136, 1172, 1444, 1656
 Ilsemanite 1363
 Imperial smelting process 585, 595, 650, 871
 Import and export of pig iron 141
 Impurities in ferronickel 459
 Impurities in the electrolyte 659
 In situ leaching 500, 526
 Incandescent lamps 1346
 Incandescent mantles 1743
 Incendiary bombs 415
 Inclusions by deoxidation 322
 INCO flash smelting 515
 INCO matte separation 735
 Increased blast temperature 61
 Inderite 1987
 Indian laterite ore 41
 Indium 10, 808, 1531
 Indium alum 1106
 Indium antimonide 1538
 Indium arsenides 815, 1538
 Indium dichloride 1537
 Indium hydroxide 1537
 Indium orthoborate 1537
 Indium oxides 1537
 Indium phosphide 1538
 Indium trichloride 1537
 Induction furnace 476
 Induction furnace linings 1028
 Industrial alumina 1095
 Inertinite 193, 194
 Information processing 1207
 Infrared detectors 6
 Ingot casting 323
 Ingot killed steel 327
 Ingot steel 280
 Inks 149
 Inquartation 1185, 1194, 1197
 Inred process 126
 Insecticides 6, 546, 815
 Inspiration converter 519, 520
 Insulating material 1027
 Insulators 1931
 Intercalation compounds 2158
 Interdendritic microsegregation 320
 Intergranular attack 1442
 Intermediate-frequency filters 1424

Intermetallic compounds 702, 837
 Internal silanols 1936
 International Bauxite Association 1090
 International Copper Association 19
 International Copper Research Association 545
 International Lead-Zinc Research Organization 19
 Inyoite 1987
 Iodargyrite 1221
 Iodite 1221
 Ion exchange 470, 527, 657, 873, 1340, 1462, 1614, 2039, 2196, 2202
 Ion exchange chromatography 1289
 Ion-exchange membranes 1200
 Ion-exchange resin for spent pickling solution 171
 Ion exchange with chelating agents 1711
 Ion exchangers 905, 1259, 1494
 Ion plating 1255
 Ionic structure of molten cryolite 1048
 Ionium 1650
 Iridium 1280
 compounds 1304
 purification 1298
 Iridium alum 1106
 Iridium(III) chloride 1304
 α -Iron
 Curie temperature 376
 lattice constant 375
 Iron
 allotropic forms 143
 atomic volume 373
 cast 341
 cast, alloyed 342
 cast, white 342
 cast, with vermicular graphite 342
 complex compounds 148
 compounds 147
 for treatment of anemia 161
 solid-state reactions 173
 compressibility 374
 elastic properties 374
 electrical properties 375
 expansion coefficient 373
 from ilmenite 103
 from pyrite cinder 102
 gray 341
 magnetic properties 374
 malleable 342
 meteoric 274
 molar heat capacity 373
 native 274
 ores 53
 Osemund 276
 oxidation 368
 pure 372
 removal 743
 specific heat capacity 373
 spheroidal graphite cast 341

sponge 283, 286
 sulfidation 370
 tellurian 274
 thermal conductivity 375
 Iron acetates 160
 Iron alum 1106
 Iron(III) ammonium citrate 160, 161
 Iron(II) ammonium oxalate 143
 Iron(II) ammonium sulfate 149
 Iron(III) arsenate 691
 Iron blast furnace 57
 Iron blue pigments 179, 181
 Iron(III) bromide 160
 Iron carbide process 116
 Iron(II) carbonate 160
 Iron carbonyl 143, 153, 752
 as antiknock agent 154
 hydride 154
 oxidation 158
 Iron chloride in water treatment 152
 Iron(II) chloride 153
 Iron(III) chloride 150
 as a chlorinating agent 152
 hexahydrate 151
 solution 161
 Iron chlorosulfate 152
 Iron chromates 1791
 Iron citrates 160
 Iron content of Al_2O_3 1084
 Iron dextran 161
 Iron disulfide 34
 Iron(III) fluoride 160
 Iron(II) fumarate 161
 Iron(II) gluconate 161
 Iron halides 160
 Iron hexacyanoferrate(II) 1104
 Iron(II) hexacyanoferrate(II) 179
 Iron(II) hydrogen carbonate 33
 Iron(II) hydroxide 162
 Iron(III) hydroxide 162, 748
 Iron(III) maltol 162
 Iron monosulfide 33
 Iron nitrates 160
 Iron ore beneficiation 39
 Iron ore production 36, 138
 Iron ore reserves 36
 Iron ore sinters 47
 Iron oxide as an extender 678
 Iron oxide hydroxide 163
 Iron oxide magnetic pigments 185
 Iron oxide pigments 150, 171, 173
 Iron oxide reduction 49
 Iron(III) oxide hydrate 33
 Iron(III) oxide pigments 152

Iron oxide-mica pigment 189
 Iron passivation 1805
 Iron(II) phosphate 144
 Iron phosphide 189
 Iron(II) phthalocyanine 161
 Iron pigments 149
 Iron silicides 416
 γ -Iron solid solutions 376
 Iron sorbital 161
 Iron(II) succinate 161
 Iron sulfate 1142
 Iron(II) sulfate 149, 161, 1147
 Iron(III) sulfate 150
 alums 150
 Iron(II) sulfide 33
 Iron technical varieties 146
 Iron(II) titanate 1172
 Iron whiskers 158
 Iron-boron alloy 465
 Iron-carbon alloys 145
 Iron-free aluminum sulfate 1096
 Iron-nitrogen compounds 144
 Irradiation of silanes 1886
 Isasmelt process 597, 600
 Ishizuka cell 992
 Isomerization 1385, 2157
 Isopolymolybdates 1382
 Isopolytungstates 1351
 Isopropyl borate 2159
 Isopropylamine 2200
 Isotope separation 2043
 Isotropic exchange 1385
 Itabirite 35, 37, 38

J

Jacobsite 1815
 Jamesonite 584, 825
 Jarosite process 654, 742
 Jasper 1912
 Jet aircraft 5
 Jet engine 7
 Jewelry 8, 1307
 Jewelry gold 1204
 Jigs 206
 Jollivet-Penarroya process 610
 Jordisite 1363
 Josephinite 32

K

Kainite 983, 1007, 1024, 1030, 2144, 2145, 2154, 2161, 2175, 2191
 Kaldo converter 520, 699
 Kalifornschungs-Institut 2160

Kalium 2142
 Kalsilite 1902
 Kaolinite 34, 1070, 1091, 1119
 Kaolinitic sandstones 1070
 Karst bauxites 1070
 Kauritil 572
 Kawasaki process 130
 Keatite 1905, 1909
 Kelex 100 1536
 Kermesite 825, 839
 Kernite 1987, 2010, 2059
 Kieselguhr 1912, 1925, 1927, 1928
 Kieselschiefer 1912
 Kieserite 983, 1006, 1007, 1019, 1024, 1030, 1034, 2145, 2152, 2165, 2174, 2175, 2193
 electrostatic separation 1031
 flotation 1031
 in fertilizers 1033
 solubility 1030, 2165
 Killed steel 325
 Kinetics of heterogeneous reactions 299
 Kinetics of precipitation 1081
 Kinglor-Metor process 114
 Kiss process 1218
 Kittquartzit 1912
 KIVCET cyclone smelting 516, 597, 598
 Klystron 1374
 Kobold 925
 Kocide 101 572
 Koehlinite 1363
 Koenerite 2145
 Kolm 1607
 Konite 2242
 Kowa-Seiko process 103
 Kroll process 991, 1000, 1162, 1439, 1463, 1464, 1672, 2057
 Kroll-Betterton process 604, 851, 2252
 Krupp Codir process 119
 Krupp-Renn process 758
 Kryptomaceral 193
 KS process 306
 Kunzite 2033
 Kupfer Nickel 716
 K-White 1121

L

Lacquers 1772
 Lactose 1031
 Ladle furnace 315
 Lambda probes 1312
 Lamellar silicates 1015
 Langbeinite 983, 1006, 1007, 1030, 1034, 2145, 2152-2154, 2175, 2194, 2212
 Lange-Mond process 753

- Lansfordite 1003
- Lanthanide contraction 1701
- Lanthanides 12, 18, 1695, 1700
- Lanthanum 12, 1749
- Lanthanum borate glasses 1424
- Lapis lazuli 1116
- Lapis magnes* 1813
- Lascas 1919, 1920
- Laser beam welding 1344
- Laser diodes 1539
- Laser isotope separation 1631
- Laser technology 1346
- Lasers 6
- Laterite 33
- Lateritic deposits 929
- Lattice constant of α -iron 375
- Laux process 173, 176
- Laves phases 1482
- Law of supply and demand 18
- Lawrencite 153
- Le Blanc process 2115, 2131, 2202
- Leaching 526
 - of chalcopyrite 152
 - of oxidic zinc ores 660
- Lead 5, 18
 - alloys 620, 627
 - anode 872
 - anode slime 853, 1229
 - as a condensing liquid 651
 - batteries 618
 - compounds 628
 - cupellation 1217
 - emissions 624
 - from scrap 615
 - in blood 625
 - in teeth 626
 - in urine 626
 - isotopes 582
 - minerals 584
 - ore reserves 584
 - pigments 635
 - poisoning 626, 634
 - powder 635
 - salts 628, 632
 - smelter flue dust 808
 - softening 607
 - statistics 621
- Lead acetates 628
- Lead alkyls 154
- Lead arsenate 813, 820
- Lead bisilicate 632
- Lead blast furnace 591
- Lead bromide 630
- Lead bullion 594, 598, 1235
 - refining 603
- Lead carbonate 629
- Lead chloride 630
- Lead chromate 1791
- Lead cyanamide 635
- Lead debismuthizing 2252
- Lead Development Association 618
- Lead fluoride 630
- Lead fluosilicate 614
- Lead furnace slags 645
- Lead glass 619
- Lead halides 630
- Lead iodide 630
- Lead monosilicate 632
- Lead oxides 630, 631, 632, 1227
- Lead silicates 632
- Lead silicochromate 1806
- Lead sulfates 632
- Lead tetraacetate 629
- Lead tin telluride 1579
- Lead vanadates 1473
- Lead Zinc Study Group 618
- Lead-antimony anodes 527
- Lead-bearing dust 624
- Lead-copper matte 807
- Lead-sodium alloy 2059
- Lead-tin coatings 359
- Leather industry 1772
- Leavening agent 2203
- Lechâtellierite 1910
- Lechâtellierites 1911
- Ledeburite 145
- Ledge 1047
- Leonardite 1030
- Leonite 1030, 2145, 2161, 2194
- Lepidocrocite 153, 163, 171, 1830
- Lepidocrocite structure 175
- Lepidolite 687, 2033, 2034, 2036, 2039, 2212
- Les Baux 1044, 1068
- Leucoxene 474, 1134, 1136, 1444
- Lewatit M 500 1199
- Liberation curves of sylvinitic ores 2150
- Light metals 3, 6, 13
- Lighter flints 1751
- Lighting industries 1346, 1374
- Lignites 200, 203
- Lignitic coal 199
- Lignosulfonates 216
- Lime 288, 2252
- Lime fusion of zircon 1437
- Lime kilns 2264
- Lime slaking 2109
- Lime/soda sinter process 1092
- Limestone 13, 54, 2252
- Limestone calcination 2109
- Limonite 33, 34

- Lindgrenite 1363
 - Linnærite 928
 - Linz-Donawitz converter 303
 - Lipowitz's alloy 875
 - Liptinite 193, 195
 - Liptinite macerals 194
 - Liquation 604, 703, 826, 1217
 - Liquefaction of coal 210
 - Liquid crystal 1539
 - Liquid-liquid extraction, see *Solvent extraction*
 - Liquid-phase chlorination 1892
 - Litharge 1227
 - Lithiophilite 2033
 - Lithiophorite 2034
 - Lithium 2029
 - alloys 2041, 2043
 - batteries 948
 - compounds 2049
 - isotopes 2042
 - Lithium acetate 2044
 - Lithium aluminate 2036
 - Lithium aluminum hydride 1113
 - Lithium amide 2044
 - Lithium azide 2048
 - Lithium benzoate 2044
 - Lithium borates 2016, 2017, 2020
 - Lithium bromide 2044
 - Lithium carbonate 2035, 2037, 2040, 2044, 2049, 2126
 - Lithium chloride 989, 2041, 2045, 2049
 - Lithium chromate 2046
 - Lithium citrate 2044
 - Lithium double oxides 2048
 - Lithium fluoride 1047, 2046
 - Lithium fluoroborate 1997
 - Lithium hydride 2042, 2046
 - Lithium hydroxide 2047, 2049
 - Lithium hypochlorite 2046
 - Lithium iodide 2047
 - Lithium niobate 1424, 2048
 - Lithium nitrate 2047
 - Lithium nitride 2048
 - Lithium oxide 2045, 2048
 - Lithium perchlorate 2046
 - Lithium peroxide 2048
 - Lithium phosphates 2033, 2048
 - Lithium sodium phosphate 2040
 - Lithium sulfate 2038, 2048
 - Lithium tantalate 1424, 2048
 - Lithium tetraborate 2048
 - Lithium tetrafluoroborate 2046
 - Lithography 149, 1110
 - Lithopone 667, 670, 672
 - Livingstonite 825
 - LIX 26 1536
 - LIX 87 QN 766
 - LIX TN 1911 1296
 - Lixivants 526
 - Local scrap 21
 - Lockalloy 971
 - Locron 1116
 - Lodestone 31
 - Loewite 1030, 2122
 - Logarithmic law 15
 - Löllingite 797, 798, 815
 - Loparite 1698
 - Lorandite 1544
 - Lorentz forces 1052
 - Low-carbon ferrochromium 438, 445
 - Low-carbon ferromanganese 436
 - Löweite 2145
 - Low-grade tin concentrates 692
 - Low-melting alloys 709
 - Lubrication 1386
 - Ludox 1947
 - Lump quartz 1917
 - Lump vein quartz 1920
 - Luppen 758
 - Lurgi-Darvo traveling grate pelletizing process 45
 - Lurgi-Ruhrgas process 251
 - Lutecium 12
 - Luzonite 798
 - Lydit 1912
- M**
- Macerals 192, 200
 - Macrinite 195
 - Macrocrystalline magnesite 1014
 - Macrosegregation 321
 - MagCan process 984, 985
 - Maghemite 33, 172
 - Magnesia 1013
 - Magnesia bricks 1023
 - Magnesia chlorination 984
 - Magnesia graphite bricks 1028
 - Magnesia negra* 1813
 - Magnesia process 2202
 - Magnesia-carbon 101
 - Magnesiochromite 1764
 - Magnesiocarbonate 1015, 1016, 1764
 - Magnesiowüstite 1026
 - Magnesite 13, 983, 1003, 1013, 1014, 1026
 - beneficiation 1014
 - chlorination 984
 - flotation 1015
 - concentrates 1021
 - Magnesium 7, 13, 981
 - batteries 1000
 - compounds 1003

- from seawater 1005
- salts 1002
- Magnesium aluminum silicates 1028
- Magnesium ammonium phosphate 1024
- Magnesium borates 2010
- Magnesium bromide 1007
- Magnesium carbonate 1003, 1014, 2092
- Magnesium chloride 1002, 1003, 1004, 1030, 1144
 - dehydration 984
 - electrolysis 983
 - hydrates 1009
 - purification 1010
 - pyrohydrolysis 1018
- Magnesium fluoride 1047
- Magnesium hydride 1000
- Magnesium hydroxide 1002, 1013, 1014, 1021, 1025, 2090
- Magnesium hydroxide separation 1016
- Magnesium nitrate 1002
- Magnesium oxide 1003, 1013
 - Magnesium oxide electrolysis 983
- Magnesium oxychlorides 1004, 1030
- Magnesium oxysulfates 1030
- Magnesium phosphate 1030
- Magnesium pyroarsenate(V) 812
- Magnesium silicates 1003, 1027
- Magnesium stearate 1030
- Magnesium sulfate 1002, 1007, 1029
- Magnesium sulfate in sugar industry 1033
- Magnesium sulfate-ammine hydrates 1030
- Magnesium sulfite 1030
- Magnesium sulfonates 1025
- Magnesium-based alloys 1000
- Magnesium-zirconium reguli 1444
- Magnetism process 993, 995
- Magnetic alloys 936
- Magnetic concentration 40
- Magnetic cores for electronic components 157
- Magnetic disturbances in Al cell 1052
- Magnetic iron oxides 164
- Magnetic minerals 1138
- Magnetic moments 374, 1703
- Magnetic pigments 153, 185
- Magnetic properties of iron 374
- Magnetic recording materials 173
- Magnetic separation 723, 1016
- Magnetite 33, 34, 148, 162, 166, 172, 802, 1069, 1472
- Magnetite anodes 1198
- Magnetite formation 518
- Magnetization curve 374
- Magnetizing roasting 40
- Magnetoresistive behavior of cobalt 927
- Magnets 6
- Magnox alloys 1000
- Malachite 498
- Malleable cast iron 2, 146
- Malleable iron 146, 342
- Manganese 12
- Manganese acetate 1846
- Manganese(III) acetylacetonate 1856
- Manganese alum 1106
- Manganese borate 1846, 2020
- Manganese(II) carbonate 1846
- Manganese(II) chloride 1846
- Manganese ethylenbis(dithiocarbamate) 1856
- Manganese(III) fluoride 1856
- Manganese hypophosphite 1856
- Manganese(II) nitrate 1847
- Manganese nodules 1828
- Manganese oxide minerals 928
- Manganese(II) oxide 1844
- Manganese(II, III) oxide 1845
- Manganese(III) oxide 1845
- Manganese(IV) oxide 12, 1838
- Manganese(II) phosphates 1847
- Manganese(II) sulfate 1847
- Manganese sulfide 478
- Manganese telluride 1577
- Manganese tungstate 1333
- Manganites 1815, 1839
- Manhattan Project 1711
- Mannheim process 2128, 2191
- Manox Iron Blue 191
- Mansfeld copper schists 1491
- Manufacture of α -FeOOH 175
- Marble 2254
- Marcasite 33
- Marignac process 1425
- Marine nodules 928
- Marine placers 687
- Marl 2254
- Marsh test 840
- Martensite 144, 147
- Mass transfer coefficients 299
- Massive iron-ore deposits 35
- Matt blue 944
- Matte 505, 594, 732
- Matte from laterites 770
- Matthiessen rule 375
- Mazarine blue 944
- McCabe-Thiele method 1714
- Mechanical and thermomechanical plating 1255
- Mechanical flotation cell 2177
- Mechanical properties of copper 494
- Mecklenburg method 1142
- Medical implants 1412
- Medium-carbon ferrochromium 438, 444
- Medium-carbon ferromanganese 434

- Megon process 1724
- Melanophlogite 1904, 1909, 1970
- Melting point of binary alumina slags 409
- Membrane cell caustic evaporation 2098
- Mendosite 1108
- 2-Mercapto-N-(2-naphthyl)acetamide 1305
- Mercury 6, 891
 - alloys 908
 - batteries 895
 - cathode 908, 2066
 - condensation 898
 - density 892
 - distillation 906
 - emissions 904
 - fluorescent tubes 895
 - in food 902
 - in fungi 902
 - in soil 901
 - in the environment 901
 - lamps 6
 - methylation 915
 - production 916
 - purification 906
 - toxicity 917
 - vapor pressure 892
 - viscosity 892
- Mercury(II) acetate 913
- Mercury(II) amidochloride 914
- Mercury(II) bromide 912
- Mercury(I) chloride 904, 907, 911, 918
- Mercury(II) chloride 904, 907, 912
- Mercury(I) cyanide 913
- Mercury(II) fluoride 911
- Mercury(II) iodide 913
- Mercury(I) nitrate 913
- Mercury(II) nitrate 914
- Mercury oxide 907
- Mercury(II) oxide 910
- Mercury oxycyanide 918
- Mercury selenide 1563
- Mercury(I) sulfate 914
- Mercury(II) sulfate 914
- Mercury(II) sulfide 911
- Mercury(I) thiocyanate 913
- Mercury(II) thiocyanate 913
- Mercury-containing antimony ores 833
- Mercury-rich mushrooms 902
- Mercury-selenium residue 898
- Merensky Reef 1271
- Merwinite 1015
- Metacinnabarite 893, 911
- Metal carbonyls 752
- Metal forming 344
- Metal hydrides 1897
- Metal production 15
- Metallex process 1671
- Metallic arsenic 804
- Metallic iron pigments 187
- Metalloenzymes 1376
- Metallothermic processes 480, 983, 993, 999, 1464, 1726
- Metallurgical alumina 1094
- Metallurgical cokes 225
- Metallurgical manganese ores 1817
- Metallurgical silicon 1863
- Metallurgical-grade silicon 1923
- Metal-producing associations 19
- Metal-producing cartels 19
- Metal-slag reactions 294
- Metastannic acid 711
- Metatitanates 1172
- Meteoric iron 31, 274
- Methane 241
- Methanol 1008
- Methionine 2126
- Methyl acetate 149
- Methyl isobutyl ketone 1406, 1418, 1423, 1462
- Methyl isobutyl ketone extraction 1437
- Methylation of mercury 915
- Methylchlorosilanes 1891
- Methylcyclopentadienylmanganese tricarbonyl 1856
- Methylisobutylcarbinol 1366
- Methylmercury 919
- Methylmercury(II) chloride 915
- Methyltrioxorhenium 1499
- Meyerhofferite 1987
- Miargyrite 1221
- Micaceous hematite 33
- Microcrystalline quartz species 1907
- Microcrystalline silver powder 1249
- Microelectronics 1255, 1256
- Microfine TiO_2 1159
- Microlite 1404, 1419
- Microscopic characterization of coal 234
- Microwave resonators 1424
- Midrex process 112, 288
- Milk of lime 2254
- Milk of magnesia 1002
- Mill scale 52
- Miller process 1195, 1197, 1198
- Millerite 719
- Millons reagent 913
- Milori blue 179, 191
- Minamata disease 919
- Mineral matter content of coal 219
- Mineral oils 1473
- Mineral reserves 1224
- Mineral resources 1224
- Mining of potash 2147

- Mintek cell 1194
 Minting silver coins 1251
 Mirabilite 2059, 2122, 2127, 2145
 Mischmetal 1743, 1748
 Mitsubishi process 519, 521
 Mixer-settler 1719
 Moa process 767
 Möbius electrolysis 1241
 Modulators 1409
 Moganite 1904, 1908
 Mohr's salt 147, 149
 Moisture indicator 941
 Molar heat capacity of iron 373
 Molecular sieves 1258
 Molten borates electrolysis 1990
 Molten salt
 distillation 1461
 electrolysis 1461
 electrolytic cell 2061
 Molybdates 1382
 Molybdenite 10, 24, 1361, 1363, 1491, 1492
 Molybdenum 9, 1361, 1589
 aqueous chemistry 1377
 by powder metallurgy 1372
 catalysts 1384
 concentrates 478
 metal powder 1371
 toxicity 1376
 Molybdenum blues 1379
 Molybdenum carbide 478
 Molybdenum(II) chloride 1381
 Molybdenum dioxide 1371, 1379
 Molybdenum disulfide 1376, 1379, 1380
 Molybdenum hexacarbonyl 1383, 1384
 Molybdenum hexafluoride 1376, 1381
 Molybdenum oxide 412, 479
 Molybdenum oxide bronzes 1379
 Molybdenum pentachloride 1376, 1381, 1383
 Molybdenum red, see *Molybdenum dioxide*
 Molybdenum selenide 1379
 Molybdenum sesquisulfide 1380
 Molybdenum telluride 1379
 Molybdenum trioxide 478, 1378
 Molybdenum trisulfide 1370, 1380
 Molybdenum-containing catalysts 1369
 Molybdophosphoric acid 1379
 Molycorp process 1723
 Monazite 1607, 1655, 1697, 1707, 1744
 Monocalcium cyanamide 2318
 Monocrystalline silicon 1880
 Monodisperse silica sols 1944
 Monogal 355
 Monohalide distillation 1053
 Monosilane 1884, 1886
 Monovalent aluminum 1042
 Monovalent mercury 910
 Montebrasite 2033
 Monticellite 1015, 1027
 Montmorillonite 45
 Montroseite 1472, 1475
 MOR process 435
 Mordant in dyeing 1105
 Mordants 546
 Mortars 2275
 Mosaic gold 711
 Mottramite 1472
 Müller-Kühne process 2307
 Mullite 103
 Multicrystalline silicon 1881
 Multilayer capacitors 1312
 Multiple-hearth furnace 504, 725, 896, 1367
 Muskovite 34
- N**
 NaK alloy 12, 2157
 Nalcoag 1947
 β -Naphthol 704
 Naphthol 2126
 National Lead Industries process 987, 1008
 Native
 antimony 825
 arsenic 796, 797
 bismuth 846
 copper 498
 iron 31, 274
 silver 1221
 tellurium 1572
 tin 686
 Natrium 2054
 Natron 2106
 Natural iron oxide pigments 172
 Natural manganese dioxide 1838
 Naumannite 1559
 Needle-shaped γ -Fe₂O₃ 178, 186
 Neodymium 12, 1749
 Nepheline decomposition 2202
 Nephelines 1092, 2116, 2212
 Neptunium 11
 Nesquehonite 1003, 1030
 Neurological effects 625
 Neutral leaching 653
 Neutralization of ammonium alum 1097
 Neutrino 1587
 Neutron 1587
 absorbers 1645
 absorption 1700
 capture 1736
 monochromators 968
 New Caledonian ores 454

- New Jersey process 649
 Niccolite 716, 719, 797, 815
 Nichrome 5
 Nickel 4, 18, 715, 1370
 alloys 775
 catalysts 772, 775
 coinage 773
 commercial forms 771
 complexes 780
 consumption 772
 electroplating 775
 electrorefining 746
 electrowinning 741, 743, 750
 laterite ores 759
 laterite process 760, 765, 770
 matte anodes 747
 matte from oxide ores 762
 smelting 732
 Nickel(II) acetate 782
 Nickel(II) acetylacetonate 782
 Nickel(II) amidosulfate 775
 Nickel(II) ammonium sulfate 775
 Nickel arsenide 716
 Nickel boron 469
 Nickel carbonate 748
 Nickel(II) carbonate 775
 Nickel carbonyl 160
 Nickel copper sulfide matte 724
 Nickel Development Institute 19, 773
 Nickel dichloride 777
 Nickel(II) dimethylglyoximate 782
 Nickel(II) formate 782
 Nickel(II) halides 777
 Nickel(II) hydroxide 777
 electrolytic oxidation 741
 Nickel(III) hydroxide 741, 748
 Nickel(II) nitrate 778
 Nickel(II) oxalate 782
 Nickel oxide 737
 Nickel(II) oxide 778
 Nickel rutile yellow 1155
 Nickel sulfamate 775
 Nickel(II) sulfate 779
 Nickel sulfides 779
 roasting 736
 smelting 726
 Nickel tetracarbonyl 718, 752, 780
 Nickel(II) tetrafluoroborate 780
 Nickel-cadmium batteries 775, 873, 874
 Nickel-chromium master alloys 448
 Nickel-cobalt alloys 947
 Nickel-containing manganese nodules 718
 Nickel-copper matte 734
 Nickel-copper-cobalt alloy 933
 Nickeliferous limonite 719, 758
 Nickeliferous pyrrhotite 719
 Nickel-niobium 472
 Nickel-steel armor plate 716
 Nicotine sulfide 704
 Niobium 9, 1403
 Niobium alkoxides 1408
 Niobium borides 1410
 Niobium carbides 1410
 Niobium consumption 1414
 Niobium hydrides 1411
 Niobium nitrides 1410
 Niobium oxide production 1405
 Niobium oxychloride 1409
 Niobium pentachloride 1407, 1409
 reduction 1411
 Niobium pentafluoride 1409
 Niobium pentoxide 1408
 optical-grade 1409
 reduction 1411
 Niobium silicides 1410
 Niobium tetrachloride 1409
 Nippon Steel process 112
 Nippon Yakin Oheyama process 758
 NiS/CoS precipitation 739
 Nitrate reductase 1376
 Nitric acid pickling solutions 169
 Nitride formers 409
 Nitrides 996
 Nitriding 371
 Nitridoactachlorodiaquodiruthenate(IV) 1313
 Nitrobenzene 177
 3-Nitrobenzenesulfonic acid 1187
 4-Nitrobenzoic acid 1187
 Nitrogen oxides 998
 Nitrogenase 1376
 Nitrogen-containing low-carbon ferrochromium 448
 Nitrogen-free operation of blast furnace 62
 α -Nitroso- β -naphthol 657
 NKK process 130
 Nodular chert 1912
 Nodular iron 1000
 Nodularization 1000
 Noise reduction 136
 Non-bronze blue 179
 Noncrystalline silica minerals 1910, 1911
 Nonferrous metals 3
 Noranda process 521, 522
 Nordstrandite 1063, 1064
 Norsk Hydro cell 991
 Norsk Hydro process 986
 Norsk Hydro refining furnace 997
 Novaculite 1912
 Nozzle process 1630
 Nuclear fission 1600

Nuclear reactor 11
 Nuclear safety 1644
 Nuclear technology 1308, 1374
 Nucleation 50, 1081
 Nutritional additives 546
 Nyacol 1947

O

Occidental pyrolysis process 255
 Octacarbonyldicobalt 939
 Odda process 2331
 Oil residues 1479
 Oil shales 1607
 Oklo mine 1600
Old Nick 716
 Oleic acid 40
 Oligodynamic effect 1264
 Olivine 983
 Onor 1806
 Oolitic ironstone 33
 Opal-A 1910
 Opal-A_N 1911
 Opal-C 1911
 Opal-CT 1911
 Opals-A_G 1911
 Open-hearth furnace 1022
 Optical fibers 1892
 Optical materials 1514
 Optical modulators 1424
 Optical switches 1424
 Optical texture of coal 238
 Optical windows 1028
 Optical-grade niobium pentoxide 1409
 Orange iron oxide 175
 Orangite 1655
 Ore beneficiation 2120
 Ore digestion 2120
 Orford process 735
 Organic binders 216
 Organic components of coal 192, 200
 Organic matter in bauxite 1085
 Organic mercury compounds 919
 Organic mercury derivatives 915
 Organic precipitation agents 1289
 Organic sulfur 219
 Organolead compounds 633
 Organolithium compounds 2042
 Organomagnesium compounds 1003
 Organophosphoric acids 1718
 Organosilanes 2229
 Organotin compounds 711, 2068
 Origin of copper ores 498
 Orpiment 795, 797, 813

Orthoclase 34
 Orthoquartzite 1912
 Orthotitanates 1172
 Oscillator quartz 1914
 Oscillators 1424
 Osemund iron 276
 Oslo crystallizer 2173
 Oslo evaporator 2091
 Osmiridium 1276
 Osmium 1280
 Osmium compounds 1304
 Osmium(VIII) oxide 1304, 1310, 1320
 Osmium tetroxide 1300
 Otavite 870
 Outokumpu 597
 ferrochromium process 443
 flash smelting 514
 process 599
 Overvoltage 1050
 Oxalic acid 1195
 Oxidation
 of aluminum 1042
 of As₂O₃ 811
 of carbon steels 368
 of Co²⁺ 937
 of ethylene 1258
 of ferrous ion 165
 of iron 368
 of iron pentacarbonyl 158
 of low-alloy steels 368
 of tetrachlorosilane 1897
 of TiCl₄ 1145
 Oxidation catalyst 1257
 Oxidation potential Ti³⁺/Ti⁴⁺ 1169
 Oxidation-resistant coatings 1374
 Oxo synthesis 1310
 Oxomolybdenum cations 1376
 Oxomolybdenum halides 1382
 Oxygen enrichment 62
 Oxygen flash smelting 734
 Oxygen in coal 205
 Oxygen potentials of oxides 462
 Oxygen sprinkle smelting 512
 Oxygen-blowing processes 302
 Oxygen-blown converter 445
 Oxygen-free copper 540
 Oxygen-releasing compounds 472
 Oxyhydration 1385
 Oxystearic acid 1031

P

Pachuca tank 1225
Pai thung 716
 Paint driers 6
 Paints 1772

Palladium 1280
 ammine complexes 1303
 compounds 1303
 purification 1297
 Palladium(II) chloride 1254, 1303, 1310
 Palladium(II) diamminedinitrite 1313
 Palladium oxides 1303
 Palladium-base alloys 1315
 Pandermite 466, 1987
 Paper industry 1096, 1105, 1110
 Parabolic law 368
 Paris blue 179
 Parkes desilvering 604, 856, 1188, 1217, 1227
 Partial roasting 504
 Partially stabilized zirconias 1446
 Particulate magnesium 998
 Pascoite 1475
 Passivation 365
 Passivation of iron 1805
 Patera process 1225
 Paterite 1363
 Patio process 1225
 Patronite 1472
 Pattinson process 1217, 1226
 Pearlite 145
 Peat 195, 200, 203
 Pedersen process 1092
 Peirce-Smith converters 519, 520, 730, 762
 Pelletizing 41, 44
 Pelletizing of UO₂ 1635
 Pellets 44
 Pen nibs 1207
 Penarroya-Leferrer vacuum distillation 613
 Peniakoff process 2131
 Penniman process 173, 175
 Pentaborane 1999, 2000, 2002
 Pentammine cobalt process 740
 Pentlandite 32, 719, 928, 1277
 Peptization of gels 1943
 Perborate anion 2015
 Perchloric acid 1287
 Percolation leaching 526
 Perenox 572
 Periclase 1013, 1022, 1026
 Peridur 45
 Periodic table 1
 Permalloys 5
 Permanent magnetic materials 377, 1752
 Perovskite 474, 1134, 1136, 1172
 Peroxide ion 164
 Peroxy group 1173
 Peroxyacid 1173
 Peroxytitanates 1173
 Peroxytitanic acid 1173

Peroxytitanyl ions 1173
 Perrhenates 1493, 1496
 Perrhenic acid 1496, 1499
 Pesticides 215
 Petalite 2033, 2036, 2049
 Petrographic studies of coal 204
 Petroleum catalysts 1369
 Petroleum coke 1045
 Petzite 1221
 Pharmaceutical preparations 1096
 Phenakite 961
 Phenanthrene 1057
 Phenol 704
 Phenylmercury 919
 Phonolite 1070
 Phosgenite 584
 Phosphate fertilizers 1460
 Phosphate rock 12, 13, 460, 1524, 1607, 1613
 uranium from 23
 Phosphates 1473
 Phosphatizing 144
 Phosphinal 1121
 Phosphine 419, 668
 Phosphinox 678
 Phosphogypsum 2290
 Phosphomolybdates 1383, 1384
 Phosphonic acids 1718
 Phosphor 1539
 Phosphorodithioates 1383
 Phosphors 1514, 1735
 Phosphorus-containing extractants 1717
 Photochromic glasses 1258
 Photodetectors 1539
 Photoelectric cells 10
 Photographic printing paper 1223
 Photographic sensitizer 1202
 Photographic slimes 1223
 Photography 8, 1258
 Photolithography 1311
 Phototropic glasses 1754
 Phtanite 1912
 Phyllites 1070
 Phyllosilicates 1014
 Pickling 149, 166, 175, 344, 349
 of stainless steel 169
 of titanium 1168
 Picromerite 1030
 Pig iron 1, 54, 137, 146
 import and export 141
 production 139
 Pigment Blue 950
 Pigments 4, 6
 Pilbarite 1655
 Pirot paulite 1544

Pirssonite 2106
 Pitch 216
 Pitchblende 1606
 Pitting corrosion 366
 Plagioclase 34
 Plasma arc remelting 338
 Plasma furnaces 438
 Plasma processes 415, 1631, 1962
 Plasma spraying 1374
 Plasmamelt 124
 Platina 1270
 Plating baths 941
 Platinized titanium anodes 1198
 Platinum 8, 1280
 allergy 1319
 coatings 1314
 coins 1271
 Platinum acetylacetonate 1314
 Platinum chlorides 1302
 Platinum(II) diamminedinitrite 1313
 Platinum group metals
 analysis 1305
 from sulfide ores 1282
 separation 1287
 Platinum metal blacks 1309
 Platinum oxide catalysts 1321
 Platinum oxides 1302
 Platinum rhodium gauze catalysts 1278
 Platinum-arsenic alloy 1270
 Platinum-group metals 1196
 Platinum-iridium alloys 1312
 Platinum-rhenium catalysts 1492
 Platinum-rhodium gauzes 1309
 Plattner process 1187
Plumbum 582
Plumbum cinerum 845
 Plutonium 11, 1685
 Plutonium isotopes 1685
 Plutonium-carbon system 1689
 Pneumatic coarse-grain flotation cell 2178
 Pneumatic free-jet flotation 2177
 Poling 529
 Polishing compounds 1753
 Pollucite 2211, 2216
 Polonides 1592
 Polonium 10, 1585, 1591
 Polonium monoxide 1592
 Poly(aluminum chloride) 1116
 Poly(aluminum hydroxychlorides) 1114
 Poly(phenylene sulfide) 2230
 Polyalcohol 470, 671
 Polyarsenides 815
 Polybasite 1221
 Polycarboxylic acids 1711

Polychlorinated biphenyls 999
 Polychloropolysilanes 1892
 Polydymite 719
 Polygermenes 1516
 Polyhalite 1030, 2090, 2145, 2175, 2286
 Polyhalogenated diphenyl ether 1025
 Polymeric borate anions 2011
 Polymerization 2157
 Polymerization catalysts 945, 1033, 1113
 Polynuclear cobaltamines 938
 Polysulfide ion 1117
 Polysulfides 2222
 Polytitanates 1172
 Polytungstates 1351
 Polyxene 1276
 Potassium continuous production 2155
 Porcelain 663
 Porcellanite 1912
 Pore-size distribution of a silica gel 1951
 Porosil framework structures 1968
 Porosils 1967, 1969
 Porphyry copper ores 10, 24, 1492
 Porter column 1615
 Portland cement 1033, 1090, 2202
 Portlandite 1915
 Positron 1586
 Pot room working conditions 1094
 Potash 2142, 2143
 deposits 2146
 fertilizers 2174
 mining 2147
 ore flotation 2179
 ore treatment 2149
 Potash Research Institute 2160
 Potash-magnesia 2152
 Potassium
 isotopes 12
 radioactive isotope ^{40}K 2184
 sulfate from kainite 2195
 sulfate from KCl and gypsum 2196
 sulfate from KCl and MgSO_4 2193
 sulfate from KCl and Na_2SO_4 2195
 sulfate from langbeinite 2195
 Potassium alkoxides 2158
 Potassium alum 1102, 1106
 Potassium aluminum sulfate 1106
 Potassium 3-aminopropylamide 2158
 Potassium amyl xanthate 1366
 Potassium antimonate 839
 Potassium arsenate(V) 812
 Potassium bases 2158
 Potassium benzoate 2204
 Potassium borates 2020
 Potassium carbonate 12, 2199
 Potassium carbonate hydrate 2202

Potassium chlorate 180
 Potassium chloride 1031, 2077, 2142, 2148, 2154, 2159, 2187
 electrolysis 2198
 flotation 2176
 Potassium chromate 1789
 Potassium chromium(III) sulfate 1785
 Potassium content of Al_2O_3 1084
 Potassium cyanamide 667
 Potassium dichromate 895, 1789
 Potassium dicyanoargentate(I) 1244, 1247
 Potassium dicyanoaurate 1199, 1208
 Potassium disulfite 2234
 Potassium ferrate 2198
 Potassium ferrocyanide 2092
 Potassium fluorogermanate 1516
 Potassium graphite 2158
 Potassium heptafluorotantalate 1421
 Potassium heptafluorotantalate, see *Potassium tantalum fluoride*
 Potassium hexacyanoferrate(II) 179
 Potassium hexafluorohafnate 1467
 Potassium hexafluorotitanate 1165
 Potassium hexafluorozirconate 1449
 Potassium hexahydroxyantimonate 839
 Potassium hexamethyldisilazane 2158
 Potassium hexanitritorhodate(III) 1298
 Potassium hexanitrorhodate(III) 1295
 Potassium hydride 2158
 Potassium hydrogencarbonate 2204
 Potassium hydroxide 2188, 2198
 Potassium manganate(V) 1848
 Potassium manganate(VI) 1848
 Potassium mercury iodide 913
 Potassium metavanadate 1484, 1487
 Potassium nitrite 2198
 Potassium osmate(VI) 1304
 Potassium pentaborate 2017
 Potassium permanganate 1848
 anodic oxidation 1850
 Potassium ruthenate(VI) 1304
 Potassium salts production 2153
 Potassium silicate manufacture 2203
 Potassium sulfate 2152, 2154, 2190
 solubility 2191
 Potassium sulfide 1173
 Potassium superoxide 2159
 Potassium tantalum fluoride 1424
 Potassium tetraborate 2017
 Potassium tetrachloroplatinate(II) 1302
 Potassium tetranitroplatinate(II) 1302, 1313
 Potassium titanate 1173
 Potassium trialkylborohydrides 2159
 Potassium tri-*iso*-propoxyborohydride 2159

Potassium tri-*sec*-amylborohydride 2159
 Potassium tri-*sec*-butylborohydride 2159
 Potassium-hafnium carbonate 1460
 Potassium-sodium alloys 2157
 Pourbaix diagram for copper 496
 Powder metallurgy 1167, 1342, 1372
 Powellite 1333, 1363, 1371
 Praseodymium 12, 1749
 Prebaked anodes 1046
 Precious metals 3, 8
 Precipitated silicas 1962, 1964, 1966
 Precipitation
 by reducing gases 528
 kinetics 1081
 of arsenic 808
 of iron hydroxide 653
 of magnesium hydroxide 1016
 of sodium bicarbonate 2111
 of sylvinit 2169
 with hydrogen sulfide 769
 Precipitation deoxidation 297
 Precision casting 1028
 Preoxidation 230
 Presses 385
 Pressure carbonyl refining process 755
 Pressure electro-slag remelting 338
 Pressure leaching 526
 Pressure leaching of sulfidic zinc concentrates 660
 Pressure operation of blast furnace 62
 Prestaminol 1031
 Pretreatment of used steel products 386
 Prevention of water pollution 136
 Priceite 466, 1987
 Prices of metals 18
 Primary amines 1718
 Printing alloys 5
 Printing industry 1772
 Printing ink industry 182
 Printing inks 1154
 Probertite 1987, 2016
 Processing
 of bauxites 1479
 of copper matte 1237
 of photographic materials for silver 1237
 of titanium sponge 1166
 Production
 of ^{233}U 1675
 of $\alpha\text{-Fe}_2\text{O}_3$ platelets 177
 of anthraquinone 1113
 of benzyl chloride 665
 of butyl rubber 1113
 of ferromanganese in blast furnaces 423
 of hafnium 1461
 of iron oxide pigments 173
 of lead bullion 1226
 of mercury 916

of MgCl_2 from seawater or brines 1007
 of niobium oxide 1405
 of potassium salts 2153
 of titanium sponge 1161
 of UF_6 1625
 Promethium 12, 1588, 1700
 Properties of barium ferrite 189
 Protactinium 10, 1594
 Proustite 797, 1221, 1225
 Proximate analysis 202, 218, 239
 Proximate analysis of coal 202
 Prussian blue 148, 149, 179
 Pseudoboehmite 1064, 1065
 Psilomelane 1815
 Pucherite 863
 Puddled steel 279
 Pure antimony trichloride 836
 Pure iron 3, 143, 372
 Pure molybdenum trioxide 1369
 PUREX process 1588, 1589, 1689
 Purgative 1002
 Purification 1461
 of crude brine 2090
 of crude phosphoric acid 905
 of iridium 1298
 of magnesium chloride 1010
 of mercury 906
 of palladium 1297
 of rhodium 1298
 of TiCl_4 1145, 1161
 of uranium concentrate 1617
 Purofer process 112
 Purple of Cassius 1201
 Putty 2254
 Pyargite 1225
 Pyargyrite 1221
 Pyrite 33, 34, 148, 164, 219, 660, 928, 1069, 1084, 1277, 1364
 Pyrite cinder 53
 analysis 103
 chlorination 2126
 Pyrite films 159
 Pyrochlore 472, 1404, 1418, 1655
 Pyrogenic silica 1944, 1954, 1958, 1959, 1961
 Pyrohydrolysis of magnesium chloride 1018
 Pyrolusite 34, 1815, 1838
 Pyrolysis
 of carboxylates 934
 of coal 211
 of trichlorosilane 1889
 Pyrometallurgical copper production 508
 Pyrometallurgical tin refining 702
 Pyrometallurgy of nickel concentrates 724
 Pyromorphite 584
 Pyrophoric properties 1733
 Pyrophoric properties of flint alloy 1750

Pyrophoric surface layer 1442
 Pyrophyllites 1028
 Pyrostibite 825
 Pyrotechnics 841, 1772
 Pyrrhotite 33, 34, 165, 660, 722, 928

Q

Q-S process 523
 QSL 597
 QSL lead smelting process 601
 Quartz 34, 1069, 1902, 1906, 1916
 Quartz arenite 1912
 Quartz for optical and oscillator devices 1924
 Quartz gravel 1917, 1921
 Quartz powder 1917, 1921
 Quartz raw materials 1917
 Quartz rock 1917, 1921
 Quartz sands 417, 1917, 1920-1925
 Quartz sandstone 1911, 1912
 Quartz single crystals 1912
 Quartz whiskers 1908
 Quartzine 1908, 1911
 Quartzite 467, 1912
 Quaternary ammonium salts 1718
 Quenching 348
 Quicklime 2258

R

Radiation shielding 1643
 Radioactive decay 1587, 1602
 Radioactive metals 3, 10
 Radioactivity 1585
 Radiogardase-Cs 184
 Radiolarite 1912
 Radium 10, 13, 1585, 1593, 1745
 Radon 10, 1593
 Railway-track material 273
 Rammelsbergite 719
 Ramsdellite 1838
 Raney cobalt 947
 Raoult's law 690
 Rare earth complexes 1732
 Rare earths 3, 12, 1695
 carbides 1731
 chalcogenides 1731
 double salts 1728
 halides 1730
 hydrides 1728
 hydroxides 1728
 nitrides 1731
 oxides 1728
 permanent magnetic materials 1733
 peroxides 1728
 separation 1708

Rare-earth bronze 1379
 Raspite 1333
 Rate of dissolution of alumina in the electrolyte 1094
 Reaction of chlorine with scrap iron 151
 Reactive alumina 1101
 Realgar 795, 797, 813
 Recovery
 of $\text{Al}(\text{OH})_3$ 1081
 of alumina from clay 1093
 of ammonia 2113
 of gold from alloys 1197
 Rectifiers 871, 1564
 Recycling 385
 of cadmium 873
 of metals 21
 of steel 381
 of various materials 381
 Red alloy 930
 Red antimony 825
 Red cake 1370
 Red hematite 33
 Red iron oxide 158, 178
 Red lead 632, 635
 Red mercury(II) oxide 911
 Red mud 173, 1088, 1104
 Red ochre 33
 Reducing agents 12, 153, 404
 Reducing power of potassium metal 2142
 Reduction
 degradation index 49
 in electric furnace 698
 in rotary kilns 698
 of aromatic nitro compounds with iron 176
 of beryllium chloride 965
 of beryllium fluoride 965
 of boron trioxide 1989
 of chalcopyrite 509
 of cobalt ions 935
 of iron oxides 49
 of KCl by sodium 2155
 of manganese oxides 993, 1818
 of niobium pentachloride 1411
 of niobium pentoxide 1411
 of noise 132
 of refractory oxides 405
 of ThF_4 1672
 of ThO_2 1669
 of TiCl_4 1160
 with magnesium 1162
 with sodium 1162
 of TiO_2 1162
 by Al 475
 of titanium tetrafluoride 1164
 of tungsten trioxide 1340
 of UF_4 1636
 of UF_6 1635
 of vanadium oxides 476, 1480

 with hydrogen under pressure 739, 742
 Refined arsenic trioxide 803
 Refining 18
 by electrolysis 1185
 of copper 529
 of ferronickel 459
 of lead bullion 603
 of nickel metal anodes 746
 of silver with nitric acid 1240
 of silver with sulfuric acid 1241
 of zinc 652
 Reforming 1100, 1309, 1492, 1498
 catalysts 1284, 1499
 of natural gas 112
 Refractories 7, 9, 943
 Refractory brick in a regenerator 100
 Refractory bricks 1022
 Refractory fibers 1946
 Refractory gold ores 34
 Refractory lining 1027
 Refractory magnesia 1003
 Refractory materials 101, 1013, 1028
 Refractory metals 3, 8
 Refractory silica 1915, 1916
 Regeneration by electrolysis 167
 Regeneration of carbon 1194
 Regeneration of HF-HNO_3 pickling liquors 170-171
 Regeneration of iron-containing pickling baths 166
 Regenerative evaporators 1088
 Reichert cone 40
 Reinforcing fillers 1959
 Relative reducibility 49
 Relays 1256
 Release of hydrogen by platinum metals 1321
 Remelting of copper cathodes 536
 Remelting processes 336
 Removal
 of pyritic sulfur from coal 209
 of vanadium oxychloride 1145
 of vanadium tetrachloride 1145
 Renal effects 625
 Renierite 1507
 Reproduction effects 625
 Residues from zinc electrolysis 645
 Resinite 194
 Resistance thermometry 1311
 Resorcinol 2126
 Retardation process 171
 Retort processes 114
 Reverberatory furnace smelting 727
 Reverberatory furnaces 510, 511
 Reynolds number 300
 Rheniform process 1499
 Rhenium 9, 10, 24, 1491
 compounds 1497

halides 1498
 oxides 1368, 1497
 powder 1495
 recovery 1494
 sulfides 1497
 Rhenium carbonyl 1498
 Rhenium(IV) fluoride 1498
 Rhenium(V) fluoride 1498
 Rhenium(VI) fluoride 1498
 Rhenium(VII) fluoride 1497
 Rhenium heptoxide 1493
 Rhenium(VII) oxide 1496
 Rhenium pentachloride 1498
 Rhenium(VII) sulfide 1497
 Rhodium 1280
 alum 1106
 chlorides 1303
 coatings 1313
 compounds 1303
 purification 1298
 Rhodium sulfate 1304, 1313
 Rhodium(III) iodide 1310
 Rhodochrosite 1815
 Rhodonite 1815
 Rinming steel 324
 Rinneite 2145
 RLE process 529
 Roast reaction 585, 596
 Roasting 503, 826
 of arsenical materials 799
 of nickel sulfide 736
 of siderite ore 41
 Rock salt 2059, 2077, 2089, 2145, 2148
 Rocket nozzles 1346
 Rockwell hydropyrolysis process 256
 Roll cladding 1255
 Rolled steel 281
 Rolling 345
 Roscoelite 1472
 Rotary grinding 967
 Rotary kiln processes 118
 Rotary kiln—electric furnace process 454
 Rotary kilns 896, 1086
 Rubber 6
 Rubidium 2211
 Russel process 1218
 Russellite 1333
 Ruthenium 1280
 Ruthenium(IV) chloride 1304
 Ruthenium compounds 1304
 Ruthenium(VIII) oxide 1304, 1310, 1320
 Rutlner process 173
 Rutile 103, 1069, 1134, 1136, 1137, 1444, 1656
 Rutile pigments 1143, 1155

S

Sachtolith 671, 672
 Safflorite 928
 Salinity 2086
 Salt harvesting 2089
 Salts of inorganic rare earth oxoacids 1728
 Samarium 12
 Samarskite 1419, 1698
 Sand-lime bricks 2275
 Sanmartinite 1333
 Sasol 213, 214
 Sassolite 1987
 Scandium 10, 1695, 1698
 Scandium alum 1106
 Scandium separation 1722
 Scattered metals 3, 10
 Schairerite 1085
 Schaphachite 1221
 Schauerteite 1507
 Scheele's green 811
 Scheelite 462, 1334, 1335, 1363, 1371
 Scheibel column 1615
 Schists 1070
 Schlippe's salt 840
 Schmidt number 300
 Schoenite 2180
 Schönite 1007, 1008, 1030, 2145, 2154, 2161, 2194
 Schroeckingerite 1606
 Schweinfurth green 811
 Scrap 283, 285, 381
 consumption 387
 external 21
 local 21
 steel 21
 substitute 22
 world market 387
 Scrap silver 1223
 Sea bitters 1007
 Sea salt 2086
 Seahostar 1947
 Seawater composition 1017
 Seawater evaporation 1007, 2086
 Seaweeds 12
 Secondary amines 1718
 Secondary metals 3, 5
 Sedema process 1841
 Seed particles 757, 1081
 Segregation process 503, 759
 Séjournet process 1373
 Selective oxidation 1385
 Selective reduction smelting 761
 Selenac 1566
 Selenate alum 1106
 Selenates 1567

Selenic acid 1567
 Selenides 1567
 Selenites 1566
 Selenium 10, 1230, 1557
 Selenium dioxide 1493, 1563, 1566
 Selenium disulfide 1567
 Selenium halides 1567
 Selenium oxide 1368
 Selenium removal 742
 Selenium trioxide 1567
 Selenocarbamic acid 1563
 Selenous acid 1566
 Selenyl chloride 1567
 Semiautogenous grinding 39
 Semiconductor industries 1374
 Semiconductor memories 1207, 1312
 Semiconductor silicon 1865
 Semiconductors 10, 1379, 1539
 Semifusinite 195
 Semikilled steel 327
 Semisplint coal 199
 Senarmontite 825
 Sensors 1311
 Separation
 of ^{233}U 1676
 of bismuth from metallic lead 850
 of cobalt from other metal ions 933
 of europium oxide 1722
 of gold from silver 1185
 of platinum group metals 1287
 of rare earths 1708
 of scandium 1722
 of yttrium oxide 1722
 of zirconium 1462
 Separation factor 1714
 Serpentine 1014, 1032
 Serpentinite 758
 Sewage treatment 2275
 Shaft furnace 113, 115
 Shaft furnace processes 110
 Shatter test 48
 Shear steel 279
 Shearing machines 384
 Sherritt ammonia leach process 739
 Sherritt Gordon process 932
 Sherwood number 300
 Shield against γ -rays 5
 Showa Denko ferrochromium process 444
 Shredders 385
 Sialic lodes 644
 Sicor 678
 Siderite 33, 34, 35, 53, 1069, 1084
 Siderite ore roasting 41
 Sideritis 31
 Sidérurgie 31

Siegenite 719, 928
 Siemens—Martin furnace 101
 Siemens—Martin process 31, 309
 Siennas 172
 Sievert square root law 292
 Silane 1866
 Silanediol groups 1935
 Silanes 672, 1884
 Silanol groups 1902, 1935
 on silica surface 1958
 Silex 1912
 Silica 101, 1902
 aquasols 1941, 1943
 bricks 102, 1916
 dust 1970
 gel 1948
 organosols 1940
 rocks 1911, 1912
 slate 1912
 sols 1933, 1939
 Silica W 1905, 1911
 Silicate precipitation 1337
 Silicides 1374, 1899
 Silicoborate 2010
 Silicochromium 446
 Silicomanganese 432
 Silicon 12, 1861
 content of Al_2O_3 1084
 rectifiers 535
 wafers 1877, 1946
 Silicon borides 1898
 Silicon bromides 1893
 Silicon carbide 101, 649, 1890
 plates 675
 retorts 675
 Silicon dioxide 1902
 Silicon fluorides 1893
 Silicon halides 1886
 Silicon hydrides 1883
 Silicon iodides 1894
 Silicon monoxide 418, 1895
 Silicon oxides 1895
 Silicon sesquioxides 1896
 Silicon sulfide 1897
 Silicon tetrabromide 1894
 Silicon tetrachloride 1462, 1889, 1955
 Silicrete 1912
 Sillimanite 1656
 Siloxane 1958
 Siloxane bridges 1935
 Siloxanes 672
 Silvanite 1221
 Silver 8, 17, 1215
 catalysts 1258
 coins 1218, 1223, 1251

complexes 1247
 crucibles 1257
 demagnetization 1218
 dissolution 1220
 drinking vessels 1264
 electroplating 1253
 electrorefining 1227
 enrichment 1226
 extraction 1217
 from copper matte 1231
 from electrolytic lead refining 1228
 extraction from gold ores 1223
 flakes 1250
 from tin ores 1223
 German 4, 5
 in medicine 1252
 plating 1253
 by chemical reactions 1254
 powder 1248
 microcrystalline 1249
 spheroidal 1250
 preparations in medicine 1264
 refining 1240
 Silver(I) acetate 1246
 Silver acetylide 1248
 Silver aluminate 1252
 Silver amalgam 909
 Silver anide 1248
 Silver azide 1247
 Silver bromide 1244
 Silver bronzes 1250
 Silver carbonate 1247
 thermal decomposition 1250
 Silver chlorate 1246, 1264
 Silver chloride 1225, 1244, 1252, 1260
 Silver chromate 1791
 Silver cyanide 1247
 Silver dichromate 1791
 Silver(I) fluoride 1246
 Silver fulminate 1248, 1264
 Silver halide 1258
 Silver halides 1224, 1244
 Silver iodide 1244, 1259
 Silver isocyanate 1247
 Silver(I) lactate 1246
 Silver nitrate 1242, 1252, 1259
 Silver nitrate for the photographic industry 1244
 Silver oxalate 1248
 Silver(I) oxide 1245, 1257
 thermal decomposition 1250
 Silver(II) oxide 1245, 1257
 Silver oxides 1244, 1245
 Silver perchlorate 1246
 Silver permanganate 1246
 Silver(I) propionate 1246
 Silver rubidium iodide 2213

Silver sulfate 1246
 Silver sulfide 1224, 1225, 1246
 coating 1220
 Silver tetrafluoroborate 1246
 Silver thiocyanate 1247
 Silver-base alloys 1315
 Silver-based materials for electrical contacts 1256
 Silver-coated copper wires 1257
 Silver-containing alloys 1253
 Silver-containing catalysts 1224
 Silver-containing scrap 1232
 Silver-containing tin deposits 1223
 Silver-copper alloys 1252
 Silver-palladium powder 1250
 Silver-tin amalgams 1253
 Silverware 8
 Silylene 1886
 Simic deposits 644
 Single crystals 1551
 Single-crystal growth 1868
 Single-crystal magnesium 997
 Single-crystal silicon 1868
 Single-phase submerged arc furnace 480
 Sinter 44
 Sinter plant 134
 Sinter roasting 646
 Sintered magnesia 1012, 1021, 1022
 Sintering 41, 47, 1342
 Sintering metallurgy of bronzes 709
 Sintering of dolomite 1019
 Sintering plants 133
 Siros melt lance 600
 Siros melt process 521
 Skin-pass rolling 348
 Skutterudite 928
 SL/RN process 119, 288
 Slag 54, 505
 Thomas 280
 Slag decopperizing 521
 Slag fuming 648
 Slag notch 59
 Slag-free ferrosilicon production 418
 Slag-fuming process 595
 Slaked lime 2254, 2271
 Slot ovens 251
 Smaltite 797, 815, 928
 Smelting
 in a rotary kiln 675
 of arsenical ores 797
 of nickel sulfide 726
 Smelting-reduction processes 123, 125
 Smithsonite 641, 644, 660
 Snowtex 1947
 Soda ash, see *Sodium carbonate*

Sodalite 1119
 Söderberg anodes 1046, 1047
 Sodium 18, 2053
 Sodium acetylide 2058
 Sodium alkoxides 2068
 Sodium alum 1108
 Sodium aluminate 1068, 1072, 1097, 1109
 Sodium aluminum silicate 2039
 Sodium aluminum sulfate 1108
 Sodium amalgams 909, 2069, 2241
 Sodium amide 2068
 Sodium ammonium vanadate 1484
 Sodium amyl xanthate 722
 Sodium antimonate 612
 Sodium arsenate(III) 811
 Sodium arsenate(V) 812
 Sodium azide 2057, 2068
 Sodium bicarbonate precipitation 2111
 Sodium borate ore 2014
 Sodium borates 2012, 2020
 Sodium borohydride 1301, 2067, 2241
 Sodium calcium borate ores 2014
 Sodium carbonate 12, 2067, 2104
 Sodium carbonate hydrates 2105
 Sodium carbonate-containing minerals 2114
 Sodium chloride 2059, 2073
 crystallization 2087
 electrolysis 2096
 solubility 2075
 Sodium chromate 1788
 Sodium content of alumina 1084
 Sodium cyanide 1190
 Sodium dichromate 1773, 1788, 2126
 Sodium disulfide 2223, 2227
 Sodium disulfite 2234
 Sodium disulfatoaurate(I) 1201
 Sodium dithionite 2239
 Sodium dithiosulfatoaurate(I) 1202
 Sodium fluoride 1054
 Sodium fluorozirconates 1449
 Sodium formate 2058, 2095, 2241
 Sodium hexachloroplatinate(IV) 1297
 Sodium hexacyanoferrate(II) 179
 Sodium hexafluorosilicate 962
 Sodium hexahydroxyantimonate 839
 Sodium hexahydroxyplatinate(IV) 1302, 1313
 Sodium hydride 1168, 2057, 2067
 Sodium hydrogencarbonate 2120
 Sodium hydrogensulfate 2132
 Sodium hydrogensulfides 875, 2228
 Sodium hydrogensulfite 2235
 Sodium hydroxide 1072, 2058, 2094
 Sodium hydroxoferrate 162
 Sodium hypophosphite 1254

Sodium isopropyl xanthate 1366
 Sodium metaarsenite 820
 Sodium metaborate 2014, 2020
 Sodium metavanadate 1484
 Sodium molybdate 1369, 1376, 1382
 Sodium monosulfide 2222, 2224, 2227
 Sodium oxalate 1085
 Sodium oxides 2058, 2067
 Sodium pentaborate 2015
 Sodium pentasulfide 2223
 Sodium permanganate 1855
 Sodium peroxide 411, 470, 2067
 Sodium polysulfides 830, 1119, 2069, 2225
 Sodium pyroantimonate 839
 Sodium selenide 875
 Sodium selenite 1562
 Sodium selenosulfate 1562
 Sodium silicate 2131
 Sodium sulfate 2121
 electrochemical decomposition 2129
 solubility 2122
 Sodium sulfhydrate 1371
 Sodium sulfide 671, 875
 leaching 830
 solubility in water 2123
 Sodium sulfite 830, 2235
 Sodium sulfoxides 1119, 1121
 Sodium tetraborate decahydrate 2012
 Sodium tetraborate pentahydrate 2012
 Sodium tetrasulfide 2223
 Sodium tetrathioantimonate 840
 Sodium thioantimonate 832
 Sodium thiosulfate 830, 1187, 1218, 1258, 2236
 Sodium zirconate 1462
 Sodium zirconium silicate 1462
 Sodium-potassium alloys 1166, 2069
 Sodium-sulfur batteries 2069
 Soft iron 146
 Soft lignite 203
 Soft magnetic steels 270
 Softening 231
 Softening of lead 607
 Softening points of coal 232
 Soil stabilization 1033, 2270, 2275
 Solar cells 6, 875, 1539
 Solar evaporation 987, 1007, 2153, 2154, 2167
 Solar silicon 1879
 Solder alloys 1538
 Solder plating 1255
 Soldering 1168
 Solders 4, 6, 708, 875, 1207, 1308
 Solidification 318
 Solidification morphology of steel 318
 Solidification of concrete 1109

Solid-state reactions of iron compounds 173
 Solid-waste disposal 546
 Solubility
 of carbon in ferrosilicochromium 441
 of carbon in molten iron alloys 290
 of gases in molten copper 497
 of hydrogen in pure iron 292
 of kieselite 1030, 2165
 of metals in mercury 909
 of nitrogen in pure iron 292
 of oxygen in cobalt 937
 of oxygen in silver 1220
 of potassium dicyanoaurate(I) in water 1200
 of potassium sulfate 2191
 of pyrogenic silica in caustic soda 1958
 of silver compounds 1231
 in water 1243
 of SiO₂ in water 1913
 of SO₂ in polyglycol 671
 of sodium chloride 2075
 of sodium sulfate 2122
 of sodium sulfate in water 2123
 Solution mining 1008, 2080, 2148
 Solution Mining Research Institute 2086
 Solution purification 657
 Solvay process 2098, 2108, 2116, 2274
 Solvent extraction 170, 657, 836, 1295, 1336, 1338, 1339, 1405, 1461, 1462, 1494, 1661, 1714
 of dilute copper solutions 526
 of indium 808
 Sorel cement 1011, 1033
 Sorelmetal 104
 Special-quality steel 2
 Specific heat capacity of iron 373
 Specular hematite 33
 Specularite 34, 35
 Speiss 594, 1234
 Spent liquors from potash industry 1005
 Sperryite 1276, 1277
 Sphalerite 644, 928, 1524, 1532
 Sphene 1134, 1136, 1172
 Spherical autoclaves 695
 Spheroidal graphite cast iron 341
 Spheroidal pig iron 140
 Spheroidal silver powder 1250
 Spheroidal titanium powder 1167
 Spheroidal ZnS 669
 Spiegeleisen 1814
 Spinels 1033
 Spiral classifier 41
 Splint coal 199
 Spodumene 2032, 2036, 2039, 2049
 Sponge iron 141, 283, 286
 Sponge iron plants 44
 Spontaneous combustion 217
 Spontaneous decomposition of some complexes of plati-

num metals 1320
 Sporinite 194
 Spray condenser 651
 Spray galvanizing 662
 Spray towers 97
 Spray-roast of metal chloride solutions 169
 Sputtering targets 1346, 1374
 Stabilizers for plastics 874
 Stainless steel 310, 451, 772
 corrosion 366
 starting sheets 535
 strip 273
 Stannates(IV) 710
 α-Stannic acid 711
 β-Stannic acid 711
 Stannite 686
 Stannous hexafluorozirconate 1450
 Stannum 683
 Starch 1079
 Starting a new furnace 59
 Starting sheet cathodes 534
 Stassfurtite 2145
 Stationary calciners 1087, 1094
 Steam power 281
 Steel 1, 146
 alloy 9, 385
 blister 279
 case hardening 370
 chemically resistant 270
 chromium-coated 359
 constructional 1
 consumption 389
 crucible 279
 cryogenic 270
 enameling 944
 high-temperature 369
 ingot 280
 ingot killed 327
 killed 325
 pretreatment of used products 386
 production 388
 environmental aspects 377
 production methods 302
 puddled 279
 recycling 381
 rimming 324
 rolled 281
 scrap 21
 semikilled 327
 shear 279
 soft magnetic 270
 solidification morphology 318
 special-quality 2
 sulfidation 370
 tool 1
 vacuum treatment 316
 world trade 389

Steel pretreatment 941
 Steel strip production 335
 Steel wool cathode 1194
 Steelmaking 52
 Stellites 471, 924
 Stephanite 1221
 Sternbergite 1221
 Stibine 840, 843
 Stibiocolumbites 1405
 Stibiopalladinite 1277
 Stibnite 825, 826, 839
 Stishovite 1904, 1905
 Stokesite 686
 Storage batteries 871
 Storage caverns 2085
 Stottite 1507
 Stoves for heat recovery 100
 Strand casting 328
 Stress corrosion cracking 364, 367
 Stromeyerite 1221
 Strontianite 2330
 Strontium 13, 2329
 Strontium carbonate 2331
 Strontium chloride 2333
 Strontium chromate 1806, 2333
 Strontium in seawater 1017
 Strontium nitrate 2331, 2332
 Structure of ultramarine 1117
 Strueverite 1419
 Studio radio tapes 186
 Stupp 896, 900
 Subbituminous coal 199, 203
 Sublimation 1461
 Submerged arc furnaces 417, 442
 Submerged combustion 2293
 Sugar refining 2275
 Sulfadiazine silver(I) 1253
 Sulfamic acid 613
 Sulfate process 1140, 1141, 1147
 Sulfated monoglyceride of coconut oil, see *Syntex VB*
 Sulfation 745, 1229
 Sulfation roasting 504, 931
 of powdered copper matte 1232
 Sulfatotitanates 1172
 Sulfidation 761
 Sulfidation of iron and steel 370
 Sulfide precipitation 321, 770
 Sulfidic copper-bismuth concentrates 848
 Sulfigran process 2228
 Sulfinic acids 915
 Sulfites 165, 2234
 Sulfomat process 2130
 Sulfur
 chromophores 1117

 dyes 2229
 from hydrogen sulfide 1100
 in coal 203, 205, 219
 in coke 53
 recovery 1100
 Sulfur dioxide 998, 1057
 Sulfur dioxide conversion to elemental sulfur 733
 Sulfur tetrafluoride 911
 Sulfur trioxide emission 133
 Sulfuric acid pickling solutions 166
 Sulfuric acid recycling 1149
 Sulfur-sulfur bonds 2221
 Sulmag II process 1019
 Sumitomo process 128, 129, 935
 Sundite 1221
 Sunshine electrolytic antimony process 831
 Superalloys 473, 1375, 1482, 1496
 Super-purity aluminum 1055
 Superquick-acting fuses 1257
 Super-VHS video 186
 Supplement for animal feeds 1024
 Supported catalysts 1279, 1284
 Surface coatings 351, 385
 Surface hardening 1374
 Surface properties of TiO₂ 1135
 Surface silanol groups 1965
 Surface siloxanes 1936
 Surface-active additives 535
 Swelling during reduction 50
 Swelling of coal 226, 233
 SX-Carbonate process 964, 969
 Syenite 1070
 Sylvinite 2162
 flotation 2178
 ores 2174, 2178
 precipitation 2169
 Sylvite 2145, 2159, 2179, 2212
 Sympathetic inks 941
 Synergistic effects 1719
 Syngenite 2145, 2196, 2286, 2310
 Syntex VB 1366
 Synthetic
 carnallite 1006
 Fe₃O₄ 162
 flocculant 1079
 iron oxide pigments 172
 kieselite 1009
 manganese dioxides 1839
 rutile 1136, 1139
 sapphire 1101
 scheelite 462, 2313
 ultramaries 1116
 zeolites 1096, 1110
 Synthol process 213
 System Ag-Pb-Zn 608

System $\text{Al}_2(\text{SO}_4)_3\text{--Al}(\text{OH})_3\text{--H}_2\text{O}$ 1103
 System $\text{Al}_2(\text{SO}_4)_3\text{--H}_2\text{O}$ 1103
 System $\text{Al}_2\text{O}_3\text{--CaO--SiO}_2$ 1916
 System $\text{Al}_2\text{O}_3\text{--Fe}_2\text{O}_3\text{--H}_2\text{O}$ 1065
 System $\text{Al}_2\text{O}_3\text{--H}_2\text{O}$ 1065
 System Au--Ag--Cu 1202
 System $\text{B}_2\text{O}_3\text{--H}_2\text{O}$ 2007
 System CaO--FeO--SiO_2 295, 594
 System $\text{CaSO}_4\text{--H}_2\text{O}$ 2282
 System C--Cr--Fe 439
 System $\text{Cu--Cu}_2\text{O}$ 530
 System $\text{Cu--Cu}_2\text{S}$ 518
 System Fe--B 465
 System Fe--C 144, 290
 System Fe--C--Cr--O 310
 System Fe--Cr 440
 System Fe--HCl--H_2 694
 System Fe--Mo 477
 System Fe--O 291
 System Fe--O--C 690
 System $\text{FeO--Fe}_2\text{O}_3\text{--SiO}_2$ 506
 System FeO--MgO--SiO_2 455
 System Fe--Si 416
 System Fe--Sn 700
 System Fe--V 476
 System Fe--W 461
 System $\text{H}_2\text{O--NaHCO}_3\text{--Na}_2\text{CO}_3$ 2120
 System $\text{K}_2\text{Cl}_2\text{--MgCl}_2\text{--Na}_2\text{Cl}_2\text{--H}_2$ 2168
 System $\text{K}_2\text{--Mg--Cl}_2\text{--SO}_4^{2-}\text{--H}_2\text{O}$ 2193
 System $\text{KCl--H}_2\text{O}$ 2160
 System $\text{KCl--MgCl}_2\text{--H}_2\text{O}$ 2167
 System $\text{MgCl}_2\cdot n\text{H}_2\text{O}$ 1005
 System $\text{MgO--CaO--SiO}_2\text{--Fe}_2\text{O}_3$ 1027
 System Mn--C 1821
 System Mn--O 1819
 System $\text{Na}_2\text{CO}_3\text{--H}_2\text{O}$ 2105
 System $\text{Na}_2\text{O--Al}_2\text{O}_3\text{--H}_2\text{O}$ 1074
 System $\text{Na}_2\text{S--S}$ 2221, 2226
 System $\text{Na}_3\text{AlF}_6\text{--Al}_2\text{O}_3\text{--CaF}_2$ 1048
 System $\text{Na}_3\text{AlF}_6\text{--AlF}_3\text{--Al}_2\text{O}_3$ 1047
 System $\text{Na}_3\text{AlF}_6\text{--Li}_3\text{AlF}_6\text{--Al}_2\text{O}_3$ 1048
 System $\text{NaCl--H}_2\text{O}$ 2075
 System Na--K 2157
 System $\text{NaOH--H}_2\text{O}$ 2095
 System Pb--Bi--Ca--Mg 851
 System Pb--Cu--S 605
 System Pb--S--O 586
 System Sn--HCl--H_2 694
 System Sn--O--C 690
 System Ti--Fe 473
 System Ti--S 1169
 System $\text{UO}_2(\text{NO}_3)_2\text{--HNO}_3\text{--H}_2\text{O}$ 1643
 System $\text{UO}_2\text{SO}_4\text{--H}_2\text{SO}_4\text{--H}_2\text{O}$ 1643
 System Zn--Fe--S--O 646

Syton 1947
 Szaibelyite 1987, 2010
 Szechtman process 2066

T

Tabular aluminas 1101
 Tachhydrite 2145, 2311
 Taconite 33, 35
 Tafel equation 658
 Tafel reaction 364, 367
 Talc 1003, 1015
 Tanning agents 1783
 Tanning of leather 9, 1116
 Tantalates 1424
 Tantalite 33, 1404, 1419
 Tantalo-columbite 1404
 Tantalum 9, 1417
 applications 1426
 capacitors 1422
 implants 1423
 powder 1421
 processing routes 1419
 scrap 1420
 Tantalum alkoxides 1425
 Tantalum carbide 1421, 1425
 Tantalum nitride 1425
 Tantalum oxides 1423
 Tantalum pentachloride 1425
 Tantalum pentafluoride 1424
 Tantalum silicide 1425
 Tantalum-boron system 1425
 Tantalum-containing tin slags 1418
 Tantalum-Niobium International Study Center 19
 Tapiolite 1419
 Tapping a molten material from the furnace 58
 Tar 202, 242, 243, 244
 Tarnishing of silver 1252
 Taunusquarzit 1912
 Teallite 686
 Technetium 1587, 1589
 Technical varieties of iron 146
 Telluric iron 31, 274
 Tellurides 1577
 Tellurium 10, 18, 1230, 1571
 Tellurium dioxide 1576
 Tellurium halides 1576
 Tellurium hexafluoride 1579
 Tellurium-lead 1577
 Tellurous acid 1577
 Tennantite 498, 797
 Tenorite 498
 Terbium 12
 Terephthalic acid from benzoic acid 2204
 Ternary molybdenum chalcogenides 1381

Terra tripolitana 1925
 Tertiary amines 1718
 Tetraborane 2000
 Tetrabromosilane 1893
 Tetrachloroaurate(III) complex 1187
 Tetrachloroauric acid 1196, 1200, 1201, 1211
 Tetrachloroferrates 151
 Tetrachloropalladate(II) 1303
 Tetrachloropalladic(II) acid 1303
 Tetrachlorosilane 1887, 1889
 Tetraedrite 498
 Tetraethyllead 633, 1000, 2068
 Tetrahedrite 825, 830
 Tetramethyltin 1499
 Tetramminepalladium(II) chloride 1303
 Tetrapentoxysilane 1944
 Textile auxiliaries 215
 Textile finishes 840
 Textile technology 1308
 Thallium 10, 1543
 Thallium(I) carbonate 1551
 Thallium(I) chloride 1549
 Thallium(I) fluoride 1550
 Thallium(I) hydroxide 1549
 Thallium(I) iodide 1550
 Thallium metasilicate 1551
 Thallium(I) nitrate 1551
 Thallium(I) oxide 1548
 Thallium(III) oxide 1549
 Thallium(I) sulfate 1550
 Thallium(I) sulfide 1550
 Thaumassite 2286
 Thenard's blue 944
 Thenardite 2122, 2145, 2162
 1-(2-Thenoyl-3,3,3-trifluoroacetone 1680
 Thermal conductivity of pure iron 375
 Thermal decomposition
 of aluminum hydroxide 1066, 1099
 of dicyanoaurate(I) complex 1198
 of $\text{Fe}(\text{CO})_5$ 177
 of ferrous oxalate 147
 of platinum group metal complexes 1299
 of silver carbonate 1250
 of silver(I) oxide 1250
 of the ammonium chloro complexes 1298
 of ThI_4 1670
 of titanium halides 1164
 Thermal dissociation of ThI_4 1669
 Thermal dissociation of zircon 1435, 1462
 Thermal expansion of refractory silica 1916
 Thermal ore beneficiation 691
 Thermal properties of copper 495
 Thermionic converters 1346
 Thermistors 948
 Thermite reaction 1043

Thermocouple elements 1346
 Thermonantrite 2106
 Thermonuclear reactions 2042
 Thermoplasticity of coal 224, 227, 231
 Thickener 1079
 Thin-film technology 1313, 1314
 Thiarsenites 797
Thiobacillus ferrooxidans 526, 695
Thiobacillus thiooxidans 526
 Thiocyanate ion 149
 Thiogermanates 1517
 Thiomolybdate 1339
 Thionalide 1305
 Thiophenes 205
 Thiosulfate leaching 1218, 1225
 Thiosulfate silver complexes 1247
 Thiosulfates 164, 2236
 Thiosulfates in waste solutions 165
 Thiourea 1254, 1305
 Thomas converter 303
 Thomas slag 280
 Thomas-Gilchrist process 31
 Thoreaulite 686
 Thorianite 1655
 Thorite 1655
 Thorium 10, 11, 1649, 1745
 decay chain 1650
 Thorium borides 1668
 Thorium carbides 1668
 Thorium carbonate 1668
 Thorium halides 1665
 Thorium hydrides 1653, 1668
 Thorium hydroxide 1668
 Thorium nitrate 1668
 Thorium nitrides 1654, 1668
 Thorium oxides 1663
 Thorium peroxide 1668
 Thorium phosphide 1668
 Thorium sulfate 1668
 Thorium sulfides 1668
 Thorogummite 1655
 Thoron 10
 Thucholite 1607
 Thulium 12
 Thyristors 1346
 Tiemannite 1559
 Tin 5, 683
 cans 21
 electrorefining 704
 from its ores 691
 from scrap 705
 refining 702
 slags 1418
 utensils 708

- vapor 684
- Tin alkyl compounds 712
- Tin amalgam 909
- Tin aryl compounds 712
- Tin(II) bromide 710
- Tin(IV) bromide 710
- Tin chloride 699
- Tin(II) chloride 709, 1254
- Tin(II) compounds 709
- Tin(IV) compounds 710
- Tin(II) cyanide 710
- Tin dichloride 704
- Tin disulfide 711
- Tin(II) fluoroborate 710
- Tin(IV) halides 710
- Tin(IV) hydride 710
- Tin(II) iodide 710
- Tin(II) oxide 710
 - hydrate 710
- Tin(IV) oxide 710
 - hydrate 710
- Tin(II) salt of ethylhexanoic acid 710
- Tin(IV) sulfide 711
- Tin tetrachloride 704
- Tincal 1987
- Tincalconite 1987
- Tin-containing alloys 706
- Tin-iron alloy 700
- Tinplate 4, 359, 705
- Tinplate packaging 386
- Titanates 1155
- β -Titanic acid 1172
- Titanic acid 1173
- Titanite 1134, 1136, 1172
- Titanium 7, 1000, 1129
 - alums 1106, 1171
 - anodes 527
 - blanks 534
 - electrowinning 1165
 - in cast iron 474
 - in tool steels 474
 - master alloys 475
 - pickling 1168
 - scrap 475, 1165, 1166
 - slag 104, 474, 1139, 1160
 - sponge 476, 1161, 1166, 1167
 - welding 1168
- Titanium borides 1173
- Titanium bromides 1170
- Titanium carbide 1165, 1173
- Titanium carbides 1170
- Titanium carbonitride 1173
- Titanium(II) chloride 1165
- Titanium(III) chloride 1170
- Titanium chlorides 1165, 1170
- Titanium(II) compounds 1170
- Titanium(III) compounds 1170
- Titanium(IV) compounds 1171
- Titanium cyanonitride 1173
- Titanium dicyanide 1173
- Titanium dioxide 149, 1134, 1165
- Titanium dioxide chlorination 1160
- Titanium dioxide pigments 1113
- Titanium dioxide reduction 1162
- Titanium disulfide 1173
- Titanium double sulfates 1171
- Titanium fluoride 1171
- Titanium fluorides 1170
- Titanium grades 1131
- Titanium(III) hydroxide 1171
- Titanium iodides 1164, 1170
- Titanium monoxide 1165
- Titanium nitride 1133, 1165, 1171
- Titanium nitrides 1170
- Titanium oxide hydrate 1142
- Titanium(III) oxide 1171
- Titanium oxides 1170
- Titanium phosphides 1170
- Titanium sulfate hydrolysis 1142
- Titanium sulfides 1170, 1173
- Titanium tetrabromide 1172
- Titanium tetrachloride 1160, 1165, 1171
- Titanium tetrafluoride 1165
- Titanium tetrafluoride reduction 1164
- Titanohematites 1134
- Titanomagnetite 1134, 1136, 1139, 1473, 1476
 - deposits 1475
 - ores 1472
- Titanyl sulfate 1172
- Ttjamunite 1606
- Todorokite 1830
- Toner in photocopiers 158
- Toning blue 179
- Tool steels 1, 461, 1345
- Toothpaste 1096
- Top-blown oxygen converter 303
- Top-blown rotary converter 519, 520, 754, 1235
- Tops and bottoms process 1282
- Torbernite 1606
- TORCO process 503
- Torpedo ladles 102
- Toscoal process 251
- Total roasting 504
- Tough-pitch copper 530, 539
- Tourmaline 687
- Toxicity of chromium 453
- Toxicity of mercury 917
- Trade in steel 389
- Transformation of β -tin 684

- Transforming coal into secondary fuels 210
 - Transistors 1346
 - Transmutation of base metals 1185
 - Transparent α -FeO(OH) 190
 - Transparent brown iron oxides 191
 - Transparent cobalt blue 950
 - Transparent cobalt green 950
 - Transparent iron blue 191
 - Transparent iron oxides 177, 190
 - Transparent red iron oxide 190
 - Transparent titanium dioxide 1159
 - Transparent yellow iron oxide 190
 - Transparent zinc oxide 677
 - Transuranium metals 10
 - Traveling grate 45
 - Treatment of nickeliferous pyrrhotite 745
 - Treatment of potash ores 2149
 - Tribasic Copper Sulfate 572
 - Tribasic copper sulfate 572
 - Tribology 1169
 - Tributyl phosphate 170, 748, 1296, 1615
 - extraction 1438
 - Tributyltin chloride 712
 - Tricalcium silicate 1015
 - Tricapryl monomethyl ammonium chloride, *see Aliquat*
 - Tricarbonatodioxouranate 1643
 - Trichlorogermane 1518
 - Trichlorooxomolybdenum(V) 1382
 - Trichlorosilane 1866, 1878, 1886, 1888
 - hydrolysis 1897
 - oxidation 1897
 - pyrolysis 1889
 - Trichlorosilanol 1897
 - Tridymite 1902-1904, 1909, 1910, 1916
 - Triethyl indium 1538
 - Triethylamine 2202
 - Triethylphosphine gold complex of thioglucose tetraacetate 1202
 - Trigermane 1516
 - Triisooctylamine 934
 - Trimercapto-s-triazine 905
 - Trimethyl borate 2067
 - Trimethyl indium 1538
 - Trimethylbismuth 863
 - Tri-*n*-butyl phosphate 1715
 - Trinuclear iron carbonyl 154
 - Trioctylamine 1296, 1339
 - Triphenyl bismuth 863
 - Triphenyl indium 1538
 - Triphyline 2033, 2036
 - Tripoli 1911, 1912, 1918
 - Tripolite 1925
 - Tri-*sec*-amylborane 2159
 - Tri-*sec*-butylborane 2159
 - Tritium 2042
 - Triuranium octaoxide 1641
 - Trona 2059, 2098, 2106, 2114, 2120
 - Troostite 645
 - Tscheffikinite 1655
 - Titanium slag 1136
 - Tube digester 1076
 - Tula process 306
 - Tumble test 49
 - Tung sten* 1330
 - Tungstates 1351
 - Tungsten 9, 1329, 1376
 - alloys 1345
 - bronzes 1352
 - in catalysis 1353
 - recycling 1355
 - scrap 1335
 - Tungsten carbide 9, 936
 - Tungsten dioxide 1350
 - Tungsten hexacarbonyl 1349
 - Tungsten hexachloride 1352
 - Tungsten hexafluoride 1357
 - Tungsten oxide 464
 - Tungsten oxytetrachloride 1353
 - Tungsten trioxide 1350
 - reduction 1340
 - Tungsten-arsenic compounds 1350
 - Tungsten-boron compounds 1349
 - Tungsten-bromine compounds 1353
 - Tungsten-carbon compounds 1349
 - Tungsten-chlorine compounds 1352
 - Tungsten-containing tin concentrates 695
 - Tungsten-fluorine compounds 1352
 - Tungsten-iodine compounds 1353
 - Tungstenite 1333
 - Tungsten-nitrogen compounds 1349
 - Tungsten-oxygen compounds 1350
 - Tungsten-phosphorus compounds 1350
 - Tungsten-rhenium alloys 10, 1496
 - Tungsten-rhenium system 1495
 - Tungsten-selenium compounds 1352
 - Tungsten-silicon compounds 1349
 - Tungsten-sulfur compounds 1352
 - Tungsten-tellurium compounds 1352
 - Tungstic acids 1351
 - Tungstite 1333
 - Turbine blades 1346
 - Turnbull's blue 148, 149, 179
 - Type metal 6
 - Tuyamunite 1472, 1475
- U**
- Ugine ferronickel process 457
 - Ulexite 1987, 2014, 2016

Ultimate analysis of coal 202, 218
 Ultracentrifuges 1629
 Ultra-high-purity niobium 1412
 Ultramarine pigments 1116
 Ultramarine structure 1117
 Ultramarines as zeolites 1118
 Umbers 172
 Uncontrolled criticality 1644
 Updraft sintering 587
 Uraninite 1606
 Uranium 10, 11, 1000, 1599
 from phosphate rock 23
 powder 1637
 Uranium carbides 1639
 Uranium dioxide 1620
 Uranium fluoride 1000
 Uranium halides 1637
 Uranium hexafluoride 1620, 1623
 Uranium hydride 1637
 Uranium nitrates 1642
 Uranium nitrides 1640
 Uranium oxides 1640
 Uranium peroxides 1642
 Uranium sulfates 1643
 Uranium tetrafluoride 1620
 Uranium trioxide 1620
 Uranium–vanadium ores 1472, 1473
 Uranophane 1606
 Uranothorianite 1655
 Uranothorite 1606, 1655
 Uranyl nitrate 1620
 Uses
 of aluminothermic processes 415
 of cobalt compounds 941
 of copper 542

V

Vacuum arc decarburization 312
 Vacuum arc furnaces 1166, 1373
 Vacuum arc remelting 338
 Vacuum cooling crystallizer 2125
 Vacuum crystallization 166
 Vacuum dezincing 854
 Vacuum distillation 806, 857, 1163, 1461
 Vacuum treatment of steel 316
 Vacuum vapor deposition 359
 Vacuum vaporization of silver 1255
 Vacuum volatilization of SnO 701
 Valentinite 825
 VAMI cell 991
 Van Arkel–de Boer process 1461, 1464
 Vanadates 1483
 Vanadinite 584, 1472
 Vanadium 9, 1069

alum 1106
 compounds 1370
 from fuel oil 23
 slags 1473, 1476
 Vanadium carbides 1484
 Vanadium halides 1484
 Vanadium hydrides 1485
 Vanadium nitrides 1484
 Vanadium oxides 1483
 Vanadium oxychloride 1141
 Vanadium oxychloride removal 1145
 Vanadium oxytrichloride 1484
 Vanadium pentoxide 1477, 1479
 Vanadium silicides 1485
 Vanadium suboxides 1483
 Vanadium tetrachloride 1141, 1484
 Vanadium tetrachloride removal 1145
 Vanadium trichloride 1484
 Vanadium–aluminum alloys 1481
 Vanadium-containing titanium alloys 1482
 Vanadium–gallium alloys 1483
 Vanadyl oxalate 1484
 Vanadyl sulfate 1484
 Vanthoffite 2122, 2145
 Vapor deposition of gold 1208
 Vapor pressure
 of mercury 892
 of MgCl_2 solutions 1006
 of SnS 691
 Vaporization of SnS 692
 Varlamoffite 686
 Varnish industries 1110
 Varnishes 215
 Vat leaching 526
 Vauquelin's salt 1303
 Venturi scrubbers 98
 Vermiculite 342
 Vernadite 1830
 Versatic 10 1718
 Versatic 911 1718
 Vertical retorts 649
 Videocassettes 185
 Violanite 719
 Violet ultramarine 1120
 Viscose manufacture 666
 Viscosity of mercury 892
 Vitamins 215
 Vitigran, Conc. 572
 Vitraints 237
 Vitreous silica 1922, 1924
 Vitrinite 193, 205, 227
 Vitroplast 234
 Vivianite 34
 Volatile matter 202, 218

Volatile organotin compounds 712
 Volatile products in coal pyrolysis 240
 Volatilization of tin from concentrates 694
 Volmer–Butler equation 364
 Voltage in Al cell 1051
 Vossen-Blue 191
 Vrbaita 1544
 Vulcanization activator 663
 Vulcanized rubber 676

W

Wacker-Kupferkalk 572
 Waelz process 595, 645, 647, 657, 660, 871
 Wafer manufacture 1876
 Wagner–Hauffe doping effect 369
 Wallisite 1544
 Warren Spring process 694
 Waste gas problems 1150
 Waste management 132, 137
 Waste sulfuric acid 2126
 Water consumption in a steel plant 379
 Water glass, see *Sodium silicate*
 Water pollution control 132
 Water protection 545
 Water purification 1096, 1098, 1099, 1105
 Water treatment 7, 152, 666, 1109, 2274
 Wave filters 1409
 Waveguides 1424
 Wavellite 1085
 Weak acid problem 1147
 Weak acid recovery 1148
 Welding 668
 Welding electrodes 1346
 Welding of titanium 1168
 Weloganite 1434
 Whisker formation 50
 White alloy 930
 White antimony 838
 White arsenic 795
 White cast iron 1, 342
 White copper 716
 White gold alloys 1205
 White metal 518
 Wiberg–Söderfors process 110
 Wickenol 1116
 Widmanstätten structure 31, 274
 Wiedemann–Franz–Lorenz law 375
 Willemite 645, 660
 Williamson ether synthesis 2068
 Willow blue 944
 Winkler gasifiers 214
 Wiser's model of coal structure 224
 Wismut 845

Wittig reaction 2068
 Wodginite 1419
 Wöhler's reduction of AlCl_3 by Na 406
 Wohlwill electrolytic refining 1196
 Wolfram, see *Tungsten*
 Wolframite 33, 462, 1329, 1334, 1336
 Wollastonite 1916
 Wood charcoal 31
 Wood industry 1772
 Wood preservatives 149, 666, 817
 Wood's alloy 875
 WORCRA process 523
 World market for scrap 387
 Wrought iron 1
 Wulfenite 1363
 Wullenite 584
 Wurtz synthesis 2059, 2068
 Wurtzite structure 671, 884
 Wurzite 644
 Wustite 166

X

Xanthates 1254
 Xanthine oxidase 1376
 Xenon short arc lamps 1346
 Xenotime 1697, 1708, 1724
 Xerography 1564
 X-ray anodes 1374
 X-ray films 1223
 X-ray screens 12
 X-ray tubes 9
 Xylolith 1024

Y

Yellow α -FeOOH 175
 Yellow antimony 823
 Yellow cake 1612, 1616
 Yellow iron oxide production 174
 Yellow mercury(II) iodide 913
 Ytterbium 12
 Ytterbium earths 1695
 Yttrium earths 1698
 Yttrium orthoaluminate 1734
 Yttrium oxide separation 1722
 Yttrium tantalate 1424
 Yttrotantalite 1419

Z

Zadra process 1193
 Zaffre 924
 Zementquarzit 1912
 Zeolite structure 1075
 Zeolites 2213

- Ziegler process 1097, 1099
 Ziegler-Natta catalysts 1466
 Ziervogel process 1218, 1231, 1232
 Zinc 5, 18, 641
 by retort process 649
 coating 355
 coating on steel 661
 dross 670
 dust 657, 662, 663, 679
 electrowinning 653
 fumes 668
 hydrometallurgy 652
 production in shaft furnace 650
 recovery rotary kilns 594
 refining 652
 soaps 665
 spray condenser 649
 Zinc antimonide 837
 Zinc blende 644
 Zinc borates 2018
 Zinc bromide 665
 Zinc bromide batteries 665
 Zinc carbonate 663
 Zinc chloride 664, 667
 Zinc chromate 667, 668, 1791, 1806
 Zinc cyanamide 667, 678
 Zinc cyanide 665
 Zinc ferrite 653
 Zinc ferrite pigment 679
 Zinc fluoride 663
 Zinc hydroxide 663
 Zinc hydroxyphosphite 678
 Zinc iodide 665
 Zinc oxide 662, 673
 Zinc oxide fume 668
 Zinc oxide in the rubber industry 676
 Zinc phosphate 144, 677
 Zinc phosphides 667, 668
 Zinc potassium chromate 1806
 Zinc protoporphyrin 626
 Zinc pyrithione 666
 Zinc stearate 662
 Zinc sulfate 666
 Zinc sulfide 10, 24, 673
 by hydrothermal process 671
 Zinc sulfide pigments 667, 668
 Zinc tetraoxycromate 1806
 Zinc thiocarbonate 662
 Zinc vapor deposition 358
 Zinc white 673
 Zincates 674
 Zinc-based chemicals 662
 Zincite 645
 Zinc-manganese dioxide batteries 898
 Zinc-mercury(II) oxide batteries 898
 Zinkchromat 1806
 Zinktetraoxichromat 1806
 Zinnwaldite 2030, 2033
 Zircaloy 1432, 1677
 Zircon 101, 405, 1138, 1434, 1444, 1445, 1460, 1656
 carbiding 1437
 carbochlorination 1435
 fluorosilicate fusion 1436
 lime fusion 1437
 thermal dissociation 1435, 1462
 Zircon sand 10
 Zirconia ceramics 1446
 Zirconium 1000
 clusters 1449
 electrorefining 1440
 electrowinning 1440
 fires 1442
 foil 1444
 powder 1442
 separation 1462
 sponge 1441
 Zirconium alkoxides 1453
 Zirconium basic carbonate 1450
 Zirconium basic sulfates 1450
 Zirconium borides 1452
 Zirconium carbide 1447, 1451
 Zirconium carbonate 1450
 Zirconium carbonitride 1437
 Zirconium dioxide 1434
 Zirconium hexafluorogermanate 1450
 Zirconium hydride 1450, 1455
 Zirconium hydroxide carboxylates 1453
 Zirconium hydroxide chloride 1448, 1450
 Zirconium monobromide hydride 1449
 Zirconium nitrate 1455
 Zirconium nitride 1451
 Zirconium orthosilicates 1434
 Zirconium oxide 1440, 1446
 Zirconium phosphate 1452
 Zirconium silicate 1445
 Zirconium sulfates 1450, 1455
 Zirconium tetrabromide 1449
 Zirconium tetrachloride 1447, 1455, 1463
 Zirconium tetrafluoride 1449
 Zirconium tetraiodide 1449
 Zirconium tetranitrate 1453
 Zirconium tungstate 1452
 Zirconolite 1434
 Zirconsilicates 1434
 Zone melting 836, 837, 857, 966, 1547, 2156